UNIVERSITY OF ILLINOIS AT
CHICAGO CIRCLE
801 SO. MORGAN
CHICAGO, IL. 60607



Digitized by the Internet Archive
in 2025

https://archive.org/details/physics-abstracts_1977-1980_80-83_cumulative-indexsof-z

S3
V. 80-83
1977-80
SUB.
INDEX
SOF-Z
N/C
Sci

Physics Abstracts

Volumes 80-83 1977-1980

Cumulative Subject Index

Sof—Z

28 July 1982

inspec
The Institution of Electrical Engineers

© 1981 The Institution of Electrical Engineers

CUMULATIVE SUBJECT INDEX 1977-80

Coverage

The present index provides a subject key to all papers abstracted in *Physics Abstracts* for the years 1977–80. It therefore comprises all relevant entries included in the six monthly subject indexes for the same period.

Subject Headings

In the course of the four years covered by this index the list of subject headings has been revised and new headings have been added. The present index uses the latest (i.e. 1980) version of the list. Entries for articles abstracted in the 1977, 1978 and 1979 volumes have been examined and, where appropriate, re-indexed under the new headings.

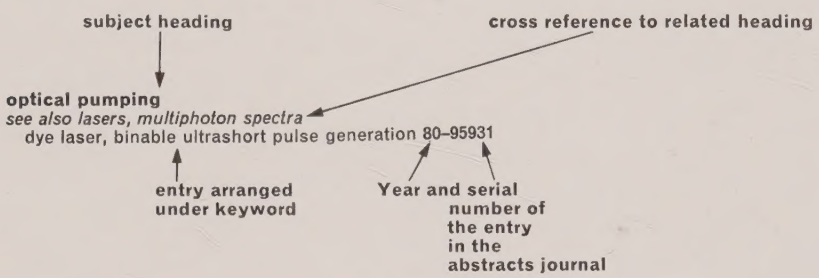
Arrangement

The subject headings are arranged in alphabetical order. The entries under each are prepared so that the most significant or 'key' words appear first and thus determine the position and grouping of entries in the alphabetical sequence under each heading.

Where the names of specific inorganic substances are significant under a given heading, the entries relating to them are found as a second alphabetical listing arranged by the chemical formulae of the particular elements or compounds.

Form of entry

The information contained in the subject index may be illustrated by an example.



How to use the index

The Subject index provides an alphabetical subject key to the articles included in the abstracts journal. Some general guidance on its use is given below:

1. Look in the index for the name of the specific subject in which you are interested. In most cases this name will be a heading in the index and you will find relevant articles listed under it. The majority of the subject headings fall into the following categories: property, phenomena, substance or named objects, instrument, device, theory, method, process, application, event.
2. Occasionally you will be directed from the subject heading chosen to a different heading under which the relevant or additional articles are listed.
3. If you do not find the subject heading you first chose, try a more general heading.
4. Each entry under the heading relates to an article appearing in the abstracts journal and gives the serial number of that article in the journal preceded by the last two digits of the current year, e.g. 78–12345; i.e. Abstract number 12345 in the abstracts journal for 1978.

   The language of the article, if it is not in English, is also indicated, e.g. optical fibre, three-wave stimulated Raman scattering (French) 0–78902.

   Each entry starts with a Keyword or Keyphrase considered to be most relevant to the heading. On sorting these Keywords, the qualifying prefixes are usually ignored (e.g. n-Ge is sorted under Ge).

   There are three main keyword lists; arabic numerals, alphabetical A–Z, and chemical symbols (organic substances are written and not given as chemical formula). More than one Keyword list may be present under each subject heading.

   For document on, say 'photoemission of silicon' at least two access points 'photoemission' and 'elemental semiconductors' are provided. Under the heading 'photoemission' the Keyword will be 'Si' and under 'elemental semiconductors' the Keyword will also be 'Si'.

   In a case like this, it is advisable and quicker to use the heading 'photoemission' and go straight to the chemical symbol list for 'Si' because there are few entries listed under 'photoemission'.

Printed by Unwin Brothers Limited, The Gresham Press, Old Woking, Surrey

Abbreviations and Acronyms

Abbreviations and acronyms are used in the modifiers in all INSPEC Cumulative Subject Indexes. Individual terms should be readily understood in the context of the subject headings. **Inorganic substances** are usually given by their chemical formulae. Iron and aluminium garnets appear in the formulae lists as MIG and MAG (where M is metal element, e.g. YIG and YAG); $(Pb,La)(Zr,Ti)O_3$ and $Ce_2Mg_3(NO_3)_{12}$ appear as PLZT and CMN respectively. **Organic substances** including **liquid crystals** are not given as formulae but common abbreviations are used.

ABS resin	acrylonitrile-butadiene-styrene
AC	alternating current
ACV	air cushion vehicle
A/D	analogue-to-digital
ADP	administrative data processing
AES	Auger electron spectra(oscopy)
AF	audio frequency
AFC	automatic frequency control
AFL	abstract family of languages
AGC	automatic gain control
AGR	advanced gas-cooled reactor
AM	amplitude modulation
ANS	Astronomical Netherlands Satellite
APACHE	accelerator for physics and chemistry of heavy elements
APR	acoustic paramagnetic resonance
APS	appearance potential spectra(oscopy)
APW	augmented plane wave
ATR	attenuated total reflection
ATS	applications technology satellite
ATWS	anticipated transients without scram
AVC	automatic volume control
BARITT	barrier injection transit time
BBEA	4-butoxybenzal-4'-ethylaniline
BCC	body centred cubic
BCD	binary-code decimal
BFO	beat-frequency oscillator
BWO	backward wave oscillator
BWR	boiling water reactor
BWT	backward wave tube
CAD	computer aided design
CAI	computer assisted instruction
CARS	coherent antiStokes Raman scattering (spectra)
CATV	community antenna TV
CB	citizen band
CBOOA	cyanobenzylidene octyloxyaniline
C-CD	charge-coupled device
CDI	collector diffusion isolation
CDM	code division multiplexing
CDW	charge-density wave
CEM	channel electron multiplier
CEPA	coupled-electron pair approximation
CERN	Conseil Européen pour la Recherche Nucléaire
CESR	conduction electron spin resonance
CGTO	contracted Gaussian-type orbital
CHF	coupled Hartree-Fock
CI	configuration interaction
CIEH	charge iterated extended Huckel
CIHY	configuration interaction Hylleras
CNDO	complete neglect of differential overlap
COC	cholesteryl oleyl carbonate
COM	computer output to microform (fiche or film)
COOB	4,4'-cyano-octyloxy-biphenyl
CP	charge, parity
CPA	coherent potential approximation
CPSK	coherent phase shift keying
CPT	charge, parity, time
CRO	cathode ray oscilloscope
CRT	cathode ray tube
CS	coupled states
CSM	continuous slowing down models
CTR	controlled thermonuclear reactor
CVD	chemical vapour deposition
CW	continuous wave
D/A	digital-to-analogue
DBR	distributed Bragg reflector
DC	direct current
DDC	direct digital control
DDL	diode-diode logic
DECENT	distribution of exact classical energy transfer
DESY	Deutsches Electron Synchrotron
DF	Dirac-Fock
DFB	distributed feedback
DH	double heterostructure
DIL	dual-in-line
DITE	divertor in torus experiment
DLTS	deep level transient spectra(oscopy)
DM	delta modulation
DMSO	dimethyl sulphoxide
DMSS	Defence Meteorological Satellite System
DOBAMBC	p-decyloxybenzylidene p'-amino 2-methyl butyl cinnamate
DODS	different orbitals for different spins
DORIS	Dopple-ring-Speicher
DOVETT	double velocity transit time
DP	data processing
DPCM	differential pulse code modulation
DPPH	diphenylpicrylhydrazyl
DPSK	differential phase shift keying
DSC	differential scanning calorimetry
DTA	differential thermal analysis
DV-Xα	discrete variational Xα method
E1,E2	electric dipole, quadrupole
EAS	extensive air shower
EB	exponential Born
EBBA	4-ethoxybenzylidene-4'n-butylaniline
EBR	experimental breeder reactor
EBT	Elmo Bumpy Torus
ECC	emergency core cooling
ECELR	epithermal critical experiment laboratory reactor
ECG	electrocardiography (-gram)
EDA	ethylene diamine
EDP	electronic data processing
EDTA	ethylene diamine tetra-acetic acid
EEBAC	ethyl-4-(4'ethoxy-benzylidene-amino) cinnamate
EEG	electroencephalography (-gram)
EELS	electron energy loss spectra
EFM	extended Flygare method
EHD	electrohydrodynamics
EHF	extremely high frequency
EHP	electron-hole potential method
EHT	extended Huckel theory
EHV	extra high voltage
ELDOR	electron electron double resonance

ELF	extremely low frequency
EM	electromagnetic
EMC	electromagnetic compatibility
EMF	electromotive force
EMG	electromyography(-gram)
ENDOR	electron nuclear double resonance
EOS	earth observatory satellite
EPEN	empirical potential energy function based on interactions of electrons and nuclei
EPMA	electron probe microanalysis
EPR	electron paramagnetic resonance
ERG	electroretinography(-gram)
ERPS	extramolecular relaxation polarisation shift
ERTS	earth resources technology satellite
ESCA	electron spectroscopy for chemical analysis
ESCAR	experimental superconducting accelerating ring
ESFI	epitaxial silicon film on insulator
ESS	electronic switching system
EUV	extreme ultraviolet
EXAFS	extended X-ray absorption fine structure
FBR	fast breeder reactor
FCC	face centred cubic
FDM	frequency division multiplex(ing)
FDNC	frequency dependent negative conductance
FDNR	frequency dependent negative resistance
FEM	field emission microscopy
FET	field effect transistor
FFHR	fusion-fission hybrid reactor
FFT	fast Fourier transform
FFTF	fast flux test facilities
FIM	field ion microscopy
FM	frequency modulation
FPT	finite perturbation theory
FSK	frequency-shift keying
FSGO	floating spherical Gaussian orbitals
FTR	fast test reactor
GAMBIT	gate modulated bipolar transistor
GANIL	grand accelerateur national a ions Lourds
GARP	global atmospheric research programme
GATE	GARP Atlantic tropical experiment
GCFR	gas-cooled fast breeder reactor
GCM	generator coordinate method
GHF-NO-CI	generalised Hartree-Fock/natural orbital/ configuration interactions
GIAO	gauge-invariant atomic orbitals
GO	Gaussian orbitals
GOO	generalised Overhauser orbitals
GPM	ground potential model
GSO	general spin orbitals
GTO	Gaussian-type orbitals
GVB	generalised valence bond
HAM	hydrogenic atoms in molecules
HBAB	hexyloxybenzylidene-p' aminobenzonitrile
HBT	N-(p-hexyloxybenzylidene)-p-toluidene
HCDA	hypothetical core disruptive accident
HCP	hexagonal close packed
HEED	high energy electron diffraction
HF	high frequency or Hartree-Fock
HFB	Hartree-Fock-Bogoliubov
HFER	hot fuel examination facility
HFIR	high flux isotope reactor
HFO	Hartree-Fock-Overhauser
HFS	hyperfine structure
HLW	high level waste (radioactive)
HMO	Huckel molecular orbitals
HOAB	heptyloxyazoxybenzene
HOBHA	p-n-heptyloxy-benzylidene-p-n heptylaniline
HOMO	highest occupied molecular orbitals
HORM	hybrid orbital rehybridisation method
HTGR	high temperature gas-cooled reactor
HV	high voltage
HVEM	high voltage electron microscopy
HWR	heavy water reactor
IAEA	International Atomic Energy Authority Agency
IBPBAC	isobutyl-4-(4'-phenylbenzylideneamino) cinnamate
IC	integrated circuit
ICDF	intermediate coupling Dirac-Fock
IDT	interdigital transducer
IEPA	independent electron pair approximation
IF	intermediate frequency
IGFET	insulated gate field effect transistor
IKO	Institute v. Kernph Ouder Amsterdam
I^2L	integrated injection logic
I^3L	isoplanar I^2L
ILS	instrument landing system
IMPATT	impact avalanche transit time
INDO	intermediate neglect of differential overlap
INDOR	internuclear double resonance
ING	intense neutron generator
INO	iterative natural orbital
INTELSAT	international telecommunications satellite consortium
I/O	input/output
IOC-ω	inclusion of the overlap charges in the omega
IR	infrared
IRDO	intermediate retention of differential overlap
ISABELLE	intersecting storage and acceleration
ISR	intersecting storage ring
ISX	impurity study experiment
ITEP	Institute of Theoretical and Experimental Physics
IU	Indiana University
IVO	improved virtual orbitals
JET	Joint European torus
JAERI	Japan Atomic Energy Research Institute
JINR	Joint Institute for Nucjear Research
KEK	Japan National Laboratory for High Energy Physics
KKR	Korringa-Kohn-Rostoker
LAMPF	Los Alamos meson physics facility
LC	inductance-capacitance
LCAO	linear combination of atomic orbitals
LCBO	linear combinations of (semi-localised) band orbitals
LCGO	linear combination of Gaussian orbitals
LCP	large coil program
LCRO	linear combination of Rydberg orbitals
LEC	liquid encapsulated Czochralski
LED	light emitting diode
LEED	low energy electron diffraction
LEP	large electron positron
LET	linear energy transfer
LF	low frequency
LMC	Large Magellanic Cloud
LMFBR	liquid metal fast breeder reactor
LMTO	linear combination of muffin tin orbitals
LOCA	loss of coolant accident
LOCE	loss of coolant experiment
LOFT	loss of flow test facility
LPE	liquid phase epitaxy
LSA	limited space charge accumulation

LSD	local spin density
LSI	large-scale integration
LTE	local thermodynamic equilibrium
LUMO	lowest unoccupied molecular orbitals
LV	low voltage
LWR	light water reactor
MADO	Mulliken approximation for differential overlap
M1,M2	magnetic dipole, quadrupole
MBBA	4-methoxybenzylidene-4'-n-butyl-aniline
MBE	molecular beam epitaxy
MBPT	many body perturbation theory
MCD	magnetic circular dichroism
MCPESCF	multiconfiguration paired excitation SCF
MCZDO	multi-centre zero differential overlap
MEDO	multipole expansion of diatomic overlap
MESFET	metal-semiconductor field effect transistor
MF	medium frequency
MFP	mean free path
MHD	magnetohydrodynamics
MIC	microwave integrated circuit
MIEHM	modified iterative extended Huckel method
MIM	metal-insulator-metal
MIS	metal-insulator-semiconductor or management information system
MIT	Massachusetts Institute of Technology
MMF	magnetomotive force
MNOS	metal-nitride-oxide-semiconductor
MO	molecular orbitals
MOCIC	molecular orbital constraint of interaction coordinates
MODPOT	model potential
MOS	metal-oxide-semiconductor
MOSFET	metal-oxide-semiconductor field effect transistor
MOST	metal-oxide-semiconductor transistor
MRD	multi-reference double excitation
MRINDO	modified Rydberg iNDO
MSI	medium scale integration
MSR	molten salt reactor
MSU	Michigan State University
MTBF	mean-time between failures
MTF	modulation transfer function
MTXα	muffin-tin Xα
MUF	maximum usable frequency
MWH	Mulliken-Wolfsberg-Helmholz-semi-empirical method
NAL	National Accelerator Laboratory
NAND	not-and(logic)
NC	numerical control
NCMET	non-closed shell many electron theory
NDDO	neglect of diatomic differential overlap
NDT	nondestructive testing
NEMO	non-empirical molecular orbitals
NEVE	non-empirical valence electron
NIC	negative impedance convertor
NMR	nuclear magnetic resonance
NNNDO	neglect of non-neighbour differential overlap
NOR	not-or(logic)
NPOST	non-perturbative open-shell theory
NPSO	non-paired spatial orbitals
NQR	nuclear quadrupole resonance
NRC	nuclear regulatory committee
NRM	natural remanent magnetisation
NTO	natural transition orbitals
OAO	orbiting astronomical observatory
OCR	optical character recognition
ODMR	optical detection of magnetic resonance
OER	oxygen enhancement ratio
OGO	orbiting geophysical observatory
OPHF	orbital polarised Hartree-Fock
OPW	orthogonal plane wave
OR	operations research
ORELA	Oak Ridge electron linear accelerator
ORNL	Oak Ridge National Laboratory
OSO	orbiting solar observatory
OTF	optical transfer function
PAA	paraazoxyanisole
PABX	private automatic branch exchange
PAC	perturbed angular correlation
PAHR	post accident heat removal
PAM	pulse amplitude modulation
PAMPUS	photons for atomic and molecular processes and universal studies
PAP	paraazoxyphenetole
PBF	power bursts facility
PBR	pebble bed reactor
PBX	private branch exchange
PC	printed circuit
PCAC	partially conserved axial currents
PCB	printed circuit board
PCGVB	pairwise correlated generalised valence bond
PCILOCC	perturbative configuration interaction using localised orbitals for crystal calculation
PCM	pulse code modulation
PCX	plasma confinement experiment
PDX	poloidal divertor experiment
PEP	positron electron proton
PETRA	positron electron tandem ringbeschle-uniger anlage
PF	power factor
PFM	pulse frequency modulation
PHWR	pressurised heavy water reactor
PID(PI,PD)	proportional+integral+differential (derivative)
PLA	phase locked arrays
PLC	programmable logic control
PLL	phase locked loops
PLT	Princeton Large Torus
PM	pulse modulation
PMMA	polmethylmethacrylate
PMDR	phosphorescence microwave double resonance
PNDO	partial neglect of differential overlap
PNO-CI	pair natural orbital configuration interaction
POL	pair orthogonalised Lowdin
POPAE	protons on protons and electrons
POPOP	phenyl-oxazolyl-phenyl-oxazolyl-phenyl
POS	point of sale
PPDP/S	Pariser-Parr-Del Bene-Pople/Segal calculations
PPI	plan position indicator
PPM	pulse position modulation or parts per million
PPP	Pariser-Parr-Pople
PRDDO	partial retention of diatomic differential overlap
PRF	pulse recurrence (repetition) frequency
PROM	programmable read-only-memory or Pockels readout optical modulator
PS	proton synchrotron (CERN)
PSK	phase shift keying
PTFE	polytetrafluoroethylene
PTM	pulse time modulation
PVC	polyvinyl chloride
PWM	pulse width modulation
PWR	pressurised water reactor

QCD	quantum chromodynamics
QDMBPT	quasi-degenerate many body perturbation theory
QED	quantum electrodynamics
QPSK	quaternary phase shift keying
RAM	random access memory
RBE	relative biological effectiveness
RC	resistance-capacitance
RCNDO	Rydberg CNDO
R & D	research and development
RF	radio frequency
RFI	radio frequency interference
RHEED	reflection high energy electron diffraction
RINDO	Rydberg INDO
RKKY	Rudermann-Kittel Kasuya-Yosida
RLC	resistance-inductance-capacitance
RMS	root-mean-square
ROM	read-only memory
RPA	random phase approximation
RPM	relaxation potential model
SAMO	simulated ab initio molecular orbitals
SAS	small astronomy satellite
SAW	surface acoustic waves
SCF	self consistent field
SCL	space charge limited
SCPT	self consistent perturbation theory
SCR	silicon controlled rectifier
SDM	space division multiplexing
SDO	shielded diatomic orbitals
SEHF	spin extended Hartree-Fock
SEM	scanning electron microscope
SFE	solar-flare effect
SGHWR	steam generating heavy water reactor
SHF	superhigh frequency
SHG	second harmonic generation
SIMS	secondary ion mass spectrometer
SIN	Swiss Institute of Nuclear Research
SINDO	scaled INDO
SISAM	spectrometer with interference selective amplitude modulation
SMC	Small Magellanic Cloud
SMS	synchronous meteorological satellite
S/N	signal-to-noise
SOG	strongly orthogonal geminal
SOS	silicon on sapphire
SPA	separated pair approximation
SPC	stored program control
SPEAR	Stanford positron electron asymmetric ring
SPHF	spin polarised Hartree-Fock
SPIN-CIPSI	spin symmetry adapted generalisation of CIPSI
SPS	super proton synchroton (CERN)
SQUID	superconducting quantum interference device
SRMCASE	symmetry-restricted-multiconfiguration annihiliation of single excitations
SSB	single sideband
SSC	sudden storm commencement
SSI	supersonic transport
STD	salinity-temperature-depth or subscriber trunk dialling
STEM	scanning transmission electron microscopy
STO	Slater-type orbitals
STOL	short take-off and landing
STP	Slater-transfer Preuss
SUHFC	spin unrestricted Hartree-Fock with local approximation for correlations
SW	short wave
SWR	standing wave ratio
SXAPS	soft X-ray appearance potential spectrum
TBBA	terephthal-butylaniline
TCNE	tetracyanoethylene
TCNQ	tetracyanoquinodimethane
TCR	temperature coefficient of resistance
TDHF	time dependent Hartree-Fock
TDM	time division multiplex(ing)
TDMA	time division multiple access
TDPAC	time differential perturbed angular correlation
TE	transverse electric
TEA	transversely excited atmospheric
TEM	transverse electromagnetic or transmission electron microscopy
TEXT	Texas Experimental Tokamak
TFTR	Tokamak fusion test reactor
TGFB	triglycine fluoroberyllate
TGS	triglycine sulphate
TGSe	triglycine selenate
TJS	transverse junction stripe
TLD	thermoluminescent dosimeter(-ry)
TM	transverse magnetic
TMMC	tetramethylammonium manganese chloride
TOP	transient overpower accident
TNS	The next step
TRAPATT	trapped plasma avalanche triggered transit
TREAT	transient reactor test facility
TRM	thermoremanent magnetisation
TSC	thermally stimulated currents
TSEE	thermally stimulated exo-electron emission
TTF	tetrathiofulvalinium
TTL	transistor transistor logic
TTT	tetrathiotetracene
TUCA	transient undercooling accident
TV	television
TW	travelling wave
TWT	travelling wave tube
UCHF	uncoupled Hartree-Fock
UHF	ultra high frequency unrestricted Hartree-Fock
UHV	ultra high voltage
UKAEA	United Kingdom Atomic Energy Authority
ULF	ultra low frequency
UMD	unitised microwave devices
UPS	ultraviolet photoelectron spectra
US	ultrasonic
UV	ultraviolet
VB	valence bond
VCR	video cassette recorder
VDM	vector dominance model
VDU	visual display unit
VHF	very high frequency
VLBI	very long base line interferometry
VLF	very low frequency
VLSI	very large scale integration
VOR	VHF omnidirectional range
VPE	vapour phase epitaxy
VRC	visual record computer
VRDDO	variable retention of diatomic differential
VSB	vestigial sideband
VSEPR	valence shell electron pair repulsion
VSWR	voltage standing wave ratio
VTOL	vertical take-off and landing
VTR	voltage transformation ratio or video tape recorder
VUV	vacuum ultraviolet
VVER	water moderated water cooled reactors
WWER	water moderated water cooled reactors
XPS	X-ray photoelectron spectra
ZEBRA	zero energy breeder reactor assembly
ZGS	zero gradient synchrotron
ZPPR	zero power plutonium reactor

soft modes continued
biphenyl, second order phase transition at 40K, Raman spectral obs. 77−32361
bis(p-toluene sulphonate)diacetylene, monomer and polymer, solid state phase transformation, far IR transmission spectra obs. 80−55077
Bloch wall, narrow, magnetic excitations, pole field effect 78−91853
catastrophe indices rel. to thermodynamic pot. function isotropy 78−14431
CDW instabilities, incommensurate struct. phase transitions, neutron scatt. study, review 79−51231
centre with close electronic levels, temp. effects 79−37804
chaotic states of anharmonic systems in periodic fields 80−22288
chloranil, mol. cryst., soft mode and central peak neutron scatt., struct. transition 79−42209
chloranil, neutron superlattice reflection, soft phonon and central peak scatt., phase transition 78−18732
chloranil, phase transition, Zeeman effect of ^{35}Cl NQR 78−59944
classical Ising model, crit. dynamics simulation in transverse field 78−59930
classification of struct. transforms., using coupled double-well model 78−14443
cluster phenomena, displacive to order disorder crossover 80−10629
coated semiconductor spheres, surface modes, plasmon oscills. 80−54730
collective modes of CDW near lock in transition 78−30879
commensurate condensations, stirrability, unstirrability, group theoret. study 78−87759
condensation, ferroic space group in transition sequence *(Japanese)* 77−43300
coupled fields in one dimension: cross-over from a continuous symmetry to a discrete one 78−87758
coupled spin $^1/_2$ phonon system, existence of sharp transition 79−69204
cubic crystal, Jahn-Teller effect, soft mode influence 80−59937
current instability, hydrodynamic modes, soft modes and fluctuation spectra 79−65491
D_{2d} crystals, structural phase transitions, soft modes, group theory 80−92638
defect structure near phase transition pt., effect on solid props. *(Russian)* 79−37838
di(methylammonium) manganese tetrachloride, LF Raman spectra and phase transitions 77−63414
dialkylammonium metal chlorides, soft modes, phase transitions 78−79723
diamantane, LF light scattering temp. depend., 40 to 340K 79−24307
diamantane, low temp. soft librational mode, Raman spectra exam. 78−30730
diamantane, Raman study of three solid-state phase transition 79−51946
diatomic linear chain, ferroelec. soft modes 80−70353
dielectric singularity, causing Kohn anomaly and soft modes 79−60470
dimethylammonium cadmium chloride, soft modes, order-disorder transition model 78−22817
dipole pseudo-spin glasses, collective excitations 80−59617
dislocation-soft mode interaction in displacive transitions *(Russian)* 80−84172
disordered systems, mode softened unified theory 79−55637
displacive phase transition, second-order, discontinuous freezing-out of local order 79−42204
displacive phase transitions, localised modes, central peak, influence of defects 78−83905
displacive phase transitions, microscopic 1/n expansion for crit. dynamics and hydrodynamics 77−76518
displacive phase transitions, role of competing forces 77−80599
displacive phase transitions in surface layers, surface phonons 79−65167
displacive transformation, defect cell and neutron scatt. central peak 77−15531
displacive transformation, dynamic critical exponents, microscopic calc. 78−10163
displacive transformation, dynamics, 1/n expansions 77−15530
displacive transformations, single defect behaviour models 78−83904
distortive phase transitions, order-disorder and displacive regimes, mol. dynamics study 80−75324
DNA, conformation changes, soft modes 77−29097
DOBAMBC, dielec. dispersion at ferroelec. smectic A-smectic C transition 79−91385
DOBAMBC, dielec. props. near ferroelec. smectic A to C transition 80−45015
doped displacive ferroelectrics, sound attenuation constant, Green's function technique 79−11397
doped narrow gap semiconductor, two-channel vibronic mechanism of ferroelectric phase transitions *(Russian)* 79−56745
elastic constants, single crystals, rel. to vibr. behavior, supercond. 78−10114
elastic phase transitions, crit. behaviour 78−79722
elastic phase transitions, crit. dynamics 80−2146
elastic phase transitions, order parameter and mode softening 80−75325
electron spin-lattice relaxation, role of soft phonon modes 79−28590
electronically driven lattice instabilities, role of p-d hybridisation 78−63835
f-band metals, mode softening and lattice instability under press. 77−51833
ferrodistortive materials, dynamics of domain walls, theory 79−73282
ferroelastic, dislocation-phonon interactions, phase transition effects 80−59600
ferroelectric, displacive, inelastic neutron scatt. cross section 77−36187
ferroelectric, H-bonded, soft and central modes, mag. reson., review 78−15108
ferroelectric, ion-ion interaction due to soft phonon modes 79−99838
ferroelectric, $KTa_{1-x}Nb_xO_3$-type, dispersion of permittivity near N-phase point 79−24276
ferroelectric, low lying vibrational modes, crit. behaviour of uniaxial materials 78−84539
ferroelectric, order-disorder, longitudinal phonon relax. *(Russian)* 79−55860
ferroelectric, photoinduced changes in refractive index and spontaneous polarisation 78−43804
ferroelectric, uniaxial, electrostrictive interaction, mode damping 80−34862
ferroelectric ferromagnet, soft modes and ferromag. reson. 80−11275
ferroelectric liquid crystal, soft modes 79−55653
ferroelectric liquid crystals, soft mode dynamics 77−7852
ferroelectric materials, H-bonded, coherent crit. neutron scatt. 79−56742
soft modes continued
ferroelectric semiconductor, electronic density of states, effect of soft phonon-electric interaction *(Russian)* 77−80718
ferroelectric semiconductor, impurity carrier effects, vibronic theory 78−43803
ferroelectric semiconductor, magnetic field influence, ferroelectric transitions 80−55049
ferroelectric semiconductor, phase transition temp., rel. to free carrier conc. 78−10860
ferroelectric semiconductor, vibronic model, fluctuation effects 77−90113
ferroelectric semiconductors, vibronic, mag. field effect on phase transition 77−40193
ferroelectric with orientational transition, coupled elastic, EM and polarisation oscill. spectrum 79−8103
ferroelectrics, improper and incommensurate phase transitions, neutron scatt. studies 80−75974
ferroelectrics, incommensurate phase transitions 80−75964
ferroelectrics, one and two dimensional displacive types, phonon relaxation 78−87761
ferroelectrics, quantum transition suppression, pyroelectric, electrocaloric effects, specific heat 80−75984
ferroelectrics, sp. ht. calc., soft mode contrib., near T_c 78−64338
ferroelectrics, temp. depend. of soft mode freq. and its damping 79−38484
ferroelectrics, vibronic, band struct. temp. depend. 80−70598
ferroelectrics and antiferroelectrics, polaron state of electron near structural instability 79−33245
ferroic phase, commensurate, form. from prototypic phase, possibility of transition being second order 78−2223
ferroic phase, second-order transition between prototypic and commensurate, thermal behaviour of soft modes 77−85662
ferroic systems, protytype temp. setting rel. to soft modes 78−63833
ferromagnetic ferroelectric, soft mode damping, temp. anomalies *(Russian)* 80−44284
ferromagnetic thin films, influence fo surface-rearrangement on soft modes 79−69702
fine particles, crystalline, freq. spectrum 79−4376
first order displacive transformations, localized soft modes and US effects 79−73281
glass, dielectric instabilities in high permittivity glass 78−52433
graphite, intercalation compound, C_8Rb, elastic and inelastic neutron scatt. 78−30597
graphite intercalation compounds with K and Cs, sp. ht., XPS 78−26693
Gruneisen parameter and eqn. of state determ. at press. induced phase transition 80−90031
helicoidal ferroelectric smectic A-smectic C phase transition, low freq. polarisation fluctuation spectrum 79−95714
heterophone sequences of transitions 77−27967
hydrogen-bonded ferroelectric, Ising model in transverse tunnelling field and proton-lattice interaction 80−7307
impurities, interaction and diffusion, near structural phase transition of matrix 79−42083
incipient ferroelectrics, mode-mode coupling 79−38464
incommensurate phase transition, equivalent directions of modulation, unmodulated soft modes 79−24271
incommensurate phase transitions, exptl. studies of soft phonons 78−75798
incommensurate structural phase transformations, recent neutron scatt. studies, review 79−42205
incommensurate structure, IR and Raman activity of soft modes, appl. to K_2SeO_4 79−28738
incommensurate-commensurate phase transition, model 78−87760
inducing soft mode transitions by IR or lower freq. EM radiation 78−7421
Invar, ferromagnetic, lattice dynamics 79−55838
Invar, influence of magnetoelastic effects on lattice vibrs., neutron scatt. meas. 78−2722
Ising model, transverse field dynamic behaviour 78−22814
Ising model with transverse field, phonon relax., soft mode and central peak roles 80−59615
Ising systems, compressible, elastic anomalies inducing first order transitions 79−47288
isotopically disordered ferroelectric cryst., thermal cond. 77−76628
IV-VI compounds, mag.-field-induced displacive phase transition 80−50278
IV-VI compounds, phase transitions induced by electron-phonon interaction 80−10656
IV-VI compounds, structural instabilities and transverse effective charges 77−27999
IV-VI semiconductors, structural phase transitions, anomalous resist., electron-soft phonon interactions 80−108167
Jahn-Teller effect, soft mode 79−69221
laser light scatt. spectroscopy, phase transitions 78−10156
lattice dynamical system, displactive structural transition anal., mol. dynamics calc. 79−86865
lattice instabilities in coupled pseudospin-phonon systems 78−10157
Lindemann's criterion and necessary condition for melting curve maximum 80−2145
lineal phase transitions, orders of 79−42206
liquid crystal, ferroelec., helicoidal, smectic-C, dynamics 79−1396
lithium ammonium tartrate monohydrate, in paraelec. phase, Brillouin scatt. 78−64373
lithium ammonium tartrate monohydrate, struct. phase transitions, light scatt. meas. 79−95774
locally distorted impurity dynamics in host lattice with displacive phase transition 80−34159
low lying lattice vibrational modes, conf., San Juan, Puerto Rico, (Dec 75) 78−10131
magnetic Debye crystal, with magnon-phonon coupling, crit. changes in vibr. modes 79−95094
magnetic ferroelectrics, mechanism of phonon relaxation *(Russian)* 79−90742
magnetic phase transitions 80−54889
malononitrile, cryst., phase transitions, Raman and IR obs. 80−88980
martensitic transformation, nonlinear mechanical model 78−87789
martensitic transformations, localised soft mode theory 78−10159
martensitic transformations, thermodynamic stability of structural states *(Russian)* 79−43246
metal, electron-phonon interaction effects on spin susceptibility 80−93108

soft modes continued
metal, quasi one dimensional, Peierls instability criterion *(Russian)* 77−89516
metallic fine particles, anharmonic lattice vibr. theory, Einstein model appl. 78−18714
mixed valence systems, phonons, effect of valence changes due to f⇄d electronic transitions 79−95104
molecular crystal, orientationally disordered, translation-rot. dynamics, soft modes 78−83906
molecular dynamics of structural phase transitions in two dimens. model 77−20038
Mossbauer radiation crit. scatt. in condensed matter 79−56635
nematic liquid crystal, coherent neutron diffr. 78−75550
neutron anomalous scatt., ferroelec. phase transitions 77−59539
$(NH_4)_2SO_4:Mn^{2+}$, ferroelec. phonon driven phase transform., reduction of spin Hamiltonian consts. 78−92033
nonstoichiometric materials, lattice instabilities, models 78−14442
one-dimensional conductor, incommensurate, IR absorpt. peak theory 77−43991
one-dimensional conductors, Peierls instability, dynamics, structural energy, pseudopot. calc. 80−54676
one-dimensional Hubbard model, antiferromag. and Peierls instability 78−23233
order parameter fluctuation spectrum, central peaks near ferroelectric phase transitions, review 79−19851
order-disorder ferroelectric, phonon damping and freq. shift *(Russian)* 79−60471
order-disorder ferroelectrics, transverse Ising models, dipolar interaction and crit. behaviour 77−81071
orthophosphates, dynamics of ferroactive cryst. 79−37801
PAA, methyl deuterated, soft-mode dynamics, proton NMR 78−79749
PAA, nonlinear soft mode at Rayleigh-Benard instability, neutron cond. spectrosc. obs. 80−79266
Peierls transition, interchain bandwidth effect at low temp. 78−10352
Peierls transition in quantizing mag. field, possibility 80−103441
periodically distorted crystals, phonon-type symmetry 77−39553
perovskites, ferroelectricity, nonlinear shell model 77−16300
perovskites, mechanisms of ferroelectric and structural phase transitions, structural distortions 79−15412
perovskites, struct. phase transitions, octahedral tilt systems 77−11655
phase transitions, obs. of crit. indices of primary and secondary order parameters using birefringence 77−28541
phase transitions soft modes and dipole relaxations 78−91409
phonon systems with quartic anharmonicity, microscopic theory of statics and dynamics 79−73260
polaronic crystals, central peak 78−47712
polyphenyls, inelastic neutron scatt. study of structural phase transitions 79−51255
pressure induced phase transitions, influence on Gruneisen parameter 79−1497
prevoskite, anisotropically-stressed, Lifshitz-point crit. and transcrit. behaviour 79−33061
pseudopsin system with dynamic long-range forces, Z-branch at phase transition 77−84887
quartz, α-β phase transition, lattice dynamical study 79−65168
quartz, incommensurate phase near $\alpha \rightleftarrows \beta$ transition pt. 79−90748
quartz, possible incommensurable phase near $\alpha \rightleftarrows \beta$ transition *(Russian)* 78−79768
quasielastic light scattering near phase transitions 80−93362
Raman spectrometer, digital control system, appl. to soft mode spectroscopy 78−86345
rare earth compounds, mixed valent, renormalisation of transversal phonons 79−90749
rare earth compounds, spinless periodic Anderson model with phonons, appl. to mixed valence systems 78−84153
rare earth intermetallics, RFe_2 and $R(Co_{0.98}\ Fe_{0.02})_2$, magnetostrictive material, changes in vibr. modes near mag. phase transition 79−90736
rare earth pentaphosphates, spectroscopy, ferroelastic/ferroelectric coupling, soft mode frequencies, phase diagram 79−19845
rare earth-Fe alloy, RFe_2 (R=Tb, Dy, Ho and Y) crit. phenomena, Mossbauer exam. 78−52403
rare gas (111) adsorbate-substrate systems, thermal expansion and stability, soft phonons 79−69352
Rochelle salt, ferroelec. phase transition, Raman scatt. study 80−97211
Rochelle salt, phase transition mechanisms by optical spectroscopy 79−15411
semiconductor, phonon spectrum in mag. field, renormalisation 79−28060
semiconductor thin films, ferroelectric properties, quantum size effect 80−97201
semiinfinite, effect of next nearest neighbour coupling 77−73014
soft, static and dynamic behaviour 77−72669
solids, disorder of NMR and soft collective lattice modes, spins and pseudospins 78−88208
soliton pinning and central peak theory 79−7668
spin system with weak exchange couplings, EPR spectrum 78−64258
spin-Peierls transition, dynamic struct. factor 78−14964
spontaneously modulated materials, Raman scatt. 79−95739
structural phase transforms. and phonons, book contrib. 77−89518
structural phase transition, computer simulation 79−77721
structural phase transition induced refractive index changes in crysts. 80−16000
structural phase transitions, crit. dynamics and quasi-elastic scatt. 80−92641
structural phase transitions, Landau theory 80−92639
structural phase transitions and anharmonic phonons 78−14433
structural phase transitions in crystals, effect of high-power visible and IR laser radiation 78−71825
structural phase transitions in crystals of D_{2d}^3 symm. 80−15986
structural transitions, dynamic aspects, nuclear quadrupole relax. studies 78−76344
structural transitions, method of self consistent phonon field 79−33065
structural transitions of antiferroelectric and displacive modulated type caused by electron-phonon interactions 78−43092
structurally incommensurate system, theory 78−79729
superconducting filament, current-carrying, mode softening near crit. current 77−72959
superconductor, high T_c, dynamic instabilities 78−10607
surface phonons and superstructures 77−62731
sym-triazine, Landau mean field description, second-order phase transition, soft modes 80−108434
soft modes continued
sym-trioxane, phase transition, polarised Raman spectra obs. 80−84742
TCNQ, lattice softening mechanism 80−6481
TCNQ-K, X-ray exam. of phase transitions 78−55933
TCNQ-Na, X-ray exam. of phase transitions 78−55933
TCNQ-Rb, X-ray exam. of phase transitions 78−55933
Teflon, bond charge model for vib. props. *(German)* 78−75781
temperature Green's function for tunnelling model, new contraction method 79−35635
tetragonal tungsten bronze structure ferroelec. mech. for ferroelec. transition 79−38481
TGS, characts. of dispersion of permittivity near phase transition 79−28695
thermal diffusion-soft mode coupling near struct. phase transition, hydrodynamical anal. 79−60468
thiourea, commensurate-incommensurate phase transition, X-ray diffuse scatt. meas. *(French)* 79−19856
thiourea, deuterated, commensurate-incommensurate phase transition, inelastic neutron scatt. 79−28098
thiourea, ferroelec., soft mode and Debye relax., IR reflection spectra 77−90111
thiourea, incommensurate phase, soft modes, condensation of even-order harmonics 80−103313
thiourea, incommensurate phase transition, X-ray and neutron scatt. study 80−75963
thiourea, IR reflectivity study of ferroelec. and antiferroelec. phases, dielec. function model 79−33686
thiourea, order-disorder transitions 78−80361
thiourea, phonon modes near phase transitions, IR and Raman spectra 80−45084
thiourea, Raman scattering spectra, soft mode frequency 79−24305
thiourea, Raman spectra of external frequencies 77−24840
thiourea, soft mode and Debye relaxations 78−80347
thiourea crystal, ferroelec., i.r. reflection spectra meas., shift of soft mode obs. *(French)* 77−4635
5d-transition metal antifluorite cryst., struct. props. and lattice dynamics, mag. struct. 80−44268
transition metal carbides, generalised susceptibilities, electronically driven phonon anomalies APW calcs. 79−42208
transition metal carbides, high temp. supercond., role of electronic struct. on obs. phonon anomalies 77−24363
transition metal carbides and nitrides, surface energy for brittle fracture from phonon frequencies 78−67790
transition metal compounds, electronically driven lattice instabilities, role of p-d hybridisation 79−7669
transition metal compounds, phonon anomalies rel. to superconductivity 77−12055
transition metal nitrides, lattice sp. ht. and phonon anomalies 78−63867
transition metal nitrides and carbides, surface energy for brittle fracture from phonon freqs., rel. to soft-mode induced supercond. 79−86837
transition metals, and their carbides high temp. superconductivity and phonon softening 78−14848
s-triazine, structural phase change, lattice energy calc. 78−55945
s-triazine, transverse elastic mode softening at structural phase transition 79−46777
tris-sarcosine calcium chloride:Mn^{2+} ferroelec. dynamics, EPR and ENDOR study 80−75972
tris-sarcosine calcium chloride, ferroelec. transitions, soft modes, Raman scatt. spectra obs. 80−80763
$TTF_{0.97}Se_{0.03}$-TCNQ, Peierls-superlattices and soft phonon anomalies, X-ray scatt. meas. 78−75795
TTF-TCNQ, band struct., soft phonon instability 77−72821
TTF-TCNQ, electronic props. and comparison with $(SN)_x$, review 78−6306
TTF-TCNQ, Kohn anomaly and Peierls-type transition, X-ray obs. 78−14435
TTF-TCNQ, neutron and X-ray diffuse scatt., phase transitions, one-dimens. behaviour and interpret. 78−10381
TTF-TCNQ, Peierls instability and consequences 78−6303
TTF-TCNQ, Peierls-superlattices and soft phonon anomalies, X-ray scatt. meas. 78−75795
TTF-TCNQ, sp. ht. meas., phase transition obs. at 46K 77−43326
TTF-TCNQ, X-ray exam. of $2k_F$ and $4k_F$ anomalies 78−10162
TTF.CuBDt, spin 1/2 Heisenberg chain, spin-Peierls transition 79−61135
TTFCuBDT, spin-Peierls transition in spin 1/2 Heisenberg chains, RPA calcs. 80−25150
two-dimensional Wigner-crystal-liquid-surface system, eigenmodes and instability of charged liq. surface 80−10896
two-electron level with quasidegenerate levels, local phase transitions and temp. effects in lattice dynamics 80−10666
uniaxial ferroelectric, acoustic attenuation near transition point 80−11350
vibronic model, fluctuations of order parameter and anharmonic interaction 77−52022
vibronic theory of antiferroelec. and struct. modulated transitions, soft modes 78−79719
weak itinerant magnetism as inhibited superconductivity 79−51715
zero-gap semiconductor, ferroelec. phase transitions, effect of Coulomb interaction on RPA calc. 79−28691
Ag_3AsS_3, and Ag_3SbS_3, Raman spectra obs. of low-temp. phases 80−93327
Ag_3AsS_3, proustite, phonons and soft modes at ferroelec. transition 80−60524
AgI, phase transition, statics and local dynamics, mean field and Mori theory 80−39347
$AgNaNO_2$, ferroelectric transitions, one-mode model 80−29702
Al, reactor irradiated, neutron inelastic scattering meas. of phonon dispersion curves 78−75758
$AlPO_4$, α-β cristobalite phase transition, Raman meas. 79−4799
Al_2SiO_5, andalusite, phonon spectra and rigid-ion model calcs. 80−11391
$As_{0.2}Sb_{0.8}SI$ cryst., ferroelec., soft mode Raman and IR spectroscopy 80−76016
$As_xSb_{1-x}SI$ mixed crystals, phonon coupling, ferroelectric phase transition, Raman study 80−108165
Au-Ag-Cd alloys, martensitic phase transition, elastic anomalies and mode softening 79−91647
Ba I-Ba II phase boundary, Ba I fusion curve peak at high press. *(Russian)* 80−2165
$BaMnF_4$, anisotropic order parameter phase fluctuations, light scatt. and thermal diffusivity meas. 80−80807

soft modes continued
$BaMnF_4$, dielec. anomaly, mechanism, spin canting 78−10744
$BaMnF_4$, incommensurate transition, Brillouin scatt. investigation 79−87406
$BaMnF_4$, mag. and structural phase transitions, neutron scatt. obs. 79−87259
$Ba_2NaNb_5O_{15}$, incommensurate refls. near ferroelastic transition, neutron and X-ray precession obs. 80−70395
$Ba_2NaNb_5O_{15}$, optical mode softenings, Raman scatt. meas., 1.5 to 600K 79−33631
$Ba_2NaNb_5O_{15}$, Raman spectra, soft oscillations, temp. depend. 78−31203
$BaTiO_3$, elastooptic effect near ferroelec. transition, temp. depend. 80−97233
$BaTiO_3$, ferroelec. phase transition, soft phonons, Raman scatt. obs. *(Japanese)* 79−65880
$BaTiO_3$, ferroelectric mechanisms, anharmonic couplings by scanning IR interferometry 80−75978
$BaTiO_3$, paraelec. phase, stabilisation of soft mode 80−75985
$BaTiO_3$, polariton and central mode softening 78−76006
$BaTiO_3$, soft mode dielec., anomalous low temp. sp. ht. 78−14423
$BaTiO_3$, soft mode exam. 79−37799
$BaTiO_3$, soft mode spectroscopy IR refl. meas. 80−88982
$BaTiO_3$, struct. phase transitions, light scatt. meas. 79−95774
$BaTiO_3$, tetragonal, over-damped soft E-polariton and dielec. dispersion 78−15111
$BaVS_3$, polycrystalline, elastic behaviour, 40 to 350K 79−60498
$Bi_xSb_{1-x}SI$, atomic substitution and ferroelec. phase transition 78−68464
$Bi_xSb_{1-x}SI$, low freq. Raman spectroscopy 78−15162
$Bi_2Ti_4O_{11}$, anomalous temp. depend. of phonon modes, Raman spectra 78−10893
$Bi_2Ti_4O_{11}$:PbO, anomalous temp. depend. of phonon modes, Raman spectra 78−10893
$BiVO_4$, ferroelastic, observation of soft optical phonon 78−2856
$BiVO_4$, ferroelastic transition, soft optical phonon mechanism 79−51230
$BiVO_4$, linear coupling between soft optical and ferroelastic acoustic modes 78−79716
$Cd(NH_3)_6X_2$, X=Br, Cl, I, orientational phase transitions, Raman spectra 80−11382
Ce, elastic properties up to 84 kbar, US vel. meas. *(Russian)* 79−60434
Ce, high press. superconductivity, phonon softening 78−14852
$CeAl_2$, mode softening due to magnetoelastic interaction, elastic consts. meas. 1.5 to 280K 77−32233
$CeSn_3$, mode softening and elastic consts., acoustic vel. meas. 80−88242
CsCN, inelastic neutron scatt. by coupled rotational and translational modes 80−70333
Cs_2CdBr_4, struct. phase transitions, NQR study 80−71343
$CsCrCl_3$, α-β phase transition, dynamical aspects and thermodynamic theory 80−70404
CsD_2AsO_4, piezoelec. coupled soft modes, Brillouin scatt. near Curie temp. obs. 77−52109
CsD_2PO_4, pseudo-one-dimensional ferrolec. and antiferroelec. transitions, phase diagram obs., soft modes 80−93245
$CsFeF_4$, two dimensional structural phase transitions, sp. ht., optical, dielec., X-ray diffr. meas. 79−69240
CsH_2AsO_4, piezoelec. coupled soft mode, Brillouin scatt. near Curie temp. obs. 77−52109
CsH_2PO_4 and CsD_2PO_4, pseudo one-dimens. ferroelec. ordering dynamics, ^{31}P NMR study 80−75971
$Cs_2LiCr(CN)_6$, room temp. struct., phase transitions 78−51491
$Cs_2MFe(CN)_6$, M=Ba, Mg, Ca, Sr, lattice instabilities 77−72668
$CsNO_3$, Raman spectra temp. depend., NO_3^- ion external librational modes, I→II transition, Raman spectra temp. depend., NO_3^- ion external librational modes 79−78662
$CsPbBr_3$, cubic-to-tetragonal phase transition, critical anomalies, phenomenological eqns. 80−39275
$CsPbCl_3$, cubic-to-tetragonal phase transition, critical anomalies, phenomenological eqns. 80−39275
$CsPbCl_3$, elastic constants and thermal expansion, near struct. transitions 78−59849
$CsPbCl_3$, n.q.r. spin-lattice relax. near cubic-tetragonal transition, soft modes 77−1616
$CsVF_4$, structural phase transitions above room temp. 80−29167
β_1Cu-Zn, structural Umklapp processes at low and high temp. lattice kinetics of phase transformation isotherms *(German)* 78−30707
$Cu_3B_7O_{13}Cl$, Raman study of ferroelec. phase transition 79−38529
$Cu_2Mo_6S_8$, phonon density of states, mode softening correl. with supercond. transition temp. 79−51714
DCN, phonons meas. by neutron coherent inelastic scatt. 79−95097
Di(methylammonium) cadmium tetrachloride, LF Raman spectra and phase transitions 77−63414
$DyFe_2$, phonon softening below Curie temp., Mossbauer effect 77−4589
α-Fe, vibrational states, phonon dispersion, phonon softening 80−88289
Fe-Ni (28 at.%), martensitic transformations, Mossbauer scattering evidence of soft modes 80−93223
Fe-Ni Invar, low temp. struct. 79−55856
Fe-Pd Invar, low temp. FCT phase obs. 80−93538
$Fe_{65}Ni_{35}$ ferromagnetic alloy, zero sound anomaly, inelastic neutron scatt. 79−46764
$Fe_{65}Ni_{35}$, ferromagnetic Invar alloy, lattice vibrations 78−91403
Fe_3O_4, multistage phonon softening in Verwey transition region, Mossbauer spectra 77−72670
Fe_3Pt Invar alloys, elec. resist. anomalous crit. behaviour 79−78067
$Fe_{72}Pt_{28}$, ferromagnetic Invar alloy, lattice vibrations 78−91403
$Gd_2(MoO_4)$, ferroelec., Raman scatt. from soft modes 77−85706
$Gd_2(MoO_4)_3$, ferroelec., anomalous damping of phonons, Raman spectra, stress and temp. effects 79−38503
$Gd_2(MoO_4)_3$, uniaxial stress effect on ferroelec. transition, Raman scatt. 78−80360
Ge, mode Gruneisen coeff. at point X, effect of lattice softening 78−38804
GeTe, electron-phonon interactin induced phase transition 79−82338
Hf, lattice dynamics, phonon dispersion, mode softening 80−107390
HfO_2, ZrO_2-HfO_2, soft phonon modes cond. monoclinic-tetragonal phase transition 77−62638
Hg_2Br_2, ferroelastic, Brillouin and Raman scatt. spectra 79−95770
Hg_2Br_2, ferroelastic phase, softening of acoustic and optical modes 79−33064
Hg_2Br_2, improper ferroelastic, soft mode props. in Raman spectra 77−36246
soft modes continued
$Hg_2Br(Cl_2)$, paraphase, Raman scatt. spectra, soft mode from Brillouin zone boundary *(Russian)* 78−2851
Hg_2Cl_2, calomel, press. depend. optical soft mode 79−55859
Hg_2Cl_2, improper ferroelastic, soft mode props. in Raman spectra 77−36246
Hg_2Cl_2, low temp. phase transition, X-ray diffr., Raman spectra 78−22849
Hg_2Cl_2, neutron and Raman scatt. studies, ferroelastic transitions 80−76015
Hg_2Cl_2 prototype phase, soft mode, inelastic neutron scattering, Raman effect 78−91411
Hg_2I_2, thermal softening of mode on Brillouin zone boundary in Raman scatt. spectra 79−73948
In-Cd, soft mode, latent heats and entropies of fusion 79−46786
In-Cd alloys, elastic-phase transition, US study 78−6919
In-Pb alloys, elastic consts. of three phases, acoustic mode softening 80−30006
In-Tl, soft mode, latent heats and entropies of fusion 79−46786
In-Tl alloy, superconducting transition temp., phonon mode softening 79−1637
KBr, doped with F-centres, Raman spectra meas. excitation in F and K bands 80−16027
KCN, elastic anomaly at 168K 78−27242
KCN, lattice dynamics and order-disorder transitions, neutron scatt. expts. 78−14434
KCN, polymorphism, high pressure, Raman spectra 78−88302
$KCaF_3$, struct. phase transitions, DSC, birefr., and neutron powder diffr. obs. 80−70149
$KCdF_3$, structural phase transitions, X-ray diffr. and differential type thermal analysis 77−80620
$KCdF_3$:Cr^{3+}, EPR, successive phase transitions 79−65717
$K_3Co(CN)_6$, Raman scatt. and electronically-induced phase transition at 130K 77−90142
KD_2AsO_4, ferrcelec., phase transition and Raman scattering 78−84540
KDP-type cryst., Raman scattering and phase transitions, deuteration effects 78−76400
KD_2PO_4, Brillouin spectrum and broad central component, depend. on scatt. wave vector direction 80−34931
KD_2PO_4, deuteron tunnelling, barrier height and energy level calc. 80−6482
KD_2PO_4, order-disorder type ferroelec., HF dynamics 77−39657
KD_2PO_4, soft ferroelec. mode anisotropy 78−14430
$KD_3(SeO_3)_2$, acoustic phonon softening and spontaneous strains 78−26652
$KD_3(SeO_3)_2$, central peak, soft acoustic shear mode, light scatt. study, isotope effects 78−52518
$KD_3(SeO_3)_2$, ferroelastic transition, EPR 80−7148
$KD_3(SeO_3)_2$, phase transition, neutron scatt. study 80−75351
$K_3Fe(CN)_6$, Raman scatt. and electronically-induced phase transition at 130K 77−90142
$KFeF_4$, struct. phase transitions obs. by dielec. const. and X-ray diffr. studies 79−95161
$KFe(MoO_4)_2$, phase transitions at 312 and 139K 80−70396
KH_2AsO_4, ferroelec., phase transition and Raman scattering 78−84540
KH_2AsO_4, Raman linewidth, isotope effect 77−8565
KH_2AsO_4, soft shear mode, Brillouin scatt. obs. 78−15176
$K(H_{1-x}D_x)_2PO_4$, polar mode softening and elastic anomaly temps. 79−28067
$KH_{2(1-x)}D_{2x}PO_4$, Raman spectra, effects of deuteration on proton tunnelling modes and coupled optic modes 77−59570
$K(H_{1-x}D_x)_3(SeO_3)_2$, Brillouin spectrum central peak, soft acoustic mode 80−2777
KH_2PO_4, and isomorphs, ferroelectric transition and Curie temp., soft mode effect, Green's function anal. 79−24269
KH_2PO_4, Bloch equations 78−64324
KH_2PO_4, Brillouin-Rayleigh scatt. studies near ferroelec. transition temp. 80−76036
KH_2PO_4, central peak susceptibility and US propag. near T_c 78−15125
KH_2PO_4, damping of transverse acoustic and ferroelec. modes 78−14413
KH_2PO_4, depolarised light scatt., dynamic central peak 78−10858
KH_2PO_4, dynamic central peak in ferroelectric phase 78−84538
KH_2PO_4, ferroelec. phase transition, soft phonons, Raman scatt. obs. *(Japanese)* 79−65880
KH_2PO_4, Green's function theory of ferroelec. phase transition 77−85669
KH_2PO_4, light scatt. in elec. field, ferroelec.-paraelec. transition 80−2707
KH_2PO_4, longit. sound attenuation, strain depend. pseudo spin coupling mechanism 77−85666
KH_2PO_4 paraelectric phase, solns. of Bloch-type eqns., soft mode freq. fluctuations 80−7304
KH_2PO_4, proton tunnelling, barrier height and energy level calc. 80−6482
KH_2PO_4, Raman scatt. near T_c, search for soft modes 78−15114
KH_2PO_4, soft branch Brillouin specta, quasielastic central peak suppression by annealing 78−95588
KH_2PO_4, soft mode behaviour, dispersive Fourier transform spectroscopy 77−7823
KH_2PO_4, strong coupling of proton-phonon system 77−7822
KH_2PO_4, struct. phase transitions, light scatt. meas. 79−95774
KH_2PO_4 type crystals, coupling between protonic E-mode and lattice vibrs. 77−7821
KH_2PO_4 type crystal, H-bonded partially deuterated ferroelectrics, order parameter fluctuation spectra, central peak calcs. 79−61316
KH_2PO_4 type crysts., evidence of non-linear behaviour of soft modes, Raman spectra 79−33639
KH_2PO_4 type ferroelectrics, isotopically disordered, collective modes, CPA 77−7825
KH_2PO_4 type ferroelectrics above T_c, soft mode and central-peak dynamics 78−87763
KH_2PO_4, variational treatment of proton-photon system 78−88261
KH_2PO_4:Fe^{3+}, ESR, anomalous temp. depend. of D tensor 79−61205
KH_2PO_4-KD_2PO_4 mixed crystals, static and dynamic props., proton-lattice coupled mode model 78−64328
KH_2PO_4-KD_2PO_4 mixed crysts., dielec. spectra, sub-mm wavelengths 80−80724
KH_2PO_4-type crystals, H bond in ferroelectricity, role of high pressure research 79−15414
KH_2PO_4-type crystal, LF dynamics 80−10602
$KH_3(SeO_3)_2$, acoustic phonon softening, US vel. meas. 78−14429

soft modes continued
$KH_3(SeO_3)_2$, phase transition, acoustic phonon softening 77−27997
$KH_3(SeO_3)_2$, thermal anomalies rel. to acoustic phonon instability 77−76545
$K_{0.75}Li_{0.25}TaO_3$, press. depend. of impurity soft modes, low energy Raman scatt. meas. 78−2852
$KMnF_3$, cubic-to-tetragonal phase transition, critical anomalies, phenomenological eqns. 80−39275
$KMnF_3$, Mossbauer gamma quanta scattering near 186K transition 80−108126
$KMnF_3$, phonon scatt., thermal cond. meas. 77−7916
$KMnF_3$, precursor order and Raman scatt. near displacive phase transitions 80−45061
$KMnF_3$, soft phonons and mag. phase transitions 80−54889
KNO_3, antiferroelec., press. induced II to IV phase transition, Raman scatt. 78−15161
$K_xNa_{1-x}TaO_3$, press. depend. of impurity soft modes, low energy Raman scatt. meas. 78−2852
$KNbO_3$, ferroelec. phase, phonon dispersion relations and lattice dynamics calcs., comparison with expt. 80−49319
$KNbO_3$, ferroelectric soft modes and order-disorder transition 77−47534
$KNbO_3$, orthorhombic, anharmonic effects 78−79721
$KNbO_3$, tetragonal phase, inelastic neutron scatt. 80−19676
K_2OsCl_6, soft rotary mode near phase transition, inelastic neutron scatt. obs. 79−60472
K_2OsCl_6, displacive phase transition, thermal expansion meas. 78−10188
K_2OsCl_6, ferrorotative transition, neutron scatt. expt., consistency with displacive and order-disorder models 78−51673
K_2OsCl_6, low temp. sp. ht. and thermodynamic props. near phase transition 77−39655
$K_2Pt(CN)_4Br_{0.3}.3H_2O$, lattice softening, temp. depend. of elastic consts., US meas. 78−14432
$K_2Pt(CN)_4Br_{0.3}.3H_2O$, specific heat and ferroelastic behaviour 78−91447
$K_2Pt(CN)_4Br_{0.3}.xH_2O$, dynamical props. near Peierls instability, neutron scatt. 78−14436
K_2PtCl_6, K_2ReCl_6, K_2SnCl_6, solid state phase transitions, lattice vibr., NMR and NQR obs. 80−34814
$K_{0.5}Rb_{0.5}I$, mixed cryst., phonons, neutron scatt. 77−1192
K_2ReCl_6, displacive phase transition, thermal expansion meas. 78−10188
K_2ReCl_6, elastic constants, softening of acoustic modes, obs. by Brillouin scattering 80−71440
K_2ReCl_6, low temp. sp. ht. and thermodynamic props. near phase transition 77−39655
K_2ReCl_6, structural phase transition, soft rotary mode, obs. by triple-axis neutron scatt. 79−1483
K_2SO_4, longitudinal-acoustic soft mode in phase transition 80−75326
$KSc(MoO_4)_2$, soft modes and Raman spectrum at ferroelastic phase transitions 79−47450
K_2SeO_4, hexagonal-orthorhombic transition, Brillouin scatt. study 80−97208
K_2SeO_4, improper ferroelec., struct., phase transform. and lattice instability neutron scatt. meas. 77−63379
K_2SeO_4, incommensurate phase transition, stress depend. of T_c 79−4391
K_2SeO_4, incommensurate phase transitions under existence of Lifshitz invariant, soft modes by Raman scatt. 79−15416
K_2SeO_4, incommensurate structure, IR and Raman activity of soft mode 79−28738
K_2SeO_4, incommensurate lattice instability, ferroelec. transition, neutron scatt. study 79−42210
K_2SeO_4, incommensurate to ferroelec. transition, hydrostatic press. effects, neutron scatt. study 80−108166
K_2SeO_4, induction of incommensurate condensations of hard modes by incommensurate condensation of soft modes 78−55931
K_2SeO_4, lattice dynamics, displacive phase transform. 80−39248
K_2SeO_4, lower freq. soft-mode in ferroelec. phase 77−81065
K_2SeO_4, non-zero wave vector incommensurate soft mode, light scatt. study 80−29754
K_2SeO_4, Raman scatt. and dielec. props. 80−11313
K_2SeO_4, Raman scattering spectra and discovery of soft mode 78−76442
K_2SeO_4, Raman spectra, 77-300K *(Japanese)* 77−43988
K_2SeO_4, Raman spectra, effects of temp., substitutional cations, and stress 80−71405
K_2SeO_4, soft modes below incommensurate transition Raman and Brillouin scatt. meas. 79−91387
K_2SnBr_6, transform. dynamics probed by Raman scatt. and microscopy 78−63832
K_2SnCl_6, elastic constants, softening of acoustic modes, obs. by Brillouin scattering 80−71440
K_2SnCl_6, phase instabilities and mode softening X-ray and neutron diffr. 77−7830
K_2SnCl_6, structural phase transitions, Raman spectra 77−73143
$KTa_xNb_{1-x}O_3$, ferroelectric transition, US attenuation, elastic consts., soft modes 78−23411
$KTaO_3$, complex refr. index meas. in far IR, by dispersive Fourier transform spectroscopy 78−92042
$KTaO_3$, ferroelec., local field determ., phase transition study by EPR 79−38471
$KTaO_3$, field depend. sp. ht. and soft modes at low temps. 79−8105
$KTaO_3$, freq. depend. of soft mode self-energy, for IR dielec. response meas. 79−33632
$KTaO_3$, incipient ferroelectric, mode-mode coupling 78−79717
$KTaO_3$, mode anharmonic self energies, freq. depend. 78−59908
$KTaO_3$ pseudodisplacive ferroelec., temp.-dependent dielectric response obs. 77−40247
$KTaO_3$, sp. ht. and electrocaloric props. at low temps. 77−84945
$KTaO_3$, stress-induced ferroelectricity, Raman scatt. obs. 77−40190
$KTaO_3:Fe^{3+}$ local phase transition, EPR line temp. broadening *(Russian)* 80−54944
$KTaO_3$:Li(Na)(Nb), microscopic distortions in paraelec. phase 78−75793
$KTiF_4$, struct. phase transitions obs. by dielec. const. and X-ray diffr. studies 79−95161
KVF_4, struct. phase transitions obs. by dielec. const. and X-ray diffr. studies 79−95161
K_2ZnCl_4, incommensurate phase transitions, ^{35}Cl NQR study 80−75968
(La,Nd)P_5O_{14}, optical props., ferroelastic phase transition induced 79−95731
La, soft phonons, f-band induced instability 78−83907
La, supercond. transition temp., press. depend., mode softening 78−14847
soft modes continued
$LaAg_xIn_{1-x}$ alloys, structural instability 78−79562
$LaAg_xIn_{1-x}$, phonon dispersion, elastic consts. and struct. instability, soft mode behaviour 80−103436
LaP_5O_{14}, coupling effects between soft optic and acoustic modes at ferroelastic transition 80−70358
LaP_5O_{14}, ferroelastic transition, soft acoustic mode 77−11656
LaP_5O_{14}, ferroelastic phase transition, thermal expansion and elastic consts. tensors 79−42236
LaP_5O_{14}, ferroelastic transition, polarised Raman study 80−16035
$La_3S_4(Se_4)$, structural transitions, symm. anal. 80−92671
$LiNbO_3$, ferroelec. phase, soft vibr. modes, far IR refl. meas. 79−87407
$LiNbO_3$, ferroelec. phase, phonon dispersion relations and lattice dynamics calcs., comparison with expt. 80−49319
$LiNbO_3$, Fourier transform Ir spectroscopy of vibr. states at high temp. 80−97256
$LiNbO_3$, X-ray diffuse scatt., temp. depend., 20 to 750°C 79−37800
$LiNbO_3$:Fe, calc. of photorefraction *(Russian)* 78−92032
$LiTaO_3$, Fourier transform Ir spectroscopy of vibr. states at high temp. 80−97256
$LiTaO_3$ high-temp. ferroelec. transition, soft mode IR reflectivity spectroscopy 79−33692
$LiTaO_3$, paraelectric phase, soft vibr. modes, far IR refl. meas. 79−87407
$LiTaO_3$, X-ray diffuse scatt., temp. depend., 20 to 750°C 79−37800
MgF_2, elastic const. C_{44}, depend. on temp. 79−73239
γ-Mn-Ni-C, elastic anomalies, martensitic transformation in Mn rich alloys 78−84807
MnAs, second-order phase transition, elastic anomalies 79−10908
$Mn_{2-x}Cr_xSb$, exchange-inversion interaction and acoustical magnon soft mode 77−40049
Mo (001) surface, electronic susceptibility and surface phase transition 79−33169
Mo and Nb-Mo alloys, superconductivity and phonon softening, between electron bands and phonons 78−14859
Mo superconducting film, amorphous and crystalline, transition temp. exam. by UPS 79−28433
Mo_6Se_8, Chevrel phase supercond., phonon spectra, neutron scatt. meas. 79−42174
Mo_6X_8 (X=S, Se), phonon density of states, mode softening correl. with supercond. transition temp. 79−51714
$(ND_4)_2BeF_4$ and $(NH_4)_2BeF_4$, incommensurate phase, ^9Be NMR study 80−75973
$(ND_4)_2BeF_4$, ferroelec. transition, Raman spectra obs. *(Russian)* 78−23408
$(NH_4)_2BeF_4$ crystals, incommensurate-commensurate phase transitions, optical props. 79−95733
$(NH_4)_2BeF_4$, incommensurate-commensurate phase transition 78−87760
$(NH_4)_2BeF_4$, phase transition at 185K, X-ray scatt. obs. 77−36186
NH_4Br, β-γ phase transition, critical anomalies, phenomenological eqns. 80−39275
$(NH_4)_2Cd_2(SO_4)_3:Mn^{2+}$, UO_2^{2+}, luminesc., vibr. modes 79−38629
NH_4Cl, acoustic absorption by soft modes of defects 80−59584
$NH_4H_2AsO_4$-$NH_4H_2PO_4$ antiferroelectric solid solution, soft-mode and energy calcs. 79−56743
$NH_4H_2PO_4$, phase transition, phonon echo method *(French)* 78−6640
NH_4IO_3, ferroelec., structural phase transition 80−7308
$(NH_4)_{2(1-x)}Rb_{2x}SO_4$, mixed crystal, dielectric and US meas. of ferroelec. phase transition *(Japanese)* 80−7305
$(NH_4)_2SO_4$, ferroelec. transition, EPR study 79−38472
$(NH_4)_2SO_4$, irrad., −50°C transition, librational mode softening, paramag. NH_3^+ probe obs. 77−20037
$(NH_4)_2SO_4$, paraelec. phase, X-ray diffuse scatt., soft mode model 77−31744
$(NH_4)_2SO_4$, phase transition mechanisms by optical spectroscopy 79−15411
$(NH_4)_2SO_4:Cd^+$, ferroelec. transition, soft mode contrib., EPR obs. 78−72469
$(NH_4)_2SiF_6$, elastic constants, softening of acoustic modes, obs. by Brillouin scattering 80−71440
$(NH_4)_2SnBr_6$, structural phase transitions study by Raman scatt. 80−93318
$(NH_4)_2SnCl_6$, elastic constants, softening of acoustic modes, obs. by Brillouin scattering 80−71440
NaCN, elastic const. temp. depend., Brillouin and US exam. 77−80572
Na_2CO_3, incommensurate structural phase transform., neutron diffr. obs. 79−86886
Na_2CO_3, struct. changes at incommensurate phase transition 79−95158
NaCl, elastic props. at press. up to 9 GPa, ultrasonic wave velocities 79−95073
NaF, anharmonicity of lattice vibrations, neutron scatt. study, rel. to melting 77−84862
$NaH_3(SeO_3)_2$, β to δ ferroelec. transition under press. Raman spectra study 80−80725
$NaH_3(SeO_3)_2$, dynamics of α-β transition, Brillouin scatt. meas. 77−8526
NaI:Cl^-, anharmonic effects on low-frequency impurity phonon resonances 78−75771
$NaNO_2$, ferroelectric transitions, one-mode model 80−29702
$NaNO_2$, incommensurate phase transitions 78−26653
$NaNO_3:Mn^{2+}$, zero-field splitting, ferroelec. soft-mode contrib., phase transition, EPR obs. 79−15344
$NaNO_3$, press. induced ferroelec. transition, soft mode dynamics, Raman scatt. meas. 78−72475
$NaNO_3$, soft mode dynamics at ferroelec. transition 78−80308
$NaNbO_3$, antiferroelec., primary order parameter, X-ray scatt. 79−51919
$NaNbO_3$, cubic to tetragonal transition, inelastic neutron scatt. study *(French)* 79−60469
$NaNbO_3$, ferroelec., local field determ., phase transition study by EPR 79−38471
$NaNbO_3:Mn^{2+}$, ESR, temp. depend., −269-750°C, fine splitting 77−51948
Na_xWO_3, metallic, light-scatt. studies 80−45071
Na_xWO_3, X>0.5, temp. depend. of Raman active soft modes, tetragonal-tetragonal transition 78−48180
Nb and Nb-Mo alloys, superconductivity and phonon softening, between electron bands and phonons 78−14859
NbC_xN_{1-x}, obs. of phonon anomalies, sp. ht. meas. and supercond. transition temp., 1.5-90K 77−39985

soft modes continued
NbC_xN_{1-x}, s.p. ht., 4.2-100K, phonon anomaly rel. to supercond. transition 78−14880
$NbD_{0.85}$, localised D vibrs., temp. depend., neutron inelastic scatt. study 80−107395
$NbH_{0.82}$, localised H vibrs., temp. depend., neutron inelastic scatt. study 80−107395
$NbSe_2$(2H), Raman spectra of soft modes at CDW transition 77−16301
Nb_3Sn, [111] transverse acoustic phonon softening near martensitic transform. 79−73283
Nb_3Sn, acoustic soft modes in high mag. fields, soft sound vel. meas. 77−43482
Nb_3Sn, Debye-Waller factor temp. depend. 79−14907
Nb_3Sn, phonon softening and T_c, strong electron-phonon coupling 78−31009
Nb_3Sn, phonon softening in [ζζζ] transverse modes, neutron scatt. obs. 79−33062
Nb_3Sn, softening of surface phonons in (100) plane 80−107627
Nb_3Sn, Young's modulus, 4.2-300K, behaviour near martensitic transition 80−66564
Nb_3Sn(Al), phonon density of states, temp. depend. 79−42183
$Nb_{0.75}Zr_{0.25}$, effect of force constant, disorder on Eliashberg function 80−29504
$Nb_{1-x}Zr_x$, supercond., McMillan-Rowell tunnelling spectroscopy 79−60985
NdP_5O_{14}, ferroelastic, spectroscopy, ferroelastic/ferroelectric coupling, soft optic mode frequencies 79−19845
NdP_5O_{14}, ferroelastic, Raman scatt. from soft phonons, 4.2-600K, monoclinic-orthorhombic transition temp. 79−51962
β-NiAl alloy, elastic soft modes preceding martensitic phase transition 79−4388
$Ni_3B_7O_{13}I$, cubic, Raman spectrum, 88-295K, vibr. anomalies 78−76479
$Ni_3B_7O_{13}I$, dynamics of ferroelec. phase transition, Raman spectra obs. 79−33630
$Ni_3B_7O_{13}I$, struct. and mag. transitions, light scatt. study 79−24308
$Ni_{1-x}S$, metal-semimetal transition, lattice dynamics and thermodynamic props. 80−29324
PLZT ceramics, sp. ht., 2-25K, field depend., phonon modes 77−47586
(Pb,La)TiO_3, soft E(TO) phonons, and phase transitions, Raman spectra, −200 to 400°C 78−15109
(Pb, Sn)Te-type semiconductors, displacive ferroelec. phase transitions, vibronic theory 80−11354
Pb, phonon softening, neutron scatt. at high press. 78−80091
Pb, transverse acoustic phonons, freq. and damping, supercond. transition temp. effects 79−42687
$Pb_{5-x}Ba_xGe_3O_{11}$, Raman spectra, temp. depend. of ferroelec. soft A-mode 79−33682
PbF_2, cubic, dielec. const., ionic cond., soft modes 78−14427
PbF_2, phonon energy dispersion relations 78−79697
$Pb_5Ge_3O_{11}$ acoustic relaxation near ferroelectric transition 78−2814
$Pb_5Ge_3O_{11}$, dynamic central peaks and phonon interactions near structural phase transitions 78−83903
$Pb_5Ge_3O_{11}$, ferroelectric transition exam. by Raman scatt. 78−56439
$Pb_5Ge_3O_{11}$, ferroelectric soft mode exam., Raman spectra 79−42202
$Pb_5Ge_3O_{11}$, ferroelectric, anharmonic effects in low freq. symm. modes, Raman study 80−25365
$Pb_5Ge_3O_{11}$, freq. and damping of ferroelec. soft mode, permittivity meas. 77−52027
$Pb_5Ge_3O_{11}$, light scatt. meas., central peak dynamics at ferroelectric transition 77−4606
$Pb_5Ge_3O_{11}$, paraelectric and ferroelectric, Raman spectra near ferroelectric transition 80−55090
$Pb_5Ge_3O_{11}$, Raman scatt., soft modes and damping near structural phase transition 79−28739
$Pb_5(Ge_{1-x}Si_x)_3O_{11}$, ferroelec. soft mode, temp. and Si impurity, effects Raman scatt. 79−1762
$Pb_5Ge_{3-x}Si_xO_{11}$, ferroelec. soft mode, temp., press. and comp. depend. 78−80304
$Pb_{1-x}Ge_xTe$, degenerate semiconducting ferroelectric, structural phase transition temp., mag. field effects 80−45017
$Pb_{1-x}Ge_xTe$, electron-phonon interaction effect on ferroelec. transition 78−76416
$Pb_{1-x}Ge_xTe$, ferroelec. phase transition, IR refl. and resist. meas. 80−11353
$Pb_{1-x}Ge_xTe$, Raman scatt. from soft TO-phonon modes 79−95773
$PbHAsO_4$, ferroelec., far IR and submillimetre dielec. dispersion 79−38528
$PbHPO_4$, ferroelec. phase transition, Brillouin and Raman spectra obs. 79−33683
$PbHPO_4$, ferroelec., far IR and submillimetre dielec. dispersion 79−38528
$PbHfO_3$, elec. quadrupole interaction, temp. depend., DPAC meas. 79−51884
$PbMo_{5.1}S_6$, high supercond. T_c, soft mode behaviour 78−14855
$PbMo_6S_8$, Chevrel phase supercond., phonon spectra, neutron scatt. meas. 79−42174
$Pb_{1.2}Mo_6Se_8$, Chevrel phase supercond., phonon spectra, neutron scatt. meas. 79−42174
$PbMo_6X_8$ (X=S, Se), phonon density of states, mode softening correl. with supercond. transition temp. 79−51714
$Pb_3(PO_4)_2$, ferroelastic, Raman scatt. by soft vibr. involved in ferroelastic phase transition 80−16040
$Pb_3(PO_4)_2$, ferroelastic transition, soft modes, inelastic neutron scatt. obs. 77−31772
$Pb_3(PO_4)_2$, ferroelastic phase transition, inelastic neutron scatt. *(French)* 80−24584
$Pb_3(P_{0.95}V_{0.05}O_4)_2$, ferroelastic transition, soft mode, inelastic neutron scatt. study 80−70357
$Pb_{1-x}Sn_xSe$, band inversion effect on phonon spectra 78−79699
$Pb_{1-x}Sn_xSe$, gapless state and phonon spectrum *(Russian)* 78−30715
$Pb_{1-x}Sn_xTe$, (x<0.35), permittivity and soft modes, carrier density and comp. effects 80−7256
$Pb_{1-x}Sn_xTe$, lattice instability and phonon lifetimes, neutron scatt. 78−55932
$Pb_{1-x}Sn_xTe$, mag. and kinetic props. near ferroelec. transition 80−11160
$Pb_{1-x}Sn_xTe$, Mossbauer investig. of phonon softening at semicond.-semimetal transition 77−43908
$Pb_{1-x}Sn_xTe$, soft mode, ferroelec. phase transition crit. temp. and dielec. const. calcs. 77−8530
$Pb_{1-x}Sn_xTe$, soft-phonon-induced Raman scatt. 77−77209
$Pb_{.87}Sn_{.13}Te$, phonon dispersion, mode softening 79−42175

soft modes continued
PbTe, electron-phonon interactin induced phase transition 79−82338
PbTe, TO phonon mode softening, sub mm spectra 78−6665
PbTe, TO phonon softening, free carriers and defects effects 78−79720
PbTe, TO-phonon mode softening, far IR Fourier transform spectroscopy 77−40248
PbTe-SnTe compound semiconductors, lattice instability by mm-wave magnetoplasma refl. 80−54336
Pb(Ti,Zr)O_3, soft E(TO) phonons, and phase transitions, Raman spectra, −200 to 400°C 78−15109
$PbTiO_3$, amorphous, crystallisation process, DTA and Raman spectroscopy meas. 80−75161
$PbTiO_3$, damping of soft E-symmetry phonon, Raman scatt. meas. 78−67799
$PbTiO_3$, soft mode decay mechanism, damping parameter freq. depend. 80−54324
$PbTi_{1-x}Zr_xO_3$, low freq. vibrational modes and ferroelec. transitions 79−33637
Pb(Zr,Ti)O_3, temp. and hydrostatic press. depend of vibr. modes, rel. to phase transforms 77−89510
$PbZr_{0.95}Ti_{0.05}O_3$, soft mode dielec., anomalous low temp. sp. ht. 78−14423
Pd-H, supercond. and phonon softening in unstable systems 79−65587
Pd-H_2, dilute soln., high temp. thermodynamics, partial molar props. 77−15597
Pd-H(D) system, superconductivity and phonon softening 79−73626
PdH_x, local, soft modes, superconductivity thermal neutron inelastic scatt. *(Chinese)* 80−70331
Pr, central peaks and soft modes, quasi-elastic mag. scatt. obs. 77−66377
Pr, magnetic ordering, stress induced 80−15776
Pr, soft mode excitation behaviour under press., long range order 80−39838
$PrCl_3$, cooperative Jahn-Teller ordering of elec. dipoles in non-Kramers doublets 78−15115
$PrCu_2$, Jahn-Teller transition, susceptibility, elec. resist., thermal expansion and acoustic meas. 77−20276
$RbAg_4I_5$, critical dynamics, role of acoustic phonons, and Z-branch 77−84887
$RbAg_4I_5$, phase transition, statics and local dynamics, mean field and Mori theory 80−39347
$RbCaF_3$, 193K phase transition, lattice dynamics 78−10160
$RbCaF_3$, 193K phase transition, crit. neutron scatt. obs. 78−10161
$RbCaF_3$, cubic to tetragonal phase transition, ^{87}NMR meas. 80−7187
$RbCaF_3$, neutron scatt. central peak rel. to soft mode 78−75794
$RbCaF_3$, precursor order and Raman scatt. near displacive phase transitions 80−45061
$RbCaF_3$, sp. ht. anomaly at struct. transform. 78−14426
$RbCaF_3$, structural phase transition, superlattice points, neutron diffr. obs. 80−19944
$RbCdCl_3$, n.q.r. spin-lattice relax. near cubic-tetragonal transition, soft modes 77−1616
$RbCrCl_3$, α-β phase transition, dynamical aspects and thermodynamic theory 80−70404
$RbCrCl_3$ crystals, β→γ structural phase transition, lattice dynamical anal. 80−84291
$RbD_3(SeO_3)_2$, DMR, electric quadrupole coupling, ferroelec. transition 79−91312
$RbD_3(SeO_3)_2$, phase transform., inelastic neutron scatt. study 78−39514
$RbFeF_4$, two dimensional structural phase transitions, sp. ht., optical, dielec., X-ray diffr. meas. 79−69240
RbH_2AsO_4, Raman scatt. near T_c, search for soft modes 78−15114
RbH_2PO_4, ferroelectric, soft mode frequency from US vel. data 78−23417
RbH_2PO_4, longit. US wave propag. near ferroelectric phase transition temp. 78−84536
RbH_2PO_4 powder, phase transition in paraelectric (upper) phase by measuring damping const. and amplitude of phonon echoes 79−19855
RbH_2PO_4, Raman scatt. near T_c, search for soft modes 78−15114
$RbH_2(SeO_3)_2$, improper ferroelectric phase transformation, neutron scattering study 78−80302
$RbH_3(SeO_3)$, ferroelectric phase transition, Raman spectra meas. 79−19871
$RbH_3(SeO_3)_2$, low temp. struct., neutron diffr. 78−38669
$RbH_3(SeO_3)_2$, order parameter 77−66460
RbI, non-linear press. depend. of phonon freq. 77−35650
$Rb_{1-c}K_c$, local mode exam. by neutron diffr. 79−37781
$RbMnCl_3$, structural phase transition 78−91442
$RbNO_2$, Raman spectra temp. depend., NO_3^- ion external librational modes, IV→III transition, Raman spectra temp. depend., NO_3^- ion external librational modes 79−78662
Rb_2ZnBr_4, incommensurate phase transition, neutron-scatt. obs. 79−4390
Rb_2ZnBr_4, incommensurate and commensurate phases, neutron scatt. meas. 79−82936
Rb_2ZnBr_4, Raman scatt., normal-incommensurate-commensurate phase transitions, soft modes 80−40071
Rb_2ZnBr_4, soft modes at phase transforms., far IR spectrum study 80−107398
Rb_2ZnBr_4, soft modes obs. by Raman scatt. 80−97283
$Rb_2ZnBr_4(Cl_4)$, Raman spectra near incommensurate phase transitions 80−76013
Rb_2ZnCl_4, ^{35}Cl NQR, incommensurate struct. phase transition 79−47401
Rb_2ZnCl_4, incommensurate phase transition, ^{87}Rb NMR study 80−75967
Rb_2ZnCl_4, incommensurate phase transitions, ^{35}Cl NQR study 80−75968
Rb_2ZnCl_4, phase transitions, soft mode, Raman scatt. meas. 79−4389
Rb_2ZnCl_4, phase transition, Raman scatt. evidence 80−40116
Rb_2ZnCl_4, US vel. and attenuation at normal-incommensurate phase transition pt. 79−55833
$(SN)_x$, electronic props. and comparison with TTF-TCNQ, review 78−6306
Sb_5O_7I, ferroelastic, Raman scatt. and symm. aspects of phase transition 77−8578
Sb_2S_3, effect of screening by conduction electrons on phase transitions 78−84537
SbSI, central mode, microwave freqs. 79−19852
SbSI, diffuse X-ray scatt., anisotropy in phonon dispersion relations 77−84866
SbSI, ferroelec. phase transition and nonlinear props. 80−75988

soft modes continued
SbSI, ferroelec. transition, inelastic neutron scatt. 77−40189
SbSI, ferroelectric, anharmonic at. pot. and temp. depend. of thermal vibrs. 80−39246
SbSI, ferroelectric semiconductor, effect of screening by conduction electrons on phase transitions 78−84537
SbSI, paraelectric-ferroelectric transition, low freq. phonon branches, neutron scatt. obs. 79−61313
SbSI, Raman scatt., near tricritical point 78−15159
SbSI-SbSBr system, ferroelec., anharmonic effects in far IR reflectivity spectra 80−76014
Se, trigonal, Raman scatt. at very high press. 80−60566
Si (111), dynamic effective charge and surface reconstruction, soft-mode theory 79−4460
SmB_6, f-d hybridisation, optic phonon anomalies 78−92080
$Sm_{0.8}La_{0.2}AlO_3$, high temp. Raman spectra, phase transition 79−61367
SmS, f-d hybridisation, optic phonon anomalies 78−92080
SmS, LO phonon freq. softening in semicond. and metallic phases 80−96619
$Sm_{0.7}Y_{0.3}S$, Debye-Waller factor, X-ray diffr. meas., evidence of optic phonon softening 77−11659
$Sm_{0.75}Y_{0.25}S$, intermediate-valence-state system, phonon dispersion meas. 79−19342
$Sm_{0.75}Y_{0.25}S$, intermediate valence compound, phonon investigation by neutron scatt. 80−6476
$Sm_{1-x}Y_xS$, effect of valence fluctuations on lattice dynamics 78−47493
$Sm_{1-x}Y_xS$, mixed valence, phonon softening and linewidths, calc. 80−75319
$SnCl_2.2H_2O$, protonic order-disorder transition, inelastic light scatt. obs. 78−68497
$Sn_{0.9}Ge_{0.1}Te$, Mossbauer spectra, soft modes 80−20550
$SnMo_5S_6$, high supercond. T_c, soft mode behaviour 78−14855
$SnMo_6S_8$, Chevrel phase supercond., phonon spectra, neutron scatt. meas. 79−42174
$SnMo_6S_8$, lattice softening, vibr. anisotropy 78−14428
$SnMo_6S_8$, phonon density of states, mode softening correl. with supercond. transition temp. 79−51714
$Sn_2P_2S_6$, ferroelec. semicond., phase transition and lattice dynamics 80−60526
$Sn_2P_2S_6$, illumination effect on soft mode and dielectric props., luminesc. study *(Russian)* 80−50420
$Sn_2P_2S_6$, soft mode, interaction of modes and crit. Rayleigh scatt. 79−99836
$Sn_2P_2S_6$, soft mode, temp. depend. of Raman spectra near phase transition 78−88263
$Sn_2P_2S_6$, soft mode props., Raman scatt. study 80−60525
$Sn_2P_2(S_{1-x}Se_x)_6$, solid solutions, ferroelectric soft mode freq., displacive transformations 80−29701
$(Sn_{1-x}Pb_x)_2P_2S_6$, solid solutions, ferroelectric soft mode freq., displacive transformations 80−29701
SnTe, bond gap, phase transform., optical dielec. const. meas. 80−10630
SnTe, carrier density depend. of soft TO-phonon, Raman scatt. meas. 78−6684
SnTe, displacive phase transition at 22K, Mossbauer spectra and elec. resist. meas. 80−6514
SnTe, displacive transform., interband electron-phonon interactions, phase diagram 80−93252
SnTe, electron-phonon interaction effect on ferroelec. transition 78−76416
SnTe, electron-phonon interactin induced phase transition 79−82338
SnTe film, polycrystalline, anomalous resist. at struct. phase transition 80−29488
SnTe, light scatt. from soft modes, theory above and below displacive transform. temp. 79−95791
SnTe, mag-props., effect of structure transition 78−6158
SnTe, Raman scatt. from soft TO-phonon modes 79−95773
SnTe, softening of TO phonon mode *(Japanese)* 78−2225
$Sr_xBa_{1-x}Nb_2O_6$, neutron and light scatt. in phase transition region 78−64336
$Sr_2Nb_2O_7$, optical mode softening in incommensurate phase 80−7352
$SrO:Ni^{2+}$, EPR line splitting rel. to Jahn-Teller coupling and soft localised mode 80−66022
$Sr_2Ta_2O_7$, soft optic phonon responsible for structural phase transition, Raman scatt. meas. 80−96618
$SrTiO_3$, anharmonic motion rel. to struct. transition 78−79718
$SrTiO_3$ ceramic, sp. ht and electrocaloric effects at low temps. 77−59518
$SrTiO_3$, complex refr. index meas. in far IR, by dispersive Fourier transform spectroscopy 78−92042
$SrTiO_3$, dynamic central peaks and phonon interactions near structural phase transitions 78−83903
$SrTiO_3$ ferroelectric modes, Raman spectra, neutron scatt. meas. 80−80727
$SrTiO_3$, freq. depend. of soft mode self-energy, for IR dielec. response meas. 79−33632
$SrTiO_3$, heavily reduced, soft mode behaviour 80−71409
$SrTiO_3$, incipient ferroelectric, mode-mode coupling 78−79717
$SrTiO_3$, phonon interactions and the dynamic central peak near structural phase transition 77−81114
$SrTiO_3$, photolum. and carrier drift mobility at ferroelec. transition 80−71469
$SrTiO_3$ pseudodisplacive ferroelec., temp.-dependent dielectric response obs. 77−40247
$SrTiO_3$, semiconductor, soft modes, zone boundary mode 80−71357
$SrTiO_3$, specific heat near structural transition 77−81072
$SrTiO_3$, struct. transition temp. from self-consistent phonon spectrum 77−89517
$SrTiO_3$, structural phase transition, intrinsic and extrinsic central peak properties 80−34168
$SrTiO_3$ under [111] uniaxial stress, neutron scatt. 78−67798
$SrTiO_3:Cr^{3+}$, nonlinear Jahn-Teller coupling, local dynamics, near struct. transition 80−2625
$SrTiO_3:Fe^{3+}$, displacive struct. transition, order-disorder behaviour, phonon softening, EPR obs. 79−23695
$SrTiO_3:Fe^{3+}$, order-disorder and central peak behaviour, EPR study 80−75970
$SrZrO_3$, high temp. phases, struct. determ., soft mode transitions 78−42942
TGS, temp. behaviour of optical phonons near T_c, evidence of non-linear pseudospin-phonon interaction 77−7824
soft modes continued
TGSe, temp. behaviour of optical phonons near T_c, evidence of non-linear pseudospin-phonon interaction 77−7824
TaS_2 (1T) and (2H), bonding and charge density wave phase transitions 80−44282
$TaSe_2$ (2H), Raman scatt. from CDW 80−93340
$TaSe_2$ (2H), softening of CDW excitation, at superstructure transition 78−79728
$TaSe_2$(2H), Raman scatt., charge density wave mode softening at superstruct. transition 77−8584
$TaSe_2$(2H), Raman spectra of soft modes at CDW transition 77−16301
$Tb_2(MoO_4)_3$, mode softening near ferroelec. transition, Raman and Brillouin spectra 79−33685
TbP, mag. excitations above antiferromag. ordering temp., inelastic neutron scatt. obs. 80−50112
TbP_5O_{14}, Raman scatt. at monoclinic to orthorhombic phase transition, soft mode behaviour 78−56486
Te, trigonal, Raman scatt. at very high press. 80−60566
Ti-V, anomalous elec. resistivity, mag. susceptibility, soft-phonon induced structural inhomogeneities 78−60104
TiN, phonon dispersion curves, soft-mode behaviour, inelastic neutron diffr. 78−43083
TiO_2, elastic const. C_{44}, depend. on temp. 79−73239
Ti_nO_{2n-1}, long-range strain and localised relax. energies of crystallographic shear structs. 79−94948
$TiO_{1.95}$iFe, quenched near melting point, transverse composition waves 79−99220
$TiSe_2$ (1T), lattice dynamics and phase transitions 78−79727
$TiSe_2$ (1T), phonons and CDWs, inelastic neutron scatt. meas. 79−28059
$TiSe_2$ (1T), Raman studies of lattice dynamics 80−103962
$TiSe_2$, optical refl. spectra obs., suppression of antiferroelectricity by excess carriers 77−59536
$TiSe_2$, semimetal, IR props. 79−24318
$TiSe_2(S_2)$ (1T), electronic and vibronic struct. 80−44500
$TlAsS_4$, struct. and soft mode behaviour 78−91327
TlBr, complex refr. index meas. in far IR, by dispersive Fourier transform spectroscopy 78−92042
TlBr pseudodisplacive ferroelec., temp.-dependent dielectric response obs. 77−40247
TlBr, soft mode dielec., anomalous low temp. sp. ht. 78−14423
TlCl, phonon dispersion relations, neutron scatt. exam. 78−51628
TlN_3, press. induced phase transition, Raman scatt. meas. 78−19468
TlN_3, press. induced transition dynamics, light scatt. 78−80362
Tl_3PSe_4, phonon dispersion temp. depend. 80−96600
Tl_3PSe_4, struct. and soft mode behaviour 78−91327
TmSe, intermediate valent, Raman scatt. 80−16038
$TmVO_4$, Jahn-Teller system, critical dynamics and acoustic phonon coupling, Z-branch 77−84887
α-U, lattice dynamics 79−95101
U, supercond., phonon-softening 78−10592
α-U, superstruct. neutron scatt. obs. near 43K 79−95116
US, phonon anomalies 79−7663
$V_3Ga_{1-x}Sn_x$, lattice props. supercond., ^{119}Sn Mossbauer shift meas., 5-300K 77−1627
V, lattice dynamics, microscopic theory 79−7664
V, supercond., soft modes, d-electron localisation 78−14872
VO_2, diffuse X-ray scatt. due to lattice instability near metal-semiconductor transition 78−56074
VO_2, phase transition, temp. variation of US attenuation and phase vel. 77−31723
VO_2, $V_{1-x}Nb_xO_2$, crysts. and polycryst. films, metal-semicond. transition, polarised Raman scatt. 77−90151
V_2O_3 phase transition, temp. variations of US attenuations and phase vel. 77−31723
V_3Si, (Ge)(Ga), phonon density of states, temp. depend. 79−42183
V_3Si, CDW instability and anharmonicity 78−79734
V_3Si, elec. resist. below 77K, phonon assisted interband scatt. 78−14703
V_3Si, neutron irrad., neutron diffraction studies 78−88076
V_3Si, neutron irrad., sound velocity, magnetic susceptibility and upper critical field 78−88074
V_3Si, phonon density of states at 300K, mode softening 77−11648
V_3Si, soft mode sound vel. in mag. field rel. to density of states 78−14647
V_3Si, sp. ht. anomaly at struct. transform. 78−14426
$W_xMo_{1-x}O_3$, mixed cryst., structural phase transition, Raman and IR spectra 78−79766
WO_3, triclinic, condensed modes 80−15211
YFe_2, phonon softening below Curie temp., Mossbauer effect 77−4589
YS, electronic instability and phonon softening, APW calc. 80−29323
YS, soft-mode behaviour in phonon dispersion, inelastic neutron scatt. meas. 78−38807
YS, supercond., phonon anomalies, inelastic neutron scatt. 78−59901
YbIG, mag. transitions at low temp., soft mode existence 77−69557
ZnF_2, elastic moduli, press. depend., 0-10 kbar 78−10117
ZnF_2, elastic props., 4.2-300K, incipient ferroelec. transition 78−30691
Zr_2Ni, search for soft phonon modes, neutron scatt. 79−23686
ZrO_2, ZrO_2-HfO_2, soft phonon modes and monoclinic-tetragonal phase transition 77−62638

software (computers) *see computer software*

software engineering
see also software portability
computer-aided software development 79−89580
high energy physics computing, CERN conf. Jadwisin, Poland (June 1978) 79−89570
nuclear plant reliability data system, quality control program in design planning 79−97774
solar heating and cooling systems, computer program validation methodology 80−35742
Spar Buoy Oceanographic Telemetry System software engineering 80−46308

software portability
CERN, software standardisation 79−89553

sogicons *see semiconductor devices*

soil
acceleration excited by 1976 May 6 Friuli earthquake 78−24260
acid waters percolating through soil, limestone bedrock erosion 77−45023
acidification by precipitation, increased by S and N filtering by trees 77−73775

soil continued
active layer, parameterisation and influence on atmosphere surface layer *(Russian)* 78−44924
aerosol size distributions, common mode struct. 77−60454
affixants, effect on germination, emergence, growth of cheatgrass, Russian thistle 79−2140
agricultural soil, losses of N_2O dissolved in drainage water 79−43797
agricultural soil and plant improvement by ferromagnetic additives *(Russian)* 77−66882
agricultural soils, phosphate leaching to groundwater 79−20901
air humidity diurnal variation over continents, absorpt. in hygroscopic soil layer 79−29825
airborne particles mass concentration rel. to visibility 77−73849
aircraft/LANDSAT scanner data delineation by digital anal., Indiana 77−78496
Alberta forests, acidity of open and intercepted precipitation and effects on soil 77−73844
alluvial soils and flooding relationship in Piedmont Lowland, SE.Pennsylvania 79−88385
alpha and beta radioactivity meas. *(Rumanian)* 77−49067
alpha-emitting contaminants in environment, field monitoring using ZnS scintillator and phoswich detector 78−70646
analysis, neutron activation, using standard reference materials as multielement irrad. standards 78−80815
aquifer delayed yield resulting from soil water hysteresis 80−61834
archaeological sites, Mossbauer and mag. susceptibility studies of Fe oxides 77−30224
arid terrain, soil zone chemistry in cyclic wetting and drying 79−62529
atmosphere soil particles in Nagoya area, characterisation via urban aerosol Si and Al concs. 80−26581
atmospheric aerosol, soil derived, extinction between 0.55 and 10.6 μm 77−91264
automatic identification from digital terrain data 77−73884
available water storage capacity with restricted subsoil permeability 77−41089
basal hills in Darling Downs, SE.Queensland, slope profiles of cycloidal form 78−44820
blocked air pore volume meas. based on volume-weight relns. 78−57231
bulk resistivity, meas. method 78−24381
buried obstacle, interaction of shock wave rel. to bulk viscosity of subsoil *(Russian)* 77−89054
Canadian soil characterisation of FeO compounds by Mossbauer and other methods 77−44986
Canterbury, New Zealsnd, evapotranspiration, comparison of methods for estimating 77−53092
capillary hysteresis model 79−53386
cement mixture for earthfill dam embankment *(Japanese)* 78−39729
chalk of S.E. England, soils and geomorphology 77−44993
chemical grout for stabilization, simultaneous tests for engng. props. *(Japanese)* 78−31596
chemical migration of radionuclides in soil 80−17144
chemical process changes caused by acid precipitation 77−73773
clay, highly plastic, compaction and lime stabilization effect on pore size distrib. *(Japanese)* 78−31365
clay mineral dispersion and swelling, effect on soil hydraulic cond. 78−53668
clay soil/sand mixtures, reflectance 80−56475
clay soils, cracking and swelling dynamics 78−73359
clays, remoulded, shear stress path, stress history rel. to shear strength characts. 78−77219
climate, soil and vegetation, annual evapotranspiration value 79−79895
climate, soil and vegetation, annual precip. distrib. from storm sequences 79−84314
climate, soil and vegetation, annual water balance dynamics 79−79896
climate, soil and vegetation, annual water yield distrib. 79−84316
climate, soil and vegetation, soil moisture movement in liquid phase, model 79−79894
climate, soil and vegetation, storm surface runoff distrib. 79−84315
climate, soil and vegetation, water balance dynamics 79−79893
coarse-grained soil, free thermal convection, effective thermal cond. 77−25705
cohesionless soil, strength, influence of high pore-water press. 77−25678
cohesionless with curved yield surfaces, elastoplastic stress-strain theory 78−18186
complex dielectric permittivity, semidisperse model 77−29288
compression in aquifer, Theis soln. deviations for groundwater flow 77−64344
conductivity measurement methods *(Spanish)* 79−96831
consolidating soil indentation effect of Poisson ratio 78−83340
consolidation, due to shear loads distributed over rectangular area 79−57936
constitutive model for critical state soil 79−16443
creep induced by freeze-thaw cycles, rate meas., lab. expt. 77−81868
crop and soil bidirectional reflectance factor calibration, remote sensing field research 80−86382
cultivated loamy soils, Belgium, splash and wash 78−73410
Cumberland Peninsula, Baffin Island, hornblende grain etching, age and palaeoclimate indicator 80−8307
cylindrical detonation waves, propag. in multicomponent media 79−86287
deformation of compressible elastoplastic ground 78−96198
desert colour, Apollo-Soyuz photographs 78−65315
desert formation mechanisms 77−70707
dew meter, β-absorpt. type, appl. to meas. on soil and plant surfaces 78−24803
diffusion eqn. soln. with exponential diffusivity comparison of iterative and perturbation techniques 77−41097
diffusive sorption of water in dry soil 77−41077
dilatation props. after expansion of gas cavity in brittle rocks 79−8608
drainage runoff hydrograph calc. for loamy soils in Lithuanian SSR 79−39781
drought effects on agriculture in United Kingdom, 1975-76 period 78−57298
drying, evaporation, solar radiation and atm. temp. effect 80−8373
dust due to soil disturbance, particle absorption contributions to mass extinction coefficients 80−61896
dust storms, Great Plains, USA, lessons 79−29486
earthquakes, two-dimensional horizontal ground motions rel. to engineering structs. design 79−48419
elastic, drained and undrained behaviour, anal. 77−3720
soil continued
elastic modulus in non-homogeneous stratum, hyperbolic variation 77−868
elasto-viscoplastic-viscous theories of granular and porous media, soil mechanics appl. 79−76982
elastoplastic deformation, volumetric constitutive equation 80−53655
elastoplastic ground motion during earthquake *(Japanese)* 79−70748
elastoplastic hardening, incremental approach 77−75818
electric soil moisture gauges, testing procedure 77−78481
electrical conductivity measurement, via HF EM induction profiling *(Polish)* 80−51547
electrical parameter measurement in SW range 80−22388
electrical properties, investigation of seasonal variations, in 10-1000 kHz band 78−88796
electrolyte flocculation of stabilised potassium 79−43638
emissivity of moist soil in microwave range, temp. effect 79−29797
England, decreasing wetness in 1969-77 period 78−65377
England, lowland soil survey, moisture content and soil discrimination from air photos 79−88504
erodibility factor rel. to aggregate stability and micromorphological props. 79−48522
erosion, wind tunnel simulation, effects on fine dust production 79−20834
erosion by Hortonian overland flow, magnitude and freq. 77−70701
erosion by wind in New Zealand, erosiveness index 79−5579
erosion prior to overland flow, time and aggregate size rel. to crusting process 79−20876
erosion processes meas. in German area of Moselle river valley 77−81937
evaporation rate from porous surfaces, wind tunnel *(French)* 77−80684
Everglades Agricultural Area, USA, soil temp. obs. in winter nighttime 80−56559
Everglades National Park and adjacent agricultural areas, polychlorinated biphenyls and chlorinated pesticides 79−92098
external environmental radiation levels of naturally of occurring radioactive sources 78−9001
filtration with partial saturation *(Russian)* 77−60433
fissionable element impurities, nature and distrib., fission track method 78−44436
fluid flow with free or artesian surface 78−92872
fluid saturated porous solid, fundamental solns., deformation, pore-fluid diffusion, soil mechs. 77−84160
forest soils, effect of acid precipitation 77−73771
forested watershed Oesling, Luxembourg, chemical erosion 77−81930
foundation calc., appl. of multilayer stress displacement calc. by double layer method *(Chinese)* 79−37162
foundation dynamic interaction with viscoelastic half-space *(German)* 78−79228
freezing, effect of moisture exchange and heaving 77−25702
freezing, migrational flow of moisture 77−25704
freezing, water migration obs. *(Japanese)* 78−88862
freezing processes, finite element simulation 79−16527
freezing soils, heat flux meas. *(Japanese)* 78−88835
freezing velocity meas., recording device design *(Japanese)* 77−82033
frost depth in soils of Urals and W.Siberia 79−57986
frost heave in Tomakomai, Hokkaido, 1976 to 1977 *(Japanese)* 78−92860
frost heaving, role of disjoining press. 79−29791
frost mounds, Bear Rock, NW Territories, Canada, obs. during 1975-76 period 78−65346
frozen, struct. changes during freezing and thawing 77−25707
frozen, theoretical basis for thermal model expts. *(Chinese)* 79−79823
frozen, water and ice envelope pressure potentials 77−78286
frozen, water transport towards ice front 77−945
frozen soil, prediction using weather records 79−88379
frozen soil, self-similar soln. of water infiltration eqns. 77−70713
fundamental period estimation for soil profile 77−9359
gas fluxes determination, chamber methods numerical evaluation 79−16700
gases, long distance migration detect. via Rn integrated emanation mapping 78−85560
geomorphological processes, conf., Louvain, Belgium (Apr. 1976) 77−81923
grassland surface temperature rel. to air temperature in summertime 77−78396
Green and Ampt infiltration eqn. parameters depend. on initial water content 79−79899
Grote Nete basin, Belgium, geomorphology *(Flemish)* 78−61452
ground surface temperature and moisture content, prediction with inclusion of vegetation layer 78−73373
groundwater, hillslope hydrographs using finite element method 77−70696
groundwater flow pattern in soil using equation of mean 80−81958
groundwater natural recharge, math. modelling 78−11934
groundwater seepage flow, Boussinesq eqn. solns. 79−2320
groundwater seepage in porous elastic soils, numerical performance of finite element schemes 77−91162
in hailstones, obs. and derivation 78−96260
hardening, anisotropic model, cyclic loading appl. 79−16441
heat and moisture transport in atmosphere-soil boundary 80−77023
heat and water coupled movement prediction in unsaturated soil math. model 78−61446
heat and water transport, force-restore method for ground surface temp. prediction 80−98469
heat recovery from nuclear plants for agriculture and pisciculture 78−37464
heavy metal adsorption and interfacial reactions 78−3832
heavy metal ion removal in clay suspensions 77−86955
hillside soils, N.Yorkshire, England, pedological features affecting permeability 77−45021
hillslope profiles in mid-Wales, sedimentological anal. 77−70666
horizontal contact resonances of vibration pickup with rectangular bases on soil surfaces 80−96160
humid temperate zone, potential effects of acid precipitation 77−73772
hummocky microrelief in Canadian north, dynamics 77−64285
hydraulic conductivity, numerical calc. from suction press.-moisture retention relation *(German)* 79−2297
hydraulic conductivity in frozen soils 77−33119
hydraulic conductivity of frozen soils 77−45035
hydraulic conductivity of unsaturated porous media 79−5526
hydraulic conductivity var. of Wisconsin soil series 78−81250

soil continued
hydraulic fracturing for stress meas. in hard and soft earthen material 77−9577
hydraulic properties, empirical eqns. 79−53385
hydraulic properties, scaling of field meas. using similar media concept 77−78278
hydraulic props., spatial var. in water budget modelling 77−73779
hydrologic behaviour of forested mountian soil, coastal British Columbia 79−84320
hydrologic infiltration model 79−16548
hydrometer particle size analysis calc. method 79−62590
hydrophys. charact., determ. method 80−85696
hysteresis effects under loading 80−21712
hysteretical models for prediction of hydraulic conductivity of unsaturated porous media 77−41088
ice-wedge casts in NE county Wicklow, distrib. and struct. 78−69379
icy permafrost in NE.British Columbia, distrib. and thickness 78−77277
in situ testing, using Camkometer self-boring pressuremeter 79−8717
industrial complex environmental impact, Whatcom County, Washinton, USA 79−57532
infiltration, parameter estimation of Green and Ampt eqn. 78−61473
infiltration, spatial var. of hydrological effects, Monte Carlo anal. 80−8363
infiltration eqn. soln., comparison of perturbation and iterative techniques 77−41096
interaction with surface mounted struct. under excitation by plane SH wave 78−22292
interblock hydraulic conductivity values for transient unsaturated flow problems, finite difference soln. 80−12460
IR spectra of hydrothermally altered area, for remote sensing 80−81871
irrigation, connection between soil and groundwater 80−26554
irrigation, kinematic model 79−5529
land-use data processing for resource planning 78−7804
landscape periodicity, slope deposits, soil pattern and erosion in small catchment area 78−11924
landscapes, soils and erosion, Wither Hills, New Zealand 78−88864
landslides due to rainwater permeation, residual strength and frictional resist. of sliding soil masses *(Japanese)* 78−11919
landslip/debris flow, Bilsdale, North York Moors, 1976 September 79−48524
lateral translocation in small valley basin in Hertfordshire 77−45026
layered, effective moduli theory appl. *(Polish)* 79−25237
life in terrestrial soils rel. to planetary soil biological search 79−40176
Lithuanian lake catchment area soil N and P distrib. *(Russian)* 79−96780
loamy sand, Flanders hilly region, quantitative rill and gully erosion study 77−81936
loess erosion and redeposition by water, expt., micromorphology 77−81925
loess geological environments, China *(Chinese)* 78−81156
loess-formed quartz silt thermoluminescence and dating *(Chinese)* 78−57226
loss factors rel. to flow, runoff creep and rainwash 77−45028
Lower Tertiary laterite on Iceland-Faeroe Ridge, rel. to Thulean land bridge 78−85514
lunar soil 15081,2, adsorpt. of methanol and water, microcrystallinity determ. 77−87292
Luxembourg Ardennes, aggregate stability and colluviation 77−44994
machine processing of remotely sensed data, conference, West Lafayette, Indiana (1980 June 3 to 6) 80−82586
Mantaro landslide, Peru, seismological and geological aspects 78−96248
mass exchange in filter medium, hydrodynamics *(Russian)* 79−37292
Matushiro fault zone, Japan, He spots caused by diapiric magma from upper mantle 79−8618
maximum molecular moisture capacity correl. with plasticity 77−78267
mechanical properties rel. to viscoplasticity under dynamic loads 78−96197
mechanics, triaxial test, limit analysis theory *(French)* 78−32073
membrane transport, physico-chemical aspects 77−29107
metal concs. in soil solns. 79−34824
micro-organism beta-particle dose rates from natural radionuclides 77−90913
microwave backscatter from ploughed soil, surface roughness meas. *(French)* 80−82072
microwave brightness spectra of layered media 77−81898
microwave emission, surface roughness effect 80−17264
mineral, dissolution under Earth surface conditions, rate control 79−20817
Moisie River, Quebec, gully flow development after heavy rainfall 77−5249
moist, dielectric relaxation model suitable at microwave frequencies 77−43930
moist, thermodynamic state functions *(German)* 80−4056
moistening, one-dimensional, surface water effects *(Russian)* 80−46209
moisture, convective-dispersive solute transport with combined equilib.-kinetic model 77−64356
moisture, effect on circulation and rainfall in a tropical model 77−45133
moisture, estimation of effective capillary press. in Green and Ampt infiltration eqn. 78−3844
moisture, freq. shift dielectric sensor 78−53739
moisture, heat and salt transport, math. model 80−26563
moisture, hydrometeorological aspects of 1975-6 drought in UK 77−70769
moisture, meas. of evapotranspiration of Douglas fir using weighing lysimeter 77−64353
moisture, microwave remote sensing, sampling techniques for ground truth data 78−65439
moisture, remote sensing by Heat Capacity Mapping Mission 79−5640
moisture, remote sensing with air temp. compensation 77−17247
moisture, stored productive, remote determ. technique 79−29795
moisture, subsoil neutron probe, lab. calibration, minimum soil sample size calcs. 77−57333
moisture and component estimation from spectral polarisation 79−16678
moisture and geology mapping, thermal inertia method 80−8344
moisture and winter wheat yield on Great Plains, Landsat data 78−65351
moisture calc. methods *(Russian)* 77−29493
moisture change-of-state front advancement in freezing and thawing 77−91163
moisture content, determ. by meas. of reflectance in ultrashort radio wave band 78−16075
soil continued
moisture content, microwave radiometer meas. over bare and vegetated surfaces, comparison 78−88851
moisture content meas., quick drying procedure 80−82109
moisture content measurement, remote sensing through agricultural crop 80−109147
moisture content measurement by microwave radiometry 80−17425
moisture deficit estimation from meteorological factors 79−20890
moisture distillation, contrib. to dew 78−73446
moisture horizontal absorption in unsaturated soils, infiltration analysis 77−29345
moisture influence on evaporation, Priestley-Taylor model 78−24314
moisture meas. by remote microwave radiometry 79−48526
moisture meas. using airborne imaging passive microwave radiometer 78−36310
moisture measurement, microwave and radar techniques 79−70896
moisture measurements, active microwave remote sensing, surface roughness and texture effects 79−12295
moisture meter, development *(Japanese)* 78−88935
moisture movement and groundwater recharge by T tagging technique 78−61438
moisture of surface, remote sensing by visible and false colour IR photography 80−56653
moisture profile development during water redistrib. after infiltration 77−29344
moisture profiles during steady vertical flows in swelling soils 79−5524
moisture sensitivity of cross-polarized radar backscatt. 79−25282
moisture surveys using microwaves and infrared heat measurement *(French)* 79−96772
moisture vars. under bare conditions rel. to rainfall at Pune and Delhi, India 79−96777
monidisperse quartz fractions from soils in completely dry state, local stability criterion 77−49060
multi-layer soils, state vector approach to one dimens. consolidation 78−3757
multiband photography for geomorphology, soils and land use study, feasibility 78−12025
multielement determ. by computerised instrumental neutron activation anal. 77−44546
natural radiation exposure, New Zealand, soil survey and air doses for ^{226}Ra and ^{232}Th daughters and ^{40}K 78−88747
natural sink for atm. N_2O 77−21772
near surface soil moisture, theory for passive microwave remote sensing 77−87105
neutron soil moisture meter, design and operation 79−44280
S New Mexico, Holocene soils and soil-geomorphic relations in semiarid region 77−78184
New Zealand, ^{238}U, ^{226}Ra, ^{232}Th and ^{40}K radionuclide conc., rel. to Fe, K content 77−86867
New Zealand, soil survey by multispectral aerial photography 78−85728
New Zealand soils, survey of naturally occurring radionuclude conc. 77−53057
noncoaxial plastic soil, steady in-plane deformation, flow conditions 79−84279
nondestructive neutron activation analysis of environmental samples using low-energy photon spectrometry 78−3995
nonhomogeneous water saturated, plane shock wave propag. 77−56607
nonlinear diffusion eqn., perturbation soln. 77−41087
nonsaturated, water infiltration, positive head effect *(French)* 79−2296
nonsaturated soil surface, water evaporation parameterisation 79−53372
Nova Scotia, polycyclic aromatic hydrocarbons 79−74555
organic C rel. to CO_2 cycle and atm. CO_2 conc. 79−58063
Otway Ranges and coastal plain, S.E.Australia 78−20418
overburden potential theory, swelling soils 77−41095
partially buried buildings, heat flux through soil, calc. *(German)* 78−55554
pathogenic fungus population reduction by 2.45 GHz irradiation 80−3719
peat, recent ombrotrophic sections, rel. to atm. fallout of magnetic particles 78−61519
perennial grasses potential yield and yield shortfall due to water deficit, agroclimatic estimate 78−61450
perennially frozen ground water cold store, struct. *(Japanese)* 78−88834
permafrost, approx. calc. of thawing zone boundaries under heat sources 77−25706
permafrost, common depth point survey technique appl. *(Russian)* 78−53751
permafrost, computer-assisted interpretation of EM soundings 77−2086
permafrost, effect of seepage flow on thawing and freezing 79−1241
permafrost, elec. props. of active layer, in situ meas. 77−64333
permafrost, neutron moisture gauge for water detection *(Chinese)* 79−34997
permafrost, obs. of sub-pingo water lenses, Tuktoyaktuk Peninsula, Northwest Territories, press. meas. 79−20873
permafrost, shallow, mapping, EM methods 79−16694
permafrost, thermal amelioration tests near Schefferville, Quebec 77−33058
permafrost, thermal and electrical conductivity, 0 to −20°C 77−24450
permafrost, two-dimens. temp. field with arbitrary temp. distrib. on subaerial surface 77−25703
permafrost, US vels. and elec. props. 77−78157
permafrost discontinuity geometry and physical props. determ., Schefferville, Canada *(French)* 77−66990
permafrost fossil patterns, S.W. Ontario, resistivity mapping 77−66991
permafrost layer thickness and temp. variations under sedimentation or denudation conditions 77−78241
permafrost mapping by audiofrequency magnetotellurics 79−58102
permafrost near Tuktoyaktuk, NWT, impulse radar obs. 77−17149
permafrost soil, compressional and shear wave vels. using US pulse technique 77−17081
permafrost soil in Yakutia (USSR), long-term studies of thaw dynamics 77−78240
permafrost terrain, EM probing, theory 78−28323
permafrost thickness determ. in wells in N. Canada 77−66989
pH and base saturation of exchange sites, acid precipitation effects 77−73774
physical properties study by US wave attenuation meas. *(Polish)* 77−9566
physics, book 80−27056

soil continued
piezoelectric sensor element for press. meas. in soil pores *(Polish)* 79−25363
plastic limit analysis with anisotropic parabolic yield function 77−91114
pollution, elemental deposition downwind of coal-fired power plant 79−20838
pollution by ^{239}Pu, ^{241}Am, Ge monitor for in situ assay 77−9546
pollution indication, by humic and fulvic acid chemistry 80−76688
pollution indication, Ca and NO_3-N loss from microcosms 78−16019
polygonal patterned ground in central New Jersey, origin during Wisconsin glaciation 79−25248
pore size distrib. estimation from moisture charact. 80−12454
pore water characteristics, modelling, similarity hypothesis 78−11941
porous elastic soil, finite consolidation theory 77−46916
porous thermoelastic matrix, slow fluid flow theory 79−7406
power plant waste heat utilisation, simultaneous heat and mass transfer governing eqns. 78−94562
pressure meas., using capacitive sensor with polyurethane foam dielectrics *(Slovak)* 80−86281
propagation velocities in subsurface soil layers 79−62460
pulverulent, homogeneous, stresses due to vertical local load *(French)* 78−61398
quartz grain source determ. from etch features 77−70650
quartz grains of podzols, surface texture, SEM study 78−36151
Quaternary loess deposits of Banks Peninsula, New Zealand, radiocarbon dating 78−24271
Quaternary profiles, SW.Slovakia, palaeomag. study *(Russian)* 79−39654
radar cross section, ground meas. for land and vegetation, influence of soil roughness *(French)* 77−49065
radiation balance of Earth surface and components, influence of irrigation 79−29863
radioactive disequilibrium, of U and AC series nuclides 80−4014
radioactive fallout effects of Nagasaki atomic bomb 78−85393
radioactive waste, low-level, radionuclide migration in soil 79−54610
radioactivity, determ. of bulk α and β radioactivity *(Rumanian)* 79−88346
radioactivity, terrestrial beta radiation field in natural environment, numerical evaluation 78−81161
radioactivity of soil samples from W.Cumbria Pu and ^{137}Cs concs. and possible maritime effect 80−108817
radioisotope sorption on USA subsoils from differing weathering intensity areas, ^{241}Am, ^{237}Np and ^{99}Tc 78−16014
radionuclide adsorption by manganese oxides and implications for radioactive waste disposal 78−69349
radionuclide contamination, ^{89}Sr and ^{90}Sr determ. using total sample decomp. 80−35808
radionuclide migration in groundwater from accelerator earth shields 79−48194
radionuclides, movement through soil *(Japanese)* 77−81593
radionuclides in sample soil and water, distrib. coeff., environmental effects 77−13092
radwaste storage, soil homogeneity evaluation by radionuclide tracer breakthrough curve interpretation 80−97821
rain infiltration into soil, theory *(German)* 80−90102
rainfall infiltration into bare soils, theoretical model and expts. 78−49058
rainfall variable infiltration, eqns. 79−53379
rainsplash erosion of sandy soils, field study 79−20879
remote sensing, relative importance of reflected and emitted flux density in 3 to 14 μm range 79−92542
resistance meter, geological and archaeological applications *(German)* 78−57361
resistivity meas., LF electromagnetic wave method *(French)* 78−24394
rigidity testing using capacitive transducer 78−19977
roadside soil and plants in Alexandria district, Egypt, contamination with Cd, Ni, Pb and Zn 78−81171
rock glaciers in southern part of Jasper National Park, Alberta, distrib. and charact. 78−77276
Rother catchment, W.Sussex, fine sediment mineralogy of source rocks and suspended sediment 79−20827
Rotoehu Ash weathering in Bay of Plenty district, New Zealand 78−85558
S-wave vel. meas. in soil and bedrock using down-hole method 80−98458
salts, dissolving and outwashing from soil and rock, hydromechanical treatment *(Russian)* 78−77279
sample control and identification system, computer operated, for neutron activation anal. of soil 79−96402
sands, poorly graded, moisture distrib. in capillary crack *(German)* 80−31066
sandy and clay soils, microwave absorption *(Russian)* 78−81162
sandy beaches, rhomboidal lattice struct. 77−37178
sandy moist, compressibility and plasticity during repeated shock loading 78−11885
sandy soil, mech. charact. under static loadings 79−88345
Santorini, soil conditions during Minoan times around 1500 BC 78−40552
saturated-unsaturated flow in deformable porous media, numerical model, appls. 79−81966
saturated-unsaturated media, hysteresis effect influence on transient flows 78−59481
seasonal freezing or thawing depth calc., eqns. eval. 77−78243
seasonal temperature, altitude effects 79−100828
seepage, free water surface behaviour in porous media 80−8349
seismic amplification functions, stochastic approach 77−9358
seismic Rayleigh surface waves, soil-structure interaction anal. 78−81109
seismic response, complete microzonation procedure importance and existing methods reliability 79−34748
seismic response and liquefaction, non-linear dynamic anal. 79−57862
shear wave velocity, meas. during standard penetration test 78−48978
sheetwash and rainsplash, soil entrainment, slope angle effects 79−74908
shield design for variable energy cyclotron 77−61622
shock wave interactions cavitation effects 79−70792
slope models and soil development models 77−81933
slope stability and valley form. in glacial outwash deposits, Norfolk, England 79−20880
slopewash and wind action, Quaternary morphogenesis in Belgium 77−81924
soil, heat and mass transfer with phase change 79−1093
soil moisture measurement, remote sensing simulator 78−49143
soil continued
soil-water system, γ-ray transmission studies, calibration 80−26629
solar energy accumulation by soil in shed hothouse 80−21373
solar energy storage, pebble layer heat exchange investigation 80−21374
solute conc. rel. to throughflow 80−31070
solute transport in soils, two-site adsorption-desorption model evaluation 77−41101
specific thermal resistance meas., theoretical basis and apparatus *(Rumanian)* 79−5461
spherical detonation waves in media with volumetric viscosity 79−14332
splash erosion and colluvium form. beneath deciduous woodland, Luxembourg Ardennes 77−81929
spring runoff from arable land and saline soils *(Russian)* 77−21811
spring-flood forecasting and runoff loss due to water absorpt. by soil 80−109178
stabilisation with granulated slag, increased compressive strength *(Japanese)* 78−31464
steel, mild, critical soil moisture content in underground corrosion 79−96186
stiffness and damping charact. for power plant design 77−3174
Straits of Malacca marine environment, radioactivity in near-short soils 79−12135
subarctic and tundra surfaces, evap. equilib. model 78−61459
subsea permafrost heat and mass transport processes, mol. diffusion and consequences anal. 79−2302
subsoil behaviour in Potsdam rel. to storms and atmospheric pressure *(German)* 79−62425
subsoil conditions, basis for seismic microzoning, maps 79−44108
subsoil liquifaction during earthquakes in Japan 78−36118
substrate core sampler, lightweight low-friction, ecological survey appls. 80−95090
subsurface drainage and irrigation, expt. evaluation of theoretical solns. 78−61465
subsurface moisture profiling, microwave probe 78−65939
surface β-activity caused by nuclear explosion products, depend. on isotope vertical migration 78−86700
surface moisture content parametrization, use in atm. prediction models 78−49052
surface moisture determination, photographic method for polarised visible light recording 79−53557
surface runoff, New Zealand, P transport, effect of fertiliser and grazing cattle 77−53094
surface temperature, rel. to sensible and latent heat fluxes influence on four-day forecast 79−96805
taluvium, residual shear tests on soil from natural slopes 78−65262
teledetection methods for determination of soil water balance *(French)* 79−96773
temperature, periodic regression model 78−73544
temperature differences and diurnal var. in Welsh soils 77−64403
temperature measuring system and data for Whiteshell Nuclear Resea-ch Establishment 79−48590
temperature prediction from winter period meteorological data 77−37418
temperatures of soil and ground surface in humid tropics, case study from Sierra Leone 80−109242
terrain classification using colour imagery, algorithms 77−78466
thawing under polar conditions using synthetic film covers, thermal balance meas. on polymeric film covered surfaces 77−78244
thermal and hydrological surveys by satellite *(Italian)* 77−81988
thermal conduction flux in situ meas., methods *(French)* 78−96331
thermal conductivity measurement by probe method, minimisation of errors 77−17259
thermal conductivity of frozen soil, thermal probe meas. method *(Japanese)* 77−82034
thermal diffusivity, Fourier anal. of temp.-depth profile 79−44264
thermal inertia, cartography in Africa by geostationary satellite (CITHARE project) 80−76980
thermal neutron constants, calibration of moisture gauges 77−25804
thermal props., transient measuring method *(German)* 78−61619
thermograph for soil temp. meas. 78−4005
thin sections, cutting method 79−80040
tilt, rel. to earthquakes and weather 77−91058
Tolaga Bay Flats basin, recent alluvial infilling estimation using tephra marker beds 78−11925
topsoil mineralogy, Ngunguru Basin, New Zealand 78−85557
transfer resistance of European soils to SO_2 77−37384
transuranic wastes, interaction with soils 79−96488
tree root potential meas. electrode earthing method *(Russian)* 80−26420
trench leachates, low-level radioactive waste disposal sites, organic carbon content 80−17145
Tuktoyaktuk Peninsula, NWT, pulsating pingos 77−53080
tundra, CO from arctic surfaces during spring thaw 80−41511
tundra surface roughness vars. with season rel. to turbulent mixing and heat flux 77−87016
Tuyuksuy moraine, Lake 2 breakthrough beneath coffer dam *(Russian)* 77−53091
two phase with viscoelastic skeleton, finite element anal. of consolidation 77−11138
unsaturated porous media flow anal. by finite element method 78−92869
unsaturated soil simultaneous heat and moisture transport analysis by finite element method 78−92868
unsaturated water flow within porous materials, obs. by NMR imaging 79−98840
unsaturated zone hydrology, United States educational effort 78−81224
urban erosion and sedimentation prediction and control 77−37282
valley incisions widening by soil fall in forested Keuper area, Luxembourg 77−81927
vegetation cover, radar backscatter meas. of surface roughness, soil moisture and texture 79−62534
vertical infiltration of water in unsaturated soils, analysis 77−29346
vertical structure, interaction effects, seismic ground motions 79−92496
viscoplastic model, eqns. and expt. determ. *(Russian)* 78−7619
viscous nonlinear, stresses and strains 78−73363
volatile trace elements determ. by RNAA 79−44276
warming of soil by using waste heat from nuclear power station 78−37463
water, hysteretic steady state profiles 77−91172
water, nonlinear diffusion eqn. via perturbation, iterative and optimal techniques 77−66943

soil continued
water absorption with exponential diffusivity, infiltration anal. and perturbation methods 77−66944
water accumulation in low-level radioactive waste burial trenches at West Valley 78−13266
water accumulation in low-level radioactive waste burial trenches at West Valley, remedial work 78−13267
water content, estimation via total solar reflectance and spectral band ratioing 77−60479
water diffusivity, scaling using universal consts. 80−8371
water flow, two-dimens. infiltration and redistrib., numerical anal. 78−11942
water flow in unsaturated noncohesive soil, modelling *(Polish)* 77−70709
water flow model with two-dimens. automatic γ-ray attenuation scanner 79−53387
water flow modelling, finite difference and Galerkin techniques 78−81249
water flow through soil with initial gradient 78−32127
water infiltration equations for simple systems 77−78282
water infiltration into frozen soil 78−16077
water infiltration into frozen soils, numerical modelling 79−39772
water infiltration into uniformly packed soil 77−2152
water percolation, sampling using plastic suction lysimeter 77−29498
water potential, detailed field monitoring of variable source areas 79−88380
water potential evaporation from soil surface, eqn. adaptable to remote sensing use 77−64334
water potential in temp. gradient, thermocouple psychrometers improvement 79−74974
water regimes near porous cup water samplers, theory 77−66942
water saturated-unsaturated flow in deformable porous media, numerical model 77−91181
water transport in soil-root system, transient analysis 77−5269
water transport through unsaturated soil, Buckingham-Darcy flux law 79−16541
water transport through unsaturated soil, conservation laws 79−16540
water vertical infiltration in dry soil 77−78279
watershed geochemistry, aqueous solns. control by soil materials 78−20445
watersheds of Eastern USA, ^{137}Cs distrib. 77−25701
wave interaction, stresses and strains 77−86801
waves propagation, theory for granular medium 77−23909
weathering, geochemical study and elemental redistrib. 78−7634
wet, complex permittivity meas. at microwave, method 77−45184
wind erosion and suspended dust deposition, wind speeds and particle concs. 78−40623
wind erosion threshold velocities, tests with portable wind tunnel 79−70826
world soil map 79−57937
Yugoslav soil medium-wave conductivity chart computation *(Slovenian)* 79−39718
Al leaching response to acid precip., effects on high-elevation watersheds in NE. United States 80−12442
^{241}Am soil concs., in situ gamma anal. and sampling data comparison, Nevada 77−64143
As determination in rocks and soils by at. absorpt. 79−88475
B abundance determ. 78−85559
^{14}C analysis and soil dating 78−36299
^{14}C dating of geological and archaeological samples 78−92993
Co and actinide adsorption by Mn and Fe oxides in soils and sediments 79−66422
Cs transport, evaluation of combined sorption model 79−8554
^{137}Cs fallout in arid watersheds, phys. and chem. parameters affecting transport 78−61461
^{137}Cs in alpine tundra habitats, effects of phys. habitat factors and plant morphology 77−37058
^{137}Cs levels in soils and vegetation of W.Malaysia 78−73263
^{137}Cs, runoff coeff. from surfaces of river basin soils 79−44212
^{3}H, environmental transport from atm. release of mol. ^{3}H 78−11987
Hg, average future content of soil in European Economic Community 79−8687
Hg levels in soil and water in Israel and Sinai 77−29337
I, radioactive, adsorption concentration depend. obs. *(Czech)* 80−12031
N fertilised soil, N_2O evolution rates 79−16656
NO_3^--N export from drainage basins, Toronto, Ontario 79−66729
N_2O, atm. life cycle, ground surface sink mechanism 77−66971
N_2O, atmospheric, prod. and consumption by soils 78−85631
N_2O emission from soils, effects of acetylene and soil water content 79−83672
N_2O emission from soils during nitrification of fertiliser 78−57313
N_2O source when soil moisture less than field capacity 78−61419
P transport in sandy soils, expt. and simulation 77−66940
Pb adsorption, in presence of Ca 77−33079
Pb adsorption, Langmuir and Freundlich isotherms 77−33078
Pb, contamination, rel. to traffic density *(German)* 79−70470
Pb, New Zealand, battery factory and smelter emissions compared with vehicle exhausts 78−85562
Pb, pollution in Christchurch, New Zealand 78−85561
Pb total in soil, comparative study of analysis methods 78−16221
Pu, Am, low conc. meas. in earth samples, appl. of Si(Li) X-ray detector 78−58505
Pu contaminated soil, nondestructive anal. 79−11879
Pu distribution in Ohio soils, local and stratospheric sources 78−16015
Pu distribution in Rocky Flats soil 78−73265
Pu dose to lung and bone from contaminated soils, statistical uncertainties 80−109028
Pu dynamics in deciduous forest ecosystem, linear compartment donor-controlled model 78−85392
Pu, inhalation hazard eval. 79−66836
Pu isotopes, in soil, determination using alpha-spectrometry 80−45601
Pu, remote contamination and total inventory from Rocky Flats, mass spectroscopic anal. 77−73739
^{239}Pu soil concs., in situ gamma anal. and sampling data comparison, Nevada 77−64143
$^{239}PuO_2$, size characts., Rocky Flats soil, autoradiographic technique 78−96102
^{226}Ra in Taiwan buffalo bone and environmental samples of N. Taiwan power reactor site 77−64142
^{226}Ra leaching from contaminated soils, investigation of Ra bearing soils from Port Hope, Ontario 79−20900
soil continued
Rn conc. in underground waters and soil-air around Asama Volcano, Japan *(Japanese)* 79−70813
Rn concentration variation, temporal (spatial), simple model 80−33671
Rn lognormal distrib. 77−5205
^{222}Rn concentration distribution under ground, effect on natural γ-ray flux density and exposure rate 80−36300
^{222}Rn exhalation meas., soil and meteorological effects *(Spanish)* 80−31082
^{222}Rn releases associated with cultivation of agricultural land 80−16850
S content and acidity of soil in Alberta, SO_2 effect 77−73843
^{90}Sr migration in aerated zones, theoretical estimation *(Japanese)* 79−9896
^{90}Sr, runoff coeff. from surfaces of river basin soils 79−44212
U environmental distribution and movement, agricultural product distrib., Japan 77−90921
U isotopes, in soil, determination using alpha-spectrometry 80−45601
U series nuclide conc. in soil particles rel. to their size 77−33073

solar absorber-convertors
absorbers, various, struct., electron reflection exam. 77−125
active collectors, design features and performance definition 80−51000
adiabatic desiccant dehumidifiers for air conditioning, performance predictions, linear modelling 80−85305
air collectors with porous absorber to reduce radiative heat transfer losses *(French)* 80−55900
air conditioning system, using evacuated tubular collectors, digital simulation and design, comparison with actual performance 79−61949
air heater buoyancy and tube inclination effects 79−62058
air heater cost-effective optimum design 79−62039
air heater transient model 79−62042
air heaters, comparative investigation of heat collectors heat-engineering characts. 80−92018
air heaters, single and double exposure, heat balance anal. 80−45734
air heating/cooling systems for buildings, review 80−45754
air-cooled solar receiver, analytical and expt. determ. of rad. and temp. distrib. 80−55894
algae, living electrode for biophotolysis of water, long-lived photoconvertor 80−104510
annular receiver heat losses by conduction and convection, reduction techniques 79−79409
antireflection coatings on metals for selective solar absorbers 79−65951
aqua-ammonia gas turbine unit, for farm power needs in India 79−62024
austenitic stainless steel thermal treatment for spectrally selective surface fabrication 80−35752
axial conduction effects on heat removal factor 80−7955
axisymmetric reflector-absorber systems with uniform flux conc. 80−94111
Baghdad insolation and meteorological data for flate plate collector design 79−62092
bi-coolant wall, heating cycle, thermosiphoning, building heating and cooling 80−72083
biological solar radiation utilisation, optical model for polar animal pelts 80−51045
black chrome solar selective absorber, microstruct., chemical comp. and reflective props. 80−7959
black Cr and Ni electrodeposit spectral selective props. 79−62036
black Cr coatings, optical props., using inhomogeneous medium theories 80−12026
black liquid collector, student apparatus 79−97140
black liquid cylindrical parabolic collector, thermal analysis 79−74539
black liquid solar collector analysis and expt. 79−62097
black liquid water, total transmittance of solar radiation 79−34441
block unit, thermal characts. experimental investigation 80−97801
Brayton cycle solar electric plant receiver, 1 MW_t bench model design and testing 80−55896
building insulation optimisation, w.r.t. internal and solar gains 79−62147
CAD of windows as passive solar collectors, using interactive program 79−62146
Cassegrainian solar concentrator, optical and thermal analysis 80−40906
cavity solar collectors with selective radiation-absorption properties, optimal geometric parameters 80−21410
cavity-type solar receivers, HEAP computer simulation program for heat energy anal. 80−30548
cavity-type surfaces for solar collectors 79−48180
central receiver gas turbine plant, using liquid metal heat pipes 79−48096
central receiver solar power stations, solar receiver tube thermal stresses, fatigue aspects 80−40908
central receiver systems for thermoelectric conversion 80−45760
ceramic solar cavity receivers for thermal electric systems 80−30549
cermet film, as solar selective absorbers, production, struct. and optical props. 79−29485
cermet film, dense, regular, optical props., rel. to appl. as selective solar absorber 79−79408
channelled solar flat-plate concentrator geometry and beam deviation 79−62072
chemical, using SO_3 gas, 'Solchem' project 80−50994
chemical treatment of cover to reduce reflection *(French)* 78−25982
chrome-black films, optical props of electrodeposited films 77−81168
coating, on to pipe *(Japanese)* 80−16834
coating development for solar energy conversion 78−79096
coaxial evaucated tubular element, with multilayer selective coatings 79−39315
collector, evacuated cylindrical, analysis 80−21415
collector absorption enhancement using multiple reflections 80−76649
collector applications for space and water heating in buildings 80−61406
collector array flow imbalance detection by thermography 79−83634
collector array performances calc., using Hottel-Whillier-Bliss equation and field-derived data 80−45724
collector arrays, calc. of performance for N collectors in series from single collector test data 80−45740
collector construction and utilisation for low-temp. heating 79−57442
collector design and operation for solar-H_2 energy systems 80−61447
collector design and suntracking control for PORSHE concept 80−61425
collector efficiency equation for corrugated steel sheet solar water heater 80−16839
collector horizontal coaxial cylinder design optimisation 79−62110
collector long-term average performance prediction method 79−62116
collector material selection and blending guidelines 79−62060

solar absorber-convertors continued
collector optimum tube pitch expt. 79−62083
collector performance eval. without flow meas. 80−61422
collector subsystem operating thresholds, quantitative effect of energy flows 80−85304
collector system for thermal power generation, with tracking cylindrical parabolic reflector *(Korean)* 80−45735
collector thermal performance test procedures 79−62066
collector transmittance-absorbtance, calc. of monthly averages 80−45742
collector-cum-storage water heater transient behaviour model 79−62088
collector-heat storage systems for solar heating and ventilating by natural means 80−45758
collectors, design, thermal performance and economic anal., review 80−51001
collectors, free convective heat transfer 80−45748
collectors, high temp., flat plate, cover system effects 80−26156
collectors, monthly mean radiation calcs. for vertical and inclined surfaces 80−45746
collectors for hot water supply system, heat collection characts. and energy conservation 80−45743
collectors for solar heating systems for use in Britain 80−35637
collectors for space and water heating systems 80−66943
collectors with absorbent selective surfaces, theoretical performance 79−29482
collectors with multilayer cylinder heat exchangers, heat balance eqn. and thermal stress anal. 80−58977
collectors with plastic covers, radiation heat loss calc. 79−74538
combined photovoltaic/thermal flat plate collectors, extended Hottel-Whillier model 80−3520
comparative efficiencies of solar energy collectors 79−24907
comparative ranking of 0.1 to 10 MWe solar thermal power systems 80−30559
compound parabolic collector glazings, effective beam rad. incidence angles for determ. of diffuse rad. transmittance 80−94112
compound parabolic concentrator collectors, prediction of thermal performance 80−55905
compound parabolic concentrator solar collector design 80−3532
concentrating collector design, economics and optical loss anal. 80−45751
concentrating collector systems, US DOE Solar Thermal Program, R and D review 80−66998
concentrating collectors, single axis, orientation, economic criterion 80−40907
concentrating flat plate solar collectors, graphical determ of working point *(French)* 80−61409
concentrating solar collectors, concentration/acceptance relationships 80−21414
concentrator flux distribution determ. using backward ray tracing 79−98457
concentrator-receiver system with selective absorbing surface, heating characts. 80−91874
conference, optical phenomena in IR materials, Annapolis, MD, USA (Dec. 1976) 78−25933
convection, free, across inclined air layer with one V-corrugated surface 79−32198
convection, natural, in compound parabolic concentrator, finite element soln. 78−90634
convective losses determ., using cryogenic heat transfer tunnel 79−83636
cooling, heating and hot water supply for hospital, evacuated glass tube solar collector system appl. 80−26155
cooling systems, residential, solar absorption-vapour compression system 80−72017
cooling systems for buildings, review 80−45756
cusp mirror−heat pipe evacuated tubular solar thermal collector 80−94110
cylindrical absorbers for solar energy collecting system, thermal power *(Korean)* 80−21380
cylindrical black body receiver design, optical and thermal anal. to reduce thermal losses 80−61428
cylindrical dioptrics, nonfocalising solar collector 78−21195
cylindrical parabolic collector geometry 79−62109
cylindrical parabolic focusing collector for distributed-collector solar power system 79−62108
cylindrical parabolic solar concentrators with flat absorbers 77−79953
DC reactively sputtered metal carbide and silicide selective surface props. 79−62029
diffraction gratings, Fredholm integral eqn. formalism, appl. to solar absorbers 78−63192
diffraction gratings and solar selective thin film absorbers, roughening effect 79−14103
diffuse radiation through series of parallel regions, transmittance calc. 79−88005
diffusion, chemical reactions, contamination, AES and SIMS 80−72066
domestic space heating in Ireland, computer simulation model of thermal performance 80−45732
double glass solar energy collection, convection in vertical rectangular channels *(French)* 80−85300
double-exposure collector system for solar water heating 79−62070
double-exposure flat plate solar collectors, mirror configurations 80−50999
drinking-straw honeycomb flat plate solar collector expts. 79−62086
dust impairment of flat plate solar collector performance 79−62054
economical photovoltaic power generation with heat recovery 77−39898
electrodeposited chrome black solar absorber surfaces, characterisation using $^{52}Cr(p,\gamma)$ 80−7878
electroplating appl., 1979 prospects w.r.t. economics 80−3490
embossed metallic film absorber for solar energy 79−29451
emissivity measurement for solar-selective coatings on flat sheet using novel calorimeter 79−80621
emittance measurement, emissometer with high accuracy for determination of the total hemispherical emittance of surfaces 80−86309
energy collection anal. using information theory 80−97799
energy collection area and carrier fluid flow rate optimisation 79−62080
energy gain analysis of flat plate and evacuated-tube collectors 80−55904
energy storage area design coefficients for consumer demand and solar radiation *(Rumanian)* 80−89670
equatorial flat plate solar collector utilisation; radiation estimation 79−57402
equitable performance comparison and economic evaluation of active and passive solar energy systems 80−94101

solar absorber-convertors continued
European Community solar collector test programme 79−62057
evacuated heat pipe solar collector, rectangular performance characts., trap mechanism 80−3531
evacuated plate-in-tube collector, heat loss characts. theory and expt. 79−88004
evacuated selective collectors, house energy conservation measures obs. and evaluation, Philips expt. house (West German project) 79−61951
evacuated tubular solar collector integration with LiBr absorption cooling systems 80−3493
evacuated tubular solar collectors, integration with LiBr absorption cooling systems 79−62135
evacuated-tube collectors, for residential heating and cooling, design 79−88002
Fe-SiO_2 cermet film, solar absorbing, production by dual cathode DC magnetron sputtering 80−16186
figure of merit for solar collectors with several separate absorber segments 80−55908
finitely conducting crossed grating applications 80−106636
finned-pipe solar energy collector, optimal material distribution 79−83631
finned-pipe solar energy collector optimal profile 79−62065
fixed collector, optimised design, radiation collection study 80−40839
fixed tilt solar collector with reversible vee-trough reflectors and vacuum tube receivers, analysis development and testing 79−100539
flat collectors, substrate plate design and construction *(Slovak)* 79−92089
flat plate, 75 to 175°C, thermal perform. predictions and sensitivity anal. 80−94109
flat plate, optimal air-flow-rate determ. 80−97805
flat plate collector, performance tests using solar simulator 80−61419
flat plate collector, transient plate temp. rise for coolant blockage 80−26154
flat plate collector anticonvective-antiradiative system model 79−62082
flat plate collector coatings, perf. comparison of flat black and selective coatings 80−61426
flat plate collector cover system and absorber heat loss rel. to angle of incidence 79−62068
flat plate collector design and optimisation for Indian conditions 79−62087
flat plate collector glazings, effective beam rad. incidence angles for determ. of diffuse rad. transmittance 80−94112
flat plate collector heater yields, computation and expt. 79−62101
flat plate collector performance evaluation 79−62091
flat plate collector systems for residential water heating 80−61311
flat plate collector technology 80−45747
flat plate collector test apparatus 79−62100
flat plate collector thermal performance testing 79−62061
flat plate collector tilt optimisation 79−62090
flat plate collector transient heat transfer models compared 79−83632
flat plate collectors, advanced non-concentrating designs 80−45749
flat plate collectors, algorithm for solar flux estimates 80−61423
flat plate collectors, appl. to space heating *(German)* 80−26152
flat plate collectors, effect of a self consistent effective ambient temp. of efficiency parameters 80−45741
flat plate collectors, effect of design and operating parameters on the performance 77−75691
flat plate collectors, fixed and fully tracking, useful energy gain comparison 79−3794
flat plate collectors, for water pumping *(French)* 80−55902
flat plate collectors, solar flux calc. for angle of optimum tilt 80−61424
flat plate collectors, use of porous construction for solar air heaters 80−35748
flat plate collectors for heating and cooling system for domestic use *(Japanese)* 80−108787
flat plate multiple pass solar collector using aqueous optical properties 80−7957
flat plate solar collector dynamic evaluation 79−62044
flat plate solar collector efficiency and heat loss characteristic meas. 79−62064
flat plate solar collector efficiency improvement by grating selective filters 79−62032
flat plate solar collector performance with fluid phase change 79−62052
flat plate solar collector performance with fluid phase change 80−35750
flat plate solar collector thermal behaviour model and performance parameters 79−62045
flat plate solar collector with flat specular mirror, optimal tilt angles with seasonal variations 80−72081
flat plate solar collector with selective transparent and absorbing plates, thermal anal. 80−61427
flat plate solar collectors, insulation damage if fluid flow stops 80−3519
flat plate solar collectors, meas. of wind speed distribution 80−94108
flat plate solar collectors, optical props. of selective surfaces, effect on collector efficiency *(French)* 80−55897
flat plate solar collectors *(French)* 79−96484
flat plate solar collectors for water heating system, collection temp. and efficiency 80−45744
flat plate solar energy collectors, efficient optical window design 79−83628
flat plate solar water heater performance comparison 79−62062
flat solar collector, energy and economic analyses 78−83236
flat solar collectors, thermal exchanges in glass absorber cavity *(French)* 79−24909
flat-plate collector, below atmospheric pressure, distributed-flow, modules integration into arrays 80−26153
flat-plate collector, no-glass, for drying agricultural crops, analytical model 79−70465
flat-plate collector, single room heating appl., efficacy evaluation 79−62142
flat-plate collector, temp. distributions under actual unsteady insolation 80−97803
flat-plate collector, transient response, efficiency evaluation 79−18676
flat-plate collector air heaters, efficiency and temp. distrib. *(French)* 80−66991
flat-plate collector design, for water heating in mine changing house 79−74503
flat-plate collector efficiency comparisons *(French)* 80−61408
flat-plate collector efficiency computation 79−3904
flat-plate collector loops with on-off control, anal. of dynamic behaviour *(French)* 80−55901

solar absorber-convertors continued
flat-plate collector utilisability calcs. ϕ curve method development 79−43786
flat-plate collectors, absorption chillers for cooling and hot water system 80−50941
flat-plate solar collector design and sizing, modified Hottel-Whillier-Bliss method 80−97806
flat-plate solar collector test facility to determine thermal performance characts. 80−45730
flat-plate solar collectors, dynamic modelling and verification 80−66992
flat-plate solar collectors, laminar mixed convection in fully developed flow *(French)* 80−61411
flat-plate solar collectors, thermal performance testing of air and liquid solar water heaters 80−55911
flat-plate solar energy collectors, optical valve design 79−81506
flat-plate water heating collectors, efficiency determ. using BSE and ASHRAE test procedures 80−85301
flate plate evacuated collector design 79−62099
flate plate solar energy collector design, props. of spectrally selective materials *(Dutch)* 78−50872
fluid circulation control in conventional and heat pipe planar solar collectors 80−66994
fluid flow in helical channel of solar receiver, determ. pressure drop factors *(French)* 79−24910
fluorescent collectors, principles and feasibility *(German)* 79−70462
fluorescent collectors for thermal energy conversion, evaluation 80−16836
fluorescent planar collector-concentrators for solar energy conversion 80−45745
forced-circulation solar water heater analysis and expt. 79−62043
German solar flat plate air collector development 79−62075
glass flat plate collector, solar energy absorption in working fluid 78−59122
glass system, layered, thermal radiative props. for solar diffuse radiation flux 79−94473
glassless flat plate solar collector efficiency rel. to air flow and other parameters 79−62089
glazed solar cooler soln. regenerator, thermotechnical characts. 79−83620
glazing hemispherical transmittance props. 79−52957
granular metal, selective solar energy absorption, particle shape depend. 78−71162
graphite film, and other solar selective surfaces, effect of Cu, Ag or Ni substrate 78−74952
graphite on Cu, interf. films deposited on diffr. gratings, for solar selective absorbers 79−14103
heat collection and storage system evolution 79−62085
heat collectors, with direct and concentrated radiation, maximum equilibrium temp. determ. 80−92031
heat mirrors, spectral selectivity of conducting micromeshes 80−26160
heat pipe, filled with porous material, glycol water circulation 80−66986
heat pipe array with common heat exchanger 79−62038
heat pump, series, flat-plate collectors, vapour compression, energy conservation 80−72078
heat pump assisted solar air heating systems, performance anal. 80−66996
heat pump evaporator using solar collector, thermal performance 80−30520
heat transfer by natural convection in an isothermal rectangular cavity open on one side *(French)* 80−61412
heating, space, with all-air systems, experiences with CSU Solar House II 79−57406
heating and cooling of buildings, Shenandoah Solar Recreational Center 80−45757
heating and cooling systems, computer program validation methodology 80−35742
heating and cooling systems design, operation, feasibility, review 80−45755
heating appl., solar power availability, Swiss meas. and collectors efficiencies *(German)* 79−48092
heating panel system, performance testing and evaluation *(Dutch)* 80−72079
heating system performance, of Toshiba Solar House No. 1 79−57458
heating systems, collector and storage efficiencies 80−45736
heating systems, economic anal. of passive and active residential designs 80−35746
heating systems, instrumentation principles for performance meas. 80−35743
heating systems with salt-water mixture and hot water storage systems 80−67006
heating systems with salt-water mixture heat storage 80−67005
heavily doped semiconductors as transparent heat reflectors *(German)* 78−79197
heliostat solar collectors, meas. of performance characts. 80−85303
heterojunction solar cell, relation between efficiency and heterojunction parameters, review 79−74523
high efficiency solar collector development 79−62051
high temp.-high flux material testing, solar power station appls. 80−40668
high temperature solar collector with optimal concentration: Non-focusing Fresnel lens with secondary concentrator 80−35753
honeycomb cell heat transfer interferometric meas. 79−62053
honeycomb structured flat plate solar collectors compared 79−62046
hot air collectors for domestic hot water heating 80−97768
hot box systems, efficiency increase by radiation reduction, dielectric/metal/dielectric coatings appl. 78−79195
hot water supply using solar collectors *(Dutch)* 80−7954
hot water system design 80−104518
hot water systems, marginal cost of electricity used for backup 80−35747
house heating, Trombe-Michel wall system design and performance, digital simulation 79−62143
house heating in Northern India, using south walls as collectors, expt. results 79−62152
house walls as passive solar collectors, assessment 79−87966
hybrid thermionic converter for space craft secondary energy source 79−92086
ideal flux concentrators, intensity variation reduction on absorbers 80−104496
ideal selective absorbing surface, absorp. and radiation coefficients calc. 80−40900
solar absorber-convertors continued
industrial solar inclined-step distiller, test results 80−40901
insolator, copper belt type tube structure, design, construction and testing *(Czech)* 79−83626
integrated collector-heat storage systems for heating and ventilation 80−51002
internal cusp reflector, optical anal. 80−101127
IR spectral emittance profiles of spectrally selective solar absorbing layers 78−25955
KS-7F solar kitchen, economic effects on economy 80−89590
laser, solar pumped, for space communications 78−46645
liquid heating flat plate solar collectors, testing consistency test program 79−74541
low temperature solar thermal systems for domestic space heating *(Czech)* 79−83566
low-temperature collector and thermal or photovoltaic concentrator development 79−62009
luminescent greenhouse solar collector materials 78−13789
materials radiation properties study, wide temperature range 79−94307
materials research and collector thermal performance tests *(Japanese)* 78−46732
materials science aspects, lecture 78−25989
maximally concentrating collectors for solar energy applications, collector performance 80−76648
metal carbide, magnetron-sputtered, solar selective absorbing surfaces 79−92079
metal-dielectric inhomogeneous selective absorpt. of solar energy 79−48181
metal-insulator composite films, optical props., rel. to solar collector appls. 78−72622
metal-insulator composite solar selective absorbers optical props. 79−52037
molten salt heat transfer fluid appl., with solar-absorbing oxide particles, absorption properties obs. 78−87112
multi-element sources of electric energy, current calc. *(Russian)* 77−39813
multiple-plate glass systems, spectral directional radiation characts. prediction 78−74956
natural convection simulation in inclined air layers 79−62056
non-selective and energy control films for enhanced photothermal solar energy collection 80−26157
nonevacuated solar collectors with compound parabolic concentrators 79−62069
nonimaging solar concentrators for different absorber shapes 78−50895
open solar regenerator, heat and mass transfer coefficients, moisture evaporation 80−38238
optical performance of absorber-reflector combinations, for photothermal conversion 78−63168
optical simulation for a fixed spherical solar collector 80−7912
optics applied to solar energy, [Conf. San Diego, CA, USA Aug. 1978] 80−7926
optics in solar energy utilization 77−53900
optics of glass tubes for thermal collective appl. 77−46684
optimal feedback controller for collector flow rate, optimal control law 80−45739
optimal insulation of solar heating system pipes and tanks 80−35745
oxide layers on high-temp. alloys, for central-receiver, solar-thermal power systems 78−18071
packed-bed absorbers for solar air heaters 79−62041
panel-type solar thermoelectric generator, water-lift appl., technical and economic eval. 79−83619
parabolic focusing collector, digital simulation 79−52911
parabolic trough collectors, incidence-angle modifier and average optical efficiency 80−85302
parabolic trough collectors, moderately concentrating, for industrial plant heating and cooling, located in Southern Europe 79−62131
passive solar heating systems design, microeconomic anal. methodology 80−35744
PCM wall thermal storage, design criteria 80−35759
PCM wall thermal storage, modelling 80−35758
performance of a collector/storage solar water heater, anal. 79−70432
photoacoustic determination of absorptance and emittance of solar selective coatings 80−77876
photoelectrolysis cells, props. of oxide-based heterostruct. photoelectrodes 80−12023
photovoltaic/thermal collector performance, comparison of theory and expt. 80−94062
pipe-and-fin solar water heating plate material economy 79−62050
planar reflector-collector array optimisation 79−62071
planar solar convertor based on uranyl Hd and Ho glasses 80−40904
planar solar energy convertor and concentrator, based on uranyl-doped glass 78−71213
Planckian black body, comparison with solar radiation absorbers *(German)* 77−35026
plastic, construction, performance and efficiency anal. 80−104516
plastic modular solar energy collector with reticulated foam 80−16833
point-focusing collectors, thermal performance trade-offs 79−52904
pond experimental and economic aspects 79−62076
ponds, computer simulation of performance 80−72080
ponds, electric power generation at Salton Sea, CA, USA 80−94113
ponds, for electric power generation in Israel 80−94114
ponds, heat transfer model to predict temp. rise 80−55912
ponds, non-convecting, review 80−61407
ponds, non-convective, operating characts. 80−45750
ponds, salt gradient, computer simulation of thermal behaviour 80−101126
power plants, solar high temp., with Stirling engine and solar thermal rocket engine, efficiency improvement by using selective radiation absorption surface 80−89589
PULSONAR polymer thick film hybrid convertor 80−55878
quantum utilizing solar energy convertor efficiency in absence of intraband thermalisation 80−26144
quarter-wave antennae solar absorber 77−39499
quasi-fixed adjustable-focus reflector array solar collectors 79−62106
R and D program at the Inst. of Engng. of the Nat. Univ. of Mexico 80−40845
radiation concentrated, absorption, solid-gas-suspensions study 79−66415
radiative losses of solar absorbers, reduction using cellular structures *(French)* 77−14890
receiver radiative loss and eye hazard evaluation by Net-Radiometer 80−89673

solar absorber-convertors continued
reflecting horizontal solar collector with inclined finned tubes 79−62049
reflector and absorber design, spherical stationary mirror, and automatic tracking absorber 80−50997
reflector-collector system all-day performance, time-integrated calc. 79−3765
refrigeration in tropical zones using flat plate collector and two-component coolant *(French)* 79−24911
refrigeration units, absorption systems with intermittent or continuous cycles 80−45729
regenerative solar still, inclined-stepped design, productivity and efficiency calc. 79−83622
regenerator, transient response for varying insolation and flow 79−62025
reverse flat plate collector, new device with high temp. collection properties 79−96485
review of solar technology, assessment and contemporary criteria, 1978-79 80−76650
salt gradient solar pond for space heating 80−94115
sandwich-type collector panels, weight minimisation 80−30547
seasonal storage devices, economic optimisation of storage capacity and collector area 80−101133
selective absorber coatings, reflectance, emittance, and thermal stability 80−12027
selective absorber design, optimal comp. profiles for max. solar absorptance of cermet layers 80−101129
selective black absorbers using sputtered cermet films 79−29483
selective coating, high-temp. resistant double layers 79−70463
selective coating electrodeposition on Al substrates 79−62079
selective coating microstructure rel. to processing parameters and optical props. 79−62033
selective film absorber, design improvements by surface roughening and refr. index grading 78−25976
selective materials for photothermal conversion of solar energy *(French)* 79−24908
selective solar absorbers, reflectance calcs. for inhomogeneous surfaces 80−12029
selective surface, thermal emissivity 80−7953
selective surface absorber coatings, technique for comparing effectiveness 80−30545
selective surface absorption and IR emissivity calorimetry 79−62098
selective surface design for solar energy collection 79−52956
selective surface for thermal absorbers, review of basic physics and requirements 80−45752
selective surface requirements and classification 79−62026
selective surfaces, hemispherical emittance of rough metal surfaces 80−70434
selective surfaces for solar-thermal conversion 77−83978
selective surfaces instrumentation for high temp. and hemispherical meas. 80−4756
selective transparent filters, Drude mirror type, efficiency 78−33836
semiconductors, Moss relation between refr. index and energy gap, rel. to solar heat absorbers 80−11357
shadow effect of adjacent solar collectors in large scale systems 80−45738
shallow pond performance with mirror on side away from Equator 79−62077
simulator design for testing solar collectors 80−50996
slat solar collector natural convection obs. 79−62055
solar collector thermal performance testing procedures *(Japanese)* 78−16795
solar collector/storage system buried in ground, heat transfer anal. 79−7275
solar energy system installation suggestions for space heating and water heating *(German)* 80−94102
solar greenhouse with soil heat accumulator, temp. conditions anal. 80−40898
solar heating systems, optimisation formulation of collector area based on TRNSYS computer code 80−61414
solar power plant, direct tracking using two-mirror unit with plane and hyperboloidal counter-reflectors 80−91875
solar thermoelectric generator panels, energy characts., estimation 80−101123
solar water heaters, aluminium alloy rolled-welded heating panels production and use 79−96421
solid state physics aspects, of solar energy conversion, book 79−74518
space heating, energy utilisation improvements using new types of construction *(German)* 80−40903
space heating, experimental installation, using solar absorbers, heat pumps, heat exchangers and measurement and control gear *(German)* 80−35741
space heating, photovoltaic and thermal collector system design and testing 80−45675
space heating, solar air heaters, aerodynamic drag investigation 80−40899
space heating by solar power, office building in Madrid, use of facade 80−89597
space heating system for intermittent heat delivery 80−89669
space heating using solar heating installation, technical and operational details *(Dutch)* 80−72013
space solar furnaces, for materials-science expts. 80−108786
spectral characteristics for improving solar collector performance 80−35650
spectral selectivity of composite materials, optical props. and fabrication of composite solar absorbers, review 79−74520
spectral selectivity of high-temperature solar absorbers 80−61403
spectrally selective coatings, physical processes, review 80−61404
spectrally selective surfaces and their impact on photothermal solar energy conversion, review 79−74519
spectrally selective surfaces for high temp. photothermal conversion, CVD 79−79400
spectrally selective surfaces for high temp. photothermal conversion, CVD 79−79403
spectrally selective surfaces for photothermal conversion of solar energy 80−101125
spectrally selective surfaces in photothermal solar energy conversion 80−45753
spherical solar still, design, operation, and appls. 80−55913
sputtered metal, silicide solar selective absorbing surfaces 78−52671
stainless steel, coloured, reflectance meas. 80−7958
stainless steel selective absorption surface props. 79−62030
standards for heating and cooling appl. 80−7915
solar absorber-convertors continued
static collector of low-conc., heat losses 80−81487
static endo-absorbent flat solar collector 80−61421
stationary solar collector design to make most of diffuse radiation 80−30517
stationary spherical solar collector design 79−62107
steady state salt gradient solar pond 80−35749
steel, stainless, carbide reactively sputtered solar selective absorbers for all-glass tubular evacuated collectors, absorptance and emittance 80−101132
steel stainless, solar energy collector optical props. rel. to heat treatment 78−94455
still, double basin, performance and periodic anal. 80−89671
stills, basin-type, periodic anal. for estimating distillate output 80−45733
stills, design and thermodynamic parameters, numerical anal. 80−55914
stills, inclined-stage type, basic parameters determ. 80−89595
storage of heat, solar collector performance analysis 80−30390
storage tank, buried, hemispherical, heat cond. to environment, series soln. 79−3891
sulphide black, on Al, solar selective coating, figure of merit 80−72082
Sun tracker, electronic, for clear or cloudy weather 80−76644
system performance rel. to duct and pipe losses 79−83633
systems analysis of solar-electric facilities 80−35685
THEK collectors, fluid transport network for solar energy to heat conversion *(French)* 79−24905
thermal balance, role of selectivity and concentration *(French)* 80−55895
thermal collector, fixed, design optimisation 80−40905
thermal collectors, prediction of long term average energy delivery 80−3533
thermal collectors, prediction of long term average performance for concentrating and non-conc. systems 80−7956
thermal conversion, collectors, storage systems, energy transport and economics, review 80−51003
thermal emittance, optical technique for meas. *(Spanish)* 80−16835
thermal energy accumulator using stones, operating principles *(German)* 80−72085
thermal insulation of a low cost solar collector 80−104517
thermal pdrformance of liquid heating solar collectors, instantaneous collector thermal efficiencies in less time 80−61416
thermal receiver utilising a small particle heat exchanger 80−30557
thermokinetics of glass and semi-transparent materials, radiative and conductive heat transfer *(French)* 80−61410
thermophotocell, design and calculations 80−97800
thermophotovoltaic convertor, parametric anal. of emitter temp., conc. ratio and cell reflectance 80−94107
thermoreceiver, solar concentrator, waste water sediments disinfection 79−83624
thermoreceiver with selective coating and vacuum thermoisolation 79−83621
thermosyphon circulation, flow rate prediction 80−66993
thermosyphon solar water heaters, transient flow meas. using laser doppler anemometer 80−61413
thin film prep. for solar energy utilisation 80−84847
thin film refractory metals, optical props. 77−55844
thin film thermal convertors 80−12011
thin sheet Fresnel solar collector-concentrators, features and economic benefits 79−79402
tilt, orientation, and overshadowing sensitivity rel. to Netherlands urban design 79−62073
transition metal carbides and silicides, reactively sputtered, solar absorbing surface, struct. and optical props. 79−79407
transparent heat-reflecting coatings utilisation 77−75642
transwall for passive solar heating of buildings, thermal performance comparison 80−40840
tri-mode solar conversion system, design and operation 80−55907
Trombe wall control strategies for passive solar heating systems 80−45737
Trombe-Michel wall using phase change materials, solar energy collection and thermal storage 80−55909
tubular cover solar collectors, performance calcs., transmittance and radiosity 80−61415
tubular solar collector, design and development 80−76646
tubular solar collectors, non-tracking, low-conc., steady state thermal anal. 80−55903
underground constant flow solar collector/storage system 80−21412
underground thermal storage in the operation of solar ponds 80−40911
USA demonstration solar heating and cooling collector thermal performances 79−62059
utilisation in human settlements, inexpensive systems, appls., function and techniques 80−51004
v-grooved surface for solar energy collection 79−39320
vacuum thermal collector with optimal conc. 78−50892
vapour absorption refrigeration flat plate solar collector tube pitch optimisation 79−62084
vapour-turbine units with organic working fluids 79−83618
water decomposition into H and O using solar energy, one-step effusional process 78−15672
water heater, low-temp., tubular heat receiver, temp. distribution, heat-balance differential equation solution 79−94464
water heater with two-fluid-circuit collector, dynamic response prediction 79−62139
water heating for swimming baths, principles, basic calcs., and economics *(German)* 79−92061
water heating systems, test procedure for performance rating 80−55910
water system for photographic processing laboratory, solar heated 80−40837
water-heating collector test procedure 79−62067
water-trickle type solar collector with massive concrete slab for heat storage 80−108814
wavelength-selective surfaces for solar energy utilization 77−54812
West German metropolitan flat plate solar collectors, outdoor efficiency meas. 79−62048
wideband selective solar absorber design optimisation 79−3793
zeolite collector for solid-gas absorpt. refrigeration system 80−35754
Al film colour anodised, selective surfaces proparation and characts. obs. *(Japanese)* 80−55893
Al-Ge-SiO selective absorber surfaces, optical behaviour at high temp. 80−101130
Al-PbS selective surfaces for solar photothermal conversion, prep., emissivity, absorptivity 80−12030

solar absorber-convertors continued
Al_2O_3 on Mo film, passivation against IR reflectance losses caused by oxidation 79−3758
Al_2O_3(Al_2O_3-MgO)-Ag(Au)(Cr)(Cu) cermet selective surfaces for evacuated solar collectors 79−43785
Au black, struct. comp. and optical props. 78−27339
Au black film, structural composition and its influence on optical props. 78−56530
Au black optical props. rel. to structural composition, appl. to solar absorption 79−83630
Au film on Al, reflectance and absorpt. obs. 80−7426
Au solar black, optical props., microstruct. influence 79−42937
C, paint type coating layer with spherical pigment, radiative transfer theory 80−61405
CO_2-Br_2-He mixture, possible gas lasers with solar excitation 80−99695
CaF_2-Ge(Si), cosputtered composite semiconductors, selective solar energy absorbers 79−56876
Cd_2SnO_4 films, optical trans. and refl. meas. 77−52191
CdTe electrolyte heterojunctions, photoelectronic props. 77−76918
CeO_2-Mo-CeO_2 thin-film selective coatings 78−94422
Co, electrodeposition for solar selective surface *(French)* 79−52133
CoO as a spectrally selective material for solar collector appls. 80−26159
CoO solar absorber surface spectral selectivity rel. to temp. and UV ageing 79−62027
$CoO_{(x)}$, black cobalt, solar absorptance of high temp. selective absorbers 80−101131
$CoS_{(x)}$, black cobalt, solar absorptance of high temp. selective absorbers 80−101131
Cr black, coating on Cu substrate, selective solar energy absorpt., model calcs. 79−57440
Cr, black, plating process for solar selective absorber 79−62031
Cr black solar absorber surfaces, determ. of O_2 content using $^{16}O(^3He, p\gamma)$ 80−45610
Cr, fine particle solar absorber, effective medium theory 80−21396
Cr particles, on reflecting substrate, selective absorpt. of solar energy, model calcs. 79−79405
Cr particles, ultrafine, for photothermal conversion of solar energy 78−71163
Cr particulate layer on Cr_2O_3, high solar absorpt. characts., selective surface electroplating 78−87111
Cr ultrafine particle selective absorption of solar energy 79−62035
Cr, ultrafine particles, coatings for selective absorpt. of solar energy, efficiency 78−18060
Cr ultrafine particles, selective solar energy absorption 78−18027
Cr-black selective absorbers, struct., elect. and optical props. of evaporated films 77−34956
Cr-Cr_2O_3, black, electrolytic deposited, characterisation and thermal stability *(French)* 80−55898
Cr-Cr_2O_3, black, solar selectivity at average temps. (100 to 250°C) *(French)* 80−55899
Cr-Cr_2O_3, black chrome, solar absorptance of high temp. selective absorbers 80−101131
Cr-Cr_2O_3, black chrome solar selective absorber, microstruct. 79−56875
Cr-Cr_2O_3, black chrome electroplating for solar energy photothermal conversion, prep. and struct. 79−74544
Cr-Cr_2O_3, black chrome electroplating for solar energy photothermal conversion, optical props. 79−74545
Cr-Cr_2O_3, black chrome selective surface, radiation props. and effect on solar collector 80−85299
Cr-Cr_2O_3, black chrome electrolytic coatings for solar collectors 80−94100
Cr-Cr_2O_3, chrome black, electroplated selective surface, thermal emittance, solar absorpt., refl., and roughness 79−79406
Cr-Cr_2O_3 black, electroplated solar collector coatings, high temp. optical and struct. degradation 80−66995
Cr-Cr_2O_3 black chrome, commercial, solar absorber coating characterisation 80−80111
Cr-Cr_2O_3 black solar absorber surfaces, microstruct. rel. to electroplating parameters 80−61418
Cr-Cr_2O_3 black solar selective absorbers, thermal degradation 80−61417
Cr_2C_3, reactively sputtered solar selective absorbers for all-glass tubular evacuated collectors, absorptance and emittance 80−101132
Cr_2O_3/Cr films, RF-sputtered, for selective block absorbers 77−58399
Cr_2O_3/Cr solar-absorber surfaces, chemical and struct. anal. 79−95283
Cr_2O_3-Cr black, selective coating, optical and topographical props. 80−26165
Cr_2O_3-Cr black, solar collector coating, microstruct., FIM and SEM obs. 80−26166
Cr_2O_3-Cr cermet films, for selective black absorbers 79−29483
Cr_2O_3-Cr film, optical degradation rel. to surface morphology, SEM and AES obs. 79−79401
Cr_2O_3-Cr film, optical props., rel. to chemical/metallurgical constitution, appl. as solar absorber 78−56531
Cu selective surfaces on Al-Cu alloy, chemical brightening and etching 79−62037
Cu tube and plate solar collector geometry optimisation 79−62040
Cu-Al_2O_3 cermet film, solar absorbing, production by dual cathode DC magnetron sputtering 80−16186
CuO, black Zn-dust pigmented solar selective coatings for solar photothermal conversion 80−66997
CuO, on Al or Cu, solar selective coating, figure of merit 80−72082
CuO selective black coatings for large area appls., prep. and props. 80−21411
CuO selective surfaces on Al-Cu alloy, chemical brightening and etching 79−62037
CuO-Ag film solar absorbers, mechanism of high-temp. instability 78−22971
CuS, black Zn-dust pigmented solar selective coatings for solar photothermal conversion 80−66997
CuS selective black coatings for large area appls., prep. and props. 80−21411
CuS-PbS, black Zn-dust pigmented solar selective coatings for solar photothermal conversion 80−66997
Cu_2S, on Cu, solar selective coating, figure of merit 80−72082
Fe-C, reactively sputtered, solar absorbing surface, struct. and optical props. 79−79407
FeC_x-CrC_y-NiC_z, stainless steel carbide, solar selective surface, fabrication, magnetron sputtering system description 80−80967
FeC_x-CrC_y-NiC_z, stainless steel carbide, graded solar selective surface, magnetron sputtered 80−81485
solar absorber-convertors continued
FeC_x-CrC_y-NiC_z, stainless steel carbide, sputtered solar selective surface, grading profile 80−81486
Fe_2O_3, paint type coating layer with spherical pigment, radiative transfer theory 80−61405
Fe_3O_4 solar absorber surface spectral selectivity rel. to temp. and UV ageing 79−62027
Ge, black, solar selective absorber characterisation 80−80112
Ge film black, solar selective absorber surface 79−29484
Ge_xSi_{1-x} amorphous semiconductor characterisation for solar cell applications 79−61983
In_2O_3:Sn films, elec. and optical props., solar energy conversion appl. 79−65945
In_2O_3:Sn solar collector selective coating resistivity obs. 79−62034
In_2O_3-SnO_2 coated Si selective absorber, temp. depend. of 10.6 μm reflectivity 77−58398
$(In_{1-x}Sn_x)_2O_{3-y}$, pyrolytic selective coating, Sn additions effect 78−43499
MgO/Au cermet films for selective black absorbers 77−1747
Mo film, CVD, with high IR refl. and large solar absorpt., prep. and props. 80−26163
Mo thin film fabrication for photothermal solar convertors using CVD 80−11573
Mo thin films for solar photothermal conversion, CVD fabrication 80−7503
NH_3 continuous absorption cooling flat plate collector design and optimisation 79−62081
NH_3-based solar thermochemical cavity absorber, design and cost anal. 80−81489
NH_3-H_2O, solar absorption refrigeration system, Seoul, Korea *(Korean)* 78−51052
NI dendrites on Al, CVD, selective solar photothermal absorber 78−52683
Nd:YAG solar pumped laser, freq. doubling 78−59045
Ni, black, solar collector selective coatings, optical and thermal props. 79−62028
Ni foil solar collector selective surface performance 79−62078
Ni solar collector coating, microstruct., FIM and SEM obs. 80−26166
Ni solar selective black coatings, electrochem. deposition on Zn surfaces 80−29885
Ni ultrafine particles for solar energy photothermal conversion 79−100538
Ni-Al_2O_3 composite film, selectively absorbing, optical props. 78−6798
Ni-Ge-SiO, solar selective absorber surfaces, optical behaviour at high temp. 80−101130
Ni-NiO_x-NiS_y, black Ni, struct.-depend. thermal and optical props., rel. to solar thermal conversion 79−79404
Ni-P coating, electroless, ultra-black surface production by chemical treatment 80−76647
Ni-pigmented anodic Al_2O_3, for selective absorpt. of solar energy, optical and struct. props. 80−55892
PbI_2:KI alloys, fundamental abs. edge, potential as solar convertor 80−101128
PbS-Al coatings, absorptivity, emissivity, as function of PbS thickness 78−46731
PbS-CuS, black Zn-dust pigmented solar selective coatings for solar photothermal conversion 80−66997
PbS+CuS selective black coatings for large area appls., prep. and props. 80−21411
Se film, gas-evaporated, selective absorpt. characts. and emissivity 80−50998
Se, thin film selective absorber coatings, prod. using an oblique vacuum deposition technique 80−81488
Si, amorphous, CVD, retarding crystn. by alloying with C,N,B or Ge, absorber life expectancy 80−44129
Si, amorphous, optical props., appl. as solar absorber review 79−74519
Si, amorphous CVD fabrication for solar photothermal conversion appl. 80−7504
Si amorphous film, anisotropic etching phenomenon, appl. as solar selective absorber surfaces 80−72054
Si, amorphous film prepared by CVD, optical props. and struct., solar absorber appl. 79−52035
Si amorphous sputtered film, solar energy selective absorber, spectral emissivity 78−83045
Si, amorphous stabilised CVD films for high temp. solar photothermal conversion 80−26161
Si, CVD amorphous films, effect of surface characts. on visible and UV optical props. 80−60698
Si, CVD prepared amorphous and polycryst., solar thermal absorber, temp. variation of absorpt. edge 80−12028
Si film selective absorber, optical consts. 78−25954
Si on Al, interf. films deposited on diffr. gratings, for solar selective absorbers 79−14103
Si plasma deposited amorphous hydrogenated film, optical props., annealing effect 79−56874
Si solar cells with concentrating collectors and integrated heat use system 80−45701
a-Si, thin film selective absorber coating 77−39907
Si thin textured tilm prep. for selective absorption 80−30544
Si-Ge sintered high temp. thermoelastic generator, performance assessment 79−74534
Si-H, amorphous, on Nb or W, spectrally selective absorber, IR spectra 80−26164
Si_3N_4 on Mo film, passivation against IR reflectance losses caused by oxidation 79−3758
SiO_2 on Mo film, passivation against IR reflectance losses caused by oxidation 79−3758
SiO_2, with embedded Au particles, thin film solar absorber 80−81490
SiO_2-Mo-SiO_2 thin-film selective coatings 78−94422
Sn, globular film, interf. and diffr., solar selective props. 79−4860
Sn globular film, solar selective props., effect of dielec. layer addition 79−4861
SnO_2 doped films for spectral-selective surfaces, refl. and elec. props. meas. 79−74013
SnO_2 films, selective, optical characterisation by thermodynamical method 80−84796
SnO_2:F films, elec. and optical props., solar energy conversion appl. 79−65945
Te film, gas-evaporated, selective absorpt. characts. and emissivity 80−50998

solar absorber-convertors continued
Te textured thin films, prep., high solar absorptivity by multiples refl. 80−11568
Te, thin film selective absorber coatings, prod. using an oblique vacuum deposition technique 80−81488
TiNx films, spectral reflectance for selective solar absorbers 77−79954
TiO_2, paint type coating layer with spherical pigment, radiative transfer theory 80−61405
W, dendritic, solar absorbing surfaces anodised interference coatings 78−13815
W dendritic surface anodisation for solar absorptance enhancement 79−34440
WO_3, antirefl. coating on textured W surface, for solar absorber appl., props. 78−63157
WO_3, antireflection coating on W dendritic surfaces, reflectance, geometrical study 79−91511
WO_3 solar absorber surface spectral selectivity rel. to temp. and UV ageing 79−62027
Zn-dust pigmented solar selective black material for photothermal conversion 80−66997
Zn-tetraphenylporphine/metal electrode, photocurrent generation mechanism 78−76868
$Zn_xCd_{1-x}S$ solid solution based devices 80−21409
$Zn(CrO_4)_2$ solar absorber surface spectral selectivity rel. to temp. and UV ageing 79−62027
ZnO, black, possible use as spectrally selective coating for low temp. solar collectors 79−994
ZnO solar absorber surface spectral selectivity rel. to temp. and UV ageing 79−62027
ZnSe solar spectrum convertor for GaAs solar cells 80−101117
ZrC, film, solar selective surface *(Japanese)* 78−90465
ZrNx films, spectral reflectance for selective solar absorbers 77−79954

solar absorbers *see solar absorber-convertors*

solar activity
see also solar flares; solar prominences; solar-terrestrial relationships; sunspots
11 and 22 year cycles, rel. to spectral anal. of geomag. activity index aa 77−87187
11 year cosmic-ray cycle, galactic and sdlar protons anal. 77−53360
11 year galactic cosmic-ray cycle, anomalous effects 77−53359
11-year and 80-year cycles, continuity *(Chinese)* 78−85925
11-year cosmic ray modulation cycle obs., review 77−13196
11-year cycle, chromospheric rot. meas. during years of declining activity 78−4186
11-year cycle, rel. to large-amplitude standing planetary waves in troposphere 78−36236
11-year cycle rel. to ^{14}C vars. in terrestrial atm. 78−92885
11-year solar cycle, double maximum features 77−49363
17th century solar activity from auroral and sunspot obs. *(French)* 77−29747
19th and 20th solar cycles, geomag. activity 27 day period amplitude var. 77−66886
22 year cycle, long period modulations by multiple-period dynamo wave oscills. 79−16813
22-year cycle, rel. to quiescent prominences mag. field orientations 78−45305
22-year magnetic cycle and dynamo theory 77−53564
30-day periodicity in sunspot activity and rainfall 79−84765
80 year sunspot period, maximum in 1944-53 period 77−17468
1971, January-April, Hα flocculi rel. to flares *(Chinese)* 77−67081
1972 August, m wavelength characts. of active region McMath 11976 *(Chinese)* 77−22156
1972 August proton event and atmospheric O_3 layer 79−35227
1972-1975 period, unusual flare and sunspots phenomena 79−16914
1973, short-term periodicity, BAA Solar Section obs. 77−78741
1973 June 15 flare in active region NOAA 131 (McMath 12379), X-ray obs. 78−53913
1978 May 7 events, radio, optical and geophysical manifestations *(French)* 80−8611
active centres, longitudinal distrib., effect on geomagnetic var. 80−82330
active complex with developing secondary region, mag. field struct. and dynamics 80−67685
active region, 1972 August, sunspots penumbral vortical pattern anal. *(Chinese)* 77−22157
active region, mag. and vel. fields config. and changes 77−17486
active region and flare plasmas, electron density from Fe IX lines intensity ratio 78−20771
active region loops, evidence for opposed currents 77−2403
active region mag. fields and noise storms *(Russian)* 77−64717
active regions, coronal and transition region temp. struct. 80−67692
active regions, nonlinear stage of instability due to local Joule overheating 78−61839
active regions, visibility at 408 MHz 80−85922
active regions and high-speed plasma streams 77−33311
active regions and interplanetary medium perturbations 77−53502
active regions and X-ray bright points, birthplaces 80−12739
active regions brightness distribs. at 2.8 cm, one dimensional aperture synthesis obs. 77−22173
active regions central meridian passage, correl. with transient cosmic ray intensity vars. 78−89022
active regions development, rel. to radio emission S-component spectrum fine struct. 80−21977
active regions distrib. during 1965-74 period 79−5803
active regions height struct., X-ray obs., OSO-8 limb crossing obs. 80−31280
active regions heliographic oscills. in longitude, sunspot zone modulation *(French)* 77−64714
active regions spectra, small line shifts meas. via automatic comparator 77−82123
active regions X-ray emission, appl. of hard X-ray imaging collimator 77−5437
active resgions, VLA synthesis maps at 6 cm wavelength 79−40157
active solar processes, manifestation in interplanetary space from data of cosmic ray variations 78−57411
analytical description of structure of an active region 77−17533
atmospheric O_3 global monthly vars. correl. with solar activity 78−85664
ball lightning correl. with solar activity, comment 77−81972
ball lightning correl. with solar activity, comment 77−87017
ball lightning in Holland rel. to solar activity 77−21840

solar activity continued
basic mechanisms, IAU Symposium 71 (Prague, 25-29 August 1975) 77−53543
biosphere and active solar processes link, role of Earth's natural electromag. field 78−61211
butterfly diagram, nonlinear MHD model of solar dynamo 78−53918
central solar disc features correl. with geomag. activity 79−40040
chromosphere active regions, bidimensional spectroscopy obs. with birefringent filter *(Italian)* 80−98568
chromosphere active regions, vels. from Si II 1816 Å line, OSO-8 obs. 77−13301
chromosphere and transition region, vel. fields in active regions, OSO-8 obs. 77−9730
chromosphere network, evolution during active regions development *(Russian)* 78−57531
chromosphere network struct. from medium resolution EUV obs. 78−20801
chromosphere plages, physical props. models based on Ca II and Mg II obs. 78−89153
chromosphere-corona transition zone of solar active regions, non-thermal velocities *(French)* 80−77371
chromospheric activity in F- and G-stars 77−53594
chromospheric flares occurrence rel. to sunspot mag. field oscills. 77−67084
chromospheric network, comparison of He II 304 Å and He II 10830 Å spectroheliograms 78−20799
chromospheric phenomena, review 79−66976
climate var. rel. to activity and solar constant change 78−28301
clock mechanism of interior driving sunspot cycle 80−17562
conference on nuclear cosmic physics, Leningrad, USSR (Oct. 1978) 80−98755
convection zone, mag. field transfer 78−96449
corona, activity complex development, Skylab soft X-ray obs. 78−12191
corona, heating above active regions by fast electron streams 80−105228
corona, high-temp. regions rel. to solar wind flows associated with hot heavy ions 80−51635
corona, latit. depend. activity long-term correl. with solar wind streams 78−93172
corona, soft X-ray obs. of large-scale active region brightening 78−20806
corona above active regions, soft X-ray and cm wavelength obs. 79−44431
corona shock waves and magnetic field above an active region 77−53512
corona tearing instability, high cond. theory 77−7527
coronal active region, differential emission measure exponential depend. on temp. and struct. 78−53917
coronal active regions, anal. of soft X-ray photographs taken with Fresnel zone plates 78−77538
coronal active regions, evidence for mag. energy storage 77−17478
coronal active regions, imaging with Fresnel zone plates 78−49342
coronal active regions, modelling of mag. field three-dimensional struct. 77−67085
coronal active regions, X-ray photographs anal. and interpretation 79−40086
coronal activity energy source; insufficiency of mag. fields interaction 77−17482
coronal and interplanetary responses, dynamic modelling 78−49418
coronal electric current systems development in active regions, rel. to filaments and flares 79−25567
coronal emission line at 5303 Å rel. to activity in 20th cycle 79−66985
coronal general mag. field evolution with solar cycle, rel. to solar wind streams and galactic cosmic ray vars. 78−7974
coronal general magnetic field evolution rel. to solar cycle 77−71087
coronal hole evolution rel. to solar activity 79−25582
coronal holes, modulation effect on cosmic ray intensity review 80−77370
coronal holes, solar wind streams and geomag. activity during 1976-77 period 79−25570
coronal holes and assoc. solar wind, sunspot cycle 20 survey 78−40911
coronal holes and solar magnetic fields, review 79−58312
coronal holes rel. to magnetic fields and model of formation in solar cycle 78−40909
coronal index of activity, for 1971-76 period 80−4322
coronal interconnecting loops transient brightenings, sudden brightenings morphology 80−21972
coronal Langmuir turbulence, rel. to quasi-stable particle accel. and type I radio bursts *(Chinese)* 80−105220
coronal line profiles above active regions, statistical anal. 78−7968
coronal long-duration X-ray event, plasma parameters from Skylab obs. 77−29741
coronal loop, plasma physics model 77−45371
coronal loops, struct. 78−89155
coronal loops, temp. and density struct. 79−8890
coronal loops, thermal instabilities in magnetically confined plasmas 80−36600
coronal loops in an active region, physical props. XUV obs. 80−90376
coronal magnetic field and current sheets above active regions 77−78757
coronal mass ejection transients rel. to other solar activity 79−44457
coronal streamers, electron densities from K-coronameter polarisation meas. 78−4182
coronal transient, broadband polarimetry obs., importance of Hα emission 77−2389
coronal transients, freq. rel. to solar activity indices 77−22181
coronal X-ray bright point and small active region fine struct. rapid vars. 80−12741
corpuscular streams, correl. with Earth troposphere instability 79−92580
correlation with interplanetary cosmic ray protons 80−77243
cosmic radiation, theoretical proton spectra at atm. depths 40 g cm^{-2}≤h≤350 g cm^{-2} *(German)* 79−12367
cosmic ray 27-day cycle and anisotropy rel. to solar activity epoch 77−53370
cosmic ray intensity var. correlation 78−69625
cosmic ray modulation and solar activity 79−80135
cosmic ray neutron component intensity delay rel. to latitude solar activity index 77−53364
cosmic ray protons at 1 AU from active regions, energy spectra from Prognoz-3 80−101512
cosmic ray variations, solar activity and neutrino fluxes, review 79−84599
cosmic rays, high-energy, modulation, anisotropy spectrum var. with solar activity cycle 80−51628

solar activity continued
cosmic rays, Z-rich particle event charcts., (1972 to 1976) 79−5717
cosmic rays long-period vars., freq. spectra 77−25892
cosmic-ray intensity variations and origin of cosmogenic isotopes 77−53361
current theories *(French)* 79−84760
currents sheets as heating source for active regions 78−28634
cycle, absence of effect on zodiacal light brightness 78−45276
cycle, as nonlinear oscill. of general mag. field driven by nonlinear dynamo 78−40889
cycle, correl. with geomag. external spherical harmonic coeffs. var. 80−85592
cycle, correl. with meteor rates and upper atm. density vars. 77−53485
cycle, correl. with vars. of geomag. field first-degree spherical harmonic components 80−85593
cycle, phase relation between poloidal and toroidal fields and location of surface magnetic fields 77−29758
cycle, rel. to mag. fields and convection and meridional motions in solar atmosphere 77−53493
cycle, rel. to polar mag. fields and cosmic ray vars. phase reversals 78−40780
cycle, var. of sunspots distrib. between N and S solar hemispheres 77−56881
cycle 20, cosmic rays modulation from neutron intensity vars. 79−84604
cycle 20, flares and cosmic ray events at minimum 79−21250
cycle 20, flares rel. to cosmic ray intensity, model 80−72914
cycle 20, Forbush decreases and geomagnetic storms rel. to interplanetary parameters 77−70956
cycle 20, geomagnetic activity recurrence tendency 79−25196
cycle 20, long-term vars. of solar wind props., Imp 6, 7 and 8 results 78−77452
cycle 20, statistical anal. of noise storms on 260 MHz and radio bursts on 29.5 MHz 80−56794
cycle 20, statistical study of Ca II flocculae and radio fluxes 77−91498
cycle 20, study of Forbush decreases and corresponding flares 78−49249
cycle 20, time-latit. occurrence of flares, 1965-76 period 79−80290
cycle 20 (1965-77), stratospheric summertime temps. 79−79936
cycle 20 descending branch, activity centres peculiarities *(Russian)* 79−96926
cycle 20 effects on cosmic ray modulation 79−53684
cycle 20 peak, corona obs. with Solwind coronagraph 80−82325
cycle 21, forecast of max. activity 78−49416
cycle 21, predicted intensity and date of max. 78−73696
Cycle 21, prediction with early 1980 max. 78−69778
cycle 21, radio communication effect 79−75181
cycle 21, sunspot effects on amateur radio communications 79−58308
cycle 21, use of dynamo theory to predict sunspot number 78−81597
cycle 21 development rel. to EUV spectrum and atmospheric absorption 79−75174
cycle dependence of F-region equatorial vertical drifts 80−31159
cycle dependence of range and freq. spread F 78−32292
cycle during classical antiquity, rel. to auroral cycle 79−92736
cycle effects in equatorial spread-F at Huancayo 78−61647
cycle effects in geomag. northward component secular var. 77−73635
cycle effects on equatorial ionospheric F-region elec. fields 78−28405
cycle influence on geomag. field 77−78090
cycle influence on geomag. solar and lunar daily vars. 77−60350
cycle irregularity, historical evidence 79−58307
cycle length, from latit. drift of sunspot groups 77−17503
cycle minimum, evolution of photospheric mag. field patterns during Skylab 78−20798
cycle minimum, H I Lyman α flux correlation 80−90393
cycle minimum, study of background corona 78−28616
cycle of activity rel. to mass motions, torsional oscillator model 80−105217
cycle parameter, sunspot variability index *(Polish)* 79−58311
cycle period-amplitude relation, hysteresis of nonlinear mag. oscill. and 55-year cyclic modulation 79−35214
cycle phase dependence of coronal rotation rate 77−87364
cycle rel. to latit. depend. of solar wind speed 77−9732
cycle rel. to solar wind speed vars. (1962-1974) 77−9734
cycle signal in surface air temp. over N.America 79−58042
cycle var. of interplanetary magnetic field 78−49274
cycle variation of interplanetary mag. field config. 80−12632
cycle variations of interplanetary mag. field intensity 80−26809
cycle vars. of stratospheric 10 mbar geopot. height 79−29824
cycles 14 to 19, large sunspot groups occurrence frequency 77−17467
cycles 19 and 20, F_2-layer ionisation, SW radiocommunication appl. 79−21102
cycles 20 and 21, solar wind structure during early phases 79−25430
cycles during 1540-1700 period, from solar and auroral obs. 79−21267
cyclic variations in cosmic rays and solar activity, detect. from radiocarbon meas. 79−16776
cyclical and secular var. 77−53558
daily cosmic ray flows during solar cycle in solar equator vicinity 78−69622
decametric noise of Jupiter, solar activity effects *(Russian)* 77−64694
decline period 1971-74, Mars spacecraft meas. of galactic cosmic ray flux 78−96365
development and structure of bright active regions at 2.8 cm 78−53910
differential rotation dependence 79−84766
Double Hale 45 yr. cycle, detect. in 8000 yr. terrestrial palaeoclimatic record 77−78401
drift pair radio burst, MHD theory 79−25558
drifting spikes, new species of solar radio bursts, obs. 79−48753
dynamo theory of solar cycle 79−44434
effect on cosmic rays, long-term var. 77−53340
effect on planetary albedos 79−75177
effects on particle accel. near Jupiter 78−57526
eleven year cycle, effects on comet brightnesses 77−25983
eleven year cycle, effects on interplanetary mag. field N-S component configurations in solar wind interaction regions 80−98529
eleven year cycle, evidence for signal in tropospheric winds 80−72604
eleven year cycle, phase rel. to convective zone cophasal regions 78−96469
eleven-year cycle, correl. with Gegenschein and relation of Danjon *(French)* 79−96968
eleven-year cycle, rel. to mag. buoyancy and Sun radius and temp. vars. 79−92749
eleven-year cycle, rel. to mag. fields floating-up time 80−101580
solar activity continued
eleven-year cycle, rel. to periodicities of Earth annual polar motion many-year var. *(Chinese)* 80−104848
emerging flux regions and evolving mag. features, rel. to flares 77−82202
energy balance of active regions 78−28633
ephemeral active regions during solar minimum 80−31279
EUV flux, changes with solar activity, rel. to ionosphere primary ion-electron prod. rates change 80−72675
EUV flux variation at end of solar cycle 20, AE-C satellite obs. 77−71075
EUV spectrum of active region, line identifications and intensities 78−96447
F10.7 index during solar cycle 21, correl. with atmospheric $O^+(^2P)$ ionisation freq. vars. 80−77195
F_2-layer ionisation through a solar cycle, SW radiocommunication appl. 80−41626
F-region, n_2F_2 annual vars. with latit. and solar activity level 78−69577
facula models, CH, CH^+ lines equivalent widths 79−66972
faculae, 1972-7 white light obs. 79−16920
faculae, direct photographs with balloon-borne 10 cm telescope *(Japanese)* 79−80292
faculae, line profile families rel. to total mag. flux 78−49408
faculae and sunspots, mag. field effects on solar luminosity 80−46515
faculae heating mechanism, convective motion interaction with mag. field 77−82193
faculae models, rot. temp. of CO mols. 77−78740
faculae rel. to sunspot cycle 80−90390
fibrils, lifetime and evolution 77−29760
filaments in 11-year cycle, activation vector space distrib. 77−53559
flare distrib. in galactic coord. system *(Russian)* 80−67689
flare mechanisms, review *(Italian)* 78−96463
flares and type I sources, evolutionary relation, 146 MHz obs. *(Chinese)* 80−8609
fluctuations, and deviations of light rays during eclipses *(French)* 80−56795
fluctuations, reln. to variation in O_3 conc. and layer temp. 80−31110
forecast for Cycle 21, comparison with previous cycles *(Chinese)* 80−8608
forecast reliability *(Russian)* 79−92742
forerunners, outer rims of coronal transients 79−25583
galactic cosmic ray intensity modulation out to 18 AU Pioneer 10 and 11 obs. 80−90297
galactic cosmic rays anisotropic diffusion in interplanetary space, 11-year var. 77−25891
galactic cosmic rays modulation, nucleonic flux and solar indices correl. 77−22026
general magnetic field evolution during solar cycle 77−53556
general problems, review 77−53544
geomagnetic activity cyclicity rel. to solar wind velocity 79−79732
geomagnetic and solar activity universal connection 79−40039
heavy-ion-rich particle events, $^3He/^4He$ ratios energy depend. and temporal evolution 80−90299
hectometric and kilometric radio emission in August 1972, satellite obs. 77−25994
high-temperature plasma, anal. using dielectronic recomb. spectra 80−46391
inactivity, ^{14}C evidence in tree rings 78−7962
influence on photoelectron fluxes in Earth's ionosphere and plasmasphere 78−16374
interchange instability, rel. to heating and reconnection magnetic flux tubes emergence 77−56894
interplanetary phenomena, solar-induced, rel. to differences between new and old comets 78−36513
intransitive Sun rel. to climate var. 79−21255
ionosphere, electron temp. var. with solar activity satellite meas. 80−26678
ionosphere, F_2-layer critical freq. vars., rel. to solar activity 77−67008
ionospheric E-region, NO var. with solar activity 78−49207
ionospheric records over Shanghai, March 1953 to June 1955, correl. of solar activities *(Chinese)* 80−77192
Jupiter decametric radio emission, correl. with solar activity 79−21222
Jupiter Great Red Spot, depend. on solar activity 79−101110
large scale variations, evidence from meteoroid data 77−82190
large-scale distrib. rel. to limb effect of redshift 77−53553
large-scale vel. features, magnetograph obs. 79−35224
latitudinal zonality, movement of material and activity cycle 77−17535
limb active regions, 1175 to 1940 Å emission-line spectra 78−96446
long term forecasting using high resolution time spectral anal. 77−33453
long-period properties, 80-90 year sunspot cycle 77−53536
long-term variations, rel. to solar cosmic-ray prod. 79−92735
long-term variations, solar activity and neutrino flux 78−45307
luminosity variation, Ca H and K behaviour at solar minimum and cycle 21 onset 79−16907
lunar spectral photometry during max. solar activity 77−37522
Lyman α albedo of Jupiter rel. to solar activity 80−98601
M-regions rel. to active regions and recurrent Forbush decreases 78−96367
magnetic activity basic props. of mag. flux tubes 77−13297
magnetic and microwave struct. in active regions 77−49361
magnetic cycle, influence on galactic cosmic ray flux semiannual var. 79−16777
magnetic field emergence and 11-year activity cycle 78−85929
magnetic field generation processes, basis for solar cycle *(Russian)* 77−60745
magnetic field in solar active regions, skinning process stability 77−53521
magnetic field lines from active regions, struct. review 80−85924
magnetic field of active regions, appl. of new approach to force-free field 80−62011
magnetic field theory, props. of mag. flux tubes 77−5513
magnetic field variations, effects on interplanetary mag. fields 77−9646
magnetic fields, flux-rope-fibre theory 78−77525
magnetic fields of active regions, zero points 78−96465
magnetic fields of active regions and spots, contrib. to solar mean field compared to background field *(Russian)* 78−57530
magnetic flux emergence, ephemeral active regions and X-ray bright spots, flux-rope theory 80−46519
magnetic flux emergence, evidence for globally coherent variability 80−51716
magnetic knots, mutual attaction 78−53898

solar activity continued
magnetised expanding plasma gaskinetic press. 77−45394
Mars thermosphere, depend. of struct. on solar activity 77−64686
mass motions in active transition zone from EUV spectra 78−85922
Maunder's paradox and the tidal theory *(French)* 77−45387
Maunder minimum, 1645-1715 period 77−71103
Maunder Minimum, catalogues of auroral obs. 80−51722
Maunder minimum, evidence for precursory solar rot. accel. from Thomas Harriot's sunspot obs. 79−75182
Maunder minimum, evidence from statistics of largest geomag. storms 77−2306
Maunder minimum, meteoritic evidence 78−57529
Maunder minimum, rel. to 11-year, 80-90 year and 600 year cycles 78−77549
Maunder minimum, solar surface rotation rate 77−2377
Maunder Minimum, solar wind state 79−75069
Maunder minimum and planetary tides 77−33376
maximum, obs. program for 1979 Apr. 1-1980 Nov. 1 period 77−17497
McMath 12686, type III burst producing McMath 12686, type III burst producing active region, overlying coronal struct. Skylab obs. 80−21976
McMath 14275, 6 cm obs. of active region and bursts with 6″ resolution 80−62096
McMath region 11976, summary of solar/interplanetary events during August (1972) 77−25991
McMath region 12336, comparison of 9.1 cm and soft X-ray emission 77−22180
McMath region 12417, X-type neutral sheet form., chromospheric activity prod. 80−98642
McMath region 13043, overlying centimetre-wave sources rapid var. rel. to optical phenomena 80−67688
McMath region 14943, optical obs., 1977 Sept. 79−48766
McMath region 15403, 5 minute oscills., SHF obs. 80−98639
McMath regions 12472 and 12474, interconnecting transequatorial loops 77−71090
McMath regions 14943 and 14979, interferometric obs. at 8.6 mm wavelength 79−48768
metre wavelength radio bursts, coronal Langmuir waves emission theory 78−57515
metre-wave radio bursts positions, correl. with X-ray emission 78−69774
metric radiobursts polarisation and location rel. to new mag. field emergence 78−61824
MHD dynamo model of solar cycle 77−17536
microwave activities associated with McMath regions 14943 and 14979, 1977 Sept.-Oct. 79−48767
microwave bursts, spectra, occurrence freq., and energy output 77−5461
microwave bursts fast structures, negligible assoc. large-scale mag. field changes 79−2536
microwave emission, sudden decreases obs. 79−101134
microwave flux decreases rel. to assoc. activity complex 77−25989
microwave impulsive bursts, superimposed fast time structs. with slowly varying polarisation 79−40173
microwaves, solar activity, lower intensity limit *(Portuguese)* 77−78729
microwaves total flux, fluctuations power spectra correl. with solar activity 80−4327
model of solar cycle driven by dynamo action 77−56903
moving type IV burst, associated pulsating struct. radioheliograph obs. 79−40171
negative bursts, absorption origin 77−53517
neutrino flux correls. 80−46522
noise storm, drift pair bursts, polarisation obs., position and freq. charcts. 80−85925
noise storm, drifting pulsations obs. 80−62105
noise storms, spectrum and position at decametre wavelengths 78−28622
north-south asymmetry of solar activity and cosmic rays 79−80137
north-south distribution of flares, sunspot mag. classes and sunspot areas, 1955-74 period 77−71088
open magnetic fields in active regions 78−28631
open magnetic structures evolution, Skylab obs. 78−16362
optical interferometry of solar phenomena 79−44378
oscillations due to rotation, effect on stratospheric circulation 77−45118
ozonosphere-solar cycle relationships 80−17342
past activity by means of cosmogenic isotope conc. in lunar samples 78−61828
Pc 2-3 pulsations with modulated amplitude, depend. on solar activity 78−69620
periodic behaviour in convective system, heated fluid bed instability *(French)* 79−84761
photosphere active region, Mg I, Mg II reson. lines obs. 79−40163
photosphere active regions, mag. flux appearance 79−40161
photosphere active regions, models from Mg II h and k line wings 78−57518
photosphere activity, energy transfer to solar wind by elec. currents 80−94768
photosphere cooling with increased sunspot activity 78−40896
photosphere faculae intensity, centre to limb var. 80−21967
photospheric faculae, models 80−12716
photospheric rotation rate, variation with activity cycle 77−13304
photospheric velocity field peculiarities in active regions *(Russian)* 77−64720
plage, absolute u.v. intensities meas. in 1750-2100 Å range 77−2405
plage Ca II K-line, peak separation due to microturbulence 80−109407
plages, correl. with Earth atmosphere vorticity area index 78−73459
plages and filaments assoc. with coronal holes, differential rot. 77−22167
planetary theory, periodicities and dissymmetries in convective layer of Sun *(French)* 79−84762
planetary theory of solar activity *(French)* 79−84759
planetary tides, mechanical interpretation of solar activity *(French)* 78−20787
plasma frequency bursts, implications of Voyager 2 coronal occultation obs., 1979 August 80−51639
polar faculae, rel. to Sun high-latit. mag. field and Earth rot. nonuniformity 80−46119
polar solar wind, variation rel. to solar activity 80−90385
pores, line profile families rel. to total mag. flux 78−49408
preflare characteristics of active regions observed in soft X-rays 79−84776
proton event of 1978 May 7, neutron monitor obs. 80−67686
pulsed microwave bursts with quasithermal spectrum, model 77−78762
quasi-biennial variation of solar activity and neutrino flux 79−44440
quiescent periods 79−2538
solar activity continued
quiet Sun, activity, microspicules obs. in Hα and He I D_3 line 79−66983
quiet Sun, electron density from EUV line intensity ratios 79−21245
radio bursts, anal. of obs. at 3.2 and 10 cm at Purple Mountain Observatory *(Chinese)* 80−105223
radio bursts, appl. of electron beam relaxation model in fluctuating plasma 78−83579
radio bursts, evidence for dense non-potential magnetic flux tubes in corona 78−28615
radio bursts of drifting pairs type, results of obs. near 25 and 12.5 MHz 78−24502
radio emission, preliminary results from Mark II Nancay radioheliograph 78−28517
radio emission from active regions, 6 cm obs. with 6 arc seconds resolution 77−33444
radio emission polarised zebra struct., interpretation 78−96467
radio noise storms, correl. with photospheric source position and mag. structs. 78−4185
radioastronomical obs. by amateurs *(Italian)* 78−7887
radiocommunication implications, historical account and predictions *(Italian)* 78−24496
rainfall pattern rel. to solar activity during N.E. monsoon in Tamil Nadu 77−70749
satellite power stations, output power variations, effects 79−29455
scattering process above active regions, propagation in fibrous medium 78−20780
sectoral struct. of interplanetary mag. field, large scale spiral waves in solar wind 80−12633
secular variations, investigation of regularities *(Chinese)* 77−71080
Shuttle/Spacelab program rel. to flare buildup studies 77−17498
Skylab obs. of quiet and active solar events 77−56891
small-scale magnetic field in active regions, size, struct. and strength 77−78738
soft X-ray bursts, statistical distrib. 80−26839
soft X-ray polychromator for Solar Maximum Mission 80−51660
solar cycle, 1959-1974, general mag. fields anal. 77−22166
solar cycle, rel. to solar wind high-speed streams outflow regions localisation and vel. 78−53919
Solar Maximum Mission GSTDN/TDRSS compatible RF system 78−45198
Solar Maximum Year project and related space experiments, review 80−90404
solar wind, evidence for solar cycle vars. 78−49266
solar wind, vel. vars. rel. to props. of interplanetary mag. field 77−17318
solar wind charcts. rel. to solar activity, review 80−94777
solar wind high-speed streams, flow parameters at 1 AU 77−9733
'spike' type radio bursts, morphological charcts. 78−65599
statistical study, X-ray radiation rel. to SEA and active areas *(French)* 78−20788
stellar activity of solar type, observational aspects 77−56918
STIP Intervals I and II, significant solar-initiated events 78−49420
submillimetre observations, of solar active regions 78−12177
Sun and heliosphere, conference, London, England (1979 April 3 to 4) 80−82574
sunspot activity periods, correlation analysis *(Chinese)* 77−67082
sunspot cycle, period rel. to solar pulsation and rot. periods 77−53519
sunspot cycle, rel. to LF radio waves signal vars. 77−78560
sunspot cycle, rel. to occurrence of range and freq. spread-F at Kodaikanal 80−72676
sunspot cycle and solar luminosity 79−75176
sunspot cycle and weather, timed by internal solar chronometer 79−16921
sunspot cycle before Maunder minimum, evidence for 11-year periodicity 78−61825
sunspot cycle morphology, theory *(Chinese)* 80−12722
sunspot cycles, relation to polar coronal holes 80−21979
sunspot cycles and effects on satellite performance 80−56812
sunspot formation, assoc. vel. field 77−2396
sunspot groups fragmentation vars., rel. to size and 11-year cycle 78−73691
sunspot minimum, correl. with afternoon counter-electrojet events occurrence in Indian region 80−56672
sunspot minimum, quiet radio Sun rel. to coronal X-ray holes radio emission 78−20805
sunspot number, rel. to tropopause height 80−77090
sunspot number and solar activity forecasting 77−29757
sunspot numbers secular course, prediction formula 77−45393
sunspot period stability investigation by periodic anal. of aurora and earthquake records in ancient China *(Chinese)* 79−21253
sunspot turning points and aurorae since (AD 1510) 80−21980
sunspots, large group sequences 77−53560
sunspots, statistics of largest number per solar cycle 77−22159
sunspots, umbral intensity rel. to phase in solar cycle 78−69773
supersecular 180-year cycle from 1610 onwards 77−53561
surface magnetic activity, role of mag. buoyancy in Sun 79−21256
surge, EUV limb spectra obs. from Skylab 80−17560
surges, dynamics of descending stage *(Chinese)* 80−105221
surges, flare-assoc. ejection mechanism 80−21975
surges and coronal heating, Skylab X-ray images examination 78−12190
SW radio noise level variation obs., as function of ionospheric perturbations *(Russian)* 77−91359
terrestrial effects, thermosphere NO and N conc. depend. on activity 80−77178
terrestrial H^+ loss during solar cycle, charge exchange processes 78−93021
terrestrial H escape flux, charge exchange induced, diurnal and solar cycle vars. 78−93022
thermal sources, microwave brightness temps. and polarisations derivation 77−22172
thermodynamic history of active region observed in X-rays 77−13303
tidal theory of solar activity 79−30034
topside ionosphere, effects of magnetic and sunspot activities 77−70918
Torun Observatory 127 MHz data since 1958, survey *(Polish)* 78−36549
transient activity and interplanetary shock waves, implications of He^+ obs. in driver gas 80−72735
transition zone, energy balance and press. for network and active region features 80−21957
transition zone instabilities rel. to preflare energy build-up, spectroscopic far UV obs. 77−17479

solar activity continued
turbulent shock wave in solar atmosphere, propag. across mag. field and struct. 79−40166
type II radio burst, 1973, May 3, fine struct. 78−24501
type II radio burst with reverse freq. drift against noise storm background, obs. 80−17567
type II radio emission prod. by coronal MHD shocks 79−92750
type III bursts, dynamics of fast electron cloud travelling through plasma 77−996
type III bursts, obs. during JIKIKEN (EXOS-B) satellite initial phase *(Japanese)* 80−94675
type III bursts, position and polarisation, VHF and HF obs. 80−105214
type III bursts, rel. to plasma waves in solar wind, Helios 1 obs. 77−37492
type III bursts, role of three dimensional Langmuir wave instabilities 77−2404
type III radio bursts, EM radiation direct generation from beam-plasma system 80−54007
type III radio bursts, fundamental emission and polarisation 80−36603
type III radio bursts, interplanetary baseline obs. 78−20808
Type III radio bursts, nonlinear Langmuir waves evolution 78−93173
type III radio bursts, nonlinear stability theory 80−26826
type III radio bursts, rel. to nonrelativistic electron beam propag. 78−28623
type III radio bursts, second harmonic radiation and related nonlinear phenomena 78−7958
type IIIb radio bursts, polarisation meas. 77−22161
type IV continuum bursts, coherent nonlinear interaction of Bernstein waves 77−53529
type IV meter bursts, continuous radiation microstruct. and source model 77−53534
type IV meter bursts microstruct., modulation of continuous emission by whistlers wavepackets 77−78761
type IV moving radio bursts, obs. and interpretation 79−40174
type IV radio burst quasiperiodic struct., anal. and interpretation 80−62097
type IV radio emission, prod. by coronal EM loss cone instability *(Russian)* 78−77528
type IV radio emission pulsations, bounce-resonance effects 78−89161
type IV solar radio events, pulsating structs. 78−96455
type U radio bursts, polarisation evolution 80−26834
type V radio bursts, dynamic spectra distinctive struct. 80−46527
type V radio bursts, position and polarisation, HF and VHF obs. 80−105215
type V radio bursts, scatt. hypothesis 77−45378
unsuspected variations, long period minima and maxima rel. to climatic vars. *(French)* 78−73695
UV brightenings in active regions, OSO-8 obs. 78−28630
UV flux variability over solar cycle, 1175-2100 Å 80−90383
UV spectra of active regions, Salyut-4 obs. 77−82211
variable Sun effects at beginning of Cainozoic era 79−75171
variations, rel. to gravitation and inertia corpuscular model *(Russian)* 79−40439
variations rel. to Earth rotation and atmospheric circulation 80−104853
Venus thermosphere, depend. of struct. on solar activity 77−64686
weather-solar activity correlation, anal. 78−40628
wind velocity, correl. with Earth diurnal rot. irregular vars. 79−8591
Wolf number data, new ARMA models 79−12442
X-ray active regions temp. and emission measure rel. to coronal mag. fields 80−12745
X-ray and 2.8 cm coordinated obs. of active regions *(Italian)* 79−21254
X-ray bright arcs and mag. flux emergence regions 78−12174
X-ray bright corona above active region McMath 12628, struct. rel. to solar atmosphere equilibria 78−53902
X-ray bright points, mag. flux emergence regions, var. out of phase with solar cycle 77−56890
X-ray bright points, mag. props. 77−91505
X-ray bright points, short-term temporal vars. 80−12740
X-ray bright points correl. with sunspot intensity, cycle var. 80−41783
X-ray complex events development, 1972 August 79−8899
X-ray corona, slowly moving disturbances 80−21971
X-ray emission spectra, differential emission measure solns. errors 79−12397
X-ray emitting active region, early evolution 78−28621
X-ray emitting coronal loops, obs. evidence of continual heating 78−61841
X-ray events with long decay times, morphology and statistics 77−60733
X-ray line emission from flares and active regions, OSO-8 obs. 79−25580
X-ray temperature-emission measure modelling of corona 80−12746
young active regions, filaments, comparison of X-ray and visible data 80−72910
Zurich relative sunspot nos. rel. to solar temp. min. in far IR 80−94769
^{14}C concentration in Earth's atmosphere, corrections with astrophysical and geophysical phenomena 78−61477
^{14}C content in tree rings correl. with solar cycle, 1744-1892 period *(Russian)* 78−16390
Ca II H and K lines cores in integrated sunlight, rel. to solar activity 78−77535
Ca II K and Hα obs. during 1969 at Kodaikanal Obs. 78−61832
Ca II K line and Hα obs. of filaments, flocculi and prominences, during 1969 at Kodaikanal Obs. 78−61833
H Balmer emission lines, Skylab obs. of active regions 77−33441
H_α high resolution obs. of active regions *(Japanese)* 78−89163
Hα activity rel. to magnetic fields and 8 and 13.5 mm radio brightness *(Russian)* 77−64724
He II 304 Å, line profiles in quiet Sun and active regions 79−12452
N IV and Ne VII emission line ratios, electron density and temp. determ. 80−17559
O_3 levels in stratosphere, solar activity, cosmic rays effects 77−53362

solar atmosphere
see also chromosphere; photosphere
5 minute oscillations, spectral lines use as temp. indicator 77−37585
absorption line formation depth *(Russian)* 77−64749
acoustic mode overstability in polytropic atmosphere 78−49413
acoustic wave propagation, radiative damping 77−53496
acoustic wave propagation until shock form., theoretical temp. min. 77−53497
acoustic waves, efficiency of one-dimens. hydrodynamic codes 78−57520
acoustic waves, energy transmission across mag. flux sheath 78−20802

solar atmosphere continued
acoustic waves, flux tubes 80−85911
acoustic waves, propag. rel. to chromosphere temp. rise 79−16911
acoustical-gravity waves in plane waveguide, interaction and self-action *(Russian)* 78−36221
active region equilibria, obs. of X-ray bright corona above (McMath 12628) 78−53902
active regions, currents sheets as heating source 78−28634
active regions, nonlinear stage of instability due to local Joule overheating 78−61839
active regions, skinning process stability of mag. field 77−53521
active regions, submillimetre obs. rel. to general atmospheric heating 78−12177
active regions magnetic field, appl. of new approach to force-free field 80−62011
Alfven wave propag. 78−53909
Alfven wave reflection at density transition region 77−29754
apparent solar diameter long period oscills., obs. 78−89138
axisymmetric convection in prescence of mag. field, solar granulation and sunspots appl. 80−12724
bound-free and free-free electron transitions, review 78−33563
centimetre wave emission, Sun radio radius and brightness distrib. across disc 80−21968
charged particles acceleration in presence of micro-turbulence, appl. to flares 77−53528
circumsolar plasma, radio signal spectral lines formation 80−92330
continuum intensities and limb darkening coeffs., synthetic and meas. 78−65590
convection, efficiency rel. to solar const. time var. 79−21262
convection zone, buoyant mag. flux tubes rel. to $\alpha\omega$-dynamo 77−45385
convection zone, mag. field transfer 78−96449
convection zone, pole-equator flux differences 77−71100
convection zone, thermal equilib. in presence of mag. flux tube 77−53581
convectively unstable atmospheres in shear flow, hydrodynamic instability 77−87253
coronal hole, atmosphere model rel. to brightness temp. obs. by λ 8-cm radioheliograph 80−4326
coronal model, rel. to Fe abundances and temps. determ. from XUV emission lines 78−4180
current sheet region during chromospheric flare development *(Russian)* 79−40159
current sheets, energetics and trigger mechanism for flares emerging flux model 78−89162
current sheets, form. during emergence of new mag. flux from below photosphere 77−22176
D abundance from SSO spectrograms 79−66982
differential rotation, from mm wave obs. 77−2378
differential rotation and giant cell circulation of Ca^+ network 77−17508
downflow, evidence from Mg II core absorpt. wavelengths 79−12451
downflow motion in mag. tubes 78−77530
dynamic response to soft X-rays from flares 78−65580
dynamics, optically thick chromospheric line formation 80−94767
electric currents, generation by solar activity rel. to solar wind energy source 80−94768
electric currents, rel. to flares energy source 77−17483
electric fields generated by motion of mag. features 78−12194
electron density, modulation rel. to centimetre and millimetre wavelengths emission oscills. 77−22175
electron density at 10^5K from O IV intersystem line obs. in EUV 78−53903
electron streams, upper limit to hard X-ray emission anisotropy 77−29742
energy balance, in solar atmosphere above coronal holes 79−92746
EUV and radio emission from chromosphere-corona transition 79−8894
EUV composite spectra of representative solar features, obs. 78−96447
evolving force-free magnetic fields, stability of configurations and motion of medium 78−12176
expansion into solar wind, higher order fluid eqns. for multicomponent nonequilib. plasma atmosphere 80−105156
faculae models, rot. temp. of CO mols. 77−78740
fast electrons cloud travelling through plasma, dynamics 77−996
filaments, multifreq. obs. at centimetre wavelengths 78−28602
five minute oscillation *(Japanese)* 80−21981
five-minute oscillations, influence of chromosphere and corona 77−91501
five-minute oscillations, observational search for large-scale organisation 78−65589
flare localisation in Sun's atmosphere, radio observations 79−88641
flare model atmospheres, reverse current effects on electron beam dynamics and X-ray bremsstrahlung 80−51711
flare particle streams, collective plasma effects associated with continuous injection model 80−21954
flare plasma, physical parameters and dynamics from X-ray and XUV emission 78−12175
flares, electrostatically unstable heat flow and its consequences 78−20804
flares, energy release processes, effect on solar atm. 77−60747
flares, Fe XXIV-XXV X-ray lines wavelengths rel. to hot plasma motions 80−21973
flares, heat transfer theory 79−40168
flares, physical processes rel. to X-ray and UV emission 78−65598
flares, physics from impulsive X-ray bursts obs. 78−93174
flares, plasma kinetic processes 78−85920
flares, polarisation and directivity of hard X-ray bremsstrahlung from thermal source 80−90374
flares, studies using optical, X-ray and radio data 78−89156
flares, unstable arch model 77−91507
flares flash phase and current sheets thermal evolution 77−17485
flares hard X-ray sources, diagnostics 78−89159
force-free magnetic fields, time evolution 78−85843
force-free magnetic fields toroidal component upper limit rel. to flares 77−33479
force-free magnetic flux tubes, dilation 78−4172
frequency response of magnetic flux sheaths 80−12743
fully ionised plasma under gravit. field, small amplitude wave motion 78−94913
gamma-rays generation, rel. to energy spectrum of 1972 Aug. 4 flare event *(Russian)* 78−12185
giant convective cells delineated by mag. fields and filaments symm. location 77−29779
global oscillations of solar brightness 77−25988

solar atmosphere continued
global solar velocity oscillation, supergranulation origin 77−13305
granulation, convection models, book contrib. 80−4329
granulation scale, physical model 78−57521
gravity waves, trapped, in solar atmosphere, obs. 80−72898
gravity waves generation by HF acoustic waves, Cherenkov radiation *(Russian)* 77−17265
heterogeneities, classification, physical mechanisms 78−16394
high-temperature plasma, anal. using dielectronic recomb. spectra 80−46391
hydromagnetic surface waves, theory 79−25462
inhomogeneous models, appl. to EUV emission lines profiles meas. near limb 79−16909
inhomogeneous solar phenomena with different porosities, line profiles *(Russian)* 78−40891
interference-phase method of mag. field meas. in solar atm. *(Russian)* 78−65509
interference-phase method of ray vel. meas. in solar atm. *(Russian)* 78−65508
IR opacity sources, rel. to IR continuous spectrum *(Italian)* 79−88638
isotope abundance, use in studies of past events 78−61829
laboratory and space plasmas, conference, Nagoya, Japan (1977 December 8 to 9) 80−4470
Langmuir waves, upconversion of ion-sound impossible 80−41716
large-scale vel. features, magnetograph obs. 79−35224
large-scale velocity field, rel. to E-W asymmetry of Fraunhofer lines central intensities 78−53916
limb darkening coefficients for quiet Sun, integrated spectrum 78−24498
limb darkening in 7404-24018 Å wavelength region 77−71099
magnetic dynamo action in slab, theory 79−44430
magnetic energy build-up, dynamic response of atmosphere 77−45391
magnetic field energy dissipation, in neutral current sheets 78−26250
magnetic field line reconnection, laboratory expts. rel. to flares 77−17494
magnetic fields, flux-rope-fibre theory 78−77525
magnetic fields, force-free fields evolution, nonequilib. states and preflare stage 80−105213
magnetic fields, non-force-free, in magnetohydrostatic equilib., anal. 79−92733
magnetic fields and motions, granulation and sunspots *(Russian)* 78−16376
magnetic flux conc. by rotational shearing motions 79−35219
magnetic flux elements vibr. modes in stratified atm. 79−16902
magnetic flux ropes, equilib. and stability *(Russian)* 80−8617
magnetic flux tubes, hydromagnetic wave modes 79−29984
magnetic fundamental flux tubes, generation, periodic field reversal 79−53792
magnetic fundamental flux tubes, rising and durability 79−53791
magnetic traps, rel. to solar radio emission polarised zebra struct. interpretation 78−96467
magnetoacoustic gravity waves 77−29752
magnetoatmospheric wave eqn., critical levels 77−78747
magnetoatmospheric waves, inhomogeneous wave eqn. 77−82189
magnetoatmospheric waves conical propag. and spicule motions 77−49351
magnetogravity waves, propag. in isothermal conductive atmosphere 79−92670
magnetospheric explosions, role of gravitational instabilities 78−28655
magnetostatic equilib. in stratified atmosphere 80−51652
mass motions in active transition zone from EUV spectra 78−85922
mass outflows, nonequilib. ionisation in solar wind 79−48751
mechanical heating of outer layers *(Italian)* 78−32431
meridional motions, rel. to mag. fields and convection 77−53493
MHD waves, propag. in mag. flux tube 78−69789
MHD-gravity wave critical levels 78−77531
models, survey of last 30 years' research 78−69764
momentum and energy transport, by acoustic, Alfven and fast mode waves 78−4162
neutral sheet two-dimens. equilib. in gravit. field 79−66919
noise storm sources, spectrum and position at decametre wavelengths 78−28622
non-LTE line formation in mag. field, two-level atom with freq. independent source function 78−61726
non-thermal vels. height variation 77−13344
nonequilibrium plasma mag. pumping as energy source for solar flares 77−78764
nonequilibrium plasmas, density diagnostics via C III EUV lines 78−53899
nonradial p mode eigenfrequencies depend. on solar envelope struct. 78−16364
nonradial p-mode oscillations 78−32428
nonrelativistic electron stream, propag. in solar atmosphere rel. to type III radio bursts 78−28623
nuclear processes in solar atm. due to charged particles accelerated in flares 78−57527
oscillations, correl. with geomag. field vars. re-examined 78−89013
oscillations, power spectra, phase spectra and coherence spectra 79−8897
oscillations, search during 1974-76 period 78−93190
p-modes stochastic excitation by turbulent convection 77−29740
particle acceleration, rel. to spectral features in hard X-ray and radio events 77−45369
penetrative instabilities in solar atmosphere, effects of thermal dissipation 80−109406
photoabsorption cross sections for positive atomic ions with $Z \leq 30$ 80−26727
physics, future progress prediction *(Italian)* 78−81606
plasma, highly ionized, ionization equilib. validity 80−21906
plasma density determination, N III and O IV intersystem multiplets appl. 80−31264
plasma effects, rel. to spectral lines in radio emission 78−96466
plasma physics, solar and solar wind, book 79−84782
plasma processes, rel. to microwave bursts and large-scale mag. fields 79−2536
plasma-neutral gas interaction in cosmic physics 78−69669
preflare current sheets search, for forecasting occurrence of flares *(Russian)* 77−60746
progressive sound waves effect on absorpt. coeff., Ca II K line with Doppler profile 77−60738
prominences, H line radiation diffusion 80−67694
pulsation, radial p-modes 77−33434
quasiperiodic oscillations inferred from 3 cm radio obs. 77−29768
solar atmosphere continued
quasiperiodic variations in solar flux at 10.7 GHz 77−17516
quiescent prominences, downward motions model 78−20779
quiet Sun, brightness temp. at cm wavelengths *(Russian)* 77−64721
radiative equilibrium departures, grey absorpt. 78−81531
radiative power loss, from plasmas in steady state ionisation balance 79−82063
radiative recombination in ions of astrophysical interest 77−78627
radiative transfer, model including OH continuum opacity 79−40162
radiative transfer, physical effects in multidimens. media, models 80−72758
radiative transfer in magnetic atmospheres, analytical soln. 80−36494
radiative transfer inversion problems, Backus-Gilbert formalism 78−89054
radio brightness distribution on quiet Sun, small-scale struct. obs. at 8 millimetre wavelength 79−40149
radio burst emission mechanisms 80−72917
radio bursts, peak flux spectra, statistical anal. source mechanisms 80−98641
radio recombination lines, high n 77−78758
rare earth rich submicron grains in Earth's atm., solar vs. terrestrial origin 78−12180
review of present knowledge 78−40895
rising magnetic field, rope struct. *(Russian)* 78−40898
shock wave dissipation in outer atmosphere 77−60740
shock waves, generation by August 1972 flare events, ground-based radio obs. 77−25993
solar oscillations, influence of Sun outer layers on detect. 79−5800
sound generation by Alfven waves with random phases 78−7979
spectral line formation depth *(Russian)* 77−64723
spectral line formation depth *(Polish)* 79−88639
spectral line formation depth in mag. field, theory *(Chinese)* 80−105159
spectral line intensity, electron impact excitation 80−36605
spectral line shifts, wave effects 80−109408
subflare, intense, compact, physical parameter anal. 79−62802
sunspot magnetic field and vel. quasiperiodic oscills. *(Russian)* 78−12186
sunspots, overlying atmosphere struct. 79−96989
superadiabatic charged particle accel. and flares 79−21251
supergranulation on quiet Sun, high-resolution obs. at 6 cm using Westerbork Synthesis Radio Telescope 80−36601
supergranulation structure in coronal holes 80−51729
supergranule network features, area var. with temp. in transition zone 78−89152
surge producing short-lived filament 77−33458
surges, dynamics of descending stage *(Chinese)* 80−105221
surges, flare-assoc. ejection mechanism 80−21975
sympathetic flares occurrence, statistical anal., negative result 77−22189
temperature fluctuations and vel. height var. 79−8891
temperature minimum, absolute brightness temp. meas. in far IR with balloon-borne interferometer 80−62095
temperature minimum, brightness temp. meas. with balloon-borne lamellar-grating interferometer 78−85921
temperature minimum, five-minute oscills. obs. 79−62808
temperature minimum region heating during solar flares, implications of Al I autosionisation lines obs. 80−26829
thin magnetic tube instability rel. to network struct. 80−12725
time intensities, dielectronic recomb. excitation effects 80−82332
transients, MHD, two-dimens. plane anal. 78−20773
transition zone dynamics 79−21247
turbulence, review 79−30056
turbulence and vel. of near Sun plasma from Venera-10 occultation obs. *(Russian)* 77−91504
turbulent shock wave propagating across mag. field, struct. 79−40166
two-dimens. model of nearly flux constant atmosphere 79−25571
type IV moving radio bursts, obs. and interpretation 79−40174
UV spectroscopy, review of high resolution obs. 78−45313
vector magnetic fields, determ. from Stokes profiles 78−28611
velocity field, estimation by measuring solar spectrum integral characts. 80−46530
velocity fields, large-scale, from Doppler line shift obs. 80−12730
velocity fields, observations *(Italian)* 78−81601
velocity fields, theory *(Italian)* 78−81600
velocity fields meas. using magneto-optical filter 79−25507
wave propagation, resonance, theory 79−84768
wave propagation in nonisothermal atmosphere, rel. to solar five minute oscills. 80−31276
waves, vertical propag., phase delay obs. 79−96981
X-ray complex events development, 1972 August 79−8899
X-ray images, quantitative interpretation by filter ratio anal. 79−40085
Be abundance 77−13332
CO IR spectrum rel. to atm. struct. and C abundance 78−28608
CO spectrum, equivalent widths of (A-X) band lines 77−17501
$^{12}C/^{13}C$ ratio from CH photospheric lines 77−5518
Ca II K-line, search for global oscillations 78−7959
Fe I lines limb shifts, effect of press. shifts in solar atmosphere 78−89150
Fe I spectrum, 300 to 900 nm, microturbulence and Fe abundance determ. using precise oscillator strengths 79−40155
Fe, Kα fluoresc. due to solar flares 80−17569
Hα output coeff. influence on source function *(Russian)* 78−73690
Hα photography 78−40833
He I, II visible and UV line radiation from model flare layer 77−22190
Li, Be, B, isoelectronic sequences, ionization equilib. balance, solar and stellar atms. appl. 79−36587
Mg II h and k lines, Skylab high-resolution obs. 78−36544
Mg VII, UV lines, theoretical intensity ratios 78−90108
$^{24}MgH^{+}$, high resolution rot.-vibr. spectra, solar atm. appl. 77−18939
O abundance, influence of diffusion on line intensities 80−4318
O I like ions emission lines, density depend. 79−40165
O^{2+}, collision strengths, radiative transition probabilities, solar atm. appl. 79−86069
S compounds presence or absence, theory 78−69765
S XI, UV lines, theoretical intensity ratios 78−90108
Si III 1892 Å emissivity, charge transfer effect on appl. of line as spectral diagnostic 80−41717
Si IX, UV lines, theoretical intensity ratios 78−90108
SiO spectrum, equivalent widths of (A-X) band lines 77−17501
Ti abundance from weak spectral lines obs. 77−29778

solar batteries *see solar cells*

solar cell arrays
see also solar power
5 kW photovoltaic generator system, analysis, design and realisation 80−45704
25 kW Fresnel lens/photovoltaic concentrator application experiment at Dallas−Fort Worth Airport 80−89647
25 kW solar photovoltaic flat panel power supply for electrodialysis water desalination unit 80−89643
50 W generator for developing nations, with simple tracking system 79−43748
100 kW peak photovoltaic power system, design, construction and capabilities 80−45705
900 mW solar battery construction and characteristics *(German)* 80−12008
aerospace photovoltaic generators, symposium, Noordwijk (1978) 79−96449
aerospace solar panels with concentrating reflectors 79−96472
aggregating cells in series and parallel, technique 80−93954
albedo contribution to satellite array perf. 78−40798
artificial satellite nonconvex solar battery panel mounting, optimal ang. determ. 79−39291
battery installation and performance in mid-European latitudes *(German)* 80−21399
bearing and power transfer assembly development status 79−96462
combined photovoltaic/thermal flat plate collectors, extended Hottel-Whillier model 80−3520
comet rendezvous mission appl., Halley's ultralow-mass designs 79−53702
concentrating array, using point focusing acrylic Fresnel lenses 79−52937
concentrator designs for space vehicle photovoltaic arrays 80−94057
concentrator systems for solar cells, economic assessment 79−43770
cost minimisation, of self-contained photovoltaic power supplies 79−48098
coverglass development, for space appl. 79−48133
DC to AC power conversion and utility interfacing, technqiues, requirements and components used 80−45703
design of high concentration solar cell arrays, components, technology and performance 80−50955
developments and new appls., cost effectiveness 80−16800
digital consumer products appl., light-power conversion problem 80−3517
direct photovoltaic conversion, future development prospects, research projects and new appls. 80−16798
dispersion of charact. effect calc. 79−87994
distributed photovoltaic systems for electricity generation, economic and technologic feasibility 80−55906
economics modelling of photovoltaic module manufacturing, SAMICS methodology developments 80−55860
efficiency of generation, solar energy conc. using Fresnel lenses, spectral adaption and fluoresc. and bifacial concentrators *(Spanish)* 80−72060
electrical system comprising DC separately excited motor and mechanical load driven by solar cell array, performance analysis 80−16801
electricity storage in solar energy plant, battery appls. potential 80−72067
ESRO IV satellite, orbital performance assessment 78−40797
ethylene-vinyle acetate lamination, solar cell encapsulation, double vac. technique 80−93510
European solar array technology status and potential 79−96463
European Space Agency lightweight hybrid solar array design and status 79−96475
European Space Agency sponsored solar arrays, predicted and achieved performances 79−96478
fabrication, review of present status and future prospects 80−61343
flat plate PV modules, elec. and environmental testing requirements for terrestrial appls. 80−61368
flat-plate non-tracking ground mounted photovoltaic array structures, cost reduction anal. 80−94038
flat-plate photovoltiac array design optimisation 80−94037
heating and cooling of buildings, Shenandoah Solar Recreational Center 80−45757
HV photovoltaic arrays, safety from high reverse voltages 80−93953
hybrid, medium power (2.1 and 3.7 kW), design for spacecraft appl. 79−48138
INTELSAT V solar array design and test results 79−96471
interconnector fatigue resistance tests 79−96457
large deployable solar array development for communications spacecraft 79−96469
large flexible solar array design analysis and verification 79−96459
lightweight hybrid solar arrays, status of development 80−94042
lightweight solar array flexible substrates with anticharging layers 79−96456
line-focus parabolic-trough photovoltaic arrays, active and passive cooling 80−93988
microcomputer controlled solar battery, charging networks and stepping motors for cell control 80−50987
monolithic solar cell panel of amorphous Si 80−45666
multikilowatt space solar array application of large-area terrestrial solar cells 79−96451
optimisation for use with concentrators 79−62001
Orbital Test Satellite solar array design and testing 79−96470
p-n homojunction integrated tandem solar cell performance 80−3521
panel design for orbiting solar observatory (OSO-8), in-orbit telemetry data, comparison with predictions 79−48652
parabolic concentrator arrays, collector end shadowing effects minimisation 80−93987
performance and thermal characteristics *(German)* 79−96443
photopile manufacture for terrestrial solar cells, review *(French)* 79−24895
photovoltaic, optimisation of total annual energy output from constant/adjustable tilt systems 80−94059
photovoltaic cells production technology, future systems efficiency and cost effectiveness 80−16799
photovoltaic cells using silicone materials, encapsulation 80−94019
photovoltaic concentrator array technology, status report 80−94024
photovoltaic concentrator cells development project, developments, performances and future trends 80−45699
photovoltaic energy system, 25 kWp, for agricultural appl., performance anal. 80−30491

solar cell arrays continued
photovoltaic modules, physical and electrical degradation in terrestrial environment 80−30492
photovoltaic modules and systems, circuit design considerations 80−93955
photovoltaic power conditioning system for professional services office building 80−89646
photovoltaic power stations, nominal costs and performance goals 79−34438
photovoltaic power system reliability assurance methods 80−61315
photovoltaic powered 20-hp DC/AC irrigation system and 3-kW N generator 80−89645
photovoltaic solar arrays and DC motors, direct coupling theory 80−3523
photovoltaic solar cell array used for supplemental power generation 80−35686
photovoltaic systems, all component optimisation, theory and appls. 79−29475
photovoltaic systems, design for intermediate-sized appls. 80−30490
photovoltaic systems, parametric cost analysis 79−100535
photovoltaic systems break-even cost anal. for rural Mexico 80−94027
photovoltaic transient analysis program for electrical and thermal anal. 80−94061
photovoltaic village power systems: the minigrid concept 80−66973
photovoltaic/thermal system powers Texas house, performance data and power conditioning equipment 80−94036
photovoltaic/thermoelectric refrigerator for medicine storage for developing countries 80−35712
plastic parabolic concentrator, for terrestrial arrays 79−14089
point-focus Fresnel lens photovoltaic arrays, active and passive cooling 80−93988
point-focus photovoltaic concentrator arrays, durability, reliability 80−93985
power loss in photovoltaic arrays due to mismatch in cell characteristics 80−16802
power satellite solar array blanket interface problems 79−96466
production, research and development, US DOE photovoltaic program 80−93879
repair, adhesive bonding, and interconnector developments 79−96455
review of US DOE R and D program 80−55874
rigid foldout solar array development for geostationary satellites 79−96468
rocket solar sensor data processing cct. *(Japanese)* 78−24423
roof shingle-type modules, for residential and commercial buildings 79−52907
rural electrification by solar power, photovoltaic arrays efficiency 80−66974
sample accelerated thermal cycling facility 79−96458
satellite appl., design for Tracking and Data Relay Satellite System 79−48136
satellite appl., Intelsat V design and development 79−48135
satellite appl., telecommunication, rigid, fold-out array prototype development 79−48137
satellite geomagnetic substorm charging simulation 79−96886
satellite photoelectric power stations, alternate favourable option 80−16791
satellite power system technology, environmental and societal impact 80−30386
satellite solar cell panel monitoring by ground station telemetry 79−62003
satellite solar power stations using solar cell arrays and microwave transmission 80−50982
semiautomatic Sun-tracking system for concentrated solar cells 79−62012
shunt regulator hot spot problem and countermeasures 79−96460
Si ribbon crystals, edge-defined film-fed growth technique 80−89633
solar voltaic power systems, comparison to fuel energy, for telecommunications 80−61381
Solarex two-axis tracking linear concentrating collector system, design and operation 80−93989
space appl., ultra lightweight panel design, development and testing 79−52940
space power generators, past developments and future trends 80−45693
space telescope appl., double roll-out array design 79−52939
Space Telescope solar array requirements and design 79−96885
space vehicle power extension package for Shuttle Orbiter fuel cell system 80−30496
spacecraft, flight perform. of Nimbus-Landsat power systems 80−30459
spacecraft, in-orbit performance, review 80−94054
spacecraft, power system perform. anal. using computer modelling 80−30497
spacecraft appls., concentrator enhanced arrays utilising thin film Kapton mirror 80−30501
spacecraft solar electric propulsion, 25 kW solar array development testing 80−30500
Spacelab and space platform solar array programmes 79−96884
spectrally selective reflectors for concentrator solar arrays, evaluation 80−94043
string disturbances, large-signal analysis 79−96461
Sun-tracking concentrator for solar cells, solar eyeball 78−66881
Suttle pallet satellite power module for Spacelab power augmentation 79−96882
table top pulsed solar simulator, design and construction, for testing solar cell arrays powering artificial satellites 80−45696
tandem solar cells, detailed balance limit of efficiency 80−72056
technological and economic barriers to be overcome for competitive power production 80−72049
terrestrial, development of glass encapsulation technique 80−94020
terrestrial flat plate photovoltaic modules, environmental testing 80−30560
terrestrial solar generators, design, fabrication, testing and economic power generation 80−45672
terrestrial solar modules, sandwich type glass encapsulation, climatic parameters effect, economic anal. 80−45673
terrestrial solar panel design, construction and operation 79−96442
testing, standard procedures for terrestrial photovoltaic performance measurements 80−66979
tracking by microprocessor-based coordinate calc. *(Spanish)* 80−89623
Ultra Lightweight Panel solar array development and testing 79−96473
water pumping solar systems using photovoltaic convertor arrays 80−61402

solar cell arrays continued
weld testing, nondestructive tech. system selection 78−35629
wraparound contact, status and space appl. 79−48132
AlGaAs/GaAs monolithic series-connected arrays 80−97794
$Al_{0.93}Ga_{0.07}As$-GaAs monolithic series-connected solar cell array 80−7939
Cu_2S-CdS integrated thin film solar cell generators, fabrication techniques 80−55857
Cu_2S-CdS solar photopiles, tunnel conduction mechanism *(French)* 79−29480
cu_2S-CdS sprayed layer solar photopiles, CdS sprayed layer props. *(French)* 79−24901
GaAs 20 kW photovoltaic dense array for central receiver concentrator appls. 80−61372
GaAs, for earth orbital and orbit transfer missions 80−94044
GaAs photovoltaic solar system for utility substation appls. 80−30493
Si, fixed-base, flat panels, possible developments for more competitive power production 80−72050
Si, for earth orbital and orbit transfer missions 80−94044
Si, high capacity arc heater production 79−11509
Si polycrystalline, low cost conversion into sheet by heat exchange method and fixed abrasive slicing technique 80−93479
Si solar cell array with concentration, design and development 80−45700
Si solar cell fabrication, R and D on low-cost processes, effect of impurities on cell performance 80−50978
Si solar cells with concentrating collectors and integrated heat use system 80−45701

solar cells
absolute efficiency meas. 79−83597
$Al_{1-x}Ga_xAs$-GaAs heterophotoconvertors, HV, investigations 80−101097
amorphous, barrier controlled charge carrier transport in structures *(German)* 79−47162
amorphous heteroface cells *(Japanese)* 79−43765
amorphous hydrogenated Si, Schottky-barrier and MIS tunnel diodes *(French)* 79−24897
amorphous materials appls. 80−107693
amorphous semiconductor appl. 79−48130
amorphous semiconductor characterisation for solar cell applications 79−61983
amorphous semiconductor role in photovoltaic and solar thermal conversion 79−61981
amorphous semiconductors applications 79−57431
amorphouse semiconductor devices 79−52932
Ansaldo, for parabolic trough concentrator systems with forced cooling 80−93982
antireflection coatings, low-cost, durable 79−14087
antireflection coatings applied from metal-organic derived liquid precursors 80−5847
applications of 100 mm diameter cells for solar modules *(French)* 79−100532
ATS-6 solar cell flight expt., radiation damage, summary results 80−94005
Auger recombination limit on efficiency at high level of illumination 80−108797
automated electronic analysis system for solar cells 80−93952
autonomous power sources with solar generators *(Slovenian)* 79−87989
autonomous solar electric systems *(German)* 80−93875
back surface field, theoretical design considerations 80−93961
back surface reflector (BSR) and back surface field (BSF) solar cell technology, compatibility 80−89650
back surface reflectors, effect on device perform. 80−93908
back-side-reflection, for future solar arrays, design and qualification 80−94040
back-surface-field n^+-p-p^+ and p^+-n-n^+ solar cells, open-cct. voltage in conc. sunlight 80−61352
back-surface-field solar cells, I-V characteristics 79−100524
batteries for solar electricity storage, Systems optimisation of solar cell/battery 80−51007
bifacial, theoretical anal. of efficiency and spectral response, fabrication and appls. 80−55856
binary alloys, detection of compositional homogeneities using ion-induced Auger electron spectroscopy 80−25514
biological photoactive components in PEC, photosynthetic bacterial reaction centres on sputtered C and SnO_2 electrodes 80−66981
book, current topics in material science 80−46747
calibration using radiometric determ. of solar radiation spectral distrib. 80−61369
carrier lifetime meas. from transient photoresponses of pulsed laser *(French)* 79−24898
carrier lifetime measurements from transient elect. photoresponses 80−61346
cascade, design for high-temp. operation using computer modelling 80−81456
cascade using two or more junctions, material and device considerations 80−81455
cast polycrystalline, ion implanted, laser annealed 80−93918
cast polycrystalline p-n junction, hydrogenation effects 80−93916
central solar receiver, struct. anal. and design considerations of superheater 79−66410
collection grid structure, optimisation of area, shape and spacing 80−72042
combined photovoltaic/thermal flat plate collectors, analysis using Hottel-Whillier-Bliss model 77−39106
communications repeater stations power supplies 79−29450
compound parabolic concentrator photovoltaic solar collector design 79−61998
concentrated Si solar cells, conducting grid, design rules *(French)* 79−24896
concentrator, Fresnel optics 79−14088
concentrator, thick film conductive ink contacts 80−93957
concentrator solar cell with tracking control information 79−29470
concentrator/photovoltaic system design for electricity and heat generation 79−61997
concentrator/photovoltaic/Rankine cycle steam turbogenerator system efficiency 79−62002
conductor-insulator-semicond. (CIS) solar cells, noncrystalline (poly and amorphous), interface importance 80−81466
conductor-insulator-semiconductor solar cell developments for low cost prod. 80−61378
conventional solar cell efficiency analysis 79−62006

solar cells continued
conversion efficiency, maximum theoretical efficiency as a function of temp. 80−81469
costs in 1985, economic forecast *(Swedish)* 80−7919
coverglass development, for space appl. 79−48133
$CuInSe_2$ thin film fabrication by RF-sputtering 80−100786
CVD $SiHCl_3$ process, for low cost solar grade Si 79−62007
dark current and photocurrent superposition 79−43769
DC-AC inverter design, effect of meteorological conditions, computer simulation 80−61373
defects, rel. to elec. parameters, SEM electron beam induced current investig. 79−43772
dendritic web growth, computer modelling and material characterisation 79−11508
desalination plant coupling to solar conversion system, technical and economic evaluation 80−55804
design and fabrication for concentrated light 79−61995
development, US DOE National Photovoltaic Program R and D 80−66999
developments and appls. for large scale electricity prod., review 80−40861
developments and new appls., cost effectiveness 80−16800
diffusion, chemical reactions, contamination, AES and SIMS 80−72066
diffusion equation, surface boundary condition 80−66975
direct photovoltaic conversion, future development prospects, research projects and new appls. 80−16798
distributed photovoltaic systems for electricity generation, economic and technologic feasibility 80−55906
distributed series resistance effects in photovoltaic devices 80−93968
Dow Corning process for Si, advances 79−8243
drift field Schottky barrier solar cell calcs. 77−15953
dye mixture planar solar concentrator for solar cell, photon trapping and energy transfer 77−88946
ecliptic-align V-grooved hyperjunction thin film cell, MIS and SIS device appls. 80−94082
economic power generation, photovoltaic modules fabrication cost analysis 80−45674
economic viability, 1979 state and future trends 79−43775
effective series resist. meas. effects of temp. variations 80−93944
efficiency, bandgap and temp. parameters relations 79−52935
efficiency degradation, sheet resistance generated loss effects 79−29473
efficiency of generation, solar energy conc. using Fresnel lenses, spectral adaption and fluoresc. and bifacial concentrators *(Spanish)* 80−72060
EFG multiple Si ribbon growth, for solar appl. 79−8245
electorn beam interaction, spatial variations effect of number density of recomb. centres on SEM meas. 80−7943
electric power sources, applications overview *(Italian)* 80−72044
electrical load feeding prospects *(Italian)* 80−60028
electricity generation with battery storage, domestic appl. *(German)* 79−39307
electrochemical, using covalently-bound dyes on semiconductor surfaces 77−4393
electrochemical liquid-junction solar cells, Schottky barrier height, photovoltage and photocurrent 80−26162
Electrochemical Society Meeting, Boston, USA, (May, 1979) 79−91959
electrochemical solar cells, design and operation, underlying theoretical principles 80−40872
electron beam depth profiling, using carrier collection models 80−70723
electron beam induced currents appl., topotaxiality and dead region determ. 80−3518
energy analysis and viability of photovoltaic conversion and OTEC 80−61358
energy conversion, Conf., San Diego, CA, USA (Aug 1978) 79−48038
enhanced carrier collection at grain-boundary barriers in cells with polycryst. material 79−92081
epitaxial polySi and amorphous Si photovoltaic thin film developments 79−74524
European nonreflective solar cell qualification 79−96477
fabrication, laser-induced p-n junction formation 80−93880
fabrication, photovoltaic process based on thick film technique 80−94016
fabrication, preliminary 'test case' manufacturing sequence for 50 cent/watt solar photovoltaic modules in 1986 80−55858
fabrication, using ionised-cluster beam deposition and epitaxy 78−11133
fabrication process, Si single cryst. cells 79−61977
failure, life prediction using physical chemical failure progression modelling 80−61370
fault analysis using scanning light spot and distrib. network model 80−81473
faulty, scanning light spot anal. 80−89625
film solar cells 78−72204
fission product detectors 79−93873
flat plate module design evolution, influence of module requirements 80−94065
fluorescent planar collector-concentrators for solar energy conversion 80−45745
fluorescent planar concentrators, efficiency and stability 80−93986
fluorescent window for semiconductor-liquid junction solar cells 80−101114
French solar energy collection, research programme, outline *(French)* 79−74498
front surface field solar cell, spectral response, theory 80−76633
G. Donegani Institute activity *(Italian)* 80−60027
GaAs, back-wall Schottky barrier solar cell with interfacial layer 77−62993
GaAs, polycrystalline, grain boundary resistance meas. effect on solar cell performance 80−93891
Galileo works activities *(Italian)* 80−60029
glazing hemispherical transmittance props. 79−52957
global calibration of terrestrial reference cells and errors involved in using different irradiance monitoring techniques 80−93951
grain boundary effects on performance 79−83603
grid lines, optimal design to reduce conductive losses 80−7945
grid patterns, optimisation of multilayer front-contact patterns 80−16803
Hall effect, theoretical anal. 79−66408
heavily doped transparent-emitter devices, analytical treatment 79−96444
heteroface, optimum design theory 80−66972
heterojunction, interface state and energy barriers effect on efficiency 78−43464
heterojunction, low resist. $Zn_xCd_{1-x}S$ films as windows 78−71200

solar cells continued
heterojunction cell, using homoepitaxial InP films prep. by MO-CVD process 79−8250
heterojunction cell production by neutralised ion beam sputtering 78−3046
heterojunction solar cell, relation between efficiency and heterojunction parameters, review 79−74523
heterojunction solar cell model, design and evaluation 80−93964
heterojunction solar cells 80−61344
heterojunction thin film solar cells, survey or semiconductor combinations 80−50974
HEWACS, high efficiency wraparound contact solar cells 80−93906
high efficiency Transcells and vertical multijunction cells for double-sided concentrated illumination 80−55855
homojunction, superposition principle 80−81449
homojunction direct gap, theoretical limit efficiency 80−97795
house retrofitting, combined heat and electricity generation, expt. results and economic assessment 79−61952
hybrid solar photovoltaic/solar thermal electric power system, simulation 80−94025
hydride concentration cells for solar conversion 80−35698
II-VI cpd. applic. in solar cells, mats. characterisation 77−77377
II-VI heterojunctions, photovoltaic effects and solar efficiency 78−52076
II-VI heterojunctions, recent results 78−39206
III-V semiconductors, p-n heterostructures, epitaxial growth techniques, appl. to optoelectronics, review 80−54770
integral glass covering of spacecraft solar cells by electrostatic bonding 80−93676
integrated photovoltaic/thermal system with faceted-mirror sunlight concentrator 79−62010
interdigitated back-contact, tandem junction cell and front-surface field cell 80−89638
introduction to the use of solar cells 80−35678
inversion layer, numerical modelling 80−81444
inversion photoconvertors, charact. 79−39299
ion implantation and annealing technology 80−93996
ion-implanted drift field Si cell 77−24615
irradiation distribution and concentration and output power conversion *(Spanish)* 80−35683
isotype heterojunction, I-V charact. anal. 80−26138
Italian National Research Council program *(Italian)* 80−72045
LAMEL activities *(Italian)* 80−60026
large-area solar cell electrical characterisation accuracy 79−96454
laser annealing, conversion efficiency improvement *(French)* 80−66976
laser scanning for display of operating charact. and detection of cell defects 80−81460
lecture on optoelectronic devices 78−25990
lensed HV vertical multijunction solar cell, efficiency error 77−32072
lensed HV vertical multijunction solar cell, modification 77−32071
lensed HV vertical multijunction solar cell, reply 77−32073
limiting efficiency 79−43764
liquid junction (Becquerel effect), fundamentals and appl. *(Spanish)* 79−96447
liquid junction cells, fill factor and stabilisation of photoanodes 80−2464
liquid junction solar cells, aqueous CO_2 photoelectrochemical reduction on p-type GaP 78−88649
low cost photovoltaic cells utilizing semiconducting thin films and advanced concentrator concepts 80−50972
low resistivity, open cct. voltage improvement 80−93910
low-cost encapsulation materials for terrestrial solar cell modules 80−3522
low-high-junction model developed for tandem cell anal. 80−89626
luminescent greenhouse collector 77−761
manufacture, alternative technology for cost reduction, review 79−74514
mass production technology, cell installation development costs *(German)* 80−72046
material parameter determ., appl. of normal modes of p-n junction devices 77−4426
material selection for solar photovoltaic cells 79−57434
materials, fabrication and research for low cost photovoltaic solar cells 80−55838
materials, use of phase diagrams 79−10922
materials and fabrication techniques to reduce the cost of Si solar cells, book 78−15306
materials science aspects, lecture 78−25989
maximum power output determ. 79−74527
merocyanine organic solar cells, photovoltaic props. in terms of exciton transport 79−43763
metal-semiconductor, practical antireflection coatings parameter determ. method 77−763
metal-semiconductor contacts, collection vel. of excess minority carriers 77−15954
metallisation patterns for higher efficiency, analytical approach 80−93943
metallisation using screen printing tech. 80−85291
minority carrier lifetime meas. from photo-induced open-cct. voltage decay 79−87990
minority carriers, diffusion length determ., using angle-lapped p-n junctions 79−42631
minority carriers life-time meas., open-cct. to short-cct. switching method 79−79392
MIS, computer simulation studies rel. to interface state meas. 80−72048
MIS, effects of nonuniformity of insulating layer 80−104507
MIS, effects of pinholes, oxide traps and surface states 78−80055
MIS, influence of interface states, efficiency improvements 78−39227
MIS, interface problems, AES, SIMS and XPS study 80−89627
MIS, interface props. and stability 79−61984
MIS, inversion layer, surface passivation 80−101098
MIS, optimal interface design using computer simulation and expt. meas. 80−16805
MIS, photocurrent depend. on thickness of Schottky barrier metals 79−34437
MIS, Si solar cells, effects on performance 78−76153
MIS, spectral response charact. and meas. of effective diffusion lengths 80−16804
MIS inversion layer, two-dimensional model 80−89641
MIS negative barrier contact for induced back surface field solar cell 80−101101
MIS Schottky barrier cells, barrier height change and current transport in presence of interfacial layer 80−61353

solar cells continued
MIS Schottky barriers, photocurrent suppression and interface state recomb. 78−39222
MIS Si solar cell, I-V curves, open circuit voltage 77−8196
MIS Si solar cells, low-temp. CVD of SiO_2 to form inversion layer 80−12019
MIS solar cell, general theory, expt. on Si 77−8197
MIS solar cell development for space applications 79−96453
MIS solar cell open-circuit photovoltage rel. to oxide thickness 79−61985
MIS solar cells, basic principles of operation theoretical charact. 80−50986
MIS solar cells, etched slotted mask for direct deposition of metal contact pattern 80−97786
MIS solar cells, fabrication and performance charact. 80−45707
MIS solar cells, review 79−39300
MIS solar cells with diffused back surface field (BSF), and diffused junction solar cells with MIS BSF 80−94074
MIS tunnel solar cell, interface states, kinetic and electrostatic props. 79−52933
MIS tunnel structures, theory of operation 77−39948
MIS-Schottky barrier solar cells, photovoltaic props. anal. 78−6448
MIS/SIS, automated surface states anal. 80−93966
modelling, rel. to optimisation 79−39297
modular, highly reliable Si cell *(Japanese)* 80−81468
monolithic III-V compound two-junction cascade solar cells, computer modelling 80−81433
monolithic solar cell panel of amorphous Si 80−45666
MOS, IV characteristics obtained under dark and illuminated conditions 79−48126
MOS solar cell, role of interface states 79−15228
MOS solar cell operation, role of interface states 79−61979
MOS solar cells, I-V charact. calc. 79−43766
MOS solar cells, theory 79−87993
MOS tunnel diodes characterisation, solar cell appls. 77−32089
MOS-inversion layer solar cells, fundamental mechanisms affecting performance 80−61377
Moss relation between refr. index and energy gap of semiconductors rel. to photovoltaic solar cells 80−11357
multi-bandgap concentrator cells, Si and $Al_xGa_{1-x}As$ systems, operation with spectrum splitting filter 80−45698
multijunction photoconvertor, prep. by zone recryst., photoelec. props. 79−39294
n^+-n-p high-low-emitter junction solar cell, open-circuit voltage in conc. sunlight 80−50957
n^+-p-n^+ double sided, optimal static concentration 80−89639
n^+-p-p^+ bifacial back surface field solar cells, optimisation of p^+ doping level by ion implantation 80−97784
n^+-p-p^+ solar cell operation anal. for concentrated illumination 79−43761
n-i-p, thin Si cells, with high output and low diffusion length damage coeff. 80−93909
n-p junction solar cell, anal. of short circuit currents generated by electron beam 79−39308
NDT of welds, mechanical strength eval. 78−35630
noise spectral density as a device reliability estimator 80−93896
nonideal Si, characterisation by lifetime and diffusion length 79−15192
numerical analysis of conb-shaped cells in 3-D 80−50973
optical detector using photovoltaic cell, background illum. effects 78−70182
optoelectronic devices and optical imaging techniques, book 80−27059
organic, photovoltaic properties of polymer films 80−60040
organic photovoltaic solar cells, solid state chem. effect on performance 79−48129
output monitoring, design and utilization of a microprocessor-controlled absolute spectral response system 80−81476
oxide semiconductor-on-semiconductor solar cell, low cost efficient 79−61980
oxide-semiconductor/base-semiconductor, optimization 80−81440
P^+-n, BN glass transfer process appl. for cell fabrication 80−107459
p^+-n, n^+-p structures on polycrystalline material, performance 80−89640
p^+-n junction, very shallow, defect free 79−15218
p-n, polycryst., grain boundary influence on recomb. 80−93913
p-n heterojunction solar cell, general formulation of current-voltage charact. 80−80361
p-n heterojunction solar cells, band structure and photocurrent collection 80−21402
p-n junction, determ. of lifetime and recombination currents 80−89637
p-n junction, influence of light scatt. through junction on collection efficiency 79−34436
p-n junction, photoinjected carrier lifetime meas. by reverse voltage pulse response 80−45664
p-n junction photodiode terminology 80−70800
p-n junction solar cell response to concentrated sunlight and partial illum. 79−61996
p-n junctions, minority carrier surface recombination velocity, lifetime, AM electron beam determ. 79−87145
p-type, illumination-and-temp. dependence 80−94046
photo-intercalation: possible application in solar energy devices 80−108803
photocatalytic prod. of H_2, TiO_2 electrodes, solar energy conversion 77−1932
photoconverter, bilateral sensitivity, n^+-p-p^+ structure, volt-ampere charact. under illumination 80−40855
photoelectric, optical methods for checking parameters of semiconductor doped layer 80−93869
photoelectric conversion, MIS structures utilisation, and manufacture, photoelectric parameters *(Czech)* 79−83595
photoelectrochemical, enhanced photoeffects by electrocatalysis and peroxide effects 80−16815
photoelectrochemical, function and construction of regenerative cell 80−26147
photoelectrochemical, review 79−52941
photoelectrochemical, semiconductor/redox electrolyte junctions, functions examples and problems 80−45714
photoelectrochemical, solar photoelectrolysis with semiconductor electrodes for solar energy conversion and storage, review 79−74533
photoelectrochemical aspects *(Japanese)* 78−53220
photoelectrochemical cells, energy conversion system, principles and appl. 80−89652

solar cells continued
photoelectrochemical cells, review of cell types and electrode props. 80−61385
photoelectrochemical cells *(Dutch)* 80−85295
photoelectrochemical regenerative and storage cells with semiconductor electrodes *(French)* 80−61386
photoelectrochemical solar energy conversion principles, review 80−35695
photoelectrochemical systems *(German)* 80−45713
photoelectrolytic, water decomp. with semicond. materials 78−2562
photoelectrolytic production of H_2 and electricity, $LaCrO_3$-TiO_2 photoactive anode 80−12024
photoemissive solar-cells, efficiency calc., use of negative affinity photoemitters 80−55876
photogalvanovoltaic cells and photovoltaic cells using glassy carbon electrodes 80−89630
photopile manufacture for terrestrial solar cells, review *(French)* 79−24895
photovoltage source in photocond. materials due to comp. and doping var. 80−7938
photovoltaic, water pumping appl., system optimisation *(Spanish)* 79−96428
photovoltaic cell efficiency calc., using irradiance-transmittance solar spectrum 80−26137
photovoltaic cell trends using Si 79−61974
photovoltaic cells in undersea environment, performance 80−93900
photovoltaic cells production technology, future systems efficiency and cost effectiveness 80−16799
photovoltaic concentrating sytems, optical and tracking systems design, performance characts. 80−72051
photovoltaic conversion, Canadian R and D program 80−55872
photovoltaic conversion, EEC R and D program 80−55873
photovoltaic conversion, French R and D program 1976-79 80−55871
photovoltaic conversion, Italian R and D program 80−55870
photovoltaic conversion comparative evaluation *(Italian)* 80−60023
photovoltaic conversion of concentrated solar radiation, feasibility assessment 79−57436
photovoltaic convertors, two junction, appl. of multijunction solar cells to photovoltaic systems 80−16812
photovoltaic effect, solar energy convertor theory with p-n junction 78−72201
photovoltaic electricity generation in India 80−21381
photovoltaic energy conversion, review 79−100530
photovoltaic flat panel procurement, qualification test results 80−94064
photovoltaic generators using optical concentration, current status and development trends review 80−45697
photovoltaic material and device meas. workshop, conf. Arlington, VA, USA, June 1979 80−77543
photovoltaic materials and devices for terrestrial solar energy applications, R and D status review 80−101112
photovoltaic mechanism, emitter-junction boundary conditions 79−100523
photovoltaic module utilising parabolic trough concentrators 80−93984
photovoltaic modules testing, reliability and performance 80−94063
photovoltaic pilot line of 15 kW under Mexican research and development 80−94022
photovoltaic power supplies, cost reduction possibilites 80−97793
photovoltaic power system, design and performance charact. 80−89644
photovoltaic power system elements, efficiency and terminology summary 80−97790
photovoltaic power systems, equipment performance and manufacturing techniques improvements and system design problems for telecommunication applications 80−55843
photovoltaic power systems for rural areas of developing countries 80−50967
photovoltaic R and D in US, National Photovoltaic Program plan 80−55868
photovoltaic R and D program in US, National Photovoltaic Program, status report 80−55867
photovoltaic receiver for parabolic trough concentrator, optimisation 80−93983
photovoltaic research and development in Japan, review 80−12012
photovoltaic research and development projects in the Federal Republic of Germany 80−55869
photovoltaic solar devices, modular system *(German)* 80−89629
photovoltaic solar energy, conference, Luxembourg (1977) 78−64106
photovoltaic solar energy conversion [conf. Berlin, West Germany, April 79] 80−30482
photovoltaic solar generators, ampere-hour efficiency, charging and discharge power 80−29434
photovoltaic system analysis computer program; SOLCEL-II 80−94058
photovoltaic system sizing anal. 80−94039
photovoltaic systems, design for intermediate-sized appls. 80−30490
photovoltaic technology, conf., San Diego, CA, USA (Jan. 1980) 80−86041
photovoltaic terrestrial systems, protection from lightning effects 80−89648
photovoltaic-solar thermal system role of high performance solar cells 79−61978
photovoltaic/thermal collector performance, comparison of theory and expt. 80−94062
photovoltaics commercialization readiness assessment by US DoE 80−55859
planar multijunction HV, technical considerations and fabrication 80−89636
planar solar energy convertor and concentrator, based on uranyl-doped glass 78−71213
Polka Dot, description and anal. 80−93959
polyacetylene, pure and doped, metal; and semicond.-semicond. junctions 79−95474
polyacetylene photoelectrochemical solar cell, fabrication and efficiency 80−50954
polyacetylene semiconductor film applic. 80−92899
polyacrylonitrile, polaris., pyroelec., electret film, solar energy conversion *(Russian)* 78−39507
polycrystalline, grain and grain boundary effects on drive characts. 80−93914
polycrystalline, influence of grain boundaries electronic structure on diode characts. 80−94068
polycrystalline, photocurrent loss in depletion region anal. 79−39309
solar cells continued
polycrystalline, physics, operation and parameters of cryst. heterojunctions 80−50985
polycrystalline, recomb. at grain boundaries, effect on photoresponse 80−108796
polycrystalline, relative orientation of grains and nature of grain boundaries 80−93915
polycrystalline, scaning optical microscopy examination of grain boundaries 78−79618
polycrystalline and tandem, for high efficiencies, using compound semiconductors 80−72052
polycrystalline heterostructure solar cells, grain boundary effects 78−52063
polycrystalline Si, amorphous Si and CdS/CuS, function and construction *(Swedish)* 80−7940
polycrystalline Si growth, ribbon to ribbon laser scanning tech. 78−35299
power conversion efficiency monitoring in photoelectrochem. and p-n junction cells 80−50989
power increase using radiation reflected from Earth 77−33318
power plant, orbiting, evaluation of current conductor mass and voltage level required 80−89616
power plants, local energy exchange dynamics and climatic boundary conditions effects, preliminary examination 78−81355
power supplies for remote telecommunication sites 80−26133
power supply appls., technology and research 79−92076
principle, construction and operation, 1979 state and world-wide research survey 80−40862
production, laser doping of perfect crystals, discussion *(French)* 79−66409
proton damage ratio obs., 2 to 10 MeV 79−96476
RAD polysilicon sheets, photovoltaic potentialities, conversion efficiencies, limitations 80−30484
recombination velocity at III-V compound heterojunctions, $Al_xGa_{1-x}As$-$GaAs_{1-y}Sb_y$ solar cells 80−12010
remote islands telecommunication repeater stations power supply 80−61382
response to intense and nonuniformly concentrated illum. 79−62000
reversible solar galvanic cell 79−62016
review, photovoltaic effects in p-n junctions, Schottky barriers *(Czech)* 77−24583
review of US DOE R and D program 80−55874
review using rational units 80−30389
ribbon growth using scanned focused CO_2 laser beams 80−66417
ribbon-to-ribbon growth method and sample characterisation Si 78−11103
satellite power plants, transmission to Earth-based utility, efficiency analysis 79−48093
satellite power plants concepts, thermal analysis 79−48094
satellite power systems concept 79−52891
satellite solar cell calibration using high-altitude balloon *(Japanese)* 78−61700
satellite solar cell power plant, operating experience 80−94055
satellite solar power systems, developments and future trends 80−45694
Schottky barrier, comparison of thin film and bulk single cryst. 78−80053
Schottky barrier, doping density effect on efficiency 80−101100
Schottky barrier, efficiency depend. on thickness of interface layer 80−76637
Schottky barrier, improvements due to Al-Si metallurgical reaction 77−72914
Schottky barrier, n-type, theoretical anal. of band edges, Fermi levels 80−50975
Schottky barrier, open cct. voltage 77−32078
Schottky barrier back-wall cell, possible peformance and potential advantages over front-wall cell 77−4438
Schottky barrier cell, optimum thickness indicator for barrier metal 78−21120
Schottky barrier solar cells, back-illuminated, theoretical performance 80−61345
Schottky barrier solar cells, interfacial layer effect 79−57429
Schottky-barrier solar cell sensitivity computation 79−62004
Schottky-barrier solar cells fabrication by electroless Ni plating 79−83591
semiconductor, n-type, thermodynamic pot. for anodic dissolution, rel. to photoelectrochem. cell efficiency 78−26948
semiconductor CVD films for solar energy conversion 77−32531
semiconductor electrodes, light energy conversion and storage 78−14813
semiconductor heterostructures, elec. and optical phenomena, discrete devices, review 78−72250
semiconductor liquid junction, efficiency, electrochemical stability and surface preparation 78−14817
semiconductor solar cells, state of the art, various installations description *(Dutch)* 80−72063
semiconductor-electrolyte solar cell, minority carrier transfer, energy levels role 78−39209
semiconductor-insulator-semiconductor device using ITO-S 78−52061
semiconductor-insulator-semiconductor solar cells, basic principles of operation theoretical characts. 80−50986
semiconductor-insulator-semiconductor solar cells, fabrication and performance characts. 80−45707
semiconductor-liquid junction type, efficiency, operation 80−72043
semiconductors, direct gap 79−92075
semicrystalline vs. single crystal Si 80−93917
series resistance evaluation 79−61972
silane pyrolysis for Si production, process design and economics 79−8234
single diode models for simulating cells with distributed series resistance 80−93962
SOC (Si on ceramic) continuous coating 80−93904
solar cells, materials aspect, review 80−50971
solar energy direct conversion to H_2 fuel by water photoelectrolysis 79−62014
solar energy direct photoelectrochem. conversion and storage 79−62015
solid state physics aspects, of solar energy conversion, book 79−74518
solid state physics rel. to solar cells, review 80−49601
solid-dielectric compound parabolic concentrator with Si solar cells, prototype 77−39107
solid-state device conference, Tokyo, Japan (Sept. 1976) 77−76901
Sophia Antipolis 5 kW photovoltaic power generator for habitat 80−61374

solar cells continued
space heating, photovoltaic and thermal collector system design and testing 80−45675
space power generators, past developments and future trends 80−45693
space qualified, high efficiency solar panel project using multiple antireflective cells 80−94056
spectral irradiance of solar simulators and its effects on cell meas. 80−93950
spectral response, enhancement by fluorescent wavelength shifting 80−26139
spectral response, pulsed measurement, test set-up and apparatus, shortcomings and planned improvements 80−45695
spectral response characterisation, 400 to 1000 nm 80−35675
sputtered amorphous film heterostructure solar cell and laser fabrication 78−64472
sputtered Cu_2S fabrication, on CdS substrate 78−39692
square Fresnel lens design for illuminating circular solar cells 78−79099
squarylium and cyanine-TCNQ dye Schottky-barrier sandwich cells 79−29468
stacked multibandgap monolithic multijunction solar cells, loss evaluation, optimum performance 80−93928
static photovoltaic concentration improvement, two-sided Transcell 79−61999
student laboratory experiment on solar energy 80−17776
substrate related problems in RAD solar cells 80−89635
Sun tracker, electronic, for clear or cloudy weather 80−76644
sunstation insolation meas. system, Si-cell based 79−5582
superposition principle application to solar cell anal. 80−76631
surface recombination velocity and diffusion length meas. 80−93965
surface texture of black solar cells *(Chinese)* 79−57435
surface-channel insulator-semicond. photocell, photoelec. characts. 78−26909
survey, solar radiation distribution in Netherlands *(Dutch)* 77−91207
tandem, detailed balance limit of efficiency 80−72056
tandem junction, Ebers-Moll transistor model 80−93911
tandem photovoltaic cell system efficiency, solar energy conc. ratio and temp. depend. 79−74516
tandem-junction, one-dimensional theoretical model 80−81450
technical and economic assessment 79−34433
temperature characts., temp. range 100-400K, for Si photoconvertors 79−39296
temperature dependence of the maximum theoretical efficiency in solar cells 80−45670
ternary semiconductor device applications, review 78−39207
ternary semiconductors, use in thin film heterojunction and homojunction photovoltaic devices 78−39208
terrestrial, self-supporting polycryst. Si film deposited by energy beam plasma 79−11523
terrestrial solar cell reliability, accelerated stress testing 79−74528
terrestrial solar cells, accelerated stress testing 79−92083
terrestrial solar generators, design, fabrication, testing and economic power generation 80−45672
test facility using plane mirror heliostat 80−45668
testing, standard procedures for terrestrial photovoltaic performance measurements 80−66979
textured surface, reflectance and transmission props. 78−1165
thermal and other tests of photovoltaic modules performed in natural sunlight 80−97789
thermoelectric air conditioner humidifier (SATEACH), solar assisted 80−108802
thermophotocell, design and calculations 80−97800
thermophotovoltaic convertor, parametric anal. of emitter temp., conc. ratio and cell reflectance 80−94107
thermophotovoltaic solar energy conversion, upper limit 80−81446
thermophotovoltaic solar energy conversion system, proposal 79−74513
thermophotovoltaics, conc. ratio and efficiency 80−7946
thick film technology, applic. to manufacture 80−93903
thin, advanced module technique 80−94041
thin film, comparison methodology 80−93920
thin film, degradation processes of electrophysical characts. during long-term operation 80−89617
thin film, performance analysis employing loss minimisation of essential characteristics 80−45682
thin film, technical and economical eval. 80−94012
thin film, unified anal. of potential 80−81436
thin film photovolt. convertors 80−12011
thin film polycrystalline, chemical and structural defects 80−93919
thin film polycrystalline materials, resistivity and Hall effect meas. 80−93899
thin film polycrystalline Si, research and develop. overview 80−93921
thin film technology, appls. in energy, optics, and electronics, review 80−78932
thin film wraparound cell, improved perform. 80−93912
thin solar cell photovoltaic and thermal props. 79−96452
thin-film solar cells, recent developments 78−80016
tilted solar cell under various atmospheric conditions, performance evaluation 79−29476
transition metal, group VIa, layered dichalcogenides, hole reactions, electrochem. solar energy conversion appl. 79−7893
transparent electrode photo-galvano-voltaic cell, using Mg-meso-tetraphenylporphine-coated glass *(Chinese)* 80−40865
transparent modules, high-efficiency, with improved glass, adhesives and heat dissipation 80−76636
tunnel MIS solar cells, grain boundary effect on performance 79−79394
two-sided photovoltaic solar cell static concentrators 80−35684
two-stage, fraction of radiation usefully converted, power prod. efficiency 80−30477
types and applications 79−74525
ultra-thin, for high-performance panel appl. 79−52938
ultrathin high efficiency coplanar back contact, design and fabrication 80−89649
V-groove multijunction solar cell 79−100519
V-I characteristics; AMO efficiency, rel. to spectral composition 80−3514
varizone photoelectric convertor efficiency anal. 80−21397
vertical junction, new developments 80−93907
vertical junction, with high radiation resistance 79−48131
water desalting by solar powered electrodialysis 80−55805
wavelength shifting, by powdered fluorescent capping layers 80−85286
wet type with semiconductor electrodes dye sensitised, effects 79−29474
wraparound contact, status and space appl. 79−48132

solar cells continued
wraparound-contact, use of printed-circuit methods 80−76635
Ag/AgCl photogalvanic cells for solar energy conversion, basic electrochemistry 80−45715
Ag-Si interfaces, solar cell contacts 80−92973
Ag-Si Schottky barrier cells, characts. of ZnS antireflection coatings 80−43414
Al/metal-free phthalocyanine Schottky barrier solar cells, photovoltaic props. 79−100527
$Al/SiO_x/p$-Si contacts for IMS solar cells, high temp. lifetesting 79−87988
$Al/SiO_x/pSi$ MIS solar cells, stability 80−85287
$Al-Al_2O_3$-GaAs backwall MIS Schottky barrier solar cell, anal. model 80−85289
Al-Ga-As heterostructure photocell with a transition layer 79−19655
Al-p-Si, MIS solar cells, interface-state Fermi level change from dark to illuminated conditions 79−66407
Al-poly-Si Schottky-barrier solar cells, grain boundary effects on electrical behaviour 80−85279
Al-Si MIS solar cells, depth conc. profiles, elec. and optical props. of Al films 80−94076
$Al-SiO_2$-Si Schottky barrier solar cells, recomb. effects 79−39310
$Al-SiO_2$-pSi, comparison of majority- and minority-carrier Si MIS cells 80−85280
$Al-SiO_x$-Si MIS solar cells, short-wavelength response 79−57428
$Al-SiO_x$-Si MIS solar cells, I-V characts. temp. depend. 80−7935
$Al-SiO_x$-Si MOS solar cells, open-cct. voltage var. with oxide layer thickness 80−81434
$Al-SiO_x$-(p-)Si barrier structs., minority carrier injection ratio meas., MIS solar cell model 80−93007
$Al-SiO_x$-p-Si MIS solar cells with back surface fields 80−12006
$Al-SiO_x$-pSi, comparison between MIS and SIS cells 80−81443
Al-Si(Ge) eutectic alloys in screened ohmic contacts for solar cells 80−94090
Al-thin oxide-Si, Schottky barrier, degradation effects, ion beam induced nuclear reactions 80−30488
n-AlAs/p-GaAs, VPE growth for solar cells 77−77391
AlAs-GaAs film heterojunction, VPE growth and characts. 78−6439
AlAs-GaAs heterojunctions, on graphite substrate, props., solar cell appls. 78−91760
AlGaAs heterojunction photocell with luminesc. wavelength converter 80−108800
AlGaAs tunnel diode, fabrication and appl. in cascade solar cell struct. 80−35682
p- (AlGa)As:Zn, MBE grown, elec. props., shallow junction solar cell use 79−91175
(AlGa)As-GaAs, large area high efficiency solar cell fabrication, LPE process 77−36410
AlGaAs-GaAs cascade solar-cell structure, fabrication and characteristics 79−43758
AlGaAs-GaAs concentrator solar cells of high-efficiency characts. 79−48125
AlGaAs-GaAs proton irradiated solar cells, deep-level defects, recombination mechanisms, performance characts. 80−81459
AlGaAs-GaAs proton irradiated solar cells, deep level defects and recombination parameters 80−94032
(AlGa)As-GaAs solar cells, theoretical perform. of multi-layer grid patterns 80−55846
AlGaAs-GaInAs cascade solar cells, AM 0-AM 5 spectra, anal. 79−79396
$Al_{0.35}Ga_{0.65}As$-GaAs cascade solar cell structs., spectral response and junction characts. 80−93926
$Al_xGa_{1-x}As$ heterostructures, photoelectric convertors of conc. solar radiation 80−12015
$Al_xGa_{1-x}As$ layer, LPE, graded bond gap solar cell, composition profile, Rutherford backscatt. 78−76612
$Al_xGa_{1-x}As$, p-n junction solar cells, effect of interface recombination on photoluminescence and current 80−93893
$Al_xGa_{1-x}As$ solar cell, intermediate wavelength conversion for operation with concentrators 79−70451
$Al_xGa_{1-x}As$-GaAs, DH photodetector, solar battery efficiency 77−87833
$Al_xGa_{1-x}As$-$GaAs_{1-y}Sb_y$ solar cells, appl. of recomb. vel. at III-V cpd. heterojunctions *(Korean)* 80−54771
p-$Al_xGa_{1-x}As$-n-GaAs heterojunction cells, optical characts. study 77−24609
p-$Al_xGa_{1-x}As$-p-GaAs-n-GaAs heterophotocells, optimal parameters for high solar-excitation level 80−93872
$Al_xGa_{1-x}AsZn$-GaAs solar cells by LPE, open circuit voltage, fill factor 80−101108
Al_2O_3 MIS Schottky structures, photovoltaic response 80−101115
AlSb, gravitational influences on liquid-state homogenisation and solidification 79−78864
AlSb Schottky barrier solar cells, characteristics and efficiency of Czochralski-grown crystals 80−61366
AlSb solar cell material, epitaxy, ionicity and bond struct. 80−61367
Au-$Al_{0.5}Ga_{0.5}As$ -GaAs heterojunction Schottky-barrier solar cells, barrier height enhancement 80−85284
Au-AlGaAs-GaAs heterojunction Schottky barrier solar cells, barrier height enhancement 80−94071
Au-GaAs, Ta_2O_5, practical antireflection coatings 77−763
Au-GaAs Schottky barrier solar cells, effect of interfacial oxide layer on cell characts. 80−61365
Au-n-$Al_xGa_{1-x}As$-n-GaAS Schottky barrier solar cells, prep. and props. 80−26140
Au-n-AlGaAs-n-GaAs Schottky-barrier solar cells, band readjustment effect 80−81458
Au-n-Si Schottky barrier solar cells, recombination in space charge region 80−61351
Au-p-n-Si Schottky barrier solar cell, photovoltaic characts., barrier heights, carrier mobility 79−83601
Au-SiO_2-n-Si, comparison of majority- and minority carrier Si MIS cells 80−85280
BP-Si heterojunctions, VPE growth of BP, device appls. 78−56585
BP-Si junctions epitaxial growth and device appls. 78−48333
Be-SiO-p-Si, MIS solar cell, performance figures 78−88030
CC Si diffused junction, n^+pp^+ or p^+nn^+, prep. using solid diffusion sources 80−35689
CdO, aqueous-deposited films, struct. and electronic props. for solar cell appls. 80−100797
CdS, aqueous-deposited films, struct. and electronic props. for solar cell appls. 80−100797

solar cells continued
CdS, film for solar cells, struct. and elec. props., thickness depend. 78−72289
CdS film solar cell yield rel. to crystallite column statistics 79−62005
CdS, for thin film and ceramic solar energy convertors 80−93870
CdS heterojunction solar cells by CVD method 80−45685
CdS, II-VI semiconductors in optoelectronics *(German)* 77−7745
CdS photoconductivity, spatial homogeneities exam. using DC and microwave techniques 80−93895
CdS photovoltaic panels, deposited by spray pyrolysis, film and junction structure studies 80−45689
CdS, review and present status 80−76638
CdS Schottky barrier solar cells, spectral distrib. and photocapacitance 80−55864
CdS, sintered film, solar cell *(Chinese)* 79−74517
CdS solar cells, construction, solar photovoltaic systems for remote communications power supply 80−66980
CdS spray pyrolysis film prep. and characterisation 78−64492
CdS sprayed thin films for CdS-Cu_2S heterojunction solar cells 79−61988
CdS thin film solar cell fabrication, HCl etching 80−81474
CdS thin film solar cells, R and D of low cost cells 80−85292
CdS thin films, growth and evaluation for fabrication of high performance photovoltaic solar cells 80−93501
CdS thin films on brass substrates, nondestructive resistivity meas. tech. 80−93898
CdS thin-film polycrystalline solar cell development 79−61993
CdS:Cu_2S sputtered solar cells, energy anal. of cell fabrication techniques 80−50966
CdS/Cu_2S, design and fabrication 80−30481
CdS/Cu_2S, formation and props. of Cu_2S thin films 79−11257
CdS/Cu_2S, polycryst. thin film photovoltaic materials, photon loss anal., expt. determ. 80−93888
CdS/Cu_2S heterojunction solar cells, optimal material props. theory and experimental verification 80−45686
CdS/Cu_2S solar cell fabrication, performance rel. to Cu_2S mats. props. 77−77426
CdS/Cu_2S thin film heterojunctions, photocapacitance meas. of solar cell parameters 80−93897
CdS/Cu_2S thin film solar cells, design and fabrication, 9.15% conversion efficiency 80−81438
n-CdS/n-InP/p-InP heteroface solar cell with ultrathin window layer, computer anal. 80−97788
n-CdS/p-$ZnIn_2Se_4$ thin film solar cell, photovoltaic props. 80−89628
n-CdS-CdSe mixed polycryst. electrode for photoelectrochem. cell 78−47867
CdS-CdTe, thin film, fabrication methods *(Japanese)* 79−87992
CdS-CdTe p-n junction screen printed thin film solar cells 80−72055
CdS-CdTe prep. by VPE, junction struct. and photovoltaic props. 77−73235
CdS-Cu_2S, design and fabrication, 8.5% conversion efficiency 80−72047
CdS-Cu_2S, effect of CdS surface stoichiometry on performance 78−2956
CdS-Cu_2S, microstructural study of heterojunction materials 80−93978
CdS-Cu_2S, props., characts. and efficiency, development costs *(Spanish)* 80−72062
CdS-Cu_2S heterojunctions, photovoltaic mechanism, model 77−43715
CdS-Cu_2S heterojunction, pilot line production 78−2525
CdS-Cu_2S solar cell, minority carrier generation and transport in emitter 77−43649
CdS-Cu_2S solar cell photovoltaic effects, self-consistent model 79−61989
CdS-Cu_2S solar cells, preparation and stoichiometric control 78−2560
CdS-Cu_2S solar cells, role of diode exponential factor 79−61990
CdS-Cu_2S solar cells, conversion efficiency improvement 80−16807
CdS-Cu_2S thin-film solar cells, low-cost manufacturing process outline, economic anal. 80−93930
CdS-Cu_2S thin-film solar cells, high open-cct. voltage and low refl. losses 80−94088
CdS-Cu_xS, electron diffusion length determ. using spectral response meas. 80−81475
CdS-Cu_xS effect in response of thermally induced changes in Cu_xS film 77−8181
CdS-Cu_xS heterojunctions produced by RF sputtering, for thin film solar cells 79−100053
CdS-Cu_xS solar cell, prep. and characts. *(Croatian)* 80−93876
CdS-Cu_xS solar cells, screen printed, prep. and photovoltaic props. 80−40863
CdS-$CuInSe_2$, solar cell, grain boundary effects on performance 79−83603
CdS-$CuInSe_2$ solar cells, grain boundary and interface recomb. effects 79−39311
CdS-$CuInSe_2$ solar cell, polycrystalline thin film, high photocurrent, characts. 80−61339
CdS-GaAs n-n voltage-enhanced photoanode, solar cell efficiency 78−14810
CdS-InP, n-p, fabrication and power conversion efficiency 77−1813
CdS-InP(CdTe)(GaAs)(Ge), solar cell heterojunctions, CVD fabrication, photovoltaic response 80−93878
n-CdS-p-CdTe heterojunctions, photovoltaic energy conversion, solar efficiency 77−43700
CdS-SiO_2-Si solar cell, I-V characteristics 80−89621
CdS(Se)-based photoelectrochem. cells, characts. 77−25287
n-CdS(Se)(Te) semicond. liq. junction solar cells, photocurrent spectra, carrier recombination 78−76142
CdSe based photoelectrochemical cell, for solar energy conversion 78−19147
CdSe, chemically sprayed thin films as photoanode in photoelectrochem. cells, power charact. meas. 80−85293
CdSe electrochem. photovoltaic cells, effect of thin film electrode prep. and conc. on efficiency 80−55847
CdSe film, electrodeposited, for photoelectrochemical cell for solar energy conversion 80−94093
CdSe film photoanodes for electrochem. photovoltaic cells, fabrication and evaluation 80−76641
CdSe, for thin film and ceramic solar energy convertors 80−93870
CdSe MIS thin film solar cell 80−45688
CdSe thin film, performance 80−93970
CdSe-Si n-p heterojunction, vacuum deposition, photovoltaic effects *(Korean)* 77−28243
CdSe(Te)-electrolyte photovoltaic cells, solar cell appls. 77−35990
$CdSe_{0.65}Te_{0.35}$, polysulphide photoelectrochem. solar cell 80−72073

solar cells continued
$CdSiAs_2$ diode, photoelec. props., potential photodetector and solar cell appl. 77−43655
CdTe cathodic deposition from aqueous electrolytes 78−64484
CdTe, film, theoretical models of impurity levels 79−82557
CdTe homojunctions from VPE growth, solar cell appl. *(French)* 77−43453
CdTe, optical absorpt. coefficient, photovoltaic determ. 77−39890
CdTe p-n homojunction, elec. and photovoltaic props. rel. to solar energy conversion 79−51668
CdTe Schottky solar cell, barrier height, open circuit voltage 77−43721
CdTe, shallow homojunctions, characteristics and surface resistance influences 80−45690
CdTe, suitability for solar photocells, photovoltaic conversion props., band gap 77−43652
CdTe thin film polycrystalline solar cells prepared by electrodeposition 80−93948
CdTe:As^{2+}, photovol. props. of p-n junction prod. by ion implantation 78−43038
CdTe/Langmuir film photovoltaic structures 80−49918
CdTe/$SnCl_2$/Pt, solar cell photoelectric props. *(Spanish)* 80−85290
CdTe-CdS p-n film heterojunction, photoelectric props. 79−39298
CdTe-CdS p-n junction, photocurrent and max. efficiency calc. 79−39295
CdTe-CdS thin film p-n solar cells, spectral response temp. depend. 80−93871
n-CdTe-electrolyte, interface changes during operation, AES, electrolum. and electroreflectance meas. 79−100525
CdTe-$SnCl_2$ electrolyte heterojunction photoelec. props., feasibility as solar energy convertors 77−76918
CdZnS thin films, growth and evaluation for fabrication of high performance photovoltaic solar cells 80−93501
CdZnS-CdS bifilm solar photocells, feasibility, study 78−76113
(CdZn)S-Cu_2S, film form. and characts. 78−68080
$Cd_{1-x}Zn_xS$, film, technical data, for low cost solar cell 79−48127
$Cd_{1-x}Zn_xS$ solar cell thin films, microprobe characterisation *(French)* 80−61349
$Cd_{1-x}Zn_xS$ spray deposited film appl. 79−7915
$Cd_{1-x}Zn_xS/Cu_2S$ thin film heterojunction solar cells, operational charact. 80−45687
$Cd_{1-x}Zn_xS$-PbS heterojunctions prepared by spray pyrolysis 79−60917
$Cd_xZn_{1-x}S$ films, chem. sprayed, carrier density and mobility 80−60121
$Cd_xZn_{1-x}S$-Cu_2S, interface chemistry modification of current-voltage charact. 79−100523
Cr MIS solar cells on Si, proton radn. effects 79−92074
Cr-MIS solar cells, on polycryst. Si, grain boundary effect and conduction mech. 80−93894
Cr-MIS solar cells on p-type wacker poly-Si substrates, high efficiency design 80−93935
Cr-MIS solar cells on Si, revised process to increase active area efficiency and reproducibility 80−81462
Cr-SiO_x-Si MIS solar cell, current cond. 80−7936
Cr-SiO_x-Si MIS solar cells, photovoltaic performance and interface states, nucl. radiation effects 80−94004
Cu/$CuGaSe_2$ Schottky-barrier cells, photovoltaic effect 79−96440
Cu-CdS, Schottky barrier, reverse differential capacitance, diffusion of Cu, solar cell appl. *(French)* 80−15424
$Cu_{1-y}Ag_yInS_{2-x}Se_{2x}$, for solar photovoltaic cells 80−10982
$Cu_{1-y}Ag_yInS_{2(1-x)}Se_{2x}$ pentenary alloy system, appl. to photovoltaic solar-energy conversion 80−35680
$Cu(Ga_xIn_{1-x})(S_ySe_{1-y})_2$, spray pyrolysis 79−70004
$CuGa_{0.5}In_{0.5}Se_2/Zn_{0.29}Cd_{0.71}S$ heterojunction solar cell, preparation and props. 80−101110
$CuGa_xIn_{1-x}Se_2$, CVD, elec. and optical props., use as heterojunction solar cell absorber 79−52095
$CuIn_{1-y}Ga_ySe_{2(1-x)}Te_{2x}$ pentenary alloy compounds for photovoltaic solar energy conversion 80−93971
$CuInS_2$ film homojunction, fabrication, performance 77−80832
$CuInS_2$ films prepared by spray pyrolysis, elec., optical and struct. props. 79−73609
$CuInS_2$ single phase thin film prep. by flash evaporation 80−100796
$CuIn(S_xSe_{1-x})_2$, spray pyrolysis 79−70004
$CuInSe_2$, spray pyrolysis 79−70004
$CuInSe_2$ thin films, prep. by spray pyrolysis, struct., elect. and optical props. for solar cell appls. 80−100781
$CuInSe_2$ thin films for solar cells, radiofrequency sputtering technique, elec. props. 80−93487
$CuInSe_2$-CdS heterojunction, photovoltaic effect, rel. to optimum conditions for solar cell fabrication 77−51810
CuO_2/Cu junction, characts. *(French)* 79−24900
Cu_2O, electrical and optical props., photocurrent anal. 80−101116
Cu_2O, front wall solar cells, chemical origin of space-charge layer 79−70449
Cu_2O MIS, with SiO_2 interfacial layers, semi-transparent layers of Au, Cu, Ag and Al 80−93946
Cu_2O Schottky cell, for barrier heights, Auger spectra obs. 79−15224
Cu_2O thin film solar cells, fabrication and anal. 80−55865
Cu_2O/Si heterojunction, using reactively sputtered Cu_2O films 79−7914
Cu_2O-Au(Mg)(Mn)(Yb) Schottky barriers, surface anal. using AES 79−43759
Cu_2S, deposited by cylindrical magnetron reactive sputtering 79−11258
Cu_2S, diffusion length meas. using scanned laser beam tech. 80−93886
Cu_2S, film preparation for solar cells, elec., optical, struct. props. 78−76602
Cu_2S stoichiometric thin films for solar cells 79−61991
Cu_2S/CdS, developments, appls., and economics of solar photovoltaic conversion *(German)* 80−26132
Cu_2S/CdS, thin film, sputtered 79−43774
Cu_2S/CdS heterojunction solar cells, diffusion length determ. using minority carrier SEM 80−61359
Cu_2S/CdS solar cells, performance, obs. 80−30480
Cu_2S-CdS, characteristics, for various solar radiation incidence angles 79−83593
Cu_2S-CdS, fabrication using solid state reaction 77−16498
Cu_2S-CdS, interface recombination phenomena and tunnel effect 80−66978
Cu_2S-CdS, optical absorption coefficient changes in Cu_2S 80−93980
Cu_2S-CdS, optical and calorimetric meas. of Cu_2S semiconductor thin films 80−55863
Cu_2S-CdS, optimised grid patterns 80−108798
Cu_2S-CdS, solar cell, photocurrent, spectral depend. 79−7853

solar cells continued
Cu_2S-CdS, sprayed, fabrication and electrical props. 80−93979
Cu_2S-CdS, with interdigitated grid, current-voltage analysis 80−93981
Cu_2S-CdS back illuminated high efficiency thin film solar cells 79−74515
Cu_2S-CdS cells, thin film fabrication processes and conduction mechanism, review 79−74522
Cu_2S-CdS film junction formation by dry-barrier process 78−64109
Cu_2S-CdS heterojunction model 78−39205
Cu_2S-CdS heterojunctions, electron trap characterisation by capacitance transient meas. 79−78163
Cu_2S-CdS heterojunction, photoelectric props. 80−29467
Cu_2S-CdS heterojunction solar cell, interface recomb. vel. determ. by capacitance/collection efficiency variation 80−50959
Cu_2S-CdS heterojunction solar cells, carrier transport, nonmonotonic band profiles 80−61361
Cu_2S-CdS heterophotocells based on CdS films of stoichiometric composition, elec. and photoelec. props. 80−93873
Cu_2S-CdS solar cell, interface recombination and junction field studies, exptl. technique 80−45683
Cu_2S-CdS solar cell applications, CdS film spray fabrication, physical props. *(French)* 80−60113
Cu_2S-CdS solar cell fabrication by magnetron reactive sputtering deposition 80−61363
Cu_2S-CdS solar cells, Cu_2S film growth methods 80−80980
Cu_2S-CdS solar cells, EBIC and capacitance measurements, stability problems 80−45684
Cu_2S-CdS solar cells in backwall configuration, model of photovoltaic effect 80−55861
Cu_2S-CdS solar photopiles, tunnel conduction mechanism *(French)* 79−29480
Cu_2S-CdS thin film heterojunction 80−93922
Cu_2S-CdS thin film planar junction devices, quantitative photon loss anal. 80−61362
Cu_2S-CdS thin film solar cells, Cu_2S layer separation, struct. 79−95282
Cu_2S-CdS thin film solar cell fabrication by electrophoresis 80−55862
Cu_2S-Zn_xCd_{1-x}, heterojunction, composition meas. near interface using aqueous ion-exchange 80−29465
Cu_2S-$Zn_xCd_{1-x}S$ and Cu_2S-CdS thin film solar cells by solid state reaction, comparison 80−101109
Cu_2S-$Zn_xCd_{1-x}S$ heterojunction, improved model of electro-optic behaviour 80−94023
Cu_2S-$Zn_xCd_{1-x}S$ solar cells, thin film photovoltaic solar energy conversion 80−61379
$Cu_{2-x}S$-CdS, collection coefficient theoretical anal. at conjunction 80−101094
$Cu_{2-x}S$-CdS, solns. cell, photo-emf, depend. on degree of doping of CdS 79−52934
$Cu_{2-x}S$-CdS ceramic solar cells, solar batteries operating characts. 80−93874
$Cu_{2-x}S$-CdS junction, low temp. growth, AES obs. 79−28924
$Cu_{2-x}S$-CdS p-n heterojunction solar cells, props., Burstein-Moss effects 80−21404
$Cu_{2-x}S$-CdS p-n heterojunction, optical energy convertor, struct. and recomb. props. 80−72065
$Cu_{2-x}S$-CdS p-n junction solar cells, fabrication and features *(Korean)* 79−60916
Cu_xS chalcocite film fabrication, characts. 78−39240
Cu_xS evaporated layer growth in vacuum, compositional and optical characterisation, solar cell appls. 80−97437
Cu_xS evaporated thin films, composition, prep. and characts. 80−25569
Cu_xS film for Cu-Cd-S solar cell, cathodolum. spectrum rel. to prod. method 79−56866
Cu_xS/CdS thin film cell, prep. by sequential evaporation 80−93902
Cu_xS/Si, Cu_xS/CdS, vacuum evaporated films, props. 79−15240
Cu_xS-CdS, cu_xS growth kinetics and composition analysis by absorbance transient and galvanic electrochemical measurements 80−92797
Cu_xS-CdS, minority carrier diffusion length, SEM determ. 77−72911
Cu_xS-CdS, p-n junction shape and struct. 77−55599
Cu_xS-CdS, post fabrication treatments, surface props. 78−39822
Cu_xS-CdS, SEM meas. of diffusion lengths, recombination vel. and junction collection efficiency 80−16808
Cu_xS-CdS heterojunction solar cells, time evolution of spectral characts. 80−30478
Cu_xS-CdS heterojunction solar cells spectral distrib. and photocapacitance 80−55864
Cu_xS-CdS large-area solar cell production pilot line 79−61994
Cu_xS-CdS solar cell improvement by Cu treatment and front contacting 79−61987
Cu_xS-CdS solar cell junction formation and open-circuit voltage 79−61986
Cu_xS-CdS solar cells, Cu_xS transform. behaviour rel. to topotaxial growth, cell efficiency 77−11814
Cu_xS-CdS solar cells, SCL current 80−76634
Cu_xS-CdS thin film, using all film vacuum deposited process 80−93977
Cu_xS-CdS thin film solar cell using chem. sprayed CdS film 78−43465
Cu_xS-CdS thin rilm heterojunction, reactively sputtered 79−11256
cu_2S-CdS sprayed layer solar photopiles, CdS sprayed layer props. *(French)* 79−24901
Fe-thionine, photogalvanic cell, photostationary state comp., current depend. 77−90629
α-Fe_2O_3, photochem. props. of sintered and doped samples for solar photoelectrochem. cell appls. 80−89651
GaAS, homojunction solar cell, temp. depend. of photovolt. solar energy conversion 79−43768
GaAS, photoluminescence in polycrystalline samples at 5K, possible solar cell material 79−99929
GaAlAs on GaAs thin film stacked multiple-bandgap solar cell structs., prep. using CVD techniques 80−94083
GaAlAs solar cells, appl. for navigational satellite power systems 80−35694
GaAlAs, solar power satellite design and evaluation, 5 GW, for Earth-based utility appl. 79−52892
GaAlAs/GaAs, Be and Zn behaviour 80−101111
GaAlAs/GaAs solar cells, efficiency optimisation at high and low current levels *(French)* 80−61348
GaAlAs-GaAs, high efficiency heterostruct. solar cell grown by metalorganic CVD 78−11118
(GaAl)As-GaAs concentrator solar cells, series resistance effects 79−57427
GaAlAs-GaAs heteroface solar cells, 1 MeV electron irrad., analytical and expt. study 79−70450
GaAlAs-GaAs heteroface solar cells, high open-cct. voltage, full-factor and efficiency 80−94081
GaAlAs-GaAs heterojunction solar cells, high temp. props. 25 to 300°C 80−94035
GaAlAs-GaAs heterostruct. solar cells, Al, P, Zn incorporation by LPE *(French)* 79−24899
$Ga_{1-x}Al_xAs$, technology advancements 79−43776
$Ga_{1-x}Al_xAs$:Si photoelectric convertors, broadband varizone creation 80−40856
$Ga_{1-x}Al_xAs$/GaAs heterostructure solar cell design for space usage 79−96450
$Ga_{1-x}Al_xAs$-GaAs, deep levels obs. 77−89834
$Ga_{1-x}Al_xAs$-GaAs, high efficiency solar cell, isothermal etchback-regrowth method 77−59701
$Ga_{1-x}Al_xAs$-GaAs, radiation resist., theoretical evaluation and optimisation 80−35681
$Ga_{1-x}Al_xAs$-GaAs high-efficiency solar cell 79−29469
$Ga_{1-x}Al_xAs$-GaAs LPE multilayer heterostructure photovolt. solar cells, fabrication and performance 79−48128
$Ga_{1-x}Al_xAs$-GaAs p-n and p-p-n heterojunction solar cells, high efficiency, prep., eval. and characters *(Japanese)* 80−61342
$Ga_{1-x}Al_xAs$-GaAs p-n structures, variable-gap front layer, photoelec. props., solar cells fabricated 79−7884
$Ga_{1-x}Al_xAs$-GaAs p-n solar cell, with thin variable gap layer, high efficiency 79−24064
$Ga_{1-x}Al_xAs$-GaAs solar cells, photoluminesc. characterisation 80−3512
$Ga_{1-x}Al_xAs$-GaAs solar cells, computer anal. of cell characts. incl. band gap variation 80−55866
$Ga_{1-x}Al_xAs$-GaAs-GaAs, p-p-n junctions, variable gap solar photocell with coordinate depend. band gap gradient 79−11213
p-$Ga_{1-x}Al_xAs$-n-$Ga_{1-y}Al_yAs$, graded band gap, solar cells, theoretical efficiency *(French)* 77−62987
GaAlAsSb-GaSb low bandgap solar subcell for high efficiency multiband-gap convertors, LPE growth 80−93927
$Ga_xAl_{1-x}P$ high-temp. solar cell with 0.3 eV band gap 80−21400
GaAs antireflecting MOS solar cells, epitaxial and polycryst. using OM-CVD techniques 80−94072
GaAs CVD for solar cell applications 77−77412
GaAs, CVD on W coated graphite, characterisation, and Schottky barrier solar cell characts. 79−28930
GaAs, developments, appls., and economics of solar photovoltaic conversion *(German)* 80−26132
GaAs, developments and trends for automatic interplanetary stations, Venus-9 and Venus-10, and mooncar program 80−89613
GaAs, efficiency improvement using ZnSe solar spectrum convertor 80−101117
GaAs, electron and proton radiation damage 80−94034
GaAs epitaxial growth, CVD-organometallics method, reactional efficiency in solar cell elaboration 80−93498
GaAs fabrication, using AMOS tech., single and polycrystalline cells 78−39935
GaAs, film, selective anodisation, grain boundary edge passivation 79−11711
GaAs, film, solar cell on large grains 79−100528
GaAs, film and solar cell on graphite, struct. and elec. props. 80−2286
GaAs film on recrystallised Ge film, solar cell appl. 78−19671
GaAs film solar cell fabrication, substrate requirements 78−11125
GaAs films for solar cells appl., deposition and characterisation 80−84853
GaAs homojunction solar cells, large-grained, passivation method to improve open-circuit voltage 80−94070
GaAs large-grained solar cell film recrystallisation 79−38737
GaAs MIS solar cells, effects of thin oxide layers on characts. 80−89624
GaAs MOS solar cells by anodisation in active region 80−101107
GaAs, minority carrier lifetime at high temp., solar cell performance appl. 80−24947
GaAs n-p homojunction, potential for high efficiencies concentrator applications 79−100534
GaAs n-p solar cells, theoretical perform. of multi-layer grid patterns 80−55846
GaAs, NTS-2 satellite experiment, radiation damage obs. 79−48134
GaAs on Ge thin film stacked multiple-bandgap solar cell structs., prep. using CVD techniques 80−94083
GaAs, photovoltaic conversion characts. *(Czech)* 77−76903
GaAs photovoltaic solar system, appl. in electric utility system 80−55875
GaAs, polycryst., wet and dry oxides, comparative study by AES, SIMS and XPS and solar cell performance 80−80116
GaAs, polycryst. Schottky barrier solar cells, effect of grain size on efficiency 80−50968
GaAs, polycryst. solar cells, thin film growth and grain size, effect on cell efficiency 80−81471
GaAs polycryst. solar cell diagnostics using IR electroluminesc. 80−93885
GaAs polycryst. tunnel MIS solar cells, grain boundary problem 80−16809
GaAs, polycrystalline, carrier transport at grain boundaries, rel. to solar cell performance 80−29411
GaAs, polycrystalline, for solar cells 78−11124
GaAs, polycrystalline, for terrestrial photovoltaic energy conversion 79−15242
GaAs, polycrystalline, props. and prep. with grain boundary edge passivation 80−81437
GaAs polycrystalline film growth for solar cells 79−33941
GaAs polycrystalline thin film solar cells, fabrication 80−94066
GaAs, props., characts. and efficiency, development costs *(Spanish)* 80−72062
GaAs prospects *(Italian)* 80−60025
GaAs, Schottky barrier solar cells, diffusion length meas. 79−61973
GaAs Schottky barrier solar cells with grain boundary edge passivation 79−83592
n-GaAs semicond. liq. junction solar cells, photocurrent spectra, carrier recombination 78−76142
GaAs, shallow homojunction solar cell, resist. to 1 MeV electron radiation 80−50953
GaAs shallow junction solar cells damaged by electron irrad., recovery of short cct. current 79−29471

solar cells continued
GaAs, shallow-homojunction solar cell by MBE, conversion efficiency 80−30476
GaAs shallow-homojunction solar cells on single crystal GaAs and Ge substrates, CVD fabrication and efficiency 80−61364
GaAs shallow-homojunction solar cells, electron radiation effects 80−97798
GaAs, simultaneous radiation damage and annealing 80−94033
GaAs solar cell, polycryst., grain boundary passivation by oxidation, AES, SIMS and XPS obs. 80−81467
GaAs solar cell polycrystalline conducting substrate, minority carrier diffusion length spatially-resolved meas. 80−94084
GaAs solar cell structs., photolum. props. 80−50958
GaAs, solar cells, electron-irrad., annealing kinetics 80−7937
GaAs solar cells, ion-implanted and laser-annealed 79−79390
GaAs solar cells, photoreactance of p-n junction diodes 80−81464
GaAs solar cells on Ge substrates, thin film shallow homojunction struct., quantum efficiencies 80−35677
GaAs solar cells with shallow homojunction on Ge substrates 80−26142
GaAs, thin film, polycrystalline, grain boundary edge passivated 80−94069
GaAs, thin film, prep. by Peeled Film Technology 79−29472
GaAs thin film growth tech. and characterisation 80−89631
GaAs thin film polycrystalline Schottky barrier solar cells, grain boundary chemistry 80−94067
GaAs:Si, heteroface solar cells, diffusion lengths 78−47849
n-GaAs:Sn-p-GaAs:Ge-p-$Al_xGa_{1-x}As$:Ge heterostructure solar cells, LPE growth techniques 80−66977
GaAs:Te Schottky barrier solar cells, diffusion length determ. using minority carrier SEM 80−61359
n-GaAs/K_2Se-K_2Se_2-KOH/C solar cell, Ru (III) chemisorption on photoanode, effect on performance 80−3516
n-GaAs/K_2Se-K_2Se_2-KOH/C liq. junction cell, effect of Ru ion chemisorption on grain boundaries 80−55879
GaAs-$(SN)_X$, solar cell fabrication and efficiency 80−26143
GaAs-AlAs, formation by VPE growth of n-AlAs on GaAs 77−1814
GaAs-AlGaAs, with valley-transferred electrons for voltage and efficiency enhancement 80−93956
GaAs-AlGaAs solar cells *(Rumanian)* 80−93877
GaAs-AlGaAs two-junction stacked solar cell, growth and characterisation 80−16811
GaAs-Au(Ag) Schottky barrier, interface problems, AES, SIMS and XPS study 80−89627
p-GaAs-$Cd_{1-x}Zn_xS$ heterojunctions, elec. and photovolt. props. rel. to growth technique 80−29466
GaAs-$Ga_{1-x}Al_xAs$, LPE growth for solar cells 77−77427
GaAs-$Ga_{1-x}Al_xAs$, variable band gap, photo-EMF, appl. to solar cells 80−20296
GaAs-GaAlAs LPE grown, parameters dependence upon impurity concentration and temp. performances for series resistance reduction 80−45692
GaAs-$In_{2-x}Sn_xO_{3-y}$ SIS heterostructure solar cells, spray-deposited 80−101106
n-GaAs-K_2Se-K_2Se_2-KOH/C thin film solar cell, 7.3% cell efficiency 80−93931
GaAs-oxide-metal structure, field shaping and barrier height 77−20454
$Ga_{1-x}As(Al,In)_x$, heterojunction solar cells, optimum bandgap, computer anal. 79−43767
p-GaP, cathode of photoelectrochemical cell 78−10552
p-GaP electrode, for solar cell, differential capacitance meas. for flatband potential determ. 78−72256
p-GaP semiconductor-electrolyte solar cells for photochemical reduction of CO_2 to organic fuel 80−55880
GaP-Si heterojunction solar cell, computer simulation 79−74529
p-GaSe, back wall Schottky barrier cells, diffusion length, RT spectral response meas. 80−107806
Ge, amorphous layer, epitaxial recrystn. by electron irrad., solar cell appl. 78−84079
n-(In-Sn)O_x-p-InP, growth efficiency 77−72910
InGaP-InGaAs solar cell, high internal collection efficiency, low bandgap 80−26134
In_2O_3:Sn films, elec. and optical props., solar energy conversion appl. 79−65945
In_2O_3:Sn/n-Si heterojunction solar cell, fabrication and charact. 78−15314
n-In_2O_3/p-InP heterojunction, photovolt. effects 80−12014
In_2O_3-Si(Ge)(GaAs)(InP) heterostructure solar cells, photovoltaic and rectifying props., electron affinity determ. 79−1618
In_2O_3-SnO_2/GaAs, solar cell, fabrication, charact. and interfacial chemistry 80−21401
In_2O_3-SnO_2/InP, solar cell, fabrication, charact. and interfacial chemistry 80−21401
In_2O_3-SnO_2/InP junction, ion probe analysis of chemical nature 79−73411
In_2O_3-SnO_2/Si, antireflection props. of oxide film 80−3513
In_2O_3-SnO_2/SiO_x/Si diode solar cells, loss mechanisms, charact., band struct. 80−26135
In_2O_3-SnO_2/polySi, response exam. using electron-beam-induced current and scanning light spot tech. 80−81477
In_2O_3-SnO_2-CdTe:P, p-n homojunction solar cell, elec., photovoltaic props., photoluminescence 80−81463
In_2O_3-SnO_2-InP solar cell junctions, efficiency, InP surface props. 80−85288
In_2O_3-SnO_2-Si heterojunctions, elec. and photovoltaic charact. 78−52070
In_2O_3-SnO_2-Si SIS heterojunction solar cells 80−85281
In_2O_3-SnO_2-Si SIS solar cells, reverse current-voltage charact. under illumination 80−89622
In_2O_3-SuO_2-SiO_x-pSi, comparison between MIS and SIS solar cells 80−81443
n-InP film appl., polycrystalline, electrical properties obs. 79−4608
InP homojunction solar cell, antirefl. coated, high-efficiency 80−104505
n-InP, MOS, electrical and photovoltaic characteristics 80−85276
InP n^+-p-p^+ homojunction solar cells, high efficiency, LPE layer growth, photolithographic fabrication 80−93929
p-InP, on foreign substrates, prep. and solar cell characterisation 77−81211
n-InP photoelectrode, stabilisation to photoanodic dissolution, in aqueous solutions of Te^{2-}/Te_2^{2-} 78−14814
InP, thin film growth tech. and characterisation 80−89631
InP thin films for photovoltaic devices 80−93972

solar cells continued
InP/CdS fabrication by reactive sputtering, anal. of technique 78−39693
InP-CdS, SiO antirefl. coatings 78−50871
InP-CdS p-n heterodiodes, junction props. study by using injection electrolum. 79−82667
InSe, photovoltaic effect, appl. to solar energy conversion 79−29481
InSe solar cells, photovoltaic conversion efficiency 80−61356
$(In_{1-x}Sn_x)_2O_{3-y}$-Si solar cells, degradation 80−94047
$In_{2-x}Sn_xO_{3-y}$, majority carrier conduction effects 80−97796
n-$In_{2-x}Sn_xO_{3-y}$/p-Si, semicond.-insulator-semicond. solar cell, performance and spectral response, fabrication 79−83596
$In_{2-x}Sn_xO_{3-y}$-CdTe(InP) photovoltaic heterojunctions, surface and interface studies, efficiency 80−45691
$In_{2-x}Sn_xO_{3-y}$-$Ga_xIn_{1-x}P$(-InP_yAs_{1-y}) heterojunction solar cells, chemistry and prep. 80−94073
$In_{2-x}Sn_xO_{3-y}$-insulator-poly-Si solar cells, photovoltaic conversion parameters 80−101093
$In_{2-x}Sn_xO_{3-y}$-n-Si, electron deposited solar cell, photovoltaic props. 79−96446
$In_{2-x}Sn_xO_{3-y}$-poly Si SIS solar cells 80−97787
$In_{2-x}Sn_xO_{3-y}$-Si solar cells, SiO_2 detection of interface, Auger anal. 79−87991
$In_{2-x}Sn_xO_{3-y}$-SiO_x-Si SIS solar cells, loss mechanisms study for improvement of efficiency to above 12% 80−94080
n-$MoSe_2$ based liq. junction solar cell, nonaqueous electrolyte system employing Cl_2/Cl couple 80−81432
$MoSe_2$, layer cryst., electrochem. solar cell, electron transfer mechanism 78−52077
$MoSe_2$ layer-type electrochem. solar cells, electrode material performance, doping effect 79−74532
n-$MoSe_2$, synthetic, performance in electrochemical solar cells 79−66412
N_2 reducing solar cells for industrial NH_3 synthesis 80−89632
Pt-Mn(III)-porphyrin electrode for possible wet solar cell 79−100529
$(SN)_x$-GaAs polymer-semiconductor solar cells 79−15219
$(SNBr_{0.4})_x$-GaAs, single crystal and polycrystalline 80−16810
Se:Te multilayer solar cell 79−43762
Si, 50 μm cell technology developments for low mass space blanket 80−30498
Si, 50 μm cells for space power systems, technology development 80−30499
Si, advanced material for space solar cell 80−94007
Si, all-plate low cost contact system 80−93992
Si, amorphous, affect of transport props. on cell efficiency 80−50961
Si, amorphous, barrier props. determ. by differential I-V charact. meas. 80−94053
Si, amorphous, current collection and electrical shorting problems 80−93969
Si, amorphous, glow discharge produced 80−12013
Si, amorphous, hydrogenated, stacked solar cells 80−55842
Si, amorphous, photovoltaic charact., rel. to appl. in solar cells 78−84253
Si, amorphous, plasma deposited, horizontally multilayered struct. 80−50964
Si, amorphous, semiconductor technology *(Japanese)* 79−57430
Si, amorphous, solar cell appl. *(Chinese)* 80−45671
Si, amorphous, solar cell construction and performance *(German)* 79−61970
Si, amorphous, solar cells, and photovoltaic devices *(Japanese)* 80−50965
Si, amorphous, technological development trends for low cost energy requirements 80−26136
Si, amorphous and polycryst. thin film solar cells, perform. parameters, review 80−93882
Si, amorphous design considerations 80−85277
Si amorphous films, RF sputtered, appl. as Schottky barrier solar cells 79−34434
Si, amorphous glow discharge films, H_2 content, elec. props., and photostability 80−25577
Si, amorphous hydrogenated, use as solar cell material 78−2565
Si, amorphous hydrogenated solar cells, field depend. quantum efficiency, electron-hole recombination 80−66971
Si, amorphous Schottky barrier solar cells, deep hole traps, spectral response and TSC meas. 80−50962
Si, amorphous vacuum deposited p/undoped photodiode and diode-voltage variable resistor combination 80−61380
Si, analysis of short-circuit current 80−85285
Si, appl. to electronic equipment and appliances *(Japanese)* 79−83599
Si, as-grown Czochralski crystal, appl. of multiple p-n junction structure obtained by heat treatment 80−101099
Si back surface field solar cell degradation at high intensity due to base cond. modulation loss 80−94085
Si, back-wall Schottky barrier solar cell with interfacial layer 77−62993
Si, base resist. influence on temp. charact. 80−89618
Si based alloys, amorphous, photovoltaic behaviour, solar cell appl. 80−94051
Si, CVD on liq. Sn layers in HCl presence, enhanced crystallinity 78−6853
Si, CVD polycryst. solar cell, grain boundary effects rel. to dopant conc. 77−7744
Si, calculations of absorption coefficient 80−7944
Si, carrier lifetime and its impact on solar cell charact. 79−74521
Si, cast, growth structure and photovolt. props. of solar cells 80−94008
Si cell fabrication, recrystallisation of CVD-grown polycryst. Si and influence of B, Al dopants on grain growth 80−54575
Si, characteristics, for various solar radiation incidence angles 79−83593
Si, coating of mullite ceramic substrate, for solar cell appl. 79−34432
Si concentrator, effects of nonuniform illumination 80−93942
Si concentrator, high efficiency, state-of-the-art design and processing 80−93958
Si concentrator, new technology for fabrication 80−81457
Si concentrator cells, high efficiency, design, fabrication and meas. 80−93938
Si conductor-insulator-semicondcutor solar cells, automated production, outlook 80−94021
Si continuous polycrystalline films on C substrates 78−64490
Si crystal growth, heat exchanger method, fixed abrasive slicing technique 80−35082
Si, crystalline sheets production, low cost, crystal growth techniques comparison 80−35083
Si, deformed, annealed and recrystallized, struct., implications for solar cells 80−60922

solar cells continued
Si, degradation processes of electrophysical charact. during long-term operation 80−89617
Si, dendritic film growth on alumina, solar cell appls. 77−77432
Si dendritic web for solar cells 80−89634
Si, design, fabrication and evaluation of a 2″ high efficiency cell for concentrator systems 80−55854
Si, design for limit conversion efficiency 80−93960
Si, developments, appls., and economics of solar photovoltaic conversion *(German)* 80−26132
Si, developments and trends for automatic interplanetary stations, Venus-9 and Venus-10, and mooncar program 80−89613
Si, device model for tandem junction solar cell 80−16813
Si diffused horizontal homojunction solar cells, effects of junction depth and impurity conc. 80−55877
Si, diffusion fabrication process, low cost, highly automated 80−30487
Si, direct conversion of sunlight into electric current, principles *(German)* 79−61971
Si, directional solidification in carbon crucibles 80−45663
Si, edge-illuminated p^+-nn^+, analytical model under concentrated sunlight 80−7942
Si, effect of Ti, Cu and Fe 80−72064
Si, effects of B and P impurities on cell performance 80−55848
Si, effects of metallic impurities 80−85278
Si, effects of nonuniform illumination and temp. profiles under concentrated sunlight 80−93941
Si, efficiency limits, comprehensive explanation 80−35688
Si, electrodeposited film, appl. in solar cell fabrication 78−76611
Si epitaxial layers on metallurgical-grade polycryst. substrates, characteris. 79−28967
Si, epitaxial layers on ribbon substrates, solar cell prod. and characterisation 77−77354
Si, experimental efficiency optimisation of n^+pp^+ and p^+nn^+ cells 80−30486
Si, fabrication overview, wafer prep., anti-refl. coatings and metallisation, efficiency *(Spanish)* 80−72059
Si, fabrication using zone melting of CVD Si on graphite, and performance 77−85945
Si film, amorphous, glow discharge deposited, for low cost solar cells 80−61355
Si film, electron beam evaporation, for solar cell appl., heat exchanges and columnar growth 79−15609
Si, film, polycryst., for photovoltaic appl., grain size effects 78−72034
Si films, electron beam evaporated, for MIS solar cells 80−93490
Si, fixed-base, flat panels, possible developments for more competitive power production 80−72050
Si, for cathode protection of submerged marine structures 80−40859
Si, for improved short-wavelength quantum efficiency 80−31874
Si, from crack-free ingots grown by directional solidification 79−8242
Si, fundamental efficiency limitations 80−93963
Si, grain boundary defects in thin semicrystalline material 80−93889
Si, grain size dependence of parameters 80−94049
Si, growth of large grain polycryst. layers on graphite substrates by CVD on liquid layers 80−55849
Si, heavily doped, excess intrinisic carrier density, deionisation of impurities as explanation, bipolar transistor/solar cell models 80−96864
Si heavily doped shallow-emitter p-n junction solar cells, diodes and transistors, Auger recombination 79−96445
Si, high efficiency, using minority carrier MISS 80−101103
Si high efficiency solar cells, laser annealing, reviews 80−93976
Si, high open circuit voltage, P implantation 80−89642
Si, high performance back-surface field with fire through contacts 80−93993
Si high-intensity solar cell, fabrication and AM1 efficiency 79−43760
Si, I-V charact. meas., effect of voltage ramp, theoretical anal. using linear model 80−61354
Si, implanted layers characteristics, laser irradiation effects 80−35692
Si, inhomogeneities and their influence on cell performance 80−93967
Si, Interdigitated Back Contact solar cells, surface recombination minimisation 80−12017
Si, ion implantation by laser annealing, characterisation, solar cell applications 80−70247
Si, ion implantation with Li^+, charact. for thin film solar cell use *(Korean)* 77−51812
Si, ion implanted, from EFG Si ribbons 80−30485
Si, ion implanted grating type 80−101102
Si, ion-implanted, expt. study of efficiency controlling factor 80−93997
Si, ion-implanted, factors controlling efficiency 80−81451
Si, ion-implanted, laser annealing, appls. to high-efficiency solar cells fabrication 79−73202
Si, ion-implanted, tailored emitter, low resistivity 80−81452
Si ion-implanted laser-annealed solar cells 80−93881
Si, junction formation techniques using spray-on polymer dopants, cost effective, high throughput 80−94014
Si large grain films on metallurgical Si substrates, chem., struct., elect. and photovoltaic props. 80−61357
Si, light trigger for slave flashguns 80−47125
Si, light-enhanced diffusion length obs. by DC photocurrent meas. 79−39301
Si, limit efficiency evaluation 80−93973
Si, liquid, interaction with die material during edge defined film fed growth 80−104060
Si, low cost, Ni contacts 80−94017
Si, low cost processes for fabrication 80−94013
Si, low cost production for solar cells, growth from melt 78−3028
Si, low series resistance photovoltaic concentrator 80−93940
Si, low-cost, starting materials technology and economics 80−30483
Si, low-cost fabrication processes *(Japanese)* 79−83600
Si, low-cost photovoltaic solar cell fabrication developments using Si on ceramics and minute spherical cells 80−55839
Si, low-cost sheet fabrication, structural defects, effect on electronic props. and cell performance 80−50977
Si, low-grade, review and current developments 80−108801
Si MIS grating solar cells on minority carrier blocking back surface field substrates 80−94078
Si MIS solar cells, 655 mV open-circuit voltage 79−79391
Si MIS solar cells, spectral response and diffusion length 79−92077
Si MIS solar cells with Cr, Hf, Be, Sc and Y as barrier forming metals, expt. investigation 80−94077
Si, MIS/inversion layer, high efficiency cell fabrication 80−94075
Si, MIS-inversion layer, low cost-high efficiency 80−76632

solar cells continued
Si MOS and oxide-charge-induced BSF solar cells, open-cct. voltage >700 mV, 20% conversion efficiencies 80−81435
Si, manufacturing cost anal. of flat plate vs. concentrator solar cells 80−93949
Si materials, advanced, preliminary evaluation for space solar cells 80−94006
Si, melt and vapour growth for integrated circuits and solar cells 79−47609
Si, metallurgical-grade, fabrication by epitaxial growth or direct diffusion 80−101104
Si, minority carrier lifetime *(Korean)* 78−23103
Si, minority carrier lifetimes determ. from spectral and transient meas. 79−100533
Si, minority carrier MIS, design and expt. results 80−81445
Si minority carrier MIS solar cells, AM1 efficiencies 80−93975
Si, minority carrier MIS diodes appl. *(Slovak)* 80−97792
Si modules, photovoltaic units combined with storage batteries *(German)* 80−55840
Si monocrystalline sheet fabrication for solar cells, CLF Czochralski furnace and enhanced slicing technology 80−93476
Si multicrystalline solar cell material prep., fast-pulled float zone, CZ and cast ingot and foil methods 80−93483
Si multielement photoelectric convertors, p-n mesa structure for investigating optical and energy charact. of solar and radiant energy concentrators 80−97783
Si n^+ pp^+ solar cells, back illuminated, internal quantum efficiency 79−34435
Si, n^+-p, Li-counterdoped, radiation damage 80−94000
Si n^+-p junction solar cells, electron irrad., DLTS spectra and defect effects 80−93999
Si n^+-p solar cell, forward and reverse bias tunnelling 80−85274
Si n^+-p solar cells, degradation mechanisms associated with Ti impurities 80−81465
Si, n^+-p-p^+ structure with two-sided photosensitivity for terrestrial applications, structure and fabrication technology requirements 80−101096
Si n^+p solar cells, effect of elec. bus during 1 MeV electron irrad. and isochronal annealing, elec. charact. and deep level pop. 80−94086
Si n-p junction vertical solar cells, Al-plated, photovoltaic effect variation with impurity conc. 79−100522
Si, Ni-Cu conductor system 80−93991
Si, nonsingle crystalline, solar cells, book contrib. 79−43771
Si on ceramic cells, growth, eval., and modelling 79−11511
Si on ceramics, coating with inverted meniscus (SCIM) technique, solar cell appl. 80−89163
Si open-circuit voltage at ultrahigh light intensities, plasma reflection effects 80−96928
Si or Si/Cu_xS manufacture w.r.t. optimum yield, Baude process appl. *(French)* 79−96448
Si, output power and sunshine conditions, correlation 80−97785
Si, p^+-i-n^+, conversion efficiency limit in concentrated sunlight 80−85282
Si p^+-n high efficiency cell, B diffusion process 77−85302
Si p^+-n-n^+ back surface field concentrator solar cells 80−93939
Si p^+-n-n^+ back-surface-field, physics underlying performance 80−85283
Si p^+-n-n^+ edge-illuminated cell, analytical model 80−12018
Si, p^+-n-n^+ high efficiency back surface field solar cells, design and fabrication 78−84283
a-Si p-i-n and c-Si p-n junction solar cells, design concept differences 80−94031
Si p-n junction, forward bias capacitance and current meas. for lifetime and band narrowing detn. 79−7892
Si, p-n junction, importance of surface recombination and energy-bandgap narrowing 79−100520
Si p-n junction diodes and solar cells, minority carrier diffusion length 80−107894
Si p-n junction solar cells, photon degradation effects 79−92078
Si, $POCl_3$ gettering of Ti, Mo and Fe-contaminated cells 80−94010
Si photoelectric convertors, photoelectric parameters under illumination 80−40857
Si photoelectric convertors, bilateral sensitivity, optical charact. anal. 80−40858
Si, photovoltaic energy conversion efficiency, photoacoustic spectra 79−15178
Si photovoltaic industry, environmental control, economic and ecological requirements 80−94026
Si, polycryst., elec. and photovolt. props., grain size effects 80−49800
Si, polycryst., p-n junction, grain boundary and intragrain recombination currents 80−81442
Si polycryst. and amorphous cell charact. 80−89619
Si, polycryst. films, transport props. and grain boundary charact. by TEM 80−50980
Si polycryst. layer, grown by ribbon-against-drop pulling process 79−8241
Si, polycryst. manufacturing methods for photovoltaic energy prod., solar cells, grain growth from melt *(Dutch)* 78−52661
Si, polycryst. rods, p-n junction appls. and transport props. 79−99612
Si, polycryst. solar cells, production problems *(Rumanian)* 80−21398
Si, polycryst. surface barrier cells, eval. for terrestial appls. 80−61376
Si, polycrystalline, electronic behaviour of grain boundaries 80−92859
Si, polycrystalline, for efficient low cost solar cells 80−21405
Si, polycrystalline, grain boundary effects on minority-carrier diffusion length and solar-cell efficiency 79−48124
Si, polycrystalline, grain boundary obs. by TEM, solar cell appl. 80−72057
Si, polycrystalline, p-n junctions, solar cell appls. 78−56220
Si, polycrystalline, refined metallurgical-grade, impurity gettering 80−94011
Si, polycrystalline, solar cells, grain-boundary hydrogenation technique for improvement 80−85273
Si, polycrystalline barrier heights and passivation of grain boundaries 80−93890
Si polycrystalline CVD film optical props. 77−77315
Si, polycrystalline Czochralski-grown, MIS solar cell characterisation using scanned laser response exam. 80−93884
Si polycrystalline film, effect of defects/grain boundaries on photovoltaic mech. 80−93883
Si, polycrystalline metallurgical grade, impurity gettering 80−81441

solar cells continued
Si, polycrystalline n^+/p, computer model of spectral response and photocurrent 80−55853
Si polycrystalline p-n junction deposition 78−10549
Si polycrystalline solar cells, ion implantation method and results 78−63784
Si, polycrystalline solar cell base material characterisation, defect states 80−50979
Si polycrystalline solar cells, recombination, electron-beam-induced current characterisation 80−81470
Si polycrystalline thin-film solar cells 79−57426
Si polycrystalline-metal Schottky barrier solar cells, elec. and photovoltaic contact props. 80−93936
Si, power transistor and solar cell epitaxy from SiH_2Cl_2 source 77−77402
Si, preparation using laser processing 80−81454
Si, prod. of polySi vapour deposited coatings for solar cells, cost anal. 80−93495
Si, production, Union Carbide Corporation Silane Process, cost analysis 80−21403
Si production from rice husk ash for solar cells 79−62008
Si, production process effect on fracture strength 80−93656
Si, props., charact. and efficiency, development costs *(Spanish)* 80−72062
Si, prospects *(Italian)* 80−60024
Si, proton irradiated, processing influence on elec. performance 80−94001
Si, proton irradiation damage 78−34556
Si, pulsed laser techniques for annealing ion-implantation damage 80−81453
Si, purification technology for the development of low cost solar cells 80−50976
Si, radiation damage annealing mechanisms and low temp. annealing 80−94003
Si, radiation damaged, origin of reverse annealing 80−76630
Si, radiation defects due to 30 MeV proton irrad. 78−71776
Si, rapidly grown RTR sheet, props. and solar cell processing 79−100048
Si, realisation by laser induced diffusion of deposited Sb 80−93998
Si, review of physics underlying recent improvements 80−93974
Si ribbon, dendritic web growth, solar cell prod. and characterisation 77−77366
Si ribbon, dendritic web growth from melt, solar cell module fabrication 80−93478
Si ribbon, EFG, diffusion length enhancement under illum. 78−14756
Si ribbon, edge-defined film-fed growth, solar cell prod. and characterisation 77−77365
Si ribbon crystal evaluation 77−76813
Si ribbon growth, ribbon-to-ribbon process, thermal environment control 80−35116
Si ribbon growth by capillary action shaping technique 80−29888
Si ribbon solar cells, defect anal. using laser scanner 80−94089
Si ribbon solar cells, var. of minority-carrier diffusion length with light intensity, heavy metal doping effects 80−93937
Si ribbons, edge-defined film-fed growth technique for solar cells 80−89138
Si ribbons for solar cells, ultra high speed growth, elec. props. 80−89162
Si ribbons grown by capillary action shaping technique, surface quality and impurity distrib. 80−108343
Si, ribbons produced through capillary action shaping, elec. and struct. charact. 78−47804
a-Si Schottky barrier, large-area RF sputtered, effect of hydrogenation, optimum barrier performance and bulk props. 80−45679
Si Schottky barrier solar cell, V-I charact. and efficiency 78−14828
Si Schottky-barrier, electron and hole drift mobility in amorphous Si 78−19027
Si, screen printed diffusion and metallisation 80−94015
Si, screen printed solar cells, effect of double exponential on efficiency and yield 80−55851
Si, second quadrant effects 80−76639
Si, semiconductor thick film cell contacts, all metal 80−30489
Si sheet casting for solar cells 80−89139
Si sheet-form solar cells, efficiency improvement, minority carrier diffusion length limitations 80−93925
Si, SiO_2 diffusion sources under oxidising ambient conditions, solar cell fabrication 78−2148
Si single crystal growth from metallurgical grade Si for fabricating terrestrial solar cells 80−59416
Si, single crystal solar cell manufacturing process, laser annealing of implanted area, energy saving 80−97791
Si, single-crystal, HV, multijunction, parameters and characteristics 80−89615
Si, solar cell, from film on foreign substrate 77−77390
Si solar cell, transition metal doped Czochralski and web crystals, measurement of impurity effects 78−35297
n-Si solar cell and concentrator manufacture *(French)* 79−83602
Si solar cell fabrication from multiple ingots using melt replenishment Czochralski method, cell anal. 80−93477
Si solar cells, capacitance transient spectra of processing- and radiation-induced defects 80−61340
Si solar cells, developments *(French)* 80−55845
Si solar cells, fabrication using continuous or pulsed lasers *(French)* 80−61350
Si solar cells, photoelectric effect and principles of operation and efficiency 80−50983
Si solar cells, photoreactance of p-n junction diodes 80−81464
Si solar cells, polycrystalline p-n junctions, recombination currents, physical models 80−93892
Si solar cells, polycrystalline, from recrystallized plasma deposited thin films 80−104509
Si solar cells, SEM electron beam induced current study, contamination effect 79−43773
Si solar cells, undergraduate teaching expts. 77−74177
Si solar cells with concentrators and heat pump 80−61371
Si solar cells with light concentrating lens, test results *(Rumanian)* 80−89620
Si solar concentration cells, concentrated sunlight effects, experimental results, interpretation 80−35690
Si, solar grade, Czochralski growth, solar cell efficiency vs. metallic impurity conc. 78−31330
Si, solar grade, prod., using Dow Corning process 80−29894
solar cells continued
Si, solar grade material economic commercial production, problems in cost reduction *(Spanish)* 80−72058
Si solar photovoltaic cells, large scale production, materials, efficiency and economics 80−50970
Si solar power cell production by capillary action shaping technique 79−34431
Si, solar-cell grade material prod., recent developments, low-cost processes *(Spanish)* 80−72061
Si, solid dielectric compound parabolic concentrator 77−7174
Si, solid source diffusion process for fabrication 80−93994
Si, spray-on TiO_2 antireflection coatings 80−80963
Si substrate, upgraded metallurgical grade, epitaxial growth 80−93905
Si substrate prep. for epitaxial solar cells, low-cost, unidirectional solidification process 80−93924
Si substrate thinness, device design, solar cell processing, empirical study of interaction 80−93995
Si, surface passivation by SnO_x films, effect on cell transport props. and short cct. current 80−61360
Si, tandem junction, operation and parameters, model 79−100521
Si, technological developments of single crystal cells and cost-effective cells 80−50984
Si terrestrial photovoltaic systems, historical developments and current research and development trends 80−45702
Si terrestrial solar cells, stress tested, contact integrity testing 80−94018
Si textured solar cell, hairline crack detect. using focused laser scanner 79−48123
Si, thin cell with back surface reflector and controlled optical absorptance 80−35691
Si, thin diffused layer, minority carrier excess charge and time const. 78−30938
Si thin film for solar cells, thermal expansion shear separation technique 80−81439
Si, thin film prep., in orbiting ultrahigh vac. facility 78−7855
Si, thin foil cells, technology developments 80−35693
Si thin p-n junction solar cells, minority carrier mirrors and optical confinement for high efficiency (27%) 80−93933
Si thin tandem junction cells, improved performance 79−39302
Si thin-film polycrystalline vacuum-deposited solar cells, TiB_2 bottom electrode, 10% efficiency 80−93489
Si, TiO_2 AR coating by spray deposition 80−104511
Si, ultrathin, electron and proton effects 80−94002
Si, unified model of fundamental limitations 80−81448
Si, updating limit efficiency 80−81447
Si, with chem. sprayed SnO_2 antireflecting films 79−72639
Si, with field-induced p-n junction, inversion layer solar convertor 77−15906
Si, with Ta_2O_5 antirefl. coating, film-substrate interaction obs. 77−1324
Si, zone refined, prep. of solar cells 78−64475
Si:Al lamellar devices, surge protector, solar cell, HV diode and negative resistor appls. 78−10068
Si:B ion implanted grating-type solar cells, var. of junction depth, collection efficiencies 80−93934
p-Si:Cu, Cn precipitation effects, for solar cells appl. 79−69249
Si:F,H, amorphous efficient carrier generation for solar photovoltaic energy conversion 80−92906
Si:Fe(Al), compensated substrates, effects of Fe and Al 80−94009
Si:H, amorphous, band tail absorpt., photocurrent meas. for Schottky barrier solar cell 80−60032
Si:H, amorphous, discharge prod., optically induced cond. changes 80−96937
Si:H, amorphous, HV photovoltaic cells, design parameters 80−101105
Si:H, amorphous, horizontal cascade type integrated photovoltaic cell module 80−94091
Si:H, amorphous, p^+-i-n^+ struct. solar cells, material parameters and deposition condition optimisation study for higher efficiencies 80−45676
Si:H, amorphous, RF sputtered, suitability as solar cell material 80−40864
Si:H, amorphous, RF sputtered, Schottky barrier solar cells, photovoltaic props. and capacitance-voltage charact. 80−45678
Si:H, amorphous, Schottky barrier, degradation mechanisms affecting stability and operation 80−45680
Si:H, amorphous, Schottky barrier diode, deposition parameter effects on elec. props. 80−45681
Si:H, amorphous, solar cell struct., photocurrent meas., absorpt. coeff. 80−50960
Si:H, amorphous, solar cells, carrier generation, recombination, and transport 80−55844
Si:H, amorphous, solar cells, trap spectroscopy using transient current techniques 80−104508
Si:H, amorphous, solar-cells, charge collection and spectral response 80−85275
Si:H, amorphous, sputtered Schottky barrier solar cells, conduction mechanism 80−104506
Si:H, amorphous, stacked solar cells, development 80−94050
Si:H, amorphous, using ultrathin active layer to increase conversion efficiency 80−94030
Si:H, amorphous Schottky barrier solar cells, depletion region, capacitance study 80−50963
Si:H, amorphous Schottky solar cells, prep. and charact. of diode RF reactive cathodic sputtered films *(French)* 80−61347
Si:H, amorphous thin film solar cells 80−81478
α-Si:H, discharge produced, electronic props. rel. to solar cell charact. 79−15241
Si:H amorphous, solar cell structure, optical absorption by gap states 80−94052
Si:H amorphous films for solar cells, optical and elec. props. of RF glow discharge deposited films 80−54576
Si:H amorphous MIS solar cell, loss mechanisms and photovoltaic parameters, overview 80−93923
Si:H amorphous semiconductors, prep. from SiH_4 and charact. 78−48326
a-Si:H highly homogeneous, for low-cost solar cell fabrication 80−72053
a-Si:H solar cells, photoexcited carrier collection efficiency 79−100526
Si:Li P/N type solar cells, irradiation obs. 79−66406
Si:P diffused solar cells, laser treatment to dissolve diffused P precipitates 80−45667
Si:P solar cell, minority carrier lifetime degradation during ion implanted processing, surface photovoltage 79−39305
Si:P solar cells, improved P diffusion using laser treatment 80−55850

solar cells continued
Si:P(O) p^+-n-n^+ solar cells, comparison rel. to resistance to 1.5 MeV electron irrad., majority carrier trapping 80−94087
Si:Sb, in solar cell struct., heavily doped, dopant striation, SEM 79−39312
Si:Ti substrate for epitaxial solar cells 80−61341
a-Si/ITO, p-i-n heteroface solar cell, device physics and design 80−101113
Si/Si-Ge alloy, amorphous multijunction structure, increased conversion efficiencies, low cost 80−45677
Si-Au Schottky barrier solar cell fabrication, doping of a-Si 80−50969
Si-C interface on polycryst. Si ribbon, effect on solar cell efficienty *(French)* 80−54531
Si-F-H amorphous solar cells, DC glow discharge fabrication 80−72041
Si-Ge, amorphous, tandem multiple gap 80−94029
a-Si-H sputtered solar cells, temp. depend. of Schottky barrier characts. 80−45669
p-Si-$In_{2-x}Sn_xO_{3-y}$ solar cells, thermal degradation mechanisms 80−55841
Si-$In_{2-x}Sn_xO_{3-y}$ SIS heterostructure solar cells, spray-deposited 80−101106
Si-In_2O_3:Sn heterojunctions 78−64107
Si-ion-ceramic, short-circuit current density meas. using light-beam-induced-current tech. 80−93887
Si-Pd_2Si, Schottky barrier, resistivity, elec. characts. 78−14825
Si-PtSi, Schottky barrier, resistivity, elec. characts. 78−14825
Si-SiO_2 interface in MOS solar cells, operational characts. and struct. 80−93901
n-Si-SiO_2-SnO_x SIS solar cell, transport props., 14% efficiency realisation 80−94079
Si-TiO_x-Ni, MIS amorphous solar cell, increase in open-circuit voltage and short-circuit current on addition of TiO_x layer 79−57425
SiC particles in EFG ribbon solar cells, EBIC and ion microprobe anal. 80−93838
Si_xGe_{1-x} diffused p-n junction, electric and photoelectric props. 80−101095
SiH_x, amorphous, short circuit currrents and collection efficiencies 80−94028
SiH_x discharge produced amorphous film, gap state role in carrier transport 79−73608
SiN_x film reactive plasma deposition enhancement 77−77405
Si_3N_4 antireflection coating for solar cells, reactive plasma process for forming metal grid patterns 80−93990
SiO_2, reduction by RF induction plasma torch., Si form. 78−11186
SiO_2, thin films on rough polycryst. Si surfaces, oxide thickness and refractive index meas. 80−93422
SiO_2-Si inversion layer solar cells, radiation effects 77−43244
n-SnO_2 pigmented solar cell for electrolysis of water, two-photon process 80−93932
SnO_2:F films, elec. and optical props., solar energy conversion appl. 79−65945
SnO_2:Sb transparent conductive coatings for Cu_2S-CdS solar cells 79−61992
SnO_2/n-Si solar cells, fabrication and characterisation 79−79393
SnO_2/n-Si solar cells subjected to different weathering conditions, stability 79−52936
SnO_2/n-Si spray-deposited solar cells 80−12007
SnO_2/n^+-pSi heterojunction solar cells, fabrication by paint-on-diffusant method 80−94048
SnO_2-polySi solar cells, fabrication, grain size effects on device parameters 80−94045
SnO_2-Si, electron-beam-deposited, fabrication, angle-of-incidence effects 79−52931
SnO_2-Si, heterojunction solar cells, anomalous photocurrent 80−3515
SnO_2-Si, solar cell, max. theoretical efficiency 79−83598
SnO_2-Si heterojunction solar cell, elec. props. *(Korean)* 80−45665
SnO_2-Si heterojunctions, elec. and photovoltaic props. 80−26141
SnO_2-Si solar cells, electron-beam deposited, struct., photovolt. props. 80−50956
SnO_2-Si solar cells, stability and degradation mechanisms 80−16806
SnO_2-SiO_2-n-Si heterojunction, cheap solar elements for ground-based appls. 80−40860
$SrTiO_3$, photoanode water photoelectrolysis at high current density 78−15679
$SrTiO_3$, transition metal doped anodes for water photoelectrolysis, response to visible and UV 79−74531
TiN layers investigation for solar-cell contacts 80−81461
n-TiO_2 electrode, near UV photon efficiency, H_2 prod. from solar energy 77−11956
TiO_2 films as solar photocatalysts, preparation 79−74530
n-TiO_2 photoanode, band bending at surface used to dissociate water under solar illumination 78−91765
TiO_2 photoanode, water photoelectrolysis at high current density 78−15679
n-TiO_2, rutile anode, water photolysis 78−2563
TiO_2, transition metal doped anodes for water photoelectrolysis, response to visible and UV 79−74531
TiO_2:Al(Y), polycrystalline photoanode, improved solar efficiency 79−96479
TiO_2-covered solar cell electrode, photoelectrolysis of water 77−1928
TiO_2-Si solar cell hybrid electrodes for photoelectrochem. H prod. 80−45775
WSe_2 d-band semicond., photoelectrochem. props., electrochem. solar cell appl. 79−66411
n-WSe_2 electrode in aq. iodide medium, high efficiency photoelectrochemical solar cell 80−72069
$Zn_xCd_{1-x}S$ film, prep. and use as heterojunction optical energy converters 79−95488
$Zn_xCd_{1-x}S$, film, single-thermal-source form. 80−2492
$Zn_xCd_{1-x}S$/Cu_2S heterojunction solar cells, fabrication and performance 79−79397
$Zn_xCd_{1-x}S$/Cu_2S heterojunction solar cells, junction anal. 79−92080
$Zn_xCd_{1-x}S$/Cu_xS, prep. by soln. spray method and characts. 78−52666
$Zn_xCd_{1-x}S$/GaAs heterojunction solar cells, meas. of minority carrier diffusion length 80−26158
$Zn_xCd_{1-x}S$-Cu_2S heterojunction solar cells, props., comp. meas. of interfacial region 80−81472
$Zn_xCd_{1-x}S$-Cu_yS, nonseries resistance limited, open circuit voltage 77−8208
ZnO, aqueous-deposited films, struct. and electronic props. for solar cell appls. 80−100797
solar cells continued
ZnO, film for solar cell appl. structural, optical and elec. props. 80−2294
ZnO sintered electrode, for dye-sensitised solar photocell 80−16816
ZnO transparent films for conductor-insulator-semiconductor (CIS) solar cells 80−93947
ZnO-Cu_2O heterojunction solar cells, prop. by RF sputtering 80−93945
ZnO-electrolyte interface, electron transfer sensitisation by salt additions 78−34894
ZnO-Ti transparent type MIS solar cells 80−45662
Zn_3P_2 large crystal growth, vapour transport perforated capsule technique, prototype solar cell appls. 80−93464
Zn_3P_2 Schottky diode 79−7839
Zn_3P_2, single crystal, growth, electronic and device props. 80−25551
Zn_3P_2 thin polycrystalline films for solar photovoltaic cells 80−97797

solar chromosphere *see chromosphere*

solar composition
abundance data for 67 elements 77−53542
chromosphere-corona transition region, diffusion effects on comp. 80−46525
D abundance from SSO spectrograms 79−66982
dirty solar models, effects of surface contamination by accretion from interstellar medium 79−44436
element abundance, atomic and mol. f-values 78−20792
element relative abundance, review 78−20793
gas diffusion into mag. tubes, lack of chem. separation 79−75184
He abundance in solar wind, evidence for chemical separation by diffusion 80−77381
heavy elements accretion periods from supernovae explosions rel. to terrestrial ice ages *(Polish)* 79−58310
initial chemical comp. discontinuity and non-radial oscills. 80−82341
interior, Fe segregation from H, ionic mixtures phase separation theory 80−77279
metal abundance and spectral type, rel. to H-R diagram appl. 78−81619
metallicity and UBV colours from spectral quantification 78−65577
metallicity meas., chromospheric activity effects 79−53784
molecular line haze opacity in sunspots 79−75188
photosphere, abundances of elements Na to Ca 78−49411
photosphere, C, N, O, abundances 78−24497
quiet corona, O/N abundance ratio from highly ionised O and N X-ray spectrum 78−45297
spectroscopic differences between solar-type cluster stars and Sun 78−36560
sunspots, alkaline earth and rare earth oxides occurrence 78−85933
surface contamination with heavy elements by accretion 77−74029
Be abundance calcs., effect of misidentification of Be I 2650 Å line 80−32636
C abundance, meas. from CO first overtone vibr.-rot. transitions 79−8889
C, radiative lifetimes of visible and near IR transitions, solar abundance 78−50506
CH, CH^+ lines in facula models, equivalent widths 79−66972
CNO, abundances rel. to Si in different solar regions 80−46518
CO IR spectrum rel. to atm. struct. and C abundance 78−28608
Cr I in photospheric spectra, solar abundance and oscillator strengths 78−69757
Fe abundance determ., Fe II oscillator strengths and choice of model atmosphere 80−56791
Fe abundance in photosphere, determ. from weak Fe I Fraunhofer lines *(Russian)* 80−12720
Fe, conc. in solar interior rel. to coalescence in centre of Sun 80−77373
Fe group elements, abundances from corrected absolute oscillator strengths 77−3310
Fe group elements abundances from singly-ionised lines 78−93189
Fe I in photosphere, line broadening, Smirnov Roueff pot. calcs. 80−98632
Fe I Kα fluorescence in solar flares, photospheric Fe abundance probe 79−75192
Fe limited solubility in central Fe-H plasma 78−89149
Fe, solar abundance from 300 to 900 nm Fe I lines using precise oscillator strengths 79−40155
He abundance in solar quiescent prominences, theoretical models 78−49405
He abundance inferred from global oscills. obs. in spectra cosmology implications 80−51724
He content of solar models, implications for convective mixing length 80−26835
He diffusion, theory 77−56888
^{3}He-rich flares, plasma mechanism 79−5795
La, photospheric abundance, new lifetime meas. of La^+ 78−17618
Li, Be and B abundances, implications for hydrodynamical instabilities in envelope 78−93202
Mn abundance, Mn^+ oscillator strengths 78−17619
Mn abundance meas. by sun model 80−91501
MnI, transition probability and solar abundance, beam foil TOF meas. 79−40154
N, radiative lifetimes of visible and near IR transitions, solar abundance 78−50506
Ni I abundance in photosphere from oscillator strengh obs. 80−98625
O, diffusion effects on photospheric and outer atmosphere abundances 80−4318
O, radiative lifetimes of visible and near IR transitions, solar abundance 78−50506
O VI gas in corona, circumstellar or interstellar origin 78−57528
OH, continuum opacity in solar atmospheric model 79−40162
Pr abundance from Pr lines in photospheric spectrum 79−44443
S compounds presence or absence, theory 78−69765
SH presence in sunspot UV umbral spectrum 79−75186
SiO (A-X) system in sunspot UV umbral spectrum 79−75187
Sm II, photospheric abundance, spectral transition probability, 3000-7000 Å 79−31453
Ti, abundance from recent Ti I oscillator strengths 78−45306
TiH in sunspot spectra, possibility 79−48789
TiO in sunspots, equiv. width meas. theoretical interpretation, line form. process 80−72902
Y I, Y II, lifetimes of excited states, rel. to solar abundance determ. 78−86815

solar composition continued
Zn, photospheric abundance, discrepancy with meteorite abundance 80−72897
Zr I, lifetimes of excited states, rel. to solar abundance determ. 78−86815

solar constant *see solar radiation*

solar corona
5 min oscillation, possible heating mechanism for chromosphere and corona 77−17519
1973, June 30 total eclipse, photographic photometry of K- and F-corona 78−89140
1973 June 30 eclipse, white light polarisation 78−20786
5303 Å emission line, photoelectric meas. by automatic coronal photometer 79−12454
abundances from X-ray obs. 77−56887
acoustic wave refl. in transition region 80−36607
active region, differential emission measure exponential depend. on temp. and struct. 78−53917
active region coronal loops, temp. and density struct. 79−8890
active region loops, gyroresonance absorption evidence 80−56792
active region surges and coronal heating, Skylab X-ray images examination 78−12190
active regions, anal. of soft X-ray photographs taken with Fresnel zone plates 78−77538
active regions, coronal and transition region temp. struct. 80−67692
active regions, currents sheets as heating source 78−28634
active regions, imaging with Fresnel zone plates 78−49342
active regions, open mag. fields 78−28631
active regions, soft X-ray and cm wavelength obs. 79−44431
active regions height struct., X-ray obs., OSO-8 limb crossing obs. 80−31280
active regions on solar limb, 1175 to 1940 Å emission-line spectra 78−96446
activity, coronal index, for 1971-76 period 80−4322
activity, effect on radar meteor rate 80−67662
activity complex development, Skylab soft X-ray obs. 78−12191
adiabatic flow in coronal loops 80−56803
Alfven and magnetoacoustic wave mode coupling in solar corona, cold plasma approx. 78−12178
Alfven waves, finite amplitude circularly polarised, instability 78−28502
Alfven waves above sunspots from forbidden line obs. 77−78732
analytical description of structure of an active region 77−17533
ancient Chinese observations of physical phenomena attending solar eclipses 80−72916
arch system, long-lived, X-ray obs. 77−71091
aureole photographs, 309 to 640 nm, validity of aerosol single scatt. 77−5448
autoionisation rate coefficients for coronal ions 78−17623
autoionisation rate coeffs. for quadruply and quintuply ionised atoms 78−74619
background corona near solar minimum, Skylab obs. 78−28616
Bernstein waves, coherent nonlinear interaction rel. to type IV continuum bursts 77−53529
bipolar magnetic region, physical conditions 78−77534
bright points, soft X-ray images 77−53557
brightness, correl. with solar activity long-period vars. *(French)* 78−73695
brightness, eleven-year cycle correl. with Gegenschein and relation of Danjon *(French)* 79−96968
brightness and polarisation obs. at 1968 September 22 eclipse *(Chinese)* 77−22154
chemical abundances, relative, in coronal hole and other solar regions 80−46518
chromosphere-corona transition region, diffusion effects on comp. 80−46525
chromosphere-corona transition region, EUV models 78−69767
chromosphere-corona transition region, interpretation of C III and O V emission line ratios 78−28598
chromosphere-corona transition region, mass motions in impulsive flarelike brightenings, OSO-8 obs. 79−35217
chromosphere-corona transition region, nonequilib. plasma density diagnostics via C III EUV Lines 78−53899
chromosphere-corona transition region, optically thin lines, OSO-8 obs. 77−9729
chromosphere-corona transition region, OSO-8 obs. of wave propag. 78−93183
chromosphere-corona transition region, persistent vel. fields, OSO-8 obs. 77−9730
chromosphere-corona transition zone, dynamics over sunspot, OSO-8 obs. 77−9728
chromosphere-corona transition zone of solar active regions, non-thermal velocities *(French)* 80−77371
collisionless conduction front production by rapid coronal heating rel. to hard X-ray bursts 79−44427
collisionless deceleration of fast electron streams rel. to type IIIb radio bursts 77−71096
colours during solar eclipse and dust composition 80−51730
compact and diffuse white-light clouds rel. to 1971 Dec. 14 type II-IV radio bursts 77−22193
conduction cooling of flare loops, magnetic structure effects 79−44451
confinement of hot electrons, hard X-ray production 79−96982
convective noise waves, dissipation in mag. struct. rel. to coronal heating 78−65600
cool corona pressure and energy balance over sunspots 77−13291
coronal hole, birth, Skylab, soft X-ray obs. 78−7967
coronal hole, differential rot. of assoc. photospheric mag. fields 77−22167
coronal hole, physical parameters defining changing struct. 78−20770
coronal hole boundary brightness in Fe XV 284 Å radiation 79−84775
coronal hole obs. at 85 GHz 77−17521
coronal holes, energy balance in overlying solar atmosphere 79−92746
coronal holes, locations, sizes and evolution during June 1973 to January 1974, EUV obs. 77−56893
coronal holes, mag. fields correl. with interplanetary mag. field structs. between 0.3 and 1 a.u. 79−25429
coronal holes, radio and EUV meas. of temp. distrib. and electron density *(Russian)* 78−16378
coronal holes, rel. to solar sources of interplanetary mag. field and solar wind 77−45275

solar corona continued
coronal holes, search for correl. with transient cosmic ray intensity vars. 78−89022
coronal holes and high-speed wind streams 78−12187
coronal holes boundary positions, 1973, May 28 to November 21, atlas 77−2349
coronal holes rel. to solar wind streams and assoc. recurrent geomag. disturbances 77−17522
coronal transient, broadband polarimetry obs., importance of Hα emission 77−2389
cosmic ray particles, origin, nature and effects, interplanetary propag., review *(Russian)* 79−66893
cosmic ray particles from E45° flare, 1973, July 29, coronal and interplanetary propag. 77−82090
cosmic ray particles motion in coronal magnetic field 79−75196
cosmic ray particles with energy below 10 MeV, propag. and acceleration 78−49246
cosmic rays, rigidity-independent propag., bird cage model 78−77443
cosmic rays with relativistic energy, review 80−56798
cosmic-ray modulation by coronal holes, during solar cycle 80−94661
current instability and mag. fields for origin and energy supply to flares 80−101571
current-free magnetic fields in active corona *(French)* 77−45388
decametric noise storms and coronal irregularities, microscopic spectral features 77−45392
decametric obs. at high resolution 80−31288
dense non-potential magnetic flux tubes, radio and soft X-ray evidence 78−28615
density structures and type III radio bursts 78−77544
dielectronic recombination 77−36751
dielectronic recombination and resonances in excitation cross sections 78−62915
dielectronic recombination rates, ionization equilib. and radiative energy loss rates for Ne, Mg, S ions in low density plasma 79−68903
digital image enhancement 78−81556
diverging coronal field effects on solar wind expansion 77−45377
downflow in supergranulation network rel. to transition region models 78−61838
drift pair radio burst, MHD theory 79−25558
drifting radio bursts, 400-500 MHz, prod. mechanism, shock wave interactions 79−53790
dust particles thermal emission, lab. expt. of Fe flakes tribothermoluminesc. 78−68570
dynamical props. from line intensities and widths of EUV forbidden lines 79−35213
eclipse obs., external occulting disc as radially-graded neutral density filter in photograph 79−80233
electric current systems development in active regions, rel. to filaments and flares 79−25567
electric currents in coronal loops and rays, as solar wind energy source 80−94768
electron beam dynamics in plasma 77−78759
electron burst relaxation in fluctuating plasma, formal dynamical model 78−83579
electron densities, from density-sensitive line ratios in N I isoelectronic sequence 79−16906
electron densities in coronal streamers, K-coronameter meas. 78−4182
electron density distrib. during solar minimum, Helios 2 expt. 80−101578
electron density distrib. from Fe XIV 5303 Å line intensity obs. 78−61843
electron density distrib. models rel. to shock wave propag. 78−16375
electron density profile from Mariner 6 and 7 time delay meas. 77−33435
electron plasma oscillations assoc. with type III radio bursts 77−37592
electron streams, three dimensional Langmuir wave instabilities rel. to type III radio bursts 77−2404
electron traps oscillations from hard X-ray data 77−17526
electrostatic ion-cyclotron heating, in coronal mag. loops 80−51708
emission line at 5303 Å rel. to activity in 20th cycle 79−66985
emission line spectrum 13.3 to 13.8 Å 77−45389
emission line strengths, computer program 77−64715
emission lines, form. in shock heated solar atmosphere 77−56889
energetic particle event history prediction using real-time particle and solar wind measurements 79−58204
energy storage, importance of photospheric mag. field, solar flare model 80−72906
equatorial K-corona radiance, temporal evolution 78−28618
eruptive prominences, assoc. coronal brightness and structure changes 80−4337
eruptive prominences, coronal manifestations, theory 80−4338
eruptive prominences and coronal transients 80−56809
EUV and radio emission from chromosphere-corona transition 79−8894
EUV composite spectra of representative solar features, obs. 78−96447
EUV emission from B-like ions, density sensitivity 79−16910
EUV holes, rot. charact. from Fe XV 284 Å spectroheliograms 77−53547
expanding arch, assoc. with pulsating struct. in moving type IV burst 79−40171
expanding coronal mag. bottle, cosmic ray accel. 80−77244
expanding loop system, long decay X-ray event 80−90402
expansion, effects of radiation heat flux 80−90377
expansion, solar wind accel. by Alfven wave flux from Sun 80−85923
expansion, steady three-fluid model for nonspherical geometries 78−57533
external occulting disc, coronograph, scattered light reduction 78−36455
F corona, radial vel. obs. at 1979 February 26 solar eclipse 80−85914
F-corona, inner, circumstellar dust cloud, model and composition 80−82162
Faraday rotation, helios 1 occultation expt. results 78−20790
Faraday rotation during PSR 0525+21 occultation 80−46526
fast drifting solar radio bursts with short decay times 77−17534
fast electrons stream, free dispersal in solar corona with nonsteady injection 80−17568
fast waves, evanescence 78−89147
Fe IX forbidden transitions, density depend. 79−66986
filament eruptions and nonflaring coronal transients assoc. with nonthermal electrons 78−65595
filament transition sheath, study from radio obs. 78−28619
filament-corona transition region, OSO-VI EUV obs. 78−28620
fine chromospheric structs. in corona, Hα obs. *(French)* 78−28607

solar corona continued
five-minute oscillations, influence of chromosphere and corona 77−91501
flare, 1973 June 15, Hα, magnetic and X-ray morphology 78−4173
flare, 1973 June 15, Skylab XUV spectra, intersystem and forbidden transitions 78−4159
flare, 1973 September 5, theoretical model for fast-mode MHD shock wave 79−92734
flare continuum events, m wavelength obs., emission mechanism 79−21248
flare cosmic ray particles, propag. model 77−2313
flare loops, mag. field config. influence on conducton cooling rate 77−17528
flare model based upon photospheric dynamo action 80−62102
flare models, high-temp. and low-temp. comparison 80−12714
flare plasma, evaporative cooling 78−40890
flare plasma nonequilibrium ionization and emergent X-ray spectrum 78−7953
flare-generated shock waves during 1972 August 79−16916
flare-like events, soft X-ray data from Skylab 78−61827
flare-produced electrons, rel. to onset and sudden reductions of type IV decimetre bursts 77−2400
flare-produced energetic particles of September and November, 1977, coronal escape time 78−77446
flare/surge events, hydrodynamic simulation 80−12748
flares, plasma heating by energetic nonthermal electrons, theory 77−53505
flares, radiative, mechanical and mag. energy release 79−53797
flares energy release and transfer, Skylab X-ray obs. 77−82208
flares of August 1972, dynamics and coronal responses 77−25992
flow in relation to solar wind long-term vars., Imp 6, 7 and 8 results 78−77452
forbidden Fe X and Ni XII line identifications 77−53511
forbidden lines in 975-3000 Å range, Skylab obs. 77−60734
force-free fields, exterior source surface 78−28600
force-free magnetic field calc. with constant α, exact Green's function method 77−33438
forerunners, outer rims of coronal transients 79−25583
general magnetic field evolution rel. to solar cycle 77−71087
global coronal magnetic field reorientation due to differential rotation 77−53515
global-scale 3-D reconstruction 80−56719
green line, polarisation obs. at 1973 June 30 total eclipse 79−66969
green-to-red line intensity ratio, improved formula 77−2391
gyro-synchrotron maser possibilities 79−48756
Hα post-flare loops dynamics, 1973 July 29 flare 80−31286
hard X-ray event, 1971, December 14, obs. 78−93177
He I, He II, XUV emission lines, intensities and gross centre-to-limb behaviour 78−40888
heating, by ion acoustic waves 78−4181
heating, dissipation of elec. currents or MHD surface waves 79−75180
heating by Alfven waves 77−29785
heating by fast. electron streams theory 80−105228
heating by sound waves 79−21246
heating mechanisms, mag. field scaling props. 80−85913
heavy ions in solar wind from flare-heated coronal plasma 79−75197
Helios 1 and 2 occultations, S-band time delay meas. 78−20791
hole, obs. with λ 8-cm radioheliograph 80−4326
hole, radio and EUV obs. 77−78753
hole boundaries, evaluation from He I IR obs. 80−72919
hole boundaries short term evolution 78−61844
hole evoluation rel. to solar activity 79−25582
hole evolution by sudden large scale changes 78−40910
hole in northern polar region, simulation, MHD eqns. 78−4168
hole model 80−8606
hole region dynamics, steady polytropic flows with multiple critical points 77−17510
hole structure from UV and radio obs. 77−53513
holes, Arecibo obs. at 11.5 and 21 cm wavelength 78−61834
holes, as sources of solar wind 77−2394
holes, dynamical model based on radio obs. 77−87359
holes, EUV and radio spectrum 80−56802
holes, hydrostatic and dynamic models 78−4167
holes, identification from 9.1 cm synoptic charts 80−98633
holes, limb brightening data anal. for EUV lines in chromosphere-corona region 80−82333
holes, link with auroral activity, 1972-1977 equatorial latitude 80−98499
holes, mag. fields rel. to interplanetary fields and flows between 1 and 0.3 AU 79−29963
holes, MHD soln. of interplanetary disturbances generated by solar wind vel. perturbations 77−29615
holes, modulation effect on cosmic ray intensity, review 80−77370
holes, nature of underlying photospheric mag. fields 78−28613
holes, obs. in Fe XIV 5303 Å line, assoc. with recurrent geomag. disturbances 79−16762
holes, rel. to large-scale solar mag. field 77−64713
holes, relation to solar mag. fields 79−58312
holes, solar wind streams and geomag. activity during 1976-77 period 79−25570
holes, temp. decrease, plasma density effect on wave absorpt. *(Russian)* 80−77374
holes, visibility at 408 MHz 80−85922
holes and arches, brightness temps. at 169 and 408 MHz rel. to UV obs. 79−8893
holes and assoc. solar wind, sunspot cycle 20 survey 78−40911
holes and large-scale structures, plasma parameters from soft X-ray obs. 78−4161
holes and quiet regions, differences 77−53514
holes physical structure, influence of mag. fields and coronal heating 80−46520
holes rel. to magnetic fields and model of formation in solar cycle 78−40909
horizontal temperature gradient in prominence/corona transition zone, meas. rel. to prominence condensation 80−26832
hot coronal regions, rel. to solar wind flows associated with hot heavy ions 80−51635
hydromagnetic surface waves, dissipation 80−21904
image enhancement by digital processing 79−25516
inhomogeneous model, for interpretation of data on quiet Sun mm wavelength emission 79−35231
inner corona polarization meas. at 1972 July 10 eclipse 77−82197

solar corona continued
interchange instability, rel. to heating and reconnection magnetic flux tubes emergence 77−56894
interconnecting loops transient brightenings, sudden brightenings morphology 80−21972
interplanetary dust and electrons spatial distrib. round Sun, contrib. to corona 80−46514
ion dynamics and abundance in coronal holes 80−41807
ion-acoustically turbulent plasma, cond., solar corona appl. 79−19027
ionisation of prominence material 80−101520
ionisation states of energetic C and O emitted by the Sun 77−49249
ions, proton excitation approximations, erratum and extension 79−35118
kink instability of loops and solar flares 80−41802
Langmuir turbulence over active regions, rel. to quasi-stable particle accel. and type I radio bursts *(Chinese)* 80−105220
Langmuir wave emission, spectra rel. to electron distribs. 78−57515
Langmuir waves, direct collapse, rel.to type III radio burst problem 78−79430
large scale magnetic field determ. from radiosource rotation meas. *(Russian)* 78−32433
latitude-dependent activity, long-term correl. with solar wind streams 78−93172
limb brightening, Abel-inverted intensities of Fe XIV and XIII EUV emission lines 77−13299
linear force-free fields in lower corona 78−40902
long distance arches, electron density from centimetric quiet Sun reinterpretation 78−28597
long-decay X-ray enhancements, physical parameters 79−44448
loop heating by fast mode MHD waves 80−41801
loop prominence knots, motions, Hα line filtergram obs. 80−67693
loop prominence system, flare assoc., high temp. corona 79−53782
loop prominences formation, kinematic model 78−7965
loop structures, temporal var., time-lapse sequence obs. 80−72909
loop transients, magnetic driving 78−61842
loop transients expansion and broadening, theoretical explanation 78−40887
loop type transients, mass flow 79−44450
loops, heating by Alfvenic surface waves reson. absorpt. 79−16905
loops, low beta model, kink instabilities 80−98636
loops, struct. 78−89155
loops, thermal instabilities in magnetically confined plasmas 80−36600
loops brightened by flares and transients, decay 78−40907
loops in an active region, physical props. XUV obs. 80−90376
loops stability, theory 79−101132
low corona, magnetic energy build-up 77−45391
low density structures and type III radio bursts 77−71095
low frequency turbulence rel. to type III radio bursts fundamental radiation 79−84778
m wavelength thermal radiation from coronal streamers and holes 77−60742
magnetic arcades and prominence formation 80−41800
magnetic arch, type III and type I-like decametric emission 78−12179
magnetic bottles, rel. to solar cosmic rays fast azimuthal transport 78−32305
magnetic energy storage in coronal active regions 77−17478
magnetic field, high resolution mapping 77−56892
magnetic field, one-dimensional, force-free, singular lines *(Russian)* 79−48670
magnetic field, potential, structs. assoc. with solar proton events and type I (metre wave) radio sources *(Chinese)* 80−105222
magnetic field, results from Crab nebula polarised radioemission occultation obs. *(Russian)* 78−77527
magnetic field above flocculus, determ. from radio obs. 80−98635
magnetic field and current sheets above active regions 77−78757
magnetic field determ., fixed mesh soln. to Laplace's eqn. 77−2392
magnetic field determ. from polarization by atomic fluorescence 77−25938
magnetic field determ. using type II burst obs. and theory 80−41785
magnetic field emergence from active region, assoc. radio burst 80−109412
magnetic field emergence rel. to metric radiobursts polarisation and location 78−61824
magnetic field evolution with solar cycle, rel. to solar wind streams and galactic cosmic ray vars. 78−7974
magnetic field geometry, influence on latit. depend. of solar wind speed 77−9732
magnetic field heterogeneities, rel. to fine struct. of type II radio burst 78−24501
Magnetic field model with non-spherical source surface 79−25577
magnetic field models, validity of Green's function solns. 80−21970
magnetic field of active corona, three-dimensional struct. modelling 77−67085
magnetic field strength above active regions 78−77533
magnetic field topology in coronal-interplanetary space 78−49273
magnetic fields, global constant-α force-free 78−85923
magnetic fields, interaction and energy release 77−17482
magnetic fields, Laplace's eqn. direct soln. using line-of-sight boundary conditions 80−12742
magnetic fields, non-force-free, in magnetohydrostatic equilib., anal. 79−92733
magnetic fields in coronal condensation obs. at 1968 September 22 eclipse *(Chinese)* 78−69762
magnetic fields in low corona, active role in solar flares 77−17474
magnetic fields in terms of thin flux tubes from photosphere, model 79−16922
magnetic fields of active regions, zero points 78−96465
magnetic flux tubes, vibration modes, general dispersion relation 80−94706
magnetic instability of coronal arcades as the origin of two-ribbon flares 80−72911
magnetic loops, downflows and convection, optical and EUV obs. 78−93175
magnetic loops, equilib. temp. and density struct. 79−92737
magnetic loops, struct., MHD stability theory 78−28632
magnetic loops, structure, equilib. theory 78−12192
magnetic reconnection and loop prominences 77−29765
magnetic struct. from solar wind energetic particles and interplanetary field osb. 77−71076
magnetic tearing instability, high cond. theory 77−7527
magnetic traps, EM loss-cone instability rel. to type IV radio emission *(Russian)* 78−77528

solar corona continued
magnetic traps, plasma instability periodical regimes *(Russian)* 80−8616
magnetic tube oscillations rel. to type IV radio emission pulsations, bounce-resonance effects 78−89161
mass ejection event, 1973 December 19, kinematics 78−28640
mass ejection events, outward vel., Skylab obs. 77−22197
mass ejection events, rel. to noncompressive density enhancements in solar wind 78−28479
mass ejection into interplanetary space 78−49417
mass ejection transients rel. to other solar activity 79−44457
mass flow and ionization equilib. 80−36608
massive slow-moving coronal transient, radio obs. 79−53796
Maunder Minimum, corona and solar wind state 79−75069
McMath region 13043, coronal mag. fields intensification rel. to centimetre-wave sources rapid var. 80−67688
meridional wind flow in midcorona, modelling 77−33452
metre-wave emission, wave ducting rel. to fundamental/harmonic source coincidence 80−21978
MHD fluctuations due to magnetosonic wave propag. in warm plasma 80−77275
MHD shock waves, propag. in solar atmosphere 78−24503
MHD wave generation and heating by prominence turbulence 80−72907
MHD waves, mode coupling, oblique incidence on stratified media 78−20775
MHD waves, mode coupling reduction of coupled eqns. 78−20776
MHD waves role in coronal heating and solar wind accel. 77−71098
microwave brightness temperatures and circular polarisations from thermal regions, derivation 77−22172
microwave radar observations 79−88635
minimum flux corona concept, appl. to quiet corona and coronal holes 78−81611
model development for chromosphere and transition zone *(Russian)* 77−64726
models, survey of last 30 years' research 78−69764
momentum and energy transport, by acoustic, Alfven and fast mode waves 78−4162
moving type IV burst at solar limb, three freq. obs. 78−69776
neutral sheet obs. during 1973 June 30 total eclipse 79−84757
north-south asymmetry from Fe XIV green line (1965-78) 80−77369
numerical model, temp. and density struct. 77−17456
observations and interpretation *(Italian)* 78−81604
observations with Solwind coronagraph 80−82325
occultation of Crab Nebula, obs. linear polarisation at 7.2 cm 77−60837
occultations of Crab Nebula, Faraday rot. obs., coronal electron density and mag. fields meas. 77−45593
open magnetic structures 78−4158
open magnetic structures evolution, Skylab obs. 78−16362
open magnetic structures rel. to solar wind flow 79−2459
open regions energy balance and solar wind generation *(Russian)* 79−21257
oscillations above active region, Fe XIV spectra obs. 80−41794
outer corona, temps. and temp. gradients from OSO-7 spectroheliograms 77−17506
particle distrib. functions following flares, radio evidence 79−48759
persistent streamer motions and mass changes 78−65594
plasma, heating by anomalous current dissipation 78−53895
plasma, inhomogeneous, electron flows stabilisation 80−109411
plasma, low-density, autoionisation contrib. to total ionisation rates 80−9738
plasma diagnostics using high-resolution spectroscopy, Skylab obs. of forbidden lines 78−14203
plasma diagnostics with broad-band X-ray imaging systems, physical parameter method 78−49414
plasma evolution during 1973 August 9 compact flare 79−5792
plasma flow along sheared magnetic arches, theory 80−62092
plasma heating during flares, ionisation and reverse currents 79−5793
plasma instabilities of trapped particles in magnetic fields 78−61823
plasma parameters in long-duration X-ray event, Skylab obs. 77−29741
plasma radiation, direct conversion of Langmuir waves into o-mode waves 80−72896
plasma radiowave fluctuations and turbulence, Venus 10 radio transmission expt. 79−80295
plasma turbulence triggering during fast flux emergence 78−45304
plasma waves conversion into transverse waves, rel to radio bursts 77−2414
polar coronal hole, EUV lines obs. anal. 79−5797
polar coronal hole, physical props. from 2 to 5 $R_\odot$ 77−45372
N.polar coronal hole at 1973 June 30 eclipse, density model 80−98627
polar coronal holes, rel. to solar cycles 80−21979
polar coronal holes rel. to galactic cosmic rays north-south gradient 78−89019
polar holes, electron density from EUV line intensity ratios 79−21245
polar holes, evolution from He I 1083 nm synoptic maps 80−56801
polar plume, X-ray anal. 79−12455
polar plumes, EUV anal. 78−4178
polar rays obs. during 1973 June 30 eclipse 77−17470
polarisation obs. at 1970 March 7 eclipse 77−33462
polarisation obs. at 1973 June 30 total eclipse *(French)* 77−74027
polarisation obs. during 1973 June 30 total eclipse 77−13313
potential magnetic fields 79−30041
pre-flare instability rel. to radio pulsations 78−53911
preflare characteristics of active regions observed in soft X-rays 79−84776
prominence interface, review 80−4333
prominence-corona interface compared with chromosphere-corona transition region 77−29786
prominences as corona condensing along mag. field lines 80−46524
properties rel. to solar wind origin *(Italian)* 78−81605
proton events and coronal mass ejections 78−77545
proton excitation of ions fine structure, approximations 77−17463
proton propag. at medium and high energies 77−53355
protons and α particles, rigidity-independent coronal propag. and escape 78−77444
quasi-static loops, numerical modelling with uniform energy input 80−21958
quiescent prominences, heating and cooling, calc. 80−12738
quiescent prominences, over sunspot umbrae, effects on Ca II H and K line profiles 77−22178
quiescent solar corona, dynamics 78−40885
quiet corona, X-ray spectrum of highly ionised O and N 78−45297
solar corona continued
quiet limb, emission measures, electron densities and nonthermal vels. from optically thin UV lines 77−17454
quiet Sun, scatt. effects on radio emission at freqs. <200 MHz 78−4183
radar signal reflection, efficiency of four-plasmon interactions 80−101582
radiative origins 78−96448
radiative transfer of X-rays, reson. scatt. 79−16904
radio bursts, type II and III theory *(Russian)* 78−16381
radio bursts of drifting pairs type, 25 and 12.5 MHz obs. rel. to coronal cyclotron instability 78−24502
radio emission, fluctuations 78−45311
radio emission, probability of occurrence of stable pulses 78−42737
radio emission, S-component local sources struct. 80−46528
radio obs. at Culgoora Observatory 79−48754
radio spectrograms, magnetoplasma, plasma wave motions *(Dutch)* 80−62101
radio wave propag. in inhomogeneous magnetic field *(Russian)* 78−16385
radiowave generation by gyrosynchrotron and Langmuir-wave processes, solar and stellar appl. 79−21172
red line, more precise wavelength *(Russian)* 78−40899
resistive diffusion of strong mag. field in tenuous conducting gas 77−78625
response to solar events, dynamic modelling 78−49418
restructurings, correl. with evolution of photospheric mag. field patterns 78−20798
reverse current in flares 78−16363
rotation, obs. methods 79−75179
rotation and lifetime of coronal features 79−75191
rotation investigation by spectroscopic method 77−53551
rotation rate depend. on solar cycle phase 77−87364
Saito density model, implications for polar solar wind flow and heavy ion abundances 77−37591
scattering process above active regions, propagation in fibrous medium 78−20780
second harmonic plasma emission polarization 78−65579
sheet-current approach to coronal-interplanetary space modelling 78−20807
SHF flux fluctuations from limited areas, rel. to coronal wave propag. 79−35222
shock wave deceleration in lower corona, numerical simulation 78−77449
shock wave dissipation 77−60740
shock waves and magnetic field above an active region 77−53512
shock waves during large solar flares, proton and electron accel. 80−21974
singular lines of one-dimensional force-free magnetic field 79−66920
Skylab obs. of quiet and active solar events 77−56891
Skylab photographic X-ray images, analysis 78−49341
Skylab X-ray obs. and mag. field correls., computer solns. 77−82198
soft X-ray bright points, lifetimes distrib. 77−17512
soft X-ray images from Skylab, atlas 79−21197
soft X-ray limb flares from Skylab 78−4164
soft X-ray obs., of large-scale coronal active region brightening 78−20806
solar wind, expansion in high-speed streams 78−45298
solar wind high velocity stream sources, high coronal struct. 77−53530
solar wind high-speed streams, outflow regions localisation on Sun 78−53919
sounding rocket expts., during 1979 February 26 total solar eclipse 79−58145
source regions of U-type bursts 78−77543
spectra, forbidden transition probabilities for ground terms of p or p^5 config. ions 77−2376
spectral line intensity ratio and temp. determ. 78−73697
spectral line profiles above active regions, statistical anal. 78−7968
spectral lines, 1175 to 1965 Å, identifications, wavelengths and intensities 79−25559
spectrum, intensity ratios of fine-struct. components of H like ions reson. lines 80−101581
spectrum, proton collisional excitation of fine struct. transitions of Ca^{14+}, Fe^{20+} and Ni^{14+} 77−19017
spicule radial velocities, and the coronal condensation mechanism of spicule formation 79−58314
spikes, obs. during 1973 June 30 eclipse, photometric anal. 77−17520
stability analysis of min. flux corona theory rel. to spicules 80−41795
stable loop, plasma physics model 77−45371
stereo radioastronomical obs. 78−49419
streamer dynamics, diffusive time scale 77−82196
streamer model based on STEREO-1 meas. of type III burst directivity 77−45382
streamers, rotational motions effects on spectral lines 78−49410
streamers and ribbon structures rel. to IMF three-dimens. structure 79−5778
streamers on image-enhanced photographs 79−16841
structure and activity, review 79−71014
structure at solar min., relation with high speed solar wind streams 77−78590
structure during 1976, October 23 eclipse, predictions v. obs. 77−25990
structure of lower corona and transition zone from Skylab NRL spectrograms 79−48744
structure prediction for 1976 October 23 eclipse 77−17471
submicron particles of solar origin 77−9727
subsonic flows, in coronal-interplanetary closed field lines regions 78−28624
supergranulation structure in coronal holes 80−51729
surge, EUV limb spectra obs. from Skylab 80−17560
surge producing short-lived filament 77−33458
temperature, determ. from spectrum of electron scatt. continuum 77−22169
temperature and coronal holes 79−2538
temperature and nonthermal motions in coronal hole, quiet and active regions 77−33449
temperature constraints in open mag. field regions 80−12744
temperature distribution 78−40908
temperature for equal green and red line intensities, improved value 77−22168
temperature gradients in inner corona 79−25576

solar corona continued
temperatures, temperature gradients and comps., from solar wind and electron densities 77−53525
thermal equilibrium of coronal loops 80−94773
thermal stability during fast mode wave heating 80−90397
thermally balanced quiescent prominence in magnetostatic equilib. in uniform gravit. field, self-consistent model 77−91509
thermally conductive flows in coronal holes, theory 78−28614
thermodynamic history of active region observed in X-rays 77−13303
trans-polar coronal hole, 1973, June 30, obs. 77−53526
transient, 1973 August 21, radio and white light obs. 79−71010
transient, 1973 June 10, numerical simulation, adiabatic response to perturbs. 77−78731
transient event, 1973 Sept. 14-15, material motions and mag. field 77 17529
transient onset, motion model 79−44449
transient phenomena, mass ejection mechanism 78−7980
transients, freq. rel. to solar activity indices 77−22181
transients, MHD, two-dimens. numerical solns. for model corona 78−20774
transients, MHD, two-dimens. plane anal. 78−20773
transients, MHD models, 1973 August 21 event simulation 79−35215
transients, MHD models in meridional plane, mag. field effect 79−5798
transients at high latitude, 1979 September 27 Solwind obs. 80−94774
transition region, Alfven wave reflection 77−29754
transition region, Bowen fluoresc. rel. to electron density determ. 78−93179
transition region, C V and O VII emission line ratios interpretation 80−98624
transition region, EUV line emission weakening short of 912 Å wavelength 80−21962
transition region, line intensities from Si VI, VIII and XII excitation calcs. 80−31273
transition region, origin for UV and radio fluctuations 80−90398
transition region, OSO 8 UV obs. of optically thick region 80−56788
transition region, theoretical network structure for coronal holes 80−85917
transition region, theoretical network structure for quiet Sun 80−85916
transition region and inner corona, temp. distrib. 79−75190
transition region in quiet Sun, evidence for overlying EUV continuous absorpt. 79−92738
transition zone, area var. of supergranule network features with temp. 78−89152
transition zone, density diagnostics for EUV spectrum 77−60739
transition zone, nonresonant heating mechanism *(Chinese)* 80−85921
transition zone, nonthermal effects assoc. with steep temp. gradients 79−84771
transition zone, search for turbulent free region 78−4174
transition zone, Si IV line profile vars., rel. to MHD disturbances 78−28626
transition zone and corona, heating 77−29766
transition zone dynamics 79−21247
transition zone instabilities rel. to preflare energy build-up, spectroscopic far UV obs. 77−17479
transition zone lines, quiet Sun, limb broadening, OSO-8 obs. 79−48752
transition-zone plasmas, electron densities and mass motions in flares 80−56804
turbulent heating role 80−12715
type I and III m wavelength bursts source heights meas. 77−33460
type I radio bursts, centre to limb vars. 77−87356
type II radio burst source region, coronal mag. struct. 78−69775
type II radio burst with reverse freq. drift against noise storm background, obs. 80−17567
type II radio bursts, fast electron tails form. 77−33439
type II radio bursts rel. to flares Hα line intensity peak 79−21252
type II radio emission prod. by coronal MHD shocks 79−92750
type III and type IV bursts from source above solar limb, heliograph obs. 79−53798
type III burst producing active region, Skylab obs. of overlying coronal struct. 80−21976
type III radio bursts, deconvolution and decay mechanism 77−45381
type III radio bursts caused by high-density electron beam, numerical simulation 79−84779
type III radio emission, head-on approximation in second harmonic plasma emission 79−41803
type III-V radio bursts, prod. by fast electrons from hard X-ray bursts 78−89157
type U radio bursts, polarisation evolution 80−26834
type V radio bursts, scatt. hypothesis 77−45378
unidentified forbidden coronal lines, emission rates for Fe X and Fe XI transitions 77−17465
UV and soft X-ray full-disc solar fluxes, rocket obs. 77−87360
UV line intensities brightness fluctuations during shock wave passage 79−66990
velocity fields, periodic oscillations, Fe XIV 5303 A line obs. 77−49362
Viking radio occultation obs. at 1976 Mars solar conjunction 78−20789
Voyager 2 occultation, 1979 August, radio signals ang. and spectral broadening 80−51639
Voyager radio science experiment 78−24430
wave reflection and wave disorder, in solar transition zone and corona 79−12453
white light intensity, rel. to solar wind latit. and longit. struct. 79−40049
white light transients rel. to type III bursts 79−48758
wind, acceleration kinetics 77−33447
X-ray active regions temp. and emission measure rel. to coronal mag. fields 80−12745
X-ray and XUV emitting structures, changes rel. to mag. reconnection 78−28635
X-ray bright corona above active region McMath 12628, struct. rel. to solar atmosphere equilibria 78−53902
X-ray bright point and small active region fine struct. rapid vars. 80−12741
X-ray bright point emergence patterns spatial and temporal vars. 77−29782
X-ray bright points, mag. flux emergence regions, var. out of phase with solar cycle 77−56890
X-ray bright points, obs. rel. to globally variability in solar mag. flux emergence 80−51716
X-ray bright points anticorrel. with sunspot number, 1970-78 period 79−53789
X-ray burst, impulsive, from coronal source, obs. 80−26836
solar corona continued
X-ray bursts, thermal models 80−94766
X-ray corona, slowly moving disturbances 80−21971
X-ray coronal arch expansion into outer corona 77−22196
X-ray coronal cavities, prominence-related, config. and dynamics 79−25565
X-ray emission, correl. with metre-wave radio bursts 78−69774
X-ray emission, obs. by S056 X-ray telescope expt. on Skylab Apollo Telescope Mount 77−60596
X-ray emission from optically thin plasmas, abundance effects on continuum spectrum 78−53814
X-ray emitting active region, early evolution 78−28621
X-ray emitting coronal loops, obs. evidence of continual heating 78−61841
X-ray enhancements assoc. with Hα filament disappearances 77−22184
X-ray holes, radio obs. rel. to quiet radio Sun at 2800 MHz 78−20805
X-ray observations, using rocket-borne real-time imagining system 80−41725
X-ray photographs, anal. and interpretation 78−4179
X-ray photographs anal. and interpretation, filter ratio method 79−40086
X-ray spectra, calibration and resolution of Leicester Bragg spectrometer 77−5442
X-ray temperature-emission measure modelling of corona 80−12746
X-ray transients rel. to hole evolution 79−12459
XUV emission lines, appl. tq coronal Fe abundances and temps. determ. 78−4180
C I isoelectronic sequence, forbidden transitions calc. 79−31444
C-like ions emission lines, density depend. 80−21963
Ca II K-line network in coronal holes 77−78752
Ca XV III, line identification in corona radiation 77−79569
Fe IX, Fe X, Ni XI, Ni XII, forbidden transitions 78−77537
Fe IX lines, appl. as coronal plasmas density indicators 79−44429
Fe IX radiative and collisional data rel. to coronal emission spectrum 77−49350
Fe XII spectrum, excitation 77−17458
Fe XIII emission line polarization from mag. sublevels statistical equilib. 77−53492
Fe XIII emission line polarisation, near IR polarimeter obs. 78−61740
Fe XIII forbidden emission lines, Si vidicon spectrometer obs. at 1973 June 30 eclipse 77−9657
Fe XIII IR lines, polarisation degree calc. 77−45373
Fe XIV, 5303 Å emission line polarisation obs. during 1973, June 30 eclipse 77−49352
Fe XIV 5303 Å emission line polarisation, coronal mag. field determ. *(Russian)* 78−16389
Fe XIV coronal depletion, 1976, April 20, photoelectric obs. 78−28617
Fe XIV emission line intensity and profile, temporal variations 77−29767
Fe XV EUV line intensities 80−51731
Fe XVIII X-ray emission lines, obs. and anal. 78−36542
Fe XXIV, line identification in corona radiation 77−79569
Fe^{11+}, proton collisional excitation in ground configuration 78−33582
Fe^{12+}, forbidden lines collisional excitation, importance of short-range pot. 77−17457
H Balmer emission lines, Skylab obs. of quiet Sun and polar coronal hole 77−33440
H Balmer emission lines, Skylab obs. of active regions 77−33441
He I, He II XUV emission lines, intensity ratios and distrib. functions 78−57516
He^{+} 304 Å radiation, theory 77−91510
He-like ions, X-ray spectra from laser plasma, comparison with solar corona 78−17596
Li, Be, B, isoelectronic sequences, ionization equilib. balance, solar and stellar atms. appl. 79−36587
Mg II UV lines obs. above solar limb from Skylab 77−33450
Mg, isoelectronic series, D-F transitions, Mg sequence, D-F transitions oscillator strengths 79−54809
N II, electron impact excitation cross sections, rel. to solar corona abundance 80−58391
N IV and Ne VII emission line ratios, electron density and temp. determ. 80−17559
N isoelectronic sequence ions, level populations and EUV line intensities for solar coronal conditions 80−51649
Ne VIII, electron impact excitation 77−537
Ni IX to Ni XII transitions, laboratory wavelengths and identifications in solar spectrum 80−99474
Ni XIX spectrum from coronal active regions X-ray spectra 77−2390
Ni XVII EUV line intensities 80−51731
O I isoelectronic sequence, excited level populations, line intensity ratios, solar corona appl. 80−32637
O III, electron impact excitation of semi-forbidden transitions in coronal holes 80−48092
O VI gas, circumstellar or interstellar origin 78−57528
O VII line intensity ratios depend. on temp. and ionization balance 79−16903
S IV observations from Skylab 80−87028
Si, dielectronic recomb. and ionization equilib., autoionization and excitation influence 78−1077
Si IV, 1393 Å line in coronal hole and quiet Sun, OSO-8 obs. 77−91511

solar corpuscular radiation *see solar wind*

solar corpuscular streams *see solar wind*

solar cosmic ray particles
11 year cosmic-ray cycle, galactic and sdlar protons anal. 77−53360
1972, August, low energy cosmic rays obs. 77−25895
1972, August cosmic ray storm, north-south anisotropies and related phenomena 78−89018
1977, September 24 and November 22, anal. of energetic particle events following solar flares 78−77446
α-particles, heating and acceleration 79−12376
accelerated nuclei from C to Fe from 20-300 MeV/nucleon 79−5802
accelerated particles escape into interplanetary space, influence of solar mag. fields 79−62807
acceleration and coronal propag. of particles below 10 MeV 78−49246
acceleration in expanding coronal mag. bottle 80−77244
acceleration in flares, power law spectrum 78−57525
acceleration in flares, X-ray and gamma-ray obs. 80−31265
acceleration into interplanetary medium during 1972, August 4 flare *(Russian)* 77−33303

solar cosmic ray particles continued
alpha-particles and protons streaming velocities relative magnitude at 1 AU 77−9643
alpha-particles in recurrent particle streams at 1 AU 79−96867
anisotropy observations, rel. to interplanetary medium characts. 77−60553
anomalous flux anisotropy, 1973 September probe meas. 77−33300
axion, astrophysical limitations on mass *(Russian)* 78−61835
bidirectional anisotropies in proton and electron events rel. to magnetic bottles 78−40778
Brookhaven experiment sensitivity to solar neutrinos, collapsing stars and cosmic neutrinos, ^{37}Cl neutrino absorpt. cross-sections 78−4929
Brookhaven solar neutrino experiment, results and solar model calcs., new solar ν-detectors 79−80286
charged-particle scatt. in interplanetary mag. field, cosmic-ray fluctuations 77−53352
complex solar particle event, 1973, April 29-30, anal. 78−20593
composition and energy spectrum meas. using multilayer metal targets 77−53391
cooling of slow protons, Helios 1 expt. 79−2463
coronal and interplanetary propagation of solar particles following E45° solar flare on 29/7/73 78−49248
coronal electron traps oscillations from hard X-ray data 77−17526
coronal particle distrib. functions following flares, radio evidence 79−48759
corotating energetic particle streams, relative abundances 78−93065
corotating events energetic particles, comp. 79−25414
corpuscular streams, correl. with Earth troposphere instability 79−92580
Cosmos 555 and stratospheric balloon obs. during solar flare 77−53350
current density and diffusion coeff. for cosmic ray scatt. in interplanetary mag. fields 77−49247
cycle 20, flares and cosmic ray events at minimum 79−21250
determ. from ^{3}He meas. in lunar rocks 80−98576
diurnal anisotropy of intensity, solar flare location effect 79−44318
Earth high-latitude magnetosphere, cosmic ray fluxes forecasting via isotropic diffusion model 77−64531
electron acceleration to mildly relativistic energies by strong plasma turbulence 77−31437
electron diffusion mechanism in interplanetary medium 77−53349
electron events not assoc. with flares, ISEE 3 obs. 80−67683
electron flux and type III radio burst intensity at 1 AU 77−2407
electron fluxes rel. to increased geomag. activity and ionospheric absorpt. after flares 79−75175
electron heating within interaction zones of simple high-speed solar wind streams 79−25426
electron nonthermal props. rel. to solar wind kinetic instabilities 80−41691
electron plasma oscills. assoc. with type III solar radio bursts, heliocentric radial var. 79−2454
electron stream, nonrelativistic, propag. in solar atmosphere rel. to type III radio bursts 78−28623
electron streams, excitation of ionospheric radio noise 79−62646
electron streams, generation of spike-type radio bursts 79−35230
electron vars. across high-speed solar wind streams 79−25425
electrons, heating of interstellar gas flowing into interplanetary space 79−16881
electrons, meas. instrumentation on International Sun-Earth Explorer spacecraft 78−85786
electrons, stable confinement in type-I burst regions 79−80296
electrons, vel. distrib. at 1 AU, steady state theory 79−101041
electrons and protons, very low temps., statistical anal., origin 78−65477
electrons assoc. with type III radio bursts, interplanetary scatt. 77−2411
electrons in solar flares, energy disposition, indirect determ. 79−25581
electrons stream, free dispersal in solar corona with nonsteady injection 80−17568
energetic charged particles transport mode in mag. fluctuations superposed on diverging mean field 79−50848
energetic flare particles, interplanetary propag. model 78−65468
energetic particle composition temporal development during flares 78−89148
energetic particle diffusion coeff., HEOS-2 magnetometer data 78−96364
energetic particle event, 1973 April 29, mean free paths near Earth 78−89017
energetic particle event history prediction using real-time particle and solar wind measurements 79−58204
energetic particle event of 1974 July 4, Fe/O charge comp. spatial and temporal vars. 77−22199
energetic particle flares rel. to type II radio burst commencements 77−37590
energetic particles from flares, interplanetary shock waves 78−49276
energetic particles in solar flares 80−31266
energetic particles in stream-structured solar wind 80−41674
energetic particles intensity meas., 1973 Sept., by interplanetary probes 77−29604
energetic protons assoc. with forward-reverse shock pair at 1 AU 78−4052
energetic protons assoc. with interplanetary active regions at 1-5 AU 78−45176
energetic storm particle events, ^{4}He/H ratio vars., theory 77−9636
energetic storm particle events, correl. with interplanetary shock wave parameters 79−35079
energetic storm particle events connection with interplanetary shock wave parameters 79−70935
energy changes of cosmic rays in the interplanetary region 79−16773
energy transfer of injected particles to lower atm. by IR emission 79−53425
energy variation in interplanetary space 80−101505
event signatures rel. to propag. and acceleration processes 78−49244
fast azimuthal transport, by coronal mag. bottle 78−32305
fast electron tails formation in type II radio bursts 77−33439
fermion nonminimal gravitational coupling and the solar-neutrino problem 79−75761
first phase acceleration mechanisms in solar flares 80−31267
flare, 1972, August, 7, charged particles accel. 79−12360
flare, 1973 April 29, cosmic ray anisotropy, Cosmos 555 obs. 77−45268
flare, particle acceleration in turbulent current sheet 79−35232
flare, particles, intensity variations, depend on interplanetary mag. field and solar wind 80−77372
flare accelerated particles, charge spectrum and comp. form. 80−46529
solar cosmic ray particles continued
flare accelerated particles, nucl. composition and Coulomb losses 80−72913
flare cosmic rays, complete model of propag. 77−2313
flare electron events, Oct. 1972 to Dec. 1974 obs. 80−56796
flare electrons, peculiarity of ejection into interplanetary space *(Russian)* 78−77445
flare energetic particle abundances, Voyager obs. 80−90382
flare energetic particle events from same active region, p/α enhancement 79−40151
flare energetic particle events obs. at 1 to 6 AU, radial transport 77−70953
flare heating by corpuscular streams, X-ray, EUV and coronal lines emission *(Russian)* 77−71071
flare increase of cosmic ray intensity during 1977 November 22 ground level event 79−48629
flare particle events, exponential decay 78−4047
flare particle events, influence of interplanetary shocks 77−49250
flare particles, 1973, July 29, coronal and interplanetary propag. study 77−82090
flare particles, 1978, May 7, Bologna, obs. by ionising component supermonitor 78−85777
flare particles, multi-stage accel. rel. to type IV radio emission 79−44437
flare particles, prod. by mag. energy direct conversion to plasma kinetic energy *(Japanese)* 80−94775
flare particles, tracks in Luna 24 core samples, thermolum. obs. 80−82246
flare particles absolute spectra for flares of 1966-76 period 79−84598
flare particles meas. and integral proton spectra anal. 79−62695
flare particles propag. in interplanetary medium, model 79−80128
flare particles pulsed accel., plasma turbulence, ion-acoustic and Langmuir waves 78−96450
flare protons, flux limit due to accel. mechanism saturation effects 80−98645
flare protons, identification from accompanying EM emission 79−12443
flare protons, interaction with zodiacal dust cloud, γ-ray and X-ray lines prod. 79−53771
flare protons, quantitative estimation from characts. of microwave radio bursts at 9 GHz 80−4323
flare protons, radiation danger during manned space flights 80−41788
flare protons, stochastic accel. 80−21953
flare protons and electrons, accel. by shock waves 80−21974
flare protons near-Earth parameters determ. from radio bursts 78−45165
flares, conf., Florence, Italy (Nov. 75) *(Italian)* 78−93191
flares, energetic Fe charge states meas. 77−2418
flares, energetic particles, convection and adiabatic decel. effects on time to max. flux 77−2420
flares, energetic particles time dispersion, vel. and species depend. 77−2419
flares, gamma-ray and microwave evidence for two accel. phases 77−17527
flares, hard X-ray time profiles and accel. processes 79−30030
flares, interplanetary scatt. mean free path, energy depend. 77−9633
flares, particle accel., injection energy concept 80−101509
flares, particle accel. by cyclotron damping of cascading turbulence 79−44433
flares, particle and EM emissions, review *(Italian)* 78−93192
flares, particle emission *(Italian)* 78−96461
flares, possible cause of ancient climatic and biological catastrophes 77−78587
flares accel. processes, obs. requirements 77−17496
flares of August 1972, particle accel. dynamics 77−25992
flares radiation dose at Earth's surface 79−25109
flares rel. to cosmic ray intensity, model 80−72914
flares relativistic electron spectra, inference from meas. of inverse Compton radiation 80−90339
Forbush decreases and solar anisotropy, 11-year vars. 79−44317
Forbush effect in intensity of solar protons 79−80126
gamma-rays, hard intensity radiation pulsations in the atmosphere *(Russian)* 80−17454
ground level enhancements, comparison of 1977 Nov. 22 and 1969 Feb. 25 events 79−40042
ground level enhancements during 21st solar cycle 79−12361
hard X-ray burst, 1972 August 4, trap-plus-precipitation model 80−12747
heavy nuclei, solar emission, Molniya 1 probe 77−53354
heavy nuclei enhancement at high energies, 1974 July 4 event 78−28641
Helios 1 measurements, 1974 Dec.-1975 Sept., quiet time spectra, radial gradients 78−20592
Homestake long-range neutrino detector research program 79−80107
intensity and anisotropy, influence of injection processes and interplanetary propag. 78−12195
intensity enhancement, diurnal var., 1973 May 22-June 4 event 80−56685
intensity variations assoc. with interplanetary mag. field disturbances 78−40779
interplanetary anisotropies, quiet time obs. from Pioneer 10 and 11 78−77442
interplanetary diffusion, Monte Carlo method 80−12623
interplanetary disturbance, 1978 January 3 to 4, Prognoz-6 energetic particle and solar wind meas. 80−90315
interplanetary ice particles erosion by low energy cosmic rays 78−45177
interplanetary particles pitch distrib. distortion by bow shock 79−35088
interplanetary propag., solar cosmic ray events, solar and interplanetary diffusion 78−28458
interplanetary propag. *(Chinese)* 79−101035
interplanetary propagation, correl. of characts. of cosmic rays detected by Mars-7 and (Prognoz-3) 77−82089
interplanetary propagation, cosmic ray flow lines and energy changes 80−82158
interplanetary propagation, diffusion in mag. fields, convection in solar wind, dimens. method soln. *(Chinese)* 78−81511
interplanetary propagation from 1 to 5 AU 78−20594
interplanetary shock waves interaction, 1973 April 29-30 events 79−21122
interplanetary transport, effects of particle drift 77−45263
ionisation states of energetic C and O emitted by the Sun 77−49249
ionosphere, ionization due to low energy solar and magnetospheric particles 79−53625

solar cosmic ray particles continued
isotope composition form., effect of ion-sonic turbulence 80−101574
isotopic composition, meas. with isotope spectrometer on International Sun-Earth Explorer C spacecraft 78−85797
Jupiter magnetosphere, Voyager 1 obs. of solar cosmic ray particles 80−26798
lepton mixing and neutrino oscillations, cosmic neutrinos, heavy leptons, μ decay 78−82193
long-lived sources, collapsing magnetic regions 80−31268
low-energy cosmic rays, origin determ. 77−53376
low-rigidity cosmic rays, weak turbulence diffusion theory rel. to mean free paths 80−98524
lunar surface, flare particles and micrometeorites in and out of ecliptic 77−29737
MeV protons associated with solar flare, May 1979 obs. 80−51627
modulation by coronal holes, review 80−77370
motion in coronal magnetic field 79−75196
muon solar harmonics, variation of upper limit rigidity, 1958-63 78−49265
near-Earth radiation hazard due to solar flares, dosage estimation technique 80−67482
neutrino detection, new expts. proposal 80−31181
neutrino emission, review and reasons for deficiency 78−77486
neutrino expts. 79−8902
neutrino flux, quasi-biennial var. and correl. with solar activity 79−44440
neutrino flux and ^{6}Be reson., ^{4}He(^{3}He,n)^{6}Be 38.61 MeV cross-section 78−619
neutrino flux calcs., neutrino oscills. constraint 80−109410
neutrino flux correls. with solar activity 80−46522
neutrino flux rel. to catalytic role of third particle in H burning 79−80287
neutrino flux rel. to solar evolution and mass changing cosmology 78−45441
neutrino fluxes, solar activity and cosmic ray variations, review 79−84599
neutrino oscillation hypothesis and time depend. of Brookhaven solar-ν counting rate 79−80288
neutrino problem, chemistry of Brookhaven expt. 77−78735
neutrino problem, proposed new expt. using ^{71}Ga detector 78−58563
neutrino problem, results versus predictions *(Polish)* 77−71081
neutrino problem and ^{3}He(^{3}He,de$^{+}\nu$)^{4}He 15, 25 MeV cross-section 77−50142
neutrino problem rel. to Fe limited solubility in central Fe-H plasma 78−89149
neutrino problem rel. to solar interior struct. *(Italian)* 78−81598
neutrino puzzle, explanations for missing neutrinos 80−51723
neutrino puzzle, lepton mixing explanation 78−16373
neutrinos, ^{37}Cl expt., theory 79−84763
neutrinos, detect. possibility using ^{81}Br(ν,e)^{81}Kr reaction 77−22160
neutrinos, proposed Earth flux determ. by mass spectrometric assay of ^{205}Pb in Tl minerals 77−5447
neutron component intensity delay rel. to latitude solar activity index 77−53364
neutron flux calc. during flares 79−80127
neutrons, detection using Aryabhata satellite payload 79−84636
neutrons, prod. in solar flares and expected fluxes 78−32306
neutrons and gamma-rays prod. in 1972 August 4 flare 79−16915
neutrons produced by (p,n) reactions with flare accel. protons 77−25997
nonrelativistic electrons coherent propag. 77−91506
nonthermal electrons assoc. with filament eruptions and nonflaring coronal transients 78−65595
nonthermal particle production during buildup and in absence of flares 77−17492
nuclear and ionic charge distrib. particle expts. on International Sun-Earth Explorer spacecraft 78−85790
nucleons, interplanetary accel. in corotating interaction regions 77−9635
origin, nature and effects, interplanetary propag., review *(Russian)* 79−66893
plasma convection in force-free mag. field, mechanism for chem. separation in cosmic plasmas 79−35125
polar cap absorption intensity and solar cosmic rays north-south asymm., riometer data 78−69629
preflare enhancement in cosmic ray intensity, rel. to solar X-ray emission 78−45166
production rate, rel. to solar activity vars. 79−92735
propagation, anisotropic diffusion-convection eqn., dimensional soln. 80−17453
propagation, equivalent diffusion coefficients of solar cosmic rays 80−85825
propagation correlations detected on Mars-7 and Prognoz-3 78−49247
propagation effects, Jokipii's diffusion coeff. computer calcs. *(Chinese)* 79−12362
propagation in interplanetary environment, study of November 18, 1968 particle event 77−29607
propagation in interplanetary medium, solns. to Fokker-Planck eqn. 80−77242
proton albedo neutron flux north-south asymm. meas. 79−75061
proton and electron events, interplanetary scatt. mean free path 78−57421
proton energy spectra slope from radio burst data 79−53683
proton event, 1969 November 2-5, HF/VHF absorption in disturbed D-region 77−53286
proton event, 1970, April 16, features in interplanetary space and magnetosheath 77−87215
proton event, 1970, April 16, pitch angle distribs. transform from solar wind into magnetosheath 77−87216
proton event, 1972 August 4, influence on stratospheric O_3 78−7732
proton event of 1972 August, effects on atmospheric O_3 layer 79−35227
proton event of 1978 May 7, neutron monitor obs. 80−67686
proton events, forecasting quality improvement *(Chinese)* 77−22158
proton events and coronal mass ejections 78−77545
proton events at large heliocentric distances, shock-assoc. 78−77451
proton events effects on HF ionospheric absorption at low latits. 78−69594
proton events forecasting rel. to microwave bursts *(Chinese)* 80−12723
proton flare, 1971 September 2, simultaneous satellite obs. 77−67083
proton flare events, relation to type I (metre wave) radio sources *(Chinese)* 80−105222
proton flare spectrum determ. from latitudinal effect, using minimal Stormer pulse 78−45308
solar cosmic ray particles continued
proton flares, excessive particle emission mechanism 78−45310
proton flares, fast particles flight time from polar cap absorpt. effects 77−17469
proton flares, particle characts. near Earth from radio burst obs., longit. attenuation function 78−45309
proton flares, pulsation instability of preceding radio emission 78−53911
proton flares, temporal ref. functions from microwave radio bursts 78−73591
proton flares, threshold effect in second-stage accel. 78−61847
proton flares 1942-76 and their prediction 78−20811
proton flares correl. with 3 cm radio emission quasiperiodic fluctuations 77−53533
proton flares in August 1972, summary of solar/interplanetary events 77−25991
proton flares rel. to IGY high latitude flares *(Russian)* 77−64729
proton flux, calc. using microwave burst parameters 80−41789
proton flux, energy and temporal spectra, influenced by interplanetary mag. field 80−41672
proton flux enhancements and solar wind speed, Mars 7 meas. 79−84620
proton flux increases, rel. to solar flares and storm sudden commencements 77−9637
proton fluxes at 1 AU during solar min., Prognoz 3 obs. 78−69769
proton generation in solar flares 80−101575
proton intensity north-south asymm. rel. to plasma sheet and daytime polar cusp dynamics 77−17297
proton parameters changes assoc. with 1972 August flares, Pioneer 9 and 10 obs. 77−33314
proton region development in 1973, September 7 flare 77−37588
proton spectra determ., comparison of methods 78−28459
proton streams after interplanetary magnetic sector boundary, effect on troposphere 79−53491
protons, as extraterrestrial source of atmospheric water vapour, Sun-weather relationships appls. 78−69416
protons, auroral zone precip. assoc. with storm sudden commencements 77−82081
protons, coronal propag. at medium and high energies 77−53355
protons, directional flux meas. in space via digital onboard processor 77−64610
protons, flux anisotropy and inhomogeneity meas. 77−53351
protons, formation of ^{3}H and ^{14}C in terrestrial atmosphere 78−92886
protons, from flare of 1972 August 4, radiation doses absorbed in near-Earth orbit 77−52892
protons, He, Ne and Ar isotopes and ^{236}U prod. in lunar materials, rate calc. 77−17311
protons, high energy, effects on middle atmosphere chemical comp. 80−109213
protons, high-energy, from 1973 April 29 flare, arrival delay at Earth 79−62694
protons, high-energy, in August 1972, review of obs. 77−25894
protons, high-energy, upper cutoff 77−17306
protons, in August 1972, role in polar cap absorpt. and auroral events 77−29567
protons, low energy, expt. on International Sun-Earth Explorer C spacecraft 78−85791
protons, low-energy, cross-sections for (p,xn) reactions 78−28504
protons, low-energy, energy spectrum shape at 1 AU *(Russian)* 78−16255
protons, low-energy events, assoc. with mag. sector boundaries 77−45265
protons, magnetotail lobe and plasma sheet, entry in 1971 April 22 event 79−101026
protons, multiplicity functions in rigidity interval 1 to 15 GV 79−66894
protons, penetration into magnetosphere, influence of magnetosheath 78−20583
protons, pitch angle distrib. in high-latitude magnetotail during 1970 April 16 solar proton event 79−53670
protons, polar cap aurora induction, secondary electrons prod. 79−53605
protons, polar region fluxes rel. to sector struct. of interplanetary magnetic field 77−49251
protons, radiation hazard in shielded spacecraft 80−8194
protons, relationships to ionospheric plar cap riometer absorpt. 78−28413
protons, spatial distrib. in Earth's mag. field 77−53357
protons, struct. of fluxes in high-latit. magnetosphere in April (1972) 77−64532
protons and α particles, rigidity-independent coronal propag. and escape 78−77444
protons and α-particles in solar wind after interplanetary shock wave passage 77−33301
protons and electrons, medium-energy, Helios 1 and 2 particle spectrometer meas. 78−20608
protons at 1 AU from active regions, energy spectra from Prognoz-3 80−101512
protons from flares, Mars 7 probe meas. 78−69624
protons from primaeval Sun, irradiation model for ^{16}O and ^{26}Al isotopic anomalies 78−93128
protons in Earth's magnetosphere, vars. and spectra (August 1970) 78−16256
protons in magnetosphere, flare-time asymmetry and anisotropy 77−33280
protons in magnetosphere (1971 September 1-16) 79−2446
protons in recurrent particle streams at 1 AU 79−96867
protons prod. by flare of 7 Aug. 1972 anal. 77−53356
protons reflected by Earth's bow shock, upstream wave boundary determ. method *(Italian)* 78−24409
quiet time comp. and energy spectra for cosmic rays between 0.6-24 MeV per nucleon 77−29609
radiation doses meas. by Molniya 1 satellite 79−8774
relativistic cosmic rays, review 80−56798
relativistic heavy nuclei, preferential accel. 77−45267
relativistic protons from flare of 1 September 1971, anisotropy 77−22022
rigidity-independent propag. in corona, bird cage model 78−77443
scatter free particles in 1978 May 7 proton event, arrival times 79−75066
shock acceleration, in corotating interaction regions in solar wind 80−82159
shock wave acceleration of protons and relativistic electrons 79−48757
solar flare proton generation 80−109413

solar cosmic ray particles continued
spectrum formation near Earth, propagation and acceleration *(Russian)* 80−4211
spherically symmetric production and modulation, analytical solns. 78−16368
St. Severin meteorite, flux of low energy particles in solar system 77−82096
stationary solar particles modulation in interplanetary space 77−25896
subcosmic rays rel. to active solar processes 78−61693
transport, solar magnetic dipole orientation effects 79−44316
X-rays and gamma-rays, obs. by Signe II MP satellite expt. 80−41696
Z-rich solar particle event characts., (1972 to 1976) 79−5717
(ν,e) reaction on ^{55}Mn, ^{71}Ga, ^{87}Rb, cross section calcs., to solar neutrino expts. *(Russian)* 77−50119
ν capture rate, disagreement between theory and expt. 78−4171
ν flux survey, inhomogeneous solar models 78−4166
ϕ meson prod. from neutrinoless fusion process 79−8898
^{26}Al, from ^{3}He-rich solar flares 80−36461
^{7}Be production in atm. and transport from Sun, tracer for terrestrial-solar relationship 80−98525
^{10}Be, from ^{3}He-rich solar flares 80−36461
CND flare particles, rel. to carbonaceous chondrite fission Kr and Xe origin 79−35199
Fe-group nuclei, energy spectrum from lunar soil samples 77−53353
H, He, interpretations of isotopic comp. 77−45266
He ions superheating and superacceleration 80−12631
^{3}He rich events during 1976 November to December, Prognoz 5 obs. 80−61972
^{3}He/^{4}He in heavy-ion-rich solar energetic particle events, energy depend. and temporal evolution 80−90299
^{3}He/^{4}He solar cosmic ray isotopic composition from Venera 9 obs. 80−72725
^{22}Na, from ^{3}He-rich solar flares 80−36461
Ne nuclei, IMP 8 obs. of flare-accelerated particles 79−92740
^{20}Ne/^{21}Ne/^{22}Ne of energetic flare particles 79−92741

solar cosmic ray photons
flare impulsive X-ray burst, spectral anal. analytical method *(Chinese)* 80−85919
gamma rays, detection using Aryabhata satellite payload 79−84636
gamma rays, theory of prod. and observational results 78−32306
gamma-ray flux calc. during flares 79−80127
gamma-ray meas. with Aryabhata satellite 77−22023
gamma-ray spectrum, 4-8 MeV range 77−53491
gamma-rays, 0.511 MeV energy, meas. with balloon-borne Ge(Li) spectrometer 77−53373
gamma-rays energy spectrum during 1972 Aug. 4 flare *(Russian)* 78−12185
gamma-rays with energy >8 MeV prod. in flares 79−53779
X-rays effects in terrestrial upper atm., ionisation, Auger electrons form. 78−53767

solar disturbances *see solar activity*

solar eclipses
1919 May 29, gravitational deflection of light, obs. reexamined 80−67553
1966, May 20, partial eclipse contacts from Belgian obs. *(French)* 77−71074
1966 November 12, ionization rates in South Atlantic geomagnetic anomaly 80−12608
1968, September 22, coordinated optical, radio, geomag. and ionospheric obs. *(Chinese)* 77−22154
1968, September 22, mag. struct. calc. of coronal condensation *(Chinese)* 78−69762
1970, March 7, coronal polarisation obs. 77−33462
1970, March 7, spectrograms of extreme limb, 4545-4579 Å 77−17472
1970 March 7, corona, colours during eclipse and dust composition 80−51730
1972, July 19, inner corona polarization meas. 77−82197
1972, July 10, chromospheric Na distrib. and nonthermal motion vels. 77−22200
1972 July 10, corona, colours during eclipse and dust composition 80−51730
1973, June 30, atmospheric waves obs. 77−53302
1973, June 30, corona polarisation obs. 77−13313
1973, June 30, coronal polar rays obs. 77−17470
1973, June 30, Dutch expedition for solar spectra exam. 80−8614
1973, June 30, equatorial electrojet irregularities drift vels. meas. 78−36365
1973, June 30, Fe XIV 5303 Å coronal emission line polarisation 77−49352
1973, June 30, ionising solar radiation meas. 79−8901
1973, June 30, ionospheric perturbations due to gravity waves generated by eclipse 77−21993
1973, June 30, IR obs. with Si vidicon spectrometer 77−9657
1973, June 30, obs. of neutral sheet in corona 79−84757
1973, June 30, obs. of trans-polar coronal hole 77−53526
1973, June 30, photometric obs. of chromospheric and coronal spikes 77−17520
1973, June 30, report of Dutch expedition 80−8615
1973, June 30, stray light meas. for sunspot intensity correction 78−28596
1973, June 30, white light corona polarisation obs. *(French)* 77−74027
1973, June 30 total eclipse, photographic photometry of K- and F-corona 78−89140
1973 June 30, atmospheric point discharge currents during eclipse 78−16094
1973 June 30, density model for N.polar coronal hole 80−98627
1973 June 30, white light corona polarisation 78−20786
1973 June 30 total eclipse, coronal green line polarisation obs. 79−66969
1975, May 11, 8 mm obs. of quiescent prominence 78−7977
1975, May 11, search for atm. Lamb waves generated by eclipse 77−29376
1975 May 11, D-region electron density variation obs. *(Russian)* 78−61652
1976, April 29, annular, direct solar radiation var. meas. 79−84781
1976, April 29, annular eclipse, obs. of Earth anomalous gravity effects *(Chinese)* 79−2174
1976, April 29, annular eclipse, zenith intensity photoelectric meas. 78−3900

solar eclipses continued
1976, April 29, annular eclipse photographic obs. for ephemeris time correction determ. *(German)* 79−44335
1976, April 29, annular eclipse shadow in Sahara, NOAA-4 picture 77−33464
1976, April 29, atm. NO_2 total content var. during eclipse *(French)* 77−2208
1976, April 29, ionospheric electron content quasiperiodic fluctuations during partial eclipse 78−24407
1976, April 29, ionospheric HF signals freq. shift 78−45111
1976, April 29, partial eclipse obs. in Poltava 78−45201
1976, October 23, atm. gravity waves obs. in ionosphere during total eclipse 77−91364
1976, October 23, atmospheric gravity wave production, predictions 77−17181
1976, October 23, atmospheric gravity waves obs. 78−88887
1976, October 23, chromosphere brightness distrib. at 3 mm wavelength 79−30042
1976, October 23, coronal struct. prediction 77−17471
1976, October 23, ionospheric total electron content meas. over Australia, rel. to induced gravity waves 78−49210
1976, October 23, mag. obs. in Australia 78−81498
1976, October 23, magnetic obs. in Australia 77−49000
1976, October 23, obs. from Zanzibar and Australia 77−33463
1976, October 23, partial eclipse in Australia, atm. surface layer turbulence response 79−70843
1976, October 23, predictions v. obs. of coronal structure 77−25990
1976, October 23, wavelike vars. in F-region in path of totality 79−66865
1976, October 23rd, upper atmos. wind obs. 80−46327
1976 April 29, atmospheric point discharge currents during eclipse 78−16094
1976 April 29, partial eclipse, obs. of granular brightness fluctuations centre to limb var. 79−66971
1976 October 23, atmospheric gravity wave production 79−92558
1976 October 23, contact timing expt. during total eclipse 78−36547
1976 October 23, in-flight obs. near Victoria, Australia 78−36548
1976 October 23, ionospheric transmissions, HF Doppler obs. over S.E. Australia 78−61662
1977, April 18, partial eclipse, radio obs. at 590 MHz 77−87362
1977, October 12, ephemeris *(French)* 77−87241
1977, October 12, photographic obs., cloudy weather 78−45315
1977, October 12, photographic obs. from North America 78−45314
1977, October 12, viewing sites in Columbia 77−64738
1977 April 18 annular and October 12 total eclipses 77−56895
1977 October 12, partial phases for N.America, predictions 78−7865
1977 October 12, ship-borne expeditions in NW.Pacific 78−32434
1977 October 12 partial eclipse, VLA 6 cm obs. of quiet Sun 80−72895
1978 April 29, limb darkening obs. during partial eclipse *(French)* 80−8612
1979, February 26, an illustrated record from N.American obs. 80−4328
1979, February 26, predictions 79−2473
1979, February 26, stratospheric response 79−100907
1979, February 26, total eclipse ephemeris 78−85928
1979 February 26, F corona radial vel. obs. 80−85914
1979 February 26, shadow band obs. 80−17372
1979 February 26, sky brightness meas., radiative transfer model 79−92588
1979 February 26, solar flash spectrum obs. 80−67687
1979 February 26, sounding rocket expts. 79−58145
1981, July 31, total eclipse, a visibility in USSR *(Russian)* 79−88640
1981 July 31, obs. of gravit. deflection of light (Einstein effect), prospects *(Russian)* 80−51651
ancient Chinese observations of physical phenomena attending solar eclipses 80−72916
ancient events as record of lunar motion 80−46182
chromosphere and prominences eclipse observations using plane grating as polar heliostat 79−84674
coronal obs., external occulting disc as radially-graded neutral density filter in photography 79−80233
effect on geostationary broadcast satellites and prediction of occurrence 80−31199
geomagnetic Ci index (1906-1976), solar eclipse perturbations 79−100811
historical accounts, solar and lunar 79−80411
ionosphere effective height change *(Russian)* 78−49201
ionosphere effects, VLF focusing during solar eclipse 80−61965
light bending by eclipsed Sun, star field obs. *(French)* 78−20634
light bending by Sun, vars. caused by solar activity *(French)* 80−56795
pre-telescopic obs., uses in modern astronomy 79−96930
predictions using vector method for intermediate level astronomy courses 80−105452
radiowaves diffraction and refl. from lunar limb during solar eclipses *(Russian)* 78−65586
Scaliger saros and condensed Canon of Eclipses *(French)* 79−2472
sky radiance during total solar eclipse, model 78−40652
stratosphere, effect of eclipse, on NO_2 and O_3 conc., and atm. temps. 80−105017
stratospheric trace species vars. during solar eclipse, theoretical study 79−58013
teaching, camera obscura demonstration *(Hungarian)* 78−36773
terrestrial heat and radiation budget during solar eclipse, above pine forest *(German)* 80−46226

solar-electric power stations *see solar power stations*

solar energy concentrators
3 m parabolic dish heliostat system design, fabrication and testing 79−62111
5 MW Solar Thermal Test Facility 79−62113
5 MWe solar thermal test facility, heliostat field design 77−23780
10 MWe pilot plant, collector field design 77−23779
50 W generator for developing nations, with simple tracking system 79−43748
accuracy characts. meas., using laser radiator and sectioned photoreceiver 79−23038
acrylic thin sheet lens construction and performance 79−62120
aerospace solar panels with concentrating reflectors 79−96472
angular misorientation, conical, spherical and parabolic reflectors 77−88891
Ansaldo solar cell for parabolic trough concentrator systems with forced cooling 80−93982

solar energy concentrators continued
array of directable mirrors as a photovoltaic solar concentrator, calc. of images 80−76609
asymmetrical ideal cylindrical solar concentrator principles 79−62119
axially symmetric hollow collectors for high temp. solar installations, radiative heat transfer computation 78−79093
axicon sun-tracking concentrators for photovoltaic conversion, conc. and cost characts. 80−93858
axisymmetric mirror class with uniform flux conc. props. along axes 80−95978
axisymmetric reflector-absorber systems with uniform flux conc. 80−94111
black liquid cylindrical parabolic collector, thermal analysis 79−74539
black Ni electrochemical coatings, characts. investigation 80−95975
black surface glass mirror as solar energy reflector, reflection coeff. determ. 77−34930
cassegrain solar collector with thermoelectric module, concentration efficiency 80−35709
cassegrain solar concentrators for photovoltaics 80−61304
Cassegrain solar furnace, determ. of concentration 80−7932
Cassegrainian solar concentrator, optical and thermal analysis 80−40906
catenary curve reflecting surfaces for concentration 78−46744
cavity-type surfaces for solar collectors 79−48180
cells irradiation distribution and concentration *(Spanish)* 80−35683
central receiver, optimisation 77−27330
central receiver program, heliostat, receiver and storage subsystems 80−30404
central receiver solar power systems, terminal concentrator concept analysis 80−26116
channelled solar flat-plate concentrator geometry and beam deviation 79−62072
chemical treatment of cover to improve collection *(French)* 78−25982
chromatic dispersion concentrator applied to photovoltaic systems 80−93862
circular film concentrator with a concentric seam of constant curvature, effect of seam on shape of reflecting surface 80−40827
coating development for solar energy conversion 78−79096
coatings and cover plates 79−24892
collapsible faceted type 77−72049
collection augmentation by planar refle-tive surfaces, calc. and expt. 79−83574
collection subsystem of 1 MW solar power station, engineering assessment 80−61305
collector absorption enhancement using multiple reflections 80−76649
collector coatings, for solar heating and cooling systems 78−30045
collector long-term average performance prediction method 79−62116
collector optical efficiency, heat loss coeff. and heat removal factors 79−100483
collector tube, bore heat flux and outside surface temp. variations 78−90629
collectors and components using total internal reflection concept 77−54813
collectors characts. and use *(Italian)* 80−101078
combined photovoltaic/thermal flat plate collectors, analysis using Hottel-Whillier-Bliss model 77−39106
composite focusing parabola and compound parabolic concentrator, sequential use 80−45638
composite heliostat, computer anal. and optimisation 79−39283
compound circular arc concentrators, optical properties 79−29453
compound elliptical concentrator, geometrical vector flux field 80−33119
compound lens-mirror parabolic collectors, optical and thermal design 77−23735
compound parabolic, cylindrical parabolic, and compound wedge solar concentrator performance 79−62117
compound parabolic, description and development 77−23727
compound parabolic concentrator, derivation of 79−72651
compound parabolic concentrator, phase space conservation for incoherent propag. 80−69491
compound parabolic concentrator collectors, prediction of thermal performance 80−55905
compound parabolic concentrator flux distrib. nonuniformity 79−62011
compound parabolic concentrator heat transport to storage 79−62102
compound parabolic concentrator photovoltaic solar collector design 79−61998
compound parabolic concentrator solar collector design 80−3532
compound versus simple parabolic 79−64304
compound wedge cylindrical stationary concentrator, charact. 78−33815
computer-based sunfollowing system, design and data requirements 79−83573
concentrating collectors, single axis, orientation, economic criterion 80−40907
concentrating solar collectors, concentration/acceptance relationships 80−21414
concentration system health hazards 80−3492
concentrator solar cell with tracking control information 79−29470
concentrator-receiver system with selective absorbing surface, heating characts. 80−91874
concentrator/photovoltaic system design for electricity and heat generation 79−61997
concentrator/photovoltaic/Rankine cycle steam turbogenerator system efficiency 79−62002
cone collectors for finite sources 78−46742
convection, natural, in compound parabolic concentrator, finite element soln. 78−90634
curvature determ. by gravity, and mobile focal axis, appls. 78−90487
curved glass mirror manufacture for linear solar concentrators 79−62124
cusplike compound parabolic collector with tubular absorber, props., construction 77−23734
cylinder-parabolic, with envelope pipe, steam generation efficiency calculation model *(German)* 80−33112
cylindrical, generalisation of 2-D optical anal. 80−101079
cylindrical absorbers, sun following reflectors, semi-parabolic reflector, thermal power and efficiency *(Korean)* 80−21380
cylindrical parabolic, with flat absorbers, intensity distribution calc. 77−23730
cylindrical parabolic concentrator, flat absorber, performance 77−79953
cylindrical parabolic concentrator, thermal regime in primary fluid heated by solar energy 78−75061
cylindrical parabolic mirror utilisation as solar receiver *(Rumanian)* 80−7914
deep cylindrical collectors, optimum depth determ. 77−88890

solar energy concentrators continued
design, economics and optical loss anal. of concentrating solar collectros 80−45751
design, effect of solar elevation angle probability distribution 80−93860
design methods, analysis and classification 78−83063
design of high concentration solar cell arrays, components, technology and performance 80−50955
design variables, optical efficiency, heat loss coefficient and heat removal factor 80−7927
designs for underdeveloped countries 79−62125
dielectric compound parabolic concentrator 78−5533
diffuse light collection onto extended absorber, mirror designs 78−22186
direct solar energy conversion to laser radiation possibility, using 20-fold concentrator 79−59688
dye mixture planar solar concentrator for solar cell, photon trapping and energy transfer 77−88946
effective series resist. meas. effects of temp. variations 80−93944
efficiency, geographic and economic aspects of solar energy utilisation 79−52888
efficiency of solar concentrators with curvature determined by gravity and a variable density distribution 80−85266
ellipsoidal concentrators, shaping errors, effects on radiant energy characteristics 79−96418
elliptical and parabolic non-imaging, comparison 77−75648
energy collection anal. using information theory 80−97799
extreme asymmetrical nonfocusing concentrators for solar energy utilisation, assessment 79−43746
facet quality evaluation for deformational forming 78−90483
faceted solar concentrator effects of reflector aperture and facet number 79−62115
fibre optics, developments and applications for concentrated solar energy transmission 80−87481
fixed focal axis large linear solar concentrators shaped by gravity field 78−9427
fixed mirror, appl. to H solar-thermochemical prod. of H_2O 80−45767
fixed mirror solar concentrator for application to a 100 MW(e) electric generating plant 80−30393
fixed mirror type, concentrated solar flux characts., expt. 77−23733
fixed spherical collector, geometrical optics *(French)* 77−83945
fixed tilt solar collector with reversible vee-trough reflectors and vacuum tube receivers, analysis, development and testing 79−100539
fixed-focal-axis solar concentrators with a curvature determined by gravity 79−74495
fixed-mirror, heat loss from heat receiver assembly meas. 79−52905
fixed-mirror, with secondary concentrator, design, construction and testing 79−52903
fixed-mirror concept, advantages 77−54774
flat energy receivers and convertors, solar radiation concentrator construction for uniform irradiation 79−83559
flat mirror materials, specular reflectance properties and appl. 77−34917
flat mirror multivalent solar concentrator 80−61420
flat plate, parabolic, and conical solar concentrator performance compared 79−62118
flat plate, performance calc. using programmable desk calculators 77−75691
flat plate collector energy yield increase by planar reflector, modelling appl. 78−33813
flat plate collector for water heater 79−39289
flat plate solar energy collectors, efficient optical window design 79−83628
flat solar plate collector cover, physical props., influence on efficiency *(French)* 79−34430
flat-plate solar energy collectors, optical valve design 79−81506
flat-sided rectilinear trough as solar concentrator, analytical study 78−74961
fluorescent planar collector-concentrators for solar energy conversion 80−45745
fluorescent planar concentrators, efficiency and stability 80−93986
fluorescent planar concentrators−performance and experimental results 80−45646
fluorescent solar collectors, second stage conc. with tapers 79−61945
flux concentrators, approach to ideality 78−66885
flux density calc. by two-dimensional Harmite function expansion 77−75647
flux density distribution on central tower receivers anal. 77−46786
flux distribution determ. using backward ray tracing 79−98457
FMDF solar-thermal-electric system, optical concentration profiles and receiver perform. anal. 80−30392
foam-film parabolic-cylindrical concentator surface fabrication 80−21372
foam-film solar energy reflector fabrication, physical and chemical processors 78−90530
focone and focline profiles calc. 77−68251
focused plate mirror, slightly curved, reflected light pattern anal. 77−23728
focusing collectors, cylindro-parabolic mirrors *(Rumanian)* 80−50934
Fresnel lens, colour-corrected linear convex, for solar concentration 80−45640
Fresnel lens, linear, high-efficiency 79−88003
Fresnel lens, plano-cylindrical, line-focusing anal., expt. 77−23732
Fresnel lens appls. 78−83065
Fresnel lens design, construction and performance 79−62121
Fresnel lenses, fabrication techniques 80−91939
Fresnel lenses, highly concentrating 79−94315
Fresnel lenses, spectral adaption and fluoresc. and bifacial concentrators *(Spanish)* 80−72060
funnel concentrator optics, ray tracing 78−58900
furnace, focal spot thermal analysis 80−21383
G. Donegani Institute activity *(Italian)* 80−60027
gases, thermal shock prod. with conc. solar energy *(French)* 78−91056
general optical concentrator, max. radiant power density at receiver 80−102794
generalised light concentrators, collection props. 78−33807
generalised optical design technique, consideration of various errors 80−95979
geosynchronous satellite plane-mirror solar concentrators 79−96474
glass components, speculiarity meas. using Fourier transform anal. 80−5804
glass tubes for absorber, vacuum, refraction effects 77−46684
glasses, high vol. low cost, as solar reflectors, compositions and weathering effects 80−106589

solar energy concentrators continued
heat collectors, with direct and concentrated radiation, maximum equilibrium temp. determ. 80−92031
heat pipe, filled with porous material, glycol water circulation 80−66986
heat transfer performance, parabolic collector, solar tracking system 77−88892
helios at mirrors, convergent, concentration of solar radiation *(French)* 79−3763
heliostat facets, optical characterisation 80−53485
heliostat field optimisation, appl. of field shape effect for power stations *(French)* 79−24903
heliostat focus and alignment system, for 5 MW Solar Thermal Test Facility 78−50894
heliostat mirror field analysis and design 79−83570
heliostat reflected beam structure 78−90482
heliostatic fields, geometry *(Spanish)* 79−23037
heliostats for central receiver solar power stations, optical analysis 79−74543
heliotherapy unit, integral concentrator, irradiation technique improvement, medical physics 79−83885
hemispherical mirror, 65 ft. dia., solar gridiron electric power generation appl. 79−87980
high-temperature solar compound parabolic concentrator requiring monthly tilt adjustments 79−62104
high-temperature solar energy installation with paraboloid concentrator, radiant flux control 79−96420
hydraulic solar collector tracking device design and evaluation 79−62123
hydride concentration cells 80−35698
hyperbolic cone-channel condenser system 78−33811
ideal, for finite sources and restricted exit angles, design 77−7168
ideal concentrators, three dimens., for distant sources 79−41334
ideal concentrators for distant radiation sources 80−35751
ideal cylindrical radiation transformers and concentrators, symm. and asymm. forms 79−55200
ideal flux concentrator design with reflector gaps 78−66880
ideal flux concentrators, intensity variation reduction on absorbers 80−104496
ideal image-forming flux concentrator design 79−55201
ideal prism solar concentrators, features 79−43745
image characteristics, non-uniform intensity distrib. 80−55816
inductive grids for solar appl., theory 77−75666
industrial applications of solar heat *(French)* 79−100486
insolation values statistical analysis, correlations between diffuse and hemispherical and between daily and hourly insolation 79−87975
insolator, copper belt type tube structure, design, construction and testing *(Czech)* 79−83626
integrated photovoltaic/thermal system with faceted-mirror sunlight concentrator 79−62010
lens-mirror combinations with max. conc. 78−9422
line focus collectors for solar thermal electric power systems, comparison 77−23775
line focus segmented mirror concentrator, features 77−54772
line focus solar collector, construction *(Japanese)* 78−30072
line-focus Fresnel lens and secondary concentrator 79−62112
line-focus parabolic-trough photovoltaic arrays, active and passive cooling 80−93988
linear echelon refractor/reflector solar concentrators 80−7929
linear focusing solar reflector, production by elastic deformation of flat sheet 80−30391
linear Fresnel lens with grooves of finite size, solar radiation concentration 80−106592
linear Fresnel solar reflector concentrator, geometrical design 80−45636
low cost photovoltaic cells utilizing semiconducting thin films and advanced concentrator concepts 80−50972
low temperature solar thermal systems for domestic space heating *(Czech)* 79−83566
low-temperature collector and thermal or photovoltaic concentrator development 79−62009
luminescent concentrators, operation theory and performance evaluation techniques 80−7913
luminescent greenhouse collector for solar cell 77−761
luminescent greenhouse solar collector materials 78−13789
materials, reflected beam profile characterisation 78−33814
materials for solar energy utilisation, review of chemical aspects 77−83977
maximal concentration from new class of radiation concentrators 80−45639
metallised polymer films and Al coatings, spectral characteristics 79−96422
mirror, performance evaluation 80−87457
mirror arrays, large Earth orbit structures reflecting sunlight for power generation, lighting, and agriculture 80−45632
mirror fabrication for projecting target surface in solar furnace *(Japanese)* 78−90534
mirror surface reflectances, expt. investigation 78−83066
mirrors, composite radiant-energy type with conical radiation sources 77−19378
mirrors, Earth-orbiting, enhanced solar energy options 79−52901
mirrors design, American and Australian practices *(Italian)* 80−50935
mirrors for distributed concentrator array, specular reflectance degradation 77−88886
modular dish solar electric system, technical feasibility 77−23777
modular solar collector development for large solar generators 79−96467
Moire fringes, rotation angles and curvature meas. appl. 78−90477
natural convection in liquid layer in flat inclined solar energy panel *(French)* 79−18894
non-tracking, optical props. and collector performance anal. 78−71193
nonevacuated compound-parabolic-concentrator solar heating prototypes 79−62105
nonevacuated solar collectors with compound parabolic concentrators 79−62069
nonimaging, optimisation for tubular evacuated receivers aligned north-south 80−72015
nonimaging concentrator design as second stages with image-forming first-stage concentrators 80−50933
nonimaging concentrators, design principles, geometrical optics theorem appl. 79−55203
nonimaging concentrators, two-dimens., with refracting optics 79−81504
nonimaging concentrators and geometrical vector flux 79−72650
nonimaging solar concentrator design, cavity enhancement by controlled directional scattering 80−45631

solar energy concentrators continued
nonimaging solar concentrators for different absorber shapes 78−50895
nontracking solar collectors, wide-angle lenses and image collapsing subreflectors 80−76603
one and two faced symmetric sidewall booster mirrors, optimal geometries 79−43743
optical and energy charact., determ. using Si multielement photoelect. conductors 80−97783
optical coatings, accelerated tests, using reliability principle 79−96419
optical concentration in solar power stations by use of conical and parabolic mirrors *(French)* 79−24904
optical simulation for a fixed spherical solar collector 80−7912
optics, conf., San Diego, USA (Aug., 1977) 78−50891
Optics applied to solar energy, [Conf. San Diego, CA, USA Aug. 1978] 80−7926
optics in energy utilisation, conf., San Diego, Calif., USA, 1976 77−53900
orbiting mirrors, solar illumination after dark appl. 78−33816
parabolic, composite, concentration characteristics 80−102793
parabolic collector system, cylindrical, transient energy removal calc. 79−52906
parabolic concentrator, use of fin receiver 80−21379
parabolic concentrator arrays, collector end shadowing effects minimisation 80−93987
parabolic cylinder at oblique incidence, cylindrical target *(Japanese)* 79−52882
parabolic cylinder at oblique incidence, flat target *(Japanese)* 79−52881
parabolic cylindrical collectors, design 77−23729
parabolic cylindrical solar concentrator, optimum direction *(Japanese)* 79−52883
parabolic dish, pointing errors effects on receiver performance 79−48097
parabolic dish thermal power systems, technology and appl. 80−30558
parabolic solar reflector for accurate and economic producibility 80−7930
parabolic trough collectors, for industrial plant heating and cooling, located in Southern Europe 79−62131
parabolic trough mirrors, concentration charact. parabolic trough mirrors, concentration charact. *(Japanese)* 79−79376
parabolic-cylinder type with moulded glass, manufacturing techniques and optical-energy charact. 77−72048
paraboloidal, axisymmetrical, mirror type, exposure to solar flux parallel to concentrator axis 79−83561
paraboloidal, flat receiver melting temp. calc. 77−45843
paraboloidal collector arrays, shading and spacing, energy loss evaluation 79−43747
paraboloidal heliostat system, energy-accuracy analysis using multimirror concentrating systems general theory 79−83560
paraboloidal mirror, image formation determ. 77−46780
paraboloidal mirror, irradiance distribution anal. 77−46779
paraboloidal mirror and paraboloidal focone system 78−90478
paraboloidal mirrors, long focus, radiant flux distribution calc. 77−50745
paraboloidal focones and parabolocylindrical foclines, radiation scattered by circumsolar parts of sky 78−83064
parallel plate channel, convective-radiative interaction, air-operated solar collectors appl. 80−96259
pendulum controlled solar tracking system and concentrator 79−62122
photovoltaic, deep well irrigation power system appl. 79−92082
photovoltaic, electrodialysis desalting plant appl. 80−55805
photovoltaic concentrating array, using point focusing acrylic Fresnel lenses 79−52937
photovoltaic concentrating sytems, optical and tracking systems design, performance charact. 80−72051
photovoltaic concentrator array technology, status report 80−94024
photovoltaic concentrator cells development project, developments, performances and future trends 80−45699
photovoltaic concentrator system for Roxborough Park 80−30408
photovoltaic conversion of concentrated solar radiation, feasibility assessment 79−57436
photovoltaic generators using optical concentration, current status and development trends review 80−45697
photovoltaic module utilising parabolic trough concentrators 80−93984
photovoltaic receiver for parabolic trough concentrator, optimisation 80−93983
planar Fresnel ring mirror, focal region, solar flux redistribution visualisation 79−68426
planar solar energy convertor and concentrator, based on uranyl-doped glass 78−71213
plane solar captors in transient regime *(French)* 77−71319
plane step lens principle and solar energy utilisation *(Chinese)* 79−81512
plano-cylindrical Fresnel plastic lens, design and performance analysis as solar collector 80−53403
point focusing, effects of tracking errors on performance, statistical anal. of intercept factor 80−61302
point-focus Fresnel lens photovoltaic arrays, active and passive cooling 80−93988
point-focus photovoltaic concentrator arrays, durability, reliability 80−93985
polyurethane foam, thermal and thermohydrolytic ageing 78−92281
pond potentialities as solar collector 80−30388
power plant, tower type, efficiency study 77−19379
power plants, solar high temp., with Stirling engine and solar thermal rocket engine, efficiency improvement by using selective radiation absorption surface 80−89589
power station, solar energy collection and conversion, pros and cons, economic prospects projection *(French)* 79−100489
power station, tower-type, heliostat field solar energy collection, achievements and projections *(French)* 79−100490
power stations, tower type, installation problems summary and current operations review *(French)* 79−100492
radiant exchange for a fin and tube solar collector 79−76955
reflecting concentrators, optical evaluation techniques 78−50893
reflecting surface formation, deformation method evaluation 78−90481
reflector and absorber design, spherical stationary mirror, and automatic tracking absorber 80−50997

solar energy concentrators continued
reflector comparison, concentrating properties of truncated hexagonal, pyramidal and circular cones 78−50896
reflector form for uniform irrad. field on receiver surface 78−90480
reflector shapes for truncation of nonimaging cusp concentrators 80−21385
reflector-collector system all-day performance, time-integrated calc. 79−3765
refrigeration, single-loop conjugate realisation 77−75644
review of energy collector developments *(Japanese)* 77−62031
segmented parabolic mirrors, optical performance anal. by THEK computer code *(French)* 80−61294
self-contained solar power installation concentrating system design and optical/energy charact. testing 80−40828
semiconductor film absorbing surface coated onto base, SiO antireflection coating over bath 78−5580
silazane protective coatings, UV exposure, ageing tests 78−79092
silicone-glass hybrid Fresnel lens for solar energy concentration 80−61303
solar air heater, Fresnel lenses concentrator 79−74493
solar cell array optimisation for use with concentrators 79−62001
and solar cell array systems, economic assessment 79−43770
solar cell response to intense and nonuniformly concentrated illum. 79−62000
solar panel, radiant props. deform. using greenhouse effect *(French)* 77−72139
solar power plant, direct tracking using two-mirror unit with plane and hyperboloidal counter-reflectors 80−91875
solar power station, tower-type, concentrating and receiving systems design modelling 80−91873
solar tower concept, ray trace approach 78−5571
Solarex two-axis tracking linear concentrating collector system, design and operation 80−93989
solid dielectric compound parabolic concentrator for photovoltaic cell 77−7174
solid-dielectric compound parabolic concentrator with Si solar cells, prototype 77−39107
space solar furnaces, for materials-science expts. 80−108786
space vehicle photovoltaic arrays, concentrator design 80−94057
spacecraft, solar energy thermionic electricity generating plants 77−78603
spacecraft appls., concentrator enhanced arrays utilising thin film Kapton mirror 80−30501
spectral characteristics for improving solar collector performance 80−35650
spectral emissivity measurement device, high-temp. materials 80−37039
spectrally selective reflectors for concentrator solar arrays, evaluation 80−94043
spherical facet concentrating capability investigation 77−68252
spherical mirror solar collector, geometrical concentration determ. *(French)* 78−33808
with spherical radiation sources, radiant-flux density distribution calc. method 77−68253
square Fresnel lens design for illuminating circular solar cells 78−79099
standard test procedure and facility for solar collectors 79−61947
static collector of low-conc., heat losses 80−81487
static photovoltaic concentration improvement, two-sided Transcell 79−61999
stationary solar collector design to make most of diffuse radiation 80−30517
with stationary spherical reflector and tracking absorber, charact. 77−54773
Stirling engine, reflector-concentrator modified, for farm power needs in India 79−62024
Sun-tracking concentrator for solar cells, solar eyeball 78−66881
sunlight reflected from polygonal heliostat, optical simulation 79−29452
surfaces, selective, for solar-thermal conversion 77−83978
symposium on solar energy, Phoenix, Az., USA (Nov. 76) 77−86329
system designs for low cost-low ratio solar concentrators 80−7928
testing, turbine flowmeters appl. 77−39387
thermal conversion, collectors, storage systems, energy transport and economics, review 80−51003
thermal deformations, computational relationships 79−39277
thermal electric power systems, line focus collectors, economic comparison 79−70435
thermal energy collection, comparative eval. of fixed and tracking collectors 80−7931
thermal generating station design, engineering problems *(German)* 80−30381
Thermal Test Facility, at Albuquerque, New Mexico, description 78−66887
thermodynamics of solar-thermal processes, second-law anal. 80−21378
thermoelectric, near-Sun missions appl. 79−48143
thermoelectric conversion, concentrators and central receiver systems 80−45760
thermoelectric generator, attainable efficiency values determ. 80−94094
thermoformed plastics for parabolic concentrators, development 77−23774
thermogravimetric method for recording mass transport of materials under action of radiant fluxes 80−17944
thermophotovoltaic solar energy conversion system, proposal 79−74513
thermoreceiver, solar concentrator, waste water sediments disinfection 79−83624
thick film conductive ink contacts for concentrator cells 80−93957
thin sheet Fresnel solar collector-concentrators, features and economic benefits 79−79402
three-step compound-wedge stationary solar energy concentrator optimal geometry 79−62103
tornado type wind energy system, wind and solar energies effect of line heat source 79−87959
tower-top focus solar receiver designs 79−62114
tower-type solar furnaces, two mirror, high power, optical charact., calc. for design 80−40824
tracking concentrator, for building interior lighting 77−62043
tracking parabolic reflecting concentrators, solar-heated water for photographic processing laboratory 80−40837
transmission solar focusing collector 77−65617
trapezoidal groove solar energy collectors, predicted daily and yearly average radiative performance 79−74540
tri-mode solar conversion system, design and operation 80−55907
solar energy concentrators continued
trough-type solar concentrator collection time rel. to orientation 79−3764
truncated hexagonal, pyramidal and circular cones, solar concentrating props. 78−83062
truncated parabolotoric focones and parabolocylindrical foclines, properties and parameters 78−79091
turntable solar arrays for electric power generation 77−23776
two-dimensional concentrators for inhomogeneous media, design procedure 78−63167
two-sided photovoltaic solar cell static concentrators 80−35684
two-stage reflecting convertor, pseudo-Lambertian, optimum configuration anal. 80−97765
vacuum thermal collector with optimal conc. 78−50892
variable-shape, fabricated from polymeric-film membrane 80−76645
wavelength-selective surfaces for efficiency improvement 77−54812
wedge concentrator, multiple reflection, concentration ratio expression 79−79395
wide aperture optical systems, irradiance field formation, comparative analysis 78−90479
Al and alloys corrosion characteristics in ethylene glycol-water mixtures 78−7095
Al-Ag alloy mirror for use as solar reflector, co-sputtering 80−20789
Au black solar absorbing film, particulate nature 77−39003
Cd_2SnO_4 film, optical transmission and reflection, evaluation for solar heat collectors 77−52191
Cr_2O_3/Cr cermet film, RF sputtered, for selective black absorbers 78−30046
Si concentrator cells, high efficiency, design, fabrication and meas. 80−93938
Si concentrator solar cells, effects of nonuniform illumination 80−93942
Si concentrator solar cells, high efficiency, state-of-the-art design and processing 80−93958
Si, effects of nonuniform illumination and temp. profiles under concentrated sunlight 80−93941
Si p^+-n-n^+ back surface field concentrator solar cells 80−93939
Si photovoltaic low series resistance concentrator for high intensity appl. 80−93940
n-Si solar cell and concentrator manufacture *(French)* 79−83602
Si solar cell array with concentration, design and development 80−45700
Si solar cells with concentrating collectors and integrated heat use system 80−45701
Si solar concentration cells, concentrated sunlight effects, experimental results, interpretation 80−35690
ZnS-Ag-ZnS coating 77−75642

solar energy conversion
see also solar absorber-convertors; solar cells
5 MW test facility, real-time computer control 80−72075
150 kW solar powered irrigation facility, design 79−96427
absorbed radiation heat conversion to chemical energy, upper limit 80−81483
absorption refrigeration machine driven by solar heat for air conditioning, math. modelling 80−76651
air conditioner, liquid desiccant, with flywheel storage system 79−52909
air conditioner appl., LiBr absorption, computer-aided performance predictions 79−62134
air conditioning system, intermittent cycle, NH_3/H_2O absorption, expt. evaluation in Florida 79−62133
air-based solar heating systems with phase-change energy storage, performance anal. using computer simulation 80−35762
alcohol fuel production from biomass 80−55773
alternative resources and technologies, Conf., Chicago, IL, USA, Nov. (1978) 80−23123
automative transport utilising stirling heat engine 80−55824
bacterial biomass production, efficiency bypasses that of photosynthesis 80−21408
Belgian solar heating systems, economic feasibility 79−57443
bioconversion of solar energy, review 80−45720
bioenergy conversion systems, efficiency improvements 80−30511
biological, energy from biomass conversion 80−61391
biomass, review of possible energy conversion processes *(French)* 80−93843
biomass conversion to fuels and chemicals, Purdue Process 80−26149
biomass energy conversion, energy sources for rural development 80−30509
biomass energy R and D 80−66922
biomass energy system for developing rural areas 79−61961
biomass options for the Big Island of Hawaii 80−66921
building heating, transient thermal flux calc. 79−62144
building heating and air conditioning, CAD w.r.t. maximum solar heat gain 79−57466
Canadian renewable energy industry, solar and biomass conversion technology *(French)* 79−87971
Canadian solar energy competitiveness rel. to government incentive policy 79−57393
central receiver program, heliostat, receiver and storage subsystems 80−30404
chemical, by NH_3 dissociation 80−30513
chemical, photo-induced electron transfer reactions in solution, organised assemblies and at interfaces 80−89677
chemical conversion and storage of solar energy, book 80−86045
chemical conversion and storage using norbornadiene-quadricyclene photoisomeric interconversion 80−89664
chemical energetics in solar energy conversion, storage and transport *(French)* 80−7917
chemical fuel production, efficiency of the conversion processes 80−61318
chemical heat pump/energy storage system 80−30512
chemical heat pumps for solar energy conversion using $LaNi_5$ hydrides 80−89667
chemical reactor theory and designs *(French)* 80−7916
chemical storage, chemical bond energy of SiO_2 and ammoniates undergoing thermal decomposition 80−76656
chemical storage, effect of micellar phase on photo-induced reactions 80−89678
chemical storage, long-term efficiency of iterative cyclic reactions 80−45764
chemical storage, photosensitization mechanisms for energy storing isomerizations 80−89679

solar energy conversion continued
chemical storage using novel photocyclization reactions of 1-alkenyl-2-pyridones 80−89680
chemistry research and developments *(French)* 80−11999
chlorophyll *a*-lecithin mixed monolayer coated electrodes, highly efficient quantum conversion, solar energy appl. 79−39314
chlorophyll a dihydrate photoelectrochemical cell 80−61387
climate, possible effects 78−81356
climate impact of thermal electric, biomass, photovoltaic and ocean thermal conversion systems 80−30612
climatic model experiments, simulated changes in albedo, surface roughness, surface hydrology, effects 78−81354
cNRS solar program and thermochemistry *(French)* 79−100485
cold water pipe designs for ocean thermal energy conversion plants 80−45725
collector system using regenerative oscills. in water columns 79−23188
composite annular wick heat pipe analysis and performance 79−62153
computer simulation for systems design 80−35679
conference, Ontario, Canada (Aug. 1978) 80−41949
conservation of nonrenewable resources 79−87976
consumer profile and application incentives 79−57391
convective losses in 2-D, differentially heated, inclined cavities *(French)* 79−24906
cooling of buildings in Turkmenian SSR, using open water evaporation, from LiCl solution 79−57463
Danish solar water heating system economics 79−62047
DC-AC inverter design, effect of meteorological conditions, computer simulation 80−61373
desalination appl., combination with greenhouse installation *(French)* 80−55806
desalination plant appl., MSF, technical and economic evaluation 80−61281
desalination plant coupling to solar collector systems, low-temperature multiple-effect type, technical and economic evaluation 80−55804
desalination plant utilising reverse osmosis, 2.5 kW solar generator 80−61282
desalination process appl., demonstration project multistage flash evaporation, demonstration project 80−61283
desalting plant appl. based on solar powered electrodialysis 80−55805
developing countries' architectural design for solar energy environmental control 79−57449
developing countries' solar energy utilisation planning methodology 79−57364
diluted black body radiation, conversion thermodynamics 79−40507
direct conversion and storage, review of developments, reviews 79−43741
direct conversion into electric current *(Italian)* 80−89612
direct conversion to H_2 fuel by water photoelectrolysis 79−62014
direct photoelectrochem. conversion and storage 79−62015
direct solar irradiance, indirect meas. 80−45644
distillation plant, 5000 lit/day, drinking water production in India 80−61280
earth storage and utilisation, technical and economic aspects 79−57475
economics, component cost of solar energy systems 80−45651
efficiency, geographic and economic aspects of solar energy utilisation 79−52888
electric generating systems, resource requirements 80−7923
electric solar pumps for water pumping 80−50942
electricity production by direct and indirect conversion schemes, review 80−50981
electrochemical heat engine for direct solar energy conversion 80−30519
electrode materials, for photoelectrolysis of water 79−29478
electromagnetics and environment, book 80−36431
electronic control of water heating system, for teachers 78−81753
energy analysis and viability of photovoltaic conversion and OTEC 80−61358
energy conservation and storage, materials needs 80−66958
energy independent houses design and construction options 79−79382
farmhouse heating solar energy collection and thermal storage system 79−57482
finned heat pipe latent thermal energy storage system performance 79−57487
flow turbine casing enclosed solar electric generator *(Japanese)* 79−88001
fluidyne pump, design and operating characts., expt. test results 80−55890
flywheel energy storage and conversion system for photovoltaic appl., economic anal. 80−94116
flywheel energy storage interface unit for photovoltaic applications 80−30571
free piston Stirling engines increase solar/thermal efficiency 79−96481
French energy research projects *(French)* 79−74497
French solar energy collection, research programme, outline *(French)* 79−74498
fuel production, by photochemical conversion and chemical storage 79−66413
ground thermal energy conversion, solar power generation 80−61313
H_2 production by H_2O pyrolysis, thermodynamics, theory 80−61448
heat generation for multipurpose utilization systems by heat of dilution converted from solar energy 80−55915
heat pump for energy storage using ammoniated salts. 80−81484
heat pump house heating system with low quality thermal flow 80−76617
heat pump plant for space heating in winter, air conditioning in summer 80−76615
heat pump system, solar ground coupled heat transfer, expt. and GROCS computer model 80−66987
heat storage by metal hydride, review 80−61455
heat storage in porous medium with circulating heat transfer fluid, solar system appl. *(French)* 80−40916
heating, water and space, Indian development 79−62140
heating and cooling of buildings, economic problems 79−57451
heating and cooling system for domestic use *(Japanese)* 80−108787
heating and cooling systems, evacuated tubular solar collectors and LiBr absorption system integration 79−62135
heating methods, collector types and insolation data *(Czech)* 79−70431
heating of buildings, types, construction and thermal and environmental parameters *(French)* 80−85268
heating of single room, heater efficacy evaluation, using stack effect 79−62142
heating system, for teachers 78−81763
heating system economic evaluation and optimisation 80−35644
solar energy conversion continued
heliostat design teaching aids and demonstrations 79−62126
high irradiance solar simulator for thermal absorptive material evaluation 79−62063
hot water systems, dyeing, in textile industry, commercial aspects 79−83576
house heating, Trombe-Michel wall system design and performance, digital simulation 79−62143
house retrofitting, combined heat and electricity generation, expt. results and economic assessment 79−61952
houses thermal environmental control in Northern India 79−62151
hydride concentration cells 80−35698
Implementation Centre proposals 79−57394
incident solar flux on arbitrarily oriented surface, computation models 79−57401
inclined-plane solar radiation design value determ. for plane-collector installations *(Spanish)* 79−79384
industrial utilisation of energy, book 80−61222
Iranian solar town conceptual development 80−35645
irrigation pump Rankine cycle solar engine and wind turbine comparison 79−57448
Jamaican solar energy training seminar programme 79−57395
large scale, climatic effects, conf., Laxenburg, Austria, Dec. 1976 78−81352
liquid thermal storage tanks, thermal stratification enhancement 80−40918
local and mesoscale weather, impact 78−81358
long-term solar energy storage in native rock 79−57474
low temperature solar energy appl. *(French)* 79−52887
low-temp. solar water heaters, tubular heat receptacles screen parameters optimisation 80−92030
major solar energy research programs, review 80−40843
materials science aspects, review 80−66957
mechanical power generation, reciprocating device development, based on vaporisation and condensation of working fluid 79−74505
metal hydride solar heat pump and power system, design and costs for space heating appls. 80−30521
micro-algae layers for various sun elevations and uniformly bright sky, capture cross sections determ. 79−23039
microbial production of energy sources from biomass 80−61392
microwave power transmission technology 80−40868
Middle Eastern research programmes 80−66939
MINI-OTEC ocean thermal energy conversion plant test 80−45727
mobile field dormitory, solar energy space and hot water heating 79−83623
modelling, of solar radiation regime energy structure 79−39285
molybdenite ore treatment using 2 kW solar furnace 80−3107
NASA space power technology program, photovoltaic energy conversion 80−30494
new materials and technical processes 79−39280
northern solar house long-term storage systems 79−57473
ocean swell and wave energy conversion system, feasibility 80−55795
ocean thermal energy conversion for electrolytic H prod. 80−30546
ocean thermal energy conversion plant, 100 MW, systems aspects 78−96235
Ocean Thermal Energy Conversion platform environmental impact assessment 80−45726
ocean thermal energy conversion systems 79−29456
oil recovery, enhanced, steam injection, cost model comparison of conventional and solar methods 80−66947
optics, conf., San Diego, USA (Aug., 1977) 78−50891
osmotic pressure utilisation, semipermeable membrane and low-head reaction turbine appl. 79−57418
OTEC; analysis of a heat exchanger−thermoelectric generator system 80−35710
OTEC, design and construction of a test plant 80−85298
OTEC, design of seacoast test facility, Hawaii 80−55888
OTEC, evaluation of alternative energy sources for the Guyana energy crisis 80−61270
OTEC, evaluation of bottom-fixed OTEC platforms on the edge of a continental shelf 80−55887
OTEC, NH_3 prod. 80−66988
OTEC, technology development, US DOE program review 80−94098
OTEC (ocean thermal energy conversion) plants, alternative forms of energy transmission assessment 79−61958
OTEC ocean engineering, status report 80−66989
OTEC ocean thermal energy conversion, American project, technical and economic fundamentals *(French)* 79−96482
OTEC ocean thermal energy conversion, commercialisation in USA 79−61957
OTEC plant development, an unfavourable analysis 80−55889
OTEC power plant, selection of working fluid (NH_3, propane and freon) 80−89665
OTEC power system development and environmental impacts 80−66990
OTEC R and D in Japan 80−35738
OTEC system performance study 80−104514
parabolic dish thermal power systems, technology and appl. 80−30558
passive rock bed storage system for domestic solar air heating 79−57490
passive solar building thermal performance modelling by passive solar test boxes, expt. 80−3494
passive solar building thermal performance modelling by passive solar test boxes, theory 80−7921
passive solar buildings, thermal heat flow modelling using model expansion methods 80−45645
phase transformation applicability using $Na_2S_2O_3.5H_2O$ and $Na_2SO_4.10H_2O$ 78−60155
phase-change, energy storage unit sizing for air-based solar heating systems 80−7922
phospholipid vesicle walls, photosensitised electron transport 78−80787
photo-electrochemical production of C-C bonds from carbon dioxide 80−21407
photobiological conversion of solar energy *(German)* 79−2013
photoelectric conversion cost reduction *(Italian)* 80−30479
photoelectrochem. processes 80−72068
photoelectrochemical cells, chlorophyll sensitised reactions 80−7948
photoelectrochemical cells, surface aspects 80−12021
photoelectrochemical cells, use of oxide semiconductors as anodes 80−101120
photoelectrochemical systems, material aspects, charge transport, energy output 80−12022

solar energy conversion continued
photoelectrochemistry, laser sources use for solar energy conversion 80 40873
photoelectrolytic production of H_2 and electricity, $LaCrO_3$-TiO_2 photoactive anode 80−12024
photogalvanic, EDTA-methylene blue cells props. and appl. 80−21406
photogalvanic, photochem. determ. of efficiency 80−89654
photosynthesis, biometric analogue 79−52914
photosynthesis, hydrocarbons production 80−89661
photosynthesis, photoelectric response of photosensitive liquid membranes and chloroplast discs 80−81482
photosynthesis, solar energy conversion and storage using artificial photosynthetic systems 80−89662
photosynthesizers, contrived, biosystems and photoelectrochem. conversion 79−52953
photosynthetic, in agricultural systems, incremental model 79−70457
photovoltaic, economic viability, 1979 state and future trends 79−43775
photovoltaic conversion of concentrated solar radiation, feasibility assessment 79−57436
photovoltaic energy conversion, review 79−100530
photovoltaic research and development in Japan, review 80−12012
photovoltaic space power systems, 25 kW power module evolution 80−30495
photovoltaic village power systems: the minigrid concept 80−66973
photovoltaic-solar thermal system role of high performance solar cells 79−61978
photovoltaic-wind hybrid alternative energy system 80−30409
photovoltaic/thermal solar energy systems, theoretical anal. 80−61375
photovoltaic/thermoelectric refrigerator for medicine storage for developing countries 80−35712
plant photosynthesis, solar energy conversion, book contrib. 79−43781
polymer films, solar energy materials, transparent, optical characts. investigation 80−20724
pond interaction with ground thermal storage 79−62093
pond viscosity stabilisation by organic thickeners 79−62094
ponds, daily performance characts. of shallow solar ponds 80−30554
ponds, economics and performance characts. of salty and saltless ponds 80−30553
power station, solar energy collection and conversion, pros and cons, economic prospects projection *(French)* 79−100489
power systems availability and reliability analysis 80−35687
primary fluid heated by solar energy in linear collector, thermal regimes and appl. 78−75061
pumps development, irrigation, 1978 status review 79−74506
quantum utilizing solar energy convertor efficiency in absence of intraband thermalisation 80−26144
R and D by US DoE 80−89674
radiation enhancement using surface polaritons 80−7941
radiation measurement requirements for energy conversion 79−57400
Rankine cycle heating and cooling system, 18-ton, analysis and design 79−52897
receiver convective losses determ., using cryogenic heat transfer tunnel 79−83636
regenerator of hygroscopic solutions, for air dehumidification 79−57464
residential applications, life cycle costing assessment 79−57445
residential heating system life cycle cost analysis 79−57444
residential solar energy systems, tax credit incentive costs and impacts 79−57450
review for teachers 78−86092
review of optical props. of composite materials with solar energy applications 78−56496
rural electrification by solar power, photovoltaic arrays efficiency 80−66974
salt-gradient solar pond absolute stability conditions 79−62095
salt-gradient solar ponds, performance characts. 80−30551
salty solar ponds, stability criteria for saturated ponds 80−30552
satellite, appl. of solid state microwave technology 80−40870
satellite, assessment for European appl. 80−40867
satellite, computer modelling of power transmission system 80−40866
satellite, microwave system perform. during startup/shutdown 80−40869
satellite photoelectric power stations, alternate favourable option 80−16791
satellite power systems concept, solar photovoltaic and solar thermal concepts 79−52891
satellite power systems review, DOE and NASA joint project 79−52890
satellite solar power stations using solar cell arrays and microwave transmission 80−50982
satellites, solar power, using microwave link, developments 79−24891
seasonal storage of solar energy 79−57472
selective surface coatings, solar energy collector appl. *(Chinese)* 79−34439
semiconductor electrodes for photoelectrolysis of water, appl. to solar energy conversion 79−29477
short- and long-term storage, stratification effects 79−57488
short-term storage monolithic structures 79−57489
simulation, testing and modelling, Conf., San Francisco, CA, USA, (Dec. 1978) 79−83635
Singapore solar energy availability, diurnal and annual variation 79−57403
Solar Assisted Gas Energy domestic hot water system installed costs 79−57447
solar energy transition and materials problems 80−26115
solar furnace, materials melting process dynamics rel. to automatic control 79−39317
solar gas turbine plant, N_2O_4 as chemically reactive working fluid 79−39316
solar power satellite, construction in space, fabrication methods, materials, tools 80−21377
solar power satellite concept, electronic systems 79−92065
Solar Power Satellites, energy anal. 80−50937
solar power satellites, solar energy conversion methods developments, general aspects *(French)* 79−100494
solar power stations, medium power heat and electricity production development program, economic requirements and technical options *(French)* 79−100493
solar still, industrial, stepped oblique type, annual operating data 79−39318
solar-electric heat pump for houses, design and tests *(German)* 80−7951
Solchem energy system, thermochemical solar energy transport, using CO_2-methane reforming-methanation cycle 80−94096
solid films and surfaces, conference, Tokyo, Japan (Jul. 78) 80−10739
solar energy conversion continued
solid state physics aspects, book 79−74518
southern Iranian solar pond performance simulation 79−62096
space heating, all-year solar energy collection and storage system 79−62074
space heating, heat pump and thermal storage system based on $CaCl_2$ and methanol vapour reaction 80−85307
space vehicle thermionic generators for solar energy conversion 80−35714
spaced metallic plate utilisation for solar thermal storage 79−57492
Stirling engine power conversion for MWe solar power system with parabolic concentrators 80−30561
storage in compressed air 79−57468
storage methods for large-scale appls., eval. 80−89675
student laboratory experiment 80−17776
subsistence-economy chicken-breeding solar energy storage regulation expt. 79−57485
sun-mill, version of dunking-bird, solar-powered, gravity-assisted heat engine 80−89672
synthetic chloroplats for H prod. 80−30508
system developments and research aims *(German)* 80−108799
system simulation, diffuse and total solar radiation relationship 79−57398
system with dual-source heat pump and long-term storage 79−57453
technology and methods for appl. of solar energy to European agriculture 80−76616
terrestrial utilisation of solar energy, scope and experience *(German)* 80−40829
testing solar thermal absorptive materials, high irradiance solar simulator *(Japanese)* 79−79185
textured surface, effects on optical props., applications in solar collectors 78−56443
THEK collectors, fluid transport network for solar energy to heat conversion *(French)* 79−24905
thermal, advanced solar thermal technology, review 80−30555
thermal, review of solar pond concepts 80−30550
thermal, Stirling heat engine, solar powered, for reverse osmosis desalination plant 80−55891
thermal chemical conversion cycles appl. to storage 79−100537
thermal electric and photovoltaic cell power plants, local energy exchange dynamics and climatic boundary conditions effects, preliminary examination 78−81355
thermal energy production, large scale, possible climatic effects 78−81357
thermal energy storage by chemically driven heat pumps 79−57476
thermal energy storage in salt hydrates for solar heating systems, storage material props. 80−101134
thermal power generation, large-scale, 1978 state and future potential 79−43749
thermal power system, open cycle air turbine *(French)* 80−45641
thermal solar pumps for water pumping 80−50942
thermal storage by molten salts *(French)* 79−70466
thermal systems, long-term perform. characts. using closed-form solns. 80−30556
thermal systems, technology status 80−40842
thermionic power plant, central thermal receiver tower concept, geometric config. and design 80−61390
thermochemical, conversion yields using $CaCO_3$ decarbonation 80−94097
thermochemical electric power generation, reversible chemical reactions 80−61394
thermochemical energy transfer, reversible reactions screening 79−87999
thermochemical receiver for solar thermal power, design 80−7950
thermodielectric effect, use in conversion of solar to elec. energy, anal. 79−43779
thermodynamic *(French)* 79−70434
thermodynamic conversion for solar water pumping 80−45728
thermoelectric, appls. to OTEC and agricultural irrigation 80−35708
thermoelectric air conditioner humidifier (SATEACH), solar assisted 80−108802
thermoelectric conversion, collector systems and thermal storage 80−45759
thermoelectric generator, high power density, with wedge-shaped electrodes 79−48100
thermoelectric generator using tubular heat-pipe with concentrator 80−89658
thermoelectric generators, efficiency evaluation and improvement 79−62017
thermophotovoltaics, conc. ratio and efficiency 80−7946
transients simulation, solar input and solar data computation for engineering of solar systems 80−94060
two-phase thermosyphon feasibility for solar energy transport and storage 79−57491
underground aquifer storage of hot water from solar energy collectors 79−57477
USA National Energy Plan, role of solar technology 79−57392
USA National Energy Plan impact on solar home heating economics 79−57446
USA solar heating and cooling R&D programme 79−57373
utilisation, conf., Cairo, Egypt (June 1978) 80−46734
utilisation, direct and indirect *(German)* 80−3489
utilisation by photobiological production of H 79−70456
utilisation via plant photosynthesis 80−3491
utility involvement in solar energy Project SAGE 79−57452
vapour turbine plants using combined thermal-power convertor and photoelectric convertor, thermodynamic efficiency for solar energy conversion 80−89614
water and space heating systems; economic feasibility 80−7920
water heater, domestic, flat-plate type, heat transfer analysis 79−62141
water heater with built-in storage 79−57454
water heater with two-fluid-circuits collector, dynamic response prediction 79−62139
water heaters, developing country (Nepal) developments 79−62137
water heaters, rural population demand fulfilment 80−89668
water heating, polyethylene low-cost unit development *(Afrikaans)* 80−7925
water heating by system of solar collectors and central hot water tank 80−55809
water heating system, solar, technical and economic anal. 80−50936
water heating systems, temperature and flow of entering water control, by thermal operated mechanical device 79−62138

solar energy conversion continued
water pumping solar systems using photovoltaic convertor arrays 80−61402
water solar photodecomposition, redox reaction thermodynamics 80−35697
water-heating systems, design method 79−83629
weather data reduction for building and solar energy system optimisation 79−57397
wind and wave power, utilisation prospects 80−61269
Al_2O_3-Au, cermet coatings, solar energy photothermal conversion, Bruggeman effective medium theory 79−83627
Al_2O_3-B_2O_3-SiO_2 sheet glass, solar energy appl., optical and mech. props. 80−87447
B-Si materials for thermoelectric conversion of solar energy *(French)* 80−89660
Bi_2Te_3 alloy thermocouples for solar thermoelectric conversion 80−94095
$CaCl_2$-methanol thermochem. cycle for solar thermal energy storage 80−30587
CdS film, chemical bath deposited, solar energy conversion by photoelectrochem. cells 80−108804
Cs-Xe vapour mixture, possibility of solar direct energy conversion into laser radiation 79−59688
$CuGaSe_2$ single crystals, elect. and optical props. for solar cell appl. 80−10981
Cu(II) complexes, reversible excited-state electron transfer reactions for solar energy conversion 80−89655
Cu_2S, polycryst. thin films, struct., optical and elect. props. for solar energy appl. 80−10837
Fe-thionine photogalvanic, cells 80−35696
H as the solar energy translator 80−30608
H biological photoprod. using sunlight, review 80−45777
H biological prod. by solar energy conversion, coupling of hydrogenase and chloroplast photosystems 80−45778
H, biophotolytic production from H_2O 80−61457
H photochemical prod. by H_2O photolysis using sunlight 80−45776
H photoelectrolytic production by H_2O decomposition using sunlight, review 80−45774
H prod. by H_2O pyrolysis using solar thermal energy 80−45770
H prod. by H_2O solar photolysis by engineering methods using biological materials *(Japanese)* 80−45765
H production by H_2O dissociation using solar energy 80−30597
H production by H_2O photocatalysis on TiO_2 using solid C 80−26150
H production for solar energy utilisation, solar-H energy system 80−51014
H, thermochemical prod. by high temp. H_2O decomposition using solar energy 80−45822
H-rich synthetic fuel prod. and transportation for solar energy utilisation 80−51015
H_2 and O_2 production from H_2O using solar energy, eval. of a hybrid process 80−104519
H_2 gas, photosynthesis prod. by green algae, turnover times and pool sizes 80−16821
H_2 generation by water solar photolysis, large-scale impracticability 80−26172
H_2, photobiological prod., key enzymes and biochem. systems, tech. problems of H_2 prod., review 80−61446
H_2 photochemical production by H_2O dissociation utilising solar energy, review 80−61452
H_2, photochemical production using visible light on aqueous solns. of a Ru complex 80−85192
H_2 photoelectrochemical production using solar energy and Zn(Mg)(Cr)(Ni) phthalocyanine dyes *(French)* 80−55936
H_2 production, by thermolysis of water in solar reactor, thermal calculations 79−39319
H_2 production, review of solar-H_2 energy systems 80−61447
H_2 production and storage utilising solar energy conversion, book 80−57017
H_2 production by biological and biochemical solar energy conversion, review 80−61454
H_2 production by direct solar energy conversion at sea, review 80−61456
H_2 production by direct thermal decomposition of H_2O utilising solar energy, thermodynamics, review 80−61450
H_2 production by H_2O decomposition, review 80−97813
H_2 production by H_2O photolysis using solar radiation, feasibility of large scale generation 80−72095
H_2 production by methylviologen photo-reduction, adsorbed on cellulose 80−81491
H_2 production by solar photochemical decomposition of H_2O 80−16822
H_2 production by solar-H_2 systems using metal hydrides 80−61464
H_2 production using Mg(Al)(Fe)(Co)(Ni)(Cu)(Zn) sulphates for solar energy storage *(French)* 80−55935
H_2, review 80−61453
H_2 thermochemical prod. by H_2O decomposition utilising solar heat 80−61451
H_2/O_2 thermochemical prod. by H_2O decomposition using solar energy 80−40919
H_2O photoelectrolysis, H_2/hydrocarbon fuel prod. via biomass conversion wastes 80−89653
H_2O, photoelectrolysis using TiO_2 and $SrTiO_3$ electrodes 79−52959
H_2O photolysis using Pt/(chlorophyll a.$2H_2O$) reaction for H_2 production 80−89663
H_2SO_4-H_2O chemical heat pump energy storage system 80−30515
In_2O_3:Sn, thin films, prep. by pyrolitic method, charact. by SEM, electron diffr. and SIMS, solar energy appl. 79−43143
KCl-CuCl eutectic fused salt, potential as intermediate temp. solar heat transfer and storage medium 80−101135
MGO-Au, cermet coatings, solar energy photothermal conversion, Bruggeman effective medium theory 79−83627
MgF_2-Au, cermet coatings, solar energy photothermal conversion, Bruggeman effective medium theory 79−83627
N_2 reducing solar cells for industrial NH_3 synthesis 80−89632
NaCl gas-droplet counterflow heat exchanger, numerical model *(French)* 80−61396
NaOH-8% $NaNO_3$ phase change thermal storage for solar total energy system 79−57481
Pt-Mn(III)-porphyrin electrode for possible wet solar cell 79−100529
Si solar cells with concentrators and heat pump 80−61371
SnO_2:F, thin films, prep. by pyrolitic method, charact. by SEM, electron diffr. and SIMS, solar energy appl. 79−43143
TiO_2-$LaCrO_3$-GaP photoelectrochem. reactor for materials synthesis using solar energy 80−45712

solar energy power stations *see solar power stations*

solar flares
1959, August 18 flare spectrum, H lines and metal emission 77−49353
1959 July 16, proton solar flare, composite plage and prominence flaring 79−75173
1967, January 29, proton spectrum in interval 1 to 5 GV 79−66894
1968, November 18, solar particle propag. in interplanetary environment 77−29607
1970 April 16 solar proton event and proton pitch angle distrib. in high-latitude magnetotail 79−53670
1970 June activity rel. to sunspots 78−89141
1971, December 14, purely coronal hard X-ray event obs. 78−93177
1971, January 14, radio emission position and polarisation 77−2393
1971, January-April, Hα flocculi rel. to flares *(Chinese)* 77−67081
1971, September 1, anisotropy of relativistic solar protons 77−22022
1972, April 18, solar protons in magnetosphere, flare-time asymmetry and anisotropy 77−33280
1972, August, anal. of dynamics 77−25992
1972, August, flares heliographic latits. rel. to cosmic rays N-S anisotropies 78−89018
1972, August, flares rel. to interplanetary shock waves and mag. fields 77−25903
1972, August, flares rel. to solar wind and magnetosheath plasma obs. 77−25904
1972, August, ground-based solar radio obs. 77−25993
1972, August, hectometric and kilometric radio emission, satellite obs. 77−25994
1972, August, high energy cosmic ray obs. 77−25894
1972, August, interdisciplinary summary of solar/interplanetary events 77−25991
1972, August, low energy cosmic rays obs. 77−25895
1972, August, magnetosphere response 77−25888
1972, August, obs. of assoc. coronal radio emission fluctuations 78−45311
1972, August, rel. to interplanetary scintillation obs. 77−25901
1972, August, solar wind plasma obs. 77−25902
1972, August 11, limb flare obs. 77−37587
1972, August 3-6, obs. at 1.9, 2.5 and 3.5 cm wavelength *(Russian)* 77−64719
1972, August 4, gamma-rays energy spectrum *(Russian)* 78−12185
1972, August 4, interplanetary flux hydromagnetic struct. 78−28475
1972, August 4, particle accel. into interplanetary medium *(Russian)* 77−33303
1972, August 4 and 7, gamma-ray obs. 78−32306
1972, August 4 to 5, interplanetary plasma flow hydromagnetic struct. rel. to mag. extra-storm 79−53653
1972, August 7, charged particles accel. 79−12360
1972, June to August, effects on comets 77−25983
1972 August, correl. with geomag. activity and microearthquakes 79−66638
1972 August, interplanetary disturbances obs. by Pioneer 9 77−2317
1972 August, m wavelength charact. of active region McMath 11976 *(Chinese)* 77−22156
1972 August, obs. of interplanetary shocks at 2.2 AU 77−45276
1972 August, solar protons auroral zone precip. assoc. with storm sudden commencements 77−82081
1972 August 2-4, ionospheric VLF sudden phase anomalies 78−40739
1972 August 4, calc. of radiation doses absorbed in near-Earth orbit 77−52892
1972 August 4, energy charact., plasma and mag. field struct. behind interplanetary shock wave 78−49268
1972 August 4, meas. of absorbed radiation by Prognoz satellites 77−29614
1972 August 4, neutrons and gamma-rays prod. 79−16915
1972 August events, shock wave form and energy 78−57534
1972-1975 period, unusual flare and sunspots phenomena 79−16914
1973, April 29, cosmic ray anisotropy, Cosmos 555 obs. 77−45268
1973, April 29, cosmic-ray particles obs. by Cosmos 555 satellite 77−53350
1973, April 29-30, anal. of complex solar particle event 78−20593
1973, July 29, E45° flare, cosmic ray particles coronal and interplanetary propag. 77−82090
1973, June 15, Hα, magnetic and X-ray morphology 78−4173
1973, June 15, high temp. plasma evolution, Fe XXIII, Fe XXIV obs. 78−28636
1973, June 15, multiple loop activations and continuous energy release 78−28637
1973, June 15, Skylab XUV spectra, intersystem and forbidden transitions 78−4159
1973, June 15, UV spectral lines list from 1000 to 1940 Å 78−89139
1973, September 5, flare pre-onset morphology 79−40169
1973, September 5, struct. and dynamics from X-ray and XUV obs. 78−12175
1973, September 5, X-ray obs. rel. to energy storage and deposition 77−17480
1973, September 7, proton region development 77−37588
1973 August 9, decay phase, X-ray and UV obs. 79−53780
1973 August 9, plasma evolution during compact event 79−5792
1973 August 9, upper flare chromosphere semiempirical model 79−40148
1973 June 15 flare in active region NOAA 131 (McMath 12379), X-ray obs. 78−53913
1973 September 5, 18:26 UT, radio data and theoretical model for fast-mode MHD shock wave 79−92734
1973 September 5, two-temp. model 80−56805
1973 September 7, Mars probe meas. 78−16252
1973 September 7, new class of transient events, X-ray, UV and visible obs. anal. 80−98643
1973 September 7, obs. of thermal phase of large solar flare 79−8886
1974, January 21, single loop obs. in Fe XV emission lines 79−66991
1974, September 10, solar mag. field var. during class 2b flare 78−89160
1974 July 3, quasiperiodic struct. of assoc. type IV burst 80−62097
1975, August 10, magnetic field reconstruction 77−13302
1975, August 22, three freq. obs. of moving type IV radio burst at limb 78−69776
1977, October 12, VLA obs. interpreted with optical, X-ray and other microwave data 79−44428
1977, September 24 and November 22, anal. of energetic particle events following solar flares 78−77446

solar flares continued
1977 April 12, gyro-synchrotron modulation in assoc. moving type IV bursts 80−26833
1978, May 7, cosmic-ray particles obs. at Bologna by ionising component supermonitor 78−85777
1978 January 1, Prognoz-6 energetic particle and solar wind meas. during assoc. interplanetary disturbance 80−90315
1979 March 25, X-ray obs. 80−85915
accelerated nuclei from C to Fe from 20-300 MeV/nucleon 79−5802
accelerated particles, nucl. composition and Coulomb losses 80−72913
accelerated particles, power-law energy spectrum problem 78−40914
accelerated particles escape into interplanetary space, influence of solar mag. fields 79−62807
acceleration mechanisms, implications for hard X-ray burst models 80−72912
acceleration phases, gamma-ray and microwave evidence 77−17527
active region flare rates and 8.6 mm brightness temps. 77−29769
active regions, 3 cm radio emission spectral slope, flare-associated variations 80−98630
active regions pre-flare X-ray morphology 77−17481
activity rel. to auroral activity equatorial latitude 80−98499
Alfven-Carlquist double layer theory 78−77526
anomalous Balmer decrement, stimulated transitions between highly excited atomic levels 78−5176
blast type cosmic phenomena, gasdynamical models and two-dimens. unsteady computs. 77−60565
blue continuum flares and D3 preflare shell obs. 80−51709
celestial chaos related to Earth's climatic and biological catastrophes 79−53509
chromosphere, emission line profiles of inhomogeneous formations 77−37586
chromosphere, long-lived radioactive nuclei generation rel. to quiet Sun γ-emission *(Russian)* 77−45390
chromosphere filaments and flare obs. 1967-9, Hα monochromatic light 78−61836
chromosphere flare, 6 cm obs. of assoc. burst source with 6″ resolution 80−62096
chromosphere flares, correl. with vars. in Earth surface atmospheric press. field 78−36245
chromosphere flares, effective time of observations *(Russian)* 78−40893
chromosphere flares, effects of soft X-ray heating 79−40170
chromosphere flares, H Lyman α direct collisional excitation rel. to profile and polarisation 80−41780
chromosphere flares, initial phase parameters determ. method 80−62104
chromosphere heating, charged particles beam collisional interaction with H target 78−93095
chromosphere impulsive flares, space-time relation to centimetre wavelength radioemission bursts *(Russian)* 79−16924
chromosphere limb flare, 1959 July 25, spectrum rel. to physical conditions 80−105227
chromospheric, effects on geomag. pulsations 78−28424
chromospheric, magnetic effects and elec. field in auroral electrojet region of ionosphere 78−69576
chromospheric, occurrence rel. to sunspot mag. field oscills. 77−67084
chromospheric, optical thickness and H ionization degree from Balmer line obs. 78−73694
chromospheric, parameters and fine struct. determ. 78−24499
chromospheric flares, rel. to pulsed microwave bursts with quasithermal spectrum 77−78762
conduction cooling of flare loops, magnetic structure effects 79−44451
conference, Florence, Italy (Nov. 75) *(Italian)* 78−93191
conference, Grenoble, France (Aug. 1976) 77−82191
confinement of hot electrons, hard X-ray production 79−96982
continuum radiation, m wavelength obs., emission mechanism 79−21248
cooling rate, nonlinear cond. effects 78−28638
corona, flares correl. with interconnecting loops transient brightenings 80−21972
corona, plasma turbulence triggering during fast flux emergence 78−45304
corona, struct. rel. to prominences and flares 79−71014
coronal and interplanetary responses, dynamic modelling 78−49418
coronal and interplanetary shock waves during 1972 August 79−16916
coronal electric current systems development in active regions, rel. to filaments and flares 79−25567
coronal flare plasma, evaporative cooling 78−40890
coronal flare-like events, soft X-ray data from Skylab 78−61827
coronal loops brightened by flares and transients, decay 78−40907
coronal mass ejection events assoc. with flares, prominences or radio bursts, outward vel. meas. 77−22197
coronal particle distrib. functions following flares, radio evidence 79−48759
coronal plasma heating during flares, ionisation and reverse currents 79−5793
coronal plasma nonequilibrium ionization and emergent X-ray spectrum 78−7953
coronal turbulent heating rel. to flares 80−12715
cosmic ray and geomag. vars. correl. with flares 79−84764
cosmic ray events with high relative ^{3}He abundances, obs. during 1976 November to December 80−61972
cosmic ray intensity diurnal anisotropy, solar flare location effect 79−44318
cosmic ray modulation by 1976 April 30 flare 80−67484
cosmic ray particle intensity variations, depend on interplanetary mag. field and solar wind 80−77372
cosmic ray particle prod. and accel. in expanding coronal mag. bottle 80−77244
cosmic ray particles, interplanetary scatt. mean free path, energy depend. 77−9633
cosmic ray particles, origin, nature and effects, interplanetary propag., review *(Russian)* 79−66893
cosmic ray particles, possible cause of ancient climatic and biological catastrophes 77−78587
cosmic ray particles emission *(Italian)* 78−96461
cosmic ray particles production and modulation, analytical solns. 78−16368
cosmic ray particles propag. in interplanetary medium, model 79−80128
cosmic ray proton flux determ. from ^{3}He in lunar rocks 80−98576
cosmic ray proton propag. in interplanetary medium 77−53502
cosmic ray protons, ≥130 MeV, April and May 1979 obs. 80−51627
cosmic ray solar modulation, semi-diurnal anisotropy on flare days 80−46356
solar flares continued
cosmic ray variations, solar activity and neutrino fluxes, review 79−84599
cosmic rays, anomalous flux anisotropy, 1973 September probe meas. 77−33300
cosmic rays, complete model of propag. 77−2313
cosmic rays, fast azimuthal transport by coronal mag. bottle 78−32305
cosmic rays, interpretations of isotopic comp. of H and He 77−45266
cosmic rays absolute spectra for flares of 1966-76 period 79−84598
cosmic rays transient intensity vars., solar flare origin 78−89021
cosmic-ray long-term var. 77−53340
cosmic-ray particles obs. during solar flares 77−53350
Cretaceous-Tertiary extinctions, effects of solar flares and stratospheric aeronomy 78−32215
current buildup prior to flares, obs. test to distinguish between slow and transient 80−31281
current layers explanation for X-ray and UV emission 80−101572
current sheet in compressible plasma, self-similar resistive decay 80−1755
current sheet models, review 77−17475
current sheet region during chromospheric flare development *(Russian)* 79−40159
cycle 20, flares and cosmic ray events at minimum 79−21250
cycle 20, flares rel. to cosmic ray intensity, model 80−72914
development, role of plasma turbulence 77−17476
development, similarities and differences with magnetospheric substorms 77−17477
disruption effects in power and communications, research progress report 79−101021
distribution in galactic coord. system *(Russian)* 80−67689
double-ribbon flares, search for auroral type brightness motions 77−60744
dynamics of flare sprays 80−56808
Earth storms, initiation and propag. from solar flares *(Korean)* 77−53335
electric currents in cosmic plasmas 78−12094
electron acceleration by strong plasma turbulence 79−4140
electron acceleration to mildly relativistic energies by strong plasma turbulence 77−31437
electron beams, diagnostic using chromospheric spectrum 80−26827
electron densities from Ca XVII line ratios 77−87358
electron density, XUV spectrum diagnostics 79−88633
electron density and temp. from Ca II/Fe I emission line ratios *(Russian)* 80−51717
electron density determ. from X-ray spectra obs. 80−82326
electron events, Oct. 1972 to Dec. 1974 obs. 80−56796
electron fluxes rel. to increased geomag. activity and ionospheric absorpt. after flares 79−75175
electron plasma oscillations assoc. with type III radio bursts 77−37592
electron streams, thick-target, relax. and bremsstrahlung, Legendre expansion, solar X-ray flares appl. 79−70950
electrons ejection into interplanetary space, correl. with flare magnitude *(Russian)* 78−77445
electrostatically unstable heat flow and its consequences 78−20804
elementary flare bursts, model, kernels excitation 80−31283
emerging flux model, trigger mechanism 78−89162
emerging flux model 77−82207
emerging flux model 78−4165
emerging flux regions and evolving mag. features, rel. to flares 77−82202
emission line profiles, from inhomogeneous solar phenomena with different porosities *(Russian)* 78−40891
emission mechanism, model *(Italian)* 78−96462
energetic flares correl. with sunspots penumbral spiral morphology *(Chinese)* 77−22155
energetic particle abundances Voyager obs. 80−90382
energetic particle composition temporal development during flares 78−89148
energetic particle event of 1974 July 4, Fe/O charge comp. spatial and temporal vars. 77−22199
energetic particle events from same active region, p/α enhancement 79−40151
energetic particle events obs. at 1 to 6 AU, radial transport 77−70953
energetic particles, acceleration 80−31266
energetic particles, convection and adiabatic decel. effects on time fo max. flux 77−2420
energetic particles, Fe charge states meas. 77−2418
energetic particles from flares, interplanetary shock waves 78−49276
energetic particles interplanetary propag. model 78−65468
energetic particles time dispersion, vel. and species depend. 77−2419
energetics depend. on flare volumes 79−25566
energy, period, radiation, future research *(Dutch)* 78−32432
energy build-up, appl. of new approach to force-free mag. field 80−62011
energy conversion mechanism, analogy with mini black holes fast explosive evaporation in plasma 78−96388
energy disposition by non-thermal electrons, indirect determ. 79−25581
energy release and transfer, Skylab X-ray obs. 77−82208
energy release processes, effect on solar atm. 77−60747
energy source, photospheric elec. currents 77−17483
energy source and current layer instability origin 80−101571
energy storage and release, model constraints 78−65491
energy transfer to chromosphere by soft X-ray photons 77−82210
ephemeral region flares and supergranulation network diffusion 79−21265
eruptive processes, onset theory 78−61840
EUV (1420-1960 Å) continua, Skylab obs. 79−30028
EUV and hard X-ray bursts interrelationship 78−61845
EUV and hard X-ray sources relationship 80−46512
EUV continuum emission, Skylab obs. 79−30046
EUV emission from B-like ions, density sensitivity 79−16910
EUV emission line spectra, analysis of Skylab obs. 78−40913
EUV impulsive bursts, characts. 78−77539
EUV radiation, detect. using ionosphere sudden freq. deviations (SFD) 80−8484
EUV structure of small flare, Skylab obs. 78−40912
evolution model, link with microwave events magnitude distrib. 80−98640
evolutionary relation to type I sources, 146 MHz obs. *(Chinese)* 80−8609
evolving force-free magnetic fields, preflare stage development 77−29739

solar flares continued
evolving force-free magnetic fields, variational formulation 78−93182
excited cosmic plasmas, review 78−69671
exposure of Luna 24 core samples, thermolum. obs. 80−82246
fast electrons scatt. in atm., X-ray spectrum 78−77542
fast electrons stream, free dispersal in solar corona with nonsteady injection 80−17568
fibril changes in small flare, high resolution obs. 79−44452
fibrils evolution rel. to flare activity 77−17487
first phase acceleration mechanisms 80−31267
flare build-up, study workshop, Cape Cod, Mass., USA (1975 September 8 to 11) 77−17473
flash phase and current sheets thermal evolution 77−17485
Forbush decreases and corresponding flares during solar cycle 20, 1965-72 period 78−49249
Forbush decreases in 1973-1974, unusual characts. 80−12624
Forbush effect in intensity of solar protons 79−80126
force-free magnetic fields evolution, field configurations stability and motion of medium 78−12176
force-free magnetic fields toroidal component upper limit rel. to flares 77−33479
gamma ray emissions study, Solar maximum mission, detector assembly and electronic assembly 80−63476
gamma-ray line emission, review 79−44641
gamma-ray line formation at 0.51 MeV 77−13292
gamma-ray lines, HEAO 1 obs. 80−67682
gamma-ray observations *(German)* 77−60853
gamma-ray spectroscopy 80−31271
gamma-rays with energy >8 MeV prod. in flares 79−53779
geocorona scattered Lα enhancement during 1972 August solar flares 77−78582
geomagnetic crochet, two-layer current model 79−44300
geomagnetic crochet type disturbances current systems and elec. fields in polar cap ionosphere 78−40733
geomagnetic effects, summary of 1978 activity 80−72919
geomagnetic solar-flare effect and ionospheric induction 79−53632
ground based observations review, flare build-up implications 77−17489
ground level enhancements during 21st solar cycle 79−12361
Hα post-flare loops dynamics, 1973 July 29 flare 80−31286
hard X-ray and radio events, spectral features rel. to particle accel. 77−45369
hard X-ray bremsstrahlung, polarisation and directivity of radiation from thermal source 80−90374
hard X-ray burst, 1972 August 4, trap-plus-precipitation model 80−12747
Hard X-Ray Burst Spectrometer on Solar Maximum Mission 80−51658
hard X-ray bursts, collective plasma effects and electron number problem 77−71094
hard X-ray bursts, intensity profiles pulsations 78−61846
hard X-ray bursts, relationship to type III-V radio bursts 78−89157
hard X-ray bursts, role of collisionless cond. front prod. by rapid coronal heating 79−44427
hard X-ray bursts, upper limit to anisotropy 77−29742
hard X-ray emission, backscatter rel. to anisotropy and polarisation 78−28594
hard X-ray emission, shot-noise character 79−96983
hard X-ray flare events, review 78−89144
hard X-ray flares, high time resolution anal., ESRO TD-1A satellite obs. 77−22185
hard X-ray flares obs. with 100 ms time resolution 77−71093
Hard X-ray Imaging Spectrometer on Solar Maximum Mission 80−51659
hard X-ray polarization 80−41787
hard X-ray radiation, elementary flare bursts props. 78−89158
hard X-ray sources, diagnostics 78−89159
hard X-ray time profiles and accel. processes 79−30030
hard X-rays obs. from 1972 August 2 and 11 flares 79−8900
heat conduction *(Russian)* 79−35229
heat transfer, influence on temp. struct. 79−40168
heating by corpuscular streams, X-ray, EUV and coronal lines emission *(Russian)* 77−71071
heavy ions in solar wind from flare-heated coronal plasma 79−75197
high latitude flares rel. to proton flares *(Russian)* 77−64729
hydrodynamic simulations of flare/surge events 80−12748
impulsive electron acceleration in solar hard X-ray flares, inferences from obs. 77−29748
impulsive electron acceleration in solar hard X-ray flares, theory 77−29749
impulsive EUV and hard X-ray emission 78−65578
impulsive flux transfer events, theory 77−17495
impulsive heating using EUV obs. *(Russian)* 77−91502
impulsive mm-wave bursts, quasi-quantization 80−94770
impulsive phase, Hα, hard X-ray and microwave emissions 78−77540
impulsive phase, hard X-ray spectrum, OSO 7 obs. 79−12440
impulsive solar flares, adiabatic heating 78−93176
impulsive X-ray burst, spectral anal. analytical method *(Chinese)* 80−85919
increase of cosmic ray intensity during 1977 November 22 ground level event 79−48629
intense compact subflare, physical parameter anal. 79−62802
interplanetary corotating nucleon fluxes separation from solar flare fluxes by radial gradients and nuclear comp. 79−25413
interplanetary flare-associated shock waves, from radiosource scintillation obs. 77−2318
interplanetary flare-generated shock wave at 9.7 AU, Pioneer 10 obs. 78−57422
interplanetary magnetic field structure within flare streams 78−7969
interplanetary manifestations, solar wind flows associated with hot heavy ions 80−51635
interplanetary matter energetic props. at Earth's orbit following solar flare 77−49261
interplanetary plasma flows from strong flares, props. and nature of mag. regions 77−91397
interplanetary plasma flux from strong flare rel. to magnetospheric disturbances 78−73600
interplanetary shock waves, flare-generated, scintillation obs., 1977 Sept. 79−48638
interplanetary shock waves during second STIP interval (1976, March 15-May 15), scintillation obs. 78−81514
interplanetary shock waves generation *(Italian)* 78−96377
solar flares continued
inverse Compton radiation, appl. to inference of relativistic electron spectra 80−90339
Io, correlation of posteclipse brightening with major solar flares 78−28573
ion-acoustically turbulent plasma, cond., solar corona appl. 79−19027
ionisation events in stratosphere, effects on NO_2, O_3 and climate, rel. to life extinction 78−96273
ionising radiation, atmospheric electrification modulation rel. to Sun-weather relationship 78−57261
ionosphere D-region interaction, relaxation after sudden cut-off of ionisation source 77−33254
kink instability obs. in XUV by Skylab 77−45370
kink instability of coronal loops 80−41802
Langmuir turbulence spectrum estimate from X-ray obs. 80−82329
Langmuir waves, upconversion of ion-sound impossible 80−41716
Langmuir waves and anisotropic particles, Legendre-expanded quasilinear eqns. appl. 79−75089
large scale variations, evidence from meteoroid data 77−82190
limb flares struct. and evolution, Skylab soft X-ray telescope obs. 77−82199
line profiles calc. for inhomogeneous emission formations 79−25562
localisation in Sun's atmosphere, radio observations 79−88641
loop prominence system, 1972 May 24, optical and X-ray obs. 79−30045
loop prominence system, flare assoc., high temp. corona 79−53782
loops, anisotropic pitch-angle distrib. of electrons generating hard X-rays 77−13314
loops, mag. field config. influence on conduction cooling rate 77−17528
Lyman continuum obs., energy transfer, chromospheric evaporation 79−21266
magnetic and velocity fields config. and changes in active region 77−17486
magnetic energy conversion 80−56682
magnetic field config., vel. fields and accel. processes, obs. requirements 77−17496
magnetic field energy dissipation, in neutral current sheets 78−26250
magnetic field evolution 77−17484
magnetic field line reconnection, laboratory expts. rel. to flares 77−17494
magnetic field lines reconnection, clouds-in-cells plasma model 77−84490
magnetic field of flare flow, anal. of struct. 78−57523
magnetic field reconnection, current instability in reconnecting current sheets 77−37486
magnetic field topology and elec. current system, similarities to auroral flares 77−17270
magnetic fields, force-free fields evolution, nonequilib. states and preflare stage 80−105213
magnetic fields, role in disparitions brusques of solar filaments *(Russian)* 80−51726
magnetic fields, skinning process stability and critical gradient in active regions 77−53521
magnetic fields in low corona, active role in solar flares 77−17474
magnetic fields meas., photographic method *(Russian)* 78−65584
magnetic flux emergency from below photosphere, form. of current sheets 77−22176
magnetic flux of colinear bipolar spot pairs 79−75185
magnetic merging during substorms and solar flares, role of O-type neutral lines 79−53665
magnetic merging effects, relevant obs. in Earth magnetotail 77−17301
magnetic pumping of energy into nonequilib. turbulence plasma, as flare energy source 77−78764
magnetic reconnection, plasma accel., heating and shock form. 78−40773
magnetic structures, models and predictions of flux rope theory 80−21955
mass ejection mechanism for transient phenomena 78−7980
mass motions in heated flare filament 77−29770
maximum activity, obs. program for 1979 Apr. 1-1980 Nov. 1 period 77−17497
mechanisms, review *(Italian)* 78−96463
mechanisms and laboratory simulation *(Russian)* 79−101135
MHD shock waves, propag. in solar atmosphere 78−24503
microwave and optical emissions comparison 80−31284
microwave burst spectra and flare mag. fields 78−7970
microwave bursts, millisecond spikes obs. 78−96464
microwave bursts, polarisation features interpretation 78−96468
microwave bursts, X-ray correlated, continuous injection model 77−17515
microwave flux decreases rel. to assoc. activity complex 77−25989
microwave radiation from thermal, hard X-ray sources 79−8892
microwave radio flares, direction pattern 78−85927
microwave spectrum, appl. of quasi-thermal electrons gyrosynchrotron emission theory 80−36602
model, nonunform current sheet breaking 77−82205
model based upon photospheric dynamo action 80−62102
model for photospheric mag. field importance in coronal energy storage 80−72906
models, current interruption and impulsive flux transfer 79−12438
models, high-temp. and low-temp. comparison 80−12714
modification of stratospheric elec. fields, direct evidence 79−48553
monitoring using global radio solar telescope network 80−82202
multiple loop activations and continuous energy release, Skylab obs. 77−82209
multiply impulsive solar bursts, spectral evolution 80−26828
near-Earth radiation hazard due to solar flares, dosage estimation technique 80−67482
negative bursts with moving filaments 1969, 19 May 77−53516
neutrons and γ-ray fluxes calc. 79−80127
non-stationary heating of solar flare plasma by non-thermal electrons 77−17455
non-thermal processes in large solar flares 77−29771
nonlinear stage of instability due to local Joule overheating 78−61839
nonrelativistic electron propag. and type III radio bursts *(Russian)* 77−78742
nonrelativistic electrons accel. by strong plasma turbulence 78−7954
nonrelativistic electrons coherent propag. 77−91506
nonthermal electron beams, effect of reverse currents on beam dynamics and X-ray bremsstrahlung 80−51711
nonthermal particle production during buildup and in absence of flares 77−17492

solar flares continued
nonthermal particles energy flux, ATM evidence for low proton/electron ratio 79−8887
north-south distribution of flares, sunspot mag. classes and sunspot areas, 1955-74 period 77−71088
nuclear processes in solar atm. due to charged particles accelerated in flares 78−57527
observation by optical and radio techniques 79−48765
observational and theoretical status, review 80−51728
occurrence frequency rel. to solar cosmic-ray prod. rate, influence of solar activity long-term vars. 79−92735
onset at m wavelengths 77−17491
onset phase, photometric anal. 77−82212
optical, X-ray and radio emission, anal. of data 78−89156
optical continuum origin, bluish-white emission knots 77−17513
particle acceleration, charge spectrum and comp. form. 80−46529
particle acceleration, injection energy concept 80−101509
particle acceleration, power law spectrum 78−57525
particle acceleration, X-ray and gamma-ray obs. 80−31265
particle acceleration by cyclotron damping of cascading turbulence 79−44433
particle acceleration in turbulent current sheet 79−35232
particle and EM emissions, review *(Italian)* 78−93192
particle events, exponential decay 78−4047
particle events, interplanetary propagation from 1 to 5 AU 78−20594
particle streams, collective plasma effects associated with continuous injection model 80−21954
particle tracks in lunar rocks, rel. to micrometeorites in and out of ecliptic 77−29737
particle trajectories at mag. neutral point 79−66886
particles meas. and integral proton spectra anal. 79−62695
particles pulsed accel., plasma turbulence, ion-acoustic and Langmuir waves 78−96450
phenomena preceding, accompanying and after flares 78−61829
phenomenological model, appl. to 1972, August 4 flare 78−49407
photosphere, force-free magnetic field bifurcation rel. to flare process 78−40901
physical mechanisms, rel. to high-energy astrophysics 77−17499
plasma, compressible magnetic-field reconnexion 80−6226
plasma, infinitely conducting, pinch effect, dynamical accumulation towards neutral line of magnetic field 80−83977
plasma column merging, simulation expt. *(Japanese)* 80−31269
plasma convection in force-free mag. field, mechanism for chem. separation in cosmic plasmas 79−35125
plasma electron density from Fe IX lines intensity ratio 78−20771
plasma flows, in strong mag. field, gas dynamics 78−57524
plasma heating by energetic nonthermal electrons, theory 77−53505
plasma instability and turbulence, review 80−62100
plasma kinetic processes, theory 78−85920
plasma physics, explosive phase 77−17514
plasma processes, magnetospheric substorm simularities 80−41671
plasma stream from flare, struct. rel. to flare location on Sun 80−41790
plasma wave electric fields meas. using Stark effect 78−12193
polarimetric observations at 3.7 and 11.1 cm wavelengths 77−71089
polarization structure of microwave bursts 79−96984
pre-flare energy build-up, role of transition zone instabilities, far UV spectroscopic obs. 77−17479
prediction by comparison of X-ray and visible data 80−72910
preflare association of mag. fields and mm wave emission 77−17490
preflare characteristics of active regions observed in soft X-rays 79−84776
preflare current sheets search, for forecasting occurrence of flares *(Russian)* 77−60746
primary energy release region, plasma radiation diagnostics 79−84777
prominence, 1979 March 27, photographic obs. *(Chinese)* 79−92744
proton and electron events, interplanetary scatt. mean free path 78−57421
proton energy spectra slope from radio burst data 79−53683
proton event, 1972 August 4, influence on stratospheric O_3 78−7732
proton events, excessive particle emission mechanism 78−45310
proton events, forecasting quality improvement *(Chinese)* 77−22158
proton events, threshold effect in second-stage accel. 78−61847
proton events and coronal mass ejections 78−77545
proton events correl. with 3 cm radio emission quasiperiodic fluctuations 77−53533
proton events effects on HF ionospheric absorption at low latits. 78−69594
proton events forecasting rel. to microwave bursts *(Chinese)* 80−12723
proton flare, 1971 January 14, assoc. complex radio emission event 79−40175
proton flare, 1971 September 2, simultaneous satellite obs. 77−67083
proton flare active regions, force free mag. field and force free factor determ. *(Chinese)* 80−77365
proton flare events, relation to type I (metre wave) radio sources *(Chinese)* 80−105222
proton flares, correl. with geomag. pulsations *(Russian)* 78−69291
proton flares, effects on ionospheric circumpolar currents 78−49198
proton flares, fast particles flight time from polar cap absorpt. effects 77−17469
proton flares, near-Earth solar protons parameters determ. from radio bursts 78−45165
proton flares, particle characts. near Earth from radio burst obs., longit. attenuation function 78−45309
proton flares, quantitative identification from characts. of microwave radio bursts at 9 GHz 80−4323
proton flares, temporal ref. functions from microwave radio bursts 78−73591
proton flares, type IV radio emission rel. to multi-stage solar particle accel. 79−44437
proton flares 1942-76 and their prediction 78−20811
proton flares rel. to sunspot mag. field motion 77−17488
proton flux increases assoc. with flares 77−9637
proton fluxes, Mars 7 probe meas. 78−69624
proton fluxes at 1 AU during solar min., Prognoz 3 obs. 78−69769
proton intensity north-south asymm. rel. to plasma sheet and daytime polar cusp dynamics 77−17297
proton long term accel., nuclear reactions, need for (p,n) cross sections 77−25997
proton parameters changes assoc. with 1972 August flares, Pioneer 9 and 10 obs. 77−33314

solar flares continued
proton spectrum determ. from latitudinal effect, using minimal Stormer pulse 78−45308
protons, flux limit due to accel. mechanism saturation effects 80−98645
protons, formation of ^{3}H and ^{14}C in terrestrial atmosphere 78−92886
protons, high-energy, from 1973 April 29 flare, arrival delay at Earth 79−62694
protons, identification from accompanying EM emission 79−12443
protons, interaction with zodiacal dust cloud, γ-ray and X-ray lines prod. 79−53771
protons, radiation hazard in shielded spacecraft 80−8194
protons, stochastic accel. by Alfven wave turbulence 80−21953
protons prod. by flare of 7 Aug. 1972 anal. 77−53356
pulses of characteristic energy, prod. and appl. to other astrophysical plasmas 77−78736
radiation, EM and particle, generation features 80−101575
radiation, microwave and protons, generation props. 80−109413
radiation danger during manned space flights 80−41788
radiation dose at Earth's surface 79−25109
radiative, mechanical and mag. energy release 79−53797
radio brightness distribution, processing in one-dimensional synthesis *(Italian)* 80−98628
radio bursts, 6 cm obs. with 6″ resolution 78−53897
radio bursts, drifting spikes obs. 79−48753
radio emission associated with chromospheric flares *(Italian)* 78−96457
radio emission preceding proton flares, pulsation instability 78−53911
radio flares and sporadic radiation, Interkosmos-Copernicus 500 obs. 77−53503
radio noise storms, spectrum and position at decametre wavelengths 78−28622
relativistic heavy nuclei, preferential accel. 77−45267
resistive magnetic tearing, energetics 79−96904
reverse currents 78−16363
S-component source spectra, correl. with flare occurrence, EHF obs. 80−101579
SCOSTEP project, Study of Travelling Interplanetary Phenomena (STIP) 77−17316
second-stage X-ray emission, spectrum beyond 200 keV 80−51710
SFE at Hyderabad, diurnal var. 77−70922
shock wave, solar flare generated, plasma enriched by O^{6+} and He^{++} 80−72740
shock wave acceleration of protons and relativistic electrons 79−48757
shock waves, coronal, during large solar flares, proton and electron accel. 80−21974
shock waves and convection in region heated by electron stream 77−71079
Shuttle/Spacelab program rel. to flare buildup studies 77−17498
simulation, expt. on merging of two current carrying plasma columns *(Japanese)* 80−94775
simulation of solar flare energy spectrum from monoenergetic incident proton beam 78−12786
Skylab obs. of quiet and active solar events 77−56891
soft X-ray and cm wavelength obs., spatial struct. 77−17524
soft X-ray emission, dynamic response of solar atm. 78−65580
soft X-ray emitting flare loops evolution 79−53781
soft X-ray flare kernel obs. by Skylab 77−29772
soft X-ray flares, emission measure 79−30047
soft X-ray flux, principal component anal. 80−41781
soft X-ray flux, Skylab obs., temporal oscills. 78−53904
soft X-ray limb flares from Skylab 78−4164
soft X-ray polychromator for Solar Maximum Mission 80−51660
soft X-ray radiation, chromospheric response 77−56885
soft X-rays affects on Earth lower ionosphere, anal. rel. to nature of flares 79−8740
Solar Maximum Year project, space expts. for flare-related subprogrammes 80−90404
solar wind shock wave, model based on Forbush decrease *(Chinese)* 80−90302
spectra, anal. of $2p^2$-$2p^23d$ transition array in Fe XX and isoelectronic ions 77−65434
spectra, He-like ions line intensities for non-stationary plasmas 78−53812
spectra, high dielectronic satellite lines analysis for plasma props. calc. 80−12728
spectra, Ni XXV, XXVI and Fe XXIII, XXIV obs. in laser-produced spectra 79−81175
spectral lines between 171 and 630 Å, obs. 78−49406
spiral sunspots, flares and prominences photographic obs., 1972 October *(Chinese)* 78−69761
spray on solar disc during radio bursts 79−80294
steady force-free dynamos, appl. to mag. fields flaring process 78−20777
stellar and solar flares, review 78−7973
subphotospheric activity assoc. with large flares, X-ray data 79−35225
sudden cosmic noise absorpt., solar Zenith angle depend. 78−12047
sudden frequency deviations and phase anomalies in ionosphere due to flares *(Italian)* 78−96345
super flares, as cause of Cretaceous-Tertiary extinctions 78−32435
superadiabatic charged particle accel. and flares 79−21251
surge of 1961, Sept. 1, rotational and turbulent motions 77−91496
surges, flare-assoc. ejection mechanism 80−21975
sympathetic flares and double-peaked flare events on red dwarf stars 77−56963
sympathetic flares occurrence, statistical anal., negative result 77−22189
temperature minimum region, heating mechanisms, theory 80−31282
temperature minimum region, struct. in flares rel. to flare heating mechanism 79−12458
temperature structures derivation from X-ray spectra, use of a priori information 78−20778
theoretical and observational considerations for understanding flares 77−82203
theory, stochastic particle accel. *(Russian)* 78−16377
thermal and nonthermal flares, nonlinear threshold phenomena during mag. field line reconnection 77−82206
third phase flare acceleration, collapsing magnetic regions as cosmic ray sources 80−31268
time-latitude, occurrence in solar cycle 20, 1965-76 period 79−80290
transient plasma X-ray spectra, electron density and temp. diagnostics 80−77368
transition region, thermal radioemission theory *(Russian)* 79−48763
transition-zone plasmas, electron densities and mass motions in flares 80−56804

solar flares continued
troposphere, lower, solar flare effects on temp. and press. 78−40615
turbulent electric fields, possible spectral diagnostics 77−17493
two ribbon flares origin from mag. instability of coronal arcades 80−72911
two-ribbon flare, assoc. umbral brightening 80−41804
two-ribbon flares, force-free magnetic arcades 80−56806
type II decameter wave burst assoc. with behind-limb flare 77−22194
type II radio burst, coronal mag. struct. in source region 78−69775
type II radio burst commencement times from energetic particle flares 77−37590
type II radio bursts rel. to flares Hα line intensity peak 79−21252
type III bursts and flare occurrence in spotless regions 80−56810
type III radio bursts, 1972 May-Aug., obs. in interplanetary space 79−62805
type IV decimetre bursts, causes of onset and sudden reductions 77−2400
type IV radio emission pulsations, bounce-resonance effects 78−89161
type IV radioemission, rel. to transient cosmic ray intensity vars. 79−40043
umbral flares 79−25579
unstable arch model, theory 77−91507
UV and X-rays contribs. to E-region ionisation, effect of neutral atmosphere seasonal vars. 79−12331
UV brightenings in active regions, OSO-8 obs. 78−28630
UV radiation spectral energy distrib. calc. from sudden freq. deviations 78−69771
UV spectra, O I 1355.6 Å and C I 1355.8 Å lines obs. 80−90381
UV spectra of active regions, Salyut-4 obs. 77−82211
X-ray and EUV emission, empirical models rel. to E-region and F-region effects 77−5515
X-ray and Hα flares comparison 78−7971
X-ray and UV emission, obs. and interpretation *(Italian)* 78−96460
X-ray and UV emission, rel. to flare physics 78−65598
X-ray and UV radiation, correl. with E-region ionization 77−25815
X-ray bremsstrahlung from energetic thermal and nonthermal electrons 77−49364
X-ray bright flares and EUV macrospicules identification with Hα macrospicules 78−16361
X-ray bright point flares, search for microwave emission 77−45384
X-ray bright points, assoc. with type III bursts 80−67681
X-ray burst, impulsive, from coronal source, obs. 80−26836
X-ray bursts, during early evolution of X-ray emitting active region 78−28621
X-ray bursts position and size compared with cm wavelength radio bursts 77−33459
X-ray directivity, Prognoz and Explorer satellite obs. in 4-24 keV range 78−69768
X-ray emission, rel. to cosmic ray intensity preflare enhancements 78−45166
X-ray emission, satellite-borne polarimeter meas. 79−25491
X-ray emission (50-100 keV) directivity 80−105218
X-ray emission rel. to optical radiation 77−22188
X-ray emitting post-flare loops, dynamics, 1973 July 29 flare 79−75193
X-ray emitting post-flare loops, physical parameters, 1973 July 29 flare 79−75194
X-ray flare, temp. distrib. models 79−35220
X-ray flare kernel, site, size, spatial stability and energetics 79−25555
X-ray flares, selected, physical parameter profiles 80−17561
X-ray line emission from flares and active regions, OSO-8 obs. 79−25580
X-ray line spectra from transient plasma 80−98626
X-ray lines during impulsive phase, nonthermal excitation and polarization 79−44453
X-ray lines from transient plasma, rate coeffs. determ. 80−72903
X-ray nonthermal emission directivity meas. 77−33461
X-ray polarisation obs. of 1974 July 5 and 6 flares 77−2397
X-ray radiation rel. to O^{2+} ions form. in disturbed ionosphere 79−62647
X-ray radiation sources, model concepts 77−17532
X-ray spectra, Fe XXIV-XXV lines wavelengths in 1.85-1.87 Å region 80−21973
X-ray spectra, high-resolution obs. 80−26837
X-ray spectra, laboratory reproduction in region of Fe XXV-XXVI reson. lines 80−18819
X-ray temperature-emission measure modelling of corona 80−12746
X-rays effects in terrestrial upper atm., ionisation, Auger electrons form. 78−53767
X-rays impulsive bursts, anal. 78−93174
XUV flare kernels, electron density meas. 79−16913
XUV spectra of 1973 June 15 flare from Skylab, allowed transitions 77−78730
Al I, 1932 and 1936 Å autoionisation lines in solar flare, Skylab obs. 80−26829
Ar fluorescent X-rays from sunlit Earth atmosphere during solar flares 77−13142
C-poor events, IMP 8 ULET sensor meas. 79−92739
CO emission lines in UV spectra of sunspots and flare 79−53795
Fe I Kα fluorescence in solar flares, photospheric Fe abundance probe 79−75192
Fe, Kα fluoresc. due to solar flares 80−17569
Fe line X-ray emission, ionization equilib. and line excitation 78−32426
Fe XIX, Fe XX, Fe XXI, forbidden lines obs. in solar flares 78−57519
Fe XIX-XII blend at 1.9 Å in flare X-ray spectra 79−96979
Fe XVIII, Fe XXII, forbidden transitions, fine struct. 79−22634
Fe XX, new atomic data for flare spectra 80−67545
Fe XXI 1354 Å line width, obs. from Skylab rel. to ionisation equilib. calcs. 80−21956
Fe XXI as electron density diagnostic 79−44435
Fe XXIV, dielectronic satellite spectra calc., solar flare spectra appl. 79−35123
Fe XXIV, dielectronic satellite spectra, solar flares appl. 80−32646
Fe XXIV, oscillator strengths, electron impact excitation collision strengths, solar flare spectra appl. 80−32647
Fe XXV, dielectronic satellite line spectra as measure of nonthermal electron energy distribs. 80−21911
Fe XXV 1.87 Å line emission effects on lower ionosphere ionisation 78−65588
H emission in gasdynamic models 77−17531
H I Lα/Hα ratio for flares, quasars and prominences 78−61826
H spectral lines, obs. rel. to flare mechanism *(Russian)* 79−16925
H_2 emission in UV spectra of sunspots and flare 79−53794

solar flares continued
Hα flares, rel. to large-scale coronal active region X-ray brightenings 78−20806
Hα flares and microwave bursts, rel. to sunspot mag. configurations 77−53527
Hα, Hβ and radio obs. of 1978 February 11 flare 78−93187
Hα off-band pre-flare activities 77−74025
Hα output coeff. influence on source function *(Russian)* 78−73690
Hα plage formation after flare 79−44445
Hα profiles from electron heated flares 78−77541
Hα-flares and microwave bursts rel. to isolated sunspot magnetic configurations 78−16387
Hα-flares rel. to radio bursts and sunspots 80−41803
He I, II visible and UV line radiation from model flare layer 77−22190
He I, levels population and emission lines optical depths 77−53538
He I, levels populations calcs. 79−62809
^{3}He rich events, description and anal. 80−101585
^{3}He-rich, plasma mechanism 79−5795
^{3}He-rich flares, 8666 MHz superfine structure line detection 80−109417
^{3}He-rich flares producing ^{26}Al and ^{10}Be cosmic ray particles 80−36461
Li I-like spectra, energy struct., accurate semiempirical formulae 79 49970
Li production in chromosphere and photosphere during white light flares 77 71092
^{7}Li and ^{7}Be gamma ray lines from αα reactions 77−87248
Mg XII, resonance line, atomic parameters calc. for dielectronic satellite lines 80−42983
Na I D-line emission and position rel. to mag. field *(Italian)* 78−96456
Ne nuclei acceleration, abundances 79−92740
^{20}Ne/^{21}Ne/^{22}Ne of energetic flare particles 79−92741
Ni XVIII XUV lines, oscillator strength meas. 79−5796
O-like ions, Fe to Zn, intercombination lines, lab. obs. 77−3289
S XIV, splitting and oscillator strengths for $2s^2S$-$2p^2P^0$ doublet 77−49348

solar furnaces *see furnaces*

solar interior
angular momentum flow, rel. to core rotation 77−45396
Boussinesq convection in deep rotating spherical shell, temp. boundary effects 79−64655
Boussinesq convection in deep rotating spherical shell, vel. boundary effects 79−64656
Brookhaven solar neutrino experiment, results and solar model calcs., new solar ν-detectors 79−80286
clock mechanism of interior driving sunspot cycle 80−17562
connection, random fluctuations rel. to stochastic evolution and oscill. props. 80−31293
convection, finite-amplitude, in compressible medium, appl. to supergranulation 79−88637
convection efficiency of Opik's cellular convection theory 80−12732
convection in deep rotating spherical shell 77−53562
convection in rotating deep compressible spherical shell, theory 78−20795
convection patterns 77−56897
convection zone, convective overstability in mag. field in downdraft in sunspot 80−21960
convection zone, cophasal regions model 78−96469
convection zone, depth rel. to high solar latits. rot. model calcs. 79−101129
convection zone, ensemble-averaged eqns. for granulation, supergranulation and giant granules 80−67698
convection zone, heat flow near obstacles 78−28609
convection zone, mag. field transfer 78−96449
convection zone, mag. fields floating-up time rel. to solar activity 11-year cycle 80−101580
convection zone, mean-field MHD 77−56900
convection zone, struct. adjustments rel. to solar luminosity short term fluctuations 80−82321
convection zone and angular vel., Boussinesq model 77−56898
convection zone dynamics, effect of rot. on turbulent viscosity and cond. 80−36612
convection zone struct. and charact. scales on solar surface 78−7981
convective collapse of flux tubes 79−66989
convective envelope, linear convective modes 80−62091
convective envelope meridional circulation and heat redistrib. 79−40150
convective instability of thin mag. flux tubes, solar convection zone model 79−75183
convective zone, dynamical struct. rel. to general mag. fields 77−22166
convective zone, nature of differential rot. mechanism 79−25556
convective zone, non-stationary mechanisms rel. to non-uniform ang. vel. distrib. maintenance *(Russian)* 79−96985
convective zone models with free parameters in mixing length theories 77−37589
core, rotational constraints 80−101576
differential rotation, due to latitude depend. convective heat transport 80−90411
differential rotation and dynamo presence 77−53582
dirty solar models, effects of surface contamination by accretion from interstellar medium 79−44436
DUMAND detector, neutrinos in the depth of the sea *(French)* 79−75104
dynamo action, interior differential rot. and meridional circulation effects 80−90378
dynamo theory and mean-field MHD 77−56901
envelope hydrodynamical instabilities, implications of Li, Be and B obs. 78−93202
fermion nonminimal gravitational coupling and the solar-neutrino problem 79−75761
global oscillations, long-period, observational evidence 79−2539
global oscillations affecting spectra, He abundance implications 80−51724
instability by magnetic buoyancy 79−75100
internal and surface processes interrelationship interpretation of neutrino data 78−61829
internal structure and solar-type stars 77−53565
lepton mixing and neutrino oscillations, cosmic neutrinos, heavy leptons, μ decay 78−82193
long-term variations, solar activity and neutrino flux 78−45307
magnetic buoyancy, effect on surface activity and solar dynamics 79−21256
magnetic core model, stability 79−44472

solar interior continued
magnetic dynamo, nonlinear MHD model 78−53918
magnetic dynamo, normal modes rel. to large-scale field and coronal holes 77−64713
magnetic dynamo, role of differential rotation 80−109414
magnetic field transfer by two-dimensional convection and solar semi-dymamo 77−49349
mass changing cosmology, solar evolution and neutrino flux 78−45441
mass distrib. from first twenty modes of radial oscill. 77−41371
MHD dynamo, convectively-driven models, solar dynamo appl. 78−42668
model tests of matter creation in Dirac cosmology 79−71163
models, H-R diagram fits rel. to He content and convective mixing length 80−26835
neutrino astrophysics, review 79−16917
neutrino capture rate problem, role of phion in composite neutron mode 80−41808
neutrino expts. 79−8902
neutrino flux, quasi-biennial var. and correl. with solar activity 79−44440
neutrino flux from standard solar model and stellar evolution calc. programme 80−67703
neutrino fluxes, solar activity and cosmic ray variations, review 79−84599
neutrino fluxes calcs., neutrino oscills. consraint 80−109410
neutrino oscillation hypothesis and time depend. of Brookhaven solar-ν counting rate 79−80288
neutrino problem, chemistry of Brookhaven expt. 77−78735
neutrino problem, conf., Washington, DC, USA (April 1978) 79−80217
neutrino problem, limitations of energy transport by mechanical means 77−17461
neutrino problem, proposed new expt. using ^{71}Ga detector 78−58563
neutrino problem, theory versus obs. 80−17566
neutrino problem rel. to solar interior struct. *(Italian)* 78−81598
neutrino puzzle, explanations for missing neutrinos 80−51723
neutrinos, detect. expts. appl. to cosmological hypothesis testing 79−16918
neutrinos production, influence of interstellar dust accretion 79−12441
non-radial oscills. with initial chemical discontinuity 80−82341
nonconvective core and origin of magnetic fields 79−53783
nonlinear dynamo model, multiple-period wave oscills. rel. to 22 year cycle long-period modulations 79−16813
nonlinear magnetic dynamos, bifurcation of steady dynamos from oscillating dynamos 78−49306
nuclear reactions explanation of solar neutrino flux obs. 77−74035
oscillations, nonradial, of 1968 nonstandard solar model 79−35218
oscillations, search during 1974-76 period 78−93190
oscillations with 160 min. period, amplitude modulation from solar rot. *(Russian)* 80−77375
oscillations with 160 min. period, magnetograph obs. 79−40156
oscillations with 160 minute period, evidence 80−82324
p-mode oscillations, tracer of radial differential rot. 79−35221
plasma diagnostics of solar interior, use of MHD pulses 80−109405
pp reactions, rel. to neutrino flux *(Russian)* 78−93195
review of present knowledge 78−40895
rotating convection zone, equilib. problem 77−56917
rotating magnetised core model, rel. to neutrino flux 77−2381
rotation, calcs. 79−75179
seismology, p-modes stochastic excitation by turbulent convection 77−29740
seismology, radial p-modes 77−33434
stability against nonradial thermal modes 80−82322
structure, implications of solar oscills. obs. 80−105226
structure of Sun and solar-type stars 77−53565
supergranulation and giant cells origin in convective zone 79−66979
thermal convection, mag. field effect on onset under const. flux boundary conditions 78−69676
torsional oscillator with 11 year period 80−105217
variability rel. to radiation and ice ages on Earth 78−12183
ν-less fusion process, model based on composite neutron model $n=p+\phi$ meson 79−8898
pp reaction, exchange current corrections π and ρ exchange 80−26733
^{37}Cl neutrino expt., theory 79−84763
Fe, coalescence in centre of Sun 80−77373
Fe limited solubility in central Fe-H plasma 78−89149
Fe segregation from H, ionic mixtures phase separation theory 80−77279
H burning, catalytic role of third particle rel. to neutrino flux 79−80287

solar magnetic fields *see solar magnetism*

solar magnetism
22-year cycle, influence on galactic cosmic ray flux semi-annual var. 79−16777
22-year cycle caused by progressive dipole waves 79−12460
22-year magnetic cycle and dynamo theory 77−53564
active complex with developing secondary region, mag. field struct. and dynamics 80−67685
active corona, modelling of mag. field three-dimensional struct. 77−67085
active region, 1978 April to May, mag. field morphology *(Chinese)* 80−8613
active region, mag. and vel. fields config. and changes 77−17486
active region, X-ray emission rel. to mag. field configuration 78−28621
active region fields rel. to line-of-sight vel. gradients *(Russian)* 77−64730
active region loops, evidence for opposed currents 77−2403
active region mag. fields and noise storms *(Russian)* 77−64717
active region magnetic field emergence into corona, assoc. radio burst 80−109412
active regions, asymmetric mag. loop rel. to type U radio bursts polarisation evolution 80−26834
active regions, currents sheets as heating source 78−28634
active regions, mag. fields and zero points 78−96465
active regions, mag. knots mutual attraction 78−53898
active regions, magnetic and microwave struct. 77−49361
active regions, magnetised expanding plasma, gaskinetic press. 77−45394
active regions, magnetosensitive line contours *(Russian)* 80−51718
active regions, nonlinear stage of instability due to local Joule overheating 78−61839
active regions, open mag. fields 78−28631

solar magnetism continued
active regions, photosphere mag. field strength rel. to submillimetre emission 78−12177
active regions, skinning process stability of mag. field 77−53521
active regions, small Zeeman shifts meas. via automatic comparator 77−82123
active regions and X-ray bright points, birthplaces 80−12739
active regions development, mag. flux changes rel. to chromospheric network evolution *(Russian)* 78−57531
active regions magnetic field, appl. of new approach to force-free field 80−62011
Alfven waves in solar atmosphere above coronal holes, rel. to energy balance and solar wind accel. 79−92746
Alfvenic surface waves in solar corona, reson. absorpt. and coronal loops heating 79−16905
atmosphere, acoustic wave energy transmission across mag. flux sheath 78−20802
atmosphere, dynamo action in slab 79−44430
atmosphere, elec. fields generated by motion of mag. features 78−12194
atmosphere, heterogeneities, classification and physical mechanisms 78−16394
axisymmetric convection in prescence of mag. field, solar granulation and sunspots appl. 80−12724
axisymmetric convection with a magnetic field 78−89165
axisymmetric magnetic flux conc. by rotational shearing motions 79−35219
bipolar magnetic group rel. to angular vel. distrib. and magnetic rope twisting 77−56904
bipolar sunspot groups, asymmetry 79−21264
buoyancy effects, rel. to Sun radius and temp. vars. 79−92749
buoyant magnetic flux tubes in supergranules 79−75170
chromosphere, effects of MHD shock wave on mag. field and density profiles 78−24503
chromosphere, fibrils evolution rel. to flare activity 77−17487
chromosphere, hydromagnetic struct. near supergranule boundary 77−13298
chromosphere, magnetic field strengths, lower limit 79−48746
chromosphere, magnetic neutral lines, assoc. with X-ray arches 77−17511
chromosphere-corona transition region, mag. force tube struct. from EUV obs. 78−20801
climatic var. induced by magnetic field screening of cosmic rays 77−78398
colinear bipolar spot pairs, mag. flux 79−75185
collapsing magnetic regions as long-lived sources of solar cosmic rays 80−31268
conduction cooling of flare loops, magnetic structure effects 79−44451
convection zone, buoyant mag. flux tubes rel. to $\alpha\omega$-dynamo 77−45385
convection zone, mag. field transfer 78−96449
convection zone, mag. fields floating-up time rel. to solar activity 11-year cycle 80−101580
convection zone, mean-field MHD 77−56900
convection zone, solar cycle driven by dynamo action of global convection 77−56903
convection zone, thermal equilib. in presence of mag. flux tube 77−53581
convective collapse of flux tubes 79−66989
convective dynamo, models 78−89090
convective element intrinsic mag. field 80−101583
convective instability in intense magnetic flux tube 79−30038
convective instability of thin mag. flux tubes, solar convection zone model 79−75183
convective zone, mag. buoyancy rel. to surface activity 79−21256
core model, rotating magnetised, rel. to neutrino flux 77−2381
core toroidal magnetic field, stability 79−44472
corona, energy source for flares 80−101571
corona, field determ. using type II burst obs. and theory 80−41785
corona, field strength rel. to coronal transients freq. and solar activity 77−22181
corona, global constant-α force-free magnetic fields 78−85923
corona, global-scale 3-D reconstruction 80−56719
corona, high resolution mapping of mag. field 77−56892
corona, influence of mag. fields on coronal holes physical struct. 80−46520
corona, large scale magnetic field determ. from radiosource rotation meas. *(Russian)* 78−32433
corona, large-scale active region X-ray brightenings rel. to field line reconnection 78−20806
corona, linear force-free fields in lower regions 78−40902
corona, mag. field effects on emission lines form. in shock-heated atmosphere 77−56889
corona, mag. field geometry rel. to localisation of solar wind high-speed streams outflow regions 78−53919
corona, mag. field heterogeneities rel. to fine struct. of type II radio burst 78−24501
corona, mag. field meas. from Faraday during occultations 77−45593
corona, mag. fields rel. to struct. and activity 79−71014
corona, mag. flux tubes ducting of metre-wave radio emission 80−21978
corona, mag. loops, downflows and convection 78−93175
corona, mag. struct. near type II radio burst source region 78−69775
corona, mag. structs. rel. to metre-wave radio bursts and X-ray emission 78−69774
corona, magnetic field model with non-spherical source surface 79−25577
corona, magnetic flux tubes, vibration modes, general dispersion relation 80−94706
corona, magnetic reconnection and loop prominences 77−29765
corona, metre-wave emission ducting rel. to fundamental/harmonic source coincidence 80−21978
corona, physical conditions for bipolar magnetic region 78−77534
corona, plasma flow along sheared mag. arches 80−62092
corona, plasma heating by anomalous current dissipation 78−53895
corona, plasma turbulence triggering during fast flux emergence 78−45304
corona, potential magnetic field structs. assoc. with solar proton events and type I (metre wave) radio sources *(Chinese)* 80−105222
corona, potential magnetic fields 79−30041
corona, radio and soft X-ray evidence for dense non-potential magnetic flux tubes 78−28615
corona, singular lines of one-dimensional force-free mag. field *(Russian)* 79−48670

solar magnetism continued
corona, X-type mag. configuration rel. to type IV radio burst quasi-periodic struct. 80−62097
corona and chromosphere, mag. field above flocculus determ. using radio obs. 80−98635
corona heating mechanisms, mag. field scaling props. 80−85913
corona magnetic traps, plasma instability periodical regimes *(Russian)* 80−8616
corona shock waves and magnetic field above an active region 77−53512
corona streamer, drift pair radio burst theory 79−25558
coronal active regions, evidence for mag. energy storage 77−17478
coronal arcades mag. instability, two ribbon flares origin 80−72911
coronal arch system, long-lived, X-ray obs. 77−71091
coronal bright points, soft X-ray images 77−53557
coronal condensation obs. at 1968 September 22 eclipse, mag. fields calc. *(Chinese)* 78−69762
coronal general mag. field evolution with solar cycle, rel. to solar wind streams and galactic cosmic ray vars. 78−7974
coronal general magnetic field evolution rel. to solar cycle 77−71087
coronal hole, physical parameters defining changing struct. 78−20770
coronal hole flows, mag. boundary conditions rel. to dynamic models 79−58313
coronal holes, lifetimes rel. to photospheric mag. fields transport 77−56893
coronal holes, mag. fields correl. with interplanetary mag. field structs. between 0.3 and 1 a.u. 79−25429
coronal holes, mag. fields rel. to interplanetary fields and flows between 1 and 0.3 AU 79−29963
coronal holes and high-speed wind streams 78−12187
coronal holes and large-scale structures, plasma parameters from soft X-ray obs. 78−4161
coronal holes and quiet regions, differences 77−53514
coronal holes rel. to magnetic fields and model of formation in solar cycle 78−40909
coronal interconnecting loops, mag. flux emergence rel. to sudden brightenings morphology 80−21972
coronal loop, mag. field and plasma phys. model 77−45371
coronal loop transients, mag. field struct. rel. to expansion and broadening 78−40887
coronal loop transients, magnetic driving 78−61842
coronal loops, struct., MHD stability theory 78−28632
coronal loops, struct. 78−89155
coronal loops, structure, equilib. theory 78−12192
coronal loops, thermal instabilities in magnetically confined plasmas 80−36600
coronal mag. field determ. from Fe XIV 5303 Å line polarisation *(Russian)* 78−16389
coronal magnetic arch, type III and type I-like decametric emission 78−12179
coronal magnetic bottles, rel. to solar cosmic rays fast azimuthal transport 78−32305
coronal magnetic field, results from Crab nebula polarised radioemission occultation obs. *(Russian)* 78−77527
coronal magnetic field and current sheets above active regions 77−78757
coronal magnetic field determ., fixed mesh soln. to Laplace's eqn. 77−2392
coronal magnetic field determ. from polarization by atomic fluorescence 77−25938
coronal magnetic field geometry, influence on latit. depend. of solar wind speed 77−9732
coronal magnetic field models, validity of Green's function solns. 80−21970
coronal magnetic field strength above active regions 78−77533
coronal magnetic fields, interaction and energy release 77−17482
coronal magnetic fields, Laplace's eqn. direct soln. using line-of-sight boundary conditions 80−12742
coronal magnetic fields, rel. to onset and sudden reductions of type IV decimetre bursts 77−2400
coronal magnetic fields in terms of twin flux tubes from photosphere, model 79−16922
coronal magnetic loops, electrostatic ion-cyclotron heating 80−51708
coronal magnetic loops, equilib. temp. and density struct. 79−92737
coronal magnetic struct. from solar wind energetic particles and interplanetary field obs. 77−71076
coronal magnetic traps, EM loss-cone instability rel. to type IV radio emission *(Russian)* 78−77528
coronal magnetic tube, bounce-reson. instability rel. to type IV radio emission pulsations 78−89161
coronal open magnetic structures rel. to solar wind flow 79−2459
coronal plasma, mag. tearing instability, high cond. theory 77−7527
coronal structure prediction for 1976 October 23 eclipse 77−17471
coronal temperature constraints in open mag. field regions 80−12744
coronal transient event, 1973 Sept. 14-15, material motions and mag. field 77−17529
coronal transients, MHD, two-dimens. numerical solns. for model corona 78−20774
coronal transients, MHD, two-dimens. plane anal. 78−20773
coronal transients, MHD models in meridional plane, mag. field effect 79−5798
coronal X-ray and XUV emitting structures, changes rel. to mag. reconnection 78−28635
coronal-interplanetary field, topological structure 78−49273
coronal-interplanetary mag. fields modelling, sheet current approach 78−20807
coronal-interplanetary space, subsonic flows in closed field lines regions 78−28624
cosmic ray intenstiy variations in midlatit. stratosphere, total solar mag. field effect 79−62696
cosmic ray particles motion in coronal magnetic field 79−75196
cosmic rays 11 year modulation cycle rel. to sunspots and solar general mag. field 79−21114
current sheets, form. during emergence of new mag. flux from below photosphere 77−22176
current-free fields in active corona *(French)* 77−45388
cycle 21, use of dynamo theory to predict sunspot number 78−81597
cycle period-amplitude relation, hysteresis of nonlinear mag. oscill. and 55-year cyclic modulation 79−35214
differential rotation of magnetic fields, solar cycle variations 78−20781
differential rotation rates for short-lived regions of emerging magnetic flux 78−20782
dipole field rel. to geomag. activity aa index *(Russian)* 79−21261
solar magnetism continued
dipole orientation effects on interplanetary cosmic ray transport 79−44316
diverging coronal field effects on solar wind expansion 77−45377
downflow motion in mag. tubes 78−77530
dynamo, nonlinear MHD model 78−53918
dynamo, role of differential rotation 80−109414
dynamo action, by large scale circulation in convective zone 77−22164
dynamo action, interior differential rot. and meridional circulation effects 80−90378
dynamo in differential rotation 77−53582
dynamo model of magnetic field, self-consistent treatment 80−81808
dynamo problem, nonlinear, small oscillatory solns. in simplified model 79−101133
dynamo theory, magnetic fields with circulation in compressible stratified medium 79−44434
dynamo theory and mean-field MHD 77−56901
emerging flux regions and evolving mag. features, rel. to flares 77−82202
emerging magnetic flux-tubes, interchange instability rel. to heating and reconnection 77−56894
ephemeral active regions and X-ray bright spots, flux-rope theory 80−46519
ephemeral region flares and supergranulation network diffusion 79−21265
equatorial, plane, large-scale spiral waves in solar wind rel. to interplanetary mag. field sector struct. 80−12633
equatorial K-corona, mag. field struct. rel. to radiance temporal evolution 78−28618
eruptive prominence, 1974, June 8, struct. rel. to mag. field 77−22182
eruptive prominence, 1974 June 8, elec. current growth obs. 77−29788
eruptive prominences, rot. motions rel. to twist transport in force-free mag. flux tubes 78−40813
evolving force-free magnetic fields, preflare stage development 77−29739
evolving force-free magnetic fields, stability of configurations and motion of medium 78−12176
evolving force-free magnetic fields, variational formulation 78−93182
experimental confirmation of Sun's magnetic field structure, Pioneer 11 obs. 77−82162
faculae, line profile families rel. to total mag. flux 78−49408
faculae, line profiles and models 77−45375
faculae, mag., vel. and brightness struct. 79−25557
faculae, models, Ca II K line wings and magnetic fields 78−16392
faculae and sunspots, mag. field effects on solar luminosity 80−46515
faculae heating mechanism, convective motion interaction with mag. field 77−82193
fast field reconnection 77−53424
fibrils, lifetime and evolution 77−29760
field components, rel. to model of heliospheric mag. field configuration 80−94670
field emergence and 11-year activity cycle 78−85929
field emergence rel. to metric radiobursts polarisation and location 78−61824
field enhancement rel. to 8 and 13.5 mm radio brightness and Hα activity *(Russian)* 77−64724
field generation by pulsations, rel. to solar rot. and sunspot cycle periods 77−53519
field line reconnection, laboratory expts. rel. to flares 77−17494
field measurement by Mt. Wilson magnetograph, effects of ang. resolution 77−22082
field measurement from saturated and blended lines, appl. of Fourier transform techniques 77−22165
fields and proper motions in sunspots *(Russian)* 77−64731
filament formation dynamics, thermal instability in sheared magnetic field 80−4319
filaments disparitions brusques, evidence for role of mag. field *(Russian)* 80−51726
filtergram or spectroheliogram observations, mag. features visibility 77−29781
flare, 1973, September 5, mag. field rel. to energy storage and deposition 77−17480
flare, 1973, September 5, mag. field struct. and dynamics from X-ray and XUV obs. 78−12175
flare, 1973, September 5, pre-onset mag. struct. 79−40169
flare, class 2b, mag. field var. meas. and anal. 78−89160
flare, flow structure and captured magnetic field 78−57523
flare, magnetic arch struct. and props. from VLA obs. 79−44428
flare, multiple loop activations and continuous energy release, Skylab obs. 77−82209
flare activity rel. to magnetic props. of active region 78−89141
flare detonations, prod. of pulses of characteristic energy 77−78736
flare loops, anisotropic pitch-angle distrib. of electrons generating hard X-rays 77−13314
flare loops, mag. field config. influence on conducton cooling rate 77−17528
flare magnetic fields and microwave burst spectra 78−7970
flare mechanisms, review *(Italian)* 78−96463
flare models, current interruption and impulsive flux transfer 79−12438
flare of 1975, August 10, magnetic field reconstruction 77−13302
flares, active role for mag. fields 77−17474
flares, Alfven wave turbulence in mag. trap rel. to protons stochastic accel. 80−21953
flares, compressible mag. field reconnexion theory 80−6226
flares, conf., Grenoble, France (Aug. 1976) 77−82191
flares, current instability in reconnecting current sheets 77−37486
flares, electrostatically unstable heat flow and its consequences 78−20804
flares, emerging flux model 77−82207
flares, emerging flux model 78−4165
flares, impulsive flux transfer events, theory 77−17495
flares, mag. field determ. from theory of gyrosynchrotron emission from quasi-thermal electrons 80−36602
flares, mag. field energy dissipation in neutral current sheets 78−26250
flares, mag. field energy source rel. to flare physics and X-ray and UV emission 78−65598
flares, mag. field evolution 77−17484
flares, mag. fields in current sheet models 77−17475
flares, mag. pumping of energy nonequilib. turbulent plasma as energy source 77−78764
flares, mag. structs. models and predictions of flux rope theory 80−21955

solar magnetism continued
flares, observational and theoretical status, review 80−51728
flares, phenomenological model 78−49407
flares, radiative, mechanical and mag. energy release 79−53797
flares, role of mag. merging, relevant obs. in Earth magnetotail 77−17301
flares, thermal and nonthermal, nonlinear threshold phenomena during mag. field line reconnection 77−82206
flares, trigger mechanism for emerging flux model 78−89162
flares, unstable arch model 77−91507
flares and prominences, mag. fields meas., photographic method *(Russian)* 78−65584
flares development, mag. field configuration and plasma turbulence 77−17476
flares experimental simulation, mag. field effects on merging of two current carrying plasma columns *(Japanese)* 80−94775
flares flash phase and current sheets thermal evolution 77−17485
flares mag. field config., obs. requirements 77−17496
flares multiply impulsive bursts, spectral evolution rel. to mag. field strengths 80−26828
flares Na I D-line emission and position rel. to mag. field *(Italian)* 78−96456
flares of August 1972, role of mag. field in dynamics 77−25992
flux elements vibr. modes in stratified atm. 79−16902
flux emergence, evidence for globally coherent variability 80−51716
flux ropes, equilib. and stability *(Russian)* 80−8617
flux tube structure 79−48755
flux tubes, basic props. rel. to mag. fields and convection 77−13297
flux tubes, hydromagnetic wave modes 79−29984
flux tubes, interaction with acoustic waves 80−85911
flux tubes, props. and restrictions on solar activity theories 77−5513
flux tubes, role of flows in prod. and maintenance of flux conc. 78−16393
flux tubes in photosphere, downdraught development at sunspot origin 80−72908
flux tubes in stratified medium, magnetic buoyancy 79−30032
flux-rope-fibre theory, appl. to solar mag. fields 78−77525
fluxtubes, polarised radiation multi-dimensional non-LTE transfer 78−69673
force free fields equilib. and stability 77−17357
force-free constant α fields, determ. from magnetograph data 79−12445
force-free fields, exterior source surface 78−28600
force-free fields, time evolution 78−85843
force-free magnetic field calc. with constant α, exact Green's function method 77−33438
force-free magnetic fields evolution, nonequilib. states and preflare stage 80−105213
force-free magnetic fields toroidal component upper limit rel. to flares 77−33479
force-free magnetic flux tubes, dilation 78−4172
force-free photospheric field bifurcation 78−40901
Fourier transforms appl. to contrast profile method of vector mag. field meas. 78−53839
frequency response of magnetic flux sheaths 80−12743
fundamental flux tubes, generation, periodic field reversal 79−53792
fundamental flux tubes, rising and durability 79−53791
galactic cosmic rays anomalous intensity during 20th solar cycle rel. to solar total mag. field 79−80132
galactic cosmic rays modulation by solar total mag. field 79−80131
gas diffusion into mag. tubes, lack of chem. separation 79−75184
gas entry into non-spot magnetic tubes 77−78749
general field evolution during solar cycle 77−53556
general magnetic field fluctuations, correl. with solar rel. oscills. 80−105226
general magnetic fields, 1959-1974, and dynamical struct. of convection zone 77−22166
generation processes, basis for solar cycle *(Russian)* 77−60745
giant convective cells delineated by mag. fields and filaments symm. location 77−29779
global coronal magnetic field reorientation due to differential rotation 77−53515
Hale solar sector boundary definition 77−17517
Hanle effect, Stokes parameters for He I D_3 line in quiescent prominences 78−85924
helical velocity and magnetic fields, stability 78−73624
high latitude field rel. to geomagnetic activity 79−44308
high-latitude magnetic field, possible connection with Earth rot. nonuniformity 80−46119
hydromagnetic surface waves, theory 79−25462
incompressible fluid flow along mag. flux tubes, stability 77−53488
inhomogeneous field, spectral line circular polarisation 79−5804
instability by magnetic buoyancy 79−75100
intense magnetic fields in weak background field rel. to umbral dots 77−29783
intense magnetic flux tube, vertical motions inside 78−40900
interference-phase method of mag. field meas. in solar atm. *(Russian)* 78−65509
interplanetary three-dimens. struct. of solar mag. field 80−31191
isolated sunspot magnetic configurations rel. to Hα-flares and microwave bursts 78−16387
K faculae as tracers of solar differential rotation 77−53501
large scale magnetic dipole and multipole progressive waves in photosphere 77−17505
large-scale fields, distrib., morphology and kinematics 77−53549
large-scale magnetic field, harmonic anal. rel. to coronal holes 77−64713
large-scale magnetic field sources, correl. with radio emission S-component 79−40172
large-scale magnetic fields, negligible changes assoc. with microwave bursts fast structures 79−2536
large-scale magnetic fields spatial distrib. rel. to interplanetary mag. field 79−84772
large-scale solar magnetic field, Stanford obs. compared with Hα synoptic charts 78−28612
line formation in unresolved magnetic element in photosphere 79−48750
longitudinal component meas. with magnetometer at Kodaikanal Obs. 78−61743
loop formation in convective regions 80−109420
loop prominence kinematics 79−84774
loop prominences form. mechanism, MHD approx. *(Russian)* 77−87363
loop prominences formation, kinematic model 78−7965
magnetic energy build-up in solar atmosphere 77−45391
solar magnetism continued
magnetic field calculation of cosmological bodies 79−12399
magnetic field transfer by two-dimensional convection and solar semi-dymamo 77−49349
magnetic flux element in horizontally stratified compressible plasma, stability 78−28610
magnetoatmospheric wave eqn., critical levels 77−78747
McMath region 12417, mag. feature producing X-type neutral sheet 80−98642
McMath region 13043, coronal mag. fields intensification rel. to centimetre-wave sources rapid var. 80−67688
mean field, 1968-74 period, obs. method, rel. to interplanetary mag. field 77−71082
mean magnetic field, contrib. of background mag. field and fields of active regions and spots *(Russian)* 78−57530
mean magnetic field, obs. at Stanford 78−20800
measurement of magnetic fields, review 78−81607
meridional motions in solar atmosphere, rel. to mag. fields and convection 77−53493
MHD dynamo, convectively-driven models, solar dynamo appl. 78−42668
MHD dynamo, mag. buoyancy effects 77−78734
MHD dynamo theory of mag. field *(French)* 79−35161
MHD oscills. ensemble, interaction with quasiuniform mag. field, sunspots 77−76041
MHD pulses, use as diagnostic technique for Sun 80−109405
MHD surface waves on cylindrical fluxtubes rel. to Sun 79−75098
MHD wave propagation in mag. flux sheath in presence of vel. field 79−62735
MHD waves, propag. in mag. flux tube 78−69789
motions in solar mag. tubes, outward wave propag. in sunspot umbras 79−16927
moving type IV radio bursts, expanding mag. arch MHD rel. to gyrosynchrotron modulation 80−26833
network features, structure and evolution 80−41793
neutral sheet obs. in corona during 1973 June 30 total eclipse 79−84757
neutral sheet two-dimens. equilib. in gravit. field 79−66919
non-force-free magnetic fields in magnetohydrostatic equilib., anal. 79−92733
non-LTE line formation in mag. field, two-level atom with freq. independent source function 78−61726
nonlinear dynamo, general mag. field nonlinear oscill. rel. to solar cycle 78−40889
nonlinear dynamo model, multiple-period wave oscills. rel. to 22 year cycle long-period modulations 79−16813
nonlinear magnetic dynamos, bifurcation of steady dynamos from oscillating dynamos 78−49306
nonspot magnetic regions, mag. field intensity determ. 78−96452
north-south distribution of flares, sunspot mag. classes and sunspot areas, 1955-74 period 77−71088
open field lines from active regions, struct. review 80−85924
open magnetic structures evolution, Skylab obs. 78−16362
origin of magnetic fields 79−53783
oscillations in mag. tubes, spectral line obs. 79−25564
phase relation between poloidal and toroidal fields and location of surface magnetic fields 77−29758
photosphere, boundary magnetic field effects on cylindrical prominences 80−90396
photosphere, dipole-like progressive wave and magnetic field analysis 77−56905
photosphere, intense mag. fields form. 77−49359
photosphere, mag. field importance for coronal energy storage, solar flare model 80−72906
photosphere, mag. fields and convection dynamic interaction 78−24458
photosphere, mag. fields and motions, granulation, sunspots *(Russian)* 78−16376
photosphere, mag. fields rel. to coronal holes 79−58312
photosphere, mag. flux appearance 79−40161
photosphere, mag. structs., models *(Italian)* 78−81603
photosphere, mag. structs. correl. with radio noise storms 78−4185
photosphere, magnetic field polarity rel. to circular polarisation of moving type IV bursts 78−53915
photosphere, press. equilib. .and energy balance of small fluxtubes 77−29780
photosphere, small-scale mag. fields and convection 78−53906
photosphere, source regions of interplanetary mag. field and solar wind 77−45275
photosphere, surface (capillary) waves in mag. field, props. *(Russian)* 80−12726
photosphere, weak and strong mag. fields, magnetogram obs. 79−44432
photosphere active region, mag. field correl. with circularly polarised 6 cm emission 80−62096
photosphere field intensity, analysis of large scale configs. 78−57522
photosphere fields, hydraulic concentration near equipartition 77−13293
photosphere fields hydraulic concentration, adiabatic cooling and conc. in downdraughts 78−45300
photosphere fields hydraulic concentration, dynamical effects in stratified atmosphere 77−13294
photosphere mag. field affecting solar proton flux 80−41672
photosphere magnetic field patterns, evolution during Skylab 78−20798
photosphere magnetic fields, influence on accelerated particles escape into interplanetary space 79−62807
photosphere magnetic fields, possible explanation for fine struct. 80−98646
photosphere magnetic fields, rel. to elec. currents and flares energy source 77−17483
photosphere magnetic fields assoc. with coronal holes, differential rot. 77−22167
photosphere magnetic fields beneath large coronal holes, nature 78−28613
photosphere magnetograms from Kitt Peak National Observatory 60 cm vacuum telescope *(Norwegian)* 77−60613
photospheric faculae, models 80−12716
photospheric facular granules, morphological props. and origin 77−78744
photospheric fluxtubes, multidimens. non-LTE radiative transfer 77−60741
photospheric granules dimensions var. rel. to sunspot mag. fields *(French)* 78−89145
photospheric network, mag. fluxes and field strength meas. 77−71083
photospheric network structure from Mn I lines obs. 79−30039

solar magnetism continued
photospheric poloidal and toroidal mag. field components near solar min. 79−66978
photospheric vertical motion in intense mag. flux tube, slender tube approx. 80−31278
Pikel'ner soln. for prominences, stationary flow in magnetic tubes of force 77−53540
plage magnetic fields, 6 cm obs. with 6 arc seconds resolution 77−33444
plage region magnetic points, vertical vel. fluctuations 77−71084
plasma convection in force-free mag. field, mechanism for chem. separation in cosmic plasmas 79−35125
plasma instabilities of trapped particles in magnetic fields 78−61823
polar magnetic features rot. rate 79−30037
polar magnetic fields, reversals rel. to cosmic ray vars. phase reversals 78−40780
polar magnetic fields strength, obs. 79−12446
polar true average field strengths 77−78743
polarity changes, skin effect of electrically conducting spherical shell 80−46389
pores, line profile families rel. to total mag. flux 78−49408
potential magnetic fields, comparison of meas. and calc. 78−77532
preflare association of mag. fields and mm wave emission 77−17490
primordial field theory, review 77−56902
primordial magnetic field 77−53494
prominence formation, Pikel'ner's thoery 77−71086
prominences, magnetic field determ. from Hanle effect 77−74024
prominences, polarimetric obs. and magnetic field determ. 80−4332
prominences weak mag. field meas. 77−71085
proton flare active regions, force free mag. field and force free factor determ. *(Chinese)* 80−77365
quiescent corona, mag. field rel. to heating and dynamics 78−40885
quiescent prominence, equipartition mag. field strength from Ca^+ K-line width and shift 80−77364
quiescent prominence, thermally balanced, self-consistent model of magnetostatic equilib. 77−91509
quiescent prominence form. by thermal instability in current sheet 77−82194
quiescent prominences, mag. field gradient 77−17466
quiescent prominences, mag. field intensity 77−87355
quiescent prominences, mag. fields orientation 78−45305
radiative transfer in magnetic atmospheres, analytical soln. 80−36494
radio bursts, high-resolution 6 cm obs. and rel. to mag. fields 78−53897
radio bursts, type I and III comparison *(Russian)* 78−16379
radio bursts, type II and III theory *(Russian)* 78−16381
radio bursts, type III and microwave, rel. to mag. config. 77−82204
radio wave propag. in inhomogeneous magnetic field *(Russian)* 78−16385
resistive diffusion of strong mag. field in tenuous conducting gas 77−78625
resonance line polarisation, non-LTE, absence of magnetic fields 79−80293
rope structure, of rising solar mag. field *(Russian)* 78−40898
Schluter Temesvary sunspot, vertically orientated mag. flux tubes, exact static equilib. 80−98637
sector changes, geomag. polar cap field responses 77−5134
sector crossings, lack of effects on troposphere 78−57244
sector structure, long term evolution 77−53389
sector structure rel. to ionosphere elec. pot., obs. over solar cycle 77−33271
singular lines of one-dimensional force-free magnetic field 79−66920
skinned magnetic flux rope, boundary sheet stability *(Russian)* 77−91503
Skylab X-ray obs. and mag. field correls., computer solns. 77−82198
small-scale fields, field amplification and magnetic flux 77−53550
small-scale magnetic fields theory 78−12197
small-scale photospheric magnetic fields 78−12196
small-scale solar magnetic field, size, struct. and strength 77−78738
solar wind, origin in coronal holes, mag. evidence 77−2394
solar wind high velocity stream sources, mag. field struct. in high corona 77−53530
spectral line formation depth in mag. field, theory *(Chinese)* 80−105159
subphotospheric activity assoc. with large flares, X-ray data 79−35225
Sun as magnetic star 77−53566
sunspot cycle morphology, theory *(Chinese)* 80−12722
sunspot decay mechanism, turbulent processes in strong mag. field *(Russian)* 78−93193
sunspot group, magnetic and vel. field evolution 78−89143
sunspot group for August 1972, force-free magnetic field 80−46521
sunspot mag. field motion rel. to proton flares 77−17488
sunspot magnetic field and vel. quasiperiodic oscills. *(Russian)* 78−12186
sunspot magnetic field gradients determ. from Zeeman line rot. and profiles *(Chinese)* 80−85920
sunspot magnetic fields higher rot. rate at photosphere, Doppler meas. 80−46516
sunspot magnetic fields spiral config. 77−82192
sunspot moats, lifetimes from magnetograph obs. 80−21966
sunspot penumbrae, fine struct. of mag. field and brightness 77−22179
sunspot umbra, spectral synthesis in mag. field 77−17459
sunspot umbrae, mag. field gradient from echelle spectrograms 77−33456
sunspots, convective propulsion of magnetic flux tubes 80−4313
sunspots, coronal mag. field struct. rel. to local sources of solar radio emission S-component 80−46528
sunspots, darkness difference, mag. and vel. field effects 78−28629
sunspots, excited states of magnetic configurations 77−29762
sunspots, heat flow in convective downdraught 80−4314
sunspots, mag. configurations rel. to Hα flares and microwave bursts 77−53527
sunspots, mag. fields rel. to thermal struct. 77−5517
sunspots, magneto-optical effects rel. to linearly polarised intensity distribs. obs. with vector magnetograph 80−21965
sunspots, origin of broad-band circular polarisation 78−45301
sunspots, running penumbral waves origin 78−93188
sunspots, stability of axisymmetric mag. flux tube 77−64734
sunspots, steady-force-free dynamos theory 78−20777
sunspots, thermal struct. and mag. fields conc. 77−64735
sunspots, twisted magnetic fields 80−41799
sunspots, two-component mag. field model rel. to overlying atmosphere struct. 79−96989

solar magnetism continued
sunspots, Zeeman line profile, mag. field determ. by radiative transfer method 80−82221
sunspots and mag. flux tube physics, connective overstability in mag. field in downdraft 80−21960
sunspots and magnetic flux tubes physics, umbral dots and longitudinal overstability 80−26825
sunspots and physics of mag. flux tubes, aerodynamic drag 79−71012
sunspots and physics of mag. flux tubes, aerodynamic lift on thin cylinder in convective flows 79−101126
sunspots and physics of mag. flux tubes, general nature of sunspots 79−75168
sunspots and physics of mag. flux tubes 79−101127
sunspots mag. field oscills., rel. to chromospheric flares occurrence 77−67084
sunspots magnetic fields and proper motions, 1968 October 20-27 complex group obs. *(Russian)* 78−65583
sunspotsand physics of mag. flux tubes, aerodynamic lift 79−101125
supergranulation, dynamics of gas and mag. field below photosphere 78−16366
supergranules, vel. and magnetic field evolution 77−53555
superlarge-scale field *(Russian)* 79−66974
surface magnetic activity, vars. rel. to solar luminosity and biological extinctions 78−32435
surges, flare-assoc. current disruption mechanism 80−21975
surges, local mag. field strength rel. to dynamics of descending stage *(Chinese)* 80−105221
thermal convection, mag. field effect on onset under const. flux boundary conditions 78−69676
thin magnetic tube instability in atmosphere rel. to network struct. 80−12725
time dependent fields, effects on interplanetary mag. fields 77−9646
transition zone, Si IV line profile vars., rel. to MHD disturbances 78−28626
turbulent diffusion of mag. field, Eulerian formalism 79−16901
turbulent shock wave propagation in solar atmosphere across mag. field, struct. 79−40166
twisted flux tube theory, stability 77−60737
twisted flux tubes, equilib. config. 77−53489
twisted flux tubes, equilib. config. 77−53490
two-ribbon flares, force-free magnetic arcades 80−56806
upper atmosphere, convective noise waves dissipation in mag. struct. rel. to heating 78−65600
vector magnetic fields, determ. from Stokes profiles 78−28611
wind and corona, mag. fields during Maunder Minimum 79−75069
X-ray active regions temp. and emission measure rel. to coronal mag. fields 80−12745
X-ray bright arcs and mag. flux emergence regions 78−12174
X-ray bright points, mag. flux emergence regions, var. out of phase with solar cycle 77−56890
X-ray bright points, mag. props. 77−91505
X-ray bright points, short-term temporal vars. 80−12740
X-ray bright points anticorrel. with sunspot number, 1970-78 period 79−53789
X-ray flare kernel, site, size, spatial stability and energetics 79−25555
Fe I lines, statistical anal., mag. line broadening 77−74028
Fe I magnetosensitive spectral lines, Stokes parameters *(Chinese)* 79−80289

solar noise *see noise; solar radiofrequency radiation*

solar power
see also solar energy concentrators
5 MW Solar Thermal Test Facility 79−62113
5 MWe solar thermal test facility, heliostat field design 77−23780
10 MWe pilot plant, collector field design 77−23779
100 MWe commercial power plant, technical feasibility and economics 77−23778
absorber, fluid flow in helical channel *(French)* 79−24910
absorber, MgO/Au selective with solar absorptivity >0.9 and IR emissivity <0.1 77−1747
absorption chillers, solar-fired, capacity modulation 80−66952
absorption cooling systems, small scale, feasibility study 79−74502
absorption refrigeration system, theoretical model 80−30413
access to sunlight, perspectives w.r.t. law and protection 79−87979
active energy systems for cooling and heating, thermal and economic anal. 80−50940
AEROSOLEC, combined solar-wind power station for telecommunication appls. 80−61306
aerospace photovoltaic generators, symposium, Noordwijk (1978) 79−96449
air conditioner appl., LiBr absorption, computer-aided performance predictions 79−62134
air conditioning, LiBr absorption, low and high temp. cycles 80−81425
air conditioning, solar cooling with air collectors by desiccant/r bed method 80−30412
air conditioning appl., NH_3/H_3O absorption unit design and performance 79−62129
air conditioning system, intermittent cycle, NH_3/H_2O absorption, expt. evaluation in Florida 79−62133
air conditioning system appl., using evacuated tubular collectors, digital simulation and design, comparison with actual performance 79−61949
air conditioning systems, stochastic simulation expts. 79−57415
air conditioning with solid absorbents, earth and underground water cooling 80−72018
air to water heat pump and solar installation for single family house *(German)* 79−87968
air to water heat pump and solar water heating, dual purpose installations for family house *(German)* 79−87969
all solar power supply for France, technological forecasting *(French)* 79−100497
alternative energy sources, feasibility and cost anal. of solar systems 80−50939
alternative energy strategies, development of solar-based renewable resources, review 80−30417
alternative fuel source, predictions for future and technical-economic possibilities 80−89591
alternative versus conventional energy sources, economic comparison *(German)* 80−72002
amorphous silicon absorber, high efficiency, for solar energy utilisation 77−39907

solar power continued
anisotropic diffuse insolation, calc. of instantaneous flux on tilted surfaces 80−101412
atmospheric attenuation, effect of O_3 and H_2O vapour content and atmos. turbidity 80−93855
Austrian solar energy R&D activities and international cooperation 79−57374
automative transport utilising stirling heat engine 80−55824
autonomous solar electric systems *(German)* 80−93875
availability concept based on climatology, Canada 77−25762
balloon project proposal, hot-air, mile-long 79−48583
barracks heating using solar energy *(German)* 79−87970
British 1977 solar energy programme 79−57369
building computer-aided analysis and design, using Cal-ERDA programs 79−57456
building design for maximum utilization *(German)* 80−93854
building heating, energy storage and power supply for system, optimal conditions *(French)* 80−61297
building insulation optimisation, w.r.t. internal and solar gains 79−62147
building solar-climate control systems, control options evaluation by simulation 80−40844
buildings, heating and cooling, solar augmented and assisted systems 80−7918
CAD of windows as passive solar collectors, using interactive program 79−62146
cellular anti-loss struct. as solar absorber, emittance distrib. at cell walls *(French)* 77−14890
central receiver system, flux density integral for reflected sunlight, numerical anal. 80−93863
chemical heat pump/storage system for air conditioning 80−55886
chemical reactors, solar thermochemistry at high temps., appls. to chemical and thermal storage *(French)* 80−55815
climatic model experiments, simulated changes, solar energy conversion effects 78−81354
climatic solar heating performance, calc. of solar fraction for building heat 80−16786
climatological design assessment of solar buildings, interactive computer aided design techniques 80−61289
climatology of global solar radiation in California and an interpolation technique based on orthogonal functions 80−67402
cNRS solar program and thermochemistry *(French)* 79−100485
coal gasification reactors using solar power, tech. and economic feasibility 80−76613
collection augmentation by planar refle-tive surfaces, calc. and expt. 79−83574
collector, appl. of forced convection heat transfer at inclined plates 78−30285
collector and task matching, thermodynamic aspect 79−57390
collector design, inclined-plane insolation computation, hourly and daily methods compared 79−83572
collectors, design and data rate requirements of computer-based sun following system 79−83573
collectors with plastic covers, radiation heat loss calc. 79−74538
complementary nature of wind and solar energy at a continental mid-latitude station 79−92062
conservation of nonrenewable resources 79−87976
convective losses in 2-D, differentially heated, inclined cavities *(French)* 79−24906
conversion effects on climate 78−81356
conversion into heat and electricity, methods of raising working temp., review 77−46903
cooling, evaporation and refrigeration units, assurance of specified energy parameter values, statistical analysis 80−93848
cooling, heating and hot water supply for hospital, evacuated glass tube solar collector system appl. 80−26155
cooling, operating systems and current developments, review 80−85265
cooling, Rankine-cycle systems, selection of working fluids 80−104515
cooling, thermodynamic anal. of sorption machines, coeff. of performance calcs. *(French)* 80−55814
cooling and hot water system, design and operation 80−50941
cooling of buildings in Turkmenian SSR, using open water evaporation, from LiCl solution 79−57463
cooling systems, residential, solar absorption-vapour compression system 80−72017
cost calculation standard procedure proposal 79−57389
crop starting tunnels for vegetable growing season increase, test results 79−70438
cyclonic, solar gas-solid chemical reactor, flash pyrolysis of wood sawdust *(French)* 80−61296
Czechsolovak radiation climate evaluation, w.r.t. solar power utilisation *(Czech)* 78−88874
daily irradiation, ARIMA modelling with constant and seasonal parameters 80−55821
daily solar total irrad. fluctuations, temporal statistical anal. *(French)* 80−61292
demonstration expt. 77−22355
desalination, solar-assisted reverse osmosis plant using Stirling heat engine 80−55891
desalination appl. reverse osmosis, expt. installations *(French)* 80−55807
desalination plant, design w.r.t. efficiency 79−87973
desalination plants for desert pastures irrigation 80−89594
desalinator appl., in combination with MHD convertor, prototype design and operation 79−74508
desiccant dehumidifier development 80−30411
design optimisation of solar energy district, systems anal. of external energy supply 80−30398
developing countries' solar energy evaluation by energy balances 79−57388
developing countries' solar energy utilisation planning methodology 79−57364
development, availability, and storage possibilities *(French)* 80−89587
development and technology, surface science rel. problem areas 78−88553
development possibilities of energy resources *(German)* 80−21355
devices, types, review 78−86092
diffuse and beam radiation, correl. with hours of bright sunshine 80−40841
diffuse irradiance measurement using shadowband, corrections 80−101410
direct conversion and storage, review of developments, reviews 79−43741
direct irradiance at the ground, parametric modelling 80−101411
direct solar air heating, theory and practice of heating strategies in Denmark 80−66945
direct solar energy, Markov chain simulation with one minute binning *(French)* 80−61293
direct solar radiation and global radiation for 69 places in West Germany, appls. *(German)* 79−70837
dispersed solar power and energy conservation 80−55811
distributed photovoltaic systems for electricity generation, economic and technologic feasibility 80−55906
distribution of solar radiation obs., at various geographical locations (1968 to 1974) 77−37313
district heating system using thermal energy storage, sensitivity anal. 80−67007
domestic applications, review 79−52889
domestic dwellings, installation practice *(Italian)* 79−100499
domestic energy units, self sufficient, for use in India's rural areas 79−74510
domestic hot water heating using hot air solar collectors 80−97768
domestic hot water system for telephone exchange 80−66940
domestic space and water heating, appraisal of solar power appl. 79−74494
domestic space heating in Ireland, computer simulation model of thermal performance 80−45732
domestic space heating using low-temp. solar thermal systems *(Czech)* 79−83566
domestic water heaters on Swiss central plateau, net heat output, economic evaluation *(German)* 79−100498
domestic water heating methods *(German)* 80−40833
domestic water heating systems, in Great Britain, design and economic aspects 80−40835
Earth satellite power stations (Powersats), economic assessment 77−91404
economic assessment of future energy schemes, domestic solar heating appl. 79−48044
economics, component cost of solar energy systems 80−45651
education, solar energy concepts, in chem. teaching 78−73805
efficiency, geographic and economic aspects of solar energy utilisation 79−52888
electric generating systems, resource requirements 80−7923
electrical energy production from solar energy, techniques and systems 79−96424
electricity generation, thermoformed plastics for parabolic concentrators, development 77−23774
electroplating appl., 1979 prospects w.r.t. economics 80−3490
energy accounting study 80−76589
energy conversion, conference, Ontario, Canada (Aug. 1978) 80−41949
energy conversion, materials used in water photolysis technique 77−20423
energy flux prediction in polluted urban areas 80−30394
energy independent houses design and construction options 79−79382
energy management system 80−66951
energy resources, overall view *(French)* 80−40804
energy resources, review of alternatives to fossil fuel *(Italian)* 80−66917
energy roof, solar energy utilisation and heat recovery *(German)* 80−61285
energy storage technology and solar energy use, worldwide trends *(German)* 80−72086
energy storage using chemical potential changes associated with drying of zeolites 80−51006
energy strategy, soft vs. hard energy technologies, review 79−24885
energy structure distrib. laws for solar-radiation regime, analytic representation 80−98378
energy system control, 16 channel data logger and serial data link 80−50947
energy system synthesis, soft solar energy option 80−76614
energy systems, electrical analogue simulator development 80−30382
energy utilisation, conf., San Diego, Calif., USA, 1976 77−53900
energy utilisation methods and overall energy resources survey *(Czech)* 79−83565
energy utilization impact on optimum plant mixes 79−87977
engine development, 1 kW, reciprocating, for rural appl. 79−74536
European Communities' solar energy R&D programme 79−57360
European Community Italian Centre activities *(Italian)* 80−785
flat collector panel, equilibrium temp. in real conditions *(French)* 77−19514
flat plate collectors, solar flux calc. for angle of optimum tilt 80−61424
flat plate solar collector low cost coating 77−32705
flat plate solar photovoltaic power system with 100 kW peak power 80−35653
flat solar collectors, thermal exchanges in glass absorber cavity *(French)* 79−24909
flux calculations, algorithm for plane surfaces 80−61423
flywheel and hot water storage systems for 10 kWe solar power pack 79−57469
flywheel energy storage and conversion system for photovoltaic appl., economic anal. 80−94116
French solar energy collection, research programme, outline *(French)* 79−74498
French solar energy development 79−57368
future energy concepts, Conf. London, England (Jan.-Feb. 1979) 79−43709
gas turbine waste heat utilisation for elec. energy generation and desalination *(German)* 79−87936
generation, system developments and research aims *(German)* 80−108799
global and net radiation distribution over Greece 80−21382
global and sky radiation estimates for Austria 80−93861
global aspects of sunlight as a major energy source 80−30385
global energy option *(French)* 79−100496
global solar radiation at Lyon and at Macon, France, for (1978) *(French)* 80−55812
global surface irradiance, effect of aerosol props. and surface reflectivity 80−76611
Great Britain, availability, collection methods, and some research projects 79−100482
greenhouse solar distillation and cultivation materials 79−74496
greenhouse with subsoil heat storage, formation of microclimate 80−89596

solar power continued
halfhour solar radiation values from hourly values for Kuwait, Markovian insolation model appl. 79−44236
harnessing, biography of A.B. Mouchot *(French)* 80−105484
harnessing tomorrow's energy sources, prospects 79−100484
Hawaii, 1977 survey 79−29454
Hawaii, wind and insolation as alternative energy resources 80−45623
heat balances of apartment house, in Dutch climate, energy conserving measures 79−61948
heat exchange in a solar greenhouse with a soil heating system 80−93849
heat pipe with active porous medium filling, for solar appl., operating characts., efficiency *(French)* 77−42725
heat pump, series, flat-plate collectors, vapour compression, energy conservation 80−72078
heat pump, solar assisted, operation 80−61395
heat pump computer simulation 79−57414
heat pump house, Dunham-Bush development 80−40830
heat pump plant for space heating in winter, air conditioning in summer 80−76615
heat pump systems, combined, performance evaluation, for residential space and water heating 79−88000
heat pumps, solar-powered absorption cycle with energy storage, theoretical anal. 80−55885
heat pumps boosting, design problems 79−57439
heat storage device, off-peak, ambient temp. observer/predictor control system 80−66950
heat storage in a solar heating system using Na salt hydrates 80−67005
heat storage in passive solar heated building using concrete block under concrete slab 80−55922
heat storage in solar heating system using Na salt hydrates, based on extra water principle 80−67006
heat storage using chemical reactions, review 77−86333
heaters of domestic hot water, commercialisation in Florida, system sizing and economics 79−57460
heating, air movement control 80−66946
heating, collector applications for space and water heating in buildings 80−61406
heating, microclimate of solar greenhouses 80−40902
heating, of building, demonstration plant in Athens 79−57410
heating, periodic heat flux through a three layered slab exposed to solar radiation 80−43598
heating, rapid implementation effect on USA energy supply 80−104497
heating, residential, in adverse climates, optimum collector slope 79−66416
heating, space, economic assessment w.r.t. auxiliary energy supply 79−57407
heating, space, Korea's expt. project 79−57409
heating, space, Markov model based computerised analysis 79−61950
heating, space, with all-air systems, experiences with CSU Solar House II 79−57406
heating, space and water, Markov model 79−74501
heating, Toshiba Solar House No. 1 performance 79−57458
heating, West German experiment, BBC Solar House (Heidelberg) design, operation and performance 79−57405
heating and air conditioning, of financial building (1100 m^2) 79−57465
heating and air conditioning 80−61290
heating and cooling appl., of mobile home, performance in Kuwait environment obs. 79−62130
heating and cooling expts., for moderately insolated regions, European research 79−57457
heating and cooling of buildings, Shenandoah Solar Recreational Center 80−45757
heating and cooling of poultry sheds, passive 79−70437
heating and cooling system, for industrial plant, located in Southern Europe 79−62131
heating and cooling systems, status and prospects 80−30384
heating and cooling systems optimisation, using continuous flow control 79−62127
heating and cooling systems performance, US national demonstration program 79−62128
heating and ventilation using integrated collector-heat storage systems 80−51002
heating appl., availability, Swiss meas. and collectors efficiencies *(German)* 79−48092
heating equipment for building, community and agricultural appl., use of heat tube 79−57412
heating expts. for performance prediction and design optimisation 80−61288
heating of buildings, thermal performance evaluation, with aid of computer 79−57467
heating of dwelling, independent of servicing networks, digital simulation 79−62149
heating of gas circulating in forced convection through porous cavity *(French)* 80−69626
heating of houses with swimming pool, Austrian development, economic aspects 79−57413
heating of housing unit, Japanese expt. and simulation results comparison 79−57455
heating of public swimming pools, feasibility 79−87978
heating of residential house, in combination with wind power, Danish design 79−57411
heating of water, Czechoslovak agricultural projects *(Czech)* 79−70430
heating panel system, performance testing and evaluation *(Dutch)* 80−72079
heating system, for administrative building, for winter use, technical and economic feasibility 79−62136
heating system, heat accumulator utilisation, calc. procedure 80−40825
heating system, performance characts. 80−61309
heating system perform. estimation using sinusoidal inputs 80−35648
heating systems, collector and storage efficiencies 80−45736
heating systems, energy conservation characteristics and resource requirements 80−45731
heating systems, performance mathematical simulation for optimal dimensioning *(German)* 80−26110
heating systems, performance modelling and simulation 80−76618
heating systems, space and water heating, application of solar energy in dwellings. A technical and economical analysis for the European Community 80−66943
heating systems analysis space and water, using stochastic modelling methods 79−57459

solar power continued
heating systems for use in Britain, collector design aspects 80−35637
heating systems performance over range of storage capacities, prediction 80−45642
heating systems simulation *(French)* 79−92063
heating systems with annual storage, performance prediction 79−70436
heating/cooling of buildings calc., w.r.t. periodic changes of solar radiation 79−62148
heliostat field optimisation, appl. of field shape effect for power stations *(French)* 79−24903
heliostat mirror field analysis and design 79−83570
heliotechnics, basic values, symbols, units and definitions *(Rumanian)* 80−57243
high temperature solar furnace for chemical appl. *(French)* 80−16784
high-temperature solar energy installation with paraboloid concentrator, radiant flux control 79−96420
hospital buildings, harnessing of solar energy 79−79383
hospital engineering, conf., Lisbon Portugal (May, June 1978) 79−79667
hot water systems, dyeing, in textile industry, commercial aspects 79−83576
hot-water supply system for residential building 80−93851
hotwater and heating systems, availability aspects 80−61314
hourly diffuse radiation predictions from meas. hourly global rad. on a horizontal surface 80−93864
hourly global radiation sequences, stochastic simulation 80−36382
house energy conservation measures obs. and evaluation, using minicomputer, Philips expt. house (West German project) 79−61951
house heating in Northern India, using south walls as collectors, expt. results 79−62152
house with integrated greenhouse design, earth-wrapped 79−62150
human health risk, comparison of conventional and nonconventional technologies 79−87956
HVAC system, thermal storage, materials, labour and insulation costs 80−72088
hybrid passive/active solar system: performance and cost 80−45635
hybrid solar/H fuel system producing high energy 80−45809
hydrocarbon oils as thermal storage media for solar central power appls., specific heat variations and their economic implications 79−100540
illumination after dark, orbiting mirror appl. 78−33816
India's 1978 development trends 79−74509
Indian national solar energy R&D programme 79−57365
industrial applications of solar heat *(French)* 79−100486
industrial process heat charact., potential for solar and nuclear power systems 78−822
industrial process heat supplied by solar energy 80−76606
industrial solar energy utilisation in UK 80−61301
industrial utilisation of energy, book 80−61222
industry, economic considerations and feasibility in Britain 80−26111
insolation modelling, review of solar radiation resource assessments 80−35640
insolator, copper belt type tube structure, design, construction and testing *(Czech)* 79−83626
installation development costs, solar cell mass production technology *(German)* 80−72046
installation for drying tobacco, solar powered 80−93850
intensity, atmospheric transmission data rehabilitation, SOLMET-2 procedures criticised 80−4071
intensity obs., global insolation on horizontal and tilted surfaces 78−81275
intensive solar energy production, albedo modification 78−85680
International Energy Agency and NATO solar energy programme status 79−57362
International Solar Energy Congress, New Delhi (1978) 79−57357
International Solar Energy Society, Australia-New Zealand section activities 79−39282
investment programme for small national state or political subdivision of large state, review 79−66403
Iran's solar town, conceptual development 79−57408
Iranian solar energy R&D approach and philosophy 79−57377
Irish solar energy developments 79−57378
irradiance on horizontal surface, estimation of totals from UK average meteorological data 80−81422
irradiation above thermal collector critical levels for 10-min and 1-hr integrals 80−16789
irrigation plant appl., comparison with wind power, w.r.t. cost, maintenance and reliability 79−70425
isotropic-distribution approximation validity, in solar energy estimations, exact procedure comparison 77−78358
Israel, estimation of solar radiation and ambient temps. 80−76607
Israeli coastal plain, weather year standardisation for solar heating simulations 79−84444
Italian national solar energy programme 79−57367
Japanese energy programme 80−3478
KS-7F solar kitchen, economic effects on economy 80−89590
Kuwaiti solar energy research, development and demonstration programme 79−57371
laminar free convection in 1-D solar induced flows, theory 80−3495
large scale solar energy conversion effects, conf., Laxenburg, Austria, Dec. 1976 78−81352
Latin American solar energy prospects and programmes 79−57363
leak-proof heat exchanger for solar water heating systems 80−30524
light water fission reactor, solar-assisted hybrid power plant 80−13561
line focus collectors for solar thermal electric power systems, comparison 77−23775
Lisbon solar radiation climate, direct, diffuse and global intensities 80−36383
local and mesoscale weather, impact 78−81358
longwave radiation incident upon inclined surfaces 80−16785
low-temperature thermal solar motor 79−96480
LWR nuclear reactors with solar collectors, SOAR power system concept 80−55820
major solar energy research programs, review 80−40843
Malawi solar energy utilisation prospects 79−57379
materials problems rel. to transition to solar energy 80−26115
measurement, microcomputer-controlled photodiode light meter and thermistors 80−50946
mesoscale mapping of available solar energy at the Earth's surface by use of satellites 80−72613
meteorological aspects of solar and wind power 78−36250
Mexican Solar Energy Experimental Center optimum site determ. 79−57380

solar power continued
microcomputer control for solar energy applications 80−50945
microwave power beaming, for long range energy transfer 79−34427
microwave power transmission system rectennas, Yagi-Uda receiving elements design, characteristics and economics 80−66938
microwave power transmission technology 80−40868
microwave telecommunication links power supply, Papua New Guinea, research 79−29449
Middle Eastern research programmes 80−66939
Minto solar wheel, effect of material properties on thermal efficiency 80−97769
mirror arrays, large Earth orbit structures reflecting sunlight for power generation, lighting, and agriculture 80−45632
mirror surfaces for solar power stations, specular reflectance obs. 78−13786
modular dish solar electric system, technical feasibility 77−23777
monthly average insolation, incident on tilted surface 77−78357
monthly mean global solar radiation maps for Japan 80−109185
monthly mean solar radiation calc. using daily time intervals 80−17353
natural gas/solar energy transition strategy 80−30414
Netherlands national solar energy programme 79−57372
Ocean Termal Energy Conversion [OTEC], the Florida Current, thermal 80−26117
ocean thermal energy, renewable power source, review 79−5503
ocean thermal energy conversion, Early Ocean Testing Platform siting considerations 79−5506
ocean thermal energy conversion, electricity to shore schemes 80−16783
ocean thermal energy conversion, OTEC power modules optimisation, computerised, w.r.t. economics 79−83615
ocean thermal energy conversion, OTEC power systems, 1978 status and development trends 79−83614
ocean thermal energy conversion, OTEC programme advancements, ocean engineering aspects 79−83616
ocean thermal energy conversion, OTEC system development, Conf. Houston, TX, USA (Nov. 1978) 79−83611
ocean thermal energy conversion, status and prospects 79−5502
ocean thermal energy conversion for electrolytic H prod. 80−30546
ocean thermal energy conversion US OTEC development programme overview 79−83613
office complex design, with up to 70% energy savings 80−40831
optical concentration in solar power stations by use of conical and parabolic mirrors *(French)* 79−24904
optical materials for solar energy appl. 77−19373
optics applied to solar energy, [Conf. San Diego, CA, USA Aug. 1978] 80−7926
optimal solar investment decision criteria, appl. to space and water heating systems 80−35643
orbital power satellites, features *(Portuguese)* 79−70452
orbital power systems, waste heat rejection development requirements for thermal control 80−30416
orientation of solar collectors, optimisation 77−81965
parabolic concentrator, use of fin receiver 80−21379
passive energy systems for buildings evaluation, use of thermal modelling and 'predicted percentage dissatisfied' 79−62145
passive heating, review and development of direct, mass wall and attached sun space systems for residential appls. 80−76619
passive measures in building design for utilizing solar energy *(German)* 80−93853
passive solar heating systems, Trombe wall control strategies 80−45737
passive solar space heating, sensitivity anal. of direct gain systems 80−35647
passive solar space heating for energy conservation 80−66948
passive systems, developments and appls. 79−96425
performance of a collector/storage solar water heater, anal. 79−70432
Philippine national solar energy development programme 79−57376
photochemical conversion and storage of solar energy 77−86330
photochemical energy conversion, nonbiological 77−86331
photochemical solar energy conversion, photoredox reactions of metal ions 77−86334
photoelectric electrodialysis desalination plant 79−39284
photoelectrochemical model energy conversion systems, evaluation 79−43777
photopile manufacture for terrestrial solar cells, review *(French)* 79−24895
photothermal conversion, closed loop systems, general design method 79−74542
photovoltaic conversion comparative evaluation *(Italian)* 80−60023
photovoltaic electricity generation in India 80−21381
photovoltaic energy generation integrations into electric grid systems, general methodology 80−45647
photovoltaic generator operation and cost simulation 79−61975
photovoltaic power system reliability assurance methods 80−61315
photovoltaic power systems for rural areas of developing countries 80−50967
photovoltaic solar cells applied to communications repeater stations 79−29450
photovoltaic solar energy, conference, Luxembourg (1977) 78−64106
photovoltaic systems break-even cost anal. for rural Mexico 80−94027
photovoltaic technology, conf., Washington, DC, USA, (June 1978) 79−7863
photovoltaic transient analysis program for electrical and thermal anal. 80−94061
photovoltaic-wind hybrid alternative energy system 80−30409
pistonless engine capable of utilising solar energy, dynamics 78−71277
plane collector, equilibration temp. in real conditions *(French)* 77−123
plant for hot water supply *(Rumanian)* 80−97766
potential energy source, short term and long term prospects 79−83569
power plant, tower type, configuration, solar energy concentrator efficiency 77−19379
practical uses of solar energy in Switzerland *(French)* 80−55808
prediction of radiation monthly mean parameters 79−48099
promotion in Austria, economic aspects *(German)* 79−87981
pump, below actuated, based on Rankine cycle principle, analysis and expt. data 79−74504
pump appl., for lift irrigation, modified design analysis, with working fluid and water separation and internal insulation 79−70440
pumping engine, irrigation, 7.5 W, with liquid piston, design and analysis 79−74537
pumping of water appl., economic comparison with wind power, petrol engine and electric water pump 79−74507
pumping of water using thermal or electric solar pumps 80−50942
solar power continued
pumping system, based on Rankine cycle, performance prediction model 79−70460
pumping system, based on Rankine cycle principle 79−70459
pumping system appl., passive, using organic working fluid 79−70439
pumps, water, air- or water-cooled, development and performance 79−70441
pumps appl., irrigation, 1978 status review 79−74506
pumps development in India, using biomass as auxiliary heat source 79−70461
pyranometers for mesoscale solar irradiance network, test and calibration experience report 79−74499
Quebec, hourly radiation values for horizontal surface 80−17354
R&D importance for university education and development in Sweden 79−57382
R and D program at the Inst. of Engng. of the Nat. Univ. of Mexico 80−40845
radiation, horizontal plane diffuse insolation from clear sky 79−83575
radiation absorption in ponds, analysis 79−16530
radiation charact. and intensity calc. 80−45649
radiation concentrated, absorption, solid-gas-suspensions study 79−66415
radiation flux density, solar and terrestrial radiation dependent on the amount and type of cloud 80−67403
radiation in Mexico using sunshine hours and meteorological data, empirical compilation 79−44237
radiation intensity oscillations, daily and seasonal, problems of power when demanded *(Croatian)* 78−3859
radiation intercepted by a tilted surface, estimation of daily, clear sky, spatial distrib. 80−81423
radiation levels on tilted surfaces, computer model validification 80−35641
radiation measurement, techniques and instrumentation, survey 77−5348
radiation on vertical and inclined surfaces, monthly mean calcs. 80−45746
radiation statistical estimate, in equatorial region (Singapore), power utilisation appl. 79−87972
radiation statistics, linear spatial interpolation 80−93859
rational use of energy in houses *(Dutch)* 80−40836
receiver surface optical properties obs., black coatings on high-temperature alloys 78−18071
recovery from soil, deep ground coil evaporators for heat pumps 79−87967
reflectivity of common building materials, effect on roof heat gain 80−55810
reflector, using black surface glass mirror, reflection coeff. determ. 77−34930
refrigeration, exam. of dry absorption using $CaCl_2$-NH_3 80−61310
refrigeration, isothermal dissociation and regeneration of $CaCl_2$-NH_3 *(French)* 80−61300
refrigeration, single-loop conjugate realisation 77−75644
refrigeration appl., H_2O-LiBr and NH_3-H_2O absorption cycles, design and optimisation 79−87974
refrigeration in tropical zones using flat plate collector and two-component coolant *(French)* 79−24911
regenerator buoyancy effects, appl. 79−68709
regenerator of hygroscopic solutions, for air dehumidification 79−57464
remote communities novel energy concepts, technical and economic aspects 79−48078
remote islands telecommunication repeater stations power supply 80−61382
renewable energy resources utilisation for the development of rural areas 80−45650
renewable energy sources, Rumania *(Rumanian)* 80−35639
renewable energy sources and the environment 79−79411
renewable solar-based energy resources for future energy strategy 80−30383
research, applications, water heating, space heating, air conditioning and hothouse heating *(French)* 79−100487
residential utilisation, conceptual development of a solar town in Iran 80−50944
review of energy resources, reactor accidents, radioactive waste disposal 78−50413
review using rational units 80−30389
rock bed storage for solar energy systems, comparison of meas. and predicted performance 80−67004
satellite, appl. of solid state microwave technology 80−40870
satellite, assessment for European appl. 80−40867
satellite, computer modelling of power transmission system 80−40866
satellite, energy anal. 80−50937
satellite, microwave system perform. during startup/shutdown 80−40869
satellite applications to solar energy monitoring 80−50982
Satellite Power Station microwave health and ecology programme 79−70443
satellite power system technology, environmental and societal impact 80−30386
satellite solar power stations, preliminary cost benefit anal. 77−87231
satellites, electronic systems 79−92065
secondary cells, Pb/acid, design and performance characteristics for remote photovoltaic applications 80−55833
selective absorbers, 10.6 μm refl. of In_2O_3:Sn coated Si 77−58398
selective materials for photothermal conversion of solar energy *(French)* 79−24908
selective surface for thermal conversion of solar energy, 80 to 200°C 77−14891
selective surfaces for high temp. photothermal conversion 78−1364
SERI, Solar Energy Research Institute, CO, USA, R and D program, organisation 80−89599
shaded vertical receivers, monthly average radiation estimates 80−35646
shadow effect of adjacent solar collectors in large scale systems 80−45738
simulations, typical weather determinations 79−16614
small village solar electrification economics 79−57387
small-state solar energy programme structuring methodology 79−57385
social and economic implications for Australia 79−83568
social implications of energy storage 80−67001
solar battery utilisation trends 79−39287
solar cell arrays, technological and economic barriers to be overcome for competitive power production 80−72049
solar cells, applications of 100 mm diameter cells for solar modules *(French)* 79−100532

solar power continued
solar cells, concentrated, conducting grid, design rules *(French)* 79−24896
solar collector-heat pump installations, meas. of efficiency under operational conditions *(German)* 80−101077
solar collectors, rectangular glass prisms with total internal reflection, appl. 77−27372
solar declination and the length of the solar day 80−45648
solar energy: four sites demonstrate potential 79−61946
solar energy and environmental heat utilization for space and water heating *(German)* 80−61284
solar energy collectors, comparative efficiency of various types 79−24907
solar energy storage as hydrogen from bromine from hydrogen bromide 79−57470
solar energy utilisation, participation of meteorology *(Czech)* 79−83567
solar enhanced oil recovery; an assessment of economic feasibility 80−40832
solar gas turbine, thermal cycle with gas reheating 79−92064
solar heating, appl. of flat plate collectors and thermal stores *(German)* 80−26152
solar heating of buildings, numerical simulation of thermal performance 80−66942
solar irradiance, model for determining the spectral quality of daylight on a horizontal surface at any geographical location 80−93856
Solar One, a 10 MW solar thermal central receiver pilot plant 80−35651
solar open cycle absorption refrigeration system, anal. and simulation 80−16788
solar panel, radiant props. deform. using greenhouse effect *(French)* 77−72139
solar power system, mathematical model, operating regimes optimisation 79−83562
solar radiation geometric Brownian distribution, implications for economical solar heating system 79−83571
solar Rankine cycle air conditioner *(Japanese)* 80−72076
Solar Thermal Electric Power System technical and economic evaluation for Japan 79−57441
solar thermoelectric generators, metallic thermo-electric materials utilisation, economic characts. 80−101122
solar tower concept, ray trace approach 78−5571
solar-electric heat pump for houses, design and tests *(German)* 80−7951
solar-radiation meter, automatic 80−89592
solarimeter, autonomous with permanent readout *(French)* 79−24893
SOLPAC energy conservation program, space heating and water heating for homes *(French)* 79−100488
Southern African solar energy resources and requirements 79−57383
space and water heating, trial *(German)* 80−108788
space heating, correspondence between solar load ratio method for passive water wall systems and f-Chart performance estimates 80−16787
space heating, heat pump house heating system with low quality thermal flow 80−76617
space heating, heat-pump assisted systems, perform anal. 80−35649
space heating, latent heat diode walls for solar energy collection and storage *(French)* 80−61298
space heating, office building in Madrid, appl. 80−89597
space heating, solar collectors combined with ground heat pumps, economic advantages *(German)* 80−76605
space heating, solar energy collection and storage *(French)* 80−61299
space heating, solar energy utilization *(Czech)* 79−83564
space heating, solar power utilisation employing solar collectors, absorbers and heat pumps *(German)* 80−76604
space heating, two-tank storage system using seasonal and diurnal tanks 80−72016
space heating in winter, solar availability from anal. of SOLMET data (1953 to 1975) 80−81421
space heating installations, case for dynamic controls on hydronic distribution systems 80−104498
space heating system optimal control study, large buildings appl. 79−87995
space heating systems, load optimisation algorithms 80−45643
space heating with air and liquid systems 80−61287
space power generators, past developments and future trends 80−45693
space stations for large orbiting energy systems, NASA philosophy 77−78602
spectral characteristics for improving solar collector performance 80−35650
spectral distrib. determ. using rapid spectral radiometer for solar cell appls. 80−61369
stations, design of village photovoltaic power systems 80−61307
status and development trends, in late 1970s 79−57347
steam production by solar power for industrial appl. 80−30401
stochastic predictions of solar cooling system performance 80−85269
stochastic weather algorithms for predictions of solar cooling performance 80−35642
storage, molten salts, heat transfer salt *(French)* 80−61434
storage, review of methods 80−55916
storage system, ammoniated salt heat pump using $MgCl_2$, $CaCl_2$, NH_4Cl 80−81484
storage tank, Markovian model of behaviour *(French)* 79−24912
sun loading on fixed, tracking surfaces, solar energy availability investig. 80−40838
sunlight absorber, struct. and thermal efficiency 77−125
sunlight reflected from polygonal heliostat, optical simulation 79−29452
Swedish energy policy up to the year 1990 *(Swedish)* 79−87982
swimming pool outdoor, heating indirect, heat pump appl. *(German)* 80−16781
synergetic aspects of solar energy and the fast breeder reactor 80−7907
systems, review 77−73798
technical-economic validation of resources as energy sources 80−89593
technological economics, current criteria based *(French)* 79−100495
technology, conf., Winnipeg, Canada, Aug. 1976 77−29412
technology and methods for appl. of solar energy to European agriculture 80−76616
temperature control systems, modern control theory appl., review 80−66949
terrestrial solar spectral irradiance distrib. variations, sensitivity of solar transmittance, reflectance and absorptance 80−82739
terrestrial utilisation of solar energy, scope and experience *(German)* 80−40829
test facilities and meas. standards in developed and developing countries 80−55819
solar power continued
test systems, elec. utility demonstration projects 80−3488
textured surface, reflectance and transmission props. 78−1165
Thai rural solar energy utilisation programmes 79−57375
Thailand, research and development in solar energy, review 80−26113
THEK collectors, fluid transport network for solar energy to heat conversion *(French)* 79−24905
thermal Albedo Energy Convertor, concept, design and testing for high altitude long endurance platforms 80−108789
thermal conversion, sputtered In_2O_3:Sn for selective transparent films *(Japanese)* 77−68247
thermal electric power technology, progress and future *(Japanese)* 79−79374
thermal energy production, large scale, possible climatic effects 78−81357
thermal energy storage 80−72089
thermal processes, digital simulation 79−24890
thermal storage, numerical simulation of energy transfer by conduction and radiation *(French)* 79−24916
thermal storage cell for high temperature solar systems 80−55923
thermal storage eutectic molten salt mixtures, enthalpy of fusion estimation *(French)* 79−24914
thermal storage of solar energy 80−51005
thermal storage using chabazitic tuff, a zeolitic rock 80−94117
thermal systems, technology status 80−40842
thermo-electrochemical H_2 prod. using solar energy *(French)* 79−24918
thermo-telemetry transistorised thermometer appl. *(Spanish)* 78−16793
thermoclines, solar thermal energy resource for enhanced hydroelectric power production 79−92060
thermoelectric generator high temp., sintered Si-Ge, performance assessment 79−74534
thin composite films, photothermal conversion efficiency film 78−2937
thin film deposition using solar furnaces 80−89148
thin sheet Fresnel solar collector-concentrators, features and economic benefits 79−79402
Third World rural development prospects 80−30399
timber dryer, forced-air, for tropical latitudes, solar heating appl. 80−21384
total radiation intensity, universal formula using climatological data 80−31108
tracking system, heliotropic fluid-mech. drive system, dynamic response anal. 80−55823
tracking system with electronic servo 79−57433
tracking systems for photovoltaic collector control *(Spanish)* 80−45637
trapezoidal groove solar energy collectors, predicted daily and yearly average radiative performance 79−74540
UNESCO solar energy programme 79−57358
UNIDO solar energy programme for developing countries 79−57359
United Nations energy program for solar and wind energy appls. 80−3496
United Nations System solar energy programmes 79−57361
units and symbols 79−12756
USA, classification of solar climates 80−76612
USA Federal solar energy programme achievements and prospects 79−57370
utilisation, conf., Cairo, Egypt (June 1978) 80−46734
utilisation, energy model anal. to 2010 cf. nuclear power *(German)* 80−26109
utilisation, review 80−16790
utilisation, solar energy planning for developing countries 80−50943
utilisation in developing countries, conf. report, Varese, Italy (March 1979) 80−40834
utilisation in Egypt for water heating and distillation, power generation and air conditioning 80−50938
utilisation in human settlements, inexpensive systems, appls., function and techniques 80−51004
utilisation in northern latitudes, insolation modelling of solar collector with thermal storage 80−66941
utilisation limits and average daily sunshine tables for Central Europe *(Czech)* 79−83563
Vietnamese rural area solar energy utilisation potential 79−57384
warm sea power plants, site limitations 77−53074
water distillation using basin-type solar stills, use of wood charcoal beds 80−7924
water heater, natural circulation, with linear and nonlinear temp. distribs. 77−75778
water heater/steam cooker, design and trials 79−66402
water heaters, rural population demand fulfilment 80−89668
water heating, flat plate system with thermosyphonic flow, investigation 79−70464
water heating, residential, combined solar systems, economic anal. 80−61311
water heating, State of Nebraska Solar Heat Pilot Project 80−55817
water heating appl., adoption in tropical countries 79−57462
water heating models comparison 80−30387
water heating system, materials corrosion 80−30131
water heating system for domestic appls. 80−93852
water heating system for mine changing house, solar collector plant design 79−74503
water heating systems analysis and optimisation 79−57461
water pump for lift irrigation, thermodynamic anal. and simulation 80−61397
water-heating systems, design method 79−83629
West German solar energy technology development status 79−57386
West German solar energy utilisation programme technologies 79−57366
Western Canadian provincial and university solar energy activities 79−57381
wood wastes, gasification, using flash pyrolysis and concentrated solar energy *(French)* 80−61226
zeolite collector for solid-gas absorpt. refrigeration system 80−35754
BaO reversible oxidation energy storage system feasibility 79−83637
CO_2, thermochem. reduction using solar energy to provide C-based fuels 80−76610
$CaCl_2.6H_2O$ heat of fusion system for solar energy storage 80−16846
$CaO-Ca(OH)_2$ reversible hydration-dehydration for solar energy storage 80−97810
Cr_2O_3-Cr, RF sputtered cermet film, selective black absorber 77−58399
H prod. by H_2O pyrolysis using solar thermal energy 80−45770
H_2 production by electrolysis of water using solar energy *(Czech)* 77−29014

solar power continued
H_2O heating, freeze-tolerant heater using crosslinked polyethylene 80−66944
Ni-Cd pocket plate batteries characteristics, solar applications 80−61332
Pb-acid battery charging from photovoltaic array energy source, problems and efficiency 80−61336
W-halogen quartz lamps with optical filters, solar simulator appls. 80−16838

solar power stations
1 MW, French CNRS plant 79−61954
3.5 m heat pipe for solar collector, charcts. *(Japanese)* 79−79378
5 GW satellite power system, power distribution design tradeoffs 79−52894
10 kW, development for rural areas in India 79−61956
10 kWe, based on freon-Rankine-process 79−62020
10 MW, Iranian design 79−57417
10 MW thermal central receiver pilot plant 80−66953
10 MWe pilot Central Receiver Solar Thermal Power System, design concept 80−16792
32 kWe total energy project, test facility 79−52912
50 W generator for developing nations, with simple tracking system 79−43748
100 kW peak photovoltaic power system, design, construction and capabilities 80−45705
100 MW, ocean thermal energy conversion, systems aspects 78−96235
100 to 1000 kWe, feasibility study *(French)* 79−52886
150 kW pilot solar pond project, Israel 80−94114
150 kW plant, Dead Sea, solar pond details 80−35638
150 kW solar powered irrigation facility, design 79−96427
600 to 800000 kW solar pond project at Salton Sea, CA, USA 80−94113
AEROSOLEC, combined solar-wind power station for telecommunication appls. 80−61306
autonomous and hybrid solar thermal electric plant energy storage requirements 79−57494
boiling two-phase flow in two parallel horizontal tubes in solar collector receiver tubes, fluctuations *(Japanese)* 79−79377
Brayton cycle solar electric plant receiver, 1 MW_t bench model design and testing 80−55896
central receiver plant, dynamic simulation of thermal-hydraulic charcts. of Na-cooled plant 80−30400
central receiver power plant, 10-MW pilot plant project 80−30405
central receiver program, heliostat, receiver and storage subsystems 80−30404
central receiver solar power systems, terminal concentrator concept analysis 80−26116
central receiver system, flux density integral for reflected sunlight, numerical anal. 80−93863
central receiver type, solar receiver tube thermal stresses, fatigue aspects 80−40908
central receiver with chemical storage, 100 MWe cogeneration 80−93857
central solar receiver, struct. anal. and design considerations of superheater 79−66410
central tower system conception and evaluation, based on heliostats 79−57416
collection subsystem of 1 MW solar power station, engineering assessment 80−61305
combined generation/storage scheme, using $Ca(OH)_2$ 79−43790
combined solar and fossil fuel systems 80−61312
comparative ranking of 0.1 to 10 MWe solar thermal power systems 80−30559
composite heliostat, computer anal. and optimisation 79−39283
concentrating collector systems, US DOE Solar Thermal Program, R and D review 80−66998
concentrator/solar array systems, economic assessment 79−43770
cylindrical parabolic focusing collector for distributed-collector solar power system 79−62108
desalination plant utilising reverse osmosis, 2.5 kW solar generator 80−61282
design, global yield and economics, current projects *(French)* 80−55803
design of village photovoltaic power systems 80−61307
direct tracking using two-mirror unit with plane and hyperboloidal counter-reflectors 80−91875
distributed microcomputer-based control system for a large scale solar total energy system 80−30396
distributed-collector, thermal-electric economic assessment 79−52908
domestic wind, solar, wind and solar heating systems, performance and economic evaluation 79−43744
Earth orbiting, economic, political, and environmental problems 80−45633
Earth orbiting, interference with space communications systems 80−45634
economic assessment, generalised methodology 79−52913
economic impact analysis of solar thermal plants in small utilities 80−30407
electric power generation in remote locations, costs comparison with diesel generators 80−55813
electric power generation technology, reviews 79−24883
electrical system comprising DC separately excited motor and mechanical load driven by solar cell array, performance analysis 80−16801
electricity storage, battery appls. potential 80−72067
energy concentrator designs for underdeveloped countries 79−62125
energy conversion, Conf., San Diego, CA, USA (Aug 1978) 79−48038
expander design and test results, valveless, using compressed air as working fluid 79−62023
farm plant, modular, 15 to 1000 kW, multiple utilisation of waste heat 79−61953
farm power supply in India, reflector-concentrator modified Stirling engine and aqua-ammonia absorber gas turbine units developments 79−62024
fixed mirror solar concentrator for application to a 100 MW(e) electric generating plant 80−30393
flat energy receivers and convertors, solar radiation concentrator construction for uniform irradiation 79−83559
flat plate solar photovoltaic power system with 100 kW peak power 80−35653
flat-plate non-tracking ground mounted photovoltaic array structures, cost reduction anal. 80−94038
flate plate evacuated collector design 79−62099

solar power stations continued
flywheel energy storage and conversion system for photovoltaic appl., economic anal. 80−94116
generation, survey, vapour-tubine units, using organic working fluids 79−83618
gridiron electric power generation, 65 ft hemispherical mirror construction 79−87980
hazards to air traffic, photometric photography of dazzling heliostat mirrors *(French)* 80−61295
heat pipe central solar receiver gas turbine plant, using open gas cycle 79−52910
heliostat field optimisation, appl. of field shape effect for power stations *(French)* 79−24903
heliostats for central receiver solar power stations, optical analysis 79−74543
heliothermal, 100 to 1000 kWhr, technical and economic feasibility 79−61960
high temp.-high flux material testing, solar power station appls. 80−40668
high temperature solar power tower plants concept considerations and operational criteria 80−55822
hybrid solar photovoltaic/solar thermal electric power system, simulation 80−94025
hybrid solar-diesel power stations for optimum energy utilisation 80−89598
hybrid solar-fossil power generation, combined cycle system 80−30406
hydro-photovoltaic plants, peak power generation economics and reliability 80−45706
ideal prism solar concentrators, features 79−43745
industrial solar total energy systems in United States 79−96426
joint operation, with wind power plant, exptl. investigation 79−39278
large scale electricity production, solar cell developments and appls., review 80−40861
Large Solar Power System Programme, in United States, progress since 1972 80−26114
medium power heat and electricity production development program, economic requirements and technical options *(French)* 79−100493
meteorological effects of solar thermal electric conversion plant, numerical modelling 80−35794
microwave power transmission technology 80−40868
military space power program, development of 10 to 50 KWe solar power systems 80−30415
modular solar collector development for large solar generators 79−96467
multi-gigawatt, in space, progress review in field since 1979 *(German)* 80−81424
new technologies 79−39279
ocean thermal energy, OTEC systems developments and 1978 status 79−83612
ocean thermal energy conversion, OTEC system development, Conf. Houston, TX, USA (Nov. 1978) 79−83611
ocean thermal energy conversion, prospects 79−87960
ocean thermal energy conversion (OTEC), 100 to 400 MW, developments survey *(Dutch)* 80−12025
ocean thermal energy conversion plants, condenser and evaporator design improvements, using internal and external flutes 79−61959
ocean thermal energy conversion systems (OTEC) turbine parameters w.r.t. working fluids 79−83617
offshore energy conversion (OTEC) plant design, technology considerations 79−5507
one and two faced symmetric sidewall booster mirrors, optimal geometries 79−43743
optical concentration in solar power stations by use of conical and parabolic mirrors *(French)* 79−24904
orbiting, American project *(Spanish)* 80−81420
orbiting, evaluation of current conductor mass and voltage level required 80−89616
osmotic pressure utilisation, semipermeable membrane and low-head reaction turbine appl. 79−57418
OTEC (ocean thermal energy conversion) plants, alternative forms of energy transmission assessment 79−61958
OTEC power plant, selection of working fluid (NH_3, propane and freon) 80−89665
OTEC system performance study 80−104514
parabolic trough mirrors, concentration charcts. *(Japanese)* 79−79376
photoelectric, for cathodic protection of pipelines 79−39286
photovoltaic, 25 kW, irrigation and grain drying appl., US expt. 79−70442
photovoltaic flat panel system, design and performance of 100 kW plant 80−61308
photovoltaic power stations, nominal costs and performance goals 79−34438
photovoltaic power systems, equipment performance and manufacturing techniques improvements and system design problems for telecommunication applications 80−55843
photovoltaic power systems for rural areas of developing countries 80−50967
photovoltaic power systems for rural areas of developing countries, technology, reliability, economics and appls. 80−61286
photovoltaic village power systems: the minigrid concept 80−66973
photovoltaic/thermal electric central solar power station 80−30410
photovoltaic/thermal system powers Texas house, performance data and power conditioning equipment 80−94036
polyurethane foam solar concentrator, thermal and thermohydrolytic ageing 78−92281
power plants, solar high temp., with Stirling engine and solar thermal rocket engine, efficiency improvement by using selective radiation absorption surface 80−89589
power systems availability and reliability analysis 80−35687
primary circuit and thermal storage tank transient thermal behaviour 80−85267
primary fluid heated by solar energy in linear collector, thermal regimes and appl. 78−75061
Rankine cycle, organic, using flat-plate collectors, cycle optimisation for turbine power package irrigation pump drive appl. 79−62019
Rankine cycle solar thermal power plants, operating experience 80−30523
Rankine cycle system simulation 79−52911
Rankine-cycle, 150 kWe, design w.r.t. economics, reliability and ambient conditions 79−62022
satellite, 5 GW, using GaAlAs cells, for Earth-based utility appl. 79−52892

solar power stations continued
satellite, appl. of solid state microwave technology 80−40870
satellite, assessment for European appl. 80−40867
satellite, computer modelling of power transmission system 80−40866
satellite, energy anal. 80−50937
satellite, Europe base-load electricity supply appl. 79−39288
satellite, in Earth orbit, survey 80−21376
satellite, microwave power transmission system design 79−52893
satellite, microwave system perform. during startup/shutdown 80−40869
satellite, photovoltaic, 10 GWe, construction and installation 79−52895
satellite, power transmission to Earth-based utility, efficiency analysis 79−48093
satellite, solid-state solar-power station spherical solar collector, enhanced power generation 80−12009
satellite, technical considerations 79−34425
satellite, technical considerations 80−72014
satellite, theoretical anal. of nonlinear interaction between strong microwaves and ionosphere *(Japanese)* 80−94634
satellite, thermal analysis 79−48094
satellite design and system engineering issues 79−96465
satellite design nomogram 79−70433
satellite ground station rectifying antenna, basic design concepts 80−16782
satellite photoelectric power stations, alternate favourable option 80−16791
satellite power systems concept, solar photovoltaic and solar thermal concepts 79−52891
satellite power systems review, DOE and NASA joint project 79−52890
satellite solar array blanket interface problems 79−96466
satellite solar cell array conception and efficiency analysis 79−96464
satellite solar power stations, review 79−8984
satellites, effect of transmissions on radio-astronomical research 80−61291
satellites, output power variations, evaluation 79−29455
self-contained solar power installation concentrating system design and optical/energy characts. testing 80−40828
solar energy collection and conversion, pros and cons, economic prospects projection *(French)* 79−100489
solar energy utilisation problems in thermal installations *(Rumanian)* 79−52884
solar gas turbine, thermal cycle with gas reheating 79−92064
Solar One, a 10 MW solar thermal central receiver pilot plant 80−35651
solar photovoltaic system feeding unusual length radio link, characteristics and design data 80−61383
solar power satellite, construction in space, fabrication methods, materials, tools 80−21377
solar power satellites, solar energy conversion methods developments, general aspects *(French)* 79−100494
solar voltaic power systems, comparison to fuel energy, for telecommunications 80−61381
Sophia Antipolis 5 kW photovoltaic power generator for habitat 80−61374
space power plant and solar energy power generator, thermionic converter proposal 80−61389
space solar electric power plants 79−39281
space-manufactured satellite power systems, costs anal. using lunar materials 80−97767
Spacelab and space platform solar array programmes 79−96884
state of art survey in solar energy utilisation *(Dutch)* 80−76608
stationary spherical solar collector design 79−62107
steam generation system for industrial appls. 80−55825
Stirling engine power conversion for MWe solar power system with parabolic concentrators 80−30561
storage of thermal energy, based on reversible dissociation of SO_3 79−48186
storage systems, 1978 development status 79−48095
storage tank, Markovian model of behaviour *(French)* 79−24912
techno-economic development of advanced plants 80−30395
terrestrial solar energy power system *(Japanese)* 79−79375
THEK collectors, fluid transport network for solar energy to heat conversion *(French)* 79−24905
Themis solar electricity generating station design *(French)* 79−39290
thermal, 1978 state and future potential 79−43749
thermal, cost estimation for Japan *(Japanese)* 79−79381
thermal, dispersed, performance and economic risk evaluation, by computer Monte Carlo simulation 79−52902
thermal, for Iran, economic evaluation 79−74500
thermal, preliminary design for Japan *(Japanese)* 79−79380
thermal, Small Power Systems Applications Project (1 to 10 MWe) 79−52900
thermal, Stirling engine appl., free-piston 79−48174
thermal electric and photovoltaic cell power plants, local energy exchange dynamics and climatic boundary conditions effects, preliminary examination 78−81355
thermal electric generation, dynamics and control of Stirling engines 80−30522
thermal electric power systems, comparative economics of small systems 80−55818
thermal electric power systems, line focus collectors, economic comparison 79−70435
thermal energy storage in aquifers for a solar power plant 80−55925
thermal energy storage systems, survey *(Japanese)* 79−79379
thermal generating station design, engineering problems *(German)* 80−30381
thermal power system, open cycle air turbine *(French)* 80−45641
thermal storage unit analysis 79−57493
thermal test facility, 400 kWth, Georgia Tech, preliminary (1979) results 79−61955
Thermal Test Facility, at Albuquerque, New Mexico, description 78−66887
thermionic power plant, central thermal receiver tower concept, geometric config. and design 80−61390
thermoelectric conversion, collector systems and thermal storage 80−45759
total energy system, for US Army base buildings, conceptual design and large-scale expt. 79−52899
total energy system, Fort Hood, control system 80−30397
total energy system, preliminary design for large building supply 79−52898
total energy system at Georgia, USA 80−35652
solar power stations continued
total energy system evaluation program 80−30402
tower type, economic aspects, power station construction and installation site *(French)* 79−100491
tower type, installation problems summary and current operations review *(French)* 79−100492
tower-top focus solar receiver designs 79−62114
tower-type, concentrating and receiving systems design modelling 80−91873
tower-type, heliostat field solar energy collection, achievements and projections *(French)* 79−100490
tower-type solar furnaces, two mirror, high power, optical characts., calc. for design 80−40824
transient temperature vars. in primary network 78−75062
turbine sizing of a solar thermal power plant, performance and economic anal. 80−30403
turbines, use of organic fluids *(French)* 79−52885
turbopack, based on low-temperature Rankine cycle, low-cost design, pump drive appl. 79−62021
undersea hot water storage system 80−45763
United States' Pacific Northwest Electric Utility, strategic solar energy planning program 79−48101
unsteady laminar heat transfer in circular duct flow in receiver tubes in solar collectors *(Japanese)* 79−77058
utilisation efficiency and feasibility criteria 80−40826
vapour turbine, using combined thermal-power convertor and photoelectric convertor, thermodynamic efficiency for solar energy conversion 80−89614
CaO-$Ca(OH)_2$ reversible hydration-dehydration for energy storage 80−97810
GaAs photovoltaic solar system for utility substation appls. 80−30493
GaAs photovoltaic solar system, appl. in electric utility system 80−55875

solar prominences
3.5 mm depression features assoc. with Hα disparitions brusques 77−78756
1959 July 16, proton solar flare, composite plage and prominence flaring 79−75173
1969, October 15, quiescent prominence macroscopic motions from Ca^+ lines 79−40167
1973 August 14 loop prominence, XUV emission and density 80−56807
1979 February 26, prominence excitation conditions determ. from flash spectrum 80−67687
active edges of quiescent prominences 79−25575
active loop prominences, numerical model 80−56787
active prominences at cm. wavelengths, RATAN-600 obs. *(Russian)* 79−16926
active region loop system, structure 77−53509
active structures and total current 80−4336
ancient Chinese observations of physical phenomena attending solar eclipses 80−72916
anomalous Balmer decrement, stimulated transitions between highly excited atomic levels 78−5176
Balmer lines, formation in bright prominences spectra *(Russian)* 80−77377
chemical abundances, relative, in prominences and other solar regions 80−46518
cm and mm wavelength obs., size and spectrum of radio filaments 79−66988
corona, struct. rel. to prominences and flares 79−71014
corona-prominence interface compared with chromosphere-corona transition region 77−29786
coronal condensation forming prominences, condensation along mag. field lines 80−46524
coronal electric current systems development in active regions, rel. to filaments and flares 79−25567
coronal interface, review 80−4333
coronal mass ejection event, 1973 December 19, kinematics 78−28640
coronal mass ejection events assoc. with flares, prominences or radio bursts, outward vel. meas. 77−22197
cylindrical prominences, photospheric boundary magnetic field effects 80−90396
destabilization rel. to coronal transient onset 79−44449
disappearance into chromosphere, appl. of mag. energy build-up theory 77−45391
eclipse observations using plane grating as polar heliostat 79−84674
electric currents as solar wind energy source, theory 80−94768
electron density and temp. from Ca II/Fe I emission line ratios *(Russian)* 80−51717
electron density of quiescent prominences in He and Na emission regions *(Russian)* 78−20784
emission line intensities rel. to model calcs. 79−44447
emission line profiles, from inhomogeneous solar phenomena with different porosities *(Russian)* 78−40891
emission line profiles of inhomogeneous formations 77−37586
eruptive, 1974 June, 8, elec. current growth obs. 77−29788
eruptive processes, onset theory 78−61840
eruptive prominence, 1974, June 8, obs. 77−22182
eruptive prominence, gyrosynchrotron modulation in assoc. moving type IV bursts 80−26833
eruptive prominence and surge, Skylab X-ray and Hα obs. 77−78755
eruptive prominence assoc. with coronal transient, Hα and He II emission 77−2389
eruptive prominences, assoc. coronal brightness and structure changes 80−4337
eruptive prominences, coronal manifestations, theory 80−4338
eruptive prominences, rel. to He^+ obs. in interplanetary shock wave 80−72735
eruptive prominences, rot. motions rel. to twist transport in force-free mag. flux tubes 78−40813
eruptive prominences and coronal transients 80−56809
EUV continuum absorption in prominences, new evidence 79−92738
EUV limb spectra of prominence, Skylab obs. 80−12717
filament, short-lived, produced by surge 77−33458
filament, synthesized map at 6 cm with about 15″ resolution 80−90380
filament eruptions and nonflaring coronal transients assoc. with nonthermal electrons 78−65595
filament features Hα contrast profiles 77−2402
filament formation dynamics, thermal instability in sheared magnetic field 80−4319

solar prominences continued
filament observations with multi-channel subtractive double pass spectrograph 78−12189
filament-corona transition region, OSO-VI EUV obs. 78−28620
filamentary prominences, radiation transfer 78−89154
filaments, multifreq. obs. at centimetre wavelengths 78−28602
filaments, radio radiation transfer 77−25995
filaments, short-lived, differential rotation 78−28642
filaments disparitions brusques, evidence for role of mag. field *(Russian)* 80−51726
filaments location symmetry, example of giant convective cells delineated by mag. fields 77−29779
filaments radio emission, obs. by RATAN 600 telescope 77−78760
fine chromospheric structs. in corona, Hα obs. *(French)* 78−28607
fine struct., small scale Doppler shifted features 77−78754
fine struct., vertical flux ropes and filamentary structure 77−29764
fine structure, obs., Hα filtergrams 77−17523
flare prominence, 1979 March 27, photographic obs. *(Chinese)* 79−92744
flare-loop prominence system, 1972 May 24, optical and X-ray obs. 79−30045
formation, by rising mag. flux ropes twisting *(Russian)* 78−40898
formation and coronal arcade structure 80−41800
hedgerow prominences, fine structure from spectral obs. 78−40906
horizontal temperature gradient in prominence/corona transition zone, meas. rel. to prominence condensation 80−26832
IAU Colloquium 44 (Oslo, 14-18 August 1978) 80−4330
line profiles calc. for inhomogeneous emission formations 79−25562
line profiles from expanding and escaping fine filaments 77−91499
line profiles of active limb filament, OSO-8 UV obs. 79−44446
loop, 1973 Nov. 3, H I, He I and He II emission line spectra 77−64736
loop, formation mechanism, MHD approx. *(Russian)* 77−87363
loop, X-ray line emission, model 77−82195
loop prominence formation mechanism 79−58315
loop prominence kinematics 79−84774
loop prominence knots, motions, Hα line filtergram obs. 80−67693
loop prominence system, flare assoc., high temp. corona 79−53782
loop prominence systems, rel. to large-scale coronal active region X-ray brightenings 78−20806
loop prominence systems rel. to coronal long-decay X-ray enhancements, physical parameters 79−44448
loop prominences formation, kinematic model 78−7965
loops, magnetic reconnection in corona 77−29765
magnetic field boundary relations 80−4335
magnetic field determ. from Hanle effect 77−74024
magnetic field meas. 77−71085
magnetic fields meas., photographic method *(Russian)* 78−65584
mass ejection mechanism for transient phenomena 78−7980
microwave radar observations 79−88635
model for quiescent prominences 80−4316
negative bursts with moving filaments 1969, 19 May 77−53516
nonthermal turbulent motions, spectral obs. 78−4174
outer regions, temp. and microturbulence *(French)* 77−53510
Pikel'ner's theory of prominence form. 77−71086
Pikel'ner soln. stationary flow in magnetic tubes of force 77−53540
polarimetric obs. and magnetic field determ. 80−4332
polarisation of D3 emission line 77−29746
quiescent, Ca II K spectra and vertical struct. of line of sight vel. field 77−53522
quiescent, EUV obs. from Skylab 79−66987
quiescent, formation by thermal instability in current sheet 77−82194
quiescent, Hα and Hβ emission line profiles 79−71011
quiescent, Hβ, He D_3 and Ca II 8542 Å line emission meas. 78−32427
quiescent, He I 10830 Å line emission obs. 77−29787
quiescent, heating and cooling, calc. 80−12738
quiescent, mag. field gradient 77−17466
quiescent, mag. field intensity 77−87355
quiescent, middle Balmer decrement meas. 80−12737
quiescent, obs. at 8 mm during 1975 May 11 eclipse 78−7977
quiescent, over sunspot umbrae, effects on Ca II H and K line profiles 77−22178
quiescent prominence, influence of spatial resolution on Ca^+ K-line width and shift 80−77364
quiescent prominence formation, support and stability 80−4334
quiescent prominence spectra, meas. of Ca^+ 8542, 8498 Å, He 4471 Å and Ti^+ 4468 Å 80−90373
quiescent prominences, Ca^+, H and He line emission 77−29750
quiescent prominences, downward motions model 78−20779
quiescent prominences, He abundance determs., theoretical models 78−49405
quiescent prominences, mag. fields orientation 78−45305
quiescent prominences, spectra meas. 78−40886
quiescent prominences, struct., and H and He spectra 77−13295
quiescent prominences, theory of Ca II emission lines 77−53523
radiative transfer, H line radiation diffusion 80−67694
radio brightness temp. depression interpretation, cm and mm data 80−90395
spectra, inclined features obs. in Ondrejov Observatory spectra 80−62098
spectra, interpretation 80−4331
spectral observations, prominence model 80−31287
spicules, line profile calcs. 77−91497
spicules, simultaneous K and D3 line obs. *(French)* 77−29763
spiral sunspots, flares and prominences photographic obs., 1972 October *(Chinese)* 78−69761
streamers, rotational motions effects on spectral lines 78−49410
surge of 1961, Sept. 1, rotational and turbulent motions 77−91496
surge prominence, 31 May, 1971, observation as continuum event 77−22183
telescope, filter type, for viewing solar prominences 79−84670
thermally balanced quiescent prominence in magnetostatic equilib. in uniform gravit. field, self-consistent model 77−91509
turbulence causing coronal heating and MHD wave generation 80−72907
UV spectra, preliminary results from OSO-8 LPSP instrument 78−49317
UV spectra of active regions, Salyut-4 obs. 77−82211
X-ray coronal cavities, prominence-related, config. and dynamics 79−25565
C III and O V emission line ratios, interpretation 78−28598
Ca II K and Hα obs. during 1969 at Kodaikanal Obs. 78−61832
solar prominences continued
Ca II K line and Hα obs. of filaments, flocculi and prominences, during 1969 at Kodaikanal Obs. 78−61833
H early Balmer lines emission, theory *(Russian)* 80−12718
H emission spectrum, last observable line, rel. to solar obs. through Earth atm. 78−77536
H I Lα/Hα ratio for flares, quasars and prominences 78−61826
H I spectra, Balmer line form. in bright prominences, theory *(Russian)* 80−36609
H lines at submm. wavelengths *(Russian)* 79−35228
Hα dark filament, study of transition sheath from radio obs. 78−28619
Hα filaments, disappearances assoc. with coronal X-ray enhancements 77−22184
Hα filaments spatial correl. with photospheric vel. field 77−2401
Hα output coeff. influence on source function *(Russian)* 78−73690
He I D_3 line, Stokes parameters for quiescent prominences, Hanle effect quantum theory 78−85924
He I D_3-line polarization in quiescent prominences, level-crossings effect 80−94772

solar radiation
see also solar cosmic ray photons; solar radiofrequency radiation; solar spectra; solar wind; sunlight
absorption, by O_2 Herzberg continuum, in stratosphere, influence of O_4 and O_2N_2 dimers 78−87429
absorption by atmospheric aerosol, spectrophone meas. 79−80027
absorption by O_2 and O_3 in terrestrial atm., heating rate parameterization, 15-120 km altitude 79−39798
absorption by stratospheric aerosols from Agung, volcano eruption 77−87072
absorption by terrestrial atmosphere, effects of gases, aerosols and clouds 77−37407
absorption by terrestrial atmosphere, radiation balance 77−33183
absorption in ponds, analysis 79−16530
absorption in stratosphere by O_2-O_2 and O_2-N_2 dimers 78−9167
active regions, submillimetre obs. 78−12177
active regions on solar limb, 1175 to 1940 Å emission-line spectra 78−96446
active regions pre-flare X-ray morphology 77−17481
Alfven wave flux, rel. to solar wind accel. 80−85923
anisotropy measurement by spinning charged particle detectors, COS approx., computer simulation 77−5457
Arctic summertime stratus clouds, solar radiation pyranometric meas. 78−32165
artificial comet interaction, proposed expt. 79−16887
artificial Earth satellite, resonance due to solar radiation pressure 79−25456
artificial satellite, eqns. of solar radiation disturbing function in nonsingular variables 77−60581
Athens and estimates for Greece, analysis 79−34930
atmosphere, daily scattered radiation totals variability over European USSR 79−29861
atmosphere, diurnal average photodissoc. rates determ. 77−78311
atmosphere, downward radiant flux obs. and predictions for urban area 78−57317
atmosphere, solar heating annual var. rel. to large-scale eddy transports linear parameterisation 80−17361
atmosphere, solar radiation absorpt., cloud and aerosol effects on heating rate 78−57319
atmosphere, spectral solar radiation and aerosols, pyranometer meas. errors 79−21050
atmosphere, surface radiative flux, clear and cloudy conditions, parametrisation accuracy 78−77325
atmosphere scattering, arrival angle statistics rel. to turbulence around solar telescope 80−26740
atmosphere-ocean system, turbidity and hydrosols refr. index effects on solar radiation flux 77−64303
atmospheric absorption, energy transport effects *(Dutch)* 79−70838
atmospheric boundary layer, radiation balance over salt marsh 78−61481
atmospheric boundary layer near water surface, diurnal characts., equatorial region, GATE meas. 78−61527
atmospheric diffuse radiation, models with aerosols and common absorbing gases, data sets 79−44235
atmospheric dust rel. to planetary radiation balance, climatological consequences 78−36242
atmospheric general circulation model, climatic characts. response to solar radiation vars. 78−36260
atmospheric spectral absorption of solar radiation by Denver Brown Cloud 78−16158
atmospheric trace gases vertical conc. from solar radiation absorpt. spectra *(Russian)* 78−69442
atmospheric turbidity, solar noon at Edmonton, in Canada 79−29858
atmospheric turbidity rel. to circumsolar radiation intensity 77−37405
atmospheric water content and turbidity in Thailand, calc. 79−5580
automatic sun sighting system, for incident solar radiation meas. *(Italian)* 77−22062
availability concept based on climatology, Canada 77−25762
availability rel. to atmospheric turbidity 79−58071
average diffuse component estimation method 79−57399
background corona, brightness near solar minimum 78−28616
Baghdad insolation and meteorological data for flate plate collector design 79−62092
balance of radiation over water surface 79−20889
Bhavnagar solar radiation, atm. turbidity and sunshine obs. 79−58072
bidirectional reflectance and transmission for space appl. 77−56809
bremsstrahlung source spectra anal. in terms of integral moments, hard X-ray burst appl. 79−16810
brightness fluctuations, correl. with solar rel. oscills. 80−105226
brightness temperature, 85-250 μm, with balloonborne lamellar grating interferometer 77−13308
brightness temperature near its minimum, meas. by balloon-borne lamellar-grating interferometer 78−85921
Canada, prairie cities increased sunshine due to natural gas use as fuel 77−17211
chromosphere, Ca II K_3-line obs. rel. to rot. during 1972-73, declining activity years 78−4186
chromosphere, continuum radiative losses 80−72924
chromosphere, H^- radiation and acoustic dissipation 78−96454
chromosphere, radiative losses effect on quiet struct. form. *(Russian)* 79−48764

solar radiation continued
chromosphere contrast profiles interpretation, embedded feature model 77−33443
chromosphere flares, effects of soft X-ray heating 79−40170
chromosphere network pattern, identification with 1.35 cm radiogranulation *(Russian)* 78−40897
chromosphere radiative losses, empirical estimate 78−40915
chromosphere-corona transition region, emission measure gradient rel. to energy balance 80−90379
circumarctic ocean temp. linked with low level cloud, climatic change study 77−29415
circumsolar, meas. instrum. 77−25767
climatic consequences of solar energy utilisation *(French)* 77−73822
clouds, horizontally inhomogeneous, albedo and refl. radiance 77−78417
clouds influence on solar radiation input in tropical ocean regions 78−3956
cloudy atmosphere, solar radiation distrib. 78−3955
cloudy skies, Cole's model extension 79−74947
conference on nuclear cosmic physics, Leningrad, USSR (Oct. 1978) 80−98755
constant measurement, take-home expt. 77−49537
continental ice sheet model, stability to insolation periodic vars. 78−28251
continuum intensity, fluctuations rel. to horizontal temp. var. in low photosphere 77−22163
corona, 1973 June 30, polarised brightness distrib. rel. to N.polar hole density model 80−98627
corona, effects of radiation heat flux on expansion 80−90377
corona, Hα emission from narrow chromospheric structs. *(French)* 78−28607
corona, radio and soft X-ray evidence for dense non-potential magnetic flux tubes 78−28615
corona, soft X-ray obs. of large-scale active region brightening 78−20806
corona, X-ray emission and mag. struct. near type II radio burst source region 78−69775
corona 5303 Å line, latit. depend. intensity long-term correl. with solar wind streams 78−93172
corona polar plumes, EUV radiation anal. 78−4178
corona radiative power loss, from plasmas in steady state ionisation balance 79−82063
corona X-ray emission, slowly moving disturbances obs. 80−21971
coronal 5303 Å emission line, photoelectric meas. by automatic coronal photometer 79−12454
coronal active region, differential emission measure exponential depend. on temp. and struct. 78−53917
coronal active regions, anal. of soft X-ray photographs taken with Fresnel zone plates 78−77538
coronal emission, rel. to solar wind high-speed streams outflow regions localisation 78−53919
coronal Fe XIV 5303 Å depletion, 1976, April 20, photoelectric obs. 78−28617
coronal green line, intensity and polarisation obs. at 1973 June 30 total eclipse 79−66969
coronal hard X-ray event, 1971, December 14, obs. 78−93177
coronal He^+ 304 Å radiation, theory 77−91510
coronal hole boundary brightness in Fe XV 284 Å radiation 79−84775
coronal holes, locations, sizes and evolution during June 1973 to January 1974, EUV obs. 77−56893
coronal holes, X-ray and radio emission rel. to quiet radio Sun at 2800 MHz 78−20805
coronal holes UV and radio emission, effect of solar wind nonequilib. ionisation 79−48751
coronal interconnecting loops transient brightenings, sudden brightenings morphology 80−21972
coronal limb brightening, Abel-inverted intensities of Fe XIV and XIII EUV emission lines 77−13299
coronal long-duration X-ray event, plasma parameters from Skylab obs. 77−29741
coronal polar plume, X-ray anal. 79−12455
coronal quasi-static loops, EUV and X-ray emission numerical modelling with uniform energy input 80−21958
coronal soft X-ray bright points, lifetimes distrib. 77−17512
coronal X-ray enhancements assoc. with Hα filament disappearances 77−22184
coronal X-ray observations, using rocket-borne real-time imaging system 80−41725
correlations between diffuse and hemispherical and between daily and hourly insolation, average distribution calc. 79−87975
cylinders, perfectly conducting arrays, transport prop. investig. 80−13011
Czechoslovak radiation climate evaluation *(Czech)* 78−88874
daily and monthly averages of solar radiation data, statistical correl. 80−8409
data base, using bright sunshine data approach 77−25763
daylight spectral quality and solar energy availability determ. model 79−58067
dielectronic recombination spectra, appl. to high-temp. plasma diagnostics 80−46391
diffuse, through series of parallel regions, transmittance calc. 79−88005
diffuse and direct radiation at Earth's surface, aerosol effects 77−37406
direct and total availability, geographic distrib., USA 77−29413
direct pressure effect on artificial satellite nodal period 77−70987
direct radiation var. during 1976 April 1979 annular eclipse 79−84781
direct solar radiation and diffuse radiation calcs. from synoptic weather obs. *(German)* 79−34925
direct solar radiation rel. to cloudiness and solar altitude 79−58073
disc centre visible continuum emission, absolute meas. *(French)* 78−96453
Earth's surface, direct radiation, turbid ideal Rayleigh atm. 78−36274
at Earth's surface, spectral distribution model 78−69456
Earth atmosphere caloric insolation long-term vars. resulting from Earth orbital elements 78−73502
Earth insolation, influence of orbital elements periodic vars. *(Russian)* 78−53605
Earth radiation balance meas. as instrument design problem 77−41173
earth radiation budget: simulation of fluxes and accelerometric measurements *(French)* 79−84482
Earth radiation budget data collection and interpretation model 77−37497
Earth radiation budget expt., Nimbus-6 obs. 77−41106
Earth Radiation Budget Expt. solar constant obs. 79−58066

solar radiation continued
effect of solar corpuscular radiation on atmos. electricity 79−79982
effect on underground temp. var. with depth and time 79−5463
electromagnetics and environment, book 80−36431
electron streams, thick-target, relax. and bremsstrahlung, Legendre expansion, solar X-ray flares appl. 79−70950
EM radiation measurement using CdS photoresistor 80−31092
emission lines propagating through interplanetary medium, profiles modification 79−66973
energy balance climate model response to parameter changes *(Russian)* 79−100938
energy flux, 770-80 Å region 78−28605
energy meas., photometric and bolometric methods 78−12470
energy system simulation, diffuse and total solar radiation relationship 79−57398
equatorial flat plate solar collector utilisation, radiation estimation 79−57402
equatorial K-corona radiance, temporal evolution 78−28618
equatorial region (Singapore), statistical estimate, solar power utilisation appl. 79−87972
eruptive prominence assoc. with coronal transient, Hα and He II emission 77−2389
estimation from meteorological data 77−73815
EUV, ionization of ionospheres of Saturn, Uranus and Neptune 78−4142
EUV, modulation of lunar ionosphere/exosphere 77−17390
EUV, spectroheliograms from Apollo Telescope Mount expt. S082A 77−60597
EUV and H Lyman-alpha, AEROS and TAIYO satellite results 80−46340
EUV and hard X-ray bursts interrelationship during flares 78−61845
EUV and radio emission from chromosphere-corona transition 79−8894
EUV and soft X-ray fluxes from quiet Sun, rel. to ionospheric ionisation 77−13307
EUV and UV radiation absorpt. by thermosphere, diurnal tide excitation 77−53260
EUV and visual obs. from Spacelab 77−22201
EUV bursts, C IV 1548 Å line profiles, OSO-8 obs. 80−90401
EUV continuum absorption above quiet Sun transition region, new evidence 79−92738
EUV emission from active regions and quiet Sun, OSO-4 spectroheliograms 77−49358
EUV emission from B-like ions, density sensitivity 79−16910
EUV flux, inferred from Atmosphere Explorer-C He^+ abundances 79−16919
EUV flux changes, AEROS spacecraft obs. and resulting ionospheric vars. calcs. 79−44293
EUV flux during solar cycle 21, correl. with atmospheric $O^+(^2P)$ ionisation freq. vars. 80−77195
EUV flux variation at end of solar cycle 20, AE-C satellite obs. 77−71075
EUV flux variations, correl. with ionosphere primary ion-electron prod. rates changes 80−72675
EUV image, obs. by Skylab Apollo Telescope Mount TV monitor 77−60600
EUV impulsive bursts, characts. 78−77539
EUV indices for solar-terrestrial relations 77−9731
EUV irradiance, cycle 21 development and atmospheric absorption 79−75174
EUV limb brightening anal., influence of spicules 77−22170
EUV line emission, contrib. of spicules 80−4325
EUV lines, medium resolution obs. rel. to chromospheric network struct. 78−20801
EUV output, present knowledge and accurate meas. techniques for aeronomy 78−57535
EUV photon fluxes from Aeros A 77−71078
F-corona, flux bump at 4 solar radii 80−82162
faculae, mag., vel. and brightness struct. 79−25557
far IR absolute brightness temperature, meas. by balloon-borne interferometer 80−62095
far IR brightness temp. minima rel. to sunspot activity 80−62035
far UV flux, origin, variations, rel. to climatology *(French)* 78−40884
flare, 1973, June 15, UV continuum and spectral lines obs. from 1000 to 1940 Å 78−89139
flare, 1973, September 5, pre-onset morphology 79−40169
flare, 1973, September 5, X-ray and XUV emission rel. to struct. and dynamics 78−12175
flare, 1973 September 7, new class of transient events, X-ray, UV and visible obs. anal. 80−98643
flare, C line profiles and continua obs. and upper chromosphere semiempirical model 79−40148
flare detonations, prod. of pulses of characteristic energy 77−78736
flare EUV continuum emission, Skylab obs. 79−30046
flare impulsive X-ray burst, spectral anal. analytical method *(Chinese)* 80−85919
flare loops, anisotropic pitch-angle distrib. of electrons generating hard X-rays 77−13314
flare plasma, evaporative cooling rel. to X-ray and EUV radiation 78−40890
flare second-stage X-ray emission, spectrum beyond 200 keV 80−51710
flare soft X-ray radiation, chromospheric response 77−56885
flare spatial structure in soft X-rays and cm wavelengths 77−17524
flare X-ray emission, rel. to energy storage and deposition 77−17480
flare X-ray radiation sources, model concepts 77−17532
flare X-rays quantitative relationship between 1-8 Å flux and D-region VLF phase deviations 77−87170
flares, acceleration mechanisms, implications for hard X-ray burst models 80−72912
flares, conf., Florence, Italy (Nov. 75) *(Italian)* 78−93191
flares, energy transfer to chromosphere by soft X-ray photons 77−82210
flares, EUV and hard X-ray sources relationship 80−46512
flares, EUV continuum obs. rel. to temp. min. region struct. and flare heating mechanisms 79−12458
flares, EUV radiation, detect. using ionosphere sudden freq. deviations (SFD) 80−8484
flares, hard X-ray time profiles and accel. processes 79−30030
flares, high-resolution X-ray spectra obs. 80−26837
flares, impulsive, Hα emission rel. to adiabatic heating 78−93176
flares, impulsive EUV and hard X-ray emission 78−65578
flares, particle and EM emissions, review *(Italian)* 78−93192

solar radiation continued
flares, polarisation and directivity of hard X-ray bremsstrahlung from thermal source 80−90374
flares, principal component anal. in soft X-ray flux 80−41781
flares, radiation props. of particle streams continuous radiation model 80−21954
flares, radiative, mechanical and mag. energy release 79−53797
flares, studies using optical, X-ray and radio data 78−89156
flares, X-ray and UV emission explanation within current layer theory 80−101572
flares, X-ray and UV emission rel. to physical processes 78−65598
flares, X-ray emission (50-100 keV) directivity 80−105218
flares, X-ray emission rel. to physical parameter profiles 80−17561
flares, X-ray fluxes rel. to peculiarity of electrons ejection into interstellar space *(Russian)* 78−77445
flares, X-ray morphology and role of mag. fields 77−17474
flares, XUV electron density diagnostics 79−88633
flares EM emission, appl. to high-energy protons identification 79−12443
flares emission mechanism, model *(Italian)* 78−96462
flares fast electrons scatt. in atm., X-ray spectrum 78−77542
flares Fe XXV 1.87 Å line emission effects on lower ionosphere ionisation 78−65588
flares hard X-ray emission, electron beams diagnostics 78−89159
flares hard X-ray radiation, elementary flare bursts props. 78−89158
flares hard X-rays, rel. to type IV radio emission and particles multi-stage accel. 79−44437
flares inverse Compton radiation, appl. to inference of relativistic electron spectra 80−90339
flares microwave and optical emissions comparison 80−31284
flares multiply impulsive bursts, spectral evolution 80−26828
flares nonthermal electron beams, reverse currents effects on dynamics and X-ray bremsstrahlung 80−51711
flares nonthermal X-ray emission directivity meas. 77−33461
flares X-ray and EUV emission, empirical models rel. to E-region and F-region effects 77−5515
flares X-ray emission, rel. to cosmic ray intensity preflare enhancements 78−45166
flares X-ray emission rel. to optical radiation 77−22188
flux distribution, comparison with stellar flux distribs. and solar B−V and U−B colours determ. 79−66970
flux mapping sensor, Si p-n junction for high intensity appl. 78−40720
flux var. rel. to Earth climate 77−21872
gamma rays, theory of prod. and observational results 78−32306
gamma-quanta flux in upper atm., short-period pulsations *(Russian)* 77−9638
gamma-ray emission, observational and physical review 79−80373
gamma-ray line formation at 0.51 MeV in flares 77−13292
gamma-rays with energy >8 MeV prod. in flares 79−53779
geometric Brownian distribution, implications for economical solar heating system 79−83571
glass system, layered, thermal radiative props. for solar diffuse radiation flux 79−94473
global daily radiation estimation for any surface 79−39805
global insolation, calc. model 79−16613
global middle UV radiation meas. at ground, cloud effects 78−92882
global oscillations of solar brightness 77−25988
global radiation calc. as function of insolation *(Spanish)* 78−49117
global radiation rel. to dew point temp., phase delay calc. *(Spanish)* 77−9477
granular brightness fluctuations, centre to limb var. 79−66971
RMS granular contrast, new meas. of centre to limb var. 78−4176
granulation, brightness fluctuations and lifetime from balloon-borne imagery 78−28601
granulation, photometric props. from balloon-borne imagery and digital image enhancement 78−7956
granule/intergranule brightness contrast, new determ. 78−20797
Great Britain, global solar radiation distrib. on horizontal surface, monthly maps 79−79959
H-R diagram fits of solar models, rel. to He content and convective mixing length 80−26835
halfhour solar radiation values from hourly values for Kuwait, Markovian insolation model appl. 79−44236
hard X-ray and radio events, spectral features rel. to particle accel. 77−45369
hard X-ray burst, 1972 August 4, trap-plus-precipitation model 80−12747
hard X-ray bursts, collective plasma effects and electron number problem 77−71094
hard X-ray bursts, intensity profiles pulsations 78−61846
hard X-ray bursts, relationship to type III-V radio bursts 78−89157
hard X-ray bursts, role of collisionless cond. front prod. by rapid coronal heating 79−44427
hard X-ray bursts, thermal model dynamic spectral characts. 80−98644
hard X-ray emission, shot-noise character of −B flare 79−96983
hard X-ray emission, upper limit to anisotropy 77−29742
hard X-ray flare events, review 78−89144
hard X-ray flares obs. with 100 ms time resolution 77−71093
hard X-ray polarization from flares 80−41787
hard X-rays, backscatter, anisotropy and polarisation 78−28594
hard X-rays, source height and anisotropy determ. 79−25568
hard X-rays from confined hot electrons in flares 79−96982
hard X-rays obs. from 1972 August 2 and 11 flares 79−8900
hard X-rays photoelectric absorpt. in photosphere, approx. formula 77−22187
heating in presence of aerosols 79−16665
heliometric station operating data 79−58069
horizontal plane diffuse insolation from clear sky 79−83575
hourly diffuse rate, horizontal surface, correlation equation, computer simulation appl. 77−81981
hourly solar radiation amounts in Thailand, statistical distrib. 78−96271
impulsive X-ray bursts, polarisation, directivity and spectrum of bremsstrahlung radiation 78−4160
incident solar flux on arbitrarily oriented surface, computation models 79−57401
inclined-plane insolation computation, hourly and daily methods compared 79−83572
inclined-plane solar radiation design value determ. for plane-collector installations *(Spanish)* 79−79384
India, solar radiation meas. and atm. transmission at high altitude stations 78−32152
solar radiation continued
input determination and irradiance maps, analytical model and simulation code 79−34426
insolation estimation over ocean, clear and cloudy skies 77−87023
insolation in equatorial region (Singapore), 1961 to 1974 data analysis 77−37315
insolation meas., field instrument calibration standard 78−88946
insolation of Saturn, rings effect on direct radiation reaching top of atm. 79−70992
insolation over tropical Pacific Ocean, cirrus cloud effects 78−92914
integrated study of various components, interpretation of neutrino data 78−61829
intensity oscillations, daily and seasonal, problems of power when demanded *(Croatian)* 78−3859
International Solar Energy Congress, New Delhi (1978) 79−57357
interplanetary dust, effect of spin and solar radiation on motion *(Japanese)* 78−20732
interplanetary dust particles, solar radiation effects on orbits 77−5493
interplanetary dust particles rot. bursting caused by solar radiation press. 77−9644
interplanetary micrometeoroid clouds, solar radiation scatt. rel. to meteoric night-glow 77−91488
intraregional variations of solar radiation in E United States 79−39804
ionisation events in stratosphere, effects on NO_2, O_3 and climate, rel. to life extinction 78−96273
ionising fluxes, correl. with seasonal var. of equatorial ionosphere radio waves absorpt. 78−85762
ionising radiation, atmospheric electrification modulation rel. to Sun-weather relationship 78−57261
ionising radiation, meas. during 1973 June 30 solar eclipse 79−8901
ionosphere, heating by solar radiation in Schumann-Runge continuum and by chem. reactions 79−62653
IR, absorption by tropospheric H_2O vapour, including multiple scatt. 78−61553
IR continuous spectrum *(Italian)* 79−88638
IR intensity, obs. in 1.5-2.4 μm range using pinhole photometer 79−101069
IR radiation brightness at crossing of sea horizon *(Russian)* 77−29438
IR solar radiance reflected from the rough sea surface *(Russian)* 79−84477
Iran, statistics 79−29815
irradiance at Table Mountain, California 1926-1977, meas. 79−29816
irradiance determination from Nimbus 7 cavity radiometer obs. 80−105225
irradiance meas. from NIMBUS 6 satellite 77−25766
irradiance meas. in upper ocean layer 78−44864
irradiance meas. using optical fibres and Si detectors 79−100960
irradiation flux determ. in 150-210 nm range 77−17509
isotropic-distribution approximation validity, in solar energy estimations, exact procedure comparison 77−78358
Italian global solar radiation obs. 79−5581
Kuwait hourly stochastic insolation model 79−58068
Langmuir waves and anisotropic particles, Legendre-expanded quasilinear eqns. appl. 79−75089
limb darkening, effects on zenith light intensities during annular solar eclipse (1976, April 29) 78−3900
limb darkening function at 5012 Å, possible vars. 80−67677
limb darkening in 3033-7297 A range 77−53507
long-term variations, solar activity and neutrino flux 78−45307
loop prominences, X-ray line emission, model 77−82195
luminosity, var. in Dirac cosmology 77−22334
luminosity and sunspot cycle 79−75176
luminosity long-term variations, correl. with sunspot struct. and Earth climate 80−31272
luminosity monitoring by photometric obs. of Uranus and Neptune 77−53500
luminosity variation, Ca H and K behaviour at solar minimum and cycle 21 onset 79−16907
luminosity variation (solar const.), direct obs. from rockets 80−90386
luminosity variations, as cause of Cretaceous-Tertiary extinctions 78−32435
luminosity variations, C I 5380 Å line response, effects of granular convection 80−85910
luminosity variations, meas. and effect on Earth climate 80−77376
luminosity variations, possible detect. from photometry of Io, Europa, Callisto and Rhea, (1976 to 1979) 80−98623
luminosity variations and global oscills., determ. via C I 5380 Å line 77−53487
luminosity variations assoc. with gravit. const. cosmological var., re-examination 80−82182
luminosity variations caused by mag. field 80−46515
lunar ancient regolith, record of solar and galactic radiations 77−60695
Lyman α radiation, high resolution filtergrams obs. 80−82323
Lyman α sky background, Copernicus high-resolution obs. 77−29963
Lyman α total flux, monthly averages vars. correl. with total atmospheric O_3 79−16571
Lyman β flux, geocoronal H conc. models and Hα emission rates 77−25808
Lyman alpha radiation pressure effects on interstellar H and D 79−92686
McMath region 12336, comparison of 9.1 cm and soft X-ray emission 77−22180
measurement, inclination dependence of pyranometer sensitivity 80−8465
measurement, multiple-filter radiometer design 78−93004
measurement requirements for energy conversion 79−57400
measurement techniques and instrumentation, survey 77−5348
measuring instrument design 79−57404
mesosphere, lower, O_3 abundance from backscattered solar radiances 78−69414
meteorological radiation reference scales 80−109206
in Mexico using sunshine hours and meteorological data, empirical compilation 79−44237
microwave radiation from thermal, hard X-ray sources 79−8892
microwave solar radiation, forward scattering from water surface 78−44872
millimetre and far IR regions, polarisation upper limit 77−49354
model year construction of solar intensity and climate 78−57241
monthly average insolation, incident on tilted surface 77−78357
natural illuminance of Earth's surface 77−70794
natural illumination of Earth's surface in European USSR 77−78422
Netherlands, surface distribution charts *(Dutch)* 77−91207

solar radiation continued
neutrino, radiochem. detectors, cosmic ray muon induced proton background effects 77−61650
neutrino emission, review and reasons for deficiency 78−77486
neutrino flux, quasi-biennial var. and correl. with solar activity 79−44440
neutrino fluxes, from dirty solar models with surface contamination resulting from accretion 79−44436
neutrino problem, limitations of energy transport by mechanical means 77−17461
neutrino problem, theory versus obs. 80−17566
neutrino puzzle, explanations for missing neutrinos 80−51723
neutrino radiation, astrophysical aspects review 79−16917
neutrino radiochemical detectors, internal contamination backgrounds 79−16827
neutrino spectroscopy at low energies, In loaded liq. scintillator 78−73639
neutrinos, detect. expts. appl. to cosmological hypothesis testing 79−16918
neutrinos, influence of interstellar dust accretion 79−12441
neutrinos measurement, cosmic ray neutrinos ^{37}Ar prod. rate estimate 79−16837
normal incidence insolation measured with RG2 filter, charcts. 77−29414
normal incidence solar intensity and total insolation rel. to weather at Fort Hood, Texas 78−57240
north-south brightness asymmetry, obs. 78−45303
numerical model based on standard meteorological observations 79−34929
oceans, received daily sums and daytime var. of solar radiation *(Russian)* 79−34922
optical continuum brightness, fluctuations rel. to trapped gravity waves in solar atmosphere 80−72898
orbital perturbation analysis for satellites in elliptic orbit due to solar radiation pressures 78−89041
orbital perturbations of space structures appl. 79−5723
Pageos 1 balloon satellite, orbital effects of direct solar and Earth albedo radiation pressure 79−88566
periodic vars., possibie solar activity-weather effects 79−34920
Peru, two-parameter statistical model of daily irradiation *(French)* 79−29812
photodissociative ionisation of cometary comae mols. 80−90370
photolysis of Eu^{2+} solutions, cyclic photoredox process, H_2 quantum yields 77−90627
photosphere, micro- and macroturbulence, spectrophotometric determ. *(Russian)* 77−56896
photosphere brightness fluctuations, two-dimensional spectral anal. of disc centre granulation 77−53520
photosphere faculae intensity, centre to limb var. 80−21967
plages, EM radiation effect on Earth atmosphere vorticity area index 78−73459
planetary atmospheres, diurnal average photodissoc. rates determ. 77−78311
polar coronal hole, radiance rel. to physical props. from 2 to 5 $R_\odot$ 77−45372
prediction of monthly mean parameters 79−48099
pressure effects on artificial satellite anomalistic period 80−77255
prominences polarisation of D3 emission line 77−29746
prominences with filamentary struct., radiation transfer 78−89154
pyranometers for mesoscale solar irradiance network, test and calibration experience report 79−74499
pyrheliometer meas., solar aureole contribution 77−2284
pyrheliometric ratioing for apparent atm. transmission determ. 79−96809
Quaternary climatic changes, insolation signature 79−74953
quiescent prominence, radiation emission and absorpt. rel. to thermal balance 77−91509
quiet Sun γ-ray emission rel. to long-lived radioactive nuclei generated in flares *(Russian)* 77−45390
radiation forces on small particles in solar system 80−17461
radiation pressure and orientation control of rotating spacecraft 77−53397
radiation pressure effects on interplanetary dust grains 78−20730
radiation pressure induced coupled librations of gravity stabilized artificial satellite 80−21888
radiative cooling by use of inverse greenhouse effect 79−25329
radiative transfer in cloudy atmosphere, model solar radiation and cloud struct. 79−21016
radiometer design for total and net exchange solar radiation meas. 79−54190
radiometric scales for solar constants 77−78737
radiometry correction for diffuse atmospheric scatt. 79−80015
reduced luminosity during Earth early history, compensation by enhanced atm. CO_2 greenhouse effect 79−39865
reduction inducing palaeoglaciation on Earth, Mars and asteroids *(French)* 79−34857
reflected irradiance indicatrices of terrestrial natural surfaces and albedo effect 79−62514
reflected radiation from Earth for satellite solar battery power increase 77−33318
resonance radiation, multiple scatt. in nearby interstellar medium 80−41874
satellite orbits perturbation by solar radiation press. general expansion of disturbing function 77−78605
scattering by clouds, dimensions and orientation effects 77−33188
short wave radiation flux, rel. to daytime F_2-layer simulation 78−45087
short-wave radiation, rel. to ionosphere O^+/n_e ratio for specific heliogeophysical conditions 79−12332
short-wave radiation flux, rel. to parameters of F-region and neutral atmosphere 77−91346
shortwave diffuse radiation intensity over daytime sky calc., semiempirical method 77−70796
simulator, non-axial type, reflector profile calc. *(Russian)* 78−63169
simulator calibration photometer 79−26103
Singapore solar energy availability, diurnal and annual variation 79−57403
Skylab X-ray obs. and mag. field correls., computer solns. 77−82198
soft X-ray bursts, statistical distrib. 80−26839
soft X-ray emitting flare loops evolution 79−53781
soft X-ray flux, Skylab obs., temporal oscills. 78−53904
solar radiation continued
soft X-rays affects on Earth lower ionosphere, anal. rel. to nature of flares 79−8740
solar constant, 1968-78 change 79−75172
solar constant, accurate determs. by avity pyrheliometers 79−2341
solar constant, effects of sunspots and faculae 78−4163
solar constant, Nimbus 6 meas., rocket calibration 78−11948
solar constant, no correl. with N.Hemisphere average temps. during Little Ice Age 80−82050
solar constant, rel. to energy-balance climate models stability theorem 80−56594
solar constant, Smithsonian Astrophysical Observatory program, (1902 to 1962) 80−36606
solar constant and the Earth's atmosphere, conference, Big Bear City, Calif. (1975, May 19 to 21) 77−2380
solar constant fluctuations, prod. by convection zone struct. adjustments 80−82321
solar constant standard data and spectral irradiance outside Earth atm. *(Chinese)* 80−4320
solar corona, mag. loops and downflows obs., rel. to convection 78−93175
solar flares, active role for mag. fields 77−17474
solar radiation budget in cloudy atm., modified two-stream approx. 79−58090
solarimeter, autonomous with permanent readout *(French)* 79−24893
spacecraft with solar sail, eqns. of motion from geocentric orbit 77−53394
spectral distrib. data, $300<\lambda<1500$ nm range 77−25764
spectral distribution of direct radiation 79−12268
spectral distribution of global and diffuse radiation 79−44229
spectral photometry using compact spectrometer 79−2396
spectrum intensities, statistical anal. 77−53537
spherically symmetric models and Mariner 10 UV obs. of interplanetary emissions 79−48736
spheroidal satellite, orbital perturbations due to direct solar radiation press. 80−4219
stochastic variation, convection efficiency and time variation of solar const. 79−21262
stratosphere, HOCl photodissoc. rel. to prospects as inert Cl reservoir 79−12207
stratospheric heating due to solar radiation absorpt. by NO_2 77−17199
summer global and diffuse solar radiation rel. to monsoon rainfall 78−32154
sunphotometer aperture effects on atmospheric turbidity meas. 79−84483
sunspot model, radiation transfer theory 80−21964
sunspots, magneto-optical effects rel. to linearly polarised intensity distribs. obs. with vector magnetograph 80−21965
sunspots, origin of broad-band circular polarisation 78−45301
sunspots, X-ray, UV, optical and radio emission rel. to overlying atmosphere struct. 79−96989
surge prominence, 31 May, 1971, observation as continuum event 77−22183
temperature variations, rel. to solar radius vars. due to mag. buoyancy 79−92749
Thailand tropical atmospheric radiation and sky temp. calc. 79−58084
thirteen-colour photometry, derived 77−22230
Tiros-N environmental spacecraft series launching 79−29973
total and net radiation intensities, power spectral anal. 78−40617
total hourly horizontal data, pyranometer data acquisition system, USA 77−25765
total optical irradiance, meas. via active cavity radiometer pyrheliometer 79−35130
trans-polar coronal hole, 1973, June 30, radial and transverse polarisation obs. 77−53526
transmission through atmosphere, Monte Carlo simulation *(Russian)* 79−12265
troposphere, solar radiation and temp. fluctuations rel. to stratospheric aerosol vars. 78−81327
troposphere, solar UV flux meas., $O(^1D)$ photoprod. rate determ. 79−12197
troposphere and stratosphere anisotropic multiple scatt. effects on solar radiation 79−80016
upper atmosphere, photoelectron spectra allowing for Auger effect 78−69557
urban-rural solar radiation and atm. turbidity, meas. in Los Angeles basin 79−80024
UV, absorption in Mars and Venus thermospheres, heat sources 77−25965
UV, atmospheric transmission calc. down to 28.7 km altitude 79−62575
UV, effects on terrestrial upper atm., review of Saha's work 79−53599
UV, intensity meas. in Earth atm. by chem. actinometer 77−45163
UV and integrated solar radiation received, influence of cloud layers 79−70883
UV and radio fluctuations in transition region, common origin 80−90398
UV and soft X-ray full-disc solar fluxes, rocket obs. 77−87360
UV and X-rays contribs. to E-region ionisation, effect of neutral atmosphere seasonal vars. 79−12331
UV continuum, absolute intensities, centre to limb vars. and Laplace inversion between 1400 and 2100 Å 79−62803
UV diffuse-direct ratios meas. with compact double monochromator 78−49144
UV flux, cyclic vars. 80−101577
UV flux variability over solar cycle, 1175-2100 Å 80−90383
UV flux variations, chemical response of Earth middle atmosphere 77−33167
UV irradiation solar flux meas. between 120 and 400 nm, current position and future needs 78−57536
UV light, polarisation at solar limb 78−45302
UV limit at Earth surface, photon counting monochromator meas. 78−49134
UV meas. and physics 80−41784
UV penetration of Earth's atmosphere, sunburn dosage spatial and temporal vars. 77−37285
u.v. radiation, absolute intensities in 1750-2100 Å range, vars. with solar activity 77−2405
UV radiation, vars. rel. to Jupiter Great Red Spot depend. on solar activity 79−101110
UV radiation effects on photochem. reactions of atm. pollutants SO_2 and NO_2 77−21894

solar radiation continued
UV radiation level measurement problems 78−37057
UV spectrum 140 to 350 nm, NASA meas. using SURF storage ring calibrations 80−94721
UV variability during solar cycle, effects on stratosphere 78−61492
variability, effect on ^{14}C prod. in atm. 80−85730
variability rel. to ice ages on Earth 78−12183
variable Sun effects at beginning of Cainozoic era 79−75171
variation of solar constant rel. to diameter meas. 79−84767
Venus, luminous flux from Sun, meas. from Venera-9 and Venera-10 77−37544
Venus atmosphere, results of solar flux radiometer expt. aboard Pioneer Venus multiprobe mission 79−48718
X-ray and EUV, satellite measurements, NRL SOLRAD, for forecasting of ionospheric disturbances 79−58134
X-ray and EUV flux estimation from thermospheric electron density and ion comp. meas. 77−87145
X-ray and Hα flares comparison 78−7971
X-ray and Lyman α, effect on ionospheric radiowave absorpt. 78−40737
X-ray and UV emission from flares, obs. and interpretation *(Italian)* 78−96460
X-ray and UV radiation from flares, correl. with E-region ionization 77−25815
X-ray bremsstrahlung from energetic thermal and nonthermal electrons 77−49364
X-ray bright arcs and mag. flux emergence regions 78−12174
X-ray bright point emergence patterns spatial and temporal vars. 77−29782
X-ray bright point flares, search for microwave emission 77−45384
X-ray bright points, mag. props. 77−91505
X-ray bright points, obs. rel. to globally variability in solar mag. flux emergence 80−51716
X-ray bright points, short-term temporal vars. 80−12740
X-ray bright points anticorrel. with sunspot number, 1970-78 period 79−53789
X-ray bright points correl. with sunspot intensity, cycle var. 80−41783
X-ray burst, impulsive, from coronal source, obs. 80−26836
X-ray bursts, thermal models 80−94766
X-ray bursts correl. with 3 cm wavelength emission *(Russian)* 78−93194
X-ray bursts position and size compared with cm wavelength radio bursts 77−33459
X-ray complex events development, 1972 August 79−8899
X-ray control of ionospheric absorpt., sweep freq. method meas. 79−84582
X-ray emission, correl. with metre-wave radio bursts 78−69774
X-ray emission, quantitative interpretation of X-ray images 79−40085
X-ray emission from coronal active regions, evidence for mag. energy storage 77−17478
X-ray emission from intense compact subflare, obs. and physical parameter anal. 79−62802
X-ray emitting active region, early evolution 78−28621
X-ray emitting features, energy or press. of plasma determ. from single filtergram 77−22186
X-ray emitting post-flare loops, dynamics, 1973 July 29 flare 79−75193
X-ray emitting post-flare loops, physical parameters, 1973 July 29 flare 79−75194
X-ray events with long decay times, morphology and statistics 77−60733
X-ray flare, temp. distrib. models 79−35220
X-ray flare kernel, site, size, spatial stability and energetics 79−25555
X-ray flares, 1974 July 5 and 6, polarisation obs. 77−2397
X-ray fluxes, correl. with ionosphere radiowave absorpt. at mag. equator 79−21099
X-ray long decay event, physics 80−90402
X-ray photographs, anal. and interpretation 78−4179
X-ray photographs anal. and interpretation, filter ratio method 79−40086
X-ray radiation rel. to O^{2+} ions form. in disturbed ionosphere 79−62647
X-ray radiation rel. to radio waves anomalous absorpt. during sudden ionospheric distrubances 79−96857
X-ray spectra, rel. to Auger electron and photoelectron spectra in ionosphere and plasmasphere 78−45094
X-ray temperature-emission measure modelling of corona 80−12746
X-rays, coronal holes boundary positions, 1973, May 28 to November 21, atlas 77−2349
X-rays, intensity in E-region meas. by rocket-borne proportional counters 78−45072
X-rays, obs. by S056 X-ray telescope expt. on Skylab Apollo Telescope Mount 77−60596
X-rays and γ-rays, spectrometric obs. from Prognoz satellites 79−21127
X-rays from flares, Prognoz and Explorer satellite obs. of directivity in 4-24 keV range 78−69768
X-rays impulsive bursts, anal. 78−93174
X-rays rel. to SEA and active areas, statistical study *(French)* 78−20788
XUV, obs. and recording of instantaneous images on ATM television monitors 77−60605
Ca II H-line emission from Sun observed as star *(Russian)* 77−64727
Fe I Kα fluorescence in solar flares, photospheric Fe abundance probe 79−75192
Fe line X-ray emission, ionization equilib. and line excitation 78−32426
H I, 584 Å reson. line profile and intensity meas. 79−40153
H I Lyman α flux near solar minimum 80−90393
H Lyman α, radiation press. depletion of satellite atoms in collisionless planetary exospheres 79−96933
H Lyman α in chromospheric flares, direct collisional excitation rel. to profile and polarisation 80−41780
Hα, hard X-ray and microwave emissions in flares impulsive phase 78−77540
Hα line radiation, high resolution solar obs. by Skylab 77−60604
Hα profiles from electron heated flares 78−77541
Hα synoptic charts, comparison with large-scale synoptic charts obs. at Stanford 78−28612
He I, He II XUV emission lines, intensity ratios and distrib. functions 78−57516
He I, II visible and UV line radiation from model flare layer 77−22190
He I 10830 Å, spectroheliograms from Kitt Peak National Observatory 60 cm vacuum telescope *(Norwegian)* 77−60613
solar radiation continued
He II 304 Å and He I 10830 Å spectroheliograms, comparison 78−20799
OH continuum opacity, influence on atmospheric model and intensity and flux 79−40162

solar radio emission *see solar radiofrequency radiation*

solar radiobursts *see solar radiofrequency radiation*

solar radiofrequency radiation
1.35 cm radiogranulation, optical identification with chromospheric network pattern *(Russian)* 78−40897
2.8 GHz quasiperiodic burst struct. rel. to burst morphological parameters 77−22191
3.2 and 10 cm emission, anal. of observational data from Purple Mountain Observatory *(Chinese)* 80−105223
3.5 mm depression features assoc. with Hα disparitions brusques 77−78756
3 cm wavelength emission correl. with X-ray bursts *(Russian)* 78−93194
10.7 cm flux, correl. with F-region temps. at Malvern and S. Santin 77−91360
10.7 cm flux, vars. during solar cycle and correl. with tropospheric winds 80−72604
10.7 cm flux rel. to O I 6300 Å airglow emission rate 77−45215
10.7 cm fluxes, correl. with ionosphere radiowave absorpt. at mag. equator 79−21099
10.7 cm radio flux peaks, correl. with Earth atmosphere vorticity area index 78−73459
27-day rotational variation, correl. with stratosphere zonal winds var. 78−88878
35 GHz emission, disc radius meas. 77−22174
50 GHz band, atmospheric attenuation, meas. 78−73494
107 cm flux, monthly averages vars. correl. with total atmospheric O_3 79−16571
146 MHz C-type bursts correl. with mag. storms *(Chinese)* 80−4321
810 MHz bursts in 1957-67 period, obs. data 77−33446
1972, August 3-6, obs. at 1.9, 2.5 and 3.5 cm wavelength *(Russian)* 77−64719
2800 MHz radio minimum (1976 February) 80−4324
active region and bursts, 6 cm obs. with 6″ resolution 80−62096
active regions, 3 cm radio emission spectral slope, flare-associated variations 80−98630
active regions, 6 cm obs. with 6 arc seconds resolution 77−33444
active regions, magnetic and microwave struct. 77−49361
active regions at 2.8 cm, development and structure 78−53910
activity levels, influence on photoelectron fluxes in Earth's ionosphere and plasmasphere 78−16374
atmospheric absorption of radio waves meas., O_2 band, at 5.6 mm *(Russian)* 77−91210
basic component, spectra 77−56884
brightness at 8 and 13.5 mm. rel. to magnetic fields and Hα activity *(Russian)* 77−64724
brightness distribution at 33 and 37 GHz, obs. 77−53524
brightness temp. in SHF, distrib. on quiet Sun, RATAN-600 obs. *(Russian)* 80−94776
brightness temperature, at millimetre wavelengths 77−22171
brightness temperature of quiet Sun at cm wavelengths *(Russian)* 77−64721
burst data and flare proton energy spectra slope prediction 79−53683
burst generation mechanism for drifting pairs 79−25587
burst intensity fluctuations at metre wavelength *(Russian)* 77−64733
bursts, 6 cm obs. with 6″ resolution 78−53897
bursts, appl. of electron beam relaxation model in fluctuating plasma 78−83579
bursts, flare spray, Hβ obs. 79−80294
bursts, night-time reception due to anomalous propag. in E-region 77−56790
bursts, peak flux spectra, statistical anal. 80−98641
bursts, stereo radioastronomical obs. 78−49419
bursts at 100-9500 MHz, obs. during 1977 Sept.-Oct. 79−48770
bursts at 26.4 MHz, struct. and evolution 78−65596
bursts at 26 MHz, obs. brightness distrib., possible ionospheric effects 80−41806
bursts at 29.5 MHz during solar cycle 20, statistical anal. and comparison with noise storms 80−56794
bursts at 30 and 60 MHz, STEREO-5 obs., ionospheric scintillation evidence 78−61822
bursts at 3.7 and 11.1 cm wavelength, interferometric obs. 80−31285
bursts at m wavelength, 169 MHz radioheliograph obs. 79−30033
bursts in 0.2-1.4 GHz range, ms fine structure 77−53499
bursts in centimetre wavelength range, space-time relation to impulsive chromospheric flares *(Russian)* 79−16924
bursts rel. to Hα-flare visual features 80−41803
catalogue of radiobursts 1966-76 having characts. predictive of proton activity 77−49356
centimetre radio waves emission, brightness var. at extreme solar limb 80−21969
centimetre wave emission, Sun radio radius and brightness distrib. across disc 80−21968
centimetre-wave sources above McMath region 13043, rapid var. rel. to optical phenomena 80−67688
centimetric quiet Sun, reinterpretation rel. to density in coronal long distance arches 78−28597
chromosphere, periodic brightness fluctuations at 2.8 cm wavelength, rel. to photospheric vel. oscills. 79−35216
chromosphere, ubiquitous structs. observed in quiet Sun at mm and cm wavelengths 79−12456
chromospheric flares and associated radio emission *(Italian)* 78−96457
chromospheric structure from brightness distrib. at mm wavelengths 79−53799
circularly polarised radioemission at 1.35 cm over bipolar sunspot groups, obs. *(Russian)* 78−57532
cm radio emission quasiperiodic fluctuations correl. with proton flares 77−53533
cm wavelength bursts, position and size compared with X-ray bursts 77−33459
collective radio-emission from plasmas 80−46392
corona, burst sources positions rel. to dense non-potential magnetic flux tubes 78−28615
corona, decametric obs. at high resolution 80−31288
corona, radio emission fluctuations 78−45311

solar radiofrequency radiation continued
corona, radio obs. at Culgoora Observatory 79−48754
corona, radio spectrograms, magnetoplasma, plasma wave motions *(Dutch)* 80−62101
coronal hole, obs. with λ 8-cm radioheliograph 80−4326
coronal holes, Arecibo obs. at 11.5 and 21 cm wavelength 78−61834
coronal holes and arches, brightness temps. at 169 and 408 MHz rel. to UV obs. 79−8893
coronal mass ejection events assoc. with flares, prominences or radio bursts, outward vel. meas. 77−22197
coronal radio emission, probability of occurrence of stable pulses 78−42737
coronal transient, 1973 August 21, radio and white light obs. 79−71010
coronal transient, massive slow-moving, radio obs. 79−53796
coronal X-ray holes, radio obs. rel. to quiet radio Sun at 2800 MHZ 78−20805
cycle 20, statistical study of Ca II flocculae and radio fluxes 77−91498
decameter wavelength spectrum of quiet Sun 78−7966
decametric emission, quasi-periodic fluctuations *(Russian)* 79−25561
decametric noise storms and coronal irregularities, microscopic spectral features 77−45392
decametric storm burst source positions, UTR-2 obs. at 25 MHz 80−90403
decimetre fluctuations, quasiperiodic components *(Russian)* 77−74034
decimetric emission quasiperiodic fluctuations 80−41791
decimetric type IV narrow-band burst with fine structure 78−36546
diffraction and refl. of radiowaves from lunar limb during solar eclipses *(Russian)* 78−65586
drift pair bursts, polarisation obs., position and freq. characts. 80−85925
drift pair radio burst, MHD theory 79−25558
drifting pairs type radio bursts, results of obs. near 25 and 12.5 MHz 78−24502
drifting radio bursts, 400-500 MHz, prod. mechanism, shock wave interactions 79−53790
drifting spikes, new species of solar radio bursts, obs. 79−48753
EHF high angular resolution obs. at 8.5 mm wavelength 79−25578
emission at 6 cm wavelength, sunspot assoc. model 80−51712
emission centre displacement measurement using alignment of antennas *(Russian)* 77−22089
emission from chromosphere-corona transition 79−8894
emission preceding proton flares, pulsation instability 78−53911
emission pulsations in 1.9-3.5 cm wavelengths *(Russian)* 80−17563
emissions from plasma waves and type III bursts 79−44454
equatorial brightness distribution at 2.8 cm, one dimensional aperture synthesis obs. 77−22173
F10.7 index during solar cycle 21, correl. with atmospheric $O^+(^2P)$ ionisation freq. vars. 80−77195
fast drifting solar radio bursts with short decay times 77−17534
fibre bursts concurrent with weak noise storm 77−2399
filament, radio spectrum rel. to transition sheath study 78−28619
filament, synthesized map at 6 cm with about 15″ resolution 80−90380
fine structure radio bursts at meter wavelengths, review *(Russian)* 78−16386
fine structure radio emission in 20-30 MHz range, theoretical freq. splitting mechanism *(Russian)* 78−16383
flare, 1971 January 14, radio emission position and polarisation 77−2393
flare, 1978 February 11, Hα, Hβ and VHF obs. 78−93187
flare continuum events, m wavelength obs., emission mechanism 79−21248
flare localisation in Sun's atmosphere, radio observations 79−88641
flare monitoring using global radio solar telescope network 80−82202
flare spatial structure in soft X-rays and cm wavelengths 77−17524
flare transition region, thermal radioemission theory *(Russian)* 79−48763
flares, 1972, August, ground-based radio obs. 77−25993
flares, conf., Florence, Italy (Nov. 75) *(Italian)* 78−93191
flares, impulsive, microwave and metre wave emission rel. to adiabatic heating 78−93176
flares, millisecond microwave spikes obs. 78−96464
flares, particle and EM emissions, review *(Italian)* 78−93192
flares, radiation generation features 80−101575
flares, radiative, mechanical and mag. energy release 79−53797
flares, radio brightness distrib. processing in one-dimensional synthesis *(Italian)* 80−98628
flares, VLA obs. interpreted with optical, X-ray and other microwave data 79−44428
flares emission mechanism, model *(Italian)* 78−96462
flares microwave and optical emissions comparison 80−31284
flares microwave spectrum, appl. of quasi-thermal electrons gyrosynchrotron emission theory 80−36602
flares onset at m wavelengths 77−17491
flares radio and hard X-ray events, spectral features rel. to particle accel. 77−45369
fluctuations, correl. with solar rel. oscills. 80−105226
flux calibration in 1970, at 2800 MHz 80−17570
flux level distrib. and oscillatory bursts 77−33451
frequency-scanning interferometry for fast-proceeding phenomena investigation *(Russian)* 77−22094
fundamental and harmonic type IV bursts in 24 to 220 MHz, range circular polarisation *(Russian)* 78−16384
gyrosynchrotron and Langmuir-wave processes for radiowave generation 79−21172
hectometric and kilometric radio emission in August 1972, satellite obs. 77−25994
impulsive microwave bursts, superimposed fast time structs. with slowly varying polarisation 79−40173
impulsive mm-wave bursts, quasi-quantization 80−94770
Langmuir wave emission and absorpt. coeffs. due to anisotropic unmagnetized particles 78−16370
Langmuir waves and anisotropic particles, Legendre-expanded quasilinear eqns. appl. 79−75089
local sources, spectral polarisation obs. at Pulkova in March (1970) 77−53535
low-contrast radio features, obs. by RATAN 600 telescope 77−78760
m and dm wavelength obs. during 1977 Sept.-Oct. 79−48769
m wavelength thermal radiation from coronal streamers and holes 77−60742
Mauna Kea, atmospheric absorpt. between 4 and 30 cm^{-1} 78−3888
McMath 12686, type III burst producing McMath 12686, type III burst producing active region, overlying coronal struct. Skylab obs. 80−21976
McMath regions 14943 and 14979, interferometric obs. at 8.6 mm wavelength 79−48768
metre wavelength radio bursts, coronal Langmuir waves emission theory 78−57515
metre-band type I-bursts, stable confinement of fast electrons 79−80296
metre-wave emission, wave ducting rel. to fundamental/harmonic source coincidence 80−21978
metre-wave radio bursts positions, correl. with X-ray emission 78−69774
metric radiobursts polarisation and location rel. to new mag. field emergence 78−61824
microbursts at 22.2 GHz rel. to lower freq. events 77−2398
microwave absolute flux, spectra of individual components 77−5461
microwave activities associated with McMath regions 14943 and 14979, 1977 Sept.-Oct. 79−48767
microwave and metre-wave bursts, correl. with impulsive X-ray bursts 78−93174
microwave brightness temperatures and circular polarisations from thermal regions, derivation 77−22172
microwave burst, 1976 March 28, superimposed 4.7 s periodic oscills. 78−7972
microwave burst and Hα-flares rel. to isolated sunspot magnetic configurations 78−16387
microwave burst data rel. to solar proton fluxes 78−73591
microwave burst emission two-component model consistent with soft and hard X-rays 77−82200
microwave burst energies correl. with ionospheric VLF sudden phase anomalies 78−77418
microwave burst spectra, source inhomogeneities, statistical analysis 80−41805
microwave burst spectra and flare mag. fields 78−7970
microwave bursts, appl. to near-Earth solar flare protons parameters determ. 78−45165
microwave bursts, assoc. with geomagnetic crochets, nature 78−69772
microwave bursts, characts. at 9 GHz freq. appl. to proton flares identification 80−4323
microwave bursts, flare protons characts. determ. near Earth, longit. attenuation function 78−45309
microwave bursts, freq. spectra 77−13311
microwave bursts, polarisation features interpretation 78−96468
microwave bursts, polarization structure 79−96984
microwave bursts, source, energetic electrons *(Russian)* 79−21258
microwave bursts, spike, rise, fall and absorpt. types, obs. 79−88636
microwave bursts, X-ray correlated, continuous injection model 77−17515
microwave bursts and Hα flares, rel. to sunspot mag. configurations 77−53527
microwave bursts fast structures, negligible assoc. large-scale mag. field changes 79−2536
microwave bursts rel. to proton events forecasting *(Chinese)* 80−12723
microwave bursts used to calc. solar proton flux 80−41789
microwave emission, sudden decreases obs. 79−101134
microwave emission at 9 cm, emission height 78−77548
microwave emission search from X-ray bright point flares 77−45384
microwave events, magnitude distrib., link with flare build up phenomenological model 80−98640
microwave flares, direction pattern 78−85927
microwave flux decreases rel. to assoc. activity complex 77−25989
microwave generation from flares 80−109413
microwaves, solar activity, lower intensity limit *(Portuguese)* 77−78729
millimetre radiation, short wave, obs. with wide-band radiometer based on superconducting point contact 79−96916
millimetre wave radiation, obs. by wide-band radiometer based on superconducting point contact 79−62750
modulated fluctuations of radio emission, probability density *(Russian)* 77−74033
moving type IV burst, associated pulsating struct. radioheliograph obs. 79−40171
moving type IV burst at solar limb, three freq. obs. 78−69776
moving type IV bursts, brightness temps. 79−48760
moving type IV bursts, circular polarisation rel. to photospheric magnetism 78−53915
moving type IV bursts, Culgoora radioheliograph obs., statistical study 79−44456
moving type IV bursts, gyro-synchrotron modulation obs. 80−26833
moving type IV radio bursts, obs. and interpretation 79−40174
negative bursts, absorption origin 77−53517
negative bursts with moving filaments 1969, 19 May 77−53516
noise storm, 1972 May 21, m wavelength pulsating bursts, model 79−25569
noise storm, drifting pulsations obs. 80−62105
noise storms, book 78−20810
noise storms, correl. with particular photospheric mag. structs. 78−4185
noise storms, spectrum and position at decametre wavelengths 78−28622
noise storms and active region mag. fields *(Russian)* 77−64717
noise storms and bursts, preliminary results from Mark II Nancay radioheliograph 78−28517
noise storms and terrestrial EM wave propag. *(Japanese)* 80−51600
noise storms during solar cycle 20, statistical anal. and comparison with radio bursts 80−56794
oscillations at centimetre and millimetre wavelengths, theoretical model 77−22175
partial eclipse, 1977 April 18, radio obs. at 590 MHz 77−87362
periodic solar microwave burst, polarisation obs. 77−29773
plasma emission appl. to radio bursts *(Russian)* 78−14139
plasma frequency bursts, implications of Voyager 2 coronal occultation obs., 1979 August 80−51639
plasma radiowave fluctuations and turbulence, Venus 10 radio transmission expt. 79−80295
polarisation characts., radio wave propag. in inhomogeneous magnetic field *(Russian)* 78−16385
polarisation in 1.9-3.5 cm wavelength region, obs. method *(Russian)* 78−65587
preflare association of mag. fields and mm wave emission 77−17490
prominence brightness temp. depression interpretation, cm and mm data 80−90395
prominences, cm and mm wavelength obs., size and spectrum of radio filaments 79−66988
prominences, H lines at submm. wavelengths *(Russian)* 79−35228
proton flare, 1971 January 14, assoc. complex radio emission event 79−40175

solar radiofrequency radiation continued
proton region of McMath 13043 active region, radio burst obs. 78−89142
pulsations, role of plasma instabilities periodical regimes in coronal mag. traps *(Russian)* 80−8616
pulsed microwave bursts with quasithermal spectrum, model 77−78762
quasiperiodic microwave bursts and adiabatic heating 80−51713
quasiperiodic oscillations at 3 cm 77−29768
quasiperiodic variations in solar flux at 10.7 GHz 77−17516
quiescent and active states, radio emission obs. *(Spanish)* 79−40160
quiet spatial structure during 1977 October eclipse, VLA 6 cm obs. 80−72895
quiet Sun, high-resolution obs. at 6 cm using Westerbork Synthesis Radio Telescope 80−36601
quiet Sun, interferometric obs. at 8 millimetre wavelength 79−40149
quiet Sun, obs. at metre and decametre wavelengths 78−4184
quiet Sun 2.8 cm emission, small-scale sources 79−5794
quiet Sun emission at freqs. <200 MHz, scatt. effects 78−4183
quiet Sun mm wavelength emission, interpretation of data, chromosphere and corona models 79−35231
radio burst emission mechanisms 80−72917
radioastronomical obs. by amateurs *(Italian)* 78−7887
radiometer harmonic generation and mm waves *(Italian)* 77−49292
recombination lines, high n 77−78758
S-component, fine spectral structure in 4.5-7 GHz range *(Russian)* 77−33457
S-component, local sources emission directivity, spectral study 78−24500
S-component emission, local sources struct. 80−46528
S-component spectrum, fine struct. in 5.0 to 7.0 GHz freq. range 80−21977
S-component spectrum in 4 to 7 GHz range, radiospectrograph for fine structure *(Russian)* 78−49320
S-component statistical anlaysis, results 79−40172
scattering process above active regions, propagation in fibrous medium 78−20780
second harmonic plasma emission polarization 78−65579
SHF emission from local sources rel. to sunspot group development *(Russian)* 79−30035
SHF flux fluctuations from limited areas, rel. to coronal wave propag. 79−35222
source localization and polarization determination using LF satellite radioastronomy *(French)* 79−70940
spectral index determ. of radio emission of individual solar regions 80−94723
spectral index of local radio sources in 1.9-3.5 cm range *(Russian)* 77−64732
spectral lines emission, plasma effects 78−96466
spectrum to 10 km wavelength 79−92748
'spike' type radio bursts, morphological characts. 78−65599
spike bursts generation by electron streams 79−35230
sporadic radiation, Interkosmos-Copernicus 500 satellite obs. 77−53503
stria burst sources ang. sizes, 24-26 MHz range 78−65597
sudden cosmic noise absorpt., solar Zenith angle depend. 78−12047
sunspot group, 1974 July, assoc. radio emission obs. at 1.9, 2.5 and 3.5 cm wavelength *(Russian)* 78−65585
sunspot group, local radiosource fine structure *(Russian)* 79−21260
synoptic charts at 9.1 cm, use to identify coronal holes 80−98633
Torun Observatory 127 MHz solar data since 1958, survey *(Polish)* 78−36549
total flux obs. at 3.2 cm wavelength at Peking Obs., 1965-75 period *(Chinese)* 78−69763
total intensity and circular polarization struct. at 21 cm 78−7957
total microwave flux, search at Toyokawa for five minute oscillations 80−4327
transition region, origin for UV and radio fluctuations 80−90398
turbulent shock wave propagating across mag. field, struct. and radio emission 79−40166
type I (metre wave) sources, relation to solar proton events *(Chinese)* 80−105222
type I and III bursts comparison *(Russian)* 78−16379
type I and III m wavelength bursts source heights meas. 77−33460
type I burst, 1972 August, m wavelength characts. *(Chinese)* 77−22156
type I bursts, centre to limb vars. 77−87356
Type I bursts, meter wave, role of coronal Langmuir turbulence and quasi-stable particle accel. *(Chinese)* 80−105220
type I bursts, microwave radar obs. 79−88635
type I bursts, photon diffusion in turbulent magnetised plasma 79−48662
type I bursts, synchronous obs. in Crimea and Cuba *(Russian)* 77−64718
type I sources, 146 MHz obs. *(Chinese)* 80−8609
type I stormburst chains, radio spectra 77−22192
type II and III bursts, plasma waves conversion into transverse waves 77−2414
type II and III bursts theory *(Russian)* 78−16381
type II and IV bursts assoc. with mag. field emergence into corona 80−109412
type II burst, 1973 September 5, theoretical model for fast-mode MHD shock wave 79−92734
type II burst, coronal shock waves and magnetic field 77−53512
type II burst commencement times from energetic particle flares 77−37590
type II burst obs. and theory for coronal magnetic field determ. 80−41785
type II bursts, fast electron tails form. 77−33439
type II bursts, radiation from MHD shock front *(Russian)* 77−87259
type II bursts data *(Russian)* 78−16380
type II bursts rel. to flares Hα line intensity peak 79−21252
type II bursts with reverse frequency drift 78−7978
type II decameter wave burst assoc. with behind-limb flare 77−22194
type II radio burst, 1973, May 3, fine struct. 78−24501
type II radio burst, coronal mag. struct. in source region 78−69775
type II radio burst with reverse freq. drift against noise storm background, obs. 80−17567
type II radio emission prod. by coronal MHD shocks 79−92750
type II radiobursts and shock waves in interplanetary medium 80−56690
type II-IV bursts, 1971 Dec. 14, rel. to compact and diffuse white-light clouds in corona 77−22193
type III and IIIb bursts, directivity in stream-plasma interaction 77−2415
type III and microwave bursts rel. to mag. config. 77−82204
solar radiofrequency radiation continued
type III and type I-like decametric emission in coronal mag. arch 78−12179
type III and type IV bursts from source above solar limb, heliograph obs. 79−53798
type III burst, stereoscopic direction finding meas., second harmonic emission 78−45312
type III burst directivity, streamer model based on STEREO-1 meas. 77−45382
type III bursts, 1972 May-Aug., obs. in interplanetary space 79−62805
type III bursts, assoc. with flaring X-ray bright points 80−67681
type III bursts, associated electron plasma oscills. 77−37592
type III bursts, conf., Berkeley, California, USA (May 1975) 77−2406
type III bursts, deconvolution and decay mechanism 77−45381
type III bursts, direct Langmuir collapse rel. to radioburst problem 78−79430
type III bursts, direction finding meas. out of ecliptic plane 77−22195
type III bursts, drift rate rel. to polarization at 237 MHz 78−36545
type III bursts, dynamics of fast electron cloud travelling through plasma 77−996
type III bursts, emitting source size and evolution 80−94771
type III bursts, enhancements assoc. with interplanetary shocks 77−2409
type III bursts, exciter theory 77−2416
type III bursts, fast electrons stream free dispersal in solar corona with nonsteady injection 80−17568
type III bursts, flaming struct. 77−74031
type III bursts, fundamental and harmonic radiation 77−2413
type III bursts, fundamental emission in 25-200 kHz range 80−56789
type III bursts, heliocentric radial var. of assoc. electron plasma oscills. 79−2454
type III bursts, high time resolution obs., instrumentation, data reduction *(Italian)* 78−96458
type III bursts, Langmuir wave-electron interactions 78−30418
type III bursts, Langmuir waves spontaneous emission 77−33455
type III bursts, LF, directivity 77−2410
type III bursts, LF obs., fast electrons interplanetary scatt. 77−2411
type III bursts, LF obs. apparent source sizes 77−2412
type III bursts, LF spectra 79−30048
type III bursts, nonlinear stability, electron exciters obs. near 1 AU 80−46513
type III bursts, obs. during JIKIKEN (EXOS-B) satellite initial phase *(Japanese)* 80−94675
type III bursts, out of the ecliptic structures 77−78592
type III bursts, position and polarisation, VHF and HF obs. 80−105214
type III bursts, radio intensity and fast electron flux at 1 AU 77−2407
type III bursts, radio mapping expt. in International Sun-Earth Explorer C spacecraft 78−85796
type III bursts, radio spectra obs., effect of interactions in ionospheric plasma 80−72904
type III bursts, rel. to plasma waves in solar wind, Helios 1 obs. 77−37492
type III bursts, role of three dimensional Langmuir wave instabilities 77−2404
type III bursts, scatt. in radiation source and fundamental-harmonic theory 77−2417
type III bursts, second and third harmonics intensity ratio 79−25588
type III bursts, second harmonic radiation and related nonlinear phenomena 78−7958
type III bursts, simulation and plasma wave excitation by fast electron cloud 79−44455
type III bursts, solitons and second harmonic radiation 79−12444
type III bursts, tracking in elevation and elongation, apparent source sizes 77−2408
type III bursts, vol. emissivity calc. 80−90384
type III bursts and coronal density structs. 78−77544
type III bursts and flare occurrence in spotless regions 80−56810
type III bursts and low density coronal structs. 77−71095
type III bursts and nonrelativistic electron propag. in solar wind *(Russian)* 77−78742
type III bursts at decameter wavelengths, longit. depend. of duration 78−81596
type III bursts caused by high-density electron beam, numerical simulation 79−84779
type III bursts during decametric storm 80−90399
type III bursts fundamental radiation rel. to coronal low freq. turbulence 79−84778
type III bursts rel. to white light coronal transients 79−48758
type III bursts with fine structure at decameter wavelengths *(Russian)* 78−16382
type III noise storms, rel. to coronal plasma heating by fast electron streams 80−105228
type III radio bursts, EM radiation direct generation from beam-plasma system 80−54007
type III radio bursts, fundamental emission and polarisation 80−36603
type III radio bursts, interplanetary baseline obs. 78−20808
Type III radio bursts, nonlinear Langmuir waves evolution 78−93173
type III radio bursts, nonlinear stability theory 80−26826
type III radio bursts, rel. to nonrelativistic electron beam propag. 78−28623
type III radio emission, head-on approximation in second harmonic plasma emission 79−41803
type III solar radio burst sources, plasma wave clumping origin 80−21959
type III U-shaped solar radiobursts, circular polarisation 77−45379
type III-like bursts, UHF obs. 80−56793
Type III-RS bursts of 1975, August 12, Hα obs. 77−29774
type III-V radio bursts, relationship with hard X-ray bursts 78−89157
type IIIb and type III bursts, harmonic struct. 79−75195
type IIIb bursts, 25 MHz obs. and theoretical model 80−90400
type IIIb bursts, polarisation meas. 77−22161
type IIIb bursts and collisionless deceleration of fast electron streams in corona 77−71096
type IV bursts, catalogue preparation *(Italian)* 78−96459
type IV bursts, rel. to mag. regions in interplanetary plasma flows from strong flares 77−91397
type IV bursts, rel. to transient cosmic ray intensity vars. 79−40043
type IV bursts and coronal gyro-synchrotron maser possibilities 79−48756
type IV continuum bursts, coherent nonlinear interaction of Bernstein waves 77−53529

solar radiofrequency radiation continued
type IV decimetre bursts, causes of onset and sudden reductions 77−2400
type IV meter bursts, continuous radiation microstruct. and source model 77−53534
type IV meter bursts microstruct., modulation of continuous emission by whistlers wavepackets 77−78761
type IV radio burst quasiperiodic struct., anal. and interpretation 80−62097
type IV radio emission, prod. by coronal EM loss cone instability *(Russian)* 78−77528
type IV radio emission, rel. to flare particles multi-stage accel. 79−44437
type IV radio emission pulsations, bounce-resonance effects 78−89161
type IV solar radio events, pulsating structs. 78−96455
type U radio bursts, polarisation evolution 80−26834
type V bursts, scatt. hypothesis 77−45378
type V bursts, theoretical model 78−53914
type V bursts, VHF obs. 78−28639
type V radio bursts, dynamic spectra distinctive struct. 80−46527
type V radio bursts, position and polarisation, HF and VHF obs. 80−105215
type-II bursts, LF and MF obs. by Prognoz satellites 78−16375
types I and III storm radiation, obs. and cut-off freq. interpretation 79−21249
U-type bursts, coronal source regions 78−77543
UHF two dimens. maps of 408 MHz 80−85922
VHF activity and auroral effects 77−67004
VHF noise registrations at Oslo Solar Obs. (1965-74) 77−53541
Voyager planetary radioastronomy experiment 78−24433
zebra structure, polarised, interpretation 78−96467
H I 9873 MHz line, chromospheric, appearance rel. to Hα seven components form 78−89151
^{3}He 8666 MHz superfine structure line detection of ^{3}He-rich flares 80−109417

solar radiowaves *see solar radiofrequency radiation*

solar rotation
12.2 day rot. period 78−16367
17th century, 1625 to 1626 and 1642 to 1644, anomalous solar rot. from sunspot drawings 78−36550
27.5 day rotation, rel. to large-amplitude standing planetary waves in troposphere 78−36236
27-day rotation, correl. with stratosphere zonal winds var. 78−88878
1611 to 1613, solar rot. determ. from Thomas Harriot's sunspot obs. 79−75182
angular momentum flow, rel. to core rotation 77−45396
angular momentum outward transport, comments 79−30036
angular momentum problem and rotation of pre-main sequence stars 79−58332
background vel. fields, anal. and instrumental effects, visible obs. 80−72915
chromosphere, rot. depend. on size of tracer features 80−12731
chromospheric feature lifetime rel. to rotation 79−44442
convection in rotating deep compressible spherical shell, theory 78−20795
convection structure, effect of differential rot., Maunder minimum nature 80−101573
convection zone, angular vel. gradients 79−53787
convection zone, momentum and energy transport using rotation model 79−25586
core, rotational constraints 80−101576
coronal features, rot. and lifetime 79−75191
coronal holes, rigid rot. rel. to nature of underlying photospheric mag. fields 78−28613
diagnostics of uniformly rotating ionised medium, appl. of MHD pulses 80−109405
differential rot. and giant cell circulation of Ca II network 77−53546
differential rot. and global-scale vel. fields 77−53545
differential rot. differences 77−53548
differential rotation, correl. with mag. fields from dynamo action 80−90378
differential rotation, due to latitude depend. convective heat transport 80−90411
differential rotation, effects of large scale circulation in convection zone 77−22164
differential rotation, from mm wave obs. 77−2378
differential rotation, gaseous polytropic configurations for const. mass solar model 80−82338
differential rotation, generation by rot. effect on convection zone turbulent viscosity and cond. 80−36612
differential rotation, influence of meridional circulation and heat redistrib. in convective envelope 79−40150
differential rotation, nature of one mechanism 79−25556
differential rotation, solar activity dependence 79−84766
differential rotation and dynamo presence 77−53582
differential rotation for unrestricted rot. rates, 2-dimens. stochastic motions 77−56899
differential rotation maintenance rel. to surface Reynolds stresses 77−2379
differential rotation meas., 1978, from recurrent and non-recurrent sunspots 79−84780
differential rotation of Ca II network and photospheric plasma 79−25585
differential rotation of magnetic fields, solar cycle variations 78−20781
differential rotation of solar wind, determ. from recurrence period as function of heliographic latit. 80−62106
differential rotation rates for short-lived regions of emerging magnetic flux 78−20782
differential rotation rel. to turbulent transport of angular momentum 78−16372
differential rotation/global convection system, modulation by nonlinear dynamo rel. to solar cycle 78−40889
dipole waves as constituents of 22-year magnetic cycle 79−12460
distortion rotating with period of 12.2 days 77−17502
effect on relativistic galactic cosmic rays, anisotropies 80−67481
elements i and Ω determ. from Doppler vel. meas. of solar plasma 78−28599
EUV flux, changes with solar rot. rel. to ionosphere primary ion-electron prod. rates change 80−72675
filaments, short-lived, differential rotation 78−28642

solar rotation continued
high solar latitude rotation, model calcs. rel. to solar convection zone depth 79−101129
induced Doppler spectral shift meas. by scanning Fabry-Perot interferometer 80−77298
interplanetary sector boundaries config. rel. to certain days of solar rot. 80−41764
longitudinal distribution of solar activity, refl. in geomagnetic var. 80−82330
magnetic buoyancy, influence of solar rot. 79−21256
magnetic core model, rot. and stability 79−44472
magnetic dynamo, role of differential rotation 80−109414
measurement technique using nonradial p-mode oscills. 79−29994
metre-wave radio bursts sources, 27 day recurrence period and correl. with X-ray emission 78−69774
MHD dynamo, convectively-driven models, solar dynamo appl. 78−42668
mixing frequency components in ionospheric electron content due to solar rot., identification 79−29929
non-uniform angular vel. distrib. maintenance throughout solar convective zone, role of nonstationary mechanisms *(Russian)* 79−96985
oblateness, rot. period and faculae 77−9735
observational determinations 79−75179
p-mode eigenfrequencies, radial rotational vel. gradient effect 79−30027
photosphere Doppler obs. in visible 80−105219
polar and equatorial rotation rates, supposed anticorrel. 78−49415
polar magnetic features rot. rate 79−30037
polar vortex, spectroscopic search 79−5801
pulsars, pulse width-period relation rel. to source of coherent radio emission 80−82403
pulsation, rotation and sunspot cycle, relationship of periods 77−53519
radial differential rotation, traced by p-mode oscill. obs. 79−35221
rapid oscillations, aspect effect due to axis of rotation inclination 77−91500
rotating convection zone, equilib. problem 77−56917
rotating magnetised core model, rel. to neutrino flux 77−2381
shape of planets and Sun due to rot., equipot. surface 77−13541
shearing motions, axisymmetric magnetic flux conc. 79−35219
sidereal equatorial rotation rate, K I 7699 Å line meas. 79−44441
solar radio emission S-component, statistical anal. 79−40172
spatial displacement pattern precession, effect on 160 min. period solar oscills. *(Russian)* 80−77375
spectroscopic Doppler rotation rates, 1966-1978 period 79−66977
sunspot, spectroscopic determ. of solar rot. 79−92745
sunspot data (1967-74), global rotation rate determ. 80−90387
sunspot group velocities, statistical distrib., depend. on solar activity cycle phase 80−72918
sunspot groups, rotation rates 80−41797
sunspot periodicity rel. to solar rot. 79−35223
supergranulation cells, equatorial rotation rate 80−90388
surface appearance of disturbances in heat flow assoc. with differential rotation 77−29751
surface oscillations and pulsations, rotation speeds 80−67676
surface rotation during Maunder minimum 77−2377
surface velocity oscillations meas., rot. effects on high-resolution spectroscopy 78−96403
theories, review 77−53563
time variations of solar angular momentum 78−7950
torsional oscillator with 11 year period 80−105217
variations in rot. pattern, correl. with evolution of photospheric mag. field patterns 78−20798
velocity, comparison with other lower main-sequence stars 80−51767
velocity fields, large-scale, from Doppler line shift obs. 80−12730
velocity fluctuations with long period 79−40152

solar spectra
see also solar activity; solar corona; solar radiation
absorption line formation depth *(Russian)* 77−64749
absorption lines formation in inhomogeneous medium, rel. to waves and convective motions *(Russian)* 80−72901
abundances from X-ray obs. 77−56887
active region and flare plasmas, electron density from Fe IX lines intensity ratio 78−20771
active region McMath 12628, EUV and X-ray obs. 80−67692
active regions, 3 cm radio emission spectral slope, flare-associated variations 80−98630
active regions, Salyut-4 UV spectra 77−82211
active regions on solar limb, 1175 to 1940 Å emission-line spectra 78−96446
aeronomical reference spectrum for solar UV below 2000 Å 79−25379
asymmetry of selected Fraunhofer lines, obs. *(Russian)* 78−40892
atmosphere, spectral line intensity, electron impact excitation 80−36605
atmospheric 5 min. oscills., spectral lines use as temp. indicator 77−37585
atomic damping constants, comparison with collisional line broadening theory 77−13237
automatic observation and data processing, by double-pass digital monochromator *(Russian)* 80−72777
Balmer lines, formation in bright prominences spectra *(Russian)* 80−77377
Balmer lines intensity fluctuations in chromosphere 79−53793
blue continuum flares and D3 preflare shell obs. 80−51709
bursts, flare spray, Hβ obs. 79−80294
Ca II network, differential rotation rel. to photospheric plasma 79−25585
chromosphere, Ca II lines, vel. and temp. disturbances, weighting functions 80−67679
chromosphere, Fraunhofer line cores formation, empirical statistical model 78−7963
chromosphere, Hα obs. close to limb 78−28628
chromosphere, Hα obs. rel. to network evolution during active regions development *(Russian)* 78−57531
chromosphere, Heζ/H8 relative intensities in spicule spectrum 78−40904
chromosphere, high resolution spectroscopy, space-time vars. 77−53498
chromosphere, limb spectra from Skylab, 2000-3000 Å region 77−45376
chromosphere, Na distrib. and nonthermal motion vels. from D-line eclipse obs. 77−22200
chromosphere, optically thick line formation, atmospheric dynamics 80−94767
chromosphere, quiet and active, Lα spectra and models based on partial redistrib. diagnostics 79−75169

solar spectra continued
chromosphere, radiative relaxation time 79−30040
chromosphere, waves in lower regions, energy transport 79−62804
chromosphere above sunspot umbrae, Ca II H, K and IR lines interpretation 78−53901
chromosphere above sunspot umbrae, obs. of emission cores in Ca II H- and K-lines 78−53900
chromosphere active regions, bidimensional spectroscopy obs. with birefringent filter *(Italian)* 80−98568
chromosphere and prominences eclipse observations using plane grating as polar heliostat 79−84674
chromosphere and transition region, OSO-8 obs. of wave propag. 78−93183
chromosphere flare spectrum, electron beam diagnostics 80−26827
chromosphere flares, H α spectra rel. to initial phase parameters determ. 80−62104
chromosphere flares, Lyman α emission obs. rel. to soft X-ray heating effect 79−40170
chromosphere Fraunhofer line cores formation, empirical statistical model 79−12450
chromosphere Hα and Ca II K emission, form. of quiet chromospheric struct. *(Russian)* 79−48764
chromosphere limb flare, 1959 July 25, spectrum rel. to physical conditions 80−105227
chromosphere line formation, C II reson. lines obs. rel. to temp. struct. 78−53896
chromosphere line profiles from OSO-8 satellite 80−67690
chromosphere lines, high-resolution obs. by LPSP expt. on (OSO-8) 77−64649
chromosphere mechanical flux determ. from Ca II lines 80−67680
chromosphere mottles, embedded feature model for contrast profiles interpretation 77−33443
chromosphere plages, Ca II and Mg II spectra rel. to physical props. models 78−89153
chromosphere-corona transition region, mass motions in impulsive flarelike brightenings, OSO-8 obs. 79−35217
chromosphere-corona transition region, optically thin lines, OSO-8 obs. 77−9729
chromosphere-corona transition region, OSO 8 UV obs. of optically thick region 80−56788
chromosphere-corona transition zone of solar active regions, non-thermal velocities *(French)* 80−77371
chromospheric flares, optical thickness and H ionization degree from Balmer line obs. 78−73694
chromospheric Hα spicules, spectra, props. 79−25563
chromospheric oscillations obs. in C II 1336 Å line by OSO-8 78−28625
chromospheric oscillations obs. with OSO-8, average phase spectra for Si II 79−62801
chromospheric oscillations obs. with OSO-8, average power spectra for Si II 79−62800
chromospheric oscillations obs. with OSO-8, basic meas. and analytical methods 79−62799
chromospheric waves, oscill. mode and vel. amplitude 79−21263
corona, 530.3 nm emission line from 1965-78, north-south asymmetry 80−77369
corona, Alfven waves above sunspots from forbidden line obs. 77−78732
corona, anal. of polar hole EUV lines obs. 79−5797
corona, approximations for proton excitation of ions fine struct. 77−17463
corona, dynamical props. from line intensities and widths of EUV forbidden lines 79−35213
corona, electron scatt. continuum spectrum, appl. to temp. determ. 77−22169
corona, EUV lines brightness rel. to temps. and temp. gradients 77−17506
corona, Fe^{12+} forbidden lines collisional excitation, importance of short-range pot. 77−17457
corona, Fe IX forbidden transitions, density depend. 79−66986
corona, Fe XII spectrum excitation 77−17458
corona, forbidden transition probabilities for ground terms of p or p^5 config. ions 77−2376
corona, intensity ratios of fine-struct. components of H like ions reson. lines 80−101581
corona, line intensity ratio and temp. determ. 78−73697
corona, N I isoelectronic sequence line ratios and electron densities 79−16906
corona, oscillations above active region, Fe XIV spectra obs. 80−41794
corona, plasma diagnostics using high-resolution spectroscopy, Skylab obs. of forbidden lines 78−14203
corona, proton collisional excitation of fine struct. transitions of Ca^{14+}, Fe^{20+} and Ni^{14+} 77−19017
corona, rotation investigation by spectroscopic method 77−53551
corona 5303 Å line, latit. depend. intensity long-term correl. with solar wind streams 78−93172
corona above active region McMath 12628, X-ray spectra rel. to solar atmosphere equilibria 78−53902
corona EUV emission lines, influence of solar wind nonequilib. ionisation 79−48751
corona polar plumes, anal. of M X and O VI EUV spectra 78−4178
coronal 5303 Å emission line, photoelectric meas. by automatic coronal photometer 79−12454
coronal emission line at 5303 Å rel. to activity in 20th cycle 79−66985
coronal emission line spectrum 13.3 to 13.8 Å 77−45389
coronal emission line strengths, computer program 77−64715
coronal Fe XIII IR lines, polarisation degree calc. 77−45373
coronal Fe XIV 5303 Å depletion, 1976, April 20, photoelectric obs. 78−28617
coronal Fe XIV emission line intensity and profile, temporal variations 77−29767
coronal Fe XVIII X-ray emission lines, obs. and anal. 78−36542
coronal forbidden lines in 975-3000 Å range, Skylab obs. 77−60734
coronal green and red lines, improved temp. for equal line intensities 77−22168
coronal green line, polarisation obs. at 1973 June 30 total eclipse 79−66969
coronal green-to-red line intensity ratio 77−2391
coronal hard X-ray event, 1971, December 14, energy spectrum 78−93177
coronal He^+ 304 Å radiation, theory 77−91510
coronal holes, EUV and radio spectrum 80−56802
coronal line profiles above active regions, statistical anal. 78−7968

solar spectra continued
coronal lines, 1175 to 1965 Å, identifications, wavelengths and intensities 79−25559
coronal loops in an active region, physical props. XUV obs. 80−90376
coronal red line, more precise wavelength *(Russian)* 78−40899
coronal X-ray spectra, calibration and resolution of Leicester Bragg spectrometer 77−5442
coronal XUV emission lines, Fe abundances and temps. determ. 78−4180
D abundance from SSO spectrograms 79−66982
damping constant and microturbulent velocities determ., study of errors *(Russian)* 80−72899
diatomic molecular lines in 7100-7600 Å range, table 78−77495
diatomic positive ions, partition functions and equilib. consts. 77−38626
Doppler shift measurements, rel. to solar oscillations and Sun internal struct. 80−105226
drifting spikes, new species of solar radio bursts, spectra 79−48753
eclipse, 1973 June 30, spectroscopic obs. by Dutch expedition 80−8615
element abundance, atomic and mol. f-values 78−20792
emission line profiles of inhomogeneous formations 77−37586
emission lines, form. in shock heated solar atmosphere 77−56889
emission lines of NeV, MgVII, SiIX, SXI, population levels as function of electron density and temp. 80−21963
emission lines propagating through interplanetary medium, profiles modification 79−66973
equivalent widths, photoelectric, appl. to stellar photographic equivalent widths calibration 78−73658
eruptive prominence, 1974, June 8, Ca II K-line spectra 77−22182
EUV, cycle 21 development and atmospheric absorption 79−75174
EUV, mass motions in active transition zone 78−85922
EUV, photometric calibration of spectroheliometer on Skylab Apollo Telescope Mount 77−60595
EUV, spectra from Skylab Apollo Telescope Mount spectrograph expt. 77−60598
EUV composite spectra of representative solar features, obs. 78−96447
EUV continuum absorption above quiet Sun transition region, new evidence 79−92738
EUV emission from active regions and quiet Sun, OSO-4 spectroheliograms 77−49358
EUV emission line nonthermal broadening near quiet solar limb 79−48748
EUV emission line spectra of flare, analysis of Skylab obs. 78−40913
EUV emission lines in different solar regions, relative chemical abundances determ. 80−46518
EUV emission-line profiles near solar limb, meas. 79−16909
EUV Fe, Si and S line intensities, OSO-7 obs. of limb brightening 78−69759
EUV forbidden lines, coronal temp. and nonthermal motions in coronal hole, quiet and active regions 77−33449
EUV line emission, contrib. of spicules 80−4325
EUV line emission, influence of spicules on limb brightening 77−22170
EUV line emission obscuration near limb 79−48762
EUV line emission weakening short of 912 Å wavelength 80−21962
EUV line intensity ratios, electron density determ. 79−21245
EUV lines, medium resolution obs. rel. to chromospheric network struct. 78−20801
EUV lines in chromosphere-corona region, anal. of coronal hole limb brightening data 80−82333
EUV spectra, appl. to transition zone energy balance and press. 80−21957
EUV spectra and solar atmosphere plasma diagnostics 79−30050
EUV spectrum, H_2 emission lines obs. 79−16908
Evershed flow in chromosphere-photosphere transition region 78−65593
extreme limb spectra, spatial struct. obs. in lines in 3398 to 3526 Å region 79−12449
extreme limb spectrograms, 4545-4579 Å, during 1970, March 7 eclipse 77−17472
F corona, radial vel. obs. at 1979 February 26 solar eclipse 80−85914
faculae, 5000 Å continuum diagnostics 80−4315
faculae, line profile families rel. to total mag. flux 78−49408
faculae, line profiles and models 77−45375
faculae, models, Ca II K line wings and magnetic fields 78−16392
faculae and pores, line profiles 78−16391
facular K line profiles, partial redistrib. 77−78748
far IR emission spectrum, meas. rel. to chromosphere/photosphere boundary temp. *(German)* 80−51721
far UV, Salyut-4 orbiting solar telescope obs. 78−53783
filament, radio spectrum rel. to transition sheath study 78−28619
filament-corona transition region, OSO-VI EUV line intensities obs. 78−28620
flare, 1973, June 15, UV spectral lines list from 1000 to 1940 Å 78−89139
flare, 1973 June 15, Skylab XUV spectra, intersystem and forbidden transitions 78−4159
flare, 1974 January 21, single loop obs. in Fe XV emission lines 79−66991
flare, C line profiles and continua obs. and upper chromosphere semiempirical model 79−40148
flare, electron density determ. from X-ray spectra obs. 80−82326
flare, EUV and X-ray obs. of thermal phase 79−8886
flare, freq. spectrum of transition region thermal radioemission *(Russian)* 79−48763
flare, Langmuir turbulence spectrum estimate from X-ray obs. 80−82329
flare, transient plasma X-ray spectra, electron density and temp. diagnostics 80−77368
flare coronal plasma nonequilibrium ionization and emergent X-ray spectrum 78−7953
flare Fe XX spectra, new atomic data 80−67545
flare impulsive X-ray burst, spectral anal. analytical method *(Chinese)* 80−85919
flare of 1979 March 25, X-ray spectra 80−85915
flare optical continuum origin, bluish-white emission knots 77−17513
flare second-stage X-ray emission, spectrum beyond 200 keV 80−51710
flare spectra, forbidden lines of Fe XIX, Fe XX and Fe XXI obs. 78−57519
flare spectra, He-like ions line intensities for non-stationary plasmas 78−53812
flare spectra, high dielectronic satellite lines analysis for plasma props. calc. 80−12728

solar spectra continued
flare spectra, Ni XXV, XXVI and Fe XXIII, XXIV obs. in laser-produced spectra 79−81175
flare time emission, shock wave and strong convection effects 77−71079
flares, anal. of $2p^3$-$2p^2$3d transition array in Fe XX and isoelectronic ions 77−65434
flares, Ca II K-line obs. rel. to temp. min. region struct. and flare heating mechanisms 79−12458
flares, EUV (1420-1960 Å) continua, Skylab obs. 79−30028
flares, Fe XXI 1354 Å line obs. from Skylab rel. to ionisation equilib. calcs. 80−21956
flares, Fe XXV dielectronic satellite line spectra as measure of nonthermal electron energy distribs. 80−21911
flares, H emission in gasdynamic models 77−17531
flares, H Lyman α asymmetry rel. to low nonthermal proton/electron energy flux ratio 79−8887
flares, H spectral lines obs. rel. to flare mechanism *(Russian)* 79−16925
flares, high-resolution X-ray spectra obs. 80−26837
flares, impulsive, X-ray spectra rel. to adiabatic heating 78−93176
flares, impulsive phase, hard X-ray spectrum, OSO 7 obs. 79−12440
flares, O I 1355.6 Å and C I 1355.8 Å lines obs. 80−90381
flares, obs. of lines between 171 and 630 Å 78−49406
flares, transient plasma X-ray lines, rate coeff. determ. 80−72903
flares, XUV electron density diagnostics 79−88633
flares microwave spectrum, appl. of quasi-thermal electrons gyrosynchrotron emission theory 80−36602
flares multiply impulsive bursts, spectral evolution 80−26828
flares spectral diagnostics for turbulent elec. fields 77−17493
flares X-ray and EUV emission, empirical models rel. to E-region and F-region effects 77−5515
flares X-ray spectra, Fe XXIV-XXV lines wavelengths in 1.85-1.87 Å region 80−21973
flares X-ray spectra, laboratory reproduction in region of Fe XXV-XXVI reson. lines 80−18819
flares X-ray spectra, use of a priori information in derivation of temp. structs. 78−20778
flash spectrum, obs. at 1979 February 26 eclipse 80−67687
forbidden coronal Fe X and Ni XII line identifications 77−53511
Fourier transform spectroscopy 80−98448
Fraunhofer line profiles for 1973 period *(Russian)* 79−92743
Fraunhofer line profiles interpretation 78−7976
Fraunhofer line shifts *(Russian)* 77−71072
Fraunhofer lines, Doppler shift meas. of solar limb local radial velocities 77−17537
Fraunhofer lines, east-west asymmetry of central residual intensities and other parameters 78−53916
Fraunhofer lines, effective form. depths calculated by various methods 79−12447
Fraunhofer lines, profiles in 4226-7700 Å range *(Russian)* 78−28606
Fraunhofer lines, progressive sound waves effect on profiles *(Russian)* 78−73689
Fraunhofer lines and continuum, solar disc polarisation meas. 78−73688
Fraunhofer lines asymmetry 78−4175
Gamma Ray Experiment on Solar Maximum Mission, spectrometer 80−51657
gamma-ray line emission in flares, review 79−44641
gamma-ray lines from flare, HEAO 1 obs. 80−67682
gamma-ray spectrum, 4-8 MeV range 77−53491
gap in 5250 Å region, spectrogram 77−49360
global oscillations affecting spectra, He abundance implications 80−51724
granular velocity vertical component, height depend., spectral obs. 79−66980
H_α high resolution obs. of active regions *(Japanese)* 78−89163
hard X-ray and radio events, spectral features rel. to particle accel. 77−45369
Hard X-Ray Burst Spectrometer on Solar Maximum Mission 80−51658
hard X-ray bursts, thermal model dynamic spectral characts. 80−98644
Hard X-ray Imaging Spectrometer on Solar Maximum Mission 80−51659
hard X-ray spectra, effects of backscatter on anisotropy and polarisation 78−28594
He I, He II, XUV emission lines, intensities and gross centre-to-limb behaviour 78−40888
He II Balmer 9 and 11 lines obs. 79−66981
hedgerow prominences, fine structure from spectral obs. 78−40906
high resolution UV spectrography appl. 79−25520
high-resolution spectroscopy, influence of solar rot. on surface vel. meas. 78−96403
inhomogeneous solar phenomena with different porosities, line profiles *(Russian)* 78−40891
IR atomic lines identification, 3.3-8 μ spectral region 77−45383
IR spectra, computer simulated, appl. to atm. fluorocarbon detect. 77−53217
IR spectral region atlas, 775 to 950 cm^{-1} and 1050 to 1300 cm^{-1} 79−48745
IR umbral intensity rel. to phase in solar cycle 78−69773
irradiation flux determ. in 150-210 nm range 77−17509
large-scale projection system at Flandrau Planetarium, Tucson 77−91433
limb darkening in 3033-7297 A range 77−53507
limb effect, Fe I line contours and shifts 77−13309
limb emission lines near Ca II H and K, spatial intensity vars. obs. 80−51720
limb spicules, time evolution study of spectra 77−2387
line asymmetries, radial movement effects 80−41792
line asymmetry meas. rel. to α Bootis (Arcturus) 80−51753
line blocking for 4006-6860 Å region 79−58306
line brightness fluctuations, statistical analysis *(Russian)* 79−21259
line formation depth *(Russian)* 77−64723
line formation depth in mag. field, theory *(Chinese)* 80−105159
line formation depth in solar atmosphere *(Polish)* 79−88639
line formation in unresolved magnetic element in photosphere 79−48750
line polarisation due to magnetic and vel. field inhomogeneities 79−5804
line polarisation in VUV, technique and data reduction 80−67691
line profiles, acoustic wave effects 80−46517
line profiles, rough reconstruction from series of narrow-band filtergrams *(Italian)* 80−98564
line profiles broadening, effects of finite sized eddies, Fourier anal. appl. 77−17500
solar spectra continued
line profiles calc. for inhomogeneous emission formations 79−25562
line profiles of active limb filament, OSO-8 UV obs. 79−44446
line shift obs. interpretation 80−51714
line shifts, meas. via automatic comparator 77−82123
line shifts, wave effects 80−109408
line shifts and asymmetries in sunspot penumbrae 80−51715
line shifts and asymmetry, appl. to solar atmosphere vel. field estimation 80−46530
line vels. and intensities of atmospheric waves, vertical propag., phase delay obs. 79−96981
line wings, polarized radiative transfer, excited state interference 80−105158
lines limb shift, effect of granular motion 79−12448
lines measured wavelengths, convective correction 78−93181
loop prominence kinematics 79−84774
loop prominence system, flare assoc., high temp. corona 79−53782
Lyman α line, wavelength and profile meas. 79−8896
Lyman alpha coronagraph 79−25486
magnetic fields measurement, multi-dimensional non-LTE polarised radiation transfer in mag. fluxtubes 78−69673
magnetic fields measurement by Fourier transform techniques, appl. to saturated and blended lines 77−22165
magnetic star phenomena *(German)* 77−67103
magnetosensitive line contours in active regions *(Russian)* 80−51718
McMath region 14943, optical obs., 1977 Sept. 79−48766
metallicity and UBV colours from spectral quantification 78−65577
micro-turbulence model test on flux spectrum 78−16365
microturbulent and macroturbulent filter functions, improved values 78−20796
microwave absolute flux, spectra of individual components 77−5461
microwave burst spectra, source inhomogeneities, statistical analysis 80−41805
microwave bursts, freq. spectra 77−13311
millimetre wavelength brightness spectrum, meas. 77−22171
molecular line haze opacity in sunspots 79−75188
multiplet lines, oscillator strength ratios calc. *(Russian)* 77−71073
noise storms, spectrum and position at decametre wavelengths 78−28622
non-LTE line formation in mag. field, two-level atom with freq. independent source function 78−61726
non-thermal vels. height variation 77−13344
observations and interpretation *(Italian)* 78−81604
oscillations in mag. tubes, spectral line obs. 79−25564
oscillator strengths of astrophysical interest 80−12656
photopshere spectrum, granulation vertical motions spatial and temporal behaviour 80−85912
photosphere, Ba II spectrum, partial freq. redistrib. 79−101128
photosphere, C, N, O, abundances 78−24497
photosphere, granular vels. around sunspots 77−29776
photosphere, line profile vars. with heliographic latit. 77−2383
photosphere, line shifts calc. from granulation vertical motion models 80−90375
photosphere, linear hydrodynamical eqns. coupled with radiative transfer, Mg I 5172 Å line interpretation 78−77529
photosphere, metallic line profiles var. with heliographic latit. 78−61837
photosphere, micro- and macroturbulence, spectrophotometric determ. *(Russian)* 77−56896
photosphere, microturbulent motions 79−75189
photosphere, spectroscopic search for polar vortex 79−5801
photosphere, struct. compared with chromosphere 77−29777
photosphere Fraunhofer lines formation, effects of 'microturbulent' vel. and damping const. *(Russian)* 80−12719
photosphere line asymmetries, appl. to vel. gradients retrieval via linearised approach 80−62093
photosphere line profiles for Na I and O I, acoustic wave effects 80−17558
photosphere lines, asymmetry appl. to stellar convection parameters meas. 79−21273
photosphere oscillations, PEPSIOS spectrometer obs. 78−93203
photosphere spectra, correction function for granulation mean vertical vel. determ. 80−62094
photosphere weak absorpt. lines, appl. to photosphere total vel. field determ. *(Russian)* 78−40894
photosphere-chromosphere transition region, spectra during eclipse June 30 1973 80−8614
photosphere-chromosphere transition region emission, spectral obs. in Hα region 79−35233
photospheric lines, response functions and contrib. functions 77−17462
photospheric network, dark component, Ca I 6103 line scan 77−29759
photospheric network structure from Mn I lines obs. 79−30039
photospheric oscillations depth depend. 80−31275
plage Ca II K-line, peak separation due to microturbulence 80−109407
plage development rel. to spectra and models *(Russian)* 77−64725
plage fragment temp. gradients determ. from equivalent width 80−98634
pores, line profile families rel. to total mag. flux 78−49408
prominence, 1969, October 15, Ca^+ lines obs. rel. to macroscopic motions 79−40167
prominence, EUV limb spectra, Skylab obs. 80−12717
prominence H I spectra, theory of Balmer line form. *(Russian)* 80−36609
prominence loop, 1973 Nov. 3, H I, He I and He II emission line spectra 77−64736
prominence model based on spectral obs. 80−31287
prominence outer regions, temp. and microturbulence *(French)* 77−53510
prominence spectra taken at Ondrejov Observatory, inclined spectral features obs. 80−62098
prominence streamers, rotational motions effects on spectral lines 78−49410
prominence-corona interface compared with chromosphere-corona transition region 77−29786
prominences, early H Balmer lines *(Russian)* 80−12718
prominences, emission line intensities rel. to model calcs. 79−44447
prominences, H line radiation diffusion 80−67694
prominences, H lines at submm. wavelengths *(Russian)* 79−35228
prominences, interpretation 80−4331
prominences, line profiles from expanding and escaping fine filaments 77−91499
prominences with filamentary struct., radiation transfer and line spectra 78−89154
pulsed microwave bursts with quasithemal spectrum model 77−78762

solar spectra continued
quiescent prominence spectra, meas. of Ca^+ 8542, 8498 Å, He 4471 Å and Ti^+ 4468 Å 80−90373
quiescent prominences, Ca^+, H and He line emission 77−29750
quiescent prominences, Ca II K spectra and vertical struct. of line of sight vel. field 77−53522
quiescent prominences, EUV obs. from Skylab 79−66987
quiescent prominences, Hα and Hβ emission line profiles 79−71011
quiescent prominences, Hβ, He D_3 and Ca II 8542 Å line emission meas. 78−32427
quiescent prominences, He I 10830 Å line emission obs. 77−29787
quiescent prominences, middle Balmer decrement meas. 80−12737
quiescent prominences, spectra meas. 78−40886
quiescent prominences, struct., and H and He spectra 77−13295
quiescent prominences, theory of Ca II emission lines 77−53523
quiet chromosphere, velocity waves propag. 77−22198
quiet corona, X-ray spectrum of highly ionised O and N 78−45297
quiet limb, emission measures, electron densities and nonthermal vels. from optically thin UV lines 77−17454
quiet-time near-IR variability 80−12729
radiation intensities, statistical anal. 77−53537
radio bursts, peak flux spectra, statistical anal. 80−98641
radio drift pair bursts, polarisation obs., position and freq. charact. 80−85925
radio emission, S-component spectrum fine struct. in 5.0 to 7.0 GHz freq. range 80−21977
radio emission spectral lines, plasma effects 78−96466
radio radiation, spectral polarisation obs. of local sources during March (1970) 77−53535
radio source spectral index in 1.9-3.5 cm range *(Russian)* 77−64732
radio spectrum to 10 km wavelength 79−92748
recorded by slit interference spectrograph 78−24866
registration using double-pass spectrophotometer with digital registration, precision *(Russian)* 79−96917
resonance line polarisation, non-LTE, absence of magnetic fields 79−80293
resonance line polarisation, non-mag., centre-to-limb var. 80−67678
resonance line scatt. from optically thin structs. located above limb 78−65591
resonance lines polarisation, theory for line core 77−29744
resonance multiplet lines, radiative transfer theory 78−24460
resonance radiation, multiple scatt. in nearby interstellar medium 80−41874
reversal wavelengths of H I, Mg II and Ca II lines, temporal var. 78−93186
rotation induced Doppler spectral shift meas. by scanning Fabry-Perot interferometer 80−77298
S-component, fine spectral structure in 4.5-7 GHz range *(Russian)* 77−33457
second-row elements, low lying levels, excitation equilib. and line intensities 79−12401
solar prominence, EUV spectrum rel. to horizontal temp. gradient meas. and prominence condensation 80−26832
spectral analogues, photoelectric scanner obs. of solar-type stars 78−40938
spectral type, from solar and stellar flux distribs. comparison 79−66970
spectral type and metal abundance, rel. to H-R diagram appl. 78−81619
spectroradiometry of daylight at sea level in Durban. 79−100955
spectroscopic differences between solar-type cluster stars and Sun 78−36560
spicules, line profile calcs. 77−91497
'spike' type radio bursts, morphological charact. and spectra 78−65599
Stokes profiles of lines, appl. to vector mag. fields determ. 78−28611
stratospheric HF acid, presence confirmed by solar spectrum obs. *(French)* 77−53105
sunspot, radiation transfer rel. to spectral lines polarisation 80−21964
sunspot, spectroscopic determ. of solar rot. 79−92745
sunspot, UV emission line spectrum obs. 77−13296
sunspot chromosphere, spectroscopic obs. rel. to radial vel. and brightness oscills. regimes *(Russian)* 80−51727
sunspot magnetic fields higher rot. rate at photosphere, Doppler meas. 80−46516
sunspot mangetic field gradients determ. from Zeeman line rot. and profiles *(Chinese)* 80−85920
sunspot penumbrae, fine struct. of mag. field and brightness 77−22179
sunspot transition region, emission meas. in far UV 77−78750
sunspot umbra, spectral synthesis in mag. field 77−17459
sunspot umbrae, Ca II H and K lines shapes and centre to limb. var. 77−22178
sunspot umbrae, IR Ca II lines 80−85918
sunspot umbrae, mag. field gradient from echelle spectrograms 77−33456
sunspot umbrae, material motions from Ti I 5713 Å obs. 77−45374
sunspot umbral spectrum, TiO rot. lines, temp. determ. 78−96451
sunspots, AlF lines intensities prediction 78−20803
sunspots, alkaline earth and rare earth oxides occurrence 78−85933
sunspots, FeH bands identification 78−7952
sunspots, FeH column densities rel. to Wing-Ford band identification 78−24507
sunspots, H_2 reson. fluoresc. with Lyman α 79−8821
sunspots, IR opacity due to molecular vibration rotation bands 80−41798
sunspots, MgO red and near UV bands calc. rel. to umbral spectrum 80−12736
sunspots, NO gamma system equivalent widths calcs. 79−12457
sunspots, O_2 Schumann-Runge band system in umbral UV spectrum 80−12735
sunspots, TiO equivalent width meas., theoretical interpretation, line form. process 80−72902
sunspots, Zeeman line profile, mag. field determ. 80−82221
sunspots umbras, outward wave propag. and motions in mag. tubes 79−16927
supergranular vels. from UV obs., height var. 79−30025
supergranule network features, emission spectra rel. to areas temp. depend. in transition zone 78−89152
surge, EUV limb spectra obs. from Skylab 80−17560
surge of 1961, Sept. 1, rotational and turbulent motions 77−91496
terrestrial atmospheric gases abundance determ. by analysing solar spectra 78−85643
time intensities, dielectronic recomb. excitation effects 80−82332

solar spectra continued
transition region instabilities, far UV spectra, relation to preflare energy build-up 77−17479
transition zone, density diagnostics for EUV spectrum 77−60739
transition zone, search for turbulent free region 78−4174
transition zone, Si IV line profile vars., rel. to MHD disturbances 78−28626
transition zone lines, quiet Sun, limb broadening, OSO-8 obs. 79−48752
type II radio burst, 1973, May 3, dynamic spectra obs. rel. to fine struct. 78−24501
type IIIb radio bursts, polarisation and spectra 77−22161
type V radio bursts, dynamic spectra distinctive struct. 80−46527
umbral spectrum in 6812-6898 Å range 79−101136
unidentified forbidden coronal lines, emission rates for Fe X and Fe XI transitions 77−17465
UV emission spectrum, beam-foil spectroscopy appls. 77−41314
UV line blending and wavelengths, spectral resolution influence 80−56811
UV line intensities brightness fluctuations during shock wave passage 79−66990
UV lines polarisation, effects on UV light polarisation at limb 78−45302
UV spectra, N III and O IV intersystem multiplets as plasma density indicators 80−31264
UV spectra, preliminary results from OSO-8 LPSP instrument 78−49317
UV spectral line identifications 78−16371
UV spectroscopy, review of high resolution obs. 78−45313
u.v. spectrum, absolute intensities in 1750-2100 Å range, vars. with solar activity 77−2405
UV vars. rel. to terrestrial climatic change 80−26607
vacuum UV centre-to-limb variation obs. *(Japanese)* 78−28604
velocity fields, large-scale, from Doppler line shift obs. 80−12730
visible spectra, balloon meas., stratospheric N_2O vertical distrib. determ. 78−61493
Voigt lines, random array, curve-of-growth function 78−89055
wavelength shift, Compton effect 77−53495
wavelength shift determ. method, appl. to C_2 molecule 78−49340
wavelengths of spectral lines and limb effect 77−49357
weak absorpt. features in Ca II H and K wings rel. to nonthermal broadening in photosphere 77−60735
weak Fraunhofer lines, effective depths of form. *(Russian)* 79−44438
weak Fraunhofer lines, effective form. depths tables *(Russian)* 79−44439
X-component sources, correl. with flare occurrence, EHF obs. 80−101579
X-ray burst, impulsive, from coronal source, spectral struct. 80−26836
X-ray emission from optically thin plasmas, abundance effects on continuum spectrum 78−53814
X-ray emission lines, differential emission measure solns. errors 79−12397
X-ray imaging spectrometer polychromator, solar obs. from Space Shuttle 80−17495
X-ray line spectra from transient flare plasma 80−98626
X-ray lines during flares, nonthermal excitation and polarization 79−44453
X-ray meas. by photometer on Prognoz satellites, description and meas. method 80−17462
X-ray spectra, hard X-ray imaging collimator 77−5437
X-ray spectroscopy with Bent Crystal Spectrometer 79−25489
XUV observations of 1973 June 15 flare from Skylab, allowed transitions 77−78730
XUV spectra, obs. by grazing incidence spectrograph on Skylab 77−60601
Al I, 1932 and 1936 Å autoionisation lines in solar flare, Skylab obs. 80−26829
B abundance, photoelectric meas. 77−29753
B-like ions, EUV emission density sensitivity 79−16910
B-like ions, highly ionised, up to Fe XXII, Breit-Pauli approximation 78−53810
Ba II 4554 A line, extreme limb obs. 77−53506
Ba II 4554 Å, obs. rel. to five-minute oscills. in solar atmosphere temp. min. 79−62808
Ba II 4554 Å solar resonance line formation, empirical NLTE analysis 78−53907
Ba III 4554 Å obs. rel. to five-minute oscills. horizontal energy flows struct. 80−62103
Be lines formation, non-LTE calc., rel. to solar Be I 2650 Å line misidentification 80−32636
C I 5380 Å, rel. to photosphere temp., luminosity vars. and global oscills. 77−53487
C I 5380 Å line sensitivity to temp. changes in static and oscill. systems 77−60743
C I 5380 Å response to solar luminosity vars., effects of granular convection 80−85910
C I isoelectronic sequence, forbidden transitions calc. 79−31444
C I multiplets at 1560 and 1657 Å, overlapping emission peaks obs. and theory 78−93178
C III 1909 Å and Si III 1892 Å emission lines, echelle obs. 80−31277
C III and O V emission line ratios, interpretation 78−28598
C III EUV lines, rel. to density diagnostics in non-equilib. plasmas 78−53899
C III line intensity ratios, Skylab obs. 79−53786
C IV 1548 Å line profiles of impulsive EUV bursts, OSO-8 obs. 80−90401
C IV 1548 Å profile in quiet region, interpretation 79−96980
C IV 1548 Å profile over sunspot, OSO-8 obs. rel. to transition zone dynamics 77−9728
C IV profiles at 1548 Å, OSO 8 time series rel. to chromospheric oscills. 79−53785
C V emission line ratios for corona transition region interpretation 80−98624
C_2 rotational temp. and photospheric models 80−62099
C_2, rotational temperatures, centre to limb behaviour 79−84758
CH, CH^+ lines in facula models, equivalent widths 79−66972
CH photospheric lines and $^{12}C/^{13}C$ atmospheric ratio determ. 77−5518
CO (A-X) band, equivalent widths of lines 77−17501
CO, centre to limb behaviour of first overtone vibr.-rot. transitions 79−8889
CO emission lines in UV spectra of sunspots and flare 79−53795
CO first overtone line centre-to-limb vars. and average facula models 79−80291

solar spectra continued
CO fluorescence in EUV solar spectrum, obs. 78−93184
CO, fourth positive system in 1115-4759 Å range 77−49291
CO IR spectrum rel. to atm. struct. and C abundance 78−28608
CO molecular layer optical depth and rotational temp. 79−96988
CO, rot. temp. of mols. in facula models 77−78740
CO, vibr.-rot. interaction, high excitation transitions in IR spectrum 77−68040
Ca I, Ca II lines, rel. to upper photosphere models, Ca abundance and damping parameters 77−33445
Ca I 6102, 6122, 6162 Å multiplet, collisional broadening 80−37777
Ca I 6573 Å and Ca II 7324 Å forbidden line, centre-to-limb behaviour 79−25572
Ca II, H and K line profiles vars. at solar minimum and cycle 21 onset 79−16907
Ca II 3737 Å emission line studies of prominences and flares *(Russian)* 80−51717
Ca II H and K line profiles rel. to temperature and electron density of chromosphere 78−53908
Ca II H and K lines cores in integrated sunlight, rel. to solar activity 78−77535
Ca II H-K and Na I D-lines, non-mag. polarisation 80−63569
Ca II H-line emission from Sun observed as star *(Russian)* 77−64727
Ca II K line emission widths 77−41373
Ca II K line with Doppler profile, progressive sound waves effect on absorpt. coeff. 77−60738
Ca II K_3-line chromospheric feature lifetime rel. to rotation 79−44442
Ca II K-line, centre-to-limb obs. of K_2 component *(French)* 80−82331
Ca II K-line, search for global oscillations 78−7959
Ca II K-line in quiescent prominence, influence of spatial resolution on line width and shift 80−77364
Ca II K-line network, giant cell circulation pattern 77−53546
Ca II K-line network in coronal holes 77−78752
Ca II line width, Wilson-Bappu effect 79−12464
Ca II network, giant cell circulations 79−8895
Ca ions, dielectronic recombination excitation in solar X-ray lines 80−51725
Co XI-XVII, $3s^23p^n$-$3s3p^{n+1}$ transition arrays, UV spectra classification 80−63570
Cr I in photospheric spectra, solar abundance and oscillator strengths 78−69757
Fe curve of growth split as function of atmospheric pressure 77−29794
Fe group elements abundances from singly-ionised lines 78−93189
Fe I, gravitational red shift, meas. 80−90391
Fe I 3737 Å emission line studies of prominences and flares *(Russian)* 80−51717
Fe I 5123.730 Å, Doppler shifts search rel. to 7 to 70 minute periods solar pulsations 78−93180
Fe I 5124 Å Doppler shift obs. rel. to oscillations 78−53905
Fe I 5250 Å line magnetic field meas. *(Russian)* 77−64724
Fe I even-odd and odd-even transitions, difference in curves of growth 77−25996
Fe I in photosphere, line broadening, Smirnov Roueff pot. calcs. 80−98632
Fe I line intensities and vel. fluctuations 79−8891
Fe I line profiles and magnetic field in quiet network regions of photosphere 78−69758
Fe I lines, 300 to 900 nm, microturbulence, Fe abundance, damping, oscillator strengths 77−5516
Fe I lines, 300 to 900 nm, of excitation pot. 0 to 1.01 eV, anal. via precise oscillator strengths 79−40155
Fe I lines, damping const. determ. preliminary results *(Russian)* 80−72900
Fe I lines, equivalent widths and microturbulent vels. determ. *(Russian)* 80−51719
Fe I lines, meas. of photospheric vel. field spatially-averaged props. 79−16912
Fe I lines, statistical anal., mag. line broadening 77−74028
Fe I lines limb shifts, effect of press. shifts in solar atmosphere 78−89150
Fe I low excitation lines, collisional broadening 80−37778
Fe I magnetosensitive lines, Stokes parameters *(Chinese)* 79−80289
Fe I weak Fraunhofer line profiles rel. to absorption coeff. *(Russian)* 78−20783
Fe I weak lines, 'microturbulent' vel. and damping const. rel. to photosphere Fe abundance *(Russian)* 80−12720
Fe II, Fe III, lifetimes, VUV beam-foil spectroscopy 79−22657
Fe II 5197.578 Å, brightness and vel. fluctuations rel. to photospheric wave propag. 77−22162
Fe II newly identified lines in limb spectrum 77−33442
Fe II spectrum, oscillator strengths and choice of solar model atmosphere rel. to Fe abundance 80−56791
Fe IX, Fe X, Ni XI, Ni XII, forbidden transitions, coronal spectrum 78−77537
Fe IX lines, appl. as coronal plasmas density indicators 79−44429
Fe IX radiative and collisional data rel. to coronal emission spectrum 77−49350
Fe, Kα fluoresc. due to solar flares 80−17569
Fe lines, equivalent widths for stellar spectral anal. 77−78771
Fe lines, wing shapes anal. 80−4317
Fe X, $3p^44s$ levels, population processes 80−47926
Fe XIII and XIV emission lines, Abel-inverted intensities rel. to coronal limb brightening 77−13299
Fe XIII coronal emission line polarization from mag. sublevels statistical equilib. 77−53492
Fe XIII forbidden emission lines, Si vidicon spectrometer obs. at 1973 June 30 eclipse 77−9657
Fe XIV 5303 Å coronal emission line polarisation obs. during 1973, June 30 eclipse 77−49352
Fe XIV 5303 Å emission line polarisation, coronal mag. field determ. *(Russian)* 78−16389
Fe XIX and isoelectronic ions $2p^4$-$2p^33d$ transition array 77−42267
Fe XIX-XII blend at 1.9 Å in flare X-ray spectra 79−96979
Fe XV 284 Å rel. to radio brightness temps. of coronal holes and arches 79−8893
Fe XV 284 Å spectroheliograms and rot. characts. of EUV coronal holes 77−53547
Fe XV coronal EUV line intensities 80−51731
Fe XVIII and XIX $2s^22p^n$-$2s^22p^{n-1}4d$ classification, for laser produced plasmas and solar spectra 77−42268
Fe XXI and isoelectronic spectra $2p^2$-2p3d transition array 77−38632
solar spectra continued
Fe XXI as electron density diagnostic in solar flares 79−44435
Fe XXII, coupling energy levels, oscillator strengths, electron collision energies 80−69068
Fe XXII, intercomb. transitions, oscill. strengths, transition probs., rel. to solar spectra 80−52935
Fe XXIV, dielectronic satellite spectra calc., solar flare spectra appl. 79−35123
Fe XXIV, dielectronic satellite spectra, solar flares appl. 80−32646
Fe XXIV, oscillator strengths, electron impact excitation collision strengths, solar flare spectra appl. 80−32647
Fe^+, gf values determ. in laboratory, for solar studies 80−42994
Fe-group elements, oscillator strengths for V I and Co I in photosphere 78−40905
FeH, partition function and equilib. const. 77−38626
H Balmer emission lines, Skylab obs. of quiet Sun and polar coronal hole 77−33440
H Balmer emission lines, Skylab obs. of active regions 77−33441
H emission spectrum, last observable line, rel. to solar obs. through Earth atm. 78−77536
H I, 584 Å reson. line profile and intensity meas. 79−40153
H I, Lyman-α and Lyman-β calibrated full disc profiles 78−93185
H I Lα/Hα ratio for flares, quasars and prominences 78−61826
H I Lyman α flux near solar minimum 80−90393
H I Lyman α profile and interstellar wind dynamics 80−8610
H Lyman α, radiation press. depletion of satellite atoms in collisionless planetary exospheres 79−96933
H Lyman α and β lines, OSO 8 disc centre obs. compared with theoretical profiles 79−8888
H Lyman α emission, absorpt. by hot interstellar H between Sun and Earth 80−31185
H Lyman α in chromospheric flares, direct collisional excitation rel. to profile and polarisation 80−41780
H Lyman-alpha, profile rel. to interplanetary H I parameters, OSO-8 meas. 79−2452
H to Ca, leading atomic lines 79−25560
H_2 emission in UV spectra of sunspots and flare 79−53794
H_2 lines, detect. in EUV solar spectra 78−12184
Hα, chromospheric, seven components form. rel. to 9873 MHz line appearance 78−89151
Hα emission line asymmetry in limb flares *(Russian)* 77−64728
Hα flocculi in 1971, January-April, flare correlation *(Chinese)* 77−67081
Hα line behaviour in photosphere, comparison with metal lines and continuum 78−57522
Hα plage formation after flare 79−44445
Hα spicules, dynamics at various heights, spectral obs. 80−90392
He I, D_3-line profile meas. with birefringent filter 78−4177
He I, He II XUV emission lines, intensity ratios and distrib. functions 78−57516
He I, in flare, levels population and emission lines optical depths 77−53538
He I 10830 Å line obs. in undisturbed chromosphere 77−71102
He I 10830 Å triplet in umbral spectrum *(Russian)* 80−36604
He I 5876 Å line emission, height distrib. in middle chromopshere 77−17525
He I 58.4 nm line profile, monitoring using resonance absorption spectrometer 80−62019
He I D_3 line, Stokes parameters for quiescent prominences, Hanle effect quantum theory 78−85924
He I D_3-line polarization in quiescent prominences, level-crossings effect 80−94772
He I in flare, lines optical depths and levels populations calcs. 79−62809
He II 304 Å, line profiles 79−12452
He II 304 Å and He I 10830 Å, spectroheliograms comparison rel. to line form. models 78−20799
He II Balmer α line components 77−33436
He-like ions, line intensities for stationary plasmas 78−53811
^{3}He 8666 MHz superfine structure line detection of ^{3}He-rich flares 80−109417
Hf abundance from Hf II spectral lines obs. 77−17518
K I 7699 Å, obs. rel. to Sun long-period global oscills. 79−2539
K I 7699 Å line meas. of sidereal equatorial rotation rate 79−44441
K I 769.9 nm line obs. of solar 5-min. oscills. 80−26838
La II, lifetimes, element relative abundance 78−17618
Li, Be, B, isoelectronic sequences, ionization equilib. balance, solar and stellar atms. appl. 79−36587
Li I-like spectra, energy struct., accurate semiempirical formulae 79−49970
^{7}Li and ^{7}Be gamma ray lines from $\alpha\alpha$ reactions 77−87248
Mg I, Mg II, reson. lines obs. in active region 79−40163
Mg I 2852 Å line sensitivity to partial redistrib. effects 78−7951
Mg I 4571 A line, extreme limb obs. 77−53506
Mg I 5172.7 Å, brightness and vel. fluctuations rel. to photospheric wave propag. 77−22162
Mg I and II line profiles comparison with theoretical spectra, visible obs. 80−82320
Mg I λ λ2852, supergranular line profile var. 79−40164
Mg II, line profiles rel. to chromosphere vel. gradients 77−17460
Mg II, reson. line fluxes rel. to chromospheric radiative losses 78−40915
Mg II core absorption, wavelengths meas. and evidence for atmospheric downflow 79−12451
Mg II h and k lines, Skylab high-resolution obs. 78−36544
Mg II h and k lines in active regions and network, wings rel. to photosphere models 78−57518
Mg II resonance-line wings, faint emission features obs. 78−32429
Mg II solar UV doublet obs. *(Japanese)* 78−61831
Mg II UV lines obs. above solar limb from Skylab 77−33450
Mg VII, UV lines, theoretical intensity ratios 78−90108
Mg XII, resonance line, atomic parameters calc. for dielectronic satellite lines 80−42983
Mg XII resonance line at 8.42 Å, new satellite line structure 78−53912
MgH rotational temp. and photospheric models 80−62099
$^{24}MgH^+$, high resolution rot.-vibr. spectra, solar atm. appl. 77−18939
Mn II, oscillator strengths, element relative abundance 78−17619
MnI, transition probability and solar abundance, beam foil TOF meas. 79−40154
N II, electron impact excitation cross sections, rel. to solar corona abundance 80−58391
N III lines for solar diagnostics 79−30031

solar spectra continued
N IV and Ne VII emission line ratios, electron density and temp. determ. 80−17559
N isoelectronic sequence ions, level populations and EUV line intensities for solar coronal conditions 80−51649
NO vibration-rotation bands, in sunspots, equivalent widths 77−2395
Na I D-line obs., Doppler width from intensity integral 80−41782
Na I D-lines, chromospheric formations beyond solar limb, filaments 79−96987
Na/Ca and S/Ca ratios, comparison with carbonaceous chondrites 77−29735
Nd II, branching ratios and transition probabilities, photospheric abundance 78−9104
Ne VIII, electron impact excitation 77−537
Ni I, effect on curve of growth of parity of spectral terms 77−53539
Ni I solar photosphere from oscillator strength obs. 80−98625
Ni IX to Ni XII transitions, laboratory wavelengths and identifications in solar spectrum 80−99474
Ni XII-XVIII, $3s^2 3p^n$-$3s3p^{n+1}$ transition arrays, UV spectra classification 80−63570
Ni XIX spectrum from coronal active regions X-ray spectra 77−2390
Ni XVII coronal EUV line intensities 80−51731
Ni XVIII XUV flare lines, oscillator strength meas. 79−5796
Ni(IX), resonance transitions, classification 80−42985
O as emission lines, Draper's 'discovery' and subsequent debate 77−37706
O I 7774.177 Å line asymmetry rel. to O isotope abundance in photosphere 77−17530
O I emission resonance triplet lines form. 78−24504
O I isoelectronic sequence, excited level populations, line intensity ratios, solar corona appl. 80−32637
O I like ions emission lines, density depend. 79−40165
O III, $^3P^e$—$^5S^0$, diagnostic studies of quiet Sun and coronal holes 80−48092
O III 374 Å, transition zone line, Bowen fluoresc. contrib. 78−93179
O IV, O VI line intensities, diffusion effects rel. to solar O abundance 80−4318
O IV solar intersystem line obs. in EUV, electron density at 10^5K 78−53903
O VII emission line ratios for corona transition region interpretation 80−98624
O VII line intensity ratios depend. on temp. and ionization balance 79−16903
O-like ions, Fe to Zn, intercombination lines, lab. obs. 77−3289
Pr lines in photospheric spectrum, Pr abundance 79−44443
S I, wavelengths of observed transitions between levels of ground configuration 78−50489
S I 1807 Å and 1900 Å lines, anal. of profiles 78−57517
S IV in solar atm., data from Skylab obs. 80−87028
S XI, UV lines, theoretical intensity ratios 78−90108
S XIV, splitting and oscillator strengths for $2s^2S$-$2p^2P^0$ doublet 77−49348
SH presence in sunspot UV umbral spectrum 79−75186
Se I lines in UV spectrum, predicted wavelengths 78−938
Si I series in UV spectrum, 3000 to 1200 Å 77−56882
Si II, Si III, chromospheric lines spectrum synthesis 78−36543
Si II, Si III, EUV emission line profiles, centre-to-limb vars. 78−28627
Si II 1816 Å line profiles and chromospheric vels., OSO-8 obs. 77−13301
Si II 1816.93 Å, line profiles and chromospheric persistent vel. fields, OSO-8 obs. 77−9730
Si II solar lines 1808-1817 Å, observed and theoretical profiles 78−49412
Si III 1892 Å emissivity, charge transfer effect on appl. of line as spectral diagnostic 80−41717
Si IV, 1122 and 1128 Å, obs. of nearby solar spectrum 78−4170
Si IV, 1393 Å line in coronal hole and quiet Sun, OSO-8 obs. 77−91511
Si IV 1393.8 Å, line profiles and transition region persistent vel. fields, OSO-8 obs. 77−9730
Si IX, UV lines, theoretical intensity ratios 78−90108
Si VI, VIII and XII, line intensities in transition region 80−31273
Si X-ray line emission from flares and active regions 79−25580
SiO (A-X) band, equivalent widths of lines 77−17501
SiO (A-X) system in sunspot UV umbral spectrum 79−75187
SiO isotopic lines in sunspots, for $^{28}Si/^{29}Si/^{30}Si$ isotopic abundance ratio determ. 79−30044
SiO vibration rotation bands in sunspots, equiv. widths at 8 μ 78−40903
Sm II, photospheric abundance, spectral transition probability, 3000-7000 Å 79−31453
Sn abundance from Sn I line intensity profiles 78−20772
Ti abundance from weak spectral lines obs. 77−29778
Ti I lines, oscillator strengths and solar Ti abundance 78−45306
Ti I lines, transition probabilities and solar Ti abundance 77−29743

solar system
see also celestial mechanics; planets; Sun
$^{129}I/^{127}I$ early solar system chronometer 80−62043
abundances of nuclides and nuclear structure 77−82130
Allende meteorite coarse-grained inclusions, trace elements and condensate phases 78−49401
angular momentum distrib. and formation *(Chinese)* 77−67049
apex of motion, correl. with long-period comets perihelion points distrib. 80−4304
asteroid concentrations in proper elements space, statistics and mapping 78−96420
asteroidal belt, cosmogony 77−13275
asteroidal belt, restricted three-body problem rel. to orbital characts. 79−8874
asteroids, early history, coalescence prevention by Jupiter 79−5774
asteroids in vicinity of 1:3 commensurability with Jupiter, orbital evolution, model calcs. results *(Russian)* 80−36486
asteroids primordial metamorphism via elec. induction in T Tauri-like solar wind 78−69728
celestial mechanics, perturbed potentials effects on libration points stability in restricted problem 80−4241
Chamberlin-Moulton cosmogony, rise and fall 78−32641
Chamberlin-Moulton cosmogony 78−86104
chemistry of primitive solar material, review 77−25959
chondrites and C1 carbonaceous chondrites origin, rel. to solar gases in meteorites 79−71008

solar system continued
coherent radio emission in nature, theory, solar system and pulsars appl. 80−46393
cold-cloud aggregates, chemical energy and meteorite chondrule origin 80−105210
collisions and interactions in early solar system 77−73977
collisions with interstellar clouds, obs. explanation *(French)* 77−74036
comet belt beyond Neptune, existence rel. to short-period comets origin 80−94759
cometary cloud, orbital evolution under perturbing influence of giant planets and nearby stars 80−98613
cometary nuclei origin in presolar nebula, dust gravit. instability 79−2523
cometary orbits, reciprocal semimajor axes accuracy 80−62074
comets, composition and struct. rel. to origin of solar system 77−78717
comets, long-period, distribs. of inclination of perihelion dynamical implications 80−101563
comets, nearly parabolic orbits, distrib. of nodes and perihelia 80−67661
comets, primordial, interiors radiogenic melting 80−67659
comets origin, implications of anomalies of orbital inclinations distrib. of original comets 80−98615
commensurabilities 80−109418
computer simulations of planetary system evolution 80−94733
conference on planetary sciences Rome, Italy (Apr. 1979) 80−77537
constants numerical values, from Joint Report of IAU Commission 4 Working Groups 78−40845
continual matter accretion, elemental heterogeneities 79−2489
cosmogony, exact soln. of general relativity eqns. for oscillatory collapse *(Russian)* 77−87256
cosmogony 80−41736
cratering, as key to system history 77−82132
critical ionisation velocity in gas mixtures, lab. expt. 78−67307
development, chemical and gravitational crystallisation of solar nebulae *(Hungarian)* 80−72795
development, rel. to distrib. of mean motions of planets and satellites 77−91451
dynamic processes on Earth, extraterrestrial causes, rel. to extinction of life 78−92820
dynamics, stability of motion 77−9679
dynamics and long-term stability 79−40095
early chronology, determ. from ^{187}Re-^{187}Os systematics in meteorites 80−41778
early chronology rel. to U-Th-Pb of Saint Severin amphoterite 78−65560
early collisional history, evidence from early lunar chronology 77−60640
early differentiation of basaltic achondrite parent body, two-step evolution 78−65561
early solar nebula, isotopic anomalies injection 79−101094
early solar nebula, primitive dust material evaporation metamorphism 79−58279
early solar system, mass removal by outer planets 78−53841
early solar system, minor planets EM heating 80−36555
early solar system magnetic fields, rel. to fields of terrestrial planets 78−12125
proto-Earth, formation of inhomogeneous Earth from nebula 80−90348
Earth and Moon origin, book 80−17266
Earth-Moon system, lunar capture hypothesis revisited 78−81570
electrostatic instabilities role in critical ionisation vel. mechanism 78−67355
elliptic motion of solid body gas drag effect 77−33362
energy loss and modulation of galactic cosmic rays 78−32308
exploration programs, United States 78−77461
extinct radioactivities in meteorites, as trapped residuals of presolar grains 77−49342
extinct radioactivities in meteorites, trapped residuals of presolar grains 77−45367
extraplanetary mission possibilities 80−17466
fluid drops as cosmological models, stellar evolution, solar system origin, planetary geology 80−73086
formation, grains ejected from supernovae rel. to isotopic abundance anomalies 77−87285
formation, numerical expts. on planetsimal aggregation 78−69713
formation, origin of Kirkwood gaps and satellite-satellite resons. 79−16867
formation, re-evaporation of condensed matter, evidence from meteorite mineral content 78−85864
formation, role of supernovae, isotopes found in primitive meteorites 79−44380
formation, supernova trigger for collapse of interstellar cloud 77−37512
formation from supernova trigger, implications for Mg and Al isotopic abundances 80−90406
formation of Jupiter, evidence from atmospheric comp. deduced from absorpt. bands in refl. sunlight 80−56758
formation of planetary system, Titius-Bode law 80−62057
formation theory based on evidence from meteorite composition *(French)* 79−92687
formation theory based on Laplacian hypothesis 80−85876
Fulton's orrery, 19th century instrument to demonstrate planetary system motions 78−69695
galactic cosmic rays access at polar heliographic latits. 77−25893
gas condensation and periodic reactions 79−62764
gas condensation chemistry 79−35155
grain accretion in protoplanetary nebula, liquid drop effects 78−85862
grain formation by nucleation, astrophysical environment 78−16501
grain motions in the solar nebula 79−84686
grain sedimentation in solar nebula 77−87284
gravitational contraction of protosun and Laplacian gas ring shedding 79−62765
gravitational potential of solid bodies 78−77550
heliosphere, solar wind interaction with interstellar matter *(Polish)* 78−61696
inner planetary systems, stability 79−70975
interplanetary dust, symmetry plane in inner solar system 80−56767
interstellar cloud encounter, terrestrial consequences 78−57292
interstellar cloud impending encounter evidence 78−93352
interstellar dense clouds encounters, effects on solar wind and comets *(German)* 80−109500
interstellar dense clouds encounters 77−87497
interstellar dust penetration, Lorentz force versus gravit. focusing 77−13315

solar system continued
interstellar gas parameters change in stellar-wind-dominated environment, rel. to solar system 78−61904
interstellar grain component in meteoritic inclusions, spectroscopic evidence 77−25987
interstellar grain streaming 80−26810
interstellar wind, Mariner 10 meas. of Lyman α and He I 584 Å interplanetary emissions 78−65474
interstellar wind properties from Lyman α and He I 584 Å interplanetary emissions 78−65475
isotopic abundances, cosmoradiogenic ghosts and origin of Ca-Al rich inclusions 78−12162
isotopic anomalies and proton irradiation in early solar system 77−49317
isotopic anomalies from neutron reactions during stellar explosive C burning 80−12651
isotopic anomalies in the early solar system 79−25522
isotopic anomalies rel. to supernova neighbour or presolar carriers model 78−12110
jet stream formation in early solar system 78−69711
Jupiter-Saturn-Sun systems, long-term numerical solns. 78−24450
Kirkwood gap 1:3, width *(Russian)* 80−36559
late heavy bombardment in inner solar system 77−71019
local interstellar medium, He component anal., UV obs. 79−30100
long-period comet loss, planetary collisions 80−77358
lunar composition determ. by solar nebula conditions and processes 79−2492
magnetic field of solar nebula, Allende meteorite chondrule record 80−36520
magnetic fields in early solar system, recorded in lunar rocks, meteorites and planets 79−5765
Mariner 10 UV spectrometry of inner solar system 77−45337
massive planet in asteroid belt, existence and removal, Ovenden's hypothesis 79−2502
massive protoplanets orbital stability in terrestrial planet region 79−66931
material distrib., effect of Jupiter close encounter with planet crossing bodies 80−77329
meteorite components primordial condensation, expt. evidence of source medium state 80−26816
meteorite condensation from solar nebula, enstatite chondrite petrology 80−51699
meteorite flux recent temporal changes, from lunar sample data 79−2534
meteorite magnetism as probe of early solar system 80− 36597
meteorites, aggregation rel. to matrix textures in unequilibrated ordinary chondrites 77−87340
model solar system, at Michigan Space Center 78−69653
motion and cosmic background radiation anisotropy 80−105407
mutual gravitational potential of N solid bodies, harmonic coeffs. expansion 79−12390
'mysterite' as late condensate in solar nebula, H6 chondrite evidence 78−7946
NASA planetary missions planning 79−5732
nearby supernova encounter, rel. to Earth ice ages and biological catastrophes 77−29662
nebula, aerodynamics of solid bodies 77−64670
nebula, charged dust accretion rel. to Fe, stone and planetesimal formation 78−28548
nebula, chondrules origin 80−4310
nebula, condensation rel. to lunar element correls. and bulk comp. 77−60637
nebula, condensation temps. rel. to Trojan asteroids comp. 80−56751
nebula, distrib. of pre-solar component in carbonaceous chondrites 77−37582
nebula, evidence for strong mag. fields from ureilites mag. props. 80−8602
nebula, fine dust grains clustering and sedimentation time 80−26937
nebula, form. of Fe-Ni-Si planetary cores 78−12112
nebula, fractionation rel. to chemical comps. of Moon, Earth and eucrite parent body 77−60636
nebula, Ga, Ge and Sb condensation rel. to Fe meteorites chemical classification 80−36594
nebula, high-energy events rel. to chondrule form. 77−29734
nebula, N isotopic comp. vars. rel. to $^{15}N/^{14}N$ ratios in carbonaceous chondrites 80−46496
nebula, particle-to-particle collisions rel. to chondrule form. 77−82178
nebula, physiochemical mechanism of planetary system form. 79−8857
nebula, primitive, interaction with giant gaseous protoplanets, computer anal. 80−56727
nebula, rare earth element condensation and fractionation 80−72796
nebula, rel. to abundance pattern of primordial noble gases in chondrites 78−32424
nebula, role of grains as isotopic anomalies carriers 80−26757
nebula collapse, supernova trigger, evidence from meteorites isotopic anomalies 78−77499
nebula cooling rate, by Allende meteorite I-Xe date 80−67666
nebula differentiation into planets, $^{15}N/^{14}N$ ratio 80−36519
nebula evolution, motion around a source whose luminosity changes 79−12394
nebula temperature, cosmothermometry via Ti^{3+}/Ti^{4+} ratios in Allende meteorite 79−12437
nebular origin NH_3 synthesis, kinetic model 80−62041
nebular primordial mag. field, meas. from Allende meteorite chondrules 78−49399
neutral gas-moving magnetised plasma interaction, Alfven critical vel. 78−69670
noble gases isotopic anaomalies in Murchison meteorite, evidence for stellar condensates 80−41772
nucleocosmochronology, model, r-process elements discrete addition to presolar cloud 78−4121
nucleosynthesis in solar nebula, possible explanation for isotopically anomalous Xe and normal Os in Allende meteorite 77−45368
Oort cloud, existence, review 77−87326
Oort comet cloud, origin 78−57502
orbit-orbit resonances, varieties and similarities 78−4093
orbital resonances, review 77−25998
organic matter origin, anal. of organic polymer in carbonaceous chondrites 78−20767
origin, accretion temp. of Tieschitz H3 chondritic meteorite 79−75166
origin, book 78−85865
origin, Earth early history 79−20739
solar system continued
origin, genetic implications of trace element distrib. in Allende inclusions mineral separates 78−49400
origin, implications of cosmic snowballs (comets) *(German)* 79−80275
origin, implications of mineralogy and petrology of isotopically unusual Ca-Al rich inclusion HAL in Allende meteorite 80−109399
origin, large, late-stage planetesimals growth 79−96931
origin, late nucleosynthetic event rel. to isotopically anomalous Ag in Santa Clara and Pinon Fe meteorites 80−85902
origin, new tidal theory 78−93131
origin, numerical simulations of collisions in Keplerian systems 80−109342
origin, particular soln. of restricted three-body problem in resisting medium *(Italian)* 80−90325
origin, planets rotation periods and relative formation times *(Chinese)* 80−105182
origin, protosolar OB association supernovae rel. to Allende isotopic anomalies and cosmochronology 80−4462
origin, relation to supernova explosions 80−17509
origin, role of nearby supernova 80−82232
origin, supernova trigger, Allende meteorite evidence 80−12683
origin, theories of 77−25957
origin, tidal model and Roche problem for polytropes in central orbits 80−82179
origin *(Chinese)* 78−20659
origin and history to earliest geological times, rel. to origin of life 78−69923
origin implications for transneptunion planets and nature of long-period comets 79−8856
origin rel. to meteorites 77−91490
origin theories critical review *(Chinese)* 77−22117
osculating elements reduction to proper elements for entire solar system 80−21897
outer asteroid belt, rel. to mini planet between Saturn and Uranus 78−20721
outer planets and satellites form. theory *(Chinese)* 78−69712
outer solar system, mass distrib. and planet form. 80−77349
periodic orbits families, existence in N-body problem 78−24449
physical parameters, determ. from Viking lander radio tracking data 78−20685
planet formation by successive contractions of solar nebula 78−85863
planet formation process, conservation laws and mass distrib. 78−81565
planetary accretion dynamics, computer simulation, sensitivity to initial conditions 77−82131
planetary accumulation, masses of largest bodies and relative vels. *(Russian)* 79−35160
planetary evolution, solar influence 78−49348
planetary exploration, neutron-gamma techniques 79−53728
planetary exploration methods, appl. to planetary atmospheres and solar nebula theory *(Czech)* 78−32374
planetary formation as adiabatic phase transition, isoentropic model 80−26763
planetary orbits major axes invariability, applicability of Poisson's theorem in heliocentric variables *(French)* 78−85829
planetary orbits stability, soln. to Poincare problem in celestial mechanics 78−28492
planetary satellites capture due to gas drag in primordial circumplanetary envelopes 79−53741
planetary sciences, AAS meeting (Honolulu, 19-22 January 1977) 78−4127
planetary system accumulation model, numerical expts. results *(Russian)* 80−8557
planetary system evolution from preplanetary gas disc, rel. to crystallisation and cryst. struct. *(German)* 78−93129
planetary system formation models 80−62058
planetary system origin, comparison with close binary systems 79−5859
planetary system origin, model comparisons 80−17508
planetesimal population, equilib. vels. 80−31219
planetesimal relative vels. and early accumulation of planets 79−58283
planetesimal theory, origin 77−87623
planetesimals in primitive solar system, statistical behaviour 78−93130
planetesimals long-term behaviour and planets formation 77−91450
planetesimals to planets: numerical simulation of collisional evolution 78−85861
planets, formation with Fe cores in early solar system 78−85869
planets and satellites formation from self-similar discs 79−80248
planets formation, appl. of statistical mechanics of perturbed Keplerian orbits 77−49269
planets growth in protoplanetary nebula *(Russian)* 78−69715
planets in terrestrial group, limiting masses, distances and accumulation times 79−8858
planets rectangular coordinates, approximation via Chebyshev polynomials *(Russian)* 80−62033
planets spin angular momentum distrib. explanation 80−41741
plasma physics, magnetospheres, book 79−84696
plasma physics, solar and solar wind, book 79−84782
plasma physics, solar system plasma processes, book 79−84625
Pluto's satellite, cosmogonical implications *(Chinese)* 79−84744
pre-stellar interstellar dust 79−84844
precondensed matter rel. to early solar system 79−58280
presolar gas components, isotopic anomalies in Murchison C2 chondrite 80−85904
presolar grains from supernova ejecta, rel. to meteorites isotopic anomalies 78−20845
presolar nebula birth, condensation sequence revealed in Allende meteorite 80−26758
presolar nebula collapse 79−58281
primaeval magnetic field intensity determ. from Jilin chrondrite *(Chinese)* 78−85917
primitive grain clumps and organic compounds in carbonaceous chondrites 77−2374
primitive nebula, magnetic field 79−16847
primitive solar nebula, equilib. chemistry thermodynamics calcs. 80−82231
primitive solar nebula, H_2 ortho-para ratio and evolution of planets 78−89233
primitive solar nebula evolution rel. to solar accretion disk 78−81566
primordial magnetic field, during meteorite parent body era 78−45293
primordial metal grains, thermal history 79−40097
primordial nebula conditions rel. to Fe meteorites comp. 79−30021
primordial refractory metal particles 80−85906

solar system continued
primordial solar nebula, struct. and evolution 80−62042
proton-associated alpha-irradiation in early solar system, search for possible ^{41}K anomaly 78−49398
protoplanet, solar wind sputtering rate 80−85835
protoplanetary cloud, ang. momentum transfer by meridional currents 77−83436
protoplanetary cloud, history rel. to Earth and planets atmospheres origin *(Chinese)* 79−16846
protoplanetary cloud blow-off by T Tauri like solar wind 78−45243
protoplanetary disc nebula disruption by T Tauri-like solar wind 80−36516
protoplanetary eruptive evolution and comets 79−70969
protoplanetary nebula, grain accretion time and mass limit 77−73976
protoplanetary orbits, effects of resisting medium 77−73978
protoplanets, isolated giant gaseous, struct. and evolution 79−75123
protosolar nebula, CO and N_2 reduction in solar nebula, kinetic inhibition 80−85875
r-process elements, abundances rel. to stellar He burning shells explosive neutron processing 79−58302
r-process nuclei, isotopic anomalies 79−5740
radar astronomy 77−25947
radiation forces on small particles in solar system 80−17461
refractory lithophile elements, condensation and fractionation 80−36517
relativistic celestial mechanics, astron. meas. and coord. systems 80−36481
relativistic effects verification, comparison of obs. results with theoretical data *(Russian)* 79−80209
ring systems around giant planets, origin 78−32373
satellite systems of major planets, form 78−69714
satellites accumulation, circumplanetary swarm model 78−28549
satellites direct and retrograde orbits, limiting radii and appl. to solar system and stellar systems 79−88572
solar companion star, evidence from pulsar period derivatives 78−12198
solar companion star effects on orbits of comets 78−81567
solar motion constants, determ. for AGK3 proper motion system in polar region *(Russian)* 80−12647
solar nebula and planetary system, mass distrib. 78−12109
solar nebula evolution, giant planet formation, gaseous envelope instability 79−12415
solar nebula fractionation, Th, U, Pu and Cm condensation 79−35154
solar nebulae, mass transport processes in rotating dust cloud 80−8556
solar terrestrial physics, symposium, Innsbruck, (May to June 1978) 79−58278
solar wind resistive effect on solid body orbits 77−73979
spaceflight and solar system colonisation 77−49263
stability, higher-order, in restricted three body problem 77−13208
stability and evolution review 80−82235
stability from origin of Solar System tidal friction considerations 80−82233
structure beyond Neptune, possible asteroid belt, cosmogony *(Russian)* 80−82237
structure of the universe, book 78−32628
Sun and heliosphere, conference, London, England (1979 April 3 to 4) 80−82574
Sun companion star, reality questioned 78−57475
Sun possible compact companion, mass, vel., and luminosity 79−2490
Sun T Tauri phase, appl. to carbonaceous chondrite fission Kr and Xe origin 79−35199
Sun-Earth-Moon system stability, Hill's problem 77−70985
Sun-Jupiter case, plane-symmetric periodic orbits 79−58235
Sun-Jupiter system, tidal torques theory for asteroid belt truncation 80−98596
Sun-Jupiter-Saturn system, stability with bifurcation theory 77−53406
swirling particle fluids, computer studies, evolution of planetary-type bodies 79−35121
teaching model for corridor display 78−86095
terrestrial planets, origin and evolution *(German)* 77−71039
terrestrial planets accretion, shock degassing rel. to atmospheres origin *(Russian)* 79−101099
three-body problem, restricted, bifurcation orbits, Sun-Jupiter case 79−84647
tidal interactions, consequences and inferences 77−87297
tidal theory for origin of solar nebula 79−84687
tidal torques on circumbinary accretion discs, theory, commensurable satellites form. appl. 79−70952
Titius Bode Rule for solar planets and planetary satellites, c.f. Bohr atomic orbitals 79−101057
Titius-Bode law, existence of space for more than ten planets 78−40851
Titius-Bode law for planet distances from Sun 80−82236
Titius-Bode law rel. to satellites of outer planets *(Swedish)* 78−85870
Twin City (Georgia) meteorite, place of origin from alloy struct. 78−65567
zodiacal cloud, symmetry plane from photopolarimetry and brightness annual vars. 78−45276
^{26}Al and partial ionization of solar nebula 79−58282
^{26}Al, as planetoid heat source in early solar system 78−65511
^{26}Al from red giant stars rel. to meteorite ^{26}Mg content 80−67712
^{26}Al in early solar system, fossil or fuel 77−17387
^{26}Al, search for effects in Allende meteorite FUN inclusion Cl 79−16896
B abundance, carbonaceous chondrites meas. 79−16897
B abundance determ. from carbonaceous chrondrites 77−49318
$BaTiO_3$ particulates coagulation in solar nebula 77−53434
C isotope ratio, in comets, stars, and interstellar matter 79−5766
^{247}Cm evidence from Allende $^{238}U/^{235}U$ ratio 80−90347
D/H ratio in early Solar Systems, H and O isotope study in chondritic meteorites 80−36518
Fe abundance rel. to nucleosynthesis 77−53435
Fe/silicate fractionation and origin of Mercury in inner solar nebula 78−85873
He during solar nebula evolution, solar He incorporated into Earth *(Russian)* 80−81856
Li, 'cosmic' abundance from sample activation anal. 78−12111
^{26}Mg negative anomalies and ^{26}Al, effects of proton irradiation on gas phase with condensation 79−13289
Ne-E, anomalous meteoritic Ne component, thermonuclear origin, supernova models 78−45292
^{22}Ne anomalous abundance in Orgueil meteorite, evidence for presolar grains 80−41773
solar system continued
^{16}O and ^{26}Al isotopic anomalies, local proton irradiation model 78−93128
^{107}Pd existence in early solar system, evidence from meteorites 79−40096
^{244}Pu, existence in early solar system 77−29663
Sr anomalies and p-process odd-A abundances 78−93101
Te, Xe and Kr isotopes in Allende meteorite, record of nucleosynthesis 79−40147
U, isotopic composition in chondritic meteorites, origin of anomalies 78−4157

solar-terrestrial relationships
20 year cycle of sunspots and climate, Greenland ice core records anal. 79−88470
1970, March 8, midlatit. ionospheric disturbances caused by high energy particles 77−60517
1971 December 14 to 21 event, pattern of 6300 Å emission over polar cap 79−75012
1972, August, polar cap absorpt. event. optical aurora diagnostics 77−29567
1972, August, solar flares, ionospheric and thermospheric responses 77−25858
1972, August 4-7 flares, incoherent scatt. radar obs. of ionosphere 77−45248
1972, August cosmic ray storm, north-south anisotropies and related phenomena 78−89018
1972 August proton event and atmospheric O_3 layer 79−35227
1977, August to October, geomag. activity assoc. with solar McMath region 14943 79−48625
1978 May 7 events, radio, optical and geophysical manifestations *(French)* 80−8611
air temp. in Tbilisi rel. to solar activity (1848-1970) 80−26595
atmosphere, solar activity effects, surface press. maps during geomag. disturbances 77−78359
atmosphere gravity waves generated during solar eclipse, obs. 78−88887
atmosphere near sea level pressure, solar influence on N.Atlantic 77−87033
atmosphere total O_3 content, monthly averages correls. with solar activity vars. 79−16571
atmosphere vorticity area index, correl. with solar plages 78−73459
atmosphere water vapour of extraterrestrial origin, possible role in Sun-weather relationships 78−69416
atmospheric circulation changes correl. with solar and interplanetary mag. sector struct. 80−17340
atmospheric electricity, potential gradient sunrise effect 77−45089
atmospheric electricity supply current, solar modulation 80−17329
atmospheric electrification, solar modulation and possible implications for Sun-weather relationship 78−57261
atmospheric O_3 global monthly vars. correl. with solar activity 78−85664
atmospheric O_3 profiles rel. to solar mag. activity 78−65373
atmospheric pressure, geographical dependence of solar-atmospheric connections 79−25315
atmospheric pressure field, vars. in periods of high and low geomag. activity 78−36245
atmospherics noise variation with sunspot number during 1600-2000 hours at Delhi 78−49083
auroral activity, equatorward extent (1973-4) during solar cycle 20 decline 79−12328
auroral changes during 18th and 19th centuries, implications for solar wind and sunspot activity long-term vars. 80−98498
ball lightning correl. with solar activity, comment 77−81972
ball lightning correl. with solar activity, comment 77−87017
ball lightning in Holland rel. to solar activity 77−21840
biosphere and active solar processes link, role of Earth's natural electromag. field 78−61211
Bombay geomagnetic and climatic (1848-1967) data rel. to sunspot nos. 80−81811
climate change, model of internal and external causes 79−16637
climate link with solar activity, from tree ring meas. of atm. ^{14}C 80−101424
climate over last 250 million years, global heat balance 80−46252
climate var. rel. to almost intransitive Sun 79−21255
climate var. rel. to solar activity and solar constant change 78−28301
climate-sunspot relations, statistical evidence from long-term temp. records 78−69439
climatic change, effect of solar convection efficiency and solar const. time vars. 79−21262
climatic changes, rel. to equatorial solar rot. 78−7960
climatic fluctuations in 1870-1969 period, statistical study of likely causes 78−7751
climatic var. induced by magnetic field screening of cosmic rays 77−78398
coronal activity effect on radar meteor rate 80−67662
coronal holes, rel. to recurrent geomag. storms 77−56893
coronal holes, solar wind streams and geomag. activity during 1976-77 period 79−25570
Cretaceous-Tertiary extinctions, effects of solar flares and stratospheric aeronomy 78−32215
Cretaceous-Tertiary extinctions, effects of solar luminosity vars. and super solar flares 78−32435
crochet associated solar microwave bursts, nature 78−69772
D-region, daytime solar proton event-disturbed model 78−93038
D-region, polar electron density profiles during solar proton event, from VLF refl. height vars. 79−8764
D-region, radiowave absorption during solar minimum, 2.5-4.1 MHz 80−41628
D-region, solar X-ray control of ionisation 80−77198
daily geomagnetic variations at Sabhawala and Hyderabad, inverse correl. with solar activity 79−44097
daytime F_2-layer simulation, selection of short-wave solar radiation flux 78−45087
E_s-layer, h-type, solar cycle var. in occurrence at Uppsala 78−81497
E-region critical penetration freq. var. with solar activity 78−7828
E-region horizontal drifts, search for solar cycle var. at Ibadan 78−36390
E-region ionisation and magnetic variations with UT, season and solar activity 77−13151
E-region ionisation by solar UV and X-rays, effect of neutral atmosphere seasonal vars. 79−12331

solar-terrestrial relationships continued
Earth annual polar motion, many-year variation rel. to solar eleven-year cycle *(Chinese)* 80−104848
Earth core torsional oscillations, induced by Sun 78−44793
Earth diurnal rotation, irregular vars. correl. with solar wind vel. 79−8591
Earth rotation modulated by solar cycle 80−56336
Earth rotation nonuniformity, possible connection with Sun high-latit. mag. field 80−46119
Earth rotation rate, sunspot numbers and K_p index, anal. of vars. in 10-100 years range 77−90980
Earth storms, initiation and propag. from solar flares *(Korean)* 77−53335
Earth tides observations, solar gravit. field screening effects *(Russian)* 78−88787
earthquakes, strong, correl. with solar activity rel. to occurrence time forecasting 79−53315
earthquakes numbers, rel. to solar activity *(French)* 77−17027
easterly gales of N.Atlantic, 1881-1970, rel. to 80-90 yr solar period 80−77101
EM field of Earth, conf., Hurbanovo, Czechoslovakia (Oct. 75) 79−39646
energy orders of magnitude in solar-terrestrial relations *(German)* 77−70940
equatorial counter-electrojet, afternoon events occurrence correl. with sunspot minimum 80−56672
equatorial counter-electrojet, geomag. aspects and solar cycle depend. 78−36367
equatorial spread-F, solar cycle effects at Huancayo 78−61647
European Grosswetterlagen, temporal vars. and correl. with solar indices 79−58081
EUV indices for solar-terrestrial relations 77−9731
evolution implications for Earth's early atmosphere 78−36285
exosphere, global temps. and densities under active solar conditions 77−33234
exosphere, solar activity influence on satellite particles 79−101097
F_2-layer, electron density long-period variation f_0 evidence 80−56667
F_2-layer, f_0F_2 vars. solar activity depend. and hemispherical differences 78−69603
F_2-layer, geometrical parameters and critical frequencies, solar activity dependence study 80−4182
F_2-layer critical frequency, forenoon bite-out solar-cycle var. 78−65453
F_2-layer nighttime ionisation latit. depend., var. in solar activity cycle 79−53617
F_2-layer thermal plasma interhemispheric flow in closed mag. flux tube, sunspot min. conditions 78−93035
F-region, equatorial anomaly, solar cycle and seasonal variation of electron content 80−41622
F-region, n_2F_2 annual vars. with latit. and solar activity level 78−69577
F-region, range and freq. spread F rel. to solar cycle 78−32292
F-region, solar activity rel. to temp. and electron density 80−46337
F-region peak electron density, diurnal and solar cycle variation 80−61949
F-region temperatures at Malvern and S. Santin, correl. with scalar 10.7 cm flux 77−91360
flare effects in ionosphere, sudden frequency deviations and phase anomalies *(Italian)* 78−96345
flare effects on geomag. pulsations 78−28424
flare effects on ionospheric circumpolar currents 78−49198
flare modification of stratospheric elec. fields, direct evidence 79−48553
flare proton intensity north-south asymm. rel. to plasma sheet and daytime polar cusp dynamics 77−17297
flare UV radiation spectral energy distrib. calc. from sudden freq. deviations 78−69771
flare X-rays effects in terrestrial upper atm., ionisation, Auger electrons form. 78−53767
flares, quantitative relationship between 1-8Å X-ray flux and D-region VLF phase deviations 77−87170
flares effects on cosmic ray and geomag. vars. 79−84764
flares Fe XXV 1.87 Å line emission effects on lower ionosphere ionisation 78−65588
flares interaction with ionospheric D-region, relaxation after sudden cut-off of ionisation source 77−33254
flares magnetic effects and elec. field in auroral electrojet region of ionosphere 78−69576
flares of 1972 August 2-4, ionospheric VLF sudden phase anomalies 78−40739
flares radiation dose at Earth's surface 79−25109
flares X-ray and EUV emission, empirical models rel. to E-region and F-region effects 77−5515
formation by solar flare particles 78−92886
gamma-rays, hard intensity radiation pulsations in the atmosphere rel. to 5-min. solar oscills. *(Russian)* 80−17454
geocorona scattered Lα enhancement during 1972 August solar flares 77−78582
geomagnetic activity, correl. with solar wind speed long-term averages 78−32301
geomagnetic activity, enhancements at passage of high-speed solar wind streams 77−37487
geomagnetic activity, rel. to Sun polar coronal holes and sunspot cycles 80−21979
geomagnetic activity 27 day period amplitude var. during 19th and 20th solar cycles 77−66886
geomagnetic activity and ionospheric absorpt. rel. to solar electron fluxes increase after flares 79−75175
geomagnetic activity and solar wind speed long-term averages correl. 77−60564
geomagnetic activity correl. with solar disc central features 79−40040
geomagnetic activity cyclicity rel. to solar wind velocity 79−79732
geomagnetic activity index aa, spectral anal. rel. to solar cycles 77−87187
geomagnetic activity indices, analysis of 100 year series rel. to 11-year and 90-year cycles *(French)* 77−52969
geomagnetic activity recurrence tendency during 20th solar cycle 79−25196
geomagnetic activity rel. to solar wind vel. 79−100813
geomagnetic activity vars. rel. to solar wind speed vars. during 20th solar cycle 77−87361
geomagnetic AE and Dst indices levels occurrence, solar cycle depend. and quietest day selection 79−66877
geomagnetic and solar activity universal connection 79−40039

solar-terrestrial relationships continued
geomagnetic annual aa index, appl. to solar cycle 21 max. intensity and date prediction 78−73696
geomagnetic crochet, two-layer current model 79−44300
geomagnetic crochet type disturbances current systems and elec. fields in polar cap ionosphere 78−40733
geomagnetic external spherical harmonic coeffs., solar cycle var. 80−85592
geomagnetic field, solar cycle vars. of first-degree spherical harmonic components 80−85593
geomagnetic field and ionospheric effects during 1968 Sept. 22 solar eclipse *(Chinese)* 77−22154
geomagnetic field pulsations before solar proton flares *(Russian)* 78−69291
geomagnetic field solar cycle modulation at Alibag 77−60354
geomagnetic field vars., correl. with solar oscills. re-examined 78−89013
geomagnetic field vars. and weather rel. to solar activity, spectral anal. 77−5308
geomagnetic H-component regular daily var. at Alibag, solar cycle depend. 79−8593
geomagnetic northward component secular var. correl. with solar cycle 77−73635
geomagnetic quasibiennial variation caused by Sun 77−21677
geomagnetic solar and lunar daily variations, solar cycle influence 77−60350
geomagnetic solar-flare effect and ionospheric induction 79−53632
geomagnetic Sq variation near mag. equator, solar control, obs. at Huancayo 1922-73 period 79−2181
geomagnetic storms, largest, per solar cycle, statistics 77−2306
geomagnetic storms and solar flares connection 80−72919
geomagnetic variation, sunspot cycle influence 77−78090
geomagnetic variations, effect of solar activity longitudinal distrib. 80−82330
geomagnetism secular variation and solar cycle, Rumanian data 80−56366
geomatnetic effects of 1976, October 23 total eclipse in Australia 77−49000
glaciation, role of solar activity vars. 79−20961
global sensitivity to solar constant vars. effect of ice albedo feedback 80−109245
gravity quasi-periodic vars. and solar activity *(Russian)* 78−69275
HF propag. in ionosphere in minimum sunspot cycle, records 79−25397
HF signals magnetospheric propag. on Earth-Earth path, depend. on solar activity 80−4195
high latitude field rel. to geomagnetic activity 79−44308
ice age, relation to Sun interstellar dust accretion and neutrino prod. 79−12441
illustrated glossary of solar and solar-terrestrial physics 78−57537
International Sun-Earth Explorer B minimum-model project 78−61702
International Sun-Earth Explorer mission 78−61701
interplanetary magnetic field, polarity changes rel. to D-region radiowave absorpt. 77−33272
interplanetary magnetic field sector changes and polar cap geomag. field responses 77−5134
interplanetary scintillation activity as precursor of solar induced geomag. activity 79−58214
ionosphere, anomalous absorption during SID rel. to solar X-ray radiation intensity 79−96857
ionosphere, electron content quasiperiodic fluctuations during 1976 April 29 partial solar eclipse 78−24407
ionosphere, electron temp. var. with solar activity satellite meas. 80−26678
ionosphere, equatorial, radio waves absorpt. seasonal var. correl. with solar ionising flux 78−85762
ionosphere, equatorial electron densities, seasonal and solar cycle changes 78−36378
ionosphere, equatorial F-region elec. fields, solar cycle effects 78−28405
ionosphere, equatorial spread-F seasonal and solar cycle vars. in American zone 80−109298
ionosphere, F_2-layer critical freq. vars., rel. to solar activity 77−67008
ionosphere, gravity waves due to total solar eclipse, detect. by radio technique 77−91364
ionosphere, linear, statistical anal. of solar flares soft X-ray effects 79−8740
ionosphere, lower, radiowave absorpt. rel. to solar X-ray flux, shortcomings in understanding 78−81492
ionosphere, mid-latit., electron density, Universal Time effect solar cycle depend. 79−25396
ionosphere, O^+/n_e relative densities at 170 km for specific heliogeophysical conditions 79−12332
ionosphere, primary ion-electron prod. rates change with solar EUV flux 80−72675
ionosphere, radiowave absorpt. at mag. equator correl. with solar X-ray and 10.7 cm fluxes 79−21099
ionosphere, range and freq. spread-F occurrence at Kodaikanal rel. to sunspot cycle 80−72676
ionosphere, SITEC events (1966-1977), rel. to solar flares 80−90276
ionosphere, sudden freq. deviations during solar flares, depend. on operating freq. 78−28373
ionosphere, topside, electron temp. models for low and medium solar activity conditions 80−67460
ionosphere, total electron content meas. during 1976 Oct. 23 solar eclipse over Australia, rel. to induced gravity waves 78−49210
ionosphere, unusual mid-latitude disturbance of corpuscular origin 78−28374
ionosphere, VLF focusing during solar eclipse 80−61965
ionosphere D- and E-regions, electron densities, diurnal, seasonal and solar cycle vars. 77−33267
ionosphere E-layer crit. freq., geomagnetic east component, and sunspot number relationships 78−65461
ionosphere electron content data, mixing freq. components identification by multiplicative homomorphic filtering 79−29929
ionosphere F_2-layer noontime critical frequency variation through a solar cycle, SW radio communication appl. 79−21102
ionosphere HF radio wave absorpt. at mid-latits., depend. on solar activity 77−53305
ionosphere HF signals, freq. shift during solar eclipse (1976, April 29) 78−45111
ionosphere hot electron layer, electron heating near Sq focus anomaly 80−51599
ionosphere LF radiowave absorpt., variation during solar cycle 80−77193

solar-terrestrial relationships continued
ionosphere relative ion comp. at midlatits., solar cycle depend. 79−21094
ionosphere S_q currents day to day variability, sunspot cycle depend. 79−44299
ionosphere sudden frequency deviations (SFD), appl. as detectors of solar flares EUV radiation 80−8484
ionosphere techniques and phenomena rel. to solar-terrestrial relationships, book 79−75040
ionosphere total electron content at Sagamore Hill, solar cycle var. 78−81496
ionosphere variations due to solar EUV flux changes meas. by AEROS spacecraft, calcs. 79−44293
ionospheric absorption, solar X-ray control, sweep freq. method meas. 79−84582
ionospheric disturbances due to gravity waves generated by 1973 June 30 solar eclipse 77−21993
ionospheric E-region, NO var. with solar activity 78−49207
ionospheric radiowave absorpt. rel. to solar activity 78−69591
ionospheric records over Shanghai, March 1953 to June 1955, correl. of solar activities *(Chinese)* 80−77192
ionospheric storm, 1972, August 4-5, in Asia-Australia-Pacific sector 77−33269
Little Ice Age, N.Hemisphere average temps. not correlated with sunspots 80−82050
long-period solar activity variations, correl. with climatic vars. *(French)* 78−73695
low latitude geomagnetic activity response to sector boundary passage 77−64206
lunar daily geomagnetic vars. at Tucson, depend. on sunspot cycle 78−96136
magnetic storm, 1972, August 4 to 5, rel. to flare interplanetary plasma flow hydromagnetic struct. 79−53653
magnetic storm sudden commencement amplitudes, equatorial enhancement, solar activity, depend. 77−78575
magnetic storms correl. with solar 146 MHz C-type bursts *(Chinese)* 80−4321
magnetic storms prediction by multivariate statistical anal. *(Chinese)* 80−12614
magnetic substorms, high-latit., occurrence freq. rel. to sunspot cycle 80−109315
magnetic variations during 23 October 1976 solar eclipse, obs. in Australia 78−81498
magnetopause altitude during geomag. reversals, solar wind stagnation point calc. 77−22019
magnetosheath, plasma props. during August (1972) 77−25904
magnetosphere, dayside, mag. flux transfer and expansions and contractions rel. to solar wind 78−96355
magnetosphere, response to solar wind vars. in August (1972) 77−25888
magnetosphere ring current plasma injection, correl. with solar wind parameters 78−96363
magnetospheric substorms rel. to solar plasma clouds and streams 77−87207
mesospheric temperature vars. rel. to solar mag. sector struct. 79−34905
meteor radar rates correl. with geomag. activity and solar wind sector struct. 78−65553
meteor rates and atm. density vars., correl. with solar activity 77−53485
meteorological index, effect of interplanetary magnetic field 77−86994
meteorological phenomena affected by solar flares 80−109230
meteorological variability mechanisms 80−51467
microearthquakes, correl. with geomag. and solar activity 79−66638
midlatitude spread-F, depend. on geomag. vars. and solar cycle 78−36389
monitoring and forecasting system, SELDADS, for radiocommunication appls. 79−58097
mutual interaction between E- and D-regions during solar flare 77−45236
neutral gas temperature at the F1-Fs transition region over Delhi during low scalar activity 79−88519
nighttime E_s, seasonal and solar cycle variations at Ahmedabad, India 79−80071
ozonosphere temp. and O_3 conc. rel. to solar activity fluctuations 80−31110
ozonosphere-solar cycle relationships 80−17342
palaeoclimatology, 8000 yr. record of 'Double-Hale' 45 yr. solar cycle 77−78401
Pc 2-3 pulsations with modulated amplitude, depend. on solar activity 78−69620
Pc 5 pulsations, features during solar cycle 78−36406
photoelectron fluxes in ionosphere and plasmasphere, solar activity effects 78−16374
photosphere cooling with increased sunspot activity 78−40896
Pi 2 pulsations, equatorial, fine struct. depend. on solar cycle 80−72721
planetary theory of solar activity *(French)* 79−84759
plasmasphere electron density, solar cycle vars. from whistler data 78−88985
polar cap riometer absorpt. and solar protons, night and day relationships 78−28413
polar thermosphere, neutral temp. during solar cycle 79−53595
proton event, 1969 November 2-5, HF/VHF absorption in disturbed D-region 77−53286
proton events effects on HF ionospheric absorption at low latits. 78−69594
proton flares, fast particles flight time from polar cap absorpt. effects 77−17469
quasi-biennial geomagnetic variation, correl. with solar activity 78−32006
radiation balance as function of atm. dust, climatological consequences 78−36242
radiation input periodic vars., possible solar activity-weather effects 79−34920
radiowave propagation in F2 layer, crit. freq., solar influence 79−2423
rainfall pattern rel. to solar activity during N.E. monsoon in Tamil Nadu 77−70749
recurrent geomag. disturbances and assoc. solar wind streams rel. to coronal holes 77−17522
resonance line splitting in Earth-ionosphere cavity during high solar activity, radiowave propag. appl. 78−77416
rotation and atmospheric circulation rel. to solar activity 80−104853
SCOSTEP project, Study of Travelling Interplanetary Phenomena (STIP) 77−17316

solar-terrestrial relationships continued
short-wave radiation flux, rel. to parameters of F-region and neutral atmosphere 77−91346
solar constant, effects of sunspots and faculae 78−4163
solar constant and the Earth's atmosphere, conference, Big Bear City, Calif. (1975, May 19 to 21) 77−2380
solar constant variation, effect on Earth climate 80−77376
solar corpuscular activity, correl. with Earth lower atmosphere instability at different seasons 80−61881
solar cosmic rays production rate, influence on terrestrial life 79−92735
solar EUV output rel. to aeronomy, present knowledge and future meas. techniques 78−57535
solar magnetic sector structure rel. to ionosphere elec. pot., obs. over solar cycle 77−33271
solar protons, struct. of fluxes in high-latit. magnetosphere in April (1972) 77−64532
solar radiation var. rel. to ice ages 78−12183
solar surface oscillations, geophysical effects 79−8777
solar wind magnetic field rel. to geoefficiency of solar flares 77−29618
solar X-ray fluxes, rel. to upper atmosphere Auger electrons fluxes and spectra 78−28376
spread-F occurrence, sunspot cycle vars. rel. to F-region irregularity model 77−41262
Sq at low latitude, hourly study of secondary effect 80−56362
STIP Intervals I and II, significant solar-terrestrial events 78−49420
stratosphere, 10 mbar geopot. height vars. rel. to solar activity 79−29824
stratosphere, intense ionisation events, effects on NO_2, O_3 and climate, rel. to life extinction 78−96273
stratosphere, long-range circulation var. in northern summer rel. to solar activity *(German)* 77−56694
stratosphere, O_3 reduction assoc. with 1972 August 4 solar proton event 78−7732
stratosphere, summertime temps. during solar cycle 20 (1965-77) 79−79936
stratosphere, temp. trends and O_3 conc. rel. to 11-yr. solar cycle 79−84443
stratosphere cosmic rays, eleven-year cycle 80−4212
stratosphere zonal winds variation, correl. with 27-day solar rot. 78−88878
stratospheric circulation rel. to solar activity oscills. 77−45118
substorms triggering by solar wind discontinuities 77−29596
Sun-induced variations in length of day, seismic activity and geomag. moment 77−90981
Sun-weather correlation, reality and nature 77−66956
Sun-weather relations, solar mag. sector crossings effect on troposphere 78−88876
sunspot activity and rainfall, 30-day periodicity 79−84765
sunspot cycle, rel. to LF radio waves signal vars. 77−78560
sunspot cycle and weather, timed by internal solar chronometer 79−16921
sunspot numbers, change in sign of relation to press., rainfall and monsoons 77−45123
sunspot numbers, geomag. vars. and Earth diurnal rot. vel. 20 year vars. 78−32005
sunspot period stability investigation by periodic anal. of aurora and earthquake records in ancient China *(Chinese)* 79−21253
sunspot structure, vars. correl. with Earth climate 80−31272
sunspots, geomag. activity and global weather data, cross-spectral anal. 77−78313
sunspots, influence on weather 77−91238
sunspots, Wolf numbers since 1665 rel. to terrestrial temp. changes, statistical study 79−8680
synoptic observation program in Sun-weather investigations 77−45088
thermosphere, middle, depend. on solar cycle vars. from incoherent scatter radar studies 80−72654
thermosphere, O^{++} photochemistry rel. to solar disturbances 77−45226
thermosphere circulation 80−56661
thermosphere ionisation and variable solar UV flux, 1974-9 obs. 80−17430
thermosphere neutral winds, seasonal vars., 1970 to 1971, and solar activity depend. 79−39996
thermosphere nighttime winds and temps., monthly vars. during solar min. 78−32263
thermosphere O and N_2 composition, seasonal-latitudinal tidal struct. and mass density, solar activity depend. 80−101467
thermosphere temperatures depend. on solar activity, incoherent scatter data comparison with global models 80−8467
thermosphere zonal mean circulation, seasonal and solar cycle vars. 78−32262
thermospheric temps., solar cycle variability 79−75002
thunderstorm activity rel. to sunspot activity, no correlation 78−57253
thunderstorms, nontropical, initiation by solar activity 78−49096
tornadoes in UK, rel. to solar mag. sector crossing, 1957-77 period 80−77094
tropopause height rel to sunspot activity 80−77090
troposphere, lack of response to solar mag. sector crossings 78−57244
troposphere, lower, solar flare effects on temp. and press. 78−40615
troposphere, press. instability connected with solar activity 79−92580
troposphere, Sun-induced large-amplitude standing planetary waves 78−36236
troposphere response to solar mag. field daily changes 78−88888
troposphere winds, evidence for solar cycle signal 80−72604
tropospheric circulation, solar cycle influences 79−34919
upper atmosphere, energetic particles precip. during mid-latit. D-region baylike disturbance 79−12333
upper atmosphere, $O^+(^2P)$ ionisation freq. vars. during solar cycle 21 from airglow meas. 80−77195
upper atmosphere and solar-terrestrial relations, introduction to aerospace environment, book 80−8466
upper atmosphere H^+ loss during solar cycle, charge exchange processes 78−93021
upper atmosphere H escape flux, charge exchange induced, diurnal and solar cycle vars. 78−93022
upper atmosphere winds, depend. on solar activity 77−13143
UV flux variations, chemical response of Earth middle atmosphere 77−33167
UV irradiation solar flux meas. between 120 and 400 nm, current position and future needs 78−57536
UV variability during solar cycle, effects on stratosphere 78−61492
UV vars. rel. to climatic changes 80−26607

solar-terrestrial relationships continued
variable Sun effects at beginning of Cainozoic era 79−75171
VLF sudden phase anomalies correl. with solar microwave burst energies 78−77418
vorticity area index, energetics of Sun-weather relation 78−81285
weather, effect of solar corpuscular radiation on atmos. electricity 79−79982
weather, effect of solar wind *(Swedish)* 79−79910
weather and climate, solar activity effects 79−16644
weather and climate, solar-terrestrial influences, symposium/workshop proceedings (Columbus, Ohio, 1978 August 24-28) 80−27037
weather effects, coincident turbulent processes 79−44219
weather forecasting skill, solar influences 79−88420
weather relation, vorticity area index to interplanetary mag. sector struct. 80−46222
weather-solar activity correlation, anal. 78−40628
weather-solar activity relationship, study of temp. and rainfall at Oxford 78−85674
weather-solar activity relationships, possible mechanisms 80−17341
weather-sunspots long-term relationships, critical review 79−48558
whistlers observed at Sofia during decreasing solar activity period 79−8779
winter temps. rel. to solar cycle 79−5596
X-ray and Lyman α solar radiation, effects on ionospheric radiowave absorpt. 78−40737
X-ray spectra, rel. to Auger electron and photoelectron spectra in ionosphere and plasmasphere 78−45094
zonal wind speed oscills., solar cycle influence 80−94562
Zurich annual sunspot number link with temp. and precipitation for USA 80−17328
^{7}Be as a tracer for helio-geophysical phenomena 80−98525
^{14}C content in tree rings correl. with solar cycle, 1744-1892 period *(Russian)* 78−16390
^{14}C formation by solar flare particles in terrestrial atmosphere 78−92886
^{14}C in atmosphere, variability due to variable Sun 80−85730
^{14}C in atmosphere content variation, past geomagnetic and cosmic ray intensity variations 78−61691
^{14}C in wines, abundance vars. with 11-year solar cycle, (1909 to 1952) 80−109249
^{14}C variations in terrestrial atmosphere rel. to 11-year solar cycle 78−92885
N_2 airglow solar activity effect on (0,0) second positive band 77−70902
N_2^+ upper atmos. photochem. rel. to solar cycle phase 80−85783
NO and N concs. in thermosphere rel. to solar activity 80−77178
O atom corona in Earth's upper atmos., during solar max. 80−101469
O I 6300 Å nightglow emission, vertical distrib. depend. on solar activity 79−53602
O_3 atmospheric vars. rel. to 11-yr. solar cycle 79−12189
O_3 content of atmos. rel. to solar activity 80−41488

solar visible radiation *see sunlight*

solar wind
see also solar cosmic ray particles
1972 August events, shock wave form and energy, satellite obs. 78−57534
α-particles, heating and acceleration 79−12376
acceleration, by Alfven wave flux from Sun 80−85923
acceleration, energy balance in solar atmosphere above coronal holes 79−92746
acceleration kinetics 77−33447
acceleration of minor species 79−96876
Alfven instabilities in streaming plasmas appl. to H and He ions vel. differences 77−49259
Alfven wave energy spectrum temporal evolution, nonlinear Landau damping 78−53813
Alfven waves, exact, nonlinear, existence of solitons 80−24159
Alfven waves, finite amplitude circularly polarised, instability 78−28502
Alfven waves, finite-amplitude circularly polarised, instability 79−4122
Alfven waves, large amplitude, propag. direction rel. to average interplanetary mag. field 80−26709
Alfven waves, non-linear interaction with compressive fast magnetosonic waves 80−105142
Alfven waves in solar wind plasma, non-WKB nature 80−72905
Alfven waves local instabilities in high speed streams 78−77546
Alfvenic variations, large amplitude, dynamic mag. struct. 80−72734
alpha component dynamics, Prognoz obs. 77−53388
alpha particle component, results of Prognoz satellite meas. 77−53385
alpha-particles and protons streaming velocities relative magnitude at 1 AU 77−9643
ancient solar wind studied by lunar regolith $^{15}N/^{14}N$ ratio 80−62046
anisotropic MHD turbulence in solar wind, obs. 80−94669
antenna in plasma, detect. of natural noises 80−24181
asteroids primordial metamorphism via elec. induction in T Tauri-like solar wind 78−69728
auroral electrojet, empirical relations to interplanetary parameters 80−105118
azimuthal vel. structure, min. variance direction of mag. field fluctuations 77−5408
blast type cosmic phenomena, gasdynamical models and two-dimens. unsteady computs. 77−60565
Chapman-Enskog description validity 77−41375
charged particle diffusion in presence of Alfven waves, perpendicular particle flux 77−84406
charged particle fluxes, electron calibration of Mariner 10 instrumentation 80−12628
charged particle interaction with linearly polarised MHD plane wave, first adiabatic invariant approximations 77−78580
charged particles transport in fluctuating mag. fields, Fokker-Planck eqn. soln. 79−27752
chromospheric boundary layer structure influence on solar wind 79−53788
coherent radio emission in nature, theory, solar system and pulsars appl. 80−46393
collisional theory of anisotropic plasma 78−53782
comet-solar wind interactions 78−49392
cometary erosion by interplanetary plasma, lab. simulation 77−87323
cometary plasma acceleration in solar wind, rel. to ion-acoustic turbulence *(Russian)* 80−106923
cometary plasma tail disconnection events, rel. to sector boundary crossings and high-speed stream encounters 80−46482

solar wind continued
cometary tials interaction effects of tail small scale turbulence 79−44411
comets interaction, mag. field line reconnection at sector boundaries rel. to plasma tail disconnection 78−93155
complex solar particle event, 1973, April 29-30, anal. 78−20593
composition and energy spectrum meas. using multilayer metal targets 77−53391
composition measuring instrument for ISEE-C space probe *(German)* 79−29974
control of geomagnetic storm development 78−85771
cooling of slow protons, Helios 1 expt. 79−2463
corona N.polar hole, electron density and solar wind speed at 1973 June 30 eclipse 80−98627
corona polar plumes as solar wind sources, EUV anal. 78−4178
coronal expansion, effects of radiation heat flux 80−90377
coronal hole flows, models 79−58313
coronal holes, as sources of solar wind 77−2394
coronal holes, influence of mag. fields and coronal heating on solar wind props. 80−46520
coronal holes, solar wind streams and geomag. activity during 1976-77 period 79−25570
coronal holes, thermally conductive flows 78−28614
coronal holes and assoc. solar wind, sunspot cycle 20 survey 78−40911
coronal numerical model, temp. and density struct. 77−17456
coronal open regions energy balance and solar wind generation *(Russian)* 79−21257
coronal temperature constraints in open mag. field regions 80−12744
coronal-interplanetary expansion, sheet-current approach 78−20807
corotating energetic particle events, origin 80−82161
corotating energetic particle streams, H, He, C, O and Fe distrib. functions 79−70938
corotating energetic particle streams, relative abundances 78−93065
corotating energetic particle streams radial var. in inner and outer solar system 79−16883
corotating interaction regions, energetic particles shock accel. 80−82159
corotating stream, compression region interaction with Comet Kohoutek (1973 XII) ion 78−49267
corotating stream interaction regions obs. by Pioneer 10 and 11, dynamic MHD modelling 79−2461
corotating streams, three-dimens. model, theory 79−35086
corotating streams and shock waves, scintillation obs. 78−49279
corpuscular activity, correl. with Earth lower atmopshere instability at different seasons 80−61881
corpuscular stream arrivals at Earth and tropospheric instability 80−109416
corpuscular streams, correl. with Earth troposphere instability 79−92580
cosmic ray 27 day modulation by solar wind *(Russian)* 78−16257
cosmic ray diffusion average properties in solar wind streams 79−75067
cosmic ray diffusion coefficients, calcs. from diurnal intensity var. 79−29952
cosmic ray effects on solar plasma flux 77−53346
cosmic ray energy changes 79−48628
cosmic ray energy loss in solar wind magnetic field 77−53347
cosmic ray modulation, effects of particle drift 77−45263
cosmic ray modulation, obs. during 1974-1975 near solar minimum 77−33304
cosmic ray particles propag. in interplanetary region, transport eqn. 79−44315
cosmic ray propagation in solar wind, latitude variation 80−12622
cosmic ray scatt. in stochastic mag. field, solar wind fluctuations, above 1 GeV 78−61689
cosmic ray solar modulation, theory 80−51629
cosmic ray steady-state transport eqn., monoenergetic source solns. 77−82088
cosmic-ray diffusion in low-latitude solar wind 77−53344
cosmic-ray long-term var. 77−53340
current sheet in compressible plasma, self-similar resistive decay 80−1755
current sheets, resistive instabilities 80−4218
current sheets struct. in mag. holes at 1 AU 79−35087
cyclotron wave growth and vel. distrib. in bi-Maxwellian two-ion solar plasma 79−101040
daily cosmic ray flows during solar cycle in solar equator vicinity 78−69622
decimetre radiowaves propagation in circumsolar plasma during flight of Venera-10 spacecraft 80−21886
deformation by interstellar medium, effect on cosmic ray diffusion 79−53680
Deimos, evidence for strong interaction with solar wind 79−8787
density fluctuations, large-scale, meas. using dual freq. phase scintillations 77−13198
density fluctuations near Sun from Pioneer 6 spectral broadening meas. 77−13199
density struct. var., interplanetary scintillation response 79−2455
diamagnetic boundary layers, kinetic theory 77−9642
differential charging and sheath asymmetry of nonconducting spacecraft due to plasma flows 79−12378
diffusion of rare gases of solar wind origin from lunar fines as bubbles 79−48695
discontinuities, substorms triggering 77−29596
dispersal of solar nebula by solar wind with Sun in T Tauri stage 77−5467
diverging coronal field effects on solar wind expansion 77−45377
early solar system, minor planets EM heating by dense solar wind 80−36555
Earth bow shock, backstreaming ions interaction with solar wind 80−101499
Earth bow shock, control by solar wind conditions from initial ISEE obs. 80−90307
Earth bow shock, current-driven instabilities in laminar perpendicular shock 78−77430
Earth bow shock, interaction with backstreaming ions 80−90287
Earth bow shock, obs. of backstreaming protons in upstream solar wind 80−90309
Earth bow shock, orientation and shape in three dimensions 79−101030
Earth bow shock, solar wind struct. in quasi-parallel, quasi-laminar shock 77−37484
Earth bow shock interaction, backstreaming ions and interplanetary mag. field 80−101500
Earth bow shock interaction, model for ion thermalisation 77−25876

solar wind continued
Earth bow shock interaction, solar wind upstream deceleration rel. to diffuse upstream ions origin 80−98528
Earth bow shock ions in upstream solar wind, two distinct populations obs. 79−21124
Earth interaction, solar wind effect on weather *(Swedish)* 79−79910
Earth magnetosheath interaction, plasma depletion obs. at dayside magnetopause 79−66876
Earth magnetosphere interaction, dayside merging rel. to substorm currents and dayside aurora 79−96852
Earth magnetosphere interaction, mag. curl in front of magnetosphere boundary 80−85804
effect on high latitude tropospheric pressure 80−56515
effects on surface chemistry of lunar grains, reply 79−12374
electric field measurements in the solar wind, bow shock, magnetosheath, magnetopause, and magnetosphere 79−40053
electromagnetic instabilities near Earth orbit, theory *(Russian)* 80−31190
electron acceleration at boundary with interstellar medium 77−17313
electron content, Pioneer 6, 8 and 9 obs., graphical summary 79−53699
electron density expt. results from ISEE 79−58210
electron density fluctuation in solar equator region, radio scintillation obs. 80−61978
electron density power spectrum, interplanetary scintillation meas. 78−77448
electron density small-scale fluctuations, interplanetary scintillation obs. 78−96376
electron exciters of type III radio bursts, obs. near 1 AU 80−46513
electron heating at Earth's bow shock, high temporal resolution obs. 79−58197
electron heating within interaction zones of simple high-speed solar wind streams 79−25426
electron kinetic instabilities 78−96369
electron of solar wind plasma, subthermal, thermal and extrathermal populations 80−41688
electron radial gradients and collisional props. 78−96374
electron vars. across high-speed streams 79−25425
electrons, energetic, of magnetospheric origin, obs. and probable source 80−90310
electrons, epithermal dumbbell distrib. Prognoz 7 obs. following-shock wave 80−109321
electrons, heating of interstellar gas flowing into interplanetary space 79−16881
electrons, penetration into magnetosphere and adiabatic motion 78−28421
electrons, vel. distrib. at 1 AU, steady state theory 79−101041
electrons and protons, very low temps., statistical anal., origin 78−65477
electrostatic fluctuations source 79−80183
electrostatic noise at solar wind plasma freq. beyond Earth's bow shock, mag. field-shock connection 79−70939
EM field in Earth magnetosphere, theory 78−28419
EM lower hybrid instability driven by electron heat flux, threshold 79−88559
energetic charged particles transport mode in mag. fluctuations superposed on diverging mean field 79−50848
energetic electrons of magnetospheric origin in solar wind, correl. with geomag. activity 79−80095
energetic heavy ions in Earth's outer radiation belt, origin in solar wind 79−40020
energetic particle acceleration mechanisms 80−31187
energetic particle coronal transport and interplanetary pitch angle scatt. 80−90305
energetic particle diffusion coeff., HEOS-2 magnetometer data 78−96364
energetic particle event history prediction using real-time particle and solar wind measurements 79−58204
energetic particles, ISEE obs. 79−40036
energetic particles in corotating events, comp. 79−25414
energetic particles upstream of Earth bow shock, review of meas. 80−90308
energetic props. at Earth's orbit following solar flare 77−49261
energetic proton bursts, simultaneous multispacecraft obs. 79−2440
energy changes of cosmic rays in the interplanetary region 79−16773
energy orders of magnitude in solar-terrestrial relations *(German)* 77−70940
energy source, direct energy transfer from photospheric activity to solar wind 80−94768
erosion of planetary and satellite atmospheres, by energetic atomic particles 80−72736
evolving streams and shocks beyond 1 AU, Pioneer 10 and 11 obs. 78−49283
expansion, higher order fluid eqns. for multicomponent nonequilib. plasma atmosphere 80−105156
expansion in high-speed streams, theory 78−45298
exposure effects measured at lunar surface 80−77556
fast ion stream front arrivals at Earth, prediction from solar wind meas. at 0.3-1 AU 79−58216
fast magnetic fluctuations, Helios 1 obs. at 1 AU 77−87225
fast mode instability growth rates, analytical results 78−96373
fast streams, Landau damping effects 79−53691
filamentary plasma elements, impulsive penetration into magnetospheres of Earth and Jupiter 77−78581
flare plasma flow rel. to Forbush decreases struct. 77−91385
flare streams, struct. rel. to flare location on Sun 80−41790
flares of August 1972, dynamics and solar wind responses 77−25992
flow features rel. to coronal open mag. structs. 79−2459
flow past planets, axisymm. implicit blunt body computation technique 78−96370
flows associated with hot heavy ions, obs. rel. to props. and origin 80−51635
flows with higher-order eqns., MacCormack's method extension 79−3987
fluid dynamical models 79−25428
flux depletion at high ecliptic latits., Mariner 10 UV obs. 78−96371
Forbush effect, 1969-1970 world data 77−53367
foreshock, energies of backstreaming protons 77−5398
geomagnetic activity cyclicity rel. to solar wind velocity 79−79732
geomagnetic activity depend. on solar wind parameters, statistical anal. 79−48402
geomagnetic field interaction, MHD waves generation and upper atmosphere absorpt. 79−53588
solar wind continued
geomagnetic field interaction, plasma dynamics laboratory simulation 79−16757
geomagnetic micropulsations, solar wind vel. and Pc 3, 4, 5 activity 80−41665
geomagnetic pulsations affected by interplanetary medium 80−77228
geometrical MHD wave coupling 78−77450
Hale sector boundary, effect on geomag. activity 79−75055
heat flux, regulation by whistler instability 77−45277
heat flux regulation at 1 AU 77−9647
heat flux regulation by ordinary mode instability at 1 AU 77−71097
heat transport in solar wind, closure relation 80−41689
heating and acceleration, implications of coronal fast waves evanescence 78−89147
heating by fast MHD waves 77−53504
heating by heat conduction driven ion acoustic instability 77−78591
heavy ions from flare-heated coronal plasma 79−75197
HELIOS 1 and 2 and STIP Intervals I and II participation 78−49295
Helios 1 and 2 mission, general aspects 78−20615
heliosphere, model of mag. field configuration 80−94670
heliosphere, props. of dust in plasma environment 80−26930
heliosphere H atom ionisation, near Sun trajectories 80−105145
Hermaean magnetosphere compression 79−96936
high latitude geophysical phenomena, fluctuations in temporal and spatial covariation 77−70950
high speed interactions, MHD model of interplanetary disturbances 79−40051
high speed stream effects on solar cycle 20 cosmic ray modulation 80−72914
high speed streams, rel. to coronal holes and solar mag. fields 79−58312
high speed streams, rel. to interplanetary accel. of nucleons in corotating interaction regions 77−9635
high speed streams, relation with coronal struct. at solar min. 77−78590
high speed streams and assoc. recurrent geomag. disturbances rel. to coronal holes 77−17522
high speed streams and galactic cosmic ray modulation 80−41673
high speed streams in outer solar system, plasma and mag. fields vars. 79−58213
high speed streams origin from coronal holes 80−72919
high velocity stream sources, high coronal struct. 77−53530
high-speed plasma streams from active regions 77−33311
high-speed stream, Helios 1 obs. of latitudinal extent 78−57419
high-speed stream, influence on cosmic ray diffusion in presence of Alfven waves 77−29606
high-speed stream, parametric decay of ion cyclotron pump wave 80−41690
high-speed streams, comets flute instability triggering and plasma tails disruptions 78−93156
high-speed streams, correl. with unusual cosmic ray Forbush decreases 80−12624
high-speed streams, flow parameters at 1 AU 77−9733
high-speed streams, long-term correl. with latit. depend solar activity 78−93172
high-speed streams, origin 80−105224
high-speed streams, proton-driven EM instabilities 79−53701
high-speed streams and coronal holes 78−12187
high-speed streams var. with solar cycle and coronal mag. field 78−7974
high-velocity quasi-steady streams, outflow regions localisation on Sun 78−53919
hydrodynamic and kinetic models 77−41374
hydrodynamic streams, 3-D model of corotating solar wind 80−72737
inert gas abundance, 500 Myr ago from lunar dust anal. *(German)* 80−51637
interaction regions, N-S mag. field component solar cycle dependent configurations 80−98529
interaction with Comet Kohoutek (1973 XII) ion tail, dynamic response 80−85897
interaction with interplanetary mag. field equatorial ionosphere elec. fields and geomag. storms 77−78578
interaction with interstellar matter in heliosphere *(Polish)* 78−61696
interaction with interstellar neutral gas, critical vel. effect 80−94666
interaction with ionospheres of Mars and Venus, electrodynamic model 79−84624
interaction with Martian atmosphere, implications of Viking data 77−87307
interaction with Moon, variable EM field calc. 77−82135
interaction with non-magnetic bodies 78−49270
interaction with Saturn magnetosphere, Pioneer 11 obs. 80−82282
interaction with surface of Mercury, planetary conductivity effects 79−101039
interaction with type-1 comet tails 78−49393
interaction with Venus, Pioneer solar wind plasma expt. results 79−48637
interaction with Venus 80−41687
interactions with lunar surface grains, O^{n+} role 80−62050
interactions with planets, magnetic field determ. *(Dutch)* 77−67054
International Sun Earth Explorer 1, electron spectrometer expt. 78−85809
International Sun-Earth Explorer 1, solar wind expt. 78−85800
International Sun-Earth Explorer 1 and 2, fast plasma expt. 78−85800
International Sun-Earth Explorer A, DC and low-freq. elec. field meas. instrumentation 78−85807
International Sun-Earth Explorer A, plasma comp. expt. 78−85810
International Sun-Earth Explorer B, EGD positive ion expt. 78−85805
International Sun-Earth Explorer mission 78−61701
International Sun-Earth Explorer-1, quasi-static and low-freq. elec. fields meas. 78−85808
International Sun-Earth Explorers 1 and 2, fluxgate magnetometers 78−85804
International Sun-Earth Explorers 1 and 2, medium energy particles expt. 78−85811
interplanetary, corotating regions, nucleon accel. and modulation of Jupiter electrons 78−61690
interplanetary ε parameter, rel. to magnetosphere ring current growth 79−75057
interplanetary collisionless shock waves, thickness 80−90314
interplanetary corotating nucleon fluxes separation from solar flare fluxes by radial gradients and nuclear comp. 79−25413
interplanetary corotating structures, MHD model 80−90304
interplanetary disturbance, 1978 January 3 to 4, Prognoz-6 energetic particle and solar wind meas. 80−90315

solar wind continued
interplanetary disturbances produced by density, temp. or vel. pulses at 0.08 AU 77−17317
interplanetary disturbances rel. to mag. and comsic ray storms 77−33313
interplanetary dust and electrons spatial distrib. round Sun, contrib. to corona 80−46514
interplanetary energy flux assoc. with magnetospheric substorms 79−48636
interplanetary flows observed by satellites, 0.6 to 1.6 AU 80−90303
interplanetary flux from flare of August 4, 1972, hydromagnetic struct. 78−28475
interplanetary ice particles erosion by solar wind particles 78−45177
interplanetary Lyman α emissions, Mariner 10 obs., rel. to solar wind latit. struct. 79−35085
interplanetary mag. field, sectoral struct. due to large scale spiral waves 80−12633
interplanetary magnetic dips in solar wind 79−75072
interplanetary magnetic field, from time-depend. solar mag. field 77−9646
interplanetary magnetic field, intensity vars. during geomag. storms with gradual commencements *(Russian)* 80−105127
interplanetary magnetic field between 0.3 and 1 AU, Helios 1 and 2 obs. 80−21887
interplanetary magnetic field structures between 0.3 and 1 a.u., rel. to high-speed streams 79−25429
interplanetary magnetic holes, theory 79−29961
interplanetary objects sputtered by solar wind 80−85835
interplanetary plasma dynamics from temporal scintillation spectra data 77−25980
interplanetary plasma inhomogeneities, anisotropy *(Russian)* 80−36468
interplanetary plasma regime, rel. to cosmic ray storm symmetrical equator-pole anisotropy obs. 78−89020
interplanetary plasma wave-solar electrons interaction, numerical anal. 78−7853
interplanetary scintillation, appl. for solar wind probing 78−45178
interplanetary scintillation, prediction of geomagnetic disturbances 79−58215
interplanetary scintillation activity as precursor of solar induced geomag. activity 79−58214
interplanetary scintillation and IMP 7 obs. during 1973 78−89033
interplanetary shock, assoc, plasma wave turbulence obs. 79−53700
interplanetary shock wave from 1972 August 4 solar flare, energy charcts., plasma and mag. field struct. 78−49268
interplanetary shock waves, three-dimens. geometry 77−22033
interplanetary shock waves at large heliocentric distances, Pioneer 10 studies 79−84621
interplanetary shocks interaction with Earth's magnetopshere, influence of solar wind rel. 78−16243
interplanetary streams, Helios 1 plasma expt. results 78−20606
interplanetary turbulent plasma, radio imagery 79−92645
interplanetary two-fluid shock waves propag., model 80−26711
interplanetary variations, correl. with proton flux rises 1973 Aug.-Sept. 79−21123
interstellar gas interaction *(Russian)* 80−36467
interstellar medium interaction, effects of solar system encounters with dense interstellar clouds *(German)* 80−109500
interstellar medium interaction region struct., rel. to H atoms penetrating solar wind 80−41686
interstellar neutral He focused by Sun's gravity, interaction with solar wind 80−105144
ion acceleration to 40 keV by shock wave disturbances 80−72738
ion acoustic waves, high-resolution spectrograms 79−96878
ion acoustic waves, Imp 6 wavelength meas. 78−40787
ion acoustic waves and related plasma obs. 79−80182
ion bombardment, lunar surface modification 80−109325
ion composition expt. on International Sun-Earth Explorer C spacecraft 78−85793
ion cyclotron instability, influence of protons non-bi-Maxwellian distrib. function 78−96375
ion cyclotron instability 78−77547
ion exchange with the solar wind for planets with negligible intrinsic magnetic fields 79−40050
ion frequencies and velocities, $^3He^{++}$, $^4He^{++}$, O^{6+}, O^{7+}, multiply charged Fe *(German)* 80−51636
ion-acoustic-like instabilities at 1 AU 78−89032
ionospheric recurrent storms, effects on HF radio communication 78−4028
irregularities impulsive penetration into magnetosphere by interplanetary mag. field direction 79−29939
ISEE-2 results from EGD plasma expt. 79−58211
Jupiter, magnetic tail, solar wind interaction with planetary field 79−96956
Jupiter, magnetosheath sunward flow, depend. on solar wind press. 80−72857
Jupiter, magnetosphere compression by solar wind 79−12429
Jupiter, outer magnetosphere, solar wind dynamic press. variations 77−71051
Jupiter, outer magnetosphere, solar wind magnetic field variations 77−71052
Jupiter bow shock, Voyager 1 plasma wave turbulence 79−96954
Jupiter interaction, decametric radio emission correl. with solar activity 79−21222
Jupiter interaction, effect on non-Io-related radio emission 78−57491
Jupiter magnetosphere interaction, influence on particle accel. 79−12428
Jupiter magnetosphere interaction, Voyager 1 studies preliminary results 80−26793
kinetic instability due to electron nonthermal props. 80−41691
Langmuir envelope solitons in turbulent plasma 78−67334
Langmuir waves, nonlinear, during Type III solar wind bursts, evolution 78−93173
latitudinal vars., Mariner 10 H I Lyman α obs. 79−48635
LF oscillations generated by accel. magnetosheath protons 77−33310
long term vars. in solar wind and sunspots, implications of auroral changes during 18th and 19th centuries 80−98498
long-term average speed, correl. with geomag. activity 78−32301
long-term variations of selected props., Imp 6, 7 and 8 results 78−77452
low energy charged particle measurements, Compton-Getting effect complications 78−49269
low frequency continuum from ISEE 3, thermal electrostatic noise, LF .obs. 80−101519
low-frequency wave packet, passage across stand-off shock front 78−45138
lunar ancient regolith, record of solar and galactic radiations 77−60695
lunar dust, inert gas conc., separation methods and methods of treatment *(French)* 80−51674
lunar EM induction, modelling, solar wind parameters limitations 78−36415
lunar grains surface chem., solar wind sputtering effects 78−77501
lunar induction, primeval and present day 77−60689
lunar interaction, enhanced mag. field fluctuations at low altitudes 78−89030
lunar ionosphere/exosphere modulation by solar wind and EUV radiation 77−17390
lunar magnetic anomalies interaction with cold solar wind 78−4125
lunar plasma wake three-dimens. struct. 77−29613
lunar regolith, solar wind and micrometeorite effects 77−60669
lunar rocks interaction, Apollo samples obs. rel. to microcrater and accretionary grain populations 80−94732
lunar rocks interaction, microcrater and accretionary grain populations temporal development 80−94731
lunar soils, Rosiwal Principle appl., solar wind implanted species, grain size dependence 77−29667
lunar surface mass fractionation by solar wind sputtering 78−49350
lunar surface sputter erosion 77−60664
lunar surface sputtering, metallic Fe prod. and element fractionation 77−29666
magnetic field, as source of field in type 1 comet tails 77−13288
magnetic field, large-scale struct. between 1 and 0.3 AU during Helios 1 primary mission 79−29962
magnetic field, reconnection with geomag. field, untenability of models 77−22007
magnetic field, southward component correl. with dayside magnetosphere mag. flux transfer 78−96355
magnetic field correl. with nighttime F-layer height vertical movement 77−13147
magnetic field obs. by Isee-1 and -3 80−85895
magnetic field rel. to geoefficiency of solar flares 77−29618
magnetic field sector boundaries at 1 AU, (1971-1973) 80−94668
magnetic fields and flows between 1 and 0.3 AU, during Helios 1 primary mission 79−29963
magnetic fluctuations, directional anisotropy and Landau damping of Alfven waves 80−21885
magnetic fluctuations, EM response of Moon 78−12113
magnetic fluctuations, Helios 1 search-coil magnetometer expt. 78−20607
magnetic holes, satellite obs. near 1 AU 77−64586
magnetopause altitude during geomag. reversals, solar wind stagnation point calc. 77−22019
magnetopause interaction, rot. simple and shock waves in anisotropic plasma 77−91369
magnetosheath burst of medium nuclei, obs. from Imp 8 (1974, Feb. 16) 80−101501
magnetosheath interaction, rel. to energetic plasma ions 79−21106
magnetosonic and Alfven waves, transfer by solar wind 80−67490
magnetosonic waves, instability driven by alpha particle beam 79−35089
magnetosphere, energy flow and current systems closure, rel. to upstream solar wind parameters 78−57400
magnetosphere, high-energy protons produced by substorms, interplanetary conditions 80−51615
magnetosphere boundary interaction, mag. fields from laboratory simulation data 78−57396
magnetosphere compression, rel. to solar cycle var. in geomag. external spherical harmonic coeffs. 80−85592
magnetosphere dynamo, energy coupling function 79−96860
magnetosphere energy coupling to solar wind, geomag. disturbances 80−85821
magnetosphere frontside boundary layer interaction, reconnection problem 78−89010
magnetosphere interaction, Akasofu substorm parameter interpretation 79−75053
magnetosphere interaction, effect of finite ion Larmor radius on magnetopause Kelvin-Helmholtz instability 79−80096
magnetosphere interaction, electron(ion)-beam instabilities 78−5888
magnetosphere interaction, energy transfer during substorms 79−12343
magnetosphere interaction, flow peculiarities rel. to magnetopause position 78−49236
magnetosphere interaction, magnetopause configuration in two dimens. *(German)* 80−31167
magnetosphere interaction, model, MHD eqns. 79−53663
magnetosphere interaction, plasma sheet slow convection and field-aligned currents theory 80−109312
magnetosphere interaction, satellite obs., comparison with laboratory plasma and simulation 78−5945
magnetosphere interaction, solar wind ion injections into morning auroral oval 80−98502
magnetosphere interaction, solar wind plasma injection at dayside cusp 78−40775
magnetosphere interaction, time-dependent global simulation 78−88991
magnetosphere interaction during August (1972) 77−25888
magnetosphere merging with interplanetary field, half-wave rectifier response 80−72710
magnetosphere micropulsations controlled by solar wind, origination region 80−85823
magnetosphere model, particle (electric current) approach 80−17442
magnetosphere penetration, nonstationary model *(French)* 78−88989
magnetosphere substorms, prediction of occurrence by solar wind and IMF obs. 80−41648
magnetosphere-solar wind dynamo, energy coupling function and substorms 80−105134
magnetosphere-solar wind dynamo affected by IMF vector 80−85824
magnetosphere-solar wind interaction, Chapman-Ferraro image method graphs correction 80−12620
magnetospheric convection driving force 79−8782
magnetospheric storm, interplanetary shock wave with increased solar wind energy deposition 80−77237
magnetotail plasma at lunar distance response to changes in interplanetary mag. field, solar wind and substorms 79−70932
Mars, heavy ions in solar wind plasma flow 80−8576
Mars, solar wind interaction region, ion flux meas. interpretation 80−8575

solar wind continued
Mars 2 plasma and magnetic meas. 77−53384
Mars atmosphere interaction, sputtering rel. to mass loss 78−53855
Mars interaction, evidence for Martian mag. field reexamined 78−49359
Mars interaction, role of planetary ionosphere and magnetosphere 80−72835
Mars interaction, satellite meas. with charged particle traps 77−13200
Mars ionosphere, solar wind interaction rel. to ion temps. 78−96419
mass loss from Sun, implications of models He content and convective mixing length 80−26835
Maunder Minimum, solar wind state 79−75069
Maunder minimum characteristics, meteoritic evidence 78−57529
McIntosh effects in geomagnetic activity, Boller-Stolov effect 77−49241
Mercury, interaction of surface with exospheric atmosphere 78−49351
Mercury, solar wind stand-off distance, erosion effects 79−80251
Mercury magnetic field-solar wind interaction, Mariner 10 obs. 78−12131
Mercury surface interaction, simple mols. prod. by solar wind irradiation 78−16324
meridional wind flow in midcorona, modelling 77−33452
MHD Bernoulli flow, singular point 78−4099
MHD discontinuities, identification method 80−109322
MHD discontinuities, single-point identification method *(Russian, English)* 79−75092
MHD dynamic modelling of disturbances during 1972 August solar flares 78−45174
MHD shock waves, numerical simulation 78−77449
MHD solitons in solar wind, nonlinear dispersion eqn. qualitative anal. 80−4217
MHD turbulence, props. 80−61977
MHD turbulence 80−85834
MHD waves, deposition of momentum and energy 77−37493
MHD waves role in coronal heating and solar wind accel. 77−71098
microinstabilities, in moderately inhomogeneous plasma 77−87223
microinstability onset and its consequences 77−87222
micropulsations Pc 3 and 4, evidence for control by solar wind vel. 78−7837
microscale fluctuations, multispacecraft obs. 77−87224
minor ions, anomalous acceleration rel. to Alfven wave emission 78−77453
models, survey of last 30 years' research 78−69764
momentum and energy transport, by acoustic, Alfven and fast mode waves 78−4162
monochromatic non-WKB Alfven waves, normals evolution 80−101521
Moon, interaction of surface with exospheric atmosphere 78−49351
multispecies flows, transport eqns. mathematical struct. 78−47084
neutrino flux explanations, nuclear reactions in Sun 77−74035
non-spherical flow of matter 77−56880
noncompressive density enhancements, props. and origin 78−28479
nonequilib. ionisation in solar wind, theory 79−48751
nonlinear Alfven waves in high-speed streams 77−33315
nonrelativistic electron propag. and type III radio bursts *(Russian)* 77−78742
north-south motions, statistical study using Explorer and Pioneer obs. 77−70966
northward magnetic field, polar cap electric field structure 79−44305
one-fluid models, Alfven waves effects 79−16789
origin, space charged particle repulsion by light *(Chinese)* 78−16388
origin in polar coronal holes, rel. to geomag. activity and solar cycles 80−21979
origin rel. to coronal props. *(Italian)* 78−81605
parameter measurement using charged-particle spectrometer, instability of analyzing voltages 80−67565
parameters influence on geomag. D_{st} vars. 79−40054
particle accel. near Jupiter, effect of solar activity on MHD oscills. 78−57526
particle acceleration by propagating interplanetary shocks 80−31188
particle telescopes with multiple view directions for pitch angle meas. from satellites 78−24425
particle trapping and acceleration during the August 1972 event 80−98532
particles accelerated by Alfven waves, distrib. function self-similar solns. 79−32757
physical processes 79−75071
plane parallel flow stability in magnetized plasma, velocity shear instability 79−37468
plasma, analyser for Pioneer Jupiter missions 77−67024
plasma, collisionless, stability of contact discontinuity, solar wind and magnetosphere boundary appls. 80−62002
plasma and mag. field parameters at 0.3 AU from meas. at 1 AU 77−53387
plasma and magnetic field parameters responsible for magnetosphere ring current plasma injection 78−96363
plasma anisotropies, alignment with mag. field direction 78−32311
plasma characteristics, vars. near D sheets 77−29616
plasma density and mag. field orientation, rel. to magnetopause three-dimensional shape 79−101029
plasma disturbances caused by charged Helios spacecraft 78−24416
plasma electron temperature, 0.5-1 AU, satellite obs. 80−12630
plasma experiment on International Sun-Earth Explorer C spacecraft 78−85788
plasma flow in curved mag. field 78−67329
plasma fluctuations, Ogo 5 meas. 78−57420
plasma fluid aspects, review 80−90313
plasma flux from strong flare rel. to magnetospheric disturbances 78−73600
plasma in external mag. field, electron beam-whistler soliton interaction, appl. solar wind 77−11360
plasma inhomogeneities evolution 79−53694
plasma inhomogeneous structure, Venera-9, 10 dispersion-interferometer meas. 79−8789
plasma inhomogeneous structure, Venera-9 and 10 radio sounding meas. 79−8788
plasma injection at dayside magnetospheric cusp 77−33288
plasma irregularities, anisotropic struct. obs. using interplanetary scintillations 80−67489
plasma kinetics, review 77−91512
plasma meas. by modulation method, amplifiers sensitvity increase 79−92676
plasma measurements near Venus using wide-angle instruments on (Venera 9 and 10) 77−91396
solar wind continued
plasma microinstabilities, review of theory 80−98530
plasma motion through comet coma 78−49391
plasma observations during August 1972 solar-terrestrial events 77−25902
plasma penetration of magnetopause 78−61675
plasma physics, solar and solar wind, book 79−84782
plasma physics basic problems 78−69672
plasma pressure rel. to magnetopause current fields 80−105123
plasma properties, review 77−41372
plasma properties during August 1972, obs. near Earth 77−25904
plasma radial expansion in 0.3-1 AU range 79−21121
plasma radiowave fluctuations and turbulence, Venus 10 radio transmission expt. 79−80295
plasma turbulence, spatial fluctuation spectra 79−53693
plasma turbulence, Venera 10 radiowave spectral width meas. 79−88560
plasma wave electric fields, Helios 1 initial results 77−37492
plasma wave propagation, magnetoacoustic wave transverse to mag. field 80−12629
plasma waves, investigation by International Sun-Earth Explorer 1 and 2 78−85802
plasma/cosmic rays energy exchange, depend. on cosmic rays radial gradient orientation *(Russian)* 79−53682
plasmadynamical processes in solar wind, reviews *(German)* 80−109323
plasmas with arbitrary orientation of mag. field, two-stream instability 80−41715
plasmasphere, characteristic size determ. from solar wind meas. 77−49224
polar coronal hole, EUV lines obs. anal. 79−5797
polar coronal hole, physical props. rel. to outflow into solar wind 77−45372
polar enhancement of interplanetary Lα through solar wind asymmetries 78−20605
polar flow and heavy ion abundances, rel. to Saito coronal density model 77−37591
polar plume, outward mass flux from X-ray anal. 79−12455
polar solar wind, variation rel. to solar activity 80−90385
preferred solar wind emitting longitudes on Sun 77−71077
Prognoz satellite studies 77−64596
properties at 1 AU, rel. to coronal temps., temp. gradients and comps. 77−53525
proton acceleration in transitional region, oscills. excitation, periods calc. 77−60563
proton flux enhancements and solar wind speed, Mars 7 meas. 79−84620
proton parameters changes assoc. with 1972 August flares, Pioneer 9 and 10 obs. 77−33314
proton streams after interplanetary magnetic sector boundary, effect on troposphere 79−53491
proton temperature heliocentric gradient, Pioneer 10 obs. 79−40052
protons, 1970, April 16, pitch angle distribs. transform from solar wind into magnetosheath 77−87216
protons, as extraterrestrial source of atmospheric water vapour, Sun-weather relationships appls. 78−69416
protons and α-particles after interplanetary shock wave passage 77−33301
protons and electrons, medium-energy, Helios 1 and 2 particle spectrometer meas. 78−20608
protons cooling, evidence from Mariner 2 data 78−40789
protons preshock perturbations, two-spacecraft study 78−12067
protons reflected by Earth's bow shock, upstream wave boundary determ. method *(Italian)* 78−24409
protoplanetary cloud blow-off by T Tauri like solar wind 78−45243
protoplanetary disc nebula disruption by T Tauri-like solar wind 80−36516
pulsations rel. to Pc 3-4 pulsations 78−65476
radial attenuation of azimuthal asymmetry rel. to 27-day cosmic ray modulation 78−73592
radial dependence of properties, results from Helios 1/2 and Pioneer 10/11 scatt. expts. 78−28595
radial expansion, appl. of MHD moment eqns. for strong mag. field 77−64584
radio bursts, type II and III theory *(Russian)* 78−16381
radio measurements of second moment field 78−16369
radio scattering, meas. of spacecraft signals 78−49277
radio wave propagation in turbulent solar wind plasma, meas. using three satellites 80−101518
radiosource structure meas., scintillation effects 79−96922
rapidly diverging flow, heat and momentum addition effects 77−29755
rare gases implantation in lunar fines 77−60672
recurrent interplanetary streams, mag. field sources 79−2457
resistive anisotropic plasma jet, stability 78−69667
resistive effect on solid body orbits 77−73979
review of theoretical research (since 1958) 78−49281
rotational shock waves as bow and return shock waves in interplanetary plasma flows 77−17315
SCOSTEP project, Study of Travelling Interplanetary Phenomena (STIP) 77−17316
sector boundary distortion in interplanetary medium 77−70967
sector structure correl. with meteor radar rates and geomag. activity 78−65553
semi-empirical model 77−13201
shock wave, magnetosphere arrival rel. to substorm-assoc. energetic ions injections obs. 79−35075
shock wave, solar flare generated, plasma enriched by O^{6+} and He^{++} 80−72740
shock wave acceleration of energetic charged particles 80−31189
shock wave fronts and Forbush effect fine structure 77−53366
shock wave produced by flare, model based on Forbush decrease *(Chinese)* 80−90302
shock waves in interplanetary plasma, MHD discontinuity, normal vector determ. *(Russian, English)* 79−75091
shock-associated energetic proton events at large heliocentric distances 78−77451
shocked solar wind viscous flow behaviour at Venus ionopause 79−75068
shocks and assoc. wave-particle interactions 78−49284
simulation studies of space 79−58217
Skylab obs. of quiet and active solar events 77−56891
slow MHD shock waves in interplanetary medium 78−12068
small-scale solar-wind inhomogeneities, whistlers model 78−45173
solar activity rel. to solar wind characts., review 80−94777

solar wind continued
solar cycle variations, additional evidence 78−49266
solar flare energy spectrum simulation from monoenergetic incident proton beam 78−12786
solar sail trajectories, long-term evaluation 79−48641
solar sources of interplanetary mag. field and solar wind 77−45275
solar wind high-speed streams, influence on geomag. activity 77−37487
solar-wind exposure effects in the lunar soil, review 79−75070
spacecraft with solar sail, eqns. of motion from geocentric orbit 77−53394
spatial struct., latit. gradients in obs. averaged over solar longit. 79−2458
speed, interplanetary magnetic field polarity and geomagnetic index 77−78593
speed, search for general gradient at low solar latits. 77−33312
speed and geomag. activity long-term averages correl. 77−60564
speed and/or southward field component at beginning of 20th century 79−2464
speed distrib. and high speed streams, evolution 78−49282
speed unusual variations during solar cycle 20 from geomag. activity vars. 77−87361
speed variations, 1962-1974, rel. to solar cycle 77−9734
speed variations power spectrum for periods >10 days 79−2462
spherically symmetric solar wind, galactic cosmic rays propag. 79−53681
spiral structures, geophysical and astrophysical 80−77287
spiral waves, effect on sector struct. of interplanetary mag. field 80−85831
sputtering of lunar surface, chemical and isotopic fractionation 78−61762
sputtering of lunar surface, comments 78−61763
stability against whistler mode, anal. of proton to α-particle vel. ratio 79−2453
stability of ordinary mode to electron heat flux 79−30049
stable solar wind and geomagnetic activity 79−53696
stream interaction regions, microscale instabilities 80−72739
stream interfaces, Imp satellite meas. at 1 AU 78−77447
stream structure, energetic solar particle events 80−41674
stream structure during solar cycles 20 and 21 early phases 79−25430
stream-associated fluctuations, effects on radial var. of average wind parameters 77−45278
stream-stream interfaces, effects of electrostatic shear flow instability 80−96359
stream/stream interaction region, rel. to correl. of solar cosmic rays detected by Mars-7 and (Prognoz-3) 77−82089
streams in inner solar systems rel. to coronal holes, mag. field and plasma obs. 79−58212
streams magnetic classification 80−41692
structure free state of high speed flows 77−53386
Sun and heliosphere, conference, London, England (1979 April 3 to 4) 80−82574
tangential discontinuities, occurrence freq. and spatial distrib. 77−9648
T Tauri type solar wind, rel. to planetary ring systems origin 78−32373
terrestrial atmos. vorticity of 500 mb rel. to sector boundary crossing 80−109199
terrestrial planets bow shock locations 78−28560
thin layered field aligned currents, distrib. in fast streams 79−12375
three-fluid model, self-consistent soln. 78−57418
transverse waves propag. along axisymm. mag. field in nonhomogeneous plasma, WKB kinetic theory 78−42740
turbulence rel. to interplanetary scintillation, synoptic anal. 79−2460
turbulence upstream of Earth bow shock, nonlinear plasma processes 80−85833
turbulent plasma conductivity *(Russian)* 79−16923
two fluid model, numerical soln. using shooting-splitting integration 77−73919
two-fluid models, spiral magnetic field inhibition of thermal conduction 78−96372
two-fluid models 77−87226
two-fluid time-dependent model with thermal cond. 79−92643
two-frequency dispersion interferometers for space plasma nonuniformity 79−70964
type II emission mechanism 78−28476
type III radio bursts, second harmonic radiation and related nonlinear phenomena 78−7958
type III solar radio burst sources, plasma wave clumping origin 80−21959
unstressed deceleration, model 79−53692
upper atmosphere heating by solar wind energy 77−37471
upstream, LF waves assoc. with suprathermal ions 79−58209
upstream particle events close to bow shock and 200 R_E upstream, ISEE-1 and ISEE-3 obs. 80−77247
upstream solar wind, energetic protons and electrons simultaneous meas. 79−16760
Uranus magnetic field interaction, plasma dynamics laboratory simulation 79−16757
variation effects on solar flare cosmic ray particle intensity 80−77372
velocities, latit. and longit. struct. from interplanetary scintillation obs. 79−40049
velocity, correl. with Earth diurnal rot. irregular vars. 79−8591
velocity, correl. with geomag. pulsations amplitudes 78−85773
velocity, determ. from Voyager 2 coronal occultation, 1979 August 80−51639
velocity, dispersion anal. 78−7852
velocity, estimation from multi-station interplanetary scintillation 78−73601
velocity, further evidence of latit. gradient 77−25900
velocity, influence on magnetosphere hydromag. energy spectra 80−67476
velocity, interpretation of influence on geomag. Pc 3-4 activity 78−73585
velocity, latitudinal depend., influence of coronal mag. field geometry 77−9732
velocity, out of the ecliptic, interplanetary scintillation obs. 77−5409
velocity and interplanetary mag. field orientation, joint distrib. rel. to geomag. Pc 3-4 pulsations 79−53672
velocity biasing in sampling 79−53698
velocity change due to interactions with galactic cosmic rays and interstellar H I 80−101506
velocity determ. from interplanetary scintillation effects on 3C 279, SHF obs. *(Russian)* 80−77248
solar wind continued
velocity determ. from interplanetary scintillation obs. *(Russian)* 79−80185
velocity dispersion analysis *(Russian)* 77−70965
velocity during August 1972, meas. by radio source scintillation obs. 77−25901
velocity meas., interplanetary scintillation obs. 78−49278
velocity meas. from scintillation obs. of H_2O and OH maser sources *(Russian)* 78−69704
velocity meas. with spacecraft phase scintillations 77−41310
velocity perturbations, MHD soln. of assoc. interplanetary disturbances 77−29615
velocity recurrence period, depend. on heliographic latit. 80−62106
velocity rel. to galactic cosmic ray flux, Mars 2-7 meas. 78−16252
velocity rel. to geomag. activity 79−100813
velocity rel. to interplanetary magnetic field vertical component origin and recurrency 80−90369
velocity rel. to plasmasphere electron content 79−16767
velocity variations, effects on large scale props. of interplanetary mag. field 77−17318
velocity variations, rel. to mag. field in magnetotail 77−22005
velocity waves formation and evolution 77−64737
Venus, flow of solar wind behind planet, model 80−98531
Venus, ionosphere, distrib. of elec. currents induced by solar wind interaction 77−64683
Venus, magnetosphere press. balance, outside dayside ionopause 80−90353
Venus, plasma meas., from Mariner 5, reexamination 79−80258
Venus 79−80181
Venus atm. interaction, mag. flux ropes nature *(Russian)* 80−77313
Venus atmosphere interaction, contrib. to exosphere non-thermal H budget 79−12416
Venus bow shock, Pioneer magnetometer obs. 80−36535
Venus bow shock, plasma absorpt. rel. to shock attachment to ionosphere 77−37541
Venus interaction, study via plasma analyser expt. on Pioneer Venus Orbiter 80−67498
Venus interaction region, struct. from meas. of ion-flux characts. by (Venera 9 and 10) 78−4051
Venus ionosphere interaction, meas. by mass spectrometers on Pioneer Venus Bus and Orbiter 80−67499
Venus ionosphere interaction, review 77−73995
Venus magnetic tail, formed by solar wind interaction 80−51679
Venus magnetic tail interaction, unipolar induction effects 80−62060
Venus plasma meas. by Venera 9 and 10 wide-angle analysers 78−96418
Venus solar wind interaction, review of present understanding 79−58288
Venus wake, Mariner 10 magnetic field obs. 78−96417
viscous boundary layer between the solar wind and cometary plasmas 80−56769
Voyager plasma experiment 78−20617
Voyager plasma wave system 78−24432
wave propagation in presence of mag. field 79−41833
whistler heat flux instability with bi-Lorentzian vel. distrib. function 77−64585
whistler soliton, interaction with electron beam 77−9649
^{26}Al from meteorites, possible 'record' of solar wind action and luminosity variations 78−61830
^{14}C abundance, meas. 77−5407
H^+, implantation in interplanetary dust grains rel. to upper atmosphere H chemistry 78−65445
^{3}H abundance, meas. 77−5407
He abundance, evidence for chemical separation by diffusion 80−77381
He III acceleration, interactions with transverse waves, comments and reply 79−80184
He ions superheating and superacceleration 80−12631
He^+ flux after interplanetary shock, Imp 7 obs. 80−101520
He^+, obs. in driver gas of interplanetary shock wave 80−72735
He^{2+} acceleration, effects of interactions with transverse waves 78−40788
^{4}He, detect. in stratosphere particles as evidence of extraterrestrial origin 77−56878
$^{15}N/^{14}N$ ratio from lunar samples 77−87354

soldering
ceramic/metal layer adhesion mechanism for metallization of electronic ceramics, elec. props. *(German)* 80−76381
diamond surface soldered to metal film, contact strength determ. device 78−60910
Eccobond solder 56 C, sp. ht., 1.3-300K 78−16804
electroless Ni deposits from Ni/P and Ni/B plating solutions, solderability by contact angle meas. study 79−88910
fusion instant recording by US method 78−44319
inspection using optical projection microscopes *(German)* 80−77849
laser material processing, IR holographic elements appl. 80−37964
lead coatings, solderability after storage at 25-400°C 78−184
optical connector for single-fibre cables 79−86253
PC fabrication, detrimental effect of aged Sn-Pb surfaces 80−108625
permanent joining techniques for vacuum components 80−82782
plasma coating, fused, strength of adhesion to base by gas flame soldering 78−23894
pressure transducer, operating temperature range extension using semicond. tensoresistors 78−4608
radio construction kits, practical hints 79−80591
solar cell fabrication, photovoltaic process based on thick film technique 80−94016
solderability of external coatings after storage at 25-400°C 78−184
space-quality solder joints, resistance to thermal fatigue 80−25831
steel, mild, solderability, annealing effect *(Japanese)* 80−89244
steel, plate, Pb-Sn soldered joint strength study *(Japanese)* 78−7166
steel, stainless, embrittlement, due to soldering with Cu alloy solder, effect of alloying additions 79−47773
superconducting wire to cryogenic leads, simple repeatable method 80−4728
thick-film conductor, adhesion meas. technique 80−50811
US exam. of solder melting point, exam. of equipment design 79−15937
US method for compatibility evaluation 77−40486
US soldering, industrial applications 77−58499
wrap-soldered tubing, inspection using UDT-6Sm us apparatus 78−3276
Ag-Cu-Zn-(Cd)(Mn), solder, UTS, room temp. to 4.2K 79−57064
Au-Pb-In solder joints, layer growth, ageing 77−32764
Cd, spreadability on Cu and brass plates *(Japanese)* 80−29252

soldering continued
Cd-Ag-Zn (96, 3, 1 wt.%) soldering alloy powder, atomised, prod. and appl. 79−100073
Cu, solderability, annealing effect *(Japanese)* 80−89244
Cu-constantan junctions with solder, shock-induced elec. response 80−75626
Cu-Ge solders for electric vacuum instruments, Mn and Ag additives effect on evaporation 79−42231
Ga, thermal contact agent for low temperatures 77−49731
In solder joints, thermal conductance at low temps. 77−30150
Nb_3Sn multifilamentary conductor production and testing 79−32809
Ni-Sn intermetallic phase growth kinetics at liq. Sn-solid Ni interface 80−71638
Pt-Au, thick film, adherence meas. and evaluation 80−50813
Sn-Pb solder, wettability on Cu and mild steel plates *(Japanese)* 80−89244
Sn-Pb solder on Cu plate, spreadability, effect of fluoride and iodide addition to $ZnCl_2$ flux *(Japanese)* 80−29251

solenoids
see also coils; electromagnets
30 T pulsed solenoid construction and life tests 79−31297
axisymmetric high flux secondary particle channel 79−45502
Bitter, optimum dimensions 79−21787
Bitter solenoid efficiency factor, allowance for cooling holes 79−30502
curved rectangular conductor magnetic field calc. 77−61895
deceleration in conducting tube 78−50678
electron beam heated solenoid reactors for fusion power and fissile fuel breeding 78−8992
ferrite-core solenoid, appl. to geomag. pulsations detect. 78−24384
football coil, absolute minimum mag. field prod., heavy ion isochronous cyclotron synergic focusing 77−83364
fusion reactor, low MP metal partially disintegrated superhigh field solenoid *(Russian)* 77−7584
fusion reactor, Shiva Faraday rot. coils, circuit and mag. anal. 78−54951
fusion reactor solenoid, orthotropic, finite element stress anal. 78−55010
galettes for cooled solenoids 77−22580
high-homogeneity coil system independent of average diameter 79−97408
homogeneous magnetic field generation, ampere turn deposition determ. 78−42253
homogeneous magnetic field generation, using thin circular current carrying coils *(Polish)* 79−98262
homogeneous magnetic field synthesis in internal region of cylindrical solenoid *(German)* 80−37923
impedance of solenoid surrounding cylindrical conductor with surface crack, eddy currents, calc. 80−23601
implosion generator of superstrong mag. fields, solenoid for generation of initial mag. flux 80−105681
inductance, minimisation, mag. induction optimum profile 79−31769
inductive oscillometer for non-intrusive LF positive-glow plasma diagnostics 78−51343
inductive oscillometry, field difference theory 78−51342
intersecting storage ring supercond. solenoid installation and performance 79−31270
laser heated fusion reactor, design of 20 tesla pulsed solenoid 77−23270
laser solenoid, fusion power appl. 77−47250
magnetic field synthesis, on the axis of cylinder solenoid 78−74814
magnetic field synthesis at mid-plane *(Polish)* 79−94123
magnetic field synthesis on axis, Tichinov's regularisation method *(German)* 77−42458
magnetic flux density calc. formula *(Norwegian)* 79−31762
magnetic sensor, high permeability metal core solenoid absolute sensitivity calibration 80−31133
magnetisation meas. using field gradient of high-field solenoid 80−31813
MHD applications, separation of two-phase flow *(Russian)* 77−7466
NMR magnetometer for solenoid calibration 78−21187
ohmic heating coil, nonuniform current density distrib., appl. to Tokamak reactor 78−17427
Proton-Electron Tandem Ring Accelerator 'transparent' solenoid superconductor 79−31274
pulsed 20 tesla solenoid design for linear laser solenoid fusion reactor 77−35373
pulsed 70-T system with long operational life, Faraday effect meas. 80−42243
pulsed eight-solenoid system, magnetic field distrib. control 77−87793
pulsed high field magnet construction *(Japanese)* 79−17456
pulsed magnetic field production, for ultrahigh acceleration of Al ring 78−5386
semiinfinite, thin, mag. field and current density distribs. near edge Wiener-Hopf calc. 78−70999
solid state physics, high mag. fields, generation and application 80−27321
superconducting, Al stabilised, design and construction, for CERN intersecting storage rings 77−46428
superconducting, as focusing element for heavy ion linac 77−38460
superconducting, automatic M-H curve recorder in high magnetic fields *(Japanese)* 79−71500
superconducting, Basque project 77−23325
superconducting, biaxial sample rot. use *(Czech)* 80−37010
superconducting, control of field-changing tasks by microcomputer 79−216
superconducting, current regulated sweep unit 78−4659
superconducting, effect of constructional features on magnetic parameters 79−21786
superconducting, for H^+ collective accelerator, Q-values and field profiles 78−46188
superconducting, for H^+ collective accelerator 78−46187
superconducting, homogeneous, for superconductor props. meas. by NMR *(Czech)* 78−29130
superconducting, in persistent mode, magnetothermodynamic meas. error anal. 79−17454
superconducting, large high current density, for use in high energy physics expts. 77−23326
superconducting, mag. field stability in persistent mode *(Czech)* 78−29131
superconducting, mag. flux conc. using Tb cryst. 78−49869
superconducting, mag. parameters, NMR study of effect of constructional features 79−71488
solenoids continued
superconducting, mag. spectrometers for colliding beam accelerators 77−26919
superconducting, magnetic field inhomogenity measurement method, Hall probe appl. *(Czech)* 80−13107
superconducting, ohmic heating, appl. to Tokamak TNS 78−54928
superconducting, square-ended design for optimum performance 78−82009
superconducting, stress-induced heating, finite element calc. 77−28342
superconducting, use of cylindrical drift chamber 79−3311
superconducting, with variable current density, optimisation 79−17450
superconducting 60 Hz AC loss meas. 77−26362
superconducting coil, electronic apparatus, for loss meas. 77−26361
superconducting magnet, pulse loss and voltage meas., elec. method 77−37949
superconducting magnet system, development for physical experiments 80−9008
superconducting multifilamentary coil, hysteresis losses 77−26363
superconducting plate, hysteresis losses 78−84345
superconducting pulsed solenoid ORPUS-1, poloidal field coil performance 77−26352
superconducting solenoid, optimisation of aperture solenoid with rectangular windings 80−4747
superconducting solenoid, with magnetometer for magnetocrystalline anistropy meas. from 4 to 300K 77−2673
superconducting solenoid design optimisation 77−147
superconducting solenoid for intense meson beam channel *(Czech)* 77−38527
superconducting transversely isotropic solenoid, electromech. stress anal. 77−79127
superconductor stability in typical coil configs. 77−26350
thin-walled solenoid and effects, mag. field max. 77−83784
Tokamak EF coil energy transfer supercond. solenoids and phase-shifting bridge 79−31213
Tokamak energy storage superconducting solenoids 78−66369
Tokamak superconducting toroidal field coils, pulsed field losses, expt. simulation 77−26871
toroidal solenoid, Aharonov-Bohm effect *(Russian)* 78−77770
toroidal solenoids, helically wound, form factor calcs. 80−100091
transient response of solenoid driven conducting cylinder 80−23599
ultrathin-coil supercond. solenoids for high-energy accelerators and storage rings 79−31260
windings, nonlinear eqn. for equal loading 79−55028
wire rope NDT, EM field perturbation by internal void in conducting cylinder 79−34213
Cu-steel composites for intense pulsed mag. field generation 80−42245
Nb-Ti superconducting magnet system, for short sample test on Tokamak superconductor 80−9010
Nb_3Sn-V_3Ga concentric solenoid magnet system, 17.5 T operation 77−26353
NbTi, operating at 9 T in He gas 77−74461
Tb single crystal flux concentrator for supercond. solenoids 78−57991

solid effect
acoustic, due to US stimulated transitions between NQR levels 77−12249
N-5-chlorosalicylideneaniline, H^+-^{14}N double reson. NQR spectra temp. depend. thermochromism and tautomeric mech. 78−70849
dynamic nuclear polarisation, review of principles 78−64297
NQR double resonance detection, principles and appl. to D 78−76354
nuclear dipolar magnetic ordering, dipole-dipole interactions review 77−85475
phonon bottleneck, influence on dynamic nucl. polarisation by solid effect 80−20511
polarised targets in high energy 79−68065
Al alloys, dil., screening charge anisotropy around impurities, nucl. quadrupole couplings meas. 77−32286
LiH, F-centres, dynamic nucl. polarisation, solid effect meas. *(French)* 77−81028

solid electrolytes *see superionic conducting materials*

solid helium
^3He, solid, two parameter model of mag. and thermal props., spin exchange 80−49461
adsorbed layers, porosity of solid gas layers, appl. to cryosorption pump *(Japanese)* 80−20031
BCC, phonon spectrum calc. 77−11766
BCC, physical origin of large four spin exchange 79−56031
book 77−47296
charge carrier mobility in strong electric fields *(Russian)* 77−62706
charge carrier mobility temp. depend., diode volt-ampere characts. meas. *(Russian)* 77−31838
charge motion, peculiarities *(Russian)* 78−95202
charge motion, singularities in temp. and time depend. *(Russian)* 78−56019
coherent diffusion of isotropic impurities 80−54468
condensed He phases, book 79−99377
crystal structure, book contrib. 77−51348
dielectric constant, 0.8-4.3K 77−8488
diffusion, of impurities and defects, review 77−7945
diffusion of ^3He, pulsed NMR exam. *(Russian)* 78−71902
diode properties 79−56021
energy absorption and size effect, point defect diffusion *(Russian)* 77−4243
FCC, lattice dynamics at high press. 78−10255
HCP, ground state props., cell model 78−14539
HCP, longitudinal sound velocity, temp. and freq. depend. 77−72742
impurities and vacancies 79−65289
interface with liq. ^4He, phonon transmission using heat pulse technique 79−56035
ion current modulation by thermal waves 78−91506
ion mobility 78−2324
Kapitza resistance at Cu boundary, heavy thermal load, 0.45-1.5K *(Russian)* 77−11767
Kapitza thermal resistance and tunnelling states of atoms, theory 77−85046
long range forces, book contrib 77−51347
low temp. mag. and thermal props. due to bound state Frenkel vacancies 79−56019
low temperature physics, conf., Grenoble, France, (Aug. 78) 79−51462
magnetic susceptibility, HF, ferromag. reson. type *(Russian)* 77−59175
melting, at ambient temp. under high pressure *(French)* 79−73373

solid helium continued
melting, at room temp. and high-press. 80−80025
melting curve shifts due to pore condensation 80−54469
melting kinetics, sound transmission at liq.-solid interface 80−92734
melting obs. at 297K and 115 kbar 79−82413
monolayer, sp. ht., low-density phase modification produced by substrate changes 77−76642
monolayer systems, book contrib. 79−99390
neutron scattering, book contrib. 80−2230
orthopositronium decay, press. up to 140 atm. 77−39713
paramagnet system, low-temp. diffusive transport for polarons and defectons 78−43174
phonons in linear chain with hard-core pot. 77−11644
plastic properties *(Russian)* 77−62705
solid-fluid, eqn. of state, melting props. under press. 80−96721
solid-superfluid interface, struct., surface tension 80−88380
specific heat anomaly, explained by hybrid cryst. model 77−65015
specific heat high temp. anomaly, quasi-average and averages, translational symmetry breakdown 78−30811
superfluidity search in ^{4}He 78−10254
surface tension and contact energy, standing waves *(French)* 80−92753
thermodynamics, book contrib. 77−47646
two body potential, theory 79−69305
vacancies, activation energy 77−28064
vacancies and dislocations *(Japanese)* 78−91507
vacancy activation energy, from high temp. sp. ht. data 77−15657
vacancy mobility *(Russian)* 77−85015
X-ray diffractometry, cryostat design 77−53921
H-He metallic, solid alloys, phase separation and thermodynamic functions calc., 0-19000K, 15-90 Mbar 77−43333
^{4}He, room temp. melting point, press. depend. calcs. 80−103463
^{4}He, superfluid against solid ^{4}He, surface tension and contact angle 79−42339
^{3}He, adsorbed film on Grafoil, NMR, intermediate and near-monolayer coverages 79−46878
^{3}He adsorbed layers, antiferromag. indirect exchange 79−99389
^{3}He, adsorbed monolayers, dipolar anisotropy effects in spin relax 77−7940
^{3}He, antiferromagnetic spin Hamiltonian with four spin interactions for BCC, lattice, mean field theory 79−1652
^{3}He, as mag. semicond., analogy to Mott insulator 80−96720
^{3}He, BCC, absence of substrate nucleation on Grafoil, 30-320 mK 79−19422
^{3}He, BCC, contrib. of vacancy mag. polarons to sp. ht. 79−56032
^{3}He, BCC, Debye behaviour of thermal cond., 0.03-0.4K 79−56034
^{3}He, BCC, first-neighbour mag. interaction sign 78−14538
^{3}He, BCC, four-spin interaction effects on ordering processes 77−39721
^{3}He, BCC, low temp. sp. ht anomalies 78−91256
^{3}He, BCC, mag. ordered phase, complicated spin-glass-like phase 78−22928
^{3}He, BCC, mag. props. near phase transition 79−65291
^{3}He, BCC, meas. from 3 to 300 mK 79−33153
^{3}He, BCC, NMR multiple echoes, soln. of eqn. of motion of magnetisation 79−86961
^{3}He, BCC, nucl. mag. order and paramag. susceptibility 80−59757
^{3}He, BCC, nucl. spin mag. ordering with four spin exchange 77−89615
^{3}He, BCC, plastic flow 79−46880
^{3}He, BCC, sp. ht. meas. for 5 molar vols. above 50 mK 77−47645
^{3}He, BCC, spin polarons in narrow almost-half-filled s-band 77−62703
^{3}He, BCC, vacancy bandwidth determ. by sp. ht. 78−79854
^{3}He, BCC, Zeeman exchange cross relax. time 78−22930
^{3}He BCC and HCP, vacancy tunnelling freq. calc. 77−80679
^{3}He, BCC lattice, quadruple exchange in Heisenberg antiferromagnet 77−89616
^{3}He, BCC solid, exptl. mag. props., four spin exchange explanation 79−69319
^{3}He, bulk and divided samples, nuclear spin-lattice relaxation meas. 78−84026
^{3}He, deform.-assisted pairing, magnetic transition interpreted 78−2334
^{3}He demountable melting curve thermometer 78−54369
^{3}He, entropy of vacancy formation 79−33156
^{3}He, FCC, vacancy induced spin polarons 80−59756
^{3}He, four spin exchange model and magnetism 80−92752
^{3}He, HCP, exchange and mag. order 80−107606
^{3}He, HCP, vacancy-induced transitions 80−88395
^{3}He, HCP solid, with ^{4}He impurities, ^{3}He nucl. mag. relax. behaviours 79−56027
^{3}He, liq. and solid., spin polarised, thermodynamical nuclear orientation 79−46879
^{3}He, locked in magnetism 79−56033
^{3}He, low temp. depend. of sp. ht., using $Ce_2Mg_3(NO_3)_{12}$ thermometry 79−88955
^{3}He, low temp. thermal cond., structural crystalline defects 80−2240
^{3}He, mag. ordering, lattice dynamical approach 78−56020
^{3}He, mag. ordering, NMR study 80−54470
^{3}He, mag. phases *(Russian)* 77−72743
^{3}He, mag. susceptibility meas. using double sample cell NMR technique 79−63225
^{3}He, mag. susceptibility near ordering temp., pulsed NMR meas. 78−18869
^{3}He, magnet, review of theory 78−38906
^{3}He, magnet, spin-lattice models 80−88394
^{3}He, magnetic polarisation around vacancies, on two-dimens. lattice 79−51368
^{3}He, magnetic susceptibility and transition, thermodynamic study 78−60003
^{3}He, magnetisation through nucl. ordering temp. meas. 78−18870
^{3}He, magnetism *(Japanese)* 79−19425
^{3}He, melting, specific heat, entropy, latent heat 78−75904
^{3}He melting curve obs. by Pomeranchuk cooling 79−7731
^{3}He, melting curves, quantum corrections, effective pair pot. calcs. 77−55347
^{3}He, monolayer on grafoil, NMR relaxation time study 78−75902
^{3}He, nuclear antiferromag. reson. 80−54471
^{3}He, nuclear spin exchange interaction at high molar vol. 77−20160
^{3}He, nuclear spin ordering in applied mag. fields 77−51568
^{3}He, phase separation of dil. ^{4}He impurities 80−88393
^{3}He, phase transition in high mag. field 79−19424
^{3}He, phenomenological treatment of exchange effects in high-temp. limit. 77−35795

solid helium continued
^{3}He, possible explanation for recently obs. phase transition in high mag. fields 80−20006
^{3}He, production and obs. of ordered state, adiabatic demagnetisation *(French)* 77−59173
^{3}He, quantum crystal, growth from melt at low temps. 78−31319
^{3}He rotating, structure of vacancies *(Russian)* 79−90843
^{3}He, solid, is level broadening due to zero point vibrs. 79−28267
^{3}He, solid, heat capacity, possible dimens. effect 78−75844
^{3}He, solid, mag. phase diagram from static magnetisation meas. 80−84342
^{3}He, solid, mag. transition, defect-melting model 79−28172
^{3}He, solid, melting, formal treatment of low temp. props. 79−69315
^{3}He, solid, Monte Carlo method of energy calc. 79−56030
^{3}He, solid, ordering obs. at melting press. in high mag. fields 80−84341
^{3}He, solid BCC, four spin exchange, susceptibility behaviour below 10 mK 78−10253
^{3}He, solid BCC, mag. susceptibility and sp. ht. 79−69318
^{3}He, spin diffusion at very low temp., multiple echo amplitudes 79−19423
^{3}He, spin diffusion coeff. *(Russian)* 77−80679
^{3}He, spin diffusion in BCC and HCP phases *(Russian)* 77−35794
^{3}He, spin ordered, melting press. and entropy 80−84340
^{3}He, spin relaxation to paramagnetic centres, in surfaces at very low temps. 79−33552
^{3}He, strongly magnetised, low-temp. melting props. 77−11765
^{3}He, struct. of vacancy induced spin polarons 79−95244
^{3}He, submonolayer on Grafoil, vacancy induced ferromag. 78−14536
^{3}He, surface ferromagnetic instability, role of attraction between liq. ^{3}He and solid substrate 79−46863
^{3}He, susceptibility along melting curve, 20 mK to nucl. ordering temp. 77−31837
^{3}He, thermal contact with powdered $Ce_2Mg_3(NO_3)_{12}.24H_2O$, below 35 mK 79−60598
^{3}He, two-dimens. solid, melting mechanism 80−10643
^{3}He, vacancy relaxational phenomena *(Russian)* 78−95203
^{3}He, vacancy struct., neighbouring ferromag. domains *(Russian)* 77−20161
^{3}He, valence band struct., zero-point motion effect 80−65333
^{3}He, variational calcs. using antisymmetric trial functions 79−65290
^{3}He:^{4}He, HCP, solid, nucl. spin-lattice relax., ^{4}He impurity effects 80−88396
^{3}He-^{4}He, mixture, isotropic phase separation temp. press. depend. 80−92751
^{3}He-^{4}He, solid soln., struct. of vacancies 80−2242
^{3}He-^{4}He mixture, ^{3}He-^{3}He and ^{3}He-^{4}He tunnelling motions, NMR meas. 78−38908
^{3}He-^{4}He solid mixture, dil. ^{3}He conc., diffusion coeff. obs. by NMR, impurity-phonon scatt. *(Russian)* 77−62701
^{4}He adsorbed on Nuclepore filter, specific heat *(Japanese)* 78−79852
^{4}He, BCC, vacancy tunnelling at finite temp. 78−38907
^{4}He, boundary limited thermal cond., Poiseuille phonon flow 80−2241
^{4}He, charge mobility, plastic deform. effect *(Russian)* 79−60599
^{4}He, crystalline, shape anal. of pulsed second sound 78−14537
^{4}He, crystallisation wave detection, solid-liquid boundary oscillation spectra *(Russian)* 79−90844
^{4}He crystals, nucleation and orientation 80−84339
^{4}He, diffusion coeff. of ^{3}He 79−56026
^{4}He, diffusion coeff. of ^{3}He, detection and study of impuriton-phonon scatt. mech. 79−56029
^{4}He, entropy, 0.1 to 0.82K, and density at freezing 77−7925
^{4}He, extension of HCP-FCC phase diagram to about 9 kbar 80−39383
^{4}He, FCC, inelastic neutron scatt., phonon spectra, dispersion curves 78−51785
^{4}He, FCC cryst., self-consistent phonon theory 79−4453
^{4}He, FCC high-density cryst., lattice dynamics by inelastic neutron scatt. 79−1539
^{4}He, FCC quantum cryst., lattice dynamics 79−77859
^{4}He, HCP, Debye-Waller factor by inelastic neutron diffraction 78−43206
^{4}He, HCP, dislocation damping, MHz sound freq. depend. attenuation 77−72739
^{4}He, HCP, elastic consts. 78−38910
^{4}He, HCP, free standing cryst., shear deform. 78−2333
^{4}He, HCP, ground-state props. 80−44389
^{4}He, HCP, ion motion in strain and unstrained cryst. 79−56020
^{4}He, HCP, lattice dynamics, neutron-inelastic-scattering obs. 79−33154
^{4}He, HCP, plastic flow 77−62702
^{4}He, HCP, US attenuation 78−47634
^{4}He, HCP, vacancy tunnelling freq. calc. 77−80678
^{4}He, HCP crystal, roughening transition 80−88397
^{4}He HCP crystals, US attenuation, dislocation damping 80−24711
^{4}He HCP crystals, US vel., temp. and freq. depend. 79−56016
^{4}He, HCP-FCC transition, near triple point, thermal anal. 79−60596
^{4}He, HCP→FCC transition, temp. hysteresis 78−56021
^{4}He, hypernetted chain generalised eqn. optimal solns. 80−75396
^{4}He, impuriton vacancy mols. 78−79853
^{4}He, impurity interaction anisotropy and quantum diffusion of ^{3}He 79−56028
^{4}He, Kapitza resist. below 1K 78−34673
^{4}He, Lennard-Jones model at 0K, props. using Monte Carlo method 79−82401
^{4}He, liq. and solid, dielec. const. meas. 77−20143
^{4}He, liquid-solid boundary, capillary sound motion, Kapitza resistance *(Russian)* 80−92737
^{4}He, melting curves, quantum corrections, effective pair pot. calcs. 77−55347
^{4}He monolayer, multicritical behaviour from triangular lattice gas model 77−74328
^{4}He, monolayer on graphite, quasi-2-dimens. quantum solid theory, lattice dynamics, thermal props. 78−84024
^{4}He, monolayer on graphite, quasi-2-dimens. quantum solid theory, vibr. props. 78−84025
^{4}He, nucleation at Grafoil/high press. liq. ^{4}He interface 77−28062
^{4}He, nucleation in Vycor under press., superfluid oscills. near melting press. 79−51388
^{4}He, phase transition 80−15333
^{4}He, plastic deform., athermal processes 79−56017
^{4}He, pure and with ^{3}He admixtures, effect of plastic deform. and impurities on internal friction *(Russian)* 79−77860

solid helium continued
^{4}He, quantum cryst., ground-state lattice vacancies and Bose-Einstein condensation 77−7943
^{4}He, quantum cryst., surface equilib. shape and vibrs. *(Russian)* 79−7732
^{4}He, quantum crystal, growth from melt at low temps. 78−31319
^{4}He, quantum diffusion of ^{3}He, tunnelling jumping approx. *(Russian)* 78−87844
^{4}He, second layer film on graphite, liquefaction 78−47632
^{4}He, solid, heat capacity, possible dimens. effect 78−75844
^{4}He, solid BCC, plastic deform., stress-strain relations and US attenuation 78−38909
^{4}He, solid-liquid interface mobility under 1 MHz sound wave *(French)* 80−100373
^{4}He, solid-superfluid interface, roughening transition 80−103536
^{4}He, spin diffusion coeff. of ^{3}He impurities, impuriton model 77−59174
^{4}He, thermal cond., 0.4 to 1.8K *(Russian)* 80−103535
^{4}He, thermodynamic props., Monte Carlo studies 79−65290
^{4}He, transition between close packed phases 79−56025
^{4}He, US finite amplitude wave propag. 80−80024
^{4}He vacancy as small liq. drop 78−51784
^{4}He:^{3}He, quantum diffusion of ^{3}He, impurity interaction anisotropy *(Russian)* 78−30810
^{4}He:^{3}He, spin diffusion coeff. and T_2, impuritons, temp. depend. 78−34675
^{4}He-^{3}He, ^{4}He impurity at. and ion interaction and mobility, in solid or liq. *(Russian)* 78−18868
^{4}He-^{3}He, quantum mobility of impurity ^{3}He atoms 78−47636
^{4}He-Cu, thermal boundary resist. meas. above 1K 77−72769
^{4}He-Cu interface, thermal boundary resist., 1-3K 77−20178

solid hydrogen
adiabatic demagnetisation, of stabilised H atoms *(Russian)* 79−82412
adsorbed layers, porosity of solid gas layers, appl. to cryosorption pump *(Japanese)* 80−20031
adsorption of atom, H, adsorpt. time and energy, hyperfine freq. meas. 79−50155
atom production in solid H_2 matrix by T decay 77−29028
atomic, spin-aligned, rapid decay mechanisms at 0K in large magnetic fields 77−72741
atomic crystalline phase, ground state energy calc. *(Russian)* 79−19426
bombardment target, construction and operation 77−6589
cluster-ion prod. on electron-irrad., lattice and fragmentation energies 77−4911
collective excitations observed by incoherent neutron scatt. 79−23690
colouring problem on randomly occupied lattice, critical conc. existence for long range order 80−80519
compressed, vibr. Raman spectrum 79−47422
crystallographic transformation below 1.5K, X-ray study 79−73374
cubic structure, mechanical stability 77−4242
dielectric constant, 4.2-15K 77−8488
dilute atomic H impurities props. calc. 79−60601
dilute para-ortho mixture, ferrorotational transition *(Russian)* 79−60597
diluted ortho-para mixtures, NMR of ortho-H_2 79−60600
discontinuous orientational phase transition, thermodynamics, isotope effects 80−6590
elastic constants and anisotropic pair correls. 79−33042
electron emission under bombard. by keV electrons, H and D ion beams 77−73196
electron localisation at surface *(Russian)* 79−60893
electronic stopping power calcs. 80−2104
energy in vol. range 10 to 60 a.u./atom, allowance for three-particle interactions *(Russian)* 78−38654
equation of state, 4.2K isotherm, ortho-para depend. 79−7670
equation of state, at high pressure 79−46781
equation of state, intramol. zero pt. energy contrib., total sublimation energy 78−71829
equation of state at megabar press. using z-pinch method *(Russian)* 79−33071
equilibrium concentration of stored atomic H, upper bound 77−46510
exciton states, intermediately bound-exciton theory 77−69234
far IR absorption by phonons and librons in ordered state 78−80331
FCC crystal, first-order shifts in electronic states 79−82510
fundamental absorption spectra, 10 to 40 eV at 2K, using synchrotron radiation 79−73967
fundamentals, static props., review 80−75403
glass phase, use of NMR *(French)* 80−93190
p-H_2, NMR study of dilute o-H_2 impurity 80−25228
HCP, density depend. of elastic consts. 80−6589
HCP, effects of internal strains on elastic consts. 77−24343
HCP to FCC transition at 80-100 atm. *(Russian)* 77−55259
heat capacity and configurational entropy at low ortho concs. 77−35706
high pressure phase, 57 kbar, 25°C, transparent crystalline mass 79−55870
highly compressed, combined representation method for use in band struct. calc. 77−89685
p-Hz:o-H_2, clustering rate and NMR obs., 25 mK-2K 78−47635
inhomogeneous many-body system integral equations 80−22732
interactions between o-H_2 molecules in nearly pure p-H_2 77−68088
interface with Cu, thermal boundary resist. meas. abov 1K 77−72769
intermolecular pair potential, from solid-state data 79−14727
IR fundamental band, U-branch transitions 78−64361
isentropically compressed, elec. cond. at Mbar press. 78−95315
Kapitza thermal resistance and tunnelling states of atoms, theory 77−85046
laser fusion research, prep. of solid H_2, D_2 targets using cryostat 78−17417
libron bound state form. in ortho-phase, Raman scatt. data 77−80600
libron spectra and conversion as function of ortho-para conc., Raman scatt. spectra 78−84570
linear chain, near Hartree-Fock limit study 79−32938
linear chain of atoms, electronic struct. calc. 78−79969
localised excitations due to p-H_2 in ordered o-H_2 lattice 79−65288
melting curve, meas. of P, V, T and longitudinal sound velocity 79−37814
melting curve up to 10 kbar *(Russian)* 77−27987
melting curves, quantum corrections, effective pair pot. calcs. 77−55347
metal phase, eqn. of state, thermodynamic pot. *(Hungarian)* 79−14909
metal phase, state eqn., correlation energy of uniform electron gas *(Hungarian)* 79−1573

solid hydrogen continued
metallic, appl. of variational approach to inhomogeneous electron liquids 79−38013
metallic, cohesive energy determ. 78−91301
metallic, defect form. energy, Einstein-Kanzaki model 78−34676
metallic, electron-lattice interaction effect on equilib. struct. form. *(Russian)* 80−34380
metallic, electron-phonon coupling const., calc., compared with expt. 79−99286
metallic, electron-phonon interaction and superconductivity, APW calcs. 78−14854
metallic, electronic band struct. using θ-function basis 79−37976
metallic, electronic struct., HF calc. using plane wave basis 79−7772
metallic, eqn. of state *(Russian)* 77−89519
metallic, expanded, Hartree-Fock and correlation energies 78−34674
metallic, ground-state energies of liq. and solid phases, variational and Monte Carlo methods 80−70502
metallic, high density, thermodynamic props. 80−88337
metallic, interion interaction *(Russian)* 78−91299
metallic, ion-electron chain, anharmonic effects, electron-phonon coupling 79−60459
metallic, phonons, supercond. transition, nonlinear self consistent screening approach 79−95537
metallic, stable phase at high press. 77−72740
metallic, struct. and stability 78−14305
metallic, total energy, self consistent harmonic phonon approx. 77−31629
metallic, transition press. and physical props. *(Chinese)* 80−54467
metallic, Wannier functions, variational calc. 77−15740
metallic and mol. crysts., X-ray scatt. factors, Hartree-Fock calc. 79−60219
metallic and molecular, transition press. and eqns. of state calc. 78−26685
microwave absorption by o-H_2 pairs 77−68034
microwave absorption of isolated pair of o-H_2 molecules in solid p-H_2, theories 78−2948
microwave spectra, orientational level struct. of o-H_2 pairs 79−47554
molar volume press. depend. at 77K *(Russian)* 79−86832
molecular, atomic H impurities, dynamic local field approx. 79−69316
molecular charge density contours for cryst. struct. 78−38645
neutron scattering, inelastic, theoretical analysis 78−34569
neutron scattering expts. 78−79693
NMR, pulsed, linewidth transition, T_1, low ortho conc. 78−43667
NMR relaxation meas. at low ortho conc. 77−81025
NMR studies on single crystals, dynamic effects 80−107608
nonlinear heat conduction 79−69317
nuclear magnetism at reduced ortho conc. 78−10787
nuclear spin-lattice relax. of in-plane and out-of-plane ortho-H_2 pairs 78−56394
nuclear spin-lattice relaxation, crystal and mag. field effects 79−42865
order-disorder phase transition for o-H_2 78−79726
orientational level structure of o-H_2 pairs, phonon renormalisation 79−47554
orientational order, phase transition, average field approx. 78−63857
orientational order parameter at reduced ortho conc., NMR spectra meas. 77−4566
orientational ordering, crit. temp. and conc. density depend. 79−86725
orientational ordering effects at low ortho conc. 79−56018
orientationally disordered and ordered state, rot. transition J=1 to J=0 79−23543
ortho-para mixtures, 10-23K, rot. Raman spectra, quantum calcs. 77−6700
ortho-para mixtures, incoherent neutron scatt. 77−47304
ortho-para mixtures, vibr. coherence decay 80−78903
para-H_2, cryst. field for ortho-H_2 impurities 77−72839
pellet ablation, in Tokamak plasma 77−89264
pellet ablation, lifetime on plasma rel. to reactor refuelling 77−23272
pellet ablation in plasma 80−19589
pellet ablation in thermonuclear plasma, electron space charge and refuelling 77−88283
pellet in plasma, transonic flow in ablation cloud 79−1322
pellet-rotating plasma interaction, spectroscopic anal. 78−18455
penetration depth of 0.5-3 keV electrons 78−56549
phantom phases 78−55946
phase transition of second kind in HCP lattice, orientational ordering 80−70410
phonon absorption line shape as function of density 80−50329
plastic deformation, controlling mechanisms *(Russian)* 77−89493
plasticity, 2-4.2K, o-H_2 content effects *(Russian)* 77−7787
quadripolar glass, relax. time and low temp. sp.ht., computer simulations 80−49377
quadrupolar glass, press. meas. 80−34271
quadrupolar glass phases, evidence from NMR study 78−84027
quantum crystal, short-range corre. and motional renormalisation of anisotropic interactions as function of density 80−34272
quantum diffusion, enhanced, below 0.3K 79−90845
quantum diffusion 80−107607
Raman active optical phonon, density depend. 79−87432
Raman active phonons, freq. depend. on ortho-para conc. and temp. 79−73918
Raman scattering meas. of rotational spectrum under press. 77−69814
renormalised pair interactions and three-body polarisation forces 77−31732
review of properties *(Dutch)* 77−62704
rotation-libration transition under press., Monte Carlo study 80−49460
rotational excitations, higher order effects 80−6591
Rydberg states 79−69425
self-induced electron emission at o-p transition 77−12506
solid- liquid mixture, nonstationary diffusion of neutrons 79−4212
solubility in high press. He 80−10674
spherical target preparation and placement in laser forces by cryogenic device 77−80335
static energy determ. taking into account three particle interactions *(Russian)* 78−9996
storage of atomic H, rate process theory 77−32770
structure transition below 1K 79−56024
substrate for liquid ^{4}He film, film transfer velocity, Van der Waals interaction *(Russian)* 80−54465
superconductivity *(Hungarian)* 77−72935
thermal boundary resistance of solid H_2-Cu and D_2-Cu interfaces, 1-3K 77−20178

solid hydrogen continued
thermal cond. at varying o-H_2 conc. 78−51786
thermodynamics, polarised spin system of H atoms, metastable in mag. field 78−30812
thermonuclear plasma, H_2 fuel pellet ablation, atomic processes effect 80−18596
uniform spheres production apparatus 77−74409
vapour pressure 2 to 4.5K, influence of thermal radiation 77−5848
vibrational energy transfer, isotopic impurities, relax. 79−6993
p-D_2, solid, roton dragging librons 78−67886
H:T solid, collision induced IR lines caused by T_2 radioactivity 80−84756
H-He metallic, solid alloys, phase separation and thermodynamic functions calc., 0-19000K, 15-90 Mbar 77−43333
p-H_2, anisotropic NMR spectra and crystalline state 78−10786
o-H_2, cohesive energy, non-additive term 79−50099
p-H_2, constant volume heat capacity and eqn. of state, temp. depend. 80−65334
p-H_2, cryst., hexadecapolar induced absorption intensities 78−88290
p-H_2, crystal field energy for o-H_2 impurities, NMR studies 80−15331
p-H_2, FCC, equation of state and lattice dynamics, temp. depend. 77−76521
O-H_2, far IR absorpt. in ordered state 79−91430
0-H_2, libron spectrum calc. 78−79677
p-H_2, local strain effects for isolated pairs of o-H_2, calc. 79−65419
H_2, metallic state, eqn. of state of solid and liq. phases *(Russian)* 79−19354
p-H_2, NMR spectra, motional-narrowing model interpretation, order-disorder transition below 0.18K 78−79855
p-H_2, NMR spectrum of isolated o-H_2 pairs 80−15332
p-H_2, neutron diffr. studies up to 5 kbar 80−59436
o-H_2, one-dimens., struct. instability 79−86885
o-H_2, order parameter temp. depend. 79−42242
o-H_2, orientational ordering, transition temp. and change of symm. 77−31609
H_2 pellet-plasma interaction, neutral gas shielding model 79−23428
o-H_2 quantum molecular crystal, quantum quadrupolar phase theory *(Russian)* 78−22929
H_2, room temp. melting point, press. depend. calcs. 80−103463
p-H_2, solid, anisotropic contribs. to ground state props. 78−83914
p-H_2, solid, elastic consts., Brillouin scatt. obs. 79−8149
p- H_2, solid, induced near IR absorption spectrum, freq. shift, intensity, up to 10 kbar 78−6658
p-H_2, solid, NMR lineshape due to unpaired o-H_2 mols. 79−47341
o-H_2, solid, NMR relax. and libron energy 78−88204
p-H_2, solid, phase diagram, HCP-FCC phase transition 79−42340
O-H_2, solid, quantum diffusion of p-H_2 impurities 80−88398
o-H_2, solid, roton dragging librons 78−67886
o-H_2, solid FCC, orientational ordering, SCF approx. 78−2029
p-H_2, time-resolved CARS, disorder effects on coherent vibr. states 80−93342
o-H_2 to p-H_2, spontaneous conversion rate anomaly obs. in heat capacity expt. 79−99392
p-H_2:o-H_2, nuclear spin-lattice relaxation, importance of Suhl-Nakamura interaction 78−52374
p-H_2:o-H_2, solid, cryst. field interactions, impurity effects 79−82562
o-H_2:p-H_2, isolated pH_2 effect on orientational order 77−47535
o-H_2:p-H_2, librons, CPA theory 77−47536
HD, enhanced nucl. polarisation of D 77−8450
HD, lattice thermal cond., 0.2 to 4K 78−75903
HD-T_2, liq. and solid, vibr.-rot. IR spectra 80−50313
HT-T_2, liq. and solid, vibr.-rot. IR spectra 80−50313
p-Hz, quantum diffusion of O-H_2 impurities 80−96719
o-pH_2, slow neutron scatt. into external radiation field *(Russian)* 80−59348

solid lasers
see also gamma-ray lasers; Raman lasers; semiconductor junction lasers
active element, circular, cooling process, variation in ambient temp. *(Russian)* 78−74915
active element temp. field calc. *(Russian)* 78−55359
active laser media, mats. search 78−63160
active mirror and disc amplifiers, laser glasses, physical props. 78−42337
active rod, effect of surface transition layer on laser action 79−50301
active solid pulsed laser cylindrical element, temp. distrib. anal. *(Russian)* 77−58332
for air pollution monitoring, electrical techniques, solid laser appls. *(Italian)* 77−82069
alkali halide, CW lasing of F_2^+-centres, 0.9-2 μm 78−29957
alkali halide crystals, tunable CW IR lasers using F_A(II), F_B(II), M and F_2^+ centres 77−88725
alkali halide CW single mode colour centre lasers, freq. behaviour and linewidth 77−88728
alkali halide host cryst. F-centre lasers, tunable IR emission 78−59030
alkali halides, coloured, light amplification at activator centres 80−2795
alkaline earth halides:Eu^{2+}, fluorescence lifetime and quantum efficiency for 5d→4f transitions 80−100681
amplifier with spatial filters, graphoanalytic determ. of energy parameters 80−48322
amplifier with spatial filters, optimal length and operating conditions 80−48323
amplifying medium interaction with laser radiation *(Rumanian)* 78−59011
anisotropic, oscill. props., rate eqns. 78−22135
antireflection coating deposition from hydrolyzable soln. 77−58495
apparatus and applications *(Japanese)* 77−68215
Argus high power system, spatial filter imaging relays 77−88760
Argus two beam system, 5 TW performance 78−46656
array spatially-coherent beam formation and mode locking 78−37898
axial mode selector for laser with active Q-switching 79−13996
beam divergence and refractive power of directly coated solid state lasers 79−59736
beam transport optics for laser fusion 78−83017
book, quantum electronics 80−105442
Bragg scattering effects 79−36901
clocks, for psec. meas., review 78−12676
coherent and nonlinear optics, conf., Leningrad, USSR (Jun. 1978) 80−98753
colour centre, tunable CW, for spectroscopy and photochemistry 78−94397
colour centre laser, progress in tunable lasers 80−43344

solid lasers continued
colour centre laser pumped by flashlamp-pumped dye laser 80−102737
colour centre laser with superfluid He cooling 80−48282
colour centre pulsed broadly tunable IR laser 79−76706
colour-centre lasers, thermal strains in active elements 80−91804
communication device research in Japan 77−75677
conference, Dresden, Germany (Mar.-Apr. 1977) 77−83881
conference, inertial confinement fusion, San Diego, USA, (Feb. 1978) 78−46171
conference, laser and electro-optical systems, San Diego, CA, USA (Feb. 1980) 80−62392
conference, laser engineering and appls., Washington, USA (May-June 1979) 80−1216
correlation function, near threshold, laser with saturable absorber 79−27266
crystal evaluation, testing and meas. instrument 77−7226
CW, actively mode-locked, picosecond pulse form., computer model 79−36939
design, construction, charact. and practical problems, book 77−71993
dibenzyl: naphthacene, cryst., ground electron state, vibr. levels, relax. time determ. *(Russian)* 78−15195
disc amplifier, amplified spontaneous radiation 77−3594
distributed aperture effect in laser rods with negative lenses 78−66857
double pulse laser oscillator with continuously variable time interval between pulses 79−10321
dye ultrafast saturable absorbers for Nd lasers 80−53386
dynamics, Auger recombination effects 80−69398
with electro-optical shutter, piezo-opt. effect on dynamics and spectral charact. *(Russian)* 77−83912
electron beam laser technology and applications 77−19262
electron beam pumped semiconductor, appl. to projection TV 77−88830
electron beam pumped semiconductor laser as TV tube screen 78−29969
electron beam pumped semiconductor laser for projection TV 77−72004
encapsulated solid-state laser based on type-IMA tube 77−38915
energy storage and nonstoring advanced lasers for fusion appls. 78−79027
F_2-centre, pulsed tunable laser, IR spectral charact., 1.1-1.26 μ region 80−91805
F II centre laser, cavity design incorporating polarisation beam splitters 79−45960
F-centre, laser, continuously tunable near IR *(German)* 80−1207
F-centre crystals utilisation, spectroscopic light sources appl. 79−36900
F-centre CW, using diffr. grating tuners 79−86183
F-centre laser used for IR optogalvanic spectrosc. of He positive column discharge 80−78563
F-centres, struct., quantum optics, laser spectra 77−52147
fibre, scattering and absorption losses, approx. theory 77−27339
fibre laser high-power stimulated emission pulses, substruct. 80−9890
fibre Raman and Brillouin laser gains, polarisation effects 80−9887
flash lamp pumping, ballast vol. effect on efficiency 77−707
fluctuations in laser theories 80−83587
fluorophosphate laser glass, highly homogeneous, production 80−14411
fluorophosphate laser glasses, low nonlinear refr. index, development 78−50870
fluorophosphate laser glasses, Nd doped, piezooptic coeffs. meas. 80−99815
four level laser, Q-switched, dynamics and lifetime of terminal energy level *(Chinese)* 78−66832
four-level laser power and relaxation oscillation, excited-state diffusion effect 77−79834
frequency spectrum, linear atom-field interaction 77−19258
fusion microexplosions appl., Nova scientific feasibility experiment 79−49863
fusion reactor laser, Shiva pulse power, isolation and control system 78−54935
fusion reactor systems 77−88763
fusion research laser, 30 TW Omega system 79−55146
fusion research lasers, advanced components and systems for beam lines 79−18466
fusion system, imaging props. of spatial filter to reduce self-focusing 77−58360
gain measurement in optically pumped materials, diffr. effect 77−19225
garnets, concentrational inhomogeneities, appl. of vacuum decoration method, laser material 79−14835
garnets development for laser cryst. matrices, spectral generation data survey 77−10928
Gekko high power glass systems, laser fusion the Japanese way *(German)* 78−66838
Gekko IV, four beam phosphate glass laser system for fusion expts. 78−46650
giant pulse lasers, passive mode-locking 79−72608
glass, beam quality and efficiency increase by using circ. polaris., phosphate glass and double-pass amplifiers 78−46654
glass, Brillouin scatt. meas. of elastic, elasto-optic consts. and extinction coeffs. 79−11429
glass, electronic nonlinearity coeff. meas. 79−27341
glass, large disc, optical homogeneity, high accuracy measurement *(Chinese)* 79−55195
glass active element, polyhedral shape *(Russian)* 77−31103
glass active elements of pulse-periodic lasers, thermal lenses 79−89914
glass cladding composition and design criteria 79−18450
glass disc amplifier assembly, necessity for dust-free environment 77−83879
glass disc amplifier output stages, energy charact. for silicate and phosphate glasses 79−64237
glass for fusion research 79−13979
glass high energy systems, conference, Reston, VA, USA (Apr. 1977) 78−50783
glass high power laser system, performance charact. of BETA 77−88761
glass high power system, with polarising optical components 77−46727
glass highly repetitive picosecond laser system, for fusion research 77−88762
glass laser, dynamic tuning of polarisation of radiation *(Russian)* 77−38945
glass laser disc interface with edge cladding glass, reflection meas. 79−27300
glass laser high power system for thermonuclear fusion *(Japanese)* 78−8970
glass laser rod, mech. strength and heat resistance obs. 79−76776

solid lasers continued
glass laser rods, silicate and phosphate, pumped in pseudoelliptic cavities, thermal effects 79−76692
glass laser self-focusing suppression through low-pass spatial filtering and relay imaging 78−74938
glass laser systems, high energy, variable ratio beam splitters 79−45952
glass rod amplifier, circularly polarised light to reduce self-focusing 77−58396
glass rod amplifier, for OMEGA system 78−46653
glass surface cleaning, liquid spraying technique 78−72921
glasses, activated, athermality criteria for laser appls. *(Russian)* 77−66485
glasses, figures of merit and physical/optical property correlations 79−13970
heat pipe apparatus for coloration of laser-quality alkali halide crystals 78−74917
HF self-modulation of laser with unstable resonator *(Russian)* 77−83911
high power, progress 77−88773
high power lasers for practical appls., conference, Reston, Va., USA (Mar. 1976) 77−34895
high power sharpened pulse form. in amplifying system 77−75584
high-efficiency, high-power lasers for fusion appl. *(Japanese)* 78−5486
high-power glass laser users' facility with computer control 77−19341
holographic method for laser radiation divergence reduction *(Russian)* 78−63147
II-VI semiconductor laser screens, for electron-hole tubes, stimulated emission mechanism 79−94237
impure molecular crystals, ground electron state, vibr. levels, relax. time determ. *(Russian)* 78−15195
instability below threshold, laser-saturable absorber system 78−94385
interlocked solid-state lasers, radiation intensity modulation for precision meas. 80−1250
inversion depletion on ultrashort pulse evolution, mode-locking behaviour 80−5736
IR source, tunable, efficient 80−5789
IR tunable laser for semiconductor multiphoton spectroscopy *(French)* 80−82836
laminated active laser element, thermal stresses produced by longit. nonuniform pumping *(Russian)* 78−5474
laser amplifier design using generalised experimental data 78−66836
laser glass inversion density, direct meas. 79−13969
lenses focal distances meas., in active elements, using Zernike interferometer 80−48268
$LiNdP_4O_{12}$, fluoresc. and oscill. characts. at 1.317 μm 78−5473
material nonlinear refractive index meas. by time-resolved interferometry 77−18088
measurement, radiation pulse width determ. using Fabry-Perot interferometer 80−23736
measurement, radiation pulses formation and stabilisation 80−23735
measurement, single-pulse, with uniform distribution of energy density, correction equipment 80−23703
Mikron high-power multichannel laser pulse system, Nd:glass rods 80−28249
miniature power pack 78−59015
mode locking, importance of active medium nonlinearity 79−13967
mode locking, longitudinal, in cavity reson., free generation region *(Russian)* 77−75572
mode self-locking 78−1283
mode-locked colour-centre, use for distortionless propagation of 5 psec-wide pulses in fibres 79−94358
modulation spectroscopy using solid-state and gas lasers 79−30572
monochromatic laser with saturable absorber driven by coherent field 79−50304
multimode, with modulated resonator losses, radiation intensity fluctuations 80−74367
multimode laser, mode interaction and radiation fluctuations 80−43338
Nd: glass, 1060 nm picosecond laser impulse, characterisation by sweeping slit cameras *(French)* 78−42366
Nd:glass, high power system for nuclear fusion 77−19338
Nd:glass 20-beam fusion laser focusing lens design 77−18706
Nd:glass multichannel laser with plasma shutter 80−64088
Nd:YAG, high-efficiency freq. doubling in CsD_2AsO_4 and KD_2PO_4 78−79071
nonlinear active medium laser, transient intracavity SHG, giant pulse generation 80−9948
nonlinear active medium laser for both stimulated emission and SHG 79−64285
nonlinear limitation for fine-scale self-focusing 79−23032
nonlinear stratified system, plane wave propagation 80−43343
Nova: the laser fusion scientific feasibility experiment 78−59040
NOVA, pulsed power control system, fibre-optic multi-tapped computer bus 80−95443
Nova 200 TW glass laser system for thermonuclear fusion, large laser control system, evolution from Shiva to Nova 80−9894
Nova Nd:glass large fusion laser system, mechanical design 80−91279
ns pulse length continuous control, appl. to Nd laser 78−1280
OMEGA laser system, design parameters, performance 78−46655
OMEGA laser system for fusion expts. 78−46649
Omega laser system for fusion studies, Rochester Univ. 78−59041
optical delay lines to control solid state laser output characts. 80−99758
optical design of laser fusion reactors 78−82518
optical fibre laser plate for digital image processing, all-optical parallel logic operation 80−106463
optical glass and single crystal production 79−94308
optical glass exposed to laser radiation, absorpt. coeff. temp. depend. 79−89979
organic dye attachment for wavelength conversion within 340 to 1200 nm 79−7147
oscillator-based powerful laser, GOS-1001 with film resonator Q-switch 79−3705
passive mode locking with fixed moment of stimulated emission 77−61973
passively mode locked, generation of ps pulses, probability of double pulse generation anal. 77−717
passively mode locked, picosecond pulse generation, pulse compression and broadening 77−31111
passively mode-locked, picosec. pulse generation, intensity maxima and their probability distrib. 77−34891
passively mode-locked laser, statistical props. of ultra-short pulses 79−36941
solid lasers continued
periodic laser with unstable resonator, single-pulse emission characts., active-medium inhomogeneities effect 80−74365
periodic mode loss, use of grating mirrors in IR laser resonators 80−28254
periodic mode without forced cooling, active element thermal deformation anal. *(Russian)* 78−66837
Pharos II, Naval Research Lab. inertial confinement fusion programme 78−59042
phosphate glass 4TW laser system for fusion ignition *(Japanese)* 79−81457
phosphate glass active-passive mode-locked oscillators at 1.054 μm 78−63139
phosphate glass laser, statistical props. and stabilisation 80−48266
phosphate glass lasers, highly repetitive, development 80−69415
phosphate glass oscillator, passively mode-locked, stabilised with acousto-optic modulator *(Japanese)* 79−13999
phosphate glasses, laser props. under pulse-periodic pumping conditions 79−64236
phosphate laser glass, Nd doped, piezooptic coeffs. meas. 80−99815
phosphate laser glass inversion density, direct meas. 79−13969
phosphate laser glasses, review 80−9888
physics of laser crystals, theoretical problems, current status *(Chinese)* 79−45948
picosecond light pulse techniques and applications, book 77−61137
picosecond pulse generation methods, book contrib. 77−61138
planar active element convective cooling *(Russian)* 78−82978
plane active element initial cooling period *(Russian)* 79−36904
plane waveguide laser, with semitransparent wall, kinetics 77−54740
planospherical resonator with internal lens, stability of caustic 79−31954
plasma Q-switch in laser cavity 80−28259
pulse generation, temporally shaped, for inertial confinement 78−50831
pulse shaping for inertial confinement fusion expts. 77−83905
pulse train stability with periodic Q-switching 80−28239
pulsed diode simulators of solid lasers $Al_xGa_{1-x}As$ and $Ga_xIn_{1-x}P_{1-y}As_y$ solid solns. 80−91816
pulsed solid laser radiation reproducibility *(German)* 77−58331
Q-switched, nanosecond and microsecond pulse generation, review 78−71130
Q-switched laser with unstable resonator, transient processes 77−75576
Q-switched operation *(Japanese)* 77−691
Q-switching by optomechanical shutter 79−72609
rare earth compounds, linear conc. quenching of luminesc. 79−31908
rare earth doped $Bi_4Ge_3O_{12}$, cryst. growth, spectral and laser props. 80−45115
rare earth ion containing inorg. materials, 3μm band stimulated radiation 80−97306
rare earth lasers, book contrib. 80−53306
rare earth lasers and excited states, book 78−29958
rare earth pentaphosphates:Ce^{3+},Tb^{3+}, energy transfer between dopants, excitation spectra, laser appls. 78−10961
rare earths in vapour and solid phases as high intensity lasers, laser line prediction 79−3700
recent advances at MIT Lincoln Lab. 78−82969
refraction effects and gain measurement 79−31905
resonantly excited laser media, possible use in wavefront reversal 79−94281
retroreflecting mirror for dynamic compensation of optical inhomogeneities 79−31970
rhodamine 6G dye in quartz glass microcomp. matrix, as tunable solid laser 80−99734
riby resonator, lasing spectrum singularities and Q-factor, for z-dimens. beam path *(Russian)* 77−88795
ring, interactions between opposite waves, self-modulation and beats 78−17983
ring, synchronisation regimes of opposite waves and beats *(Russian)* 79−3717
ring, with weak external signals 77−23702
ring laser, generation of microsecond pulses 80−9913
ring laser, mode locking theory 79−41399
ring laser, single-freq., spontaneous antiphase fluctuations, theory 80−91821
ring laser, solid state, with intracavity bleachable filter, conditions for CW stimulated emission 80−14368
ring laser, synchronisation modes of colliding waves and beats 79−72602
ring laser, travelling-wave, linear stage of field development 80−23724
ring laser with additional mirrors, stabilisation by external signal 78−82998
rods, with negative lenses, distributed aperture effect 80−38046
rods and mirrors, optical fabrication techniques 77−65600
ruby, μs pulse laser with negative feedback 77−714
ruby, application to high-speed photography of fast processes 77−68236
ruby, battery powered, pulsed, based on electronic flash, for portable holo-camera 79−3711
ruby, beam characts. using DC induced SHG in gas 77−7093
ruby, coherence for holographic interferometry rel. to pumping energy 77−75440
ruby, concentrational inhomogeneities, appl. of vacuum decoration method, laser material 79−14835
ruby, continuously pumped, repetitive self-Q-switching 78−50781
ruby, cryst., excited state absorpt. and energy output 77−65595
ruby, cryst., lasing action, spectrum, luminesc. spectrum effects *(Russian)* 78−13716
ruby, cryst., optical properties, effect of annealing near melting point 78−90419
ruby, crystal defects influence obs., on energetic effectiveness *(Czech)* 78−79022
ruby, CW operation, pumping by Ar ion laser 78−1253
ruby, CW operation 77−38901
ruby, effect of unexcited part of rod on generation 79−18422
ruby, EPR method of predicting cryst. characts., laser appl., working element parameters 79−11345
ruby, fabrication of optics 79−23099
ruby, far IR lasing feasibility, pumping via ruby laser 79−81435
ruby, focusing effects during laser emission in relaxed state *(French)* 77−34896
ruby, for high freq. holography *(German)* 77−79779
ruby, freq. synchronisation and locking by passive modulator 80−1249
ruby, frequency-stabilised using Fabry-Perot interferometer 80−58566
ruby, gain probing by intracavity dye laser spectroscopy 77−7092
ruby, giant pulse self-modulation at 90K 77−38961

solid lasers continued
ruby, giant pulses, time of appearance control with KS-19 glass passive switch 77−38959
ruby, graphical method for pumping coeff. estimation 80−14343
ruby, HF holography, appl. to laser-prod. cavitation bubbles *(German)* 77−75437
ruby, laser, variable radiation loss 77−50685
ruby, lasing spectrum fine structure form. in transparency microwindows of gaseous media 79−3722
ruby, low-temp., with optical delay line inside resonator, cooling system 79−36922
ruby, microsecond pulse production, with quadratic loss in laser cavity 77−7147
ruby, mode synchronisation during loss modulation on freq. difference *(Russian)* 77−61989
ruby, modulation by US surface waves on resonator mirror 77−50699
ruby, negative feedback, external perturbations effect, spectral depend. 77−83908
ruby, negative feedback, ultrashort pulse generation 78−13714
ruby, nonlinear optical freq. transform. of variously polarized laser radiation 79−55181
ruby, nonuniform amplification effects *(Russian)* 77−14722
ruby, one-freq. tunable one-pulse, selector parameter optimisation 78−74935
ruby, output spatial charact. using FTIROS material 79−68414
ruby, passive Q-switching by colour centres in SrF_2 78−71157
ruby, passive Q-switching by I_2 vapour bleaching 77−79872
ruby, peak generation for active mode phasing *(Russian)* 79−14000
ruby, picosecond pulse generation by electrooptic shutter passive switching 79−36942
ruby, power enhancement by intracavity plasma 80−53330
ruby, pulse generation by electrooptic gating *(Russian)* 77−79871
ruby, pulsed, laser annealing to round edges of Si structures 80−25742
ruby, pulsed, with active spectrum phasing, dynamics and energy charact. *(Russian)* 78−9387
ruby, Q-factor passive modulator, unloading, in resonator with prism *(Russian)* 77−68234
ruby, Q-switched, power dependent freq. sweep 77−19256
ruby, Q-switched, semicond. wafer laser annealing, review and anal. 80−25741
ruby, Q-switched, spectroscopic props., operation modes, pulse amplification *(Rumanian)* 80−48265
ruby, Q-switched laser, laser induced damage, influence of pores 77−83918
ruby, Q-switching, theory 77−38948
ruby, radiation self-modulation with passive closing of electro-optic shutter 79−64258
ruby, rotating beam generation 80−1258
ruby, single pulse formation kinetics with self-modulation of quality factor *(Russian)* 77−27312
ruby, single-pulse laser, controllable phototropic shutter design 80−23699
ruby, slot method for radiation extraction 77−50694
ruby, spark control cavity dumping 78−59053
ruby, spatial coherence meas. with holographic coherence meter 80−9837
ruby, threshold pumping energy depend. on loss coeff. *(Russian)* 77−46723
ruby, total mode self-synchronisation 79−64259
ruby, treatment of chromatic maculae of the skin *(German)* 78−24177
ruby, ultrashort pulse generation by internal phase and amplitude modulation 80−106551
ruby, unstable Q-switched resonator in negative branch confocal config. 79−13980
ruby, use of KS glasses as passive shutters for generating subnanosec. pulses 80−102728
ruby, weak passive Q-switching in spherical resonator 78−50834
ruby, with electrooptical shutter, emission spectrum narrowing and single freq. giant pulse lasing 80−78877
ruby and Nd:glass lasers placed parallel in cavity, for efficiency increase *(Russian)* 77−10954
ruby cryst. R-line absorpt. and dispersion spectra, mag. field effects *(Russian)* 78−92056
ruby crystal, radiation amplification, spatial coherence 80−99737
ruby fibre laser, room temp. continuous operation without cooling, crystal growth, heating effects 78−66833
ruby laser, double mode locking using dye saturable absorber 80−99763
ruby laser, generation, amplification of high power picosecond pulses depend. on superluminescence 80−53305
ruby laser, negative feedback, cavity Q insertion effect on parameters of modulated pulses 80−43376
ruby laser, passively mode-locked, output charact. 79−18424
ruby laser, pulsed, electronic speckle pattern interferometry 78−65961
ruby laser, Q-switched, parameter depend. on ruby quality 78−46608
ruby laser, radiation automodulation with passive switching of electro-optical shutter *(Russian)* 78−74936
ruby laser, radiation charact. rel. to pumping intensity in long-time operation *(Russian)* 77−68214
ruby laser, radiation effects on Xe plasma *(Russian)* 78−22514
ruby laser, self-synchronisation of modes *(Russian)* 78−74937
ruby laser, spherical cavities, Q-switching by rotating mirror 80−28261
ruby laser, spiked regime, dynamic theory 79−27260
ruby laser, two single-pulse generation *(Russian)* 77−46725
ruby laser, with stimulated Brillouin scatt. complex conjugate mirror 80−87438
ruby laser beam amplifiers, induced distortion removal by dynamic holographic correction *(Russian)* 78−55326
ruby laser beam spatial coherence interferometry 79−14003
ruby laser elements, laser backscatt. by bulk damage zones 79−23000
ruby laser generating ultrashort light pulses, saturating absorber efficiency increase 80−23700
ruby laser holocinematography for cavitation bubble dynamics recording 79−86147
ruby laser operation principles 79−27265
ruby laser rod, absorption coeff., loss coeff. and population inversion *(Japanese)* 78−37888
ruby laser rod, exoemission parameter rel. to optical strength 77−732
ruby laser third harmonic generation in Tl vapour, focusing degree influence 80−48348
ruby laser with bisanthene phototropic Q-modulator *(Russian)* 77−83910
solid lasers continued
ruby laser with high-frequency control of lasing conditions 80−74363
ruby laser with nonorthogonal resonator, rotating laser beam generation *(Russian)* 79−10330
ruby laser with optical delay line inside cavity resonator 77−42552
ruby laser with small active volume, mode-locked ultrashort pulse generation 79−89932
ruby laser with special resonator Q-switching 77−38958
ruby lasers and $LiNbO_3$ cryst. in difference freq. laser, tunable MM range emission 80−5764
ruby NMR laser, ^{27}Al nucl. spin system, collective ordering phenomena, instabilities 80−11278
ruby NMR laser, dynamic props. from point of view of synergetics 80−43341
ruby NMR laser, spontaneous nucl. spin system self organisation 79−916
ruby oscillator-amplifier compact system for satellite ranging 79−966
ruby passive Q-switched oscillator, damage limited pulsewidth 78−83004
ruby passively mode-locked laser, subnanosecond pulse generation using saturable absorber 79−86197
ruby pulsed laser radiation action on polydisperse water aerosols 80−14378
ruby pulsed laser real-time holographic interferometry 80−74319
ruby Q-switched, with stable operation in pure transverse natural oscillations *(German)* 77−14761
ruby Q-switched laser, photographic film calibration for energy meas. 78 5517
ruby raser, instabilities and first order phase changes *(German)* 80−48263
ruby ring laser with forced mode locking 80−95915
ruby rods, quality control, EPR method 79−14047
ruby sweep generator, spectral-kinetic charact., singularities *(Russian)* 77−83894
sapphire, concentrational inhomogeneities, appl. of vacuum decoration method, laser material 79−14835
satellite rings, energy losses caused by diffusion, refl. in cavity 79−89911
scanning laser microscope, electron beam excited 80−52303
self-synchronising modes, saturated filter relax. time reduction *(Russian)* 77−7145
semiclassical theory of stability, generalised entropy 79−3699
semiconductor DFB laser excited by electron beam, radiation coupling out 79−90038
semiconductor DFB laser pumped by electron beam, temporal and spectral charact. 79−94238
semiconductor electron-beam-scanned laser quantoscope, large-screen colour projection TV system 80−99783
semiconductor laser, longit. pumped by electron bombard., variable-gap struct. threshold charact. 79−59703
semiconductor sealed scanning laser with transverse electron-beam pumping, for projection TV systems 79−89936
semiconductor single crystal, CRTs with semiconductor laser screens, scanning optical microscopy appl. 80−86398
semiconductor streamer lasers 77−79831
semiconductors, low carrier density, lasing action, exciton Bose condensate charact. function 79−64233
SHIVA, 30 TW Nd glass laser system for inertial confinement fusion 79−22978
Shiva, laser-target and laser isolation 78−59035
Shiva alignment systems 78−59033
Shiva fusion laser, development of components and subsystems 78−5491
Shiva high-radiance nd-doped disc laser amplifiers 78−59036
Shiva laser, 25 MJ energy storage and delivery system 78−59038
Shiva laser beam diagnostics 78−59037
Shiva laser computer control system 78−59034
SHIVA laser for fusion reactors, fluorphosphate glass development 78−37440
Shiva laser fusion facility construction, optical engineering problems 78−82989
SHIVA laser optical component manufacture and testing 79−22980
Shiva laser performance, nominal interstage beam energy, power 78−59032
Shiva mechanical systems 78−63135
Shiva Nd:YAG short-pulse oscillator 78−63134
Shiva optical system 78−59039
short pulse generation, subnanosecond and picosecond operation 80−28262
single-mode face pumped laser, resonant-mode analysis 77−58350
SL100, commercial Nd laser glass, props. 78−74912
solid Nd:YAG, picosec. pulse freq. doubled laser system, for satellite ranging 77−21933
spectrally inhomogeneous active medium, giant external pulse 78−17897
stability, using resonator without external mirrors 80−33024
stimulated emission threshold of semiconductor, surface recombination influence 79−10311
survey of solid state lasers, book contrib. 80−106529
system performance and machine idealisation 77−19326
thermo-optic lens temp. distrib. and focal length calc. 79−72575
thermostabilization by liquid flow past laser active element *(Russian)* 79−27268
tunable IR lasers, principles and operating charact., review 79−98376
tunable IR lasers with $F_A(II)$ and $F_B(II)$ colour centres 78−90420
tunable IR solid-state laser characteristics and principles 80−87406
tunable laser with microcomposition matrix active medium 79−64238
tunable medium IR down conversion in GaSe using Nd^{3+}:YAG and dye lasers 79−55183
TV image formation using laser projection electron-beam tubes 79−59743
two-standing mode operation with stationary ats., saturation effects and stimulated scatt. 79−68398
ultra-short light pulse generation, review *(Japanese)* 79−45973
ultrashort laser pulses, form. dynamics and self-stabilisation *(Russian)* 77−19259
ultrashort light pulse optimum generation, solid laser with brightening filter 79−36903
ultrashort pulse duration control rel. to forced mode synchronisation *(Russian)* 77−46735
ultrashort-pulse generation by lasers with saturable absorbers 78−46687
undamped spiking, dynamical theory 77−14724
unstable telescopic resonator laser, energy parameters calc. 77−75577

solid lasers continued
UV laser possible pumping by synchrotron radiation, NaCl:I(Br) luminesc. 78−66835
vacuum UV laser possibility for crystals pumped by X-ray synchrotron radiation 79−41387
wavelength identification using reference absorber 78−5513
YAG highly repetitive picosecond laser system, for fusion research 77−88762
Ar pumped CW ruby laser 77−68227
CO, solid, CO laser excited, strong vibr. population inversion 80−58547
CaF_2 crystal active element for colour-centre laser, thermal strain anal. 80−91804
$CaF_2:D^{2+}$ submm. magnetospectroscopy, tunable far IR laser potential 78−52481
CaO, tunable optical gain at 3600 Å using F^+ centres 79−45947
CdS, CdS_2Se_{1-x}, single cryst. ingot, as CRT screen 77−75561
CdS, CdS_xSe_{1-x}, scanning semiconductor laser with transverse electron-beam pumping 80−9904
CdS crystals, one-photon pumping, active layer structure, light amplification 80−78858
CdS, doped laser mechanism and output study 80−43340
CdS, electron beam pumped, catastrophic and gradual degradation 77−61960
CdS, electron-beam pumped, excitation of short cavity rhodamine 6G laser 78−25887
CdS, electron-beam-pumped laser, basis of scanning optical microscope 80−31864
CdS, generation of optical radiation in direction of propag. of streamer 80−69401
CdS, highly excited, stimulated emission process at 80K 80−97307
CdS, laser, petal shaped cryst., high-temp. spectral charact. *(Russian)* 79−13968
CdS, laser action in dense exciton systems 77−75531
CdS, laser thresholds and stimulated emission, intrinsic recomb. processes 79−15489
CdS monocrystal petal lasers, single-photon excitation *(Russian)* 80−99736
CdS platelet laser, emission spectra, optical coupling between partial resonators 80−69400
CdS platelet lasers, optically pumped, spatial and spectral distribution of laser emission 80−64032
CdS screen, laser electron-beam tube under scanning conditions 79−13983
CdS screen for laser CRT, stimulated emission with TV type operation 78−59028
CdS semiconductor laser, longitudinally pumped, electron beam scanning vel. rel. to output parameters 80−9889
CdS, single cryst., laser emission following single-photon excitation *(Russian)* 78−37889
CdS single cryst., lasing action excited by ruby laser picosecond pulses 80−64035
CdS single crystal, laser emission at one-photon excitation *(Russian)* 77−79835
CdS, single crystal, subnanosecond light pulse generation by laser radiation pumping 79−64234
CdS single crystal laser screen, photolum., determ. of layer depth disturbed by polishing 78−17977
CdS single crystals, depend. of radiative props. on equilib. carrier density 79−19932
CdS, stimulated and spontaneous emission from degenerate electron-hole plasma at 300K 80−29762
CdS, stimulated emission under N_2 laser excitation 77−14723
CdS streamer laser, generation of ps. light pulses 80−9908
CdS, submillimetre laser emission due to transitions between free exciton level 79−27261
CdS, superluminescence due to pulsed X-rays, 170 and 295K 78−42338
CdS, two-photon-excitation, tunable laser emission, luminesc. processes 80−55127
$CdS_{1-x}Se_x$ monocrystal petal lasers, single-photon excitation *(Russian)* 80−99736
$CdS_{1-x}Se_x$, spatial distribution and lasing modes under one photon optical excitation *(Russian)* 78−59012
CdS_xSe_{1-x} laser electron-beam tube, possibility of acceleration voltage lowering 79−89929
CdS_xSe_{1-x}, strongly excited by electron beam, determ. of nonequilibrium carrier lifetime 80−39603
Ce:LaF_3 286 nm laser, optically pumped 80−99738
Ce:$LiYF_4$, tunable UV laser at 325, 309 nm, KrF laser excitation 80−38022
Ce^{3+}:LaF_3, UV fluoresc. potential tunable laser 2760 to 3220 Å 78−15206
Ce^{3+}:$LiYF_4$, UV laser at 325 nm, stimulated emission obs. 79−72574
Ce^{3+}:LuF_3, UV fluoresc. potential tunable laser 2760 to 3220 Å 78−15206
Ce^{3+}:YAG, excited-state absorpt. meas., tunable laser model system 79−42994
Co:MgF_2, laser, broadly tunable CW operation, output powers, optical pumping 80−32995
Co:MgF_2, tunable transition-metal-doped solid state lasers 80−58549
Cr^{3+}:Al_2BeO_4, Alexandrite, tunable laser sources development and appl. 80−48262
Cr^{3+}:$BeAl_2O_4$, alexandrite, potential laser material, stimulated emission and absorpt. spectrum 79−33734
Cr^{3+}:$BeAl_2O_4$, tunable laser performance, 701 to 794 nm, long-pulse and Q-switch operation 79−72573
Cr^{3+}:$BeAl_2O_4$ alexandrite laser, high gain performance 80−53299
Cr^{3+}:$BeAl_2O_4$ alexandrite laser, wavelength-tunable CW laser action 80−53300
Cr^{3+}:YAG, radiation colour centres, absorpt. and thermolum. spectra 78−48206
Cu laser with excitation by transverse discharge, construction of cuvette 80−106532
Dy^{3+}:oxide glass, intensity parameters and laser transitions 79−50300
Er^{3+},Yb^{3+}:glass, laser pumped, stimulated emission 77−50675
Er^{3+} implanted crystals, laser active media, nonradiative losses due to $^4I_{11/2}$-$^4I_{13/2}$ transition 79−31911
Er^{3+}:CaF_2, laser-induced damage in alkali halide and other crystals at 2.76 μm 79−91539
Er^{3+}:CaF_2 crystal laser, hologram form. at 2.76 μm, laser emission linewidth meas. 79−10270
Er^{3+}:ErAG, 3 μm stimulated emission at room temp. 77−42541
solid lasers continued
Er^{3+}:$Gd_3Ga_5O_{12}$, stimulated emission 79−91466
Er^{3+}:$KGd(WO_4)_2$, stimulated emission by subsidiary transitions 79−3696
Er^{3+}:$KLu(WO_4)_2$, room temp. stimulated emission obs. 80−106527
Er^{3+}:$La_2S_3.3Ga_2S_3$ glass, fluoresc., and possibility of lasing 78−23514
Er^{3+}:$Lu_3Al_5O_{12}$, 3-μm crystal laser functional scheme, stimulated emission 80−43339
Er^{3+}:$Lu_3Al_5O_{12}$ 3 μm stimulated emission at room temp. 77−42541
Er^{3+}:trifluoride, VUV fluoresc., tunable source, 1650-2600 Å 77−688
Er^{3+}:YAG, 3 μm stimulated emission at room temp. 77−42541
Er^{3+}:YAG pulse periodic laser with high activator conc. 79−10320
Er^{3+}:YE+AG, radiative and nonradiative transitions, conc. quenching 77−16391
Er^{3+}:YErAG, $^4I_{11/2}$ to $^4I_{13/2}$ laser transition cross section, luminesc. energy 77−79833
$Er_3Al_{5-x}Ga_xO_{12}$, LPE, spectroscopic props. 80−93419
Eu^{3+}→Nd^{3+} diffusion-limited energy transfer in Na borate glass 78−31238
GaAs, density of states, spontaneous emission rate calcs., 120, 160, 200K 77−4292
GaAs, electron beam pumped laser, far-field radiation pattern, optical confinement effects 79−86181
GaAs, electron-beam excited, efficient generation of electron-hole plasma 80−76051
GaAs electron-pumped uncooled laser, degradation rel. to dislocation density 80−14344
GaAs excited by HV pulses, stimulated emission and luminesc. obs. 79−59704
GaAs, image emission platelet laser, for optical information processing 77−58268
GaAs, N_2 laser pumped under appl. elec. field, gain anisotropy 77−61958
GaAs, optically pumped DFB laser, with two-dimens. Bragg reflectors 78−1252
GaAs ribbon whiskers, photopumped, laser action 80−91801
GaAs, stimulated and spontaneous emission from degenerate electron-hole plasma at 300K 80−29762
p-GaAs, wavelength depend. of gain saturation 78−1229
n-GaAs:Sn, Te, compact IR laser source pumped by electron beam from field emission tube 79−59725
GaAs:Zn optically pumped ribbon-whisker laser, picosecond pulses 80−99771
$GaAs_{1-x}P_x$, continuously tunable electron beam pumped laser 78−50802
$GaAs_{1-x}Sb_x$-$Ga_{1-x}In_xP_{1-y}As_y$ multilayer structure, continuously tunable electron beam pumped laser 78−50802
$GaAs_xSb_{1-x}$, spontaneous and stimulated emission, electron beam excitation 77−58333
GaInAs, electron-pumped laser, far-field radiation pattern, optical confinement effects 79−86181
$Ga_xIn_{1-x}As$, spontaneous and stimulated emission, electron beam excitation 77−58333
$Ga_xIn_{1-x}As_{1-y}P_y$, spontaneous and stimulated emission, electron beam excitation 77−58333
GaSb, electron beam excited, spectral and power charact. 77−50676
Gd_2O_2S, compact specimen prep. 77−85951
Ge^{3+}:YAG, excited state absorpt. loss, 5d→4f rare earth lasers 78−90417
$Hg_{1-x}Cd_xTe$, LPE-grown and optically pumped crystal, continuous lasing at 2.79 μm 79−68397
HgI_2, stimulated emission and optical gain, 80K 78−33738
Ho^{3+} in oxygen-containing crysts., stimulated emission at low temps. 80−106526
Ho:$LiYF_4$, 750 nm laser oscill., flashlamp and dye laser pumping 78−9386
Ho:$LiYF_4$ laser, TEM_{00} mode and Q-switched operation 80−74395
Ho^{3+}:$BaYb_2F_8$ 80−95902
Ho^{3+}:$ErVO_4$, CW and pulsed laser emission at 2.0416 μm 77−19254
Ho^{3+}:$Gd_3Ga_5O_{12}$, stimulated emission and Ho^{3+} cascade laser action 79−91466
Ho^{3+}:$LiEr_{0.945}Tm_{0.05}Ho_{0.005}F_4$ laser, tuning at 2.06 μm 80−83611
Ho^{3+}:$LiYF_4$, 1.392, 1.673 and 3.914 μm stimulated emission, laser cascades 80−9886
Ho^{3+}:$LiYbF_4$, active medium for Nd laser freq. convertor, cascade stimulated emission 80−102727
Ho^{3+}:$LiYbF_4$, laser converter for 2.06 μm radiation, ND primary laser 79−18427
Ho^{3+}:YAG, 2.09 μm stimulated emission, resonant pumping by Nd laser 78−17944
Ho^{3+}:YVO_4, CW and pulsed laser emission at 2.0412 μm 77−19254
$Ho^{3+}KGd(WO_4)_2$, stimulated emission by subsidiary transitions 79−3696
InAs, electron beam excitation, luminesc. and stimulated emission 77−16339
InAs, electron-beam-pumped 77−50689
InAs, epitaxial, laser action mechanisms with electron beam excitation 80−28240
$InAs_xP_{1-x}$, continuously tunable electron beam pumped laser 78−50802
$InAs_xSb_yP_{1-x-y}$, efficient electron-beam-pumped laser at 3.1-3.7 μm 80−5738
n-InSb, stimulated recomb. radiation 78−90456
$K_5Bi_{1-x}Nd_x(MoO_4)_4$ solid soln., growth, spectroscopic and laser props. 78−2901
KCl crystal active element for colour-centre laser, thermal strain anal. 80−91804
KCl:Li $(F_2^+)_A$ centres, tunable CW laser action 80−87399
KCl:Li F_A(II) centre laser, pumped by flashlamp-pumped dye laser 80−102737
KCl-OH^-, electron irrad., F_2^+ centre stabilisation and tuneable laser operation 80−54231
$KEr(WO_4)_2$, crystallisation cond., stimulated emission in 2.8 μm band 80−53301
KF F_2^+-centre laser, picosecond pulse generation 1.24 to 1.45 μm, mode locking 79−89925
KF, tunable CW laser, using F_2^+ centres for 1.26-1.48 and 0.82-1.07 μm bands 78−79023
KF:Pd^{2+}, pure and doped, two-step photoionisation, laser-active F_2^+ centre form. 79−963
$K_5NdLi_2F_{10}$ (KNLF), spectroscopy and lasing 80−5737
$K_5NdLi_2F_{10}$, high yield luminesc., potential miniature Nd laser 79−1784
$K_5Nd(MoO_4)_4$, Ar^+ laser pumped, quasi-CW laser action 79−18421

solid lasers continued
$KNdP_4O_{12}$, CW laser oscill., near 1.32 μm 77−61957
$KNdP_4O_{12}$, determ. of fluoresc. quantum efficiency and laser emission cross sections 80−48264
$KNdP_4O_{12}$ epitaxially grown waveguide, laser operation at 1.051 μm 79−18423
$KNdP_4O_{12}$, laser emission cross sections, fluorescence spectra, radiative lifetimes, quantum efficiency 80−23694
$KNdP_4O_{12}$, laser waveguide, fabrication by LPE 79−36925
$KNdP_4O_{12}$ laser waveguide, epitaxial growth 79−91597
K_2O-BaO-SiO_2-Ti(Ce)O_2 laser glasses, TiO_2 and CeO_2 antisolarisation additive effects 79−94309
KY_3F_{10}:Eu^{2+}, luminescence 79−78746
$La_2Be_2O_5$:Nd^{3+}(Pr^{3+}), cryst. growth, spectral and laser properties in $^4F_{3/2}\rightarrow{}^4I_{11/2}$ and $^4F_{3/2}\rightarrow{}^4I_{13/2}$ transitions 80−80853
$La_{1-x}Nd_xP_5O_{14}$, Nd^{3+} luminesc. anomalously weak quenching 77−75533
La_2O_2S, compact specimen prep. 77−85951
Li^+,Na^+:KCl(RbCl), F_A(II) to F_B(II) centre crystals, CW laser oscill. with extended tuning range 80−32997
Li^+:KCl, F_A (II) colour-centre laser, mode locking and tunable picosecond IR pulse generation 80−43364
Li-$La_{1-x}Nd_x$ phosphate glasses, stimulated emission spectroscopy of $^4F_{3/2}$ to $^4I_{11/2}$ and $^4F_{3/2}$ to $^4I_{13/2}$ transitions 79−38573
Li-Nd-La phosphate glass active elements, laser characts., comparison with Nd:YAG 80−33002
$LiBi_xNd_{1-x}P_4O_{12}$ waveguide laser layer epitaxially grown on $LiNdP_4O_{12}$ substrate 80−23709
LiF, coherent freq. tunable radiation generation in F-centres, 0.6 to 1.26 μm range 79−36902
LiF, coherent radiation generation in F_2-centres 78−50782
LiF crystal, tunable laser via F_2^+, F_2^--centres, 0.88 to 1.25 microns 77−75529
LiF crystal active element for colour-centre laser, thermal strain anal. 80−91804
LiF crystal with F_2^+ centres, periodic pulsed tunable laser, Nd laser second harmonic excited 80−38021
LiF, laser action of M-centres at 700 nm 78−82972
LiF OH-stabilised F_2^+-centre laser, appl. to intracavity laser spectroscopy 80−32999
LiF, picosecond generation on F_2^+ colour centres, induced mode synchronisation *(Russian)* 80−64033
LiF tunable laser production, F_2^+ centre accumulation and generation *(Russian)* 80−28238
LiF-OH, γ-irrad., colour centre lasing at 0.84-1.13 μ at 300K 80−5739
$LiNd_{0.5}La_{0.5}P_4O_{12}$, stabilised dual-polarised oscill. 77−54723
$LiNd(PO_3)_4$ laser with external and Fabry-Perot resonators, 1.05, 1.32 μm CW oscill. 80−23693
$LiNdP_4O_{12}$ (LNP), optical transmitter appl., properties and LED pumping 79−3712
$LiNdP_4O_{12}$ CW laser oscill., near 1.32 μm 77−61957
$LiNdP_4O_{12}$ efficient miniature laser pumped with GaAlAs laser diode 80−32994
$LiNdP_4O_{12}$ electroluminescent diode pumped miniaturized laser for optical transmission system 79−41395
$LiNdP_4O_{12}$, glass clad, slab waveguide laser 78−46625
$LiNdP_4O_{12}$ glass-clad rectangular waveguide, laser performance 80−32996
$LiNdP_4O_{12}$, grown by top seeded pulling technique, possible laser material 80−25542
$LiNdP_4O_{12}$, intensity fluctuations due to external perturbations 79−81437
$LiNdP_4O_{12}$, LED and semiconductor laser pumped 77−75552
$LiNdP_4O_{12}$ laser, fluctuations in bath of strong Gaussian noise 79−55166
$LiNdP_4O_{12}$ laser, relaxation oscillations and mode spectra, high density pumping effect 80−69396
$LiNdP_4O_{12}$ laser, spontaneous phase locking obs. 78−83005
$LiNdP_4O_{12}$, laser emission cross sections, fluorescence spectra, radiative lifetimes, quantum efficiency 80−23694
$LiNdP_4O_{12}$ laser material, optical props. and crystal growth *(Japanese)* 79−27259
$LiNdP_4O_{12}$ laser material, crystal growth and optical props. 79−41386
$LiNdP_4O_{12}$ miniaturised lasers for optical communication systems *(Japanese)* 79−27278
$LiNdP_4O_{12}$, simultaneous oscillations of different transitions in lasers 79−22927
$LiNdP_4O_{12}$ single crystal growth, study of Li_2O-Nd_2O_3-P_2O_5 phase diagram 80−25668
$LiNdP_4O_{12}$, single-transverse-mode slab waveguide laser, characts. 79−55141
$LiNdP_4O_{12}$ stable miniature laser with compact resonator, single mode operation 79−50305
$LiYF_4$, host material, prep. and cryst. growth 77−55879
$LuAlO_3$:Nd^{3+}, spectral-generation characts., expt. and theory *(Russian)* 77−7090
$Lu_3Al_5O_{12}$:Er^{3+}, absorpt., luminesc., stimulated emission 77−32402
$Lu_3Al_5O_{12}$:Ho^{3+}(Er^{3+}), sensitized stimulated emission at 3 microns 80−53302
MgF_2:Ni electronic transition laser, tunable IR emission 78−59030
ND:fluorozirconate glass, prep. and optical props. 78−27304
ND:glass, sub ns periodically Q-switched 78−17995
NI:MgF_2, laser, broadly tunable CW operation, output powers, optical pumping 80−32995
Na:CaF_2, tunable room temp. laser action of M-centres, luminesc. and absorpt. spectra 79−31907
Na:SrF_2, tunable room temp. laser action of M-centres, luminesc. and absorpt. spectra 79−31907
Na^+:KCl, CW laser action of $(F_2^+)_A$-centres, tunable from 1.62 to 1.91 μm 80−32998
Na^+:KCl, F_B(II) colour centres, tunable CW laser action obs. 77−83877
Na^+:RbCl, F_B(II) colour centres, tunable CW laser action obs. 77−83877
NaCl:I, UV laser generation by optical pumping 78−82973
NaCl-OH^-, electron irrad., F_2^+ centre stabilisation and tuneable laser operation 80−54231
NaF, F_2^+-like colour centre, room temp. stable, CW laser, 0.99-1.22 μm tunable 80−69399
NaF:Mn^{2+}, two-step photoionisation, laser-active F_2^+ centre form. 79−963
$NaNdP_4O_{12}$, CW laser oscill., near 1.32 μm 77−61957
solid lasers continued
$NaNdP_4O_{12}$, laser emission cross sections, fluorescence spectra, radiative lifetimes, quantum efficiency 80−23694
$Na_2Nd_2Pb_6(PO_4)_6Cl_2$, laser material, flux growth *(French)* 78−35288
$Na_2Nd_2Pb_6(PO_4)_6Cl_2$, high-Nd conc. laser material, oscillator strengths and laser effect 79−55140
Nd,Cr:Li-La phosphate glass, Nd luminesc. quantum efficiency meas., Nd-Cr nonradiative transfer 80−66296
Nd^{3+},Cr^{3+}:glass, nonradiative energy transfer from Cr to Nd, optical pumping efficiency improvement 80−33001
Nd, 3rd and 5th harmonic generation in Cs vapour *(Russian)* 78−25926
Nd activated laser glass characts., review 79−27262
Nd Argus 4 TW laser system, damage history 79−18463
Nd, bleaching-spectrum widths for dyes used in Q-switching 77−42573
Nd compound optically pumped miniature lasers, for fibre optical communication system 78−50786
Nd compounds, diode pumped miniature laser 78−9392
Nd, cryst. struct. of $Na_3Nd(PO_4)_2$ laser mat. 78−79582
Nd crystals, determ. of fluoresc. quantum efficiency and laser emission cross sections 80−48264
Nd disc amplifier, inductive energy source, operational characts. 77−31109
Nd doped (fluoro) phosphate laser glass piezo-optic coeffs. meas. at 0.6328 and 1.15 μm 80−34888
Nd, emission freq. conversion by method of reson. pumping of active media 80−1206
Nd, for optical communication, characts. *(German)* 78−37902
Nd garnet ring laser, with return mirror, mode locking 80−99764
Nd glasses, luminesc. obs. by chronospectroscopic technique 79−11467
Nd laser, continuously tunable, pulsed, operation and output, characts. 79−18448
Nd laser, excited stimulated Mendelstam-Brillouin scatt. phase fluctuations *(Russian)* 80−89014
Nd laser, freq. conversion using rare earth:YAG crystal and reson. pumping *(Russian)* 79−10314
Nd laser, giant nanosecond pulse chain stabilisation 79−13998
Nd laser, review of fibre optical communication devices 77−58446
Nd laser, stable passive switch using phthalocyanine dye, bleaching and relaxation 80−74368
Nd laser freq. conversion, resonant pumping of Tm^{3+}, Ho^{3+} activated YAG 78−17944
Nd laser glasses, gain coefficient meas. and modelling 79−81436
Nd laser Mikron system, ultimate Xe pump lamp module operating conditions 80−91815
Nd laser plasma diagnostics, probing radiation Raman scatt. *(Russian)* 80−19618
Nd laser produced plasma, nonlinear scattering of laser radiation by fast ion waves in plasma 80−106916
Nd laser pulse irrad. expts., German laser fusion programme 78−63136
Nd laser pumping, Na plasma optical props. 79−4115
Nd, lasers, efficiency enhancement by pump radiation conversion in luminesc. liq. 80−48293
Nd miniature laser, optimum design 79−22966
Nd, multifreq. laser, coherence time meas. using bleaching dyes 80−23739
Nd, nonlinear optical freq. transform. of variously polarized laser radiation 79−55181
Nd pulsed garnet lasers, pulse repetition frequency, optimal operating regime 80−53303
Nd pulsed laser sources 78−50784
Nd, reproducible active-passive mode locked oscillators 77−88810
Nd, second harmonic doubling with $KD_{2x}H_{2(1-x)}PO_4$, 90° synchronism *(Russian)* 77−58386
Nd stoichiometric laser crysts., oscill. props., rate eqns. 78−22135
Nd, with mirror plasma-optical Q-switch *(Russian)* 80−33028
Nd^{3+} activated laser matrices, luminesc. quantum efficiency, conc. depend. 79−27263
Nd^{3+} auto-extinction, fundamental mechanism and predicative criterion *(French)* 79−59702
Nd^{3+} based stoichiometric laser materials, comparison with GaAs based lasers 77−7088
Nd^{3+}, Bi^{3+}:glass, energy transfer between impurities 77−90183
Nd^{3+}, containing laser crystals *(Japanese)* 79−3697
Nd^{3+} in glass and cryst. hosts, fluoresc. branching ratios 78−29956
Nd^{3+} ion miniature phosphate glass lasers with high ion concentration 80−19038
Nd^{3+} ions in solids, anti-Stokes effects 78−80405
Nd^{3+} laser crystal efficiency 79−50302
Nd^{3+} miniature laser principles, materials and integrated optical design 80−33004
Nd^{3+}, tricarbocyanine dye passive Q-switch 79−10333
Nd^{3+}, UO_2^{2+}:BaO-B_2O_3 glass, radiative and nonradiative energy transfer 78−60508
Nd: glass laser operating Ge optical switch, picosecond pulse generation at 10.6 μm 79−7159
Nd:AlG, laser, mode locked, output stabilisation 77−61986
Nd:BeF_2 glass lasers for fusion expts. 78−46661
Nd:$CaLa_4(SiO_4)_3O$, laser rod, laser damage initiating inclusions 77−68246
Nd:$CaY_2Ge_3O_{12}$, energy levels and laser action, fluoresc. meas. 79−81438
Nd:$CaY_2Mg_2Ge_3O_{12}$, CW room temp. laser operation, 0.941 and 1.059μm 78−66842
Nd:$CaY_3Mg_2Ge_3O_{12}$, CAMGAR low threshold CW room temp. laser operation at 0.941 μm 78−1234
Nd:garnet, freq. axial mode shift, two-mirror resonator synchronisation, stabilisation *(Russian)* 78−22154
Nd:glass, 0.92 μ laser action at room temp. 78−1236
Nd:glass, Argus two-beam laser system, performance 77−88759
Nd:glass, CW SELFOC, actively initiated quasi-passive mode-locking 77−19306
Nd:glass, chirp-free picosecond pulse generation 77−79869
Nd:glass, coaxial digital pulse compression 77−7101
Nd:glass, comparative lasing characts. of silicate and phosphate laser glasses 80−74364
Nd:glass, continuous dynamic freq. tuning of pulse radiation 78−29986
Nd:glass, controlled-inversion-profile amplifier as soft aperture 79−98427
Nd:glass, disc amplifier for nuclear fusion expts. 77−19340

solid lasers continued
Nd:glass, disc laser, using deuterated water as coolant, 1% efficiency 77−23695
Nd:glass, dye passive switch for laser pulses, transmission coeffs. 77−23686
Nd:glass, dynamic mode sweep-laser, freq. tuning 78−66851
Nd:glass, fluoresc. decay data from minicomputer-operated spectroscopy equipment 77−74526
Nd:glass, fluorophosphate glass for fusion lasers 78−46660
Nd:glass, for fusion, comparative review of Nd:glass, CO_2, HF and I lasers 77−7062
Nd:glass, for laser fusion 77−88764
Nd:glass, gain coeff. for fusion laser amplifier 77−19261
Nd:glass, gain coeffs. meas. and modelling for different glasses 77−88726
Nd:glass, γ-ray induced absorbing layer form. in optical medium 77−50688
Nd:glass, high efficiency short pulse laser, coaxial flashlamp pumping 77−75558
Nd:glass, large laser effect phosphate and fluorophosphate glasses 78−79021
Nd:glass, laser bulk damage rel. to temp. and conc. 79−14023
Nd:glass, laser material, luminesc., population inversion depend. on pump pulses 77−23679
Nd:glass, laser rod amplifier of 4 cm diam., design and performance 77−19339
Nd:glass, line narrowing and tuning using intracavity Brewster angle birefr. filter 77−38916
Nd:glass, linear expansion coeff. and r.i., temp. depend. 77−733
Nd:glass, luminesc. absolute quantum efficiency 77−34893
Nd:glass, luminesc. quantum yield meas., relative method *(Russian)* 78−35203
Nd:glass, microsecond pulse production, with quadratic loss in laser cavity 77−7147
Nd:glass, mode locked, picosec. pulse form., expt. technique 77−38957
Nd:glass, mode locked laser, self-focusing effect on output power 77−751
Nd:glass, OMEGA fusion laser system 78−50811
Nd:glass, OMEGA-10 multibeam laser system, automatic alignment system 78−50847
Nd:glass, optical inhomogeneity cancellation using $LiIO_3$ parametric convertor 80−33049
Nd:glass, oscillator, short laser pulses *(Rumanian)* 79−7165
Nd:glass, passive mode-locking by optical Kerr effect modulator 78−9403
Nd:glass, passively mode locked, picosecond pulse generation, pulse compression and broadening 77−31111
Nd:glass, picosecond pulse time behaviour, background free meas. using SHG in $LiIO_3$ 79−59758
Nd:glass, ps pulse amplification, self-focusing brightness limitation 77−14725
Nd:glass, pulsed, beam quality *(Slovenian)* 78−63137
Nd:glass, pumping efficiency improved using Xe flashlamps with interf. coatings 79−10316
Nd:glass, Q-switched laser, radiation polarisation 77−27293
Nd:glass, Q-switched with stable operation in pure transverse natural oscillation *(German)* 77−14761
Nd:glass, repetitively pulsed, high efficiency 77−72005
Nd:glass, silicate and phosphate glass, comparison of gains 80−19039
Nd:glass, slot method for radiation extraction 77−50694
Nd:glass, spectral distrib. kinetics rel. to intracavity spectroscopy 78−1293
Nd:glass, status of large JANUS, CYCLOPS, ARGUS and SHIVA systems 77−38929
Nd:glass, stimulated emission cross sections and absorpt. coeffs. at 1.06 μm, calorimetric meas. 77−71987
Nd:glass, stimulated emission cross section by absorpt. meas. from thermally populated $^4I_{11/2}$ levels 78−71107
Nd:glass, subnanosecond pulse oscillator, investigation by high-speed oscillography 80−74411
Nd:glass, TEM_{00} mode operation *(Rumanian)* 78−50798
Nd:glass, thermal distortion of active element during pumping pulse *(Russian)* 77−50696
Nd:glass, thermal distortion induced by optical pumping *(Chinese)* 78−50779
Nd:glass, third harmonic generation in phase matched Rb-Xe mixture 77−27318
Nd:glass, tunable-wavelength mode-locked, with instant recording of temporal and spectral characts. 77−54732
Nd:glass, ultimate power characts. at high pulse repetition freqs. 80−64036
Nd:glass, with metallic grating in cavity, Fourier spectrum and periodic mode fields distrib. *(Russian)* 79−31915
Nd:glass, with nonlinear absorber, pulsed Q switching 78−9400
Nd:glass 2 TW laser for fusion expts. 80−33035
Nd:glass amplifier, large aperture, active mirror design 78−46659
Nd:glass amplifier, pump radiation pulse shape influence on stored energy 79−64235
Nd:glass and ruby lasers placed parallel in cavity, for efficiency increase *(Russian)* 77−10954
Nd:glass Argus laser system, performance summary 78−55361
Nd:glass composite tunable laser at 1.89, 3.39 and 16 μm 79−72596
Nd:glass conical fibre optics quantum amplifier parameters 78−59024
Nd:glass disc amplifier design 78−46633
Nd:glass disc amplifiers, possibility for efficiency improvement 80−33000
Nd:glass disc laser amplifier with immersion medium 78−1262
Nd:glass fibre laser plate for optical parallel processing 79−76695
Nd:glass fibre optical quantum image amplifier 78−1261
Nd:glass high energy laser amplifier, nonlinear pulse propag. 78−50780
Nd:glass high energy system for fusion expts., multi-lens focusing systems 78−50848
Nd:glass intracavity laser spectrometer with dispersive resonator 77−74530
Nd:glass intracavity laser spectrometer for 1.35 μm 79−63316
Nd:glass large-aperture disc amplifier, optical distortions of light beam 79−10338
Nd:glass laser, blue tunable picosecond pulse generation by synchronous mixing with sideband radiation in $NH_4H_2PO_4$ 80−87431
Nd:glass laser, enhanced performance by double doping with Cr 79−31906
solid lasers continued
Nd:glass laser, Fabry-Perot etalons tuning, narrow linewidth 79−76707
Nd:glass laser, generation of picosecond light continua depending on various nonlinear processes 80−33095
Nd:glass laser, influence of neutron and γ irrad. on generating characts. *(Russian)* 80−69402
Nd:glass laser, luminesc. filters efficiency 80−1213
Nd:glass laser, mode locking characts. using polymethine dye No. 3955 in solid host 78−17989
Nd:glass laser, mode-locked, ultrashort pulse duration meas., two-photon fluoresc. 79−27302
Nd:glass laser, new rapid-relax. passive trap *(Russian)* 77−54714
Nd:glass laser, output spatial characts. using FTIROS material 79−68414
Nd:glass laser, resonant reflectors in laser cavity, freq. selection 78−55369
Nd:glass laser, short pulse mode-locked, using prisms 80−83617
Nd:glass laser, spherical cavities, Q-switching by rotating mirror 80−28261
Nd:glass laser, stable ultrashort light pulses generation *(German)* 80−91823
Nd:glass laser amplifier, small scale self-focusing effects, exam. 78−55415
Nd:glass laser amplifier, terminal level lifetime effect *(Chinese)* 79−89913
Nd:glass laser amplifiers, self-focusing and suppression by spatial filtering 80−14406
Nd:glass laser array, mode locking, spatially coherent beam form. 77−88811
Nd:glass laser array, spatially coherent beam form., mode locking 78−29989
Nd:glass laser beam distrib. in focal region, transmission monitoring through pinhole 78−90441
Nd:glass laser cooling and index-matching liquid props. 80−33015
Nd:glass laser development and laboratory work 78−94395
Nd:glass laser fusion systems, optical developments 77−19289
Nd:glass laser in Tl vapour, output conversion from 1.06 micron to 388.1 nm 80−91850
Nd:glass laser irradiated fusion targets, time and space resolved harmonic emission 79−82095
Nd:glass laser materials, intensities of optical transitions 77−689
Nd:glass laser operation, self-focusing influence 79−13997
Nd:glass laser output, passive-mode locked, resonator length effect 78−79044
Nd:glass laser performance and reliability developments 80−78869
Nd:glass laser picosecond pulses, background energy content meas. with saturable absorbers 78−59062
Nd:glass laser prep. and fundamental characteristics *(Japanese)* 79−7133
Nd:glass laser pulses, plasma closure phenomena in irradiated pinholes 79−89946
Nd:glass laser radiation, spatial coherence of fundamental and second harmonic 80−69442
Nd:glass laser resonator deform. due to polarisability change of excited Nd ions 79−10313
Nd:glass laser rod, piezoelectric detection of photoacoustic signals 78−54467
Nd:glass laser rod, pumped, thermal relaxation 80−69397
Nd:glass laser six beam system, output characts. *(Chinese)* 80−83612
Nd:glass laser system, beam spatial profile optimization in amplifier channel 80−74407
Nd:glass laser system, multichannel, for fusion experiments, model 80−58557
Nd:glass laser system, oscillators operating at 1.054 μm 78−46657
Nd:glass laser system, pulse shaping 78−46658
Nd:glass laser system, Thompson scattering diagnostics of low density plasmas 80−96388
Nd:glass laser system 400 MW, output characts., plasma production appl. 79−41384
Nd:glass laser system for optical wave mixing expts. 78−5521
Nd:glass laser system with parametric freq. conversion 80−1277
Nd:glass laser UV coherent pulse, 45 GW, for laser fusion 80−69450
Nd:glass laser with active mode locking, ultrashort pulses 80−64087
Nd:glass laser with continuously tunable ps output, polaris. filter 79−22985
Nd:glass laser with freq. doubling compatibility, for glaucoma surgery 78−40403
Nd:glass laser with grid mirror, emission field 79−55142
Nd:glass laser with numerical programmed control *(Russian)* 80−91811
Nd:glass laser with periodic Q-switching, mathematical model 80−33043
Nd:glass laser with US modulated emission 80−48309
Nd:glass laser with US Q-switch 80−64034
Nd:glass laser with unstable resonator and additional feedback, angular divergence 80−48307
Nd:glass laser/parabolic mirror lidar for airborne aerosol mass conc. meas. 77−21937
Nd:glass lasers, optimisation for 1-10 ns pulses operation 78−46651
Nd:glass lasers, performance, Nova system design 78−46652
Nd:glass mode locked ring laser, unidirectional travelling wave operation 77−88812
Nd:glass off-axis multipass laser system 78−50813
Nd:glass passively mode-locked laser, obs. of external feedback influence 80−23729
Nd:glass Q-switched laser, feasibility of tuning range widening 79−59724
Nd:glass Q-switched laser controlled by external signal, stimulated emission characts. 79−10312
Nd:glass Q-switched laser emitting polarised radiation 79−45974
Nd:glass resonator, lasing spectrum singularities and Q-factor, for z-dimens. beam path *(Russian)* 77−88795
Nd:glass ring laser, actively mode-locked and Q-controlled, props. 79−18445
Nd:glass ring laser, holographic dispersion element *(Russian)* 78−59051
Nd:glass ring laser, mode-locking, unidirectional travelling wave operation 77−61976
Nd:glass ring laser, single synchronizable ps pulse generation 77−14739
Nd:glass saturated amplifier, direct meas. of gain recovery 78−71104
Nd:glass Shiva laser system, for fusion expts. 78−50812
Nd:glass Shiva laser system for fusion expts. 78−50820
Nd:glass solid state laser, giant emission pulse prod. 80−91803

solid lasers continued
Nd:glass telescopic small-signal amplifier with a Brillouin mirror 80−69420
Nd:glass travelling-wave sweep laser, emission spectrum dynamics 78−50829
Nd:glass type, periodic monopulse energy output *(Russian)* 78−50787
Nd:glass ultrashort pulse length, passive switch relax. time effect 77−38960
Nd:glass:CeO_2, TiO_2, lasing action, stabilisation *(Russian)* 78−13715
Nd:glass-YAG composite medium master oscillator, 1.06 μm stable conversion into fourth harmonic 78−46724
Nd:$La_2Be_2O_5$, laser crystal properties 77−19260
Nd:$La_2Be_2O_5$, passive mode locking, ps pulse generation 77−7118
Nd:$La_2Be_2O_5$, two-photon pumping of Cs vapour for IR image upconversion 77−10968
Nd:P_2O_5 glass, stimulated emission cross section, Verdet const. 78−25885
Nd:phosphate glass, high-power laser, design and performance 80−48270
Nd:phosphate glass, single ps pulse props. 77−19273
Nd:phosphate glass amplifier for pulse shaping 77−14758
Nd:phosphate glass double pass amplifier with circular polarisation 77−88774
Nd:phosphate glass laser, CW oscillation 79−50311
Nd:phosphate glass mode-locked oscillator and amplifier system 79−81446
Nd:phosphate glass oscillator, bandwidth-limited picosecond pulses 77−79830
Nd:silicate glass, resonance laser excitation, inhomogeneously broadended emission spectra 80−66295
Nd:Y_2O_3 single crystal fibre laser, room temp. CW operation at 1.07 and 1.35 μm 78−63121
Nd:YAG, 1 Gb/s satellite communication system 77−19440
Nd:YAG, acousto-optic Q-switches 79−7166
Nd:YAG, actively AM mode-locked Q-switched laser, pulse compression by liq. Kerr cell 79−22990
Nd:YAG, actively mode locked laser, short pulse generation for fusion 77−88809
Nd:YAG, amplifier, gain increase by parasitic oscill. suppresion 77−14720
Nd:YAG, appl. of pulse gas-discharge lamp to optical pumping *(Bulgarian)* 78−33795
Nd:YAG, beam divergence in short interferometers 77−27310
Nd:YAG, CW laser gain switching for intracavity pulse amplification 77−88771
Nd:YAG, CW mode-locked, diagnostics of radiation using nearly online picosecond streak camera 79−49314
Nd:YAG, cavity dumping single mode-locked pulses 77−7137
Nd:YAG, crystal defects influence obs., on energetic effectiveness *(Czech)* 78−79022
Nd:YAG, electro-optical extraction of ps laser pulse *(German)* 80−87416
Nd:YAG, flash lamp discharge development effects on pumping efficiency 78−71114
Nd:YAG, for optical fibre transmission system at 1.32 μm 79−94331
Nd:YAG, for space communications system, optical coatings 79−86248
Nd:YAG, freq. doubled, blue-green laser technology for ocean optics 77−78458
Nd:YAG, freq. doubled, pump for efficient oscillator-amplifier dye laser 79−41389
Nd:YAG, frequency-doubled, thermooptical instabiliites and bistable behaviour 77−71998
Nd:YAG, frequency-doubled operation, effects of absorpt. loss in $Ba_2NaNb_5O_{15}$ 79−36957
Nd:YAG, glass clad fibre LED end pumped, 1.3 μm CW operation 77−7120
Nd:YAG, grown from melt, in Mo crucibles, laser props. 80−48261
Nd:YAG, heat capacity and thermal diffusivity meas. 80−19956
Nd:YAG, high brightness 1 J freq. doubled laser 77−88776
Nd:YAG, high brightness 1 J freq. doubled laser 78−46615
Nd:YAG, high repetitive picosecond laser system and broad range wavelength tuning *(Japanese)* 79−3698
Nd:YAG, hole burning elimination in active medium 77−79851
Nd:YAG, injection locked oscillator, pulse duration var. 77−88772
Nd:YAG, intense fourth harmonic generation, pulse periodic conditions 78−17972
Nd:YAG, intracavity modulation, sum freq. mixing, 212.8 nm pulse burst generation 78−74934
Nd:YAG, LED end pumped laser, cavity loss, efficiency 77−14740
Nd:YAG, laser cryst., dislocations density and propag., rel. to Czochralski growth *(Chinese)* 77−11552
Nd:YAG, laser fusion system, short pulse generation, active mode-locking and Q-switching 77−79868
Nd:YAG, laser transition cross sections, modulation *(Chinese)* 78−90418
Nd:YAG, linear expansion coeff. and r.i., temp. depend. 77−733
Nd:YAG, low power, appl. for space communications 77−75567
Nd:YAG, materials processing appls. *(German)* 78−1294
Nd:YAG, miniaturized, end-pumped by superlum. diode, CW operation 77−10938
Nd:YAG, mode locked, Na multiphoton ionisation in third harmonic generation 78−94413
Nd:YAG, mode locked oscillator, operation at 1.052 μm 80−33017
Nd:YAG, mode self locking with combined Q-switching 78−1284
Nd:YAG, mode-locked, picosecond pulse parameter meas. 77−19271
Nd:YAG, mode-locked frequency-doubled laser efficiency 77−19264
Nd:YAG, mode-volume matching of oscillating modes of laser containing several active elements *(Chinese)* 79−50325
Nd:YAG, negative feedback external perturbations effect, spectral depend. 77−83908
Nd:YAG, operational characts. of $LiNbO_3$ Q-switch for generating single laser pulse *(Korean)* 77−704
Nd:YAG, optical pumping, using room temp. CW superluminesc. diode 77−7122
Nd:YAG, passive mode-locked, picosecond pulse duration, determ. from luminesc. intensity 78−71134
Nd:YAG, positive branch, unstable oscillator 78−66845
Nd:YAG, ps pulse amplification, self-focusing brightness limitation 77−14725
Nd:YAG, pulse exchanges with plasma *(German)* 80−48918
Nd:YAG, pulse shaping for laser fusion 77−88806
Nd:YAG, pulse synchronisation system for fusion laser 77−88807

solid lasers continued
Nd:YAG, pump for IR dye laser 78−22139
Nd:YAG, pumped by Kr arc lamp, conductive cooling, for space operation 77−88775
Nd:YAG, pumped laser rod, quantum efficiency 77−88724
Nd:YAG, repetitively pulsed, high efficiency 77−72005
Nd:YAG, semicond. convertor in pump system 77−7129
Nd:YAG, semicond. wafer laser annealing, review and anal. 80−25741
Nd:YAG, single freq. laser with waveguide resonator 78−1277
Nd:YAG, single mode pulsed oscillator, control of temporal and spectral jitter 78−46629
Nd:YAG, single mode Q-switched oscillator with short build up time 77−7091
Nd:YAG, space communications appl. 78−28483
Nd:YAG, spherical resonator diffraction losses, expt. meas. 78−29980
Nd:YAG, thermal lens effect on emission stability 80−19064
Nd:YAG, three-way mixing in low dispersion wavelength region in optical fibre 80−99792
Nd:YAG, unstable resonator oscillator, 12 ns 200 mJ output 77−42548
Nd:YAG, unstable resonator, Q-switched laser, operating characts. 79−36928
Nd:YAG, using flash lamp pumping source 77−50679
Nd:YAG, with improved fluoresc. lifetime of $^4F_{3/2}$ state 77−687
Nd:YAG acousto-optically mode-locked CW laser performance and stability criteria 77−38934
Nd:YAG acousto-optically mode-locked CW laser, optical spectra obs. by interferometer 79−7134
Nd:YAG actively mode-locked laser, short pulse generation for laser fusion 78−9404
Nd:YAG CW laser, active stabilisation, laser noise 80−48295
Nd:YAG CW laser, longit. mode number reduction 79−72576
Nd:YAG CW laser, mode locking, 30 W average power 80−87419
Nd:YAG CW mode-locked laser, negative feedback power stabilization 80−69435
Nd:YAG crystal, orientation influence on thermally induced birefringence *(Chinese)* 80−88958
Nd:YAG FM laser, pulse compression in Nd:YAG laser dispersive delay line 77−88815
Nd:YAG fibre laser, self-contained LED-pumped single-crystal 78−1264
Nd:YAG for 100 Gbit/s transmission rate over optical fibres expt., review *(French)* 80−69525
Nd:YAG giant pulse lasers, energy characts., superradiance effects 80−64031
Nd:YAG high performance laser system efficiency and beam uniformity 77−19327
Nd:YAG K vapour arc lamp as optical pump source 79−86261
Nd:YAG laser, actively modelocked and Q-switched, fusion reactor appl. 79−45980
Nd:YAG laser, CW, with high output coupling modulation 80−9917
Nd:YAG laser, CW mode-locked and intracavity freq. doubled, anal. 80−58548
Nd:YAG laser, coherence time meas. of picosecond pulser by light-induced grating method 80−53347
Nd:YAG laser, conductively cooled pulsed design 78−46647
Nd:YAG laser, influence of birefraction and cooling on output characteristics *(Italian)* 79−50299
Nd:YAG laser, intracavity freq. doubling by $LiIO_3$ long pulse emission 80−102736
Nd:YAG laser, kinematic mode synchronisation *(Russian)* 77−34892
Nd:YAG laser, Kr-pumped for space optical communications 77−19328
Nd:YAG laser, min. amplitude noise for high-sensitivity meas. 79−63317
Nd:YAG laser, passive Q switching at 1.3 μm 79−72610
Nd:YAG laser, phase conjugation using gain saturation 79−64272
Nd:YAG laser, Q-switched, pulse stretching using Pockels cell 80−95927
Nd:YAG laser, radiation characts. rel. to pumping intensity in long-time operation *(Russian)* 77−68214
Nd:YAG laser, reduction of passive Q-switch output jitter 78−46648
Nd:YAG laser, subnanosecond pulse generation at 100K 80−74397
Nd:YAG laser as optical pulse generator, mode locking by acoustooptic loss modulation 79−64260
Nd:YAG laser as source for airborne lidar system for atmospheric expts. *(Italian)* 80−109278
Nd:YAG laser freq. doubled output for dye laser pumping 78−59090
Nd:YAG laser frequency tripling 79−14030
Nd:YAG laser integration into optical systems 80−78887
Nd:YAG laser multipass cell for Raman scatt. diagnostics 80−1231
Nd:YAG laser oscillator, mode-locked, pulse splitting 79−7160
Nd:YAG laser oscillator-amplifier coupled to Nd:glass amplifier, programmable electro-optical pulse form. *(German)* 78−33753
Nd:YAG laser pulse tailoring/synchronization system for laser-plasma interaction expt. 79−98404
Nd:YAG laser pumping system, heterostructure spectrum convertor, opaque and sapphire heat sink 79−27272
Nd:YAG laser radiation, Q-switched, temporal power variation of second and fourth harmonic generation 78−25922
Nd:YAG laser range finder, performance in radiation environments 80−38054
Nd:YAG laser stabilisation by T-shaped four-mirror resonator *(Russian)* 78−13730
Nd:YAG laser third harmonic pumping a tunable picosecond UV dye laser 79−31927
Nd:YAG laser with internal SHG in coupled resonators, CW coherent UV-source *(German)* 79−98438
Nd:YAG lasers, sun-pumped and lamp-pumped, for space communications 79−86194
Nd:YAG long laser resonator, active and passive mode-locking 78−50832
Nd:YAG long-pulsed laser, resonator config. for relax. oscills. suppression 79−72599
Nd:YAG master oscillator, spectral comp. form. of high-power laser radiation 78−71115
Nd:YAG mode-locked laser picosecond pulse profile and power meas. 77−7112
Nd:YAG mode-locked laser pulse, quadratic phase evolution direct meas., time resolved interferometry 80−48318
Nd:YAG mode-locked unstable laser, p-branch unstable resonator config. 79−31928
Nd:YAG oscillator, flashlamp pumped, const. gain Q-switching to improve stability 78−50837
Nd:YAG oscillator, output stabilisation by Q-switching 78−83003

solid lasers continued
Nd:YAG oscillator, Q-switched, generation of high-power ns pulses 80−23730
Nd:YAG oscillator-amplifier system, synchronised diagnostic pulses for laser fusion 78−51365
Nd:YAG passively locked laser, pulse width meas. by SHG method *(Chinese)* 80−87432
Nd:YAG passively mode-locked unstable oscillator 79−45953
Nd:YAG pumped $LiNbO_3$, parametric oscillator, picosecond IR pulse generation 78−71151
Nd:YAG pumped $LiNbO_3$ parametric oscillator, for tunable IR source 77−46767
Nd:YAG pumped tunable sources, appl. to spectroscopy 80−58576
Nd:YAG Q-switched laser, ohmic contacts on n-GaAs produced by laser alloying of Ge films 80−58546
Nd:YAG Q-switched laser beam and waist, knife-edge profiling 79−45982
Nd:YAG Q-switched oscillator for underwater appls. 80−8461
Nd:YAG regenerative amplifier, variable-duration synchronized pulse generator 79−45967
Nd:YAG regenerative amplifier, expt. studies 80−95909
Nd:YAG repetitively Q-switched laser, fifth harmonic generation for mW 213 nm source 79−55178
Nd:YAG short-pulse oscillator, for Shiva 78−63134
Nd:YAG single crystal fibre laser, self-contained LED pumped 79−59711
Nd:YAG solar pumped laser for space communications 78−46645
Nd:YAG solar pumped laser, freq. doubling 78−59045
Nd:YAG space laser communication system, K-Rb arc lamp pump 78−46646
Nd:YAG two beam laser irradiation facility for nuclear fusion 77−18705
Nd:YAG unstable resonator design 79−13988
Nd:YAG unstable-resonator oscillator, stable single-axial-mode operation by injection locking 80−53331
Nd:YAG waveguide resonator laser, time characts. 77−58345
Nd:YaG laser reflection resonator with hole coupling 80−58597
Nd^{+3}: glass laser for stimulated Raman scatt. Dewar cell 80−99799
Nd^{3+}:Al_2O_3-P_2O_5 glass, high Nd conc., spectroscopy and lasing obs. 78−46609
Nd^{3+}:$Ca_3Ga_2Ge_3O_{12}$, stimulated emission at 300K 80−38019
Nd^{3+}:$CaLa_4(SiO_4)_3O$, stimulated emission, absorpt. and luminesc. spectra 77−85755
Nd^{3+}:CaO-Li_2O-Al_2O_3-SiO_2, CaO enriched, laser type glasses, spectroscopic behaviour 78−60497
Nd^{3+}:$Gd_3Ga_5O_{12}$ pulse-pumped laser action at 1.054 μm 80−64030
Nd^{3+}:glass, $^4I_{11/2}$ level population, absorpt. and relax. rate meas. 77−36290
Nd^{3+}:glass, analysis of antireflection layers 77−58340
Nd^{3+}:glass, ED-2 laser glass, transition probabilities and quantum efficiency 77−58330
Nd^{3+}:glass, fluoresc. line narrowing, hole burning and ion-ion energy transfer 79−89912
Nd^{3+}:glass, giant laser pulse-induced luminesc., spectral shape temp. depend. *(Russian)* 77−19257
Nd^{3+}:glass, laser props., uncorrelated inhomogeneous broadening of 1.06 μm band induced luminesc. quenching 79−31914
Nd^{3+}:glass, oscillator, narrow bandwidth ps. laser operation using Nd^{3+}:YAG as amplifier 78−37894
Nd^{3+}:glass, Q-switching by exploding PbS film 78−42361
Nd^{3+}:glass, quantum efficiency for upper laser level, photoacoustic meas. 79−19924
Nd^{3+}:glass, spectral behaviour under narrow-line excitation 79−33747
Nd^{3+}:glass based on alkali metal metaphosphates, luminesc. and lasing *(Russian)* 77−46724
Nd^{3+}:glass energy transfer processes, radiative transitions *(Chinese)* 79−61431
Nd^{3+}:glass laser, stabilised, single-mode, Q-switched, continuous frequency scanning 79−31922
Nd^{3+}:glass laser, with contacted mode-locking-dye cell 79−18454
Nd^{3+}:glass luminesc. band profile deform. under free-oscillation conditions 80−71487
Nd^{3+}:inorganic glass, energy transfer processes, nonradiative transitions *(Chinese)* 79−64232
Nd^{3+}:$La_2Mg_3(NO_3)_{12}.24H_2O$, proton raser, self-radiating nuclear spin system *(German)* 80−53298
Nd^{3+}:Li-Nd-La phosphate glass, nonradiative losses, pulse periodic stimulated emission and luminesc. 77−83878
Nd^{3+}:$LiNd_{0.3}La_{0.7}$ phosphate glass, stimulated emission characts. 79−18426
Nd^{3+}:$LiYF_4$, pulsed free running laser action at 1053, 1046 nm, passive mode locking *(French)* 78−79048
Nd^{3+}:$NdTa_7O_{19}$, fluorescence intensity and lifetime rel. to mini laser prod. *(French)* 77−71988
Nd^{3+}:P_2O_5-K_2O-CdO-Na_2O glass, spectroscopic props. and CW laser action *(French)* 79−41385
Nd^{3+}:phosphate glass, physicochem., spectral, luminesc. and stimulated emission props. 77−54715
Nd^{3+}:phosphate glass laser, brightness enhancement by spatial filtering in amplifying channel 80−48321
Nd^{3+}:quartz fibre, stimulated radiation generation and amplification 77−88729
Nd^{3+}:TeO_2-Li_2O glass, spectroscopic props. and CW laser action *(French)* 79−41385
Nd^{3+}:trifluoride, VUV fluoresc., tunable source, 1650-2600 Å 77−688
Nd^{3+}:$Y_3Ga_5O_{12}$($YGaO_3$), spectroscopic characts. 77−12427
Nd^{3+}:YAG, 1.05 to 1.44 μm tunable high-power laser emission on 18 CW transitions 77−88727
Nd^{3+}:YAG, CW, 1.05 to 1.44 μm tunability, performance 78−22142
Nd^{3+}:YAG, CW, intensity fluctuations in single-freq. mode 80−91802
Nd^{3+}:YAG, CW laser with planospherical resonator, freq. degeneracy of modes 79−31953
Nd^{3+}:YAG, CW operation 77−38901
Nd^{3+}:YAG, contrast and configs. of $LiNbO_3$ electrooptic switches 80−33012
Nd^{3+}:YAG, energy transfer between Nd^{3+} ions, laser-excited time-resolved site-selection spectroscopy 79−95839
Nd^{3+}:YAG, laser characts., comparison with Li-Nd-La phosphate glass active elements 80−33002
Nd^{3+}:YAG, Q-switching mechanism by intracavity stimulated Brillouin scatt. 80−106552

solid lasers continued
Nd^{3+}:YAG, Raman laser with optical-fibre resonator, expt. investigation 79−31913
Nd^{3+}:YAG, running pulse mode of operation, exptl. obs. 77−7089
Nd^{3+}:YAG, spontaneous mode locking necessary conditions, quadratic nonlinearity influence 79−64261
Nd^{3+}:YAG, stabilised laser with longitudinal mode synchronisation *(Russian)* 77−19315
Nd^{3+}:YAG, stable periodic-pulse, with CW pump 80−74400
Nd^{3+}:YAG, with intracavity SHG, amplitude- and phase-freq. characts. 78−25884
Nd^{3+}:YAG, with nonstationary resonator, axial mode synchronisation *(Russian)* 77−75582
Nd^{3+}:YAG CW linear laser, longit. mode self-locking 79−72611
Nd^{3+}:YAG CW ring laser, axial mode locking by electrooptic $LiNbO_3$ phase modulator 78−50835
Nd^{3+}:YAG CW ring laser, fluctuation spectrum 80−9914
Nd^{3+}:YAG continuous laser, radiation freq. stabilisation system using Fabry-Perot interferometer 80−78871
Nd^{3+}:YAG continuously pumped pulse-periodic laser, stability 80−28241
Nd^{3+}:YAG electro-optically Q-switched pulse-periodic laser 79−45975
Nd^{3+}:YAG electrooptically Q-switched laser pulse duration increase by intracavity SHG 79−94255
Nd^{3+}:YAG fibre laser pumped by single LED, optimum geometry *(German)* 78−55366
Nd^{3+}:YAG laser, analysis of antireflection layers 77−58340
Nd^{3+}:YAG laser, conc. determ. of ^{137}Cs fission product in coated-particle fuel 80−18416
Nd^{3+}:YAG laser, high repetition rate electrooptic Q-switching, birefringence 80−69430
Nd^{3+}:YAG laser, improved efficiency with $Al_xGa_{1-x}As$-GaAs LED pump system 79−41396
Nd^{3+}:YAG laser, pumping by alkali metal vapour arc discharge 80−78924
Nd^{3+}:YAG laser, second harmonic used to pump NdP_5O_{14} microlaser 79−98377
Nd^{3+}:YAG laser active element, linearly polarised light depolarisation due to thermally induced birefr. 80−106528
Nd^{3+}:YAG laser frequency stability improvement using active interferometer *(Russian)* 80−64043
Nd^{3+}:YAG multimode laser radiation noise 80−74366
Nd^{3+}:YAG Q-switched picosecond laser radiation, pulse duration and energy fluctuations 79−89949
Nd^{3+}:YAG stabilised single-freq. travelling wave laser 79−18449
Nd^{3+}:$YAlO_3$, $^4F_{3/2}\rightarrow{}^4I_{13/2}$ transition, stimulated emission wavelength, continuous tuning 77−58334
Nd^{3+}:$YAlO_3$ biaxial laser cryst., anisotropy of spectral characts. 79−50303
Nd^{3+}:$YAlO_3$ laser double-pulse flashlamp trigger cct. 78−55378
Nd^{3+}:YVO_4, absorption and fluoresc. spectra of laser states 77−38900
Nd^{3+}:YVO_4, optical absorption intensities 79−24335
Nd-glass, mode-locked, measurement of picosecond pulses using two-photon photoconductivity detector 80−77872
Nd-YAG laser, Q-switched, freq. doubled, 200 kW output 80−33026
$Nd(Al,Cr)_3(BO_3)_4$, CW laser action, CR^{3+} cross pumping, Nd^{3+} direct pumping 79−64231
$Nd(Al,Cr)_3(BO_3)_4$, efficient cross pumping of Nd^{3+} by Cr^{3+} 78−59010
$NdAl_3(BO_3)_4$ (NAB), optical transmitter appl., properties and LED pumping 79−3712
$NdAl_3(BO_3)_4$, cw laser action at 1.3 μm 79−27258
$NdAl_3(BO_3)_4$ miniaturised crystals with directly applied mirrors, laser emission 79−22958
$NdAl_3[BO_3]_4$, luminescence and lasing characts., solubility 79−31910
$Nd(Ga,Cr)_3(BO_3)_4$, cryst. growth by LPE, Nd^{3+} fluorescence, lattice constants 80−29883
$Nd_{0.5}La_{0.5}P_5O_{14}$ laser, FM mode-locked 79−86184
$Nd_{0.75}La_{0.25}P_5O_{14}$, miniature laser system bonded mirrors, side pumped by LEDs 78−87058
$Nd_xLa_{1-x}P_5O_{14}$, crystal growth, laser generation characts. 80−38020
$Nd_xLa_{1-x}P_5O_{14}$ laser, pumped by nanosecond pulses, performance 77−38897
$Nd_xLa_{1-x}P_5O_{14}$, laser properties 79−22957
$Nd_xLa_{1-x}P_5O_{14}$, Nd^{3+} stoichiometric materials, luminesc., conc. quenching 78−27315
$Nd_{0.75}La_{0.25}P_5O_{14}$, laser side-pumped by LED arrays, design procedure and functioning 79−22966
Nd_2O_3-Y_2O_3-As_2O_5 glass, spectroscopic props., rel. to possible appl. in lasers 78−84624
NdP_5O_{14} (NPP), optical transmitter appl., properties and LED pumping 79−3712
NdP_5O_{14}, cw laser action at 1.3 μm 79−27258
NdP_5O_{14}, flash-lamp excitation, room temp., operation 77−88779
NdP_5O_{14}, flash-lamp-excited, operation 77−83883
NdP_5O_{14} laser, flashlamp excited, emission cross section at 1.32 μm 79−59701
NdP_5O_{14}, laser materials, linear conc. quenching of luminesc. 79−31908
NdP_5O_{14}, luminesc. excited by LED radiation 79−24366
NdP_5O_{14} microlaser pumped by second harmonic of Nd^{3+}:YAG laser 79−98377
NdP_5O_{14}, XeF excimer pumping 79−7130
$Nd_xR_{1-x}P_5O_{14}$ (R=La, Y: $0.1<x<1$), laser quality cryst. growth, morphology 80−66412
$Nd_{0.14}Y_{0.86}P_5O_{14}$ epitaxial layer an $Gd_{0.33}Y_{0.67}P_5O_{14}$, growth lasing 77−46722
$Nd_{1-x}Y_xP_5O_{14}$, laser emission at 1.32 μm, Ar laser pump source 79−31909
$Nd_xY_{1-x}P_5O_{14}$, fluoresc. conc. quenching, decay rate consts. 78−64404
$Nd_xY_{1-x}P_5O_{14}$, NdP_5O_{14}, laser materials, flux evaporation growth, dislocation etch tunnels 77−35560
Nd;YAG, Raman shifted, frequency conversion appl. 80−69451
Ni:glass, amplifier module inversion investigation, active element with rectangular cross section 79−27264
Ni:MgF_2, efficient CW optically pumped laser, 1.63 to 1.75 μm operation 79−18425
Ni:MgF_2, tunable transition-metal-doped solid state lasers 80−58549
Ni:MgO, heavily doped, defect charcterisation rel. to use as laser material 80−65000
Ni:MgO, tunable transition-metal-doped solid state lasers 80−58549
Ni^{2+}:MgO laser system, optical parameters 80−48260
$Pb_xSn_{1-x}Se$, electron-beam-pumped 77−50689

solid lasers continued
n-$Pb_{0.88}Sn_{0.12}Te$ spin flip Raman laser pumped by TE CO_2 laser, charcts. 80−87397
$Pb_{1-x}Sn_xTe$, continuously tunable electron beam pumped laser 78−50802
Pr^{3+}:$LiYF_4^-$, blue light emission, room temp. operation 77−38899
Pr^{3+}:oxide glass, intensity parameters and laser transitions 79−50300
PrF_3, laser action of Pr^{3+} 80−95901
$Pr_xLa_{1-x}P_5O_{14}$, laser emissions, fluoresc. 79−72572
PrP_5O_{14}, chemical synthesis and crystal growth of laser quality 78−92184
PrP_5O_{14}, laser emissions, fluoresc. 79−72572
$Pr_xY_{1-x}P_5O_{14}$, laser emissions, fluoresc. 79−72572
RbCl:Li F_A(II) centre laser, pumped by flashlamp-pumped dye laser 80−102737
SrF_2:Na, γ-irrad. cryst., spontaneous and induced colour centre emission 79−7131
Tb^{3+},Ho^{3+}:calibo glass, diffusion limited energy transfer 78−31235
Tb^{3+}:glass, luminesc. and laser props. 79−33798
Te, energy gap, laser emission study of press. depend. 79−82521
Tm:$LiYF_4$, XeF pumped, excimer excited storage laser 80−33003
Tm^{3+}:trifluoride, VUV fluorescence and tunable coherent sources from 1650 to 2600 Å 77−688
Tm^{3+}:YAG, 2.014 μm, stimulated emission, resonant pumping by Nd laser 78−17944
Xe film, possible ablation laser, intrinsic luminesc. decay times meas. 77−59619
YAG, high yield triggered laser *(French)* 78−37916
YAG laser, resonator length effects on loss coeffs. and ouptut energy *(German)* 78−66849
YAG laser, trimmer for wafer level products 80−87428
YAG rods, thermally induced birefringence in (001) direction, transmission loss *(Chinese)* 77−77166
YAG, single pulse formation kinetics with self-modulation of quality factor *(Russian)* 77−27312
YAG stable resonator, yielding high output energy and very low divergence beam 80−23721
YAG, transient colour centres caused by UV radiation 77−84744
YAG:Ho^{3+}, spectroscopy, stimulated emission 80−93374
YAG:Nd,Ce,Cr, effect of γ-rays, fast electrons on optical props., annealing and colour centre destruction 77−8608
$Y_3Al_5O_{12}$, laser cryst., struct. inhomogeneity obs. by vac. decoration 77−35701
Y_2O_2S, compact specimen prep. 77−85951
$Y_{1-x-y}R_xEr_yAlO_3$, $Y_{1-x-y}R_xEr_yScO_3$, stimulated emission of Er^{3+} ions 78−6705
$Zn_xCd_{1-x}S$, lasing modes and spatial distrib. under one-photon excitation, cavity model 78−74913
$Zn_xCd_{1-x}S$ monocrystal petal lasers, single-photon excitation *(Russian)* 80−99736
$Zn_xCd_{1-x}S$, platelet single cryst. one-photon optical excitation, spatial distrib. and mode struct. of laser emission 79−31912
ZnO epitaxial film, UV luminesc. due to one-, two-photon excitation, laser possibility 79−11468
ZnO, laser thresholds and stimulated emission, intrinsic recomb. processes 79−15489
ZnO, optical gain spectra, direct recording using laser modulation 78−66834
ZnO single cryst., UV laser, electron beam excited 80−53304
ZnO, two-photon-excitation, tunable laser emission, luminesc. processes 80−55127
ZnO UV laser, electron-beam pumped 80−99753
ZnS single cryst., UV laser, electron beam excited 80−53304
ZnS UV laser, electron-beam pumped 80−99753
ZnS:Mn, electroluminescent film, stimulated emission *(Russian)* 77−19255
ZnS_xSe_{1-x}, electron-beam pumped, end-pumped config., 415-430 nm emission 77k 77−14745
ZnSe, optically pumped stimulated emission at 4580 Å, near band edge luminesc. 78−71105
ZnSe single cryst., lasing action excited by ruby laser picosecond pulses 80−64035
ZnSe, single cryst. ingot, as CRT screen 77−75561
ZnTe, laser thresholds and stimulated emission, intrinsic recomb. processes 79−15489
ZnTe single cryst., lasing action excited by ruby laser picosecond pulses 80−64035

solid-liquid transformations
see also crystallisation; freezing; melting; solidification
AB-type compounds, high-press. and high-temp. behaviour, review 78−22850
acoustic levitation technique, for phase transition studies and props. of liqs. 80−43565
air based solar heating systems, phase charge energy storage, optimum physical properties 79−43742
alkali isoalkanoates, thermal behaviour, differential scanning calorimetry 78−34600
alkanoate, Li, Na, K and Rb salt mixtures, DSC anal. 78−10192
alloy, binary and ternary interdiffusion parameters, possibility of correl. with solidus temp. *(Russian)* 77−24426
alloy, solidus temperature determ. by method of moving specimen boundary projected on screen 78−35353
asymmetrical Ising model, phase transitions 80−17891
binary alloy, numerical calc. and simulation of nonsteady mass transfer by moving phase boundaries *(German)* 77−8811
binary alloys, pseudopotential theory 78−6144
binary metallic system, conc. profiles across solid-liq. interfaces 80−55382
borophosphate glasses, effect of F on props. 78−67657
t-butyl bromide, elec cond., temp. depend. in liq. and plastic phases 80−1944
t-butyl chloride, elec cond., temp. depend. in liq. and plastic phases 80−1944
$CaO-SiO_2-CO_2$, subsolidus and liquidus phase relationships to 30 kbar 80−85643
carbon tetrachloride, dual melting curves and metastability 80−92647
carbon tetrachloride, in porous medium, allotropic and liq.-solid-solid transformations *(French)* 78−83944
carbon tetrachloride, Rayleigh scatt. from liq. near solidification temp. 79−4807
chlorobenzene-cis-decalin mixtures, phase transitions and dielec. behaviour study in 77-330K 80−29680
collagen-water system, phasic transition invesitgation by calorimetry and NMR 79−62167
computer built random model for simulation of cryst.-melt interface 77−20165
Coulomb gas, 2-dimens., dissociation at low temp. 77−31748
crystal nucleation and symmetry, interaction pots. effect 80−34169
cyclohexane, differential thermal anal. under high press. 78−51669
cyclohexanol, orientationally disordered phase, Brillouin scatt. study 80−93351
cylindrical annulus phase-change energy storage simulation 79−57478
degree of dissociation of congruently melting compound, calc. from liquidus curve 77−84892
diamond solid-fluid interface roughening transition, Monte Carlo simulation 79−99088
diemthyl sulphoxide-H_2O-NaCl system, DTA exam. of primary ice phase field 78−48382
2,2′-dimethylbutane, differential thermal anal. under high press. 78−51669
dodecylamine (−NH_2)/H_2O_2 and deuterated cpd., liquid crystal, phase relationships, isotope effects 79−19358
dynamic Ginzburg-Landau theory 80−44292
elastic stress field shape change kinetics depend. on inclusion-edge dislocation interaction 79−86815
equilibrium liq.-solid coexistence line, phase instability and direct correl. function integral eqn. 80−65196
ethanol-H_2O mixture, liq. and solid, US vel., −80 to 20°C, 1-5 MHz 78−59933
experimental methods of investigation 79−73291
fluid stability towards solid formation, integral eqn. calcs. 77−35671
fluid-solid type phase transition, one dimens. model 78−63838
frequency distribution function, Debye temp., intermol. energy distrib. 77−4183
furan, adsorbed on NaCl, evidence of new condensed phase, IR spectra *(French)* 80−16028
Gaussian core model, high temp. expansion for fluid-crystal transition 79−65172
hard disk system, solid-fluid transition 79−88900
hard sphere system in equilibirum 80−86225
hard sphere system in three dimens., thermodynamic props. 80−86226
hard spheres with square-well attraction, Percus-Yevick eqn. soln. 79−37599
hard-sphere fluid, liq.-solid instability, bifurcation anal. 79−27888
hard-sphere system, liquid-solid transition, chem. pot. calcs. 80−54088
heat conduction and natural convection in phase change region, numerical method 79−41563
heat transfer and interface motion 80−53609
p-n-heptylhydroxybenzylidene-p'-n-butylaniline, phase transition study from 22 to 80°C 79−14679
ice-water system dielectric additive dissolution, interphase phenomena obs. *(Russian)* 77−8486
interface instability in presence of chemical potential gradients *(French)* 80−75338
interphase mass flux and mass fluxes within phases 80−48561
kinetic coefficient of two-phase transitional region between A+B melt and crystalline bulk phase A 80−96455
lattice gas model, three phase eqns. of state 78−22818
lattice models, LJD model, fine-grained lattices and continuum, Monte Carlo methods 79−12734
leghaemoglobin, thermal denaturing in cryst. and soln. 80−108849
Lennard-Jones fluid, thermodynamic props. calc. by modified Monte-Carlo method 77−35662
lipid bilayer phase transition, semiphenomenological model 77−35670
lipid monolayers and bilayers, phase transitions, model 78−44460
lubricant, shear rheological behaviour at high press. 80−35342
macromolecular systems, phase transitions, temp. and press. depend. theory, Ising model appls. 78−43105
metal-H, phase transitions 80−50631
metastable states below freezing point, fluctuation theory 77−24377
method and alloys, liquidus and solidus temperatures, determ. by γ-ray method 80−65193
methylcyclohexane, differential thermal anal. under high press. 78−51669
mixed salt aerosols, phase transform. and droplet growth in moist atmosphere 79−52783
mixtures, binary and ternary, solid-liq. phase equilib., excess Gibbs free energy 78−30736
molecular dynamics calc. at solid-liq. interface 79−42395
molecular dynamics calc. of liq. struct. up to solid surface 78−26764
molecular dynamics simulation 78−67803
molecular geometry, orientational order and melting 79−37810
monodisperse latex, simulation study of eqn. of state of simple liquid 77−63964
neopentane, Brillouin scatt. near liq.-plastic cryst. transition 78−19495
non-linear elastic thermal stress analysis with phase changes 78−79218
nonergodic hard parallel squares, with Maxwellian vel. distrib., mol. dynamics calcs. 80−100156
nonlinear heat cond. problem with phase change, finite element anal. 78−75030
phase change material, melt time and heat flux relations, appl. to thermal energy storage 79−74546
phase change material physical and chemical props. for space heating and cooling 79−57479
phenanthrene-d_{10}, oriented in biphenyl, triplet zero-field splittings, conc. depend. 78−2773
phenylenediamine-dihydroxybenzene mixtures, solid-liquid equilibria, phase diagrams 77−27986
phospholipid bilayers, low temp. transition from fluid state 80−97871
phosphoric acids, glass transition temps. 77−4050
polymers, solid-liquid state transitions, state before breakdown 78−63842
potassium alkanoates, phase transitions, differential scanning calorimetry 77−43319
potassium n-alkanoates, thermal behaviour, differential scanning calorimetry obs. 80−92650
protein-water system dynamic model 77−21470
quantum crystal translational symmetry spontaneous breakdown, quasi-averages and averages, phase transitions 78−30811
soils, non-linear seismic response and liquefaction 79−57862

solid-liquid transformations continued
solid solutions, congruent transformation pt., regular soln. theory 79−60477
solloidal solution droplets, solid, particle form., heat and mass transfer 78−95967
stability limit of liquid and crystal phase, three-parameter law of corresponding matter 80−49340
Stefan problem, generalised, soln. for slab-shaped body 77−46891
Stefan problem, two-phase, with varying specific heat coeffs. 77−69070
thermal energy storage by latent heat of fusion *(French)* 79−3893
thermal phase change storage medium, new type, thermal properties 79−43787
thermodynamic potential calc., liquid-solid transition determ. 77−20049
thermohydrodynamic equations for two-phase polydisperse medium with phase transformations and size distrib. 79−41743
transition metal solid solutions, max. or min. liquidus temps. 78−39741
1,1,2-trichloroethane, phase diagram, 0-10 kbar 77−72679
triethylacetic acid, high resolution ^{1}H and ^{13}C NMR spectra at liquid-solid phase transition 80−11281
trimethylacetic acid, high resolution ^{1}H and ^{13}C NMR spectra at liquid-solid phase transition 80−11281
US wave freezing effect, creation of const. volumetric periodic struct. *(Russian)* 78−63843
vacancy cell model and BGY integral eqn. 80−38887
virial series divergence for hard discs and spheres at closest packing 79−94859
water, amorphous solid, spontaneous electric polarisation rel. to solid struct., 20 to 100K 79−65791
water, continuity of state between liquid and amorphous solid, IR obs. 79−8130
water-ethylenediamine, liq.-solid equilibrium *(French)* 79−51236
water-propylene 1.3-diamine, liq.-solid equilibrium *(French)* 79−51236
Al-Si (2.4 wt.%), liq. fluidity in solid-liq. zone 80−108429
Al-Sn alloy, conc. profiles across solid-liq. interfaces 80−55382
Al_2O_3-BaO system, T-x phase diagram, phase transformation temps. in conc. range 100-65 mole% Al_2O_3 79−24428
Ar monolayer adsorbed on graphite basal planes, heat capacity anomaly rel. to phase transition 80−6636
Ar, solid-liq. transition and mech. props., modified cell theory 79−23703
BaF_2-NiF_2-CrF_3, X-ray crystallography study, phase identification at 700°C, cryst. symm. *(French)* 78−95733
Be, transformation enthalpies for α-β and β-liquid transitions 77−35690
Bi-Sb (1 at.%) alloy single cryst. growth solid-liq. interface study 80−107073
$CaAl_2O_4$, phase transform. accompanying hydration, US and X-ray obs. 79−39115
Cu-P-Se system, glasses, semicond., density, microhardness, softening point rel. to conc. 77−7674
cyclopentane, plastic cryst. and liq. phases, thermal cond. and sp.ht., 100-300K, 0-2.1 GPa 78−34663
e-D_2, solid-liquid coexistence curve anomaly *(Russian)* 78−75824
Fe, cast, grey eutectic transform. mechanism *(Russian)* 80−20924
Ga, collective mode dynamics, quantum corrections 77−15554
Ga, photoacoustic detection of phase transitions 78−75810
Ga photoacoustic effect at first order phase transitions at increasing and decreasing temp. 80−70320
Ga, transition from ordered solid to disordered liquid, viewed by photoemission 80−45217
Ga-Al-Si, solubility of Si at 500-800°C liquidus lines *(French)* 77−51498
GaP(As), liquid interaction parameters determ., 580-670°C 80−65197
Ge-P-Se system, glasses, semicond,, density, microhardness, softening point rel. to conc. 77−7674
Ge_xSe_{1-x}, vitrification, liquid-solid phase diagram, viscosity var. *(French)* 77−72680
GeTe-MnTe-SnTe system, compds., GeTe phase transition temp., elec. props., thermal cond. 79−43220
H_2 and isotopes, 4 to 30K 77−72674
H_2O, photoacoustic detection of phase transitions 78−75810
He liquid, plane surface layer, density profiles and pair correlation asymptotics *(Russian)* 80−88371
^{3}He, submonolayer on Grafoil, vacancy induced ferromag. 78−14536
^{4}He solid-liquid interface mobility under 1 MHz sound wave *(French)* 80−100373
Hg, thermal switching at solid-liquid transition 77−8154
Hg, transition from ordered solid to disordered liquid, viewed by photoemission 80−45217
In, transition from ordered solid to disordered liquid, viewed by photoemission 80−45217
InP(As), liquid interaction parameters determ., 580-670°C 80−65197
KCl-NaCl solid solns., equilib. decay curve *(Russian)* 79−90760
$(K_xNa_{1-x})NbO_3$ single crystals, growth and phase transitions 79−33915
Kr absorption on graphite, monolayer regime phase diagram 80−49507
Kr adsorbed monolayer, on graphite basal face, fluid-registered solid transition 80−49491
Kr, near solidification, 50°C, up to 6500 bar, meas. and simulation using Lennard-Jones pot. *(French)* 78−67301
Li soaps, n.C_{13}-n.C_{20}, phase transition temps. and enthalpies, DSC obs. 80−45544
NaOH-8% $NaNO_3$ phase change thermal storage for solar total energy system 79−57481
$Na_2SO_4.10H_2O$, solid-liq. transform., solar energy conversion applicability 78−60155
$Na_2S_2O_3.5H_2O$, solid-liq. transform., solar energy conversion applicability 78−60155
Ni-Pb alloy, conc. profiles across solid-liq. interfaces 80−55382
Ni-Sn intermetallic phase growth kinetics at liq. Sn-solid Ni interface 80−71638
PbO-B_2O_3-Al_2O_3 system melts and glasses, viscosity, phase separation, and supercritical fluctuations effects 79−65235
$Pb_{1-x}Sn_xTe$, solid-liq. phase equilib. above 750°C 79−82316
$Pr_{0.75}Sm_{0.25}Co_5$ magnets, struct. and props. sintering temp. depend. *(Russian)* 79−82819
$SbCl_5$, phase diagram to 43 kbar 80−2144
Se, acoustic props. near first-order phase transition 77−20014
Se, liquid-crystal phase transition, elec. cond. changes 79−33310
Si_3N_4-AlN-SiO_2-Al_2O_3 solid-liquid equilibria 78−92247
SiO_2, three-component glass, liq. phase separation, with two oxide modifiers 80−103250
SiO_2-Al_2O_3-FeO-CaO-MgO pyroxene glasses, phase changes 80−15013
SiO_2-base cores, for superalloys, high temp. characterisation 80−10640

solid-liquid transformations continued
$Te_{80}Ge_{15}Pb_5$, DSC sensitivity to controlled ageing in glass transition region 80−71673
Tl, transition from ordered solid to disordered liquid, viewed by photoemission 80−45217
V_2O_5 type liquid semiconductor, elec. props. control, by O_2 partial press. *(Russian)* 78−72142
Y_2O_3, calorimetric meas. of enthalpy, heat of fusion, heat of high temp. phase transition 77−28020
Zn aerosol condensation, prismatic and spherical particle form. 77−9135
Zn-Al, splat quenched and bulk specimens, eutectoid decomposition 77−63628
Zn-Bi(Sn) alloys, specific elec. resist., temp. and conc. depend., 20-800°C 79−82571
Zn-Cd alloys, liq. and solid, ultrasound speed and compressibility meas. 80−102941
Zn-In alloy, solid-liq. equilib. roughening transition 80−96630

solid mechanics *see mechanics*

solid solubility
alkali metal alloys, dil., binary, equilib. at. vol. and compressibility 80−70295
alkaline earth silicate glasses, morphology effects on props. 80−49118
alkaline earth silicates, Cr^{2+} solid solubility 77−76564
alloys, rapidly quenched crystalline, struct., and heat treatment effects 80−76292
BCC transition metals, of C 78−71861
binary melts, appl. of quasichem. method of cluster components *(Russian)* 77−80623
binary system, distribution coeffs., estimation from Van Laar and Hayes-Chipman relations 80−84293
cemented carbides, physical and chem. nature 80−76265
cluster components method, quasichem. variant, for multicomponent solid solns. *(Russian)* 77−80622
coalescence of gas-filled pores *(Russian)* 78−18679
conference, Masnuy-St-Jean, Mons, Belgium, Oct. 1979 80−82570
Cu, of O_2 77−69089
cubic margules solution model, miscibility gap and crit. point behaviour 78−59925
divalent metal alloy, solid solubility 79−60514
durene-p-dibromobenzene system, phase diagram and X-ray diffr. expts. 78−79774
entropy of solubility of substitutional impurities 77−4202
finite single- and two-phase systems, atomic diffusion, iterative solns. 77−4224
impurity diffusion profiles, influence of limited solubility 78−55989
KCl-$BaCl_2$ system, solid solns., phase diagram, enthalpy of soln., vibr. entropy. 78−39751
metal refining by crystallisation and reflux, three component Raoultian behaviour 77−28799
metallic system, compound formation rel. to heat of mixing 80−55689
metals, overbarrier states of H and D, subsystem heat capacity, equilibrium props. *(Russian)* 80−79998
methane-O_2, solid mixture, electron diffraction study *(Russian)* 78−83953
pigeonite, inverted, from SW Norway, precipitation temp. estimation 80−72500
PMMA-spirobenzopyran mixed monolayers, photoresponsive effects 79−66316
polystyrene, correlation between fatigue lifetime and solubility parameter for organic media 79−43455
precipitate free zones, X-ray microanal. 80−108768
rare earth intermetallic, $R(Fe_{1-x}Mn_x)_2$, phase struct., mag. and Mossbauer meas. 77−20563
refractory compound fibre reinforced cpd. materials, diffusional reaction, effect of alloying calc. 80−20851
restorational carbonisation in one and two phase states *(Russian)* 80−65225
semiconducting binary compound, third component solubility 78−43124
sesquioxides solubility in periclase and monticellite systems 79−69253
steel, austenitic, strength, ductility and fracture toughness, N and Cr effects 80−100878
steel, B concentration and solubility depend. on introduction of rare earth metals *(Russian)* 80−65226
steel, carbide and nitride phases dissolution *(Russian)* 80−20888
steel, Cr-C and C, carbide coating by CVD, interlayer form. 80−11574
steel, ferritic, of graphite, high temp. vacuum metallography determ., 545 to 750°C *(Russian)* 77−55359
steel, high-speed cutting, carbide solubility in austenite, Co addition effects *(Russian)* 77−21177
steel, HSLA type 4340, hydrogen diffusivity and solubility, correl. with embrittlement and SCC phenomena 79−83323
steel, maraging, solubility of Fe-Mo-Co (10, 0 to 20 wt.%) Laves phase, depend. on Co *(Russian)* 79−100145
steel, maraging alloy, intermetallic compound solubility, thermodyanmic calcs. *(Russian)* 80−40363
steel, medium C, 40MnB, dissoln. and precipitation of $M_{23}(C,B)_6$ *(Chinese)* 80−66511
steel, stainless, ferrite to austenite decomp. 80−93554
steel, stainless Kh18N11, MnS solubility determ. method 80−84910
steel, tempered, kinetics of solution of Mn in precipitated cementite *(Russian)* 78−6891
steel, V, N effect on precip. and transform. kinetics 80−97485
stress corrosion cracking, role of H_2, state of art review 80−61017
ternary alloy, metastable miscibility gap determ. by small angle scatt. 77−28780
transition metal carbides and nitrides, solid soln. formation, elastic lattice deform. energy 77−84927
transition metal compounds, $(M,M')Cr_2S_4$ and (M,M')S, where M,M'=Mo,Co,Zn,Cd, solid-state equilib. *(German)* 77−36486
transition metalloid atom solubility and electronegativity difference correl. with phase stability and d-electron/atom ratio 78−6914
Ag-Ni supersaturated metastable solid solns. formed by ion beam mixing 80−107425
AgBr layer, of Ag, solubility and transport 79−23742
AgBr NaBr, thermodynamic props., metastable states and demixing 80−96660
AgBr-NaBr, phase diagram, miscibility, binodal curve and demixing kinetics, X-ray meas. 80−96659
$AgInS_2(Se_2)$-$SnS_2(Se_2)$, degree of solid solubility and phases characts. 78−35377

solid solubility continued
Ag_2S-In_2S_3-SnS_2 system quaternary and ternary sulphide spinels, solid solubility and struct. 78−35376
Al, heat of soln. of H, electron charge distrib. calc. 78−51689
Al, powder, liquid phase sintering, solid-state solubility effect on vol. change 78−35332
Al-Ag_2Al, eutectic alloy, exam. of terminal solid solubility limits 78−76633
Al-Mg-Zn, neutron small angle scatt. study 79−43255
Al-Mn alloys, study of solidification by rapid cooling *(Japanese)* 78−88459
Al-Sc, solid solubility and residual resist. 79−51265
Al-Zn, neutron small angle scatt. study 79−43255
Al-Zn-Mg, metastable miscibility gap determ. by small angle scatt. 77−28781
Al-Zr (1-13 wt.%), rapidly quenched, extended solid solubility, grain refinement and age-hardening 80−76266
$Al_yGa_{1-y}As_{1-x}Sb_x$, LPE, strain effects near miscibility gap, importance 79−7759
Al_2O_3, in $Mg_2Si_2O_6$, enstatite, rel. to palaeogeotherm uncertainties 78−65283
As_2S_3, amorphous film, photodissolution of Ag, struct. changes 77−11815
As_2Se_3-Sb_2Se_3, phase relns. 77−21118
Au, Co-hardened, characterisation by Mossbauer spectroscopy, Co precip. formation 80−80108
Au, in Si, gettering by P 78−83961
B-Si, (0 to 14.3 at.%), phase charact., regions of existence *(French)* 80−104117
$BaAl_2Si_2O_8$-SiO_2, celsian solid solns., effects on polymorphic transform. kinetics 78−68677
$BaO.6Fe_2O_3$, solubility of CaO 80−100333
$(Ba_xSr_{1-x})SO_4$:Eu mixed crystal series, X-ray diffr. study of miscibility 80−2168
$Ba_2TiGe_2O_8$-$Ba_2TiSi_2O_8$, pseudobinary system, pyroelectricity and related props. 78−95553
Be, of Al, diffusion mobility and solubility 77−35758
Be, of V, Nb, Ce, diffusion coeffs. and solubility 77−35757
Bi-Sb, bicrystal rearrangement of grid of nonconformity dislocations on (111) interface during heating 79−28215
Bi-Se system, high-temp. calorimetry *(French)* 77−44501
BiI_3-Sb(As)I_3, phase diags. 78−6905
BiTeI-SbTeI solid solns., form., crystn., elec., thermal props. 78−44003
Ca-Mn-S-Se system, multicomponent solubilities 80−108416
$CaAl_2O_4$-$SrAl_2O_4$-BaA_2O_4, binary and ternary systems, solid solubility *(Japanese)* 80−35174
$(Ca_xCd_{1-x})CO_3$, cryst. struct. and cation isomorphous miscibility 80−33972
CaF_2-CaO, elec. cond. meas., CaO solubility, O^{2-} diffusion const. 78−30760
CaF_2-ScF_3, phase relationships at 100 kbar and 1200°C 77−43335
$Ca_{0.5}Gd_{0.5}H_n$, H_2 dissociation press., phase behaviour and struct. 78−2260
$Ca_{0.5}Nd_{0.5}H_n$, H_2 dissociation press., phase behaviour and struct. 78−2260
CaO-MnO system, solid soln. form. and analysis 80−28996
$Ca_{0.5}Pr_{0.5}H_n$, H_2 dissociation press., phase behaviour and struct. 78−2260
Ca_2SiO_4-BaO, conditions and mechanism in cryst.-chemical stabilisation of unstable phases 80−39302
Ca_2SiO_4-FeO, conditions and mechanism in cryst.-chemical stabilisation of unstable phases 80−39302
Ca_2SiO_4-MgO, conditions and mechanism in cryst.-chemical stabilisation of unstable phases 80−39302
CaX-MnX, X=S, Se, Te, solubility limits 80−44320
$Ca_{0.5}Y_{0.5}H_n$, H_2 dissociation press., phase behaviour and struct. 78−2260
$CdGa_2S_{4(1-x)}Se_{4x}$, solid soln., crystallographic studies 78−15301
CdSb:Au, solubility, thermal anal., microhardness, microstruct., elec. charcts. 77−16557
CdSe, of Cu and Ga 78−22856
CdTe, amphoteric behaviour and solubility of Sn 79−33008
CdTe, of Ge, 630-800°C, prep. conditions depend. 80−103519
CdTe-CdS solid solution phase diagram *(Russian)* 79−100120
CdTe-Co(Mn) systems, reaction of components, DTA, microstruct. and microhardness obs. 79−38804
CdTe-ZnS system, phase diagram and solid solubility 80−20909
$CdTl_2Se_4$:Au, solubility meas. by microhardness method 80−96650
Ce-Mn-Ni system, phase diag. 77−52283
$CeMg_{11}$V(Cr)(Mn)(Fe)(Co), hydriding and appl. in H_2 storage 80−51009
$CeNi_2$, of Cu, Ag, Au, absence of obs. 78−6032
$CeNi_2$-$CePt_2$ system, structural and mag. studies on valence behaviour of Ce 80−103809
CeO_2:Nb_2O_5, sintered, elec. cond. and solid solubility, 800 to 1329°C 79−99546
$CeRh_{3-x}Pd_x$, electronic and cryst. struct. comparison, catalytic behaviour 78−84398
Co-WC hard alloys, rapidly quenched struct. 80−76233
Co_2GeO_4-Mg_2GeO_4, solid solubility and cation distrib., free energy 77−35700
Cr-C, binary alloy formation of nonequilib. Cr_3C in alloys quenched rapidly from melt 80−7581
Cr-Ge system, phase diagram, thermal anal., X-ray diffr., microhardness, and electron probe anal. *(French)* 80−97462
Cr-Si-Cu, struct. and supercond., Cu influence 80−50592
Cu, of Fe, study at high temp. using molten salt electrochemistry 77−84997
Cu/Al film system, interdiffusion and phase growth kinetics 77−69122
Cu-Ag interface, interdiffusion, X-ray and electron microprobe data 77−4225
Cu-Ag(Ta) metastable alloy form. by ion implantation, combined TEM and ion channelling obs. 78−34530
Cu-Cd, structure, electrolytic deposition on monocrystalline Cu cathodes *(Polish)* 80−44435
Cu-Cd alloys obtained by electrolysis, struct. 78−91552
Cu-Cr alloy, laser irrad., structural changes *(Russian)* 80−100247
Cu-Fe (0.2 at.%), clustering, precipitation, and oxidation, 298 to 919K, Mossbauer study 80−7242
Cu-Fe (<4 wt.%), solubility determ. by thermoelectric power meas. *(French)* 77−62644
solid solubility continued
Cu-Fe alloy, cluster form., Fe solubility determ., 450 to 1000°C, Mossbauer spectra obs. *(German)* 79−29021
Cu-Ga porous solid formed by shock compression 80−29905
Cu-Mn-P alloys, phase diagram *(Russian)* 80−20891
Cu-Ni (20-80 at.%), clustering, diffuse neutron scatt. study, conc., temp. depend., miscibility gap location 78−47529
Cu-Ni-Nb (30, 0.9 at.%), precipitate free zones, X-ray microanal. 80−108768
Cu-Sb alloy, splat-quenched, energy dispersive X-ray diffr. 78−23728
Cu-Ti, solubility of Ti, exam. using NMR of ^{63}Cu *(French)* 80−7179
$CuInS_2(Se_2)$-$GeS_2(Se_2)$, degree of solid solubility and phases charcts. 78−35377
Er_2O_3:CaO, elec. cond. and nonstoichiometry 79−11112
Eu-B-C ternary and binary boundary systems, preparation techniques, X-ray analysis 80−60840
EuB_6-CrB_2 quasibinary cross section 77−86001
α-Fe, Armco, determ. of H solubility 80−54390
Fe, chem. diffusion coeffs. and solubility limits for Cu, 690-1050°C 77−59146
Fe, diffusion and solid solubility of Sb, 773-873K, ion backscatt. anal., rel. to intergranular embrittlement 78−71880
Fe, effect of H_2 on phys. and mech. props. 80−101657
Fe, segregation of impurities, physico-chemical aspects *(Czech)* 80−60866
Fe, trapping of H, average trapping depth and trapping sites density 80−84297
Fe, white cast, migration of C to the surface, solubility *(Russian)* 80−92720
Fe:C, solubility at transition temp. between α and γ phases 79−11611
α-Fe-Be(P)(Mo)(W)-Co, effect of Co on solubility anomaly due to mag. transition *(Japanese)* 79−42257
α-Fe-Be(Ti)(Mo)(P)(Sb), effect of mag. transition on solubility of alloying elements *(Japanese)* 79−42256
Fe-C system, FCC, austenite field thermodynamics, re-anal. 80−89201
Fe-Cr-Co permanent magnets, phase diagram, miscibility gap 77−89984
Fe-Cr-Co permanent magnet system, miscibility gap, microstruct. and mag. props. obs. 80−76228
Fe-Cr-Co-Mo high energy permanent magnets, mag. props. 80−97119
Fe-Mo-C system, isothermal sections, 973 to 1273K, thermodynamic analysis 78−6895
Fe-Nb-V-C-N, equilibrium comp. and solubility in steels, model of ideal solns. *(Russian)* 80−60832
Fe-NbC, exam. of phase diagram, and mech. props. *(Russian)* 79−20028
Fe-Ni (6-8 at.%) 80−75888
Fe-Ni-Al alloys, phase diagram, miscibility gap, DTA meas. 78−92237
Fe-Pd (1-2 wt.%), solution of ^{119}Sn, study by Mossbauer spectroscopy 80−75888
Fe-Sb-Ti(V)(Cr)(Mn)(Co)(Ni), dil., interactions and precip., Mossbauer study 80−39997
Fe-Sb-Ti(V)(Cr)(Mn)(Co)(Ni), interactions and segregations, Mossbauer and X-ray diffr. study 80−70415
Fe-Ti-V-C-N, equilibrium comp. and solubility in steels, model of ideal solns. *(Russian)* 80−60832
α-Fe_2O_3, solubility in BeO, Al_2O_3 and synthetic chrysoberyl Mossbauer studies 77−7867
$Fe_{1+x}Sb$-CoSb solid soln., mag. props., Mossbauer spectra, solubility limits, and lattice consts. *(Russian)* 77−59394
$Fe_{1+x}Sb$-NiSb solid soln., mag. props., Mossbauer spectra, solubility limits, and lattice consts. *(Russian)* 77−59394
GaAs, of Se, SIMS 78−67830
GaAs:Cr, carrier equilibrium effects, impurity states, elec. resistivity 80−65488
GaAs:Cr diffusion profile meas. 80−6554
GaAs:Na, impurity solubility and diffusion 79−55930
$GaAs_ySb_{1-y}$, miscibility gap, rel. to LPE 79−33090
$Ga_xIn_{1-x}P_yAs_{1-y}$, ($0.5<y<0.9$), LPE on InP, Ga, As distrib. coeffs., lattice matching 78−47673
GaP:Au, diffusion, solubility, and electrotransport of Au 78−91489
GaP:Cr, diffusion parameters and solubility and influence on elec. and optical props. 79−73343
GaP:Fe, diffusion, solubility, elec. activity and energy levels 77−55395
GaS-YbS system, phase diagram, reacts., thermal, mag. and elec. meas. 79−11578
GaSb, separate and combined solubilities of donors and acceptors 77−15434
GaSb-Ag, phase diag. 77−90327
$(GaSb)_{1-x}Ge_x$ films, single-cryst. metastable semicond., growth and phase stability 80−80115
Ge, n- and p-type, solubility and diffusion of Na, vacancy mechanism 77−89592
Ge:Al, limiting solubility, rel. to charge carrier conc. 80−24596
Ge:Ba distrib. pattern, partition coeff., limiting solubility and energy levels 77−15444
Ge:Cu, solubility and behaviour of Cu, internal friction investigations 80−92678
Ge:Sb, limiting solubility, rel. to charge carrier conc. 80−24596
Ge-In-Te system, homogeneity region, struct., electrophysical props. 78−44091
Ge-In-Te system, region of solid soln. of In in GeTe 77−51499
Ge-metal film, polycryst., struct. props. determ. 79−4494
Ge-Si system, solubility of Au, thermodynamic calcs. 79−86890
Ge-Sn solid solution, cooling rate effect on partition coeff. of Sn between liq. phase and crysts. 77−12510
GeS_xSe_{1-x}, form. of solid soln. and phys. props. *(Russian)* 77−1232
GeTe-Ga_2Te_3, electrophys. props. 77−48403
GeTe-In, solubility, thermo-EMF coeff. meas. 78−43124
H solid solution with Pd-Cu(Ag)(Au) alloys, superconducting transition temp. behaviour *(Russian)* 80−70879
H_2, solubility in high press. He 80−10674
Hf-M-B systems (M=Rh,Ir), phase equilib. and cryst. structs. 80−15072
Hf-O, phase props. 77−40415
HgSe-MnSe system, phase exam., solubility limit 77−36488
InAs, individual solubilities and cosolubilities of Zn, Cd, Te, microhardness 77−16552
InAs-CdTe quasi-binary system, temp.-comp. diagram, physicochem. and thermodynamic analysis 80−104127
In_2O_3, grown from Sn-In melt, Sn solubility 77−11697
In_2O_3-SnO_2, X-ray and optical meas. of solubilities 79−55894

solid solubility continued
$InSb_{1-x}Bi_x$ films, single-cryst. metastable semicond., growth and phase stability 80−80115
$InSb_{1-x}Bi_x$, metastable epitaxial film, phase diagram 80−76238
In_2Se_3-Cu_2S system, electrophys. props., influence of 1-4% Cu_2S 80−20219
In_2Te_3, of PbTe 78−35361
Ir, diffusion of C from surface into bulk, theory 80−6562
$(K_{0.5}La_{0.5})_xBa_{1-x}TiO_3$, cryst. struct., dielec. and IR spectral meas. 79−46614
$KMg_2LiSi_4O_{10}F_2$-$NaMg_2LiSi_4O_{10}F_2$, solid soln., solid solubility and swelling characts. 80−59660
K_2O-CaO-B_2O_3:CuII, immiscibility, ESR detect. 78−80200
La_2O_2S-R_2O_2S (R=rare earth), solid solubility, differences in ionic radii 77−15593
La_2Se_3, La_2Te_3, mutual solubility 77−21113
Li, impurity and conduction electron scatt. at 4.2K *(Russian)* 77−35931
Li-Al system, Li solubility and chem. diffusion in Al, electrochem. study 80−107432
LiF:Mg^{2+}, TLD-100, precipitation reactions and ionic cond. 77−56479
$Li_{0.5}Fe_{2.5}O_4$-$CuFe_2O_4$-$MnFe_2O_4$, structural characteristics and mag. props. of solid solutions 77−35696
$(Li_{0.5}La_{0.5})_xBa_{1-x}TiO_3$, cryst. struct., dielec. and IR spectral meas. 79−46614
$LiNbO_3$:Na structure field stability limits, LPE film growth, SAW velocity 80−80102
Li_2O-B_2O_3-SiO_2 glass systems, phase separation effect on the diffusion processes 78−26734
Mg, heat of soln. of H, electron charge distrib. calc. 78−51689
Mg-Ag-Cu, phase comp. in Mg-rich region *(Russian)* 80−40331
Mg-Al-Tl(Pb) systems, phase diags., electrode pots. *(Russian)* 78−80516
Mg-Ga-In(Tl) and Mg-In-Tl, phase diagrams and electrochem. props. *(Russian)* 80−40330
Mg-Ho, phase diagrams and transformations, Ho solubility *(Russian)* 79−52162
Mg-Tb, (up to 45 wt.%), phase diagram, and mech. preps. 80−16277
Mg-Y-Zn alloys, phase equilib. *(Russian)* 80−16271
MgO, solid solubility of Sc_2O_3, Al_2O_3, Cr_2O_3, SiO_2 and ZrO_2 80−15247
Mn-Ga system, X-ray struct. investigation, solubility *(Chinese)* 80−88084
$Mn_xCr_{3-x}O_4$ spinels, miscibility gap boundaries, annealing expts. 77−86012
$(MnTe)_{1-x}(Bi_2Te_3)_x$ ($x \leq 0.05$) solid solution, electrophys. props. 80−24925
Mo chalcogenides, layered, soln. mechanism of metals 79−42249
Mo, high-pressure studies of N_2 solubility 77−15592
Mo, TEM exam. of Mo_2C precipitates, exam. of crystallographic relationships 78−52811
Mo:N, ion implanted proton-irradiated, annealing behaviour 78−91362
Mo-N system, phase diagram of solid and liq., high and low press. 78−44083
Mo-Si-Cu, struct. and supercond., Cu influence 80−50592
Mo-W-N system, nitrided annealed samples, W replacement of Mo 80−76227
Mo_2C, free energy of form. and thermodynamic props. of C in solid Mo 80−15266
$NaCaPO_4$-$Ca_3MgSi_2O_8$(CaO) systems, phase diagrams of partial system 78−35369
$NaCaPO_4$-$CaMgSiO_4$ system, phase diagram 78−35370
NaCl:Sr, free and assoc. Sr by elec. cond. and ionic thermocond. meas. 77−62645
NaCl-KCl, interdiffusion and demixing, electron microprobe anal. *(French)* 80−54444
NaCl-KCl system, interdiffusion, miscibility, Kirkendall effect 80−107568
NaCl+Pb, Pb aggregation effect on yield stress, incoherent precipitates, solubility determ. method 80−50645
Na_2O-B_2O_3:Au glasses, Au solubility, oxidation state and opt. absorpt. 80−44321
Na_2O-CaO-SiO_2 glass, effect of phase on liquids and gas diffusion *(German)* 80−38931
Na_2O-CaO-SiO_2 glass, redox phenomena evaluation in melting-fining process, SO_2 evolution 80−84900
Na_2O-Ga_2O_3 system β and β'' phases, fast ion cond., prep. and phase comp. 80−59716
Nb chalcogenides, layered, soln. mechanism of metals 79−42249
Nb, of O_2 steady state *(German)* 78−38851
Nb-Ga-Ir system, phase equilib. at 1000°C and supercond., Nb-rich portion 77−36480
Nb-Ge-Cu, phase equilib. and supercond. props. *(Russian)* 80−40332
Nb-H(D) system, isotope effects 77−20069
Nb-O solid solution, interaction with O_2 at low press., segregation equilib. and chemisorpt. *(French)* 77−24483
Nb-Pd constitution diagram, metallographic and X-ray diffr. anal. 80−89204
Nb-Re-(Ru)-N system, N_2 solubility and solubility limit *(German)* 77−4205
Nb-Re(Ru)-N system, spectral emissivity, lattice parameter, initial rate of N_2 absorption *(German)* 77−4204
Nb-Si-Cu, struct. and supercond., Cu influence 80−50592
Nb-Sn-Si(As), ternary A15 phase regions, solubility 77−44215
Nb-TiN(HfN)(ZrN), BCC solid soln., nitride solubility, alloying effects *(Russian)* 79−51262
$NdCl_3$-$SnCl_4$-$POCl_3$, complex formation, struct. and comp. 77−89413
Ne solid, solubility in high press. He 80−10674
Ni, diffusion and solubility of S *(Russian)* 80−70465
Ni, grain boundary internal friction, B solid solubility as function of grain size 80−60903
Ni, of C *(Czech)* 79−77757
Ni-B, grain boundary internal friction, B solid solubility as function of grain size 80−60903
Ni-Mn, permeability, diffusion and solubility of H 80−107573
Ni-Ta(Sn)(Er)(La) ion implanted surface alloys, solid solubility and radiation-induced disorder, backscatt. obs. 79−46692
NiO, undoped and Al doped, Ni self-diffusion, vacancy-impurity complex effects 80−107493
NiTaC eutectic superalloy, casting, furnace atm. effects 80−84880
NiZn ferrite, ZrO_2 additions influence on sintering and physicochem. props. 80−108369
solid solubility continued
Pb, diffusion and saturation solubility of Pt, melting curve, conc. profiles 80−88365
Pb, ion implanted, diffusion of Co, exam. by activation analysis 78−91488
Pb, of ^{64}Cu, electromigration and thermomigration obs. 78−71882
Pb, of Au, elec. resist. meas. 80−39298
Pb-Bi, splat quenched, solubility limit, vacancy conc. and supercond. transition temp. 77−12046
Pb-Zn, pressure effect on solubility and diffusion of Zn 77−43385
$PbCO_3$-$BaCO_3$($SrCO_3$)($CaCO_3$), solid soln. form., regions of existence 79−11581
$Pb_{1-x}Ge_xTe$, solubilities, elec. and optical props. 77−35940
$Pb_{0.8}Sn_{0.2}Te$:Cd, defect struct., Hall effect and solubility meas. 77−11571
$Pb_{1-x}Sn_xTe$, diffusion of Cd, Hall effect, cond. and solubility meas. 79−69292
$Pb_{1-x}Sn_xTe$:Cd, Cd diffusion obs. using Hall mobility and Cd solubility expts. 78−26584
PbTe, diffusion of Cd, Hall effect, cond. and solubility meas. 79−69292
PbTe:Cd, Cd diffusion obs. using Hall mobility and Cd solubility expts. 78−26584
PbTe:Cd, defect struct., Hall effect and solubility meas. 77−11570
PbTe:Zn, defect struct., Hall effect and solubility meas. 77−11572
PbTe-Ga_2Te_3, phase interaction, DTA, XPA and microstructural anal. 80−96625
PbTe-InTe system, phase interactions and solid soln. form., physicochem. and elec. characteris. 80−104129
PbTe-PbS, solid-phase solubility, use of diffusion couple 77−12602
$Pb(Zr,Ti)O_3$:Cr_2O_3 ceramics, reson. freq. comp. and temp. depend. 80−70413
Pd-Al(Si) melts, appl. of quasichem. method of cluster components *(Russian)* 77−80623
Pd-H, low temp. transport props., heterogeneous-mixture model 80−24871
Pd-H system, effect of α-β phase change on β-phase solubility of H 77−89544
PdAl-Fe(Ni), phase diagrams, eutectic points and solubility *(Russian)* 80−40333
$Pd_{77.5}Cu_6Si_{16.5}$, ternary miscibility gap, simulation, dispersed phase composite form. 80−54379
Pr-Ga (0 to 50 at.%), phase diagram and cryst. structs. of intermetallic cryst. 80−3002
PuC-TaC, solubility study 78−83956
PuC-ZrC, solubility study 78−83956
Sb-Te-Bi, miscibility limits, computer study 78−79773
SbI_3-AsI_3, phase diags. 78−6905
Sc-M-B systems (M=Rh,Ir), phase equilib. and cryst. structs. 80−15072
Si, hole localisation, solid solubility, excitonic Auger lifetime of acceptors 80−20216
Si laser annealed, nonequilibrium solubility and segregation 80−84296
Si, of Co, 1000-1270°C, radiotracer obs. 77−51500
Si solubility in Mg, depend. on impurity inclusions *(German, English)* 80−97492
Si:Al(Ga), O_2 diffusion, conc. profile meas. 80−79990
Si:As, high-dose implanted, irrad. time and subsequent heat treatment effects on laser annealing 80−29041
Si:As, solid solubility and thermal behaviour of metastable 80−75359
Si:As, solid solubility of As determ. by ion implantation, CW laser annealing 80−6517
Si:Au, diffusion of Au anal. 79−23786
Si:B, high conc. effects in ion implantation 80−75245
Si:B, solubility and precip., and supersat. resulting by thermal predeposition 78−11232
Si:Fe, solubility study by EPR and neutron activation anal. 80−75361
Si:Fe(Cu)(Pt), implant redistrib. and enhanced solubility following laser irrad. 79−69129
Si:Ga^+, carrier conc., influence of Ga solid solubility 79−69152
Si:Ir, Ir diffusion and solubility 77−15448
Si:O, impurity solubility and diffusion props. 78−6093
Si:P(As)(B), nonequilibrium solid solutions obtained by heavy ion implantation and laser annealing 80−92544
Si:Sb, high dose implanted, orientation dependent annealing effects 78−18665
Si:Sb vacuum deposited coating, p-n junction, pulsed electron beam annealing doping, diffusion 80−75480
Si:Sb(Ga)(Bi)(In), dopant solubility limit, laser irrad. effects 80−84295
Si:Se, diffusion coeff., solubility and energy level determ. 79−35825
SiC, exam. of N solubility, in epitaxial layers 80−6520
SiC, solubility, partition coeff. of Be 79−10951
SiC:Al epitaxial layers, growth, Al distrib. and solubility 80−15391
SiTe-GaTe, thermo-EMF, elec. cond. and solubility 77−20346
Sn-Bi alloy, splat-quenched, energy dispersive X-ray diffr. 78−23728
SnO_2, grown from Sn-In melt, In solubility 77−11697
SnTe-In, solubility, thermo-EMF coeff. meas. 78−43124
SnTe-InTe, SnTe-In_2Te_3, solid soln. region, lattice constant variation 77−35697
$SrAl_2O_4$-$BaAl_2O_4$ system, solid solubility, α-β transition 78−63860
Ta chalcogenides, layered, soln. mechanism of metals 79−42249
Ta-Si-Cu, struct. and supercond., Cu influence 80−50592
Te-based eutectics, crystn. rate effect on electrophys. props. mutual solubility effect 80−60774
Ti alloys, hydrogenation at 200-600°C and up to 10000 kPa 80−107435
α-Ti/Fe, retrograde solid solubility 80−79950
Ti-B-C system, complex carbide phase synthesis by crystallisation from gas phase 77−16526
Ti-$C_x(N_x)(O_x)$, solid soln. film prep. by reactive sputtering, solubility and effect on props. 79−28231
Ti-Cu solid solution, determ. of Cu solubility, stability by thermoelec. power meas. 79−77753
Ti-H, H diffusion and phase consistution, V influence, proton spin-lattice relax. meas. 78−27484
Ti-Mo binary system, solid state phase transform. and miscibility gap, phase diagram 79−8298
Ti-Si-C system, complex carbide phase synthesis by crystallisation from gas phase 77−16526
TiO-VO, solid soln. formation 77−89541
Ti_2O_3-$MgTiO_3$, phase analysis 78−3103
Ti_3O_5-Al_2TiO_5 ($MgTi_2O_5$), solid solubility, X-ray phase and optical microscopic exam. 80−59657
U alloys, strengthening rules, high temp. 77−21157

solid solubility continued
U, of Y, solubility at 1700K 77−89545
UP-PrP (NdP) systems, mag. phase diagrams 78−84424
V, H solubility and diffusivity around room temp. 80−29225
V-H system, DTA, phase diagrams, low temp. phase 78−6903
V-Nb(Ti)(Zr)(Cr)(Mo)(Fe)(Cu), H solubility and diffusivity around room temp. 80−29225
V-O solid solutions, solubility and thermodynamic props. 77−7866
V-Si-Cu, struct. and supercond., Cu influence 80−50592
W, chalcogenides, layered, soln. mechanism of metals 79−42249
W-Ni system, liq. phase sintering, 1640°C, solubility and vol. diffusion of Ni in W 79−86895
W-Si-Cu, struct. and supercond., Cu influence 80−50592
Y, solubility of H_2 and D_2 *(Japanese)* 78−18784
YO_x-ZrO_2, YO_x-rich, phase equilibria 77−21117
Y_5Si_3, $YSi_{1.56}$ solubility of Re 79−38806
Zn-Cu-Se system, region of existence of ZnSe phase 77−16554
Zn_3As_2-2ZnTe, solid soln., sphalerite-antifluorite struct. stability, cation distrib. 77−43334
ZnS, wurtzite, ZnO solubility, 1444-1240°C 80−15248
ZnSe:Ga,As, characts. of simultaneous incorporation, by Mn^{2+} ESR and X-ray fluoresc. anal. 80−34017
α-Zr, H terminal solid solubility, optical metallographic study 80−34195
Zr, of H, optical metallography, internal friction meas. 78−83962
Zr-M-B systems (M=Rh,Ir), phase equilib. and cryst. structs. 80−15072
Zr-Ru, alloy Zr rich, Ru solubility, eutectic decay, $\alpha \rightleftarrows \beta$ transform., struct. *(Russian)* 80−65227
Zr-W-Cr, Zr-rich corner of phase diag. *(Russian)* 78−80517
$((ZrO_2)_{0.92}(Y_2O_3)_{0.08})_{1-x}(Fe_2O_3)_x$, Fe solubility and elec. cond. 79−99354
$ZrRh_{3-x}Pd_x$, electronic and cryst. struct. comparison 78−84398

solid solution hardening
alkali halide conc. solid solns., hardening theory, dislocations, stress effects 79−32994
alloy, $L1_2$ ordered, yield stress 77−52392
alloy, solid soln. strengthening, HTR appl. 79−15688
alloy, strengthening mechanism anal. by thermal activation theory 79−78987
BCC lattice, low temp. interstitial hardening 79−20060
brass, theory 78−19771
chemically hardening material cast in elastic cylindrical mold, transient thermal stresses 80−7589
computer simulation 78−31420
concentration gradient soln. hardening 77−55974
dislocation, straight line, motion in conc. solid soln. computer simulation 77−81268
dislocation motion, straight line, in concentrated solid soln., computer simulation 77−15413
dynamic simulation, normalised crit. stress 79−11635
eutectic alloy, yield point analysis 77−8875
Hastelloy-X, fatigue crack propag. at elevated temps. in solid solution strengthened superalloys 78−39895
Haynes alloy 188, fatigue crack propag. at elevated temps. in solid solution strengthened superalloys 78−39895
ionic crystal, solid soln. hardening by aliovalent cations 77−44265
lattice hardening due to dissolved H_2 in Fe, and ferritic steel 78−76656
metal, BCC, solution hardening and softening 77−12635
metal, review of theories *(Czech)* 80−3084
metals, BCC, crystal resolved shear stress depend. on dislocations 80−40373
metals, FCC, hardened, plasticity, review 79−11683
model comprising work hardening and solid solution hardening 79−34051
Multi-component intrinsic solid solution softening and hardening 78−19774
multicomponent, model, compared with expt. results 77−44262
multicomponent, model 77−44261
Multimet, fatigue crack propag. at elevated temps. in solid solution strengthened superalloys 78−39895
obstacle strength determ. in solid soln. 78−68704
statistical behaviour analysis, with aid of computer *(Japanese)* 80−11658
steel, austenitic, corrosion-resistant, strengthening by alloying with N_2 78−95757
steel, austenitic stainless, metastable, Si effects, unlubricated adhesive wear, oxidation resistance, solid soln. hardening 77−59949
steel, austenitic stainless, yield strength, effect of N_2 additions and grain size, solid soln. strengthening 77−52430
steel, CC Cr-Mo (2.25, 1 wt.%) effect of heat treatment on tensile props. 78−23745
steel, cold rolled, high strength, mech. props. 77−36527
steel, Cr and Mn, softening during hardening, austenitising effect 79−96052
steel, Cr-Mo, annealed, interaction solid soln. hardening, precipitation effects on creep 79−4974
steel, Cr-Mo (2.25, 1 wt.%), annealed, heat treatment effect on tensile props. 78−11243
steel, high-speed tool, Nb addition effect on hardening 79−34048
steel, low C, alloy, structural transform. during deform. and annealing *(Russian)* 79−91707
steel, low C, impact and tensile props., effect of Si 77−36526
steel, low-alloy, props. with nitride and Cu hardening at low temps. *(Russian)* 80−40372
steel, low-C, phosphorus effect on annealing texture, plastic anisotropy and mech. props. 77−25069
steel, Mn-C (1, 0.1 wt.%) strip, hot rolled, P effect on mech. props. 78−27532
steel, quenched-tempered, relationship between half value breadth and hardness *(Japanese)* 77−52366
steel, Si-P-C, low C, varying Si content, cold rolled annealing 80−3090
steel, type 20 CND 10-10, temper brittleness and intercrystalline segregation *(French)* 77−81316
steel nitride phase hardening, precipitation and solution kinetics after heat treatment 78−95756
steels, austenitic, microdefect accumulation during creep, effects of heat treatment, hardening 79−24550
texture influence on stress/strain curves, prestrain, solid soln. and particle hardening effect on inhomogeneous deform. *(German)* 80−30014
theory 77−36530

solid solution hardening continued
theory 78−19771
AgCl:Ba^{2+}, plasticity, impurity hardening effect 78−47466
AgCl:Li^+(Na^+)(K^+)(Rb^+), impurities effect on plasticity, brittleness 78−14398
Al, non-elastic deformation, phenomenological model with solute strengthening effect incorporation 78−39832
Al-Cu, work hardening under tension at 1.6-900K 79−38842
Al-$CuAl_2$, directionally solidified eutectic alloy, effect of heat treatment 77−55977
Al-$CuAl_2$ eutectic, heat treatment and interlamellar spacing effect on tensile deformation 80−29979
Al-Mg, work hardening under tension at 1.6-900K 79−38842
Al-Mg (2.4 wt.%) alloy, solution-treated, grain size effects on fatigue strength 77−4839
Al-Zn, work hardening under tension at 1.6-900K 79−38842
α-Al_2O_3:Cr^{3+}(Ti^{3+})(Ti^{4+}), solid soln. hardening, yield stress conc. depend. 77−28823
Au-Cu(Ag)(Pt), cold worked, impurity conc. rel. to internal friction Bordoni peak, solid soln. hardening mech. 80−16363
BN:C, hardening by doping, p-T diagram, cryst. struct. *(Russian)* 77−77491
CaF_2, impurity effects on strengthening 77−63682
Cd-Mg, solid solution hardening of Cd single crysts. with Mg 79−87647
Cd-Mg single crystals, exam. of critical resolved shear stress from 77 to 300K *(Czech)* 79−91741
Co-transition metal, transition metal additives influence on struct., specific resistance, microhardness, mech. props., magnetic props. 79−29078
Cu-Al, cold worked solid soln., anneal hardening, grain boundary effects 78−48420
Cu-Ni-Sn (10, 6 wt.%), temp. depend of yield stress and work hardening 80−21026
Cu-O single crystals, shear stress measurement, solid solution strengthening 79−52225
Cu-Ti(Ag) alloys, activation vol. stress depend., single crysts. 77−48499
(Cu-Au)-Co, single crysts., solid soln. and particle strengthening, superposition 80−97495
Fe alloy, martensitic transform., critical driving force, effect of alloying elements 77−48437
Fe-Al, Al effect on softening in solid soln. *(French)* 79−52226
Fe-C, softening by C in solid soln. *(French)* 77−36660
Fe-Cr-Ni, solid soln. strengthened and precipitation hardened, in-reactor creep 79−43327
Fe-N, BCC, solution hardening and softening 77−12635
Fe-N, single cryst., solid soln. softening, effect of interstitial N 80−97496
Fe-Ni (1 to 5 at.%), mech. props. below 300K *(French)* 79−8314
Fe-Ni solid solution, deformation mechanism, softening phenomena, dislocation-solute atom interactions *(French)* 80−45344
$(Fe_{1-x}Mn_x)_3Si$, $(Fe_{1-x}Co_x)_3Si$, order distrib., hardening effect *(Russian)* 77−89410
GaAs:Cr(Te)(Zn), dopant influence on hardness 77−84777
Hf-O(N), solid soln. hardening, impurity cluster and interstitial mechanisms 77−36523
KCl:RbCl, $SrCl_2$, laser window material, prep., grain boundary stability 77−46774
KCl-KBr, solution hardening and softening at low temp. 78−31414
KCl-KBr, solution hardening and softening at low temp. 80−108462
KCl-KBr single crysts., yield strength and dislocation mobility, solid soln. hardening model 77−72649
Mg-Cd, single crysts., temp. depend. of crit. resolved shear stress *(Czech)* 80−29112
Mg-Cd single crysts, crit. resolved shear stress, temp. and comp. depend. 79−91659
$MgZn_2$, solid soln. softening in homogeneity range, dislocation density and velocity *(German)* 77−44264
Mo alloy:Re, effect of Re on mechanical props. 80−35196
Mo and Mo superalloys high temperature properties 78−44173
Mo-W-Mo (4.74, 2.17 wt.%), creep resistance in ultrahigh vacuum 79−5027
Nb alloys, solid solution hardening, crystal resolved shear stress depend. on dislocations 80−40373
Nb-N, BCC, solution hardening and softening 77−12635
Nb-N, dil., low temp. interstitial hardening 79−20060
Nb-O system, solid soln. hardening and softening 80−71665
Nb-ZrN alloy, high temp. hardness and short duration tensile strength *(Russian)* 77−44266
Ni alloys, welding crack resist. during welding, heating, stress reduction by hardening 79−24618
Ni alloys EhP539L, heat-resist., heat treatment effect on props. and hardening phase morphology 80−29995
Ni based alloys, hot hardness and oxidation resistance meas. 78−31588
Ni, dislocation intersection and solution strengthening, effect of solute on obstacle profiles 80−7590
Ni/Cr-Fe-C, Inconel, dislocation intersection and solution strengthening, effect of solute on obstacle profiles 80−7590
Ni-Al, solid soln. and solid soln. hardened, stead state creep 78−27578
Ni-base superalloy, IN-738, microstruct. changes during isochronal heat treatment, 773-1467K 78−27531
Ni-Co, dislocation intersection and solution strengthening, effect of solute on obstacle profiles 80−7590
Ni_3Al, substitutional soln. and defect hardening mechanisms 77−21155
Pb-Ag, solid soln. hardening due to metal interstials 77−52337
Pb-Sn(Ag), dil. alloys, dislocation motion and electron-dislocation interactions 77−7728
Pb(Ag) alloys, effect of Ag content on yield strength 80−76322
Pd alloys, controllable hydrogen phase naklep, hardening and phase-strengthening 80−16323
Th, strengthening with C to $ThC_{0.063}$, effect on elastic consts., 4.2-300K 77−90386
Ti, nitriding kinetics at 1230 to 1500°C, diffusion and struct. investig. *(French)* 77−36683
Ti-Al, hardening of Ti by addition of Al *(French)* 78−23715
Ti-Al(Sn) alloys, thermal and athermal solid solution strengthening 77−4787
Ti-Cu-Al(Zr)(Sn)(Nb)(Mo), heat treatable alloys, effect of alloying on strength, tensile props. 78−56671
Ti-transition metal, transition metal additive effect on struct., specific resistance, microhardness, mech. props. 79−29078
Ti-Zr-W-(Al) alloys, phase struct. and props. *(Russian)* 80−16270
U alloys, strengthening rules, high temp. 77−21157

solid solution hardening continued
UC-NbC, UC-ZrC and UC-ZrC-NbC, solid soln. strengthening rules, physicomech. prop. changes 77−28826
V and V-Mo, mechanical properties, O, N_2 and C addition effects 79−52356
V, polycrystalline, strength, ductility, 4.2 to 400K, O_2 effect 77−36529
V, pure and with O_2 additions, single cryst. elastic consts., 4.2 to 300K, and hardening 79−90712
Zr-Al (4.6 wt.%), microstruct. effect on mech. props. 79−20080
Zr-Cu, dil. martensites, struct. and strength 79−29077
Zr-Ir hardened alloys, metastable phases *(Ukrainian)* 79−34000

solid solutions
solid solutions such as Au-Cu are indexed under alloys of the named elements i.e. 'gold alloys' and 'copper alloys' in this example see also alloys; solid solubility
β-eucrypite, glass-ceramics, internal stresses 79−15770
β-spodumene, glass-ceramics, internal stresses 79−15770
A15 type compounds, A_3B type, supercond. transition temp.-solid solution range correlation 77−85373
alkali alloy, dil. solid solution, atomic displacement near solute atom and in asymptotic range 79−65162
alkali earth halides, spectroscopy, investigations by F. Klement *(Russian)* 80−8767
alkali feldspars, TEM study of exsolutions, review *(French)* 78−28224
alkali halide crystals, mixed, impurity centre local vibrs., comp. depend. of spectral parameters 80−79898
alkali halide solid solns., lattice parameter and heat of form. 80−79739
alkali halides, spectroscopy investigations by F. Klement *(Russian)* 80−8767
alkali metals, dil. binary solns., heat of formation 78−75840
alkali-alkaline earth ceramic solid solutions, with tetragonal tungsten bronze struct., low freq. optical modes 78−76477
alloy, binary, theory for initial stage of grain growth and unmixing kinetics 78−19714
alloy, large grained, creep ductility 78−48479
alloy, solid soln., grain boundary mobility 79−46676
alloy, solid substitutional soln., diffusive creep *(Russian)* 79−55816
alloy, substitutional solid soln., irradiated creep rate enhancement theory 77−63739
alloy steel, rel. to special carbide formation *(Russian)* 77−21153
alloys, binary, calibration line introduction for comp. determ. by AES 79−56892
alloys, creep behaviour at intermediate stresses and creep power law breakdown 79−57058
alloys, interstitial solid solns., HCP, ordering type transitions within thermodynamics theory framework 80−49162
almandine-pyrope-grossular garnet, exsolution obs. 78−32074
Approximation of the phase diagrams of complex binary systems with unlimited solid solutions and peritectic transitions 78−23680
azeotropic and two terminal solid solution type binary diagrams, synthesis 80−19901
BCC, SRO and LRO 77−43178
bimetal system, diffusion kinetics taking into account nondiagonal coeff. of Onsager matrix *(Russian)* 78−38871
binary, diffusion, correl. effects and jump freq. ratios 79−99350
binary, growth-disorder model, three-dimensional, phase transition 78−26462
binary, order-disorder transition, long range order parameter and chemical potential 80−6487
binary, tolerance classes in system of elements with α-Fe type struct. 78−2053
binary, tolerance classes in system of elements with Cu structural type 78−9988
binary, tolerance classes in system of elements with Mg and α-La structural type 78−9989
binary alloys, acoustic modes in random and correlated alloys, order-disorder transform. 80−65189
binary alloys, diagrams of state, component interaction parameters *(Russian)* 80−55354
binary alloys, diagrams of state, component interaction parameters, computer calcs. *(Russian)* 80−55355
binary alloys, diffusion-controlled growth of solid soln. scales 77−70232
binary alloys, two phase region calcs. in solidifying melt *(Russian)* 80−65195
binary BCC and FCC solid solns., short range order rel. to comp.-prop. relations *(Russian)* 78−47280
binary disordered continuous solid solns., thermal cond. calc. method, struct. model 77−43394
binary oxide, cluster form., high temp. equilib. 79−60511
binary systems of eutectic type, phase diagrams, approximations, appls. 78−43094
binary triangular lattice solution, phase stratification statistical modeling 80−65239
brass, LANKMts, solid soln. range of existence 77−12653
carbide, decomposition temp. expression 80−55398
3-carboxy-2,2,5,5-tetramethylpyrrolidinyl 1-oxyl system, enantiomer solid soln., cryst. struct. and phase diagram 79−86778
chalcopyrite compounds, ternary, review 79−70048
p-chloronitrobenzene-p-bromonitrobenzene system, growth rate depend. of solid soln. supersaturation 77−1804
chlorophyll, and related mols., in solid solns., fine-structured vibronic spectra under tunable dye laser excitation *(Russian)* 80−74164
chlorophyll, fluoresc. detection of triplet state kinetics 77−30903
classical solid solutions, beyond-mean-field approx. 77−20039
conc. tetragonal substitutional, dislocation impurity segregation *(Russian)* 79−65114
congruent transformation pt., regular soln. theory 79−60477
$(1-x)Cr_2O_3$-$x\alpha Fe_2O_3$, mag. phase diagram, EPR method *(Russian)* 79−28521
cubic, at. mean sq. displacement and critical voltage effect 79−60236
decomposition, two-phase, X-ray diffr. anal., exam. of method 79−52510
density of states in forbidden band and band edge smearing 79−73418
dichalcogenides, pyrite-type, ^{57}Fe isomer shift, quadrupole splitting, Mossbauer study 80−15832
p-dichlorobenzene-naphthalene alloys, solid solns., NQR study 80−66063
diffusion, chemical, highly defective solids, steady-state computer simulation method for lattice gas 80−49401
diffusion, influence of conc.-induced stresses *(Russian)* 78−55969
diffusion equation, during a decomp. process, role of non-linearised terms *(Japanese)* 80−92723

solid solutions continued
diffusion equation, with non-linear terms, Fourier transform 80−103514
diffusion in force field 78−10211
diffusive creep, theory *(Russian)* 80−40437
p-dihalobenzene, mixed cryst., Raman spectra, phonons and vibr. excitons, criteria for solid solns. 78−43840
p-dihalobenzene alloys, successive perturbation of phonon bands 77−35653
dilute alloy, equilibrium distrib. coeff. relationship *(Russian)* 79−83186
dislocation motion, straight line, in concentrated solid soln., computer simulation 77−15413
dislocation motion activation energy, from crit. resolved shear stress data 77−55289
dislocation-core movement and frictional stress 80−92529
disordered alloy, conc. depend. of superconducting transition temp. *(Russian)* 79−28427
disordered multicomponent solid solutions conc. fluctuation waves, microscopic theory 80−44327
dissolution in water *(French)* 79−52734
Elinvar, γ to γ′ transformation and γ′ phase form. kinetics, lattice consts. 80−35191
enstatite-wollastonite system, solid solns. at high press. and temps. with emphasis on diopside 79−79825
exciton theory, qual. tests, energy denominator depend. of naphthalene reson. pairs 77−39783
FCC, modelling, computer program 78−26475
FCC crystal, interstitial and solute concentration gradients, flux expression derivation *(French)* 80−54219
flow stress, temp. plateau 79−14877
2-fluoronaphthalene-2-naphthol system, phase relations, X-ray diffr. and DTA study 80−45287
formation in heat of combustion process *(Russian)* 77−66765
formation kinetics of solid layer on surface in reaction diffusion 78−63938
free energy extrema characterised by two long-range order parameters *(Russian)* 77−76576
freeze drying of solid solutions, solvent choice in semiconducting powder prep. 80−11583
fusibility diagrams, assessment of cryoscopic calc. accuracy 77−25010
geikielite, solid soln., phase transform. during reduction *(Russian)* 78−44042
glass-ceramics and photosensitive glass, microstructure rel. to properties *(German)* 80−38926
grain boundary self-diffusion co-eff. meas. in single phase 77−7886
heterogeneous short-range order parameters, Mossbauer meas. *(Russian)* 79−4418
heterovalent, use of expt. data to estimate energy of soln. 80−54380
homogeneous precipitation of supersaturated soln., phenomenological theory, in liquid and solid soln. 78−67833
homogeneous solid solution crystallisation crucible 80−45224
3-hydroxymethyl-2,2,5,5-tetramethylpyrrolidinyl 1-oxyl system, enantiomer solid soln., cryst. struct. and phase diagram 79−86778
IIIiV semiconductor solid solutions, interaction parameters 78−51688
ilmenite, solid soln., phase transform. during reduction *(Russian)* 78−44042
impurity atoms diffusion and impurity-vacancy interactions *(Russian)* 80−19985
impurity centres, internal mol. vibrs., inhomogeneous band broadening 78−92103
inert gas in metal in gas discharge, model, lattice const. 79−65202
inhomogeneous, with conc. expansion, thermodynamics, energy defect diffusion calcs. 80−24618
instability zone rel. to new phase preformation and nucleation 78−10169
interstitial, chemical diffusion in presence of solute atom gradient 77−76612
intersitial, deform. interaction of atoms, pseudopot. calc. *(Russian)* 78−18636
interstitial, with repulsive interactions, statistical treatment 77−72611
interstitial ideal solution const. press. and vol. effect on nonideality 79−7697
interstitial phase struct., reconstructive transition struct. symm. relationships 79−69246
interstitial solid solution, growth rate of layer of new phase containing impurity atom traps 77−76620
interstitial solid solutions, self-diffusion activation energy rel. to partial molar energy 80−15291
interstitial solute in multicomponent substitutional solvent, quasi-chemical approach to thermodynamics 77−28784
interstitial-FCC soln., thermodynamics based on kinetic considerations 77−62651
interstitials, in body centred refractory metals, thermodynamic study *(Ukrainian)* 79−37845
interstitital ideal solution, const. press. and vol. effect on nonideality 79−7698
ionic compounds, monovalent, surface comp. calc. using monolayer model 80−6607
isotropic solid soln. cryst. surfaces, surface stress and chem. equilib. 80−107628
ketone-paraffin solid soln., dielec. relax., temp. and lattice const. depend. *(German)* 78−76383
liquid phase sintering, elementary mechanisms, soln.-reprecipitation 80−50571
metal, HCP, regular soln. model for interstitial soln. 77−15591
metal, interstitial soln., conversion of thermodynamic functions from const. press. to const. vol. 77−7877
metal and alloy polycrystals, internal friction amplitude depend. *(Russian)* 79−90726
metal-NH_3 solid solutions, phase comp., dissoc. *(Russian)* 77−35665
metal-NH_3 solutions, optical and microwave props. of microscopically inhomogeneous materials 77−77161
metallic, diffusion by press. *(Russian)* 78−18833
metallic alloys, supersaturated solid solution decomposition, model *(Russian)* 79−47656
metallic solution, α-parameter approach to thermodynamics 77−4207
metallic solution, thermodynamics of solutions, α-parameter approach 77−4208
metallic system, compound formation rel. to heat of mixing 80−55689
metals, FCC, under H_2 press., crit. phenomena and isomorphic transitions 80−49367
molecular crystal with disorder, mean field approx. 78−22688

solid solutions continued
molecular crystals of solid replacement solns., NQR investig. of impurity distrib. 77−12222
Mossbauer spectra interpretation allowing for at. interaction in lattice *(Russian)* 77−69738
mullite-corundum refractories, reactions with FeO in different media 77−24994
multicomponent, diffusion processes *(Russian)* 78−47552
multicomponent solid soln., diffusion mass transfer *(Russian)* 77−41552
naphthalene $^1B_{2u}$ resonance pairs, energy denominator depend. of excitons absorpt. 77−39783
naphthalene-coumarin solid solution, struct. parameters and phase diagram 77−11532
naphthalene-naphthol solid soln. system, excess thermodynamic functions 80−107445
nondiagonal disordered system, excitation spectrum 80−15429
nonstoichiometric solid solutions, ordering 78−87794
ordering, characterisation by long range order parameters *(Russian)* 79−1489
ordering, many particle correls., coupled Green function eqns. *(Russian)* 77−72675
ordering and disordering under irradiation 79−87626
organic, cell parameters calc. *(Russian)* 77−72687
oversaturated solid solution, directed decomposition *(Russian)* 80−97458
paradibromobenzene-paradichlorobenzene solid solutions, mol. cryst., NQR study 80−25242
perovskite structure oxides, solid soln., crystal lattice parameters, conc. depend. calc. 78−95041
polarised photochromism in solid solutions 78−64859
polycomponent metallic solid soln., creep and diffusion of vacancies *(Czech)* 79−43340
polyhedrisation of quinary metallic systems with isomorphic intermediate phases *(Russian)* 80−45270
pseudobinary alloy, use of parallel and monochromatic beams for comp. determ. by X-ray fluorescence 79−48000
pyroxene-garnet solid-soln. equilibria in $Mg_4Si_4O_{12}$-$Mg_3Al_2Si_3O_{12}$ and $Fe_4Si_4O_{12}$-$Fe_3Al_2Si_3O_{12}$ systems 77−81895
quasi-particles method in solid solution theory 80−24560
rare earth oxide-ZrO_2 (HfO_2), cubic solid soln., lattice parameters 79−82186
refractory carbides, borides and nitrides, wetting by and interactions with liq. metals, solid soln. form 80−54473
rhombic distortion of cryst. lattice at low temp. 78−2253
schoenite-type salt, formation of single phase ferrite powders 77−16524
semiconducting, growth of homogeneous single crystals 77−12518
semiconductor supersaturated solid solns., decomp., surface impurity content 78−51681
semiconductors, ternary and quaternary solid solutions with nearly perfect sublattices, stoichiometry invariants 79−51270
short-range order, size effect in electronic theory *(Russian)* 77−15339
short-range order parameters, AC-BD, X-ray diffr. determ. 80−38875
single crystal growth from melt, role of composition fluctuations 79−8239
solid soln., ductility, comp. effect *(Japanese)* 79−43334
solid solution, binary, radiation-induced instability, contrib. of dissipative processes 80−65039
solid solution, interstitial and substitutional, ordering 78−79744
solute interaction energy, const. press. and const. vol. condition effects 78−38856
spectroscopy investigations by F. Klement *(Russian)* 80−8767
spinel solid solutions, $A_xB_{3-x}O_4$ type, quasichemical method of cluster components, electron exchange allowance 79−51475
spinel systems, prop.-comp. relationship, electron exchange effect *(Russian)* 78−47524
statistical treatment by first order approx. *(French)* 77−9117
steel, austenitic, Ni-Ti, alloy N35T5, ageing, magnetisation and Curie temp. depend. on plastic deform., Mossbauer studies *(Russian)* 79−69669
steel, austenitic solid solution, chem. evaluation of B and its correlations with hardenability and hardness *(German)* 79−39230
steel, austenitic stainless B-containing, decomp. of solid solns., effect of cooling conditions 77−44256
steel, B concentration and solubility depend. on introduction of rare earth metals *(Russian)* 80−65226
steel, Cr-Mo(-V), ductility and heat resistant prop. prediction rel. to fine struct. and solid soln. state 79−15751
stepped ordering in binary solid solutions 78−67807
substitutional, energy spectrum, of impurity mol. crystals *(Russian)* 79−78720
substitutional, with immobile cryst. lattice, chain of models *(Russian)* 79−46588
substitutional alloy, disorder description within supercell model 78−26479
substitutional impurities in solids, entropy and volume of solution 80−15253
substitutional impurity, model parameters, determ. from low temp. data *(Russian)* 79−33007
substitutional solid solution comp. from X-ray integral intensities 77−84584
substitutional solid solutions, new phase nucleation mechanism 80−61135
superionic-electronic solid solution electrodes, partial cond. meas. technique 80−44360
supersatuated diffusive decomposition, universal distrib. function in dimension space for new-phase particles 78−48372
supersaturated, cellular precip. features, review *(Russian)* 80−84937
supersaturated, dissoc. kinetics determ. method 77−52317
supersaturated, isomorphic decomp., elastic interaction of dilating particles *(Russian)* 79−47691
supersaturated multicomponent systems, theory of diffusive decomposition 77−76565
supersaturated solid solution, diffusive decomposition 78−76653
surface enrichment for perfect and regular solutions, broken bond model 79−90849
surface segregation, miscibility gaps, reg. soln. theory 78−18882
TCNQ anion radical salts, phase transition $\alpha\gamma \rightarrow \beta\gamma$, volume change 78−26684
TCNQ anion radical salts, phase transitions, solid solns., thermodynamic props. 77−47571
TCNQ anion radical salts, solid solns. phase transition, heats of mixing 78−47519
solid solutions continued
TCNQ salt, $TTF_{1-x}TSeF_x$-TCNQ, mol. substitutional disorder 80−24438
technical superconductor requirements and main properties 79−30511
ternary systems, triangulation parameters correl. with isomorphic intermediate phases *(Russian)* 79−52203
o-terphenyl, dipolar solutes, reorientational motions, dielectric relax. below glass transition 80−19706
thermodynamic activity meas., Knudsen method appl. 78−79783
thermodynamic functions calc., ternary alloy of quasi-binary cross sections 80−16265
$\alpha+\beta$-Ti alloy, singularities of decomposition of β solid solutions, low temp. range *(Russian)* 79−1867
tolan-mercury diphenyl, energy charact. determ. of mol. interaction and short range order parameters 79−14794
tolan-mercury diphenyl solid soln., anal. of diffusely scatt. intensity distrib. of X-rays 78−95048
transition metal based, relationships involving max. or min. liquidus temps. 79−78934
transition metal carbides, complex phases with NaCl struct., microhardness rel. to electronic structure 77−90438
transition metal carbides and nitrides, solid soln. formation, elastic lattice deform. energy 77−84927
transition metal carbonitrides, physicochem. props., comp. depend. 80−55370
transition metal solvent, max. or min. liquidus temps. 78−39741
transition metal-H dilute solns., pair potential anal., unrelaxed lattice model 79−65070
TTF_x $TseF_{1-x}TCNQ$ solid soln., DC conductivity, struct. 78−10423
tungsten-bronze ferroelectrics, $A_5B_{10}O_{30}$- and $A_6B_{10}O_{30}$-type, phase relations 78−35100
volume, electron correl. effect 77−28133
wustite solid solns., props. connected with localised electron state 80−107734
wustite solid solutions, miscibility data rationalisation classification of ternary fields and postsaturation reactions 80−79948
X-ray diffraction studies of high temp. solid state reactions 77−47303
$XY_{1-c}Z$ mixed crystals, impurity centre local oscill. spectral distribution *(Russian)* 80−60643
$3Al_2O_3$-GeO_2-SiO_2, reduction by C, mixed diffusional-kinetic regime *(Russian)* 80−66771
Ag:He, implanted films, solid solutions radiation induced polymorphism 79−86810
Ag-Cu (50 at.%), splat-cooled, struct. of γ' extended solid solution 78−3147
Ag-Cu metastable solid soln., form. by ion-beam mixing 80−75244
Ag-Ga solid soln., internally oxidised, hardness *(Japanese)* 78−60744
Ag-Ga(Ge)(In), α-phase, lattice sp. ht. calcs. 80−65246
α-Ag-In solid solutions, lattice dynamics parameters *(Russian)* 80−96477
Ag-Mg (18.5 wt.%), rheological study of crystallographic order on creep *(French)* 80−97548
Ag-Ni, reversible surface segregation, radioactive tracer, LEED, and AES expts. *(French)* 77−69155
Ag-Ni supersaturated metastable solid solns. formed by ion beam mixing 80−107425
Ag-Pt, sintering, limited solid solubility, peritectic diagram 77−28754
$AgGa_xIn_{1-x}Se_2$, X-ray diffr. cryst. data 80−84147
$AgGa(Se_{1-x}S_x)_2$, crystal growth, phase studies, optical props. 78−48305
$(Ag_{x/2}Pb_{1-x}Bi_{x/2})Te$ solid solution, preparation and thermoelectric props. 77−47839
$(Ag_{x/2}Pb_{1-x}Sb_{x/2})Te$ solid solns., Hall coeff., thermoelec. power, and thermal cond., 100 to 500K 79−82614
$Ag_2S+Ln_2S_3$, powdered mixtures, reaction rate, production of ionic semiconductors 80−93741
Al alloy D16, supersaturated solid soln., decomp. process, electron microscope obs. and acoustic anal. *(Russian)* 79−15650
Al substitutional solid solution alloys, volumetric effect and props. *(Russian)* 80−39293
Al-(Mn), effects of Mn on electrode or free corrosion potentials 80−100942
Al-Ag, nonhomogeneity of deform. 78−84888
Al-Ag, type-II superconductor, torque oscillations in mag. field *(Russian)* 80−103800
Al-C interstitial solid solns., atomic static displacements and deform. interaction *(Russian)* 80−64953
Al-Cu solid soln., supersaturated, plastic deform. effects *(French)* 79−91748
Al-Cu-Mg-Si-Fe-Mn-Ti, Si, Fe, Mn and Ti effect on precipitation in solid soln. *(Korean)* 79−66064
Al-Cu(Mg)(Zn), cold working causing preprecipitation, thermoelec. power *(French)* 79−8306
Al-Fe (0.02 at.%), rapidly quenched, ^{57}Fe Mossbauer spectrum associated with vacancy 78−23378
Al-Ga-In system, thermodynamic anal. 79−60512
Al-Ga(In) systems, thermodynamic anal. 79−60512
Al-Mg, homogenisation process, effect of solidification rate and alloying *(Polish)* 79−78949
Al-Mg (1 to 11 wt.%), alloy A99, dissociation in solid soln., effect of treatment of liquid Al *(Russian)* 78−15353
Al-Mg (5.5 at.%), applied stress change effect in creep *(Czech)* 79−70126
Al-Mg (5.5 at.%), stress change expt. on creep 79−24584
Al-Mg solid soln., AE during plastic deform. 78−64592
Al-Mg solid solns., decomposition studied by ultrasonic meas. of elastic props. 80−35184
Al-Mg supersaturated solid soln., spinodal decomposition at 20°C *(French)* 77−85987
Al-Mg_2Si (1 wt.%), precipitation reactions 80−11652
Al-Mg-Be, solid soln. decomposition, metallographic study 77−16577
Al-Mg-Li-Si system, phase diag. *(Russian)* 78−80515
Al-Mg(-Zn)(-Zn-Cu), exam. of precipitation struct. by neutron scattering 78−92270
Al-Mn, direct chill-cast, struct. changes during heat treating *(German)* 80−40408
Al-Mn alloys, study of solidification by rapid cooling *(Japanese)* 78−88459
Al-Mn(Cr), quenched, thermal stability *(Russian)* 80−20976
Al-Mn(0.6 wt.%), supersat. solid solns., isothermal decomp., Zr addition effects 77−63626
Al-Ni solid, liquid mixture, diffusion processes *(Russian)* 80−107563

solid solutions continued
Al-Sn-U alloy, phase equilib. exam. by metallographic and X-ray anal. 77−21102
Al-Zn, nonhomogeneity of deform. 78−84888
Al-Zn, resistivity anomalies in Guinier Preston zones *(French)* 78−6937
Al-Zn (10 wt.%), solid soln., decomposition meas. by resistivity meas. under isothermal conditions *(French)* 79−20025
Al-Zn (20 (30) (35) (40) (60) at.%), effect of UTS on cyclic creep strength *(Korean)* 80−25778
Al-Zn (8-25 wt.%), solid solns., residual resist. during clustering 80−97483
Al-Zn solid soln., controlling creep mechanisms, role of diffusion 78−31469
Al-Zn solid soln., controlling creep mechanisms role of diffusion 78−31470
Al-Zn-Mg, polygonized struct. in extrusions, thermal stability and mech. props. 80−50659
Al-Zn-Mg (4.8, 1.2 wt.%), quenched, Guinier Preston zones formation 80−45273
Al-Zn-Mg granules and bands rolled from them, heat treatment 80−100862
Al-Zn(10 at.%), supersaturated solid soln., structural charact. of decomposition 77−70027
Al-Zr solid soln., discontinuous precipitation of metastable Al_3Zr 78−3130
$Al_{12-4x}Be_2C_{10-3x}(-1\leq x\leq 1)$, solid soln., comp. vs lattice constants 80−45284
$Al_4C_3.3Be_2C$, X-ray difr. and TEM study 80−14973
AlGaAs, heteroepitaxial waveguides for image transmission *(Russian)* 77−11037
$Al_xGa_{1-x}P$, solid solutions, refr. index dispersion charcts. *(Russian)* 77−81080
$Al_xGa_{1-x}Sb$, solid soln., epitaxial layer growth from liq. phase 77−85089
$Al_xGa_{1-x}Sb$ solid solns., freq. dependences of form of luminesc. spectra 80−40160
Al_2O_3-Ca_3SiO_5, solid solution, exam. of lattice defects 79−95167
Al_2O_3-Cr_2O_3, crystalline soln., microstrain rel. to lattice energy and strain energy 77−24411
Al_2O_3-Cr_2O_3, microstrain correction 78−59852
Al_2O_3-Cr_2O_3, solid soln., thermal expansion anisotropy, lattice consts. 80−54411
Al_2O_3-Fe_2O_3:Cr^{3+}, dil. paramag. system, Cr^{3+} conc., effect on cross relax. 79−15387
β-Al_2O_3-K_2O/K ferrite, interfaces and solid soln., thermal expansion and lattice parameter variations 78−55959
Al_2O_3-TiO_2-MgO.2TiO_2, exam. of solid solutions by X-ray phase analysis 79−95981
$Al_2O_3+TiO_2$, reaction on sintering in reducing media 78−27457
(Al_2O_3-Fe_2O_3):Cr^{3+}, (0.04 mol.% Fe_2O_3), paramag., cross relax., annealing temp. effect from Mossbauer meas. 80−44983
$Al_2O_3.3H_2O$-H_3PO_4-CaO(ZnO), phase equilib., $AlPO_4$ solid soln. 79−11586
$As_xSb_{1-x}SI$, solid solns., ferroelec. props. 78−23409
AsSe-GeSe$_2$-PbSe, glass form., struct. defects, elec. cond., assoc. *(Russian)* 80−54144
Au-3d transition metal alloys, UPS study, localised states 80−93449
Au-Co solid solution, mag. susceptibility 79−61081
Au-Ga, dil. alloys, dHuA meas. and phase shift analysis of electronic scatt. anisotropy 77−35932
Au-Ge-Te ternary system, solid soln. in vicinity of GeTe, phase diagram *(French)* 77−85994
Au-Ni solid soln., creep 78−15475
Au-Ni-Cu-Zn, white gold, metallographic struct., heat treatment and plastic working effect 80−40403
Au-transition metal alloys, ^{197}Au Mossbauer isomer shift cellular atomic model 80−84673
AuCu-Al thin film bilayer system, phase formation, backscattering spectra 80−96728
B-Si alloys, B-rich, prep., anal. and cryst. growth *(French)* 80−104091
B-Zn solid soln., struct. changes on Zn incorporation into α- and β-rhombohedral B 78−79596
BN-AlB, cubic phase solid soln., crystallographic and metallographic study, thermal resist. *(Russian)* 78−30599
$BaAl_2Si_2O_8$-SiO_2, celsian solid solns., effects on polymorphic transform. kinetics 78−68677
$BaCO_3$-$SrCO_3$-TiO_2(ZrO_2), ternary systems, solid-phase synthesis 78−52733
$BaFe_{12}O_{19}$, Ca^{2+} substitution effect on hexaferrite lattice and mag. props. 80−60243
$Ba_{1-x}La_xF_{2+x}$, enhanced ionic motion in solid solutions 80−107491
BaO-MoO_3, solid phase reaction, thermal analysis 80−55639
BaO-WO_3, solid phase reaction, thermal anal. 80−55639
BaS-CaS:Cu phosphors, X-ray diffr. and fluoresc. spectra 80−40148
$BaSi_{2-y}Ge_y$, solid solution with type $SrSi_2$ struct., lattice parameters at high press. 80−54203
$BaSiO_3$-$BaGeO_3$, phase diag. 77−48404
$Ba_{1.35}Sr_{0.65}NaNb_5O_{15}$ crystals, struct., dielec. and pyroelectric charcts. 79−51913
$Ba_xSr_{1-x}Nb_2O_6$ crystals, struct., dielec. and pyroelectric charcts. 79−51913
$Ba_xSr_{1-x}Nb_2O_6$ crystals, defects and their characteristic features 80−88138
$BaTiO_3$-$Ba_{1/2}NbO_3$, defective solid solns., reduction 77−81395
$BaTiO_3$-$BaNb_2O_6$ system, solid solns. of tungsten bronze struct. of type $BA_{5+x/2}Nb_{10-x}Ti_xO_{30}$ 77−52021
$Ba_{1-x-y}U_xCe_yF_{2+2x+y}$, solid soln., ionic cond. 79−99356
Be, metastable alloy form. by ion implantation 79−82252
Be, plastic strain mech., effect of impurities *(Russian)* 79−34101
(Bi, Sb)$_2$Te$_3$ solid soln., semiconductor film, oxidation, electrophysical props. 80−45407
Bi:Sb, solid soln. struct., growth rate effects 77−52246
Bi-MnBi, directionally solidified composite, processing parameter role on mag. props. 80−35352
Bi-Sb, conditions for dendritic crystallisation, accompanying rapid cooling *(Russian)* 79−34020
Bi-Sb, solid solns., thermoEMF in transverse mag. field 77−47841
$Bi_{2-x}La_xWO_6$, synthesis and crystallography 80−66459
Bi_2S_3-CuPbBi$_5$S$_9$, solid solution, semiconductor and dielectric props. 79−69511
$Bi_{1-x}Sb_x$, galvanomag. props., energy spectrum *(Russian)* 79−56248

solid solutions continued
$Bi_{1-x}Sb_x$, growth by horizontal zone refining, low charge carrier conc. 77−21020
$Bi_{0.52}Sb_{1.48}Te_3$ thermoelec. solid soln., homogeneity, effects of prep. method 78−52698
$Bi_{2-x}Sb_xTe_{3-y}Se_y$, elec. cond. and thermoelec. props., neutral defects influence 80−60017
n-Bi_2(Te,Se)$_3$ semiconducting solid solns., plastic deform. during hot extrusion 79−20143
Bi_2Te_3-based solid solns., decomp. kinetics under flux layer 77−81205
Bi_2Te_3-Bi_2Se_3-Sb_2Te_3, single crystal, elec. cond., thermoelectric props. 80−88550
Bi_2Te_3-Sb_2Te_3, plastically deformed by hot extrusion, diffusion meas. using micro-X-ray spectrum anal. 79−14954
p-Bi_2Te_3-Sb_2Te_3 semiconducting solid solns., plastic deform. during hot extrusion 79−20143
Bi_2Te_3-$SbTe_3$, ordered structure formation, heat treatment effect on thermal cond. 80−54448
$Bi_{1-x}Te_xO_{3/2+x/2}$ ($0.33\leq x\leq 0.50$), phase transformations, dielectric and differential microcalorimetry *(French)* 79−55886
$Bi_2Te_{3-x}Se_x$, thermoelec. mat., prep. effects on inhomogeneities 78−51576
α-brass, solid soln., ductility, comp. effect *(Japanese)* 79−43334
Ca-Mn-S-Se system, multicomponent solubilities 80−108416
$Ca_{0.2}Ba_{0.8}TiO_3$:Nb, conductive single cryst. growth by Verneuil method 77−85928
(Ca_xCd_{1-x})CO_3, cryst. struct. and cation isomorphous miscibility 80−33972
$Ca_{1-x}Eu_xSi_2$, solid solns., α-$ThSi_2$ struct. type, comp. and press depend. 78−91322
CaF_2-LaF_3, solid soln. with fluorite struct., phase diagram 79−100119
CaF_2-rare earth trifluoride, charcts. of ordering of solid solns., superstructure form. 79−14725
CaF_2-SrF_2-BaF_2:Gd^{3+}, luminescence spectrum of Gd^{3+} ion and solid solution region obs. 78−84638
CaF_2-YF_3, fluorite- and tysonite-related ordered phases *(German)* 79−23725
$CaF_{2-x}H_x$, solid soln. prep. and struct. determ. *(French)* 78−51505
$CaMg(Si, Ge)_2O_6$, solid solns., IR spectra 77−48156
$Ca_2Nb_2O_7$-Sm_3NbO_7 system, phase equilib. 80−20907
CaO-Fe_2O_3-Al_2O_3 system, solid soln. of $Ca_2Fe_{2(1-x)}Al_{2x}O_5$ *(Russian)* 80−16284
CaO-MnO system, solid soln. form. and analysis 80−28996
CaO-SiO_2/GeO_2-H_2O system, phase relations, influence of Si/Ge isomorphous substitution 79−52180
$(CaO)_3SiO_2$, effects of polymorphism on hydration, X-ray and TEM obs. *(Japanese)* 79−20046
ZCaO.SiO_2-2CaO.$Na_2O.P_2O_5$ system, polymorphism and solid soln. 78−19731
CaS-Y_2S_3 (1 wt.%), solid electrolyte, elec. cond. under low partial pressures of S *(Japanese)* 80−49409
$CaSO_3.1/2H_2O$-$CaSO_4$ solid solution, prepared by coprecipitation from solns., exam. 79−20034
$CaSO_4.2H_2O$-$CaHPO_4.2H_2O$ system, solid solns., IR study *(French)* 80−66165
Ca_2SiO_4-BaO, conditions and mechanism in cryst.-chemical stabilisation of unstable phases 80−39302
Ca_2SiO_4-$CaSO_3$-CaO, region of homogeneity of Ca_2SiO_4 77−90332
Ca_2SiO_4-FeO, conditions and mechanism in cryst.-chemical stabilisation of unstable phases 80−39302
Ca_2SiO_4-MgO, conditions and mechanism in cryst.-chemical stabilisation of unstable phases 80−39302
$Ca_{1-x}Sr_xSi_2$, solid solns., α-$ThSi_2$ struct. type, comp. and press depend. 78−91322
$CaTiO_3$-$Ca_2Fe_2O_5$, Mossbauer resonance exam. of structure, phase equilibrium 78−76640
$CaTiO_3$-$LaAlO_3$ solid soln., phase redistrib. during roasting in H_2 78−52735
Ca_2TiO_3-La_3AlO_3, synthesis of solid solution by coprecipitation 79−1836
$Ca_{1-x-y}U_xCe_yF_{2+2x+y}$, solid soln., ionic cond. 79−99356
CaX-MnX, X=S, Se, Te, solubility limits 80−44320
$CaZrO_3$-$CaHfO_3$, solid soln. formation obs. 77−86003
$Cd_{1-x}Cu_xCr_2Se_4$ solid solution, spinel struct., X-ray investigation 79−78940
$CdGe(As_{1-x}P_x)_2$, crystal growth, phase studies, optical props. 78−48305
$Cd_xHg_{1-x}Te$, comp. determ. by electroreflection method 77−52708
$Cd_xHg_{1-x}Te$, solid solns., role of stoichiometry defects 77−47813
$Cd_xHg_{1-x}Te$, vacancy mech. of resorption of Hg droplets 80−39070
$Cd_{1-x}M_x$ (M=Mg, Ca, Sr), solid soln., phase equilib. diagrams 80−108412
$Cd_{1-x}M_xS$ (M=Sr, Ca, Mg, Pb, Sn), solid soln., prep. and semicond. props. 80−2383
$Cd_{1-x}Ni_xFe_2O_4$, solid soln., mag. and structural characterisation 80−103906
CdO-WO_3, phase rels. and cryst. struct. 80−108410
CdS:M, M=Zn, Te, doping and solid soln. prep. during VPE 77−85353
CdS-CaS, rock salt struct., high press. phase equilibrium study 78−52777
CdS-MgS, rock salt struct., high press. phase equilibrium study 78−52777
CdS-SrS, rock salt struct., high press. phase equilibrium study 78−52777
CdSe:Fe, exciton electroreflectance spectra, impurity effects 77−16335
$CdSe_xTe_{1-x}$, solid solns., epitaxial layer prod. 78−23619
$CdSnP_2$-$CdSnAs_2$, and $CdSnP_2$-$CdGeP_2$, solid solution form. and elec. characterisation 78−43125
CdTe-CdS solid solution phase diagram *(Russian)* 79−100120
CdTe-HgTe, semicond. solid solns., effect of reactor irrad. on electrophys. props. 77−51744
CdTe-ZnS ternary mutual system, phase diagram 80−20904
$CdTe_{1-x}Se_x$ solid solution films, prep., struct., and photocond. 80−54541
$Cd_{1-x}Zn_xSe$, epitaxial layer growth with Zn content from doping to solid soln. formation 77−85094
Ce-Nd-Si, phase diagram, X-ray anal. *(Ukrainian)* 79−38792
$Ce_xDy_{1-x}C_2$, solid solns., mag. props. 80−108008
CeO_2-Y_2O_3 solid soln. phases, synthesis 80−104132
$CeO_2La_2O_3$, ceramic, thermal stability, sintering, deform., effect of La_2O_3 79−11532
CeSe:Fe, long-wavelength fundamental absorpt. edge formation, role of Fe 77−16351
Ce_2Se_3-$SnSe_2$, solid-solution region, physical properties 78−43391

solid solutions continued
Co base alloy, creep-fatigue interaction in aligned eutectic and solid soln. 80−108554
Co-Al solid soln., lamellar spacing in discontinuous precipitation, expt. proof of Gaussian distrib. *(German)* 77−36517
Co-Ga binary system, lattice consts., phase transform *(Chinese)* 80−88108
Co-Mo, sintering, limited solid solubility, peritectic diagram 77−28754
Co-Sb-Te ternary system, crystn., heat treatment and phase equilib. 79−52156
Co-Zn, physical-chemical metallurgy *(German)* 80−108390
$Co_xMg_{1-x}O$, EPR of Co^{2+} *(Russian)* 80−11251
$Co_xMg_{1-x}O$ system, thermodynamic investigation, 1100 to 1300K *(German)* 80−107430
Co_2NiO_4, powder prep. by freeze drying of solid solutions, solvent choice 80−11583
$Co_{3-x}Ni_xO_4$, $0 \leq x \leq 1.1$, struct., semicond.-semimetal transition, Seebeck coeff. 78−87972
$(Co_yNi_{1-y})_{1-x}O$ and O_2 prep. props., and reactions 77−12569
CoO-MgO, cryst. oxide demixing in O pot. gradient 79−37849
CoO-MgO, solid solns., determ. of degree of imperfection 77−80624
CoO-MgO-Al_2O_3-Cr_2O_3-TiO_2, form. and colour of spinel solid soln. *(Japanese)* 77−32550
CoO-MgO-Cr_2O_3-Fe_2O_3-TiO_2, form. and colour of spinel solid soln. *(Japanese)* 80−16059
CoO-ZnO-Al_2O_3-Cr_2O_3-TiO_2 system, form. and colour of spinel solid soln. *(Japanese)* 77−25001
CoO.Al_2O_3-Al_2O_3, solid soln. *(Japanese)* 77−32567
$Co_{1-x}Zn_xFe_{2(1-y)}Cr_{2y}O_4$ spinels, solid solns., struct. 80−19764
$(Co_{0.001}Zn_{0.189}Ni_{0.143}Fe_{0.667})SO_4.(NH_4)_2SO_4.6H_2O$, schoenite-type salt, formation of single phase ferrite powders 77−16524
Cr binary substitutional solutions, thermodynamics 80−54410
Cr-Fe-Ni, γ-solid soln., thermodynamic activity determ. at 1500K 80−108397
Cr-Mo, elec. resist. and thermo-EMF, conc. depend., 4.2 to 1500K *(Russian)* 80−80247
Cr-Mo-N system, at high-pressure, temp., X-ray anal., phase diagram 80−50607
Cr-N, interaction with dense stream of N ions, metallography, microhardness, specific volume *(Russian)* 80−15169
Cr-Os, magnetic transition T-P-C diagram, triple points *(Russian)* 80−54895
$Cr_xFe_{2-x}CaO_4$ mag. phase transitions meas. *(Russian)* 79−75556
$Cr_{1-x}Fe_xOOH$, $0 \leq x \leq 10$, prep., Mossbauer effect, Neel temp. 80−108134
$Cr_xMo_{1-x}O_2$ ($x \leq 0.5$), solid soln., trivalent Cr, X-ray powder diffr. anal. 80−70177
CrN-MnN, synthesis and props. 77−40405
Cr_2O_3-Al_2O_3, solid soln., effect of Cr on point of zero charge 78−61021
CrS-FeS, sulphorspinel, struct. and elec. props. 80−49834
$Cr_2S_{3-x}Se_x$, elec. resist., thermal cond. and Seebeck coeff. meas. 80−24958
$Cr_{1-x}V_xN$ solid solution, X-ray diffr. structure exam. at low temp., deformation study *(French)* 78−2069
CsBr-TlBr, phase diagram and pt. defect parameters 79−96017
CsCl-TlCl, determ. and computation of phase diagram 80−55379
CsCl-TlCl solid soln., point defect parameters 80−54224
$CsGa_{1-x}Fe_xS_2$, tetrahedrally coordinated Fe atoms in low spin state, mag. props. and neutron diffr. study *(German)* 80−88714
CsI:Na, crystal, kinetics of decay of surface solid soln. 79−23810
CsI:Tl, precipitation of Tl solid solns. 80−70419
$CsNO_2$-$CsNO_3$, cryst. struct. and phase changes 79−51082
Cu alloy solid solution condensed films, influence of alloying components on phase composition and lattice spacing *(Russian)* 80−20047
Cu dilute binary solid solutions, enthalpies of mixing and excess free enthalpies *(French)* 80−107427
Cu, metastable alloy form. by ion implantation 79−82252
Cu solid soln., wear 78−3233
Cu solid solutions, single phase FCC metal, stacking fault energy and delamination wear 78−3239
Cu-Ag, nonhomogeneity of deform. 78−84889
α- Cu-Al (6 to 17 at.%), short-range order investigated by diffuse X-ray scatt. *(Russian)* 80−104187
Cu-Al solid soln., internally oxidised, mech. props. *(Japanese)* 77−52411
Cu-Al-Ti, formation of modulated structure rel. to barrier nucleation of new phase *(Russian)* 77−32580
Cu-Au single crystals, precipitation hardening by misfitting Co particles 80−97495
Cu-Au solid soln., Cu rich, elastic const. 79−87681
Cu-Au system, two-phase mixtures, long-period superlattices 80−84140
Cu-Be solid solutions, local oscill. conc. depend., impurity bands *(Russian)* 80−75318
Cu-Co, solid soln., mag. susceptibility near solubility boundary *(Russian)* 79−15281
Cu-Fe, metastable solid solutions, production by explosive plasma compressor *(Russian)* 77−90289
Cu-Fe-O system, ternary phases, activities in spinel solid soln., phase equilibria and thermodynamic props. 78−6910
Cu-Ga porous solid formed by shock compression 80−29905
Cu-Ge solders for electric vacuum instruments, Mn and Ag additives effect on evaporation 79−42231
Cu-Ge solid soln., isotope effect for Ge diffusion 78−2285
Cu-Mg(Sn) precipitating phase nuclei, diffuse X-ray scattering intensity determ. *(Russian)* 77−86031
Cu-Sb solid soln., finely lamellar discontinuous precipitation, ternary addition effects 77−36510
Cu-Sn solid soln. steady state deform. *(Japanese)* 78−19832
Cu-Ti, lattice parameter change during ageing *(Japanese)* 78−35411
Cu-Ti (3.5 wt.%), aged by US strain, struct. and props. *(Russian)* 80−21003
Cu-Zn, rheological study of crystallographic order on creep *(French)* 80−97548
α-Cu-Zn(Al), solid soln., intermediate temp. embrittlement *(Japanese)* 79−20158
Cu-Zn(Ge)(Ni)(Ga), α-phase alloys, lattice sp. ht. calcs. 80−65246
$(Cu_xAn_{1-x})_2AsO_4(OH)$, olivenite-adamite solid soln., ordering 78−42962
CuBe, Be distrib. in vicinity of oxidation boundary *(French)* 80−11984
CuBr-AgI system, ionic cond. and phase diagram 80−2198
CuCr alloys, supersaturated solid soln. dissociation *(Russian)* 79−52201
$CuCr_2O_4$-$MgCr_2O_4$, X-ray investig. 77−44224
solid solutions continued
$(CuCr_2S_4)_x$-$(Cu_{0.5}In_{0.5}Cr_2S_4)_{1-x}$, piezoelectric effect, X-ray struct. anal. *(Russian)* 80−15978
$CuCr_2Se_4(S_4)(Te_4)$, binary and ternary solid solns., mag. and elec. props. 80−2407
$CuFeO_2$-Fe_2O_3, decomposition kinetics and mechanism of spinel solid soln., composition and precipitation effects *(Japanese)* 77−77489
$Cu_{0.5}Fe_{2.5}O_4$-$ZnFe_2O_4$, cation distrib., mag. moment, Mossbauer spectra, chem. anal. 80−75210
$CuGa_xIn_{1-x}Se_2$, X-ray diffr. cryst. data 80−84147
$CuInSe_2$-$CuInS_2$, solid soln., photo-EMF spectra 80−20248
$CuInSe_{2-x}S_x$, phase equilibria 77−90328
$Cu_2S+Ln_2S_3$, powdered mixtures, reaction rate, production of ionic semiconductors 80−93741
$Cu_{2-x}Se$(Te) crystals, struct. 79−90608
Dy_2O_3-HfO_2, kinetics of initial stages of formation of solid soln. 77−48617
Er_2O_3-ZrO_2, subsolidus phase relations, X-ray diffr. and thermal expansion exam. 78−31382
Eu solid solutions with lanthanides, monosulfides, and oxides, vacant d states, X-ray absorpt. 80−103623
Eu-Ce(Pr)-Fe-O system, solid solns. of ferrogarnet and ferroperovskite type 78−27488
$Eu_{1-x}La_xS$, electron struct., lattice consts., X-ray spectral study *(Russian)* 80−100432
$Eu_2Nb_2O_7$-$Sr_2Nb_2O_7$, new system preparation 78−42994
Eu_2O_3-Y_2O_3 solid soln. phases, synthesis 80−104132
$Eu_{1-x}Sm_xS$, ESR, exchange interaction, susceptibility, elec. cond., thermoelectric power 80−93174
$Eu_xSr_{1-x}M_4O_{11}$, M=Nb, Ta, electrophys. and mag. props. 77−89760
$Eu_{1-x}Sr_xSi_2$, solid solns., α-$ThSi_2$ struct. type, comp. and press depend. 78−91322
$Eu_2Ta_2O_7$-$Sr_2Ta_2O_7$, new system preparation 78−42994
(Fe, Mn)B and (Fe, Mn)$_2$B, lattice constants of solid solns. *(Italian)* 77−48402
(Fe, Mn)O_x, thermodynamic characts. deduced from Wustite reaction *(Italian)* 77−48401
Fe base ternary soln., containing interstitials and substitutional solutes, thermodynamic and kinetic props. 78−2297
Fe, cast, interdendritic dispersed graphite, dissolution kinetics on heating, excess time *(Russian)* 77−52360
Fe, metastable alloy form. by ion implantation 79−82252
Fe solid solution, substitution strengthening by Cr and Mo *(Czech)* 80−30080
Fe-bearing binary, substitutional liq. and solid solns., statistical thermodynamics 80−11630
Fe-C, softening by C in solid soln. *(French)* 77−36660
Fe-C interstitial solid solutions, self-diffusion activation energy rel. to partial molar energy 80−15291
Fe-C solid solution, martensite, carbide decomposition, electron microscopy and X-ray diffr. obs., review *(Russian)* 79−33998
Fe-C solid solution, volume effects on enthalpy and internal energy 78−75839
Fe-C system, FCC, austenite field thermodynamics, re-anal. 80−89201
α-Fe-C(N), C and N migration at low temps., monograph 80−22149
Fe-Co-Ni-Al-Nb (15-20, 14, 9, 0.1-5.5 at.%), Nb effect on magnetic props., lattice parameter *(Russian)* 77−55689
Fe-Co-Si, BCC solid soln. interchange energies, high temp. neutron diffr. 80−29166
Fe-Co-Si solid solutions, BCC, atomic configs., Mossbauer study 80−39006
α-Fe-Cr solid soln., thermodynamic activity of components 79−38797
Fe-Cr-C solid solns., ordering and γ to α transforms, effect of heat treatment *(Russian)* 79−24520
Fe-Cr-(Co), decomposition of solid soln. in mag. field, neutron and X-ray diffr. study *(Russian)* 78−68694
Fe-Ga, solid soln., order-disorder transform. *(French)* 78−3121
α-Fe-Me-C(N), C and N migration at low temps., monograph 80−22149
Fe-Mn-S, thermodynamics, activity of FeS-MnS solid soln., 1100 to 1400°C 78−6902
Fe-Mo (3 wt.%), substitutional solid soln. with cubic faced symmetry, Portevin-Le Chatelier effect *(French)* 78−23785
Fe-N, interaction with dense stream of N ions, metallography, microhardness, specific volume *(Russian)* 80−15169
α-Fe-N, supersaturated solid solns., N atom precip. kinetics, resist. meas. 80−60864
Fe-N single crystals, N effect on hardening 80−97496
Fe-N single crystals, plastic deform. in temp. range 4.2 to 300K 80−76321
Fe-N single crystals, solid soln. stress assisted nucleation of α″ precipitates 78−52810
α-Fe-N solid soln., N precipitation kinetics, defects effect 77−59789
Fe-N(C), solid soln., metastable and stable, interstitial atom config. 77−36512
Fe-Ni, influence of hydrogen press. on temp. of martensitic transform. *(Russian)* 78−27514
Fe-Ni solid soln., thermodynamic study 78−6904
Fe-Ni solid solution, deformation mechanism, softening phenomena, dislocation-solute atom interactions *(French)* 80−45344
Fe-Ni-C-Mn (3.56, 3.25, 0.6 wt.%), solid soln., quenched, changes during annealing to crystal structure, mech. props. *(Russian)* 79−34076
γ-Fe-Ni-Cr solid soln., thermodynamic activities determ. in Ni rich corner at 1500K 77−32561
Fe-Ni-Pt system, ordered phase fields of equilibrium diagram 78−48373
Fe-Ni-Ti (25.9, 2.15 wt.%), exam. of effect of inhomogeneous solid soln., on martensitic transformation *(Russian)* 79−34034
Fe-Ni(Mo), solid soln., cyclic stress-strain props., depend. of fatigue crack growth rate 77−4853
α-Fe-P, grain boundary adsorption of P, internal friction *(Russian)* 77−32609
Fe-Si(Cr)(Ni)(Mn)(C), alloy layers formed by reaction with molten Al, X-ray, EPMA anal., hardness meas. *(Japanese)* 78−72926
Fe-V (10 to 50 at.%), solid soln., tempered, exam. of long and short range order, using Mossbauer effect *(Russian)* 79−29105
Fe-Zn, physical-chemical metallurgy *(German)* 80−108390
Fe-Zr, dilute solid solution, surface segregation, AES exam. 77−43413
Fe_3-Al, solid soln., rheological study of crystallographic order on creep *(French)* 80−97548
Fe_3Al-M, ternary ordered solid solns. with M=Ti, Mn, Ni, Cu, Ge substituent 77−43177

solid solutions continued
$FeBO_3$-MBO_3 solid soln., (M=Mn, Cr, Al, Ga, In), synthesis, crystal chem. and mag. props. 78−31058
$Fe_xCo_{1-x}S_2$, ferromagnetic, electronic props. 79−7990
$Fe_{1-x}Co_xSi$ solid solution, semiconductor-metal transition 80−103627
$(Fe_xCr_{1-x})_2O_3$ corundum-type solid solution single crystal growth, chem. vapour transport 80−93465
$FeGa_2Se_4$, elec. cond., mag. susceptibility 80−88301
$(Fe_{1-x}Mn_x)_3Si$, $(Fe_{1-x}Co_x)_3Si$, order distrib., hardening effect *(Russian)* 77−89410
Fe_4N growth kinetics in Fe-N system *(Korean)* 80−93540
$Fe_xNb_xV_{2-2x}O_4$ complex solid solns., synthesis and phase diagram, semicond.-metal transition temp. 79−43214
$Fe_{65}(Ni_{1-x}Mn_x)_{35}$, H solid solutions magnetisation behaviour in pulsed mag. fields 79−65674
$Fe_{1-x}O$-ZnO, solid solns., determ. of degree of imperfection 77−80624
γ-Fe_2O_3:Fe_3O_4, magnetite impurity determ. by C_p calorimetry 78−2152
Fe_2O_3-Al_2O_3, solid solns., effect on Fe on point of zero charge 78−61021
Fe_2O_3-Al_2O_3 mixed oxide, X-ray diffr. and elec. cond. 80−79954
α-Fe_2O_3-Li_2O, structural and thermal phase behaviour from mag., spectral and thermal studies 80−2673
Fe_2O_3-MgO-NiO, tie-lines between solid solns. of oxide and spinel at 1273K *(French)* 79−100124
Fe_3O_4-$ZnFe_2O_4$, spinel type solid soln., thermodynamic study by EMF meas. 78−15379
FeSb solid solution, supersaturated, mag. hyperfine field, Mossbauer study 80−44961
$Fe_xTa_xV_{2-2x}O_4$ complex solid solns., synthesis and phase diagram, semicond.-metal transition temp. 79−43214
α-$FeTiD_{0.057}$, solid soln., interstitial D, neutron diffr. study 80−39071
$Fe_xV_{2-x}O_4$, specific heat near semiconductor-metal transition 80−24612
$Fe_{1-y}Zn_{3y/2}O_3$, solid soln. prep., struct. and mag. moment 78−52228
^{57}Fe interstitial cpds. and solid solns., Mossbauer spectra 80−20557
Ga-AlSb-GaSb, phase diagram, LPE of $(AlSb)_x(GaSb)_{1-x}$ solid soln. 77−40392
Ga-In(Al) systems, thermodynamic anal. 79−60512
Ga-Sb-Te, props. of ternary solid solution based on GaSb 79−7826
$Ga_{1-x}Al(In)_xAs$, $GaAs_{1-x}P_x$, substit. solid solns., comp. determ. from X-ray integral intensities 77−84584
GaAs:Cu, supersaturated solid solns., decomp., surface impurity content 78−51681
GaAs-AlAs, epitaxial layer, partition coefficients of impurities 77−15443
GaAs-ZnSe, solid solution crystals, grown by Bridgman method, exam. of resistivity and Hall effect 79−95919
$GaAs_{1-x}P_x$, solid soln. comp. control during gas-phase heteroepitaxy 77−85091
$Ga_xIn_{1-x}As$, recombination mechanisms of excess carriers 80−97337
$Ga_xIn_{1-x}P$ solid solutions, single cryst prep. and props. 80−16162
$Ga_xIn_{1-x}P$:Si, solid soln., splitting of ground state 79−51527
$Ga_xIn_{1-x}Se$, fabrication, struct., elec. and optical props. 80−44180
Ga_2O_3-Fe_2O_3 system, anomalous Mossbauer line shapes, incomplete annealing 78−92006
β-Ga_2O_3-K_2O/K ferrite, interfaces and solid soln., thermal expansion and lattice parameter variations 78−55959
GaP-based III-V solid solns., bonding and energy gap, mag. meas. 78−18580
GaP-ZnS, solid solns., microstruct. investig. 78−2128
$(GaP)_x(ZnSe)_{1-x}$, reaction of Zn with Se during Czochralski growth and LPE 79−8238
GaS-SmS system, phase diagram 79−78939
$GaS_{1-x}Te_x$, solid soln., single cryst., crystallography and optical props. 79−55711
$Ga_2S_{2-x}Te_{1+x}$ ($0 \leq x \leq 0.17$), solid soln., Ga_2S_3-Ga_2Te_3 phase diag. *(French)* 78−76635
GaSb, solid solns., impact ionisation, cond. and valence band effects 80−65583
GaSb-GaAs-Ge system, props. and struct. 80−20232
GaSb-InSb solid solns., heavily doped, electronic props. 77−80727
Ga_2Se_3, elec. cond. 80−88301
Ga_2Se_3-FeSe, phase diagram, elec. cond., mag. susceptibility 80−88301
$GaSe_{1-x}Te_x$, Raman spectra, phonon freq. 80−97286
Ga_2Te_3-Cu system solid solns., elec. cond. 78−51988
GdCa garnets, solid soln., mag. and cryst. chem. props. 77−16057
$GdCrO_3$-$GdAlO_3$ solid solutions 80−20887
$Gd_xEu_{1-x}B_6$, solid solns., mag. susceptibility, 80 to 1000K *(Russian)* 80−88713
GdF_3-RF_3, R=Tb, Ho, Er, Yb, stabilisation of rhombic β-YF_3 type struct. 78−67700
$Gd_xLa_{1-x}B_6$, solid solns., mag. susceptibility, 80 to 1000K *(Russian)* 80−88713
$Gd_xZr_{1-x}O_{2-x/2}$, fluorite and pyrochlore solid solutions, electrical conductivity meas. 80−65287
Ge, As impurity precipitation from solid soln., neutron irrad. effect 80−29177
Ge:Al, solid solns. decomp. 80−15249
Ge:Li, supersaturated solid solns., decomp., surface impurity content 78−51681
Ge:metal, polycrystalline film, electron transport props. 79−99642
Ge:Sb, solid solns. decomp. 80−15249
Ge-Ag, exam. of structure using electron microscope *(Russian)* 79−14738
Ge-Al (1.15 wt.%), US wave vel. meas. for anal. of solid soln. breakup 78−23887
Ge-Ga (1.13 wt.%), US wave vel. meas. for anal. of solid soln. breakup 78−23887
Ge-GaAs, crystallisation at superhigh cooling rates 80−54349
Ge-GaSb, metastable continuous solid solutions 79−8284
Ge-In-Te system, region of solid soln. of In in GeTe 77−51499
Ge-Si, solid soln., local IR transmission 80−7357
Ge-Si solid solution film, elec. props. in range 4.2 to 500K 77−8214
Ge-Si:Sb, prepared in Universal Furnace expt. in Soyuz-Apollo programme, melting and crystn. 80−19737
Ge-Si:Te, solid solns., donor states energy spectrum 80−88516
Ge-Si-Sb solid soln., distrib. of components in universal furnace expt. in Soyuz-Apollo programme *(Russian)* 78−31381
Ge-Si-Sb solid soln., prod. by 'Universal Furnace' expt. Sb and Si distrib. *(Russian)* 78−23692
Ge-Si-Sb solid soln., struct. peculiarities and mech. props. under weightlessness *(Russian)* 78−23693
solid solutions continued
Ge-Sn-M, M=Cu, As, Sb, formation of Ge-based solid solns. during crystallisation 77−80625
$Ge_{0.8}(GaAs)_{0.2}$, metastable solid solns., decomp. kinetics 79−38789
GeO_2-SiO_2, reduction by C, mixed diffusional-kinetic regime *(Russian)* 80−66771
GeS-GeSe, limits of solid soln. region, microstructural, X-ray and DTA meas. 78−47530
GeS_2-$GeSe_2$ cross section, $GeSe_2$ single cryst. growth 77−52305
Ge_2S_3-Ge_2Se_3, glass, photoluminesc. spectra, solid soln. form. *(Russian)* 78−23525
GeS_xSe_{1-x}, IR spectra, differential calorimetry, phase diagram *(Russian)* 78−52513
$GeSe_xS_{1-x}$ long-wavelength optical phonons, Raman spectra 80−25378
Ge_xSi_{1-x}:Cu, solid soln., single cryst., photocond. spectra 79−24015
GeTe-Ga_2Te_3, electrophys. props. 77−48403
GeTe-Sb_2Te_3, cond., density of states 80−88472
H solid solution with Pd-Cu(Ag)(Au) alloys, superconducting transition temp. behaviour *(Russian)* 80−70879
^3He-^4He, solid soln., struct. of vacancies 80−2242
Hf-C-N-O-H, solid solns. of H, exam. of props. 80−29172
Hf-O, phase props. 77−40415
HfO_2, Y_2O_3-stabilised, solid soln., Raman scatt. anal. of struct. transform. 78−88312
HfO_2-CeO_2, system 77−16549
HfO_2-Eu_2O_3, phase composition in HfO_2-rich region, X-ray anal. 77−12609
$Hf_xTa_{1-x}C$, thermal cond. and diffusivity, 1000-2200°C, elec. cond. 78−91491
HfV_2D_4, disordered solid solution, order-disorder transition 80−88321
Hg-HgTe-CdTe system, equilib. phases comp. by dew point method 79−78941
$Hg_{1-x}Cd_xTe$, CESR *(Russian)* 78−23344
$Hg_{1-x}Mn_xTe$, transverse magnetoresistance in quantised mag. fields 80−96922
HgTe-HgSe film, optical spectra in fundamental absorption edge 79−74012
HgTe-MnTe, growth from two-phase melts, crystallisation characts. 77−36393
In-Ga-P system, solvent choice for InP and GaP LPE 79−87589
In-GaP, phase diag. cross section 77−48410
In-Sb-Te, region of In-Sb-based solid solutions 77−36466
InAs, exam. of decomposition of donors 79−1605
InAs:Zn,S,(Se)(Te), exam of microhardness, Hall effect as function of dopant 79−95038
InAs-CdTe, preparation, microhardness rel. to component interactions 77−24350
InAs-InP, phase equilib. and dissoc. 80−35170
$(InAs)_{1-x}(CdSe)_x$ solid solution, elec. props. 79−15146
$InAs_xSb_{1-x}$, recombination mechanisms of excess carriers 80−97337
$In_{1-x}Ga_xP$, solid soln., evaporation of P during LPE 79−95948
InP-GaP, solid soln. crystallization from stoichiometric melt, solidus construction 77−85927
InSb-CdTe solid solns., electroreflectance spectra, Brillouin zone transitions 80−7330
In_2Se_3-Cu_2S system, electrophys. props., influence of 1-4% Cu_2S 80−20219
$(In_2Te_3)x$-$(Hg_3Te_3)_{1-x}$, $0.15 \leq x \leq 0.37$, E_g-comp. depend., spectral photo EMF meas. 77−47851
KBr-KI, mixed crysts., microhardness, theory 80−75298
$KCaCl_3$ impurity in NaCl cryst., precipitation and dissolution 79−42259
KCl:Ba solid solution decomposition, elastic ordered structure formation 79−86896
$KCl:Ba^{2+}$, localised stress relaxation in excess vacancy system, prismatic loops *(Russian)* 80−88160
$KCl:Br^{2+}$, solid solution periodic precipitation in inhomogeneous conc. field 80−103485
$KCl:NH_4Cl$, PMR, NH_4^+ ion proton spin-lattice relax. time temp. depend. 78−27104
KCl:Pb, solid solution, electron microscope exam. of decomposition, of naturally aged specimens 79−96030
$KCl:Pb^{2+}$ crystals, precipitation, density changes, nucleation mode, lattice relaxation, heat treatment 79−66066
KCl-$BaCl_2$ supersaturated solid soln., deformed, $BaCl_2$ precipitation kinetics, metastable region *(Russian)* 78−60673
KCl-CuCl solid solution supersaturated, precipitation, impurity aggregation 80−29174
KCl-KBr, mixed crysts., microhardness, theory 80−75298
KCl-KBr, solid soln., negative muon capture ratios 80−55007
KCl-KBr solid solution, yielding model on plateau stress 78−27568
KF-ErF_3, phase diagram 80−92645
$K(H_{1-x}D_x)_2PO_4$, ferroelec., dielec. susceptibility, pseudo-spin model 77−52024
$KMg_2(AlSi_3O_{10})F_2$-$KMg_{2.5}Si_4O_{10}F_2$, solid soln., melting and crystn., quenching and DTA study 80−39263
$KMg_2LiSi_4O_{10}F_2$-$NaMg_2LiSi_4O_{10}F_2$, solid soln., solid solubility and swelling characts. 80−59660
K_2ReCl_6-K_2ReBr_2 solid soln., mixed ligand complexes 77−72585
$K[(OH)_{0.42}(O_2)_{0.50}]$, cubic solid soln., structural and mag. study *(French)* 80−107177
(La, Y, Sc)B_6, electron work function, thermal emission technique 80−20755
$La_{1-x}Eu_xB_6$ solid solutions, cryst. lattice defectiveness, mag. susceptibility and elec. conductivity 80−15083
LaB_6:Y, Sc effects of impurities thermionic emission 78−60542
La_2C_3, solid solution, lattice const. and superconducting transition temp. *(Russian)* 80−92496
$La_{1-x}Ca_xCrO_3$, heating elements for high temp. furnaces *(French)* 77−52524
La_2O_3-Mn_2O_3-Cr_2O_3, synthesis and properties of solid solutions 78−44038
La_2O_3-Y_2O_3, phase diagram at high temps. *(Japanese)* 77−70038
$LaRu_xFe_{1-x}O_3$ perovskites, cryst. struct., elec., mag. and Mossbauer behaviour 77−55274
$LaS_{1.500}$-$LaS_{1.333}$, density meas. 80−95075
La_2Se_3-Ga_2Se_3-$GeSe_2$ ternary system, phase diags., glass formation *(French)* 78−3109
$La_xSm_{1-x}B_6$, mag. susceptibility meas. *(Russian)* 79−28501
Li ferrite, phase transitions during reduction 80−55642
Li-Al system, Li solubility and chem. diffusion in Al, electrochem. study 80−107432

solid solutions continued
- LiF:Co_x flow stress changes during precipitation 80−92594
- LiF:Co^{2+}, solid soln. decomp., precip. of new phase, electron microscope expt. 79−11619
- LiF-MgF_2, high-pressure phase relations rel. to mixed oxide zone of Earth mantle 77−37193
- $Li_{0.5}Fe_{2.5}O_4$-$CuFe_2O_4$-$MnFe_2O_4$, structural characteristics and mag. props. of solid solutions 77−35696
- Li_4GeO_4-Zn_4GeO_4, solid electrolyte system, phase diagram 80−66489
- $Li_{1-x}Hf_{2-x}Ta_x(PO_4)_3$, new solid ionic conductors 77−35953
- Li_2MgGeO_4, high temp. modif., struct. derivation *(French)* 77−47433
- Li_2MgSiO_4-Li_2ZnSiO_4, form. of solid soln. *(Japanese)* 77−25037
- $Li_xNi_{1-x}0$ (x=0 to 0.03), solid soln. effect of Li on densification during sintering 80−25638
- LiO_2-Al_2O_3-SiO_2, anal. of composition by IR reflection spectra 80−40783
- Li_2O-Al_2O_3-Cr_2O_3 system, subsolidus equilibria 80−60843
- Li_2O-Ta_2O_5 system phase diagram 79−47668
- Li_2O-TiO_2, pseudobinary phase rotations, DTA and X-ray anal. 80−108411
- $Li_2O.nAl_2O_3(7.3\text{-}n)SiO_2$, metastable solid soln., Al^{3+} vacancy incorporation 77−12593
- $LiTaO_3$-$CaZrO_3$, struct. and dielec. props. 78−80298
- $Li_{1+y}Ta_{1.5y}Ti_{6y}O_3$ ($0 \leq y \leq 0.028$), non-stoichiometric phase, crystallographic and dielec. props. 80−75212
- $Li_{1-x}Zr_{2-x}Ta_x(PO_4)_3$, new solid ionic conductors 77−35953
- $M_{1-x}Sr_xSi_2$ (M=Ca, Eu, Ba), solid solution with type $SrSi_2$ struct., lattice parameters at high press. 80−54203
- Mg-Sm, solid soln., phase diagram *(Russian)* 77−25015
- $(MgAl_2O_4)_x(AMn_2O_4)_{1-x}$, A=Mg,Mn,Zn,Cd, $0<x<1$, mixed oxide spinels, chemical shifts of Mn K-absorpt. edge 80−29828
- $MgCu_{2-x}Ni_x$, X-ray and neutron diffr. investigation of Laves phases of $MgCu_2$-type *(German)* 80−15050
- $MgCu_{2-x}Zn_x$, X-ray and neutron diffr. investigation of Laves phases of $MgCu_2$-type *(German)* 80−15050
- $Mg_xFe_{1-x}O$, diffusion of ^{59}Fe and elec. cond. 80−59700
- $MgGeO_3$-$Ca_{0.5}Fe_{0.5}GeO_3$, solid solns., physicochem. props. 77−44223
- $MgNi_{2-x}Zn_x$, X-ray and neutron diffr. investigation of Laves phases of $MgCu_2$-type *(German)* 80−15050
- MgO solution in UO_{2+x}, shell model calcs. of enthalpy, computer program for formation energies 79−42251
- MgO:LiF_3 accretive recrystallisation during hot pressing 77−36421
- MgO:Mn^{2+}(Fe^{2+})(Cr^{2+}), redox behaviour of ions, ESR and X-ray diffr. 78−52341
- MgO-NiO, crystalline soln., microstrain rel. to lattice energy and strain energy 77−24411
- MgO-NiO, solid soln. formation, initial stage obs. 77−81243
- $Mg_2P_2O_7$-$Mg_2As_2O_7$ solid solns., formation of mixed anions $PAsO_7$, IR absorption spectra exam. 79−1508
- $MgTi_1O_5$, formation of solid solutions, on chemical reduction, X-ray analysis of phases *(Russian)* 79−33072
- $Mg_yU_{1-y}O_{2+x}$, thermodynamics from EMF meas., high Mg conc. 78−43143
- $(MgV_2O_4)_c(FeFe_2O_4)_{1-c}$, struct. parameters, IR spectra, cluster-component analysis 77−47425
- MgZn ferrites and ZnO in MgO, thermodynamic props. 77−21116
- Mn chalcogenides-II-VI compound solid solutions, cryst. growth and physicochem. props. 79−14711
- Mn-Ga system, X-ray struct. investigation, solubility *(Chinese)* 80−88084
- Mn-Y-Zn-Cd alloy,phase equilibria, plastic deformation, microhardness *(Russian)* 80−40334
- $Mn_{1-x}Fe_xSi_{1.7}$, solid soln. system, temp. depend of conductivity and thermo-EMF, conc. depend of Hall const. 77−11913
- $Mn_xMg_{1-x}O$, EPR, mag. interactions *(Russian)* 80−44908
- MnO-CdO(ZnO), solid solns. prep., struct. 78−95157
- MnO-CoO-O_2, semicond. solid solns., ageing effects on elec. cond. 78−23085
- MnO-MgO, EPR concentration dependence in magnetically diluted crystals with strong spin-spin interaction 79−42826
- MnS-$CuInS_2$, phase relations, 400 to 1300°C, X-ray and microscopic exam. 79−1853
- $Mn_5(Si_xGe_{1-x})_3$ solid solution, mag. ordering, magnetisation and neutron scatt. meas. 78−27023
- Mn_2SnO_4-Mn_3O_4 system, spinel solid soln. form., atm. effects 77−43332
- $(MnTe)_{1-x}(Bi_2Te_3)_x$ ($x \leq 0.05$) solid solution, electrophys. props. 80−24925
- Mo, cast and low alloy, C distrib. between solid soln. and precipitate *(German, English)* 79−20059
- Mo, chromizing, formation of ordered solid soln. *(Russian)* 78−11402
- Mo-(Zr+V+C) (1.1 wt.%) alloy, phase composition, carbide phase microhardness *(Russian)* 80−60834
- Mo-Be solid solutions, superconducting transition, temp. changing peculiarity due to press. *(Russian)* 80−70878
- Mo-low alloys, C enrichment mechanism of intercrystallite zones *(Russian)* 80−20963
- Mo-N, thermodynamic props., 1618 to 1883K 80−65230
- Mo-N solid solution, exam. of enthalpy of solution, variation with temp. 79−10947
- Mo-Nb solid solutions, enthalpy of soln. of H meas. 80−2166
- Mo-Re, solid soln., dislocation internal friction *(Russian)* 78−23748
- Mo-V, elec. resist. and thermo-EMF, conc. depend., 4.2 to 1500K *(Russian)* 80−80247
- Mo-W solid soln., joint solubility of C and Zr 77−25025
- $NH_4H_2ASO_4$-$NH_4H_2PO_4$, EPR spectra of central peak fluctuations 78−91932
- $(NH_4)_{1-x}M_xX$, and $(ND_4)_{1-x}M_xX$ M=Tl, Rb, Cs, X=Cl, Br, phase diagrams birefringence obs. *(German)* 79−83185
- (Na,K)NbO_3, struct. transitions, neutron powder diffr. 78−38649
- Na-rich plagioclase microstructure and exsolution 80−72501
- $NaAl_2O_4$-$MgAl_2O_4$ spinel solid solns., activities rel. to cation distrib. 77−15377
- NaCl-KCl-$CaCl_2$, solid soln., X-ray examination of final decomp. stage *(Russian)* 77−63681
- NaCl-NaBr, mixed crysts., microhardness, theory 80−75298
- NaCl-NaBr, solid soln., negative muon capture ratios 80−55007
- NaF-AlF_3 system, thermodynamics, solid soln. in cryolite 79−52183
- Na_2MoO_4-$CaMoO_4$, phase diagrams, solid soln. form. 77−36467
- Na_2MoO_4-Na_2SO_4, phase diag. and isomorphism 78−27486
- $Na_2(MoO_4)_3$-$Nd_2(SO_4)_3$ system, sulphatomolybdates and isomorphous substitution 80−19763

solid solutions continued
- Na_2O-M_2O_3-TiO_2, (where M=Al, Cr, Fe or Mn) ternary systems, X-ray anal. 79−51067
- Na_2O-SiO_2-Ga_2O_3-Al_2O_3 glasses in mixed $AgNO_3$-$NaNO_3$ melts, ion exchange 80−21282
- Na_2SO_4-$Y_2(SO_4)_3$, solid solution, effect of defect concentration on ionic conductivity 78−75870
- Nb-C-N-O-H, solid solns. of H, exam. of props. 80−29172
- Nb-H, interstitial position of H from entropy of soln. 77−65989
- Nb-H system, accommodation effects during hydride precipitation, TEM 80−89218
- Nb-Mo, BCC, struct. singularities rel. to solid solution behaviour *(Russian)* 77−11696
- Nb-O, cyclic creep, effect of O_2 conc. and temp. 78−48466
- Nb-O system, solid soln. hardening and softening 80−71665
- Nb-O(N), dislocation pinning, impurity interactions, strengthening *(Russian)* 80−92532
- Nb-Re-(Ru)-N system, N_2 solubility and solubility limit *(German)* 77−4205
- Nb-Re(Ru)-N system, spectral emissivity, lattice parameter, initial rate of N_2 absorption *(German)* 77−4204
- Nb-Ta alloys, terminal solubility of H and characts. of solid solns. 79−86894
- Nb-TiN(HfN)(ZrN), BCC solid soln., nitride solubility, alloying effects *(Russian)* 79−51262
- Nb-V-O solid soln., thermodynamics of O_2 78−68673
- Nb-Zr-C welding solid solutions, ageing kinetics, influence of inclusion elements *(Russian)* 80−100853
- NbH, H impurity screening, lattice deformation, dipole force tensor component calcs. 79−77611
- NbO_x, interstitial O, diffuse neutron scatt. 78−83809
- Nd-Gd-Te alloys of R_2Te_3-T_3Te_4 region, physicochem. props. 78−52017
- Nd-H, possibility of H ordering, DTA meas. 79−52174
- $Nd_{1-x}Ca_xVO_3$, elec. props., thermo-EMF 80−96866
- $Nd_xEu_{1-x}B_6$ solid solution, mag. susceptibility, lattice parameters, Weiss temp. 80−29535
- $Nd_xY_{1-x}Zn$ system, solid soln., mag. susceptibility, 77 to 600K *(Russian)* 80−65776
- $Nd_2Zr_2O_7$-$Nd_2Hf_2O_7$, struct., elec. cond. and melting point 80−54197
- $Nd_xZr_{1-x}O_{2-x/2}$, fluorite and pyrochlore solid solutions, electrical conductivity meas. 80−65287
- Ni alloy, ZhS6K, diffusion layer form. on Nb addition, struct., comp. *(Russian)* 78−56814
- Ni, dissolution and passivation in acid medium, effect of S in solid solution *(French)* 78−64771
- Ni heat resistant alloys, orientational correspondence between γ solid solution, and $\gamma+\gamma'$ eutectic precipitation *(Russian)* 79−11621
- Ni, metastable alloy form. by ion implantation 79−82252
- Ni-Al, rheological study of crystallographic order on creep *(French)* 80−97548
- Ni-Al, solid soln. and solid soln. hardened, stead state creep 78−27578
- ζ Ni-Al system, solid soln., interdiffusion *(Japanese)* 80−70476
- Ni-Al(Ti)(Mo)(Si), effect of solute misfit and temp. on irradiation induced segregation 78−72779
- Ni-bearing substitutional binary solutions, thermodynamics 80−44336
- Ni-C. exam. of metastable phase diagrams, at high temp. and pressure *(Russian)* 79−56955
- Ni-Co-C solid solution, C precipitation, Ni_3Co ordering, Ni-Co lattice parameter meas. *(Czech)* 80−60867
- Ni-Cr, solid soln., lattice parameter meas. rel. to conc. and temp. depend. *(Czech)* 80−28949
- Ni-Cr, solubility limit determ., X-ray method 79−43199
- Ni-Cr(Mo), solid soln., US effect on mech. props. *(Russian)* 78−23819
- Ni-Cu-X (X=Sn, Nb, Ti), spinodal decomp. alloys, linear expansion coeff. influence on morphological anisotropy *(Japanese)* 80−70431
- Ni-H, thermally charged, serrated yielding 80−85007
- Ni-Mn (10∼40 wt.%), γ solid soln., interdiffusion 80−100366
- γ-Ni-Mn solid soln., interdiffusion 1073 to 1323K *(Japanese)* 79−99374
- Ni-Mn-H solid solutions, mag. props. 80−88753
- Ni-Mo, sintering limited solid solubility, peritectic diagram 77−28754
- Ni-Mo-W, diagram of state, W solubility, dispersion hardening *(Russian)* 80−66477
- Ni-Ni_2B eutectic, high temp. X-ray anal. 80−71639
- Ni-Ni_4Mo system, deformation microstruct. 80−93591
- Ni-NiAl solid soln., high temp. transforms *(Russian)* 79−56973
- Ni-P, electrodeposited film, thermal anal., occlusion of gases rel. to mag. props. 80−59823
- Ni-Pd-Mn, ternary FCC solid soln., saturation magnetisation and Curie temp., medical appl. *(Japanese)* 79−61114
- Ni-Pd-Mn ternary alloys, mag. characts., use for thermoseed 80−107995
- Ni-Re, sintering, limited solid solubility, peritectic diagrams 77−28754
- Ni-S, electrodeposited film, thermal anal., occlusion of gases rel. to mag. props. 80−59823
- Ni-S, phase diagram calc. and thermodynamic props. of liq. phase 80−108401
- Ni-Ti (1.6, 7.64 wt.%), monophase high temp. scaling, metallography study 80−21159
- Ni-V, solid soln., diffusion and thermodynamic props. 80−65278
- α-Ni-Zn, solid soln. diffusion annealing effect *(Japanese)* 80−34255
- Ni-Zn solid soln., lamellar spacing in discontinuous precipitation, expt. proof of Gaussian distrib. *(German)* 77−36517
- Ni-Zn-Co ferrites, synthesis from solid solns. of schoenite-type salts 80−93511
- $Ni_{0.5-x}Co_xZn_{0.5}Fe_2O_4$ ferrospinal solid solutions, cryst. lattice defects and props. 80−19796
- $Ni_{1-3x}^{2+}Fe_{2+2x}^{3+}Vac_xO_4^{2-}$ (Vac=cation vacancy), solid solns., cryst. lattice imperfections 80−39069
- $NiFe_2O_4$-Fe_2O_3, effects of excess Fe_2O_3 on mag. props. 77−85495
- $(Ni_{1-x}Fe_x)S$, solid solns., electronic props., X-ray, thermal and Mossbauer study 79−78376
- NiH, H impurity screening, lattice deformation, dipole force tensor component calcs. 79−77611
- NiH_x, formation and decomp. studies 80−71626
- $Ni_{1-x}Li_xO$, $0.01 \leq x \leq 0.08$, mag. susceptibility in region 80 to 800K *(Russian)* 78−2664
- $Ni_xMg_{1-x}O$, EPR in magnetoconcentrated solid solution *(Russian)* 80−39856
- NiO:Cr, effect of Cr additives on structure parameters *(Bulgarian)* 80−44319
- NiO-Al_2O_3, Verneuil-grown crysts., phase comp. 77−66586

solid solutions continued
NiO-MgO, ESR and refl. spectra, Ni^{2+} distrib. 79−33745
NiO-MgO solid solns., surface comp. study by XPS 80−104035
NiO-MgO-ZnO, solid soln. form and colour *(Japanese)* 77−63647
NiO-$NiAl_2O_4$-Al_2O_3, heterogeneous solid state reactions, role of phase boundaries, dynamic equilib. at interfaces 78−71848
NiO-TiO_2, solid soln. series, between rocksalt and spinel structure 78−51513
NiO-ZnO, solid solution, exam. of mechanism and kinetics of reaction with Fe_2O_3 ferrite formation 80−3309
$(NiV_2O_4)_c(MgFe_2O_4)_{1-c}$, struct. parameters, IR spectra, cluster-component analysis 77−47425
$Ni_{1-x}Zn_xO$, reaction with Fe_2O_3, microstruct. 79−87834
PCl_5-HCl_2, Raman spectra, solid and melt, species identification *(German)* 80−45083
$(Pb,Ba)_5Ge_3O_{11}$ ferroelectric crystals, influence of Pb replacement by Ba on props. 79−87402
$(Pb,Sr)_5Ge_3O_{11}$, single crysts., growth and X-ray and dielec. investigations 80−88127
Pb chalcogenide, solid solution, thermoelectric efficiency 79−95429
Pb-As (~0.01 wt.%), enhanced precip. phenomena, invest. of mechanism by elec. resist. meas. 80−104162
Pb-Bi (4.1 at.%) solid soln., tetragonal distortion field for substitutional Bi atoms, neutron scatt. 78−51568
Pb-In (40 wt.%), solid soln., single phase, superplastic behaviour 80−21048
Pb-Sb-As (1.1-1.8, ~0.01 wt.%), enhanced precip. phenomena, invest. of mechanism by elec. resist. meas. 80−104162
Pb-Si superconducting solutions, effect of hydrostatic compression on tunnelling *(Russian)* 80−65746
Pb-Sn-Te system, solvent choice for PbTe and SnTe LPE 79−87589
Pb-Zn, unmixing alloys, mathematical model for solidification process *(Russian)* 80−81047
Pb(Ag) alloys, effect of Ag content on yield strength 80−76322
$(Pb_{1-x}Ba_x)_5Ge_3O_{11}$, ferroelec. transition blurring, US relax., dielec. and opt. props. 78−95559
$Pb(Fe/Al/Ga)_{12}O_{19}$, solid soln., crystallographic charact. *(German)* 79−94972
$2PbFe_{1/2}Nb_{1/2}O_3$-Pb_2FeReO_6, comp., struct., dielec. and mag. props. 80−2704
$2PbFe_{1/2}Ta_{1/2}O_3$-Ba_2FeReO_6, comp., struct., dielec. and mag. props. 80−2704
$2PbFe_{1/2}Ta_{1/2}O_3$-Pb_2FeReO_6, comp., struct., dielec. and mag. props. 80−2704
$Pb(Fe_{2/2}U_{1/3})O_3$-$PbZrO_3$ solid solns., phase transition 77−48138
$PbFe(_{2/3}W_{1/3})O_3$-$Pb(Co_{1/2}W_{1/2})O_3$ solid soln., crystallographic, dielectric, magnetic props., Mossbauer spectra 78−43807
$Pb(Fe_{2/3}W_{1/3})O_3$-$Pb(M_{3/2}W_{1/2})O_3$, (M-Mn, Co, Ni), ferroelec. phenomenological theory 79−99831
$xPb_5GeO_4(VO_4)_2$, $(1-x)Pb_5SiO_4(VO_4)_2$, solid solution of centrosymmetric crystals, electrically induced optical activity 80−108180
$Pb_5(Ge_{1-x}Si_x)_3O_{11}$, electrogyration, phase transition and dielectric props. 80−93269
$Pb_5(Ge_{1-x}Si_x)_3O_{11}$ solid solutions, dielec. props., ferroelec. phase transitions 80−15988
PbI_2-$PbBr_2$, optical spectra, solid soln. struct. 78−48247
$PbMg_{1/3}Nb_{2/3}O_3$-$BiMg_{2/3}Nb_{1/3}O_3$, dielectric polarisation of solid solutions 78−43776
$PbNb_2O_6$-$NaNbO_3$, DTA *(French)* 77−44234
$15PbO.3B_2O_3.2WO_3$, struct. and electrophys. characts. 77−84716
$Pb_3(P_{1-x}V_xO_4)_2$, x=0.1, 0.2, Raman scatt. by low freq. vibrs. 80−55111
PbS-CdSe, phase boundary processes 78−71857
PbS-$CuS_{1.8}$-ZnS, phase equilib. *(Russian)* 77−28786
$PbSc_{2/3}Te_{1/3}O_3$-$PbSc_{2/3}W_{1/3}O_3$($PbFe_{2/3}Te_{1/3}O_3$) ferroelec. props. and lattice consts. 80−60520
$Pb_{1-x}Sn_xSe$, single crystal and film, X-ray spectral investigation of solid solution 77−16477
$Pb_{1-x}Sn_xSe$ solid solns., photoluminesc. spectra, energy band parameter determ. 80−71484
$Pb_{1-x}Sn_xSe$, transport phenomena in solid solutions with band inversion 80−107792
$Pb_{0.84}Sn_{0.16}Te$ single cryst., anelastic relax., helicon wave dispersion *(Russian)* 77−51437
$Pb_{1-x}Sn_xTe$, hole effective mass near zero bandgap, IR refl. study 80−108205
$Pb_{1-x}Sn_xTe$, reststrahlen band, reflection spectra 79−8162
$Pb_{1-x}Sn_xTe$, single cryst. grown from vapour, photocond. meas. 79−24016
$Pb_{1-x}Sn_xTe$: Mn, Mn mag. and elec. active states, mag. impurity behaviour 80−44627
$Pb_{1-x}Sn_xTe$:In epitaxial layers, growth, elec. props., and luminesc. 80−54542
$Pb_{1-x}Sn_xTe_{1-y}Se_y$, narrow-gap solid soln., lattice parameter, energy gap and Hall mobility of carriers 79−73154
$Pb_{1-x}Sn_xTe_{1-y}Se_y$ solid solutions with constant lattice parameter, phase comp. 80−108417
$Pb_{0.95}Sr_{0.05}(Zr_x, Ti_{1-x})O_3$-$Nb_2O_5$, phase coexistence range, lattice consts. 80−92680
$Pb_{0.95}Sr_{0.05}(Zr_{0.53}.Ti_{0.47})O_3$, low temp. internal friction in ferroelectric ceramic 77−21200
PbTe-Ga_2Te_3, phase interaction, DTA, XPA and microstructural anal. 80−96625
PbTe-InTe, solid solns., anomalies in electron mobility 77−80772
PbTe-PbSe system, thermodynamic props. 80−11635
PbTe-SnTe, solid soln. single crysts., TSM growth and elec. characts. 78−68625
PbTe-SnTe solid solns., directional solidification 77−44149
$Pb_{1-x}Th_xF_{2+2x}$, solid soln., anionic cond. *(French)* 78−91481
$Pb(Ti,Zr)O_3$ solid solutions, phase coexistence discrepancies 80−96662
$PbTiO_3$-$CaFe_{2/3}W_{1/3}O_3$, solid solutions 78−43816
$PbTiO_3$-$PbZrO_3$-$PbNb_{2/2}Zn_{1/3}O_3$(-$PbNb_{2/3}Co(Mg)_{1/3}O_3$) solid solutions, dielec. and piezoelec. props. 79−87393
$PbTiO_3$-$Pb(Fe_{1/2}Nb_{1/2})O_3$ based modified ceramics, struct. and elec. props. 79−87392
$PbTiO_3$-$Pb(Ni_{1/2}W_{1/2})O_3$ system, solid soln. form., struct., dielec. props. and thermal expansion *(Japanese)* 78−27501
$xPbTiO_3+(1-x)PbCd_{1/3}Nb_{2/3}O_3$, phase transition spread, polarisation relaxation, dielectric susceptibility *(Russian)* 80−75922
Pb(Zr, Ti)O_3 internal struct., prep. effect, ionic shadowing obs. *(Polish)* 80−11612

solid solutions continued
$PbZrO_3$, ferroelec. solid solns., atom shifts, polarisation and Curie temps. 80−100636
$PbZrO_3$-$PbCd_{0.5}W_{0.5}O_3$, phase transitions 78−43817
$1-xPbZrO_3$-$xPbSc_{0.5}Nb_{0.5}O_3$, $0\leq x\leq 1$, phase transitions, X-ray, dielec., and thermal anal. 80−45020
$Pb(Zr_{1-x}Ti_x)O_3$ solid solution, piezoelectric ceramic, prop. improvement by multiple substitution 80−80702
$PbZr_xTi_{1-x}O_3$ ceramics, morphotropic phase boundary 80−81035
$PbZr_xTi_{1-x}O_3$, tricritical behaviour 78−80296
Pd:H, elastic props. of dilute solid solutions 78−75706
Pd-Ag thin-walled tubes, for thermal diffusion apparatus H diffuser 80−100358
Pd-Ag-Cu (35,25 at.%), determ. of ageing transformations by resist. meas., metallography, TEM and X-ray diffr. 79−4967
Pd-C solid solution, dechannelling of α-particles by C atoms *(French)* 79−7643
Pd-Cu-H(D) dilute alloy soln., thermodynamic props. at high-temp. 79−99334
Pd-H, H phase hardened, recrystallisation study 80−60883
Pd-H, interstitial position of H from entropy of soln. 77−65989
Pd-H_2, dilute soln., high temp. thermodynamics, partial molar props. 77−15597
Pd-noble metal solid solns., with dissolved H, thermodynamic props. 80−108402
Pd-Si-H(D) alloys, superconductivity in solid solution and amorphous phase regions, isotope effect 79−56347
Pd-W, elect. resist., mag. susceptibility, Hall coeffs., in plastically deformed state and after annealing *(Russian)* 79−66174
$Pr_2(MoO_4)_3$-$Pr_2(SO_4)_3$ system, sulphatomolybdates and ismorphous substitution 80−19763
Pt-Au(Al)(In)(Sn)(Zr), solid soln., magnetic props. and lattice parameters *(German)* 79−87236
Pt-H solid solutions, thermodynamics 79−77756
RbCl:NH_4Cl, PMR, NH_4^+ ion proton spin-lattice relax. time temp. depend. 78−27104
RbF-CsF, solid solution, fundamental absorption 79−11433
$(Rb_xK_{1-x})AgI_3$, cryst. struct. 77−51360
$(Rb_xK_{1-x})Ag_4I_5$, cryst. struct. 77−51360
$RbNi_xMn_{1-x}F_3$, powder, mag. props. 80−2560
S-Ni-Fe system containing monosulphide solid soln., elec. and struct. relations 80−90038
Sb-Bi, melting kinetics of solid soln. during high heating rates, superheating *(Russian)* 78−15358
$Sb_{1-x}Bi_xSI$, SHG at microwave freqs. 79−55188
$Sb_{1.5}Bi_{0.5}Te_3$, electrical, thermoelectric and thermal properties, temp. influence obs. *(Slovak)* 78−30946
$SbS_{1-x}Se_xI$, SHG at microwave freqs. 79−55188
$(Sb_2Se_3)_x$-$(Bi_2S_3)_{1-x}$ single crystals, elec. and photoelec. props., stoichiometry deviations influence 79−60870
$(Sb_2Se_3)_{0.7}(Bi_2Se_3)_{0.3}$, solid soln., prep. and elec. properties of layered crystals 80−70762
Sb_2Te_3-Bi_2Te_3, low-temp. thermoelectric mats., growth of microhomogeneous crysts. 77−48337
Sb_2Te_3-Sb_2Se_3, ordered structure formation, heat treatment effect on thermal cond. 80−54448
ScH_x thin films, struct. and elec. props. 80−107931
Sc_2O_3-Ho_2O_3 (Dy_2O_3), solid solution, use of segregation phenomena to exam. solidification phase diagrams *(French)* 79−8293
Sc_2O_3-ZrO_2 (HfO_2), cubic solid soln., lattice parameters 79−82186
Sc_2O_3+Sb(V) reaction, phase formation, structs. 77−84712
Se-Te crystallised glasses, struct. transforms. and IR spectra 80−19712
Si, O impurity precipitation from solid soln., neutron irrad. effect 80−29177
Si, supersaturated solid sol., form. by laser annealing 79−69247
Si:Au, precipitation of solid soln., effect of gamma irradiation 80−59515
Si:Bi, ion-implanted, solid phase epitaxial growth during annealing, supersaturated solid soln. form. 80−103384
Si:Fe^0, solid soln. decomp., Fe deposition on dislocations 77−51943
a-Si:H alloys, sputter deposited thin film coatings, property-comp. relationships 80−80975
Si-Au, solid soln., influence of precip. on relax. of ^{29}Si nucleus 80−11287
Si-C-Al-O-N and related systems, new materials 78−95159
Si-Ge, solid soln., vol. effect on bulk modulus 80−24526
Si_2B, equilib. with B_2H_6 80−97721
$SiF_4Cl_{4-n}^-$ in γ-irradiated solid solution of tetramethysiline, EPR spectra obs. 80−80611
$SiF_3Cl^-(Br^-)(I^-)$ in γ-irradiated solid solution of tetramethysiline, EPR spectra obs. 80−80611
β-Si_3N_4 solid soln., form. from SiO_2-AlN sintering 78−23655
β-Si_3N_4 solid soln. prod. by reaction sintering SiO_2-AlN mixture 80−25645
Si_3N_4/Al_2O_3, powder compact, electron microprobe investigation of reactions *(French)* 80−26009
β-Si_3N_4-AlN-Al_2O_3-MgO, insolubility of Mg in β-Si_3N_4 79−10953
Si_2N_2O-Al_2O_3, solid soln., prep., effect of Si_3N_4 powder reactivity 80−45256
SiO_2-BPO_4, glasses and devitrificates prep., IR spectra *(Polish)* 80−71624
$(SiTe)_{1-x}(ATe)_x$, A=Ge, Sn, Pb, solid soln. with small substitution, mag. susceptibility *(Russian)* 80−70933
$Sm_xLa_{1-x}B_6$, solid solns., exam. of structure, elec. props. 80−39290
$Sm_{1-x}La_xS$, electron struct., lattice consts., X-ray spectral study *(Russian)* 80−100432
$SmS_{1-x}As_x$, intermediate valence phase, lattice const. and mag. susceptibility meas. 79−87245
$Sm_xTb_{1-x}FeO_3$, mag. reorientation, temp. *(Russian)* 79−87263
Sn-Sb (10 wt.%), decomposition of supersaturated solid soln. 80−29960
$Sn_{1-x}Ge_xTe$, solid soln. series, Mossbauer study 80−39985
SnO_2-TiO_2 solid solns., X-ray diffr. and thermogravimetric meas. 79−90792
$Sn_2P_2(Se_xS_{1-x})_6$, ferroelec. props. *(Russian)* 80−25313
$Sn_{1-x}Pb_xTe$, film, production under quasi-equilibrium conditions 80−45241
SnS-SnSe, solid soln. comp. calcs. 77−44230
SnS-SnTe, solid solns., synthesis, Mossbauer spectra 77−24768
$SnS_{2(1-x)}S_{2x}$ solid soln. system, long-wavelength optical phonons, Raman scatt. study 80−80794
SnSe-SnTe, solid solns., synthesis, Mossbauer spectra 77−24768
$SnSe_2$-$GeSe_2$, phase diag., electrophys. props. of solid solns. 77−52306

solid solutions continued
SnTe-PbTe solid solns., defects from susceptibility meas. 77−84737
SnTe-Tl_2Te, phase and elec. props. 77−48406
$(SnTe)_{1-x}(PbSe)_x$ films on glass-ceramics, struct. and elec. props. 77−52251
$Sn_xTi_{(1-x)}O_2$, solid soln., thermal reaction with V(V), Cr(III), Cr(VI), Mn(II), Fe(III), Co(II), NI(II), Cu(II), Sb(III) 80−16674
$(Sr/Ba)(Fe/Al/Ga)_{12}O_{19}$ solid soln. crystal for hexaferrite layer substrate *(German)* 78−23672
$SrCl_2$-$GdCl_3$, prep. and purification 78−88420
$SrCl_2$-$PrCl_3$, prep. and purification 78−88420
$Sr_{2x}Eu_{2-2x}NbO_4$, synthesis and props. 77−52265
$SrFe_{12}O_{19}$, Ca^{2+} additives effect on hexaferrite lattice and mag. props. 80−60243
$Sr_2Fe_xRu_{1-x}O_4$ solid soln., Mossbauer spectrosc. study 80−50235
$SrGa_2Si_2O_8$-$SrGa_2Ge_2O_8$, solid solution, exam. of elastic and electrical props. 79−96057
Sr_2GeO_4-$Sr_3(PO_4)_2$, phase equilibria and struct. 77−85999
$Sr_x(Na_{0.5}Bi_{0.5})_{1-x}$ solid solutions, piezoelec. and ferroelec. props. *(French)* 80−108158
$Sr_{1.8}Na_{0.1}Nd_{0.1}Ta_2O_7$, solid soln., ferroelectric phase transitions, dielec. constant and thermal expansion rel. to temp. 80−88934
$SrO.R_{1-x}Sr_xVO_{3-0.1x}$, R=Nd, Eu, Gd, solid solns., elec. and mag. props. 77−89819
$Sr_{1-x-y}U_xCe_yF_{2+2x+y}$, solid soln., ionic cond. 79−99356
Ta-Cr (15 wt.%), solid soln., discontinuous precipitation *(German)* 80−45314
Ta-D, dil. soln., high temp. thermodynamics 78−43128
Ta-Ga, crystal struct. at high press., polymorphism 80−88112
Ta-H, dil. soln., high temp. thermodynamics 78−43128
Ta-H, fracture modes *(Japanese)* 80−66636
Ta-H, interstitial position of H from entropy of soln. 77−65989
Ta-N (0.6 to 6.5 at.%), supersaturated solid soln., precipitation 79−96028
Ta-O, dil. soln., high temp. thermodynamics 78−43128
Ta-O solid soln., interstitial ordering and precipitation at 100 to 270°C, exam. 78−52813
Ta-O(N), dislocation pinning, impurity interactions, strengthening *(Russian)* 80−92532
Ta-W-Hf (8,2 wt.%), T-111, O_2 absorption, effect on lattice parameter and specimen dilation 78−83958
TaH_x, H diffusion and electronic struct., pulsed NMR obs. 80−54967
Tb-Dy-Ho, phase diagram, alloy struct. *(Russian)* 77−25016
TeO_2-NaCl(-NaBr), condition diagram, thermographic obs. *(Russian)* 80−55377
$(Th,U)O_2$ fuel conversion to $(Th,U)C_2$ for reprocessing 79−54579
$Th_{0.25}NbO_3$-$xNaNbO_3$ solid soln., cryst. struct., perovskite-type phases, X-ray diffr. obs. *(French)* 79−1413
ThO_2-UO_2 solid solns., props. of importance for use as nuclear fuels 79−54506
Ti alloy in Al alloy melt, raction zone formation, component interaction *(Russian)* 80−54377
α-Ti based alloys, deform. twinning effect on mech. props. at low temps. *(Japanese)* 78−6979
Ti fibres, high-temp. nitriding kinetics *(Russian)* 80−21166
α-Ti, solid soln., strain ageing *(Japanese)* 78−6953
α-Ti/Fe, retrograde solid solubility 80−79950
Ti-C-N-O-H, solid solns. of H, exam. of props. 80−29172
Ti-Mn base beta alloys, H effect on stability solid soln., hardness *(Japanese)* 77−81261
Ti-O, dil. HCP solid soln., O interstitial distrib. effect on lattice parameters 78−30588
Ti-O alloys+Li melt, ternary solid soln. formation *(Russian)* 78−11396
α-Ti-O solid soln., hexagonal, thermodynamics 78−3098
Ti-TiO_2-ZrO_2-Mo, sintered struct. and mech. props. 78−60618
Ti-V-C-N, solid solns., quasibinary cross sections 78−23676
α-Ti-Zr-W, effect of W impurity on mech. preps. 80−16392
$TiAl_3$ crystals dissolution in pure Al liq., grain refinement of α-Al solid-solution by Ti addition 80−35178
TiC-ZrC, solid soln., conc. and temp. dependence of props. 80−39736
Ti_8C_5, X-ray order struct. determ. 80−103295
TiC_xN_y, powder preparation, physical, chemical props. *(Russian)* 80−76212
TiC_xO_y, structural mechanism of O inclusion into lattice 78−22707
TiN-MnN, solid solns., electrophys. props. 77−35914
TiO-VO, solid soln. formation 77−89541
TiO_2:Nb, rutile, elec. cond., 1273-1623K, O_2 press. depend., charge compensation mechanism 77−85217
TiO_{2-x}, nonstoichiometric and Nb_2O_5 doped, defect struct. and thermodynamic props. 79−90650
Ti_2O_3-$MgTiO_3$, phase analysis 78−3103
$Ti_{1-x}Ta_xO_2$, solid soln. formed in TiO_2-Ta_2O_5-Ta at 1100°C *(French)* 78−35375
$(Ti_{1-x}V_x)_2O_3$ solid soln., struct. changes comp. depend. 77−55275
TlBr-TlCl, photoelastic consts. dispersion 79−65136
TlCl-TlBr, single cryst., composition determ. by reflection spectrophotometry 77−1961
$TlCl_xBr_{1-x}$, $TlBr_xI_{1-x}$, polymorphous mixed cryst. layers, opt. props. 78−23490
$TlGaS_{2x}Se_{2(1-x)}$, solid soln., fundamental optical absorpt. edge 80−25408
Tm-H solid solution, struct., 20-500°C 79−90643
U-Pu carbides, advanced LMFBR fuels, equilib. thermodynamics 79−67862
U_3O_8-$Y_2O_3(Sc_2O_3)$, solid soln. electrode, high temp. electrochem. appl. 80−6828
$U_{0.75}Pu_{0.25}O_{2-x}$, variation in O_2 potential with simulated burnup 78−70597
$U_{1-x}Th_xO_2$, solid solution, single crystal growth by chemical transport reactions 78−72708
$(V,Fe)_3M$, M=Si, Ge, Ga, solid soln. form. and supercond. T_c *(Russian)* 78−80512
V-based ternary solutions, containing H, thermodynamics 80−19961
α-V-N solid solns., quenched ordered structures *(Ukrainian)* 77−69088
V-O, dislocation pinning, impurity interactions, strengthening *(Russian)* 80−92532
V-O solid soln., BCC, modelling of interstitial solute behaviour 79−77748
V-O solid solutions, solubility and thermodynamic props. 77−7866
V-O system β phase BCT, X-ray diffr. study of additional scatt. effect *(Russian)* 80−10537
solid solutions continued
VN-Mn, solid solns., electrophys. props. 77−35914
VO_2-$CrNbO_4$, solid solns., synthesis and phase diagram 80−35171
α-$V_{0.97}O_{0.03}$, impurity vibrs., inelastic neutron scatt. study 80−92635
V_2O_3-M_2O_3, M=Ti, Cr, struct. and mag. props. 78−27041
V_2O_5-CsV_2O_5 system, phase comp. and phase diagram for conditions of inert atmosphere 77−25030
V_2O_5-MoO_3, small polaron cond., elec. resist. and thermoelec. power meas. 80−34447
V_2O_5-MoO_3, solid soln. thermogravimetric anal., ion formation on crystallisation 77−20076
V_2O_5-MoO_3 solid soln., number of V^{4+} ions, magnetic and thermogravimetric exam. 78−52199
V_2O_5-WO_5, solid soln. thermogravimetric anal., ion formation on crystallisation 77−20076
V_3O_5-Ti_3O_5, DTA, mag. susceptibility and X-ray diffr. study 80−70970
V_xO-M_xO, (M=Ni, Co, Mn), solid solutions, exam. of thermal conductivity 78−79827
$(V_2O_5)_{0.93}(MoO_3)_{0.07}$, struct. transform. in oxidizing and reducing gas atm. 79−23740
$VSe_{2-x}S_x$ (0<x<2) solid solutions, characterisation 80−88730
$V_{1-x}Ti_xO_{1.75}$, synthesis and mag. susceptibility obs. 78−23243
$(V_{1-x}Ti_x)_2O_3$, solid solution, phase transition exam. 77−15590
W-Cr, 1200-1700°C *(French)* 77−48393
W-Cr solid solution, precipitation behaviour, reaction front motion, lattice parameters *(German)* 80−55401
W-Ni-Cr, high-temp. phase diag. *(French)* 77−48393
W-ThO_2-B, thermocathodes diffusion mobility, based on deboronation kinetics 80−39349
W-Ti(Zr)(Hf)-C, cubic solid soln., form. and props. 78−48348
Y-H system, solid soln. phase, wide-line PMR 80−25226
Y-Si-Al-O-N solid soln., based on α-Si_3N_4 struct., comp. and struct. 79−74136
YC_2-DyC_2, solid solution, antiferromag. props. 79−91230
YCa garents, solid soln., mag. and cryst. chem. props. 77−16057
$YCrO_3$-$MgCr_2O_4$ sintered ceramics, elec. cond. 80−24927
$Y_3Ga_5O_{12}$-$Y_3Fe_5O_{12}$ garnets, EPR spectra of ferric ions 77−66414
$Y_{3-x}Gd_xFe_{5-y}Al_yO_{12}$, solid solns., IR absorpt. spectra, physical props. 80−55082
$Y_{3-x}Gd_xFe_5O_{12}$, solid solns., IR absorpt. spectra, physical props. 80−55082
YIG-rare earth garnet solid solutions, magnetisation temp. depend. calcs. 80−20388
YN-UN, decomp. press.-temp. relations 78−52780
$YO_{1.5}$-PrO_x, phase relns. and electrophys. props. of solid solutions 78−23686
YO_x-ZrO_2, YO_x-rich, phase equilibria 77−21117
Y_2O_3-ZrO_2 (HfO_2), cubic solid soln., lattice parameters 79−82186
$YbCr_{1-x}Al_xO_3$ solid solutions 80−20887
$YbNi_{(2)}$-$YbCu_{(2)}$, valency state, Yb behaviour *(French)* 80−45277
YbPd-YbAg, valency state, Yb behaviour *(French)* 80−45277
YbPt-YbAu system, valency state, Yb behaviour *(French)* 80−45277
Zn-Ti-Fe-O, spinel solid solns. 77−48409
$ZnAl_2S_4$-$ZnCr_2S_4$, nonstoichiometric spinel solid solns., synthesis and cryst. chemistry 77−35526
$ZnAl_2S_4$-$ZnIn_2S_4$, phase relationships, 800 to 1050°C 79−1852
Zn_3As_2-ZnSe(ZnTe) solid solutions, single cryst., phase equilib. and props. 80−16283
$Zn_xCd_{1-x}S$, thin solid soln. films, vapour deposited, elec. and optical charcts. 80−60110
$Zn_XCd_{1-X}S(Te)$, solid soln., broadening of exciton states, depend. on conc. 79−73449
$(Zn_{0.2}Co_{0.8}(Ni_{0.8}))O.Al_2O_3$, ZnO evaporation in vac. 80−59640
$ZnFe_2O_4$-Fe_3O_4 solid solns., form. of α-Fe_2O_3 during oxidation 80−25889
$Zn_xHg_{1-x}Se$, current carrier scattering mechanism 80−65546
$Zn_xHg_{1-x}Te$, vacancy mech. of resorption of Hg droplets 80−39070
$Zn_cM_{1-c}Fe_2O_4$, M=Ni^{2+}, Co^{2+}, Fe^{2+}, $Zn_cMFe_{2-c}O_{4-c}F_c$, M=Ni^{2+}, Co^{2+}, calc. of saturation magnetisation by cluster components 77−43817
ZnO, vaporization from spinel solid solns. 77−76541
ZnO-WO_3, phase rels. and cryst. struct. 80−108410
ZnO-Zn_2TiO_4, solid soln. formation 78−27490
ZnS-Al_2S_3, phase relationships, 720 to 1110°C 79−1852
ZnS-CdS, equimolar solid soln. formation kinetics 80−39289
ZnS-CdS films, prep. by atomisation 80−16176
ZnS-$CuInS_2$, phase relations, 400 to 1300°C, X-ray and microscopic exam. 79−1853
ZnS-MgF_2 alloy films, struct. and optical props. 79−90910
ZnS-MgS, solid solution, prep. of single crystals with wurtzite structure, exam. 79−1821
ZnS-MnS, phase relations, 400 to 1300°C, X-ray and microscopic exam. 79−1853
ZnS-MnS-$CuInS_2$, sobsolidus equilib., phase diagrams 80−3016
ZnS-ZnO_x solid solns., edge emission and exciton spectra *(Russian)* 77−24899
$(ZnSe)_{1-x}(GaAs)_x$ solid solns., photoluminescence spectra 80−40159
Zn_2SiO_4-Mg_2SiO_4, melt solidification behaviour 77−90337
ZnTe-CdSe, solid soln. formation and effects 78−27489
ZnTe-CdSe system, phase equilibria *(Russian)* 79−43224
$(ZnV_2O_4)_c(MgFe_2O_4)_{1-c}$, struct. parameters, IR spectra, cluster-component analysis 77−47425
Zr base alloys, formation of phases precipitated from β solid solutions *(Russian)* 79−1869
Zr fibres, high-temp. nitriding kinetics *(Russian)* 80−21166
α-Zr, H location in HCP phase 78−18637
Zr-C, exam. of metastable phase diagrams, at high temp. and pressure *(Russian)* 79−56955
Zr-C-N-O-H, solid solns. of H, exam. of props. 80−29172
Zr-Nb solid solutions, BCC, direct imaging of linear defect using diffuse scatt. 78−22726
Zr-Nb-Fe (13 wt.%, 5 wt.%), struct. changes during decay of BCC β solid solution 79−15669
Zr-Nb-V-Fe (12 wt.%, 6 wt.%, 4 wt.%), struct. changer during decay of BCC β solid soln. 79−15669
Zr-Ru, alloy Zr rich, Ru solubility, eutectic decay, $\alpha \rightleftarrows \beta$ transform., struct. *(Russian)* 80−65227
Zr-Y (15 wt.%), decomp., during heating and cooling cycles, solid solubility changes *(Russian)* 78−92267
$ZrB_{\sim 51}$, X-ray powder profile refinement 79−23574
ZrC-NbC-MoC_{1-x} alloys, physicomech. props., comp. depend. 79−66097

solid solutions continued
ZrC-NbN, mag. susceptibility, zone struct., conc. and temp. depends. 77−8788
$ZrC_{0.97}$-$NbN_{0.93}$, $Zr_{0.5}Nb_{0.8}C_xN_{0.98-x}$, solid solns., elastic props. expansion and hardness 77−52380
ZrC(Re), adsorption of H 79−19467
$Zr_{0.5}Nb_{0.5}C_xN_{1-x}$, mag. susceptibility, zone struct., conc. and temp. depends. 77−8788
ZrO_2, R_2O_3-stabilised (R=La, Gd, Y or Yb), solid soln., Raman scatt. anal. of struct. transform. 78−88312
ZrO_2-based solid solutions, effect of added B_2O_3 and Nb_2O_5 on sintering and stability 77−40410
ZrO_2-CaO-Y_2O_3, formation, stability and elec. props. of fluorite-like solid solutions 77−16550
ZrO_2-CaO(Y_2O_3) ceramics with grainy structure, props., effect of heating to 2000°C 80−104194
ZrO_2-Gd_2O_3, solid solution with fluorite and pyrochlore structure; exam. of elec. conductivity *(German)* 79−23766
ZrO_2-HfO_2, monoclinic solid soln., ceramic prep. and use 80−55338
ZrO_2-HfO_2, soft phonon modes and monoclinic-tetragonal phase transition 77−62638
ZrO_2-HfO_2-CaO, cubic solid solutions, thermal expansion 77−15598
ZrO_2-TiO_2 solid solns., X-ray diffr. and thermogravimetric meas. 79−90792
ZrO_2-Y_2O_3, stabilised, struct. of single crysts. 77−35527
ZrO_2-Y_2O_3 monocrystalline solid solutions, struct. and phase form. 79−52188
ZrO_2-Y_2O_3-CaO(MgO), long term firing effect at 2100 to 2200°C on solid soln. conc. and microstruct. 77−90309
ZrO_2-Y_2O_3-Nd_2O_3, spectral determ. of crystal stabilisation 78−27203
ZrO_2-Y_2O_3-Nd_2O_3(CeO_2), solid solns., form. by coprecipitation, struct., X-ray, electron diffr. anal. 77−12583
ZrO_2-Y_2O_3(Nd_2O_3)(Ce_2O_3), stabilised, reaction with Cr_2O_3 77−36438
ZrO_2-$YO_{1.5}$ solid solutions, ZrO_2 rich side, X-ray spectroscopic study 78−95617

solid-state microwave circuits
see also Gunn oscillators; microwave integrated circuits
cryogenically cooled mixer for 80 to 120 GHz, improvements 79−40073
frequency multiplier, for superhigh frequencies, high multiplication factor 78−4636
Josephson mixers, mm wave, using Nb point contacts 79−26123
Josephson mixers for heterodyne reception at submillimetre wavelengths present expt. status, future developments 79−26120
low-noise 115 GHz receiver 79−53718
preamplifier, for ESR/ENDOR spectrometer sensitivity enhancement 78−82014
solar power satellite, appl. of solid state microwave technology 80−40870
submillimetre wave mixers 78−45712
subMM wave mixing in metal-metal and metal semiconductor point contact diodes 80−4769
superconducting tunnel junctions as low noise 10 GHz mixers 79−82714

solid-state microwave devices
see also BARITT diodes; IMPATT diodes
aerospace systems and electronics, IEEE conference, Washington D.C., USA, 26-29 Sept (1976) 77−5420
coherent tunable Josephson radiation generation, 2-18 GHz, with narrowed linewidth 78−88078
conference contributions, Tokyo, Japan (Sept. 1976) 77−76901
cryogenically cooled C-band p-i-n diode integrated switch matrix for radio astronomy applications 78−96392
device fabrication by MBE 79−43154
ferrites suitability characterisation, spin waves line width parameter meas. 77−20571
gyrotron efficiency, CW and pulsed power achievements 79−31849
hyperabrupt varactors, fabrication from vapour phase epitaxial GaAs 80−29288
information storage in piezoelectric semiconducting single crystals 78−15101
International Microwave Symposium, San Diego, Calif., USA (June 1977) 78−5478
Josephson junction, coherent microbridges coupled by external shunts, props. 79−28460
Josephson junction, radiation power spectrum 78−43522
Josephson low noise mixers at 115 GHz using recyclable point contacts 78−62224
Josephson microbridge, thin-film, millimeter-wave conversion 79−73644
Josephson microwave source, short term emission fluctuations 79−15263
Josephson mixer receiver, at millimetre and long submillimetre wavelengths 77−34027
Josephson point contact junctions and microbridges, HF props. 79−28461
Josephson self-oscillator mixer, submillimetre and far IR detector 77−34026
low-level microwave power detector 79−54189
microbridge, thin film, nonreson. detection of Josephson radiation 78−43523
MM-wave and sub MM-wave receiver elements 80−11558
multilayer structure of semiconductor, dielectric and mag. film, constant EMF 79−69583
p-i-n diode, design technique for specific reverse bias characts. 78−34890
parametric amplifiers for radioastronomy at 18 and 1.35 cm wavelengths, characts. *(Russian)* 77−9658
photon detection in nonlinear tunneling devices, theory 79−6177
point contact microwave detector/receiver 77−79153
Schottky-barrier diode, sub-micron size, for submillimetre wave detection 77−34024
Schottky-barrier diode, submillimetre heterodyne detection 77−34028
semiconductor thin films, MBE, device appls. *(German)* 78−68630
SQUID magnetometer, broadband and higher-power, for small signal A-D convertor 78−62211
superconducting mm wave devices, present status 79−26119
superconductor-semiconductor contact amplification props. 79−7941
tunnelling and negative resistance phenomena in p-n junction devices, book 78−26947
Au-GaAs Schottky barrier diode, X-band applications 77−8192
GaAs and related cpds., conf., Edinburgh, Scotland (Sep 1976) 78−3039
GaAs, chem. etched surface, Auger characterisation 77−25169

solid-state microwave devices continued
GaAs devices and their use for generation and freq. conversion of microwave oscillations 80−15534
GaAs, diode chips, elec. characterisation 78−91791
GaAs FET, ion implantation, trends 80−39132
GaAs, laser-annealed ohmic contacts for microwave devices 79−73584
GaAs MBE physical characteristics and applications *(German)* 79−7618
GaAs, MBE prep., device props. 77−77417
GaAs MESFET fabrication using dual-bubbler CVD system 78−6856
GaAs, MIS structures, dielec. and interfacial characts. appl. to microwave MISFETs 79−60933
GaAs Schottky-gate FET and GaAlAs injection DH laser, monolithic integration 80−58593
GaAs thin film growth by MBE process, military appl. 79−52129
GaAs:Si(Se), ion implanted, laser annealing, appl. to microwave devices 79−69139
GaAs:Sn films, MBE power MESFETs 80−50563
n-GaAs/N-GaAlAs heterojunctions, microwave detection 79−54186
In-In_2O_3-Pb, Josephson tunnel junction fabrication for MM-wave detector 80−100427
$In_{1-x}Ga_xAs$, LPE, electron mobility and max. drift vel., microwave device appls. 77−77431
InP, MIS structures, dielec. and interfacial characts. appl. to microwave MISFETs 79−60933
InP, transferred electron device, relationship between microwave efficiency and metallurgical state of cathode contact 80−6981
n-InSb Corbino disc power meter for 3 cm wavelengths 79−71428
InSb film cyclotron-frequency submillimetric oscillation generation model 77−80801
Nb bridges, variable thickness, microwave mixing 77−85390
Nb superconducting C-band cavities for linear accelerator appl. 79−36432
Nb superconducting variable thickness bridges, mm wave response 79−28463
Pb-PbO-Pb, Josephson tunnel junction fabrication for Mm-wave detector 80−100427
n-Si, microwave and far IR hot carrier mobility, Monte Carlo calc. appl. to mm. transit time oscill. efficiency 78−72184
Si semiconductor switch using laser-excited solid-state plasma for pulse shaping, expt. 77−19397
Sn thin-film superconducting bridge microwave impedance anomalies 79−7942
W-Ni(Co) point-contact diodes as harmonic generators and mixers, DC bias dependence 80−75653

solid-state phase transformations
see also ageing; decomposition; ferroelasticity; ferroelectric transitions; glass transition; high-pressure solid-state phase transformations; martensitic transformations; order-disorder transformations; polymorphic transformations; precipitation; segregation; spinodal decomposition
ϕ^4 kink behaviour in presence of inhomogeneous perturbation 79−75692
A15 structure, O_h^3-Pm3n, group theory of phase transition 78−9992
A15 superconductors, electronic instabilities and phonon softening 79−95115
A^4-phonon theory, free energy and phase transition 78−41257
A-15 compounds, density of states model for lattice transforms. 80−65219
A-15 compounds, structured phase transition, renormalisation group theory 78−79743
A-15 compounds, superconducting props. and structural transition *(Russian)* 77−12052
A-15 space group struct., phase transitions, renormalisation group theory comparison with Landau theory 80−6489
ABO_3 and ABO_4 crystal types, transition *(Chinese)* 77−76553
absorption edge anomalies, phenomenological anal. 80−2718
AC induction at high temp., apparatus for transform. detect. 77−39674
actinide, compounds, f-electron systems with fluctuating valence, phase transitions 80−6789
actinide compounds, mag. ordering and struct. transforms. 77−20596
adamantane, plastic and solid-solid transitions, Raman study 80−60590
adsorbed layers, commensurate-incommensurate transitions, substrate defects effect 80−75437
alkali alkanoates, phase relationships and thermal behaviour branching effects 78−43111
alkali alkanoates, solid-state transitions, diffractometric and conductometric meas. 79−60507
alkali fluoantimonates, dielectric props. and structural phase transitions *(German)* 80−25274
alkali halides, polymorphic phase transition 77−80618
alkali hexahalogeno compounds: $ReCl_6^{2-}$($ReBr_6^{2-}$), low symm. splittings in vibronic spectrum due to phase transitions 80−55161
alkali hyperoxides, ionic π-electron systems, magnetogyration 80−93155
alkali metal fluo-perovskites, weakly discontinuous phase transition, linear birefringence obs. 80−11362
alkali metal hexachlorotellurates, $A_2(TeCl_6)$, (A=Cs, Rb, K), IR and Raman spectra, lattice and internal modes, phase transition 78−6659
alkali metal hexacupronitrates, incommensurate Jahn Teller phase transitions 79−95156
alkali tungsten bronzes, dynamic fluctuations between local struct. states in supercond. TI phase 78−26981
alkaline trihydrogen selenites, ferroelec. phase transitions, Raman spectra 77−8525
alkanoate, Li, Na, K and Rb salt mixtures, DSC anal. 78−10192
di-alkylammonium copper tetrachloride, weakly discontinuous phase transition, linear birefringence obs. 80−11362
alkylammonium tetrachloromanganate (II) IR and Raman spectroscopic exam. 78−31189
alkylene di-ammonium cadmium tetrachlorides, sp. ht. anomalies at phase transitions 80−70421
alkylene-di-ammonium cadmium chloride, influence of C atoms and metal ions on structural phase transitions 78−2256
allanite, metamict, phase changes on heating, age determ., x-ray fluoresc. anal. 77−51493
alloy, diffusive phase transform., boundary conditions 77−11693
alloy, quenched to sufficiently low temp., struct. function, long time behaviour 77−84886
alloy, role of phase boundaries in phase transformations 78−72772
alloy, struct. transform. during ageing, book contrib. 78−11199
alloy, temp. calibration of X-ray diffractometer furnace *(Japanese)* 79−6128

solid-state phase transformations continued
alloys, phase transition premonitory phenomena, exam. by electron diffr. and microscopy *(French)* 80−59651
alloys, precipitated phases, size, shape, distrib., diffusion controlled changes 80−3072
alloys with twinned martensite, crystallog. singularities in reverse martensitic transform. *(Russian)* 77−32571
almost commensurate structures, phase transitions and oscillation spectra *(Russian)* 79−4397
alumina gel, hydrated, prep. by homogeneous precipitation method, phase change by heating *(Japanese)* 77−25046
amethyst quartz, α-β phase transition, interaction of Dauphine and Brazil twins 77−62641
ammonium halides, phase transitions by Monte Carlo method using cubic Ising model 80−70408
ammonium hydrogen oxalate hemihydrate, low temp. dielec. and thermal props. 77−28510
amorphous alloys, struct. phase transition *(Chinese)* 79−82336
analyticity breaking in crystallographic model 79−77544
anharmonic crystal, lattice dynamics and stability, self-consistent phonon theory 79−51209
anharmonic phonons and structural phase transitions 78−14433
aniline hydrobromide, ferroelastic phase transition, Raman scatt. study 80−108195
aniline-HBr, ferroelasticity, orthorhombic to monoclinic phase transition, X-ray scatt. 80−39276
anthracene, electron diffr. of topochem. conversion and phase transition 78−83680
anthracene-phenanthrene-tetracyanobenzene, CT-cryst., mini-excitons and lattice dynamics, ESR, optical and Raman spectra 80−60406
anthracene-tetracyanobenzene, charge transfer complex, phase transitions, deuteration effect, mag. reson., spectral and thermal meas. 79−4412
anthracene-tetracyanobenzene charge-transfer complex, EPR of triplet excitons, phase transitions 77−28425
anthracene-tetracyanobenzene crysts., deuteration effect on phase transition, triplet state EPR study 80−50163
anthracene-trinitrobenzene complex, neat and mixed cryst. and glass opt. spectra 77−40274
aragonite, transform. to calcite in marine gasteropod 79−62485
asymmetrical Ising model, phase transitions 80−17891
atom probe techniques for phase transformation studies 80−3000
austenite, quenched and tempered, effect of bainitic decomp. products on mech. props. 77−56007
austenite formation, dislocation density effects, $\alpha \rightarrow \gamma$ transform. temp. *(Russian)* 77−8813
austenite transformation in hot rolled strips 80−55407
austenitic steel, 17G1S struct. and austenite transformation kinetics variation on deform. *(Russian)* 79−70060
austenitic steel, pearlitic transformation incubation effect, Mossbauer spectra *(Russian)* 79−70061
austenitizing during continuous heating, qualitative anal. *(French)* 77−81260
2-azanoradamantane N-oxyl, crystal-plastic transition, plastic crystal struct. exam. 78−2100
B-32 superstructure, instability in absence of many-particle interactions 77−58972
bainitic transformation, suppression in steels *(Russian)* 80−76247
benzene-fluorobenzene system, phase transitions, Raman spectra 79−91449
benzene-hexa-n-hexanoate, phase transitions and mesophase form., sp. ht. and IR spectra, 13 to 393K 80−79955
benzil, crystallographic study of solid-solid phase transition *(French)* 78−55939
benzil, ENDOR study of phase transition 79−73855
benzil, heat capacity near phase transition 78−2250
benzil, high temp. ODMR obs. of cryst. phases 79−38407
benzil, phase transition, far IR spectroscopy meas. 80−71407
benzil, phase transition study be simultaneous Raman-scatt. and domain-struct. investigations 79−60504
benzil, structural transition model, cryst. symm. spontaneous strain components 80−2161
benzylideneanilines, thermal parameters for cryst.-mesophase and cryst.-cryst. transitions 77−11679
bifurcation approach to phase transitions, external field inclusion 78−14446
binary alloy, quenched, time evolution of struct. function free energy 78−55937
biotite, temp. transformations, spinel formation 77−78163
1,1′-biphenyl, heat capacity anomalies due to successive phase transitions 80−96664
biphenyl, incommensurate phases, elastic neutron scatt. study 79−86887
biphenyl, phase transitions at 40 and 16K, transmitted light intensity meas. 78−51663
biphenyl, second order phase transition at 40K, Raman spectral obs. 77−32361
biphenyl-d_{10}, phase transitions at 38 and 24K, transmitted light intensity meas. 78−51663
bis(p-toluene sulfonate) diacetylene polymer cryst., second order phase transition 79−73922
bis(p-toluene sulphonate)diacetylene, monomer and polymer, solid state phase transformation, far IR transmission spectra obs. 80−55077
bis(propylammonium)tetrachlorocadmate, first-order phase transition, X-ray diffr. meas. 78−55826
bis-(p-toluene-sulphonate) of 2,4 hexadiyne 1,6 diol, X-ray scattering obs. of polymerisation mechanism and phase transition *(French)* 80−70399
bis-p-toluene sulphonate of 2,4-hexadiyne-1,6-diol, X-ray scatt., incommensurable modulated struct. obs. 80−70185
bis-tetraethylammonium tetrachloronickelate, heat capacity, structural transitions 79−65209
bis-tetraethylammonium tetrachlorozincate, heat capacity, structural transitions 79−65209
brass, massive transform. in presence and absence of special orientation relationships, nucleation kinetics 77−28808
brittle material, phase transform., plane stress anal. 77−86024
brittle solids, microfracture resulting from anisotropic shape changes 80−88254
9-bromo-meta-carborane, mol. reorientation, ^{1}H and ^{11}B NMR 77−16185
bromoform, solid, phase transform., dielec. dispersion and differential scanning calorimetric obs. 80−24582

solid-state phase transformations continued
caesium alkanoates, phase transitions, differential scanning calorimetry 77−43315
caesium propanoate, solid state transitions and melting process, diffr. and conductometric meas. 80−10670
dl-2,3-camphanedione, elec. cond., brittle-to-plastic region, cond. jump 78−39169
dl-camphor oxime, elec. cond., brittle-to-plastic region, cond. jump 78−39169
carbazole, birefr. meas., 20 to 190°C, crystal-to-crystal phase transform. 80−45031
carbon tetrabromide, phase I cryst. struct. 78−18626
carbon tetrabromide, phase II cryst. struct. 78−18623
carbon tetrachloride, cryst. phase transformations at atm. pressure *(French)* 77−84920
carbon tetrachloride, phase transform. process, energy-dispersive X-ray diffractometry 80−96631
carbon tetrachloride, solid, Raman study of phase transition and dynamic struct. 80−34916
carborane, ortho- and para-, phase transition and mol. reorientation, isomer effects, PMR obs. 80−80628
cast iron, hypereutectic, transform. of cementite to austenite 77−52318
CDW transitions, layer cpds. 77−59116
cell-preserving, space group theory of translation, twin and translation-twin boundaries 77−19892
cell-preserving phase transitions, new group theoretical approach 77−80619
cellular phase separation rate, extremum condition 80−2137
central peak phenomena and incommensurate structures, non-linear physics in crystals 80−10631
central phonon peaks, droplet model 77−43302
ceramics, microstructural consequences of phase transformation 80−3034
cetyliodide, cryst. phase transitions, mol. dynamics, spectroscopic and dielectric meas *(Russian)* 79−51965
chain-molecule crystals, phase transitions in semiflexible long-chain molecular crystals 78−91439
chevkinite and perrierite from Oslo region, Norway, phase change depend. on comp. 78−85533
chloral hydrate, phase transform. rate, ^{35}Cl NQR rate 80−54983
chloranil, mol. cryst., soft mode and central peak neutron scatt., struct. transition 79−42209
chloranil, neutron superlattice reflection, soft phonon and central peak scatt., phase transition 78−18732
chloranil, phase transition, Zeeman effect of ^{35}Cl NQR 78−59944
2- chloro-1,3,2-dioxa-arsolane, temp. depend. of NQR spectra parameters of ^{75}As and ^{35}Cl 80−20494
o-chlorobomobenzene, phase transition evidence from far IR absorption and Raman spectra 79−33693
cholesterol, solid-solid phase transitions, positron annihilation study 80−84289
cholesteryl oleate, solid-solid phase transitions, positron annihilation study 80−84289
cholesteryl oleate (linoleate), solid-solid transition, glass transition, cryst. nucleation temps., DSC obs. 78−34604
classical Ising model, crit. dynamics simulation in transverse field 78−59930
classification, according to mechanism and kinetics 78−26683
classification , using coupled double-well model 78−14443
coherent domain structures from crystal transitions with related space groups 79−42002
coherent phase form. at stress concentrators, effect of dislocation splitting, dislocation pile-ups, and phase elastic moduli *(Russian)* 80−49356
collective modes of CDW near lock in transition 78−30879
commensurable-incommensurable transition, Devil's staircase and harmless staircase, oscillating interactions through elastic stairs or other harmonic fields 80−88296
commensurate and incommensurate charge-density wave states, nearly half-filled Frohlich model 80−107723
commensurate and incommensurate structural phase transitions in Jahn-Teller system 80−70403
commensurate phases, spatially modulated, in simple Ising model 80−79909
commensurate-incommensurate transition in the quasi-one-dimensional Frohlich model with a nearly half-filled band 80−80199
commensurate-incommensurate transitions, conical points, Lifschitz invariants and superspace group characterisation 80−70367
composite growth by eutectoid or solid-state decomposition 78−44056
computer coupling of phase diagrams and thermochemistry 77−77460
conference, Masnuy-St-Jean, Mons, Belgium, Oct. 1979 80−82570
conference, phase transformations in metallurgy, York, England (Apr. 1979) 80−2994
conical points in the dispersion relation and related phase transitions 79−4393
continuous crystalline transitions, counterexample to maximal subgroup rule 80−59428
continuous phase transitions in structurally complex crysts., Landau theory, subgroup approach 78−14441
continuous spin model, exactly soluble, for mag. and distortive systems 77−85470
continuous transformations 77−8817
cooperative Jahn-Teller T-systems dynamics vibronic excitation branches 80−10934
coupled fields in one dimension: cross-over from a continuous symmetry to a discrete one 78−87758
coupled oscillator problem, crit. dynamics, renormalisation group approach 77−76522
Cr-Re binary system, isomorphous transition region, phase diag. *(Russian)* 77−55945
critical dynamics and quasi-elastic scattering, structural phase transitions 80−92641
critical fluctuations, classical and quantum scaling 79−35626
critical indices of primary and secondary order parameters using birefringence 77−28541
crossover exponents, crit. behaviour of quadrupole ordering parameter 77−66339
crystal irreducible problems, use of Clebsch-Gordan reduction 78−2052
crystal orientational disordering, thermodynamic props., stat. mech. model 80−96453
crystal stability and three-body interactions 80−79740
crystal symmetry changes due to structural phase transforms. 78−2056

solid-state phase transformations continued
crystalline films, dispersion law and struct. transition, Fermi line geometry, acoustic spectrum, resist. min. *(Russian)* 79−7764
crystalline substance, sequences of phase transitions *(Japanese)* 79−65194
crystals, coupled hydrodynamic modes near structural phase transitions 77−1203
cubic compounds of A15, C15 and B2 types, struct. phase transitions 77−4198
cubic compressible lattice, directional phase instability near 2nd-order transition 77−62616
cubic crystal, phase transitions with three-component order parameter, elastic anomalies *(Russian)* 79−37837
cubic crystal with antiferrodistortive interactions, Jahn-Teller induced structural phase transitions 77−11657
cubic crystals, commensurate nonLifshitz phases 78−18772
cubic crystals, tensile deform. induced transitions 80−59653
cyclobutane-$d_0(d_8)$, cryst. modifications, low. freq. Raman and IR spectra 80−7342
cyclohexane, solid, Raman spectra near 186K phase transition 78−56480
cyclohexane crystals, luminesc. emitted at 55 cm^{-1} near phase transition point 77−52180
cyclohexane-$d_0(d_6)$, plastic crystal phase transition, mol. reorientation, Raman scatt. phonon spectra 80−20631
cyclohexanol, low temp. solid phases, far IR absorpt. spectra, 93 to 303K 79−56785
DL-cysteine, phase transition obs. at 10°C *(French)* 80−49355
n-decylammonium cadmium chloride, perovskite-type layer cmpd. n-decylammonium chain dynamics 79−99313
defect influence on solid props. near phase transition 80−75334
defect structure near phase transition pt., effect on solid props. *(Russian)* 79−37838
detection techniques, review 80−2996
di(alkylammonium)$CdCl_2Br_2$, solid-solid phase transitions 80−84290
di(methylammonium) manganese tetrachloride, LF Raman spectra and phase transitions 77−63414
diacetylene monocarboxylic acids, multilayers, struct. phase transitions and polymerisability 80−80129
dialkyl ammonium cadmium chloride, influence of C ions and metal ions on structural phase transition 78−2256
dialkyl ammonium manganese chloride, influence of C ions and metal ions on structural phase transition 78−2256
dialkyl ammonium manganese chloride, phases and structural phase transitions, DSC and X-ray diffr. meas. 77−47574
dialkylammonium compounds, $(C_nH_{2n+1}NH_3)_2MX_4$, cryst. growth solubility, and props. 78−43999
dialkylammonium manganese tetrachloride, lattice consts. and phase transition temps. 79−86779
diamagnetic perovskites, AMF_3, Fe^{3+}-O^{2-} pair EPR probe for struct. phase changes 77−36113
diamantane, low temp. soft librational mode, Raman spectra exam. 78−30730
diamantane, plastic and solid-solid transitions, Raman study 80−60590
diamantane, Raman study of three solid-state phase transition 79−51946
diamantane, sp. ht., thermodynamics of transition and fusion 79−55899
diamond polycrystals, phenomenon of catalyst movement *(Chinese)* 77−77806
diatomic lattice, solitary wave solns., ϕ^4 kink, struct. phase transition, phonon dispersion curves 79−80544
p-dibromo-tetrafluorobenzene mol. cryst., in commensurate phase, quasielastic neutron scatt. 80−107386
dicalcium lead strontium propionate, mixed cryst., phase diagram, dielec. and dilatometric anomalies 77−11689
dicalcium strontium propionate, ferroelasticity and opt. activity rel. to transition 78−76420
dicalcium strontium propionate, ferroelasticity and optical activity rel. to transition 77−76547
1,5-dichloroanthraquinone, solid state transformation, X-ray powder anal. 79−51251
p-dichlorobenzene, lattice dynamics, thermodynamic functions and phase transitions 78−67777
o-dichlorobenzene, phase transition evidence from far IR absorption and Raman spectra 79−33693
4,4′-dichlorobenzophenone, phase changes, Raman spectra *(French)* 80−2756
Dicke model, modification for long wave photons 80−1169
dielectric singularity, causing Kohn anomaly and soft modes 79−60470
diethylammonium cadmium tetrachloride, dielec. props., phase transition 80−80675
p-dihalobenzenes, apparent NQR spin-spin relax. times obs. 80−54991
dihalobenzenes, IR and Raman spectra, phase transitions *(French)* 78−84557
p-diiodobenzene, far IR single cryst. transmission spectrum, temp. and polaris. depends., assignments 78−72498
dimethyl ammonium cadmium tetrachloride, dynamics of structural phase transitions 79−73309
dimethyl tin difluoride, crystallographic phase transition, 70K, Mossbauer obs. 79−47366
dimethyl tin difluoride, solid, methyl group motion, neutron scatt. study 80−10607
dimethylacetylene, solid-solid phase transition, NMR meas. 78−6583
dimethylammonium cadmium chloride, proton-^{14}N double reson. exam. of struct. phase transitions 77−4583
dimethylammonium cadmium tetrachloride type compounds, structural phase transition model 79−37829
dimethylammonium cadmium tetrachloride-type compounds, theory struct. phase transitions 80−10668
dimethylammonium iron tetrachloride, Mossbauer study of struct. phase transition 80−39278
dimethylammonium manganese chloride, perovskite-type layer structure submillimetric-wave spectroscopy 79−33540
dimethylammonium manganese tetrachloride, H-bonding, struct. transition, neutron diffr. study 79−42004
dimethylammonium manganese tetrachloride-d_6, structural and mag. phase transitions, neutron scatt. and AC susceptibility meas. 80−44825
2,2-dinitropropane, specific heat meas., adiabatic calorimetric method 78−71854
dipalmitoyl lecithin dihydrate, phase transforms., 20 to 70°C, X-ray diffr. obs. *(French)* 78−91436
dipolar lattice, 2-D, Monte-Carlo calc., lattice energy 78−14308
direct observation using TEM 80−2997

solid-state phase transformations continued
dislocations and lattice transformations, book contrib. 80−107242
disordering systems, multiple phase transitions 78−34595
distortive transition, three-dimens. one-component model, mol. dynamics 78−51646
double phase transitions, physical value anomalies *(Russian)* 80−59622
dynamic aspects, nuclear quadrupole relax. studies 78−76344
Earth interior, polymorphic phase transforms. rel. to geosynclinal processes energy sources *(Russian)* 78−96182
Earth mantle, phase boundary motion rel. to vertical crustal movements 77−49040
Earth mantle, phase transitions and gravit. differentiation effects on convection 80−51371
EBBA, liq. cryst., Raman and calorimetric evidences for existence of three solid modifications 77−77207
n-eicosane-n-docosane binary mixture, solid-solid phase transform. rate, positron annihilation meas. 77−20066
n-eicosane-n-docosane mixtures, positron lifetime spectra, temp. depend., phase depend. 78−18768
eight-vertex three dimensional phase transition model, disagreement with scaling law *(Chinese)* 77−35661
elastic anomalies near phase transition point *(Russian)* 77−80621
elastic constants, crit. behaviour near elastic phase transitions 80−100299
elastic constants anomalies near struct. transition, phenomenological theory 78−67765
elastic constants crit. behaviour near non-elastic phase transitions 80−100298
elastic phase transitions, crit. behaviour 78−79722
elastic phase transitions, crit. dynamics 80−2146
elastic phase transitions, order parameter and mode softening 80−75325
electron microscopy, conf., Nice, France (May 1977) 78−24889
electron microscopy, quantitative analytic studies 80−2998
electron probe microanalysis for high-temp. applic. *(French)* 77−29074
electron spin echo investigations 78−84476
electron-phonon interaction, matrix element calculation 78−79703
electron-phonon interactions, structural phase transitions *(Japanese)* 79−4384
electron-phonon interactions and phase transitions *(Japanese)* 79−65195
electronically driven phonon anomalies and phase transforms. 78−63834
EPR spectra, above crit. temp., cluster theory for dynamic crit. phenomena 78−6566
equilibrium conditions of solid phases 78−10171
ethane, solid, PMR line shape, band width and second moment, phase transition 77−85584
ethane, solid, thermodynamic props. between double solid-to-solid transition and triple point temp. 78−75828
ethylammonium tetrachloromanganate, dielec. props. in phase transition region 80−55011
ethylene, IR spectra, 15-85K 79−36638
eutectoid reaction, degenerate 77−52320
excitonic wave-phonon coupling, struct. transitions 77−15775
excitonic waves, role in distortive transform. 77−11861
FCC crystal, electron diffr. anal. of twin and HCP phase *(Chinese)* 79−10763
FCC to BCC transition, under [100] tensile loading, theory 80−39279
ferrite, transform. kinetics, grain size, alloying element effect, carbide precip. 80−93560
ferrite-austenite transition, C diffusion const. determ., rate const. of carburization and decarburization 78−48396
ferrocene, cryst., stable low-temp. phase 80−34185
ferrodistortive spin-phonon systems, crit. props. 80−88315
ferroelastic second-order transitions, cryst. unit cell modification, group theoretical anal. 79−37830
ferroelectric, $BaTiO_3$ type, thermodynamic analysis of struct. phase transitions *(Russian)* 80−103473
ferroelectric and other structural phase transitions at low temps. 80−75990
ferroic phase, commensurate, form. from prototypic phase, possibility of transition being second order 78−2223
ferroic phase transitions, non-mag., unified classification 80−70387
ferroics, nonmagnetic secondary and higher-order, order-parameter symmetries for the phase transitions 77−85668
ferrous alloys, phase transforms. and ordering, Mossbauer spectroscopy 77−12619
$FeSb_2S_4$ crystal, berthierite, at 348K 77−47821
film, phase transition dynamics, investigating device 78−22967
FIM atom probe technique, suitability for continuous phase transforms. obs. 78−35621
fine fragmented crystals, complex struct. analysis by electron microscopy 80−104416
first order transitions induced by single irreducible representation 80−70365
first-order phase transitions, clusters, metastablility, nucleation 78−54326
first-order transitions, finite-size rounding rel. to entropy, system size 80−59623
Fischer-Tropsch wax, NMR investigation 80−7186
fission reactor materials, constitution changes due to radiation effects 80−34048
furan, adsorbed on NaCl, evidence of new condensed phase, IR spectra *(French)* 80−16028
gamma-ray diffractometry, phase transitions, domain structures, twinned texture studies 80−19678
geikielite, solid soln., phase transform. during reduction *(Russian)* 78−44042
glasses, inorganic, struct. by X-ray scatt. diffr. obs. 80−84069
glasses, inorganic, thermal expansion coeff. rel. to phys. props. 80−49389
grain and phase boundaries between crystals, conf., Konigstein, Germany (Oct. 1977) 78−72762
graphite, intercalation compound, C_8Rb, elastic and inelastic neutron scatt. 78−30597
graphite, self focusing high current relativistic electron beam for structural and chemical transformations *(Russian)* 80−15190
graphite intercalation compounds, props. and appls. 78−71711
graphite intercalation compounds, two-dimensionality, structural phase transitions 80−19938
graphite-nitrate residue compounds, phys. props. 78−10199
graphite-Rb, intercalation cpd., superlattice struct., electron diffr. study 80−75214

solid-state phase transformations continued
Green's function theory in quadrupolar-coupled quasi-Heisenberg system 79−38340
gypsum, struct., vibr. spectroscopic obs. *(Russian)* 78−15175
gyrotropic phase transitions 78−71852
H-halide, phase transition theory 77−15580
haematite reduction to magnetite, stress development mechanism *(Russian)* 80−93553
hard disc thin layer, solid-solid phase transformation 80−79908
heat-resisting alloys, VM-1 and VX-4, thermal fatigue rel. to struct. changes *(Russian)* 78−11302
heterogeneous solid state reaction, Avrami parameter calc., modified Kissinger method 78−92239
hexamethylbenzene, IR polarised spectra 79−28758
hexamethylethane, crystal structures and phase transitions, X-ray diffr. study 79−73158
hydroxyapatites, dipolar reorientations, TSC study 80−60491
ilmenite, solid soln., phase transform. during reduction *(Russian)* 78−44042
impurities, interaction and diffusion, near structural phase transition of matrix 79−42083
impurity centres and phase transitions *(Russian)* 80−10907
incommensurably distorted structures, review 80−10665
incommensurate phase, light scatt., order parameter fluctuation *(Russian)* 80−93354
incommensurate phase transitions, exptl. studies of soft phonons 78−75798
incommensurate phase transitions under existence of Lifshitz invariant 78−22822
incommensurate structural phase transition, and phason *(Japanese)* 78−30758
incommensurate structural phase transitions and phason interpret., review *(Japanese)* 78−22827
incommensurate structures, defectibility and frustration, devil's stair case transform 80−75333
incommensurate structures phase transitions *(Czech)* 80−88294
incommensurate-commensurate phase transition, model 78−87760
incommensurate-commensurate transition, Ginzburg criterion and crit. behaviour 80−70368
induced electron tracks and structural phase changes in MCr_2O_4 type cryst. *(Dutch)* 79−1585
inert gas adsorbed on graphite, phase transitions using Landau model 79−69243
intermediate valence compounds, phonon produced instabilities, periodic Anderson model 78−79964
interstitial solutions, impurity subsystem free energy, impurity distrib., temp. depend. 80−44232
Invar, phase stability, spinodal decomposition 80−88327
ionic crystal defects, mag. reson. studies 80−108066
Ising chain with several phase transitions, Monte Carlo simulation 79−12732
Ising models, generalised with degeneracy, Lee-Yang theorem 78−65879
Ising universality class, structural phase transform., real-space renormalisation calc. 80−39255
isomorphic transformation, characterisation of hysteresis processes *(Russian)* 80−80562
itinerant magnets and superconductors, structural instabilities, phase diagrams 78−14922
IV-VI compounds, conditions for structural transitions 77−51497
IV-VI compounds, phase transitions induced by electron-phonon interaction 80−10656
IV-VI compounds, structural instabilities and transverse effective charges 77−27999
IV-VI mixed compounds, structural phase transition 80−15242
IV-VI semiconductors, crystal structure and symmetry of electron spectra, doping effects *(Russian)* 79−7696
J-ferroics, rotational-invariant classification of structural phase transitions 80−70369
Jahn-Teller cooperative phase transition, helical ordering 79−46778
Jahn-Teller cooperative system, US attenuation, appl. to TmZn 79−78053
Jahn-Teller system, thermodynamic properties, internal stress effects 80−59679
Johnson-Mehl and cellular microstructure, comparative analysis, computer simulation 80−54392
kaolinite, optical spectroscopy study of structural changes at 700-1000°C 79−65193
kaolinite to mullite reaction series, reexam. of solid state phase transformations 78−64535
kaolinite-mullite thermal sequence, intermediate cubic phase 80−25652
KCN, relax. times of F-centres meas. at 83K phase transition 77−59458
Landau theory, thermodynamic potential models, mag. reorientation 80−103456
Landau theory of structural phase transitions 80−92639
laser light scatt. spectroscopy 78−10156
latex films, surface struct., vulcanisation, radiothermoluminesc. obs., 100-230K 78−75575
lattice constant fluctuations, influence on thermal props. of cryst. 79−77715
lattice dynamics, conf., Paris, France (Sept. 1977) 78−59869
lattice dynamics of centre with close electronic levels, temp. effects 79−37804
lattice internal rearrangement modes, correlation betwen lattice structural and magnetic structural transitions 78−47987
lattice oscillation modes nonlinear reson. induced struct. transition *(Russian)* 77−31746
lattice-dynamical model, crit. exponents calc., statistical mech. treatment 77−84880
layered structure metals, transport props., book contrib. 77−43566
Lifshitz's criterion for symmetry changes in second-order phase transitions 79−4392
Lifshitz invariant, time-reversal prop. 78−67679
light scattering near phase transition pts. in pure and defect containing crysts., review 80−93361
light scattering on central peaks *(Japanese)* 78−52522
light scattering studies, in book 80−2774
linear diatomic rigid mol. chain, mol. dynamics, rot. phase transformation, struct. factors 78−26635
lithium n-alkanoates, long-chain, thermal and phase props. 77−62619
low temperature depend. of elec. resist., mag. suscept., heat capacity, Hall const. *(Russian)* 78−30900
solid-state phase transformations continued
low-lying vibrational modes and theory of local and transport props. at transitions 78−14425
lunar pyroxenes, cation distrib. and exsolution as chronological indicator of thermal history 78−45246
macroscopic quadrupole effects as method of obs. of struct. transforms in crysts. 80−71321
magnetic binary alloys, phase separation, double Ising system 78−91835
magnetic field effect on critical temp. *(Russian)* 77−11667
magnetic materials, transparent, optical studies of phase transitions 77−66481
magnetically ordered cryst., dislocation drag, magnetoelastic waves 80−103332
malonic acid, phase transition at 360K, IR study 80−44311
malononitrile, cryst., phase transitions, Raman and IR obs. 80−88980
massive transformations, free energy, microstruct., growth and nucleation 77−4776
materials interactions, stability, phase transformations, thermodynamics and corrosion 78−88444
melting curve extrema from repulsive step potential, molecular dynamics calc. 77−59102
memory alloy, pseudoelastic, model for first-order phase transition 80−92642
mercury carboxylates, phase transitions, DTA 79−90759
metahalloysite, dehydration, lattice transformation mechanism 77−31780
metal, dislocations rel. to electron gas thermodynamics at $2^1/_2$th order transition *(Russian)* 78−51910
metal, electron-phonon interaction, magnetism influence 77−73040
metal, Fermi surface topological transition, electron-phonon interaction contrib. calc. 80−6697
metal, sound absorpt. coefficient at phase transition of order $2^1/_2$, effect of geometry of const. energy surfaces 77−39769
metal halides, fluorite structure, retarded ionic motion 80−88361
metal-H system, solubility, mobility, and phase transitions, book contrib. 79−82350
metal-insulator transition study, electron microscopy *(French)* 78−26815
metals, FCC, 'brass to copper' transition in rolling textures 80−76246
metals, ferrous and non ferrous, exam. of abnormal deformations and transformations *(French)* 78−60714
metals, wave movement, resonance phenomena in deformation zone during rolling *(Russian)* 80−65123
metals and alloys, critical temperatures determination, elec. resist. method, IMASh-5S-69 installation 80−71827
metals and alloys, thermodynamic and mechanistic classification review 80−2995
metals and alloys, use of dilatometric methods *(French)* 79−5100
methane, and $-d_4$, solid-phase transitions, hysteresis effects 79−99316
methane, solid, phase II, Raman spectrum, vol. and temp. depend. 80−97260
methane, solid, phase II, theory of phase transitions 77−51494
methane, solid, thermodynamic props. from US velocity obs. 79−46753
methane-d_1, tunnelling states and nuclear spin conversion 79−10944
methane-d_4, solid, sound velocity meas., 4-77K 78−75734
methane-d_4, solid, thermodynamic props. calc. using significant structures method, 6 to 87K 80−24616
5-methyl-1-thia-5-azacyclooctane-1-oxide perchlorate, single cryst. transform., evidence for intermediate state 80−88078
methylammonium bromide, solid, phase transitions, PMR, DTA study 80−107421
methylammonium hexahalometallates (IV), halogen NQR obs. of struct. phase transition 79−95673
methylcyclohexane, differential thermal anal. under high press. 78−51669
microcline, maximum, room temp. phase transition, heat capacity meas. 80−54373
microcline, maximum room temp. phase transition, unit cell parameters, thermal expansion 80−54208
microscopic approach to theory 78−51460
migrating orientable lattice defects 2D systems 79−77719
mixed valence compounds, structural phase transitions, effect of electron-phonon coupling 79−33265
mode condensation, ferroic space group in transition sequence *(Japanese)* 77−43300
modulated ordered phases, superspace group description *(Chinese)* 80−8942
molecular crystal, anomalous thermoelastic behaviour and orientational transition 77−76334
molecular crystal, semiflexible long-chain mols., phase transition 77−80615
molecular crystal, two-dimensional, with random pairwise interactions orientational phase transition 79−60478
molecular dynamics of structural phase transitions in two dimens. model 77−20038
molecular substances, positron annihilation and phase transitions, review 78−95614
montmorillonite, Co^{2+} form, optical spectroscopy study of structural changes at 700-1000°C 79−65193
Mossbauer isomer shift at phase transitions, book contrib. 79−87352
Mossbauer radiation crit. scatt. in condensed matter 79−56635
Mossbauer spectra, struct., electronic and mag. props. 79−91320
multicomponent diffusional impregnation, role of phase transformations 77−62686
naphthalene, single crystal, anomaly in permittivity, Costa Ribeiro effect 80−7258
naphthalene-tetracyanobenzene, charge transfer complex, phase transitions, deuteration effect, mag. reson., spectral and thermal meas. 79−4412
naphthalene-tetracyanobenzene, Raman spectra, phase transition and isotopic substitution 78−80364
nepheline containing ceramic masses, phase transform. during firing 77−66611
neutron scattering conference, Gatlinburg, TN, USA (June 1976) 79−41910
nitrocomplexes, planar dynamic Jahn-Teller effects 77−15804
N-nitrodimethylamine-do,(-d_6), structural phase transition, Raman study 80−34911
NMR near second order struct. transition, effect of crit. slowdown 79−73846
noble metal complexes, hexafluoro, review of struct. obs., pseudorot., press. effects 78−6045
non-ferroic phase transitions, group theoretical methods 80−70388

solid-state phase transformations continued
non-ideal systm, generalisation of scaling hypothesis 79−19356
non-IPS geometric surface relief effects rel. to diffusional phase transform. 77−15667
non-linear elastic thermal stress analysis with phase changes 78−79218
nonlinear elastic media, second order phase transitions *(Russian)* 80−24583
nonlinear lattice dynamics, mol. dynamics simulation 78−59921
nonlinear lattice dynamics, molecular dynamics studies 79−77713
nonlinear system, kink-phonon interaction 79−73262
nonstoichiometric materials, lattice instabilities, models 78−14442
NQR studies, elec. field effects 80−20488
nuclear quadrupole splittings in phase transitions 80−20489
nucleation, kinetics for parallelepiped crit. nucleus shape 77−31773
nylon 6, influence of monomer and water diluents on mech. relax. 79−4993
nylon II, high-press. X-ray structural study 78−14296
octafluoronaphthalene, struct. phase transition exam. 77−47572
octafluoronaphthalene crystals, phase transition, Raman spectra 77−24829
octaphenylcyclotetrasiloxane, phase behaviour and nucleation kinetics 80−29168
oil shales, review of thermophysical properties 79−100479
olivine to spinel transition kinetics, rel. to deep-focus earthquake genesis 77−5190
one-dimensional metallic systems, theory of structural phase transitions 78−38830
opaque minerals alteration states correl. with temp. in active geothermal system 78−40551
ordered regions near macroscopic defects and percolation phase transform. in crystals *(Russian)* 80−92665
ordering solid solution, many particle correls. coupled Green function eqns. *(Russian)* 77−72675
organic charge transfer crystals, transport props., phase transitions, mol. dynamic *(German)* 80−39507
organic compounds, investig. by Rayleigh scatt. of Mossbauer radiation *(Russian)* 77−69760
organic crystal, appl. of TEM 80−24327
organic reactions in solid state 80−21309
orientation relations, from relative orientations of final phase, diffractometric determ. *(Russian)* 77−44240
orthovanadates, centrosymmetric exhibiting cooperative Jahn-Teller effect, dielec. props. 79−28694
PAC method appl. *(German)* 80−2679
n-paraffin, cryst., first-order phase transition 77−80615
n-paraffin, crystals, phase transitions, statistical theory 80−44290
paraffin, polymer modelling, mol. motion, thermal expansion and phase transitions 78−51436
paraffin crystals, molecular motion, thermal expansion and phase transitions *(German)* 78−67837
passive microwave radiometry as a tool for investigating phase transitions 79−23729
pearlitic transformation, effect of ultrasound *(Russian)* 78−67823
Peierls transition in quantizing mag. field, possibility 80−103441
periodically distorted crystals, phonon-type symmetry 77−39553
Permalloy film, implanted with C ions, HCP struct. formation, electron diffr. study *(Russian)* 79−82469
perovskite, ABO_3, crit. dynamics, nuclear relax. 78−75805
perovskites, instability and phase transition splitting at non-ferroelec. structural phase transitions 80−44314
phase boundaries in first-order phase transitions, dynamics stability 80−107403
phase diagram with first-order transition close to second-order transition 80−59625
phase diagrams, step pot. particles, 2- and 3-dimens., mol. dynamics 79−28072
phase transformation, $\alpha \rightleftarrows \beta$, influence on mech. props. *(Russian)* 78−68681
phase transition to incommensurate excitonic phase 80−75510
phase transitions, appl. of TEM 79−68988
phase transitions, induced by several order parameters, thermodynamic parameters 80−103457
phenanthrene, crystalline, Raman band intensity temp. depend. 77−59564
phenanthrene, low freq. Raman spectra intensity temp. depend., phase transition, conformation change 77−36211
phenanthrene, phase transition, Raman spectral obs. 77−59112
photoacoustic effect 80−69615
photoemission electron microscopy, use in phase transformation continuous obs. 80−2999
phyllosilicates, struct. inheritance in transforms. under hydrothermal conditions *(French)* 79−34802
physics of transitions, introduction 78−26660
pigeonite, high-low transformation rel. to antiphase domains exptl. coarsening 80−81886
pivalic acid, ^{13}C NMR chem. shift, plastic-brittle transition 80−2652
plastic crystal-crystal transition, mol. and lattice symm., Landau theory 78−42929
plastic deforms ands rupture mechanisms, depend on B additives *(Russian)* 79−61650
Pm3n space group struct., phase transitions, renormalisation group theory comparison with Landau theory 80−6489
polaronic crystals, central peak 78−47712
poly(vinylidene fluoride) films, poled, piezoelec. activity and field-induced cryst. struct. transitions 80−20592
poly(vinylidene fluoride) phase II, field induced phase transitions 80−96640
poly [nitrilo-bis(phenylamino)phosphoranetriyl]s, synthesis and characterisation *(Italian)* 77−66755
poly-p-xylylene, α-β phase transition, electron microscopy study 79−69241
polyarylates, sorpt. kinetics of tetrahydrofuran, struct. transform *(Russian)* 79−51432
polybutylene terephthalate, hysteresis of stress-induced cryst. phase transition 78−31404
polydiacetylene, reflection spectra, thermochromism, temp. hysteresis and phase transformation 78−19452
polydiacetylene cryst., electronic struct. change at phase transition, Raman spectra 78−2833
polyethylene, crystalline struct. transitions 77−51496
solid-state phase transformations continued
polyethylene, struct. transform. under tension in liqs. *(Russian)* 77−51492
polyethylene terephthalate, amorphous state change by heat treatment below glass transition temp. 78−30550
polyhedrisation of quinary metallic systems with isomorphic intermediate phases *(Russian)* 80−45270
polyimide, influence of monomer and water diluents on mech. relax. 79−4993
polymer film, conformational transitions, activation energy determ. *(Russian)* 78−48186
polymer glass, isothermal struct. relax., in high elasticity transition region, mol. model *(Russian)* 78−87629
polymer systems, binary, high mol. wt., phase transform. assoc. with spinodal decomposition 79−70062
polymer-filler system, glass transition *(Japanese)* 77−51479
α,ω-polymethylene diammonium metal (II) tetrahalides, cryst. growth, solubility and props. 78−43999
polyorganosiloxane-talc composites, high-temp. transitions 79−52152
polyphenyls, inelastic neutron scatt. study of structural phase transitions 79−51255
polysulphur nitride:bromine, struct. and phase transition 80−24382
polysynthetic phases, thermodynamics of formation in stress field 78−67808
polyvinylidene fluoride, elec. field induced phase changes 79−11387
polyvinylidene fluoride, structural phase transitions, statistical mech. theory 79−82331
polyvinylidene fluoride-PMMA blends, dynamic mech. props. and sonic velocity, cryst. phase transitions 78−26454
potassium acetate, thermal expansion 79−51280
potassium alkanoates, phase transitions, differential scanning calorimetry 77−43319
potassium chloranil, IR spectra, mag. and optical props., phase transition and solvation 77−43983
potentially incommensurate but eventually commensurate phase transition, Verwey transition in Fe_3O_4 as example 79−95120
1,3-propylenediammonium manganese tetrachloride, vibr. study of phase transitions, IR and Raman spectra 80−40103
proteins, globular, crystalline, intermol. interactions, denaturation, DSC and X-ray diffr. obs. 80−16897
protohaematite, transformation to maghaemite in CsI discs 79−69259
prototype and prototypic phase explained 78−38833
pseudo-one-dimensional system, Ginzburg-Landau theory of phase transitions 77−15529
pseudoion form factors, rel. to energy differences in phase transitions 77−62617
pseudopsin system with dynamic long-range forces, Z-branch at phase transition 77−84887
pseudospin-phonon system exam. 78−10157
PTFE, shape change during 19°C phase transform. 78−76646
pyrazine, cryst. phases, entropy changes and struct. implications 80−54397
pyrazine, phase transitions, sp. ht., X-ray diffr., LF vibr. spectra 78−43122
pyrene, far i.r. spectra, phase transition effects 77−1685
pyrene, low temp. phase transform., TEM obs. 78−22851
pyrene crystal, mechanism of structural phase transition 78−30757
pyrene crystals, anomalous emission excited near absorption edge 80−100682
pyrene-tetracyanobenzene, charge transfer complex, phase transitions, deuteration effect, mag. reson., spectral and thermal meas. 79−4412
pyridinium pentasilver hexaiodide, sp. ht. and cond., gradual solid electrolyte transition 77−76604
pyridinium silver iodide, fast ion conductor, phase transitions, thermoelec. power meas. 80−107540
PZT, polycrystn., thermal expansions, elasticity and internal friction 80−35238
quantum crystal, ground-state lattice vacancies and Bose-Einstein condensation 77−7943
quantum effects in second order phase transition described by $\mu\phi^3+\lambda\phi^4$ model 78−24752
quartz, birefr. and opt. rot. near structural phase transition points 78−75823
quartz, fundamental and second harmonic light scattering by α-β coexistence state 77−69086
quartz, incommensurate phase near $\alpha \rightleftarrows \beta$ transition pt. 79−90748
quartz, light scattering polarisation props. at α-β phase transition 80−108220
quartz, optical SHG and γ-ray diffr. results 78−14459
quartz, phase transform. in brittle materials, plane stress anal. 77−86024
quartz-cristobalite transform. kinetics 78−11223
quasi-one-dimensional electron-phonon system, electron jump effect on phase tansition *(Russian)* 80−92673
quasi-one-dimensional system, first and second order phase transitions, qualitative theory 78−31086
quasielastic light scattering near phase transitions 80−93362
quasione dimensional crystal, phonon spectrum change due to struct. transition 78−67789
quasione dimensional crystals, effect of band filling on features of struct. transition 78−2424
p-quaterphenyl, Raman spectra, struct. transitions 79−19870
random system, crit. behaviour near 2nd order phase transition lines intersection 78−68276
rare earth alloys, RCo_2, elec. resistivity, thermopower, X-ray struct. meas. 80−24874
rare earth compounds, $RThNbTiO_8$, synthesis and cryst. struct. *(French)* 78−83799
rare earth dicarbides, solid solns., phase transformation, strain energy 78−51672
rare earth intermetallic cpds., cryst. field effects rel. to mag. props. 80−59933
rare earth intermetallics, structural instabilities 80−24587
rare earth metals and some alloys, X-ray diffraction obs. of magnetostriction and phase transitions 77−73068
rare earth orthovanadites, phase transitions and Jahn-Teller distortions 79−28548
rare earth orthovanadites, RVO_3, magnetic and cryst. struct., Jahn-Teller effect 77−32169
rare earth oxide film, short-range order to long-range order transition 78−10288

solid-state phase transformations continued
rare earth pentaphosphates, spectroscopy, ferroelastic/ferroelectric coupling, soft mode frequencies, phase diagram 79−19845
rare earth perovskites, prep. and props. book contrib. 80−44193
rare earth zircons, Jahn-Teller cooperative phase transition, crossover effects 80−88316
rare earth-Al, RAl_2, spontaneous cell distortion due to cryst. field, magnetoelastic consts. 77−63255
rare earths, compounds, K X-ray line shift associated with valency change and isomorphous phase transitions 79−47553
rare-earth $CaWO_4$, phase transitions of fergusonite-scheelite *(French)* 80−19942
rare-earth germanides, R_5Ge_3, thermal expansion, phase transition effects 80−70433
rare-earth oxides, non stoichiometric phases in thin films 79−7755
rare-gas monolayer, adsorbed on graphite, commensurate-incommensurate transition 79−69244
Rayleigh critical surface wave velocity near phase transitions 77−35803
$RBCaF_3$, cubic to tetragonal X-ray diffr. examination of temp. depend. lattice consts. *(French)* 78−10184
Recalloy, Fe-Nb, semihard magnetic alloy, magnetic props., hardness, microstruct. 78−56660
refractive indices and electro-optics at ferroelectric and structural phase transitions 79−19850
refractory films, stability, high temp. and electron irrad. effects 77−39747
reinforced plastics, equations of state, taking account of mech. damage 80−97553
rigorous bounds, quantum anharmonic phonon model 77−15541
rotational phase transition in ferroelectrics and other crysts., Ising model 77−4605
rubidium propanoate, solid state transitions and melting process, diffr. and conductometric meas. 80−10670
second order phase transition, nonvalidity of Lifshitz condition, appl. to heavy lanthanides *(Chinese)* 78−51643
selection principles, unitary groups appl. to cryst. tensor components 79−46589
self consistent theory in exactly soluble model *(Russian)* 79−95121
self-consistent phonon field method 79−33065
semi-infinite systems, critical behaviour 78−4563
semicarbazide hydrochloride, phase transition, IR spectra and thermal study 79−37833
semiconductor, compensated, phase transition of impurity electrons interacting with lattice 77−24535
semiconductor, homologous series, semicond.-metal transitions, homeomorphous, polymorphous and morphotropic transitions 79−37988
semiconductor, phonon spectrum in mag. field, renormalisation 79−28060
semiconductor film, laser-induced transmittance oscills. and struct. phase transitions 79−87516
semiconductor physics, conf., Edinburgh, Scotland (Sept. 1978) 79−95303
semiconductor-metal transition, structural transformations 79−23897
short-term local phase and polymorphic transforms. and changes of inner states in solids 79−14913
silicate rocks, quartz-stishovite transitions, shock wave processes 79−88347
single crystal growth during massive transformations 78−56629
single-particle properties of systems undergoing struct. phase transitions 78−26654
sodium n-alkanoates, long-chain, thermal and phase props. 77−62619
solid electrolyte dielectric permeability, phase transition to superionic state *(Russian)* 80−49403
solid electrolytes, phase transitions and thermodynamic states 77−84975
solid solutions, congruent transformation pt., regular soln. theory 79−60477
solid solutions, interstitial phase struct., reconstructive transition struct. symm. relationships 79−69246
soliton solutions to nonlinear phenomena 78−59880
spectroscopic properties of crystals of C_{4h}, D_{2d} and D_4 symmetry at second-order structural transform. 78−22845
spherical system of transition parameters, reducible but unreduced 77−31751
spherical-like model, isolated impurity behaviour near displacive phase transition 78−71821
spinel solid solutions, $A_xB_{3-x}O_4$ type, quasichemical method of cluster components, electron exchange allowance 79−51475
spinel-garnet peridotite transitions in upper mantle, evidence from harzburgite xenolith 78−65309
squaric acid, 2-dimens., phase transition studied by Raman scatt. 79−82330
squaric acid, $C_4H_2O_4$ and $C_4D_2O_4$, theory 77−15585
squaric acid, dielec. const. and PMR near struct. phase transition 79−10946
squaric acid, ferroelasticity, elastic hysteresis loop and domain struct. 79−55814
squaric acid, structural phase transition, US vel. meas. as function of temp. below and above T_c 79−14927
squaric acid, two dimensional antiferroelec., Brillouin scatt. at structural phase transition 80−71430
squaric acid, two-dimens., phase transition, elastic neutron scatt. 78−6155
stearic acid, single cryst., characterisation *(Japanese)* 79−46587
steel, 0.2 to 0.8% C, ferrite-pearlite transformation, tensile strength, cooling rate effect 80−7549
steel, 12Cr2MoWVTiB, transformation mechanism and fine structure of (M-A) phase, TEM study *(Chinese)* 80−66500
steel, 18KhNMFA, transform. of austenite during continuous cooling 77−44245
steel, 34KhN1MAR structural heterogeneity of 70 ton ingots γ to α transform, in dendritic section 77−70047
steel, 35KhN3MFA, 25KhN3MFA, bainite transform. kinetics and mech. props. *(Russian)* 78−80539
steel, 7.1% Cr, $\alpha \rightarrow \gamma$ transformation, studied by internal friction meas. *(French)* 77−25043
steel, α to γ phase transform., during rapid resistance heating, apparatus for investigation *(Slovak)* 78−19742
steel, alloy, Fe-C-Zn (0.45, 1.56 wt.%), pearlite transformation during continuous cooling 78−80538
steel, alloy, mechanical properties, morphology, transform. kinetics and composition interrelations 77−86146
solid-state phase transformations continued
steel, alloy, transform. from austenite 77−25045
steel, alloy, type HSLA, exam. of NbCN precipitation by elec. resistivity meas. 78−84822
steel, alloy, type ST.5, structural and phase changes after high temp. heating *(Russian)* 80−55439
steel, alloy, V-W-Mo-Cr, exam. of carbide transformation 80−16299
steel, austenite form. from ferrite-cementite mixtures, HVEM obs. 77−66639
steel, austenite hot deformation influence on phase transformations 80−7606
steel, austenitic, 16H2NMB, struct., texture and mech. props. of product of transform. 78−92273
steel, austenitic, Cr-Mn-B-N, phase composition and struct. transformations 80−104171
steel, austenitic, deform., struct., transform. kinetics hot working effects *(Russian)* 77−52361
steel, austenitic, low-C, transform. kinetics rel. to temp., deform., struct., mech. props. 79−24519
steel, austenitic, metastable, 0Kh14AG12M, Cr-Mn and Cr-Mn-Ni, phase transform. kinetic effect on mech. props. *(Russian)* 79−34024
steel, austenitic, pearlite transform. kinetics, effect of US deform. *(Russian)* 77−21136
steel, austenitic, phase transform to pearlite and martensite, kinetics, stresses due to quenching, anal. *(Japanese)* 78−27508
steel, austenitic, supercooled ShKh15, stability, effect of spheroidising carbides *(Russian)* 77−25074
steel, austenitic→pearlitic transformation, partitioning, atom probe microanal. 80−3079
steel, austenitic 30KhGSN2A, bainite transform., US strain effects *(Russian)* 77−73269
steel, austenitic stainless, Cr-Ni, elec. resistivity and struct.-mag. transitions at low temp. 79−99527
steel, austenitic stainless, fracture toughness and transition temp., T_{50}, effect of cooling rate and supercooling temp. 78−84987
steel, austenitic stainless, plastically deformed, TEM obs. *(French)* 77−44302
steel, austenitic stainless, tensile fracture, phase transform. effect, comparison of stable and metastable phases 78−60798
steel, austenitic stainless, weld, ferritic-austenitic solidification mode 80−89214
steel, austenitic supercooled, transformation kinetics into spheroidised pearlite *(Russian)* 78−95742
steel, austenitic type KO 34, microstruct. changes on electron beam welding *(Hungarian)* 80−104252
steel, bainitic, invariant plane strain theory, determ. of habit planes and orientation relationships 80−55388
steel, C, autectic, sintered, isothermal transformation behaviour, porosity effects 80−3031
steel, C, ferritic-pearlitic transform., kinetics, struct. aspects *(French)* 78−68685
steel, C, mech. props. rel. to heat treatment, ferrite-pearlite transform. *(French)* 79−20043
steel, C, structural transform. and surface hardening by laser treatment 77−70233
steel, C, thermal stresses in submerged arc welded joint, consideration of phase transformations 79−61683
steel, C and Co, carbide transitions during post-strain ageing and tempering *(Russian)* 78−95741
steel, C content influence on brittle and tough fracture, heat treatment *(Russian)* 80−40500
steel, C-Mn-(Cr), structural changes during stress cycling after heat treatment and cold rolling *(Russian)* 78−19787
steel, C-Mn-Cr-Mo (0.4, 0.8, 1.1, 0.25 wt.%) C, Ni, Mo, Cr addition effects on toughness of bainite 78−11327
steel, carbide form. depend. on Mn, Cr, V additions, cementite stabilisation, microstruct. *(Russian)* 80−55399
steel, case carburised, residual stress effect in mech. performance 79−24659
steel, Cr, lower bainite transform., significance of carbide precip. 80−97476
steel, Cr, phase transform., effect of high temp. plastic deform. *(Slovak)* 78−19837
steel, Cr (0.5 wt.%), austenite-pearlite transformation 80−97480
steel, Cr (1 to 5 wt.%), effect on transform. of Cr content and all round press. of 25 kbar *(German)* 78−11219
steel, Cr (3.51, 3.74, 3.56 wt.%), bainite transform. of deformed austenite 77−32574
steel, Cr-C (13, 0.15 wt.%), bainitic transform. *(German)* 78−11218
steel, Cr-C (3.74, 0.86 wt.%), stress assisted bainitic transform. *(Czechoslovakian)* 77−32573
steel, Cr-Mn, carbide transform. *(Russian)* 79−33997
steel, Cr-Mo (2.8, 1.6 wt.%), atom probe anal. of bainitic phase boundaries 80−71990
steel, Cr-Mo-V, creep, effect of microstruct., heat treatment, transform. temp. 78−11248
steel, Cr-Mo-V pressure vessel, microstruct. parameters and yielding rel. to plastic deform. 80−89318
steel, Cr-Ni, carbide transform. *(Russian)* 79−33997
steel, Cr-Ni-Mo, handbook data for type 34KhN1M 79−78960
steel, Cr-W(Mo), quenched, carbide reactions during tempering 80−89229
45 steel, current pulse effects on struct. at crack tip *(Russian)* 77−44332
steel, En 24, Cr, V, deform. effect on decomp. of austenite, carbide precipitation 80−84938
steel, eutectoid, anisothermal strain with phase transform., effect on tensile strength *(Russian)* 80−40431
steel, eutectoid, U8, cold hydraulic press. forging effect on transform. and heat treatment *(Russian)* 79−52235
steel, eutectoid and hypoeutectoid stress relaxation during rapid heating transform. *(Japanese)* 78−11258
steel, Fe_2O_3, transformation to Fe_3O_4 in oxide scales conversion kinetics 80−7561
steel, Fe-Mo-C low-alloy, photoelectron microscopy of diffusional transformations 77−44242
steel, Fe-V-C (1, 0.2 wt.%), austenite formation 80−84927
steel, ferritic, Cr-Mo (2.25, 1 wt.%), C and Nb influence on structural transformations *(French)* 80−84925
steel, ferritic containing N, continuous transformations 80−7585

solid-state phase transformations continued
steel, ferritic-bainitic welded by electron beam, morphology and struct. of heated zone *(French)* 77−73292
steel, first order phase transformations, in non-isothermal conditions, exam. of kinetic parameters *(Russian)* 79−34028
steel, free plate elastoplastic stress condition 78−95781
steel, high alloy, strain induced martensite and austenite influence on crack formation *(Russian)* 80−21007
steel, high Mn alloy G22, phase transform. during plastic deform. 77−16576
steel, high-C martensite, struct. transforms. during low temp. tempering *(Russian)* 77−59737
steel, hypereutectoid, austenite dissociation depend. on strain at intercritical temps., pearlite transform. *(Russian)* 80−40362
steel, Kh2G2P, high-temp. plastic strain influence on austenite transformation kinetics *(Russian)* 80−21004
steel, low alloy, bainite transform. behaviour, struct., toughness 78−27513
steel, low alloy, bainitic transform., isothermal studies 77−36497
steel, low alloy, sintered, isothermal transformations, porosity effects 80−3032
steel, low alloy and C, bainite morphology 78−68682
steel, low alloyed (Mo,Cr,B), structural and mech. props., report *(French)* 80−25691
steel, low C, austenite transform., TTT diagrams 77−70031
steel, low C, Cr-Ni (25, 25 wt.%), σ phase form., prestrain effects *(Japanese)* 78−92260
steel, low C, high C, bainite transform. heat treatment effects *(Czech)* 77−63661
steel, low C, transition behaviour, bending speed effect *(Japanese)* 78−11222
steel, low C, with Mo and B, proeutectoid γ to ferrite transform. *(French)* 77−73270
steel, low C (0.01-0.05 wt.%), structural and mech. props., report *(French)* 80−25691
steel, low pearlite, Ti addition effect on transform. behaviour *(German)* 77−90343
steel, low-alloy, transform. of austenite, cooling rate effect 79−38821
steel, low-C, transformed by cooling in ferritic-pearlitic range, relations between cooling rate, struct. and mech. props. *(French)* 77−32570
steel, maraging, Fe-Cr-Co-Mo, phase transforms. during high temp. austenitisation and solid soln. decomp. *(Russian)* 80−66524
steel, maraging, Hart's model in hydrogen embrittlement 79−24621
steel, maraging, steady state unidirectionally solidified, austenite reversion and determ. 77−25118
steel, maraging stainless, phase transformation and mech. props. rel. to heat treatment *(Chinese)* 80−66501
steel, martensite, high C, tempering, nuclear gamma reson. meas. *(Russian)* 79−1883
steel, martensitic, Cr-Ni, grain refining and phase transforms. effect on plasticity *(Russian)* 78−39837
steel, medium C, Nb addition, effect on transformation and strength 80−7607
steel, Mn, H_2 embrittlement mechanism *(Korean)* 78−68774
steel, Mn-B-V, low alloy, transform. singularities *(Russian)* 80−104116
steel, Mn-Ni-Cr-C, supercooled austenite, influence of constant mag. field on diffusional decomp. *(Russian)* 79−4964
steel, Mn-Si-Cr-Mo, dual phase, as-rolled, continuous cooling transformation diagram to optimize composition 80−100829
steel, Ni(9 wt.%), isothermal bainitic transform., thermomechanical effects on mech. props. *(German)* 80−40383
steel, Ni-Mn (16, 2 wt.%), 40N16G2, single crystal, stabilisation and destabilisation mechanisms *(Russian)* 78−23732
steel, Ni-Mo-C (2.0, 0.2, 0.4 wt.%) sintered, struct. transforms. and mech. props. after quenching 80−66557
steel, Ni-S-(Mn), ferrite to austenite transform. effect on sulphide precipitation 77−86025
steel, pearlitic, strength, fracture, microstructure effect 77−40449
steel, pearlitic and bainitic transformations in austenite, processes during incubation period 80−40348
steel, phase separation, effect of plastic deform. and heat treatment *(Polish)* 78−92295
steel, proeutectoid reaction, review 77−4777
steel, rimming, cold rolled, low alloy, radiation capacity *(Russian)* 78−14486
steel, Si, metallography of bainitic transform., carbide precipitation 78−27527
steel, stainless, 0Kh13N7, 0Kh13AN7, thermocyclic treatment effects, on struct. phase composition and mech. props. 78−44204
steel, stainless, 18-8 type polycrystal, strain induced γ to α' transform. *(Japanese)* 78−11221
steel, stainless, austenitic, H_2 induced transformation obs. *(Japanese)* 80−11640
steel, stainless, austenitic, precipitation hardening and N_2 effects obs. *(Rumanian)* 77−55973
steel, stainless, constitution changes due to radiation effects 80−34048
steel, stainless, ferrite to austenite decomp. 80−93554
steel, stainless, ferrite to austenite decomposition 80−3073
steel, stainless, high-strength 0Kh11N10M2T, phase transform. 77−70046
steel, stainless, stress relieved, microstruct. transformations resulting from ageing 80−71644
steel, stainless, type 304L, neutron irradiated, in-reactor precipitation and ferritic transformation 79−77644
steel, stainless, wire, effect of stress on phase transformations 78−44119
steel, stainless 316, ion implanation produced crystalline phase transitions 80−7558
steel, stainless volume changes during phase changes, meas. using low temp. differential scanning dilatometer *(Russian)* 79−34224
steel, strengthening by rapid electrothermal treatment 78−84870
steel, structural, austenite form. during heating *(Russian)* 77−32572
steel, structural recrystallisation, phase and struct. transformations during heating 77−55990
steel, tempered martensitic, type AISI 410, role of C in embrittlement phenomena 80−93652
steel, Ti (0.1 to 0.55 wt.%), strengthening by carbide precipitation 77−25062
steel, tool, NC6, carbide lattice, kinetics of its destruction *(Polish)* 78−92280
steel, transformations, influence of type of cold plastic strain *(Russian)* 79−52232
solid-state phase transformations continued
steel, type 30KhGSN2A, influence of US on γ-α transformation kinetics *(Russian)* 79−74148
steel, V, precip. and transform. kinetics, effect of N 80−97485
steel, Zi, high permeability grain-oriented, AlN precip. study 79−83337
steel 12Kh1MF, fine struct., effect of isothermal transform. temp. 77−21137
steel 18Kh2N4MA, phase transformations and props. 77−12614
steel ball bearing, fatigued, phase changes, nomenclature 80−89198
steel low C, γ-α transform. kinetic rel. with self-diffusion characts. *(Russian)* 78−67850
steel Ni-Cr-Ti-C (2.8, 0.9, 0.2, 0.73 wt.%), ferrite, orientation in pearlite, rel. to austenite *(Russian)* 80−81072
steel stainless, plastic deform. of single crystal, contribution of $\gamma \rightarrow \varepsilon$ transform. 77−52394
steel transition temp. determ. from fibrous structure in fracture, exam. of method 78−85080
steel VNS-2, damping capacity, magnetomechanical, phase transform. effects 78−31445
steel XC80 isothermal and pearlitic transform. mech. prop. meas. using dilatometer *(French)* 78−31598
steels, thermal hardening stress determ. by thermoplasticity theory 79−29076
stepped ordering in binary solid solutions 78−67807
structural phase transformations, static critical behaviour 80−92640
structural phase transition, computer simulation 79−77721
structural phase transitions, applicability of thermodynamic theory 80−2139
structural phase transitions from hypothetical phase 78−83938
structurally incommensurate systems, commensurate-incommensurate phase transitions 78−91418
structurally incommensurate systems, disordered-incommensurate phase transitions 78−91417
structurally incommensurate systems, fluctuation spectrum, incommensurate phases 78−91419
structurally incommensurate systems, transition and excitations 80−44293
styrene acronitrile copolymer, glass transition temp. determ. by elec. meas. 78−47506
succinonitrile, defects in plastic phase, positron annihilation obs. 80−11504
succinonitrile, phase transition, Raman spectrosc. obs. using low-temp. sample holder 78−86342
sulpholan, molecular solid, laboratory frame and rotating frame spin-lattice relax., pulsed NMR meas., phase transitions obs. 80−93197
superconductivity, effect on cubic to tetragonal structural transition due to two-fold degenerate electronic band 79−4615
superconductivity and lattice distortion, three-dimens. models anal. 77−8225
superconductivity and structural instability 79−38294
superionic conductor, statics and local dynamics near phase transition 80−107542
superionic conductors, microscopic theory 78−79809
superionic conductors, phase transitions and dynamics 78−59924
superionic crystals, phase transitions 78−75826
superionic fluorites, structure and transport 80−84318
sym-triazine, Landau mean field description, second-order phase transition, soft modes 80−108434
sym-trioxane, phase transition, polarised Raman spectra obs. 80−84742
symmetry determined phenomena, ferroicity 79−46800
1T-TaS_2, nearly commensurate phase, harmonics effect on phase transitions 78−14462
TBBA, dielec. const. in cryst. and smectic phases 79−78607
TBBA, new cryst. phase, calorimetric meas. 79−51254
TCNQ alkali salt spin-Peierls transition 80−29395
TCNQ alkaline salts, phase transitions, vibronic intensity enhanced IR spectra 78−23441
TCNQ anion radical salt, $[(C_6H_5)_3PCH_3]_{1-x}{}^{+}[(C_6H_5)_3AsCH_3]_x{}^{+}(TCNA)_2{}^{-}$, phase transition and phase diagram 77−76555
TCNQ anion radical salts, phase transition $\alpha\gamma \rightarrow \beta\gamma$, volume change 78−26684
TCNQ anion radical salts, solid solns. phase transition, heats of mixing 78−47519
TCNQ ion radical salt, DECA$(TCNQ)_2$, IR absorpt. spectra obs. of first-order transition 80−71397
TCNQ salt, alkali transition metal, elec. cond. and phase transition 78−43370
TCNQ salt, DECA $(TCNQ)_2$, struct., phys. props. and irreversible phase transition 78−6273
TCNQ salt, HMTSF-TCNQ, lattice phase transitions and conduct. anomalies obs. 77−1226
TCNQ salt, MEM$(TCNQ)_2$, phase transition electronic struct. interpretation 80−24781
TCNQ salt, MEM$(TCNQ)_2$, phase transitions, elec. cond., ESR, mag. susceptibility study 80−24981
TCNQ salt, N-propyl-quinolinium$(TCNQ)_2$, defect conc. depend. phase transition 80−44577
TCNQ salt, NH_4-TCNQ, crystal structure and phase transition 78−91330
TCNQ salt, NMeQn$(TCNQ)_2$, phase transition, role of acetonitrile solvent 78−60119
TCNQ salt with MDCA cation, first order phase transition 79−73122
TCNQ salts, Mn$(TCNQ)_2$ and hydrates, mag. and elec. props. 79−82767
TCNQ salts, modulated struct., dynamical processes, X-ray and neutron scatt. 79−95155
TCNQ-K, X-ray exam. of phase transitions 78−55933
TCNQ-Na, X-ray exam. of phase transitions 78−55933
TCNQ-Rb, X-ray exam. of phase transitions 78−55933
TCNQ-TSeF, crit. behaviour at electronically driven struct., phase transition 77−80767
TEM, appl. to organic solid-sate chemistry, review 79−60235
ternary systems, triangulation parameters correl. with isomorphic intermediate phases *(Russian)* 79−52203
p-terphenyl, carrier generation and transport, temp. depend. around phase transition at 180K 78−47783
p-terphenyl, far IR absorption spectra, 300-1.3K, phase transition obs. *(French)* 77−90140
p-terphenyl, long range order at phase transition, neutron diffr. exam. 77−1228

solid-state phase transformations continued
p-terphenyl, phase transition, heat capacity meas. 79−46801
p-terphenyl, Raman spectra, struct. transitions 79−19870
tetraalkylammonium tetrahalometalates, opt. lifetimes rel. to thermal transitions 77−28608
tetracene, cryst., solid-state transitions, Raman spectra, prompt fluoresc. in mag. field 79−99865
tetracene, photoluminescence spectra, 4.2-300K, phase transition and excitons 79−4847
tetracene single crystals, exciton refl. spectra, 4.2 to 300K 79−47478
1,2,4,5-tetrachlorobenzene, lattice dynamics, thermodynamic functions and phase transitions 78−67777
sym-tetrachlorobenzene, LF Raman bands and space symmetries 77−66504
tetramethylammonium cadmium chloride, EPR of Mn^{2+} meas., near structural phase transition 77−59452
tetramethylammonium hexabromotellurate, far IR and Raman spectra and phase transitions 80−11376
tetramethylammonium hexachlorotellurate, IR and Raman spectra, lattice and internal modes, phase transition 78−6659
tetramethylammonium manganese(II) tribromide, cryst. struct. at 235 and 115K 78−63745
tetramethylammonium octahydrotriborate, NMR study of proton and B dynamics 80−93200
tetramethylammonium tetrachlorocuprate, incommensurate phase, neutron diffr. study 80−79935
tetramethylammonium tetrachlorocuprate crystal, incommensurate-ferroelastic (commensurate) phase transition obs. 80−75352
tetramethylammonium tetrachlorozincate, incommensurate phase study, ferroelectric-paraelectric phases *(French)* 80−88318
tetraphenyldithiapyranylidene triiodides, elec. cond. and thermoelec. power 79−56207
(TETTF)$(TCNQ)_2$, charge transfer complex, phys. props. and phase transition 78−64032
theory, lattice dynamical aspects 78−75797
theory, using differential geometry 78−67805
thermal conductivity, anomalous temp. behaviour near structural phase transition *(Russian)* 80−75394
thermal conductivity, quasi-elastic scattering of phonons near transition 79−82299
thermal diffusion-soft mode coupling near struct. phase transition, hydrodynamical anal. 79−60468
thermal expansion of crystals, book 80−73115
thermodynamic relations, appl. to K_2ReCl_6 80−29164
thermodynamic theory for cryst. props. behaviour near structural transitions *(German)* 78−38809
thiourea, deuterated, commensurate-incommensurate phase transition, inelastic neutron scatt. 79−28098
thiourea, incommensurable phase transitions. thermodynamic pot. 80−79941
thiourea, lock-in phase transform. 80−29698
thiourea-cyclohexane inclusion compound, phase changes, molecular motion exam. 78−31116
three dimens. pure substance with two critical points, model 79−69239
Ticonal with Sm, magnetic props., phase transform. after thermomagnetic treatment 78−3155
tilted perovskites, influence of ionic radii on transition temp. 80−24590
TMMC phase behaviour, DTA using Ge-Ag thermocouple 79−65186
TMNC, phase transition, low temp. far IR spectra 79−24309
TMTSF-DMTCNQ, role of individual stacks in phase transition 79−73307
tool steel transformation hardening by CO_2 laser 80−16483
transition element compounds, supercond. props., lattice symm. and instability 77−8224
transition metal, dichalcogenide layer cpds., bonding and phase transitions 80−34186
transition metal alloys, ω-phase transform, structural model 77−77472
5d-transition metal antifluorite crystal, struct. props. and lattice dynamics, mag. struct. 80−44268
transition metal complexes, A_2MX_6, d-electron config., effects on phase transitions 77−35687
transition metal compounds, Jahn-Teller effect in solid state chem. 79−47061
transition metal dichalcogenides, periodic lattice distortions, charge density waves 79−82536
transition metal film, chemical compound formation by ion bombardment 78−30846
transition metal layer compounds, Fermi surface anisotropy effect on struct. transitions 77−51661
transition points determination via AC conductance meas. 77−55341
translational symmetry changes in struct. phase transitions 77−62500
Tremolite, fibrous, high temp. phases, transformations, DTA 79−77742
n-triacosane, chain axis cryst., quasi-elastic neutron scatt., plastic phase transform 78−6023
triamantane, plastic and solid-solid transitions, Raman study 80−60590
s-triazene, second order phase transition, mol. reorientation, ^{14}N NQR 78−48074
s-triazine, mol. cryst., low temp. mol. reorientation, phase transition, ^{14}N NQR 77−36150
s-triazine, sp.ht. 130-380K, melting enthalpy and solid-state transition 79−46812
s-triazine, structural phase change, lattice energy calc. 78−55945
s-triazine, structural phase change, sp. ht. meas. 78−55944
s-triazine, structural phase changes, X-ray diffraction and NQR reconciliation 79−46798
s-triazine, structural transitions, low temp. phase 78−55943
trimethylammonium cadmium chloride, $(CH_3)_3NHCdCl_3$, struct. phase transitions 79−1502
tris-sarcosine calcium chloride, ferroelec., ferroelasticity and hypothetical hexagonal to orthorhombic phase transition 77−63377
n-tritriacontane, non periodic molecular motions, neutron scatt. study 79−51024
TSCC ferroelastic monodomain crysts., dielec. behaviour 79−42888
$(TSeF)_x(TTF)_{1-x}TCNQ$, struct., cond., phase transitions 78−47770
TTF(MBDT) spin-Peierls transition, mag. exchange interactions, mag. props. 80−25138
TTF-$CuS_4C_4(CF_3)_4$, quasi-one-dimens. antiferromag., spin-lattice dimerisation, X-ray scatt. obs. 77−85464
TTF-DETCNQ, metal-insulator transition, struct., elect. cond. and sp. ht. expts. 78−14662
solid-state phase transformations continued
TTF-halides, conductors with chain struct., lattice phonons and distortions, incommensurability transitions 80−24549
TTF-TCNQ, CDW and phase transition exam. 78−6283
TTF-TCNQ, CDW transition with tripling of period along chains 80−96805
TTF-TCNQ, commensurate ordering 77−7829
TTF-TCNQ, coupled Peierl's systems, model, phase transitions 77−69230
TTF-TCNQ, crit. behaviour at electronically driven struct. phase transition 77−80767
TTF-TCNQ, deuterated, phase transition exam. by elastic neutron scatt. 77−4194
TTF-TCNQ, divergent mag. responses at $2k_F$ and structural phase transitions 80−20376
TTF-TCNQ, Landau theory of phase transitions 78−30914
TTF-TCNQ, Landau theory of phase transitions 80−92666
TTF-TCNQ, lattice distortion, displacive transform., Landau theory 77−31743
TTF-TCNQ, lattice phase transitions and cond. anomalies obs. 77−1226
TTF-TCNQ, neutron and X-ray diffuse scatt., phase transitions, one-dimens. behaviour and interpret. 78−10381
TTF-TCNQ, ordering types below 54K, perp. phase depend. 78−6300
TTF-TCNQ, periodic lattice distortions, charge density waves 79−82536
TTF-TCNQ, phase transition model, interchain coupling of CDW 77−76558
TTF-TCNQ, phase transitions, thermoelec. power meas. 79−65464
TTF-TCNQ, phason instability at 49K phase transition 77−4303
TTF-TCNQ, possible Lifshitz point, struct. transitions exam. 78−2423
TTF-TCNQ, single cryst., mag. susceptibility in phase transition region, two-gap model 78−6511
TTF-TCNQ, sp. ht. meas., phase transition obs. at 46K 77−43326
TTF-TCNQ, struct. phase transitions, coupled phasons model 78−83942
TTF-TCNQ, symmetry changes and phase transitions 78−6299
TTF-TCNQ, theory of structural phase transitions 78−38831
TTF-TCNQ, X-ray exam. of $2k_F$ and $4k_F$ anomalies 78−10162
TTF-TCNQ, Young's modulus, temp. depend., rel. to transition points 77−15475
TTF-TCNQ phase transition, press. depend., longitudinal lockin, stacking axis resistivity meas. 78−47520
TTF-TCNQ powder, phase transition at 49K 77−89539
tungsten bronze, tetragonal, type structure cpds, transition sequences *(French)* 77−89538
two-dimensional triangular octopolar array, orientational order and phase transitions 79−95257
two-electron level with quasidegenerate levels, local phase transitions and temp. effects in lattice dynamics 80−10666
two-level tunnelling system, phonon interaction theory 77−15525
unijunction transistor, negative resistance as phase transition, critical exponents *(French)* 80−49746
unsteady heat conduction accompanied by an endothermic solid reaction *(Japanese)* 79−76939
urea, low temp. phase transition, X-ray diffr. expts. 79−1501
V-Ru, electronic states calculation 78−95255
valency change, sound vel. renormalisation *(Russian)* 78−79963
Vicalloy 1, dilatometric anomalies and α to γ transform., effect of heating rates *(Russian)* 78−39762
vicalloy-2, high heating rate effect on mag. props. *(Russian)* 77−81328
vinylidene fluoride-trifluoroethylene film, cryst. phase transition 80−66120
viscoelastic materials, glass-transition temp., thermodynamic criterion 77−59783
waves, finite amplitude, in solid undergoing phase transitions *(Russian)* 79−28100
wavevector reversed ultrasound studies 80−75306
weak Lifshitz condition, allowed types of ordering in second-order transitions 78−87769
white cast iron, plasticity in impact toughness, bending angle tests 77−56039
X-ray diffractometry of struct. transitions in single crysts. 79−52483
X-ray studies at low temp., automatic system 77−15281
xylideneaniline-p′-benzonitri 80−44328
zeolites, Na, Cs, Sr types, processing radioactive waste soln., thermal transform. 77−10477
SnTe-PbTe-GeTe, alloy semiconductor, phase transition *(Japanese)* 78−91443
Ag complex, dioxane perchlorate, cryst. struct., phase transitions, X-ray study 80−59646
Ag-Al, dislocation interactions with migrating interphase boundary electron microscope obs. 77−55963
Ag-Al, plastic flow enhancement during massive transformations 78−48468
Ag-Al (26 at.%), massive transform, $\beta \rightarrow \zeta$, crystallography and morphology 80−97475
Ag-Cd (approx. 50 at.%), disordered hcp to ordered bcc transition, meas. of activation energy 78−72773
Ag-Cu-Sn(Zn)(Au), effect of additions on eutectic and peritectic temp., of binary alloys 78−84801
Ag-Ga (27 at.%), cooling rate depend. of thermal arrest, transform. temp. 79−29053
Ag-Ga(In)(Sn)(Te) thin film couples, room temp. interactions, struct. transformations 80−2220
Ag-Te amorphous films, effect of annealing on elec. resist., phase transitions 79−11241
Ag-Zn (27-48 wt.%), interphase β'-ζ transform., thermal expansion exam. 77−63630
Ag-Zn alloy, deposited under controlled potential, spontaneous transformations obs. 78−51853
Ag_3AsS_3, low temp. struct. transition 79−69245
Ag_3AsS_3, phase transition near critical pt., spin-lattice relax. *(Russian)* 79−38397
Ag_3AsS_3, proustite, structural changes in low temp. phase transition, NQR study 80−19935
Ag_3AsS_3, rel. to US absorpt. and vel. anomalies, 4.2-100K 77−24361
Ag_7AsS_6, thermal, crystallographic and elec. props. *(French)* 80−40338
Ag_7AsSe_6, thermal, crystallographic and elec. props. *(French)* 80−40338
$AgClO_3$, NQR and thermal expansion investig. of phase transform. 77−12229
$AgClO_3$, NQR freq. of ^{35}Cl, temp. depend., phase transition 77−12228
$AgClO_3$, structural phase transition, ^{35}Cl NQR meas. 80−15819

solid-state phase transformations continued
$AgFeSe_2(S_2)(Te_2)$, elec. props., band gap *(Russian)* 79−11116
$AgFeTe_2$, Mossbauer parameters in phase-transition region 80−11308
α-AgI, fast ion conductor, phase transitions, thermoelec. power meas. 80−107540
AgI group superionic conductor, phase transition detection by thermoelectric power method 80−92669
AgI solid electrolyte α-phase stabilisation 80−29209
α-AgI, superionic conductor, soft-core model, Monte Carlo study 80−54430
α-AgI type superionic conductors, struct. and phase transition *(Japanese)* 79−65250
$Ag_{26}I_{18}W_4O_{16}$, solid electrolyte, anisotropic elec. cond., low temp. phase transitions 80−65289
$Ag_{26}I_{18}W_4O_{16}$, struct. phase transition, dielectric, cond. and Raman obs. 79−19368
$Ag(NH_3)_2Ag(NO_3)_2$, phase transition, mol. motion, PMR obs. 78−88203
$AgNbO_3$, cryst. growth and phase transitions 80−40243
Ag_3SBr, ionic conductivity in temp. range 93-573K, X-ray diffr. and DTA 80−79988
Ag_3SBr, superionic conductor, phase transition, struct. 80−107144
Ag_3SI, ionic conductivity in temp. range 93-573K, X-ray diffr. and DTA 80−79988
Ag_3SI, superionic conductor, struct. and phase transition *(Japanese)* 79−65250
Ag_2SO_4, enthalpies of transition and fusion 79−10925
Ag_2Se, X-ray determ. of inclusion function 77−76559
Ag_8SnSe_6, phase transition, thermal expansion meas. 78−14466
Al alloy, columnar to equiaxed transition on solidification 77−63655
Al complex, Al $urea_6(ClO_4)_3:Cr^{3+}$ structural phase transition, ESR meas. 77−20681
Al film, vacuum deposited, structural changes during annealing at temp. near melting point 78−84096
Al, struct. stability 77−8015
Al-Al_2O_3, amorphous crystalline phase transition, effect on electronic states 79−69595
Al-Al_3Ti, directionally solidified, thermal stability during annealing, 435-660°C 80−108393
Al-Cu (4 wt.%), non IPS geometric surface relief effects associated with diffusional phase transform. 77−32575
Al-Ga, face centred cubic struct. stability, melt equilib., α-Ga effects 78−18766
Al-Mg, homogenisation process, effect of solidification rate and alloying *(Polish)* 79−78949
Al-Mg-Si, heterogeneous precipitation studies using differential scanning calorimetry 80−3062
Al-Mn, cooling after recrystallisation, phase transform., X-ray and thermal anal. *(Russian)* 77−66663
Al-Zn (30 wt.%), metastable phases, transformation kinetics, quenching rate effects meas. 77−55960
Al-Zn (30 wt.%), precipitation sequences and transformation kinetics, X-ray diffr. and TEM obs. 77−55959
Al-Zn alloy, small-angle neutron scatt. in crit. point regions, 324-435°C *(German)* 77−85993
Al-Zn alloy, solid state eutectoid transformation 79−74146
Al-Zn-Mg, plastic deform. influence on structural transform. and mechanical props. *(Russian)* 80−7623
Al_3Mg_2, diffusionless phase transformation 80−104150
Al_2O_3, thermal anal. using solar heating *(Ukrainian)* 79−77725
β-Al_2O_3-Ag_2O, stoichiometric A phase, X-ray diffuse scatt. obs., sublattice phase transition 80−64944
Al_2O_3-CaF_2, phase relns. 78−23700
Al_2O_3-Na_2O-Li_2O, phase transformations during firing 80−3036
β-Al_2O_3-$Na_2O(Ag_2O)$, Raman scatt., 12-400K, 2nd order phase transition 77−81091
β″-Al_2O_3-NaO-LiO_2, stabilised, effect of phase composition, grain size, on Na ion cond. 78−47582
Al_2O_3-Pr_2O_3, phase diagram at high temps. *(Japanese)* 78−88449
Al_2O_3-SiO_2 system, solid state transform. of andalusite to mullite 80−16281
Al_2O_3-Sm_2O_3, phase diagram at high temp. *(Japanese)* 78−92253
Al_2O_3-ZrO_2 dispersed system, thermal diffusivity/conductivity, effect on microcracking resulting from phase transform. 78−10231
$Al_2O_3(H_2O)_3$, gibbsite, synthetic, crystallinity and topotactic reactions, X-ray diffr. obs. 78−63851
o-$As_2B_{10}H_{10}$, ^1H and ^{11}B CW NMR, mol. reorientation in cryst., phase transition 77−85583
As_2Te_3, phase transitions and elec. cond. 78−10440
Au small particles in glass, transition cluster-solid state 79−33593
Au-Cu (50% at.), pretransitional fluctuations *(French)* 80−2160
Au-Cu-Ag, phase transform. effect on mech. props. *(Russian)* 78−3122
Au-Cu-Ga, solid soln., phase systems, valence electron density effects *(French)* 78−19724
AuCu II plates, growth mechanisms 77−48423
$Au_{11}Mn_4$ ordered phase formation, electron diffr. and microscopy study 80−107418
Au(110), spin polarised LEED 78−18508
BN, cubic, growth pressure-temp. region in system BN-Mg 79−66053
BN, rel. to artificial production of growth twins 78−30641
BN, self focusing high current relativistic electron beam for structural and chemical transformations *(Russian)* 80−15190
BN, wurtzite-type, lattice distortions 77−11636
BN:C, hardening by doping, p-T diagram, cryst. struct. *(Russian)* 77−77491
$Ba_2Bi^{3+}Bi^{5+}O_6$, structure and elec., mag., thermal props. vs. temp. X-ray and neutron powder diffr. study 79−19189
$BaCl_2(F_2)$, sp. ht. meas., Schottky-type diffuse phase transitions, defect form. energies and entropies 80−107441
$Ba(ClO_4)_2$, anhydrous, phase transition obs. *(French)* 78−83939
$BaCl_2.2H_2O$ rel. to artificial production of growth twins 78−30641
$BaMnF_4$, antiferromag., dielec. anomalies at low temp. obs. 77−20791
$BaMnF_4$, incommensurate phase, Brillouin spectra 79−42981
$BaMnF_4$, low temp. dielec. props. and phase transitions 77−20790
$BaMnF_4$, low temp. phonon, and exciton effects on polarisation 79−42905
$BaMnF_4$, mag. and structural phase transitions, neutron scatt. obs. 79−87259
$BaMnF_4$, struct. and mag. transitions, magnon dispersion curves, nearest neighbour exchange consts. 79−42760
$BaMnF_4$, struct. phase transition, optical parameters obs. 80−100328

solid-state phase transformations continued
$Ba(NO_3)_2$, low temp. struct. changes, elec. props. 79−87377
$Ba_2NaNb_5O_{15}$, ferroelastic transition sequence, cooperative pseudo-Jahn-Teller model 77−35689
$Ba_2NaNb_5O_{15}$, incommensurate refls. near ferroelastic transition, neutron and X-ray precession obs. 80−70395
BaO film, depend. of struct. on thickness 78−2391
$BaO.Al_2O_3.2SiO_2$, hydrothermal synthesis, phase transitions 77−48378
$BaSnF_4$, thermal expansion and phase transitions 79−77781
$Ba_2TiGe_2O_8$-$Ba_2TiSi_2O_8$, pseudobinary system, pyroelectricity and related props. 78−95553
$BaTiO_3$, 3d element doped, phase stability, phase transition temp., mag. susceptibility meas. 78−38835
$BaTiO_3$, piezoceramic, elastic normal wave propagation, phase transitions *(Russian)* 80−40067
$BaTiO_3$, polycryst., phase transition obs. in −170 to 220°C range *(Russian)* 80−103474
$BaTiO_3$ type crystal, thermodynamic analysis of struct. phase transitions *(Russian)* 80−103473
$BaTiO_3Fe_2O_3$, photoacoustic effect, first order phase transitions at increasing and decreasing temp. 80−70320
$BaVSe_3$, one-dimensional, struct. and mag. props. 80−28993
$Ba(V_{1-x}Ti_x)S_3$, synthesis and struct. phase transitions 80−107415
Be-bronze BrB2, struct. and phase transform. during mechano-thermal treatment *(Russian)* 80−11667
$BeO+SiO_2+V_2O_5$, reaction kinetics and mechanism, phenakite formation 78−23608
Bi_2MoO_6, superplasticity during phase transitions 80−108498
Bi_2O_3-Sm_2O_3 eutectoid system, isothermal deformation 77−63625
Bi_2O_3-SrO, solid state phase diagram, thermal and high temp. X-ray anal. *(French)* 79−65190
Bi_2S_3-Bi_2Se_3 and Bi_2Te_3-Bi_2Se_3 systems, thermal cond. change during phase transitions 80−100368
$Bi_{1-x}Te_xO_{3/2+x/2}$, solid solutions, phase transformations, dielectric and differential microcalorimetry *(French)* 79−55886
$BiVO_4$, ferroelastic domains, electron microscopy and electron diffr. obs. 80−100254
$BiVO_4$, ferroelastic phase transition, thermodynamic theory 79−37832
$BiVO_4$, ferroelastic phase transition, birefringence meas. using rotating-analyser method 80−80742
$BiVO_4$, ferroelastic transition, soft optical phonon mechanism 79−51230
$BiVO_4$, struct. and ferroelastic phase transition 80−29004
Bi_2WO_6, superplasticity during phase transitions 80−108498
C foil, ion irrad., graphitisation rel. to lifetime, relevance to beam-foil spectroscopy 80−15166
C foil, ion irradiation, correlation of energy loss and crystallographic transform. 80−23215
C shock compression, diamond production 80−11613
CO, press. depend. of melting and α-β phase transition temp. 77−69075
Ca film, vac. deposited, photoionisation coeff. from photoemission meas., granular-lacunar transition 79−91569
$CaCO_3$, aragonite-calcite transformation, effect of impurities, DTA and IR studies 78−51662
$Ca_2Nb_2O_7$, crystal struct. rel. to isomorphous crystals *(Japanese)* 80−49208
$CaSO_4$, hexagonal-orthorhombic transition kinetics 79−23724
$CaSO_4.1/2H_2O$, transition to gypsum, mechanism 77−48390
$CaSiO_3$, structural transform. during hydration, IR spectra and X-ray diffr. meas. 77−76548
Ca_2SiO_4, structural transform. during hydration, IR spectra and X-ray diffr. meas. 77−76548
Ca_2SiO_4, structurally related phases, high-temp. X-ray powder diffr. 80−81050
Ca_3SiO_5, structural transform. during hydration, IR spectra and X-ray diffr. meas. 77−76548
$CaSnCl_6$, Cl NQR anomalous temp. depend., crystal struct. and phase transitions 80−54977
$Ca[B_3O_4(OH)_3].H_2O$, differential thermal X-ray anal. of phase transitions in non isothermal conditions 79−52205
$Ca[B_3O_3(OH)_5].4H_2O$, differential thermal X-ray anal. of phase transitions in non isothermal conditions 79−52205
Cd-Sb alloy condensate film, phase transform. kinetics 77−15721
$Cd(ClO_4)_2.6H_2O$ and $Cd(ClO_4)_2.6D_2O$, single crystals, EPR study of phase transitions 80−66025
$Cd(ClO_4)_2.6H_2O:Mn^{2+}$, phase transition, EPR of Mn^{2+} meas. 79−56604
$Cd_xHg_{1-x}Se$, phase transition and elastic consts., US vel. study 80−75354
$Cd(NH_3)_6(BF_4)_2:Ni^{2+}$, EPR of $[Ni(NH_3)_6]^{2+}$, temp. depend. at phase transition 77−20685
$Cd(NH_3)_4Cl_2$:Cu, EPR dynamical effects 79−61204
$Cd(NH_3)_6X_2$, X=Br, Cl, I, orientational phase transitions, Raman spectra 80−11382
$CdTe_{1-x}Se_x$, Raman scatt. spectra, two-mode behaviour 78−60450
Ce and Ce-Nd, reversible mech. memory effect, α to γ transition *(Russian)* 78−15396
Ce, energetics of γ-α phase transform, rel. to atomic excitation $fds^2 \rightarrow d^2s^2$ in atomic Ce 77−62639
Ce, high temperature transport props., scatt. mechanisms, phase transitions 77−15825
Ce, isostructural solid-solid phase transitions, core collapse, cell theory 80−59620
Ce, phase transitions, shouldered hard-sphere pots. calcs. 77−2600
$Ce_{0.74}Th_{0.26}$, mixed valence alloy, spin dynamics 78−10708
$Ce_{1-x}Th_x$ solid mixture, isostructural phase transitions 77−84884
Co complex, $[Co(NH_3)_6]I_3$, enantiotropic phase transition obs. 80−107412
Co complex, $Co(NH_3)_6I_3$, phase transition investig. by NMR 77−1608
Co, deformed, microstruct. singularities in pre-transform. temp. range *(Russian)* 80−45347
Co, phase transformations and vacancy form. by positron annihilation 80−2155
Co, steady state creep rate, stress depend. rel. to FCC to HCP phase change 78−64598
Co, X-ray diffraction investig. near FCC to HCP transform. *(Russian)* 77−47570
Co-Fe alloy, Invar characts. 77−1550
Co-Fe alloy, plastic deform. effects on phase comp. *(Russian)* 78−19743
Co-Ga binary system, lattice consts., phase transform *(Chinese)* 80−88108

solid-state phase transformations continued
Co-Ni-Cr-Mo (35, 20, 10 wt.%), MP35N, TEM study of phase transformations 80−81054
$CoMoO_4$, formation and phase transition in CoO-MoO_3-Al_2O_3 system 79−61569
$Co(OH_2)_6(SiF_6)$, phase transitions, spectrometric exam. *(French)* 78−88291
$CoSiF_6.6D_2O$, phase transition, mag. anisotropy and IR absorption spectra 77−89537
$CoSiF_6.6H_2O$, anomalous thermal expansion near transition temp. 78−47516
$CoSiF_6.6H_2O$, elec. resist. anomaly near struct. phase transition 79−95401
Cr coatings, electrodeposition, conditions rel. to H_2 conc., internal stresses 77−1933
Cr-Mo-V rotor steel, austenite to bainite transformation under cooling conditions, effect on creep 80−3033
Cr_5Al_8, γ-phase, microstruct., transform. strains, TEM obs. 79−11614
CrAs, heat capacity, enthalpy increments, thermodynamic props., 5 to 1280K 78−91450
$CrCl_3$, electronic struct. and struct. phase transition 80−59644
Cr_2O_3, US wave vel. near mag. transition 78−84263
$CrSe_2$, layered, phys. and elec. props. 80−44594
Cs, isostructural transition and lattice vibrs., relativistic LMTO calc. 80−20074
Cs, phase transitions, shouldered hard-sphere pots. calcs. 77−2600
$CsBi(MoO_4)_2$, low temp. phase transition, permittivity meas. 79−28698
$CsCaCl_3$ crystal, cubic→tetragonal phase transition 80−10681
CsCl, luminesc. in vac. UV range above and below phase transition temp. 80−93399
CsCl, phonon dispersion, temp. induced phase transition, deformable shell model calcs. 79−77698
CsCl, twin form. by compressive stress during phase transform. 80−49358
$CsCrI_3$, Mossbauer spectra, struct., electronic and mag. props. 79−91320
$CsCrI_3$, Mossbauer spectra, struct., electronic and mag. props. 80−15908
$CsCrI_3$, neutron diffr. expts. at 300, 77 and 1.2K 80−107163
$CsCuCl_3$, birefr. and opt. rot. near structural phase transition points 78−75823
$CsCuCl_3$, cooperative Jahn-Teller transition with trebling of period *(Russian)* 77−76557
$CsCuCl_3$, Jahn-Teller effect induced phase transitions 79−47439
$CsCuCl_3$, Jahn-Teller induced phase transitions 80−70391
$CsCuCl_3$, phase transition, refr. index, electrooptic coeff., pyroelec. signal, and NQR meas. 80−70386
$CsCuCl_3$, piezoelectricity, Jahn-Teller type phase transform. 80−40065
$CsCuCl_3$ submillimetre spectra phasons, low freq. modes, phase fluctuations *(Russian)* 80−50333
$Cs(D_{1-x}H_x)_2AsO_4$, high temp. nondestructive phase transform. at 170°C 77−12337
$CsDy(MoO_4)_2$, effect of 38K phase transition on phonon spectrum, IR reflection spectra *(Russian)* 79−10902
$CsDy(MoO_4)_2$, trivalent ion impurity effects on structural phase transition temp., new transition 20-30K *(Russian)* 79−19367
$CsDy(MoO_4)_2$:Eu^{3+}, anomalous effect of impurity on struct. phase transition temp. *(Russian)* 77−69083
$CsFeF_4$, struct. phase transition at 250K 80−10663
$CsFeF_4$, two dimensional structural phase transitions, sp. ht., optical, dielec., X-ray diffr. meas. 79−69240
$CsHF_2$, heat capacities, transitions and melting 79−10967
$CsHF_2$, struct. and phase transformation, NMR study 77−90047
CsH_2PO_4, Raman scatt. and high temp. props. 80−16024
Cs_2HgBr_4, phase transitions and singularities of cryst. struct., NQR study 80−19936
$CsInCl_3$, mixed-valence cpd., structural phase transition *(German)* 80−70406
$Cs_2MFe(CN)_6$, M=Ba, Mg, Ca, Sr, lattice instabilities 77−72668
$CsNO_2$-$CsNO_3$ solid solns., cryst. struct. and phase changes 79−51082
$CsNO_3$, phase transition, IR spectra 80−7350
$CsNO_3$, Raman spectra temp. depend., NO_3^- ion external librational modes, I→II transition, Raman spectra temp. depend., NO_3^- ion external librational modes 79−78662
$Cs_2NaM^{3+}Cl_6$ (M^{3+}=Bi,Nd,Pr), ferroelastic phase transitions, thermal expansion, elasticity, and X-ray anal. 80−70393
$Cs_2NaM^{3+}Cl_6$, (M=Bi,Nd,Pr), struct. transitions, polarisation optical expts. 79−99318
$CsPbBr_3$, US vel. around successive phase transition points 77−80581
$CsPbCl_3$, electronic struct. and optical props. in fundamental absorpt. region 80−93367
$CsPbCl_3$, refr. index and birefr., struct. transition effects 77−90126
$CsPbCl_3$, struct. phase transitions, NMR obs. 78−83943
$Cs_2PbCu(NO_2)_6$, α-modification, Jahn-Teller induced α to β transition, neutron diffr. obs. 79−1498
$Cs_2PbCu(NO_2)_6$, incommensurate Jahn-Teller transition, Huang scatt. 80−70401
$Cs_2PbCu(NO_2)_6$, successive Jahn-Teller phase transitions, neutron and X-ray diffr. 78−95154
Cs_2SnCl_6:$ReCl_6^{2-}$, luminesc. and absorpt. spectra, relax. processes 77−85779
$CsSrCl_3$, dilatometric and press. studies 77−15578
$CsSrCl_3$, refr. index and birefr., struct. transition effects 77−90126
$CsSrCl_3$:Mn^{2+}(Gd^{3+}), structural transitions, EPR meas. 78−34619
$Cs_2(TeBr_6)$, far IR and Raman spectra and phase transitions 80−11376
$CsVF_4$, structural phase transitions above room temp. 80−29167
$CsVI_3$, Mossbauer spectra, struct., electronic and mag. props. 79−91320
Cu, theoretical strength, rel. to FCC⇌BCC transitions 80−104229
Cu-Al, heat capacity of phases, 233 to 800K, heat of transform. and entropy 77−47589
Cu-Al (11.47 wt.%), high temp. phase transforms., effect of pre-exposure to neutrons 79−20045
Cu-Al films, elec. cond. of vacuum condensates depend. on composition, annealing *(Russian)* 80−65709
Cu-Al-Fe (11, 2 and 1 wt.%), Fe effects on microstruct. and mech. props. *(Korean)* 77−28807
Cu-Al-Fe-Mn (10,3,2 wt.%), phase comp. struct., continuous cooling from β-phase effect 79−24499
Cu-Al-Mn, Heusler alloy, magnetic prop. investig. of struct. transitions *(German)* 77−8289
β_1-Cu-Al-Ni (14.2, 4.3 wt.%), quenched, metastable 2H type phase charcts., TEM and electron diffr. study 79−74149

solid-state phase transformations continued
Cu-Al-Ni (14.3, 4 wt.%), ω-phase form. during quenching and ageing *(Russian)* 80−25686
Cu-Al(In), lamellar eutectoids, calorimetric determ. of interfacial enthalpy 78−60668
Cu-Ga, plastic flow enhancement during massive transformations 78−48468
Cu-Ga alloy, periodic antiphases obs. *(French)* 77−4772
Cu-Mn, positrons as probe of phase transforms. 78−31401
Cu-Ni-Mn (20,20wt.%), structural transform., X-ray and hardness study *(French)* 78−39760
Cu-Ni-Sn (15, 9 wt.%), age hardening accompanying phase transition 78−64551
Cu-Sb (24-45 wt.%), phase transform. exam. by thermal expansion 77−63629
Cu-Ti, deform. effect on precipitation and recrystallisation, electron microscope study 77−70115
β_1Cu-Zn, structural Umklapp processes at low and high temp. lattice kinetics of phase transformation isotherms *(German)* 78−30707
β_1-Cu-Zn mixed crystal, metastable structural Umklapp process, isothermal phase transform. *(German)* 78−22798
Cu-Zn-Ga martensite, thermally produced large single crystals 77−12615
CuAu, electrical resistivity meas. to detect phase changes 77−48425
CuAu, exam. of streaming due to intrinsic fluctuations 79−11602
$CuBeF_4.5H_2O$, NMR investig. of mag. props. and crystallographic transitions 77−63295
$CuCr_2O_4$, quadratic-cubic transformation, X-ray diffr. study *(French)* 79−47452
CuI and CuI:CdI_2, ionic cond., vacancy and interstitial mobilities, phase transitions 77−20116
CuI, γ and β phases, phonon contribs. to Gibbs free energy and entropy 77−80633
CuI solid electrolyte α-phase stabilisation 80−29209
$CuInS_2$, region of existence, determ. by quenching and X-ray anal., phase transition 79−66054
$Cu_xMo_3S_4$, superconductivity, lattice transforms., electronic instabilities 77−39990
$Cu_{0.7}Mo_3Se_4$, Chevrel-phase, low temp. struct. instability rel. to supercond. 77−47919
$Cu(NH_3)_5(ClO_4)$, EPR parameters and dilatometry 80−39850
$Cu(OH)_2$-α-$Mn(OH)_2$, phase transition during ht. treatment 78−23659
$CuO.Al_2O_3.2SiO_2$, hydrothermal synthesis, phase transitions 77−48378
$CuPbBiS_3$ aikenite, rel. to electrophysical props. 77−47822
$Cu_{1.8}S$-Cu_2S thin films, phase transforms kinematic electron diffr. study 80−29295
Cu_2S, optical and calorimetric meas. of thin films for Cu_2S-CdS solar cells 80−55863
Cu_7S_4, alternative transform. behaviour, direct obs. by TEM 77−1227
Cu_xS, $1 \leq x \leq 2$, quantum temp. size effect and magnetism *(Russian)* 80−103764
CuSe, lattice expansion, elec. cond. and sp. ht. at 326K transition 77−51491
CuTe, Cu_2Te and $Cu_{2-x}Te$ alloys, struct., electron diffraction investigation 79−51066
CuTeBr, ionic cond., phase transition obs. by millimetre wave spectroscopy 78−22855
$Cu_xZn_{1-x}SiF_6.6H_2O$, heat capacities and thermodynamic props., 14 to 300K, cooperative Jahn-Teller transition 80−21314
cyclopentane, plastic cryst. and liq. phases, thermal cond. and sp.ht., 100-300K, 0-2.1 GPa 78−34663
p-D_2, order parameter temp. depend. 79−42242
n-D_2, solid, nucl. spin-lattice relax. and evidence for low temp. phase transition 79−56022
DBr, orientational phase transitions, effective field approx. calcs. 77−24404
DCN, phonons meas. by neutron coherent inelastic scatt. 79−95097
$D_3O.ClO_4$, specific heat anomalies, investig. of solid phases 77−47591
Di(methylammonium) cadmium tetrachloride, LF Raman spectra and phase transitions 77−63414
Dy, hexagonal-orthorhombic transition temp., effects of press. and crystallinity 80−24585
$DyAsO_4$, cooperative Jahn-Teller transition, optical study 80−15240
$DyAsO_4$, cryst. struct. by X-ray diffr. co-operative Jahn-Teller transition 77−89411
$DyAsO_4$, first order Jahn-Teller phase transition, sp. ht. and refr. index meas. 80−59645
$DyAsO_4$, first-order cooperative Jahn-Teller phase transition, dielec. suscept. studies 80−19940
$DyAsO_4$, phase transitions obs. 80−70412
$DyCo_2$-$DyAl_2$ system, mag. and structural studies 80−108006
Dy_2O_3 film, phase transforms. on annealing 79−95285
$Dy_2Ti_2O_7$, neutron irrad., structural and volume changes 77−51416
$DyVO_4$, antiferromag.-ferromag. structural phase transition induced by elec. field *(Russian)* 79−46802
$DyVO_4$, cooperative Jahn-Teller distortion, mag. field depend. 77−47777
$DyVO_4$, cooperative Jahn-Teller transition, optical study 80−15240
$DyVO_4$, cooperative Jahn-Teller phase transition, linear birefr. meas. 80−88960
$DyVO_4$, dielec. anomaly and improper antiferroelectricity at Jahn-Teller transition 77−24802
$DyVO_4$, Jahn-Teller distortion, mag. field depend. 78−79733
$DyVO_4$, phase transitions obs. 80−70412
Er, US attenuation, longitudinal, in mag. ordered region and at phase transitions 77−28422
$ErFe_3$, 47K magnetic anomaly, point charge crystal field model 77−20517
$ErFe_3$, Mossbauer and magnetisation investig. of 47K mag. anomaly, atomic rearrangement 77−20766
ErO_x films, amorphous to cryst. and cryst. to cryst. transform. 77−62784
ErO_x, nonstoichiometric film, short-range order charact. and its effect on elec. behaviour 79−99435
Eu, high temperature transport props., scatt. mechanisms, phase transitions 77−15825
Eu_5As_3, cryst. struct. of high and low temp. phases 78−75626
$Eu_{1-x}La_xS$, electron struct., lattice consts., X-ray spectral study *(Russian)* 80−100432
Fe and its alloys, austenite formation kinetics during accelerated heating model, kinetic curves *(Russian)* 79−70058

solid-state phase transformations continued
Fe, α and γ phase, transition temp., influence of C interstitials 79−11611
Fe, cast, dispersed with interdendritic graphite, eutectoid transformation of austenite during cooling 78−84800
Fe, cast, nodular, hardenability, isothermic transition *(Czech)* 77−59778
Fe, cast, pearlitic, nodular graphite type, struct. evolution *(French)* 80−93551
Fe film, implanted with C ions, HCP struct. formation, electron diffr. study *(Russian)* 79−82469
Fe, phase transformations and vacancy form. by positron annihilation 80−2155
Fe, pure, nitrided layers obtained by ion bombardment, microstruct. exam. *(French)* 78−15581
Fe-Al-Si alloy, order-disorder transform. exam. by Mossbauer spectroscopy 77−63334
Fe-Al(Cr)(V)(Ti), hardness after nitriding, metallographic, electron microscopic and microprobe anal. 78−51608
Fe-B_4C powder mixtures, phase changes and struct. of sintered materials *(Russian)* 78−6872
Fe-C, lamellar eutectoid, calorimetric determ. of interfacial enthalpy 78−60668
Fe-C alloys, thermodynamics of proeutectoid ferrite transform. re-exam. 78−84763
Fe-C-Mo, dynamics of transform. interface, ferrite-austenite interface 78−52795
Fe-C-Mo, dynamics of transform. interface, at intermediate temps. 78−52796
Fe-C-O, sintered, ferritic struct. obtained by Ar_3 transform. *(Japanese)* 78−6874
Fe-C-Si-Mn, cast, high C, K_1 phase formation due to peritectoid transitions *(Russian)* 79−11548
Fe-C-Si(Co), eutectoid alloy, Si and Co addition effects on pearlite growth rate 77−16575
Fe-C(C-B)(C-Si), splat cooled, formation of metastable crystalline phases and glasses 78−88461
Fe-Co alloy, order-disorder and α-γ transitions 77−25042
Fe-Co-C (0.8 wt.%), unidirectional transformation process per struct. relationship, pearlite interlammellar spacing meas. 77−70045
Fe-Co-Cr, 25KKh15 alloy, atomic redistrib. during annealing, α to γ transform. *(Russian)* 77−12640
Fe-Co-Cr, alloy K25Kh15, phase tranforms., nucl. gamma reson. and X-ray diffr. meas. *(Russian)* 77−44241
Fe-Co-V, Vicalloy 1, α-γ transformation, γ-phase morphology and structural inheritance depend. on heating rate *(Russian)* 79−70059
Fe-Co-V-Cr alloys, struct. transform., appl. of mag., thermomag. methods *(French)* 79−20318
Fe-Cr, high purity binary alloy, isothermal decomp. of austenite 78−64525
Fe-Cr, role of C in transform. by heating in (α+γ) phase *(French)* 78−52798
Fe-Cr (2 at.%), plastic flow enhancement during massive transformations 78−48468
Fe-Cr-C (10,0.2 wt.%) isothermally transformed, carbide distrib., microstruct. development 80−3076
Fe-Cr-C alloy, bainitic struct. morphological changes, due to external stress, plastic deform. 78−44120
Fe-Cr-Co-Mo alloys, struct. transform. and mag. props. *(Russian)* 77−76543
Fe-Cr-Mo, grey cast, pearlitic, isothermal transform. of austenitic in bainitic range *(Rumanian)* 78−23698
Fe-Cr-Ni, cold-rolled foils, dilatometric study 80−21033
Fe-Cr-Ni (18, 14 wt.%), single strain induced γ to α' cryst. transform. *(Japanese)* 78−11221
Fe-Cr-Ni based alloys, Ni^+ ion and neutron irradiated, γ' particle redistrib. and phase stability 79−78977
Fe-Cr-Ni system, austenitic, energetic particle bombardment, thermodynamic and dimensional stability 77−27904
Fe-Cr-Ni-C (23.19, 4.91, 0.025 wt.%), two phase alloy, effect of prestrain above Md temp. on Ms temp. 78−80543
Fe-Cr(Ni), use of electrochemistry in understanding $\alpha \rightleftarrows \gamma$ transform., interstitials role *(French)* 77−63662
Fe-Cr(6 to 9 wt.%), transform. study during (α+γ) region reversion *(French)* 77−59780
Fe-Cu alloys, transform. substruct., lath microstructure after quenching 80−16298
Fe-Ga, constitution between 10 and 50 at.% Ga, heat treatment depend., BCC phases *(German)* 77−90325
Fe-Ga, Mossbauer effect for phase transitions, 20-720°C, 25.7-28.3 at.% Ga *(German)* 78−68437
Fe-Ga, volume change during solid state transformation *(German)* 78−84802
Fe-M, (M=Cr,W,Mo,V,Ti), morphology and growth kinetics of δ-pearlite formed by carburisation 80−108485
Fe-Mn, annealed, α-γ phase transformation obs. 78−75831
Fe-Mn, stacking fault energy, Mn conc. depend. *(Russian)* 77−1836
Fe-Mn (9 to 20 wt.%), ^{57}Fe Mossbauer spectroscopy in phase transformations 80−29948
γ-Fe-Mn alloys, antiferromag., mag. and crystallographic transformations 77−55964
Fe-Mn-C, austenitic, strain induced γ to ε transform., active slip systems 77−48427
Fe-Mn-C-Si alloy, G20 type, vol. effects during $\gamma \rightarrow \varepsilon$ transform., lattice parameters of γ-and ε-phases, Si and Mn effects *(Russian)* 78−6918
Fe-Mn-C-Si alloy G20, effect of Si and Mn additions on phase composition in multiple $\gamma \rightleftarrows \varepsilon$ transitions *(Russian)* 78−95743
Fe-Mn-Cr(Ni), mag. and crystallographic transformation depend. on Cr-Ni addition *(Russian)* 79−83334
Fe-Mn-Ni-V-C (0.5, 3.0, 1.0, 0.2 wt.%), austenite decomp., isothermal transform. characts. 80−97477
Fe-Mn-V-C (0.5, 1.0, 0.2 wt.%), austenite decomp., isothermal transform. characts. 80−97477
Fe-Mn(Sb)(Sn), additive effect, on eutectoid transformation of Fe 78−52799
Fe-Mo system, α-γ transform. rel. to Mo diffusivity in pure Fe 77−4214
Fe-Mo-C, eutectoid transform. of δ-ferrite 77−16570
Fe-Ni, FCC alloy, thermoelec. power, anomalous conc. depend. at high temp. 79−4548
Fe-Ni, thermal diffusivity during martensitic and austenitic transform. *(French)* 77−59781
solid-state phase transformations continued
Fe-Ni alloy, N27T2 and N28, internal friction peaks after reverse martensitic transform. *(Russian)* 78−92287
Fe-Ni alloy, ordered, low temp. $\alpha \rightarrow \gamma$ transform. *(Russian)* 78−19740
Fe-Ni alloy, rod-shaped martensite→austenite transform, struct. mech. *(Russian)* 77−66636
Fe-Ni alloys, enthalpy change between $\alpha' \rightarrow \gamma$ and $\alpha \rightarrow \gamma$ transformations 80−93550
Fe-Ni film, $\alpha \rightarrow \gamma$ transition, Mossbauer effect *(Russian)* 77−40154
Fe-Ni-Al-Co-Cr-Ti, YuNDK35T5BA, exam. of hypodissociation process *(Russian)* 79−11547
Fe-Ni-C martensite morphology, butterfly-lenticular transition temp., Cr addition effect *(Japanese)* 80−81053
Fe-Ni-Co alloys, struct., appl. of mag., thermomag. methods *(French)* 79−20318
Fe-Ni-Co-Mo alloys, struct. transform. produced during tempering 77−86058
Fe-Ni-Cr, Elinvar, struct. and mag. props., singularities during tempering *(Russian)* 80−50627
Fe-Ni-Cr vapour deposited film metastable phase formation *(German)* 78−38984
Fe-Ni-Te alloy system, first-order phase transformation obs. 78−64533
Fe-Ni-Ti martensitic alloy, γ' particle effect on crystallisation struct. *(Russian)* 78−44129
Fe-Ni-V-(CO) alloy, lattice parameter variation during ageing *(Russian)* 78−39812
Fe-Si cast alloy with spheroidal graphite, transform. investigation during tempering *(Russian)* 80−97479
Fe-Ta alloy, mech. drawn and aged, exam. of electrical resistivity, hardness, microstruct., and mag. props. *(Japanese)* 78−48545
Fe-W-Cr-Mo-Co (18,12,3,x wt.%) alloy, γ-α transformation, effect of cold working on magnetisation and hardness obs. *(Japanese)* 77−40428
$(Fe_{1-y}{}^{3+}Al_y{}^{3+})_2O_3{}^{2-}$, γ to α transform. elec. cond. study, oxidation initial stage kinetics, lacunar spinel form. 78−92384
$(Fe_{6-y}Al_y)O_9$, IR spectra, lacunar γ-phase to corundum α-phase transform. 80−108199
$Fe_{80}B_{20}$, amorphous to cryst. transorm. 80−34188
$Fe_{80}B_{20}$, binary amorphous ferromagnet, Mossbauer spectra 79−4749
$Fe(BF_4)_2.6H_2O(6D_2O)$, phase transition, mag. susceptibility and anisotropy and permittivity meas. 79−23718
$Fe_x(C,N)$, obtained by ion bombardment thermochemical treatment of Armco Fe *(French)* 77−86229
$(Fe_2Cr_{4-y}Al_y)O_9$, IR spectra, lacunar γ-phase to corundum α-phase transform. 80−108199
$Fe_{65.4}Cr_{20.5}Al_{10.7}V_{3.4}$, effect of Al and V on form. of $L2_1$ superstructure and stratification 77−77474
$(Fe_{1-y}{}^{3+}Cr_y{}^{3+})_2O_3{}^{2-}$, γ to α transform. elec. cond. study, oxidation initial stage kinetics, lacunar spinel form. 78−92384
$(Fe_{6-y}Cr_y)O_9$, IR spectra, lacunar γ-phase to corundum α-phase transform. 80−108199
$FeCr_2S_4$, Mossbauer spectra, second order phase transition 80−20539
$Fe^{2+}{}_{1+x}Cr_{2-2x}Ti_xO_4$ spinel, low temp. crystallographic transitions 77−15589
$Fe^{2+}{}_{0.2}Fe^{3+}{}_{1.8}Cr^{3+}O_4$, acoustic props. rel. to cooperative Jahn Teller effect and structural phase transform 80−24538
β-Fe_5Ge_3 formation in isothermal sintering, phase transition kinetics 80−89197
$Fe_{3-x}Mg_xO_4$, Verwey transition, Mossbauer study 80−39942
$(Fe_{1-x}Mn_x)Si$, US vel. rel. to mag. struct. and phase transforms *(Russian)* 77−47976
$Fe_2(MoO_4)_3$, ^{57}Fe Mossbauer effect obs. 77−48108
$(Fe_{100-x}Ni_x)_{100-y}B_y$, metallic glass, embrittlement and crystn. transformation products 80−7685
Fe_2O_3 based γ defective spinels, elec. cond. behaviour during transform. to α rhombohedral phases *(French)* 80−49354
α-Fe_2O_3, hematite, high temp. anomalous behaviour of cryst. lattice 77−69087
Fe_2O_3 reaction with NiO, ZnO, and (Ni,Zn)O solid soln., microstruct. 79−87834
γ-Fe_2O_3, struct. vacancy distrib., effect on $\gamma \rightarrow \alpha$ transform. heat 78−6051
Fe_2O_3-FeO, sinter, heating and reduction effect of phase transform. and fracture *(Russian)* 78−15375
Fe_2O_3-TiO_2 system, high temp. intergrowth struct., metal atom ordering in intergrowth boundaries 78−79573
Fe_3O_4, magnetite, change in state due to applied mag. fields obs. in magnetoresistance meas. 77−43623
Fe_3O_4 magnetite, low temp. phase transition, diffuse electron scattering *(Japanese)* 80−24591
Fe_3O_4, magnetite, phase transition, X-ray diffr. meas. 80−15238
Fe_3O_4, neutron diffuse scatt. due to molecular polarons 80−88488
Fe_3O_4, typical spontaneous symmetry breakdown in solid state 80−34737
Fe_3O_4, Verwey transition, electron-phonon versus Coulomb interaction effects 80−39280
Fe_3O_4, Verwey transition, charge density-phonon condensation 80−65217
Fe_3O_4:$Cd^{2+}(Zn^{2+})$, Verwey transition 80−6513
$Fe_3O_{4-x}F_x$, specific heat in neighbourhood of Verwey temp. 79−33500
$Fe(OH_2)_6(SiF_6)$, phase transitions, spectrometric exam. *(French)* 78−88291
δ-FeOOH, structure and phase transform., Mossbauer, X-ray, DTA study *(Chinese)* 80−54368
FeS, zinc blende type, crystallographic and Mossbauer obs. 78−87650
$FeSiF_6.6H_2O$, phase transform. exam. by X-ray and DSC methods 78−83948
Ga complex, $Gaurea_6(ClO_4)_3$:Cr^{3+} structural phase transition, ESR meas. 77−20681
Ga, FCC hypothetical struct., stability calcs. 78−18766
Ga-In-Sn, thermal analysis, determination of liquidus and reactions 78−88446
$GaMn_3(C_{1-x}N_x)$, mag. struct., phase transition, rel. to valence instabilities in rare earth compounds *(French)* 80−34596
GaS_xSe_{1-x}, grown by iodine vapour transport, X-ray struct. studies 79−4411
GaS_xSe_{1-x}, IR reflectivity and transmission spectra, stacking transform. 77−32371
GaS_xSe_{1-x}, indirect exciton spectrum and phase transition, luminesc. and absorption spectra 79−8160
GaSe, layer compounds, lattice instability, deformation dipole model 80−39249
$GaSe_{1-x}Te_x$, Raman scatt., optical phonons and phase transition 80−66202

solid-state phase transformations continued
$GaSe_{1-x}Te_x$, Raman spectra, phonon freq. 80−97286
$GaSe_{1-x}Te_x$, zone-centre optical phonons, Raman scatt. meas., structural phase transition obs. 78−10141
GdB_6, crystal preparation, elec. resistance, phase transitions 80−97427
GdB_6 single crystals, mag. behaviour and structure change at low temp. 80−71018
$Gd_xEr_{1-x}Rh_4B_4$, ferromag. and structural transitions, low temp. calorimetric meas. 79−55888
$Gd_3Ga_5O_{12}$, garnet-perovskite transform 80−15239
$GdMn_2$-$GdAl_2$ system, mag. and structural studies 80−108006
$Gd_2(MoO_4)_3$, electron microscope exam. 78−15134
Gd_2O_3-Ga_2O_3 system, phase diagram relationships of garnet-perovskite transform. 80−97460
Ge, evaporated film, lattice parameters and phase transition temp., surface influence of glass substrates 78−94996
Ge, order-order type phase transition at surface *(Russian)* 77−39728
Ge-Bi-Te system, thermal cond. change during phase transitions 80−100368
Ge-Te system, microstruct. in phase transform. region 79−52177
GeH_4, IR spectral obs. 77−36226
GeH_4:$SiHD_3$, symmetries of GeH_4 cryst. phases, IR spectra meas. 79−19886
GeS, photoelectron spectra, rel. to ionicities and phase transitions 77−69960
GeSe, photoelectron spectra, rel. to ionicities and phase transitions 77−69960
γ-GeTe, anisotropy of elec. props. near to structural phase transition 79−73515
GeTe, bond orbital model of band struct. 80−59853
GeTe, effect of phase transition on mech. and elec. props. 77−51746
GeTe, electron-phonon interactin induced phase transition 79−82338
GeTe, heterophase state, plasma refl. spectra, twinning domain distrib. study 79−69845
GeTe, structural transitions 77−51497
α-$Ge_{1-x}Te_x$, anisotropy of elec. props. rel. to cubic phase transition and band struct. 77−76820
H bond lattice with diamond struct., 3D statistical model of phase transition *(Chinese)* 80−8924
o-H, one-dimens., struct. instability 79−86885
o-H_2, order parameter temp. depend. 79−42242
H_2, orientational order, phase transition, average field approx. 78−63857
H_2, orientational ordering effects at low ortho conc. 79−56018
H_2, phase transition of second kind in HCP lattice, orientational ordering 80−70410
H_2, solid, crystallographic transformation below 1.5K, X-ray study 79−73374
H_2, solid, phantom phases 78−55946
p-H_2, solid, phase diagram, HCP-FCC phase transition 79−42340
H_2, solid, structure transition below 1K 79−56024
HCN, hydrogen bond distance, stretching freq. calc. 78−10183
H_2S frost, near IR reflectance spectra, tetragonal to cubic phase transition 77−81094
$H(UO_2P(As)O_4)4H_2O$, H motion, PMR obs. 78−80239
^{3}He, solid, phase transition in high mag. field 79−19424
^{3}He, solid, possible explanation for recently obs. phase transition in high mag. fields 80−20006
^{4}He, FCC high-density cryst., lattice dynamics by inelastic neutron scatt. 79−1539
^{4}He, HCP-FCC transition, near triple point, thermal anal. 79−60596
^{4}He, phase transition 80−15333
^{4}He, quantum cryst., ground-state lattice vacancies and Bose-Einstein condensation 77−7943
^{4}He, solid transition between close packed phases 79−56025
$(Hf,Zr)V_2$, phase transition, sp. ht. anomalies meas., 70-150K 77−35691
Hf, solid state phase transformation $\alpha \rightarrow \omega$, exam. of phase transformation kinetics under static, and dynamic pressures 78−80541
Hf-O, phase props. 77−40415
Hf-Zr (3 wt.%), $\alpha \rightarrow \beta$ transform. temp. and entropy, emissivity 77−48424
HfO_2, thermal anal. using solar heating *(Ukrainian)* 79−77725
HfV_2, C-15 struct., phase transitions, elec. cond., crystal lattice parameters *(Russian)* 80−54826
HfV_2, elec. resist. and mag. suscept., anomalous temp. depend. 79−69491
HfV_2, latent heat of structural transform. 80−24589
HfV_2, supercond. compound, thermal expansion at low temp. 78−76189
HfV_2O_7:^{181}Ta, EFG temp. depend., TDPAC 77−59488
$Hg_{3-\delta}AsF_6$, one dimensional phonons and chain ordering 80−24544
$Hg_{3-\delta}AsF_6$, theory of phase transitions 80−6486
Hg_2Br_2, sp. ht. near phase transition region meas. 78−38855
$Hg_2Br(Cl_2)$, paraphase, Raman scatt. spectra, soft mode from Brillouin zone boundary *(Russian)* 78−2851
$HgCl_2$, second order phase transition, elastic consts. meas., Brillouin scatt. 78−10908
Hg_2Cl_2, ferroelastic transition, refr. index, 80 to 300K 79−82941
Hg_2Cl_2, neutron and Raman scatt. studies, ferroelastic transitions 80−76015
Hg_2Cl_2 prototype phase, soft mode, inelastic neutron scattering, Raman effect 78−91411
HgI_2, single cryst. elec. and thermal props. 79−11111
$HgSb_4S_8$, photosensitive semicond., US attenuation, phase transition obs. 79−65518
Ho, phase transition along mag. field, X-ray obs., 77-292K *(Russian)* 77−4504
IF_6, NMR and NQR of ^{127}I and ^{19}F, solid-solid transitions and mol. motions 79−99784
In-Cd alloys, elastic-phase transition, US study 78−6919
$InSb_{1-x}Bi_x$, metastable epitaxial film, phase diagram 80−76238
InSe, layer compounds, lattice instability, deformation dipole model 80−39249
KAg_4I_5, ionic conductivity and heat capacity near T_c 78−47584
KAg_4I_5, solid electrolyte, Raman spectra 79−73934
KB_3H_8, NMR study of proton and boron dynamics 80−71210
KC_{24}, intercalated graphite, struct. phase transitions, X-ray diffr. 79−65189
KCN, dipolar impurity tunnelling model, elastic interaction and const. 78−71826
KCN, elastic functions meas. by US pulse-echo method and Brillouin scatt. 77−84829
KCN, F-centres, optical props., rel. to structural phase transition 78−2892
KCN, optical F centres and phase transitions 78−56504
KCN, phase transition at 168K, neutron inelastic scatt. line shapes for phonons obs. 78−38840
$K(CN)_{1-x}Cl_x$, elastic functions meas. by US pulse-echo method and Brillouin scatt. 77−84829
$(KCN)_x(KBr)_{1-x}$, Brillouin scatt. of elastic anomaly 79−28779
KCN_xKCl_{1-x}, phase transition and OCN^- vibr. spectrum 78−43093
$KCaF_3$, struct. phase transitions, DSC, birefr., and neutron powder diffr. obs. 80−70149
$KCdF_3$, structural phase transitions, X-ray diffr. and differential type thermal analysis 77−80620
$KCdF_3$, structural phase transitions using linear birefringence studies 78−76424
$KCdF_3$:Cr^{3+}, EPR, successive phase transitions 79−65717
$K_2Cd_2(SO_4)_3$, ferroelastic phase transition, X-ray diffr. and dielec. temp. depend. meas. 79−55882
$K_2Cd_2(SO_4)_3$, piezoelec. langbeinite-type, cryst. struct. and ferroelastic transform. 78−6036
KCl:Ba^{2+}, localised stress relaxation in excess vacancy system, prismatic loops *(Russian)* 80−88160
$KCl_{1-x}CN_x$, dipolar impurity tunnelling model, elastic interaction and const. 78−71826
$K_3Co(CN)_6$, Raman scatt. and electronically-induced phase transition at 130K 77−90142
$KCoF_3$, lattice parameter temp. depend., phase transitions and thermal expansion coeff. 80−1988
$K_2Co_2(SO_4)_3$, phase transition behaviour with respect to lattice constants and ionic radii of constituent ions 78−6643
$K_2Co_2(SO_4)_3$ polycryst., growth and phase transitions 79−33918
$KCr(SO_4)_2.12H_2O$, phase transition associated fluctuations, Cr^{3+} EPR obs. 77−32247
$KD_3(SeO_3)_2$, phase transition, neutron diffr. 80−2158
$KD_3(SeO_3)_2$, phase transition, neutron scatt. study 80−75351
$KDy(WO_4)_2$, Jahn-Teller transition, permittivity behaviour 80−55012
$KDy(WO_4)_2$, low temp. phase transitions *(Russian)* 78−87787
$KDy(WO_4)_2$, phase transition mechanism, absorpt. spectra, symmetry props. *(Russian)* 80−55130
$K_3Fe(CN)_6$, Raman scatt. and electronically-induced phase transition at 130K 77−90142
$KFeF_4$, struct. phase transitions obs. by dielec. const. and X-ray diffr. studies 79−95161
$KFe(MoO_4)_2$, phase transitions at 312 and 139K 80−70396
$KFeO_2$, cryst. and mag. struct., neutron and X-ray powder diffr., and Mossbauer effect meas. 77−84722
K_2GeF_6, first order phase transition, X-ray diffr. and IR spectra 79−73945
KH_2PO_4 optical SHG and γ [quartz, struct. transitions, optical SHG and γ-ray diffr. results]-ray diffr. results 78−14459
KH_2PO_4, soft branch Brillouin specta, quasielastic central peak suppression by annealing 78−95588
$KHSO_4$, pure ionic cond., proton mobility, irreversible phase transition 77−59141
$KH_3(SeO_2)$, $KD_3(SeO_3)_2$, second-order ferroelastic phase transitions, piezo-opt. props. obs. 78−95558
$KH_3(SeO_3)_2$, acoustic phonon softening 77−27997
$KH_3(SeO_3)_2$, ferroelastic transition under uniaxial press., EPR study 80−59562
$KH_3(SeO_3)_2$, phase transitions *(Japanese)* 79−65812
$KH_3(SeO_3)_2$, proton NMR study about paraelastic-ferroelastic transition 78−23363
$KH_3(SeO_3)_2$, thermal anomalies rel. to acoustic phonon instability 77−76545
$KLiSO_4$, phase transition, lattice parameter variation with temp. 78−79767
$K_2Mg_2(SO_4)_3$, langbeinites, structural phase transitions 78−83938
$KMnF_3$, 185K structural transition, wavevector reversed ultrasound study 80−75306
$KMnF_3$, birefr. and opt. rot. near structural phase transition points 78−75823
$KMnF_3$, dynamic scaling and US attenuation at structural phase transition 80−44260
$KMnF_3$, lattice parameter temp. depend., phase transitions and thermal expansion coeff. 80−1988
$KMnF_3$, mag. props. and struct. transitions, antiferromag. reson. meas. 79−8052
$KMnF_3$, Mossbauer effect in ^{57}Fe, struct. and mag. transition investig. 77−20779
$KMnF_3$, width of central peak in crit. scatt. of γ-rays 77−1623
$KMnF_3$:Rb, phase transition and atomic motions, NMR study 80−75872
$KMn_{0.9}M_{0.1}F_3$, (M=Co,Ni), lattice parameter temp. depend., phase transitions and thermal expansion coeff. 80−1988
$K_2Mn_2(SO_4)_3$, phase transition, X-ray diffr. study of high and low temp. phases 78−38832
K_2MoO_4, hysteresis of phase transitions and modulated structures 80−29169
KNO_3 characteristic features of electronic structure by infrared spectroscopy 79−47436
KNO_3(II), Raman spectral study of struct. props., disordered groups 77−66486
$KNbF_6$, NMR, quadrupole effects and struct. distortion 80−15809
$KNiF_3$, lattice parameter temp. depend., phase transitions and thermal expansion coeff. 80−1988
$K_2O_sCl_6$, soft rotary mode near phase transition, inelastic neutron scatt. obs. 79−60472
K_2OsCl_6 powder, spin-lattice relax., dynamic clustering near struct. transition 77−48079
$K_2PbCu(NO_2)_6$, incommensurate Jahn-Teller transition, neutron scatt. meas. 77−69065
$K_2PbCu(NO_2)_6$, incommensurate Jahn-Teller phase transition 78−79730
$K_2PbCu(NO_2)_6$, incommensurate Jahn-Teller transition, Huang scatt. 80−70401
$K_2PbCu(NO_2)_6$ Jahn-Teller phase transitions, X-ray and neutron measurements 78−91438
$K_2PbCu(NO_2)_6$, US vel. near cooperative Jahn-Teller phase transitions 79−23680
$K_2Pb(MoO_4)_2$, and isomorphs, domain struct. and phase transition *(Russian)* 78−6159

solid-state phase transformations continued
$K_2Pt(CN)_4Br_{0.3}.3H_2O$, quasi-one-dimens. conductor, Br distrib. long-range Coulomb interaction, effect on structure and CDW 79−7591
K_2PtCl_6, K_2ReCl_6, K_2SnCl_6, solid state phase transitions, lattice vibr., NMR and NQR obs. 80−34814
K_2ReCl_6, elastic constants, softening of acoustic modes, obs. by Brillouin scattering 80−71440
K_2SO_4, α-β phase transition, Raman scatt. study *(French)* 80−55096
K_2SO_4, hexagonal orthorhombic phase transition 78−2251
K_2SO_4, longitudinal-acoustic soft mode in phase transition 80−75326
K_2SO_4, phase transform., mech. of thermal hysteresis, DTA, dilatometry and dielec. meas. 80−75353
β-K_2SO_4 type crystals, structural transitions 80−75349
$K_2S_2O_8$, thermal transitions, catalytic effects of CuO and ZnO 79−15983
$KSc(MoO_4)_2$, quadrupole interaction const., influence of phase transition, NMR meas. 77−16206
$KSc(MoO_4)_2$, soft modes and Raman spectrum at ferroelastic phase transitions 79−47450
K_2SeBr_6, rotational phase transitions, cryst. struct., X-ray diffr. study 80−70400
K_2SeO_4, hexagonal orthorhombic phase transition 78−2251
K_2SeO_4, incommensurate modulation along axis perpendicular to x-axis 78−6154
K_2SeO_4, non-zero wave vector incommensurate soft mode, light scatt. study 80−29754
K_2SeO_4, phenomenological theory of transition sequence 77−76546
K_2SeO_4, Raman spectra, 77-300K *(Japanese)* 77−43988
K_2SeO_4, structural transition, polarised Raman spectra 80−75349
K_2SeO_4, ultrasonic study in temp. range of incommensurate phase transform. 80−88276
K_2SnCl_6, elastic constants, softening of acoustic modes, obs. by Brillouin scattering 80−71440
K_2SnCl_6, phase-transition-induced dipolar relax. 80−66107
K_2SnCl_6, photoacoustic detection of phase transitions 78−75810
K_2SnCl_6, structural phase transition exam. by neutron powder diffr. 78−55940
K_2SnCl_6:$ReCl_6^{2-}$, (K_2PtCl_6:$ReCl_6^{2-}$), luminesc. and absorpt. spectra, relax. processes 77−85779
$K_2(TeBr_6)$, far IR and Raman spectra and phase transitions 80−11376
$KTiF_4$, struct. phase transitions obs. by dielec. const. and X-ray diffr. studies 79−95161
K_2TiF_6, anion motion and phase transition, NMR spectra 79−99788
KVF_3, antiferromag. ordering points, thermal anal. and X-ray diffr. meas. *(French)* 78−84421
KVF_4, struct. phase transitions obs. by dielec. const. and X-ray diffr. studies 79−95161
K_2WO_4, hysteresis of phase transitions and modulated structures 80−29169
K_xWO_3 bronze, oxidation to $K_2O(WO_3)_n$, struct. changes 78−68925
K_2XY_6 (X=Sn, Te, Y=Cl, Br), low temp. vibr. spectra, lattice dynamics and phase transitions 79−73917
K_2ZnCl_4, ^{35}Cl NQR study of incommensurate phase transition 80−60450
$K_4Zn(MoO_4)_3$, domain struct. and phase transition, ferroelastic behaviour 77−62581
$K_2[SnCl_6]$, defects determ., dipole relax. in phase transform. *(German)* 78−22711
Kr, epitaxial monolayer on graphite, second order phase transform. obs. by LEED 77−76687
Kr monolayer, on graphite, phase transition from localised to nonlocalised solid 77−11787
Kr, monolayer on graphite, commensurate-incommensurate transition, X-ray scatt. 79−73382
(La,Ce)Ru_2, supercond. transition temp., its press. depend., and structural phase transform. 78−6473
$LaAg_xIn_{1-x}$ alloys, structural instability 78−79562
$LaAg_xIn_{1-x}$, phonon dispersion, elastic consts. and struct. instability, soft mode behaviour 80−103436
$La_{1-x}Ca_xVO_3$, struct., elec. and mag. props., temp. and conc. depend. *(French)* 77−4293
$LaCoO_3$, structural phase transition involving changes in spin and valency 78−79765
LaD_3, stoichiometric, structural phase transform., neutron diffraction evidence 80−88319
La_2O_3, elec. cond. and dielec. const., 400-1180K, phase transition 79−56224
La_2O_3-Mn_2O_3-Cr_2O_3, synthesis and properties of solid solutions 78−44038
LaP_5O_{14}, continuous ferroelastic transition elastic and mechanical props. 80−92668
LaP_5O_{14}, coupling effects between soft optic and acoustic modes at ferroelastic transition 80−70358
LaP_5O_{14}, ferroelastic phase transition, thermal expansion and elastic consts. tensors 79−42236
LaP_5O_{14}, ferroelastic transition, polarised Raman study 80−16035
$La_2(SO_4)_3.9H_2O(D_2O)$, cryst., polarised Raman spectra, phase transition *(French)* 77−66497
$La_{1-x}Sr_xCoO_3$, specific heat meas., using laser-flash method, high-order and ferromagnetic transitions obs. *(Japanese)* 80−54898
$La_2Ti_2O_7$, crystal struct. rel. to isomorphous crystals *(Japanese)* 80−49208
$LaVO_3$, successive phase transitions, X-ray anal. 80−108437
Li, struct. stability 77−8015
β-$LiAlSiO_4$, eucryptite, one-dimensional ionic conductor, neutron scatt. study 80−49361
$LiCd_{1-x}Tl_x$, intermetallic, X-ray and Knight shift meas. of ^{205}Tl and ^{113}Cd 79−42851
$Li_xCr_yV_{1-y}S_2$, Mossbauer and mag. studies 79−73869
$LiFe_5O_8$, hysteresis and other mag. props. rel. to microstruct., TEM investig. 77−20636
$LiFe_5O_8$, material loss and high-temp. phase transition 78−64534
$Li_{0.5}Fe_{2.5}O_4$-$CuFe_2O_4$-$MnFe_2O_4$, structural characteristics and mag. props. of solid solutions 77−35696
$Li_xFe_yV_{1-y}S_2$, Mossbauer and mag. studies 79−73869
$LiGaO_2$, Raman scatt., optical modes determ., 65K phase transition obs. 79−15463
α-$LiIO_3$, temp. depend. studies of Raman spectra of polaritons in region of phase transition 78−76467
$LiKSO_4$, uniaxial crystal, pyroelectric, thermal expansion, phase transition 80−19966
solid-state phase transformations continued
β-$LiNH_4SO_4$, lattice modes and phase transition, polarised Raman meas. 77−20859
$LiNH_4SO_4$, phase transitions, temp. depend. of NMR, spontaneous polarisation, birefringence and SHG 78−10191
$LiNbO_3$, piezoceramic, elastic normal wave propagation, phase transitions *(Russian)* 80−40067
Li_2O-SiO_2, glass ceramics, phase transformation processes 80−3025
$Li_{1-x}Ti_{2-x}O_4$, struct. phase transition and thermal expansion 78−14465
$Li_{1+x}Ti_{2-x}O_4$, high temp. spinel-Ramsdellite transform. 80−70407
lithium ammonium tartrate monohydrate ferroelastic phase transition *(Japanese)* 79−77747
Mg cast iron, effect of heating temp. on microstruct. and mech. props. 77−56005
Mg cast iron, effect of heat treatment on phase comp., microstruct., wear resistance 77−56006
Mg ferrite, sintered, cation redistribution, microstructural effects 77−55356
Mg-Ho alloys, phase diagrams and transformations, Ho solubility *(Russian)* 79−52162
Mg-Li-Al (31, 1 at.%), heat treated, precipitation 80−40364
Mg-Sm, solid soln., phase diagram *(Russian)* 77−25015
$MgAl_2O_4$ spinel, anomalous thermal expansion, second order transition 80−84307
$MgAl_2O_4$, structural phase transition obs. by electron diffr. 77−66020
$MgFe_{2-y}Al_yO_4$, with added Co, effect of Na_2O admixture on props. 77−36423
$MgFe_2O_4$, Mossbauer effect determ. of cation distrib. temp. depend. 77−8481
$Mg(IO_3)_2.4H_2O$, struct. and phase transition using X-ray diffr. and thermal anal. *(Chinese)* 79−51059
$MgMn_2O_4$, cation migration, neutron diffr. investig. 77−7896
$Mg(NH_3)_6(ClO_4)_2$, phase transition, group theoretical anal. 80−65218
$Mg(NH_3)_6(ClO_4)_2$, solid, mol. rot., Raman contour, quasielastic neutron scatt., and PMR obs. 79−87444
MgO-Al_2O_3-Fe_2O_3-SiO_2, cordierite, in ceramic, effect of heat treatment on cordierite content 79−20039
MgO-Al_2O_3-SiO_2, glass ceramics, phase transformation processes 80−3025
MgO-$Ca_3Mg(SiO_4)_2$($CaMgSiO_4$)-$NaPO_3$, phase conversions 77−66641
MgO-Nb_2O_5-Al_2O_3, equilibria at 1400°C phase diagram *(Italian)* 78−23671
$Mg(OH)_2$-α-$Mn(OH)_2$, phase transition during ht. treatment 78−23659
$Mg(OH_2)_6(SiF_6)$, phase transitions, spectrometric exam. *(French)* 78−88291
MgO.Al_2O_3.$2SiO_2$, hydrothermal synthesis, phase transitions 77−48378
$MgSiF_6.6H_2O$:Ni^{2+}, EPR meas., low temp. phases 77−63269
$MgTiF_6.6H_2O$:Ni^{2+}, EPR meas., low temp. phases 77−63269
Mn cast Fe, W effect on transform. in thin surface layers during dry sliding friction 77−21289
Mn-Cu, mag. and cryst. struct., neutron and X-ray diffr. meas. *(Russian)* 78−22694
Mn-Cu (25 wt.%) alloy, critical shear stresses of twinning and glide 79−87693
Mn-Cu-Al alloy under torsion, anomalous elasticity and transformation plasticity obs. *(Russian)* 78−75834
γ-Mn-Fe, FCC→FCT transform. temp. and Neel temp., X-ray and neutron diffr. expts. *(Russian)* 78−84797
Mn-Ni alloys, γ-phase antiferromag., lattice distortion and elastic props., ΔE effect interpret. 77−20671
Mn-Ni alloys, Mn-rich, structural changes associated with antiferromag. ordering 77−69085
Mn-Ni(Pd), atomic and mag. order, neutron diffr. exam. 79−73697
MnAs, struct. and mag. props., temp. depend., neutron study 79−47246
MnBi films subjected to pulse heating, phase trans. rate const. temp. depend. *(Russian)* 78−88282
$Mn_xCr_{3-x}O_4$, cubic and tetragonal structs., neutron diffr. obs. 79−19369
$Mn_3Ga_{1-x}Mn_xN$, perovskite struct., phase transformations *(French)* 80−81048
Mn_3GaN, sp. ht., 6 to 350K, mag. and crystallographic phase transitions 80−71060
$Mn_3GaN_{1-x}C_x$, perovskite struct., phase transformations *(French)* 80−81048
$Mn_{1-x}Mg_xSe$, mag. and struct. phase transitions, mag. susceptibility and X-ray diffr. study 80−71022
$Mn_2N_{0.86}$, cryst. and mag. struct. at low temps. *(French)* 77−73003
MnO, elastic props. singularities near phase transition 77−16093
MnO-MgO-ZnO-Fe_2O_3, grade 1.3 VT ferrite formation from hydroxides 77−90302
Mn_3O_4, hausmannite, tetragonal-cubic transform., X-ray anal. 80−103288
$Mn(OH_2)_6(SiF_6)$, phase transitions, spectrometric exam. *(French)* 78−88291
MnS, phase transform. at 200°C, diffusive and deformational mechanisms 80−65216
α-MnS, polycryst. and oriented single cryst., phase transition at 131K 78−6157
α-MnSe, mag. and struct. phase transitions, mag. susceptibility and X-ray diffr. study 80−71022
Mn_5Si_3, elastic moduli, phase transitions, ultrasonic velocity 80−92589
$MnSiF_6.6H_2O$, specific heat, thermal cond., simultaneous meas., method, 90-300K, near phase transition 77−37892
Mn_3ZnN, sp. ht., 6 to 350K, mag. and crystallographic phase transitions 80−71060
Mo (100), chemisorption of H, phase changes, LEED obs. 79−77911
Mo (100) surface, phase transition exam. of LEED 77−55433
Mo and Mo superalloys high temperature properties 78−44173
Mo:N film, implantation effect on supercond. and struct. transform. 77−4462
Mo_5GaS_6, struct. transform. below 50K, mag. permeability and elec. cond. meas. *(Russian)* 77−7864
MoO_3 topotactic transform into MoO_2, electron microscopy, X-ray anal. 80−107417
β-$MoTe_2$, domain struct., dislocation fine struct., phase transitions 79−82332
β-$MoTe_2$, low-temperature structural phase transition, X-ray meas. 79−14928
Mo(001) surface, atomic displacements and electronic struct. 78−30963
N_2, α-β transition obs., thermometric fixed point applicability 80−13076
N_2, solid, Raman spectra vibron and lattice freq. shifts, librational force consts., α- and γ-phases 78−19460

solid-state phase transformations continued
$(N(CH_3)_3H)_2SnF_6$, phase transition and temp. effects, Mossbauer and NMR spectra 78−88236
$ND_4D_2AsO_4$, ND_4 role in antiferroelec. transitions, D NMR 77−52025
ND_4NO_3, low temp. phase, Raman scatt. meas. 78−84568
$(NH_4,Cs)Cl$, negative isotope effect on II-III phase transition *(German)* 78−95155
$N_2H_6^{2+}$ salts, NMR spin lattice relaxation study, ^{14}N-^1H dipole-dipole contrib. to relax. 80−75878
$NH_4Ag_4I_5$, ionic conductivity and heat capacity near T_c 78−47584
$NH_4Ag_4I_5$, solid electrolyte, Raman spectra 79−73934
$(NH_4)_2BeF_4$ crystals, incommensurate-commensurate phase transitions, optical props. 79−95733
$(NH_4)_2BeF_4$, incommensurate-commensurate phase transition 78−87760
NH_4Br, ^{14}N NMR obs., rel. to structural transforms. 79−15368
NH_4Br birefr. and opt. rot. near structural phase transition points 78−75823
NH_4Br, dislocation influence on phase transition and light scatt. *(Russian)* 80−59648
NH_4Br-NH_4I mixed crysts., far IR spectra, phase transition and NH_4^+ libration 77−85719
$NH_4Br(Cl)$, anomalous sound attenuation above lambda point 78−51617
$(NH_4)_2Ca_2(SO_4)_3$, phase transition behaviour with respect to lattice constants and ionic radii of constituent ions 78−6643
NH_4Cl, acoustic absorption by soft modes of defects 80−59584
NH_4Cl, order-disorder transition exam. by optical second harmonic generation 78−51671
NH_4Cl, piezoelec. effect near nonferroelastic phase transition 80−66116
NH_4Cl, specific heat, thermal cond. simultaneous meas. method, 90-300K, near phase transition 77−37892
NH_4Cl, thermal cond. and heat capacity of solid phases under press. 80−2225
$NH_4Cl_{1-x}Br_x$, US exam. of order-disorder phase transform. 78−38841
NH_4ClO_4, photothermochemical process, influence of phase transition 79−24770
NH_4CoF_3, susceptibility and magnetisation meas. 77−85432
$(NH_4Eb)Cl$, negative isotope effect on II-III phase transition *(German)* 78−95155
NH_4FeF_4, Mossbauer and optical evidence for crystallographic transition 79−14931
$(NH_4)_2HPO_4$, NH_4^+ motions, PMR relax. times obs., 77-430K, struct. transition 77−85599
$(NH_4)_3H(SO_4)_2$, press.-temp. phase diagram, dielec. and DTA meas. 77−81067
NH_4HgCl_3, high resolution heat capacity meas. *(Japanese)* 80−52218
αNH_4HgCl_3 quasione dimensional type cryst., phase transition statistics, molecular field approx. calcs. 80−34190
NH_4IO_4, high order phase transition, quadrupole coupling temp. depend. 80−54371
$NH_4IO_3.2HIO_3$, dielec. constant, elec. cond. phase transition and cryst. struct. 80−1999
$((NH_4)_xK_{1-x})_2SnCl_6$, mixed cryst., NQR relax. and reson. 80−54990
NH_4LiSO_4, PMR line shape and spin-lattice relax., phase transition obs. 78−88205
$(NH_4)_2Mg_2(SO_4)_3$, phase transition behaviour with respect to lattice constants and ionic radii of constituent ions 78−6643
NH_4MnCl_3, X-ray single crystal analysis, phase transitions, Mossbauer effect 79−19366
NH_4NBeF_4, successive phase transitions, dielec. and optical props. obs. 80−50275
NH_4NO_2, thermal anal. by energy-dispersive X-ray diffr. 78−91440
NH_4NO_3, low temp. phase, Raman scatt. meas. 78−84568
NH_4NO_3, phase transition, IR spectra 80−7350
NH_4NO_3, Raman scatt. in region of extended IV-V phase transition 79−99887
$(NH_4)_2Ni_2(SO_4)_3$, phase transition behaviour with respect to lattice constants and ionic radii of constituent ions 78−6643
$(NH_4)_2PtI_6$, crystal symm., struct. phase transition, ^{127}I NQR freq. 80−34815
NH_4ReO_4, high order phase transition, quadrupole coupling temp. depend. 80−54371
NH_4ReO_4, ND_4ReO_4, Raman spectrum, temp. depend. 78−80335
NH_4ReO_4, nuclear quadrupole coupling, NQR temp., press. depend., continuous phase transition 78−27109
$(NH_4)_2SO_4$, phase transition mechanisms by optical spectroscopy 79−15411
$N_2H_6SO_4$, orthorhombic, low-temp. phase transition, Raman spectra meas. 77−24849
$(NH_4)_2SO_4.Al_2(SO_4)_3.24H_2O:Cr^{3+}$, and deuterated derivative, structural transition studied by EPR 77−85553
NH_4SbF_5, dielectric props. and structural phase transitions *(German)* 80−25274
$(NH_4)_6Sb_4(SO_4)_3F_{12}$, dielec. props. and phase transitions 79−69765
$(NH_4)_2SeO_4:Mn^{2+}$, single cryst., EPR and phase transition 79−73805
$(NH_4)_2SiF_6$, cryst. phases, Raman obs. 20-290K 77−66495
$(NH_4)_2SiF_6$, elastic constants, softening of acoustic modes, obs. by Brillouin scattering 80−71440
$(NH_4)_2SnBr_6$, structural phase transitions study by Raman scatt. 80−93318
$(NH_4)_2SnCl_6$, elastic constants, softening of acoustic modes, obs. by Brillouin scattering 80−71440
$(NH_4)_2(TeBr_6)$, far IR and Raman spectra and phase transitions 80−11376
$(NH_4)_2(TeCl_6)$, IR and Raman spectra, lattice and internal modes, phase transition 78−6659
NH_4X, (X=Cl, Br, I), tricritical points 79−7695
NO, first monolayer on MgBr cleavage face, triple point 78−6227
NaCN, optical F centres and phase transitions 78−56504
Na_2CO_3, elec. cond., 270-830°C, and transition points 78−10216
Na_2CO_3, incommensurate structural phase transform., neutron diffr. obs. 79−86886
Na_2CO_3, quasicrystalline state, incommensurate phase transformation 79−99310
Na_2CO_3, single cryst. growth from melt, thermal expansion meas. 79−4913
$Na_2CO_3+CaCO_3$ solid state reactions, Hedvall effect 79−96300
$NaCaPO_4$-$Ca_3MgSi_2O_8(CaO)$ systems, phase diagrams of partial system 78−35369
$NaCaPO_4$-Ca_3MgSiO_4 system, phase diagram 78−35370
Na_2HAsO_4, ^{75}As NQR, phase transition mechanism 78−52375

solid-state phase transformations continued
$Na_{1-x}Li_xNbO_3$, dielec. const. and X-ray diffr., for Curie temp. and phase diagrams 78−72768
$Na_4Mg_2Si_3O_{10}$, orthorhombic to cubic phase transformation at 198K 80−19765
NaN_3, lattice dynamics and phase transition, theory 77−76501
$NaNO_3$ characteristic features of electronic structure by infrared spectroscopy 79−47436
$NaNO_3$, low temp. struct. changes, elec. props. 79−87377
$NaNO_3$, rel. to ^{23}Na spin-lattice relax. time −75.5 to +320°C *(Japanese)* 77−43897
$NaNbO_3$, cubic to tetragonal transition, inelastic neutron scatt. study *(French)* 79−60469
$NaNbO_3$, X-ray and Mossbauer γ-ray scatt., near phase transition, energy width of central peak 78−79724
Na_2SO_4, topotaxic phase change obs. 77−51340
$Na_2S_2O_8$, thermal transitions, catalytic effects of CuO and ZnO 79−15983
$Na_3Sc_2P_3O_{12}$, fast-ion conductor, struct. phase transition 80−88362
$NaTaO_3$, high temp. structs. neutron powder diffr., comparison with $SrZrO_3$ and $NaNbO_3$ 80−88094
Na_2UBr_6, phase transformations, elec. cond. and entropy meas., synthesis *(French)* 78−79763
β-$Na_{0.33}V_2O_5$, quasi-one-dimensional conductor, NMR studies 80−93204
Na_xVS_2, intercalation cpd., mag. phase transitions 77−69558
$Na_xVS_2(Se_2)$, mag. and elec. props. rel. to struct. transitions 78−91848
Na_xVSe_2, intercalation cpd., mag. and structural phase transitions 77−69558
Na_xWO_3, dynamic fluctuations between local struct. states in supercond. TI phase 78−26981
Na_xWO_3, X>0.5, temp. depend. of Raman active soft modes, tetragonal-tetragonal transition 78−48180
$Na_5W_3O_9F_5$, phase transitions obs. *(French)* 80−6516
$Na_2[B_4O_6(OH_4)].8H_2O$, differential thermal X-ray anal. of phase transitions in non isothermal conditions 79−52205
Nb, H_2 embrittlement, microscopic obs. at low temps. 77−32666
Nb-H, coherent α-α' phase transition, sample shape depend. 79−34005
Nb-H system, phase diagram and transforms., struct. obs. of various phases 80−104125
Nb-H(D) system, incoherent phase transition 79−73304
Nb-Pd constitution diagram, metallographic and X-ray diffr. anal. 80−89204
Nb-Ti (60 at.%), aged, TEM exam. of precipitation process *(Japanese)* 78−48409
Nb-Zr alloy, BCC-ω phase transition, electronically driven nature 80−103433
Nb-Zr-N, deformed and annealed, internal friction, rel. to structural state *(Russian)* 78−6957
Nb_3Al superconductors, sputter deposited, BCC to A15 transition, microstruct. investig. 78−27512
$Nb_3Al(Ge)$, bonding, electronic charge distribs. and struct. transform. from self-consistent pseudopotentials 79−69054
Nb_3Ge, band struct. and density of states from self-consistent pseudopotentials, struct. transitions 79−69401
NbH_x, coherent α-α' phase transition 80−71641
NbH_x, HF phonons, neutron spectral obs. 80−49317
Nb_2N, supercond. props. and structural phase transform. induced by C^+ and N^+ implantation 80−107942
NbO_2, electronic band struct., optical props., generalised susceptibility, struct. transition 79−95328
NbO_2, Lifshitz point behaviour 80−70402
NbO_2, structural fluctuations at high temps., inelastic neutron scatt. 78−55947
NbO_2, structural phase transform., neutron scatt. obs. 78−14458
Nb_3Sn, softening of surface phonons in (100) plane, rel. to structural phase transition 80−107627
$Nb_{1-x}W_xSe_2$ x=0 to 0.15, elec. resist., mag. suscept., heat capacity, structural, supercond. transition *(Russian)* 78−31006
Nd, high temperature transport props., scatt. mechanisms, phase transitions 77−15825
$NdCl_3$, aqueous frozen soln., phase transformations, optical absorpt. spectra, Nd^{3+} Stark splitting 79−1777
NdP_5O_{14}, ferroelastic, spectroscopy, ferroelastic/ferroelectric coupling 79−19845
NdP_5O_{14}, ferroelastic, hydrostatic press. effect on phase transition temp. 80−70293
NdP_5O_{14}, sp. hts. near ferroelastic phase transitions 78−63863
$Nd_2Ti_2O_7$, crystal struct. rel. to isomorphous crystals *(Japanese)* 80−49208
Ni (111) surface, C interaction, monolayer form. and struct. stability 80−10756
Ni alloy, GAB 286, austenitic energetic particle bombardment, thermodynamic and dimensional stability 77−27904
Ni alloys, constitution changes due to radiation effects 80−34048
Ni based superalloys, sigma phase prediction techniques 80−7567
Ni complex, 1,2-benzoquinonedioximates, refl. spectra, 0.5-2.5 eV, Young's modulus and internal friction 78−39562
Ni complexes, $[Ni(NH_3)_6](ClO_4)_2$ and $[Ni(ND_3)_6](ClO_4)_2$, phase transitions, Raman spectra meas. 77−66501
Ni film, implanted with C ions, HCP struct. formation, electron diffr. study *(Russian)* 79−82469
Ni, ion implantation produced crystalline phase transitions 80−7558
Ni perfect crystal, stability under various stresses 80−104208
Ni, phase transformations and vacancy form. by positron annihilation 80−2155
Ni-Al (51 to 55 at.%), vacancy defective, TEM exam. of structure 78−76677
Ni-Cr-Mo-W-Al-Ti, heat-resist., phase comp. 80−76250
Ni-Mo-W, type N55M20V25, quenched at various cooling rates *(Russian)* 79−66052
Ni-Ti (12 wt.%), dil. alloys, transform. early stages 78−3096
Ni-Ti (12 wt.%), early stages of transformation 80−76251
Ni-V, interdiffusion coeffs. in phase transform. range, 810-1175°C *(Russian)* 78−91490
β-Ni-Zn, eutectoid decomposition kinetics *(German)* 77−8819
$Ni_3B_7O_{13}I$, 10K mag. transition and accompanying struct. transition 77−69565
$Ni_3B_7O_{13}I$, unit cell parameters and struct. transitions, 20 to 293K, X-ray diffr. study 80−24431
$Ni_3B_7O_{13}I$, X-ray diffr. obs., 77-300K, rel. to mag. susceptibility anomaly 77−47573

solid-state phase transformations continued
$Ni(CN)_2$-dodecylamine, lamellar paraffinic system, phase transitions, wide-line NMR obs. *(French)* 80−44929
$Ni(ClO_4)_2.6H_2O$, EPR and IR spectra, 98-298K, phase transition at 224K 78−84477
$NiCr_2O_4$, acoustic props. rel. to cooperative Jahn Teller effect and structural phase transform 80−24538
$NiCr_2O_4$, cooperative Jahn-Teller phase transition, channelling obs. 78−38839
$NiCr_2O_4$ single crystal, appl. of particle channelling to the study of a cooperative Jahn-Teller phase transition 79−4413
$NiCr_2O_4$:Fe, Mossbauer effect 80−15874
$Ni_{0.6}Fe_{2.4}B_7O_{13}I$, boracite, orthorhombic-trigonal transition region, Mossbauer investig. 79−87342
$Ni_xFe_2O_4$ series, chem. and mag. transformation, X-ray diffr. and mag. susceptibility study 79−51774
$Ni^{2+}Fe_{0.75}^{3+}V_{1.25}^{3+}O_4$, acoustic props. rel. to cooperative Jahn Teller effect and structural phase transform 80−24538
$Ni(H_2O)_6(ClO_4)_2$, specific heat meas., 90 to 376K, phase transitions 78−83970
$Ni_7I_2B_{16}O_{30}$, isomorphous phase transition ~120K 78−79764
Ni_4Mo, coherent phase form. at stress concentrators *(Russian)* 80−49356
$Ni(NH_3)_8(BF_4)_2$, phase transition, group theoretical anal. 80−65218
$Ni(NH_3)_6(ClO_4)_2$, phase transition, group theoretical anal. 80−65218
$Ni(NH_3)_6I_2$, EPR of Ni^{2+} ion near structural phase transformation 80−11248
$Ni(NH_3)_6I_2$, phase transition and rot. excitation 80−96642
$Ni(NH_3)_6(NO_3)_2$, Raman spectra exam. of orientational phase transitions 78−31184
$Ni(NH_3)_6(PF_6)_2$, EPR investig. of struct. transition 77−20679
$Ni(NH_3)_6X_2$, (X^-=Cl^-, BF_4^-, ClO_4^-) spin dynamics at struct. phase transition 79−15309
$Ni(OH_2)_6(SiF_6)$, phase transitions, spectrometric exam. *(French)* 78−88291
NiS, struct. mechanism of low-temp. phase transition in hexagonal modification 78−71855
NiS_2, thermal expansion and cryst. distortion below antiferromag. Neel and weak ferromag. Curie temps. 77−15579
Ni_7S_6, alternative transform, behaviour, direct obs. by TEM 77−1227
$NiTiF_6.6H_2O$, mag. and struct. transitions 78−68257
$Ni_xZn_{1-x}Mn_2O_4$, mag. props. 78−43573
$Nz(ClO_4)_2.6H_2O$:Mn^{2+}, EPR obs. of high temp. phase transition 79−28598
O_2, density of solid in equilib. with vapour 78−93656
O_2 solid, α-β transition, mag. susceptibility *(Russian)* 80−6592
O_2, solid, mag. susceptibility, temp. depend. as function of press. and mag. field, α-β transition obs. 77−47991
O_2 solid-solid transition point, international practical temp. scale precision appl. 78−87786
PF_3, cryst., mol. motion, ^{19}F NMR investig. 77−73093
γ-$PH_{3-x}D_x$, Raman and IR spectra, phase transition, internal and external modes 77−77191
PLZT ceramics, diffuse phase transitions and thermodynamics 80−29694
PLZT ceramics, ferroelectric and struct. transitions, crystallographic, thermal, and dielec. anal. 80−29693
PLZT ceramics, phase transitions induced by elec. fields 80−29695
P_4S_3, ^{31}P NMR spectrum and spin-lattice relax. time, 77 to 500K and 7 to 25 MHz 79−8064
(Pb,Ba)Nb_2O_6, polycryst., orientational polarisation and phase comp. in strong field 78−27157
Pb-Bi, peritectic reaction, microstruct. changes 78−52753
PbF_2, cubic and orthorhombic, press. and temp. depends. of ionic cond. 79−95207
PbF_2, sp. ht. meas., Schottky-type diffuse phase transitions, defect form. energies and entropies 80−107441
Pb_2GaTaO_6, transition from pyrochlore to imperfect fluorite struct. 80−19939
$PbGeO_3$, cryst. struct., dielec. and optical props. 77−1118
Pb_3GeO_5, cryst. struct. dielec. and optical props. 77−1118
$Pb_{1-x}Ge_xTe$ epitaxial layers, phase transition obs. by far IR reflectivity spectroscopy 79−33691
p-$Pb_{1-x}Ge_xTe$ film, cyclotron reson. above and below struct. phase transition 80−88879
$Pb_{1-x}Ge_xTe$, n- and p-type, effective masses 80−44481
$Pb_{1-x}Ge_xTe$ solid solns., phase transition influence on elec. props., 77 to 450K 80−103689
$Pb_{1-x}Ge_xTe$, TO phonon interaction with acoustic phonons near phase transition temp. 79−90776
PbI_2 direct gap polar semicond., electron hole liquid phase diagram *(Russian)* 80−93314
$PbMg_{1/3}Nb_{2/3}O_3$, ferroelec., crit. electron-phonon phenomena and diffuse phase transition in elec. field 79−38497
$PbMoO_4$, vibr. props. and struct., effect of hydrostatic press. 77−28571
$Pb(NO_3)_2$, low temp. struct. changes, elec. props. 79−87377
PbO, reactively evaporated photoconductive film, phase transform. induced by water vapour 79−78233
$PbO_{1.57}$, thermal expansion tensor, phase transitions, X-ray diffr. obs. *(French)* 79−1515
Pb_3O_4, cryst. struct., 5-240K, symm. change at 170K *(French)* 78−34618
Pb_3O_4, IR and Raman study of structural phase transitions *(French)* 78−84582
Pb_3O_4, phase transition, texture of tetragonal and orthorhombic phases *(French)* 79−23726
$Pb_3(PO_4)_2$, crit. behaviour of polar modes near ferroelastic phase transition 79−95750
$Pb_2(PO_4)_2$, ferroelastic, Raman scatt. by soft vibr. involved in ferroelastic phase transition 80−16040
$Pb_3(PO_4)_2$, ferroelastic, dielectric anomalies, phase transitions, permittivity, relaxation *(Russian)* 80−71293
$Pb_3(PO_4)_2$, ferroelastic phase transition, thermodynamic theory 79−37832
$Pb_3(PO_4)_2$, ferroelastic phase transition, inelastic neutron scatt. *(French)* 80−24584
$Pb_3(PO_4)_2$, temp. depend. of lattice parameters and spontaneous strain 80−29170
$Pb_3(PO_4)_2$:Gd^{3+}(Eu^{2+}), EPR spectra of α- and β-phases 80−11261
$Pb_3(PO_4)_2$-$Pb_3(VO_4)_2$ mixed crystal, crit. stress and phase diagram temp. depend. 78−26623
solid-state phase transformations continued
$Pb_3(P_{0.95}V_{0.05}O_4)_2$, ferroelastic transition, soft mode, inelastic neutron scatt. study 80−70357
$Pb_3(P_xV_{1-x}O_4)_2$, ferroelastic phase transitions, lattice dynamics, dielec. and optical props. meas. 77−55334
$Pb_3(P_xV_{1-x}O_4)_2$, ferroelastic phase transition, DTA, dilatometric and Brillouin scatt. study 80−70398
$PbSnF_4$, anionic conductor *(French)* 79−1523
$PbSnF_4$, thermal expansion and phase transitions 79−77781
$Pb_{1-x}Sn_xTe$, thermoelectric effects, characteristics at low temps. 80−107831
$Pb_{0.95}Sr_{0.05}(Zr_x, Ti_{1-x})O_3$-$Nb_2O_5$, phase coexistence range, lattice consts. 80−92680
PbTe, electron-phonon interactin induced phase transition 79−82338
PbTe, structural transition 77−51497
PbTe, TO-phonon mode softening, far IR Fourier transform spectroscopy 77−40248
Pb(Ti,Zr)O_3, polycryst., orientational polarisation and phase comp. in strong field 78−27157
Pb(Ti,Zr)O_3 solid solutions, phase coexistence discrepancies 80−96662
$PbTiO_3$, phase transition study by X-ray powder structural refinement 80−40075
$PbTiO_3$, soft mode decay mechanism, damping parameter freq. depend. 80−54324
$PbTiO_3$, struct. changes with temp. variation, rel. to elec. cond. 78−91437
$xPbTiO_3+(1-x)PbCd_{1/3}Nb_{2/3}O_3$, phase transition spread, polarisation relaxation, dielectric susceptibility *(Russian)* 80−75922
$Pb_3(VO_4)_2$, ferroelastic, phase transitions, boundary walls 80−107419
$Pb_3(VO_4)_2$, ferroelastic phase transition, thermodynamic theory 79−37832
Pb_2WMO_6, M=Cd, Mg, synthesis, struct., phase transitions 77−84715
$PbWO_4$, thermal expansion tensor, phase transitions, X-ray diffr. obs. *(French)* 79−1515
Pb_2WO_5, phase transformation study by high temp. X-ray diffr. and differential scanning calorimetry 79−43244
Pb(Zr,Ti,Ge)O_3, antiferro-ferroelectric transition 78−95565
Pb(Zr,Ti)O_3, X-ray anal. of phase transform. at 163K *(Ukrainian)* 77−69082
$PbZrO_3$, struct. phase transition 79−61312
$PbZrO_3$-$PbCd_{0.5}W_{0.5}O_3$, phase transitions 78−43817
Pd complex, 1,2-benzoquinonedioximates, refl. spectra, 0.5-2.5 eV, Young's modulus and internal friction 78−39562
Pd-H system, controlled H phase-induced strain hardening *(Russian)* 79−1878
Pd-H system, effect of α-β phase change on β-phase solubility of H 77−89544
Pd-H(D) alloy, low temp. ordering 79−14654
PdAl.r, cryst. struct. determ. 77−84700
$PdD_{0.64}$, neutron scatt. exam. of 50K transition 78−55942
PdGdH, diagram of state elec. props., indirect exchange interaction, EPR study *(Russian)* 80−50179
$PdH_{0.73}$, 50K transition, γ-ray and neutron diffr. study 79−14932
PdH_x, incoherent phase transition, lattice gas model 80−29171
$Pd_{1-x}M_xSe_2$ (M=Ru,Co,Ni), high pressure phase transformation studies, lattice constants and densities 79−65187
Pr, high temperature transport props., scatt. mechanisms, phase transitions 77−15825
$PrAlO_3$, ^{27}Al NMR, electronic spin dynamics at Jahn-Teller phase transition 78−68403
$PrAlO_3$, mechanism of 118.5K phase transition 77−47532
$PrBr_3(Cl_3)$, cooperative Jahn-Teller antiferroelec. ordering, struct. phase transition 77−66144
$PrCu_2$, mag. excitations and cooperative Jahn-Teller transition 79−65196
$Pr(OH)_3$, electronic heat capacity, 0.45 to 4.2K, phase transition at 1.21K 80−59673
$Pr(OH)_3$, Jahn-Teller antiferroelectric ordering 78−10859
PrP_5O_{14}, sp. hts. near ferroelastic phase transitions 78−63863
Pt, (100) surface, phase transition and relax. by MeV ion backscatt. and channelling 79−86970
Pt complex, 1,2-benzoquinonedioximates, refl. spectra, 0.5-2.5 eV, Young's modulus and internal friction 78−39562
Pt complex, KCP, periodic lattice distortions, charge density waves 79−82536
Pt complex, $Mg_{0.82}Pt(C_2O_4)_2.xH_2O$, X-ray diffuse scatt., 1-D Peierls-Kohn anomaly and struct. transforms. 78−14680
Pu and other actinides, conf., Baden-Baden, Germany (Sept. 1975) 77−19807
Pu, β to α, phase transformation kinetics anal. 77−70044
$RbAg_4I_5$, ionic conductivity and heat capacity near T_c 78−47584
$RbAg_4I_5$, solid electrolyte, neutron scattering study 78−79696
$RbAg_4I_5$, solid electrolyte, Raman spectra 79−73934
$RbAg_4I_5$, static and dynamic NMR effects at 208K and 122K phase transitions 80−108105
$RbAg_4I_5$, struct. transition at 209K, Ising like behaviour 78−14460
$RbAg_4I_5$, superionic conductor, evidence for first-order phase transition 78−83949
$RbAg_4I_5$, superionic conductor, phase transition detection by thermoelectric power method 80−92669
$RbAg_4I_5$, US attenuation near 208K phase transition 79−33085
β-$RbAlF_4$, struct. and irreversible and topotactic phase transition $\beta\rightarrow\alpha$ mechanism 80−107132
$RbCaCl_3$, Raman scatt. study of phase transitions 80−71411
$RbCaF_3$, ^{87}Rb NMR at cubic to tetragonal phase transition 79−82885
$RbCaF_3$, 193K phase transition, lattice dynamics 78−10160
$RbCaF_3$, 193K phase transition, crit. neutron scatt. obs. 78−10161
$RbCaF_3$, crit. scatt. at phase transition, Mossbauer diffraction 79−1733
$RbCaF_3$, critical scatt. at struct. phase transition, Mossbauer diffr. 80−20546
$RbCaF_3$, cubic to tetragonal phase transition, neutron diffr. obs. 79−23730
$RbCaF_3$, cubic to tetragonal phase transition, ^{87}NMR meas. 80−7187
$RbCaF_3$, cubic to tetragonal phase transition, ^{87}Rb NMR study 80−70392
$RbCaF_3$, elastic consts. near phase transition by Brillouin scatt. 78−38844
$RbCaF_3$, first order improper ferroelastic phase transition at 194K, phenomenological description 80−70397
$RbCaF_3$, influence of domains on struct. phase transition 79−28097
$RbCaF_3$, NQR obs. of struct. transition at 198K 79−65191

solid-state phase transformations continued

$RbCaF_3$, phase transitions due to octahedra rots. in perovskite struct., order-disorder model 80−70151
$RbCaF_3$, structural phase transition, superlattice points, neutron diffr. obs. 80−19944
$RbCaF_3$:Gd^{3+}, O_h^1-D_{4h}^{18} struct. transition, ESR obs. 80−50178
$RbCaF_3$:Gd^{3+}, struct. phase transition, EPR study 80−71171
$RbCaF_3$:Gd^{3+}, uniaxially stressed, transcrit. behaviour, EPR obs. 79−33086
$Rb_2Ca_2(SO_4)_3$, phase transition behaviour with respect to lattice constants and ionic radii of constituent ions 78−6643
$RbCdCl_3$, struct. phase transitions, NMR obs. 78−83943
$RbCdF_3$, Fe^{3+}-O^{2-} pair EPR probe for struct. phase changes 77−36113
$RbCdF_3$:Gd^{3+}, O_h^1-D_{4h}^1 struct. transition, ESR obs. 80−50178
$RbCdF_3$:Gd^{3+}, struct. phase transition, EPR study 80−71171
$Rb_2Cd_2(SO_4)_3$, ferroelec., X-ray study on phase transition 77−85665
$Rb_2Cd_2(SO_4)_3$ single cryst., growth and phase transitions 79−33918
$RbDy(MoO_4)_2$, Dy^{3+} doublets, temp. anomaly in splitting separation due to structural phase transformation *(Russian)* 80−39274
$RbDy(MoO_4)_2$, low temp. phase transitions *(Russian)* 78−87787
$RbFeF_4$, Mossbauer and optical evidence for crystallographic transition 79−14931
$RbFeF_4$, two dimensional structural phase transitions, sp. ht., optical, dielec., X-ray diffr. meas. 79−69240
$RbH_3(SeO_3)_2$, phase transitions *(Japanese)* 79−65812
$Rb_3H(SeO_4)_2$, phase transitions, dielec. behaviour 79−90777
$Rb_2Hg(CN)_4$, spinel, ferroelasticity and phase transformation 79−7646
$Rb_xK_{1-x}MnF_3$, struct. transitions, NMR and birefr. expts., 60-300K 77−47577
$Rb_2KMO_3F_3$, (M=Mo, W), low temp. phase transitions *(French)* 78−92036
$RbLiSO_4$, field induced ferroelec. phase 79−78633
$RbMnCl_3$ crystal, structural phase transition 80−15243
$RbMnCl_3$, structural phase transition 78−91442
$Rb_3MoO_3F_3$, ferroelec., phase transitions, crystallographic, DTA, dielec. and pyroelec. meas. *(French)* 77−85671
RbN_3, lattice vibration Raman study, tetragonal-cubic phase transitions 79−77743
$RbNO_2$, Raman spectra temp. depend., NO_3^- ion external librational modes, IV→III transition, Raman spectra temp. depend., NO_3^- ion external librational modes 79−78662
$RbNO_3$, phase transition, IR spectra 80−7350
$RbNO_3$, single cryst., DC cond., dielec. and thermophys. props., temp. depend., transitions interpret. 78−26682
$RbNO_3$, struct., high temp. phases, neutron diffr. study 80−79756
$Rb_2PbCu(NO_2)_6$, incommensurate Jahn-Teller phase transitions 79−65185
$Rb_2PbCu(NO_2)_6$, incommensurate Jahn-Teller transition, Huang scatt. 80−70401
$Rb_6Sb_4(SO_4)_3F_{12}$, dielec. props. and phase transitions 79−69765
Rb_2SnCl_6:$ReCl_6^{2-}$, luminesc. and absorpt. spectra, relax. processes 77−85779
$Rb_2(TeBr_6)$, far IR and Raman spectra and phase transitions 80−11376
Rb_xWO_3, phase transitions, supercond. transition temp. and elec. props. 79−28431
Rb_xWO_3, resistivity, Hall effect and Seebeck coeff. from 1.5 to 300K 80−6879
Rb_2ZnBr_4, incommensurate phase, ^{87}Rb NMR lineshape 80−93191
Rb_2ZnBr_4, quasicrystalline state, incommensurate phase transformation 79−99310
Rb_2ZnBr_4, soft modes at phase transforms., far IR spectrum study 80−107398
Rb_2ZnCl_4 single crystals, Raman scatt. spectra, temp. range covering two phase transitions 80−7340
$Ru_2Ge_{3-x}Sn_x$, and $Ru_2Ge_{3-y}Si_y$, diffusionless phase transitions, elec. and mag. props. 80−96871
S, orthorhombic-monoclinic heat of transition, by mass spectral determination of sublimation heat 79−73302
SF_6, cryst., IR and Raman spectra at 9 and 97K, cryst. struct. 79−87427
Sb, liquid-quenched, stabilisation and transformation kinetics of metastable phases 80−3022
Sb_2O_5 hydrate, cryst. struct., P_H phase, dehydration effects 77−35540
Sb_2O_5 hydrated, preseparation stage in dehydration, phase transformation 80−35524
Sb_2S_3 crystals, X-ray and DTA methods phase transitions *(German)* 78−43119
Sb_2S_3, NQR freq. of $^{121,123}Sb$, temp. depend., phase transition 77−12228
SbSI, birefr. and phase transitions 78−60405
SbSI, ferroelec. semicond., nature of low-temp. phase transition 77−69784
Sb_2Te_3-Bi_2Te_3 and Sb_2Te_3-Sb_2Se_3 systems, thermal cond. change during phase transitions 80−100368
$Sc_{0.995}Gd_{0.005}H_{1.9}$, low temp. anomaly, Gd^{3+} EPR linewidth and X-ray meas. 77−69687
Se, monoclinic to trigonal transform., DTA, X-ray diffr. and optical microscopy meas. 78−14461
Si, (111) surface structure phase transform, screw dislocations RHEED study 80−88153
Si, chemically etched, model of structural transforms. during thermal oxidation 78−79557
Si, order-order type phase transition at surface *(Russian)* 77−39728
Si, phase transformation, lattice dynamics, microscopic theory 80−107387
Si-Te structural changes rel. to memory effect *(Russian)* 78−71679
SiC crystals, 2H to 6H solid-state transformation, X-ray diffraction study 80−28943
SiC, uncommon mode of morphological development among coherent phases, optical and electron microscope exam. 78−80544
Si_3N_4 amorphous, crystallisation and sintering under pressure 79−87596
Si_3N_4, α to β transform., TEM and electron diffr. obs. 78−27507
Si_3N_4, α/β phase transform. 78−56632
Si_3N_4, hot pressed, effect of powder composition and sintering temp., on phase transformation kinetics, microstructure and mech. strength *(German)* 79−4939
Si_3N_4, mechanism of α-β transition under annealing 79−87629
SiO_2-Al_2O_3, coprecipitated gel, Si-Al spinel formation during transformation on heating 79−78958
SiO_2-Li_2O-K_2O-ZnO-P_2O_5, glass ceramic, phase changes and crystn. processes 80−7562
Si_2O_3-TiO_2 system, phase transform. at high temp. 77−84926
Si(110), clean surface structural transitions, LEED obs. 78−6203
$Sm(Co,Cu)_5$, eutectoid transform. 77−8799
$SmCo_5$ films, struct. transformations effect on coercive force and mag. reversal *(Russian)* 80−20436
$SmCo_5$, vacuum-deposited, eutectoid decomp. *(Russian)* 77−66621
$Sm_3Ga_5O_{12}$, garnet-perovskite transform 80−15239
$Sm_{0.8}Gd_{0.2}S$, low temp. phase transition, X-ray diffr. expts., 110-293K 77−59115
$Sm_{1-x}La_xS$, electron struct., lattice consts., X-ray spectral study *(Russian)* 80−100432
Sm_2O_3-Ga_2O_3 system, garnet-perovskite transform., phase diagram relationships 80−97460
Sn, acoustic emission rel. to effect of cold work on struct. transitions 77−63659
α-Sn, compact prep., from β-Sn containing 0.1 at.% Ge 80−55320
Sn-Ni, electrodeposited, thermal stability 77−52319
Sn-Ni, equiatomic, metastable, transformation kinetics, Avrami parameters calc. method 78−92239
$SnCl_2(H_2O)_x(D_2O)_{2-x}$, high resolution heat capacity meas. *(Japanese)* 80−52218
$SnCl_2.2H_2O$, Brillouin scatt. and thermal expansion 80−97289
$SnCl_2.2H_2O$, high temp. entropy of ionic model for phase transition 78−55949
$SnCl_2.2H_2O$, isomorphous transition, Landau type thermodynamic potential 80−107413
$Sn_{1-x}Eu_xMo_6S_8$, supercond., Mossbauer effect, struct. phase transition 77−12290
$Sn_xGe_{1-x}Te$ ($0.62<x<0.91$), specific heat anomaly at struct. phase transform. 77−69095
$Sn_xGe_{1-x}Te$, structural transitions 77−51497
SnS photoelectron spectra, rel. to ionicities and phase transitions 77−69960
SnSe, photoelectron spectra, rel. to ionicities and phase transitions 77−69960
SnTe, bond orbital model of band struct. 80−59853
p-SnTe, elec. resist. anomaly in vicinity of struct. phase transform. 79−19597
SnTe, electron-phonon interactin induced phase transition 79−82338
SnTe, NMR of ^{119}Sn and ^{125}Te, low hole conc., 64-440K *(Russian)* 79−15365
SnTe, phase transition obs. by Mossbauer spectroscopy 77−55740
SnTe, sp. ht. mean field behaviour at phase transition 77−66023
SnTe, structural phase transition threshold instability in strong EM field 80−103477
$SrAl_2O_4$-$BaAl_2O_4$ system, solid solubility, α-β transition 78−63860
$Sr_{1-x}Ba_xZrO_3$, struct., X-ray powder diffr. study for different phases 80−1989
$SrCl_2$, sp. ht. meas., Schottky-type diffuse phase transitions, defect form. energies and entropies 80−107441
$Sr(NO_3)_2$, IR reflection spectra, dynamical props. and phase transition 77−16303
$Sr(NO_3)_2$, low temp. struct. changes, elec. props. 79−87377
$Sr_2Nb_2O_7$, crystal struct. rel. to isomorphous crystals *(Japanese)* 80−49208
$Sr_2Nb_2O_7$, normal-incommensurate phase transition, electron microscopy and diffraction study 80−39277
$Sr_2Nb_2O_7$, phase transition at 215°C, physical props. obs. 79−56744
$SrSnF_4$, thermal expansion and phase transitions 79−77781
$Sr_2Ta_2O_7$, crystal struct. rel. to isomorphous crystals *(Japanese)* 80−49208
$Sr_2Ta_2O_7$, soft optic phonon responsible for structural phase transition, Raman scatt. meas. 80−96618
$Sr_2Ta_2O_7$, structural phase transition to superlattice, electron microscopy and diffraction study 80−39277
$SrTiO_3$, crit. behaviour under stress 77−31745
$SrTiO_3$, critical elastic compliance, acoustic resonance meas. 80−65118
$SrTiO_3$, H_2 reduced, neutron scatt. study of structural phase transition, central-peak enhancement 78−30755
n-$SrTiO_3$, magnetoresist. meas., band struct. exam. 77−85242
$SrTiO_3$, neutron quasi-elastic scatt. above structured phase transition 79−27877
$SrTiO_3$, phonon interactions and the dynamic central peak near structural phase transition 77−81114
$SrTiO_3$, semiconductor, soft modes, zone boundary mode 80−71357
$SrTiO_3$, specific heat near structural transition 77−81072
$SrTiO_3$, structural phase transition at 110K, theory 78−80300
$SrTiO_3$:Fe, photochromic Fe^{5+} in non-cubic local fields, EPR spectra near structural phase transition 77−40127
$SrTiO_3$-$Bi_2Ti_2O_7$-$CaTiO_3$ system, solid solns., elec., optical props. 79−11375
$SrWO_4$, vibr. props. and struct., effect of hydrostatic press. 77−28571
Ta BCC lattice, strain ordering in interstitial solutions 80−107420
Ta-chalcogenides, domain-like incommensurate CDW states and first order incommensurate-commensurate transition 78−26824
Ta-H system, phase diagram and transforms., struct. obs. of various phases 80−104125
TaS_2 (1T), domain-like incommensurate CDW states and first order incommensurate-commensurate transition 78−26824
TaS_2 (2H), sp. ht. and resist. near CDW phase transitions 78−34786
$TaSe_2$ (2H), broken hexagonal symm., incommensurate charge-density wave struct. 80−96646
$TaSe_2$ (2H), domain-like incommensurate CDW and first order commensurate-incommensurate transitions 78−56084
$TaSe_2$ (2H), first-order phase transition, thermal expansion meas. 79−51256
$TaSe_2$ (2H), Raman scatt. from CDW 80−93340
$TaSe_2$ (2H), sp. ht. and resist. near CDW phase transitions 78−34786
$TaSe_2$(2H), layer cpd. commensurate-incommensurate transition 79−69244
$TaSe_2$(2H), Raman scatt., charge density wave mode softening at superstruct. transition 77−8584
$TbAsO_4$, cryst. struct. by X-ray diffr. co-operative Jahn-Teller transition 77−89411
TbBi, type II antiferromag., trigonal lattice distortion, temp. depend. 79−23732
$(Tb_{1-x}Gd_x)_3Co$, intermetallic cpd. mag. props., phase transform, and mag. hystersis *(Russian)* 80−93113
$Tb_xGd_{1-x}VO_4$, cooperative Jahn-Teller effect, linear birefringence 77−76550

solid-state phase transformations continued
Tb_2O_2S, tunnelling effect and mag.-cryst. transition, neutron diffr. expts. 77−63180
$TbPO_4$, phase transitions at low temp. 80−15237
TbS, type II antiferromag., trigonal lattice distortion, temp. depend. 79−23732
TbSe, type II antiferromag., trigonal lattice distortion, temp. depend. 79−23732
TbTe, type II antiferromag., trigonal lattice distortion, temp. depend. 79−23732
$TbVO_4$, co-operative Jahn-Teller transition, low freq. dynamics, light scatt. study 80−88317
$TbVO_4$, cooperative Jahn-Teller effect, linear birefringence 77−76550
$TbVO_4$, dielec. meas. at Jahn-Teller transitions 77−24802
$TbVO_4$, Jahn-Teller distortion, mag. field depend. 78−79733
$TbVO_4$, Jahn-Teller phase transition, γ-ray diffractometry 78−91205
$Tb_pY_{1-p}AsO_4$, crystallographic, mag. phase transition as function of temp. and Tb conc. 78−43334
TbZn, ferromag. transition, transport coeffs. critical behaviour 80−15498
Te-In system, enthalpies of fusion, peritectic decomp. and allotropic transition, DTA *(French)* 80−76226
$Te_{80}Ge_{20-x}Sb_x(Bi_x)$, DSC studies of struct. phase transformation 80−66505
Ti (10$\bar{1}$1) surface, HCP→BCC transition He II UPS study 79−42345
Ti alloys, metallurgical characterisation using thermoelec. power meas. *(French)* 80−45462
Ti, fracture mechanism at different temps. 77−63785
Ti, heating and cooling rate effects on α to β phase transform. and recrystallisation 77−90379
Ti, solid state phase transformation α→ω, exam. of phase transformation kinetics under static, and dynamic pressures 78−80541
Ti, surface struct., HCP to BCC type struct. transition, FEM obs. *(Japanese)* 78−22938
Ti-Ag (10 to 17.5 wt.%), eutectoid system, $\beta \rightarrow \alpha_m$ transform., nucleation kinetics 80−97474
Ti-Ag(Au)(Si), thermodynamics and kinetics of β to α_m transformation 78−84795
Ti-Al-Mo, type BT22, phase transformations under step-by-step heat treatment *(Russian)* 80−108436
Ti-Al-Mo (31, 13 wt.%), transform. microstruct. 78−48394
Ti-Al-Mo-Cr-Fe (6.4, 2.7, 1.6, 0.4 wt.%), quenched VT3-1, decomposition kinetics of α″ and β in annealing *(Russian)* 77−66662
Ti-Al-V-Fe-Si, alloy VT6, phase transform. kinetics and Young's modulus *(Russian)* 77−81258
Ti-Al-Zr alloy, TA6Zr5D, structural evolution during continuous cooling at different rates *(French)* 80−45300
Ti-alloy, VT16, volume and phase changes during continuous heating *(Russian)* 77−77470
Ti-Au, (9.9 wt.%), eutectoid system, $\beta \rightarrow \alpha_m$ transform., nucleation kinetics 80−97474
Ti-Cu-Si alloy system, transforms. in Ti-Ti_3Si_3-TiCu region, 800-1600°C *(Russian)* 77−21099
α-Ti-Fe(0.22 wt.%), ω phase form. during ageing 77−52355
Ti-Mn base beta alloys, H effect on stability solid soln., hardness *(Japanese)* 77−81261
Ti-Mo (20 at.%), incommensurate struct., stacking soliton 80−107109
Ti-Mo binary system, solid state phase transform. and miscibility gap, phase diagram 79−8298
Ti-Mo-V-Al-Cr-Fe (4.8, 4.7, 5.2, 1.1, 1.0 wt.%), structural changes during heating up to 1000°C, DTA study *(Russian)* 80−93552
Ti-Mo-Zr-Sn, alloy, βIII, struct. transform. in thermally affected zones after electron beam welding 78−23919
Ti-Mo(Nb)(Ta), BCC struct., tetragonal phase form. by cold deform. *(Russian)* 78−88462
Ti-N system, phase relations, struct. rel. to heat treatment 79−11552
Ti-Nb alloys, Fe, Mo, V, Ta alloying additions on microstruct. after combined treatment *(Russian)* 77−59826
Ti-Nb-Mo(V)(Ta)(Al)(Zr), BCC struct., tetragonal phase form. by cold deform. *(Russian)* 78−88462
Ti-Nb-Zr-Fe-Mo-V, cold worked, struct. and phase transform. during ageing 78−3153
Ti-V-Si (30, 1 at%), quenched and aged, hardness, tensile behaviour and phase transform. 79−11646
βTi-V-Si (40, 1 at.%), Si effect of precipitation and age hardening 77−63676
Ti_3Al, phase transitions and physical props. 77−25068
TiC, ageing and ordering phenomena *(Russian)* 78−39807
TiC, X-ray diffraction study of struct. of ordered phase and phase transform. *(Ukrainian)* 79−37660
$TiCl_3$, electronic struct. and struct. phase transition 80−59644
$TiCl_3$, layer compound, theoretical study of phase transition 79−10945
$TiCl_3$, phase transition, phonon dispersion curves 80−2130
TiCo-H system, thermodynamic rels. and struct. transformations 80−49385
$Ti_{1-x}Hf_xSe_2$ mixed cryst., elec. resist. and phase transition temp. 80−24928
TiN, precipitation of ordered δ′-phase *(Russian)* 78−6929
TiNi alloys, structural transform., physical props. and memory effects *(Russian)* 79−1856
TiNi-H system, thermodynamic rels. and struct. transformations 80−49385
TiO_2, thermal anal. using solar heating *(Ukrainian)* 79−77725
TiO_2-SiO_2 powders, anatase-rutile transition, mechanism investigation *(Japanese)* 78−95746
Ti_2O_3, structural changes associated with semicond.-metal transition 77−15583
$TiSe_2$ (1T), lattice dynamics and phase transitions 78−79727
$TiSe_2$, electronic instability, ^{77}Se NMR 78−10790
$TiSe_2$, IR reflectivity, phonons and free carriers 79−61379
$TiSe_2$, mechanism for 200K transition, sp. ht. meas. 78−22853
$TiSe_2$, structural distortion, band Jahn-Teller type mechanism 77−62875
$TiSe_2$ Young's modulus and internal friction obs., 1.3 to 300K 79−46750
$TiSe_2$:Ta(V), transport props. and phase transition 78−72149
$Ti_{1-x}V_xSe_2$ ($0 \leq x \leq 0.1$), elec. resist. and Hall effect 80−2386
Tl, photoemission studies 80−45217
$TlAsS_4$, struct. and soft mode behaviour 78−91327
$TlCdF_3$, elastic consts. near phase transition by Brillouin scatt. 78−38844
solid-state phase transformations continued
$TlCdF_3$, third and fourth order elastic consts., press. depend. near phase transition *(French)* 80−34116
$TlCdF_3$, weakly discontinuous phase transition, linear birefringence obs. 80−11362
$Tl_2Cd_2(SO_4)_3$ single cryst., growth and phase transitions 79−33918
$Tl_2Cd_2(SO_4)_3$, structural phase transition, phenomenological theory 79−7693
TlH_2AsO_4, proton spin-lattice relax. study of structural phase transition 79−19796
TlH_2PO_4, high resolution heat capacity meas. *(Japanese)* 80−52218
TlH_2P0_4, calorimetric and dielectric exam. of phase transition, nearly crit. case. 77−40171
Tll, XPS and UPS study of phase transforms. 80−45210
$TlMnCl_3$, refr. index and birefr., struct. transition effects 77−90126
$TlMnCl_3$, specific heat in region of struct. phase transition 77−7862
TlN_3, lattice vibration Raman study, tetragonal-cubic phase transitions 79−77743
$TlNO_3$, boiling and melting pts., heats of transformation, solid-solid transformation 78−91441
Tl_3PSe_4, struct. and soft mode behaviour 78−91327
$Tl_2PbCu(NO_2)_6$, incommensurate Jahn-Teller phase transitions 79−65185
$Tl_2PbCu(NO_2)_6$, incommensurate Jahn Teller phase transitions 79−95156
$Tl_2PbCu(NO_2)_6$, incommensurate Jahn-Teller transition, Huang scatt. 80−70401
Tl_2SeO_4, structural transition, polarised Raman spectra 80−75349
$Tl_2(TeCl_6)$, IR and Raman spectra, lattice and internal modes, phase transition 78−6659
TmCd, struct. phase transition driven by quadrupolar pair interaction 79−61583
TmCd(Zn), quadrupolar phase transitions, magnetoelastic and quadrupolar coupling consts. 80−15744
$TmVO_4$, dielec. meas. at Jahn-Teller transitions 77−24802
$TmVO_4$, Jahn-Teller system, critical dynamics and acoustic phonon coupling, Z-branch 77−84887
TmZn, struct. phase transition driven by quadrupolar pair interaction 79−61583
α-U, CDW at 43K 80−80198
α-U, charge density wave, first order transition 80−10664
α-U, pseudo-single cryst. and polycryst., low temp. sp. ht. 78−83972
α-U, superstruct. neutron scatt. obs. near 43K 79−95116
U, vacancy formation and phase transformation by positron annihilation 80−49215
U-Al, transform. and struct. changes, cooling, cooling rate effect *(Korean)* 77−63660
U-Ti (0.75 wt.%), quench rate sensitivity, effect on microstruct., mech. props., ageing 77−70077
UAs_xSe_{1-x}, lattice distortion below Curie temp. 77−63252
UMn_2, structural transition from cubic to monoclinic, neutron and X-ray obs. 78−75833
UMn_2, transport props., influence of lattice distortion 80−100452
UO_2, mag. ordering lattice internal rearrangement transition, theory 80−20402
U_4O_{9-y}, doped, phase transitions, heat capacity meas. 77−18664
U_4O_{9-y}, thermal conductivity and diffusivity, 250 to 415K 77−50234
$U(OH)_2SO_4$, cooperative Jahn-Teller effect, mag. susceptibility meas. 78−72121
V-N α-solid solution, struct. transform. during annealing and quenching *(Russian)* 77−81257
V-Si, A15 cpd., Hall coeffs., effect of tetragonal distortion on band struct. 79−33281
VCl_3, electronic struct. and struct. phase transition 80−59644
$(V_{1-x}Cr_x)_2O_3$, Raman scatt. and phase transitions 80−71420
$(V_{1-x}Cr_x)_2O_3$, thermal props., rel. to phase transition 77−35709
$V_{1-x}Fe_xO_{2-x}F_x$, $0<x<0.2$, phase diagrams, ^{57}Fe-Mossbauer spectra, X-ray diffr. studies *(German)* 80−29663
$V_{1-x}Ga_xO_2$, phase transitions, semicond. metal transition, antiferromag. props. 77−11969
VH_x, NMR, phase transition obs., activation energy for H diffusion meas. *(Russian)* 78−27506
VH_x, positron annihil. lineshape Doppler broadening, H conc. and temp. depend., 20-500K 79−61463
$V_{1-2x}M_x^{2+}N_x^{6+}O_2$, (M=Ni,Cu,Mn, N=W,Mo,Te) cryst. struct., transitions and thermal effects 77−68950
$V_{1-2x}M_x^{3+}Nb_xO_2$, (M=Fe,Cr) cryst. struct., transitions and thermal effects 77−68950
VO_2, amorphous thin films, phase transition, resistivity and opt. transmission discontinuities 77−47871
VO_2, ferroelastic metal-insulator transition, electronically triggered crystallographic phase transition 80−70614
VO_2, film, optical consts. and electrical props. near phase transition *(Russian)* 77−59631
VO_2 interference films, colour valency change at phase transition temp. *(German)* 78−56533
VO_2, metallic, electronic struct., lattice instability 78−14664
VO_2, phase transition, temp. variation of US attenuation and phase vel. 77−31723
VO_2, photoacoustic effect at first order phase transitions at increasing and decreasing temp. 80−70320
VO_2:Al, photoacoustic effect study of phase transitions 80−69615
VO_2:Ga, Mo, phase behaviour with Mo content, Ga constant 78−76121
VO_2:Ga(Al)(Fe), phase transforms., influence of nonstoichiometry 77−85274
V_2O_3, crystallographic structure changes due to phase transition, electron microscope study *(French)* 79−7688
V_2O_3, impurity doping effects, elec. props. obs. 80−75609
V_2O_3, lattice parameter anomalies at high temp. 78−47522
V_2O_3, lattice parameters and anomalous high temp. behaviour 78−87790
V_2O_3 phase transition, temp. variations of US attenuations and phase vel. 77−31723
V_2O_3, phase transitions, Raman scatt. expts., 20-300K 78−39538
V_2O_3, thermal expansion tensor, phase transitions, X-ray diffr. obs. *(French)* 79−1515
V_2O_5, thermal expansion tensor, phase transitions, X-ray diffr. obs. *(French)* 79−1515
V_3O_5, heat capacity anomaly near 425K, and enthalpy change 77−47576
V_3O_5, high-temp. phase transition, resistivity, valence photoelectron spectra 80−49357

solid-state phase transformations continued
V_3O_5, insulator-metal phase trnasition at 450K, properties 78−39023
V_3O_5, phase transition, X-ray diffr. and DTA meas. 77−28001
V_3O_5, resistivity switching due to phase transition, 154°C 79−19642
$(V_2O_5)_{0.93}(MoO_3)_{0.07}$ solid soln., struct. transform. in oxidizing and reducing gas atm. 79−23740
VSe_2 (1T), incommensurate periodic lattice distortion, X-ray diffraction study 80−107414
VSi_2 thin film growth rel. to annealing environment and interposed layers 78−2395
V_3Si, electron spectrum characts., mag. susceptibility depend. on resistivity ratio 79−95320
V_3Si, magnetic susceptibility, density of states model for lattice transformation in A-15 compounds 80−65219
V_3Si, NMR meas. near struct. transform. *(Russian)* 80−44942
V_3Si, NMR of ^{51}V above and below 21K struct. transition *(Russian)* 80−34796
V_3Si, phase transition and transition temp., chemical comp. effects, defect struct. exam. 78−18651
V_3Si plastically deformed cryst., lattice transform., Kossel technique 78−95153
V_3Si volume changes during phase changes, meas. low temp. differential scanning dilatometer *(Russian)* 79−34224
$(V_{1-x}Ti_x)_2O_3$, solid solution, phase transition exam. 77−15590
$V_2Zr(Hf)$, struct. transform. at low temp., X-ray diffr. anal. *(Russian)* 80−45298
W (001), surface phase transition, electronic contribs., surface susceptibility, ab initio self-consistent thin-film energy band calc. 80−29255
W (100), chemisorption of H, phase changes, LEED obs. 79−77911
W (100) surface, phase transition exam. by LEED 77−55433
W, field cathode with (001) orientation preparation technique 80−15241
W-Nb (0-30 at.%), average thermal expansion coeff., 500-1200K 78−14483
WC-Co hardmetals, β-SiC to turbostratic graphite transformation 79−74150
$W_xMo_{1-x}O_3$, mixed cryst., structural phase transition, Raman and IR spectra 78−79766
WO_3, acoustic instability near monoclinic orthorhombic phase transition, X-ray scatt. 80−65215
WO_3, orthorhombic phase struct., rel. to struct. of other phases 77−24297
WO_3, semiconductor-metal transition, structural phase transition 80−107870
WO_3, triclinic, condensed modes 80−15211
Xe monolayer on graphite, phase transition from localised to nonlocalised solid 77−11787
Xe substrate, thin Ar films, phase transitions 79−42244
YIG, substituted, magnetite nucleation in transitional zone, ionic process, lattice imaging 80−107424
Y_2O_3-Al_2O_3, thin film, electron diffraction exam. of phase transformations *(Russian)* 79−34025
$YThNbTiO_8$, synthesis and cryst. struct. *(French)* 78−83799
$Y_2[Pt(CN)_4]_3.21H_2O$, first order phase transform., spectroscopic and thermodynamic anal. 78−38829
YbAg, mag. susceptibility, thermally excited interconfiguration crossover 77−16042
YbAu, mag. susceptibility, thermally excited interconfiguration crossover 77−16042
Zn, internal friction anomalies in temp. initiated brittle-plastic transition *(Russian)* 80−96648
$Zn(BF_4)_2 6H_2O$:Ni, phase transition study, EPR of diluted Ni^{2+}, 98-298K 80−75846
$Zn_2Ba_2Fe_{12}O_{22}$, phase transition, mag. props. *(Russian)* 79−51837
$Zn_{0.005}Fe_{2.995}O_4$, phase transitions, neutron elastic scatt. and resist. meas. 77−28000
$ZnGeF_6.6H_2O$:Mn (II), phase transition, ESR meas. 77−62636
$ZnMo_5S_6(Se_6)$, Chevrel-phase, low temp. struct. instability rel. to supercond. 77−47919
$Zn(NH_3)_4(ClO_4)_2$:Mn, EPR study of Mn^{2+} detection of structural transition 79−87308
$Zn(OH_2)_6(SiF_6)$, phase transitions, spectrometric exam. *(French)* 78−88291
ZnS, plastic deform., metastable to cubic sphalerite struct. conversion 77−80573
ZnS, with CdS or Cu_2S addition, phase transform. during crystn., 850 or 1150°C 77−48362
ZnSe, phase transition, differential thermal analysis 77−7863
Zr, solid state phase transformation $\alpha \rightarrow \omega$, exam. of phase transformation kinetics under static, and dynamic pressures 78−80541
Zr-Al (14 wt.%), transformation sequence from Zr-Al martensite to Zr_3Al phase 80−3027
Zr-Al (8.6 wt.%), dimensional stability struct. and mech. props, effects of neutron irrad. 80−92563
Zr-Al martensite, DO_{19} phase formation, selected area diffr. obs. 78−84779
Zr-Ir hardened alloys, metastable phases *(Ukrainian)* 79−34000
Zr-Mo-Nb-V-Sn (1,2,2,2 wt.%), heat treatment, transform. reactions and mech. props. 79−24545
Zr-Mo-Sn (3,2 wt.%), heat treatment, transform. reactions and mech. props. 79−24545
Zr-Nb, phase transformation sequences, prediction using free energy composition diagrams 79−4951
Zr-Nb, singularities of $\beta \rightarrow \omega$ transform. in alloy, with high content of β-stabiliser *(Russian)* 78−76644
Zr-Nb (1 and 2.5 wt.%), annealed, thermal expansion, α/β transition *(Russian)* 78−26702
Zr-Nb (20 wt.%), ω-phase form., diffuse Mossbauer scatt. 80−25324
Zr-Nb (20 wt.%) ω-phase transform., structural model, intensity distrib. in neutron diffr. 77−77472
Zr-Nb (2.5 wt.%), superplasticity 77−12669
Zr-Nb-Ge, singularities of $\beta \rightarrow \omega$ transform. in alloy, with high content of β-stabiliser *(Russian)* 78−76644
Zr-Nb-V-Al (Fe) alloys, decomp. of β solid soln., metastable and equilib. phases 79−11632
Zr_3Al base alloy, forming press. tubes 77−8784
ZrCu, constitutional and struct. studies, by mag. susceptibility, metallography and X-ray diffr. 80−70166
$ZrH_{1.5}$ and $ZrH_{1.75}$, low temp. phase transitions in H sublattice 77−24405
ZrO_2 ceramics, microstruct. and props., monoclinic to tetragonal transition 80−3035

solid-state phase transformations continued
ZrO_2, polycrystalline, tetragonal phase, stabilisation 78−15392
ZrO_2, thermal anal. using solar heating *(Ukrainian)* 79−77725
ZrO_2-$GdO_{1.5}$ (80 mol.%), X-ray diffr. exam. of continuous transition 78−68684
ZrO_2-P_2O_5, hydrated, heat treatment and coprecipitation, phase transitions 77−90335
ZrO_2-Zr cermet composite, hot pressed, fracture toughness 78−27604
ZrV_2, C-15 struct., phase transitions, elec. cond., crystal lattice parameters *(Russian)* 80−54826
ZrV_2, elec. resist. and mag. suscept., anomalous temp. depend. 79−69491
ZrV_2, latent heat of structural transform. 80−24589
ZrV_2, Laves-phase, cubic to rhombohedral transition, lattice electron instability 78−92261
ZrV_2, supercond. rel. to struct. instability *(Russian)* 78−23196

solid-state plasma
see also helicons; plasmons
A15 compounds, plasma energies, tight-binding energy-band model 78−84159
Alfven wave in stochastic mag. field Markovian approx. 77−51168
alkali metal, plasmon line width variation due to interband transitions 78−47822
alkali metal anions and trapped electrons formed by evaporating metal-ammonia solutions which contain cryptands 79−100340
alkali metals, line shape of plasma reson. 77−39765
amplifying Gunn diodes, nonlinear effects 79−51622
bimetallic junction, dispersion formulae for interface plasma oscill. 79−24048
charged-particle stream, wave interaction, nonlinear effect 80−80310
classical one-component plasma, dynamical struct. factor and velocity autocorrelation function 78−71430
classical one-component rare plasma, non-linear electron distrib. around massive positively charged particle 79−55458
coherent excitation of microwaves by electron beam 77−24579
coherent microemission excited by relativistic electron beam in solid-state plasma *(Russian)* 77−15205
complex dielectric function long wave limit, Coulomb systems with bound states, elec. cond. 80−33738
conductor, MHD kink instability 80−6307
conference, Masnuy-St-Jean, Mons, Belgium, Oct. 1979 80−82570
Coulomb screening in presence of two EM waves 79−15107
crystallisation of electron-hole plasma in strong mag. field *(Russian)* 78−79955
degenerate magnetoactive solid state plasma, enhancement of self focusing of laser beams 77−83934
degenerate semiconductor, Coulomb collisions in quantising mag. field, photon absorpt. *(Russian)* 78−55715
degenerate semiconductor, phonon-assisted Auger recomb. 77−59292
dichalcogenide layer compounds, interface plasmon-phonon interactions, transverse cond. 80−49641
dielectric crystal, uniaxial, wave propag., polarisation relations and dispersion eqns. 80−64723
dielectric function of electron-hole plasma, influence of two-particle states 79−56154
dielectric ionization density distrib. meas. during pulsed electron beam irradiation 77−20810
dielectric solids, quasiequivalence of annihilative e^+e^- and ionisative e^-e^- interactions 78−72633
dielectric-plasma like medium interface, image potential 78−14794
direct gap semiconductors, gain spectrum of electron-hole liquid 80−66279
dislocations and microplasma sites, STEBIC/STEM/EELS correlation 80−96528
doped conducting media, low-freq. props., EM wave reflection 80−103715
doped semiconductor plasma, inelastic light scatt., spin diffusion 77−36241
drift wave instability 79−15175
drifting hot carriers, EM wave amplification, linear theory *(Russian)* 79−69539
elastic ion lattice-electron gas binary mixture, continuum theory 79−51503
electric response function, two-component quantum plasma 79−37452
electron gas, layered, with random inhomogeneities, plasma wave damping 77−51689
electron gas, quantised in mag. field, plasma oscill., light scatt. 77−28134
electron plasma in presence of EM wave, DC mag. field, Coulomb screening, dielec. const. 80−15464
electron plasma with nonparabolic energy dispersion relation, EM fluctuations 80−2413
electron transport in dense nondegenerate plasma, thermal cond. *(Russian)* 79−98865
electron-hole plasma, created by pulse, hydrodynamics 79−65389
electron-hole plasma, striation form. during homogeneous heating 80−6889
electron-hole plasma, strongly degenerate, helical density waves 80−15550
electron-hole plasma, subject to crossed fields, propagation and spreading 78−76102
electron-hole plasma current layering, electron cooling length, momentum scatt. 80−6890
EM surface wave, normal mode propag. at drift vel. tangential discontinuity 77−24076
EM wave penetration into plasma, permittivity sign changes *(Russian)* 80−100477
equation of state, asymptotic method 77−24527
equation of state, quantum statistical theory, degeneration, electron-hole plasma thermal instability 78−91627
excitation of plasma column by ring source of elec. and mag. currents 77−27677
excitons, influence of dynamical effects 78−76004
excitons in electron-hole plasma, dynamical screening and self-energy 79−15093
extraordinary electron cyclotron waves, transverse propag. in quantising mag. field 77−59298
Fermi system, excitons in electron-hole plasma 79−90969
fermion one-component plasma ground state, two and three dimens. Monte Carlo study 79−33248

solid-state plasma continued
ferromagnet, harmonic rotator, Coulomb plasma and related models, renormalisation group treatment 78−88135
ferromagnet, harmonic rotator, Coulomb plasma and related models, case of dimensions D<2 and D>2 78−88136
ferromagnet, harmonic rotator, Coulomb plasma and related model, two dimens. case 78−88137
ferromagnetic semicond., spin-helicon wave parametric amplification 79−69665
ferromagnets with conduction electron spin, EM wave propagation with discrete spectrum 80−92923
free electron Compton scatt. of spectrally narrow radiation flux 80−20731
frequency dependent dielectric function of gapless semiconductors in a magnetic field 78−63994
graphite, IR optical properties, refl. data and complex dielec. function 78−10889
HF wave dispersion for complex wave numbers, ordinary waves 80−70740
highly degenerate multicomponent plasma thermodynamic props. 80−33739
hybrid bulk-surface polaritons for solid plasma slabs 79−60904
hybrid mode interaction in inhomogeneous semiconductor plasmas 78−63995
image charge pot. at interface of two semi-infinite media, Thomas-Fermi soln. 79−87155
inelastic light scattering, single particle excitations in many valley semiconductors 80−29749
inhomogeneous electron and electron hole systems, plasma oscills. 79−99496
inhomogeneous semiconductor plasma filled rectangular waveguide propagation 79−68928
inhomogeneous semiconductor structures, instability of plasma oscills. 79−11167
n-InSb, impact ionised plasma, three stream instability 77−55557
instabilities, magnetohydrodynamic, in nonequilibrium plasmas, theory and expt. *(Japanese)* 78−10493
instability, sausage, in linearly pinched plasma, theory and expt. *(Japanese)* 78−10492
ionic crystal, electron beam excited, luminesc. and cond. of nonideal degenerate electron-hole plasma 78−10488
jellium, one-dimensional, wall effects 79−46468
Kane semiconductors, parametric excitation of surface waves 79−38014
Kolmogorov Arnold Moser theorems, appl. to struct. problems in condensed matter 80−59878
linearized Boltzmann equation for semicond. plasma, carrier wave phase vel. 77−43634
localized electromagnetic pulses in a collisional medium 79−23999
low temp. plasma in mag. field, periodic signal generation, I/V characts. *(Russian)* 77−20352
low-dimensional systems, infrared problems and phase transitions of continuous order 78−6286
magnetic semiconductor, sound-like plasma oscillations in electron gas *(Russian)* 78−23125
magnetised, theory of neutron scattering 79−38015
magnetised semiconductor plasma, EM wave amplitude modulation and demodulation 80−84482
magnetoplasma, two-carrier, mag. and elec. dimens. reson., gyrotropic sphere problem 79−42570
metal, normal and magnetic, temp. depend. of plasma freq. 78−56100
metal, pair potential between two ions in electron gas 78−47723
metal clad dielectric slab waveguide, longit. plasma wave 77−777
metal conductivity, plasma model 80−80311
metal electrodes, plasma-type electroreflection, mechanisms 77−1659
metal film, ion sound velocity in mag. field *(Russian)* 78−18982
metal lattice heating by radiation, plasma effects, degenerate electron gas calcs. 80−70742
metal slab, relativistic electron beam exciting Langmuir turbulence 79−10878
metal-dielectric interface, p-polarised light total absorpt. by surface plasma waves 78−88373
metallic aggregated system, optical props., interband transitions and optical cond. reson. 77−44016
metallic film, steady-state Langmuir turbulence spectrum and turbulent energy absorption 78−26899
metallic surface, effect on cooperative Lamb shift 77−3317
metals, collective modes of void-surface coupled systems, surface plasmons 80−49642
metals, proper EM radiation on inelastic electron tunnelling with photon emission, cond. *(Russian)* 80−54765
molecular crystal, dipole plasma 77−85168
molecular crystal, dipole plasma oscillations, Bose-Einstein condensation of excitons *(Russian)* 78−84155
molecular crystal, dipole plasma oscillations, scattering of light 79−33723
molecular crystal, stimulated Mandelshtam-Brillouin scatt., dipole-plasma oscills. 80−1278
multicomponent electron-hole plasma correlation energy by RPA and mean component approx. calc. 80−24824
multilayer semiconductor structures, plasma-wave beams 80−49795
multivalley semiconductor, domain instability, two-beam model 79−47116
n-type semiconductor, inelastic light scatt. from magnetoplasma oscills. 77−12385
narrow gap semiconductor, plasma frequency, effect of electron spin, in quantising mag. fields 79−95436
narrow gap semiconductor with symmetrical carrier spectra, hot electrons 79−23982
narrow-gap semiconductor, recomb. instability of electron-hole plasma 80−39621
noble metal aggregated film, absorpt. peaks, collective oscills. of electrons 78−80428
nondegenerate semicond. plasma carrier wave energy characts. *(Russian)* 79−7849
nonlinear surface-wave interaction, in plasmalike media, theory 80−107839
nonlinear theory of stationary strata *(Russian)* 78−57884
nonuniform electron plasma, singularities of Landau attenuation and radiation width of collective levels *(Russian)* 78−56088
nonuniform plasma in high mag. field, elec. fields and transp. props. 79−60862
solid-state plasma continued
one component plasma, semi-analytic theory for static properties 79−38115
one dimensional Fermi gas model in relation to spin and field theoretical models 80−24816
one-component plasma in two and three dimens., static props., semi-analytic theory 80−87853
opaque semi-infinite crysts., dynamical light scatt. from dielec. bulk waves, phenomenological theory, appl. to n-InSb 79−69829
p^+-ν-p^+ structure, expt. determ. of lateral spreading vel. of electron-hole plasma 77−4428
p-n junction, HV, microplasma position determ. 77−20407
p-n junctions, microplasma noise, stochastic model, breakdown voltage of microplasma 78−47854
p-n junctions microplasma formation, influence of imperfections in Si crystals 77−8177
p-type epitaxial layer, thermalisation of electron-hole plasma, photolum. meas. 78−80408
parametric excitation of charge density fluctuations in classical and quantum electron-hole plasmas 79−50856
photo-excited semiconductor plasma, optical props. 79−43040
photodiode, switching process and plasma effects, theory 80−65667
piezoelectric, magnetised heavily doped semicond., hybrid mode parametric excitation 80−29427
piezoelectric semiconductor, acoustic waves parametric excitation 79−47128
piezoelectric semiconductor, dissipative, amplification of spin waves 79−24000
piezoelectric semiconductor, n-type, heavily doped, laser beam modulational instability 79−99570
piezoelectric semiconductor, n-type, magnetoactive, Brillouin instability in magnetostatic field 80−78909
piezoelectric semiconductor, transversely magnetised, parametric instability of acoustic waves 79−65521
piezoelectric semiconductor-plasma, parametric excitation of helicon and acoustic waves 80−107837
pinch effect in semiconductors and Bi, review 77−1441
plasmon-acoustic wave interactions due to deformation potential *(Russian)* 80−15356
polar semiconductor, EM wave propag. in solid-state plasma, DC electric field effect 79−82620
polar semiconductor, free carrier magnetoabsorpt. by photon-ionised impurity magnetoplasmon processes 79−38117
polar semiconductor, highly excited, optical dielec. function of electron-hole plasma 80−92847
polar semiconductor, n-type, hybrid mode instability 77−80800
γ-quanta channelling effect in periodic struct. *(Russian)* 80−96584
quantum insulator, plasma oscillation spectrum charges, continuum approx. free electron surface state binding energy 79−69575
randomly inhomogeneous cond. medium in mag. field 80−19558
Schottky diode, effect of thin oxide layer between metal and semicond. 77−20432
Schottky layers, homogeneous avalanche breakdown instability mechanism, microplasma form. 78−72262
screened interaction in electron plasma of cryst. 78−79561
secondary breakdown, microplasma effect *(Russian)* 79−56722
semiconductor, 2-dimens. plasma formed by quantising surface channel *(Russian)* 77−15936
semiconductor, anisotropic conductivity and ambipolar drift noise 77−20375
semiconductor, coexisting phases in electron-hole plasma 77−1374
semiconductor, crit. points for electron-hole system 80−44511
semiconductor, damage by 10.6 μm CW CO_2 laser beam 77−63497
semiconductor, electron-hole plasma and elec. field, stratification at low temp. 80−60020
semiconductor, electron-hole plasma drift due to carrier mobility gradients 78−26896
semiconductor, electron-hole plasma in crossed fields, renormalised diffusion coeffs. 79−87123
semiconductor, EM wave instability, effect of density gradient 79−1607
semiconductor, EM wave propag., temporal instability in crossed elec. and mag. fields 79−4577
semiconductor, EM wave propag. in external alternating mag. field 77−20350
semiconductor, exciton-plasma transition 79−28295
semiconductor, frequency shift of combined resonance, influence of plasma oscills. of conduction electrons 79−7850
semiconductor, hot electron waves in transverse mag. field 77−4387
semiconductor, hot plasma, wave instability 78−84245
semiconductor, inhomogeneous, radiation from a line source 77−66178
semiconductor, instabilities of electron-hole plasma under impact ionization and microwave emission 79−65508
semiconductor, intrinsic and injected electron-hole plasmas, one-dimensional drift and diffusion of carriers 79−11163
semiconductor, IR plasma reflectivity spectra analysis 78−52480
semiconductor, Kane's, parametric excitation 78−52023
semiconductor, layered, electron-hole liq. and metal-dielec. transition *(Russian)* 78−2425
semiconductor, light scatt. spectra, interference effects 79−82977
semiconductor, magnetised plasma, theory of EM surface waves 80−88584
semiconductor, n-type, carrier waves instabilities electron relax. time 77−4382
semiconductor, non-equilibrium, acoustic plasma oscills. generation 80−96811
semiconductor, nondegenerate, polarisation description 78−56176
semiconductor, nonhomogeneous hot solid state plasma, transverse EM instabilities 77−66177
semiconductor, normal transverse waves in longitudinal mag. field 80−80309
semiconductor, optical generation of carriers under Franz-Keldysh effect conditions, instability 79−24017
semiconductor, optical props. under intense laser fields 78−72513
semiconductor, oscillatory overheating instability 77−76855
semiconductor, overheating magneto-optic instability 77−1661
semiconductor, parametric amplification of plasma waves 78−43428
semiconductor, photoexcitation phenomena, low density 78−27319
semiconductor, piezoelectric, modulational instability of far IR laser 79−47117
semiconductor, plasma model of exciton gas *(Russian)* 77−11860

solid-state plasma continued
semiconductor, plasma self-oscillations within submillimetre freq. range 80−84473
semiconductor, quantum electron-phonon system, theory of parametric excitation 78−10489
semiconductor, single cryst., current-convective instability kinetics 77−32031
semiconductor, size effect, influence of space-charge regions on boundary conditions 77−89790
semiconductor, sound-induced anomalous transmission of light below plasma edge 78−68475
semiconductor, spatially periodic, natural oscillations of nonequilibrium plasma 77−20355
semiconductor, with superlattice, plasma resonant interaction with Stark oscills. 80−107842
semiconductor dielectric interface, surface wave propag. in presence of radial density gradient 79−7875
semiconductor electron-hole-plasma, instability in heating elec. field 80−15552
semiconductor EM wave propag. in electric field 77−43636
semiconductor in quantizing mag. field, plasma surface states of electrons 79−11195
semiconductor magnetically active plasma, longit. propag. of surface waves 77−15934
semiconductor plasma, isotropic heated, temp. plasmon oscills. 78−26898
semiconductor plasma, longitudinal oscillations 80−88583
semiconductor plasma, magnetised, stimulated Brillouin scatt. 80−33085
semiconductor plasma, solitons in radiophysics 80−48124
semiconductor plasma, strongly elongated electron distrib., normal oscills. 80−60021
semiconductor plasma, surface helicons, theory 80−60019
semiconductor plasma, surface waves 79−1612
semiconductor plasma, surface-helical instability *(Russian)* 77−15885
semiconductor plasma, unstable EM wave propagation, hot carriers, Hall effect, calc. 80−39620
semiconductor sandwich structure, magnetoplasmon-type surface polaritons at interface 77−85292
semiconductor stable electron-hole plasma, diffusion in magnetic field 79−24001
semiconductor surface, electron beam prod. of plasma oscillation instabilities *(Ukrainian)* 79−33318
semiconductor surface, resonance inelastic light scattering by carriers 80−20655
semiconductor surface plasma, van der Waals interaction with neutral atom, mag. field effects 77−59316
semiconductor with carrier mobility gradients, electron-hole plasma drift *(Russian)* 77−35948
semiconductor with electron heating by constant electric field, magnetoplasma wave instabilities 77−43639
semiconductor with superlattice, nonlinear plasma oscills. 78−26897
semiconductor-metal boundary, magnetoplasma polaritons at the interface 79−38163
semiconductor-plasma with two-hole species, parametric instability 80−2410
semiconductors, anomalous phonon induced light transmission below plasma edge 78−80368
semiconductors, ferromag. and nonferromag., paramag. waves travelling near the paramag. resonance freq. 78−88168
semiconductors, narrow-gap, recomb. instability under crossed elec. and mag. fields 80−70712
semiconductors, surface magnetoplasma wave spectrum in HF mag. field 80−24995
semiconductors with negative differential conductance, surface EM wave excitation, helicon and Alfven waves 79−69543
semiconductors with superlattice, plasma waves *(Russian)* 77−1439
semimetal in strong mag. field, metal-dielectric transition of electron-hole fluid *(Russian)* 77−80731
semimetals, modulational instability of finite amplitude Alfven wave 79−47118
shear waves, rotary activity under helicon-phonon interaction 80−2412
slab-shaped magnetoplasma excitation by magnetic current line sources 78−55717
small overdense plasma particle Thomson-like RF scatt., linear perturbation theory 80−48858
stratification on heating by light or elec. field *(Russian)* 77−11951
strongly degenerate plasma, double injection, vol. controlled current regime 79−51658
superionic conductors, ionic plasma oscills. 80−29212
superlattice, nonlinear plasma oscillations in high freq. elec. field 79−19612
superlattice, plasma oscillations 77−72878
surface modes, LF degenerate, of electron-hole plasma 77−28137
surface piezoelectric shear wave, two-dimens. electron plasma interaction *(Russian)* 79−19842
test charge bounded by solid state plasma, analytic expression for pot. energy 78−84154
three-dimensional rotator and vortex models 78−95266
transverse dynamic magnetoresistance and cyclotron reson. damping 79−4576
transversely magnetised semiconductor plasma, instability of EM waves 80−2411
two-dimensional quantum plasma de Haas-van Alphen oscill. in correlation energy 79−60738
two-valley semiconductor, hot electron instability, intervalley scatt. *(Russian)* 80−92921
vibronic ferroelectric carriers, dependence of plasma frequency on spontaneous lattice distortion *(Russian)* 79−15410
wave-divergence criteria 77−4389
weakly-ionised, three-component, ionis. equilib. instability 80−10877
Wigner electron crystal, melting curve 79−19531
Wigner lattices in one component plasma, H-stability and energy, numerical anal. 77−66129
Ag film, bounded by dielectric slabs, attenuated total refl. angular spectra 78−92135
Ag film, reflection coeff. minima and surface plasma wave dispersion curve comparison *(French)* 78−80429
Ag film, with thin transparent and absorbing coatings, surface plasma oscills. 78−43951
Ag film coated with dye monolayer, anomalous dispersion of surface plasma oscills. 79−8203

solid-state plasma continued
Ag, microcrystals on C foil, size distrib. from electron micrograph obs., UV absorpt. spectra obs. 80−55121
Ag, photoemission yield anomalies, quantitative analysis, dielec. response nonlocality *(French)* 79−61489
Ag, surface plasma waves, dispersion curves, attenuated total reflection spectra 78−88015
Ag, surface plasma waves 79−47151
Ag-LiF, alternating plasma-dielec. five layer system, ATR angular spectra 79−19943
Ag-MgF_2 layered system, optical excitation of surface plasma waves 78−6803
Al caesiated thin film, surface plasma wave excitation by polarised light, photoemission obs. 80−50518
Al film, dispersion curve of surface plasma waves, rel. to refl. power minimum curve *(French)* 78−88372
Al, plasma oscillations in oxide free Al clusters 78−2510
Au, surface plasma waves, dispersion curves, attenuated total reflection spectra 78−88015
Au, surface plasma waves 79−47151
Bi, Alfven wave dispersion, non-local, freq. and relax. time depend. effects 80−29429
Bi, Alfven-like waves, new branch obs. at 300 GHz 80−49794
Bi, Bernstein waves, electrostatic wave dispersion relation in mag. field 80−34471
Bi, EM wave dispersion and damping, Voigt configuration, non-local calcs. 80−100475
Bi, HF EM wave propagation in Voigt configuration 78−68045
Bi hole pocket, far-IR magnetospectroscopy, electron-electron interaction effects 77−77211
Bi, instability induced by microwave field, carrier overheating 78−19076
Bi, magnetoplasma effects at 300 GHz in Voigt configuration 80−39619
Bi, magnetoplasma waves, freq. doubling in propag. 79−28367
Bi, magnetoplasma waves at 9 to 100 GHz microwave freqs. 79−78127
Bi, magnetoplasma waves in strong mag. fields at 300 GHz 79−38116
Bi, microwave frequency shift associated with magnetosonic electric effect 79−60865
Bi, mode mixing of Alfven waves 77−4381
Bi, plasma echo for elliptic Fermi surface, echo coordinates *(Russian)* 80−44633
Bi-Sb, magnetoplasma waves in strong mag. fields at 300 GHz 79−38116
Bi-Sb, semimetallic, magnetoplasma effects at 300 GHz in Voigt configuration 80−39619
Bi-Sb (0 to 6 at.%), semimetal, magnetoplasma waves at 9 to 100 GHz microwave freqs. 79−78127
$Bi_{0.89}Sb_{0.11}$, effect of band structure on the dispersion of magnetoplasma waves 77−47845
$Bi_{0.924}Sb_{0.076}$, doped, optical, oscillation and galvanometric effects *(Russian)* 77−85247
$Bi_{1-x}Sb_x$, non-ellipsoidal Fermi surface, cyclotron reson. meas. at 35 and 70 GHz 77−62804
$Bi_{1-x}Sb_x$, semiconductor, anomalous conductance in strong electric and longit. quantised mag. field *(Russian)* 78−76084
$Bi_{1-x}Sb_x$, semimetallic, plasma effects, submm. wave expts. 77−35881
$Bi_{1-x}Sb_x$:Te(Sn), band struct., plasma refl. spectra and galvanomag. tensor 77−16315
$Bi_{86}Sb_{14}$:Te, single crystal, dispersion of magnetoplasma waves *(Russian)* 80−70739
Bi_2Se_3:Hg point defects in crystal lattice, Hall coefficient and IR spectra determ. 80−55129
$Cd_xHg_{1-x}Te$, electron mobility and conc. near gapless state, influence of hydrostatic press. 79−65486
$Cd_xHg_{1-x}Te$ epitaxial graded gap layers, plasma reflection and magnetoreflection 80−71391
CdS crystals, electron-hole plasma, carrier optical orientation 80−100689
CdS, electron-hole plasma, gain and refl. spectra study 80−66227
CdS, highly excited, stimulated emission processes, electron-hole plasma recomb. 80−97307
CdS, highly excited cryst., biexciton, impurity transition and electron-hole plasma 79−15092
CdS, nonequilibrium electron-hole plasma, optical orientation of carriers *(Russian)* 78−2904
CdS, parametric action of strong radiation field 78−14752
CdS, spatial diffusion of excitons under intense excitation 77−44061
CdS, stimulated and spontaneous emission from degenerate electron-hole plasma at 300K 80−29762
CdS, time-resolved spectra of spontaneous luminesc. from high density electron-hole plasma 80−40156
CdS type direct semiconductor, high excitation 77−48202
CdSe crystal, stimulated emission from electron-hole plasma, temp. depend. 78−88331
CdSe, luminesc. of high density electron-hole plasma at elevated temps. 80−20696
CdSe, optical gain spectra, exciton collision processes and electron-hole plasma 79−28814
CdSe, photocond. film, plasma reson., IR refl. obs. 80−11037
CdSe, single crysts., luminesc. of electron-hole plasma 80−60675
CoSi, plasma refl., 80 to 300K, energy overlap of valence and conduction bands 79−28366
Cr, ferromagnetic surface layer on antiferromag. bulk, determ. by surface magnetoplasma wave detect. 78−68356
Cr-Co (4 wt.%) alloy, antiferromag. transitions effect on opt. props. 77−12371
Cu, surface plasma waves 79−47151
Fe film, transverse Kerr magneto-optical effect enhancement by surface magnetoplasma waves 77−52056
Fe granular deposits, plasma reson., rel. to interstellar dust extinction curve 79−21387
Fe, optical and electronic props., temp. depend., 20, 1400 and 1600°C 79−87412
Fe_2O_3, haematite, anal. of refl. spectrum by Kramers-Kronig relations 80−16058
GE, microwave cyclotron resonance lineshape, magnetoplasma interference effect, reinterpretation of excitonic polaron 78−43287
GaAs, electron-beam excited, efficient generation of electron-hole plasma 80−76051
GaAs, electron-hole plasma, ground state energy 78−84244
GaAs, electron-hole plasma, Coulomb effects on gain and absorption spectra 80−50371

solid-state plasma continued
GaAs, epitaxial layers, high density electron-hole plasma luminesc. 78−19537
p-GaAs epitaxial layers, electron-hole plasma, quantum effects in magnetoluminesc. 78−72591
GaAs, insulating, optically pumped electron-hole plasma, Raman scatt. 77−40236
GaAs, magnetoplasma reflectivity effects, difference method *(German)* 77−12363
GaAs p-n homojunctions, microplasma elec. breakdown mechanism 79−87147
GaAs, spontaneous luminesc. due to high density electron-hole plasma under nano- and picosecond pulse excitation 80−40157
GaAs, stimulated and spontaneous emission from degenerate electron-hole plasma at 300K 80−29762
GaAs, thermalisation of electron-hole plasma 79−95439
GaAs, two photon absorpt., hot electron-hole plasma, relax. time depend., picosecond spectra 79−51979
n-GaAs, two stream instability 78−2509
GaAs:Be, ion-implanted, IR refl. and transmission meas. 80−34908
GaN, magnetoplasma reflectivity effects, difference method *(German)* 77−12363
GaP, electron-hole plasma photolum. obs. 78−52559
GaP, first order Mott transition of exciton gas 78−76535
GaP, stabilisation of electron-hole liquid by camel's back 80−6740
GaSb, electron-hole plasma, ground state energy 78−84244
GaSe, absorpt. spectra, electron-hole system at high densities 77−69854
GaSe, stimulated eimission due to electron-hole plasma recomb. 80−50374
n-Ge, anomalously enhanced plasma diffusion transverse to mag. field 80−96931
Ge, carrier density in electron-hole drops, plasma reson. determ. 77−24522
Ge, carrier relaxation rate temp. depend. and pair density in large electron-hole drop 80−75509
Ge, compressed electron hole plasma, luminesc. 78−72592
Ge, drift velocity of plasma cloud, at high elec. field 80−6887
Ge, elec. cond., optically injected carrier density and temp. depend. 78−68046
Ge, electron-hole drop and exciton atmosphere 80−6748
Ge, electron-hole drop freq. depend. damping 80−88482
Ge, electron-hole drop magnetoplasma resonance 79−60722
Ge, electron-hole drop recombination radiation due to heat pulse action *(Russian)* 80−16087
Ge, electron-hole droplet cloud kinetics, thermalisation phonons 80−88483
Ge, electron-hole droplets, conc. in mag. field, magnetoplasma absorpt. spectra meas. *(Russian)* 77−24854
Ge, electron-hole droplets, magnetoplasma reson. with submillimetre circularly polarised waves 77−89712
Ge, electron-hole droplets, luminesc. and absorpt. lineshapes, RPA theory 80−49613
Ge, electron-hole drops, appearance of plasma at high excitation rates 78−26821
Ge, electron-hole drops, IR magnetoplasma absorptions 80−6728
Ge, electron-hole drops, magnetoplasma resonance at arbitrary crystallographic orientation in mag. field 79−78018
Ge, electron-hole drops, resonant power absorpt., Alfven wave anal. 79−42569
Ge, electron-hole liquid, pinch effect 78−87993
Ge, electron-hole liquid in magnetic fields, expt. and theoretical investigations, review 79−60720
Ge, electron-hole plasma, destruction of pinch channel by longit. mag. field *(Russian)* 77−80802
Ge, electron-hole plasma, helical instability excitation in strong. mag. field *(Russian)* 77−69368
Ge, film, dense electron-hole plasma, negative differential resistance 77−89794
Ge, free carrier, intervalence band indirect absorpt., at high optically created carrier densities 79−42961
Ge, free-carrier plasma edge, fast transient spectroscopy 77−8558
n-Ge, HF plasma oscills. in external mag. field 80−54731
Ge, highly excited, theory of electron-hole plasma 78−10363
Ge, hot phonon influence on energy relax. of high-density carriers 79−82608
Ge, nonequilibrium charge carrier-mag. field interaction electron-hole drops, recombination *(Russian)* 80−75511
Ge, optically stimulated, electron-hole drops and appearance of dense plasma *(Russian)* 77−4688
Ge, oscillistor effect in strong mag. fields, ambipolar drift and breakdown 78−2511
Ge, p-n junction, I-V curve for microplasma breakdown, at. size difference effect 78−2550
Ge, plasma excitation, ultrafast optical props. 78−31248
Ge, reflectivity, picosec. laser pulses and electron-hole plasma 79−47463
Ge, solid-state plasma, ultrafast transient response, theory and expt. 77−80748
Ge, stressed, metal-insulator transition, luminesc. 80−20695
Ge, transport props. of high density electron-hole plasma at low temp. 77−47864
p-Ge-n-GaAs diode, microplasma breakdown 79−91140
GeTe, heterophase state with nonuniform distribution of free carriers *(Russian)* 78−2849
GeTe, heterophase state with nonuniform free carrier distrib. 79−56798
$Hg_{1-x}Mn_xTe$, microwave helicon propag. and helicon excited EPR 77−43637
In-Bi, vacuum UV optical props., surface and vol. plasma reson. 77−1697
InGa-GaSe interface, microplasma electrolum. at 300K 79−11469
InGaAsP-InP photodiodes, microplasma-limited avalanche multiplication at 1 to 1.3 μm 79−26128
InP avalanche photodiodes, microplasmas, investigation 80−60018
InP, electron-hole plasma, ground state energy 78−84244
InSb, absorpt. saturation by nonequilib. electron-hole plasma, luminesc. 78−9418
InSb, Auger-governed decay of laser-induced plasma, optical probing 80−76105
n-InSb, Brillouin instability in magnetostatic field 80−78909
n-InSb, coherent microwave emission in high mag. field 79−60863
n-InSb, degenerate plasma, Coulomb collision photon absorpt. dynamic screening *(Russian)* 80−92924
solid-state plasma continued
InSb, depletion layer, plasma and vibr. plasma type guided polaritons *(Russian)* 80−96933
n-InSb, drift induced insolubilities, carrier temp. effects 77−35949
InSb, drift wave instability 79−15175
InSb, EM wave instability, effect of density gradient 79−1607
n-InSb electron heating and energy relaxation time in quantising mag. field 80−10996
n-InSb, electron-hole plasma, LF instabilities in crossed fields 78−39146
InSb, electron-hole plasma instabilities, impact ionisation conditions, microwave emission 80−107840
InSb, intrinsic, photoinjected electron hole pairs, Auger lifetime, photoconductive decay obs. 80−39629
InSb, intrinsic and n-type, elec. cond., carrier wave instability in elect. and mag. fields 79−82617
InSb laser with two photon pumping by CO_2 laser radiation 79−86182
n-InSb, microwave helicon resonances, carrier density, mobility, dielectric const. 80−96930
n-InSb, microwave magnetoplasma and heliconlike reson., sample shape effects 77−85252
InSb, microwave magnetoplasma matching effect 78−14750
n-InSb, millimetre rare modulation in semicond. plasma, use of effects of high elec. field. 78−60149
InSb n-type, heavily doped, effects of hydrostatic pressure on electron mobility and conc. 77−4390
InSb, parametric amplification of plasma waves 78−43428
n-InSb, parametric excitation of plasma oscills. 77−66179
n-InSb, photoconductivity meas. in crossed fields 79−7852
InSb, pinch effect at room temp. 80−65615
n-InSb, plasma filament form. under impact ionisation conditions 78−60147
n-InSb powder, microwave propag., 90-300K, magnetoplasma and helicon wave excitations 78−72183
n-InSb, propagation of magnetoplasma waves, Faraday geometry, effect of strong electric field 79−65510
n-InSb, SBS of laser radiation in presence of mag. field, ion acoustic wave nonlinearity 80−45091
n-InSb, semicond. plasma, Raman scatt. of waves of fluctuations *(Russian)* 79−94299
n-InSb, semiconductors, plasma oscills. within submillimetre freq. range 80−84473
n-InSb, stationary energy transport velocity of light scattered from bunched solid-state plasma 79−95720
InSb, surface magnetoplasma waves, reson. spectrum and dispersion charcts. 79−38148
n-InSb, surface polaritons, excited by microwave magnetoplasma 79−19530
n-InSb, transversely magnetised, parametric instability of acoustic waves 79−65521
InSb:Te, periodically laminated plasma, 56.5 GHz transmission, helicon diagrams *(German)* 77−20348
InSb-GaAs semiconductor plasmas, surface wave instabilities, temp. effects 79−78125
InSb-insulator boundary, surface wave resonance in transversely magnetised semicond. plasma 78−30948
KCl, cryst., optical breakdown plasma effects 77−66558
La compounds, plasma light reflection by free charge carriers 80−11403
$MgF_2/In/MgF_2$ struct. surface plasma wave optical excitation in In 79−91516
NaCl, cryst., optical breakdown plasma effects 77−66558
Nb_3Ge, electron-lifetime effects on props. 80−10951
Nb_3Sn, electron-lifetime effects on props. 80−10951
Ni film, surface magnetoplasma waves, ATR meas. 77−69639
Ni film, transverse Kerr magneto-optical effect enhancement by surface magnetoplasma waves 77−52056
$Pb_{1-x}Ge_xTe$ magnetoplasma reflectivity and transmission spectra 80−71428
PbS, dispersion relation for magnetoplasma waves 79−51506
n-PbS, natural galenite, IR reflectivity obs. of plasma freq. 79−42975
PbSe, dispersion relation for magnetoplasma waves 79−51506
$Pb_{1-x}Sn_xTe$, lattice and electronic props. and g-value 80−80161
PbTe, asymm. strip line wall, EM wave propag. in mag. field 77−76854
PbTe, dispersion relation for magnetoplasma waves 79−51506
PbTe, lattice permittivity determ. by magnetoplasma waves method 78−19075
PbTe, microwave magnetoplasma exam. of lattice and electronic props. 77−69364
PbTe-SnTe compound semiconductors, lattice instability by mm-wave magnetoplasma refl. 80−54336
Pr compounds, plasma light reflection by free charge carriers 80−11403
Pt-n-GaAs Schottky diode, microplasma breakdown 79−91140
Sb, magnetosonic waves propagating in Voigt configuration obs. 78−23126
n-Si, appearance of high-field domain in pinch channel 78−26900
Si, As-doped, effect of elec. and struct. parameters on avalanche breakdown localisation 77−11926
Si, dense plasma dynamics during pulsed laser annealing, carrier density, recombination 80−84479
Si detector, α-particle dense track charge losses 77−3233
Si, exciton-plasma Mott transition, luminescence spectra 77−62836
Si, exciton-plasma transitions, dense electron-hole system portrait composition *(Russian)* 80−49622
n-Si, HF plasma oscills. in external mag. field 80−54731
Si, highly excited, theory of electron-hole plasma 78−10363
Si, inversion layer, magnetoplasmon reson. lineshape theory 79−1615
Si, ion implanted amorphous layers, free carrier plasma effects 77−73133
Si, laser-excited plasma, elec. signal pulse shaping expt. 77−19397
Si n^+-p junction, microplasma sites, SEM and TEM characterisation 77−43702
Si, non thermal laser induced ordering, plasma life time, phonon interactions 80−84481
Si, nonequilib. electron-hole system, gas-liq. phase diagram *(Russian)* 77−43509
Si, p-n junction, ellipsometric method of temp. meas. rel. to secondary breakdown *(Russian)* 80−11074
Si p-n junction, high-voltage, microplasma characts. 77−11997
Si p-n junction, mesoplasma formation, light-emitting properties of secondary breakdown region *(Russian)* 79−91131
Si p-n junction, microplasma characts., temp. depend. 77−4430

solid-state plasma continued
Si p-n junction, microplasma instability, effect of space-charge field of mobile carriers 78−19140
Si p-n junction, reverse bias high voltage, secondary surface breakdown 80−70813
Si p-n junctions, secondary breakdown, pre-mesoplasma state expsn. *(Russian)* 79−56723
Si, plasma effects during pulsed laser annealing 80−84480
Si, pulsed laser annealing, nonthermal, plasma annealing 80−25498
Si, reflectivity time dependence during pulsed laser annealing 80−66214
Si, solar cell, open-circuit voltage at ultrahigh light intensities, plasma reflection effects 80−96928
Si:P, amorphised by Ne^+ implantation, high fluence P implants, plasma region obs. 79−86807
n-Si:Zn,P, local deform. of cryst. lattice, charact. parameters or recomb. waves 77−4386
SmS, metallic, thermal modulation of reflectivity, 1.2-3.8 eV 79−99909
SnO_2 film, doped, electron effective mass and elec. props., carrier density depend. 77−43750
SnO_2 films, selective, optical characterisation by thermodynamical method 80−84796
Ti-V-Cr, electron-lifetime effects on props. 80−10951
TiS_2, evidence for semicond. props., Hall coeff., refl., cond., thermoelec. power 80−20220
ZnO, electron-hole plasma, gain and refl. spectra study 80−66227
ZnO epitaxial film on Al_2O_3 substrate, recombination radiation in intense single photon excitation 80−7410
ZnO, reflection spectra, exciton reflection at high excitation levels 77−69853
ZnTe, resonance Raman scatt. at high excitation levels *(Russian)* 80−55109

solid-state rectifiers
see also copper-oxide rectifiers; thyristors
34MW 120MJ pulsed DC supply for Divertor & Injection Tokamak Expt. 79−31214
CTR neutral beam source, SCR series switch and impulse crowbar 78−66395
fusion reactors, PDX, shaping field-equilib. field power supply rectifier upgrade study 80−91290
half-wave, RMS ripple current calc. *(German)* 77−20405
mass spectrometer magnetic analyser constant current solid-state power unit 80−86499
Schottky barrier, theory, technology and appl. 78−52089
Au/(Zn-)phthalocyanine/Al(In), photovoltaic effects, illuminated thin-film cell props. 79−4605
Au/(Zn-)phthalocyanine/Al(In), photovoltaic effects, dark elec. props. of rectifying cells 79−4604
Cu, electrolytic refining power supplies appl. 77−9089
GaAs-GaAlAs-GaAs rectifying semicond. struct., prep. by MBE and charcts. 80−65657
n-Si-Ni structure formed by elec. explosion of metal, rectifying barrier 78−72263
Te-Se-Cd, sandwich structure, fabrication and characteristics 80−60089

solid structure
see also crystal structure; long-range order; noncrystalline state structure; short-range order
atom/molecule effective volumes and electron correls. in one- and two-electron systems 77−3286
hard-sphere solid, correl. function model 79−23541
hard-sphere solid, disordered, lattice energy 79−23542
hard-sphere solid, radial distrib. function, Monte Carlo calc. 78−6022

solid theory
computer modelling of matter, conf., Anaheim, USA (March 1978) 80−51954
Frohlich, H., biographical notes rel. to solid state physics develop. 80−57059
Gottingen school, contrib., 1920-40 80−57070
hard-disc solid, free vol. props. 79−46534
hard-sphere solid, correl. function model 79−23541
hard-sphere solid, disordered, lattice energy 79−23542
hard-sphere solid, radial distrib. function, Monte Carlo calc. 78−6022
historical aspects, symposium, London, England (Apr.-May 1979) 80−56999
history since first appls. of quantum mechanics 80−57072
introduction to solid-state theory, book 79−33215
macromolecular, star-shaped molecules with branched nuclei, statistics 77−89383
Pohl, R., recollections of solid state physics 80−57060
SCF theory, orbital and pot. functions calc., eq. of state 80−44463
schools of thought, 1930 to mid 1960s 80−57069
Seitz, Frederick, biographical notes on early solid state physics 80−57058
sine-Gordon soliton dynamics, numerical simulation in presence of perturbations 77−76714
theoretical physics at Kharkov Inst., Ukrainian SSR *(Russian)* 79−12558
thermodynamics of polarisable and magnetisable solids in EM fields 77−57291
variational approach, hard sphere melting law 77−47359

solid-vapour transformations
see also sublimation
AES, effect of Coster-Kronig energy changes 78−56548
air-vapour flow in channel, laminar, with wall vapour-ice transition 79−94617
fluid-solid type phase transition, one dimens. model 78−63838
frost formation, struct. model of frost layer growth 78−79200
frost growth rate prediction eqn. for cooled surfaces 78−87248
high-current, graphite cathode vaporisation, composition and temp. spectral determ. 78−14228
inert gas adsorbed monolayer, Percus Yevick theory 77−7968
ions, mol. clustering, gaseous-condensed state, nucleation and solvation 80−28129
lattice gas model, three phase eqns. of state 78−22818
plane evaporation boundary instability in laser radiation-matter interactions *(Russian)* 80−76111
propane, vapour-liquid and vapour-solid equilib. data, mass spectroscopic tracer pulse chromatography 80−37115
tetrachloroisophthalonitrile, vapour press. by effusion method, solid phase eqn. of state 80−49350

solid-vapour transformations continued
Van der Waals film adsorbed on graphite, two-dimensional phase transitions 80−107653
water vapour, desublimation under vacuum, rate of ice form. 77−24402
Ar, adsorbed on graphite, monolayer two-dimensional phase change, calorimetric investig. 77−47669
Ar, phase transition, anharmonic cryst.-gas transition 80−6510
As(111), thermal accommodation coeffs. of As_4 determ., vibr. surface method 77−1319
CO_2, vapour-liquid and vapour-solid equilib. data, mass spectroscopic tracer pulse chromatography 80−37115
Cd, equilibrium condition, quantum statistical mechanics viewpoint *(Croatian)* 79−95154
In_2Se_3, vapour press. temp. depend., heat of evap. and form. 80−59642
KOH gas-crystal system, isotopic equilibrium near phase transition points *(Russian)* 80−91697
N_2, adsorbed on graphite, monolayer two-dimensional phase change, calorimetric investig. 77−47669
N_2, solid low-press. diffusion of vapour 78−22842
NaOH gas-crystal system, isotopic equilibrium near phase transition points *(Russian)* 80−91697
Pb, evaporation under action of laser beam, recoil press. behaviour 80−25501
Sc_2S, high temp. vaporisation, enthalpy, atomisation, dissoc. energies 77−1223
SiO vapour, refractory silicates nonequilib. phases condensation 79−60497
Xe adsorbed on Cu, NaCl, stepped and disordered surfaces, two-dimens. phase transformations 80−103580
$ZnGeP_2$ dissoc. press., vapour comp. and press., thermodynamic charcts. 77−24934

solidification
see also segregation
alloy, binary, crystallisation under parabolic stability *(Russian)* 79−70054
alloy, binary, nonequilib. crystn. dynamics, eqns. for supercooling, supersaturation of melt *(Russian)* 78−95736
alloy, binary, solidification, predicted volume change 77−28802
alloy, binary, solidification, transition from diffusion controlled to diffusionless, solute drag treatment 77−16563
alloy, binary, with curved solid-liq. interface, lateral solute segregation during unidirectional solidification 79−47692
alloy, crystallising, impurity distrib. under suppressed natural convection temp. *(Russian)* 77−28795
alloy, rapidly solidified powder, nucleation, undercooling and homogeneous struct. 79−11598
alloy, role of phase boundaries in phase transformations 78−72772
alloy, solidification mechanisms, contribution of microgravity expts. 78−88457
alloy, solidified, thermophysical charact. in region of special points of phase diagram *(Russian)* 78−44082
alloy, splat-quenched, grain size, isothermal transform. 77−77463
alloy solidification, interface stability, interfacial wave 77−86019
alloy solidification, kinetic model, appl. to liquisol quenching 78−44116
alloys, binary dilute, solidification, planar interface stability *(Czech)* 80−89212
alloys, complex, method for evaluating influence of each element on microsegregation of solidification *(French)* 79−74159
alloys, continuously cast, numerical study of optimal solidification conditions 79−83188
alloys, heterogeneous nucleation activity, and melting point ratio correlation 78−92255
alloys, heterogeneous nucleation during solidification 79−28077
alloys, multidimensional three-phase free boundary problems 80−75340
alloys, rapidly quenched crystalline, struct., and heat treatment effects 80−76292
alloys, review of theory, industrial techniques *(French)* 77−73268
amorphous solid, rapid quenching, techniques for determ. very short room temp. lifetimes 80−84981
amorphous solid, supercooled liquid-glass transition region, short-range order, simulation 80−44127
arc welding, molten pool solidification and bead formation 80−75341
arc welding, pool metal solidification kinetics in welding with electromag. stirring 80−71636
binary alloy, solidification chemical inhomogeneity *(Russian)* 80−75335
binary alloy indirectional solidification, convective and interfacial instabilities 80−60851
binary alloys, directional solidification, theory of dendritic growth 80−70145
binary alloys, initial transient segregation during unidirectional solidification in a furnace with thermal damping 80−70146
binary alloys, solidification calc. using compensation system *(Russian)* 80−16292
binary alloys, two phase region calcs. in solidifying melt *(Russian)* 80−65195
binary eutectic alloys, solidification anal. considering temp. and solute distrib., numerical soln. *(Japanese)* 78−39757
binary eutectic system, steady state lamellar solidification, self consistent theory 77−70041
binary melt, analytic description with melt diffusion consideration 80−24390
binary melt, crystallising, thermoconcentrational convection in liq., core 80−6043
binary melt, thermoconcentration convection in solidification, influence on impurity distrib. *(Russian)* 79−73292
binary melt-crystal phase transformation kinetics, stat. modelling of cryst. growth mechanism 80−24389
brass leaded, effect of Al, Sn, Fe on solidification, differential thermal analysis exam. *(Russian)* 79−29041
bubble departure radii at solidification interfaces 80−44295
carnauba wax, thermoelectret orientation parameters, solidification with different cooling rates 79−38444
casting, closed mould horizontal continuous, mathematical model 77−28801
casting, impurity distrib., effect of thermal-gravitational convection, numerical study *(Russian)* 78−19734
casting, solidification and cooling in mold *(Russian)* 79−29038
casting considerations 79−78952
casting in space environment, dendrite remelting and macrosegregation in low-gravity 79−47669

solidification continued
casting solidification simulation, use of general purpose software 77−52312
cellular and cellular dendritic growth, general microsegregation eqn. 80−84921
cellular phase separation rate, extremum condition 80−2137
ceramic, directionally solidified eutectic 78−27503
chemical compatibility with Ni base directionally solidified eutectic alloys 79−87623
chemically hardening material cast in elastic cylindrical mold, transient thermal stresses 80−7589
classical liquids, phase transitions, book contrib. 79−60481
continuous casting cylindrical ingot, development of elastic-plastic temp. stresses and deformations *(Russian)* 79−29151
continuous ingots, two phase zone critical parameters during casting *(Russian)* 80−93549
continuously cast billet with cubic cross-section, solidification *(Russian)* 78−19735
cooling bodies, thermal stresses and temps. determ. by finite elements 77−14881
Cotac 74, directionally solidified composite, creep behaviour prediction *(French)* 78−68754
crystal growth, capillary phenomena during solidification 78−30564
crystallisation from melt, nucleation on supercooling, inter-nuclear separation distrib. function *(German)* 77−19885
cylindrical ingot, continuous casting, elastic-plastic temp. stresses and deformation *(Russian)* 79−61576
cylindrical ingot, shrinkage effects on solidification rate under radiative heat transfer 80−66493
cylindrical mould, heat cond. with phase change 79−37108
dendritic growth, diffusion in semi-solid region 80−15281
dendritic growth, fluid flow effect 78−11215
dendritic solidification during welding 79−87625
dilute alloy, equilibrium distrib. coeff. relationship *(Russian)* 79−83186
dilute alloys solidification, numerical soln. model 79−69228
dilute binary alloy, unidirectional growth, morphological stability of planar interface 80−84920
directional, dendrite growth *(German)* 79−34023
directional, effect of thermal parameters, two-dimens. heat transfer model 78−88456
directional solidification, processor-operated segregation of minority atoms 80−29941
Earth core, dynamics of fluid core with inward growing boundaries 80−76934
electron probe microanalysis for high-temp. applic. *(French)* 77−29074
engineering structures, welded exam. of fracture processes, review 78−60777
epoxy resin ED-5, specific heat during solidification *(Russian)* 78−38816
epoxy type adhesives, solidification temp. conditions rel. to strength *(Russian)* 79−56972
eutectic, anomalous, acicular, nonequilib. crystn. anal. *(Russian)* 80−25678
eutectic, irregular, branching limited growth 80−81042
eutectic 78−23694
eutectic alloy, multiphase solidification theory 78−95740
eutectic alloy, rim zone formation *(Russian)* 77−85988
eutectic alloy directionally solidified, contact melting kinetics, mass transfer during solidification *(Russian)* 77−52310
eutectic alloys, unidirectionally solidified, solidification and morphology relationship 80−25684
eutectic containing enhanced amounts of reinforcing phase, unidirectional crystallisation *(Rumanian)* 79−29035
eutectic crystallisation kinetics, transient temp. effects *(Russian)* 77−1215
eutectic morphology modification, state-of-the-art 78−31394
eutectic structure coarsening during and after unidirectional growth 78−35379
FCC crystal-melt interfaces, mol. dynamics simulation 80−79913
fixed boundary condition modal, phase interface velocity *(Russian)* 78−15390
flow through channels and into cavities, Stefan problem 77−7383
foreign particle trapping during solidification anomalous influence of body force 78−2045
formulated as heat conduction problem with moving heat source 78−91420
front propagation, residual stress levels, polymerisation 80−59635
glass, solidification kinetic eqn., derivation from heat transfer and viscosity eqns. 80−25679
glass-ceramic, aligned, hot extrusion method for prep. 77−32552
glass-forming systems, thermodynamic origin of microstructure 78−88442
grain refinement during unidirectional solidification, effects of addition of powdered cpds. *(Japanese)* 78−35395
graphite, crystallisation from molten metal solns. *(Chinese)* 79−91634
gravity level effects, direct obs. 77−36494
Hastelloy X, mech. props. effect of solidification substruct. 77−25040
heat balance integral method, transformations 77−24380
heat flow, macroscopic, use of anal. approx. for description 80−104142
helical impurity distrib. produced by hydrodynamic instability, vertical solidification 78−30567
horizontal macrosegregation during solidification with a heterogeneous zone *(German)* 78−15381
ice, growth beneath water film, air bubble precipitation 78−83922
ice-water interface, local temp. meas. and convective flow 79−73293
ingot, continually cast, optimum conditions for variable drawing rate *(Russian)* 79−70056
ingot, hollow cylindrical, temp. field and crystallisation front calc. *(Russian)* 78−63690
ingot, temp., strain and stress distrib. *(Russian)* 77−25041
ingot formed in EM crystalliser, control of metal melt circulation *(Russian)* 78−84790
ingot forming from melt, liq. containment by EM field 80−35120
ingot solidification and reheating, thermal model 77−73340
ingots, cooling regime in conditions of minimal thermal stress, modelling *(Russian)* 80−65194
ingots, quenching technique, for studying formation of macrosegregations 78−52793
inorganic hydrate, heat transfer processes *(Japanese)* 80−6372
interfacial stability theory, moving symmetric model 78−2230
interfacial stability theory, stationary symmetric model 78−2229
solidification continued
inward cylindrical solidification, uniformly valid soln. 80−48564
inward solidification with black body radiation at boundary, asymptotic and perturbation solns. 77−55346
isotropic solidification, plane slip line fields, construction by characteristic net method *(German)* 79−91640
lamellar eutectic diffusion problem, numerical solns. determ. using elec. analogue 78−3116
laminar forced flow in convectively cooled parallel plate channel, asymmetric solidification anal. 78−38404
laminar heat transfer in tube, liq. solidification in thermal entrance region 78−18346
Landau theory, solidification and cryst. nucleation 78−83761
linear elastic solid with mass addition, stresses and displacement eqns. 77−55955
linear polycrystal, grain length statistics *(German)* 79−86872
liquid metal, cooling, new technique 77−36493
liquid metal, nucleation undercooling meas. in small drops 77−7851
liquid metal alloys solidification temp. range meas. technique 79−12799
liquid metal continuous casting, solidification process, convective heat transfer, anal. 78−84789
liquid metallic thin film, supercooling, electron diffraction study *(French)* 79−7676
liquid metals, flow in two-phase zone 79−81953
liquid solidification about cold cylindrical pipe 80−19383
liquid solidification on moving sheet 77−39201
liquid solidification press. meas., dielectric loss method 77−45868
liquid-glass transition, free volume approach, thermodynamic behaviour 80−1940
LMFBR, hypothetical core disruptive accident, molten fuel relocation dynamics, simulant fluids 79−30980
LMFBR single component and mixed oxide fuel solidification anal. 78−74435
low gravity solidification expts., use of metallic analogue materials 80−71635
low temp. melt spinning device 80−100825
low thermal conductivity material, solidification, dispersed high conductivity particles effects 77−80602
lubrication film temp. and traction, rel. to solidification and glass transition temp. 79−28041
magnetoelectric composite, growth from melt, gas bubble form. ahead of solidification front 79−29044
materials interactions, stability, phase transformations, thermodynamics and corrosion 78−88444
materials processing in space 78−35296
materials science and technology, space flight appl., conf., Gaithersburg, USA (April 1977) 79−47881
melt, solidifying, concentration convection 79−14237
melt, thermal convection as function of Grashof no., solidification kinetics 77−65661
melt extraction technology, advances 80−76207
melt near solid-liquid interface, diffusion during crystallisation *(German)* 79−29046
melt solidification, heat and mass transfer 79−14236
meltspinning, theoretical anal. of ribbon thickness formation 80−104143
metal, continuous coating of slab, solidification interface shape 79−15656
metal, eddy current response to solidification in one dimension 80−104140
metal, grain boundary groove migration at solid-liquid interface, simulation and with camphene 78−52789
metal, ingot solidification and shrinkage cavity form., model *(Russian)* 77−16566
metal, mathematical model for unidirectional solidification, massive moulds 79−56971
metal, pore form. mech. investigation by directional solidification 77−28800
metal, simulation by NH_4Cl cryst. growth from soln. *(Korean)* 77−73266
metal, solidifying, heterogeneous nucleation 78−39754
metal, weld pool solidification under EM agitation 79−24510
metal, welded joints, pore formation mechanism evaluation, rel. to solidification 80−3017
metal and alloy crystallisation, apparatus for decanting solid and liquid phases 78−56597
metal foams, solidification in space environment, fluid flow effects 79−47674
metal growth in space, theoretical models, comparison with ground expts. 78−84786
metal ingots, phase interface motion and variational Biot method 79−83189
metal metal system, glass formation 80−64921
metal refining by fractional solidification 79−61536
metal Taylor wires, texture and metastable phases 77−8812
metallic coatings, electric field atomisation from melt 80−76174
metallic glass formation, generalised kinetic treatment 77−52315
metallic glasses, electronic structure rel. to elec. cond., supercond. and mag. props. 80−65429
metallic glasses, formation, model based on nearly-free-electron approx. 77−52316
metallic one component systems, normal cryst. growth fluctuations theory 80−15025
metallic systems, in-situ obs. of solidification interfaces with 1 MeV electron microscope 79−87574
metals, unidirectional solidification, heat flow model 80−79914
metals, unidirectional solidification, in cooled mould, mathematical model 79−11600
metals, variational formulation of stationary free boundary problem *(French)* 80−96626
metals and alloys, crystn. process, X-ray fluoroscopic obs. 80−50620
metals and alloys, solidification models for high cooling rates 79−91639
microcrystal, temp. gradient, mol. dynamics model calc. *(German)* 77−76527
microsegregation, method for evaluating influence of each element *(French)* 79−74159
microsegregation and macrosegregation, relevance of processes in front of solidification front *(German)* 77−90342
mixture, binary, time-depend. solidification, series soln. 78−75058
molecular liquids and their binary solns., glass transition temps. 79−51239

solidification continued
molten salts, cellular convection, drastic viscosity, change *(French)* 78−14004
monotectic composite growth 79−56970
multi-dimensional solidification, dominated by thermal cond., similarity calc. method 80−38243
multidimensional conduction phase change problems, effect of density change, enthalpy model 77−42699
naphthalene-p. chloronitrobenzene system, eutectic, solidification 78−64530
Nimonic, IN100, γ' precipitates, casting conditions effect on morphology 80−7548
Nimonic 80A, rapidly solidified, struct. and initial precipitation, field-ion and TEM study 79−78982
m-nitroaniline single crystal fibre waveguide core, melt growth and charact. 77−34965
nucleation of crystallization centres, low frequency vibration effects on rate *(Russian)* 78−15383
numerical treatment of axisymmetrical conduction phase change 79−33073
off eutectic solidification, stage II transient, approx. soln. for composition variation 78−60665
off-eutectic alloy growth from stirred melt 77−8808
oils, viscosity and solidification press., 0-10^4 Pa, 20-180°C 77−43266
oxide eutectics, directionally solidified, crystallography and microstruct. 79−78950
PAA, nematic liq. cryst., thermomagnetic behaviour *(French)* 78−87612
PAP, nematic liq. cryst., thermomagnetic behaviour *(French)* 78−87612
paraffin plate heat storage element, fusion, periodic solidification, heat transfer kinetics *(French)* 80−40913
parallel-plate channel, convectively-cooled, liq. solidification 77−68666
particle engulfment, thermodynamic aspects 77−4184
particle rejection by solidifying melts, appl. of net repulsive van der Waals forces 80−34274
pattern selection in non-equilib. processes, marginal stability theory, eutectic solidification model 80−60852
peritectic structure formation criteria *(Ukrainian)* 80−11636
plasma sprayed coating, ultramicrostructure and porosity 79−82500
polyethylene, partially crystalline test body prep. and charact. *(German)* 78−31398
polyethylene fibre, high-strength high-modulus, morphology and tensile prop. relations 80−103264
polyethylene fractions, quasi-binary systems, solidification and crystn. 80−84108
polyethylene terephthalate, induced crystn. on metallic nucleating particles 79−15658
polyethylene-paraffin wax, blends, rapid cooling processing techniques 80−84905
polymer, crystallisation rates from melt, universal relation 79−10816
polymeric solidification of low level radioactive waste, Dow process 80−37502
polymers, solidification, as dissipative process 80−65205
polypropylene, partially crystalline, test body prep. and charact. *(German)* 78−31398
polyvinylidene fluoride, melt-solidified, crystn. and morphology 80−103461
powders, rapidly solidified, nucleation, undercooling and homogeneous structs. 78−52708
pyroelectricity, role in Costa Ribeiro effect 78−56431
radioactive high level waste, ceramics for solidification and storage 77−6542
radioactive high level wastes at Karlsruhe nuclear research centre 77−61545
radioactive liquid wastes, solidification 77−83046
radioactive nuclear reactor waste solidification 77−67836
radioactive waste, anal. of concentrating and drying processes in thin-film evaporator 79−59215
radioactive waste, from commercial LWRs 79−59207
radioactive waste, high-level, evaluation of products for solidification 77−61555
radioactive waste, high-level, new waste calcining facility 79−59211
radioactive waste, high-level, solidification production facility 80−83201
radioactive waste, low-level, developments and studies for marine disposal 77−61578
radioactive waste, low-level, from nuclear power plants 79−54540
radioactive waste, medium-level, cementation and bituminisation methods 77−65313
radioactive waste, reprocessing, solidification vitrification of liquid waste, review 79−9762
radioactive waste, spray calcination system 79−59212
radioactive waste, volume reduction and solidification systems, economics 78−17396
radioactive waste calcination and vitrification 77−61546
radioactive waste calcining at Idaho Chemical Reprocessing plant, design criteria 77−61549
radioactive waste fixation using sol-gel technology 80−83207
radioactive waste glasses, high-level, charact. of glasses for solidification 79−63779
radioactive waste portable vol. reduction and solidification system 80−37515
radioactive waste solidification, Sandia process 77−61551
radioactive waste solidification in concrete, polymer impregnation 77−6537
radioactive waste solidification system, Dow, state-of-the-art 80−5259
radioactive waste solidification to phosphate glass-metal matrix blocks 77−61550
radioactive waste solidification using a drum drier, FIPS method 77−61548
radioactive waste storage, high-level waste glass 77−6540
radioactive wastes, leach behaviour of hydrofracture grout 77−10478
radwaste, current concerns, treatment system design changes 80−5258
rare earth $Zr_{1-x}O_{2-x/2}$ growth from skull melting, directional solidification 78−60567
real liquids, quenched to glassy state, struct., one dimens. Ising model appl. 80−54134
reduced gravity, solidification interface, bubble interactions 78−84787
refractory composites, fibre reinforced, directionally solidified tensile tests, in HVEM, deform. and fracture *(French)* 78−68785
repulsion of foreign particle from solidification front of weak electrolyte soln. 77−84899
ribbon-form material, rapid quenching from melt *(Japanese)* 78−92210
solidification continued
rotated remelted ingots, macrosegregation 79−52196
sapphire, growth angle determ. from cryst. lateral face shape and solidified separation drops 80−103282
secondary boundary formation during crystn. *(Russian)* 77−59767
semi-infinite medium, solidification problems including density jump at moving boundary 79−77727
semi-infinite solid, laser surface melting and subsequent solidification, computer heat flow models 79−69916
semiconductor, dynamics of surface melting and resolidification during laser annealing 79−69918
shell forming solidification, hot tearing, model 79−79062
silicone liquids, viscosity and solidification press., 0-10^4 Pa, 20-180°C 77−43266
skin technology, industrial appl. of space processing 79−28991
slab, bounds and approximate solns. 78−67810
slab, zeroth order variable eigenvalue approach to melting or solidification 77−67392
solid-liquid interface shape, effect on temp. distrib. in cryst. growth from melt 79−61513
solid/melt interfacial tension and contact angles of small particles, determ. from crit. vel. of engulfing 80−79915
solidifying melt, two phase zone formation, convection *(Russian)* 80−93547
solidifying sphere, thermal contraction and density change effects upon freezing 79−64517
space environment, bubbles thermal migration and interaction with solidification interfaces 79−47670
space environment experiments, priorities 79−46787
spherical particle, growing from a binary alloy melt, morphological stability 80−29943
spherical particle growing from stirred melt, stability 77−47365
splat cooling process, using piston and anvil technique, mathematical model 80−11679
stability analysis, interfacial surface entropy effect in heat balance 78−26464
steel, 12% W, eutectic carbides struct. and comp. during heating 80−76283
steel, austenitic, Cr-Ni (20, 25 wt.%), containing B and Ti additions, splat quenching, X-ray and TEM study 79−74186
steel, austenitic, type 12Kh18N10T, pool metal solidification kinetics in welding with electromag. stirring 80−71636
steel, austenitic and austenitic ferritic, welds, rel. between solidification and microstructs. 79−61579
steel, austenitic stainless, ferritic, single phase ferritic solidification in welds, exam. 80−7546
steel, austenitic stainless, microstructural effects on US attenuation 78−11455
steel, austenitic stainless, weld, ferritic-austenitic solidification mode 80−89214
steel, boride coatings, form. mechanism and struct. during crystn. of castings 80−35412
steel, C, casting by C diffusion solidification 78−52792
steel, cast, effect of non-uniform struct. on props. 78−84850
steel, cast, high speed, solidification, $(Fe,Mo)_6C$ form., struct. 79−24514
steel, cementite precipitation from binary alloys, hardness and Mossbauer effects 77−70054
steel, continuous casting machine design, based on heat flow analysis, review 77−21048
steel, continuously cast slab, liquid-solid interface obs. by Pb additions to mould 77−21128
steel, Cr, high C, ingot, macrostruct., effect of diffusion annealing, solidification condition *(Chinese)* 78−15429
steel, Cr-Ni, pendant drop melt extracted, struct. and props. 80−76242
steel, Cr-W(Mo), quenched, carbide reactions during tempering 80−89229
steel, cylindrical ingot, continuous casting, elastic-plastic temp. stresses and deformation *(Russian)* 79−61576
steel, high speed, made by liquid infiltration 77−55906
steel, high speed, props. after electroslag remelting 80−104139
steel, high speed M2, charact. of solidification struct. within dendritic core 78−27504
steel, high speed S6-5-2 Si content effect on solidification *(German)* 78−11213
steel, high speed tool rapidly quenched, exam. of solidification struct. 78−39758
steel, high-speed, solidification cycle, thermal anal. 80−29945
steel, killed, microsegregation and macrosegregation, relevance of processes in front of solidification front *(German)* 77−90342
steel, low alloy, S and Mn influence on high temp. strength and ductility after solidification from melt *(German)* 80−81106
steel, low C, rapidly solidified laser surface alloyed, electron microprobe obs. 79−70201
steel, low C, structurally free cementite formation 78−23697
steel, low impurity, peritectic transformations, influence on initial struct., solidification, grain boundaries *(Russian)* 80−66621
steel, low-alloyed, C-content influence on high temp. strength and ductility after solidification from melt *(German)* 80−81105
steel, maraging, steady state unidirectionally solidified, austenite reversion and determ. 77−25118
steel, melting and solidification *(French)* 77−66635
steel, MHD industrial smelting, techniques, economics *(Russian)* 77−24980
steel, molten, heat loss during solidification hydrodynamic eqns., hardening front kinetics *(Russian)* 80−55385
steel, Ni-S-(Mn), ferrite to austenite transform. effect on sulphide precipitation 77−86025
steel, oxide inclusions 78−23648
steel, residual stress influence on mech. props. *(German)* 78−27587
steel, Rheocast, struct. and props. 77−28804
steel, rimming, continuous casting and solidification *(French)* 80−25685
steel, rimming, teeming and solidification *(French)* 80−16296
steel, SiO_x inclusion formation on introduction of solid SiO into molten steel *(Russian)* 78−80530
steel, solidification of castings in mould *(Russian)* 78−27502
steel, solidification singularities in C and low-C steels *(Russian)* 78−80532
steel, solification during continuous casting, cooling regime comparison *(Russian)* 80−93548
steel, steady state unidirectionally solidified, dendrite morphology 77−16569

solidification continued
steel, undirectionally solidifying melt, horizontal macrosegregation during solidification with heterogeneous layer *(German)* 78−19733
steel, V, carbide eutectic presence, solidification and struct. 80−50624
steel, W-Mo-V-Cr(6,5,2,4 wt.%), 56-5-2, microstruct. produced by melting and powder metallurgy *(German, English)* 77−63591
steel forgings, expt.-calc. model of quenching, temp. meas. across cross section 80−16345
steel ingot, state of viscoelasticoplastic stress deformation, in process of solidification *(Russian)* 80−45295
steel shell, mech. behaviour during solidification 80−81043
stress, and dislocations, creation during crystal growth *(Russian)* 80−103277
styrene solutions, polymerisation initiation by intense pulsed electron beam 79−15997
succinonitrile, low entropy of fusion plastic crystal, dendritic growth, expt. test of theory 77−35842
superalloy, laser melted, epitaxial resolidification 77−90491
supercooled, struct. refinement mech. *(Russian)* 80−20975
supersaturated soln., shape stability of growing cylindrical particle due to diffusion and interface kinetics 80−79720
surface tension driven convection, solidification effects 80−43703
SYNROC-B sintered ceramics for high-level radwaste fixation, comp. and phase charact. 80−106126
theory development 77−4185
thermal contact resistance, determ. for solidifying metal and mould 78−39759
thermal gravitational convection, impurity distrib. and transfer processes 80−19367
thermal storage, high temp., latent heat method using heat exchanger *(French)* 80−40912
TNT, role of HNS in grain modification 79−100129
turbulent flow of liquid at its freezing temp. into a convectively cooled tube 78−34001
turbulent heat transfer and press. drop in tube, internal solidification effect 79−32512
two-dimensional inward solidification, in prisms, front movement obs. 78−95134
Udimet 700, microstruct. of resolidified zones formed by laser melting single crysts. 79−78953
weld pool, preferred growth direction of cellular-dendritic crystallites *(Russian)* 77−44236
white Fe castings, morphology of eutectic M_3C and M_7C_3 80−108427
working equations and simple anal. for cylinders and spheres 77−52313
zone refining-cascade purification, theoretical solute redistrib. computational results 79−74083
Ag, adsorbing species in melt effect on solidification 78−23695
Ag-Bi, discrete eutectic form. mechanism *(Russian)* 77−66634
Ag-Cu, directionally solidified, obs. of cutting deform. zone *(Japanese)* 78−15422
Ag-Cu (39.9 at.%), eutectic composites, solidification and deform. *(Czech)* 77−59773
Ag-Cu eutectic alloy, mechanism of lamellar spacing adjustment 78−31395
Ag-Ge alloy, liq.-quenched, metastable phase formation and evolution 77−90338
Ag-Ge eutectic alloys, unidirectional solidification, electron microscope study of twinning 79−61574
Ag-O system, melt, blow hole form. during solidification 79−43238
Ag-Sn, splat-quenched, X-ray diffr. study 80−81094
Al alloy, cast struct. form. in continuous casting *(German)* 78−92256
Al alloy, columnar to equiaxed transition on solidification 77−63655
Al alloy, sheets, type 7004, asymmetrical solidification structures, fluid flow, in W arc welds 78−84794
Al alloy welded joints, hot cracks in mutual solidification zone 79−24594
Al alloys, columnar struct. of alloys solidified in flowing melt in centrifugal casting 80−71640
Al and Al alloys, solidification of castings, electrical modelling study *(Rumanian)* 79−74142
Al and Al-Cu (0.5, 2 and 4.5 wt.%), solidification, apparent solid region *(Japanese)* 77−63653
Al binary alloys, rapid quenching, struct. and decomp. 80−76244
Al, cast and directionally solidified, porosity 79−74145
Al, crystallisation thermokinetics calc. of pure cylindrical specimen *(Czech)* 77−63654
Al ingot, dendrite arm spacing through heat flow control 77−73267
Al ingot solidification by HV pulses, impurity distrib. and conc. region formation *(Russian)* 80−20919
Al, ingot struct., effect of mould rotation and electromagnetic stirring *(Japanese)* 77−63652
Al, molten, showering cryst. form. in mould cooled from top *(Japanese)* 80−66498
Al, perfect single crystal growth from melt, different orientations of crystallisation front *(Russian)* 77−55881
Al powder, liq.-solid phase transforms. *(French)* 80−45294
Al, pure, dendritic growth, fluid flow effect 78−11215
Al, rapid melting and solidification of surface layer, exam. using computer heat flow model 78−83228
Al, solidification, high press. effects 80−66499
Al-A_3Ni eutectic, effect of some thermal parameters on the directional solidification process 78−88456
Al-$Al_{21}Pt_5$ eutectic alloys, unidirectionally solidified, struct. study 80−108394
Al-Al_3Ni directionally solidified eutectic alloy, struct. and mech. props. *(Korean)* 80−29944
Al-Al_3Ni eutectic composite, structural response to shape variations 79−83190
Al-Al_3Ti, directionally solidified, thermal stability during annealing, 435-660°C 80−108393
Al-Al_3Ti, peritectic transform. 77−16564
Al-Al_4Ca, eutectic alloy, unidirectionally solidified, exam. of growth and crystallography 78−72771
Al-Al_6Fe eutectic, thermal stability rel. to soaking times 77−21131
Al-alloy ingots, crystallisation condition effects on fan-shaped zone struct. *(Russian)* 78−3114
Al-B, manufacture, use of $NaBF_4$, transfer of B 78−27453
Al-based eutectic alloys, unidirectionally solidified, solidification and morphology relationship 80−25684
Al-Be-Mg (30, 5wt.%) alloy, weld solification parameters 79−24511

solidification continued
Al-Bi-(Fe), directionally solidified monotectic, growth parameters for aligned microstructs. 79−43236
Al-Bi(In)(Pb), monotectic system, rapid cooling from melt, effect on struct. *(Russian)* 79−70053
Al-Cd hypomonotectic alloy, rapid solidification and decomposition 80−50638
Al-Cr (3 to 11 at.%), cooling rate effect on solidification struct. and mech. props. *(Japanese)* 78−39755
Al-Cr dilute alloy, morphological stabilities of planar solid-liquid interfaces during unidirectional solidification 79−4960
Al-Cu, binary, solidification, predicted volume change 77−28802
Al-Cu, cast and directionally solidified, porosity 79−74145
Al-Cu, dendritic growth, fluid flow effect 78−11215
Al-Cu, isothermal coarsening of liquid inclusions 77−21166
Al-Cu, melt near solid-liquid interface, diffusion during crystallisation *(German)* 79−29046
Al-Cu, molten, showering cryst. form. in mould cooled from top *(Japanese)* 80−66498
Al-Cu, partially solidified, viscosity and struct. *(Japanese)* 79−14950
Al-Cu, solidification, solid-liq. interface, solute conc. effects 80−59632
Al-Cu, stir cast microstructure, turbulent flow and solidification 79−20036
Al-Cu (Mg), vertically solidified, effect of fluid flow on solidification struct., and macrosegregation *(Japanese)* 78−48391
Al-Cu (Mg)(Zn), corrosion of chill zone, solidification microstruct. effect 77−36687
Al-Cu (0.1 wt.%) alloy, unidirectional solidification, stability of planar solid liquid interface 77−86020
Al-Cu (0.5 to 40 wt.%), morphology of quenched solid-liquid interface *(Czech)* 77−86021
Al-Cu (33 wt.%) eutectic, solidification under reduced gravity, behaviour of suspended Al_2O_3 particles *(German)* 80−60853
Al-Cu (4.5 wt.%), growth structs. with dendrite growth directions differing from heat flow direction during solidification 79−43235
Al-Cu (4.5 wt.%), volume contraction accompanying solidification 78−52791
Al-Cu (4.5 wt.%) cast alloy, press. effect during solidification on struct. and mech. props. *(Korean)* 77−77469
Al-Cu (4.8 wt.%), secondary arms in dendritic growth, solidification effects *(Japanese)* 78−15387
Al-Cu (5.7wt.%), unidirectionally solidified, dendritic morphology and dendrite arm spacing 79−29043
Al-Cu alloy, cast, chilled zone composition and thickness obs. *(Japanese)* 80−7541
Al-Cu alloy dendritic solidification kinetics 80−81041
Al-Cu alloys, coarsening mechanisms of secondary dendrite arm, and organic analogue 80−81049
Al-Cu alloys, hypo- and hyper-eutectic, dendrite coarsening during solidification 77−63651
Al-Cu dilute alloys, vein closing mechanism in fluidity tests 80−84924
Al-Cu eutectic alloy, cooling rate in rapid solidification, estimation from cell spacing 80−50623
Al-Cu hypoeutectic, solidification cycle, thermal anal. 80−29945
Al-Cu-Mg, string ghost form. during solidification *(Japanese)* 79−100130
Al-Cu-Ni, directionally solidified, exam. of struct. of two phase alloys 78−80537
Al-Cu-Si, Al rich, unidirectionally solidified, microstruct. 79−34021
Al-Cu-Zr, superplastic alloy Supral, solidification and recrystallisation 80−7550
Al-$CuAl_2$, directionally solidified eutectic alloy, effect of heat treatment 77−55977
Al-$CuAl_2$, directionally solidified eutectic, structural changes during strength tests *(Russian)* 80−7543
Al-$CuAl_2$, interface undercooling-growth vel. relationship, horizontal and vertical solidification 79−8294
Al-$CuAl_2$ eutectics, microstruct. after solidification, heat pipe influence 80−76243
Al-Cu(Mg), dil. binary alloy, planar interface stability during solidification *(Slovak)* 80−108424
Al-Cu(Mg), macrosegregation during solidification *(Japanese)* 79−100150
Al-Cu(Mg)(Cu-Mg), normal and gravity segregation in ingots, expt. study *(Japanese)* 79−24526
Al-Cv (0.3 wt.%), moving solid-liq. interface, diffusion in liq. 80−107456
Al-Fe, cast, influence of Zr on precipitation, solidification and grain size *(Rumanian)* 78−84813
Al-Fe-Si, eutectic alloy growth, by twinning plane propagation *(French)* 78−60667
Al-Fe-Si, Fe phase form., solidification condition effects *(French)* 77−70030
Al-$FeAl_3$, unidirectionally solidified eutectic, α-liq. interface stability 77−63650
Al-In (40, 70 wt.%), liq. phase immiscible system, solidification in microgravity 78−84770
Al-In alloys within miscibility gap, agglomeration in space environment 79−47672
Al-In emulsion, solidification mechanisms at zero gravity, review 78−88458
Al-Mg, crystallization interface *(Slovak)* 79−78951
Al-Mg, homogenisation process, effect of solidification rate and alloying *(Polish)* 79−78949
Al-Mg, rapidly solidified, metastable phases *(German)* 79−34011
Al-Mg, solidification, solid-liq. interface, solute conc. effects 80−59632
Al-Mg, type AMg6, pool metal solidification kinetics in welding with electromag. stirring 80−71636
Al-Mg alloy, cast, chilled zone composition and thickness obs. *(Japanese)* 80−7541
Al-Mg alloy, crystallisation front form. props., casting in EM field *(Russian)* 80−55384
Al-Mg alloys, distrib. of liquid Mg at liquid-solid interface *(Slovak)* 79−91637
Al-Mg-Fe-Mg-Si-Cr, alloys, dendritic segregation with Fe, Mg, Si and Cr additions *(Polish)* 79−56980
Al-Mg-Ti-Zr alloy AL23-1, nucleating cellular dendritic crystallisation *(Russian)* 79−70055
Al-Mg(Cu)(Si), (5.0(4.5)(11.8) wt.%), ingots, vibr. effect during solidification on porosity formation 80−108426
Al-Mn alloys, study of solidification by rapid cooling *(Japanese)* 78−88459

solidification continued
Al-Ni, solidification in mag. field, crystallite obs. *(Russian)* 77−4770
Al-Ni (3-18wt.%), gun-quenched from melt, struct. 80−76225
Al-Ni eutectic alloy, directional solidification using electroslag remelting 79−61578
Al-Ni-Co, directionally solidified ternary eutectic morphology *(Czech)* 77−59772
Al-Ni-Si, eutectic, unidirectional solidification 77−16565
Al-Pd eutectic, microstruct. morphology 80−3018
Al-Pt (2 at.%), splat cooled, $AlPt_2$ phase, electron diffr. obs. 79−15657
Al-Pt (2 wt.%), rapidly solidified alloy, metastable phase formation and decomposition 79−52194
Al-Si, hypereutectic Ostwald ripening of Si crystals during solidification *(Japanese)* 79−4962
Al-Si, off-eutectic alloy growth from stirred melt 77−8809
Al-Si (25.4 wt.%), solidification, high press. effects 80−66499
Al-Si (2.4 wt.%), liq. fluidity in solid-liq. zone 80−108429
Al-Si (8 wt.%), threshold H_2 for pore form. during solidification 78−52794
Al-Si alloys, penetrability coeffs. for two-phase zone of solidifying castings *(Russian)* 77−55956
Al-Si eutectic, directionally solidified, tensile props. 78−64531
Al-Si eutectic, pressure effect on metal-die heat transfer coeffs. during solidification 80−7544
Al-Si eutectic alloy, banded struct., SEM and optical microscopy 80−104144
Al-Si-P (19, 0.02 wt.%), primary Si crystals in Al melt, Ostwald ripening and solidification growth 80−35179
Al-Sn, discrete eutectic formation mechanism *(Russian)* 77−66634
Al-Ti, manufacture, use of Na_2TiF_6, transfer of Ti 78−27453
Al-Ti, molten, showering cryst. form. in mould cooled from top *(Japanese)* 80−66498
Al-Ti, solid soln., unidirectionally solidified, segregation patterns revealed by etching 79−47693
Al-Ti alloys, growth crystallography and morphologies of Al_3Ti primary dendrites 79−43230
Al-Ti dilute alloy, morphological stabilities of planar solid-liquid interfaces during unidirectional solidification 79−4960
Al-Ti dilute alloys, solute distribs. during unidirectional solidification 79−4961
Al-Ti-C, grain refinements study using centrifugal force *(Japanese)* 79−20035
Al-Zn alloys, interfacial stability of planar solid-liq. interface during solidification 80−104145
Al-Zn alloys, interfacial holes distrib. at beginning of interfacial instability in solidification 80−104146
Al-Zn-Mg powder, selected-area electron diffr. ring patterns 80−50642
Al-Zn(Cu)(Ni), ingots, solidified, formation of equiaxed eutectic grains *(Japanese)* 78−39756
Al-Zn(Cu)(Ni) eutectic alloy, mechanism of lamellar spacing adjustment 78−31395
Al-Zr, cast, precipitation and solidification *(German)* 77−36519
Al-Zr, interphases, formed during precipitation and solidification *(German)* 79−29062
Al-Zr, solidification and precipitation, Zr effect on cast struct. *(German)* 77−36518
Al-Zr (0.8 and 1.5 wt.%), hyperperitectic, non equilibrium solidification 78−3113
Al-Zr (1-13 wt.%), rapidly quenched, extended solid solubility, grain refinement and age-hardening 80−76266
(Al-Zn):Cd eutectic system, cellular growth, unidirectional solidification investig. *(Korean)* 77−28805
Al_2O_3, Mo-refined single crysts., fabrication 80−16250
Al_2O_3, molten, structural, conform. and solidification 77−36491
Al_2O_3-Sm_2O_3, phase diagram at high temp. *(Japanese)* 78−92253
Al_2O_3-Y_2O_3, melting behaviour and metastability determ. by optical DTA 80−92648
Al_2O_3-ZrO_2 cast refractories, nucleation processes reconstruction by SEM, TEM and STEM 78−35380
AlSb, gravitational influences on liquid-state homogenisation and solidification 79−78864
$AuSn_4$-Sn, eutectic struct., faceting and morphological regularity 79−61573
$AuSn_4$-Sn, unidirectionally solidified, X-ray diffr. anal. of crystal struct. 78−91308
B-Al cast braid, crystallisation and structuring of Al matrix *(Russian)* 78−52725
Be, cast, crystallographic orientation of columnar grains 77−59774
Be casting produced in zero gravity environment, BeO particles uniform distrib. 78−72753
Be, containerless grain refinement using BeO in space environment, melting and solidification 79−47673
Be, containerless melts in terrestrial and space environment, thermodynamic props. calc. from solidification and cooling curves 79−70052
Bi-Cd, solidification in mag. field, crystallite obs. *(Russian)* 77−4770
Bi-Cd eutectic alloy, directionally solidified, contact melting kinetics, mass transfer during solidification *(Russian)* 77−52310
Bi-MnBi, directionally solidified composite, processing parameter role on mag. props. 80−35352
Bi-MnBi directionally solidified eutectic alloys, struct. and mag. props. 79−51815
Bi-MnBi eutectic, directional crystallisation and microstruct. *(Russian)* 77−55915
Bi-Pb(Sn)(Tl), complex-regular eutectics, structural modification 78−23695
Bi-Sb, solidification, predicted vol. change 77−28802
Bi_2O_3-Si(Ge)O_2 melts, phys. props. 77−89566
$Bi_2Te_{3-x}Se_x$, thermoelec. mat., prep. effects on inhomogeneities 78−51576
CBr_4, bubble departure radii at solidification interfaces 80−44295
CBr_4, low gravity solidification, bubble behaviour 80−15219
(Cd-Bi)-Sn, eutectic alloy, directionally solidified, contact melting kinetics, mass transfer during solidification *(Russian)* 77−52310
Cd-Cd_3Ag, peritectic transform. 77−16564
Cd-$CuCd_3$, off-eutectic alloys, controlled grain growth *(Japanese)* 77−55958
Cd-Zn, solidification in mag. field, crystallite obs. *(Russian)* 77−4770
Cd-Zn alloys, splat-quenched, X-ray diffr., SEM and TEM study of struct. 79−66077
Cd-Zn eutectics, microstruct. after solidification, heat pipe influence 80−76243

solidification continued
(Co,Cr,Ni)-TaC, eutectic alloy, directionally solidified, struct. defects, autoradiographic investig. *(Russian)* 77−25038
(Co,Cr)-$(Cr,Co)_7C_3$, eutectic alloy, directionally solidified, struct. defects, autoradiographic investig. *(Russian)* 77−25038
Co-C-TaC directional eutectic, high-strength, interphase boundaries *(Russian)* 79−38812
Co-Cr-C-Al (39, 2.2, 2 wt.%), directionally solidified eutectic alloy, Larson Miller C const. 79−70162
Co-Cr-NiTaC eutectic, directionally solidified, microstructural stability 79−38815
Co-Cr(VC)((Ti,V)C)-(Al), eutectic alloy, unidirectional solidification, oxidation and tensile tests 78−52790
Co-Gd-B, rules of cmpd. form. in related systems 79−34010
Co-Nb(W)(Mo)(Ti)-Si, directionally solidified eutectics 79−61575
Co-Ni-Cr-Ta-C (10, 10, 14, 1 wt.%), aligned eutectic, directionally solidified, fatigue crack propag. 78−27624
Co-Si, directionally solidified eutectic composite alloy, form. and strength 77−90294
Co-WC hard alloys, rapidly quenched struct. 80−76233
25Cr-20Ni stainless steel dendritic solidification, growth morphology and solute redistrib. *(Japanese)* 80−81045
Cu and Cu alloy, unidirectionally solidified, morphology of solid liquid interface and solute redistribution *(Japanese)* 77−21133
Cu, continuous casting, heat transfer and surface temp. meas. apparatus *(Russian)* 77−66631
Cu, continuously cast, O free, effect of nonmetallic inclusion on microstruct. and props. 77−81280
Cu ingots, quality and optimal modes of solidification, prediction from temp. fields 79−83187
Cu melts, supercooled, solidification and melting rates from elec. cond. meas. 79−29042
Cu, preferred crystallographic orientation of unidirectionally solidified polycrystals *(Czech)* 79−43233
Cu surface melt of spherical crysts., microscopic obs. 78−34599
Cu-Al, directionally solidified eutectic composite alloy, form. and strength 77−90294
Cu-Al eutectic alloy, unidirection transform. controlled by heat flow *(Japanese)* 78−15386
Cu-Al spherical crysts. grown from drop of melt, topography 80−84353
Cu-Al-Ni Marmen alloys, rapid solidification and ageing 80−76245
Cu-Al(Si)(Fe)(Ni)(Pb), preferred crystallographic orientation of unidirectionally solidified polycrystals *(Czech)* 79−43233
Cu-Cr, eutectic, effect of comp. and solidification conditions on microstruct. *(Russian)* 79−29037
Cu-Cr (1.45 wt.%), unidirectionally solidified eutectic, cooperative growth 77−90341
Cu-Cr-Zr-Ti-B alloy system, solidification cracks formed during welding, reduction by microalloying with B 79−96148
Cu-Cu_6Y eutectic alloy, cast and directionally solidified, struct. and props. *(Russian)* 80−104138
β-Cu-In, directionally transformed eutectoid, morphology exam. by metallography *(German)* 78−92257
Cu-Nb, exam. of monotectic reaction, using chill casting technique 78−68679
Cu-Nb, supercond. wire, directional solidification of melts, supercond. ionisation temp. *(Russian)* 78−76596
Cu-Nb (7 wt.%), solidification microstruct., SEM 77−12611
Cu-Nb alloy, chill casting, consumable arc melting, ingot prep. techniques 80−84879
Cu-Ni, melt, accel. by shock wave treatment, crystallisation *(German)* 77−86022
Cu-Ni-Al, review 80−7564
Cu-Ni-W melt, solubility of W, primary solidification 78−19726
Cu-SO_2 system, melt, blow hole form. during solidification 79−43238
Cu-Zn-Al, memory alloy wire and ribbon reversible martensitic transformation, ageing effect, review 80−7564
Cu-Zn-Al alloys, dendritic struct. obs. 77−8810
Cu-Zn-Al wire, rapidly solidified, X-ray diffr. and therm. anal. comparison of martensites before and after solidification 79−43227
$CuInTe_2$ single crystals, directional freezing growth and doping, resist. changes on annealing 80−60768
Cu_2S, molten, oxidation, exam. of product phase composition by X-ray anal. *(Russian)* 79−34166
Fe alloy YuNDK35T5, mag., solidification, direct elec. current effect 79−78954
Fe and steel, macrosegregation of S and form. of equiaxed crystals, autoradiographic study, cast struct. effect 77−63658
Fe, cast, Ce hypoeutectic, new phase formation sequence during crystallisation, X-ray obs. *(Russian)* 78−95731
Fe, cast, eutectic solidification, expt. study by quantitative metallography 79−24516
Fe, cast, fused metal solidification enhancement using Bi and Te *(Italian)* 80−7540
Fe, cast, grey, density variation during slow crystallisation *(Russian)* 78−95737
Fe, cast, grey, solidified in oscillatory and rotating moulds, metallographic study 80−89213
Fe, cast, hypoeutectic, primary crystn. features by means of apparent viscosity meas. in early stages of solidification *(Japanese)* 79−43231
Fe, cast, inoculated with Ce, exam. of phase composition 78−56620
Fe, cast, mech. props., demodification influence of isothermal holding and Mg additions *(Bulgarian)* 79−15707
Fe, cast, nodular, solidification *(Japanese)* 78−11217
Fe, cast, white, freezing rate and Si content effect on graphitisation *(Japanese)* 77−56009
Fe, cast, with Mn, high S, exam. of sulphide phases, cocrystallisation during solidification 78−56646
Fe, cast, with spheroidal graphite, crystn. *(German, English)* 80−97473
Fe, pure, splat-quenched, martensite morphology, SEM study 80−7547
Fe, rapid melting and solidification of surface layer, exam. using computer heat flow model 78−83228
Fe smelting, Si-Q apparatus for solidification temp., Si correction, %P correction *(German)* 80−76450
Fe, splat-quenched, microhardness and martensite 80−76359
Fe-(Ni)(Si)-C, cast, spheroidal graphite, metallography of solidification 78−19737
Fe-B, rapidly quenched, metastable phases 80−76234
Fe-B, rapidly solidified, metastable phases *(German)* 79−29045
Fe-B amorphous ribbons formation, high-speed photography investigation 80−76216

solidification continued
Fe-C, binary, solidification, predicted volume change 77−28802
Fe-C, pearlite, eutectoid alloy, efficiency of directional transformation on orientated growth 78−76642
Fe-C, pre-eutectic melt, struct. anomalies *(Russian)* 77−28794
Fe-C eutectic, solidification cycle, thermal anal. 80−29945
Fe-C hypoperitectic, solidification cycle, thermal anal. 80−29945
Fe-C-S-Mg melt, S and Mg effect on graphite growth shape 79−38817
Fe-C-Si, effects of Si on matrix struct. of spheroidal graphite cast iron *(Korean)* 78−60666
Fe-C-Si, high purity, vacuum melted, nodular graphite form. 80−108452
Fe-Cr-Al-TaC (13.5, 3.7, 9 wt.%) eutectic alloy, directionally solidified, thermal cycling effects on microstruct. 77−32686
Fe-Cr-Ni, melting and solidification *(French)* 77−66635
Fe-Cr-Ni-Nb-C, austenitic, splat quenching 78−72798
Fe-Cu-C, phase equilibria, 950 to 1500°C 80−60836
Fe-Mn-C, cast iron and steel, Mn effects on struct. 78−23696
Fe-Mn-O melts, formation of oxide inclusions, cryst. pulling, Bridgeman tests *(German)* 80−35074
Fe-Mn-Si-C, cast, Mn effect on struct. during solidification 79−83191
Fe-MuS eutectics, unidirectional solidification *(German)* 80−100827
Fe-NbC, exam. of phase diagram, and mech. props. *(Russian)* 79−20028
Fe-Ni, segregation of inhomogeneities during crystallisation *(Russian)* 78−27521
Fe-Ni (25%), solidification of powder or large ingot, heat losses 77−12612
Fe-Ni (30 wt.%), Ni segregation singularities during dendrito-cellular solidification *(Russian)* 80−7542
Fe-Ni alloy, cellular-dendrite struct., effect of temp. gradient and crystallisation rate on morphological singularities *(Russian)* 78−3115
Fe-Ni-Al-Co-Cu-Ti, 38 to 40 wt.% Co, 8 to 8.5 wt.% Ti, alloy YuNDKT tempering and thermomagnetic treatments 78−3154
Fe-Ni-Cr-Al-Ti-W-Mo (35, 15, 2.4, 2.3, 2.2 wt.%) wrought superalloy, freckles *(Chinese)* 80−104137
Fe-Ni-P-B amorphous ribbons, form. by melt spin technique 80−76215
Fe-P-C alloys, amorphous, mag. anisotropy, Mossbauer obs., prior cooling effects *(Russian)* 77−32300
Fe-Si (3 wt.%), tertiary products from deoxidation, electron emission microscope study *(Russian)* 78−11214
Fe-SiO_2, slowly and rapidly solidified, coarsening of SiO_2 77−86023
Fe-Ti-C, rapidly quenched by splat-cooling 80−84923
Fe-V-S-(C), sulphide nature exam. by X-ray spectral anal., solidification effects *(Russian)* 79−52191
FeCoC, unidirectionally transformed eutectoid, crystallography of herringbone pearlite, TEM obs. 78−31399
Fe_2O_3 haematite platelets, growth and cross-connection in consolidation of haematite pellet *(Chinese)* 80−104186
α-Fe_2Si_5-ε-FeSi eutectic, orientation relationships 78−31397
Fe_2Ti-Fe eutectic alloy, directional solidification singularities *(Russian)* 78−68678
Ga-Al, effect of Al on solidification kinetics, and morphology of Ga 78−56628
Ga-In-Sb system, precipitation of solid phase from liq. phase, thermodynamical formulation *(French)* 77−28003
GaAs, laser-induced recrystallisation and damage of ion-implanted amorphous samples 79−47557
Ge film recrystallised by unidirectional solidification, GaAs film deposition 78−19671
Ge, solid-liquid interfacial tension determ., glassy sphere nucleation by rapid cooling 77−51570
Ge-Sb, eutectic alloy, exam. of morphology during solidification *(Russian)* 79−34022
Ge-Si-Sb solid soln., prod. by 'Universal Furnace' expt. Sb and Si distrib. *(Russian)* 78−23692
H_2, solid, high pressure phase, 57 kbar, 25°C, transparent crystalline mass 79−55870
^{4}He monolayer, theory 77−20158
^{4}He, solidification at room temp. under high press. 79−82413
^{4}He, superfluid, negatively charged vortex rings, nucleation near solidification press. 78−55997
^{4}He, superfluid, nucleation on Grafoil 77−28062
Hg, inductively stirred, convective flow rate controlled by Lorentz's number rel. to solidified struct. 79−10444
Hg, optical and elec. effects during solidification 78−47502
Hg-HgTe-CdTe system, equilib. phases comp. by dew point method 79−78941
In surface, impurity precipitation and resolution at melting point 78−14553
$In_xGa_{1-x}Sb$, influence of annealing on microstruct., exam. 78−56669
InP-GaP, solid soln. crystallization from stoichiometric melt, solidus construction 77−85927
InSb, growth angle determ. from cryst. lateral face shape and solidified separation drops 80−103282
InSb-GaSb, directionally solidified, determination of non-constant distrib. coeffs. 78−76641
InSb-GaSb alloy, directionally solidified, orientation, twinning and orientation depend. reflectance 79−28001
InSb-GaSb alloys, directionally solidified, composition variations, electron probe anal. 79−24513
InSb-Sb eutectic solidification, interface demarcation expts. 79−43228
$Li_{0.5}Fe_{2.5}O_4$-LiNb(Ta)O_3, in situ composite growth, phase diag., melting relns. 77−21132
$LiInS_2$, single cryst. growth by directional solidification, photoluminescence meas. 79−61514
Li_2O-SiO_2 glass ceramic, aligned, prep. by hot extrusion and microstruct. 77−32552
$Li_2O.2SiO_2$ ceramics unidirectionally solidified, porosity *(Japanese)* 79−38816
$Li_2O.2SiO_2$, ceramic, prep. of oriented microstructure by unidirectional solidification of melts 80−71614
$Li_2O.2SiO_2$, directionally solidified, thermal and mech. props. *(Japanese)* 80−16295
$Li_2O.2SiO_2$ melt, bubble form. during unidirectional solidification *(Japanese)* 79−70057
$Li_2O.2SiO_2$, polycrystalline, oriented, fabrication by unidirectional solidification from melt *(Japanese)* 78−31371
$100(Li_2O.2SiO_2).3B_2O_3(3Na_2O)(3MgO)(3Al_2O_3)(3SiO_2)(3P_2O_5)$, directionally solidified, thermal and mech. props. *(Japanese)* 80−16295
$LiY_{0.416}Er_{0.5}Tm_{0.067}Ho_{0.017}F_4$, Stockbarger single cryst., charact. of solidification behaviour 77−24948
solidification continued
Mg-Al, unidirectional solidification, method for determ. of diffusion and thermal diffusion coeffs. in molten Mg 78−30772
Mg-Fe, unidirectional solidification, method for determ. of diffusion and thermal diffusion coeffs. in molten Mg 78−30772
Mg-Si, unidirectional solidification, method for determ. of diffusion and thermal diffusion coeffs. in molten Mg 78−30772
Mg-Zn-Zr rare earth alloy, mech. props., effect of microshrinkage during solidifaction 79−43234
Mn-Bi alloy, melting and solidification under microgravity, mag. props. *(German)* 80−45296
Mn_2SiO_4-MnO eutectic composite, EFG die-top geom. effect on solidification interface shape 77−48420
NH_4Cl transparent soln., basaltic equiaxed solidification, visualisation of convection *(French)* 80−44297
NH_4Cl-H_2O, binary dendritic system, exam. of solidification 79−11599
NH_4Cl-H_2O, solidification microstructs., effect of reduced gravity 80−96632
NH_4Cl-H_2O solidification model for showering cryst. form. in molten metal cooling *(Japanese)* 80−66498
$NaNO_3$, crystallite boundary structural instability during solidification *(Russian)* 78−95738
$NaNbO_3$-$BaTiO_3$, unidirectionally solidified transparent ceramics 80−25677
Na_2O-B_2O_3-SiO_2-MoO_3 glass containing high level radioactive waste, phase separation 80−25683
Na_2O-PbO-SiO_2 glass-ceramic composite, directionally crystallised 80−107058
Na_2O-SiO_2-Ga_2O_3-Al_2O_3 glasses in mixed $AgNO_3$-$NaNO_3$ melts, ion exchange 80−21282
$Na_2S_2O_3.5H_2$, heat transfer processes *(Japanese)* 80−6372
$(Nb,Ti)N_x$, metastable supercond. phase, effects of rapid quenching on transition temp. 78−2611
Nb-Nb_2C, directional crystn. using plasma heating 78−60569
Nb-Nb_2C eutectic composites, directionally solidified, growth crystallography and lamellar to rod transition 77−32569
Nb_3Sn multifilament superconducting composites, alternative technologies for fabrication 79−38756
Nb_3Sn superconducting wire, fabrication from Cu-Nb-Sn alloy using controlled high temp. gradient 80−25056
Ni alloy Mar M200, directionally solidified Hf additions, effect of vol.% γ' on creep rupture 78−27526
Ni base superalloy, directionally solidified, struct. and props. *(Chinese)* 80−20918
Ni base superalloys, rapid solidification, use in gas turbine engines 80−84888
Ni, rapid melting and solidification of surface layer, exam. using computer heat flow model 78−83228
Ni, solidified from supercooled condition, Si conc. influence on struct. *(Russian)* 77−16567
Ni superalloy, transient liq. phase diffusion bonding and mechanism *(Japanese)* 78−2279
Ni, supercooled, struct. refinement mech. *(Russian)* 80−20975
Ni/Ni_3Al+Ni_3Nb, directionally solidified eutectic alloy, crack growth rate under creep fatigue conditions 79−52361
Ni-Al-Cr, IN-100, growth geometry of carbides in dendritic monocrystals, solidification effects 79−11597
Ni-Al-Cr alloy IN 100 powder, rapidly solidified, effect of high melt superheat on microstructure 79−52195
Ni-Al-Cr-Ti-W-Mo, US vibration applied during solidification, improved strength, corrosion resistance *(Russian)* 78−15382
γ-αNi-Al-Mo eutectic, γ' precipitation 77−12629
Ni-Al-Ta (7.5, 2.0 wt.%), dendritic monocrystal, microsegregation and nonhomogenisation 79−37940
Ni-Al-Ta dendritic monocrysts., directionally solidified, coarsening kinetics 80−108425
Ni-Al-Ti-(W) (Cr) (Co) (Mo) (Ta) (Nb), heat resist., solidification range 80−35177
Ni-based eutectic alloys, struct. and props. *(Russian)* 77−21129
Ni-based eutectic alloys, unidirectionally solidified, solidification and morphology relationship 80−25684
Ni-Cr-Al-Cr-Hf-Zr-C, directionally solidified eutectic with (Hf,Zr)C reinforcement, precipitation, and thermal cycling 78−44057
Ni-Cr-Mn alloy solidification, effects of Si, Mo and Co alloying 79−83193
Ni-Cr-NbC eutectic composite, unidirectional solidification, thermal cycling, temp. range effect on microstructural degradation 80−89272
Ni-Cr-TaC directional eutectic, high-strength, interphase boundaries *(Russian)* 79−38812
Ni-Cr-Ti rapidly solidified superalloys, surface segregation 80−76263
Ni-Mo-Al eutectics, unidirectional solidification 77−4769
Ni-Nb-Al, unidirectionally solidified γ/γ'-δ eutectic, fatigue crack propag. 79−29184
Ni-Nb-Al (25, 2.5 wt.%), directionally solidified γ/γ'-δ eutectic, growth conditions on struct. 80−11639
Ni-Nb-Al-Cr, directionally solidified, exam. of growth and morphology 79−11601
Ni-NbC (10 wt.%) eutectic alloy, directional solidification and struct. *(Russian)* 80−84922
Ni-NbC eutectic, microstructure and strength depend. on composition and crystallisation conditions *(Russian)* 79−100128
Ni-Ni_2B eutectic, high temp. X-ray anal. 80−71639
Ni-Ni_3Al-Ni_3Nb, directionally solidified, role of twinning in cyclic stress strain behaviour 78−80605
Ni-Ni_3Ti eutectic alloys, solidification 77−70042
Ni-P(B), amorphous, thermal anal. and X-ray diffr., solidification struct. development *(French)* 78−91253
Ni-Ti-Al superalloy, pendant drop melt extracted, struct. and props. 80−76242
Ni-W-Co-Cr, superalloy MAR 200, with Hf, cellular composite prod. by isothermal dendrite ripening 78−44150
NiAl-Cr, eutectic, directionally solidified, temp. behaviour of misfit dislocations *(German)* 78−3119
NiAl-Cr eutectic alloy, directional solidification singularities *(Russian)* 78−68678
NiAl-V join, phase relations and eutectic directional solidification 78−31396
$NiFe_2O_4$-$BuTiO_3$, in situ composite growth, phase diag., melting relns. 77−21132
NiTaC, eutectic alloys, chem. incompatibility of ceramic nitrides for directionally solidifying 80−81046

solidification continued
NiTaC eutectic superalloy, casting, furnace atm. effects 80−84880
Ni_3Ti-Ni eutectic alloy, directional solidification singularities *(Russian)* 78−68678
O_2, EPR temp. depend. *(Russian)* 78−31103
P, white, dendritic growth, fluid flow effect 78−11215
Pb, changes in electron image contrast 80−100147
Pb, grain refinement, and structural stability by S, Se and Te additions *(German)* 80−55387
Pb, variations of energy of the ⟨111⟩ torsion joint as a function of the angle of torsion in metallic seeds [dendritic structure] *(French)* 80−25682
Pb-Bi, temp. regime of crystn. on rapid cooling *(Russian)* 80−66495
Pb-Cu, hypoeutectic, grain refinement, and structural stability by S, Se and Te additions *(German)* 80−55387
Pb-Sb, thermal analysis in non-faceted/faceted eutectic systems 80−71637
Pb-Sb eutectic alloys, solidification in space environment 79−47671
Pb-Sn, controlled solidification, monograin growth, selection and struct. *(French)* 77−16568
Pb-Sn, eutectic alloy, spiral growth phenomenon 77−48419
Pb-Sn, ingots, solidified, formation of equiaxed eutectic grains *(Japanese)* 78−39756
Pb-Sn, lamellar eutectic stability and growth struct., fault formation 79−96019
Pb-Sn, off-eutectic alloy growth from stirred melt 77−8809
Pb-Sn, solidification, predicted vol. change 77−28802
Pb-Sn, undercooled eutectic, compositional variations at various gravity levels 77−52314
Pb-Sn (20wt.%), eddy current study of solidification 80−104141
Pb-Sn directionally solidified eutectic alloy, morphology and crystallography 77−90340
Pb-Sn eutectic, directionally solidified, perfection and stability of lamellar struct. *(French)* 77−77468
Pb-Sn-Cd, eutectic and monovariant eutectic, ingot struct. 78−15388
Pb-Sn-Cd, monovariant eutectic and eutectic alloys, ingot struct. 77−63656
Pb-Zn, off-eutectic alloys, controlled grain growth *(Japanese)* 77−55958
Pb-Zn, unmixing alloys, mathematical model for solidification process *(Russian)* 80−81047
$Pb_{1-x}Sn_xTe$, segregation during solidification by Bridgman technique 79−38735
PbTe-SnTe solid solns., directional solidification 77−44149
Rb, liq., cryst. nucleation and growth, mol. dynamics calcs. 79−74144
Sb-crystals, in binary or ternary alloys, shapes on solidification *(German)* 80−3020
Sb-Ge, unidirectionally solidified, exam. of compressive props. and struct. 78−68730
Sc_2O_3-Ho_2O_3 (Dy_2O_3), solid solution, use of segregation phenomena to exam. solidification phase diagrams *(French)* 79−8293
Sc_2O_3-R_2O_3, regular soln. approx. of solidification diagram *(French)* 79−24505
Se, amorphous and liquid state, Raman spectra, crystn. processes 80−60608
Si, cast, growth structure and photovolt. props. of solar cells 80−94008
Si, coating of mullite ceramic substrate, for solar cell appl. 79−34432
Si, crack free ingots, by directional solidification using heat exchanger method 79−8242
Si, dislocation growth during laser melting and solidification 80−2022
Si, large single crystal production, using directional solidification tech. 78−35298
Si laser annealed, nonequilibrium solubility and segregation 80−84296
Si, laser annealing, nonequilib. incorporation of impurities during rapid solidification 80−55286
Si, metallurgical grade, purification and charact. 78−56573
Si polycrystalline, low cost conversion into sheet by heat exchange method and fixed abrasive slicing technique 80−93479
Si sheet, high speed growth, heat transport analysis 80−107669
Si sheet casting for solar cells 80−89139
Si single crystal ingot growth from metallurgical grade Si, inhomogeneities 80−59416
Si, solar grade, directionally solidified using C crucibles, TEM study 79−47617
Si, web dendritic ribbon growth, thermal analysis of solidification 78−72770
Si:Te, laser melting, surface Te atom accumulation, profiles 80−100258
SiC-B_4C eutectic, directional solidification, growth and mech. props. 79−91638
Sm, metastable phase modification formation during quenching from molten state *(Russian)* 79−91636
Sn droplets, on Bi, Zn and Al, heterogeneous nucleation 80−44294
Sn melt, highly supercooled, dendrite growth *(Russian)* 77−81253
Sn melt fragmentation on quenching in n-pentadecane and water 79−15706
Sn, molten rotating stream, vortical filament generation during solidification *(Russian)* 78−88460
Sn, undercooled, dendrite growth rate 77−90339
Sn-Bi, thermal analysis in non-faceted/faceted eutectic systems 80−71637
Sn-Bi (Pb) alloys, supercooled, dendritic growth rates *(Russian)* 78−80533
Sn-Bi(Pb)(Ga), temp. regime of crystn. on rapid cooling *(Russian)* 80−66495
Sn-Pb, dil., undercooled alloy, solidification 78−3120
Sn-Pb, refining by fractional solidification 79−61536
Sn-Pb (15 wt.%), partially solidified slurry, exam. of structure, viscosity 78−84793
Sn-Sb-Ag, splat cooled foils, TEM study 80−40344
Sn-Zn, ingots, solidified, formation of equiaxed eutectic grains *(Japanese)* 78−39756
Sn-Zn alloy, planar and cellular solidification interfaces, distrib. coeffs. and conc. profiles *(German)* 77−32568
Sr radioactive waste solidification process *(Japanese)* 77−54319
Te amorphous and liquid state, Raman spectra, crystn. processes 80−60608
Te-$(Bi_xSb_{1-x})_2Te_3$ eutectic, electrophys. props., directed crystn. conditions influence and comp. depend. 80−107827
Te-based eutectics, crystn. rate effect on electrophys. props. mutual solubility effect 80−60774

solidification continued
Te-Bi_2Te_3 oriented eutectic, microhardness, influence of size of phases *(Russian)* 78−92322
Te-Sb_2Te_3 oriented eutectic, microhardness, influence of size of phases *(Russian)* 78−92322
Ti alloys, ingots, produced by vacuum arc smelting, exam. of crystallisation process *(Russian)* 79−34019
Ti base alloys, melt-extracted polycryst., mech. props. 80−76360
Ti, type VT1-0, pool metal solidification kinetics in welding with electromag. stirring 80−71636
Ti-Ag (10 to 17.5 wt.%), eutectoid system, $\beta \rightarrow \alpha_m$ transform., nucleation kinetics 80−97474
Ti-Al (27.3 wt.%), arc melted, microstruct. 79−61577
Ti-Au, (9.9 wt.%), eutectoid system, $\beta \rightarrow \alpha_m$ transform., nucleation kinetics 80−97474
$TiAl_3$ crystals dissolution in pure Al liq., grain refinement of α-Al solid-solution by Ti addition 80−35178
TiC-base alloys, anomalous phase flaky precipitation *(Japanese)* 78−48401
TlS_x, amorphous, composition-dependent solidification 79−23527
UO_2, condensate solidification onto steel struct. in above-core region of LMFBR after HCDA 78−17364
V-Ni-Mo, structure in alloy crystallisation region, peritectic equilibria *(Russian)* 80−50622
VC, metastable supercond. phase, effects of rapid quenching on transition temp. 78−2611
V_3Ti, metastable supercond. phase, effects of rapid quenching on transition temp. 78−2611
W, containerless melts in terrestrial and space environment, thermodynamic props. calc. from solidification and cooling curves 79−70052
W-W_2C, directional crystn. using plasma heating 78−60569
W-Zr (2.92, 7.42 and 10.02 wt.%), and W_2Zr, thermal expansion, elec. resistance, 100-900°C, crystallisation 78−91455
YAG, molten, complexity in solidification behaviour, SEM electron images 79−43229
Zn-Al, unidirectional eutectic, FCC phase, preferred orientation 80−29973
Zn-Al, unidirectionally solidified eutectic, morphology and crystallography 77−48421
Zn-Ga, temp. regime of crystn. on rapid cooling *(Russian)* 80−66495
Zn-In(Bi) interfacial tension and microstruct. 79−74132
Zn-Pb composite, production under conditions when gravity forces are balanced out by EM forces 78−31363
Zn-Sn-Hg, diagram of state, melting temp., peritectic and eutectic phases *(Russian)* 80−55350
Zn-Sn(Bi), discrete eutectic formation mechanism *(Russian)* 77−66634
Zn-Sn(Bi) alloys, morphology and mechanism of formation of eutectic *(Russian)* 78−6916
Zn_2SiO_4-Mg_2SiO_4, melt solidification behaviour 77−90337
ZrO_2-CaO, stabilised microspheres, structure, mechanical props. *(Russian)* 80−100379
ZrO_2-Nd_2O_3(Sm_2O_3)(Dy_2O_3) eutectic, unidirectional solidification, microstruct. and crystallographic characterization 80−35176
ZrO_2-Ta and ZrO_2-Y_2O_3-Ta aligned eutectic composites, solidification and fracture behaviour 77−48387
ZrO_2-ThO_2, high temp. study of phase diagram using X-ray and thermal anal. *(French)* 79−70049
ZrO_2-Y_2O_3, stabilised microspheres, structure, mechanical props. *(Russian)* 80−100379
ZrO_2-Y_2O_3 monocrystalline solid solutions, struct. and phase form. 79−52188

solids
Generalities only; for specific aspects see appropriate headings see also crystals; quantum solids; solid hydrogen; solid structure; solid theory
conference, condensed matter physics, Sarajevo, Yugoslavia (Oct. 1976) 77−51629
conference, Taiwan (April 1977) 78−10314
conference on solid-state physics, Munster, Germany (Mar. 1977) 78−2401
experimentation in solid state physics, review *(Spanish)* 80−82624
quantum theory basis for shaping ideas on solid state phys. *(Hungarian)* 77−87608

solions *see transducers*

solitons
(1+1) dimensional field theoretic models with soliton behaviour, exact S-matrices and form factors 79−26240
(1+1) dimensional model field, fermion-boson correspondence, Klein transformation 80−42379
$\lambda\phi^4$, extended objects in quantum systems and soliton solns. 79−35945
$(\lambda|\phi|^4)_2$ quantum field model, soliton mass and surface tension 78−58109
τ-vacuum for ϕ^4 and sine-Gordan theories, stationary solitons *(Chinese)* 80−101932
$\phi_2{}^4$ field theory, coupled states of solitons *(Russian)* 77−6037
ϕ^4 behaviour in presence of an impurity potential, collective coordinate method 80−31528
ϕ^4 kink behaviour in presence of inhomogeneous perturbation 79−75692
ϕ^4 two-dimens. model, kink-antikink collisions 79−85218
ϕ^4-theory, soliton soln., fluctuation renormalisation and extended particles 77−5996
adiabatic perturbations of solitons and shock waves 80−46830
adsorbed layers, two dimensional incommensurate crystal theory, thermodynamics *(Russian)* 80−49524
Alfven waves, circular polarisation, propagation in mag. field, spiky soliton 80−28662
Alfven waves, circularly polarised, spiky soliton soln. to nonlinear evolution eqn. 80−38590
Alfven waves, exact, nonlinear, existence of solitons 80−24159
Alfven waves, finite amplitude 78−83551
Alfven waves modulational instability, solitons 78−59576
amorphous magnets, disclinations and solitons 80−75786
amplification in modified Korteweg-de Vries eqn. 80−27145
anharmonic, one dimensional ferromagnet, magnon and lattice deformation, bound state 79−78357
anharmonic lattices, quasisoliton solns., influence of pair pot. shape 80−22297
anisotropic ferromagnet, one-dimensional Landau-Lifshits eqn. multisoliton solutions *(Russian)* 80−71014
anisotropic Heisenberg chain, nonlinear excitations 80−70927

solitons continued
annual review of fluid dynamic, book 80−94927
antiferromagnet, acoustic nuclear resonance, self-induced transparency *(Russian)* 79−91304
antiferromagnet, linear-chain, sine-Gordon solitons 80−80543
antiferromagnet, magnetoelastic soliton propag. 80−66003
antiferromagnet, nonlinear magnetisation waves *(Russian)* 79−91251
antiferromagnet, one-dimens., nonlinear dynamics 80−80521
antiferromagnets, nonlinear waves 80−84612
antisoliton-soliton reflection in sine-Gordon model, single-loop approx. 79−21960
asymptotic behaviour for propag. through two different mediums, K-dV eqn. 80−43924
atmosphere, internal solitary waves, obs. 79−8656
avalanche breakdown as nonlinear wave of soliton type 77−47824
Backlund transformation, discrete-time Toda eqn. 78−73829
Backlund transformation for higher order Korteweg-de Vries equations 77−78999
baroclinic fluid, rapidly rotating, sine-Gordon eqn. model 80−46820
Belousov-Zhabotruskii reaction, existence of solitary travelling wave solns. 80−35525
Benjamin Ono eqn., exact multi-soliton soln. 79−40379
Benjamin-Ono eqn., conservation laws 80−31524
Benjamin-Ono eqn., multi-soliton like solns. 78−28960
Benjamin-Ono eqn., props. 79−63050
Benjamin-Ono equation, Backlund transform. and conservation laws 80−4540
Benjamin-Ono equation, higher order, solns. 80−62482
Benjamin-Ono equation, internal wave solitons, linear stability 80−53802
Benjamin-Ono equation, meromorphic solns. 79−62998
Benjamin-Ono equation, meromorphic solutions 80−31980
Benjamin-Ono equation, N-soliton soln. 79−92929
Benjamin-Ono equation, periodic wave and soliton solns. 79−35570
Benjamin-Ono solitons, interactions 80−73181
Bethe-Salpeter eqn., quantised solitons 78−32985
bilinear soliton equations, method of constructing generalised soliton solns. 80−4541
bilinearisation method of analysing soliton eqns. 80−46813
bilocal Lie groups and solitons 77−67194
bioenergetics, solitons, muscle contraction mechanism 79−96508
black solitons and hadronic temperature 77−26498
boomeron equation, asymptotic behaviour (in t) of solutions 79−9082
boson soliton collisions in plasma, nonlinear scatt. 79−27768
boson system, 1-D, with δ-function interactions, time-depend. Hartree approx. 79−9184
Boson theory, quantum soliton and classical soliton 80−12986
boson-soliton scatt., sine-Gordon model 80−9109
Boussinesq type eqn., reduction to modified Hirota eqn. 80−8804
breather generation, inverse scatt. technique 80−78913
bremsstrahlung emission 77−59240
canonical description of solitary quantum decay 78−36881
canonical transformation for eqn. of form $\phi_{xt}=h(\phi)$ 77−33875
canonical transformations theory for nonlinear evolution eqns. 77−29993
caviton dynamics at crit. density 80−106909
CDW, one-dimensional, commensurability pinning versus impurity pinning 79−11075
CDW condensates, soliton pair creation and low temp. elec. cond. 79−4550
CDW condensates, soliton pair creation by elec. fields 77−69309
chain of coupled nonlinear oscillators, large amplitude motion, numerical study 79−25993
chaotic states of anharmonic systems in periodic fields 80−22288
charge density wave condensate high freq. cond. at low temps. 79−95392
charge-density waves, lock-in transition, effect of thermal fluctuations on harmonics 79−19338
charged, stability, relativistic complex scalar field, direct Lyapunov method 80−62827
charged scalar solitons, electrodynamics 80−42078
charged soliton long range interactions 79−63373
chiral nonlinear field eqns., exact solns. 78−54527
chiral solutons and current algebra 79−40680
chiral SU(3)×SU(3) models, soliton solns. 78−4761
circular solitary wave on shallow water 79−55397
classical field theory, string-like solitons, 2-sphere range for variables 79−53988
classical Q solitons, two space dimens. interaction 79−45015
classical soliton dynamics in nonintegrable systems 78−28996
cluster walls and phonons in structural phase transitions 79−77720
coherent excitations interacting in dispersive medium, envelope-soliton propagation 79−2639
coherent phonons and photons, soliton study 79−64291
coherent pulse propagation, soliton creation by chirped initial profiles 79−72632
cold nuclear matter, stationary finite amplitude motions, quantum shock waves and solitons 80−42573
collapsons, new form of nonlinear excitations 80−4876
collisionless gravitating systems, gravitational pot. nonlinear eqns. determ., astrophysical appl. 80−67560
commensurable-incommensurable transition, Devil's staircase and harmless staircase, oscillating interactions through elastic stairs or other harmonic fields 80−88296
commensurate-incommensurate transition, coupling between phase solitons and strain 79−28073
computer calculations 80−46832
condensation of extended structures 78−78141
condensation of the vortex solitons in a 2+1 dimensional Abelian Higgs model 80−99048
condensed matter, a paradigm, review 80−77632
condensed matter, propag. and decay due to interaction with medium 79−25871
condensed matter physics, theory 80−50122
condensed Peierls phase, non-linear modes 78−56087
conference, group theoretical methods in physics, Austin, Texas, USA (Sep. 1978) 80−4474
conference, nonlinear problems in theoretical physics, Jaca, Gain 1978 80−4478
conference on solitons and condensed matter physics, Oxford, England (June 1978) 79−75364
conservation laws, quantum field theory approaches *(German)* 79−9274
continuum spin system, as exactly solvable dynamical system 77−47960
solitons continued
converging ion acoustic soliton excitation in double plasma type device 80−106907
correlation functions, dielectric function 79−85071
coupled fields in one dimension: cross-over from a continuous symmetry to a discrete one 78−87758
coupled intensity deviations from stationary nonlinear state, space and time soln. 80−48882
coupled Langmuir and ion-acoustic solitons, instability 78−75294
coupled linear chain system 77−43463
coupled localized electron-plasma waves and oscillatory ion-acoustic perturbations 78−67349
coupled non-linear field eqns., soliton solns. 80−68338
coupled nonlinear evolution eqns., L-operator factorisation 79−44751
coupled nonlinear oscillators, Brownian motion, thermalised solitons and nonlinear response 78−29053
coupled scalar field theories in 2-dimens., exact soliton solns. 79−21920
coupled solitary waves in neurophysics 80−51067
covariant quantisation of solitons in gauge theories 78−16916
covariant scheme of quantisation for one-soliton sector 78−8265
cubic nonlinearity, effect on soliton stimulated Raman scatt. 79−15103
cyclotron, generation of km wavelength terrestrial radn. *(Russian)* 78−40764
cylindrical, exact solutions to equation 79−75359
cylindrical waves in variable depth water 78−40578
damped double solitons in the nonlinear Schrodinger equation 79−64853
damped nonlinear Schrodinger equation, exact soln. for parabolic profile 79−17278
damping in nonlinear line, nonadiabatic stage, intermediate asymptotics *(Russian)* 77−68769
deep water gravity waves, two-dimens. nonlinear wave eqn., exact envelope soliton solns. 80−43725
delta function fermion gas, solitons and HF solns. 78−49755
derivative nonlinear Schrodinger eqn, soliton solns. 79−44773
derivative nonlinear Schrodinger eqn., under nonvanishing conditions, exact solns. 78−62093
Derrick's theorem in curved space 79−12658
development of soliton physics, anal. based on INSPEC tapes 79−62990
diatomic lattice, solitary wave solns., ϕ^4 kink, struct. phase transition, phonon dispersion curves 79−80544
diatomic lattice system, soliton solns. in continuum limit 80−4668
diatomic lattice system with cubic nonlinearity, soliton solns. 79−93076
dielectric medium, steady propag. of coherent light pulse, effect of spatial dispersion 79−72480
diffraction by circular island in ocean, shallow-water theory *(French)* 80−83803
dimensioned profile for propagation *(French)* 77−35155
Dirac field, linearly rising soliton trajectories, Lorentz and gauge invariant 78−4791
Dirac nonlinear eqn., soliton solns. 79−71591
Dirac self-interacting field, soliton solns. in three-dimens., quark confinement 77−26461
Dirac spinor solitons or bags 78−12817
dislocation motion, soliton-like, piecewise linear force model 78−2119
dispersive media, nonlinear, with weak dissipation, soliton propagation, tail generation 78−75287
dispersive media, nonlinear evolution eqns. soln., review 78−60
dispersive nonlinear wave eqn., soliton like solns. 78−93538
displacive transformations, connection to dislocations and solitons 79−82300
displacive transformations, one-dimensional model, interaction of solitary wave soln. with phonons 78−22813
dissipative structures in quasi-one-dimensional superconductors, soliton solns. 79−87186
dissipative Toda lattice, soliton propag. using nonlinear transmission line 80−27228
double quadratic chain, statistical mech., nonreflectionless solitary wave 80−22518
double quadratic kink soln. to ferroelec. domain wall dynamic polarisability 80−66135
double sine Gordon equation, exact multiple soliton solutions 78−20978
double sine-Gordon equation, perturbation theory 79−75403
double soliton solutions for multidimensonal eqn., quasiclassical quantisation 78−54569
driven sine-Gordon chain, periodic and solitary states 80−82881
dynamic stability of solitons and general nonlinear wave phenomena *(German)* 80−4544
education, soliton solns. to nonlinear wave eqns. 80−17737
education, topological solitons in physics, vortices and mag. monopoles as examples 79−25793
effective Lagrangian, soliton form-factor and intersoliton asymptotic force 79−45010
effective-potential approach to the quantization of the sine-Gordon theory in 1+1 dimensions 80−73608
Einstein gravitational eqns., integration by inverse scatt. method, soliton solns. *(Russian)* 79−25940
Einstein gravitational eqns. and nonlinear scalar field, time-depend. solns. with localised energy 80−46888
Einstein-Maxwell eqn., N soliton solutions *(Russian)* 80−105556
Einstein-Podolsky-Rosen paradox, de Broglie's physical waves, solitons 80−90710
electron beam-plasma system, soliton characts., reson.-like struct. 78−79429
electron gas, one-dimens., with backward scatt., soliton Green's functions 78−10386
electron holes, theory, anal. soln. 80−48879
electron plasma wave, computer simulation of modulational instability 79−32766
electrostatic envelope solitons in plasma 77−39420
electrostatic solitary drift waves, modulational instability 78−91105
elementary particle theory, mathematical method, conf., Liblice, Czechoslovakia (June 1978) 79−21891
elementary particle theory, real scalar fields, solitons with particle props. 77−45936
EM soliton in weak and EM unified field theory 79−9323
EM soliton propagation in nonequilibrium dispersive media *(Russian)* 80−106933
energy loss of a modified Korteweg-de Vries solitary wave in a varying medium 80−90683
envelope soliton of random phase waves 78−26282

solitons continued
envelope solitons and holes for sine-Gordon, nonlinear Klein-Gordon eqns. 77−2553
equation, geometrization 79−75358
equations, Hirota and inverse spectral methods 80−71
equilibrium turbulence, soliton role as liquid drops *(Russian)* 80−98804
euclidean image of soliton coherent state 78−32989
evolution, perturbation effects 80−46824
evolution equation with linearly x-depend. coeffs., spectral transform, single soliton soln. 78−57746
evolution equations, symplectic operators and hereditary symmetries 80−82650
evolution equations solvable by inverse spectral transform of rank 4 matrix Schrodinger eqn. 78−41187
evolution of modified Korteweg-de Vries eqn. under action of perturbations 79−84970
exact from factors in field theoretic models with soliton behaviour 78−82211
exchange vortexes of magnetisation, micromagnetic bubble domains 80−71138
exciton solitary waves, damping and modification 77−62833
extended objects, quantum statistical mech., correl. functions in one-dimens. kink-bearing systems 80−86204
extended particle, quantisation, degeneracy of eigenstates 80−73594
extended structures described by Z(N) spin and gauge models, applications 79−67479
extension of nonlinear evolution equations of the K-dV (mK-dV) type to higher orders 80−105508
factorised gauge solitons for compact gauge groups in n dimens. 79−21944
factorized U(n) symmetric S-matrices, two dimens., scatt. of solitons 78−45802
fast Langmuir solitons existence in non-equilibrium plasma 80−38604
Fermi gas, one dimensional with backward scatt., gap renormalisation 80−24818
Fermi gas model in 1-D, review 79−58636
fermion interactions, eigenvalue spectrum 77−8035
fermion zero modes in soliton fields 78−8517
fermionic solitons in gauge theories and their quantum corrections 80−101927
fermions as solitons in extended particle field theory 77−26454
ferroelectric domain wall struct., and stability under competitive phase transitions 79−78639
ferromagnet, Landau-Lifshitz eqn., two soliton solns. for nonlinear dynamics *(Russian)* 78−43646
ferromagnet, localised nonlinear oscillations, unidimensional magnetisation soliton, analytic soln. *(Russian)* 79−78437
ferromagnet, magnon drops and mag. solitons 79−61093
ferromagnet, nonlinear localised wave of magnetisation as bound state of magnons *(Russian)* 77−63160
ferromagnet, one-dimens., algebraic soliton in mag. field directed along anisotropy axis 80−75785
ferromagnet, one-dimensional, with biquadratic exchange, solitary excitations 78−76232
ferromagnet, topological solitons, localised *(Russian)* 79−69661
ferromagnet, uniaxial, magneto-dipole interaction influence on one dimensional magnetisation soliton *(Russian)* 80−54880
ferromagnetic chain, characts. of soliton-like mag. excitations 80−39762
ferromagnetic chain, isotropic solitary waves 78−64180
ferromagnetic domain wall, soliton theory and dynamics 80−29569
ferromagnetic domain wall dynamics, soliton theory appl. 79−82813
ferromagnetic domain wall dynamics and soliton theory, coercive force determ. 79−42796
ferromagnetic domain wall pinning, planar defects, coercive force and correl. length, soliton theory 78−31092
ferromagnetic Heisenberg chain, weakly bound magnon states *(Russian)* 80−100591
ferromagnetic one-dimensional chain, solitary magnon propag. 77−63146
ferromagnets, magnetic solitons propagating along anisotropy axis *(Russian)* 79−73798
ferromagnets, magnetic vortex as topological soliton in Landau-Lifshitz eqns. *(Russian)* 80−7097
field theory, construction of Green's functions from an exact S matrix 79−71629
ϕ^4 field theory, dynamics of collisions of two space-dimensional pulsons 78−8250
field theory, existence of non-one-dimensional soliton-like solns. 77−67560
finite, exponential waves, solitons formation through nonlinear coupling 79−5967
finite amplitude solitary Alfven waves 80−53973
finite amplitude whistler wave solitons and filaments, properties and propagation 79−41836
finite depth stratified fluids, internal wave solitons, infinite depth limit 80−64574
finite ion temperature effects on strongly nonlinear ion acoustic solitons 79−41811
finite-depth stratified fluid, internal-wave solitons 79−80450
flexural EM waves in magnetoactive plasma *(Russian)* 80−83918
flowing viscous film of fluid, horseshoe-shaped solitons 79−18906
fluids of finite depth, N-soliton soln. of higher order wave eqn. 80−48724
flux line collapse, invisible string 77−57451
formal series solutions, rational solns., soliton eqns. 78−57747
formation, mth order parametric interaction, using Klein-Gordon eqns. 80−12917
formation in warm magnetised Vlasov plasma 79−90396
free and pinned, dynamical struct. factor for one-dimens. $\lambda\psi^4$ model 79−7668
free energies calcs., WKB approx. failure 80−42073
galaxies, nonlinear phenomena in gas subsystems *(Russian)* 77−74143
gas, soliton, interaction with nucl. spin 79−69736
gauge field nontopological solitons in three dimens. space 77−18167
gauge phase factor operators, extended Higgs models and 't Hooft algebra 80−42324
gauge theory solitons, quantisation, Feynman rules 77−2734
gausson collisions, logarithmic nonlinear Schrodinger eqn. solns., resonance energy interval 78−89357
gaussons, logarithmic nonlinear Schrodinger eqn. solns. 80−46865
general relativistic nonlinear field, kink soln. in generalised geometry 79−21922
solitons continued
general relativity, coupled scalar-vector-tensor eqns., axially symmetric soliton solns. 80−31635
generalized solitons of the Schrodinger equation with unitary nonlinearity 79−71294
geometric interpretation, Lie group theory 79−54266
geometrical field theories 80−27390
geometrical interpretation, rigid body motion along helical space curves 78−24684
Ginzburg-Landau (ϕ^4) field theory, solitary waves and electron localisation in disordered one-dimensional systems 78−14646
glasses, nuclear quadrupole spin-lattice relax., soliton-nucl. quadrupole moment interaction, temp. depend. 80−50220
grain boundary soliton-like features, molecular dynamics computer simulation study 79−77610
gravitating disc, rotating, nonlinear stability theory 80−17488
gravitational fields, stationary, axi-symmetric, soliton solutions 80−73253
gravitational solitons 79−44838
gravitational solitons with axial symmetry *(Russian)* 79−93030
gravity wave evolution for very weak nonlinearity 79−10575
gravity waves, interfacial and internal long, dissipation, Korteweg-de Vries eqns. 80−90686
gravity waves, nonlinear oblique interactions 77−23970
gravity waves, resonant interaction between three waves 77−27543
gravity waves, soliton fission in channel of varying width 80−46816
gravity waves, weakly nonlinear, long, on two-layer fluid 78−83419
gravity-acoustic waves, self-localisation, non-linear effect in non-uniform atmosphere 79−8761
Gribov's ambiguities and horizons 79−71639
guided lightwave propag., soliton techniques 80−58760
guided solitary waves from Boussinesq eqns. 80−92298
hadron models, semiclassical approach to quantum field theory 77−5981
hadrons, extended, second-quantisation of strongly interacting fields, meson state regarded as non-topological soliton 80−13270
Hamiltonian, completely integrable relativistic system 77−57450
harmonically coupled particle chain in double-minimum potential well exact soln. for soliton propag. in discrete case 80−34166
Hartree eqn., quasiclassical soliton soln., Newtonian interaction with screening 80−68569
head on collisions between two solitary waves 80−87780
heat pulses, soliton-like props. 78−22808
Heisenberg, ferromagnet, three-dimens. solitons 79−82741
Heisenberg chain, classical, solitons and magnons 80−60161
Heisenberg chain, classical continuous, magnon-soliton phase shift 80−107998
Heisenberg continuous chain, quantum solitons as magnon bound states 80−60162
Heisenberg continuous spin chain, soliton scatt. process 78−19203
Heisenberg ferromagnet, quasiclassical description, soliton solutions 78−39282
Heisenberg model, nonlinear excitations 79−78286
Heisenberg one-dimensional magnet, classical, nonlinear dynamics 80−71056
Heisenberg spin chain, continuous, solitons 77−55654
helical curve motion and soliton eqns., scaling invariance 78−49667
α-helical protein molecules, solitons *(Russian)* 78−68990
higher order Benjamin-Ono equation, N-soliton and N-periodic wave solns. 80−12915
higher order Korteweg de Vries eqn., Backlund transform 80−105510
higher order modified KdV eqns., bilinearisation 80−105509
history in mathematics of solns. to nonlinear evolution eqns. 79−75365
hollandite, one dimensional ionic and solitary wave conduction 79−23954
homotopy theory for soliton solns. classification *(German)* 78−78062
Hubbard chain, modified, solitary solns. derived step-by-step 80−10849
Hubbard model, one-dimensional modified 78−87895
hydraulic surge phenomena *(Norwegian)* 80−27141
incommensurate Peierls systems, amplitude solitons, implications for TTF-TCNQ 80−92841
incommensurate systems, discrete lattice effects 80−107402
incommensurate systems, transitions, solitons 79−77714
inelastic interaction, examples and Boussinesq. eqn., computer investigation 78−51
infinite constituent bound states, quantum correction soliton states 79−2903
inhomogeneous waveguide, nonlinear pulse (soliton) propag. theory 79−72617
initial-value problem for zero-area pulses, anal. props. 80−23756
instability in one-dimensional nonlinear systems *(Russian)* 80−52039
instanton applications in statistical mechanics 79−75450
insulator, modulation oscills. of travelling EM wave 80−24962
integrable nonlinear evolution equation, soliton soln. from inverse scatt. method 80−73186
interacting Dirac and Klein-Gordon fields, absence of solitary waves 77−30226
interaction dynamics and nontopological stability in nonlinear model of complex scalar field 80−101719
internal solitary waves in linearly stratified fluid 78−79332
internal solitary waves in stratified flows, cubic and quadratic nonlinearity 80−69856
internal solitary waves prod. by tidal flow over three-dimens. ridge, ocean appl. 79−46332
internal waves with finite fluid depth, inverse scatt. problem, Backlund transformation 80−31517
intersoliton forces in weak-coupled quantum field theories 77−71430
inverse method for solving differential-difference and difference-difference eqns. 80−105513
inverse scatt., generalised problem prolongation structs., soliton solns. 77−3833
inverse scatt. method, N-dimens. resolvent of linear problem, soliton theory 79−12643
inverse scattering and solitons, geometric considerations 80−4550
inverse scattering method for equation $\sigma_{xt}=e^{\sigma}$, soliton soln. 78−389
inverse scattering method for nonlinear evolution eqns. under nonvanishing conditions 78−57808
inverse scattering problem, N-soliton of eqn. $\sigma_{xt}=e^{\sigma}$ 78−8269
inverse scattering technique of soliton theory, Lie algebra, Poisson-Moyal bracket, rotating rigid body 77−9908
3×3 inverse scattering transform, soliton perturb. scheme 80−27151
ion acoustic, interpretation of expt. 78−38474
ion acoustic soliton propag. in strong RF electric field 77−31454
ion acoustic soliton propag. in two-electron temp. plasma 80−33767

solitons continued
ion acoustic soliton reflection and transmission at plasma interface 80−106899
ion acoustic solitons, density gradients effect 77−31456
ion acoustic solitons in beam plasma system with nonisothermal electrons generated by ion-beam 80−103151
ion acoustic solitons in collisionless multi-ion plasmas 79−77351
ion acoustic solitons in plasma, props., related theories 80−48877
ion acoustic wave soliton soln., LF, multicomponent plasma 77−35336
ion acoustic waves, diverging cylindrical, recurrence investigation 80−79474
ion acoustic waves, soliton-like, obs. of slow and fast cylindrical waves 79 37484
ion acoustic waves, soliton-like, slow and fast, obs. 80−28654
ion beam-plasma system with nonisothermal electrons, ion-acoustic solitary waves 80−33784
ion sound soliton-Langmuir wave interactions *(Russian)* 80−100077
ion wave packet, nonlinear, modulational instability, expt. 77−65853
ion-acoustic, coupled-wave and envelope solitons 78−75334
ion-acoustic cylindrical soliton, scatt. collapse 79−32544
ion-acoustic cylindrical solitons 79−19015
ion-acoustic Korteweg de Vries solitary waves in plasma with density, temp. gradients 78−55720
ion-acoustic large-amplitude solitons, nonstationary theory *(Russian)* 78−1820
ion-acoustic solitary wave excitation in collisionless plasma *(Russian)* 78−26267
ion-acoustic solitary waves, ion temp. and higher order contrib. effects 79−46439
ion-acoustic soliton, in nonuniform plasma, theory 78−30436
ion-acoustic soliton, refl. from sheath around negatively biased grid 78−38479
ion-acoustic solitons, dressed, dynamical processes 77−80286
ion-acoustic solitons, temporal development, initial value problem; 80−33771
ion-acoustic solitons, two-dimens. interaction 80−106908
ion-acoustic solitons in electromagnetically irrad. magnetoplasma 78−22485
ion-acoustic solitons with a temperature gradient 80−79490
ion-acoustic-solitons, dissipative effect on formation 77−84419
ion-sound soliton-resonant plasma particle interactions *(Russian)* 80−14880
ionosphere, solitary drift waves excitation and propag. *(Russian)* 77−70915
Ising model, modulated phase with solitons, phasons and devil's staircase 80−95044
Ising model, nonlinear excitations and coherent states in transverse field 80−68143
Ising model with competing interactions, solitons and phasons 80−34653
Ising-Heisenberg linear ferromagnet, excitation spectrum and thermodynamic props. 80−50118
Josephson point junction chain, solitary wave solns. 79−87212
Josephson transmission line oscillators, soliton solns. 79−87211
Kadomtsev-Petviashvili eqn., appl of variation of action method of one field solitons 80−331
Kadomtsev-Petviashvili eqn., inverse scatt. problem, separation of variables 78−62087
Kadomtsev-Petviashvili equation, two-dimensionaL solitons and their interaction 78−12575
KdV eqn., particular N-soliton soln. 80−31971
Keller's solitary wave, capillary force effect 77−72313
kinematic characteristics of travelling waves 78−67205
kink theories, approximately straight 80−82871
kinklike multisolitons in polynomial field theories 78−21014
Klein-Gordan equations with logarithmic nonlinearities, classical theory 79−5996
Klein-Gordon kinks with fourth order derivative self coupling 78−32970
Klein-Gordon nonlinear eqn., generalised susceptibility of solitary wave 79−75357
Klein-Gordon nonlinear eqn., solitary wave exist. in higher dimens. 77−74232
Korteweg de Vries eqn., periodic multi-soliton solns. and Toda lattice 77−30109
Korteweg de Vries eqn., second modified, exact multi-soliton soln. 80−73180
Korteweg de Vries eqn., soliton soln., Hugoniot conditions for gas dynamics 80−42069
Korteweg de Vries equation, Pade approximants, soliton solns. 80−42071
Korteweg de Vries equation, shock-like solns. for plasma response to piston driver 77−51187
Korteweg de Vries equations, higher order, soliton solns., inverse scatt. problems 77−45741
Korteweg de Vries integrals and Poisson's theorem 79−69
Korteweg de Vries modified eqn., solitary wave solns. 80−46818
Korteweg de Vries soliton, collapse into weak noise shelf 78−57792
Korteweg de Vries soliton, in slowly varying medium, theory 78−30436
Korteweg-de Vries, complex modified eqn., dispersion, self-propagation in anisotropic medium 79−75371
Korteweg-de Vries eqn., exact soln. 77−26138
Korteweg-de Vries eqn., higher order, prolongation struct., Lie algebra, soliton solns. 78−8249
Korteweg-de Vries eqn., initial value problem, soliton region determ. 80−62490
Korteweg-de Vries eqn., quasi-solitary wave soln. 80−70
Korteweg-de Vries eqn., slowly varying solitary wave solns. 80−72
Korteweg-de Vries eqn., weak dissipation effect on two soliton soln. 80−27143
Korteweg-de Vries eqn. difference analogue 78−55
Korteweg-de Vries eqns., perturbed solns. and soliton production 80−42074
Korteweg-de Vries equation, algebraic soliton 77−9858
Korteweg-de Vries equation, invariances and conservation laws 79−26244
Korteweg-de Vries equation, modified, N-soliton soln., matrix trace method 80−36871
Korteweg-de Vries equation, perturbation theory 77−33852
Korteweg-de Vries equation, soliton soln. using matrix trace 80−36870
Korteweg-de Vries equation, solns. for slowly decreasing boundary conditions 80−36872
Korteweg-de Vries equation, two-dimens. distrib. soliton soln., asymptotic anal. 79−49376
solitons continued
Korteweg-de Vries equation and nonlinear waves 79−92956
Korteweg-de Vries equation solns. 79−84964
Korteweg-de Vries equation with loss and nonuniformity terms, N-soliton solns. 77−13600
Korteweg-de Vries equations, N-soliton soln., functional integral representation 80−4542
Korteweg-de Vries solitary wave, energy loss 80−62489
Korteweg-de Vries solitary waves for cylindrical and spherical symmetric ion acoustic waves 79−77371
Korteweg-de Vries soliton solutions, perturbations 80−105511
Korteweg-de Vries-Burgers eqn., invariant solns. 79−63052
Korteweg-de Vries-Burgers equation, self-similar solns., quasi-solitons 78−93537
Korteweg-de-Vries eqn., exact soln. via a generalisation spectral transform 78−65786
Korteweg-de-Vries eqn., solitons and rational solns. 79−67
Kortweg-de Vries equation, perturbations conserving solitons 78−49642
Landau-Lifshitz nonlinear equation, N-soliton solutions *(Russian)* 79−24184
Langmuir, one-dimensional, propag., interactions and generation 77−43057
Langmuir bounded wave solns. in self-consistent density cavity *(Japanese)* 77−42973
Langmuir envelope finite amplitude soliton form., in plasma-beam systems 77−84422
Langmuir envelope solitons in turbulent plasma 78−67334
Langmuir multidimensional nonlinear waves 78−63555
Langmuir oblique solitons, self-contraction in free path regime *(Russian)* 80−43921
Langmuir soliton EM wave scatt., theory *(Russian)* 80−38564
Langmuir soliton formation with ion-acoustic densiton emission 78−75328
Langmuir soliton solns. with high nonlinearities, energy principle 80−24156
Langmuir soliton theory, Lagrangian density and conservation laws, strongly turbulent plasma 77−51169
Langmuir soliton weak EM wave scatt., Doppler shift and reflection coeff. calc. *(Russian)* 79−7467
Langmuir solitons, electron beam interaction in turbulent plasma 79−14563
Langmuir solitons, generation and collapse, numerical study 77−68784
Langmuir solitons, in inhomogeneous plasma, accel., theory *(Russian)* 78−26269
Langmuir solitons, in nonequilib. plasma, nonlinear Landau damping effects *(Russian)* 78−22479
Langmuir solitons, large amplitude, props. 79−10656
Langmuir solitons, non-neutral soln. 80−33763
Langmuir solitons, prolongation struct. 79−88814
Langmuir solitons, transverse instability 80−6250
Langmuir solitons *(Russian)* 79−46451
Langmuir solitons in magnetised collisionless plasma *(Russian)* 78−47122
Langmuir solitons nonlinear interaction in magnetised plasma 79−14540
Langmuir solitons with opposite vel., collisions 77−68776
Langmuir standing waves instability, one dimens., soliton and collapse, numerical expt. 80−38619
Langmuir turbulence, modulating instability wave, nonlinear dynamics, solitons *(Russian)* 77−47196
Langmuir turbulence in upper hybrid resonance region, external electric field effects *(Russian)* 79−73010
Langmuir waves, modified decay, collisions effect *(Russian)* 77−27672
Langmuir waves, modulated, nonlinear damping 78−51301
Langmuir waves, modulated, nonlinear Landau damping effect 78−81849
Langmuir waves, numerical modelling of 1-D turbulence, acoustic oscillations effect *(Russian)* 80−103135
large radius polaron model, soliton excitations 79−42470
laser physics appls. 80−48333
lattice, scattering theory from mass impurity in cubic nonlinear lattice 79−4385
lattice models of screw dislocation high velocity motion, lattice model effects 79−77600
lattice of solitons, dynamic and stochastic oscills. *(Russian)* 77−74324
lattice quantisation of Sine-Gordon system, single-site approx. 79−17603
lattice soliton, scatt. by mass interface, reductive perturbation method 78−18889
lattice soliton scatt. from mass interface in 1D nonlinear lattice, simulation *(Japanese)* 77−43306
lattice solitons, scatt. from mass impurity 80−46992
lattice stability in coupled linear chain system 80−73282
lattice thermal conductivity theory 80−46991
lecture 78−24690
Liapunov stability of generalized Langmuir solitons 80−38631
Lie algebras, solitons and pseudopotentials 77−26131
Lie group framework for soliton eqns., Lund-Regge model generalisations 79−17605
light beam self-action in nonlinear media, soliton solns. 80−14404
linear equation associated with solitons, Green's function using scatt. theory 78−4507
Liouville equation, nonlinear solutions and their stability 80−68374
liquid crystal, thin layer, symmetry defects and solitons, topological classif. 80−107044
liquid film solitons, draining behaviour 80−96272
liquid layers, immiscible Kelvin-Helmholtz instability, nonlinear wave packets 79−46289
liquid with gas bubbles, soliton interactions *(Russian)* 79−14419
liquid-vapour flow, wave pattern and liq. film burnout 78−90985
local field theory of solitons 79−12953
logarithmic Schrodinger equation, soliton dynamics 80−57130
long waves in dispersive media, solitary wave interaction 80−59062
long waves in inviscid compressible isothermal atmosphere 79−29811
low temperature physics, importance of solitons 79−63057
lower hubrid, envelopes in magnetic fields 80−59224
lower hybrid cones, stability anal. 80−48880
lower hybrid waves, modulation instability growth rates 80−48881
lower hybrid waves, two-dimens. self-modulation in inhomogeneous plasmas 79−90403
Lund-Regge system, prolongation structures and connection forms 78−93805
Mach reflection of solitary wave 80−79340

solitons continued
magnetic, in one-dimensional mag. systems, obs. *(Japanese)* 80−2555
magnetic flux annihilation in a large Josephson junction 80−11139
magnetic gap, soliton bound states in Ising model, quantum double sine Gordon eqn. solns. 79−78288
magnetic monopole soliton solns., gauge particles 78−16920
magnetic semiconductor, conduction electron spectrum, influence of nonlinear spin waves 79−28270
magnetised collisionless plasma, oblique Langmuir solitons under free path conditions *(Russian)* 80−79477
magnetised plasma loaded waveguide, interaction between solitary structures 80−38661
magneto-acoustic macroscopic soliton instability growth rate, dispersion eqn. *(Russian)* 78−59562
magneto-acoustic solitons, macroscopic instability *(Russian)* 77−47200
magnetoplasma, solitary ion-acoustic wave propag. exact stationary solns. 79−19010
many-dimensional solitons, gauge invariant theory of nonlinear chiral field 77−34082
mass formula for solitons with quantized charge 79−93282
mass of solitons, surface tension, in $(\lambda|\phi|^4)_2$ quantum field theory 77−30240
massive elementary particle, maintenance of size and shape 79−71643
massive Thirring model, complete S-matrix, sine-Gordon solitons 78−16936
massive Thirring model, multisoliton solns. in Pohlmeyer-Lund-Regge system 80−47195
massive Thirring model, quantized renormalized, dynamical charges, soliton, antisoliton, breather states 77−18171
massive Thirring model, sine-Gordon eqn., soliton struct., Coleman correspondence 78−8509
massive Thirring model, two-dimens., inverse scatt. method 80−4840
Maxwell-Bloch equations, breakdown of soliton behaviour 77−72024
mechanics, short-wave asymptotics 77−37763
melting, dislocation generation, anharmonicity and solitons 78−79746
meson interactions, LSZ reduction formulae, soliton asymptotic theory 78−4774
MHD, solitary fluid transient compression wave in rectangular duct in transverse mag. field 78−59503
MHD perturbations, formation of upper hybrid solitons 79−90348
MHD solitons in solar wind, nonlinear dispersion eqn. qualitative anal. 80−4217
microscopic system mechanics, solitons and 1-dimens. Schrodinger eqn. 79−12934
Miura transformation, Backlund transform. and problem of collision 77−9881
mode converted lower hybrid solitons, stability in parametric regions 80−92303
modified Benjamin-Ono eqn., N-periodic wave and N-soliton solns. 80−28518
modified Korteweg-de Vries eqn., N-soliton solns. 80−36876
modified Korteweg-de Vries solitary wave in a slowly varying medium 80−36873
modulation instability and strong turbulence in materials with inverse dispersion *(Russian)* 77−62359
modulational instability expt. using nonlinear transmission line 77−82397
modulational instability growth, for randomised initial conditions 78−18406
molecular chain, 1-D electron motion, electron-phonon interaction, acoustic solitons 80−70628
molecular chain, radiative lifetime of solitons, theory *(Russian)* 77−66539
molecular systems, biophys. effects of solitons and excitons 80−51044
monatomic three dimensional FCC lattice, solitary wave effect on shock profile 80−79874
monopole-dyon system in nonAbelian gauge theories, Georgi-Glashow model 77−79213
motion in nonuniform, sinusoidally varying media 80−42072
multi-soliton solutions of a derivative nonlinear Schrodinger equation 80−105528
multi-soliton solutions of nonlinear partial differential eqns. 80−105763
multicomponent nonlinear Schrodinger equation, soliton solns. 77−9907
multidimensional, additive topological laws of conservation *(Russian)* 77−74601
multidimensional nonlinear eqns., N-soliton solns. by Hirota's method 80−105797
multidimensional stable relativistic solitons *(Russian)* 80−13224
multisoliton breakdown criteria and implications 77−29994
multisoliton formula for completely integrable two-dimensional systems 79−67166
multisoliton solutions in two-layer finite depth fluid 78−55621
multisoliton solutions of nonlinear Klein-Gordon eqns. 79−12617
N-soliton evolution eqns. generated from Boussinesq eqn. Backlund transform. 77−53748
N-soliton solns. of nonlinear evolution eqns., Wronskian representation 79−25867
narrow magnetic domain wall material, theory of intrinsic coercivity 80−2597
neutron scattering observation of solitons near critical point 80−34650
non-Abelian gauge group theory, relationship with solitons 80−4549
non-Abelian internal symmetry in 3+1 dimensional space-time, quantisation, collective coord. and Lorentz covariant methods 80−47199
non-linear one dimensional, solitons and kink Schrodinger eqns., general method for soln. 80−46871
non-linear wave equations in a curved background space 78−65827
nonAbelian gauge fields *(Chinese)* 78−24917
nonequilibrium plasma, fast Langmuir soliton possibility 78−75340
nonlinear 1D system, ϕ^4 chain dynamical props. 80−4655
nonlinear σ model in two dimensions, geometry 77−41496
nonlinear complex scalar field with nontrivial asymptotic behaviour of soliton solns. 80−4867
nonlinear difference-difference equations, derivation of infinite number of conservation laws 78−89324
nonlinear differential evolution eqns., 3+1 dimens. 80−46828
nonlinear Dirac eqn. in four dimens., asymptotic solns. 77−6016
nonlinear Dirac equation with SU(3) colour symmetry, vanishing soliton solns. 79−71693
nonlinear dispersive systems, 2-D lumps 79−92955
nonlinear dispersive systems, classical mechanics 79−75449
solitons continued
nonlinear dispersive wave eqns., modulational instability and envelope solns. 78−54199
nonlinear elastic dispersive media, interaction of solitary waves *(Russian)* 80−42076
nonlinear electrodynamics, three-dimensional soliton solution *(Russian)* 79−22884
nonlinear electrostatic drift solitary waves in two species plasma 77−55135
nonlinear equations, multi-soliton soln. construction, direct method 79−75360
nonlinear equations with soliton solns. 78−45467
nonlinear evolution, instability, self-refraction *(Russian)* 77−11212
nonlinear evolution eqns., multi-soliton solns. 79−58556
nonlinear evolution eqns., soliton connection 78−16661
nonlinear evolution eqns., solitons and rational solns. 79−67
nonlinear evolution eqns., solitons on moving space curves 77−74254
nonlinear evolution equation, exact inverse scattering solution 79−84965
nonlinear evolution equation class solvable by spectral transform technique 79−75370
nonlinear evolution equations, inverse scattering method 80−12919
nonlinear evolution equations simulating pair production and annihilation, solitary wave solns. 78−86167
nonlinear evolution of three-wave interactions in inhomogeneous medium 77−74272
nonlinear fermion system of self-interacting particles, field patterns 78−16909
nonlinear field theory, two-point function 77−65078
nonlinear hydrodynamical eqn. of Kaup, periodic and N-soliton solns. *(French)* 80−31521
nonlinear hyperbolic eqn., special classes of solns. *(German)* 79−21526
nonlinear internal wave solitons, Calogero-Moser-Sutherland N-body problem 79−27679
nonlinear kinetic equation, structural stability, soliton collisions 80−10382
nonlinear Klein-Gordon equation, solitary wave collisions 79−80761
nonlinear Klein-Gordon equations, three dimens. multiple soliton-like solns. 78−49955
nonlinear lattice, wave propagation 77−13707
nonlinear lattice dynamics, molecular dynamics studies 79−77713
nonlinear long waves on liq. layer adjacent to gas stream 77−11203
nonlinear magnetostatic modes and twisting modes with magnetic islands 80−106900
nonlinear magnons 78−6523
nonlinear normal mode theory 80−48875
nonlinear one-dimens. lattice with Lennard-Jones potential, soliton soln. 79−54069
nonlinear partial differential eqns., pure soliton solutions 77−82368
nonlinear refraction and self-focusing effects *(Russian)* 80−98805
nonlinear Schrodinger eqn., appl of variation of action method of one field solitons 80−331
nonlinear Schrodinger eqn., slowly varying solitary wave solns. 80−73
nonlinear Schrodinger eqn., soliton solns. 80−27173
nonlinear Schrodinger equation, adiabatic invariants, deep water and spiral density waves 80−48874
nonlinear Schrodinger equation, soliton soln. *(Chinese)* 79−92987
nonlinear Schrodinger equation, spectral transform soln., charact. behaviour of solitons 78−70005
nonlinear Schrodinger equation, transverse instability of soliton solns. 79−58561
nonlinear self dual network, with saturable property Korteweg-de Vries eqns. 79−21560
nonlinear shallow water waves, deformation, disintegration into solitons 77−84266
nonlinear solvable models, common features 77−67573
nonlinear spinor eqns. with localised solns. 78−49964
nonlinear string dynamics, rigid body motions, space curves, prolongation structures, fiber bundles, and solitons 79−97213
nonlinear system, chopping phenomena induced by solitons 77−30111
nonlinear system, kink-phonon interaction 79−73262
nonlinear three wave interactions, space-time evolution in homogeneous medium 79−84966
nonlinear three wave interactions, space-time evolution in inhomogeneous medium 79−84967
nonlinear transmission line, solitary waves 80−4543
nonlinear wave and soliton propagation, arbitrary density profile, adiabatic approx. 78−49676
nonlinear wave equations, soliton applications in physics 80−8813
nonlinear wave equations, symm. of solitons and general solns. 79−85210
nonlinear wave equations solns., classical, quantal, appls. 78−57793
nonlinear wave packets propagation, finite depth effects 79−48510
nonlinear waves, appls. of soliton *(Japanese)* 79−80418
nonlinear waves and solitons, stability in three dimens. 79−97211
nontopological, and appls. to hadrons 78−32968
nontopological, hadron appl. 80−47191
nontopological soliton solutions, conservation laws 79−45022
nonuniform states, stability in systems exhibiting continuous bifurcation 79−84972
nuclear matter, elongated soliton type wave solutions, finite amplitude wave propagation *(Russian)* 80−13397
nuclear potential, solitons as model 80−83081
numerical studies, historical review 79−75367
numerical study of solitons *(Chinese)* 79−35529
oblique collision of ion-acoustic solitons 80−83934
ocean, stability of solitary Rossby waves over variable relief, analytical theory 80−101371
ocean, stability of solitary Rossby waves over variable relief, numerical expts. 80−101372
one dimensional condensate, nonlinear oscillating dipolar excitations 79−38007
one dimensional magnet with easy plane, solitons and magnons 78−23260
one dimensional systems with resonance interaction, collective particle like excitations, Schrodinger eqn. 80−46868
one-dimensional ϕ^4 and double quadratic systems, kinks, quantum statistical mechanics 80−47197
one-dimensional complex scalar fields with phase anisotropy, statistical mech. 80−22517
one-dimensional conductor, quantum solitons 77−39792
one-dimensional conductors, quantum solitons 78−6285

solitons continued
one-dimensional ferromagnet with biquadratic exchange, solitary bound states of magnons and lattice deform. 79−19732
one-dimensional field, complex, solitary-wave soln. 77−5707
one-dimensional ionic conductors, cooperative diffusion and soliton Brownian motion 78−95177
one-dimensional lattice, shock propag., soliton like behaviour 78−59859
one-dimensional materials, nonlinear transport due to bound quantum solitons 79−51558
one-dimensional materials, nonlinear transport due to bound quantum solitons 79−78089
one-dimensional molecular chain, collective excitations, solitons *(Russian)* 77−4305
one-dimensional molecular chain, collective model for conformons 80−15456
one-dimensional molecular crystal, soliton-like solns. of eqns. for excitations 78−84149
one-dimensional molecular lattice, soliton motion, thermal vibrations *(Russian)* 80−54321
one-dimensional quiescent lattices, shock profiles, end condition effects 80−34138
one-dimensional sine-Gordon system, kinks 80−46969
one-dimensional solitary-wave-bearing scalar fields, statistical mechanics, ideal-gas phenomenology 80−105792
one-dimensional spin 1/2 chain, soliton excitation in strong spin-phonon interaction 80−103842
one-dimensional system, electron-phonon interaction, soliton solns. 79−23691
one-dimensional systems, electron trapping and transport by supersonic solitons 78−72139
one-dimensional systems, with reson. interaction, soliton-like solns. 80−46831
one-soliton sector, covariant functional approach 78−78092
optic mode-EM mode coupled systems, soliton relation to polaritons 79−77707
optical fibre, soliton pulse propag. 80−58759
optical fibres, nonlinear pulse propagation 79−18536
optical pulses, one-dimensional transparent, in resonant media, transverse instability 79−46010
optical waveguides, nonlinear pulse propag. theory 80−83669
optical zero-area pulse output, by self-induced transparency, initial conditions 79−41424
orthorhombic ferrimagnets, domain wall motion at near sonic velocity, magnetoelastic interactions 80−34683
oscillatory shock waves in soliton system under perturbation *(Russian)* 79−92959
overtaking solitons of high energy in a one-dimensional Lennard-Jones chain 80−73182
$P(\phi)_2$ models, soliton solns. 80−42333
parametrically excited spin waves system *(Russian)* 77−59401
parametrically unstable plasma eqns. and solitons 78−75324
particle model based on stringlike solitons 78−62294
particle stability in nonlinear scalar field theory 80−91004
partition function for two-dimensional solitons 79−6039
patching solitons in 2+1 dimens, Coleman's rules 77−82678
path-integral quantisation using zero-mode Feynman rule 78−70276
Peierls dielectric, one dimensional, selftrapped excitations in Peierls-Frohlich state *(Russian)* 80−54678
Peierls-Frohlich condensate, attracting solitons and discontinuous lock-in transition 80−92840
periodic exponential lattice, soliton quantum theory 77−30110
periodic solutions to classical field equations 80−46822
perturbation theory, evolution eqns. for nonlinear waves *(Russian)* 77−79005
perturbation theory, evolution theory, tail struct. *(Russian)* 78−86197
perturbations, variational calcs. 80−46825
perturbed, interaction, and struct. of oscillatory shocks 79−64868
perturbed soliton equations, variational approach 78−89366
phase-locked solutions, comparison of single and double sine-Gordon solns. 79−58552
planar ferromagnetic chain, soliton dynamic struct. factors 80−7125
planar Langmuir solitons, 3-dimens., stability 80−46827
plasma, cartons induced by soliton flash 78−91104
plasma, caviton, dissipative three-dimens. Langmuir soliton, formation *(Russian)* 80−83943
plasma, diverging cylindrical ion acoustic soliton, transition to disperse wave 77−89257
plasma, diverging cylindrical solitons excited by probe 77−7522
plasma, effect of ion beam propag. on ion acoustic soliton characts. 77−89271
plasma, electron beam delay, strong turbulence, ballistic modes and Langmuir solitons *(Russian)* 77−76111
plasma, electron-acoustic mode, two-temp. electrons 78−14141
plasma, electrostatic high freq. oscills. damping, nonlinear Schrodinger eqn. calcs. 77−7530
plasma, electrostatic ion cyclotron waves 77−80291
plasma, envelope solitons of relativistically strong electromagnetic waves *(Russian)* 79−37503
plasma, helicon, soliton form., acoustic wave emission, interactions 77−7537
plasma, HF soliton interaction with ion-acoustic waves and plasmons *(Russian)* 77−19682
plasma, inhomogeneous, modulated nonlinear ion acoustic waves 79−86576
plasma, ion acoustic soliton, Boussinesq eqn. description 79−46449
plasma, ion-acoustic, amplification by an ion beam 78−83554
plasma, ion-acoustic, ionic thermal effects 77−47191
plasma, ion-acoustic holes in a two-electron-temperature plasma 80−59205
plasma, ion-acoustic Korteweg de Vries solitons 79−46446
plasma, ion-acoustic solitary wave, third-order corrections, reductive perturbation method 80−43898
plasma, ion-acoustic solitary waves *(Czech)* 80−1764
plasma, ion-acoustic solitons, 3-dimens. interactions 78−59570
plasma, ion-acoustic solitons, strongly non-linear 78−5858
plasma, ion-acoustic solitons launched from plate, distortion in density gradient 79−64863
plasma, ion-acoustic wave packets, nonlinear distortion 79−46448
plasma, ion-acoustic waves, Korteweg-de Vries soliton, higher order terms in reductive perturbation theory 78−1824
solitons continued
plasma, Korteweg de Vries waves and solitons, three-dimens. stability 78−83540
plasma, Langmuir soliton excitation by monoenergetic electron beam *(Russian)* 79−77381
plasma, Langmuir solitons 78−51302
plasma, Langmuir waves, cascade and collapse in 2-D 79−1308
plasma, laser irrad., soliton generation at resonance, density modification 78−14172
plasma, laser irrad. pellet, role in two-plasmon decay instability 78−1842
plasma, laser-irradiated, Langmuir soliton generation at crit. density 80−6267
plasma, LF drift solitons, 2D stability 77−84431
plasma, lower hybrid cones, nonlinear development 78−34306
plasma, magnetised, electrostatic single wave, particle trapping, detrapping and acceleration 77−68738
plasma, magnetosonic solitons, one-dimens., helicon perturbation 79−7454
plasma, modulation instability and nonlinear waves *(Russian)* 78−22476
plasma, near-Alfvenic upper-hybrid envelope solitons 79−98898
plasma, negative solitons rel. to current interruption in collisionless plasma 79−75052
plasma, nonlinear electron-beam self-induced transparency modulation mechanism 78−34341
plasma, nonlinear evolution eqn., bifurcation of solitary waves *(French)* 78−38465
plasma, nonlinear MHD mode struct. in pinch 77−974
plasma, nonlinear quasioptics in DC mag. field *(Russian)* 79−98914
plasma, nonlinear surface density wave 79−98896
plasma, nonlinear theory of unstable plane waves and solitons 80−87888
plasma, nonlinear wave propag., soliton form. 79−46442
plasma, nonlinear wave propag., solitons and envelope solitons 78−14158
plasma, one-dimens. coupled Langmuir-ion acoustic waves, dynamics and stability 78−34296
plasma, parametrically unstable 78−63563
plasma, photon soliton and fine structure due to nonlinear Compton scattering 80−10363
plasma, solitons in convective motion 79−46443
plasma, solitons in convective motion 79−46444
plasma, stabilisation of modulation instability, fast Langmuir solitons generation *(Russian)* 78−38470
plasma, stability to transverse perturbations 77−51180
plasma, strong Langmuir turbulence, soliton flash, turbulent ion heating and relax. oscills. 78−1834
plasma, transverse wave packets, momentum, mass and energy transport, solitons 78−1812
plasma, trapped electrons in ion acoustic waves and solitons 77−19690
plasma, upper hybrid solitary waves, existence and propag. 78−83555
plasma, wave excitation in relativistic electron beam heating 78−26307
plasma 79−98884
plasma and other dispersive media, review 79−44755
plasma electrostatic wave interaction, upper-hybrid envelope solitons 77−76074
plasma flow, steady, shock and soliton solutions 77−15172
plasma in external mag. field, electron beam-whistler soliton interaction, appl. solar wind 77−11360
plasma ion-acoustic waves, K-dV eqn. with coord. stretchings 77−58859
plasma Langmuir turbulence, numerical modelling, solitons, nonlinear interactions 80−70030
plasma Langmuir turbulence driven by constant pumping 78−75341
plasma low-hybrid wave nonlinear eqns. and solitons 78−75323
plasma media with inverse dispersion, soliton solns. 80−103152
plasma nonlinear lower hybrid solitary waves 78−51291
plasma parametric instability and Langmuir quasicollapse, two-dimensional calc. 78−75329
plasma soliton propag. and deformation in magnetised plasma filled waveguide, modification by reson. particles 79−77395
plasma surface waves, nonlinear behaviour 79−1302
plasma wave, finite amplitude, stability criteria 79−64860
plasma wave, radially symm., Korteweg-de Vries eqn., spike soln. 78−47109
plasma wave propagation, nonlinear Schrodinger equation, modified Zakharov-Shabat inverse scatt. problem 80−59200
plasma waves, localised density depressions travelling at subthermal speeds 77−19692
plasma waves, nonlinear, using perturbation theory 79−10662
plasmapause, shocks and solitons 77−25840
plasmas, cylindrical ion-acoustic soliton propagation 80−28632
plasmas, soliton damping 79−64869
polyacetylene:AsF_5, soliton doping mechanism, mag. susceptibility meas. 80−107979
polyacetylene, continuum model for solitons 80−65472
polyacetylene, lightly doped, phenomenological theory of soliton formation 80−103644
polyacetylene, mag. soliton defect ESR study 80−80590
polyacetylene, metallic, mixed Peierls phase, Hartree-Fock calcs. 80−70689
polyacetylene, pristine and acceptor doped isomers, EPR, DC cond., evidence against solitons 80−15782
polyacetylene, soliton form. 79−76540
polyacetylene, soliton formation and cis trans isomerization 80−76505
polyacetylene, vibr. excitations of charged solitons 80−108201
polyethylene, crystal, dielectric α-relax., soliton as crystal defect 80−45004
polynomial field theories, N-soliton states 77−18174
polynomial field theories, nonlinear Klein Gordon eqn., exact multiple solution solns. 78−45773
polyvinylidene fluoride, poling process, solitary wave propagation model 79−87398
Prasad-Sommerfield soliton, excited states, SU(3) generalisation 80−4877
Prasad-Sommerfield soliton mag. monopole, excited states and SU(3) generalisation 79−40665
propagation, cloud generation, in nonlinear dispersive media with weak dissipation 78−47123
pseudospherical surfaces in soliton eqns., conservation laws, Backlund and scale transformations 79−75688
pulsar coherent radiation, relativistic soliton model *(Russian)* 78−77568
pulsars, relativistic Langmuir soliton appls. 79−17004
pulsating, classical and quantum appls. *(Russian)* 77−74267

solitons continued
pulse propag. in nonlinear media, linear approx. 79−94390
pulsons, spherical symm., large amplitude, dynamics *(Russian)* 77−30274
pulsons, spherically symmetric; cascade evolution in multivacuum field theory models 77−61192
quantisation, cancellation of zero-mode singularities 77−49838
quantisation in infinite volume 77−13865
quantisation of soliton solution of a generalised discrete non-linear equation 79−17261
quantisation using Bogolyubov transformation 78−16695
quantised states in non-perturbative field theory 77−67564
quantum, connection with fermion fields for $(\sin \phi)_2$ interaction 77−41780
quantum corrections to soliton mass in QFT, Feynman rules 78−78069
quantum crystal, one-dimensional, solitary defectons 78−2332
quantum expansion generalisation *(Chinese)* 78−24915
quantum field theory, nonperturbative, resonance states, solitons 78−380
quantum field theory, quasiclassical expansion and solitons 78−94
quantum field theory, solitons and instantons 78−8495
quantum fluid, hydrodynamics equations in presence of vortices *(Russian)* 79−33141
quantum mass corrections to supersymmetric soliton theories in two dimensions 79−54254
quantum mechanical mass in supersymmetric theories 80−22536
quantum soliton operators for monopoles and Fermionization mechanism of dyons 79−35940
quantum theory of solitons, review 78−70288
quantum two-loop corrections of soliton mass in scalar field theories 77−10175
quark model, bag-like soliton solns. 78−8609
quasi one dimensional charge transfer salts, soliton model for dielectric permeability 80−40036
quasi one-dimensional charge transfer salts, soliton model for dielec. permeability 79−91338
quasione dimensional structures, collective excitation of CDW 78−18981
quasisoliton pulses, head-on stimulated scatt. 79−27332
radiophysics theory 80−48124
random surface wave field, wave groups presence modelling 79−2245
recurrence of solitons, coupled mode approach to nonlinear dispersive wave *(Japanese)* 77−41471
regularised long wave equation, anelastic collision of solitary waves, numerical anal. 78−77724
regularised long wave equation, solitary wave solns. 77−13616
relativistic charged particle beams in storage rings, soliton soln., phase locked states 78−50425
relativistic field eqns., two-soliton solns. 78−74124
relativistic scattering theory, a covariant approach for the one-soliton sector 79−17640
relativistically invariant two-dimens. models, classification method *(Russian)* 78−70291
relaxation times in solid-state theory and one-dimensional molecular systems *(Russian)* 80−100640
renormalisation and quantum corrections 80−82884
resonant interaction of long and short waves, envelope pulse solitons and breather state 80−1616
resonant production in regularised long wave eqn. 79−97216
resonant three-wave process, Backlund transform. 77−68609
review, classical soliton solns. and semi-classical quantisation techniques 78−8255
review of concepts and methods in theory *(Polish)* 80−68057
review of soliton theory 80−47204
ring of torsion coupled overdamped pendulums, nucleation theory of overdamped soliton motion 80−12899
Rossby solitary waves, theory 78−1678
Rossby waves in two-layer system, theory 80−17293
Rossby waves in zonal shear flows, interactions, terrestrial atm. appl. 79−7379
rotating baroclinic fluid, soliton behaviour 79−72898
scalar complex field, Lorentz invariant system, exact many soliton solns. *(Russian)* 77−30275
scalar field, complex, one-dimens., with fourfold phase anisotropy, solitary-wave solns. 79−58553
scalar field interacting with Dirac field, soliton solns. in three space dimensions 77−26453
scale invariance and solitons 79−58866
scattering by impurities in Toda lattice, localised modes 78−14420
scattering of quantised solitons in non-linear Schrodinger theory, seminar 78−8256
scattering of quantised solitons in nonlinear Schrodinger theory 77−49842
Schrodinger derivative nonlinear eqn., exact. soln. using inverse scatt. technique 78−49703
Schrodinger eqn., cubic, perturbed plane-wave solns. 79−58587
Schrodinger eqn., nonlinear, perturbed, soliton interactions 77−87661
Schrodinger eqn., perturbation expansion, nonlinear Landau damping influence 78−62110
Schrodinger equation, nonlinear, conservation laws soln. method 79−63066
Schrodinger equation, nonlinear, perturbation expn. 78−47124
Schrodinger equation, soliton solutions, stability, nonlinear term of form $\psi|\psi|''$ 78−70013
Schrodinger equation, strongly nonlinear, variational approach 79−58583
Schrodinger equation with variable coefficients, differential-difference analogue, single-soliton solution behaviour 80−8819
Schrodinger nonlinear eqn., damped, soliton soln. 78−12605
Schrodinger nonlinear eqn., exact stationary soliton soln. 78−12604
Schrodinger nonlinear eqn., soliton-like soln. 79−44790
Schrodinger nonlinear eqn. three dimens. stability of solns. 80−57141
Schrodinger nonlinear mixed eqn. and soliton solns., inverse method 80−68065
Schrodinger S3-equation, perturbed by reson. interac., soliton-like soln. 79−7765
Schwinger generating function in terms of non-Gaussian functional measure, soliton soln. appl. 79−21892
self-diffusion via sine-Gordon solitons 80−70443
self-dual network eqn., shock wave and hole type soliton 78−27
self-induced transparency and superfluidity phenomena rel. to soliton wave packet propag. 78−22178
semiclassical fields in soliton sectors 78−29232
semiclassical soliton solns. in quantised field theories 80−4874
solitons continued
semiconductor, ferromag., polaron solitary waves 80−70625
semiconductor, nonlinear coherence phenomena in exciton region 80−99806
semiconductor superlattice, soliton propagation 78−72162
semiconductor with superlattice, EM wave propagation, solitons *(Russian)* 78−79999
shallow water solitary waves, shelves and Korteweg-de Vries eqn. 80−92166
shallow water waves strong interaction in channel 78−46989
sigma model, nonlinear, soliton stability in S^2 80−37165
$(\sin \phi)_2$ interaction in box, soliton soln. fermionisation 79−88840
sine Gordon equations, complex solitons and poles 79−30264
sine Gordon field, thermodynamics 77−87913
sine Gordon theory, equivalence to z-dimens. ferromag. classical X-Y model low temp. behaviour 77−13873
sine-Gordon, dynamic polarisability 77−9880
sine-Gordon ϕ-particles, quantum dynamics and statistical mechanics 79−42475
sine-Gordon breather soliton dynamics, rel. to special relativity 80−46801
sine-Gordon chain, classical, low freq. dynamics 80−108020
sine-Gordon chain, displacement fluctuations, long-time behaviour and dynamic scaling props. 80−101764
sine-Gordon chain, effect of external field 78−62145
sine-Gordon chain, evidence for breather excitations 79−63054
sine-Gordon chain, long-term behaviour 80−68051
sine-Gordon chain, mass diffusion, soliton solns. 79−85102
sine-Gordon chains, role of breather solns. in statistical mechanics 79−85212
sine-Gordon eqn., inverse method for solving differential-difference and difference-difference eqns. 80−105513
sine-Gordon eqn., return effect for rotationally symmetric solitary wave soln. 79−5986
sine-Gordon eqn., soliton creation-annihilation operators as canonical transformation 77−30041
sine-Gordon eqn., solitons and separable elliptic solns. 79−97215
sine-Gordon eqn. and Laplacian invariant, separable solns., complex solitons 80−90680
sine-Gordon eqn. two dimens. solns., Josephson junction phase calcs. 79−82725
sine-Gordon eqns.,.2- and 3-dimens., ring-shaped quasisoliton solns. 80−46829
sine-Gordon equation, 3 and 4 dimens., exact solns. 80−86091
sine-Gordon equation, approx. rotationally symmetric solns. 80−8807
sine-Gordon equation, approx. treatment of two soliton solns. 79−88838
sine-Gordon equation, Backlund transform., physical space-time solitons 80−77629
sine-Gordon equation, difference analogue 78−20976
sine-Gordon equation, discretisation 79−21931
sine-Gordon equation, double, multidimensional multisoliton kink solutions 80−73184
sine-Gordon equation, in one and more dimensions, break-up of quasi-soliton solns. 80−8806
sine-Gordon equation, multidimensional soliton solns. 79−49383
sine-Gordon equation, N-soliton construction, domain walls appl. 78−19198
sine-Gordon equation, polynomial field theories, solitary wave solns. 77−2726
sine-Gordon equation, rotationally symmetric breather-like solns. 80−77955
Sine-Gordon equation, soliton solns., boson transformation 79−17611
sine-Gordon equation, soliton solns. and appl. to solid state physics *(Japanese)* 77−30025
sine-Gordon equation, two soliton solutions, breather solution 80−12945
sine-Gordon equation and nonlinear σ model on a lattice 79−21932
sine-Gordon equations for 3-D solitons, classical $\lambda\phi^4$, double and single eqns. 78−45785
sine-Gordon field, topology and static-soliton solns. 77−49850
sine-Gordon finite-energy two-dimens. solns. and Yang-Mills pseudoparticles, transformation 77−65100
sine-Gordon interaction solitons and classical particles 77−74589
sine-Gordon kinks, nonequilib. props. using mol. dynamics techniques 79−12737
sine-Gordon model, quantum solitons, exact two-particle S-matrix *(Russian)* 77−57463
sine-Gordon model, supersymmetric, exact soliton like solns. 79−30643
sine-Gordon model, supersymmetric solitons and monopoles 80−31991
sine-Gordon model for large coupling consts., soliton scatt. matrix *(Russian)* 80−13221
sine-Gordon N-soliton quantum scatt. 77−34084
sine-Gordon pendulum eqn. and $\lambda\phi^4$ model, generalisation 77−49610
sine-Gordon perturbed equation, soliton mass formulae 80−22200
sine-Gordon problem, soliton mass, renormalisation 79−40678
sine-Gordon soliton, adiabatic behavior in presence of perturbations 79−49093
sine-Gordon soliton dynamics, numerical simulation in presence of perturbations 77−76714
sine-Gordon soliton form factors, massive Thirring model S-matrix 77−45952
sine-Gordon soliton mass, higher order correction 77−61188
sine-Gordon soliton mass, thermal renormalisation 79−54036
sine-Gordon solitons, boundary effects 80−62481
sine-Gordon solitons, dynamics, in presence of perturbations 77−37751
sine-Gordon solitons, exact two-particle S-matrix 77−74608
sine-Gordon system, bion dissoc. 80−13201
sine-Gordon system, solitons and bion dissoc. 79−63048
sine-Gordon system with winding-number density, low temp. soliton gas phenomenology 80−105589
sine-Gordon theory, soliton mass 77−13848
sine-Gordon type field eqn., two-dimens., solitons, quark confinement 78−74160
single Langmuir solitons, perturbation anal. 80−69999
single soliton cosmological waves, Friedmann cosmological model background *(Russian)* 80−17708
singular perturbation theory, solitons as particles, oscills. 78−73882
Skyrme gauge model, topological solitons 80−9086
SL(2,R) and solitons 78−57748
slow Langmuir solitons, low amplitude and wavenumber behaviour 78−75293

solitons continued
SO_4, $SL_{2,C}$ classical gauge field eqns., isotropic and solitary-wave solns. 78−93795
solar wind Langmuir waves, two-dimensional soliton collapse during Type III radio bursts 78−93173
solid state physics, lattice dynamics and distortive transitions 78−59880
solids, kinks, solitons, and nonlinear transport 80−65421
solids with chain structure, role of soliton *(Chinese)* 79−90931
solitary solutions collision in nonlinear field theory, variational anal., ϕ^4 appl. 79−35922
solitary structures in magnetised plasma loaded waveguide 80−48878
solitary water wave amplitude, in slowly varying channel 77−39302
solitary wave diffraction in water, amplitude and direction determ. 78−22361
solitary wave exchange potential in pseudoscalar and scalar meson fields 79−71617
solitary wave propagation in 3-dimensional lattice 80−8929
solitary wave stability in shallow water 79−90270
solitary wave transport, nontrivial example soln., numerical method 80−77971
solitary waves, review, book contrib. 80−94962
solitary waves in Born-Infeld electrodynamics 80−4554
soliton lattice melting, functional integral method 80−17883
soliton model of ψN interactions and ψ photoprod. *(Russian)* 77−46071
soliton perturbations and nonlinear focusing, anal. method for fluid dynamics 79−75369
soliton-antisoliton pair interaction in double sine-Gordon eqn., numerical simulation 80−46821
soliton-soliton scattering amplitudes, three dimens., semi-classical approx. 79−49091
sonic-Langmuir solitons, formation, interaction, inverse scatt. method 77−27664
space charge ionising waves, high velocity propagation 80−87889
spherical ion acoustic soliton excitation by conducting probe 79−90461
spherical ion-acoustic solitons, inelastic collision 79−77373
spherically symmetric solitons for nonlinear or scalar field-gauge field interactions 79−97521
spinor soliton as elementary particle, wave packet-soliton equivalence 78−12814
spinor soliton stability 79−97532
spiral density waves in plane galaxies *(Russian)* 77−87553
stability, gauge theories, nonlinear Schrodinger equation 80−4881
stability and dynamic behaviour for one- and two-dimensional cases 78−47621
stability in nonlinear propagation of lower hybrid waves in three dimensions 78−30424
stability of a plane soliton to infinitesimal two-dimensional perturbations 78−83420
stability of nonlinear ion sound waves and solitons in plasmas 79−60128
stability of soliton-like solns., nonperturbative methods 77−2750
stability of three-dimensional nonrelativistic solitons *(Russian)* 80−4583
static form factor, quantum correction in 2-D field theory with classical lump, asymptotic behaviour 80−52395
static gravitational solitons, singularities, horizons, field behaviour at infinity *(Russian)* 80−73229
static soliton, mass formula in two-dimens. scalar field theory 77−204
stationary connected multisoliton formations, Schrodinger eqn. with nonlocal nonlinearity *(Russian)* 80−57105
stationary multisolitons, existence 80−13218
stationary nonlinear waves in stratified rot. fluid, periodic solns., solitary waves *(Russian)* 79−7378
statistical mechanics, classical, universal features for continuum-field nonlinear Hamiltonians 78−93543
stimulated Raman scatt., semiclassical eqns., two-level mol. *(German)* 77−79889
stimulated Raman scattering, soliton regimes *(Russian)* 77−3634
stratified fluid, internal solitary waves 77−75963
stratified fluid, internal wave solitons, numerical computation 78−59410
stratified fluid in channel, wake collapse in the thermocline and internal solitary waves 80−53787
stratified fluid of finite depth, exact multi-soliton soln. for nonlinear waves 80−22199
stratified fluid wave propag., modified finite depth fluid eqn., exact N-soliton soln. 80−28517
strings and vortices with soliton solns. 77−5674
strongly dispersive system, higher order approx., reductive perturbation method 78−73926
structural phase transition, computer simulation 79−77721
structural phase transition, intrinsic and extrinsic central peak properties, review 80−34168
structural stability in physics (conference, Tubingen, Germany, May and Dec. 1978) 80−8739
structurally incommensurate systems, commensurate-incommensurate phase transitions 78−91418
structurally incommensurate systems, fluctuation spectrum, incommensurate phases 78−91419
studies in mathematical physics 79−75366
SU_N/Z_N gauge invariant theory, phase factor operators and soliton fields 80−77947
SU(2) gauge group, magnetic monopole as finite energy smooth soliton soln., review 78−89625
SU(2) Yang-Mills-Higgs system, soliton solns. 79−26218
SU(2)/U(1) nonlinear theory, solitons with nonvanishing Hopf index 78−86410
SU(3) gauge field nontopological soliton in three dimens. space 77−18168
submagnetosonic, lower hybrid wave solitons 79−14537
superionic conductor, one-dimens., soliton Brownian motion and impurity effects 79−77814
superposition of solitons from same nonlinear differential eqns. 80−67
supersymmetric quantum theory construction around supertranslated soliton soln., Dirac's method 78−45783
supersymmetric solitons in four space-time dimens., the mag. monopole 79−21896
supersymmetric theories with solitons, algebra including topological quantum numbers as central charges 78−89630
surface waves on water, soliton solns. of Davey-Stewartson eqn. for long waves 78−38351
synchronised solitons for sine-Gordon eqn. with perturbative term 77−57204

solitons continued
synchronous standing soliton infinite chain, stability and kinetic effects *(Russian)* 77−80299
tachyon solitons and their interactions, Backlund transformations in nonlinear systems 78−54181
teaching, classical nonlinear field eqns. exact solns., review 80−17756
thallium hexanoate, soliton conduction, elec. cond. field and temp. depend. anomaly *(Russian)* 80−103703
theory and applications 78−36811
Thirring model, 2-D, complete integrability 78−49685
Thirring model Lagrangian, generalised, interacting fermions, interacting solitons 77−45937
three-dimens. solitons 78−62053
three-frequency soliton solns. in second approximation *(Russian)* 78−57789
three-frequency wave interaction, waveguide and soliton solns. 78−41167
three-level molecular system, cooperative evolution, transient effects of dephasing and relax. 80−28184
three-soliton interactions, resonant triads of Korteweg de Vries eqn. 78−67207
TMMC, antiferromag., nuclear spin-lattice relax. by solitons 80−97159
TMMC, classical Heisenberg antiferromagnet, one-dimens., dynamic props., review 80−15737
TMMC, one-dimensional antiferromag., solitons, neutron inelastic-scatt. meas. 80−44810
Toda equation, difference analogue 78−20975
Toda lattice, excitation spectrum, molecular dynamics study 80−105588
Toda lattice, generalised eqn., solitons 80−95040
Toda lattice, nonlinear network eqns. generated from Backlund transformation 77−30107
Toda lattice, poles, soliton solns. 79−75368
Toda lattice, scatt. of solitons from mass impurity 79−12739
Toda lattice, statistical mechanics and solitons 79−49176
Toda lattice, surface impurity localised mode vibr. 79−60462
Toda lattice, transformation theories 77−30106
Toda lattice, wave behaviour in nonlinear LC equivalent circuit 80−105577
Toda lattice soliton, interaction with impurity atom 78−75772
topological solitons and instantons 79−12924
topological solitons graded Lie algebras, appl. to obstructions for crossing defect hypersurfaces 79−42062
transparency, self-induced, perturbed soliton solns., finite relax. time 80−58643
transverse envelope solitons, strongly non-linear 77−84421
transverse instability of breathers in resonant media 80−62485
transverse pure gauge fields and nonlinear chiral solitons, Coulomb condition 78−78068
trapped particles and waves in plasma solitons, theory and appls. 80−48876
TTF-TCNQ, pure and irrad. crystal, nonlinear transport at low temp. 79−4552
tunnelling of soliton pulse 78−57811
tunnelling of solitons and CDWs through impurities 78−51913
turbulence in a system with weak dispersion, stochastisation of soliton motion 78−41169
two soliton sectors of two dimens. canonical quantum fields, semiclassical approx. 79−12939
two-dimens. Thirring and Schwinger models, solitons and confinement *(German)* 77−82665
two-dimensional classical field theory, nontrivial interaction between solitons *(Russian)* 78−32698
two-dimensional interface, sine-Gordon chain model 80−29272
two-dimensional lattice, solitons and nonlinear resonances *(Russian)* 80−52041
two-layer fluid, finite depth, solitary waves, exact stationary wave soln. to Whitham eqn. 78−22355
type II superconductors, resistive domain existence, current generation *(Russian)* 80−44776
U(1) solitons, many-dimens., interactions, resons. and bound states 80−46823
undamped spiking of lasers, equivalent cct. used for soliton line 79−3673
uniaxial ferromagnet, Landau-Lifshitz eqns., self-localised solns., accidental degeneracy *(Russian)* 79−33444
unstable states, semiclassical calc. of half-life 77−45953
upper hybrid solitons, in warm magnetised plasma, kinetic anal. 80−38595
Van der Pol oscillators, diffusion-coupled active medium, nonlinear waves 80−4546
velocity and linear dispersion relation, higher order corrections 80−46826
viscous fluid layer, solitary waves *(Russian)* 77−51070
Volterra competition eqn., inverse scatt. soln., N-soliton solns. 77−49565
Volterra soliton, collapse into weak monotone shock wave 78−49673
vortex solitons, nonlocal field theories 79−49384
water wave packet evolution, Schrodinger and Korteweg-de Vries eqn. models 79−72902
water waves modulation near kh=1.363, Stokes wave stability 77−84265
wave eqns. with infinite components, soliton solns. 77−26180
wave functionals, soliton sector and asymptotic vacuum states, Creutz quantisation method 80−68340
waveguides with prescribed propag. consts., design 80−48419
weak ferromagnet, domain wall dynamics, nonlinear waves, mag. solitons *(Russian)* 80−75793
weak ferromagnets, Landau-Lifshitz eqn. solutions, moving domain walls, struct. *(Russian)* 80−100596
weakly damped, mechanical model 78−86192
weakly dispersive system, higher order approx., reductive perturbation method 78−73925
Werle type confining models, soliton-soliton interactions 79−85272
whistler soliton in solar wind, interaction with electron beam 77−9649
whistler wave solitons, classification of descriptions 78−75286
whistlers, supersonic large amplitude electron whistler-wave-ion density perturbation coupling, solitons 77−58854
WKB wave function, systems with many degrees of freedom, solitons and pseudoparticles 78−29255
X-Y model, one-dimens., with symmetry-breaking fields, thermodynamics and static props. 79−73742
X-Y model, two-dimensional, with quartic anisotropy, mol. dynamics study 78−75739
X-Y model with quartic anisotropy, soliton-like features 79−78429

solitons continued
Yukawa and Georgi-Glashow models with dynamical spontaneous symmetry breaking 79−6264
Z(2) and Z(3) cyclic symmetric vector field theories, 1-dimens. solitons 80−77950
zero frequency mode contributions in soliton quantisation general scatt. amplitude 78−29234
π field, nonlinear chiral models, many dimensional solitons 78−4792
Ar-He plasma, ion acoustic soliton form., mechanism 78−18457
$CsNiF_3$, 1-dimens. ferromag., evidence for solitons, inelastic neutron scatt. study 79−78430
$CsNiF_3$, anisotropic Heisenberg chain, nonlinear excitations 80−70927
$CsNiF_3$, easy-plane ferromagnet, one-dimens., dynamic props., review 80−15737
$CsNiF_3$, low frequency dynamics in external mag. field 80−108020
$CsNiF_3$, nonlinear excitations, 1D-ferromag., neutron scatt. 80−70949
$CsNiF_3$, one dimensional planar model with symm. breaking fields, thermodynamics, static props. 80−97111
$CsNiF_3$, one-dimens. ferromag., solitons in external mag. field 79−19724
$CsNiF_3$, one-dimens. ferromag., collective excitations in mag. field 80−44822
$CsNiF_3$, solitons in one-dimens. ferromag., inelastic neutron scatt. 78−95450
$CsNiF_3$, stochastic motion of Sine-Gordon-solitons, spin-correlation function 80−93105
Cu complex, dichloro-bis-pyridine copper II, one-dimens. antiferromagnet, dynamic props., review 80−15737
H, unmagnetised, completely ionised plasma, soliton-like struct. in 3-D, instability against adiabatic collapse 79−37496
He, liq., electron-charged surface, nonlinear wave propag., theory 78−67879
He, parametric plasma turbulence, soliton struct. obs. 79−60143
^{3}He, superfluid, A to B phase nucleation 80−100371
^{3}He, superfluid, A-phase, solitons in the vicinity of the transition to A_1-phase *(Russian)* 78−87840
^{3}He, superfluid, B-phase, n-solitons, and NMR freq. calcs. 78−34670
^{3}He, superfluid, creation of mag. solitons 77−15653
^{3}He, superfluid, magnetic solitons and monopoles 77−66065
^{3}He, superfluid, particle like solitons *(Russian)* 77−80675
^{3}He, superfluid, planar and linear solitons 79−33146
^{3}He, superfluid, soliton solns. for spin orbital freedom wave eqns. *(Japanese)* 78−38904
^{3}He, superfluid, spin wave interactions 79−86957
^{3}He, superfluid A-phase, composite magnetic solitons 77−31832
^{3}He, superfluid A-phase, composite solitons and mag. reson. 77−80674
^{3}He, superfluid A-phase, composite solitons, mag. reson. 78−51779
^{3}He, superfluid A-phase, composite solitons in presence of superflow 80−2233
^{3}He, superfluid A-phase, composite soliton in narrow circ. cylinder, satellite freq., thermal fluctuations 80−34266
^{3}He superfluid A-phase, exptl. studies of solitons 80−88386
^{3}He, superfluid A-phase, orbital motions 79−19416
^{3}He, superfluid A-phase, planar-twist soliton near A-A_1 transition, NMR props. 79−33145
^{3}He, superfluid A-phase, soliton lattice, flow induced 79−82407
^{3}He, superfluid A-phase, soliton lattice for NMR behaviour 80−2234
^{3}He, superfluid B phase, soliton-like spin waves 80−44385
^{3}He, superfluid B phase, spin waves creation 79−82411
^{3}He, superfluid B-phase, bound spin wave states associated with n-solitons 78−67884
^{3}He, superfluid B-phase, n solitons in crossed mag. field and superflow 80−44386
^{3}He, superfluid textures 79−82410
^{4}He monolayer superfluid films, third sound modes, superfluid solitons 79−10998
^{4}He, superfluid, three-dimensional solitons *(Russian)* 78−63892
^{4}He, superfluid film, solitons at low temps., Korteweg-de Vries eqn. 80−96717
$Hg_{3-\delta}AsF_6$, one-dimens. liq., fluctuations and freezing in order-disorder transitions 79−82301
K hollandite, one-dimens. ionic and solitary wave conduct. theory 79−86924
K_2SeO_4, elastic props. at commensurate-incommensurate transition, Brillouin scatt. and US study 80−93248
Na vapour, soliton interactions, self-induced transparency, numerical plane wave simulations 80−64117
$Pb_{1-x}Sn_xTe$, lattice instability and phonon-width, modulation effect due to intrinsically non-linear solitary wave 79−14906
$Pb_{1-x}Sn_xTe$, soliton modulation widths for TO-phonons 77−80588
Pt complex, $(C(NH_2)_3)_2Pt(CN)_4Br_{0.23}.H_2O$, pseudo-one-dimens. cpd., solitary wave excitations, and cryst. struct. 78−6307
SF_6 glow discharge, non-linear effects on self-exciting wave 78−83633
SbSI, ferroelec. phase transition and nonlinear props. 80−75988
TMMC, antiferromagneric chain, 3-D ordering temp. controlled by solitons and defects, mag. field depend. 80−60275
TTF-TCNQ, pure and irrad., nonlinear transport, ESR study, 1.2-4.2K 80−20167
Ti-Mo (20 at.%), incommensurate struct., stacking soliton 80−107109
Zr-Nb, stacking solitons in ω-phase systems and quasielastic scatt. 79−38822

sols
see also colloids; sedimentation
Aerosil, diffusion coeffs. and characterisation by photon correl. spectrosc. *(German)* 79−29418
agarose-water systems, gel-sol transition, thermal hysteresis and reversibility 79−66361
amphoteric latex coagulation, reversibility and specific ion effects 80−45567
coagulated, viscoelastic props., elastic floc model 79−37270
colloidal, electrically charged unstable, flow props., energy dissipatation in flow units 77−3862
colloidal, expt. props. of flow curve parameters 77−938
colloidal, flow props., elastic floc model 77−939
diepoxide-diamine network polymers, chem. props. and average mol. wt. 80−37915
diepoxide-diamine network polymers, reaction mechanism investigation using gel permeation chromatography 80−40789
ferromagnetic, relaxation of mag. birefr. and dichroism 79−57301
gelatin sol-gel transition, viscosity meas. method 80−85219

sols continued
geomagnetic field effects on charged particles in ocean *(Russian)* 77−60416
heterocoagulation, interaction energy of two unequal spheres 79−29411
hydrosols, separation, chainlike form. of particle deposits 77−77813
latex, sol, diffusion coeff. meas. by photon correl. spectroscopy 77−10117
light scattering matrix of artificial hydrosol, influence of form of scatt. particles *(Russian)* 78−5420
liquid particles, aerosol and hydrosol, separation by size in thermal fields 80−101044
Lyophobic sol stability in mixed media 78−11570
magnetic hydrosols, struct. and stability *(Russian)* 78−80794
photographic gelatin, gel-sol transition, gel characts. 78−35724
polymer statistics of long chains in solns. or melts 79−31758
polymers, based on oligodienehydrazides and diepoxides, A-copolymerisation, sol-fraction *(Russian)* 80−58431
polysaccharide gels and sols, PMR relax. times rel. to temp., pH and conc. 78−56952
polystyrene, sol, light scatt. data, Fourier inversion anal. 78−76932
primary and secondary coagulation and heterocoagulation, role of surface chemistry 80−45551
sheared coagulated sols, energy dissipation during sheared flow 78−63461
silicic acid sol., gel formation, characteristics of light scattering 78−53269
silicic and aluminosilicic acids, effect of increased size of scattering centres in sols 78−53270
size distributions, transient electric birefringence 80−85223
sol crystals, grain boundary struct. and boundary diffusion obs. *(Japanese)* 78−15721
sol-gel transition, incoherent light scatt. 79−61915
sol-gel transition, theory, polycondensing system, mol. size 79−57303
sol-gel transition, US attenuation meas. 80−101043
sol-gel transition kinetics 80−85218
solgel scintillators for liq. scintillation counting of aqueous and non-aqueous samples 77−38546
soya protein gels and sols, PMR relax. times rel. to temp., pH and conc. 78−56952
structure determ. by neutron diffr. and small angle scatt. 80−40748
thoria sol-gel processes for nucl. fuel fabrication 79−13503
viscosity near sol-gel transition, Rouse approx. *(French)* 78−61054
Ag halide hydrosol models of photographic emulsions 79−20470
AgBr, electrophoresis of spectral sensitising dyes, dye layering obs. 77−56240
AgCl microcrystals in sol., cryst. growth, optical absorpt. 77−12835
AgI hydrosols, appl. of radiometric method for particulate processes characterisation 80−45579
AgI hydrosols, kinetics and mechanics of colloid systems formation 80−101045
AgI, interfacial electrochem., review 78−80748
AgI nascent hydrosol absorption spectra and microcrystal growth 79−100449
AgI, sol, water PMR meas., 3 to 60°C 78−76930
Ag_2S, red-IR photoluminescence obs. at 77K 80−103982
Al_2O_3, transparent, polycrystalline, prep. by sol-gel method *(Japanese)* 78−19698
Au, monodisperse sol, ordered struct. obs. 78−3384
Au sol, grain boundary struct. obs. and boundary diffusion 78−51552
CuO, mixtures with TiO_2 and α-FeOOH sols, differential surface coagulation 79−79303
α-FeOOH, mixtures with CuO and TiO_2 sols, differential surface coagulation 79−79303
Se, amorphous film, photodeposition by Selor process, kinetics 78−75963
Se, amorphous film, photodeposition by Selor process, struct. and kinetics 78−75964
Se amorphous thin film photodeposition from hydrosols 78−11109
Se, amouphous film, photodeposition by Selor process struct. 78−75962
SiO_2 colloidal sol, particle size distrib., small-angle X-ray scatt. obs. 77−44516
SiO_2, condensed, electron microscopy and diffraction studies 77−29049
SiO_2 hydrosols, diffusion coeffs. and characterisation by photon correl. spectrosc. *(German)* 79−29418
$(Th,U)O_2$ microspheres, fabrication 80−801
ThO_2, sol-gel, for nucl. applics., sorption of water, CO_2 and N_2 77−4940
TiO_2, mixtures with CuO and α-FeOOH sols, differential surface coagulation 79−79303
UO_2 sol-gel particles, low temp. sintering and props. 79−100101

solubility
see also phase equilibrium; solid solubility; solutions
aerosol, mixed-salt particle suspension in moist air, phase transform. growth 77−12832
2-(4-n-aklylphenyl)-5(4-nalkoxyphenyl)-pyrimidines, smectic polymorphism, miscibility meas. 79−86678
alcohols in organic solvents, H_2O absorption 80−66788
alkali bromides, soln. in propylene carbonate, dissociation, radius and no. of ion solvation *(French)* 79−70319
alkali germanate glasses, He permeability, diffusivity and solubility 79−51308
alkali halides, solubility press. coeffs. and solvent isotope effect 80−96649
alkali metal/alkali halide liquids, high temp. furnace for small-angle neutron scatt. expts. 77−84591
alkali metals, liq., solubility and solns. of nonmetals 77−51505
alkali metals, liquid, O_2 pot. and O_2 distrib. coeffs. between alkali and struct. metals 80−65231
alkali n.-alkanoates, long-chain, ethanolic solns., temp. depend. 78−15724
alkanes, in liquid O_2, estimation by Preston-Prausnitz method 80−39285
alkenes, in liquid O_2, estimation by Preston-Prausnitz method 80−39285
4′-n-alkoxybiphenyl-4-carboxylic acids, 4-(2′-methylbutyl)phenyl esters, smectic phases 79−86684
4-n-alkoxyphenyl 4-n-alkylcyclohexanecarboxylates, smectic polymorphism, miscibility meas. 79−86678
n-alkyl 4′-n-alkoxybiphenyl-4-carboxylates, smectic polymorphism, X-ray diffr. and miscibility meas. 79−27912
4′-n-alkylbiphenyl-4-carboxylic acids, 4-(2′-methylbutyl)phenyl esters, smectic phases 79−86684
n-(4-n-alkyloxybenzylidene)-4-n-alkylanilines, smectic polymorphism, miscibility meas. 79−86678

solubility continued
alloy, coarsening by temp. cycling 79−29111
anaesthetics, general, rel. to site of action on lipid bilayers 78−77008
anthraquinone pleochroic dyes in liq. cryst. soln., photostability, appl. to liq. cryst. displays 80−88961
aromatic hydrocarbons, in liquid O_2, estimation by Preston-Prausnitz method 80−39285
As-S-Se glasses, solubility, photostimulated changes 80−24602
benzene, vapour, solubility in polystyrene *(Japanese)* 80−59667
benzene-d_6, solubilization in hexadecyltrimethylammonium bromide aq. soln., D NMR 78−24015
benzene-hexa-n-alkylanoates, disc-like molecules, miscibility studies of mesophases 80−19696
binary heterogeneous vapour-liquid equilibrium, student experiment demonstrating miscibility effects 77−82352
binary mixture, Kerr effect near crit. pt. 79−61336
binary ordering alloy, gas absorption, correl. effects *(Russian)* 78−47525
binary solid-liquid equilibria, student experiment, phase diagram computer program 78−89285
binary system, effect of mutual solubility of auxiliary solvent on liq.-liq. equilib. for activity coeff. 77−63945
bombardment, simultaneous with He, H_2, heavy ions to simulate microstruct. damage from fission or fusion neutrons 79−46723
butadiene copolymers, diffusion and solubility of S and 2,2′-dioxy-3,3′-di(α-methylcyclohexyl)-5,5′-dimethyldiphenylmethane *(Russian)* 79−33092
butene-1, in liquid N_2 80−39286
calcium oxalate trihydrate and monohydrate, dissolution kinetics charact. by SEM 79−42250
calculation, from eqn. of state 77−11660
n-caproic acid, colloidal dissolution in water 79−66358
carbonatite magmas, origin by liq. immiscibility 79−57928
carbonatitic igneous rocks, apatite comp. vars. rel. to liq. immiscibility 79−57929
cellulose acetate, solubility of CO_2, 0-70°C, up to 45 atms. 78−83957
chalcogenide melts, glass-forming, miscibility criteria and phase separation 77−76569
classical nucleus in liq.-liq. miscibility gap, undercooling in binary system 77−28002
cryogenic liquid, of light alkanes, IR spectroscopy obs. 80−59654
crystal habit, modifications control in growth 80−49150
crystallisation from solution, same complex effects 80−100189
cubic Margules solution model, miscibility gap and critical point 79−65199
4-cyanobenzoyloxy-4′-pentylstilbene, nematic, smectic A, and orthogonal smectic B phases 80−64890
cyclohexane-d_6, solubilization in hexadecyltrimethylammonium bromide aq. soln., D NMR 78−24015
DBS micelle solution, hydrophobe molecule solubility, NMR 79−83517
trans-decahydronaphthalene-polystyrene system, press. and mol. wt. depend. of polymer solubility 79−23734
dextran fractions, production, characterisation and solution properties 80−59368
2,3-dialkoxynaphthalene, H_2O and D_2O solns., solubility and ht. of soln. 79−66333
dialkylammonium compounds, $(C_nH_{2n+1}NH_3)_2MX_4$, cryst. growth solubility, and props. 78−43999
1,4-dialkylbenzene, H_2O and D_2O solns., solubility and ht. of soln. 79−66333
dichloromethane, solidified, solubility in liq. N_2 at 77.4K 80−10673
dielectric, dipolar point defects, studied by ITC 80−6405
dilute alloys, solubility of H, isotope effect 78−14470
disperse systems, solubility increase, phase composition, size effect calcs. 80−70418
elastomer reinforcement, carbon black-polymer interaction 79−83171
electrolytes in non-ion-exchange polymers *(Russian)* 80−54391
ethylene, in liquid N_2 80−39286
ethylene-polyethylene mixtures, phase behaviour under high-press., polymer mean mol. wt. influence 79−24745
exciton-phonon system, spectral parameter calcs. 78−43113
α-Fe alloy, ferromagnetic, thermodynamic analysis of solubility and miscibility gap 79−60508
Fe-Si melts, high Si, O solubility *(Russian)* 80−15252
fission products, solubility rules based on lattice parameter differences 78−59953
flux growth, crystn. conditions expt. method *(French)* 77−63552
fused, solubility of GaP, thermodynamics, rel. to epitaxial growth 78−34721
GaAs:O, growth, O_2 solubility determ. rel. to temp. 78−34624
gas solubilities near solvent critical point 79−51258
gas solubility, entropy of soln. in binary nonpolar solvent mixtures 79−52745
gas-gas immiscibility in binary fluid mixtures 78−34627
gas-liquid metal reactions, mixed transport control 77−72709
gases in liquids, Henry's constants, modified Pierotti theory 79−51259
gases in liquids, perturbation theory of convex mols. 79−77749
gases in liquids, Weeks-Chandler-Andersen theory 77−84931
gases in rabbit brain and blood, solubility and partition coeffs. 80−46116
glass, melt, bubble behaviour during refining, math. model 80−81277
glass fibre, surface struct. effect in solubility in water *(Japanese)* 80−34198
glass-forming multicomponent systems, phase behaviour, miscibility, tie lines 80−84294
group VIII and nearly related elements, cmpd. and superlattice form. 79−94955
H_2 absorption in thin film hydriding alloys, $LaNi_5$ and $SmCo_5$ 80−65238
halobenzenes, aqueous molar solubilities and partitioning, 25°C obs., rel. to melting pts. 80−40803
n-hexane, colloidal dissolution in water 79−66358
n-hexyl alcohol colloidal dissolution in water 79−66358
hydrophobic interaction, solubility and solvent struct. changes 78−83705
hydrothermal synthesis and growth, selection of mineralisers 78−72715
ice single crystals, solubility of HF, 180-270K 77−28007
ijolitic igneous rocks, apatite comp. vars. rel. to liq. immiscibility 79−57929
Incoloy 903, H_2 permeation and diffusion 78−26730
Inconel 718, H_2 permeation and diffusion 78−26730

solubility continued
inert gas solubility in liquid solvents, temp. depend. from scaled particle theory 80−24604
inert gases, solubility in homogenates of canine lung tissue 80−46117
inorganic gases, in liq. O_2, estimation by Preston-Prausnitz method 80−39285
isobutyric acid-d_{10}-D_2O, coexistence curve, liq. densities 78−18780
Kordes eqn. for estimating impurity partition coeff. between liquid/solid phases 78−2258
Laves phase AB_2 intermetallic compounds, H_2 sorption, capacity and preferred location 79−43791
liquid, solubility parameter estimation method 77−9158
liquid metals, N solubility, droplet weighing method 79−86889
liquid metals, of inert gases 77−51506
liquid metals, solubility of H rel. to that in solid phase *(Russian)* 80−65222
liquid metals and binary alloys, relationships between activity coeff. of nonmetallic solutes 78−52766
liquid mixture, crit. soln. point, sedimentation and density gradients in high gravit. field 77−59121
liquid phase elution chromatography for determining solubilities of organic liqs. in H_2O 80−71958
liquid-liquid, critical phenomena in binary mixtures 80−54376
liquid-liquid nonpolar regular solution, symmetry and crit. consts. 78−34623
liquids, unassociated, estimate of props. 79−51232
lung, intrapulmonary haematocrit maldistrib., effect on O_2, CO_2, inert gas exchange 80−8033
medical polymers, chem. problems, conf., Prague, Czechoslovakia (Aug. 1977) 80−56996
metal, liq., of oxygen, electrochem. obs. using solid oxide electrolytes 80−59669
metal, of H_2, deviations from Sievert law 77−76567
metal-H system, basic props., book 79−82349
metal-H system, solubility, mobility, and phase transitions, book contrib. 79−82350
metallic glass, continuous-biased sputter-deposited Kr entrapment 80−24603
metals, FCC, under H_2 press., crit. phenomena and isomorphic transitions 80−49367
metals, gas saturation, apparatus 80−61039
methane, liq., estimation of solubility of solidified substances, by Preston-Prausnitz method 79−37842
methanol, in liq. O_2, estimation by Preston-Prausnitz method 80−39285
methanol+water mixtures, solubility of AgCl 77−47579
α methyl styrene-acrylonitrile, molecular mass determ., solubility studies *(German)* 80−23590
4-2′-methyl-butylphenyl-4′-n-octyloxybiphenyl-4-carboxylate, smectic F phase, characterisation and struct. 79−86707
9-methylanthracene, solubilisation in water by hypercoiled polymethacrylic acid 80−91591
2-methylpyridine+D_2O, p-T-X miscibility dome critical point, US vel. meas. 77−27979
3-methylpyridine-D_2O soln., consolute points, crit. soln. temps., light scatt. obs. 77−77230
micellar aggregate, solubilisation parameters and dynamics, photoluminescence obs. 79−79297
micellar systems, solubilisation 80−89546
micelle forming detergent solutions, fluoresc. quenching by O_2, dynamic parameters and solubility charact. 79−83513
micelles, reversed, solubilisation and catalysis, review 80−45545
migration in Na_2O-Al_2O_3-SiO_2 glass 77−7902
multi-ion system, strong electrolytes, phase diagrams and solubilities calcs. 80−25665
mutual solubility of LaN, CeN, NdN and GdN *(German)* 79−19374
naphthene hydrocarbons, in liq. O_2, estimation by Preston-Prausnitz method 80−39285
nitrobenzene/n-hexane (n-heptane), critical exponent β, phase coexistence curve anal., viscosity coeff. meas. 80−100327
o-nitrotoluene-saturated hydrocarbon soln., critical exponent, permittivity meas. 78−22858
nonpolar binary systems, generalized correl. for Henry's constants 78−67827
4″-n-octylphenyl-4′-n-octylbiphenyl-4-carboxylate, orthogonal smectic B to tilted smectic B (smectic H) transition 79−94881
oil-water microemulsions, US attenuation and structural transitions 79−61917
organic compounds, correl. between solubility and mol. polarities *(Chinese)* 79−37847
organic pollutants in water, influence of detergent traces on hydrosolubility and maintenence in suspension *(French)* 80−7961
Ostwald ripening kinetics, depend. on particle vol. fraction 79−46806
oxide fuel, of fission produce Ba 79−19373
oxides in molten alloys 77−72692
PAA, nematic phase, solubilisation of poly-ethylen-oxide chain, effect on twist viscosity 78−67642
phlogopite, solubility in basic aqueous solns. under hydrothermal conditions 78−43127
pitch, mesophase 78−67831
plasma arc heating, equilib. in gas-melt system *(Russian)* 79−37512
pleochroic dyes, dissolved in nematic liq. crysts., guest-host interactions, appl. to electrooptic displays 80−44113
PMMA electron resists, molecular weight depend. of developed contours 79−87859
cis-polybutadiene and butadiene-styrene copolymer mixture, effect of temp. on phase composition 79−96005
polybutadiene miscibility with butadiene/styrene copolymers, viscometric method *(Polish)* 79−42260
polyether sulphone, evidence for crystallinity 80−28928
polyethersulphone dissolution in chloroform 80−21353
polyethylene, high-press., solubility coeffs. of propane and propene *(German)* 79−33093
polyethylene, migration and solubility of antioxidants *(French)* 79−46839
polyethylene, molten, N_2 and ethylene solubilities, statistical thermodynamical method, sorption data 78−71859
polymer mixtures, thermodynamics, review 79−1506
polymer protonated and deuterated mixtures, partial miscibility 80−107037
polymer soln., dilute, equilibrium theory *(German)* 80−33872

solubility continued
polymeric films, gas solubility, gas chromatographic determ. *(Russian)* 79−65205
α,ω-polymethylene diammonium metal (II) tetrahalides, cryst. growth, solubility and props. 78−43999
polyphenylene oxides, high temp. ageing effect on struct. and props. *(Japanese)* 77−70078
polyquinazolones containing pendant imide groups, prep. and props. *(Japanese)* 80−104111
polyquinazolones with N-phthalimide groups in side chain, prep., props. *(Japanese)* 79−15642
polysiloxene, irrad., linear, IR and solubility obs. 80−93775
polystyrene, star branched in cyclohexane, upper and lower critical soln. temp. 79−90789
polystyrene-cyclohexane, polymer solns., coexistence curve 79−28101
polystyrene-polyisobutylene, solns., incompatibility, binodal and spinodal calcs. 77−28005
polystyrene-polyisobutylene, solns., incompatibility, light scatt., conc. and angle depend. 77−24407
polystyrene-polyisobutylene, solns., incompatibility, light scatt., crit. opalescence 77−24408
polytrifluoroethylene and copolymer, γ-irrad., Ar diffusion and solubility *(Russian)* 79−51315
polyurethane foams, elastic, stability against organic solvents *(German)* 80−85074
polyvinyl imidazolium sulphobetaine, aq. soln. props. 79−32879
polyvinyltrimethylsilane, diffusion, sorption, solubility, permeation of hydrocarbons, Xe *(Russian)* 80−6564
polyvinyltrimethylsilane, sorption, diffusion, solubility of hydrocarbons, Xe rel. to temp. *(Russian)* 80−6565
porous material, press. soln. thermodynamics, chem. and mech. forces interaction 77−60369
precipitation kinetics, effect of particle solubility and inhomogeneities 78−27530
propylene, in liquid N_2 80−39286
PTFE, $H_2(D_2)$ solubility and diffusion, activation enthalpy 78−79775
PTFE, Ne, Ar, Xe and He diffusion and solubility 80−6561
PVC, plasticized, solubility of O_2, N_2 and CO_2 *(Polish)* 79−69252
quartz sand, press. soln. expt. 77−60370
rare earth iron garnets, (Ca,Ge)-substituted, flux growth in regular soln. approx. 79−78907
rare-earth Fe garnets, solubility model in PbO/B_2O soln. 79−46807
rubber, blooming by waxes 80−104109
scaled particle theory results for dense mixtures of convex shaped mols. 78−1969
seawater synthetic, solubilities and activity coeffs. of $CaSO_4$ and $SrSO_4$ 79−91986
segregation, nonequilibrium, during pulsed laser annealing, model 80−108451
semiconductors, electron traps, degeneracy factors, energy level estimates 78−14691
serpentine, solubility of inert gases, meteoritic abundance 80−12712
silicates, liq. immiscibility rel. to spheroidal pyroxenite aggregates in Bushveld Complex 79−88351
simple liquids, thermodynamic props. and solubility parameters 78−2265
Sitalls, soln. rate in alkali soln. 80−16531
sodium lauryl sulphate micelles, chlorophyll-a, soln., dilution expts., solubilisation anal. 80−35587
solid solution form. in heat of combustion process *(Russian)* 77−66765
solid-liquid equilibrium, UNIFAC group contrib. method 79−42247
solubility of group III and V elements 77−84928
solute solubilities, and Meyrick criterion for incidence of discontinuous precipitation 79−78983
β-spodumene-mica glass ceramics, phase evolution and TiO_2, MgF_2 additive effects, exam. 78−44089
steel, austenitic, Cr-Ni (20, 25 wt.%), containing B and Ti additions, splat quenching, X-ray and TEM study 79−74186
steel, austenitic stainless, type 316, irradiated with 46.5 MeV Ni^{6+} ions, soluble C effect on void swelling and low dose dislocation structs. 80−49280
steel, C-Ni-Cr (0.6, 1, 1 wt.%), grain boundary segregation of S, N, P, As, Sb and Bi *(Japanese)* 78−15405
steel, carbide form. depend. on Mn, Cr, V additions, cementite stabilisation, microstruct. *(Russian)* 80−55399
steel, complex alloy, carbonitride comp. and solubility calcs. *(Russian)* 77−70052
steel, Cr-Mo (2.25, 1 wt.%), quenched and tempered, diffusion and solubility of H_2 *(Japanese)* 79−65255
steel, maraging, investigation with lower Ni and Co contents *(Chinese)* 78−84812
steel, microalloyed, types V1599, V1600, V1286, NbCN precipitation in undeformed austenite 80−89230
steel, Ni, maraging, H_2 diffusion, diffusivity and solubility *(Japanese)* 79−42311
steel, solubility of W and Mo in $Ti(C,N)_x$ 80−16276
steel, stainless, martensitic 403, heat treated struct. effect on H_2 diffusion 77−63703
steel, V high strength low-alloy, low temp. use, $VC_{0.75}$ and VN solubility 79−70118
steel Cr-Mo, Ni-Cr, Ni-Cr-Mo, Cr, quenched and tempered struct. effect on H diffusion coeff. and solubility *(Japanese)* 78−52857
supersaturation, of H, produced by dislocation motion 77−36640
TBBA/n-hexyl-4′-n-dodecyloxy-biphenyl-4-carboxylate, mixtures, orthogonal smectic B to tilted smectic B (smectic H) transition 79−94881
terephthalylidenebis-4-n-pentylaniline, smectic F phase, characterisation and struct. 79−86707
terephtylidene-bis-(4-nalkylanilines), smectic polymorphism, miscibility meas. 79−86678
ternary alloy, combined inner adsorption *(Russian)* 77−76568
ternary and higher order, activity coeff. of nonmetallic solutes 80−107433
toluene, solid, solubility in liq. N_2 79−37843
transition metals, BCC, H impurity, calc. 78−6160
transition metals, solubility of H_2 and bulk modulus 78−55950
triphenylene, hexasubstituted, thermotropic mesophases 79−86681
trivalent metal phosphates, condensed, synthesis in polyphosphoric acid melts, physicochem. equil. considerations 80−97419
UO_2, polycrystalline, 400-600°C, Ar solubility and diffusion 77−20130
Ventersdorp lavas, Ni partitioning between immiscible picritic liqs. 78−32069
water, liq., solubility in compressed air 78−34631

solubility continued
wustite solid solutions, miscibility data rationalisation classification of ternary fields and postsaturation reactions 80−79948
Zircaloy, H absorption, Sn(Fe)(Cr)(Ni) effect 80−49527
Zircaloy, steam oxidised, partitioning behaviour of O_2 78−68839
Zircaloy-4/stainless steel type 304 diffusion junction, hydriding behaviour 79−65200
Ag growth in Ag-Bi and Ag-Pb melts, transition from round to face forms *(Russian)* 79−28906
Ag halide emulsion crystal growth, complex solubility computation 79−83516
Ag-As chalcogenide glass systems, reaction and diffusion 79−77826
Ag-As-Se system glasses, soln. rate 79−43456
Ag-Bi-S, ternary phase diagram, DTA and X-ray diffr. investigation 80−84917
Ag-Cd alloys, internally oxidised, thermal stability of CdO, exam. of particle coarsening 78−76789
Ag-Cu, metastable solubility lines on Ag side 78−39737
AgBr, crystal growth behaviour, influence of Gibbs-Thomson effect 78−24883
$AgCl_xBr_{1-x}$, binary melt, Ag solubility, temp. and conc. depend. 80−10677
$AgReO_4$, solubilities and chem. reactions, comparison with $AgClO_4$ 79−15976
$Ag_2S_2O_3$ solubility limit below 0°C 79−19376
Al alloys, liquid, kinematic viscosity temp. depend., porosity, H solubility, supercooling *(Russian)* 80−54425
Al chalcogenate and chalcogenite double salts, form. laws and acid-base props. 80−101070
Al in surface water on granite, mineral-controlled solubility *(French)* 77−41029
Al kinematic viscosity temp. depend. porosity, H solubility, supercooling *(Russian)* 80−54425
Al, liq., of Co and Fe, 700-900°C *(Russian)* 77−59119
Al, liquid, kinematic viscosity temp. depend., porosity, H solubility, supercooling *(Russian)* 80−54425
Al, molten, viscous flow, H dissolution temp. depend. X-ray anal. 79−91628
Al, of H_2 *(Japanese)* 79−99370
Al-Ag, low-conc. alloy, spinodal curve and metastable miscibility gap 77−63680
Al-Au melt, Si solubility *(Russian)* 77−66024
Al-Cr-Zn (2.5, 1.5 wt%), phase equilibrium, solubility *(Russian)* 78−19723
Al-In alloys within miscibility gap, agglomeration in space environment 79−47672
Al-Li system, δ' coherent miscibility gap determ. by small-angle X-ray scatt. 77−77483
Al-Si-Li alloy system, Al-rich, phase comp., limits of solid solubility *(Russian)* 77−21097
Al-Zn, miscibility gap, spinodal region, thermodynamic data transferability *(German)* 79−20027
AlBr solution, in propylene carbonate, dissociation, radius and number of ion solvation *(French)* 79−70319
Al_2O_3, permeability and solubility of H_2, 1200-1450°C 80−39351
Al_2O_3 single crystals, soln. in M_2O-V_2O_5 (M=Li, Na, K) and $NaVO_3$-KVO_3 melts 80−20910
Al_2O_3-SiO_2-P_2O_5, refractory glasses, exam. of liquid immiscibility and crystallisation 78−55814
$AlPO_4$ solubility, in H_3PO_4 hydrothermal soln., conditions for cryst. growth *(French)* 79−77539
Am-La, solubility, heat of mixing and vaporisation of Am, 1200 to 1600K 80−15232
Ar-He(Kr)(Ne), solubility in Ar, and related functions, three-body forces 79−10776
As, inorganic, in freshwater environment, stability and solubility theoretical aspects 79−16553
As-S(Se) glasses, solubility, photostimulated changes 80−24602
$AsSe_{1.5}Bi_{0.05}$ glasses, soln. rate in alkali solns. 80−16531
Au-Cu-Ni, computer characterisation, exam. of phase equilibria and miscibility gap 79−11561
B-C system, electron probe microanalysis and destructive chem. methods of study *(French)* 80−11982
B_2O_3-BaO, liquid immiscibility region, equilibration and quenching expts. 80−45288
Ba, liq., of Ti *(Russian)* 78−80513
Ba-Al-Si, exam. of phase diagram, confirmation of $BaAl_2Si_2$ and $Ba(Al,Si)_2$ *(Russian)* 79−29019
Ba-H_2 system, equilib. H_2 press. and enthalpy of forml of BaH_2 79−86893
$BaSO_4$, in water, effect of ^{35}S tracer, particle size and imperfection 78−43126
$BaTiO_3$, of Al estimation by conductivity meas. 79−69250
$BaTiO_3$:C, solubility of C at low O_2 potentials, 800°C 80−100334
Be-Al-Fe system, solubilities in α-Be for Fe-rich three phase condition 79−43203
BeF_2 glass, durability in water 79−95171
BeF_2-LiF, thermodynamically predicted miscibility gap 78−11209
$BeSO_4.2H_2O$, composition of saturated solutions from 360 to 570K 78−22857
Bi-$BiBr_3$ liquid system, miscibility gap, elec. cond. meas. 79−90790
C black, graphitized, theory constant for sorbed cyclohexane and benzene 78−6216
C in CaO-Al_2O_3 melt in presence of graphite 78−38850
C, pyrolytic, tritium diffusion coeffs. and deuterium solubilities 80−37443
C/epoxy laminates, moisture solubility coeff. 79−65252
CO, in water and seawater at 10^{-5} atm partial press., 0-30°C 79−100870
CO_2, under magma genesis conditions, petrological implicatons 78−11886
CO_2(g), standard enthalpies of solution and formation, standard Gibbs energies of formation and standard entropy 79−57285
$C0_2$ solution in ocean surface waters, role of homogeneous buffer factor 80−21783
CaC_2, solubility in CaF_2 and $CaCl_2$-CaF_2-CaO system *(French)* 79−70050
$CaCO_3$ polydisperse particles, in $Ca(HCO_3)_2$ soln., growth, soln. in mag. field 78−53260
CaF_2, fluorite, solubility equilibria in geothermal waters 77−60368

solubility continued
CaF_2-(Y,R)F_3 systems (R = rare earth), phase diagrams, limiting solubilities and non-stoichiometry 79−47665
CaO-Al_2O_3 melt, solubility of H_2O at 1600°C 78−51687
CaO-Al_2O_3-CaF_2, electroslag remelting slag, solubility of N_2 and C, equilibria 78−44110
$Ca_{10}(PO_4)_6(OH)_2$, hydroxyapatite, aq. solution system, interfacial props. and equilibria 79−77751
$Ca_{10}(PO_4)_6(OH)_2$, solubility in aq. media 79−82341
$Ca_{10}(PO_4)_6X_2$ (where X is F, Cl, OH or Co), influence of mech. treatment on struct. and reactivity *(German)* 79−43272
$Ca_{10}(VO_4)_6(OH)_2$, solubility in aq. media 79−82341
CdF_2:Eu, role of solution and precipitation phenomena on ITC spectra 80−7265
CdS, solution growth, using Te solvent 79−65993
CdSe, of Cu 77−52303
$CdSnAs_2$, solubility in Sn melt, temp. depend., enthalpy of melting 80−59658
CdTe:Fe, dopant solubility 77−90334
$(CdTe)_{1-x}$-$(ZnSe)_x$ system, mutual solubility and band gap energy *(Japanese)* 77−51501
Ce-Ga (Al)(In)(Sn)(Pb)(Bi)(Zn) liquid, solubility and thermodynamic props. *(Russian)* 78−19717
Ce-Ni, hydriding characts., applicability for H_2 storage material 78−83955
Ce-S-O equilibrium in molten Fe *(Chinese)* 80−104423
Co-W-C system at 1150°C, phase equilibria, isothermal reactions and thermodynamic study 78−31385
Co_2, in liq. solutions of $ZnCl_2$ in NaCl and KCl 79−90785
$CoCO_3$, monocryst. solubility under hydrothermal conditions 77−12512
CoO, solubility of S at 1000°C 78−63858
Cr, molten, N_2 absorption at high temps., Cr-N phase diagram, solubility-temp. relation *(Japanese)* 79−43201
Cr, solubility in liq. Li, impurity effects of O_2, N_2 and C 79−77760
Cu, liquid, of S, Se and Te 77−21096
Cu liquid/liquid CuS, miscibility gap *(German)* 80−49370
Cu, low temp. in Be, Be-Al, and Be-Si, ion implantation and backscattering 77−62646
Cu, solid, solubility and diffusivity of F, electrochem. meas. 79−46808
Cu-Ag, liquid alloy, solubility and activity of O_2 79−29028
Cu-Ag-S, computation of component activities from ternary miscibility gap data 79−11591
Cu-Au, dil., O_2 solubility, thermodynamic and residual resist. study 78−59952
Cu-Cd(2.7 wt.%), cellular precipitation kinetics and dissolution *(German)* 80−11651
Cu-Fe, dil. alloy solubility and diffusion of Fe 78−43170
Cu-In, of O, liq., solubility and activity 77−43331
Cu-In solid/liquid interface, laws governing diffusive interaction *(Russian)* 78−95156
Cu-Ni-Ti system, phase equilibria in Cu rich region and Cu-T quasi-binary constitution *(Japanese)* 80−89203
Cu-Ni-W melt, solubility of W, primary solidification 78−19726
Cu-Pb (Fe), liq., thermodynamic props. *(Polish)* 80−89199
Cu-Pb-S system, at 1473K, thermodynamic anal. 78−39746
Cu-Sb, peculiarities in temp. behaviour of internal adsorption *(Russian)* 79−55890
$CuCl_xBr_{1-x}$, binary melt, Cu solubility, temp. and conc. depend. 80−10677
Dy_2O_3, soln. in $K_2O.2(3)MoO_3$, rel. supersaturation and supercooling 80−40245
Er-Co-Ni, cryst. struct. and H_2 capacity 77−89543
Er-Fe-Al(Mn)(Co), cryst. struct. and H_2 capacity 77−89543
$ErFe_3(BO_3)_4$, solubility in Bi_2O_3-B_2O_3 melt and crystallisation 80−19736
Fe alloys, component interaction parameters, enthalpy and mixing energy *(Russian)* 80−54382
Fe alloys, liquid, complex, diffusivity and solubility of N_2 at 1600°C 77−39684
Fe and alloys, liq., C solubility, donor-acceptor mechanism 80−49365
Fe, H_2 solubility in 600-1500°C temp. and 0.1000 atm. pressure ranges *(Russian)* 78−59948
Fe, liquid, N solubility and AlN precipitation 79−11630
Fe, liquid, N solubility depend. on added elements, mechanism *(Russian)* 80−65223
Fe, of P, alloying element effects *(Russian)* 79−69248
Fe, permeability, solubility and diffusion of H and D, 9 to 73°C 77−76560
Fe, pure, of H and D at 10 to 60°C 78−75887
Fe, solubility in liq. Li, impurity effects of O_2, N_2 and C 79−77760
α-Fe, solubility of H_2 at press. up to 67 kbar *(Russian)* 79−51260
Fe-Ag-Cu melts, phase interface props., Cu influence *(Russian)* 79−51261
Fe-Co-Ni, liquid, H solubility meas., 1400 to 1800°C 77−1231
Fe-Cr alloy, Cr rich, solubility of S *(French)* 78−30761
Fe-Cr alloy, N solubility investigation *(Russian)* 80−92675
Fe-Cr-Mn, Cr and Mn effect on N_2 solubility above 1000°C *(Bulgarian)* 79−65203
Fe-Cr-Ni liquid alloy, N_2 soln. and TiN precipitation 78−6931
Fe-Cr-Ni melts, S solubility and solid soln. precipitation *(Russian)* 80−15251
Fe-Cr-Ni-Mn-Mo, liquid, N_2 solubility 78−44087
Fe-Cr-Ti(Al) liquid alloys, thermodynamical anal. of O_2 solubility *(Russian)* 80−92676
Fe-FeS-MnS-Mn reciprocal system, interaction between three liq. miscibility gaps 77−7865
Fe-Ga-C melts, thermodynamics and C solubility *(Russian)* 80−39292
Fe-H system, influence of H press. on Fe crit. points and H solubility 78−52758
Fe-H system, specific heat 7 to 60K 79−99332
Fe-M alloys, of H, 850-1150°C, M = Co, Ni, Mn, Cr, conc. depend. *(Russian)* 77−59120
Fe-Mn (22 wt.%), $\varepsilon \rightarrow \gamma$ transformation, effect of H_2 pressure up to 23 kbar on transition temp. *(Russian)* 79−24517
Fe-Mn-S, thermodynamics, solubility of S and Mn in γ-Fe, 1100 to 1300°C 79−47662
Fe-Mo, ferritic, thermodynamics and solubility of C and ferrite 77−36456
Fe-Ni, influence of hydrogen press. on temp. of martensitic transform. *(Russian)* 78−27514
Fe-Ni Invar alloy, virtual miscibility gap and interdiffusion coefficient 79−55891
solubility continued
Fe-Ni liquid alloy, physical and chemical props. deviations from Raoult's law *(Russian)* 78−95729
Fe-Ni-Al, liq. alloys, N solubility and AlN precipitation 80−11648
Fe-Ni-C, Redlich-Kister eqns., activity coeffs., phase equilib. 78−23664
Fe-Ni-Cr melts, O solubility *(Russian)* 80−15250
Fe-Ni-Ge, liquid alloy, H_2 thermodynamic interaction, solubility *(Russian)* 78−11202
Fe-Pt alloys, solubility of H_2 at press. up to 67 kbar *(Russian)* 79−51260
Fe-S system, solubilities in aqueous H_2S and mass transport role in girdler-sulphide heavy water plants 78−83963
Fe-Sb system, α-phase, interdiffusion 79−73349
Fe-Si (3 wt.%) alloy, solubility of MnS, 950-1200°C, C conc. depend. *(Russian)* 77−16541
Fe-Si (3.1 wt.%), solubility product of BN 79−10955
Fe-Ti, solubility and diffusivity of H and D in mixed crystal phase, elec. cond. meas. *(German)* 80−107575
FeO, wustite, simultaneous solubilities of Na and Ca *(French)* 78−31392
FeO-Fe_2O_3-SiO_2-Al_2O_3-$CuO_{0.5}$ slag, and Cu, distribution equilibria of Sn, Se, Te 77−51502
$Fe_{1-x}O$-ZnO at 900°C, some peculiarities *(French)* 77−70037
α-Fe_2O_3 crystal flux growth, solubility and relative supersaturation in Fe_2O_3-PbO-V_2O_5 fluxed melt system 80−64934
Fe_2O_3 films, DC reactively sputtered, for selectively semitransparent photomasks, struct., mech. and chem. props. 80−59835
Fe_3O_4, solubility in H_2 saturated LiOH soln., meas. 150 to 300°C 77−60179
α-FeSe, prep., solubility of Se in α Fe 79−24239
Fe_3Si, 3d transition metal substituted, limits of solubility, mag. props. and electron conc. 78−10670
Fe_2SiO_4-$KAlSi_2O_6$-SiO_2, phase relations at 1 atm., and low temp. liq. immiscibility 79−47664
Ga chalcogenate and chalcogenite double salts, form. laws and acid-base props. 80−101070
Ga liquid, solubility and activity of O_2 77−59122
Ga-Al-Si, solubility of Si at 500-800°C liquidus lines *(French)* 77−51498
Ga-Cu liquid alloy, solubility and activity of O_2 77−59122
Ga-In, liq., O diffusion coeff., thermodynamic activity and solubility 78−38860
GaAs epitaxial layers, from mixed Ga solns., C solubility 80−15392
GaAs, solubility in Ga-Al alloys in multilayer LPE of $Ga_xAl_{1-x}As$ 78−52690
GaAs:Ge, solubility and point defect-dopant interactions 79−90689
GaAs:Sn, solubility and point defect-dopant interactions 79−90688
GaAs:Te, solubility and point defect-dopant interactions 79−90687
GaAs:Zn, surface conc. control 79−55758
$GaAs_ySb_{1-y}$, miscibility gap, rel. to LPE 79−33090
$Ga_{1-y}In_yAs_xSb_{1-x}$, LPE on GaSb, miscibility gap in liq. phase and lattice mismatch 80−15404
Ga_2O_3 in H_3PO_4, $GaH_2P_3O_{10}$ and $Ga(PO_3)_3$ crystn. 79−52641
GaP, diffusivity and solubility of Cu 78−51743
GaP, impurity behaviour during crystallisation from melt 77−84772
GaP-Sb, Sb solubility in region of GaP primary crystn. 79−86891
GaSe, ^{110}Ag diffusion, temp. depend. and solution *(Russian)* 80−70467
GaSe:Sn, ^{113}Sn diffusion, temp. depend. and Sn solubility *(Russian)* 80−70466
GaTe, ^{110}Ag diffusion, temp. depend. and solution *(Russian)* 80−70467
Gd-C-N system, isothermal section at 1200°C, X-ray investigation *(German)* 80−93543
$GdFe_3(BO_3)_4$, solubility in Bi_2O_3-B_2O_3 melt and crystallisation 80−19736
Ge alloy, amorphous film, formation and stability criteria 79−10799
Ge, liquid, solubility and activity of O_2, 1233 to 1397K 78−44109
Ge:Be single crystals, grown by Czochralski method, exam. of Be distribution ratios and solubility 79−95043
Ge:P, solubility and segregation of electrically active P 77−15442
Ge-Cu, liquid, solubility of O_2 at 1373K, in equilibrium with GeO_2 78−44109
Ge-S(As)-Se glasses, solubility, photostimulated changes 80−24602
GeO_2, amorphous, obtained by hydrolysis of $GeCl_4$, exam. of props. 79−95956
GeO_2-K_2O, glass composition effect on solubility in H_2O 80−39303
GeO_2-Na_2O, glass composition effect on solubility in H_2O 80−39303
H diffusion, and solubility in solid metals 80−49422
H_2 in Fe-Ni, effect of magnetic ordering *(Russian)* 77−24435
H_2, in molten alkali acetates, fuel cells technology appl. 79−57244
H_2, in Nb-V system 80−59808
H_2, in water and seawater at 10^{-5} atm partial press., 0-30°C 79−100870
H_2, metallic, solubility of He, Gibbs energy, fluid state model, He conc. in giant planets 79−60602
H_2, solubility in Ni, Ni-Cr, Ni-Mo, 500-1000°C *(Japanese)* 78−38845
H_2 solubility rel. to electron density in transition metals 79−51266
H_2-N_2, liquid-vap. equilib., 63-110K and up to 57 MPa 79−55881
H_2O, under magma genesis conditions, petrological implications 78−11886
H_2S, solubility in water, 10 to 180°C 78−18776
Hg, of CdTe and $Cd_xHg_{1-x}Te$, rel. to LPE 78−35359
$Hg_{1-x}Mn_xS$, phase studies and hydrothermal synthesis 77−48333
$Hg_6O_4Cl_4$, cryst. struct. determ. 78−26516
In chalcogenate and chalcogenite double salts, form. laws and acid-base props. 80−101070
In, of O, liq., solubility and activity 77−43331
InAs:Zn,S(Se), solubility and donor-acceptor interaction 80−54263
InP surface decomposition prevention in LPE growth 80−96749
InP:Co(Fe), diffusion solubility and elec. activity of Co and Fe 77−43240
K, in Fe-S liquid, silicate-K-(Fe-S liq.) equilibria and planetary implications 78−11843
KCl:Pb, lead aggregation effect on yield stress, incoherent precipitates, solubility determ. method 80−50645
KCl-NaCl solid solns., equilib. decay curve *(Russian)* 79−90760
$K(D_xH_{1-x})_2PO_4$, monoclinic and tetragonal forms, existence in aq. soln. 78−47262
KH_2PO_4, kinetics of crystn. from soln., activities, interfacial energy and solubility 77−76340
$KLa(MoO_4)_2$, solubility in aq. K_2MoO_4 solns., hydrothermal conditions 80−96651

solubility continued
KNCO, fused, soln. mechanism of Fe and Cr 79−39271
K_2O-Al_2O_3 system, high temp. thermodynamics and phase equilibria 78−80521
K_2SO_4, kinetics of crystn. from soln., activities, interfacial energy and solubility 77−76340
Kr, in liq. scintillator solvents, meas. using radioactive tracers 77−57808
La-H, phase equilibria 80−66492
La-Ni, hydriding charact., applicability for H_2 storage material 78−83955
La-Ni(-Ce)(-Co), H absorption for storage appls. 80−45790
$LaCo_5$, N_2 absorpt. at low temps. 80−24599
$LaNi_5$/H system, thermodynamics of H trapping 80−107444
$LaNi_5$-H, thermodynamics of solution of H at small content 77−21104
$LaNi_4Al$, solubility and sorption props. of H_2, effect of Al 80−103482
$La_7Ni_3D_2$ storage material, neutron, X-ray diffr. study 78−83954
La_2O_3-P_2O_5-H_2O, solubility, regions of crystallisation, 100-500°C 77−16483
Li, blanket, isotopic exchange equilib. for H and D 79−49845
Li, liquid, of LiD, activity coefficient 78−2259
Li-LiH system, H isotope solubility thermodynamic singularities 80−81356
Li-LiH system, liquid Li, dilute solns., equilib. H press., solubility, heat of soln., CTR materials 77−14266
Li_2C_2 solubility in Li, for fusion reactor appls. 80−13840
LiF-NaF-KF molten mixture, diffusivity and solubility of H_2 78−34640
$Li_{0.5}Fe_{2.5}O_4$ Ru substitution effect on struct. and mag. props., and max. solubility determ. 80−75364
$LiNdP_4O_{12}$, single crysts. flux growth and cryst. morphology, solubility curve 79−43124
Li_2O in liquid Li, solubility determ. by neutron activation anal. 78−11601
Li_2O solubility in liquid Li, determ. by fast neutron activation 79−42252
Li_2O-Al_2O_3-SiO_2 glass, He migration, struct. effects 77−55389
Li_2S, solubility in LiCl-KCl and LiCl-LiF molten eutectic mixtures 80−54387
Mg, H_2 dissolution, resistometric study under press. 80−70417
α-Mg, solubility of H_2 77−25024
Mg-$MgNi_2$-Zn, diagram of state, Zn solubility, initial phase precipitation *(Russian)* 80−66478
Mg-Sm, solid soln., phase diagram *(Russian)* 77−25015
Mn, liq., of N_2, exam. 78−51685
Mn, of N_2, 650-1030°C, 13-25 at.% N range 79−90783
Mn-Cu, alloying behaviour and high damping capacity 80−35160
Mn-Ni(Cu)-S, solubility and activity of S *(Russian)* 77−25012
MnO-SiO_2 slag, SiO_2 solubility and MnO activity 79−52184
Mo and alloys, absorption of N_2 in induction and plasma-arc heating *(Russian)* 77−16732
Mo, diffusion and solubility of C *(French)* 79−55932
Mo, impurities, interaction mechanism and saturation limit *(Russian)* 77−55358
Mo-N system, phase diagram of solid and liq., high and low press. 78−44083
Mo-Ti-Zr, diffusion and solubility of C *(French)* 79−55932
Mo-W solid soln., joint solubility of C and Zr 77−25025
N, in CaO-Al_2O_3 melt in presence of graphite 78−38850
N_2, liq., of solidified hydrocarbons and halogen-hydrocarbons, calc. by Preston-Prausnitz method 78−26686
N_2O_4, solid, solubility in liquid N_2 at 77.4K 77−32827
Na-K-H system, H influence on component interactions *(Russian)* 80−54383
Na-Li (19.2 wt.%), elec. resistivity, immiscibility region 79−1593
Na_2CO_3, molten, of O_2 and CO_2, manometric technique 79−69251
Na_2CO_3(s), $NaHCO_3$(s), standard enthalpies of solution and formation, standard Gibbs energies of formation and standard entropy 79−57285
NaCl-KCl, molten, alkaline earth oxides solubility products, potentiometric determ. 80−76488
NaCl-KCl mixture, electrical, electromag., and acoustic props. *(Russian)* 78−30759
NaH solution in liq. Na, elec. resist. and solubility 79−14934
$NaNO_{3(2)}$, precipitation from mixed aq. solns. 80−100191
β-Na_2O-Al_2O_3, isomorphous replacement of Al^{3+}, solubility of Cr^{3+}, Ti^{3+}, Fe^{3+} 77−85926
Na_2O-B_2O_3-NiO melts, NiO activity and solubility meas. by EMF method *(Japanese)* 80−92677
Na_2O-B_2O_3-SiO_2 glass, phase-separated, leaching 79−66394
$2Na_2O$-CaO-$XSiO_2$ glass, He mobility, interconnectivity, miscibility limits, effect of morphology 78−67864
Na_2O-P_2O_5-SiO_2 glass, metastable liquid immiscibility 80−100331
Na_2O-P_2O_5-SiO_2 glass, substitution of Li^+, Mg^{2+}, Sr^{2+}, Ba^{2+}, Zn^{2+} for Na^+ 80−100332
Na_2SO_4, molten, of O_2 and SO_2, manometric technique 79−69251
Nb liquid, exam. of O_2 solubility using thermodynamic analysis *(Russian)* 79−55889
Nb, of O_2, temp. depend. 79−99326
Nb, oxidation in imperfect vac., solute O_2 level change and ductility loss 79−52452
Nb-D-H, equilib. H/D separation factors 80−59668
Nb-H, incoherent spinodals, meas. by Gorsky effect 78−19712
Nb-H, spinodals and diffusion coefficients of H, sample shape depend. 78−19713
Nb-Mo alloy, solubility of H_2 77−89542
Nb-Sn-Cu, Cu effect on Nb solubility and peritectic transform. temp. in Sn bath *(Czech)* 77−59754
Nb-Ta alloys, terminal solubility of H and charact. of solid solns. 79−86894
$Nb_2C_2O_7$, H solubility 80−34191
NbO and NbO_2, H solubility 80−34191
Nb_2O solution in liq. Na, elec. resist. 79−14934
$Nb(OR)_2Cl_3$.L, halo-alkoxide complex, prep. and props. 78−18605
Nb_3Sn film formation, solubility, precipitating processes *(Russian)* 80−92792
$NdFe_3(BO_3)_4$, solubility in Bi_2O_3-B_2O_3 melt and crystallisation 80−19736
Ni, β-phase form., H enriched, at surface and grain boundaries, during H_2 absorption *(Russian)* 78−31410
Ni, electrical resistance and H solubility at high press. *(Russian)* 79−91018
Ni, of H, D and T 79−77823
Ni, of H *(Japanese)* 78−51739
Ni, solubility in liq. Li, impurity effects of O_2, N_2 and C 79−77760
solubility continued
Ni-Al, liquid, diffusion coeff. differences, rotating-disc determ. 80−39330
Ni-C, exam. of metastable phase diagrams, at high temp. and pressure *(Russian)* 79−56955
Ni-Co, electrical resistance and H solubility at high press. *(Russian)* 79−91018
Ni-Co-Al alloys, continuous precip., SEM, TEM, X-ray diffr. study 80−89220
Ni-Co(Cu) alloys, of H, 850-1150°C, conc. depend. *(Russian)* 77−59120
Ni-Mo-W, diagram of state, W solubility, dispersion hardening *(Russian)* 80−66477
Ni-Ni_2B eutectic, high temp. X-ray anal. 80−71639
Ni-Zn-Mn-Fe spinel, solubility curve in melt of BaO-B_2O_3-Bi_2O_3 80−2945
$NiFe_2O_4$-Fe_2O_3, effects of excess Fe_2O_3 on mag. props. 77−85495
$Ni_xFe_{3-x}O_4$, solubility in high-temp. aqueous soln., appl. to PWR 78−4987
$Ni_{98}M_2$, M=impurity metal, solubility of H_2, formation of MH(D)-complexes 80−65236
NiO, solubility of FeO at 1273K *(French)* 79−33089
NiO, solubility of S at 1000°C 78−63858
$Ni_2P_2O_7$-$H_4P_2O_7$-H_2O system, solubility isotherm at 0°C 77−25027
$Ni_2P_2O_7$-$K_4P_2O_7$-H_2O solubility at 25 degrees C, double phosphates formation 80−54381
Ni(s, l)+NiO(s)+NiX_2O_4 (X=Al, Ga), chem. potential and solubility of O_2 80−92679
OH-ion solubility in silica glass, 1900°C, OH-ion distribution in optical fibre preforms 79−14121
P-Se glasses, solubility, photostimulated changes 80−24602
Pb complex, $Pb(C_2O_4)_2^{2-}$, stoichiometry, form. const. determ., teaching appl. 79−84916
Pb, melt, of Th, 676-770°C *(Russian)* 77−25011
Pb-Fe(Cu), liq., thermodynamic props. *(Polish)* 80−89199
Pb-Zn, liquid phase immiscibility determ., DTA 78−64523
PbS, solubility products in LiCl-KCl and LiCl-LiF molten eutectic mixtures 80−54387
Pd alloys, H_2/D_2 solubility ratios 79−99325
Pd, electrical resistance and H solubility at high press. *(Russian)* 79−91018
Pd mechanical props., effect of H diffusion 79−65138
Pd, of H, lattice defects influence, extended core model 80−88326
Pd, of S, 600-1000°C, H_2-H_2S gas phase composition depend. *(French)* 78−87791
Pd, soln. of $H_2(D_2)$, isotope effect model 77−66026
Pd-Ag, Fermi energy influence on soln. behaviour of H, B and C *(German)* 80−44323
Pd-Ag (25 at.%) H_2 permeability and solubility, comparison with other Pd solid soln. alloys 79−23738
Pd-Ag(V), H mobility and solubility, appearance pot. spectra obs. 80−55231
Pd-Ce (5.75 at.%), H_2 permeability and solubility, comparison with other Pd solid soln. alloys 79−23738
Pd-Cu, H solubility enthalpy and entropy, effect on elec. cond. 77−35699
Pd-Cu-Si, metallic glass, miscibility limits, computer study 79−65198
Pd-D-H, equilib. H/D separation factors 80−59668
Pd-Fe, dil., anomalous lattice parameters and H_2 solubilities 79−33091
Pd-H, solid soln., excess entropies, variation of H solubility with pressure 79−46846
Pd-H system, solvus hysteresis 80−71659
Pd-Pt alloys, soln. of H_3, partial thermodynamic parameters determ. 77−66027
Pd-Rh alloys, soln. of H_2, partial thermodynamic parameters determ. 77−66027
Pd-W (20 wt.%), permeability, diffusion, and solubility of H_2, elec. resist., heat treatment effects *(Russian)* 79−51307
Pd-Y (8 at.%), H_2 permeability and solubility, comparison with other Pd solid soln. alloys 79−23738
Pd_3P_{1-x}, nonstoichiometric, $H_2(D_2)$ solubility 80−59662
Pt, diffusivity permeability and solubility of H_2 79−95170
Pt, electrical resistance and H solubility at high press. *(Russian)* 79−91018
Pt, solubility of H_2 at press. up to 67 kbar *(Russian)* 79−51260
Pt-Pd system, sorption of H_2 during cathodic charging, deflection technique meas. 79−51427
Pu in Irish Sea, oxidation state rel. to solubility and sedimentation 79−16516
RPO_4-$Pb_2P_2O_7$, R=Tb-Lu, solubility curves for high temp.-melts for growth of single crysts. 78−95687
RbCl, diffusion by $^{20}Ne(^{22}Ne)$, isotope effect 78−18841
SO_2-seawater, thermodynamics 77−52660
Sb, liquid, solubility and activity of O_2 *(German)* 79−90793
Sb-Te-Bi, computer study of miscibility limits, 273 to 300K 78−52781
Sb_2O_3-$SiO_2(GeO_2)$-Na_2CO_3-H_2O, crystallisation 77−12605
$Sc_2(WO_4)_3$:Er^{3+}, growth, solubility, absorption spectrum and thermal expansion meas. 77−36391
Se, amorphous, correl. between mol. struct. and props. 77−11484
Se-Ge amorphous films, obliquely deposited, photoinduced chem. changes 80−76385
Si, Czochralski growth, equilib. of dissolved C and O with CO in ambient atm. 80−1949
Si, impurity solubility limit after laser induced melting 80−107426
Si, liq. solubility in metallic solvents *(French)* 77−27978
Si solubility and transport behaviour of water, dissolution 80−93801
Si:In, gradient transport soln. growth, IR monitoring, 950-1300°C 79−100040
Si:Se,B(Ga)(Al)(In), diffusion of Se, solubility and ionization levels, Hall effect and photocond. meas. 79−42486
β′-Si-Al-O-N, Mg-containing phases, crystn. 80−39297
Si-Al-Si, isothermal version of the moving solvent method 79−1824
Si-Au-P system, partition coeff. of P, temp. depend. 79−43158
SiC, exam. of T_2 diffusion coeffs. and D_2 solubility 78−79816
SiC, permeability and solubility of H_2, 1200-1450°C 80−39351
SiO_2, fused, He solubility and diffusion above transform. range 80−79965
SiO_2, three-component glass, liq. phase separation, with two oxide modifiers 80−103250
SiO_2, vitreous, D_2 diffusion and solubility, 0-800°C, interaction with structural OH 77−89585

solubility continued
SiO_2, vitreous, He solubility, 100 to 1350 atm., 5 to 80°C 79−4414
SiO_2, vitreous and cristobalite, interstitial struct. anal. from gas solubility data, review 79−23525
Si_2O_3-TiO_2 system, phase transform. at high temp. 77−84926
Sm-H, phase equilibria 80−66492
SnO-SiO_2 glass, exam. of immiscibility 78−75837
SnO_2-TiO_2 solid solns., X-ray diffr. and thermogravimetric meas. 79−90792
Sr, liq., of Ti *(Russian)* 78−80513
Sr-Y, phase diag. *(Russian)* 77−59745
T, in Pd, isotherms at low equilib. press. 79−14935
Ta, of H_2, solubility at high temp. 77−84934
Ta-H, incoherent spinodals, meas. by Gorsky effect 78−19712
Ta-H, N interstitial trapping of H, hydride precip., resist. meas. 77−20293
Ta-H, spinodals and diffusion coefficients of H, sample shape depend. 78−19713
Ta-Nb(Re)(W) (50,20,0 at.%), with N_2, spectral emissivity, N_2 absorption rate, N_2 solubility, thermodynamic data *(German)* 77−25026
Ta-O, steady state O_2 solubility *(German)* 80−44322
TaC-TaB_2, phase diag., solubilities, reactions 77−63643
TaC_x, solubility of H, X-ray diffr. exam. 80−44318
Ta_2C_x, solubility of H, X-ray diffr. exam. 80−44318
$Ta_2C_xO_y$, solubility of H, X-ray diffr. exam. 80−44318
$Ta(OR)_3Cl_3L$, halo-alkoxide complex, prep. and props. 78−18605
Tb_2O_3-H_3PO_4-H_2O system, cpd. form., comp. and props. 80−100832
TeO_2-P_2O_5, electron microscope exam. of phase equilib. and immiscibility 78−52779
TeO_2-P_2O_5 system, glass struct., neutron diffr. study 80−70128
Ti alloy in Al alloy melt, raction zone formation, component interaction *(Russian)* 80−54377
Ti alloys, fusion reactor, first wall and blanket structure, impact of H_2, phase stability and solubility 80−32435
β-Ti, dilute soln. of H and D 79−99322
α-Ti, of V, 400-700°C 78−83959
α-Ti, solubility of H, neutron diffr. study 80−15254
Ti-Al-Kh18 steel, O_2 solubility thermodynamical anal. *(Russian)* 80−92676
α-Ti-Fe, solubility, resistivity variation rel. to quenching temp. 79−99324
TiC-WC-TaC carbide mixture in plasma reactor *(German)* 77−1819
TiCo-H system, thermodynamic rels. and struct. transformations 80−49385
$TiCr_{1.8}$, H and D soln., enthalpy, solubility and mol. vibr. determ., comparison with soln. in metals and binary alloys 80−79951
TiNi-H system, thermodynamic rels. and struct. transformations 80−49385
TiO, powder solubility of H_2 77−11698
TiO-ZrO_2, pseudo binary system, effect of Ti addition on struct. and props. of zirconia 79−11583
TiO_2, solubility in KF aq. solns. 80−34197
Tl-Se phase diagram, 73-100 at.% Se 79−96018
Tl-Te, liquid alloy, miscibility gap 79−10952
Tl_5Te_3-Tl_4SnTe_3-Tl_4PbTe_3, phase equilib., DTA, SPA and microhardness meas. 80−96628
U BCC alloys, solubility of H_2 and D_2 gas 79−96302
U, liq., O_2 solubility and comp. of lower phase boundary of UO_2 at 1950K 80−49366
U solubility in the Oklo reactor 80−21756
U-Ce-C system, phase equilibrium exam. *(German)* 78−23670
U-Nb-C system, phase equilibrium exam. *(German)* 78−23670
UC, miscibility with rare earth nitrides *(German)* 80−96654
UO_2-SiO_2, 1000-1400°C, Ar solubility and diffusion 77−20130
US-UC_2, solution studies 77−21120
V, pure and with O_2 additions, single cryst. elastic consts., 4.2 to 300K, and hardening 79−90712
V-Ga-Sc, phase diagram, metallographic and X-ray meas., solubility boundaries *(Russian)* 78−56618
V-H, incoherent spinodals, meas. by Gorsky effect 78−19712
V_2O_5, amorphous semicond., solubility and fibrous texture 80−75162
W-ZrC(-Re) eutectic alloy, Re effect on breaking stress, lattice parameters, electron struct. *(Russian)* 79−1845
Xe, in liq. scintillator solvents, meas. using radioactive tracers 77−57808
^{133}Xe solubility coefficients in water, saline, dog blood and organs 80−56331
Y, of T, 250-400°C, rel. to possible appl. for T recovery from molten Li blanket in fusion reactor 79−90784
YAG, melting behaviour and metastability determ. by optical DTA 80−92648
YAG, solubility in solvent $PbO_{-x}PbF_2$, phase form. in system Y_2O_3-Fe_2O_3-PbO-PbF_2-B_2O_3 78−95247
$YAl_3(BO_3)_4$, solubility in fused potassium trimolybdenate and seeded cryst. growth 77−43330
$YAl_3(BO_3)_4$ solubility in $K_2Mo_3O_{10}$ melt 80−65211
$YAlO_3$, melting behaviour and metastability determ. by optical DTA 80−92648
$YCo_5(Ni_5)$, H_2 solubility *(Russian)* 78−15356
$YFe_3(BO_3)_4$, solubility in Bi_2O_3-B_2O_3 melt and crystallisation 80−19736
$YFeO_3$, solubility in aq. KOH under hydrothermal conditions 77−39677
YPO_4-$Pb_2P_2O_7$, solubility curves for high temp.-melts for growth of single crysts. 78−95687
$YVO_5$4-$NaVO_3$, solubility curves for high temp.-melts for growth of single crysts. 78−95687
Zn-Bi, liquid, inconsistent conjugated liquidus 80−76232
Zn-Ca, liquid alloy, exam. of thermodynamic props., using EMF method *(Russian)* 79−34003
Zn-Ti-Fe-O, spinel solid solns. 77−48409
Zn_3As_2, solubility in Bi, LPE on $(Cd_xZn_{1-x})_3As_2$ 78−35324
ZnS, of Ag_2S 78−22753
ZnS, solution growth, using Te solvent 79−65993
ZnSe, solution growth, using Te solvent 79−65993
Zr and Zr alloys, cracking, H_2 induced delay, strain energy effect on H_2 solubility 78−92364
β-Zr, diffusion and solubility of H, above 1000°C and below 1×10^{-4} mm Hg *(Russian)* 80−24671
Zr, dissolution of γ-ZrH, in situ study, HVEM obs. 78−55951
α-Zr, of O, solubility limit meas. 78−11211
Zr-C, exam. of metastable phase diagrams, at high temp. and pressure *(Russian)* 79−56955
ZrC, solubility, diffusion and permeation of Cs 78−51684
ZrC_xO_y, ZrN_xO_y, $ZrC_xN_xO_y$, of H 77−84930
solubility continued
ZrO_2, glaze, liq. phase separation rel. to cryst. in glassy phase 80 103252
ZrO_2-SiO_2, liquid immiscibility, microstruct. of plasma dissociated $ZrSiO_4$ 80−107429
ZrO_2-TiO_2 solid solns., X-ray diffr. and thermogravimetric meas. 79−90792

solute clustering *see segregation*

solution annealing
chemically stabilised, sensitisation and corrosion resist., heat treatment depend., precipitation steel, stainless, Cr-Ni 79−38827
Incoloy 800, mechanical props., heat treatment and appl., conf., Petten, Netherlands (March 1978) 79−43296
Incoloy 800, review of structural charact., heat treatment and comp. effects 79−43297
Incoloy 800, sensitisation and intergranular corrosion 79−47721
Incoloy 800, solution annealed, low and high cycle fatigue correlation 79−43439
Incoloy 800H, high temp.-low cycle fatigue, ageing and cold working effect on initial stress/strain curve 79−47720
Nimonic PE16, Ni ion irradiated, Ni segregation to voids 79−28020
products for nuclear power stations, research and development *(Russian)* 79−34080
steel, 18% Ni maraging, fatigue strength, effect of soln. treatment and inclusions 78−23805
steel, austenitic, Cr-Ni (18,12 wt.%), containing coarse grain boundary precipitates, thermomechanical treatment 78−27545
steel, austenitic Cr-Ni (18,12 wt.%), containing coarse irregular carbide precipitates along grain boundaries, ductility 78−60718
steel, austenitic stainless, 304, solution annealed, tensile flow behaviour after exposure to flowing Na, in temp. range 550 to 700°C 78−35463
steel, austenitic stainless, cold worked, 20%, heat treatment effects on mech. state, load-relaxation expts. 77−52350
steel, austenitic stainless, Cr-Ni (16, 16 wt.%), in-pile rupture strength, cold work and soln. annealing effects 77−63687
steel, austenitic stainless, sensitivity of intergranular corrosion, effect of Mo content, heat treatment and degree of stabilization *(Czech)* 79−70095
steel, austenitic stainless, sensitized, type 304, intergranular corrosion fatigue crack growth in oxygenated pure water at 85°C 79−47814
steel, austenitic stainless, sensitized forgings, corrosion resistance restoration, computer calc. *(German)* 79−66074
steel, austenitic stainless, type 304, exam. of continuous cooling sensitization 79−29098
steel, Cr and Mn, softening during hardening, austenitising effect 79−96052
steel, Cr-Mo-V, creep fracture, microstruct. effects 78−64668
steel, Cr-Ni-Mo-Cu-Nb, martensitic precipitation hardenable, corrosion resistant, heat treatment, structure and props. 79−74169
steel, maraging, (18 wt.% Ni), solution annealed, exam. of cryogenic tensile, fatigue, and fracture props. 78−92311
steel, maraging Ni-Co-Mo, strengthening by repeated strain ageing *(Japanese)* 79−100157
steel, martensitic, age hardening with Cu, Nb additions, exam. of hardness 80−7681
steel, Mn-Cr-V, study of structural changes *(Czech)* 78−84864
steel, Nb, controlled-rolled into ferrite temp. range, soln. temp. and rolling effects 80−11678
steel, stainless, 1Kh18N10T, solution annealed effect of cyclic stresses on corrosion rate in acid environments *(Russian)* 78−31577
steel, stainless, 304, shot peened, stress corrosion cracking, const. strain rate investig., cold work, sensitisation effect 79−20259
steel, stainless, 316, creep and rupture, 525 to 900°C 79−8328
steel, stainless, 316L, corrosion, comparison of powder metallurgy and conventionally produced specimens 79−15863
steel, stainless, δ-ferrite, isothermal decomposition and transform. of heating at 550 to 950°C *(Chinese)* 79−43239
steel, stainless, critical cooling rate for sensitization and intergranular stress corrosion cracking in high temp. water 79−47807
steel, stainless, neutron irrad., solution-annealed and cold-worked, swelling 78−13229
steel, stainless, Ni-Cr-Mo, two-phase, compositional charge of ferrite and austenite *(Japanese)* 79−4948
steel, stainless, solution annealed 304L, in-reactor deform. 77−42076
steel, stainless, solution treated, irradiated to low doses with 22 MeV C^{2+} and 46.5 MeV Ni^{6+} ions, interstitial loops 79−14855
steel, stainless, solution treated FV 548, irradiated with 22 MeV C^{2+} and 46.5 MeV Ni^{6+} ions void swelling 78−22771
steel, stainless, stress corrosion cracking in high temp. water, surface prep. effect 79−5088
steel, stainless, Ti modified 316, uniaxial tensile behaviour, Na environment effect 78−52916
steel, stainless, type 304, corrosion fatigue and stress corrosion cracking, in boiling NaOH 80−7719
steel, stainless, type 304, low temp. sensitization 79−74181
steel, stainless, type 304, solution-annealed and thermally aged, correl. of high- and low-cycle fatigue data 78−15532
steel, stainless, type 304 welded, low temp. sensitisation, nucleation of CR carbide nuclei along grain boundaries TEM, SEM study 79−38851
steel, stainless, type 316, stress-free swelling at high neutron fluence, rel. to LMFBR core environment 78−13239
steel, stainless, XM19, stress corrosion resistance 80−16558
steel, stainless 304, sensitized electrochemical polarisation in high temp. water *(Japanese)* 79−15868
steel, stainless 304, stress crack initiation in chloride soln., role of corrosion pits *(Japanese)* 78−92397
steel, stainless 304 sol. of annealed and thermally-aged, high-cycle fatigue behaviour 80−100923
steel, stainless 316, soln. annealed, cavity alignment and precipitation during dual ion bombardment 80−70273
steel, stainless cold-worked austenitic, fatigue and creep crack growth at elevated temp. 78−48524
steel, TRIP, powder processing, tensile strength, ductility 78−64499
superconducting composites, Kirkendall void elimination by solution anneals 80−7520
Al alloy 2024, relief of residual quenching stresses *(Korean)* 79−70091
Al alloy 2024-T3, work hardening in surface layers and bulk during fatigue 78−48428
Al alloy 2036, thermomechanical treatment on struct. and props. 79−29109

solution annealing continued
Al alloy 6061, thermomechanically treated elev. temp. mech. props. 79−8310
Al alloy 7001, ageing effect on hardness and tensile props. rel. to delay time till quenching 78−92286
Al alloy RR58, low cycle fatigue at 423K, prior treatment effect 80−104254
Al alloys 2024, thixoforging into net-shapes 80−16339
γ′-Al-Ag (15 wt.%), dislocation splitting mechanism, cessation above critical temp. 78−26572
Al-Cu (1.7 at.%), EXAFS study of precipitation 79−100151
Al-Cu-Mg type 2036, thermomech. treatment, flow stress anal., effect in mech. props. 80−93584
Al-Si(Cu)(Zn-Mg-Cu), extraction and phase anal. 79−15673
Al-Zn-Mg, precipitation of η′ phase, heat treatment, electron microscope obs. 78−68699
Al-Zn-Mg (4.8, 1.1 wt.%), second phase dissolution, calorimetry study 79−100193
Al-Zn-Mg-Ti, Ti effect on microstructure during ageing 78−64568
Au-Fe-Ni layer coating, Fe and Ni conc. meas. by X-ray diffr. *(German, English)* 80−34330
Co-Ti-C, secondary precipitation and allotropic transform., TEM obs. 80−108453
Cr-Co-Fe cold formable mag. alloys for use in telephone receiver 79−52227
Cu-Ag(Se)(Sn)(Ag-SeSn), Ag, Se, and Sn effects, singly and together, on recrystallisation 79−100164
α- Cu-Al (6 to 17 at.%), short-range order investigated by diffuse X-ray scatt. *(Russian)* 80−104187
Cu-Be, SCC in NH_3 80−104326
Cu-Be-Ni (1.9, 0.32 wt.%) solution treated alloy, age induced vol. changes in structural transformations *(Russian)* 79−100179
α-Cu-Ni-Zn-Pb, fire cracking, effect of pores and impurities 79−29207
Fe-Cr (28 wt.%), intergranular corrosion and anodic polarization at grain boundary groove *(Japanese)* 79−15869
Fe-Cr-Co, mag. alloys, Mossbauer spectra 78−19386
Fe-Ni-Cr (10, 6 to 14 wt.%), electrochemical polarisation in high temp. water *(Japanese)* 79−15868
Fe-Ni-Cr (35, 15 wt.%) superalloy, stress rupture and tensile props., C and B additions effect *(Chinese)* 80−104244
Fe-Ta alloy, mech. drawn and aged, exam. of electrical resistivity, hardness, microstruct., and mag. props. *(Japanese)* 78−48545
Ga_2O_3-Fe_2O_3 system, anomalous Mossbauer line shapes, incomplete annealing 78−92006
(In+InP) melt, critical undercooling determ. and P content change after annealing *(Slovak)* 80−55430
LiF:Mg^{2+}, TLD-100, treatment temp. effect on thermolum., 210 to 470°C 77−56480
Nb-Nb-Al-(Cr), γ/γ′-δ type eutectic, fatigue, effect of composition and microstruct. 78−48520
Nb-Ti (60 at.%), aged, TEM exam. of precipitation process *(Japanese)* 78−48409
Ni alloy Mar M200, directionally solidified Hf additions, effect of vol.% γ′ on creep rupture 78−27526
Ni base superalloy, directionally solidified, struct. and props. *(Chinese)* 80−20918
Ni-Al (6.05 wt.%), prediction and meas. of precipitate number density 78−19756
Ni-Al-Ti, soln. temp. of hardening intermetallic phase in heat resistant alloys 78−52865
Ni-base alloy, age hardened, stress corrosion cracking resistance, plastic deform. and microstruct. relation 77−63829
Ni-Fe-Cr superalloy 718, heat treatment effect on room temp. : nd elevated temp. fracture toughness response 80−100922
Pb-Sb (1 wt.%), highly averaged, fracture behaviour 79−8356
β IIITi alloys solution treated and aged, estimation of precipitate volume fraction using Young's modulus 78−39781
Ti-Al-V (6, 4 wt.%), cavitation induced erosion, under mill annealed, soln. treated and aged, and beta annealed conditions 79−8371
Ti-Al-V (6, 4 wt.%), solution treatment temp. effect on fracture morphology 79−61620
Ti-Hastelloy-N, homogenization 79−61606
Ti-M-V-Cr-Mo, RMI 38644, shock loaded, age hardening 79−29112
Ti-Mo-V-Fe-Al (8,8,2,3, wt.%), exam. of stress controlled fatigue response 79−61734
β-Ti-Mo-Zr-Sn (10.2, 5.8, 4.7 wt.%) heat treated, tensile yield, fracture behaviour, primary deform. mode, exam. 78−60724
β-Ti-Mo-Zr-Sn(11.5, 6, 4.5 wt.%), metastable phase III, microstruct. and age hardening response 80−84945
W-Ni-Fe(Cu), liquid phase sintered, interfacial embrittlement 79−57101
Zr-Nb (2.5 wt.%), strain ageing 77−77511

solution energy *see heat of solution*

solutions
see also critical mixtures; Debye-Huckel theory; heat of solution; liquids; polymer solutions; solid solutions; solvation
acetic acid, in cyclohexane soln., Raman scatt. near crit. stratification, temp. depend. *(Russian)* 79−11420
acetone in mixed protic-aprotic solns., C=O stretching, IR spectra 80−45056
acetone-benzene(cyclohexane), vap.-liq. equilibria 78−30745
acetone-chloroform solution, Monte Carlo calcs. for interface struct. with directed intermol. forces *(Russian)* 78−1975
acetonitrile, Raman spectral study of aq. soln. struct., H-bond effects 77−88454
acid, weak, ionisation in aq. soln., rate const. meas., elec. field jump method errors 79−43611
activity coeffs. at infinite dilution, Wilson and UNIQUAC eqns. correl. 78−64875
adsorbed film on cryst. surface, NMR investig. 77−8426
adsorption isotherm and solute activities from spreading pressure-surface charge data 78−14576
albumin, bovine serum, five-component dielec. dispersion 78−15759
alcohol binary mixtures, nonlinear dielec. effects, shift in assoc. equilib. 77−73108
alcohol-active soln., assoc. soln. thermodynamics, H^E, V^E curves 78−31671
alcohol-alkane dilute system, electron solvation, picosecond spectral obs. 77−44573
alcohol-H_2O solutions, structure, luminesc. probe obs. 78−84636
alcohol-inert soln., assoc. soln. thermodynamics, enthalpy, Gibbs free energy 78−31670
alcohol-solvent, associated, excess free energy and enthalpy of mixing 78−31680
alcohol-water solutions, containing radioisotopes, radiochemical purification *(Russian)* 77−86432
alcohol/water mixtures, NMR and IR obs., low temp., shifts, interpretation 77−52065
alcohols, dil. aqueous solns., isentropic compressibility behaviour from sound vel. meas., dissolution mechanism 80−30269
aliphatic amine mixtures, ionis. consts. determ. by gas-chromatographic anal. *(Russian)* 79−61921
alkali bromides, soln. in propylene carbonate, dissociation, radius and no. of ion solvation *(French)* 79−70319
alkali chlorides, aq. soln., ion-solvent and solvent-solvent interactions, X-ray obs. 80−44107
alkali halide solns. with H_2O and D_2O, struct. and O isotope fractionation 78−22629
alkali halide solutions, tetrahedral hydration of ions from Raman bands obs. 78−55804
alkali halide solutions, US determ. of hydration numbers 78−20027
alkali halide solutions in DMSO, modelling of interactions 79−77469
alkali halides, aqueous area solutions, conc., viscosity meas. 79−23759
alkali halides, ion hydration numbers in aq. solns., mol. dynamics calcs. 77−62464
alkali iodides in acetone, press. effects on Walden products, ion-solvent interactions 80−3398
alkali metal cation pairs, lumiensc. with dichromate anion 80−83409
alkali metal-ammonia solns., elec.-cond. and thermopower 77−1370
alkali metal-ammonia solns., metal-insulator transition, h.f. and u.s. props. 77−1369
alkali metal-ammonia solns., spin site exchange mechanism for electron relax. times 78−27077
alkali metal-ammonia solutions containing cryptands, metal anion and trapped electrons form. by evap. 79−100340
alkaline, O electrode reaction on transition metal oxides prepared by thermal decomposition 79−61864
alkaline, silicate glass decomp. by ion exchange 77−48637
alkaline frozen solutions, polycryst. and glassy, photocond. and radiometric obs. 80−45531
n-alkane binary mixtures, infinite dilution activity coeffs. 78−15695
alkylammonium iodides, solns., MCD spectra of iodide ions 78−94268
4-amino-N-methylphthalimide-decalin-n-propanol, translational relax. kinetics, luminesc. obs. 79−8180
4-aminomethylphthalimide-decalin-n-propanol, electronic spectra of 3-component solns., temp. depend. 79−4822
anilines, substituted, in benzene, dielectric relax. and mutual viscosity, obs. 79−38449
anthracene-2-methyltetrahydrofuran, glassy solution, site-selective impurity phonon coupling 77−81142
anthraquinone-xanthone liq. soln., upper excited singlet state, delayed fluoresc. 80−106345
aqueous, free energy parameters for reverse osmosis separations of inorganic ions 77−32831
aqueous, hydrophobic apolar spheres interaction, Monte Carlo simulation 80−6335
aqueous, hydrophobic hydration around apolar species pair, Monte Carlo simulation 80−6336
aqueous, ionic crysts. precipitation, induction period 80−50882
aqueous, neutron scattering, book contrib. 79−60232
aqueous, nucleate boiling, bubble growth, saturation press.-temp. relation 77−46892
aqueous electrolyte solution, activity coeff. at 298.15K 77−60074
aqueous electrolyte solutions, thermal diffusion, Soret coeffs. meas. 78−18811
aqueous electrolyte solutions, vel. correls., improved representation 80−59360
aqueous fluids, statistical mech., book contrib. 79−60250
aqueous heterogeneous systems, thermal anomalies 77−32829
aqueous metals, adsorption on inorganic minerals 78−49006
aqueous micelle form., kinetics, relax. process 78−76928
aqueous mixtures, lower crit. soln. pt. theory 79−4415
aqueous multicomponent multiphase equilibria, free energy minimisation method, comput. algorithm 80−40724
aqueous nonelectrolyte solutions, thermodynamic excess functions at high press. 78−18793
aqueous nonelectrolytic soln. microheterogeneous struct., X-ray diffr. study 78−87608
aqueous organic solns., 25°C, solute/water rel. evap. rates 78−34614
aqueous solns., max. density temp., structural interpretation 77−58933
aqueous solns., max. density temp., structural interpretation 77−58934
aqueous solutions, electrode effects, high-speed camera obs. *(French)* 79−24751
aqueous solutions, influence of cooperative effects on props. 80−28906
aqueous solutions, Monte Carlo simulation, convergence of new algorithm 78−63649
aqueous solutions reactions and chemical evolution on primitive Earth 77 - 33189
aragonite, transform. to calcite in marine gasteropod, role of soln. films 79−62485
associated, characteristic sums method in stat. theory 80−10480
associated, H bonding and anomalous saturation 78−52426
Backlund transformation, simple structure of superposition formula, 79−12616
bead solutions, quasielastic light scatt. in small wave vector limit 80−45088
benzene, benzene-d_6 soln. excess thermodynamic props. 78−53245
benzene, in Br_2-carbon tetrachloride soln., complex form., IR spectra 78−70828
benzene, in polar solvent, excess thermodynamic props., Rayleigh scatt. meas. 78−52523
benzene solutions, liq. and solid, positron and positronium annihilation 77−1152
benzene-cyclohexane, solution, self-diffusion, capillary cell meas. 78−34637
benzene-cyclohexane, vap.-liq. equilibria 78−30745
benzene-I_2, binary soln., charge transfer spectrum 78−90183
benzene-toluene, solution, self-diffusion, capillary cell meas. 78−34637
binary and ternary systems, pred. of isothermal vapour-liquid equilibria, heat of mixing, viscosity 77−31761

solutions continued
binary electrolyte solns. thermodynamics using US props. 78−73946
binary liquid solutions, surface cluster functions 78−67631
binary mixture, pretransitional effects near convective instability 77−41536
binary mixtures, excess surface tension calc. and theories of solns. 78−91508
binary mixtures, models, distance parameter geometric averaging, excess free enthalpies *(German)* 77−32825
binary mixtures, US props., molecular interaction between components 78−63657
binary molten salt mixture, excess free energy of mixing, conformal ionic soln. theory 77−1230
binary solutions of dense liquids and gases, isothermal eqn. of state calcs. *(Russian)* 80−88292
binary system, distribution coeffs., estimation from Van Laar and Hayes-Chipman relations 80−84293
binary system, effect of mutual solubility of auxiliary solvent on liq.-liq. equilib. for activity coeff. 77−63945
biomolecular aqueous solution, attractive and repulsive dispersion forces 78−44447
brine, Dead Sea, KCl and H_2O activities 78−31673
bubble homogeneous nucleation in gas-liq. soln., press., expt. and theory 78−91430
buffer solution, effect of EDTA, ethyl alcohol and sugar in leach soln., chem. durability 79−74269
buffer solutions, of corrosion resistance of glass 79−74268
n-butane in liq. solvents, conformational structure 80−28115
t-butanol-CCl_4, excess thermodynamic functions, 15, 30 and 45°C, composition depend. *(Russian)* 78−31677
t-butanol-water, X-ray scatt. intensity composition depend., soln. struct. 78−6005
t-butyl alcohol, struct. determ. from vibr. spectra, H-bonding and heat of mixing *(Russian)* 78−3368
caffeine in aq. electrolyte, adsorpt. isotherm and solute activities from spreading pressure-surface charge data 78−14576
carbocyanines, dye laser appls., soln. chem. 77−40568
carbon tetrachloride soln. of Br, adsorpt. of Br on C 78−10273
carbon tetrachloride-ethanol (methanol), binary soln. with mol. assoc., interdiffusion anal. 79−55912
carboxylic acid-ethanol systems, proton exchange process kinetics, effect of H bond strength in intermediate state *(Russian)* 79−96306
chain molecules in soln., thermodynamic props. related to chem. pot. 80−3394
chemical reaction rate constants, in solution, short-range caging effects 79−96286
chemical reactions, Brownian dynamics simulation in soln. 80−104422
chemical reactions rate constants, in solution, escape probability and time-depend. reactivity 79−96287
chemically coupled equilibria, thermodynamic theory of solvent-jump relax. method 79−39186
chlorobenzene, in CCl_4 soln., quadratic changes in elec. permittivity, intermol. interactions 77−73107
colligative properties of simple solns. 77−21466
colloidal cylinders, charged, electrophoresis in salt solns., in transverse elec. field 79−1955
component quantity automatic determination, two-coordinate potentiometer appl. 78−93657
concentrated electrolyte, solutions, viscosity, mixture law 78−18818
concentrated electrolyte solution, cond. model 77−84957
concentration, interconversion during crystn. 80−100773
conductive samples, superconducting NMR spectrometer, efficient decoupler coil design to reduce heating 80−31828
coronene trimer radical cation, spin densities in CH_3Cl_2-CH_3NO_2 solvent mixture, −100°C 80−5565
correlation functions, mono- and multi-molecular, for liquids and solutions *(French)* 79−50971
correlation range behaviour in gravitational field *(Russian)* 77−62633
Coulomb systems, equilib. distrib. functions expansion in power of density 80−64681
critical point of unmixing, acoustic relax. *(Russian)* 79−95085
critical vapour form. phenomena, in binary soln. and pure material, isomorphism *(Russian)* 77−13723
cryogenic solutions, spectrosc. and photochem. 80−16713
crystalline, binary, isostructural, thermodynamic mixing parameters computation 77−86344
n-decanol-CCl_4, excess thermodynamic functions, 15, 30 and 45°C, composition depend. *(Russian)* 78−31677
degree of dissociation of congruently melting compound, calc. from liquidus curve 77−84892
diatomic molecular dilute solns., IR and Raman spectra temp. depend. anal. model *(French)* 77−88456
diazonium salts in aqueous solns. and polymer matrices, IR absorpt. spectra 80−76030
dibenzylketone, photolysis in micellar soln., quantum yield and ^{13}C enrichment 80−97711
dichromate solutions for low-level dosimetry 79−29633
diffusion of small light solutes in solvent of larger heavier mols., isotopic mass effects 78−34639
diffusion rate processes, effect of intermol. force field 77−35733
diffusion to drop (bubble) chain at large Peclet nos. of dissolved substance 79−86489
difluoroacetic acid, soln., polarisable H bonds, IR spectrosc. obs. 80−58408
p,p′-dihexyloxyazoxybenzene-fluorobenzene, solute orientational order, NMR obs. 77−84627
dilute, associated, lattice model, chem. equilib. laws 79−82139
dilute, electron paramag. relax. theory 77−80998
dilute, picosecond reson. Raman spectroscopy, appl. to β-carotene and cytochrome c 79−98102
dilute, spheroid-cylindrical mols., dynamics 80−44090
dilute solutions, Monte Carlo algorithm for preferential sampling near solutes 77−51287
dilutor method extension to meas. of high activity coeffs. at infinite dilution 79−19372
dimethylformamide binary systems, critical mixing temp. *(German)* 79−77762
dioxan(-oxalic acid)(-benzoic acid), solns., compressibility, internal press., US vol., H-bonding 79−82272
dioxan-acetone, dioxan-chloroform, US props., molecular interaction between components 78−63657
solutions continued
dioxan-$H_2{}^{16}O(H_2{}^{18}O)(D_2{}^{16}O)$, solns., FP determ., equilib. method 77−20048
dioxane, Raman spectral study of aq. soln. struct., H-bond effects 77−88454
p-dioxane-H_2O at 11 and 25°C, US absorption 80−65171
dipolar solvent, ionic mean force, pot. anal. 77−56234
dipole solvation, one polar mol. dissolved in 499 moderately polar particles 78−47221
Disjoining pressure of thin layers of binary solutions 78−15716
dispersion eqn., solns. 79−41649
DNA, phase transitions in water-ethanol solns. *(Japanese)* 80−89709
DNA conformation, influence of intermol. interactions 80−16900
DNA-type macromolecule, melting, low mol. wt. impurity effect 80−12050
drop, drying of solute skin-covered soln. drop *(Russian)* 79−68561
drop moving in hot gas, solvent evaporation 77−65783
drop moving in hot gas, solvent evaporation 77−68673
drop of solution, slow evaporation 79−90847
droplets of soln. vaporisation in high-temp. gas flow, heat and mass transfer 78−75191
dye solution, induced birefringence as result of illumination dichroism 79−28709
dye solutions, liq. scintillation counting, rel. to colour quenching ability 79−1790
dynamic orientational correlation functions, coupled translational-rot. diffusion model 77−84604
EBBA, binary systems with non-nematic solutes, phase transition behaviour and ^1H NMR anal. 80−34174
EBBA, mematic, orientational order, effect of hexa-n-alkoxy-triphenylene disc-like solutes 80−79682
elastic stress field shape change kinetics depend. on inclusion-edge dislocation interaction 79−86815
electrical force between permeable charged sheets, in electrolyte soln. 79−43605
electrolyte, aq. soln., field-induced ion evap. from liq. surface at atm. press. 80−29859
electrolyte, Debye-Huckel ionic atmosphere, number density of ions 79−29369
electrolyte, electron energy 80−66812
electrolyte, interionic radial distrib. function approx. scheme 77−32796
electrolyte, ion solvation, stat. theory 79−91966
electrolyte, polarisable dielectric spheres model, struct. around ions in soln. rel. to ionic solvation and activity coeff. 79−29368
electrolyte, precipitation processes, study by particle site anal. 80−50883
electrolyte, solutions, 1-1 and 1-2, extended mean spherical approxs. 79−4216
electrolyte, strong, conc. solns., thermodynamic props. of mixed electrolytes and Harned rule basis 79−90506
electrolyte, tracer and mutual diffusion, open-end capillary method 79−28119
electrolyte dipolar hard sphere solvent with charged hard spheres, hypernetted chain approx. 80−61130
electrolyte solution, two-dimens., theory 77−86323
electrolyte solutions, diffraction expts. and theory *(German)* 78−95935
electrolyte solutions, fluctuations rel. to acoustic relaxation and light scatt. 77−15497
electrolyte solutions, preferential solvation, NMR obs. 78−95919
electrolyte solutions, preferential solvation and mol. motion, NMR obs. 78−95920
electrolyte solutions, thermodynamics, transport props., semi-phenomenological approach including short range forces 80−3353
electrolytes, aq., water struct., differential IR spectral investig. 77−52651
electrolytes, aq., X-ray, neutron diffr. data, termination errors, Fourier anal. 77−47299
electrolytes, aq. solns., CO_2 diffusivities 79−95190
electrolytes, diffusion coeffs. meas., conductometric method 79−23753
electrolytes, electrified interfaces, theory 77−48649
electrolytes, mixed, solns., electrical transport 80−3354
electrolytes, osmotic coeffs., mean spherical approx. refined model 79−1965
electrolytes and non-electrolytes, aq. soln., apparent molal isochoric heater capacities at 25°C 80−59671
electrolytic, struct. of free surface, single ion hydration energies 78−26752
electrolytic, thermodynamics and correlation functions 80−24132
electrolytic aqueous solution, US study of apparent molar compressibility 78−10125
electronic bands statistical broadening depend. on intermol. interaction 77−71837
electronic excited state transport, Green function soln. 79−68994
enzyme-substrate interaction forces influence on reaction rates 78−31765
ESR, bibliography of 1975-76 literature 80−51979
estuarine particle dynamics, math. model, phys. and chem. processes 77−21793
ethanol, aq. soln., conc. fluctuations, shear and longit. relax., Brillouin scatt. and pulse techniques 78−71792
ethanol, aq. subcooled soln., acoustic phenomena during nucleate boiling 78−10181
ethyl alcohol, solution, struct. determ. from vibr. spectra, H-bonding and heat of mixing *(Russian)* 78−3368
ethyl ether-N_2, bubble homogeneous nucleation in gas-liq. soln., press., expt. and theory 78−91430
ethylcellosol, aq. soln., light scatt. rel. to conc. fluctuations *(Russian)* 78−3450
ethylene glycol solution, flow boiling and pool boiling critical heat flux, effect of flow passage geometry 77−62250
ethylene glycol-water, uninhibited soln., corrosion of Al 79−70222
fatty acids in anhydrous solvents, partial molar volume from density meas. 79−43616
ferrocene derivatives in smectic B phase liquid cryst. BBOA, ^{57}Fe Mossbauer study 78−27136
fluidised beds, dehydration of solutions and suspensions, rel. to granulation 80−81373
fluoride-oxide-SiO_2 system, containing Mg^{2+}, Ca^{2+}, Ba^{2+}, Pb^{2+}, cryoscopy 77−28798
fluoride-oxide-SiO_2 system, containing Na^+, K^+, Li^+, cryoscopy 77−28797
fluoroform(-d_1)-trimethylamine-Ar(Kr), cryospectroscopic IR study of association 77−468

solutions continued
formaldehyde, solid soln. in Xe, precipitation, IR spectra obs. 80−45059
formamide-water soln. permeability of cellulose membrane 78−11557
formic acid, soln., polarisable H bonds, IR spectrosc. obs. 80−58408
frozen acid solutions, aq., irrad., at. H trap struct., spin echo obs. 79−42824
frozen alcohol solutions, aqueous, H atom stabilisation, EPR obs. 79−47325
frozen salt solutions, aq., irrad., at. H trap struct., spin echo obs. 79−42824
Gibb's excess energy, thermodynamic restrictions on analytic expression 78−27817
glass, complex raw material, hydrothermal prep. 80−104106
glycol-alkane systems, interfacial tensions, regular soln. theory and Antonow's rule 79−14983
group contribution mol. model of liqs. and solns., thermodynamic props. 77−58932
Hand and Othmer-Tobias correlations, critical anal. 79−1504
hard disc fluid, infinite dilution solute chemical pot. by Monte Carlo simulation 80−88009
hard sphere macromolecule dil. soln. viscosity, Thorne-Enskog theory 78−91467
hard sphere solvent, dense, solute test hard sphere kinetic energy relax. 80−33864
heat transfer across low aspect enclosure, solute layering effect 77−75776
heterophase fluctuations 78−91444
n-hexadecane-β,β'-dichlordiethyl ether exfoliating mixture, light scatt. and hypersound vel. 77−28586
histones, H2a and H4, aggregation ionic strength effect *(Russian)* 80−55697
homogeneous precipitation of supersaturated soln., phenomenological theory 78−67833
hydration, hydrophobic, of nonpolar mols. in dilute aq. soln., Monte Carlo simulation 80−3314
hydrocarbons, thermodynamic props., multiparameter conformal solution theory 78−18796
hydrophobic effect, dil. soln. struct. and thermodynamic props., semi-empirical model 78−20060
hydrophobic solutions molecular properties, one dimensional soluble models 79−46536
inert gases, liquid phase mixtures, dipole autocorrelation function, IR absorpt. spectra obs. 80−28903
ion-selective liquid chloride electrodes, solvent effects *(Russian)* 79−91972
ion-water interactions, survey of diffr. studies 80−24347
ionic, elec. field statistics 78−87601
ionic and multipolar liq., thermodynamic perturbation theory 77−47316
ionic diffusion in naturally-occurring aqueous solns., use of activity coeffs. in transition-state models 78−57224
ionic equilibria in water and mol. dynamics of pure liqs. using high-press. Raman spectroscopy 79−24301
ionic fluid, equilib. props. using corresponding states concepts 79−27889
ionic liquids, struct. determ., summer school lecture series 80−6349
ionic solute hydration, thermodynamic and transport props., review 78−27815
ionic solution, charged square well model, virial osmotic coeffs. 79−4217
ionic solution, in mol. polar solvent, charged sphere model, statistical mechs. 78−71655
ionic solution in molecular polar solvent, stat. mech. 78−30527
ionic solution theory, variational approach 77−7645
ionic solvation, spectroscopic data comparison for methanolic and aqueous solns. 80−26099
ionic-polar mixture, equilib. props., generalised electrostatic model 79−68995
ionisation, induced ion pair separation, Coulomb cage pair 79−11811
ionizing liquids, non-aqueous, review *(French)* 79−69255
IR ν_s absorption band profile of isotopically diluted OH groups, rel. to crysts. 79−69821
4-isocyanate-trans-stilbenes, donor substituted, anisotropic fluoresc. in low viscosity solvents *(German)* 80−93401
isotopic isomers, solns. (one in another), excess thermodynamic props. 78−53245
kinetics of reacting solns., diffusional barrier crossing processes, trajectory simulation 80−81280
Langmuir wave quasicollapse, one-dimens., under parametric and modulation instabilities 77−42982
lattice model directionality depend., solns. with closed loop coexistence curves 78−95158
Lennard-Jones liq. mixtures, mol. dynamics calc. 78−55794
liquid, boiling at wall, nucleation, influence of dissolved gases 77−76537
liquid crystal, isotropic phase, orientation pair correl. obs. using depolarised Rayleigh light scatt. *(Russian)* 79−90552
liquid solutions, reaction rates, mol. mobility effects, review, book contrib. 77−40526
liquid solutions containing dust particles, light scatt. meas. techniques 77−37959
liquid-liquid nonpolar regular solution, symmetry and crit. consts. 78−34623
lysozyme, aq. solns., H_2O ordering, NMR relax. investig. 79−62171
macroionic solution, plus counter ions, Kirkwood theory, mean field phase transition 78−38812
macromolecular, alternating elec. field light scatt., low angle approx. 80−84721
macromolecular, dynamic light scatt. by flexible macromols. in fluctuating elec. field 80−84722
macromolecular, gel conc. and diffusivity at gelling determ. by ultrafiltration 80−21325
macromolecular, rigid ellipsoidal macromols. in cond. soln. at low ionic strength, specific Kerr consts. 80−84718
macromolecular, rot. diffusion coeff. calc. method w.r.t. mol. struct., elec. birefringence relax. time data interpret. 80−85331
macromolecular, transient elec. birefringence in reversing fields of arbitrary strength and duration 80−84719
macromolecular liquids and solutions, statistical thermodynamics 78−18528
macromolecular solns., self-diffusion coeff. 78−6168
macromolecular solutes, finite conc., isothermal diffusion and quasielastic light scatt. 79−82367
macromolecule in soln., spectroscopic meas. of energy barrier to electron transfer 77−38766
solutions continued
macromolecules, orient. in laser beam elec. field, anisotropic light scatt. 79−1768
macromolecules, Rayleigh scatt., elec. reorient. rel. to spectral line rot. broadening 79−1774
magnetic phenomena classification *(Russian)* 77−8384
material systems containing aqua solns., heat cond. with freezing 79−50565
matter concentration in solution, determ. using FL luminescence photometer 79−30575
metal refining by crystallisation and reflux, three component Raoultian behaviour 77−28799
metal-ammonia soln., ionis. equilib. instability of weakly-ionised 3-component plasma 80−10877
metallic, small ion currents, mag. scanning type spectrometer 78−8464
methane, dil. aqueous soln., Monte Carlo calcs. on struct. 79−32874
methanol, dil. soln. in nonpolar solvent, lattice models, association consts. 79−82141
methanol solns., IR spectroscopic detection of free lone-pair groups or terminal methanol mols., PMR 79−19869
methanol solution in benzene, dielec. relax. time by RF cond. meas. 80−71302
methanol-benzene solutions, adsorption on carbon 78−14568
methanol-water (propylene glycol), proton medium effects, ferrocene redox couple reference obs. 77−77786
methanol-water soln. permeability of cellulose membrane 78−11557
methine dyes, spectral props., solvent effects 80−69181
3-methoxybenzanthrone in ethanol, photoprotolytic reactions, spectra, rate consts. and lasing thresholds 80−43327
methylene chloride-cyclohexanol system, acoustic props. 77−51450
micellar dye soln., energy transfer 80−45581
micellar systems, solubilisation 80−89546
mixed freshwater, seawater and brine solutions, chemical speciation of Cd, Cu, Pb and Zn 78−20409
mixed salt solutions, apparent and partial molal volumes, ternary systems 77−9114
molecular dynamics simulation of chemical reactions in solution 80−40673
molecular orientation, cooperative, rel. to OH proton chem. shift 78−1974
molecular theory, comment on two-centre expansion 77−60920
molten salt, metal dilute solns., optical absorption 79−19899
naphthalene in nonpolar solvent, vibr. and reorientational relax., correl. function 80−45065
Nernst distribution law, use of thermodynamic excess functions 78−43123
nitrobenzene:n-hexane, depolarised Rayleigh scatt., crit. anomalies 78−68524
nitrobenzene-hexane, soln., dielec. permitt. in two phase region 80−2682
nitrobenzene-hexane critical solutions, crit. exponent determ. by nonlinear dielec. method 79−87373
nitroethane, crit. soln. in cyclohexane, nonlinear dielectric effect 78−27152
NMR, ^{89}Y spin-spin relax. times, no pH depend. 80−2657
NMR of solutions exhibiting chemical exchange, spin 5/2 and 7/2 nuclei 79−65750
nonaqueous electrolyte solutions, ionic nuclei, quadrupolar interaction, mag. relax., infinite dilution limit 78−35692
nonaqueous electrolyte solutions, thermal diffusion, Soret coeffs. meas. 78−18811
nonaqueous solutions, conf. Leeds, England (July 1976) 78−73036
nonaqueous solutions, Raman spectrosc. obs. techniques 78−72514
nonelectrolyte aqueous solns., X-ray diffr. meas. of struct., scatt. curves 79−10785
nonelectrolyte aqueous solutions, temp. of max. density rel. to partial compressibility, struct. strengthening 80−30270
nonelectrolyte solutions, liq. theory, review, book contrib. 77−39523
nonelectrolytes, aqueous, excess heat capacity, H bonding 78−3362
organic N bases, solutions in organic solvents, IR spectra and struct. 79−38534
organic solute rejection by reverse osmosis, regular soln. theory appl. *(Japanese)* 80−101041
osmotic pressure, teaching, solvent tension, dilution explanations 78−73803
packing densities for liquids, solutions and random assemblies and spheres 77−58937
pair distrib. functions, modification of regular solution theory 78−67829
pair potential of attractive dispersion interaction in dense media 77−66787
pancreatic trypsin inhibitor tyrosine residues in soln., laser photo-CIDNP as surface probe 78−73138
partial molar quantities, calc. from molar quantities *(German)* 78−85191
particle size meas. of crystallites in soln. by line-broadening meas. 78−18488
pentofuranosyl nucleosides, isomeric, ^1H NMR coupling consts., SCF FPT INDO approx. calc. 80−14156
peptides, α-aminoisobutyric acid containing, ^1H NMR conform. obs. 79−81311
phase equilib. prediction, simplified molecular models of soln., study 79−19351
phenol(-d_1)-dioxan(-acetonitrile), in carbon tetrachloride ($CDCl_3$) solns., H-bonds vibr. relax. bands anal. 78−84560
photoelectron emission theory 77−21403
phthalocyanines, dye laser appls., soln. chem. 77−40568
β-picoline-water solution, light scatt. spectra, ultra- and hypersonic absorpt. *(Russian)* 80−93353
piperidine solution of PbI_2, crystn. of intercalation cryst. 80−16170
plasmid DNA and DNA-histone chromatin-like complexes, conform. and soln. props. by laser light scatt. 80−55987
polar liq. in nonpolar solvent, dipole moment extrapolation procedure 79−33650
polar liquids, H bonding, dielec. theory, apparent dipole moment, chem. model 77−48671
polar liquids soln., mol. electric dipole moments, extrapolation formula 79−38437
polar molecular solution, local order and vibr. coupling, Raman bands, dielec. const. 79−99868
polar molecule, dipole moment determ. from soln. data 77−6956
polar molecule in soln., broadened band contour anal. 77−496

solutions continued
polar solvent reorganisation energy in inner sphere complex charge redistrib. 80−40730
polar/nonpolar mixtures, pot. of mean force, approx. theories, clustering of solute mols. 78−26401
polarisable fluid containing charged particles, mol. dynamics theory 78−91214
polyatomic asymmetric top molecules, solns., IR spectra 78−58694
polydisperse rod suspension, elec. birefringence relax. 78−23430
polyelectrolyte solutions, counterion nucl. mag. relax., quadrupolar mechanism 80−2659
polymer mixtures, solns., viscosity *(Russian)* 79−65236
polymethine dye solutions, photochem. transformations and short-wavelength luminesc. 80−100686
polypeptides, poly-L-lysine based, comb-like, struct., physicochem. props. *(Russian)* 79−55644
positronium chemistry, in soln., form., inhibition and reactivity 77−44499
pressure solution thermodynamics, interction between chemical and mechanical forces 78−57194
propylene glycol-water (methanol), proton medium effects, ferrocene redox couple reference obs. 77−77786
protein solutions, quasielastic light scatt. in small wave vector limit 80−45088
protein-water interactions in aq. solns., Raman spectroscopy 77−6792
proteins, globular, crystalline, intermol. interactions, denaturation, DSC and X-ray diffr. obs. 80−16897
proteins, laser photo-CIDNP as surface probe 78−73138
pyridine, in carboxylic acid soln., stimulated Raman scatt., H-bonded complex effects *(Russian)* 77−3625
pyridine, vibr. reson. lasing threshold, complex form. and solvent effects *(Russian)* 77−75507
pyridine-N-oxide, in benzene, dipolar assoc. investig. 80−107035
pyridine-water soln., reorientational relax. and activation energy of pyridine, depolarised Rayleigh scattering 80−76037
quasilattice theory of solutions, use in mol. spectroscopy, thermodynamic parameters determ. 79−96350
radiochemicals in aqueous soln., use of revised MIRD eqn. for dosimetry calcs. 77−66851
Raman line intensity conc. depend. 79−56786
refractive index transients, laser-induced, low-temp. solns., excited triplet state polarisabilities role 79−87411
rhodamine 6G in ethanol, photobleaching mechanism *(Russian)* 78−48680
rhodamine (6G-DTDC and 6G-CV) in alchohol solns., energy transfer by means of photobleaching 79−23031
rhodamine B in aq. LiCl soln., absorpt., pH, electric conductance 77−27079
rhodamine-B, thermochromic and hyperchromic effects 79−91977
ribonuclease A, thermodynamics of interaction and unfolding in transfer to aq. consolute solns. 79−24939
ruthenium trisbipyridyl ions in surfactant solns., excited state decay kinetics 80−83407
salt solutions, in liquid alkali metals, phase equilib. and chemistry 78−73040
salts, aq. solns., mechanical and electro-optical anharmonicity *(Ukrainian)* 78−2830
saturated liq. low press. enthalpy function, corresponding states and pseudocriticals 78−31672
seawater, dissolved trace metals concs. in Laccadive Sea 80−104997
sedimentation and density gradients, near liq.-liq. crit. soln. point, high gravit. field 78−47526
serum albumin, human hydration, pH depend., water self-diffusion obs. *(French)* 79−34475
sodium dodecyl sulphate micelles, diarylalkane intramolecular excimer formation, microfluidity and fluoresc. meas. 78−80791
solute molecules in 1-dimensional fluid, forces due to solvent struct. 79−73080
solute transport in porous media, statistical theory 80−28899
solute-solute-solvent interaction, dielec. behaviour problems, review 80−25298
solute-solute-solvent interactions, introduction to symposium in Vienna, Austria (1978) 80−26098
solute-solvent interaction, discrete, continuum and discrete-continuum models 78−73130
solutes, differential concentration by cryoscopic effect 77−36856
solvation effects and Gurney cosphere overlaps, conductimetric approach 80−21354
solvent mediated interactions−solute size effects and predictions of mean field theory 78−75513
solvent struct. around ions as hard spheres, mean spherical approx. 79−70335
solvent structure, in particle interactions, short range forces 78−83709
solvent structure in particle interactions, asymptotic regime 78−83708
solvophobic effect in simple fluid mixtures 77−31569
spectrochemical analysis of biological solns. using wall stabilised arc source 80−41343
spheroidal macromolecules solutions, quasielastic light scatt. 79−24325
spray drying, of highly viscous conc. solns., heat and mass transport *(Russian)* 78−83230
strong II-I electrolytes, aq. soln., Raman spectrum, local order 78−84563
surface tension of concentrated aqueous solutions of 1.1-electrolytes measured by means of Wilhelmy and laser light scattering methods 77−72745
surfactant, aq. subcooled soln., acoustic phenomena during nucleate boiling 78−10181
surfactant solutions, aggregation, micelle and microemulsion form. 80−89547
symmetrical electrolytes, conductance and model for ions in soln. 80−29197
TCNE, K salt, in nematic liq. crystal solvent, ion pairing, EPR spectra 78−73020
ternary dil. soln., free energy of transfer determ. by vapour press. method 78−64871
ternary liquid mixtures, shear viscosity at plait points 77−35685
ternary solution phases, empirical methods of predicting and representing thermodynamic props. 80−70423
tetrabutylammonium halides, solutions in organic solvents, IR spectra and struct. 79−38534
solutions continued
tetrabutylammonium iodide, alcoholic soln., repulsion phenomena in thin layers 80−107619
thermodynamic functions, endostatic transformations 77−28022
thermodynamic functions for characterising structural changes 77−25301
thymine+muonium, radical form. in aq. soln., spin reson. obs. 78−74679
toluene, in polar solvent, excess thermodynamic props., Rayleigh scatt. meas. 78−52523
toxic gas microconcentration determ. by automatic belt photometer *(Russian)* 78−28347
trace elements, in acid solns., solvent extraction, chelation and thermodynamic activity *(French)* 78−27816
trans-Pu solvent extraction recovery and purification by trioctylphosphine oxide chromatography 80−93826
transuranium cpds. in aq. soln., electrochem. 77−29040
trifluoracetic acid-water, molecular dynamics simulation of chemical reactions in solution 80−40673
trifluoroacetic acid, soln., polarisable H bonds, IR spectrosc. obs. 80−58408
trifluoromethanesulphonic acid, and salts, electrochem. characts. in nonaqueous solvents 80−89499
trioxane, in nitrobenzene soln., polymerisation, polyoxymethylene morphology 80−59403
uracil in aq. electrolyte, adsorpt. isotherm and solute activities from spreading pressure-surface charge data 78−14576
vibrational relaxation, nonrandom sequential coupling influence 78−90205
viologens, electrochromic, for display appl., oxidant impurities elimination 80−78922
vitrified conc. aq. solns., ionic hydration and secondary dielec. relax. 79−24882
volatile trace organics, aqueous environmental samples, head space anal. 80−40763
water, cavitation, gas supersaturation thresholds under high press. 77−16861
water, solutions in organic solvents, IR spectra and struct. 79−38534
water containing dissolved gases, sonoluminesc. theory 77−85818
water-ethanol, inversion of Kirkwood-Buff theory 78−27807
water/magma solutions, appl. of Gibbs-Duhem eqn. 78−57205
X-ray scatt. intensity composition depend., soln. struct. 78−6005
acetone-d_0, d_6, Raman spectral study of aq. soln. struct., H-bond effects 77−88454
Ag(I) ions, in methyl cyanide, electron loss and capture, ESR spectra 79−33531
AlBr solution, in propylene carbonate, dissociation, radius and number of ion solvation *(French)* 79−70319
$AlCl_3$, aq. solns., order phenomena, X-ray diffr. obs. 80−1915
$AlPO_4$ solubility, in H_3PO_4 hydrothermal soln., conditions for cryst. growth *(French)* 79−77539
Ar, aqueous soln., dil., energy and struct., pair pot. energy function, Monte Carlo calc. 80−54107
Ar-Kr liq. and gas. solns., collision-induced dipole moment, far IR band obs., self-diffusion coeff. 77−38627
As(III) and As(V), redox stability in aq. soln. 80−61068
$BaCl_2$ aq. soln., vel. correls., time integral calcs. 80−59360
BaF_2-xBaO.ySiO_2, activities rel. to liquidus comp. 77−28798
BeF_2 aqueous solns., mag. and quadrupole relax. 80−71226
CO_2, aqueous solution, photoelectrochemical reduction on p-type GaP in liq. junction solar cells 78−88649
$CaCl_2$ aq. soln., vel. correls., time integral calcs. 80−59360
$CaCl_2$, aqueous soln., ion hydration 80−35518
$CaCl_2$, $CaCl_2$-CaF_2-CaO eutectic melts, specific cond. meas. 77−59131
$CaCl_2$-NaCl-H_2O, conc. solns., vap. press. meas. 79−23713
CaF_2-xMgO.ySiO_2, activities rel. to liquidus comp. 77−28798
$Ca(NO_3)_2$-H_2O solns., ice I homogeneous nucleation temp., slow vitrification mechanism 78−26666
$CdCl_2$-KCl-H_2O, water activity, 0 and 50°C, conc. depend. *(Russian)* 78−31679
$Cr(H_2O)_6Cl_3$, aq., solute structuring 77−15298
$Cr(H_2PO_4)_3$-$Al(H_2PO_{43})$-H_2O system, IR spectra 79−87428
$^{51}Cr_2O_7^{2-}$ tracer solution preparation *(French)* 79−29385
Cs-NH_3, Cs-ND_3, solns., US absorption, metal-nonmetal transition 79−69194
Cu complexes with dipeptides, EPR spectra of high pH aq. solns. 77−32248
$CuBr_2$, highly conc. aqueous soln., local ordering, extended X-ray absorb. fine struct. spectra 78−79520
$CuBr_2(Cl_2)$, aq. soln., structural transition, neutron diffr. study 80−64872
$CuCl_2$, aqueous soln., nonlinear conversion of acoustic pulses with thermooptic excitation 80−14510
$CuCl_2(Br_2)$, aq. solns., EXAFS meas. 80−60714
$Cu(NO_3)_2$, frozen aq. soln., phase transitions, struct., ESR 77−16154
$CuSO_4/H_2SO_4$ electrolytes, densities, elec. cond., viscosities 80−107455
Dy_2O_3, soln. in $K_2O.2(3)MoO_3$, rel. supersaturation and supercooling 80−40245
Fe based ternary solutions, liquid, exam. of thermochemistry 78−80782
Fe^{3+}-Fe^{3+} distances, in aq. NO_3^- and ClO_4^- solns., from small-ang. X-ray diffr. maxima 78−42880
$Fe(CO)_5$, solns. with dissolved NO, photolysis, $Fe(NO)_3CO$ form. 80−53024
Fe^{3+}(III) water-glycerine solution-U(IV) cationic resin, inverse break through study on U isotope separation 79−41025
$Fe(NO_3)_3$ conc. aq. solns., struct., X-ray scatt. investig. 77−31576
GaAs in Sn, vap. press. of P and As 77−51485
GaP in Sn, vap. press. of P and As 77−51485
H-bonded species, in soln., vibr. relax. model 78−84559
H_3BO_3, aq. soln., dielec. props. and struct. 77−89369
HCl aqueous soln., H^+ mobility, 15, 25, 40°C, up to 5000 atm 78−10207
HCl aqueous solutions, diffusion coeffs. at 298K, conductimetric obs. 80−24628
HCl in DMSO-H_2O soln., ion assoc., US absorpt. obs. 79−23513
HCl-$CoCl_2$-H_2O, activity coeffs., 298.15K, electrostatic terms effects 79−24812
HCl-H_2O, p-V-T relations up to 773K and 1500 bars 78−43096
HNO_3, aq. soln., heat capacity at 298.15K 78−3364
H_2SO_4, suspension-electrolysis leaching of β-ZnS, PbO_2(Pb) electrode anodic impedance *(Japanese)* 79−43594
H_2SO_4:Fe^{2+}, frozen soln., photo- and radiation-produced H-atoms obs. 79−39162

solutions continued
Hf complex, Hf-EDTA 80−34837
$HfOCl_2$, aqueous solns., rotational diffusion, TDPAC study 80−34837
Hg, atoms, in aq. soln., transient spectra 79−6899
K isotope separation in solution by thermal diffusion 80−87236
K solution, in KBr, conc. fluctuations, neutron small-angle scatt. study in electrolyte-metal transition range 79−14668
K-ethylamine-ethylenediamine, soln., ion-pairing and EPR 79−78502
$KCl-KNO_3-H_2O$, apparent and partial molal volumes in mixed salt solns. 77−9114
$K_2Cr_2O_7$, acidic soln., UV absorbance standard verification 78−21092
$KF-3K_2O.2SiO_2$, activities rel. to liquidus comp. 77−28797
KNCO, fused, soln. mechanism of Fe and Cr 79−39271
KNO_3, aq. soln., heat capacity at 298.15K 78−3364
$Li-NH_3$ solution, small angle X-ray scatt. meas. 79−14667
LiCl aq. soln., vel. correls., time integral calcs. 80−59360
LiCl aqueous soln., ion-water clusters, electronic struct., Compton profile 78−47227
LiCl, concentrated aqueous soln., IR absorpt. to high press. and temps. 80−80803
$LiCl-LiNO_3-H_2O$, mixed salt solutions, apparent and partial molal volumes 77−9114
$LiCl+NaNO_3$, apparent and partial molar volumes in aq. soln. 78−44396
$LiF-Li_2O.SiO_2$, activities rel. to liquidus comp. 77−28797
Li_2O-CaF_2 melts, component activities *(Russian)* 77−60104
LiOH, anodic oxidation of Cu amalgam at room temp. 79−61865
$MgCO_3^0$, ion-pair relaxation rel. to acoustic absorpt. 79−74914
$MgCl_2$, aq. solns., X-ray diffr. study 79−37608
$MgCl_2$ solution, initiation of SCC and pits in austenitic Cr-Ni steel at 40-90°C 80−50748
$MgCl_2-NaCl-H_2O$, conc. solns., vap. press. meas. 79−23713
$MgCl_2CaCl_2$, aq. soln., hydration, X-ray diffr. 77−43126
$MgF_2-xMgO.ySiO_2$, activities rel. to liquidus comp. 77−28798
Mn^{2+} in soln., EPR relax. probe 78−31104
Mn^{2+} ions, solvation enthalpies in various solvents *(French)* 79−69264
$MnSO_4+H_2O$ solutions, relaxation freq. and activation energy depend. on conc. 78−55913
Mo complexes, aquo ions in solutions, isolation, characterisation 77−77847
MoF_6(l), enthalpy of form. by soln. calorimetry 79−47962
$MoO_{4-n}Sn^{2-}$, (n=0-4), $^{17}O(^{33}S)(^{95}Mo)(^{97}Mo)$ NMR investig. 80−53022
NH_3 and ND_3, UV absorpt. of solvated electron 79−87935
NH_3-metal, thermophysical props., review 79−77758
NH_4Cl, aq. soln., dynamical props., mol. dynamics simulation 80−1918
NH_4Cl, aq. soln., struct. props., mol. dynamics simulation 79−82142
$(NH_4)_2SO_4-H_2O$-ethanol-benzene, tricritical mixture, light scatt. 79−15473
NO_3^-, aq. soln., vibr. width and dephasing, conc. depend. 80−43029
N_2O aqueous solution, loss from agricultural land in drainage water 79−43797
Na-In, dilute soln., thermodynamic props. 77−89553
$Na-NH_3$, nonmetal-metal transition, thermodynamics 78−18964
$Na-NH_3$ solns., UV absorpt. *(German)* 77−24869
$Na-NH_3$ solution, small angle X-ray scatt. meas. 79−14667
NaCl aq. soln., vel. correls., time integral calcs. 80−59360
NaCl, aqueous soln., Lennard-Jones parameters, mol. dynamics and X-ray obs. 78−9939
NaCl aqueous soln., mol. dynamics simulation, central force model 80−49077
NaCl dilute solution, US vel. meas. by differential velocimeter 77−78065
NaCl solution, ionic hydration for cations 77−62460
NaCl, solution, seawater, with trace quantities of Cs, adsorption behaviour on paper *(Russian)* 77−73766
NaCl, stratified solutions, elec. cond. meas. instrument 77−52718
NaCl, supersaturated soln., H_2O activity prediction 79−23713
$NaCl-NaNO_3-H_2O$, apparent and partial molal volumes in mixed salt solns. 77−9114
$NaClO_4:Fe^{2+}$, frozen soln., photo- and radiation-produced H-atoms obs. 79−39162
$NaCo(CO)_4$, soln., ion sites, cryptand C221 doping effects 80−70102
$NaF-3Na_2O.2SiO_2$, activities rel. to liquidus comp. 77−28797
$NaNO_3$, aq. soln., heat capacity at 298.15K 78−3364
$NaNO_3$, aqueous soln., X-ray diffraction, radial functions and positional correl. 80−79665
Na_2O-SiO_2, aqueous solns., Raman and IR spectra, pH depend., species at equilib. identification 79−87866
NaOD solution in D_2O, collective excitations in liquid and amorphous state, 77 to 300K 80−92636
NaOH water solution, struct. props. of disordered systems, Raman spectral study 77−4631
Na_3PO_4 solution, in tap water as corrosion inhibitor of Fe 80−45424
Na_2SO_4 in aqueous soln., diffusion coeffs. and Onsager-Fuoss theory disagreement 80−40729
Ni^{2+} ions, solvation enthalpies in various solvents *(French)* 79−69264
$NiCl_2$, aq. soln., Ni^{2+} coordination from extended X-ray absorption fine struct. 80−1913
$NiCl_2$, aq. soln., structural transition, neutron diffr. study 80−64872
$NiCl_2$, aq. soln., viscosity meas., struct. props. 78−75863
$NiCl_2$ aqueous solution, hydration of Ni^{2+} 78−79518
$NiCl_2$ solution, ionic hydration for cation 77−62460
$NiCl_2-D_2O$ solution, hard-sphere model 77−62461
$NiCl_2$-heavy water solution, inelastic neutron scattering 78−91203
$NiCl_2(Br_2)$, aq. solns., EXAFS meas. 80−60714
O_2 singlet in solns., luminesc. duration following pulsed laser excitation 80−76070
O_2+muonium, aq. soln., reaction rate const., spin-conversion 79−100422
Pb, determ. in aqueous solns. by Delves Cup technique and flameless atomic absorpt. spectrometry 78−68973
$PbF_2-xPbO.ySiO_2$, activities rel. to liquidus comp. 77−28798
PbO/B_2O solution, solubility model in PbO/B_2O soln. 79−46807
Pt anode, impedance behaviour study in β-ZnS suspension-electrolysis leaching in 1N H_2SO_4 soln. *(Japanese)* 79−24754
Rb anions, THF soln., photolysis, appl. to photogalvanic cell 80−85294
$RbCl-KCl(H_2SO_4)-H_2O$, water activity, 0 and 50°C, conc. depend. *(Russian)* 78−31679
$RbX-CdX_2-H_2O$, X=Cl,Br,I, Gibbs free energy, H_2O activity, 25°C *(Russian)* 78−31678

solutions continued
SF_6, dissolved in O_2 and Kr, cryogenic liqs., mol. motions, IR and Raman spectra 79−69823
SiO_2-water system, inorg. polymer struct. form., globular crystn. 80−101042
$SrBr_2$, aq. solns., EXAFS meas. 80−60714
$ThCl_4$, in LiCl-KCl and Na-K eutectic solns., thermodynamic props. 77−86345
ThO_2, particle size of crystallites in soln. by line-broadening meas. 78−18488
$TlNO_3$, Tl_2SO_4, TlOH, aq. solns., viscosities at 25°C 77−20104
U, in alkali, chloride eutectic melts, interdiffusion, chronopotentiometric meas. 77−80637
$UF_6-MF_5(MF_6)$, dil. solns., (M=Te, Mo, W, V, Sb, Ta), liq.-vapour equilib. 77−62632
$UO_2(NO_3)_2$ solutions, cryoscopy and activity coeffs. 78−11544
YAG solutions, in $PbO/PbF_2/B_2O_3$ solvent systems, density, surface tension and expansivity data, effect of B_2O_3 conc. 79−19985
Zn-Ti, environmental factors affecting pitting corrosion potential in NaOH solns. 80−45423
$ZnBr_2$, aq. solns., EXAFS meas. 80−60714
$ZnCl_2$, aq. soln., structural transition, neutron diffr. study 80−64872
$ZnCl_2$, aq. solns., complex IR refr. indices, IR spectra, mechanisms, spectrometer system 78−43831

solvated electrons
absorption spectrum in polar solvents, interpretation by simple model 79−87934
acridine, aqueous soln., laser induced two-photon ionisation investig. 80−32780
alcohol-alkane dilute system, electron solvation, picosecond spectral obs. 77−44573
alcohols, electron solvation dynamics, rel. to interaction pots. 77−9052
alcohols, optical spectra of solvated electrons, band resolution 79−78698
alkali metal anions and trapped electrons formed by evaporating metal-ammonia solutions which contain cryptands 79−100340
alkali metal cation-electron pair in ethers, optical spectra, coordination effects 77−66788
alkali metal cryptand complex, with anion or solvated electron, optical absorpt. spectra 78−52526
alkali metal solutions cation-electron interactions 78−73037
alkali metal-ammonia solns., elec.-cond. and thermopower 77−1370
alkali metal-hexamethylphosphoramide, low temp. glass, EPR of solvated K, Cs and Rb 78−91927
alkaline glass: tryptophan (tyrosine), γ-irrad., electron traps, stimulated luminesc. 78−11536
alkanes, electron localisation and solvation, radical ion theory 78−87936
alkanes, liq. and glassy, semicontinuum model with structured first solvation shell for excess electrons 77−90711
amino acids, aq. solns. EPR of spin-trapped radicals, hydrated electron reactions 78−27796
ammoniated electron+R^{3+}, reaction kinetics meas. by ns. pulse radiolysis 79−52638
ammoniated electrons, reaction rate consts. with hydroquinone, phenol, propionamide 77−9043
aqueous glass, γ-radiolysis, photolysis of trapped electrons, quasi-free electron IR absorpt., luminesc. 77−21401
aromatic hydrocarbons, singlet energies, correlation with anion radical protonation 78−40064
chondromucoprotein, effects of ^{60}Co γ-irrad. 78−7400
Compton profiles 79−29339
condensed media, electron localisation and solvation, radical ion theory 78−87936
continuum model for polar liquids 77−60178
cytochrome c conformationally-nonequilibrium state reactivity obs. by pulse radiolysis 79−43816
cytochrome c-phospholipid interaction, studied by pulse radiolysis 78−48746
diffusion controlled reactions in polar solvents, reaction parameters 80−97687
dilute polar fluid, electron solvation, picosecond spectral obs. 77−44573
dimethylsulphide, liq., solvated electrons, optical absorpt. spectrum obs. 80−97250
dipole polarisability, Compton profiles 78−27877
electrochemistry 77−16829
electrolyte solutions, electron energy 80−66812
energy characteristics, absorpt. spectra analysis 79−34320
ethanol, glassy matrix, absorpt. spectra after X-irrad., solvated electrons 79−65903
ethanol, pulse radiolysis, solvated electrons decay kinetics 79−66319
ethanol glass, trapped and solvated electrons produced in presence of applied electric field 80−7379
ethanol-d_0,-d_1, solvated electrons reacting with scavengers, inverse isotope effects 78−31751
ethanol-$d_1(d_2)(d_3)$, glassy state, solvated electron geometry, electron spin echo modulation obs. 80−66009
excess electron ground state energy and solute ionisation pot. calcs. 77−83508
excess electrons, optical absorpt. spectra, moment theory anal. 78−73072
excess electrons in condensed media, migration in dilute mol. solns. 77−81457
excess electrons in liquid inert gas-propane systems, ground state energy 79−57346
fibrinogen solution, effect of scavengers on radiation-susceptible sites 78−11701
fluorobenzene in liq. NH_3, solvated electrons reaction kinetics 77−73434
fractional charge MO model 78−31752
glass, alcoholic and aq., 4.2K, trapped electron photocond. and optical spectra following radiolysis 79−29378
haemoglobin, dynamic characts. of conformational nonequilib. states, radiolysis investig. 78−58877
n-hexane, liquid, ground state energy of excess electrons 78−68976
hydrated electron+O_2, rate const., Arrhenius parameters 78−20041
indole, aq. solns., flash photolysis, transient absorpts., 600 to 800 nm 78−53228
inorganic anions, solns. in aromatic solutes photochem. hydrated electron decay kinetics 77−52656
interaction, Coulombic component intense long-wave field effects 80−43141
methanol, aq., radiolysis, CIDNP, methoxy radical involvement 78−53223

solvated electrons continued
methanol, dry-electron localisation, impurity trapping, solvated electron rate consts. 79−1990
methanol, glassy matrix, absorpt. spectra after X-irrad., solvated electrons 79−65903
methanol, solvated electron lifetime and reaction with hydroxymethyl radical, dose and base effects 78−20043
methanol, solvated electron yield and spur decay following electron irrad. 78−20042
methanol glass solvated electrons, EPR, ^1H spin flip satellites, geometrical model 80−7146
methanol-2-methyltetrahydrofuran glasses, electron solvation conversion, pulse radiolysis obs. 77−77795
methanol-H_2O matrix, 77K, electron solvation and presolvation, electron spin-lattice relax. 79−57260
methylamine liquid, 293K, solvated electron decay kinetics obs., IR spectra 80−71928
13-methylpentane-d_{14}, glass, γ-irrad., solvated electron struct. obs. 77−9101
2-methyltetrahydrofuran glass, solvated electrons by electron spin echo modulation spectra 79−88991
model, statistical distrib. of trapped electron energies 79−66395
MTHF, localised excess electrons, semicontinuum models 78−73129
muonium chemistry, radiolysis effects 78−88653
myoglobin conformationally-nonequilibrium state reactivity obs. by pulse radiolysis 79−39353
β-naphthol, aq., solvated electron prod. using laser excitation 77−60087
optical absorption spectra, temp. depend. moments, many-particle theory 79−72301
optical absorption spectra evolution for localisation in trapping and solvation 77−90173
optical absorption spectrum, shape, temp. depend. 77−65489
optical excitation energies, correlation with solvent props. 78−53309
optical spectra and model potentials 80−30318
optical spectrum broadening in polar liquids 77−21465
organic liquid mixtures, positronium form., spur process 78−1113
picosecond chromodynamics 79−35850
picosecond spectroscopy using ultrashort laser pulses, appls. 79−54195
polar fluid, improved model of long range electron solvent interaction of localised electron 77−90710
polar fluid mixtures, two-absorber model of solvated electrons, spectra 78−85284
polar fluids, electronic energy levels for photoinjection 80−30319
polar liquid, solvated electron optical props. and thermodynamic characts., polaron model 78−85170
polar liquids, electron solvation, spectral changes 77−73501
polar solvent mixtures, solvated electron diffusion, 2-absorber model 80−85206
in polar solvents, absorpt. spectra, intrasolvent and intersolvent correls. 80−93840
polar solvents, equilib. electronic states, basic eqn., broken symmetry 78−37535
positron+halide ion, competitive reaction in water, ang. correl. obs. 79−61846
positronium chemistry, in soln., form., inhibition and reactivity 77−44499
positronium formation, in liq. hydrocarbons, mechanism, rel. to electron solvation 78−70980
positronium formation inhibition by solvated electron precursor scavenging, line shape Doppler broadening, lifetime spectroscopy 80−93784
positronium oxidation react. in aq. soln., positron hydration energy 78−61039
propane-d_8, liq., solvated electron optical absorpt. band 78−72544
1-propanol, dry-electron localisation, impurity trapping, solvated electron rate consts. 79−1990
1-propanol, low temp. pulse radiolysis, solvated electrons, absorpt. spectral changes 77−12813
n-propanol-3-methylpentane mixtures, pulse radiolysis, solvated electrons 79−66321
Raman spectrum modification, polarisation CARS obs. 80−5549
reaction rates, solvent effects 77−25259
snowballing effect for electron solvation in dilute solutions of polar molecules in nonpolar solvents 78−85283
solvated electron+ion, in ethanol, reactivity, ion pairing effects 78−85147
spectral broadening in alcohols, laser saturation 78−31750
statistical model, distrib. function of hydrated electron energy 80−30271
tetrahydrofuran, optical spectra of solvated electrons, band resolution 79−78698
tetramethylsilane, liquid, ground state energy of excess electrons 78−68976
tetraphenylcyclobutane, in hexamethylphosphoric triamide soln., pulse radiolysis, optical absorption decay obs. 79−16019
thiamine (vitamin B_{12}), aq. soln., radiation induced reactions 80−93779
time resolved ESR, time profile meas. and anal. 77−5878
trapped electrons in glassy hydrocarbons, gamma ray irrad., relax., spectral obs. 80−23416
2,2,4-trimethylpentane, liquid, ground state energy of excess electrons 78−68976
tryptophyl peptides, pulse radiolysis, hydrated electron reaction 78−48679
virtual charge model representation of solvent polaris. 78−74593
water, I^- charge transfer to solvent spectra, water struct., solvated electron 77−50447
water, liq., electron solvation dynamics 80−85205
water, optical spectra of solvated electrons, band resolution 79−78698
water, solvated electron, polaron coupling const. from dipolar plasmon freq. 77−89720
water, solvated electrons, photon-induced electron transfer transitions 79−8154
wavefunctions, approx. single parameter var. calcs. 78−66467
BeF_2, aq. glass, 76K, solvated electron spectrum evolution, following ns radiolysis 78−88295
D_2O, IR and vis. spectra, 292 to 445K 78−74672
H_2O, liq. and ice, localised excess electrons, semicontinuum models 78−73129
H_2O, pulse radiolysis, hydrated electron absorbance, spur overlap 77−86328
$H_2O(D_2O)$, solvated electrons, optical absorpt. spectra. temp., isotope effects 80−55124
solvated electrons continued
K_2CO_3-D_2O, glassy matrix, absorpt. spectra after X-irrad., solvated electrons 79−65903
$KOH.xH_2O$, pulse radiolysis, absorpt. spectra of electrons 79−16013
LiCl aqueous glass, X-irradiated, localised electron optical, IR and photoconductivity spectra 78−73064
LiCl-D_2O, aq. 10 M glass, optical absorpt. spectra after X-irrad., electron scavenging efficiency 79−83476
LiCl-D_2O glass, trapped and quasifree electrons optical transitions, bound-continuum character 78−6660
NH_3 and ND_3 solutions, UV absorpt. of solvated electron 79−87935
NH_3, liq., localised excess electrons, semicontinuum models 78−73129
NH_3 liq., solvated electron optical absorpt. spectra anal., method of moments 77−50436
NH_3, solvated electron, polaron coupling const. from dipolar plasmon freq. 77−89720
Na-ice condensate, EPR lineshape second moment, electron solvation struct. 78−3440
Na^+-solvated electron, reversible capture by 1,1-diphenylethylene, equilib., kinetics 78−7177
$NaClO_4$-D_2O, glassy matrix, absorpt. spectra after X-irrad., solvated electrons 79−65903
NaOH-D_2O, glassy matrix, absorpt. spectra after X-irrad., solvated electrons 79−65903

solvated protons *see hydroxonium ion*

solvation
see also hydroxonium ion; solvated electrons
acetic acid-pyridine, H-bonding, proton transfer, isolated system, solvent effect, MO calc. 80−55629
acetone, macroscopic model for solvated ion dynamics, cation conductance calcs. 80−65261
acetonitrile, macroscopic model for solvated ion dynamics, cation conductance calcs. 80−65261
adsorption of liq. mixture on solid, equilib. thermodynamics 78−84045
albumin, bovine serum, diffusion, hydration and soln. environment effects 77−19116
albumin, bovine serum, diffusion, hydration effects, finite conc. 77−19115
albumin, bovine serum, diffusion, hydration effects 77−19114
alkali bromides, soln. in propylene carbonate, dissociation, radius and no. of ion solvation *(French)* 79−70319
alkali halide solns. with H_2O and D_2O, struct. and O isotope fractionation 78−22629
alkali halide solutions, ionic hydration, review 78−92501
alkali halide solutions, tetrahedral hydration of ions from Raman bands obs. 78−55804
alkali halide solutions in DMSO, modelling of interactions 79−77469
alkali halides, ion hydration numbers in aq. solns., mol. dynamics calcs. 77−62464
alkali halides, solns. in methanol, halide ion solvation, IR obs. 79−22703
alkali metal-H, liq. and solid, mol. orbital approach, solvation energies 77−4201
alkali metals, liq., soln. chemistry as elucidated from elec. resist. studies 77−52636
alkali metals, liq., solubility and solns. of nonmetals 77−51505
2-anilinonaphthalene, excited state solvation dynamics in polar solvent 77−44572
anthracene anion radicals, enthalpy of disproportionation, calorimetric determ. technique 79−96296
aqueous-organic mixed solvent structure, solvation, cation exchange *(Dutch)* 79−83500
bacteriorhodopsin photocycle hydration effects, in thin purple membrane layers 78−7320
benzene, in inorganic frozen solns., structured phosphoresc. spectra 77−65504
binary solution, ion solvation, thermodynamic description *(Russian)* 78−31676
biomacromolecules, nonpolar groups, correl. function anal. 80−30644
biomolecules electrostatic model of solvation, SCF MO calc. 79−96305
t-butyl acetate, rot. isomerism, dielect. and Raman spectra 80−106328
t-butyl formate, rot. isomerism, dielect. and Raman spectra 80−106328
chain molecule in solutions, finite concentrations, different solvent conditions, simulation 79−45872
chlorophyll, and related mols., in solid solns., fine-structured vibronic spectra under tunable dye laser excitation *(Russian)* 80−74164
chlorophyll-a, hydration, field desorpt. mass spectral obs. 80−71936
colloids, solvation force between particles, Monte Carlo calc. 80−21328
competitive preferential solvation theory of weak mol. interactions 79−27051
dense fluids, solvation forces between two solids 80−64855
dense Lennard-Jones fluids, solvent struct. and solvation forces between rigid particles 80−30287
p-dioxane, aq. soln., excess molar heat capacities, 298.15K, US vel. obs. 80−6523
dipole solvation, one polar mol. dissolved in 499 moderately polar particles 78−47221
DNA, gamma-ray effects on hydration, PMR of frozen and liq. solns. 78−27900
DNA, oriented films, hydration, slow neutron scatt. obs. 79−57572
DNA and polynucleotide hydration, γ-irrad effects, NMR of frozen H_2O and D_2O solns. 77−21484
DNA hydration characts. in H_2O/D_2O frozen solns., γ irrad. effects, PMR 78−31772
dynamics of solvated ions, mol. theory 78−35695
educational model 77−26110
electrical double layer theory, Poisson-Boltzmann eqn. including hydration forces 78−48668
electrode-electrolyte systems, absolute half-cell EMFs and single ion free energy of solvation 77−73449
electrode-solution interfaces, role of water 78−40058
electrolysis, solvent transport by ions, kinetic hydration and viscosity mechanisms 78−3347
electrolyte, free surface struct., single ion hydration energies 78−26752
electrolyte, polarisable dielectric spheres model, struct. around ions in soln. rel. to ionic solvation and activity coeff. 79−29368
electrolyte solution, ion solvation, stat. theory 79−91966
electrolyte solutions, preferential solvation, NMR obs. 78−95919
electrolyte solutions, preferential solvation and mol. motion, NMR obs. 78−95920

solvation continued
electrolytes, dil. solns., Hall const., ion solvation and dynamics *(French)* 77−4910
electron reaction rates, solvation effects 77−25259
empirical potential model EPEN/2 for conform., intermol., solvation studies 79−50102
ethanol, electron solvation, ps laser study 80−101032
ether-water mixtures, miscibilities, enthalpy of mixing, solvation *(German)* 78−18779
ettringite, expansion by H_2O adsorption, exam. 78−64806
fluorescein dye laser, solvation effects on tunability 80−53285
formaldehyde-water, heuristic intermol. pot. function, ab initio MO calcs. 78−33566
formamide, hydration by H_2O mol., point charge model 77−34569
gaseous univalent ions, solvation entropy, one-layer continuum model 79−47959
glass dating by hydration layer thickness meas. by NMR 77−74567
glass fibre reinforced cement, durability in wet and dry conditions, fibre length and content effect 80−71726
glasses, electron scavenging, hopping controlled time-depend. reaction rates 80−108723
Gurney cosphere overlaps and solvation effects, conductimetric approach 80−21354
hard particle fluids, short range solvation forces 80−38885
heavy lanthanide perchlorator, aq. solns., US vel. and solvation numbers meas. 79−19319
hexamethylene tetramine, cryst. growth kinetics from soln., role of solvent-solute interactions 77−24282
hydrated ions in stratosphere, comp. abundance meas. 78−88877
hydration number of electrolyte, determ. by vapour press. meas. 79−87868
hydrides, aq. dissoc., solvation, MINDO/S calcs. solvation theory 80−97708
ion dynamics, kinetic dielectric decrement, microscopic theory 80−7801
ion dynamics, mol. theory, fluid struct. and ionic mobility 80−7800
ion-molecule equilibria in solvolysis, secondary β ^{2}H isotope effects, hyperconjugation 80−50874
ion-selective electrodes, liq. membrane, free and supported, ion transport, interfacial kinetics, time depend. phenomena 79−83535
ionic solute hydration, thermodynamic and transport props., review 78−27815
ionic solutions, in liq. HCl, coord. sphere radius, vibr. spectrosc. investig. 80−50843
ionic solvation, electrostatic free energy, multilayered continuum model 79−57282
ionic solvation, in methanol, spectroscopic study *(French)* 79−70363
ionic solvation, spectroscopic data comparison for methanolic and aqueous solns. 80−26099
ionic solvation energy, statistical calc., gas approx. 80−40731
ions, in polar media, continuous charge distrib. model, quantum mech. calcs. 78−68913
ions, mol. clustering, gaseous-condensed state, nucleation and solvation 80−28129
isopropyl vinyl ether, chem. initiated soln. polymerisation and radiation-initiated bulk polymerisation 79−91952
kaolinite, hydration, lattice deform., vol. expansion due to adsorbed H_2O 80−45555
large complex systems, mixed electrostatic-quantum chemical approach 79−89605
Lennard-Jones liquid mixtures, equimolar, mol. dynamics, struct. and thermodynamic props. 78−18517
Lennard-Jones solutes, hydration, mol. dynamics obs. 79−34294
liquid-liquid phase equilibria, theory, chem. models 78−18781
lysozyme, aq., Raman intensities, interac. 78−58704
lysozyme bound water, thermally-stimulated press. and current 78−15757
macromolecular hard-sphere system, diffusion, hydration and soln. environment effects 77−19116
macromolecular hard-sphere system, diffusion, hydration effects 77−19114
macromolecular hard-sphere system, diffusion, hydration effects, finite conc. 77−19115
mean spherical approx. for arbitrary hard ions and dipoles, soln. for electrolytes 79−1380
methacrylic acid-methyl methacrylate statistical copolymer suspension polymerisation, stabilisation effects, viscosity 78−85157
methanol, electron solvation, ps laser study 80−101032
methanol, solvation in water, discrete, continuum and discrete-continuum models 78−73130
methanol-H_2O matrix, 77K, electron solvation and presolvation, electron spin-lattice relax. 79−57260
methanol-methyltetrahydrofuran glass:β-naphtholate, electron solvation, laser flash photoionis. compared with pulse radiolysis 79−74405
methanol-water, assoc. mixture, rot. barrier solvent effect, CNDO/2 calc. 78−29861
methanol-water (propylene glycol), proton medium effects, ferrocene redox couple reference obs. 77−77786
methyl cyanide-water (methanol), Ag^+ ion solvation, γ-irrad., ESR obs. 80−97726
micelles, surfactant, H_2O penetration, hydration 80−45572
molecular dynamics study of solvation of large dipoles 79−77470
molecules, in polar media, continuous charge distrib. model, quantum mech. calcs. 78−68913
monatomic ions, stoichiometric water mixtures, struct. changes due to hydration thermodynamic props. 78−7225
non-aqueous ionizing liquids, review *(French)* 79−69255
nuclei acid phosphate group, analytical atom-pair pot., SCF-LCAO calc. 79−70516
nucleic acid purine, pyrimidine bases, base pairs, hydration scheme 79−92127
nucleic acids, bases and base pairs, water struct. in soln., Monte Carlo simultion 80−76709
oil-water interface, fatty alcohol adsorbed layer phase transition, high-press. effect 79−99395
organic liquids, electrohydrodynamic ionisation, solvated ion mass spectroscopy, anal. appl. 78−73102
Ornstein-Zernike and Percus-Yevick temperature dependent fluids, solvation forces 80−64862
phosphatidylcholine hydration, adsorpt.-desorpt. isotherm and PMR 78−15781
solvation continued
polar liquid solns., H bonding, dielec. theory, apparent dipole moment, chem. model 77−48671
poly-N-vinylcarbazole, soln., picosecond time-resolved fluoresc. by pulse radiolysis 80−28122
polymer solutions, order, conf., Midland, USA, (Aug 1973) 79−10769
polymer solutions, solvation, preferential, effect on polymer dimensions 79−10771
polynucleotide hydration characts. in H_2O/D_2O frozen solns., γ irrad. effects, PMR 78−31772
polynucleotides, gamma-ray effects on hydration, PMR of frozen and liq. solns. 78−27900
polystyrene-benzene-methanol system, preferential solvation 79−10772
polystyrene-tetrahydrofuran-water system, thermodynamic and hydrodynamic props. 79−96353
Portland cement, absorbed H_2O, pulsed NMR study 80−84665
positronium formation, inhibition processes, role of solvation properties of solvents 80−93786
positronium formation in polar liquids, unsolvated electron effects 78−17826
potassium chloranil, IR spectra, mag. and optical props., phase transition and solvation 77−43983
preferential solvation, effects on reaction kinetics 78−73017
propylene glycol-water (methanol), proton medium effects, ferrocene redox couple reference obs. 77−77786
pyrene-3-sodium sulphonate solubilised in didodecyldimethylammonium bromide-benzene inverted micelles 80−3417
pyridine, macroscopic model for solvated ion dynamics, cation conductance calcs. 80−65261
radical ion pair formation, ESR spectroscopic obs. 78−73038
rare earth chlorides, glass transition temp. meas., inner-sphere coordination number change effect on soln. props. 80−83239
rare earth perchlorates, glass transition temp. meas., inner-sphere coordination number change effect on soln. props. 80−83239
reaction field theory modification for solvent polarities 79−91913
serine, neutral and zwitterion, water solvation, Monte Carlo simulation 80−76707
skin components, rheological props. under compressive load 80−35945
solute-solute-solvent interactions, introduction to symposium in Vienna, Austria (1978) 80−26098
solutions, dilute, Monte Carlo free energy calcs. in isothermal-isobaric ensemble 78−92498
solutions in alcohols, ultrasonic vel. and density meas. used to calc. compressibility, intermol. free length and salvation no. 80−96150
solvation, classical mean space charge model 78−76841
surfactant micelles, hydration 80−89518
tetrabutylammonium iodide, in aq. proline soln., elec. conductance investigation 80−10692
tetracene anion radicals, enthalpy of disproportionation, calorimetric determ. technique 79−96296
tetracyanoethylene in acetone-d_6, anion solvation, electron spin echo modulation 80−63676
tetracyanoethylene in dimethylsulphoxide-d_6, anion solvation, electron spin echo modulation 80−63676
tetracyanoethylene in methanol-$d_3(d_1)$, anion solvation, electron spin echo modulation 80−63676
tetramethylammonium chloride in HCl, Cl^- solvation no., Raman spectra 79−96410
tetramethylammonium iodide, in aq. proline soln., elec. conductance investigation 80−10692
thermodynamic data, characteristic vector analysis 77−21409
thiourea, struct., hydration, ab initio SCF calcs. 80−58142
transferrin, human anal. density gradient equilib. centrifugation for determ. of mol. wt., sp. vol., preferential hydration 77−64160
triethylamylose-solvent complexes, conform. and packing analysis 78−75654
trifluoromethoxide gas phase ion reactions with carboxylic acids, ion cyclotron reson. obs. of competitive solvation 79−79227
trimethylammonium chloride in HCl, Cl^- solvation no., Raman spectra 79−96410
univalent gaseous ions, free energy of solvation, 1-layer continuum model 78−95944
vinyl polymers quenched with electron donor (acceptor) in soln., ionic photodissoc. 79−11800
vitrified conc. aq. solns., ionic hydration and secondary dielec. relax. 79−24882
water, free surface struct., single ion hydration energies 78−26752
^{205}Tl, chem. shift and nuclear relaxation *(Rumanian)* 79−82888
Ag, and Ag^+, solvation in deuterated-ice matrices, electron spin echo obs. 80−15780
Ag atom solvation in methanol, geometrical model, electron spin-echo modulation obs. 80−63682
Ag in ice matrix, ESR and irrad. at 4.2 and 77K 79−8444
Ag, in ice matrix 79−5166
Ag solvation in ice matrix, electron spin echo modulation 78−39396
$AgNO_3$-KF in ice matrix, γ-irrad., Ag at., form., solution, ESR 77−59454
AlBr solution, in propylene carbonate, dissociation, radius and number of ion solvation *(French)* 79−70319
$Al(NO_3)_3$, aq. soln., X-ray diffr. obs. 77−72541
$Br(H_2O)_n$, geometric and electronic struct., CNDO/2 calcs. 77−79542
$Br^-(H_2O)_n$, hydration energies, orientation, ab initio-LCAO SCF MO calcs. 80−27944
CN^- ion, gaseous, heat of form., solvation, proton affinity calc. 77−1092
$CN^-.H_2O$, redox processes, MINDO/3 calcs. 79−47895
CO-He-O_2-H_2O laser discharge, stability, influence of recombination and ion chem. 78−17915
$Ca_3Al_2O_6$, retardation of hydration by sulphates 77−56249
$CaCl_2$, aqueous soln., ion hydration 80−35518
β-Ca_2SiO_4-CaO-SiO_2 paste, hydration, compression strength and composition 80−50584
Ca_2SiO_5, hydraulic reaction observed by microwave dielectric meas. 78−80745
Ca_3SiO_5-$Cr_2O_3(Al_2O_3)(Fe_2O_3)$ solid solns., elec. cond., 800-1000°C, hydration 80−54683
$CoCl_4^-$ formation kinetics, in nonaqueous systems, rate constants and temp. change determ. *(German)* 79−70300
$Co(NH_3)_5Br^{2+}$, aquation, polyelectrolyte catalysis, high pressure effect 80−55656

solvation continued
$Co(NH_3)_5Br^{2+} + OH^-$, polyelectrolyte catalysis, high pressure effect 80−55657
$CoSO_4$, aq. soln., viscosity meas., viscous flow activation energy, entropy *(Japanese)* 77−43363
Cr^{3+} hydration model, external water interactions 78−78772
$Cr(NO_3)_3$, aq. soln., X-ray diffr. obs. 77−72541
CsCl, activation coefficients and solvation numbers in mixed methanol solvents 80−81334
$CuSO_4$, aq. soln., viscosity meas., viscous flow activation energy, entropy *(Japanese)* 77−43363
$EuCl_3$, coord. in aq. Cl^- soln., X-ray diffr. obs. 80−92445
F^- hydration, ab initio MO calcs., fractional charge model 77−34547
$F^-(H_2O)_n$, complex struct., coord. numbers 79−7049
Fe complex, tris-(4-morpholinecarbodithioate-S,S')Fe(III), and dichloromethane solvate, Mossbauer and EPR spectra, spin 3/2 state 78−9169
$FeCl_3$, nonaq. solns., solvent-solute interactions, Mossbauer investig. of equilib. consts. 79−1729
$Fe(ClO_4)_3$, soln., struct., X-ray scatt. obs. 78−34421
$Fe(ClO_4)_3$-DMSO, solvation spheres, exchange kinetics, PMR *(French)* 77−58045
Ge dissolution by oxidation and solvation, hole injection effect 80−26051
H-bond, symmetric $AHA^{(\pm)}$, A-H stretching vibr., liq. IR band shape, strong coupling phonon model 78−64358
HCl(-acetone)(-acetonitrile), soln., IR absorption, H-bonding, solvent effect 78−29778
$H_2O.H_2O$ and $H_2O.Ne$, excited, first order interaction energy, ab initio calc. 80−32598
$Hg(CN)_2$, solvation by NH_3 and ND_3, Raman spectroscopic study 78−90172
$Hg(CNS)_2$, solvation by NH_3 and ND_3, Raman spectroscopic study 78−90172
I^-, aq., in supercooled water, and glass forming solns., charge transfer to solvent spectra 77−50447
$I(H_2O)_n^-$, geometric and electronic struct., CNDO/2 calcs. 77−79542
K^+ salts, diamag. ion solvation in methanol soln., NMR relax. obs. 78−56389
KBr, activation coefficients and solvation numbers in mixed methanol solvents 80−81334
$KBrO_3$, KIO_3 and K_2SO_4, in dioxane-water mixtures, ion-solvent interaction and conductance 79−34315
KCl, activation coefficients and solvation numbers in mixed methanol solvents 80−81334
$K_2Mg_4Mo_4O_{16}.(OH)_2(H_2O)_2$, dehydration processes rel. to stoichiometry *(French)* 79−24734
KNO_3, activation coefficients and solvation numbers in mixed methanol solvents 80−81334
$LaCl_3$, aq. soln., H_2O coordination of metal ion, X-ray diffr. 79−69000
Li^+, hydrated, polarisation model, review 80−54115
Li^+ hydration, ab initio MO calcs., fractional charge model 77−34547
Li^+ salts, diamag. ion solvation in methanol soln., NMR relax. obs. 78−56389
Li-H, liq. and solid, mol. orbital approach, solvation energies 77−4201
$LiBF_4$, $LiHBF_3$, spin-spin coupling and T_1 in non-aq. solns. 77−23512
$Li(CO)_n$ (n=1,2,3,4,5,6,8), semiempirical CNDO calcs., solvation struct. 78−82649
^7LiCl, heavy water soln., anionic hydration, 1 bar and 1 kbar, neutron diffr. obs. 80−30212
$MgCl_2CaCl_2$, aq. soln., hydration, X-ray diffr. 77−43126
Mn^{2+} ions, solvation enthapies in various solvents *(French)* 79−69264
$MnSO_4$, aq. solns., viscosity meas., viscous flow activation energy, entropy *(Japanese)* 77−43363
NH_3, gas phase proton solvation energetics, mol. beam-photoionis. obs. 79−29345
NH_3, liq., irradiated, solvated electron yield, partially diffusion-controlled ion recomb. 79−100409
NH_4^+, solvation in water, discrete, continuum and discrete-continuum models 78−73130
NH_4Cl, activation coefficients and solvation numbers in mixed methanol solvents 80−81334
NH_4NO_3 conc. aqueous soln., X-ray scatt., NO_3^--H_2O interactions 78−42881
$NO_3^-.(HNO_3)_n$ clusters, form. studied by mass spectrometer, thermodynamic functions, sol. struct., 80−95754
Na^+ ion solvation number determ. for sodium tetraethylaluminate-benzene (cyclohexane)-donor two-phase system 78−95987
Na^+ salts, diamag. ion solvation in methanol soln., NMR relax. obs. 78−56389
Na-H, liq. and solid, mol. orbitals approach, solvation energies 77−4201
Na-ice condensate, EPR lineshape second moment, electron solvation struct. 78−3440
$NaBF_4$, spin-spin coupling and T_1 in non-aq. solns. 77−23512
$NaBrO_3$, $NaIO_3$ and Na_2SO_4, in dioxane-water mixtures, ion-solvent interaction and conductance 79−34315
NaCl, activation coefficients and solvation numbers in mixed methanol solvents 80−81334
NaCl, aq. soln., isothermal compressibility, hydration parameters, up to 350°C and 10^3 kg cm^{-2} 78−10112
Na_2O-CaO-SiO_2, soda-lime glass, hydration 79−87877
^{23}Na, relax. in polyelectrolyte solns. 79−20353
$NdCl_3$, aq. soln., H_2O coordination of metal ion, X-ray diffr. 79−69000
$Ng(NO_3)_2$, solvation by NH_3 and ND_3, Raman spectroscopic study 78−90172
Ni^{2+} ions, solvation enthalpies in various solvents *(French)* 79−69264
$NiCl_2$, heavy water soln., anionic hydration, 1 bar and 1 kbar, neutron diffr. obs. 80−30212
O_2^-, in nonpolar liqs., laser photodetachment, elec. cond. obs. 79−64057
$OH^- + CO_2 \rightarrow HCO_3^-$ react., MO-LCAO-SCF calcs., energy barrier 78−76846
$PrCl_3$, aq. soln., H_2O coordination of metal ion, X-ray diffr. 79−69000
R^{3+} ions, coord. in aq. Cl^- soln., X-ray diffr. obs. 80−92445
Rh complexes, Rh(III) halopentaammines, solns., luminesc. and excited state lifetimes, photoaquation 79−8175
Ru complexes, $Ru(NH_3)_6^{2+}$ and $Ru(en)_3^{2+}$ in soln., UV spectra, solvent effects 79−94010
$Sc_2(SO_4)_3 + Al_2(SO_4)_3$ aq. solns., complex form. reacts., kinetics, US relax. investig. 79−1942
$SmCl_3$, coord. in aq. Cl soln., X-ray diffr. obs. 80−92445
$TlNO_3$, ion pair, in Ar matrix, solvation effects, IR spectra 77−46563
V_2O_5, amorphous, hydration and fibrous texture, EPR study *(French)* 79−24826
solvation continued
XeO, excited state spectra, subpicosec. predissoc., solvation, in solid rare gas hosts 77−68050
Zn^{2+}-H_2O clusters, solvation, Monte Carlo simulation 80−44102
$ZnSO_4$, aq. solns., viscosity meas., viscous flow activation energy, entropy *(Japanese)* 77−43363
$Zn^{2+}.CO_2$-H_2O clusters, solvation, Monte Carlo simulation 80−44102

solvent effects
ABA poly(styrene-b-butadiene) copolymer, physical props., casting solvent effects 77−55935
acenaphthene in n-alkane matrices, Shpolskii spectra fluorescence 78−9190
acetaldehyde, soln., C-O stretching band intensity calcs., intermol. interaction effects 77−68081
acetone, solvent effects on oscillator integrated strength, IR absorpt. bands 78−84575
acetonitrile, ν_2, ν_3 and $2\nu_3$ bands, vibr. relax., Raman spectra of liq. and dil. soln. 78−9154
acetonitrile, electrolyte solns., IR and Raman spectra interpretation, CN-stretching region 79−73941
acetonitrile, liq. and solns., IR absorpt. band intensity, temp. depend., CC and CN bonds 77−75157
acetonitrile, soln., vibr. relax., isotropic Raman spectrosc. obs. 79−50025
acetylenic compounds, 1- and 4-octyne, hydrogen bonding effects on Raman line $\nu(\equiv C\text{-}H)$, solvents effects *(French)* 77−71805
acridine, solvent depend. of radiationless relax., singlet lifetime, picosecond spectroscopy 78−66582
acridine orange, solvent effect on fluoresc. polaris. 79−41191
acriflavine, fluoresc. polaris., solvent effect 77−50468
alcohol homologous series, $^1HT_1$-relax. time, paramagnetic, diamagnetic shift reagent effects *(German)* 78−43673
alcohol/water mixtures, NMR and IR obs., low temp., shifts, interpretation 77−52065
alkali halide:CrO_4^{2-})(MoO_4^{2-})(MnO_4^-)(ReO_4^-), frozen solns., absorption spectra, 4.2-300K 79−87467
alkali iodides in acetone, press. effects on Walden products, ion-solvent interactions 80−3398
alkali metal solutions cation-electron interactions 78−73037
alkanes, solvent effects, quantum mech., macroscopic electrostatic contribs. 77−30801
alkylbenzenes, intramol. hydrophobic interactions, direct meas. 79−45648
amide group in soln., interactions, IR, Raman spectral investigs., peptide, protein struct., review 78−90330
2-amino, 7-nitrofluorene, in 2-propanol, Stokes fluorescence shift time resolution 77−58060
4-amino-4'-nitrostilbene, fluoresc. emission anisotropy, solvent effects 79−3489
4-amino-4'-nitrostilbene, thermal motion of prolate luminescent molecules in solvents with different viscosities 79−83029
7-amino-4-methylcoumarin, fluoresc., solvent depend., shift of max. wavenumber 79−85997
4-amino-N-methylphthalimide-decalin-n-propanol, translational relax. kinetics, luminesc. obs. 79−8180
4-aminomethylphthalimide-decalin-n-propanol, electronic spectra of 3-component solns., temp. depend. 79−4822
4-aminophthalimide, soln. in n-propanol, fluoresc., orient. relax. of solvent 79−24357
aminoquinoline derivatives, solvent effect on absorpt. and fluoresc. spectra 79−59494
anilines, substituted, in nonpolar solvent, dielec. relax. obs. 80−55022
8-anilino-1-naphthalenesulfonic acid, fluoresc. probe mol. in mixed solvent 79−45746
1,8-anilinonaphthalene sulphonate, aq. and ethanolic solns., excited singlet state decay pathway 78−17703
anion-water H-bonds, nature, from IR and Raman OH(OD) splittings 78−62811
anthracene, aromatic solvents, two-photon absorption cross section meas. by energy migration 77−58204
anthracene, fluorescence spectra in aq. and surfactant solns. 77−83639
anthracene, in stretched polyethylene film, UV-visible and fluoresc. spectral shifts 78−62852
anthracene, melt and dil. soln., UV spectra, line broadening and shift vibr. struct. 78−17684
anthracene, pure and d_n, PMMA soln., triplet lifetimes, 77-300K 78−25594
anthracene derivatives in solution, polarisability and dipole moments, emission and absorpt. spectra obs. 80−69256
anthracenes, anthronyl substituted, solvent-assisted form. of luminesc. intramol. exciplexes 78−25589
4-(9-anthryl)-N,N-dimethylaniline, fluoresc., dipole moments and polarisabilities 80−1019
p-(9-anthryl)-N,N-dimethylaniline derivatives, excited emitting states in polar solvents, fluoresc. 78−5263
aromatic hydrocarbons, ethanol-KI solns., fluoresc. affected by I^- 79−13749
aromatic hydrocarbons, excimer decay dynamics, rate const. rel. to solvent 78−58729
aromatic hydrocarbons, rot. anisotropy and solvent-fluorophase bonds, differential polarised phase fluorimetric investig. 77−61779
aromatic molecule, in aromatic (aliphatic) solvent, 77K, triplet-triplet absorption spectra, anomalous broadening 77−88502
aromatic solutions, triplet-triplet absorption, anomalous broadening 79−54842
2-aryl-3-benzylidenamino-4-thiazolidones, IR and NMR spectra, solvent effects and isomer conform. *(Italian)* 79−3596
azoalkanes, fluoresc., solvent isotope effect 78−25591
azoethane, in hydrocarbon glass, 77K, photoisomerisation, matrix memory effect, quantum yield 78−7213
BBOT, time-depend. fluoresc. depolarisation, mol.-rot., slip boundary conditions in soln. 78−9179
1,2-benzanthracene, monomer and excimer fluoresc. in soln., triplet-triplet annihilation and mag. field depend. 78−78738
benzene, $\pi\pi^*$ and Rydberg bands, cryogenic solvent effects 78−55182
benzene, fluoresc. quantum yield in soln., dipole-dipole interaction 78−25598
benzene, unlabelled and ^{13}C labelled PMR, oriented in liq. crysts., r_α struct., solvent effects 79−94017
benzene in 3-methylpentane glass, phosphoresc. polarisation and intensity, 77K 77−46588

solvent effects continued
benzene in dilute cyclohexane solution, fluoresc. quenching on pulsed proton irrad., temp. depend. 80−21307
benzimidazole, excited states, solvent interactions, fluoresc. obs., rel. to chromophore 78−37670
benzoic acid, in acidic solns., room temp. fluoresc. 78−50568
Benzophenones, substituted solvent independence of radiative rate constant 77−30904
1,4-benzosemiquinone, monoprotonated radical, spin distrib., INDO calcs. 77−14357
3,4-benzpyrene, monomer and excimer fluoresc. in soln., triplet-triplet annihilation and mag. field depend. 78−78738
benzylidene t-butylamine N-oxide, amphiphilic liq. cryst. solvent effect on hydrolysis 79−100355
bilayer membranes, permeation of water mols. meas. using fluoresc. quantum yield solvent-isotope effect 79−34710
bilirubin, anomalous solvent shift effect and phosphoresc. 77−30899
bimolecular mixed-valence metal complex, intramol. intervalence charge transfer 79−76405
binary liquid mixtures, dispersion interactions, struct. effects 79−46535
biological macromolecules, computer simulation of solvent struct. 78−40113
biological molecules, improved method for calc. the contrib. of solvent to X-ray diffr. pattern 79−16355
biomolecule conformational anal., solvent effects 80−3583
biphenyl, carbonyl derivatives, absorpt. and luminesc. spectra, solvent effects and triplet lifetimes 77−24889
biradical, photogenerated in Norrish type II reaction, solvent effects on lifetime 79−11804
butene-1, solubility in liq. N_2 80−39286
4-n-butoxybenzylidine-4′-n-octylaniline, liquid cryst., smectic B phase lattice vibr. anisotropy, Mossbauer anal. 77−7666
n-butyl acetate, alkaline hydrolysis in water-alcohol mixture, solvent polarity effects 77−48639
d-camphor, optical rot. dispersion spectra, solvent effects 77−10684
β-carotene, excitation profile of ν_2 line in resonance Raman spectrum, solvent effects 80−74173
β-carotene, in CS_2, reson. Raman spectra, room temp. 78−35803
l-carvone, optical rot. dispersion spectra, solvent effects 77−10684
cellodextrin alditols, alkali solns., hydrodynamic props., frictional envelope form. 77−28031
cellulose acetate, solvent effect on lyotropic mesomorphicity 80−70121
chain molecule, influence of solvent struct. on conformations 80−91700
charge transfer transitions, solvent effect, appl. to Ru complexes 77−75127
charge-transfer, excited, ps. kinetics, geometrical and solvent polarity effects 77−30986
chemical outer sphere electron transfer reactions, generalised Landau-Zener model 79−34278
chemical reaction kinetics of dense fluid, correlated binary collisions 78−44347
chemical reactions, Hammett correlation, explanation of solvent effects by frontier orbital method *(French)* 78−11604
chemical reactions, semiempirical model 80−25986
chemical reacts. in condensed phase at low temps., at.-mol. transforms. 77−25253
3-chlorodiphenyl, in dipolar aprotic solvent, internal rot. barrier, ^{13}C T_1, obs. 78−29860
chloroform, and d, polar soln., Raman line shape of ν, band 78−74705
chloroform, in isotropic MBBA, nucl. spin-lattice relax., reorientation 79−4735
chloroform, solns., vibr. dephasing and reorientational relax., solvent depend., Raman spectra 79−85968
chlorophyll, a and b, lowest singlet-singlet transition, solvent effects 79−24952
chlorophyll, and related mols., in solid solns., fine-structured vibronic spectra under tunable dye laser excitation *(Russian)* 80−74164
chlorophyll a-water interaction, NMR obs. in CCl_4 and trichloromethane 79−34501
chlorophyll photochemical activity, rel. to microviscosity of detergent micelles 77−21478
chlorophyll solutions, photolum. of singlet O_2 78−80831
chlorophyll-a, solns., vis. absorpt. spectra of monomer, dimer and oligomers 77−29101
chloroquinolines, photophys. behaviour, substituent and solvent effects 80−106342
cholesteric esters, effect of nature of organic solvent on gamma radiolysis 80−7835
cholesteric products, gamma irradiation, effect of presence of organic solvents 79−24777
cholinesterase-acetylcholine soln., anion-cation site interactions, solvent effects on aggregate stability 80−61070
chromone, solns., pH dependent fluorescence spectra, pK_a and tautomerism 79−59506
chromophore, excited state, solvent interactions, fluoresc. obs. 78−37670
Coordination equilibria in non-aqueous solvents. I 80−66860
coumarin laser dyes, fluoresc. quantum yields and lifetimes, polar solvent effects 80−87054
coumarin laser dyes, in methanol, ethanol, and water, fluoresc. lifetimes meas. 79−27252
coumarin laser dyes, solvent effects on photophysical parameters 80−91598
p-cyano-N,N-dimethylaniline in polar solvents, double fluorescence, theoretical model 80−58296
4-cyanobiphenyl and 4′-alkyl- or 4′-alkoxy-substituted liq. cryst. derivatives, soln., absorpt. and fluoresc. spectra 80−87164
cyanomethane-d_0,-d_3, soln., for IR spectra, band shape and moment anal. 80−58252
cyclohexane-d_{12}, Raman linewidth and molecular diameter meas. 80−69153
Debye screening length, solvent effect in diffuse double layer problem 78−53211
decane: pyrene (coronene), quasiline spectra, multiplet struct., freezing conditions and solvent effects 79−1786
deuterochloroform, solns., vibr. dephasing and reorientational relax., solvent depend., Raman spectra 79−85968
2,5-di(4-biphenylyl)oxazole, fluoresc. emission anisotropy, solvent effects 79−3489
di-tert-butyl nitroxide, N hyperfine coupling const., solvent effect, model 79−54870
solvent effects continued
di-tert-butyl radical, ^1H NMR in organic solvents, press. depend. 79−31546
dialkylanilines, p-substituted, twisted internal charge transfer excited state form. 79−22683
diatomic liquid, vibr. dephasing calc., diatom anharmonicity 78−94959
diatomic molecule in strongly interacting solvent, IR band shape, field theoretic methods appl. 79−27038
diatomic Morse mol., inhomogeneous broadening in liqs., temp. depend 77−61803
1,2-dibromoethane in various solvents, dipole moments, concs. of anti and gauche forms 79−27106
dicarbaclosododecaboranes, icosahedral, electron transfer phenomena in isolated borane units 80−18871
dicarbonitrile-anthracene solutions, absorpt. and emission spectra 80−43083
2,3-dichloro-1,4-napthoquinone in EBBA, PMR obs., mol. struct., orientation and solute-solvent interactions 77−27806
dichloromethane, vibr. population lifetimes in liqs. anti-Stokes Raman scatt. 78−74665
dichloromethane-d_0,-d_2, soln., far IR spectra, band shapes and moment anal. 80−58252
dicyanoacetylene, solns., NMR and mol. reorientation 79−73840
9,10-dicyanoanthracene, exciplexes, electronic struct. by electro-optical expts. 78−25581
dielectric attenuation of substituent effects, field transmission in partially occluded cavities 78−2789
dielectric model for electronic spectra solvent effects 77−26991
2,5-dihydroxy-p-benzoquinone, proton tautomerism dynamics, ^{13}C NMR obs., CNDO calc. 79−52632
dilutor method extension to meas. of high activity coeffs. at infinite dilution 79−19372
dimethyl mercury, coupling consts., solvent depend., ^1H, ^{13}C and ^{199}NMR 78−76334
4-dimethyl-amino-4′-nitrostilbene, in EBBA, nematic ordering influence on fluoresc., temp. depend. *(German)* 79−81235
4-dimethylamino-4′-nitrostilbene, thermal motion of prolate luminescent molecules in solvents with different viscosities 79−83029
4-dimethylamino-4′-nitrostilbene in solvent fluorescence lifetime meas. by picosecond optical amplification 79−81227
7-N-dimethylamino-4-methylcoumarin, fluoresc., solvent depend., shift of max. wavenumber 79−85997
p-dimethylaminobenzonitrile, picosecond relax., fluoresc. spectroscopy, solvent effects 78−58737
dinaphthylamine, fluoresc. in soln., intramol. excimer and exciplex form. 78−62836
2-(2′,4′-dinitrobenzyl)-pyridine, photochromism, ns laser absorption spectra 78−48138
2,2′-dinitrodiphenylmethane, nanosecond laser flash photolysis and absorpt. spectra, photochromism, solvent polarity 78−61029
1,6-diphenly-1,3,5-hextriene, mol. derivatives, absorpt. and fluoresc. spectral props. 79−72344
9,10-diphenylanthracene, luminesc. quantum yield, fluoresc. spectra polarisation effect, solvent viscosity depend. 78−27303
diphenylene sulphide, phosphoresc. vibronic struct., solvent heavy at. effect 78−17710
1,6-diphenylhexatriene, radiationless transitions and natural lifetimes, solvent effects 80−63622
2,5-diphenyloxazole, phosphoresc., 77K, solvent effect 78−42118
diphenylpolyenes, two-photon absorptivities via three wave mixing 79−68416
diphenyltriafulvenes, absorpt. and fluoresc. spectra, dipole moments, solvent effects 77−75169
dipolar solvent, ionic mean force, pot. anal. 77−56234
diquinolyl cyanomethane, fluoresc. quantum yields, viscosity effects 80−60646
divalent transition metal halides, Coordination equilibria in non-aqueous solvents. I 80−66860
DNA, gamma-ray effects on hydration, PMR of frozen and liq. solns. 78−27900
dye molecules, dissolved, influence of environment on luminesc., intense laser excitation 78−84622
dye molecules, long wavelength conc. shift in luminesc. 79−64032
dye solutions, mixed, fluoresc. conc. quenching, sensibilisation 79−24347
dyes in organic solvents of high viscosity, diffusion coeffs. 78−10203
dyes in rigid matrices, solvent reorientation relax. effect on luminesc. 79−43009
electrolytes, aq. solns., ion-solvent interactions, transport props. *(German)* 78−79790
electron exchange reactions, stochastic solvent model 79−68312
electron transfer reactions, damping mechanisms effects calcs. 77−21381
electronic bands statistical broadening depend. on intermol. interaction 77−71837
electrostatic interactions in liquid state, effect on frontier orbitals and chem. reactivity 80−84046
eosin, fluoresc. polarisation, solvent effects 79−36678
eosin, in glycerine-water mixture, excitation and emission peaks, concentration shifts 78−33540
erythrosin, aq. soln., polarisation of fluoresc. spectra, aggregation of mols. 78−31227
esterification kinetic study by monitoring pitch changes in cholesteric liq. cryst. solvent 80−7786
ethanol, vibr. population lifetimes in liqs. anti-Stokes Raman scatt. 78−74665
ethyl-furan-2-carboxylate, skeletal vibr. of IR spectra, conformational props., solvent polarity effect 80−87118
ethylene, solubility in liq. N_2 80−39286
ethylene carbonate, Fermi reson., isotopic substitution meas. 78−86870
ethyleneglycol dye laser, conversion efficiency and tuning, solvent effect 79−55131
exciplexes, electronic struct. by electro-optical expts. 78−25581
excited molecular systems, relax. processes, nanosecond time-resolved spectra 77−26992
flavins, phosphoresc. props. 77−12885
fluoradene, absorpt. and fluoresc. in solvents, excimer form., aggregation 77−79625
fluorenone, intersystem crossing rates, ps time-resolved spectra 77−6821
fluorenone fluoresc. in plastic, high press. effects., quantum yield 78−25601
fluorescence solvatochromism kinetics 77−30898

solvent effects continued
fluoroethanes, mol. liqs., dielectric solvent effects, quantum chem. calcs. 77—14375
fluoromethane, in liq. O_2(Ar), vibr. energy relax. obs. 78—5208
formaldehyde, in Ar, medium perturbations of extravalence excitations, VUV absorpt. 78—1002
formamide, hydration by H_2O mol., point charge model 77—34569
free radical reactions, liquid phase, cage model, solvent effects 77—16811
fumaronitrile exciplexes, photoisomeris. and photoionis, dissolved O_2 effect 78—27789
gels, dynamic light scattering in poor solvent 78—88318
glassy polymer, solvent osmotic stresses, prediction of Case II transport kinetics 80—26049
glycine, neutral and zwitterion interaction with water, Monte Carlo simulation 79—53026
halobenzenes, in potassium laurate mesophase, NMR, proton distance ratios and order tensor elements calcs. 80—63672
hexafluorobenzene+bisdiphenylenephenylallyl radical, solvent effects on collisions, dynamic nucl. polaris., spin-lattice relax. 77—63303
hexamethylene tetramine in water-acetone soln., crystal growth kinetics 78—30554
hexamethylenetetramine in oriented mesophases, mol. distortion, PMR 77—6802
hexane:pyrene (coronene), quasiline spectra, multiplet struct., freezing conditions and solvent effects 79—1786
hydrides, aq. dissoc., solvation, MINDO/S calcs. solvation theory 80—97708
hydrophobic effect, dil. soln. struct. and thermodynamic props., semi-empirical model 78—20060
hydrophobic interaction, solubility and solvent struct. changes 78—83705
7-hydroxy-2-methylchromone, solns., pH dependent fluorescence spectra, pK_a and tautomerism 79—59506
p-hydroxyazobenzene, acidic soln., reson. Raman spectra, ring deuterated derivatives 79—26987
in cyclohexane-ethanol mixtures, UV spectra, solvent effect 79—22770
incorporation of solvent effect, Germer's model 79—93935
indigo dye, excited state lifetime, influence of inter- and intramol. H bonding 77—79659
indocyanine green fluoresc. spectrum in blood and other solvents, rel. to angiography 78—28057
indole, and derivatives, temp. fluoresc. quenching, rel. to H_2O solvent struct. 78—5265
indole, fluoresc. polaris., solvent effects 78—33542
indoles, excited states, solvent interactions, fluoresc. obs., rel. to chromophore 78—37670
indoles, fluoresc. anomalies, mixed valence-Rydberg states 78—17707
intramolecular hydrophobic interactions, direct meas. 79—45648
iodide, charge transfer to solvent spectra, spectral shift data, Madelung const. determ. 80—85204
iodoform, soln., MCD spectra, assignments 79—31567
iodomethane, liq. (liq. mixtures), vibr. relax. and reorientation, symmetric C-H bending mode 1st overtone 78—62884
iodomethane, vibr. population lifetimes in liqs. anti-Stokes Raman scatt. 78—74665
iodomethane-d_1, ^{13}C enriched, NMR, oriented, symmetry related isotope effects 77—61772
iodomethane-d_1, in nematic soln., D NQR coupling const., isotope effect 79—27009
ion-selective liquid chloride electrodes *(Russian)* 79—91972
IR band moments, effect of dipole induction 77—75143
isoquinoline, solns., dielec. polarisation, π-electron system effects 77—90096
ketocyanines alcohol solns., spectral-luminesc. props. 80—2835
ketones, rigid, optical rot. dispersion spectra, solvent effects 77—10684
ketyl radical+benzophenone, triplet-doublet energy transfer, viscosity and mag. field effects 77—71850
Kramers chain, mol. dynamics calc., incorrectness of random walk description confirmed 77—561
lanthanide(III) complexes, f-f transition intensities, general theory of solvent effect 80—18811
large molecules, picosecond relax., fluoresc. spectroscopy, solvent effects 78—58737
lipid planar bilayers, Ca^{2+} interaction with negative lipids, solvent effect 77—77871
liquid alloy, dil., partial interference functions of solutes 79—19139
liquid crystal nematic to isotropic transition, effect of quasispherical and chainlike solutes 80—65202
liquid mixtures, associating, mol. hyperpolarisability, SHG 77—552
Longuet-Higgins-Pople theory extension using isotropic polarisability 79—31617
luminescent system, orientation factor in conc. effects due to nonradiative energy transfer 80—25425
lysozyme spin-labelled preps., water-protein layer microstruct. study by mag. relax. 78—76980
macromolecular interactions, effects of intervening medium and polar mode energy feeding 79—13857
magnesium alginate, light scatt., wt.-average mol. wt., charge density 77—61882
magnesium porphin, ESR study of metastable triplet state, in n-octane matrix, 1.3K 79—72340
malachite green leucocyanide, photoionization in polar solvents, mechanism 77—25295
MBBA, nematic-isotropic transition, intermolecular forces, IR N_2O mol. probe obs. 80—29155
mercurochrom, fluoresc. polarisation, solvent effects 77—14470
merocyanine dye, solvent-depend. hyperpolarisability, polar (nonpolar) solvents 78—70962
methane, ^{13}C and proton medium shifts in gas phase and in soln. 77—88467
methane, liq. and solns., Raman spectra, vibr. anal. 79—27001
methanol, H-bonded struct., IR spectra, assignments 78—62800
methanol, IR spectra in soln., OH group fundamental and first overtone bands *(French)* 77—27071
methanol-water, assoc. mixture, rot. barrier solvent effect, CNDO/2 calc. 78—29861
methanol-water (propylene glycol), proton medium effects, ferrocene redox couple reference obs. 77—77786
methine dyes, spectral props., solvent effects 80—69181
methyl furan-2-carboxylate, skeletal vibr. of IR spectra, conformational props., solvent polarity effect 80—87118
solvent effects continued
methyl furan-2-thiolcarboxylate, skeletal vibr. of IR spectra, conformational props., solvent polarity effect 80—87118
methyl iodide, in Ar and Kr, medium perturbations of extravalence excitations, VUV absorpt. 78—1002
methyl iodide, solns. with liq. Ar, Kr, Xe, CH_4 and CF_4, Rydberg band positions, temp. depends. 78—17686
methyl isothiocyanate, in benzene (tetrachloromethane), nonlinear dielectric solvent effect 79—28702
methyl propionate—$H_2O(Ba^{2+})$ mixtures, in DMSO, acetonitrile solns. IR, assoc., solvent, catalytic effects *(French)* 79—87827
methyl protons, NMR relax. in presence of chem. exchange 78—13515
methylbixin, low-lying forbidden π-electronic state, spectral evidence 77—58029
2-methylchromone, solns., pH dependent fluorescence spectra, pK_a and tautomerism 79—59506
methylene iodide, soln., MCD spectra, assignments 79—31567
2-methylPOPOP, soln., anisotropic fluoresc. of prolate mol. *(German)* 80—1018
molecular electron-donor-acceptor complexes, solvent effect on charge transfer absorpt., thermodynamic props. 77—83615
molecular electronic spectra, effect of polarisation structure of solvent 80—43062
molecular IR spectra, vibr. freq. shift, press. and solvent effects 78—74709
molecular liquid, dielectric solvent effects, quantum chem. calcs. 77—14375
molecular liquid, hot bands, vibr. correlations, dephasing 79—85966
molecular radiative rate consts., solvent depend. 78—66587
molecular solution, excess electron optical absorption spectrum model, band shape 78—33500
molecular spectral solvent shifts, electrostatic model, semi-empirical PPP calcs. 77—83507
molecular struct., self consistent reaction field theroy, proton potentials 78—58608
molecular vibr. freq. shifts in polyatomic solutes 78—58654
molecular vibronic interaction on electronic spectrum 79—54839
molecules in strong solvents, spectral band shape, rot. diffusion model 79—64048
molybdate solution, ^{95}Mo and ^{97}Mo Fourier transform NMR, chem. shifts and Larmor freqs. *(German)* 77—59473
3-monomethylamino-N-methylphthalimide solns., fluoresc. and excitation spectra 79—61425
multicomponent solutions, solvatofluorochromism kinetics, orientation-concentrational relax. 77—65506
multinuclear magnetic resonance spectroscopy, universal referencing, solvent effects 80—73402
naphthalene, fluorescence quenching by biacetyl, effect of viscosity 78—29810
naphthalene, in nonpolar solvents, IR absorpt. bands 79—6939
naphthalene in EBBA, PMR obs., mol. struct., orientation and solute-solvent interactions 77—27806
naphthalenes, heavy atom effects on phosphorescent triplet states 78—70858
1,4-naphthoquinone in EBBA, PMR obs., mol. struct., orientation and solute-solvent interactions 77—27806
β-naphthylmethyl amine, solvent-induced intramol. exciplex fluoresc. 78—25592
2-nitrofluorene, $^1A \rightarrow {}^1L_a$ transition, electronic absorpt. spectra, solvent effects 77—58028
o-nitrophenol, solvent effects on oscillator integrated strength, IR absorpt. bands 78—84575
nitroxide free radicals, neutral, EPR spectra, localised solvent-radical adducts 79—96290
nonaqueous solutions, conf. Leeds, England (July 1976) 78—73036
nonradiative transitions, solvent effects, dynamic coupling model, quantum mechanical theory 80—29787
Norrish type II reaction biradicals, spectra, extinction coeffs., solvent effect on lifetime 77—90617
nucleic bases, interactions and self-organisation, ionisation and solvent salt comp. effects 80—55985
nucleotides, interactions and self-organisation, ionisation and solvent salt comp. effects 80—55985
octane: pyrene(coronene), quasiline spectra, multiplet struct., freezing conditions and solvent effects 79—1786
1,3,5,7-octatetraene, UV, visible, and fluoresc. spectra and assignments, evidence for ^1A_g state 78—33518
optical activity, dispersion-induced, new theory of olfaction 77—56393
organic compounds, solns., line struct. of broad absorption bands 79—54841
organic liquids, NMR spin energy transfer using zero mag. field, spin echoes 79—95675
organic molecules, C-H Raman stretching bands in soln., vibr. freqs. and linewidth 80—78622
organic molecules, complexes with rare earth ions, energy transfer in strong donor solvents 79—54930
oscillatory forces between two solid surfaces arising from struct. in intervening liquid, meas. 80—70521
pentamethinemerocyanine dye, electronic spectrum and struct., solvatochromism, microstructural model 77—61817
perfluorotertiarybutanol, IR spectra in soln., OH group fundamental and first overtone bands *(French)* 77—27071
perturbation energy, second order, environmental effects, SCRF theory 78—58609
perylene in EBBA, nematic ordering influence on fluoresc., temp. depend. *(German)* 79—81235
phenetole, in cyclohexane-ethanol mixtures, UV spectra, solvent effect 79—22770
phenol, in cyclohexane ethanol mixtures, UV absorption, solvent effects 79—22767
phenol(-d_1)-dioxan(-acetonitrile), in carbon tetrachloride ($CDCl_3$) solns., H-bonds vibr. relax. bands anal. 78—84560
phenol-cyclohexane (-ether), UV spectra, solvent effects, matrix rank anal., species determ. 79—22768
phenol-organic solvent mixtures, UV spectra, solvent effects 79—22769
phenols, orthosubstituted, proton acceptor soln., PMR of H-bonding 78—13517
phenols, substituted, in cyclohexane-ethanol mixtures, UV spectra, solvent effect 79—22770
phenols, substituted, proton NMR chem. shift in aprotic solvents 79—47342

solvent effects continued
phenyl acetylene, liq., phase relax., vibr. dephasing, Raman spectra obs. 80−91567
phenyl isothiocyanate, in benzene (tetrachloromethane), nonlinear dielectric solvent effect 79−28702
pheophytin solutions, photolum. of singlet O_2 78−80831
photoluminescence of solutions, decay and self-depolarisation 79−24351
photophysics, solvent effects, energy differences calc. methods 78−61031
photosynthetic pigment, intersystem crossing 77−58057
phthalimide, soln., triplet state accumulation and deactivation depend. on solvent polarity 79−85982
phthalimide acetyl derivatives in polar solvents, luminesc. kinetics and phosphoresc. quenching 80−18885
phthalimide derivatives, hidden vibr. band determ. method, fluorescence and excitation spectra meas. 80−40158
phthalimides, solns., solvent effects on absorpt. spectra and fluoresc. 77−34650
pigment associations, conc. effects, luminesc., absorpt. spectra and dichroism obs. 80−1007
pinacyanol, picosecond photobleaching and absorpt. recovery, solvent effects 77−44493
pivalophenone, organic soln., triplet reactivity solvent depend., flash photolysis study 80−11902
PMMA, methanol crazes, grown from cracks, exam. of growth criteria 78−48551
PMR, tunable notch filter for solvent elmination 80−22405
polar molecule in soln., broadened band contour anal. 77−496
polar molecules, fluoresc. emission anisotropy, solvent effects 79−3489
poly(butadiene-co-styrene), rubber, radiation cured, dynamic phys. props. 77−69003
poly-γ-benzyl-L(D)-glutamate, soln., liq. cryst. and pretransitional regions, optical rot. 80−66145
poly-L-ornithine solution, ^{15}N NMR, coil-helix transition, solvent effects and pH depend. 80−74275
polyacrylamide, gels and single chains, phase transitions and crit. behaviour 80−40759
polyacrylamide gels, structural collapse in solvent, crit. endpoint 78−48702
polyaromatic hydrocarbons, n-alkane solvent effect on low temp. fluorescence spectra 77−36274
polybutadiene, dil. soln., viscosity, temp. depend., solvent effects 80−59686
polydimethyl siloxane-b-styrene-b-dimethyl siloxane block copolymer, morphology, mech. props. 80−64930
polyenes, linear, radiative rate consts., environmental effects 79−72348
polymer, chain molecule, excluded vol. theory based on fifth-power eqns. for unperturbed mol. dimensions 77−50578
polymer, dil. soln., light scattering charact. of thermodynamic props., solvent and mol. wt. effect 80−16717
polymer chains, θ-domain, tricrit. props. in poor solvent 80−103450
polymer solution, configurational props. of model lattice chains under varying solvent conditions 77−89364
polymer solution, diffusion of a chain, conc. effects 80−70103
polymer solution, intermolecular interaction phenomena *(Russian)* 77−21414
polymer solution, semidilute, chain size 78−87607
polymer solutions, dielectric relaxation time, diluent effects 78−10843
polymer solutions, dilute, depolarised light scatt., solvent effects 77−20862
polymer solutions, viscosity, intrinsic, friction coeff., porous sphere model, solvent quality effect 78−71301
polymer-solvent interaction from gas-liquid chromatography, open tubular column expts. 78−35753
polymethinecyanines, symm. solvent effects on electronic struct., ^1H, ^{13}C NMR 78−13516
polymethylsiloxane-polyarylate block copolymer, soln., viscosity, rel. to film mech. props. and microstruct. *(Russian)* 79−23762
polynucleotides, gamma-ray effects on hydration, PMR of frozen and liq. solns. 78−27900
polynucleotides, interactions and self-organisation, ionisation and solvent salt comp. effects 80−55985
polynucleotides and components, temp. depend. of UV absorpt. spectra 77−21475
polystyrene, in solns., intrinsic viscosity rel. to mol. wt., unperturbed dimensions 80−65268
polystyrene, solns., sedimentation behaviour, branching effects determ. 80−66887
polystyrene, spin-labelled, EPR, end group mobility, temp. and solvent depend. 78−56368
polystyrene in solns., unperturbed dimensions rel. to temp., solvent composition 79−64132
polystyrene photophysical behaviour, solvent effect obs. *(Spanish)* 79−57267
polyurethanes, vapour press. of solvent above swollen crosslinked networks rel. to rubber elasticity theory 80−45536
poly[(R)-oxypropylene], opt. rot. dispersion and vac. UV circular dichroism 80−40084
POPOP, soln., anisotropic fluoresc. of prolate mol. *(German)* 80−1018
porphin, free base, in n-octane crystal, S_1 from S_0 transition, freq. shift and dephasing temp. depend. 78−25584
porphin ($-d_2$,d_4,d_6,d_8,d_{10},d_{12},d_{14}), nonradiative transition probabilities, deuteration effects 79−3485
porphyrin, dication and dianion, spectra, quantum chem. calcs. 79−36597
porphyrins, solid solns., phosphoresc. rel. to solvent heavy ats. *(Russian)* 77−40286
propionitrile-hydrocarbon systems, critical solns., Kerr electrooptical Kerr effect meas. 80−100645
n-propyl alcohol-α-picoline, donor-acceptor complex form., solvent effects, IR spectra 77−38660
propylene, solubility in liq. N_2 80−39286
propylene glycol-water (methanol), proton medium effects, ferrocene redox couple reference obs. 77−77786
protein chromophores, fluoresc. props., use in macromol. equilib. struct. mobility investigs. 79−64130
protein dynamic states, role of geometry and elastic strains 78−48745
proteins, conform. changes in aqueous soln. and in mixed solvents, IR absorpt. spectra 78−15762
proton relay model systems, reaction field theory of solvent effects 78−44346
protoporphyrin IX, triplet states, flash photolysis, obs. 80−95555
solvent effects continued
protoporphyrin IX dimethyl ester, triplet states, flash photolysis, obs. 80−95555
pyrene, fluorescence spectra in aq. and surfactant solns. 77−83639
pyrene, in alcohol solns., polar fluid electrons optical absorption coeffs., ns laser ionis. obs. 78−84600
pyrene, monomer and excimer fluoresc. in soln., triplet-triplet annihilation and mag. field depend. 78−78738
pyrene, S_1, fluoresc. decay in micellar and homogeneous liq. dispersions 77−75199
pyrene+N,N-dimethylaniline (deuterate)(3,5 dimethoxy-N,N-dimethylaniline), geminate recomb., solvent, isotope, mag. field effects 78−56888
pyrene-N,N-diethylaniline exciplex, visible spectra obs., picosec. laser photolysis, solvent polarity depend. 77−38677
pyridine, cyclohexane soln., depolarised Rayleigh scatt. 79−47467
pyridine, solns., dielec. polarisation, π-electron system effects 77−90096
pyridine, vibr. reson. lasing threshold, complex form. and solvent effects *(Russian)* 77−75507
pyridinium salt solns., electrochromism in visible absorpt. spectra 77−77244
pyridinyl radicals, hyperfine splitting consts., vibronic effects 77−57890
pyrylium salt solns., electrochromism in visible absorpt. spectra 77−77244
quinine sulphate, acid soln., edge excitation red shift and proton migration 78−1028
quinoline, solns., dielec. polarisation, π-electron system effects 77−90096
quinolines, heavy atom effects on phosphorescent triplet states 78−70858
quinones, spectral solvent shifts, electrostatic model and semi-empirical PPP calcs. 77−83507
quinoxaline, in organic solvent, excited state absorpt. spectra, 422 and 533 nm, picosec. relax. 79−89683
radiationless transitions in solute-solvent system, solvent effect 77−6842
radiative transitions, proximity effects, role of vibronic coupling and static crystal field interactions model 80−69126
radical ions, conjugated, solvent effect in π-approx. calcs. of electronic transitions and spin densities 77−38623
radical ions, conjugated, solvent effect in CNDO and INDO calcs. of electronic spectra by restricted methods 77−38624
radical ions and mols., solvent effect in π(PPP-like) and CNDO calcs. 77−38622
rare earth perchlorates, in solvents with high dielectric const., spectra and struct. 79−65860
reaction field theory modification for solvent polarities 79−91913
resonance Raman excitation profiles, vibronic state short lifetime determ. 79−98103
resonance Raman spectra intensity distribs. in soln. 79−22763
trans-retinal, ground and excited state dipole moments, permittivity, solvent effects, spectrophotometry 78−27883
retinal, in ethanol soln., methyl groups effect optical absorpt. 79−53047
retinal, isomers, intersystem crossing quantum efficiencies, solvent effects 79−22751
trans-retylidene-n-butylamine, ground and excited state dipole moments, permittivity, solvent effects, spectrophotometry 78−27883
rhodamine, soln., triplet state accumulation and deactivation depend. on solvent polarity 79−85982
rhodamine 6G, aqueous soln., absorpt. spectra, ground and triplet state photoprotonation pH depend. 80−42961
rhodamine 6G, delayed fluoresc. of simple associates in polar and nonpolar solvent mixtures *(Russian)* 78−48185
rhodamine 6G, fluoresc. polarisation, solvent effects 80−32755
rhodamine 6G, in glycerine-water solns., anti-Stokes fluoresc., conc. quenching 79−24349
rhodamine 6G, orientated relax. times, streak camera meas. 80−14168
rhodamine 6G, rot. diffusion, fluoresc. spectra, solvent effects 77−75198
rhodamine 6G dye laser, degree of polaris., solvent effect 79−41375
rhodamine B and 6G, fluoresc. decay time meas. in different solns. 80−9637
rhodamine B lactone, dual fluoresc., solvent polarity depend. 77−3394
rhodamine C and 6G, strong base solns., electronic spectra, temp. depend. 79−85987
rhodamine dye solutions, vibr. relax. in S_1-state 77−6826
rhodamine dyes in soln., bleaching, electronic and vibr. absorpt. spectra, fluoresc. 80−42960
rhodamine solution, picosec. spectroscopy with antiStokes excitation, orientational rearrangement *(Russian)* 79−42984
rhodamine-B fluoresc. polarisation, solvent effects 77−54569
$tRNA_{yeast}^{phe}$, Fourier transform PMR in aq. soln., ^1H exchange and relax. rates meas. method 78−15049
rose bengal, excited state orientational relax., in protic and aprotic solvents 78−46383
rose bengale, fluoresc. polaris., solvent dipole moment effect 78−25596
Schulze-Hardy rule, theory 80−89540
scintillator systems, liq., organic, energy transfer, fluoresc. intensity-max. solvent depend. 78−21966
semiquinones in protic solvents, saturation behaviour, ESR 77−6808
sodium alginate, light scatt., wt.-average mol. wt., charge density 77−61882
solute molecules in 1-dimensional fluid, forces due to solvent struct. 79−73080
solute-solute-solvent interaction, dielec. behaviour problems, review 80−25298
solute-solute-solvent interactions, introduction to symposium in Vienna, Austria (1978) 80−26098
solute-solvent interaction, discrete, continuum and discrete-continuum models 78−73130
solute-solvent interactions, moment anal. of IR absorpt. bands 78−58766
solvated electron, optical excitation energies, correlation with solvent props. 78−53309
solvated electron, optical spectrum broadening in polar liquids 77−21465
solvated electron reaction rates in alcohols and water 77−25259
solvation, classical mean space charge model 78−76841
solvatochromism, microstructural model 77−61817
solvent extraction device using radioactive tracers 77−32819
spectra, electronic and vibr. absorpt., repulsive intermol. forces 77−79671
trans-stilbene, excited state orientational relax., sub-picosec. pulse obs. 79−50006
stilbene, two-photon absorptivities via three wave mixing 79−68416
stilbenes, substituted, dipole moment calcs., in excited singlet state *(German)* 77−50367

solvent effects continued
strongly interacting solvents, IR band shapes, solvent-induced chirality, field theoretic Green's function method 79−27037
sulphonyl compounds, H-bonding by methyl groups, Raman spectra obs. 79−24320
ternary electrolytes, viscosity and ion-solvent interactions in dioxane-water mixtures 78−18817
p-terphenyl, fluoresc. quenching by 4-aminobenzophenone in different dielec. const. solvents *(German)* 79−83030
p-terphenyl solns., mag. field effects on scintillation pulse shape, ion pair recomb. 77−16835
tetraalkylammonium halides in methanol, struct., IR spectra 77−23500
1,1,4,4-tetrachloro-1,3-butadiene, reson. Raman intensities, mol. struct., excited states, vibr. anal. 77−65470
tetrachlorotetraiodofluorescein, rot. diffusion, fluoresc. spectra, solvent effects 77−75198
tetraethylammonium triiodide, solvent effects on electronic transitions of I_3^- 77−27080
N,N,N′,N′-tetramethyl-p-phenylenediamine-p-chloranil, soln., optical spectra, temp. and environment effects 79−54861
tetramethylammonium chloride solns., aq. and methanolic, Raman spectra 79−28750
thermodynamic data, characteristic vector analysis 77−21409
thin-layer phosphorimetry, solvent enhancement effects 78−61082
TMPD, fluoresc. in nonpolar organic liqs. for excitation energies above and below photoionis. threshold 78−1018
toluene, fluoresc. quantum yield in soln., dipole-dipole interaction 78−25598
transition metal complexes, reaction mechanisms and solvent effects 80−26012
tri-O-ethylamylose-solvent complexes, cryst. struct., chain conforms. 79−65067
triatomic mol. in solvent, rot. induced vibr. energy relax., Coriolis effect 80−47921
1,1,2-trichlorethane, soln. in acetone, US relax., solvent effects 79−99275
1,1,1-trichloroethane, Raman spectra, vibr. dephasing 79−59465
trichloroethane, vibr. population lifetimes in liqs. anti-Stokes Raman scatt. 78−74665
trichloromethane, vibr. population lifetimes in liqs. anti-Stokes Raman scatt. 78−74665
trichloromethane-d_0,-d_1, soln., far IR spectra, band shape and moment anal. 80−58252
triethylamine, gas (soln.), fluoresc. quenching by 'inert' perfluoromethylcyclohexane 78−46438
triethylenediamine, aq. soln., stimulated Raman scatt., struct. enhancing solute 78−27222
trifluoroiodomethane, solns. with liq. Ar, Kr, Xe, CH_4 and CF_4, Rydberg band positions, temp. depends. 78−17686
2,4,6-trimethoxy-s-triazine, thermal isomerisation, nematic solvent effects 79−91944
triple-ion species of alkali metals, ESR spectral hyperfine multiplets, linewidth effects 77−83624
trypsin, in suspension, radical form. and inactivation after Γ-irrad. 78−3564
tryptophan, Fourier transform PMR in aq. soln., ^1H exchange and relax. rates meas. method 78−15049
two-level system coupled to thermal bath, relax. quantum dynamics 77−3437
umbelliferone, excited state tautomeric forms, solvent polarity effects 79−59377
vanadyl alkanoates, ^{51}V NMR, quadrupole splitting in nematic phases 79−28637
vanadyl triisopropylate, chem. shifts, NMR line widths, temp. and solvent depend. 78−70853
virtual charge model representation of solvent polaris. 78−74593
water, H-bonded struct., IR spectra, assignments 78−62800
xanthene dye, solute-solvent hydrogen bonding and temp. effects on internal conversion 77−3402
xanthene dyes, hidden vibr. band determ. method, fluorescence and excitation spectra meas. 80−40158
xanthene dyes, internal heavy atom effect on radiative and non-radiative rate consts. 80−32765
xanthione, solns., triplet state quenching by ground state xanthione 78−42180
zinc porphin, ESR study of metastable triplet state, in n-octane matrix, 1.3K 79−72340
Ag complexes in organic solns., ^{109}Ag NMR, solvent effects 77−16191
$AlBr_3$, Raman IR spectra, organic solvent effect *(German)* 77−3370
BN, cubic, high pressure synthesis, solvent effects 80−40310
Br_2 in Ar, solvent effects on equilibrium props. 80−61128
Br_2, organic solvent effects on Raman parameters 79−26998
$(C_6H_5)_3AsI_3$, solvent effects on electronic transitions of I_3^- 77−27080
CO group, NMR chem. shift, solvent's dielectric const. effect, mag. anisotropy 79−42847
CO-alkane, liq. soln., vibration-rot. IR spectra, rot. diffusion 77−83584
CO-cycloalkane solns., CO IR vibr.-rot. spectra, solvent mol. struct. 77−83585
CO_2, in various solvents, IR absorpt. spectrum, Fermi-reson. doublet and intermolecular interactions 80−18856
CS_2, in Ar, medium perturbations of extravalence excitations, VUV absorpt. 78−1002
CS_2, liquid, dilution in inert solvent, Raman spectra, effects of intermolecular forces 79−41177
CS_2, $\pi\pi^*$ and Rydberg bands, cryogenic solvent effects 78−55182
CS_2, solns. with liq. Ar, Kr, Xe, CH_4 and CF_4, Rydberg band positions, temp. depends. 78−17686
Cl^-, far UV spectra in solns. 78−94208
ClCF, radical in Ar matrix, vibr. relax., multiphonon processes, fluoresc. 77−65430
^{35}Cl NMR, medium effects 77−1612
Cr^{3+} hydration model, external water interactions 78−78772
$Cr(CO)_6$, ν(CO) region, IR and Raman spectra in organic solvents 79−41169
Cs^+, glycerol solns. quadrupole interactions, nucl. mag. relax., correl. time determ. 77−14449
CsI_3, solvent effects on electronic transitions of I_3^- 77−27080
Cu II complex, bis(pyrrolidonecarbodithioato) copper II, ESR, solvent effects 78−1008
Cu II complexes, 5-coord., ESR, optical absorpt., solvent effects 78−5253
solvent effects continued
D_2/CCl_4, inhomogeneous broadening of Morse oscillator, temp. depend. 77−61803
DCl, vib.-rot. spectra in hexadecane solvents of different mol. shapes 77−34623
DCl-cycloalkane solns., CO IR vibr.-rot. spectra, solvent mol. struct. 77−83585
4-dimethyl-amino-4′-nitrostilbene, fluoresc. emission anisotropy, solvent effects 79−3489
Dy complex, acetoacetic ether, luminesc. spectral band intensities, solvent effects *(Russian)* 78−84653
Dy^{3+}, in soln., non-radiative transitions as Forster's energy transfer to solvent vibrations 80−1014
$Dy(NO_3)_3$ in nonaqueous solvents, anharmonic vibrs. in electronic energy degradation 77−23541
Eu ions, solvent effects on band intensities *(Russian)* 77−55828
Eu^{3+}, in soln., non-radiative transitions as Forster's energy transfer to solvent vibrations 80−1014
$EuCl_3$, solns., $^7F_0 \rightarrow {}^5D_1$ and $^7F_1 \rightarrow {}^5D_0$ transitions, MCD 79−31566
F, spin-spin coupling constants, review 77−23511
^{19}F NMR solvent shifts, charge transfer contribs. 77−50454
Fe complex, Fe (III) acetylacetonate, solvent effects on oscillator integrated strength, IR absorpt. bands 78−84575
Fe complex, halobis(morpholyldithiocarbamato)Fe(III), solvation effects, mag. susceptibility and Mossbauer spectra 78−27129
Fe^{2+} and Fe^{3+} hydrate clusters, aq. electron exchange reaction, ab initio RHF MO calc. of inner shell reorganisations, vibr. freq. 80−102564
$FeBr_4^-$, in various solvents, $^4A_1\ {}^4E$ d-d band reson. Raman spectra, solvent depend. 80−55085
$FeCl_3$, nonaq. solns., solvent-solute interactions, Mossbauer investig. of equilib. consts. 79−1729
$FeCl_4^-$ in organic solvents, dilute, ESR linewidths *(German)* 80−11258
H-bond complex formation, enthalpy change due to electronic excitation, spectroscopic determ. 78−92496
H_2 dissolved in Ar, far IR spectra, density narrowing of rot. line 79−50086
H_2 in organic solvents, proton chem. shift, Van der Waals solvent effect contrib. 77−68062
H_2/CCl_4, inhomogeneous broadening of Morse oscillator, temp. depend. 77−61803
HBr, fundamental IR band, solvent effect *(Russian)* 78−13501
HCN, IR and Raman vibr. intensity changes due to Li^+ interaction 79−45712
HCl, in dil. solution IR absorpt. fundamental shape temp. depend., solvent-solute interaction 79−26977
HCl, Raman spectra in various solvents, depolaris. ratio and profiles 79−59464
$HCl/SF_5(CCl_4)$, inhomogeneous broadening of Morse oscillator, temp. depend. 77−61803
HCl(-acetone)(-acetonitrile), soln., IR absorption, H-bonding, solvent effect 78−29778
$H_5O_2^+$, aq. soln., IR continua with polarisable H-bonds 79−26979
$^4He_2$ and $^3He_2$ dimers in liquid ^4He, non-additive interactions in solvent effect 79−41120
Hf complex, tetrakis (tropolonato) hafnium (IV), mol. interactions in solid, perturbed γ-γ ang. correl. obs. *(French)* 79−8076
Hf complex, with N-benzoyl N-phenyl hydroxylamine, mol. reorientation in soln. 77−16218
HgI_2, Raman spectra, in high-temp. $CsNO_3$, metaterphenyl, and paraterphenyl solns. 78−86876
HgX_2 (X=Cl,Br), aprotic donor solns., Raman spectra, mol. vibr. and solvent strength 78−29788
HgX_3^- (X=Cl,Br), aprotic donor solns., Raman spectra, mol. vibr. and solvent strength 78−29788
HgX_4^- (X=Cl,Br), aprotic donor solns., Raman spectra, mol. vibr. and solvent strength 78−29788
I radical recombination in dense liquids, stochastic trajectory simulation 80−45487
I_2, in CCl_4 and cyclohexane solns., higher vibr. levels, dephasing lifetimes, from reson. Raman spectrum 78−42068
I_2, picosecond relax., fluoresc. spectroscopy, solvent effects 78−58737
I_2, solns., visible absorpt. spectra, temp. effects 77−61760
I_2 solutions, vibr. and rot. relax., reson. Raman lineshape meas. 79−31616
$^{129}I_2$, frozen soln. in o- or p-xylene, Mossbauer effect obs. 80−78637
I_2-quinoline (pyridine) complexes, stability const. determ. by spectrophotometric methods 80−87056
$I_2(B^3\pi_{0^+u})$, ps excitation, in CCl_4 soln., ultrafast decay and spectrum 78−9184
Ir(III) complex, cis-dichlorobis(4,4′-dimethyl 2,2′-bipyridine) iridium chloride 80−97319
LiCNS, ether solns., dimer struct. and force consts., IR and Raman spectra 79−72442
LiCl glycerol solns. quadrupole interactions, nucl. mag. relax., correl. time determ. 77−14449
$LiNO_3$, soln. in organic liq. or D_2O, Raman lineshape, solvent-solute interaction 78−76448
Mn II complex with amino acids and peptides in D_2O, NMR line widening 77−56328
Mn^{2+}, in soln., non-radiative transitions as Forster's energy transfer to solvent vibrations 80−1014
$Mn(CO)_5Br$, ν(CO) region, IR and Raman spectra in organic solvents 79−41169
$MnCl_2$ in soln., luminesc., strong vibronic coupling 79−65922
N_2, liquid, in Kr, methane, and CO, Raman scatt. parameters, high-resolution coherent active spectroscopy 80−66207
N_2/CCl_4, inhomogeneous broadening of Morse oscillator, temp. depend. 77−61803
NH_3, symmetric bending mode, Raman intensity, electrolyte solvent effects 77−34638
NO, EPR line shape in solvating mixtures 78−33532
NO_2, Ne matrix isolated, 6K, B←X band system 78−993
NO_2^-, solvated, in H_2O, ethanol, cyanomethane, and DMF lowest n-π^* transition 79−85960
^{14}N NMR chemical shift, external neat nitromethane scale 78−24834
$NdCl_3$, aqueous frozen soln., phase transformations, optical absorpt. spectra, Nd^{3+} Stark splitting 79−1777
O_2 in chloroform and carbon tetrachloride solns., sensitized luminesc. 80−32762
O_2, lifetimes and reactivity in aq. micellar system 78−46398

solvent effects continued
O_2, singlet state lifetime in D_2O soln., decay of micellar system 78−46301
OCS in Ar soln., IR spectra, solvent shifts, vibr. band assignment and anharmonic force consts. 80−9607
OCS in n-alkane, rot. relax., solvent hydrodynamic props., Raman and IR spectra 80−45055
OH, in inert gas matrix, H-bonding and charge transfer, fluoresc. 78−25602
$OH^- + CO_2 \rightarrow HCO_3^-$ react., MO-LCAO-SCF calcs., energy barrier 78−76846
$POCl_3$-$SnCl_4$, Sm^{3+} fluoresc. quenching temp. depend., near reson. interaction 79−65915
PSF_3, in orienting smectic solvent, ^{19}F and ^{31}P mag. shielding anisotropies, F-P-F bond angle 77−18942
Pt phthalocyanine, reson. Raman excitation profiles, solvent effects 80−102512
Ru complex, Ru(II)-polypyridine, excited charge transfer states, multiple emissions 79−3468
Ru complexes, $Ru(NH_3)_6^{2+}$ and $Ru(en)_3^{2+}$ in soln., UV spectra, solvent effects 79−94010
$SbCl_3$, dynamic coeff., molecular interaction effects of media *(Russian)* 77−83601
o-semiquinone, radicals, intra- and intermolecular H^+ transfer, ESR 77−16840
Tb complex, acetoacetic ether, luminesc. spectral band intensities, solvent effects *(Russian)* 78−84653
Tb^{3+} in $POCl_3$:$SnCl_4$, $^5D_3 \rightarrow {}^5D_4$ transition, solvent depend. 79−22644
$^{205}Tl^+$ ion, solvent effects on spin-lattice relaxation time 77−48073
UO_2^{2+}, in $HClO_4$ soln., photoluminesc. intensity, conc. depends. of uranyl and H^+ 77−68069
$UO_2(DMSO)_5^{2+}$ in DMSO soln. kinetics of DMSO exchange by NMR method 79−81214
UO_2(acac)DMSO, in DMSO soln. kinetics of DMSO exchange by NMR method 79−81214
Xe, extravalence excitations, VUV spectra, solvent perturbations 77−50386
Xe in inert gases at high press., extravalence excitation solvent perturbation 77−75099
^{131}Xe, in poly-γ-benzyl-L-glutamate liq. crystal solution, quadrupole splitting 79−4741
Yb^{3+}, in dessicated (nondessicated) and protonated (deuterated) solvents, photoluminesc. energy degredation 78−19544
Yb^{3+}, in soln., non-radiative transitions as Forster's energy transfer to solvent vibrations 80−1014
Zn-porphin($-d_4$,d_8,d_{12}), nonradiative transition probabilities, deuteration effects 79−3485

sonar
see also bioacoustics; navigation; underwater sound
2D linear prediction for freq. and bearing estimation 79−64409
32 kW Doppler sonar for ocean internal wave meas. 80−46296
acoustic backscattering from very rough water surfaces 79−41499
acoustic Doppler sodar, appl. to atmospheric temp. fluctuations heat flux and struct. functions meas. 80−105023
acoustical tracking, ocean current profiling 80−67427
acousto-optic deflector for TV and oscillograph displays 77−39099
acousto-optic real-time radar and sonar signal processing 79−72515
active detection range, Adriatic Sea refract. effect *(Croatian)* 79−57945
adaptive beamformer for optimal directional spectra 79−18621
adaptive beamforming introduction 79−18620
aerospace systems and electronics, IEEE conference, Washington D.C., USA, 26-29 Sept (1976) 77−5420
air pollution meteorology, use of sodar acoustic echo sounder, low level stability and wind velocity monitors 80−108828
angle of arrival sodar and acoustic Doppler wind detect., comparison with direct meas. 79−39884
array gain, sampling error effect anal., Bryn processor 78−66975
array paired element delay meas. with sequential state estimation 80−96128
array processing using freq.-wavenumber approach 78−66974
atmosphere acoustic and radio acoustic exploration, effects of sound nonlinear absorpt. *(Russian)* 80−94567
atmosphere acoustic sounding technique, appls. to siting studies 78−81467
atmosphere sound ranging, rangers and source on same level not assumed *(German)* 77−54824
atmospheric boundary layer, Doppler sodar obs. of turbulence struct. 79−66762
atmospheric mixing depth and stability regional patterns, sodar network meas. 79−100965
atmospheric sounding, influence of varying system parameters 77−70863
atmospheric turbulence simultaneous meas. using sodar and aircraft 79−20923
AUTOBUOY directional array, ambient sea noise directionality meas. and processing 78−16025
backscattering cross-sections of live fish, probability density function and aspect 80−64260
bat, simulation in anechoic chamber, coherent processor performance estimation appl. *(French)* 80−56072
bats, biosonar signals, fine freq. anal. via phase-locked loop device 77−56392
beam steering, time delay and integrate CCDs 79−18623
beamformer, serial phase shift, using charge transfer devices 80−96078
beamforming by CCD scan conversion for SAW chirp-Z transform 80−43552
beamforming when the sound velocity is not precisely known 80−96123
blind children's CW FM sonar 79−70708
bottom reverberations picked up by hydroacoustic dipoles, spatial correlation functions *(Russian)* 78−53659
broadband target classification using bionic sonar 78−18123
C-CD appls. in sonar systems 80−53535
C-CD beamforming and signal processing systems 80−33325
C-CD implementation of chirp Z-transform 79−18626
cable-laying using ship hull-mounted sub-bottom profiling 78−5620
camera, SX-70, automatic focusing by US echo ranging 79−93239
capped sphere partially insonified at circular spot, monostatic and bistatic sonar cross sections 77−62081
coherent optical processing techniques 78−75018

sonar continued
computerised fibre optic system, geological and hydrographic survey applications 78−88947
Continental Shelf sediment sonar signal processing 78−61622
correlation sonar for ship's velocity meas. 79−27474
cross-section of coated hollow cylinder in water 77−46844
curved face parametric projector for marine sediment penetration 78−51032
CW FM sonar with aural displays, improvements 78−87221
cylindrical arrays, vertical sidelobe suppression 77−46848
cylindrical receiving arrays with nonuniform hydrophone response directional characts. 77−88979
data processing, testing for multivariate normality 79−59865
deep ocean hydrophone array 77−62087
deep ocean navigation, acoustic beacon-aided 79−32166
deep ocean navigation by Parametric Array Doppler Sonar 77−3698
deep ocean seamount detection using reconnaissance sonar 78−69551
deep sea floor mapping instrumentation 77−5358
deep-tow and digital techniques 77−73882
deep-water acoustical analysis of stationary and moving broadband sound sources 78−63226
delay parameter estimation following robust detection 79−55267
digital beam forming 80−91950
digital beamforming 78−50989
digital distributed signal processing, fifth generation concept 77−88995
digital phase shift beamformer, design and implementation 79−1034
digital techniques for beamforming and signal processing 79−18619
distributed sensor concept for underwater detection 78−33944
dolphin, Phocoena phocoena, props. of low freq. sonar signals *(French)* 77−52809
Doppler phased array coherent imaging and processing by metaxial optics 79−72521
Doppler sodar antenna configs. for horizontal wind meas. 78−65410
Doppler sonar, digital processing of signals 77−46856
Doppler sonar, range-gated, obs. of strongly nonlinear internal motion in open sea 80−51422
Doppler sonar controller 80−43575
Doppler sonar fish counting system, feasibility study 78−50980
Doppler sonar for ship's velocity meas. in deep water 79−27475
Doppler sonar ocean current profiles 80−46311
dual-beam sonar system for individual fish target strength meas. 77−3704
echo sounders, Koden SR651 depth indicator *(Italian)* 79−14168
echo sounding and seismic profiling 77−70865
echoes scattered by random fluctuating surface, statistical model *(French)* 77−11066
echosonde antennas, echo carrier freqs. and antenna dimensions rel. to performance 78−1474
electronic sector scanning sonars, signal generation 79−18622
end-fire arrays, exponentially shielded, nearfield axial levels 77−39127
epoxy material, filled, US props. for sonar transducers 78−59867
fibre optic sonar link, multichannel 78−42446
fish density and backscattering cross section determ. 77−817
fish target strength functions, model for averaging 80−43512
FM-CW acoustic sounder resolution rel. to modulation noise *(Japanese)* 78−30137
Gulf Stream ring tracking with buoyant SOFAR floats 77−17245
HF transducers, lumped bandpass filter equiv. ccts., quarter-wave matching characts. 80−1397
high-resolution, using parametric transducer 80−14539
hologram matrix image reproduction expt. 79−55271
hologram matrix sonar 79−41526
holographic passive sonar, new system using polyspectral anal. 77−39124
holographic piezoelectric integrated acoustic array, system anal. 80−79067
horizontal array shape measurement, active/passive acoustic techniques 80−23824
icebergs underwater profiling using unmanned submersibles, echo sounder and scanning sonar 79−5673
identifiable sound source location from time differences of arrival 80−91951
imaging, techniques and characts. 79−64462
imaging, using elasto-optic material and laser interferometer 77−58501
imaging with synthetic aperture technique 78−33943
incoherent and coherent processing against echo fading in shallow water 80−19142
interference rejection, by amplitude shading of sonar transducer arrays 77−62094
interference rejection by amplitude shading of transducer arrays 78−38151
interference to propag. by marine organisms, review 80−64269
lake surface reverberation, statistical props. 79−1020
linear feedback AGC with input-level-invariant response times for sonar signal processing 78−30130
linear sonar array processor finite impulse response digital filter design 80−43549
lower atmosphere dynamics study, optical and acoustic techniques *(Italian)* 77−91327
mapping of lake bottom sapropel and sea shelf sediments *(Russian)* 77−9562
marine photography and side-scan sonar image processing 77−5357
marine profiling images, recording, signal amplitude preservation 78−36326
meteorology, sodar appl. to weather analysis and local forecasting 80−85713
mobile sonar technology (MOST), technical document information system 78−45003
monostatic Doppler sodar system, meas. method, wind obs. appl. *(German)* 79−16710
moving target indicator, removal of periodic waves from reflecting signals 80−69585
multibeam hydrographic sonar system, deterministic and random error model 79−3873
multibeam sonar systems, data flow requirements 77−3697
multichannel wide-range oceanographic sonar 80−46295
multisignal time difference estimator for transient sound source location 80−96127
nearfield array for use in acoustic backscattering cross section meas. 77−14862
nearfield performance of passive correlation processing sonars 79−10433
object pattern classification using A-scan data 78−66980

sonar continued
ocean bottom profiling, narrow beam scanning sonar 79−88509
ocean mapping, bottom return signal model and signal processor 77−2272
ocean multipath propagation effects on sonar design and performance 78−5602
ocean surface waves remote sensing, theory 80−12564
ocean-bottom subsurface layered media, spatial parameter estimation 80−77134
oceanic internal struct. exploration using remote probing techniques *(French)* 79−44274
oceanographic research techniques used in survey ships *(French)* 78−65434
oceanography, integrating optics and sonar for deeply towed vehicle 78−45045
Oceans '77, conf., Los Angeles, USA (Oct. 77) 78−36193
optical hydrophone using optical fibre, development 79−3832
optical signal and image processing, conference, San Diego (1977) 78−74853
output fluctuation modelling, stochastic process 78−66981
Pacific Ocean floor relief meas. by side-scan sonar 78−36142
parametric acoustic array max. conversion efficiency anal. 78−71242
parametric sonar performance calculator 80−33392
passive, directional transducer arrays appl., underwater location of acoustic sources *(Spanish)* 80−69586
passive, errors in range and bearing estimation 80−79030
passive, prediction of post-detection data load 80−96125
passive bearing estimation, removal of bias and 2π ambiguities 78−38150
passive coherence processing sonars, near-field performance 80−33346
passive range estimation from array of sensors 80−53583
passive ranging of acoustic source 78−71241
passive sonar system adaptive processor 78−5622
piezoceramic tubes with capped or shielded ends, sensitivity above omnidirectional freq. range 78−1534
portable acoustic Doppler detector, buoy sonar system 77−7273
portable monolithic IC sonar unit *(French)* 78−13868
position location system, for ocean mining 78−45046
Proteus, advanced signal processor system 77−65648
Radar-Acoustic Sounding Systems, range limitation due to atmospheric refractive turbulence 77−41195
radio-acoustic sounders for remote sensing of lower atmosphere *(Japanese)* 78−16209
range prediction, inherent errors 78−66977
ranging systems, pulse compression techniques 80−33350
rare earth iron magnetostrictive underwater sound transducer 78−13881
remote sensing imagery, spatial filtering 78−90385
scattering from marine organisms, appl. of fluid sphere theory 77−46846
sea floor analysis with deep tow techniques 78−33942
sea floor mapping on Mid-Atlantic Ridge, integrated approach 77−5360
sea ice, sidescan sonar imagery, Arctic Ocean 79−25339
sea surface inhomogeneities sensing via sound scatt., phase function shape in shadowing conditions *(Russian)* 80−94530
sea-floor mapping in real time, sonar-microprocessor equipment 80−26646
sector scanning sonar, use in fish heart rate telemetry 80−8225
sediment refraction of sound, importance for sonar studies 80−81902
shallow ocean water propagation, Naval Research 79−25258
shallow-water sound propagation 79−5493
ship speed determ., new acoustical method 79−14178
side looking sonar, picture improvement 79−84516
side looking sonar for sand wave study in White Sea 78−3999
side scan sonar, review 77−70866
side scan sonar data, adaptive sample set construction 80−43554
side scan sonar surveys, tow line depth increase 77−64490
side scan sonar system capability improvements 80−43574
side-scan obs. of sedimentary sea bottoms, machine classification 79−92626
side-scan sonar with selective textural enhancement 77−5371
signal processing, algorithms soln. with multi-microprocessor network 78−45044
signal processing, conference, Portovenere, Italy (Aug./Sept. 1976) 78−5614
signal processing, hydroacoustic scatterers identification, system optimisation *(German)* 78−42487
signal processing by chip slice microcomputer 79−94408
signal processing in ultrasonics, conf., London, England, Jan. 1980 80−33351
signal processing technology for sonar, conf., London, England 1978, Nov. 79−18618
signal processor, 36-channel, programmable 78−66976
signal time delay estimation using parameter estimation of FIR filter 79−59867
small, medium resolution, for underwater vehicles 79−3834
small ring arrays, directional sccuracy 77−31181
for smaller ships, clutter spatial correlation signal processor 79−3833
sodar, appl. for acoustic detection in lower atmosphere *(French)* 80−8435
sodar application in aviation 80−31132
sodar meas., improved quantitative display techniques 78−77332
sodar obs. of lower atm. thermal struct. at Delhi, India 79−53428
sodar system tone-burst protector, cct. design, micrometeorological appl. 79−18641
sodar techniques, theory and appl. of acoustic sounding 79−64466
SOFAR, anal. of source-motion effects on sound transmission in deep ocean 77−62088
sofar floats for POLYMODE 78−45047
sonobuoys for anti-submarine warfare, design 79−3829
source-receiver and target transfer function, in homogeneous fluid 78−75012
sparse line array, cross-sensor beam forming 77−39126
statistical model for backscattering from a randomly fluctuating surface 79−27459
sub-bottom profiling, using nonlinear sound source 77−45198
surveying underwater transducers by acoustic method, computer simulation model 79−32165
synthetic aperture imaging using acoustical holography 79−3863
synthetic aperture radar underwater mapping, array processing 78−69549
synthetic aperture sonar in turbulent media 79−90058
synthetic aperture sonar system prototype 77−46867
sonar continued
synthetic-aperture sonar systems in turbulent medium 80−96080
synthetic-aperture systems, characts. and comparison with nonsynthetic-aperture systems 77−62092
system design requirements 77−27441
target recognition expt., comments 80−58866
target recognition expt. 79−64389
target recognition expt. 79−86298
target transfer function estimation in presence of noise and clutter 77−62110
technology development, review 78−55500
telemetering methods for deep sea nodules deposits *(German)* 80−26623
telephone equipment for underwater sonar communications type 2008 system 78−94478
thermocline depth determination, appl. of sonar in Caspian Sea *(Russian)* 77−13132
time delay and integrate CCD device for pulse sector scanning in sonar 79−18624
time delay design using CCD 80−43570
time delay estimation, cross-correl. and smoothed coherence transform methods compared 80−96086
towed array system modelling, steady-state and transverse dynamic motion study 78−30112
towed type, portable, for ocean acoustic meas., features 78−69550
tracking of slowly sinking floats, meas. vertical profiles of oceanic current and Richardson number 80−67378
transducer, magnetostrictive, hollow spherical scatterer effects on radiation resistance at air-water surface 77−39125
transducer array directional response anal., model 78−66973
transducer arrays, image prod., signal processing methods comparison 78−18122
transducer arrays, numerical calc. method for acoustic interaction *(Japanese)* 78−9521
tropospheric studies, FM-CW radar, microbarograph, review 77−91332
underwater communication systems 79−18574
underwater electric cable terminations 78−45041
underwater horns, directivity 78−18138
underwater objects, depths determ. in presence of refr. 77−34986
underwater obs. of glaciers by side-scan sonar 77−5270
underwater offshore acoustic test range construction 79−16720
underwater sound, broadband detection system, anal. 79−3827
US echo sounding equipment *(Italian)* 78−55530
US imaging sonar, design and construction 79−3831
US pulse-echo systems, improved sensitivity using pseudo-random binary-code phase-modulated signals 80−38182
US receiver, multiple use *(French)* 79−64457
velocity meas. sonar system, transfer function model 77−7275
velocity resolution with linear-period-modulated pulse 77−54825
vertical processing sonar, concept 79−3830
water pollutant particles, diffusion and scattering theory *(Italian)* 77−91335
wideband acoustic characterisation method for fish schools and long-range propag. channels 80−43551
wideband equation for pulse distortion estimation 79−3837
Woodhead seabed drifters, acoustic tracking 77−5366
Ni-Fe polycrystalline film cross-tie memory for shipborne radar/sonar 80−42204

sonic boom *see shock waves*

sonic propagation *see acoustic wave propagation*

sonoluminescence
alkali metal salt solution, Ar saturated, sonoluminesc. as acoustic cavitation probe 79−60437
blood plasma, sonoluminescence generation by US therapy equipment 77−77930
bulk solution temperature effect on sonoluminescence intensity 80−76090
EHD visible sonoluminescence, due to collapse of cavity in liquid 80−45158
fluid, radio band pulse radiation due to spark initiated cavity dynamics, sonoluminescence *(Russian)* 80−66313
nematic liquid crystal, laser breakdown, plasma-acoustic cavitation phenomena *(Russian)* 77−65947
US cavitation, production of pressure and light impulses *(French)* 80−33297
water, sonoluminescence generation by US therapy equipment 77−77930
water, sonoluminescence spectrum in visible region *(French)* 79−33855
water containing dissolved gases, sonoluminesc. theory 77−85818
Ar saturated solutions, NO_3^- effects on spectral distribution and intensity of sonoluminescence 80−76091
CdS, Lamb US wave induced luminesc., green edge radiation *(Russian)* 79−91509
CdS, single crysts., US luminesc. obs. 80−76092
N_2 cryogenic liq., laser sonoluminesc., at elevated hydrostatic press. 80−71498

Soret effect *see thermal diffusion in liquids*

sorption
see also adsorption; chemisorption; desorption; surface diffusion
ABA poly(styrene-b-butadiene) copolymer, physical props., casting solvent effects 77−55935
absorbed layer, commensurate-incommensurate transition 80−49494
absorbed molecules from medium, Raman spectrosc. technique 79−42364
accommodation coefficients, effects on evaporation and condensation *(Japanese)* 78−81933
albumin, of fatty acids, rel. to struct. lability of biomembranes, using fluoresc. probes 77−25381
amorphous surface-molecule interaction, model pot. 79−46919
anisothermal physical sorption kinetics in porous granules, integration of nonlinear eqns. 77−7967
AVEhD 40/800 arc-sorption pumping system 78−227
bentonite, selective sorption props., thermodynamics of ion-exchange reactions 79−39203
bentonite, selectivity of ion-exchange reactions 79−34360
bentonite, sorption props., appl. to radioactive fallout water deactivation 79−43995
bentonites, granulation, appl. to deactivation of radioactive waste waters *(Russian)* 77−38369
binary ordering alloy, gas absorption, correl. effects *(Russian)* 78−47525
biporous sorbent, internal diffusion 80−44414

sorption continued
bispenol-A epoxy resin, glass transition temp., effect of absorbed water, PMR line width 79−90766
bitumen-filler systems, selective sorption 79−100437
blood metabolites, dynamics of depend. sorption by C sorbents 77−70487
Brunauer, Emmett and Taylor surface area meas. apparatus 79−35666
butyl rubber ethylene propylene ternary copolymer mixture, permeability, diffusion of gases and solvents 79−95217
cation-exchange sorption microcalorimetry, automatic micro-injection system 78−24777
chromatography, liquid, sorption materials, characteristics and development trends *(Czech)* 78−64904
chromatophores of photosynthesising purple bacteria, sorption and desorpt. of water 78−69012
cleaning techniques review, for atomically clean surfaces preparation 80−11804
clinoptilolite, of ^{106}Ru and ^{59}Fe *(Russian)* 77−38370
clinoptilolite, sorption props., appl. to radioactive fallout water deactivation 79−43995
cobalt phthalocyanine film, sorption of O_2 and water, AES obs. 78−91531
concrete and containment uptake of fission product I, sorption and diffusion 79−67898
conference, Eindhoven, Netherlands (June 1976) 77−62708
contact film absorption on plastic deform. of contacting bodies *(Russian)* 80−93596
cryosorption pumping of He by charcoal, cryopump design for fusion reactor 80−105654
dextran structural modifications, I_2 sorption, porosity depend. *(Russian)* 79−23535
diffusion coefficient estimation for sorption process 77−80696
diffusion coefficient time depend. from single (de)sorption expt., step-by-step calc. method 78−87859
directional time-lag asymmetry in media with position-dependent sorption and diffusion props. 78−3372
Dowex 50 W×8 cation exchange resin, sorption of Zn^{2+} from HCl soln., temp. depend. *(Bulgarian)* 79−87004
drying intensification, thermolabile porous material in contact with sorbent, in vac. 77−89641
electron irradiation effects on surface prop. of solids 80−70261
endosseous implant material, radiation processed alumina-polyacrylic acid composite 77−60308
epoxies, Ablefilm, Dupont, EPO-TEK and Eccobond, water vapour sorption 79−82454
ettringite, expansion by H_2O adsorption, exam. 78−64806
ferrogel, reaction with $MnCl_2$ solution, production of MnMg ferrites 77−12582
fission reactor primary circuits, nonlinear surface absorption activity *(Russian)* 80−9340
fluid in contact with wall, nonuniform Percus-Yevick and hypernetted chain eqns. 80−15370
gas, analyser error anal. using mean risk criteria *(Russian)* 78−70088
gas absorption, into accelerating thin falling liq. film on inclined surface 78−93632
gas absorption by liquid, exothermicity altering solubility and reaction rate 79−74341
gas absorption in liquid, soln. to nonlinear Volterra integral eqn. 77−72754
gas absorption with second-order irreversible chem. reaction, enhancement factors 78−80727
gas implantation and deposition rate, simultaneous irradiation, injection expts. 78−83855
gas sorption measurement at 12-150K, He cryostat system 78−32823
gas-liquid interface, absorption rate, diffusion coeff., stat. thermodynamics anal. 77−76644
gas-solid barrier permeability, absorption dissoc. anomalous temp. depend. 77−7977
gas-solid energy transfer, test of first order distorted wave Born approx. 77−85876
gas-solid interaction dynamics, energy transfer and sticking calcs. 77−51593
gas-surface energy accommodation, hard-cube model anal. 80−50888
gas-surface interactions, mathematical description based on reciprocity 77−31868
gelatin layer, dry, aqueous soln. penetration 80−85221
glass, viscoplastic, gas-vapour interlayer problem 80−49490
glass fibre reinforced plastics, exposed to liq. media, dynamic high-speed Young's modulus determ. *(German)* 80−85123
glassy polymers, films and spheres, transport props., film thickness and sample history effects 78−76917
graphite fibre reinforced epoxy, mositure absorption in liquids and humid air 79−61897
graphite-epoxy composites, Thornel 300/Fiberite 1034, effects of thermal spiking on moisture absorpt. characts., tensile strength and buckling modulus 79−43330
gravimetric measurement of sorption isotherms, errors 78−67905
haemodialysis and haemoperfusion, joint system, evaluation of novel sorbent systems 78−7542
haemoperfusion systems, characterisation of solute removal 78−44689
heterogeneous catalysis, conference, Varna, Bulgaria (Oct. 1979) 80−82578
hydrocarbon gas, sorption and transport in ethyl cellulose membrane 78−76913
hydrogen storage materials *(French)* 79−66419
hydrous mixed oxides, sorption props. 80−92781
interface of two phases or liquids, selective processes induced by resonance laser radiation 78−64867
interfacial tension minima, dynamic, equilibration of surface-active solute between two liquid phases 80−80026
intermetallic compounds, containing d-transition metal, hydrogenated, magnetism 80−34609
Invar, absorption of H_2, mag. props. effects 80−65787
Invar, magnetic structure, absorbed H_2 effect 80−20534
ionically pumped inert gases, thermal release 77−67450
jet, liquid, turbulent, gas absorpt. *(Japanese)* 80−38473
kinetics, time-lag theory, diffusion coeff. 78−38937
laminate, fibre reinforced composites, moisture diffusion, 3-D Fick's law 78−10218
laminates, exposed to liq. media, dynamic high-speed Young's modulus determ. *(German)* 80−85123

sorption continued
laser calorimetry for absorption meas. 79−55308
laser induced reactions 77−25308
Laves phase AB_2 intermetallic compounds, H_2 sorption, capacity and preferred location 79−43791
Laves phase pseudobinary alloys, absorption capacity of H_2, phenomenological model 77−84935
liquid film, falling, theory of mass transfer 79−65309
liquid film, influence of waves on mass transfer *(Russian)* 79−64677
liquid film, vapour absorption, combined heat and mass transfer 79−19430
lunar soil, of N_2 and water, surface props. of North Ray Crater soil 77−87287
mass transfer mechanism, formation of new crystalline phases 80−6625
melting of plate with internal continuously-active source, influence of absorpt. coeff. *(Russian)* 79−37811
membrane transport sorption and desorption time lag meas. apparatus 78−38428
metal, H_2 absorpt. determ. by mag. sound technique *(Russian)* 77−60009
metal, O_2 diffusion and dissolution effects on optical props. in radiative heating, appl. to Ti 79−65884
metal, with stored H, electronic struct., many electron theory 80−49667
metal surface, sticking coeff. and transmission problem, quadratic phonon coupling effects 80−39424
metal surface, sticking rate, transmission problem, model Hamiltonian 80−107640
metal surface interaction with external mol. complex 79−47140
metal-H_2 systems, determ. of absorption/desorption isotherms, high press. 78−51679
metal-H system, multiplateau absorpt. isotherms, theory 80−103564
metals, gas saturation, apparatus 80−61039
metals, of gas ions, ion collector for expt. investigation of absorpt. and reliberation 79−99254
microporous graphite compact, anomalous diffusion of N_2, time-lag and transient-state kinetic analysis 78−34655
mischmetal-$Ni_{5-x}Al_x$ ternary alloys, Al addition effects on structural and H_2 absorp. props. 79−52761
mischmetal-Ni-Al alloys, H_2 absorpt.-desorpt. characts. 79−95168
Mischmetall-Co_5, absorpt.-desorpt. characts. for H_2 77−89640
molecular gas flow through tube, transmission probability 77−7417
molecules, physisorbed on homogeneous surfaces, NMR study 80−97732
nitrosamine, air sampling sorbents testing 80−77026
nonisothermal mixture motion through porous media, sorption dynamics and heat exchange kinetics 77−7447
oscillating surface, thermal accommodation coeffs., translational and internal energy 77−86354
photographic fixing solutions, Ag extraction using sulphide-containing cellulose fibres *(Russian)* 79−58835
physical chemistry of surfaces, book 77−25310
piezoelectric quartz cryst. microbalance for sorption studies under dynamic conditions 80−73323
PMMA, diffusion-controlled penetration by monohydric normal alcohols 78−76918
PMMA, in distilled water, influence of liquid environmental media on mech. behaviour 78−52902
Polimal 109, polymer resin laminate, density porosity, water vapour diffusion sorption and permeation *(Polish)* 80−59665
pollutants, hydrophobic, sorption on natural sediments 79−83651
poly(m-xylylene adipamide), crystallisation induced by water absorption *(Japanese)* 79−90573
poly(m-xylylene adipamide), water induced crystallisation *(Japanese)* 79−90574
poly(tetrahydropyran-2, 6-diyliminocarbonyl), permeability to H_2O liq. and vap. *(Japanese)* 79−70376
poly-2-hydroxyethyl methacrylate, glass transition temp., water content and tacticity effects 79−37817
poly-n-hexyl L-glutanate, sorption and permeation mechanism 80−26048
polyacrylonitrile glassy polymer, energetics of gas sorption 80−29270
polyarylates, sorpt. kinetics of tetrahydrofuran, struct. transform *(Russian)* 79−51432
polycarbonate, amorphous morphology, from NMR obs. of swelling penetrant mol. motion 79−27929
polycarbonate, glassy polymer, energetics of gas sorption 80−29270
polycarbonate, sorption of water and its effect on dielec. behaviour 79−11383
polyester film, cross-linked, low-mol. wt. substance sorption effect on struct. *(Russian)* 80−59405
polyester-E glass composites, types SMC-25, SMC-65 and SMC-30EA, moisture absorpt. 80−93799
polyesters, linear, H_2O absorption and electric loss factor *(German)* 80−34849
polyethylene, drawn low-density, sorption and diffusion of methylene chloride 79−74210
polyethylene, environmental stress cracking correl. with liq. sorption for low-swelling liqs. 80−81165
polyethylene, in toluene, pressure crystallised, swelling behaviour, rel. to densities 80−2167
polyethylene, molten, N_2 and ethylene solubilities, statistical thermodynamical method, sorption data 78−71859
polyethylene sorption properties, γ-ray effects in N_2O_4 medium *(Russian)* 77−72796
polyethylene terephthalate, glassy, energetics of CO_2 sorption 80−29270
polyethyleneterephthallate, sorption of low MW solvents on struct. and mech. props. *(Russian)* 78−11358
polymer, glassy, gas sorption and transport, review 80−15360
polymer film, swollen, diffusion-relax. cojpling, two-stage sorption correl. 79−94864
polymer films, diffusion coefficients of organic vapours calc. from sorption data 79−77831
polymer films, instrument for studying sorption and diffusion of low-molecular liqs. 79−100305
polymer membrane, penetrant sorption kinetics, transverse differential swelling stresses 78−76923
polymerisation, from emulsion, homogeneous nucleation 79−29354
polymers, glassy, of solvents, sample dimension effects 79−52766
polymers, water absorption, osmotic effects 80−65366
polysiloxane dizwitterionomers, of H_2O, effect on dielec., mech. relax. 80−50261
polysiloxane dizwitterionomers, of H_2O, mechanism 80−49506

sorption continued
polystyrene, of organic vapours, glassy-state relaxation induction and meas. 80−44415
polystyrene-benzene-methanol system, preferential solvation 79−10772
polystyrenecobutadiene, vapour sorption isotherms for benzene and n-heptane 78−68912
polyurethanes, rigid foamed, cellular struct. effect on water absorpt. 80−39416
polyvinyl alcohol, absorption of H_2O mols. from liq., Raman spectrosc. technique 79−42364
polyvinyltrimethylsilane, of hydrocarbons, Xe, permeation selectivity *(Russian)* 80−6564
polyvinyltrimethylsilane, of Xe, hydrocarbons, sorpt., diffusion rel. to temp. *(Russian)* 80−6565
porous media, nonisothermal multicomponent sorption dynamics 77−65793
porous media, sorption dynamics for nonlinear isotherm 77−39734
porous medium with stagnation zones 80−6139
Portland cement, absorbed H_2O, pulsed NMR study 80−84665
Potts model, critical dynamics 80−101766
PTFE fibres, US effects on structure *(Polish)* 78−68702
pump, design, rel. to rotary oil pumps 79−63255
PVA, H_2O swollen, of $TiCl_4$ from benzene solns. *(Polish)* 79−4471
PVC, of organic vapours, glassy-state relaxation induction and meas. 80−44415
PVC, sorption of monomer vapour, effects of previous history, time and temp. 79−4470
pyrazine absorbed on electrode, surface enhanced Raman spectra, symmetry and polarisability changes 80−50310
pyrimidine bases, water vapour effect on struct. and amorphous-cryst. transition 77−70408
radioactice waste storage, interaction of actinides and humic acid 80−13715
radioactive gas distrib. in porous medium, diffusion and sorption effects 79−81964
radioactive substances, numerical soln. of dynamical sorption eqns. *(Russian)* 79−61907
radioactive waste, geological disposal, chemical factors controlling environmental actinide sorption 80−13713
radioactive waste, shallow land disposal, radionuclide sorption 80−16851
radioactive waste storage, Am sorption on major rock-forming minerals 80−13716
radioactive waste storage, mineral-contributed anion effects on the retention of trivalent actinides in the environment 80−13717
radioactive waste storage Sr, Cs, Co sorption meas. on soil sediment 80−95482
rare earth, of $H_2(D_2)$, adsorpt. and absorpt. 77−4257
rare earth alloys, RM_x (R=La, Ce, Pr, Er, M=Co, Ni), H(D) sorption at press. up to 1500 atm. 80−97819
rare earth-Co, RCo_3 (R=Gd, Dy and Ho), effect of absorbed H_2 on mag. behaviour 79−33483
rare earth-Fe_2, mag. props. changes due to H_2 absorption, unit cell vol. 77−63178
rare earth-transition metal alloy, of H_2 77−35812
rare earth-transition metal alloys, H_2 absorption, effect on mag. props. 78−68231
rarefied gas of fast particles interacting with cryst., kinetic eqn. *(Russian)* 77−55440
sediments in laboratory-scale aquatic ecosystem, radioisotope behaviour 78−3831
selective interactions of laser radiation, photoionisation [-] elementary processes 77−27034
shale investigation as radioactive waste repository, vermiculite role 80−32354
silica, colloidal, liquid imbibition characteristics *(Japanese)* 78−95963
sintered composite-liq. metal interaction, mass transfer eqn. approx. soln. 78−67262
skin, human, permeation of scopolamine in vitro 77−21487
soil water absorption with exponential diffusivity, infiltration and perturbation methods 77−66944
solid sorption systems, spectroscopy via IR cell with Si windows 78−299
solid-gas and solid-liquid interfaces, struct. rel. to reactivity 77−72775
specific heat meas., 4.2 to 90K, USSR special standard 77−31207
stainless steel oxides, of Cs, meas. of contamination using washing test 78−62597
stearic acid films, evaporated, vac. effects 80−97435
steel, austenitic, neutron irradiated, He absorption 77−51414
steel, C, accelerated deform. by to H_2 absorption *(Japanese)* 79−70121
steel, H_2 absorption, effect of organic inhibitors *(Russian)* 78−35570
steel, hydrogen absorption, anilines surfactants effectiveness, HCl conc. effect 80−108638
steel, hydrogenation and cracking in H_2S, cathodic polarization and surface layer effects *(Russian)* 77−52528
steel, low-alloy hydrogenation and embrittlement under neutron irrad. in contact with water *(Russian)* 77−52529
steel, mech. strength, effect of H_2 sorption and Al and N_2 surface treatment *(Russian)* 78−31570
steel, stainless, dissolution kinetics of Ti *(Russian)* 80−34193
steel, stainless, oxidised, of Cs 78−84061
stratum corneum of rat, surfactant diffusion and sorption phenomena, model for human skin 78−77007
subsoil, ^{241}Am, ^{237}Np and ^{99}Tc sorption on USA subsoils from differing weathering intensity areas 78−16014
surface energy, theory and appls., symposium, New York, USA (Apr. 1976) 77−55422
surface reactions, kinetics and dynamics, conf., La Jolla, CA, USA (Aug 1979) 80−105415
thermal accommodation coefficients determ. using modified Knudsen manometer 77−26320
thermal radiation detector sorbent test 79−29403
thermodynamics, equilib. and nonequilib. processes, review 77−44505
transient diffusion of gas in highly dispersed sorbing porous solid 77−15114
transition metal ferrocyanide selective sorbents for alkali metals, sorptive props. w.r.t. struct. 80−101051
transition metal intermetallic cpds., H absorption and mag. props. 80−60224
transpiration, thermal, effect of gas-surface interaction, dusty gas theory 77−19634
turbulent liquid film, gas absorpt. accompanied by first order reactions 79−69327
vacuum deposition, evaporation source mol. distrib. and effect of accommodation coeff. *(French)* 77−69999
vacuum gap electrode surface sorption, mass spectroscopic obs. 78−75466
Vacuum Society conf., San Francisco, USA (Nov. 1978) 79−77862
vermiculite, of ^{106}Ru and ^{59}Fe *(Russian)* 77−38370
vermiculite, sorption props., appl. to radioactive fallout water deactivation 79−43995
work function fast variation meas., photoelectric method 79−91561
zeolite, hydrated Na-Y, ^{23}Na pulsed NMR free induction decay 80−84660
zeolite interface, ionic conduction bands 77−35745
Zircaloy, H absorption, Sn(Fe)(Cr)(Ni) effect 80−49527
Zircaloy-4/stainless steel type 304 diffusion junction, hydriding behaviour 79−65200
$^{239,240}Pu(V)$ in alkaline freshwater pond, determ. by coprecipitation technique 80−71988
Ag, of pyridine, surface enhanced Raman scatt., mol.-surface separation depend. 80−92775
AgBr absorption of gelatine *(Russian)* 79−100420
AgBr:Pb^{2+}, cubic microcryst., ion influence on ionic cond. and space charge characts. 79−55928
Al, reaction with H_2, influence of surface reactions on rate *(Russian)* 80−66863
Al_2O_3-B_2O_3 system, phase comp. and sorption props., Al salts chem. nature influence 79−51426
β-Al_2O_3-H_2O, stability and dehydration 78−51693
β''-Al_2O_3-Na_2O, absorbed water effect on NMR lineshape and spin-lattice relax. time 80−108098
Ar^+, in rarefied plasma stream, energy accommodation coeffs. meas. by thermoanemometric sounding 80−16722
C allotropes, diamond, graphite, gas-solid interface, electronic struct. HFR calc. 80−54745
C, impregnated, reaction steps in gas sorption 78−68916
CO_2 absorption in H_2O, aq. solns. with interfacial turbulence due to microstirrers 80−64527
Ce, gettering of H, mass spectrometry and microgravimetry study, rel. to HTGR gas purification 80−73374
Ce-M intermetallic cpds., M=3d transition metal, of H_2, structural charges 80−88429
Ce_3Co, of D, heats of reaction and equilib. press., T-getters for CTR 78−51683
$Ce_{5.3}Co$, of D, heats of reaction and equilib. press., T-getters for CTR 78−51683
$Ce_{8.5}Fe$, of D, heats of reaction and equilib. press., T-getters for CTR 78−51683
Ce_xMg_y, hydrogen storage materials *(French)* 79−66419
$CeMg_{11}V(Cr)(Mn)(Fe)(Co)$, of H_2, and appl. in H_2 storage 80−51009
$Ce_{4.5}Ni$, of D, heats of reaction and equilib. press., T-getters for CTR 78−51683
Ce_2O_3, hydrated, sorption props. rel. to dehydration conditions 79−66345
$CeRu_2$, H absorption induced Ce valence change, mag. and supercond. props. 80−50042
Cs, in nuclear graphite, sorption kinetics modelling 80−102244
Cs sorption in Ba-impregnated nuclear graphite, thermodynamic modelling of multicomponent sorption behaviour 80−102243
Cs, transport in soil, evaluation of combined sorption model 79−8554
^{137}Cs conc. meas. in ocean, sorbent props. *(Russian)* 79−39763
Cu, crysts., absorbed H, strain anal., X-ray divergent beam method 78−15463
Cu, liquid, absorption of gaseous O_2 78−51686
D-T fusion reactor, tritium recovery using Zr, Y *(Japanese)* 78−29646
D_2, sticking and accommodation on low-temp. substrate, mol. beam expts. 80−84368
Dy, and $DyMn_2(Fe_2)(Co_2)(Ni_2)$, H_2 absorpt., Mossbauer study 80−44987
Er film, work function, effects of O_2 sorption 78−19125
$ErCo_3$, absorption of H_2, 77-300K 79−23737
$EuRh_2$, H_2 absorbing, degradation by cycling 78−34628
Fe alloys, liquid, complex, diffusivity and solubility of N_2 at 1600°C 77−39684
Fe, liquid, absorption of gaseous O_2 78−51686
Fe, of water, visualisation using THO and autoradiography 78−26761
Fe, single crysts., absorbed H, strain anal., X-ray divergent beam method 78−15463
Fe, zone melted, H_2 diffusion, reversible lattice dilation 77−11732
Fe-C, levitated drops, carburisation and decarburisation in CO-CO_2 gas mixture, exam. of reaction kinetics 78−85053
Fe-Ti, magnetism and H_2 storage 80−70941
Fe-Ti alloys, of H_2, appl. to industrial hydride reservoirs for H storage 80−45792
Fe-V(Cr)(Mn)(Ni), unlimited component solubility, intercrystallite internal adsorption *(Russian)* 80−39294
ε-FeTi, Ce addition effect on H_2 absorption capacity 79−61899
ε-FeTi, effect of Ce on H_2 absorption 79−73315
FeTi, surface and mag. props., heat treatment and hydrogenation effects 80−75447
$FeTiD_x$ ($0 \leq x \leq 1.9$), structural phase transitions, absorpt. and desorpt. isotherms 80−19948
^{57}Fe paramagnetic ions sorbed on cation exchange resin, chem. information from relax. Mossbauer spectra 77−70332
^{59}Fe on natural sorbents clinoptilolite and vermiculite *(Russian)* 77−38370
Gd-Al-Co, H sorption props. for H storage, influence of Al 80−45794
GdM_2, (M=Mn, Fe, Co, Ni, Rh, Ru, Ir, Al), H_2 sorption props. 79−86980
H^+, energetic beam direct cryosorption pumping 80−105655
H_2 absorption and desorption kinetics in $LaNi_5$-type ternary alloys 80−55932
H_2, solubility in Ni, Ni-Cr, Ni-Mo, 500-1000°C *(Japanese)* 78−38845
H_2 sorption kinetic studies using high-accuracy volumetric device 79−56071
H_2 sorption/desorption by ternary $LaNi_5$ type alloys, reaction kinetics 80−45813
H_2, sticking and accommodation on low-temp. substrate, mol. beam expts. 80−84368
H_2, v.p. meas. 2 to 4.5K, influence of thermal radiation 77−5848
Hf based intermetallic compounds, of H_2 79−77754
Hf_2Fe, moment form. on H_2 absorpt. 79−87343

sorption continued
$HfV_2H_{2.1}$, proton NMR relax. time and Knight shifts, diffusional activation energies meas., sorption props. 80−75871
Hg, determ., cold vapour atomic absorption method, sorption effects *(Russian)* 78−73122
Hg determination by cold vapour at. absorpt. spectroscopy, effect of sorption on sensitivity 79−52829
^{166}Ho electrosorption on anodically polarised Pt surface 79−52684
I_2 adsorption on steel in HTGR He environment 80−44233
^{129}I, in reactor waste, sorption by minerals 79−49721
^{131}I, dynamic sorption from gas phase of dissociating N_2O_4 *(Russian)* 78−58356
La-Ni alloys, D_2 absorption, 500-700°C 79−23736
$La_{1-x}Ca_xNi_5$, H_2 sorption props. 78−91533
$La_{0.003}Ba_{0.66}Sr_{0.34}TiO_3$, water absorpt., mech. strength, stability, TCR *(Russian)* 80−16511
$LaCo_5$, N_2 absorpt. at low temps. 80−24599
La_2Co_7, mag. props. changes upon H_2 absorpt. 80−71270
$La_{0.9}Eu_{0.1}Ni_{4.6}Mn_{0.4}$, absorption-desorption props. of H_2, degradation mechanism, Mossbauer study 80−88431
LaM_2, (M=Rh, Ru, Pt, Ir, Al), H_2 sorption props. 79−86980
La_2Mg_{17}, of H_2, characts. on H_2 carrier 77−84933
La_xMg_y, hydrogen storage materials *(French)* 79−66419
$LaNi_5$, of H_2, absorption rates, diffusion consts. 78−14508
$LaNi_4$, absorption and desorption of H_2 77−81400
$LaNi_5$, absorption of H_2, 77-300K 79−23737
$LaNi_5$, activated, slow step for H_2 absorpt. (desorpt.) 78−18894
$LaNi_5$, appl. as H storage system for heat engines *(Ukrainian)* 78−67022
$LaNi_5$, H_2 absorption in thin film hydriding alloys 80−65238
$LaNi_5$, magnetism and H_2 storage 80−70941
$LaNi_5$, of H, rel. partial absorption (desorption) enthalpies 80−50881
$LaNi_5$, of H_2, for storage appls., effect of Ni, Ce, Co alloying additions 80−45790
$LaNi_5$, of H_2, kinetics *(Chinese)* 80−103561
$LaNi_5+3H_2 \rightleftarrows LaNi_5H_6$ reaction, absorpt. capacity and reaction kinetics 79−43626
$LaNi_4Al$, solubility and sorption props. of H_2, effect of Al 80−103482
$LaNi_{5-x}Al_x$, H_2 absorpt.-desorpt. kinetics rel. to metal hydride appls. 77−86308
$LaNi_{5-x}Al_x$ ternary alloys, Al addition effects on structural and H_2 absorpt. props. 79−52761
$LaNi_{4.4}B_{0.6}$, H_2 absorpt. props. 80−88432
$La(Ni_{1-x}Cu_x)_5$, H_2 sorption props. 78−91533
$LaNi_5H_{\geq 3.0}$, H diffusion coeff., neutron scatt. obs. 80−24643
$LaNi_{4.6}In_{0.4}$, H_2 absorption props., desorpt. pressure calc., and decomp. pressures 79−24827
$LaNi_{4.6}Sn_{0.4}$, H_2 absorption props., desorpt. pressure calc., and decomp. pressures 79−24827
$LaRu_2$, H absorption induced Ce valence change, mag. and supercond. props. 80−50042
Li-Bi(Al), of tritium, for appl. in thermonuclear reactor 77−1301
LiBr absorption air conditioner, solar powered, computer-aided performance predictions 79−62134
$LuFe_2$, mag. props. changes upon H_2 absorpt. 80−71270
$LuMn_2$, Lu_6Mn_{23}, H_2 absorption effect on mag. props. 77−89931
Mg, vaporised, evidence for gas-surface exchange 78−91532
Mg-$Mg_{17}Y_{13}$, of H, high temp. hydrides for H storage 80−45793
Mg-Mg_2Ni, of H, high temp. hydrides for H storage 80−45793
$MgCu_2$, of H_2, appl. to industrial hydride reservoirs for H storage 80−45792
Mg_2Cu sorption capacity, grain size distrib., and compactness for H_2 storage appl. 79−74547
Mg_2Ni, magnetism and H_2 storage 80−70941
Mg_2Ni sorption capacity, grain size distrib., and compactness for H_2 storage appl. 79−74547
Mn film, vacuum-evaporated, H(D) uptake kinetics and energetics 80−88430
Mo and alloys, absorption of N_2 in induction and plasma-arc heating *(Russian)* 77−16732
Mo film, work function, effects of O_2 sorption 78−19125
N_2^+, in rarefied plasma stream, energy accommodation coeffs. meas. by thermoanemometric sounding 80−16722
NH_3/H_2O absorption unit for solar air conditioning, design and performance 79−62129
$(NH_4)_{0.8}Ni_{1.1}PO_4.xH_2O$, of Cs^+ ion, ion exchange 77−9121
Na_3AlF_6 film on Si, fused quartz substrates, absorption of H_2O, IR anal. 80−75446
$Na_2O-B_2O_3$ glass, absorptivity of OH determ. 79−52763
$Na_2O-B_2O_3-SiO_2$, optical waveguide glass, molar absorptivity of water 80−80066
Nb, H uptake rates, enhancement by thin surface overlayers of Pd or Pt 79−82345
Nb, of H, rate, metallic film effect 80−49525
Nb-V system, H_2 absorpt. 80−59808
Nb-Zr-C (0.1, 0.01 wt.%) plastic deform. influence on electronic state of Nb atoms 80−40463
$NdCo_5$, absorption of H_2, 77-300K 79−23737
Ni, liquid, absorption of gaseous O_2 78−51686
Ni, of Na, Rb and Cs, accommodation coeffs., 685-1095K 77−47666
Ni to NiH_3 transition, magnetic study of activation energy 78−71860
Ni-Mn, hydrogenation kinetics, magnetisation, interstitial H influence 80−35528
$Ni_{62}Ti_{29}Zr_9$, amorphous, H-sorption, X-ray and DSC obs. 80−49526
$Ni_{64}Zr_{36}$, amorphous and cryst., H-sorption, X-ray and DSC obs. 80−49526
O_2 by water in rotor-pulsated disc apparatus *(Russian)* 77−84312
^{233}Pa removal from ^{237}Np by coprecipitation with MnO_2 or sorption on silica gel 79−52733
PbS(Se) film, moisture drift origin 77−20187
Pd film, discontinuous, on rocksalt, elec. cond., H_2 absorpt. effects 77−47905
Pd layer, adsorption and absorption of H_2, kinetic analysis of models 77−47679
Pd membrane, gaseous H quasiequilib. processes, 100-500°C, 10^{-4}-10^{-2} torr 77−29047
Pd membrane, H atom interaction, superpermeability 80−81365
Pd membrane, of H_2, adhesion and penetration probabilities, extreme values 80−101040
Pd-Ag(Cu) systems, positron annihilation, absorbed H_2 effect *(Russian)* 79−91528

sorption continued
Pd-D, crystallite size effects, simultaneous sorption and X-ray study 80−65237
Pt, electrosorption of H_2, oxidation, effect of soluble prods. *(German)* 80−55717
Pt wire, O_2 covered, accommodation coeff. meas. of Ne(Kr), 400-1400K 77−63948
Pt-Pd system, sorption of H_2 during cathodic charging, deflection technique meas. 79−51427
Re-O-Cl system, gas-transition metal interaction, kinetic model *(French)* 80−108740
ReO_3, absorpt. of H_2, electron diffr. obs. of H_xReO_3 phase 79−60513
^{106}Ru on natural sorbents clinoptilolite and vermiculite *(Russian)* 77−38370
Si amorphous film, vacuum deposited, microscopic voids, gas absorpt., crystn. study 80−49534
$SmCo_5$, H_2 absorption in thin film hydriding alloys 80−65238
T, in Pd, isotherms at low equilib. press. 79−14935
T, removal from liq. K and Li by sorption onto Y, fusion reactor breeder blanket 78−66411
Ta, absorption kinetics of H_2, 77-700K, effect of O_2 sorption layers 79−95169
Ta, H uptake rates, enhancement by thin surface overlayers of Pd or Pt 79−82345
Ta, of H, rate, metallic film effect 80−49525
Ta wire, H-absorption kinetics between 500 and 700K 80−49528
Ta-W-Hf (8,2 wt.%), T-111, of O_2, effect on lattice parameter and specimen dilation 78−83958
$Ta_2O_5-H_2O_n$, influence of preparation on pore structure and ion exchange props. 79−1970
^{99}Tc in reactor waste, sorption by minerals 79−49721
^{99}Tc, reduction and sorption in granitic bedrock, biological hazard estimation 79−79415
$Th_7Co_3(Ni_3)$, effect of absorbed H_2 on mag. behaviour 80−60184
$ThMn_2$, Th_6Mn_{23}, H_2 absorption effect on mag. props. 77−89931
Th_6Mn_{23}, absorption of H_2, influence on mag. behaviour 77−85423
$ThNi_{5-x}Al_x$, absorption of H, form. of hydride 77−84932
ThO_2, sol-gel, for nucl. applics., sorption of water, CO_2 and N_2 77−4940
Ti, film, CO surface contamination effect on deuteriding 77−35814
Ti, film, isotope effect on pumping speed of H_2 and D_2 78−51819
Ti film, work function, effects of O_2 sorption 78−19125
Ti, gettering of H, mass spectrometry and microgravimetry study, rel. to HTGR gas purification 80−73374
Ti, of H_2 and N_2, gas-discharge device appl. 80−10796
Ti sheets, porous, absorpt. of gases 78−60602
Ti sorption pump for molecular beam detector 78−21150
Ti thin films, H absorption and desorption, Tokamak gettering, Auger electron spectrosc. 80−75092
Ti-Co(Ni) alloys, of H_2, thermodynamic parameters calc. 80−2268
Ti-Co(Ni) alloys, press.-composition-temp. relationships, enthalpy, entropy 80−2267
$Ti(Al_xB_{1-x})_2$ (B=Cr, Mn, Fe, Co), $0<x<0.4$, influence of Al on H sorption props. X-ray cryst. struct. determ. 79−28198
$Ti_{0.75}Al_{0.25}H_x$, $x<1.5$, metastable hydride form. 78−51682
$TiCo_{1-x}Mn_x$, H absorption-desorption characteristics 80−96735
TiO_2, nonstoichiometric anodic films, O incorporation kinetics 80−97733
$Ti_{1-x}Zr_xMn_2$, hydride formation, hydriding characts. of reversible uptake 78−44402
U extraction from natural seawater, by sorption techniques 79−29902
U ore processing by filtration-free sorption method 79−26664
UO_2, of gaseous fission products 77−46291
V-Cr alloys, absorption of H_2, thermodynamic parameters 78−87862
W, N_2 and CO_2 thermal accommodation coeffs., gas saturated system 77−70335
W, of He, gas-solid interaction dynamics, energy transfer and sticking calcs. 77−51593
W, of Ne, He, tangential momentum accommodation coeff. meas. by acoustic vel. and absorpt. obs. 80−66867
Y, of T, 250-400°C, rel. to possible appl. for T recovery from molten Li blanket in fusion reactor 79−90784
Y, of T, recovery from liq. Li fusion reactor blanket 80−95434
Y-M intermetallic cpds., M=3d transition metal, of H_2, structural charges 80−88429
Y-Mn system, absorption of H_2, lattice consts. and mag. props. 77−36061
YMn_2, Y_6Mn_{23}, H_2 absorption effect on mag. props. 77−89931
Y_6Mn_{23}, absorption of H_2, influence on mag. behaviour 77−85423
YNi_3, loss of ferromagnetism after H_2 absorpt., Pauli paramag. props. 80−34588
$YNi_{5-x}Al_x$ ternary alloys, Al addition effects on structural and H_2 absorpt. props. 79−52761
^{90}Y electrosorption on anodically polarised Pt surface 79−52684
^{169,175}Yb electrosorption on anodically polarised Pt surface 79−52684
Zn-Al, dil., isotherm of internal adsorption at dislocations 79−37733
ZnS film on Si, fused quartz substrates, absorption of H_2O, IR anal. 80−75446
Zr based intermetallic compounds, of H_2 79−77754
Zr, gettering of H, mass spectrometry and microgravimetry study, rel. to HTGR gas purification 80−73374
Zr pseudo-binary alloys, $Zr(A_xB_{1-x})_2$ (A=V, Cr, Mn; B=Fe, Co), H_2 absorpt. capacity 80−88433
Zr-3d Laves phase binary and pseudobinary intermetallics, mag. props. H absorpt. effect 80−88821
Zr-Al-Cr H sorption props. for H storage, influence of Al 80−45794
Zr-Al-V, H sorption props. for H storage, influence of Al 80−45794
Zr-Al-(Fe,Co), H sorption props. for H storage, influence of Al 80−45794
Zr-N system, hydrogenation, phases form. 79−43200
$Zr(Al_xCo_{1-x})_2$, Laves phase, H_2 absorption capacity meas. 78−87866
$Zr(Al_xFe_{1-x})_2$, Laves phase, H_2 absorption capacity meas. 78−87866
ZrC, of O_2, effect on work function, thermionic emission and thermal desorption obs. 79−56285
ZrC-W, eutectic alloy, H_2 adsorption and dissolution 79−69951
$Zr(Co_xM_{1-x})_2$ (M=V,Cr,Mn) H absorption and desorption props. 77−55448
$Zr(Fe_xM_{1-x})_2$, (M=V,Cr,Mn), H absorption and desorption props. 77−55448
$ZrMn_2H_x$, proton NMR relax. time and Knight shifts, diffusional activation energies meas., sorption props. 80−75871

sorption continued
$ZrS_2Cs_{0.37}$, lamellar cpd., gas absorpt. 80−44418
$Zr(V_{1-x}Co_x)_2$, of H_2, relation between electronic struct. and H_2 storing props. 80−76662
sorting
see also merging
arrhythmia sorting, oesophageal electrode for atrial electrogram 79−39574
cell sorting, automated, with flow systems, review, book contrib. 79−5435
multi-parameter expt., one-pass sorting method 77−87748
multispike signal detection and sorting hardware 79−79711
sorting programs *see sorting; utility programs*
SOS integrated circuits *see field effect integrated circuits*
sound *see acoustic waves; acoustics*
sound amplification *see acoustic wave amplification*
sound broadcasting *see radio broadcasting*
sound field *see acoustic field*
sound generators *see acoustic generators*
sound intensity *see acoustic intensity*
sound measurement *see acoustic variables measurement*
sound propagation *see acoustic wave propagation*
sound ranging *see sonar*
sound reproduction
see also audio acoustics; audio recording; pick-ups
accuracy of reproduction determ., w.r.t. ear props. *(German)* 80−106703
acoustic feedback's influence on speech intelligibility 80−23859
acoustical research laboratory design for the Rensselaer Polytechnic Institute 77−80036
artificial head stereophony, tone meas. *(German)* 80−106702
artificial head system, transmission errors causes and improvements *(German)* 80−106700
artificial heads with stereophonic intensity signals, directional effects *(German)* 80−106701
automatic control in cinema *(Russian)* 80−38212
cinefilm, Dolby stereo procedure for optical sound prints *(German)* 80−18030
concert halls, hearing impressions of loudspeaker reproductions and orchestras *(German)* 78−94485
digital systems for use in cinematography *(Russian)* 79−27487
domestic room acoustics, speaker positioning for optimum frequency response 77−54845
dual language, Super 8, airborne cinematography appl. 80−4785
dummy head design comparisons 79−18656
electronic modification of room acoustics in a concert hall 77−3702
equalisers as universal sound quality control instruments *(German)* 79−64399
fidelity, comparison of acoustic measurements and hearing tests 79−83792
hearing and pain thresholds, cassette recorder noise and music levels *(German)* 80−81616
high fidelity, components and characts. 80−77582
high fidelity sound, perception of sound and music 80−42014
home cinefilm sound track using stereo tape recorder 78−16883
impulsive noise reduction on gramophone records 80−87689
lateral, phantom sources generated by two loudspeakers, localisation 77−54849
lip synchronised recording technique for speech translation in cinefilms *(Russian)* 80−105737
listener's perception thresholds, mono, stereo, pseudo-quadrophonic, quadrophonic systems study *(Polish)* 80−5906
listening room, reverberation time and reproduced sound definition 79−18606
living room loudspeaker performance problems *(German)* 79−90081
loudspeaker design for domestic appls. *(Italian)* 80−91960
loudspeaker measurement, by application of digital techniques 77−68345
loudspeaker reproduction at home, characts. and problems *(German)* 79−72755
loudspeaker vented alignments, providing fourth order responses 77−68356
magnetic stripes on professional cinefilm, construction, coating techniques, reproduction quality 79−85188
magnetic tape synchronisation with cinefilm, digital technique *(German)* 79−35866
mobile sound reinforcement system for musical performances in New York City parks 78−1509
monitoring, acoustic factors in cinemas, dubbing theatres 78−33961
motion picture, methods of improving sound reproduction in cinemas *(Russian)* 79−10430
motion picture sound recording and reproduction using a holographic method *(Russian)* 79−10273
motion picture sound track, freq. distortion and two dimens. sound record scatt. *(Russian)* 80−95175
motion picture theatres, acoustic response measurements and standards 77−19496
multidimensional audio, meas. and hearing sound quality 79−64458
music, in small rooms, acoustic theory *(Spanish)* 78−38155
noise eval. in motion picture studio recording room *(Russian)* 78−55518
optical sound track reproduction using photodiode as current source 79−10439
Pfield principle, Hi-Fi music reproduction *(German)* 80−87685
photographic sound track, cine film KINTEK 7 channel system 80−28403
photographic sound track quality increase *(Russian)* 80−22464
psychoacoustic and sound recording, book 77−826
psychoacoustics and the perception of space, stereo reproduction appl. 79−100623
in review rooms and theatres, meas. standard, calc. 77−54844
room acoustic effects transmission, uniplanar and biplanar eidophony *(German)* 80−106699
room acoustics analyser using public telephone line and computer 77−35004
room influence on music rendering, unified sound field anal. *(German)* 77−11092
sound differences in sensory space *(Russian)* 78−55521
stereo perception space, in intensive stereophony (quadrophony) *(Czech)* 79−68491
sound reproduction continued
stereophonic cinefilm, 4-channel photographic sound track, CCD, system Colortek *(Russian)* 79−58818
stereophony, reproduction of sound effects using microphone and headphones *(German)* 79−37106
studio equipment for film, TV studios, circuit diagrams *(German)* 80−18031
subjective evaluation tests of audio perception thresholds from front and rear *(Polish)* 79−55288
synchroniser cct. for image, sound in amateur cine films *(Russian)* 79−6210
teaching a physics course based on the fundamental principles of hi-fidelity 77−33733
theatrical sound effect for cine films *(Spanish)* 79−41550
transistorised system Century, cinematography appl. *(Russian)* 79−14194
triphonic system using coincident microphones 80−28405
sound waves *see acoustic waves*
space charge
see also limited space charge accumulation; space-charge-limited conduction; space-charge limited devices
AC corona meas. using field-filter probes 80−47082
acetone, rel. to transient pressure-drop fluctuations in electroviscous effect 80−15286
air, predischarge-stabilised breakdown voltage *(German)* 78−63608
air, rod-to-plane gap, impulse voltage meas. *(Japanese)* 80−87970
air, Trichel corona, negative ion form. 77−35425
air gap between electrodes, conducting body and space charge effect on breakdown 79−50919
air HF corona discharge ignition characteristics 78−67589
alkali metal seeded plasma, calc. of thermal nonequilib. near-electrode region 77−55186
alkali metal tungsten bronzes, enhanced supercond. T_c, possible explanation 78−14850
amorphous solid, anomalous transient-time dispersion 78−31155
anodic oxide films, space charge, TSC obs. 77−32326
anodisation, high space charge conditions in large elec. field, single carrier steady state theory 77−48561
anthracene, off-diagonal electron mobility and lateral space charge drift 78−72192
arc with emitting cathode, ignition, rel. to Cs diode 77−7623
arc with emitting cathode, ignition 77−7622
atmosphere, space charge generated by surf, meas. 78−36235
atmosphere electrode effect obs. at mountain 79−25307
atmosphere over oceans, space charge and elec. field short period fluctuations 79−39816
avalanche growth in space charge stabilised nonuniform fields, formative time-lag calc., physical model 80−49038
beam-plasma system, explosive instability due to helical electron beam 77−68807
benzene cation+benzene, fragment ions trapped in electron space charge 80−89470
biological sample electron probe microanal., charging effect in electron-irrad. ice 78−57141
blocking electrode, statics and dynamics of space charge regions, numerical anal. 79−51670
boundary conditions for space charge surface layer at electrode plasma boundary, particle flux *(Russian)* 78−55736
breakdown wave propagation in ionised gas in nanosecond discharges 80−87890
carrier traps in polymeric insulating materials, investigation by X-ray induced thermally stimulated current and thermoluminescence methods 80−93240
cathode lens, transient processes, finite-particle method 77−61909
cathode sheath, ion field effect on field emission characts. 77−66582
cathode spot of a vacuum arc, space-charge layer at electrode surface 80−24290
cavity plane magnetron, averaging method, electron tongues *(Russian)* 78−37037
charged particle acceleration in nonadiabatically varying uniform mag. field 77−27236
charged particles, plane-symmetric finite-emittance beams, combined effect of space-charge and external fields 77−23605
chloroform HV polarisation and space charge obs. *(Russian)* 80−25277
cholesteric liquid crystal with anisotropic dielec. permeab., transient electrodynamic instability *(Russian)* 78−51418
cholesterol, dielectric props. under UV excitation 80−6912
cholic acid, dielectric props. under UV excitation 80−6912
collective ion acceleration by cyclotron of space charge waves in relativistic electron beam 77−24204
collective ion acceleration in relativistic electron beam diode, intense slow space charge generation 78−9863
collective ion acceleration using space charge waves on electron beams 80−13995
conducting medium, inhomogeneous, anisotropic, thermal fluctuations of current density, EM fields, and charge density 78−23067
corona, AC, obs. at 50 Hz, DC electric field influence *(German)* 80−70052
corona, multifluid behaviour between elec.-stressed spherical cathode and spherical anode 80−10443
corona AC, point-plate arrangement, behaviour near threshold voltage obs. *(German)* 80−70051
corona discharge, anomalous athode drop, elec. field form. *(German)* 77−43088
corona discharge, computing process for electrons and ions distribution determ. 79−4204
corona system, under neg. direct and pulsed voltage, characts. 79−19107
current runaway in insulators affected by impact ionisation and drift 78−39501
cyclic accelerators, parametric resonance of betatron oscills., space charge influence 77−67923
DC corona discharges in coaxial cylinder electrode, time variation of ionic mobility 80−33837
degenerate junctions with position-dependent band struct., density-voltage relations 79−87150
dielectric, electron beams as virtual electrodes, review 80−6861
dielectric, ion implantation, space charge elec. field effect 79−82250
dielectric, mean potential and electric field determ. 79−24262
dielectric block, solid, between point-plane electrodes, treeing inception conditions calc. *(French)* 77−38771

space charge continued
dielectric electret effect, homo and heterocharge charge distribution 80−11317
dielectric electron irradiation and space charge accumulation *(Russian)* 79−38450
dielectric film, space charge quantity meas. by Maxwell stress method 80−22389
dielectric fluid, space charge transfer by slow flow, in strong nonuniform elec. field *(Russian)* 78−75223
dielectric liquid, charge generation and transport from contacting surface, Mach-Zehnder and Schlieren obs. 80−20589
dielectric liquid, elec. stressed, motion due to Coulomb, electromech. forces, schlieren image obs. 80−100037
dielectric liquid, polarity effect on breakdown voltage in inhomogeneous field 77−52018
dielectric liquid, stationary EHD instability, charge carrier mobility temp. induced variations effects 79−77269
dielectric liquid with electrolytic dissoc. of additive, weak conductivity *(Russian)* 78−27161
dielectric solid, resorption current calc., boundary conditions using method of joint characts. 80−40055
dielectric solid, resorption current due to space charges 80−40053
dielectric solid, resorption current for steplike charge distribs. 80−40054
dielectric solid, space charge density distrib. and I-V characts. from current injection coeff. 80−39589
dielectric solid, space charge distribs., indeterminability limits 80−40056
dielectric solid, space charge problems by analogue modelling on field analyser 80−40058
dielectric solid, space-charge behaviour, effect of relax. processes 80−40057
dielectric solid, space-charge distrib., investigative method 80−40059
dielectric solids, space charge phenomena, decay function and resorption current 80−40052
dielectric space charge distrib., carrier mobility and interface injection mechanism identification 80−15974
dielectric trapping, bremsstrahlung shielding meas. 78−78507
dielectrics, fast electron effects, space charge build up, range reduction 77−72636
dielectrics, field induced thermally stimulated polarisation-depolarisation currents, relaxation, book contribution 80−80687
dielectrics, potential distrib. determ., non-destructive method *(French)* 80−40060
dielectrics, props., model of relax. phenomena 77−63366
dielectrics, radiation induced charging and discharging, analytic solution 79−78612
dielectrics, space charge static states and evolution dynamics *(French)* 79−69774
dielectrics, space charge studies of elec. phenomena 80−24939
direct energy space charge based convertor, numerical simulator 77−35406
discharge current induced by charged particle motion in space charge filled gap 80−24283
double injection p-i-n structures in magnetic field 80−107899
electret discharge model, injection relaxation mechanism, space-charge cond. 78−80279
electrets and dielectrics, conf., Sao Carlos, Brazil, Sept. (1975) 80−7251
electric discharge in transverse magnetic field, anode sheath, theory 77−35432
electric field, variable space charge density, design, between hyperboloidal conic electrode and grounded plate *(Czech)* 80−87258
electric field averaging at cathode in space charge sheath 77−19806
electro-optic crystals, hologram formation arbitrary transport length anal., photovoltaic effects 80−78802
electrochemical kinetics at interface with space charge layer, appls. *(German)* 77−32807
electrode flashover voltage, effects *(Japanese)* 79−50917
electrode-insulator boundary, current injection in presence of space charge 79−1619
electrographic development, electrostatic calc. 80−77888
electron beam, in inhomogeneous plasma, space charge wave generation 79−41845
electron beam, intense, ns, production in linear accelerator, space charge and radiation field effects 78−70654
electron beam, ion neutralisation, probe beam diagnostics 79−27157
electron beam, relativistic, high-current, in microwave linear accelerator, transient behaviour 80−32541
electron beam, relativistic, solid, vac. propag. 79−59625
electron beam, relativistic, space-charge limiting current simulation 79−59626
electron beam, wave amplification by spatially periodic mag. field, space charge waves 77−19158
electron beam broadening effects caused by discreteness of space charge 80−69309
electron bunch, relativistic, instability in reson. storage chamber 77−54381
electron layer, low density, in homogeneous mag. field orbital motion instability 77−65561
electron plasma relax. characts., 3-30 eV 80−79612
electron probe devices, space charge effects 79−27154
electrostatic double layers, review 78−67368
electrostatic ion analysers for laser prod. plasma detection, space charge effects 80−96392
electrostatic mirror, second order focusing space charge effects 77−50598
elliptic beam in cylindrical conducting pipe of circular cross section, space charge potential and field *(French)* 78−42261
epoxy-resin, Nomex-filled, space charge polarisation, thermal depolarisation current study 80−7282
free space charge motion, exact solution 77−10809
gas discharge, electron beam excited, space charge and inhomogeneous ionisation *(Russian)* 77−47281
glasses, high-resistivity, uniform and space charge polarisation, thermally stimulated depolarisation anal. 78−15085
Green's function for perfectly conducting cylinder *(French)* 78−25770
gyrotrons, space charge phenomena 80−28868
gyrotrons and gyrokylstrons, small signal theory, fusion reactor appl. 78−70633
haemoglobin, dielectric props. under UV excitation 80−6912
helical electron beams, extended and intense with space-charge forces, trajectory anal. *(Russian)* 79−918
space charge continued
helical electron beams, trajectory anal. with allowance for space-charge forces 79−86127
n-hexane, subjected to charge injection, low stress mobility, induced motion effects 79−91063
HF discharges, near-electrode layers of space charge effect on electrodynamic props. 78−30510
hollow beam in magnetically insulated beam, characts. 80−5398
hologram writing by photorefractive effect, Gaussian beam at const. voltage 77−3552
II-IV p-n amorphous heterojunction, phenomenological model 80−54769
III-V semiconductor based layered multielectronic systems, electronic process investig. survey *(Russian)* 80−107891
image convertor tubes for nanosecond, subnanosecond photography, dynamic range 78−38034
implanted space charge effect on heavy charged particle range distrib. 77−24340
insulator flashover in HV vacuum transmission line, mag. effects 77−24236
insulators, nondestructive acoustic elec. field probe 80−47076
intense low energy ion beam transportation, space charge blow up 79−44982
interfacial polarisation effect on dielectric props., sandwich capacitor model 80−15614
ion beam, overneutralisation, by electrons in mag. field 79−10256
ion beam, space limited positive charge compensation by electrons 77−71916
ion beam in plasma, reactive medium instability of space charge wave 78−18421
ion beam transport, shape of beam envelope, beam space charge and emittance effects 80−32901
ion beams, intense, space charge field 79−41325
ion beams, space charge neutralisation 79−45507
ion beams, transport, space charge effects, computer simulation 78−50328
ion bunching in electronic space-charge regions 77−3955
ion multiaperture sources, beamlet-beamlet interactions, effect on ion optics 78−46507
ion optical focusing in cylindrical mirror analyser, space charge effects 78−25791
ion optical system, expt., theory 78−9020
ion source, accelerator system computer solns. 77−88309
ion space charge neutralisation, influence on mass separator transmission 78−82073
ion trajectories calc. in a 3-dimens. beam subjected to a space charge *(French)* 78−82902
ionic crystal, space charge polarisation involving electrode reaction with surface adsorption 77−12019
ionising waves in plasma, high velocity propagation 80−87889
iris loaded waveguide relativistic electron beam interaction, electron energy distrib. space charge effects 78−46190
irradiated MIS device positive space charge formation kinetics 78−76155
junction devices, generation recombination current, noise reduction, SRH centres in space-charge layer 77−76905
laser, free electron type, small-signal gain, space charge effect 79−920
lens development, electrode geometries and current status 79−68071
linac particle tracing simulations 79−71999
liquid dielectric, intensity of elec. field and space charge 80−11339
liquid dielectric, Sumoto effect under transient conditions 80−97198
longitudinal carrier waves in solids, coupled mode anal. *(Korean)* 78−43403
magnetic Faraday's law analogue, appl. to slow charge convection, for teaching 78−49607
magnetron, oscillations spectra, average freq. depend. on anode voltage 77−49747
magnetron sputtering, appl. to sputtered thin compound films, review *(Japanese)* 80−25561
many-valley semiconductors, space charge, contrib. of different charge carriers *(French)* 80−34458
MBBA, positive space charge influence on texture, domain form. factor, polarised light study 80−88037
metal, compensated, transport of spatially inhomogeneous current under mag. fields, pot. and current distribs. 79−87081
metal-amorphous Si barrier, electronic props. 80−11089
metal-insulator-semiconductor structure, DC cond. and Shubnikov-de Haas effect 80−11012
methylene chloride HV polarisation and space charge obs. *(Russian)* 80−25277
microscopic metal points, explosive emission characts. 77−7624
MIM systems, TSC, space-charge layer model 80−93009
mixed positive and negative ion beams, space charge neutralisation 79−27159
molecular charge distrib., quantum topology, bonding theory and molecular structure 80−5463
molecular crystal, band structure, excitonic processes, trap distrib. 80−6720
molecular crystal/electrolyte interface, illuminated, space charge behaviour 78−84290
MOS structure, space charge layer physics 80−92980
n-n^+ junction point contacts, I-V characts. 77−1480
naphthalene, single crystal, anomaly in permittivity due to thermodielectric space charge 80−7258
negative ion beam space-charge neutralisation, ion beam in gas 79−55048
nematic-liquid crystal, space charge freezing, electro-optic effect meas. 78−34436
neutral beam, charged particle separation by space target blowup 78−9018
non-self-maintaining gas discharge, oscill. of space charge in cathode layer 79−86641
nonattaching gas, irrad., in infinite cylindrical cell, space charge and wall effects 77−68737
noncylindrical symmetric space-charge flow, Coriolis and centripetal accel. 78−91182
noncylindrical symmetric space-charge flow, momentum eqns. 78−91181
nonlinear free electron laser dynamics with space charge and wiggler effects 80−58500
nonpolar organic liquids, field emission 275-334K 78−88406
n-octadecane, surface charge decay 78−43463

space charge continued
orbitron device, electronic injection, ionisation phenomena and space charge influence 79−40587
orbitron device, optimum injection condition for electrons, influence of end effects 80−82784
oxide electrodes, electron transfer reactions, tunnelling through a space charge barrier 78−80050
oxide film, thermal and anodic, space charge effects on steady-state transport 80−11124
p^+-i-n^+ double-injection struct., regional approx. 78−14805
p-n heterojunction differential admittance theory in the presence of surface electron states 80−96981
p-n hot carrier functions, effect of space charge layer defects on characts. 80−25001
p-n junction, abrupt, forward-biased, transition region behaviour anal. 77−76909
p-n junction, abrupt, space-charge layer capacitance, approximation eqns. 77−35989
p-n junction, current-voltage charact. effect of generation-recombination *(Rumanian)* 78−2553
p-n junction, diffused, space-charge recombination current 80−88623
p-n junction, HV, current induced by electron probe in space charge region 79−24065
p-n junction, US wave effect on effective current relaxation time in base 77−4434
p-n junction boundary conditions 80−20295
p-n junction with inhomogeneous impurity distrib., space-charge layer 78−30982
p-n junctions, linearly graded, characterisation 80−6962
p-n junctions, variable gap, recombination currents in space charge layer 80−20303
p-n-p-n structures, turn-on at high voltages and high currents 77−1475
paper capacitor, dielec. loss, effect of simultaneous application of AC and DC voltages, freq. and temp. depend. 78−15091
particle beam transport, role of space charge 79−30610
particle diagnostics of laser-produced plasma, space charge effects 78−63581
particulate detector, ionisation type, space charge effects 77−41587
Perspex, dielec. breakdown and space charge, treeing 78−27160
piezoelectric semiconductors, surface phonon acoustoelectric interaction, elastic anisotropy effects 80−6610
plasma, electron beam space charge wave in mag. field, cyclotron damping 79−46459
plasma, magnetised, double-layer characts. meas. 80−43874
plasma, streaming, in laser vac. diode, electron emission temp. 78−91162
plasma, uniform mag. field, relativistic electron beam injection *(Russian)* 77−19719
plasma confinement, space potential on Elmo bumpy torus 78−67414
plasma double-layer, steady-state, fluid theory 80−43873
plasma sheath edge theory is weakly ionised collision dominated plasma 80−43935
plasma waves in straight-line electron beam, collective accel. of ions 80−103166
plasmatrons, mono- and duo-, anode space-charge sheath characts. rel. to ion source 79−55576
PLZT, optically induced birefr. change 78−43832
PMMA, electret, dielectric meas. at ultralow freq. by reheating 80−4741
PMMA, nondestructive acoustic elec. field probe meas. 80−47076
PMMA, treeing effects on electric breakdown *(Korean)* 77−81053
poly(N-vinylcarbazole) layers, supermol. struct. effect on elec. props. 80−44606
poly-γ-benzyl-L-glutamate, preliq. cryst. mol. alignment, space charge effect, electro-optical obs. 77−40206
polyacrylonitrile, film, dielectric polarisation 78−52431
polycarbonate films, high temp. relaxations 80−97187
polyethylene, accumulated charge profile during fast electron irradiations 77−4600
polyethylene, corona charged, direct drift mobility meas. 78−10837
polyethylene, electrical capacitance under high DC elec. field 80−54705
polyethylene, high density corona charged, TSC, oxidation effect 78−26882
polyethylene, relation between electrostatic capacity and electronic space charges induced by high field 79−15154
polyethylene, space charge effect on local electric breakdown 77−69773
polyethylene, space charge injected from electrode at low temps., luminesc. obs. 80−25464
polyethylene, space-charge storage under high DC voltage condition, TSC meas. *(German)* 80−75576
polyethylene, tree initiation under impulse voltage, effect of needle electrode materials 77−73112
polyethylene cables carrying DC current, TSC and space charge effects *(French)* 80−40042
polyethylene film, high density, corona charged, thermally stimulated surface pot. 80−11327
polyethylene film, surface pot. decay, drift mobility determ. 77−11979
polyethylene surface field strength under DC stress 80−15967
polyethylene terephthalate, TSC due to mobile ions and ionic conduction *(Japanese)* 80−54432
polyethylene terephthalate, TSC meas., space charge and injected surface charge effects 80−11320
polyethylene terephthalate electrets, formed by electron injection, TSC meas., space charge drift 80−11321
polyethylene terephthalate film, nonlinear elec. cond. effect 77−39980
polyethylene terephthalate film, space charge quantity meas. by Maxwell stress method 80−22389
polyethylenenaphthalate, elec. cond., appl. of model 80−24940
polymer, dielec. breakdown theories, mol. and morphological features rel. to elec. strength, review *(Japanese)* 80−60501
polymer, in MIS struct., charge movement study using capacitance-voltage characts. *(French)* 80−39575
polymer electret, charge dissipation, transport mechanisms 80−7268
polymer film, space charge, thermal expansion and pyroelectricity 77−4603
polymers, space charge behaviour and luminescence at 77K 79−99947
polymethine semiconducting films, surface photovoltage 80−70857
polymethyl methacrylate, direct obs. of zero field surface 80−16133
polymethylmethacrylate, effect of accumulated charge on depth dose profile of electron beam 79−90700
polymonochloro-p-xylylene, γ-ray-induced cond., hole injection effects 80−34452
space charge continued
polypropylene film, corona-charged, TSC and space charges 80−40041
polypropylene film electret, space charge injection induced pyroelectricity 77−12324
polypyromellitimide, thermal depolarisation current 78−52429
polystyrene, γ-ray-induced cond., hole injection effects 80−34452
polystyrene films on metal substrates, electrode effect on carrier injection, TSC, I-V characts. 80−34463
positive columns composed of mixed ion plasma, general ambipolar diffusion theory 78−94897
positive impulse sparkover, unipolar space charge effects 78−87542
positive ion beam dynamic decompensation in absence of mag. field *(Russian)* 80−106993
proportional counters, counting rate depend. gain shift and space charge 78−74536
proportional counters, peak shifts and space charge effects 78−74537
proton dynamics in linear accelerator with variable phase focusing, space charge effect, simulation 79−13561
pulseless corona, space-charge limited current flow, computer solutions of Poisson and current continuity equations 79−86627
pyrene, band structure, excitonic processes, trap distrib. 80−6720
quadrupole ion storage trap (quistor), relative confinement efficiencies of Ar^+ and Ar^{2+} 79−2869
quadrupole ion store, spatial distribution of ions derived by phase space anal. 80−95185
quartz, surface space-charge layer form. on γ-irrad. 80−10575
p-quaterphenyl, polycryst. thin layer-metal sandwich, elec. cond. 80−34526
quinoxaline in durene (naphthalene) crystal, Stark effect, space charge, local field tensor and dipole moment 77−28601
QUISTOR, space charge and ion stability 80−86487
radiotracer diffusion rates in ionic solid, influence of transmutation products 77−89568
random dielectric, mean pot. and field 78−55271
reflex discharge, diocotron-instability pulses, current and electron loss effects 77−62423
relativistic electron beam, excitation of slow cyclotron and space-charge waves 79−86118
relativistic electron beam, inhomogeneous, space charge oscills. 80−78759
relativistic electron beam, propag., Poukey-Rostoker model 78−5412
relativistic electron beam, technique for amplitude and phase vel. meas. of slow space charge wave 78−54508
relativistic electron beam injected into drift tube, limiting currents 79−10699
relativistic electron beams, slow space-charge wave propag. 80−1115
relativistic free-electron wave generators, electrically pumped 80−91742
RF discharge, electrode sheath 80−44052
rotating electron-plasma column space-charge wave propagation 77−55137
schlieren method for the determination of electric field distributions in dielectrics 80−31720
Schottky injection currents, effect on time depend. 78−14735
secondary electron emission, from plane electrode, space-change limitation 79−4871
semi insulating layer with conductivity gradient, charge storage 77−80784
semi-insulating material, elec. stressed, storage of charge caused by cond. gradient 80−25306
semiconductor, charged impurity diffusion 80−6563
semiconductor, doped photoemission, calc. of escape probability of electrons *(Russian)* 79−24408
semiconductor, energy relaxation of photoexcited hot electrons in near-surface region 80−92928
semiconductor, energy spectrum of discrete centre in high inhomogeneous electric field of space charge region 80−10873
semiconductor, inhomogeneous elec. fields in oscillatory photocond. 80−2421
semiconductor, phonon induced hopping between Stark levels 80−92900
semiconductor, photocond., influence of surface space-charge layer 80−15563
semiconductor, quasiunipolar, elec. field screening 77−55605
semiconductor, size effect, influence of space-charge regions on boundary conditions 77−89790
semiconductor, space charge region thickness, deep level props., determ. by γ-ray absorpt. 80−59995
semiconductor, superficially illuminated, space charge effect on Dember effect 77−8133
semiconductor, surface space charge layer spectroscopy 77−20386
semiconductor coatings, space charge effects on triboelec. charge exchange 80−54763
semiconductor cyclotron resonance 78−6575
semiconductor electrode, charge injection, space charge region, simulation 77−15949
semiconductor electrode, open-circuit photopotential, simulation 77−15950
semiconductor of simple geometries, field penetration and band bending in high elec. fields 79−87106
semiconductor resistivity meas., influence of space charge 78−23076
semiconductor step l-h junction, elec. struct. analytical methods, review 80−100507
semiconductor structures, s-type switching at high current densities 77−20417
semiconductor surface, electron beam prod. of plasma oscillation instabilities *(Ukrainian)* 79−33318
semiconductor surface, electron-electron interaction and electronic props. of space charge layers 78−60210
semiconductor surface, resonance inelastic light scattering by carriers 80−20655
semiconductor surface and adsorbate states, charge injection into space charge layers 80−100496
semiconductor surface space charge layer study using SAW convolver 77−46871
semiconductor surface space charge layers, subband struct., perturbation theory 80−84497
semiconductor with arbitrary energy spectrum of trapped states, surface region of space charge 80−107811
semiconductor-electrolyte junction photovoltaic cells, interface charge transfer, recombination rate, C-V characts. 80−70818
semiconductors, current instabilities, theory and expts. *(Hungarian)* 77−39857

space charge continued
semiconductors, deep level carrier trapping and emission, transient spectroscopy, book contribution 80−80216
SF_6 discharge inception voltage affected by avalanche growth space charge *(German)* 80−75109
silastic tubular electret, mag. polarised, thermal currents 80−40037
silicate glass, space charge distrib. after 2.1 MeV electron irrad. *(Russian)* 77−69772
small Hall effect transducer potential, elec. field and majority carrier density distrib. 79−67290
solid dielectrics, conference, Karpacz, Poland (Sept. 1977) 80−36766
solid dielectrics, electric breakdown mechanism, discharge development, electron impact ionisation 80−15961
solid electrolytes 78−71877
solvation, classical mean space charge model 78−76841
space charge lens for high current ion beams 78−55075
space charge limited current with diffusion theory, for exponential trap distribution 80−10992
spacecraft surface plasma sheath, space charge neutralisation 77−87240
spatio-temporal distrib. determ. in breakdown 80−38771
spherical particle, max. charge imparted by pulse-charging 80−6945
static probe for electric field meas., in presence of space charge 79−17448
steady-state space charge blowup and recovery of intense ion beams 79−1323
surface charge decay due to time dependent bulk cond. 78−23397
swarm in fluid, transient currents 80−106869
synchronous slow space-charge wave accelerator 78−17448
synchrotron, effects of induced voltage and forces of space charge on motion *(Bulgarian)* 80−47792
TEA laser discharges, inhomogeneities 77−14687
Teflon FEP, electron beam charged film, charge centroid location 78−15095
temporal space-charge field change meas. at high voltage electrodes in negative corona 80−38770
testosteron, dielectric props. under UV excitation 80−6912
tetrode system, two-dimens., algorithm for solving space-charge problems with thermally-emitted electrons 80−100743
thermally degenerated Schottky diodes, resonant tunnelling 80−100503
thermally stimulated currents, effect of space charges 79−65793
thermionic diode, non-Boltzmann distribution of free electrons under high space charge conditions 78−56555
thermionic diode, uniformly heated, non-Boltzmann distrib. of free electrons, high space charge conditions 77−84390
thermionic diodes, planar low press. gas discharges, space charge regime, volt-ampere characts. 79−77434
transformer oil, nondestructive acoustic elec. field probe meas. 80−47076
transient and AC steady-state response of solid with recombining space charge 77−51737
trapped-ion cyclotron reson. spectra, intensity oscills. characterisation 78−48716
triode and diode guns, electron optics numerical determ. of beam profile 80−106435
two-dimensional semiconductor, Gunn instability 78−84305
two-temp. electron-ion plasma with mirror reflection, EM fluctuations, space charge correl. *(Russian)* 78−59548
ultrathin doping levels as model for 2-dimens. systems 78−60182
very thin films, tunnelling currents, temp. and space charge effects 80−70799
vinylidenechloride-acrylonitrile copolymer, amorphous, pyroelectricity due to space charge mechanism 79−87400
wave propagation along rotating relativistic electron beam 79−55047
wave propagation on rippled electron beams 77−3933
waves propagation along moving magnetoplasma slab 80−38700
Ag-halide microcryst., space charge characts. 78−15097
AgBr and AgBr:$PbBr_2$, emulsion grains, dielec. loss, ionic cond. and surface space charge 77−28038
AgBr emulsion grains, edge length dependence of ionic conductivity 80−88360
AgBr film, surface space charge region 77−1508
AgBr microcrystals, influence of Pb^{2+} ions on ionic conductivity and space charge characts. 79−23778
AgBr, thin epitaxial layer, surface ionic cond., lattice disorder, space charge region 77−11730
AgBr thin film interstitials, Frenkel and space-charge contributions 79−18494
AgBr:Pb, ionic space charge model, rel. to impurity distrib. 77−19979
AgBr:Pb^{2+}, cubic microcryst., ion influence on ionic cond. and space charge characts. 79−55928
AgCl, ionic space charge and dissolution 80−107431
Al-SiO_2-Si, MIS diode, neutralisation of mobile ions in insulating film *(Japanese)* 79−73591
Al-SiO_2-Si structures, effect of β-radiation on fast surface states and space charge 77−55610
n-$Al_xGa_{1-x}As$, electrical props. 78−6381
$Al_xGa_{1-x}As$, electron mobility illumination, compensation, space charge regions, carrier scatt. 80−70691
Al_2O_3 polycrystalline, effects of space charge, grain-boundary segregation and mobility differences on conductivity 80−79979
Al_2O_3-Si boundaries, insulator charges evaluation *(German)* 79−82682
Al_2O_3-SiO_2-Si boundaries, insulator charges evaluation *(German)* 79−82682
Ar breakdown voltage and voltage-current characts. obs., up to 2400°C 78−87510
Ar discharge, optogalvanic and excited state photoionisation signals, space charge effects 80−14947
$As_{35}Te_{28}Ge_{16}S_{21}$, chalcogenide semiconductor study of electric properties *(French)* 80−29414
$BaTiO_3$, ferroelec. inhomogeneous impurity distrib., distrib. of spontaneous induction 77−28530
$BaTiO_3$, X-ray irrad. effect on dielec. props. 78−15082
$BaTiO_3$-KCl composite cryst., F-centres, thermoluminesc., DC field and X-irrad. effects 78−2926
BeO, field-assisted thermally stimulated exoelectron emission 80−100761
Bi, liquid, field ion source emission characts. 80−74059
CdF_2, electrical transport limitation by electrodes, polarisation effects 80−96689
CdS, obs. of acoustically induced space charge gratings 77−7203
CdS, piezoelectric semiconductor, space charge distribution at elastic wave propag. *(Russian)* 77−77150

space charge continued
CdS, quasimonopolar semicond., recombination in near surface space charge region *(Russian)* 80−88574
CdS-Cu_2S, thin film, heterojunction, space charge in CdS, depend. on heat treatment 79−56294
CdS-metal interface, chemical reactions and local charge redistrib. 79−19661
CdSe-metal interface, chemical reactions and local charge redistrib. 79−19661
p-CdTe diodes, X-ray escape peak variations 77−71723
CdTe-metal, diode contact, elec. characts., generation-recombination space charge region *(Russian)* 78−39214
Cu_2O, front wall solar cells, chemical origin of space-charge layer 79−70449
Cu_2S-CdS, solar cell, CdS space charge layer, photohole generation 79−7853
Cu_2S-CdS heterojunction solar cells, carrier transport, nonmonotonic band profiles 80−61361
$Cu_{2-x}S$/CdS heterostructures, heat treated, capacitance voltage meas. anal. 80−20292
EuO:La, photothreshold reduction by mag. induced space charge layer 78−72692
Ga, liquid, field ion source emission characts. 80−74059
Ga liquid metal field emission ion source, characts. 80−108326
p-$Ga_{1-x}Al_xAs$ crystals, spectral characts. of photosensitivity, mechanism 80−44735
GaAs, chemisorption of Li, charge injection into space charge layers 80−100496
GaAs, deep trap study by free exciton refl. spectra 79−60761
GaAs, electron mobility illumination, compensation, space charge regions, carrier scatt. 80−70691
GaAs MOS structures, leakage current for anodic oxide layers, space charge trapping effects 80−60091
GaAs p-n junction, HV, current induced by electron probe in space charge region 79−24065
p-GaAs/electrolyte soln., electrode photoemission, energy diagram, Volta pot. 77−62990
GaAs-$Ga_{0.7}Al_{0.3}As$ n-n heterojunction, LPE, rectification 80−49888
GaP, n-, p-type, electrode, impedance in alkaline medium *(French)* 79−43586
Gd_2O_3, B-type monoclinic, DC(AC) elec. cond., thermoelectric power, dielectric const., temp. depends. 80−59980
Ge (111) surface, n-channel inversion layer, subband energies 80−11063
Ge, field effect characts. rel. to surface inhomogeneity 78−26933
Ge, spectrum of photocapacitance current near fundamental absorpt. edge 77−28217
Ge, surface, high freq. cond. and cyclotron reson. 80−11273
Ge, voltage-current curves, specimens of variable cross-section 77−8113
Ge/electrolyte soln., photoemission, energy diagram, Volta pot. 77−62990
Ge-Au eutectic alloys, field ion sources 80−97414
H, ionised gas, H_α-, H_β-line Stark broadening, space charge field 77−39409
H, pellet ablation in thermonuclear plasma, electron space charge and refuelling 77−88283
H^-, production by Hall accelerator in Cs vapour, space-charge effects 78−67375
He constricted glow discharge, space charge double layer influence obs. 78−67492
He, liquid, electrical strength, breakdown voltage depend. on electrode configuration 80−7293
Hg 40.8 MHz discharge electrode space-charge sheath thickness obs. 78−67547
InAs, surface space charge investig., reson. enhanced Raman scatt. 77−20849
n-InP, compensated, elec. props., space-charge effects 80−65569
InP, deep trap study by free exciton refl. spectra 79−60761
InP, surface space charge layers and Schottky barrier form., Raman scatt. study 80−50319
InSb n^+-p junctions, photocurrent spectrum near long wavelength edge of fundamental absorption band 80−100483
InSb surface, IR spectroscopy of subband levels 80−20277
KCl, low temp. space charge polarisation 78−43789
KCl:Sn^{2+}, thermally stimulated space charge decay 78−48111
K_2O-SiO_2, glass, influence of electric charge phenomena on AES *(French)* 80−50478
$KTaO_3$, rel. to crit. dielec. and optical props. and storage, 4K 77−24805
Li, vap., multiphoton absorption, space-charge ion detect. 79−54827
$(Li_2B_4O_7)_{1-x}(WO_3)_x$ dipolar glass, space charge injection, thermally stimulated depolarisation currents 80−66103
LiF, space charge distribution meas. in solid dielectrics 80−50271
α-$LiIO_3$, defects decorated by space charge, X-ray topography study *(Chinese)* 80−107204
α-$LiIO_3$, single crysts., light diffr. under DC field 80−11367
$LiNbO_3$ crystal, elec. cond., optical quality, impurity depend., space charge pyroelectric field compensation 79−64295
$LiNbO_3$, hologram storage depend. on envelope field, space charge field 80−78801
$LiNbO_3$, photoinduced grating contrib. to acoustic wave vel. 77−77154
$LiNbO_3$:Fe, intensity enhanced bulk photovoltaic effects 79−19616
$LiNbO_3$-gap coupled Schottky diode memory correlator, grating coupled optical imaging 80−64143
MOS, photocurrent-voltage characts., insulator bulk trapped charge 78−30991
MgO crystals, dipolar defects, thermally stimulated depolarisation 80−66101
N_2 breakdown voltage and voltage-current characts. obs., up to 2400°C 78−87510
N_2, electric breakdown in long high-voltage gaps with gamma and alpha particle irrad. 79−18993
N_2-methane, rapidly developing discharge, streak camera records interpretation 80−59280
NaCl, F-centres near monoenergetic proton stopping region, space charge effect 78−18640
NaCl, low temp. space charge polarisation 78−43789
NaCl, surface charge meas. in ultra high vac. 80−20287
NaCl:Sn^{2+}, thermally stimulated space charge decay 78−48111
$NaZnGeO_4$:Mn, electrolum., ionisation domains 80−84787
Nb-Nb_2O_5-Al structures, oxide film space charge density obs. *(Russian)* 78−10579

space charge continued
p-n junction space charge region, thermally stimulated current, impurity centre parameters 77−85237
PLZT ceramic;, visible light scatt. depend. on photoferroelectric space charge fields 80−80806
PLZT composition, effect on its switching characts. 79−42917
PMMA, resonance size effect in space charge relaxation 80−75937
PbI_2, dielectric props., elec. cond., space charge polarisation 80−100631
PbS-Si heterojunction, space charge capacitance, PbSn film thickness depend. 80−88630
n-PbTe, accumulation layer, quantised surface states 80−20279
p-PbTe, MIS struct. inversion layer sub-bands, IR magnetoreflectance obs. 80−44731
PbTe, magnetoreflectance of surface space charge layers 78−52475
PbTe surface space charge layers, far IR magnetoreflectance meas. 78−64349
$Pb(Zr,Ti)O_2$ ceramic, surface barrier electroreflectance, hysteresis, ageing 80−80752
$Pb(Zr,Ti)O_3$ ceramic, permittivity and resonant frequency ageing, space charge field effects 77−85657
$Pb(Zr,Ti)O_3$ ceramics, space charge field meas. by ferroelec. domain switching current, piezoelec. reson. freq. ageing characts. 80−7296
Pt-Si thermally degenerated Schottky diodes, resonant tunnelling 80−100503
SF_6 and SF_6-air mixture gas under impulse voltage, discharge phenomena *(Japanese)* 80−96409
SF_6, compressed in space-charge stabilised nonuniform fields, corona threshold computation 79−19118
SF_6, predischarge-stabilised breakdown voltage *(German)* 78−63608
Se-binding agent electrophotographic film characteristics and sensitivity *(German)* 80−4789
Si (100), surface space charge layer, inter-subband optical transitions 77−15931
Si (100) surface, cyclotron reson. of electrons in surface space charge layers 77−8169
Si (100) surface, intersubband optical absorption in space-charge layers 77−35984
Si (100) surface, surface cyclotron resonance, freq. depend. 77−8170
Si, (100) surface space-charge layer, intersubband cyclotron combined resonances 79−69571
Si, accumulation layer, intersubband-cyclotron combined resonance, theory 80−20278
Si, amorphous, Schottky barrier and p-n junction props. 79−28407
Si, field effect characts. rel. to surface inhomogeneity 78−26933
Si MOS capacitors, pulse response anal., lateral depletion region around gate area 79−38187
Si p^+nn^+ reverse-bias struct. with confined space-charge region, field profile 79−73581
Si p-n junction, high-voltage, microplasma characts. 77−11997
Si p-n junction, microplasma instability, effect of space-charge field of mobile carriers 78−19140
Si photodiode, avalanche, $n^+p\pi p^+$-type, primary photocurrent anal. by noise measurements *(French)* 80−88624
Si, photovoltaic and photomagnetic effects, rel. to intervalley electron transfer 80−60034
Si, plastically deformed, spin-depend. charge transport 80−6895
Si, surface space charge layer, electron subbands, mag. field effect 77−20393
Si surface space charge layers, cyclotron reson. of holes 77−76932
Si, surface space charge layer, anisotropic and tilted valley systems, absorption 77−85726
n- Si, surface space-charge layer, intersubband-cyclotron combined reson. 78−68063
Si, voltage-current curves, specimens of variable cross-section 77−8113
Si:Au p^+-i-n^+ diode, double injection switching, effect of trapped space charge 77−1473
Si:Au p-n junction, forward-biased, recombination current variation *(Rumanian)* 78−19131
a-Si:H Schottky barrier diodes, capacitance studies 80−49908
Si:Na^+, inversion layer, far IR optical spectroscopy 80−20680
n-Si:Sm,P rel. to electron irrad. effects on carrier conc. and mobility *(Russian)* 77−66168
Si-Au eutectic alloys, field ion sources 80−97414
Si-insulator structures, space-charge density determ. from contact pot. difference meas. *(German)* 79−11232
Si-$NaNO_3$ aq. soln., anodic polarisation of semicond. electrode 77−11999
Si-SiO_2, flat-band voltage due to fixed surface charge density, modified expression 79−56317
Si-SiO_2 boundary, origin of interface states and oxide charges generated by ionising radiation 77−20380
Si-SiO_2 interface, electron injection into oxide due to mobile ion induced internal field 77−15963
Si-SiO_2-Al, internal photoemission, pot. barrier height determ. 80−65699
$Si_{1-x}H_x$, amorphous, gap states, DLTS 80−49656
Si_3N_4, low press CVD film, steady-state electron and hole space charge distrib. 80−29493
SiO film, electrode effects in TSC and capacitance meas. 79−78203
SiO supermultilayer dielectric film, elec. strength *(Russian)* 77−85648
SiO_2, numerical anal. of kinetics of space charge formation, rel. to irradiation *(Russian)* 79−78243
SiO_2-Si boundaries, insulator charges evaluation *(German)* 79−82682
Sm_2O_3, B-type monoclinic, DC(AC) elec. cond., thermoelectric power, dielectric const., temp. depends. 80−59980
$Sr_{1-x}Ba_xNb_2O_6$, photorefraction in space charge field, phase transitions 80−97229
$SrTiO_3$, rel. to crit. dielec. and optical props. and storage, 4K 77−24805
Tb_2O_3, B-type monoclinic, DC(AC) elec. cond., thermoelectric power, dielectric const., temp. depends. 80−59980
TiC, TiN and VC, charge distrib. and bond ionicity 78−63961
TiO_2 rutile ceramics, capacitors, elec. cond. meas., anomalous conduction, ageing effects 78−14836
VC, TiC and TiN, charge distrib. and bond ionicity 78−63961
W-EuS, amorphous, memory effect in field emission 80−89126
XeF_6 seeded mol. beam, transverse ionisation, space charge, mass spectra and vel. 80−78725
ZnO (0001) surface, hardness, electrolyte pH and bias voltage effect 78−47654
ZnO, electrophotographic layer, fatigue recovery 79−63321
ZnO, photodielectric effect, space-charge polaris. 79−60872

space charge continued
ZnO, surface phenomena, interpretation by compensation model 78−95323
ZnTe, photoinduced dielec. loss and capacitance changes, rel. to space charge polarisation 80−2417
ZnTe-electrolyte interface, electrochem. behaviour of single crysts. 79−91138
ZnTe-In Schottky diodes, photocapacitance determ. of electron-hole recomb. *(French)* 79−47119

space-charge-limited conduction
see also limited space charge accumulation
2,4-hexadiyne-1, 6-diol, bis(p-toluene sulphonate), dark-current meas. 80−15520
air positive point-to-plane corona, continuous and pulse components 79−19119
aliphatic unsaturated poly(1,3,4)-oxadiazole films, electrode and bulk limited currents 77−69436
anthracene, photo-enhanced currents 79−82599
bulk trap energetic distribution props., space charge limited current meas. use 80−80293
bulk trapping processes and trap occupancy 77−39876
cellulose acetate, I_2 doping effect on elec. props. 80−49757
chalcogenide glass, threshold switch, high resist. state 77−15924
charge injection between concentric cylindrical electrodes 77−59514
coaxial cylinders, potentials up to 15 MV, space charge limited current flow, diode laser appls. 77−39477
Compton currents, historical aspects and recollections 78−80018
concentric spheres, space-charge-flow theory 80−75573
cryogenic liquid, ionic mobility measurement, pulsed spacecharge technique 77−74420
current charge distribution discharge, with shorted and open electrodes 80−6863
current jump region, I-V characts. *(Russian)* 77−39875
current-voltage characts., steady state, validity of anal. eqns. 80−107800
deep fast trapping dielectric, SCL current injection 80−6862
dielectric, electron beams as virtual electrodes, review 80−6861
dielectric, radiation induced currents and cond. 78−30927
dielectric, SCL cond., field ionisation and annihilation of traps of different elec. nature *(Russian)* 77−69330
dielectric, solid, energetic struct. of traps, from SCL currents 80−24941
dielectric diode, Joule instability under space-charge-limited current conditions 80−15618
dielectric solid, current limitation in injected beam of fast electrons, stationary MFP *(Russian)* 77−4349
dielectrics, current injection method appl. *(Portuguese)* 80−20179
diode, with local ionisation, critical conditions for SCL current *(Russian)* 77−15255
electrets and dielectrics, conf., Sao Carlos, Brazil, Sept. (1975) 80−7251
electrode and volume controlled photocurrents 80−6908
electron beams, annular, space-charge limiting current, upper bound 80−43245
gas, low density, space charge limited current flow 80−79605
high field conduction in solids, effect of collision ionisation space charge 80−84469
high pressure effect on space charge limited current in N_2 and air 79−32735
homogeneous insulator with traps, SCLC characts. 78−39122
homogeneous solid, arbitrary trap energy distrib., SCL current-voltage characts. 78−84224
hopping, equivalence with transport via extended states 79−95399
indanthrone film, SCL conduction, trapping 77−15978
insulating films trap analysis, influence of spatial trap distrib. on SCLC charact. 79−56343
insulating particles in insulating liquids, high-field electrophoresis, basic transport mechs. 80−93767
insulator, arbitrarily distributed traps, SCL currents anal. 79−11132
insulator, current carrier trapping, SCL current-voltage characts. 80−39588
insulator, extension of theoretical description of space-charge-limited currents 78−39128
insulator, inhomogeneity effects 78−19047
insulator with two sets of traps distributed in energy, theory and expt. test 77−89768
malononitrile, plasma-polymerised, in Ag-polymer-Ag struct., SCL currents and carrier trapping 79−51687
MIM struct., space charge controlled cond., transport eqns. 80−97002
naphthalene, electron trapping, one-carrier TSC and SCL currents 80−70715
naphthalene, space charge transport 80−20209
nickel phthalocyanine, ohmic and space-charge-limited currents in vacuum ambient 77−20323
ohmic contact, exponential trap distribution limited current with diffusion theory 80−10992
one-carrier SCL currents in solid with two sets of traps distributed in energy 78−72158
organic insulator, photo-enhanced currents 79−82599
[p-]quinquaphenyl film between metal electrodes, memory switching 80−2484
pentacene, evaporated film elec. cond. meas. for various temps., SCL 78−10584
perspex, electric conduction and isothermal dielectric relax. 80−80285
photoconductivity-controlled imaging systems, limitations on sensitivity 80−6907
photocurrent, under bulk generation conditions 77−8137
phthalocyanine metal free films, TSC, ferroelectric-semiconductor transition 80−66105
phthalocyanine thin layers, metal-free, mobility and thermally stimulated polarisation meas. 79−73527
PMMA film, in Al-PMMA-Al struct. SCL currents and cond. mechanism 79−51686
poly-α-naphthol film, nonlinear I-V characts. obs. 77−47910
polyethylene, non-isothermal currents and space charge build-up 80−39590
polyethylene film, high density, anomalous transient currents around 50-70°C 79−33368
polyethylene films, low density, γ-irrad., elec. cond., effect of elongation 79−4564
polyferrocene, in MSM sandwich, I-V and I-d characts. 78−80064
polypropylene, film, isotactic, ion injection, space-charge-limited currents 79−69775

space-charge-limited conduction continued
polyvinylacetate film, in MIM struct., DC cond. phenomena 80−25020
polyvinylcarbazole, fast hole transport 79−51628
pyrene-TCNE, vapour-grown cryst., transit-time meas. of photocarriers 78−39149
quasi-two dimensional space charge layers, transport phenomena 79−95508
relaxation semiconductor, theory of carrier transport in p^+-ν junction 79−60914
semiconductor, contact emission limited current with weak harmonic distortion of steady bias 78−39127
semiconductor, high resist., continuous energy distrib. of trapping centres, dynamic charact. of SCL current 78−56153
semiconductor structures, grain boundary barriers, sudden change in current 78−56246
semiconductor-on-piezoelectric SAW convolver saturation phenomena 78−2358
semiconductors, high-resistivity, carrier transport *(Japanese)* 80−6850
silicon oil, behaviour under HV stress 79−91368
sisal wax, space-charge-limited currents, thermoelectret state 79−51901
steady-state I-V charact., differential method of anal. 77−69333
strongly degenerate plasma, double injection, vol. controlled current regime 79−51658
tetracene, photo-enhanced currents 79−82599
tetracene, polycryst., SCL currents and trap distrib. 79−1603
thermionic diodes, planar low press. gas discharges, plasma regime, plasma charact. 79−77435
thin insulator, SCL currents, effects of finite contact energy barriers and traps 79−38209
transient SCL current problem 77−69331
Al-Al_2O_3-Al structure, elec. cond. 261 to 418K *(Russian)* 78−64144
Al-Fe_2O_3-Al, space charge limited current, current density as function of elect. field and temp. 79−51688
Al-Sb_2O_3-In films, negative resistance charact. 80−11103
Al-Si-SiO_2-Al structure switching and memory effects 78−95385
$Al_xGa_{1-x}As$:O, appl. as insulating layer in MIS struct. 78−64115
Al_2O_3, elec. props. meas. in MIM struct 79−99646
Al_2O_3, porous film, elec. cond. charact. 78−76179
As-Te-Ge-Si sandwich type amorphous films with metal electrodes, space-charge-limited switching, pre-breakdown charact. *(Japanese)* 77−69385
As_2Se_3 glassy films, current-voltage charact., temp. depend., SCL current 80−92902
As_2Te_3-GaAs, amorphous-monocrystalline heterojunctions, space charge limited conduction 78−64099
Au-tetrathiotetracene-Al systems, dark cond., photocond. mechanisms rel. to contact phenomena *(Russian)* 78−52103
B film, elec. field effect on struct. 80−20050
BN films, elec. resist., depend. on relative humidity 79−4609
BN films, humidity sensitive elec. props. and switching charact. 80−107938
$BaTiO_3$, SCL currents, carrier mobility and trapping 77−15863
$Bi_{12}GeO_{20}$ wide-zone dielectric injection contact characteristics *(Russian)* 78−60236
Bi_2O_3 film, thermally grown, I-V charact., current controlled neg. resist. 80−15637
$CdInGaS_4$, TSC and SCL cond. investig. of electron trap parameters, 120 to 350K 77−69341
CdS epitaxial film, with grain-boundary barriers, field charact. of elec. cond. 77−55626
CdS-Cu_2S solar cell, minority carrier generation and transport in emitter 77−43649
CdSe evaporated films, elec. props. 80−2498
n-CdTe, detector material, single crysts., activation energy anal. of defect levels 78−6321
CdTe, film, theoretical models of impurity levels 79−82557
CdTe:Cl, cryst., high resist., SCL currents, DC meas. 77−66170
p-CdTe:Cl, deep level characterisation, gamma-ray detector parameters 77−39802
CdTe:Cl(In), photoelectronic investig. of trap depths, TSC and SCL cond. 77−39893
CdTe-Si heterojunctions, epitaxy and electrical props. *(Japanese)* 77−32074
Cu_xS-CdS solar cells, SCL current 80−76634
GaAs anodic oxide film, direct current-voltage charact. 78−23186
GaAs, DC biased, filamentation of laser radiation 80−74428
n-GaAs, electrical instability, negative differential cond., electron heating by static and alternating elec. fields 79−11165
GaAs:Cr, current voltage characterisation, deep levels and Fermi level determ. 79−7823
GaAs:Cr, semi-insulating, I-V charact. and surface currents 79−56234
GaAs:Cr, semi-insulating, I-V charact. and photocond. spectra dependencies on Fermi level 79−99576
GaAs:Cr, semiinsulating, I-V charact., photocond., Fermi level, and deep levels 78−39118
GaAs-$Ga_{1-x}Al_xAs$ n^+-ν-n junction, avalanche carrier multiplication *(Russian)* 78−76140
GaP:Zn, growth, I-V charact., electroluminesc. *(Korean)* 78−52653
n-GaS, TSC, electron traps 80−11002
GaSe, space-charge-limited currents at different temps. 77−43607
n-GaSe:I, expt. test of theory for insulator with two sets of traps distributed in energy 77−89768
GaSe-SnO_2 heterojunction, elec. props. and electrolum. spectra 77−59328
GaTe, transport anisotropy 79−23975
Ge-GaAs p-n junction, microparameters determ. 79−11216
Ge(Li) not ideally compensated coaxial detectors, elec. field distrib. and charge collection process 78−94164
Ge_xSe_{1-x}, amorphous semicond., elec. props. 78−84219
HgI_2, single cryst. elec. and thermal props. 79−11111
p-InAs-Au contacts, influence of free surface on elec. behaviour 78−95362
n-InSe, layered semiconductor, current-voltage charact. investig., 130 to 400K 77−4342
KBr, electrolytically coloured single cryst., ionic SCL transient and steady elec. currents 77−62937
KCl, electrolytically coloured single cryst., ionic SCL transient and steady elec. current 77−62937
$KHSO_4$, pure ionic cond., proton mobility, irreversible phase transition 77−59141

space-charge-limited conduction continued
KI, electrolytically coloured single cryst., ionic SCL transient and steady elec. current 77−62937
Nb_2O_5, polycryst. film, switching processes, dielec. breakdown 77−39981
Sb_2S_3 film, coevaporated, elec. cond. meas. 80−65726
$(Sb_2S_3)_{0.95}(Na_2S)_{0.05}$, condensate, local states and switching effect 80−20336
Se powder compacts, sintered, electrical cond. 80−70693
Se:As, amorphous, pure and doped, photoelectronic preps. in glass transition region 79−4583
Se-poly(N-vinylcarbazole), double layer polymeric photoreceptor, potential discharge kinetics 78−72194
$Se_{1-x}Te_x$ amorphous films, sublinear and superlinear I-V charact. 79−82695
Si, high resistivity, specific resistance depend. determ. using impedance freq. depend. *(Czech)* 80−15536
Si MOS struct., space-charge generation props. of Au 80−2475
Si, quasi-two dimensional space charge layers, transport phenomena 79−95508
Si, uncompensated, influence of carrier transit time on small-signal admittance of SCLC diode 77−85305
Si:As, p-n junction form. by laser annealing, space charge region, effects on reverse current 80−54772
Si:H, amorphous, plasma deposited, cond. adsorbate and insulating layer effects 80−49749
Si-SiO_2 interface, trapping props. from electrochemical current-voltage behaviour 79−69597
Si-V_2O_5 p-n heterostructure, photocond. *(Russian)* 79−42622
n-SiC, saturation of electron drift velocity in strong electric field 77−76840
$Si_{12}Ge_{10}As_{30}Te_{48}$ chalcogenide glass threshold switch conductivity in high ohmic state *(Russian)* 78−43502
Si_3N_4, film, cond. mechanism, double injection, trap SCL current 77−32099
SiO_2 film electron beam induced conductivity theory and expts. 80−15640
SiO_2 layers, thermally grown, undoped and ion implanted, elec. props. 78−23187
SiO_2 MOS capacitor, defect current obs. 80−92987
$Si_{12}Te_{48}As_{30}Ge_{10}$, amorphous film, elec. cond. mechanisms, temp. depend. *(Japanese)* 78−80078
$SnCl_2.2H_2O$ layered single cryst., protonic cond. and crit. behaviour 79−28136
$SnCl_2.2H_2O$, protonic cond. in layered single cryst. 80−19983
SnO_2-copper phthalocyanine-Ag systems, elec. and electroluminescent behaviour 80−80864
Ta_2O_5 anodic film with Au counterelectrodes, conduction process 78−84312
Ta_2O_5 film, for MIS device, CVD and characterisation 77−4742
Ti-anodic oxide-Au(Al), electronic cond. *(French)* 79−95512
TiO_2, rutile ceramics, space charge effects 80−24945
Tm_2O_3 film, between Al electrodes, prep. and elec. props. 80−60103
Tm_2O_3 film, electron beam deposition, elec. props., and struct. 79−87580
V_2O_5 single crystals, contact-limited conduction 79−95493
$Zn_{1-x}Cd_xS$ films, polycryst., reactively sputtered, MSM struct. obs. of dielec. props. and cond. mechanism *(French)* 78−14841
$ZnIn_2S_4$, and $ZnIn_2S_4$-In_2S_3 alloys, SCL currents, trap distrib. 78−52000
$ZnIn_2S_4$ switching investigation, negative resistance state instability, resistivity transitions 80−6920
ZnO, polar faces, space charge layers, anomalous electron mobility 77−62981
ZnO-Bi_2O_3-ZnO structure, injection currents obs. *(Russian)* 77−32068
ZnO-CdSe thin film n-n heterojunctions, prep. elec. and optical props. *(Korean)* 77−28244
n-ZnS based heterojunctions, epitaxial, elec. props. *(Russian)* 78−88023
ZnSSe:Cu, Br, SCL currents and electrolum. via rad. recomb. 77−44065
p-ZnTe film, current-voltage charact. 77−66214
ZrO_2-CaO (12-19 mole%), AC elec. behaviour, 300-900°C, grain size, electrode material, and sintering effects 78−34649

space-charge limited devices
see also limited space charge accumulation
coaxial cylinders, potentials up to 15 MV, space charge limited current flow, diode laser appls. 77−39477
diode, influence of carrier transit time on small-signal admittance 77−85305
diode, space-charge limited, rigorous Poisson eqn. soln. for electron beam 77−50605
diode with traps, small-signal admittance in high freq. range, negative conductance 79−11221
electron beam propagation in dielectric guide due to space charge neutralisation 80−18716
junction lasers, transport phenomena, junction effects and devices, book 80−98766
planar relativistic diode, Poisson eqn. 79−10700
precise diode method for recording contact potential changes caused by gas adsorption 79−88982
thermal noise, effects of hot carriers 79−24036
Pt-Cu_2O-Cu single carrier space charge limited diodes, I-V charact. 77−47901

space-charge limited solid state diodes *see space-charge limited devices*

space-charge limited solid state triodes *see space-charge limited devices*

space communication links
see also satellite links; space vehicles; telemetering
1 Gb/s laser space communication system 77−7213
CETI, 1.5 mm as optimum wavelength region 79−40094
CETI from Earth satellite orbit 78−61758
CETI from Earth satellite orbit 80−4275
conference on laser and fibre-optics communications, San Diego, CA, USA, Aug. (1978) 79−86203
dipole antennas entering planetary atmosphere, plasma wake model and radiation patterns 79−48647
Earth-space radio propagation paths, rain attenuation joint statistics 78−73490
European Space Agency activities *(German)* 80−8516
extraterrestrial intelligence, telecommun. technology 78−32319
extraterrestrial intelligence communication, international conference discussion and conclusions *(German)* 77−56845
fibre optics tasks of NASA, review 78−42441

space communication links continued
Ganymede image restoration by maximum entropy method 77−60624
interstellar communication, signalling strategy 78−61757
interstellar communication, theory 80−4271
interstellar probes, communications philosophy 79−21133
interstellar travel and communication, bibliography 80−101677
Jupiter probe-to-relay communication MFSK frequency acquisition and tracking 77−64613
laser modulator, 1 Gb/s 77−79965
laser pumping, K-Rb arc lamp development 78−46646
laser space communication, 1 Gb/s 77−88831
Mars 6 descent vehicle, communication loss on entry into Martian atm. 77 64597
Mars 6 descent vehicle radio signal parameters meas. by retranslation method 77−67020
Mars entry probe, communication black-out due to shock induced plasma flow 77−5413
Mars Viking Lander communications 77−9650
million channel 300 MHz bandwidth digital spectrum analyser for Deep Space Network and SETI 78−73642
MM wave space applications and technology in 100-1000 GHz range 79−92650
near-space radio noise environment characteristics and sources 78−89034
optical, 10.6 μm laser data relay link transmitter/receiver optical design 77−19442
optical, CO_2 waveguide laser development for space link transceiver 77−19322
optical, Nd:YAG laser appl. 78−66859
optical communications systems for naval appls. 79−86133
optical tracking system for space laser communication 80−33068
outer planet research requirements 78−32318
path diversity performance, for Earth-space communication links 78−69424
phase-coherent dual-freq. link for high-precision Doppler tracking between spacecraft 77−60576
Pioneer Venus spacecraft programme 78−61707
plasma antenna system, multilayered, electronically scannable, for space communication 79−4151
search for extraterrestrial intelligence, implications for telecommunication 77−33361
solar pumped laser 78−46645
Space Shuttle/Orbiter S-band communication development problems 78−45197
Spacelab, communications R and D project management 77−17321
spin-scan imaging photopolarimeter for Pioneer Jupiter missions 77−41303
standard transmissions stability on transionospheric paths 79−84577
Viking Ground Reconstruction Equipment for facsimile picture recording 77−38051
Viking Lander camera design 77−41285
Viking Lander camera performance and data reduction 77−41286
Viking Orbiter uplink command generation and validation simulation 77−22040
Voyager, telecommunications system and broadcast from Jupiter 80−26715
Voyager planetary probes for outer planets, review 78−24435
Voyager project, microwave communications from outer planets 80−77263
Voyager Project, spacecraft communication system 80−26718
Nd:YAG laser, appl. in space communications 78−28483
Nd:YAG laser, Kr-pumped for space optical communications 77−19328

space groups
see also crystal atomic structure
$\bar{4}3m$ symmetry geometric units, cryst. structs. 80−107087
α-quartz, constitutive eqns. by group theoretic methods 80−1954
A15 compounds, elec. struct., 3-D k.p model 78−2405
A-15 space group struct., phase transitions, renormalisation group theory comparison with Landau theory 80−6489
adamantane crystals, relative stability of ordered $F\bar{4}3m$ and disordered $Fm3m$ 79−73119
algebraic definition of cryst. symmetry on n-dimens. space *(French)* 78−55824
alunite-jarosite, spcae group refinement by means of vibr. spectroscopy 79−94981
anti ferromagnet, spin arrangement of field-induced phases, mag. space aroups 77−32166
Belov's classes, and subclasses, distrib. of symmetry groups 79−14721
Bravais classes and superspace groups for the classification of structures with a one-dimensional modulation 79−94938
Bravais problem for n-dimensions (n>3) 77−15334
cell-preserving phase transitions, new group theoretical approach 77−80619
cellulose II, unit cell parameters, neutron diffr. 77−1086
centrosymmetric in close-packed MX_2-type structs. 77−31618
centrosymmetric molecules in centrosymm. space group statistical anal. *(German)* 78−42940
chiral molecules, mol. symmetry rel. to cryst. space group *(French)* 77−31621
cholesteryl ethyl carbonate, unit-cell dimensions and space group 80−84165
Clebsch-Gordan coeff., crystallographic space groups 80−1955
Clebsch-Gordan coeff. of symm. group, arranged into eigenvectors of propagation matrices 79−19175
Clebsch-Gordan coefficients for Pn3n 79−60293
Clebsch-Gordan coefficients for space groups 79−60292
coherent domain structures from crystal transitions with related space groups 79−42002
colour symmetry groups, of coloured polyhedra and coloured simple forms 79−60294
coloured lattices, rot. symmetry effect, appl. to mag. structs. 79−90587
commensurate-incommensurate transitions, conical points, Lifschitz invariants and superspace group characterisation 80−70367
complex conjugation of space group representations 79−90583
conjugated elements, classes, of crystallographic groups *(French)* 79−7564
continuous crystalline transitions, counterexample to maximal subgroup rule 80−59428
convergent beam electron diffraction, determ. of crystal point groups and space groups *(Japanese)* 79−77461
coupling coeff. 79−90584
'crystal data space-group tables', anal. of population freq. 77−80434
crystal symmetry, 230 or 1651 space groups 78−30572
crystal symmetry, implications in charge density studies 78−71694
cubic space groups, classification by geometrical units 80−15028
diamond-type structures, second kind phase changes, table of space groups *(Russian)* 78−63692
dibromomaleic acid thioanhydride, mol. and cryst. structs., X-ray obs. *(German)* 80−44199
dicalcium strontium propionate, ferroelasticity and opt. activity rel. to transition 78−76420
1,2-diidobenzene, vibr. spectra, packing calcs. and crystal structure investig. 80−28938
diiodomaleic acid thioanhydride, mol. and cryst. structs., X-ray obs. *(German)* 80−44199
dipole interaction energy, group theoretical reduction 78−87639
direct methods, survey as number and kind of solved acentric equal atom structs. 80−38865
double space group O_h^1 selection rules 78−51456
double space groups O_h^6 (Fm3c) and O_h^8 (Fd3c), selection rules 80−10518
elastic dielectrics, group theoretic methods 80−1954
enantiomorphic space group identification by electron diffr. 78−9917
enantiomorphously related space groups, identification by electron diffr. 77−19848
equivalent subgroups, and supergroups of the space groups 79−99098
extended unit cell-contracted Brillouin zone model, group-theoretical anal. 80−107093
factored irreducible symmetry operators and space groups 79−73121
Fedorov groups, translationally centred, theory 78−79546
Flodmark-Blokker method for irreducible representations of crystallographic space groups 80−6376
four-dimensional space, crystallographic groups, book 79−27942
group theory, space and point group factorization, appl. to crystallography and spectroscopy 79−60295
holosymmetric double space groups based on body-centred cubic Bravais lattice, selection rules 79−65019
homogeneous linear structures, systemisation according to charact. numbers of position symbols 78−95009
incommensurate crystal phases, symmetry, superspace-group approach, commensurate basic structs. 80−79726
incommensurate crystal phases symmetry, incommensurate basic struct., superspace group approach 80−79727
incommunsurate crystal phases, lattice dynamics, harmonic approx. 80−29147
independent tensor components enumeration method for trigonal and hexagonal point groups 80−79730
internal dimensions in crystal space group symmetry 80−38983
irreducible linear representation, image struct. 80−6377
isomorphic subgroups, of P1 and p1 *(French)* 80−49155
joint probability distribs. of struct. factors for space group P bar 1 from corresp. distribs. for space group P1 77−19811
Karl-Hauptman matrix, joint probability distrib. of struct. factors in space group P1 79−23480
Lifshitz invariant, time-reversal prop. 78−67679
low symmetry, comments on struct. refinement 79−90582
magnetic double point groups, Clebsch-Gordan coeffs. determ. 77−19886
magnetic group, finite, irreducible tensor operators and Wigner-Eckart theorem 78−22678
magnetic point groups, simplified calc. and tabulation of tensorial covariants belonging to same Laue class 79−19174
magnetic space group, reality criterion for corepresentations 78−22677
magnetic space groups, Clebsch-Gordan coeff. calcs. 80−79731
magnetic space groups, minimal supergroups 77−85417
magnetic structs., group theoretical anal. of second order phase transitions 79−91239
magnetic structure, neutron determ., book contrib. 79−61064
magnetic structure, neutron diffr. study, symm. anal., polarisation effects 80−93083
magnetic structures, symmetry anal. in neutron studies, phase transition concept 79−99679
marcasite structure, space group selection rules 79−99099
maximal subgroups, with increased unit cells 77−1090
metals, FCC, (001) twist boundaries symmetry and struct. 79−82242
mode condensation, ferroic space group in transition sequence *(Japanese)* 77−43300
Molien function, new algorithms, space group representations 77−72575
Molien generating function calc., irreducible representation of cryst. space group 77−72576
monoclinic space groups, use of Σ_1 relation 77−43165
monocrotaline sulphite hydrochloride, struct., space groups from X-ray crystallography *(Chinese)* 80−49210
4-nitrophenyl 4-n-octyloxybenzonate, space group unit-cell and crystallographic props. 80−6399
noncentrosymmetric structures, correlation between third cumulants in refinement 78−91288
nonevident subgroups of double crystallographic point groups, theory 79−32933
nonsymmorphic, multiplicities for space group representations 79−60291
octahedral molecule MX_6 with close-packed arrangement of X-atoms, possible cryst. struct. *(German)* 79−27940
order-disorder groupoid family, parameters, stacking 80−38982
organic compounds, crystallographic pedigree 78−91287
P1 group, and its subgroups, reticular conservation *(French)* 80−107086
P1 subgroups, mathematical tools, automorphism and matrix factorisation *(French)* 79−51037
$P2_1$, pairs, probability distribs., for two phase struct. semiinvariants 78−38643
$P2_1$, pairs, probability distribs. for two phase struct. semiinvariants 78−38641
$P2_1$, pairs, probability distribs. for two phase struct. semiinvariants 78−38642
P2 space group, compensation of excess intensity 80−107088
Patterson functions, identification of double peaks, $P\bar{1}$ space group 79−32859
Patterson method, multiple solutions for low symm. systems *(Chinese)* 80−87986
Patterson synthesis, partial, derivation of 57 black-and-white symmetry groups, interpretation 79−60296
periodically distorted crystals, symmetry 77−39553

space groups continued
perovskite-like structures, some remarks on the 'family tree' of Barnighausen 79−7565
phase determination, appl. of quartet and quintet invariants 79−51034
Pm3n space group struct., phase transitions, renormalisation group theory comparison with Landau theory 80−6489
Pn3n, Clebsch-Gordan coupling coefficients 79−90585
point groups, allowable representations of appropriate small groups 79−2595
polymers, structure classification, according to rel. between chain symmetry and space group *(French)* 79−51058
polymers, symmetry props., classification using line groups 77−51327
polytrimethylene terephthalate single crystals, X-ray and electron diffr. obs. of cryst. struct., packing analysis 79−94924
powder reflections, an error in several published tables of the multiplicities for Laue class $\bar{3}1m$ 79−14720
powder reflections, computer program for determining multiplicities, correction for $\bar{3}1m$ Laue symmetry 79−10759
quartet invariants in space group P1, least-squares analysis 77−84570
quintet, conditional probability distribution 77−43166
quintets, conditional probability 77−84689
quintets, phase sum 77−55253
quintets in space group $P\bar{1}$, probabilistic theory of invariant five phase struct. 77−84687
representation domain, completeness of identification of stars 77−76345
revolution manifold isometric stereohedra 79−82170
Rochelle salt, phase transitions, free energy in symm. group representation of parent phase 79−69790
second order phase transitions, superspace group description *(Chinese)* 80−8942
seminvariants in space groups P312, $P3_112$, $P3_212$, $P\bar{6}$, $P\bar{6}m2$ and $P\bar{6}c2$ 78−91290
sequences of maximal subgroups 78−9987
sextets in P1, joint probability distrib. of 31 struct. factors 77−84685
sextets in P1, probabilistic theory of six-phase struct. invariants 77−84686
spinel, electron diffr. pattern anal. 79−7594
spinel structure, space group ambiguity rel. to multiple diffr. 77−84592
subgroups and changes of standard setting for monoclinic and triclinic space groups 78−9984
subspace groups, systematic determ. *(French)* 78−55823
superspace groups, mathematical struct. and props. 80−17884
symmetry coordinate generation using multiplier representations of space groups 79−37646
symmetry operations, program for deducing from symbolic notation 79−94942
symmorphic space groups, irreducible representations, multiphonon IR and Raman spectra *(Japanese)* 79−77541
tables of irreducible representations, construction and use 77−68938
thiourea, incommensurate phase, soft modes, condensation of even-order harmonics 80−103313
three phase struct. invariant, in $P2_1$, probabilistic theory 79−51033
transition, cell-preserving, space group theory of translation, twin and translation-twin boundaries 77−19892
triclinic, cryst. struct. refinement by least squares 78−75607
TTF-TCNQ, modulated phases in terms of four-and five-dimens. superspace groups 78−47310
two-dimensional space groups, subgroups, standard settings, complete list 78−75610
two-phase and three-phase structure semiinvariants, estimation in $P\bar{1}$, via first representations 78−26473
two-phase seminvariants, of first rank, probabilistic theory via method of representations 79−32848
unitary representations, Takagi construction 80−28940
vector symmetry, in crystallography, basic theorems 79−23556
vector system interpretation by symmetrisation, Patterson function, Harker peaks 80−33914
vibrational spectroscopy, possibility of appl. to space group refinement 78−79507
wave vector selection rule table construction, use of induced compatibility tables 77−19887
wreath groups, symm. of crysts. with struct. distortions 80−75196
Wyckoff family association, changes in conventional space group setting and passages to spatial subgroups *(French)* 78−91289
Wyckoff site description of cryst. struct., depend. on labelling of axes 79−23557
X-ray intensites variation, effect of dispersion and higher symmetries 79−7520
$AgIn_5S_8$ thiospinel, space group assignment by X-ray diffractometry 79−99141
$AgNbO_3$, single crysts. flux growth, space group determ. 80−55282
$AgTaO_3$, single crysts. flux growth, space group determ. 80−55282
γ-AlOOH and γ-AlOOD, IR and Raman spectra obs., struct. and D_{2h}^{17} space group anal. 80−89000
γ-AlOOH, boehmite, lattice vibrs., evidence for $C_{2v}^{1}{}_2$ space group 79−28756
$Ba(NO_2)_2.H_2O$, hexagonal, piezoelec., electro-optic, dielec., elastic, thermoelastic props., space groups 78−76388
Cd_3P_2, band struct., rel. to symmetry props. of D_{4h}^{15} space group 80−34357
Ce-Co-Al (0-33.3 at.% Ce), isothermal section, X-ray study *(Ukrainian)* 80−39002
Cl_2 solid, space group, anisotropic atom-atom forces 79−73127
$Cs_2S_2O_6$, hexagonal, piezoelec., electro-optic, dielec., elastic, thermoelastic props., space groups 78−76388
$Cu_3As_2S_3I$, space group, determ. by convergent-beam electron diffr. 80−49154
Cu_2FeGeS_4, crystallographic and magnetic structure *(French)* 80−28998
$CuIn_5S_8$ thiospinel, space group assignment by X-ray diffractometry 79−99141
Cu_2O, space group selection rules, symm. points and lines 77−35499
GaS, space group, determ. by convergent-beam electron diffr. 80−49154
$Hg_{3-\delta}AsF_6$, space group symmetry and phase ordering 80−6396
$KAlCl_4$, cryst., Raman spectra, orthorhombic space group, Cl splitting of $AlCl_4^-$ 77−85700
$KDy(WO_4)_2$, phase transition mechanism, absorpt. spectra, symmetry props. *(Russian)* 80−55130
$KIO_3.HIO_3$, I atom electronic struct. in X-ray-neutron difference synthesis 79−90595
KSO_3F, disordered cryst., IR and Raman spectra, internal modes assignment, space group *(French)* 79−95742
$K[B(SO_3Cl)_4]$, space group 80−33913
$LaNbO_4$, space group determ. using convergent beam electron diffr. 80−79723
$La_3Ru_3O_{11}$, crystal struct., X-ray diffr. study 78−67688
$La_3S_4(Se_4)$, structural transitions, symm. anal. 80−92671
$LiAl_5O_8$, ordered single cryst., struct. determ. *(French)* 80−15074
$LiClO_4.3D_2O$, hexagonal, piezoelec., electro-optic, dielec., elastic, thermoelastic props., space groups 78−76388
$LiClO_4.3H_2O$, hexagonal, piezoelec., electro-optic, dielec., elastic, thermoelastic props., space groups 78−76388
$LiCsSO_4$, space group from optical second harmonic generation, pyroelectric meas. 80−34860
$MgAl_2O_4$, lattice dynamics, rel. to space group of spinel 78−59898
$MgAl_2O_4$ spinel, optic frequencies, evidence for membership of F43m space group 78−48168
$MgAl_2O_4$, spinel, space group 80−28937
MnF_2 antiferromag., mag. space groups, Clebsch-Gordan coeff. calcs. 80−79731
$NdNbO_4$, space group determ. using convergent beam electron diffr. 80−79723
SiC (6H), piezoresist. meas. 78−2090
SiC polytype 6H, space group 80−1956
lett-SiC, space group refinement, P3 ml 78−47299
Sn_2S_3, mixed valence semicond., long wavelength phonons, full space group theoretical anal. 79−65873
$Sr(NO_3)_2$, Raman and infrared spectra, structure of nitrate ion from space groups 78−43002
α-$ThSi_2$-AlB_2 series, struct., symm. and rel. to other linear structs. 77−11525
TlSe type crystals, possible second-order phase transitions, group-theoretical anal. 80−92672
$U_{10}Co_{51}Si_{33}$, crystal struct., dimensions, space group and coord. *(Russian)* 80−88085
W {001}$(\sqrt{2}\times\sqrt{2})$R45°, low temp. surface struct., space group determ. by LEED 77−85037
β-W structure Clebsch-Gordan coeffs. 79−37645
β-W type (A-15 type) structure, double space group selection rules 77−39551
YIG film, surface pinning parameter, symm. props. 79−28570
$ZnSeO_4.6H_2O:Cu^{2+}$, crystal struct. orientational degeneracy removal scheme, space groups, ESR spectra 78−47267
Zn_2SiO_4, willemite, cryst. struct. 78−83804

space heating
air based solar heating systems, phase charge energy storage, optimum physical properties 79−43742
air to water heat pump and solar installation for single family house *(German)* 79−87968
air to water heat pump and solar water heating, dual purpose installations for family house *(German)* 79−87969
air-based solar heating systems with phase-change energy storage, performance anal. using computer simulation 80−35762
all-year solar energy collection and storage system 79−62074
Baghdad insolation and meteorological data for flate plate collector design 79−62092
barracks heating using solar energy *(German)* 79−87970
Belgian solar heating systems, economic feasibility 79−57443
British 1977 solar energy programme 79−57369
building solar-climate control systems, control options evaluation by simulation 80−40844
buildings, passive solar heating, transwall thermal performance 80−40840
climatic solar heating performance, calc. of solar fraction for building heat 80−16786
diesel-driven chiller system, with multi-tank thermal storage system, computer simulation 79−48187
district heating from Kaiseraugst nuclear power station 78−37462
district heating in Stockholm, nuclear power and oil-fired plant comparison 78−37458
district heating systems, combined generation by fossil fired and nuclear power plants 78−37457
domestic, heat pump appls. *(German)* 80−94099
domestic, mass spectrometer leak detection probe with He-permeable membrane 80−98994
domestic space heating using low-temp. solar thermal systems *(Czech)* 79−83566
domestic wind, solar, wind and solar heating systems, performance and economic evaluation 79−43744
domestic wind power system including storage, simulation analysis 79−92058
duplex chemical system for storage and transport of heat from LWR, district heating 78−37460
dwellings, single family, heat pump appl., computer-aided analysis 79−43784
energy roof, solar energy utilisation and heat recovery *(German)* 80−61285
energy utilisation improvements using new types of construction *(German)* 80−40903
experimental installation, using solar absorbers, heat pumps, heat exchangers and measurement and control gear *(German)* 80−35741
fossil fuel heat pumps for domestic, commercial and industrial space heating 80−89666
gas research with a view to energy savings in France *(French)* 79−39272
geothermal, coaxial well for space heating and cooling 80−66933
geothermal, system design and economic anal. 80−30379
geothermal energy, exploitation in France 79−79372
geothermal energy, utilisation for thermal and electric energy, geochem. engineering and materials 80−61275
geothermal power for heating purposes *(Slovak)* 79−87963
German solar flat plate air collector development 79−62075
greenhouse heating, using thermal effluent from heavy water plant, feasibility study 78−86678
heat balances of apartment house, in Dutch climate, energy conserving measures 79−61948
heat pump, chemical, hydride conversion and storage system 80−72077
heat pump water-to-water, school with gymnasium, heating appl. *(German)* 80−16831

space heating continued
heat pumps, domestic applications *(French)* 80−30518
heat recovery/heat pump combination for sports centre heating system, operating experience *(German)* 80−16830
heat-loss index incorporating solar, temperature wind and cloud cover effects 80−53605
heating systems, performance mathematical simulation for optimal dimensioning *(German)* 80−26110
hot water supply systems using solar collectors, technical problems *(German)* 80−94106
Iceland, geothermal energy exploitation 78−57181
indoor sports centre heating, heat pump appl. *(German)* 80−16829
industrial solar total energy systems in United States 79−96426
low temp. heat extraction from nuclear power plants for district heating 78−37456
metal hydride solar heat pump and power system, design and costs for space heating appls. 80−30521
mobile field dormitory, solar energy space and hot water heating 79−83623
noise survey at Liverpool University 77−7251
nonevacuated compound-parabolic-concentrator solar heating prototypes 79−62105
nuclear energy for combined electricity and district heating prod. 78−37459
nuclear heat appl. to space heating at Karlsruhe Nuclear Research Centre *(German)* 79−87943
nuclear power appl. to centralised heat supply and central heating 79−26730
nuclear power appl. to district heating systems 78−37454
office building in Madrid, solar power appl. 80−89597
passive solar heating systems, Trombe wall control strategies 80−45737
passive solar heating systems design, microeconomic anal. methodology 80−35744
passive solar space heating, sensitivity anal. of direct gain systems 80−35647
passive solar space heating for energy conservation 80−66948
phase change material physical and chemical props. for space heating and cooling 79−57479
photovoltaic and thermal collector system design and testing 80−45675
photovoltaic power conditioning system for professional services office building 80−89646
PWR nuclear steam supply system for district heating and elec. prod. 78−37466
residential, in adverse climates, optimum collector slope 79−66416
solar, active and passive systems, Indian development 79−62140
solar, analysis by stochastic modelling 79−57459
solar, CAD of windows as passive solar collectors, using interactive program 79−62146
solar, CAD w.r.t. maximum solar heat gain 79−57466
solar, combined photovoltaic and house heating system, existing residence retrofitting, expt. results and economic assessment 79−61952
solar, computer-aided analysis and design, using Cal-ERDA programs 79−57456
solar, correspondence between solar load ratio method for passive water wall systems and f-Chart performance estimates 80−16787
solar, demonstration plant in Athens 79−57410
solar, domestic, economic assessment of future energy schemes 79−48044
solar, economic assessment w.r.t. auxiliary energy supply 79−57407
solar, evacuated tubular solar collectors and LiBr absorption system integration 79−62135
solar, for moderately insolated regions, European research 79−57457
solar, heat-pump assisted systems, perform anal. 80−35649
solar, heating and air conditioning 80−61290
solar, Korea's expt. project 79−57409
solar, Markov model-based computer-aided analysis 79−61950
solar, natural environmental control of houses in Northern India 79−62151
solar, of dwelling independent of servicing networks, digital simulation 79−62149
solar, of financial building (1100 m^2) 79−57465
solar, of houses with swimming pool, Austrian development 79−57413
solar, of Japanese multi-family housing unit, expt. and simulation results comparison 79−57455
solar, of North Indian houses, using south walls as collectors, expt. results 79−62152
solar, of single room, heater efficacy evaluation, using stack effect 79−62142
solar, office complex design, with up to 70% energy savings 80−40831
solar, passive, of poultry sheds 79−70437
solar, performance modelling and simulation 80−76618
solar, periodic heat transfer analysis 79−62148
solar, salt gradient solar pond for space heating 80−94115
solar, thermal performance evaluation, with aid of computer 79−57467
solar, Toshiba Solar House No. 1 performance 79−57458
solar, Trombe-Michel wall system design and performance, digital simulation 79−62143
solar, types, construction and thermal and environmental parameters *(French)* 80−85268
solar, US national demonstration program 79−62128
solar, West German experiment, BBC Solar House (Heidelberg) design, operation and performance 79−57405
solar, with all-air systems, experiences with CSU Solar House II 79−57406
solar air heaters, aerodynamic drag investigation 80−40899
solar air heating/cooling systems for buildings, review 80−45754
solar and wind energy combination, low-energy house in Denmark design 79−57411
solar augmented and assisted systems 80−7918
solar availability for winter space heating, anal. of SOLMET data (1953 to 1975) 80−81421
solar collector applications for space and water heating in buildings 80−61406
solar collector construction and utilisation for low-temp. heating 79−57442
solar collector wall, bi-coolant, heating cycle, thermosiphoning, building heating and cooling 80−72083
solar collector-heat storage systems for heating and ventilation of buildings 80−45758
solar collectors combined with ground heat pumps, economic advantages *(German)* 80−76605
space heating continued
solar domestic space heating in Ireland, computer simulation model of thermal performance 80−45732
solar energy: four sites demonstrate potential 79−61946
solar energy, Markov model 79−74501
solar energy, research, applications, water heating, space heating, air conditioning and hothouse heating *(French)* 79−100487
solar energy, storage and power supply for building heating, optimal conditions *(French)* 80−61297
solar energy and environmental heat utilization for space and water heating *(German)* 80−61284
solar energy collection and storage, latent heat diode walls, space heating *(French)* 80−61298
solar energy collection and storage, space heating *(French)* 80−61299
solar energy earth storage and utilisation, technical and economic aspects 79−57475
solar energy system installation suggestions for space heating and water heating *(German)* 80−94102
solar energy systems evaluation, passive, use of thermal modelling and 'predicted percentage dissatisfied' 79−62145
solar energy transition and materials problems 80−26115
solar energy utilization, all year domestic heating, in Europe *(Czech)* 79−83564
solar heat collection and storage system evolution 79−62085
solar heat pump house, Dunham-Bush development 80−40830
solar heat pump house heating system with low quality thermal flow 80−76617
solar heat pump plant for space heating in winter, air conditioning in summer 80−76615
solar heat pump systems, combined, performance evaluation 79−88000
solar heating, air movement control 80−66946
solar heating, passive systems 80−76619
solar heating and cooling of buildings, economic problems 79−57451
solar heating and cooling of buildings, Shenandoah Solar Recreational Center 80−45757
solar heating and cooling system for domestic use *(Japanese)* 80−108787
solar heating and cooling systems design, operation, feasibility, review 80−45755
solar heating equipment, for building, community and agricultural appl., use of heat tube 79−57412
solar heating expts. for performance prediction and design optimisation 80−61288
solar heating installation, technical and operational details *(Dutch)* 80−72013
solar heating of buildings, numerical simulation of thermal performance 80−66942
solar heating panel system, performance testing and evaluation *(Dutch)* 80−72079
solar heating storage device, off-peak, ambient temp. observer/predictor control system 80−66950
solar heating system, heat accumulator utilisation, calc. procedure 80−40825
solar heating system economic evaluation and optimisation 80−35644
solar heating system for dwellings, temp. regime investigations 80−97802
solar heating system optimal control, large buildings appl. 79−87995
solar heating system optimal controllers 80−45739
solar heating system perform. estimation using sinusoidal inputs 80−35648
solar heating systems, economic anal. of passive and active residential designs 80−35746
solar heating systems, instrumentation principles for performance meas. 80−35743
solar heating systems for heating and hot water *(German)* 80−108788
solar heating systems for use in Britain, collector design aspects 80−35637
solar heating systems performance over range of storage capacities, prediction 80−45642
solar hot water system design 80−104518
solar hot water systems, marginal cost of electricity used for backup 80−35747
solar hot-water supply system for residential building 80−93851
solar hotwater and heating systems, availability aspects 80−61314
solar house heating system, possibilities of integrating heat pump *(Rumanian)* 80−97804
solar house with integrated greenhouse, earth-wrapped 79−62150
solar installations for utilisation of solar radiation and heat from outside air *(German)* 80−94104
solar investment decision criteria, appl. to space and water heating systems 80−35643
solar pond viscosity stabilisation by organic thickeners 79−62094
solar power, appl. of flat plate collectors and thermal stores *(German)* 80−26152
solar power and other energy conservation measures obs. and evaluation, using minicomputer, Philips expt. house (West German project) 79−61951
solar power systems with annual storage, performance prediction 79−70436
solar power utilisation employing solar collectors, absorbers and heat pumps *(German)* 80−76604
solar power verus heatpumps for domestic space and water heating, appraisal 79−74494
solar powered system for intermittent heat delivery 80−89669
solar residential heating system life cycle cost analysis 79−57444
solar space and water heating rapid implementation effect on USA energy supply 80−104497
solar space heating, two-tank storage system using seasonal and diurnal tanks 80−72016
solar space heating installations, case for dynamic controls on hydronic distribution systems 80−104498
solar space heating systems, load optimisation algorithms 80−45643
solar space heating with air and liquid systems 80−61287
solar storage tank, buried, hemispherical, heat cond. to environment, series soln. 79−3891
solar system, for administrative building, for winter use, technical and economic feasibility 79−62136
solar systems installation for domestic heating *(German)* 80−94103
solar thermal energy storage in salt hydrates, material props. 80−101134
solar total energy system, for US Army base buildings, conceptual design and large-scale expt. 79−52899

space heating continued
solar total energy system, preliminary design for large building supply 79−52898
solar town in Iran, conceptual development 79−57408
solar transition region and inner corona, energy balance 80−90379
solar water and space heating, economic feasibility 80−7920
solar-electric heat pump for houses, design and tests *(German)* 80−7951
SOLPAC energy conservation program, space heating and water heating for homes *(French)* 79−100488
sports centre all-electric, heating requirements, heat pump appl. *(German)* 80−16827
sports facilities and indoor swimming pools, two heat pump appls. *(German)* 80−16832
storage of thermal energy, annual cycle, ice storage and three-coil heat pump 80−55917
swimming baths and associated buildings, heat pump appls. *(German)* 79−92088
technical meteorology, technical and commercial appls. *(German)* 80−46231
thermal, waste heat utilization with annual aquifer storage for space heating appls. 80−97809
two-phase thermosyphon feasibility for solar energy transport and storage 79−57491
USA National Energy Plan impact on solar home heating economics 79−57446
wall with one-way heat flow, vertical inclined cavity stack 79−3899
water heating system using solar collectors *(German)* 80−94105
wind energy conversion system, low-cost, for domestic premises appl. 79−43716
wind furnace systems, advanced, for residential and agricultural heating and power supply 79−48070
wind power for domestic use, Cambridge project 79−48076
wind turbine appl., electricity generation in dwelling, independent of servicing network 79−61943

space research
see also artificial satellites; astronomy and astrophysics; space vehicles
1946 to 1978 review, satellites and space probes 79−80195
1975 launchings *(French)* 77−29624
active and planned spacecraft and expts., 1977 to 1978, report 79−5726
ALSEP-quasar differential very long baseline interferometry, for lunar position meas. 78−45245
American Astronautical Society 25th conference, Houston, Texas, (30 October to 2 November 1978) 79−75077
American space programme, benefits 77−73930
Apollo and Amor asteroids, mining, to provide raw materials for space manufacture 77−91467
Apollo Telescope Mount and solar instruments of Skylab, overview 77−60593
Apollo tradition, object lesson for management of large-scale technological endeavours 78−93071
applications and benefits of US and USSR space programmes 77−87227
Ariane launch vehicle, model firing tests, acoustic field, heat flux, press. distrib. 78−4062
ASSESS II: a simulated mission of Spacelab 78−85813
asteroid 1943 Anteros, spacecraft rendezvous potential target, request for photometry and spectrophotometry 80−90356
asteroid missions: goals for elemental abundance analysis 80−36474
asteroid multiple flyby mission in main belt, feasibility study 80−36473
asteroids 1976 AA and 1973 EC, manned and unmanned round-trip mission requirements 77−82101
astrodynamics conf. (Provincetown, MA, USA, June 1979) 80−82583
Astrometric Satellite and stellar parallaxes 79−30051
astrometry from space vehicles, general principles 78−12082
astrometry from space vehicles, limitations and prospects 78−12083
astronautical congress, Anaheim, Calif., USA (Oct. 1976) 78−4054
astronauts and UFO phenomena 77−64607
astronomers in space, prospects for Space Shuttle 77−56806
astronomy, NASA prospects 78−69654
astronomy, optical systems of space telescopes *(Russian)* 77−17367
astronomy, planned studies from space shuttle telescope 79−21183
astronomy and space age progress *(Spanish)* 79−62719
astronomy and space exploration, first 20 years *(Russian)* 78−16267
astronomy from Space Shuttle, payload specialist experience 77−64588
astrophysical obs. by space vehicles (1966-76) *(Japanese)* 78−24417
aviation and astronautics, conf., Tel Aviv and Haifa, Israel, May 1976 77−31319
balloon space obs. (1966-76) *(Japanese)* 78−24419
biological materials separation in space environment, electrokinetic phenomena and electrophoresis 79−48351
biology and medicine in space 80−41265
biomedical parameters interference, caused by space motion sickness medication 78−53536
biophysics in space, Soviet research programme *(Russian)* 78−40354
blood viscosity and red cell aggregation at zero and 1G, instrumentation for Space Lab 3 80−61716
blood volume regulation, effects of space flight, review 80−3826
British space prospects 79−84644
Canadian space activities from 1950s 79−84631
charged particle-beam interactions, space and laboratory plasma workshop 78−7821
charged particles, meas. instruments review *(Russian)* 77−17368
circumsolar plasma, Venera 10 radio signal spectral meas. 80−109326
colonisation, preliminary cost benefit anal. 77−87231
colonisation, two new propulsion systems 77−87232
colonisation consequences 78−4187
comet fly-by mission, impact mass spectrometer for chemical analysis 78−93112
comet fly-by mission, low vel. dust particle meas. using capacity type detector 78−93113
comets, direct investigation by space probes 77−37494
comets mission, US space agency plans for 1980 research 80−46492
communications requirements for outer planets exploration 78−32318
computerised planning in ESA 80−4223
conference, COSPAR 22nd plenary meeting (Bangalore, India, May-June 1979) 80−77549
conference, Tel Aviv, Israel (June 1977) 79−25448
construction of large structures in space 80−98533
cosmic ray nuclei, Z=30-40, fractional cell loss, Earth orbit expt. 80−3828
cosmic rays, meas. instruments review *(Russian)* 77−17368

space research continued
cryogenic hybrid cooler for space flight appl. 78−89484
cryogenics appl. *(French)* 79−70942
cryogenics appls., 1 mK to 10K temp. range, survey 78−93712
Deimos, spacecraft imaging 78−89102
Deimos, surface morphology, comp. and props. 78−89103
directional charged particle flux meas. in space, digital onboard processor appl. 77−64610
DMSP auroral photographs, new auroral pattern 77−13146
dual magnetometer method, extension for use on dual spinning spacecraft 78−77459
Earth observations by astronauts, potential appls. and results *(Russian)* 78−40795
economics, forward-looking financial planning in ESA 80−4221
economics, investment planning in ESA 80−4222
El Paso/Juarex Space Shuttle research projects 79−53952
electron beam injection, beam-plasma discharge at low press. and mag. field strengths 78−42769
electron beam interaction expts. planned for space shuttle 78−9796
electronic units development, on-board, used in rockets and satellites *(Spanish)* 77−91401
EM environment, microwaves effect on animals *(French)* 77−44716
EM slingshot system for space propulsion 78−77462
equipment for spacelab, costs, safety 80−41267
ESA programmes in infrared astronomy *(Italian)* 79−48646
ESTEC European Space Research and Technology Centre, role within ESRO framework 79−5722
European Space Agency, status of certain privileged non-member states *(French)* 80−72633
European Space Agency activities *(German)* 80−8516
European Space Agency cyrogenic programme and superfluid He cryostat for spacelab 79−63239
European Space Agency programmes, developmental or operational status 80−72742
European Space Agency projects (Dec. 1977) 78−61703
European Space Agency satellite, programmes and projects 79−12377
European Space Agency scientific programme trends and prospects 79−2468
European Space Agency spacecraft, Ariane and Spacelab 79−88565
European Space Research and Technology Centre (ESTEC) 78−69651
European space technology developments, Swiss role *(German)* 80−4234
Excede 2 test, artificial auroral expt., ground-based optical meas. 78−89038
experimental precision, gravitation and general relativity 78−8333
exploration, American and Soviet space programs, book 77−57149
exploration, concepts and effects 78−81792
extraterrestrial intelligence, telecommun. technology 78−32319
extraterrestrial space travellers, characts. 78−69708
fabrication of ionisers for electric propulsion *(French)* 79−56946
fibre optic dosimeter on Navigational Technology Sattelite 2 79−22487
finance, the role of private funding in European space ventures 80−77121
flight factors combined effects on man 78−53537
fluctuations generation with arbitrary power spectrum, algorithm 78−73927
forecast of space technology 79−66905
future space travel and astronauts, technical problems *(Italian)* 79−80244
Galilean satellites, diameters from Pioneer data 78−85893
GEOS, dynamics response study mission 78−4072
Geos mission, launch malfunction, experimental program procedure 77−70979
geostationary satellite, orbit determ. by single ground station tracking 80−109329
graphite fibre epoxy composites, eutectic coating moisture barriers 80−81228
graphite fibre epoxy laminates, low thermal expansivity, design considerations 80−81031
graphite fibre filled polyimide composite laminates, space environment, phys. and mech. response 80−81140
gravitational Doppler effect explored using geostationary satellite 80−109351
Halley-Venus mission, Planet-A project for mag. meas. in interplanetary space *(Japanese)* 80−94672
HELIOS spacecraft, problems for Sun flyby mission 77−70969
High Energy Astronomy Observatory (HEAO) programme 79−44368
High Energy Astronomy Observatory Program, mission 79−5730
high speed spectrum analysis method appl. 77−73896
high-temperature materials for space power systems, mech. props. 79−57045
Hipparcos astrometric satellite project and space telescope astrometric program, review *(French)* 80−46365
Houston area getaway special experiments 79−53951
incoherent response method for space plasmas nonstationary processes, phase fluctuations effects 78−45184
India's domestic satellite, positioning agreement and interference problems 77−82099
industrial projects in space 80−90319
industrialisation of space, introductory outline *(French)* 78−77454
industrialization, prospects 78−36435
industrialization programme 77−78765
inner planets exploration programme, US, telemetry data rate improvement appl. 78−32317
instrumentation, use of solid cryogens *(French)* 77−134
international astronautical Federation, 29th Congress (Dubrovnck, Yugoslavia, 1-8 October 1978) 80−46723
International Magnetosphere Research programme, review *(Russian)* 80−17467
International Solar Polar Mission, predictions for zodiacal light and local interstellar dust obs. 79−92717
International Space Hall of Fame Dedication Conference, Alamogordo, New Mexico (Oct. 1976) 77−56814
International Sun-Earth Explorer, three-spacecraft programme for magnetosphere study 78−28485
International Ultraviolet Explorer, geosynchronous satellite 78−89060
interplanetary electron shield anal. 77−78604
interplanetary H, Lyman α radiation meas. with absorpt. cell spectrophotometer 78−28519
interplanetary low energy charged particle measurements, Compton-Getting effect complications 78−49269

space research continued
interplanetary missions, trajectory analysis computing, ESTEC program 79−21129
interplanetary space, use of comets as probes 77−25983
interstellar exploration programme considerations 77−2319
interstellar flyby missions, relativistic effects 78−61729
interstellar ramjets infeasibility 78−81520
interstellar space travel 78−61699
interstellar travel and communication, bibliography 78−81564
ion beam, fast, production technology, use in laboratory and space expts. 78−5889
ionosphere, space vehicle obs. (1966-76) *(Japanese)* 78−24402
ionosphere probes, plasma disturbances creation rel. to Spacelab proposed low-energy meas. 78−77458
IR measurement facility, low-background large-aperture, design 79−21125
IR measurement facility, low-background large-aperture, performance 79−21126
IR observation technique 78−61738
Japanese space projects *(Japanese)* 77−87237
Jovian atmospheric probe, mass loss, shape change, real-gas aerodynamic effects 78−4055
Jovian entry, Rankine-Hugoniot eqns., soln. using reduction-of-ionisation-pot. 77−9651
Jovian system, Voyager 1 encounter 80−26716
Jupiter, data from Voyager 2 on Jovian system 79−84740
Jupiter, magnetopause motion longit. control from Pioneer magnetopause crossings 78−49375
Jupiter, magnetosphere, low-energy charged particle environment, Voyager 1 first look 80−26797
Jupiter, orbiter probe mission, 1981, planning 78−4056
Jupiter, Voyager 1 mission 79−96948
Jupiter, Voyager 1 photographic obs. of atmosphere ring and major satellites 80−26788
Jupiter, Voyager 1 planetary radio astronomy obs. 80−26796
Jupiter, Voyager telecommunications system 80−26715
Jupiter atmosphere, future spacecraft missions 77−37564
Jupiter atmosphere and ionosphere, Voyager 1 preliminary radio profiles 80−26791
Jupiter colour pictures from Voyager space probes, 800 line scan TV system, land based receiver systems *(German)* 80−101549
Jupiter flyby by Voyager 1 *(German)* 79−96961
Jupiter magnetic field studies by Voyager 1, preliminary results 80−26793
Jupiter magnetosphere, Voyager 1 obs. of energetic ions and electrons 80−26798
Jupiter magnetosphere plasma observations, Voyager 1 initial results 80−26794
near-Jupiter plasma, Voyager 1 plasma wave obs. 80−26795
LANDSAT, proposed parameters 78−7858
life support system with autonomous control employing plant photosynthesis 77−25563
low gravity development of vitroceramic-metal composite materials, Spacelab appl. *(French)* 78−92229
Lunar and Planetary exploration programs, United States 78−77461
lunar exploration, status after 18 years 78−61767
lunar mass-catcher for large-scale material transport 79−16844
lunar probe tracking data processing, for geocentric and selenocentric gravit. constants refinement *(Russian)* 77−73940
magnetosphere, appl. of impulsive plasma accelerators, tests under cosmic conditions 77−53399
magnetosphere, high-latit., Echo 4 electron beam expt. and artificial auroral streaks obs. 78−89036
magnetosphere, research via front-end electroreactive plasma accelerators 77−53400
magnetospheric plasma as energy source for space instrumentation 77−64605
mankind's future needs and aspirations in space, conf., Washington USA, 1976 Oct. 78−4078
Mare Crisium, view from Luna 24, conference, Houston, Texas (1977, December 1 to 3) 80−17710
Mariner 10 expedition to Venus and Mercury *(Norwegian)* 78−49291
Mariner Jupiter/Saturn 1977 mission, navigation strategy 77−5411
Mars, biological implications of Viking mission 79−8872
Mars, Mariner 9 maps compared with canal system 78−16326
Mars, using Viking Orbiter visual imaging system, slow-scan TV cameras appl. 77−45282
Mars, Viking 1 landing sites selection 77−13271
Mars, Viking biological expts. findings 78−65542
Mars, Viking gas exchange reaction simulation on UV irradiated MnO_2 substrate 80−72831
Mars, Viking lander sites spectrophotometric and colour estimates 78−85881
Mars, Viking Landers and unsuccessfull search for life 78−49367
Mars, Viking orbiter images IPL processing 78−20679
Mars, Viking project and search for organic life *(Swedish)* 77−22128
Mars, Viking results from early meas. on surface 77−33383
Mars, Viking-1 photography rel. to tectonics and volcanism *(Russian)* 79−48726
Mars magnetic field, Mars 2 and 3 evidence 78−49361
Mars magnetic field, Mars 3 evidence re-examined 78−49359
Mars magnetic field, Mars 5 evidence 78−49362
Mars magnetic field, Mars 5 evidence re-examined 78−49360
Mars upper atmosphere, H Lyman α radiation meas. with absorpt. cell spectrophotometer 78−28519
material sciences development, future interest and expectations, Spacelab era influence (1981) 79−19981
materials processing experiments 79−1817
materials science and technology, space flight appl., conf., Gaithersburg, USA (April 1977) 79−47881
materials sciences in space, first Skylab mission, review 77−36377
Mercury orbiter missions, new concepts 79−80197
metal foam solidification, fluid flow effects 79−47674
Michigan Space Center, space vehicles exhibition and model solar system 78−69653
microwave and IR detectors, space appl. of superconductivity 80−85836
miniaturised turbo-molecular pump, for space appl. *(French)* 80−42234
molecular shield for Shuttle Orbiter, effect of expts. on density distrib., model 78−22374
Moon, exploration and post-Apollo prospects 77−17329
Moon landing, effects on space exploration and science 79−96881
space research continued
MOS dosimetry unit development for use in space 79−22485
multiple-launch space research program, choice of vehicles 80−8512
nammed spacecraft, data acquisition and logging system incl. speech 80−61979
NASA astrophysics activity 79−5729
NASA budget rel. to 1979 missions 78−45195
NASA planetary missions planning 79−5732
NASA solar Maximum Mission, hard X-ray imaging collimator 77−5437
NASA solar terrestrial programme, planning 79−5731
NASA space power technology program 79−96883
NASA-ESA mission for Periodic Comets Halley and Tempel 2 rendezvous 80−82168
near-Earth radiation hazard due to solar flares, dosage estimation technique 80−67482
near-Sun missions, solar thermoelectric generators appl. 79−48143
optical instrument space qualification using long duration exposure facility 78−85826
optical instruments, testing, using NASA Long Duration Exposure Facility 79−5725
optical studies from space, Soviet, review 78−85815
orbiting ultrahigh vacuum facilities, appls. and characts. 78−7855
OSO-8, LPSP expt. instrumentation, laboratory calibration and pre-launch performance 77−64649
otolith sensitivity assoc. with habituation to linear accels. capable of inducing motion sickness 78−44621
out-of-ecliptic mission, optical detection of local interstellar particles 78−85906
outer planets, Voyager spacecraft mission 78−49289
particle anisotropies in space, multiple telescope meas. techniques 77−82103
Periodic Comet Halley mission *(Polish)* 80−67516
Phobos, spacecraft imaging 78−89102
Phobos, surface morphology, comp. and props. 78−89103
Pioneer Jupiter missions, solar wind plasma analyser 77−67024
Pioneer Venus, initial results 79−48699
Pioneer Venus a first report 79−84701
Pioneer Venus mission, first results 79−66945
Pioneer Venus program, 1978 mission 77−73926
Pioneer Venus program, spacecraft, objectives and payloads 77−73927
planet thermal radiation intensity field modelling; principles 80−62056
planetary atmospheres, improved small Mattauch-Herzog mass spectrometer appl. 79−8795
planetary atmospheres, light scatt. process meas. via laser beam *(Russian)* 79−44365
planetary atmospheres, research developments 78−69720
planetary atmospheres, results from space missions 78−32377
planetary atmospheres, review 78−69719
planetary exploration, invited discourse before sixteenth general assembly of IAU 78−12076
planetary exploration, neutron-gamma techniques 79−53728
planetary exploration 79−62710
planetary exploration by spacecraft 80−105146
planetary exploration programme, US 78−32316
planetary exploration using impact spacecraft imagery, crater morphology investigations 80−62052
planetary lander, biological and soil chemical testing system 77−45284
planetary surfaces exploration, radar appl. 78−73663
planets gravitational spectra, determ. from planetary orbiters tracking 80−41744
plasma electron energy distrib. function meas. by probe *(Japanese)* 78−28474
plasma simulation chamber, design and appls. *(Japanese)* 77−22039
plasmapause, displacements meas. via radiowave phase shifts 77−22034
plasmas, new concept for EM and electrostatic waves detect. 77−9549
Pluto encounter in mission beyond planets 80−17466
Precede, artificial auroral expt., summarised results 78−89037
Project Daedalus: an analysis of the photometric data on Barnard's star, and its implications 78−81657
Project Daedalus: astronomical data on nearby stellar systems 78−81612
Project Daedalus: payload design for stellar flyby mission 78−81524
Project Daedalus: the evidence for planetary companions of Barnard's star 78−81656
Project Daedalus: the mission profile 78−81523
Project Daedalus: the ranking of nearby stellar systems for exploration 78−81522
Project Daedalus, origins and objectives 78−81521
pulmonary function test automated apparatus for use on Space Shuttle 78−31912
radiation doses absorbed in near-Earth orbit from 1972 August 4 solar flare 77−52892
radiation environment of space vehicles electronic components, laboratory simulation 80−94689
radiation safety, in high-altitude air traffic 78−44620
radiobiological studies in space and at ground-based accelerators 80−41266
raw materials for space manufacturing, comparison of terrestrial practice and lunar availability 77−87233
recording satellites and instrumentation, 1976-8 launchings *(German)* 80−36471
remote programming, real time computers, space flight on-board expts. *(German)* 78−53791
review, 1976-77 period 79−25449
rocket and satellite space obs. (1966-76) *(Japanese)* 78−28481
rocketless space science, ionosphere props. meas. at Arecibo Observatory 78−81488
Salyut 6, aspects of system and scientific investigations 79−29970
SAS-3, general description 77−2324
satellite, India's participation 77−13203
satellite Fourier spectroscopy, mechanical disturbance effects on optical elements *(German)* 80−36478
satellite Fourier spectroscopy methods and problems *(German)* 80−36477
satellite range measurements, formula for refr. effects computation 78−73609
satellites studying wave-particle interactions in magnetosphere, X-ray, γ-ray astronomy, Ariel series, Geos, ISEE, Cos-B satellites 80−90317
scientific instrument development problems and solns. 77−82111
SEPAC (Space Experiments with Particle Accelerators), program for first Spacelab mission 79−48650

space research continued
SEPAC for ionosphere and magnetosphere studies from Space Shuttle/Spacelab 77−73925
Shuttle/Spacelab, platform for cooled IR astronomical telescope 77−73921
Shuttle/Spacelab mission, instrumentation requirements and provisions 77−70972
Shuttle/Spacelab program rel. to solar flare buildup studies 77−17498
simulation studies of space 79−58217
Skylab, review of manned expts. in space 78−36429
Skylab astronauts, high-LET particle exposure 77−29212
Skylab contaminant particulate environment, coronagraphic technique 77−78633
Skylab simulator visual displays and training for joint obs. programmes 77−60566
sled programme, Spacelab, weightlessness expts. on man 80−94381
SNIA Viscosa SpA contrib. to European space programmes *(Italian)* 77−82109
solar electric propulsion stage applications 78−4059
solar furnaces, for materials-science expts. 80−108786
Solar Maximum Mission, XUV spectroheliometer described 79−25487
Solar Maximum Year project and related space experiments, review 80−90404
solar radiation induced orbital perturbations, space structures appl. 79−5723
solar thermal aerostat research station (STARS) 80−17471
solar wind, studies from Prognoz satellites 77−64596
solar wind composition measuring instrument for ISEE-C space probe *(German)* 79−29974
solar wind turbulent plasma, radio wave propag. meas. using three satellites 80−101518
Soviet achievements survey *(German)* 77−41283
Soviet lunar and planetary exploration, handbook 80−62398
Soyuz programme, analysis of Soyuz 1-18 achievements 78−12071
space environment effect on coatings 78−85827
space research programmes *(Japanese)* 78−24418
space science instrument testing, modular, CAMAC based computer controlled ground support equipment 79−25434
Space Shuttle, astronomy and space science research tool 79−40057
Space Shuttle, small planetary missions 80−109339
Space Shuttle, tethered satellite system 79−8794
Space Shuttle, use for science and engineering, Symposium, California (May 77) 78−36426
Space Shuttle and deep space missions 80−109336
Space Shuttle and Spacelab, expected mission results *(French)* 78−53784
Space Shuttle first orbiter dedication 77−17326
Space Shuttle project, space-oriented experimental programme 80−17465
Space Shuttle/Spacelab utilisation, conference, Washington, DC, USA (8 to 10 March, 1978) 79−80203
Space Transportation System, integration with deep space mission 80−109337
spacecraft communication antennas, composite material for fabrication 78−4063
spacecraft surface material performance modelling 78−4061
spaceflight and solar system colonisation 77−49263
Spacelab, biomedical expts. 77−16999
Spacelab, communications R and D project management 77−17321
Spacelab, contributions of Germany to payload 77−17323
Spacelab, development and integration of payloads 77−17322
Spacelab, space applications missions 77−17324
Spacelab, technical description 77−17320
Spacelab 2 mission, astrophysical payload summary 78−85816
Spacelab and artificial satellites appls., conf., Rome, Italy (Mar. 1978) 78−96384
Spacelab and European expts. on Space Shuttle 79−44332
Spacelab and services to users 80−31194
Spacelab and Space Transportation System, management and programme 77−45280
Spacelab development of operational Earth observation systems 77−22037
Spacelab of European Space Agency 80−85837
Spacelab pressurised model development for future space missions 80−90318
Spacelab project, ESRO/NASA cooperative programme 79−8792
Spacelab project, zero gravity physics review 77−29619
spectral reflection characts. transformation of natural formations 79−48640
status and development, reviews 79−80190
stratospheric balloons for IR astronomy *(Italian)* 79−48683
Sun, out-of-ecliptic space probes 77−87228
superconducting magnets, appl. 80−37058
superconductivity, space applications 80−41694
superluminal space travel and ballistic theory of light 79−80204
technological payoffs 77−17328
telemetry, space technology appl. *(German)* 78−93073
TLD system for meas. of cosmic dose on board a spacecraft 80−109047
universal telemetering system *(German)* 77−73924
USA planetary exploration programme 77−33324
USA space science missions and satellites 77−29630
USSR space base at Plesetsk 77−73929
UV and visible astronomy from space 78−61704
UV astronomy, new era with International Ultraviolet Explorer (IUE) 79−48671
Venus, description of expts. on Pioneer Venus 77−73928
Venus, luminous flux from Sun, meas. from Venera-9 and Venera-10 77−37544
Venus, Pioneer and Venera, spacecraft 79−62721
Venus, Pioneer obs. *(German)* 79−96961
Venus, Pioneer radar data, planet's topography *(German)* 80−105190
Venus, Pioneer-Venus, Venera 11 and 12 research results on atmosphere and surface topography *(German)* 79−80260
Venus, program for exploration 77−73990
Venus, wind speed meas. by anemometers on Venera-9 and Venera-10 probes 77−37542
Venus atmosphere, anal. by automatic interplanetary stations (Venera-4, 5, 6 and 8) 78−28520
Venus atmosphere, struct., and light, heat and wind regimes from space vehicles 80−62062
space research continued
Venus atmosphere and surface, investigation by radiosounding from Venera 9 and 10 satellites 80−101543
Venus cloud layer, struct. according to Venera 9 televised pictures 80−67604
Venus nighttime ionosphere, two-freq. sounding by Venera-9 and Venera-10 probes 77−37543
Venus rock density, method, equipment and results of Venera 10 meas. 78−28564
vibrational effects in weightlessness and prospects for space technology 77−58597
Viking, surface sampler subsystem 79−48651
Viking biological investigations, review and status 79−80263
Viking entry vehicle, aerodynamic behaviour, ground test and flight results 79−16821
Viking Lander I, Martian life search project 77−33321
Viking landers, locations and Mars physical ephemeris from radio tracking data 78−20685
Viking Mars, extended mission 80−67514
Viking mission, radio science investigations 78−20684
Viking mission to Mars, review 77−73933
Viking mission to Mars, review of planetary data 80−72839
Viking missions, example of planetary exploration 78−12076
Viking missions, review of results *(Russian)* 78−20667
Viking missions, scientific results review 77−56852
Viking programme, biological expts. *(Hungarian)* 79−44329
Viking project, imaging expts. on orbiters and landers 77−56851
Viking project, summary 78−20611
VLF signals, preprocessing on spacecraft 77−64609
Voyager 1, IR obs. of Jupiter and satellites 80−26790
Voyager cosmic ray detector system, energetic particle studies in outer heliosphere 78−24434
Voyager images, automatic technique for planet centre location 80−101534
Voyager imaging experiment 78−24427
Voyager IR spectroscopy and radiometry experiments 78−24428
Voyager low energy charged particle experiment 78−20618
Voyager magnetic field experiment 78−24431
Voyager mission objectives 78−24426
Voyager mission to Jupiter, Galilean satellites improved ephemerides 80−62066
Voyager mission to outer planets 79−62718
Voyager photopolarimeter experiment 78−20616
Voyager planetary probes for outer planets, review 78−24435
Voyager planetary radioastronomy experiment 78−24433
Voyager plasma experiment 78−20617
Voyager plasma wave system 78−24432
Voyager project, Jupiter and Saturn *(Norwegian)* 79−92646
Voyager project, microwave communications from outer planets 80−77263
Voyager radio science experiment 78−24430
Voyager UV spectrometer experiment 78−24429
Voyagers 1, 2, interplanetary probes, projected itineraries *(French)* 77−70976
WARC 1979 regulations impact 80−105147
water loss, evaporative, by man in a gravity-free environment 79−57779
weightless liquid systems, acoustic manipulation in space 77−49716
weightlessness, prophylaxis for external breathing disturbances due to water immersion 77−52893
weightlessness expts., metallurgy and electrolysis, ERNO space research, with vertical Skylark rocket *(German)* 79−19980
Zarnitsa.2 electron injection expt., circumrocket glow spectral obs. *(Russian)* 80−12596
zero-gravity environment, possible expts. for films 78−12507

space science *see space research*

space-time configurations
see also general relativity
$\lambda_0\Phi^4$ field theory, 3 space-time dimensions, renormalisation, analytical continuation to imaginary time 80−86563
σ-model, nonlinear, curved space, spontaneous compactification, Grassmann manifold 80−57467
σ-model, nonlinear, superconformal invariance in 4-dimens. space-time 80−37154
$\phi^{3,4}$ theory, conformal anomalies for interacting scalar fields in curved spacetime 79−49396
$\mathcal{H}$-space formalism 78−21018
absolute space time theory, criticism 78−86210
absolute space time theory, reply to criticism 78−86211
absolute space-time theory 78−36921
adiabatic regularisation, quantum field in Robert-Walker metric 78−73916
affine motion in recurrent Finsler space 78−57797
algebraic type of space-times possessing a nonsingular killing horizon 78−62126
amorphous spaces, affinely-rigid motion 77−60991
angular momentum in general relativity, defn., asymptotic behaviour 77−49650
anisotropic fluid in spherical space-time, high freq. null radiation state 78−21016
anomalous currents in curved space 78−62336
anomalous Einstein coefficients representation with effective space-time metric *(German)* 77−82118
anti de Sitter space, supersymmetry nonlinear realisation 77−87915
asymptotic Minkowskian space-times 79−97263
asymptotic symm., conformal struct. 78−21023
asymptotically flat initial data for vacuum spacetimes 78−16702
asymptotically flat space-times, approx. H-spaces 78−105
axial symmetric space-times, canaonical forms 80−105545
axiomatic formulation of six dimens. phys., 3+3 dimens. spacetime 78−81834
axisymmetric spacetime, ang. momentum and Dirac charge quantisation 78−70045
b-boundaries of special space-time models 80−31602
b-boundary definition, modifications 80−31606
Bach field equations, jump relations and associated transport equations *(German)* 79−9162
background curved space-time in indefinite metric QFT 79−85049
BI-SPR-F_n space, theorems 80−8866
Bianchi cosmologies, classification in conformal flat space times 80−56985

space-time configurations continued
Bianchi model universes, hypersurfaces of transitivity, Riemann curvature 80−67922
Bianchi type I space-time gravitational field, particles eqn. of state 80−77664
Bianchi type II exact cosmological model with matter and EM field 80−105560
Bianchi type VIII spatially homogeneous cosmologies 77−17729
Bianchi V LRS dust space-times, intermediate singularities, whimpers, instability 80−36750
Bianchi-type I universe, causally connected DeWitt's two vacuum states 78−12608
Bianchi-V cosmological space-time, Einstein-Weyl equations, neutrino currents 80−86023
bimetric general relativity theory, space-times 79−67198
bimetric gravitation, rel. to cosmological models 77−17352
bimetric gravitation theory, cosmological basis, closed universe 78−65844
Birkhoff's theorem generalisation 80−27187
black hole, charged, motion in EM field, EM and gravitational perturb. of Reissner-Nordstrom space time 80−82407
black hole, definition 79−2555
black hole, generation of pairs by collapsing body *(Russian)* 77−13234
black hole, point source spherical model, Schwarschild coord. frame, nature of interior universe 77−67107
black hole, slow rot., weakly charged, space-time and physical fields perturbs. *(Russian)* 78−36634
black hole collisions, time-asymmetric initial data from nonsingular vacuum Cauchy hypersurfaces 80−82408
black holes, Hawking's effect, quantum field theory applied in curved space-time 78−12268
black holes, primordial, ingoing Vaidya metric rel. to radiation accretion in early Universe 80−67918
black holes, reversible and irreversible transforms in Torimatsu Sato space times 79−2554
black holes, thermodynamics and space-time distortion 78−8041
black holes and particle detectors 78−12287
black-hole, Kerr-Newman, quantised massless field, instability 80−82409
black-hole evaporation, unified gravit. and electromag. field theory 78−53979
black-hole space-times, mass positivity 80−8880
Bondi-Metzner-Sachs group, lifting of projective representations 78−21028
boundary definitions for space time configurations 80−31605
bundle boundaries, Schwarzschild and F-R-W solns. 77−57248
bundle boundary for the Schwarzschild and Friedmann solutions 80−31603
bundle completion for parallelisable space-times 80−31604
canonical systems, geometric approach to space-time struct. and symm. 77−17885
Cartan spacetime, pseudoscalar action 79−12691
Carter separable spacetimes, characteristaion 78−36867
Cauchy surface topology restriction in general relativity 77−9921
Cauchy surfaces, determ. from intrinsic props. 78−70023
causal struct., covariant representation of Galilean logic 77−5619
causal structure and four-momenta conservation law *(Rumanian)* 80−46887
causality and relativity 78−81901
causality structure, relativistic, representations by operator density current 77−45767
causality violation region, positive- and negative-energy states 78−29024
causally continuous closed universes, props. 78−29011
causally symmetric spacetimes 77−74281
caustics and singularities, gravitational converging effects 80−77654
charge quantisation in curved spacetime, Kaluza-Klein background, Mandelstram field 79−2695
charged black hole, QED effects, Cauchy horizon *(Russian)* 80−51803
charged fluid, orthonormal tetrads in general relativity 78−54269
charged fluid sphere, general relativity soln., Einstein-Maxwell eqns. 80−68088
charged particle motion in an electromagnetic field on Kerr background geometry 79−9167
charged particle trajectories in static Ernst space-time 79−17291
charged particles, motion in relativistic fields 80−57146
charged stationary axially-symm. metric 78−62131
charged tachyon, gravitational field 78−54282
charm, elementary particle theories, properties *(Spanish)* 80−73681
chronogeometry and diaric method *(Russian)* 78−54265
class-A spacetimes, nonexistence of charged solns. to Maxwell eqns. 79−25767
class-two space-time of product spaces 77−22457
classical domain transformation groups and invariants *(Chinese)* 78−54162
classical space-time model *(Chinese)* 77−9889
classical spontaneous breakdown of symmetry and induction of inertia 79−40417
classification of space-time structures 77−30057
Clifford-Klein space times, effective Lagrangian and vac. stress-energy tensor 79−2674
clock retardation, absolute space, and special relativity 79−67156
coherent beam interference, phase shift in gauge and grav. fields 80−4627
collapsing shell, Schwarzschild-de Sitter space-time, thermodynamics and radiation 80−17607
colliding plane gravitational waves 80−101741
colour geometrodynamics, eightfold way, review 80−95243
compact spinor space-times, parallelisation 78−65828
complex potential eqns., all solns. to nonlinear system 80−46795
complex potential equations, special relativity, and complexified Minkowski space-time 80−52018
complex relativity and double KS metrics 77−2580
complex space-times, real geom. 78−77684
conformal Killing horizons 79−49123
conformal Killing tensors in Riemannian space 78−4534
conformal relativity, bare mass theory 80−27417
conformal space-time group, invariant tensors for maximal subgroups 79−85239
conformal symm. breaking, quantisation in curved space-time 78−41434
conformal transformations in spinor space-time 79−30674
conformally, related space times, field theories, global considerations 79−67473
space-time configurations continued
conformally flat Einstein-Maxwell spaces, Newman-Penrose formalism 80−62559
conformally flat Robertson Walker space-time, explicit dimensional renormalisation of QFT 78−54539
conformally flat space-time, space tensors, trace anomalies 78−12623
conformally flat space-times of divergence free Riemann tensor 78−41220
conformally flat spacetime, singularities 78−16703
conformally flat spherically symmetric space-time 80−8867
conformally invariant gravitation theory and space-time singularities 77−74286
conformally symmetric spaces with positive definite metric forms 77−49574
conformally-recurrent Ricci-recurrent spaces, existence 77−49573
constant curvature spaces, Kepler problem and geodesic flows theory 78−40807
constant mean curvature and canonical time, concept generalisation 78−98
contracted Ricci collineations, timelike mapping characterisation 77−67345
coordinate identification in line elements, isometries, Killing solns. 78−54252
coordinate transformations of the absolute space-time theory 79−67157
cosmic time functions, smoothing and extending 78−21020
cosmological dimensionality and the generation of matter 79−101231
cosmological generic singularity studies by Belinskii, Khalatnikov and Lifschitz 80−31399
cosmological model without big-bang, spherical space metric *(German)* 80−51927
cosmological models with Hoyle's hypothesis 78−86045
cosmological principle, new look 78−86042
cosmology, Lagrangian or Hamiltonian formulations, shift vector field restrictions, symmetry group 80−67923
cosmology, space-time metric, quantised field influence, external grav. field *(Russian)* 80−86027
Cosserat continuum in space with torsion *(Russian)* 78−24715
covariant conservation eqns., relation to energy-momentum concept in general relativity 79−25933
covariant perturbed wave equations in arbitrary type-D backgrounds 79−30314
covariant quantum equations in curved spacetime, Lorentz covariance and tachyons, book contrib. 79−44725
covariant quantum field theory, geometric quantization theory appl. curved space-time 78−12637
curvature invariants and space-time singularities 77−57249
curvature of tridimensional orientations, issued from a point in a four-dimensional space S_4 *(Italian)* 79−30203
curved space, number and location of symmetric vectors 79−71166
curved space of const. curvature, Dirac eqn. 77−87898
curved space path integral, quantal Lagrangian and Hamiltonian for harmonic oscillators system 78−41193
curved space-time, high-freq. EM waves propag. through magnetised plasma 80−48894
curved space-time, neutrino fields with geodesic and shear-free rays, zero rest-mass fields 77−17890
curved space-time, post geometric optics, dispersive effects of EM polaris. 78−96
curved space-time, propag. of photons and neutrinos 77−79011
curved space-time of rotating star, instability of quantum field, particle creation 78−69790
curved space-time quantum stochastic processes, covariant Kolmogorov-Klein-Fock eqn. 80−18083
curved static space-times, quantisation of conformally coupled scalar fields, particle emission *(French)* 78−77771
cut points, conjugate points and Lorentzian comparison theorems 79−93009
cylindrically symmetric space-time, coupled EM and scalar fields 79−85035
D type perfect-fluid solutions of Einstein's equations, classification 78−21019
de Broglie wave packet, nondispersive 78−36858
de Sitter curved spacetime, particle detection 77−30040
de Sitter fibre bundle, wave eqns. for extended hadrons 77−18189
de Sitter space, conservation laws from action principles in five-space 77−22451
de Sitter space, dynamics of free particle systems 78−20958
de Sitter space, quantised fields 78−92
de Sitter space-time, QFT, relativistic wave eqns. *(German)* 77−82666
de Sitter space-time, wave eqns. for arbitrary spin 77−30234
De Sitter symm. space, gravit. interaction and spinning electron eqn. 78−103
de Sitter universe, uniticity conditions for $\Delta^1(x,y)$ propagator of scalar field *(French)* 77−5704
de Sitter universe and mechanics 78−21034
decoupled eqn. solns., EM and gravitational perturbation eqn. soln. construction 78−70029
defect dynamics, field equations, four dimensional space-time setting 80−96521
deformations of the embedded Einstein spaces 78−54254
degenerate spacetime class, props. 78−36902
dielectric const., space-time dispersion, causality principle *(Russian)* 78−56418
differentiability of space time, singularities 77−53815
differential forms in general relativity 79−44818
differentiation with respect to spinors 80−105551
diffusion equation, from space-time transport eqn., for anisotropic random media 80−62595
dimensionality of physical space, assumption of three-dimensionality 78−93515
dimensionality of space, relation to homogeneity of universe 77−64893
Dirac equation generalized total ang. momentum operator in curved space time 79−49128
Dirac equation solution in class of type D vac. space-times 77−74578
Dirac field in curved spacetime, geometrodynamical superHamiltonian and supermomentum 78−45518
Dirac field in Kerr metric, absence of superradiance 77−67578
directional singularities, poles in Voorhees metrics 78−65837
discrete space structure dynamics 80−52392
discrete space-time, geometric formulation of electrodynamics and general relativity 77−26184

space-time configurations continued
discrete spacetime, quantum numbers, uncertainty and min. entropy 77−87659
distant synchrony and the one-way velocity of light, thesis of conventionality 79−67153
distribution valued curvature tensors 80−86163
divergence free tensor densities in 3-space 80−103
divergence free vector fields and Bochner's theorems 79−63003
diverging type-D metrics 77−45761
domains of stationary communications in space-time 78−62133
dual charged solution in curved space time, Dirac quantisation, SU(2)×U(1) gauge theory 78−12827
dual theory space-time geometry, graviton coupling to fermion string 77−18242
Dubourdieu's space-times which admit holonomy groups 79−120
dust, Einstein equations, nonexistence of solutions 78−49736
dynamical lattice theory 79−21933
dynamical properties admitting Gaussian foliation 79−88845
dynamical space and gravitation within a purely geometrical framework including Machian ideas 78−93587
edge geometry, geometrical singularities 79−44807
education, Mach's principle, Einstein's equation and classical physics anal. 77−49524
Eguchi Hanson metric equivalence to Gibbons Hawking metric 79−58612
Einstein's eqns. for dust, gravit. collapse and radiation 78−99
Einstein's equations, local and global props., Universe matter density 78−61942
Einstein's field eqns. on curved background metric, approximation method 78−109
Einstein's theory of gravitation generalised using tetrad field to avoid singularities 78−57833
Einstein's unified field theory, field equations soln. for H-atom space-time struct. 79−21634
Einstein's vacuum field eqns., general static soln. 77−49649
Einstein 4-D manifolds, characteristic classes 80−46886
Einstein action of Riemannian metrics, rel. to quantum gravity and thermodynamics 77−45778
Einstein black hole, existence, local instantaneous symm. of space-time, variable vel. *(Chinese)* 77−13381
Einstein eqn. spherically symm. solution in presence of conformally invariant scalar field 80−17846
Einstein equation, asymptotically flat stationary solns., space-time generation 79−30321
Einstein equations, [(2+1)+1]-formalism, apparent horizons in space-time with rotational Killing vector 80−73222
Einstein field equations, plane symmetric static and homogeneous vacuum solns. 80−86164
Einstein Maxwell space-times with symms., nonnull EM fields 78−65823
Einstein Universe, with source-free EM field 79−85036
Einstein vacuum and Einstein-Maxwell space-times, infinitesimal holonomy group structure and geometrization 80−73252
Einstein-Cartan theory of gravitation, homogeneous isotropic cosmological model *(Russian)* 77−49510
Einstein-de Sitter model, singularity problem, book contrib. 80−46891
Einstein-de Sitter model and metric, book contrib. 80−22248
Einstein-de Sitter universes, adiabatic density perturbations evolution 79−25769
Einstein-Kaehlerian conharmonic recurrent spaces 79−63096
Einstein-Klein-Gordon eqn. solns. in stationary axially symmetric space-time *(French)* 79−25921
Einstein-Maxwell, homogeneous fields admitting transitive group of motions 79−40437
Einstein-Maxwell eqn., N soliton solutions *(Russian)* 80−105556
Einstein-Maxwell equations, EM and gravitational wave spacetimes, similarity solutions 80−57154
Einstein-Maxwell equations, static electrovac solns., complexification technique 80−68114
Einstein-Maxwell fields with cosmological constant, null strings 78−21033
Einstein-Maxwell null fields in Newman-Penrose formalism 80−17853
Einstein-Maxwell space times, symmetry mappings 79−49139
Einstein-Maxwell theory, energy-momentum tensor, invariance transforms. 78−21036
Einstein-Yang-Mills system in six dimensions, static solution 80−8883
Einsteins eqns., algebraically special space-times with nontwisting rays 80−42114
elastic spacetime rel. to black holes and gravitational waves 78−73625
electrodynamics *(Italian)* 78−12840
electrodynamics in general relativity 78−45471
electron pair production by photons in constant electromagnetic field in general relativity 78−8568
electrovac spacetimes, Kinnersley-Chitre transforms., homogeneous Hilbert problem 80−86162
elementary axiomatisation of spacetime, particle, signal, transmission, reception concepts 78−70044
elementary particles, physical fields, symmetry, causality props. 79−6270
EM fields in Godel universe 80−42125
EM fields of embedding class one 78−36914
EM fluids and Ricci collineations 79−35605
EM null point source intensity in stationary spherically symmetric space-time 78−57839
EM tensor fields in space-time V_4 of general relativity 80−77674
empty space Einstein eqn. solns., Mach's principle in spatially homogeneous spacetimes 79−17295
empty space-times, four-parametric set of solutions to $G_{\mu\nu}=0$ 80−95007
empty space-times with separable Hamilton-Jacobi eqn. 77−45755
energy conditions and space-time singularities 80−31608
energy-momentum tensors in locally isotropic space-times 80−31631
equations of motion for a class of space-time singularities 79−49114
equivalence of projective representations 77−17863
equivalence principle according to Mach 79−44823
ergosphere instability to scalar and EM perturbations 79−12489
evolution equations for Killing fields, vac. and Einstein Maxwell space-times 78−8279
expanding universe effect on quantum mechanics of electromag. bounded spin 1/2 particles 78−54271
extended conformal spacetime interactions and dynamical groups of elementary particles 78−8290
Fermi normal coords., expansions of the affinity, metric and geodesic eqns. 80−104

space-time configurations continued
Feynman propagator in curved spacetime, momentum space representation 80−32004
fibre bundle with Cartan connection, group contraction 77−74573
fibre bundles, almost complex manifold approach to elementary particles 78−12915
fibre bundles, internal affine symm. of Dirac fields 78−24697
field equations for spatially homogeneous space-times 80−52083
field theory in 2+ϵ dimensions, critical dimen. in string model 77−57503
finite Lorentzian distance space-time singularity theorem *(French)* 78−62075
Finsler space and affinities for external EM fields in general relativity 77−57256
Finsler space with Kropina metric 78−54264
Finsler spaces, curvature tensors P_{hijk}, S_{hijk}, special conditions, Ricci tensors 78−12625
Finsler spaces, structurological remarks on field theory 79−12660
Finslerian relativity, development and basic theoretical principles review 79−35596
Finslerian struct. and absolute parallelism 78−54262
Finslerian struct. of EM field, rest frame of electric charge defined 77−60995
Finslerian structure of space-time, defined by its absolute parallelism 77−82416
five-dimensional theory, conditions of existence of horizons 78−73907
flat space time, conservation laws based on traceless energy momentum tensors 80−52085
flat space-time describing perfect fluid distrib. of matter, embedding class one 78−54272
flat superspace with supertorsion, supergravity, quantisation, renormalisable theory 79−2705
fluid cylinders, static, and plane layers, general relativity solns. 80−68090
fluid space-time including EM fields admitting symmetric mappings of contracted Ricci collineations 77−74277
foam-like struct., mathematical framework 79−9172
foam-like structure, Bjorken scaling violation due to gravitational field 80−77939
foliation of space-time by spacelike hypersurface of const. mean curvature 77−64970
formalism of external forms and non-inertial reference systems *(Russian)* 78−81894
four-dimensional symmetries and laser expts. 77−37791
with four-parameter groups of motions acting on null hypersurfaces 77−57247
frequency solutions of massive vector field eqns. in curved static space-time 78−36909
Friedmann background universe, shock damping and entropy prod. in relativistic simple waves 77−17725
Friedmann cosmological models, relativity of space finiteness-infiniteness 78−96582
Friedmann model, large distance meas. by triangulation 78−86047
Friedmann model with eqn. of state of non-ideal hadron gas, evolution *(Russian)* 79−44649
Friedmann-Lemaitre universes, adiabatic density perturbations evolution 79−25769
function spaces with asymptotic conditions, noncompact spacelike hypersurfaces *(French)* 77−13583
fundamental dimensionless numbers and possibility of life, Machian variational cosmology 79−80246
gauge field theory, de Sitter invariant Lagrangian 80−82868
gauge field theory, space-time symmetry, Higgs model 80−52385
gauge theories for space-time symmetries 77−2723
gauge theory, space-time inversion, classical approach 78−41416
gauge-invariant perturbations on most general spherically symmetric space-times 79−71322
Gauss-Codazzi-Ricci eqns. of local isometric embedding 77−57162
general relativity, indefinite metric quantum field theory, Poincare generators 79−35618
general relativity, quantum spinors and singularity theorems 78−70027
general relativity, space-like infinity, conformal structure 78−8293
general relativity, spherical symmetry in a 4-dimens. space-time 79−35590
general relativity, the Dirac equation, and higher symmetries 79−25931
general relativity, vacuum field equations, fifth dimension, ratio of EM to gravitational force 80−77679
general relativity canonical formulation by analogy with elementary particle string model 78−8287
general relativity conference, Trieste, Italy, 1975, July 78−8285
generalised axisymmetric spacetimes, Einstein vacuum eqn. solns. 80−22243
generalised Goldberg-Sachs theorems in complex spactimes energy-momentum and conformal tensors 79−71300
generalised Peres space-time, geometric and mathematical props. 80−22246
generalised Peres space-time plane wave-like solns. of weakened field eqns. 78−57827
generalised Takeno space-time, coupled EM and zero-rest-mass scalar meson fields 78−70020
generalized macro-causality in relativity theory 79−85021
geodesic balls, volume, and geometry of Riemannian manifold *(French)* 80−68085
geodesic property of general space time *(French)* 78−16701
geodesically complete space time, topology change of edgeless acausal spacelike hypersurface 79−6029
geodesics in black hole space-times 80−4602
geometric quantisation and general relativity 78−8288
geometric struct. of charged fields, Aharanov-Bohm effect 78−28994
geometric style of explanation 80−18
geometrical spacetime perturbation theory: regular first-order structures 79−2678
geometrodynamics, inclusion of observer in wave function 78−54234
geometrodynamics and Gauss-Codazzi eqns. in affine 5-space 79−35595
geometrodynamics with tetrad fields 79−30304
geometry and quantisation of space-time 77−33924
geometry of space-time at coordinate infinity 79−49111
geometry of spacetime 78−36895
geometry of spacetime founded on spacelike metric 79−63102
global structure of space-time, classical bremsstrahlung problem 80−105547

space-time configurations continued
globally hyperbolic spacetimes, conformal deform., Ricci curvature and energy condition 79−9159
Godel's metric 78−62125
Godel's space-time, rotating universe with successive causal and noncausal regions, solns. to Einstein eqns. 79−67200
Goldberg-Sachs generalized theorems in complex and real space times 79−80475
Goldberg-Sachs spacetimes, zero rest mass field perturbations, spinar framework for Hertz/Debye potentials 79−58597
gravitation, canonical many-time quantisation 78−8328
gravitation, metric-affine theory as gauge theory of affine group 78−32746
gravitation, modified theory with regular solns. *(German)* 79−88844
gravitation and dynamical space, geometrical framework, Mach's principle 80−95001
gravitation and inertia in general relativity 78−8317
gravitation and space-time, general relativity 80−68104
gravitation bimetric theory, flat metric election 80−62004
gravitation metric theories, appl. to gravit. dipole radiation from binary systems 77−60589
gravitation theories derived from nonlinear Lagrangian with limiting curvature 78−81897
gravitational, mass defect in Reissner-Nordstrom metric, charge conservation *(Chinese)* 80−86182
gravitational bubbles, radiative corrections to covariant massless quartically self-interacting meson theory 80−62826
gravitational constant rel. to cosmological parameters 79−48974
gravitational dual charge 78−36906
gravitational effects in 6-D general relativity, Schwarzschild metric, orbital precession 80−62550
gravitational energy, torsion of spacetime included in a quadratic Lagrangian 78−8316
gravitational field, quantisation, Hilbert space of quantised system 80−52113
gravitational field, spherical symmetric, spin ang. momentum tensor calc. 80−42107
gravitational field, thermodynamic comments 79−2701
gravitational field and arbitrary gauge field, equations of motion, Heisenberg and classical, force term, spin-curvature coupling 80−57158
gravitational field asymptotic flatness of spacelike infinity 78−45532
gravitational field at spatial infinity asymptotically Minkowskian space-times 80−46885
gravitational field theory, ten-dimensional manifold of local inertial reference frames 80−46903
gravitational field with flat spacetime, extended body weight, Einstein eqn. soln. 79−85015
gravitational fields, axially symmetric, Weyl's class of static vacuum solutions 80−68089
gravitational interaction of spin-1/2 particles, Lorentz invariant theory 80−22257
gravitational radiation and invariants of curvature tensor in general relativity 78−57836
gravitational theory based on Weitzenbock space-time 79−85022
gravitational wave detection, astrophysical sources, resonant mass, laser interferometer and Doppler ranging methods 80−68122
gravitational wave field, conformal coupling to curvature 80−68105
gravity in ray gauge 78−8313
group structure of space and field *(Russian)* 77−13650
growth of curvature near a space-time singularity 80−31612
H space, the manifold of complex asymptotically shear free light cones 78−8292
H-space of Robinson-Trautman type II soln., world-line 77−79010
hadron microstructure, de Sitter microuniverse, relativistic Hooke group and nonrelativistic quark model 80−27480
hadrons, extended, Lorentz deformation props., O(4) and light-cone coordinate systems 80−68354
Hauser space-time in General Relativity *(French)* 79−25919
Hertz-Bromwich-Debye-Whittaker-Penrose potentials in general relativity 79−88858
historical development *(Hungarian)* 80−46784
homogeneous collapsing star, orthogonal vector and tensor harmonics, matter and field asymmetries 79−5841
homogeneous cosmologies, dipole and quadrupole anisotropies 80−109572
homogeneous isotropic space-time, with const. curvature, wave eqn. of nonrelativistic spin-s particle, Galileian limit 78−32740
homogeneous space-times of the Godel type 80−105553
homothetic Killing trajectories, stationary limit surface geometry 79−40424
homothetic maps of the space-time distance function and differentiability 79−116
Huyghens' principle, validity for spinor field eqns. *(French)* 77−41487
ideal liquid, generalised Lagrangian energy density, nonsingular cosmological space-time model *(Russian)* 79−9040
incomplete space-times 77−2572
incompressible minimal surfaces, 3-dimens. manifolds with nonneg. scalar curvature, positive mass conjecture 79−30318
inertial frames in classical space time 78−81826
infinity of time and space in Universe, various problems in cosmology *(Polish)* 78−61948
inhomogeneous cosmologies, anal. of conformally flat slices 80−17704
inhomogeneous cosmologies, conformally flat slices and invariant classification 80−17703
inhomogeneous cosmologies, intrinsic symmetries 80−17702
inhomogeneous local gauge transformations in spacetimes with torsion 79−71330
inhomogeneous metrics, approx. symmetry groups 77−71248
inhomogeneous metrics, approx. symmetry groups 78−62129
instantaneous Cauchy surfaces, existence 78−65832
instantons, gravitational, flavour currents of QCD, Green's functions, foam-like structure of space-time 80−62825
intrinsic metrics on continuous spatial manifolds 77−41459
intrinsic symmetries in general relativity 80−12955
invariance group instability, spacetime, group contractions and models of Universe 79−9041
invariant field equations solns. in (4,1) de Sitter space-time 78−93563
IR regularisation of massless scalar free field in two dimens. space time, Lorentz expansion 78−12818
isolated systems, integral conservation laws, privileged vector fields method, general relativity, external Kerr metric *(German)* 78−16698

space-time configurations continued
isometries compatible with asymptotic flatness at null infinity 79−2675
isotropic and pseudoisotropic subvarieties of n-dimensional hyperbolic variety *(French)* 77−53818
isotropic universe, particle creation and vacuum polarisation, cosmological models 80−90582
Jacobi fields, four-dimens. Riemannian manifold 77−60983
Kaehlerian concircular recurrent and Kaehlerian concircular symmetric spaces 79−35592
Kasner spacetime, conformal energy-momentum tensor trace anomaly calc. 79−21603
Kerr, Dirac eqn., anomalous Zeeman splitting of energy level 77−74081
Kerr associated metric, solution of Einstein's eqns. 77−5713
Kerr black hole, orbits of spinning particles 80−31326
Kerr black hole in thermal equilibrium and the ν vacuum 79−97022
Kerr geometry, wave mechs. of electrons 78−12622
Kerr metric, angular momentum, separation const. 80−77658
Kerr metric, charge accretion *(French)* 77−71257
Kerr metric, geometrical optics appls. to light propag., analytical results 77−29637
Kerr metric, stationary axisymmetric test fields 77−41515
Kerr metric, test particle motion *(Russian)* 77−45752
Kerr metric, vortical type geodesics, causality non-violation 78−54251
Kerr metric in cosmological background, event horizon radius 77−74082
Kerr metric sources, ellipsoidal space-times 78−54249
Kerr naked singularity, classical instability 78−57834
Kerr space-time, EM quadripotential of point change at rest on symmetry axis *(French)* 78−45541
Kerr-Newman background, charged top exact solns. 77−64978
Kerr-Newman background space, nonstatic nuclear forces, meson field at black hole event horizon 78−61880
Kerr-Newman black hole, scalar and electric charge at rest *(French)* 77−67108
Kerr-Newman geom., equatorial circular geodesics 78−4533
Kerr-Newman space of black hole, Dirac eqn. class of solns. 77−49828
Kerr-Newmann, black holes, stress-energy tensor 77−71126
Kerr-Schild congruences and Kerr's theorem 77−60989
Kerr-Schild metric, generalised, for gravit. waves *(French)* 77−71255
Kerr-Schild metric, Maxwell-Hamilton-Jacobi-, and Dirac-eqns. Minkowski covariance 77−64977
Killing horizon as event horizon, a necessary condition in general relativity 78−8295
Killing structures and complex $\mathcal{L}$-potentials 77−82418
Killing tensor quantum nos. and conserved currents in curved space 78−29249
Killing tensors and Killing-Yano tensors 77−33926
killing vectors and maximal slicing 80−77667
Killing-vector five-space, Einstein eqns. 77−49651
kinematical conditions in construction of spacetime 78−70033
kinematical groups and coord. transformations using light-cone frame 78−81796
Klein Gordon lattice field eqn. in 4-D space-time, Lorentz covariance 78−54184
Klein-Gordon equation for massive scalar meson field, Kerr-Newman metric 77−22262
Klein-Gordon field in naked-singularitiy background 78−70274
Kruskal extension from vacuum field eqns. in Schwarzschild metric 80−42112
Kruskal space time, algebraic isometric embedding 79−80478
Laplacian on pseudo-Riemannian manifold, conformal quasi-invariance 77−13654
left-flat space-times, null tetrad and restrictive conditions 80−62545
Lemaitre Universes, Jeans instability 78−12445
length prescription for generalised radial observer, Schwarzschild and Reissner-Nordstrom line elements 80−73223
Lewis metric and flat space-time 80−46877
Lie algebras, BRS transform. 78−93591
Lie group broken symmetry of transformation generating general relativistic theories 80−98836
Lie theory and wave eqn. in space-time, SO(4,C) group 79−12968
Lifshitz-Khalatnikov time functions in gravitational collapse 80−31615
light Doppler effect, absolute spacetime theory 78−69979
limits, co-ordinate dependent investigation 80−95003
locally de Sitter invariant gravitational theory *(Chinese)* 77−26219
locally flat space-time, quantised metric, spontaneous dilatation asymm. 78−16713
long-range scalar field in conformally flat space-time 79−71303
lorentz gauge invariant vacuum functionals for quantized spinor fields in non-simply connected space-times 79−89061
Lorentz groups on skew symmetric tensor space, nonlinear realisations of direct product 78−62329
Lorentz-covariant model of the system of two gravitating particles 80−8865
Lorentz-Minkowski space, extremal surfaces *(French)* 77−67369
Lorentzian manifolds, almost Hermite and almost product (2×2) structures 79−119
Lorentzian manifolds structured by flat conform connection *(French)* 78−77683
M_4 factorisation, spinor algebra, Dirac equation geometrical, interpretation 80−62838
Mach's principle, gravity and inertia, Leibniz invariant theory 77−41426
Mach's principle, modification of general relativity theory *(German)* 79−88843
Mach's principle, the cosmological constant, and the scale-covariant theory of gravity 79−25774
Mach's principle and general principle of relativity, elementary physical approach and observational basis 80−52080
mach principle and the quantal response of the Universe 79−12549
Machian argument in Friedmann models of Universe 77−74168
Machian effects in compact rapidly spinning shells 79−2684
Machian framework, purely geometrical, for describing gravity and inertia 79−44651
magnetic symmetry, improper symm. and Neumann's principle 78−38646
magnetofluid, relativistic, and space-like conformal mappings 80−75001
magnetofluid space-times, imperfect, spacelike, family of contracted Ricci collineations symmetry mappings 80−51650
marginally bound dust collapse, time functions in numerical relativity 79−71321
Marinov coupled mirrors expt., a critique, preferred cosmological reference frame 80−27120

space-time configurations continued
mass operator in Riemannian spacetimes 80−82683
massive particle production in anisotropic space-times 80−90583
massive quantum field theory in two-dimensional Robertson-Walker space-time 79−25962
massive spinning particle in Minkowski space equivalence to massless particle in de Sitter space 80−119
massless field theory, conformally invariant struct. 79−30656
massless particles wave eqns., positive freq. solns., generally covariant defn. 77−49644
massless quantum fields in curved asymptotically flat space-time, particle creation near black hole *(Russian)* 78−57846
massless scalar and spinor field theory in curved space-time 78−21321
matter field space-times, timelike symm. props. 78−24698
matter field spacetimes, symm. mappings satisfying vanishing contraction of Lie deform. of Ricci tensor 79−113
matter-antimatter symmetric universe, random geometry 78−86046
matter-filled universe, relativity of space and time finiteness-infiniteness 78−96581
maximal surfaces in closed and open spacetimes 78−8294
maximally symmetric space with torsion 79−115
Maxwell equations in Riemann-Cartan space, spin-torsion coupling const. 80−82697
Maxwell fields, time depend., in stationary geometry 78−8308
memory geometric-dynamic model in four-dimensional pseudoRiemannian space *(Russian)* 78−27923
mesonic test fields and spacetime cohomology 78−78065
metric existence in 2-D affine manifolds 79−85039
metric fields, generally invariant Lagrangians 79−44708
metric relativity, appl. to EM dipole fields 77−64988
metric tensor components interpretation, astrophys. implications 78−93097
metric topology for causally continuous completions 77−71245
metric-affine gravit. theory, vol. preserving and canonical transform. 79−44826
metrical fluctuations induced by cosmic turbulence 80−82557
metrical forms which admit [(11)(11)] Killing forms 78−32738
miniphantom geometrodynamics for 2+2 resolution of space-time 78−62132
Minkowski space, causal logic 78−16739
Minkowski space, complex, superluminal boost in x-direction, Lorentz transformation, tachyonic connections 80−105497
Minkowski space, tensor spherical harmonics and tensor multipoles 77−5717
Minkowskian spacetime, asymptotic, rel. to asymptotically simple space-time 78−29019
Minskowski space time, real analytic local extension 80−77656
momentum space techniques for curved space-time quantum field theory 79−71341
Morse theory on timelike and causal curves 77−13649
motion of continuous medium in given space-time, four-velocity 80−68091
multiparticle S-matrix factorisation in two dimens. space-time models 79−281
multiply-connected space-time, black holes and tachyons 79−30315
N-type vacuum space-times as special functions in C^2 78−21021
naked Kasner type singularity, motion of particles in field 78−70028
naked singularity solutions, gravit. collapse with axial symm., geodesics, particle orbits 78−41215
natural theory of continuous media 79−25917
negative mass and positive mass matter, hypothetical coexistence, causal paradoxes 80−82685
net cohomology over Minkowski space 78−93561
neutrino-generated static space-times 80−52107
neutron stars, electrodynamics in curved space 80−90465
Newtonian theory of gravitation, tensor pot. and Cartan's four-dimens. represent. *(Russian)* 77−49658
non-compact maximal submanifolds of Lorentzian manifold 77−74287
non-expanding shear free normal null congruence soln. of Einstein eqns. 80−42111
non-flat space time, Ferraro's theorem validity 80−4247
non-inertial framed space-time configurations, gauge theory appl. 80−22262
non-Minkowskian space-times, mass generation by self-interaction 79−45014
non-Minkowskian spacetime, EM polarisation plane rot. 79−35115
nonequatorial tachyon trajectories in Kerr spacetime, and second law of black hole phys. 79−71244
nonhomogeneous space-time in Brans-Dicke cosmology 80−86024
noninertial frames, cotangent bundle approach, Lie derivative 80−62468
noninertial reference system, electrodynamics eqns. *(Russian)* 78−81895
nonlinear de Sitter symmetry and restricted space-time regions for gravity and supergravity 79−85043
nonlinear Einstein field eqns., numerical soln. algorithm 79−93011
nonlinear Heisenberg-Klein-Gordon equation, localised solns. in flat Schwarzschild space-time 80−4620
nonlinear Lagrangians and Einstein spaces 80−36915
nonlinear scalar field theory, space-time metric *(Russian)* 78−74127
nonlocal field theory and space-time quantisation 77−34078
nonlocalisability of space-time events 80−94972
nonrelativistic Markoff field, stochastic quantisation 79−67181
nonspreading wave packets 79−44672
nonstandard vector connections given by nonstandard spinor connections 77−57250
nonsymmetric field struct., generalised gravit. theory 77−74296
nonuniqueness of solutions to Einstein's equations, symmetries in T_{ij} 80−12953
nonvacuum stationary Einstein space-times, analyticity 77−71
Nordstrom field timelike and null geodesics 77−67350
Novikov coordinates, equivalent to Kruskal, transformaton from Schwarzschild coordinates 80−68098
nuclear forces in Kerr-Newman metric 77−60999
null infinity and Killing fields, local isometries, space-times, asymptotic conditions 80−62832
null infinity as poor initial data surface 78−62127
null strings, geometry in complex space-times 80−22241
NUT spacetimes, completely singularity free 77−13657
odd-parity perturbations, junction conditions on spherically symmetric space-times 80−42127
one-electron atom in curved space-time 80−78509
space-time configurations continued
operational analysis of spacetime struct. in quantum-relativistic theory 77−67322
orbits for interacting relativistic particles, syntactic versus semantic observables 79−21976
orthometric monad formalism, rel. to chronometric and kinematic invariants 77−77
particle creation in curved space, covariant description 77−13857
particle creation in curved space-time, covariant treatment 78−12443
particles with isotopic spin, kinematics, geometric quantisation 80−62871
path integrals for a particle in curved space 79−35598
path integrals in curved spacetime, zeta function regularisation 77−74302
path integration in phase space 78−128
path structures on manifolds, analytic characterisation 78−4535
Pauli-Villars regularisation trace anomalies 78−45548
Peirce's theory of the geometrical structure of physical space 78−28906
Peres space-time, generalised, algebraic props. and solns. 80−106
perihelion precession as Machian effect 77−26098
periods on manifolds, quantisation, gauge, comments on Kiehn's work 78−8508
Petrov homogeneous vacuum space time source 80−31632
Petrov type {3,1} vacuum solns. with twist, Killing struct. of family 78−54253
Petrov type N vacuum metrics and homothetic motions 79−75421
photon decay in curved space-time, Hubble red shift and solar limb effect explanation 79−35606
physical operations, diagram operations 80−46846
physical system, model of space-time from set theory concepts 80−82660
plane symm. space-time of class 1 77−57239
plane symmetric space-time of class-1 and electromagnetism 80−22252
plane symmetric space-times, kinematical aspects 78−65834
plane-symmetric containing perfect fluid, evolution 80−94999
plasma processes, neutron stars and black holes 79−84873
Plateau problem in Minkowski space, existence theorem *(French)* 78−86209
point mass alternative space-time 80−31638
point mass space-time singularity 80−82690
point splitting in curved space-time background 79−80491
polarised light beams in gravitational fields, Dirac-spinor form of Maxwell's eqns. 78−50696
positive mass conjecture proof for general relativity 79−40420
pregeometry, gravity with composite metric 79−35619
primordial continuum, principle of least action 77−60921
projective affine motion in recurrent Finsler space 78−73893
projective geometry, Langrangian subspaces, and twistor theory 80−52112
projective invariance in general space times with spinor, torsion and Yang-Mills fields 78−57832
projective space-time, geom. of (N+1) particle system 77−74221
projective symmetries of dynamical systems, infinitesimal symm. transforms of vector field 78−32650
proper homothetic maps and fixed points 79−12662
pseudo Riemannian manifold, maximal submanifold props. 78−12624
pseudo-Riemannian curvature spaces, group struct. 78−57829
pulsars, EM vars. in curved space-times 80−56866
QED, massless, energy-momentum tensor anomalies in spherical space-time 80−73628
QFT, regularisation and renormalisation 77−87890
quadratic Lagrangian in space with torsion *(Russian)* 78−24714
quantisation, projective geometry for polarisations 80−52053
quantisation of space time, based on quantum mechanics and general covariance 79−71343
quantised gravitational perturbations, invariant states under symmetry transformations 79−136
quantum field theory, conformal-invariant, composite field operators 78−81886
quantum field theory, degree of freedom, cutoff and space time struct. 78−66031
quantum field theory, Euclidean approach in curved spacetime, functional anal. 80−27181
quantum field theory, Lagrangian formulation, conservation laws, relativistic gravitation *(Russian)* 80−68337
quantum field theory, relativistic, discrete symmetries 80−68387
quantum field theory in de Sitter space, renormalisation by point-splitting 78−29035
quantum fluctuations near the classical space-time singularity 80−8893
quantum gravity theory at very short distances, nonlinear sigma model 80−12979
quantum many-particle systems in curved spacetime 80−98751
quantum mechanics, space-time operators incompatibility in special relativity 79−12592
quantum mechanics and relativity, interrelations between truth space and time space, holistic analysis of theory of measurement 80−27177
quantum numbers for Dirac spinor fields on a curved space-time 79−97277
quantum scalar field in Bianchi I anisotropic space-time, particle prod. anal. 77−30238
quantum stress energy in nearly conformally flat spacetimes 80−57170
quantum theory, origins of 80−27176
quantum theory, physical geometry, group manifold 80−105522
quantum theory and structures of time and space conference, Starnberg, W.Germany (July 1978) 80−27044
quantum topology, spacetime code 78−36859
quasicurrent pairing of vector fields 77−87669
quasispherical spacetimes of Szekeres, collapse without gravit. radiation 78−28510
quaternion limitations on higher dimension spacetimes for unified field theories 78−45545
radiating Demianski-type space-times 79−30309
radiating systems, gravit. field, twisting free type II metrics 77−71256
radiation damping in general relativity 78−8310
radiation damping in universe with topologically closed space sections 78−57828
Randers' hypersurface, induced and intrinsic connections 79−30204
Randers space of scalar curvature 78−4469
real miniheaven 78−93570
recurrence conditions in space-time, Riemann, Ricci and Weyl tensors 77−17883
red-shift effect, local, relativistic 78−28788

space-time configurations continued
reduced gravitational field eqns., on algebraically special space times with twisting rays 79−30302
reference system contraction or Universe expansion 79−101228
Reissner naked singularity, spontaneous pair creation 78−24990
Reissner-Nordstream black holes, stress-energy tensor 77−71126
Reissner-Nordstrom metric, charged black holes 78−12277
Reissner-Nordstrom naked singularity as quantum mech. scatterer 77−57267
Reissner-Nordstrom perturbations, coupled Einstein-Maxwell eqns. 80−68108
Reissner-Nordstrom spacetime, spin coeffs. and electromagnetism 78−8309
relativistic kinetic theory, thermodynamics, symmetry props. role 80−27117
relativistic mechanics, generalised, spacetime quantisation and Mach's principle 78−73867
relativistic quantum mechanics, semigroup 80−27180
relativistic quantum mechanics, space-time formalism for spin-zero particles 79−21974
relativistic quantum mechanics formulation of space and time 78−65796
relativistic quantum theory, space-time states, book contrib. 79−58886
relativistic star, curved space-time, vac. stability, polarisation, phase transition 77−49290
relativistic wave equations derivation, elementary domains theory, stochastic quantisation procedures 77−41502
rescaling problem of space-times admitting groups of conformal motions 78−36920
Ricci-flat Riemannian spaces, six dimens. single-loop divergences 77−38081
Riemann curvature tensor and closed geodesic paths, for teachers 78−24600
Riemann geometry with torsion, space-time struct. using spin 1/2 elementary particle probes 77−41517
Riemann gravitational theory, cosmic time asymmetry *(German)* 79−35610
Riemann space-time, symmetrisation of energy-momentum tensor of spinor field *(Russian)* 77−82422
Riemann space-time metric construction for given props. of trial particle motions 79−85025
Riemann spaces, conformal correspondence tensor *(Russian)* 77−53814
Riemann-Cartan space-time with cosmological principle, torsion tensor 80−31633
Riemannian curvature and classification of Riemann and Ricci tensors in space-time 80−36914
Riemannian curvature and the Petrov classification 78−54266
Riemannian geometry, Onsager-Machlup Lagrangian, functional integration 80−68102
Riemannian manifolds, quantisation in spaces of constant curvature 78−12602
Riemannian manifolds, symmetric vectors and algebraic classification 80−68094
Riemannian metric description, of gravit. and EM interactions 78−36904
Riemannian space-time cut locus 80−36910
Riemannian struct. on states of quantum-like system 78−67
Riemannian submersion of Lorentzian manifold onto Riemannian manifold of 1 lower dimens. 77−37803
right translation invariant metrics and variational principles on principal bundle, gauge theories *(Chinese)* 80−101743
rigidly rotating relativistic dust cylinder, Riemann tensor, ultrarelativistic case 80−86158
Robertson Walker metric, pair prod., propagator method appl. 80−105564
Robertson-Walker and Petrov G_4 VIII cosmologies, general relativistic kinetic theory 78−24586
Robertson-Walker cosmologies, radiation damping and expansion of universe 77−33717
Robertson-Walker expanding universe, energy spectrum of H-atom 78−73869
Robertson-Walker metric, origin of matter in universe 78−20918
Robertson-Walker spacetime, energy-momentum tensor and particle state definition 79−25934
Robertson-Walker spacetime, path integral quantisation and cosmological particle prod. 78−12440
Robertson-Walker spacetime, trace anomaly of energy-momentum tensor of quantised scalar fields 79−63360
Robertson-Walker spacetime, vacuum expectation values, perturbation technique in curved space 79−97286
Robertson-Walker universe, stress tensor and conformal anomalies for massless fields 77−78903
Robertson-Walker universes, field interaction effects on particle creation 80−42130
Robinson-Trautman space-times, cosmic time functions 80−42113
Rosen's bimetric theory of gravity, orbital topoography and other astrophysical consequences 78−54274
rotating disc experiments, absolute space-time theory 78−36823
rotating pressure-free space-time, thin self-similar disc config. 78−96387
rotating star, interior Kerr metrics, tests 78−28666
rotating systems, Einstein equations 80−68101
S_2 separable space-times, algebraic props., Weyl tensor 79−63093
S-PRF_n-space of first kind 79−17294
Sasakian manifold with recurrent curvature tensors 77−71191
scalar and EM fields struct. in tangent bundle of spacetime with absolute parallelism *(Russian)* 78−49741
scalar electrodynamics in nonsimply connected space-time, topological mass generation 80−82924
scalar field vacuum fluctuations in curved space-time localised region 80−42116
scalar quantum field in curved spacetimes, particle detection and creation 77−67597
scattering operator, analyticity in nonlinear relativistic classical and prequantised field theories 80−73611
scattering processes, Penrose graph representation 78−49983
Schwarzschild field, Papapetrou eqn. motion of spinning particles, Wigner-Lubanski integral 78−108
Schwarzschild radial coord. as measure of proper distance 78−70034
Schwarzschild space time, algebraic embeddings in R^7 space *(Italian)* 79−17284
Schwarzschild space-time, distant stars distrib. seen by freely falling observer *(Polish)* 80−26897

space-time configurations continued
Schwarzschild space-time, electrostatics, electric fields and black holes *(French)* 79−40432
Schwarzschild space-time, EM waves diffr. theory appl. to gravit. lens 80−90750
Schwarzschild space-time, vacuum polarisation induced by gravitation 80−82410
Schwarzschild space-time parallel transport of vector along circular orbit 79−71313
Schwarzschild space-time zero rest mass scalar wave eqn. solns 79−93010
Schwarzschild-Kruskal space-time, role in developing Maxwell field non-zero vacuum expectation value 80−62828
segmented structures, space-time point segment 78−32
self-dual Yang-Mills fields, complex, in Minkowksi space time 78−41424
self-gravitating charged relativistic fluid, space-time permeation 79−2689
self-similar space-times, perturbation scheme 78−54099
self-similar space-times, solutions to general relativity eqns. 78−54098
semiclassical theory of scalar field in globally hyperbolic universe 78−54250
sigma model, nonlinear, soliton stability in S^2 80−37165
sine-Gordon equation, Backlund transform., physical space-time solitons 80−77629
singletons and massless, integral-spin fields on de Sitter space 80−110
singular holonomy group 78−41206
singular space times, classification scheme 80−31609
singular space-times, classification scheme for boundary points 78−24699
singularities, heuristic discussion 78−93568
singularities, incompleteness and the Lorentzian distance function 79−30317
singularities, native and classes 80−31610
singularities 78−8291
singularities and causality violation 80−31607
singularities and energy conditions 78−70032
singularities and invariants 80−31611
singularities in general relativity theory 79−35591
singularities in spatially homogeneous cosmologies 80−36747
singularities in stationary, cylindrically symmetric dust solutions 80−31613
singularities in the $\delta=3$ Tomimatsu-Sato space-time 80−86170
singularity avoidance and quantum conformal anomalies 77−67148
six dimensional space time formalism of electromagnetism, mag. monopole behaviour of electrically charged tachyons 78−54182
six-dimensional space-time 78−89394
six-dimensional space-time theory, experimental tests 79−58538
SO(1,3)-gauge theory of gravity 79−129
solution generating theorem, appl. to general relativity 78−21027
some thermodynamical remarks on the theory of gravitational field 78−81899
space like hypersurfaces of const. mean curvature 78−21025
space-like geodesics in fields of charged mass point and uncharged static cylinder 77−53805
space-times admitting a three-parameter isometry group with two-dimensional null orbits 79−85019
spacelike dust, 4-parameter Lie isometry groups 77−57246
spacelike motions admitted by the magnetofluid space-times 79−80481
spacially homothetic space-times, 3-surface intrinsic curvature 78−29018
spatially homogeneous anisotropically expanding universe, Heckmann-Schucking models 79−88768
spatially homogeneous universes 78−8318
spatially homothetic, intrinsic scalar curvature *(French)* 78−36893
special relativistic theory with locally anisotropic space-time 77−67279
special relativity, discrete space-time and fundamental length 80−27122
special relativity, group hypothesis, transformations with singularities 78−49655
special relativity test theory, dynamical aspects 80−17798
special-relativistic theory of locally anisotropic space-time 77−67278
spherical spacetime anisotropic fluid, compact star radiation 77−56821
spherical spacetimes for gravit. collapse to neutron stars and black holes, computer generation 80−46385
spherically symmetric, Einstein gravit. field eqns., static solns. and Birkhoff's theorem 79−71340
spherically symmetric metric, charged particle gravit. field 77−53806
spherically symmetric space-times with vanishing curvature scalar 80−68096
spin half field theory in Rindler space, Green's functions 78−12826
spinless EM charge, geom. theory 78−45533
spinning particles interacting with gravit. field 77−71261
spinor affine, general relativity reformed as gauge theory 77−22470
spinor electrodynamics in Riemann-Cartan space, dynamical theory of axial vector torsion propag. in vac. 78−73889
spinor field geometrodynamical superspace, quasi-catastrophe theory 78−41137
spinor field theory, generalized spin structures on 4-D space-times 80−62564
spinor fields in four dimensional space-time 79−6271
spinor gauge field in spinor space-time formalism 78−41401
spinor geometry for Friedmann space, space-time quantisation *(Russian)* 77−33909
spinor structure of space-time 80−52081
spinor theories in curved space-time, nonlinear invariances 79−54029
spinorial structs., and EM hyperheavens 77−74283
spinorial structure of hyperheavens, Einstein's vacuum eqns. fracture 77−22454
spinors, geometrical interpretation 80−46880
spinors, visual geometry and algebraic props. 80−31625
spontaneous compactification of arbitrary space-time dimens., SO(N) gauge group 77−22458
static axially symmetric electrovac universes, Einstein-Maxwell field eqns. exact solns. 79−85034
static general relativistic stellar models, props. 80−86165
static space-times, finite temp. and boundary effects 78−54526
static space-times with horizons, alternative vacuum states 77−57243
static spherically symmetric stellar models, admissible coord. system 78−28665
static Universe model with two centres, red shift explanation 78−57706
static Weyl solutions, for Brans-Dicke Maxwell fields 79−85033
stationary charged C-metric 80−17849
stationary Einstein-Maxwell space-times, conserved quantities determ. 78−49737

space-time configurations continued
Stokes' theorem in non-orientable manifolds, relation between charge and topology anal. 77−45776
stress tensor vacuum expectation value, renormalisation, curved spacetime, covariant geodesic point separation 78−54246
string moving in uniform static external field, 2-D space-time surface 80−57087
strings in the embedding space 78−89654
SU(2) dual charges, 4-D space of constant curvature *(Chinese)* 80−68392
SU(2) gauge fields in Minkowski space-time reparametrisation invariant formulation 78−70257
sublcass of vac. metrics admitting Killing motion 78−36911
subluminal and superluminal transformations in six dimens. special relativity 78−41154
super Riemannian space quantisation, perturbation theory rule derivation 78−77790
super Riemannian space-time, differential forms 77−82441
superconformal invariant two- and three-point functions, and invariant equations in 2-D space-time *(Bulgarian)* 80−47206
supergravity, Bianchi identities and supercovariant derivative 80−17852
supergravity, extended, with gauge internal symmetry in de Sitter space 77−79021
supergravity, superspace-time local symmetry, Ferru torsion preservation, renormalisability 79−12689
supergravity theories, background metric, conformal anomalies calc. 78−70043
superluminal and subluminal causal transformations through transformations of metrics 78−28943
superluminal phenomena and frames in special and general relativity 78−36825
superspace Bianchi identities and 6-dimens. spacetime 79−67204
supersymmetry formulation on space-time lattice 77−82689
supertwistors and conformal supersymm. 78−29015
surface deformations, their square root and the signature of spacetime 80−8874
symplectic struct. on Einstein metrics, general relativity, canonical formalism 77−9922
synchronization in special relativity and related theories 79−71243
syntopic spacetime meas., time dilatation and Lorentz contraction meas. 78−73896
systems with curved phase space, quantisation and global props. 79−74
systems with Killing's property *(French)* 80−31601
T-spheres with homogeneous mag. and elec. fields *(Russian)* 77−60993
tachyon magnetic monopoles, existence in 6 dimens. space, superluminal transforms. in Dirac theory 78−54183
tachyonic matter and curved space times, book contrib. 79−44822
tachyons, complex physical quantities and space-like states, book contrib. 79−44723
tachyons, Lorentz group and relativistic semigroup *(Russian)* 77−82386
tachyons, quaternionic formulation superluminal transformation, in complex space-time 79−53973
Taub's metric non-empty space-times *(French)* 78−45527
Taub-Nut spacetime, thermal particle prod. spectra 77−13382
teaching demonstration of curved space 77−57130
telescopic principles in the theory of gravitation *(German)* 79−40416
tensor fields invariant under subgroups of the conformal group of space-time 79−2603
tensors, metric and Ricci, for D-type spacetime class 78−36903
test particle mass in gravitational field, rel. to Mach's principle 79−12670
test particles, with internal struct., conservation laws 77−67338
tetrad formalism of empty static space-times 79−30328
thermodynamics in multiply connected spaces 80−4606
Thirring model of massless scalar field, conformal transformations 80−52428
time's arrow and the structure of spacetime 79−97173
time asymmetries and classical and quantum physics 80−22216
time quantisation, discrete space-time model 78−20999
time varying inhomogeneous media, space-time considerations for Doppler effects 78−20965
Tomimatsu Sata space-times, Einstein eqns. soln., effective pot. for equatorial motion 78−32621
Tomimatsu-Sato $\delta=3$ metric, Weyl conform tensor, invariants 80−68087
Tomimatsu-Sato soln., symmetry axis extension 77−72
topological spaces for formalising representation of discrete space time 80−98837
topology of space-time determ. from class of continuous timelike curves 77−71250
torsion enables metric to allow gravit. field 78−73902
torsion singularities, Bianchi-V cosmology with Proca field 77−67149
torsions in Riemann Cartan space times, U_4 reinterpretation, gravit. radiation solns. 78−45537
torsions in Riemann Cartan space-times, physical props., torsion classification scheme 78−45538
torsions in Riemann-Cartan spacetime, U_4 reinterpretation of null EM Einstein eqns. solns. 78−41212
total mass positivity of a general spacetime 80−12965
trace anomalies in a two-dimensional de Sitter metric and black-body radiation 78−65841
trace anomaly for neutrinos in Ricci-flat space-time of six dimens. 78−57847
transformations, superluminal and subluminal 77−74224
transformations leaving Einstein eqns. invariant *(French)* 78−62123
translations as gauge transformations using fibre bundles formalism 78−12808
trichromatic theory and time vector in relativity theory *(French)* 78−57006
trouser type universe metric 77−45623
twisted quantum fields in a curved space-time 78−73913
twisted scalar and spinor strings in Minkowski spacetime 80−57480
twisted scalar field, vacuum solns. 78−93804
twistor space, Kahler struct. in asymptotically flat space-time with gravit. radiation 77−26218
twistor surfaces and right-flat spaces 79−49119
twistor theory and particles, book 79−97485
twistor theory of space-time 80−17843
twistors and SU(2,2) induced representations 78−8229
unified field theory, five-dimensional theory of interacting scalar, electromagnetic, and gravitational fields 80−105833
unified field theory, nonsymmetric, metric hypothesis, spinor analysis 80−68404
unified gauge theory of gravitational and strong interactions 80−95016
uniform electrovacuum space time, observer dependent effects, Bertotti-Robinson line element 79−122
universe early metric, effect of primordial short-wave turbulence and quantum turbulence near singularity 78−77629
vacuum definition in curved space-time 80−73613
vacuum Einstein spaces with axial symm. *(Russian)* 77−5714
vacuum space-times, principal null directions without spinors 77−70
vacuum spacetimes, stationary and axially symmetric, homogeneous Hilbert problem, Kinnersley-Chitre transformations 80−68349
vacuum structure for a quantum field theory in curved space-time 79−21638
vacuum superfluidity near anisotropic singularity, phase transitions *(Russian)* 80−94905
vacuum tunnelling of gauge theory in Minkowski space 78−41425
Vaidya's metric, complexification, radiative and nonradiative, parts of energy-momentum tensor 80−68093
van Est theorem for groups of diffeomorphisms 78−93811
van Stockum metric, axially symmetric gravitational fields of bounded sources 79−21597
vector field with zero covariant deriv., general metric 80−68092
velocity matrix in six-dimensional space-time 80−86171
velocity of light Markov process, Klein-Gordan quantum statistic, quantum mechanics 80−98808
viscous fluid cosmological model in general relativity 78−61944
wave equation in curved space-time, compact and noncompact sources 80−73571
Weinberg-type fields in curved spacetime, stress tensor conformal anomaly 79−25960
Weyl and Papapetrou axisymmetric space-time as geodesics of hyperbolic complex plane 79−49126
Weyl-type vacuum space-time, new solns. of Einstein eqns. 77−22459
Wheeler's superspace, correspondence eqns., variational principles 78−24696
whimper singularities, Newman-Penrose formalism 78−41205
whimper space-time solns. to Einstein eqn. 80−31614
white holes spectral features in Nordstrom and Kerr-Newman metrics 77−29967
Whiteheadian approach to quantum theory and the generalized Bell's theorem 79−30276
world time, reference systems, invariant content *(Russian)* 78−45530
Yang's gravit. field eqns., reduced spinor formalism *(Chinese)* 78−119
Yang-Mills fields, finite, Feynman diagram theory, analogy with space-time approach 80−52400
Yang-Mills instantons, space-time topology 78−8522
Yang-Mills theory, broken symmetry soln., Higgs fields and Einstein gravity action 80−101746
York data, specification of asymptotically flat space-time 79−97264
zero mass surfaces, rel. to cosmological singularities 79−25772
zero-mass limit of point-mass space-times 80−82691
ν emission in gravitational collapse, Liouville line element 78−57437

space vehicle power plants
air-scooping nuclear-electric propulsion for advanced orbital transportation missions 78−45188
bearing and power transfer assembly development status 79−96462
Brayton isotope power system, dynamic power convertor 79−48167
dynamic isotope power system, PuO_2 fuelled, organic Rankine cycle turbine power system for space appls. 80−18692
electrochemical advanced energy sources, 1979 state of art and development trends 79−100506
energy conversion, Conf., San Diego, CA, USA (Aug 1978) 79−48038
European solar array technology status and potential 79−96463
European Space Agency lightweight hybrid solar array design and status 79−96475
European Space Agency sponsored solar arrays, predicted and achieved performances 79−96478
fast spectrum reactor space power system with thermoelec. conversion, baseline design 80−37441
fuel cell appls. in space power systems 80−30465
geosynchronous satellite plane-mirror solar concentrators 79−96474
ground-to-satellite power transfer by laser beam 79−62724
heat-pipe nuclear power plants for reliable space power 80−18377
hybrid thermionic converter for 10 GW space power plant 79−92086
integral glass covering of spacecraft solar cells by electrostatic bonding 80−93676
Intelsat V, solar array design and development 79−48135
INTELSAT V solar array design and test results 79−96471
isotope-powered satellite design for Shuttle launches 78−61709
large deployable solar array development for communications spacecraft 79 - 96469
large flexible solar array design analysis and verification 79−96459
lightweight solar array flexible substrates with anticharging layers 79−96456
magnetospheric plasma motion to elec. power conversion, concept 77−64605
migmacell advanced fuel fusion appl. to manned space propulsion 77−87236
NASA space power technology program 79−96883
NASA space power technology program 80−30494
Nimbus-Landsat spacecraft power subsystems, flight performance 80−30459
nuclear dynamic power systems, thermally-integrated spacecraft design 79−48166
nuclear elec. propulsion vehicle, planetary exploration appl. 77−87235
nuclear electric spacecraft propulsion, fast spectrum reactor core design 80−37440
nuclear integrated multimission spacecraft, definition and evaluation 80−18715
nuclear pulse propulsion, historical review of advanced consent 80−36475
nuclear reactor plant elements for space electric power systems 80−32339
nuclear space power, missions and planning, elect. and propulsion power requirements 80−30428
orbital power systems, waste heat rejection development requirements for thermal control 80−30416
Orbital Test Satellite solar array design and testing 79−96470

space vehicle power plants continued
photovoltaic generators, symposium, Noordwijk (1978) 79−96449
photovoltaic solar arrays, appl. of thin film Kapton mirror concentrators 80−30501
photovoltaic space power systems, 25 kW power module evolution 80−30495
power system perform. anal. using computer modelling for geosynchronous spacecraft 80−30497
radioisotope power system, using Rankine conversion cycle, emergency cooling by multifoil insulation melting 79−48168
radioisotope thermoelec. generators, design optimisation for Solar-Polar Mission 80−40880
radioisotope thermoelectric generator, heat pipes design and testing, Cu/H_2O, axially-grooved 79−48144
radioisotope thermoelectric generator, selenide technology evaluation at JPL, for Galileo (NASA) spaceflight mission 79−48147
radioisotope thermoelectric generator 78−85824
radioisotope thermoelectric generator cooling in the Schuttle bay 80−40881
radioisotope thermoelectric generators, power degradation predictions using DEGRA code 80−40879
radioisotope thermoelectric generators, SNAP 19 performance update for Pioneer and Viking missions 80−40883
radioisotopic generator, selenide, for Galileo mission 79−52951
radiosotope thermoelectric generator cooling, in Shuttle 79−48142
reactor hybrid-organic Rankine cycle power system 78−8993
rigid foldout solar array development for geostationary satellites 79−96468
satellite appl., telecommunication, rigid, fold-out array prototype development 79−48137
satellite solar cell calibration using high-altitude balloon *(Japanese)* 78−61700
satellite solar cell panel monitoring by ground station telemetry 79−62003
satellite solar cell power plant, operating experience 80−94055
satellites photovoltaic generators, low-orbit, D2B and Signe 3, performances comparison 80−3524
Shuttle Orbiter, solar cell array power extension package 80−30496
solar array, double roll-out, for space telescope 79−52939
solar array design, for Tracking and Data Relay Satellite System 79−48136
solar array for Halley's comet rendezvous mission, ultralow-mass designs 79−53702
solar array shunt regulator hot spot problem and countermeasures 79−96460
solar arrays, in-orbit performance, review 80−94054
solar arrays appl., hybrid, medium power (2.1 and 3.7 kW) 79−48138
solar battery panel mounting, optimal ang. determ. 79−39291
solar battery power increase using solar radiation reflected from Earth 77−33318
solar cell array, ultra lightweight panel, development and testing 79−52940
solar cells, space qualified multiple antireflective cells 80−94056
solar cells and arrays appl., wraparound contact 79−48132
solar cells appl., coverglass development 79−48133
solar cells radiation damage obs., GaAs and Si, on NTS-2 satellite 79−48134
solar concentrator designs for photovoltaic arrays 80−94057
solar electric propulsion, 25 kW solar array development testing 80−30500
solar energy power generators with advanced thermionic converters for space craft applications 80−61389
solar energy thermionic electricity generating plants 77−78603
solar observatory, orbiting (OSO-8), solar panel design and in-orbit performance 79−48652
solar power satellite, Europe base-load electricity supply appl. 79−39288
solar thermoelectric generators, near-Sun missions appl. 79−48143
space craft thermionic reactors, reflector drum control mechanism, fuel and moderator 79−17988
space shuttle-tethered balloon subsatellite, current collection by long wire 77−25859
space shuttle-tethered balloon subsatellite for ionospheric plasma studies and power generation 77−25912
spacecraft, power system perform. anal. using computer modelling 80−30497
Spacelab and space platform solar array programmes 79−96884
Stirling isotope power system for space appls., development and test results 80−18693
Suttle pallet satellite power module for Spacelab power augmentation 79−96882
thermionic convertor array, efficiency optimisation using heat transfer computer modelling 80−40886
thermionic generators for solar energy conversion 80−35714
thermionic reactor, ^{233}U fuel and Be moderator, neutron physics analysis 77−50281
thermionic reactors with const. emitter heating, reflector drums as control mechanism 80−42784
thermionic spacecraft reactors with ^{233}U as fuel, reflector drums as control mechanism 80−47686
thermoelectric generators, Voyager and LES 8/9 flight performance 80−40882
thermoelectric power generation, 1978 state of art and development trends 79−43780
Ultra Lightweight Panel solar array development and testing 79−96473
Ag-H_2 energy storage system, long-life, light-weight 79−48108
GaAlAs solar cells, appl. for navigational satellite power systems 80−35694
Ni-Cd, sealed aerospace cells, H_2 recombination during over discharge 80−30461
Ni-Cd batteries development, lightweight, long-life 79−48106
Ni-Cd battery reconditioning and long term performance, in geosynchronous orbit spacecraft 79−52929
Ni-Cd battery system design for tracking and data relay satellite system 80−30460
Ni-H_2 50 Ahr battery for low earth orbit satellite appls. 80−30463
Ni-H_2 battery appl., to Navigation Technology Satellite-2, first-year operating experiences 79−48107
Ni-H_2 battery for satellite energy storage 80−81430
Ni-H_2 secondary cells, characterisation and simulated low earth orbit cycling 80−30462
Si solar cells, low mass space blanket using 50 μm cells 80−30498
Si solar cells, technology development of 50μm cells 80−30499
U plasmas, fissioning, for space vehicle power, propulsion, terrestrial appls. 77−3145

space vehicles
see also artificial satellites; rockets; space vehicle power plants
1946 to 1978 review, satellites and space probes 79−80195
1975 launchings *(French)* 77−29624
acoustic excitation, analysed by Statistical Energy Method 77−58502
active and planned spacecraft and expts., 1977 to 1978, report 79−5726
aerobraking for planetary orbit missions 80−109338
aeromanoeuvering orbit transfer vehicles, for space transport system 78−4060
Apollo 16, magnetometer meas. rel. to elec. cond. anomaly beneath Mare Serenitatis 80−56730
Apollo landers, magnetometers data errors and lunar induction studies 79−96932
Apollo Soyuz mission report, book 77−82106
Apollo-Soyuz Test Project, phase-coherent dual-freq. radio link for Doppler tracking 77−60576
astronautical congress, Anaheim, Calif., USA (Oct. 1976) 78−4054
astrophysical obs. by space vehicles (1966-76) *(Japanese)* 78−24417
Atmospheric Cloud Physics Laboratory on Shuttle/Spacelab, droplets optical motion control appl. 80−12634
attitude control and navigation systems, instruments reliability enhancement 77−29623
attitude determination, real time, star pattern recongition using CCD star sensors 78−96380
autonomous space rendezvous and docking with 10.6 μm ladar 78−57428
ball bearing surface CVD coating expts. 79−83366
ballistic axisymmetric vehicle, spin during atmospheric entry 77−64591
ballistic descent, stabilisation transient processes 77−53395
base flow at supersonic vel., rockets and re-entry vehicles appl. 78−67243
bidirectional reflectance and transmission for optical diffusers use in space projects 78−36438
body shape for minimal radiative heat inflow, spacecraft atmospheric entry *(Russian)* 78−77457
British space prospects 79−84644
charge neutralisation, electron emitter neutralisation *(Japanese)* 80−94673
charging in ionosphere due to positive ion emission 79−84633
charging problems in plasma, PICPAB ion source on Spacelab 80−85840
in close near-circular orbits, optimal multimomentum transfers 77−41290
conductor-like behaviour of photoemitting dielectric surface 79−101046
coupled motion of rigid bodies about their center of mass 79−40065
cruise engines optimal thrust in interorbit flights, analytical determ. 78−4069
cryogenic systems for spacecraft 80−86319
debris and jettisoned boosters as UFO phenomena 77−64607
Deep Space Net, appl. of spacecraft tracking technology to experimental gravitation 80−8895
descent into atmosphere, eqns. of motion, analytical soln. 79−84628
detumbling, using movable telescoping appendages 77−54868
dielectric materials, charging and discharging 80−71315
dielectric materials, surface discharge arc propag. and damage 80−71314
differential charging and sheath asymmetry of nonconducting spacecraft due to plasma flows 79−12378
dipole antenna entering planetary atmosphere, plasma wake cylindrically stratified model 79−48647
disordered rotation damping by elastically suspended ballast *(Russian)* 77−45287
Doppler tracking of spacecraft, gravit. radiation detect. possibility 79−30345
dual spinning spacecraft, extension of dual magnetometer method 78−77459
Dyson spheres, mass and energy requirements rel. to IR emission 78−69710
Earth resources rocket, enriched air propulsion system 77−2259
Earth-Mars min. time orbit transfer, conjugate gradient method 77−87244
Earth-Mars-Venus orbital transfer minimal flight time calc. 78−4090
electric charge build up in sunlight, model of photosheath 80−90316
electronic components, space radiation environment effects, laboratory simulation 80−94689
entry into Jupiter atmosphere, modelling by H_2-He mixture 78−71413
entry probes objectives, atmospheric composition and structure obs. 77−49267
European Space Agency spacecraft, Ariane and Spacelab 79−88565
European Spacelab, remote sensing appls. for 1980s 78−69494
fibre reinforced polymer matrix composites, space environmental effects 80−71721
final descent vel. control in Mars atmosphere, autonomous navigation algorithm 77−29620
fission-engined series-staged, numerical results 77−2321
fission-engined series-staged, overall payload-optimal control 77−2320
flexible spacecraft, eigenvalues and eigenvectors for hybrid coordinate eqns. of motion 79−75085
flight trajectories to Jupiter using Mars gravit. field 79−62712
flight trajectory between satellite orbits of Earth and Moon, variational problem 80−72754
four-impulse planetary landing and return under time constraints 79−62711
future space travel and astronauts, technical problems *(Italian)* 79−80244
Halley probe, cometary micrometeoroid hazard workshop proceedings (Noordwijk, Netherlands, 18.10 April 1979) 80−36782
Halley-Venus mission, Planet-A project for mag. meas. in interplanetary space *(Japanese)* 80−94672
heat shield ablation, effect on blunt body heat transfer near stagnation point 78−94736
HELIOS 1 and 2 and STIP Intervals I and II participation 78−49295
Helios 1 and 2 mission, general aspects 78−20615
Helios 1 primary mission, interplanetary mag. field large-scale struct. between 1 and 0.3 AU 79−29962
HELIOS spacecraft, problems for Sun flyby mission 77−70969

space vehicles continued
Helios zodiacal light expt., data processing and evaluation 79−80235
HELIOS-1, HELIOS-2, onboard shock identification computer 79−92679
Helois 1 primary mission, mag. fields and flows between 1 and 0.3 AU 79−29963
Hermes, flight results on structural dynamics 80−12639
hypersonic re-entry vehicle heat transfer meas. in separated laminar base flow 78−61708
infinite vertical limiting surface with suction, Stokes free convection effects, spacecraft reentry appl. 80−19364
International Comet Mission, proposed fast flyby of P/Halley P/Tempel 2 rendezvous 80−82166
International Solar Polar Mission 80−109335
International Space Hall of Fame Dedication Conference, Alamogordo, New Mexico (Oct. 1976) 77−56814
International Ultraviolet Explorer (IUE), spacecraft and instrumentation 78−96382
interplanetary electron shield anal. 77−78604
interplanetary trajectories, perturbed boundary-value problems, variational formulae 79−21161
interstellar appls. of electrostatic/EM ion collection techniques 77−70974
interstellar arks, cosmic-ray shielding 77−49264
interstellar flight, vehicle erosion by dust and particles 77−49266
interstellar flyby missions, relativistic effects 78−61729
interstellar probes, communications philosophy 79−21133
interstellar rocket, laser powered, mass ratio and instantaneous efficiency 79−21134
interstellar rocket relativistic navigation problem, three-dimensional eqn. of motion 79−21136
interstellar space travel 78−61699
interstellar travel, optimum transfer in uniform motion 78−20614
ion-propelled space tug optimisation 78−53798
ionosphere, space vehicle obs. (1966-76) *(Japanese)* 78−24402
ionospheric flight conditions simulation 79−16796
ISEE 3 gamma ray burst instrument, first results 80−98546
Jupiter atmosphere probe, ballistic and navigation aspects of spacecraft braking problem 80−61981
Jupiter entry probe, heat shield, C vaporisation into nonequilib. stagnation point boundary layer 79−1264
Jupiter fly-bys and orbiters, radiation effects on materials 79−92648
Jupiter orbiter, nuclear-electric propulsion, fast numerical analysis 78−45189
Jupiter orbiter motion and risk of collision with Galilean satellites 77−2322
Jupiter probe, mass and shape var. due to aerodynamic heating 79−84630
Jupiter Voyager electrostatic discharge protection 78−89042
laser-powered interstellar ramjet 77−70975
launch vehicle, guided, effect of misalignments on static aeroelastic characts. 79−14313
launching directions, influence on pencil of orbits 80−26723
location determ. on planetary surface from Sun's azimuth meas. 78−49287
long duration exposure facility, utilisation of vacuum developed in wake zone 78−36433
louvres in thermal radiating panel, temp. distrib. 80−10124
Luna 16-24, equipment and expt. procedures for radar obs. of Moon 80−77302
Luna 18, automatic lunar station, radar expts. 77−53438
Luna 24, Mare Crisium core sample return and analysis 77−29673
Luna 24 and Mare Crisium, conference, Houston, Texas (1977, December 1 to 3) 80−17710
Luna-22 for lunar bistatic radar surveillance with FM signal 79−5758
Luna-24 site, Fahrenheit crater ejecta emplacement 80−8564
lunar mass-catcher for large-scale material transport 79−16844
lunar polar orbiter, NASA 1980 global survey study 78−4064
Lunokhod 2, magnetometer meas. rel. to elec. cond. anomaly beneath Mare Serenitatis 80−56730
magnetic damping of rotation, shielding effects 78−69646
magnetic field effects, exponential damping 78−69645
magnetoaeroelastic stability of thin panels, space vehicle re-entry *(French)* 77−65702
manned interstellar flight and colonisation of other systems 77−71017
Mariner 10, UV spectrometer airglow expt. 77−64611
Mariner 10 expedition to Venus and Mercury *(Norwegian)* 78−49291
Mariner 10 radio occultation by Venus, atmospheric profile statistical and computational uncertainties 79−96938
Mariner 10 UV spectrometer, Mercury occultation expt. 77−67023
Mariner 2, data anal. rel. to solar wind protons cooling 78−40789
Mariner Jupiter/Saturn 1977 mission 77−73932
Mariner-5, Venus microrelief irregularites mean height, determination from radio transillumination data 80−72807
Mariner-Jupiter-Saturn low energy charged particle expt. 77−70971
Mars 4-7 meas. of interplanetary integrated electron content 77−53383
Mars 4-7 space probes, meas. with H absorption-cell spectrophotometer for Lyman α radiation 78−28519
Mars 6 descent vehicle, communication loss on entry into Martian atm. 77−64597
Mars 6 descent vehicle radio signal parameters meas. by retranslation method 77−67020
Mars descent spacecraft, ballistics 77−33319
Mars descent trajectories using parachute-rocket system for soft landing 78−69640
Mars descent vehicle, aerodynamic braking arc control algorithm 79−84629
Mars entry probe, communication black-out due to shock induced plasma flow 77−5413
Mars entry vehicle, lifting spacecraft control and ballistics 78−16264
Mars lander, effectiveness of min. final vel. criterion in spacecraft descent trajectories synthesis 77−64590
Mars lander sterilisation and biological expt. containment 77−17327
Mars orbit emplacement using atmospheric braking, control algorithm 78−69639
Mars probe, optimal atmospheric entry trajectories with two-dimensional control 77−91400
Mars rover laser rangefinder accuracy estimate 78−24437
Mars Viking surface sampler subsystem, acquisition assembly 79−12380
Mars-7 and Prognoz-3, correl. of solar cosmic rays propag. characts. 77−82089

space vehicles continued
materials failure, metallurgical exam. 80−71868
materials in space environment, conf., Noordwijk, Netherlands (Oct. 1979) 80−67933
Mercury orbiter missions, new concepts 79−80197
metal and metal oxide thermal control materials low-energy proton effects 80−70288
metallic tethers in ionospheric plasma, electrodynamics 78−69652
meteoroid impacts effect on attitude motion, analytical model 78−73608
meteoroid shield, destructive effect and meteoroid vel. 78−53788
mission analysis mathematical background, orbit selection and mission constraints 78−40790
motion determ., guaranteed accuracy characts. 79−2467
motion in gravitational and mag. dipole fields *(Russian)* 80−36487
motion in vicinity of collinear libration point, semianalytical method 78−4066
motion in vicinity of collinear libration point, statistical estimates in control problem 78−4067
multi-mission spacecraft, modular satellite 77−73931
multiple-launch space research program, choice of vehicles 80−8512
NASA-ESA mission for Periodic Comets Halley and Tempel 2 rendezvous 80−82168
navigation, celestial reference coord. system 78−49346
navigation, planetary mission, Givens transformation techniques for Kalman filtering 78−4473
navigation to Venus, distance determ. from radar obs. 80−109386
non-gravitational foci and apexes, of paths with common launching point and common apsidal distances 79−16804
nonstationary spacecraft, coordinate-parametric control via multidimensional asymptotically stable adaptive systems 80−101522
nosetip ablation holography in 10 MW plasma arc facility 78−20621
nosetip recession meas. using implanted radioactive sources, error analysis 78−16272
nuclear elec. propulsion vehicle, power system design, planetary exploration appl. 77−87235
O'Neill space colonies, prospects for realisation 77−87230
oblate planet orbiter, optimal low-thrust takeoff from orbit 77−60580
occultations by turbulent planetary atmospheres, effects of inhomogeneous background on radiation propag. 78−69679
optical materials and components, space charged particle environment effect 80−69472
optimal accel. with electroreactive engine with bound on thrust vector 77−53393
optimal attitude control of descent to surface of atmosphere-less planet 78−16265
optimisation of geometrically imperfect stiffened cylindrical shells under axial compression 79−3916
optimum body conformation for radiative heating along a prescribed trajectory 79−80189
optimum low-thrust multiple rendezvous between inclined orbits 78−4086
optimum vehicle family selection for space study programs 79−8790
orbit determination optimization with incomplete inform. on error covariance matrix and expectation 79−8808
orbital transfer, optimal, low-thrust, limited power, elliptical orbits 78−4087
orbital transfer using two fixed-magnitude impulses 78−81518
orbits near Jupiter and Saturn, post-Newtonian effects 79−101054
orientation control of rotating spacecraft by solar radiation pressure 77−53397
particle emission from charged sphere into mag. field, theory 80−69304
payload optimisation using parametric modelling 77−5410
perturbed motion about centre of mass, element formulation 78−41150
Pioneer 10 and 11, Jupiter cloud configurations obs. interpretation in time-depend. framework 80−26787
Pioneer 10 and 11, radio signals spectral broadening by ionospheres of Jupiter and Saturn 80−109391
Pioneer 10 and 11 obs. of solar wind streams and shocks 78−49283
Pioneer 10 and 11 photographs and Earth-based obs. of Jupiter 77−67064
Pioneer 11, experimental confirmation of Sun's magnetic field structure 77−82162
Pioneer 11, meteoroid detector particle flux at Saturn 80−82291
Pioneer 11 at Saturn, trajectory var., carrier freq. Doppler shift, Saturn mass determ. 80−82294
Pioneer 11 investig. of Saturn 80−46476
Pioneer 11 post-Jupiter trajectory midcourse manoeuvre sequence for Saturn targeting options 78−7857
Pioneer Jupiter missions, solar wind plasma analyser 77−67024
Pioneer Venus, cloud particles size distrib. meas. 79−48717
Pioneer Venus, expts. descriptions 77−73928
Pioneer Venus, initial results 79−48699
Pioneer Venus, large probe IR radiometer expt. results 79−48719
Pioneer Venus, nephelometer expt. preliminary results 79−48716
Pioneer Venus, Orbiter and Multiprobe missions 79−75076
Pioneer Venus, preliminary results on Venus lower atmosphere comp. 79−48720
Pioneer Venus, radio interferometric obs. for wind vels. vector determ. 79−48722
Pioneer Venus, Solar Flux Radiometer 80−82198
Pioneer Venus, study of Cytherean ionosphere and solar wind interaction 77−73995
Pioneer Venus, study of dynamics, winds, circulation and turbulence in Cytherean atmosphere 77−78706
Pioneer Venus, Unified Abstract Data Library and Quick Look Data Delivery System 80−67494
Pioneer Venus 1978, prospects 78−36436
Pioneer Venus a first report 79−84701
Pioneer Venus Bus and Orbiter, Bennett ion mass spectrometers 80−67499
Pioneer Venus Bus neutral gas mass spectrometer 80−67513
Pioneer Venus Differential Long Baseline Interferometry expt. 80−67578
Pioneer Venus entry probes, atmosphere structure instruments 80−67562
Pioneer Venus entry probes, results on Venus atmosphere struct. up to 110 km 79−48715
Pioneer Venus large probe neutral mass spectrometer for measurement of composition and abundance of atmospheric gases 79−88563
Pioneer Venus mission to study planetary atmosphere 79−44331
Pioneer Venus Multiprobe entry phase, telemetry recovery 80−67493
Pioneer Venus multiprobe mission, solar flux radiometer expts. preliminary results 79−48718

space vehicles continued
Pioneer Venus Multiprobe mission 79−84632
Pioneer Venus occultation experiment, radio science data generation 80−67492
Pioneer Venus orbiter, cloud photopolarimeter investigation 79−48713
Pioneer Venus Orbiter, electron temp. probe 80−67500
Pioneer Venus orbiter, IR radiometer 80−36469
Pioneer Venus Orbiter, magnetometer expt. system 77−87229
Pioneer Venus orbiter, magnetometer obs. of Venus bow shock 80−36535
Pioneer Venus Orbiter, neutral gas mass spectrometer expt. 80−67502
Pioneer Venus Orbiter, planar retarding potential analyser plasma expt. 80−67501
Pioneer Venus Orbiter, plasma analyser expt. 80−67498
Pioneer Venus Orbiter, plasma wave investigation 80−67497
Pioneer Venus Orbiter, radar mapper design and operation 80−67495
Pioneer Venus Orbiter, study of Cytherean surface and interior 77−73996
Pioneer Venus orbiter, Venus middle atmosphere IR remote sounding 79−48712
Pioneer Venus orbiter, Venus radar mapping 79−48723
Pioneer Venus orbiter, Venus UV spectroscopy initial results 79−48711
Pioneer Venus Orbiter fluxgate magnetometer design and operation 80−67496
Pioneer Venus Orbiter Gamma Burst Detector 80−67505
Pioneer Venus Orbiter radiometer (VORTEX) 80−67504
Pioneer Venus Orbiter UV spectrometer, design and operation 80−67503
Pioneer Venus program, 1978 mission 77−73926
Pioneer Venus program, spacecraft, objectives and payloads 77−73927
Pioneer Venus Programme stable quartz oscillator 77−41288
Pioneer Venus results, surface and atmosphere 80−17523
Pioneer Venus small probes net flux radiometer experiment 80−67512
Pioneer Venus Sounder and small probes nephelometer instrument 80−67511
Pioneer Venus Sounder Probe gas chromatograph 80−67507
Pioneer Venus Sounder Probe IR radiometer 80−67509
Pioneer Venus Sounder Probe neutral gas mass spectrometer 80−67506
Pioneer Venus Sounder Probe Particle Size Spectrometer 80−67510
Pioneer Venus Sounder Probe Solar Flux Radiometer 80−67508
Pioneer Venus spacecraft, design and operation 80−67491
Pioneer Venus spacecraft programme 78−61707
Pioneer Venus study of thermal balance of Cytherean atmosphere 77−73994
Pioneer-Venus large probe infrared radiometer optical system 78−81543
Pioneer-Venus Orbiter Mission, retarding potential analyzer 79−58251
Pioneers 10 and 11, tracking data rel. to gravity field of Jupiter and satellites 77−37554
planetary atmosphere entry, transport props. of monatomic C rel. to heat shield ablation 78−87424
planetary atmosphere probes, flight characts., scale model expts. 78−7854
planetary exploration 79−62710
planetary lander, biological and soil chemical testing system 77−45284
planetary probe entering Jupiter atmosphere, subliming boundary layer flow, simulation 78−65545
planetary probe heat shield ablation, C excited electronic states contrib. to transport props. 80−23326
planetary probes, possibility of satellite aided capture by planets 79−75087
planetary spacecraft, Jovian environment simulation, materials hardening and mass shielding 80−36472
plasma rarefied flow around spacecraft, ion density computation accuracy 79−50849
polymer composite matrix materials, space radiation effects evaluation 80−70263
polymer materials, electron and proton irrad. effects 80−70262
position determination on planetary surface, optimal navigation meas. 77−29621
Project Daedalus: payload design for stellar flyby mission 78−81524
radiation exposure, charged particle flux-at-a-point in complex geometries, numerical method 77−26249
radiation protectio design considerations for man in geosynchronous orbits 78−28096
ram effect for conducting cylinder in drifting plasma 80−54029
re-entry, thermal stress analysis 77−35031
re-entry vehicle acoustic/vibration environment expt. 78−20620
re-entry vehicle flight tests, boundary layer acoustic meas. 78−16275
reentry, mass loss and shape change with radiative heating 80−31198
reentry vehicle, ablation embedding in inverse heat cond. problems, finite difference algorithm 78−94508
reentry vehicle, laminar compressible boundary layer flow in mag. field 79−14489
reentry vehicle aerodynamic heating problems with shape change, review 78−94735
reinforced organic composite, graphite, or C-C, ablation, mathematical modelling 79−41564
relative motion around orbiting station, guidance method 78−16263
relative motion computation using time transformations 77−22050
relative motion computation with increased precision 77−22048
rescue and safety considerations, conf., Lisbon, Portugal (Oct. 1975) 77−25913
robot probes for hostile planetary atmospheres and surfaces 78−4065
rocket attitude measurement using laser system 79−12763
rotating, eigenvalue problems solution, with real symmetric matrix of same dimension 80−12895
rotation control by mass ejection 77−41278
RPV, high-altitude, for environmental appls. 80−17470
Salyut, international spaceport, review 80−31196
Salyut 6, aspects of system and scientific investigations 79−29970
Salyut space stations, review 80−31195
Salyut-4, equipment for measuring X-ray emission from extraterrestrial sources 78−28521
Salyut-4, ITS-4 IR telescope-spectrometer 77−78635
Salyut-6 orbital station, cosmic radiation dose field meas. 80−89876
Salyut-6 spacelab, data acquisition and logging system incl. speech 80−61979
SEPAC (Space Experiments with Particle Accelerators), program for first Spacelab mission 79−48650
series-staged fission powered starship, direct propulsion 78−61706
shape factors in space thermodynamics, determ. using shape factormeter *(German)* 78−73610

space vehicles continued
shock absorption of docked spacecraft after coupling 77−33317
shuttle insulation coating, combined load testing at 1100°C 79−34261
Shuttle IR telescope facility 77−49297
shuttle operations, stratospheric aerosol modification and climate implications 80−98408
Shuttle Orbiter, skin electrical charging during electron gun operator 77−22042
Shuttle payload preparation at Kennedy Space Center 78−12073
Shuttle programme details *(Norwegian)* 78−49292
shuttle reentry trajectory optimisation method 77−67021
Shuttle/Spacelab, platform for cooled IR astronomical telescope 77−73921
Shuttle/Spacelab mission, instrumentation requirements and provisions 77−70972
Shuttle/Spacelab missions, low power CAMAC and NIM modular systems for spaceflight use 77−70973
Shuttle/Spacelab platform in near Earth ionospheric plasma, aerodynamics 80−8517
Skylab, anticipated motion for revisit mission, digital computer simulation 79−16794
Skylab, low energy cosmic rays meas. 80−56689
Skylab, spacecraft-produced neutron fluxes meas. 78−28486
Skylab 1, orbital elements, determ. of air density var. at 435 km altitude 79−5694
Skylab simulator visual displays and training for joint obs. programmes 77−60566
small geophysical vehicles, aspect sensor 77−45279
soft landing guidance algorithms based on terminal control principles 78−73602
solar electric propulsion stage applications 78−4059
Solar Maximum Mission GSTDN/TDRSS compatible RF system 78−45198
solar probes, out-of-ecliptic space research 77−87228
solar radiation pressure for maximization of orbital momentum and energy 80−12640
solar sail trajectories, long-term evaluation 79−48641
solar thermal aerostat research station (STARS) 80−17471
Soviet achievements survey *(German)* 77−41283
Soviet space astronomy developments 77−45289
Soyuz 22 and MKF-6 multispectral camera 78−40794
Soyuz programme, analysis of Soyuz 1-18 achievements 78−12071
Soyuz-Apollo launching, lower ionosphere disturbances obs. 78−45110
Space lab integrated UV and X-ray astronomical payload proposal *(Italian)* 77−82112
Space Shuttle, Am. Astronaut. Soc. 21st meeting (Denver, 26-28 Aug. 1976) 77−78614
Space Shuttle, astronomy and space science research tool 79−40057
Space Shuttle, contaminant environment effect on IR telescope 77−91398
Space Shuttle, design and missions 79−66904
Space Shuttle, design of Space Telescope as long-life free flyer 80−109364
Space Shuttle, development, reusable orbiter vehicle programme 79−84640
Space Shuttle, environmental effects during launch and reentry 78−85681
Space Shuttle, features, development 77−33320
Space Shuttle, first free flight test 78−7860
Space Shuttle, first tests *(Norwegian)* 77−70968
Space Shuttle, flight schedule and Spacelab 2 mission 78−85816
Space Shuttle, history, principle features and uses 78−36427
Space Shuttle, international cooperation *(Japanese)* 77−87238
Space Shuttle, Kennedy Space Center preparations for launch 78−85820
Space Shuttle, long duration exposure facility 78−36432
Space Shuttle, methods of improving vacuum for expts. 78−32825
Space Shuttle, operational features, review 78−36428
Space Shuttle, orbital environment 78−36430
space Shuttle, pre-debut review 77−56811
Space Shuttle, prediction of acoustic environment in payload bay 80−102919
Space Shuttle, progress report 80−12644
Space Shuttle, prospects for astronomers in space 77−56806
Space Shuttle, remote manipulator arm, dynamics of chain of flexible bodies 80−94953
Space Shuttle, remote sensing appls. for 1980s 78−69494
Space Shuttle, small planetary missions 80−109339
Space Shuttle, tethered satellite system 79−8794
Space Shuttle, use for science and engineering, Symposium, California (May 77) 78−36426
Space Shuttle, wake shield expt., true and net outgassing rates 79−48645
Space shuttle, X-ray astronomical instrums. and expts. 80−109363
Space Shuttle and deep space missions 80−109336
Space Shuttle and Spacelab, development and appls. 77−91406
Space Shuttle and Spacelab, expected mission results *(French)* 78−53784
Space Shuttle and Vandenberg Air Force base 77−64608
Space Shuttle capabilities STS utilization planning 79−58223
Space Shuttle carrying reusable satellites 80−61985
Space Shuttle components, missions, financial aspects *(French)* 78−93067
Space Shuttle external insulation, acoustic emission inspection 78−16276
Space Shuttle external tank for main propulsion system 77−73922
space shuttle features and instrumentation 78−61710
Space Shuttle first orbiter dedication 77−17326
Space Shuttle laser expts. for atmospheric meas. 78−53793
Space Shuttle lightning current distrib., circuit modelling and exptl. verification 78−49293
Space Shuttle Orbiter, flow angle and mass flow rate meas. in unknown flowfield 79−77306
Space Shuttle Orbiter, hypervelocity impact tests on RCC thermal protection material 79−16795
Space Shuttle orbiter, remote manipulator system 79−21150
Space Shuttle orbiting molecular beam laboratory 78−35242
Space Shuttle payload verification requirements 78−85812
Space Shuttle Program description and status 79−21130
Space Shuttle project, basic elements and space-oriented experimental programme 80−17465
space shuttle reentry, unsteady nonequilib. chemically reactive flow, parallel computation 78−47065

space vehicles continued
Space Shuttle reusable orbiter vehicle programme, project planning 79−84641
Space Shuttle technology, payloads and operations 80−101528
Space Shuttle tethered subsatellite, current collection by long wire 79−25438
Space Shuttle/Orbiter S-band communication development problems 78−45197
Space Shuttle/Spacelab, SEPAC for ionosphere and magnetosphere studies 77−73925
Space Shuttle/Spacelab utilisation, conference, Washington, DC, USA (8 to 10 March, 1978) 79−80203
Space Shuttles, Gamma Ray Observatory launch instrums. and operations 80−109365
space station motion, mechanical model, rotational stability *(Russian)* 79−35095
space stations for the international future, review 78−32322
Space Transportation System, integration with deep space mission 80−109337
space-shuttle thermal-protection coating, testing techniques at 870°C 78−35604
spacecraft, flexible, in gravitational field, stability 77−25906
spacecraft data processing and analysis 77−78650
spacecraft orbital plane, autonomous determ. via landmarks on central planet surface 77−64595
spacecraft spin system, convection heat transfer in rot. curved pipe 78−94737
spacecraft with solar sail, eqns. of motion from geocentric orbit 77−53394
spacecraft-artificial satellite closest approach times calc. 79−62713
Spacelab, alloy solidification expts. 78−88457
Spacelab, ASSESS II, simulated mission 78−85813
Spacelab, atmospheric physics, ESLAB Symposium (Frascati, Italy, 11-14 May 1976) 77−21775
Spacelab, biological and medical appls. 77−45281
Spacelab, biomedical expts. 77−16999
Spacelab, communications R and D project management 77−17321
Spacelab, contributions of Germany to payload 77−17323
Spacelab, crystal growth, preparatory experiments for first Spacelab flight 78−88414
Spacelab, crystal growth expts. 78−52647
Spacelab, data communications, systems, 79−84643
Spacelab, deep photographic sky survey 79−25474
Spacelab, development and integration of payloads 77−17322
Spacelab, ESA material science experiments 78−88618
Spacelab, Federal Government of Germany promotion 78−53790
Spacelab, general design and operation 78−12072
Spacelab, grille spectrometer for first payload *(French)* 79−80202
Spacelab, holographic interferometry feasibility study *(German)* 78−33711
Spacelab, integrated UV and X-ray astronomy facility 79−25475
Spacelab, material processing facilities and expts. 78−36431
Spacelab, material processing facilities and expts. 78−53789
Spacelab, materials processing 78−35295
Spacelab, materials research and processing programme, German Federal Republic 78−88620
Spacelab, metal adhesion expt. 78−88621
Spacelab, microwave remote sensing expt. operation 80−109332
Spacelab, past and future cryst. growth in space 78−80462
Spacelab, payload data path from user input (on-board) to user ouput (laboratory) 79−21137
Spacelab, proposed French metallurgy programme 78−57423
Spacelab, role in cometary obs. 77−33425
Spacelab, space applications missions 77−17324
Spacelab, technical description 77−17320
Spacelab, use of ion beams in near-surface anal. 78−35755
Spacelab and artificial satellites appls., conf., Rome, Italy (Mar. 1978) 78−96384
Spacelab and European expts. on Space Shuttle 79−44332
Spacelab and services to users 80−31194
Spacelab and Space Transportation System, management and programme 77−45280
Spacelab as orbiting atmospheric laboratory 77−21941
Spacelab crystal growth expts. 78−52648
Spacelab development in Europe, space transportation system Orbiter vehicle program appl. 79−84642
Spacelab development of operational Earth observation systems 77−22037
Spacelab development progress 78−81519
Spacelab Instrument Pointing Subsystem 79−25447
Spacelab launch conditions for absorption spectroscopy *(French)* 79−8791
Spacelab lidar for atmospheric topside sounding 77−21942
Spacelab metallurgical experiments, possible influence on current procedures 78−88619
Spacelab of European Space Agency 80−85837
Spacelab pallet, C fibre reinforced plastic appl. 78−45186
Spacelab pallet, meas. of mol. streaming fields 80−82173
Spacelab passive atmospheric sounders 77−82113
Spacelab pressurised model development for future space missions 80−90318
Spacelab project, ESRO/NASA cooperative programme 79−8792
Spacelab project, zero gravity physics review 77−29619
Spacelab simulation, OH submicron air-glow bands correl. studies 79−25381
spin-stabilised spacecraft, optimal aerodynamic attitude controlZ 80−77250
starship, single-stage constant-power, optimal exhaust vel. programming 78−20613
starship flight optimisation, time plus energy minimisation criterion 79−44330
starships, detectability 77−49265
station-keeping manoeuvre, operational requirements and geometry 78−45180
supersonic re-entry into atmosphere ablation reduction 79−32780
surface material performance modelling 78−4061
surface plasma sheath, space charge neutralisation 77−87240
surface transport vehicle, stability in weak gravity field 77−64594
system acceptance testing, evaluation 79−16797
telescope-observatory 2.4 m, instrumentation and appl. *(French)* 80−17493
space vehicles continued
terradynamic penetrators as planetary landers 77−78601
Texus 1 and 2 sounding rockets for Swedish materials science expt. 80−104362
thermal control coatings, electron and proton irrad. effects 80−70262
thermal control systems, spray evaporator for transport fluid cooling 80−29160
thermoregulative coatings, radiation effects on reflectivity *(Russian)* 78−76542
three-impulse min.-time orbital transfer generation, numerical method 78−73607
thrust limited relativistic, interstellar drag effects on minimum time trajectory 78−49286
thrust-aided sub-orbits 78−45181
trace contaminant concentration, toxokinetic/toxodynamic model 79−83952
trajectory measurement errors, motion parameters estimation 77−29633
trajectory measurement process optimisation, visibility limitations 77−29632
trajectory optimal correction, pulse count constraint, combinatorial method 77−64598
trajectory optimisation using closed soln. of constant thrust-accel. motion 77−25926
trajectory prediction errors for geocentric motion of apparatus with solar sail *(Russian)* 79−88576
transfer flights between orbits, energy-weight effectiveness 79−2466
transpiration-cooled system, thermal response in radiative and convective environment 78−32323
unmanned (or manned) vehicles, automatic rendezvous with space station 80−77249
unnamed space probes, recent achievements, financial restrictions and their effect on future programmes 80−72743
unpowered spaceprobe ejected from circularly orbiting space station, trajectories calc. 80−36484
USA planetary exploration programme 77−33324
USA space science missions and satellites 77−29630
UV astrophysical studies from space vehicles 79−25519
Venera, surface bistatic radar survey 77−87304
Venera 10, Venus rock density meas. method and results 78−28564
Venera 11 and 12 first results *(Russian)* 79−35165
Venera 9 and 10, aerodynamics and dynamics during motion in Venus atmosphere 77−91399
Venera 9 and 10, descent vehicles and atmospheric parameters meas. 77−78597
Venera 9 and 10, flight control 77−78598
Venera 9 and 10, ion-flux charact. meas. in solar wind/Venus interaction region 78−4051
Venera 9 and 10, meas. of interplanetary background due to low-energy particles 78−4049
Venera 9 and 10, plasma meas. using wide-angle instruments, preliminary results 77−91396
Venera 9 and 10, preliminary results 77−78596
Venera 9 and 10, results of two-freq. radioscopy of Venus daytime ionosphere 78−4129
Venera 9 and 10, results of two-freq. radioscopy of Venus nighttime ionosphere 77−91454
Venera 9 and 10, TV surface expts. on Venus 77−78599
Venera 9 and 10 construction, instrumentation and preliminary results 77−41339
Venera 9 and 10 probes, successful Venus surface pictures *(Russian)* 77−25967
Venera 9 and 10 satellites, Venus atmosphere and surface radiosounding 80−101543
Venera 9 and 10 satellites, Venus atmosphere radio occultation and surface bistatic radiolocation 79−48698
Venera 9 and Venera 10 probes, cosmic ray meas. 77−91388
Venera radio transirradiation of Venus atmosphere 77−82140
Venera spacecraft, anal. of wind vel. meas. 77−29683
Venera station orbiter, TV observation of Venus cloudy layer in UV, violet region *(Russian)* 79−53747
Venera-4, 5, 6 and 8, gas anal. equipment 78−28520
Veneras 9, 10, dual-freq. radio occultation expts. rel. to Venus daytime ionosphere profiles 79−96939
Venus entry probes and orbiters, spectral photometric data rel. to cloud layer optical model 78−4130
Viking, estimation of payload loads using rigid-body interface accelerations 80−10135
Viking, extended mission 80−67514
Viking, first mission to Mars 77−13262
Viking, initial exp. analysis of Mars environment 77−41341
Viking, Mars geological evolution data *(French)* 80−8578
Viking, surface sampler subsystem 79−48651
Viking 1, Mars landing site selection 77−13271
Viking 1 and 2, surface photography on Mars 77−2361
Viking 1 and 2 expeditions, scientific results *(Hungarian)* 78−73666
Viking 1 lander, location on surface of Mars 78−65479
Viking 1 Orbiter encounter with Phobos, trajectory analysis 80−12641
Viking 2 landing and first photographs of Mars' surface 77−9689
Viking 2 landing site search 77−17404
Viking biological investigations, review and status 79−80263
Viking entry vehicle, aerodynamic behaviour, ground test and flight results 79−16821
Viking lander biology instrument 78−49347
Viking Lander environmental test programme 77−56810
Viking lander gas chromatograph-mass spectrometer 78−77460
Viking Lander I, Martian life search project 77−33321
Viking lander radar system mechanical design 78−57427
Viking lander remote diagnostic techniques 78−57426
Viking landers, imaging obs. during one Mars year 79−80265
Viking Landers 1 and 2, 1977 winter survival prospects 77−74001
Viking landers 1 and 2, Mars atmospheric press. annual cycle meas. 80−72812
Viking landers on Mars, longitude determ. 78−16327
Viking Mars lander, hydrazine terminal descent engine, thermal design 77−87234
Viking Meteorology Experiment and Mars atmospheric meas. 77−33384
Viking mission, review of surface sampling and landing of second vehicle 77−17403
Viking mission operations strategy 77−17325
Viking mission to Mars, optical equipment 77−29627
Viking mission to Mars, review 77−73933

space vehicles continued
Viking missions, scientific results review 77−56852
Viking orbiter, imaging obs. of dust in Martian atmosphere 79−84707
Viking Orbiter uplink command generation and validation simulation 77−22040
Viking Orbiter visual imaging system, for Mars research, use of slow-scan TV cameras 77−45282
Viking orbiters, radio occultation meas. of Mars atmosphere and topography and atmosphere 80−72836
Viking orbiters, scientific missions 78−20612
Viking programme, biological expts. *(Hungarian)* 79−44329
Viking project, imaging expts. on orbiters and landers 77−56851
Viking project, instrumentation, scientific experiments and results 79−16865
Viking spacecraft, Doppler and range data rel. to geocentric gravit. const. evaluation 80−3891
Viking spacecraft, Mars atm. struct. expt., techniques, instruments and accuracy 77−13205
Viking-1 meteorological meas. on Mars 77−29686
Vikings 1 and 2, results before 1976, November superior conjunction 77−29701
Voyager, electrostatic discharge testing, JPL, Pasadena, USA 80−92415
Voyager, Jupiter low energy charged particle expt. results 80−98605
Voyager, receiver for measuring LF planetary radio emissions 78−4075
Voyager, telecommunications system and broadcast from Jupiter 80−26715
Voyager 1, currently active volcanism discovery on Io 80−26789
Voyager 1, encounter with Jovian system 80−26716
Voyager 1, mission to Jupiter 79−96948
Voyager 1, photographic obs. of Jupiter atmosphere ring and major satellites 80−26788
Voyager 1 encounter with Jupiter, ground-based IR imaging at 5 microns wavelength 80−26799
Voyager 1 Jupiter cloud configurations obs. interpretation in time-depend. framework 80−26787
Voyager 2, data from Jovian system 79−84740
Voyager 2, Jupiter's mag. tail, traversal during 1981 Saturn encounter 80−12706
Voyager 2, Jupiter magnetosphere, energetic ions and electrons obs. 80−77342
Voyager 2, Jupiter magnetosphere HF and LF radio events obs. 80−77344
Voyager 2, Jupiter magnetosphere obs., hot plasma environment 80−77341
Voyager 2, Jupiter magnetosphere plasma waves, radio obs. 80−77343
Voyager 2, obs. of solar coronal occultation, 1979 August 80−51639
Voyager 2, plasma obs. near Jupiter 80−77340
Voyager 2 at Jupiter, 1979 J 1 satellite discovery 80−77334
Voyager 2 at Jupiter, atm. 2400 Å map 80−77336
Voyager 2 at Jupiter, H I Lyman α and Io torus, EUV obs. 80−77338
Voyager 2 at Jupiter, ionosphere struct. from occultation radio obs. 80−77337
Voyager 2 at Jupiter, magnetometer obs. of bow shock and magnetosphere 80−77339
Voyager 2 encounter with Jupiter, trajectory and sequence modifications 80−77265
Voyager 2 encounter with Jupiter system, IR obs. 80−77335
Voyager 2 obs. of Jupiter and Galilean satellite/features visible 80−72871
Voyager cosmic ray detector system, energetic particle studies in outer heliosphere 78−24434
Voyager Cosmic Ray Experiment 79−48643
Voyager design and flight loads comparison 79−80196
Voyager I and Jupiter encounter 80−12642
Voyager imaging experiment 78−24427
Voyager IR spectroscopy and radiometry experiments 78−24428
Voyager low energy charged particle experiment 78−20618
Voyager magnetic field experiment 78−24431
Voyager mission objectives 78−24426
Voyager photopolarimeter experiment 78−20616
Voyager planetary probes for outer planets, review 78−24435
Voyager planetary radioastronomy experiment 78−24433
Voyager plasma experiment 78−20617
Voyager plasma wave system 78−24432
Voyager project, colour photographs of Jupiter, Amalthea and four Galilean satellites *(German)* 79−96959
Voyager project, Jupiter and Saturn *(Norwegian)* 79−92646
Voyager Project, spacecraft communication system 80−26718
Voyager radio science experiment 78−24430
Voyager reconnaissance missions to Jupiter and Saturn *(German)* 78−20619
Voyager spacecraft, journey to outer planets 78−49289
Voyager Sun sensor, CdS detector, radiation effect test, simulator 79−23644
Voyager UV spectrometer experiment 78−24429
Voyagers 1 and 2, missions and prospects 78−7859
wake, use of vacuum for conducting expts. 78−74013
weight and cost parameters, statistical analysis 79−84635
C fibre reinforced composites for spacecraft use, prep., props. and struct. 80−71625

spacecraft *see space vehicles*

spallation (nuclear) *see nuclear spallation*

spark chambers
see also position sensitive particle detectors
2-gap chamber with wire electrodes and stereoscopic cameras, 6 m^2 79−725
1200 pF fast-response pulse voltage generator 77−54444
amplifier-discriminator for magnetostriction spark chambers 78−868
beta-ray cameras, gas replacement monitor 80−95502
Cherenkov light photograms, automatic scanning by TV digitiser 80−52822
cosmic ray spark calorimeter, for locally generated penetrating-particle beams obs. 79−84603
Crystal Ball data acquisition system 79−89531
data readout cct. for magnetostriction spark cameras 78−78576
demonstration 80−77596
electron-photon shower recording, single-particle background suppressing method 78−78573
EM delay lines readout in spark, proportional, and drift chamber appl. 78−74547

spark chambers continued
emulsion stack connected with ionis. calorimeter for high energy cosmic ray obs. 78−25386
filmless, multipulse HV supply 78−78565
filmless chambers in high energy physics, review *(Russian)* 77−67938
flash chamber calorimeter, fine grain 78−37496
flash chambers for neutrino detection, construction and performance 80−58026
flash chambers of plastic material 78−55106
flash tube chamber, high press., γ-ray energy and spatial coords. meas. 77−57794
flash tubes, effect of induced clearing field on performance 78−50438
formation time of sparks for different initial charges 80−9460
gamma ray shower detector of low press. flash tubes 78−70697
gamma ray spark chamber telescope for range 10-100 MeV 78−36459
gamma-ray telescope, spark chamber, scintillation counter time-of-flight system 80−62017
gas discharge converters of X-ray pictures with Ne filling, memory time 79−26827
gas monitor, used in Rutherford multiparticle spectrometer 79−3318
high current pulse generator for flash chamber particle detector arrays 80−69039
high-energy particles detection by electronic method, principles of spark, streamer, proportional, drift and hybrid chambers *(Czech)* 77−42213
highly stabilized hybrid spark chamber for β-ray imaging 80−102398
holographic gas discharge chamber 77−10551
hybrid spark chamber for radioisotope distrib. meas. 78−46227
imaging alpha detector, radioactive contamination monitoring appl. 80−102384
low mass wire film spark chambers, capacity readout 78−29715
magnetic detector, SPEAR, PbO-SiO_2 wall addition 78−37494
magnetic large acceptance spectrom. using wire chambers 78−46207
magnetic spark spectrometer, high-speed photorecorders 80−87014
magnetostriction, multichannel time-digit conversion modules of 'Summa' system 77−3236
magnetostrictive wire readout system, transducer S/N ratio improvement 77−79518
MEA, magnetic detector at Adone 78−33367
missing data reconstruction in principal component anal. 78−17537
multigap, HV supply cct. for parallel feeding 80−63456
multilayer γ-telescope spark chamber, 5-200 MeV e^+e^- track anal. 80−63469
multilayer wide-gap spark chamber for a gamma telescope 79−76267
multiwire proportional spark chamber and wide gap spark chamber for photonuclear reaction use 79−68133
narrow gap chambers, effect of high gas density and energy control on spark width 78−33390
neutrons from extended source, meas. in spark chamber+time of flight detector 77−83447
noise, protection of Geiger counters in hodoscope 77−18742
optical, automatic data digitisation using CCD 79−89517
optical, thin Mylar film as window material 77−65395
optical chamber digitisation using CCD 80−27902
parallel plate, efficiency characteristics calc. 78−33393
parallel recording system for magnetostrictive spark chambers 78−867
particle identification by spark formation time meas. 77−83457
particle trajectory reconstruction using optical wedges 79−68132
photographs, automatic and semiautomatic handling, comparison 77−23371
photographs analysis with PA-BESM-4 system, exchange apparatus 78−9045
plasma memory and read-out *(French)* 78−46223
plastic total absorption track detector of high energy particles 78−55107
pre-triggered flash tubes for particle detection 78−82579
proton spectrometer/polarimeter for photoreactions below 1 GeV 80−18751
pulse generator, high speed HV, eff. irradiation of spark gap 77−34511
rectangular electrode frame prestressing and deformation 78−29708
self-triggering wide-gap spark chambers for recoil alpha-particles 77−30710
track displacement, operational frequency dependence *(Russian)* 77−83451
track shifts as function of actuation frequency and HV pulse time delay 77−6618
unstable systems, repeated measurements effects, primary decay law in spark chamber 77−41562
voltage pulse generators, Arkad'ev-Marx type, time characteristic stabilisation 77−34512
wide-gap, Tskhra-Tskaro (USSR) 80−87016
wide-gap, with Mylar film walls 77−65394
wide-gap chamber for gamma-ray astronomy, Soviet-French design 78−17503
wide-gap spark chamber used as a vertex detector in a high energy neutrino experiment 79−45569
wire, CAMAC standard ferrite matrices data read-out device 77−46473
wire, with decoupling resistors, transients calc. 77−65396
wire ferrite ring matrix, CAMAC-VECTOR standard readout system 77−46474
wire spark chambers, capacitive read-out system 80−102407
wire type, operation in extreme conditions 78−5094
X-ray camera, Ar filled, device description and performance evaluation 79−13598
γ-ray position determination using high press. flash tube chamber 77−57795
Ar filled low-pressure spark chambers, short pulses, spark track structure 77−3230
Fe calorimeter, hadronic cascade curves between 20 and 8000 GeV 80−36464
He-O_2 chambers, ionisation discrimination 80−37700
Ne circulation, purification system 77−14309
Ne flash tube chambers for electron and photon detection 78−58552
Ne flash tubes, appl. of alternate polarity HT fields 77−10539
Ne flash tubes, decay of clearing fields 78−94166
Ne-He high press. flash tubes, digitisation pulse characteristics 80−9455

spark counters
automatic, for through tracks in organic films 79−97941
corona counter, determ. of U content in solid waste mats. by α-detection *(Russian)* 80−27904
corona counter resolution rel. to current, gas pressure and anode wire diameter *(Russian)* 78−90018

spark counters continued
corona counters, exptl. results *(Slovak)* 78−33388
corona flow counter, multi-filament *(Slovak)* 78−55094
fission track spark counter, correction for track-hole densities in aluminised mylar film 77−3231
jumping spark counter, rapid determ. of counting parameters 77−30725
localised-discharge spark counter, as new particle detector 79−81119
sonic location spark counter system for mag. spectrometers 79−68162
wide gap, π^0 photoprod. on ^{4}He meas. 78−29694

spark erosion machining *see spark machining*

spark-gap voltmeters *see voltmeters*

spark gaps
air gap discharge zone probabilistic features 78−67582
air insulation, critical impulse voltage stress determ., test 77−4018
alloying powder particle interaction obs. *(Russian)* 79−83146
arc gap with displacement by mag. field 78−87513
arc with semimetallic cathodes, spark gap resist. 79−23471
automobile ignition RFI suppression at distributor rotor gap 79−55586
COMBI SPARK, single or multiple spark gap 78−42401
discharge in positive point-to-plane air gaps, obs. 77−35414
discharges, effect on plastic track detectors 78−86742
electric breakdown in gases, optical investigation *(German)* 78−30497
electric strength recovery after impulse current passage 78−67565
electrical breakdown of air gaps, 1 to 9 cm, with heated electrodes, investigation *(German)* 80−107010
electrode shape effect on SF_6 dielectric strength, overvoltage protection *(Czech)* 80−10444
electrodes, acoustic phenomena in erosion 80−64796
electron beam triggered, charact., investig. 80−107001
electronic spark source, adjustable-waveform, thyratron-diode switch element 77−63998
failure modes study, design of extended life high current spark gap 79−90481
flashover voltage calc. of uniform-field gaps under steep-front impulse voltages *(Japanese)* 79−64932
flowing gas, electric breakdown study, improved method 80−64821
four-electrode field emission pre-ionised triggered spark-gap switches, 10 to 30 kV, parallel operation 80−70075
generator for dust explosion hazard assessment and gas ignition 78−57983
graphite, impurity analysis, laser emission spectroscopy, material evaporation, auxiliary spark gap effects 79−87924
grouping technique for spark sources of elastic waves *(Russian)* 77−7630
n-hexane, trigatron spark gap, time-lag charact. 77−1030
high-voltage pulse generator, controlled spark gaps 78−5965
HV heavy-current arc gap 78−87514
HV laboratory ion density due to repetitive impulse generation 78−65913
HV pulser for discharge into CS_2 laser cavity, with triggered spark gap 79−13973
HV switching surges, influencing factors *(German)* 80−87958
laser triggered solid dielectric switches with low jitter and inductance 80−54066
laser triggered spark gaps, pressure depend. of rise time 78−55764
laser triggered switching of solid insulated spark gap 80−54065
laser triggered vacuum gap for high energy appl. 80−78888
laser triggering through fiber optics of a low jitter spark gap 80−107000
laser-triggered breakdown in gases, basic processes responsible studies 80−38794
lightning, stepped leader, spark gap+parallel R-C network simulation 77−17155
long, effects of neutral gas density reduction on negative pulseless glow-spark transition 80−33850
long air, disruptive voltage calc. with positive switch voltages *(German)* 80−87964
long air gap minimum breakdown voltage and time estimation 78−67575
long rod-to-plane air gap voltage/time characteristic for switching impulses 78−67576
long spark in reduced air density 77−35428
long spark-gaps, breakdown voltage *(French)* 80−33828
low-inductance spark gap switch for Blumlein-driven N_2 laser 80−33010
multichannel commutator for nanosecond generators, Torus accelerator investigation appl. 77−71708
multichannel high-energy switch 78−55770
multichannel surface spark gaps 79−18436
needle gaps, spark voltage charact. *(Korean)* 78−1931
needle to plate, laser triggered in nonuniform field, breakdown mechanism 77−7614
overpressure of spark gaps, 0.2 MA, design and appl. in fusion reactor technology 78−75456
parallel-plane electrode erosion charact. at atmos. and vacuum press. 80−70076
plasma confinement, Eta Beta machine, spark gap switches charact. *(Italian)* 79−55533
point-to-plane gap corona and breakdown in supersonic airstream 78−67573
positive point-plane gap, critical press. prediction, v_c/press. charact. 78−87583
pressurized spark gap switch with high repetition rates in multimegawatt average power range 77−23275
quarter-wave spark source, 323MHz, appl. stable spark discharge production 77−80394
resistance measurement during breakdown, time-resolved resist. meas. 80−19639
rod-plate, switching surge, long spark modelling *(Czech)* 77−1028
rod-plate arrangement, sliding flashover at switching-wave *(Czech)* 77−47278
rod-rod and rod-plane gaps, influence of positive and negative impulses on breakdown voltage, obs. *(German)* 78−5981
rod-to-plane air gap impulse-voltage delayed streamer and leader formation 78−67570
rod-to-plane air gap impulse-voltage primary and secondary streamer obs. 78−67569
rod-to-plate system, initial corona voltage calculated according to Townsend's Theory *(Czech)* 80−87961
sphere spark gap, impulse wave investigation *(French)* 79−50900
sphere-plane gap with lightning voltage impulse, photomultiplier and fluxmeter obs. 78−87580
spherical electrodes, breakdown voltage calc. 78−55763
spark gaps continued
square cut irradiated rod-rod gap sparkover under nonstandard impulse voltage 78−67564
square shaped fluid shock wave pulses with variable time duration 80−74593
switch for high voltages and currents, thyratron-spark gap hybrid 80−54067
switches, for main capacitor banks switching in ZT-40 fusion reactor, development 78−55036
time lag statistical distribution 77−62417
trigatron gap, transient glow discharge obs. and simulation *(Japanese)* 77−43097
trigger system, optically isolated, for pulsed high voltage plasma expt. 77−41650
vacuum, long, with static uniform fields, breakdown time interval determ. 77−15267
vacuum gap, electrically stressed, evidence against micro-particle initiated breakdown 77−4011
vertical single-pole earthed sphere gap, voltage measurement influence of neighbouring surfaces *(German)* 78−29880
very long gap anomalous discharge phenomena 78−67568
Cs, pulsed vapour source for ion sources in heavy ion accelerators 80−63423
Cu halide laser driving ccts., parametric study 80−83610
H arc discharges, laser-triggered, electron density meas. 80−64822
He rise time and time-depend. spark-gap resist., microwave meas. technique 77−31538
N_2, electric breakdown in long high-voltage gaps with gamma and alpha particle irrad. 79−18993
N_2, rise time and time-depend. spark-gap resist., microwave meas. technique 77−31538
SF_6 coaxial gap breakdown probability determ., influence of meas. procedure 78−67579
SF_6, limiting sparkover voltage values determ. and dielectric strength testing in power equipment *(Czech)* 80−87962
SF_6, spark gap, KrF laser triggered, low jitter timing 80−106999
SF_6-air mixture impulse discharge characteristics of 30 cm gaps 78−67572

spark machining
alloy, layer microhardness and thermal stability, effect of alloying additions in dielectric *(Russian)* 78−64760
carbide, effect of mech. props. on erosion resist. under spark machining conditions 78−11421
complex profiled surface alloying, automatic electrode feeding *(Russian)* 78−19936
computerised control, conference New Delhi, India (1977) 78−4590
control cct. for wire spark erosion machine for hard metals 79−35695
dielectrics break-up, mathematical model, non-ore materials milling appl. *(Russian)* 78−27653
electrical discharge machining, workpiece craters, electron microscopic study 80−30157
electroerosion, anode dissolution by pulsed current *(Russian)* 78−27652
electrospark coating formation factors *(Russian)* 78−19908
electrospark coating improvement by laser action *(Russian)* 79−15850
electrospark coating of Ti alloy, frictional charact. obs. *(Russian)* 79−1916
erosion and aggregate condition near discharge, cellular structure effects *(Russian)* 79−37557
Fe, Armco, electron microscope object prep. method 80−50789
heat and mass transfer 79−1369
melting crater propagation and material erosion, calc. method *(German)* 78−59282
metal, electroerosion and electrochemical treatments compared *(Russian)* 79−15846
metal electrospark deposition mechanism regularities *(Russian)* 78−19932
metallic powder, spark erosion prep. 78−27452
metallic surface alloying methods *(Russian)* 78−19931
metallic system, thermodynamically unstable, produced by spark discharge *(Russian)* 78−19933
micro-slit production method by elec. discharge machining *(Japanese)* 77−84015
refractories, erosion resistance during action of highly concentrated energy fluxes 80−55562
solid-alloy-liquid-metal systems, surface layer spreading and formation kinetics *(Russian)* 78−27668
steel, appl. of W_2B_5- and Mo_2B_5-based alloys as electrodes 80−21174
steel, corrosion resistance rel. to electroerosion treatment conditions *(Russian)* 79−15848
steel, surface hardening during electrospark alloying with transition metals IV-VI *(Russian)* 78−95849
steel, unalloyed, electric metallisation, corrosion resistance tests *(Russian)* 78−19935
surface strengthening by electrospark alloying *(Russian)* 79−96198
thin film microstructures, with and without stencils *(Russian)* 78−27651
Al alloys, use of electrospark cutting for preparing thin foils for electron microscope exam. 77−52590
Al-Ti alloy spark alloying, cathode weight change and hardened layer obs. *(Russian)* 80−61005
$CdFe_2$, $GdCo_2$, cubic Laves-phase cpds. 77−90501
Cr, fracture during electrospark cutting *(Russian)* 79−87719
Cr-Fe (1 wt.%), fracture during electrospark cutting *(Russian)* 79−87719
Fe and Fe alloys, polymorphism effect on failure accompanying electrospark action *(Russian)* 79−74236
$Fe_{72}Ni_8P_{13}C_7$, glass, erosion craters produced by spark machining, scanning microscopy obs. 78−44268
Gd-Y alloy, metal sphere prod. by spark erosion technique 78−81956
Mo, dislocation structure inhomogeneity in electromachining crater zone *(Russian)* 80−16326
Mo-Cu, electrical erosion resistance during electrospark machining 78−35531
$Pd_{781}Gi_{35}Si_{164}$ glass, erosion craters produced by spark machining, scanning microscopy obs. 78−44268
Ti, surface layer alloying element distrib. *(Russian)* 78−19934
TiN-AlN, composite, erosion resist. in electron stream 78−11365
W, monocrystalline cylindrical component surface finish, electroerosion polishing *(Russian)* 79−15847

spark machining continued
W-Cu, electrical erosion resistance during electrospark machining 78−35531
ZrN-AlN, composite, erosion resist. in electron stream 78−11365

sparks
see also electric breakdown; lightning
air, compressed, uniform field gap spark breakdown 77−11410
air, DC point-to-plane elec. discharge, temp. patterns, Michelson interferometry 80−54061
air, discharge, high-current, nanosecond, explosive cathode processes and contraction 80−10449
air, elec. discharge, effect of long laser spark ionis. channel 78−67468
air, electric breakdown between coaxial cylinders in crossed elec. and mag. fields 78−5963
air, electric breakdown by long laser spark 79−64822
air, laser breakdown, very long spark prod. *(Russian)* 77−1031
air, laser-initiated ionisation channels, form., characts. 77−89345
air, method of controlling growth and formation of parallel sliding spark channels 77−80389
air, multichannel spark form. 80−87976
air, negative pulseless corona to spark breakdown transition condition 80−54062
air, spark discharge, numerical simulation 77−89340
air, streamer to spark transition *(French)* 79−73053
air-H_2 (methane) mixtures, ignition energy by capacitive discharge *(French)* 80−10446
atmospheric pressure sparks, chemical species stroboscopic extraction into high vacuum regions 77−77858
atomic emission spectroscopy, discharge localisation with oxidised electrodes *(Russian)* 77−52728
ball lightning explanation by water electrolysis and combustion 78−69436
bipolar oscillatory spark discharges, vapour mixing and energy transfer 79−73050
calorimeter for routine use 78−37010
cathode spot pinning with pulsed discharge current 79−55601
ceramic substrate, surface spark discharge, channel spreading and substrate vaporisation 77−89336
channel formation in strong mag. field, Kerr cell obs., plasma model *(Russian)* 78−59693
COMBI SPARK, single or multiple spark gap 78−42401
corona to spark transition, cathode zone activity, Schlieren obs. 78−87585
dielectric spark discharge, conditions for building up compression rings 78−38493
discharge, appl. to multielement spectrochem. anal. 78−40103
discharge, correl. relations in spectrochem. anal. *(Russian)* 77−70379
discharge plasma electron temperature, time development 77−11394
discharge sparking potential dependence on nature of the wall 78−67552
distributed spark discharge for volume photoionization laser appls. 79−14634
dye laser, spark pumped compact modular design with high peak power 77−10950
dye laser emission, from laser spark, nonlinear absorpt. meas. 79−64922
effects of neutral gas density reduction on negative pulseless glow-spark transition 80−33850
electrical field of laser spark ignited near conducting target *(Russian)* 78−9884
electrodynamic mechanisms of limitation of the electron concentration in a laser spark *(Russian)* 80−59333
electron neutral collision frequency from breakdown measurements in crossed electric and magnetic fields 79−14517
electron-beam sliding spark device, C^{4+} plasma, soft X-ray emission, no superradiant gain 78−79444
electronegative gas mixture, spark breakdown current growth gas dynamic processes 78−87588
electronically controlled spark source, for anal. emission spectroscopy 78−16857
electrostatic, charged powder in container anal., hazards identification and control 80−69291
electrostatic, detection and characts., by radio methods 80−68217
electrostatic discharges from body nature and incendiary behaviour obs. 80−72406
energy determ., using mathematical and physical model 80−70065
excimer laser preionisation techniques, spark and corona preionisers 80−33016
extended high-current discharge, initiation by long laser spark *(Russian)* 80−10404
fast electron beam, transition from non-selfmaintained volume discharge to spark discharge *(Russian)* 79−23466
fireball plasma formation, transmission line model 78−59702
fluid, radio band pulse radiation due to spark initiated cavity dynamics, sonoluminescence *(Russian)* 80−66313
fluorocarbon vapours, sparking potential meas. 77−65922
fusion, TFTR, neutral beam sources overcurrent protection during spark down 80−102331
gas breakdown, cross-field, in coaxial cylinder geometry 79−82029
gas mixtures, ignition energy by capacitive discharge and through discharge of person charged with static elec. *(French)* 80−10446
gases in metals, detection by vacuum spark technique, appl. to Al wire 78−61094
grouping technique for spark sources of elastic waves *(Russian)* 77−7630
high current leader channel radial expansion, numerical model 78−87543
high current particle beam prod. by low pressure spark discharges, accelerator 79−31247
high voltage high frequency spark, with electronic control, for emission spectral anal. *(Russian)* 78−35771
high voltage unipolar spark discharge, spectrochem. anal. *(Russian)* 78−15750
high-degree ionized spectra excited by spark source and its application *(Chinese)* 79−80695
high-voltage, strong transverse air blowing, anal. appls. *(Russian)* 78−91183
high-voltage spark source, characterisation, computational method 78−45717
high-voltage spark sources, calibration meas. methods 78−49908
hydrocarbon liquids, electrostatically charged, incendivity of sparks from surface 80−6303

sparks continued
ignition of gas mixture, Kasaev cathode call formation 80−70066
incendiary sparks of minimum ignition energy, spark formation 79−10729
industrial stack plumes, electrically charged, fire and explosion danger 77−5315
ion acceleration mechanisms in vacuum spark 80−92417
ion energy distribution, of late stage, mass spectrometer meas. 79−55596
ionised atoms, prod. by low inductance vacuum spark, spectroscopy *(Japanese)* 80−52911
laser gas breakdown, shock and ionisation waves, photographic absorpt. obs. 80−87967
laser radiation absorpt. mechanism in deionis. stage *(Russian)* 78−22583
laser spark, diagnostics using hologram interferometer 79−64921
laser spark, photographic study by picosecond techniques 78−42826
laser spark in focused beam, numerical study 79−14632
laser-produced, light pulse narrowing and power density increase 80−28862
leader-stoke velocity, significance for lightning and long sparks 77−76234
light emission from high-current surface-spark discharges, book contrib. 79−77449
light source, with Kerr cell, construction and operation *(Russian)* 77−72042
light sources, reproducibility for emission spectroscopy 78−3429
lightning and spark discharge leader-stroke velocity comparison 78−94947
long, at switching surge, modelling *(Czech)* 77−1028
long, in reduced air density 77−35428
long spark form. mechanism 80−59326
mass spectrometer using spark source, elemental sensitivity 79−57314
miniature triggered spark switch, high repetition rate 80−103203
minimum breakdown potentials in crossed elec. and mag. fields 78−67554
negative impulse corona and sparkover, background ionisation effects 78−87540
optical discharge maintenance by giant laser pulse with extended tail 79−23478
perfluorocarbon-SF_6 mixtures, sparking C inhibition, decomp. product investig. 80−89478
plasma, electrically-initiated, laser-driven, attenuation of 10.6 μm beam 77−34424
plasma, laser prod., holographic study at 10.6 μm 80−38685
plasma, local high-press. regions production in vac. spark, diagnostics 79−19104
plasma deionisation stage, laser radiation absorption obs. 78−75398
plasma ion source effects on mass spectroscopic quantitative anal. 79−14631
Plexiglas, spark energy balance 79−23474
Plexiglass, spark press. field in solid dielectric 77−24233
positive impulse sparkover, unipolar space charge effects 78−87542
powders, spark elutriation into plasma spectrochem. anal. *(German)* 78−68959
pressure depend. of spark constant 78−30504
pressure wave generation and propagation by spark discharges in liquids *(Japanese)* 80−70060
pressurised field distortion spark gaps, arc voltage waveforms, electrode material effects 78−87549
probee investigations of the electric fields produced in air near a laser spark *(Russian)* 80−59334
propane, ignition by small sparks 79−55587
pulsed discharge, air, elec. wind and sonic wave (350 mis) initial growth, Schlieren obs. 78−87587
repetitive electric discharge, time-gated spatially resolved spectrometric obs. 78−45727
RF spark ion source, multiply-charged species rel. abundance distribs. 77−61151
selfluminous, schlieren system for time and space resolved photography 80−87471
shock wave degeneration to sound waves in highly-conducting spark channel 80−38428
shock wave degeneration to sound waves in highly-conducting spark channel 80−38429
shock wave detection 78−87586
silhouette photography, high-speed, of small biological subjects 78−44743
simulated combustion gases, mode and sparking characts. of back discharges, NO conc. effects 80−6301
sliding, in air, development on dielec. film covering cond. 79−86634
sliding discharge, guided, explosive emission phenomena 80−19649
sliding spark capillary discharge and electron beam device, physical props. 78−5974
small spark form. mechanism 78−18469
solid breakdown, pulsed, plasma form., blow off, shock waves 77−27688
spark tracing, high frequency, application in engineering and aerodynamics 78−38434
sparking potential in longit. mag. fields 80−106996
spectral emission source, effect of strong transverse blowing 80−3441
spectroscopic spark sources, air gap or rotary gap types 77−40584
sphere-plane gap with lightning voltage impulse, photomultiplier and fluxmeter obs. 78−87580
stable discharge production using 323MHz quarter-wave spark source 77−80394
Stark broadening of spectral lines, electron density, determ. in stages of spark discharge *(Russian)* 80−28859
streamer-induced spark form. model based on neutral dynamics 79−55588
striated filamentary sparks produced by a CO_2 TEA laser 80−24288
subsonic electron fluid and small spark formation 80−38792
switches, high repetition rate, with Al and brass electrodes, surface ageing 80−106997
switching surge, modelling, voltage and flashover distance conversion factors *(Czech)* 77−15254
Tesla discharge temperature diagnostics, from OH A→X intensity meas. 79−64939
triggered spark gap switch system, long life, high repetition rate 80−106998
underwater, current pulse characts. in RCl circuit 78−9886
underwater, induced cavity collapse 78−42636
underwater, integrated bulk plasma characts. 79−27857

sparks continued
underwater spark discharge, vapour cavity development, bounding surface effects 80−49022
underwater spark discharge, vapour-gas cavities generation and space-time evolution characts. 80−19650
underwater spark induced axisymmetry unsteady motion betweeen shock wave front and contact surface *(Russian)* 79−77323
underwater steam cavity during spark discharge *(Russian)* 77−31345
UV light source, surface spark discharge type, for H_2/F_2 laser initiation 80−78923
UV spectral efficiencies of surface-spark discharges, appl. to I laser 77−75496
vacuum, form. mechanism of $H_3O^+(H_2O)_n$, mass spectrometer expt. 79−32844
vacuum gap, long, with static uniform fields, breakdown time interval determ. 77−15267
vacuum spark, electron density, interferometric meas. 78−5962
water spark, high voltage, resistive phase 78−67453
X-ray emission, of RF spark source mass spectrometer 79−90480
Al suspension in Ar stream, Nd laser radiation interaction, spark form., breakdown intensity *(Russian)* 77−35435
Ar, atmospheric press. with Mg cathode, evidence for ionic toroidal post discharge environment 77−84551
Ar plasma, 14000K, continuum emission coeff., laser spark temp. meas. 77−31527
Ar supersonic jet, spark line emission, 300-1000 Å 77−19793
Au wire-semiconductor, elec. contacting method, spark welding *(German)* 79−49215
B, filament, light emission during fracture 77−28896
CO_2 laser, vac. UV preionisation source spectral characts. 79−31938
CO_2 laser gas mixture, vol. photo-preionisation by VUV radiation 80−87966
Cu-Al (0.5-17.6 at.%), mol. ions in spark source mass spectra 78−44427
Cu-Al alloys, spark-source mass spectrosc. chem. anal., using mol. ions 79−92031
H, laser-triggered, electron densities meas. 80−106975
H-inert gas laser spark, emission spectra 79−82119
He, cathode spot conversion kinetics 80−44067
He condensed spark discharge, integrated luminosity, pulsed longit. mag. field 77−76233
He, spark prod. by short laser pulses, spectroscopic meas. of temp. and electron density 77−43086
He-Ne mixtures, spark channel formation 78−1936
He+Ar+polyatomic fluorides, VUV spark emission spectra 79−3457
N_2, dense gas near metallic target, laser spark *(Russian)* 80−38682
N_2, electric breakdown, vol. discharge with external photoionisation, plasma focus spark channel *(Russian)* 80−38738
N_2, electric breakdown between coaxial cylinders in crossed elec. and mag. fields 78−5963
N_2 laser, high-power, TE, UV, using Blumlein transmission line, construction characts. *(Korean)* 79−22971
N_2 plasma, 18000-45000K, continuum emission coeff., laser spark temp. meas. 77−31527
N_2 positive corona into spark, prebreakdown phase, spectroscopic anal. 80−38790
SF_6-N_2-Ar mixture high-current multispark discharge switching characteristic 78−67444
Si, controlled dislocation formation, struct. density *(Russian)* 80−107244
Zr VIII spectra, reson. transitions in UV 80−91479

spatial filters
acoustic logging, optical filtering appl. in data processing *(Russian)* 79−39942
acousto-optic modulator, improved contrast using spatial filtering 78−9448
acousto-optical wideband programmable filter 80−102842
adaptive holographic matched spatial filter for pattern recognition 77−7011
aerial photograph statistical spatial filtering 79−13908
aerial reconnaissance film interrogation by optical matched filtering 77−78484
algae recognition by coherent spatial filtering with simulated input 79−79696
alignment system for Helios CO_2 fusion laser 80−33070
alkali halide photodichroic crystals use for coherent opt. data processing 77−68248
alkali halides, photodichroic, as optical processing elements 78−83056
amplitude filtering for superresolution, maximum central irradiance under energy constraint 80−91914
amplitude filters, optimum function analysis 77−58453
analogue image processing, Japanese achievements 77−50634
apertures with triangular and assoc. filters, variable apodisation 80−63914
apodisation filters, atm. turbulence effects on central irradiance in Fraunhofer diffr. by slit apertures 78−25796
apodisation filters in optical systems with residual aberrations, image optimisation 80−53223
apodiser, optimum, simulation by binary filters 78−5539
apodization and image contrast, MTF evaluation 79−59640
apodized optical systems, frequency response and point image irradiance distrib. 80−9819
applications *(Japanese)* 80−99851
axially symmetric filters, Fresnel diffr. field, series representation 77−46696
axially symmetric filters, two-point resolution evaluation method 77−46697
background noise attenuation, spectrum anal., geological appl. *(French)* 78−9338
binary computer generated holograms 77−50774
binary digital hologram as matched filter, Fourier domain quantization effect 77−3544
binary filters simulating apodizers, expt. results 78−46780
biological pattern recognition, rotational matched spatial filter 80−76866
biological specimen pattern recognition via matched spatial filtering 78−69261
biological specimen recognition with partially matched spatial filter 80−46113
biomedical image optical differential operation processor 77−52911
bipolar, review of techniques appl. to incoherent optical systems 80−95821
spatial filters continued
bipolar spatial filtering, incoherent, review 80−102822
character identification, use of holographic filter *(German)* 77−88668
chromatic Fourier hologram as matched filter, for spatially coherent white light correlator 79−3642
circularly symmetric positive filter function realisation by transparent rings 78−94448
circularly symmetric positive filter function realisation by transparent rings 80−87343
coded-aperture image deconvolution, single-emulsion-layer holographic inverse filters 79−76647
coherent, operating principles, appl. in instrum. production *(German)* 78−71208
coherent feedback, flexible filter operations 80−87337
coherent image deblurring using computer generated holographic filters 77−14669
coherent optical compensation of post-detection spatial distortion, optimal spatial filters 79−98302
coherent optical correlators, filter plane resolution requirements 77−34828
coherent optical feedback analogue computer for partial differential eqns. with inhomogeneous terms 79−76870
coherent optical feedback technique, multiplicative disturbance suppression 78−22094
coherent optical matched spatial filter correlator, for microfilm data base word recognition 80−43279
coherent optical processor, input object vibr. effects on spatial freq. spectrum 77−46686
coherent optical processor for vehicle tracking and identification using laser diode light sources 80−37957
coherent optical system, impulse response for image multiplication by spatial sampling filtration 80−33126
coherent optical systems, spatial filtration, freq. characts. *(Russian)* 77−71927
coherent optics fundamentals 78−78910
coherent optics system, amplitude and phase spectra analysis *(Russian)* 80−28164
colour coding of spatial freq. using incoherent optical processing 80−37956
colour encoded aperture masks used for incoherent filtering of images 79−41348
colour sensitive, using volume holograms 78−87150
colour spatial filtering for image enhancement 80−87341
complex controllable nonholographic image filter production and implementation *(Russian)* 78−46516
complex correlation function between two signals, interferometric method, with spatial filtering *(Spanish)* 79−76611
complex Fourier spectra, interferometric determ. 80−87327
complex signal addition by matched spatial filtering 78−29905
complex spatial filters for image deconvolution 77−10860
computer contouring method using digital filter, bathymetry appl. 79−39894
computer generated holographic spatial filters for large objects 77−23753
computer-generated hologram spatial filter for large object formats, interpolation 78−22099
computerised tomography, dose reduction using a generalised filter 79−66557
contemporary optics, book 79−81353
contrast improvement, noise-free, with LF polarising filter 77−75656
Controlled phase transparencies in coherent-optical systems performing Walsh and Hilbert transformations 78−50931
correlation filtering for increasing diffr. efficiency 80−96028
correlation reduction, spatial filtering and variation of resolution 80−102850
correlator, estar base reconnaissance film, birefringence effects 77−74538
correlator, nonlinear t-E curve effects for matched spatial filter material 80−95812
correlator with matched filtering using band-limited illumination 80−69531
corrugated waveguide filters, sidelobe suppression 77−84008
cytological preparation image processing, filter construction *(German)* 78−36026
data extraction from film using optical and/or digital and/or electronic devices 78−63024
deblurring filter, space-bandwidth product 77−83959
differential operator processor, filter fabrication feasibility studies 78−58925
differentiation by spatial filtering 78−1171
differentiation coherent spatial filtering, phase bias introduction 77−83821
direct picture transmission in single optical fibre, restoration with holographic filters 79−89871
directional filtering two-dimensional patterns, hybrid character recognition system *(German)* 77−83819
double-beam interferometry with optical background suppression 79−75576
dynamic, for optical image enhancement 77−79769
dynamic spatial filtration of coded optical image signals from noise 80−95826
edge filters for phase contrast imagery, theoretical design 79−86250
elastomer storage device evaluation for optical signal processing 80−48444
electron micrograph optical and digital spatial freq. filtering, expt. results 78−82079
electron micrographs, image reconstruction and spatial filtering 79−97477
exponential transformation using film nonlinearity for optical homomorphic filtering 80−58467
feature enhancement using noncoherent optical processing 80−99651
feedback systems for analogue and digital optical image processing 80−102650
filamentary, for multipass interferometer 78−77975
filamentary for use with interferometry in phase measurement 79−71518
filamentary spatial filter interferometer, appl. to phase meas. 78−49890
film-grain noise degraded image estimation 78−54479
fingerprint identification, matched filtering on basis of thick holograms 77−79781
flexible band-pass filtering using coherent optical feedback 79−94166
fogged photograph restoration by optical spatial filtering 78−74857

spatial filters continued
Fourier plane spatial filtering, real time operations on spectral and temporal envelopes 78−22093
Fourier transform microscope, with optical spatial filtering 78−58028
Fourier transform of half-tone picture, spatial filtering using photographic replica 79−27184
Fraunhofer diffraction pattern of circular apertures with triangular apodisation filters, encircled energy 80−14277
frequency plane filtering by dynamic coherent illum. 80−95825
frequency sampling by phase modulation, multiple image generation 77−79759
frequency spatial filters, laser intensity spectral distrib., contrast magnification *(Russian)* 77−747
generalised matched filters for coherent optical pattern recognition 80−99654
generalised sampling theorem for Dirac Δ functions, appl. to computer-generated transparencies 78−42284
generalized sampling theorem with application to computer-generated transparencies 79−41343
halftone images, histograms meas. 80−23631
hologram, computer generated, as space-variant optical elements 78−37856
hologram filter for three dimens. object recognition *(French)* 79−18359
holographic, CAD, optimisation method *(Russian)* 80−28171
holographic, for electron micrography image improvement 80−99680
holographic, invariance of diffr. correlators to optical element shifts 80−106471
holographic, optical images analysis appl. *(Russian)* 78−37809
holographic character identification *(German)* 77−88668
holographic correlator, noise sources, accuracy improvement 77−23636
holographic correlators, expts. to improve accuracy 77−65583
holographic Fourier transform lenses for matched-filter optical processor 79−45913
holographic matched filter, increasing information capacity 78−25815
holographic matched filtering system adjustment by diffraction gratings 78−87027
holographic pattern recognition for 'simple' objects 80−53230
holographic pattern recognition of Korean alphabets, discrimination enhancement using phase modulated matched filters 80−95854
holographic pattern recognition of the Korean alphabet using matched spatial filters *(Korean)* 79−22920
holographic picture scrambling for confidential picture taking technology, method 77−19208
holographic pseudocolor encoding technique 79−18370
holographic Vander Lugt filters, optical correlation for pattern recognition 77−79765
hybrid image processing 78−25810
image classification by orthogonalised spatial filtering 77−50635
image deblurring by convolution with impulse response operator 77−65580
image enhancement for objects embedded in scatt. media, mammary growth diagnosis appl. 78−40288
image filter with noncoherent incandescent source, model and expt. *(Russian)* 79−7083
image filtering using prism and incoherent light *(French)* 80−14450
image generation using 2-D elec. filters 77−79772
image reconstruction by modified back projection methods, reconstruction error determ. 78−33682
image reconstruction from projections, filtering 77−68176
image restoration by Wiener filtering, signal dependent noise 77−88645
imaging relays in high power lasers 77−88760
improvement of cross-correlation peaks by image filtering 79−76610
in-plane strain meas. by holographic modulated diffr. grating 79−90202
incoherent complex signal detection, spatial filtering technique 79−3639
incoherent complex spatial filtering 80−95834
incoherent diffraction correlator with a holographic filter 80−37955
incoherent image optical matched filtering 80−14286
incoherent optical processing via spatially offset pupil masks 78−82917
integral equations soln. by optical spatial filtering 79−3643
integrated optical spatial digital filter based on Bragg effect 80−96036
interferential spectrometry, matched filtering, real time spectral recognition 78−37822
interferometric spatial filtering system 78−90515
inverse filters, simplified holographic fabrication 79−23077
IR optical system input diffr. effects and use of spatial apodisation 78−79113
kinoform method, for filtering and image synthesis 77−58295
LANDSAT imagery, spatial filter analysis 78−69490
Laplacian formation by holographic zone plate moire patterns 79−13917
laser amplifier system, small-scale self-focusing 80−106580
laser amplifier with spatial filters, graphoanalytic determ. of energy parameters 80−48322
laser amplifier with spatial filters, optimal length and operating conditions 80−48323
laser fusion apodised apertures, Faraday rotators, and spatial filters 77−19290
laser fusion experiments, Nd:glass laser with high flux spatial filters 80−33035
laser line art optical processor, optimal enhancement filter 79−59648
laser line scanning sensor, spatial filtering design considerations 78−85752
laser self-focusing suppression through low-pass spatial filtering and relay imaging 78−74938
least-mean-square spatial filter for IR sensors 80−38092
lens-pinhole spatial filter, student laboratory apparatus appl. 79−62976
lensless matched filter, operating principle, third order holographic aberration 77−7013
line scanning sensor, spatial filtering design 79−53527
liquid crystal polarization rotator for intermodulation spatial-bandwidth reduction holography 80−53439
liquid crystals, as tunable spatial filters in optical signal convertors 78−50930
liquid-crystal devices, variable-grating-mode, optical logic operations on binary images 80−106613
logarithmic filtering using inherent film nonlinearity 77−88646
low spatial frequency enhancement with triangular and associated filters, incoherent transfer functions, equiv. passband 79−94168
Mach-Zehnder interferometer 77−42616
matched filter, multicapacity, for correlator appl., using birefr. object film 80−74478
matched filter correlator memory techniques and capacity 80−43280
spatial filters continued
matched filter visibility effects on the correlation function 80−96031
matched filtering improvements for coherent optical pattern recognition 80−78786
matched filtering using binary digital hologram, Fourier domain quantization 77−3544
matched filters for optical signal and pattern recognition 80−48392
matched holographic filters with Pockels readout optical modulators 80−53456
matched spatial filter optimisation for diatom recognition 80−48180
matched spatial filter synthesis, parameter optimisation 77−71925
maximum likelihood spatial filtering examples 78−63038
metallic film apodising and attenuating filters, phase shifts and aberrations 78−90514
metallic thin film apodising and attenuating filters, phase shifts and aberrations 80−87552
micropattern array multiplication by sampling spatial filtering 77−65581
microscopy, spatial freq. filtering 77−79760
multi-aperture system imaging props. 80−87332
multiactuator mirrors, wavefront error compensation capabilities 79−59797
multiband image spatial domain filtering by Karhunen-Loeve transform 78−78952
multiple hologram appl. to variable size 3-D object recognition *(French)* 77−46705
multiple image formation by sampling Fraunhofer diffr. patterns 78−1334
multiple imaging with thin phase filters, signal processing approach 78−66772
multiple spatial filters, imaging props. to reduce self-focusing in fusion lasers 77−58360
multislit spatial filtered pseudocolour holographic imaging 80−53236
multispectral size-averaged incoherent spatial filtering 80−33146
noise problems in image processing by spatial filtering 78−37817
noisy blurred image restoration by smoothing spline filter 78−33679
non-contact rotational speed measurement and integrated spatial filter detector *(Japanese)* 79−93107
nonlinear, adaptive spatial filter for image classification *(Russian)* 78−42292
nonlinear, two-dimensional high accuracy signal processor 78−46532
nonlinear medium, loss formation with spatial filtering 80−53357
nonlinearity recorded matched filter, false alarm rate reduction 77−62037
object-plane Fourier processing with volume-hologram filters 79−94172
one-dimensional signal bilinear transformation by 2-D coherent optical processors 79−13909
optical, pattern recognition by means of holography *(Japanese)* 80−5699
optical diffraction analysis, in microscopy 80−32926
optical image processing using dynamic spatial filters to remove multiplicative noise 79−59650
optical material inspection procedure using holographic filter technique *(German)* 77−31142
optical pattern recognition, discriminant hypersurface prod. by average filters 80−99649
optical pattern recognition by thermoplastic complex filter 80−99656
optical processor, real-time, for pattern recognition of biological specimens 78−40454
optical pseudo-colour processing of height and flow velocity *(Japanese)* 80−9826
optical spatial domain filter theory, gas molecule images by electron holography 80−10016
optical spatial filtering, of visualised results of flaw detection monitoring, rational regions of appl. 80−7751
optimum filter for image restoration *(Ukrainian)* 78−55308
optimum spatial filter, for noise degraded image restoration 77−10857
OTF, two pupil synthesis, incoherent spatial filtering 78−58919
OTF synthesis, pupil function replication 79−27182
parallel matched filtering, vol. effect minimisation 77−7012
pattern recognition, multiclass, multivariant technique 80−87320
pattern recognition using wavelength-multiplexed matched spatial filters 79−76603
patterned optical filters for solid-stage imager spectral encoding 78−66945
periodic structure defect detect. using optical processing 80−95829
periodic-pattern-defects omnidirectional-spatial-filter optical detection system 80−69333
phase contrast objective, point spread functions of annular phase filters 78−25805
phase delay measurement using Fourier optical synthesis of Zernike's three-slit interferometer 78−65960
phase determination of amplitude modulated complex wavefront 78−55305
phase filter with specified pulse response modulus, design *(Russian)* 78−13813
phase object differentiation by spatial filtering 77−65579
phase recovery from single intensity distrib., using spatial filter 77−83825
phase stripe, for optical surface testing by caustic method 79−72722
phase-inverting grating construction, use in deblurring filters 80−48398
photochemical adjacency effect for spatial high pass filtering 77−71929
Photoelectric recording of optical fields by correlation processing 78−71048
pick-up tube aperture distortion correction, optical method 80−95827
pinhole closure due to intense laser radiation 77−79877
pinhole plasma shutter for optical isolation in high-power glass lasers 80−23733
pinholes irradiated by Nd:glass laser pulses, plasma closure phenomena 79−89946
plasma, high density, directed, source design, characts., numerical model 80−38538
plasma spatial filter for high power laser system 77−72056
plasma spatial filter for high-power lasers, mechanism 77−19269
pockels readout optical modulator, for optical/digital processing systems 78−79125
Pockels readout optical modulator, optical processing appls. 78−83100
processor, for filtering airborne and ground geomag. data 77−25797
pseudo colour equidensitometry, analogue optical method 78−32903
pseudocolour encoding of spatial frequency information 78−87018
pulse shaping and compression using electrooptic deflector with Fourier optical elements 80−53421

spatial filters continued
radar and sonar coherent optical processing techniques 78−75018
radar signal processing, multichannel optical correlator 78−74847
radiographic image analogue processing by photographic spatial filtering 78−57070
Raman spectroscopy, high local resolution, optical energy and spatial filter 79−35838
random, pattern generation using coherent optical spatial filtering 79−98462
random spatial phase modulation for speckle elimination 78−58920
raster scanned images, matched filter processing 77−7018
real time image restoration through Walsh filtering 77−27264
real-time filtering of cytological preparations *(German)* 78−36025
real-time optical processing using the liquid crystal light valve 80−63936
real-time spatial modulators for optical/digital processing systems 78−63025
remote sensing imagery, spatial filtering 78−90385
rotating circular involute reticle used in optical searching systems 79−98505
rotating wedge spatial filter, pattern recognition of biological speciemens (algae) 78−33837
scene principal vector analysis by multiple spatial filtering 80−48179
schlieren system, phase object projection, imaging characts., recording conditions 78−25977
schlieren techniques represented by phase contrast function 80−9813
scintigraphy, multichannel, collimated, Compton effect on spatial resolution, digital spatial filtering 78−69182
shift invariant linear matched filter for optical correlator 80−37962
side band spatial elimination associated with acoustooptical pulse-picking 79−59732
sine-cosine motion converters, optimal parameters of filter with unit transmission function 78−79133
single-mode optical fibre interferometry 80−73442
sinusoidal amplitude grating, with apodisation filter, coherent imagery 79−55067
sky image coherent-optical processor for moving object location 78−78944
slotted aperture for Moire photography 77−65053
smeared photographic image restoration by white light processing 79−18352
space variant optical transfer with Fourier filter in extrapupilar position 77−10846
space-variant linear processing of 1D signals 77−42490
space-variant processing of 1D signals, direct output and output spectrum displays 77−42491
spatial electric filters, 2-D image formation book contrib. 77−79772
speckle coded image subtraction configs., optimal distrib. of exposures 79−55071
speckle reduction, moving aperture method and incoherent spatial filtering 77−42489
speckle reduction in coherent imaging, two-step process 78−37819
speckle spatial filtering, detection of binary images 79−36849
square root, phase image differentiation with linear intensity output, theory 78−33839
statistical filter for image feature extraction 80−99636
Straubel apodisation filter, rot. symmetric, circ. aperture diffr. pattern, pupil functions 79−81530
straubel apodisation filter systems, effects of defocusing on point spread function 78−25804
Straubel apodisation filters, equivalent passband of optical system 78−50880
Straubel apodisation filters, for straight edge coherent imagery 78−25808
summing luminescence spectrometer using polychromators and spatial filtering 77−74517
texture pseudocolouring, single pass by spatial filtering 80−95809
thermoplastic-photoconductor films for optical data processing 78−50875
thermoplastic-photoconductor image transducer, input to coherent optical processor 78−83098
thermoplastic-photoconductor tape for holographic recording, spatial filter prod. 78−90391
thin phase structure detection method spatial filtering props., under partially coherent illum. 80−95828
transaxial tomography, simple pupil function for OTF synthesis 79−41349
transaxial topography, optical method, optical fibre, refr. index meas. *(French)* 78−66778
transverse analogue tomography, cross-sectional imaging of X-rays 80−56201
triangular apodiation filter system, rectangular and triangular wave-response 79−59645
tunable spatial filtering with a Fabry-Perot etalon 80−58668
turbulent atmosphere spatial filtering function for collimated laser beam amplitude fluctuations 80−9810
Two-stage holographic rejector filter *(Russian)* 77−75675
uneven interface of media with different refractive indices, statistical characts. of images 80−87331
unstable resonator with spatial filter, mode discrimination, phase modification 79−76719
US low-pass spatial filtering 79−47869
Vander Lugt filter, effect of recording errors 77−23624
Vander Lugt holographic filters, optical correlation for pattern recognition 77−79765
variable threshold zonal filtering 77−71926
vernier sine-cosine angle convertors, output signal eqn. 80−10031
visual perception appl. 80−30731
visualization of light propagation, hologram construction 79−81391
visually optimised image restoring filter 79−3644
volume diffraction gratings as filter, for image restoration 78−94378
volume hologram representation of space-variant systems 78−33696
volume hologram spatial filtering props. 79−27211
volume holograms for image restoration 80−83566
wavefront reconstruction, linear filtering influence 80−99670
Wiener filters, bilinearly distorted image linear restoration 80−83557
wind velocity lidar meas. by spatial filtering 79−29901
CO_2 laser Antares fusion system power amplifier optics 80−74394
CO_2 laser Helios fusion system alignment 80−74420
KCl:LiCl photodichroic crystals as adaptive spatial filters 79−72713
KF:LiF, photodichroic, real time recording medium, for optical spectrum analyzer 78−71174
spatial filters continued
KF:LiF, photodichroic real-time recording medium, for optical spectrum analyser 78−66878
KF:LiF photodichroic crystals as adaptive spatial filters 79−72713
$LiNbO_3$ volume holographic grating as spatial-freq. selector for tunable dye laser 80−53240
Nd:glass laser amplifiers, self-focusing and suppression by spatial filtering 80−14406
Nd^{3+}:phosphate glass laser, brightness enhancement by spatial filtering in amplifying channel 80−48321

spatial orientation control *see attitude control*

spatial variables measurement
see also angular measurement; area measurement; curvature measurement; diameter measurement; displacement measurement; distance measurement; height measurement; length measurement; level measurement; particle size measurement; position measurement; surface topography measurement; thermal expansion measurement; thickness measurement; volume measurement
3-dimensional probes, meas. errors *(German)* 79−80574
aerosols, monodisperse, mass concentration, laser monitoring 80−98878
afocal projection measuring system, moire fringe techniques, large lathes, milling machine appl. 77−71295
amplitude, using pneumoacoustic transducer, for linear dimens. control 79−17387
anatomical surface shape meas. method 80−3882
attitude determ. for artificial satellites, meas. errors 79−88561
attitude of rocket, meas. using Hall-effect magnetometers 79−21148
automation of real-time optical meas. of small structures 79−85115
bidirection laser rod gauge, development program *(Chinese)* 79−64239
centre of gravity coordinates of optical images, measurement accuracy analysis 79−36850
coded grating method for measuring three dimensional objects 78−86240
coherent light use *(French)* 80−23641
combined length, angle measuring procedure for spur-gear measurement *(German)* 78−77855
complex shape, of components, contactless method using gap transducer in local EM field 78−93648
computerised coordinate measuring technique, plane, prismatic workpieces, mating simulation *(German)* 78−77846
concentric round parts, profile determ., concentricity errors *(German)* 80−57249
contour mapping of 1st and 2nd derivatives of plate deflection using modulated diffr. gratings 79−6086
coordinate measurement, computerised problem oriented language MAUS *(German)* 78−89432
coordinate measurement error with scanistor, sweep voltage nonlinearity effect 77−14808
coordinate measuring apparatus calibration, errors evaluation *(German)* 78−77854
dimension meas. and control in-process using laser sensors and microprocessor 79−80577
dimensional metrology, light diffraction patterns, technical structures *(German)* 79−30415
dimensional metrology of large objects by projection moire techniques 79−85122
dithered-beam metrology 79−30408
E-glass fibre, pore size distrib. anal. method 79−87805
electron microscope samples, geometric stability *(Ukrainian)* 77−67536
endoscopic contour technique for meas. dimensions of object detail *(German)* 80−31839
engineering metrology, measurements by optically generated patterns 79−3648
fibre sizing using light scatt., error contour charts 80−4689
gauge blocks, WC, determ. of thermal expansivity using interferometric dilatometer 79−12767
gauging of intermittently present surfaces, possible solution 78−93649
gear profile testing, new method for discontinuous kinematic errors 80−95068
gear tooth profile, portable meas. instrum. for large gears, interchangeable standard profiles 80−57259
glass fibre reinforced polyacetal mouldings, injection, shape testing, projection of optical gratings *(German)* 79−29322
hardwired image analyser software control 78−57917
helical motion of rigid body, meas. by double exposure speckle method 78−16775
holographmetric plotter for three-dimensional meas. 79−7103
image counting and sizing using TV-microprocessor system 78−94377
internal diameter, caliper standard accuracy determination 77−71296
internal gauge, microinterferometer IZK-61 78−89438
intervertebral joints, painful, meas. of movement by biplanar radiography 80−98079
IR detector dimensions, rapid meas. by Fresnel diffr. *(French)* 78−89435
laser fusion targets, X-ray meas. using least squares fitting 80−32425
light beam deviation from straight line meas., optoelectronic arrangement *(German)* 78−77850
linear dimensions, measured on production line by optical techniques 80−82746
linewidth measurement using optical microscope 77−79147
Mekometer additional equipment design, manufacture and calibration for more complete utilisation *(Italian)* 80−64129
micrometer slides, for linear meas. in range of 100 mm to 1 μm accuracy 77−5808
micromovement measurement, hologram repositioning by an interferometric technique 80−23640
moire topography for 3-D shape meas., opto-electronic processing technique 79−86146
multicoordinate measurements, correction for bending of feelers *(German)* 79−49197
neutron radiography accurate dimensional meas. 78−60926
object dimension meas. by computer-controlled laser beam scanning 79−98431
object geometric param. single meas. in image linear space quantification, random error calc. *(Russian)* 77−37838
optical fibre, elliptical, unclad, ellipticity meas. 77−14797
optical fibre dimensional nonuniformity, automatic measuring techniques *(Japanese)* 78−37982
optical fibres, preformed rods, automatic nondestructive dimensional nonuniformity meas. 79−18541

spatial variables measurement continued
optical fibres, single-mode and multimode, automatic geometric meas. 79−36988
orientation determ. of unstabilized slightly perturbed satellite 78−69642
particle porosimetry by inverse gel permeation chromatography 77−90659
physical objects, instruments, types characteristics *(German)* 77−75702
polymer film, dimensional changes meas. using stroboscopic-disk tester 79−17386
pore size in porous and microporous materials, resonant ion beam backscatt. method 79−2747
powders, surface area, meas. by Monosorb surface-area analyser using Brunauer-Emmett-Teller eqn., reproducibility 80−36979
precision measurement, image analysis of precison components *(German)* 80−42193
precison measuring table with hollow rotor asynchronous motor, digital control system 80−105607
production process linear dimensions, contactless digital system appl. *(Polish)* 78−93652
profile, using electro-optical instrument 79−21701
projection microscope measurement gauge 77−5904
rectilinearity measurement, laser transit prototype parameter optimisation 79−76745
shape factors in space thermodynamics, determ. using shape factormeter *(German)* 78−73610
sighting telescope and autocollimator, general-purpose optical string 79−81510
silicone elastomers, for teeth impressions, holographic interferometric meas. of dimens. variations 79−94195
sonic laser radiation detector *(Polish)* 79−85113
spacecraft trajectory meas. errors, motion parameters estimation 77−29633
spacecraft trajectory meas. process optimisation, visibility limitations 77−29632
stereophotogrammetry, meas. of deforms. in human body *(Croatian)* 80−108997
stereophotogrammetry of objects at close range, integral photography method 77−61148
straight line meas. using laser, LINOMETER *(German)* 77−87727
straightness, varifocal moire zone plates 77−88902
straightness meas. using laser beam as reference line *(German)* 77−87726
surface defects in metals estimation, Rayleigh wave scattering technique *(French)* 80−55612
surface structure and dimensions, using laser beam, Selcom System 1000 *(Swedish)* 78−63402
surface tables, maintenance, positioning, and possible sources of error 78−93651
telemetry system, totally implantable, for dimensions meas., animal physiological research 80−67294
thread parameters meas., Fraunhofer diffr. coherent optics method 78−89439
threaded article parameter measurement by spatial spectra analysis 79−30409
three-coordinate measuring machine, dynamic acquisition and automatic reduction of data 79−75507
three-dimensional measurement on image reconstructed by holographic process 78−58958
three-dimensional shapes, scanning Moire method, automatic meas. *(Japanese)* 78−77865
transparent fibre, geometrical parameter meas., laser method 77−18062
two-coordinate measuring device calibration, interference band-object scanning and precision gauge block *(German)* 78−89433
two-coordinate measuring microscope, supplementary unit 79−75588
two-coordinates measuring microscope, ZKM 02-250 79−75587
US shadow immersion exam. of defects, dimension determ., error anal. 78−44305
water depth measurement using airborne pulsed Ne laser system 80−61908
AgBr microcrystals in dispersed photographic emulsions, dimens. determ., specific turbidity method *(Russian)* 79−26027
Al, anodic oxide film, porosity determ. by pore filling method 79−47848

speakers *see loudspeakers*

special purpose computers
see also digital differential analysers; process computers
algorithms and data structs. for array processing 80−83530
biomedical computer, low cost 78−36045
Fourier analyser system for vibrs., shock and noise 77−68335
heart rate on-line statistical anal. 78−35984
horological microprocessor, design and circuit architecture, functions *(French)* 80−90822
nuclear medicine, buyer's guide to current performance and future promise 78−48883
pulmonary measurement system, HP model 47804A 80−36163
real-time computer for first- and second-order Wiener kernels 79−12046
scientific calculating system with number-oriented microprocessor 78−36983
wave data analyser system for buoys 77−5362

special relativity
see also Lorentz transformation
ψ collapse and locality 80−372
A-topology for Minkowski space 79−92933
Abraham-Minkowski controversy, EM momentum in static fields, teaching 80−101678
absolute space, soln. 79−58514
accelerated observer, proper reference frame and local coords. 78−42
accelerated observer with rotating tetrad 79−80430
additivity, rapidity, relativity, teaching 80−41984
advanced solutions of relativistic eqns., interpretation as antiobjects 77−26170
aether drift experiments, nonuniformity of background radiation 78−93482
anholonomic frames, relativistic rot. 77−49592
appearance of objects moving at relativistic speeds, computer programs 78−12484
approximately relativistic Lagrangians for classical interacting point particles 78−54179
arbitrary moving frames of reference 80−98797
arithmetic basis, force law 77−74220
arithmetic basis, numerical eqns. computer solvable 77−57185

special relativity continued
artificial satellite tracking, relativistic Doppler shift meas. 80−46951
atomic clocks and relativity theory *(Hungarian)* 77−67277
ballistic theory of light based on EM force laws and Newtonian mechanics 80−50
bounded velocity postulate for special relativity 79−53972
bradyons and tachyons, unified approach by conformal transformations 77−67282
broken Lorentz invariance and conventionality of clock synchronization 79−63030
Caldirola equations, generalised, for classically radiating electron 77−82401
causal interpretation of quantum mech., superluminal propag. of quantum pot. 79−40400
causal unification of relativity, gravitation and quantum mechs. 77−33923
causality, comparison with substratum theory, Lorentz transforms. 77−57184
causality, problems in theory of tachyons 78−28945
causality for tachyons in macrophysics, extended relativity 77−22411
causality for tachyons in macroscopic processes 77−2542
causality laws, violation with tachyon discovery, book contrib. 79−44720
causality problems in special relativity, tachyons in an expanding universe 79−67155
causality recovered for tachyons 77−82387
causality recovery in special relativity for tachyons 78−73843
causality violation in controlled creation and absorpt. of tachyons 77−22413
causally connected events, obs., means of perception 78−28944
charged particles in external fields, classical Dirac, Klein-Gordon eqns. 77−49829
Cherenkov losses of relativistic neutron in conducting medium 78−5410
Christoffel symbols and inertia 77−64946
circular motion for a time-asymmetric relativistic two-body problem 79−75336
classical charged particles with spin 78−65790
classical interacting fields, virial theorem and stability of localised solns. 78−21342
classical null strings, free Nambu strings 78−12560
classical predictive dynamics of two charges with radiation 79−88817
classical predictive electrodynamics, energy and 3-momentum balance and scatt. cross sections 79−88818
classical relativistic particles, presymmetry, Fermi-Walker transport 79−12593
classical special relativity mechanics, classical particles with unusual props. 80−77615
classical tachyon theory, appl. of quasi-catastrophe theory, imaginary units 77−22414
clock paradox, conventionality of simultaneity 77−74222
clock problem, perception and meas. by accelerated observer 78−4482
clock rates (undergraduate level) 77−22404
clock retardation, absolute space, and special relativity 79−67156
clock signal, light signal synchronisation, one-way light velocity meas. 80−42055
clock synchronisation, distant simultaneity 80−27125
clock synchronisation for VLBI, influence of relativity theory *(Russian)* 77−5664
clock synchronisation in uniformly rotating frame, one way speed of light 79−49034
clock synchronisations comparison, first order tests of special relativity 78−44
clock synchronization in a rotating frame 79−49037
collisionless plasma, current responses of all orders 79−90449
common time in a four-dimensional symmetry framework 80−52016
complex potential equations, special relativity, and complexified Minkowski space-time 80−52018
Compton effect, analogy to reflection from moving mirror 78−82218
conducting sphere, rot. in mag. field relativistic, co-rot. frame 79−53714
conformal relativity, bare mass theory 80−27417
conformal relativity, unified description of bradyons and tachyons based on dynamical SO(4,2) 77−67352
consistency of postulates, comment on recent paper 77−9883
continuity equations, for transverse multipole amplitudes, EM and gravitational fields 79−58609
coordinate conventionalism 77−60930
coordinate transformation formulas for massive reference frame 80−90673
coordinate transformations of the absolute space-time theory 79−67157
cosmological objects in nonradial motion, redshifts, special and general relativistic anal. 79−80212
Coulomb law and relativity theory in electromagnetism, Horak method approach *(Polish)* 78−13639
coupled inertial and gravitational effects in the proper reference frame of an accelerated rotating observer 79−93007
covariant formalism for a relativistic string in a constant homogeneous electromagnetic field 79−21546
covariant representation of the causal logic 79−97235
CPT invariance, quantum mechanical interpretation 80−105805
creation and gnosiological lessons 80−98780
crystal, spherical integral reps. for cond. of abruptly activated current 80−42080
crystal optics, relativistic phenomena 80−46839
cube moving at relativistic speed, two-dimens. appearance 79−97142
de Broglie wave, relativistic Doppler shift for teaching 78−49613
deformable media, electrodynamics, relativistic field equations 78−49678
derivations, without Einstein's second postulate *(Russian)* 77−30009
didactical challenge for the future *(German)* 80−101714
didactical treatment, use of the invariancy of the Maxwell eqns. for vacuum 78−81835
dilatational degree of freedom, six-dimensional space V_6 80−57088
discrete space-time and fundamental length 80−27122
discrete special relativity, bases 77−71208
discrete spectrum of singular velocities 78−8239
distant synchrony and the one-way velocity of light, thesis of conventionality 79−67153
Doppler effect, for teaching 78−24609
Doppler effect, relativistic dynamics, teaching 79−97164
Doppler effect 80−82637
Doppler effect expt. to test special relativity 78−20963
Doppler redshifts in oblique approach of source and observer, for teaching 79−58475

special relativity continued
dynamics of continuum in generic motion, action of volume and surface forces, second cardinal equation of dynamics 80−31501
education, acoustical second-order Doppler effect, introductory expt. for special relativity 78−49584
education, Bohr-Einstein weighing of energy debate, time and gravity 79−97152
education, gauge invariance, analogy with relativity, particle internal symmetry 78−49595
education, moving vertical line, apparent appearance for v>c, v=c and v>c 78−69935
education, radar echo Doppler shift formula by wave superposition, appl. special relativity transformation props. 79−97147
education, relativistic statics, covariant formulation 78−49593
education, rotations, Lorentz transformations, and arbitrary axes 79−97155
education, simplified relativistic force transformation equation 79−25791
education Einstein's principle of equivalence, source of confusion 77−45646
educational course, for general students 78−73791
Einstein, light quanta, radiation, relativity in 1905 77−31
Einstein's 1907 essay, discussion 78−12454
Einstein's 1907 essay-translation 77−87619
Einstein's 1907 paper, retranslation 77−71173
Einstein's contribution to development of science *(Russian)* 79−84926
Einstein's first paper, retranslation, comments 77−33811
Einstein's relativity paper (1905) and the electromagnetic world picture 78−16616
Einstein's second postulate 77−2
Einstein's special relativity and Pauli's exclusion principle, verification within a hadron 78−89655
Einstein's spectral relativity, Lorentz's rod contraction-clock retardation ether theory, possible equivalence 78−49654
Einstein's velocity addition theorem using invariant double ratio 78−36822
Einstein postulates, inconsistency, comment 77−41476
Einstein postulates, inconsistency, comment 77−41477
Einstein postulates, inconsistency, comment 77−41478
Einstein postulates, inconsistency, reply to comments 77−41479
Einstein relativistic two-particle systems 78−41152
Einstein simultaneity, meas. methods 79−8
Einstein theory in relation to Newton and Maxwell *(Norwegian)* 80−27119
Einstein-Podolsky-Rosen paradox, causal superluminal interpretation 80−45
Einsteinian vel. addition and phase vel. 78−16665
elasticity of dissipative media, wave propagation modes 78−4485
electrodynamics of moving bodies, nonequivalency of 'right' and 'left' 79−25841
electrodynamics of moving media, drag effect involving dispersion term *(Chinese)* 78−12558
electron beam, relativistic, fields excited near plane magnetoedielectric slab 80−18986
electron charge and velocity, independence limit, atomic neutrality 79−97549
electron currents in vac. relativistic generalisation of Child/Langmuirs laws *(German)* 78−36843
electron rest energy, using X-ray photoelectron spectrometer, student expt. 79−25802
elementary particle theory, relativistic centre of mass of extended particle with interacting constituents 79−17701
EM contributions to energy-momentum tensor 80−105495
EM induction law from view point of relativistic mechanics *(German)* 79−41287
EM permeability of vac. and light-cone structure 80−36879
EM plane wave propagation in moving dielectrics, contradiction with Einsteinian addition of velocities, geometric resolution 78−24673
EM propagation between physical source and constant vel. receiver in vacuo 80−105502
EM radiation from accelerated charge 80−31497
EM tachyon, prep. of three-dimens. superluminal light spot in vacuum 80−42058
EM theory based on additive light velocity and gaseous ether theories 80−51
EM wave dispersion equations in moving media, relativistic electrodynamics 80−57089
EM wave propag., birefringence in moving anisotropic media 79−80432
energy flow velocity, rel. to energy momentum tensor, for teachers 79−21498
equations of motion and radiation reaction 80−73232
equipartition theorem generalisation, for teaching 78−49603
equivalence principle, quantification relationships 79−25842
ether as a neutrino sea 77−53728
ether as neutrino sea, materialistic basis for physical explanation 77−53729
ether drift, historical review 80−49
ether drift expt., magnetic shielding of low temp. torsion pendulum 79−88988
ether drift expts., using coupled mirrors interferometer 80−22193
ether theory, relativistic formula for Doppler effect *(French)* 80−105494
ether wind first-order expt. with stabilised lasers 77−5665
ether-relativity polemic, nominalism and realism 80−42110
excitable ether composed of neutrinos, anomalous structural interactions explained 77−53730
experimental test from high-γ electron g-2 meas. 79−58540
experimental test recently proposed, criticism 77−22408
experimental verification of special relativity 78−57777
extended relativity, absorpt. of tachyons 78−32672
extended relativity, macroscopic tachyons absorpt., paradoxes 77−57188
extended relativity, T-violation and new particle 80−37182
extended theory, introduction to extended projective and conformal relativities 79−21547
faceless linear cones, orders, gauge, and distance, appl. to continuum mechanics and special relativity 78−57753
faster than light phenomena in special and general relativity, book contrib. 79−44817
faster than light processes, causality 77−54061
Feshbach-Villars transformation, bosons, fermions 77−87647
fibre bundles and relativity principles 80−8783

special relativity continued
field theory, interpretation of advanced solns., relativistic eqns. 77−22410
first-order effects, test by measuring electric field inside rotating electric screen 80−46796
fluid system, electric conduction in relativistic thermodynamics 80−105498
forces and accelerations, directional relationships 79−63028
foundational problems, philosophical aspects 80−12906
free particle in special relativity, state-ket formulae 77−41480
fundamentals of relativity, general, special and cosmological, book 78−29007
g-2 experiments as a test of special relativity 79−58539
g-2 experiments as special relativity tests 80−52019
gas, arbitrarily moving, discontinuities propagation 78−73842
gedankanexperiment, special relativity and the ether 77−82360
general Sagnac effect, ring laser and interferometer study of accelerated systems 80−4520
geometry conventionality and the ontology of special relativity 80−4521
gravitation, gauge theory, special relativistic limit 80−22256
gravitational compression of a body within the approximation of the special theory of relativity 80−4611
gravitational mass change in two point charges system, for teaching 79−35460
gravitational Michelson-Morley expt., proposed, experimental and Schwarzchild metrics, black holes 79−97289
gravitational time dilation according to absolute space-time theory 77−43
gravity mass invariance 78−57778
Hamiltonian formulation for an extended particle with interacting constituents 79−63022
harmonic oscillators, relativistic two-body interaction, exactly soluble system 78−16955
historical background *(Hungarian)* 77−22407
history, Einstein's theory of relativity and Lorentz's theory compared 77−3
Huygens' principle and Broglian waves *(French)* 79−21545
impulse equilibrium correction in continuum Ott's transformation *(Hungarian)* 77−74223
inertial navigation equations based on relativistic effects 77−67276
infinite diffusion velocity and causality in special relativity 79−63027
isotropy of space, improved laser test 79−30229
joint distributions and tachyons 79−58541
k-calculus approach and the generalized Lorentz transformations 79−17212
Kennedy-Thorndike expt., Lorentz-transformation validity 77−78975
Kennedy-Thorndike expt., on Janossy's interpretation 77−78976
Kerr source, energy extraction by tachyon injection 79−48844
kinematics and dynamics of faster than light motions *(Russian)* 79−71247
Klein Gordon equation, propag. of solns. with arbitrary complex mass 79−21924
Klein-Gordon eqn. with step nonlinearity, jetlike solutions 80−17813
Lagrangian for a system of charged particles to higher-order terms 79−97219
laser experiment verifying Special Theory of Relativity 80−27118
length contraction and time dilatation, de Broglie waves explanation 77−60932
length paradox in three dimens., for teachers 78−62015
Lewis-Tolman paradox, soln. in relativistic states 80−86083
Lie algebras associated with classical relativistic planar motion in axisymmetric EM fields 79−49064
Lienard-Wiechert eqns., rel. to electron mass *(Spanish)* 80−82654
light Doppler effect, absolute spacetime theory 78−69979
light induced mechanical effects connected with Fresnel coeffs. of drag 80−32908
light power, relativistic transformations 79−84887
light propagation, a ballistic theory 80−4524
light propagation in Earth rotating frame, time discontinuity obs. in clock synchronisation 77−60333
light reflection from transversely moving mirror, attempt to find freq. shift 77−30006
light signals on closed path, relativistic expts. 80−82645
light velocity in vacuum, quantised space, special relativity and relativistic field theories 80−82869
light velocity meas., Marinov's expt. 78−32673
light velocity measurement, one-way, and light signal synchronisation 80−82644
light-like motions of particles in gravitational fields 78−4480
linearity postulate of the 'special theory' of 1905, 1907 79−97195
linearity postulate of the 'special theory' of 1905, 1907 80−105503
Lobachevskii space vector and relativistic kinematics 78−62076
locally anisotropic space-time, motion group and metric 77−67278
Lorentz and Einstein theories, experimental indistinguishability 77−45695
Lorentz covariance test and relativity of simultaneity, one way light velocity 79−2625
Lorentz groups, homogeneous and inhomogeneous, teaching method to illustrate difference 80−17766
Lorentz invariant clock 77−37755
Lorentz transformations, derivation by Ives, review 80−4523
Lorentz-invariant Newtonian mechanics, kinematic const. nonexist. 77−74216
low velocity motion, further problems of special relativity 79−67152
magnetospheric ether-drag theory and the reference frames of relativistic physics 80−12905
Marinov absolute space, velocity aberrational test method 80−82646
Marinov coupled mirrors expt., a critique, preferred cosmological reference frame 80−27120
mass and momentum density transform. 77−30005
mass velocity dependence without momentum principle, for teaching 78−24613
massive reference system, transform. of coords. *(Russian)* 78−65769
Maxwell equations covariance, comparison of electrodynamic systems 77−87680
measurement standards and structure of physical knowledge 77−74347
measuring instrument readings depend on massive reference system 80−73171
mechanics and electrodynamics, Euclidean space, Galileo transformation 80−62467

special relativity continued
mechanics and electrodynamics in theory with locally anisotropic space-time 77−67279
Michelson experiment seen 90 years after first execution *(Italian)* 79−17175
Michelson-Morley and Kennedy-Thorndike expts., logical equivalence 79−88801
Michelson-Morley experiment, history of physics, role in education 80−8759
Michelson-Morley experiment, modern version *(French)* 80−12904
microcosm and macrocosm, discrete modelling 80−82643
minimum measurable intervals and classical mechanics 80−90668
Minkowski space and special relativity rel. to Brownian motion *(French)* 77−67377
monatomic gas, propagation eigenmodes, Marle's 14-moment description 77−27626
moving target for coherent radiation test of k-factor of Bondi's calculus 79−75435
Nambu mechanics, reln. to Lagrange, and Hamilton-Dirac mechanics 78−54180
neo-Lorentzian relativity of G. Builder, review 80−46
neutron interferometer, rotating, phase shift due to Doppler effect 80−18006
Newton-Huygens problem of circular rotation 80−105501
Newtonian force and EM field, relativistic transformations, for teaching 78−49601
non Euclideans Lorentz transformations and special relativity 79−97194
nonequatorial tachyon trajectories in Kerr spacetime, and second law of black hole phys. 79−71244
noninertial acceleration of observers, equivalence relations 79−97193
noninertial frames, cotangent bundle approach, Lie derivative 80−62468
noninertial systems, new synchronisation procedure 79−53975
noninertial systems, new test of synchronization procedure, comment 79−53974
noninertial systems, synchronization of clocks 78−24665
nonparallel force-acceleration paradox, negative acceleration component 77−13547
nonrelativistic transformations giving invariant Maxwell's EM theory laws 78−77738
null hyperspace initial data 80−101740
ondulatory radiation sources, theory and appl. 80−37947
one way velocity of light, anisotropic effect detection using stellar aberration 80−86081
optical tests, second order 78−20964
Ott relativistic temperature variation, comment on derivation 80−86084
paradox on frequencies of light emitted by hydrogen 77−49530
paradoxes, cardinal equations of dynamics 80−12903
parallel velocities, addition, theory 77−67274
particle decay in six-dimensional relativity 80−27121
particle dynamics 78−93529
particle moving in external field, eqns. of motion *(Russian)* 77−45690
particle moving in gravitational field, eqns. of motion *(Russian)* 77−45691
particle spectra line shapes after γ emission in flight 78−41665
particle speed when approaching Schwarzschild metric 78−57776
path-dependent Lagrangians in relativistic electrodynamics 80−90670
phase locked cavities as particle models 78−77705
photon-tachyon interactions and the isotropic photon flux 80−446
physical nonexistence of signals going backwards in time 80−42094
plane EM waves, relativistic invariance of complex phase 77−37764
plasma, magnetised Vlasov-Maxwell plasma, current responses 79−90450
Poincare discovery?, discussion *(Hungarian)* 79−80431
Poincare generators, timelike, spacelike and lightlike realisations 78−86150
Poincare transformations and Galilei transformations 78−69981
point particle description 79−63026
position operators, systems exhibiting special relativistic relation between momentum and vel. 78−89335
postulate consistency, reply to recent paper 77−9900
probabilistic anal. of unification of quantum theory and relativity 78−86176
projective relativity based on De Sitter universe 77−41423
projective space-time, geom. of (N+1) particle system 77−7422i
proper time and eqn. of motion for particle 77−67280
protophysics of time and relativity principle 77−67176
pulsar models, relativistic clock error effects 77−64786
pulsars, superfluid liquid rotation, theory, relativistic effects in vortices *(Russian)* 78−61876
quantum field theoretical study of tachyons, book contrib. 79−58887
quantum kinematics on stochastic phase spaces for massive particles 79−2648
quantum mechanics of relativistic spinless particles 79−17255
quantum theory and special relativity 77−26192
quasars redshifts, relativistic Doppler formula rel. to transverse vels. and distances *(Chinese)* 80−105379
quasi-Newtonian interpretation of special relativistic dynamics 80−4519
quaternion quantum mechanics as the description of tachyons and quarks 79−30273
radiating electron, stability of motion 78−65789
radiation from a uniformly accelerated charge 80−31495
radiation temperature of moving bodies *(German)* 77−37830
radiation temperature of moving bodies 78−57775
radiation with spin, minimum size using special relativistic centroid theorem 78−69995
radiative transfer, comoving-frame transfer eqn. soln. in spherically symmetric relativistic flows 80−82181
Ramakrishnan's approach, velocity addition theorem 79−71242
reducible relativistic wave eqns. 79−45003
reference frames and the velocity of light, book contrib. 79−58542
reflection and elastic scatt., Compton scatt. and special relativity 80−46756
reflection from a corner reflector moving at high velocity 79−30228
relative simultaneity; empirical determ. 78−16642
relative simultaneity 80−27126
relativistic continuum thermodynamics, dynamical approach 79−58661
relativistic contraction of moving bodies 77−13605
relativistic ether hypothesis, generalised Galilean transformations 80−86085
relativistic field eqns., two-soliton solns. 78−74124
relativistic invariance in classical limit 79−21586
relativistic Lagrangian with variable mass *(French)* 77−9882
special relativity continued
relativistic magneto thermo viscoelastic medium, effect of mag. and thermal fields on plane wave propag. 79−2637
relativistic particles in EM field, conservation of angular momentum 80−48129
relativistic quantum mechanics, space-time formalism for spin-zero particles 79−21974
relativistic quantum theory, space-time states, book contrib. 79−58886
relativistic synchronization procedures, geophysical tests in rotating frame 78−24662
relativistic thermodynamics, temp. transforms., invariance and meas. 79−92935
relativistic two-body electrodynamics 78−54112
relativity principle verification by new Michelson-Morley expt. in Space Lab 80−27124
rest frames for tachyons and photons 77−60928
restricted relativity in a space-like region 79−30225
restricted relativity theory, vel. of light postulate 78−41153
retrocausation and formal assimilation of classical electrodynamics to Newtonian mechanics 79−97175
retrocausation in classical electrodynamics 79−97174
Riemannian metric description, of gravit. and EM interactions 78−36904
rigidily connected accelerated clocks, teaching approach 79−58487
rigidity and indeformability, new theoretical concept *(Spanish)* 79−80429
rotating disc experiments, absolute space-time theory 78−36823
rotating disc expt., second-order effects 77−60933
rotating disc with ang. accel. 79−67154
rotating disk, uniform motion without tangential strain 80−82641
rotating disk problem 80−82640
rotating frames, generalised theory 80−57086
rotating frames anal. 78−36824
rotating system, cylindrical cardboard model, teaching 79−44661
rotating systems, ang. velocity anal. 77−78977
rotational motion in special relativity 77−45692
rotations in space-time 79−97190
scalar potential inter-relation between non-relativistic and relativistic wave eqns. 78−58110
second postulate of Einstein's theory of special relativity 80−90669
simple waves, shock damping and entropy prod. 77−17725
simultaneity, distant, conventionality, standard synchronisation 80−77612
simultaneity and clock synchronization, test theory of special relativity 78−43
simultaneity and conventionality 77−53778
sine-Gordon breather soliton dynamics, rel. to special relativity 80−46801
singular speeds in special relativity, group hypothesis 78−49655
six-dimensional, centre-of-mass frames of pairs of particles, bradyons, luxons, tachyons 80−77614
six-dimensional space-time theory, experimental tests 79−58538
solid angle, relativistic transformation, teaching 80−101683
sound propagation, influence of relaxation phenomenon *(French)* 77−37754
space isotropy test, special relativity, laser version of Michelson-Morley expt. 80−52021
space-time models causal foundations *(Russian)* 77−37759
space-time operators, quantum mechanics incompatibility in special relativity 79−12592
space-time relationship generalisation to cover small velocities of motion 79−30224
space-time structure operational anal. in quantum-relativistic theory 77−67322
space-time test theory, dynamical aspects 80−17798
spacetime, elementary axiomatisation, particle, signal, transmission, reception concepts 78−70044
spatially dispersive media, generalised Kramers-Kronig formula, vac. polarisation tensor 77−17798
speed of light independence of source vel. extraterrestrial test 78−8241
spin-2 field theory of gravity, locally Lorentz invariant 77−5725
spin-s tachyons and tachyon wave propag., book contrib. 79−58890
spinless particle, point form of quantum dynamics and 4-vector coord. operator 79−17213
spinning tachyons as particle constituents, free spinning point particle theory 78−41155
starfield, appearance from relativistic spaceship, nonexistence of 'starbow' 79−62955
statics, synchronous formulation 77−87648
statistical mechanics of relativistic gas in thermal equilibrium 77−58830
steady rotation about fixed axis in relativity 79−9106
Stephenson-Sanduleak 433, nature, special relativistic effects, binary model 79−88679
subluminal and superluminal transformations in six dimens. special relativity 78−41154
superluminal and subluminal causal transformations through transformations of metrics 78−28943
superluminal antimesons in 1955 antiproton-discovering time-of-flight expt.? 79−67158
superluminal bodies, apparent dimensions and apparent velocity 77−78978
superluminal communication through wave function collapse in quantum theory 80−27166
superluminal frames and tachyons, introductory view, book contrib. 79−44719
superluminal frames and tachyons 79−58543
superluminal particles and rods, visual appearance 78−89334
superluminal phenomena and frames in special and general relativity 78−36825
superluminal relative velocities, thought expts., tachyon Cherenkov radiation 77−57186
superluminal transformations 78−8240
superluminal velocities in extragalactic radiosources, review 77−78882
superluminal wave propagation, causality criteria 78−73861
superluminous velocity 79−75335
surface currents induced by perpendicularly incident point charges, anal. *(German)* 77−42461
symmetries revealed through rewritten transform. formulas 78−77704
symplectic formulation of relativistic particle dynamics 77−57237
synchronization in special relativity and related theories 79−71243
Synge's triads of null rays 80−73146

special relativity continued
tachyon, field model, Lee-like *(Korean)* 78−50058
tachyon and tardyon causal and noncausal wave propag. 77−49593
tachyon classical field theory 77−64949
tachyon quasi-catastrophe theory, tachyon existence, imaginaries, and causality, book contrib. 79−44815
tachyon theory, information flow, causality 78−82261
tachyon theory, information flow, causality 79−9429
tachyon universe, open time-symm. model, momentum flux, press. 78−86153
tachyon wave propag. and spin-s tachyons, book contrib. 79−58891
tachyons, absence in supergravity and classical Einstein gravity 79−67208
tachyons, causality, recovery in macrophysics 77−26172
tachyons, causality in macrophysics, paradoxes, extended relativity theory 77−22406
tachyons, causality violation 77−22412
tachyons, charged, Cherenkov radiation in vac. 77−57210
tachyons, charged extended EM radiation, collison with neutral particles 80−4522
tachyons, classical theory of Recami and Mignani, rigorous approach, formal proof 77−26171
tachyons, complex physical quantities and space-like states, book contrib. 79−44723
tachyons, direction of light emission 77−33862
tachyons, electromagnetic and hadronic props. 79−44721
tachyons, emission and absorpt. in six dimensional relativity 80−31502
tachyons, free falling body in field of black hole 77−78816
tachyons, Lorentz group and relativistic semigroup *(Russian)* 77−82386
tachyons, monopoles and related topics, book 79−44718
tachyons, quaternionic formulation superluminal transformation, in complex space-time 79−53973
tachyons, search for preferred frame of reference, book contrib. 79−44722
tachyons, spinless, propagator determ. 77−74263
tachyons and bradyons, unified description using dynamical SO(4,2) symmetry, book contrib. 79−44834
tachyons and causal paradoxes, reinterpretation principle 79−84949
tachyons and magnetic monopoles in the de Sitter universe, book contrib. 79−44726
tachyons in field theories, conventional treatment book contrib. 79−58888
tachyons interaction with gravity, rel. to cosmology and black holes 79−25839
tachyons without paradoxes 77−60931
teaching, developments and changes 80−8758
teaching, event method 80−31450
teaching, secondary-school course not relying on historical approach 78−86096
teaching approaches 77−33810
teaching course 79−21483
temperature, special relativistic transformation thought expt. 80−86086
tensor formulation, dual observers 77−22405
test, macroscopic and local, Stokes-Planck theory discriminated from special relativity, length contraction measurement 80−46797
testing by light reflection from moving corner reflector, Doppler effect 77−37758
theory, derivation of two variants *(Russian)* 78−49657
theory of motion, electromagnetism, gravitation 80−105500
thermodynamic implications 80−47003
thermodynamic quantities, Voigt-Palacios-Gordon transformations 77−9970
thermodynamics and hydrodynamics, time conventions effect on fundamental eqns. 77−67275
Thomas precession, new simple deduction 77−67281
three dimensional time eqn. 79−92934
three time dimensions, use in relativity 80−68042
three-dimensional time, expt. test 80−105499
time, the concept in physics 78−28946
time, uniform scale in astronomy rel. to relativity and Ephemeris time 77−53402
time analysis, universal and relativistic time 79−30299
time and frequency, conf., Helsinki, Finland (Aug. 1978) 80−46728
time as three dimensional vector, arguments against the hypothesis 80−12901
time dilation, fivefold hypothetical struct., review 79−25840
time dilation, verification of time transformation at $\gamma \sim 29.3$, in $\mu^{\pm}$ CERN storage ring 79−45088
time dilation and twin paradox, intuitive understanding, for teaching 78−86093
time dilation meas. for relativistic muons 77−71210
time quantisation, discrete space-time model 78−20999
time scales and signal transmission, relativistic effects 80−46802
time signal transmission by radio, Einstein's theory 78−86154
time spending and space exploring 80−90671
time varying inhomogeneous media, space-time considerations for Doppler effects 78−20965
topology, propagation of surfaces of weak discontinuity, broken extremals in classical field theory 78−93541
transformation formulae with discrete spectrum of singular velocities 79−97189
transformations, superluminal and subluminal 77−74224
transformations between inertial and rotating frames of reference 79−84950
transient relativistic thermodynamics and kinetic theory 79−17330
transport equation for discontinuity wave amplitude, quasi-linear hyperbolic system *(French)* 80−90667
transverse contractions of moving bodies 78−69980
twin paradox teaching 80−105465
two body correlations through tachyon exchange 80−42367
two point charge system, electrostatic pot. energy and inertial mass change 78−54116
two-body interaction with radiation damping 77−30022
two-body problem, initial segment problem forward and backward extensions 79−71241
ultrabaric matter, must it be superluminal 80−17796
ultrahigh velocities in special relativity, superspace concept 79−88802
ultrarelativistic electron bunch in free space, lateral spreading 80−53196
ultrarelativistic particle channelling in crystal lattice *(Russian)* 79−30690
special relativity continued
ultrarelativistic particles, Lorentz factor determ. by ionisation loss 79−35551
unified approach to bradyons and tachyons by conformal transformations 77−60934
unified model for description of subluminal and superluminal objects 78−73845
unitary group representations, appl., book 79−30198
vacuum instability, tachyon existence 77−9884
variations in light velocity due to motion of earth 78−24666
Vavilov-Cherenkov effect in motion of source with velocity exceeding velocity of light in vacuum *(Russian)* 78−12582
vector constants and their algebras for classical Hamiltonians 79−56
velocity composition laws derivation 80−42056
velocity of light, constancy, four dimens. symm. 78−69978
velocity of light, constancy 78−65768
velocity of light meas. by stable clocks 78−54185
weakly relativistic gas, equilib. distrib. and eqn. of state 79−21649
Wigner elementary particle in external homogeneous field 77−37756
world line conditions for spinning particles, spin orbit forces 80−36844
zero-rest-mass fields, boundary conditions at past null infinity 78−24661
H weak decay rate as Einstein special relativity test 79−2624

specific gravity *see density*

specific gravity measurement *see density measurement*

specific heat
see also Debye temperature; Gruneisen coefficient; specific heat of gases; specific heat of liquids; specific heat of solids
absolute zero, vanishing of specific heat without invoking 3rd law, objections 80−8940
AC calorimeter, computer-controlled, for sp. ht. meas. 79−85142
AC calorimeter, construction and design *(Japanese)* 78−89481
AC calorimetry, appl. *(German)* 77−82518
adiabatic calorimeter for continuous specific heat meas. 800 to 1800K, design and calibration 80−57299
adsorbed gas layers on solid adsorbent, thermodynamics *(Rumanian)* 80−10786
adsorbed monolayer, vibr. contrib. to thermodynamic props. *(French)* 77−4261
Anderson model, asymmetric, perturbation theory, impurity sp. ht. 80−6766
Anderson-localised states, intrastate and interstate interactions 80−20113
anharmonic oscillator, classical, variational method test, sp. ht., elec. susceptibility and oscillation freq. *(Portuguese)* 80−77611
anharmonic oscillator, energy eigenvalues, partition function 79−55321
atomic nuclei, level density rel. to eqn. of state at subnuclear densities 80−77278
biological macromolecules, conformation studied by calorimetry, review 80−97870
biopolymers, reversible unfolding, mol. field theory 79−34479
bolometer, ^{3}He-cooled, low heat capacity, differentiated-structure, performance 79−30544
Bose gas, with anisotropic dispersion laws, phase transitions, sp. ht. and excitons *(Russian)* 77−4229
Bose interacting gas, energy spectrum and specific heat 77−15656
boson system, plane rotator model, Hamiltonian and mol. dynamics 80−52122
C_p/C_v resonance apparatus for physics teaching laboratory 79−84885
calorimeter, adiabatic heat capacity small sample low temp., with automatic data acquisition system 78−12697
charged two-dimensional isotropic Fermi liq., static and dynamical props. 79−19532
classical magnet, random one dimens., thermodynamic quantities 77−48002
classical planar spin model, two-dimens., Monte Carlo study 80−25147
classical spins, linear chain, with random Dzyaloshinski-Moriya interactions, exactly soluble model 79−61118
clusters of atoms, phase transitions, thermodynamics calcs. 77−59096
computer generated phase diagrams 78−83928
confluent singular term for systems with continuous symmetry, crit. amplitude ratio, calc. to order ϵ^2 80−57235
continuous phase transition, universal combination of critical amplitudes from field theory 80−95051
digital automatic thermodynamic enthalpy and specific heat determ. equipment 78−57951
dilatometric determination method 79−86327
DSC curves correction for thermal lag effects, sp. ht. determ. case 80−37035
Earth surface, Heat Capacity Mapping Mission 79−5640
Einstein and the quantum theory, review 80−22237
elastic body, non-negativity of specific heat, rel. to dynamic stability 77−42723
electrically insulating media, heat capacity and thermal cond. from pulsed wire probe meas. 77−41613
electron gas, 2D, intermediate density region 79−60110
electron gas, one-dimens., with backward scatt., soliton Green's functions 78−10386
electron gas, two-dimensional, study in intermediate mag. field 79−60743
energy density fluctuation, at fixed wavevector, max. below T_c 79−69225
epoxy resin ED-5, specific heat during solidification *(Russian)* 78−38816
Fermi systems, disordered in two dimensions, interaction effects 80−75655
fermions, independent, set of systems, depend. of sp. ht. on spectrum fluctuations 77−61010
finite system, order parameter and sp. ht. for epitaxial ordering renormalisation-group calc. 80−17862
fluids interacting with Kihara potential, thermodynamic props. using cell theory with holes *(Spanish)* 77−72400
gas-particle mixture, shock wave structs., particle specific heat effect 78−14072
glass fibre reinforced epoxy, thermal cond., diffusivity and sp. ht., determ. 80−24613
glass transition, soft-sphere model, mol. dynamics study 80−49343
glass-C fibre reinforced epoxy, thermal cond., diffusivity and sp. ht., determ. 80−24613
glycerol, high press. heat capacity and thermal cond. meas. 77−41613
gravothermal catastrophe and negative specific heat of self-gravitating systems 78−93593

specific heat continued
heat capacity evaluation, electrical analogy 79−10453
Heisenberg ferromagnet containing nonmagnetic impurity, local mean spin deviations 77−66236
Heisenberg magnet, relaxation-shape function, specific heat series 78−31036
Heisenberg model, operator formulation of renormalisation transformation 77−59376
Heisenberg open finite chains, mag. and thermodyn. props., temp. dependence 77−72971
Hubbard model, cluster-variation method in two-site approx. at high temp. 80−7071
Hubbard model, single band with infinite repulsion on 2×2×2 lattice, thermodynamic props. 79−87225
humid materials, diffusivity and specific heat, transient temp. changes *(French)* 80−64355
inert gas solid, adsorption of inert gases sp. ht. of adsorbates calc. 77−1302
interstellar dust grains, specific heat rel. to temp. fluctuations 80−26938
inverse problems, numerical method *(Ukrainian)* 79−41560
Ising chain, spin-1, sp. ht. in presence of impurities and mag. field 80−93128
Ising chain of alternating spins of 1/2, and general S, appl. of transfer matrix method 80−80529
Ising lattice, triangular, antiferromag. to ferrimag. transition 77−20522
Ising lattice, two-dimens. finite square, sp. ht. anomaly 80−27230
Ising model, bond-dilute two-dimensional, crit. behaviour 79−8009
Ising model, effective field theory 80−7116
Ising model, exact renormalisation group equations 79−73749
Ising model, ferromag. and antiferromag. in mag. field, new perturbation approach 78−56336
Ising model, one dimensional, with infinite radius of interaction in transverse magnetic field 80−2587
Ising model, random-bond, upper bond to sp. ht. on Nishimori's line 80−71068
Ising model, randomly dilute, crit. and thermodynamic props. 79−8005
Ising model with competing interactions, critical properties and exact results 80−93129
Ising O(2), O(3) and O(4) spin systems, Hamiltonian string-coupling expansions 80−20426
Ising spin glass, three-dimensional mag. correlations 80−103849
Ising system with S=1, thermodynamics, uniaxial anisotropy 79−49173
Ising systems, finite thickness, renormalization-group transformation, real-space 80−15749
Kadanoff lowerbound renormalization transformation for the q-state Potts model 79−44876
laser-flash calorimetry for small sample thermal capacity meas. *(Japanese)* 77−49725
linear chain of classical spins with logarithmic nearest neighbour pair potential 77−36085
liquid isobaric heat capacity, experimental apparatus using stationary flow-through calorimetry *(Russian)* 79−30480
liquid-gas system, scaling equation of state derived from the pseudospinodal 80−44286
localised electronic system, sp. ht., singularity at Anderson-Mott transition 80−34381
low-temperature meas. via adiabatic calorimeter 77−41614
macromolecular systems, statistical thermodynamic analysis, heat capacity function 80−61514
macromolecules, linear, heat capacities, scanning calorimetry meas. 80−61134
measurement, high temp., modulation method, thermal losses compensation 79−85144
measurement, precise method using analogue simulator 77−49721
measurement at low temps., calorimetric and electronic system *(French)* 80−27305
measurement method at arbitrary temp., simple and accurate 78−62202
measurement technique, computer controlled AC calorimetry *(Japanese)* 80−27306
membrane system, closed, vesicular, mechano-chemistry 77−60189
metallic particles, spectrum fluctuations in two-dimens. model, specific heat calc. 77−82447
micellar systems, aqueous, thermochemistry 80−61133
mixed valence impurity model, Fermi liq. theory, Ward identities 80−34401
molecule-molecule reaction, ergodic energy transfer, vibr. quantisation effects 78−85137
molecules, without internal rot., ground state heat capacity and entropy MINDO/3 calc. 78−33450
monolayer on graphite, sp. ht. and u.p., size and steric effects 77−85073
n-component spin system, energy-energy correl. function calc. 80−31697
negative specific heat paradox, astronomical and physical appls. 78−9557
nonlinear thermal diffusion equation, parameter calcs., numerical calcs. *(French)* 78−94584
one dimensional fermion system, thermodynamics by cluster expansions 77−41535
one-dimensional crystal, Debye, Einstein and exact heat capacities, theory 77−68376
one-dimensional system, Bose-Einstein condensation at const. press. 80−22276
one-spin ferromagnet, high temp. series expansion for mag. susceptibility and sp. ht. 80−25148
Potts model, Monte Carlo simulation in three dimens. 80−163
propylene, computer generated phase diagrams 78−83928
pure material, in two-phase solid-liq. melt regime, eqns. 77−55342
random exchange Heisenberg antiferromagnetic chain, exchange-coupled pair model 80−20423
random magnet, Ginzburg-Landau model 78−10704
renormalisation group eqns. and thermodynamic anomalies near tricritical point *(Russian)* 80−13027
renormalisation theory, variational principles 78−73951
spin-one Ising model with bilinear and biquadratic interactions 79−65677
standards choice and certification, for liquids and vapours in 90 to 273.15K range 80−23877
thermophysical measurements, sample shape determ. 79−30457
third law of thermodynamics, vanishing of specific heat at absolute zero 80−73294
triangular and honeycomb lattice gases, order-disorder transitions to 2×2 struct. 80−4674

specific heat continued
triangular lattice, self-avoiding walks 79−40478
tricritical points and thermodynamic quantity singularities, renormalisation group method *(Russian)* 77−69071
turbulent pipe flow, heat transfer, fluid props., var. calcs. 77−27527
two state approximation, for sp. ht. anomalies associated with phase transition 79−26013
two-dimensional Ising system, crossing over to two-dimensional Heisenberg system 80−93123
X-Y model, on linear chain in random fields, thermal props., appl. to praseodymium ethyl sulphate 79−65679
X-Y model, second order Green's function theory 80−54913
XY model, Monte Carlo simulation, phase transition with vortices 77−43799
Ar monolayer adsorbed on graphite basal planes, heat capacity 80−6636
Ar, solid, desorption heat capacity of adsorbed ^{3}He 80−10735
BeCu pressure clamp cell, for low temp. specific heat and magnetisation meas. 80−17956
C fibre reinforced epoxy, thermal cond., diffusivity and sp. ht., determ. 80−24613
Cu-In liquid alloys, heat of form meas. *(Korean)* 77−9116
HSO, thermochem. props. 79−5173
He, adsorbed on graphite, band struct. effects in heat capacity 80−59788
He, thermodynamic props., in range 20 to 1500°C and 1 to 100 bar *(German)* 79−69266
^{3}He, adsorbed monolayers on solid Ne, desorption heat capacity 79−51383
^{3}He film adsorbed on graphite 78−87842
^{3}He monolayer film, adsorbed on Grafoil, phase determ. by sp. ht. meas. 77−11764
^{3}He, specific heat second layer adsorbed on Grafoil 78−87843
^{4}He film, adsorbed on disordered substrate, heat capacity meas. 0.08-1.3K 80−2239
^{4}He films, adsorbed on graphite substrate, layering and thermal cond., heat capacity and vapour press. meas. 79−51386
^{4}He, in Vycor glass, finite size scaling of sp. ht. 79−56015
^{4}He monolayer film, adsorbed on Grafoil, phase determ. by sp. ht. meas. 77−11764
^{4}He submonolayer film adsorbed on Grafoil coated with monolayer Ar, sp. ht. 0.4-4.0K 79−51379
^{4}He-^{3}He film, low temp. heat capacity, ^{3}He surface states 79−51380
Mo, temperature standard reference material, USA National Bureau of Standards 80−47009
Ne, solid, desorption heat capacity of adsorbed ^{4}He 80−10736
UO_2 rate-dependent heat capacity, rel. to fast reactor safety 79−31035

specific heat at constant pressure *see specific heat*

specific heat at constant volume *see specific heat*

specific heat of gases
adsorbed gases, cryostate for sp. ht. meas. 79−58695
air flows in triple point shock configurations, anal. thermodynamics *(Russian)* 79−32569
atmospheric oscillations and Ruchhardt's experiment, theory, for teachers 79−71198
benzene, vapour-flow calorimetry 78−91058
2,3-benzo-1,6-methano(10)-annulene, mol. geom. and gas phase thermodynamic props., minimisation scheme 78−78829
Bose systems, interacting, sp. ht. at low temps. 77−15651
Bose-gas model, dil. hard sphere, calc. of low density atomic H gas props. 80−87194
α,βbromonaphthalenes, thermodynamic functions calcs. 298-1500K 77−31418
caloric function derivation for liquids and gases 80−13017
β-chloronaphthalene, thermodynamic functions calcs. 298-1500K 77−31418
cresols, ideal gas thermodynamic props. 78−75250
diphenyl mixtures, press. depend. at 298K 78−42702
ethane, dense gas and liquid, meas. of C_p and C_v 77−69093
free-electron gas, n-dimens., specific heat and density of states 78−12466
hydrocarbons, thermodynamic props., optimum incremental diagram calc. method *(German)* 78−51702
measurement using transient hot-wire technique 79−200
methane, liq. and gas, mol. dynamics simulation, thermodynamic props., struct. factors, etc. 79−50976
1,6-methano(10)-annulene, mol. geom. and gas phase thermodynamic props., minimisation scheme 78−78829
molar heat capacities, correlation coeffs., data collection 78−85188
phenol, ideal gas thermodynamic props. 78−75250
polyatomic gas viscosity related to Cp and molal vol. 78−34248
real gas version of de Saint Venant and Wantzel gasdynamic formulae *(German)* 79−18974
simple fluid, sp. ht. on liq. branch of coexistence curve, rel. to sp. ht. in gas branch 77−39670
simple fluid near crit. point, homogeneous phase sp. ht. at const. vol. 78−71832
steam-air mixture, condensation, transport and thermodynamic props. *(Japanese)* 78−34251
water vapour, dissociated, thermodynamic props. *(Japanese)* 77−80263
CO, heat capacity, calc. by modified Redlich-Kwong eqn. of state 80−69963
CO_2, specific heat, meas., near crit. point 77−51490
Cs vapour, thermodynamic props. calc. from Joule-Thomson data 78−94886
H_2 occlusion in MoO_3, molar heat content *(French)* 80−45247
H_2, rot. energy, specific heat, temp. depend. determ., demonstration 78−12465
^{4}He, heat capacity of liquids and dense gases at low temps. *(Russian)* 80−65324
K_2SO_4, vaporisation thermodynamics, MHD generation appls. 77−9112
$Mn(CO)_5Cl(Br)(I)$, thermodynamic props. tabulation 79−24808
$Re(CO)_5Cl(Br)(I)$, thermodynamic props. tabulation 79−24808
S_7, Raman and IR spectra, vibr. anal., force consts., thermodynamic functions 78−50545
ScI_3, vaporisation thermodynamics, sublimation and formation 80−54366
$Tc(CO)_5Cl(Br)(I)$, thermodynamic props. tabulation 79−24808
WO_3, force field, normal coord. anal., kinetic consts. method, thermodynamic props. 78−25504
Xe lamp, pulsed, effect of gas heat capacity on characts. 78−42838

specific heat of liquids
acetic acid, liq., sp. ht. of 2nd relax. step *(German)* 79−37766
adiabatic scanning microcalorimeter specific heat capacity meas. of small samples 78−86274
air-water droplet, heat capacity meas. *(Russian)* 80−54395
alcohols, aliphatic, dilute aqueous solns., excess partial molal heat capacities 79−57280
alkali nitrates, molten, pVT data, internal energies, eqn. of state 78−43098
alkali nitrates, molten, thermodynamic study *(French)* 77−31781
aniline, determ. from US velocity meas. *(Japanese)* 77−59068
anthracene, chemical thermodynamic props. 80−21312
aqueous organic binary mixture, pseudophase transition, heat capacity evidence 78−83937
benzene, tables of thermodynamic props. 77−24419
benzene-cyclohexane(carbon tetrachloride), binary liq. mixtures, molar heat capacity isothermal compressibility 79−66328
binary fluids, universal const. R_ξ^+ meas. 80−19952
binary liquid mixtures, nonassociated, thermodynamics 78−18797
binary liquid mixtures, sp. ht., light scatt., two-scale-factor universality 79−42267
binary mixtures, calc. methods 78−63862
biopolymer soln. heat capacity, conformational props. temp. depend. 80−8009
borate glass melts, struct. determ. using graph theory 79−64980
Bose systems, interacting, sp. ht. at low temps. 77−15651
α,βbromonaphthalenes, thermodynamic functions calcs. 298-1500K 77−31418
t-butanol aq. soln., heat capacity anomaly, struct. phase transformation 79−10959
2-butoxyethanol, aq. binary mixture, pseudophase transition, heat capacity evidence 78−83937
t-butyl alcohol, aq. soln. 80−88237
n′-n-butyl-n-methoxyazoxybenzole, specific heat anomaly and isotropic liquid to nematic liquid cryst. transition *(Russian)* 77−62624
calculation method 78−67834
caloric function derivation for liquids and gases 80−13017
calorimetry at high state parameters 78−57953
carbon tetrachloride-benzene(cyclohexane), binary liq. mixtures, molar heat capacity isothermal compressibility 79−66328
CBOOA, US absorpt. and dispersion at nematic-smectic-A transition 79−82287
CBOOA, US attenuation near nematic-smectic A transition 78−87773
ceramic, calc. for solids and liqs. 77−43348
ceramic, high temp. eqn. 77−51510
β-chloronaphthalene, thermodynamic functions calcs. 298-1500K 77−31418
configurational heat capacity, correlation formula, corresponding states method 78−30766
configurational properties near glass transition 78−26662
cryogenic binary mixture, ultrasonic velocity, compressibility, heat capacity, at 298.15K 79−10898
crystallisation, percolation theory, Lindemann melting criterion and thermodynamic props. 79−28081
cyclohexane, determ. from US velocity meas. *(Japanese)* 77−59068
1,2-dichloroethane+benzene(toluene)(p-xylene), liq., molar heat capacities 78−18787
dilatometric determ. of liquid specific heat and thermal expansivity 77−87758
dilatometric method for simultaneous heat capacity and thermal expansion meas. 77−84131
p-dioxane, aq. soln., excess molar heat capacities, 298.15K, US vel. obs. 80−6523
DOBAMBC, specific heat determ., temp. depend. 78−91250
electrolytes and non-electrolytes, aq. soln., apparent molal isochoric heater capacities at 25°C 80−59671
esters, SLC, ferroelectric behaviour, specific heat, spontaneous polarisation 80−75958
ethane, dense gas and liquid, meas. of C_σ and C_v 77−69093
ethane, fluid, saturated, compressed, sound velocity meas., compressibility, sp. ht. determ. 77−76488
ethane, thermophysical props. from 90 to 600K at press. up to 700 bar 77−84940
ethane, use of high press. recycle-flow calorimeter 80−42228
ethanol, config. and vibr. heat capacities, H-bonds 79−99331
ethanol, plural glass-transitions, thermodynamic functions 78−38820
furan, liq., US relax., light scatt. meas. relaxing part of sp. ht. calc. 77−77231
glass-forming melts exam. of isobaric-isothermal pots. in glass transition interval 79−7681
glass-forming systems, structure and thermodynamics *(German)* 80−38924
glycerol, relaxing fluid, thermally induced light scatt., dispersion of sp.ht. 77−32388
p-n-heptyloxybenzylidene-p-aminobenzoic acid, smectic C to nematic transition 79−33076
n-hexane, superheated, thermodynamic props. from ultrasound speed 80−92036
n-hexane, superheated liq., US wave vel., adiabatic compressibility, heat capacity 78−2198
p,n-hexyloxybenzylideneamino-p′-chlorobenzene, liq. cryst., sp. ht. meas. 78−22831
HOAB, liq. cryst. phase transitions, specific ht. meas. 79−33075
hydrocarbon liquid, residual energy and entropy, rel. to liq. and mol. structs. 78−71869
hydrocarbon oils as thermal storage media for solar central power appls., specific heat variations and their economic implications 79−100540
hydrocarbons, saturated open-chain, transport behaviour of excess electrons and props. 80−39643
hydrocarbons, thermodynamic props., optimum incremental diagram calc. method *(German)* 78−51702
Ising model and config. heat capacity 79−33096
laminar convection in vertical tube, thermophysical prop. temp. depend., effects 78−90895
liquid crystals, thermodynamic props. calc. 80−103464
liquid metal, bulk modulus, calc. using press. fluctuation in microcanonical ensemble 80−2106
liquid-glass transition, glass transition depend. on heating and cooling rates 80−79920
MBBA, nematic-isotropic transition, isothermal compressibility and thermal expansion coeff. meas. 79−99301

specific heat of liquids continued
MBBA, specific heat anomaly and isotropic liquid to nematic liquid cryst. transition *(Russian)* 77−62624
measurement using transient hot-wire technique 79−200
mesophase pitch, magnetically-oriented, phys. props., mol. struct. 80−64885
metal, high temp. eqn. 77−51510
metal, interatomic forces and thermodynamic props., hard-sphere model 77−47321
metal, thermal press. coefficients and sp. ht. 79−65207
metal, thermophysical properties meas. by submicrosecond-pulse-heating method 80−52220
metal calc. for solids and liqs. 77−43348
metal halides, calc. for solid and liq. phases 77−43349
metals, heat capacity near melting point, vacancy mechanism of melting 80−10641
metals, radial distrib. function and thermodynamic characts., interparticle interaction pot. *(Russian)* 80−49086
metals, tunnel theory 79−33095
methane, liq. and gas, mol. dynamics simulation, thermodynamic props., struct. factors, etc. 79−50976
methanol-cyclohexane, crit. exponents *(Russian)* 79−77766
mixtures, binary, excess isentropic compressibilities and isochoric heat capacities 80−21313
molecular dynamics simulation, sp. ht., thermal press. coeffs., compressibilities 77−28013
nematic liquid cryst., tricritical behaviour near transition to isotropic fluid *(Russian)* 80−15001
nematic liquid cryst., two-dimensional, Monte Carlo simulation 80−100168
nematic liquid crystals, sp. ht., thermodynamic props. 77−39678
nematic-isotropic phase transition and short range orientational order 77−27832
nitrobenzene-aniline, US vel., sp. ht. and compressibility 79−33037
nitroethane-iso-octane (hexane), crit. exponents *(Russian)* 79−77766
nonelectrolytes, aqueous, excess heat capacity, H bonding 78−3362
nuclear reactor core melt from LOCA, viscosity, thermal cond., specific heat 77−14247
p-n-octadecyloxybenzoic acid, thermal props. 77−47345
octylcyanobiphenyl, crit. heat. capacity near nematic-smectic A transition 80−100323
octyloxycyanobiphenyl, nematic-smectic A transition, heat capacity study 80−88033
octyloxycyanobiphenyl, nematic-smectic-A transition sp. ht. 79−42225
organic compounds, enthalpies and related thermodynamic functions 79−42276
organic compounds, partial molar heat capacities, in aq. solns., additivity schemes calcs. 78−22861
oxtyloxycyanobiphenyl, nematic-smectic-A transition, high-resolution 80−10649
4-n- pentyl-phenylthiol-4′-alkoxybenzoate, homologous series, specific heat meas., nematic-smectic-A tricritical point 80−15227
4-n-pentylphenylthiol-4′-n-octyloxybenzoate, sp. ht. and crit. behaviour of liq. cryst. phases 78−67816
perfluoromethylcyclohexane-tetrachloromethane, specific heat temp. depend., critical composition mixture near critical temp. 78−26689
phase transition and critical phenomena in fluids, low gravity expts. 77−39658
phenanthrene, chemical thermodynamic props. 80−21312
polymer solution, aqueous, meas. of thermal props. 77−51555
polymers, specific heat, conform. effects 80−24607
polymethylsiloxane-2, liq., thermodynamic props. at high press., US propag. meas. *(Russian)* 80−65157
potassium oxyacid salts, aq. electrolytes, apparent molar heat capacities and vols. 79−23744
propane, saturated and compressed liq. 79−86898
rare earth metals, heat capacity near melting pt., vacancy mechanism of melting 80−15221
salicelidenanilines, SLC, ferroelectric behaviour, specific heat, spontaneous polarisation 80−75958
silicate glasses from igneous rocks, high temp. thermal props. 77−33055
simple fluid, sp. ht. on liq. branch of coexistence curve, rel. to sp. ht. in gas branch 77−39670
simple fluid near crit. point, homogeneous phase sp. ht. at const. vol. 78−71832
simple fluids, hard-core equations of state, C_p extrema loci 79−60474
sodium oxyacid salts, aq. electrolytes, apparent molar heat capacities and vols. 79−23744
soft discs, two-dimens. melting, phase transition boundary 80−96629
specific heat meas. near λ transition, universality test of α and α′ 79−51364
steel, Ni-Co-C (9, 4, 0.2 wt.%) enthalpy, sp. ht. to 2000K 79−10960
Stefan problem, two-phase, with varying specific heat coeffs. 77−69070
superheated liquid, rel. to effect of spinodal singularities on evaporation *(Russian)* 77−89533
TBBA, US absorpt. and dispersion at nematic-smectic-A transition 79−82287
tetramethylsilane, 3-300K, γ- and liq. phases 77−84943
thermophysical properties rel. to compressibility 78−83964
thermotropic systems of rodlike molecules with orientation-depend. interactions 80−33883
toluene, tables of thermodynamic props. 77−24419
transition metals, 3d, effect of d-band on heat of vaporisation and sp. ht. 77−76539
transition metals, 3d, liquid, electronic contrib., Percus-Yevick eqn. soln. *(Japanese)* 77−76579
transition metals, thermophysical data at high temps., submicrosecond-pulse-heating method 80−103459
triethylamine-water, critical mixture, specific heat anomaly 79−42268
triethylamine-water, near crit. soln. pt., sp. ht. at const. press. and crit. conc., −1-22°C 78−38847
vinyl monomers, calorimetric method based on ^{60}Co source *(Italian)* 77−72694
viscous liquid, glass transition, mol. mechanism for thermodynamic second order transition 78−2237
water, config. and vibr. heat capacities, H-bonds 79−99331
water, enthalpy of ionisation, 273 to 323K, from HCl neutralisation meas., sp. ht. changes 77−48676
water, heat capacity and structure, isomerisation reaction role 79−33097
water, molar heat capacity under high press. near solidification point 78−51695

specific heat of liquids continued
water, Monte Carlo simulation 80−54113
water, physical props., two-state model approach 80−75144
water, random network model, liq. and ice polymorphs enthalpy and heat content 80−64869
water, relax. compressibility and heat capacity 80−92580
water, superheated, specific heat estimation 77−24413
water, thermal activity coeff., rel. to density, heat cond., sp. heat and viscosity meas. 77−7883
water, transport and thermodynamic props. *(Japanese)* 78−34251
water, tunnel theory 79−33095
p-xylene, heat capacity rel. to temp. 80−44335
xylideneaniline-p'-benzonitri 80−44328
Ag-Ge eutectic alloy, heat capacity meas. over temp. range 800-1200K *(French)* 80−88331
Ag-Te, liquid alloys, Ag_2Te solid compound, calorimetric, investigation at high temp. 79−61893
Al, liquid, bulk modulus, calc. using press. fluctuation in microcanonical ensemble 80−2106
Ar, crit. exponents *(Russian)* 79−77766
Ar, tunnel theory 79−33095
$AuM_{(2)}$ cpds., M=Ga,In,Sn,Sb,Te, and derivation of ΔG^E of mixing for liq. alloys 77−4920
B, thermoelastic props. near melting point 80−19862
Ba, thermophysical properties, up to 1800K 78−30767
Bi, US vel. and thermophysical props. meas., 500-1000K 78−38778
CO_2, specific heat, meas., near crit. point 77−51490
$Ca(NO_3)_2$, aq. electrolyte, apparent molar heat capacity and volume, of 298.15K 79−65208
$CaO-SiO_2$ liquid, anal. expressions for heat capacities 79−77765
Cd, US vel. and thermophysical props. meas., 500-1000K 78−38778
Cd-Bi, US vel. and thermophysical props. meas., 500-1000K 78−38778
Cd-Zn(Pb)(Sn), binary metallic melt, deviation from the Kopp law, specific heat *(Russian)* 80−39305
$Co(NO_3)_2$, aq. electrolyte, apparent molar heat capacity and volume, of 298.15K 79−65208
Cs, specific heat meas., at temp. up to 1700K under pressure 78−51696
Cu-In liquid alloy, thermodynamic props., potentiometric exam. *(French)* 77−59126
$Cu(NO_3)_2$, aq. electrolyte, apparent molar heat capacity and volume, of 298.15K 79−65208
cyclopentane, plastic cryst. and liq. phases, thermal cond. and sp.ht., 100-300K, 0-2.1 GPa 78−34663
DI, thermodynamic properties 78−47517
D_2O, eqn. of state, up to 380°C and 1000 bar, derived functions 78−26655
D_2O, heat capacity, compressibility and speed of sound 79−82284
D_2O, liq., ionisation const., thermodynamic props. determ., 298-523K 77−32821
D_2O, liquid, volumetric and derived thermal characteristics at low temp. and high pressure 80−107352
Fr, properties from melting point to 7500K, prediction *(Russian)* 80−44296
Ga, liq., thermal props. at high temp. 80−75536
$Ge_{0.5}Te_{0.5}$, heat capacity in solid and liq. phases, enthalpy of form. *(French)* 80−35565
p-H_2, equil. bulk props., perturbation theory approach and quantum effects *(Russian)* 77−89551
H_2, liq., thermodynamics below Debye temp., thermal capacity temp. depend. *(Russian)* 79−10999
H_2, perturbation theory and quantum effects, thermodynamic props. and quantum stat. corrections *(Russian)* 78−22867
HCl, liq. struct. simulated by a Lennard-Jones pot. 80−1917
$HClO_4$, aq. soln., thermal capacity at 25°C 78−83965
HI, thermodynamic properties 78−47517
HNO_3, aq. soln., heat capacity at 298.15K 78−3364
$H_2O-H_2O_2$, isolation of singular component for heat capacities of supercooled H_2O 80−107437
$H_2O-N_2H_4$, isolation of singular component for heat capacities of supercooled H_2O 80−107437
He films, physisorbed low-density submonolayer thermodynamics, potential scatt. theory calcs. 79−95243
He monolayer, sp. ht., low-density phase modification produced by substrate changes 77−76642
He, superfluid, statistical thermodynamics of cubic system below 0.5K 79−86939
^{4}He, superfluid, sp. ht. of confined sample, near superfluid transition 79−46859
^{3}He adsorbed on solid Ne, desorption heat capacity 79−4452
^{3}He, B-phase, textures effect on sp. ht. 78−75900
^{3}He, $Ce_xLa_{2-x}Mg_3(NO_3)_{12}.24H_2O$, magnetically diluted thermometer for sp. ht. meas. 79−17420
^{3}He, liq., exchange model 80−88387
^{3}He, liq., in contact with dielec. surface, mag. susceptibility enhancement, thermodynamics 80−54460
^{3}He, liq., normal phase, Landau Fermi liquid theory and low temp. props., book contrib. 79−99386
^{3}He, liq., thermal contact with Pd sinter down to 0.4 mK, anomalous Kapitza boundary conductance 79−69312
^{3}He, normal and superfluid 78−75904
^{3}He, significant structure theory, thermodynamic props. 78−51774
^{3}He, superfluid, fountain press., sp. ht. and thermal cond. meas. 77−35782
^{3}He, superfluid, heat capacity, spin susceptibility, NMR and viscosity *(Danish)* 78−22921
^{3}He, superfluid, in weak-coupling-plus model 79−46867
^{3}He, superfluid, meas. of A⇄B transition in mag. field near polycritical point 77−11760
^{3}He, superfluid, near transition, anomalous heat capacity, 0.8-20 mK 80−15326
^{3}He, superfluid, order parameter, sp. ht., mag. props., sound propag., hydrodynamic props., book contrib. 79−99388
^{3}He superfluid, phys. props. *(Danish)* 78−2325
^{3}He, superfluid, sp. ht. discontinuities, rel. to Ginzburg-Landau parameters 80−54459
^{3}He, superfluid, sp. ht. jump at superfluid transition and effective mass, press. depend. 80−65331
^{3}He, superfluid, strong coupling effects 78−47626
^{3}He, superfluid, strong-coupling effects 77−11758
^{3}He, two-dimensional, in ^{4}He film, sp. ht. meas. 80−39382
^{3}He-^{4}He, at λ transition, universality 78−51782

specific heat of liquids continued
^{3}He-^{4}He, dil. solns., sp. ht. and ^{3}He quasiparticle excitation spectrum 78−71901
^{3}He-^{4}He solutions, crit. and tricrit. exponents from light scatt. data 77−20152
^{3}He-He II mixture, dil., possibility of obs. of weak bound state for ^{3}He quasiparticles 78−22925
^{4}He, adsorpt. and sp.ht. in 0.2 μm Nuclepore filters 77−35773
^{4}He, confined film near T_λ, sp. ht. scaling 78−38894
^{4}He film, Bose-Einstein condensation, thermodynamic functions 79−82399
^{4}He film, specific heat near Tλ 77−80664
^{4}He, heat capacity of liquids and dense gases at low temps. *(Russian)* 80−65324
^{4}He, liq., two-dimens., excitation spectrum and thermodynamic props. 79−86959
^{4}He, liquid comprehensive theory 79−73361
^{4}He, monolayer adsorbed on Kr-plated graphite, possible Ising transition 80−34298
^{4}He, sp. ht. near lambda point, under press., exptl. tests of scaling laws and universality 78−84017
^{4}He, sp.ht., 65-850 mK, and phonon dispersion 79−4442
^{4}He superfluid, acoustic vibration field density of states in piecewise const. parameter media 80−6483
^{4}He, superfluid, liq.-vap. sound propag., crit. props. of sp. ht. 79−33134
^{4}He, superfluid, thermodynamic props. determ. from sound velocity data 77−15649
^{4}He, superfluid, thermodynamic properties, at very low temps., rel. to interacting boson systems 78−2320
^{4}He, superfluid, two-dimens., microscopic theory, excitation spectrum and thermodynamics props. 80−24709
^{4}He, thermal expansion coeff., scaling and universality near superfluid transition 77−7927
Hg, P-V-T relations for temperatures of 40 to 240°C and press. up to 1400 kg cm^{-2} 78−6140
Hg, thermophys. props. rel. to clustering in liqs. 77−1065
Ho, thermophysical properties at high temps., exam. *(Russian)* 79−28105
In, liq., thermal props. at high temp. 80−75536
In-Sb(Sn), binary metallic melt, deviation from the Kopp law, specific heat *(Russian)* 80−39305
KCl, solution, apparent molar heat capacity and volume, at 298.15K 80−29179
KCl-CuCl eutectic fused salt, potential as intermediate temp. solar heat transfer and storage medium 80−101135
KNO_3, aq. soln., heat capacity at 298.15K 78−3364
KNO_3, solution, apparent molar heat capacity and volume, at 298.15K 80−29179
$KO_{0.5}-SiO_2$ liquid, anal. expressions for heat capacities 79−77765
$K_2O-Al_2O_3$ system, high temp. thermodynamics and phase equilibria 78−80521
Li, thermophys. props. rel. to clustering in liqs. 77−1065
Ln, thermophysical properties at high temps., exam. *(Russian)* 79−28105
$Mg(NO_3)_2$, aq. electrolyte, apparent molar heat capacity and volume, of 298.15K 79−65208
$Mn(NO_3)_2$, aq. electrolyte, apparent molar heat capacity and volume, of 298.15K 79−65208
Mo, liquid, thermophysical measurements up to 4300K 78−43136
NH_3-metal, soln., thermophysical props., review 79−77758
Na, thermophys. props. rel. to clustering in liqs. 77−1065
NaCl, soln., sp. ht. capacity at high press., temp. jump method 77−69092
NaCl, solution, apparent molar heat capacity and volume, at 298.15K 80−29179
$NaNO_3$, aq. soln., heat capacity at 298.15K 78−3364
$NaO_{0.5}-SiO_2$ liquid, anal. expressions for heat capacities 79−77765
$Ni(NO_3)_2$, aq. electrolyte, apparent molar heat capacity and volume, of 298.15K 79−65208
Pb, thermodynamic characterisation, by isobaric expansion meas. 80−103494
Pb, thermophys. props. rel. to clustering in liqs. 77−1065
PbSe, enthalpy, heat capacity, 300 to 1480K 79−60523
Pt, thermodynamic characterisation, by isobaric expansion meas. 80−103494
Pu, liq., hard-sphere model, phys. prop. meas. interpret., adjacent solid phase implications 77−19866
Pu, meas. using neutron heating 77−20078
Rb, molten, meas. in 320 to 1220K range 77−35711
$RbHF_2$, molten-salt region, heat capacities, transitions and melting 79−10967
Se, heat capacity and chem. equilib. 80−103486
Se, liq., heat capacity, 500-700K, dynamic differential calorimeters comparison 78−89482
Sn, US vel. and thermophysical props. meas., 500-1000K 78−38778
Sn-Bi, US vel. and thermophysical props. meas., 500-1000K 78−38778
Ta, heat capacity, 10^8-10^9 K s^{-1} pulsed heating, (2-4)×10^3K 78−14473
Ta, liquid, thermophysical measurements up to 7500K 78−43136
TcF_6, heat capacity, entropy Gibbs energy, 2.23-350K 78−38852
Te, and enthalpy, 0 to 750°C 77−11705
Tl, liq., thermal props. at high temp. 80−75536
U, liq., hard-sphere model, phys., prop. meas. interpret., adjacent solid phase implications 77−19866
U, meas. using neutron heating 77−20078
UO_2, thermal and transport props., electronic contrib. 80−15432
Y, thermophysical properties at high temps., exam. *(Russian)* 79−28105
$ZnCl_2$, liq., glass, cryst., sp. ht. meas., glass transition temp. rel. to press. 77−66029
$ZnCl_2$-LiCl(NaCl)(KCl)(CsCl), molten, US velocity, thermodynamic quantities and struct. *(Japanese)* 80−88270
$Zn(NO_3)_2$, aq. electrolyte, apparent molar heat capacity and volume, of 298.15K 79−65208

specific heat of solids
see also Schottky anomaly
2-chloronaphthalene, heat capacity from 4.2-300K, polymorphism 78−87641
2-fluoronaphthalene, heat capacity from 4.2-300K, polymorphism 78−87641
4f substances, rel. to electronic props. at config. crossover 77−47775

specific heat of solids continued
A 15 type superconductors, acoustic phonon spectra, electronic density of state function *(French)* 80−80444
A-15 compounds, radiation induced damage, TEM and heat capacity meas. 79−56349
A-15 high-T_c supercond., apparent T^2-depend. of normal-state resist. and lattice sp. ht. 77−47921
actinide, transport props. and sp. ht., role of optical and acoustic phonons 77−15821
actinide compounds, specific heat meas., review 80−6524
actinide metals, specific heat, Debye temp. 80−15258
actinide systems, nearly ferromag., coupled d- and f-band model 77−63211
actinides, spin fluctuation theory, for mag. and elec. props. 78−91869
adamantane, thermal cond. and heat capacity under press. 80−80008
adiabatic calorimetry, high resolution heat capacity meas. *(Japanese)* 80−52218
adiabatic scanning microcalorimeter specific heat capacity meas. of small samples 78−86274
aerodynamic ablation of melting bodies, effect of temp.-depend. heat capacity 79−37431
alkali halide:NH_4^+, hindered rot. energy levels calc. 80−10514
alkali halides, anomalous sp. ht. Ising model and Monte Carlo calcs. 78−47989
alkali halides, premelting elec. cond., heat capacity 78−91445
alkali halides, strain defects, low temperature props., heuristic model 79−82245
alkali metal, bulk properties, computer simulation 78−30729
alkali metal based liquid coolants, sp. ht. 79−86902
alkali metal halides, ionic crysts., impulse compression temps. 80−100307
alkali metals, anharmonic effects in thermodynamics *(Russian)* 78−43145
alkali metals, elastic and thermal props. by pseudopotential method 80−19899
alkali metals, lattice anharmonicity 79−19341
alkali metals, lattice sp. ht. and thermal vibrs. 78−30768
alkali metals, thermal properties and Gruneisen parameters, employing model pot. 78−71815
alkylammonium copper halides, mag. sp. ht., two-dimens. S1/2 Heisenberg ferromag. behaviour 77−32206
alkylene di-ammonium cadmium tetrachlorides, sp. ht. anomalies at phase transitions 80−70421
alloy, dilute, sp. ht., electronic, mass renormalisation and band density of states influences 78−43137
ammonium hydrogen oxalate hemihydrate, low temp. dielec. and thermal props. 77−28510
amorphous dielectric solids, low energy atomic motions and anomalies at low temps. 78−30724
amorphous mag. substance with rare earth ions, low temp. specific heat, elec. resistance and US absorpt. *(Russian)* 79−19734
amorphous magnet, random anisotropy axis model in the infinite-range limit 80−88761
amorphous magnets, random anisotropy axes, high-temp. expansion for sp. ht. 80−71041
amorphous polymers, localised low-energy excitations 79−73322
amorphous polymers, specific heat rel. to rate of heating *(Russian)* 77−85986
amorphous semiconductor, non-polar, mobility gap temp. variation calcs. 78−10339
amorphous solids, structure and low temp. props. 79−37631
amorphous solids, vibr. sp. ht. enhancement from force-const. variations 80−88333
amorphous systems, mag. props. effect of random anisotropy 79−4686
amorphous systems, origin of thermal anomalies, struct. model 78−91256
Anderson impurities, interacting, pair, Fermi-liq. theory 80−44803
Anderson localised states, electron correlation effects 79−23919
anharmonic crystal, thermal expansion contribution to free energy and heat capacity to order λ^4 78−6138
anharmonic crystals, Debye-Waller factor, specific heat thermal behaviour 80−54335
anisotropic 3-D Ising lattice 79−156
anisotropic multilayer solids, macroscopic fields anal. 77−89547
anthracene, chemical thermodynamic props. 80−21312
anthracene, thermal cond. and heat capacity, meas. under press. 79−90796
anthracene, thermodynamic function calc. using cell model 77−7879
antiferromagnet, anisotropic correction to scaling in specific heat 78−80168
antiferromagnet, cluster approximation, Neel temp. and specific heat calc. 80−54901
antiferromagnet, linear chain, biquadratic exchange interaction effects 77−63062
antiferromagnet, mag. moment and sp. ht. fluctuations near critical temp. 78−91867
antiferromagnet, residual stress induced domains, specific heat meas. anal. 78−60286
antiferromagnetic chain, random, quantum spin-1/2 Heisenberg soln. 80−11148
antiferromagnetic degenerate semiconductor, thermal and mag. props. 78−19224
antiferromagnetic triangular cactus tree, bond-diluted, ordered phase 80−71037
antiferromagnets, reln. between temp. depend. of mag. susceptibility and sp. ht. *(German)* 77−69567
apparatus for meas. thermophysical characts. by composite method, wide temp. range 77−26285
apparatus to meas. thermophysical props. at high temps. 80−37458
Araldite AW106/Hardener HV953U epoxy resin, thermal props. at high press., glass transition 77−59160
Ashkin-Teller-Potts model, renormalisation group anal. 79−154
austenitic stainless steel, sp. ht., 4-300K 77−24416
baddeleyite-corundum refractories, thermophysical props. 79−82398
benzene, thermal cond., heat capacity, 105-375K, up to 2.4 GPa 79−90839
benzene, thermal cond. and heat capacity, meas. under press. 79−90796
benzene-hexa-n-hexanoate, phase transitions and mesophase form., sp. ht. and IR spectra, 13 to 393K 80−79955
benzenechromium tricarbonyl, sp. ht. and thermal expansion tensor meas. *(French)* 78−79788
specific heat of solids continued
benzil, heat capacity near phase transition 78−2250
bicrystal interface vibrational props., different-interface phonons and low-temp. sp. ht. 77−76656
binary alloy with BCC type lattice, order-disorder transition 79−78957
binary alloys, random, specific heat enhancement and electron-phonon interaction 80−65242
1,1′-biphenyl, heat capacity anomalies due to successive phase transitions 80−96664
biphenyl, heat capacity near phase transition regions 80−44330
bis-tetraethylammonium tetrachloronickelate, heat capacity, structural transitions 79−65209
bis-tetraethylammonium tetrachlorozincate, heat capacity, structural transitions 79−65209
borides, ternary, struct. classification, props., book contrib. 78−47309
borosiliate glasses, thermal conductivity meas. by laser flash method *(Japanese)* 77−69124
β-brass order-disorder transition, crit. temps. and exponents rel. to composition 77−8818
butyloxybenzylidene octylaniline, liq. cryst., phase transitions, calorimetric obs. 80−103466
carbon tetrachloride, freezing and melting of stable and metastable phases 77−27984
carnauba wax thermoelectret, charge behaviour 80−7276
ceramic, calc. for solids and liqs. 77−43348
chalcogenide spinels, specific heats 79−11315
chalcogenide spinels, thermal stability, thermochemical, thermodynamic and crystallochemical props. 77−51519
chromocene, heat capacity meas., phase transitions 78−38853
classical quadrupole solids, correl. effects 80−10628
composites, bounds for effective thermal conductivity and specific heat 79−23745
constant power source method, for therm. characts. 79−95222
continuous heat source, sphere, boundary conditions of second kind, temp. field 77−23851
copper, benzoate, one-dimens. antiferromag., heat capacity, field-induced crossover of spin-dimensionality 80−97099
copper benzoate, mag. heat capacity and Neel temp. in mag. field 79−61147
copper tetrammine sulphate monohydrate, evidence for exchange coupled quadratic nets 77−24705
covalent crystals, lattice dynamics, unpaired forces effects 79−95096
covalent semiconductors, displacement correlations, adiabatic bond charge model 80−70350
critical indices for systems with strong dipole interactions *(Russian)* 77−28390
cryolite, hydrothermal synthesis of large synthetic single crystal, props. 78−19654
crystal, anharmonic contribs. to sp. ht. and thermal expsn. 79−82354
crystalline materials, sp. ht. rel. to binding energy temp. depend. 80−54403
crystallisation, percolation theory, Lindemann melting criterion and thermodynamic props. 79−28081
cubic crystal, surface contribution to low temp. sp. ht., elasticity theory 78−18790
cubic Ising ferromagnet, three spin interaction effect on mag. props. 80−54910
curve-fitting method based apparatus for thermal props. meas. at cryogenic temps., performance characts. 77−67441
cyclo-hexyl-ammonium-copper-trichloride, specific heat, ferromagnetic chain system 80−103491
cyclohexane, thermal cond. and sp. ht. under press. 78−22906
Debye heat capacity, calc. using Einstein heat capacity formula 80−24608
diamagnetic ionic cubic lattice in homogeneous mag. field, oscillations 78−91868
diamantane, sp. ht., thermodynamics of transition and fusion 79−55899
diammonium layer compound, $(CH_2)_2(ND_3)_2MnCl_4$, mag. and optical props. 79−51760
diammonium layer compound, $(CH_2)_n(NH_3)_2CuCl_4$, mag. and optical props. 79−51760
diammonium layer compound, $Mn(NH_3)_2(CN)_42C_{12}H_{10}$, mag. susceptibility and sp. ht. meas. down to antiferromagnetic state 79−7999
diamond-structure crystals, cubic and quatic anharmonic contribs. to sp. ht. 77−89549
dibenzene chromium, heat capacity meas., phase transitions 78−38853
dielectric, regulated, thermal capacity, strong US waves effects *(Russian)* 80−65240
differential scanning calorimetry, meas. of accurate heat capacities 80−8987
1,5-difluoronaphthalene, IR and Raman study of crystal dynamics 78−80346
digital instrument for measuring average heat capacity 79−71453
dilute alloy, perturbation expansion for the asymmetric Anderson Hamiltonian 80−80202
dilute alloy, rel. to force const. changes due to substitutional impurities 77−24374
dilute alloys, mag. impurity ordering 77−28370
dilute mag. alloy, density of energy states from sp. ht. as function of temp. 79−19741
dilute magnetic alloy, sp. ht. evaluation role of fluctuations 77−69580
dilute random magnet, one-dimens., low temp. behaviour of susceptibility, sp. ht. and correl. length 79−69682
dimethyl ammonium manganese chloride, sp. ht., quasi-one dimens. behaviour 78−52293
dimethylammonium copper tetrabromide, quasi two-dimensional antiferromag., mag. behaviour 80−97098
2,2-dinitropropane, temp. dependence, adiabatic calorimetric method 78−71854
disordered one dimensional chains, low temp. electronic sp. ht. 79−51275
disordered one-dimensional conductors, interacting electron thermodynamics *(Russian)* 80−54679
disordered solid, low temp. sp. ht., linear function of temp. 77−69097
disordered substitutional alloy, mag. props., Heisenberg model 79−38342
disordered systems, localisation using random series, Anderson transition for extended states 80−44542
disordered systems, phonon-like excitations, dispersion and damping 80−49331
DNA film, in range 4.2-400K *(Russian)* 77−51511
DOBAMBC, ferroelec. props. 79−32884

specific heat of solids continued
doped semiconductors, correlation effects on Anderson localised states 79−95337
double Ising chain, model in zero external field *(Russian)* 78−84430
DPPH-benzene complex, ht. capacity, 0.55-20K, mag. susceptibility, 0.4-300K 78−56317
dynamical properties of solid surfaces, analytic approach 78−71929
Eccobond solder 56 C, 1.3-300K 78−16804
education, specific heat curves, exact, Einstein and Debye for one-dimens. crystal 78−86076
elastic surface waves at hexagonal surface and interface, thermodynamic and dynamical props. 79−69338
electrically conducting materials, at high temps., improved apparatus 79−86326
electrolyte, ionic conductivity, phenomenological theory 78−83994
electron, and effective mass, temp. depend. *(Russian)* 78−59958
electron gas, two dimens., exchange interaction contrib., calc. 80−44331
electron gas, two-dimensional, internal energy, specific heat effective mass, temp. depend. 80−75513
elemental superconductors, review and table of props. 77−4460
elements, monotonous series based on atomic bond energy, for mech. and phys. props. calc. *(Russian)* 80−19740
entropy, free energy, sp. ht., electron-phonon interaction corrections 80−49387
epoxies, Epo-Tek H31LV, 4 to 25K, and H62, 4 to 40K 78−43138
epoxy resin, low temp. thermal props., phonon states and crosslinked struct. *(German)* 78−75846
epoxy-resins, sp. ht. and thermal cond., 0.1 to 80K, phonon scatt. 79−65215
ethane, solid, thermodynamic props. between double solid-to-solid transition and triple point temp. 78−75828
ethanol, plural glass-transitions, thermodynamic functions 78−38820
ethylene copolymers, partially cryst. pseudoeutectoid, swelling, thermodynamics 80−39311
FCC crystal containing substitutional impurities, low temp. heat capacity *(Russian)* 77−84941
FCC lattice, uncorrelated-pairs approximation for anharmonic free energy, tests 78−59920
ferrite, two-sublattice, thermodynamic functions in mag. field *(Russian)* 77−32197
ferroelectric, anomalous sp. ht. Ising model and Monte Carlo calcs. 78−47989
ferroelectric, Debye temp., tabulation of calorimetric values 78−51639
ferroelectric, SAW propagation along domain boundaries, low temp. sp. ht. contrib. 77−77158
ferroelectric, $T^{3/2}$ contrib. 77−59528
ferroelectric, uniaxial, dipolar crossover effects from Ising crit. behaviour 77−89961
ferroelectric, uniaxial, static and dynamic crit. phenomena, Larkin-Khmelnitzkii theory 78−64327
ferroelectric dipole waves, low temp. sp.ht. and spontaneous polarisation calc. 79−33614
ferroelectric materials for dielectric power conversion, dielectric prop. anal. 80−80712
ferroelectrics, meas. by dynamic method at high hydrostatic pressures 80−47059
ferroelectrics, properties near phase transition point, influence of defects 79−42918
ferroelectrics, quantum transition suppression, pyroelectric, electrocaloric effects, specific heat 80−75984
ferroelectrics, soft mode contrib., near T_c 78−64338
ferroelectrics, surface sound waves on domain boundaries, low temp. sp. ht. 78−71937
ferromagnet, dislocation effects on phys. props. at $T \neq 0K$ *(Russian)* 77−8378
ferromagnet, impurity uniaxial, thermodynamics below Curie point *(Russian)* 77−43801
ferromagnet, Ising model, diamond lattice, phase transition, crit. props. 80−93127
ferromagnet, itinerant, mag. props., temp. depend., functional integral approach 80−60170
ferromagnet, magnetic moment fluctuations and sp. ht. near crit. point 77−28388
ferromagnet, uniaxial, dipolar crossover effects from Ising crit. behaviour 77−89961
ferromagnet, uniaxial, with flat-parallel domain struct., classical phenomenological description 78−56316
ferromagnet with admixture of antiferromag. bonds, thermodynamic functions *(Russian)* 79−87224
ferromagnetic alloy, temp. depend. of mag. props. and sp. ht., mag. phase transition region 78−64207
ferromagnetic classical vector model, extension of high temp. free energy series 80−7062
ferromagnetic metals, thermodynamic props. 79−91245
ferromagnetic semiconductors with doubly charged donors, quasiphase transition 79−65684
ferromagnetic system, singularity in sp.ht., random spherical model in non-zero mag. field 77−55677
ferrous formate dihydrate, mag. sp. ht. 79−91235
ferrous formate dihydrate, paramagnetic specific heat, decoration iteration transformation anal. 80−70938
ferrous-formate dihydrate, mag. system model, mag. sp. ht. *(Japanese)* 78−31091
filled samples, sp. ht., density 78−5645
finite disordered Hubbard cluster, thermodynamic and mag. props. 77−85409
finite one-dimensional lattice finite length effects, Debye-Waller factor and sp. ht., for teaching 77−33798
fluorite crystals, Brillouin scatt. and high temp. disorder 78−80365
fluorite type crystal, effects of anharmonicity and disorder on Raman scatt. at high temp. 78−80349
frozen food, hydrostatic press. effect on phys. props. 78−26706
garnet:Nd^{3+}, doped, Schottky specific heat and mag. susceptibility calcs. 79−51759
garnet, specific heat meas., elastic type of antiferromag. ordering *(Russian)* 77−55686
Gaussian-to-Heisenberg crossover, specific heat, renormalised perturbation theory 80−60356
Gibbs equilibrium thermodynamic pot. second derivatives, discontinuity surfaces rel. to phase boundaries of q-component systems 79−82304
glass, anomalous sp. ht. at low temp. 77−80631
specific heat of solids continued
glass, equilib. thermodynamics, sp. ht., refr. index and glass transition *(German)* 78−83745
glass, inorganic, specific heat in anomalous region near vitrification temp., simple relax. model 77−43341
glass, insulating, thermal, acoustic props., low temp. anomaly microscopic model 80−28921
glass, time depend. sp. ht. rel. to US props., at low temps. 78−59957
glass ceramic, low temp. heat capacity, glassy and devitrified states 78−22862
glass ceramic, machinable, elastic moduli press. and temp. derivatives, specific heat 78−52873
glass fibre reinforced epoxy, heat ageing effect on thermophys. props., 10-400K 77−59161
glass fibre reinforced epoxy resins, thermal props., 80-300K *(German)* 79−10990
glass-ceramic, machinable, elastic const. temp. depend. 80−79852
glasses, low temp. props., two-electron excitons 77−15786
glasses, strain interactions, low-temp. props. 79−42269
glasses, thermal, acoustic, and dielec. props. at low temps. 79−65164
glasses, time-dependent sp. ht. at low temps. 79−60520
glasses, US properties and short-time sp. ht. relationship 79−60440
glasses and amorphous solids specific heat at low temps. 77−11703
glassy state, one-dimensional disordered harmonic system, heat capacity from spectral moments 79−28107
L(+) glutamic acid halogen acid salts, crystallographic, optical and calorimetric meas., halide effect 78−34505
glycerol, cryst. and glassy states 80−2176
graphite, adsorbed layers of O_2, heat capacity meas. 80−49511
graphite, frequency distribution based on unfolding technique 80−92619
graphite, intercalation compounds with K and Cs, low temp. 78−71868
graphite, neutron-irrad., sp.ht., 0.4-4.5K, rel. to localised spin transition 77−28389
graphite, Poco AXM-5Q1, thermal and elec. transport props., 4-3000K 78−6375
graphite, polycryst., neutron irrad., low temp. sp. ht. anomalies, spin-spin interactions 79−15307
graphite, pure, anomalies around 1.45K in 13.7 T mag. fields 79−42270
graphite, pyrolytic commercial, high-temp. thermal and mech. props. 80−75372
graphite, with physisorbed Xe monolayer, dynamical and thermal props. 80−34292
graphite intercalation compounds with alkali metals and halogens, physical props. 78−31050
graphite intercalation compounds with K and Cs, low temp. specific heat meas. and XPS 78−26693
graphite intercalation compounds with K and tetrahydrofuran *(French)* 78−26692
graphite-ICl intercalation compounds, anomalous sp. ht. due to order-disorder transform. 79−42235
graphite-nitrate residue compounds, phys. props. 78−10199
graphited, exfoliate, sp. ht. low temp. meas. 79−73317
Griffiths singularity in specific heat of random spherical model 77−8325
guanidinium vanadium sulphate hexahydrate, mag. behaviour in applied fields below 1K 77−66376
guanidinium vanadium sulphate hexahydrate, singlet ground state system, low temp. mag. props. 80−44843
harmonic crystals, cell cluster method, Einstein heat capacity 78−51636
harmonic crystals, thermodynamic props., effects of vacancy defects determ. by cell cluster method 80−79959
heat capacity meas. low temp., mag. fields to 4.5 T 78−16798
heat-insulating material, simultaneous determ. of temp-depend. thermal cond., heat capacity 77−11120
heat-pulse experiments, nonlinear effects, theory 80−96182
heavily doped semicond., electronic sp. ht. and transport coeff., influence of band-tail parameters 79−14941
Heisenberg, ferromagnet, classical, with dipole-dipole interaction, renormalisation group and crit. exponents 80−60351
Heisenberg antiferromagnet, disordered, magnetic atom-conc. near percolation threshold, mag. props. *(Russian)* 78−80171
Heisenberg antiferromagnet, quadratic spin 1/2, sp. ht. and susceptibility, comparison with $Cu(C_5H_5NO)_6(BF_4)_2$ data 77−66353
Heisenberg antiferromagnetic chain, random, low temp. thermodynamic props. in zero mag. field 80−34657
Heisenberg ferromagnet, consistent linearised Green's function theory for $s=1/2$ 79−4685
Heisenberg ferromagnet, density of states and heat capacity near percolation threshold 77−77021
Heisenberg ferromagnet, with single-ion anisotropy, correlation functions calc. 78−31076
Heisenberg ferromagnet in critical region, Bloch renormalised spin wave approx. 79−82784
Heisenberg linear chain, alternating spin quantum numbers, mag. and thermodynamic props. 80−34578
Heisenberg linear chain, with nearest and next-nearest neighbour interactions 77−63059
Heisenberg magnet, dil. three dimensional, static behaviour at finite temps., Monte Carlo calc. 79−73752
Heisenberg model, critical behaviour, high temp. susceptibility and internal energy series 78−34987
Heisenberg model, planar, classical, with biquadratic interactions, theory 77−72970
Heisenberg model, specific heat, high-temp. expansions, numerical investigation *(German)* 77−59420
Heisenberg model magnets, high-temperature specific heat *(Russian)* 80−88757
Heisenberg-Dzyaloshinsky-Moriya model, high temp. expansions for zero-field susceptibility and specific heat 79−33497
hexagonal crystal, surface contrib. to low temp. sp.ht. 77−1233
hexamethylenetetramine, thermal cond. and heat capacity under press. 80−80008
high heat-conductance materials, method for determ. of thermophys. charcts. on thin samples 77−61063
high vacuum, HV bushings, for cryogenic appl. 78−81977
HMTTF-TCNQ, quasi-one dimensional conductor, sp, ht. 79−55897
Hubbard Hamiltonian, two-site, half-filled band, thermodynamic props. 77−24505
Hubbard model, computer renormalisation-group technique 79−19716
Hubbard model, half-filled, mag. couplings 78−52192
Hubbard model, one-dimens. half-filled band Holstein-Frolich modified, transport props. 78−23237

specific heat of solids continued
Hubbard model, one-dimensional, elementary excitation with complex wave vector 80−75783
Hubbard model, two-point doubly degenerate in half-filled case, thermodynamics 77−4492
Hume-Rothery Phases, electronic struct., main features 79−23883
ice, random network model, liq. and ice polymorphs enthalpy and heat content 80−64869
ice, VII to VIII transition, lattice model 78−10187
ice, vitreous, sp. ht., entropy and 'glass transition' 77−51520
Inconel 718, heat capacity 313 to 1053K 79−10964
inert gas, calc., using model theory of free vol. and Lennard Jones potential 77−62653
inorganic compounds, empirical estimation, 298K to melting point 78−43140
insulating solids, transient hot-wire method 77−67428
insulating systems, magnetic, review of expts. 78−68240
insulator, mag. transition sp. ht. anomaly, photoacoustic meas. 80−4773
insulators, appl. of cryogenic calorimetry 79−40577
interface specific heat at low temp., vibr. contribution, elasticity theory 77−1234
intermediate valence, phase diagram and Kondo behaviour 80−29366
intermediate valence, theory, electronic sp. ht. calc. 80−79956
intermediate valence, three-site, six-electron, even-parity model 80−20125
intermediate valence compounds, mag. susceptibility and sp. ht., mean-field theory of periodic Anderson model 78−47937
interstellar grains, exact Debye theory for max. temps. 77−49449
Invar, AC calorimetry at high press. 77−41616
Invar, ferromagnetism and antiferromagnetism coexistance at low temp. 77−66320
Invar, specific heat, temp. depend. *(Russian)* 78−56341
Invar, stainless, thermal expansion, elastic props. and Mossbauer effect 79−56502
ionic cryst., polymorphic transition due to disordering, behaviour of sp. ht. as function of cryst. parameters 79−14724
ionic crystal, surface vibrational properties, review 78−71928
ionic crystals, vibrational surface modes, vibrational contributions to surface thermodynamic functions 77−47659
iron (II) formate dihydrate, mag. sp. ht., S_z^4-term 79−61127
iron formate dihydrate, mag. sp. ht., S_z^4-term 80−60289
iron tetraphenylporphyrin chloride, electron spin pairs, low and ultralow temps. 77−77092
Ising antiferromagnet, BCC, in mag. field, Monte Carlo calcs. 78−31032
Ising chain, amorphous, finite, thermodynamic behaviour 79−61028
Ising chain, linear, three dimensional phonon field 77−73036
Ising chain, one-dimens., with generalized molecular field 79−91242
Ising chain, random one-dimensional, in transverse field, thermodynamics 77−77019
Ising chain, with next-nearest neighbour interactions, mag. responses to spin-Peierls transition 80−71054
Ising chain with random bonds, remanence and non-exponential relax. 79−73751
Ising dilute magnetic alloys, local mag. fields and fluctuations 77−40061
Ising double chain, compressible, mag. susceptibility and thermodynamic props. 79−15320
Ising ferromagnet, FCC, cluster variation approx. 78−27049
Ising ferromagnet, one-dimens., with phase transition, thermodynamic props. calc. 80−80536
Ising ferromagnet, renormalised crit. behaviour 78−52272
Ising ferromagnet, S=1, single-ion type uniaxial anisotropy, cluster-variation method appl. in pair approx. 78−68281
Ising like model, tricritical two-dimensional behaviour, finite size effects, model depend. 79−35641
Ising model, 2-dimens., sp. ht. divergence, calc. using Kadanoff's variational approx. 77−37822
Ising model, adiabatic susceptibility and specific heat at const. magnetisation 80−7114
Ising model, bond random, ferromagnetic-antiferromag. mixture, triangular cactus tree, statistical theory 80−75702
Ising model, dipolar antiferromag., phase transition at negative absolute temp. *(Russian)* 78−43594
Ising model, finite, statistical mechanics 77−36081
Ising model, magnetic specific heat, effect of spin-lattice coupling 78−80157
Ising model, quantal and finite-sized, dimensional crossover 78−95444
Ising model, random band, cumulant expansion to glass-like phase 77−8319
Ising model, random bond, susceptibility and specific heat of glass like phase, cumulant expansion 78−6533
Ising model, random chain, low temp. sp. ht. calc. 79−56562
Ising model, randomly diluted, on honeycomb lattice, thermodynamic props. 80−54902
Ising model, spatially nonhomogeneous, correl. functions 80−60314
Ising model, spin glass, mean field theory 79−4680
Ising model, spin glass in Bethe-Peierls-Weiss and other mean-field approximations 79−65682
Ising model, spin-s, corrections to scaling for spin-pair correls., series anal. 77−16027
Ising model, three dimensional, free energy, lower bound approx. 78−10707
Ising model, three-dimens. mag. susceptibility and sp. ht., high temp. series anal. 80−22295
Ising model, with regularly spaced blocks of impurities, crit. temp. and sp. ht. 77−69576
Ising model spin glass, phase transitions 77−8327
Ising or ϕ^4 ferromagnet, rigorous inequality for sp. ht. 79−78413
Ising quadratic two-dimensional ferromagnet with three spin interactions 80−2542
Ising spin glass, with RKKY interaction, props. 79−24177
Ising system, cubic $S=^1/_2$ model, lattice dimensionality crossovers anal. 78−39347
Ising system, finite, statistically layered, crit. phenomena 78−95446
Ising system, periodically layered, cooperative effects in crit. phenomena in sp. ht. 78−23284
Ising two-dimens. lattice, next-nearest neighbour interaction, impurity effect on sp. ht. 77−89957
Ising-like ordered phases, calcs. of bicritical crossover scaling functions 77−55678

specific heat of solids continued
isopropyl ammonium chloroplatinate and chlorostannate, ferroelastic transition, thermal, optical, and elastic meas. 79−28096
isotropic spin system, cubic lattice, step model of phase transitions, critical behaviour 78−60290
itinerant electron ferromagnetism, press. effects on mag. props. 77−66241
itinerant-electron systems with narrow bands, single-site spin fluctuation theory 80−97049
Jahn-Teller system, thermodynamic properties, internal stress effects 80−59679
kinetic Ising model of ferromagnetism, simulation of equilib. critical props. 78−89410
Kondo lattice, electron dynamics, additional sp. ht. 80−15688
lattice constant fluctuations, influence on thermal props. of cryst. 79−77715
lattice vibrations and cryst. heat capacity, historical review 80−57071
layered crystal, electron gas statistical and thermodynamic props. *(Russian)* 79−87051
layered structures, sp. ht. rel. to phonon spectrum *(Russian)* 79−90794
linear chains, monatomic, anharmonicity in surface and size effects in sp. ht. 77−1236
linear defects, local phonon modes and structural instability *(Russian)* 79−73275
liquid-glass transition, free volume approach, thermodynamic behaviour 80−1940
liquid-glass transition, glass transition depend. on heating and cooling rates 80−79920
lithium thallium tartrate, sp. ht., 0.3 to 25K, second-order ferroelec. transition 80−59674
localised magnetic impurity problem, functional-integral approach, sp. ht. calc. 77−77026
logarithmic singularities, phys. models of 1/f noise 77−71272
low temperature depend. of elec. resist., mag. suscept., heat capacity, Hall const. *(Russian)* 78−30900
low temperature measurement, dynamic differential calorimetry 77−74405
lysozyme, cryst., dynamic sp. ht. capacity meas. 80−21447
mag., heat capacities refrigerant materials, low temp. 78−37012
magnetic dipoles on a lattice, theory at low temps. 80−50082
magnetic model systems, computer simulations 80−65924
magnetic superconductor, thermodynamics of magnetism and supercond., mol. field theory 80−34668
magnetically ordered materials, specific heats and spin wave theory, review 79−42763
manganese formate dihydrate, 2-D Heisenberg antiferromag., sp. ht. 78−14965
manganese formate dihydrate, Zn- and Mg-substituted, anomalous crit. phenomena 80−60316
manganese zinc formate dihydrate, two-dimens. antiferromag., anomalous crit. phenomena, neutron scatt. and PMR obs. 80−50104
measurement, 4.2 to 90K, USSR special standard 77−31207
measurement, 90 to 273.15K, USSR special standard 77−31206
measurement, differential method 78−57952
measurement using heat pulse technique, down to 25 mK 77−45850
measurement using resistive SQUID 79−63213
measuring installation for pressures up to 250 MPa and 150-350K temps. 77−76572
melting, dislocation model 78−26657
mercury carboxylates, phase transitions, DTA 79−90759
metal, allotropic transform., anharmonicity, effects due to thermal expansion and Gruneisen parameters 79−52207
metal, Arrhenius plot of diffusion, curvature, disappearance under press. with single-vacancy model 79−10975
metal, atomic heat capacity change during polymorphic transformations 79−29055
metal, degree of deform. effect on thermophys. props. at high temps. 78−26694
metal, electrical method of measurement 77−51513
metal, electronic sp. ht., Gutzwiller theory of electron correl. at finite temp. 77−43527
metal, entropy/free energy relation 78−15368
metal, equilibrium vacancy conc. 78−38694
metal, FCC, vibr. behaviour of self interstitials 77−4175
metal, many-electron theory 79−46991
metal, monovalent, low temp. eqn. of state 78−22820
metal, one component substances, surface energy, temp. depend. 77−72753
metal, quasimagnetic impurity, exact solution of Wolff's model 78−56105
metal, supercond. as probe of mag. state of local moments 77−20491
metal, thermodynamic properties, outer electron contributions *(French)* 78−43091
metal, vacancies, energy charact. *(Russian)* 77−24314
metal calc. for solids and liqs. 77−43348
metal film, electronic density of states, sp. ht. and spin susceptibility 77−15730
metal film, quench-condensed, 0.6-4.4K 78−41309
metal halides, calc. for solid and liq. phases 77−43349
metal heating by laser radiation, calc. allowing for thermal props. temp. depend. 78−30770
metal particle, 9 Å, in zeolite matrix, melting temp. 77−59103
metal particles, thermodynamics and paramag. props. of electrons 78−31051
metal-hydrogen system, electronic sp. ht. meas. 80−49378
metal-metal interface, simple, electronic props., interface sp. ht., single-particle contrib. 78−72234
metallic chains, weakly coupled, Ginzburg-Landau theory 78−60068
metallic crystal, phonon density of states determ. from heat capacity *(Russian)* 80−29131
metallic crystals, HCP, Brillouin zone representative points 79−33044
metallic glass, stability, hole theory of liquids appl. 80−100174
metallic glasses, elec. and thermal props. 78−72131
metallic glasses, mats. props. review 77−4043
metals, appl. of cryogenic calorimetry 79−40577
metals, heat capacities meas., undergraduate experiment 79−84915
metals, heat capacity, ultra-low temp., anomalies due to CDWs 79−42271
metals, heat capacity near melting point, vacancy mechanism of melting 80−10641
metals, low temp. and high pressure techniques 80−52246

specific heat of solids continued
metals, nonstationary temperature fields due to moving heat sources, heat capacity, thermal cond. *(Russian)* 80−107448
metals, overbarrier states of H and D, subsystem heat capacity, equilibrium props. *(Russian)* 80−79998
metals, simple, expansion coeff. rel. to heat capacity 77−43354
metals, spin fluctuations, mag. field effect, electronic sp. ht. and elec. resist. 80−108026
metamagnetic phase diagram, determ. method 78−68254
methane:O_2, crystal field, O_2 catalysis of spin-species conversion 77−51706
methane, entropy and sp. ht., 0.4 to 28K, spin-species conversion 77−28015
methane-d_1, tunnelling states and nuclear spin conversion 79−10944
methane-d_1(-d_2,-d_3), solid, struct. of phase III from thermodynamic meas. 79−82193
methane-d_2, orientational ordering and tunnelling states meas. 79−10963
methane-d_4, solid, thermodynamic props. calc. using significant structures method, 6 to 87K 80−24616
methane-d_4, solid, tunnel splittings, heat capacity meas. 80−96451
methanes, solid, heat capacity, possible dimens. effect 78−75844
$Mg_{70}Zn_{30}$, amorphous alloy 77−27835
microcline, maximum, room temp. phase transition, heat capacity meas. 80−54373
microcrystallites, sp. ht. calc. 77−72696
Migdal-like approximation, quantum spin systems 80−34649
mixed alkali silicate glasses, heat capacity *(Japanese)* 78−55954
mixed valence compounds, periodic Anderson model self-consistent treatment, specific heat, susceptibility 79−99514
mixed valence cpds., mag susceptibility and sp. ht., periodic Anderson model, CPA alloy analogue method 80−15474
mixed valence metals, elementary excitation damping, electron specific heat 79−95180
mixed valence model, spinless, isolated f-level problem 80−107750
$MnCl_2.4H_2O$, isothermal and adiabatic susceptibilities near antiferromag. transition, vel. to sp. ht. 77−69561
model, exactly soluble *(Russian)* 77−80944
modified heat pulse method, 0.2-4.2K range 78−21143
molecular crystal, quadrupole ordered phase, thermodynamic props. *(Russian)* 79−82353
molecular crystals, rot. and sp. ht. anomalies 80−28932
molecular solid, heat capacity, possible dimens. effect 78−75844
molecular solids, intermol. forces and eqn. of state, pseudoharmonic approx. calcs. 78−30731
molybdenum chalcogenides, multicomponent, physical props. 80−84577
naphthalene, thermal cond. and heat capacity, meas. under press. 79−90796
naphthalene, thermodynamic function calc. using cell model 77−7879
naphthalene charge transfer complexes, orientational disorder, spt. ht. meas. 79−46813
naphthalene-tetracyanobenzene, order-disorder transition, heat capacity and thermodynamic props., 5 to 300K 79−33100
Nb_3Ge, supercond., single phase, sp. ht. meas., 4-29K 78−72307
Neel ferrimagnets, phase transitions, field-induced spin-orientational 80−75767
neodymium ethyl sulphate, cryst. c-axis demag. from 25000G, magneto-hydrodynamic props. to 0.01K 77−20599
neodymium ethyl sulphate hydrate, spherical single crystal, magnetothermodynamic props. 77−55365
$Ni(OH)_2$, quasi-two-dimensional antiferromagnet 79−11317
nickel hexapyridol perchlorate, $Ni(C_5H_5NO)_6(ClO_4)_2$, sp. ht., mag. ordering transition 77−48004
nitromethane, solid, tunnel states investig. 80−103274
NMP-TCNQ, low temp. specific heat 78−52297
noble metals and their dil. alloys, electronic struct., de Haas-van Alphen studies, book contrib. 79−37967
nonconducting solids, technique for thermal cond. and sp. ht. meas. 77−10015
nonlinear diffusion equations, identification of thermal cond. and sp. ht. *(French)* 77−47614
nuclear reactor materials, thermal properties at elevated temps., determ. method 77−73402
nuclear reactor materials, thermophys. prop. meas. at RFL Springfields 77−14230
oil shales, review of thermophysical properties 79−100479
oligocarbonatemethacrylates, and their cross-linked polymers, thermophysical characts., temp. depend. anal. 80−19721
one-dimens. disordered solid, anomalous specific heat 79−23746
one-dimensional classical spin chain with random interactions, exact calcs. 79−4687
one-dimensional dilute Heisenberg system, mag. props. 78−64179
one-dimensional disordered systems, magnetism 80−25152
orbital degeneracy, one dimensional two spin models *(Russian)* 80−54899
orbitally degenerate interacting impurity thermodynamics, stress field depend. due to point defects, dislocations 79−69477
ordered and isotopically disordered lattices, sp. ht. at constant vol. calc. 79−1509
ordered regions near macroscopic defects and percolation phase transform. in crystals *(Russian)* 80−92665
oxovanadium carboxylates, near one-dimensional antiferromagnetism, thermal and mag. props. calc. 77−20602
paramagnet, narrow-band with strong Coulomb correlations, electron. sp. ht. *(Russian)* 80−103487
phase transformations, thermodynamic relations, appl. to K_2ReCl_6 80−29164
phenanthrene, chemical thermodynamic props. 80−21312
phenol formaldehyde resin reinforced with chrysotile asbestos fibres 79−55908
phenol-formaldehyde resin, thermodynamic props. 78−91452
phenolformaldehyde resin, sp. ht. obs. *(German)* 78−75845
phonon density of states determ. from sp. ht. temp. var. 77−84871
picrite, calculation using measurement of US vel. 80−41436
plane rotor model, static and dynamic crit. behaviour, Monte Carlo simulation 79−38334
Plexiglas, spark energy balance 79−23474
PMMA, amorphous, thermophysical props. depend. on hydrostatic press. 78−47612
PMMA, filled amorphous polymer, heat capacity meas. *(Russian)* 79−65211
PMMA, Gruneisen const. and thermal props., temp. depend., 4-300K, Brillouin scatt. obs. 80−100662
PMMA, thermophysical props. at high hydrostatic press. 78−2317
PMMA and PPMA, glassy state, cyclic loading effects on internal damping, shear modulus, heat capacity and density 77−43275
poly(alkyl methocrylates), US determ. of relax. 77−51449
polyacrylonitrile and copolymers with polyisobutylene, specific heat and glass transition temp. meas. *(German)* 78−34603
polyalkaneimide, mech. and thermophys. props. at liq. He temps. 80−3117
polyamide single crysts., struct. *(Russian)* 77−43158
polybutadiene, thermal cond. and sp. ht. 79−65265
polycarbonate, amorphous, thermophysical props. depend. on hydrostatic press. 78−47612
polyethylene, extruded semicryst., thermal cond. and specific heat, <1K 80−59742
polyethylene, irrad., thermophys. characts. of amorphous phase, effects on crystallinity 77−7870
polyethylene, linear, after annealing at low temps. 77−39679
polyethylene, partially crystalline, far IR absorption and thermal props. 79−33690
polyethylene (orthorhombic), intermol. pot. functions, force consts., vibr. assignments, thermodynamic props. 77−39639
polyethylene terephthalate, low temp. sp. ht., effect of cooling rate 80−100336
polyisobutylene and copolymers with polyacrylonitrile, specific heat and glass transition temp. meas. *(German)* 78−34603
polymer, 223 to 383K 77−7871
polymer, conformational sp. ht. determ. method 78−14474
polymer, constant sp. ht. at glass transition, rot. degrees of freedom 79−69029
polymer, glass transition kinetic nature, sp. ht. 79−10929
polymer, glassy, ageing, scanning calorimeter meas., theoretical prediction 79−10810
polymer, packing coefficient determ. from acoustical meas. data 80−38959
polymer, thermosetting *(German)* 78−75845
polymer blends, two-component, glass transition, calorimetric investig. *(Russian)* 80−39268
polymer glass, sp.ht. discontinuity at glass transition 80−19954
polymer properties of glass transition, conformational effects anal. 79−69231
polymers, effect of glass transition temp. on thermal props. *(German)* 78−30742
polymers, glassy, Gruneisen const. calc. from thermoelastic meas. 79−14945
polystyrene, amorphous, low temp. sp. ht. calcs. 77−28014
polystyrene, amorphous, thermophysical props. depend. on hydrostatic press. 78−47612
polystyrene, filled amorphous polymer, heat capacity meas. *(Russian)* 79−65211
polystyrene, solid, low freq. Raman scatt., vibr. density of states, 29-300K 78−72516
polystyrene, sp. ht. determ. by differential scanning calorimetry 79−33101
polystyrene, sp. ht. meas. by differential scanning calorimetry 77−51515
polytrivinyl benzene, thermal and mech. props. rel. to high-press. polymerisation conditions 79−70326
polyvinylidene fluoride, heat capacity, 5 to 200K 79−86900
Potts model on square lattice, specific heat critical exponents 77−20606
powders, meas. apparatus for 4.3-300K 80−227
praseodymium ethyl sulphate, one-dimensional X-Y model, hyperfine contrib. to specific heat 79−1678
praseodymium ethyl sulphate, specific heat, electric suscept. and thermal cone., one-dimens. electric dipolar XY system 77−32148
pressurised metal, containing dislocations, quantum oscillations of thermodynamic props. *(Russian)* 79−86899
proximity sandwiches, thermodynamics of second order phase transitions 79−56408
PVC, different stereoregularities, heat treatment effect on glass transition temp. and c_p changes 79−4985
PVC, heat capacity and thermodynamic props., 6 to 375K obs. 78−79779
PVTE, heat capacity, 5 to 200K 79−86900
pyrazine, cryst. phases, entropy changes and struct. implications 80−54397
pyrazine, phase transitions, sp. ht., X-ray diffr., LF vibr. spectra 78−43122
pyridinium manganese chloride, anhydrous, quasi one-dimensional mag. behaviour, heat capacity meas. 80−80549
pyridinium nickel chloride, anhydrous, quasi one-dimensional mag. behaviour, heat capacity meas. 80−80549
pyroelectric glass, low temp. behaviour 78−56432
quantum crystal, role of defectons 77−35796
quartz, smoky, gamma-irradiated, short-time-scale sp.ht. meas. 80−59672
quartz, smoky, sp. ht. 78−71867
quartz ceramics, thermal and temp. cond. in range 500-1900K 80−39370
quasi-one-dimensional systems, free energy of Ginzburg-Landau field, equiv. Hamiltonian 78−6293
quenched random magnets, thermodynamic behaviour from position-space renormalisation group 78−68244
random anisotropy model in Ising model, Monte Carlo simulation 80−80546
random annealed one-dimensional Ising spin system, site model, specific heat, susceptibility 77−32139
random binary system, mag. transition temp. and sp. ht. 77−77065
random harmonic chain model, essential singularities of sp. ht. and density of states 77−72665
random Ising bond interactions, paramag. phase, thermodynamic props. 77−20523
random n-vector model, renormalisation group analysis, crossover behaviour 77−85459
random system, density of states, essential singularities, sp. ht., free energy 78−18729
rare earth alloy, amorphous, ferromag. state, non-axial elec. field gradient effect 80−75728
rare earth alloys, amorphous, mag. props. rel. to struct., review 79−15298

specific heat of solids continued
rare earth alloys, cryst. field effects on thermal props. 77−12072
rare earth alloys, RFe_2, (R=Gd, Tb, Dy, Ho, Er, Tm, Lu), electronic heat capacity coeffs. 80−39787
rare earth ethyl sulphates, sp. ht., susceptibility 79−24129
rare earth garnets, prep. and props. book contrib. 80−44193
rare earth impurities in s-band metals, Kondo anomaly 78−52208
rare earth intermetallics, low temp. sp. ht. 80−15259
rare earth intermetallics, RMg_2, cryst. and mag. props., ordering 78−68185
rare earth metals, heat capacity near melting pt., vacancy mechanism of melting 80−15221
rare earth metals, low temperature heat capacity, review 79−69263
rare earth metals and alloys, ferromag. props., book contrib. 80−75725
rare earth molybdenum selenides, $R_xMo_6Se_8$, coexistence of superconductivity and long-range magnetic order 79−11264
rare earth orthochromites, mag. interactions and weak ferromagnetism 78−52220
rare earth orthoferrite, stripe domain struct. near spin-reorientation points 77−24707
rare earth orthovanadites, phase transitions and Jahn-Teller distortions 79−28548
rare earth pnictides, prep. and props., book contrib. 80−54212
rare earth rhodium boride system, ternary, supercond., phase diagrams at upper crit. fields 80−2531
rare earth rhodium borides, RRh_4B_4, NMR and sp. ht. in supercond. and mag. ordered phases 80−7037
rare earth sesquisulphides, $RS_{1.5}$ (R=La,Ce,Pr,Nd,Gd,Tb,Dy,Ho,Er,Tm,Lu), sp. ht. between 2 and 20K 79−60518
rare earth systems, metallic, with unstable valence, model for thermodynamic props. 77−69487
rare earth trihydrides, light, low-temp. sp. ht., mag., elec., and cryst. field splitting effects 80−49379
rare earth-Al_2, cubic Laves phases, prep. and phys. props. *(German)* 78−23075
rare earth-Co system, spin reorientation and sp. ht. anomaly *(Japanese)* 79−47287
rare earth-transition metal alloys, amorphous, anomalous low-temp. props. 78−91872
rare gas crystals, lattice heat capacity, thermal vibrations, Lindeman parameter, lattice dynamic model *(Russian)* 80−29141
rare-earth compounds, antiferromag., mag. props., cryst. field theory 78−27006
rare-earth compounds, antiferromag., mag. props., cryst. field theory 78−27007
refractory, thermophysical props. in rarefied gaseous medium 78−34664
RKKY spin glass, conc. depend. of low temp. sp. ht. 77−12135
Rochelle salt, ferroelec. phase transition, Raman scatt. study 80−97211
Rochelle salt, high resolution heat capacity meas. *(Japanese)* 80−52218
Rochelle salt, phase transitions, high-resolution sp. ht. meas. 78−48128
rubber, natural, stretching effects on glass transition, sp. ht. obs. *(German)* 78−79753
rubber, natural, thermal properties depend. on temp. and press. 79−95223
S=1, singlet ground state systems, mag. props. 80−11157
scaling and multiplicative renormalising in solid state physics, review *(Hungarian)* 79−11289
schultenites, ferroelectric, sp. ht. 79−19853
semi-metal or degenerate semiconductor, beta effect of sp. ht. due to impurities, in external mag. field 78−10401
semiconductor, electrical method of measurement 77−51513
semiconductor, phonon conduction and relaxation times 80−107585
semiconductors, elementary excitations in disordered systems with localised electrons, polarons *(Russian)* 80−49632
semiconductors in metallic region, elec. heat capacity 79−42273
shock waves in material with linear shock wave-particle vel. relation 77−69042
silicate glass, containing ZnO and TiO_2, thermal capacity 80−88335
silicate glasses from igneous rocks, high temp. thermal props. 77−33055
silicate minerals, heat capacities rel. to simple lattice vibrational models 80−4005
silicate minerals, thermodynamics and lattice vibr. props. 79−100830
silicate minerals, thermodynamics and lattice vibrs. 79−100831
simultaneous measurement method for thermal props. of plane-shaped solids using iterative calcs. 77−42713
single-ion anisotropy, magnetic systems, high temp. series expansion 80−34576
small samples, meas. using thermal relaxation method 79−49231
smoky quartz, thermal props. at very low temp. 80−24610
soft discs, two-dimens. melting, phase transition boundary 80−96629
solid-on-solid representation, planar model Monte Carlo simulation 80−96727
spin glass, and mictomagnet, computer simulation 77−66365
spin glass, classical, Heisenberg, Monte Carlo calc. of internal energy and sp. ht. 77−20612
spin glass, cluster mean field theory 77−80949
spin glass, cluster mean field theory and evidence for spin clusters 79−78382
spin glass, cluster mean-field model, static props. 79−4689
spin glass, dipolar, anomalous sp. ht. Ising model and Monte Carlo calcs. 78−47989
spin glass, Edwards-Anderson model, appl. of Migdal's recursion relations 77−40070
spin glass, effective field distrib., time dependent order parameters 77−43843
spin glass, generalised mean field theory with spin correls. 78−2691
spin glass, infinite-ranged model, mean field theory hypothesis 80−97104
spin glass, mean field approx. 78−52280
spin glass, nonmagnetic defects, sp. ht., susceptibility and resist. determ. 79−19738
spin glass, phenomenological theory 78−19263
spin glass, self-consistent mean random field approximation, comparison with $n\to 0$ expansion 77−20622
spin glass, Sherrington-Kirkpatrick model, thermodynamic props. 79−51797
spin glass, thermodynamics, virial expansion vs. T^{-1} expansion 77−66362
spin glass behaviour, 3-dimens., using real space scaling transform. 77−69570
spin glass in d dimensions, Ashkin Teller model 79−65691

specific heat of solids continued
spin glass systems, experimental props. and theories 79−65688
spin glass transition in random bond Ising model in 2-D, and 3-D, renormalisation group approach 78−68275
spin glass with nonmagnetic defects *(Russian)* 78−60298
spin glass with short range interaction in neighbourhood of percolation threshold *(Russian)* 78−68282
spin glasses, 2-dimens., computer expts. 77−80945
spin glasses, dilute ferromagnets, ferromagnetic modes 80−93133
spin glasses, excitation exam. 79−78419
spin glasses, fluctuation theory, mag. susceptibility and sp. ht. 79−24176
spin glasses, free energy, order parameter expansion, random bond model 80−84609
spin glasses, Ising type random bond, scaling, eqn. of state and instability 79−73753
spin glasses, mag., transport props. *(Czech)* 78−80149
spin glasses, phase transition, mag. susceptibility, specific heat, Ising model calcs. *(Russian)* 80−34671
spin glasses, recent progress in numerical simulation 79−69689
spin glasses, review 77−69578
spin glasses, RKKY Ising, sp. ht. 1/T behaviour 80−11210
spin glasses, sp. ht. and susceptibility, random series method 80−44542
spin glasses, thermodynamic props., cluster mean-field theory using Ising Hamiltonian 79−33499
spin glasses, towards a mean field theory 79−99704
spin glasses (C211), collective excitations 78−56322
spin glasses with short-range interaction in mag. field 79−28539
spin model, random mag. bonds, phys. props. near crit. point 78−84440
spin system, disordered, commutator and anticommutator Green's functions 79−51792
spin system, random thermodynamic props. using Bethe-Peierls-Weiss approx. 79−78387
spin systems, random annealed, crit. amplitudes for specific heat 78−43600
spin-glass, one-dimens., sp. ht. and mag. susceptibility calcs. 80−7120
spin-Peierls transition in mag. field, phonon freq., Heisenberg model calcs. 80−25151
squaric acid, antiferroelec., struct. phase transition mechanism 80−75969
squaric acid, sp. ht. near phase transition 79−91389
standard unit, 1800-2800K, USSR 78−12665
static properties of spin systems with truncated secular dipolar coupling 78−88130
steel, alloy, thermal and electro-physical props. of various heat resisting stampings *(Russian)* 78−51698
steel, Cr, hypereutectic, ShKh15, exam. of thermal props., 298 to 1173K *(Russian)* 79−28334
steel, maraging, Ni-Co-Mo, ageing and evolution peak at 470°C, calorimetric anal. *(Japanese)* 79−100156
steel, maraging Ni-Co-Mo, strengthening by repeated strain ageing *(Japanese)* 79−100157
steel, martensitic, sp. ht. and magnetisation meas. 1.2 to 10K 80−71059
steel, Ni-Co-C (9, 4, 0.2 wt.%) enthalpy, sp. ht. to 2000K 79−10960
steel, stainless, sp. ht. 4 to 30K 79−61115
steel, stainless, specific heat, low temp. 78−83966
Stefan problem, two-phase, with varying specific heat coeffs. 77−69070
step model critical behaviour high temp. susceptibility and internal energy series 78−34987
stored energy, and increment in heat capacity due to plastic deform. 80−54302
strong-coupling superconductors, meas. of small changes in sp. ht. 77−33988
structural phase transitions, applicability of thermodynamic theory, temp. depend. of specific heat 80−2139
substitutional impurity, model parameters, determ. from low temp. data *(Russian)* 79−33007
superconducting alloys, Kondo effect, specific heat jump at transition temp. 78−6479
superconducting composites, granular, Ginzburg-Landau theory, props. 80−88673
superconducting critical temp., generalised moments of phonon spectrum *(French)* 80−39702
superconducting proximity effect, McMillan tunnelling model, sp. ht. jump 79−87201
superconductor, composite, normal zone propag. calcs. 77−43778
superconductor, effect of mag. impurities with high Kondo temp., in Anderson model 77−63023
superconductor, high T_c, dynamic instabilities 78−10607
superconductor with mag. impurities, Shiba theory consequences beyond s-wave scatt., sp. ht. discontinuity 80−2516
superconductors, granular, percolation model, specific heat, elec. resistance 80−93025
superconductors, granular, percolation theory, crit. props. 80−84575
superconductors, high T_c, anal. of data 79−38247
superconductors, magnetic impurity low temp. behaviour, transition temp., specific heat, free energy 80−88691
superconductors, relationship between crit. field and energy gap 79−65621
superconductors with Ce impurities, sp. ht. jump, unified description of demagnetisation of Ce impurities 77−69450
superionics, with fluorite structure, Brillouin scattering and lattice defect energetics 78−80369
superlattice, electron gas statistical and thermodynamic props. *(Russian)* 79−87051
surface, effects of roughness on dynamical props. 78−75923
TCNB, 10-300K 77−11702
TCNB-pyrene 1:1 charge transfer complex, 10-300K 77−11702
TCNQ alkali salt, spin-Peierls transition 80−29395
TCNQ complexes, low temps. 77−51514
TCNQ complexes, $Qn(TCNQ)_2$, NMePh.TCNQ, and Li^+TCNQ^-, mag. susceptibility and sp. ht. 78−43556
TCNQ salt, $(TMA^+)_3(I_3^-)(TCNQ^-)_2(TCNQ^0)$, struct., phys. props. and lattice distortion evidence 78−6305
TCNQ salt, acridinium $(TCNQ)_2$ low temp. heat capacity, Debye temp. 80−2180
TCNQ salt, HFTTF-TCNQ, phase transitions, calorimetry study 79−51253
TCNQ salt, HMTTF-TCNQ, metallic organic charge transfer complex, chemical prep. and phys. props. 78−2471
TCNQ salt, HMTTF-TCNQ, sp. ht., 30 to 80K 80−24614
TCNQ salt, $MEM(TCNQ)_2$, phase transitions, elec. cond., ESR, mag. susceptibility study 80−24981

specific heat of solids continued
TCNQ salt, N-methyl-N-ethyl-morpholinium-$(TCNQ)_2$, spin-Peierls transition 79−82803
TCNQ salt, quinolinium $(TCNQ)_2$, random-exchange Heisenberg antiferromag. chain, 0.07-5K 78−14976
TCNQ salt, tetramethylhexamethylenediammonium-TCNQ-iodine, elec. and mag. props., struct., specific heat 80−24898
TCNQ salts, sp. ht. meas., 0.2-300K, extended Hubbard model *(French)* 77−35710
p-terphenyl, phase transition, heat capacity meas. 79−46801
tetramethylsilane, thermodynamic props. of polymorphic phases 77−84943
tetranuclear cluster, eigenvalues spectrum of spin Hamiltonian calc., thermodynamics props. *(French)* 77−35902
tetrebromomethane, thermal resistivity, heat capacity and phase diagram under pressure 80−65316
TGFB, deuterated, single crysts., specific heat data 79−24422
TGFB, high press. influence on anomalous specific heat, tricritical point 80−25322
TGS, calorimetry, sp. ht., 0-80°C 78−15122
TGS, critical region in sp. ht. 79−28106
TGS, deuterated and undeuterated, pyroelectric, dielectric and thermal props., temp. depend. 78−43809
TGS, ferroelec., meas. of sp.ht. at constant elec. flux density by AC method 79−33098
TGS, ferroelec., phonon contributions to anomalous sp. ht. near phase transition temp. 77−52023
TGS, gamma irrad. effects on heat capacity, Curie temp., permittivity 78−67737
TGS, perfect and imperfect, sp. ht. and sound vel., crit. anomalies 80−71331
TGS, temp. depend. and effect of Cr and α-alanine impurities 78−91448
TGS γ-ray irrad. cryst., heat capacity anomalies near phase transition *(Russian)* 80−49375
TGS $(-d_5)$, sp. ht. near ferroelec. phase transition 80−70420
TGS crystals, thermal props., γ-radiation defects and inhomogeneity of domain deposition 79−46810
TGSe, acoustic and thermal anomaly correlation near ferroelec. transition 79−4775
TGSe, behaviour under press. near tricritical point 79−95716
TGSe, deuterated, thermal and dielectric props. at high hydrostatic press. 80−34864
TGSe, ferroelec., meas. of sp.ht. at constant elec. flux density by AC method 79−33098
TGSe, sp. ht. anomaly, AC calorimetric obs. 78−23414
thermal insulation on metal backing, thermophys. characts., expt. determ. technique 80−4707
thermal penetration property ρck meas. instrum. 78−70120
thin coated wire, specific heat of coating, meas. using transient acoustic Doppler effect 79−81706
thiophenechromium tricarbonyl, sp. ht. and thermal expansion tensor meas., order-disorder phase transform. obs. *(French)* 78−79788
tissue-equivalent plastic, A-150, thermal diffusivity, sp. ht., thermal cond. obs. 80−34258
TMMC, effect of impurity spins on three-dimensional ordering 79−24159
TMMC, linear antiferromag., mag. phase diagram, expt. and theoretical study 80−71038
TMMC, mag. heat capacity and Neel temp. in mag. field 79−61147
TMTTF salts, $(TMTTF)_2$-X, $(X=BF_4^-, ClO_4^-, SCN^-, PF_6^-, Br^-)$, physical props. 79−47085
transition metal, electronic sp. ht. calc. 79−73323
transition metal alloy, electronic structure, mag. props. 78−95254
transition metal alloys, electronic specific heat, near and weak ferromagnetics 78−80158
transition metal alloys, low temp. sp. ht. 79−61155
transition metal alloys and cpds., sp. ht. and electronic structure *(French)* 77−28400
transition metal borides, narrow band types, electronic density of states, many-electron Hubbard model calcs. 80−20064
3d-transition metal complexes, low spin-high spin paramag. transition, Ising model calc. 80−93073
transition metal glasses and amorphous films, supercond. and electronic props. 79−73612
transition metal magnetic alloys, dilute, props., review of theory 79−15282
transition metal nitrides, lattice sp. ht. and phonon anomalies 78−63867
transition metal sulphides, selenides and phosphides, NaCl struct., supercond. props. 79−4613
transition metal superconductors, specific heat anharmonic components, phonon freq. temp. shift *(Russian)* 79−91183
transition metals, electrnic sp. ht. and heat conduction, temp. depend. 78−71865
transition metals, group V, low temp. sp. ht. anomalies 77−77002
triangular lattice, thermodynamic props., effect of vacancy defects determ. by cell cluster method 80−79959
s-triazine, sp.ht. 130-380K, melting enthalpy and solid-state transition 79−46812
s-triazine, structural phase change, sp. ht. meas. 78−55944
triglycine fluoberyllate, pyroelectric, dielectric and thermal props., temp. depend. 78−43809
trimethylammonium cobalt trichloride:CU, bound impurity effect, heat capacity meas. 79−61146
trimethylammonium cobalt trichloride, mag. heat capacity and Neel temp. in mag. field 79−61147
trimethylammonium copper chloride dihydrate, mag. props., evidence for lattice dimensionality 77−89967
trimethylammonium manganese trichloride, Heisenberg antiferromag. chain, specific heat and EPR 80−65931
$TSeTBr_{0.5}$, phase transition, mag. props., thermal capacity and cond. *(Russian)* 79−99537
TTF(MBDT) spin-Peierls transition, mag. exchange interactions, mag. props. 80−25138
TTF-BDT(M), BDT=$S_4C_4(CF_3)_4$, M=Cu, Au, spin-Peierls transition, sp. ht. meas. 77−28401
TTF-DETCNQ, heat capacity, elec. cond., cryst. struct., metal-insulator transition 77−8077
TTF-DETCNQ, metal-insulator transition, struct., elect. cond. and sp. ht. expts. 78−14662
TTF-TCNQ, Landau free energy function, CDW-libron interaction, sp. ht. near phase transitions 80−19963
specific heat of solids continued
TTF-TCNQ, sp. ht. meas., phase transition obs. at 46K 77−43326
TTF-TCNQ and derivatives, 1.8 to 40K, three dimens. state, specific heats 80−44333
TTF-TCNQ complex, trans-diethyl-dimethyl TTF-TCNQ, one-dimens. cond. 80−96853
TTF-TCNQ powder, phase transition at 49K 77−89539
TTFCuBDT, spin-Peierls transition in spin 1/2 Heisenberg chains, RPA calcs. 80−25150
$TTF.PtS_4C_4(CF_3)_4$, quasi-one-dimensional cpd., exchange, thermal and mag. study 78−68209
TTT_2-$(I_3)_{1+x}$, physical props., elec., mag. and optical meas. 80−24908
two dimensional periodic lattice, electron ordering, CDW-disordered state transition, Hubbard model *(Russian)* 80−6754
ultrasonic method 77−89015
uniaxial ferromagnet, domain struct. in mag. field 80−103853
unsteady heat conduction accompanied by an endothermic solid reaction *(Japanese)* 79−76939
vacancy, sp. ht., macroscopic calc. 79−32989
vacancy contribution to const. press. sp. ht., pressure variation 79−1510
vacancy formation parameters from specific heat data 80−75221
valence transition, entropy and phase diagram 80−59877
vanadocene, order-disorder phase transition, sp. ht. and crystallographic study *(French)* 80−84131
weakly disordered uniaxial ferromagnet, phase transition *(Russian)* 78−23291
Wigner crystal, lattice quantum oscills. in mag. field, specific heat, mag. moments *(Russian)* 80−49636
Wolff model, thermodynamic props., local moments in dil. alloys, var. method 80−65781
X-Y magnetically dilute ferromagnet, two dimens. lattices 77−63056
X-Y model, rigorously solvable, numerical computations 77−1534
X-Y model, spin 1/2, thermodynamic props. in three dimens., high temp. series expsn. 78−47930
X-Y model, spin Peierls transition in mag. field 79−56537
X-Y model, two-dimens., vortex formation in Monte Carlo calcs. 77−63224
X-Y model critical behaviour, high temp. susceptibility and internal energy series 78−34987
xylideneaniline-p′-benzonitri 80−44328
ytterbium ethyl sulphate, crystal field effects on mag. and hyperfine props. of Yb^{3+} 80−97101
Zircaloy-2 and associated oxide layers, thermal property meas. 77−8063
$Zn_3B_7O_{13}Br$, ferroelec. 43m-mm2 phase transition, molar heat capacity meas. 80−93249
Ag, cyclotron mass and Fermi velocity meas. by de Haas-van Alphen effect 77−76734
Ag, modified CGW model calcs., phonon dispersion, sp. ht. and equiv. Debye temp. 78−10135
Ag, specific entropy and surface heat determ. as function of temp. *(German)* 80−6619
Ag, two-parameter dynamical model appl 80−10597
Ag-Ga(Ge)(In), α-phase, lattice sp. ht. calcs. 80−65246
Ag-Ge eutectic alloy, heat capacity meas. over temp. range 800-1200K *(French)* 80−88331
AgAu, quenched, short range order effects on specific heat 80−29181
AgBr NaBr, thermodynamic props., metastable states and demixing 80−96660
$AgClO_4$ benzene, complex, heat capacity 78−75843
AgCr, dil., specific heat, impurity contrib. Kondo temp. 80−65903
$AgGaTe_2$, Debye temp., standard entropies and enthalpies, sp. ht. meas. 78−30769
$Ag_2H_3IO_6$ crystal, growth, specific heat, antiferroelec. transition 77−69781
AgI type solid electrolytes, sp. ht. anomaly, theory *(Russian)* 78−10198
$AgInTe_2$, Debye temp., standard entropies and enthalpies, sp. ht. meas. 78−30769
$AgNa(NO_2)_2$, crit. sp. ht. near ferroelec. transition 79−38474
$AgNa(NO_2)_2$, Landau behaviour of sp. ht. close to nearly tricritical ferroelec. phase transition 78−10861
$AgNa(NO_2)_2$, single cryst., specific heat anomaly, −90-55°C, ferroelec. transition entropy 77−77157
Ag_3SI, superionic conductor, ordered phase struct. 78−83792
Ag_3SI, superionic cond., phase transition and cryst. structs., sp. ht., neutron and X-ray diffr. obs. 80−10662
Al, 0-100 kbar, press. depend. 77−51512
Al alloy, 51S, modified by misch metal, for space appl. 80−55466
Al film, lattice and bulk heat capacity meas. for normal and supercond. states 80−92684
Al, granular film, heat capacity, 0-4.5K, crit. coupling between grains 78−84348
Al, Nernst-Ettingshausen coeff., transport heat capacity 78−26848
Al, phonon density of states by neutron scatt., sp. ht. and Debye temp. 80−2132
Al, phonon dispersion relations and lattice heat capacity calc. 77−20023
Al, phonon dispersion relations and lattice heat capacity, modified Bhatia model 77−20024
Al, specific entropy and surface heat determ. as function of temp. *(German)* 80−6619
Al, superconducting band gap anisotropy and Fermi surface anisotropy *(Spanish)* 80−84544
Al, two-parameter dynamical model appl. 80−10597
Al, validity of Nernst-Lindemann eqn. over temp. range 293 to 925K 77−72695
Al-3d transition metal, dil., transport props., sp. ht. and supercond. ant. temp. calcs. 77−1393
Al-Ce, very dil. alloy, low temp. sp. ht. 79−51745
Al-Li alloy, thermal anal. of precipitation 78−15417
Al-Mg-Zn solid solution, thermophysical props., 0-400°C *(Russian)* 77−89548
Al-transition metal alloys, anomalous sp. ht. and nuclear spin-lattice relax. 79−46814
Al_3Ce, thermal expsn. below 1K 79−90803
Al_2O_3, heat capacity laser-flash calorimetry 80−4716
α-Al_2O_3, synthetic sapphire, heat capacity, 300 to 550K 79−21754
Al_2O_3, therm. characts. using constant power source method 79−95222
β-Al_2O_3-M_2O, M=monovalent metal, superionic cond., phonon spectra and sp. ht. calc. 77−24368
β-Al_2O_3-M_2O_3 (M=Li,Na,K,Ag), 0.1-1 K, evidence for localised low-energy excitations 78−34632

specific heat of solids continued
Al_2O_3-SiO_2-Na_2O-CaO-MgO-Fe_2O_3-SO_3 glass, thermal capacity meas. at low temps. 80−44334
β-Al_2O_3.$Li_2O(Na_2O)(K_2O)(Rb_2O)(Ag_2O)$, low temp. sp. ht., tunnelling states and diffusion theory 77−43345
$Al_{10}V$, well defined local modes, low temp. heat capacity meas. 78−26648
$Al_{10}V$-Ga, dil., well defined local modes, low temp. heat capacity meas. 78−26648
$(Al_xV_{1-x})_2O_3$, heat capacity anomalies, metal-insulator transition, phase diagram 77−11701
Am, elec. resist. and sp. ht. 78−47762
Am, superconducting critical field, sp. ht. 80−11136
^{241}Am metal, specific heat, 15 to 300K 77−28019
Ar, solid, equilib. props., uncorrel. pairs approx. 80−84303
Ar, solid, heat capacity, possible dimens. effect 78−75844
Ar, solid, phonon freqs., lattice heat capacities, and Debye charact. temps. 79−10905
Ar, solid, phonon spectrum, effect of 3-body forces and anharmonicity 79−77706
Ar, solid, thermodynamic props. under press., multiparametric pairwise and Lennard Jones potential calcs. 80−39316
Ar, solid, vibr. and thermal props., effect of polarisability 78−71807
As, amorphous, 2 to 23K, phonon frequency distrib. 78−30723
As, amorphous, low temp. thermal cond. and sp. ht. 79−28161
As, amorphous, optical, vibr., transport and defect-related props., review 79−51935
As, amorphous, sp. ht. and thermal cond. at low temp. 79−65213
As, bulk amorphous, sp ht. meas., 1.8-20K 78−22866
As-S, amorphous, glass transition and specific heat, intermolecular bond saturation 80−15011
As-Se, amorphous, glass transition and specific heat, intermolecular bond saturation 80−15011
As_2S_3, vitreous, thermal capacity, 300 to 600K 80−103492
As_2Se_3 glass, heat capacity and struct. relaxation of enthalpy 77−55360
As_2Se_3, vitreous, thermal capacity, 300 to 600K 80−103492
$(AsSe)_{1-x}Te_x$ glasses, thermal props. and viscosity, temp. and conc. depend. 77−76324
As_2Te_3, vitreous, thermal capacity, 300 to 600K 80−103492
Au, cyclotron mass and Fermi velocity meas. by de Hass-van Alphen effect 77−76734
Au, modified CGW model calcs., phonon dispersion, sp. ht. and equiv. Debye temp. 78−10135
Au-Cd alloy, α and ζ phase, low temp. sp. ht. 78−18789
Au-Fe (1 at.%), spin glass, specific heat 80−60355
Au-Fe spin glass, long-time relax. processes, heat capacity expts. 77−66374
Au-Ni, fast liq. quenched, anomalous sp. ht. near ferromag. crit. comp. 77−80947
Au-Ni, heat capacity, 1.5 to 15K 78−95452
Au-Ni, magnetisation and sp. ht., ferromag., paramag. and crit.-conc. regions 79−38330
$Au_{1-x}Fe_x$, $0.14<x<0.28$, ferromagnetism study by specific heat meas. 80−7121
$AuGa_2$, supercond., press. depend., theor. *(Russian)* 77−51843
BAs and B_6As, temp. depend., 55 to 310K 77−24414
B_4C, thermophysical props. and neutron absorpt. 80−103488
BN, hexagonal, parallel to basal planes, thermal conductivity 78−22907
BN, wurtzitic, temp. charcts. of thermodynamic props., 5-320K 77−55361
B_2O_3glass, effect of thermal treatment on low temp. specific heat 80−54401
BP, sp. ht., Debye temp., compressibility and Gruneisen coeff. meas. 78−63865
$BaCo_2(AsO_4)_2$, quasi 2D XY helimag., sp. ht. meas. 79−61151
$BaCo_2(PO_4)_2$, quasi 2D XY helimag., sp. ht. meas. 79−61151
Ba_2NiF_6, specific heat capacity, critical amplitude, cross-over from 2-D Ising to Heisenberg behaviour 80−39791
$BaNi_2(PO_4)_2$ and $BaNi_2(AsO_4)_2$, mag. props., neutron diffr. and sp. ht. meas. 80−70948
BaO, lattice dynamics, sp.ht., Debye temp. and Raman spectra calc. 77−1195
$BaTiO_3$, soft mode dielec., anomalous low temp. sp. ht. 78−14423
$BaTiO_3$, thermodynamic props. 77−39680
$BaZrO_3$, high-temp. enthalpy and specific heat, method of mixtures 77−35712
Be, HCP, electron-phonon interaction, thermal effects 79−33057
Be, spin susceptibility, electronic effective mass, spin density functional calcs. 78−43291
$Be_5(Fe_{1-x}Mn_x)$, mag. and calorimetric props. 77−63083
Bi, phonon density of states by neutron scatt., sp. ht. and Debye temp. 80−2132
$Bi_3Sr_{1-x}Eu_x$, supercond. and mag. ordering 78−56252
C, amorphous, anomalous low temp. mag. and thermal props. 78−10647
C, anthracene char, density fluctuations effect on physical properties 78−51420
C, soft, low temp. sp. ht. anomalies, spin-spin interactions 79−15307
C, soft, sp. ht., 0.4-4.5K, rel. to localised spin transition 77−28389
C, soft and hard, sp. ht. anomalies and spin-spin interactions, review 79−69261
C, synthetic mats., 50-3000K 77−84942
C, vitreous, low temp. sp. ht., thermal cond. and US vel. meas. 78−47533
CMN-^{3}He(^{3}He-^{4}He), heat capacity and heat transfer meas. instrum. *(French)* 79−1097
$C(NH_2)_3V(SO_4)_2.6H_2O$, low temp. mag. props., mag. sp. ht. *(Japanese)* 78−19268
$C_{24}Rb$, intercalated graphite, resistivity and specific heat anomalies 80−107440
$Ca_3Al_2Si_3O_{12}$, garnet, thermophysical props., 5 to 600K 79−60517
CaBr(Cl)(I), Gruneisen γ and other thermodynamic props. at zero and elevated press. 78−43142
CaF_2, lattice dynamics in ang. force model, Debye-Waller factors, sp. ht., dispersion relations 77−59081
CaF_2:Dy^{3+}, cubic cryst. field effects 80−2368
CaF_2+Yb^{3+}, Stark level Zeeman energies, mag. susceptibiltiy, Schottky specific heat, crystal field splitting 78−26831
$CaNi_5$, Haucke compounds, low temp. heat capacity, Debye temp. 80−96663
$Ca_{10}(PO_4)_6(OH)_{2-2x}O_x\square_x$ polycryst. sintered bodies, prep. and thermal props. 80−25624

specific heat of solids continued
$CaV_{12}O_{30}$, phase transitions, elec. cond., susceptibility and sp. ht. meas. 78−14776
$CaWO_4$:Er^{3+}, magnetocaloric behaviour, cryst. field theory 77−4520
Cd, phonon dispersion relations, specific heat by modified Cheveau model 78−38792
$CdAs_2$, thermodynamic functions 79−10961
$Cd_3Cr_2Ge_3O_{12}$, antiferromagnetic ordering of Cd^{3+}, sp. ht. and mag. susceptibility meas. 77−16062
$CdCr_2S_4$, thermodyn. props. 78−51703
p-$CdCr_2Se_4$, resistivity anomalies at mag. transitions, sp.ht. 80−39785
CdF_2, low temp. heat capacity 78−47490
$Cd_{0.010}Fe_{2.990}O_4$, heat capacity investigation of dopant effects on mag. disordering temp. 80−25143
$CdNb_2O_6$, sp. ht. and Debye temp. meas., 2-25K 79−73319
$Cd_2Nb_2O_7$, ferroelec., sp. ht. and Debye temp. meas., 2-25K 79−73319
CdP_4, thermodynamic functions, 55-300K 80−34203
Cd_3P_2, Cd_3As_2, sp. ht., thermodyn. props. 78−22863
$Cd_3(PS_4)_2$, synthesis by roasting, and exam. of props. 79−4926
$Cd_{1.6}Pd_{0.4}Nb_2O_7$, ferroelec., sp. ht. and Debye temp. meas., 2-25K 79−73319
$Cd_2Re_2O_7$, specific heats, electronic and lattice contrib. below 20K 80−34200
$Cd_2Ru_2O_7$, specific heats, electronic and lattice contrib. below 20K 80−34200
CdSb, thermodynamic props. 79−77767
$CdTl_2Te_4$, single and polycryst. samples, linear expansion, heat capacity and thermodynamic props. 80−103489
(Ce, La)In_3, heat capacity and elec. resist. 80−71049
Ce, 0-16 kbar, press. depend. 77−51512
Ce binary and pseudobinary intermetallics, struct. and mag. data 80−20129
Ce, determ. at 300K, up to 20 kbar *(French)* 79−95177
α-Ce, exchange-enhanced, elec. resist. T^2 depend., press. effect 80−96845
β-Ce, heat capacity redeterm. 77−20617
γ-Ce, lattice and spin dynamics, inelastic neutron scatt. obs. 79−86859
Ce, sp. ht. and temp. coeff. of resist., 20 kbar at 300K 78−83973
α-Ce, susceptibility, sp. ht. and magnetisation 79−28512
Ce-alloys, abnormal ordered Kondo lattice 78−47947
Ce-La, mag. ordering, sp. ht., susceptibility and resist. 78−68238
Ce-Th, mag. suscept. and sp. ht. 79−78411
$CeAl_2$, and $CeAl_3$, magnetisation and sp. ht. 80−20418
$CeAl_2$, antiferromag. ordering between 4f shells, Kondo effect 80−20417
$CeAl_2$, conf. Kondo system, sp. ht. meas. 78−52210
$CeAl_2$, pure and $LaAl_2(YAl_2)$ diluted, collective phenomena 80−65933
$CeAl_2$, sp. ht. in high mag. fields, Kondo effect 78−52284
$CeAl_2$, specific heat between 0.02 and 1K 79−1680
$CeAl_3$, sp. ht., Kondo effect and ferromag. order coexistence 80−65927
$CeAl_3$, sp. ht. anomalies due to presence of $CeAl_{11}$ 79−19745
Ce_3Al_{11}, sp. ht., Kondo effect and ferromag. order coexistence 80−65927
CeB_6, anomalous sp. ht. intrinsic mag. phase transitions obs. 80−108027
CeB_6, mag. and electronic props. 80−71048
$CeCu_2Si_2$, collective phenomena 80−65933
$CeH_{2.70}$, low temp. phase transition, sp. ht. meas. 78−47535
$CeH_{2.70}$, sp. ht., 2 to 260K, second-order phase transitions and cryst. field splitting 79−82355
Ce(In, Sn)$_3$, heat capacity and elec. resist. 80−71049
$CeIn_3$, magnetisation and sp. ht. 80−20418
$Ce_2Mg_3(NO_3)_{12}$, heat capacity meas., 0.15 to 0.6K, origin of anomaly 77−35707
$Ce_2Mg_3(NO_3)_{12}$ thermometry, for sp. ht. meas. below 10 mK 79−88955
CeP(As), single crystals, low temp. thermal, electrical and mag. props. meas. 78−27051
$CePd_3$, susceptibility, sp. ht. and magnetisation 79−28512
CeS, mag. props., sp. ht. and thermal expansion 78−60292
$Ce_2(SO_4)_3.9H_2O$, grown from solution, exam. of Raman spectra and physical props. 79−52104
CeSe, mag. props., sp. ht. and thermal expansion 78−60292
CeTe, mag. props., sp. ht. and thermal expansion 78−60292
$CeTl_3$, mag. susceptibility, magnetisation, neutron diffr., elec. resist., and sp. ht. meas. 80−75733
ClO_3F, heat capacity, permittivity, thermodynamic props., 2.7 to 160K 77−35713
Co, Co alloys, electrical resistivity and specific heat meas., anomalies rel. to thermally excited states 80−6809
Co complex, $CoCl_2.2$ pyrazine, mag. sp. ht. below 2K 79−61152
Co complex, $Co(C_3H_4N_2)_6(NO_3)_2$ and $Co(C_{11}H_{12}ON_2)_6(ClO_4)_2$, paramag., hyperfine sp. ht. 77−55683
Co complex, $Co(C_5H_5NO)_6(ClO_4)_2$ and $Co(C_5H_5NO)_6(BF_4)_2$, $S=^1/_2$ XY magnet, sp. ht. below 1K 77−55682
Co complex, $Co(C_5H_5NO)_6I_2$, simple cubic X-Y mag., specific heat, mag. exchange anisotropy meas. 78−39346
Co complex, Co(II)(1,2,4-triazole)$_2$$(NCS)_2$ quasi two-dimens. canted S=1/2 antiferromag. 80−70976
Co, ferromagnetic, anomalies in thermal expansion and heat capacity 79−73744
Co, lattice sp. ht. calc. 79−69262
Co, Stoner model, mol. field coeff., temp. and field depends. 77−72975
CoB, thermophysical props., 296-2000K 78−14477
CoB_{12}, growth from melt and phys. props. 80−20782
$CoCl_2$, antiferromag., phase diagram, heat capacity meas. 80−93126
$CoCl_2.2NC_5H_5$, quasione dimens. Ising system, thermodynamic props. 78−27042
CoMn(Cr)(V)(Ti), dil., low temp. specific heat and magnetisation 80−65925
$Co(NH_4)_2(SO_4)_2.6H_2O$ Tutton salt, low-temp. spin orientation, mag. props. 0-0.1K, sp. ht. temp. depend. 79−15286
$Co_xNi_{1-x}Cl_2.6H_2O$, calorimetry, γ-type transitions of sp. ht. 78−68256
CoSb alloys, sp. ht. and thermal expansion 77−47587
$CoSe_2$, paramag. metal, sp. ht., Mossbauer effect, absence of ordering 77−16036
$CoTi_{1-x}Al_x$, mag. and electronic props., ferromag. and paramag. state 80−65814
CoZn, complex, $Co_pZn_{1-p}(C_5H_5NO)_6(CPO_4)_2$, dilute simple-cubic antiferromag., sp. ht. near crit. conc. 79−38336
$Co_{1-x}Zn_x$hexa(pyridine-N-oxide)$(ClO_4)_2$, dilute cubic S=1/2 XY antiferromag., sp. ht. data 77−66358
$Co(urea)_2Cl_2.2H_2O$, two-dimens. mag. props., cryst. struct., specific heat 80−75777

specific heat of solids continued
Cr complex, $[Cr_3(CH_3COO)_6(OH)_2]Cl.8H_2O$, mag. sp. ht. *(Japanese)* 79−33501
Cr complex, trimeric clusters, low temp. mag. props. 78−76261
Cr, enthalpy and specific heat, empirical eqn. *(Russian)* 80−92683
Cr, lattice dynamics, and sp. ht., extended de Launay model 79−46762
Cr, lattice sp. ht., Clark-Gazis-Wallis ang. force model 78−22799
Cr, specific heat of strained and annealed samples 79−38331
Cr, thermal vacancies, energy of form. and conc. 80−29014
Cr-Fe, antiferromag. sp.ht. around Neel point 79−73750
Cr-Fe (0.8-8 at.%) alloy, mag. phase transforms obs. *(Russian)* 77−80941
Cr-Fe alloy, mag. phase transition, sp. ht. meas. 77−12120
Cr-Fe-Si alloy, 1.4-4.2K 77−20079
Cr-Mn (0.5 at.%) alloy, mag. phase transforms. obs. *(Russian)* 77−80941
Cr-V, itinerant electron antiferromag., spin fluctuations, low temp. specific heat 80−107439
CrAs, heat capacity, enthalpy increments, thermodynamic props., 5 to 1280K 78−91450
CrB_2, CrB, and Cr_5B_3, mag. and thermal props. at low temps. 80−20385
$Cr_3B_7O_{13}Cl$, ferroelec. 43m-mm2 phase transition, molar heat capacity meas. 80−93249
CrCo, dil., low temp. specific heat meas., 1.5 to 4K 80−60328
CrF_2, heat capacity, entropy, 10-300K, mag. ordering effects 79−87264
CrH, electronic props., H alloying effects, book contrib. 79−82522
Cr_2O_3, specific heat near. Neel temp. 77−63207
Cr_2S_3, enthalpy and specific heat, temp. depend. 80−54406
$CrSb_2$, heat capacity and thermodynamic props., mag. transition, enthalpy of decomposition 78−43591
Cr_3Se_4, mag. susceptibility and sp. ht. meas. *(French)* 79−56507
$Cr_3Se_xS_{4-x}$, mag. susceptibility and sp. ht. meas. *(French)* 79−56507
Cr_3Si, specific heat at low temps., electron density of states, Debye temp. *(Russian)* 80−54398
$CrVO_4$, temp. depend. of heat capacity, 60-1080K, Debye temp. 77−7869
CsBr, thermodynamic props., lattice dynamical calc. 77−20090
$CsCaCl_3$ crystal, sp. ht. and thermal expansion coeffs. 80−10681
$CsCoCl_3.2H_2O$, pseudo one-dimens. Ising-like system, mag. heat capacity and metamag. transitions 77−66351
Cs_2CoCl_4, heat capacity below 1K, rel. to S=1/2 linear chain XY model 77−59415
Cs_2CoCl_4, paramag. mag. exchange rel. to low temp. mag. characts. 77−55669
$Cs_2Co_{1-x}Zn_xCl_4$, mag. sp. ht., effect of dilution, comparison with linear XY antiferromag. 77−66354
$CsFeF_4$, two dimensional structural phase transitions, sp. ht., optical, dielec., X-ray diffr. meas. 79−69240
CsI, thermodynamic props., lattice dynamical calc. 77−20090
$CsMnBr_3.2H_2O$, pseudo-one-dimensional mag. system, low-temp. sp. ht. 77−85471
$CsMnCl_3.2H_2O$, Heisenberg antiferromag., linear mag. birefringence meas., rel. to mag. sp. ht. 77−16277
$CsMnCl_3.2H_2O$, linear antiferromagnet, specific heat, exchange interactions and anisotropy effects 77−1556
$CsMnCl_3.2H_2O$, pseudo-one-dimensional mag. system, low-temp. sp. ht. 77−85471
$CsMnCl_3.2H_2O$, spin wave anal. 77−8292
$CsMn_{1-x}Co_xCl_3.2H_2O$, random mag. mixture, mag. torque and sp. ht. expts. 80−60323
$CsMnF_3$, ordering temp., virtual bicritical pt. 79−61128
$CsMnF_3$, specific heat, crossover from Heisenberg to XY like behaviour 77−85461
CsN_3, heat capacity from 5 to 350K 79−55901
$CsNiBr_3$, double ordering in mag. linear chain system, sp. ht. and NMR data 79−28545
$CsNiBr_3$, nearly one-dimensional antiferromag., thermal and mag. props. meas. 77−77041
$CsNiCl_3$, double ordering in mag. linear chain system, sp. ht. and NMR data 79−28545
$CsNiCl_3$, nearly one-dimens. antiferromag., mag. sp. ht. determ. 77−24702
$CsNiF_3$, one dimensional planar model with symm. breaking fields, thermodynamics, static props. 80−97111
Cs_2O-SiO_2 glass, low temp. heat capacity 80−49373
Cu, 0-100 kbar, press. depend. 77−51512
Cu complex, hexa(pyridine-N-oxide)$(BF_4)_2$, Heisenberg antiferromag., mag. props. and sp. ht. 78−23287
Cu, cyclotron mass and Fermi velocity meas. by de Haas-van Alphen effect 77−76734
Cu, heat capacity, 2 to 6.5K, using resistive SQUID 79−63213
Cu, high-cond., high spt. ht., for cryogenic appl., prep. 78−76670
Cu, lattice specific heat, from two-parameter lattice dynamical model with dispersion 80−10678
Cu, modified CGW model calcs., phonon dispersion, sp. ht. and equiv. Debye temp. 78−10135
Cu, nonlinear diffusion eqns., identification of thermal cond. and sp. ht. *(French)* 77−47614
Cu, recrystallisation of room-temp. deformed torsion samples, microcalorimetry 77−28827
Cu, standard sample, 2-30K *(German)* 77−87763
α-Cu-Al, binary substitutional, short-range ordering kinetics, vacancy behaviour 78−55867
Cu-Al, heat capacity of phases, 233 to 800K, heat of transform. and entropy 77−47589
α-Cu-Al, kinetic behaviour of vacancies and atoms 79−28129
Cu-Au, dil., enhanced lattice sp.ht. 78−51699
Cu-Fe, dilute, low temp. heat capacity in mag. field, superparamagnetism 80−39804
Cu-Gd_2O_3, high sp. ht. metal for supercond. composite 77−40404
Cu-Mn, classical RKKY model, thermodynamic props. 78−39333
Cu-Mn, dil., mag. heat capacity, conc. and temp. depend. 79−61164
Cu-Mn (3.%), specific heat below 3K 79−61165
Cu-Mn spin glass, specific heat below 3K, spin glass freezing temp. 79−95600
Cu-Pt, ordered equiatomic, lattice specific heat meas., Debye temp. 80−54396
Cu-Zn alloy, molecular dynamic exam. of perfect and imperfect cryst. 77−39647

specific heat of solids continued
Cu-Zn-Al cubic alloy, phonon sp. ht. near martensitic transform. 79−60521
Cu-Zn(Ge)(Ni)(Ga), α-phase alloys, lattice sp. ht. calcs. 80−65246
CuAu I, ordered equiatomic, lattice specific heat meas., Debye temp. 80−54396
$Cu_3B_7O_{13}Cl$, ferroelec. 43m-mm2 phase transition, molar heat capacity meas. 80−93249
CuBr, specific heat and lattice dynamics 79−37798
$Cu(C_5H_5NO_6)(BF_4)_2$, sp. ht. and susceptibility, comparison with quadratic spin 1/2 Heisenberg antiferromag. calcs. 77−66353
CuCl, polycryst., meas. at low temps., Debye temps. 77−55367
CuCr, dil., specific heat, impurity contrib. Kondo temp. 80−65903
$CuCr_2O_4$, heat capacity, entropy, polymorphic transition, 298-1000K 78−10196
CuF_2, heat capacity, entropy, 10-300K, mag. ordering effects 79−87264
$Cu_{0.5}Fe_{2.5}O_4$, ferrite, determination of specific heat at 298-800K 80−2579
CuI, ionic motions nature, mol. dynamics calcs., sp. ht. anomaly due to order-disorder transform. 80−107533
CuI, specific heat and lattice dynamics 79−37798
$Cu_{1/2}In_{1/2}Cr_2S_4$, transition from long-range to short-range mag. ordering 77−36087
$CuInSe_2(S_2)(Te_2)$, Debye temp., standard entropies and enthalpies, sp. ht. meas. 78−30769
CuMn spin glass, specific heat and entropy 80−60354
$Cu_2Mo_6S_8$, normal state and superconducting property measurements 78−91660
$Cu_xMo_6S_8$, $1.5 \leq x \leq 3.55$, low temp. phase diagram, 1.2-320K 77−85371
$Cu(NH_4)_2Br_4.2H_2O$, Heisenberg ferromag., corrections to scaling in sp. ht. 77−66328
$Cu(NH_3)_4(NO_3)_2$, single cryst., low temp. susceptibility and sp. ht., 10 behaviour 77−89929
$Cu(NO_3)_2.2^1/_2H_2O$, singlet ground-state system, mag. props., short-range ordered state 78−23289
$Cu(NO_3)_2.2^1/_2H_2O$, singlet ground state system, mag. props. 80−44850
$Cu(NO_3)_2.2.5H_2O$, linear Heisenberg antiferromag., mag. and thermodynamic props. 79−61136
CuPt, specific heat, Debye temp. below 30K 78−55956
CuSe, lattice expansion, elec. cond. and sp. ht. at 326K transition 77−51491
$CuSeO_4.5H_2O$, $CuSO_4.5H_2O$ and $CuBeF_4.5H_2O$, linear-chain antiferromag., mag. phase transition investig. 77−55684
$Cu_xV_2O_5$, nonmetallic bronze, low field sp. ht. and mag. suscept. 78−72357
$Cu_xZn_{1-x}SiF_6.6H_2O$, heat capacities and thermodynamic props., 14 to 300K, cooperative Jahn-Teller transition 80−21314
cyclopentane, plastic cryst. and liq. phases, thermal cond. and sp.ht., 100-300K, 0-2.1 GPa 78−34663
D-T, estimated heat capacity, enthalpy, thermal cond. and diffusivity 77−4228
D_2, effect of Ne impurities 79−33099
DI, thermodynamic properties 78−47517
$D_3O.ClO_4$, specific heat anomalies, investig. of solid phases 77−47591
DX, X=Cl, Br, I, thermodynamic properties, phase transitions 78−47518
Dy, critical exponents and amplitude ratios from elec. cond. data, theoretical model 80−50126
Dy, mag. contrib. to sp. ht. 79−28538
Dy, resistivity anomalies at mag. transitions, sp.ht. 80−39785
Dy-Cu, amorphous, mag. phase diagram, magnetisation and sp. ht. meas. 80−80532
Dy-Cu amorphous mag. alloy, linear sp. ht. due to single-ion excitation 78−91874
DyAG, cubic antiferromagnet, multiaxis phase transitions 79−78377
$DyAl_2$, sp. ht. and thermal props., 5 to 300K 77−43342
$DyAsO_4$, first order Jahn-Teller phase transition, sp. ht. and refr. index meas. 80−59645
$DyAsO_4$, phase transitions obs. 80−70412
$Dy_3Ga_5O_{12}$, dipolar magnet, sp. ht. and magnetisation meas. 80−60344
$Dy_3Ga_5O_{12}$, sp. ht. meas., 0.4-90K 77−55680
$Dy_3Ga_5O_{12}$, sp. ht. meas, 37mK-2K 77−85476
$Dy_{1.2}Mo_6S_8$, low temp. heat capacity anomaly rel. to antiferromag. transition in supercond. state 80−25044
$Dy_2O_2SO_4$, antiferromag., specific heat, 0.6 to 30K 79−33487
$DyVO_4$, phase transitions obs. 80−70412
Dy_2ZrS_5, mag. and sp. ht. meas. on polycrystalline samples 78−23253
Er, mag. contrib. to sp. ht. 79−28538
Er, specific heat and compression curves 79−51272
$ErAl_2$, sp. ht. and thermal props., 5 to 300K 77−43342
$ErFe_2$, crystal field interaction contribution to specific heat 80−39788
$Er_{1-x}Ho_xRh_4B_4$, ferromagnet, sp. ht anomaly at lower superconducting transition temp. 79−47194
$Er_xLa_{1-x}Be_{13}$, mag. sp. ht. and ESR, cryst. field interactions 80−60290
$Er_xLa_{1-x}Cu$, and $Er_xY_{1-x}Cu$, antiferromag., mag. and resist. behaviour 80−34412
$Er_xMo_6Se_8$, long-range antiferromag. order and supercond. coexistence 78−10715
$ErNi_{0.6}Cu_{0.4}$, sp. ht. and modulated mag. struct. 77−32167
$Er_2O_2SO_4$, antiferromag., specific heat, 0.6 to 30K 79−33487
$ErPd_3$, specific heat at low temp. 80−20413
$ErRh_4B_4$, ferromag. superconductor, vortex phase 80−80441
$ErRh_4B_4$, superconducting and normal state props. 79−73632
$ErRh_{1.1}Sn_{3.6}$, synthesis, supercond. and mag. props. 80−100547
Er_2ZrS_5, mag. and sp. ht. meas. on polycrystalline samples 78−23253
EuB_6, electronic struct., transport and mag. props. 80−96782
EuB_6, ferromag. and antiferromag. sp. ht meas., 1.8-77K 80−65948
EuB_6, mag., transport and thermal props. 79−73738
$EuCl_3$, heat capacity and Schottky anomaly, 5 to 350K, entropy 77−47588
$Eu_3Ga_5O_{12}$, sp. ht. meas., 0.4-90K 77−55680
$Eu_{1-x}Gd_xO$, mag. semicond., magnetocaloric effect 79−69688
$Eu_{1-x}Gd_xS$, concentrated system with ferromag. and antiferromag. interactions, spin-glass props. 80−34639
$Eu_2Ir_2O_7$, pyrochlore, sp. ht. below 20K, Debye temp. 80−65241
EuO, Heisenberg ferromagnet, exchange interactions, neutron scatt. expts. 77−20579
EuO:Gd, critical specific heat depend. on doping, microwave cond. 79−95602
$EuO_{1.05}$, specific heat, mag. phase transition 77−36077

specific heat of solids continued
Eu_2O_3, mech. and physical props. rel. to reactor control rod appl. 78−21641
Eu_2O_3, thermophysical props. and neutron absorpt. 80−103488
$Eu(OH)_3$, heat capacity from near 5 to 350K, lattice and Schottky contribs. 80−49374
$EuPO_4$, enthalpy and heat capacity, 298.15-1600K 77−12559
EuS, heat capacity near ferromag. transition 78−47986
EuS, Heisenberg ferromagnet, exchange interactions, neutron scatt. expts. 77−20579
$EuSO_4$, sp. ht. and susceptibility meas. 78−14977
$Eu_{1-x}Sm_xO$, mag. semicond., thermodynamics of mag. quasimols. 78−19266
$EuSm_2S_4$, mag. props. 78−68237
$Eu_5Sn_3S_{12}$, mag. and thermodynamic props., metamagnetism 80−60273
$Eu_xSr_{1-x}S$, Heisenberg spin glass system, excitations 80−84610
$Eu_xSr_{1-x}S$, insulating spin-glass, sp. ht. near ferromag. onset 80−34667
$Eu_xSr_{1-x}S$, insulating spin glass, sp. ht. near ferromag. onset 80−97106
$Eu_xSr_{1-x}S$, spin glass, spin wave modes and low temp. sp. ht. 80−80538
Fe alloys, magnetic sp. ht., Curie temp., alloying effects model 79−61116
Fe complex, bis(N,N-diethyldithiocarbamato)-iron chloride, ferromag., sp. ht. meas., 0.4-20K 78−19258
Fe complex, Fe(1,2,4-triazole)$_2$(NCS)$_2$, quasi-2-dimens. S=$^1/_2$ antiferromag., mag. props., hidden canting 80−107986
Fe complex, hexa(pyridine-N-oxide)$(ClO_4)_2$, sp. ht., comparison with simple cubic S=1/2 Ising magnet 78−23290
Fe, electronic heating in modulation meas. method 80−24609
Fe, heat capacity temp. depend. meas., internal energy and entropy, anharmonic theory calcs. *(Russian)* 80−54402
α-Fe, lattice sp. ht., Clark-Gazis-Wallis ang. force model 78−22799
Fe, phase transition thermodynamics 78−18769
Fe, point defect estimation from specific heat and volume in plastically deformed pure metals *(Russian)* 80−54223
Fe, resistivity anomalies at mag. transitions, sp.ht. 80−39785
Fe, Stoner model, mol. field coeff., temp. and field depends. 77−72975
Fe-alloy, FCC, Invar, thermally excited electron transitions 79−56559
Fe-Co-Ti(V)(Cr)(Mn), sp. ht. in ordered and disordered phases 80−71061
Fe-Cr-Al alloys, low temp. sp. ht., resistivity and coercive force 78−63866
Fe-Cu-C alloy, sintered with added S, thermophys. props. 79−61541
Fe-H system, specific heat 7 to 60K 79−99332
Fe-N (10 at.%), structural transforms., expt. investig. *(Russian)* 77−12613
Fe-Ni alloy, diffusivity, heat capacity and thermokinetic behaviour, simultaneous meas. *(French)* 77−1235
Fe-Ni alloys, FCC, mag. props. calc. 79−65659
Fe-Ni alloys, lit. review *(Russian)* 78−18805
Fe-Ni binary alloy, specific heat temp. depend., α to γ transformation *(Russian)* 79−83198
Fe-Ni-Cr, mag. props. in weak mag. fields *(Russian)* 80−75771
Fe-Ni-Mn martensitic alloy, precipitation 77−12630
Fe-O, exam. of thermodynamic data, using a computer aided strategy 79−11592
Fe-Pt Invar alloy, homogeneous strong ferromagnet, thermal expansion and mag. props 79−91278
Fe-Ti (V)(W), dil., thermophysical props. and elec. cond., temp. depend. 80−96842
Fe-V(Cr)(Mo)(W)(Ti)(Nb) alloys, split bands evidence from sp. ht. and elec. transport data 77−24515
FeB, thermophysical props., 296-2000K 78−14477
$Fe_{80}B_{20}$, elastic, magnetoelastic and thermal props. 79−19759
$Fe_{80}B_{20}$, metallic glass, low temp. specific heat, metalloid effects 80−34654
$Fe_3B_7O_{13}I$, ferroelec. 43m-mm2 phase transition, molar heat capacity meas. 80−93249
$Fe_3B_7O_{13}I$, spontaneous polarisation, dielec. const., d.c. resist., sp. ht. 77−1643
$Fe_{82}B_{15}Si_3$, metallic glass, low temp. specific heat, metalloid effects 80−34654
$FeCl_2$, metamagnet, scaling props. of magnetisation and heat capacity, test of tricritical scaling 80−60336
$FeCl_2.2H_2O$-$CoCl_2.2H_2O$ random mixture, phase diagram 79−73748
FeCo, ordered alloy, 550°C change, study through elec. cond. and specific heat meas. 78−56633
$Fe_{(1-x)}Co_xCl_2.2H_2O$, random mixture of anisotropic antiferromags., isotropic state obs. 78−84396
$Fe_{(1-x)}Co_xCl_2.2H_2O$, antiferromag. random mixture, sp. ht. meas. 79−65678
$Fe_xCo_{1-x}S_2$, ferromagnetic solid soln., electronic sp. ht. coeffs., calc. by CPA and Hartree-Fock approx. 79−7990
$Fe_{1-x}Co_xSi$, mag. props., sp. ht., n.m.r. and Mossbauer effect meas. 77−12129
$Fe_xCo_{1-x}Si$(Ti), magnetic props., sp. ht. and resist. meas. 79−61120
$(Fe_{98}Cr_2)_{79}P_{13}B_8$ and $(Fe_{96}Cr_4)_{79}P_{13}B_8$, amorphous, low temp. sp. ht., mag. contribs. 80−80552
FeF_2, mag. sp. ht. near Neel temp. mag. susceptibility meas. 80−60341
$Fe_5(Fe_{1-y}Co_y)$, mag. and calorimetric props. 77−63083
$Fe(HCOO)_2.2H_2O$, heat capacity 78−22865
$FeMgBO_4$ and $FeMg_2BO_5$, mag. props., spin glass behaviour 79−61145
$(Fe_{1-x}Mn_x)_3Si$, mag. phase diagram determ. 77−24697
$(Fe_{1-x}Mn_x)_3Si$, sp. ht. at low temps., mag. transitions *(Russian)* 77−32189
$Fe_{0.49}Mn_{0.01}Ti_{0.5}H_x$, localised vibrs., sp. ht. obs., room temp. 80−65248
$Fe_{1-x}Ni_x$, FCC, anomalies in sp. ht. and thermal expansion 79−19739
$Fe_{40}Ni_{40}B_{20}$, metallic glass, low temp. specific heat, metalloid effects 80−34654
$Fe_{65}(Ni_{1-x}Cr_x)$, microhardness and specific heat, depend. on Cr content *(Russian)* 79−100240
$Fe_{32}Ni_{36}Cr_{14}P_{12}B_6$, elastic, magnetoelastic and thermal props. 79−19759
$Fe_{40}Ni_{40}P_{14}B_6$, elastic, magnetoelastic and thermal props. 79−19759
$Fe_{40}Ni_{40}P_{14}B_6$ glass, ferromagnetic, low temp. meas., electronic, phonon contribution 78−10689
$Fe_xNi_{80-x}P_{14}B_6$ (x=0, 20, 40, 60, 80), metallic glass, low temp. sp. ht. 80−2588
$Fe_xNi_{80-x}P_{14}B_6$, amorphous, sp. ht. and susceptibility meas., spin glass and mictomag. props. 78−68274
$Fe_xNi_{80-x}P_{14}B_6$, metallic glass, low temp. sp. ht. for spin-glass and spin-cluster-glass regime 80−71071

specific heat of solids continued
$(Fe_yNi_{100-y})_{79}P_{13}B_8$, metallic glass, low temp. sp. ht. for spin-glass and spin-cluster-glass regime 80−71071
$Fe_{29}Ni_{49}P_{14}B_6Si_2$, Metglas 2826B, Hall, elec. resist., magnetisation and heat capacity meas. 78−68019
FeO based slag, thermophysical props., effect of basicity, rate of heating *(Russian)* 77−25009
γ-Fe_2O_3:Fe_3O_4, magnetite impurity determ. by C_p calorimetry 78−2152
$(Fe_2O_3)_x$-$(3B_2O_3.PbO)_{1-x}$ glass, thermal cond. and diffusivity obs. 79−60561
Fe_3O_4, anomalous sp. ht. obs. at 10K 77−85454
Fe_3O_4, electron energy band theory, thermodynamic functions *(Korean)* 79−7785
Fe_3O_4, low temp. phase, sp. ht. and elec. cond. 77−59308
Fe_3O_4, magnetite, oxidation rate anomaly at Curie temp. 79−96298
$Fe_3O_{4-x}F_x$, specific heat in neighbourhood of Verwey temp. 79−33500
$Fe_{90}P_{14}B_6$ glass, ferromagnetic low temp. meas., electronic, phonon contribution 78−10689
$Fe_{75}P_{15}C_{10}$, glassy ferromag., crit. sp. ht. meas. 78−10716
$Fe_{34}Pd_{46}P_{20}$, amorphous, sp. ht. and resist. near ferromag. phase transition 78−56333
FeS_2, marcasite and pyrite phases sp. ht., thermodynamics of transform. 77−28016
FeS_2, pyrite, heat capacity meas. by differential scanning calorimetry 80−8987
$FeSb_2$, heat capacity and thermodynamic props. from 5 to 1021.2K, heat of decomposition 77−90636
η-Fe_5Si_3, thermal and mag. props. 77−36080
Fe_2TiO_5, anisotropic spin glass behaviour 79−99707
Fe_2TiO_5, anisotropic spin glass type behaviour 80−60296
$FeVO_4$, temp. depend. of heat capacity, 60-1080K, Debye temp. 77−7869
$Fe_xV_{2-x}O_4$ solid solutions, specific heat near semiconductor-metal transition 80−24612
Ga II, superconducting high pressure phase, sp. ht. 80−70894
Ga metastable states, supercooling and polymorphism *(French)* 78−14325
GaP, moments of phonon spectra from specific heats 80−15203
GaS, 2-30K, expt. compared with theory 78−18791
GaS, anisotropic phonon dispersion 77−84864
GaS, lattice dynamics parameters, X-ray diffr. study *(Russian)* 80−29146
GaS, sp. ht., vibr. spectra and Debye temp. 78−87796
GaSe, lattice dynamics parameters, X-ray diffr. study *(Russian)* 80−29146
GaSe, sp. ht., vibr. spectra and Debye temp. 78−87796
GaTe, sp. ht., vibr. spectra and Debye temp. 78−87796
Gd, appl. of AC specific heat method to bulk samples 77−71317
Gd, ferromagnetic, crit. sp. ht. and thermal expansion 80−60343
Gd, mag. contrib. to sp. ht. 79−28538
Gd, scaling behaviour near T_c 77−66333
Gd-Fe amorphous alloys, mag. props. and crystn. 79−90557
$GdAl_2$, amorphous, mag. heat capacity 77−89969
$GdAl_2$, thermal expansion and heat capacity Curie temp. determ. 77−1559
$GdAlO_3$:La, antiferromag., random-field crit. and multicritical behaviour 80−65939
GdB_6, thermophys. props., 700 to 1200K 79−37850
$GdCl_3$, heat capacity, 5 to 350K entropy 77−47588
$Gd_xEr_{1-x}Rh_4B_4$, ferromag. and structural transitions, low temp. calorimetric meas. 79−55888
$Gd_3Ga_5O_{12}$, magnetic interactions and short range order 79−78401
GdMg, sp. ht., magnetisation and stability of canted struct. 79−78412
$Gd_{1.2}Mo_6S_8$, low temp. heat capacity anomaly rel. to antiferromag. transition in supercond. state 80−25044
$Gd_{0.1}Mo_6Se_8$, mag. supercond., low temp. sp. ht. meas. 79−56380
$Gd_{1.2}Mo_6Se_8$, coexistence of supercond. and long range antiferromag. order 80−84534
Gd_2O_3, C-phase, specific heat, 1.4 to 18K, antiferromag. ordering 79−38351
$Gd(OH)_3$, heat capacity from near 5 to 350K, lattice and Schottky contribs. 80−49374
$Gd_2O_2SO_4$, antiferromag., specific heat, 0.6 to 30K 79−33487
Gd_2ZrS_5, mag. and sp. ht. meas. on polycrystalline samples 78−23253
Ge, amorphous, tunnelling states simulation and sp. ht. 79−37791
Ge, heat capacity and phonon dispersion, using five force schemes *(Russian)* 77−62649
n- Ge, heavily doped, extrinsic sp. ht. in metallic regime 78−59956
Ge, lattice dynamics using Born-van Karman model 79−73271
Ge, phonon density of states determ. from sp. ht. 77−7809
Ge, thermodynamic functions and normalised moments 79−51279
Ge-As-Se system glasses, thermal capacity, 300-600K 79−65210
Ge-Sb-Se system glasses, thermal capacity, 300-600K 79−65210
Ge-Te binary glass, eutectic, DSC obs., thermodynamic and thermokinetic characts. 80−39309
GeH_4, heat capacity, dielectric const., thermodynamic props. 78−83967
GeO_2, amorphous, 2 to 23K, phonon frequency distrib. 78−30723
GeP, thermodynamic characts. 10-300K, interatomic bond elasticity 80−59677
GeS_x amorphous semiconductor, neutron irrad. effects on thermal parameters 77−11597
GeS_x glass, x=1.25 to 1.5, softening and crystallization kinetics 79−32906
GeS_x, neutron irrad., thermal and elec. conductivity and heat capacity 78−2165
Ge_xS_{1-x} glasses, sp. ht., 2 to 18K 79−65214
GeTe, enthalpy and specific heat, 0 to 860°C, polymorphic transitions obs. 77−43350
$Ge_{0.5}Te_{0.5}$, heat capacity in solid and liq. phases, enthalpy of form. *(French)* 80−35565
p-H_2, FCC, equation of state and lattice dynamics, temp. depend. 77−76521
H_2, solid, heat capacity and configurational entropy at low ortho concs. 77−35706
H_2, solid quadripolar glass, relax. time and low temp. sp.ht., computer simulations 80−49377
o-H_2 to p-H_2, spontaneous conversion rate anomaly obs. in heat capacity expt. 79−99392
HI, thermodynamic properties 78−47517
HX, X=Cl, Br, I, thermodynamic properties, phase transitions 78−47518

specific heat of solids continued
He, anomaly, explained by hybrid cryst. model 77−65015
He monolayer, sp. ht., low-density phase modification produced by substrate changes 77−76642
He, solid, theory and thermodynamic props., book contrib. 77−47646
He, solid, vacancy tunnelling freq. calc. 77−80678
He, specific heat high temp. anomaly, quasi-average and averages, translational symmetry breakdown 78−30811
He, vacancy activation energy, from high temp. sp. ht. data 77−15657
^{4}He, FCC quantum cryst., lattice dynamics 79−77859
He-H_2 mixtures, isobaric sp. ht. 78−18788
^{3}He, BCC, low temp. sp. ht anomalies 78−91256
^{3}He, BCC, meas. from 3 to 300 mK 79−33153
^{3}He, BCC, nucl. spin mag. ordering with four spin exchange, vel. to sp. ht. 77−89615
^{3}He, BCC, sp. ht. meas. for 5 molar vols. above 50 mK 77−47645
^{3}He, BCC, vacancy bandwidth determ. by sp. ht. 78−79854
^{3}He, BCC solid, exptl. mag. props., four spin exchange explanation 79−69319
^{3}He on graphite, two dimensional quantum crystal *(Russian)* 78−60001
^{3}He, solid, heat capacity, possible dimens. effect 78−75844
^{3}He, solid, low temp. mag. and thermal props. due to bound state Frenkel vacancies 79−56019
^{3}He, solid, low temp. thermal cond., structural crystalline defects 80−2240
^{3}He, solid, two parameter model of mag. and thermal props., spin exchange 80−49461
^{3}He, solid BCC, contrib. of vacancy mag. polarons to sp. ht. 79−56032
^{3}He, solid BCC, mag. susceptibility and sp. ht. 79−69318
^{4}He adsorbed on Nuclepore filter, specific heat *(Japanese)* 78−79852
^{4}He film adsorbed on graphite, transition temp., entropies, internal energies and heats of desorption 80−2238
^{4}He, isobaric 78−18788
^{4}He, solid, heat capacity, possible dimens. effect 78−75844
$(Hf,Zr)V_2$, phase transition, sp. ht. anomalies meas., 70-150K 77−35691
Hf, HCP, lattice dynamics, thermal and elastic props., model 80−34155
Hf-Ni(Co), amorphous, formation, decomposition and elec. transport props. 80−20143
$HfB_{2.036}$, $HfC_{0.968}$, ht. capacity, thermodyn. props., 5-350K 77−47590
HfS_2, enthalpy and specific heat, temp. depend. 80−54406
Hg superconducting filament, ultrathin, rel. to resist., 2-9K 77−8234
$Hg_{2.86}AsF_6$, linear chain, anomalous low temp. sp. ht. 78−14476
$Hg_{3-\delta}AsF_6$, low-temp. sp. ht., lattice dynamics, 1- to 3-dimens. crossover 79−86864
Hg_2Br_2, sp. ht. near phase transition region meas. 78−38855
Hg_2Cl_2, ferroelastic, 100-273K 77−59064
$HgCr_2S_4$, cooling efficiency near 60Kas mag. refrigerant 80−71034
$Hg(NH_3)_2Br_2$, $Hg(NH_3)_2Cl_2$, thermodynamic study of disorder 79−28109
HgTe, 1.5 to 30K, thermal expansion and heat capacity meas. 80−59681
Ho, sp. ht., using lattice dynamical model for HCP metals 79−51273
Ho, thermophysical properties at high temps., exam. *(Russian)* 79−28105
$HoAl_2$, heat capacity, 1.5-12K, magnetocryst. anisotropy effects 78−68236
$HoAl_2$, spin reorientation, sp. ht. meas. 79−73724
$HoFe_2$, crystal field interaction contribution to specific heat 80−39788
$Ho_{1.2}Mo_6S_8$, re-entrant ferromag. supercond., heat capacity and AC mag. susceptibility 79−60948
$HoNi_{0.5}Cu_{0.5}$, sp. ht. and modulated mag. struct. 77−32167
$Ho_2O_2SO_4$, antiferromag., specific heat, 0.6 to 30K 79−33487
$HoRh_4B_4$, low temperature magnetic properties 80−88728
$HoVO_4$, RF susceptibility below 1K, mag. sp. ht. 80−84585
$Ho_cY_{1-c}Sb$ system, magnetisation, elec. resist., and sp. ht. meas. 80−60213
In films, supercond., sp. ht. discontinuity and transition temp. meas. 79−60969
In, heat capacity and enthalpy of fusion, 300-1000K 79−14939
In-Bi(Tl)(Pb), small κ supercond., phase transitions higher than second order 80−88668
In-Cr(Mn) films, supercond., sp. ht. discontinuity and transition temp. meas. 79−60969
In-Mg, ordered equiatomic, lattice specific heat meas., Debye temp., superconducting transition 80−54396
In-Mn, discontinuity in sp. ht. at supercond. transition 79−60971
InSe, $InSe_{1.2}$, In_2Se_3, molar heat capacity and enthalpy of transition, 129 to 920K range 77−29030
In_2Se_3, temp. depend., 55 to 330K 77−24417
In_4Se_3, layered cryst., sp. ht. rel. to phonon spectrum *(Russian)* 79−90794
$In_{0.69}Tl_{0.31}$, supercond. transition temp., specific heat, pseudopotential form factor 80−97026
KAg_4I_5, ionic conductivity and heat capacity near T_c 78−47584
KAg_4I_5, superionic phase transition, dynamical and crit. pt. props. 80−107535
$K_2BaCu(NO_2)_6$, antiferromagnetic Heisenberg spin 1/2 simple quadratic lattice, mag. and caloric meas. 79−78397
KCl, thermodynamic props., lattice-dynamical calc. 77−35715
KCl:$Cs^+(I^-)$, low-temp. heat capacity enhancement due to impurities 80−107442
KCl:Kbr(KI), enhancement in sp. ht. due to anion impurities 79−51274
KCl:Pb^{2+}, low temp. sp. ht. 80−2178
KCl-CuCl eutectic fused salt, potential as intermediate temp. solar heat transfer and storage medium 80−101135
K_2CoF_4, specific heat capacity, critical amplitude, cross-over from 2-D Ising to Heisenberg behaviour 80−39791
$K_2Co_2(SO_4)_3$ polycryst., growth and phase transitions 79−33918
$K_2Cr_2O_7$, polymorphic behavior, depend. on thermal and prep. history 80−34184
K_2CuF_4, layered, mag. sp. ht., two-dimens. $S^1/_2$ Heisenberg ferromag. behaviour 77−32206
KDP-type crystals, polarisation, dielec. const. thermodyn. props. 77−59527
$K_4Fe(CN)_6.3H_2O$, ferroelec., sp.ht. and spontaneous polarisation, −65 to 0 degrees C, mol. field model 78−64333
$K_3Fe(Cn)_6$, mag. and thermodynamic props. below 0.4K in mag. fields 79−56542
$KFe(MoO_4)_2$, phase transitions at 312 and 139K 80−70396
KH_2PO_4, one-dimensional Slater model, with random impurities due to partial deuteration, thermodynamic behaviour 77−59537
specific heat of solids continued
KH_2PO_4 type ferroelectrics, Green's function theory of phase transitions with pseudo-spin-lattice coupled mode model 80−71354
$KH_3(SeO_3)_2$, thermal anomalies rel. to acoustic phonon instability 77−76545
K_2IrCl_6, sp. ht. meas. at low temp. 80−7119
$KMnF_3$, specific heat near Neel temp. *(Russian)* 80−100340
K_2MnF_4, specific heat capacity, critical amplitude, cross-over from 2-D Ising to Heisenberg behaviour 80−39791
KN_3, heat capacity from 5 to 350K 79−55901
KNO_2, polymorphism, calorimetric investigation 78−75827
K_2NiF_4, specific heat capacity, critical amplitude, cross-over from 2-D Ising to Heisenberg behaviour 80−39791
K_2O-Al_2O_3 system, high temp. thermodynamics and phase equilibria 78−80521
K_2O-SiO_2 glass, low temp. heat capacity 80−49373
$K_2O_sCl_6$, sp. ht. meas. at low temp. 80−7119
K_2OsCl_6, low temp. sp. ht. and thermodynamic props. near phase transition 77−39655
$K_2PbCu(NO_2)_6$, antiferromagnetic Heisenberg linear spin 1/2 chain, mag. and caloric meas. 79−78397
$K_2Pt(CN)_4Br_{0.3}.3H_2O$, specific heat, 0.75 to 25.7K 78−87795
$K_2Pt(CN)_4Br_{0.3}.3H_2O$, specific heat and ferroelastic behaviour 78−91447
K_2PtCl_6, diamag. sp. ht. meas. at low temp. 80−7119
K_2ReCl_5, sp. ht. meas. at low temp. 80−7119
K_2ReCl_6, low temp. sp. ht. and thermodynamic props. near phase transition 77−39655
K_2ReCl_6, thermodynamic relations at solid state phase transitions 80−29164
$KReO_4$, heat capacity and thermodynamic props., 8 to 304K 80−100335
$KTaO_3$, pure and Gd_2O_3 doped, elec. cond. and sp. ht. 79−78097
$KTaO_3$, sp. ht. and electrocaloric props. at low temps. 77−84945
β-$K_{0.27}V_2O_5$, heat of form. and sp. ht., 450 to 900K 80−61129
Kr absorption on graphite, monolayer regime phase diagram 80−49507
Kr layer on graphite, heat capacity 79−60621
Kr, solid, vibr. and thermal props., effect of polarisability 78−71807
$(La,Ce)Al_2$, conf. Kondo system, sp. ht. meas. 78−52210
(La, Ce)Sn_3, dil. alloys, supercond. and normal state props. 78−76184
(La, Gd)Al_2 spin glass, suscept. and sp. ht., mag. field depend. 79−61173
(La,Na)Sn alloys, supercond. transition temp. 79−78254
(La, Nd)Sn_3, cryst. field effects, normal and supercond. props. 79−60973
(La, Nd)Sn_3, superconducting props. 79−60958
La, $(SO_4)_3.9D_2O$, soln. growth, struct., props. 77−77363
La, FCC, NMR 4.2 to 296K, mag. susceptibility and sp. ht. 80−15813
La, heat capacity and supercond. props. 80−65247
LaAg, band calcs., rel. to mag. and electronic props. and martensitic transform. 77−8014
LaAg, electronic struct., susceptibility, sp. ht. and Knight shift meas. 77−43485
$La_{1-x}Au_x$, supercond. splat cooled amorphous alloy 78−19182
$(La_{0.8}Ca_{0.2})MnO_{3+y}$, mag. sp. ht. and Debye temp. 79−61124
$(La_{1-x}Ce_x)Al_2$, Kondo system, antiferromag., specific heat 79−24179
La(Ce)$Sn_{3-x}Pb_x$ system, mag. impurities in supercond., supercond. transition temp. and sp. ht. 78−39244
$LaCrO_3$, sp. ht., enthalpy, entropy, 298-900K, polymorphic transition 77−69094
LaF_3, heat capacity of 350K, enthalpy to 1477K, calorimetric determ. 78−79781
$La_{1-x}Ga_x$ foils, amorphous, splat cooled, calorimetric and resistive meas. 79−33417
$(La_{1-x}Gd_x)_{1.0}Mo_6Se_8$, Gd-rich, supercond. state, phase transition, lambda-type sp. ht. anomaly obs. 78−6480
$LaGe_x$, specific heat in range $0.07 \leq T \leq 10K$, comp. depend. 78−43517
$LaH_{2.69}$, low temp. phase transition 78−14665
$LaMnO_3$, ferromag.-paramag. phase transition, neutron diffr., calorimetric investigs. 78−31072
$LaMo_6X_8$ (X=S, Se), supercond., sp. ht., 1 to 14K 79−51720
(LaNd)Sn_3, containing Nd impurities, supercond. and normal state props. 80−49967
$LaNi_5$, crystal field investigation from inelastic slow neutron scatt. expts. 80−39538
$LaNi_5$, Haucke compounds, low temp. heat capacity, Debye temp. 80−96663
$La(OH)_3$, heat capacity from near 5 to 350K, lattice and Schottky contribs. 80−49374
LaP_5O_{14}, continuous ferroelastic transition elastic and mechanical props. 80−92668
$LaPd_3$, heat capacity at low temps. 79−28547
$LaS_{1.33}$-$LaS_{1.40}$, low temp. sp. ht. 80−15259
La_3S_4, high crit. mag. field supercond., elec. resist., sp. ht. and magnetisation 80−2532
La_3S_4-La_2S_3, low temp. sp. ht. 80−15259
$La_{1-x}Sr_xCoO_3$ meas., using laser-flash method, phase transitions obs. *(Japanese)* 80−54898
$La_{1-y}Tb_yAg$, crystal field effects, normal and superconducting states 78−2621
$La_{0.9}Tm_{0.1}Se$, sp. ht. meas., 1.6 to 20K, mag. contrib. 80−65934
$La_{10}W_2O_{21}$, enthalpy and heat capacity at high temp. 80−70424
α-La_2WO_6, enthalpy and heat capacity at high temp. 80−70424
$La_6W_2O_{15}$, enthalpy and heat capacity at high temp. 80−70424
$La_{1-y}Y_y$(Ce) system, mag. impurities in supercond., supercond. transition temp. and sp. ht. 78−39244
$LiAlH_4$, molar heat capacity, thermodynamic props., 10 to 300K 80−44329
Li_3AlH_6, molar heat capacity, thermodynamic props., 10 to 300K 80−44329
LiC_6, intercalation compound with graphite, sp. ht. meas., 4-300K 80−44332
$LiCsSO_4$, thermal and dielec. props. 80−34860
LiH, cryst., specific heat at const. vol., isotopic modifications effects 80−103490
$LiKSO_4$, thermal and dielec. props. 80−34860
$LiMSO_4$, M=Li, Na, K, Li_2SO_4-$ZnSO_4$, ht. capacity and ht. of transform. 78−26690
Li_3N, heat capacity 5 to 350K, thermochem. props. to 1086K 78−92500
Li_3N, superionic conductor, cryst. growth and struct., phys. props., book contrib. 79−42308

specific heat of solids continued
$LiNH_4SO_4$ and $LiND_4SO_4$, dielec. pyroelec., and thermal props. 80−60509
LiO_2-Na_2O-MgO-TiO_2-Al_2O_3-SiO_2, exam. of specific heat and thermal conductivity *(Russian)* 79−55898
Li_2O, heat capacity 306 to 1073K 79−10965
Li_2O_2, thermal decomposition and heat capacity 301 to 566K, enthalpy 80−3322
$LiRbSO_4$, order-disorder phase transitions with many-minimum potential, thermodynamic props. 80−96623
$LiTbF_4$, ferromag., susceptibility, sp. ht., renormalisation group theory test 77−16087
$LiTbF_4$, mag. props., crit. behaviour at marginal dimensionality 80−54906
β-$Li_{0.27}V_2O_5$, heat of form. and sp. ht., 450 to 900K 80−61129
$LiYF_4$:Er^{3+}, magnetocaloric behaviour, cryst. field theory 77−4520
$LiYF_4$:Tm^{3+}, cryst. field parameters, appls. 77−20277
Lu, lattice dynamics, heat capacity, thermal expsn. 79−86857
Lu, specific heat from 1.6 to 18K, electronic coeff., Debye temp. at 0K 79−7700
Lu, thermophysical properties at high temps., exam. *(Russian)* 79−28105
Lu-H alloy, influence of H on low temp. sp. ht. 78−38854
$LuAl_2$, sp. ht. and thermal props., 5 to 300K 77−43342
$LuFe_2$, crystal field interaction contribution to specific heat 80−39788
$(Lu_{1-x}Ho_x)Rh_4B_4$, interaction between superconductivity and magnetism 79−38248
$Lu_2Ir_2O_7$, pyrochlore, sp. ht. below 20K, Debye temp. 80−65241
$LuMO_6X_8$ (X=S, Se), supercond., sp. ht., 1 to 14K 79−51720
$LuRh_4B_4$, superconducting and normal state props. 79−73632
Mg, KKR calc. using potentials with exchange and correlation 79−11060
Mg, lattic dynamics and sp. ht. in extended de Launay model 79−51217
Mg, phonon spectrum and thermodynamic functions, inelastic coherent cold neutron scatt. *(Russian)* 78−55917
Mg, spin susceptibility, electronic effective mass, spin density functional calcs. 78−43291
$Mg(AlH_4)_2$, prep., thermal decomposition, molar heat capacity, heat of form. 80−3325
$MgAl_2O_4$ spinel refractory, enthalpy and specific heat determs. 80−88334
$MgCr_2O_4$, spinel refractory, enthalpy and specific heat determs. 80−88334
$MgCu_2$-$MgNi_2$, electronic sp. ht. 1.5 to 4.2K, Fe impurity effects *(German)* 77−59125
$Mg(NH_3)_6(ClO_4)_2$, phase exam. by adiabatic calorimetry and X-ray diffr. methods 78−63854
MgO, lattice dynamics and vibr. sp. ht. 78−47482
MgO, thermal characts. using constant power source method 79−95222
Mg_2Sn, lattice dynamics, angular force model 77−4166
$MgUO_4$, standard enthalpy of formation, high-temperature thermodynamic functions 78−27811
Mn, complex, $Mn(C_5H_5NO)_6(BF_4)_2$, mag sp. hit below 1K 77−89968
Mn complex, $Mn(SCN)_2(C_2H_5OH)_2$, two-dimens. Heisenberg magnet, cryst. struct. and mag. props. 79−60337
β-Mn, spin fluctuations effect on sp. ht. 79−82788
Mn-V(Cr)(Fe)(Co)(Ni), spin fluctuations effect on sp. ht. 79−82788
MnB_{12}, growth from melt and phys. props. 80−20782
$MnBr_2.4H_2O$, high-resolution sp. ht. meas. near Neel temp. 77−28393
$Mn_xCd_{1-x}(NH_3)_2.Ni(CN)_4.2C_6H_6$, Hofmann type mixed cryst., mag. props. 79−4659
$MnCl_2$, lattice dynamics, density of states and sp. ht. calc. 80−92624
$MnCl_2$, $MnBr_2$, mag. phase diagram, optical absorption meas. 77−4514
$MnCl_2.4H_2O$, biaxial antiferromag., bicritical region, sp. ht. meas. 78−68246
α-$MnCl_2.4H_2O$, crossover from divergent to non-divergent nature of paramag. transition 79−73735
$Mn_{0.27}Co_{0.73}Cl_2.6H_2O$, antiferromag., sp. ht. meas., phase transition obs. 79−78415
$Mn_3Cr_2Ge_3O_{12}$ garnet, antiferromag. ordering *(Russian)* 78−80146
$(Mn_{0.95}Cr_{0.05})_3Si$, sp. ht. at low temps., mag. transitions *(Russian)* 77−32189
MnF_2, heat capacity and entropy, 10 to 300K, mag. ordering contrib. 77−16080
MnF_2, mag. susceptibility, crit. behaviour near Neel point, rel. to mag. sp. ht. 79−91217
MnF_2, specific heat, Heisenberg to Ising crossover near Neel temp. 78−47980
$(Mn_{1-x}Fe_x)_5Si_3$, solid soln., mag. transitions sp. ht., magnetisation and thermal expansion meas. 77−16075
Mn_3GaN, sp. ht., 6 to 350K, mag. and crystallographic phase transitions 80−71060
$Mn(NH_3)_2Ni(CN)_4C_{12}H_{10}$, phase transition, mag. susceptibility, sp. ht. 79−91234
$Mn(NH_3)_2.Ni(CN)_4.(benzene)_2$, antiferromag. ordering, mag. susceptibility, sp. ht. and Neel temp. meas. 77−12128
$Mn_xNi_{1-x}Cl_2.nH_2O$, antiferromag., sp. ht. meas. 79−91226
MnP, and Mn_2P, enthalpy and heat capacity at high temp. 77−11704
MnP, sp. ht., 1.5-8.0K 79−91236
MnP, spin polarised energy band struct., electronic specific heat, APW calcs. 80−65431
Mn_2P, heat capacity, mag. entropy and thermodynamic functions 77−80630
MnSi, amorphous, sputtered, mag., elec., struct. and thermal props., spin glass behaviour 80−50124
$MnSiF_6.6H_2O$, specific heat, thermal cond., simultaneous meas., method, 90-300K, near phase transition 77−37892
MnTe, resistivity anomalies at mag. transitions, sp.ht. 80−39785
$Mn_{1-x}Zn_xF_2$, linear mag. birefr., crit. behaviour 77−52061
$Mn_{1-c}Zn_cFe_2$, Heisenberg antiferromag., linear mag. birefringence meas., rel. to mag. sp. ht. 77−16277
Mn_3ZnN, sp. ht., 6 to 350K, mag. and crystallographic phase transitions 80−71060
Mo, specific heat near melting point, rapid pulsed heating method 77−35704
Mo, standard ref. material, enthalpy and heat capacity 78−18792
Mo ternary chalcogenide, MMo_6X_8 (M=metal, X=chalcogen) Chevrel phase, supercond. and normal state props. 78−56267
Mo ternary chalcogenides, supercond., compared with band struct. calcs. 78−51871
specific heat of solids continued
Mo-Fe, spin glass and mictomag. regimes, sp. ht., resist. and susceptibility meas. 77−69581
Mo-Re (5 at.%), enhanced lattice sp. ht. due to LF reson. modes 78−14882
MoFe, occurrence of spin glass and mictomagnetic regimes, props. meas. 77−16085
Mo_5GaS_6, specific heat temp. depend. 77−63199
Mo_6NaS_8, specific heat and supercond. critical field *(Russian)* 77−77004
Mo_xRe_{1-x}, (x=0.4 and 0.6), search for strong coupling superconductivity 79−28441
MoS_2, enthalpy and specific heat, temp. depend. 80−54406
MoS_2, entropy, enthalpy and specific heat, temp. depend. 500 to 1700K 80−15260
$Mo_6S_8(Se_8)$, heat capacity and mag. props., 2-30K 79−42692
$Mo_6S_8(Se_8)(Te_8)$ and halogen substituted cpds., sp. ht. capacity 80−49986
$Mo_5SnGa_{0.5}S_6$, specific heat temp. depend. 77−63199
$Mo_5SnGa_xS_6$ heat capacity from 2 to 25K 78−43518
Mo_5SnS_6, supercond., at 2 to 25K, lattice and electron contrib. to sp. ht. 77−77003
$Mo_{0.18}Tc_{0.82}$, search for strong coupling superconductivity 79−28441
$Mo_{0.4}Tc_{0.6}$, A15 and BCC, sp. ht., 4-20K 78−68111
$Mo_{1-x}Tc_x$, BCC, sp. ht. in normal and supercond. phases 79−87190
ND_4Cl, order-disorder transformation, elasticity and heat capacity temp. depend., US obs. 78−71851
ND_4Cl, sp. ht. at high press. meas., near order-disorder transition 77−84944
NH_3, ND_3, crystals, rotation mol. motion *(Russian)* 78−87762
NH_4^+, libration and tunnelling freq. rot. heat capacity, hindered rot. energy level calcs. 79−98058
NH_4^+, tetrahedron, hindered rot. energy levels in orthorhombic crystalline field, rot. heat capacity 77−76332
$NH_4Ag_4I_5$, ionic conductivity and heat capacity near T_c 78−47584
$NH_4Ag_4I_5$, superionic phase transition, dynamical and crit. pt. props. 80−107535
NH_4Br, heat capacity meas. near order-disorder transition 80−88332
$NH_4Br_xCl_{1-x}$, heat capacity meas. near order-disorder transition 80−88332
NH_4Cl, AC calorimetry at high press. 77−41616
NH_4Cl, molar heat capacity near order-disorder transform. under high press. 78−51697
NH_4Cl, sp. ht. at high press. meas., near order-disorder transition 77−84944
NH_4Cl, specific heat, thermal cond. simultaneous meas. method, 90-300K, near phase transition 77−37892
NH_4Cl, thermal cond. and heat capacity of solid phases under press. 80−2225
$(NH_4)_3H(SO_4)_2$, phase transitions, sp. ht. meas. 80−2157
NH_4HgCl_3, high resolution heat capacity meas. *(Japanese)* 80−52218
NH_4ReO_4, heat capacity and thermodynamic props., 8 to 304K 80−100335
$(NH_4)_2SO_4(BeF_4)$, order-disorder phase transitions with many-minimum potential, thermodynamic props. 80−96623
$NH_4Zn(Co)F_3$, sp. hts., librational and reorientational 77−84946
NH_4ZnF_3, hindered rot. sp. ht. of NH_4^+, 2.5-300K 77−62648
Na alloys, very dilute, sp. ht. meas. close to melting point 78−47501
Na, phonon dispersion curve, sp. ht. and Debye temp., ang. force model 77−15509
$NaAlH_4$ and Na_3AlH_6, molar heat capacity and thermodynamic functions, 10 to 300K 80−65243
NaBr, heat capacity, Gruneisen parameters, 2 to 20K 80−29180
Na_2CO_3, phys. props. related to phase transitions 80−96643
$NaCa_2Mn_2V_3O_{12}$, antiferromag., spin wave contrib. to sp. ht., λ-anomaly at 25.05K T_N 77−77068
NaCl, Gruneisen γ and other thermodynamic props., vol. depend. 77−76577
NaCl, sp. ht., meas. by pulse method, influence of press. 79−7701
NaCl, thermodynamic props., lattice-dynamical calc. 77−35715
$NaClO_3$, lattice vibrations and sp. ht., neutron spectroscopic study 80−107388
NaF, heat capacity, Gruneisen parameters, 2 to 20K 80−29180
$NaNH_4SO_4.2H_2O$, ferroelec. and thermal props. 78−83968
$NaNO_2$, ferroelec., dielec. and thermal behaviour 80−80680
Na_2O-Cs_2O-SiO_2 glasses, thermal diffusivity, heat capacity and thermal cond., laser flash method study 80−65310
Na_2O-SiO_2, Na_2O-CaO-SiO_2 glasses, thermal capacity meas. at low temps. 80−44334
Na_2O-SiO_2 glass, 2-20K, comp. effects 77−20097
Na_2O-SiO_2 glass, low temp. heat capacity 80−49373
Na_3RuO_4, mag. props., isolated tetranuclear cluster model 79−24180
$Na_3Sc_2P_3O_{12}$, fast-ion conductor, struct. phase transition 80−88362
$NaTl_3(SO_3)_2$, heat capacity and thermodynamic functions, 10 to 300K 80−65244
$NaUO_3$, ht. capacity and thermodyn. props., 5-350K 77−43343
β-$Na_{0.27}V_2O_5$, heat of form. and sp. ht., 450 to 900K 80−61129
$Na_{1.9}V_{12}O_{29.7}$, phase transitions, elec. cond., susceptibility and sp. ht. meas. 78−14776
$Na_xV_2O_5$, nonmetallic bronze, low field sp. ht. and mag. suscept. 78−72357
Na_xWO_3 enhanced T_c, interband coupling 78−91804
$Na_3Zr_2Si_2PO_{12}$, NASICON, phase transition, X-ray diffr., ionic cond. and sp. ht. meas. 80−19979
Nb, enthalpy and heat capacity determ. 78−71866
Nb, mixed state, sp. ht., 0.03-0.3K, electronic and nucl. contribs. 78−10621
Nb, plastic deformation effects on superconducting specific heat transition 80−20352
Nb, spin fluctuations effect on T_c, from sp. ht. and mag. suscept. 80−7030
Nb, supercond. mixed state, low temp. sp. ht. meas. 77−24638
Nb:N, H, atomic tunnelling of interstitial pair, specific heat meas. 78−47600
Nb/H, heat capacity and supercond. between 1.5 and 16K 80−2521
Nb-H (30 at.%), specific heat at $\varepsilon \rightarrow \zeta \rightarrow \beta$ phase transition 77−12616
Nb-Ti, superconductivity after heavy ion irradiation at low temps. and high fluence 77−69437
$Nb_3Al_{0.8}Ge_{0.2}$, supercond., sp. ht. meas. 77−28296
$Nb_3Al_{0.83}Ge_{0.21}$, A-15 phase, sp. ht. meas. 79−19689
Nb_3As, electronic and supercond. props. 77−16011

specific heat of solids continued
Nb_3Au, BCC, density of states, comparison with A-15 78−80095
NbC, true heat capacity meas. by pulse method 80−19953
NbC_x, thermophys. props. 77−89600
NbC_x, thermophysical props. at high temp., thermal vacancies form. 78−43141
NbC_xN_{1-x} 4.2-100K, phonon anomaly rel. to supercond. transition 78−14880
NbC_xN_{1-x}, obs. of phonon anomalies, sp. ht. meas. and supercond. transition temp., 1.5-90K 77−39985
$Nb_{0.75}Ga_{0.25}$, A 15 phase high transition temp., sp. ht. determ. 80−60140
Nb_3Ge, amorphous film, supercond., flux flow resist., vortex pair dissoc. 80−88701
Nb_3Ge, amorphous nongranular thin superconducting film, thermodynamic and resistive transitions 80−34571
$NbH_{0.3}$, α-α' phase transition, sp. ht. anomaly 78−39764
NbN, opt. consts. and physicochem. spectra 77−85677
$Nb_3Nb_{1-x}Si_x(Ge_x)$, impurity stabilised A15 supercond., transition temp., lattice consts., specific heat 80−93026
NbO_2, low temp. elastic consts. and Debye temp. 78−47463
NbO_2, low temp. sp. ht. and Debye temp., role of phonon-like CDW excitations 77−80632
NbS_2, enthalpy and specific heat, temp. depend. 80−54406
Nb_3S_4, anisotropic superconductor, critical field and specific heat meas. 80−44779
$NbSe_2$, 2H polytype, layered cpd., thermal props. at CDW transitions 77−47750
$NbSe_2$ (2H), layered, anisotropy and electron-phonon coupling effects on sp. ht. 77−51844
$NbSe_2$ (2H), supercond., thermodynamic props., exhibiting anisotropy and strong-coupling effect 77−12062
$NbSe_3$, phase transitions, phys. props. meas. 77−8005
$NbSe_2$(2H) layered supercond., effect of Fe impurities on sp. ht. 79−60972
$NbSe_2$(2H), specific heat and critical field, anisotropy and strong coupling effects 77−36021
Nb_3Si, electronic and supercond. props. 77−16011
Nb_3Si, high T_c, supercond. props. from extrapolation of sp. ht. meas. on A-15 Nb-Si 80−25045
$Nb_{1-x}Sn_x$, sp. ht., supercond. T_c and martensitic transform. *(French)* 78−43508
Nb_3Sn composite superconductor, 4-24K, calorimetry 77−32116
$Nb_{1-x}W_xSe_2$ x=0 to 0.15, elec. resist., mag. suscept., heat capacity, structural, supercond. transition *(Russian)* 78−31006
$Nb_{20}Zr_{80}$, supercond. and normal, sp. ht. meas., 2-20K 80−70893
Nd, 1.5-10K, in applied fields 0-1.3T 79−61158
Nd, anomaly at 773K *(Russian)* 77−28017
Nd, mag. struct., heat capacity meas., 2 to 10K 79−51788
Nd^{3+}:scheelite-type crysts., magnetic, thermal properties, cryst. field calcs. 78−91875
Nd-La, mag. ordering, sp. ht., susceptibility and resist. 78−68238
$Nd_{1-x}Dy_xCo_5$, rotational type spin reorientation, appl. to thermomagnetic generator 77−85451
NdF_3, enthalpy, entropy, heat capacity and Planck function from 5 to 350K 80−15257
$NdH_{2.70}$, low temp. phase transition 78−14665
$Nd(OH)_3$, heat capacity from 10 to 350K, lattice and Schottky contribs. 80−84300
NdP_5O_{14}, sp. hts. near ferroelastic phase transitions 78−63863
NdP_5O_{14}, thermal cond. and specific heat 79−42325
$NdRh_4B_4$, possible obs. of coexistence of supercond. and long-range mag. order 79−82730
Ne, lattice vibrs., heat capacities 79−42169
Ni, 0-100 kbar, press. depend. 77−51512
Ni complex, $[Ni(OCH_3)(acac)(CH_3OH)]_4$, sp. ht., 0.4-285K, methyl group internal rotation 78−47531
Ni complex, $[Ni(en)_2Cl]_2Cl_2$, heat capacity, X-ray diffraction and mag. meas., phase transition 78−47515
Ni complex, hexa(pyridine-N-oxide)$(ClO_4)_2$, field-induced mag. ordering in S=1 singlet ground-state 78−23288
Ni complex, tris(ethylenediamine)nickel(II) nitrate, mag. props. from susceptibility and sp. ht. meas., 0.3-3.0K 78−91877
Ni crystals, at mag. crit. temp., sp. ht. rounding 79−95595
Ni, ferromagnetic, anomalies in thermal expansion and heat capacity 79−73744
Ni, heat capacity temp. depend. meas., internal energy and entropy, anharmonic theory calcs. *(Russian)* 80−54402
Ni, high purity single cryst., sp. ht. near crit. temp. 78−64212
Ni, magnetisation in pulsed field up to 320 kOe, 283 to 693K, band theory *(Russian)* 77−80920
Ni, point defect estimation from specific heat and volume in plastically deformed pure metals *(Russian)* 80−54223
Ni, specific heat, temp. depend. *(Russian)* 78−56341
Ni, Stoner model, mol. field coeff., temp. and field depends. 77−72975
Ni-Al alloy, solid phase reaction kinetic parameter calcs., defect formation *(Russian)* 80−54399
Ni-Cr, low temp. sp. ht. near ferro-paramag. transition 77−63218
Ni-Cr alloys, low temp. transform. mechanism, electrophys. props. obs. *(Russian)* 77−59777
Ni-Cu, nearly ferromag., heat capacity meas. in mag. field 0.3 to 4K, superparamag. clusters 77−69579
Ni-Cu alloy, nearly ferromag., spin-glass-like distrib. of interaction fields 79−91243
Ni-Cu alloy, sp. ht. in mag. field, 1.2-15K 78−68262
Ni-Fe, split bands rel. to sp. ht., g-factor and magnetostriction data 77−72977
Ni-Fe based metallic glasses, Curie pt. anomalies 80−60256
Ni-NiAl solid soln., high temp. transforms *(Russian)* 79−56973
Ni-Pd alloys, mag. props., average and local density of states, CPA calc. 77−59242
Ni-V, low temp. sp. ht. near ferro-paramag. transition 77−63218
Ni_3Al, refractory transition metal alloying effects 78−26691
$Ni_3B_7O_{13}Br$, ferroelec. 43m-mm2 phase transition, molar heat capacity meas. 80−93249
$Ni_3B_7O_{13}Cl$, specific heat anomaly at $F43c \rightarrow Pca2_1$ transition 79−28690
$NiBr_2.6H_2O$, antiferromag. transition, susceptibility and sp. ht. meas. 77−69587
$NiBr_2.6H_2O$, antiferromag. ordering and paramag. behaviour 78−14941
$Ni(ClO_4)_2.6H_2O$, sp. ht. between 2 and 17K 78−47532
$NiCl_2.6NH_3$, low temp. sp. ht. and mag. ordering 80−75784

specific heat of solids continued
$(Ni_{1-x}Cu_x)Ti$, martensitic, shape memory effect kinetics and thermodynamics 80−3021
Ni_3Fe alloys, low-temperature specific heat, long and short range order effects 80−100339
$(Ni_{99}Fe_1)_{79}P_{13}B_8$, amorphous, low temp. sp. ht., mag. contribs. 80−80552
$(Ni_{1-x}Fe_x)_{1-\delta}S$, anisotropic spin glass, mag. props. 80−39793
$Ni(H_2O)_6(ClO_4)_2$, specific heat meas., 90 to 376K, phase transitions 78−83970
NiI_2, antiferromagnetic, neutron diffr. and sp. ht. meas. 77−55663
$Ni_xMn_{1-x}Cl_2$, 2-28K, anomalies *(Russian)* 77−89970
$Ni(NH_3)_2Ni(CN)_4.2C_{12}H_{10}$, mag. susceptibility, sp. ht., spin arrangements and transition obs. 77−20590
$Ni(NO_3)_26NH_3$, specific heat discontinuity at Neel point 77−51912
$Ni(NO_3)_2.4H_2O$, two spin ordered states under mag. field 79−15308
$Ni(NO_3)_2.6H_2O$, susceptibility and specific heat meas., spin ordering, antiferromag. spin pair coupling 80−7084
NiO, bulklike powder, sp. ht., 14-280K 79−69260
NiO, phonon dispersion relations, neutron scatt. meas. 79−42181
NiO, temp. and stoichiometry depend., antiferromag. T-domain influence 77−8332
$Ni_{78}P_{14}B_8$, $Ni_{80}P_{12}B_8$, amorphous mag. clusters, sp. ht. meas. 78−68274
$Ni_{80}P_{14}B_6$ glass, low temp. meas., electronic, phonon contribution 78−10689
$Ni_{1-x}S$, metal-semimetal transition, lattice dynamics and thermodynamic props. 80−29324
$NiS_{2-x}Se_x$, sp. ht. and elec. resist. in metallic regime 77−69589
$NiSe_2$, paramag. props., NMR, mag. susceptibility 80−60175
$NiSiF_6.6H_2O$, ferromag. ordering, susceptibility and heat capacity obs. 79−61080
$NiSnF_6.6H_2O$, ferromag. ordering, susceptibility and heat capacity obs. 79−61080
NiTi, martensitic, shape memory effect kinetics and thermodynamics 80−3021
$NiTiF_6.6H_2O$, mag. and struct. transitions 78−68257
$Ni_3(VO_4)_2$ temp. depend. of heat capacity, 60-1080K, Debye temp. 77−7869
$NpIr_2$, itinerant antiferromagnetism 79−61154
$NpOs_2$, band magnetism due to f-electrons, T_c 77−73039
$NpOs_2$, itinerant ferromagnet, 3-25K 77−63212
$NpRu_2$, spin fluctuation cpd., 3-25K 77−63212
$NpSn_3$, band magnetism due to f-electrons, T_N 77−73039
$NpSn_3$, itinerant f-electron antiferromag. obs. 77−8315
O_2, antiferromagnetic, internal sublattice fields, nucl. heat capacity meas. of ^{17}O 79−95597
β-O_2 crystal, thermodynamics of mol. libration motion *(Russian)* 80−70328
P-S, amorphous, glass transition and specific heat, intermolecular bond saturation 80−15011
P-Se, amorphous, glass transition and specific heat, intermolecular bond saturation 80−15011
PLZT ceramics, 2-25K, field depend., phonon modes 77−47586
$P_2Se_xS_y$ glass, thermophysical props., 303-413K, struct. interpretation 78−47615
Pa, phonon density determ. and heat capacity *(Russian)* 77−24415
Pb, phonon dispersion relations and lattice heat capacity, modified Bhatia model 77−20024
Pb-Bi film, amorphous and polycrystalline, specific heat meas. 77−80715
PbF_2, orthorhombic and cubic, heat capacity, 3 to 22K 80−19955
PbF_2, sp. ht. anomalies, phase transition 79−86901
$Pb_5Ge_3O_{11}$, ferroelectric, anharmonic effects in low freq. symm. modes, Raman study 80−25365
$PbH(D)PO_4$, $PbH(D)AsO_4$, ferroelectric, sp. ht. 79−19853
PbI_2, low temp. thermal props. 79−95178
PbI_2-piperidine(aniline)(pyridine), intercalation cpds., heat capacity of low temp., intercalation effect *(Russian)* 80−92682
$Pb(Mn_{1/2}Ta_{1/2})O_3$, ceramic, for thermal and dielectric isolation at low temp. 80−39365
$PbMo_5S_6$, high supercond. T_c, soft mode behaviour 78−14855
$PbMo_6S_8$, normal state and superconducting property measurements 78−91660
$PbNb_2O_6$, ferroelec., sp. ht. and Debye temp. meas., 2-25K 79−73319
$PbNb_2O_6$, sp. ht. and Debye temp. meas., 2-25K 79−73319
$Pb_2Nb_2O_7$, sp. ht. and Debye temp. meas., 2-25K 79−73319
PbO, sintered, pure, prep. and props. 77−48361
Pb_3O_4, tetragonal to orthorhombic transition, heat capacity meas. 80−20929
PbSe, enthalpy, heat capacity, 300 to 1480K 79−60523
$PbZrO_3$ pyroelectric detector, low temp. behaviour, expt. 80−31869
$PbZr_{0.95}Ti_{0.05}O_3$, soft mode dielec., anomalous low temp. sp. ht. 78−14423
Pd, phonon dispersion curves, freq. spectrum, specific heat calc. 77−15516
Pd, ultrafine particles, size effect on vibr. sp. ht. 78−10153
Pd-Ag(Mo)(Nb)(Rh)(Ru), dilute, low temp. sp. ht and mag. susceptibility 77−62650
Pd-Fe-Mn, ferromagnet-spin glass, thermal expansion forced, magnetostriction and magnetisation under high press. 80−65255
Pd-H, dil. α-phase, influence of deform. on low-temp. sp. ht. 77−31783
Pd-H alloy, 50K transition, sp. ht. and thermal relax. meas., diffusion effects 77−15596
Pd-H(D), isotope effects in supercond. properties 78−6471
Pd-Mn, spin freezing in spin glass phase, susceptibility meas., sp. ht. analysis 77−69582
Pd-Mn (10 at.%), spin glass, inelastic neutron scatt. exam. 79−61170
Pd-Mn dilute alloys, mag. ordering, sp. ht. calc. by Monte Carlo method 77−77030
Pd-Pt alloys, mag. props., average and local density of states, CPA calc. 77−59242
Pd-Si amorphous alloy, heat treated, low temp. lattice sp. ht. 80−75368
Pd-Si(-Cu) amorphous ribbons, low temp. sp. ht., density of states trends 80−79957
$(PdAg_{0.2})H_2$, molar heat capacity, 2-6K, absence of supercond. transition 77−1516
$Pd_{0.775}Cu_{0.06}Si_{0.165}$ alloys, glassy and crystallised, low-temp. specific heat 79−60516
PdD_x, superconducting, molar sp. ht., γ-coeff. and Debye temp., 2 to 12K 77−1517
PdH_x, 55K heat capacity anomaly relation with vibrational spectrum modification of Pd 77−51516

specific heat of solids continued
PdH_x, electronic props., H alloying effects, book contrib. 79−82522
$Pd_{1-x-y}Si_xCu_y$, glassy, low temp. specific heat 78−83969
$Pn_2Nb_2O_7$, relax. phenomena, meas. of dielec. const., polarisation and sp. ht. 77−4597
Pr, anomaly at 700K *(Russian)* 77−28017
$Pr_{21}Ag_{79}$, amorphous, sp. ht. at low temp. 80−75780
$PrAl_2$, cryst. field interpretations of inelastic neutron scatt. meas. and mag. props. 79−56174
$PrCl_3$, cooperative Jahn-Teller ordering of elec. dipoles in non-Kramers doublets 78−15115
$PrCl_3$, one and three dimensional antiferroelec. ordering 77−4607
$PrCu_6$, nucl. mag. ordering, heat capacity and magnetisation obs. 79−87272
PrF_3, heat capacity from 5 to 350K, entropy enthalpy, Planck function 79−46811
$Pr_3Ga_5O_{12}$, sp. ht. meas., 0.4-90K 77−55680
$PrH_{2.65}$, sp. ht., 2 to 260K, second-order phase transitions and cryst. field splitting 79−82355
$PrIn_3$:Gd, indirect nuclear exchange interactions, ESR-linewidth meas., sp. ht. determ. 80−103825
$PrIr_2(Pt_2)(Rh_2)(Ru_2)$, sp. ht., differential susceptibility and elec. resist. meas., 1.4-40K 80−71063
$Pr_xLa_{80-x}Au_{20}$, amorphous, low temp. excitations, specific heat 80−100337
$PrMg_3$, cryst. field study, inelastic neutron scatt. and sp. ht. meas. 80−59939
$Pr_2Mg_3(NO_3)_{12}$, sp. ht. and elec. susceptibility 77−85642
$PrNi_5$, crystal field investigation from inelastic slow neutron scatt. expts. 80−39538
$PrNi_5$, crystal-field effects, comparison of calcs. with expts. 79−87071
$PrNi_5$, powder, in contact with liq. ^3He, thermal relaxation and heat capacity, mag. susceptibility 79−44909
$Pr(OH)_3$, electronic heat capacity, 0.45 to 4.2K, phase transition at 1.21K 80−59673
$Pr(OH)_3$, low temp. heat capacity, thermophys. props. optical spectra, anal. of Schottky contributions, review 80−24611
PrP, 20-300K, cryst. field effects contrib. 77−16092
PrP_5O_{14}, sp. hts. near ferroelastic phase transitions 78−63863
$PrPd_3$, heat capacity at low temps. 79−28547
Pr_3Tl, hyperfine interactions, sp. ht. and magnetisation meas. 79−28531
Pr_3Tl, resistivity and sp. ht. near threshold 79−78399
Pt, heat capacity, 80 to 1000K, laser flash calorimetry 79−95179
Pt, lattice dynamics, ang. forces and normal vibrs. 78−22810
Pt, phonon dispersion, vibr. spectrum, sp. ht., modified ang. force model 77−69054
Pt, sp. ht. at const. vol., high temp., dilation convection 79−14940
Pt, specific heat, electron-phonon effects and anharmonic contrib. 79−90795
Pt, specific heat meas., 0.4 to 30K, Debye temp. 78−55955
Pt-Mn, dil. alloy spin glass, mag. sp. ht. 78−14966
Pt-SiO_2 granular sputtered film, size effects in electronic sp. ht. 77−43346
$Pt_{90}Ir_5Au_5$, $Pt_{80}Ir_{10}Au_{10}$, low temp. sp. ht. 79−73320
PtMn, spin glass, nonlinear susceptibility and sp. ht. 80−60304
Pt_3Mn, obs. of magnon sp. ht. 77−63217
$Pt_3Mn_xCr_{1-x}$, electronic specific heat meas. comparison with band model calcs. 80−54400
$Pt_{86}Rh_9Au_5$, $Pt_{74}Rh_{17}Au_9$, low temp. sp. ht. 79−73320
Pu-Ga (1-8.56 at.%) alloys, enthalpy sp. ht. determ. at elevated temp. 78−78458
$PuAl_2$, low temp. sp. ht., spin fluctuation phenomena 77−28405
PuC, high temp. heat capacity 80−49384
PuC_{1-x} and Pu_2C_3, 10 to 300K, mag. ordering 77−28403
PuC_x (x=0.8, 1.44, 1.67), low temp. sp. ht., mag. ordering obs. 80−49372
PuN, heat capacity, at low temps. 79−24168
PuN, high-temperature enthalpy, heat capacity 79−24809
PuO_2, thermal and transport props., electronic contrib. 80−15432
Rb, specific heat at high temp., Monte Carlo calc. 80−29182
$RbAg_4I_5$, ionic cond. near order-disorder transition 77−11728
$RbAg_4I_5$, ionic conductivity and heat capacity near T_c 78−47584
$RbAg_4I_5$, nonequilibrium thermodynamic description, variation of ionic cond. with temp. 79−61391
$RbAg_4I_5$, struct. transition at 209K, Ising like behaviour 78−14460
$RbAg_4I_5$, superionic cond., US absorpt., ionic cond., relaxing sp. ht. 78−14505
$RbAg_4I_5$, superionic phase transition, dynamical and crit. pt. props. 80−107535
$RbCaF_3$, first order improper ferroelastic phase transition at 194K, phenomenological description 80−70397
$RbCaF_3$, sp. ht. anomaly at struct. transform. 78−14426
$RbCaF_3$, thermal props. near phase transition 78−75850
$Rb_2Cd_2(SO_4)_3$ single cryst., growth and phase transitions 79−33918
RbCl, sp. ht. at low temps., Debye temp. determ. 80−2177
RbCl, thermodynamic props., lattice-dynamical calc. 77−35715
$RbCoCl_3.2H_2O$, Dzyaloshinsky-Moriya linear chain magnet, spin counting 79−38304
$Rb_2Co_cMg_{1-c}F_4$, magnetic specific heat, dilution on a two-dimensional Ising-like antiferromagnet 78−91871
Rb_2CuCl_4, layered, mag. sp. ht., two-dimens. $S^1/_2$ Heisenberg ferromag. behaviour 77−32206
$RbFeCl_3.2H_2O$, pseudo one-dimens. Ising-like system, mag. heat capacity and metamag. transitions 77−66351
$RbFeF_4$, two dimensional structural phase transitions, sp. ht., optical, dielec., X-ray diffr. meas. 79−69240
$RbHF_2$, heat capacities, transitions and melting 79−10967
$RbHSO_4$, acoustic and dielectric props. near phase transition 80−55053
$RbHSO_4$, phase transition, sp. ht. and dielec. permittivity meas. 77−85672
$RbMnCl_3$, specific heat near Neel temp. *(Russian)* 80−100340
α-$RbMnCl_3.2H_2O$, pseudo-one-dimensional mag. system, low-temp. sp. ht. 77−85471
RbN_3, heat capacity from 5 to 350K 79−55901
$RbNO_3$, single cryst., DC cond., dielec. and thermophys. props., temp. depend., transitions interpret. 78−26682
$RbNiF_3$, high-temperature mag. sp. ht. *(Russian)* 80−88757
Rb_2NiF_4, specific heat capacity, critical amplitude, cross-over from 2-D Ising to Heisenberg behaviour 80−39791
Rb_2ZnCl_4, commensurate-incommensurate phase transition, crit. behaviour, sp. ht. meas. 80−71342

specific heat of solids continued
Re, plastic deform. rel. to low temp. sp. ht., supercond. *(Russian)* 78−31005
Re, specific heat, elec. cond., emissivity, 1600-2400K 78−67835
Ru 79−69262
Ru, kinetic and thermal props. at high temp., anisotropy 77−43563
Ru, lattice dynamics, sp. ht., thermal expansion 79−82363
$(SN)_x$, lattice and electronic sp. ht. contribs. density of states 77−43344
Sb-Ge-Se system glasses, thermal capacity, 80 to 300K 79−42272
$SbGe_xSe_y$ glasses with const. Sb content, heat capacity, thermal expansion, US vel. and elastic moduli 77−76574
Sc, HCP, lattice heat capacity, third order elastic consts., thermal expansion 79−82352
Sc, lattice dynamics, sp.ht. and bulk modulus 78−71814
Sc, sp. ht. data rel. to electronic props. 78−83971
Sc-Ag(Cu)(Pd)(Rh)(Ir)(Ru), electronic struct., susceptibility, sp. ht. and Knight shift meas. 77−43485
Sc-Fe alloy, electrotransported, low temp. sp. ht. meas. 77−7872
Sc-Gd, spin glasses, low temp. sp. ht. and magnetisation 80−65913
Sc-Gd spin glass, sp. ht., 0.3-10K 80−25145
Sc-Zr(Mg), low-temp. heat capacity 80−75370
Sc_3In, itinerant electron ferromag., low temp. sp. ht., mag. field depend. 79−42765
$ScMo_6X_8$ (X=S, Se), supercond., sp. ht., 1 to 14K 79−51720
$ScPO_4$, enthalpy and heat capacity, 298.15-1600K 77−12559
$(Sc_xTi_{1-x})_2O_3$, semicond.-metal transition, sp. ht. meas., 300-600K 77−43347
Se amorphous films, structural relax., viscosity, creep, heat capacitors, and IR spectra meas. 79−42424
Se, glass, sp. ht. excess rel. to far IR absorption 77−84874
α-Se, monoclinic, heat capacities and thermodynamic properties, 3-300K 78−95162
Se, monoclinic to trigonal conversion, thermodynamic stability and associated investigs. 80−24592
Se, trigonal, low temp. sp. ht. and elastic consts., piezoelec. effect influence on phonons 80−54404
Se, trigonal and vitreous, sp. ht. and thermal cond., 3 to 300K 80−59676
Se, trigonal or amorphous, thermal expansion and Gruneisen coeffs., 10-300K 78−22870
$Se_{0.84}Ge_{0.16}$ glass, sp. ht. excess rel. to far IR absorption 77−84874
Si, amorphous, tunnelling states simulation and sp. ht. 79−37791
n-Si, heavily doped, extrinsic sp. ht. in metallic regime 78−59956
Si, lattice dynamics using Born-van Karman model 79−73271
Si:P, heavily doped, electronic sp. ht. meas., rel. to metal-nonmetal transition 78−6162
Si:P, heavily doped, sp. ht. near metal-nonmetal transition, generalized Matsubara-Toyozawa theory 79−73321
Si:P, heavily doped, sp. ht., calc. using AMO-MT scheme for impurity bands 79−95182
β-SiC, thermodynamic props., temp. depend., 5 to 300K 80−96666
Si_3N_4, and thermodyn. props. 77−80629
Si_3N_4, hot-pressed, thermal cond. by laser flash method 79−69302
Si_3N_4, pyrolytic, crystn. and amorphous, thermal diffusivity, thermal cond., specific heat 79−69303
SiO_2, amorphous, fast-time heat capacity, heat pulse propagation 78−51700
SiO_2, amorphous, sp. ht., time-dependent, 0.1 to 1K 80−100338
SiO_2 glass, thermal capacity meas. at low temps. 80−44334
SiO_2, vitreous, electron irrad. effect on sp. ht. 79−65212
SiO_2, vitreous, existence of gap in low-energy density of states 79−60769
SiO_2, vitreous, low temp. sp. ht., effect of heat treatment 78−59955
SiO_2, vitreous, low temp. thermal props. and intrinsic defects 80−29057
SiO_2, vitreous, low temperature heat capacity enhancement model 80−75369
SiO_2, vitreous, neutron irrad. effects on heat capacity, thermal cond., US velocity temp. depend. 78−83851
SiO_2, vitreous, Suprasil-W, short time scale transient temp. profiles, time-depend. sp. ht. 79−60519
SiO_2-Al_2O_3-Cu_2O glass alkaline durability, corrosion rate, heat capacity and elastic moduli 80−93673
SiO_2-Al_2O_3-Fe_2O_3-CaO-MgO-Na_2O-SO_3 glass, thermophysical props. 78−18849
SiO_2-PbO system glass, thermal capacity, temp. depend. 79−95181
Si_2ON, and thermodyn. props. 77−80629
SiO_2glass, effect of thermal treatment on low temp. specific heat 80−54401
SiP, thermodynamic characts. 10-300K, interatomic bond elasticity 80−59677
$Sm_{21}Ag_{79}$, amorphous, sp. ht. at low temp. 80−75780
SmB_6, specific heat anomalies 80−34199
SmB_6, thermophys. props., 700 to 1200K 79−37850
SmB_6, valence fluctuating state, sp. ht. 80−20127
$SmCl_3$, heat capacity and Schottky anomaly, 5 to 350K, entropy 77−47588
$SmCo_5$, specific heat and kinetic props. at elevated temp. *(Russian)* 79−28530
$SmCrO_3$, spin reorientation phase transition, second order nature 77−80950
$Sm_{1-x}Gd_xS$, calorimetric exam. of metal-semiconductor transition 78−18967
SmH_2, low temp. sp.ht., antiferromag. ordering and cryst. field splitting effects 78−84439
$SmH_{2.84}$, sp. ht., second-order phase and cryst. field splitting effects 79−87279
$SmRh_4B_4$, coexistence of supercond. and antiferromag. order 80−11140
Sm_2S_3, mixed valence compound, mag. and thermal props. 79−78400
Sm_3S_4, mixed valence compound, mag. and thermal props. 79−78400
Sm_3S_4, sp. ht. anomaly 77−89550
Sm_3Se_4, mixed valence compound, mag. and thermal props. 79−78400
Sm_2WO_6 and $Sm_{14}W_4O_{33}$, high-temp. enthalpy and specific heat 80−34205
Sm_2ZrS_5, mag. and sp. ht. meas. on polycrystalline samples 78−23253
Sn, low temp. under pressure, meas. method 78−77915
Sn, low temperature heat capacity measurement, of metals under pressure 78−81979
Sn, supercond. fine particles, sp. ht., fluctuations under mag. field, crit. field and transition temp. 77−80873
Sn, superconducting fine particles, specific heat exam., fluctuations in zero mag. field 77−28295

specific heat of solids continued
Sn-Bi(Sb), small κ supercond., phase transitions higher than second order 80−88668
Sn-Pb alloy, dil., lattice dynamics, sp. ht., resist., thermal expansion and nuclear γ reson. expts. *(Russian)* 78−87749
Sn-Pb alloys, dil., low-freq. phonon spectrum peculiarities 79−60463
$(Sn)_x$, superconducting polymer, elec. cond., heat capacity and optical props. 80−7028
$SnCl_2(H_2O)_x(D_2O)_{2-x}$, high resolution heat capacity meas. *(Japanese)* 80−52218
$SnCl_2.2H_2O$, isomorphous transition, Landau type thermodynamic potential 80−107413
$SnCl_2.2H_2O$-type layer cpds., two dimens. ferroelec. ordering sp. ht. obs. 78−92034
$Sn_{1-x}Ga_xMo_6S_6$, heat capacity meas., singularities at low temp. 80−49985
$Sn_xGe_{1-x}Te$ ($0.62<x<0.91$), specific heat anomaly at struct. phase transform. 77−69095
$SnMo_6S_6$, high supercond. T_c, soft mode behaviour 78−14855
SnTe, low-temp. sp. ht., thermal expansion and Gruneisen parameter 77−15601
SnTe, sp. ht. mean field behaviour at phase transition 77−66023
p-H, solid, constant volume heat capacity and eqn. of state, temp. depend. 80−65334
Sr, specific heat and thermodynamic props. 5-350K 78−47534
$Sr_{0.5}Ba_{0.5}Nb_2O_6$ crystals, ferroelec., dislocation free, pyroelec. props. 79−42907
$SrCl_2$, fast ion cond., specific heat anomaly, mol. dynamics study 80−65283
$SrCl_2$, specific heat anomaly and sublattice disorder, neutron diffr. meas. 79−42238
$SrF_2:Tb^{3+}$, mag., thermal and hyperfine props. 80−29368
$SrSm_2S_4$, mag. props. 78−68237
$SrTiO_3$ ceramic, sp. ht and electrocaloric effects at low temps. 77−59518
$SrTiO_3$, field depend. sp. ht. and soft modes at low temps. 79−8105
$SrTiO_3$, heat capacity crit. behaviour 78−10857
$SrTiO_3$, specific heat near structural transition 77−81072
$SrTiO_3$, thermodynamic props. 77−39680
$Sr_{1.1}V_{12}O_{29.9}$, phase transitions, elec. cond., susceptibility and sp. ht. meas. 78−14776
$SrZrO_3$, high-temp. enthalpy and specific heat, method of mixtures 77−35712
Ta, heat capacity, 10^8-10^9 K s^{-1} pulsed heating, $(2\text{-}4)\times10^3$K 78−14473
Ta, internal equilibrium, cryst. dynamics, lattice dynamical theory of BCC metals 78−79688
Ta, thermophysical props. and neutron absorpt. 80−103488
Ta-Nb-V, solid solutions, superconductivity and charge transfer 79−7926
Ta-Nb-V BCC solid solutions, supercond. and normal state, sp. ht. meas. 78−84347
$TaB_{2.11}$, heat capacity thermodynamic properties from 5 to 350K 78−91446
TaC, true heat capacity meas. by pulse method 80−19953
$TaH_{0.75}$, calorimetric study of phase transform. 77−48426
TaS_2 (2H), sp. ht. and resist. near CDW phase transitions 78−34786
TaS_2 (2H) single crystal, specific heat meas. in mag. field, 0.3 to 3K, AC calorimetry technique 78−43516
TaS_2, enthalpy and specific heat, temp. depend. 80−54406
$TaS_2(Se_2)$, 2H and 4Hb polytypes, layered cpd., thermal props. at CDW transitions 77−47750
$TaSe_2$ (2H), sp. ht. and resist. near CDW phase transitions 78−34786
$TaSe_2$ (2H), thermal and elastic props., X-ray diffr. exam. 79−37754
$TaSe_2$(2H), plasmon behaviour at charge density wave onset 80−10900
$Ta_{22}W_4O_{67}$, Ta_2WO_8, and $Ta_{16}W_{18}O_{94}$, characterisation of thermally contracting tungstates 78−63869
Tb, sp. ht., using lattice dynamical model for HCP metals 79−51273
$TbFeO_3$, thermodynamic props. 77−36078
$Tb_{1.2}Mo_6S_8$, low temp. heat capacity anomaly rel. to antiferromag. transition in supercond. state 80−25044
$Tb(OH)_3$, heat capacity from 10 to 350K, lattice and Schottky contribs. 80−84300
$Tb_2O_2SO_4$, antiferromag., specific heat, 0.6 to 30K 79−33487
TbP (As)(Sb)(Bi), mag. transitions, quadrupolar interaction effects 80−80512
$TbPO_4$, phase transitions at low temp. 80−15237
$TbPO_4$, sp. ht., 0.5-10K 78−52298
$TbPO_4$, specific heat from 1.2 to 6K 78−14475
$TbPO_4$, zircon struct., cryst. field analysis 80−80232
$TbPd_3$, specific heat at low temp. 80−20413
Tb_2ZrS_5, mag. and sp. ht. meas. on polycrystalline samples 78−23253
Tc, Fermi surface, constant-energy-search KKR band theory calc. rel. to low-temp. sp. ht. 77−89689
TcF_6, heat capacity, entropy Gibbs energy, 2.23-350K 78−38852
Te alloy, intermetallic, melting entropy and molar specific heat 79−29024
Te, and enthalpy, 0 to 750°C 77−11705
Te-based chalcogenide glass, 373-600K 77−20138
Te-Si glassy alloys, IR transmission and sp. ht. changes in glass interval, vibr. modes, struct. models 78−23474
Te_2Br, specific heat, 1.5-300K 79−91991
$Te_{0.81}Ge_{0.15}As_{0.04}$, amorphous and cryst., 1-20K 78−22864
α-TeI, specific heat, 1.5-300K 79−91991
Th metallic, heat capacity from 80 to 1000K 80−34201
Th, phonon dispersion relations and lattice heat capacity calc. 77−20023
Th, phonon dispersion relations and lattice heat capacity, modified Bhatia model 77−20024
Th-Gd spin glass, low temp. sp. ht. 79−51795
Th-Y-Ce, supercond., magnetisation of Ce impurities, sp. ht. meas. 78−47904
Th_3As_4, 5-300K 80−88769
$ThC_{0.75}$, specific heat, Fermi level density of states 80−10680
$ThC_{0.6}N_{0.4}$, specific heat, Fermi level density of states 80−10680
ThC_xN_y, NMR, Knight shift and spin-lattice relax. 80−100621
ThH_2, $ThH_{3.75}$, heat capacity and thermodynamic props. to 1000K 78−91451
$Th_4H_{15}(D_{15})$ normal and supercond., low-temp. sp. ht., Debye temp. and supercond. props. 77−4466
$ThMg_2$, cubic Laves compound, sp. ht. rel. to supercond. 79−82356
$ThNi_5$, Haucke compounds, low temp. heat capacity, Debye temp. 80−96663
ThO_2, thermal and transport props., electronic contrib. 80−15432
specific heat of solids continued
ThP, specific heat, Fermi level density of states 80−10680
$Th_{65}Sc_{35}Ce$, supercond., magnetisation of Ce impurities, sp. ht. meas. 78−47904
Ti alloys, data handbook of low temp. mech. and phys. props. 80−22153
Ti alloys, VT5 and VT5-1, specific heat, 4 to 290K *(Russian)* 79−14938
Ti, HCP, lattice dynamics exam. by inelastic neutron scatt. 79−60447
Ti, heat capacity near polymorphic transition, temp. depend., vacancy mechanism 79−86884
Ti, high purity, data handbook of low temp. mech. and phys. props. 80−22153
Ti, lattice specific heat and thermal expansion 79−73318
Ti, point defect estimation from specific heat and volume in plastically deformed pure metals *(Russian)* 80−54223
Ti, pulse heating method, 1500 to 1900K 78−43139
Ti, specific heat and thermal expansion, 4-290K *(Russian)* 79−51276
Ti, VT1-0 and 99.8% pure sample, specific heat, 4 to 290K *(Russian)* 79−14938
Ti-Al, Ti-Al-Sn, specific heat and thermal expansion, 4-290K *(Russian)* 79−51276
Ti-Al-Mo-Cr (5.9, 2.5, 2.2 wt.%), heat capacity meas., 25-960°C *(Russian)* 77−66030
Ti-Al-Sn (3.7, 0.8 at.%) alloy, specific heat, 4 to 290K *(Russian)* 79−14938
Ti-Al-V alloy, thermophysical meas. above 1450K, using subsecond transient technique 78−95161
Ti-Al-V-Sn-Zr (5.9, 2.0, 2.0, 2.0 wt.%), heat capacity meas., 25-960°C *(Russian)* 77−66030
Ti-Mo (5 at.%) based alloy, supercond. transition temp. enhancement by varying struct. state 77−20483
Ti-Mo-V-Al-Cr-Fe (4.8, 4.7, 5.2, 1.1, 1.0 wt.%), structural changes during heating up to 1000°C, DTA study *(Russian)* 80−93552
Ti-Ni-Co cubic B_2 alloys, phonon enhancement of electronic sp. ht. near martensitic transform. 79−60522
$TiB_{1.964}$, heat capacity thermodynamic properties from 5 to 350K 78−91446
TiB_2, low temp. radiation damage, calorimetric investigation 77−27916
$TiBe_2$, cubic Laves compound, sp. ht. rel. to intinerant antiferromag. 79−82356
TiC-C composites, hot pressed, thermophys. props. at high temps. 80−59675
TiN, opt. consts. and physicochem. spectra 77−85677
$Ti_{1-x}Nb_xH_{1.94}$, x=0.25, 0.50, low temp. specific heat meas. 80−2179
$Ti_{50}Ni_{47}Fe_3$, premartensitic phases, neutron scatt., sp. ht. and electron microscopy obs. 79−96025
TiO_2:Nb, rutile, low temp. sp. ht. 78−55957
Ti_4O_7 and $(Ti_{1-x}V_x)_4O_7$, metal-insulator transitions, EPR, elec. and mag. props. 80−2336
Ti_5O_9, phase transitions, elec. cond., mag. susceptibility, sp. ht., EPR and struct. aspects 78−10526
TiS_2, stoichiometric, heat capacity from 100 to 700K 80−10679
$TiSe_2$, mechanism for 200K transition, sp. ht. meas. 78−22853
$Ti_{1-y}V_yH_x$, electronic props., H alloying effects, book contrib. 79−82522
$(Ti_{0.99}V_{0.01})_2O_3$ spin glass, sp. ht. anomaly and entropy change 79−56546
$(Ti_{1-x}V_x)_2O_3$, spin glass, nonlinear susceptibility and sp. ht. 80−60304
$(Ti_{1-x}V_x)_2O_3$, spin-glass props., 0.05-300K 80−25149
$(Ti_{1-x}V_x)_4O_7$, metal-insulator transition investig. by resist., sp. ht. and X-ray diffr. 77−43497
Tl, band struct. by LMTO method, electronic sp. ht. calc. 77−39773
Tl films, supercond. amorphous, effective phonon spectrum and lattice sp. ht. 80−70895
Tl, thermal and elastic props., lattice heat capacity, elastic constants and thermal expansion, model 80−39321
Tl-Pb-Bi, critical field and specific heat 79−73631
Tl-Pb-Bi alloys, supercond., electronic density of states from heat capacity meas. 79−56383
TlBr, soft mode dielec., anomalous low temp. sp. ht. 78−14423
$TlCdF_3$, thermal props. near phase transition 78−75850
$Tl_2Cd_2(SO_4)_3$ single cryst., growth and phase transitions 79−33918
TlH_2PO_4, high resolution heat capacity meas. *(Japanese)* 80−52218
TlH_2PO_4, thermodynamics props. of solid phase transitions, heat capacity 79−10966
TlH_2P0_4, calorimetric and dielectric exam. of phase transition, nearly crit. case. 77−40171
$TlMnCl_3$, sp. ht. and latent heat, under press. 79−7694
$TlMnCl_3$, specific heat in region of struct. phase transition 77−7862
$TlMnCl_3$, specific heat near Neel temp. *(Russian)* 80−100340
TlN_3, heat capacity from 5 to 350K 79−55901
Tl_3PO_4, heat capacity and thermodynamic functions, 5 to 320K 80−65245
TlSe, heat capacity, at low temp. and Debye temp. *(Russian)* 79−10962
Tm, lattice dynamics, thermal expansion, spt. ht., mag. contrib. 79−37778
$TmCu_5$, crystal field level scheme, neutron inelastic scatt. and specific heat meas. 79−51536
$Tm_2O_2SO_4$, antiferromag., specific heat, 0.6 to 30K 79−33487
$TmRh_4B_4$, mag. and supercond. props., mag. susceptibility and sp. ht. meas. 79−78344
TmZn, cooperative Jahn-Teller effect 78−67998
U, anomalous thermal prop. behaviour at low temp. 77−28018
U dipnictides, elec. and mag. props. 78−84399
U metallic, heat capacity from 80 to 1000K 80−34201
α-U, polycrystalline, low temp. sp. ht. anomalies 77−35708
α-U, pseudo-single cryst. and polycryst., low temp. sp. ht. 78−83972
α-U-Mo, dil., electronic properties depend. on $2^1/_2$-th order phase transition under high press. *(Russian)* 80−11128
UAL_2, band magnetism due to f-electrons, T_{sf} 77−73039
UAl_2, low temp. sp. ht., spin fluctuation phenomena 77−28405
UAl_2, spin fluctuations, mag. field effect, electronic sp. ht. and elec. resist. 80−108026
UAl_2, transport props., susceptibility and sp. ht. 80−11174
UAs, sp. ht. meas., 5-300K, mag. transition obs. 80−50101
U_3As_4, 5-300K, ferromag. transition obs. 80−88769
U_3As_4, ferromagnetic transitions and heat capacities from 5 to 950K 78−14955
$UAs_2(Sb_2)$, heat capacities, antiferromag.-paramag. transitions 78−76253
β-UD_3, electronic props., metallic character 80−6693

specific heat of solids continued
UO_2, crystn., specific heat anomaly 80−84299
UO_2, electronic contribution to thermodynamics, sp. ht. 79−7699
UO_2 fuel, density, thermal conductivity, specific heat, thermal diffusivity, flash method 77−55362
UO_2 phase, thermodynamic props. 80−13594
UO_2, spin wave spectrum, mag. susceptibility, sp. ht. *(Russian)* 79−33470
UO_2, thermal and transport props., electronic contrib. 80−15432
U_3O_8, λ-type heat capacity anomalies 77−20080
U_4O_{9-y}, doped, phase transitions, heat capacity meas. 77−18664
U_4O_{9-y}, thermal conductivity and diffusivity, 250 to 415K 77−50234
$U(OH)_2SO_4$, mag. susceptibility, heat capacity anomalies at 21K 80−11151
$UP_{1-x}S_x$, sp.ht. and electronic struct. 79−91240
UPd_3, anomalous behaviour in low temp. props. 79−28108
UPt, weak ferromag., magnon heat capacity, magnetisation and mag. entropy 77−24685
U_2S_3, sp. ht. at low temps., mag. behaviour 80−60353
U_3Sb_4, ferromagnetic transitions and heat capacities from 5 to 950K 78−14955
U_3Si, heat capacity and thermodynamic props., 1 to 1203K 77−72697
$U_{1-x}Th_xAl_2$, ferromag. spin fluctuation system, sp. ht. and elec. props. 77−20604
$(U_xTh_{1-x})S$, mag. props. rel. to elec. struct., 1.5-300K 77−1557
V complex, $[C(NH_2)_3]V(SO_4)_2.6H_2O$, mag. sp. ht., low-temp. crit. behaviour *(Japanese)* 78−56340
V, electronic density of states, effective mass, electron-phonon interaction, Coulomb pseudopot. *(Russian)* 78−26804
V, enthalpy and heat capacity determ. 78−71866
V, lattice dynamics, vibr. spectrum and sp. ht., CGW model 78−22793
V, lattice dynamics and cryst. equilib. 78−75753
V, spin fluctuations effect on T_c, from sp. ht. and mag. suscept. 80−7030
V, ultrafine particles, 1.3-10K, supercond. transition 77−12061
V/H, heat capacity and supercond. between 1.5 and 16K 80−2521
V-Pt, sp. ht. and mag. meas. in ordered and disordered phases 80−70422
V-Re system, discovery of supercond. A-15 phase 78−88060
V-Zr-Nb alloy, rel. between density of states and martensitic and superconducting phase transition temps. 78−10594
$(V_{1-x}Cr_x)_2O_3$, thermal props., rel. to phase transition 77−35709
VF_2, nearly one-dimensional, paramag. susceptibility, sp. ht. calc. 79−15278
VF_2, prep., struct., heat capacity 5-300K, mag. ordering 79−86746
$V_{1-x}Fe_x$, low temp. sp. ht. and mag. props. 80−2548
$V_{1-x}Fe_xH_n$, low temp. sp. ht. and mag. props. 80−2548
$V_3Ga(Si)$, high T_c supercond., rel. to density of states sharp struct. effect on electron-phonon coupling 78−14877
VH_x, electronic props., H alloying effects, book contrib. 79−82522
$V_2Hf_{1-x}Ta_x$, C15 supercond., electronic and lattice props. 78−68110
$V_2Hf_{1-x}Zr_x$, normal and supercond. state, transition temps., mag. susceptibility and specific heat determ. *(Russian)* 80−60132
VN, opt. consts. and physicochem. spectra 77−85677
$VN_{0.74}$ and $VN_{0.89}$, low-temp. specific heat and superconducting critical temp. meas., density of states 80−54835
VO_2, metallic phase, electronic props., plasma freq., Hall coeff. 78−84195
V_2O_5-P_2O_5 based glasses, specific heat effect of fast neutron irradiation 77−69096
V_6O_{11} single crystals, heat capacity anomaly at 172K 78−10197
V_6O_{11}, sp. ht., 0.4-50K 78−72358
V_nO_{2n-1}, insulating Magneli phases, mag. susceptibility and sp. ht. meas. 80−34604
V_nO_{2n-1}, Magneli phases, sp. hts. 0.4 to 50K 79−42774
V_2S_3, enthalpy and specific heat, temp. depend. 80−54406
VSe_2, 1T polytype, layer cpd., thermal props. at CDW transition 77−47750
V_3Si, heat capacity rel. to temp. *(Russian)* 78−52152
V_3Si, low temp. sp. heat and thermal cond. 77−15995
V_3Si, mixed state, ultrasonic anomaly 77−55644
V_3Si, neutron irradiated single crystal, superconducting transition temp. widths, resistivity and heat capacity meas. 78−91802
V_3Si, neutron-irrad., ht. capacity and resistivity 78−88075
V_3Si, normal, mixed and supercond. state, specific heat meas., thermodynamic and superconducting props. 80−49987
V_3Si, sp. ht. anomaly at struct. transform. 78−14426
V_3Si, supercond., sp. ht. meas., internal heating effect obs. in mixed state 77−12067
V_3Si, supercond. mixed state, low temp. tetragonal-domain-reorientation phenomena, US expts. and thermal props. 80−60141
V_3Si, thermodynamic study, intrinsic type II superconductivity 79−47193
W filament, appl. of noise thermometry *(Russian)* 77−76573
W, from calorimeter meas. of enthalpy in 1500-2800K range *(French)* 77−13754
W, high-temp. specific heat, 2300-3600K, meas. of wire cooling in vacuum 77−35703
W, lattice sp. ht., Clark-Gazis-Wallis ang. force model 78−22799
W, relative enthalpy, 273 to 1173K, electronic heat capacity coeff. 80−103496
W, sintered metal reference standard, sp. ht. at high temp. 78−89427
W, specific heat near melting point, rapid pulsed heating method 77−35704
W-Mo alloys, thermal conductivity and diffusivity, sp. ht., 100-2400°C 78−75842
WB_{12}, growth from melt and phys. props. 80−20782
$W_{0.65}Re_{0.35}$, search for strong coupling superconductivity 79−28441
Xe, lattice vibrs., heat capacities 79−42169
Y, thermal and elastic props. 79−33027
Y, thermophysical properties at high temps., exam. *(Russian)* 79−28105
Y-Gd, spin glasses, low temp. sp. ht. and magnetisation 80−65913
Y-Gd spin glass, sp. ht., 0.3-10K 80−25145
$Y_{0.7}Th_{0.3}C_{1.58}$, specific heat 78−91813
YAG:Nd, heat capacity and thermal diffusivity meas. 80−19956
YB_6, thermophys. props., 700 to 1200K 79−37850
$Y_3(Co_{1-x}Al_x)_{17}$, low-temperature sp. ht. meas. 79−56541
$Y_{0.98}Dy_{0.02}$, spin glass, calorimetric exam. 78−68270
$Y_3Fe_{5-x}Al_xO_{12}$, $Y_{3-x}Gd_xFe_5O_{12}$, linear expansion 77−48024
specific heat of solids continued
$YFe_{3-x}Ni_x$, electronic sp. ht., saturation magnetisation and lattice parameter meas. 78−68261
$Y(Fe_{1-x}Co_x)_2$, electronic sp. ht. meas., rel. to mag. props. 77−63197
YIG, thermodynamic props. 77−36078
Y_6Mn_{23}, low temp. specific heat determ. 80−65896
$Y_2Mo_2O_7$, pyrochlore compounds, sp. heat meas. 80−107438
YMo_6X_8 (X=S, Se), supercond., sp. ht., 1 to 14K 79−51720
YNi_3, magnetism resurgence, neutron diffr. and mag. props. study 80−65819
YNi_5, Haucke compounds, low temp. heat capacity, Debye temp. 80−96663
$Y_{0.22}Ni_{0.78}$ amorphous alloy, low temp. sp. ht. 79−65680
YRh, electronic struct., susceptibility, sp. ht. and Knight shift meas. 77−43485
$Y_2Ru_2O_7$, pyrochlore compounds, sp. heat meas. 80−107438
$Y_{0.8}Tm_{0.2}Se$, sp. ht. meas., 1.6 to 20K, mag. contrib. 80−65934
$YVO_4:Nd^{3+}$, zircon struct., cryst. field analysis 80−80232
$YVO_4:Tm^{3+}$, cryst. field parameters, appls. 77−20277
$Y_2[Pt(CN)_4]_3.21H_2O$, first order phase transform., spectroscopic and thermodynamic anal. 78−38829
Yb, FCC, Fermi surface parameters, de Haas-van Alphen effect, press. depend. 77−28092
$YbAl_3$, susceptibility, sp. ht. and magnetisation 79−28512
YbCuAl, mixed valence behaviour, mag. props. 78−68150
YbCuAl, mixed-valence behaviour, mag. susceptibility and sp. ht. 77−80939
YbCuAl, susceptibility, sp. ht. and magnetisation 79−28512
$YbFe_xMo_6S_8$, singularities in mag. and supercond. props. 79−51710
YbGaG, mag. props. between 44-600 mK 80−80517
$Yb_3Ga_5O_{12}$, dipolar magnet, sp. ht. and magnetisation meas. 80−60344
$YbMo_6S_8$, supercond., low temp. thermal and mag. props. 78−14904
$YbS_{1.387}$, magnetic and thermal props. 80−34586
Zn, heat capacity meas. by computer-interfaced differential scanning calorimetry 78−65935
Zn, mean square displacement of atoms in cryst. lattice, rel. to sp. ht. *(German)* 80−79902
Zn-Al-Cu-Mg (4.1, 3.1, 0.05 at.%), thermal cond. and sp. ht. meas. below 4.2K 77−20081
$ZnCl_2$, liq., glass, cryst., sp. ht. meas., glass transition temp. rel. to press. 77−66029
$ZnCr_2O_4$, mag. phase with short range order *(French)* 77−63203
$ZnFe_2O_4$, heat capacity investigation of dopant effects on mag. disordering temp. 80−25143
$Zn_xFe_3O_4$, heat capacity investigation of dopant effects on mag. disordering temp. 80−25143
$ZnGa_2S_4(Se_4)(Te_4)$, low temp. obs. 77−35705
$Zn_3(OH)_4(NO_3)_2$, sp. ht., 5-300K, thermodynamic props. 79−55900
$Zn(OH)(NO_3).H_2O$, sp. ht., 5-300K, thermodynamic props. 79−55900
$Zn_5(OH)_8(NO_3)_2.2H_2O$, sp. ht., 5-300K, thermodynamic props. 79−55900
Zn_3P_2, Zn_3As_2, sp. ht., thermodyn. props. 78−22863
$Zn_3(PS_4)_2$, synthesis, structural and thermodynamic props. 77−24304
ZnSb, thermodynamic props. and elastic moduli 79−77767
ZnSe, moments of phonon spectra from specific heats 80−15203
ZnTe, moments of phonon spectra from specific heats 80−15203
Zr, HCP, normal vibr. modes, temp. depend. 79−19339
Zr, lattice sp. ht. calc. 79−37851
ZrC, true heat capacity meas. by pulse method 80−19953
ZrC-C composites, hot pressed, thermophys. props. at high temps. 80−59675
ZrC_x, thermophysical props. at high temp., thermal vacancies form. 78−43141
$Zr(Fe_{1-x}Co_x)_2$, low temp. sp. ht. and mag. props. 79−61153
$Zr(Fe_{1-x}Co_x)_2$, mag. props. and Mossbauer effects 79−91322
ZrI_4, high-temp. enthalpy, X-ray powder diffr. data 80−107446
ZrN, in homogeneity range, high-temp. thermodynamic characts. 77−77464
ZrN, opt. consts. and physicochem. spectra 77−85677
ZrO_2, enthalpy and heat capacity at 1100-2500K 80−103472
ZrO_2:Y_2O_3, low-temp. specific heat, oxygen vacancy effects 80−49376
$Zr_{0.7}Pd_{0.3}$, amorphous supercond., sp. ht. and thermal cond., 0.1-10K 78−26991
ZrS, electronic struct., bonding effects, photoelectron spectroscopic and low temp. heat capacity cal. 80−96780
$ZrZn_2$, itinerant electron ferromag., NMR exam. of effect of spin fluctuations 77−16192

specific volume *see density*

specimen preparation
see also biological specimen preparation; metallography; replica techniques
adhesion testing of coating to substrate, specimen prep. device 79−43518
aerosols, atmospheric, automatic time sequence filter sampler for proton induced X-ray emission anal. 77−60171
air-lock system for reactive sample transfer to Philips 300S electron microscope 78−41382
alkali halide crystals, ultrahigh vacuum equipment for surface charge and pot. meas. 78−12708
alkali halide pelleting technique for solid sampling in IR spectroscopy 78−87171
alkali metal alloys, for thermal analysis up to 1500°C 77−28948
amosite in calcium silicate matrix, detection limit in X-ray diffr. analysis 77−84578
anthracene, polariton effects in transmission and absorpt. spectra in thin crysts. 77−20886
apparatus for solid/liquid metal interaction determ. under controlled conditions 79−43526
archaeometry, sampling stylus for use with electron probe 78−70246
asbestos fibres concentration meas., in air and liquid, analytical methods review 80−72120
baryta crystal gas-liquid inclusion meas. with microscope heating stage 80−76967
brittle materials specimen prep. for strength determ. 80−40632
bronzes, ancient, chem. polishing and etching for metallographic exam. 78−356
capillary-syringe method for prep. of air-sensitive samples for MP determ. 77−67419
carbides, sintered, sample prep. for metallographic structural anal. 80−13048

specimen preparation continued
ceramic, brittle, specimen prep. for optical and SEM obs. *(German, English)* 80−35457
ceramic, specimen prep., time saving methods *(German, English)* 80−35459
ceramic material specimens, prep. with Pedemax-Planopol automatic grinder and polisher 79−74333
ceramic thin sections, for optical microscopy 79−52562
ceramics, and metal-ceramic mixtures, metallographic method for polishing specimens 78−56850
ceramics, mounting and polishing technique, for microstruct. exam. 78−48580
chalk, grain size determ., sample preparation methods 79−24694
chemical, analyser design impact of microprocessors *(German)* 78−61096
chemical analysis, ashing methods critical anal. rel. to environmental radioactivity and microelements determ. *(Bulgarian)* 79−88043
clamp for holding and stretching fibrous sheet microscope specimens 77−26396
clay, isotropically consolidated sample prep. with random fibres 77−90531
coal, polished section prep., structural anal. 79−15924
coal, synthetic, microsection prep. and struct. *(German, English)* 80−35458
coating techniques, for SEM and X-ray microanalysis 79−12783
coke, preparation for ESR exam. 77−90517
colloid freeze-fracture, for electron microscopy 78−337
compact specimen, for plane strain crack arrest toughness testing 80−76433
composites, thermal stresses investigation, using polymer models 80−40639
compressing device for single crysts. at low temps. 78−49809
corrosion science, surface analytic techniques 80−31929
corrosion test samples, specimen holder for surface prep. 77−28937
corrosive materials, freeze-drying 77−41580
crystal, single, jig for precise orient. and grinding *(Czech)* 79−26047
crystal heater supply using controlled electron bombardment 78−181
crystal turning in common lathe 78−18482
crystallisation process, effect of solid and liq. boundary layers 79−23544
cytology, digital picture analysis 77−21650
decoration methods, electrical relief, on crystal surface during cleavage 79−24045
decoration technique, surface step struct. determ. 80−103554
dehydration of specimens, for SEM, bibliography (1974-8) 80−73544
deposit-substrate systems, adhesion testing 80−50814
device for making plane and plane-parallel specimens 80−85104
device for producing fatigue cracks in specimens 80−61051
diffusion batcher for preparing air and vapour mixtures 79−67275
diffusion sampling method for ambient aerosol size discrimination with chemical comp. determ. 77−37349
dispersion staining method for refr. index meas. of a thin crystal section 80−8433
dispersion staining technique for microscopical particle anal. 78−24855
distillation apparatus incorporating vaporizer which induces vapour flow pattern producing centrifugal field 80−86274
electron diffraction camera, convergent-beam, contamination suppression 78−14252
electron inelastic tunnelling spectrometer, construction and operation 79−40646
electron microscope filaments, micrometer clamp meas. device 79−21700
electron microscope heating stage, double tilt design for structural anal. of metals 77−57430
electron microscope specimen contamination problems 79−71577
electron microscope specimens, vacuum pipette for processing groups 80−18052
electron microscope specimens, VUP-2K vacuum station improvement 77−38058
electron microscope study, book 78−19989
electron microscopy, cold-stage system for fast-frozen liquids 79−71573
electron microscopy, decoration method, rel. to crystal growth *(German)* 80−103222
electron microscopy, high resolution shadowing by sputter deposition 77−55219
electron microscopy, ion techniques 78−32947
electron microscopy, possibilities and limits, review *(German)* 77−82652
electron microscopy, sample preparation effects on decoration patterns 79−86658
electron microscopy, specimen deposition and fabrication by ion beam sputtering 80−82855
electron microscopy, staining and X-ray microanal., book 78−4739
electrothinning, laser-monitored, for preparing ultrathin metal foils 78−53074
EM tensile adhesion test method 80−50804
emission spectrometry, current developments *(Japanese)* 78−86356
environmental cell for 3MV-class microscope, and its appl. to metallurgical problems 77−10141
EPR, CO_2 laser-heated sample holder for high-temp. EPR spectrometer 80−68233
fatigue and fracture toughness testing, fastening materials 80−61050
Fe, Armco, electron microscope object prep. method 80−50789
ferrite powder, grain size meas. by electron microscopy, sample prep. *(German)* 78−56833
ferrous material fractured surface exam., oxide scale removal 78−95886
field desorption mass spectroscopy, new sample supply technique 77−56279
field ion (emission) microscope tip prep. from sheet and block metal 78−7155
film casting method for electron microscopy samples, particularly elastomers 78−29213
filter fabrics, specimen prep. techniques to optical microscopy anal. of dust distrib. 77−56191
fluorescence microscopy, incident light, specimen prep. method 80−82755
fluorite crystal gas-liquid inclusion meas. with microscope heating stage 80−76967
foil, preparation apparatus, for X-ray diffr. study of lattice defects 79−37585
foil for TEM, preservation technique *(German, English)* 79−96263
foil mounting technique, wrinkle-free 80−77767
foil thinning for transmission electron microscopy, monitoring by PP-8 radiometer (USSR) 80−73525

specimen preparation continued
formaldehyde-glutaraldehyde-OsO_4 mixture as fixative for electron microscopy 79−17404
formaldehyde-OsO_4 mixture as fixative for electron microscopy 79−17404
fracture preservation and cleaning, for fractography 80−71866
freeze drying microscope stages 78−45681
freeze etching and related techniques, resist. monitor for automatic film thickness regulation 78−49810
frozen hydrated specimens, mass loss and etching by electron microscopes 80−47147
fuel cell pellet sample holder for high-temp. meas. 79−88928
gas chromatograph modification for capsule dosing system attachment 79−70407
gasoline, sample preparation for P determ. by at. absorpt. 78−31729
geological samples, prep. for SEM 79−12785
glass, ancient, X-ray fluoresc. anal. 77−34064
glass, heat treated, thin foil prep. for TEM obs. 78−7154
glass fibre reinforced plastic, tubular specimen manufacture, apparatus 79−15906
glass fibre reinforced plastics, winding device for mech. test specimens prep. 78−7138
glass-fibre reinforced plastic, three-layer cylindrical with syntactic foam base 80−3267
glasses and fragile materials, fracture energy, direct meas. *(French)* 80−104376
GMA-Quetol 523, ultraviolet polymerisation in embedding procedure for semithin sections prod. 78−92767
goniometer, universally adjustable polishing device 79−2755
graphite, thin support films, 2 nm, prep. for high resoln. electron microscopy 77−87880
graphite composites containing refractory carbides, electrochem. etching for microscope section preparation 77−28949
grid handling, of semi-thin sections of GMA-Quetol 523 embedded tissue, with reference to O_5O_4 78−92766
grinding device for radioactive tracer diffusion studies in hard ceramics 78−41291
hard and brittle materials, microsection prep. technotron and polishing systems *(German, English)* 80−11859
high performance liquid chromatography, automating preparatory techniques 77−52719
high pressure preparation lock for surface analysis in ultrahigh vacuum chamber *(German)* 80−52261
hydrothermal etching method 80−50790
II-VI semiconductors, thin foils, electron microscopic investigations 79−32864
III-V semiconductors, film, sample preparation for TEM studies 78−14258
incubator, choice 80−68187
involatile molecule thin films, electrospray deposition for ^{252}Cf plasma desorption obs. 80−35584
ion beam sputtering, application to high resolution electron microscopy 78−32925
ion beam techniques for SEM, TEM and optical microscopy 78−24778
ion bombardment equipment, IBMA, for electron and optical microscopy *(Czech)* 77−61161
ion implantation in samples colder than 0.5K, low temp. nuclear orientation studies 80−34033
ion sputtering deposition of coatings for ultrahigh resolution SEM 80−76184
lamellar eutectic, specimen thinning for TEM *(German, English)* 78−95885
laser-heated miniature oven, for prop. of matrix isolation samples for Raman studies 78−45737
latex samples, extraction method, gas chromatographic determ. of residual monomers 77−77845
liquid chromatography, preparative, freely programmable fraction collector with automatic repetitive injection 79−79338
liquid mixer, consisting of rotating cylindrical tube 79−71434
liquid nitrogen cooler, for specimen manipulator of LEED-AES experiment *(Japanese)* 78−45639
magnetic domain, SEM obs., method of removing fine magnetite particles from surface *(Japanese)* 80−108655
major element whole rock anal. using sample fusion technique with electron microprobe 77−64494
Mars Viking surface sampler subsystem, acquisition assembly 79−12380
mechanical system for multi-specimen cleavage and rotation in secondary electron emission studies 78−36987
metal, load-bearing surfaces, secondary structures obs. by electron microscopy, specimen thinning method 79−52484
metal coatings, electrolytic cell for making standard samples 80−85106
metal hydride, oxide, nitride prod. in electron diffr. camera 77−65937
metal sample preparation facility 79−180
metal sample preparation furnace for remelting prior to spectrochem. analysis 77−44556
metal specimen preparation for TEM, two-stage, jet-stagnant electrolytic thinning, Ti, Mo appls. 77−71405
metal ultrathin foils, laser monitored electrothinner *(German)* 79−34219
metallographic, specimen preparation for edge profile microscopy 78−57921
metallographic sample preparation, procedures 80−57272
metallographic specimen prep. using micromilling device *(German)* 78−19980
metallographic specimens, automatic machine and procedure for prep. 80−13050
metallographic specimens, grinding and polishing apparatus 78−23889
metallography, quantitative methodology *(French)* 80−30205
metallurgical coke, mech. behaviour charact. *(French)* 80−104371
metals, cryogenic fracturing, appl. to surface layer struct. investig. 77−30219
meteorites, diamond-containing, polished thin section preparation technique 78−65566
micro-sample handling device, various appl. 80−62642
Microcell for polishing TEM specimens 79−96248
microgrid preparation as specimen support for high resoln. electron microscopy 77−87879
micron thick, for high pressure study 79−17408
microparticles, quantitative anal. with electron beam instruments 79−21866
micropipet, digital high precision device 78−24774

specimen preparation continued
microscope cold stage for vacuum etching and freeze drying, comments and replies 78−54450
microscopy, plastic surface coatings as alternative to standard thin section cover glass 78−73974
microtome, automatic for cutting 400 μ fibre snippets 77−9999
mineralogy, application of TEM, sample prep. methods *(French)* 79−5629
miniature electron bombardment sample evap. source for ESCA 77−90248
mixing cell for indirect meas. of excess volume 77−29032
molecular beam mass spectrometric sampling, high press., high temp. mols., review 80−52355
molecular beam mass spectrometry, in situ anal. in crystal growth ambients 80−52357
molecular beam mass spetrometric sampling system, ion concs. in coal-fired MHD plasmas 80−52358
multilayer heterostructures, prep. and ion etching of thin foils for electron microscopy 79−12779
neutron diffraction crystallography, liquid sample freezing with quartz wool 78−18502
nuclear ceramics, quantitative image anal. using light and SEM obs. 79−12912
nuclear targets, techniques used in preparation 79−85201
nylon 6,6, drawn fibre, selective degradation, gel permeation chromatography, TEM 78−71683
nylon 6,6, selective degradation, mol. wt. determ., gel permeation chromatography, TEM 78−71682
optical fibre characterisation techniques compared 80−64202
organic compound luminescence spectrometer attachment for recording at liquid N_2 temp. 79−67394
organic compounds, ^{35}S-labelled, liquid-scintillation counting, automatic sample prep. 78−70688
organic media, sample preparation for P determ. by at. absorpt. 78−31729
organic specimens, calcination methods, for spectrochem. anal. *(Russian)* 78−23997
particles, collecting, handling and mounting for SEM characterisation 79−21867
particulate analysis, aspects of specimen prep. and a limitations of precision by SEM and TEM 79−17574
photoelastic models, 2D, simple procedure for casting plates from Epon 828 79−39061
plastic, load-bearing surfaces, secondary structures obs. by electron microscopy, specimen thinning method 79−52484
poly(4-methylpentene-1), permanganic etchant for TEM obs. 80−21132
polyacrylonitrile fibres, section cutting, technique *(Russian)* 80−7754
polyethylene, electron microscopy with chlorosulphonation aid 77−89351
polyethylene, partially crystalline test body prep. and charact. *(German)* 78−31398
polyethylene, permanganic etchant for TEM obs. 80−21132
polymer, partially cryst., electron microscope struct. anal., soln. and melt-grown films as model specimens 78−30523
polymer blend morphology, methods for study and specimen prep. 78−75580
polymer materials, characterisation, by TEM 80−103270
polymer multicomponent systems, selective electron beam etching 78−45603
polymer sections of min. thickness 5 μ, microtome based on MBR-1 microscope 77−71306
polymer treeing resistance assessment 80−15971
polymeric materials, partially crystalline, comparative evaluation of various prep. techniques for morphology visualisation 80−13049
polymers, vacuum dispersed carbon replicas, for fast electron wide-angle scatt. *(Russian)* 79−32923
polypropylene, partially crystalline, test body prep. and charact. *(German)* 78−31398
polypropylene, permanganic etchant for TEM obs. 80−21132
polypropylene film and fibre, plasma etching 78−95871
pore-channel marking, electron microscopy of polymer films 80−103271
postcontamination avoidance using room with controlled microclimate, for electron microscopy 78−54350
potassium formate, IR absorpt. spectra, sampling effects, Davydov splitting and struct. 78−52508
powder for spectral anal. 78−23884
powder pressing for refr. index meas. 77−156
powder sample isoformation for X-ray fluoresc. anal. 79−87930
powders, spark elutriation into plasma spectrochem. anal. *(German)* 78−68959
pulsed condensation of matrix mixture for spectroscopic investigations 79−36799
pyroelectric polymer film for electron microscope sample preparation, rapid cooling effects *(German)* 80−13185
radioactive aqueous samples in scintillation cocktails prior to counting, mixing device 79−93116
radioactive samples for TEM, jet electropolishing equipment 79−87766
randomised X-ray powder diffraction patterns, adjustable sample holder 80−6317
rare earth oxide, lattice images *(French)* 78−26397
refractory metal-H alloy prep. technique for TEM studies 77−90544
Reichert FC-2 cryomicrotome attachment, improved sectioning reproducibility 80−47149
remotely controlled computer-guided preparation facility for X-ray fluoresc. anal. at fuel reprocessing plant *(German, English)* 78−17399
rocks, preparation for petrographic description, suggested method 78−81431
rubber, crystallising, tensile test specimen prep. 80−71838
scanning electron microscopy; pellet mould for bulk specimen anal. 80−95191
sectioning diffusion specimens in liquid N 79−67276
SEM, cryogenic stage for sample preparation for X-ray microanalysis 80−42306
SEM, low-temp., review 78−54510
SEM, multispecimen holder for materials processing and critical point drying 77−57429
SEM, powder scintillators, type P-47 80−22487
SEM, sample preparation, for materials microanal. 80−37129
SEM, thin film coating techniques 80−68308
SEM, wet objects, use of gas microchamber 79−21855
SEM circle mounts for elemental anal. or morphological studies 77−45921
specimen preparation continued
SEM conductive treatment of specimen to prevent charging 80−101883
SEM insulating specimen charge neutralization using very low energy ions 80−68309
SEM preparation technique for emulsion particles, freeze drying 80−62799
SEM sample preparation apparatus for freeze drying and vacuum evaporation 78−335
SEM samples, metal coating by sputtering, specimen heating *(German)* 80−73338
SEM specimen mounting epoxies, aerosols, and adhesive tapes 79−71580
semi-automatic grain size separation apparatus 78−54351
semiconductor crystal defect obs. by TEM *(Japanese)* 77−84752
semiconductor TEM 90° cross-section and 1° angle-lap specimen prep. 80−71881
semiconductor thin sample etching for electron microscope exam. 80−86272
silicate glass, low voltage electron microscopy of heated surfaces using C replica technique 80−25974
small particle analysis, step-wise procedure 79−97369
spark-cutter, elec. resistivity meas. *(Japanese)* 80−22339
spectrophotometric automatic sample prep. 78−81960
spherical crystal marking for identical remounting 78−18497
splat quenching, electron transparent area prod., comment 77−4755
splat quenching, electron transparent area prod. 77−4754
spray-freezing unit for prep. of specimens for freeze-etching 77−41581
sputtering coating in oil-contamination free vacuum for SEM 79−12784
steel, chemical polishing for opt. microscopy 77−9021
steel, cleaning corroded surfaces for electron microscope exam. by cathodic polarisation 79−70242
steel, high alloy, preparation for instrumented anal., HF induction melting, casting 78−48607
steel, high strength, H_2 embrittlement due to cathodic charging during specimen prep. for SEM *(German, English)* 80−11760
steel, low C, mech. charact., specimen size and shape effects 80−66715
steel, mild, semi-killed, tempering, effect of microstruct. and hardness 77−21184
steel, stainless, Cr-Ni-Mo, surface, scraping, mech. (electrolytic) polishing, ion etching, effects on ESCA 78−53037
steel, surface state influence on etching effect 80−81235
STEM contamination and countermeasures 79−71578
STEM specimen support using C film, prep. and observation 80−93496
Technotron system for specimen prep. *(German, English)* 80−30199
TEM, cold cathode ion gun for sputter etching 80−105748
TEM, plasma etching use for foil thinning *(Slovak)* 80−45405
TEM, specimen thinning, ion beam penetration switch 78−70228
TEM, thinning of objects for exam. 77−82644
TEM, welding technique, grain boundaries in Si 80−103364
TEM contamination exam. and specimen cleaning methods 79−54232
TEM fine grained coating prep., sputter source design 80−99015
TEM specimen preparation by chemical etching 77−52589
TEM specimen preparation using photochem. etching *(German, English)* 77−56202
TEM tensile specimen preparation, stress distrib. 78−73973
tensile test specimen prep. for TEM *(German, English)* 78−60936
thin foils, electropolishing technique for transmission electron microscope specimen preparation 78−57919
thin metal films, for electron microscopy, production by jet polishing apparatus 78−86247
thin metallic foil prep. for TEM obs. *(German, English)* 79−91885
thin specimen preparation by sputter-etching 78−24893
transition metal hydrides and deuterides, $MH_x(D_x)$, M=gp. V metal, single cryst. prep. and characterisation 79−95910
transPu elements, chem., phase anal., X-ray powder diffr. techniques 77−70388
tree rings, ^{14}C radial flow and chemical pretreatment for ^{14}C meas. 78−28346
ultrafine particles, VEROS prep. method and superparamag. props. *(Japanese)* 77−85954
ultramicrotomy in corrosion and protection TEM 77−81358
ultrasonic separation method, for TEM 79−52561
ultrathin cryo-section stabilization by freeze-drying 78−54349
ultrathin serial section transfer and orientation, accessory equipment 78−73976
US test samples of different materials with equivalent vibration charact. 80−11847
vacuum decoration, anal. of patterns by dark-field microscopy 79−23506
vacuum instrumentation, specimen manipulator 79−63245
vacuum-sealed specimen stage for scanning microscopy of air-sensitive materials 79−17571
vibration polishing microsections for metallography 79−87786
water, trace metal anal. by energy dispersive X-ray fluoresc., enrichment procedures 77−60174
water swollen membrane, rapid prep. technique, obs. using SEM with cryo-unit 79−89047
water-in-oil-in-water emulsions, electron micrography 78−7245
wcrn ball, metallographic micro prep. method 78−3274
wear test specimen, metallographic technique 80−35496
weld, specimen prep. for TEM obs. 77−60029
X-ray diffractometry handling problems, survey 80−1898
X-ray fluoresc. multielement anal., sample dispersion into film-forming polymer soln. 77−56316
Ag and alloy electron microscope specimens, noncyanide electropolishing method 80−100967
Ag halide photographic emulsions, SEM investig. of grain props., specimen prep. technique 77−41715
Ag membrane filters for sample collection for X-ray diffr. chem. anal. 77−63972
Ag. surface Au decoration, appl. to electrodeposits *(French)* 80−44445
Ag-Cu (6.2 at.%), with discontinuous precipitates, quantitative struct. anal. using SEM 79−43527
Al alloy, age-hardenable, extraction of precips., electrochem. method 77−32735
Al alloys, specimen preparation for electron microscopy 80−40636
Al alloys, use of electrospark cutting for preparing thin foils for electron microscope exam. 77−52590
Al, anodic layers, coloured, prep. by ultramicrotome without embedding, for TEM and X-ray obs. 79−39074
Al powder thin foil, prep. for TEM study 80−42310
Al, surface film electronoptical exam., appl. of ultramicrotomy to specimen prep. 79−47847

specimen preparation continued
Al wire, specimen preparation for TEM by ion beam thinning *(German, English)* 80−11861
Al-Ge, directionally solidified lamellar eutectics, specimen prep. for TEM *(German, English)* 78−95885
AlCu, electron microscope spot prep. of deform. bands 79−15922
Al_2O_3 supermicrogrid for high resolution electron microscopy 79−17563
Au, Au-rich alloys, electropolishing for electron microscopic examination 78−35589
Au, epitaxially grown bicrystalline thin films, preferred inclinations of (100) grain boundaries 80−103367
Au, thin disc prep. and electropolishing for TEM 78−88601
Au-Zn(Cu) alloys, electrolytic thinning for use in transmission electron microscopy 78−57918
BC, specimen preparation for TEM by ion beam thinning *(German, English)* 80−11861
$BaTiO_3$, Mossbauer spectroscopy, sample prep. and results 80−66078
C, pyrolytic, specimen preparation for TEM by ion beam thinning *(German, English)* 80−11861
$Ca_5OH(PO_4)_5$, prep. of dry powder specimens for TEM diffr. *(French)* 79−37594
Cd, metallographic prep. at room temp. *(German, English)* 77−9026
Cd-Ag (3 wt.%), metallographic prep. at room temp. *(German, English)* 77−9026
Cd-Zn, directionally solidified lamellar eutectics, specimen prep. for TEM *(German, English)* 78−95885
CdTe foils, prep. for TEM, ion sputtering technique *(Czech)* 80−16619
CsI, 5-30 μ thick single crysts., for channellography 78−80658
Cu complex Cu (II) ammonia, phenanthroline complexes, ion exchanged, EPR anal. precision 77−56261
Cu, cracks in fatigue early stages, direct obs. of substruct. by electron microscope *(Japanese)* 78−7028
Cu-decoration technique, lattice imperfection characterisation, of Si wafer *(Japanese)* 79−65069
Eu pellets, specimen preparation for TEM by ion beam thinning *(German, English)* 80−11861
Fe, cast, nodular graphite, welded, struct. exam., heat treatment effects 78−80703
Fe-base samples, for working curves, HF induction melting and centrifugal casting 80−22340
FeTi, H storage alloy, prep. for TEM *(German, English)* 80−30197
GaAs foils, prep. for TEM, ion sputtering technique *(Czech)* 80−16619
GaSb, thin film prep. for TEM 77−9027
Gd-Y alloy, metal sphere prod. by spark erosion technique 78−81956
Ge, epitaxial growth of very thin electron microscopy specimens 80−100793
Ge foil, thinning for electron microscopy 79−49217
Ge, thin crystal, SEM, contrast features, variation of specimen thickness 79−23508
Ge, thin single crystal, (110) orientation, preparation technique 79−95930
Ge-Si alloy foil production by jet thinning apparatus, improved design 78−88589
In, electrodiffusive conc. of impurities for analysis 78−22752
KBr, 5-30 μ thick single crysts., for channellography 78−80658
La-N-C system, metallographic investigation *(German, English)* 77−52600
$LiNbO_3$, ion-bombardment erosion of single cryst., prep. for TEM exam. 79−38996
Mg-Al single crystal growth, specimen for tensile testing in corrosive medium *(Russian)* 80−20774
Mo foils, device for electrolytic thinning from wire, for electron microscopy 80−85105
Mo, high rate sputter deposition for TEM specimens 78−47451
NaCl, 5-30 μm thick single crysts., for channellography 78−80658
Nb, plastically deformed single crystal, foil, damage free prep. for TEM and X-ray topography *(German, English)* 80−30200
Nb_3Ge film, supercond., TEM obs. of microstruct. foil prep. method 77−55642
Nb_3Sn multifilamentary composite supercond. wires, transverse sections prep., ion milling, TEM obs. of grain size 80−101000
Ni alloy, oxide film isolation and obs. method 77−52563
Ni base superalloy, preparation for instrumented anal., HF induction melting, casting 78−48607
Ni single crystal foil, H_2 induced deform. during thinning, electron-optical obs. 79−57059
Ni superalloy powder, thinning technique for microstruct. obs. using analytical electron microscopy 78−48587
Ni-base superalloys, technique for replication of γ' 80−79648
Ni-W directionally solidified eutectic composite, foil prep. for TEM 78−53072
PbSb foil production for TEM by electrolytic and ion beam thinning *(German, English)* 77−49812
Pd-Cu-Si, laser melting and splat quenching to form foils for TEM obs. 80−29986
Pr tinted glasses, transparency, dichroism and colour effects *(Polish)* 80−71371
Si, foil, thinning for electron microscopy 79−49217
Si, spreading resistance calibration, effect of specimen preparations 78−10450
Si wafers, preparation of preselected areas for TEM 78−24887
Si-SiO_2 wafer thinning for TEM 77−89352
SiC, diffusion tracer deposition, using travelling solvent zone 78−51742
SiC, specimen preparation for TEM by ion beam thinning *(German, English)* 80−11861
$SrTiO_3$, Mossbauer spectroscopy, sample prep. and results 80−66078
Ti, electron microscope specimen prep. technique for dynamic straining expt. 78−88602
Ti, metallographic specimen prep. for chem., mech. electrolytic polishing 78−80705
Ti-Mo (15 wt.%) alloy, metastable β-phase, deform. characts. 78−6975
β-Ti-Mo alloys, thinning transformation 77−44438
Ti-Ni, laser melting and splat quenching to form foils for TEM obs. 80−29986
$^{235}UO_2$ single crystals, electrochemical prep. 78−37478
W on graphite for bright field TEM 77−62456
W, polishing technique as prep. for TEM 80−71851
W support film for high resoln. electron microscopy, phase contrast, computer modelling 78−1144
Zr, FIM, specimen prep. and results 77−11449

specimen preparation continued
Zr, microstructure exam. by electron microscopy, oxide film appl. 79−70243
Zr-Nb (2.5 wt.%) alloys, microstruct investigation by electron microscopy using oxide films 79−70243
ZrO corrosion layer, specimen preparation for TEM by ion beam thinning *(German, English)* 80−11861
ZrO_2 foils, production for TEM 79−74087

speckle
1978 P 1, speckle obs. rel. to orbital radius and system mass and density 80−109394
acoustic holograms, speckle size 78−13864
adaptive optical systems, speckle effects 77−19410
affine geometry, tilt topology 77−19176
amorphous materials, thin, dark field speckle patterns in high resolution electron microscopy 78−34402
amphibian middle ear dynamics using laser speckle interferometry 78−40198
amplitude and intensity statistics, general relations 79−27176
analogue video transmission feasibility using laser diode, over 30 km at 1.3 μm 80−58737
astronomical doublet system resolution, random speckle structure model and expt. *(Russian)* 79−7082
astronomical image processing digital techniques 78−81555
astronomical image reconstruction 77−37508
astronomical IR interferometry, high spatial resolution methods, speckle and aperture synthesis *(French)* 80−46405
astronomical optical intensity and speckle interferometry, review *(German)* 77−56835
astronomical speckel interferometry with multiple mirror telescopes, laboratory expts. 79−80237
astronomical speckle camera, Kitt Peak National Obs., design, double star meas. 79−62745
astronomical speckle imaging for diffr. limited image recovery 77−45318
astronomical speckle interferogram masking, holography and phase flipping 80−109373
astronomical speckle interferometry, defocusing effects 78−40834
astronomical speckle interferometry, image reconstruction by speckle masking 77−49308
astronomical speckle interferometry, obs. using linear digicon detector 77−78648
astronomical speckle interferometry, stellar image recovery, photon noise limitations 77−49309
astronomical speckle patterns, interference, point spread function 77−22101
astronomical telescope image, phase var. due to atm. turbulence 77−45317
astronomical telescope speckle interferometry, online digital autocorrelator 78−81548
astrophotography, isoplanicity meas., speckle holography 80−56717
astrophysical applications of image restoration, conf., Bordeaux, France (Mar. 1979) 80−41935
atmosphere, speckle propagation through turbulence 78−66758
atmospheric isoplanation measurement using speckle interferometry 78−65385
atmospheric turbulence, research progress on speckle propag. 79−66803
α Aurigae (Capella) AB, angular diams. by two telescope interferometry 78−8055
averaging in imaging step, sub-channel holography 79−22918
axial structure, Fourier description 79−72494
Benard convection, transient, laser speckle photography obs. 79−32508
bibliography of laser speckles (1976 to 1978) 80−82593
binary image in noise, corruption by multiplicative speckle 79−36848
binary stars, obs. by speckle interferometry 80−90477
binary stars, speckle interferometry appl. 77−71011
binary stars, speckle interferometry at 5200 Å for 30 objects 78−65656
biological objects, electronic speckle pattern interferometry in vivo 80−109083
birefringent slice, isoclinics and isochromatics, speckle pattern visualization 77−2687
Bragg diffraction imaging systems, speckle size 78−13864
camera and analyser for surface displacement and tilt meas. 78−32790
circular particle size determ., complete histograms, diffraction spectrum anal. 79−86130
circular surface trueness testing by laser speckle photography 79−86266
coherent background-speckle pattern superposition, statistical props. *(Chinese)* 78−90368
coherent imaging, speckle power spectrum, effect of moving diffuser 79−31811
coherent imaging, two step laser speckle reduction process 78−37819
coherent noise reduction by freq.-modulated zone plate fabricated by holographic techniques 79−86134
colour reproduction of objects by speckle interferometry in white light 80−47094
combustion phenomena deflection mapping, speckle superposition techniques 78−44379
component inspection by speckle pattern interferometry 77−37975
concrete, stress determ. by holographic and speckle techniques *(French)* 79−27603
contour slope meas. of an object, coherent optical method 78−32862
contrast, off-axis, of laser light transmitted through multimode fibres 78−90513
contrast in speckle pattern, method of meas. *(French)* 80−14284
contrast measurement in and near image plane 78−42287
contrast of time-averaged speckle patterns produced by small vibrations of diffuse objects 79−94169
contrast patterns rel. to surface roughness, polarisation effects obs. 80−43258
crack front, stress intensity factor, three dimens. speckle interferometry 77−84196
crack initiation determ. 78−60933
curved rotating surface of Gaussian roughness, laser spot illumination 77−19173
curved surface contouring, two-wavelength speckle imaging methods 79−85121
cylindrical rough surface, speckle image for radius of curvature meas. *(French)* 77−34020
cylindrical surface two-wavelength speckle pattern intensity distrib. at optical transform plane 80−106487

speckle continued
decorrelated diffusers interferometer, description, exam. of interference phenomena 78−37051
deflection contour generation by white light projection speckle method 80−98881
defocused speckle photography, topological information extraction technique 77−41676
deformation measurement, out-of-plane, using holographic interferometry and speckle photography, comparative accuracy 80−78804
diffuse object, under Gaussian beam illum., laser speckles produced by longit. motion 80−48156
diffuse object longitudinal motion under Gaussian beam illum., laser speckle dynamic statistical props. 80−99628
diffuse object real-time velocity meas. using laser speckle zero-crossings 80−77760
diffuse object vel. meas. by speckle intensity fluctuations 79−97366
diffuse objects, fringe loci and visibility in holographic interferometry 78−58951
diffusely reflecting objects, deformation meas. by lasers, appl. of holography and speckle, review *(Japanese)* 80−9832
diffuser, weak, speckle pattern, spherical aberration effect 80−87476
diffuser form. of simple known statistical props. 78−90539
diffusing object axial displacement detection, image plane speckle 79−85118
diffusing object axial displacement meas. in speckle photography 77−57301
diffusing object surface state study by double speckle photography 79−85120
diffusing surface determ. by speckle photography 79−85117
diffusing surface inclination determ. rel. to viewing direction, speckle photography 79−2815
digital filtering of speckle-photography data 80−27338
displacement determination in special alloys by holographic and speckle interferometric methods 78−27688
displacement meas. by combined holographic and double-aperture speckle interferometry *(Japanese)* 79−80670
displacement meas. of curved surface, using laser speckle interferometry 80−31712
displacement measurement, 3-dimens., from single image hologram, combined holographic and speckle interferometry 77−83831
displays speckle noise, min. detectable contrast 77−19411
double exposure interferometry through speckle photography *(French)* 80−83568
double exposure photographic technique, strain, small displacement measurement appl. *(German)* 78−1616
double-exposure speckle photography, analysis using electro-optical readout system 80−62708
dye laser multimode beam, spectral distrib. meas. using speckle patterns 77−14730
dynamic laser speckle due to in-plane object motion, theory and appls. 77−50618
dynamic laser speckle interferometry, appl. to transient flexure 78−32861
dynamical properties study using light scatt., principles spectra derivation and applics. 80−53218
ear drum, human, vibr. meas. using electronic speckle pattern interferometry 79−53205
education, scatter plate prod. using laser speckle, for scatter light interference expt. 79−9063
electronic speckle pattern interferometric system based on a speckle reference beam 80−58472
electronic speckle pattern interferometry, appl. to NDT 77−74491
electronic speckle pattern interferometry, optimal signal processing 78−16837
electronic speckle pattern interferometry, phase modulated, principle 79−85167
electronic speckle pattern interferometry, small vibr. detection and meas. 77−72253
electronic speckle pattern interferometry, small vibrations meas. 78−32865
electronic speckle pattern interferometry, vibr. phase mapping 77−5897
electronic speckle pattern interferometry, vibrating object meas., use of chopped laser light 79−85165
electronic speckle pattern interferometry apparatus with multichannel data acquisition 79−80671
electronic speckle pattern interferometry for NDT 79−24702
electronic speckle pattern interferometry of surface shapes 78−94380
elimination using random spatial phase modulation 77−71923
engineering struct. surface deform. meas. by laser speckle photography 79−40534
extrasolar planet detect. using speckle interferometry 77−41309
eye, human, pupil diameter and depth-of-field as meas. by laser speckle 78−15826
Fabry-Perot rings, effect of freq. chirping of light from Q-switched ruby laser 79−41340
fibre optical illuminator output speckle, smoothing methods 79−7209
fibre transmission of laser light, speckle contrast 77−62057
flow velocity distrib. meas., by speckle photography 78−67288
fluid flow patterns from speckle interference fringes 77−84346
fluid section flow pattern speckle photography 80−103096
fluid velocity distribution meas. by speckle photography, expt. 79−86543
fluid velocity measurement by speckle photography and interferometry 78−26221
focus-position sensing using laser speckle 79−59785
Fresnel plane interference fringe generation by correlated speckle patterns 80−106462
fringe contrast analysis, in electronic speckle pattern interferometry 79−72506
fringe shifting technique application in speckle photography 79−54210
fringe visibility, recovery from recorded images quantised to two levels 78−12104
fundamental properties 77−19168
general object deformation decomposition by speckle displacement 80−106486
helical motion of rigid body, meas. by double exposure speckle method 78−16775
high-resolution astronomical imaging, results 80−82225
hologram, redundant Fourier, speckle noise for one class of diffusers 78−50734
hologram, strain meas. near stress conc. in life size specimen 77−119
holographic images, diffuse noise, statistical characts. calc. 80−28176
speckle continued
holographic interferometry and speckle photography, scatt. geometry, topology vector fields theory 80−87347
holographic interferometry for hydrostatic stress/deformation meas. 79−7353
holographic microscopy using image plane holograms, speckle reduction 78−58944
holographic NDT system application of laser speckles 77−75457
holographic projection of speckle patterns applied to remote metrology 80−14299
holographic reader-copier development and speckle suppression 79−81395
holographic speckle reduction by complementary spatial sampling 77−58290
holographically stored X-ray images, grey-tone reproduction 78−65120
holography, astronomical, isoplanicity and temporal correlation meas. *(German)* 79−75116
holography measurements of stars ζ Cancri and ADS 3358 78−93120
image detection in the presence of speckle 79−45909
image digital processing 78−71053
image information processing and evaluation *(Czech)* 78−29147
image plane speckle noise, integration with finite aperture, logarithmic transform 77−19188
image plane speckle patterns, statistical props. 80−63940
image plane speckle statistics 77−19182
image processing technique requiring no reference point 80−98556
image quality of coherently illuminated objects, speckled background smoothing *(Russian)* 80−28168
image reconstruction of single stars, by speckle interferometry 78−32350
image reconstruction of solar features 77−33354
image sharpening telescope, observatory results 77−49295
image speckle contrast, depend. on object surface profiles 78−1168
image speckle pattern, point spread function effect on average contrast 77−46702
image speckle pattern rel. to object surface profile, simulation 77−19175
image speckle patterns rel. to object surface profile, computer simulation 78−13660
image structure of coherently illuminated objects, moving random mask effect 78−82922
image subtraction configs., speckle coded, optimal distrib. of exposures 79−55071
image subtraction through speckle modulated by Young fringes 80−95813
image-shearing camera for surface strain direct meas. 79−58773
imaging, photon by photon, diffr. limited performance for large telescopes 79−53729
imaging phase estimation, FFT-based algorithm 79−76605
imaging system, speckle statistics, gaussian approximation 77−46701
imaging through turbulence with telescope array, speckle interferometry 77−5458
in-plane mechanical vibrs. meas. by speckle imaging, sub Å range 78−30247
in-plane stress waves in solids, mapping by laser speckles 79−27608
in-plane vibration measurement, real-time interferometry with aid of liq. cryst. light valve 80−53734
information processing and correlation 77−19189
information processing experiment set for undergraduates 78−28885
integrated speckle pattern statistics due to mixed coherent and diffused light 80−14285
intensity and phase of speckle pattern, second-order conditional statistics 80−37951
intensity correlation for general scattering objects 79−89851
intensity level crossings, expected number in normal speckle pattern 80−99629
interference fringe localisation, by double exposure speckle photography 78−37803
interference fringes, lens aberration effects 80−105700
interference phenomena generated by two radially shifted speckle patterns 78−90359
interferometer, electronic speckle pattern, TV, principle and appl. 78−58014
interferometer, subsystems and S/N ratio 77−41678
interferometer construction, review 77−71369
interferometric analysis of transient phenomena 80−105701
interferometric meas. of ang. diameters of asteroids Vesta and Pallas 79−35172
interferometric meas. of Pluto diameter 80−41763
interferometric measurement method, appl. to oil instrumentation *(French)* 77−71365
interferometric measurements of binary stars 79−71065
interferometric obs. of binary stars with Haute-Provence 1.93 m telescope 80−90475
interferometric obs. of Pluto's satellite (1980 June) 80−101553
interferometric obs. of solar photospheric granulation *(French)* 80−46523
interferometric obs. of spectroscopic binary 17 ξ Cephei A 80−56874
interferometry, ang. diameter of asteroid Vesta 78−20712
interferometry, astron. appls. *(French)* 80−46404
interferometry, astronomical, isoplanicity and temporal correlation meas. *(German)* 79−75116
interferometry, atm. nonisoplanicity meas. using double stars 78−65387
interferometry, binary stars ang. separations meas. 79−40215
interferometry, binary stars obs. with 1 m telescope 78−69831
interferometry, book contrib. 79−75584
interferometry, decorrel. effects, contouring and surface roughness meas. 77−45886
interferometry, decorrel. effects, machine induced strain obs. 77−45887
interferometry, displacement meas. errors rel. to camera displacements during exposure 79−17479
interferometry, double-exposure, with instant Polaroid film 79−221
interferometry, effects of spectral bandwidths and exposure times 78−69701
interferometry, electronic, using digital image processing techniques 80−87322
interferometry, focused radiation scintillations freq. correl. 79−94153
interferometry, lens aberration effects, optical system pupil complex amplitude changes *(French)* 79−50237
interferometry, meas. of astronomical objects, simulated multiple mirror telescopes 80−56716
interferometry, meas. of binary stars 78−85973

speckle continued
interferometry, one beam laser speckle, smallest measurable displacement 79−97427
interferometry, orbital inclination and masses determ. for triple star β Persei (Algol) 80−36668
interferometry, real-time meas. of vibrations and displacements *(Italian)* 78−54336
interferometry, S/N ratio improvement, image subtraction method 79−86144
interferometry, speckle shearing, fringe parameters 79−220
interferometry, stellar diameters and close binary star separation meas. *(Russian)* 78−40922
interferometry, stellar imaging through randomly fluctuating media 77−13248
interferometry, two-point, astron. appls. and disadvantages *(Russian)* 79−16840
interferometry bandwidth extension using simple optical system 79−26114
interferometry for looking at star surfaces 77−9675
interferometry fundamentals and appl. *(Czech)* 78−29148
interferometry of binary stars, computer simulations in photon-counting mode 78−53836
interior displacement and strain measurement using white light speckles 80−95064
IR speckle images of α Orionis, two-dimens. obs. *(French)* 80−46553
IR speckle interferometry, principle, performance and appl. to NML Cygni 80−31216
IR stellar speckle interferometry, modulation transfer function and evidence for log-normal statistic 79−101079
laser, appl. to vibrational charact. 79−94569
laser beam spatial coherence control by progressive US wave 80−78885
laser heterodyne signals from moving object, bandpass filtering by finite apertures 78−55306
laser pulse power meter, speckle effect on diffuser used as attenuator 79−86202
laser refraction, speckle motion, expt. obs., vision appls. 80−45879
laser refraction theory, speckle movement, ocular refr. determ. 80−41001
laser speckle and surface roughness 80−102622
laser speckle granularity growth, appl. to surface inspection 78−12750
laser speckle in presence of spherical aberrations in imaging geometry 79−81373
laser speckle interferometry, anal. of double aperture speckle and shearing camera techniques 79−6169
laser speckle interferometry, vibration anal. of plate and shell 77−10008
laser speckle interferometry of periodic nonsinusoidal vibrs. 77−41673
laser speckle pattern obs. through finite-size scanning apertures, extreme-value statistics 78−66759
laser speckle photography, double-exposure, magnification change effect 79−40607
laser speckle photography, for nondestructive testing 77−67515
laser speckle photography, review *(Chinese)* 79−35880
laser speckle photography for fluid flow vel. meas. 78−14112
laser speckle photography for in-plane displacement sign detect. 77−79140
laser speckle produced in diffr. field, statistical props. 77−71918
laser speckle reduction, moving aperture method and incoherent spatial filtering 77−42489
laser speckle reduction by US modulation 79−3638
laser speckle reduction in image plane by US modulation of spatial coherence 80−106459
laser speckle suppression during magneto-optical tests 80−85093
laser speckle velocimeter, differential type 79−31975
lens aberrations, effect on speckle photography 78−32866
lens aberrations determination by speckle interferometry *(French)* 79−72653
measurement, control and testing, coherent light appl. *(French)* 80−23641
mechanical translations (10^{-11} to 10^{-3} m) meas. using real-time speckle method *(German)* 80−17924
metal rough surface, speckle pattern statistics 77−75421
metal surface, rough, orthogonally polarised speckle images, cross correlation, effect on fringe visibility in speckle interferometry 78−37808
metal surface roughness meas. using laser speckle 78−8383
metrology applications *(French)* 77−67494
mixed integrator processors, comparison of continuous and discrete types 77−19190
modal noise in multimode optical fibre systems 79−46083
model based on exponential type entire functions 78−50701
moderately rough surface, probability density function of refl. light intensity in far field 79−36837
moire method, speckle shearing, qualitative appl. for structural flow detect. *(German)* 78−82015
monochromatic pattern, amplitude and intensity spatial derivatives, statistical props. 80−53216
monochromatic speckle patterns, statistical props. 80−53215
motion, combined and general forms, laser speckle interferometric obs. 78−74054
motion paths display, speckle photography, holographic reconstruction 77−18084
moving random phase screen, enhanced fluctuations 77−19171
MTF, two-dimensional, meas. by second order speckle statistics calc. 80−63937
multiaperture method, strain analysis by one-beam laser speckle interferometry 79−81821
multidither adaptive optics, speckle cancellation techniques 80−48161
multidither adaptive optics system, speckle interactive effects 77−46797
multifold independent partially polarised speckle fields, and coherent background, superposition statistics 78−1155
multimode optical fibres, freq. depend. of modal noise, speckle theory 80−102817
multiple image shearing interferometric camera, displacement derivative meas. 80−33549
multiplex image coding, astronomical IR speckle interferometry appl. *(French)* 80−67580
nematic liquid crystal, elec. field suppression of fluctuations, laser speckle picture 77−7660
noise and object contrast, detection thresholds eval. technique 78−5434
non-Gaussian, contrast variation 80−83554
non-Gaussian statistics, correlated weak scatterers, computer simulation 80−28159
speckle continued
noncircular Gaussian speckle patterns, statistical distrib. of phase 78−66761
nondestructive evaluation by laser speckle interferometry 78−60976
nondestructive testing of steel, using laser speckle photography 78−76797
object geometries comparison, speckle pattern interferometry, holographic illum. elements 78−66785
one-dimensional stellar and solar speckle interferometry 77−64662
ophthalmology and vision research, appl. of lasers, holography 80−12210
optical coherence applications, seminar, San Diego, CA, USA (Aug. 1979) 80−77542
optical fibre, mode scrambler characts. from speckle contrast 79−98283
optical fibre, multimode, speckle pattern visibility of transmitted light 77−19413
optical fibre modal noise anal. and meas. 80−10003
optical fibres, step-index, modal-noise probability distrib. meas. and anal. 80−99859
optical heterodyne line-scan imagery, speckle noise model 79−50337
optical information processing, photography and interferometry appls., review 77−83820
optical information retrieval, speckle and quantum noise effects 79−76606
optical stress analysis using moire fringe and laser speckles 80−10217
optical systems and speckle 78−46515
α Orionis, speckle interferometry diameter, limb darkening 77−91525
out of plane tilts measurement, Fourier speckle technique 77−13735
partially coherent beam intensity fluctuation calc. in turbulent atmosphere 80−78775
partially coherent light propagating through atm. turbulence, intensity fluctuations 79−58087
partially correlated speckle sum of two patterns, statistical props. 77−83813
partially developed speckle patterns, effect of occupation no. fluctuations 78−74842
pattern holographic projection, metrological applications 80−106493
pattern interferometer for measurement of displacements and surface tilt, book contrib. 79−20334
12 Persei, masses and luminosities from speckle interferometric obs. 78−93305
phase problem, zeroes of entire functions 78−29900
phase screen statistical features from scatt. data, book contrib. 79−36851
phase statistics in coherently superposed Gaussian speckle patterns 80−102626
phase values reconstruction from phase differences, matrix formulation 79−59642
phased array US imaging with multiscan processing 79−57736
photoelasticity, three-dimensional, appl. of speckle pattern props. *(French)* 77−23920
photographic emulsion evaluation 78−49922
photographic recordings, fringes generated in Fresnel plane 78−66763
photographically recorded speckle patterns, contrast 77−604
photography, combined with holographic interferometry for stress anal. 78−70095
photography, defocusing problem, rel. to holographic interferometry 77−18083
photography, double exposure, anal. technique 80−62718
photography, meas. of longit. rot. and lateral motion of diffuse surfaces 78−21235
planar deformation analysis, speckle correlation method *(Dutch)* 80−32930
plane slice optically isolated in three dimens. photoelasticity, plane and circular anal. 77−68540
plane strain field meas. using speckle pattern interferometer 77−26388
polarised pattern, first-order statistics from information theoretical method 78−58908
polychromatic light, short detector integration times 77−14660
polychromatic speckle pattern, dominant eigenvalues to evaluate intensity probability density function 80−106451
polychromatic speckle technique for 3D nondestructive photoelasticimetry 77−58623
polypropylene, transparent film, strain anal. by scattered-light speckle photography 79−32399
polypropylene film, double-exposure speckle pattern obs. of tensile deform., displacement, Poisson's ratio and stress relax. 80−84795
pressure vessel, defect detection, strain evaluation laser holographic and speckle photography methods 77−81365
principle surface strain determ. of arbitrarily deformed objects using tandem speckle photography 79−32408
properties and applications *(Japanese)* 78−22085
Pulsed lasers in electronic speckle pattern interferometry 78−65961
radar processors, synthetic aperture, speckle reduction by moving diffuser 77−34838
random phase screen, geometrical focusing, speckle effects 77−79755
random spatial phase modulation for speckle elimination 78−58920
randomly rough target, laser radar cross section statistics 77−19169
Rayleigh-Benard flow, equal velocity fringes by speckle photography 80−75005
real-time measurement of in-plane translation and tilt by electronic speckle correlation 80−57252
real-time optical processing using the liquid crystal light valve 80−63936
rear projection screen, speckle free 77−19412
resolution, speckle effects 77−19183
rigid body, parallel displacement meas. using polychromatic speckle patterns 77−41568
rigid-body movement induced speckle motion 79−76590
rotating object, vibration anal., image detector in hologram interferometry and speckle photography 78−59351
rotation measurement, in-plane, speckle photography appl. 80−31714
rough laser illuminated rotating cylinders, far field speckle and Doppler shifts 79−50216
rough laser illuminated surface, no. of random point sources, RMS phase depend. 79−59635
rough metal surfaces, diffuse and specular refl., empirical representation 80−87315
rough moving object, cross correl. functions 77−19172
rough object motion measurement, real time, speckle pattern correl. 77−10098
rough surface, exact multiple scatt., speckle contrast 80−53217

speckle continued
rough surface, far field polychromatic speckle, external angular dispersion effect 78−22086
rough surface small vibrs., light scatt. meas. 80−1494
rough surface speckle contrast, depend. on laser spot radius with surface height variance 79−59636
rough surfaces, reflection light, division into specular and diffuse components *(Japanese)* 80−106457
roughness measurement, image speckle contrast 77−18082
roughness measurement, real time speckle pattern correl. 77−18081
S/N ratio in speckle interferometry, photon counting autocorrelation mode at low light levels 79−76613
sandwich speckle interferometry 79−30537
sandwich speckle photography for stress meas. *(German)* 80−10216
satellite laser ranging, scintillation statistics 77−88900
scalar diffusor autocorrelation *(French)* 78−90369
scattering object, coherently illuminated, speckle pattern statistics in diffr. field 80−63924
scatterplate interferometer, scalar diffraction theory 80−73432
semi-Lambertian reflecting surface, laser speckle interferometry 78−82910
serrated apertures, monochromatic light diffr. 80−43260
shearing interferometer for studying aberration of optical system *(French)* 77−65616
shearing interferometer using Savart plate 77−30199
signal and image processing, US Air Force research programme 80−78791
size variation with film density, example of Babinet's principle 79−76592
solar granulation, one-dimensional speckle interferometry 78−45299
solar photosphere, granulation statistical properties and seeing, speckle interferometry obs. 79−88634
solar speckle interferometry calibration, atm.-lens MTF changes 79−2370
space-time optics, speckle phenomena and white light correlations 80−106460
space-time optics in shape and surface metrology 79−6093
space-time random speckle pattern optical analysis 80−102682
spatial coherence meas. by correlated diffusers 80−74296
spatial filtering, detection of binary images buried in speckle 79−36849
spatial power spectra estimation in speckle interferometry S/N ratio calc. 79−76608
speckle patterns, image retrieval 77−22100
spot size estimate in diffr. pattern of scattered field 80−95789
star cluster high resolution imaging by speckle interferometry, simulation 78−77492
stars, interferometry of 155 binary systems 79−17017
statistical analysis, second-order, speckle patterns 78−63011
statistical properties, of the sum of partially developed correlated speckle patterns 79−3629
statistical properties of sum of partially developed patterns 78−1162
statistical props. and coherence aspects 80−78773
statistical theory foundations, comment 79−7077
statistical theory foundations, reply to comment 79−7078
statistics for general scatt. objects, mean, covariance and power spectrum 79−31802
statistics from mixture of moving and stationary scatterers 78−66765
statistics of speckle focused through a hard-edged pupil 79−76594
statistics of speckle patterns, surface depend. features, book contrib. 77−31070
stellar, speckle patterns and plane scintillation, statistics 79−100948
stellar digital speckle interferometry 77−53641
stellar interferometry, high ang. resolution obs., review 77−33355
stellar interferometry 78−77491
stellar interferometry data processing method 80−17498
stellar speckle interferometry, appl. to image reconstruction of α Oriionis 77−22222
stellar speckle interferometry, atmospheric effects, laboratory simulation 79−53730
stellar speckle interferometry, lens-atmosphere modulation transfer function meas. 79−101078
stellar speckle interferometry, S/N ratio 78−12102
stellar speckle interferometry, two aperture pupil plane 79−35145
stellar speckle interferometry, wave correlation scale meas. 78−65388
stellar speckle interferometry data processing method 79−12409
stellar speckle interferometry in near IR 79−53734
stellar speckle interferometry lens-atm. MTF meas. 77−22103
stellar speckle interferometry on 2.5 m Isaac Newton telescope 77−22102
stellar speckle pattern statistics, photon counting techniques 79−25324
step height determ. by two-wavelength speckle pattern method 80−105614
Steward Observatory speckle camera 80−4254
strain meas. by speckle photography technique, accuracy assessment 79−86389
strain meas. speckle photography with hybrid optical/electronic image processing 80−106768
strain measurement, full field optical method having postrecording sensitivity and directional selectivity 78−57892
strain measurement by speckle photography, hybrid optical and electronic image processing 80−99976
strain studies on flat metal plates, holographic interferometry, high-freq. moire technique, and speckle correlation 79−32421
stress-strain state, of machine parts, speckling application 80−19300
structural deformation meas. by holographic speckle interferometry *(French)* 78−30249
submillimetric imaging, speckle effects and specular reflections 77−39071
subspeckle size changes meas. by laser-speckle photography 80−31853
subtraction of speckle coded images, optimal distrib. of multiple exposures 77−34834
surface displacement and strain anal. by speckle interferometry 80−14635
surface displacement and vibration meas. µsing laser speckle *(French)* 78−4686
surface inspection, defocused speckle photography, tilt topology technique 77−26419
surface inspection appl. 77−26385
surface light scattering rel. to microtopographic features 79−59639
surface relief obs. by speckle topography 79−54096
surface roughness dependence 77−19174
surface roughness meas., non-gaussian statisics 78−66762
surface roughness meas., speckle correlation of diffuse surface image *(French)* 77−61115
surface roughness measurement by speckle wavelength decorrelation 79−30418
surface roughness measurement using dichromatic speckle 77−79056
surface roughness measurement using dichromatic speckle pattern 78−89428
surface roughness measurements by means of polychromatic speckle patterns 80−31708
surface roughness properties meas. using polychromatic speckle 78−21210
surface roughness statistics, optical estimation from light scatt., review 77−61916
surface structure influence on image speckle pattern contrast 80−17985
synthetic aperture radars, speckle reduction 77−19191
T-density for speckle and photocounting statistics 78−50700
51 Tauri, Hyades spectroscopic binary, speckle interferometry 77−29876
telescope with severe aberration, MTF for speckle interferometry 78−12103
temporal, appl. to spectral anal. and roughness 77−10836
temporal frequency dependence of modal noise in fibres [optical] 80−58687
theory of speckle, comments 79−50226
theory of speckle, comments 79−50227
thermal expansion, speckle interferometric meas. apparatus 80−68170
thermal radiation sources for speckle interferometry 78−49891
thermoplastic moulding quality assurance using holography and speckle photography 78−27720
three-dimensional intensity distrib., longit. correl 77−75420
time-averaged image speckle pattern, contrast for vibrating object 78−50703
time-averaged patterns, contrast at defocused image plane 79−72491
time-space cross-correlation of speckle patterns under double-crossed laser beam illum. 79−81363
topogram sensitivity, wavefront correl. effect 80−69345
tuning fork for clock, vibr. anal. using speckle method 79−21737
turbulent atmosphere, speckle propag. statistics 77−19170
turbulent atmosphere speckle propag. statistics, log-amplitude covariance function effect 80−82058
two-dimensional optical system MTF meas. by second-order speckle statistics computation 80−74304
two-dimensional structure in-plane vibr., stress analysis by laser speckle method 80−103006
two-scatter-plate low-speckle-noise integrator for atmospheric laser beam transmission meas. 80−90252
ultrasound B-mode scans, speckle reduction 78−22233
US B-mode images of human tissue, real-time speckle reduction 80−74634
velocimeter, non-contact, using laser produced speckle patterns *(Japanese)* 78−178
velocity contour generation by speckle photography 77−2638
velocity measurement application using laser beam, operation *(German)* 77−9991
velocity measurement by first order statistics of time-differentiated laser speckles 80−82750
velocity measurement using time-space cross-correlation of speckle patterns 80−105623
vibrating laser speckle in diffr. field, dynamic statistical props. 79−22895
vibrating membrane speckle pattern analysis 80−106769
vibrating panel laser speckle patterns, interpretation for mode shape information 77−51004
vibration analysis using diffraction field laser speckle dynamic statistical props. 79−76595
weak diffusers with small number of correlation areas, speckle contrast 78−90370
white light, contrast at defocused image plane 80−23621
white light image speckle statistical props. 80−106461
white light image speckles, contrast depend. on surface roughness 79−13903
white light images, speckle patterns, average contrast meas. 80−9808
white light speckle method of experimental strain analysis 79−37255
white light speckle patterns, contrast near image plane 80−102624
wideband speckle interferometry, true imaging of astronomical objects 80−53226
Young's experiment with n holes, appls. *(French)* 78−42274
zero-crossing study on dynamic properties of speckles 80−63923
Al plate, thermal strain meas. by one-beam laser speckle interferometry 80−103005
GaAlAs DH laser coherent light, propagating in multimode optical fibre, speckle contrast 80−78978
Pt-electrolyte interface laser speckle movements related to electrode pot., H_2 adsorb. 78−40052

spectra
see also alpha-particle spectra; astronomical spectra; atmospheric spectra; atomic spectra; beam-foil spectra; beta-ray spectra; Brillouin spectra; cosmic ray energy spectra; electron spectra; energy level crossing; gamma-ray spectra; light scattering; luminescence; mass spectra; matrix isolation spectra; microwave spectra; molecular spectra; multiphoton spectra; neutron spectra; nonradiative transitions; optical double resonance; oscillator strengths; proton spectra; quantum beat spectra; Raman spectra; spectra of inorganic liquids and solutions; spectra of organic molecules and substances; spectra of solids; spectral line breadth; spectral line shift; spectrochemical analysis; Stark effect; stimulated scattering; time of flight spectra; time resolved spectra; transition moments; tunnelling spectra; X-ray spectra
condensed phases, picosec. relax. polarisation spectrosc. meas. 78−68530
demonstration of continuous spectrum, optical filters to audiences, students 77−45649
flare spectrum, H lines rel. to metal emission 77−49353
IR absorpt. spectra, broad, anal. by nonlinear conversion to optical freq. *(Russian)* 77−49793
quantum system, nonintegrable, irregular part of discrete energy spectrum, statistical theory 80−82667
radial integrals calc. in Coulomb approx., use of semiclassical wavefunctions 80−43025

spectra of diatomic inorganic molecules
see also infrared spectra of diatomic inorganic molecules; radiofrequency and microwave spectra of diatomic inorganic molecules; Raman spectra of diatomic inorganic molecules
alkali bromides, photofragment spectra, 266 nm, bond energies and excited state symmetries 80−53072
alkali metal chlorides, photofragment spectra, bond energies and excited state symmetries 80−87190
astrophysical molecule, review of spectroscopic information in visible and UV regions 77−88459
band strengths of electronic spectra, calc. method 77−61810
Born-Oppenheimer approximation, breakdown, electronic isotopic shift 79−3497
bound, hybrid potential function 80−69209
C_2, vibr. and rot. anal. of vis., UV spectra, RF discharges in N_2, H_2, CH_4 mixtures 78−5241
diatomic hydrides, quantum mechanically calculated observables, reliability determ. 80−63505
diatomic molecule, wave functions and intensity factors, using effective Hamiltonian *(French)* 78−5114
diatomic molecule Hamiltonian, homogeneous derivation for spectrum anal. *(French)* 78−5113
generator coordinate method, nonadiabatic mol. dynamics 79−31495
halide vapour, discharge, potential fusion laser systems 78−63074
halogen molecule negative ion, transition energies from pot. curve 77−10596
homopolar molecules, light scatt. *(Hungarian)* 77−50442
inert gas, electron beam pumped, visible absorpt. rel. to visible laser development 78−63057
inert gas dimer ions, $A^2\Sigma_{1/2u}^+ \rightarrow D^2\Sigma_{1/2g}^+$ system, theoretical absorption spectrum 80−32734
inert gas halide laser, discharge excited, gas composition and lifetime studies 80−53268
inert gas halides, B(1/2)-A(1/2) system, emission spectra 79−6934
inert gas halides, electronic transition dipole moments, excited state alignment 77−38698
inert gas halides, emission spectra, open-shell closed-shell interaction, electron gas model 77−30879
inert gas oxides, low-lying electronic states, ab initio CI calcs. 77−57888
inert gases, electron beam excited, transient absorpt. at XeF laser wavelengths 80−32644
ion beam, from saddle-field ion source, gas depend. characts., at. spectroscopy appls. 78−78039
metal oxides, absorption spectra, in flame, optogalvanic spectrosc. obs. 79−18202
parity nonconservation effects and Λ doubling *(Russian)* 79−3432
periodic table, spectrophysical props. 79−45621
periodic table of diatomic molecules, internuclear separation 79−45859
r-centroid approximation accuracy 79−89661
superheavy quasimolecules, Bang Hansteen scaling rule, $K\alpha_1$ line anal. 79−10126
Zeeman effect, calc. for doublet transitions 78−58740
Ag_2, dispersion absorption spectra, 1500 to 5300 Å, rot. anal. 78−42089
AgO, $A^2\Pi$-$X^2\Pi$ blue system, rot. anal. 77−38678
AgO, electronic spectra in rare gas matrix 78−996
AlBr, UV emission spectrum, vibr. consts., isotope displacement and dissoc. energies 77−3381
AlD, $A'\pi$, spectral lifetime and predissociation 79−59515
AlF, $a^3\Pi$-$X^1\Sigma^+$ transition, rot. anal. 77−18938
AlF, hyperfine structure simulated by computer programme 78−50538
AlF, radical, form. in arc plasma, spectra 77−28989
AlH, (1,1)-band emission of $b^3\Sigma$-$a^3\Pi$ system 78−42092
AlH, $A'\pi$, spectral lifetime and predissociation 79−59515
AlH^+, spectrum at 3632 Å, rot. anal. 80−78632
AlI, electronic spectrum, Franck-Condon factors, r-centroids 78−62817
AlO, $D^2\Sigma$-$X^2\Sigma$, Franck-Condon factors and V-centroids *(Russian)* 78−74642
AlO, ground state dissoc. energy, normalised temp. method *(German)* 77−476
AlO, spectra, vibr. consts., pot. curves, Franck-Condon factors and r-centroids 78−42243
AlS, $B^2\Pi$-$X^2\Sigma^+$ transition, assignment of UV bands, vibr. and rot. anal. 80−58278
AlSe, $A^2\Sigma^+$-$X^2\Sigma^+$ transition, rot. anal. 79−72325
Ar_2, electron-beam pumped, visible absorpt. rel. to laser development 79−59671
Ar_2, emission spectra, VUV region 79−31543
Ar_2, VUV emission spectrum, rot. anal. 79−98119
Ar_2^+, bound-free absorpt. cross section for Π and Σ states 78−5140
Ar_2^+, near UV absorption spectra, config. interaction methods 78−17680
ArBr, emission spectrum and chemiluminesc. 80−45508
ArBr, pot. curves, population distribs. and chemiluminesc. for B(1/2) and C(3/2) electronic states 80−45509
$ArKr^+$, absorpt. spectra, ab initio calc. of potential energy curves 78−74568
ArXe, continuous VUV emission spectrum 80−43066
Ar^*+N_2, excitation transfer collision, vibronic energy partitioning 77−75264
AsF, molecular constants determ. from $b^1\Sigma$-$X^3\Sigma$ transition, nonlinear least squares procedure 79−798
AsF, UV band system, $e0^-$-X_21 and $f0^+$-X_21 rot. anal. 77−27083
AuO, electronic spectra in rare gas matrix 78−996
BH, PE curve, spectroscopic consts., perturbation theory appl. 80−23341
BaBr, visible spectrum, $C^2\Pi_{1/2,3/2}$−$X^2\Sigma^+$ transition, laser induced fluorescence 79−98072
BaH, 3800 angstrom absorption band, concave grating spectrograph obs. 80−14154
BaH, new absorpt. band at 2991 Å, electronic transition, rot. consts. 77−83616
BaI molecule UV band systems 79−22728
BaI, visible emission spectrum, vibr. consts. 77−34643
BaI, visible spectra, 5200-5700 Å, vibr. consts. 78−25549
BaO, $A\ ^1\Sigma^+$ state, dipole moment, level crossing spectroscopy obs. 79−94040
BaO, $C^1\Sigma^+$-level, perturbation, extra lines, assignment 79−18213
BaO, recoil velocity spectra from crossed-beam spin-forbidden $Ba+SO_2$ reaction 79−74361
BaO, recoil velocity spectra from form. in crossed beam system 80−76500
spectra of diatomic inorganic molecules continued
BaO_3, visible absorpt. and reson. Raman spectra in Ar and N_2 matrices 77−65487
BeI, reinvestigation of $A^2\Pi$-$X^2\Sigma^+$ band system 77−23503
$BeKr^+$, $A^2\Pi_r$-$X^2\Sigma^+$ system, rot. anal., Λ-doubling consts. 77−27078
Bi_2, in Ar matrix, electronic states, vis. and near IR absorption spectra 78−5213
BiF, fine-structure in C_1-X and C_2-X systems 79−810
BiF, spectrum, 5800-6600 Å, vibr. anal., electronic transition assignment 80−992
Br_2, $2g^3\Pi$-$2u^3\Pi$ UV laser transition, vibr. anal. 77−75170
Br_2, $A^3\Pi_{1u}$-$X^1Sigma^+{}_g$ continuum absorptivity meas. 79−68238
Br_2, absorpt. spectrum, laser isotope separation *(Japanese)* 77−34649
Br_2, absorpt. spectrum, rel. to laser isotope separation 77−10683
Br_2, air pollutant, spectroscopic analysis using scanning tunable dye laser 78−81362
Br_2, and isotopic forms, new rot.-vibr. lines, laser reson. fluoresc. obs. 78−991
Br_2, dissoc. and recomb. rate consts. meas., 1200-3000K, techniques comparison 77−63892
Br_2, laser-induced photodissoc. spectroscopy 77−90614
Br_2, vac. UV absorpt. cross section 80−91574
Br_2, vibrational relaxation and dissoc. behind a shock front, absorpt. spectroscopy *(Russian)* 77−88536
BrCl laser induced fluoresc., quantum resolved level dynamics in $B^3\Pi(O^+)$ state 80−74188
BrF, $B^3\Pi(0^+) \leftarrow X^1\Sigma^+$ absorption spectrum, high-resolution anal. 79−59478
BrO, free radical, Ar matrix absorpt. spectra, mol. vibronic states obs., spectroscopic const. determ. 80−83387
$^{81}Br_2$, visible, vibr.-rot. absorption, fluoresc. decay, predissoc. quantum yield 77−18962
C_2, $(A^3\Pi_g$-$X'\ ^3\Pi_u)$ band system, vibr. and rot. intensity distrib. 77−42332
C_2, $A^3\ pi_g$-$X'^3\ pi_u$ bands, rot. struct., intensity alternation 79−41158
C_2 absorption bands in stellar spectra, 876 nm obs. 80−12805
C_2, calc. of bands strengths of Swann bands 77−61810
C_2, in comets, synthetic spectra calcs. 78−28579
C_2, in southern mag. white dwarf LP 790-29, spectrophotometric obs. 79−92765
C_2 interstellar (0-0)R(0) transition at 2312 Å, UV obs. of ζ Ophiuchi cloud 78−41022
C_2 molecule in solar spectrum, wavelength shift determ. method 78−49340
C_2 molecule produced by laser irrad. of polyethylene 78−42777
C_2, solar rotational temperatures, centre to limb behaviour 79−84758
C_2, Swan bands identification in mag. degenerate star LP 790−29 79−5815
C_2 Swann band profiles in spectra of two comets 78−85909
C_2, transition moments of Swan band system, SCF-CI calc. 78−58746
C_2, triplet ground state dissoc. continuum obs. in UV spectrum of C_2 white dwarf (LP 145-141) 80−67715
C_2^-, matrix isolated, vibr. relax., absorpt. spectra 77−75172
CD^+, $A^1\Pi$-$X^1\Sigma$ band system, spectroscopic consts. and isotope shifts 79−59485
CH^+, photodissociation to C^+ and H, wavelength depend. and photofragment kinetic energies, visible obs. 80−58275
CN, $(A^2Pi_i \rightarrow X^2\Sigma^+)$ and $(B^2\Sigma^+ \rightarrow X^2\Sigma^+)$ yields from HCN photodissoc. 80−87141
CN $(A^2\Pi$-$X^2\Sigma^+)$ transition, Franck-Condon factors, r-centroids, by Langer's approx. method 78−37685
CN, $B^2\Sigma^+ \leftarrow A^2\Pi$ 0-0 and 1-0 bands, laser excitation spectra 80−91588
CN, form. by photodissoc. of parent mols., possible detect. in comets 78−61798
CN in F- and G-type stars, bands oscillator strengths rel. to C and N abundances 77−91530
CN molecular bands in N_2 and air-O_2 arcs, CN origin, band identification 80−38803
CN, r-centroids for $B^2\Sigma^+$-$X^2\Sigma^+$ transition 78−70811
CN, radical, nonradiative transition rates, matrix isolated molecule 78−78740
CN, red spectral system anal., mol. consts. 79−13728
CN, spectral absorpt. coeffs. for fundamental and first overtone vibr.-rot. bands 77−14405
CN, vibr. and rot. anal. of vis., UV spectra, RF discharges in N_2, H_2, CH_4 mixtures 78−5241
CN violet $(B^2\Sigma$-$X^2\Sigma)$ band system, photoelec. intensity meas., transition probabilities 78−37649
CN violet system, rotational and vibrational analysis 80−52961
$CN+O \rightarrow CO+N$, flash photolysis, absorption spectrosc. obs. 79−66289
$CN(B^2\Sigma)$ shock wave excitation, emission, excited state populations, in CO-N_2-Ar mixtures *(Russian)* 78−74638
CO, (4+) system, electronic transition probability 80−106332
CO adsorbed on Al_2O_3-Ni catalyst in He-H_2 effect of H_2S on IR spectrum 78−71945
CO, adsorption on alkaline earth oxides, reflectance spectra obs. 79−28781
CO, CO^+, emission spectra, 2100-5600 Å, electronic band systems and assignments 80−5560
CO, $d^3\Delta_i$ v=4 state dipole moment, laser-induced transition in mol. beam 78−25513
CO, Doppler-free two-photon vac. UV absorption spectra 78−86882
CO, elec. and mag. props., mol. beam elec. reson. spectroscopy 77−61791
CO emission from late-type galaxies 78−89250
CO, fourth positive system in 1115-4759 Å range 77−49291
CO, freq.-depend. polarisabilities and Verdet consts., calcs. 78−62781
CO, high order vib. matrix elements, for dipole moment function and transition moments 77−6757
CO in Venus' atmosphere nighttime luminescence spectra 77−78702
CO isotopes in Ar matrix, vibr. energy accumulation 78−13485
CO, K-shell photoabsorption coeffs., 500-600 eV 80−9617
CO, output spectra from CS_2-O_2-$CO_2(N_2O)$ flame lasers 80−83601
CO, photoabsorpt. cross-section, 50-340 Å, as sum of empirical at. cross-sections 78−58718
CO, photoabsorption , photoionisation cross section, separated channel static exchange Stieltjes-Tchebycheff calc. 79−3502
CO, photoabsorption and photionisation, UV region meas. 78−42087
CO, vac. UV absorpt. spectrum, Doppler-free two-photon excitation 79−41185
CO, valence excitation energy and UV spectra, HAM/3 calc. 78−25453

spectra of diatomic inorganic molecules continued
CO^+ ^{14}C and ^{18}O isotope shifts, vibr. anal. of first negative, comet-tail and Baldet Johnson systems 80−28029
CO^+, $A^2\Pi$-$X^2\Sigma^+$ system, (2,0) band, rot. anal., $^2\Pi$ state Λ-doubling *(French)* 77−10681
CO^+, electronic transition moments for ($B^2\Sigma^+$-$X^2\Sigma^+$) and ($b^3\Sigma^+$-$a^3\Pi$) systems and matrix elements for ($X^1\Sigma^+$) and ($B^2\Sigma^+$) 77−38696
CO^+, fluoresc. spectra of ion beam, laser and electron excitation 79−45743
CO^+, violet-degraded B-A bands, rotational analysis 79−18199
$^{12}C^{18}O$, Herzberg system of $C^1\Sigma^+$ state 78−90185
$^{14}C^{16}O$, fourth positive band system, near UV meas. 78−66559
$CO+He_2$, collisionally excited neutral and ionic emission, flowing afterglow 77−51248
$CO^+ + H_2$, ion-molecule reaction detection of laser-induced ion spectrum, rot. components 78−74671
CS, near UV spectra, rot. anal. of $a^3\pi_r = X^1\Sigma^+$ transition 78−5242
CS, ultraviolet vibronic spectra, for ^{34}S isotopic anal. *(Russian)* 79−50041
Ca_2, in Kr matrix, 1- and 2-photon fluoresc. excitation 78−50567
Ca_2, matrix isolated, vis. and near IR spectra 78−5214
Ca_2, optical spectra, inert matrices 78−58712
Ca_2, van der Waals mol., in Kr matrix, absorpt. and emission spectra 77−83611
Ca_2, vibr. relax. in rare gas matrices 78−58711
CaBr, thermally excited mol. emission spectrum 77−3377
CaCl, $B^2\Sigma^+$-$X^2\Sigma^+$ system, laser excitation spectroscopy, rot. anal. 77−65500
CaCl, $E^2\Sigma$-$X^2\Sigma$ transition, rot. anal. 78−37652
CaCl, form., spectral bands, dissoc. energy calcs. 77−16816
CaCl, free radical, $A^2\Pi$-$X^2\Sigma^+$ system obs. by saturation spectroscopy 78−46353
CaCl, laser excitation and ODR spectra 78−82757
CaCl, laser excitation and fluorescence spectra, rotational anal. of $A^2\Pi = X^2\Sigma$ transition 80−43098
CaD, absorption spectra, extension of F-X system 79−18205
CaF molecule, vis. spectrum, $B^2\Sigma$-$X^2\Sigma$ system 80−18863
CaH absorpt. spectra 2480 to 2550 Å, new electronic states and rot. anal. 79−36662
CaH, absorption spectra, extension of F-X system 79−18205
CaH, $D^2\Sigma^+$-$X^2\Sigma^+$ band system 80−18847
CaI, electronic band spectrum 6100 to 6600 Å 78−90176
CaO $B^1\Pi$-$X^1\Sigma$ and $C^1\Sigma$-$X^1\Sigma$ transition strengths, shock tube spectroscopic absorpt. meas. 80−53053
CaO, $B^1\Pi$-$X^1\Sigma$ and $C^1\Sigma$-$X^1\Sigma$ electronic transition strengths meas. 80−78602
CaO_3, visible and absorpt, and reson. Raman spectra in Ar and N_2 matrices 77−65487
CaS, $A^1\Sigma^+$-$X^1\Sigma^+$, Franck-Condon factors and r-centroids 79−36700
Cd_2 as 470 nm absorber, multiconfig. SCF calcs. 80−32731
Cd_2, in Ar and Kr matrices, 10K, UV spectrum, vibr. assignments 77−58038
CdF, mol., ESR spectra in inert gas matrix 79−76455
CdHg, excimer kinetics and transmission meas. 80−37832
CdHg excimer system, absorpt. meas. 80−48007
CdHg(Mg), Ar matrix absorpt. spectra, vibronic spacing and bonding 79−3453
$C_2(d^3\Pi_g)$ shock wave excitation, emission, excited state populations, in CO-N_2-Ar mixtures *(Russian)* 78−74638
$^{113}Cd_2$, two-level system, absorpt. spectrum, subradiative struct. *(Russian)* 80−28008
CeO, dissoc. energy, rel. band strengths of a_2-X_2 and b_2-X_2 systems 80−99495
CeO, gas, electronic spectrum 79−41178
Cl_2, B-X transition, predissoc., laser-induced fluoresc. obs. 80−43093
Cl_2, B-X transition, rotationally resolved excitation spectra and predissociation in excited state 79−45754
Cl_2, isotope shift and absorption spectrum for laser isotope separation 77−34701
Cl_2, vac. UV absorpt. cross section 80−91574
Cl_2^-, gas phase photodissoc. spectrum 77−58098
Cl_2^-, photodissoc. and photodetachment, pot. curves. 79−64060
$ClF^*(B^3\pi_0^+)$, electronically excited, chem. generation, B→X emission spectrum 79−57216
ClO, $A^2\Pi$-$X^2\Pi$, UV absorpt. spectrum 78−74673
ClO $A^2\Pi$-$X^2\Pi$ system, electronic transition moment and dissoc. cross-section meas. 77−38679
ClO, $A^2\Pi$-$X^2\Pi$ system, photoabsorpt. cross sections 77−79624
ClO, free radical, Ar matrix absorpt. spectra, mol. vibronic states obs., spectroscopic const. determ. 80−83387
ClO, UV absorpt., lab. spectra rel. to atmos. identifications 77−34653
ClO, UV spectra of $C^2\Sigma^- \leftarrow X^2\Pi$ system, rot. anal. 80−996
ClO^-, photodissoc. and photodetachment, pot. curves. 79−64060
$^{35}Cl^{35}Cl$, $B^3\Pi(0^+) \rightarrow X^1\Sigma^+$, 6300 to 9900 Å, rot. anal., mol. consts., equilib. internuclear separation 78−42082
$^{35}Cl^{37}Cl$, $B^3\Pi(0^+) \rightarrow X^1\Sigma^+$, 6300 to 9900 Å, rot. anal., mol. consts., equilib. internuclear separation 78−42082
Co, vacuum UV molecular photoabsorpt. cross-section meas. 80−37096
CrMo molecule, electronic absorpt. spectrum from flash photolysis 77−6796
CrO, $A^5\Pi$-$X^5\Pi$ transition, rot. anal. laser induced fluoresc. and discharge emission spectra 80−69173
Cs excimer states, mol. satellites of 6^2S-7^2P doublet 78−17632
Cs-inert gas molecule, excimer transitions, absorpt. spectra 77−475
Cs_2, 4800 Å absorpt. band, classical method anal. 80−106330
Cs_2, 6^2S-7^2P doublet, mol. satellites 79−85956
Cs_2, absorpt. spectra, ground state pot. curves 77−75171
Cs_2, absorpt. spectrum in visible and near visible 78−46356
Cs_2, fluoresc. at 6270 Å, rot. consts. 79−45744
Cs_2, ground state consts., pot. curve, laser spectroscopy 79−98247
Cs_2, rot. consts., Doppler-free polarisation spectrosc. 80−5555
CsAr, 6dσ states, multiphoton laser spectrosc. obs. 79−85974
CsHe absorption bands associated with forbidden Cs transitions 79−27005
CsKr, 6dσ states, multiphoton laser spectrosc. obs. 79−85974
CsX, (X=F, Cl, Br), absorpt. fine struct. at Cs^+ 4d threshold 77−18940
Cu_2, emission band spectra and vibr. const. 79−36656
Cu_2, in supersonic free jet expansion, laser induced excitation spectrum obs. 80−14151
CuBr, new bands in emission spectrum 77−68052

spectra of diatomic inorganic molecules continued
CuCl, mol. emission spectrum, 5900-6800 angstrom, rot. anal. of A-X system 80−58273
CuF, from gas phase reaction, photon yields, chemi- and photo-luminesc., excitation spectra 79−5157
CuH, UV absorpt. spectra 80−87143
CuI, visible spectra, A-X system, rot. anal. 79−72326
CuO, $^4\Sigma_{1/2}$-$^2\Pi_{1/2}$ transition, rot. anal. 78−82748
CuO, 4182 Å band spectrum, rot. anal. 79−89685
CuO, $C^2\Pi_i$-$X^2\Pi_i$ and $D^2\Delta_i$-$X^2\Pi_i$ band systems, rot. anal. 78−82747
CuO, electronic spectra in rare gas matrix 78−996
CuO, red $^2\Delta$-$x^2\Pi_i$ transition, $^2\Delta_{5/2}$ state consts. 78−9163
CuO, rot. anal. of red $A'\,^2\Sigma^+ - X\,^2\Pi_i$ system 78−13508
CuS, emission spectra, rotational analysis of O-O band of green system *(French)* 77−3372
D_2, Lyman bands, Morse Franck-Condon factors and R-centroids 77−58088
D_2, photoabsorpt. spectra, rovibronic interactions 78−992
D_2, predissoc. linewidths and shapes for $3p\pi D^1\Pi_u^+$ state 80−53066
$DBr^+(A^2\Sigma^+)$ vibrational states, lifetimes, emission cross sections, prod. by electron impact 77−3419
DyO, UV emission spectrum, high resolution, band systems and isotopic shifts 80−87146
F_2, continuous UV absorpt. spectrum, temp. depend. 77−23506
F_2, eqns. of motion method, transition energies, oscill. strengths, electron impact Born cross section 77−18983
F_2, PE curve, spectroscopic consts., perturbation theory appl. 80−23341
F_2, pot. curves and electronic phototransitions 79−63935
F_2, valence electronic states, $^1\Pi_u \leftarrow X^1\Sigma_g^+$ absorption spectrum 79−63920
FH, freq.-depend. polarisabilities and Verdet consts., calcs. 78−62781
FeF, electronic states, ab initio calcs., UV spectrum elucidation 78−74570
FeF, electronic states, anal. of rot. struct. 78−74674
FeH, wavelengths and line intensities for 4920 Å, 5320 Å and 8690 Å bands 77−10680
FeS, X-ray and visible spectra, SCF-Xα scatt. wave anal. 78−5138
GaI, $A0^+$-$X0^+$ and B1-X0$^+$ transitions, isotope shifts, UV and visible spectra obs. 80−53005
GaO, B-X band system, electronic spectrum, struct. and anal. 79−45732
GdO, high resolution visible emission spectrum 77−18932
GeCl, mol., UV spectra, band assignments and rot. consts. 80−997
GeO, Franck-Condon factors and r-centroids of A-X band system 77−65513
GeO, RKRV Franck-Condon factors and r-centroids, ($A^1\Pi$-$X^1\Sigma^+$) transition, pot. energy curves 78−29817
GeO, UV spectra of mol., rot. anal. 79−81210
GeS, band system vibr. anal. 80−48009
GeTe, matrix isolated absorpt. and emission visible spectra, electronic states 80−28026
H_2 3s, 3d: $^3\Sigma$, $^3\Pi$, $^3\Delta$ complex, fine struct., Doppler-free laser spectroscopy 80−1087
H_2 4-0 S(1) 6368 Å quadrupole line strength and pressure shift 80−43108
H_2 (4,0) and (3,0) S(1) lines, absorption strengths 79−16852
H_2, (4,0) S(1) quadrupole line intensity and pressure shift 78−90178
H_2, $B^1\Sigma_u^+$ state, selectively excited continuous vac. UV emission obs. 79−13667
H_2, Balmer radiation production by electron impact 0-2000 eV 79−76521
H_2, electron impact dissoc. excitation, cross sections, mechanisms 80−37895
H_2, electron impact excited singlet-g states, optical and time resolved spectra, radiative lifetimes, quenching rates for rovibronic levels 80−23564
H_2, excitation energy, pot. curves, oscill. strength, Hartree-Fock calcs. 77 -6685
H_2, Fulcher bands, radiative decay consts. 79−22722
H_2, Fulcher system ($3p^3\Pi_u \rightarrow 2s^3\Sigma_g^+$), electronic-rot.-vibr. emission spectra, relative intensities calc. 79−6932
H_2 in solar EUV spectrum, mol. fluoresc. spectrum 79−16908
H_2, long-range force effects on photon and electron impact excitation 79−10170
H_2, Lyman bands, Morse Frank-Condon factors and R-centroids 77−58088
H_2, metastable state, Doppler-free linear single-photon spectroscopy 78−50487
H_2, optogalvanic spectroscopy in discharge, 570 to 620 nm 79−54862
H_2, photoabsorpt. spectra, rovibronic interactions 78−992
H_2, photoabsorption, photoionisation, predissoc., high resolution obs. 77 -477
H_2 plasma satellites, mol. lines mole, in afterglow 80−44053
H_2, predissoc., interference effects, lineshape obs. 80−83432
H_2, predissoc. linewidths and shapes for $3p\pi D^1\Pi_u^+$ state 80−53066
H_2, reson. fluoresc. with Lyman α, astronomical appls. 79−8821
H_2 , free free absorpt. coeffs. dipole length formulation and two centre close coupling calc. 80−83345
H_2^+, grazing incidence collision with surface, Balmer radiation, elliptical polarisation 78−86804
H_2^+, restricted quantum-mechanical three-body problem 80−42083
H_2+H, reactions and collisions in IR laser field, collision-induced absorpt. spectra 80−76499
H_{22} quadrupole vibration-rotation transition probabilities 78−25512
HBr, Balmer radiation production by electron impact 0-2000 eV 79−76521
HBr, spectral intensity, vibr.-rot. bands, dipole-moment expansion 77−75228
$HBr^+(A^2\Sigma^+)$ vibrational states, lifetimes, emission cross sections, prod. by electron impact 77−3419
HCl, 6,0 band, highly forbidden optical transitions using intracavity laser spectroscopy 77−42331
HCi, Balmer radiation production by electron impact 0-2000 eV 79−76521
HCl, $C^1\Pi$-$X^1\Sigma^+$ system, (0, 0) and (0, 1) bands, oscillator strength determ. and UV spectra 80−91570
HCl, electronic spectrum, vac. UV absorpt. 80−9616
HCl, linewidths and shifts in fundamental band broadened by D_2 and H_2 *(French)* 78−972
HCl, overtone vibr.-rot. bands, intracavity dye laser techniques meas. 80−91532
HCl^+, emission cross sections for $A^2\Sigma^+,v' \rightarrow X^2\Pi_i,v''$ on electron impact and lifetime of $A^2\Sigma^+,v'$ state 77−38697
HCl(Br)(I), vac. UV absorpt. cross section 80−91574

spectra of diatomic inorganic molecules continued
HD 4-0 and 5-0 bands, absorption strengths 80−43059
HD, dipole moment and rot. spectrum, perturbation theory calcs. 77−65454
HD, dipole spectrum, influence of intracollisional interference 78−33492
HD, elec. dipole vibr.-rot. spectrum, line strengths, ab initio calcs. 78−25514
HD, Lyman bands, Morse Franck-Condon factors and R-centroids 77−58088
HD, nonadiabatic effects in the B, C and E, F states, rot. line strengths 78−5148
HD, $\nu=0$ to $\nu=5$ rot.-vibr. band, photoacoustic spectrosc. obs. 80−9589
HD, predissoc., interference effects, lineshape obs. 80−83432
HD, predissoc. linewidths and shapes for $3p\pi D^1\Pi_u^+$ state 80−53066
HD^+, HT^+, DT^+, accurate rot.-vibr. energy and transition moment calcs. 77−14412
HD-inert gas mixtures, $R_1(J)$ and $P_1(J)$ absorpt. spectra, positive intercollisional interference 79−54843
HD-Kr, $R_1(1)$ absorpt. spectra, positive intercollisional interference 79−54843
HF, electronic spectrum, vac. UV absorpt. 80−9616
HI, Rydberg states, quantum defect theory applic. 80−32700
HI, UV absorpt. spectra, ionis. limit region, assignment 78−21940
HS_2 radical, ab initio calcs. of geometry and spectra 77−34552
He_2, 600 Å emission continuum struct., in 700-900 Å region in glow discharge 80−95641
He_2, form. in early afterglow of pulsed discharge, time-resolved spectra 78−63585
He_2 formation of He_2 in afterglow of pulsed discharge 77−15259
He_2, laser-driven transitions to high Rydberg states 80−106360
He_2, metastable states, laser excitation spectra 80−5578
He_2, molecular spectrum and structure, singlet Π states $4p\pi$-$9p\pi$ 78−42080
He_2 optical absorpt. spectra and kinetic behaviour 80−95635
He_2, spectra, struct., triplet states, $4p\pi$, $5p\pi$ UAO's 77−34647
HeH^+, excitation energy, pot. curves, oscill. strength, Hartree-Fock calcs. 77−6685
$HeNe^+$, visible spectrum obs. in discharge 79−13729
$He_2(1\sigma_g)^2(1\sigma_u)np\lambda$ triplet levels, multichannel quantum defect anal. 80−91542
Hg_2, absorpt., fluoresc. and two-photon spectroscopy 78−998
Hg_2 and Hg_3 metastable states in flash photolysis of Hg vapour, electronic absorpt. spectra 79−76438
Hg_2, dissociative recomb. and optical transmissions meas. in high press. discharge 80−37816
Hg_2, emission bands, pot. energy surface calcs. 77−10601
Hg_2, fluoresc. and absorpt. spectra anal., pot. energy curves 78−999
Hg_2, model calc. of electronic struct. and spectroscopy 79−3352
Hg_2 vapour, high-press., selective refl. meas. up to 700 bar 80−28031
Hg_2^+, electronic struct. and photoabsorpt. calcs. 80−27932
HgCl, $B^2\Sigma^+$ state, produced in photochem. of $Hg/Cl_2/Ar$ 79−39154
HgCl, HgBr, HgI, $B^2\Sigma$-$X^2\Sigma$ systems, Franck-Condon factors and r-centroids 79−64051
$Hg_2(Hg_3)$, violet emission, formation and decay kinetics, luminesc. time resolved spectra 79−76464
HgXe, excited molecule formation 77−23519
HgZn(Cd), Ar matrix absorpt. spectra, vibronic spacing and bonding 79−3453
I_2, 2-step reson. scattering, subnatural linewidths in vapour 79−76419
I_2, $2g^3\Pi$-$2u^3\Pi$ UV laser transition, vibr. anal. 77−75170
I_2, 5350 Å band rot. anal., Fourier transform spectroscopy 77−27081
I_2, air pollutant, spectroscopic analysis using scanning tunable dye laser 78−81362
I_2, B-X band system, intensity factors 78−25551
I_2 B-X transitions near 5145 Å, reassignment 77−3374
I_2, B←X(0-0) band, visible spectrum obs. 78−5238
I_2, band system, MC SCF pseudopot. calcs. 78−78632
I_2, Doppler-free optoacoustic spectra 80−995
I_2, doubly resonant third harmonic generation, spectrosc. 79−93984
I_2, electron diffraction parameters, spectrosc. calc. 78−70932
I_2, energy levels near B-state dissoc. limit, two-photon spectra 78−9210
I_2 folded Doppler broadened system, interaction with two reson. laser fields 80−53007
I_2, high-dispersion polarisation-labelled spectrum 80−990
I_2, high-resolution saturated absorpt. spectroscopy with short light pulse coherent trains 80−64110
I_2, hyperfine predissoc., Doppler-free spectrosc. obs. 78−89558
I_2, hyperfine structure, 612 nm and 640 nm, saturated absorpt. expt. 78−66871
I_2, in Ar, emission spectrum interpretation 80−95634
I_2, laser saturation spatial spectroscopy of diffusion coeff., interaction pot. 77−75341
I_2, lifetime of R(127) line of 11-5 band of $B^3\Pi_{ou}^+$-$X^1\Sigma_{og}^+$ transition 77−6861
I_2, matrix samples, laser spectroscopy, evidence for $(I_2)_2$ species 78−58735
I_2, molecular absorption spectra, line identification band atlas, 19000 to 18000 cm^{-1} 78−42079
I_2, picosecond relax., fluoresc. spectroscopy, solvent effects 78−58737
I_2, RF optically heterodyned saturation spectroscopy, reson. degenerate four-wave mixing 80−74211
I_2, reson. CARS spectrum, electronic resonance enhancement 79−14033
I_2, saturated absorpt. obs. using interferometric spectroscopy 78−74079
I_2, solns., visible absorpt. spectra, temp. effects 77−61760
I_2, stepwise two-photon excitation, E-state vibr. bands, B-state vibr. rot. levels 79−26962
I_2, transition moment of BO_u^+-$X^1\Sigma_g^+$ system in I_2 laser 79−54917
I_2, use as test mol. in modern spectroscopy, review 78−90317
I_2, vac. UV absorpt. cross section 80−91574
I_2, vibrational relaxation and dissoc. behind a shock front, absorpt. spectroscopy *(Russian)* 77−88536
I_2, visible absorpt. spectra, Fourier transform spectroscopy appl. 78−58060
I_2, visible region, wavenumber meas. by Fourier transform spectroscopy *(French)* 77−57407
I_2 visible spectrum, Fourier transform spectroscopy, B-X system 79−94007
I_2, $X^1\Sigma_g^+$ ground state, Le Roy's theory, continuous wave oscillation 79−94006
I_2+I_2, collisional energy transfer, ground and excited states, polarisation spectra 80−32805

spectra of diatomic inorganic molecules continued
IBr, magnetic rot. spectrum, rot. and vibr. anal. 78−70861
IBr, predissoc. and photodissoc., intermed. coupling strength 77−16850
ICl, two photon UV absorpt. spectrosc. 79−89687
IF, in solid Ar, emission and excitation visible spectra at 12K 80−87137
IO, free radical, Ar matrix absorpt. and emission spectra, mol. vibronic states obs., spectroscopic const. determ. 80−83387
$^{127}I_2$, B-X band system, nucl. HFS, coupling consts. 77−6794
$^{127}I_2$, B-X band system, nucl. HFS, octupole coupling const. effects 77−6795
$^{127}I_2$, hyperfine struct. in electronic spectrum, saturated absorption spectroscopy 78−37645
$^{127}I_2$, visible spectra, HFS at 586.82 nm 78−9395
$^{127}I_2$ wavelengths at 633 nm and H_α, precision interferometer calibration for wavelength meas. 79−80696
$^{129}I_2$, $^{129}I^{127}I$, $^{127}I_2$ high resolution saturated absorption spectra at 633 nm using He-Ne laser 80−95637
$^{129}I_2$, complete hyperfine spectrum obs. at 612 nm 80−95638
InCl, B→X system, rot. anal. 79−36619
InCl, discharge excited spectrum 4100-3900 Å, vibr. anal. 80−32732
InKr, low-lying electronic states, PE curves, transition moments, emission coeffs. 79−6894
IrO, ground state, matrix isolation spectra 78−46352
KXe, fluoresc. excitation and emission spectrum 79−6947
Kr_2, electron-beam pumped, visible absorpt. rel. to laser development 79−59671
Kr_2^+, near UV absorption spectra, config. interaction methods 78−17680
KrF, laser spectrum, discharge-pumped, absorption bands and lines, assignment 78−79004
KrF, matrix isolated, absorpt. and emission spectra 77−14446
KrF, UV bound-free emission after electron excitation 77−27279
KrF*, oscillatory bound-free emission spectra, semiclassical anal. method 80−7799
KrX, (X=He, Ne, Ar, Xe), VUV absorpt., van der Waals mols. props. 78−13513
Kr_2*, VUV time resolved spectra, formation and decay kinetics 79−31544
LaF, Franck-Condon factors and R-centroids, rot.-vibr. effects 78−50596
LaO, absorption spectra, in flame, optogalvanic spectrosc. obs. 79−18202
LaO, spectral intensity of $B^2\Sigma$-$X^2\Sigma$ bands, Rydberg-Klein-Rees pot. 79−31611
LaS, chemiluminesc. vibr. analysis of $C^2\Pi\rightarrow X^2\Sigma^+$, D_0^0 determ. 77−48645
Li_2, far UV photoabsorpt. spectra, core-excited states and CI calcs. 78−37655
Li_2, triplet absorpt. bands, 6215-5875 Å, after two-photon excitation 79−50035
Li_2^+, $X^2\Sigma_g^+$, $^2\Sigma_u^+$, $A^2\Pi_u$ and $^2\Pi_g$ states, electronic struct. vibr. spectra, ab initio calcs. 79−36507
$^7Li_2$, $B^1\Pi_u$-$X^1\Sigma_g^+$ band system, absorpt. and laser fluoresc. spectra 79−68256
$Li_2(A^1\Sigma_u^+)$, state multipoles transfer following rot. inelastic He collisions, polarised emission obs. 80−5608
LiH, isotopic species, $A^1\Sigma^+\rightarrow X^1\Sigma^+$ bands 78−42091
^7LiH, $A^1\Sigma^+$ state, vibr. levels, radiative and nonradiative lifetimes 78−66604
^7LiH, $A^1\Sigma^+$-$X^1\Sigma^+$ bands, radiative transition probabilities calcs. 78−66603
^7LiH, radiative transition probability, from pot. curves, $B^1\Pi$ curve calc. 78−78752
LiI, electron-mol. beam collisions, autoionising states, electronic spectra *(Russian)* 78−22023
LiO, struct., spectra, SCF MO calcs. 78−17559
Li_2O (LiOLi, LiLiO), struct., spectra, SCF MO calcs. 78−17559
LiOO, struct., spectra, SCF MO calcs. 78−17559
LuF, $^1\Pi$ hyperfine struct. parameters, bonding 77−58036
LuF, mol. electronic states, 3000-6500 Å *(French)* 77−23502
Mg_2, Ar matrix isolated laser photoluminescence spectra, electronic absorpt., emission, vibronic and vibr. relax. 78−82744
Mg_2 matrix isolated, vis. and near IR spectra 78−5214
MgD, emission spectra, 600 to 850 nm, rot. anal., dissoc. energies 78−62815
MgH, $A^2\pi$−$X^2\Sigma^+$ system, dissoc. energy 77−10686
MgH, emission spectra, 600 to 850 nm, rot. anal., dissoc. energies 78−62815
MgH(D), spectra in 230-235 nm region 80−48012
MgO, electronic transition strengths, shock tube meas. 80−87183
MgO, new electronic band system in UV 77−14447
MgO, red and near UV bands calc., rel. to sunspot spectra 80−12736
MgO, visible-near UV triplet-triplet transition moments and intensities 77−58085
MgO_3, visible absorpt. and reson. Raman spectra in Ar and N_2 matrices 77−65487
MgZn(Cd), Ar matrix absorpt. spectra, vibronic spacing and bonding 79−3453
$^{24}MgH^+$, high resolution rot.-vibr. spectra, solar atm. appl. 77−18939
MnH(MnD), $^7\Sigma$-state, mol. parameters, ESR and optical spectrosc. 78−94264
$^{98}Mo_2$, electronic spectra after flash photolysis of $Mo(CO)_6$ 79−36622
N_2, 1^- system bands, line broadening and shift 80−87138
N_2, 250 MW 0.53 micron laser pulse scatt., spectra, vibr.-rot. transitions *(Russian)* 77−46570
N_2, absorpt. spectrum, using vacuum UV storage ring source 77−7165
N_2 airglow solar activity effect on (0,0) second positive band 77−70902
N_2, asymptotic expansion for Morse-Pekeris oscillators, band strength factors, electronic transition moment 78−78755
N_2, B^3pi_g state vibr. levels, obs. in Lewis-Rayleigh afterglow 77−6797
N_2, B-state collisional transfer, press. effects, oscillator strengths, time resolved spectra 79−36744
N_2, diffuse plasma, population densities of triplet states, correl. with electron impact processes 80−43966
N_2, discharge excited vibr.-rotation states meas. by CARS *(Russian)* 79−3429
N_2, electrical discharge excitation, vibr. level population distrib., electron beam fluoresc. obs. 80−48031
N_2, first negative system, Deslandres table 79−98118
N_2, first positive system, electronic transition probabilities 80−78603
N_2, fission fragment excitation, delayed coincidence spectroscopy 77−24189

spectra of diatomic inorganic molecules continued
N_2 gas, electron impact ionisation, electronic fluoresc. spectra 80−95664
N_2, high resolution absorpt. in VUV 77−61762
N_2, isotopic forms, visible spectra, rovibronic and rot. anal., $C'\,^3\Pi_u$ and $C\,^3\Pi_u$ interaction 77−18933
N_2, Lewis-Rayleigh afterglow, spectrum 77−61757
N_2, liq. and gas, induced absorpt. spectral moment, mol. calcs. 80−63737
N_2, mol. spectra, 500-1300 Å, matrix isolated 79−33724
N_2, multiphoton absorpt., spectroscopic evidence 80−63726
N_2, optogalvanic spectroscopy in discharge, 570 to 620 nm 79−54862
N_2, oscill. strengths of $W^3\Delta_u$-$X^1\Sigma_g^+$ band system 79−59486
N_2, PE curve, spectroscopic consts., perturbation theory appl. 80−23341
N_2, photoabsorpt. cross-section, 50-340 Å, as sum of empirical at. cross-sections 78−58718
N_2, photoabsorption, moment anal. 78−46321
N_2, photoabsorption and photionisation, UV region meas. 78−42087
N_2, positive column, flowing, visible spectrum obs. 80−49026
N_2, spectroscopic data review 77−38680
N_2, transition moments between excited electronic states 78−5204
N_2 triplet-triplet transitions, Einstein-A coeffs., oscill. strengths, lifetimes, theory and experiment comparison 80−47876
N_2, UV dayglow on Mars 77−53452
N_2 UV spectra, new band, $^3\pi_u$ state lower vibronic levels 78−17682
N_2, VUV absorpt. spectrum, homogeneous perturbation between $c_4'(0)\,^1\Sigma_u^+$ and $b'(1)\,^1\Sigma_u^+$ levels 77−83618
N_2, valence excitation energy and UV spectra, HAM/3 calc. 78−25453
N_2, vertical electronic spectrum, MRD-CI method calcs. 78−42033
N_2, vibr. and rot. anal. of vis., UV spectra, RF discharges in N_2, H_2, CH_4 mixtures 78−5241
N_2^+, 1NG: $B^2\Sigma_u^+ \rightarrow X^2\Sigma_g^+$, 3800 to 4750 Å spectra, mol. consts. 78−42081
N_2^+, 3914 Å band spectra, fluoresc. efficiency 79−81226
N_2^+, A- and B-states interactions, time-resolved obs. 80−18862
N_2^+, deperturbation of first negative group, $B^2\Sigma_u^+$-$X^2\Sigma_g^+$ 79−59481
N_2^+, first negative spectra, modelling 77−61758
N_2^+ Meinel system, high resolution spectrum to 11 250 Å 80−99497
N_2^+, reson. absorpt., 1st negative band, in irrad. air, calcs. 77−30850
N_2^+, spectrum, appl. air arc temp. meas. 80−59314
N_2^+, UV spectral line width in rarefied free jet, for rot. temp. 80−6184
N_2-CO, electrical discharge excitation, vibr. level population distrib., electron beam fluoresc. obs. 80−48031
N_2+Ar, metastable atom excitation of $C^3\Pi_u$ state, symmetry, propensity rules and alternation intensity, rot. spectrum 80−87135
N_2+He, collisionally excited neutral and ionic emission, flowing afterglow 77−51248
$N_2^+(A^2\Pi_u$-$X^2\Sigma_g^+)$ system in aurora, vibr. development and quenching effects 78−88967
$N_2(B^3\Pi_g$-$A^3\Sigma_u^+)$ system in aurora, vibr. development and quenching effects 78−88967
$N_2^+(B^2\Sigma_u^+)$, $N_2(C^3\Pi_u)$ and $N_2(C'^3\Pi_u)$ molecules, emissions obs. in yellow N_2 afterglow 80−63649
NBr, mol. pot., r-centroids, $A^1\Sigma^+$-$X^1\Sigma^-$ band system 77−3373
ND $c\,^1\Pi$-$a\,^1\Delta$ system, new bands, spectroscopic consts. 80−9612
ND, $d^1\Sigma^+$-$c^1\Pi$, spectra, equilib. consts., dissociation energy 78−33517
ND radicals, metastable, production in discharge, spectra, rot., vibr. consts. determ. *(German)* 77−34642
ND, singlet-triplet transitions, high resolution spectrosc. with new emission source *(French)* 80−57383
NH, $d^1\Sigma^+ - c^1\Pi$, $d^1\Sigma^+$-$b^1\Sigma^+$, spectra, equilib. consts., dissociation energy 78−33517
NH in F- and G-type stars, bands oscillator strengths rel. to N abundances 77−91530
NH radicals, metastable, production in discharge, spectra, rot., vibr. consts. determ. *(German)* 77−34642
NH, rot.-vibr. anal. by finite difference perturbation method 77−50420
NH, singlet-triplet transitions, high resolution spectrosc. with new emission source *(French)* 80−57383
NH_3-NO mixtures, combustion emission spectra, identification of NH_2, NH, OH, NO by rapid scanning spectra *(French)* 79−52665
$N_2(N_2^+)$, UV, visible spectra in Ar plasma, 230-620 nm 78−13456
NO, $A^2\Sigma^+$ state, two-photon excitation and emission spectra 77−83666
NO, absorpt. characts. of γ-O band, rel. to atm. meas. 78−57316
NO, absorpt. characts. of γ-0 band 79−39845
NO, chemisorption on Rh, reactions with CO over Rh, flash desorption spectra, titration, reaction kinetics calcs. 78−61045
NO, electronic spectrum, press. induced config. demixing 78−42090
NO electronically excited photofragment of VUV photodissoc. methylnitrite, identification and quantum yield 80−99527
NO, fluoresc. spectra, $3s\sigma(A^2\Sigma^+)$ Rydberg state, vibr. relax. 79−13759
NO, γ (1,0) band auroral emission at 2150 Å probably N_2 feature 78−45083
NO, γ and β system, electronic transition probability 80−106332
NO, γ-band collisional broadening parameters from resonance line absorpt. 77−10704
NO γ-bands at 2259 Å, shock wave effective absorption coeffs., empirical determ. 79−64799
NO, high frequency discharge 79−82105
NO, $I^2\Sigma^+$ state, valence bands, absorpt. spectra 78−46361
NO, mol. beam tunable diode laser sub-Doppler spectra, $^2\Pi_{1/2,3/2}$ Λ splittings 79−41180
NO, mol. parameters determ. 77−83571
NO nonlinear laser spectroscopy, VUV harmonic generation 80−74175
NO, photoabsorpt. cross-section, 50-340 Å, as sum of empirical at. cross-sections 78−58718
NO, photoabsorption and photionisation, UV region meas. 78−42087
NO, Rydberg absorpt. bands 800-850 Å, isotope shift 79−13734
NO, simultaneous one- and two-photon spectroscopy, Λ-doubling, spin-rot. splitting 78−66560
NO, spectroscopic data calc., 2-0 and 3-0 overtone bands 79−36623
NO, UV absorpt. spectra, 600-1000 Å, Rydberg series, ionisation energy 77−75180
NO vibr. overtone band, mag. rot. spectrosc. obs. 80−86446
NO^+, R_e-function of A-X system, rel. to astrophysical meas. 78−13554
NO+CO(N_2), electronic energy transfer, spectroscopic obs. 78−82716
NO+N_2(CO_2)(CO)(CH_4)(Ar), NO γ(0,0) band, oscillator strength and line broadening 80−106356
N_2O, photoabsorpt. cross-section, 50-340 Å, as sum of empirical at. cross-sections 78−58718
N_2O, satellite struct. and momentum distrib., binary (e,2e) spectroscopy 80−69125

spectra of diatomic inorganic molecules continued
NS_2 spectrum, perturbations in $A^2\Pi_{1/2}$-$X^2\Pi_{1/2}$ transitions, constants of $B''^2\Sigma^+$ state 78−70845
$N_2(^1\Sigma_g^+)$, exact collinear calcs. of $N_2O(X^1\Sigma^+)$ photodissociation 77−30937
N_2*, metastable, collisional form., C-B emission spectrum 77−19019
N_2*+CO, vibr. excitation and quenching, long contact time effect 79−86040
Na_2, $^1\Sigma_g^+$-$^1\Pi_u$ transition moment as function of internuclear separation 77−18838
Na_2, $A^1\Sigma_u^+$ state, spectroscopic consts. and RKR pot. calcs. 77−75130
Na_2, dimer, $B'\Pi_u$-$X'\Sigma_g^+$ band system obs. 78−62837
Na_2, mol. spectroscopy by photodeflection in supersonic nozzle beam 79−54995
Na_2, triplet satellite band obs. in self-broadened D-line very far blue wing 80−95688
Na_2, two-photon transition, Doppler free vs. Doppler broadened absorpt. 79−13779
Na_x, matrix-isolated, formed in supersonic nozzle beam, 400-800 nm absorption and mass spectra obs. 79−76439
NaH, $A^1\Sigma^+$-$X^1\Sigma^+$ electronic transition, spectroscopic anal. and potential energy curves 80−48102
NaK, $^1\Pi$ state perturbations, circular polarisation fluoresc. meas. 79−76462
NaK, $a^3\Sigma^+$ state, laser induced fluorescence, $D^1\Pi$ to $a^3\Sigma^+$ transition, molecular constants, dissociation energies 79−98143
NaK, $a^3\Sigma^+$ state, $X^1\Sigma^+$ state, fluorescence, visible spectrum 79−98114
NaK, mol. transition dipole moment, from laser-induced fluoresc. spectra 79−94034
NaKr, red wing radiation and pot. 80−87180
NaNe, van der Waals mol., form., laser spectroscopy 78−29797
Ne+HD, j=0 to 1 rot. excitation, differential cross sections, time of flight obs. 80−48104
Ne_2, van der Waals mol., vibr.-rot. spectrum 79−13698
Ne_2^+, near UV absorption spectra, config. interaction methods 78−17680
Ni+Ni, 12-90 MeV, molecular orbital K X-rays ang. distrib. 79−10125
Ni_2, UV Ar matrix spectra theory 77−75178
Ni_3, UV Ar matrix spectra theory 77−75178
Ni_n clusters, Ar matrix, UV-visible spectra pot. energy curves 77−65552
$NiBr_2$ band system in near UV, vibr. analysis 80−32733
NiF $^2\Delta$-$^2\Pi$ system, rot. anal. 79−98115
O_2 0.762 μ band absorption coeff. in atmosphere *(Russian)* 78−28315
O_2, 2,0 band, highly forbidden optical transitions using intracavity laser spectroscopy 77−42331
O_2 7594 Å telluric A-band on objective prism spectra of stars, radial vel. meas., appl. *(Japanese)* 78−89083
O_2, $(C^3\Delta_u$ to $a^1\Delta_g)$ bands in Venus nightglow spectrum 79−16856
O_2 (0-1) band at 8645 Å, nightglow intensity var. 77−73899
O_2, $A^3\Sigma_u^+$, $C^3\Delta_u$ and $C^1\Sigma_u^-$ states in van der Waals solids, electronic spectra, dynamics 78−1000
O_2, $A'^3\Delta_u$ state, inversion, presence in nightglow and discharges 80−63616
O_2, atmospheric, electric quadrupole transitions detection in A band 80−85746
O_2 $b^1\Sigma_g^+$ state prod. and deactivation following $O(^1D_2)$ quenching 80−76493
O_2 $C^3\Delta_u$−$a^1\Delta_g$ band system, vibr. anal. 80−5556
O_2, EUV absorpt. cross sections from thermosphere occultation profiles 78−28356
O_2, electron diffraction parameters, spectrosc. calc. 78−70932
O_2, electronic spectra, parity nonconservation effects *(Russian)* 78−13488
O_2, gas, temp. meas., vibr. Raman intensity, 500-2000K 79−37436
O_2 Hertzberg II bands, Venus night airglow excitation 77−41340
O_2, inert gas matrix, visible emission spectra, $c^1\Sigma_u^- \rightarrow a^1\Delta g$ and $C^3\Delta u \rightarrow X^3\Sigma_g^-$ transitions 77−14444
O_2, K-shell photoabsorption coeffs., 500-600 eV 80−9617
O_2, liq. and gas, induced absorpt. spectral moment, mol. calcs. 80−63737
O_2, mag. dipole transitions, line positions and strengths from stratospheric emission spectra 80−78604
O_2, metastable emission bands 79−64015
O_2 metastable states obs. in electron-beam controlled discharges *(French)* 77−30880
O_2 molecule, effect of spin orbit interaction on magnetic dipole transition intensity *(Russian)* 79−6948
O_2, oscillator strengths and linewidths, Schumann-Runge bands 78−90186
O_2, photoabsorpt. cross-section, 50-340 Å, as sum of empirical at. cross-sections 78−58718
O_2, photoabsorption and photionisation, UV region meas. 78−42087
O_2, photoabsorption cross-section, 55-350 Å 78−46364
O_2, Schumann-Runge band system, oscill. strengths and linewidths 79−98120
O_2, Schumann-Runge band system in sunspots UV spectrum 80−12735
O_2, Schumann-Runge bands, predissoc. linewidths and oscill. strengths, vibr. level depend. 79−45735
O_2, Schumann-Runge bands, atmospheric absorpt. model 79−96823
O_2, Schumann-Runge continuum, oscill. strength and electron impact excitation 80−69121
O_2, Schumann-Runge system, electronic transition probabilities 80−78603
O_2, singlet-triplet transitions, external theory at. selective effect 79−98159
O_2, spin-forbidden transition intensities, selective heavy atom effects 80−58240
O_2, UV absorpt. into $^3\Pi_u$ state, calc., atmos. opacity 80−12582
O_2, vac. UV absorpt. spectra of excited states 78−82749
O_2, vacuum UV molecular photoabsorpt. cross-section meas. 80−37096
O_2^+, 1NG bands spectral synthesis, for auroral obs. anal. 77−2296
O_2^+, $b^4\Sigma_g^-$-$a^4\Pi_u$ band, rot. lines, rel. intensities, theoretical and exptl. results 78−13505
O_2^+, first negative system, high-resolution photofragment spectroscopy 80−47971
O_2^+, laser-induced predissoc. spectrum, rot. anal. 77−71839
O_2^+, predissociated $b^4\Sigma_g$ state, high resolution laser spectroscopy in fast ion beam 80−9656
O_2^+, quartet states, predissoc. photofragment spectroscopy 78−82794
O_2^+, radiative lifetimes and UV spectra, $b^4\Sigma_g$-$a^4\Pi_u$, $A^2\Pi_u$-$X^2\Pi_g$ transitions 78−17724

spectra of diatomic inorganic molecules continued
O_2^+, second negative ($A^2\Pi_u$-$X^2\Pi_g$) band system, rot. anal. 77−18911
O_2+Ar, gas, intermol. pot. for spectral props. and rot. energy transfer 79−68224
O_2+Ar(O_2), collision induced UV absorpt. in Herzberg continuum, dimer form. 77−30883
O_2+N_2, collision induced UV absorpt., Herzberg continuum, dimer form. 78−9167
OD, spectra, A-X system Einstein coeffs. 79−36703
OH, $^2\Pi$ states, $^2\Delta$ states, $^2\Pi$ ground state, g-factor, Zeeman effect 79−98149
OH 1222 Å, f-value from obs. of UV interstellar lines 77−45509
OH, (0,0) UV transitions, band oscill. strength 80−69162
OH (6-2) and (8-3) nightglow bands, rotational temps. and intensities 79−58147
OH, band oscill. strength, rot. excitation effects 80−23460
OH, continuum opacity oscillator strength rel. to solar atmosphere model 79−40162
OH emission as recorder of internal gravity waves near mesopause 78−12031
OH, excitation and band rot. temp. of plasma jet light source 77−44555
OH formation in H_2-NO flame, OH collisional broadening parameter, curve of growth method 80−53052
OH, free radical, vibr.-rot. level population determ., including unresolved doublet struct. *(Russian)* 77−68033
OH, fundamental vibr. band, mag. rot. spectrosc. obs. 80−86446
OH, radiative lifetimes of $A^2\Sigma$ state and A-X Einstein coeffs. 79−36703
OH rotational temp. determ., successive approx. 80−23389
OH, spectra rel. to celestial masers physics 79−21455
OH, UV light absorpt. at 3080 Å, for Gibbs free energy of mol. 79−100425
OH, vibr. ground-state, MFS, rot. spectra and electronic band anal. 78−5206
OH+H_2O, OH linewidth rot. depend. on UV transitions 80−91606
OH+OH→H_2O+O, rate meas. by UV absorpt., 1200 to 1800K 78−35642
OH(8-3) 7274 Å band rel. to O_2 and forbidden O I atmospheric spectra 78−61639
O_2(0-1) 8645 Å band rel. to OH and forbidden O I atmospheric spectra 78−61639
$^{13}O^{16}O$ and $^{12}C^{18}O$, emission bands of $E^1\Pi$-$A^1\Pi$ transition 78−90177
^{16}O, $^{18}O_2$, vac. UV absorpt. spectra, band intensities and designations 78−5245
$^{18}O^{16}O$, Schumann-Runge bands line positions rel. to atmospheric photodissoc. and O_3 prod. 80−94559
$O_2(c^1\Sigma_u^-)$, in Ar(Kr)(Ar-Kr) matrices, multiphonon vibr. relax., time-resolved emission obs. 80−18861
P_2, intersystem transition obs. in absorpt. spectrum 80−48008
P_2 radical, $A^1\Pi_g$-$X^1\Sigma_g^+$ transition, vibr. consts. *(French)* 77−75176
P_2 radical, emission spectrum, perturbations in $c^3\Pi_u$ and $C^1\Sigma_u^+$ states *(French)* 77−23484
PCl, visible and near IR emission, $A^3\Pi$→$X^3\Sigma^-$ and $b^1\Sigma^+$→$X^3\Sigma^-$ systems vibr. anal. 78−21938
PH, $b^1\Sigma^+$ band emission visible and UV regions 78−46357
PN, absorpt. and emission spectra, electronic transition and vibr. obs. 80−91573
PO, in Ar matrix, IR and UV absorpt. spectra 80−47985
PO, rot. struct. of absorpt. bands 1850-1600 Å, valence $^2\Pi$ state 79−13739
PO, Rydberg states, UV absorption spectrum 78−90184
PO, $SiCl_2$ band system reassignment to PO and P_2 radicals 77−23505
^{18}PO, spectral intensity of $E^2\Sigma$-$X^2\Pi$ transition 79−50084
$P^{18}O$, UV absorpt. spectra, valence and Rydberg states, rot., vibr., anal., predissoc. 79−41184
PS, electronic transition $B^2\Pi$-$X^2\Pi$, vibr. and rot. anal. *(French)* 78−78716
PS, UV bands, rotational anal. 79−76443
Pb_2, in Ar matrix, excitation and emission spectra, vibr. freq. 78−13507
PbF, visible spectra, A-X_1 and B-X_1 fine struct. anal. 79−36657
PbI, $^1S_0$-$^3P_1$ to $^1S_0$-$^3P_2$ multipole line intensity ratio 79−36658
PrO, 0-0 band in XVII system, hyperfine splitting, visible excitation spectra 80−28028
PrO, hyperfine structure, rotation, electronic spectrum obs. 79−98061
PrO, visible spectra, 7500-8500 Å, VII and X systems, rot. anal. *(French)* 78−46355
PtO, ground state, matrix isolation spectra 78−46352
PtO, ground state identification from 3800-7000 Å emission spectrum 78−21937
Rb-inert gas molecule, excimer transitions, absorpt. spectra 77−475
Rb_2, absorpt. spectrum in visible and near visible 78−46356
Rb_2, mol. spectra, population inversion, high-power laser appls. 77−3406
S_2 and S_3, absorpt. spectra in Ar matrix 79−5149
S_2, in Ar matrix, fluoresc. and excitation spectra 78−94271
S_2 mol. $B^3\Sigma_u^-$→$X^3\Sigma_g^-$ fluorescence induced by N_2 laser *(Japanese)* 80−14175
S_2, v.u.v. absorpt. spectrum, Rydberg transitions 77−3382
SN, struct., vibr. spectra, ab initio calcs. 78−66475
SN^+, struct., vibr. spectra, ab initio calcs. 78−66475
S_2N_2, struct., vibr. spectra, ab initio calcs. 78−66475
SO, S isotope composition, vibronic spectroscopic determ. *(Russian)* 79−10124
SbI, decay branching ratios meas., transition probabilities derivation 80−95642
SbN, 3300-4000 Å, rot. and vibr. perturbations and rot. anal. *(French)* 78−37651
SbO, B-X system fine struct. 79−50030
SbO^+, visible region band spectrum 79−72328
ScD, emission bands in 5580 and 8603 Å regions 78−990
ScF, Franck-Condon factors and R-centroids, rot.-vibr. effects 78−50596
ScH, emission bands in 5580 and 8603 Å regions 78−990
ScO, absorption spectra, in flame, optogalvanic spectrosc. obs. 79−18202
ScO emission spectrum, intensity distribution, spin decoupling, theory, expt. 77−23504
Se_2, 3d absorption spectra, mol. damping of centrifugal barrier effects 77−61736
SeD, ground state, spin-orbit coupling const. vac. UV determ. 78−70847
SeH, ground state, spin-orbit coupling const. vac. UV determ. 78−70847
SeH, isotope effects, Rydberg levels-ground state transitions, rot. const., VUV spectra obs. 80−58279
SeO, $A^3\pi$-XO^+, 1 band system 77−58039

spectra of diatomic inorganic molecules continued
SeO, molecular constants determ. from $b^1\Sigma$-$X^3\Sigma$ transition, nonlinear least squares procedure 79−798
SiC, Si K_α X-ray emission spectra chemical shifts, linewidths and intensities 78−13461
SiCl, ($A^2\Sigma^+$-$X^2\Pi$) transition, rot. anal., equilib. consts. 78−37648
SiF, D-X transition, rot. anal. 79−72331
SiH, ground state, Λ-type doubling 80−23431
SiH, transition moments of $A^2\Delta$-$X^2\Pi$ band, 150-650 nm 79−45767
SiH^+, time resolved precision spectroscopy rel. to oscillator strengths and dissoc. energy 80−58272
SiO, $d^2\Pi_i$-$b^3\Pi_r$ transition, 0-1 band rot. anal. 77−18961
SiO emission, $A^1\Pi$, $b^3\Pi$ and $a^3\Sigma$ states, Si+N_2O flame chemiluminesc. 77−77767
SiO in Ar matrix, vac. UV spectrum, vibr. progression 80−23432
SiO, interaction between $G^1\Pi$ and $I^1\Pi$ states 79−50040
SiO, low-lying electronic states, vib. assigned perturbations 77−27082
SiO, nearly degenerate $G^1\Pi$-$I^1\Pi$ energy spectra, predissoc., extended virial theorem 79−22771
SiO, nonmaser emission lines from expanding envelopes around evolved stars 78−28650
SiO, test of perturbation method for vibr. assignments, low lying electronic states 77−34645
SiO, transition moment of $A^1\Pi$-$X^1\Sigma^+$ band, 260-290 nm 78−13552
SiO, VUV absorpt. spectra of mol., Rydberg, series and ionis. pot. 79−81213
SiO, valence-excited bound states, spectroscopic consts., radiative lifetimes 77−6752
SiO^+, rot. spectrum, isotope shift, mol. consts. 79−59483
SiS, electronic spectra, parity nonconservation effects *(Russian)* 78−13488
Sn_2, in Ar matrix, absorpt., fluoresc. and reson. Raman spectra 80−95640
SnF, rotational struct. of UV (O,O) bands 77−34658
SnO, D $^1\Pi$-$X^1\Sigma$ transition 79−41179
Sr_2, matrix isolated, vis. and near IR spectra 78−5214
SrD, UV absorpt. spectra, rot. consts. 77−14448
SrF, $B^2\Sigma^+$-$X^2\Sigma^+$ system, rot. anal. using a cw tunable dye laser 78−9165
SrH, absorption UV spectra, (0,0)-band at 2680 Å 78−50554
SrO_3, visible absorpt. and reson. Raman spectra in Ar and N_2 matrices 77−65487
TaN, matrix isolated, electronic and vibr. absorpt. spectra 79−64014
TbF, absorption spectrum, vibr. and rot. anal. 78−55181
TeF, chemiluminesc. from oxidation in F_2+H_2Te(D_2Te) emission spectrum obs. 80−43058
ThO, $L^1\Pi$-$^1\Sigma^+$ and $N^1\Pi$-$X^1\Sigma^+$ systems, spectra, rot. anal. 80−23430
TiN, electronic absorpt. spectrum, rot. anal. 80−78601
TiO 7120 Å band strength in metal-rich globular star clusters 78−49487
TiO band absorption effect on stellar photometry with broadband filters 80−41811
TiO β system, electronic transition moment and effective vibr. temp. 77−68078
TiO, $e^1\Sigma^+$-$d^1\Sigma^+$ transition rel. to cool star spectra 77−67089
TiO, γ'-system, Franck-Condon factors, r-centroids and Einstein coeffi-cients calcs. 80−74163
TiO in Ar matrix, meas. of absorpt. and magnetic circular dichroism spectra 80−86356
TiO, rot. anal. of (0,0) (1,0) (0,1) (1,1) bands of $\gamma'(B^3\Pi$-$X^3\Delta)$ 79−22719
TiO, rot. temp. in sunspots, rel. to photospheric and sunspot models 78−69766
TiO, solar lines in 7100-7600 Å range, table 78−77495
TiS, $C^3\Sigma_2$-$X^3\Sigma_2$, Franck-Condon factors and r-centroids 79−36700
Tl-Hg, excimer band emission from electron beam initiated discharge in Tll-Hg 80−78841
Tl-Xe, excimer band emission from electron beam initiated discharge in Tll-Xe 80−78840
V_2, formation, spectra, electronic struct. 77−54642
^{186}WO, electronic spectra following flash photolysis, intracavity laser technique, rot. consts. 79−31538
Xe, atom-diatom paradox, phenomenological description of spectroscopic props. 78−78766
Xe-rare gas mixtures, far UV absorpt., at. and quasimol. spectra 77−61698
Xe_2, e-beam excited, 193 nm absorpt. studies 80−43323
Xe_2, electron beam excited, 193 nm absorpt. meas. rel. to 172 nm laser pulse termination 80−28200
Xe_2, electron-beam pumped, visible absorpt. rel. to laser development 79−59671
Xe_2, time and energy resolved fluorescence, radiative lifetime, collisional mixing, pulsed synchrotron radiation obs. 79−98136
Xe_2^+, near UV absorption spectra, config. interaction methods 78−17680
XeBr, UV bound-free emission after electron excitation 77−27279
XeCl, B-X and D-X band systems, vibr. anal. 79−59482
XeCl, excimer emission band at 235.5 nm 77−18935
XeCl* emission spectrum obs., in Xe(6s,$^3P_2$)+RCl reactive quenching 79−100344
XeCl* spectra, for Xe(6s,$^3P_2$)+RCl vibr. energy disposal assignment 79−100345
XeF,(Cl)(Br) matrix isolated, absorpt. and emission spectra 77−14446
XeF, 3500 Angstrom band, vibr. anal. 78−70843
XeF, B-X transition vibr. anal., flash photolysis UV absorpt. spectroscopy 78−42088
XeF, C-A blue-green band, gain meas. at 488 and 475.9 nm 79−45929
XeF, X, B, and D-states, spectra, vibr. and rot. consts. 78−70844
XeI, UV bound-free emission after electron excitation 77−27279
XeO, Ar-matrix-isolated, UV absorpt. spectra 77−3375
XeO, $d^1\Sigma^+$→$a^1\Sigma^+$($b^2\Pi$), green band emission spectroscopic anal., RKR pot. curves, bond lengths and dissoc. energies 79−41181
XeO, excited state spectra, subpicosec. predissoc., solvation, in solid rare gas hosts 77−68050
XeX, (X=F,Cl,Br,I), Ar matrix isolated, MCD, low temp. depend., spectroscopic parameters calc. 77−38682
XeX, (X=He, Ne, Ar, Kr), VUV absorpt., van der Waals mols. props. 78−13513
YD, electronic spectra *(French)* 77−14442
YF, Franck-Condon factors and R-centroids, rot.-vibr. effects 78−50596
YH, electronic spectra *(French)* 77−14442

spectra of diatomic inorganic molecules continued
YH, YD, 3800-9000 Å negative glow spectra, triplet and singlet systems 77−79608
YO, $A^2\Pi-X^2\Sigma^+$ and $B^2\Sigma^+-X^2\Sigma^+$ systems, Fourier transform spectroscopy anal. 79−22718
YO, absorption spectra, in flame, optogalvanic spectrosc. obs. 79−18202
YO, spectra, 4500-6900 Å, mol. consts. 78−50551
$Y^{16}O$ and $Y^{18}O$, vibr. anal. of blue and red system 79−809
YS, $A^2\Pi-X^2\Sigma$ and $B^2\Sigma-X^2$Sigma transitions vibr. anal. and B-X(0,) band rot. anal. 79−31537
YbBr, emission spectra in arc discharge, vibr. anal. 78−74670
YbCl, emission spectra in arc discharge, vibr. anal. 78−74670
YbI, emission spectra in arc discharge, vibr. anal. 78−74670
Zn_2, in Ar and Kr matrices, 10K, UV spectrum, vibr. assignments 77−58038
ZnF, mol., ESR spectra in inert gas matrix 79−76455
ZnHg(Mg), Ar matrix absorpt. spectra, vibronic spacing and bonding 79−3453
ZrN, absorption spectra, isolated in rare gas matrices 78−78652
ZrO, band identifications in $^1\pi-X^1\Sigma^+$ system 77−18931
ZrO bands, integrated intensity meas. and effective vibr. temp. 80−43111
ZrO, $C^3\Delta-X^3\Delta$ system, electronic transition moment depend. on internuclear dist. 77−68079
ZrO, γ system anal., isotopic band shifts in stellar spectra calc. 79−50029
ZrO, singlet-triplet separation meas. 80−78623

spectra of inorganic liquids and solutions
see also Raman spectra of inorganic liquids and solutions
alkali halides, aq. solns. with extrinsic O_2 ions, spectral props. *(Russian)* 78−6766
alkali-haloid salts, aqueous solutions, IR absorpt. ν_1 (CN) band parameter temp., conc. study *(Russian)* 80−80801
anharmonic molecules in condensed media, vibronic dephasing, intra- and intermolecular processes 80−2127
cell, thin-wedge-shaped, for highly absorbent liqs., Lambert absorpt. coeffs. meas. 78−45720
cholesteric liquid crystal, stabilisation, multicomponent mixtures, refl. spectra, clarification temp. and melting point meas. 78−9951
complex refractive index, 5 to 500 cm^{-1}, Fourier transform interferometric determ. 77−13798
cryogenic solutions, spectrosc. and photochem. 80−16713
cryolite, molten, struct. charact. by IR spectroscopy and splat cooling *(French)* 79−69835
diatoms in solution, IR band profile, memory function approach 79−11414
dilute metal solutions in molten salts, optical absorption 80−89023
electrolyte aq. solns., IR librational bands, struct. making and breaking 78−56476
electrolyte solns., aq., water struct., differential IR spectral investig. 77−52651
electrolyte solutions, fluctuations rel. to light scatt., spectra 77−15497
far IR absorpt., statistical functions of motion *(French)* 78−39534
Fourier transform spectroscopy appl., far IR 78−58069
heavy water, optical consts., 6-450 cm^{-1}, 19°C 78−6649
heavy water, VUV reflectance, refr. index, absorpt. coeff., isotope effects 78−6695
hydrates, vibrational spectra, H^+ and OH^n aq. soln. 79−73916
hydrogen bonded liquids, elec. anharmonicity on H-stretching bands 78−48167
inert gas liquid mixtures, collision induced absorpt. 77−4638
inert gases, liquid phase mixtures, dipole autocorrelation function, IR absorpt. spectra obs. 80−28903
interaction induced light scattering and IR absorption in liquids 80−60561
intermolecular interactions in condensed medium, long-wavelength IR spectroscopy 80−34927
ionic solutions, in liq. HCl, coord. sphere radius, vibr. spectrosc. investig. 80−50843
ions in aqueous soln., absolute absorpt. coeff. meas. using photoacoustic spectroscopy 80−82828
IR band moments, effect of dipole induction 77−75143
IR continua, phonon theory 80−29729
lanthanides in molten $LiNO_3$-KNO_3, transition probabilities in absorpt. and fluoresc. spectra 79−50085
linewidth, vibr. dephasing and gas-liq. crit. density fluctuations 79−51954
liquid metal, electron states, esp. opt. and mag. props., review 78−2882
lossy liquid, for IR refr. spectrum meas. 77−2700
metal chloride aqueous solns. with NO_2^- impurities, luminesc., absorpt. and Raman spectra *(Russian)* 77−36291
molecular liquids, IR absorpt. lineshape, orientation density fluctuation effects 78−48171
molecular liquids, IR spectra, calc. involving vibr. and reorientational relax. 78−48170
molecular reorientation, autocorrelation functions 77−80400
molecular rotation, model for IR and Raman studies in liqs. and gases 80−11390
molten salt, metal dilute solns., optical absorption 79−19899
molten salt heat transfer fluid with solar-absorbing oxide particles, solar absorber appl. 78−87112
molten salts, IR, Raman, EPR and NMR spectroscopy, review *(French)* 79−69832
nitroxide free radicals, neutral, EPR spectra, localised solvent-radical adducts 79−96290
orientational correlation functions for dipolar and induced dipolar absorpt. in far IR 77−11451
photon correlation spectroscopy, liquid surfaces, effect of instrumental broadening 77−87852
polar fluid mixtures, two-absorber model of solvated electrons, spectra 78−85284
polar fluids, Debye and far IR absorpt. theory 77−69829
polar liquid, integrated absorpt., microstruct. effect *(French)* 78−10823
polar liquid, IR absorpt. spectra and hydrodynamic model *(Russian)* 79−78689
polar liquid, solvated electron optical props. and thermodynamic characts., polaron model 78−85170
polar solvents, solvated electron absorpt. spectra, intrasolvent and intersolvent correls. 80−93840

spectra of inorganic liquids and solutions continued
polyatomic fluid, local dynamics, spectroscopic studies, summer school lecture series 80−6343
polyatomic liquids, vibr. relax. and energy transfer, ultrafast dynamics obs. 77−50506
polyatomic molecule vibrational mode obs. with picosecond laser pulses 77−58007
quartz, cryst. and melt, irrad., optical absorpt. spectra, computer calcs. *(Russian)* 78−92091
rare earth complexes, formation and props., book contrib. 80−43204
rare earth ions in soln., absorpt. and fluoresc. spectra, book contrib. 80−45112
rare earth perchlorates, in solvents with high dielectric const., spectra and struct. 79−65860
saline environmental waters, IR relative reflectance and complex refr. index 77−45013
salts, aq. solns., mechanical and electro-optical anharmonicity *(Ukrainian)* 78−2830
semiconductors, normal refl. data and model densities of states 80−50364
solutions, electronic and vibr. absorpt. spectra, repulsive intermol. forces 77−79671
solvated electrons in polar solvents, interpretation by simple model 79−87934
solvated excess electrons, optical absorpt. spectra, moment theory anal. 78−73072
spectrophotometer attachment for fused salt absorption spectrum registration 78−86353
transition metal complex ions, MY_4^{n-4}, MY_6^{n-6}, alkali metals and alkaline earth outer-sphere cations, spectroscopic splitting parameters 78−39075
transition metal halide-alkali halide binary melt, spectra by cryst. field theory 79−4820
water, absorpt. coeffs. meas. using far IR laser source 77−5932
water, absorption coefficient at 488 and 541.5 nm, adiabatic laser calorimetry 77−73123
water, collision-induced far IR absorpt., depolarised Rayleigh scatt. 77−81100
water, continuity of state between liquid and amorphous solid, IR obs. 79−8130
water, deionised filtered, attenuation coeffs. meas. by split-pulse laser method, visible region 79−17505
water, far IR transmission spectrum 78−4713
water, in quartz pores, H^- excess mobility IR spectroscopic study 79−51955
water, IR spectrum, influence of Cu^{2+} ions 78−72501
water, mag. treatment affecting props., proposed mechanism 78−84827
water, optical absorption coeff. 79−82992
water, optical consts., 400-5000 cm^{-1}, 1, 16, 27, 39 and 50°C, rel. to intermol. struct. 77−66469
water, optical consts., 6-450 cm^{-1}, 19°C 78−6649
water, optical spectra of solvated electrons, band resolution 79−78698
water, solvated electrons, photon-induced electron transfer transitions 79−8154
water, turbid, spectral scatt. props. 80−72560
water, UV absorpt. spectra 80−76043
water, VUV reflectance, refr. index, absorpt. coeff., isotope effects 78−6695
water cluster evidence from phase transition changes in IR mol. absorpt. coeff. 79−10100
water sorbed on DNA, temp. anomaly, IR spectroscopic obs. 80−51046
water-carbon tetrachloride soln., fundamental H_2O IR spectrum, liq. struct. 80−23419
AgBr, molten, freq. depend. ionic cond. 77−7882
AgBr-NaCl(Br) solutions, UV spectra 78−39560
AgCl in alkali chlorides aq. soln., absorpt. spectra 79−65895
AgCl, molten, freq. depend. ionic cond. 77−7882
AgCl, molten and solid, visible absorption spectra *(Japanese)* 79−4816
AgI, molten, freq. depend. ionic cond. 77−7882
AgI nascent hydrosol absorption spectra and microcrystal growth 79−100449
$AgNO_3$, cryst. and molten salt, Raman and IR spectra, vibr. anal. 77−16311
$AlCl_3$, soln., IR spectra 78−74649
$Al(OH)_xCl_{3-x}$, soln., IR spectra 78−74649
Ar, liquid, depolarized Rayleigh scatt. at triple point, mol. dynamics simulation 80−60617
Ar, liquid and solid, absorpt. and luminesc. spectra of self-trapped excitons 79−65893
Ar:Xe, 0-1.4 g cm^{-3}, vac. UV absorpt. spectra, Wannier impurity states 77−77232
Ar-H_2 solution, far IR spectra, density narrowing of rot. line 79−50086
Ar-HCl, liq. density fluctuations, far IR absorpt., neutron scatt. mol. dynamics calc. 78−19461
Ar-Kr liq. and gas. solns., collision-induced dipole moment, far IR band obs., self-diffusion coeff. 77−38627
AsSe, molten semicond., pseudogap, elec. cond. and optical absorption meas. 77−8160
As_2Se_3, molten semicond., pseudogap, elec. cond. and optical absorption meas. 77−8160
$Au_{81}Si_{19}$, optical refl., 0.5 to 6 eV, hall coeff. and elec. resist. 80−29755
Ba^{2+}-methyl propionate mixtures, in DMSO, acetonitrile solns. IR, assoc., solvent, catalytic effects *(French)* 79−87827
CO_2, liq. and gas, state of aggregation effect on 1-4 μm absorpt. bands intensities 79−27042
COF_2, soln. in liquid Ar, transition freq., halfwidths and relative intensity, IR absorpt. spectra 80−55101
CS_2, liq., electronic optical Kerr effect, subpicosec. optical gating 79−46548
CS_2, liq., Kerr effect in UV region, mol. optical anisotropy dispersion 78−72488
CS_2, liq., props. from allowed light scatt. spectra 80−25364
CS_2, liquefied gas solns. bound exciton model for Rydberg bands 78−31214
$CaCl_2(Br_2)$, aq. solns., IR spectral reflectance meas., Kramers-Kronig anal. 77−4633
$Ca(No_3)_2.3.91H_2O$-$NiCl_2$ melts, glass forming, transport behaviour 78−59963
CaO-Al_2O_3-B_2O_3-SiO_2-FeO, glass, IR spectra at room and melt temp. 80−88986

spectra of inorganic liquids and solutions continued
CaO-SiO_2-NiO-MgO glass melt, interaction of NiO and MgO, elec. cond. and IR spectra obs. *(Japanese)* 80−24632
Ce complex, Ce (III) 1,2-dioxy-3-sulphoanthraquinone, soln., absorpt. spectra *(Russian)* 78−76975
Cl_2, Ar matrix, vibronic dephasing 80−6469
Cl_2-O_3-H_2 dilute mixtures, photolysis products, Fourier Transform IR kinetic obs. 80−26033
$CoCl_2$, electronic absorpt. spectra and coord. in cryst., soln. and melt 79−38570
$CoCl_2$-LiCl-glycerin-water system, Co^{2+} ion coordination transition, spectral investig. 79−42953
$Cr(CO)_6$, linear dichroism, distortion and local field contribs. 79−87415
$Cr(H_2PO_4)_3$-$Al(H_2PO_4)_3$-H_2O system, IR spectra 79−87428
CrO_2Cl_2+carbon tetrachloride+acetone, intermediate complex form., electronic spectra 80−61075
CsAu, optical absorpt. in liq. and solid 79−61397
Cu complex, catena-μ-isothiocyanato-(N′-pyridylmethylene-N″-salicyloylhydrazinato-NN′O) copper (II), EPR and visible spectra 80−5566
Cu complex, Schiff-base, ESR and optical absorpt. in soln. and powder 79−65892
$CuCl_2$, aq. solns., IR spectral reflectance meas., Kramers-Kronig anal. 77−4633
D_2O, effect of phase density on ionisation process and electron localisation 77−89731
D_2O, IR spectral refl. and complex index of refr. 78−68501
D_2O-H_2O, IR absorption spectra, statistical charact., continuous model of liq. struct. confirmation 78−6671
Eu^{3+} in aq. soln. MCD spectrum, sign inversion 77−34669
$EuCl_3$, solns., $^7F_0 \rightarrow {}^5D_1$ and $^7F_1 \rightarrow {}^5D_0$ transitions, MCD 79−31566
$Eu(ClO_4)_3$, aq. soln., Eu^{3+} $^5D_{0,1,2} \leftarrow {}^7F_{0,1,2}$ transitions, MCD and absorpt. spectra 78−19446
Fe complex, Fe (III) acetylacetonate, solvent effects on oscillator integrated strength, IR absorpt. bands 78−84575
Fe complex, haemoglobin in salt. soln., diffusion rel. to intermol. interactions, light scatt. investig. 77−44585
Fe, optical and electronic props., temp. depend., 20, 1400 and 1600°C 79−87412
Fe^{3+} solutions, UV absorption spectrosc. obs. of equilib. 80−93812
Fe-Si alloys, liq., refractive index, absorpt. coeff., elec. cond. 78−43830
$Fe(CO)_2(NO)_2$, vib. assignment using ^{15}N isotopic substitution, solid, liq. and soln. spectra 77−48152
Ga-Te, reflectance, 0.65-3 eV, comp. depend. 78−72549
GeH_3NCS, liq. and solid, IR and Raman spectra 79−89663
$Ge_{0.08}Se_{0.92}$, molten semicond., pseudogap, elec. cond. and optical absorption meas. 77−8160
H-bond, symmetric AHA$^{(\pm)}$, A-H stretching vibr., liq. IR band shape, strong coupling phonon model 78−64358
HBr, aq. solns., IR spectra, H_3O^+ ion 77−30868
HCl, aq. solns., IR spectra, H_3O^+ ion 77−30868
HCl, in dil. solution IR absorpt. fundamental shape temp. depend., solvent-solute interaction 79−26977
HCl, liq., IR spectral intensity and Raman cross-section meas. 80−2742
$HClO_4$-H_2O, aq. soln., IR and Raman spectra, conc. depend. *(Russian)* 80−53002
HD-T_2, liq. and solid, vibr.-rot. IR spectra 80−50313
HF, aq. solns., IR spectra, H_3O^+ ion 77−30868
HI, aq. solns., IR spectra, H_3O^+ ion 77−30868
HNO_3, aq. soln., H bonds, IR spectra 78−94243
HNO_3, aqueous soln., reflectance and complex refractive index, IR spectra, vibr. modes 80−66168
$HN(SO_2Cl)_2$, physical props. meas. 79−51293
H_2O, and aq. solns., IR spectral investigations of assoc. 79−65847
H_2O, band spectra after HF combined mag. treatment *(Russian)* 79−15682
H_2O, D_2O, visible absorpt. meas., pulsed dye laser optoacoustic spectroscopy 80−11426
H_2O, liquid, far IR optical consts. meas. with optically pumped laser 80−40082
H_2O reorientation in H-bonding free solvents, IR absorpt., dielectric loss 77−36233
H_2O vapour and liquid far IR spectroscopy 80−60610
$H_5O_2^+$, aq. soln., IR continua with polarisable H-bonds 79−26979
HOD, IR spectra in D_2O, combination vibr. 80−9609
$H_2O(D_2O)$, solvated electrons, optical absorpt. spectra. temp., isotope effects 80−55124
H_3PO_4, aq. soln., elec. cond. and Raman spectra at high-press., 25°C 79−56220
H_2S, liq., optical absorption transients produced by ns pulse radiolysis 79−11803
H_2SO_4 soln., opt. consts. in far IR 77−8574
HT-T_2, liq. and solid, vibr.-rot. IR spectra 80−50313
He, liq., surface local disorder, for IR transmittance meas. 80−75395
He:Xe, 0.04-0.1 g cm^{-3}, vac. UV absorpt. spectra, Wannier impurity states 77−77232
^{4}He, superfluid, Raman expts., interpretation 79−73362
Hg complex, trihalogenomercurate II ions in amide solvents, config. equilib. 79−26997
Hg, expanded fluid, opt. gap, KKR band calcs. 77−1354
Hg, expanded fluid, optical props. 79−19902
Hg fluid, expanded, optical absorpt., excitonic and continuum states 79−95801
Hg halides in aq. soln., pulse radiolysis, emission species 79−24764
$Ho(NO_3)_3$ solns., f-f transitions, intensity anal., correl. with cond. and US absorpt. 80−97292
I^-, aq., in supercooled water, and glass forming solns., charge transfer to solvent spectra 77−50447
IO_4^- ion in solns., UV spectra 80−2786
In-Te, reflectance, 0.65-3 eV, comp. depend. 78−72549
$InX(X_2)(X_3)$, $InAlX_4$, X=Cl,Br, Raman spectra, up to 1200K 80−48003
KCl-$CuCl_2$ solution, optical absorption of complex ions *(Russian)* 77−28592
K_2CrO_4, investigation by diffuse reflectance spectroscopy 78−88326
$K_2Cr_2O_7$, acidic soln., UV absorbance standard verification 78−21092
KH_2PO_4, aq. soln., elec. cond. and Raman spectra at high-press., 25°C 79−56220
$K_2(RuCl_5NO)$, polarised Raman and IR spectra, vibr. anal. 77−69819
Kr, liquid and solid, absorpt. and luminesc. spectra of self-trapped excitons 79−65893

spectra of inorganic liquids and solutions continued
LiCl, concentrated aqueous soln., IR absorpt. to high press. and temps. 80−80803
LiF, molten, charge fluctuations, collective dynamics, from IR reflectivity 78−67841
Mg-Bi alloy, liq., far IR reflectivity rel. to possible transport processes 78−2827
Mg-Bi alloys, liq., far IR reflectivity meas. 77−52105
$MgCl_2$, aq. solns., IR spectral reflectance meas., Kramers-Kronig anal. 77−4633
$Mo(CO)_6$, in nematic matrix, linear dichroism, distortion and local field contribs. 79−87415
$MoCl_5$-MoF_5 system, magnetochem. and IR study of phase struct. 77−85710
ND_3, effect of phase density on ionisation process and electron localisation 77−89731
NH_3 and ND_3 solutions, UV absorpt. of solvated electron 79−87935
NH_3, and solid, vibr. spectra 77−32360
NH_3 liq., solvated electron optical absorpt., spectra anal., method of moments 77−50436
NH_2O_2, long-lived radical prod. by photolysis of ammoniacal KO_3 soln. 77−16838
$(NH_4)_2(RuCl_5NO)$, polarised Raman and IR spectra, vibr. anal. 77−69819
$(NH_4)_2SO_4$ aqueous soln., photoacoustic spectra in middle IR 77−81101
NH_4X, X=OH, Cl, Br, aq. soln., IR reflectivity spectra, Kramers-Kronig anal. 78−68500
NO_2^-, solvated, in H_2O, ethanol, cyanomethane, and DMF lowest n-π* transition 79−85960
NO_3^-, in aq. nitrate solns., vibr. dephasing process, Raman obs. 79−51936
N_2O, in soln., IR and Raman band shapes, mol. dynamics, ν_3 band 77−36238
Na, electronic structure, optical absorption 79−38566
Na, liquid, optical conductivity 77−63425
Na-NH_3 solns., UV absorpt. *(German)* 77−24869
NaCN, aq. solns., IR spectral reflectance meas., Kramers-Kronig anal. 77−4633
NaCl:Bi^{3+}, complex form. in soln., absorpt. spectra 77−28591
Na_2O-CaO-SiO_2-Fe_2O_3 molten glass, optical props., temp. depend. *(French)* 80−100667
Na_2O-SiO_2, aqueous solns., Raman and IR spectra, pH depend., species at equilib. identification 79−87866
Na_3PO_4, aq. soln., elec. cond. and Raman spectra at high-press., 25°C 79−56220
$Nd(NO_3)_3$, aqueous soln., single photon absorpt. band struct., electronic resons. coherent ellipsometry 80−90881
Ne, liquid and solid, absorpt. and luminesc. spectra of self-trapped excitons 79−65893
Ne:Xe, 0.1 to 0.65 g cm^{-3}, vac. UV absorpt. spectra, Wannier impurity states 77−77232
Ne-Ar liquid mixtures, collision induced absorpt. 77−4638
$NiSO_4$, aq. soln., UV transmission filter characts. 77−3679
Np V, absorpt. spectra in aq. solns. 79−65899
OCS in Ar soln., IR spectra, solvent shifts, vibr. band assignment and anharmonic force consts. 80−9607
PCl_5-HCl_2, Raman spectra, solid and melt, species identification *(German)* 80−45083
PCl_5-$SnCl_4$, mixtures, liq. and solid, Raman spectra study *(German)* 79−91451
PH_3, liq. and solid, Raman spectra., vibr. correl. functions, rot. motions 80−55087
$PO(SCN)_3$:Nd^{3+} solns., spectroluminesc. props. 77−16362
PbO-SiO_2 melt, behavior of MgO and NiO *(Japanese)* 79−52746
PbO-SiO_2-NiO-MgO glass melt, interaction of NiO and MgO, elec. cond. and IR spectra obs. *(Japanese)* 80−24632
Pd complex, $Pd^{II}Pt^{II}(CNCH_3)_6(PF_6)_2$, vibr. spectra, M-M bonds. *(French)* 80−47997
Pd complex, $Pd(C_{18}H_{25}O_3)_2$, synthesis and props., possible mesomorphism 78−18749
Pm^{3+}:$POCl_3$-D_2O soln., absorption and fluoresc. spectra *(French)* 77−66514
Pt complex, $Pt^{II}(CNCH_3)_4(PF_6)_2$, $Pt_2^{I}(CNCH_3)_6(PF_6)_2$, and $Pt^{I}Pd^{I}(CNCH_3)_6(PF_6)_2$, vibr. spectra, M-M bonds. *(French)* 80−47997
Ru complex, $Ru(bpy)_3^{2+}$, excited, in aq. soln., optical absorption spectrum 79−50032
Ru complexes, $[Ru(bipy)_n(pq)_{3-n}]^{2+}$ mixed-ligand, electronic absorpt. and emission spectra meas. 80−71441
Ru complexes, $Ru(NH_3)_6^{2+}$ and $Ru(en)_3^{2+}$ in soln., UV spectra, solvent effects 79−94010
S, liq., optical absorption spectrum, up to supercrit. conditions 78−88320
S, liq., temp. depend. of absorption edge 77−66515
SF_6, dissolved in O_2 and Kr, cryogenic liqs., mol. motions, IR and Raman spectra 79−69823
SF_6, in cryogenic liqs., vibr. kinetics, IR spectrosc. obs. 79−18182
SF_6, soln., cryosystem, vibr. relax. times, pulsed IR absorpt. spectral obs. 80−66188
SF_6-N_2O solution, IR and Raman rot. correl. functions, expt. and theory 79−46541
S_4N_4, solid and soln., IR and Raman spectra, vibr. assignment 78−74659
$S_3N_3Cl_3$, solid and soln., IR and Raman spectra, vibr. assignment 78−74659
$S_4N_4H_4$, and -d_4, solid and soln., IR and Raman spectra, vibr. assignment 78−74659
S_7NH, solid and solns. vibr. spectra, force consts. isotope effects 77−66490
$S_{8-x}(NH)_x$, (x=1,2,3,4), and deuterates, IR and Raman spectra, isotope shifts, mol. vibr. assignment 79−10110
SeO_4^{2-} ions in aqueous solns. of halides at 4.2-290K *(Russian)* 77−28624
SnI_4 in cyclohexane, far IR absorpt. using band shape absorpt. 77−71794
Tl-Te, reflectance, 0.65-3 eV, comp. depend. 78−72549
UO_2F_2, in soln., UV-visible spectra, ^{18}O isotope effects 77−52116
$W(CO)_6$, in nematic matrix, linear dichroism, distortion and local field contribs. 79−87415
Xe, liq., UV reflection spectra, density depend., excitonic band evolution 77−77246
$ZnCl_2$, aq. solns., complex IR refr. indices, IR spectra, mechanisms, spectrometer system 78−43831

spectra of inorganic molecules
see also spectra of diatomic inorganic molecules; spectra of polyatomic inorganic molecules
aggregates, optical spectra, near strong coupling limit, Green's function model 77−83774
discharge lasers, use of surface discharge for gas preionisation 79−46504

spectra of inorganic solids
see also impurity and defect absorption spectra of inorganic solids; infrared spectra of inorganic solids; luminescence of inorganic solids; radiofrequency spectra of inorganic solids; Raman spectra of inorganic solids; visible and ultraviolet spectra of inorganic solids
alkali metal compounds, A_nCY_6, spectra by cryst. field theory 79−4820
alkali metal granular films, multipole oscillations in small hemispherical particles 79−78774
alkali-alumino-phosphate:U, rontgenoluminesc. and fluoresc., radiative transitions obs. 80−103977
ceramic, B content by emission spectrosc. with high freq. plasma excitation *(French)* 80−76477
cermet film, as solar selective absorbers, production, struct. and optical props. 79−29485
crystals, line-shape distortion on anisotropic absorpt. meas. in unpolarised light 80−2765
ferromagnetic semiconductors, s-f interaction on conduction band, red shift effect theory 80−59872
garnets, photoinduced phenomena 79−99718
inert gas crystal, exciton-phonon interaction, absorption and luminesc. data *(Russian)* 77−62831
lead chalcogenides, interband absorption under linearly polarised light excitation 78−92089
magnetic semiconductors, excitation spectrum, temp. and band occupation depend. 80−49588
magnetic system, amorphous, microwave absorption spectra 80−50469
magneto-optical spectra appls., review 77−52050
many-valley semiconductors, inversion layers, optical props. of CDW ground states 77−43732
metal film, optical absorption due to particle-hole excitations 80−45160
metallic thin films, granular, optical props. rel. to multipole oscills. in hemispherical particles 80−7431
mixed semiconductor with comp. fluctuation, kinetics of intraband absorpt. and magnetoabsorption coeff. 79−19865
molecular crystals, spectroscopy, bibliography for 1976 78−72585
narrow band gap semiconductors, conference, Warsaw, Poland (Sept. 1977) 79−82582
narrow band gap semiconductors, conference, Warsaw, Poland (Sept. 1977) 80−49703
picosecond interactions, book contrib. 77−65057
polar dielectric interface, phonon-polariton modes, ATR spectroscopy detect. 77−24474
random alloy, optical absorption and photoemission spectra 80−45216
rare earth compounds, cooperative Jahn-Teller phase transition, theory of optical side-bands 77−1398
rare earth ion garnets, spectra calc. using exact microscopic Hamiltonian 77−8553
rare earth metals, optical props., review 77−40259
rare earth metaphosphates, glasslike, spectral intensity, effect of number of 4f electrons 78−84602
rare earth orthovanadates, covalency, chemical bonding and opt. spectra 77−80442
rare earth pnictides, prep. and props., book contrib. 80−54212
rare-earth ion spectra, effect of coordination polyhedron struct. 77−55807
rocks, laboratory spectra appl. to Landsat filters assessment for rock type discrimination 79−16791
semiconducting alloy, two-band, electronic and optical props., multiband theory 79−37952
semiconductor, disordered, absorption edges, temp. depend. 77−77160
semiconductor film, quantised, indirect interband absorption rel. to surface irregularity 78−39618
Si, multiple bound exciton states, valley-orbit splitting 79−60725
spessartine garnet, measurement of absorpt. spectra using automated microscope-spectrophotometer 80−18010
transition metal complex ions, MY_4^{n-4}, MY_6^{n-6}, alkali metals and alkaline earth outer-sphere cations, spectroscopic splitting parameters 78−39075
vibrational spectroscopy review 80−55093
YIG, optical absorption and magneto-optic spectra 79−99860
Ag clusters on Si substrates, opt. spectra investig. of struct. *(German)* 80−25492
Ag, ellipsoidal small particle assembly absorption spectra, optical model *(Russian)* 78−60483
Ag halide emulsions, ultra-fine-grain, spectral absorption 79−24793
AgBr thin films, influence of bromine vapour on spectral props. 77−71393
α-AgI, superionic conductor, microwave absorption spectrum 80−11515
β-Al_2O_3-Ag_2O, superionic conductor, microwave absorption spectrum 80−11515
β-Al_2O_3-Na_2O, superionic conductor, microwave absorption spectrum 80−11515
$Al(OH)_3$ gel, coprecipitated with $Cr(OH)_3$, mixed valency phase of partially oxidised Cr 79−47995
As_2S_3 coatings, transmission and refraction dispersion spectra *(Russian)* 77−48264
Be-Mg, two-band alloy, electronic and optical props., multiband theory 79−37952
Cd, photon interactions, energy role 77−36305
$CdCr_2S_4$ ferromag. semicond. film, props. 78−76175
$CdCr_2S_4$, ferromagnetic semiconductor films, prep. and props. *(Japanese)* 79−47308
$CdGa_2Te_4$ film, effect of thermal annealing on struct., optical absorpt. and photocond. 79−65342
CdS film, chemically deposited, cond. and absorpt. edge meas. *(Russian)* 77−8210
CdS, granulated films, optical reson. 79−4863
$CdS_{1-x}Se_x$ mixed crystals, free excitons, disorder effects 80−34365
CdSe, direct gap, picosec. time resolved reflectivity obs. 78−76495
CdTe, luminescence and reflect. investig. of excitons, stress and Zeeman splitting 77−40281
Co, 3p excitation spectra 79−22633
Co^{2+} complex, ammoniated zeolite, oxygenated product form., electronic spectrosc. obs. 80−991

spectra of inorganic solids continued
CrF_6^{3-}, spectra, cryst. field least squares fitting interpretation 80−44548
$Cr(OH)_3$ gel, coprecipitated with $Al(OH)_3$, mixed valency phase of partially oxidised Cr 79−47995
$CsMnCl_3.2H_2O$, antiferromag. insulator, self-trapping of excitons 80−70619
Cu, 3p excitation spectra 79−22633
$CuGaS_2$, exciton absorption energies, appl. of modulated phase-shift-difference method 78−39565
CuTeBr, superionic conductor, microwave absorption spectrum 80−11515
Er_2O_3, solid, photoacoustic spectra 78−58044
Fe, 3p excitation spectra 79−22633
Fe_3Al, order-disorder transform. effect on optical props. *(Russian)* 77−39820
$Fe(ClO_4)_2.6H_2O$, single cryst. polarised opt. spectra 77−48188
Fe_3O_4, optical cond. anisotropy calcs. below Verwey transition 80−50289
GaAs, direct gap, picosec. time resolved reflectivity obs. 78−76495
GaAs, electron-hole plasma, Coulomb effects on gain and absorption spectra 80−50371
GaAs:Si(Te)(S), vapour phase epitaxial grown layers, photoluminesc. and emission spectra 80−29774
GaAs:Sn, surface segregation of Sn during MBE, SIMS and AES 78−72031
GaP, ground state of indirect free exciton 77−51670
GaSb, vibr. spectra, lattice dynamics ang. force model 80−29127
GaSe, group theoretical anal. of phonon assisted optical transition 78−39564
Ge, electron hole droplets, intervalence band absorption 80−6742
Ge, inter-valence-band absorption in electron-hole droplets 79−4515
Ho_2O_3, solid, photoacoustic spectra 78−58044
InAs, three-photon absorption, transition effects *(Russian)* 78−35147
InS, prep., and elec. and optical props. 77−77361
K_2O-BaO-SiO_2 glass, rare earth ion activated, spectral intensity, effect of number of 4f electrons 78−84602
$LaF_3:Pr^{3+}$, optical free induction decay exam. of dephasing time 77−3637
Na_3AlFe_6 coatings, transmission and refraction dispersion spectra *(Russian)* 77−48264
$NaMnCl_3$, antiferromag. insulator, self-trapping of excitons 80−70619
$NaSbSe_2$ films, struct., photoelec. and opt. props. 78−51834
Nd^{3+}:scheelite-type crysts., transition probabilities, cryst. field calcs. 78−91875
Ni, 3p excitation spectra 79−22633
$(NiF_6)^{4-}$ complex, open-shell cluster calcs., semiempirical LCAO-MO method 80−54583
NiF_6^{4-}, spectra, cryst. field least squares fitting interpretation 80−44548
NiO, bulk props., initial state MO Ni_4O_4 and $Ni_{13}O_{14}$, cluster model, lattice and force consts., photoemission and CT absorpt. spectra 80−84828
Pb chalcogenide mixed crystals, intraband absorption due to chemical disorder 79−56789
Pb chalcogenides, interband absorpt., optical absorpt. coeff., two- and six-band models 79−33728
PbF_2 coatings, transmission and refraction dispersion spectra *(Russian)* 77−48264
$Pb_{1-x}Sn_xSe$, X=0.03-0.07, monocrystal film, edge of intrinsic absorpt. *(Russian)* 80−71368
$Pb_{1-x}Sn_xTe$, X=0.2, monocrystal, edge of intrinsic absorpt. *(Russian)* 80−71368
$(SN)_x$, polymeric, electronic structure, semi-empirical pseudopotential calc. 77−72812
Si (100) surface, intersubband optical absorption in space-charge layers 77−35984
Si (100) surface accumulation layer, subband struct. and inter-subband absorption in strong mag. field 78−39177
Si, ground state of indirect free exciton 77−51670
Si polymorphs, optical props., orthogonalized LCAO calc. 78−10345
SiC crystal, energy band struct. and optical spectra 78−18962
SiO_2, vitreous, and quartz, impurity C determ. by isotopic spectral method 80−26093
Te thin film, optical props. *(French)* 77−44076
$(TiF_6)^{3-}$ complex, open-shell cluster calcs, semiempirical LCAO-MO method 80−54583
TlBr, resonant polaron coupling and excitons under mag. field 80−71383
TlCl, piezoreflectance spectra of first exciton band 77−12357
UF_4, solid, photoacoustic spectra 78−58044
V_2O_5, electronic and band struct. and spectra, CNDO CI cluster method 79−11091
$Zn_xCd_{1-x}S$, granulated films, optical reson. 79−4863
ZnS, granulated films, optical reson. 79−4863

spectra of organic molecules and substances
see also infrared spectra of organic molecules and substances; luminescence of organic solids; radiofrequency and microwave spectra of organic molecules and substances; Raman spectra of organic molecules and substances; Shpolskii spectra
absorption bands, vibronic intensification obs., floating-orbital method 80−63619
acenaphthene, vibronic spectra, electronic-vibr. interactions 78−1021
acetaldoxime, photoelectron and far UV absorpt. spectra 78−17712
acetic acid amides, polarisabilities and π-π^* transitions, dipole interaction calcs. 80−23411
acetic acid-aliphatic amide intermol. H-bonded systems, charge transfer bands 77−58041
acetone, ab initio CI valence and Rydberg states, spectral assignments 77−14346
acetone, absorption bands, vibronic intensification obs., floating-orbital method 80−63619
acetone complex with Br_2, electronic absorpt. spectral calc. *(Russian)* 78−37628
acetone oxime, photoelectron and far UV absorpt. spectra 78−17712
acetones, fluorinated, absorpt., fluoresc. spectra, quantum yields, decay times meas., mechanism 77−3410
acetonitrile, submillimeter rotational spectrum, laser generation line identification 79−64210
acetonitrile-phenol-(d_1), in CCl_4 ($CDCl_4$) solns., H-bonds vibr. relax. bands anal. 78−84560
acetophenones, di- and trisubstituted, π^*-π systems, UV electronic absorpt. spectra 80−74132

spectra of organic molecules and substances continued
acetyl radical, absorpt. spectrum obtained by flash photolysis and kinetic spectroscopy 79−13731
2-acetylanthracene solutions, excitation spectra rel. to absorption spectra, 77-300K 79−85970
9-acetylanthracene subpicosecond laser photolysis and time resolved absorpt. spectra *(Japanese)* 79−79272
acetylene, adsorbed on Ni(111), benzene form., vibr. spectra 78−95952
acetylene, excited state, photochem. and spectrosc. investig. 80−95553
acetylene, relationships between higher-transition frequencies 80−69119
acetylene, valence excitation energy and UV spectra, HAM/3 calc. 78−25453
acetylene ($-d_1,d_2$), and isotopic forms high resolution absorption spectra, Renner-Teller interactions 79−72332
acetylene ketones, absorpt. and phosphoresc. spectra 79−54865
acetylene smoke, optoacoustic meas. of absorpt. at 0.5145, 10.6 μm 80−43060
acetylperoxy radicals, absorpt. spectrum and reaction kinetics 80−91571
acridine, Ar matrix-isolated, lowest triplet state IR and visible absorption spectra 79−68228
acridine, nonradiative electronic relax., picosecond absorption spectrosc. obs. 78−82053
acridine, singlet state absorption profile, time resolved spectra 79−45769
acridine, T-T absorpt. build-up, following picosec. pulse singlet excitation, in gas phase 78−9161
acridine C-radical, polarised absorpt. and ESR spectra, dichroism and HF-CI calc. 78−50563
acridine orange dye soln., dimerisation equilib., absorpt. spectra least squares anal. 79−50007
acrylonitrile, semiempirical CNDO calcs. of electronic struct. and absorpt. spectra 78−995
actidine orange, interaction of cationic dyes with mitochondria, absorpt. spectra 77−52752
acyloxy radical ion, in irrad. Rochelle salt, decarboxylation, pulse radiolysis and EPR obs. 78−70854
2-adamantanone, absorption and fluoresc., high-press. 77−52113
adenine, hydroxy and methoxy derivatives, absorption UV spectroscopy and electronic struct. of ionic and tautomeric forms 80−74177
adrenaline, acid aq. solns., pulse radiolysis, H., OH. react. kinetics, UV spectra 77−16841
aggregate organic photoconductor, composition prep., struct. and optical props. 79−24006
alchohols, glassy, spectra shift of trapped electrons, after γ-irrad. 79−78709
alcohol-alkane dilute system, electron solvation, picosecond spectral obs. 77−44573
alcohols, liq., picosec. mol. dynamics and electron localisation 79−46548
alcohols, optical spectra of solvated electrons, band resolution 79−78698
alkali metal cation-electron pair in ethers, optical spectra, coordination effects 77−66788
alkali metal cryptand complex, with anion or solvated electron, optical absorpt. spectra 78−52526
alkanes, overtone spectra, local mode anal., discrete excitation of nonequivalent CH oscills. 78−78688
alkyl aryl ketones, in homogeneous n-heptane solns., quasi-isoenergetic triplet energy migration, photolysis obs. 79−61878
alkyl benzenes, jet-cooled, intramol. vibr. relax., reson. fluoresc. and excitation obs. 80−14152
alkyl iodide-$I_{(atom)}$ complex, multiple charge-transfer bands in liquid-phase 77−32776
alkyl silanes, far UV and He I photoelectron spectra 79−18204
alkyl substituted diacetylene radical cations, optical emission and photoelectron spectra, fragmentation decay 80−53004
alkylammonium iodides, UV spectra 79−36663
alkylbenzenes, jet-cooled, vibr. relax., absorpt. spectra 80−74236
alkylbenzenes, jet-cooled, vibr. relax., fluoresc. spectra 80−78694
alkylphosphonium iodides, UV spectra 79−36663
allene, gas and soln., UV absorpt. and MCD spectra 79−50056
allyl isocyanide, state-selected, visible absorption spectra and photoisomerisation kinetics 80−11879
allylamine, anomalous Stark effect for torsional splitting 79−64040
amines, caged, multiphoton ionisation, two-photon transition resons. 78−33558
4-amino-N-methylphthalimide, reversible induced absorpt. spectra in binary solvents 79−98117
m-aminoacetophenone+t-amyl alcohol, in soln., fluoresc. and absorpt. spectra, excimer form. 78−78737
aminochlorotoluenes, UV aborpt. spectra 79−36660
4-aminomethylphthalimide-decalin-n-propanol, electronic spectra of 3-component solns., temp. depend. 79−4822
p-aminophenol, gas phase, near UV absorpt. spectra 79−22725
3-aminophthalimide, continuous spectra, electronic transition freq. determ. 77−50425
4-aminophthalimide, soln. in n-propanol, fluoresc., orient. relax. of solvent 79−24357
3-aminophthalimide-ethanol soln., luminesc. quantum yield, photoacoustic method 77−86335
aminoquinoline derivatives, solvent effect on absorpt. and fluoresc. spectra 79−59494
ammonium bioxalate monohydrate spontaneous parametric scatt. spectra, polariton wave vector and Stokes lines analysis 78−43885
amphotericin B in H_2O and hydroalcoholic solns., circular dichroism, Rayleigh scatt., absorpt. spectra, temp. depend. *(French)* 78−62807
aniline, gas phase electrochromism studies in vacuum UV 77−50562
aniline, singlet-singlet electron transitions, modified CNDO-CI method exam. 78−25552
aniline, vibronic perturbations of UV spectrum 78−37654
aniline black, superconductivity at room temp. 78−80089
anils, cryst., high-press. optical effects 78−31170
anils, polystyrene soln., high-press. optical effects 78−31171
anisotropic media, molecular distrib. determ., using polarised absorption and emission spectroscopy 78−27298
anthracene:2-aminoanthracene, polarised guest absorpt. spectra, transition dipole moment direction, cryst. packing 77−8610
anthracene:chloranil, charge transfer spectra line shape 79−78700
anthracene:cyclohexadienyl type radicals, charge transfer reactions 78−52535
anthracene:tetracene, electronic absorpt. spectrum, host-cryst. field effect 80−100669
anthracene, 340-310 nm absorption spectrum dichroism, masked ^1L_b-$^1A_1$ transition 78−17685
spectra of organic molecules and substances continued
anthracene, cryst., radiation induced radicals, optical absorpt. bands, SCF-CI MO calc. 79−91463
anthracene, electronic vibr. spectra, stochastic description, numerical modeling, comparison with expt. 80−63620
anthracene, Faraday spectrum, sign rel. to mag. field strength *(German)* 77−36204
anthracene, fluoresc. from (001) surface and sub-surface excitons 79−33763
anthracene, in stretched polyethylene film, UV-visible and fluoresc. spectral shifts 78−62852
anthracene, irradiated, optical absorption and EPR meas., low temps. 78−68538
anthracene, melt and dil. soln., UV spectra, line broadening and shift vibr. struct. 78−17684
anthracene, molecular crystal, exciton-phonon coupling, absoprt. band profile in first singlet system 78−83888
anthracene, monocryst., additional absorpt. spectrum at low temp. 78−92096
anthracene, orientated in nematic liq. cryst., UV-visible dichroism meas. *(German)* 77−34668
anthracene, polarised refl., surface excitons, Davydov splitting 77−16327
anthracene, polariton effects in transmission and absorpt. spectra in thin crysts. 77−20886
anthracene, pulsed electron excitation, triplet excitons, spectral and electrical investigations 80−92828
anthracene, radiation-induced radicals, EPR and optical absorpt. obs. 77−12816
anthracene, reflectivity and fluoresc. of (001) surfaces, sub-surface exciton states 79−15508
anthracene, single cryst. triplet excitation form. 79−69437
anthracene, singlet-triplet absorpt. spectra, 2-300K, photoexcitation spectra 78−43890
anthracene, spectra, PPP approx., CI clacs. *(German)* 79−36602
anthracene, surface polaritons, attenuated total refl. 77−63423
anthracene, thin film vacuum deposited, exciton reflection spectra *(Russian)* 78−15194
anthracene, total reflection spectra, site shift surface exciton dispersion 77−77233
anthracene, triplet exciton absorpt. lines 79−47475
anthracene, triplet-exciton fine struct., high resolution optical meas. 80−45099
anthracene, vibronic absorpt. spectra in soln. and cryst., universal mol. interactions effects 77−68031
anthracene crystals, and thin films, electroabsorption in disordered solids 78−95590
anthracene derivative, Langmuir-Blodgett multilayer film, semiconducting props., optical and elec. meas. 80−11122
anthracene derivatives in solution, polarisability and dipole moments, emission and absorpt. spectra obs. 80−69256
anthracene films, optical props., comparison between free and optical contact mounting 80−89079
anthracene in PVC film, photodichroism at 257 and 383 nm 79−31539
anthracene iostopic mixed crystals, exciton spectra 79−38602
anthracene like crysts., optical transitions to electron-exciton bands 78−10365
anthracene single cryst., Frenkel exciton spectra at dielectric and conducting layer interfaces 80−44510
anthracene vapours, shape of absorpt. bands, temp. depend. 78−82743
anthracene-β-sulphonic acid, 340-310 nm absorption spectrum dichroism, masked ^1L_b-$^1A_1$ transition 78−17685
anthracene-PMDA, charge transfer cryst., 2K, zero-phonon lines, singlet spectra 78−23484
anthracene-pyrometallitic dianhydride cryst., refl. and absorpt. spectra of singlet charge transfer excitons 80−71442
anthracene-trinitrobenzene complex, neat and mixed cryst. and glass opt. spectra 77−40274
anthracenes, bridged, photochemistry and spectra 77−77793
anthraquinone-xanthone liq. soln., upper excited singlet state, delayed fluoresc. 80−106345
9,10-anthraquinones, Π-Π^* electronic transitions, substituent effects calcs. 80−28006
4-(9-anthryl)-N,N-dimethylaniline, fluoresc., dipole moments and polarisabilities 80−1019
arachidate monolayers, optical props. integrated optics meas. 78−35214
aromatic, absolute fluorescence quantum yield, calorimetric determ. 80−43092
aromatic esters, in ethanol, luminescence spectra, phosphoresence and fluorescence 79−54899
aromatic hydrocarbons, absorpt. spectra, electronic-vibr. sequence band broadening 77−65453
aromatic hydrocarbons, catacondensed, photoelectron spectra, correlations with UV absorpt. spectra 77−34690
aromatic hydrocarbons, in organic glasses, nonphotochemical burning, impurity site relaxation 78−25548
aromatic hydrocarbons, mol. struct. determ. from electronic spectra, oscill. strengths *(French)* 77−71888
aromatic hydrocarbons, struct., UV absorption band calc. *(French)* 77−18989
aromatic hydrocarbons, vibronic coupling model, nontotally symm. harmonic mode 77−3337
aromatic hydrocarbons in Shpolskii matrices, $S_0 \rightarrow T_1$ absorpt. spectra 79−85995
aromatic molecule, in aromatic (aliphatic) solvent, 77K, triplet-triplet absorption spectra, anomalous broadening 77−88502
aromatic molecules in O_2 matrices, singlet-triplet absorpt. spectra 78−17683
aromatic nitroso compounds, fluoresc. from upper singlet 79−6958
aromatic solutions, triplet-triplet absorption, anomalous broadening 79−54842
aromatics, electronic absorpt. spectra absolute intensities estimation 77−34702
1-azaphenanthrene H-bonded complex formation, enthalpy change due to electronic excitation, spectroscopic determ. 78−92496
azo dyes, UV-visible spectrophotometric 80−61207
azo polyamide, solutions, spectra and viscosity 79−68340
azomethine compounds, nonaromatic, photoelectron and far UV absorpt. spectra 77−58079
p-azoxyanisole, orientated in nematic liq. crysts., UV-visible dichroism meas. *(German)* 77−34668

spectra of organic molecules and substances continued
azulene, induced circular dichroism of π-π^* bands in presence of (+)-nopinone 80−53058
azulene, soln., laser-excited $S_2 \rightarrow S_1$, $S_1 \rightarrow S_0$ emission and $S_2 \rightarrow S_n$ absorption 79−10131
azulene vapour, IR and CO_2-laser absorpt. spectra 80−87120
bacteriochlorophyll electronic transition moment directions 79−100572
bacteriochlorophyll of green bacteria, resolution of absorpt. and fluoresc. spectra into components 78−20152
bacteriorhodopsin, 13-cis and trans isomers, photochem. and dark equilib. 77−90798
bacteriorhodopsin, Debye rot. relax. times, modulation excitation spectrophotometric obs. 79−3532
bacteriorhodopsin, effect of high press. on absorpt. spectrum and isomeric composition 80−67041
bacteriorhodopsin 580 nm ultrafast transient, psec kinetics 78−44455
bacteriorhodopsin Br570, bathochromic shift of absorpt. band in external elec. field 80−35838
bacteriorhodopsin emission lifetime, using picosec. meas. method 77−17009
bacterioviridin, photochem. oxidation mechanism 77−25370
BBOT dye, vapour phase, optical props. *(Japanese)* 80−9879
benzaldehyde, and substitution products, spectral props. 79−27007
benzaldehyde, electronic spectra, Cl and F substitution effects 80−23456
benzaldehyde gas, nonradiative electronic transition 80−83413
benzaldehyde in methylcyclohexane, $n^3\pi^*$ spectra 80−63627
benzaldehydes, o- and m-substituted fluoro- and chloro- forms, rot. isomerism, $n\pi^*$ spectra obs. 80−5631
benzene:I_2, charge transfer spectra line shape 79−78700
benzene, 260 nm absorpt. spectrum, band contours, vibr. ang. mom. components 79−13736
benzene, 260 nm absorpt. spectrum, band maxima positions and intensities 79−13735
benzene, 260 nm absorpt. spectrum, vibronic anal. 79−13737
benzene, $^1A_{1g} \rightarrow {}^1B_{2u}$ absorption band, Franck-Condon factors calc. 79−36701
benzene, $^1B_{2u}$-$^1A_{1g}$ transition, vibronic coupling, Duschinsky effect 77−88439
benzene, $\pi\pi^*$ and Rydberg bands, cryogenic solvent effects 78−55182
benzene, adsorbed on porous vycor glass, adsorpt. spectrum 80−9615
benzene, and methyl derivatives, $^1E_{1u}$ N-V state mag. moments, MCD obs. 80−23575
benzene, C-H stretching overtones, thermal lensing spectrosc. obs. 79−35851
benzene, cryst., molecular exciton cluster states and spectra 77−66123
benzene, derivatives, calc. of second-order susceptibility, using electronic spectra data 80−29756
benzene, extinction coeff. in 4.6-36 eV range 78−86877
benzene, Faraday spectrum, sign rel. to mag. field strength *(German)* 77−36204
benzene, first-ionisation Rydberg spectrum assignment via John-Teller splitting 80−69155
benzene, Jahn-Teller active states, vibronic struct., vibr. perturbation, spectral obs. 78−13440
benzene, liq., light scatt. coeff. determ., absolute method 78−2868
benzene, liq., two-photon spectra, $^1E_{2g}$ state 79−11431
benzene, liq., visible region absorpt. spectra, overtones meas. 80−78625
benzene, liquid, C-H stretch, seventh harmonic, absorption profile 79−56806
benzene, liquid, visible absorpt. expt. using wavelength-modulation spectroscopy 78−24868
benzene, nanosecond laser photolysis 80−66825
benzene, optoacoustic spectroscopy, weak visible absorpt. spectra, pollution monitoring in liquid phase 79−58797
benzene, optoacoustic spectroscopy using cell with ultimate corrosion resistance 80−42269
benzene, overtone spectrum, intramol. lineshape narrowing 79−45705
benzene, photoelectron and optical spectra, occupied virtual orbital energies and eigenvalue ordering, CNDO/S calc. 77−61796
benzene, photoexcitation, triplet factor group states assignment 77−85741
benzene, Rydberg series, second ionis. process assignment, vibronic coupling 77−42333
benzene, S_0-S_1 transitions, two-photon absorpt. spectra by nozzle beam-multiphoton ionisation method 80−63728
benzene, semiempirical CNDO calcs. of electronic struct. and absorpt. spectra 78−995
benzene, solid and isolated in rare-gas matrices, spectroscopic study 79−3455
benzene, substituted benzenes, liq., Kerr effect in UV region, mol. optical anisotropy dispersion 78−72488
benzene, substituted cations, spectroscopy, substituent effects 78−58709
benzene, symmetry forbidden transitions in MCD and electronic spectra 77−65494
benzene, thermal lensing effect, absorptivity meas. at 607 nm 80−34900
benzene, UV laser photolysis, electronic 3-wave mixing spectra of transient fragments 79−68223
benzene, UV photoelectron spectra, valence electron shake up approx. methods 80−18788
benzene, visible absorpt. spectra, local mode overtone intensity of C-H stretching mode 79−81207
benzene and deuterates, highly vibr. excited intramolecular V-V transfer, visible and photoacoustic spectra 80−32729
benzene cryst., electron irrad., phenylcyclohexadienyl radical form., absorpt. and fluoresc. spectra study 80−89035
benzene excimer, nanosecond laser photolysis 80−66825
benzene in CCl_4, weak 607nm absorpt. band obs. by optoacoustic spectroscopy 79−35855
benzene liquid, two-photon absorption spectra and cross-section meas. 79−82993
benzene p-dihalogen derivatives, electron-vibr. spectra *(Russian)* 79−89686
benzene phenol crystal, asymmetry of phonon side bands, absorption, luminesc. and specular spectra 77−1730
benzene radical cation in solid Ar, fluorescence spectra obs. 80−83382
benzene-d_0, -d_6, electronic relax., absorpt. spectra 77−75129
benzene-d_0, -d_6, vapour absorpt. spectrum, band intensities meas. 79−81212
benzene-d_0(-d_3)(-d_6), vibronic coupling, hot band absorpt. spectra 78−58708

spectra of organic molecules and substances continued
benzene-d_5, C-H vibr. states, thermal lensing spectra, local mode model test 77−71812
benzene-d_6:benzene-d_0, phonon side bands of specular optical transitions 78−26649
benzene-I_2, binary soln., charge transfer spectrum 78−90183
benzened$_0$:phenol, phonon side bands of specular optical transitions 78−26649
benzenes, trisubstituted, UV aborpt. spectra 79−36660
benzenoid hydrocarbons, triplet state decay, kinetic spectroscopy, 220-250 nm 78−62820
1,3-benzodioxole, geometry, electronic absorpt. spectra 80−971
1,12-benzoperylene, in n-paraffin solns., quasiline spectra, press. effects *(Russian)* 77−68053
benzophenone: diphenylmethylene, mixed cryst., emission and absorpt. spectra, 2-30K, excitation-phonon coupling 79−99900
benzophenone, in DDE at 2K, vibr. overtone characterisation and local modes by emission spectroscopy 79−89682
benzophenone, laser spectroscopy by cascade photoionisation method in mass spectrometer 80−99496
benzophenone, triplet exciton absorpt. lines 79−38563
5,6- and 7,8-benzoquinoline trapped in n-paraffins at 77K, quasilinear absorption spectra 78−90179
p-benzoquinone, hydroxy substitutions effect on $^1B_{1g} \leftarrow {}^1A_g$ transition 79−18200
benzoxazole, polarisation of 274 nm absorpt. system, band contour analysis 79−27043
9-benzoylanthracene, subpicosecond laser photolysis and time resolved absorpt. spectra *(Japanese)* 79−79272
2-benzoylpyridine crystals, optical spectra of lowest triplet state 80−16081
3,4-benzphenanthrene cation radical, in boric acid glass, spectrum 200-1400 nm, MO calcs., assignments 77−75174
benzyl, $1^2B_2 \rightarrow 2^2B_2$ electronic excitation, natural orbital occupation numbers calcs. 79−45638
benzyl, circular dichroism 78−27178
benzyl radical, 1^2B_2-3^2B_2 transition in absorpt. spectrum, extinction coeffs. 80−102523
benzyl radical, in solid Ar, absorption and photodissociation spectra 80−69156
benzyl radicals, monomtheyl- and dimethyl-substituted, electronic spectra and electron affinity 80−63618
biacetyl, lower excited electronic states, ab initio SCF and CI calcs., absorption band assignment 78−74589
biacetyl, multiphoton excitation of triplet state, fluoresc. decay 79−31632
1,1′-bianthryl derivatives, dimer optical activity, vibronic circ. dichroism, theoretical anal. 78−62821
1,1′-bianthryl derivatives, theoretical analysis of UV, circular dichroism and optical rotating dispersion vibronic spectra 77−34652
biaryls, dimer optical activity, vibronic circ. dichroism, theoretical anal. 78−62821
bilirubin, aq. soln., pulse radiolysis 78−48761
1,1′-binaphthyl, conformational changes, picosec. dynamics 78−25625
1,1′-binaphthyl, $T_n \leftarrow T_1$ absorption spectrum in rigid and fluid media, CNDO/A study 79−76355
biological macromolecules, picosec. and subpicosec. relax. and dephasing, reson. light scatt. obs. 79−45876
biphenyl:tetracene, electronic absorpt. spectrum, host-cryst. field effect 80−100669
biphenyl, carbonyl derivatives, absorpt. and luminesc. spectra, solvent effects and triplet lifetimes 77−24889
biphenyl, cryst., electronic absorpt. and refl. spectra 78−64377
biphenyl crystals, electronic and vib. states, cryst. field mixing, two-photon spectra 77−59603
biphenyl single crysts., γ-ray induced radicals, EPR and optical absorpt. studies 80−44921
bis-merocyanine dye, intramol. dimer soln., Stark effect, optical absorption and density 78−50573
1,4-bis[2-(5-phenyloxazolyl)]benzene, saturated vap. press., absorpt. and fluoresc. spectra 79−76442
blood, high-resolution optical props. 77−36869
Bowman-Birk soybean proteinase inhibitor, gamma irrad. 78−53343
o-bromobenzene, electronic absorpt. spectra, vibr. anal. 77−3379
bromobenzene, optoacoustic spectroscopy using cell with ultimate corrosion resistance 80−42269
bromoethane, and -d_5, first s-Rydberg transitions 78−42094
bromoethylene, and perfluoro analogue, VUV spectra, perfluoro effect on Rydberg states 77−61764
bromoethylene, vac. UV spectra 77−23507
p-bromofluorobenzene, UV electronic absorption spectrum, band shape and molecular geometry 80−87147
bromofluoromethane cations in solid Ar, absorpt. spectra and photochem. 79−96339
bromoform, highly excited vibr. states, thermal lensing spectrosc. and local mode model 80−87140
4-bromoisoquinoline, UV and IR spectra, f-values and ground state vibr. freqs. 78−58714
bromomethane, mol. Rydberg transitions mag. circular dichroism 80−43081
bromotrichloromethane, vac. UV absorpt. cross section 80−91574
bromotrifluoromethane, vac. UV absorpt. cross section 80−91574
bromoxylenes, near UV absorpt. spectra 79−31542
bromoxylenes, near UV absorption spectra, assignments 79−81209
trans-butadiene, $^1B_{1u}$-state dynamics in cooled supersonic expansion, electronic absorpt. spectra obs. 80−78629
trans-butadiene, all-valence-electron CI calcs. of electronic spectrum 77−10654
butadiene, UV and photoelectron spectra, first Rydberg states, vibr. components 77−46573
1,3-butadiene, UV spectra, polarisation of strongest Rydberg transitions 78−46360
trans-butadiene, weak low-energy band, S and T levels by fragment method 78−82625
butadiene chromophores, cis- and trans- (α- and β-phellandrene) absorpt. and CD spectra 78−62834
n-butane, vertical electronic spectra, limited CI calcs. 79−13693
n-butyl retinal Schiff bases, absorpt. spectral props., rel. to bathochromic shift in visual pigments 78−40117
tert-butyl sulphide, UV spectra, assignments 78−46359
n-butyraldoxime, photoelectron and far UV absorpt. spectra 78−17712

spectra of organic molecules and substances continued
caesium tartrate, optical rot. dispersion, dichroism and spectra, in soln. and cryst. *(Russian)* 77−90124
calcium tartrate tetrahydrate:Cr^{3+}, optical absorpt. spectrum, cryst. field parameters 80−16067
calcium tartrate tetrahydrate:Cu^{2+}, spin-orbit coupling, optical absorpt. spectra 80−45120
calcium tartrate tetrahydrate:VO^{2+}, optical absorption spectrum 78−6713
(X)-D-camphor, circularly dichroic band at 3000 Å, RPA calc. 78−94267
d-camphor, optical rot. dispersion spectra, solvent effects 77−10684
carbamides, electronic absorpt. spectra, expt. and CNDO calcs. *(Russian)* 78−37647
carbazole:tetracene, electronic absorpt. spectrum, host-cryst. field effect 80−100669
carbazole cation radical, optical absorpt. spectra 77−40564
carbazole H-bonded complex formation, enthalpy change due to electronic excitation, spectroscopic determ. 78−92496
carbon tetrachloride, vac. UV absorpt. cross section 80−91574
carbon tetrachloride, vac. UV absorpt. spectra, 250-115 nm 77−79628
carbonaceous meteorite extract, UV spectrum rel. to interstellar grains 77−25987
carbonmonoxyhemoglobin, spectroscopic meas. after pulsed optical excitation 79−92150
carbonyl group, mag. rot. strength of spin-forbidden transitions 77−14468
β-carotene, optical absorpt., theory 79−62189
β-carotene, orientated in nematic liq. crysts., UV-visible dichroism meas. *(German)* 77−34668
carotenoid pigments, radical ions, radiolysis generation, absorpt. spectra, MO calcs. 77−65488
carotenoids related to visual chromophore, electronic struct., band shape model 78−20142
l-carvone, optical rot. dispersion spectra, solvent effects 77−10684
catechol borane, geometry, electronic absorpt. spectra 80−971
cellulose acetate, gamma-ray effect on light absorption used as dose meas. technique 78−13345
chain, collective excitations and optical absorpt. 79−47019
charge-transfer and hydrogen-bonded complexes, electronic absorpt. spectra calc. *(Russian)* 78−37628
charge-transfer organic salts, strongly correlated, interband absorpt., long-range Coulomb interaction 79−4525
chlorin, ab initio CI calcs. on ground, singlet and excited states, visible spectrum 79−16139
chlorin, UV absorption and photoelectron spectra, CNDO/S3 calcs. 77−75210
chlorobenzaldehyde, $a^3A'' \rightarrow X^1A'$ phosphoresc., conformations and ground state fundamentals 80−78642
chlorobenzene, optoacoustic spectroscopy using cell with ultimate corrosion resistance 80−42269
chlorobenzene, S_0-S_1 transitions, two-photon absorpt. spectra by nozzle beam-multiphoton ionisation method 80−63728
chlorofluorobenzene cations in gaseous phase, emission spectra and lifetimes in B(0°) states 80−63711
chlorofluoroethanes, gas, photoabsorption cross-sections, 46-100 Å 78−42095
chlorofluoromethane cations in solid Ar, absorpt. spectra and photochem. 79−96339
chlorofluoromethanes, gas, photoabsorption cross-sections, 46-100 Å 78−42095
chloroform, highly excited vibr. states, thermal lensing spectrosc. and local mode model 80−87140
chloroform, liq., light scatt. coeff. determ., absolute method 78−2868
1-chloronaphthalene, A^1A'-X^1A' electronic transition, rot. band contour 79−6935
β-chlorophenetole, UV and IR electronic and vibr. spectra, model assignments 77−10673
chlorophyll, a and b, lowest singlet-singlet transition, solvent effects 79−24952
chlorophyll, and related mols., in solid solns., fine-structured vibronic spectra under tunable dye laser excitation *(Russian)* 80−74164
chlorophyll a, absorpt. and fluoresc. spectra, observance of Stepanov relation 80−81554
chlorophyll a and protochlorophyll a, optical transitions anisotropy 79−43825
chlorophyll and analogues, role of O_2 in regeneration of photoreduced pigments in soln. 78−68980
chlorophyll c absorpt., fluoresc. and fluoresc. excitation spectra in alga cell at −196°C 78−53329
chlorophyll mixed associates, intermol. interaction, energy transfer, luminesc. and absorpt. spectra 78−64924
chlorophyll photo-oxidation, spectral detect. of exciplex in triplet state 77−25368
chlorophyll photo-oxidation mechanism, effect of spectral composition of light 77−25369
chlorophyll pigments, aggregated forms in soln., spectral-luminesc. charcts. *(Russian)* 78−23529
chlorophyll-a, mols. and complexes in PMMA and MTHF matrices, optical spectra 79−3433
chlorophyll-a, solns., vis. absorpt. spectra of monomer, dimer and oligomers 77−29101
chlorophyll-a, spectral props. of liquid crystal solutions 78−27291
chlorophyll-a, triplet and excited singlet optical absorpt. spectra 79−59477
chlorophyll-a adsorbed on aerosil, absorpt. spectra 78−53327
chlorophyll-b, mols. and complexes in PMMA and MTHF matrices, optical spectra 79−3433
chlorophylls, mag. reson., site selected fluoresc. detection 80−69164
chloroplasts and subchloroplast particles, optical absorpt. at 700 nm and EPR spectra 77−25394
chlorotrifluoroethylenes, electronic transitions, electron impact spectra 77−10775
chlorotrifluoromethane, photoabsorpt. cross-section, 175-770 Å 77−88462
chloroxylenes, UV absorpt. spectra 78−86879
chloroxylenes, UV absorpt. spectra 79−22727
cholesta-4,6,8(14)-triene, fluoresc. and absorpt. spectra in UV, lifetimes 79−27017
cholesta-5,7,9(11)-triene-3β-01, fluoresc. and absorpt. spectra in UV, lifetimes 79−27017

spectra of organic molecules and substances continued
cholesteric liquid crystal, thermosensitive, props. *(Hungarian)* 78−59755
cholesteric liquid crystal coatings, superimposed left- and right-handed, peak refl. and colour gamut 80−74472
cholesteric mixtures, optical props., temp. meas. *(German)* 77−44013
cholesteryl esters, isotropic mesophase, optical props. 79−65891
cholesteryl myristate, two blue phases demonstrated by selective refl., 300-400 nm 79−90553
cholesteryl nonanoate, polymorphism of blue phase, optical rot. and refl. 79−37820
chromophore aggregates, optical absorpt. and circular dichroism spectra, degenerate ground state model 79−70523
cinnamaldehydes, electronic spectra, CNDO CI calcs. 78−29774
cofacial diporphyrins, electron transfer reactions following picosecond excitation, CT state lifetimes, optical difference spectra 80−25995
complex mixtures in solid-state matrices, dip shape saturation effects on nonuniformly broadened spectra 79−95799
computer applications in organic struct. chem. and mol. spectroscopy in USSR 78−88624
conjugate heterosystems, UV spectra, substituent effects 79−27006
conjugated double bonds, 2200 Å signature rel. to organic mols, in interstellar dust 77−57074
conjugated molecules, conformation, electronic spectra, NDDO calcs. 79−85901
conjugated molecules, triplet-triplet excitation, atomic localisation calcs. 79−54830
contact charge transfer complexes of organic molecules with O_2, CNDO/S calcs., absorpt. spectra obs. 80−69076
continuous relaxation spectra, direct anal. 80−104831
copper (II) carboxylates, magnetic and spectroscopic props. 79−91204
copper (II) complex, bis(dithiocarbamate), HF-Slater-LCAO calcs., mag. coupling parameters and optical spectrum 80−99447
copper phthalocyanine, polycryst. film, charge transfer state and optical spectra *(Russian)* 78−84607
copper porphine, Xα multiple scatt. calcs., EPR and electronic spectra 78−13426
coronene, in n-paraffin solns., quasiline spectra, press. effects *(Russian)* 77−68053
coronene-TCNQ, solid complexes, spectra, stoichiometry 78−23435
coumaran, geometry, electronic absorpt. spectra 80−971
coumarin 6-diethylamine, soln. fluoresc. induced by laser, vibr. relax. 79−26984
cresyl violet, excited singlet-singlet absorpt. *(Russian)* 79−42985
critical mixture, multiply scatt. light, LF spectrum 77−52125
cryogenic solutions, spectrosc. and photochem. 80−16713
cryptocyanine-methanol, soln., nonlinear optical absorpt., 310-815 nm 79−85973
cryptopleurine derivatives, absorpt. and fluoresc. obs. of photodecomp. processes, dye laser relevance 80−55686
crystal violet, soln., picosec. relax., wavelength depend. 79−99921
crystals, line-shape distortion on anisotropic absorpt. meas. in unpolarised light 80−2765
CTIP, exciton surface polaritons at room temp. 79−47476
cyanine dye, crysts., extraordinary exciton polaritons in refl. spectra, macroscopic dielec. theory 77−89715
cyanine dye sensitisers, J-aggregate formation, spectral changes of UV bands 77−70318
cyanine dye sensitisers, J-aggregates, circular dichroism and induced Cotton effect 77−70319
cyanine dye sensitisers, J-aggregates, meso substituents effect on mol. assoc. 77−70320
9-cyanoanthracene, cryst., excimer emission, spectra, photochem. and multiphonon processes 78−10914
cyanobenzenes, weak triplet-triplet absorpt. spectra 77−58027
4-cyanobiphenyl and 4′-alkyl- or 4′-alkoxy-substituted liq. cryst. derivatives, soln., absorpt. and fluoresc. spectra 80−87164
4-cyanobiphenyl/4-cyano-p-terphenyl liq. cryst. mixture, order parameters of dissolved dyes 80−100167
cyanodiacetylene cation, gas phase, UV emission spectra of $\tilde{A}(\pi^{-1}) \rightarrow \tilde{X}(\pi^{-1})$ band system 80−95636
cyanomethane, matrix-isolated, VUV photolysis, CNC radical vibr. and electronic spectra 78−85180
cyanomethane-d_0, -d_3, vacuum UV photodissociation spectroscopy 79−834
cyanotrifluoromethane, vacuum UV photodissociation spectroscopy 79−834
9-cycanoanthracene, subpicosecond laser photolysis and time resolved absorpt. spectra *(Japanese)* 79−79272
cyclic π-electron systems, magnetic circular dichroism 77−88481
cyclobutanone, ring puckering in $^1B_2(n,3s)$ Rydberg state, VUV spectrum 78−74675
β-cyclodextrin-azulene complex, circular dichroism spectra 78−58713
1,3-cycloheptadiene, electron impact, electronic spectra 79−45855
1,3-cyclohexadiene, electron impact, electronic spectra 79−45855
1,4-cyclohexadiene, excited electronic states, electron impact spectrosc. 79−45842
cyclohexane, excited electronic states, electron impact spectrosc. 79−45842
cyclohexane, visible absorpt. spectra, local mode overtone intensity of C-H stretching mode 79−81207
cyclooctatetraene, anions, in condensed media, electronic spectra 79−22723
1,3-cyclopentadiene, electron impact, electronic spectra 79−45855
cyclopenta[h]cycl[4.2.2]azine, photoelectron and visible, and UV spectra 78−5286
cyclophosphazene-DNa complex, spectrofluorometric and spectrophotometrics investig. 80−95643
cyclopropyl silane, rotational spectrum (9.0-35 GHz), transitions of ground vibrational state 79−98077
cytidine monophosphate, aq. soln., spectra, 300-450 nm, polarisation study 78−96015
cytidylyl-3′,5′-cytidine, aq. soln., spectra, 300-450 nm, polarisation study 78−96015
cytochrome c-serotonin soln., UV effect on optical props. 80−30663
cytochrome P-450, non-equilib. states formed by low-temp-reduction, absorpt. spectra 80−35837
cytochrome P-450-CO complex, absorpt. spectrum, electronic transitions, PPP calcs. 77−71811
cytosine, hydroxy and methoxy, derivatives, absorption UV spectroscopy and electronic struct. of ionic and tautomeric forms 80−74177

spectra of organic molecules and substances continued
Davydov splitting theory, excitonic parameters, split absorption bands, organic molecular aggregates *(Spanish)* 79−59437
deca-2,4,6,8-tetraene, fluoresc. and absorpt. spectra, forbidden transition 78−82764
decacyclene, MCD and absorpt. spectra 79−54875
deuteronaphthalene:β-deuteromethylnaphthalene crystal, asymmetry of phonon side bands, absorption, luminesc. and specular spectra 77−1730
di(thiomethyl)methane, vapour, far ultraviolet spectra, valence-shell and Rydberg transition interpretation 79−50037
diacetylene, near UV band system, rot. and vibr. anal., rot. fine struct. 77−61761
diacetylene, UV spectra of mol. excited states 79−31540
diacetylene (TSHD), low temp. photopolymerisation, short chain intermediates obs. 80−93754
diacetylene chains in partially polymerised diacetylene cryst., temp. depend. optical absorpt. 78−64376
diacetylene radical cation, and deuterated forms, electronic spectrum in solid inert gases 79−94026
diacetylene single crystals, photopolymerisation, optical transmission spectroscopic exam. 78−27757
dialkylammonium manganese tetrachloride, quasi two-dimensional antiferromag., temp. depend. of absorption spectra 78−43894
diammonium layer compound, $(CH_2)_2(ND_3)_2MnCl_4$, mag. and optical props. 79−51760
diammonium layer compound, $(CH_2)_n(NH_3)_2CuCl_4$, mag. and optical props. 79−51760
9,9'-dianthryldisulphide, UV/visible absorption spectrum *(German)* 79−59487
1,3-diazaazulene, vibronic coupling, Duschinsky effect, mixed cryst. spectra 77−79622
1,3-diazaazulene-azulene, Stark spectra, vibronic perturbations in mixed cryst. 77−79623
4,10-diazachrysene, absorpt. spectra and luminesc. in cryst. and glassy matrices, 77K 78−37650
diazanaphthalenes, excited state absorpt. spectra and intersystem crossing kinetics 80−74176
dibenzofuran, single cryst. 2-photon excitation spectrum, 4.2K 79−56807
dibromodifluoromethane, vac. ultraviolet photodissociation, CF_2 emission 79−47955
p-dibromodiphenylether surface, normal and ultra-Brewster refl. spectra 80−25400
cis-dibromoethylene, vac. UV spectrum, Rydberg transitions, ionisation limits 78−78718
trans-dibromoethylene, VUV and photoelectron spectra, Rydberg series, vibr. fine struct. 77−6799
dibromoethylenes, vac. UV spectra 77−23507
dibromomethane, highly excited vibr. states, thermal lensing spectrosc. and local mode model 80−87140
1,4-dibromonaphthalene:octafluoronaphthalene, absorpt. and phosphoresc. spectra, intermol. reson. 79−33764
1,4-dibromonaphthalene, optical props., struct. disorder effects 78−52525
1,4-dibromonaphthalene, S_0 to T_1 exciton transition, optical dephasing time and lineshape function 78−15183
1,4-dibromonaphthalene, substitutionally disordered, energy localisation, optical and ODMR spectra of triplet Frenkel excitons 80−54996
(1,4)-dibromonaphthalene, triplet exciton scatt., absorpt. spectra 78−6696
1,3- and 1,4dibromotetrafluorobenzene cations in gaseous state, emission spectra 80−63648
dicarbocyanine solns., photoisomerisation, fluoresc. and absorpt. spectra of photoisomer 78−85181
dicarbonitrile-anthracene solutions, absorpt. and emission spectra, solvent influence 80−43083
2,4-dichloroaniline, UV aborpt. spectra 79−36660
9,10-dichloroanthracene, cryst., singlet-triplet absorpt. spectra, delayed fluoresc. 77−8619
9,10-dichloroanthracene, quasi 1D α-cryst., exciton transitions, optical refl. spectra obs. 77−81116
p-dichlorobenzene-p-dibromobenzene, mol. cryst., intermol. mixing of electronic states 77−85768
p-dichlorobenzene-p-dibromobenzene, solid soln., local struct. and triplet energy migration 78−60489
4, 4'-dichlorobenzophenone, triplet exciton absorpt. band, zero phonon line *(French)* 79−33726
4-4' dichlorobenzophenone, triplet exciton absorpt. lines 79−38563
2,4-dichlorobromobenzene, UV absorpt. spectra of vap. phase, vibr. anal. 79−81211
2,4-dichlorobromobenzene, vap. phase UV absorpt. spectra 79−22726
dichlorocarbene, electronic spectrum, ab initio CI calcs. 79−85948
dichlorofluoromethyl peroxynitrate, UV absorpt., spectra, photodissoc. lifetime meas. 80−83386
dichloromethane, highly excited vibr. states, thermal lensing spectrosc. and local mode model 80−87140
dichloromethylene, radical, emission and excitation spectra, in Ar matrix 77−34657
dichloropyrimidines, UV-vis. absorpt. spectra, anal. 77−50445
dichroic dye guest, depend. of absorption and optical contrast on chiral nematic host pitch 77−90164
dichroic dye in chiral nematic host, visible absorpt., pitch relationship 78−48193
dicyanoacetylene radical cation, $\tilde{A}^2\Sigma_g^+ \rightarrow \tilde{X}^2\Pi_u$ emission band system 79−22721
dicyanodiacetylene radical cation, photoelectron and emission spectra 80−5558
1,1'-diethyl-2,2'-cyanine iodide, neat and mixed crysts., visible absorption and emission spectra assignments 77−1692
1,3'-diethyl-2,2'-quinolylthiacarbocyanide iodide, soln., 78−68530
diethylammonium manganese tetrachloride, quasi two-dimensional antiferromag., magnon sideband in absorption spectra 78−43895
3,3'-diethylthiacarbocyanine iodine-rhodamine 6G, energy transfer with increased local conc., Forster mechanism 80−69220
1,3- difluorobenzene radical cation, and deuterated forms, laser-induced fluoresc. matrix. study 79−98138
difluorodiacetylene radical cation, $\tilde{A}$-$\tilde{X}$ band emission spectra, $\tilde{A}$ state lifetime 79−72327
difluoroethylene, cis-, trans- and perdeuterated isomers, absorpt. spectra, 120 to 165 nm 78−94256
difluoromethane, triplet state emission spectra, phosphoresc. and energy transfer 78−53196

spectra of organic molecules and substances continued
diglycine barium chloride monohydrate:Cu^{2+}, optical absorpt. and EPR, lattice sites, hybridisation 77−43872
dihalodiacetylene radical cations, $A^2\Pi_u$-$X^2\Pi_y$ system, emission spectra and state lifetime 79−10121
dihalogenoacetylene radical cations, $C_2X_2^+$, emission spectra, $A^2\Pi \rightarrow X^2\Pi$ band systems 78−17679
dimesitylboranes, phenyl substituted, absorption and emission 78−27311
dimethyl ether, low-lying excited states, improved virtual orbitals calcs. 77−14372
dimethyl sulphide, sulphoxide and sulphone, electronic struct. and spectra *(Russian)* 78−66460
4-dimethyl-amino-4'-nitrostilbene, in EBBA, nematic ordering influence on fluoresc., temp. depend. *(German)* 79−81235
1,5-bis dimethylamino pentamethinium perchlorate, refl. spectra calcs. 77−85154
trans-4-dimethylamino-4'-nitrostilbene, mol. hyperpolarisability in soln., UV dispersion of charge transfer contrib. 79−31986
p-dimethylaminobenzonitrile, picosecond relax., fluoresc. spectroscopy, solvent effects 78−58737
4- dimethylaminochalcone fluorescence, distrib. of hydrophobic mols. in artificial lipid membrane 77−16912
dimethylammonium copper chloride, magneto-optical props., 0.03-13.5 eV 77−52132
6,6'-dimethyloxyindigo, picosec. kinetics, and photostability, spectrosc. obs. 79−45748
2,6,dimethylpyrazine, PMMA soln., fluoresc. and phosphoresc. quantum yield and lifetime, 20-120 kbar 79−54902
2,10-dimethylundecapentaene, optical spectra, vibr. anal., rel. to visual chromophore 77−29102
α,α-dinaphthylalkanes, absorpt. spectra and phosphoresc. in soln., triplet excimers 78−62816
dinitrobenzene, adsorption on alumina, adsorption isotherm, ESR and electronic spectra 77−48681
4-(2',4'-dinitrobenzyl)-pyridine, photochromism, nanosec. laser absorpt. spectrosc. obs. 80−85193
2-(2',4'-dinitrobenzyl)-pyridine, photochromism, ns laser absorption spectra 78−48138
2,2'-dinitrodiphenylmethane, nanosecond laser flash photolysis and absorpt. spectra, photochromism, solvent polarity 78−61029
N,N'-dioctadecyloxacarbocyanine monolayers on Ag surface, attenuated total refl. 79−11480
9,10-dioxa-anti-bimanes, fast intersystem crossing, picosecond spectrosc. obs. 79−85998
dioxan-phenol($-d_1$), in CCl_4 solns., H-bonds vibr. relax. bands anal. 78−84560
1,6-diphenly-1,3,5-hextriene, mol. derivatives, absorpt. and fluoresc. spectral props. 79−72344
diphenyl anion salts, sublimed layer, electronic and IR absorpt. spectra 80−66189
diphenyl butadiene, absorption recovery lifetime, use in UV mode-locked lasers 80−19075
3,5-diphenyl-1,2,4-oxadiazole, saturated vap. press., absorpt. and fluoresc. spectra 79−76442
1,6-diphenyl-1,3,5-hexatriene and derivatives in n-paraffins, electronic spectra and fluoresc. 78−13509
2,6-diphenyl-1,4-benzoquinone+aromatic amine, triplet exciplex quenching, H-transfer mechanism 79−79228
3,6-diphenyl-pyridazine, valence electronic structure 79−72360
3,6-diphenyl-s-tetrazine, valence electronic structure 79−72360
diphenylamine, in nitrobenzene soln., dry hole capture in pulse radiolysis expt. 79−79266
diphenylethylene, UV spectra, quantum-mechanical investigation of isomerisation pathways 80−43065
1,6-diphenylhexatriene, radiationless transitions and natural lifetimes, solvent effects 80−63622
diphenylpolyene molecules, excited electronic states, vibronic mixing, wave functions, method of fragments anal. 80−63615
diphenyltriafulvenes, absorpt. and fluoresc. spectra, dipole moments, solvent effects 77−75169
dispersion induced circular dichroism, determ, of mag. dipole allowed transitions 80−14163
dissolved organic matter in seawater, fluoresc. spectra *(Russian)* 77−13083
p-ditertiarybutylbenzol electron absorption spectra and struct. *(Russian)* 77−16338
DNA binding to ethidium bromide derivatives, competitive and non-competitive bonds *(German)* 79−79446
DNA from mouse tissue, UV irrad. studies, UV absorpt. spectra 78−11702
DNA interactions with cations, UV difference spectrosc. and Marcus theory 80−94153
DOBAMBC, smectic liquid crystal, ferroelectric, colour switching in elec. field 80−29719
DODCI, ps absorption relax. lifetime, isomers, pulse excitation 77−9098
DTTC, subpicosecond laser photolysis and time resolved absorpt. spectra *(Japanese)* 79−79272
dye absorpt. spectra, observation using oscillating beam spectrometer 80−31907
dye in nematic liquid crystals, order parameter 77−83614
dye in polymer matrices, electrochromic props. and use as probe of matrix softening around T_g 80−84724
dye molecules, dissolved, influence of environment on luminesc., intense laser excitation 78−84622
dye molecules adsorbed on Ag, Au and Cu films, absorpt. and luminesc. study 80−103981
dye solns., single and two-photon spectroscopy, using pulsed acousto-optical effect 77−68087
dye solutions, short-wavelength stimulated emission limit, induced absorpt. spectra 79−59696
dye-polymer system, diffusion based direct marking process, laser induced, spectral thermal characteristics 79−76779
dyes, absolute fluorescence quantum yield, calorimetric determ. 80−43092
dyes, solns., polarisation spectroscopy 78−89559
elastomers, relax. transitions from relax. spectrometry and internal friction *(German)* 80−34136
electron microprobes and scanning electron microscopy, conf., Orsay, France, Dec. (1978) 80−11979
electronic transitions, obs. by inelastic tunnelling spectroscopy 77−38704

spectra of organic molecules and substances continued
epoxy, Stycast 1266, very low temp. thermal conductivity and optical props. 78−55992
ester+amine, consecutive reactions, reaction rate constants, absorbance meas. using isosbectic points 77−73433
ethane, diode laser spectra, baseline variations, elimination by ultra-low freq. filtering 80−90901
ethane, long path photoelec. absorpt. spectra 4200-10600 Å, appl. to Uranus 77−83592
ethane, photoabsorption cross sections, 1380 to 1600 Å, at 295 and 200K 78−90181
ethane, vertical electronic spectra, limited CI calcs. 79−13693
ethane gas, local mode overtone bands 80−83444
ethane-propane, binary mixture near crit. point, conc. fluctuation decay rate, spectrosc. obs. 77−81108
ethanol, glassy matrix, absorpt. spectra after X-irrad., solvated electrons 79−65903
ethanol glass, trapped and solvated electrons produced in presence of applied electric field 80−7379
N-ethyl carbazole, CNDO/S spectrum calc. rel. to poly-n-vinylcarbazole solid state spectrum 79−89815
ethyl carbazole, in nitrobenzene soln., dry hole capture in pulse radiolysis expt. 79−79266
ethyl substituted ammonium halides, exciton absorpt. spectra 79−28782
ethylcyanodiacetylene cation, gas phase, UV emission spectra of $\tilde{A}(\pi^{-1})\rightarrow\tilde{X}(\pi^{-1})$ band system 80−95636
ethylene, adsorbed on ZnO, adsorption rate spectra, freq. response method 78−51817
ethylene, electronic struct., CNDO/S2 calc., photoelectron and UV absorpt. spectra 77−30783
ethylene, excited states, spectral assignments 79−85915
ethylene, excited states, V←N spectrum 77−50446
ethylene, near vac. UV MCD obs., assignments, new transition 77−38684
ethylene, planar, V-N vertical transition, SCF and correlation energies 77−68032
ethylene, S_0,S_1-states, twisting vibrs., pot. curve calcs., absorpt. spectra 77−83576
ethylene, UV photoelectron spectra, valence electron shake up approx. methods 80−18788
ethylene, V←N transition origin determ. 78−13510
ethylene, vacuum ultraviolet absorption spectra 80−63653
ethylene, vertical $^1(\pi\text{-}\pi^*)$ V-N transition, MRD-CI calc. 79−27004
ethylene dibromide, photoabsorption and photodissociation, 190-300 nm 79−50038
ethylene-d_0, -d_4, hindered internal rotation, vibronic luminesc. and absorption spectra 79−54883
ethylene-O_2 complex, CI calcs., singlet-triplet transitions 79−63923
N-ethylphthalimide+olefins, photochemical reaction, absorpt., fluoresc., phosphoresc. and triplet-triplet absorpt. spectra 80−85197
ethynyl radical, emission spectra and pot. energy surface, ab initio MRD CI calc. 79−41099
ethynyl radical, vertical electronic spectrum, CI calcs. 77−34656
excited molecular systems, relax. processes, nanosecond time-resolved spectra 77−26992
ferricytochrome c structure, effect of different phospholipids 78−68981
ferrocene, multiphoton dissoc. and ionisation by tuneable dye lasers 80−99524
ferrocytochrome c, picosec. and subpicosec. relax. and dephasing, reson. light scatt. obs. 79−45876
ferrous porphyrin, intermediate spin, reson. Raman spectra 79−69820
fibrinogen solution, effect of scavengers on radiation-susceptible sites 78−11701
films, X-ray induced luminesc. and optical absorpt. rel. to γ-induced free radicals 77−5033
flavin adenine dinucleotide, resonance CARS line shapes, excited state parameters 79−3448
fluoradene, absorpt. and fluoresc. in solvents, excimer form., aggregation 77−79625
fluoranthene, single cryst. and in fluorene matrix, polarised absorption spectra, assignments 80−55122
fluorescein 27, rot. diffusion and level kinetics separation in transient absorpt. spectroscopy 77−30877
fluorinated organic iodides, absorpt. spectra and primary photolysis processes, near and vac. UV 79−20393
3-fluoro-4-methyl aniline, near UV electronic absorpt. spectra, line shift, vibr. anal. 77−10682
2-fluoro-5-methyl aniline, near UV electronic absorpt. spectra, line shift, vibr. anal. 77−10682
fluoroacetylene, laser Stark and IR-microwave double resonance, E1 moment, vibr. states 77−6813
fluoroaromatics, CH stretching, vibr. force fields, substitution pattern effects 77−54550
fluorobenze, optoacoustic spectroscopy using cell with ultimate corrosion resistance 80−42269
fluorobenzene, 2644 Å band system, rovibronic anal., isotope effects 79−6949
fluorobenzene, cryst., absorpt. spectrum, vibronic states 77−59588
fluorobenzene, multiphoton ionisation spectrum in one-photon wavelength region 80−63727
fluorobenzene, multiphoton reson, ionis. spectrum, 51000 cm^{-1} assignment 79−86021
fluorobenzene, S_0-S_1 transitions, two-photon absorpt. spectra by nozzle beam-multiphoton ionisation method 80−63728
fluorobenzene, singlet-singlet electron transitions, modified CNDO-CI method exam. 78−25552
fluorobenzene cations, emission spectra, Jahn-Teller effects and vibronic coupling 79−10120
fluorobenzenes, electronic struct., CNDO/S2 calc., photoelectron and UV absorpt. spectra 77−30783
fluorobenzenes, UV spectra calc., oscill. strengths 79−18203
fluorobenzenes in Ne matrices, molecular cation electronic absorption spectra, new photolytic technique 80−58415
fluorocarbon polymer film, prep. by RF sputtering and plasma polymerisation, props. 77−55890
fluoroethylenes, electronic transitions, electron impact spectra 77−10775
fluoromethanal, visible spectrum, rot., vibr. and vibronic anal., double min. pot. 79−41182
fluorosilanes, far UV and He I photoelectron spectra 79−18204
p-fluorostyrene, 288 nm electronic absorpt. spectra, vibr. assignment 79−13738

spectra of organic molecules and substances continued
formaldehyde, 4_0^1 band anal., isotope effects 78−86878
formaldehyde, a^3A_2-X^1A_1 system, rot. anal. 78−62818
formaldehyde, electrochromism of 1749 Å band, electric dipole moment and polarisability 78−66572
formaldehyde, electronic excited states, GO calcs., $\pi\rightarrow\pi^*$ transition 79−22616
formaldehyde, emission spectrum, forbidden n-π^* transition, electronic-vibr. struct., CNDO/2 calcs. 77−58035
formaldehyde, excited state photodecomp., rotationally resolved spectra 77−60088
formaldehyde, in Ar, 0.17-1.4 gm cm^{-3}, VUV absorpt. spectra, Rydberg excitations 77−79627
formaldehyde, in Ar, medium perturbations of extravalence excitations, VUV absorpt. 78−1002
formaldehyde, mag. rot. spectrum, singlet-triplet perturbations 78−25580
formaldehyde, mol., UV absorpt. cross-section, and stratosphere chem. 80−109209
formaldehyde, photoabsorpt. and ionis., intensities, assignments, ST, IVO calc. 79−31614
formaldehyde, rot. struct. of 3500 Å transition, large amplitude vibr. effect 79−93976
formaldehyde, selective laser photolysis for ^{14}C enrichment 80−108720
formaldehyde, UV photolytic separation of D from H in cryogenic solns. 78−95937
formaldehyde (−d_1,d_2), isotopic forms. vac. UV Rydberg spectra, vibr. assignments origin isotope effect 77−61763
formaldehyde and its isotopic species, rot. spectra of ground vibr. state, rot. const. determ. 80−83350
formaldehyde UV spectrum, selective laser photolysis for ^{14}C enrichment 79−10220
formaldehyde-^{13}C, A^1A_2-X^1A_1 system, UV absorpt. spectra, rot. anal. 80−9614
formaldehyde-d_0,-d_2, higher Rydberg states, vac. UV transitions assignments 77−42334
formaldoxime, photoelectron and far UV absorpt. spectra 78−17712
formamide, and related cpds., INDO-CI calc., transition moments 79−45637
formamide, valence ionisation energy and electron affinity, HAM/3 calc. and photoelectron, UV spectra 79−50081
formic acid amides, polarisabilities and π-π^* transitions, dipole interaction calcs. 80−23411
1-formyl 2(4-nitrophenyl) hydrazine, preparation, optical and electro-optical props. 77−36201
formyl radical, form., vibr. relax., spectrosc. 79−36746
free radicals determ., on polymer surfaces *(German)* 80−7892
free-base porphin, S_2-S_0 transition vibronic bands, photochem. hole-burning 79−36631
furan, resonantly enhanced multiphoton ionisation 80−106362
gelatin-Pd II complex formation, circular dichroism and absorpt. spectra meas. 79−61881
germanium phthalocyanine, elec. cond. temp. depend. 80−80271
glass, alcoholic and aq., 4.2K, trapped electron photocond. and optical spectra following radiolysis 79−29378
glyceraldehyde 3-phosphate dehydrogenase, EPR, saturation transfer EPR 79−98124
glycerol, liq., reflectivity, in VUV region, for optical and dielec. functions 79−15475
glycine-d_3, pulse radiolysis, primary reaction product optical and EPR spectra 79−79265
glyoxal, 4550Å bond system, rot. anal. mol. consts. and geometry 77−42330
glyoxal, ^1A_u state energy transfer, D effects 77−58066
glyoxal, $S_0\rightarrow S_1$ band, opto-acoustic phase angle meas. 80−68256
gold complex, AuI (triphenylphosphine)$_n$ chlorates (n=2,3,4,), Mossbauer spectra 79−54874
haematoporphyrine, complexed with chloranil and tryptophane, energy spectra, transition moments and intermolecular distances 80−72127
haemoglobin, absorpt. spectra, light scatt. method meas. *(Russian)* 78−21939
haemoglobin, dynamic characts. of conformational nonequilib. states, radiolysis investig. 78−58877
haemoglobin, in salt soln., diffusion rel. to intermol. interactions, light scatt. investig. 77−44585
haemoglobin-CO complex, absorpt. spectrum, electronic transitions, PPP calcs. 77−71811
haloacetylene cations, electron impact excitation A→X band system assignment 80−32766
halobenzene type ions, high resolution spectrosc. with new emission source *(French)* 80−57383
halogenoacetylene radical cations, C_2HX^+, emission spectra, $A^2\Pi\rightarrow X^2\Pi$ band systems 78−17678
halomethanes, synchrotron radiation photoabsorption cross sections, Rydberg states 80−28033
α-(β-)heptacyclene, vibronic spectra, electronic-vibr. interactions 78−1021
4-n-heptyl-4′-cyanobiphenyl, linear dichroism spectra in nematic and isotropic phases 80−25336
heterocyclic compounds, bond lengths, fifth overtone of C-H stretching vibrs. obs. 80−91528
heterocyclic conjugated compounds, electronic struct., spectra, ionisation pot., INDO-CI LACO-MO-SCF calcs. 79−54834
hexabenzocoronene, MCD and absorpt. spectra 79−54875
hexafluorobenzene, γ-radiolysis, matrix isolation spectra of radical anions 79−52704
hexafluorobenzene, cation, visible emission spectra of gas, Jahn-Teller effect 79−50034
hexafluorobenzene, IR multiphoton excitation, vibr. energy redistrib. and hot band spectrum 80−95656
hexafluoroethane, photoabsorpt. cross-section, 175-770 Å 77−88462
hexahydrohexahelicene, in Shpolskii matrix, absorpt., fluoresc., phosphoresc. spectra 79−76463
hexamethyl indatricarbocyanine iodide-ethanol soln., luminesc. quantum yield, photoacoustic method 77−86335
hexamethylbenzene in tetrachloromethane soln., local mode overtone bands 80−83444
1,3,3,1′,3′,3′-hexamethylindotricarbocyanine iodide, laser dye, ultra-fast excited state absorpt. spectroscopy 77−30876
n-hexane, visible absorpt. spectra, local mode overtone intensity of C-H stretching mode 79−81207

spectra of organic molecules and substances continued
trans-hexatriene, multiphoton ionization spectrum in 6.2 eV region 77−27133
1, 3, 5-hexatriene, radical cations, emission spectra of cis and trans isomers 77−6793
trans-hexatriene, weak low-energy band, S and T levels by fragment method 78−82625
1,3,5-hexatriene radical cation, in Ne matrix, laser induced fluoresc. and emission spectra 80−87163
hydrogen maleate ion, electronic spectra, CNDO/S CI calcs. 77−75128
1-hydronaphthyl radical, 4.2K absorpt. spectrum *(French)* 80−80809
1-hydronaphthyl radical, in naphthalene single cryst., anisotropic oscill. strength 78−50591
hydronaphthyl radicals embedded in naphthalene cryst., optical transition energies and ionisation energies 80−78595
2-hydroxy, 3-allyl, 4,4′-dimethoxybenzophenone, methyl methacrylate copolymer, excitation singlet, internal H^+ transfer, visible spectra 80−32728
β-hydroxyacrolein, intramol. H bonds, orbital and transition energies, ab initio SCF and SCF CI calcs. 77−14345
2-hydroxybenzophenone, excitation singlet, internal H^+ transfer, visible spectra 80−32728
ortho-hydroxybenzophenone, soln., intramol. proton transfer and energy relax. photostability, transient absorption obs. 80−28032
7-hydroxycoumarin, absorpt. and emission spectra, ionic forms 78−21955
7-hydroxycoumarine, one- and two-photon absorption, fluoresc. obs. 78−46407
7-hydroxycoumarine, two-photon visible absorpt. spectra, fluoresc. obs. 78−42147
hydroxygallium phthalocyanine, exciton electroabsorpt., optical density spectra 77−85746
2-hydroxytropone, in β-cyclodextrin complex, UV circ. dichroism spectrum assignments, complex struct. 78−46358
in cyclohexane-ethanol mixtures, UV spectra, solvent effect 79−22770
indane, 271 nm spectrum, rot. band contour anal., puckering vibr. 78−1001
indigo, picosec. kinetics, and photostability, spectrosc. obs. 79−45748
indigo dyes, triplet state config., laser flash absorpt. spectrosc. obs. 80−5557
indole, aq. solns., flash photolysis, transient absorpts., 600 to 800 nm 78−53228
indole, oriented in polyethylene film, dichroism spectrum 79−54864
indole, UV absorpt. spectra, low-lying Rydberg band 77−58037
indoles, in glassy hydrocarbons, complexation vs. aggregation, absorption and fluoresc. obs. 79−98132
indoline spiropyrans, methoxysubstituted, activated solns., photochromism, laser nanosecond spectroscopy 77−70317
inhomogenously broadened absorption spectra, linear struct. detect. *(Russian)* 78−76504
iodoethylene, and perfluoro analogue, VUV spectra, perfluoro effect on Rydberg states 77−61764
iodoform, soln., MCD spectra, assignments 79−31567
iodomethane, dressed mol., ν_6 band, saturated absorption spectrosc. 79−54844
iodomethane, first s-Rydberg transitions 78−42094
3-iodopropene, rot. spectra, quadrupole hyperfine struct. 80−91545
iodotrifluoromethane, continuous absorpt. band contour, temp. depend. 78−70876
isopropyl ammonium chloroplatinate and chlorostannate, ferroelastic transition, thermal, optical, and elastic meas. 79−28096
isoquinoline, quasilinear absorpt. spectrum, in Shpolskii system 77−46571
isorhodopsin, physiological activity in rat rods 77−60204
Kapton, optical, elec. props., struct., ion textured surface 78−72904
ketones, rigid, optical rot. dispersion spectra, solvent effects 77−10684
ketones, triplet-triplet absorption carbonyl group role 77−83641
lactate dehydrogenase+free radicals, reactions, pulse radiolysis 78−7214
lanthanum ethyl sulphate nonahydrate:Pr^{3+}, 400-700 nm, 78K, 22 kbar press. effects 77−81133
larch arabogalactan solns. as optical cement 77−75723
large molecule, electronic struct., photoemission and optical absorpt. spectrum, CNDO/S3 model 80−53172
latex, monodisperse, reflectivity obs. of phase separation into ordered and disordered phases 77−70345
lipid bilayer thermal excitations detect. by light beating spectroscopy 77−48762
local vibration inhomogeneous broadening, organic mols. in solid matrices 77−58087
lycopene, soln., depolarised Rayleigh light scatt. in absorpt. bands 79−87451
lysozyme protein solution, spectra and dye laser threshold power 79−68391
macromolecular solution, quasielastic light scattering from rigid mols. 79−64127
magnesium chlorin, ab initio CI calcs. on ground, singlet and excited states, visible spectrum 79−16139
magnesium porphine, ab initio CI calcs., electronic absorpt. spectra 78−78639
malachite green, soln. picosec. relax. polarisation spectrosc. meas. 78−68530
malondialdehyde, UV electronic absorpt. spectra, G_4 mol. symmetry group 77−6798
masked antifoggants, hydrolysis stability, photographic process depend. *(German)* 80−45530
MBBA, electronic spectra 78−52530
mesitylene:tetracyanoethylene, charge transfer spectra line shape 79−78700
metallophthalocyanines, α-phase solid, absorpt. and MCD spectra 79−73964
metalloporphyrin triplet state quenching by Fe II- and Fe III-porphyrins 78−76992
methane, 4350-10600 Å bands, intensity profile, vibr. assignments, rel. to major planets spectra 78−42084
methane, 6190 Å spectral line, press. broadening detected by photoacoustic 79−94033
methane, 6825 Å band obs. in Uranus and Neptune 77−78715
methane, ν_2 and ν_4 bands Coriolis interaction, using a general Hamiltonian formalism *(French)* 78−5192
methane, ν_4 band, high resolution spectrosc. 80−5529
methane, ν_4 band Q-branch spectrum 80−5530

spectra of organic molecules and substances continued
methane, absorption and press. coeffs., 4500-10500 Å, band model calcs., astronomy appls. 77−83593
methane, absorption spectra, 6000-6500 Å, intracavity laser detection 79−89684
methane, and isotopic forms, ν_4 band, line parameters, Jovian atmosphere transmission, 7.7 micron 78−85894
methane, appl. of band-model parameters to Uranus visible and near IR spectrum 80−98609
methane, Balmer radiation production by electron impact 0-2000 eV 79−76521
methane, $F_2^{(2)}$ doublet Zeeman effect obs., nonlinear reson. *(Russian)* 77−38027
methane, liquid, opto-acoustic study of weak optical absorpt. 80−93278
methane, liquid, vibrational overtone spectrum, planetary appls. 79−2497
methane, photoabsorpt. cross sections, 1400-1850 Å spectral region 77−46572
methane, photoabsorpt. cross-section, 175-770 Å 77−88462
methane, photoabsorption cross sections, 1380 to 1600 Å, at 295 and 200K 78−90181
methane, recoil effect, optical resolution by saturated absorpt. spectroscopy 77−18937
methane, shock-tube oxidation, equilibrium and nonequilibrium radiation emission 78−27760
methane, vertical electronic spectra, limited CI calcs. 79−13693
methane+methane and methane+monatomic collisions, photoacoustic study of vibr. relaxation *(French)* 77−30969
methane(-H_2), long path photoelec. absorpt. spectra 4200-10600 Å, appl. to Uranus 77−83592
methane 7300 Å band of Uranus, limb brightening obs. 78−85902
methane (methane-^{13}C) band strength, spectral line breadth in ν_3 bands 79−98069
methane-d_1, high resolution spectra, line intensities, ground-state rot. const. determ. 80−83517
methanol, free O-H overtone absorpt. in vis. region, thermal lensing spectra 77−34644
methanol, glassy matrix, absorpt. spectra after X-irrad., solvated electrons 79−65903
methanol, low-lying excited states, improved virtual orbital calcs. 77−14372
methine dyes, spectral props., solvent effects 80−69181
methoxy radical fluoresc. spectra induced by laser, UV region 79−59498
methoxy radical UV emission spectra from methanol+Ar(Kr) reactions 80−91572
methoxy thiomethyl methane 79−50037
3-methoxybenzanthrone in ethanol, photoprotolytic reactions, spectra, rate consts. and lasing thresholds 80−43327
methyl allenyl sulphide, UV absorpt. spectra, role of 3d valence-shell and 4s Rydberg-type atomic orbitals 80−83384
methyl bromide, photoabsorption and photodissociation, 190-300 nm 79−50038
methyl bromide, submillimeter rotational spectrum, laser generation line identification 79−64210
methyl chloride, vacuum UV absorpt. spectrosc., Rydberg transitions obs. 80−5561
methyl cyanide, linewidth parameters in rot. spectrum, multiple differentiation calcs. 79−98070
methyl fluoride, rot. absorpt., Stark modulation expt. 79−59396
1-methyl indole, UV absorpt. spectra, low-lying Rydberg band 77−58037
methyl indoles, UV and IR absorpt. spectra, f-values and ground state vibr. freqs. 78−58716
methyl iodide, in Ar, 0.25-1.38 gm cm^{-3}, VUV absorpt. spectra, Rydberg excitations 77−79627
methyl iodide, in Ar and Kr, medium perturbations of extravalence excitations, VUV absorpt. 78−1002
methyl iodide, liquefied gas solns. bound exciton model for Rydberg bands 78−31214
methyl iodide, mag. circular dichroism, mol. Rydberg transitions 78−66573
methyl iodide, Rydberg states, quantum defect theory applic. 80−32700
methyl iodide, solns. with liq. Ar, Kr, Xe, CH_4 and CF_4, Rydberg band positions, temp. depends. 78−17686
methyl iodide, UV absorpt. spectra, ionis. limit region, assignment 78−21940
methyl isocyanide, vacuum UV photodissociation spectroscopy 79−834
3-methyl lumiflavin, in soln., absorpt. spectrum 80−58277
3-methyl lumiflavin in soln., optical absorption, theory 78−74569
methyl peroxynitrate, UV absorpt., spectra, photodissoc. lifetime meas. 80−83386
N-methyl pyrrole, resonantly enhanced multiphoton ionisation 80−106362
methyl radicals, reactions behind shock waves, UV absorpt. obs. 78−46362
methyl salicylate, vapour phase, absorption and fluorescence spectra 79−81232
methyl substituted ammonium halides, UV exciton absorpt. bands 78−72547
methylalkanes, CH stretching local mode anharmonicity, intramol. perturbation overtone spectra 79−18171
methylbenzene cations, photodissoc. spectra, substituent effects 78−58710
methylbenzene sulphinate, vapour and soln. UV spectra, solid IR spectrum, assignments 77−50444
methylbenzenes, 3p Rydberg transitions, multiphoton ionis. spectrosc. obs. 80−95644
methylbixin, low-lying forbidden π-electronic state, spectral evidence 77−58029
methylchloroform, vapour phase, UV absorpt. spectrum, photodissoc., stratospheric appls. 79−81208
methylcyanodiacetylene cation, gas phase, UV emission spectra of $\tilde{A}(\pi^{-1})\rightarrow\tilde{X}(\pi^{-1})$ band system 80−95636
methylene blue in methyl blue, concentrated solutions, Nd laser radiation absorption spectra *(Russian)* 77−54753
methylene diiodide, in 3-methyl pentane, γ-radiolysis 79−24776
methylene iodide, soln., MCD spectra, assignments 79−31567
methylene radical, vibronic bands obs. in pulsed supersonic jet 80−28024
3-methyleneoxetane, electron structure, orbital-O interaction, MO calcs., UV photoelectron spectra 80−28058
methylhydroperoxide, UV absorpt. spectra of vap. 80−69159
1-methylindan, circular dichroism, rot. strengths, CNDO/S calc. 79−3452

spectra of organic molecules and substances continued
3-methylisoquinoline, quasilinear absorpt. spectrum, in Shpolskii system 77−46571
3-methylpentane, C-H stretching diagonal local mode anharmonicity, intermol. perturbation 78−25524
3-methylpentane-d_{14}, glass, trapped electron optical spectra, wavelength selective bleaching 79−83480
1,4-Bis(2-methylstyryl)benzene, laser dye, picosec. laser obs. 79−36891
2-methyltetrahydrofuran, glass, trapped electron optical spectra, wavelength selective bleaching 79−83480
2-methyltetrahydrofuran-methanol mixed glasses, annealed, γ-ray produced electrons transfer from IR to bisible traps 80−11440
β-methylumbelliferone in ethanol solns., spontaneous luminesc. kinetics 80−74192
methyoxy radical, electronic absorpt. spectra, visible, vibr. freqs., vibronic intensities and oscill. strengths 80−28025
molecular crystal, impurity reson. interaction effects 77−1396
molecular crystal, optical transitions to electron-exciton bands 78−10365
molecular crystal, singlet and triplet biexciton spectra, optical transitions 78−10366
molecular crystals, intermolecular interactions, spectroscopic studies, review 80−103958
molecular crystals, spectroscopy, bibliography for 1976 78−72585
molecular crystals, struct. disorder effect on optical props. 77−90165
molecular crystals, thermal modulation spectroscopy, electron-phonon interaction 77−32392
molecular electron-donor-acceptor complexes, solvent effect on charge transfer absorpt., thermodynamic props. 77−83615
molecular mixed crystals, electronic transition props., Redfield theory 79−46008
molecular solution, excess electron optical absorption spectrum model, band shape 78−33500
monohalonaphthalenes, electronic transition spectra forbidden charact., symmetric vibr. interaction 78−58663
2(4)-monooxopyrimidines, gaseous, matrix, soln., tautomeric equilib., IR and UV absorpt. spectra 80−58256
myoglobin , oxyhaeme complex, single cryst., visible spectrum, electronic struct., coord. geometry 78−44456
N-substituted amides, liquid, acoustic spectroscopy method for H-bond studies 79−96303
naphthalene:1-hydrodynaphthyl, cryst., charge transfer optical transitions 77−44027
naphthalene:tetracene, electronic absorpt. spectrum, host-cryst. field effect 80−100669
naphthalene, β-naphthol impurity mol. distrib., spectral obs. *(Russian)* 79−82253
naphthalene, a-exciton temp. depend. scatt., optical absorpt. profile 78−72088
naphthalene, absorption spectrum in rare-gas matrices 79−3454
naphthalene, $C_{10}H_8$ and $C_{10}D_8$, optical absorpt. spectra of hydronaphthyl radicals, isotope effects 78−60487
naphthalene, cryst., radiation induced radicals, optical absorpt. bands, SCF-CI MO calc. 79−91463
naphthalene, cryst., vibronic absorpt. spectrum with totally symm. phonons 79−4817
naphthalene, deformation potential consts. of exciton-phonon interactions *(Russian)* 78−56498
naphthalene, Faraday spectrum, sign rel. to mag. field strength *(German)* 77−36204
naphthalene, fluorescence and absorpt. spectra, deviations from Condon approx. 80−28004
naphthalene, molecular cryst., phonon scatt. and exciton linewidths 78−15185
naphthalene, Rydberg spectra, antireson. lineshapes 77−50424
naphthalene, singlet-singlet transition, Born-Oppenheimer approx., CNDO/S calcs. 77−27045
naphthalene, solid, high-energy vibr. overtone spectra, local modes, intramol. relax. 79−28052
naphthalene, solution, structured UV spectrum obtained by ultrafast two-pulse excitation 80−78630
naphthalene, spectra, PPP approx., CI clacs. *(German)* 79−36602
naphthalene, spectra of directionally deformed crystals and phonon-exciton interaction constants 79−78703
naphthalene, UV spectra and extinction coeffs. for $S_n \leftarrow S_1$ absorption 80−18866
naphthalene $^1B_{2u}$ resonance pairs, energy denominator depend. of excitons absorpt. 77−39783
naphthalene anions, electron affinities, transition energy, comparison for gaseous liquid and solid 80−29731
naphthalene TCNE π-π three mol. complexes, absorpt. spectra, assoc. consts., extinction coeffs. *(German)* 77−35465
naphthalene vapour, fast obs. of primary triplets with tandem laser pulse absorption 77−58056
naphthalene-β-naphthol, concentration effects in exciton absorption region 80−108241
naphthalene-β-naphthol mixture, exciton absorpt. depolarisation 80−103972
naphthalene-d_8:β-methylnaphthalene -d_{10}, phonon side bands of specular optical transitions 78−26649
naphthalene-d_8:naphthalene, symmetry reduction obs. of deformed crysts. by absorbt. spectrum method 79−15504
naphthalene-TCNE π-π three mol. complexes, UV-visible spectra assoc. const., extinction coeff. determ. *(German)* 77−35464
naphthalene-tetrabromophthalic anhydride, complex cryst., visible spectra, singlet-triplet absorpt. 79−19897
naphthalene-tetrachlorophthalic anhydride, complex cryst., visible spectra, singlet-triplet absorpt. 79−19897
naphthalenes, substituted, electronic singlet-singlet spectra 77−3378
1,2-naphthalocyanine-rare earth ion complexes, electronic excitation deactivation mechanism 79−85988
β-naphtholate in methanol-methyltetrahydrofuran glasses, electron solvation, laser flash photoionis. compared with pulse radiolysis 79−74405
1,4-naphthoquinone, $T_1 \leftarrow S_0$ transition, elec. and mag. field spectra 78−88322
naphthoxazole derivatives, elec. cond., thermoelec. power, energy gap, absorpt. spectra 77−32053
β-naphthylamine-cyclohexane soln., luminesc. quantum yield, photoacoustic method 77−86335
nematic liq. cryst. with luminesc. impurity, luminesc. and absorpt., order parameter determ. 79−4240

spectra of organic molecules and substances continued
nematic liquid crystal, electronic spectra, influence of order in liq. cryst. struct. 78−71675
neodymium ethyl sulphate, electronic spectra Stark pattern, crystal elec. field and mag. props. 77−12084
neodymium oxydiacetate, magneto-optical rotatory dispersion and oxid absorption spectra 79−91409
neopentane liq., local mode overtone bands 80−83444
nickelocene, multiphoton dissoc. and ionisation by tuneable dye lasers 80−99524
Nile blue, excited singlet-singlet absorpt. *(Russian)* 79−42985
nile blue, interaction of cationic dyes with mitochondria, absorpt. spectra 77−52752
Nile Blue, subpicosecond spectroscopy, tunable probe, spectral dynamics 80−23429
p-nitroaniline, cryst., electronic excited states, config. interaction calcs., UV spectrum 78−10913
p-nitroaniline, exciton level directional dispersion, absorpt. band profiles 78−48192
p-nitroaniline, mol. hyperpolarisability in soln., UV dispersion of charge transfer contrib. 79−31986
nitroanilines electronic states, CNDO/s-CI correlative calcs. 78−58604
9-nitroanthracene, subpicosecond laser photolysis and time resolved absorpt. spectra *(Japanese)* 79−79272
nitrobenzene-n-hexane, crit. mixture, multiply scatt. light, LF spectrum 77−52125
nitrobenzene-n-hexane, crit. mixtures, reorientation spectra, linewidths and intensities 79−28777
2-nitrofluorene, $^1A \rightarrow {}^1L_a$ transition, electronic absorpt. spectra, solvent effects 77−58028
3-nitropyrene, triplet state, absorption spectra in soln. 78−33440
nitrosomethane, mol., spectra 600-720 nm, and geom. change on excitation 79−72329
nitrosomethane-d_3, electronic excitation, conformational changes obs. 79−98233
n-nonane:H_2-tetra-4-tert-butylphthalocyanine, thermal broadening of zero phonon lines, hole burning 78−71803
norbornadiene, excited electronic states, electron impact spectrosc. 79−45842
norbornene, excited electronic states, electron impact spectrosc. 79−45842
Norrish type II reaction biradicals, spectra, extinction coeffs., solvent effect on lifetime 77−90617
nucleic acid component pulse sonolysis obs. 79−53186
nucleic acid components, low-intensity US effects 77−32874
nucleic acids, electronic absorpt. and emission spectra 80−55989
nucleic acids and related compounds, photoemission rel. to absorpt. and luminesc., 120 to 250 nm 77−81466
nucleotide bases, electronic absorpt. and emission spectra 80−55989
octafluorotoluene, γ-radiolysis, matrix isolation spectra of radical anions 79−52704
n-octane-3,4,6,7-dibenzpyrene impurity, fluorescence impurity spectra, phonon free line broadening *(Russian)* 80−108279
1-octanol, dielec. consts., solvent struct., effect of H bonding solutes, chain length 77−48674
trans, trans-1,3,5,7-octatetraene, high-resolution one and two photon excitation spectra 80−78669
1,3,5,7-octatetraene, lowest excited singlet state, dipole forbidden character 79−27024
1,3,5,7-octatetraene, UV, visible, and fluoresc. spectra and assignments, evidence for ^1A_g state 78−33518
trans-octatetraene, weak low-energy band, S and T levels by fragment method 78−82625
of monocarboxylic acids, tunnelling spectroscopy 78−91545
organic charge transfer complexes, refl. spectra, excitons 79−47477
organic mixed crystals, transverse relax. and freq. shifts of optical transitions 78−84599
organic molecular crystal, doped, two-particle electronic excitation, optical cooperative excitation 80−93368
organic molecules, electronic transitions polaris. determ. by dichroism in nematic solvents 77−42344
2′-oxaindan (dihydroisobenzofuran) spiropyrans, photochromic transforms, spectrokinetic study 80−30259
α-oxalic acid dihydrate, low-lying excited states, ODMR and optical obs. 79−41188
3- oxetanone, electron structure, orbital-O interaction, MO calcs., UV photoelectron spectra 80−28058
oxy- and deoxyhaemoglobin, optical spectra, dichroism 79−20514
oxyhemoglobin, spectroscopic meas. after pulsed optical excitation 79−92150
2-oxyphenylbenzoxazol, proton intramolecular transfer, light absorpt. and emission, dichroism, polarised fluoresc. 80−87166
palladium porphin, in n-alkane crystal, Zeeman and crystal field effects, absorpt. vibr. anal. 80−7372
palladiumporphin, in n-alkane, $S_1 \leftarrow S_0$ absorpt. spectrum, vibronic coupling and avoided crossing, field splitting 78−84613
papain inactivated by OH radicals and H_2O_2, optical density, amino acid composition and fluoresc. 78−53344
pentacene, ATIR spectra, Davydov splitting 77−24865
pentacene, disordered solid layer, absorpt. spectra 80−93417
pentacene, evaporated on quartz, optical absorption, substrate temp. depend. 78−2932
pentacene, in p-terphenyl, electronic excitation transport, acousto-optical effects 78−72079
pentacene, in p-terphenyl mixed cryst., low temp. optical phase relax. obs., mechanism 77−52112
pentacene in naphthalene (p-terphenyl), mol. mixed crysts., optical dephasing and vibronic relax. 80−95957
pentacene in naphthalene crystal, relax. of vibronic states, photon-echo and ab absorpt. relax. expts. 79−95807
pentafluorobenzene, C-H vibr. states, thermal lensing spectra, local mode model test 77−71812
pentafluorobenzene, cation, visible emission spectra of gas, Jahn-Teller effect 79−50034
pentamethinemerocyanine dye, electronic spectrum and struct., solvatochromism, microstructural model 77−61817
pentyl cyanobiphenyl nematogen, depolarised light scatt. 79−95790
peptide-Cu II interaction, EPR and optical absorpt. 78−27881
perfluorohexadiyne radical cation, $\tilde{A}$-$\tilde{X}$ band emission spectra, $\tilde{A}$ state lifetime 79−72327

spectra of organic molecules and substances continued
perfluoropentadiyne radical cation, $\tilde{A}$-$\tilde{X}$ band emission spectra, $\tilde{A}$ state lifetime 79−72327
peroxidase, low-temperature radioreduction, MCD and absorpt. spectra 78−31763
perylene, α- and β-crysts. and soln., polarised reflection and absorption spectra 77−8598
perylene, solid soln. in ethanol, fine struct. in absorpt. spectra, laser technique 77−90178
(perylene)$_3$TCNQ, prep. and spectra, electron-mol. vib. coupling 77−16290
perylene in EBBA, nematic ordering influence on fluoresc., temp. depend. *(German)* 79−81235
perylene-tetracene in liquid crystals, temp. depend. of absorption and fluoresc. *(German)* 80−18887
petroleum samples, extinction coeff., refractive index meas., 0.25-25 microns 79−65818
phenanthrene, cryst., refl. spectra of first singlet transition 78−88323
phenanthrene, molecular cryst., phonon scatt. and exciton linewidths 78−15185
phenanthrene, subpicosecond laser photolysis and time resolved absorpt. spectra *(Japanese)* 79−79272
phenazine, substitutionally disordered, energy localisation, optical and ODMR spectra of triplet Frenkel excitons 80−54996
phenazine, T-T absorpt. build-up, following picosec. pulse singlet excitation, in gas phase 78−9161
phenazine, triplet state intersystem crossing, picosec. singlet excitation 77−6824
phenetole, in cyclohexane-ethanol mixtures, UV spectra, solvent effect 79−22770
phenol, in cyclohexane ethanol mixtures, UV absorption, solvent effects 79−22767
phenol, singlet-singlet electron transitions, modified CNDO-CI method exam. 78−25552
phenol(d_1)-dioxan(-acetonitrile), in carbon tetrachloride ($CDCl_3$) solns., H-bonds vibr. relax. bands anal. 78−84560
phenol-cyclohexane (-ether), UV spectra, solvent effects, matrix rank anal., species determ. 79−22768
phenol-organic solvent mixtures, UV spectra, solvent effects 79−22769
phenols, substituted, in cyclohexane-ethanol mixtures, UV spectra, solvent effect 79−22770
phenothiazine derivatives, semicond. elec. props., optical spectra, and EPR 80−103693
6-phenoxy-5,11-napthacenequinones, photochromism, molar extinction coeffs. meas. 80−66220
phenyl isocyanate, electronic absorpt. spectrum, vibr. struct., f-values, spectroscopic moment and config. 78−58715
(+)-(S)-2-phenyl-3,3-dimethylbutane, optical activity, circular dichroism, polarisability model 80−43082
phenylene compounds in n-paraffins, electronic spectra and fluoresc. 78−13509
phlorin, UV adsorption and photoelectron spectra, CNDO/S3 calcs. 77−75210
phthalamide derivatives, solutions, excitation spectra rel. to absorption spectra, 77-300K 79−85970
phthalan, geometry, electronic absorpt. spectra 80−971
phthalimide P derivatives 79−56836
phthalimides, solns., solvent effects on absorpt. spectra and fluoresc. 77−34650
phthalocyanine, optical density spectra, charge transfer states 79−95800
phthalocyanine, polycryst. film, charge transfer state and optical spectra *(Russian)* 78−84607
phthalocyanine, quasiline emission spectra using low temp. laser luminesc. spectrosc. *(Czech)* 80−86445
picosecond transient spectroscopy of molecules in solution 79−36621
pigment associations, conc. effects, luminesc., absorpt. spectra and dichroism obs. 80−1007
pigment molecule organisation and interaction in reaction centres of Rhodopseudomonas viridis 80−35843
pinacyanol, picosecond photobleaching and absorpt. recovery, solvent effects 77−44493
pinacyanol in ethanol, electronic relax., analysing light ps spectroscopy 80−99517
pleochroic dyes, dissolved in nematic liq. crysts., guest-host interactions, appl. to electrooptic displays 80−44113
PMMA, glassy, optical absorpt., visible region, determ. by laser calorimetry 80−66218
polar fluid mixtures, two-absorber model of solvated electrons, spectra 78−85284
polar glasses, aq. and alcoholic systems, trapped electrons, photocond., optical spectra 77−85742
polar liquid, integrated absorpt., microstruct. effect *(French)* 78−10823
polar liquid, solvated electron optical props. and thermodynamic characts., polaron model 78−85170
polarised photochromism in solid solutions 78−64859
poly(2-vinyl pyridine), dil. solns., translational diffusion, chain conformation influence 80−103508
poly(5,7-dodecadiyne-1, 12-diol-bis phenylurethane), visible refl. spectra, photocond., excitons 77−81117
poly(9-vinyl anthracene), struct. *(German)* 79−98256
poly O-carbobenzoxyl-L-tyrosine, in soln., conformation, helix-coil transition, circular dichroism, NMR spectra 77−31037
poly-1,2-bis 4-isopropylcarbamoyloxy-n-butyl-1-buten-3-ynylene, cryst., UV refl. spectra, 25-160°C 79−82991
poly-1,6-di-N-carbazolyl-2,4-hexadiyne, synthesis, thermal expansion, photocond., optical transition 78−76858
poly-2,4-hexadiyne-1,6-diol bis (p-toluene sulphonate), cryst., exciton surface polaritons, reflectivity of (100) face, 295K 78−80372
poly-2-vinylnaphthalene, soln., lowest triplet props., flash photolysis and radiolysis obs. 80−32861
poly-γ-benzyl-L-glutamate helices, optical activity 80−48113
poly-n-vinylcarbazole, higher-lying singlet states, CNDO/S study 79−89815
polyacenes, S_1-T_1 interconversion, excitaiton indices calcs. 79−54830
polyacenes, spectra, correlation effects 79−81199
polyacetylene, pure and heavily doped, optical and IR studies, electronic struct. calcs. 80−7347
polyacetylene pure and doped films, anisotropic optical properties 78−92137
polyatomic mol. quasi line spectrum in paraffin matrix, electronic-vibr. interaction 79−85971
polyatomic molecules, structure recognition, from IR, UV, NMR and mass spectra, computer method 78−25737
st-1,2-polybutadiene, oriented film, anisotropic C 1s XUV absorpt. spectra 80−55207
polycarbonate, colour appearance during oxidation *(Russian)* 79−24643
polycarbonate film dosimeter for high-level electron dose meas., optical density 77−25559
polydextran, γ-irrad. frozen gel, electron trapping, EPR and optical obs. 78−20030
polydiacetylene, cryst., one-dimens. conjugated semicond., vibronic coupling, Fano interference effects 80−34939
polydiacetylene, extended chains with realistic model side groups, self-consistent electronic band structs. 77−39776
polydiacetylene, reflection spectra, thermochromism, temp. hysteresis and phase transformation 78−19452
polydiacetylene, single cryst. piezomodulated and specular refl. spectra 77−20869
polydiacetylene crystals, electronic spectra and struct. 79−73923
polydiacetylene polymer crystals, optical nonlinearities, chain pairing effects, one dimens. band model 77−69851
polydiacetylene PTS crystal, Davydov splitting in spectra at 15000 to 19000 cm^{-1}, at low temp. 78−31212
polydiacetylene-bis(toluenesulphonate), refl. spectra, 0-15 kbar, doublet press. shift 78−43891
polydiacetylene-bis(toluenesulphonate), single cryst., thermal expansion and optical band splitting 77−8594
polydiacetylenes substituted with urethane, solid and film, visible spectra, refl. and absorpt. 79−87460
polyenals related to visual chromophores, absorpt. spectra rel. to chain length 79−34494
polyenals related to visual chromophores, emission spectra 79−34495
polyene chromophones, band broadening in electronic-vibr. absorpt. spectra 80−28003
polyenes, absorpt. spectra, electronic-vibr. sequence band broadening 77−65453
polyenes, conjugated, homologous linearity rule for electronic spectra 79−6933
polyenes, electronic absorpt. spectra, charact. spectral band criteria 80−63651
polyenes, electronic absorpt. spectra, intensity distrib. anal. 77−58034
polyenes, electronic absorpt. spectra absolute intensities estimation 77−34702
polyenes, electronic struct., spectra interpretation, CNDO/S2 calcs. 79−6870
polyenes, substituted, spectra, four-level state scheme 79−54840
polyenones related to visual chromophores, absorpt. spectra rel. to chain length 79−34494
polyenones related to visual chromophores, emission spectra 79−34495
polyethylene low density flame treatment of surface, XPES study 79−66179
polyethylene photochemical aerosol, absorbance rel. to presence in Titan atmosphere 80−31249
polymer, polydispersity anal. in photon correlation spectroscopy 78−27247
polymer spectral sensitivity and photochem. stability using Xe high press. lamp *(German)* 80−61119
polymer-Cu(II) complexes in poly(vinyl alcohol), polyacrylamide and poly(vinyl pyrrolidone) films, ESR or optical study 79−61199
polymers, synthetic, chiral, with aromatic side chains, conform. from circ. dichroism 79−55014
polymethine dye solutions, photochem. transformations and short-wavelength luminesc. 80−100686
polymethine dyes, excited mols., photoisomeric transformations 79−87854
polymethine dyes, ultrafast absorpt. spectra 77−18934
polymethinium dye, excitonic fluoresc., absorpt. trapping spectra 78−27302
polynucleotides and components, temp. depend. of UV absorpt. spectra 77−21475
polyoxyethylene, semidilute and dilute soln. behaviour crossover, UV spectrometry 78−80375
polypeptide chains, struct. of conduction and valence band 80−76700
polypeptides, α-helical, π-π^* absorpt. and circular dichroism spectra 80−23398
polypeptides, β-form, vibronic exciton approach to NV_1 absorption band 77−79626
polyphenylacetylene, cryst., resonant Raman scatt., opt. absorpt. 77−4630
polyphenylene oxide-polystyrene blends, spectroscope exam. of chain conform. and bonding 78−42925
polyphenyls, S_1-T_1 interconversion, excitaiton indices calcs. 79−54830
polystyrene, and copolymers, optical fibre waveguides, spectral characts. 80−14461
polystyrene, film, optical props. from near IR to X-ray, sum rules 77−48195
polystyrene, glassy, optical absorpt., visible region, determ. by laser calorimetry 80−66218
polystyrene, intermol. interaction, conform. *(Russian)* 79−23539
polystyrene, semidilute and dilute soln. behaviour crossover, UV spectrometry 78−80375
polystyrene solutions, dilute, diffusion coeff., solvent effect 80−19971
polystyrene-PMMA-benzene, soln., polystyrene diffusion, photon correl. spectroscopy 80−34220
polyvinylquinazoline-I_2 complexes, absorpt. spectra and elect. cond. 80−92891
poly[(R)-oxypropylene], opt. rot. dispersion and vac. UV circular dichroism 80−40084
porphin, hypersurface of adiabatic pot. calc. by CNDO/2 method, vibr. freqs., absorpt. spectra calc. 80−95543
porphin free base in cryst. anthracene, site selective optical spectra, vibronic freqs. 79−13730
porphine, ab initio CI calcs., electronic absorpt. spectra 78−78639
porphins, UV absorption and photoelectron spectra, CNDO/S3 calcs. 77−75210
porphins orientation in n-alkane Shpolskii hosts, spectra 80−48035
porphyrin, dication and dianion, spectra, quantum chem. calcs. 79−36597
porphyrin-pyridine complex, 4.2K, visible absorption spectrum gap burning-out 78−53232

spectra of organic molecules and substances continued
potassium acetylacetonate, polycryst., elec. cond., pyroelectricity, phase transition, UV spectrum 78−76392
praseodymium β-ketoesters, Pr^{3+}, visible spectrum, interaction, intensity and bonding parameters 80−993
praseodymium oxydiacetate crystal, opt. rot. dispersion 77−36193
propane, vertical electronic spectra, limited CI calcs. 79−13693
propane, vertical electronic spectrum, ab initio MRD-CI calcs. 78−70810
propane-d_8, liq., solvated electron optical absorpt. band 78−72544
β-propiolactone, electron structure, orbital-O interaction, MO calcs., UV photoelectron spectra 80−28058
propiolyl chloride(-d), 357-333 nm absorpt. system 80−69161
propiolyl fluoride(-d), 290 nm absorpt. system 80−87142
propyleneimine, circular dichroism, optically active Rydberg transitions 77−18952
protein secondary structure determ. by circular dichroism spectra 80−30653
proteins, UV irradiated, luminesc. quenching, EPR and absorpt. spectra 78−15768
protochlorophyl, mag. reson., site selected fluoresc. detection 80−69164
protoporphyrin IX, triplet states, flash photolysis, obs. 80−95555
protoporphyrin IX dimethyl ester, triplet states, flash photolysis, obs. 80−95555
pseudoisocyanine bound by sulphated polysaccharides, dil. aq. soln., visible and circular dichroism spectra 80−45107
PTFE film electret, optical spectra, band theory interpretation *(Russian)* 78−88376
PTFE films, sputtering conditions effect on comp. and optical props. 79−52115
PTS, exciton surface polaritons at room temp. 79−47476
PTS polydiacetylene single cryst. reflection spectra, exciton site splitting 78−31211
PTZ:PMDA, purification, growth, struct., optical and elec. props. 80−54216
purple membrane of halobacterium halobium, aggregate optical spectra, moment anal. 79−2007
purple membrane structure, effects of bleaching and regeneration, H-halobium 77−86532
PVA, semidilute and dilute soln. behaviour crossover, UV spectrometry 78−80375
PVC:Fe(Cu) film, struct. and optical props., soln. growth technique 78−51837
PVC, thermal stabilisation by triazine dithiols *(Japanese)* 80−108386
PVC thermal degradation, reinitiation mechanism of HCl catalysis 80−71944
pyrazine, dispersion induced circular dichroism, determ, of mag. dipole allowed transitions 80−14163
pyrazine, PMMA soln., fluoresc. and phosphoresc. quantum yield and lifetime, 20-120 kbar 79−54902
pyrazine, reson. Raman and absorpt. spectra to $S_2(\pi,\pi^*)$ state, excited state geometry 79−76433
pyrazine, vibr. struct. and nonlinear vibronic coupling, pseudo Jahn-Teller effect 78−94234
pyrazine complexes with H_2O, Br_2 and I_2, electronic absorpt. spectra calc. *(Russian)* 78−37628
pyrazine H-bonded complex formation, enthalpy change due to electronic excitation, spectroscopic determ. 78−92496
pyrene, fluoresc. quenching by 1,4-diazabicyclo[2-2-2]octane in cyclohexane soln. 79−31575
pyrene, in alcohol solns., polar fluid electrons optical absorption coeffs., ns laser ionis. obs. 78−84600
pyrene, orientated in nematic liq. crysts., UV-visible dichroism meas. *(German)* 77−34668
pyrene, triplet exciton absorpt. lines 79−47475
pyrene excimer formation in micelle, time-resolved spectra 79−79298
pyrene-3-sodium sulphonate solubilised in didodecyldimethylammonium bromide-benzene inverted micelles 80−3417
pyrene-N,N-diethylaniline exciplex, visible spectra obs., picosec. laser photolysis, solvent polarity depend. 77−38677
pyrene-naphthalene complex radical cation, in γ-irrad. glass, visible spectrum obs. 78−44385
pyridazine, elec. field induced spectrum, 0_0^0 band near 3752Å 78−17700
pyridine, $\pi\rightarrow\pi^*$ transition, 1800 Å, electronic absorpt. spectrum 77−71813
pyridine, dispersion induced circular dichroism, determ, of mag. dipole allowed transitions 80−14163
pyridine, in benzene single cryst., electronic spectrum Stark modulation, dipole moment 78−29814
pyridine cation radical in trichlorofluoromethane matrix, gamma irrad., EPR and optical obs. 80−23442
pyridine in aliphatic alcohol solns., relationship between stimulated Raman scatt. and complex formation *(Russian)* 77−48174
pyridine in rare gas matrices, absorpt. spectra, 1700-2900 Å, progressions 77−3376
pyridine N-oxide, 341 nm band system, out-of-plane modes assignment 77−34646
pyridine-d_0-d_5, $n\pi^*$ excited state vibronic coupling, vis. and Raman spectra 77−14438
pyridines, monosubst., H_2O complexes, n-π^* transitions, H bonding, MO theory 80−95550
pyridinium salt solns., electrochromism in visible absorpt. spectra 77−77244
pyridizine, 0-0 bands in n-π^* absorption, rot. contour anal. 78−55184
2-pyridyl phenyl sulphide, dipole moments, absorpt. spectra, meas. and calcs. 77−46574
2-pyridyl phenyl sulphone, dipole moments, absorpt. spectra, meas. and calcs. 77−46574
pyrimidine derivatives, absorpt., luminesc. and polarisation spectra, electronic struct. 79−85993
pyrimidine in cyclohexane at 77K, absorption and phosphorescence spectra 78−61138
pyrimidines, substituted analogues, absorption UV spectroscopy and electronic struct. of ionic and tautomeric forms 80−74177
pyromellitic dianhydride-anthracene, cryst., charge transfer exciton transitions, refl. spectra obs. 78−72540
pyrrole, resonantly enhanced multiphoton ionisation 80−106362
pyrylium dye J-aggregate species, circular dichroism spectropolarimetric characts. 79−3456
pyrylium salt solns., electrochromism in visible absorpt. spectra 77−77244

spectra of organic molecules and substances continued
trans-quinacridones, absorpt. and emission spectra, struct. and solvent effects 77−478
quinones, spectral solvent shifts, electrostatic model and semi-empirical PPP calcs. 77−83507
quinoxaline, in organic solvent, excited state absorpt. spectra, 422 and 533 nm, picosec. relax. 79−89683
quinoxaline, solns., excited state absorpt. kinetics 79−45734
quinoxalinones, new class of high-efficiency laser dyes 78−46597
radical ions, conjugated, solvent effect in π-approx. calcs. of electronic transitions and spin densities 77−38623
radical ions, conjugated, solvent effect in CNDO and INDO calcs. of electronic spectra by restricted methods 77−38624
rare earth ions, ligand-induced pseudoquadrupole absorpt., vibronic contribs. 80−52978
rare earth oxydiacetate, spectra, energy level patterns 79−38561
resorufin, in PMMA, site selection spectra, hole burning and Stark effect 78−9159
retinal, in ethanol soln., methyl groups effect optical absorpt. 79−53047
retinal, isomeric triplets, low temp. spectrosc. and kinetic flash photolysis obs. 79−85972
retinal, isomers, intersystem crossing quantum efficiencies, solvent effects 79−22751
retinal electronic structure 78−15764
rhodamine, dye soln., photoinduced dichroism and vibronic relax. 77−14465
rhodamine 3B solutions in polyvinyl alcohol matrix, spectrum-luminesc. characts. 79−13761
rhodamine 640, subpicosecond spectroscopy, tunable probe, spectral dynamics 80−23429
rhodamine 6G, aggregation, modulation Stark spectrosc. obs. 79−27030
rhodamine 6G, aqueous soln., absorpt. spectra, ground and triplet state photoprotonation pH depend. 80−42961
rhodamine 6G, fluoresc. polaris. spectra in glycerol soln. 79−76458
rhodamine 6G, in organic solvent, hot luminesc. 79−4842
rhodamine 6G, in rigid matrix, conc. effects in spectra 80−83347
rhodamine 6G, solns., delayed fluoresc. of simple associates and T-T absorption spectra 79−56847
rhodamine 6G, solns., electronic absorpt. spectra, mol. assoc. effects *(Russian)* 77−88460
rhodamine 6G and 3B, excited singlet-singlet absorpt. *(Russian)* 79−42985
rhodamine 6G ethanol soln., absorpt. and luminesc. spectra using picosecond excitation 80−106351
rhodamine 6G polar solution, conc., temp effect on spectral props. 79−87505
rhodamine 6G soln., hot luminesc. and vibr. relax. 79−22752
rhodamine 6Zh, electronic spectra, intermol. interactions effect *(Russian)* 77−48237
rhodamine B, 6G, spectra of lowest excited singlet states 79−81424
rhodamine B, double Davydov's splitting of visible absorpt. band 78−82746
rhodamine B in aq. LiCl soln., absorpt., pH, electric conductance 77−27079
rhodamine B-ethanol soln., luminesc. quantum yield, photoacoustic method 77−86335
rhodamine C and 6G, strong base solns., electronic spectra, temp. depend. 79−85987
rhodamine dye, photodecomposition of laser dyes *(Russian)* 77−29017
rhodamine dyes, phosphoresc. quantum yields determs. 79−8179
rhodamine dyes, soln. induced singlet-singlet absorption spectra 78−46363
rhodamine dyes in soln., bleaching, electronic and vibr. absorpt. spectra, fluoresc. 80−42960
rhodamine R derivatives, water (heavy water) detergent solns., luminesc., lasing 79−56836
rhodamine solution, picosec. spectroscopy with antiStokes excitation, orientational rearrangement *(Russian)* 79−42984
rhodamine-B, fluorescence decay meas. via modulated gain spectroscopy 79−64025
rhodamines, solns., amplification and induced absorpt., cross-sections, spectra 77−68208
rhodamines, solutions, electronic absorption spectra and dimeric props. 77−88458
rhodanines, tautomeric, electronic struct. and spectra, MO calcs. 79−13629
rhodopsin, bovine, conform. in situ and solubilised with detergent 77−44587
rhodopsin, bullfrog, thermosensitive prop. 77−25431
rhodopsin, conformeric states, spectrophotometry 77−90725
rhodopsin and intermediates, absorpt. spectra and orientational change of chromophore 78−7321
rhodopsin in digitonin, isolation of 3 isochromic forms 77−52951
rhodopsin kinetics at room temp. meas. by picosec. spectroscopy 77−64036
rhodopsins of oceanic decapods, absorpt. spectra 78−61182
riboflavin, transition moments in 300 nm region 79−53042
riboflavin in various solvents, absorpt. spectra, relative quantum yields, electronic transitions 77−52149
Rochelle salt, optical characteristics in UV region *(Russian)* 78−84550
Rochelle salt, spectra of absorption edge, low-temp. 79−4819
Rose Bengal, appl. of nsec. time resolved photoacoustic spectroscopy 77−74511
rotational diffusion and level kinetics separation in transient absorpt. spectroscopy 77−30877
rubeanic acid, in ethanol and water solns., UV transmission filter characts. 77−3679
rubidium tartrate, optical rot. dispersion, dichroism and spectra, in soln. and cryst. *(Russian)* 77−90124
saturated organic molecule, photolysis, primary step prediction using Rydberg and valence-shell transitions 77−21404
selenophene, flash photolysis, transient absorpt. spectra 80−14153
self-consistent many-body theory, self-energy effect 79−63901
shift in electron levels, method for estimating *(Russian)* 78−46403
silicon phthalocyanine, elec. cond. temp. depend. 80−80271
simple molecules, conformation, electronic spectra, NDDO calcs. 79−85901
sodium uranyl acetate, absorpt. spectra, MCD and natural dichroism, UV and visible 79−69853
solids, cryst. and amorphous, optical spectra, Urbach rule, struct. disorder effect 78−23479

spectra of organic molecules and substances continued
solids, XUV photoabsorpt. spectra, at. effects 80−2785
solutions, electronic and vibr. absorpt. spectra, repulsive intermol. forces 77−79671
solutions, electronic energy level shift estimation 79−54919
solutions, line struct. of broad absorption bands 79−54841
solvent effects, rel. to polarisation structure 80−43062
spiropyrane, triplet-triplet absorpt. by laser photoexcitation 77−10685
spiropyron solutions, nitro-substituted, electronic state participation in photochromy 80−81347
trans-stilbene, cryst., triplet excitons, $S_0 \rightarrow T_1$ transition 78−76518
stilbene, direct photoisomerisation theory, from fluoresc. and absorption spectra 79−79262
trans-stilbene, excited state orientational relax., sub-picosec. pulse obs. 79−50006
stilbene, ps photoisomerisation, time-resolved spectra obs. 79−57252
stilbene, pulsed electron excitation, triplet excitons, spectral and electrical investigations 80−92828
stilbene, radiolysis, electron transfer and protonation, vis. spectra, isomer effects 77−60085
stilbene, trans-, cis-forms, singlet excited state, picosecond dynamics 78−17677
trans-stilbene, two-photon excitation, phantom photochemical singlet, assignment 77−75247
trans-stilbene photoisomerisation, ps dynamics under collision-free conditions 79−91975
strontium formate dihydrate:Cr^{3+}, optical absorption spectrum 80−50380
strontium formate dihydrate, EPR and optical absorption spectra of VO^{2+} ion 77−40112
styrene, anions, in condensed media, electronic spectra 79−22723
styrene, styrene-β-d_2, 288 nm electronic absorpt. spectra, vibr. assignment 79−13738
styrene anions, electron affinities, transition energy, comparison for gaseous liquid and solid 80−29731
styrene-acrylonitrile copolymer solutions, dilute, diffusion coeff., solvent effect 80−19971
styrene-methacrylic acid copolymer, intermol. interaction, conform., composition depend. *(Russian)* 79−23539
sucrose, single cryst., absorption spectrum of electron traps, pulse radiolysis obs. 80−93369
TCNE, semiempirical CNDO calcs. of electronic struct. and absorpt. spectra 78−995
TCNE-substituted benzene complexes, isomers, stability, rel. to charge transfer band intensity 77−68051
$TCNQ^0$, crysts., extraordinary exciton polaritons in refl. spectra, macroscopic dielec. theory 77−89715
TCNQ, adsorption on alumina, adsorption isotherm, ESR and electronic spectra 77−48681
TCNQ, anions, screened INDO model, appl. to UV-visible spectra 79−765
TCNQ, exciton surface polaritons at room temp. 79−47476
TCNQ, metallic reflection band, vibronic struct. 78−19502
TCNQ, salt, $(NMe_3H)(I)(TCNQ)$, semicond. 'metal-like' complex, optical props. 79−95761
TCNQ, semiempirical CNDO calcs. of electronic struct. and absorpt. spectra 78−995
TCNQ, single crystal, exciton surface polaritons, attenuated total reflection spectra 79−91460
$(TCNQ)_2TEA$, refl. spectra 77−90154
TCNQ charge transfer complexes, elec. cond. 79−38058
TCNQ complex salts, optical absorption spectra 79−15486
TCNQ derivatives, intramol. charge transfer, electronic absorpt. spectra obs., electron density calcs. 77−65490
TCNQ donor-acceptor complexes, refl. and absorpt. spectra 79−73965
TCNQ polycation salts, chem. stability determ. from electronic spectra 79−83456
TCNQ salt, HF-TCNQ in acetonitrile, absorpt. spectra, 200-1200 nm 77−83617
TCNQ salt, HMTTF-TCNQ, electron-electron interactions, mag. susceptibility and optical reflectivity 77−81104
TCNQ salt, K^+TCNQ^- particles, light scatt., absorpt. spectra 79−24332
TCNQ salt, MeDABCO$(TCNQ)_2$, elec. cond. and IR and visible spectra meas. 79−42526
TCNQ salt, MeDABCO$(TCNQ)_2$, optical, elec., and mag. props. 80−65539
TCNQ salts, complex, optical absorption meas. 79−4824
TCNQ salts, elec. and optical props. 79−73498
TCNQ salts, electron arrangement in ground state, optical spectra interpretation 78−47715
TCNQ salts, K(TCNQ), Ba$(TCNQ)_2$ and Ca$(TCNQ)_2$, electronic absorpt. spectra, vibronic struct., charge transfer bands 79−24331
TCNQ salts, vibr. and electronic spectra 79−45704
TCNQ salts with alkali metals, optical absorpt. spectra of small particles 78−19505
TCNQ-HMTSeF, polarised single cryst. reflectance obs. and one-dimens. behaviour interpret. 78−6690
TCNQ-perylene, electronic absorpt. spectra, vibronic struct., charge transfer bands 79−24331
TCNQ-TSeF, Drude optical edge, press. depend. 79−19882
Teflon, optical, elec. props., struct., ion textured surface 78−72904
p-terphenyl, saturated vap. press., absorpt. and fluoresc. spectra 79−76442
p-terphenyl, valence electronic structure 79−72360
p- terphenyl cryst., low lying single state 80−97320
tetrabenzo[a, cd, j, lm]perylene evaporated film, crystn., time depend. as function of purity 80−88449
tetracene, disordered solid layer, absorpt. spectra 80−93417
tetracene, in p-terpheny. mixed cryst., low temp. optical phase relax. obs., mechanism 77−52112
tetracene, intrastate scrambling in large mol. bound level struct. 80−63696
tetracene, polycryst. film, thermoelec. absorpt. spectroscopy 79−61451
tetracene in liquid crystal, absorption, fluorescence and polarisation, temp. depend. study *(German)* 80−18887
tetracene single crystals, Davydov splitting, press. depend., phase transition obs. 78−27250
1,2,3,4-tetrachloro-7,8-diphenylcalicene, excited states, moments anal. of electro-optical spectra 79−22698
tetrachlorobenzene, triplet exciton spectral line shape, 2-45K 78−19498
spectra of organic molecules and substances continued
tetrachloromethane, UV laser photolysis 80−66826
di-(tetraethylammonium)tetrahalomanganate, mag. circular and linear dichroism obs. 80−29725
tetraethylammonium triiodide, solvent effects on electronic transitions of I_3^- 77−27080
tetrafluorobenzene, cation, visible emission spectra of gas, Jahn-Teller effect 79−50034
tetrafluoroethylene, electronic struct., CNDO/S2 calcs., photoelectron and UV absorpt. spectra 77−30783
tetrafluoromethane, gas, DID Rayleigh and Raman depolarised scatt., lattice-gas model 80−10356
tetrafluoromethane, photoabsorpt. cross-section, 175-770 Å 77−88462
tetrahedral molecules, vibr.-rot. spectral parameters 77−3341
tetrahydrofuran, optical spectra of solvated electrons, band resolution 79−78698
tetramethyl-1,3-cyclobutanedithione-h_{12} and -d_{12}, visible spectra, $n\pi^*$ transitions obs., mol. vibr. 80−97297
N,N,N′,N′-tetramethyl-p-phenylenediamine-p-chloranil, soln., optical spectra, temp. and environment effects 79−54861
tetramethylbutane in hexachlorobutadiene soln., local mode overtone bands 80−83444
2,2,4,4-tetramethylcyclobutane-1,3-dione, Rydberg transitions, spectra, LCRO calcs. 77−34659
3,6-tetramethyldiamino-N-methylphthalimide soln., hot luminesc. and vibr. relax. 79−22752
3,6-tetramethyldiamino-N-methyphthalimide, in organic solvent, hot luminesc. 79−4842
tetramethylpyrazine, PMMA soln., fluoresc. and phosphoresc. quantum yield and lifetime, 20-120 kbar 79−54902
tetramethylsilane, IR and visible spectral intensity data and the universal intensity concept 80−28066
tetraoxomanganese compounds, electronic spectra of tetrahedral $[MnO_4]^{m-}$ chromophore 77−58032
1,3,6,8-tetraphenyl-pyrene, UV absorpt. spectra, SCF CI method 79−59479
tetraphenylcyclobutane, in hexamethylphosphoric triamide soln., pulse radiolysis, optical absorption decay obs. 79−16019
tetraphenyldithiapyranylidene mixed valence polyiodides, crystalline struct. and optical props. 80−92516
tetraphenylporphyrin, dispersion induced circular dichroism, determ, of mag. dipole allowed transitions 80−14163
s-tetrazine, fluoresc. excitation spectra, 1K rot. struct. 78−1020
sym-tetrazine, mol., isotope spectra, from unseparated natural mixture, spectrosc. technique 79−31736
s-tetrazine, visible absorpt. band assignment, vibr. anal. 78−994
s-tetrazine(-d_1), and $^{15}N_2$-substituted, rot. consts., ground and $^1B_{3u}$ excited states geometries 78−82862
TGFB, IR and UV absorpt. spectra, temp. var. of fund. absorpt. edge 78−84604
TGFB, refl. spectra 4-22 eV, optical consts. 79−4821
TGFB, refractive dispersion, absorpt. spectra characteristics 78−68469
TGS:Fe^{3+} and aq. solns., optical absorpt. spectra 79−82997
TGS, refl. spectra 4-22 eV, optical consts. 79−4821
TGS, refractive dispersion, absorpt. spectra characteristics 78−68469
TGSe, IR and UV absorpt. spectra, temp. var. of fund. absorpt. edge 78−84604
TGSe, refractive dispersion, absorpt. spectra characteristics 78−68469
thermoplastics, wideband optical transmission meas. 79−76771
thermotropic polymers, cholesteric with mesogenic moieties and flexible spacers in main chain, synthesis and light reflection 80−88028
thieno(3,2-b)thiophene, electronic and vibr. spectra, vapour phase and cryst. 77−34654
thiocarbonyl chlorofluoride, second excited singlet state emission spectroscopy, resonance fluorescence obs. 80−69158
thioformaldehyde, and -d_2, $\tilde{A}^1A_2$-$\tilde{X}^1A_1$ visible electronic absorpt. spectra, vibr. anal. 79−45733
thioformaldehyde, elec. dipole moment determ. using elec. field spectroscopy 78−70870
thioformaldehyde-d_0, -d_2, A^1A_2-X^1A_1 vis. absorpt. system, rot. anal. 80−5559
thioformaldehyde-d_0,-d_2, far UV spectrum meas. 2200 to 1800 angstroms 78−25553
thioformamide(-d_2), photoelectron and absorption spectra, vibr. struct., excited state configs. 77−6847
thioindigo dyes, triplet state config., laser flash absorpt. spectrosc. obs. 80−5557
thionine in sodium lauryl sulphate micellar solns., absorpt. spectra and fluoresc. yield, local dye conc. depend. 80−106343
thiophene, flash photolysis, new transient absorption spectrum, C_4H_3 radical, assignments 78−46354
thiophene, mag. circ. dichroism, vis. transitions 77−83628
thiophene, single cryst., UV spectrum, ab initio CI calcs. 79−19898
thiophosgene, a^3A_2-X^1A_1, dye laser excitation spectra, 539 to 610 nm 78−42083
thiophosgene, second excited singlet state emission spectroscopy, Franck-Condon anal. 80−69157
thiophosgene, vibronic anal. of electronic transition, inversion doubling splittings obs. 80−83388
1,2,3-timethoxybenzene, weak electronic transition, solid, and in rigid glass, UV assignments 78−17681
toluene, electronic-vibr. spectra calcs., Franck-Condon and Herzberg-Teller approx. 80−37735
toluene, optoacoustic spectroscopy using cell with ultimate corrosion resistance 80−42269
toluene, visible absorpt. spectra, local mode overtone intensity of C-H stretching mode 79−81207
toluene cation in solid Ar, absorption and photodissociation spectra 80−69156
bis p-toluene sulphonate diacetylene, low-temp. spectral line splitting 77−32397
toluene sulphonate diacetylene, strain dependence of dominant electronic excitation 78−80373
TP-C-DMP, new bifluorophoric laser dye with intramolecular energy transfer, lasing characts. 78−74899
TP-CSC-DMP, bifluorophoric mol. ultrafast intramolecular energy transfer 78−74900
transition metal trinuclear carbonyl complexes, electronic structures, and spectra 79−59480
triacetylene, UV spectra of mol. excited states 79−31540

spectra of organic molecules and substances continued
trialkylammonium, iodides, absorpt. and luminesc. spectra of self-localized excitons 80−97340
triallylarsine, vibr. spectra 79−22696
triallylphosphine, vibr. spectra 79−22696
tribenzo [12] annulene, monovalent anion, MCD and absorpt. spectra 78−70859
tribromomethane-propyl alcohol conc. fluctuation kinetics, holographic study *(Russian)* 78−19508
1,3,5-tribromotrifluorobenzene in gaseous state, emission spectra 80−63648
tricarbocyanine solns., photoisomerisation, fluoresc. and absorpt. spectra of photoisomer 78−85181
sym-1,3,5-trichlorobenzene, cation, emission spectrum, Jahn-Teller effect 79−89681
trichlorobenzene cation, selectively excited wavelength resolved emission spectra 80−87136
trichlorobenzene radical cation, gas and matrix isolated vibr. resolved electronic spectrum 79−68252
trichlorobenzene radical cation, symm. substituted, fluoresc. and emission spectra in Ne matrix 79−89702
trichlorofluoreomethane, UV laser photolysis 80−66826
trichloromethyl peroxynitrate, UV absorpt., spectra, photodissoc. lifetime meas. 80−83386
trichloronitromethane, visible and near UV spectra, 295K, photoabsorpt. cross-section 79−22720
trichloronitrosomethane, visible and near UV spectra, 295K, photoabsorpt. cross-section 79−22720
triethylamine-perfluoro-T-butanol, photoelectron and Rydberg bands, UV spectra study 80−18865
trifluorobenzene, cation, visible emission spectra of gas, Jahn-Teller effect 79−50034
trifluorobenzene cation, selectively excited wavelength resolved emission spectra 80−87136
trifluorobenzene radical cation, symm. substituted, fluoresc. and emission spectra in Ne matrix 79−89702
1,3,5-trifluorobenzene-d_0($-d_3$), cation, emission spectrum, Jahn-Teller effects 79−89680
trifluoroiodomethane, highly excited, intermol. vibr. energy transfer, transient UV absorpt. spectra 80−106381
trifluoroiodomethane, liquefied gas solns. bound exciton model for Rydberg bands 78−31214
trifluoroiodomethane, solns. with liq. Ar, Kr, Xe, CH_4 and CF_4, Rydberg band positions, temp. depends. 78−17686
trifluoroiodomethane, UV absorpt. spectrum broadening by laser-induced vibr. excitation 80−53050
trifluoroiodomethane, vac. UV absorpt. cross section 80−91574
trifluoronitrosomethane, visible and near UV spectra, 295K, photoabsorpt. cross-section 79−22720
1,3,5-trimethoxybenzene, solid, and in 77K glass, electronic absorption spectra interpretation 79−36659
2,4,6-trimethyl pyridine-N-oxide, linear dichroism in liq. cryst. matrix, out-of-plane components 78−17701
trimethylammonium manganese chloride dihydrate, optical absorpt. spectrum, 300K, 90K, cryst. field parameters 78−27253
1,2,4-trimethylbenzene, visible absorpt. spectra, local mode overtone intensity of C-H stretching mode 79−81207
2,2,4-trimethylpentane, visible absorpt. spectra, local mode overtone intensity of C-H stretching mode 79−81207
trimethylsilyl sulphide, UV spectra, assignments 78−46359
triphenyl phosphonium ytterbium chloride, $Yb^{3+}(4f^{13})$ absorpt. spectrum, cryst. electric field splitting 77−73151
triphenylene, triplet state, MIDP and T-S excitation spectrosc. 79−81233
triphenylene positive ion, MCD spectra, test of pairing theorem 79−31565
tris (N,N'-diethyldithiocarbamate) iron II, high field Mossbauer study 79−54873
trypaflavine solutions in polyvinyl alcohol matrix, spectrum-luminesc. characts. 79−13761
TSeF salts, mol. props., one-dimens. cond. salts form. 78−6363
(TTF^+) radical cation, optical props. in mixed-valence and monovalent halide salts and solns. 79−61399
TTF-I_n, single cryst. optical props., polarised specular reflectance meas. 77−12400
TTF-TCNQ, optical evidence for Coulomb interactions, review 78−6704
TTF-TCNQ, Drude optical edge, press. depend. 79−19882
TTF-TCNQ, reflectance meas. at press. to 70 kbar by micro-optic system 77−61133
TTF-TCNQ derivatives, transport props., reflectance spectra 78−91683
TTT salts, charge transfer salts, optical props. 79−61403
TTT salts, charge transfer salts, optical props. 79−73970
TTT-I_n, charge transfer salt, electronic spectra in soln. and solid state 78−2878
umbelliferone, excited states, in ethanol-water soln., absorption and emission spectra 79−13763
uracil film, far vacuum UV transmission spectrum 77−8671
uranyl acetates, cubic crysts., optical spectra fine struct. 77−1693
uranyl propionates, cubic crysts., optical spectra fine struct. 77−1693
UV photoelectron spectroscopy, systematic review 80−28057
vanadium hexacarbonyl, EPR in frozen glasses, optical spectra in soln., solid, assoc., bonding 77−6807
vibrational combination states, ultrashort two-pulse spectroscopy 79−828
vibrational states, visible region thermo-optical spectroscopy 79−50036
vinyl copolymers, containing fluorescent groups, optically active 80−102594
vinyl polymers quenched with electron donor (acceptor) in soln., ionic photodissoc. 79−11800
vinyl sulphides, divalent S linking with multiple bonds, spectrosc. obs. *(Russian)* 78−21929
visual excitation, mol. mechanism for initial process, optical activity in rhodopsin and bathorhodopsin 77−52783
visual photopigments and pseudo-pigments, spectral sensitivity and neural interaction 77−25425
visual pigment and photoproduct spectral absorpt., crayfish rhabdom, pH sensitivity 78−65008
visual pigment long-lived photoproducts, in frog green rod 77−25433
visual pigment model systems, spectroscopy and photochem. 77−32871
visual pigment spectra nomograms, wavelength depend. 77−25430
visual pigments, oil droplets and spectral sensitivity, pigeon 78−11655
visual pigments in isolated retina of chicken and pigeon 77−44667

spectra of organic molecules and substances continued
visual pigments of Gekko, ionochromic behaviour 77−36928
vitamin B_{12} derivatives, vis. and UV reson. Raman spectra, rapid flow method 77−66796
xanthione in benzene, second excited singlet state, ps spectra 77−3399
xanthone, single cryst., polarised UV absorpt. spectra 78−19500
p-xylene, electronic-vibr. spectra calcs., Franck-Condon and Herzberg-Teller approx. 80−37735
p-xylene, visible absorpt. spectra, local mode overtone intensity of C-H stretching mode 79−81207
y_1-base, ground and excited states, dipole moment, CNDO/S and INDO/S calcs. 79−36534
ytterbium etiophorphyrin, electronic energy transfer with porphines and metalloporphyrins, luminesc. 77−474
zinc porphin, in anthracene, triphenylene, n-octane, fluoresc. and optical absorpt. spectra 79−68240
zinc porphin, in n-alkane crystals. at 4.2K, Zeeman spectra for Jahn-Teller instability 78−27256
Ag complexes, Ag(II) porphyrins, picosec. flash photolysis, transient absorpt. 80−52976
anthracene, polycrystalline, optical props., 3.2-9.3 eV 80−76097
2-azaanthracene and methyl derivatives, electron-vibr. props., UV spectra *(Russian)* 77−75177
BeF_2, aq. glass, 76K, solvated electron spectrum evolution, following ns radiolysis 78−88295
CCO radical, heat of form. calc., geometries excitation energies and vibr. freq. calc. using POL-CI wave functions 80−89512
CF_2, time-resolved optical absorption obs. in IR multiphoton dissoc. of CF_2HCl 80−16702
CF_3I, I laser medium, UV absorption profile modification by vibr. excitation, for fusion ignition 78−58717
CH, $A^2\Delta$ state, radiative lifetime 77−34698
CH, C-X system f-values, from obs. of UV interstellar lines 77−45509
CH in F- and G-type stars, bands oscillator strengths rel. to C abundances 77−91530
CH^+, CD^+, $A^1\Pi$-$X\ ^1\Sigma^+$ band system, spectroscopic consts. and radiative lifetimes 78−5237
CH^+, predissociation transition obs. 80−37838
CH_2 radical, fluoresc. induced by laser 588.9-595.6 nm, ($a^1A_1-X^3B_1$) energy separation 78−42121
C_4H_3, in flash photolysis of thiophene, transient absorption spectrum 78−46354
$(C_6H_5)_3AsII_3$, solvent effects on electronic transitions of I_3^- 77−27080
CH_3O_2, radical, form. and decay rates, UV absorpt. spectra 77−48631
CH_3PF_4, nonrigid mol., tunnelling mechanisms, spectrosc. theory 80−78605
CNC radical vibr. and electronic spectra, in VUV photolysis of matrix-isolated cyanomethane 78−85180
CO^+, electronic absorpt. spectrum, rot. lines, laser/ion beam reson. 77−54564
CS_2 in cooled supersonic expansion, electronic absorpt. spectra obs. 80−78629
Cd etiochlorin complex, visible spectrum, intracomplex electron phototransfer, vibr. effects 79−72330
Cl_2, Ar matrix, vibronic dephasing 80−6469
ClCF radical in solid Ar, emission and excitation spectra, vibr. anal. 78−9164
ClFCS, second excited singlet state photophysics, laser excitation obs. 80−32758
Co(II) Schiff base complexes, structure and bonding, book contrib. 80−972
Cr complex, (−)$_D$-tris(ethylenediamine) chromium (III), solid-state circular dichroism spectra, phase modulation spectrosc. obs. 80−93271
Cu complex, L-alanyl-L-serine, PMR, EPR and absorpt. spectra 78−46367
Cu, effect of impurities 80−50925
Cu II complexes, 5-coord., ESR and optical absorpt. spectra 79−64020
Cu(II) complex, 2,2',2"-triaminotriethylamine, EPR and optical absorpt. obs. 80−108055
Cu(II) complex, hexamethyltriaminotriethylamine, EPR and optical absorpt. obs. 80−108055
Cu(II)-DL-proline complex, ESR, magnetic susceptibility and optical absorption 80−93167
1,4-di-[2-(5-n-tolyloxazolyl)] benzene, absorption spectra and stimulated emission dependence on pressure of extraneous gas *(Russian)* 77−50660
2,5-dichloro-p-benzoquinone, adsorption on alumina, adsorption isotherm, ESR and electronic spectra 77−48681
2,12-dimethyltridecahexaene, optical spectra, vibr. anal., rel. to visual chromophore 77−29102
Fe complex, tris (1,10-phenanthroline) iron(II), transient bleaching, excitation wavelength absorpt. 78−73060
p-fluorobenzaldehyde, vap., high-resolution electronic emission spectrum assignments 78−78742
Gd^{3+} in solution, absorpt. spectrum intensity *(Russian)* 78−35169
HCCN, matrix isolation IR and UV spectra, vibr. anal., struct. 77−65457
HCO, prod. by formaldehyde photolysis, vibr. relax., chem. kinetics and spectra 79−11808
HCO, UV matrix isolation spectra, 14K, 210-260 nm, C-X transition 78−62819
Ir complex, tetraethylene iridium chloride, ligand-ligand interactions; low freq. vibr. obs. 78−94255
$Na_3Pr(C_4H_4O_5)_3.2NaClO_4.6H_2O$, single cryst., forbidden $A_1 \rightarrow A_1$ transition, mag. field induced intensification 80−50302
Nd^{3+} complexes, hypersensitive transitions 79−36620
Ni complex, bis-4-dimethylaminodithiabenzyl nickel, tetrachlorethane soln., photochem. and thermal stability 80−16708
Ni complex, bis[3,4,-benzo-N-(S)-sec butylsalicilaldiminato] nickel (II), stereochemistry, De Voe theory 77−14600
Ni complexes, Ni(II) porphyrins, picosec. flash photolysis, transient absorpt. 80−52976
O_2, $b'\Sigma_g^+$-$X^3\Sigma_g^-$ electronic transition, absorpt. coeffs. and transition moments 80−43061
OCS, motion, regular and irregular spectra, theory 80−9590
Pd complex, L-alanyl-L-serine, PMR, EPR and absorpt. spectra 78−46367
Pt complex, $[Pt(dapn)_2][Pt(dapn)_2Br_2](ClO_4)_4$, (dapn=1,2-diaminopropane), optical absorpt. spectra of small particles 79−56812
pyrene, UV spectra and extinction coeffs. for $S_n \leftarrow S_1$ absorption 80−18866

spectra of organic molecules and substances continued
Ru(II) complex, carbonyl(pyridine)-phthalocyaninatoruthenium(II), optical hole burning, matrix effects 80−102522
S compounds, unstable, forbidden transitions, laser optoacoustic spectroscopic obs. 77−61756
Zn porphin, in triphenylene, single site fluoresc. and visible spectra, vibr. assignments 77−58031
Zn-tetraphenylporphine/metal electrode, photocurrent generation mechanism 78−76868

spectra of polyatomic inorganic molecules
see also infrared spectra of polyatomic inorganic molecules; radiofrequency and microwave spectra of polyatomic inorganic molecules; Raman spectra of polyatomic inorganic molecules
Ar_3^+, visible photoabsorpt., pot. energy surface 79−98112
$^{12}C^{16}O_2$, Herman-Wallis coeff. for band affected by reson. *(French)* 77−61805
cryogenic solutions, spectrosc. and photochem. 80−16713
Doppler-limited spectroscopy, $3\nu_3$ band of SF_6 80−58244
electronic absorpt. spectra, band assignments 78−50553
fluorides+He+Ar, VUV spark emission spectra 79−3457
hydrated electron, optical absorpt. spectrum, shape, temp. depend. 77−65489
ice, D_2O, H_2O, intramolecular potential from overtone spectrum anal., H-bonding dependence 79−93972
ice, D_2O-H_2O, intramolecular stretching spectrum, role of Fermi resonance 79−93973
inert gas halide laser, discharge excited, gas composition and lifetime studies 80−53268
inert gas halides, triatomic, optical emission 78−66558
metal hexafluorides, MF_6(M=W,Re,Os,Ir,Pt), ionisation energies and optical spectra in Dirac-Slater model 77−83488
photoabsorpt. cross-section, 175-770 Å 77−88462
strontium halides, absorpt. spectra in air-acetylene flame, using AAS with data processing 78−20102
structure recognition, from IR, UV, NMR and mass spectra, computer method 78−25737
tetrahedral molecules, vibr.-rot. spectral parameters 77−3341
transition metal chlorides, 4d-series, electronic struct. and spectra, multiple scatt. calcs. 77−83486
transition metal cluster carbonyls. fluxionality, collective oscills. and low energy spectra 80−78738
transition metal complexes, mol. dissymmetry, book 80−27057
transition metal tetrahalogeno anions, ligand field spectra, MO model 78−17654
trifluoroiodomethane, UV absorption induced by excitation of ν_1 vibrational mode 78−50552
trihalide anions, VB pseudopot. calcs. on electronic states 77−26984
uranyl complexes, MCD spectra, electronic struct. of lowest excited states *(Japanese)* 79−27014
water, oscill. strengths of UV lines, rel. to abundance in interstellar clouds 78−90104
water vapour, atmospheric, spectral transmission at wavelengths 0.7 to 1 μm 78−85685
XY_2, symmetric triatomic molecules, photodissoc., time depend. theory 78−66610
XY_4 spherical top mols., general rot.-vibr. Hamiltonian formalism *(French)* 78−5192
Ag_n, (n<10), uv-visible absorpt. spectra in Kr matrices 79−13858
AlI_3, UV absorbance, dimer-monomer dissoc. equilib., vap. press. of solid 78−13511
Ar:OCS, liq., dissoc. studies 80−78716
Ar_2F, low-lying electronic states 77−65491
BO_2, laser saturation spatial spectroscopy of diffusion coeff., interaction pot. 77−75341
BrCN, vacuum UV photodissociation spectroscopy, quantum yield, fluoresc. polarisation 80−32736
$BrCl_2^-$, photodissoc. and photodetachment, pot. curves. 79−64060
$BrONO_2$, stratospheric photolysis, UV and IR spectra 78−53227
C_3, electron spectrum, ab initio MRD CI calcs. 78−90089
C_3, Swings band system, absorpt. cross section, oscill. strength meas. 79−98116
CF_2 radical, UV emission in microwave discharge, assignments 77−50461
C_2N_2, and $C_2N_2^+$, electronic struct. UV and PE spectra 80−23304
C_3N_2, valence excitation energy and UV spectra, HAM/3 calc. 78−25454
CNN, matrix isolation spectrum, 2600-1900 Å 78−86880
CO_2 7883 Å band in Venus spectrum, high-dispersion obs. 78−53851
CO_2 gas, electron impact ionisation, electronic fluoresc. spectra 80−95664
CO_2, induced absorpt. spectral moment, mol. calcs. 80−63737
CO_2, K-shell photoabsorption coeffs., 500-600 eV 80−9617
CO_2 laser, transverse double-discharge, spectral characts. *(Russian)* 77−656
CO_2 nighttime luminescence, Venera 9 and 10 spectroscopic obs. in Venus atmosphere 77−78701
CO_2, photolysis, O(^{1}S) absolute quantum yield spectral depend. meas. using XeO luminesc. 80−35561
CO_2 plasma, atm. press. opt. props., 400-1200 nm spectral range and 10^3-2×10^4K temp. 80−33753
CO_2, Π_u symmetry transition probabilities, dipole moment and electro-optical consts. calc. 80−43115
CO_2, spectra, Fermi reson. and classical motion 80−28000
CO_2, valence excitation energy and UV spectra, HAM/3 calc. 78−25454
CO_2 vibr. and translational temp. fields, in gas flow laser, panoramic spectrosc. obs. *(Russian)* 79−12868
CO_2^+, $A^2\Pi_u$-$X^2\Pi_g$ band emission spectrum, rovibronic anal. 80−9613
CO_2^+, photoelectron and ion emission quantum yields, interelectronic state effects 79−6967
CO_2-water vapour mixtures, 2.7 micron band absorption, 1000 to 2200K, 0.25 to 3 atm. 77−58006
CO_2+He, collisionally excited neutral and ionic emission, flowing afterglow 77−51248
CS_2, $^3A_2$ state, triplet bands, MCD spectrum, near UV absorpt. spectrum 80−48010
CS_2, $^3A_2$-state, MCD and UV spectrum, theoretical anal. 80−48011
CS_2, absorpt. spectra, Rydberg series converging to $A^2\Pi_u$ states of CS_2^+ 78−90182
CS_2, as candidate for 3150 Å Venus band 79−40108

spectra of polyatomic inorganic molecules continued
CS_2, electronic transitions, solid phase UV spectra 77−3380
CS_2, high resolution X-ray emission, valence electron struct. and chemical bonding 79−31545
CS_2, in Ar, medium perturbations of extravalence excitations, VUV absorpt. 78−1002
CS_2, laser transition, rel. dipole strengths calcs. 77−61937
CS_2, $\pi\pi^*$ and Rydberg bands, cryogenic solvent effects 78−55182
CS_2, shock heated, visible emission 80−58274
CS_2, solns. with liq. Ar, Kr, Xe, CH_4 and CF_4, Rydberg band positions, temp. depends. 78−17686
CS_2, UV spectra, Stark modulation of a^3A_2-$X^1\Sigma_g^+$ system 79−86003
CS_2^+, electronic transitions, solid phase UV spectra 77−3380
CS_2^{2+}, photodissociation cross section, UV and visible spectral obs. 80−28077
C_3S_2, electronic struct., optical and photoelectron spectra 78−70745
C_3S_2, electronic struct., optical and photoelectron spectra 78−70982
$CdGa_2$, excimer visible emission spectra in RF discharge, vibr. struct. 79−18201
Cl_3^-, photodissoc. and photodetachment, pot. curves. 79−64060
ClCN, vacuum UV photodissociation spectroscopy, quantum yield, fluoresc. polarisation 80−32736
ClNO, phys. and chem. data 78−27727
$ClNO_2$, phys. and chem. data 78−27727
$ClNO_3$, phys. and chem. data 78−27727
ClO_2, predissoc. mechanism determ. from rot. level lifetimes 79−13732
ClO_2, solns., reson. Raman effect and absorption spectra 77−71807
$Cl_2O+H_2O\rightarrow2HOCl$, equilib. const., UV spectrum investig. 79−79238
ClONO, near UV absorpt. spectrum, rel. to atm. chem. 77−30881
$ClONO_2$, form., photolysis in stratosphere, photochem. absorpt. cross sections, UV spectra 77−33154
$ClPF_4$, nonrigid mol., tunnelling mechanisms, spectrosc. theory 80−78605
Co complex, X-ray K-absorpt. edge, ligand field splitting, spectrochemical series 77−10688
Co complexes, Co II tetraphenylporphyrins, constraint, ESR and optical detect. 80−83394
Co complexes, Co(III) mixed complexes, orbital angular momentum reduction, ^{59}Co NMR chemical shift 80−58137
Co_2, electrooptical consts., $2\nu_3$ band induced component 80−78626
$CrAl_3Cl_{12}$, gas, mol. struct., ligand field spectrum *(German)* 78−37762
$Cr(CO)_6$, electronic spectra following flash photolysis, intracavity laser technique 79−31538
$CrCl_2O_2$, electronic transition origin band identification with the van der Waals complex 78−5239
CsI_3, solvent effects on electronic transitions of I_3^- 77−27080
$CsNpF_6$, optical spectrum anal. 79−26963
Cu complexes, electronic transitions polaris. determ. by dichroism in nematic solvents 77−42344
Cu II complexes, 5-coord., ESR, optical absorpt., solvent effects 78−5253
$Cu(CN)_3^{2-}$, UV absorpt. spectra, electronic struct., MO calcs. *(French)* 77−34655
CuCl-Cl^- complex formation, UV absorpt. spectra 77−60064
Cu(II) complexes, electronic transitions, dispersion induced circular dichroism spectra 77−27101
D_3, emission spectra, rot. struct. obs. mol. const. determ., predissociation 80−106331
D_3^+, vibr. spectra, ab initio calcs. 77−83562
DCN, electronic spectra, vibr. struct., ab initio calc. 78−9166
D_2O, Rydberg states, visible spectra 78−9162
D_2O, UV and VUV spectra, 180-790 Å, absolute photoabsorpt. cross-section 77−75182
D_2O, vac. UV absorption spectra, Rydberg series vibr. anal. 78−42093
Er^{3+} amino acid complexes, supersensitive transition intensities, spectra *(Russian)* 77−88461
$ErCl_3(AlCl_3)_x$, vap. complexes, absorpt. spectra, 6000-44000 cm^{-1}, relax. props. 78−62799
FNO, electronic transitions, limited GSMO and ESMO CI calcs., oscillator strengths, spectra 78−70750
FNO_2, UV photoabsorption spectrum 79−10123
Fe complex, $[Fe(CN)_6]^{3-}$, electronic struct., optical transitions, XPS, Mossbauer isomer shift, valence ionisation pot., SCF-MSX calc. 79−6864
Fe_2B_6, UV-visible absorpt. spectrum 78−13512
$FeBr_2$, UV-visible absorpt. spectrum, vaporisation thermodynamics 78−13512
$FeBr_3$, UV-visible absorpt. spectrum 78−13512
Fe_2Br_4, UV-visible absorpt. spectrum 78−13512
Fe_2I_4, vapour phase, UV-visible absorpt. spectra, absorbance peaks 80−994
FeS_2, X-ray and visible spectra, SCF-Xα scatt. wave anal. 78−5138
$GaCl_3(I_3)$, gaseous, Raman spectra, struct., Fermi reson. and thermodynamic functions 77−18929
GaX_3, (X=Cl,Br,I), charge transfer spectra 79−76441
$GeBr_4$, vac. UV absorpt. spectra, 130-270 nm 77−75183
$GeCl_4$, vac. UV absorpt. spectra, 250 to 115 nm 77−79628
GeF_4, ($GeCl_4$), X-ray absorpt. spectra struct. 80−37819
$(GeH_3)_2S$, UV spectra, assignments 78−46359
H^{3+} amino acid complexes, supersensitive transition intensities, spectra *(Russian)* 77−88461
H_3, discrete Rydberg spectrum in hollow cathode discharge 79−68239
H_3, emission spectra, rot. struct. obs. mol. const. determ., predissociation 80−106331
H_3, Rydberg spectrum , theory 80−5528
H_3^+, grazing incidence collision with surface, Balmer radiation, elliptical polarisation 78−86804
HCN ($A^1A''\rightarrow X^1\Sigma^+$), fluoresc. spectrum, using ArF laser excitation 79−36675
HCN, electronic spectra, vibr. struct., ab initio calc. 78−9166
HCN, photodissoc., photoabsorpt., photoemission and CN form. obs. 80−87141
HCN, relationships between higher-transition frequencies 80−69119
HCN, self-assoc., matrix isolation vibr. spectroscopy, complex form. studies 78−62952
HCN, valence excitation energy and UV spectra, HAM/3 calc. 78−25453
HCO, radical formation in acetaldehyde photodissoc., wavelength depend. 79−83490
HD_2^+, vibr. spectra, ab initio calcs. 77−83562
H_2D^+, vibr. spectra, ab initio calcs. 77−83562

spectra of polyatomic inorganic molecules continued
HDO, line strengths and intensities, ab initio calcs. 79−72300
HNF, $\tilde{A}^2A'$-$\tilde{X}^2A''$ emission spectrum 79−50033
HNO^+, vertical spectra, heat of form., ab initio MRD-CI calcs. 79−49934
HO_2, vertical electronic spectrum, MRD-CI calcs. 78−37646
H_2O absorption lines at ruby laser wavelengths, saturation effect 80−4098
H_2O, anharmonic vibr. spectroscopic coeffs. contribs. 78−86846
H_2O, Balmer radiation production by electron impact 0-2000 eV 79−76521
H_2O, excited stretching vibrs., quantum mechanics. 80−91535
H_2O, higher ro-vibr. levels, high resolution flame spectra 77−58033
H_2O, intracavity laser spectroscopy sensitivity, saturation absorpt. influence 79−63312
H_2O, line strengths and intensities, ab initio calcs. 79−72300
H_2O, low-lying excited states, improved virtual orbital calcs. 77−14372
H_2O, Rydberg states, visible spectra 78−9162
H_2O, UV and VUV spectra, 180-790 Å, absolute photoabsorpt. cross-section 77−75182
H_2O, vac. UV absorption spectra, Rydberg series vibr. anal. 78−42093
H_2O vapour, spectral line broadening by N_2, CO_2, Ar, intraresonator laser spectroscopy method 79−54863
H_2O vapour, visible absorpt. spectrum, fine struct. acoustooptical determ. 80−86450
H_2O, weak spectral absorpt. of vap., visible and near IR 80−82062
H_2O^+, electronic spectrum, vibr. levels, rot. consts. 77−473
$H_2O^+ + H_2$, ion-molecule reaction detection of laser-induced ion spectrum, rot. components 78−74671
H_2O_2, UV absorpt. cross sections 78−42086
H_2O_2, Zeeman effect and mol. quadrupole moment, beam maser spectrosc. 78−90152
HOCl, 3200 Å absorpt. rel. to photodissoc. and atmospheric Cl reservoir prospects 79−12207
HOCl, form in Cl_2O+H_2O equilib., UV spectrum 79−79238
HOCl, UV spectrum, stratospheric lifetime rel. to photodissoc. 79−36661
$H_2O(D_2O)$, VUV absorption spectra, Rydberg series, rot. line shapes, quantum defect 78−5244
HO_2NO, UV absorpt., spectra, photodissoc. lifetime meas. 80−83386
HO_2NO_2, gas phase, UV and IR absorpt. cross sections 79−13733
HO_2NO_2, in stratosphere, UV absorpt. spectrum rel. to abundance 78−20467
HPO, in Ar matrix, IR and UV absorpt. spectra 80−47985
H_2S, Balmer radiation production by electron impact 0-2000 eV 79−76521
H_2S, electronic struct., ab initio CI SCF calc., spectra assignments 77−10586
H_2S, ground and excited states, SCF and CI calcs. 77−414
H_2S, liq., optical absorption transients produced by ns pulse radiolysis 79−11803
H_2S, VUV absorption spectrum, Rydberg series assignments 79−64016
H_2S+Ar^+, emission spectra obs. 78−50622
HSO radical, Doppler-limited dye laser excitation spectroscopy, rot., distortion and spin-rot. interaction const. determ. 80−83383
H_2Se, UV absorpt. spectra, 148.3 nm band, rot. contour anal. 77−75179
He+OCS, emission spectra in He afterglow 80−87139
Hg_2 and Hg_3 metastable states in flash photolysis of Hg vapour, electronic absorpt. spectra 79−76438
$HgBr_2$, UV absorpt. cross-sections of vapour 78−25554
$HgCl_2(Br_2)(I_2)$, vac. UV absorpt. cross section 80−91574
$Hg_2(Hg_3)$, violet emission, formation and decay kinetics, luminesc. time resolved spectra 79−76464
HgI_2, UV absorpt. cross-sections of vapour 78−25554
ICN, vacuum UV photodissociation spectroscopy quantum yield, fluoresc. polarisation vacuum UV photodissociation spectroscopy, quantum yield, fluoresc. polarisation 80−32736
$I_2Ne_aHe_b$ van der Waals complexes photodissoc. 80−50864
InX_3, (X=Cl,Br,I), charge transfer spectra 79−76441
IrF_6, in mixed crysts., Jahn-Teller effect, $\Gamma_{8g}(t_{2g})^3$ state, 6800 Å 78−76032
IrF_6, ligand field theory analysis of spectra 79−72248
KCl, spectral interference in at. absorption spectroscopy in C tube atomiser and flames *(Japanese)* 79−48019
$KClO_4$, spectral interference in at. absorption spectroscopy in C tube atomiser and flames *(Japanese)* 79−48019
KNO_3, spectral interference in at. absorption spectroscopy in C tube atomiser and flames *(Japanese)* 79−48019
KOH, spectral interference in at. absorption spectroscopy in C tube atomiser and flames *(Japanese)* 79−48019
K_3PO_4, spectral interference in at. absorption spectroscopy in C tube atomiser and flames *(Japanese)* 79−48019
Kr_2F, absorpt. in near UV wing of 410 nm band, fluoresc. efficiency 80−14323
LiCl, spectral interference in at. absorption spectroscopy in C tube atomiser *(Japanese)* 79−48018
$LiNO_3$, spectral interference in at. absorption spectroscopy in C tube atomiser *(Japanese)* 79−48018
$Li^+NO_3^-$ ion pairs and hydrated ion pairs, MO calcs., matrix isolation data 78−46267
LiOH, spectral interference in at. absorption spectroscopy in C tube atomiser *(Japanese)* 79−48018
Mg complex, bis-pyridal-Mg-tetrabenz-porphyrin, disagreement with diffuse interstellar bands 80−56905
$MnH_2(MnD_2)$, $^6A_1$ state, mol. parameters, ESR and optical spectrosc. 78−94264
MnO_4^{m-} chromophore, tetrahedral, electronic spectra 77−58032
Mo complexes, dinuclear, chem. and spectroscopic props. 77−77239
$Mo_2Br_8^{4-}$, electronic and reson. Raman spectra, Mo-Mo band 78−82745
$Mo_2(CH_3)_2P(CH_3)_2$, δ-$\delta^*(^1A_{2u}$-$^1A_{1g})$ transition, vibr. struct. anal. 80−53006
$Mo(CO)_6$, electronic spectra following flash photolysis, intracavity laser technique 79−31538
$Mo(CO)_6$, polarised absorption, field effects in condensed media 78−997
N_2, spectroscopic data review 77−38680
N_3, spectroscopic data review 77−38680
ND_3, Einstein A coeff. for A→X transition 77−27127
ND_3, hyperfine structure of inversion transitions, molecular beam electric resonance 79−98071
ND_3, predissoc. mol., rot. resolved IR reson. scatt. 77−30882
spectra of polyatomic inorganic molecules continued
ND_3, relax. rates determining the inversion spectra 77−454
N_2D_2, near UV spectrum, vibr. assignment 78−78717
NH_2, A^2A_1-X^2B_1 absorpt. spectrum, 6250-9500 Å, rot. and vibronic anal. 77−472
NH_2, ground state mol. consts., absorption spectra 80−28030
NH_2, optogalvanic spectroscopy in discharge, 570 to 620 nm 79−54862
NH_3, absorption spectra, 6000-6500 Å, intracavity laser detection 79−89684
NH_3, Balmer radiation production by electron impact 0-2000 eV 79−76521
NH_3, $\tilde{C}'$-state, 3-photon gas phase spectroscopy obs. 79−89715
NH_3, excited vibr. states, transition dipole moments, laser Stark spectrosc. 79−68261
NH_3, inversion spectra, ν_4 state 80−47965
NH_3, inversion spectrum collisional line broadening, general theory 80−87184
NH_3, inversion spectrum press. broadening by He and Ar, linewidths calc. 80−95599
NH_3, optical band strengths and curves of growth rel. to spatial distrib. on Jupiter 80−46386
NH_3, relax. rates determining the inversion spectra 77−454
NH_3, self-assoc., matrix isolation vibr. spectroscopy, complex form. studies 78−62952
NH_3-NO mixtures, combustion emission spectra, identification of NH_2, NH, OH, NO by rapid scanning spectra *(French)* 79−52665
N_2H_2, near UV spectrum, vibr. assignment 78−78717
$NH_2^+(^1B_1 \leftarrow {}^1A_1)$ optically-allowed transition position estimation, from UPS data 80−53047
NHD, electronic absorption spectrum, 5750-6450 Å, rot. assignments 79−64013
NHD radical, dipole moment determ., optical Stark spectroscopy 80−23455
$NH_3(ND_3)$ in solid Ar, matrix isolated spectra, temp. dependence 80−63652
NO_2, 6480 Å absorption, rot. anal. 79−45731
NO_2, A-X band system, visible absorption, fluoresc., vibronic coupling 77−58030
NO_2, air pollutant, spectroscopic analysis using scanning tunable dye laser 78−81362
NO_2, core-electron excitation, absorpt. spectrum and CI calcs. 77−75181
NO_2, electronic states, pot. energy surface calcs. 77−6673
NO_2, electronic struct., $A^2B_2 \leftarrow X^2A_2$ and $B^2B_1 \leftarrow X^2A_1$ absorpt. bands 77−3257
$(NO)_2$, heat of form., UV spectrum temp. depend. 78−64872
NO_2, inter and intramolecular radiationless transitions, relax., time resolved excitation and fluoresc. spectra 80−27966
NO_2, laser spectroscopy by cascade photoionisation method in mass spectrometer 80−99496
NO_2, lowest quartet state theoretical excitation energy 79−68221
NO_2, minor atm. components, visible absorpt. spectra, temp. depend. *(French)* 80−36355
NO_2, Ne matrix isolated, 6K, B←X band system 78−993
NO_2, optogalvanic spectroscopy in discharge, 570 to 620 nm 79−54862
NO_2, reson. coherent antiStokes Raman and absorpt. spectra 79−54860
NO_2, shock heated, visible emission 80−58274
NO_2, Stark spectroscopy using CW dye laser 77−38026
NO_2, sub-Doppler spectra, laser-beam system, HFS excitation, radiative, non-radiative decay 78−90210
NO_2, UV photodissoc. quantum yield, absolute absorption cross section 77−90616
NO_2, VUV absorption spectra, Rydberg states assignments 77−58040
NO_2, vacuum ultraviolet absorpt. spectra, absorpt. coeffs. 78−70846
NO_2, vertical electronic spectrum, SCF and CI calcs. 77−30878
NO_2, vertical electronic spectra, ab initio calcs. 78−66538
NO_2, visible fluoresc., rotational structure of vibronic bands 79−98146
NO_2^-, vertical electronic spectra, ab initio calcs. 78−66538
NO_2^+, vertical electronic spectra, ab initio calcs. 78−66538
$^{15,14}NO_2$, predissoc. rot. struct. in 2490 Å band 80−87192
N_2O, absorption spectrum anal. press., temp. quantity and spectral resolution retrieval 79−100462
N_2O, electron impact excitation, ionisation, emission spectrum 77−50469
N_2O gas, electron impact ionisation, electronic fluoresc. spectra 80−95664
N_2O, K-shell photoabsorption coeffs., 500-600 eV 80−9617
N_2O ν_3-fundamental at 4.52 μ, shock wave effective absorption coeffs., empirical determ. 79−64799
N_2O, photoabsorption and photionisation, UV region meas. 78−42087
N_2O, photolysis, $O(^1S)$ absolute quantum yield spectral depend. meas. using XeO luminesc. 80−35561
N_2O, synthetic absorption spectra rel. to quantitative anal. 79−100461
N_2O, valence excitation energy and UV spectra, HAM/3 calc. 78−25454
N_2O+He, collisionally excited neutral and ionic emission, flowing afterglow 77−51248
NOBr, photoabsorption and photodissociation, 190-300 nm 79−50038
NOH^+, vertical spectra, heat of form., ab initio MRD-CI calcs. 79−49934
Na_3, absorpt. spectra, 405-690 nm, mol. beam expt. 79−50031
Na_x, matrix-isolated, formed in supersonic nozzle beam, 400-800 nm absorption and mass spectra obs. 79−76439
Nd complex, with ortho-phenanthroline and $\alpha\alpha'$-dipyridyl tris-trifluoroacetate, absorption spectra 79−98113
Nd^{3+} amino acid complexes, supersensitive transition intensities, spectra *(Russian)* 77−88461
Ni complexes, with CO, O_2 and NO ligands, in NiCa-Y zeolite, EPR, UV obs. 77−63949
Ni_n clusters, Ar matrix, UV-visible spectra pot. energy curves 77−65552
$Ni(CO)_4$, ppb in air meas. by chemiluminesc. detector 80−40692
$(O_2)_2$, struct., energy transfer, high resolution electronic spectra 78−25550
O_3, CI calc., ground and excited states, energy locations, transition probabilities 78−74584
O_3, Hartley band during formation, metastable states, vibr. excitation and relax. 80−55632
O_3, Huggins bands, vibr. anal. 78−42085
O_3, in atmosphere, Chappuis-band absorpt. rel. to conc. determ. 80−77063
O_3, UV absorpt. spectra, IR laser induced changes 80−83385
O_3, UV absorpt. spectrum, Hartley continuum, IR laser induced changes 80−95639

spectra of polyatomic inorganic molecules continued
O_3, UV absorption bands, new vib. quantum no. assignments, based on isotope effect 79−94008
O_3, UV photofragment spectroscopy 79−10122
O_3, vibr. energy anal., form. by recomb. 77−75119
OCS^+, photodissociation cross section, UV and visible spectral obs. 80−28077
ONF, vertical electronic spectrum, CI and SCF calcs. 77−75123
OPCl radical, absorpt. spectra, PO (β and B′-X) systems, vibr, numbering 77−75173
OPF_3, forbidden transitions, mol. beam elec. reson. obs. using avoided crossings 78−29775
O_4* van der Waals complex, radiative lifetime, dimole intensity press. depend. 78−58741
OsO_4, HFS and fine struct., saturation spectroscopy obs. visible spectra 80−53008
PH_3, conc. meas. by vacuum UV absorpt. spectra 80−71972
PH_3, core-excited states, valence-Rydberg mixing and term values, XUV spectra and CI calc. 79−76444
PH_3, vac. UV photolysis, emission spectra 78−46357
$PdBr_n(H_2O)_{4-n}^{2-n}$, electronic absorpt. spectra, band assignments 78−50553
Pr complex, with ortho-phenanthroline and $\alpha\alpha'$-dipyridyl tris-trifluoroacetate, absorption spectra 79−98113
$PtCl_n(H_2O)_{4-n}^{2-n}$, electronic absorpt. spectra, band assignments 78−50553
$Re_2Cl_8^{2-}$, spectral assignment, metal-metal bonds, SCF Xα SW calcs., relativistic corrections 80−53006
ReO_3Cl, near UV absorpt. spectra, dynamical Jahn-Teller effect 78−86881
Ru complex, ruthenium(II) tris(2,2′-bipyridine), absorption spectrum and quantum yield of formation *(French)* 80−5554
Ru complexes, $Ru(NH_3)_6^{2+}$ and $Ru(en)_3^{2+}$ in soln., UV spectra, solvent effects 79−94010
S compounds, unstable, forbidden transitions, laser optoacoustic spectroscopic obs. 77−61756
S_2 and S_3, absorpt. spectra in Ar matrix 79−5149
S_2Cl, blue absorpt. in Ar matrix 79−5149
SF_6, $3\nu_2$ vibr. spectra 78−55183
SF_6, absorpt. structs. in VUV region 79−3458
SF_6, collisionless multiphoton excitation, anharmonic oscill. model rot. effects 78−86845
SF_6, electronic props., (e,2e) spectrosc. obs. 80−5527
SF_6, $L_{II,III}$-absorption spectrum, prethreshold range fine struct. 78−86847
SF_6, multiple-photon absorption, experimental conditions and mol. parameters depend. 80−32790
SF_6, ν_3 bands, rot. fine struct., HFS spectroscopic consts. determ., saturation spectroscopy obs. 80−53008
SF_6, ν_3 mode 2nd vibr. overtone absorpt. spectrum 77−88463
SF_6, population of excited vibr. level, nonequilib. absorpt., 140K *(Russian)* 79−36708
SF_6, rot. spectra, asymptotic level clusters, quantum model 77−23490
SF_6, spectroscopic consts. calc. from saturated absorption spectrum *(French)* 78−971
$S^{16}O_2$,$S^{18}O_2$, (0,0) band rot. anal., a^3B_1 state electron spin fine struct. consts. 77−10687
SO_2, absorption spectrum, meas. using frequency doubled pulsed dye laser 80−87144
SO_2, absorption spectrum, meas. using frequency doubled CW dye laser 80−87145
SO_2, minor atm. components, near UV absorpt. spectra, temp. depend. *(French)* 80−36355
SO_2, shock heated, visible emission 80−58274
SO_2, spin-forbidden singlet-triplet transition, appl. of high-resolution spectroscopic technique 77−22601
SO_2, UV absorpt. meas. using lithium formate monohydrate freq. doubling system 79−31979
SO_2, UV absorpt. spectrum, triplet states, phosphoresc. lifetime 79−50042
SO_2, UV excitation spectra, mol. fluoresc. meas., mol. predissoc. obs. 80−83389
SO_2, X→A electronic absorpt. band system, non Condon effects study 80−18837
SO_2+Ar^+, emission spectra obs. 78−50622
SO_3^{2-}, SO_4^{2-}, O K-emission spectra, electron struct. 80−87099
S_2O, 3400 Å bands, rot. anal., upper state struct. 78−13506
S_2O, UV excitation spectra, mol. fluoresc. meas. 80−83389
$SOCl_2$, photoabsorotion and photodissociation, 190-300 nm 79−50038
SO_2Cl_2, photoabsorption and photodissociation, 190-300 nm 79−50038
SeO_3^{2-}, SeO_4^{2-}, O K-emission spectra, electron struct. 80−87099
Sf_6, high resolution X-ray emission, valence electron struct. and chemical bonding, LCAO comparison 79−31545
$SiBr_4$, vac. UV absorpt. spectra, 130-270 nm 77−75183
$SiCl_2$, band system reassignment to PO and P_2 radicals 77−23505
$SiCl_4$, vac. UV absorpt. spectra, 250-115 nm 77−79628
SiF_3, 2100-2700 Å spectra 77−54512
SiF_4, ($SiCl_4$), ($SiBr_4$), X-ray absorpt. spectra struct. 80−37819
SiF_4, XUV spectra, overlapping core-valence and core-Rydberg transitions and resons. 80−32735
SiH_4, core-excited states, valence-Rydberg mixing and term values, XUV spectra and CI calc. 79−76444
$(SiH_3)_2S$, UV spectra, assignments 78−46359
SiO_2, Si K_α X-ray emission spectra chemical shifts, linewidths and intensities 78−13461
Sm complex, with ortho-phenanthroline and $\alpha\alpha'$-dipyridyl tris-trifluoroacetate, absorption spectra 79−98113
$SnBr_4$, vac. UV absorpt. spectra, 130-270 nm 77−75183
$SnCl_4$, vac. UV absorpt. spectra, 250 to 115 nm 77−79628
SnX_2 (X=Cl, Br, I), UV absorpt. cross-sections of vapour 78−25554
$TbCl_3$-$AlCl_3$, vap., high-energy laser medium props., for fusion ignition 78−63075
$Tc_2Cl_8^{3-}$ ion, visible spectra, electronic struct. 78−5240
TcO_3Cl, near UV absorpt. spectra, dynamical Jahn-Teller effect 78−86881
TeO_3^{2-}, TeO_4^{2-}, O K-emission spectra, electron struct. 80−87099
ThF_4, absorpt. spectrum of vapour, Th reson. localised 5,epsilon f state 80−91467
$TiCl_4$, optical and Ti 2p core photoemission spectra, SCF Xα anal. 79−94032
$TiCl_4$, photoelectron and UV spectra, SINDO theory 77−50360

spectra of polyatomic inorganic molecules continued
$U(BH_4)_4$, IR and UV spectra of gas phase 78−62798
UF_4, absorption spectrum indicating presence of resonantly localised continuum state 80−58173
UF_6, 360 to 420 nm absorpt., intraresonator laser spectroscopy technique 77−50448
UF_6, $3\nu_2$ vibr. spectra 78−55183
UF_6 ($^{235,238}U$), vibrational overtone spectra calc. 78−66534
UF_6, electronic struct., relativistic MS Xα calc. 79−85911
UF_6, emission and absorpt. spectra at 80 to 600 nm, decomp. products 77−23212
UF_6, fission fragment excitation of optical radiation 77−23665
UF_6, gas, laser-induced fluoresc., A-X band 78−94275
UF_6, matrix isolation spectra and photolysis 79−50043
UF_6, multiphoton irradiation, spectra and modeling of laser induced emission 80−69160
UF_6, photophysical props., laser study 80−28040
UF_6, UV spectra, electronic and vibronic states in gas and solid phases 77−14445
UF_6, vap., high-resolution spectroscopy by density modulation and UV spectrum 77−31023
UO_2F_2, ^{18}O isotope effects on electronic spectrum, temperature effect 79−31541
$UO_2(NO_3)_2.6H_2O$, 420 nm absorpt. band, electronic-vibr. struct. calc. 79−10119
VCl_4, photoelectron and UV spectra, SINDO theory 77−50360
$W(CO)_6$, electronic spectra following flash photolysis, intracavity laser technique 79−31538
WF_6, electronic structure, SCF-Xα-SW calcs. 77−26974
XeF_2, photodissoc. yield in solid Xe and Kr, time-resolved photolum. excitation obs. 80−3372
XeOH exciplex, UV emission 78−37653
Zn complex, Zn-TMP-pyridine, burning out of valleys in absorpt. spectra 79−76440
Zn complex, Zn-tetraphenylporphine, absorption spectra fine struct., hole-burning method 77−88594
$ZnGa_2$, excimer visible emission spectra in RF discharge, vibr. struct. 79−18201

spectra of solids
see also impurity and defect absorption spectra of solids; luminescence of solids; Shpolskii spectra; spectra of inorganic solids; spectra of organic molecules and substances
absorption band struct. resolution by using complex dielectric const. 78−72546
absorption coefficient under laser irrad. 80−34940
absorption spectra meas. using compact vacuum vessel-cryostat 77−41689
adsorption behaviour at solid/liq. interface, IR spectra study 80−40733
amorphous semiconductor, configuration-coordinate model, Urbach rule 80−34948
amorphous semiconductor or insulator, optical absorption 77−90167
amorphous semiconductor with Gaussian random pot., exciton effects on absorpt. spectra 77−16273
amorphous semiconductors, props., principles and appl., w.r.t. electronic band states *(Japanese)* 79−23979
amorphous solids, optical absorption tail, shape 80−34946
anisotropic crystal, refl. spectra, phase difference determ., Fresnel formula validity 77−43956
anisotropic transition layer, surface polariton spectra in presence of resonance 80−88484
antiferromagnet, 1-dimens., two-spin IR absorpt., Green's function and classical moments theories 77−40025
antiferromagnetic, light absorption in freq. region of exciton and exciton-magnon transitions 77−48149
antiferromagnetic extended Hubbard chain, excitonic effects on optical absorption 79−61323
aromatic compounds and oxygen, at 10K, contact charge transfer interactions 77−46637
band shape, quadratic electron-phonon interaction effect 77−32342
biexcitons, nonlinear laser spectrosc., multiphoton transitions 80−84433
bistability and anomalies in absorption and resonance scattering of intense light 79−95803
Brillouin zone scheme 78−15190
broadening, inhomogeneous and homogeneous, of optical and ODMR transitions in solids 80−32750
chemical reacts. in condensed phase at low temps., at.-mol. transforms. 77−25253
chemisorption systems, IR spectral linewidth and sticking coeffs., nonadiabatic effects 80−39423
composite materials, review 78−56496
composite materials, small particle, optical props. 78−56445
conference, basic optical props. of materials, Gaithersburg, MD, USA (May 1980) 80−101668
conference, Krusevac, Yugoslavia, Sept. 1978 79−56104
convalent crystals, fundamental absorption band struct. in quasimolecular model 77−24868
cubic crystal Zeeman anisotropy in absorpt., emission and MCD, eigenfunctions 77−55773
cubic crystals, Raman scatt. from tunnelling of substitutional molecules 80−40107
diamagnetic excitons in crossed mag. and elec. fields, optical absorption 78−10874
dielectric, photon induced relativistic band struct. 77−32462
dimerized interrupted strand model, optical absorption 77−16271
dipole absorption due to electron-electron interaction of electrons occupying Landau levels 78−27195
disordered, optical props. 79−42936
disordered solid, IR and Raman spectra, analytic models 80−7336
disordered solids, harmonic approx. for vibr. spectra 78−51635
disordered systems, optical energy transfer 78−92105
dust, soil derived atmospheric, IR spectra, Christiansen effect, Rayleigh limit 80−105046
dynamic Jahn-Teller systems, calc. of absorption band shapes, use of Lanczos algorithm 80−45023
electronic states determ. using synchrotron radiation 77−20882
electronic transitions, optical dephasing times and line shape functions 78−35162
exciton absorption peak, temp. depend., calc. 80−59885
exciton absorption range, spatial dispersion theory *(Russian)* 79−61405
exciton reflection of light for arbitrary surface pot. 79−38568

spectra of solids continued
exciton resonance region, energy density and flux 78−48201
exciton resonance region, energy transfer by normal modes 77−89705
exciton system, Bose condensation and optical props. of condensate 77−55485
exciton-phonon parameters from absorption band shape *(Russian)* 77−28533
exciton-phonon system, exciton peak position, temp. depend. *(Russian)* 79−37777
exciton-phonon system, spectral parameter calc. *(Russian)* 78−43311
exciton-photon interaction, exciton absorpt. lineshape, polariton and wave models 79−38564
excitonic state of assembly of double mol. chains oriented in non-reson. matrix, optical response *(French)* 78−10358
excitons, optical absorption 77−80734
excitons and related states, conf., Tomakomai, Japan (Sept. 1975) 77−43510
excitons in semi-infinite crystals, microscopic calc. of optical refl. 79−69430
Fermi resonance theory 77−1666
ferroelectric semiconductor, vibronic, interband light absorption 78−72555
ferromagnetic semiconductors, giant blue shift of absorption edge *(Russian)* 77−32401
Fourier transform spectroscopy appl., far IR 78−58069
Frenkel biexcitons, eigenstates and transition spectra 80−88480
Frenkel excitons, kinematical interaction at light absorption and luminesc. 78−10359
g-shifts, correl. with optical absorption spectra 78−23485
gelatine films containing AgBr, effect of AgBr comp., aging, UV exposure *(Russian)* 79−67408
gravitational radiation, HF, by normal modes of crystalline solids 77−2586
high density excited system, population instability and optical anomalies 79−28826
homogeneous linewidths in ODMR and optical transitions, connection 79−91316
Hubbard chain, half-filled band, strong coupling, low temp. absorpt. lineshape 77−59546
Hubbard chain, low-density, intraband absorption 77−24809
Hubbard model, extended, optical absorpt. spectra 77−20812
inner level spectroscopy with synchrotron radiation, theoretical aspects, book contrib. 80−4778
interband light scattering in semimetals and semiconductors *(Russian)* 78−60485
interstellar grains, interaction of light with small-particle system 77−74111
ion beam heated thin targets, soft X-ray and VUV spectra 80−2907
ionic crystals, lattice defects, conference, Canterbury, England (Sept. 1979) 80−105420
IR ν_s absorption band profile of isotopically diluted OH group in crysts. 79−69821
IR absorption mechanisms 78−60460
IR absorption mechanisms for crystals 78−80329
IR and Raman two-phonon, morphic effects, appl. of irreducible representations in symmorphic space groups *(Japanese)* 79−77541
IR reflection spectrum, dispersion formula fitting, Kramers-Kronig anal. 80−50311
Jahn-Teller effect, equal coupling to ε and τ_2 vibrs., Γ_8 quartet 78−2454
Jahn-Teller system, lattice relax., photo-absorpt.-luminesc. polarisation correl. 77−51708
Jahn-Teller system of E-e species optical response 77−35898
layered compounds, book 77−39757
layered crystal, light absorption by excitons, interlayer hoppings *(Russian)* 78−68532
layered semiconductor plate, exciton light absorption *(Russian)* 77−85750
lectures on interaction of radiation with condensed matter, Trieste, Italy (Jan.-March 1976) 78−27172
linear conductor, diagrammatic calc. of IR props. 77−32374
linear conductor, IR absorption, amplitude and phase mode dynamics 77−16313
localisation criteria 79−15110
localised centres, reson. scatt. and absorpt. *(German)* 79−65848
localised electron nonequilibrium vibration interaction secondary radiation spectrum 80−2778
low temperature absorption spectra, thermal detection 77−74522
magnetic chains with X-Y symmetry, anharmonic effects and IR singularity 77−32146
metals, chemisorption of gases, book 79−69370
mixed crystal, line profile of absorpt. and Raman spectra, calc. 78−48183
molecular crystal, calc. of second-order susceptibility, using electronic spectra data 80−29756
molecular crystal, light absorpt. with excitation of singlet and double triplet excitons *(Russian)* 77−15773
molecular crystal, principal axes of tensor of polarisability derivs., spectroscopic determ. *(Russian)* 77−85683
molecular crystal, Stark modulation of Lorentzian line shapes, Fourier anal. 77−1691
molecular crystal spectroscopy, 1975 bibliography 77−77159
molecular crystalline slab 77−8534
molecular crystals, biexcitonic level splitting 78−10362
molecular crystals, charge transfer exciton-phonon interactions 77−84857
molecular crystals, energy transport dynamics, picosec. transient-grating method 78−72079
molecular crystals, exciton interband transitions absorpt. band shapes 77−20876
molecular crystals, optical absorpt. line shape of excitons, two-time correl. function calcs. 79−44795
molecular crystals, optical props., struct. disorder effects 78−52525
molecular crystals, spectroscopy, bibliography (1977) 80−7317
molecular crystals, two particle exciton-phonon interactions, optical absorpt. line shapes theory 80−55120
molecular crysts., extraordinary exciton polaritons in refl. spectra, macroscopic dielec. theory 77−89715
molecular motion, submillimetric-wave spectroscopy obs. 79−31517
monoclinic crystal, refl. spectra dispersion anal. 79−99877
monoclinic crystals, IR refl. spectra 79−78676
monomolecular layers, Langmuir-Blodgett, mol. orientation determ. by IR absorpt. 79−11423

spectra of solids continued
Mott transition, optical criterion 78−75996
multiphoton absorption, intense field effects 78−10921
non-equilibrium phonon distrib., in cryst., spectral line shape theory 80−60530
noncrystalline materials, optical props., lecture 78−27263
noncrystalline materials, optical props., lecture 78−31219
nonequilibrium free carrier distrib. in EM wave field, luminesc. intensity and IR scatt. cross section 79−69888
nonpolar molecular crystal phonon sidebands, Green's function mol. model 79−37779
one dimensional Hubbard chain, optical spectrum 78−10920
one-dimensional conductor, incommensurate, IR absorpt. peak theory 77−43991
optical transitions, radiation induced, choice of gauge 77−27001
phonon-assisted radiative electronic transitions 79−24348
phonon-assisted radiative transfer 77−90192
phonons and polaritons, general lecture 78−26638
photoacoustic measurement of spatially varying absorpt., theory 77−32341
photoacoustic spectroscopy, freq. depend., surface and bulk absorpt. coeffs. 77−53981
photoacoustic spectroscopy of solids, theory 78−65975
photoacoustic spectroscopy of solids immersed in transparent liquids 80−22452
photon echo spectroscopy of crysts., review 80−83648
piezoelectric semiconductor, optical absorpt. by free polaron 77−59547
piezoelectric semiconductor, polaron optical absorpt., external static elec. field depend. 77−85158
plastic crystal, dipolar autocorrelation function, phonon contrib., IR absorption 78−42928
polariton kinematical levels resulting from excitons interaction, optical absorption line broadening 80−10892
polariton systems with minimum group velocity, time-depend. optical spectrosc. obs. 78−80376
polarons, effective mass and optical absorpt. spectrum, f-sum rule 77−43520
quantum EM processes, population var. and natural radiative decay *(Russian)* 77−32343
quasi-Jahn-Teller optical absorption line shape due to transition from A_{1g} to $(A_{1g}+T_{1u})\times t_{1u}$ system 80−92862
reflectance spectra, correction for spectrometer polarisation 77−22603
reflection spectra, phase correction in Kramers-Kronig anal. 79−56815
resonant secondary radiation of excitons strongly interacting with phonons 79−60724
second order optical processes, stochastic models of intermediate state interaction, stationary response 77−85769
second order optical processes, stochastic models of intermediate state interaction, stationary response 77−85770
self-diffraction of light by excitons 80−53389
semiconducting solid solutions, optical transitions, review 78−2908
semiconductor, absorption of EM and sound waves in strong coupling case, effect of acoustic superlattice 78−26630
semiconductor, carrier concentration distribution by scanning IR absorption 79−61356
semiconductor, characts. of two-photon absorption under reson. conditions 77−90170
semiconductor, conjugated, one-dimens., vibronic coupling, Fano interference effects 80−34939
semiconductor, core level spectra, electronic polaris. effects 79−90985
semiconductor, cubic, noncentrosymmetric, electrooptic effect 79−69812
semiconductor, diamagnetic excitons, odd states, oscillator strengths and optical absorption line positions 79−11072
semiconductor, direct-gap, final state interactions in gain and absorpt. spectra of electron-hole liq. 78−43305
semiconductor, disordered, electroabsorption, contact excitons influence 80−10882
semiconductor, electron excitation spectra in field of two travelling waves 80−65514
semiconductor, electron excitation spectrum in resonance field of standing EM wave *(Russian)* 77−63386
semiconductor, EM properties, general lecture 78−27173
semiconductor, excitonic surface potential 78−76000
semiconductor, film or wire, intraband light absorpt. by degenerate electron gas *(Russian)* 77−44077
semiconductor, fundamental light absorption, in field of strong EM wave 77−52032
semiconductor, impurity-level assisted two-photon interband absorption of laser radiation 78−23464
semiconductor, interband absorpt. in strong parallel mag. and elec. fields 79−78063
semiconductor, interband optical absorption with one-dimensional electronic superlattice 79−15483
semiconductor, IR absorpt. and optical relax. time of free carriers 80−66206
semiconductor, light absorption, temp. depend., exciton-exciton and -phonon interactions *(Russian)* 77−40265
semiconductor, light pulse propag. inducing transitions between bands with different effective masses 80−34871
semiconductor, many-photon absorption by intraband transitions in mag. field 78−27261
semiconductor, optical parameters in strong EM field, effects of finite wavelength of light 77−44050
semiconductor, optical phonon generation on intraband absorpt. of EM radiation *(Russian)* 77−48235
semiconductor, optical transform. of biexcitons 77−62844
semiconductor, quasi-one-dimensional, light absorpt. and Raman scatt., large exciton form. 77−16272
semiconductor, reson. in fundamental absorpt. region, quasi-mol. model interpretation 78−76490
semiconductor, self-oscillatory medium, modelling 77−20811
semiconductor, three-band, absorpt. of weak EM wave in presence of intensive one 79−61325
semiconductor film with surface states, light absorption under superhigh vac. *(Russian)* 78−72618
semiconductor solid solution, compositional disorder, free carrier absorpt. 78−64387
semiconductor with nonspherical bands, diamag. excitons and Franz-Keldysh effect 78−72554
semiconductor with superlattice, two-photon absorpt. 77−16331

spectra of solids continued
semiconductors, disordered, phonon-assisted interband optical absorption 80−34947
semiconductors, IR absorpt. of light by polarons 79−56799
semiconductors, quasienergy spectrum, polarisation depend. in field of strong EM wave 79−69415
semiconductors and insulators, nonequilib. electron Coulomb collisions during optical pulse interband interaction 80−76049
semiconductors free-carrier concentration, contactless meas., IR polarimeters, Faraday effect 77−73135
small metal particles, inorganic and organic, review 80−45106
small particles, optical absorpt., sum rule for polarisability 77−28532
solid state spectroscopy using synchrotron radiation, book contrib. 80−7375
solid-state theory, introduction, book 79−33215
solid/gas interfaces, in situ Fourier transform IR spectroscopy 80−37100
spatially dispersive medium, exciton polaritons, absorption theory 80−54618
spin-Peierls dimerised Hubbard chain, optical absorption spectrum 79−60677
sputtered coatings, optical props. *(Russian)* 77−69924
surface, light interaction effects and spatial dispersion role *(Russian)* 78−23481
surface, rough, optical emission due to electron irrad. 78−60529
surface analysis, atomic beam scatt., SIMS, and vibr. spectra, book contrib. 79−42357
surface polaritons, nonlinear optical spectroscopy, stationary and nonstationary, theory *(German)* 80−6922
surface science conference, Cambridge, England (March 1979) 80−36773
surfaces, optical examination and monitoring, review 79−67375
temperature dependence, transport eqn. 78−23421
tetrahedron method for evaluating spectral props. of solids 80−10855
thermal broadening, inhomogeneous, of crystal vibr. spectrum 80−55100
thin crystal, interference spectra, size quantisation of excitons 78−47708
thin film heterostructures, optical transition selection rules 80−66319
thin films, IR absorption spectra rel. to microporosity and absorptivity 80−9053
transmission and reflection spectra, 100 to 400 nm, using vac. double-beam spectrophotometer 79−75624
triclinic crystals, polarized IR spectra, vibr. transition moments 77−85720
triple optical reson. in crystal, weak absorpt. struct. in IR field 77−24808
two-phonon transitions, phonon assisted, in mag. field, four-band model 77−36260
two-photon absorption coeff., polarisation depend. 78−80379
Urbach's rule derived from thermal fluctuations in the band-gap energy 79−33729
vibration spectra and crystal symm., book 77−24365
vibrational relaxation of molecules in condensed media, survey, book contrib. 77−36295
wave vector selection rule table construction, use of induced compatibility tables 77−19887
wire, exciton energy spectrum and light absorption *(Russian)* 77−62832
zero-gap semicond., IR absorption coeff., theoretical anal. 80−20641
H-bonded crystal, IR absorpt. spectra band shape, X-H stretching vibr. temp. depend., isotope effect 78−76445

spectral analysers
see also spectral analysis; transient analysers; wave analysers
4-channel analyser for use in Thomson scattering diagnostics of plasmas 80−31905
32-channel filter analyser for radioastronomical investigations *(Russian)* 77−29653
40-channel quartz filter analyser for radio spectrometer *(Russian)* 77−22566
acoustic noise meas., unsteady, from letter-handling machines, automatic classification of noise levels 80−79085
acousto-optic parallel channel wideband receiver 80−48447
acousto-optic spectrum analyser for radar signal processing 78−78942
acousto-optical processors for wideband electronic signals 78−79137
acousto-optical snapshot Pockels Readout Optical Modulator 77−19193
acousto-optical spectral analyser at RATAN-600 radio telescope, first test *(Russian)* 80−51668
acousto-optical spectrum analyser for radioastronomy, expt. *(Russian)* 77−29652
acoustooptic snapshot PROM, real-time optical, signal spectrum analyser 78−90494
advantageous use 77−34005
amplitude accuracy limitations 79−1042
arc discharges, periodic processes, spectral emission characts., vidicon system investig. *(Russian)* 78−9848
astronomical automated spectrum scanner, 3000-11000 Å region 79−53724
audio spectrum analyser HP3582A using digital signal processing 80−43567
carotid artery imager, CW Doppler US and spectrum analyser 79−57731
circuit component LF noise meas. arrangement 77−13776
coherent light valve optical processor for GHz bandwidth signals 78−78937
coherent light valve processor, two-dimens. optical modulator 80−102840
coherent optics system, use of spatial filtration *(Russian)* 80−28164
CROs, plug-in type used for spectrum and logic analysis, timers, computer interfaces 77−41648
cross-power spectrum analysers, satellite-borne, appl. to ionospheric plasma wave meas. 80−94621
curve synthesizer SK-2 for resolving spectral curves into components 78−73980
digital, noise.vibtation meas., Bruel & Kjaer products review 78−94493
direct readout system for clinical and research purposes 78−3488
directive acoustic spectrum analyser using moving microphones 78−66992
Doppler US decompression data, divers, spectral anal. of bubble transients 77−70513
Doppler-shift blood-velocity waveforms, real-time spectrum analyser 79−88145
double-exposure technique improves spectrum analyser photographs 78−12714
EEG, absolute value of amplitude, hold facility 77−44792

spectral analysers continued
EEG monitor using Walsh transform on standard microprocessor 80−26399
electroacoustic, analytic and diagnostic equipment 78−63249
EM analyser control, automatic registration of the back-scattered ions 80−18042
EM waveforms, utilisation theory and practice 77−65029
EMG quantitative analysis instrument 78−81041
equalizing and coherence measure correlators 79−13911
FFT analysers, high real time, applications 79−1041
film waveguide spectrum analyser with prism coupling 77−62071
Fourier, using light polarization discrimination technique combined with chirp-Fourier transform algorithm 80−74310
frequency analyzing equipment, device for scientific education in oscillatory phenomena 78−41126
frequency meas., accuracy improvement *(French)* 77−65023
frequency overlap requirements and detectability 79−1032
frequency-variant signal waveform processing using 2-D optical processors 80−48178
gated optical multichannel analyzer for tune resolved spectroscopy 77−74516
GenRad 2512, simplicity of operation due to interactive display, technical specifications 80−64326
geodesic lens design for integrated optics signal processing 80−33247
guided-wave optical systems and devices, seminar, Washington, USA (April 1979) 80−31418
HF, Anritsu Electric MS62A/A3/B/B3 instrums., operation and characts. 77−37927
high speed, vessel noise freq. anal., comparative advantages *(Croatian)* 79−55278
image Fourier transform correlator using US light modulator *(Russian)* 77−58264
improved RF instruments 77−41585
integrated acousto-optical spectral analyser waveguide geodesic lens correction 79−50241
integrated optic, design of Bragg cells 80−74515
integrated optic Bragg spectrum analyser design 80−33237
integrated optic spectrum analyser design and fabrication 79−72720
integrated optical circuit for Fourier transform 77−39111
integrated optical RF spectral analyser acousto-optical readout scheme 79−50446
integrated optical RF spectrum analyzer, feasibility 78−5431
integrated optical spectral analyser design and fabrication 79−50445
integrated optical spectrum analyser, 1978 advancements 79−46086
integrated optical spectrum analyzer dynamic range, waveguide scatt. effect 78−59163
integrated optics, broadband chirp transducers 80−74514
integrated optics version, SAW Broadband modified chirp transducers appl. 80−58802
integrating real-time noise analyser for portable field operation 79−1037
Josephson junction, discriminating props., use in microwave spectral anal. 77−49748
kit of instruments for statistical research 78−87215
laser emission power fluctuation statistical meas. system 77−79881
laser flash absorption change kinetics spectroscopy at 820 nm, photosynthesis study appl. 78−92769
laser output spectrum, high resolution meas. 80−95891
LF, operation and appls. 77−37926
LF real-time spectral analyser design and operation *(French)* 78−20538
LF spectral analyser with HF SQUID, threshold sensitivity 78−41328
low-temp. plasma diagnosis by laser scatt. method, image convertor and spectral analyser device 79−4180
microwave, portable, type 7L18, 1.5 GHz to 60 GHz 78−93675
microwave spectrum analyser model 7L18 79−30487
microwave spectrum analysis, using microcomputer 78−41329
million channel 300 MHz bandwidth digital spectrum analyser for Deep Space Network and SETI 78−73642
modulation-interference spectrum analyser 77−79161
MS62 series description 78−49861
multichannel, 1 to 300 kHz range, plasma diagnostics appl. 77−39455
multiple beam spectral analyser with thin film waveguide feed, prism radiation tap 77−34944
ocean wave measurements, analogue spectrum analyser system for operational buoys 79−5662
operation and applications 79−50516
optical, log-freq. variable resolution system using holographic mapping 77−638
optical, synchronous dual-channel processing 79−72499
optical analogue processing system appl. *(Spanish)* 80−95822
optical laser oscillator radiation, spectrum analyser for 77−26403
optical line image transmission through single fibre using spectral instrums. 80−102820
optical mixing spectra, real-time analysis system 79−67392
optical power spectrum sampling and nonparametric pattern recognition algorithms 78−63032
optical spectra meas. using SAW spectrum analyser 79−21819
optical superheterodyne spectrum analyzer with triggered photon counting method 79−80691
optical waveguide lens technologies for RF spectrum analyser 77−34961
phoneme discriminator for automatic discrimination of fricative consonants based on human audition 79−55286
photodetector noise power spectrum density meas. 78−21197
plasma turbulence meas. with spectrum analyzer and differential amplifier 77−43081
portable digital spectrum analyser by GenRad, Model 2512 78−57933
principal error classification and assessment 78−41326
real time anal., FFT appl. *(Spanish)* 80−90825
real-time analyser with on-line definition of confidence levels 77−73959
real-time frequency analysers for acoustic noise control 78−83192
repetitive photoelec. scanning system for high resolution optical spectra accumulation 78−54456
RF frequency spectrum visible display using optically pumped cell 77−65027
RF spectral analyser using integrated optics 77−27389
SAW chirp filters based Fourier transformation processors 79−7270
SAW integrated optics spectrum analyser, development progress 80−58803
SAW spectrum analyser, digital signals processing 78−26007
SAW spectrum analysers in photon-counting mode, statistical props. 80−105712

spectral analysers continued
self-scanned photodiode array, evaluation for integrated optics spectrum analyser 80−58806
signature analysis systems with Fourier analyzer 78−87195
six channel radiometer for spectral investigations of terrestrial and planetary atmospheres *(Russian)* 77−29468
spectrum analyzer employing SAW chirp filter *(Japanese)* 80−79065
speech disorder evaluation using basilar membrane electronic model 78−40206
survey of currently available models 79−1040
swept-frequency heterodyne receiver with CRT display *(Spanish)* 77−37875
TAC-MCA systems, distortion of spectra by measuring process 79−63877
teaching apparatus, evaluation of Pasco Model 9302 77−9842
time- and space-integrating, acoustooptic system 80−9983
US blood flow spectral anal. using coherent optics 78−53459
US blood flow spectrum, coherent optical anal. 77−40722
US Doppler signal, calc. of blood flow 78−44573
US Doppler signals, real-time spectrum analyser, medical appls. 80−36040
US light modulators, multichannel optical processing and spectral anal. of radio signals 77−23763
vidicon spectrograph for multichannel detection of Raman spectra 77−74518
visual speech vocoder as teaching aid for deaf 78−36069
weak light fluxes with slowly varying intensity detector 79−2806
whistler analyser, semiautomated, using spectrum analyser and programmable tracking filter 79−74975
wideband electron spectrum analyser, 10 to 275 keV electron energy 78−86719
KF:LiF, photodichroic, real time recording medium, for optical spectrum analyzer 78−71174
KF:LiF, photodichroic real-time recording medium, for optical spectrum analyser 78−66878
$LiNbO_3$, bulk, Ti-diffused integrated optical spectrum analysers, H implantation effects, pot. uses 80−43486
Si photodiode array for integrated optical spectrum analyser 80−33241
TeO_2, cryst., acousto optical RF spectrum analyser, double diffr. *(Russian)* 77−7263
TeO_2 rapid optical spectrum analyser *(Japanese)* 77−27360
TeO_2 time-integrating acousto-optical correlator for chirp spectrum analyses 80−106474

spectral analysis
see also spectral analysers
2D linear prediction for freq. and bearing estimation 79−64409
acoustic, directive spectral analysing system using moving microphone *(Japanese)* 80−33348
acoustic attenuation coefficient slope for liver tissue, statistical estimation from refl. US signals 80−46000
acoustic bispectral holography, theory 77−84086
acoustic CW line spectra, determination of struct. using integration time and acoustic multipaths 79−59860
acoustic emission pulse signature anal., optimal design and eval. criteria 77−48596
acoustic emission pulses evaluation, freq. anal. appl. 78−18126
acoustic emission source identification using signal anal. 77−44415
acoustic emission source mechanism identification by energy spectrum anal. 77−19489
acoustic high resolution cross sensor beamforming for uniform line array 78−50988
acoustic noise, spectral anal. rel. to unified index formulation 77−50823
acoustic noise meas., unsteady, from letter-handling machines, automatic classification of noise levels 80−79085
acoustic noise spectrum meas. in ocean for small observation baseline 80−102902
acoustic signal characterization using spectral microanalysis 80−74607
acoustic signature anal. for noise source identification 77−68336
acoustic spectra, appl. of cepstral techniques to ground refl. effects 77−31165
acoustic system identification, from multiple input/output data, comment and reply 78−83179
acoustical data anal. using digital techniques 78−83193
acoustics, discernibility of amplitude changes in harmonic signals *(Polish)* 80−38193
acoustics, echo time delay detection, effect of zero singularity smoothing 78−90605
acousto-optic spectrum analysis, wideband high-resolution, hybrid technique 79−76597
adaptive estimates of random processes and fields, ocean and atm. waves appl. *(Russian)* 77−29475
Aegean Sea, spectral anal. of tidal data 77−86905
aerial photography rapid screening by optical power spectrum analysis 78−63033
AES/APS self-convolution inversion, FFT and digital signal processing 79−71430
alkali halides, photodichroic, as optical processing elements 78−83056
analogue data processing systems, polarised modulation of light *(Russian)* 80−91884
aneurysm detection using one-bit correl. 80−17175
angiographic I imaging using spectral anal. 80−36122
apparatus spectrum decomposition, universal method 77−57800
arc spraying, frequency analyses application 79−83359
aspectrogram filtering, multiplying mask prod., photographic method 79−27196
aspherical geodesic lenses for integrated optical circuits, signal spectral analysis appl. 79−27437
asteroid belt, Kirkwood gaps, spectral anal. 77−60711
astronomical time measurements, spectral anal. appl. to study of forced nutation 77−52956
N.Atlantic sea surface temp. fluctuations at tidal frequencies 77−2170
atmosphere, freely convecting, above water surface, oscills. spectral density function *(Russian)* 78−11964
atmosphere, refr. index struct. parameter from refractivity and amplitude scintillation meas. at 36 GHz 78−81316
atmosphere, turbulence and internal waves spectra in stably stratified boundary layer *(Russian)* 78−81297
atmosphere echo sounding, Doppler shift extraction hy adaptive linear-prediction filtering 77−64453

spectral analysis continued
atmosphere flow, aperiodic trajectories and stationary points in three-component spectral model 77−5287
atmosphere general circulation model, space-time spectral anal. of mid-latit. disturbance 77−66951
atmosphere spectral energetics, determ. via numerical filtering anal. 80−26577
atmosphere submillimetre emission and absorpt., freq. spectrum of fluctuations 77−41308
atmospheric infrasound waves recording method and computer anal. *(Russian)* 78−65407
atmospheric mean daily pressure over Mediterranean 78−3913
atmospheric parameters over vegetated surface in sensible heat advection conditions 80−17343
atmospheric penetrative convection, AMTEX obs. 79−58028
atmospheric precip.-time struct., daily precip. amounts modelling with Markov-I chain 80−101401
atmospheric temperature, daily maximum on mountain slope, time series anal. 78−73457
atmospheric temperature data for central England, 1659-1973 period 77−17208
atmospheric temperature records, sunspots and volcanic dust effects on climate 78−69439
atmospheric variables, spectra deduced from ground-based radiometry 79−92567
atmospheric wave propag. in distorted background flows, spectral series convergence 77−29375
atmospheric waves and winds, midlatits., 52-110 km altitude 79−5565
auditory electrophysiology, spectral analysis of cochlear and brain stem evoked potentials 80−16957
auditory evoked pots. with pseudorandom noise excitation 79−83795
auroral pulsations, spectral anal. rel. to interplanetary mag. field fluctuations 79−8736
automated pattern recognition with hybrid optical/digital systems 78−63037
autoregression order selection 77−2270
autoregressive spectral estimates, geophysical applications 77−29471
autoregressive spectrum analysis, sources and remedies for spectral line splitting 79−59871
autoregressive technique, appl. to astronomy and geodynamics *(Chinese)* 80−85869
baseline recognition and baseline flattening algorithm 78−262
Bayesian deconvolution, appl. and algorithm implementation 78−70103
Bayesian deconvolution, convergent props. 78−57861
Bayesian deconvolution, noise props. 78−57862
beam generation, quasi-homogeneous Gaussian sources, spatial coherence 80−48145
biased spectral decomposition in glass, ^{11}B NMR spectroscopy 78−88198
bifurcation and reaction-diffusion spectroscopy 78−95910
biological rhythm research, second-order correlation functions and bi-spectra 78−3441
biological shape pattern recognition, average similarities of Fourier spectra 80−104818
bioluminescence sensor, moving linear, for ocean light field meas. 79−20732
biomedical applications, review of anal. methods 80−21560
biomedical signal high efficiency freq. anal. and data compression through digital filtering 78−31939
biomedical signals, short-length, maximum-entropy correlation and spectral analysis 79−66577
biophysics, deconvolution of exponential response functions 80−16894
bird song spectrum anal. rel. to Western musical scales 77−50840
blood velocity waveform display by spectrum analysers, direction Doppler signal preprocessing 79−34611
brainstem auditory evoked potentials, human, freq. comp. 80−16956
bubble size spectra, acoustical determs. 78−9735
Burg maximum entropy method, possible instability 79−80045
C-CD implementation of chirp Z-transform in sonar system 79−18626
cardiac event sequence following mental loading 79−29516
cepstral method improvement from spectral envelope extraction 79−81659
cepstrum performance, improvement through windowing of log spectrum 78−89303
climatic change, spectral anal. rel. to astronomical theory 77−13114
climatological power spectra computation technique 77−91305
climatology, anal. of 500 mb geopotential height in N.Hemisphere 77−5311
clustering of extragalactic radiosources, power spectrum anal. of Parkes and Bologna catalogues 77−60838
clustering of extragalactic radiosources, power spectrum anal. of 5C surveys 77−60839
cochlea model, for signal analysis 77−26281
coda waves from local earthquakes, spectral anal., decay charact. 79−66639
coherent and incoherent optical spectrum analysis techniques in image evaluation 78−78928
coherent optical hybrid space- and time-integrating spectrum analysis 80−48177
coherent optical power spectrum analysis for image evaluation, contrast effect 79−81367
coherent optics system, use of spatial filtration *(Russian)* 80−28164
colour photography of accidental thermal burns, diagnosis appl. 78−3648
completely monotonic operators, spectral props., resolvent 78−8226
complex contour resolution into components, Fourier method 77−31561
computerised tomography, two-component spectral analysis 77−25548
condensation nuclei, size spectrum meas. via counter with inherent size resolution capability 78−81470
constant-Q spectral analysis and Mellin transforms 79−98551
continental ice sheet model, spectral response to insolation vars. 79−2300
correlation TOF technique, real modulation 79−49898
cosmic ray diurnal variation, power spectrum anal. 79−25416
cosmic ray fluctuations at 250 GV 79−75062
cosmic ray intensity diurnal variation, power spectral method 79−29953
cosmic ray intensity fluctuations, spectra rel. to interplanetary mag. field spectra 78−28457
cosmic ray neutrons, maximum entropy spectral anal. rel. to short-period vars. *(Russian)* 79−96865
cosmic rays long-period vars., freq. spectra 77−25892
cosmological turbulence, short-wave spectra and non-linear interactions effect on universe expansion 78−77629

spectral analysis continued
coupled nonlinear oscillators under modulation conditions in intestinal modelling, spectral analysis 78−44754
cumulative spectrum distortion with random scanning errors, digital processing 77−38028
cumulonimbus cloud drops, size spectra study from mobile ground station 78−92943
curve synthesizer SK-2 for resolving spectral curves into components 78−73980
CW signals in white noise, influence of data window shape 80−64300
61 Cygni, unseen companions, max. entropy spectral anal. of period data *(Russian)* 78−69841
Cygnus X-1, optical and X-ray evidence for 78/39-day period 78−89274
data extraction and classification from film, conf., San Diego, USA (Aug. 1977) 78−63023
data extraction from film using optical and/or digital and/or electronic devices 78−63024
decay time coincidence spectra, anal. 77−38575
decomposition of two-dimensional spectra, eval. of peak volume, position and width 80−18890
deconvolution method for use in small computers 79−76321
deconvolution of experimental spectra using moments method 78−29094
deconvolution of IR spectra in real time 77−38034
deformable shell containing compressible fluid and gas, spectral anal., vibr. modes *(French)* 77−72209
deterministic signals spectral anal., comparison of max. entropy method and nonrecursive technique 79−58112
differential operator with highly oscill. pot., spectrum *(French)* 77−71180
diffraction pattern sampling for optical power spectrum meas., error sources 78−63030
diffuse reflectance spectra interpretation 77−53982
digital filtration in correlation time-of-flight spectrometry 79−49894
Dirac operator, virial theorem and spectral shift function 79−17339
discrete time series, spectral estimation techniques 78−53734
discrete time series spectral estimation novel aspects 77−91336
display-equalised filter for freq.-time anal. of seismic waves 77−73650
diurnal latitude vars. spectra based on obs. at Gor'kii 79−35100
dolphin boundary layer pulsations, results of spectral anal. *(Russian)* 80−41063
dolphin communication signal spectrum, fine struct. anal. 78−20197
Earth crust, spectrum characts. appl. to seismic stations calibration *(Russian)* 78−49158
Earth daily free nutation determ., spectral anal. technique 78−96126
Earth gravitational potential, amplitude spectrum rel. to anomalies sources depths 79−16366
Earth mean pole position from star pair latitude obs. anal. 80−21892
Earth orbital vars., support for astronomical theory of climatic change 77−87058
Earth secular polar motion, low frequency spectrum anal. *(Chinese)* 80−104849
Earth strain-tides, spectroscopy 78−73301
earthquake aftershocks off Izu Peninsula 77−56606
earthquakes, New York State, spectral anal. 79−48412
earthquakes, spectral analysis of 1976 Friuli aftershocks 78−24240
ECG, diagnostic, classification in terms of spectral characts. 80−56264
ECG data analysis for data compression 77−40862
ECG frequency spectrum anal., clinical usefulness 79−25147
ECG in contusive myocardial injury 79−43997
ECG R-R intervals, time series analysis using autoregressive model 79−83972
eclipsing variable stars light curves, power spectra of Fourier transforms 77−49428
edge waves in NW.Pacific Ocean, wavenumber-freq. spectrum *(Russian)* 78−44841
EEG, event-related, sequential freq. anal., hybrid method 77−81759
EEG, eye movement artifacts, spectral method for removal 79−16184
EEG, infant, ordinary and partial coherences of bipolar and quasi-unipolar derivations 77−44828
EEG, nonstationary, anal. by approx. canonical expansion method 78−53555
EEG, normal children 6-16 yrs. 79−70653
EEG, rel. to haemodialysis 78−31968
EEG, spectral band analysis, contrib. to attentional processes study *(French)* 80−61721
EEG 80−3619
EEG activity comparison in right and left cerebral hemispheres by power spectrum analysis 80−45922
EEG alternations, power spectral analysis 80−30924
EEG artifact automatic detect. during sleep 79−100759
EEG automatic analysis using adaptive segmentation of EEG records 77−25581
EEG automatic classification, parametric ARMA time series models 77−90944
EEG development in rat, power spectral analysis 79−83742
EEG dynamic evolutionary spectral analysis 78−57102
EEG frequency spectral analysis, physiological aspects 77−25627
EEG multivariate analysis, parametric time series models 77−40830
EEG power spectral analysis to determine stage of anaesthesia in normal dogs and cats 77−37066
EEG signals, Fourier-Haar transform 77−44823
EEG signals, Walsh power spectra estimation 77−40823
EEG spectral parameter analysis operating system 77−9291
EEG spectrum analysis, LF activity isolation by autoregressive filter 79−96672
electromyogram envelopes, study of muscular control 78−92750
electrostatic sparks detection and characts., by radio methods 80−68217
EM wave propagation through turbulent medium, space-time anal. 77−42472
EM wideband freq. response conversion to transient response using segmented transform. 78−77349
EMG, inspiratory diaphragmatic 79−88071
EMG, surface, digital simulation, spectral anal. 78−80863
EMG envelopes, Parkinson's disease diagnosis and treatment appl. 79−5390
EMG index for localised muscle fatigue 78−57093
EMG of muscular exterior carpi radialis, form recognition by freq. spectrum 78−15939
EMG of Vastus medialis for graded isometric torque tensions, power spectrum distrib. 78−44673
EMG power spectrum, contrib. of individual motor units 77−29129
EMG power spectrum analysis, in neuromotor speech disorders 77−29161
EMG spectra, effect of motor-unit firing time statistics 78−31804
EMG spectra, factors affecting interpretation, stochastic process model 77−44825
energy spectra, deconvolution, modified method of statistical regularisation 78−54164
EPR spectrum analysis, polynomial regression and nonderivative search technique 77−14461
equally spaced time series of finite length, power spectrum computing methods 77−45190
equatorial electrojet, type II gradient drift irregularities, power spectrum studies 79−75016
equatorial stratopause, planetary wave disturbances 79−5557
erythrocyte-rouleaux formation, US detect. by spectral anal. 78−40280
esophageal speech, long-time spectral and intensity characts. 80−74643
ESR, conc. determ. and resolution of multiple-component spectra 78−259
estimators, statistical parameters in cross-spectral anal. 78−83180
Eurasian earthquakes and explosions, discrimination using P codes spectral characts. 78−7576
European air temperature change patterns 78−92957
European Grosswetterlagen, temporal vars. and possible causes 79−58081
exponential distrib. parameter estimates under poor statistics, computer program 78−57863
F-region critical frequency small scale fluctuations at Kodaikanal 79−16745
fast breeder reactor floor response spectra direct calc. 77−38327
fast Fourier transforms, for teachers 78−81750
FFT, analysis of oscillatory data, appl. to de Haas-van Alphen effect 79−42434
filtered image, geological appl. *(French)* 78−9338
first-heart-sound spectra, temporal and heart-size effects 80−41276
flue gas optical density spectral analysis, smoke density meter maximum sensitivity determination appl. 78−69500
fluid dynamics, sinusoidally perturbed flow meas., photon correlation technique 77−42945
foetal heart rate variability anal. using spectral anal. 78−28111
forest aerial photograph spectral investigation *(Russian)* 77−34041
Fourier and Fresnel images, spatial freq. analysis *(German)* 77−79764
Fourier transform NMR spectroscopy, clipped free induction decay signal anal. 77−63976
Fourier transform signal processing in integrated optical format 78−50950
Fourier transform systems, discrete-time windows, optimum low-order 77−5631
Fourier-Autoregressive spectral estimation 79−59872
frequency variant optical signal analysis 77−19180
frequency variant optical signal processing 77−71934
frequency-time filtering of ULF signals and magnetospheric channel characterisation *(French)* 79−70920
Fresnel diffraction pattern, spatial freqs., spectral analysis *(French)* 77−58269
Friuli earthquakes, response spectra analysis for different sites 78−24248
gamma spectra anal., software system VAT-69 79−9949
gamma spectra from Ge(Li) spectrometers, set of computer programs SPECTRAN for anal. 79−9947
gamma-ray detection, scintillator response, pulse height spectra unscrambling, computer program 78−55092
gamma-ray spectra, automatic analysis, fast program 79−9948
gamma-ray spectra, background subtraction, direct method 79−723
gamma-ray spectra, Ge(Li) detector, IAEA intercomparison of computer processing methods 79−9954
gamma-ray spectra, linear least-squares peak search algorithm 79−754
gamma-ray spectra multiplet resolution, semiempirical approach 79−234
gamma-ray spectra using FFT *(Japanese)* 78−90047
gamma-ray spectrometry, data analysis, theoretical foundations 79−233
garnet:Nd^{3+}, spectral, structural regularities, anal. 78−51948
gastrointestinal electrical rhythm freq. estimation using autoregressive modelling 78−80855
gear noise, real-time bispectral anal. appl. to contactless diagnosis 77−84066
generalized framework for power spectral estimation 80−83703
geodesy, altitude obs. Fourier transform. *(German)* 78−61312
geodetic measuring instruments, periodic errors determ. via spectral anal. *(German)* 77−87131
geoid spectrum from altimetry 80−3904
geomagnetic activity aa index, maximum entropy spectral anal. over 107 year interval 77−87187
geomagnetic anomalies, spectral anal. of step model total anomalies 79−5450
geomagnetic dipole field vars. and length of day fluctuations, spectral line similarities 77−32993
geomagnetic energy spectra, depend. on solar wind vel. and interplanetary mag. field direction 80−67476
geomagnetic field annual oscillation 78−40470
geomagnetic field fluctuations at synchronous orbit, power spectra 78−96358
geomagnetic field long-period variations, spectra anal. methods *(Russian)* 79−34743
geomagnetic field variations, spectral anal. rel. to solar oscillations correl. 78−89013
geomagnetic field variations during quiet conditions, spectral characts. 77−87179
geomagnetic fluctuations, spectral stacking and smoothing rel. to Earth global elec. cond. character 80−17231
geomagnetic micropulsations, 0.3-300 s periods, integrated power spectra 77−9622
geomagnetic pulsations, cross-correlation and cross-spectral analyses *(French)* 79−70928
geomagnetic pulsations, numerical frequency-time anal. 79−39990
geomagnetic pulsations, problems in appl. of spectral-temporal anal. 77−13188
geomagnetic S_q var. at mag. conjugate points and interplanetary mag. field var. 78−69287
geophysical time series anal. *(Italian)* 77−70841
geophysical time series statistical processing, spectral estimators *(German)* 77−70852
graphics display terminal for spectral data analysis 78−54473

spectral analysis continued
gravity and magnetic anomalies due to rectangular prismatic bodies, spectral anal. 77−53222
gravity waves, spectral decomposition 80−36319
Gulf Stream meanders, GOES IR meas., time series anal. 79−34842
harpsichord sounds, time-varying amplitude-freq. structs. in attack transients 77−14858
HD 101065, Przybylski's star, light variability freq. anal. 80−62152
HDE 226868 (Cygnus X-1), anal. of linear polarisation vars. 77−9810
Heisenberg ferromagnet, one-dimensional infinite model, ground state representation 77−72967
HF coda waves of local earthquakes, Stone Canyon, California, temporal trend in attenuation 79−57861
HF diffraction of arbitrary incident field by half plane, asymptotic techniques 78−42264
HF diffraction phenomena, spectral domain interpretation 77−83788
HF P_n and S_n phases obs. at great distances in W.Pacific 78−77195
Hilbert spaces, nested, spectral props. in class of operators and group representations 78−4459
holographic passive sonar, new system using polyspectral anal. 77−39124
hydrometeorologic elements in coastal zone, long-term vars. from spectral anal. *(Russian)* 78−77258
hydrometeorological large scale processes, spectral density, evaluation *(Russian)* 77−5337
hydrometeorological time series, spectral analysis for United States 77−64341
image evaluation, coherent and incoherent optical spectrum analysis 78−63031
images in optical-electronic processor, discretisation using holographic filter *(Russian)* 78−37809
Indian monsoon, spectrum anal. appl. 78−44957
Indian Ocean equatorial waves, evidence for continuous spectrum 80−98331
Indian summer monsoon, oscill. with one month period 77−53118
industrial X-ray film information processing methods *(German)* 78−15637
infrasound signals, dynamic spectral anal. by FFT *(Chinese)* 78−1453
inhomogeneous lossless dielectric slab, permittivity profile reconstruct. from reflection coeff. spectral anal. 79−36819
interferential spectrometry, matched filtering, real time spectral recognition 78−37822
interplanetary magnetic field, power spectra from radial or transverse mean field meas. 77−29617
interplanetary plasma turbulence, spatial fluctuation spectra 79−53693
interplanetary scintillation, mathematical anal. in weak scatt. approximation 77−9706
interpolation by zero fill or convolution 78−25803
intestinal motility study by computerised anal. of sounds and EMG wall pots. *(German)* 78−31944
intracortical EEG relationship model *(German)* 79−16180
ionosphere amplitude scintillations, multifreq. spectra 77−87161
ionosphere EM wave propagation, backscatter echo spectral analysis and radio transmission forecasts *(French)* 79−29912
ionosphere night-time scintillations at mag. equator, power spectra and freq. indices 79−44292
ionosphere scintillation, power spectra rel. to VHF/UHF satellite communication 77−41264
ionosphere waves in D- and F-regions, spectral anal. and temporal vars. 80−8483
ionospheric f_0F_2 vars. correl. with stratospheric O_3 content vars. 78−45098
ionospheric wave spectrum measurements using cross-power spectrum analyzer on space shuttle *(French)* 79−70912
land-use photo classification, scale and resolution effects 78−12023
LANDSAT data high-level computer processing 78−69546
landscape multispectral data, Karhunen-Loove analysis 80−48164
laser beam, spectral analysis, photomixing method 78−46698
laser Doppler anemometer signals operating in burst mode 80−100041
laser Doppler particle meas. system, using nonsinusoidal forced vibr. and bispectral analysis 78−41285
laser Doppler velocimeter with direct spectral anal., for instantaneous vel. meas. 80−99782
laser Doppler vibr. meas. system using bispectral anal. 80−38357
laser radiation, pulsed, measurement of energy using multichannel instrum. 79−76731
laser radiation energy, spectral and time range meas., instruments 79−35687
laser velocimeter, 3D Doppler, using cross-bispectral analysis 79−30426
lasers, measurements of 3-dim. energy characts. in IR region and imaging methods 79−76842
lateral geniculate nucleus of cat, periodic stimulation, neural activity transient persistence 80−56021
Ligurian Sea, sea level spectral anal. rel. to free oscill. correl. with meteorological perturbations 79−34826
linear motion blurred picture, motion estimate, spectrum anal. 77−3547
linear systems with multiple inputs and outputs, comment 79−17344
locally stationary time series *(Japanese)* 77−67238
long-term spectra, computerised meas. method, English and Finnish data comparative study 80−104688
loudspeakers, constant-Q analysis using chirp Z transform 79−64407
low intensity data recording, estimation of reliable spectral information 79−21724
lunar and solar tide generating potentials, spectroscopy, rel. to ocean tide features 77−86904
lunar geomagnetic tidal variation in Indian region 77−60541
magnetic field, atmospheric, induced by sea waves, spectral anal. and attenuation 77−13058
magnetic field anomalies, comparison of Moon and Earth 78−4122
magnetosphere, ULF waves anal. techniques using spectral matrix 77−13137
magnetospheric waves, digital techniques for ULF wave polarisation analysis *(French)* 79−70923
magnetotelluric data, tensor anal. for two-dimensional geological structs 78−40471
matched spatial filter optimisation for diatom recognition 80−48180
maximum entropy method, appl. to seismic waves *(Japanese)* 77−2260
maximum entropy method, model data anal. situation study 79−8843
maximum entropy method and appls. 80−37006
maximum entropy method appl. to inverse problems, short data records anal. and Earth density determ. 77−64465
maximum entropy method confidence limits 80−22284
spectral analysis continued
maximum entropy method for spectral analysis of digital data *(Japanese)* 77−17227
maximum entropy method of period determ., accuracy 80−56712
maximum entropy power spectrum anal., soln. to problem of spontaneous line splitting 77−45187
maximum entropy spectral analysis, power estimation method 79−16691
maximum entropy spectral analysis, prediction filter error length determ. for artificial samples 79−66829
maximum entropy spectral analysis of multiple sinusoids in noise 79−48579
measurement system noise spectra determ., simultaneous eqns. soln. method 78−57354
mechanical light modulator, harmonic anal. of noise spectrum 78−1362
membrane noise analysis by integral spectrum procedure 77−48958
membrane noise spectral density measurement, use of octave filters 77−48957
mesoscale motion in western North Atlantic Ocean, space and time scales 78−49035
metal defect meas. using US cepstral processing 78−73010
meteor trails, struct. function of effective linear electron density fluctuations 78−73687
meteorological historical series spectral anal. using maximum entropy method *(Chinese)* 79−79958
method of moments in spectral analysis 80−68137
Michelson experiment seen 90 years after first execution *(Italian)* 79−17175
microoptic signal processing research, review 78−38073
microphone signals, cross-spectral density for acoustic intensity meas. 78−9514
microprocessor in real-time Fourier analysis *(German)* 79−67266
microseismic events in Badra area, Iraq, spectral anal. 80−56413
modal anal. dynamic anal. program *(Japanese)* 77−86784
modified-triggered photocounting and its application to optical superheterodyne spectrum analysis 80−31865
molecular fluorescence, nonexponential decay, method of moments for data anal. 80−55975
monsoon system oscillations, spectral anal. of obs. records 77−33148
multicomponent HF skywave arrival elevation angle meas. 78−24408
multidimensional power spectral anal., new method, radioastron. appl. 77−17378
multidimensional power spectral analysis, note 79−12406
multiple input/output data, system identification 77−37750
multispectral analysis by NOAA and METEOR satellites 77−82009
multivariate random process, consequences of non-negative definiteness of spectral density matrix 79−80511
muscular activity in pasture maintenance, control mechanisms study 79−5306
musical complex tone classification according to shape of spectrum envelope 80−102939
musical instruments, natural tones, short-time spectral analysis *(Japanese)* 77−88994
musical scale, 12-tone, tempered Fourier transform 80−87671
narrowband optical signal, spectral width estimation 80−102627
natural seismic events using autoregressive techniques 77−29470
nested variance technique, space physics appl. in FORTRAN 77−87275
nested variances method for power spectrum calc. 80−8965
neurophysiological activity in olfactory system of rabbits, and pheromones 77−90816
neutron crystal spectrometer superposition spectral recording method 78−78548
neutron moderation, linear Boltzmann operator, in various geometries, contributions to spectral theory *(Rumanian)* 78−46128
NMR analysis system, LAOCOON3-type, reliability efficiency and error estimates 78−258
noise across sample-hold system *(Portuguese)* 77−31174
nonnegative spectral densities, moment-theory approx. 77−49563
nonstationary data, dynamic spectral comparisons, EEG anal. 77−44827
nonstationary time series, Fourier-Haar transform 77−44823
NRM in deep sea sediments, time series anal. 79−29757
nuclear power system and fuel channels stochastic identification and parameter estimation 79−3201
nuclear reactors, process monitoring and parameter estimation, multivariate signal analysis algorithms 80−47585
ocean current spectra interpretation, dynamical hypotheses testing 79−21045
ocean current spectra interpretation, three-dimens. vector time series kinematics 79−21044
ocean current velocities, spectral anal. of vector time series 79−39757
ocean horizontal current, mesoscale horizontal turbulence problem *(Russian)* 79−39741
ocean inertial currents, wind-driven, Gulf of St. Lawrence 79−20845
ocean internal wave climate near NW.African coast during JOINT-I 79−20840
ocean internal waves and mesoscale eddies, weak interaction 77−9433
ocean mixed layer, vel. spectrum induced by internal waves 78−73395
ocean quarter-diurnal tides loading effects by Ligurian Sea 78−61308
ocean random hydrophysical processes, quantification *(Russian)* 78−77359
ocean salt fingers spectral signature 77−25686
ocean semidiurnal internal waves in Polygon-70 test area of Atlantic, spatial spectra 80−31051
ocean short period internal waves, spatial spectrum 78−3800
ocean small scale turbulence, anal. of spectra *(Russian)* 79−88360
ocean surface gravity waves during Tropical Storm Delia, directional spectra and kinematics 79−48506
ocean trapped waves, adaptive wavenumber-frequency spectrum analysis *(Russian)* 78−81189
ocean wind wave energy spectrum, spectral-correl. anal. *(Russian)* 77−73752
ocean wind waves, high-freq. spectra meas. in presence of currents in shallow sea 80−31053
ocean wind-generated waves, power spectrum, wave height calc. *(German)* 77−17137
oceanic finestructure, spectral anal. rel. to wave-induced and intrusive structs. separation 79−48502
oceanic magnetic anomalies recorded during deep-water mag. surveys, statistical anal. 80−36233
oceanographic scalar quantity undergoing advection, temporal and spatial spectra 79−48507

spectral analysis continued
oceanography, spectral anal. of temp., salinity and sound vel. gradients in western N.Pacific 80−51429
offshore environmental and platform data processing from Norwegian continental shelf 79−12273
optical analogue computer performance advantages 78−78949
optical coherent, smoothing energy estimate using multimode laser radiation 78−55311
optical correlation instrument field-of-view, intensity distrib. selection 79−72688
optical image quality, scene power spectrum moment as merit factor 77−7019
optical power spectrum, system design approach 78−63029
optical power spectrum sampling and nonparametric pattern recognition algorithms 78−63032
optical processor, time- and space-integrating, for spread spectrum appl. 80−78777
optical signal processing, one- to two-dimensional (and vice versa) mappings 78−78948
optical wave, log-amplitude fluctuations spectra, turbulence spectra parameters determ. 80−95797
P-wave signals, multivariate autoregressive model, short-period discrimination appl. 79−16385
paediatric EEG reactivity, spectral and temporal analysis 77−9293
Parkes radiotelescope, spectral baseline ripple reduction 78−69703
partial differential operator, unified approach 78−73827
particle counting by size, optical-digital training method 77−71305
particle size and density determ., bispectral anal. of laser Doppler vibr. meas. 80−98880
Pc 1 geomagnetic pulsations, chevron struct. 79−58193
Pc 3-4 pulsations, effect of doubling period in vertical elec. component meas. in air 77−41270
periodic waveforms using programmable pocket calculator, Simpson's rule appl. *(Spanish)* 78−86121
phonocardiogram classification, linear prediction analysis appl. *(Japanese)* 78−36010
phonothyreogram and phonocardiogram frequency spectrum analysis by minicomputer, ECG reference time signal 79−83966
photoelectric photometry at Trieste, real time spectral analysis *(Italian)* 79−62756
photographic image optical power spectra anal., S/N concepts 78−63028
photon correlation spectroscopy, spectral analysis with short data batches 79−41346
photon-correlation spectroscopy, spectral parameter extraction 78−77993
physiological signal pre-forming system for automatic freq. anal. 78−3621
physiological signals, gastro-intestinal tract, spectral analysis 80−41269
Pi2 micropulsations, morphology of spectra 77−87209
Pi 2 geomagnetic pulsations, complex demodulation appl. 79−84588
Pi 2 micropulsations, harmonics in power spectra assoc. with plasmapause 77−25885
piano sounds, time-varying amplitude-freq. structs. in attack transients 77−14858
Pisarenko and Prony methods, comparison 79−55269
plasma coherence wave spectra, freq. averaging effects, digital simulation 77−35390
plasma diagnostic real-time spectral analysis methods, applicability and constraints *(Russian)* 77−31525
point process sampling for spectral analysis 79−68498
polarised light, spectral analysis, polychromatic and coherent optics *(French)* 79−50209
polished surfaces, smoothness parameter meas. using spectral analysis optical system 80−86261
Poltava latitude differences from obs. of bright zenith stars 78−28488
potential fields due to vertical circular cylinder and dike, statistical anal. 79−34972
potential fields from arbitrary 2-, $2^1/_2$- and 3-dimensional bodies, wavenumber domain expressions 79−5634
power density spectrum estimation from finite length signal 77−91337
power spectral density and coherence functions, leakage and reduction, resolution increase 79−18097
power spectrum of a random process, computing using data segmentation 77−60912
precipitation, seasonal, in Jerusalem, temporal fluctuations 80−72618
prediction methods based on autoregressive or maximum-entropy-method 79−55268
programmable calculator as alternative to minicomputer-based analyser 79−9985
progressive and retrogressive waves coherence and space-time power spectra partition 77−91306
pulse height analyser data, on-line method for peak area determ. 79−755
quantum freq. standards, output signal sidebands/resonator detuning effects on accuracy 77−87743
quasar redshifts distributions, periodicity from correl. and power-spectrum anal. 80−62313
Quaternary palaeomag. data from British Columbia, rel. to geomag. secular var. 78−11806
radar measurement of clouds and precipitation, correl. and spectral anal. 80−12529
radio auroral signals, maximum entropy spectral anal. 78−93006
radiosonde meas. and spectral anal. of LOS fading 80−56568
radiosource scintillation obs., ionospheric irregularities determ. 79−84579
radiosources isotropy in B2 catalogue 78−73766
radiowave reflection from ionosphere, large-scale screen speed determ. 77−9602
radiowave scattering signals, incoherent, use of general-purpose computer with intermediate spectral base *(Russian)* 79−5621
rainfall at Madras, India, periodicity 79−84426
rainfall in England and Wales, long-period records spectral and filter anal. 80−4080
rainfall short-period fluctuations for New Zealand 77−25746
random data, effects of detrending and smoothing 78−40685
random field spatial spectrum, use of reference sensor in autoregression evaluations *(Russian)* 78−61578
random signal analysis, conf., London (April 1977) 77−44822
randomly sampled records by direct transform 77−30134
randomly sampled signal analysis 77−9961
randomly sampled signals, variability reduction by filtering out parts of spectral energy 80−57193

spectral analysis continued
real-time Fourier spectrum analysis, using acousto-optic devices 77−58285
real-time multichannel optical spectral analysis, by liq. cryst. display 78−38042
real-time optical Fourier spectrum analysis using acousto-optic diffr. 78−5430
recording of spectral lines in presence of intense background, techniques, appls. *(Russian)* 77−40613
recursive multichannel max. entropy method 77−91338
recursive multichannel max. entropy spectral estimation 78−53735
reflection seismograms signal anal., use of kepstrum 78−81425
reticulocyte blood count data analysis by maximum entropy spectral estimate 77−78017
reticulocyte production rhythm investigation by spectral analysis 78−73279
RF technique, instrument improvement and development trends 77−41585
rivers monthly average water discharge cycles and prediction 77−78264
road traffic noise poly-freq. spectral anal. based on filtered Poisson process model 79−52998
rough surface power spectrum measurement 80−36989
SAW and optical signal processing techniques compared 80−48173
scalar ocean wave spectra estimation by maximum entropy method 79−74900
scanning signal, influence of resonance filter on wave form *(Russian)* 79−55265
Schumann resonances, atmospheric, averaged power spectra from stratosphere balloon obs. 79−44221
sea upper layer, wind waves components of temp. fluctuations spectrum *(Russian)* 78−53655
SEASAT radar altimeter data, spectral coherence rel. to geoid features resolution capability 80−72645
second derivative UV absorpt. spectrometry, improving analysis 78−45731
seismic background noise detect. by Viking Lander 2 site seismometer, wind activity determ. 79−84703
seismic body waves in upper mantle, parameters from spectral amplitude curves *(Russian)* 79−53316
seismic body waves spectra, free surface effects on moments and corner freqs. determ. 78−85492
seismic body waves spectral anal., earthquake source parameters, Himalayan region 79−39660
seismic data, maximum entropy spectra, choice of operator length 79−84134
seismic fields, decomposition algorithm from charact. numbers and vectors of spectral matrices 77−9370
seismic ground motion spectra 79−88311
seismic long-period P-waves, spectral-ratio anal. rel. to Moho depth under NORSAR array 77−86814
seismic P_s waves rel. to crustal struct. under Sainte-Marie-aux-Mines observatory *(French)* 77−73666
seismic Pn,Sn phases, high-freq., recorded on ocean bottom seismographs, spectral anals. 79−16400
seismic prospecting problem soln. *(Russian)* 79−74859
seismic records, combined spectral anal. for determ. of geologic section props. *(Russian)* 78−40696
seismic reflected waves, spectral characts. in region of bright spot anomalies *(Russian)* 79−53319
seismic response from local earthquakes at Lipari, Eolian Islands, anal. 78−40494
seismic sources, spectral theory and determ. of parameters of earthquake foci 77−21687
seismic transverse waves in rocks, spectral anal. rel. to waves identification 77−21682
seismic waves, absorpt.-conditioned transition functions estimation and props. *(Russian)* 79−53318
seismic waves, dynamic spectral ratios with variable freq. bands as seismic discriminants 77−81834
seismic waves, integral spectrum parameters appl. to geological section prediction *(Russian)* 79−8705
seismic waves, of explosion earthquakes assoc. with 1973 eruptions of Asama Volcano *(Japanese)* 80−67340
seismic waves, spectral anal. rel. to attenuation in earthquake aftershock region 80−76926
seismic waves primary signals, amplitude spectrum and partial multiple refl. effect *(Russian)* 78−85484
seismograms, algorithms for true Earth tremor vels. determ. 79−96743
seismology, higher-order refl. moveout spectra computation procedure 79−92501
seismology, optimal vel. anal. in common depth point method *(Russian)* 78−40698
shoreline periodicities, spectral anal. rel. to edge waves 80−12375
signal level fluctuations on long-distance radio paths, energy spectra 79−53629
skin IR radiation 79−88057
solar activity long term forecasting using high resolution time spectral anal. 77−33453
solar activity-weather correlation, anal. 78−40628
solar activity-weather relationship, study of temp. and rainfall at Oxford 78−85674
solar and geophysical parameters, power spectrum anal. 79−16705
solar Ba II 4554 Å filtergrams, two dimensional anal. rel. to five-minute oscills. in temp. min. 79−62808
solar chromospheric oscillations obs. with OSO-8, average phase spectra for Si II 79−62801
solar chromospheric oscillations obs. with OSO-8, average power spectra for Si II 79−62800
solar chromospheric oscillations obs. with OSO-8, basic meas. and analytical methods 79−62799
solar flares, principal component anal. in soft X-ray flux 80−41781
solar granulation, morphological interpretation of spatial power spectrum 78−65581
solar granulation, power spectrum from one-dimensional speckle interferometry 78−45299
solar photosphere, granulation statistical properties and seeing, speckle interferometry obs. 79−88634
solar radiation, total and net intensities, power spectral anal. 78−40617
solar radio emission S-component, statistical anal. 79−40172
solar wind, electron density spectrum from interplanetary scintillation 78−45178

spectral analysis continued
solar wind speed variations power spectrum for periods >10 days 79−2462
solar wind velocity, dispersion anal. rel. to spatial and temporal spectra 78−7852
solid state detectors spectra, fast analysis, LIZA program 80−37706
solid-state convection in planetary interiors, numerical methods 79−84693
sound analysis, reversible computer method adapted to bioacoustical expts. 78−57137
sound pattern recognition in foreign languages, optical methods 77−68337
source radiation in presence of smooth convex bodies, spectral domain approach 79−64151
space physics, high speed spectrum analysis method appl. 77−73896
space-time optics, speckle phenomena and white light correlations 80−106460
space-time optics in shape and surface metrology 79−6093
spatial frequency analysis with incoherent optical approach, using LED light panel 80−78779
spatial power spectra estimation in speckle interferometry S/N ratio calc. 79−76608
spectra-colour ultrasonography, instantaneous power spectra, theoretical anal. 80−51190
spectral anal. of flaws, theoretical study 78−95897
spectrograms, detection, estimation and classification 80−64296
speech, power spectrum peak extraction for signals with pitch 79−98563
speech, speaker identification by long-term spectra under normal and distorted conditions 78−11677
speech analysis, PES method for formant freqs. extraction 78−11674
speech recognition using spectral peaks *(Japanese)* 77−64053
spermatozoa mobility, photon correlation study 80−12063
spoken word recognition method using nonlinear spectral matching *(Japanese)* 80−69605
stars, dynamical spectra rel. to local stellar stability theory 77−5521
stellar atmosphere waves, spectrum determ. via spectral line anal. 79−44465
storms secular variation in tropical N.Atlantic and E.Pacific Oceans 79−100929
stratiform cloud radar obs. 78−7686
stratigraphic data, spectral density anal. rel to astronomical theory of climatic fluctuations 80−72509
stratosphere, lower, power spectral anal. of meteorological data 78−40616
stratosphere, wave-mean flow interaction rel. to sudden warmings, numerical model 77−5297
Sun total microwave flux, search at Toyokawa for five minute oscillations 80−4327
sunspot activity and rainfall, 30-day periodicity 79−84765
sunspot periodicity rel. to solar rot. 79−35223
surface texture assessment, Walsh function method 80−36995
Sutlej catchment annual rainfall and Bhakra dam site annual runoff statistics 77−53082
systematic errors in astrometric obs., spectral anal. of obs. series *(Russian)* 78−73614
T-E curve classification, appl. in spectrum analysis and holography 78−82916
thermosphere, tides and midnight temp. anomaly 79−84556
threaded article parameter measurement 79−30409
time and frequency stability, characterisation and meas. 80−47025
time dependent Fourier transforms, time dependent spectrum density *(Korean)* 77−22384
time series, rest frame spectra deduction from spectra computed in moving frame 77−25795
time-delay spectrometry, practical appl. in field of acoustics 80−79082
TOF spectra, parameter estimation and gain of correlation method 79−49895
Tokyo, winter temps., spectral anal. of data for 1443-1970 period 77−45128
tone quality determ. by spectral anal. of violins and guitars 77−50841
traffic noise spectra, simulation model 77−46865
transducer signals, flow noise rejection using coherence function method 77−84067
travelling ionospheric disturbances, spectral comp. meas. 77−25824
troposphere, eddy transport of sensible heat and momentum, time spectral anal. 78−92899
tsunamis, power spectra rel. to transform. in coastal zone 78−77192
tuned equipment-structure systems, response spectra design methods 79−3952
turbulence dynamics, Fourier transform ambiguity 77−5300
underwater illumination fluctuations, nonstatistical model *(Russian)* 77−2173
underwater sound, background ambient noise estimation from spectral anal. of time series 77−84046
underwater sound, estimation and interpretation of acoustic CW phase fluctuation spectra 77−46850
underwater sound meas., FM signals power spectra and correl. methods 77−62086
underwater sound scattered by rough surface of upward-refr. ocean, sideband struct. 77−46847
unfolding of spectra with continuum and discrete components 79−9946
Universal Time, short period terms anal. *(Chinese)* 79−8589
universal time system (TU2) differences, spectral anal. rel. to Earth rotation nonuniformities 78−65174
UPEAK spectral decomposition routine 78−32798
upper atmosphere, neutral waves determ. from AE satellite meas. 79−58139
US, tissue identification by colour-coded B-scan display 77−64112
US, transcutaneous CW Doppler signals, for arterial physio/pathological data 77−44731
US, using frequency-tracked gated RF pulses 80−79079
US A-mode echo computer spectral anal. 80−51193
US Doppler signal LF spectral analysis for blood flow model 79−62312
US Doppler vascular diagnostic system 77−29190
US tissue characterisation, clinical spectrum anal. techniques 80−45998
variable stars, short-period, max. entropy method appl. 78−16436
vector wind meas., principal components anal. 79−39807
Vela supernova remnant, rot. measure correl. function and assoc. power spectrum rel. to turbulence 80−51836
ventilation fan acoustic noise *(Russian)* 80−53584
ventricular fibrillation recognition using ECG power spectrum 78−81032

spectral analysis continued
vibrating string, density determ. from spectral data 77−9856
vibration data, manufacturing machines, failure prediction 80−79048
violins, long time averaged spectra and rated qualities 79−50537
visual cortex, image description model 78−40143
visual evoked human-scalp EEG data monitoring, processing and displaying system 77−90936
visual evoked potential spectrum, short term vars. 77−48795
visual images, model of local spectral description 79−79545
visually evoked nonstationary EEG, anal. using max. entropy method 80−26397
VLF signal variations in Earth-ionosphere waveguide *(Russian)* 77−78305
volcanic activity dust veil index, stochastic simulation rel. to apparent periodicity 79−92514
Walsh transformation processing, matrix relationship with discrete Fourier transformation *(Russian)* 78−26
water inflow to Clutha Lakes rel. to atm. circulation indices and rainfall 78−11926
water waves, wind-generated, cross-spectral density rel. to freq. independent phase vels. 80−98333
watersheds, runoff kinetic energy spectra, urbanisation effects 79−25275
wave groups modelling in random wave field, power spectral density calcs. 79−2245
wave perturbations in ionospheric D-layer and F-layer 80−21873
wavenumber-frequency anal. of 500 mb geopotential at 50°N 79−5578
weather, anal. rel. to geomag. field vars. and solar activity 77−5308
weather satellite data, complex demodulation 78−49177
Weiner spectrum, fast Fourier digital quantum mottle anal. for radiography 77−52868
whistler propagation times eqn., inversion via spectral expansion 80−8495
whistler sonograms, anal. of quasiperiodic struct. 77−53316
whistlers, spectral-temporal anal. by digital methods 80−4175
wide-band spectrum analysis with area modulation 79−36840
wideband acousto-optic radiometry 78−77983
wideband spectrum analysis with area modulation 79−94159
wideband spectrum analysis with area modulation 79−94160
Wigner distribution function, optical production, speech signal analysis 80−48521
wind, tropospheric, flow periodicities during NE monsoon season 79−20917
wind field temporal and spatial scales over N.Pacific and N.Atlantic Oceans 79−79942
wind speed and atm. elec. field near ground, spectra and cospectra 78−11950
wind velocity spectra, determ. from cup anemometer meas. *(Russian)* 77−13102
wind waves, spectra via similarity theory *(Polish)* 77−21795
Wolf sunspot numbers, freq. anal. and forecasting 80−56797
X-ray analysis, high-speed, profile fitting method 78−75492
X-ray computerised tomography, energy-dependent reconstruction 77−12991
X-ray source counts, spectral anal. rel. to binarity detect. via Doppler effect *(Russian)* 78−77623
CO_2, atmospheric, conc. vars., cycles and trends 79−84381
^{13}C, improved techniques in spin-echo spectroscopy using chemical shift 77−48086
^{14}C concentration in Earth's atm. with variations of geomag. field, spectral anal. 78−61478
D_2O far IR laser pulses, real-time spectral anal. using SAW dispersive delay line 79−45983
Fe, conversion spectrum anal., outer-shell s-electron density, ACSEMP program 80−7208
SO_2 conc. and wind in Venice, Italy, spectral anal. 77−73824

spectral line breadth
see also atomic spectral line breadth; chemical shift; Davydov splitting; Doppler effect; EPR line breadth; molecular spectral line breadth; NMR line breadth; Stark effect; Zeeman effect
0254−334/2, high redshift QSO, P Cygni type absorpt. lines obs. 79−92886
1309−216, probable BL Lacertae object, absorpt. lines intrinsic widths and red shifts 80−67856
A-type stars, line profiles rel. to differential rot. 77−45409
A-type supergiant stars, reson. line profiles from IUE and Copernicus spectra 80−90424
absorption band shape model for mols. in damping medium 77−71794
absorption bands, optical activity, scatt. formalism treatment 78−72481
absorption spectra, collision-broadened lines, information anal. 80−22433
absorption spectra in QSOs, line shape analysis 78−36718
acetic acid, cryst., and isotopic species, H-bond, ν_s-ν_σ coupling and ν_s anharmonicity, IR spectra at 10K 79−15450
acetic acid, in cyclohexane soln., Raman scatt. near crit. stratification, temp. depend. *(Russian)* 79−11420
acetic acid and isomeric methyl formate, Compton profiles 77−30928
acetic acid-d_0(-d_1), Fermi reson., IR spectra band profiles 80−60569
acetonitrile, Rayleigh linewidth, in crit. region 79−24329
acetylene, He-Ne laser line, high temp. absorpt., anal. by high resolution IR spectra 80−91554
active polarisation spectroscopy by combinational light scatt. *(Russian)* 78−78006
adsorbed molecules, photoelectron line shapes, vibr. excitation and hole delocalisation effects 79−95905
adsorbed species, relax. shifts, line shapes and satellites in XPS and X-ray absorption spectra 77−90242
AES, background interferences in inductively coupled plasma discharges 80−22435
alkali halide: Ge^{2+}(Sn^{2+})(Pb^{2+}), T-centres, absorpt. spectra, energy level diagram 77−73157
alkali halide:O_2^-, frozen soln., impurity luminesc., zero-phonon lines interpretation 79−87488
alkali halide crystal, containing mol. centres, IR absorpt. spectra, 77-630K 79−99863
alkali halides, photoemission, energies and lineshapes 80−89119
alkali halides, spectra of O_2^-, S_2^- and NO_2^- mol. ions, electron-phonon interaction 77−52174
alkali intercalated graphite, C XVV Auger lineshape anal. 80−104019
alkali nitrites, molten, combination scatt. spectra, freq. shifts, jumps at melting, line widths *(Russian)* 77−40241

spectral line breadth continued
alkali-haloid salts, aqueous solutions, IR absorpt. ν_1 (CN) band parameter temp., conc. study *(Russian)* 80−80801
alkaline earth metals, atomic interaction effects in X-ray emission spectra *(Russian)* 79−69905
alkaline earth nitrites, molten, combination scatt. spectra, freq. shifts, jumps at melting, line widths *(Russian)* 77−40241
n-alkanes, depolarised Rayleigh spectroscopy 79−4808
allene, rot. diffusion in CS_2 soln., IR spectral profiles 79−87426
alloy, comp. modulation spectra, line shape 78−76491
alloys, oxidation, Auger spectra 78−14600
aluminophosphate glass, multicomponent, 3.2 micron broad absorption band computer anal., residual H_2O vibr. 78−52478
amorphous semiconductor, optical absorpt. edge shape, band edge fluctuations 77−20880
amorphous solids, electron-phonon interactions, fluoresc. line broadening and spectral diffusion 78−84655
analysis, digital computer method 79−83522
analyte emission characts., inductively coupled plasma, effect of emission spatial profiles 80−89557
anisotropic motion, and reson. line shape 80−7144
anisotropic NiAs-CdI_2 type structure, Mossbauer line broadening due to diffusion 77−12281
anthracene:chloranil, charge transfer spectra line shape 79−78700
anthracene, cryst., exciton aggregate possible form. under intense optical pumping, fluoresc. spectra 80−84772
anthracene, cryst., fluoresc. spectra, press. tuning 77−28612
anthracene, singlet-triplet absorpt. spectra, 2-300K, photoexcitation spectra 78−43890
anthracene, triplet exciton absorpt. lines 79−47475
anthracene, triplet excitons, phosphoresc. and delayed fluoresc. excitation spectra 78−63986
anthracene in 2 methyl-THF glass, low temp. fluoresc. bandshape, excess energy effects 78−76509
anthracene mol. cryst., exciton-lattice interaction and exciton absorption line shape 78−18968
anthracene vapour, conc. depend. of diffuse component of fluoresc. spectrum *(Russian)* 77−46601
anthracene-TCNB, charge transfer cryst., Raman study of phase transition 79−19885
antiferromagnetic extended Hubbard chain, excitonic effects on optical absorption 79−61323
antiferromagnetic polaritons, dispersion relation and light scatt. 77−35871
antiferromagnetic resonance linewidth theory, multimagnon processes contrib. 77−69708
antiresonance line shapes and radiationless decay, compatibility restrictions 80−48040
R Aquarii, Hα and forbidden O III emission line profiles 80−85946
α Aquarii, spectral line profiles vars. rel. to chromospheric event 80−31299
aromatic molecules in cryst. lattice, phosphoresc. intensity and optical nuclear polarisation, level anticrossing effects 78−91992
L-ascorbic acid, cryst. isolated OH iscillators, IR absorption, temp. and H-bond effects 80−7351
astronomical line profile measurements, accuracy 80−26751
astronomical spectra, Doppler broadening parameters meas. without spectrograph 78−20646
atom+diatomic molecule, collinear collision, light absorption 79−76486
atom pairs in solids, cooperative two-photon absorpt. lineshape 80−84706
atomic motion in resont fluctuating laser radiation 80−43310
atomic spectra in intense mag. fields, theory and appl. to dense stars atmospheres 80−105160
Auger line shape changes effect on depth profiles, correction 77−40605
Auger lineshape anal. of molecules and solids 80−76113
AR Aurigae, eclipsing binary Hg star, Hg II 3984 Å profile vars. during eclipse 80−98679
B 1 Ia-0 supergiants, P Cygni line profiles and mass loss 79−16948
band shape of IR spectra, slit width effect 80−86463
Bartels' theory of radiation from an inhomogeneous layer, appl. to plasma temp. meas. 80−53948
Be stars, electron scatt. effects on Balmer emission lines 80−17589
Beer-Lambert modified law calc. 78−82906
benzene:I_2, charge transfer spectra line shape 79−78700
benzene, in benzene-d_6 soln., IR and Raman spectra, line breadths, rot. diffusion consts. 79−56772
benzene, liq., spectral broadening of mol. transitions, librational broadening 79−51939
benzene, vib. relax. and Raman line widths 77−32359
benzene-d_6, liq., Raman spectra vibr. relax. and band widths 78−23440
benzene-d_6, splitting of vibrationless level in Jahn-Teller active state of D_{2h} symmetry 77−58080
1,12-benzoperylene in n-alkane, zero-phonon lines in luminesc. spectra 78−56512
beta spectra, response function correction for magnetic spectrometer 78−74532
beta-spectrometer, spectral line shape, electrostatic prism design effects 77−27239
biexciton, indirect band gap semiconductors, excitonic absorption band shape calc. 79−78015
biexcitons recombination, polariton effects 78−23033
biological cell suspension, electrophoretic analysis, Doppler spectra line shape smoothing 79−84053
blue variable stars at high galactic latit., spectral line profiles 78−32482
ξ Bootis A, G8 V star, line profiles Fourier deconvolution and mag. field obs. 80−72949
Brillouin spectra, multipass Fabry-Perot spectroscopy, linewidth correction 77−59583
broadening by photon interaction with new field and red shifts 79−48663
3C 120, radio galaxy, search for vars. in emission lines equivalent widths and profiles *(Russian)* 80−90540
3C 286 radio absorpt. line, profile rel. to cosmological deceleration meas. 78−20902
3C 33, radio galaxy, optical emission lines widths rel. to physical conditions in compact heads 80−51892
calcium alginate gels, Raleigh scatt., spectral broadening, density fluctuations 79−1776
α Camelopardalis (O9.5 Ia), variable Hα P Cygni profile 80−41818

spectral line breadth continued
UW Canis Majoris, O7f supergiant, UV lines P Cygni profiles rel. to mass loss rate 80−67736
α Canis Majoris (Sirius), Ca II K line high resolution profile obs. 80−56830
CARS spectroscopy linewidth parameter from laser mode structure 80−33083
U Cephei, eclipsing binary, gas stream effects in UV spectrum, IUE obs. 80−26898
VV Cephei, Mg II reson. lines profiles and absolute visual magnitude 80−109498
chemical laser, low pressure, line-shape flattening resulting from hypersonic nozzle wedge flow 80−91783
chemisorption systems, IR spectral linewidth and sticking coeffs., nonadiabatic effects 80−39423
chromosphere flare spectrum, line broadening as electron beam diagnostic 80−26827
coherent anti-Stokes Raman scatt., linewidth determ. by integrated power meas. 79−3744
coherent antiStokes Raman scattering, reson. excitation, lineshape 78−9415
coherent optics, T_2 as collision time, dephasing time, or reciprocal linewidth for teaching 80−27075
collision model for spectral line shapes, explicit parity considerations 77−58110
collisional linewidths and shifts determ. by convolution method 80−102541
colour-centre-phonon many-mode interaction, absorption band shape, adiabatic approx. 78−2883
complex band shapes, resolution by IR polarisation meas. 79−12873
condensed phase, reson. Raman and reson. fluoresc. spectra 78−80323
condensed phases, picosec. relax. polarisation spectrosc. meas. 78−68530
contour breakdown into two components *(Russian)* 79−49989
S Coronae Austrinae, a bright southern YY Orionis star, line profiles 77−29818
Crab Nebula, possible line feature at 73 keV, intensity and width 79−92829
critical fluid, Rayleigh linewidth meas., double scatt. effect 77−20865
crystal impurities, zero-phonon transitions, spectral characts. 78−2884
crystal vibrational spectrum, inhomogeneous thermal broadening effect 80−55100
crystalline solid of two-level atoms, resonance fluorescence 79−56844
crystals, line-shape distortion on anisotropic absorpt. meas. in unpolarised light 80−2765
crystals, theory of phononless line broadening for impurity center 78−35180
cyclotron absorption in mag. white dwarfs, Doppler and collisional broadening effects 80−4351
cyclotron lines in Hercules X-1 spectrum, first harmonic splitting 78−20912
cyclotron resonance lineshape for two-dimensional electron-phonon system, quantum theory 79−47336
P Cygni, H Paschen α equivalent width 80−62156
V1329 Cygni (HBV 475), symbiotic variable, nebular and Balmer line profiles 80−62148
V1500 Cygni (Nova 1975), Balmer line emission profiles evolution in early decline phase 80−82371
V1500 Cygni (Nova 1975), models for 3 hour line profile vars. 79−8920
V1668 Cygni (Nova 1978), Hα emission line profiles obs., (1978 to 1979) *(Russian)* 80−109444
cytochrome-c, coherent reson. Raman scatt. and incoherently broadened reson. fluoresc., condensed phase 78−60429
Dawson function for Voigt and Doppler profiles *(Japanese)* 78−58623
deconvolution by Fourier analysis 79−12861
DFB laser, limiting spectral characts. 79−64197
DFS-8 spectrograph, attachment for oscillographic recording of line shapes 80−105721
diamond, two-phonon Raman peak linewidth, bond polarisability model 77−77212
diamond, two-phonon Raman spectrum, harmonic pot. and bond polarisability model 77−77213
diamond, valence electrons XPS spectrum, OPW calc. 77−4715
1,4-dibromonaphthalene, k-k scatt., exciton dephasing time-resolved phosphoresc. obs. 80−11458
1,4-dibromonaphthalene, S_0 to T_1 exciton transition, optical dephasing time and lineshape function 78−15183
(1,4)-dibromonaphthalene, triplet exciton scatt., absorpt. spectra 78−6696
4,4′-dichlorobenzophenone, cryst., $T_1 \leftarrow S_0$ singlet-triplet absorption profiles, temp. depend., phonon-exciton anal. 78−60436
4, 4′-dichlorobenzophenone, triplet exciton absorpt. band, zero phonon line *(French)* 79−33726
1,1′-diethyl-2,2′-cyanine iodide, neat and mixed crysts., visible absorption and emission spectra assignments 77−1692
1,3′-diethyl-2,2′-quinolylthiacarbocyanide iodide, soln., 78−68530
diethylammonium cadmium tetrachloride, first order phase transition, optical phonon line broadening, spin-phonon coupling model 80−7335
dimethyl ether, condensed multilayers, electron bombard. effects, AES line-shape anal., XPS, and desorption meas. 80−7450
1,6-diphenylhexatriene soln., light quenching effect on fluoresc. band shape 79−98148
discharge, low-pressure, shape and width of ion line, use on diagnostic 77−35386
discharge tube, hollow cathode type, with conical bottom, spectroscopic and elec. characts. 80−31891
disordered systems, optical excitation spectral transfer. generalised models 79−43027
dispersion vs. absorption curve method for distinguishing peak position distrib. from linewidth distrib. 80−4775
Doppler broadened laser amplification line frequency characteristics meas. 78−59060
Doppler broadening, elimination problem, parametric soln. 80−62730
S Doradus, Hubble-Sandage variable in LMC, visual line profiles rel. to mass loss 80−101595
dye CW laser, spectral narrowing and continuous tuning by grating beam-expansion 79−59720
dye CW laser, spectral narrowing by intracavity Na atomic beam 79−55159
dye laser, difference frequency generation, degree of conversion depend. on linewidth 80−48347

spectral line breadth continued
dye laser, flashlamp-pumped high-energy, spectral narrowing by two-stage injection locking 79−81450
dye laser, line width using high dispersion rutile prism for tuning 77−7107
dye laser, self frequency locking, strong field effect on intracavity atoms 79−86198
dyes, saturable, for Nd laser, bleaching spectra 77−42573
dynamic Jahn-Teller systems, calc. of absorption band shapes, use of Lanczos algorithm 80−45023
early-type stars, H and He^+ synthetic line profiles in stellar winds 80−85926
early-type stars, line profiles Fourier anal. for photospheric expansion meas. 78−93224
education, hadronic atom strong interaction induced level widths and shifts, WKB calc. 77−78923
electron cyclotron reson. lineshape analysis for cylindrical cavity field inhomogeneities 78−13560
electron spectroscopy of core levels in solids, lifetime broadening 80−80938
electronic line profile, narrowing and oscill. *(Russian)* 79−56859
emission line shapes from a rotating ring radiator 80−83998
emission lines in Be-stars, V/R var. rel. to gaseous ring 77−37604
emission spectra and phonon relax. 77−77279
emission-line profile computations for Be-stars 77−56920
ethane-1,1,1-d_3, gas-phase IR spectra, rot. fine struct. obs. 80−83359
ethylammonium cadmium tetrachloride, order-disorder transition, far IR reflectivity obs. 79−65870
ethylene, He-Ne laser line, high temp. absorpt., anal. by high resolution IR spectra 80−91554
excitation energy transfer and migration, spectral line broadening 80−2841
exciton absorption spectra, dislocations effect on band profile 80−16070
exciton line shapes and migration with stochastic exciton lattice coupling 79−11070
exciton-phonon parameters from absorption band shape *(Russian)* 77−28533
exciton-photon interaction, exciton absorpt. lineshape, polariton and wave models 79−38564
F-centre optical absorption bandshape calc. for transition to state with Jahn-Teller and spin orbit couplings 80−55135
Fabry-Perot interferometer, instrumental convolutions, linewidth anal. determ. 80−31904
Fabry-Perot spectrometer, instrumental function influence on spectral profiles 77−67503
Fabry-Perot spectrometer instrumental function determ., Voigt function assignation *(Spanish)* 80−52322
far IR transmission spectral bandshape 77−32363
far wing line broadening, quasistatic theory, appl. to alkali-rare gas mols. 79−22762
ferrimagnetic resonance near mag. compensation temp. 77−51963
ferroelectric, susceptibility, Raman line shape of overdamped mode 79−91426
ferromagnet, shape of Mossbauer line 80−71251
ferromagnetic, thick film, reson. transmission of EM energy via phonons 80−60382
ferromagnetic polariton linewidths, theory 78−87918
ferromagnetic resonance absorpt. lineshape 24 GHz microwave transmission apparatus 77−49755
ferromagnetic resonance line, uniform, at finite temps., dislocation broadening 78−19334
ferrous rubredoxin, high spin, spin fluctuation rates from Mossbauer spectra 79−29506
fluid, dense, isotropic Raman polaris., correlation function, kinetic eqn. 77−28567
fluorescence line narrowing, line-shape deconvolution 80−89039
formaldehyde, pressure-broadened linewidths in microwave region, temp. depend. 77−34694
Fourier transform ion reson. spectroscopy of ions undergoing collisions with mols. 80−35598
G200-39, hot hybrid white dwarf, H and He I line profiles 80−26852
Galatry profile convolved with Fabry-Perot instrument function 77−78642
galaxies, H I profiles appl. to mass determ. 80−56937
galaxies, IR magnitude/H I vel. width relation rel. to distance scale and Universe expansion rate outside Local Supercluster 80−105325
galaxies active nuclei, Balmer line ratios rel. to ionised gas and dust 79−88730
galaxies H I lines, widths rel. to distance determ. 77−29920
galaxies velocity dispersions and redshifts survey, data reduction techniques 80−22074
n-GaP, quasidirect radiative recombination of free holes at neutral shallow donors 78−64410
garnets, magnetic relaxation phenomena 79−99776
gas, inhomogeneous layer, transmission calc. for spectral line with Voigt profile 80−59164
gas laser regeneration mode with saturation effect taken into account 77−650
giant stars, circumstellar line profiles rel. to mass loss 77−9743
glass, fluoresc. linewidth 80−34978
glass, fluorescence linewidth, anomalous of impurity ions, theory 80−50404
glass, linewidth and anomalous dispersion of ultrasound 77−39636
glass targets, laser-produced plasma X-ray spectral lines identification *(Chinese)* 80−54036
graphite, reflectivity in near IR under hydrostatic press., lineshape anal. 79−91424
graphite intercalation compounds, C_8M, (M=K, Rb, Cs), Breit-Wigner line shape anal., Raman spectra 80−50336
graphite interclation with Li, Raman scatt. study 80−88999
HD 168607 (B9 Ia^+), S Doradus type star candidate, spectral line profiles *(Russian)* 80−90456
HD 34452, Si Ap star, spectrum and line profiles vars. 78−65634
HD 50896, WN5 star, emission-line profiles vars. 80−51791
heavily doped semicond., photoemission lineshapes of impurity levels, p-wave resonance 80−76154
Hercules X-1, X-ray cyclotron line features width calcs. 80−86015
AM Herculis, X-ray binary, vel. curves for emission lines broad and sharp components 78−32513
heuristic model for line profiles, general Lorentz function *(German)* 78−37074
high resolution spectroscopy of atoms and mols., without Doppler broadening, laser techniques 77−54631
high-resolution laser spectroscopy, techniques and applications 77−57403
high-Z emitters in ultradense plasmas, hydrogenic profiles, perturbing ion effects 80−79566
hollow cathode lamp, spectral lines width and intensity, high freq. field effects 78−16856
HR 8752 (HD 217476), superluminous supergiant, line profile vars. rel. to expanding shell 79−80308
Hubbard chain, half-filled band, strong coupling, low temp. absorpt. lineshape 77−59546
hydrates, vibrational spectra, H^+ and OH^n aq. soln. 79−73916
hyperfine spectra lineshapes, stochastic model for classical bath variables 77−85631
IC 4329A, Seyfert galaxy, optical spectrum and line profiles 80−36706
ice, pure and acidic, electron irrad., ESR of H atoms, motional narrowing and spin polarisation 77−20706
ICR spectra, line shapes, linear response theory appls. 79−2874
II-VI semiconductor mixed crystal, comp. disorder-induced broadening for free excitons 79−15479
II-VI semiconductors, highly excited blend type involving free particle scatt. 79−38648
impurities in solids, absorpt. and emission line shapes, quantum-mechanical moments 78−72566
impurity absorption and emission in solids, Poisson distrib. moments 80−25419
impurity absorption and fluorescence spectra, quadratic electron-phonon interaction and impurity-ion band shape 78−6731
impurity centres, electron-phonon coupling from structured optical spectra, review 80−89038
inert gas, dense, depolarised Rayleigh scatt. 79−69851
inert gas crystal, lattice vibrs. and radiative transitions of implanted ions *(Russian)* 80−69098
inhomogeneous semiconductor, impurity opt. absorpt. and photocond. spectral line profile variation 77−16352
inhomogeneously broadened spectrum, saturation kinetics *(Russian)* 79−86222
inhomogeneously broadened systems, spectral-spatial diffusion 77−77280
intensity fluctuation linewidth, Jakeman-Pike approx., black-body and laser models 78−58960
interplanetary H I, Lα emission profiles reanal. rel. to local interstellar gas temp. and vel. 80−105141
interstellar absorption lines towards 30 Doradus central object (HD 38268), profiles 80−51839
interstellar clouds, spectral line widths rel. to vel. fields 79−12398
interstellar formaldehyde, absorpt. line widths in small dust clouds 77−5558
interstellar H_2O *(Russian)* 80−105320
interstellar matter towards ζ Ophiuchi, narrow-lined cloud obs. from RF mol. emission spectra 80−26958
interstellar molecular clouds, line profiles rel. to radiation transport and kinematics 78−93347
interstellar spherically symmetric radially moving clouds, spectral line shapes 78−20865
intracavity spectroscopy, laser output spectrum, lineshape 79−55155
iodide, charge transfer to solvent spectra, spectral shift data, Madelung const. determ. 80−85204
ion bombardment-induced photon emission, spectral features, mechanisms band struct. depend., review 77−44072
ionic halide crystals, mol. model for V_k centre 77−85567
ions, positive, dielectronic recomb. in plasma generalised cascade theory 80−43851
ions in solids, time resolved fluoresc. line narrowing 79−38611
IR ν_s absorption band profile of isotopically diluted OH group in crysts. 79−69821
IR intensity measurements, by band contour anal. 78−29182
IR spectral lines, intensities and half widths, nonlinear least squares calcs. 77−52682
Ising model, 2-D, mag. reson., appl. to $FeCl_2$ 79−47323
isopropyl benzene, mol. solid, temp. depend. UPS linewidths 80−89115
Jahn-Teller multimode effect for E-term with strong vibronic coupling, IR and Raman spectra band shapes 80−20139
Kerr effect, Raman-induced, line shape calc. *(German)* 79−50358
EV Lacertae, flare star, Balmer emission lines vars. rel. to starspots and rot. period 80−98665
laser, single-mode, modal noise suppression by dithering laser's operating point 79−94357
laser diode, spontaneous emission linewidth, calcs. 77−10927
laser spectroscopy, finite bandwidth laser excitation, line shapes, non-perturbative effects 80−52332
late-type supergiant stars, line widths rel. to luminosity 77−60753
latex, sol, diffusion coeff. meas. by photon correl. spectroscopy 77−10117
48 Librae, Be star, shell spectrum line profiles 80−62146
light echo angular spectroscopy, inhomogeneously broadened lines 80−43406
line broadening theory, screening process dynamics *(Russian)* 80−69988
line contours in incoherent scatt. 79−88590
liquid, barrier to internal rot., IR spectral linewidths meas. 78−72507
liquid, induced Raman scatt., anomalous line broadening 78−56490
liquid, Raman band profile, vibr. dephasing and intermolecular interactions 80−60556
liquid, US-induced birefringence, Brillouin scatt. linewidth, sound absorption coeff. 78−27180
liquid, VH depolarised light scatt., orientational and translational motion coupling const., shear viscosity depend. 77−59584
liquid, vibr. dephasing and gas-liq. crit. density fluctuations 79−51954
liquid, vibr. relax., line widths, intermol. forces dephasing 77−47315
liquid mixture, anomalous broadening of excited Raman scatt. lines *(Russian)* 77−52103
liquid phase band contours, data processing, band shape corrections 78−27215
liquid solution, nonlinear reson. processes, influence of spectral line broadening mechanism 79−7181
lithium acetate dihydrate, γ-irrad., methyl radical, ENDOR, line-shape model appl. 79−73853
localised centres in strong EM fields, multiquantum transitions 78−10936
longitudinally detected ESR, lineshapes, density matrix formalism calcs. 79−82894

spectral line breadth continued
Lorentz function convolution with spectral line data, accelerated convolution algorithm 79−81239
Lorentz function of n-th degree represent. of line profiles *(German)* 78−37075
Lorentzian lines, calculation of modulation broadened 77−48029
lower main-sequence stars, line profiles Fourier anal. rel. to rot. vel. 80−51767
LS I+61°303, radio, optical, X-ray, gamma-ray Be star with very broad Balmer lines 79−88755
luminescence, nonuniform broadening profile, optical excitation migration effects 78−48215
luminescence line profile, microscopic theory 79−28832
Lyman-α line shape of high-z emitters, effect of fine struct. splitting in ultradense plasmas 79−64912
β Lyrae, H emission profiles rel. to pattern of gaseous flow in system 78−57576
macromolecular, solutions, Rayleigh scatt., elec. induced variations, spectral width and intensity meas., review 78−48187
macromolecular relaxation time spectra rel. to luminesc. depolarisation function *(Russian)* 77−31040
macroradical, electron spin echo spectra, instantaneous and conventional spectral diffusion 79−15355
magnetic crystal, with impurity centre, anomaly of width and lineshape of light absorpt. 78−76499
magnetic DA white dwarfs, spectral line and circular polarisation profiles 80−62123
magnetic resonance, line shape for inhomogeneous mag. field 79−38365
magnetic resonance line width, theory of exchange narrowing 77−66411
malachite green, soln. picosec. relax. polarisation spectrosc. meas. 78−68530
maser with beam of inflying atoms, spectral line broadening mechanism 80−106503
measurement accuracy, apparatus function effects *(Russian)* 77−13800
mesitylene:tetracyanoethylene, charge transfer spectra line shape 79−78700
metal, 3d, X-ray emission and XPS broadening, many-body effects and intra-atomic exchange 77−44090
metal, cyclotron reson. line shape in inclined mag. field *(Russian)* 77−36136
metal, ferromagnetic resonance linewidth, interaction of spin waves with conduction electron current 80−25216
metal, K- and L-emission bandwidths from characteristic electron energy loss values 79−83057
metal, narrow-band, quasiatomic Auger spectra and electron correl. effects 77−81183
metal, XPS and X-ray absorption spectra, thermal broadening of core levels, many-electron effects 78−31284
metal cavity, lifetime of trapped excited atom, broadening mech. for optical absorption line 79−38578
metallic ferromagnetics, two-magnon scatt. on dislocations, resonance linewidth broadening 77−20708
metallic system, X-ray line shapes for core levels, phonon broadening 77−12464
metallophthalocyanines, α-phase solid, absorpt. and MCD spectra 79−73964
metals, narrow-band, Auger line shape 80−60719
methane, ^{12}C and ^{14}C, line parameters for ν_2 and ν_4 bands, isotope shifts, appln. to planetary atmospheres 80−95622
methane, Compton profiles, high energy electrons impact spectroscopy 77−27188
methanol, condensed multilayers, electron bombard. effects, AES lineshape anal., XPS, and desorption meas. 80−7450
methanol, Rayleigh linewidth, in crit. region 79−24329
methanol dehydrogenase, spin echo powder ENDOR, line shape aspects 79−34485
methyl alcohol IR transitions, saturated absorption spectroscopy 77−38874
methyl bromide, pressure-broadened linewidths in microwave region, temp. depend. 77−34694
methyl formate and isomeric acetic acid, Compton profiles 77−30928
methyl iodide, vib. relax. and Raman line widths 77−32359
3-methylpentane-nitroethane, binary fluid, Rayleigh linewidth meas. near crit. point 78−48190
2-methyltetrahydrofuran glass, 77K matrix ENDOR line shape model and expt. 78−6600
mixed crystal, line profile of absorpt. and Raman spectra, calc. 78−48183
mixtures, Rayleigh line narrowing near critical mixing pt. 79−56803
molecular crystal, exciton scatt. by lattice defects, absorpt. line shape 79−38576
molecular crystal, Stark modulation of Lorentzian line shapes, Fourier anal. 77−1691
molecular crystal IR spectral line shape and polarisation temp. depend. 80−88991
molecular crystals, barrier to reorientation of mols. from LF lattice vibr. spectra 77−69824
molecular crystals, exciton interband transitions absorpt. band shapes 77−20876
molecular crystals, exciton-lattice interaction and exciton absorption line shape 78−18968
molecular crystals, optical absorpt. line shape of excitons, two-time correl. function calcs. 79−44795
molecular crystals, struct. disorder effect on optical props. 77−90165
molecular crystals, thermal modulation spectroscopy, electron-phonon interaction 77−32392
molecular glass, density of states for IR active internal modes of tetrahedral mols. 78−75788
molecular liquids, IR absorpt. lineshape, orientation density fluctuation effects 78−48171
molecular liquids, vibr. line broadening, Zwanzig-Mori theory and quasielastic processes 78−27221
molecules in strong solvents, spectral band shape, rot. diffusion model 79−64048
Mossbauer line broadening due to correlated diffusion 77−73097
Mossbauer line broadening due to Mossbauer atom diffusion via vacancies 79−73868
Mossbauer line narrowing by resonant filter 80−77922
Mossbauer line narrowing due to motion of emitting atoms in periodic field 77−43914
spectral line breadth continued
Mossbauer line profile, effect of diffusion in external force field *(Russian)* 78−19382
Mossbauer line shape, in presence of ionic charge relax., perturbation calc. 77−28495
Mossbauer line shape, Liouville relax. supermatrices 79−28649
Mossbauer line shape in presence of external periodic perturbation 78−84502
Mossbauer lineshape, in presence of electronic relaxation *(Rumanian)* 78−60368
Mossbauer linewidth, thermal motion effect, second order Doppler effect *(German)* 77−43924
Mossbauer relaxation spectra, interference effects 77−63326
Mossbauer relaxation theory 80−39954
Mossbauer spectra, line-broadening 80−93221
multi-pulse spectroscopy with Ramsey fringes, resolution and signal strength 78−82869
N70, giant filamentary shell in LMC, line profiles rel. to dynamics 80−90511
naphthalene: pentacene, intermol. interaction dynamics and optical dephasing 80−64112
naphthalene, a-exciton lineshape, exciton-photon coupling 79−33243
naphthalene, a-exciton temp. depend. scatt., optical absorpt. profile 78−72088
naphthalene, cryst., fluoresc. spectra, press. tuning 77−28612
naphthalene, doped, zero-phonon lines and absorpt. spectra, temp. depend. of shift and broadening 79−69866
naphthalene, molecular cryst., phonon scatt. and exciton linewidths 78−15185
naphthalene, solid, high-energy vibr. overtone spectra, local modes, intramol. relax. 79−28052
naphthalene, triplet excitons, phosphoresc. and delayed fluoresc. excitation spectra 78−63986
naphthalene, vibr. dephasing and Raman active localised internal mode temp. depend. 80−45060
naphthalene, vibr. relax. studied by four wave mixing (CARS), spectral lineshapes obs. 80−80762
naphthalene-d_0, (-d_4), (-d_8), inequivalent local C-H modes, subpicosec. dephasing, high energy overtones 79−86850
naphthalene-h_8 and -d_8 mixed crystal, two-dimens. lattice, cluster-cluster interactions, model inhomogeneous distribs. 79−23922
naphthalene-TCNB (PMDA), Raman spectra orientational disorder, charge transfer cryst. 78−19459
naphthalenes, phonon satellite narrowing in local exciton luminesc. *(Russian)* 79−47507
narrow linewidth meas. using Fabry-Perot interferometer of limited resolution 77−26408
neopentane:tetramethyltin, Mossbauer exam. of plastic phase transition 77−69759
Neptune reflected spectrum, effects of seeing rel. to rot. period determ. 80−46479
NGC 3516, Seyfert galaxy, emission line breadths and intensities 77−26052
NGC 604, 5471, giant extragalactic H II regions, P Cygni line profiles in UV spectra 80−77467
NGC 604, H II region in M 33, Hα line profile width rel. to core-halo struct. 80−85984
NGC 650/1, planetary nebula, emission line profiles and internal kinematics 80−17639
NGC 6888, ring nebulae around Wolf-Rayet star HD 192163, filaments and smooth gas linewidths *(Russian)* 80−90515
nitrobenzene, liq., induced Raman scatt., anomalous line broadening 78−56490
nitrobenzene-n-hexane, crit. mixtures, reorientation spectra, linewidths and intensities 79−28777
nitrobenzene-n-hexane crit. mixture, depolarised Rayleigh linewidth meas. 77−81112
nitroethane-3-methylpentane, binary liq., depolarised light scatt. at crit. point 78−39558
NMR, Voigt profile analysis, Fourier transform approach and least-squares curve fitting 77−20729
NMR spectral lineshape analysis of two-site exchange kinetics, student expt. 77−26118
noble metals, many-body effects in X-ray photoemission 77−28684
non-equilibrium gas, Doppler broadened spectral and time correl. functions 78−14122
non-equilibrium phonon distrib., in cryst., spectral line shape theory 80−60530
non-Lorentzian laser lineshape and reversed peak asymmetry in double optical reson. 80−69443
nonafluoroisobutane, IR spectra, spectral bandshape and intensity of C-H chromophore 80−83355
nongrey radiation, IR band model correls. 77−57286
nongrey two-dimens. medium, band or line shape effect on radiative transfer 77−62139
nonlinear absorption method in magnetic field for spectral line width and shift meas. 80−37066
nonlinear crystals for frequency conversion of optical radiation, review *(Russian)* 80−38068
nonlinear laser spectroscopy, gravitational effects 79−67391
nonlinear optical phase conjugation, compensation for channel dispersion 79−45993
nonlinear spectroscopy, recoil effects on Doppler-free lineshapes 80−82829
nonmetal, impurity optical absorption and emission, anharmonic effects 78−56503
Nova Cygni 1978, P Cygni lines widths and atmosphere expansion vel. 78−89213
Nova Delphini 1967 (HR Delphini), emission lines widths var. rel. to circumstellar envelope *(Russian)* 78−77564
NQR precision thermometry, freq. meas. improvement 80−22356
nucleon-nucleus inelastic scatt. leading to resonant states, line shape 77−54211
Nylon 66, stress-oriented NMR expt. using multiple impulses to achieve line narrowing *(German)* 77−28457
O3 to O5.5 type stars, equivalent width and line profiles 77−33481
4-octyloxy-4′-cyanobiphenyl, CN stretching in liq. cryst. phases, vibr. spectra 78−80325
opaque semi-infinite crysts., dynamical light scatt. from dielec. bulk waves, phenomenological theory, appl. to n-InSb 79−69829

spectral line breadth continued
70 Ophiuchi A, K0 V star, line profiles Fourier deconvolution and mag. field obs. 80−72949
ρ Ophiuchi dark cloud, atomic and mol. line widths rel. to contraction 78−41013
optical absorption band shapes, reconstruction from moments 78−37686
optical free induction decay, subnanosecond, with novel laser freq. shifting 80−38075
optical frequency standard, collision shift and broadening *(Russian)* 79−59783
optical glasses, Brillouin scattering meas., sound vels., Pockels coeffs., phonon damping 79−95792
optical line broadening owing to kinematical exciton and polariton levels 79−56134
organic compounds, inhomogenously broadened absorption spectra, linear struct. detect. *(Russian)* 78−76504
organic molecule, complex mixtures in solid-state matrices, dip shape saturation effects on nonuniformly broadened spectra 79−95799
organic solids, cryst. and amorphous, optical spectra, Urbach rule, struct. disorder effect 78−23479
organic solids, vibr. relax. and dephasing Raman spectra, review 80−88987
ζ Orionis, Reticon obs. of Hα P Cygni profile 80−82365
YY Orionis stars line profiles, spectral line form. in axisymmetric moving envelopes 80−41813
oscillating arc plasma, optical characts., H_α spectral line profile *(Russian)* 77−19775
overlapping components of spectral line, numerical method for separation 78−21227
paramagnet, Heisenberg, two-spin Raman scatt. 77−85715
particle shape, in laminar flow, by optical mixing *(Russian)* 79−10619
β Persei (Algol), UV line profiles obs. rel. to primary component rot. 80−72996
perylene in n-alkane, zero-phonon lines in luminesc. spectra 78−56512
PET, IR, spectra of prefractured state 77−69032
phenanthrene, cryst., refl. spectra of first singlet transition 78−88323
phenanthrene, molecular cryst., phonon scatt. and exciton linewidths 78−15185
phenol(-d_1)-dioxan(-acetonitrile), in carbon tetrachloride ($CDCl_3$) solns., H-bonds vibr. relax. bands anal. 78−84560
phonon-assisted radiative electronic transitions 79−24348
Phonon-cyclotron absorption in a transverse electric field 78−2741
phosphoric acids, n.m.r. linewidths rel. to glass transition temps. 77−4050
photoelectron, and hole recoil and vibrational shake-up, in mols. and solids 80−55265
photoelectron spectra, lineshape transformations for Fourier transform resolution enhancement 77−90250
photoemission, many-body effects, book contrib. 78−95667
photoemission spectra calc. using wave mech. scatt. techniques, book contrib. 78−95666
photon correlation spectroscopy, liquid surfaces, effect of instrumental broadening 77−87852
photon correlation spectroscopy, using jet stream dye laser 77−10117
photon echo, anomalous time shape, induced by two successive light pulses 78−18021
photon kinetic equation for Doppler line broadening, soln. 78−9751
photon-correlation spectroscopy, spectral parameter extraction 78−77993
photosynthetic systems, discovery of phase transitions, Stokes Raman scatt. 80−81539
phyllosilicates, IR band widths comparison with interstellar 10 micron absorpt. band 79−80344
Pioneer 10 and 11 radio signals, spectral broadening by ionospheres of Jupiter and Saturn 80−109391
plasma, Lyman-α, line broadening calc. 80−43984
plasma, model of non-thermal RPA plasma 79−46433
plasma, nonthermal, two-temp. electron gas, collective elec. field fluctuations estimation 80−43882
plasma, photoabsorpt. cross sections 77−7515
plasma, spectral lines, complex level shift 78−26253
plasma, turbulently heated, electron cyclotron radiation spectral line width collisional broadening 78−34369
plasma discharge, spatially-resolved spectrometry, radial emission line profiles, Abel inversion 77−12841
plasma electron density, determ. by spectral line width, at. oscill. strength effects 77−51230
plasma line broadening, correlations in quantum theory 77−7514
plasma optical transparency evaluation, line broadening effect 80−79453
Pleione (28 Tauri), metallic shell lines widths correl. with ionisation potential 80−8637
PMMA, molecular interaction in frictional-contact zone, absorpt. spectra 79−78688
polar molecule in soln., broadened band contour anal. 77−496
polariton kinematical levels resulting from excitons interaction, optical absorption line broadening 80−10892
polycaproamide, molecular interaction in frictional-contact zone, absorpt. spectra 79−78688
polyethylene, molecular interaction in frictional-contact zone, absorpt. spectra 79−78688
polyethylene terephthalate, molecular interaction in frictional-contact zone, absorpt. spectra 79−78688
polymer solutions, random coil, intramol. fluctuations by photon correl. spectroscopy 77−48184
polypeptide hormones, conformations, ODMR investig. 78−76356
polypropylene, molecular interaction in frictional-contact zone, absorpt. spectra 79−78688
polypropylene glycol, Rayleigh-Brillouin spectra calcs. 79−47465
polystyrene, O treated, interaction with vapour-deposited Cr and Ni atoms 80−3407
polystyrene, soln., laser light scatt. Rayleigh linewidths anal., intramol. motion 77−3500
polystyrene-cyclohexane mixture, Rayleigh and Brillouin scatt. and struct. relaxation 80−63640
positron annihilation and vacancy formation, Doppler broadening study 80−60708
positron annihilation gamma-ray lineshape parameters 77−69929
positron annihilation line broadening, Ge detector 77−16418
positron annihilation lineshape measurement, simple correction technique 77−63482
positron-annihilation, Doppler broadened line shapes 79−19947
positrons, planar channelled, radiation characts. 79−55797
spectral line breadth continued
pressure broadening asymmetry factor in unified Franck-Condon method 77−46536
pressure line shape in impact approx. with Debye screening, semiclassical and quantum calcs. 78−37591
pressure-broadening cross-sections, averaged j_z-conserving coupled states approx. 77−54585
profile correction for instrumental influence, numerical methods, astron. appl. 79−35148
profile recording, high resolution, using Fabry-Perot interferometer and monochromator 80−42268
profile recording with high time resolution 78−86351
propylene, He-Ne laser line, high temp. absorpt., anal. by high resolution IR spectra 80−91554
PTFE, molecular interaction in frictional-contact zone, absorpt. spectra 79−78688
pulsed hollow cathode lamp characteristics 78−67530
RX Puppis, peculiar emission-line object, P Cygni profiles 79−44497
ζ Puppis, Reticon obs. of Hα P Cygni profile 80−82365
pyrene, triplet exciton absorpt. lines 79−47475
Q 2240.9−3702, Q 2238.9−4115, QSOs, broad-lined absorpt. systems widths 80−4456
QSOs high-redshift, emission-line profiles and emitting regions props. 79−21458
quadratic electron-phonon interaction effect 77−32342
α-quartz, Raman spectral lines, radiation and temp.-induced changes in width and intensity 78−2859
quasars, spectral line profiles interpretation *(Russian)* 79−101203
quasi-Jahn-Teller optical absorption line shape due to transition from A_{1g} to $(A_{1g}+T_{1u})\times t_{1u}$ system 80−92862
quasi-stellar objects, H emission line ratios implications 80−56968
radiation redistrib., diffuses reflection effects 78−53819
radiative transfer, calc. methods for line broadening by electron scatt. *(Russian)* 77−17347
radiative transfer, non-LTE, asymptotics of partial redistrib. 80−62008
Raman effect in solids, interacting elementary excitations, review 78−43846
Raman scattering investig. of polaritons in solids 77−40238
Raman scattering of light by polaritons, reviews 80−34928
Raman spectral line shape, quantum field theoretic formulation 78−31187
Raman spectroscopy, resolution enhancement, using polarisation data 78−74062
Ramsey fringes in saturation spectroscopy 78−82868
random arrays of grains, spectral properties 80−12727
rare earth metals, atomic interaction effects in X-ray emission spectra *(Russian)* 79−69905
rare earth tellurides, electron density distrib. from Mossbauer spectra 78−23374
Rayleigh scattering linewidth near pt., simple fluid, gravity effect 77−85735
recoil effects in nonlinear spectroscopy, quantum representation of mol. motion 77−39000
recombination lines in primordial microwave radiation, intensities and profiles 78−54097
relativistic gas, Doppler shift distribs. 78−65492
resolution, refinement of initial parameters by least-squares procedures 79−41198
resonance filter of defect SnO_2 for Mossbauer line width reduction 77−24767
resonance fluorescence, Doppler-free obs., fluorescence-line-narrowing method and improvement 79−13840
resonance Raman lineshape studies of vibrational and rotational relaxation in soln. 80−60560
resonance Raman lineshapes and fluorescence in strong radiation fields 80−87074
resonance Raman scattering, appl. to ultrafast dephasing and relax. obs., phonon scatt. effects 80−7337
resonance scattering line, Monte Carlo calcs. for line width with absorpt. or differential expansion 80−21901
resonant Brillouin scatt. as form of modulation spectroscopy 79−91456
resonant-pulse propagation method for line-shape parameters analysis 79−55168
rhodamine B activated waveguide, amplification of narrow-band signal 79−36930
rhodamine dye polar frozen solns., luminesc. broadening 80−2834
Rochelle salt, cryst., oriented intrinsic absorpt. edge shape 77−66505
Rochelle salt, ferroelectric, Raman and IR study 80−71406
rotational effects on spectral lines 79−97050
ruby, cryst., lasing action, spectrum, luminesc. spectrum effects *(Russian)* 78−13716
ruby, fluorescence line narrowing, energy transfer studies 78−84642
ruby, R-lines breadths and shifts rel. to high press. calibration 77−18106
ruby, radiative spectral transfer, time resolved fluoresc. 78−2900
ruby, Raman ^2E and phosphorescence transitions, line widths, time correl. study 80−20621
ruby, selection rules and absorpt. line widths of 10^{12} Hz phonons, optical meas. 77−36272
ruby R_1 zero phonon line, resonance fluoresc. meas. 80−89055
WZ Sagittae, recurrent nova, Balmer emission lines double-component struct. during 1978 outburst 80−56849
saturation spectroscopy, lineshape, vel. changing collisions *(French)* 78−12765
ζ^1 Scorpii, extreme B1 supergiant, UV reson. lines profiles 80−4349
second order optical processes, intermediate state interaction stochastic models 77−48243
second order optical processes, stochastic models of intermediate state interaction, stationary response 77−85769
second order optical processes, stochastic models of intermediate state interaction, stationary response 77−85770
selective excitation spectroscopy, particle kinetics 78−82046
semiconductor, donor van der Waals interactions, spectral lineshapes 80−11450
semiconductor, impure, exciton absorpt. line shape calc. *(Russian)* 78−10934
semiconductor, light absorption, temp. depend., exciton-exciton and -phonon interactions *(Russian)* 77−40265
semiconductor, photoluminescence, deep level recombination temp. depend. 79−47497
semiconductor, Wannier-Mott polaritons in mag. fields, review 78−2437

spectral line breadth continued
semiconductor, weakly inhomogeneous, impurity absorpt. and impurity photocond. line profiles 78−19098
semiconductor, wurtzite-type, emission lineshape of excitonic mols., polariton states 77−20918
semiconductors, high density excitons and biexcitons, recomb. radiation bands profiles, time depend. 80−45140
semiconductors, luminesc., electron beam or optically excited, quasi-equilib. approx. 80−84779
semiconductors, quantum limit cyclotron resonance linewidth 80−7171
semiconductors and metals, Mossbauer spectra of implanted ^{83}Kr, line widths, isomer shifts 80−39899
Seyfert galaxies, broad H lines prod. by suprathermal protons passing through neutral gas *(Russian)* 78−57642
Seyfert galaxies, nearby, Hβ line width correl. with morphology 80−82478
Seyfert galaxies, spectral line profiles interpretation *(Russian)* 79−101203
Si:P(As)(Sb)(Bi), high resolution study of group V impurities absorption 80−7388
signal to noise improvement by numerical procedure 78−65981
silicate galss:Eu^{3+}, fluoresc. linewidth variation, electron-phonon coupling 78−19531
silicate glass: Cr^{3+}, optical props., 88-273K, energy levels in crossing region 78−6709
single-mode gas laser with slightly anisotropic resonator, output polarization stability 80−43370
solar corona, intensity ratios of fine-struct. components of H like ions reson. lines 80−101581
solar corona, temp. determ. from line breadths in electron scatt. continuum 77−22169
solar corona green and red lines, intensity ratio rel. to coronal temp. 77−22168
solar emission line profiles of inhomogeneous formations 77−37586
solar EUV emission lines, near-limb profiles meas. 79−16909
solar faculae and pores, Fe I line profiles families 78−49408
solar flare, 1973, June 15, UV lines wavelengths and widths from 1000 to 1940 Å 78−89139
solar Fraunhofer lines, asymmetry rel. to photospheric waves and convective motions *(Russian)* 80−72901
solar Fraunhofer lines, east-west asymmetry of central residual intensities and other parameters 78−53916
solar H Lyman-alpha, profile rel. to interplanetary H I parameters, OSO-8 meas. 79−2452
solar limb flare, 1959 July 25, Balmer line profiles rel. to physical conditions 80−105227
solar line profiles, broadening by finite sized eddies, Fourier anal. appl. 77−17500
solar Mg II,reson. line profiles rel. to chromosphere vel. gradients 77−17460
solar Mg II h and k lines in active regions and network, wing profiles and photospheric models 78−57518
solar photosphere, 'microturbulent' vel. and damping const. rel. to lines equivalent widths *(Russian)* 80−12719
solar photosphere line asymmetries, appl. to vel. gradients retrieval via linearised approach 80−62093
solar photospheric lines, brightness and vel. fluctuations rel. to wave propag. 77−22162
solar quiescent prominence spectra, meas. of Ca^+ 8542, 8498 Å, He 4471 Å and Ti^+ 4468 Å 80−90373
solar resonance radiation multiply scattered by nearby interstellar medium, line profiles 80−41874
solar S I 1807 Å and 1900 Å lines, anal. of profiles 78−57517
solar spectra, line profiles, rough reconstruction from series of narrow-band filtergrams *(Italian)* 80−98564
solar spectra, local macroturbulent broadening by granulation vertical vel. component 80−62094
solar spectral lines, improved value for microturbulent broadening filter function 78−20796
solar spectrum, lines integral characts. rel. to solar atmosphere vel. field estimation 80−46530
solar spectrum, photospheric lines damping const. determ. methods errors *(Russian)* 80−72899
solar UV spectra, evidence, for chromosphere nonthermal line broadening 78−45313
solid solutions, impurity centres, internal mol. vibrs., inhomogeneous band broadening 78−92103
solid solutions, inhomogeneity and site selective impurity-phonon coupling effects 78−84625
solvated electron, optical spectrum broadening in polar liquids 77−21465
solvated electrons in alcohols, spectral broadening, laser saturation 78−31750
spark discharge, electron density determ. from Stark broadening of spectral lines *(Russian)* 80−28859
spectrophotometer recording errors caused by discrete removal of information 79−49301
spectrum profiles in the presence of Stark, Lorentz and Doppler broadenings 78−86820
spin waves in absorptive mag. material, light scatt. lineshape 78−23476
spontaneous emission, line widths and energy shifts *(Chinese)* 79−89874
spontaneously modulated materials, Raman scatt. 79−95739
squaric acid, two-dimens. phase transition, Raman scatt. study 80−71401
Stark effect, two photon absorption spectroscopy 80−43126
stars, line profiles in spherically symmetric flows, scatt. source functions 77−22056
statistical profile, theory 77−18850
steel, austenitic, Cr-Ni, ion-implanted N, chem. state study by AES and XPS 80−79825
steel, high C, type 7KhFNSh, plastic deform. influence of X-ray interference line breadth *(Russian)* 80−93599
stellar Ca II and Mg II reson. lines profiles, effects of high-press. transition regions in model chromospheres 80−26847
stellar expanding spherical atmosphere, line form. with partial freq. redistrib. function R_I 79−88643
stellar line profiles, non-isotropic redistrib. theory in chromospheric-type stellar atmospheres 77−5522
stellar line profiles, rot. vel. determ. via appl. of Bessel transform 77−49369
stellar spectra, combined effects of atmosphere expansion and rot. on line shapes 78−53920
stellar spectra, line asymmetry appl. to convection parameters meas. 79−21273
stellar spectra, line formation in turbulent media 80−77387
stellar spectra, line profiles anal. using linear filtering theory *(Italian)* 80−90340
stellar spectra, lines form. and profiles in radially symmetric accreting envelopes *(Russian)* 78−57544
Stepanyan's star, eclipsing binary, Hβ emission line width 80−67788
Stokes parameters and mag. field vector profiles *(Chinese)* 80−77386
strongly coupled Jahn-Teller system, cluster model for optical absorption spectrum 80−89034
sub-Doppler line shapes, saturation and two-photon spectra, elastic collisions, review 78−82697
Sun, line profiles in mag. fluxtubes, multi-dimensional non-LTE polarised radiation transfer 78−69673
sunspot, widths of UV emission lines rel. to mass motions 77−13296
sunspot umbrae, chromosphere Ca II H- and K-lines emission cores obs. 78−53900
Supermalloy, 9, 24 and 38 GHz ferromagnetic reson. absorpt., line shapes 77−51958
supernova in MCG 10-16-117, H emission lines P Cygni profiles 78−69818
superparamagnet, magnetodipole broadening of reson. line *(Russian)* 79−38385
symmetrical lines, profile measurable deform. by cause of anomalous astron. redshifts 77−13458
synchronous excitation spectrofluorometry *(Japanese)* 80−86452
DR Tauri, T Tauri star, Balmer line profile changes and inverse P Cygni profiles 80−101591
T Tauri stars, spectral features synthesis from photosphere and low chromosphere model 80−36623
T Tauri stars, spectral types, radial vels. and line profiles 77−56921
Taurus Molecular Cloud 2 (TMC-2), HC_5N and NH_3 lines widths 80−26957
TBBA, smectic and cryst. phases, far IR absorpt., struct. and dynamical props. 77−84636
tetrachlorobenzene, triplet exciton spectral line shape, 2-45K 78−19498
TGS, cryst., characteristic absorption edge shape 77−85712
thiourea, ferroelectric, Raman and IR study 80−71406
three two-level atoms system, continuously incoherently-pumped, radiation rate, spectrum 80−5716
three-level system, adiabatic following in two-photon transitions refr. index, line asymmetry 77−57956
three-level system, strongly-excited, statistical broadening and population loss 79−41359
three-level system in strong nonmonochromatic radiation field, linear susceptibility 78−70877
time-resolved laser saturation spectroscopy and coherent transients survey 80−9965
tobacco mosaic virus, solutions, Rayleigh scatt., elec. induced variations, spectral width and intensity meas. 78−48187
bis p-toluene sulphonate diacetylene, low-temp. spectral line splitting 77−32397
toroidal diffraction grating, spectral lines width and astigmatic curvature *(Russian)* 78−57452
transition metal ion, in inert medium, electronic relax., theory 79−76465
transition metal ions in crystals, thermal broadening and shift calcs. 77−48208
transition quasilinear spectra of resonant secondary emission *(Russian)* 80−16102
transition-metal compounds, effects of electron transfer on shake-up satellites, model calc. 78−95650
trichloromethane, and -d_1, depol. Raman scatt. line shapes in liq., density effects 79−4796
trifluoroiodomethane, UV absorption induced by excitation of ν_1 vibrational mode 78−50552
trifluoromethane, IR spectra, spectral bandshape and intensity of C-H chromophore 80−83355
triple optical reson. in crystal, weak absorpt. struct. in IR field 77−24808
tunable diode laser spectrometry for line profile determination in second derivative spectra 80−86435
tunable diode laser spectrometry for line profile determination of second derivative spectra, expt. results 80−86436
turbulent plasma, magnetised, line shape of optical satellites 80−75098
TV recording of interference images, spectral line contours 79−2833
two coupled oscillators, decaying in the same bath, absorpt. line shape 79−10088
two-level molecular gas, nonlinear absorption near gas-medium reson. 79−41409
two-particle bound state, lifetimes and level shifts 78−75265
Uranus reflected spectrum, effects of seeing rel. to period determ. 80−46479
urea in NaI aq. soln., Raman scatt., mol. reorientation relax. time 79−8136
urea-$NaNO_3$(KNO_3) solid eutectic mixtures, Raman, IR spectra, line shifts, widths 77−55793
W Ursae Majoris stars, rot. line broadening functions rel. to stellar shapes 80−109494
vibrationally hot molecules, local mode relax. in cold environments 79−86851
vidicon based apparatus for spectral line contours investig. 79−93226
vidicon spectrometer, spectral line contour investig. *(Russian)* 78−74075
78 Virginis, magnetic Ap star, high resolution polarisation obs. inside spectral lines 80−51772
viscoelastic liquids, structural relax., fast and slow relax. limits 79−47465
Voigt contour of spectral line, nomogram for parameters determ. 80−52321
Voigt contour parameters determ. 80−943
Voigt function and its derivatives, complex probability function 79−45675
Voigt functions, nonlinear least square algorithm 80−90900
Voigt functions, partial derivatives 78−89052
Voigt line width, empirical fits 77−22059
Voigt lineshape, evaluation and characterisation 80−73401
Voigt profile, expansion into components 80−83427
Voigt profile, fast calculational algorithm, line-by-line transmittance 78−7767

spectral line breadth continued
Voigt profile, Lorentz component true halfwidths and line intensities 80−87943
water, condensed multilayers, electron bombard. effects, AES line-shape anal., XPS, and desorption meas. 80−7450
water, low-density amorphous solid, OH stretching spectrum 79−11413
water, solvated electrons, photon-induced electron transfer transitions 79−8154
wave-broadened spectral line profiles, anal. of Fourier transforms 79−80229
wavefront reversal by stimulated Brillouin scatt., four-wave process 80−53382
wavelength modulation spectrometry, computer modelling 77−63974
weak lines in stellar atmospheres, macro-and microturbulent filter functions 79−53803
white dwarfs, DB-type, model atmospheres rel. to line profiles and equivalent widths 80−51761
X-ray diffraction and spectral line breadth, anal. method using Voigt function 78−34387
X-ray diffraction instrumental line broadening with non-ideal standard specimen, anal. 78−41391
X-ray diffraction line profiles, corrections for angle depend. of Lorentz, polarisation and structure factors 77−72526
X-ray fluorescence, energy-dispersive, direct meas. of net peak areas 79−1989
X-ray spectral lines profile evolution due to Comptonisation, Monte Carlo computations 79−66916
XPS, achromatic X-ray source, spectrum iterative deconvolution 78−72689
XPS, prediction model for ang. distrib. intensity and lineshape 77−41734
XPS line shapes, phonon broadening, and independence of hole state lifetimes 77−48313
$XY_{1-c}Z$ mixed crystals, impurity centre local oscill. spectral distribution *(Russian)* 80−60643
YIG, optical absorption and magneto-optic spectra 79−99860
Zeeman resonance lineshapes, motional narrowing, lineshape in absence of motion 77−38636
Zeeman resonance lineshapes, motional narrowing, Monte Carlo simulation 77−38635
Zeeman resonance lineshapes, motional narrowing 77−38634
I Zw 92, III Zw 77, compact galaxies with broad emission lines, line profiles 78−73760
Ag foils, polycryst. and bicrystals, grain boundaries, ^{119}Sn Mossbauer anal. 80−7229
Ag, N-shell vacancy state widths, X-ray photoelectron, Auger spectra 77−18875
AgBr, highly excited, time resolved luminesc., recomb. of excitonic mols. 77−69889
Ag_2HgI_4, Raman line shape and ionic cond., coupled mode model 80−66171
α-AgI, superionic, continuous order-disorder transition, Raman spectroscopic evidence 80−45070
$AgNO_3$, molten, Brillouin scatt. meas. 77−8592
$Ag_2SO_4:CrO_4^{2-}$, polarised electron spectrum assignments, red colour explained 77−85753
Al, positron annihilation, effects of quenching, annealing and neutron irrad. 80−20732
Al, valence band Auger spectra, surface effect 80−80915
Al-Co, electron irradiated, self-interstitials trapped at Co impurities, Mossbauer line shape anal. 78−6615
Al-Sn alloys, heat treatment effect on ^{119}Sn Mossbauer spectrum 80−7228
$Al_xGa_{1-x}As$ pulsating DH laser, spectral broadening 80−23686
$Al_xGa_{1-x}As$-GaAs heterostructure photoluminesc., origin of large dark spots 77−85763
AlN, absorpt. edge shape interpretation, Wannier excitons absorpt. in charge impurity elec. field 80−66233
$Al_2O_3:Cr^{3+}$, Jahn-Teller system, zero-phonon line broadening due to non-radiative transitions 80−108258
^{241}Am, α-radiation self-damage effect on hyperfine interaction and Debye-Waller factor, Mossbauer meas. 80−7230
Ar, fluid, light scatt., collision-induced, line-shape theory and mol. dynamics 79−41921
Ar, liq., depolarised scatt. lineshape correlation function theory 77−40253
Ar plasma, Ar III and IV lines, Stark broadening, Gaunt factor calcs. 77−51231
Ar, plasma, vac. UV emission profile, temp., spectroscopic meas. 77−51229
AsD_3, solid and liq., vibr. relax., Raman ν_1 band, 54, 160K 78−27198
$As_{0.2}Sb_{0.8}SI$ cryst., ferroelec., soft mode Raman and IR spectroscopy 80−76016
As_2Se_3, amorphous chalcogenides, optically broadened lattice vibration spectra 79−77712
a-As_2Se_3, doped film, photoluminescence intensity and lineshape study 80−50448
$As_4Se_5Ge_1$, amorphous chalcogenides, optically broadened lattice vibration spectra 79−77712
BN, hexagonal, electronic struct. from X-ray emission and XPS 79−47009
BaF_2, superionic conductor, theoretical investigation of Raman scatt. 78−80351
$BaMnF_4$, incommensurate phase, Brillouin spectra 79−42981
$BaSnO_3$, powder, electron scatt. from ^{119}Sn, effective range, Mossbauer obs. 77−63345
$Ba_{0.54}Sr_{0.46}Nb_2O_6$, line broadening effect in Rayleigh scatt. of Mossbauer radiation 80−50238
$Ba_xSr_{1-x}Nb_2O_6$, single crystal, Mossbauer diffraction *(Russian)* 79−56644
$BaTiO_3$, ferroelec. temp. depend. of broad A_1 (TO) phonon Raman linewidth 78−2857
$BaTiO_3$, line broadening effect in Rayleigh scatt. of Mossbauer radiation 80−50238
Be:Ar, ion-implanted, high resolution LMM Auger spectra 79−83066
$BeF_2:Pr^+$, glass, optical homogeneous linewidths 80−7395
Bi, hole relaxation time, temp. depend., cyclotron reson. 79−47108
Bi, optical phonon anharmonicity and melting, light scatt. study 80−60621
Bi, solid and liq., core-level line shape, high-resolution XPS meas. 77−59668
spectral line breadth continued
BrCN, pressure-broadened linewidths in microwave region, temp. depend. 77−34694
C IV, solar reson. lines profiles, OSO-8 obs. 77−9729
CF_4 Nd laser excited stimulated Mendelstam-Brillouin scatt. phase fluctuations *(Russian)* 80−89014
CO, condensed film, UPS linewidths 78−31294
CO liq. and CO-O_2 (N_2)(Ar) mixtures, polarised vibr. Raman scatt. lineshapes 78−27199
CO_2, isotopically mixed crysts., IR spectra ν_2 vibr. exciton band 77−73136
CO_2, liq., 100 to 3000 atm., depolarised Rayleigh spectra, orientation dynamics, wings 78−92084
CO_2, Rayleigh linewidth, vap. near crit. pt., gravitationally induced effects 79−82035
CO_2, vibr.-rot. transitions power broadening by laser irrad. 77−3420
COF_2, soln. in liquid Ar, transition freq., halfwidths and relative intensity, IR absorpt. spectra 80−55101
Ca and Ca^+, spectral lines collision broadening and shifts 78−58624
Ca II, H, K and IR line profiles in sunspot umbrae rel. to chromosphere models 78−53901
Ca II, H and K lines in sunspot umbrae, shapes and centre to limb var. 77−22178
Ca II, in A0ep star HD 190073, nightly vars. and line profiles interpretation 77−17578
Ca II, K-line profiles in four late-B stars 78−73722
Ca II K-line profiles in α Centauri A and B, rel. to model chromospheres 77−13326
Ca, laser saturation broadening in flames, fluoresc. excitation profile obs. 80−95568
CaF_2, superionic conductor, theoretical investigation of Raman scatt. 78−80351
$CaF_2:Co^{2+}$, designation of optical transitions near 5.40 nm, temp. evolution of absorption spectra meas. 77−55806
$CaF_2:Sm^{2+}$, coherent population oscills. and hole burning observed using polarization spectroscopy 80−71457
$Ca(PO_3)_2:Eu^{3+}$, amorphous, phonon-assisted site-to-site electronic energy transfer, fluoresc. line narrowing obs. 77−81140
$Ca(PO_3)_2:Eu^{3+}$, anomalous spectral props. 79−38614
$Ca_5(PO_4)_3F:Nd^{3+}$, luminesc. and absorpt. spectra, line shift and broadening 77−4678
$CaSnO_3$, powder, electron scatt. from ^{119}Sn, effective range, Mossbauer obs. 77−63345
$Ca_{1-x}Sr_xF_2:Er^{3+}$ mixed crystal, luminesc. transition, inhomogeneous line broadening calc. 80−97332
$CaWO_4:Nd^{3+}$, thermal behaviour of shape and width of 9145 Å laser line 78−6755
Cd, Auger MNV lineshapes, hole-hole interaction 80−45177
$CdCr_2Se_4$, resonant Raman scatt. 79−4802
$CdCr_2Se_4$:Ag, ferromag. linewidth and eddy current losses 79−33541
CdO, Auger MNV lineshapes, hole-hole interaction 80−45177
CdS, biexciton fluoresc. line shape 77−44059
CdS, emission lineshape of excitonic mols., polariton states 77−20918
CdS, high intensity excited, exciton reflection spectra, reflection struct. 80−20692
CdS, spin-flip line shape 78−88307
CdS, study of electron dynamics by spin flip Raman scatt. 79−95789
CdS, wurtzite crysts., calc. spectra compared piezoemission meas. 77−52038
$CdS_{1-x}Se_x$, comp. disorder-induced broadening for free excitons 79−15479
$CdS_{1-x}Se_x$ mixed crystals, free excitons, disorder effects 80−34365
CdSe, high intensity excited, exciton reflection spectra, reflection struct. 80−20692
CdSe:Fe, exciton electroreflectance spectra, impurity effects 77−16335
CdSe:Li, pure and doped, reson. Raman and Brillouin scatt., elastic exciton-defect scatt. 80−80788
CdTe, shallow impurity spectral linewidths, 4-10K 77−63443
CdTe, undoped and donor-compensated, cathodoluminesc. of 1.4 eV bands 77−40291
CdTe(Se):Co, impurity luminescence no phonon line depend. on temp., Debye temp. 80−66273
Cl_2, liq., mol. reorientation, Raman spectra obs. *(French)* 78−31192
$Co^{2+}[Fe^{III}(CN)_6]^{3-}$, time depend. linewidth of Mossbauer spectrum 80−15911
Cs atoms, exp. multiphoton ionisation through $9D_{3/2}$ resonant level 77−34602
Cs, photoplasma, optical excitation in radiation diffusion conditions 78−55227
CsF, F-centre optical absorption bandshape calc. for transition to state with Jahn-Teller and spin orbit couplings 80−55135
CsI:Na, photoluminescence spectra and lineshapes anal., exciton energies 77−77281
CsI(Br), IR active and silent modes, hyper-Raman scatt. obs. 79−61376
CsI(Br)(Cl), electronic struct. anal. by reflectance and thermoreflectance studies 79−69855
$CsMnCl_3.2H_2O$, subthreshold two-magnon absorpt., depend. on freq., temp. and mag. field, exchange coupling const. *(Russian)* 80−71184
$CsNO_3$, molten, Brillouin spectra, 420-520°C, hypersonic vel. and sound absorption freq. depend. 77−28589
$CsNiF_3$, 1D ferromag., optical absorption and spin dynamics 80−71417
$Cs_2SO_4.Al_2(SO_4)_3.24H_2O$, $^{53}Cr^{3+}$ ENDOR Lines, RF ENDOR power and modulation freq. effects 80−75884
Cu alloy, comp. modulation spectra, line shape 78−76491
Cu, Auger M_1VV line shape, bandlike and atomiclike features 79−43075
Cu, LMM Auger spectra, rel. to L_{23} photoelectron spectra 77−77348
Cu, laser-produced plasma X-ray spectral lines identification *(Chinese)* 80−54036
Cu, plastically deformed, containing dislocation distribs., X-ray diffr. line broadening 77−43218
Cu, prevacancy temperature depend. of positron annihilation, Doppler broadening lineshape parameters 80−60709
Cu-Mn alloys, Mn K X-ray emission and XPS lines, width and asymm. 78−19605
Cu-Ni, soft X-ray emission and local densities of states 79−83059
CuCl, phonon interaction of excitonic molecule 80−50316
CuCl, phonon-assisted two-photon absorpt. of excitonic mol., bare-exciton approach 79−78702
Cu_5FeS_4, S and S^{2-} states, identification from Auger line shapes 79−92034

spectral line breadth continued
CuO_2, width of reson. Raman scatt. enhancement profiles, phenon-lifetime contrib. 79−19883
Cu_2O, 1s yellow exciton, lineshape studies by reson. Raman scatt. 78−76465
Cu_2O, yellow exciton series, silver impurity influence on spectrum 78−64388
$Cu_2O:Ag^+$, yellow series line width, exciton-impurity scatt. 78−64386
Cu_2S, S and S^{2-} states, identification from Auger line shapes 79−92034
Cu_3VS_4, Raman linewidth of A_1 mode under high press., reson. effects 80−108210
D_2, solid, compressed, anomalons double peaked one-phonon for IR absorption 79−56788
D_2O far IR laser pulses, real-time spectral anal. using SAW dispersive delay line 79−45983
D_2O, single 1.06 μm picosecond pulse superbroadening, concurrence with dielec. breakdown 79−86223
Dy_2FeSbO_7, Mossbauer spectra, temp. depend. line broadening due to ^{57}Fe 77−59494
$Dy_2Sn_2O_7$, Mossbauer spectra, temp. depend. line broadening due to $^{119}Sn^m$ 77−59494
Eu complex, Eu(III) β-diketonates, Mossbauer studies 79−61286
Eu^{3+} compounds, chloride, sulphate, nitrate, carbonate, oxalate and acetate, Mossbauer study 79−99801
Eu^{3+} fluoresc. lineshape in glass, temp., time and conc. depend., two-phonon Raman scatt. 78−64406
$EuAsO_4$:Gd, dynamical interactions, EPR meas. 80−7162
EuO nonstoichiometric film, ESR spectra and exchange interaction 80−93176
$Eu_{1-x}Sm_xS$, ESR, exchange interaction, susceptibility, elec. cond., thermoelectric power 80−93174
$EuVO_4$:Gd, dynamical interactions, EPR meas. 80−7162
F spectral lines, neutral, in shock tube plasma, Stark widths and shifts 78−9117
Fe armcotype, Mossbauer spectrum linewidth, influence of dislocations 79−99806
Fe complexes, $M[Fe(C_2O_4)_3].XH_2O$, M=Li, Na, K, Rb, Cs, NH_4, Mossbauer studies of electronic relax. phenomena 80−44973
Fe particles, lunar matter, FMR study, effective linewidth method 78−95523
α-Fe-V, dilute alloy, Mossbauer diffusion line broadening, exponential fitting evaluation 78−52379
Fe-V alloys, Mossbauer study, hyperfine field effect on formation of local moments 78−27134
FeF_2:Mn, mag. polariton, impurity mode enhancement and superradiance effects 79−28622
FeI, self-absorption-free spectral lines for temp. meas. in DC C-arc 80−87965
α-Fe_2O_3 microcrystals, surface phonon modes, IR study 80−55089
FeS, S and S^{2-} states, identification from Auger line shapes 79−92034
FeSb alloy films, vapour-deposited, formation of metastable phase 80−44437
$Fe_{0.96}Se$, Mossbauer diffusional line-broadening 77−55734
Fe_3Se_4, Mossbauer diffusional line broadening 77−43370
$FeSiF_6$, phase transform. and relax., EFG and quadrupole spectra 77−51995
$FeSnO_3$ particles in EBBA liq. cryst., Mossbauer study of Brownian motion 79−95691
Ga, LMM Auger spectra, rel. to L_{23} photoelectron spectra 77−77348
Ga, liq., Brillouin scatt. obs. 77−24858
GaAs, absorption edge broadening by piezoelec. phonon fields 77−16302
GaAs, donor van der Waals interactions, spectral lineshapes 80−11450
GaAs, electron-exciton collision influence on luminescence line profile due to bound excitons 80−29800
GaAs, exciton quenching, obs. at room temp. using electrolyte electroreflectance 80−60546
GaAs laser, broadening mechanism, limitations to single mode power emission 79−961
GaAs, reson. polariton fluoresc. obs. 77−85785
GaAs, shallow impurity spectral linewidths, 4-10K 77−63443
n-GaAs, spectra, light induced, electrolyte and Schottky barrier techniques of meas. 80−76046
n-GaAs tunable far IR Landau emission with subnanosecond rise time 79−32015
GaAs, two-photon electroabsorption by excitons 79−42944
Ga_2O_3-Fe_2O_3 system, anomalous Mossbauer line shapes, incomplete annealing 78−92006
GaP, complex ^{119}Sn impurity-defect, Mossbauer study 80−75898
GaP, donor-acceptor pair spectra, electron-phonon interactions 79−38631
GaP, electron-hole plasma luminesc. 79−38651
GaP, light scatt. by LO phonons, high-resolution study 80−80798
p-GaP, Raman scatt. by coupled plasmon-phonon oscills. 78−6687
GaP, Raman spectra, press. depend. optical phonon anharmonicity 77−8586
GaP:S, effects of uniaxial stress on luminesc. 79−78739
GaSb, accumulation layer localised carriers interaction with LO phonons, Raman interference lineshapes 80−93338
p-GaSb, heavily doped, LO phonon-carrier interaction, Raman interf. lineshapes 80−93319
GaSb, interaction of exciton recombination with LO phonons 79−38647
GaSe, electron-phonon interaction and optical props. 80−34942
GaSe, exciton absorption under intense excitation 77−77235
$GaSe_{1-x}Te_x$, room temp. electroreflectance meas. 77−12361
Gd, ferromag. reson. line width *(Russian)* 78−39406
Gd-Al, amorphous film, microwave mag. reson. 78−91948
Gd-Al, amorphous film, microwave mag. reson. 78−92060
$GdCoO_3$, spin state of Co^{3+} ion, X-ray photoemission line broadening 79−82751
$GdRh_4B_4$, magnetic and electrostatic props., NMR study 80−93195
Ge (111), spectroscopy of electron subbands 80−71422
Ge, direct gap recombination, at high excitation level and low temp. 79−38650
Ge, electron-hole droplets, luminesc. and absorpt. lineshapes, RPA theory 80−49613
Ge, electron-hole liq. thermalisation between mag. field split valleys 80−25444
N-Ge, electrorefl. spectra, light induced, electrolyte and Schottky barrier techniques of meas. 80−76046
Ge, impurity spectral linewidth meas., free electron effects 80−71463
Ge, LMM Auger spectra, rel. to L_{23} photoelectron spectra 77−77348
spectral line breadth continued
Ge, luminescence line shape of free exciton, electron-hole droplet binding energy 77−44041
Ge, magnetoluminescence of electron-hole liq. 80−29790
Ge, stressed cryst., props. of strain-confined electron-hole liquid 79−7787
Ge, surface energy effect on electon-hole drop luminesc. 77−48239
n-Ge:As, heavily doped, luminesc. from electron-hole drops 77−81144
GeO_2:Pr^+, glass, optical homogeneous linewidths 80−7395
$GeSe_2$, glassy and single-cryst., photoluminesc. at 77K 77−63456
H I, line profiles in giant H I envelope of irregular galaxy (IC 10) 79−67094
H I 21 cm line, width in elliptical galaxy (NGC 4278) 77−22312
H I in field of elliptical galaxy NGC 1052, 21 cm emission mapping and line profiles 80−98719
H I regions, 21 cm line profile rel. to galactic shocks 78−54042
H lines, in Nova Cygni 1975, rapid vars. of emission line profiles 77−45434
H plasma, Stark broadening, model microfield methods calcs. 80−92274
H-bonded crystal, IR absorpt. spectra band shape, X-H stretching vibr. temp. depend., isotope effect 78−76445
H-bonded species, in soln., vibr. relax. model 78−84559
H-bonded systems, frequency shift rel. to IR bandwidth 80−99502
H_2 dissolved in Ar, far IR spectra, density narrowing of rot. line 79−50086
H_α and H_β spectral profiles from neutral beams and plasmas in high mag. fields 80−83999
H_b line profiles for white dwarfs with dipole and quadrupole magnetic fields 78−8004
HCl, cryst., internal vibr. electrostatic interactions and IR bandshape 79−91417
HCl, linewidths and shifts in fundamental band broadened by D_2 and H_2 *(French)* 78−972
HCl, liq., IR spectral intensity and Raman cross-section meas. 80−2742
HCl-DCl mixed crystal, IR spectra, freqs., bandwidths and ν_{01} simultaneous transition 77−28564
HCl-inert gas rot.-vibr. line pressure broadening and shift calc. 80−69124
HCl+H_2 (o- and p-), press. broadening and alternate ang. momentum coupling, rot. excitation 77−42375
HD+Kr(Xe), collision-induced fundamental band in room temp. IR absorpt. spectra 77−34627
H_2O, IR absorpt. spectra, band profile temp. depend. 77−30869
H_2O, single 1.06 μm picosecond pulse superbroadening, concurrence with dielec. breakdown 79−86223
H_2O vapour absorpt. coeffs. at HF laser wavelengths 79−80010
Hα, Hβ emission lines in γ Cassiopeiae, P Cygni and Nova Cygni 1975, equivalent widths 77−2430
Hα in eclipsing binary EM Cephei, emission line profile rel. to circumstellar shell *(Russian)* 78−57587
Hα line profile in Tycho SNR, model of optical emission from fast shock wave 80−46631
Hα, line profiles and polarisation in mag. white dwarfs 77−2427
He, 3^3D_1-2^3P_0 line, press. broadening studies by saturated absorpt. techniques 80−52939
He, emission line profile, hollow cathode source 77−23469
He II 4686 Å line, Stark profile meas. in high density plasma 80−96390
He, liq., surface with trapped electron, parallel mag. field effect on interband transition 78−87835
He, liquid, velocity autocorrel. time in surface electron liq. from spectral line broadening 77−20146
He-Cd single-mode laser, linewidth meas. and population calc. 77−14694
He-Ne discharge, striation oscills., spectral width variations 77−62429
He+NO, multiphoton ionisation spectra in supersonic expansion, laser entranced collisional effects 80−83459
^4He, liq., cyclotron reson. of hot electrons 80−88377
^4He, liq., Rayleigh linewidth meas. 78−14522
Hg, liq., Brillouin scatt. obs. 77−24858
$HoCoO_3$, spin state of Co^{3+} ion, X-ray photoemission line broadening 79−82751
I^-, aq., in supercooled water, and glass forming solns., charge transfer to solvent spectra 77−50447
n-In Ar:Te(Sn), heavily doped, cathodoluminescence, doping effect on luminesc. band position and spectral profile 80−45153
In, Auger electron spectra, solid state effects 80−20739
In, laser saturation broadening in flames, fluoresc. excitation profile obs. 80−95568
$In_{1-x}Ga_xP$, quantitative characterisation of chemical disorder from wavelength-modulated no-phonon absorpt. 79−15482
InP:Bi, isoelectronic impurity states, emission and absorpt. obs. 79−42491
InSb, accumulation layer localised carriers interaction with LO phonons, Raman interference lineshapes 80−93338
n-InSb, cyclotron reson. of conduction electrons, strong mag. field, hot electrons 80−2640
n-InSb, cyclotron reson. study of conduction electrons, strong mag. field 80−2639
p-InSb, heavily doped, LO phonon-carrier interaction, Raman interf. lineshapes 80−93319
InSb, interaction of exciton recombination with LO phonons 79−38647
n-InSb tunable far IR Landau emission with subnanosecond rise time 79−32015
α-In_2Se_3, X-ray diffr. line broadening 80−49047
$(In_2SnTe)_x$-$(2InSb)_{1-x}$ system, semicond., Mossbauer absorption line of ^{119}Sn 78−27146
Ir(III) complex, cis-dichlorobis(4,4′-dimethyl 2,2′-bipyridine) iridium chloride 80−97319
^{191}Ir, excited nuclei mean precession time depend. on γ-spectral width, g-factors *(Russian)* 80−78211
K I 7699 Å, emission line profiles in α Orionis (Betelgeuse) circumstellar shell 77−22210
KBr, intra impurity local oscill. composition tone absorpt. band anharmonic temp. broadening *(Russian)* 80−60642
KBr:HS^-(Hf_2^-), anharmonic interaction of impurity intramol. vibrs. with cryst. phonons 77−77217
KBr:In^+, B-band, optical absorpt. and mag. circular dichroism calcs. 80−29765
KBr:Tl, A-emission, line shapes and relative efficiencies 79−83011
KCN, Brillouin line width of phonons 78−80370
KCN, dynamics of CN^- ions near phase transitions at 83K 80−80717

spectral line breadth continued
KCl, F-centre first order reson. Raman spectra, line shape freq. depend. 77−32370
KCl, F-centre phonon many-mode interaction, absorption band shape 78−2883
KCl, single cryst., electron beam irrad. optically simulated exoelectron study 79−95908
KCl:Au^-, absorption band shape in D-mode model 79−47485
KCl:Ca, optical studies of Z_4 centres 79−24336
$KCl_{1-x}Br_x:NCO^-$, absorpt. band defect broadening *(Russian)* 78−72526
$KCl_{1-x}I_x:NCO^-$, absorpt. band defect broadening *(Russian)* 78−72526
$K_3Co(CN)_6$, Raman scatt. and electronically-induced phase transition at 130K 77−90142
$KCoF_3$, strain sensitive props., Mossbauer spectra obs. 77−20765
$KCr(SO_4)_2.12H_2O$, phase transition associated fluctuations, Cr^{3+} EPR obs. 77−32247
KF(Br)(Cl)(I), K^+3p core excitons, refl. spectra study, low temp. 80−29759
$K_3Fe(CN)_6$, Raman scatt. and electronically-induced phase transition at 130K 77−90142
$KFeF_3$, strain sensitive props., Mossbauer spectra obs. 77−20765
KH_2AsO_4, ferroelec., temp. broadening of hard mode Raman lines near Tc 78−88296
KH_2AsO_4, Raman linewidth, isotope effect 77−8565
$KH_{2(1-x)}D_{2x}PO_4$, Raman spectra of overdamped mode 79−91427
KH_2PO_4, E-symmetry Raman spectra 79−38535
KH_2PO_4, ferroelec., Raman internal-mode line broadening by proton jumps 77−43981
KH_2PO_4, ferroelec., temp. broadening of hard mode Raman lines near Tc 78−88296
KI, luminesc. due to free excitons, line shapes 79−33803
KI, surface, 420 nm band laser-stimulated emission, V_2 centres 78−84633
KI, zero phonon and LO phonon assisted luminesc. of free excitons 79−28799
$KMnF_3$, exciton dynamics by time resolved emission spectroscopy 80−54615
K_2MnF_4 and K_2NiF_4, two-dimens. antiferromag., two-magnon Raman scatt. linewidth, finite temp. 77−66508
K_2MnF_4, quadratic layer antiferromag., intrinsic emission obs. 77−20906
KNO_3 polycrystalline specimens, effect of cryst. size on parameters of LF Raman spectrum *(Russian)* 77−28581
$3KNO_3-2Ca(NO_3)_2$, glass form. from liq., struct. transform., Raman spectrum obs. 80−64916
$3KNO_3-2ZnCl_2$, glass form. from liq., struct. transform., Raman spectrum obs. 80−64916
$K_5Nd(MoO_4)_4$, spectral and struct. props. *(Russian)* 79−52020
K_2O-SiO_2 glasses, IR reflection spectra, computer resolution *(Japanese)* 77−69832
$K_xRb_{1-x}Cl:HF_2^-,SO_4^{2-}$, nonuniform broadening of IR vibr. absorpt. bands of impurities *(Russian)* 77−16357
K_2SeO_4, phase mode in incommensurate phase, Raman scatt. obs. 80−80766
$KTaO_3:Fe^{3+}$ local phase transition, EPR line temp. broadening *(Russian)* 80−54944
Kr, 3p core hole spectrum, many electron description 78−50517
$LaCl_3:Np^{3+}$, phonon-induced relax. in excited optical states, linewidth temp. depend. meas. 80−100688
$LaCl_3:Pr^{3+}$, hyperfine struct. of 6011 Å line, laser-induced absorpt. line narrowing 78−15196
$LaF_3:Pr^{3+}$, laser-induced fluoresc. line narrowing 77−40280
$LaF_3:Pr^{3+}$, optical line narrowing by nuclear spin decoupling, photon echo meas. 80−48353
$LaF_3:Pr^{3+}$, optical transition, spin decoupling and magic angle line narrowing 80−28286
$LaF_3:Pr^{3+}$, ultrahigh resolution photon echo spectroscopy 80−28285
$La_2O_3-Al_2O_3-SiO_2:Sm^{3+}$, luminesc. selective laser excitation line narrowing 80−25434
Li, Auger line shape KVV, energy band theory 79−43074
Li I lines in C stars, line form. theory and profiles 78−65615
Li, valence band Auger spectra, surface effect 80−80915
LiC_6, intercalation compound, electronic struct., XPS meas. 80−59850
$LiClO_4-CsNO_3(RbNO_3)(KNO_3)(KClO_4)(RbClO_4)(CsClO_4)$, binary melt, Raman spectra, polarised line width, temp. depend. 78−84578
LiF, R core exciton thermotransmission and absorpt. spectra, line shapes, forbidden and allowed excitons 79−73968
LiF:$Mg^{2+}(CO^{2+})$, X-ray induced UV absorpt., band shapes, F- and Z-centers 77−20889
$LiNO_3$, soln. in organic liq. or D_2O, Raman lineshape, solvent-solute interaction 78−76448
$LiNO_3-NaNO_3(KNO_3)$ solid eutectic mixtures, Raman, IR spectra, line shifts, widths 77−55793
$LiNbO_3$, optical parametric oscillator threshold parameters and linewidth control 79−81480
$LiNbO_3$, y-z crystal, line shape of light scattered by SAW upon total internal refl. 79−24287
$Li_2O-B_2O_3:Eu^{3+}$ glass, laser induced fluoresc. line narrowing, struct. 79−38613
$LiYF_4:Ce^{3+}$, laser transition at 325 nm, large fluoresc. linewidth 79−72574
$LuRh_4B_4$, magnetic and electrostatic props., NMR study 80−93195
Mg II, h and k emission in luminous M-type stars, profiles and line widths 78−53945
MgF_2, optical absortion following pulsed electron irrad., 100-500K 79−8164
MgO:Cr, high resolution far IR spectroscopy of lower energy levels of Cr^{2+} 80−80822
MgO:Fe^{2+}, phonon-induced transition interf. in EPR and IR spectra, ion-lattice coupling 77−51945
MgO:V^{2+}, Jahn-Teller system, zero-phonon line broadening due to non-radiative transitions 80−108258
$MgSiF_6$, phase transform. and relax., EFG and quadrupole spectra 77−51995
$Mg_xZn_{1-x}Te$, temp. depend. of energy gap, near band gap reflectivity spectra 79−28786
MnO, absorption line shape, magnon sidebands 77−52128
MnO, antiferromag. reson. linewidth below and above T_N 77−40133
MnO, magnon-sideband lineshape, exciton-phonon interaction effects 80−65846

spectral line breadth continued
$MnSiF_6$, phase transform. and relax., EFG and quadrupole spectra 77−51995
MnZn ferrite, high cond., magneto-microwave Kerr effect, ferromag. reson. linewidth determ. 77−43888
$Mn_{1-x}Zn_xF_2$, antiferromagnetic reson. freq. from far IR transmittance spectra 77−69695
Mo-Fe, local magnetisation from Mossbauer meas. 77−20549
N_2, condensed film, UPS linewidths 78−31294
N_2, liq., Raman lineshape 80−11384
N_2, liq., vibr. line broadening, Zwanzig-Mori theory and quasi-elastic processes 78−27221
N_2, solid, electron impact excited, luminesc. spectra 77−48252
N_2, solid, UV spectra, phonon induced exciton fine struct. 79−15477
α-N_2, solid, $w^1\Delta_u-X^1\Sigma_g^+$ intensity and band shape 79−47427
$(N(CH_3)_3H)_2SnF_6$, phase transition and temp. effects, Mossbauer and NMR spectra 78−88236
NH_3, inversion spectrum press. broadening by He and Ar, linewidths calc. 80−95599
NH_4Br, partially disordered, librational modes below 235K, Raman scatt. obs. 78−72500
NH_3D^+, IR spectrum in NH_4ClO_4 and weakly H-bonded cpds., mol. motion 77−36232
$((NH_4)_xK_{1-x})_2SnCl_6$, mixed cryst., spectroscopic study 79−33712
NO_3^-, in aq. nitrate soln., vibr. dephasing process, Raman obs. 79−51936
Na, laser saturation broadening in flames, fluoresc. excitation profile obs. 80−95568
Na, overlapping autoionisation lines, interference effects 80−91677
Na-He model pot. calcs., fluoresc. line profile 79−36723
Na+inert gas, non-Lorentzian spectral line shape 80−106297
Na_2, liq., vibr. line broadening, Zwanzig-Mori theory and quasi-elastic processes 78−27221
NaCl film, UPS linewidth, phonon broadening of core levels 77−36371
NaCl, plastically deformed, containing dislocation distribs., X-ray diffr. broadening 77−43218
$NaClO_4$ aqueous soln., IR absorpt. spectra, band profile temp. depend. 77−30869
NaF, F_3^+ centre zero-phonon line, photochem. and population hole burning 79−42997
$NaFeF_2$, Mossbauer and low-temp. dilatometry study *(French)* 80−80662
$NaNO_3$, disordered, temp. depend. of Raman spectra, Rayleigh wing scatt. 78−31209
$NaNO_3$, lattice vibration neutron diffusion study *(French)* 80−103429
NaSCN, cryst., Raman spectral lines, temp. depend., anion disorientation *(German)* 78−52514
Nd glasses, GLS-1 and GLS-22, luminesc. band, forced transition cross sections, laser meas. 80−40152
Nd, threshold pot. spectra, $N_{4,5}$ absorpt. widths 79−69578
Nd:glass laser, resonant reflectors in laser cavity, freq. selection 78−55369
Nd:silicate glass, resonance laser excitation, inhomogeneously broadended emission spectra 80−66295
Nd:YAG laser, subnanosecond pulse generation at 100K 80−74397
Nd^{3+}:glass, fluoresc. line narrowing, hole burning and ion-ion energy transfer 79−89912
Nd^{3+}:glass, inhomogeneously broadened spectra, struct., selective laser excitation obs. *(Russian)* 78−35181
Nd^{3+}:glass, laser induced fluoresc. line narrowing, site depend. 79−33819
Nd^{3+}:glass luminesc. band profile deform. under free-oscillation conditions 80−71487
$Nd^{3+}:LaCl_3$, laser-induced fluoresc., hyperfine structs. 80−100677
Ne spectral line broadening as diagnostic for compressed laser fusion targets 79−98979
Ni, ferromagnetic reson. determ. of first three anisotropy consts. 77−8414
Ni, $M_{2,3}$ edge, temp. depend. 80−50463
Ni-Fe film, oligatomic, ferromag. reson. and torsion magnetometry, 123-373K 77−59461
NiF_2, ESCA, charge transfer satellite struct., hole state localisation intensity depend., MS-MO calc. 77−66139
Ni_3Mn, ferromagnetic reson. field and line width temp. depend. 3-300K 79−95651
$Ni_{0.25}Zn_{0.75}Fe_2O_4$, Mossbauer study, noncollinear spin struct. 80−60472
^{237}Np, lineshape analysis of 60 keV Mossbauer resonance, interference effects 79−28644
O I 5577 Å nightglow line profiles, thermospheric temp. vars. determ. 77−9584
O_2, $^3\Sigma_u^-$-$^3\Sigma_u^+$ spin-orbit mixing in Schumann-Runge predissoc. 77−6875
O_2, gas, vibr. Raman spectrum, anomalous behaviour near crit. point 78−55179
OCS, pressure-broadened linewidths in microwave region, temp. depend. 77−34694
PbF_2, superionic conductor, theoretical investigation of Raman scatt. 78−80351
$Pb_5Ge_3O_{11}$, dynamic central peaks and phonon interactions near structural phase transitions 78−83903
PbTe, far IR magnetorefl., band struct. 80−76010
Pd-Fe, scatt. and transmission Mossbauer spectra near Curie temp. 80−15864
Pd-H system, many-body contrib. to XPS line asymm. 77−66575
β-PdH_x, diffusion-induced reduction of ^{57}Fe Mossbauer fraction 80−108131
Pt oxidation, XPS spectra study 80−3254
Pt, single cryst., oxidation, Auger spectra 78−14600
$RbFeCl_3.2H_2O$, 2D Ising system, crit. fluctuations, Mossbauer spectra study 80−44842
RbI, IR active and silent modes, hyper-Raman scatt. obs. 79−61376
RbI, intra impurity local oscill. composition tone absorpt. band anharmonic temp. broadening *(Russian)* 80−60642
RbI, zero phonon and LO phonon assisted luminesc. of free excitons 79−28799
RbI:HF_2^-, anharmonic interaction of impurity intramol. vibrs. with cryst. phonons 77−77217
RbI:ReO_4^-, IR absorpt., half width, temp. depend. *(Russian)* 79−78722
$RbMnCl_4$, quadratic layer antiferromag., intrinsic emission obs. 77−20906

spectral line breadth continued
RbN_3, lattice vibration Raman study, tetragonal-cubic phase transitions 79−77743
$3RbNO_3-2Ca(NO_3)_2$, glass form. from liq., struct. transform., Raman spectrum obs. 80−64916
S^{4+}, travelling in solids, Kα X-ray spectra 80−100706
SF_6, long-range correlation length near liquid-vapour transition, Rayleigh scatt. 77−8593
Sb, Auger electron spectra, solid state effects 80−20739
Sb, optical phonon anharmonicity and melting, light scatt. study 80−60621
Si (100) surface, intersubband optical absorption in space-charge layers 77−35984
Si (111), (100) and (110) ideal surfaces, valence-band Auger lineshape theory 77−48286
Si, Auger line shape $L_{2,3}$ VV, energy band theory 79−43074
Si, bound-exciton spectral lines, conc. broadening at high impurity concs. 80−80826
Si, dielectric function spectra, ellipsometric determ., many-particle effects at E_1-transition 80−93363
Si, electro- and thermo-reflectance spectra, line-shape anal. 79−24296
Si, electron-hole drops, thermodynamical parameter determ. from luminescence data 80−2845
n-Si, heavily doped, self energy of phonons interacting with free electrons, Raman scatt. 78−64366
Si IV, solar reson. lines profiles, OSO-8 obs. 77−9729
Si, intrinsic, phonon replicas of electron-hole liq. luminesc. line 79−28831
Si, single cryst., oxidation, Auger spectra 78−14600
Si, surface inversion layers, intersubband optical absorpt., Auger-type transition 80−29741
Si, symmetry analysis of E_2 structs., low-field electroreflectance meas. 77−40209
Si, valence electrons XPS spectrum, OPW calc. 77−4715
Si:Al, absorpt. line broadening 78−95594
Si:Ar, ion-implanted, high resolution LMM Auger spectra 79−83066
Si:P, excitation spectrum of P donors introduced by neutron transmutation, high resolution study 79−47460
Si:P, exciton complexes bound to impurities, resolved fine structure 77−62843
Si:P, photolum. obs. of donor pairs 79−52014
Si-type, semiconductor, interimpurity radiative recomb. with phonon cooperation 77−16385
α-SiC, wurtzite type cryst., temp. depend. of one phonon Raman spectra, Gruneisen parameters 77−66500
SiO_2:Au(Ag)(Cu), XPS line broadening and extra-atomic relax. energies 80−71561
Si; Ar ion bombarded, projectile energy depend. and line shape of Ar-L AEs 80−16139
Sn, Auger electron spectra, solid state effects 80−20739
SnF_2, Mossbauer effect 77−85626
SnO_2, powder, electron scatt. from ^{119}Sn, effective range, Mossbauer obs. 77−63345
Sr, laser saturation broadening in flames, fluoresc. excitation profile obs. 80−95568
$SrF_2(Cl_2)$, superionic conductor, theoretical investigation of Raman scatt. 78−80351
$SrNO_3$, single cryst., normal Raman modes, temp. effects *(French)* 77−43998
$SrTiO_3$, forced thermal Rayleigh scattering 78−80371
$SrTiO_3$, IR active and silent modes, hyper-Raman scatt. obs. 79−61376
$SrTiO_3$, phonon interactions and the dynamic central peak near structural phase transition 77−81114
Ta, surface layers, Mossbauer conversion electron studies 78−15068
$Tb(OH)_3$, exciton dynamics within an inhomogeneously broadened line, luminesc. spectra 80−50407
Te, Auger electron spectra, solid state effects 80−20739
Te, intervalence band absorption, press. and defects influence 80−55149
Ti I, in Sun, line profiles and solar Ti abundance 77−29743
TiO_2 anatase, Raman spectrum, temp. depend. 80−76027
TiO_2, ESCA, charge transfer satellite struct., hole state localisation intensity depend., MS-MO calc. 77−66139
Tl+inert gas, $6^2P_{1/2}$-$7^2S_{1/2}$ and $6^2P_{3/2}$-$7^2S_{1/2}$ line broadening 77−50475
TlN_3, lattice vibration Raman study, tetragonal-cubic phase transitions 79−77743
TlN_3, press. induced phase transition, Raman scatt. meas. 78−19468
V, X-ray band spectra calcs. 79−33860
Xe, fluid, near crit. point, correl. range and Rayleigh linewidth 80−93352
YAG:Cr^{3+}, absorption and luminesc., spectra, Cr conc. depend. 77−12435
$YAlO_3$:Nd^{3+}, thermal broadening and shift calcs. of Nd^{3+} energy levels 77−48208
$YAlO_3$:Pr^{3+}, ultrahigh resolution photon echo spectroscopy 80−28285
$Y_3Al_5O_{12}$:Yb^{3+} (Nd^{3+}), one-phonon satellites in luminesc. spectra, rel. to effective phonon density 78−6730
$YCoO_3$, spin state of Co^{3+} ion, X-ray photoemission line broadening 79−82751
$Y_3Fe_{5-x}Ga_xO_{12}$, substituted garnet, floating zone grown, FMR line width, saturation magnetisation 80−29626
YIG, porous and fine grain polycrystalline, temp. depend. of effective linewidth 77−85574
YIG:La film, for microwave applics., growth and ferromag. reson. meas. 78−3008
Yb, 4f levels, hole lifetime and chemical shift, UHV study 80−20762
^{170}Yb, Mossbauer line shape, Liouville relax. supermatrices 79−28649
Zn, $L_{2,3}M_{4,5}M_{4,5}$ Auger spectra, solid state and oxidation effects 77−63501
Zn, LMM Auger spectra, rel. to L_{23} photoelectron spectra 77−77348
Zn, optical phonon anharmonicity and melting, light scatt. study 80−60621
Zn, oxidation, MVV Auger spectra, line shape, relax. energies 77−73195
$Zn_xCd_{1-x}S$, bound-exciton lines, compositional fluctuation-induced broadening 80−2846
ZnO, self-activated phosphor, band width and shift, temp. depend. 77−8623
ZnO, wurtzite type cryst., temp. depend. of one phonon Raman spectra, Gruneisen parameters 77−66500
ZnO:Er, phosphors, photo- and electroluminesc. 77−12428
ZnS, time differentiated Mossbauer spectra from ^{57}Co impurities, relaxation processes *(Russian)* 80−34834
spectral line breadth continued
ZnS, wurtzite type cryst., temp. depend. of one phonon Raman spectra, Gruneisen parameters 77−66500
ZnS:^{57}Co Mossbauer sources, Fe^{1+} transient charge state 80−108128
ZnS:Cl, shape of self-activated cathodoluminesc. band 80−34987
ZnS:Pb^{2+} (Mn^{2+}), high press. luminesc., localised excitations 78−19534
ZnS(Se)(Te):Co, impurity luminescence no phonon line depend. on temp., Debye temp. 80−66273
ZnSe, exciton emission, halfwidths, thermal and optical activation energies obs. *(French)* 80−66268
ZnSe, reson. Raman scatt. meas. 77−66510
ZnSe:Cr^{2+}, stress-induced alignment of Jahn-Teller centres 79−78651
ZnTe, magnetoreflectance meas. on Γ_6-Γ_8 exciton 78−6656
ZnTe, radiative recombination involving free particle scatt. 79−38648
ZnTe, single cryst., electron-hole drop conc. *(Russian)* 79−11460
ZnTe, spin-flip plus phonon scatt., line shape and shift in peak position 79−73907
Zr complexes, X-ray K-absorption edge, shift and width meas. 77−8683
Zr, two-phonon Raman scatt. at low temps. 79−87433

spectral line profiles *see spectral line breadth*

spectral line shift
see also chemical shift; isomer shift; isotope shifts; Lamb shift; radiative shifts; red shift; Stark effect; Zeeman effect
acetic acid-aliphatic amide intermol. H-bonded systems, charge transfer bands 77−58041
acetonitrile, adsorbed on ZnO, IR spectrum species identification *(French)* 79−82967
2-acetylanthracene, soln., excitation spectra rel. to recording wave length *(Russian)* 77−12438
acetylene-d_2, microwave spectrum, P-branch transitions, Stark shifts 77−27057
acridine, dye solns., luminesc. spectra, conc. depend. effects 79−54885
acridine, methanol soln., edge excitation red shift, excited state proton association 79−18228
active ions in crystals, spectral thermal line shift mechanism *(Chinese)* 80−7385
alchohols, glassy, spectra shift of trapped electrons, after γ-irrad. 79−78709
alkali halides, spectra of O_2^-, S_2^- and NO_2 mol. ions, electron-phonon interaction 77−52174
alkali metal, ground state coherence, transversal relaxation rates, Zeeman shifts 77−6888
alkali metal, modulated optical absorption transients weights, transversal relaxation effects 77−6887
alkali metal, two-photon S-S transitions, press. broadening and shift by rare gases 79−6916
alkali metal+inert gas, collisional shifts and broadening of Voigt contour 80−27983
alkali metal+inert gas, line profiles, width, shift and asymmetry, square well pot. approx. 80−52936
alkali metal atom+inert gas, collisional broadening and shifts, semiempirical pots. calcs. 77−10727
alkali metal atom+inert gas atom, hyperfine transition spectral line shift, quantum corrections 78−82655
alkali metal Stark profiles, of reson. lines, model microfield method appl. 79−26931
alkali nitrites, molten, combination scatt. spectra, freq. shifts, jumps at melting, line widths *(Russian)* 77−40241
alkaline earth nitrites, molten, combination scatt. spectra, freq. shifts, jumps at melting, line widths *(Russian)* 77−40241
alloys, oxidation, Auger spectra 78−14600
2-amino, 7-nitrofluorene, in 2-propanol, Stokes fluorescence shift time resolution 77−58060
7-amino-4-methylcoumarin, fluoresc., solvent depend., shift of max. wavenumber 79−85997
2-amino-7-nitrofluorene, in binary solvent soln., time-resolved fluoresc. spectroscopy 79−36680
4-amino-N-methylphthalimide-decalin-n-propanol, translational relax. kinetics, luminesc. obs. 79−8180
aminophthalimides, dynamic dipole induced interactions in absorption spectra 78−13553
aminoquinoline derivatives, solvent effect on absorpt. and fluoresc. spectra 79−59494
anthracene, cryst., fluoresc. spectra, press. tuning 77−28612
anthracene, in stretched polyethylene film, UV-visible and fluoresc. spectral shifts 78−62852
anthracene, melt and dil. soln., UV spectra, line broadening and shift vibr. struct. 78−17684
anthracene, singlet-triplet absorpt. spectra, 2-300K, photoexcitation spectra 78−43890
anthracene-PMDA crysts., phosphorescence blue shift of charge transfer config. 77−36278
astronomical spectra, Doppler shifts meas. without spectrograph 78−20646
atom, Bloch-Siegert shift, photon beam interaction, QED calcs. 77−27033
atom, Doppler broadening compensation with laser induced light-shifts 79−3405
atom, Doppler-free multiphoton excitation, light shift and saturation 79−76399
atom, multiphoton transitions, continuum level shift effects 79−26956
atom, pressure effects on spectral lines 78−82690
atom, relativistic, level shifts, transition probabilities, perturbation theory 79−10067
atom, RF spectroscopy, nonlinear and parametric effects, review 80−18816
atom, Rydberg states, use as spectroscopic probe for resonances in mol. electron elastic scatt. 77−58162
atom, spin-1/2, general higher-order effects of freq. shifts in optical-RF double reson. 78−21884
atom+atom anisotropic collisions, spectral line breadth and shift, polarisation depend. 78−46305
atom+charged particle anisotropic collision, spectral line shift and broadening, polarisation depend. 78−82695
atom+foreign gas, absorpt. spectrum shift near series limit, K-matrix anal. 77−10731
atom level light shifts, model pot. calcs. 77−31017
atom-ion core level shifts, ΔSCF calcs. 80−87176
atomic bibliography on atomic line shapes and shifts (June 1975-June 1978) 79−49990

spectral line shift continued
atomic emission lin profiles, ultrarelativistic charged particle EM field effects 77—3313
atomic excited state collisional relax., line broadening, interat. interactions, review 80—43149
atomic ground state shift, limited nonreson. moderately strong laser field 79—18157
atomic hyperfine components of spectral line 77—34587
atomic hyperfine transitions in buffer gas, quantum theory *(Russian)* 78—21881
atomic level field splitting, resonant cooperative light scatt. *(Russian)* 80—74148
atomic level shift and width in light field, higher order perturbation theory *(Russian)* 79—3414
atomic level shifts in laser fields and space-translation Hamiltonian 77—34858
atomic spectral line shifts for heavy quark atoms 78—62965
atomic spectral lines, impact broadening HFS considerations 77—83541
atomic spectrum, relaxation shift by laser action freq. 79—18150
atomic system, reson. fluoresc. with recoil effects, quantum statistical theory 78—78660
ATR spectroscopy, Goos-Hanchen shift and effective sample thickness 77—49791
autotype detector, spin resonance detection 80—22397
azobenzene, parasubstituted derivatives, reson. Raman spectra *(French)* 79—59472
bacterial cells, active, reson. between 10^{11} and 10^{12} Hz obs. by laser Raman spectroscopy 77—36893
bacteriorhodopsin, dynamics, of pH-induced spectral changes 79—57587
benzene, $\pi\pi^*$ and Rydberg bands, cryogenic solvent effects 78—55182
benzene, electron impact-induced generalised oscill. strength, 400 eV, 500 eV, momentum change depend. 78—1088
benzene, photoluminesc. at 5K, N_2 and inert gas matrices 77—6838
benzene cryst., electron irrad., phenylcyclohexadienyl radical form., absorpt. and fluoresc. spectra study 80—89035
benzenes, para-disubstituted, liq., 2nd order hyperpolarisabilities, regularities, intramol. charge transfer 79—10353
benzoic acid, spectral shift due to electron-repelling substituents 79—72362
1,12-benzoperylene in n-alkane, zero-phonon lines in luminesc. spectra 78—56512
p-benzoquinone, hydroxy substitutions effect on $^1B_{1g} \leftarrow {}^1A_g$ transition 79—18200
2-benzoylpyridine crystals, optical spectra of lowest triplet state 80—16081
biexcitons recombination, polariton effects 78—23033
bilirubin, anomalous solvent shift effect and phosphoresc. 77—30899
black hole, spherical, with thin accretion disc, image and spectral shifts 79—67049
blending effects 78—62851
Block-Siegert shifts and multi-quantum transitions, spin-one systems, RF and DC fields 77—75103
bromanil and radical anion, Raman and IR freq. shifts 78—33516
bromomethane, and isotopic forms, self-broadening and self-shifting of rot. spectra 78—13551
4-n-butoxybenzylidine-4′-n-octylaniline, liquid cryst., smectic B phase lattice vibr. anisotropy, Mossbauer anal. 77—7666
N-tert-butylacrylamide-styrene copolymers, struct., composition, IR, DTA investigs. *(Polish)* 79—31751
carotenoid pigments, radical ions, radiolysis generation, absorpt. spectra, MO calcs. 77—65488
chamber calibration using ruby R_1 luminescence line shift, 80 to 550K 78—86284
chloranil and radical anion, Raman and IR freq. shifts 78—33516
chloromethane, microwave spectrum, width and shift parameters 77—18985
chlorophyll, a and b, lowest singlet-singlet transition, solvent effects 79—24952
chlorophyll-a, solns., vis. absorpt. spectra of monomer, dimer and oligomers 77—29101
cholesteric liquid crystal, nonmesomorphic solutes, effect on cholesteric pitch, max. refl. wavelength shift *(Russian)* 78—38620
cholesteric liquid crysts., light reflection by crysts. with tilted molecular struct. 80—29713
chromocene, solid, Raman transition assignments, mag. susceptibility, mag. moment 78—43861
collisional linewidths and shifts determ. by convolution method 80—102541
complex molecules, vibr. spectra, stochastic description, appl. to optically active Brownian oscillator 80—52974
conjugate heterosystems, UV spectra, substituent effects 79—27006
coronene, n-alkane matrix, up to 1.8 kbar emission multiplet struct. shift 77—34677
coumarin 102, excited state interaction dynamics, picosec. time-resolved spectral shift obs. 80—78624
crystal impurity centres, quadratic Stark effect, quantum mech. band shape calcs. 77—69863
crystal vibrational spectrum, inhomogeneous thermal broadening effect 80—55100
4-cyanobiphenyl and 4′-alkyl- or 4′-alkoxy-substituted liq. cryst. derivatives, soln., absorpt. and fluoresc. spectra 80—87164
cyanomethane, collisional rot.-line widths and shifts, microwave region 78—25619
cyclophosphazene-DNa complex, spectrofluorometric and spectrophotometrics investig. 80—95643
degenerate atomic level perturbation by neutral particles 79—792
dense plasma, H_β line red shift expt. 78—67473
dense polyatomic molecular systems, vibr. correl., HF band exchange dephasing 80—37803
dianthronylidene ethane, luminescent excimer geometries, intermol. shift 78—27294
diatomic+polar diatomic, vibr.-rot. absorpt. line shift 77—27160
diatomic molecular dilute solns., IR and Raman ~~spectra~~ temp. depend. anal. model *(French)* 77—88456
diatomic molecule, Autler-Townes power splitting of rovibr. lines, direct obs. using intense IR laser 79—54854
diatomic molecules, matrix isolated, vibr. spectrosc., IR line shape calcs. 79—72307
diatomic molecules, shifts and widths of predissoc. levels 78—5304
2,4-dichlorobromobenzene, UV absorpt. spectra of vap. phase, vibr. anal. 79—81211

spectral line shift continued
1,1-dichroethane and d, IR and Raman spectra, βCH stretching interaction force consts. 77—79616
dielectric model for electronic spectra solvent effects 77—26991
1,1-difluoroethane, rot. relax., anharmonic shifts and excited state absorpt. 80—43154
digital processing techniques applied to astronomical images 77—60626
dilute atomic gas, weak at.-at. interaction pot. from master eqn. for coupled radiation 80—23484
7-N-dimethylamino-4-methylcoumarin, fluoresc., solvent depend., shift of max. wavenumber 79—85997
diphenyl styryl pyrazoline-active electrolyte system, electrochemiluminesc. spectral shift 77—20929
1,6-diphenylhexatrienes, electronic and fluoresc. spectra, solvent effects, 77K 78—21959
2,5-diphenyloxazole, phosphoresc., 77K, solvent effect 78—42118
DNA, Na salt, freeze-dried layers, unpolarised IR spectrum, temp. dependent spectral shift 77—48755
double Mossbauer spectrometer for small resonance line shift meas. 78—82560
dye energy transfer laser, intermol. interactions and spectral shifts 78—74902
dye molecules, long wavelength conc. shift in luminesc. 79—64032
education, hadronic atom strong interaction induced level widths and shifts, WKB calc. 77—78923
electron cyclotron reson. lineshape analysis for cylindrical cavity field inhomogeneities 78—13560
electron localisation, evolution of optical spectra 77—90173
eosin, in glycerine-water mixture, excitation and emission peaks, concentration shifts 78—33540
EPR, introductory student expt. 78—41119
ESCA expt., charging and rotational dependence of time position 78—21970
ethane, in air, IR spectra, optical-acoustic investig. *(Russian)* 78—74663
ethylene, in air, IR spectra, optical-acoustic investig. *(Russian)* 78—74663
F-centre electron levels, temp. depend. shift calcs. 77—28599
ferromagnetic semiconductors, giant blue shift of absorption edge *(Russian)* 77—32401
fluorescence solvatochromism kinetics 77—30898
3-fluoro-4-methyl aniline, near UV electronic absorpt. spectra, line shift, vibr. anal. 77—10682
2-fluoro-5-methyl aniline, near UV electronic absorpt. spectra, line shift, vibr. anal. 77—10682
fluoromethanes, soft X-ray absorpt. spectra, fine struct. above K-edge of C 78—42096
fluorophosphate glasses, rare-earth activated, luminesc., bonding 78—64415
foreign gas induced line shifts, thermodynamics 80—106295
formaldehyde, in Ar, medium perturbations of extravalence excitations, VUV absorpt. 78—1002
Franck-Condon effects in resonance Raman spectra and excitation profiles, appl. to CrO_4^{2-} and β-carotene 80—14129
free-base porphin, Zeeman shift meas. by photochem. hole-burning 80—83416
frequency shifts, determ. by Raman difference spectrosc. 80—78654
n-GaP, quasidirect radiative recombination of free holes at neutral shallow donors 78—64410
gas pressure depend. 80—87185
gas-pressure shifts of molecular lines, Stark displacements 80—23463
glass, alkali-alkaline earth nitrates, Raman spectra, vibr. perturbations effect 79—8132
glycerol($-d_3$), single cryst., glassy, and supercooled, polarised Raman spectra, anharmonic multiphonon interactions 79—91419
graphite-alkali metal intercalation cpds., IR, active lattice mode obs. 80—45072
gravitational, review of laser appl. to precision meas. 78—42246
group frequencies shift, rel. to bond props. 79—98057
harmonic oscillator, $v=0$ level predissociation, by linear pot., line width and shift 77—75239
harmonic oscillator model in predissoc., level widths, shifts and curve crossing 78—90239
HD 168607 (B9 Ia^+), S Doradus type star candidate, absorption lines differential shifts *(Russian)* 80—90456
heteroatomic cpds., paramag. reagents for ligand mol. struct. determ. from NMR 79—13741
heterocyclic compounds, bond lengths, fifth overtone of C-H stretching vibrs. obs. 80—91528
high-sensitivity multipurpose remote sensor 78—40684
highly excited atoms, blackbody radiation effects 80—58176
hydrogenic orbitals, Compton shift *(French)* 78—42012
hydroxyquinones, H-bonded, zero-phonon photochem., hole burning obs. 79—11802
hyper-Raman scattering, saturation effects, resonant three photon processes 80—38069
I_2He, I_2He_3, and I_2He_3, photodissoc. products energy distrib. 79—100410
ice, hexagonal, Raman spectrum of translational lattice vibrs., press. effects 79—24304
indole, and derivatives, temp. fluoresc. quenching, rel. to H_2O solvent struct. 78—5265
inert gas, spectral line width and shift in shock-tube plasma 77—23467
inorganic molecular crystals, metal complexes electronic spectra and intermolecular interactions 80—55137
iodoethylene, and perfluoro analogue, VUV spectra, perfluoro effect on Rydberg states 77—61764
iodomethane, and isotopic forms, self-broadening and self-shifting of rot. spectra 78—13551
iodomethane, collisional rot.-line widths and shifts, microwave region 78—25619
ions, positive, dielectronic recomb. in plasma generalised cascade theory 80—43851
IR molecular absorption spectra, effect of rotational coupling on torsional bands 78—13497
isobutylene, liq., vibr. phase relax. and freq. shifts, density and temp. effects 80—74235
isoquinoline semiperchlorate, H-bonding, strong, stochastic model and IR spectra temp. effects 78—62805
Lamb dip, transit time broadening, perturbation theory calcs. 77—647
laser-induced line shifts and double-quantum Lamb dips 78—86825
linear conductor, dynamical aspects of fluctuations 79—33715

spectral line shift continued
LP 790-29, mag. degenerate star, C_2 Swan bands broadening and shifting 79−5815
luminescence of solutions under powerful excitation, intermol. relax. effect 79−85985
magnetic resonance expts. in weak magnetic fields with zero-field splitting 77−48034
manganese minerals, photoluminesc., cryst. field theory *(Russian)* 78−84654
matrix isolated impurities, freq. shift anal. 79−91472
measurement accuracy, apparatus function effects *(Russian)* 77−13800
methane, in air, IR spectra, optical-acoustic investig. *(Russian)* 78−74663
methane, nonlinear optical reson. shift in mag. field, vibr.-rot. transition 78−13549
methane, saturated absorpt. reson. shape, geometry and field intensity effects *(Russian)* 80−32778
methane, saturated absorpt. resonances, shift and broadening due to curvature of laser wave fronts 77−18981
methanol laser, CW, optically pumped, 170-μm emission, press. shift 80−106510
methyl chloride, pressure-induced shift of the J=0→1 transition, 193 to 366K 77−14497
methyl iodide, in Ar and Kr, medium perturbations of extravalence excitations, VUV absorpt. 78−1002
1-methylindole-n-butanol (ethyl acetate), soln., ground state complex form., fluoresc. spectra, Stoke's shift origin 80−58299
3-methylisoquinoline, semiperchlorate, H-bonding, strong, stochastic model and IR spectra temp. effects 78−62805
molecular beam spatio-temporal modulation near mol. reson. *(French)* 79−49299
molecular crystal, polar guest, stark shift, point-dipole approx. 77−1701
molecular electronic spectra, high press. effects 78−78754
molecular far IR line shift, meas. using Michelson spectro-interferometer *(French)* 77−61875
molecular interaction anisotropy, small angle scatt., spectral evidence 80−78600
molecular IR spectra, vibr. freq. shift, press. and solvent effects 78−74709
molecular nonrigidity effect on line shift 77−50473
molecular press. broadened width and shift, temp. depend. 77−61807
molecular solid, intermolecular interactions, laser induced phonon probe 80−79891
molecular transition identification, coherence resonances for hyperfine struct. interpretation 79−54920
molecular vibr. freq. shift during gas-soln. phase change, intermolecular interaction pot. 77−23487
molecular vibr. freq. shift during gas-soln. phase change, Onsager-Bottcher model 77−23488
molecular vibr. freq. shifts in polyatomic solutes 78−58654
molecule, elastic scatt., nonlinear reson. freq. shift in rot.-vibr. transitions 79−36731
molecule, method for estimating shift in electron levels *(Russian)* 78−46403
Mossbauer line, cubic cryst., second-order Doppler shift 79−56633
multi-level atomic systems, reson. lineshapes and shifts in rot. mag. field 77−68010
Nafion cation exchange membranes, IR spectrum assignment 79−89818
naphthalene, cryst., fluoresc. spectra, press. tuning 77−28612
naphthalene, doped, zero-phonon lines and absorpt. spectra, temp. depend. of shift and broadening 79−69866
naphthalene, phosphorescence spectra in rare gas matrices, multiplet struct. and pot. energy functions 80−106341
naphthalene, vibr. dephasing and Raman active localised internal mode temp. depend. 80−45060
naphthalene vapour, fast obs. of primary triplets with tandem laser pulse absorption 77−58056
neutral+high Rydberg atom, thermal collisions, review 80−63756
neutral atom collisions, hyperfine component broadening and shift of spectral lines 80−74136
nitrobenzene, spectral splitting of stimulated Raman scatt. 78−50860
n-nitrophenol, H-bonded complexes, IR absorpt. band struct., freqs. and intensities *(Russian)* 77−18928
noble metal, matrix-isolated, matrix-induced changes in opt. spectra 77−57913
nonlinear absorption method in magnetic field for spectral line width and shift meas. 80−37066
octachlorofulvalene, electronic structs., semi-empirical MIEHM calcs. and photoelectron spectra 77−75057
optical frequency standard, collision shift and broadening *(Russian)* 79−59783
organic impurity crystals, press. effect on shift of zero-phonon lines 79−95824
organic mixed crystals, transverse relax. and freq. shifts of optical transitions 78−84599
organic molecules in solution, electronic energy level shift estimation 79−54919
organic ortho compounds, solid, H bonding, wide line NMR obs. 78−52362
orthocarboranes, IR spectra, CH intra-, intermol. perturbations, hydrogen bonds *(French)* 77−68044
pentacene in naphthalene (p-terphenyl), mol. mixed crysts., optical dephasing and vibronic relax. 80−95957
pentacene in p-terphenyl, intermolecular interactions, laser induced phonon probe 80−79891
perylene, intermolecular interactions, laser induced phonon probe 80−79891
perylene in n-alkane, zero-phonon lines in luminesc. spectra 78−56512
phenol, H-bonded complexes, IR absorpt. band struct., freqs. and intensities *(Russian)* 77−18928
photon echoes, mixing collisions and quantum beats 77−34914
photon-correlation spectroscopy, spectral parameter extraction 78−77993
phthalimide, soln., excitation spectra rel. to recording wave length *(Russian)* 77−12438
phthalimide solutions, fluoresc. optical quenching by ruby laser rad. *(Russian)* 77−12437
pionic atoms, 2p level shifts and widths 78−46469
plasma negative ions, broadening of free-bound radiation threshold, quasistatic theory 80−53941
plasma reson. lines regularities in Stark widths and shifts, He^+-Ca^+ 80−43881
polar liquids, electron solvation, spectral changes 77−73501
polar molecule in soln., broadened band contour anal. 77−496
Polaroid K, oriented analogue of polyacetylene, reson. Raman spectroscopy 80−66208
polyacetylene:I, pure and doped, reson. Raman spectroscopy 80−66208
polyatomic mol., fluoresc. spectrum excitation depend., proportionality coeff., vibr. redistrib. 77−23518
polyatomic molecules in condensed phases, origin of vibr. dephasing 79−27069
polydiacetylene, urethane substituted, conjugated polymer soln. spectral shift on planar-nonplanar conformational transition 79−64129
polydiacetylene-bis(toluenesulphonate), refl. spectra, 0-15 kbar, doublet press. shift 78−43891
polydiacetylenes, electronic structure, bond length variations effect, Xα SCF calc. 78−5378
polyethylene, H bonding effects on skeletal optical and longitudinal acoustical modes 80−34914
polyethylene, linear, far IR absorpt. spectrum, temp. depend., 14K to melting pt. 79−1758
polymer, deformation of interatomic bonds, IR spectral meas. 79−38918
porphin, free base, in n-octane crystal, S_1 from S_0 transition, freq. shift and dephasing temp. depend. 78−25584
positronium hyperfine press. shift in buffer gas, calc. 77−557
predissociated two-channel model, resonances with complex rot. method 80−58327
predissociating harmonic oscillator, relative line widths and level shifts 80−23469
predissociation, reflection method of calculating energy shifts and linewidths 77−75237
pressure-induced spectral linewidth and line shifts, vibr. depend., IOS scatt. approx. 79−68267
1-propanol, electron traps, prestabilised electron relax. model 78−27803
propylene/butene-1 copolymers, coisotactic shift contribs. in ^{13}C NMR spectra 80−29635
protonium, atomic X-ray yields 1s and 2p level shifts and widths, cascades, calc. 80−78730
quadrupolar nuclei in solids, enhanced resolution NMR interferometric correl. of shifts 80−57355
quinine sulphate, acid soln., edge excitation red shift and proton migration 78−1028
Raman spectra, Stokes radiation freq. diffr. shift 79−72625
Raman spectral line shape, quantum field theoretic formulation 78−31187
rare earth ion energy separation, $4f^N$-$4f^{N-1}$ nl, host depend. 80−49676
resonance spectral broadening in high density gas, many body shielding 77−79579
rhodamine 6G, in rigid matrix, conc. effects in spectra 80−83347
rhodamine 6G, solns., electronic absorpt. spectra, mol. assoc. effects *(Russian)* 77−88460
rhodamine 6G dye laser, induced radiation spectral characts., effect of vibr. relax. 80−64008
rhodamine 6G in dimethylsulphoxide, concentratational red shift and luminesc. spectra 80−83426
rhodamine dye polar frozen solns., luminesc. broadening 80−2834
Rochelle salt, cryst., oriented intrinsic absorpt. edge shape 77−66505
Rochelle salt, ferroelectric, Raman and IR study 80−71406
rotational spectral line shift and widths, collision induced phase shifts 77−75222
ruby, fluoresc. spectrum, appl. to glass transit fluid press. determs. 77−26321
ruby, optical spectra freq. shifts press. depend., nonperturbative theory 78−23499
ruby, R-lines breadths and shifts rel. to high press. calibration 77−18106
ruby fluorescence line shift, appl. to press. distrib. meas. in diamond anvil press 78−12710
ruby fluorescence line shift, condensed gas phase transitions obs. in diamond-anvil cell 80−73381
self reversal contours, use in determ. of line broadening and shift consts. 80−52940
semiconductor, light absorption, temp. depend., exciton-exciton and -phonon interactions *(Russian)* 77−40265
semiconductors, indirect interzone absorpt. in presence of strong EM waves *(Russian)* 80−66217
solar lines limb shift, effect of granular motion 79−12448
solar Mg II core absorption, wavelengths meas and evidence for atmospheric downflow 79−12451
solar photosphere line shifts, granulation contrib. spatial and temporal depend. 80−85912
solar photospheric line shifts, calc. from granulation vertical motion models 80−90375
solar rotation induced Doppler spectral shift meas. by scanning Fabry-Perot interferometer 80−77298
solar spectra, small line shifts meas. via automatic comparator 77−82123
solar spectral lines, improved value for macroturbulent displacement filter function 78−20796
solar spectrum, convective correction to measured wavelengths 78−93181
solar spectrum, lines integral characts. rel. to solar atmosphere vel. field estimation 80−46530
solution, electronic bands broadening rel. to Stokes shift of lum. 77−71837
solutions, dilute, freq. shift, method of local field calcs. 78−13553
solvent effects, electrostatic model for mols., semi-empirical PPP calcs. 77−83507
spontaneous emission, line widths and energy shifts *(Chinese)* 79−89874
SS 433, Hα blue component wavelength obs. and weak lines interpretations 79−67023
SS 433, reality of 6-day periodicity in spectral lines wavelengths var. 80−67743
SS 433, wavelength shifts 164[d] period as precessional motion, massive black hole and pulsar models 80−62138
Stark, width and shift depend. on ionisation potential 80−58211
statistical evaluation and measuring strategy for extremely small line shifts 78−86234
Stokes fluorescence shift time resolution, obs. of 2-amino, 7-nitrofluorene in 2-propanol 77−58060
TCNQ salts, PMR, electron-proton couplings, local susceptibilities 79−82883
tetrachloromethane in dilute soln., dynamic dipole induced interactions in absorption spectra 78−13553

spectral line shift continued
tetramethylammonium chloride solns., aq. and methanolic, Raman spectra 79−28750
thiourea, ferroelectric, Raman and IR study 80−71406
three level absorber, two-photon transition, self-induced transparency 79−27337
TMMC, crossover transition, effects on susceptibility and EPR shift 80−71047
transition metal ions in crystals, thermal broadening and shift calcs. 77−48208
transition potentials, for ESCA and Auger spectra, equiv. cores and Hellmann-Feynman calcs. 77−61724
trichloromethane in dilute soln., dynamic dipole induced interactions in absorption spectra 78−13553
trifluoromethane, rot. transitions, self-broadening and self-shifting meas. 79−59426
D-tryptophan, soln., excitation spectra rel. to recording wave length *(Russian)* 77−12438
TTF salts, PMR, electron-proton couplings, local susceptibilities 79−82883
TTF-TCNQ, charge transfer determ. from spectral line shift using Raman scatt. 80−25392
TTF-TCNQ, one-dimensional conductor, Raman scatt. 78−80355
TTF-TCNQ, plasma reflectance edge shift, meas. from 0 to 62 kilobar 77−61133
two-atom resonance fluoresc. spectrum, cooperative effects 80−78570
two-level atom, EM radiation interaction, elec.- and mag.-dipole contribs., reaction field 78−94215
two-level atom, phase shifts in weakly amplitude modulated light scatt., linewidth effect 78−50505
two-level atoms, dynamics and spontaneous radiation in bichromatic EM field 80−91502
two-level molecules in low press. gas, nonlinear power reson., field broadening and shifts 79−45768
two-photon absorption, semiclassical theory, finite-state model 77−58109
two-photon light shift and two-photon Lamb dips 79−36591
umbelliferones, 3-substituted, fluoresc. spectra, pH depend. 77−88492
unimolecular predissociation, type I, level widths and shifts, quantum-mech. method 79−31629
urea-$NaNO_3(KNO_3)$ solid eutectic mixtures, Raman, IR spectra, line shifts, widths 77−55793
vanadyl porphyrins, anion radicals and dianions, reson. Raman spectra 77−471
variational study, non-relativistic general formulation *(French)* 79−75093
visual pigment model systems, spectroscopy and photochem. 77−32871
visual pigments of Gekko, ionochromic behaviour 77−36928
water, low-density amorphous solid, Raman spectra, OH stretching region 79−11410
X-ray, lineshifts in nonrelativistic and relativistic approxs. 78−951
X-ray absorption edge-shifts, empirical relations, effective ionic charge for isoelectronic series 78−55136
X-ray spectral lines profile evolution due to Comptonisation, Monte Carlo computations 79−66916
xanthene, dye solns., luminesc. spectra, conc. depend. effects 79−54885
Zeeman resonance lineshapes, motional narrowing, analytical results 77−46524
Zeeman resonance lineshapes, motional narrowing, expt. 77−46525
Zeeman resonance lineshapes, motional narrowing, lineshape in absence of motion 77−38636
Zeeman resonance lineshapes, motional narrowing, Monte Carlo simulation 77−38635
Zeeman resonance lineshapes, motional narrowing 77−38634
zinc porphyrins, anion radicals and dianions, reson. Raman spectra 77−471
Ag, matrix isolated, fluoresc. spectra. excimeric bond effects 78−50498
Ag_2HgI_4, polycryst., Raman spectra, press. depend. 77−73137
$Ag^{+14}N^{n+}$, 7-35 MeV, K-shell X-ray production cross sections 77−75090
Al I line broadening and shifts by van der Waals interaction with Ar and He atoms 79−6912
Al I resonance line profiles, influence of boundary layer of Al-seeded shock heated plasma 80−43876
α-$Al_2O_3:Cr^{3+}$, electronic Raman transition from optically pumped excited state 78−39531
Ar, photoionisation, Auger processes, decay lifetime, line shift, profile, X-ray photoelectron spectra 80−37798
Ar, spectral line collisional broadening and line shift 77−10641
Ar-Kr(Xe), UV absorption spectra, induced lines and line-shift meas. *(French)* 77−61697
As_2S_3, amorphous, time resolved luminesc. 80−66288
As_2S_3 glass, melt-quenched, reversible photostruct. change 77−68925
Au, K-shell X-rays, energy shifts and excitation mechanism 78−41990
Au thermal modulation reflectance spectrum, temp.-dependent shift 77−81121
AuLi, vibr. freq. determ., IR spectra, matrix depend. 77−75146
B, amorphous, X-ray Raman scatt. 78−48157
BCl_3, intense IR radiation absorption singularities 79−76432
Ba I, laser-excited, absorpt. spectra, press. shifts 77−27007
Ba II, Stark half-widths, line shifts, calcs. *(Russian)* 78−62764
Ba, quadratic Zeeman effect, diamagnetic shift, Rydberg series, strong field mixing 78−946
Ba, reson. lines, emission and absorpt. core profiles 77−50389
Ba^+, electron and ion Stark effects in plasma, widths and shifts 77−46526
BaS-CaS:Cu phosphors, X-ray diffr. and fluoresc. spectra 80−40148
Be, Doppler effects in X-ray spectra excited by accelerated ions 78−86808
BeF_2, aq. glass, 76K, solvated electron spectrum evolution, following ns radiolysis 78−88295
Bi phosphates, X-ray electron spectra 77−36352
^{209}Bi, pionic 4f→3d transition, pionic 3d state strong interaction level shift and width 79−98251
Br_2, Ar matrix reson. Raman excitation profile, red shift rel. absorption spectrum 77−14440
Br_2, organic solvent effects on Raman parameters 79−26998
C, reson. transitions, Stark widths and shifts of UV and VUV Lines 77−88425
C_2 molecule in solar spectrum, wavelength shift determ. method 78−49340
CF_3I, I laser medium, UV absorption profile modification by vibr. excitation, for fusion ignition 78−58717
CO, Autler-Townes power splitting of rovibr. lines, direct obs. using intense IR laser 79−54854
CO, pressure-induced spectral linewidth and line shifts, vibr. depend., IOS scatt. approx. 79−68267
CO, Xe matrix-isolated and solid, UPES obs. 79−45762
CO_2 IR Zeeman spectra utilizing copropag. wave reson., diamag. shift obs. 80−53055
CO_2 laser line, electro-optic frequency shift *(Chinese)* 80−43379
CS_2, in Ar, medium perturbations of extravalence excitations, VUV absorpt. 78−1002
CS_2, $\pi\pi^*$ and Rydberg bands, cryogenic solvent effects 78−55182
CS_2, spectral splitting of stimulated Raman scatt. 78−50860
Ca II K-line in quiescent solar prominence, influence of spatial resolution on line width and shift 80−77364
Ca^+, electron and ion Stark effects in plasma, widths and shifts 77−46526
Ca+He(Ne), press. broadening, line shifts 78−5290
$CaCO_3$, calcite, spectral splitting of stimulated Raman scatt. 78−50860
$Ca_5(PO_4)_3F:Nd^{3+}$, luminesc. and absorpt. spectra, line shift and broadening 77−4678
Cd, $5s5p^3P_1$-$5s^2\ ^1S_0$ intercombination line, press. broadening and shift 80−95564
^{114}Cd λ326.1 nm reson. line, self-broadened, temp. depend. of parameters 79−63964
^{114}Cd+He, collisional effects on 326.1 nm line rel. to temp. and conc. 78−5336
Cd_3As_2 film, optical absorption edge 80−50450
CdS, Raman shift dispersion near exciton reson., two-phonon cascade processes 80−11405
CdS, wurtzite crysts., calc. spectra compared piezoemission meas. 77−52038
CdS(Se), ps. spectra, high density exciton system 78−19554
CdSe:Fe, exciton electroreflectance spectra, impurity effects 77−16335
^{114}Cd, resonance line contant., effect of Xe temp. and conc. 79−63945
Cd_2^* excimer, fluoresc. band shape, decay rates 78−70866
chloromethane, collisional rot.-line widths and shifts, microwave region 78−25619
Cl^- (Br^-) (I^-), in plasma, broadening of free-bound radiation thresholds 80−53940
Cr complex, tris(2,2′-bipyridine)Cr(III), excited states, Raman spectra 80−97263
Cs, discrete level raising into far continuum, oscillator strength to shape reson. transfer 78−78624
Cs, four-photon ionis., strongly interacting resons. theory 80−52955
Cs, HFS of first doublet, He, Ne and Ar press. effects 77−38638
Cs, hyperfine struct. density and temp. shift coeffs., at high buffer gas densities 79−18138
Cs vapour, general higher-order effects of freq. shifts in optical-RF double reson. 78−21884
Cs+Ar(Kr)(Xe), spectral line breadth and shift, Van der Waals pot. calc. 78−90126
Cs+Ar(Xe)(He), shift, halfwidth, satellite and absorpt line in square-well pot. 80−42993
Cs+inert gas, D_2 line collisional broadening and shift, and HFS 79−22664
Cs+inert gas, hyperfine struct., broadening and shift calcs. 77−58153
$CsNO_3$, molten, Brillouin spectra, 420-520°C, hypersonic vel. and sound absorption freq. depend. 77−28589
$CsNiF_3$, one-dimensional ferromagnet, optical absorpt. and static spin correlation functions 80−71415
Cu complex, Cu(II) acetylacetonates, X-ray K-absorpt. edges, edge widths and shifts 78−50556
Cu-Cr, Kondo alloy, NMR of Cu satellites, 1 to 4K 79−73837
Cu+Cu collisions, Kα X-ray energy shifts, target thickness depend. 80−83311
Cu_2HgI_4, polycryst., Raman spectra, press. depend. 77−73137
D_2 matrix shift, CoM freq., in solid Ar, Kr and Xe 79−6969
D_2, Raman spectra, vibr. freq. press. shifts 78−78703
D_2O superradiant laser, Raman shifts of 99 μm output, Fabry-Perot freq. meas. 79−55120
Dy, isotope shift meas. using laser atomic beam technique specific mass shift determ. 80−91497
Eu_2O_3-Sc_2O_3-Ta_2O_5 system, orthotantalate section, X-ray diffr. and luminesc. obs., conc. depend. 80−54205
F, pionic X-ray transitions, strong interaction line widths and shifts 77−23586
F spectral lines, neutral, in shock tube plasma, Stark widths and shifts 78−9117
FCN, IR laser Stark spectra, C-F stretching mode, dipole moments, rot. consts. 78−1022
$(Fe,Cr)_3C$, reln. between bond energy and X-ray emission line shifts 78−50555
Fe I 3719.94 Å line broadening by He, line width and shift meas., astrophys. significance 77−73942
Fe I lines limb shift in solar atmosphere, pressure shifts effect 78−89150
Fe XXIV, dielectronic satellite spectra, solar flares appl. 80−32646
$(Fe_xMn_{1-x})_3C$ in steel, X-ray K-absorpt. spectra *(Russian)* 78−6813
FeOOH, H-bonding, strong, stochastic model and IR spectra temp. effects 78−62805
Ga complex, photoluminesc. spectra, $\pi\rightarrow\pi^*$ and charge transfer L→M transitions, Stokes shift 78−64407
Ga+inert gas atom, diffuse series head lines, hyperfine components, broadening calcs. 80−32632
$Ga_{1-x}Al_xAs$, optical detection of CESR 77−36155
GaAs laser diodes, junction temp. meas. method 79−36895
GaAs, optical detection of CESR 77−36155
GaAs, photoconductivity, impurity induced, low energy edge spectral shift 80−65630
$Ga_{1-x}In_xAs$, optical detection of CESR 77−36155
p-GaP, Raman scatt. by coupled plasmon-phonon oscills. 78−6687
GaP:S, effects of uniaxial stress on luminesc. 79−78739
GaSe, exciton absorption under intense excitation 77−77235
Ge, effect of pressure on the Raman shift 78−92064
Ge, electron-hole drops size effect on far IR absorption and scatt. *(Russian)* 78−10903
$Ge+^{14}N^{n+}$, 7-35 MeV, K-shell X-ray production cross sections 77−75090

spectral line shift continued
GeS_2 glass, melt quenched, reversible photostructural change, optical transmission spectra obs. 80−45109
$GeSe_2$, glassy and single-cryst., photoluminesc. at 77K 77−63456
H Balmer-α fine struct. lines, anomalous shifts, in He-H_2 DC discharge 79−45677
H, He atmosphere, hyperfine press. shift, MCSCF-variational procedure 77−6735
H, hyperfine freq. and wall shift, 4.2K gas in solid H_2 coated bulb 79−50155
H, hyperfine shift and interatomic pots. in inert buffer gas 80−5491
H, hyperfine shift in He buffer, exchange perturbation theory 77−6736
H, in hot plasma, elementary excitation spectrum, exchange and polarisation effects 80−43892
H, maser hyperfine transition, affected by coherently excited Zeeman transitions 79−72544
H, mesic, atomic X-ray yields 1s and 2p level shifts and widths, cascades, calc. 80−78730
H, multiphoton absorpt., reson. shift and power broadening, truncated model semiclassical calcs. 78−17644
H, n=4 level shift induced by laser radn. 79−98036
H, quasi-stationary states in field of strong monochromatic wave, perturbation theory calcs. *(Russian)* 80−58145
H, scatt. in reson. line wings and hyperfine struct. levels excitation *(Russian)* 77−57930
H-bond complex formation, enthalpy change due to electronic excitation, spectroscopic determ. 78−92496
H-He, H hyperfine struct. shift, commutator computational method 78−78608
H-like ions in laser-produced plasma, Balmer fine struct. (broadening) 80−48860
H+D, excitation transfer, spectral line broadening and shift 77−46531
H+He, H Balmer-α fine-struct. line shift and broadening 80−37783
H+He(Ar), press. effects on H_α and H_β Balmer series 77−18845
H_2 4-0 S(1) 6368 Å quadrupole line strength and pressure shift 80−43108
H_2, (4,0) S(1) quadrupole line intensity and pressure shift 78−90178
H_2, Compton defect, high energy electron impact spectroscopy 77−71876
H_2, D_2 and HD, intermol. collision process obs. using light scatt. expts. 80−53001
H_2, Λ doubling, $C^1\Pi_u$ states, calc. methods 78−90227
H_2, Raman spectra, vibr. freq. press. shifts 78−78703
p-H_2, solid, elastic consts., Brillouin scatt. obs. 79−8149
p- H_2, solid, induced near IR absorption spectrum, freq. shift, intensity, up to 10 kbar 78−6658
HBr, far IR Ar matrix isolated spectra, 4.2K, press. and conc. effects 78−62801
HCl, far IR Ar matrix isolated spectra, 4.2K, press. and conc. effects 78−62801
HCl, linewidths and shifts in fundamental band broadened by D_2 and H_2 *(French)* 78−972
HCl, mol., XPS and KLL Auger effect, line shifts 79−31602
HCl, pure rot. lines, press. induced shift perturbed by Ar 77−79652
HCl, vibr.-rot. lines broadening and shifting by SiF_4 perturber 77−23521
$H^{35}Cl$, collision broadened vibr.-rot. linewidths and shifts in fund. band, low temp. obs. *(French)* 77−68076
$H^{35}Cl$, $H^{37}Cl$, IR Fourier absorption spectra, press. induced shifts 78−74706
HCl-inert gas rot.-vibr. line pressure broadening and shift calc. 80−69124
HCl+Ar(Xe), spectral line shift of vibr.-rot. lines. press. shift 79−18237
HCl+iert gas, weak collisions, HCl spectral line broadening of IR spectra 80−74161
HCl+N_2, IR spectral line parameters 79−22766
HCl+$N_2(O_2)(D_2)(H_2)$, HCl ν_0-ν_1 band perturbations, linewidth and shifts calcs., IR spectra obs. *(French)* 80−58251
HCl(-acetone)(-acetonitrile), soln., IR absorption, H-bonding, solvent effect 78−29778
HF, aq. solns., IR spectra, H_3O^+ ion 77−30868
HF, far IR line shift, meas. using Michelson spectro-interferometer *(French)* 77−61875
HF, IR Fourier absorption spectra, press. induced shifts 78−74706
HF rotational line shift, far IR Fourier transform spectrometry improvement 79−30582
HF+inert gas, press. broadening and shifting of vibr.-rot. absorpt. lines 77−27161
H_2O, linewidths and press. shifts, in N_2 and air, Anderson theory and quantum many-body theory 78−74708
H_2O, mol. nonrigidity effect 77−50473
$H_2{}^{16}O$, laser spectroscopy using an optothermal receiver 80−37810
H_2O-HCl(HBr)(DBr) complexes, IR matrix isolation spectra, struct. 78−29781
$H_2O(D_2O)$, solvated electrons, optical absorpt. spectra. temp., isotope effects 80−55124
H_2S, mol., XPS and KLL Auger effect, line shifts 79−31602
Hα(Dα) plasma red shift meas. in Ar arc, ion dynamic depend. 80−10364
He, 3^3D levels shift induced by laser radn. 79−98036
He, 3^3D_1-2^3P_0 line, press. broadening studies by saturated absorpt. techniques 80−52939
He, 504.7 nm line excited in discharge 77−18848
He, Compton defect, high energy electron impact spectroscopy 77−71876
He, emission line profile, hollow cathode source 77−23469
He I, spectral line shift and Stark broadening in plasma 77−18843
He I lines in B-type stars spectra, wavelengths 77−25999
He I plasma lines, Stark broadening, quantum mechanical calcs. 80−43880
He II, Paschen lines, red shift in plasma 80−103128
He II, plasma polaris. red shift, Stark profile, temp. depend. 77−18842
He II plasma, spectral line shifts, electron collision induced 80−106879
He, isoelectronic series, ground state specific mass shift, HF variation perturbation calc. 80−47889
He, laser induced level shift 78−58627
He plasma, Stark shift and line broadening in 3-D stochastic laser field 78−50502
He, shift of 4^3S-2^3P line by CW CO_2 laser beam 77−30829
He, Stark broadened 4121 Å and 4437 Å lines in plasma, electron impact effects 77−27025
spectral line shift continued
He, Stark effect on optically excited plasma atoms in static mag. field 78−66505
He-H_2, rot. relax and spectral line shapes, coupled states calcs. 77−50500
He-Ne-methane stabilised ring laser, freq. stability calcs. *(Russian)* 78−9401
He+Cs(Rb), interatomic pots., hyperfine shifts, diffusion coeffs., perturbation exchange theory 79−41220
^{4}He, kaonic and pionic X-rays, strong interaction widths and shifts 79−98253
Hg, 1849 Å absorption line broadening and shift in inert gases *(French)* 77−30825
Hg doubly K ionised, energy shift between K_α X-ray and its hypersatellite line 78−9107
Hg, line profile and shift at 546.1 nm, high-press. discharge *(French)* 79−785
Hg_2-Pt, ^{199}Hg Mossbauer meas., isomer shift and quadrupole splitting calcs. 80−28039
Hg_2Br_2, improper ferroelastic, soft mode props. in Raman spectra 77−36246
Hg_2Cl_2, improper ferroelastic, soft mode props. in Raman spectra 77−36246
Hg_2F_2, ^{199}Hg Mossbauer meas., isomer shift and quadrupole splitting calcs. 80−28039
Ho, K X-rays, energy shifts, role of atomic struct. 78−70777
I+Ar, press. induced freq. shifts in I photodissociation laser 78−37875
$I_2Ne_aHe_b$ van der Waals complexes photodissoc. 80−50864
n-In Ar:Te(Sn), heavily doped, cathodoluminescence, doping effect on luminesc. band position and spectral profile 80−45153
In, Auger electron spectra, solid state effects 80−20739
In complex, photoluminesc. spectra, $\pi \rightarrow \pi^*$ and charge transfer L→M transitions, Stokes shift 78−64407
In+inert gas atom, diffuse series head lines, hyperfine components, broadening calcs. 80−32632
p-InSb, photoexcited exciton spin-flip scatt. 80−74434
IrF_6, in mixed crysts., Jahn-Teller effect, $\Gamma_{8g}(t_{2g})^3$ state, 6800 Å 78−76032
K, 5^2P to 4^2S resonance line, rare gas perturbations, broadening, shift and dipolaris. 78−9126
K, hyperfine struct. density and temp. shift coeffs., at high buffer gas densities 79−18138
K, resonance lines broadening and shift by noble gases 79−10070
K, resonance spectral lines, Stark broadening and shift 77−75097
K salt of β-ketoaldehyde, configurations of anions in solutions studied by IR spectroscopy, H-bond form. 80−87117
K+He(Ar)(Ne)(Xe), K 5^2P level broadening and collisional relax., quantal, semiclassical and expt. comparison 80−18903
KCl absorption and emission of F_A(Li) centres under hydrostatic pressure 78−92117
$KMnF_3$, exciton dynamics by time resolved emission spectroscopy 80−54615
K_2O-SiO_2 glasses, IR reflection spectra, computer resolution *(Japanese)* 77−69832
$La_{3-x}V_xS_4$:Gd^{3+} localised moment-conduction electron interact., ESR obs. 78−88183
Li, resonance spectral lines, Stark broadening and shift 77−75097
Li salt of β-ketoaldehyde, configurations of anions in solutions studied by IR spectroscopy, H-bond form. 80−87117
Li+He, press. broadening, line shifts 78−5290
LiH, finite-field method calcs., dipole moment gradients, polarisability gradients and elec. field effects 77−88589
$LiNO_3$-$NaNO_3(KNO_3)$ solid eutectic mixtures, Raman, IR spectra, line shifts, widths 77−55793
Li_2O-TeO_2 glasses, struct., IR reflection spectra 78−68516
Li*+He(Ar), Li principal series line broadening and shift, interat. pot. consts. 78−42165
LuCl, LuBr, LuI, visible emission spectra, detection and characteris. 79−6963
Mg, Doppler effects in X-ray spectra excited by accelerated ions 78−86808
Mg I, Mg II lines, broadening and shift by van der Waals interactions and electron impact 77−3303
Mg I, press. shifts of $^1D_2$ Rydberg states 77−61711
Mg, pionic X-ray transitions, strong interaction line widths and shifts 77−23586
Mg^+, electron and ion Stark effects in plasma, widths and shifts 77−46526
Mn^+, in soln., EPR relax. probe 78−31104
Mo^{32+}, dielectronic recomb. rate coeffs. in plasma 80−43853
Mo^{38+}, dielectronic recomb. rate coeffs. in plasma 80−43852
N_2, 1^- system bands, line broadening and shift 80−87138
N_2, liq., spectral splitting of stimulated Raman scatt. 78−50860
N_2, solid, α- and γ-forms, Raman spectra, vibron and lattice freq. shifts, libration 80−16020
N_2, solid, Raman spectra vibron and lattice freq. shifts, librational force consts., α- and γ-phases 78−19460
N_2, Xe matrix-isolated and solid, UPES obs. 79−45762
N_2-Ar, liq. mixture, isotropic Raman line shape theory 78−88298
N_2-Ar(Kr)(O_2)(CO)(CH_4), liquid, high resolution CW CARS spectra 80−63635
NH_3, dynamic Stark shift, microwave obs. 79−72352
NH_3, microwave spectra, press. shift of inversion lines 79−31615
NH_3, microwave spectrum, width and shift parameters 77−18985
NH_3, molecular rotational transition, collision induced shift 77−484
$^{14}NH_3$, J=13, K=13 inversion line displacement as function of pressure *(French)* 78−70815
NH_3-$N_2(H_2)$(Ne)(Ar)(Kr)(Xe), as R(1,1) vibr-rot. line parameters, ν_2 band, using CO_2 laser light 79−3444
NH_3+H_2, NH_3 inversion transition, linewidths and T_1/T_2 ratio 80−99499
NO_2, Ne matrix isolated, 6K, B←X band system 78−993
N_2O, rot. transitions, self-broadening and self-shifting meas. 79−59426
Na, 3S-4D and 3S-5S two-photon lines, broadening and shift by inert gases 77−75105
Na, pionic X-ray transition strong interaction line widths and shifts 77−23586
Na, resonance spectral lines, Stark broadening and shift 77−75097
Na salt of β-ketoaldehydes, configurations of anions in solutions studied by IR spectroscopy, H-bond form. 80−87117
Na, two-photon transition broadened by Ar impact 79−22681

spectral line shift continued
Na+He(Ar)(N_2), collision broadening and shift of 3S-4D and 3S-5S lines 79−3406
Na+Kr(Xe), reson. line broadening, press. depend. 78−66596
NaCN, Raman spectrum, hydrostatic press. effects 78−6663
NaCl, inelastic light scattering of localised vibration of interstitial H atom in alkali halides 80−88998
NaCl, thermoluminesc. and optical absorpt., simultaneous DC field and X-irrad. 79−99956
$NaD_3(SeO_3)_2$, ^{23}Na NQR, second-order quadrupole shift, temp. depend. 78−15055
$NaMO_2$, Stark shift of visible absorpt. of NO_2 78−19499
Nb_3Ir, A-15 struct. ^{93}Nb NQR spectra 80−20496
Nb_3Os, A-15 struct. ^{93}Nb NQR spectra 80−20496
Nb_3Pt, A-15 struct. ^{93}Nb NQR spectra 80−20496
Ne, at. spectra, Doppler broadening compensated by light shifts 79−41136
Ne, reson. obs. in saturated absorpt. spectroscopy 79−89972
Ne, X-ray line shift for high density laser produced plasma diagnostics 80−64778
Ne+Ne(He), 7d′ states, isotope shift, press. shift, press. broadening, two-photon spectra obs. 78−55155
Ne* 5882 Å line, Doppler free spectra, press. broadening and shifts, saturation spectroscopy 80−78565
Ni, UV matrix freq. shifts, ionis., pot., assignments, appl. to Ni_2, Ni_3 77−75178
O_2, $^3\Sigma_u^- - ^3\Sigma_u^+$ spin-orbit mixing in Schumann-Runge predissoc. 77−6875
O_2, $(0,0)b^1\Sigma_g^+ - X^3\Sigma_g^-$ band, press.-induced line shift 79−98160
O_2, gas, vibr. Raman spectrum, anomalous behaviour near crit. point 78−55179
OCS, collisional rot.-line widths and shifts, microwave region 78−25619
OCS, microwave spectrum, width and shift parameters 77−18985
OCS+OCS(He)(Ar), rot. spectral line shift and widths, collision induced phase shifts 77−75222
$O_2(c^1\Sigma_u^-)$, in Ar(Kr)(Ar-Kr) matrices, multiphonon vibr. relax. time-resolved emission obs. 80−18861
P, Stark widths and shifts, visible and UV 77−57927
PH_3, mol., XPS and KLL Auger effect, line shifts 79−31602
$PdBr_n(H_2O)_{4-n}^{2-n}$, electronic absorpt. spectra, band assignments 78−50553
$PdCl_n(H_2O)_{4-n}^{2-n}$, electronic absorpt. spectra, band assignments 78−50553
Pt, single cryst., oxidation, Auger spectra 78−14600
$PtCl_n(H_2O)_{4-n}^{2-n}$, electronic absorpt. spectra, band assignments 78−50553
Rb, $5^2P_{1/2} \rightarrow 5^2S_{1/2}$ resonance line perturbed by inert gases, depolaris., broadening and shift 78−21880
Rb Doppler-free two-photon lines, self-broadening and shift meas. 80−5506
Rb, hyperfine struct. density and temp. shift coeffs., at high buffer gas densities 79−18138
Rb, resonance spectral lines, Stark broadening and shift 77−75097
Rb, Zeeman resonance lineshapes, motional narrowing 77−46525
Rb+$^{14}N^{n+}$, 7-35 MeV, K-shell X-ray production cross sections 77−75090
Rb+Ar(Kr)(Xe), spectral line breadth and shift, Van der Waals pot. calc. 78−90126
Rb+inert gas, D_2 line collisional broadening and shift, and HFS 79−22664
Rb+inert gas, hyperfine struct., broadening and shift calcs. 77−58153
Rb+inert gas, mag. scanning technique for broadening and shift 79−22663
Rb+Kr, STS components shift and broadening 77−68014
Rb+Rb**, freq. shift, line broadening, phase interference effects, Doppler free two photon spectra 80−58200
^{85}Rb cell filtering action, press. shift and broadening by foreign gases 79−3403
^{85}Rb, ground state dipole HFS diamagnetic shift, high field optical pumping expt. 78−90129
^{87}Rb, hyperfine transition, light shifts, buffer gas shifts, rel. to maser freq. stability 79−98029
^{87}Rb resonant frequency change, due to spectral profile of pumping light 78−45590
^{87}Rb+Kr, D_1 line broadening and shift 77−38640
^{87}Rb+inert gas, D_1-line hyperfine components perturbation, interferometer obs. 80−32635
Re, pionic 4f→3d transition, pionic 3d state strong interaction level shift and width 79−98251
S, He-like ions, X-ray emission passing through thin foils 77−3293
SF_6 gas, CO_2 TEA laser-excited, slow intermol. redistrib. of vibr. energy 80−53039
SF_6, IR absorption peak shift at high intensity *(Russian)* 77−42327
Sb (III) compounds, orbital population anal. using ^{121}Sb Mossbauer data 78−21953
Sb, Auger electron spectra, solid state effects 80−20739
Se, Doppler effects in X-ray spectra excited by accelerated ions 78−86808
Si, absorpt. spectrum red shift, spectrum temp. depend. 79−78699
Si, single cryst., oxidation, Auger spectra 78−14600
Si:H(B)(P), amorphous, UV absorpt. spectra 80−25420
Si:O,H amorphous, time resolved luminesc. 80−66288
Si:P, EPR line shift, 0.56 to 4.2K, investig. of interacting donor clusters 77−77084
Si:P, heavily doped, IR bound-exciton luminesc. spectra 78−15211
SiF_6, saturation absorpt. spectra, evidence of tumbling multiplets 79−36637
$Si_{1-x}Ge_x$ amorphous, ESR centres, g-shift rel. to annealing 77−55701
SiH_4, mol., XPS and KLL Auger effect, line shifts 79−31602
SiO_2, amorphous forms, surface struct. ESCA, X-ray line shift meas. *(Russian)* 77−66775
Sn, Auger electron spectra, solid state effects 80−20739
Sr, 4607 Å reson. line shape, width and shift in Ar, press. depend. 79−22653
Sr, 4607.33 Å line, broadening and shift in H_2-O_2-Ar flames 77−18849
Sr, quadratic Zeeman effect, diamagnetic shift, Rydberg series, strong field mixing 78−946
Sr, reson. lines, emission and absorpt. core profiles 77−50389
Sr^+, electron and ion Stark effects in plasma, widths and shifts 77−46526
Ta, K X-ray energy, excitation mode depend. 78−17597
Ta, K X-ray energy, excitation mode depend. 78−17598
^{181}Ta, pionic 4f→3d transition, pionic 3d state strong interaction level shift and width 79−98251
Te, Auger electron spectra, solid state effects 80−20739
Te, Te cpds., Auger spectra 78−58638
Tl, 535.0 nm line shift by H_2 perturber 80−91506
Tl+inert gas atom, diffuse series head lines, hyperfine components, broadening calcs. 80−32632
Tl($^2S_{1/2}$)+inert gas, long-range interaction, spectral line shifts and broadening 79−10174
UF_6, gas, laser-induced fluoresc., A-X band 78−94275
V, atom and ions, shell energy struct., SCF calc. by Dirac-Fock-Slater method 80−52877
WSe_2, refl. spectra and photovoltaic effect, 1.5-3.2 eV, 4.1-300K 79−47470
Xe, atom and ions, relativistic Dirac-Fock-Slater calc., fluoresc. yield, X-ray energies shift 78−25450
Xe, extravalence excitations, VUV spectra, solvent perturbations 77−50386
Xe I, arc spectrum, press. shifts and broadenings in visible and near i.r. 77−440
Xe, K X-ray energy shifts following electron capture beta decay, role of nucl. hyperfine struct. 78−5166
Xe, photoelectron-Auger electron post collision interaction, Auger peak shift obs. 77−27039
Xe-Kr, UV absorption spectra, induced lines and line-shift meas. *(French)* 77−61697
^{136}Xe laser amplifier, pressure shifts of 3.51 μm line 79−76669
Y+$^{14}N^{n+}$, 7-35 MeV, K-shell X-ray production cross sections 77−75090
YAG:Cr^{3+}, absorption and luminesc., spectra, Cr conc. depend. 77−12435
$YAlO_3$:Nd^{3+}, thermal broadening and shift calcs. of Nd^{3+} energy levels 77−48208
Y_2O_2S:Eu, phosphor, temp. meas. by line shift method 77−13750
ZnO, self-activated phosphor, band width and shift, temp. depend. 77−8623
ZnO:Er, phosphors, photo- and electroluminesc. 77−12428
ZnS, green-blue luminesc. charact., model of luminesc. centres 79−73999
ZnS, interimpurity high press. luminesc. 78−19532
ZnS, time differentiated Mossbauer spectra from ^{57}Co impurities, relaxation processes *(Russian)* 80−34834
ZnSe:Cr^{2+}, stress-induced alignment of Jahn-Teller centres 79−78651
ZnSe:Cu, Cl, high press. luminesc. 78−19532
ZnTe, spin-flip plus phonon scatt., line shape and shift in peak position 79−73907
Zr complexes, X-ray K-absorption edge, shift and width meas. 77−8683
Zr+$^{14}N^{n+}$, 7-35 MeV, K-shell X-ray production cross sections 77−75090

spectral linewidths *see spectral line breadth*

spectral methods of temperature measurement
see also pyrometers
absolute radiation, receiver-coating thermal resist. effect on accuracy 77−87836
absorption spectroscopy principle, appls. 78−54375
absorption spectrum, press., temp., quantity and spectral resolution retrieval, appl. to N_2O 79−100462
acetylene-air flames, local temp. profiles and at. fluoresc. intensity profiles meas. 77−52680
air, rot. Raman spectra 78−62200
air, unipolar HF discharge, determ. of gas and rotational temperature *(German)* 77−1033
air arc temp. meas. by N_2^+ integrated emission coeffs. 80−59314
air-H_2 flame, temp. profile, two-line at. fluoresc. method meas. 77−71328
arc plasma temp. meas., electro-optical device *(Polish)* 79−82121
atmospheric temp., surface to orbit gas laser, absorpt. of vibr.-rot. band 78−12015
atmospheric vertical temp. profiles using ground based IR spectroradiometer *(Japanese)* 77−29499
atomic vapour excitation temperature in graphite furnace AAS 78−7298
camera spectrometer, for colour temp. meas. in cinematography and TV *(Russian)* 77−38050
CARS spectrometer for gases and flames 80−95154
cavity emissivity meas. in thermophysical investigation 78−74005
cholesteric mixtures, optical props., temp. meas. *(German)* 77−44013
chopping pyrometer for remote meas. below 200°C *(German)* 80−86313
circuit breaking arcs, HV, AC, switching, spectroscopic measurement of temp. distribution in constant pressure axial air flow *(Czech)* 80−86296
coherent antiStokes Raman scatt. *(German)* 79−27321
combustion, coherent Raman spectrosc. obs. 80−16691
combustion diagnostics, laser appls. 80−16688
combustion diagnostics, laser Raman and fluoresc. techniques 78−88635
combustion flame temperature profiles, using nonlinear inversion techniques 79−85140
combustion flow, passive optical diagnostics of temps. and species concs. 77−44527
combustion gas flow, spectroscopic temp. meas., cold boundary layer effects 77−31399
comparator of spectral radiances, use in realising temp. scale above 1337.58K *(Japanese)* 78−8407
comparators, integrated arc optoelectronic, automatic testing standard temperature-calibrated lamps appl. 77−53907
contactless, IR techniques and detectors *(German)* 80−86314
contactless, using pyrometer, problems *(German)* 77−82507
contactless temp. meas. by EM radiation *(German)* 77−79099
detonation temp. meas., theory and expt. results *(French)* 77−53917
diatomic gas, transient flow, temp. and conc. profiles, by rot. Raman scatt. 77−75995
dielectrics, surface heating by laser, optical temp. meas. 79−55911
digital pyrometry in solar furnace *(Japanese)* 78−32821
EHD contacts, asperity interactions 79−20215
electric arcs, temperature estimation from self-reversed spectral lines 80−75110
emissive medium, local equilib. temp. fields reconstruction 79−41874
evaluation by computer 78−91150

spectral methods of temperature measurement continued
flame, containing light scatt. particles, optical props. and temp. meas. method *(Russian)* 78−56894
flame, determ. by laser Raman optical multichannel analyser 78−73098
flame, laser Raman spectroscopy 77−5833
flame, laser Raman spectroscopy method *(German)* 78−32900
flame, spectral remote sensing 78−32818
flame, temperature and OH concentration, simulatenous determ. by high-resolution laser absorpt. spectroscopy *(German)* 78−35776
flame diagnosis, CARS appls. 80−16689
flame diagnostics using multichannel pulsed Raman spectroscopy 80−30237
flame temperature, meas. using unresolved rot. struct. of mol. spectra 80−86300
flame temperature meas., 5 laser-excited fluoresc. methods, theoretical basis 80−101793
flame temperature meas. by Raman scattering 77−16822
flame temperature meas. using laser induced fluoresc. spectrosc. of OH 80−90839
flame temperature measurement, spatially resolved, spectroscopic method 79−71446
flame temperature measurements, role of transition probability factors 77−1925
flames, anal., small vol. temp. meas. by two-line at. fluoresc. 77−40594
flames, gas temperature measurement, spectral technique *(Chinese)* 79−35749
flames, local temperature measurement, by two-line at. fluoresc. and photon counting method 79−71447
flames, temp., OH conc., spectrosc. determ. 77−32853
gas or plasma, Raman Q-branch intensity 79−37545
gas sample, IR spectra, nonlinear least squares method 78−15738
gas temperature measurement by spectrum line reversal 80−73358
geological materials, spectrographic thermometry and manometry using DC arc 78−16796
glow discharge, temp. meas. using electronic rot.-vibr. mol. spectra *(Russian)* 78−71575
high temperature gas diagnostics by spectral remote sensing 78−74002
high-current, graphite cathode vaporisation, composition and temp. spectral determ. 78−14228
HV equipment temperature meas. by IR instrument 77−10039
hypersonic flow, excitation temp. meas., hook method 77−58200
hypersonic wake, excitation temp. meas. by atomic spectral line relative intensities 80−43732
ICP plasma source, 9.2 MHz, temp. determ. by monitoring N_2^+ bands 79−12858
internal combustion engine, CARS noninvasive temp. and species meas. 80−30293
IR and UV temperature units, USSR special standards 77−30148
IR determ. of temp. increase in tension tests *(German)* 79−61806
IR multidetector spectrometer for atm. temp. sounding 79−25365
IR plasma temperature unit, 10000 to 15000K, USSR special standard 77−31519
IR pyrometer, portable, principles *(German)* 80−42229
IR pyrometer for remote temp. meas. of high-power radiation-generating equipment 78−24799
IR pyrometry, calc. method for true temp. from expt. readings 80−13081
IR radiation thermometer, −10 to +600°C range, solid-state, features *(German)* 77−82513
IR radiometric meas. of object true temp. 77−57326
IR remote sensing measurements, conceptual considerations and surface temp. estimation, review 79−34984
IR thermometry, semiconductor material temperature measurement *(Spanish)* 80−47062
IR tunable diode laser technique, temp. meas. of high-temp. gases 78−86268
laser fluorescence temperature measurement of Na in flames 80−11893
laser fluorescence temperature measurements in flames 80−11892
laser heated surface colour temp. meas. pyrometer 78−57956
laser Raman spectroscopy, flame temp. meas. 80−13074
leucosapphire, supercooling and crystn. temp. determ. 79−51237
light scattering diagnostics for combustion gases 77−47124
line shift method, internal temp. of Y_2O_2S:Eu phosphor 77−13750
line-reversal method, effect of fluctuations and nonuniformities 78−8404
line-reversal method, turbulent fluctuation effects 77−30147
low-temperature star automatic recognition by two-channel IR systems 79−75118
melting pool surfaces, temp. meas. by ratio pyrometers 78−82471
microwave thermography, current status for medical appls. 79−66503
multiplicative comparator of spectral radiances, systematic errors *(Japanese)* 78−29139
multispectral radiance method for temp. distribution meas. *(Japanese)* 78−77912
multiwavelength optical pyrometer for shock compression experiments 80−52229
multiwavelength radiation pyrometry where reflectance is measured to estimate emissivity 80−31757
neutral particle spectrometer for measuring ion temperatures *(Chinese)* 79−37553
NMR meas. at ultra-low tapes, S/N ratio, appl. to thermometry 80−73400
NMR thermometer, for multinuclear Fourier transform NMR 80−57292
optical and photoelectric pyrometry, measurement correction, reference wavelength 77−45847
optical meas. of semicond. temps. *(French)* 79−35743
Oxford spectroscopic furnace, temp. meas. by photoelectric pyrometer for Fe I oscillator strengths 79−36584
passive microwave radiometers 77−56775
photoelectric pyrometer for domestic oven temp. meas. *(Russian)* 78−70128
photoelectric pyrometer using non-cooled $Hg_{1-x}Cd_xTe$ detector, 0-700°C range *(Polish)* 78−41313
photoresistor contactless temperature indicator *(Russian)* 77−10023
photosphere, excitation temp. meas. from Ni I lines, effect of parity of spectral terms 77−53539
plasma, CO_2-TEA laser breakdown, average temp. depend. on physico-chemical target props. 77−19738
plasma jet light source, intensity distribs., OH band rot. temp. 77−44555
plasma temperature field determ., asymmetrical *(Czech)* 80−38704
spectral methods of temperature measurement continued
precision, with filament and optoelectronic transducers, 400-900°C range 77−87766
premixed H_2-O_2-N_2 laminar flames, temp. profiles, Raman, absorpt. and line reversal obs. 80−42227
pulsed plasma source temperature calibration spectropyrometer 77−7590
pyrometer, 3 wavelength for flame temp. meas. 79−93141
pyrometer, photon counting, 1400K to above 2200K within 0.5K and 1.0K 80−52232
pyrometer, scale correction by electric method *(Russian)* 80−37040
pyrometer, wide spectral range, temp. scale calc. 78−217
pyrometer calibration, near-infrared using standard temp.-calibrated lamps with filter 77−53915
pyrometer giving emission factor and luminance temp. *(French)* 79−17424
pyrometer operating principles survey and error sources *(German)* 78−49841
pyrometers, potential and limitations, charact. *(German)* 78−62203
pyrometers, two-colour, operation and appls. 78−65937
pyrometers, two-colour, principle, appls. 79−6129
pyrometric system image quality in temp. meas. of nonisothermal objects 78−41312
pyrometry, effect of scattered light 77−26301
pyrometry, photoelec., radiance temp. direct calc. 80−73367
pyrometry, true temperature rel. to object emission *(German)* 77−22546
radiation pyrometers, principles and appl. *(German)* 78−32819
radiation thermometers and appls. *(Dutch)* 77−53916
Raman spectroscopy, remote spontaneous, new trends in recording of signals 80−73485
Raman techniques for gas mixture concentration and temp. meas. *(French)* 79−17425
remote technique for meas. temp. fields by IR radn. detection 77−41606
ribbon-filament temperature lamps, measurement of charact. 80−4720
rotation of spectral lines, optical system *(Russian)* 77−53913
sea ice and surface temp. meas., enhanced IR satellite imagery 77−37422
sea surface temp. meas. using IR radiometry and visible spectrometry 78−69535
SEASAT-A satellite scanning multichannel microwave radiometer 77−5416
small volume flames, temp., temporal meas., two line at. fluoresc. technique, Raman scatt. 80−42226
solar far IR brightness temp. minima rel. to sunspot activity 80−62035
solar furnace, digital pyrometry system 77−37896
sooty diffusion flame, CARS obs. 80−16690
spectral emissivity measurement device, high-temp. materials 80−37039
steel against Al_2O_3, elastohydrodynamic contact, lubricated by naphthenic hydrocarbon, IR meas. of surface temp 79−15807
surface temperature meas., emissivity effect elimination 77−5840
temperature regulation, thermography in environmental physiology 78−58043
thermal radiation receiver load limits *(German)* 78−49840
thermal receiver with temp. readout by laser beam 77−82605
thermogrammetry, charact. *(Hungarian)* 78−65924
thermography, skin temp. meas. appl. 78−61280
thermovision equipment, thermograms anal. *(Hungarian)* 78−65923
transition metal spectral emissivity variation with temp. *(Japanese)* 79−1517
two-dimensional spectral line emission reconstruction as a plasma diagnostic 78−67415
visual pyrometric systems, optoelectronic convertor characteristics *(Russian)* 78−77919
Ar, plasma, vac. UV emission profile, temp., spectroscopic meas. 77−51229
Ar-air arc, stabilised, spectroscopic methods of temp. meas. *(Russian)* 80−38854
CO_2 4.3 μ band radiance meas. of internal combustion engine gas temp. *(Japanese)* 78−29119
CO_2 conc. and temp. in flames, Raman spectroscopy 80−32720
CO_2, fast flow laser, meas. of N_2 vibr. temps. 80−32955
CO_2 gasdynamic laser, vibr. temp. meas. method 80−9854
CO_2-N_2 mixture, temperature measurement by spectrum line reversal 80−73358
Cu vapour laser, gas temp. meas. using Doppler broadening of Ne buffer gas lines 80−19020
FeI, self-absorption-free spectral lines for temp. meas. in DC C-arc 80−87965
H_2 diffusion flame, Rayleigh temp. profiles meas. 80−16692
H_2O, low density flow temp. and density meas. by submillimetre spectroscopy 80−43816
Hf, 0.3 wt.% Zr, melting pt. and radiance temp. meas. by pulse heating method 77−53914
N_2, flame temp., CARS spectra diagnostic investigation 80−43404
N_2, high-speed Raman spectroscopy, condensed discharge vibr. excitation, vibr. temp. 78−82740
N_2 in premixed laminar methane-air flame, Raman scatt. meas. of vibr. temp. 79−80622
N_2, rot. temp. meas., rocketborne electron beam fluoresc. meas., reflected mol. effects 77−29519
N_2, rot. temps. determ. in diffusion flames using CARS 79−29358
Na D-line in shock-heated gases, collision mechanism 77−23539
O_2, gas, temp. meas., vibr. Raman intensity, 500-2000K 79−37436
OH, methane-air flame, conc., temp. and rot. temp., laser absorption spectroscopy 78−76862
OH radical in premixed laminar methane-air flame, fluoresc. meas. of rot. temp. 79−80622
OH radicals in glow discharge, rot. levels distrib., temp. meas. 78−47169
PbS detector, contactless thermometer appl., for 600 to 1200°C *(Slovak)* 78−54366
SF_6, 40 kA arc, time-resolved temp. and radius meas. using rapid-scanning polychromator 79−50907
SF_6, arc, temp. determ. accounting for demixing 80−70057
SF_6, ν_3 band, IR spectra, in supersonic mol. beam 78−66541
Si, temperature during CW laser heating, Raman scatt. meas. 80−76109
W filament lamp, temp.-calibrated, standard, charact. 78−218
W ribbon-filament temperature lamps, radiation error estimation 80−64128
ZrC-Re, spectral emissivity, 1400 to 2500K, surface relief and composition 77−24420

spectrochemical analysis
see also atomic absorption spectroscopy; atomic emission spectroscopy; X-ray fluorescence analysis
ABS polymers, deposited in internal magnet magnetron sputtering system, adhesion of Cu films 79−83121
absolute mass detection limits using laser microprobe anal. with cross excitation 78−7297
absorbing solutions, anal. by fibre optic filter fluorometer 77−36813
absorptiometer with parameter modulation appl. *(Russian)* 77−29070
absorption spectra, collision-broadened lines, information anal. 80−22433
absorption spectroelectrochemistry at Pt electrode 79−74395
absorption spectroscopy in scattering samples using integrated optics 77−29232
absorption spectrum, press., temp., quantity and spectral resolution retrieval, appl. to N_2O 79−100462
acetaldehyde photolysis products, time resolved Fourier transform spectrum 78−58071
acetylene smoke particles, optoacoustic meas. 80−50895
acetylene-air flames, local temp. profiles and at. fluoresc. intensity profiles meas. 77−52680
acid oxygen carbon electrodes, electrochemical measurements and surface studies, ESCA method appl. 78−31651
acrylamide-acrylic acid (acrylic acid salts) copolymers, composition determ., IR spectra *(Russian)* 80−7358
adenylate kinase, photokinetic microassay using the firefly luciferase reaction 80−56306
adsorbed species, catalytic reaction, high temp. IR obs. 78−88655
aerosol solid particles, diffusive evaporation, laser spectrochemical analysis 79−92040
aerosols, atmospheric, individual microparticles identification via micro-Raman spectrometer 78−68970
aerosols, particle size fractionated, Cd, Pb, Mn determ. by flameless atomic absorpt. 78−69434
AES, depth profile analysis, influence of impurity gases in UHV systems 78−76958
AES, qualitative and quantitative surface analysis appls., review 77−90704
AES, quant. depth profile *(Japanese)* 80−16751
AES, quantitative analysis *(Polish)* 78−76967
AES, surface composition, quantitative anal., review 79−24854
AES principles, developments and applics. 78−35781
AES quantitative anal. of impurities *(Japanese)* 78−91356
air, nonlinear least squares method for IR spectra 78−15738
air pollutant emission and emission meas. by laser *(German)* 78−40665
air pollutant gas detection by dye laser and Fourier transform method 79−57558
air pollutant measurement by absorption spectrum Fourier transform 80−81514
air pollutants, determ. by Stark modulated microwave spectroscopy 78−57337
air pollutants, laser spectroscopic detection 80−17366
air pollutants remote sensing by correl. spectroscopy, instrumental response characts. 79−5623
air pollution, detection by analytical spectroscopy using dye laser 78−81362
air pollution, laser-Raman microprobe anal. of suspended particulates 80−76687
air pollution, particulate C and SO_4^{2-} species identification by Raman spectroscopy 79−5625
air pollution, X-ray photoelectron spectroscopy *(French)* 77−36837
air pollution detection using lasers, review 77−9569
air pollution measurement by Fourier transform spectroscopy 78−61564
air pollution photoacoustic detector characts. at CO_2 laser freqs. 79−100554
air pollution studies, laser absorpt. techniques 77−9570
alkali metal anions and trapped electrons formed by evaporating metal-ammonia solutions which contain cryptands 79−100340
alkali tetrachloroaluminates, vapor characterisation by photoelectron spectrosc. 80−81388
alkali tetrafluoroaluminates, vapor characterisation by photoelectron spectrosc. 80−81388
Allende, S content, neutron capture gamma-ray spectroscopy 80−94728
alloy, surface layer anal. with emission spectrochemical anal. *(Japanese)* 78−92570
alloy films, deposition processes, rate controlling and composition analysis by electron impact emission spectroscopy 77−44165
alloys, liq., composition determination during electron bombardment furnace fabrication, X-ray emission spectrography *(French)* 78−3427
alpha spectrometry using liquid, scintillation methods appl. to nuclear materials safeguards 80−78379
ammonium tetrachloroaluminate, vapor characterisation by photoelectron spectrosc. 80−81388
analyte emission characts., inductively coupled plasma, effect of emission spatial profiles 80−89557
arc discharge, spectrum, correl. rels. *(Russian)* 78−70196
arc light sources in graphite tubes, plasma form. and rot. 79−43676
archaeometry, laser microspectral analysis *(German)* 80−55750
asphaltenes, from coal liquefaction, IR characterisation 77−52683
atmosphere, mol. complexes presence and role in residual absorpt., light scatt. obs. 80−56607
atmosphere contaminant tele-detection apparatus using combination light scatt. spectra *(Russian)* 77−49193
atmospheric analysis, using laser, from orbiting satellite 77−9571
atmospheric NO_2 total content meas. by absorption spectroscopy *(Japanese)* 80−12469
atmospheric pollutant interferential detector 80−108830
atmospheric pollutants, selective quantitative meas. using CO and CO_2 lasers 78−69526
atmospheric reactions, IR Fourier transform spectroscopic obs. 79−66785
atom, resonance ionization spectroscopy with amplification 79−54996
atom detection technique 79−26950
atom distribution, in flame spectrometry, moving point source model 78−61084
atomic detection, saturated optical nonresonant emission spectroscopy 77−60137
atomic Faraday effect, analytical appl. 80−9538
atomic forward reson. scatt. spectrometry using magneto-optical effect *(Japanese)* 78−76956
atomic spectrochemical measurements using Michelson interferometer Fourier transform spectrometer 78−3399

spectrochemical analysis continued
atomiser chamber electrode-diffusion flame, atoms distrib. in absorpt. zone, convection currents role *(Russian)* 79−34420
Auger spectra, digital methods for film anal. using computer-controlled spectrometer 77−56268
Auger spectra development for derivation of chem. information 80−3434
Auger spectroscopy, quantitative, effect of electron escape depth 77−21452
autoanalyser chart peak height digitiser 78−44431
automatic initiator for microwave induced plasma 78−88682
automobile exhaust, multigas analyser 77−49198
benzene, bromination on zeolite adsorption complex, Raman spectroscopic anal. 80−16670
benzene, plasma polymerisation in glow discharge, thin film IR and free radical EPR obs. 80−2964
benzo(a)pyrene, distrib. with respect to particle size in submicron atm. aerosols 79−74563
benzophenone, sensitised crosslinking, polymerisation, UV curing, IR investig. 78−35709
bilge water oil pollution monitoring system development 77−5246
binary alloy, relative sensitivity factors for quantitative Auger analysis 77−32861
binary mixtures, anal. by computer decomposition of mol. fluoresc. spectra 78−15735
binary mixtures, qualitative anal. by fluoresc. polarisation spectroscopy 79−34396
binary mixtures, qualitative anal. using fluoresc. polarisation 79−24849
biological molecules, chem. reactions, Raman difference spectroscopic obs. 78−44368
biological solutions, using wall-stabilised arc plasma source 80−41343
biological tissue, laser Raman probe microanalysis 78−88773
biomedical low light level video fluorimetry and microscopy 77−44874
biophysical substances, chemical and structural anal. by fluorescence and phosphorescence spectroscopy *(Norwegian)* 78−92596
blood alcohol determ., spectrophotometric method *(German)* 79−5415
blood analysis in vivo, noninvasive spectroscopic method 77−60234
blood erythrocyte count and haemoglobin determ. by mobile miniphotometer *(German)* 79−5416
blood indicator dye microconcentration meas. instrument 79−39565
bone elemental analysis by prompt γ-ray spectra due to ^{252}Cf neutron irrad. 80−17065
bone powder and ash, PMR and IR spectra, chem. anal., bond lengths 78−3414
brass, Auger spectral anal. of oxide corrosion films, quantitative methods 78−35557
buffers, effect on transit time and diffision of atoms in discharge *(German)* 79−79360
butadiene-nitrile elastomers, high temp., and press. chem. transformations *(Russian)* 79−52659
cadmium arachidate monolayer, Ag(Au) substrate, reson. surface plasmon reflection 78−56536
carbon steel, S determ., flame chemiluminesc. method 78−48711
carboxyhaemoglobin, redox investig. using reson. Raman, visible absorption and electrochem. methods 78−76832
CARS, reson.-enhanced, and coherent anti-Stokes hyper-Raman spectroscopy 78−86980
CARS, review 79−16051
CARS, theory and applications 79−97444
CARS spectrometer for gases and flames 80−95154
catalysis research, heterogeneous IR spectroscopy appl. literature review *(German)* 78−53256
catalytic surface phenomena, Raman spectroscopy using rot. vacuum cell 78−16852
cell nuclei staining parameters, evaluation regarding reproducibility of fluorescence measurements 80−21590
ceramic, B content by emission spectrosc. with high freq. plasma excitation *(French)* 80−76477
cerebral cortical microfluorometry at isosbestic wavelengths for correction of vascular artifact 80−56322
chalcogenide semiconductor amorphous film comp. monitoring by EPR 77−51940
chemical laser, combustion driven nozzle, F_2 absorption meas. 78−79011
chemiluminescence, analytical, flow cell design 78−73090
chemiluminescence analyser, process industry appl., air pollutants monitoring 78−40094
chemiluminescence in solution, anal. appls. 79−24874
chemistry and spectroscopy 78−89556
Cherenkov radiation light source in pulse radiolysis 80−42267
chlorodifluoromethane, IR multiphoton dissoc., CF_2 form., time-resolved optical absorption obs. 80−16702
chlorophyll a in benzene solns. and monolayers, chem. stability 79−47912
chromatogram scanning spectrofluorimeter-densitometer 80−31901
chromatography, liquid, detector characts. and use, book 78−15751
cigarette smoke, diode laser meas. of methane, ethane and H_2O vapour concs. 80−97847
citric acid, single cryst., X-irrad., EPR and ENDOR, 4.2K radical identification 79−65764
clathrate hydrates, identification from NMR line shapes 78−27861
coal, chem. struct., NMR and IR obs. 77−40590
coal and mineral content characterisation by Fourier transform IR spectroscopy 80−104474
coal liquids characterisation, analytical use of dialysis 80−30334
coherent anti-Stokes Raman scattering, for quantitative gas anal. 78−68968
coherent anti-Stokes Raman scattering integrated power, press. depend. 78−59081
coherent anti-Stokes Raman spectroscopy, anal. capabilities, rel. to other methods 77−40589
coherent anti-Stokes Raman spectroscopy system, using freq. doubled Nd+YAG laser 78−64906
coherent antiStokes Raman spectroscopy use, three-wave mixing phenomenon 80−40802
coherent Raman loss spectroscopy, appl. to conc. meas. and fundamental spectrosc. 80−89580
colorimetric techniques, on-line developments 80−81378
coloured compounds, trace amount determ. by reson. Raman spectometry, appl. to methyl orange, amaranth and new coccine *(Japanese)* 79−48017
combined retrieval system for IR, ^{13}C NMR and mass spectral data 78−31717

spectrochemical analysis continued
combustion, coherent Raman spectrosc. obs. 80−16691
combustion diagnostics, laser appls. 80−16688
combustion diagnostics, space- and time-resolved coherent anti-Stokes Raman spectroscopy 79−76757
combustion flow, passive optical diagnostics of temps. and species concs. 77−44527
combustion gases, high resolution spectroscopy using tunable IR diode laser 77−81434
combustion products, Raman scatt., fluoresc. interference 78−15728
compilation of computer-readable spectroscopic reference data 78−64894
complex biological systems, Fourier transform. IR obs. 78−68945
complexes, differentiation between poly-, mononuclear, stability consts., graphical method 79−87927
composition and structure of engineering and industrial materials, instrumentation 77−4882
computer controlled ESCA for nondestructive surface characterization utilizing a TV-type position sensitive detector 78−76969
computer routine, element identification and quantitation 79−43658
computer-simulated laboratory experiments, teaching 79−40339
computers and optimisation, conf., Amsterdam, Netherlands (April, 1978) 79−52791
concentration fluctuations, chem. species in unsteady flow, Raman spectrosc. obs. 79−66379
condensation chamber, for flame photometric analysis, exam. of design 80−21342
conduction cooling device for low temp. phosphorimetry 80−90855
conference, Grenoble, France (Sept. 1975) 78−3424
continuum source atomic fluorescence spectrometer, wavelength modulated, appls. 78−70190
contour plotter, automated, 3-dimens., for fluoresc. meas. 78−58046
controlled generators, spectra, rel. to quantometric meas. *(Russian)* 78−74072
conversational data processing system for instrumental analysis *(Japanese)* 77−82496
core level ligand field splittings 80−43106
coronene, distrib. with respect to particle size in submicron atm. aerosols 79−74563
corrosion science, surface analytic techniques 80−31929
cryogenic substances, Doppler method for dispersion analysis of cryosols and suspended microadmixtures 79−75535
crystals, electron spectroscopy, book 80−36786
cuvette, heated for IR spectroscopy, exam. of design. 80−18025
CVD film growth, inelastic light scatt. as in situ probe of chem. reaction 77−40383
CW intracavity dye laser spectroscopy, enhancement, pumping power depend. 80−13155
cyanide, on Ag, at electrolyte interface, enhanced Raman effect 79−28767
cyanide containing deposits in CO_2 lasers with amine additives 77−71991
cyanoethylene, photofragment recoil, state selective time of flight- fluoresc. method 79−11809
cystic fibrosis diagnosis by in situ sweat Na concentration meas. using elec. field 77−73554
Dancer microphotographic emulsion identification 79−17177
DC arc, anode spot temp., buffer cpd. effect 79−48029
DC arc, vaporization processes, thermochem. reagents effect *(German)* 79−48030
DC arc techniques, transport mechanism 78−22464
DC discharge plasma, inverted V, industrial analytical appl. 78−76944
DC plasma arc, for elemental anal., review 77−73478
DC plasma echelle spectrometer system, anal. capabilities 79−12854
DC rotating arc as spectrochem. light source 79−52856
decomposition products of CO in corona discharge, IR absorption spectra 78−60992
deconvolution of spectra by least-squares fitting 78−64897
derivative spectra, informational content 79−96390
derivative spectrometer, vidicon-based, for spectrochem. anal. appls., design, evaluation 77−77827
derivative spectrophotometry, theory and appls. *(Japanese)* 80−86451
derivative spectroscopy, fundamentals and practical examples *(French)* 78−58055
diamond, powders, oxidised surfaces, thermal desorpt. spectra 78−47661
diamond anvil cell, for high press. far IR obs. 79−12874
dibromodifluoromethane, UV laser fluoresc. and photochem., CF_2, CF and Br_2 fluoresc. obs. 80−16703
dicyclopentadiene, liq., CO_2 laser pulse induced chem. reactions 80−66821
diesel smoke particles, optoacoustic meas. 80−50895
differentiated UV quantitative spectroscopic analysis using RC device 79−87901
differentiation, filtering props. of polynomial methods 80−66900
diffracted stimulated emission induced by coherent crossed laser beams for conc. meas. 80−35585
diffuse reflectance, FT IR spectrometric meas. 79−35858
diffuse reflectance spectrometry, continuum models 77−21430
digital lock-in detection technique and appls. 79−49303
dihalogenated benzene derivatives, 77K, gamma radialysis radical pair formation, EPR 79−29334
dimethylnitrosamine, in aq. soln., detect. and meas. by laser Raman spectroscopy 78−15725
direct solution analysis, using arc source, with two rot. plasmas in graphite tube 78−40105
discharge lamp, HF, with hollow electrode, for atomic spectroscopy 80−26090
discharge-flow systems, noise reduction in EPR studies 79−39256
discharges, high-freq., unipolar and electrodeless capacitively-coupled, excited at atm. press., appls. 80−1861
dispersive IR spectrophotometry, on-line minicomputer system, design, appls. 77−63975
dithiocarbamate complexes of Cr, Mn, Sn and Pb IR, electronic and mass spectra, mag. susceptibility, cond. meas. 80−97270
double-beam fluorescence spectrophotometry 77−21435
dual wavelength spectrophotometer detector use in high performance liquid chromatography 79−92023
dual wavelength spectrophotometric measurement, precision optimisation 79−92019
dual-grating direct-reading spectrograph mirror system design and performance 80−81397

spectrochemical analysis continued
dual-wavelength spectrophotometry, precision, theoretical assessment 78−29163
dust analysis using LMA 10 laser microspectral analyser 78−24385
echelle grating monochromator, spectral efficiency 79−98461
Eimac arc lamp, 300 W, spectral and noise charact. 78−32878
electrification phenomena obs., surface analysis techniques appl. 80−80354
electrochemical reaction intermediates, at rot. disc. electrodes, spectroscopic obs. 78−53210
electrode-electrolyte interface, solid film props., review of expt. techniques 77−77780
electrodeless discharge lamp, microwave excited, fabrication and operating conditions effects 78−29179
electrodeless discharge lamps, for elements forming gaseous covalent hydrides, spectrosc. appls. 77−67500
electrodeless discharge lamps, pulsed, RF excited, anal. at. spectrometry appls. 78−74061
electrogenerated chromophores, electrochemical conc. profiles, mass transfer, charge transfer, laser absorpt. spectroelectrochem. obs. 80−40765
electron beam particulate analysis of air samples 80−40785
electron energy analyser based on retarding field method for use in gas medium 80−45598
electron energy loss spectrometry, thin specimen sections, electron microscopic chemical analysis, review *(French)* 79−8469
electron microprobe Auger spectrometer with ultra high vac. SEM capability *(Japanese)* 78−27849
electron spectroscopy for chemical anal., appls. to materials for electrophotography 78−92565
electron spectroscopy of surfaces, review 78−92169
electronic absorption spectra, digital anal. appls. 78−8448
electronically controlled spark source, for anal. emission spectroscopy 78−16857
electrothermal atomisation, atom form. and dissipation 80−57388
emission spectrographic analysis system, minicomputer based, using scanning microphotometry 80−22436
emission spectroscopy, literature review 1976-1977 78−80797
enamel-metal interface, diffusion phenomena, spectroscopic investig. *(Russian)* 77−90508
enantiomers, discrimination using liq. crystalline solns., IR rot. dispersion meas. 79−16064
energy loss spectrometry microanal. using field emission STEM 78−53286
enhancement using alumina cup electrode *(Japanese)* 77−86418
entrance slit mask, for rotating step sector or 8-step filter for emission spectrography 78−29165
environment materials, multielement anal. by rotrode direct reading spectrometry 77−70355
enzyme activity, kinetic assay, progress curve algorithm for spectrophotometric meas. 78−20083
eosin-erythrosin, soln., qualitative anal. using fluoresc. polarisation 79−24849
EPR, ns time-resolved, in pulse radiolysis, via spin echo method 80−43075
EPR anal., precision investig., Cu (II) complex appl. 77−56261
EPR analysis, accuracy improvement 79−52827
eriochrome cyanine R, spectophotometric agent for Be, Al, Ga determ. in aq. organic medium 77−36829
ESCA, appls. in industrial research 79−39232
ESCA, chem., technical and industrial appls., lecture 78−27875
ESCA, conf., Uppsala, Sweden (May 1977) 78−53297
ESCA, electrostatic quadrupole prism spectrometer charact. 77−1970
ESCA, insulator charging, line energy corrections 80−50898
ESCA, intermediate X-ray sources, Y Mζ and F Kα 78−53301
ESCA, polymer surface oxidation process 79−76344
ESCA, quantitative surface anal., limitations, depth profiling, catalyst surface anal. 78−53298
ESCA, surface anal. and electronic structure *(French)* 80−7891
ESCA, X-ray (132.3 eV) source for 77−4958
ESCA, X-ray type, C 1s contaminant buildup on conductors and insulators 78−95981
ESCA appl. to Ni-Cr resistor layers *(Hungarian)* 77−4951
ESCA appl. to thin film production, surface analysis *(Hungarian)* 80−54537
ESCA chemical shift, indirect evaluation of Coulombic contribution to ionis. pots. for nonbonding electrons 78−92572
ESCA chemical shifts and modified Sanderson electronegativity calcs. 77−83656
ESCA of film on thermally aged Co hardened Au 77−4436
ESCA photoionisation cross section, relative intensities calcs., comparisons 78−50464
ESCA spectra automatic analysis by top down method *(Japanese)* 77−40598
ESCA using monochromated UV discharge lamp and XPS spectrometer 78−89601
ESCA-ion scatt. spectroscopy-SIMS, review, chem. appls. 79−43701
ethane, X-irradiated, 4.2K, pairwise radical trapping mechanism, EPR obs. 79−100412
ethylene, ^{13}C substituted, isotope analysis by CO_2 laser absorpt. spectroscopy 77−44529
ethylene, air pollution monitoring, computer controlled CO_2 laser absorpt. system 80−89699
ethylene, high pressure polymerisation investig. using near IR spectroscopy *(German)* 77−21384
ethylene, pure, IR absorption obs. of C-H stretching fundamentals up to 2 kbar and 200°C 79−22701
ethylene in exhaust gas, optoacoustic detect. using line-selectable CO_2 laser 78−56947
ethylene in gas mixtures, optoacoustic detect. in urban areas and fruit storage chambers 79−87886
explosive vapours, laser optoacoustic absorpt. spectra 78−76941
far IR spectroscopy, variable path length solution cell, for use in vacuum 78−45736
fast kinetics studied by NMR, review 80−55662
fast reaction kinetics meas. by ESR of free radicals 80−21286
fibre light guide for lighting inlet slit of metal spectroscope *(Russian)* 79−41456
fibre optic micro-spectrophotofluorimeter for in vivo animals studies 77−60327
fibre-optic microfluorimeter for animal haemodynamic and pharmacokinetic meas. 79−92455

spectrochemical analysis continued
fission reactor materials, anal. using plasma jets 80−19624
flame, bluff-body stabilised diffusion, CARS meas. 79−85964
flame, OH concentration measurement, local and instantaneous, by laser induced fluoresc. obs. *(French)* 79−15999
flame, temperature and OH concentration, simulatenous determ. by high-resolution laser absorpt. spectroscopy *(German)* 78−35776
flame diagnosis, CARS appls. 80−16689
flame diagnostics using multichannel pulsed Raman spectroscopy 80−30237
flame emission, atomic absorption, and atomic fluorescence spectrometry, review of literature 1975-1977 78−85224
flame spectrometry, analyte reduction by heterogeneous reactions 79−48026
flame spectrometry with laser enhanced ionisation 78−92528
flame spectroscopy, free atom fractions and equilib. comp. calcs. 80−22438
flames, temp., specie conc. meas., CARS and laser induced saturation fluoresc. spectroscopy obs. 80−45617
flow microfluorometry instrumentation, rapid data collection, analysis and graphics 78−86348
fluorescein-rose bengale, soln., qualitative anal. using fluoresc. polarisation 79−24849
fluorescence, spectrophotometric detection system for HPLC 78−48737
fluorescence anal., computerised correction for excitation beam absorpt. 77−77818
fluorescence analysis using pulse-delay data acquisition sampling system 80−37004
fluorescence correlation spectroscopy, profile of focused collimated laser beam near focal minimum 80−43386
fluorescence detection system for HPLC 78−48735
fluorescence polarisation meas., T-format photon-counting polarisation photometer 78−54423
fluorescence quenching measurements, inner filter effects for different illumination geometries 78−92548
fluorescence spectra, synchronously excited, peak wavelength and intensity prediction 78−20082
fluorescence spectral files for chem. characterisation, data compression by Fourier transformation 78−35744
fluorescence spectrometry, anal. appls., historical review 78−93507
fluorescence spectrometry, beam splitter and cell window errors 80−31897
fluorescence spectrometry with optoelectronic image detectors 79−21815
fluorescence spectroscopy, advantages at low quantum efficiency 77−52684
fluorescence spectroscopy in study of biochem. processes review 78−11784
fluorescence versus concentration, Maclaurin series truncation errors 79−43649
fluorescent measuring equipment, selection of standard testing substances 80−7882
fluorescent sample, multicomponent anal. method 77−70350
fluorescent tagged reagents, time integrated emission, quantum efficiency independ. 77−21440
fluorescent tracers in hydrology, conc. meas., synchronous excitation method *(French)* 77−77840
fluorimeter for medical sample anal. 79−92323
fluorimetry, weak fluoresc. detect., analogue method 77−40581
fluorometric and phosphorometric analysis, review of literature 1975-1977 78−85220
fluorometric flow cell, using fibre optic system, design and evaluation 78−32879
fluorometric system, nanosec. time-resolved spectrometry with tunable dye laser and pulse-gated photon counter 80−11968
fluorometry, meas. technique for radiation detection in UV, visible, IR range *(Czech)* 79−71535
fossil bones from N. Greece, conc. of U and daughter prods., γ-spectroscopy, activation anal. 77−60161
Fourier transform, IR spectroscopy, microscopic technique for sub-ng level anal. 78−32901
Fourier transform gas chromatograph-IR system, trace organic pollutants detect. 78−68967
Fourier transform interferometric IR spectrometer, performance evaluation 78−29181
Fourier transform IR spectrometry, absorbance compensation technique, anal. appls. 78−74083
Fourier transform IR spectrometry, absorbance subtract, wedging errors diagnosis and correction 80−11967
Fourier transform IR spectrometry, chem. and environmental anal. appls. 78−20100
Fourier transform IR spectroscopy, least squares curve fitting, appls. to polymer systems 78−15726
Fourier transform IR spectroscopy, use in atm. chem. 80−55743
Fourier transform IR spectroscopy, use in polymer research as vibr. spectroscopy tool 80−55744
Fourier transform IR spectroscopy, variable field of view techniques 77−40586
Fourier transform IR spectroscopy appls. to analytical chemistry 78−61092
Fourier transform IR system, km pathlength, for trace pollutants detect. and meas. 79−5624
Fourier transform NMR spectroscopy, clipped free induction decay signal anal. 77−63976
Fourier transform spectrochemical measurements, using modular Michelson interferometer 78−29177
free radicals, high resolution spectroscopy *(Japanese)* 79−79355
free radicals determ., on polymer surfaces *(German)* 80−7892
free surfaces, apparatus for Mossbauer effect emission and AES, appl. to ^{57}Co on Ni (111) 79−80735
galvanic detection of optical absorpt. in gas discharge 77−15251
garnierite, high-temp. reactions, spectrochem. anal. 77−70294
gas, photoacoustic spectroscopy, resonant cell design optimisation 78−56924
gas analysis, laser optical-acoustic spectroscopic method 79−66383
gas analysis, using IR absorptiometry, modern trends 79−8458
gas analysis by computer-controlled microwave rotational spectrometry 78−85227
gas analysis by polarised coherent active Raman scatt. spectroscopy *(Russian)* 77−56295
gas cells for high temp. and press. IR spectroscopy 77−38033
gas chromatograph-second derivative UV spectrometer system 77−86394
spectrochemical analysis continued
gas chromatographic effluents, FT IR spectrometric identification 78−73091
gas chromatographic fractions, collection on activated charcoal, IR identification 79−79328
gas chromatographic fractions, on-line identification using multichannel Raman spectrometer 79−83524
gas chromatography interfaced with IR or PMR spectroscopy 77−52690
gas chromatography-IR spectroscopy interface, optimised sampling techniques 77−77831
gas chromatography-IR spectroscopy using Sadtler CIRA 101 analyser, vapour phase spectra of liqs. and solids 80−93809
gas chromatography-IR-PMR optimised method anal. 77−86392
gas chromatography/Fourier transform IR spectroscopy, review 80−55729
gas jet, conc. profile determ. by laser Raman optical multichannel analyser 78−73098
gas matrix sample, electronic and reson. Raman spectra, simultaneous meas. 78−66554
gas mixtures, kinetic studies rel. to gas lasers and pollutant detect. 79−48013
gas phase concentration, meas. to $10^4/cm^3$, analytical photon catalysis 77−52685
gas sample, nonlinear least squares method for IR spectra 78−15738
gas sampling to mass spectrometers, fast-response, using quartz tube orifice leaks 80−35609
gas-solid adsorption, spectrophotometric obs. using IR vacuum cell 79−80703
gases, derivative spectroscopy, measurement based on 2nd derivative optical absorption spectrum *(German)* 77−21459
gases, nondispersive IR anal., semiautomated, solid-state programmable switching device 77−77830
gases, nondispersive IR analyzer with compensation for optical bias 79−16103
gases, rotational Raman spectra, interferometry 77−73494
geochemical sample anal. by gamma-spectrometry, data bank system 80−31120
glass, boric acid content, differential-photometric determ. using SPEKOL spectrocolorimeter 78−23984
glass, medieval, simulated, durability anal. using IR reflection spectroscopy 80−40777
graphite cups for solid sample introduction into eletrothermal atomiser 80−62734
graphite furnace, HGA-2200, operating parameters 79−34384
halide dioxide radical form., H_2O_2 decomposition of halide-coated surface, EPR obs. 80−7851
hazardous chemicals, water pollution detect. using reson. Raman spectrosc. 79−74581
heated closed quartz cell for spectroscopic anal. of metal vapours 78−77996
hexane-cyclohexane mixtures, quantitative IR spectrosc. anal. 79−96377
high resolution scanning resonant Raman spectrometer 79−6185
high temperature gases, characterisation, reactive flow in shock tubes, laser absorpt. spectroscopy 80−45618
high-concentration alloy analysis by optical emission spectrometers 80−104477
high-purity substances, analysis methods 79−39241
homogeneity investigations with LMA 10 laser microspectral analyser 78−23983
humidity trace detection in H_2 and air by CO laser driven spectrophone 79−20477
hybrid chromatographic system techniques for unique identification 79−70403
hydrocarbons, aromatic, ultrasensitive detection by two-photon photoionisation 80−104473
hydrocarbons, substituted, chemisorbed monolayers on Pt (100) surface, AES quantitative anal., calibration 78−31724
hydrophilic polymers, ESCA evaluation of surface layer water structuring and protein adsorpt. 80−108758
ICP background emission, highly structured 80−73467
ICP unit, 5 kW, for 3.4 metre Ebert spectrograph, commissioning, operation 80−86453
image analysis device, Chromotron 80−83683
immersion microsampling technique for Fourier transform IR spectroscopy 78−12777
immunochemical analysis, standardisation of light scatt. meas. 78−36081
immunochemical analysis, standardisation of light scattering meas. 77−56548
immunofluorescence diagnosis using AR laser *(German)* 79−5335
impurities from graphite powder, diffusion into arc discharge plasma, kinetic characts. 77−72514
impurity microconcentrations in liquids analysis using opto-acoustic effect 80−50916
Incoloy 600 and 800, surface film in hot conc. NaOH, XPS study 80−11824
indole decapeptide luteinising hormone, high-press. liq. chromatography, fluorometric detect. 78−20096
induction-coupled plasma system, use for spectrochem. anal., calibr. 77−90708
inductively coupled Ar plasma emission source, appls. 79−35839
inductively coupled plasma, spectral characteristics 79−70394
inductively coupled plasma emission spectrometry, with programmable monochromator, intensity meas., data processing 80−62728
inductively coupled plasma emission spectroscopy, using photodiode array spectrometer with correl. readout system 78−31726
inductively coupled plasma source, emission spatial profiles, self-scanning photodiode array obs. 78−16850
inductively coupled plasmas, optical emission spectroscopy 80−42266
industrial atmospheric pollutant remote analysis by Raman lidar 80−12047
industrial IR analysis using Fourier transform spectrometer 78−61091
inelastic electron tunnelling spectroscopy appls. to trace substance detection 78−92589
information processing, television methods appls. 80−89568
infrared intensity reference meas., spectrophotometric data reduction, modular computer programs appl. 80−3471
inorganic compounds, electronic spectroscopy, KBr matrix method 77−40597
inorganic compounds, XPS chem. anal., chem. shift, core binding energy 78−20134

spectrochemical analysis continued
inorganic solids, anal. of H_2 in solids by sputter induced emission spectroscopy 79−5231
insulating film, Auger depth profiling by angle lapping 78−53287
insulators, chemical state identification, Auger and photoelectron lineshapes and chem. shifts 77−32855
interferometric IR spectroscopy-gas chromatography data, chromatogram reconstruction method 78−35737
internal combustion engine, CARS noninvasive temp. and species meas. 80−30293
internal combustion engine, conc. fluctuation meas. 80−71973
internal reflection spectroscopy, effective thickness calc. 80−89558
intracavity laser Raman spectrometer, appls. 78−65973
inverse Raman scattering spectroscopy and chem. appls. 80−37094
ion backscattering, material characterisation technique 79−96407
ion beam material characterisation, conf., Aleria, Corsica (Sept. 1976) 79−96403
ion beam-surface impact effects, ESCA obs. 79−33020
ion-induced photon emission spectroscopy 77−48740
ionic reaction products, laser induced fluoresc. detect. and characterisation 79−1978
IR, computerised dispersion system as alternative to Fourier transform method 77−82631
IR, dispersive, industrial applications, for analysis in soln. 79−49305
IR, quantitative, microprocessor appl. and sampling technique advancements 80−16746
IR, techniques, detectors, appls. 77−5934
IR absorption gas analyser, portable model, molecular resonance effects *(German)* 80−98990
IR absorption meas. using quasi-tunable I_2 laser 77−42551
IR analyser, Infralyt 4, dynamic charact. *(German)* 78−88676
IR analyser, microcomputer controlled, for multicomponent anal. 77−36822
IR analytical instrumentation using tunable diode lasers 80−16762
IR data files, hierarchical preprocessing 78−15731
IR diffuse reflectance spectrometer, for anal. of catalyst surface, design and construction 79−79319
IR diffuse reflectance spectrometry, appls. 79−34387
IR file searching, ASTM, algorithm using peak intensity data 80−30295
IR laser photolysis of polyat. mols. photochem. appls. 80−66835
IR reference spectra, for GC-IR, presentation specifications 80−31908
IR reference spectra, library retrieval based on intensity data 79−96380
IR spectra, computer-assisted interpretation, pattern recognition and artificial intelligence methods 78−15732
IR spectra, feature selection, using numerical taxonomy and information theory 79−50012
IR spectra, interference fringe elimination, computer method 79−12872
IR spectra differentiation using Fourier transforms 79−67397
IR spectral analysis, background and overlapping of absorpt. bands influence on accuracy 80−55748
IR spectral identification, computer-assisted 77−4948
IR spectral lines, intensities and half widths, nonlinear least squares calcs. 77−52682
IR spectrometer performance testing using CO line parameters 77−91275
IR spectrometry, review of literature 1976-1977 78−85223
IR spectrophotometers, grating and FT types, rel. advantages of interferometers and monochromators 78−16861
IR spectroscopic data, using minicomputer and IR spectrophotometers 79−49304
IR spectroscopy microsampling, computerised data enhancement 77−36821
IR spectroscopy of gas chromatographic peaks, high resolution 78−20101
IR technique, for in situ identification of TLC spots 78−15727
isopropylbenzene, IR spectra of oxidation products *(Rumanian)* 78−23838
isotope dilution alpha spectrometry for determ. of Pu concentration in irrad. fuel dissolver solns. 80−78428
K-vitamins, IR absorpt. spectra, vibr. anal., quinonoid struct. 78−61139
kaolinite-mullite reaction sequence, interpretation from IR absorption spectra, comment 78−48720
Kevlar-49, chemical characterisation 78−95725
lakes, suspended solids, anal. using Landsat multispectral data 79−16523
lanthanide complex, struct. and equilib. by time resolved Eu(III) spectrosc. 80−78736
lanthanide ion bound to macromol., struct. and equilib. by time resolved Eu(III) spectrosc. 80−78736
lanthanide ion fluorescent probes, spectroscopic obs. system 78−11573
laser analytical instrument, industrial appl. of tunable diode lasers 78−61133
laser beam applications, survey *(German)* 77−698
laser chemical analysis systems, modular component optics system 79−1974
laser fluorosensor performance, sea-state effect 78−92990
laser fusion microsphere targets, nondestructive anal. using rot. Raman spectroscopy 80−50896
laser gas analysers, freq. modulation appls. 80−85246
laser induced fluoresc. spectroscopy in flames, detectability limit 78−73096
laser induced fluorescence spectroscopy, saturation effects 77−44526
laser intracavity absorption method, sensitivity investig. 79−57328
laser intracavity adsorption spectra of surface-active substances and aerosols *(Russian)* 79−57343
laser microprobe system *(Italian)* 77−25323
laser microspectral analyser, sample chamber with supply module 80−85241
laser microspectral analysis, forensic appl. 80−81385
laser PROBE technique, density profile meas. of specific constituent 78−28320
laser Raman molecular microprobe (MOLE) 80−21330
laser selective detection of ultralow concentrations of atoms 78−3407
laser selective detection of ultralow concentrations of molecules 77−90669
laser spectroscopy, conf., San Diego, USA (Aug. 1978) 80−13153
laser spectroscopy, selective detection of ultra-low concs. of atoms and molecules 79−24869
laser spectroscopy applications, conf., Anaheim, USA (Mar. 1978) 80−36781
laser-based methods for transient chem. events meas. 80−40801
laser-excited luminescence spectrometry, review 80−40800

spectrochemical analysis continued
laser-generated plasma, time-resolved spectroscopy and microanalysis 77−43015
lasers for industrial chemistry 80−87427
lasers in metrology, review *(German)* 77−14734
light scattering diagnostics for combustion gases 77−47124
line pair intensity ratio stability, internal standard variability 79−39247
linuron, herbicide, interaction with soil, Fourier transform IR spectra 77−9142
liquid chromatography, real time Fourier transform IR detector 78−86357
liquid chromatography, spectrometric detect., computer control of data acquisition, reduction and display 78−27850
liquids, trace anal., freq. modulated laser optoacoustic technique 77−70349
lubrication, spectroscopic methods for surface anal. *(French)* 80−26095
lunar rock, S content, neutron capture gamma-ray spectroscopy 80−94728
lunar surface elemental composition, analytical determ. from Apollo X-ray and γ-ray spectrometer data 79−2495
matrix effect on arc temperature and electron pressure 79−37565
matrix isolation microsampling procedure for quantitative IR Fourier transform spectrosc. 79−100460
matrix isolation Raman spectroscopy, water pollution detect. appl. 80−108829
matter concentration in solution, determ. using FL luminescence photometer 79−30575
measurement theory, anal. function optimisation, appl. to spectrometry 80−62614
meat, biochemical procedure for detect. of radiation treatment 78−65075
metal, C content determ., isotope-spectral method *(Russian)* 80−55766
metal, quantitative spectral anal., appl. of microdensitometry *(Czech)* 79−30524
metal atom reactions, cryogenic techniques and matrix isolation spectroscopy 77−9080
metal species, identification and determ. by chromatographic-at. spectrosc. method 78−68972
metal substrate, thin film form., appl. of AES and ESCA *(French)* 80−50903
metal surface, spectroanalytical investig. of friction processes and subst. transfer products *(Russian)* 79−34418
metal-containing plasma polymerised fluorocarbon films, deposition, struct., and polymerisation mechanism 79−78928
metal-poor dwarf stars, abundance anals. of yellow spectra 79−92760
metallic corrosion anal. using luminesc. discharge *(Spanish)* 79−92029
metallurgical substances, standard specimens for spectral analysis, review 78−7273
metastable reaction products, laser induced fluoresc. detect. and characterisation 79−1978
methane, concentration along line in jet, spatially resolved coherent anti-Stokes Raman spectra 79−74476
methane, X-irradiated, 4.2K, pairwise radical trapping mechanism, EPR obs. 79−100412
methane-air flames, OH conc. profile 80−35534
methoxy detection by submillimetric laser spectrometer 77−40623
8-methoxypsoralen detection in ocular lens, rel. to psoriasis treatment with photosensitising agent 78−15937
4,4′-methylenebis(2-chloroaniline), air sampling and anal. method 79−79420
methyltin compounds, separation and determ. in environmental samples 79−79416
MHD laser, admixture atom conc., automatic meas. system *(Russian)* 78−73123
micro-Auger analysis, ratio technique 77−32862
microanalysis, limit of detection 77−40602
microanalysis by energy loss spectrometry *(Japanese)* 78−85244
microanalysis of light elements by electron energy loss spectrometry 78−80441
microchemical environment, anal., electron and photon beam appls. 78−44434
microfluorimeter design for medical-biological research 79−57818
microfluorometric measurements of DNA dye complex using cryostat 80−17949
microphotometry, photographic emulsion calibration method 79−79321
Microprobe Mole/plasma chromatograph system, for anal. of compounds on micron scale 80−101049
microsampling techniques, for IR spectroscopy 78−16862
microspectrofluorometry of biogenic amines, automatic correction of excitation spectra, on-line system 77−9308
microthin film chromatogram evaluation by scanning fluorimetry and digital image analysis *(German)* 79−5188
microwave spectrometry, characts., instrumentation, automation, review 77−56260
mild steel, S determ., flame chemiluminesc. method 78−48711
mineral prospecting by tunable laser spectroscopy 77−60500
minerals, by Kler method, increased accuracy 79−70393
minerals, electrodes and paste specimens for emission spectrographic anal. *(French)* 78−92563
mixture, multicomponent, quantitative analysis from absorpt. spectra, review 79−52811
mixtures, anal. by retrospective computer subtraction of gas phase IR spectra 77−77824
mixtures, determ. of number of compounds present 79−43657
mixtures, quantitative IR spectrosc. anal. 79−96377
modulation spectroscopy, of wavelength modulation and derivative 79−79317
moisture measurements using NMR, reference materials 79−34403
molecular absorption spectrophotometric detection, using CCD photoarray 79−80689
molecular emission cavity anal., vapour generating systems, cool flame spectroscopy 80−81396
molecular microprobe, microscope system 78−45686
molecular microprobe using laser, MOLE 77−60141
molecular spectroscopic laboratory strategies, queueing theory and digital simulation use 80−30299
molecule, method for estimating shift in electron levels *(Russian)* 78−46403
molluscan shells, IR spectral anal. 78−3413
monochromator accessory module, microcomputer-controlled for dual wavelength operation 79−74440

spectrochemical analysis continued
Mossbauer effect, appl. in chemical analysis *(Hungarian)* 79−16070
Mossbauer spectroscopy, review of literature 1976-1977 78−84501
multi-element ultratrace analysis of solutions using inductively coupled HF plasma 79−39257
multicomponent, multipoint infrared ambient air monitor, microcomputer-controlled 80−40945
multicomponent analysis by synchronous luminesc. spectrometry 78−73089
multicomponent deposition processes, monitoring and controlling techniques, review 78−11113
multicomponent fluorescent mixtures, quantitative anal. of data 78−27833
multicomponent meas. NDIR analyser *(Japanese)* 78−61117
multicomponent spectra, numerical anal., least squares, optimisation methods, acid base indicator anal. appls. 77−56264
multicomponent spectra, resolution by multiple regression and linear programming 79−74443
multicomponent systems, video fluorometer anal., rank annihilation method appls. 78−92546
multielement, using coherent forward scatt. at. spectrosc. 80−57389
multielement analysis, by ICP emission spectrometry, compromise conditions 78−76937
multipass-systems for Raman spectroscopic gas analysis *(German)* 80−81393
β-naphtholate in methanol-methyltetrahydrofuran glasses, electron solvation, laser flash photoionis. compared with pulse radiolysis 79−74405
naphthylamines, abnormal fluorimetric titration behaviour, kinetic anal., fluoresc. quantum yields and lifetime meas. 80−89560
narrow absorption lines, fluoresc. recording, intracavity at. spectrosc. method *(Russian)* 78−73124
natural rubber latex ^{13}C NMR spectra 80−15816
near IR diffuse reflectance analysis anomalies 80−86383
nebuliser, for ICP system 79−12860
negative photoresist, RF O_2 plasma stripping, visible spectra 77−40591
negative photoresists, RF O_2 plasma stripping, optical detect. systems 77−40585
neutral density filters, for UV-vis. spectrophotometry, calibration 78−45734
nitroxide free radicals, neutral, EPR spectra, localised solvent-radical adducts 79−96290
NMR, literature review July 1975-July 1977 78−85217
NMR spectrometer, for quantitative analysis, microprocessor-controlled digital integrator 80−11971
NMR spectroscopy, appl. to organic compounds anal. 80−16756
noble metals, spectral detection limits, line increase cathode effect appls. *(Russian)* 79−11868
noise and signal-to-noise ratios 79−43672
noise and signal-to-noise ratios 79−43671
non-crystalline solid, surface and thin film chem. anal. techniques *(French)* 77−73495
non-dispersive IR photometer for gas anal., function and design *(German)* 80−108772
nonconducting powders, emission spectrographic anal. using plastic bounded electrode 78−48714
nonuniform samples, Fourier transform IR spectroscopic meas. 78−15730
nuclear energy materials, anal. techniques 80−93834
nuclear spectra, model uncertainty and bias in evaluation, smoothest consistent baseline theory 78−11591
nucleic acid optical measurements in presence of phenol and protein impurities 77−56546
oil, remote characterisation by time-resolved laser fluorosensors, lab. expt. 78−73097
oil pollution on sea, remote sensing using laser radar 78−77373
oil slicks, use of FFT in evaluation of laser Raman and fluoresc. decay times 78−81444
oil spill detection by airborne laser fluorosensor 80−67024
on-stream analysers development, w.r.t. speed and reliability 77−66778
one-atom detection, reson, laser spectrosc. obs. 80−22441
online spectroscopic data base system status 80−104475
optical system simulation for luminescence spectroscopy 77−34036
optoacoustic signals, polymer film thickness effect on signal magnitude 80−11969
optoacoustic spectroscopy, direct exam. of solid and liq. samples 80−7886
optoacoustic trace gas analyser with CO_2 laser 79−5245
optogalvanic effect, using tunable gas laser, appls. 78−95977
optogalvanic spectroscopy, analytical appls., elec. meas. 78−62231
organic compounds, elemental anal., by ICP optical emission spectrometry 78−76936
organic compounds, IR spectra, binary coded, feature selection for automated interpretation 80−3428
organic compounds, spectroscopic identification, computer methods 78−88679
organic molecules, struct., computer-assisted interpretation, using fluoresc. spectra 77−36805
organic phosphors, continuous sampling system at room temp. 79−43647
organic sample preparation in HF discharge 80−1855
organic specimens, calcination methods, for spectrochem. anal. *(Russian)* 78−23997
organo tin polymers, glow discharge formed, interface composition and adhesion 79−82467
oxyanions, in nuclear waste materials, laser Raman spectrometric determ. 78−35743
oyster shell, IR and atomic mineral anal. 78−61116
paddy leaves, spectrochem. anal., mineral constituents rel. to brown spot disease resistance 80−12055
paper, coating type and extent, attenuated total refl. spectrosc. obs. 79−79329
particle analysis, using laser-Raman microprobe 79−43696
passivation films, on Sn plate, lacquer adhesion, ESCA exam. of constitution and effects 80−40776
pathological samples, mol. microanal. in situ with laser-Raman microprobe 80−81683
pentachlorotoluenes, positional isomers, ^{13}C Fourier transform NMR spectrometry, struct. and compositional anal. 80−91576
petrols, optical consts. in 0.25 to 25 micron region, sea pollution detection appl. *(Russian)* 78−76976
phase fluorometry as a probe of diffusion-controlled molecular encounters in dense fluids 80−32799
spectrochemical analysis continued
phase resolved phosphorimetry, analytical possibilities 77−90663
phase-compensating fluorometers, Hall effect transducer appl. 79−8459
phenol (oestrogen) compounds, high-press. liq. chromatography, fluorometric detect. 78−20096
phenol-cyclohexane (-ether), UV spectra, solvent effects, matrix rank anal., species determ. 79−22768
4-phenyl-3-thiosemicarbazide, single cryst., X-irrad., EPR, ENDOR, radical identification 79−31560
phosgene, spectrophone meas. at selected CO, CO_2 laser wavelengths 78−57310
phosphates, uranium content, alpha-ray autoradiography, comparison of results 78−20414
phosphorimetric instrument, automated, for room temp. phosphorimetry with continuous filter paper device 77−90654
photoacoustic detection, gas trace conc. meas., spectroscopy and photochem. appls. 79−74474
photoacoustic double-beam spectrometer, for use in UV, visible and near IR regions 79−79320
photoacoustic FT IR spectroscopy of liquid and solid samples 80−90911
photocounting pulse fluorimetry, mol. rot. correl. times determ., statistical accuracy 77−61777
photodissociating small molecules in solid matrix, cage effect 79−52728
photoelectric concentration meter, acceptable error determ. for automatic biochemical anal. 79−92435
photoelectric spectrometer, drift correction procedure 78−29178
photoelectron spectroscopy, biological appls., review 77−56558
photoemission, many-electron theory, in electron spectroscopy book 78−17714
photographic emulsion, for spectrographic anal., calibration curve computer calcs. 78−4706
photographic paper print residual thiosulphate, methylene-blue and Ag densitometric meas. correlation 79−74472
photographic spectral detection, using roll film back 79−12857
photographically recorded spectra, semi-automatic interpretation, mass, at. spectra appls. 77−48708
photometric analysis, reproducibility and lower detection limit 79−87899
photometric analysis methods, review 79−43660
photometric determination and control of solution components, automatic method 79−79350
photon counting spectrometer, computer controlled, rapid scanning of low light level spectra 78−86338
photosynthesis, picosec. spectroscopic investig. 78−68964
photosynthesis, picosecond spectroscopy appls. 78−53601
photosynthesis, primary events, picosec. fluorometric obs. 79−8476
photosynthetic systems, computer assisted scanning and kinetic spectrophotometry 78−68963
picogram analysis using microwave excitation with sealed atomisation cells, buffer effects 78−48729
picosecond phase shift measurements at 358 MHz using synchrotron radiation 79−44949
picosecond spectroscopy, appl. to chem. and biological reactions 79−80697
pipette, multichannel, for parallel aliquoting into centrifugal analyser minidiscs 78−7267
pitch weathering processes, IR multiple internal refl. obs. 79−74461
plasma emission spectroscopy, background and developments 80−45588
plasma radiation, ionis. and excitation processes 79−55475
plasma source, 40 MHz inductively coupled, Ta I and Ta II oscill. strength determ. 79−48031
polarisation of fluorescence spectrum for enhanced resolution 77−6827
polarisation relaxation of materials, meas. using synchronously mode-locked dye lasers 79−44952
pollution plume transport and diffusion studies using fluorescence lidar 80−101139
pollution samples, X-ray anal., absolute sensitivity and detection limits 78−7261
polyacrylamide, conversion to poly-N-dimethylaminomethacrylate, Raman method meas. 79−74460
polybutadienes, epoxidised, epoxide content, ^{13}C NMR determ. 79−51872
polycarbonate films, effect of UV and visible mono- and polychromatic radiation, stability *(Russian)* 79−57268
polycyclic aromatic hydrocarbons, detect. using laser-induced mol. fluoresc. 77−81431
polyethylene terephthalate fibres, high freq. US effects on physical and chem. structs. *(Polish)* 78−51446
polyisocyanides, solns., struct. and acidification 80−19915
polyisoprenes, epoxidised, epoxide content, ^{13}C NMR determ. 79−51872
polymer, degradation products, chem. anal. by UV photoelectron spectroscopy 78−53300
polymer film, formation, time-lapse IR spectroscopic obs. 79−74458
polymer impregnating soln. concentration meas. by transmission photometer *(Russian)* 77−73484
polymer mixtures, IR difference spectra, dispersion effects 79−96379
polymer primary structures ESCA and EHCO methods 78−52630
polymer surfaces, appl. of ESCA to struct. and bonding 79−57344
polymers, paints, testing, modern analytical methods appl. *(Polish)* 78−85253
polymers, pyrolysis-IR anal. 78−3404
polymers, struct., bonding, reactivity by ESCA 78−53299
polynuclear aromatic compounds, second derivative UV absorption spectrosc. anal. 79−83526
polystyrene, thermal polymerisation, kinetics, Rayleigh scatt. 79−57228
polystyrene lattice cleaning, dialysis, steam stripping and ion exchange effectiveness 80−3414
polystyrene microspheres, dye impregnated, fluoresc. spectra struct. resonances 80−50914
polyurethane foam, rigid, gaseous thermal decomposition products, IR anal. *(German)* 79−29348
pottery composition from Ayios Stephanos, rel. to Minoan potters on Greek mainland 78−355
powdered sample, in graphite tube, anal. using double plasma DC arc 78−16858
powders, analysis by photoacoustic and photothermal spectroscopy 79−61929
powders, emission spectrometric anal., suspension sampling method 77−86393
powders, spark elutriation into plasma *(German)* 78−68959
principal component anal., statistically weighted, of rapid scanning wavelength kinetics 77−77826

spectrochemical analysis continued
PROBE, profile resolution obtained by excitation 78−76938
programs for identification of chem. compounds from mol. spectra *(Russian)* 77−52727
propane-air flame, chem. anal. of reaction zone by Raman spectra 78−64837
propanolol, (adrenergic blocking agent), high-press. liq. chromatography, fluorometric detect. 78−20096
propylene copolymers, ethylene incorporation meas. by ^{13}C NMR and IR spectrosc. 79−39225
protein detection in implanted cardiac pacemaker epoxy housing 79−25156
proton transfer reactions, excited state, laser pH jump analysis method 79−47922
proton-induced γ-ray emission, appl. to obsidian characterisation 79−74442
pulse counting detection, high precision, limitations, optimal conditions 77−54463
pulse NMR technique, chem., anal. appls. 77−29975
pulsed laser induced molecular fluorescence, exptl. configs. 78−58045
pulsed photoacoustic Raman spectrosc., gaseous trace anal. 80−40769
pulsed spontaneous Raman scattering technique for luminous environments 78−89549
PVC, gaseous thermal decomposition products, IR anal. *(German)* 79−29348
quality control appl. *(French)* 77−90703
quantitative analysis of absorption spectra, appl. to N_2O 79−100461
quantitative depth profile, by AES *(Japanese)* 80−16751
quantitative laser micro-spectrochemical analysis, of samples with high concentrations 78−40099
quantometer output data processing, regression anal. *(Russian)* 77−21461
quartz, excitation in inert gas medium, detection limits of contaminants 80−55746
γ-quartz, reaction, with NaCl-kCl melt, exam. of struct., IR absorption spectra 80−55706
α-quartz, synthetic, growth, defects induced by seed orientation 80−96454
quartz spectrograph, Littrow, appls. 77−86396
Raman effect optical microscope *(French)* 77−56290
Raman laser uses in molecular spectroscopy and atmospheric constituents detection 80−55762
Raman microprobe for micron size particle anal. and cryst. state determ. 77−86421
Raman photoluminescence and cathodoluminescence 80−108774
Raman scattering analytical techniques using tunable lasers 78−61134
Raman scattering diagnosis, laser modulated particulate incandescence effects 78−20117
Raman spectra of hydrocarbon flames, computer processed spectra 79−43652
Raman spectroscopic direct identification of substance fixed on silica gel *(French)* 78−88664
Raman spectroscopy, chemical species anal. in conjunction with liq. phase chromatography *(French)* 80−93823
Raman spectroscopy, diamond anvil cell method, weak Raman signals obs. 77−71383
Raman spectroscopy, literature review, 1975-1977 78−85218
Raman spectroscopy, recent advances, reivew 78−41359
Raman spectroscopy, vap., medium resolution, appls., review 78−42065
Raman spectroscopy and liq. chromatography anal. *(French)* 80−45595
rapid scanning spectrometer application to continuous-flow analysis 79−70406
rare earth elements, spectral determination using hollow cathode discharge in mag. field *(Russian)* 79−52859
rare earth elements spectral determ. in luminescent materials 77−73485
rare earth sulphides L-X-ray absorpt. spectroscopy, conc. of ions with various numbers of f electrons 77−28646
reaction products, weak excitation spectra, computerised spectrometer meas. 80−76574
reducing agents, spectrophotometric determ. by $K_2Cr_2O_7$ and H_2SO_4 79−39234
refractory alloys, spectrochem. anal. using high-voltage unipolar spark discharge *(Russian)* 78−15750
residual carbonaceous material, in urban airborne particulates, Raman microprobe obs. 78−69441
resonance ionisation spectroscopy, generalisation of one-atom detection 79−52800
resonance Raman spectra, adsorbed species anal. 78−42066
resonance Raman spectroscopy, uses in analytical chem., review 79−92014
resonant ionisation spectroscopy, chem.-physics appls. 80−68259
resonant optoacoustic cells for trace gas analysis 79−11840
respiratory gas analyser utilising glow discharge selective spectral emission, microprocessor based 79−100772
rhodamine, anal. by fluoresc. spectrophotometry, optics 77−34030
rhodamine dye mixtures, qualitative anal. by fluoresc. polarisation spectroscopy 79−34396
rocks, multielement analysis with DFS-36 quantometer and ES-1020 computer 79−70392
rocks, trace element content, direct-reading spectrometer 78−85738
room temperature phosphorimetry, anal. technique, review, methodology, instrumentation, appls. 78−95972
rubrene film, photooxidation in solid, UPS obs. 79−52693
ruby, Cr content determ. *(Russian)* 77−48745
saline environmental waters, anal. via IR relative refl. and complex refr. index 77−45013
sample changer, automatic, for semi-automatic photometric anal. systems 77−48705
saturated fluorescence excitation, transition probabilities and particle density determ. 78−58871
saturated laser-induced fluoresc., rot. redistrib. effect 79−81259
scanning dye laser, microprocessor controlled, for spectrometric anal. systems 78−20081
scanning fluorescence spectroscopy, new rapid technique and instrument 77−90650
scintillation counter appl., liquid, use of miniature ^{14}C and ^{3}H standards 80−21346
secondary laser cavity for weak absorptions 78−92551
selective excitation of probe ion luminesc. technique development 80−40797
spectrochemical analysis continued
selective volatilisation, in DC arc, direct-reading spectrometer obs. 77−73480
selective volatilisation, spectrographic anal. method using Hartmann diaphargm time resolution device 77−49775
selective volatilisation in DC arc, in external mag. field 78−68938
self-scanning silicon photodiode array with microcomputer control 80−35612
SEM cathodoluminescence detection system for transmission optical fluorescence analysis 78−23999
SEM cathodoluminescence microscopy, mirror detector system 78−24000
semiconducting film, on dielectric backing, spectrochem. anal. 80−66904
semiconductor surface, depth profiling, optoacoustic technique 80−65337
SEMIDS, (selectively modulated interferometric dispersive spectrometer) anal. capabilities 77−44521
serum bilirubin conc. rel. to skin reflectance, neonatal jaundice screening 79−92328
shock wavefront molecular process kinetics, IR absorption meas. installation 79−70389
Shpolskii spectra, identification and struct. anal. of unknown compounds in organic mixture 79−87891
Shroud of Turin, IR reflectance spectrosc. and thermographic investigations 80−87578
Shroud of Turin, scientific investigation 80−87576
Shroud of Turin, spectral props. 80−87577
Shroud of Turin, UV-visible reflectance and fluoresc. spectra 80−87579
silicate: Yb_2O_3 glassy film, Yb laser spectral microanalysis 80−76585
silicate materials, additive method of analysis, Fe determ. by flame emission and absorption spectrometry *(German)* 79−39235
silver clouds, visible spectroscopic investig. from Salyut-4 orbit 80−82014
single atom detection, laser reson. fluoresc. method 80−26096
single atom detection, using resonance ionisation spectroscopy 80−3422
single-photon fluorimetry, time-correlated, data acquisition rate optimisation 79−20494
SIT image detector, for anal. fluoresc. spectrometry 77−61134
sodium lauryl sulphate micelles, chlorophyll-a, soln., dilution expts., solubilisation anal. 80−35587
soil moisture and component estimation from spectral polarisation 79−16678
solid and liquid samples, composition determ. using Neva spectrofluorometer 79−30576
solid materials, anal. using microcomputer assisted single beam photoacoustic spectrometer 78−58044
solid sorption systems, use of IR cell with Si windows 78−299
solid surface fluorescence analysis, calibration curves 78−31719
solid surfaces, electron spectroscopy, quantitative, electron inelastic mean free path 79−92041
solutions, emission spectrochem. anal., problems *(Japanese)* 79−29429
sooty diffusion flame, CARS obs. 80−16690
source fluctuation, automatic correction using simultaneous split beam ratio meas. system 77−10115
spark discharge, appl. to multielement anal. 78−40103
spark discharge, correl. relations in spectrochem. anal. *(Russian)* 77−70379
sparks, effect of strong transverse blowing on a high-voltage spark *(Russian)* 78−91183
spectra, deconvolution and background subtraction by least-squares fitting with prefiltering 78−31718
spectra registration system for spectrophotometers, graphical and digital forms 80−47113
spectra search systems, computer-aided, efficiency eval. using information theory *(German)* 80−37003
spectral decomposition, generalised algorithm, appl. to UV, IR, at. emission spectrometry 77−12842
spectral line breadth, analysis, digital computer method 79−83522
spectral lines intensity and plasma parameters dependence on Li additive 80−73478
spectral subtraction in Fourier transform IR spectroscopy 79−83525
spectrofluorimetric system, multifunctional, for luminesc. meas. 78−80811
spectrofluorimetry, effects of bandpass intensity distrib. spectrum 77−29071
spectrofluorometer, scanning photon-counting, construction and data acquisition and manipulation system 77−2698
spectrofluorometers, state of the art *(Slovak)* 78−56940
spectrogram evaluation by I-transformation, accuracy of transform. parameters *(German)* 79−43674
spectrographic anal., signal near detect. limit 80−85244
spectrophotometer, automated clinical/analytical system 77−52687
spectrophotometer characteristic curve, stray light interference effect *(German)* 79−44938
spectrophotometer performance parameters, advanced analytical chem. expt. 79−30170
spectrophotometer transmittance transfer standards 78−45728
spectrophotometric determination of aluminium in iron alloys *(Polish)* 80−35604
spectrophotometric standards, glass filter SRM 930 by NBS, clinical laboratory appl. 78−54331
spectrophotometric titration, equivalence point determ. by computerised curve fitting 78−7258
spectrophotometry, uses and limitations of standard additions methods 78−3405
spectroscopy, fundamental techniques, spectrographs and spectrochem. anal. *(Japanese)* 78−8452
spent reactor fuel burnup determ. using anal. chem. [conf. Piestany, Czechoslovakia (Sept. 1978)] 79−89371
stable molecules, matrix isolation spectroscopy obs., appls. 78−46320
stainless steel determination of 0.001 to 0.01% by extraction and photometry 77−56275
standard paper density scaling, line spectrum intensity determ. *(Portuguese)* 80−11965
standard samples, metrology *(Russian)* 77−70380
standard specimens, optimum sets *(Russian)* 77−48743
standards, for instrumental methods 77−70346
steel, bar, and wire rod, small sample prep. and spectrometric anal. *(German)* 80−93704
steel, carbide phase determ. by annealing in moist H_2 *(German)* 79−39231
steel, construction type, spectrochem. determ. of Ca 78−7275

spectrochemical analysis continued
steel, emission spectrometric determ. of Al *(Japanese)* 80−16750
steel, for nuclear reactors, trace element anal., spectra of laser plasma 78−88691
steel, high speed, fixed time integration-emission spectral anal. and employment of high freq. induction melting-centrifugal casting samples *(Japanese)* 80−89567
steel, impurity spectral lines, intensity, temp. and conc. effects 80−64774
steel, low alloy, Mn determ. by AES and APS 79−48001
steel, low alloy 79−43487
steel, medium C, hardened, Mossbauer spectroscopy study of austenite and carbide 79−56646
steel, mild, laser microspectral anal. 80−108769
steel, mild, surface analysis rel. to annealing *(French)* 77−32857
steel, spectrophotometric determ. of Nb and Ta, Zr, in mixed ligand complex 77−16878
steel, stainless, metallic element depth distribution, in passivation layer, luminescent discharge spectrometry exam. *(French)* 78−31585
steel, surface dacarburation, luminescent discharge spectrometry exam. *(French)* 78−31585
steel, surface hardened, luminescent-discharge optical emission spectrometry appl. to surface anal. *(French)* 79−79164
steel, trace element UV emission, spectrochem. anal. *(French)* 80−71997
steels, low C conc. determ. using laser excitation in vac. UV *(Russian)* 77−12867
steelworks computerised spectrometric analysis and management information system 80−89574
stopped flow temperature jump apparatus with spectrophotometric detection of fast chem. reactions 77−3892
stopped-flow spectrometer performance with viscous solutions 77−32852
stopped-flow spectrometry for kinetic meas. of fast chem. reaction 78−56925
stratosphere, laser spectroscopy relevant to photochem. 78−88951
stratosphere trace molecule Fourier transform spectrometer optical design 80−82099
stratospheric composition, IR meas. radiometer, H_2O vapour profile 79−8718
stratospheric composition, simultaneous IR meas., of NO and NO_2 through dawn 79−8671
strontium halides, absorpt. spectra in air-acetylene flame, using AAS with data processing 78−20102
styrene, plasma polymerisation in glow discharge, thin film IR and free radical EPR obs. 80−2964
styrene, thermal polymerization, PMR obs. 80−3342
submillimetre Stark shift laser spectrochemical analysis 77−40622
substance evaporation in laser torch *(Russian)* 79−52858
subsurface layers, attenuated total refl. Fourier transform spectra 77−71379
subway air pollutants, (sulphates, nitrates, bromates, SiO_2, acrolein $(NH_4)_2SeO_4$) IR anal. 78−36273
sulphide determination by gas-phase molecular absorption spectrometry 79−29430
sultams, characteristic band in IR region, Raman obs. 78−29784
super modified simplex, appl. to flame spectrophotometry 78−3397
surface analysis, spectroscopic methods, review *(Chinese)* 79−34414
surface analysis techniques, AES, ESCA, and photoelectron spectroscopy 79−95252
surface and bulk microanalysis, electron spectroscopy apparatus *(French)* 80−47151
surface composition, ion beam sputtering, spectrochem. anal. 77−48701
surface composition anal. by Penning ionisation electron spectroscopy, metastable He impact, electron energy distrib. 79−52060
surface contamination due to polishing determ. by luminescent-discharge spectrometry *(French)* 79−52839
surface layer, ion beam-modified, ESCA obs. 78−52612
surface techniques, AES, ESCA and SIMS 77−56187
surface trace analysis *(Japanese)* 78−40102
synchronized flash photolysis and pulse deposition in matrix isolation experiments 78−73120
synchronous excitation spectrofluorometry *(Japanese)* 80−86452
synchronous luminescence spectroscopy in multicomp. anal. 79−74452
dl-tartaric acid, radiation products, ESR-ENDOR OBS. 80−55682
tartaric acid salts, and deuterated forms, irrad.-crysts., primary reactions, EPR obs. 80−3370
teaching, mobile spectroscopy, chem. anal. laboratory 78−93502
techniques, review 80−98989
temperature jump sample cell 78−32881
tetramethyltetraphenyltrisiloxane film, DC-704, on Ge, Al and KRS-5, IR refl. spectra anal. 77−59630
thick liquid films, absorbance ratio, IR spectra determ. 78−48710
thin film sample, electronic and reson. Raman spectra, simultaneous meas. 78−66554
thin layer chromatography, luminesc. meas. methods 78−53305
thin layer chromatography, luminescence quantitation, solvent effects 78−53306
thin surface layers, depth and composition determ. by depth-selective photoelectron spectroscopy 79−43090
thin-layer phosphorimetry, solvent enhancement effects 78−61082
thiosulphate determ. in photographic gelatine, spectrophotometric method *(Hungarian)* 80−66905
time-dependent fluorescence, anal. by method of modulating functions 78−48715
time-dependent fluorescence depolarisation, anal. appls. 79−24846
time-of-flight spectra, fibre optic waveguides 80−23767
time-resolved fluorimetry, cross-correlation method 79−79331
time-resolved resonance Raman spectroscopy and vidicon Raman spectrography, vibr. spectra on nsec scale 80−37095
tin inorganic compounds, separation and determ. in environmental samples 79−79416
tissue reflectance oximetry, exptl. and theoretical models 79−79624
Tokamak discharge chamber, AES anal. *(Russian)* 79−4163
total luminescence spectroscopy, mixture anal. appl., practical values 78−56927
toxic gas monitor based on laser photoacoustic spectrometer *(German)* 80−12046
toxic micro-concentration, photo-colorimetric lens technique *(Russian)* 77−40610
toxic organic substances, detect. in water, Raman matrix isolation spectrosc. method 80−30616
spectrochemical analysis continued
toxic substances identification using online computerised infrared system 77−90709
trace analysis by IR spectroscopy, preconcentration, separation and computer techniques 78−31730
trace analysis in gases by laser-induced schlieren technique 80−3436
trace element analyzer, TABLASER, based on laser ablation and selectively excited radiation 79−39228
trace element determination, using DC plasma echelle spectrometer, automated 78−53277
trace gas analysis, with reson. optoacoustic cell operating inside CO_2 laser cavity 78−27836
trace gases in atmosphere, airborne lase-induced fluorescence systems 80−36425
trace impurities in gasses, IR spectrometric detect., cryogenic method 79−16053
trace metals, determ. by microwave plasma spectrometry with the discharge 79−16052
trace organic gases, using IR laser 79−43653
trace-gas remote analysis, optoacoustic radiometry limitations 80−108759
transient species, detection by dielectric loss meas., microwave method 79−74467
transmission spectroscopy, interference fringe 78−16851
transuranic trace analysis using resonance ionisation spectroscopy of inert gases 80−93833
trapped atmospheric contaminants, IR anal., solvent extraction technique 77−73479
trichlorofluoromethane, matrix radiolysis and photoionis. at 15K,IR spectrochem. anal. 78−76893
triglycerides, diacid and triacid, IR spectra, diathesis (vibr. moieties) anal. 77−44525
Trombay IR pneumatic detector, operational characteristics 79−12843
troposphere, O_3 distribs. meas. with airborne laser absorpt. spectrometer 79−2344
tunable-diode-laser IR spectroscopy applics. 80−40798
tunnelling spectroscopy, appls., review 78−92588
turbulent combustion processes, conc. fluctuations, Raman meas. using Fourier anal. 78−92564
two-photon excited molecular fluorescence, in optically dense media 78−33534
two-photon excited molecular fluorescence technique 80−40799
UHF-plasma torch emission spectrometry by metal hydride generation *(Japanese)* 78−92582
ultrapure water, trace metal determ. 80−81394
ultratrace inorganic ion determination by laser excited fluoresc. 79−34372
unknown spectra identification, computer systems, performance evaluation 78−3398
urban aerosols, optically absorbing component identification as graphitic C 79−34939
urine glucose analyser with audible output 77−52909
UV absorption and fluorescence spectrophotometry, practical standards 77−49783
UV and light absorption spectrometry, review of literature 1975-1977 78−85222
UV and X-ray photoelectron spectroscopy, review of literature, 1975-1977 78−85225
UV monitor for column chromatography design, construction 79−1973
UV photoelectron chemical anal., appl. to conjugated carbonyl cpds. *(French)* 78−90215
UV spectrophotometry, $K_2Cr_2O_7$ in H_2SO_4, nicotinic acid in HCl as standards 77−77819
UV vacuum spectrofluorimeter design for luminescience meas. from thin films 79−71538
vapour cell, single pass, for GC/IR spectrometer appls. 80−16743
vibrational spectroscopy−gas chromatography, method of trapping fractions 77−4960
video fluorometer, computer-controlled, multichannel, features 79−20495
vidicon-based spectrometer, with autoranging amplifier, performance characts. 79−21817
vinyl chloride, air pollution monitoring, computer controlled CO_2 laser absorpt. system 80−89699
vinyl chloride, IR laser induced photoreactions, product identification 79−57257
vinylidene chloride copolymer, stretched, free radical form., meas. using indirect scavenger method 79−61923
Voigt effect, reson. absorpt. description 80−30302
VUV spectrography using electric discharge 79−43675
water media, remote determ. of impurity conc. by laser spectroscopy, calibration by Raman scatt. 79−16090
water pollution, analytical methods comparison 77−90685
wavelength modulation spectrometer for chem. anal. *(Japanese)* 78−76957
X-ray, energy-dispersive, with aid of computer 80−3433
X-ray, specimen particles dimensions effect on X-ray intensity excited by protons 80−85238
X-ray, spectral line superpositioning, calc. 80−85240
X-ray intensity ratio $L\beta/L\alpha$, atomic number dependence 80−62818
X-ray microscopy, high resolution, with synchrotron radiation, for chem. microanal. 80−81416
X-ray photoelectron spectra, surface chemical analysis through even derivatives 79−100463
X-ray spectral analysis, energy dispersive, using semicond. detectors 80−85237
X-ray spectral analysis of minerals calibration method 79−87904
XPS, analytical potential, book contrib. 80−16761
XPS, graphite plate sample holders 80−11972
XPS, quantitative, rel. to subshell photoionis. cross-sections and electron mean free path 80−81389
Ag, adsorption of O, surface species identification by XPS, high press. 79−28191
Ag, development of standard specimen 77−90680
Ag statuette of Mercury from Bonn 1896, particle induced X-ray emission analysis 80−85228
Ag-Cu solid soln., spectral determ. of comp. using UHF plasmotron as source 79−52812
Al, adsorption of NH_3, KVV Auger spectra, deconvoluted spectra 80−50508
Al, high purity, spectrographic determination of trace impurities *(Polish)* 80−35603

spectrochemical analysis continued
Al, plasma etching in CCl_4, end point determ. by spectroscopy 78−76786
Al-Ni(Si), optical emission spectrographic analysis of some binary alloys by a glow discharge of Grimm lamp *(Japanese)* 79−99015
Al_2O_3, adsorption of NH_3, KVV Auger spectra, deconvoluted spectra 80−50508
α-$AlPO_4$, berlinite, H_2O conc. determ. by Raman scatt. 80−76572
Au, by scintillation method in geological samples 79−70391
Au film, ionic sputtering and AES anal. *(French)* 78−76959
Au in thin Ag objects, quantitative analysis by γ-ray differential absorpt. 80−85227
Au-Co electrodeposits, Co hardened, high temp. film formation 79−91848
Au-Cu solid soln., spectral determ. of comp. using UHF plasmotron as source 79−52812
B, amorphous, microimpurities determ. using hollow cathode discharge 80−85247
B determ. in high purity Al 77−90707
B, dissolved, in water, determ. via azomethine H colorimetric method 79−92115
B-Si alloys, B-rich, prep., anal. and cryst. growth *(French)* 80−104091
BFHOH, transient mol. form., microwave spectroscopic obs. 78−74643
$BF(OH)_2$, identification, rot. and centrifugal consts., mol. struct., microwave spectra obs. 80−32705
$BH(OH)_2$, transient mol. form., microwave spectroscopic obs. 78−74643
BN, cubic, growth pressure-temp. region in system BN-Mg 79−66053
Ba^{2+}, on calcite surface, ESCA, calibration 77−81432
$BaTiO_3$, pure and doped, cryst. growth and chemical composition 77−40349
$BaTiO_3$ surface voids, Auger spectrochem. anal., organic contamination 79−24467
Br, determ. using $Ar^* + Br_2$ lamp, line absorpt. meas. 78−46466
BrO_2, detection in oscill. Belousov-Zhabotinskii system *(German)* 79−29351
C, determ. by DC arc optical emission spectroscopy 79−83527
C, oxidation kinetics on Ni (110), AES meas. 79−79291
C, surface groups, spectroscopy 78−68919
C_2, concentration in oxy-acetylene flame, $^3\pi_u$ state, saturation spectroscopy 77−77832
CF_2, in Ar matrix, conc. determ. by intensity calcs. 78−68941
CF_3, in Ar matrix, conc. determ. by intensity calcs. 78−68941
CH_3O_2, radical, form. and decay rates, UV absorpt. spectra 77−48631
$CH(X^2\Pi)$ radical, prod., detect. and reactions 79−61842
CO, chemisorbed on supported Rh surface, activated surface processes, IR spectra 80−16724
CO concentration meas. in coal pulverising plant, IR gas analysers 80−89572
CO, determ. by portable IR tester 80−89569
CO, nondispersive IR analyzer with compensation for optical bias 79−16103
CO_2, $^{12,13}C$, $^{16,17,18}O$ isotope analysis by PbS diode laser absorpt. spectroscopy 77−44529
CO_2 conc. and temp. in flames, Raman spectroscopy 80−32720
CO_2, gaseous reactor coolant, monitoring of U, Pu and fission products by gamma spectrometry 79−89374
CO_2, isotope ratios, optical anal. method 78−85228
CO_2 single and multiple free jet conc. meas., CW laser Raman spectroscopy 79−97447
^{13}C NMR intensity meas. technique, chem. anal. appl. 77−51981
$^{14}CO_2$, tunable diode laser spectroscopy, absorption coeffs., appls. 77−83583
CaF_2, trace impurities, carrier distillation-spectrographic determ. 78−3412
CaO, determination of contents in sintering charge, using X-ray spectral anal., assessment of error 79−52823
$CaO-Fe_2O_3-B_2O_3$ glasses, phys. props. rel. to struct. and comp. 78−23331
(Cd,Hg)Te epitaxial structures, comp. profile depend. on deposition parameters 80−100795
Cd, detection, using forward scatt. of reson. radiation with Voigt effect 78−23993
Cd-Sn alloy, spectral determ. of comp. using UHF plasmotron as source 79−52812
$Cd + N_2$, electronic-vibrational process, state-resolved products distrib. determ. 79−6956
$Cd_xHg_{1-x}Te$, comp. determ. by electroreflection method 77−52708
Ce complex, Ce (III) 1,2-dioxy-3-sulphoanthraquinone, soln., absorpt. spectra *(Russian)* 78−76975
$^{249}CfCl_2$, prep. by reduction of $CfCl_3$, spectrochem. anal. 78−27756
Cl, determ. in refractory metals, spectrosc. method *(Russian)* 79−16095
ClONO, prod. via $Cl + NO_2$ react., FT IR obs. 79−8427
Co, effects of interfering metals on absorption in flameless atomisation 77−90675
Co-Cr orthopedic implants, surface oxide layer investigations using ESCA technique 79−25157
Cr $^7P_0$ state, radiative lifetime in matrices, meas. using laser ablation and selective excitation 80−71959
Cr in urine, determ. by electrothermal atomic absorpt. spectrophotometry 80−61175
Cr, oxidation, Cr-O bonding, characterisation by high resolution AES *(French)* 79−100468
Cr powders (60 to 70%), spectral determination of Al and Fe 77−90679
Cr trace quantity analysis, based on laser ablation and selectively excited radiation 79−39228
$Cr-Cr_2O_3$ black chrome, commercial, solar absorber coating characterisation 80−80111
Cr-Y coatings, spectral determ. of Y content 77−90681
CrO_2Cl_2 + carbon tetrachloride + acetone, intermediate complex form., electronic spectra 80−61075
Cu corrosion inhibition, by mercaptobenzothiazole, spectro-electrochem. studies 80−30138
Cu, determ. in salt *(Russian)* 79−29440
Cu glow discharge sputtering redeposition, in noncond. compound chem. anal. 77−77860
Cu vapour, conc. determ. in hollow-cathode discharge from autoionised line intensity *(Russian)* 77−84547
Cu-Ni, sputter-induced subsurface segregation, Auger electrons obs. 80−10757
Cu-Sn alloy components, photometric determ. *(Russian)* 79−11842

spectrochemical analysis continued
$CuF_2.2H_2O$, synthesis, appl. for carrier-distillation emission spectroscopy 80−89164
$EsCl_2(Br_2)(I_2)$, prep., characterisation and decay of Es(II) 80−16727
F_2 absorption diagnostic, sensitive technique, for chem. laser flow 78−74896
FO free radical, detection by CO_2 laser mag. reson. 80−45594
Fe and Al alloys, Mn content determ. *(Polish)* 80−31889
Fe corrosion products, Raman spectroscopic detect. 79−16063
Fe, determ. in salt *(Russian)* 79−29440
Fe, determ. in waters, colorimetric-acid digestion method 78−61088
Fe, effects of interfering metals on absorption in flameless atomisation 77−90675
Fe film, vacuum-evaporated contamination, conversion electron Mossbauer spectroscopic obs. 78−23985
Fe^{3+} solutions, UV absorption spectrosc. obs. of equilib. 80−93812
Fe/ZrB_2, metal-like cpd. form. in diffusion layer during solid phase saturation 80−19994
Fe-C, optical emission spectrographic analysis of some binary alloys by a glow discharge of Grimm lamp *(Japanese)* 79−99015
Fe-Cr-Al-Y, oxidation resistance, heat treatment and Al^+ ion implantation 80−71785
Fe-Ni alloy, fluorination kinetics and fluoride film form., chem. nature obs. 80−101035
Fe-Si, grain oriented, phosphate coating anal. by IR spectroscopy 80−89570
$Fe_{1-x}Al_xOOH$, Mossbauer study, determ. of Al content and mag. props. 80−39938
$Ga_{1-x}Al_xAs$:Si, Si determ., spectrochem. method, photoluminesc. spectra, Hall effect meas. *(German)* 77−77851
GaAs/III-V solid soln. heterostructure composition profile by photoemission microanalysis 80−44717
GaP LED, N content by photovoltage meas. 77−11993
Ge, film, epitaxial growth on Si, interdiffusion, plasmon energy loss anal. 77−31916
Ge, impurity determ. in very pure sample by photoelec. spectroscopy 77−39888
Ge(Li) gamma-ray spectra, interfering peak anal., using resolution enhancement filters 78−11590
Ge(Li), well-type detectors for low-level radiochemical analysis 78−37119
H, determ. in metals, spectrochemical method *(Russian)* 78−31748
H_2 flame in air, laminar diffusion flame, Raman spectra 79−47928
HBr, and DBr, in monatomic matrices, near IR spectra and aggregate structs. 79−89667
HCN in smoke, tunable diode laser meas. 80−89559
HCl, and DCl, in monatomic matrices, near IR spectra and aggregate structs. 79−89667
HCl + Ba, beam-gas reaction, multiphoton ionisation, product identification 78−23946
HF, IR resonance absorpt. of CW chemical HF laser radiation, pollution monitoring appl. 79−48200
$HNO_2 + O_3$, rate consts. determ. with diode laser 79−70310
HNO_3, atmospheric monitoring, chemiluminesc. method 79−16062
$HNO_3 + NO$, rate consts. determ. with diode laser 79−70310
HO fluorescence detection, interference suppression by sampling method 80−8431
H_2O, determ. in lower stratosphere, far IR spectrosc. method 79−39790
H_2O, determ. in organic solvents, IR spectrophotometric method 78−31731
H_2O isotopes, spectrophone meas. at selected CO, CO_2 laser wavelengths 78−57310
H_2O, trace element anal. by ESCA 77−66779
HPO_3^{2-}, in NaH_2PO_2-Na_2HPO_3, quantitative anal. by relative Raman intensities obs. *(Japanese)* 78−23991
$H_2PO_2^-$, in NaH_2PO_2-Na_2HPO_3, quantitative anal. by relative Raman intensities obs. *(Japanese)* 78−23991
H_2SO_4 and SO_4^{2-}, air pollution determ. in Netherlands, 1971-76 period 79−21031
H_2SO_4, dissociation and absorpt. consts., ultrahigh resolution obs. of 8.2, 11.3 μm bands 78−70825
H_2SO_4, gaseous, IR absorpt. coeffs., partial press. variations 78−56922
He glow discharge, spectroscopic element detector for gas chromatography 78−31721
He-Cs mixture, Cs ion conc. determ. by radn. absorpt. 79−34395
He-O_2-acetylene flame atom cell, for at. spectrometry, characterisation 78−32876
^4He, ion, backscattering anal. 79−96408
Hg, detection by forward scatt. of reson. radiation in mag. field and Voigt effect *(Japanese)* 77−60155
I laser, photochem. changes in CF_3I, $(CF_3)_3CI$ active media 77−14704
I molecular cell, impurity gas detection, He-Ne laser stability appl. *(French)* 77−73496
I_2 vapour concentration monitoring, secondary laser cavity for weak absorptions 78−92551
I_2 vapour low conc. detect. by laser fluoresc. excitation 78−27871
$^{129}I_2$ radioisotope detection in nuclear fuel cycle, intracavity selective absorpt. analysis 78−46182
n-InP, epitaxial layer, (100) surface chemistry, ESCA study 80−103552
InP-SiO_2 interface, CVD problems, ESCA profiles 80−93497
Ir, spectrophotometric methods of determination, review 78−61115
KBr pellet, appl. to IR spectroscopy of inorganic species 80−22455
K_2CO_3-SiO_2-As_2O_3, laser Raman spectrosc. study of ions in quenched reaction mixtures 80−25357
$KCl:KNO_2(KNO_3)$, anion exchange during tablet pressing, IR spectroscopy appl. 80−2764
$KEuHP_3O_{10}$ acid, exam. of thermal decomposition 80−55638
K_2O-SiO_2 glass, Raman scattering of dissolved CO_3^{2-} ions 78−27848
KOH, beam, formed at 300-800°C, electron elastic scatt. obs., species identification 80−14231
Kr^+ ion laser, mode-locked near UV output, chem. and appls. 79−45966
LaF_3-$La(OH)_3$, high pressure phases, X-ray diffr. and IR spectroscopic anal. 79−47679
Li, natural isotope ratio, spectroscopic determ. *(Russian)* 78−23996
$LiNbO_3$, optically active centres, form. by electron and γ-irrad. 78−18642
LiO_2-Al_2O_3-SiO_2, anal. of composition by IR reflection spectra 80−40783
Mg alloy trace element determ., emission spectrographic method 78−48713

spectrochemical analysis continued
MgO single crystals, chem. polishes for {100}, {110} and {111} surfaces, spectrochem. anal. for impurity content 79−29241
Mn, determ. in salt *(Russian)* 79−29440
Mn VI, colorimetric determ., appl. to Egyptian Mn ores 78−53285
Mo film on Si surface, $MoSi_2$ form. conditions *(French)* 78−43270
Mo ion incorporation into TiO_2 matrix, ESR, UV, and ESCA spectral anal. 79−43670
Mo, oxidation, IR emission spectrosc. obs. 78−68942
Mo, sintered, thermally induced surface composition variations 79−5078
Mo-Si, film deposition by reactive sputtering, characteris. *(Japanese)* 80−93485
Mo_2, matrix isolated visible absorpt. spectra, electronic, vibronic and vibr. states 80−28027
MoN, matrix isolated visible absorpt. spectra, electronic, vibronic and vibr. states 80−28027
MoO, matrix isolated visible absorpt. spectra, electronic, vibronic and vibr. states 80−28027
N I, detect. using Ar ICP emission spectrosc. 80−91474
N, in water, total content trace anal. by isotopic dilution and optical spectroscopy 77−5253
N_2, isotopic composition, spectrosc. determ. in systems below natural ^{15}N levels *(Russian)* 77−68130
N_2 single and multiple free jet conc. meas., CW laser Raman spectroscopy 79−97447
N_2-Cu thermal plasma, effect of Cs on intensity of spectral lines, quantitative spectral anal. appl. *(German)* 78−30417
N_2^+ +Group IV elements and oxides, XPS and UPS prod. determ. 78−73084
N_3, absolute conc. determ. in NaN_3 thermal decomp. from O/NO afterglow 79−100351
NH_2 fragments, multiple photon dissoc. of CH_3NH_2 and NH_3, laser-excited fluoresc. obs. 80−11938
NO, absorpt. characts. of γ-O band, rel. to atm. meas. 78−57316
NO, chemisorption on W (110) surface, chemical changes detected by AES 80−10787
NO, combustion gas sampling system and valves for sampling during engine expansion process 78−24380
NO concentration meas. in gas mixtures, chemiluminescence method *(Russian)* 79−16094
NO detection using optoacoustic cell with improved performance 77−66987
NO, in exhaust gas, direct optical detect., transverse sensitivity *(German)* 78−35751
NO isotopes, spectrophone meas. at selected CO, CO_2 laser wavelengths 78−57310
NO measurements in CH_4-O_2-N_2 flame by laser fluorescence 80−61178
NO, nondispersive IR analyzer with compensation for optical bias 79−16103
NO, optical detection in air, gamma band fluoresc. *(German)* 77−60494
NO, photofragment of NO_2, Doppler spectroscopy 80−53124
NO, press.-broadened linewidths of $R(9.5)_{3/2}$ transition 78−70824
NO_2, cyclic chemiluminescent monitoring device, NO conc. effects 77−49177
NO_2 fluorescence monitor with flashlamp pumping atm. tests 77−64443
NO_2, laser and flash lamp fluoresc. monitors, comparison 80−17367
NO_2 laser fluoresc. meas. in flames 78−56923
NO_2, optoacoustic detect. using pulsed dye laser 78−27835
NO_2, quantitative intracavity laser detect. by optical multichannel anal. 77−77846
NO_2 spatial distribution, detectivity estimation of DAS lidar 78−92991
NO_3^-, determ. in waste and treated waters by laser Raman spectroscopy 79−92113
NO_x, atmospheric monitoring, chemiluminesc. method 79−16062
NO_x source, continuous chemiluminescent analysis, using diffusion interface module 78−40095
$^{14}N^{16}O$, $^{15}N^{16}O$ isotopic species determ. using Zeeman scanning of atomic line, vibr.-rot. line profiles 79−49983
Na, single atoms, fluoresc. selective detect. by laser radiation 80−83312
Na zeolite, molten salt inclusion in intracrystalline canals, spectrosc. charact. *(Rumanian)* 79−74463
NaCl:Pb, Pb determ. by optical absorpt. in aq. soln. 78−85232
NaCl:$PbCl_2$ crysts., melt grown, Pb distrib. determ., UV spectrochem. anal. 78−40101
NaCl-kCl melt, reaction with LiO_2-$2SiO_2$ X-ray, IR exam. 80−55706
$NaClO_4$, aq. glass, formation of trapped H-atoms and electrons on X-irrad. 80−35559
Na_2O-SiO_2-B_2O_3 glasses, phase separation meas. by optical absorption spectra of VO^{2+} *(Japanese)* 79−70414
$NaPO_2$, mol. identification by matrix isolation IF. spectrosc. 80−104485
$NaPO_3$, mol. identification by matrix isolation IF. spectrosc. 80−104485
Nb_3Ge superconducting films, quantitative Auger anal. 80−55740
Ni (100), catalysis of CO+H_2, reaction rate, AES and UPS obs. 79−79290
Ni, effects of interfering metals on absorption in flameless atomisation 77−90675
Ni-base superalloys, emission spectral anal. with fixed time integration technique *(Japanese)* 80−71974
Ni-Cr, film, quantitative anal. by DC arc optical emission spectroscopy 78−68940
Ni-Si, Cs ion-bombarded, surface Cs concs., AES meas. 79−83073
Ni-Si-B powder, oxidation at 850°C, SEM, ESCA, and elec. cond. meas. 80−7717
Ni-Sn alloy, spectral determ. of comp. using UHF plasmotron as source 79−52812
Ni_3C films, form. by carburisation, characterisation 80−34337
Ni_3C films, on graphite, thermal decomp., AES lineshape study 79−79293
NiO electrodes, effect of $Co(OH)_2$ on self-discharge, IR spectra obs. 80−21295
Nz pulsed laser stroboscopic fluorimeter 80−35593
O, conc. in lower ionosphere, fluorescence spectra 80−36434
O_3, determ. in lower stratosphere, far IR spectrosc. method 79−39790
O_3, in atmosphere, monitoring apparatus, chemiluminescence reaction with ethylene 78−96310
O_3+ethylene, dioxirane form., identification by microwave spectra 78−15659
OD radical, in $NiSiF_6.6D_2O$, optical absorption spectrum, 300 and 80K 79−73966
spectrochemical analysis continued
OH, atm. conc. meas. by laser fluoresc., O_3 dissoc. interference 77−49110
OH local concentration in flame, direct meas. from single laser pulse induced fluoresc. 79−39229
OH, methane-air flame, conc., temp. and rot. temp., laser absorption spectroscopy 78−76862
OI, detect. using Ar ICP emission spectrosc. 80−91473
P containing compounds, analysis by spectrophotometry 79−34379
P-SiO_2, film, quantitative anal. by DC arc optical emission spectroscopy 78−68940
PCl_5-HCl_2, Raman spectra, solid and melt, species identification *(German)* 80−45083
PCl_5-$TiCl_4$, gas, melt, and solid, dimer-monomer conversion, Raman spectra obs. *(German)* 79−70320
PH_3, conc. meas. by vacuum UV absorpt. spectra 80−71972
Pb, determ. in aqueous solns. by Delves Cup technique and flameless atomic absorpt. spectrometry 78−68973
Pb^{2+}, on calcite surface, ESCA, calibration 77−81432
Pd, spectrophotometric methods of determination, review 78−61115
Pd-Si (111) interface, microscopic Pd_2Si form., UPS obs. 80−24743
Pd_2Si, Cs ion-bombarded, surface Cs concs., AES meas. 79−83073
Pt, spectrophotometric methods of determination, review 78−61115
Pt-Pb fibre, CO adsorption and oxidation, AES and ESCA obs. 79−52469
Pt-Si, Cs ion-bombarded, surface Cs concs., AES meas. 79−83073
Pu analysis in irradiated fuel reprocessing solns., spectrophotometric determ. in near IR 80−78433
Pu, determ. in soln., on-line γ-ray spectrometric meas. 79−11872
Pu extraction-spectrophotometric determination in spent fuel of first Czechoslovakian nuclear power station *(Czech)* 77−3105
Pu, isotope compositon, determ. using gamma spectrometry 80−66915
Pu, isotopic composition, determ. using thermal ionisation spectrometry with automatic data eval. 80−66913
Pu, isotopic composition, determ. using precise absolute gamma spectroscopic meas. 80−66916
Re surface, interaction with N_2^+ beam, reaction dynamics studied by XPS and thermal desorpt. spectrometry 80−93797
Rh, spectrophotometric methods of determination, review 78−61115
Ru (001), dissociation of adsorbed H_2S, chemisorption and electronic struct. of S layer 79−79292
Ru (~001) stepped surface, O_2 chemisorption, LEED and AES obs. 80−11947
S adsorption in coal, content meas., using X-ray radiometric analysis 80−26077
S, concentration and valence state in pollution samples, X-ray fluoresc. anal. 79−48027
S containing aerosols, continuous in situ meas. by flame photometry and thermal analysis 78−96296
S isotopic composition in CS, spectroscopic meas. *(Russian)* 80−91696
S, total conc. meas. using pulsed electrostatic precipitator and flame photometer 78−95975
S_2 in flames, laser induced fluoresc. meas. 78−61132
SF_6 detection in air, photoacoustic spectroscopy, resonant cell design optimisation 78−56924
SF_6-Ar, condensing flow, gasdynamic and IR meas. 80−6501
SH, in flames, laser induced fluoresc. meas. 78−61132
$(SN)_n$* radicals polymerisation to $(SN)_x$ in thin films, optical spectra 80−16656
SO, SO_2 in flames, laser induced fluoresc. meas. 78−61132
SO_2, atmospheric, fluoresc. monitoring using NO γ-bands 78−73121
SO_2, atmospheric pollution detect., interferential Fourier correl. of spectrum *(French)* 79−21059
SO_2, nondispersive IR analyzer with compensation for optical bias 79−16103
SO_3, gaseous, IR absorpt. coeffs., partial press. variations 78−56922
SO_3^- +BrO_3^-, fast oxidation in acid medium, laser Raman multichannel spectroscopy 78−27754
SO_4^{2-} aerosols, ambient, laser-Raman monitoring 78−69532
Se, spectral determination of trace impurities after solvent extraction 77−90676
Se trace amount determ. by hydride generation-nondispersive flame at. fluoresc. spectroscopy 80−89553
Se-Ni-Mylar multilayered struct., interfacial bonding effect on adhesion, ESCA obs. 79−95274
Si, Cs ion-bombarded, surface Cs concs., AES meas. 79−83073
Si film, epitaxial growth on Si, impurities, plasmon energy loss anal. 77−31916
Si, impurity determ. in very pure sample by photoelec. spectroscopy 77−39888
Si, O content determ. by spectral analysis, phonon absorpt. effects *(Russian)* 77−48177
Si polycryst., end point detection in plasma etching by optical emission spectroscopy 80−50733
Si:As, ion implanted, glow discharge optical spectroscopy 78−22755
Si:B, impurity conc. from photoluminesc. anal. 78−63785
Si:H, amorphous, dopant conc., glow discharge optical spectroscopy 80−49546
Si:P, impurity conc. from photoluminesc. anal. 78−63785
Si-Al, film, quantitative anal. by DC arc optical emission spectroscopy 78−68940
$SiCl_4$+O_2 in modified CVD process for optical fibre prod., reaction IR spectra 78−80472
Si_3N_4, CVD films, chemically trapped H reflection spectrometry 78−10081
Si_3N_4, end point detection in plasma etching by optical emission spectroscopy 80−50733
Si_3N_4 film, high temp. annealing effect on struct. and comp. 77−15714
SiO_2 glass, AES anal. *(French)* 79−39236
SiO_2, plasma-chemical etching, spectroscopy 80−85243
SiO_2, vitreous, and quartz, impurity C determ. by isotopic spectral method 80−26093
Sn, oxidation, exam. by ESCA 78−72920
Sn, oxidation kinetics, in high-temp. fast flow reactor, chemiluminesc. titration meas. 77−48623
SnO_2, from rocks, quantitative determination by Mossbauer effect *(Rumanian)* 78−49178
SrO-Al_2O_3-B_2O_3-SiO_2, glass, corrosion by Cs vapour or liq. 77−16706
Ta film, determ. of thickness and O, N content 78−80824
Th, determ., in natural waters, spectrophotometric method *(German)* 78−70952

spectrochemical analysis continued
Ti alloys, surface layers examination using vacuum UV spectrograph *(French)* 80−71987
Ti, corrosion inhibition in acid medium, electrochem., Auger investigs. *(French)* 78−44430
Ti, oxide layer growth by dry oxidation at 25°C, ESCA obs. *(French)* 80−45434
Ti, surface layer, study using vac. UV spectrograph *(French)* 80−71987
TiD_2, film, AES detection of decomp. 79−91937
TlI powders, photoacoustic spectroscopy obs. 79−12855
U, assay in fuel rods, by passive gamma-ray spectrometry 78−92576
U concentration in fuel reprocessing streams, acid-compensation dual-wavelength spectrochem. anal. 80−78430
U, determ., automated spectrophotometric method for sub-milligram amounts 79−11870
U, determ., in natural waters, spectrophotometric method *(German)* 78−70952
U, determ. in environmental samples, neutron activation, neutron assay and fluorometric methods 78−61087
U, determ. using automated fluorometer 79−11871
U from urine separation, meas. by fluorometry 79−57788
U in natural waters, field meas. technique 78−85705
U safeguarding, determ. of trace amounts by pulsed laser fluorometry 80−78382
U-Pu mixed oxides, impurities, emission spectrometric anal., single carrier method 78−68944
UF_4, photoacoustic spectra determ. of amorphous deposits from plasma 78−53303
UN, identification in AR matrix, IR spectra, vibr. freqs. 77−9066
UO_2, quantitative spectrographic anal. of rare earth and other impurities 79−59232
$UO_2(NO_3)_2$, aq. soln., pulsed NMR relax. time, ^{235}U enrichment depend. 80−2658
V, determ. by chelating agent, synergic extraction and photometric determ. 79−79345
V-Ti-C, elemental anal. by EELS 80−101069
W-Mo-Co high-speed cutting steels, Co determ. 78−3416
Y_2O_3 reactions, with Cr surface, IR spectroscopy 79−100297
Zn protoporphyrin, solns., anal. by fibre optic filter fluorometer 77−36813
$Zn_3(PS_4)_2$, synthesis, structural and thermodynamic props. 77−24304
ZrC powders produced by various methods, impurities 80−11615
ZrC_x, micro X-ray spectral anal. of boundary zones 79−8301

spectrography *see spectroscopy*

spectrometer components and accessories
see also mass spectrometer components and accessories
30 MHz amplifier for EPR spectrometer 80−98955
1024-channel particle spectrometer power supply 79−68169
β-ray interference elimination by mag. deflection, for X-ray meas. following neutron activation 78−74101
absorbance standards, UV, using $K_2Cr_2O_7$ acid solns. 77−53990
absorption cell, for microwave double reson., rel. to collision induced transition 79−58764
acousto-optic modulator, for single sideband Doppler-free double reson. Stark spectroscopy 79−44935
acousto-optical modulators, for laser freq. changes 78−74932
acousto-optical tunable filter spectrometer development 80−101848
adjustable angle beam-crossing system, for coherent anti-Stokes Raman spectroscopy 77−82613
alumina cup electrode, for spectrochem. anal., enhancement *(Japanese)* 77−86418
analogue storage register, for fast transient recording 77−45827
analogue-digital convertor taking into account nonselective absorption 79−57331
analogue-digital function generator, for pulsed AAS *(Russian)* 78−70199
analyser, hemispherical, low KE electrons, in appl. of UV discharge lamp to XPS spectrometer 78−89601
anastigmatic mounting for ellipsoidal concave grating 80−106634
appearance pot. spectrometer design, demonstrations 80−105477
astronomical grating spectrometer, transmission efficiencies of EUV and soft X-rays 77−60621
atomic absorpt., continuum source, wavelength modulated monochromator for spectral interference correction 77−77825
atomic absorption, resonance monochromator detector with continuum source 79−83540
atomic absorption spectrophotometry, equipment design, for anal. appls. *(Russian)* 77−70378
atomic absorption spectroscopy, adjustable read delay device for sampling system 77−32846
atomic absorption spectroscopy, using filament in furnace atomisation 79−79322
atomic absorption spectroscpy, cathode preparation by electroplating 79−43655
atomic emission spectrometer, interference filter, stray light reduction 79−43645
atomic fluoresc. spectroscopy, atomisation cell, inductively coupled plasma appls. 77−12839
atomiser, absorption zone atom distrib. convection effects calcs. *(Russian)* 77−68730
attachment for meas. reflecting powers of materials subject to hemispherical radn. 78−65985
attachment for recording reflection spectra with SF-8 spectrophotometer 78−74070
automatic background-correcting spectrometer 77−29061
automatic compensator for background and dark current in output of photomultiplier 77−87851
automatic control unit for discrete recording 78−58049
automatic initiator for microwave induced plasma 78−88682
automatic multiphase sampling device 78−89548
automatic NMR field-freq. lock, pulsed phase locked loop approach 78−74041
automatic sampler, for flame at. absorption 78−65974
autoranging amplifier, for vidicon based spectrometer, performance charcts. 79−21817
beam brightness modulation, in Auger scanning microscopy 79−16097
beam splitter and reflection reducing coatings on ZnSe for 3-14 μm 79−76811
beam splitter using diffr. grating combination, for Michelson interferometer 78−70205

spectrometer components and accessories continued
beamsplitter using ultrathin metal grids, polishing technique to improve reflectivity 78−55459
bell-jar cryostat for low temp. optical spectrometry *(French)* 77−175
bit-oriented I/O structure applications to laboratory automation 77−44532
blanking resistive heating for Auger spectroscopy and LEED using retarding field analyzer 78−54509
bolometer for IR spectrophotometer, spectral and freq. charcts. 79−6195
Bragg mode analyser potassium acid phthalate, Bragg refl. coeff. obs. 80−95204
broadband transmit/receive circuit for NMR 78−89520
burner system for atomic absorpt. spectrophotometers 80−73468
capacitor discharge temperature jump apparatus, nanosec. resolution 77−79159
Cassegrain mirror system with high light grasp for Raman spectroscopy 78−78000
catalytic surface phenomena, Raman spectroscopy using rot. vacuum cell 78−16852
cathode lamps for atomic absorpt. spectrometry, method of modifying used lamps 80−90898
cell, for liquid differential absorpt. meas. in far IR 78−24872
cell, IR, with Si windows for solid sorption systems 78−299
cell, thin-wedge-shaped, for highly absorbent liqs., Lambert absorpt. coeffs. meas. 78−45720
cell, UV, for meas. of liquids at high press. and temp. 77−53992
cell for adsorption spectra meas. of gases *(French)* 78−58056
cell for investigation of IR spectra of liquid crystals 79−93238
charge coupled device photoarray, as mol. absorpt. spectrophotometric detector 79−80689
chopper for deep space IR interferometer/spectrometer 78−81545
chromatographic-IR analyser, appl. to vapour phase spectrosc. 80−93809
combination light scattering spectrometer temp. regulating attachment *(Russian)* 77−53987
compact vacuum vessel-cryostat for absorption spectra meas. 77−41689
compressed air purging system, continuous flow, for IR spectrophotometer 78−65984
computer automation of multichannel AutoAnalyzers 77−41686
concave diffr. grating, astigmatism compensation, comparative charcts. 79−32067
concave grating efficiency in VUV region, diffusion pump oil contamination effect 80−14429
concave holographic grating, for slitless optical fibre laser Raman spectrometer 77−71380
condensation chamber, for flame photometric analysis, exam. of design 80−21342
conduction cooling device for low temp. phosphorimetry 80−90855
confocal interferometer light-scattering sample cell 79−6182
continuous jet dye laser, appl. to intracavity spectrometer *(Russian)* 78−70197
continuously tunable filter for reson. Raman spectroscopy 77−22604
contour plotter, automated, 3-dimens., for fluoresc. meas. 78−58046
cooled and intensified array detectors 78−65983
cooling of Si/Li spectrometer, using Peltier elements *(Czech)* 78−49947
cooling system, for light sources and detectors in low-light level systems 78−45718
cooling system for sample introduction in low temperature phosphorimetry 80−87158
correlation readout system for photodiode array spectrometer for ICP emission spectroscopy 78−31726
Coude spectrograph of 188 cm reflector, integrating exposure meter *(Japanese)* 77−73961
cryostat, variable temperature for MCD spectroscopy 77−22554
cryostat for Raman scatt. meas. 78−290
crystal analyser optical alignment for X-ray fine spectral structure study 77−18148
cuvette, heated for IR spectroscopy, exam. of design. 80−18025
cuvette attached to UR-20 spectrophotometer for recording refl. spectra of adsorbed mols. 78−298
cuvette chamber, enlarged and thermostatted 77−5925
CW dye laser spectrometer with computer control 79−75618
cylindrical He absorption cell, multiple scatt. effects near reson. 80−16049
cylindrical mirror analyser, design and use with synchrotron radiation, autoionisation obs. 80−18049
cylindrical mirror analyser, transmission props. viewed in energy-angle space 78−15745
cylindrical mirror analyser system for AES, Auger electron appearance pot. spectroscopy and disappearance pot. spectroscopy 78−23986
data handling attachment for UR-20 spectrophotometer 77−26409
DC arc, for emission spectroanal., transport mechanism 78−22464
DC arc, selective volatilisation of elements, in external mag. field, anal. appls. 78−68938
DC discharge lamp, coupling to photoelectron spectrometer using differentially pumped isolating collimator 80−13156
DC plasma arc, for elemental anal., review 77−73478
decoupler coil, for supercond. NMR spectrometers 80−31828
detector systems, for near IR Raman spectroscopy *(German)* 77−65059
deuterated polyethylene target holders for (n,γ) studies 80−99402
DFS-8 spectrograph, attachment for oscillographic recording of line shapes 80−105721
diamond anvil cell, for high press. far IR obs. 79−12874
diamond anvil gasketed cell, for mid IR ultramicrospectroscopy at very high press. 79−44955
diamond selection for anvils in high-press. devices for IR and Raman spectroscopy 77−57413
diaphragm scanning system for Michelson interferometer 78−12764
differential optical spectra recorder using wavelength modulation method 79−2832
differential retarding field analyser charcts., photoelectron and Penning ionis. spectrometry 77−41735
differentiated UV quantitative spectroscopic analysis using RC device 79−87901
differentiator attachment for IR spectrometers 77−73487
diffraction grating monochromator for UV-visible spectrophotometer, stray light 78−94445
diffraction grating mounting for concave grating 78−50913
diffraction gratings, first, second and third order blazes 77−79945
diffraction gratings, for wavelength tuning of SISAMs 79−26143
diffraction gratings, VUV and XUV, simple selection rules 78−55435

spectrometer components and accessories continued
diffraction mountings, conical and classical, for XUV gratings 79−3780
diffuse reflectance Fourier transform IR spectroscopy using diamond anvil cell 80−101855
digital calibration device for mag. field, appl. to EPR spectroscopy *(French)* 77−152
digital integrator, automatically triggered, for flame AAS with discrete nebulization 80−35610
digital integrator, for flameless at. absorpt. spectrometry 77−38014
digital interface for remote control and data transmission 77−2697
digital peak reader, drift compensating, for direct atomisation graphite furnace AAS 78−68939
direct sample insertion device for inductively coupled plasma emission spectroscopy 80−42264
discharge lamp, UV inert gas-type, monochromated, addition to XPS spectrometer 78−89601
dissector pickup tube operating as a counter 80−95153
Doppler-free two photon and saturation spectroscopy, using thermionic detector 78−46465
double nuclear magnetic resonance, probe cct. with transmission line tuning 77−26375
double plasma arc source, for powdered sample analysis in graphite tube 78−16858
double-disc chopper with improved gating characts. for TOF spectrometer 80−37120
drift chamber for multitrack particle identification 79−3276
dual-grating direct-reading spectrograph mirror system design and performance 80−81397
duplexing switch with high isolation, for pulsed NMR spectrometer 80−86363
dye lasers as light sources, props. and appls. *(German)* 79−12864
dynamic feedback system for stabilisation of double-crystal X-ray spectrometer 79−97482
Ebert parabolised monochromator, coma compensation 79−81526
Ebert-Fastie monochromator, alignment using He-Ne laser and Fresnel diffraction pattern 80−99853
echelle efficiencies, theory and expt. 80−102802
elastic parallelogram mechanism 78−16859
electrodynamic scanning mirror drive system for fast-scanning Fourier spectrometer 79−75630
electron beam guiding system including automatic capture circuitry 80−99005
electron energy analyser, electrostatic, appls. 79−44990
electron gun, pulsed, for electron spectroscopy 78−5413
electron irrad. of LiH at 90K, closed liquid Ar circuit *(French)* 78−62214
electron source, for pulse radiolysis, Febetron 708 type 77−88319
electron spectrometer entrance slit 77−54018
electron spectrometer multichannel detector system 77−23520
electron spectroscopies, low-energy, temp. controller 79−44987
electron spectroscopy, sample manipulator and heater for ultrahigh vac. 79−44988
electronic setting comparator, direct viewing *(French)* 78−86354
electronic spark source, adjustable-waveform, thyratron-diode switch element 77−63998
electronically controlled spark source, for anal. emission spectroscopy 78−16857
electrophotographic spectrographs with electronic pulse readout 79−26147
electrostatic cylindrical electron vel. analyser, 127°, relativistic effects 80−86506
electrostatic electron energy analysers, cylindrical mirror appls. 78−21265
electrostatic prism, electron optics for Auger spectrometer 79−29437
electrothermal atomiser, for AAS 78−31715
electrothermal atomiser using graphite braid, for at. absorpt. spectrosc. 79−34377
ellipsoidal mirror display analyzer system for electron energy and angular measurements 80−90908
EM vel. drive for Mossbauer spectroscopy 78−66022
emission quantum yield spectrometer and program system *(Japanese)* 79−89008
emission spectroscopy signal-to-noise ratio improvement and data processing *(Japanese)* 77−21448
ENDOR cavity constructed from X-band rectangular waveguide 79−80653
ENDOR cavity for electron spin echo experiments 78−82013
entrance slit mask, for rotating step sector or 8-step filter for emission spectrography 78−29165
EPR, digital block for electronic sweep of mag. field 77−26371
EPR, magnetic field stabiliser using directly coupled IC op. amps *(Czech)* 79−26095
EPR cavity matching device for use at low temperatures 78−54420
EPR Dewars containing liq. N_2, bumping elimination 79−40600
EPR multipurpose cavities, 1.6-1300K appl. 78−8430
EPR sample tube, gas-permeable 78−260
EPR spectrometer, second harmonic extsn. for saturation transfer meas. 79−40599
EPR spectrometer attachment for studying materials in 120 to 350K. 1-10^4 atm. range 80−105686
ESCA spectrometer retarding lens system, computer optimisation 77−13827
ESR dual sample cavities for Q-band and spectrometers with small magnets 79−58761
Fabry-Perot interferometer, for Raman spectrometers 78−74063
Fabry-Perot interferometer, for remote sensing rot. Raman spectrosc., background rejection method 77−71384
Fabry-Perot prefilter for Raman spectroscopy 79−71532
Fabry-Perot spectrometer, reference channel for path difference determ. of interfering beams 80−77882
far IR gas cell, high press., low temp. 77−30207
far IR modular Fourier interferometer construction, very high resolution 80−57401
far UV transmission grating monochromator for use with reson. radiation lamps 77−27364
fibre light guide for lighting inlet slit of metal spectroscope *(Russian)* 79−41456
field-frequency lock, for a superconducting spectrometer 78−86312
filter, single mesh narrow bandpass, IR to submm. region 78−50911
filters, multielement reciprocal grid interf., far IR transmission characts. 77−46789

spectrometer components and accessories continued
fine wire free standing grids for mm and sub mm waves 78−5559
fixed groove depth lamellar grating Fourier transform spectrometer 80−77885
flameless atomic absorption spectrometer, modification for background correction 78−11581
flow cell, for anal. chemiluminesc. 78−73090
flow microfluorometry instrumentation, rapid data collection, analysis and graphics 78−86348
flowing gas He cryostat for Raman spectroscopy 79−67312
fluorescence cell, IR laser induced for multiple photon processes 78−54475
fluorescence life time decay curve meas. and anal. 78−54465
fluorescence spectrophotometer, optics modifications, for improved sensitivity 77−34030
fluorometric flow cell, using fibre optic system, design and evaluation 78−32879
focal plane IR detector arrays for planetary missions 80−85862
Fourier spectrometer reflector displacement precision meas., photoelectric method 77−18107
Fourier transform IR spectrometer, linear guide way and driving motor *(German)* 79−63313
Fourier transform spectrometer performance, instrumentation for assessment 80−95165
Fraunhofer spectra line position, instrument for meas. *(Russian)* 77−38029
frustrated total internal reflection adaptors optical consts. meas. 77−34039
fused silica fibre link from telescope to spectrograph, operation and prospects 79−53721
gamma spectrometer protection and operation simplification, by relay device attachment 80−57447
gamma-ray guide using total external refl., Mossbauer spectroscopy 80−7200
gamma-ray spectrometer self-stabilising peak detector *(Russian)* 79−26814
gas cell, for gas chromatography-IR spectroscopy interface, optimised sampling techniques 77−77831
gas cell, heatable long path for IR, of light pipe type, design and efficiency 79−58807
gas cell, multiple-path, for Fourier spectrometer, small f-number optics 79−58805
gas cells, for high press. and temp. IR spectroscopy 77−38033
gas diffusion samplers, Fick's law comparison with Ohm's law 80−43819
gas tube, as radiation source for soft X-ray spectrometer 77−18152
gated constant-fraction discriminator for use with fast-focused photomultiplier tubes 78−58063
Girard grille, holographic simulation 80−69337
glass capillary for high resolution NMR measurements at pressures up to 400 MPa 78−65950
glow discharge, cathodic sputtering atomisation for AAS 78−44415
graphite atomiser, for atomisation under pressure in graphite furnace AAS 78−11600
graphite boat for furnace-flame atomic absorption analysis *(Russian)* 77−29080
graphite cups for solid sample introduction into eletrothermal atomiser 80−62734
graphite disc atomiser, for flameless atomic absorption spectrophotometer, exam. 78−54463
graphite furnace, HGA-2200, operating parameters 79−34384
graphite furnace-flame atomic absorption technique, for thermoanalytical investigs. 79−100477
graphite grids for X-ray microanalysis of biological materials 80−8232
graphite platform atomisation system, for graphite furnace AAS 78−32877
graphite thermal atomiser, sample vapour supply and removal rates meas. 78−29164
graphite tubes, for at. absorpt. spectroscopy, pyrolytic coating method optimisation 78−76940
grating, double blazed, for IR spectrophotometers *(Japanese)* 79−40633
grating double monochromator, GDM 1000, spectral anal. of low intensity emissions 79−80701
grating or prism separated elements for increased spectroscopic resolution 80−43271
grating polariser for IR spectral region 79−55221
grating spectrograph, self-calibrating, for light wavelength meas. 78−24869
gratings for UV space instrumentation, comprehensive analysis 79−8839
grazing incidence spectrograph-monochromator with focusing toroidal mirror 79−75617
grids of fine W wire, production, use in IR spectroscopy, polarization interferometry 80−9052
grille filtering method and associated spectometers, capability study, double grille monochromator 80−48427
Hall effect transducer, phase-compensating fluorometer appl. 79−8459
Hartmann diaphragm device, for time resolution during selective volatilisation, spectroscopic anal. 77−49775
heat-pipe oven, disc-shaped, used for Li excited-state lifetime meas. 80−52941
heated closed quartz cell for spectroscopic anal. of metal vapours 78−77996
heated vacuum monochromator for 40-280 nm spectroscopy 80−33176
heater cell for IR high temp. amplitude-phase spectroscopy 79−35860
heating block and high-temperature cell, for spectrophotometric research of solutions, in UV and visible range 80−31899
helical cathode position sensitive proportional counter system for use in a broad range spectrograph 78−82578
helical delay line position sensitive proportional counters for mag. spectrometers 79−68160
high pressure cell, quantitative absorpt. meas., variable thickness *(German)* 78−12769
high pressure cell for matrix isolation Raman spectroscopy 80−272
high pressure optical cell for Raman studies of gases, liquids and molecular solids 78−12767
high pressure sample container for thermal neutron inelastic scattering on fluids 80−37681
high temperature accessories for Fourier spectrophotometer, far IR emission meas. 77−45900
high voltage high frequency spark, with electronic control, for emission spectral anal. *(Russian)* 78−35771

spectrometer components and accessories continued
high voltage unipolar spark discharge, spectrochem. anal. *(Russian)* 78−15750
high-intesnity arc, anal. appls. *(Russian)* 78−35772
high-pressure chamber for pulsed NQR spectrometer 78−86308
high-pressure optical cell for Raman scattering at low temps. 79−49247
high-speed amplitude spectrometry, overlapping pulse elimination 78−78544
high-temp. spectral vessel for adsorbed molecule spectra meas. 77−41690
holographic diffr. gratings, Wadsworth mountings, astigmatism compensation 80−48428
holographic grating, blazed, spectral performance, numerical anal. 77−42617
holographic grating, transparent 80−57395
HV pulse generator for modulation spectroscopy 78−77995
hybrid focal plane detectors for heavy ions 79−68163
ICP torch design method, using hydrodynamic flow patterns 80−24256
ICP unit, 5 kW, for 3.4 metre Ebert spectrograph, commissioning, operation 80−86453
IKS-21, high temp. attachment for reflection and absorption coeff. meas. 80−105720
image detector, Si intensified vidicon target tube for inductively coupled plasma emission spectrometer 80−86439
image dissector spectrometry, magn. disturbances 80−73476
image dissector tube design, with high resolution and large deflection angle 80−73475
image rotator, reflective 78−74065
induction-coupled plasma system, use for spectrochem. anal., calibr. 77−90708
inductively coupled plasma torch configurations 77−82608
instrument developments, overview *(French)* 78−293
integrating sphere, for high-resolution UV and visible spectrophotometry of solids 80−61188
integrating sphere, for reflecting power meas. 77−38037
integrating sphere accessory, spectrosc. meas. of horizontal surface from above 80−86443
Intensified Silicon Intensified Target (ISIT) tubes, medium speed gating 78−12766
interference filters for field of view shaping of optical probe 77−58456
interference filters for wavelength calibration of UV-visible range spectrophotometers 77−33808
interferometer, appl. to dual beam Fourier transform spectrometer, sensitivity improvement 80−90910
interferometers, in IR spectrophotometers, optical and digital advantages 78−16861
ion trap sensitivity for spectroscopic applications, $^{137}Ba^{+}$ ground state hyperfine splitting 80−22447
IR absorption spectrometer cryostat 79−67396
IR broadband spectra upconversion 78−55406
IR cell, low temp. for use with hydrated films 79−6193
IR cell, variable-temp., for studies of adsorption on alkali halides, 80 to 300K 79−80604
IR detector-preamplifier for cryogenic spectrometer, optimization 80−95164
IR emission spectroscopy, double-beam reflectance measuring device 79−80704
IR filter, elmination of near from far IR, LiF Brewster angle plates *(French)* 79−3772
IR filters, transmission characts. of polyethylene mixtures 77−39020
IR polariser grid prod. process *(Russian)* 78−46795
IR reflectance accessory, for obs. of surface films on medium size crysts. 78−35591
IR spectrophotometer, digital data acquisition/analysis system 80−73482
IR spectrophotometer data processing system applications 80−90912
IR spectrophotometer multiple reflection attachment, for surface films on metals 79−71543
IR spectroscopy of solids, inert atmosphere cell, for teachers 79−40338
IR window mounting for ultrahigh vac. appl. 80−82778
iris, for variable field of view Fourier transform IR spectroscopy 77−40586
jig, for precise orient. and grinding of single crysts. *(Czech)* 79−26047
large capacity sample changer for fully automated gamma ray spectroscopy 80−58021
large spectrometer calibration chamber for SURF-II storage ring 80−91339
laser heterodyne, for high resolution optical spectrometer *(Russian)* 78−29180
laser microprobe, for thickness meas. using AAS 80−27355
laser microprobe, modification for transmitted light illumination 77−5902
laser microprobe analyser assessment for quantitative analysis in AES 80−30313
laser microspectral analyser, LMA 10, combined atomic absorption and emission 79−79344
laser microwave double resonance spectroscopy, wide-band intracavity microwave cells 77−82580
laser Raman spectrometer, 180° microscope sampling and viewing attachment 80−13150
laser spectrometer based on Pb and Sn tellurides injection lasers 80−102504
laser-heated miniature oven, for prop. of matrix isolation samples for Raman studies 78−45737
lens objectives, visible and UV, for microscopes and microspectrophotometers 79−75591
LF module reference signal shaper 78−57924
light pipe device for obtaining reference beam with single far IR spectrometer or interferometer 77−38035
light polaris. dynamics in nanosecond band, spectrometer system 79−2834
linear pulse amplifier for X-ray spectrometer, cct., features 78−78595
liquid sample cell, thermostatted, for Raman spectrometer 77−38016
lock-in amplifier, for NQR spectrometer 78−256
lock-type cell for high pressures and low temps. for NMR 78−54416
long-wavelength IR optical filter development status 79−27423
low temp. cooling device with DRON or URS-50 spectrometers 78−24910
luminescence spectroscopy, image devices and photomultiplier detectors, signal-noise calcs. 77−81433
luminescence spectrum recording monochromator wavelength reference marker generator 78−58050

spectrometer components and accessories continued
'magic angle' spinning apparatus in solid NMR spectroscopy 80−17983
magic-angle rotor, using forced air bearing for NMR of solids 80−47083
magnetic flux stabiliser, for NMR radiospectrometers 80−52286
magnetic tape recorder, for NMR spectra recording processing and accumulation *(Russian)* 79−26097
matrix isolation spectroscopy, of sputtered products, low temp. apparatus 77−26407
MCD spectroscopy, permanent mag. interface, rot. system 78−62232
micro sampling cell, for coherent anti-Stokes Raman spectrometry 77−79169
microchannel plate detector for far UV spectrograph, rocket-borne astronomy appl. 77−22086
microphotometer with micrometer attachment, for absorpt. or emission band wavelength meas. on Ebert plates 78−16853
microprocessor controlled data acquisition system, for pulsed laser spectroscopy 78−86341
microprocessor-based spectroscopic instrumentation 80−9047
microreactor assembly to study heterogeneous catalyst system, IR emission spectra anal. 80−98988
microspecimens photo-, X-ray and thermally stimulated luminescence obs., installation for specimens ≥0.8 mm 80−57381
microspecular reflectance apparatus, for Cary 14 and 17 series spectrophotometers 77−5926
microwave 'stripline' absorption cell, for use in microwave Stark spectrosc. 79−81305
microwave cavity for EPR at high hydrostatic pressures 78−89518
microwave discharge lamp for atomic resonance absorption/fluorescence spectrometry 78−89586
microwave preamplifier for ESR/ENDOR spectrometer sensitivity enhancement 78−82014
microwave spectrometer, RE1301, wide-range magnetic current regulator 79−21779
microwave spectrometer control pulse shaper for two-pulse relaxation time meas. 79−67363
microwave spectrometers, modern aspects, book contrib. 80−52328
microwave spectroscopy Stark cell, broadband and low insertion loss, performance 79−17460
mirror mount for optical instrumentation 79−80690
modification, for faster response time to flameless atomiser absorption signals 78−82044
modular Michelson interferometer for Fourier transform spectrochemical meas. 78−29177
modulator, EPR radiospectrometer having discrete set of modulation frequencies 80−52285
monochromator, constant-deviation, defocusing compensation with concave diffr. grating 78−46792
monochromator, glancing incidence, with corrections for astigmatism and spectral-line curvature 80−43466
monochromator, minicomputer controlled, with repetitive optical scanner 78−27843
monochromator, multiple, construction *(Hungarian)* 80−102812
monochromator, near IR meas. of parameters 79−75625
monochromator, normal incidence, intensity calibration by double monochromator method 79−94341
monochromator, programmable, for ICP emission spectrometry, intensity meas. 80−62728
monochromator, tunable vacuum UV photofragment 78−90316
monochromator, vacuum UV 6 m, photoabsorpt. obs. in atm. gases 78−37969
monochromator, very rapdily scanning, for IR and MM wavelengths 80−5829
monochromator accessory module, microcomputer-controlled for dual wavelength operation 79−74440
monochromator drive, using high-speed digital servo 78−36992
monochromator for investigating scattering objects in vacuum UV 77−74523
monochromator scanning control system using microprocessor, spectral line shift correction *(Japanese)* 80−57384
monochromators, construction, spectrosc. appl. *(Hungarian)* 80−43478
monochromators, in IR spectrophotometers, optical and digital advantages 78−16861
monochromators with off-axis mirrors, distortion and split-image curvature 78−59141
Mossbauer furnace for amorphous alloy investigations 80−98916
Mossbauer nuclear gamma-resonance, electronic control block for moving system 77−38075
Mossbauer spectrometer drive systems, improved interferometric calibration 77−18151
Mossbauer spectroscopy, glass liquid He cryostat 79−58853
Mossbauer spectroscopy drive system, low cost, using μA747 ICs 79−89049
mount grating efficiency, triangular and sinusoidal groove gratings 78−32889
moving-condenser electrodynamic unit, for fast scanning microspectroscopy 77−5903
multi-sample wheel for far-infrared dichroism measurements 80−47086
multichannel analyser interface cct. providing full synchronisation for picosec. spectroscopy 77−38022
multichannel analysers for X-ray spectroscopy *(Hungarian)* 80−95205
multichannel digital correlator for optical mixing spectroscopy 79−93234
multichannel spectrometer, quantometer, design trends for computerised control 79−80694
multigap proportional wire chamber system for multiparticle spectrometer 79−3271
multilayer broadband dielectric mirror coatings for Fabry-Perot spectroscopy 77−18101
multiparameter focal plane detector, development of capacitively coupled distributed parameter delay lines 80−78491
multipass cavity for IR spectroscopic meas. of thin polymer films 77−57414
multiple optical cell for absorbance meas. of aqueous solns. 80−22450
multiple reflection cell, 2 m, for mol. IR spectra in liq. Ar soln. 77−83766
multiple reflection cell, laser spectroscopy, meas. on N_2O, SF_6 78−86359
multiple-reflection attachment for UR-10 and UR-20 spectrophotometers 77−45905
multiplex and high throughput spectroscopy 80−95145
multistrip β semicond. detectors for magnetic spectrometers 78−78545
multiwire and drift chambers for the Omicron spectrometer 79−3277

spectrometer components and accessories continued
MWPC appl. as focal plane detection system for mag. spectrograph 79−3295
MWPC appl. in multiparticle spectrometer, description and performance 79−3275
MWPC in synchrotron beam spectrometer, performance under very high fluxes 79−3272
nanosecond pulse stretcher, appl. to laser-excited time-resolved fluorescence spectrometer 79−67390
nebuliser, for ICP system 79−12860
nebuliser, modified cross-flow type, for inductively coupled plasma spectrometry 78−58048
nebuliser, US, in plasma jet emission spectroscopy, parameter, Mn determ. appl. 78−68960
neutral density filters, for UV-vis. spectrophotometry, calibration 78−45734
neutron activation, epithermal, coaxial Ge(Li) and low-energy photon detector systems 78−20123
neutron beam charged particle spectrometers, appl. of drift chambers 79−3278
neutron mechanical velocity selector for small angle scatt. instrument on pulsed source 79−13586
neutron spin-echo attach. for three-axis neutron spectrometer, theory 79−3270
NMR, double, probehead based on crossed slotted tube resonator 78−265
NMR, double, simple single-coil probe 78−264
NMR, Faraday screen for crossed coil instrument 78−4670
NMR, IC Robinson oscillator for detection 77−74475
NMR, magic angle spinner, high-speed 78−89516
NMR, pulsed, analysis of RF field delay line probe 77−49758
NMR high-pressure probe, high-resolution proton NMR 78−89517
NMR lines, analogue calc. of various integrals *(French)* 77−18061
NMR low-noise broadband transmit/receive circuit 80−62706
NMR probe, for combined homonuclear multiple pulse decoupling and magic angle spinning 78−12735
NMR probe double-tuned matching boxes for experiments at 94 and 100 MHz 77−45874
NMR pulsed spectrometer wideband preamplifier 79−71502
NMR Q-meter spectrometer modification, servomechanism for automatic tuning *(French)* 77−18061
NMR sample tube self-positioning anti-vortex plug 77−21434
NMR spectrometer, programming device for control of frequency synthesizers 80−22400
NMR spectrometer, slotted tube resonator as probe head at high freqs. 77−30192
NMR spectrometer interfacing 79−12828
NMR spectrometer modification for high pressures 78−45664
NMR spectroscopy, auto-increment cct. for digital pulse programmer 77−79134
NMR spectroscopy, digital pulse programmer cct. 77−74474
NMR thermometer, for multinuclear Fourier transform NMR 80−57292
non-spectral interference using graphite mini-tube furnaces 79−48028
nonflame atomiser, programmed unit for at. absorpt. anal. 78−54462
NQR, multichannel synchronous detector 77−61098
NQR, panoramic pulsed spectrometer programmer 77−61100
NQR, signal register for pulsed two-freq. instrument 77−61099
NQR, transmitter for LF pulsed spectrometer 77−61101
NQR pulse spectrometer modulator 80−17971
NQR scanning spectrometer, improved super-regenerative oscillator and quench generator 78−8429
NQR spectrometer, programming device for a spin-echo installation 80−17972
nuclear spectrometry, 4k, using 2k ADC with two biased amplifiers 78−46234
null line stabiliser of NMR spectrometer with time division 79−2800
off-resonance nuclear spin-lattice relaxation time, pulsed NMR method for mol. motion in condensed phases 79−78554
on-line dual-wavelength spectrometer for automatic correction of light scattering interference in atomic fluorescence analysis 77−70377
one-beam spectrophotometer with two radiation detectors 79−71536
optical beam-splitter of variable ratio 79−40078
optical bed, referenceable and vibr. isolated 78−83129
optical cuvette, high temp., for transmission spectra meas. over 2-13 μm, 300-1600K ranges 79−2839
optical detectors, for spectroscopic monitoring of negative photoresist stripping by RF plasma 77−40585
optical energy and spatial filter, for high local resolution Raman spectroscopy 79−35838
optical fibre scatt. cell for inverse Raman scatt. 79−9249
optical multichannel detection system for modulation spectroscopy 77−41693
optical transfer functions, direct meas. 78−74849
optical vacuum furnace for Raman and Brillouin spectroscopy 78−58062
optoelectronic image detectors, for mol. fluoresc. spectrometry 79−21815
optothermal detector with pyroelec. sensitive element, absorpt. coeff. meas. of formaldehyde 79−40634
organic compound luminescence spectrometer attachment for recording at liquid N_2 temp. 79−67394
oven, for laser induced fluorescence spectroscopy of U 78−21230
phase splitting circuit, for pulsed NMR spectrometer 80−62704
phosphorimetric instrument, automated, for room temp. phosphorimetry with continuous filter paper device 77−90654
photoacoustic, sample cell, appl. to solids, liqs. 77−74520
photoacoustic cell design, reson. enhancement, background signals 78−4700
photoacoustic cell for liqs. and solids, one-dimens. model generalisation 80−82827
photoacoustic cell for mirror scan Michelson interferometer 80−68277
photoacoustic cell resonances from standard ultrahigh vacuum components 79−12862
photoacoustic cell with improved performance for NO detect. 77−66987
photoacoustic gas cell with weakly absorbing windows 77−5920
photoacoustic high-performance cell 78−8451
photodiode array for radiation detection in AES and analytical appl. *(German)* 80−11992
photoelastic modulators, appl. to polarisation spectroscopy 79−93224
photoelectric concentration meter, acceptable error determ. for automatic biochemical anal. 79−92435
spectrometer components and accessories continued
photoelectric detector for photographic plate holder replacement *(French)* 79−75623
photoelectric pyrometer, for Oxford spectroscopic furnace temp. meas. 79−36584
photoelectric stellar radial velocity spectrometry, use of echelle grating *(French)* 77−91438
photoelectric systems for recording spectral and temporal characteristics of pulsed light 80−73471
photoelectric transducers with astatic characteristics, statistical error determ. 78−93760
photographic emulsion, for spectrographic anal., calibration curve computer calcs. 78−4706
photometer, computer-controlled, for meas. of Raman spectra on photographic plates 77−65051
photometer, digital, laser Raman and spectrofluorometer systems appl. 77−5881
photomultiplier FEU-49, time resolution improvement for Cherenkov spectrometer 77−87831
photon counter design for low light detection systems, spectroscopy, cathodolum. materials appl. 80−105711
photon counting spectroscopic system, error optimisation of dead time determ. *(Spanish)* 79−80693
photothermophone, device for absolute calibration of photoacoustic spectrometers 78−16854
physiocochemical meas., modular equipment and microprocessor control *(French)* 80−30304
pipette, multichannel, for parallel aliquoting into centrifugal analyser minidiscs 78−7267
plane gratings, in series, angular amplification 79−90014
plasma atomisers, high-temp., efficiency and appls. *(Russian)* 77−67506
plasma jets, spectral analysis of dissolved materials 80−19624
plasma torch design, inductively coupled, high-power operation 79−40621
plastic bounded electrode, for emission spectrometric anal. of nonconducting powders 78−48714
pneumatic nebuliser efficiency enhancement through appl. of elec. field 78−95966
polarisation scrambling device, for Raman spectroscopy 77−82612
polariser, rotating triple-reflection, for UV discharge lamps in photoelectron spectroscopy 78−94443
polarising attachment with disrupted total internal reflection for UR-10 and UR-12 IR spectrophotometers 77−74528
polychromators and spatial filtering for summing luminescence spectrometer 77−74517
potassium acid phthalate 80−95204
preamplifier, universal low-noise spectrometric design 77−14315
preamplifier modernisation by input FET operating regime control 80−32579
predisperser for large plane-grating spectrograph 80−73477
premonochromator for stray light rejection in Raman spectroscopy 77−58438
pressure cell for IR investigations of gases 80−83522
printing scalar, single channel, for photon counting 77−5919
prismatic double monochromator 80−23796
programmable gain amplifier, for chem. anal. instruments 79−43644
programmable timer for pulsed NMR spectrometers 79−40598
pulse aspiration sampling system, for flame AAS of small sample vols. 78−27838
pulse field gradient for Fourier transform NMR spectrometer 80−57353
pulse generator, HF oscillator with single coil transducer, for NMR spectrometer 79−2802
pulsed excitation sources, for at. fluoresc. spectroscopy, signal-to-noise ratio effects 77−79158
pulsed NMR, digital integrator 77−26372
pulsed NMR spectrometer incorporating microprocessor, operational, software and hardware details 78−45666
pulsed NMR spectroscopy, extremely fast recovery time receiver 77−26376
pulsed NMR transmitter, for relaxation time meas. in biological samples, construction and operational details 78−93745
quartz analyser crystal, oblique-cut, for Cauchois focusing of X-ray spectrometer 79−52815
quick access sample system for low temp. K-band ESR and ENDOR 80−57352
quick sample change probe for magic-angle-spinning NMR in a superconducting magnet 80−31834
radiation source, VUV He reson. line, for UHV photoelectron spectroscopy 78−89602
radiospectrometer electromagnet field uniformity rel. to pole piece shape and material 78−86309
radiospectrometer resonator uniaxial crystal deformation unit 80−31822
Raman scattering spectrometer, multiple transmission attachment 77−38036
Raman spectrometer, monochromator adjustable intermediate slit, Zeiss GDM 1000 *(German)* 79−9245
rapid-scan spectrometer control unit 78−74067
RC filters, iterated, for signal recording in pulse atomisation AAS *(Russian)* 78−3436
readout system for MWPC of focusing spectrometer 79−3280
recoil spectrometer, use of MWPC in elastic polarisation expts. 79−3274
rectangular groove grating efficiency optimisation for visible, IR regions 79−81525
reflectance measurement attachment for spectrophotometer 77−174
reflection dispersive Fourier interferometer window eliminating backlash error 80−57402
refractometer, SP-129, for UV region 80−31846
resolution enhancement filters, for interfering peak anal. of Ge(Li) γ-ray spectra 78−11590
resonance cell for ENDOR spectrometer, 120-350 G field 78−4671
resonance filter of defect SnO_2 for Mossbauer spectroscopy 77−24767
resonant cell design optimisation, for photoacoustic gas spectroscopy 78−56924
respiratory gas analyser utilising glow discharge selective spectral emission, microprocessor based 79−100772
retroreflecting multipass cell for Raman scatt. 77−74510
RF coil, CW operation, signal intensity for NQR and NMR 78−89515
RF oscillator, marginal, for size effect meas. 77−26377
RF preamplifier, tunable, low-dissipation, for low temp. NMR appls. 79−17458

spectrometer components and accessories continued
rigid W collar, for sensitivity enhancement in flameless atomisation systems 78−35770
roll film back for photographic spectral detection 79−12857
rotation device for producing small angular displacements with multicrystal X-ray spectrometer 79−35905
RYa-2308 radiospectrometer, attachment for obs. of DNMR in ^{31}P 80−98957
sample cell for photoacoustic spectroscopy 77−5921
sample cell for photoacoustic spectroscopy of powdered solids *(Korean)* 79−9247
sample chamber with supply module, for laser microspectral analyser 80−85241
sample changer, automatic, for semi-automatic photometric anal. systems 77−48705
sample heating apparatus, for laser Raman spectroscopy 80−22439
sample holder, for low temp. Raman spectroscopy of crystals 78−86342
sample holders for use with dispersive refl. interferometer 79−30587
sample introduction, high solids aerosol, for flame at. absorpt. 78−3396
sample introduction method, for ICP emission spectroscopy *(Japanese)* 78−82045
sample transfer system for transferring samples between chambers in UHV 79−12809
sample vessel for 400-5000 cm^{-1}, appl. to adsorption meas. 77−41704
scanning dye laser, microprocessor controlled, for spectrometric anal. systems 78−20081
scanning spectrometry, submillimetre, modern aspects, book contrib. 80−52329
sealed atomisation cells, for picogram anal. by microwave excitation, buffer effects 78−48729
self-scanned photodiode array as multichannel spectrometric detector 80−73466
SEM/energy dispersive X-ray spectrophotometry, carousel stage for multisample anal. 77−40611
sequential/parallel track selector, 1 μs hardware pre-analyser for CERN Omicron spectrometer 80−91364
shutter model, ultrafast, for resonant gamma rays 80−31955
shutter system, digitally controlled, for spectroscopic appls. 77−82609
signal shape reconstruction from derivative using synchronous filter 77−37870
signal shaper-discriminator 78−33387
silica cell and photochemical assembly 77−67512
simulated spherical capacitor for use in electron spectrometers 79−89043
SISAM employing contracircular design 80−31894
SIT image detector, for anal. fluoresc. spectrometry 77−61134
slit, digitally controlled 77−34035
slotted tube resonator, pulsed ESR and ODMR expts. 80−86360
Soller slit collimators for 1 eV neutrons 78−82564
solution cell, variable path length, for IR spectroscopy in vacuum 78−45736
sonic location spark counter system for mag. spectrometers 79−68162
Space Telescope spectrograph Digicons 80−85858
spark chamber gas monitor, used in Rutherford multiparticle spectrometer 79−3318
spark discharge, appl. to multielement anal. 78−40103
spark discharge, correl. relations in spectrochem. anal. *(Russian)* 77−70379
spectrofluorometer components, state of the art *(Slovak)* 78−56940
spectrograph focal plane counter with sub-mm position resolution 80−91399
spectrograph lenses, optical parameters 79−97440
spectrophotometer, cutoff system for filtering out higher spectral orders in 400 to 200 cm^{-1} region 80−28334
spectrophotometer accessory for digital absorption and transmission meas. *(German)* 77−57408
spectrophotometer attachment for fused salt absorption spectrum registration 78−86353
spectrophotometer dip probe bubble formation prevention 80−13154
spectrophotometer head with fibre-optic bundles 79−93201
spectrophotometer head with small-spot fibre-optic viewer 79−30525
spectrophotometer IR rejection polariser system 79−63314
spectrophotometer kinetic curve recording unit 78−86352
spectrophotometer reflectivity measuring attachment, for type SF-16 79−85160
spectrophotometer universal cryostat attachment 80−31765
spectrophotometer-type filters of highest possible performance, 2.5-40 μm 80−14438
specular reflectance accessory, IR, small samples 77−2702
specular reflection attachment, PZO-1, for SF-4A spectrophotometer 77−13804
spherical concave gratings, off-plane stigmatic imaging 77−38808
spherochromatism correction system for high-speed spectrographs *(Russian)* 77−61129
spin-echo Fourier transform NMR spectroscopy, multiple pulse technique 80−37063
split beam ratio meas. system for automatic correction of source fluctuations 77−10115
square wave modulator, bidirectional, for NQR spectrometer 78−256
standard spectrometric source conversion peak half-width determ. 77−79499
Stark modulator, zero-based half-sine wave, for analytical microwave spectrometer 77−13802
stigmatic spectrograph image intensifier system, appl. to plasma diagnostic work at low light levels 78−93767
stroboscopic installation for recording luminesc. decay curves 77−74512
stroboscopic integrator for studying NQR relax. processes 80−17969
superheterodyne spectrum analyzer with triggered photon counting method 79−80691
synchronous detector for ESR spectrometer 79−35802
synchrotron radiation spectroscopy, vapour absorpt. cells and beam generating ovens 78−66688
tapped delay line focal plane detectors for mag. spectrometers 79−68161
Teflon, powder pellets for near-IR spectra 78−3401
Teflon sampling manifold for use with small injections 79−34383
temperature controller for ESR and NMR spectrometers 79−35803
temperature jump sample cell 78−32881
temperature variator coupling to EPR radiospectrometer 78−58003
temperature-controlled multireflection absorption cell design and performance 77−18108
ten-channel differential discriminator for radiation detection spectra 78−78593

spectrometer components and accessories continued
thermocouple installation in IR spectroscopy and reaction cells 80−57398
thermoluminesc. signal amplification, with high impedance IC amplifier 79−99955
thermostatic control for radiospectrometer, Diapazon temperature variator 80−47160
three-mirror system as IR broadband polarisation rotator 77−58413
thyristor temp. regulator for pulsed NMR spectrometer 80−105687
thyristor thermostabiliser for at. absorpt., spectroscopy with non-flame atomisation, power supply *(Russian)* 78−76977
time resolved EPR spectroscopy, stopped flow EPR apparatus for biological appl. 80−36206
toroidal diffraction grating, monochromatic image of entrance slit, form., theory *(Russian)* 78−12770
toroidal diffraction grating, spectral image at point at spectrometer entrance slit *(Russian)* 78−57452
toroidal mirror as focusing element for stigmatic grazing incidence spectrometer 79−71539
transmittance standards, use of metallic thin films 77−53991
transmittance transfer standards 78−45728
transmitting TV camera, scanning nonlinearity cancellation 80−52318
triple monochromator a spectrometer in Raman scatt. *(French)* 80−96007
triple NMR technique for N-containing molecules, ^{13}C-{^{1}H,^{14}N} triple reson. 79−81219
tubes design with hollow cathode, for Mo, Fe and Si analysis *(Bulgarian)* 80−85232
tunable acoustooptic narrow band optical filters, appl. computer-controlled spectroscopy 77−75705
TV optomechanical scanner for panoramic spectroscopy *(Russian)* 79−12868
TV type position sensitive detector, for nondestructive surface characterisation by ESCA 78−76969
two crystal diffractometer, neutron spectrometer component, luminosity 78−21807
two-way EPR cavity, for Stark effect meas. on NO_x 80−90872
two-way ESR cavity for magnetic- and electric-dipole transitions 79−17459
ultrahigh vacuum chamber for Raman studies of gases adsorbed on metals 78−81991
unclipped digital correlator constr. for photon correlation spectroscopy 80−57387
UPS, ultrahigh vacuum, apparatus *(Japanese)* 80−37125
US nebuliser, for inductively coupled plasma-atomic emission spectrometry, detect. limits, efficiency 77−68361
UV absorption detector for HPLC 78−45707
UV detector, high sensitivity, for HPLC 78−45709
UV detectors, for high-press. liq. chromatography 78−45706
UV high-resolution optical telescope design 80−90335
UV monitor, variable wavelength, for HPLC 78−45708
vacuum cell, for IR spectrophotometric obs. of gas-solid adsorption 79−80703
vacuum seal, with thermomechanical drive of Ti-Ni 80−31773
variable-thickness cell for liquid MM-wave Fourier transform and laser spectroscopy 80−57403
Varian Model 63 C rod atomiser, device for positioning and dispensing samples into C rods 80−42206
vidicon based apparatus for spectral line contours investig. 79−93226
vidicon based rapid scan spectrometer, for anal. appls., design, evaluation 77−77827
vidicon camera attachment, appl. to anal. of trace metals in Au 77−21453
vidicon spectrometer, spectral line contour investig. *(Russian)* 78−74075
vidicon tubes, detect. sensitivity, at. spectrometry appls. 77−41695
Wadsworth improved mounting with aspherical holographic grating 80−99824
water purification system for at. absorpt. anal. 77−52688
wavelength calibration device for large dispersion spectrographs 80−41728
Woodriff furnace, for SO_4^{2-} determ. in natural water by at. absorpt. spectroscopy 77−40595
X-ray collimators for soft region, test procedures using laboratory sources 77−5436
X-ray diffractometer specimen holder for reactive and toxic materials 79−63863
X-ray electron spectrometer reference voltage supply 78−21307
X-ray energy-dispersive detector, simplex method for fitting Gaussian profiles 79−722
X-ray focal plane spectrometer, high voltage power module and charge amplifier design 78−40826
X-ray imaging collimator for hard region spectroscopy of solar active area 77−5437
X-ray modulation collimators, design and construction 77−5434
X-ray multigrid collimators, design and fabrication 77−5435
X-Y recorder for Auger spectrometer using pulse height analyser, computer interfaces 78−49942
XL-100 spectrometer, design of voltage-controlled oscillator 80−71211
XPS azimuthal angular-depend. studies, using electron spectrometer 80−57428
zone plate with circular sensor, spectral resolution 77−42591
Al filters, for use on Apollo Telescope Mount XUV spectrograph, fabrication 77−60602
Ar plasma source in TM_{010} cavity, for soln. anal. 79−48032
Be film, opt. filter in He discharge lamp for photoelectron spectroscopy 78−79115
C atomizers, problems associated with atomization 79−34386
C electrodes, used in emission spectrography, isotopic labelling study *(Hungarian)* 80−106976
C furnace, for at. emission spectrometry, atomisation temp. effects 77−40583
C rod atomiser, for Ni determination, in heavy crude oil, by at. absorpt. spectroscopy 77−52681
CaF_2 photoelastic modulator, for vibrational circular dichroism spectrometer 78−54476
CdTe low temp. detector, rel. to TGS room temp. detector, for Fourier transform IR emission studies 79−67399
F Kα, 676 eV X-ray source for ESCA 78−53301
HF absorption cell, appl. to precision stellar radial vels. meas. 80−12681

spectrometer components and accessories continued
He discharge, atmospheric press., for microwave plasma spectrometry 79−16052
He I polarised radiation source for surface studies 78−74959
He thin-window gas cell, calibration of magnetic quadrupole spectrometer 79−93859
He-O_2-acetylene flame atom cell, for at. spectrometry, characterisation 78−32876
I_2 filter, absorpt. lines removal from 514 nm excited Raman spectra 78−70200
KBr pellet, appl. to IR spectroscopy of inorganic species 80−22455
KBr, pellets, appls. in inorganic electronic spectroscopy 77−40597
LiF dispersing crystal, X-ray source, synchrotron-like intensities, EXAFS expts. 78−86398
Nd:YAG laser multipass cell for Raman scatt. diagnostics 80−1231
Pu-Be neutron source, for activation anal., β-ray meas. 78−73114
^{242}Pu preparation by EM isotope separation, for use as α-spectrometry and mass spectrometry tracer 78−9011
Si Kα source, sensitivity factors, cross section and resolution data 80−77920
Si spectroscopic applications of structures produced by orientation-dependent etching 80−93668
Si vidicon-image detector system, for atomic emission echelle spectrometer 78−61081
Si(Li) detector for energy dispersive analysis *(French)* 77−26445
SiO_2-Si film-substrate refl. polariser, operation at Hg spectral lines 77−75655
Ta foil lining of graphite furnace, at. spectrosc. 78−74078
Ta treated, graphite atomiser tubes, for high temp. AAS 78−73093
W electrode, method for sealing into quartz 79−71463
W filaments as electrothermal atomisers 78−27860
W filaments as electrothermal atomisers, choice of solvent, gases and nebuliser assembly 78−44432
W filaments as electrothermal atomisers, design of atomiser and power supply 78−44433
W filaments on electrothermal atomiser, atomic absorption spectrophotometry appl. 78−86346
Xe, discharge lamp, RF excited electrodeless, atomic fluoresc. spectrometry 77−86395
Y Mζ, 132 eV X-ray source of ESCA 78−53301
ZnS-Na_3AlF_6 layer achromatic interference polarizers, design, fabrication 79−55222
^{67}Zn spectrometer, double freq. interferometer for absolute velocity calibration of piezoelectric transducer 80−37146

spectrometers
see also interference spectrometers; magnetic resonance spectrometers; mass spectrometers; microwave spectrometers; particle spectrometers; radiofrequency spectrometers; X-ray spectrometers
absorption spectrometer for gas phase samples, computer controlled 80−86459
AC cataphoresis meas. techniques and apparatus 79−8442
acousto-optic spectrograph, for radioastronomy *(Russian)* 79−25506
acousto-optical solar radio spectrograph 78−73631
acoustooptical laser spectrometer, high resolution, appl. to H_2O vapour spectrum 80−86450
aerosol particle size spectrometer, microcomputer-modified 79−39329
aerosol spectrometer using two-pulse Fraunhofer holography, fibrous particle motion anal. 80−58476
aerosols, atm., size distrib. meas. with particle Doppler shift spectrometer 78−69515
airborne far IR Fabry-Perot spectrometer for astronomical fine structure lines 80−62026
analytical atomic spectrometry, sensitivity and detection limit, review *(Japanese)* 80−11990
angle resolved photoelectron spectrometer for atoms and molecules using synchrotron radiation 80−90932
anti-Stokes Raman, microcomputer-controlled 80−24111
Apollo Telescope Mount and solar instruments of Skylab, overview 77−60593
applied IR spectroscopy, instrumentation, sampling techniques and appl., book 80−46745
astronomical, for prime focus of parabolic mirror, new design *(Chinese)* 79−80226
astronomical, horizontal spectrograph for solar mag. and vel. field meas. 77−17366
astronomical, with holographic and ruled diffr. gratings 78−40831
astronomical acousto-optical radio spectrograph for spectral integration 78−69694
astronomical compact echelle spectrograph 77−87271
astronomical grating spectrographs, physical principles *(German)* 77−56830
astronomical IR instrumentation on NASA airborne observatories 78−45224
astronomical monochromatic imaging using filters, slitless (multislit) spectrograph, and interferometers 79−8840
astronomical spectrograph, slow scan SEC vidicon system 77−25945
astronomical spectrographic camera shorter than Schmidt 77−73951
atomic absorption, HF field Zeeman modulation 79−57341
atomic absorption spectrometer, graphite furnace, modified for Li at. emission obs. 78−31727
atomic emission echelle spectrometer with image dissector and vidicon tubes, for multielement determ. 78−61081
Auger gridless cylindrical mirror analyser for electron energy meas. 79−71563
Auger spectrometer, with electrostatic prism electron optics 79−29437
automatic, for examining semicond. two-photon absorpt. spectra 79−17503
automatic scanning integrating spectronephelometer 77−79165
automatic system for near IR stellar spectra obs. *(Russian)* 80−51664
balloon borne interference spectrometers operation and appl. to solar UV obs. *(Japanese)* 78−57442
blood analysis in vivo, noninvasive spectroscopic method 77−60234
calibration between 180 and 500 nm via microwave lamps photoelectric spectra 77−45899
calibration samples, homogeneity investigations with LMA 10 laser microspectral analyser 78−23983
CARS spectrometer for gases and flames 80−95154
Cassegrain echelle spectrograph 79−62749
Cassegrain echelle spectrograph at Mt. John Observatory, New Zealand 78−69689

spectrometers continued
circular dichroism meas. in vacuum UV 78−49913
circular polarisation of emission, magnetically induced, appl. to inorganic complexes 78−78005
coherent anti-Stokes Raman spectroscopy system, using freq. doubled Nd+YAG laser 78−64906
collisional photoionisation emission spectroscopy and apparatus 79−55001
computer control of spectrometers in microanalysis lab. *(German)* 77−52686
computerised rapid-scan spectroscopy, at NAVWPNSUPPCEN Crane 78−41362
concave grating, spectral line aberration deconvolution appl. *(Japanese)* 79−26141
concentric spectrograph using holographic grating 78−32896
continuum source atomic fluorescence spectrometer, wavelength modulated, appls. 78−70190
correlation spectrometer, computer assisted, for remote sensing of air pollution 78−4002
Correlation Spectrometer Remote Sensor, baseline drift minimisation 78−16167
Coude spectrograph for 2.6 m Shajn Telescope *(Russian)* 77−64644
cryogenic etalon-spectrometer on Space Shuttle for atmospheric meas. 79−58232
data sampling process for dielec. dispersion meas. in freq. range $<10^{-1}$ Hz *(French)* 79−49257
DC plasma echelle spectrometer, automated, for trace element determ. 78−53277
DC plasma echelle spectrometer system, anal. capabilities 79−12854
differential reflectance, for study of small liquid-solid interfacial effects 79−58804
diode laser correlation, low SO_2 conc. meas. 77−91301
diode laser dual-beam, long-term temporal and scanning characts. 80−90902
diode laser-CO_2 laser, heterodyne spectrometer, meas. of 2sQ(1,1) in NH_3 2ν-ν_2 79−75626
directional spectral reflection on plane surfaces meas. device *(German)* 78−12745
Doppler shift, particle sizing devices for research and calibration 80−4827
Doppler-free high-resolution spectroscopy, instrument, appls. 78−89558
double-beam, for very low absorption coeffs. measurement 77−13801
double-beam single-detector wavelength-modulating, AGC 80−86447
double-pass, appl. to meas. of electron cyclotron emission in plasma device JIPP T-II 80−54035
dual beam fibre optic time-of-flight spectrometer 80−52347
dual-beam diode laser spectrometer with sweep integration, $^{12}CH_4$ absolute line strengths meas. 80−101853
dye laser, high resolution, for meas. of isotope, isomer shifts and hyperfine struct. 77−61141
dye laser spectrometer, computer controlled, time averaging to improve sensitivity 80−101850
echelle Czerny-Turner spectrometer, 5 m, instrumental functions 78−8449
echelle spectrograph, high-resolution, for far UV and visible astronomy, design and performance 80−26744
echelle spectrograph, moderate resolution, wide band 77−33351
echelle-type grating spectrograph, advantages *(Polish)* 80−26745
efficiency, S/N ratio formula 80−31881
electron impact spectrometer, low energy, computer controlled, for mol. energy loss spectra 78−25756
electron inelastic tunnelling spectrometer, construction and operation 79−40646
electron microprobe Auger spectrometer with ultra high vac. SEM capability *(Japanese)* 78−27849
emission background corrections obtained with oscillating refractor plate, modulation waveform effect 77−90653
emission spectrometry, current developments *(Japanese)* 78−86356
energy calibration, 110-280 nm 77−71386
ESCA 36 spectrometer, advanced data anal. 77−90684
EUV spectrograph, Skylab Apollo Telescope Mount expt. S082B 77−60598
EUV spectroheliometer for photometry of dynamic phenomena 78−53825
EUV spectroheliometer on Apollo Telescope Mount 77−60594
EUV spectroheliometer on Skylab Apollo Telescope Mount, photometric calibration 77−60595
Fabry-Perot spectrometer, high-contrast multipass 77−22602
Faint Object Spectrograph for Space Telescope 79−25483
Fick Observatory rasdial velocity spectrometer 78−12098
field meas. Fourier transform spectrometer 80−86470
fisheye field spectrograph design 79−8698
flame atomic absorption spectrometer, multielement, time multiplex multiple slit type 79−40617
flame emission spectrometer, automatic spectral interference registration, for trace element determ. *(Russian)* 78−35775
flat-field spectrograph design, holographic grating appl. 80−68264
fluorescence life time decay curve meas. and anal. 78−54465
Fourier spectrometer, mirror oscills., mathematical error corrections *(Russian)* 77−87849
Fourier spectrometer for recording holograms 79−68369
Fourier transform far IR spectrometer 80−86461
Fourier transform IR spectrometer, dual beam 78−70201
Fourier transform IR spectrometer, for satellite, optical design problems *(German)* 78−86360
Fourier transform IR spectrometer, sensitivity 78−74082
frequency controlled saturation spectrometer, description 80−53008
frequency-crossing phonon spectrometer for measuring magnetothermal conductivities 80−31741
Gamma Ray Experiment on Solar Maximum Mission 80−51657
gas luminescence spectrometer, for examining emission spectra of gas mixtures produced by α-particles 79−35852
Golay-type static multi-slit spectrometer 78−295
grating spectrographs, anamorphic magnification and appl. 79−66927
grating spectrometer, liquid He cooled, for far IR astronomical obs. 79−66925
grazing incidence, construction, and appl. to extreme UV spectra of light impurity ions in linear pinch plasmas 80−59276
grazing incidence spectrometer, 1.0 m, photometric calibration for plasma fusion diagnostics 80−92386

spectrometers continued
grazing-incidence spectral region, beam-gas and beam-foil excitation obs. 80−14250
grille spectrometer efficiency, effect of aberrations 78−70195
grille spectrometer for first spacelab payload *(French)* 79−80202
Hadamard spectrometer, curved slits used to increase throughput 80−95149
Hadamard transform, with computation and superposition procedure for multielement atomic absorpt. anal. 77−70376
Hadamard transform optical instrument, systematic errors 78−94375
heat of vaporisation spectrometer, multilayer desorption meas. 79−82453
high energy electron spectroscopy techniques 80−62740
high resolution laser spectrometer, 10^{13} resolving efficiency *(Russian)* 77−38027
high speed, emissivity measurement of partially transparent materials to thermal radiation appl. 79−7280
high speed, for μs range, 380 to 780 nm *(German)* 77−79166
high-resolution, with dye laser, meas. of isotopic, isomeric shifts and hyperfine struct. 79−6191
high-resolution electronic emission spectrum, N_2, 15300 Å 78−66549
image analysis device, Chromotron 80−83683
image dissector echelle spectrometer use in flame atomic fluoresc. and emission meas. 80−11993
image intensifier spectroscope appl. for low intensity spectroscopy of triboluminescence 78−58061
image-intensifier spectrograph, astronomical, description and use 78−73647
imaging device anamorphoses in spatio-temporal optics *(French)* 77−68179
inductively coupled plasma , determination of minor impurities and alloying constituents in steel 80−90903
inductively coupled plasma spectrometer, data processing using APL 79−17501
infrared high resolution spectrometer, used for satellite astronomical measurements, cryogenically cooled 80−90914
instrument for quenching studies on rare gas and metal halide excited complexes 79−17511
instrument function of spectral devices with multiple diffraction 80−37093
International Ultraviolet Explorer (IUE), spectrograph in-flight optical performance 78−96383
International Ultraviolet Explorer (IUE) spacecraft 78−96382
intracavity dye laser spectrometer, double beam, flash lamp pumped 79−75620
intracavity laser Raman spectrometer, appls. 78−65973
intracavity Nd:glass laser spectrometer for 1.35 μm 79−63316
intracavity Nd:glass laser spectrometer with dispersive resonator 77−74530
intracavity spectrometer, using continuous jet dye laser *(Russian)* 78−70197
ion mobility, multielectrode, for atm. elec. meas. 80−31145
ion scattering spectrometer, for surface anal. 79−12883
IR, instrumental distortion computation without measuring apparatus function 80−95159
IR, measurements and control, Meteor 25 satellite appl. *(German)* 78−32321
IR, performance testing using CO line parameters 77−91275
IR, UR-10, attachment for investigation of small objects at low temps. 79−21822
IR absorption gas analyser, portable model, molecular resonance effects *(German)* 80−98990
IR and sub-MM spectroscopy, conf., Bonn, Germany (Mar. 1977) 78−12778
IR astronomical instrumentation at U.C. Berkeley, current status 78−16293
IR correlation process analyser, non-dispersive instrument 77−82628
IR diffuse reflectance spectrometer, for anal. of catalyst surface, design and construction 79−79319
IR double-beam, using diode laser 79−17510
IR Fourier spectrometer, lamellar grating type, for balloon-borne telescope 78−16294
IR Fourier transform spectrometers for astronomy 78−16309
IR INFRAMEK-E system operational principles *(Hungarian)* 78−54474
IR instrumentation of Calar Alto telescopes 78−16295
IR laser absorption, monitoring of atm. O_3 77−91303
IR laser spectrometer, PbSe diode, for air pollution monitoring and mineral prospecting 77−82044
IR scanning, for spectrally-resolved radiance 80−13164
IR space sensors, low-background large-aperture, meas. facility for evaluation 79−21126
IR space sensors, low-background large-aperture, meas. facility for evaluation 79−21125
IR spectrometers, on Viking orbiters 78−20612
IR-array, low resolution, for 7-25 μ astronomy 77−22081
isochromat vacuum UV spectrometer using Geiger Muller phonon counter 77−74521
ITS-4 IR telescope-spectrometer on Salyut 4 station 77−78635
laser, high-speed, high-resolution, short-wave region *(Russian)* 78−45735
laser absorption, for high sensitivity pollution detect. 78−57373
laser absorption, for point monitoring of atm. gases ambient concs. 78−61607
laser absorption polarising spectrometer, for meas. of small absorpt. coeffs. *(Russian)* 78−29175
laser absorption spectrometer, detection of atmospheric SO_2 concs. 79−96497
laser absorption spectrometer, long path length, effect of scintillation and multiwavelength coherence 78−40653
laser beam focusing, wave front convolution effect *(Russian)* 79−45990
laser correlation spectrometer for virology and immunology 80−56158
laser photoelectric spectrometer for large condensation nuclei meas. *(Russian)* 78−65408
laser Raman spectrometer, Chinese WFL model design *(Chinese)* 79−30573
laser scattering system for marine aerosol meas. 78−36316
laser spectrometer, methane-stabilised for saturated absorpt. profile meas. 79−98446
laser spectrometer based on Pb and Sn tellurides injection lasers 80−102504
spectrometers continued
laser spectrometer with intracavity atomic beam for low intensity spectral lines 77−19107
laser system, for high resolution optical spectrometry, separate laser heterodyne *(Russian)* 78−29180
laser-ion coaxial beams spectrometer 78−12775
laser-radiation, type SKL-2 80−13151
Lexan spectrometry, relativistic projectile fragments, imaging and identification 80−63442
light scattering, quasielastic, power spectrum analyser biological appls. *(German)* 80−12314
light scattering spectrom., polymer characterisation 80−95753
light-scattering apparatus, low-angle for polymer films investigation, calibration 79−58803
logarithmic convertors and amplifiers appl. *(German)* 79−9233
magnetic prism beta spectrometer for low energies 80−99403
magnetic scanning spectrometer, appls. 79−2835
magnetic spark, high-speed photorecorders 80−87014
magnetic spectrometer, precision magnetic measurements by the floating wire analog technique 79−67354
Michelson Fourier transform stellar spectrometer 80−98552
micro-Raman spectrometer, for individual aerosol microparticles identification 78−68970
microwave cavity Q-factor meas. appl. *(Polish)* 78−93728
microwave wavemeter molecular rotational resonance investigation, calibration *(Polish)* 78−29866
microwave-optical, microcomputer-controlled 80−86448
monochromator with random rasters, S/N ratio 79−54193
Mossbauer spectrometer based on Motorola MEK 6800D1 microprocessor 78−37120
multi-purpose instrument for biochemical and related undergraduate studies 78−73816
multichannel digital correlator for optical mixing spectroscopy 79−93234
multielement flameless atomic absorption spectrometer, multiple slit, time multiplex, design and performance 79−12859
multimode, single or double channel operation 77−10116
multiplex and high throughput spectroscopy 80−95145
multislit spectrometer, data processing *(Japanese)* 78−58053
near IR mapping spectrometer design and testing for Galileo Jupiter Orbiter 80−90336
NMR low-noise broadband transmit/receive circuit 80−62706
objective-prism spectrograph, for UV stellar spectral obs. from Skylab 77−60609
on-line dual-wavelength spectrometer for automatic correction of light scattering interference in atomic fluorescence analysis 77−70377
optical, instrumental advances and new designs *(Polish)* 80−101847
optical parametric oscillator spectrometer for IR linear absorpt. meas. 79−7180
optical single-particle-size spectrometer calibration and testing, monofilament fibres as substitute particles 80−58819
optical spectral instrument CAD status and prospects 79−44939
oscillating beam spectrometer for detection of very small transmission and reflection differences 80−31907
oscillating beam spectrometer for organic thin film transmission 80−18022
OSO-8 Univ. of Colorado UV spectrometer expt., optical design 78−49326
peak outputs, distortion due to electronic time consts. 77−2667
photo-acoustic spectrometer for powdered solids *(Korean)* 79−9247
photoacoustic double-beam spectrometer, for use in UV, visible and near IR regions 79−79320
photoacoustic spectrometer, single beam, for near IR region 79−14167
photoacoustic spectrometer, single-beam, microcomputer assisted, for solid materials anal. 78−58044
photoacoustic spectrometer design considerations for spectroscopy of solids 77−41687
photodiode array spectrometer, for ICP emission spectroscopy, correl. readout system 78−31726
photodiode array spectrometer for David Dunlap Obs. 78−12097
photoelastic modulator spectrometer, for 78−58058
photoelectric scanning spectrometer for vacuum UV molecular photoabsorpt. cross-section meas. 80−37096
photoelectric spectrometer, drift correction procedure 78−29178
photoelectrons ang. distrib. meas. by fully automated spectrometer 77−58202
photoionisation collision radiation spectrometer, for absolute intensity distrib. meas. of light sources 79−93233
photon counting spectrometer, computer controlled, rapid scanning of low light level spectra 78−86338
photon-counting multichannel spectrometer 77−22079
photophoretic, spectral dependence meas. of radiometric force on micron sized particle 80−105719
Pioneer Venus Orbiter UV spectrometer, design and operation 80−67503
plane grating spectrometer with off-axis parabolic mirrors, slit curvatures 78−24865
planetary spectrograph 77−73954
plasma emission, background and developments 80−45588
plasma-optical emission spectrometer, inductively coupled, light scatt. effect 80−86455
prism IR spectrometer, calibration curve, non-min. deviation effect 77 13809
pseudorandom noise dielectric spectrometer, appl. of Fourier synthesis 78−16813
pulsed dye laser double beam spectrometer, instrumental noise sources 78−88662
radial velocity spectrometer, on McDonald Observatory 2.1 m telescope 80−51667
radiation meas. bibliography (1972-76) *(German)* 80−95510
radio spectrograph, appl. to interplanetary scintillation spectra obs. 80−72741
radiospectrograph for 25-50 MHz range 79−21077
Raman, digital control system, appl. to soft mode spectroscopy 78−86345
Raman, efficiency quality factor from Q-branch resolution of O_2 vibr.-rot. spectrum *(German)* 79−85967
Raman, interferometric accessory, for resolution enhancement 78−74063
Raman, spectral sensitivity calibration 77−5930
Raman spectrometer, monochromator adjustable intermediate slit, Zeiss GDM 1000 *(German)* 79−9245
Raman spectrometer calibration using AR ion laser lines 79−97446

spectrometers continued
rapid scanning spectrometer application to continuous-flow analysis 79−70406
rapid-scanning Si vidicon, IR capability for solar research 77−9657
reflectometer, spherical, calibration of lustrous colour standards appl. *(German)* 77−18066
remote sensing field research, refl. factor calibration, spectrometer system performance 80−86382
repetitively pulsed dual beam thermo-optical absorption spectrometer 78−77999
resonance absorption spectrometer for monitoring profile of solar He I 58.4 nm line 80−62019
rocket borne resonant absorption spectrometer and photometer for geocoronal and interplanetary He obs. 80−4155
rocketborne IR spectrometer 78−81460
rocks, trace element content, direct-reading spectrometer 78−85738
Rowland concave grating spectrometer, component alignment using optical bench *(French)* 79−98514
scanning spectrometer, programmable, appl. to weak airglow emissions meas. 80−8469
selective spectral line modulation AAS 78−89546
self-scanned photodiode array spectrometer, for flame at. absorpt. meas. 78−70191
SHG, computer controlled intracavity, in CW ring dye laser 80−91841
single photon decay spectrometers with pile up correction, performance 77−61126
single-photon counting fluorescnece decay-time spectrometer 77−82620
slitless optical fibre laser Raman spectrometer, with concave holographic grating 77−71380
small-angle intensity fluctuation spectrometer, appl. to Rayleigh linewidth meas. in liq. ^{4}He 78−14522
solar spectrometer, reson. scatt., apparatus and instrumental errors 78−96393
space telescope, design features 78−45229
spectrofluorimetric system, multifunctional, for luminesc. meas. 78−80811
spectrofluorometer, for composition determ. of solid and liq. samples 79−30576
spectrofluorometer design and development criteria *(Russian)* 77−45898
spectropyrometric unit, for vibr. relax. meas. in supersonic flow 78−9275
spectroradiometer for reflectance measurement 80−56658
spectroradiometers, for atm. meas. 77−9568
spin-flip Raman laser spectrometer as source for high resolution mol. spectroscopy and photochem. review 78−32894
stellar echelle spectrograph, balloon-borne UV 78−49318
stellar spectrograph for large azimuthal telescope 77−91431
stellar spectrograph with electron optical convertor for large azimuthal telescope 77−91432
stellar spectrography with crossed dispersion 78−49337
stopped-flow spectrometer performance with viscous solutions 77−32852
stopped-flow spectrometry for kinetic meas. of fast chem. reaction 78−56925
stroboscopic absorpt. spectrometer, dye laser appl. with forced mode synchronisation 80−78873
summing luminescence spectrometer using polychromators and spatial filtering 77−74517
Sun photometry using compact spectrometer 79−2396
with synchrotron emission channels *(Russian)* 77−82623
Tandem Wadsworth spectrographs, horizontal foci calcs. 79−49298
telescope-spectrometer combination, optical props. 80−87455
thermoluminescence measurement apparatus, lunar samples and meteorites appl. 77−13803
thin three-lens optical systems, secondary spectrum investigation *(Russian)* 78−57456
thin-film spectrograph for guided waves 80−58778
time resolved spectroscopy with streak camera, picosec. operation 79−44945
time- and space-resolved spectrometry, instrumental advances, optical spectrometers *(Polish)* 80−90906
time-gated, spatially-resolved system, for repetitive elec. discharge obs. 78−45727
transmission, appl. to optical props. of metastable CuFe solid solns. 79−83044
tunable diode laser spectrometer, rapid-scanning computer-controlled 80−101854
two-photon, based on flashlamp-pumped dye lasers 78−16860
Ultraviolet Spectrometer and Polarimeter on Solar Maximum Mission 80−51661
unit magnification system, improved field coverage 77−88881
UV calibration, using acidic $K_2Cr_2O_7$ soln. as absorbance standard 78−21092
UV optics, high intensity solar irrad. testing 77−5431
UV spectrometer in airglow expt. on Mariner 10 spacecraft 77−64611
UV spectrometer on Mariner 10, Mercury occultation expt. 77−67023
UV stellar spectrograph BUSS, optical system, appls. *(Dutch)* 78−7880
vacuum grating 3-m IR spectrometer with digital recording, description 80−95157
vacuum monochromator spectrograph with plane diffraction grating, for 120 to 700 nm region 80−82831
vacuum spectrograph, 6.600 m grazing incidence, construction, adjustment and performance 79−26146
vacuum UV, quantum efficiency determ., branching ratio method with ion impact excited Ne III, Ne IV 79−22848
vibrational circular dichroism spectrometer, using CaF_2 photoelastic modulator and Xe lamp 78−54476
vidicon spectrometer, spectral line contour investig. *(Russian)* 78−74075
vidicon-based spectrometer, with autoranging amplifier, performance charcts. 79−21817
vidicon-echelle spectrometer with random access, design and eval. for multielement determs. in atomic absorpt. spectrometery 77−90652
visible IR spectrometer, on Skylab, for Earth surface remote sensing 77−60567
VUV Eagle spectrometer, 2 m, design, construction, operation *(German)* 78−45732
VUV isochromat spectrometer for surface anal. 79−54197
wavelength modulated spectrometer for reflectivity meas. in 150-900 nm range 77−13807
wavelength modulation reflectivity spectrometer using transmission chopper 80−13157
spectrometers continued
wavelength modulation spectrometer for chem. anal. *(Japanese)* 78−76957
wavelength modulation spectrometers, modulation depth 78−89551
wavelength-modulating spectrometer implemented with photovoltaic photodiodes for studying optical props. of semiconductors 79−80699
CO_2 laser heterodyne spectrometer for examining wave-number stability of laser diode mounted in closed-cycle He refrigerator 80−31906
He-cooled LWIR, for exo-atmospheric airglow measurements, caibration 79−97450
TeO_2 rapid optical spectrum analyser *(Japanese)* 77−27360

spectrophotometers
see also spectrophotometry
8450A spectrophotometer, microcomputer system based on MC5 SOS processor 80−68272
AAS, microcomputer based, 2-channel spectrometer 79−24864
absorption bands in solids at low temps., spectrophotometer for meas. 80−86456
accessory for digital absorption and transmission meas. *(German)* 77−57408
amplifier improved design, for SF-4 and SF-4A spectrophotometers 80−31882
astronomical automated spectrum scanner, 3000-11000 Å region 79−53724
astronomical EUV system, obs. of He in interplanetary space 77−45309
astronomical for short term variability obs. in stellar spectra 78−73643
astronomical multi-channel spectrophotometer, polarimeter attachment *(Japanese)* 78−89072
atomic absorption, 'Saturn-2' double-beam type, illuminating system *(Russian)* 77−87850
atomic absorption, dual wavelength, using pulsed hollow cathode lamp 77−40593
atomic absorption, positioning device for dispensing samples into C rod atomiser 80−42206
atomic absorption analysers, with nonflame atomisation, programmed unit, exam. 78−54462
atomic absorption double-beam spectrophotometer operation and applications *(Russian)* 78−27864
atomic absorption fluid-analytical spectrophotometers *(Russian)* 78−27863
atomic absorption spectrophotometer, AAS 1N 78−37084
atomic absorption spectrophotometer, microcomputer control and data reduction 78−35762
atomic absorption spectrophotometer, pulsed hollow cathode lamp *(Japanese)* 78−45669
atomic absorption spectrophotometer using Zeeman effect and polarisation characts. 77−90651
atomic absorption two-channel type, microcomputer-based, appls. 78−56926
atomic absorption two-wave and dispersionless spectrophotometric systems *(Russian)* 78−27862
attachment for fused salt absorption spectrum registration 78−86353
attachment for recording reflection spectra with SF-8 spectrophotometer 78−74070
automated atomic absorption spectrophotometer, operation and specifications *(Russian)* 78−27865
automated clinical/analytical aystem 77−52687
automatic, film thickness and optical consts. evaluation by computer program *(French)* 77−13808
automatic processor for atomic absorption signals 80−105694
biochemistry university course spectrophotometer/fluorimeter 77−33807
bolometer for IR spectrophotometer, spectral and freq. characts. 79−6195
Brewster's angle, refined absolute refl. technique for film thickness meas. 79−21820
calibration in visible range, photometric accuracy verification *(Czech)* 80−13159
calibrator, nonlinearity of transmission coeff. scale 79−30571
Cary 118C spectrophotometer, universal computer interface 78−73972
Cary 14, remote control via digital interface 77−2697
Cary 14 and 17 series spectrophotometers, microspecular reflectance apparatus 77−5926
characteristic curve, stray light interference effect *(German)* 79−44938
circular dichroism spectrophotometer, near IR, microprocessor controlled 80−22454
colour meas. appl., metrological qualification *(Hungarian)* 78−24841
colour measurement, flexible instrument with microprocessor 78−54428
colour measuring, spectrophotometer, ACS Spectra Sensor 78−54429
combined double modulation of source, modulation functions 77−57400
controlled rapid-scan spectrophotometer for turbidity meas. 77−41700
CORAVEL, Cassegrain spectrophotometer for stellar radial vel. determ. 80−82210
cutoff system for filtering out higher spectral orders in 400 to 200 cm^{-1} region 80−28334
data handling attachment for UR-20 spectrophotometer 77−26409
derivative, vidicon-based, for spectrochem. anal. appls., design, evaluation 77−77827
didymium glass filters for spectrophotometer wavelength scale calibration 80−43417
differential spectrophotometer for hydro-optical studies 78−3997
diffraction grating monochromator for UV-visible spectrophotometer, stray light 78−94445
diffuse-reflection spectra recording instrum., 200 to 2500 nm 80−57382
digital colour integrator 78−29138
dip probe bubble formation prevention 80−13154
dispersive IR spectrophotometry, on-line minicomputer system, design, appls. 77−63975
diver-operable multiwavelength spectroradiometer 80−90251
Dobson, direct Sun meas. for atm. O_3 estimates 77−45049
Dobson O_3 spectrophotometer, automation *(Dutch)* 77−70867
Dobson spectrophotometer for atmospheric O_3 meas., installation in Seychelles 77−17250
Dobson spectrophotometer for O_3 determ., aerosol attenuation effect 77−45186
double beam atomic absorption spectrophotometer, electronic-mechanical modulator *(Russian)* 80−68262
double wavelength rapid scanning spectrophotometer, appls. 78−4699
double-beam, for examining circular dichroism for scattering objects 79−35853
double-beam, measurement reproducibility 77−49792

spectrophotometers continued
double-beam UVI spectrophotometer specifications 79−26144
double-pass spectrophotometer with digital registration, spectrum registration precision *(Russian)* 79−96917
dual wavelength detector use in high performance liquid chromatography 79−92023
dual wavelength spectrophotometer, computer-controlled, for UV-vis. mol. absorpt. meas. 79−40620
dual wavelength spectrophotometric measurement, precision optimisation 79−92019
dual-wavelength spectrophotometer/fluorometer, high-performance 80−98198
Ebert-Fastie spectrophotometer for airglow and aurora studies 77−70903
electronics appl. in chemical technology *(German)* 77−77841
errors and calibration procedures 78−32849
fibre optic micro-spectrophotofluorimeter for in vivo animals studies 77−60327
field averaging spectrograph camera for remote sensing 77−45161
field double-beam differential spectrophotometer *(Russian)* 79−49269
field of view shaping with interf. filters 77−58456
FL luminescence photometer, for determ. of matter conc. in soln. 79−30575
flame, multigrating, for simultaneous determ. of five elements 77−21455
fluorescence, spectrophotometric detection system for HPLC 78−48737
fluorescence spectrophotometer, optics modifications, for improved sensitivity 77−34030
four-channel photon-counting spectrophotometer, for stellar Ca II H and K flux meas. 78−73646
Fourier, for far IR thermal emission meas. 77−45900
Fourier emission IR microspectrophotometer for surface anal., lubrication problem appls. 80−13162
Fourier transform IR, underlying principles 80−36812
Fourier transform IR spectrometers, spectral compensation, instrument line shape and resolution effects 79−40631
Fourier transform IR spectrophotometer *(Japanese)* 79−75627
frustrated total internal reflection adaptors optical consts. meas. 77−34039
functional elements of spectroradiometer, accuracy optimisation in light and colour 79−12836
goniospectrophotometer, high angular resolution recording, for visible and UV 78−45671
graphite disc atomiser, for flameless atomic absorption spectrophotometer, exam. 78−54463
grating spectrophotometer, stray light sources 77−41701
head with fibre-optic bundles 79−93201
head with small-spot fibre-optic viewer 79−30525
Hewlett-Packard 8450A UV/Vis, beam director 80−68271
Hewlett-Packard 8450A UV/Vis, design and performance 80−68267
Hewlett-Packard 8450A UV/Vis, input section 80−68270
Hewlett-Packard 8450A UV/Vis, user interface 80−68268
Hewlett-Packard 8450A UV/Vis optical measurement system 80−68269
high-energy, 0.25-2.4 μm, for rapid food constituents qual. 79−17508
high-resolution spectroscopy of gases, density modulation and UV spectrum of UF_6 77−31023
HP 8450A, UV/visible computerised spectrophotometer 80−31883
IL 282 CO-Oximeter for measurements on whole blood 80−56159
intracavity spectroscopy, spectrometer based on continuous jet dye laser 79−52831
IR, continuous flow purging using oil-pumped compressed air 78−65984
IR, digital data acquisition/analysis system 80−73482
IR, effective energy distrib. in light beams 77−61145
IR, effective spectral slit width determ. using NH_3 absorpt. line 80−95167
IR, for small particle spectral diffuse IR reflectivity meas. 80−68276
IR, IKS-12 type illumination system improvement 79−2838
IR, SPECORD 61 recording-type grating spectrophotometer with LT1 air drier 77−45906
IR, using double blazed grating *(Japanese)* 79−40633
IR diffuse reflectance, Fourier transform spectrophotometer 77−5929
IR heterodyne radiometer using tunable diode laser local oscillator 78−267
IR rejection polariser system 79−63314
IR spectrophotometer data processing system applications 80−90912
IR spectrophotometer multiple reflection attachment, for surface films on metals 79−71543
IR spectrophotometers, grating and FT types, rel. advantages of interferometers and monochromators 78−16861
IR spectroradiometer systematic error calc. 79−75629
IR spectroscopy microsampling, computerised data enhancement 77−36821
isolation of set of signals, 'electrical' ratio cct. 77−57401
kinetic curve recording unit 78−86352
laser microspectral analyser, LMA 10, combined atomic absorption and emission 79−79344
laser optical microprobe, MOLE 77−60141
lens objectives, visible and UV, for microscopes and microspectrophotometers 79−75591
light beam size shape and position, light sensitive material determ. method 78−58047
low-temperature device for SPECORD UV VIS spectrophotometers 78−21229
materials analysis spectrophotometer with linear output 78−86344
Michelson Fourier transform spectrophotometer for stellar obs. 78−81550
microcomputer appls. 79−54192
microcomputer interfaced spectrophotometer for kinetic studies 80−62726
microphotometer, with rebuilding struct., for registration of spectra in terms of intensities *(Russian)* 77−13244
microprocessor based data acquisition and control system 80−22335
microprocessor controlled optical spectrophotometer operational principle 79−26104
microprocessor controlled spectrophotometric colorimeters *(Hungarian)* 80−101851
microprocessor-based spectroscopic instrumentation 80−9047
microscope-photometer for visible region absorpt. of single living cell *(German)* 79−66588
microscope-spectrophotometer, computer processed, for measurement of absorption spectra of rock-forming minerals 80−18010
microwave temperature-jump apparatus, with spectrophotometric detection, biological appl. 79−20733
spectrophotometers continued
minicomputer-controlled high-speed transient recording system *(Russian)* 77−9992
modification, for faster response time to flameless atomiser absorption signals 78−82044
modulation excitation spectrophotometer, kinetic anal. appl. 79−12866
monochromator stray light transmission meas. and evaluation 77−38030
multielement atomic spectrum anal. under computer control 80−27357
multiple-reflection attachment for UR-10 and UR-20 spectrophotometers 77−45905
non-dispersive IR photometer for gas anal., function and design *(German)* 80−108772
observatory scanning spectrophotometer *(French)* 78−20638
one-beam spectrophotometer with two radiation detectors 79−71536
one-channel double-beam microspectrophotometer 78−89563
optical density, normalisation of meas. error 79−54091
optical feedback stabilised photometer, compensation for thermal drift 77−2695
optical parameters, measurement errors, normalisation *(Russian)* 78−70198
optical spectral instrument CAD status and prospects 79−44939
optical-null spectrophotometers, photometric scale nonlinearity 80−101816
opticophysical and physicochemical meas. instrum. 80−13121
optimum colour appearance anal using spectrophotometers in quality assurance laboratories 80−90877
performance evaluation tests 79−67371
performance parameters, advanced analytical chem. expt. 79−30170
phase modulation spectrophotometer, for polarisation spectroscopy, optical calculi 78−45715
phase-measuring recording system, double modulation of source 78−29174
phosphorimetric instrument, automated, for room temp. phosphorimetry with continuous filter paper device 77−90654
photochromic materials, spectrosensitometer for spectral-kinetic characts. meas. 80−27358
photoelectric spectrophotometer, accurate absolute calibration in wide spectral region 79−96919
photoelectronic, using p-n junction photovoltaic cells and inherent compensation 79−54200
photometric scale calibration using fluorite 1200-800 cm^{-1} transmission 79−12837
photon counting microspectrophotometer for study of single vertebrate photoreceptor cells 80−12323
photopic response sensor, calibration rel. to photopic handbook data 80−62732
plasma diagnostic instrumentation, 300 to 2500Å 79−64904
polarisation sensitive spectroradiometer, methods for overcoming refl. spectra meas. problems 79−40623
portable dual-channel instrument for rapid optical spectral reflectance measurements 80−13158
prism instruments, Beckman Instrument Inc., historical review 77−61125
pulsed atomic absorption, analogue-digital function generator *(Russian)* 78−70199
pulsed Xe spectrophotometer with parallel wavelength sensing 78−54427
Pye Unicam SP8-100 for colour and UV/vis. transmission meas. 78−93768
radiation heating of specimen in spectrophotometer, effect on meas. accuracy 79−30589
rapid scanning, UV-vis., computerised, automatic absorbance calibration method 77−67509
rapid scanning microspectrophotometer, rhodopsin photoproduct kinetics in frog retinas 78−92763
recording errors caused by discrete removal of information 79−49301
reference for analysis of diffuse transmittance and reflectance 77−38023
reference level periodic autocorrection error due to additive noise, minimisation *(Russian)* 77−2703
reflectance, non-contact, 300 to 1100 nm range *(German)* 79−12865
reflectance measurement attachment 77−174
reflectance spectrophotometers, old geometry problems *(German)* 78−54431
reflectivity measuring attachment, for type SF-16 79−85160
reflectometry of 0.1 mm surface elements *(Japanese)* 78−89527
remote sensing, spectral reflectance, scene composition, instrument for simultaneous recording 78−81443
Reticon spectrophotometer at Asiago Observatory, data anal. procedure *(Italian)* 80−98565
Reticon spectrophotometer at Cima Ekar Observatory, first obs. 79−58254
RETICON spectrophotometer at Cima Ekar Observatory *(Italian)* 79−21190
review of modern instrums. 78−93747
scanning interferometric multiplex photometer, airglow appls. 78−62216
Schumann UV spectrophotometer system for absorpt. and refl. meas. on thin films and solids 78−12772
self-calibrating automatic ranging spectrophotometer/colorimeter 79−30574
sickle cell anaemia sickling kinetics, multiangle laser scatt. spectrophotometer 79−79494
single beam, enlarged and thermostatted cuvette chamber 77−5925
single-beam, holographically recorded concave diffraction grating appl. 78−54468
single-beam absorption-emission flame spectrophotometer design *(Russian)* 78−27866
single-beam microspectrophotometer, for visible absorbance and linear dichroism meas. 80−37097
single-beam spectrophotometer, EPROM for automatic baseline control 79−35691
single-beam UVI, multiple reflections as source of errors 77−49788
small-spot scanning IR spectrophotometer head 78−29133
solid state image sensor, photometric characts. *(Japanese)* 78−4677
SPECORD UV VIS, mag. micromixer attachment for immobilised cytochrome C investigs. 80−56302
spectral slit width determ., method comparsion, IR spectrophotometers 80−86472
spectrocolorimeter, SPEKOL, meas. of diffuse reflectance spectra, of differently matted polyamide fibres 80−77836
spectrofluorometer, scanning photon-counting, construction and data acquisition and manipulation system 77−2698
spectrograph DFS-13 wavelength modulator 78−74069

spectrophotometers continued
SPECTROMOM 190 A for flying dust lead content determ. *(Hungarian)* 77−21893
Spectronic 2000 spectrophotometer, interactive microprocessor-controlled instrument 80−105716
spectropyrometer effective wavelength value, narrowband interference filter background transmission effect 79−72687
specular reflection coeff. meas. on SF-4A spectrophotometer, 0.5% accuracy 77−13804
specular reflectometer-spectrophotometer, NBS reference, mirror refl. meas. 80−68236
SPEKOL 20 routine spectrophotometer 79−54167
stray light by scattering 79−32056
stray light obs., optical techniques 79−30569
stray radiation level during 280 to 350 nm region operation, SF-26 spectrophotometer 80−101852
teaching, mobile spectroscopy, chem. anal. laboratory 78−93502
thin film thickness meas., automatic Brewster angle spectrophotometer 79−6078
two-beam, with compensated 100 percent line 78−74068
ultra short-time spectrophotometer *(German)* 78−89523
universal cryostat attachment 80−31765
UR-10 and UR-12 IR spectrophotometers, disrupted total internal reflection polarising attachment 77−74528
UR-20 spectrophotometer, cuvette for recording IR multiple refl. spectra of adsorbed mols. 78−298
UR-20 with two-channel cryostat 78−24800
UV, aircraft-borne, for columnar atm. O_3 meas. 78−73522
UV, second derivative, combination with gas chromatograph 77−86394
UV, visible and near IR, certification of neutral light filters 80−273
UV absorbance standards, $K_2Cr_2O_7$ in perchloric acid soln. 78−32851
UV and visible spectra of solids using integrating sphere 80−61188
UV spectrophotometer cell, for meas. of liqs. at high temps. and press. 77−53992
UV-visible, high throughput, optical and optomechanical design 80−95155
UV-visible, Hitachi 100- and 200-series, modification, Japan 77−13794
UV-visible, HP 8450 system, using reversed optic method 80−68273
vacuum double-beam spectrophotometer, VM-3, principle and assembly 79−75624
Zeeman effect appls. to atomic absorpt. spectrophotometer, development of spectral-line sources 80−76583
Zeiss DMC 25 automatic recording instrument errors 78−54430
H absorption-cell spectrophotometer for Lyman α radiation, on Mars 4-7 space probes 78−28519
UV, liq. chomatography detector, effect of wavelength 77−44535

spectrophotometry
see also colorimetry; spectrophotometers
absolute luminescence quantum yields, actinometric meas. 77−41691
absorbance measurement, UV-visible region, rel. to spectral slit width 77−30206
absorption spectroelectrochemistry at Pt electrode 79−74395
accuracy, linearity and Beer's law 77−38015
Al-Fe alloys, spectrophotometric determ. of Al content *(Polish)* 80−35604
alloy colour and colour stability as alloy design criteria 80−101005
aluminoborate glass, Fe and Cr ion interaction, mag. and spectral props. 80−103883
Am-stars, scanner obs. 79−5827
analysis, uses and limitations of standard additions methods 78−3405
analysis instrumentation in clinical enzymology 78−88675
aqueous soln. reaction kinetics meas. microwave apparatus 80−3470
astronomical, using intensifier Si vidicon 78−32356
atmosphere, total O_3, spectrophotometric determ. using interference filters 78−16180
atmosphere vacuum UV background, meas. 80−90221
atomic absorption analysis, nonselective interferences 79−87900
atomic absorption methods, trends *(Russian)* 77−57396
atomic absorption/emission, applied to pharmaceutical analysis 79−96397
atomic fluorescence spectrophotometry, review 77−66780
automatic fluorescence microscope photometry data processing and display *(German)* 80−86369
blood alcohol determ., spectrophotometric method *(German)* 79−5415
borosilicate glass, Fe and Cr ion interaction, mag. and spectral props. 80−103883
burner system for atomic absorpt. spectrophotometers 80−73468
calibration standards, glass filter SRM 930 by NBS, clinical laboratory appl. 78−54331
candoluminescence, flame technique for trace metal anal. 78−61093
capacitor discharge temperature jump apparatus. nanosec. resolution 77−79159
cement raw-material mix, main component determ. by atom absorption spectrophotometry 80−45615
chemical analysis methods, review 79−43660
cine camera lens characteristics, measuring techniques for zoom lenses *(Russian)* 79−49322
coated substrate, transmittance and reflectance, film refr. index meas. 78−56534
colorimeter short-time stability, colour measurement repeatability appl. *(Hungarian)* 77−26404
colorimetry for 0° illumination/diffuse observation measuring geometry *(Hungarian)* 78−93750
colour difference meas., spectrophotometric random errors effect 78−12741
colour measurement, computer aided 79−67372
colour sicence contributions, collection of papers by D.B. Judd 80−98761
computer-controlled double-beam scanning microspectrophotometry for rapid microscopic image reconstructions 80−18008
computerised colour matching, spectrophotometry 80−17995
continuous light source, applic. in UV and visible *(Japanese)* 79−80702
cool stars in near IR, spectrophotometry and Cassiopeia 79−88658
crystal, low temp. spectrophotometry *(Russian)* 79−40635
crystalline material optical absorption meas. 80−105718
derivative spectrophotometry, theory and appls. *(Japanese)* 80−86451
derivative spectroscopy, understanding its appl. 80−77875
dielectric thin films, refractive index and thickness, spectrophotometric determ. 78−29144

spectrophotometry continued
differentiated UV quantitative spectroscopic analysis using RC device 79−87901
diffuse reflectance, in near IR, spectrophotometric method 77−82625
digicons, image detection with semicond. array for multichannel photon counting 77−83989
DNA-Au (III) interaction, rate consts., activation energies, pH, spectrophotometric obs. 80−30228
double wavelength rapid scanning spectrophotometer, appls. 78−4699
double-beam fluorescence spectrophotometry 77−21435
dual wavelength spectrophotometric measurement, precision optimisation 79−92019
dual-wavelength spectrophotometry, precision, theoretical assessment 78−29163
electrogenerated chromophores, electrochemical conc. profiles, mass transfer, charge transfer, laser absorpt. spectroelectrochem. obs. 80−40765
emission spectrophotometry, review of data processing systems *(Japanese)* 78−88685
enzyme-linked immunosorbent assay, apparatus for meas. light absorbance of small vols. of liquids 80−72387
eriochrome cyanine R, spectophotometric agent for Be, Al, Ga determ. in aq. organic medium 77−36829
errors and calibration procedures 77−53988
errors and calibration procedures 78−32849
erythrocytes, gas reactions, shape changes microspectrophotometry obs. 79−8488
ethidium bromide E-DNA, intercalated birefringent fibres, microspectrophotometric investig. *(German)* 80−57392
excited atoms fast reactions, optical absorbance laws 79−52667
film, non-absorbing, with randomly rough boundaries, optical anal. by immersion spectrophotometry 79−75572
film thickness meas., lattice absorption method *(Czech)* 77−172
fluorescence decay, nanosec., meas by squirrel-cage photomultiplier, base design 77−30204
galaxies, irregulars and blue compacts, chemical comp. and evolution from spectrophotometry 80−36711
glass, boric acid content, differential-photometric determ. using SPEKOL spectrocolorimeter 78−23984
glass, white-surface, spectral reflection coeffs. and colour coordinate comparison 77−71358
grating type monochromators, errors caused by polarisation of meas. system *(Japanese)* 80−101815
halogen tungsten lamp as radiation source for investigation of weakly reflecting materials 80−22456
ICP emission spectrometry, compromise conditions for multielement anal. 78−76937
inductively coupled plasma optical emission spectrometry, for elemental anal. of organic compounds 78−76936
infrared, lead germanate glass, crystallisation study 80−6499
integration over cylindrical luminous volumes, using calibrated piston source 77−5923
internal reflection spectroscopy, effective thickness calc. 80−89558
IR internal reflection spectroscopy, high reliability, simplified theory 80−105722
IR spectra differentiation using Fourier transforms 79−67397
IR spectrophotometers, meas. errors of polarising objects 80−86471
IR transmission spectrophotometry of solid sorption systems, via cell with Si windows 78−299
Jupiter, spectrophotometry in 0.6 to 1.1 μ region, Jovian atmosphere optical parameters latit. vars. 80−46468
laser intraresonator absorption technique, 360 to 420 nm obs. in UF_6 77−50448
light source development support spectroradiometric system *(Japanese)* 78−45733
liquid chromatography effluents on line anal., micro liq. chromatograph-interfaced Fourier transform IR spectrophotometer 80−73483
mask correlation spectrophotometry, long horizontal path appls. 79−12277
micro, laser in metrology, review *(German)* 77−14734
mid IR ultramicrospectroscopy at very high press., using gasketed diamond anvil cell 79−44955
modulation excitation, kinetic anal. of multiple lifetime meas. 80−86449
MOM integrator description for atomic absorption *(Hungarian)* 77−18102
multichannel photon counting image detector arrays 78−65970
narrow band interference filter, spectral transmission curve meas. 78−297
negative corona discharge effects over surfaces investigation *(French)* 77−4014
nitrocellulose fibres, polarised light study 80−80736
noise meas. in atomic absorpt. flame spectrometry, single and double beam instrum. comparison 80−76584
Nylon 12 melt, diffusion coeff. meas. by microspectrophotometry using dye-tagging *(Japanese)* 79−23756
optical spectra recording with UR-20 spectrophotometer 80−105693
Orion Nebula, spectrophotometric obs., ion abundances, and thermal balance 77−67121
photodiode array, self-scanned, for high dispersion astronomical spectrophotometry 78−45230
photometric analysis, reproducibility and lower detection limit 79−87899
photoresist, negative, as phase profile material for near IR, IR spectrophotometric meas. 78−37953
photosynthetic systems, computer assisted scanning and kinetic spectrophotometry 78−68963
photosynthetic systems, computer-assisted scanning and kinetic spectrophotometry 78−48950
PKS 2126−15, bright quasi-stellar object with neutral colour and redshift of (3.27) 78−93450
planetary nebulae, 8 to 13 micron spectrophotometry 80−22057
planetary nebulae, low excitation, of small ang. size, spectral studies 80−17646
polymers, pyrolysis-mol. wt. chromatography−vapour phase IR spectrophotometry, on-line system, reviews 80−55768
pulsed hollow cathode lamp, transient emission charact. in microsecond region for atomic absorption spectrophotometry *(Japanese)* 77−70365
purine and pyrimidine, γ-irrad. investig. by diffuse refl. spectrophotometry 77−48756
quasars, optically selected, with $3.0<z<3.5$, spectrophotometry rel. to absorpt. line problem 79−25746
quasars of Michigan-Tololo survey, spectrophotometry 80−22105
radiation power of lines, appl. *(Japanese)* 78−8453

spectrophotometry continued
rainwater, multielement anal. 78−69512
reducing agents, spectrophotometric determ. by $K_2Cr_2O_7$ and H_2SO_4 79−39234
reflecting power meas. using integrating sphere 77−38037
trans-retinal, ground and excited state dipole moments, permittivity, solvent effects, spectrophotometry 78−27883
retinal cone pigments, human spectrophotometry, annotated bibliography *(Italian)* 79−62256
trans-retylidene-n-butylamine, ground and excited state dipole moments, permittivity, solvent effects, spectrophotometry 78−27883
river chemical gauging using food colour additives *(French)* 77−41688
rocket instrument for far-UV spectrophotometry of faint astronomical objects 80−62014
sample preparation, automatic, for spectrophotometric anal. 78−81960
scanning photoluminescence, coupled with IR microscopy 80−73447
scintillation counter appl., liquid, use of miniature ^{14}C and ^{3}H standards 80−21346
Seyfert galaxy nuclei, absolute spectrophotometry 79−12508
sheet with chipped surface, spectral transmission curve meas. 78−297
signal controller for photomultiplier output in magnetic circular dichroism 77−67511
solar irradiance, multispectral measurements, atm. total ozone determ. 79−53401
spectra registration system, graphical and digital forms 80−47113
spectral coefficient error numerical calc. 79−75571
spectral irradiance scale, 1973 NBS standard 77−83942
spectrochemical analysis, photographic emulsion calibration technique 79−79321
spectrophotometric titration, equivalence point determ. by computerised curve fitting 78−7258
spectroradiometry, principles *(Japanese)* 78−4678
spectroradiometry automation and applications 78−12740
specular reflectance meas. with double-beam spectrophotometers 78−45674
spread function, graphical representation, stray light concept 80−33198
standardisation in spectrophotometry and luminescence meas., conf., Gaithersburg, USA (Nov. 1975) 78−32846
standardisation to ensure original calibration 77−38020
stellar absolute spectrophotometry, comparison with UBV photometry 78−96476
stellar spectrophotometry at Moscow and Alma-Ata, comparison 79−58273
structural colours of beetles, analysis using reflectance measurements from macro- and microspectrophotometers 80−18023
sulphates in atmospheric particulates, analysis 79−83685
Sun photometry using compact spectrometer 79−2396
sunlight, spectral actinometric obs. for atmospheric aerosol turbidity charcts. determ. 78−92986
super modified simplex, appl. to flame spectrophotometry 78−3397
synchronous excitation spectrofluorometry *(Japanese)* 80−86452
thiosulphate determ. in photographic gelatine *(Hungarian)* 80−66905
tissue reflectance oximetry, exptl. and theoretical models 79−79624
total luminescence spectroscopy, mixture anal. appl., practical values 78−56927
translucent blurring effect, evaluation and estimation method 77−38024
transmission, standardisation in UV and visible regions 78−32850
transmission meas. of neutral absorbers of NS glass, when irradiated with laser radiation 80−105692
transmission spectrophotometry in visible and UV regions, standardisation 77−53989
transmittance standards, semi-transparent metallic thin films use 78−32852
transmittance standards, use of metallic thin films 77−53991
TU-20 turbine oil, 4-methyl-2,6-ditertiarybutylphenol determ., using IR spectrophotometry *(Polish)* 80−13161
two-beam, solutions in UV and visible range, high-temperature cell and heating block design 80−31899
ultramicrospectrophotometry techniques in intravital microcirculatory studies 80−21589
UV absorption and fluorescence spectrophotometry, practical standards 77−49783
UV/vis, use of automation in achieving improved accuracy 80−27356
vacuum UV photometric measurements, spectrosc. eqpt. appls. *(Russian)* 78−32897
Venus, data from entry probes and orbiters rel. to optical model of cloud layer 78−4130
visual pigments, slow flash photolysis using conventional spectrophotometer 78−68904
zone plate with circular sensor, spectral resolution 77−42591
As determination in seaweed and related products, hydride generation system, at. absorpt. spectrometry 80−30294
Cr in urine, determ. by electrothermal atomic absorpt. spectrophotometry 80−61175
Cu complex, polyacrylic acid-polyethyleneimine-Cu(II), struct. *(Russian)* 79−55018
Fe and Al alloys, Mn content determ. *(Polish)* 80−31889
H_2SO_4 and SO_4^{2-}, air pollution determ. in Netherlands, 1971-76 period 79−21031
I+HCl, quenching of $I(5^2P_{1/2})$, temp. depend., time resolved at. absorpt. spectrophotometry 80−32655
I_2-quinoline (pyridine) complexes, stability const. determ. by spectrophotometric methods 80−87056
$K_2Cr_2O_7$ acidic solns. as UV absorbance standards 77−53990
Mn VI, colorimetric determ., appl. to Egyptian Mn ores 78−53285
$Ni(H_2V)_2(H_2O)_2$, synthesis and characterisation *(French)* 80−45225
Pu analysis in irradiated fuel reprocessing solns., spectrophotometric determ. in near IR 80−78433
Pu extraction-spectrophotometric determination in spent fuel of first Czechoslovakian nuclear power station *(Czech)* 77−3105
SO_2 optical depths, mask correlation, advanced methodology, remote sensor 77−82066
Si, epitaxial layer thickness meas. using phase correction function of substrate resistivity *(Rumanian)* 80−90812
Si, photovoltaic cell, absolute spectral sensitivity calibration, radiometry, photometry *(Chinese)* 80−86367
TaF_x complex, with 4-(2 pyridylazo)-resorcinol, stability investig. by spectrophotometry 77−36782
TlCl-TlBr, single cryst., composition determ. by reflection spectrophotometry 77−1961

spectrophotometry continued
W filament as electrothermal atomiser, Zn in acetone determination appl. 78−86346
Xe lamp spectral radiation density, 400 to 1000 nm obs. 79−14072

spectroscopes *see spectrometers*

spectroscopic light sources
acousto-optical modulators, for laser freq. changes 78−74932
arc, DC, AC, for spectrochem. anal., correlation between anal. signals, plasma parameter changes 79−52828
arc discharge, spectral line intensity changes due to plasma comp. changes 79−94838
arc discharge, spectrum, correl. rels. *(Russian)* 78−70196
arc lamps, for UV spectrometry, highly regulated power source 79−40629
arc light sources in graphite tubes, plasma form. and rot. 79−43676
arc source, with two rot. plasmas in graphite tube, for direct solution analysis 78−40105
atomic absorpt. spectroscopy, RF-excited hollow cathode lamps as Zeeman-modulated sources 78−85275
atomic absorption spectroscopy, cathode preparation by electroplating 79−43655
atomic absorption spectroscopy, pulsed lamp supply, optical, elec. charcts. 79−57329
atomic emission spectroscopy, graphite arc, anal. signal, axial distrib. rel. to additives, atms. 79−87922
atomic emission spectroscopy, quantometric meas. of spectra of controlled arc, spark generators, correls. 79−66382
atomic emission spectroscopy, RF induction discharge excitation source anal. curves, detection limits 79−87919
atomic emission spectroscopy spark source, linear Si photodiode array detector, appl. *(German)* 79−87926
atomic fluorescence spectrometry, hollow cathode lamp, pulsing conditions optimisation 78−65972
bipolar oscillatory spark discharges, vapour mixing and energy transfer 79−73050
black body, imperfect, for Fourier transform IR, effects calcs. 77−38032
BRV source, emission at 34 nm, absolute radiometric meas. 77−75636
capacitively coupled RF sources, for Zeeman effect anal. at spectroscopy 77−61135
capillary discharge mode selection for IR brightness standard *(Russian)* 79−55198
cathode lamps for atomic absorpt. spectrometry, method of modifying used lamps 80−90898
charged particle oscillator, high resolution photoelectron spectra, stability 78−74700
charged particle oscillator He II photon source 79−58845
Cherenkov radiation light source in pulse radiolysis 80−42267
commercial circular dichroism instruments, magnetic shielding problems 77−87807
composite wall hollow cathode lamp, for study of mol. electronic spectra 77−19376
continuous light source, applic. in UV and visible *(Japanese)* 79−80702
continuous spectrum light source, for at. absorpt. anal. *(Russian)* 77−61136
continuum source, for at. absorpt., selective spectral line modulation method 77−44520
continuum source, for at. absorpt. spectroscopy, charact. conc. meas. 77−67501
continuum source, for at. fluoresc. spectroscopy 78−11578
controlled generators, spectra, rel. to quantometric meas. *(Russian)* 78−74072
CW dye laser spectrometer with computer control 79−75618
CW source, for at. and mol. luminesc. spectrometry, signal-noise ratio 77−71381
DC arc as spectroscopic light source, mag. field effect on line intensities 78−87550
DC plasma excitation source, interference effects 80−86434
DC rotating arc as spectrochem. light source 79−52856
diode laser, pressure-tuned, appl. to high-resolution spectroscopy 80−82835
diode lasers, tunable IR, appls. to high resolution spectroscopy 80−58562
discharge, pulse, low voltage, radial temp. distrib., chem. composition determ. 79−50845
discharge lamp, cold-cathode, current-regulated power supply design 77−57409
discharge lamp, HF, with hollow electrode, for atomic spectroscopy 80−26090
discharge lamp, high intensity, for UV angle-resolved photoemission spectroscopy 79−12870
discharge lamp, high intensity VUV inert gas mixture low-voltage tubular design 79−64300
discharge lamp, hollow cathode type, discharge excitation charcts. obs. 80−42260
discharge lamps, electrodeless, for at. fluoresc. spectrometry, twin-port power divider 79−43681
discharge simulation, interactive programme, adaptation to disc supported microcomputer 80−24269
discharge tube, hollow cathode type, with conical bottom, spectroscopic and elec. charcts. 80−31891
discharges, inductively-coupled, and unipolar HF, spectrum excitation 80−1855
double plasma arc source, for powdered sample analysis in graphite tube 78−16858
dual-grating direct-reading spectrograph mirror system design and performance 80−81397
dye CW commercial laser, freq. stabilisation for ultrahigh resolution spectroscopy 77−88802
dye CW frequency-locked mode-locked laser, for high resolution spectroscopy in freq. domain 80−43350
dye CW mode-locked lasers for ultra-fast spectroscopic studies 79−31960
dye laser, capabilities extension and appl. 79−18495
dye laser, CW freq. stabilised, spectroscopic and metrological appl. 78−9395
dye laser, flashlamp-pumped, linear, thermal effects on spatial mode struct. 79−36943
dye laser, N_2-pumped subnanosecond pulse generation, design 80−87403
dye laser, narrow band CW oscillator/pulsed amplifier system for precision nonlinear spectrosc. 80−53318

spectroscopic light sources continued
dye laser, narrowband CW, high output power, piezoelec. mirror translator for stabilisation 80−33036
dye laser, two-wavelength pulsed, spectroscopic applications 80−28246
dye laser appl. *(German)* 78−89552
dye laser for at. and mol. spectroscopy *(Japanese)* 77−58341
dye laser oscillator-amplifier MW system for high resolution spectroscopy 79−41393
dye laser pulsed absorption spectroscopy of metastable and excited Hg atoms 79−26924
dye laser short-cavity design, picosecond spectroscopy appl. 79−41390
dye laser spectrometer, computer controlled, time averaging to improve sensitivity 80−101850
dye lasers, flashlamp pumped, nanosecond pulse shaping 77−5928
dye lasers, props. and appls. *(German)* 79−12864
dye lasers, single-mode and multimode CW, as sources for obtaining power-squared corrected two-photon spectra 80−78849
dye tunable lasers, for high resolution laser spectroscopy *(German)* 79−26138
Eimac arc lamp, 300 W, spectral and noise characts. 78−32878
Eimac Xe arc lamp, radiant power rel. to hollow cathode lamp 78−89547
electrodeless discharge lamps, for elements forming gaseous covalent hydrides, spectrosc. appls. 77−67500
electrodeless discharge lamps, pulsed, RF excited, anal. at. spectrometry appls. 78−74061
electrodeless discharge lamps, pulsed RF excited, for at. absorpt. and at. fluoresc. spectrosc. 79−21816
electronically controlled spark source, for anal. emission spectroscopy 78−16857
emission source for high resolution spectrosc. *(French)* 80−57383
emission spectrometry, current developments *(Japanese)* 78−86356
exploding thin film excitation, anal. spectrosc. appls. 79−40618
F-centre lasers appl. 79−36900
far IR laser spectroscopic sources and applications 77−57415
far IR laser spectroscopy in liquid and solid states 77−38041
far IR-submm spectroscopy using tunable laser 78−4713
far UV source, 1150-3100 Å, for spectrometer calibration 77−41696
flame atomic absorpt. spectroscopy, background light losses, correction 77−12838
flow lamp, for ionised and neutral metal spectra 79−27355
fluctuations, automatic correction using simultaneous split beam ratio meas. system 77−10115
fluorescence, nonexponential resonance decay, role of exciting light source 77−42348
frequency locked single mode pulsed dye laser appl. to tunable UV generation 77−42547
gas jet source, emission spectrographic analysis appl. *(French)* 79−34390
gas mixture, reacting, atom conc. reson. absorb. meas., microwave discharge lamp calibration 79−92032
glow discharge, for optical spectroscopy of ion implanted Si:As 78−22755
glow discharge plasma line emission intensity calc. and meas. 78−67526
glow discharge type, characts. using Ar(He) carrier gases, Al(graphite) cathodes 78−82047
Grimm lamp, glow discharge, for emission spectrographic anal. of binary alloys *(Japanese)* 79−99015
heterogeneous plasma discharge, spatial information modelling and processing algorithms 78−14229
high-frequency bulb tube, Hg linewidth meas. *(Russian)* 78−4708
high-frequency discharge, appl. to anal. of semicond. film on dielec. backing 80−66904
high-resolution spectroscopy using tunable lasers 80−101849
high-voltage spark source, characterisation, computational method 78−45717
high-voltage spark sources, calibration meas. methods 78−49908
hollow cathode, HF modulated for atomic absorption 79−57341
hollow cathode discharge, electron temp meas. 78−67445
hollow cathode discharge, for spectrochem. anal. of microimpurities in amorphous B 80−85247
hollow cathode discharge, LTE and non-LTE conditions effects *(German)* 78−32891
hollow cathode gasdynamic jet carrying excited metal atoms as spectral light source and chemical reactor 79−46493
hollow cathode lamp, cooling system 78−45718
hollow cathode lamp, pulsed, for at. absorpt. 77−40593
hollow cathode lamp, spectral lines width and intensity, high freq. field effects 78−16856
hollow cathode lasers, high voltage, spectroscopy appls. 79−27274
hollow cathode spectroscopic light source, characts. using Ar(He) carrier gases, Al(graphite) cathodes 78−82047
hollow cathode tubes noise levels for at. absorpt. spectroscopy, pulsed *(Russian)* 77−71385
hollow sintered cathode spectral lamp *(Rumanian)* 79−17509
hypersonic plasma jet discharge, highly effective radiation sources prod. using freq. doubled pulses 79−93235
hypersonic plasma jet discharge, pulsed radiation source *(Russian)* 78−74073
ICP plasma source, 9.2 MHz, temp. determ. by monitoring N_2^+ bands 79−12858
ICP plasma source, axially viewed, for atomic emission spectroscopy 80−22434
illuminating system for double beam at. absorpt. spectrometer *(Russian)* 77−87850
inductively coupled Ar plasma 79−35839
inductively coupled plasma, spectral characteristics 79−70394
inductively coupled plasma discharge, gas flow injection system modifications 78−3400
inductively coupled plasma source, emission spatial profiles, self-scanning photodiode array obs. 78−16850
inductively coupled plasmas, optical emission spectroscopy 80−42266
industrial IR instrumentation sources and optical components 80−87453
inert gas halide lasers, operation and use in photochem. 80−9860
intensity modulated vacuum UV source 77−39009
ionised atoms, prod. by low inductance vacuum spark, spectroscopy *(Japanese)* 80−52911
IR, freq. tunable, using difference freq. method, appl. to PH_3 spectroscopy 79−59484
IR continuum source, improved design 77−39008
IR diode laser for double-beam spectrometer 79−17510
spectroscopic light sources continued
IR Fourier spectrometer, choice of radiation source 80−27362
IR laser absorpt. spectroscopy with ATR prism 79−98480
IR lasers, and laser techniques in mol. spectroscopy 78−8455
IR radiation source, for Fourier spectrometer, stability *(Russian)* 79−26150
IR tunable laser for semiconductor multiphoton spectroscopy *(French)* 80−82836
laser, intensity modulated, 0.01 Hz to 1.2 GHz 79−41400
laser and electro-optical systems, conf., San Diego, CA, USA (Feb. 1980) 80−62392
laser chemical analysis systems, modular component optics system 79−1974
laser light sources, appl. in atomic and mol. optics *(Polish)* 79−36951
laser spectral characteristics measurements, high resolution spectroscopy appl. 78−89555
laser spectroscopy, picosecond processes, review 79−54194
laser-cum-discharge source for spectrochemical analysis *(Russian)* 77−21464
laser-microwave two-photon spectroscopic tunable source 79−30579
lasers, tunable, reson. Raman scatt., review, appls. 78−94247
lasers, tunable diode, for far-IR region, optical coupling arrangement 80−73481
lasers application in Raman spectroscopy, review 78−65979
lithium formate monohydrate frequency-doubling system, automatic phase-matched, for 240-350 nm region 79−31979
LSP type, construction and operating characts. *(Russian)* 79−50364
luminescence discharge, appl. in spectrochem. anal. of metallic corrosion *(Spanish)* 79−92029
magnetoplasma compressor, radial limitation of focal zone, dynamic, energy, spectral characts. 79−55477
metal atom conc. determ. by reson. lines broadened by Hg press. 80−43883
microarc atmospheric pressure glow discharge, operating characts, obs. 79−82106
microwave induced plasma discharge, emission source appls. 78−32880
microwave lamps, UV photoelectric spectra for spectroscopic calibration 77−45899
microwave plasma detector as element analyser for gas chromatography *(German)* 78−64895
microwave surface wave plasma at atmospheric press., production and appls. 79−50868
microwave-excited electrodeless discharge lamps. fabrication and operating conditions effects 78−29179
mode-locked lasers for picosecond spectroscopy 80−9046
monochromatic, electronically variable wavelength 80−102791
nanosecond light pulser with Hg vapour, quenching rate constants determ. 80−100111
National Synchrotron light source magnetic component system 79−68038
noise, flicker or shot, noise power spectra 77−53980
optical parametric oscillators, 0.3-20 μm 77−27319
parametric amplifier for ps spectroscopy 77−27320
parametric generator-amplifier system, for ps pulse duration adjustment, spectroscopy appl. 79−46003
parametric oscillator for intracavity absorpt. spectroscopy 77−10976
Penning discharge as photoelec. UV spectroscopy source 120-300 Å 77−75637
photodetector spectral response determ. using calibrated lamp and interference filters 79−71528
picosecond, laser mode-locking 80−42263
picosecond parametric light source, narrow output spectrum, high pulse rate 78−33780
picosecond pulse sources for time resolved spectroscopy, book contrib. 77−61138
picosecond spectroscopy, broadly tunable repetitive laser system using parametric oscillator 79−46006
picosecond spectroscopy techniques *(Japanese)* 79−71541
plasm torch, inductively coupled plasma optical emission and at. absorpt. appls. 77−51243
plasma, microwave induced, excitation source for at. emission anal. 77−56262
plasma arcs, influence of additive substance *(German)* 79−54196
plasma continua, laser-produced, for absorpt. spectroscopy in VUV and XUV 80−75094
plasma jet light source, intensity distribs., OH band rot. temp. 77−44555
plasma light source, inductively-coupled, for optical emission spectrometry *(Japanese)* 79−48020
plasma quantometer, quantitatively coupled, for emission spectrochem. anal. *(Japanese)* 78−83624
plasma source for at. emission spectrometry 80−26068
plasma torch, reduced size inductively coupled, operation mode and detection limit 80−43994
Pockels cell system, with 2.25 cm^2 aperture, for IR pulsed radiation production 80−5806
power supply for Hg-Ar high press. DC 125 W lamp 78−12722
pulse generator, variable duration and synchronised, Nd:YAG regenerative amplifier 79−45967
pulsed, circuitry and characts., AAS applic. *(Russian)* 78−46740
pulsed EIMAC source, for at. fluoresc. spectrometry 77−61144
pulsed hollow cathode lamp, transient emission characts. in microsecond region for atomic absorption spectrophotometry *(Japanese)* 77−70365
pulsed hollow cathode lamp characteristics 78−67530
pulsed laser excitation source for time-resolved fluoresc. spectroscopy 80−9051
pulsed laser induced molecular fluorescence, exptl. configs. 78−58045
pulsed laser spectroscopic instrumentation 77−18105
pulsed source, for at. and mol. luminesc. spectrometry, signal-noise ratio 77−71381
pulsed Xe light source, programmed command unit 77−79163
radiation energy meas., spectral slit width correction 80−96020
radio-frequency excited pulsed hollow-cathode lamp, absorpt. and emission characteristics 80−89550
rare earth metal plasmas, absorpt. spectra continua, 40 to 2000 Å 78−54471
reproducibility for emission spectroscopy, hollow cathode, glow discharge and sparks 78−3429
semiconductor, physical principle and appl. *(German)* 78−71108
single-beam absorption-emission flame spectrophotometer design *(Russian)* 78−27866

spectroscopic light sources continued
solid laser wavelength identification using reference absorber 78−5513
spark, high-voltage, effect of strong transverse blowing 80−3441
spark BRV source, time resolved meas. of far UV output 79−98454
spark source, electronically controlled, adjustable waveform, spectrometric obs. 78−45727
spark source for high degree ionised spectra *(Chinese)* 79−80695
spark sources, air gap or rotary gap types 77−40584
sparks, effect of strong transverse blowing on a high-voltage spark *(Russian)* 78−91183
spectrochemical analysis with glow-discharge lamp *(Japanese)* 78−85262
spectrofluorometer components, state of the art *(Slovak)* 78−56940
spectrophotometer, combined double modulation of source, modulation functions 77−57400
storage ring synchrotron radiation far IR source 79−30577
stratified pulsed discharge, struct. and emission 79−64946
street lights, high press. vapour lamps, spectroscopic expts. 77−22356
submillimetre laser sources for magnetic resonance spectroscopy, standard frequencies 77−13788
submillimetre laser spectroscopy, complete freq. coverage with CH_3OH, CH_3OD, CD_3OD, CH_2CF_2 78−25860
submillimetric waveguide laser for gas spectroscopy 80−33022
surface spark discharges high current, light emission props. and appls., book contrib. 79−77449
synchronously pumped dye laser, freq. doubled, appl. to reson. Raman spectroscopy 79−12869
synchrotron and laboratory discharge light sources comparison 79−10371
synchrotron radiation, appl. to elec. struct. determ. of solids 77−20882
synchrotron radiation, appls., review 78−9010
synchrotron radiation, for X-ray fluorescence analysis 79−48009
synchrotron radiation for VUV and X-ray spectroscopy, lecture 78−24870
synchrotron radiation source, monochromatic, for fluorescence spectroscopy 78−296
synchrotron radiation sources, props. and characts. 80−62729
synchrotron radiation spectroscopy, review *(German)* 79−40624
synchrotron radiation spectroscopy instrumentation and appls., book contrib. 80−4782
synchrotron radiation used for fast fluoresc. obs. 80−62736
synchrotron radiation with single photon counting or phase shift techniques, for fluoresc. lifetime meas. 79−13841
synchrotron sources for low energy AES 80−77913
tesla discharge as spectroscopic source for excimer laser transition study 80−274
three-electrode DC Ar plasma source for optical emission spectrometry 80−62735
time-resolved fluorimetry, cross-correlation method 79−79331
tunable diode laser, for high resolution matrix IR spectroscopy 78−45739
tunable diode lasers, construction and operating characts. 77−27304
tunable dye laser, for picosec. spectroscopy, 400-500 nm 78−82988
tunable dye laser, N_2 pumped, setting up, high resolution spectrosc. obs. 79−86177
tunable IR solid-state laser characteristics and principles 80−87406
tunable laser spectroscopy, of semiconductors, review 79−93231
tunable lasers, conf., Tsakhkadzor, USSR (Jan. 1976) 77−23706
two-wavelength double-pulse tunable dye laser for differential absorption lidar 77−21939
undulator radiation source, specified spectrum 79−10251
UV, broadly tunable, using stimulated Raman scatt. in H_2 80−9963
UV, comparison of sources for 120 to 200 nm range *(German)* 79−85186
UV, LV deuterium lamp as secondary radiation standard 78−77998
UV, miniature long lived cold cathode discharge 77−19375
UV, syncyrotron orbital radiation appl. *(Japanese)* 78−25941
UV continuum source, use of laser generated plasmas 79−94314
UV glow discharge source, appl. in spectrochem. anal. of steel products *(French)* 80−71997
UV inert gas monochromated discharge lamp, addition to XPS spectrometer 78−89601
UV light source, laser plasma using grooved Ta target 79−19096
UV radiation standard sources *(French)* 77−61142
UV spectral emission scales, synchrotron radiation appl. 78−78001
vacuum far-ultraviolet, hypersonic dense plasma *(Russian)* 77−49789
vacuum UV energy brightness spectral standard source, 0.05-0.25 μm range 77−79909
vacuum UV line source, He lamp, for photoelectron spectroscopy 78−94419
vacuum UV pulsed controlled source 78−87115
vacuum UV radiation from DORIS storage ring, high resolution monochromator 77−7165
vacuum UV source, 60-200 nm 79−32014
vacuum UV source chamber, US gas jet evacuation system 77−13763
vacuum UV tunable anti-Stokes light source, He 1s2s $^1S_0$ isotopic shift meas. 79−18149
VUV and soft X-ray source, using anti-Stokes emission 79−46024
VUV light source, transfer standard, low-current AR arc with MgF_2 window 79−35856
VUV low voltage lamp, prod. using Xe-Kr-Ar mixture continuous spectrum *(Russian)* 78−75451
VUV source, laser induced two photon blackbody radiation from He atoms in glow discharge 78−58102
windowless AR discharge VUV lamp, for matrix isolation spectroscopy, spectrosc. evaluation 78−45730
Ar flash lamp, for vacuum UV spectral region 79−93236
Ar ICP plasma, excitation source for flame at. fluoresc. spectrometry 80−37089
As continuum source, for atomic fluorescence spectrometry 78−45716
Br_2+Ar* lamp, for meas. of Br atom concs. 78−46466
CO_2, continuously tunable high press. monochromatic laser for spectroscopy 80−5762
CO_2 high stability CW waveguide laser, for high resolution saturation spectroscopy 78−71112
CO_2 lasers for selective interactions with matter 77−27296
Cs vapour tunable IR source using stimulated electronic Raman scatt., appl. to HCN (001) relax. obs. 80−9696
D_2 gas discharge lamp as UV continuum source, space appls. 80−36505
D_2 lamps, influence of Ne and Ar on spectral parameters 80−86460
D_2-Ne capillary-arc lamp, optimum parameters 80−95971
F Kα X-ray line, from KF, for excitation of electron spectra 78−29865

spectroscopic light sources continued
Fe Zeeman tuned mag. confined arc lamp, appl. to U 78−17593
H and D atom concentration, using UV H_2-D_2-He microwave discharge lamp, Lyman-α line shape 79−80698
H, discharge lamp, Doppler effects *(German)* 79−44946
H high power arc, standard source of continuum radiation, 53-92 nm 80−44054
H high-power arc as continuum radiation standard source, 53 to 92 nm, VUV radiometry 79−94311
H lamp, organic film form. on windows 77−58412
H lamp using hollow lightguides, optical and operational characts. 80−53395
H-He, discharge lamp, Doppler effects *(German)* 79−44946
H_2 flashlamp light pulse shape calibration, using synchrotron radiation excitation standard 79−72642
H_2 high power tunable IR compressed laser, for spectroscopy 80−48277
H_2 plasma, UV spectral radiance calibration *(French)* 78−12774
HCN, 337 μm tunable radiation in laser-klystron link through Schottky diode or metal-semicond. point contact 78−46714
HCN CW laser, for semicond. magnetospectroscopy *(German)* 77−10948
H_3PO_4, broad-band picosecond light generation by mode-locked ruby laser 79−31989
He I polarised radiation source for surface studies 78−74959
He II, hollow cathode, high resolution photoelectron spectra, stability 78−74700
He II resonance discharge lamp, for UV photoelectron spectroscopy 79−58847
He II resonance lamp for UV photoelectron spectroscopy 79−93232
He II resonance radiation intensity, He gas press. depend. 77−84553
He, low press. discharge lamps, reson. line broadening of O I and N I 78−9123
He, pulsed microwave discharge, vac. UV emission characts. 77−35408
He resonance source for photoelectron spectroscopy, impurity lines 77−14787
Hg high pressure sources, spectral distribution of irradiance, 240 to 600 nm *(German)* 77−79910
Hg vapour DRT-220 lamp temp. and Hg 253.7 line intensity relationship 79−2836
I_2 laser, quasi-tunable IR emission, appl. to absorption meas. 77−42551
Kr_2 resonance lamp in vac. UV, new developments 79−32017
Kr^+ ion laser, mode-locked near UV output, chem. and appls. 79−45966
KrF* laser, generation of high-spectral-brightness tunable XUV radiation at 83 nm 80−91846
Li heat-pipe arc lamp as spectroscopic source 80−102787
$LiIO_3$, pulse-period parametric oscillator, tunable 0.63 to 3.4 μm, for nonlinear spectroscopy 78−59083
$LiNbO_3$ computer-controlled IR parametric oscillator source 77−19365
$LiNbO_3$ computer-controlled Nd:YAG-pumped parametric oscillator 77−54758
$LiNbO_3$, optical parametric oscillator, for IR linear absorpt. spectroscopy 79−7180
$LiNbO_3$ parametric generator, producing high power tunable ps visible and IR pulses, spectroscopy appl. 79−46003
N_2 high power tunable liq. Raman laser, for spectroscopy 80−48277
N_2 laser, TEA, for sub ns spectroscopy, modified elec. field 78−17964
NH_3 laser, resonantly pumped, for spectroscopy 80−48277
Nd:YAG pumped tunable sources, appl. to spectroscopy 80−58576
Ne hollow cathode discharge tube, spectral line intensities, rise time 80−103212
Ne-filled discharge lamp, for AAS isotope anal. of B 78−20097
Pb salt DH lasers for IR gas spectroscopy 77−19325
$Pb_{1-x}Sn_xSe$ CW and pulsed diode laser spectroscopy of $^{14}NH_3$, $^{15}NH_3$ mols. 79−26980
$Pb_{0.93}Sn_{0.07}Te$ tunable diode laser for IR spectroscopy 78−33511
Rb vapour D-line profiles for spherical lamp *(French)* 78−18032
SiC cavity radiator, spectral emissivity and radiance 77−83939
U emission standard, wavenumber meas. by Fourier transform spectroscopy *(French)* 77−57407
Xe, discharge lamp, RF excited electrodeless, atomic fluoresc. spectrometry 77−86395
Xe discharge lamp, tubular, with short discharge, characts. *(Russian)* 79−32019
Xe, discharge lamps, 147 nm resonance line production 77−39497
Xe high pressure lamp for polymer spectral sensitivity determ. *(German)* 80−61119
Xe lamp, for vibrational circular dichroism spectrometer 78−54476
Xe optical discharge radiation source 78−87116
Xe, resonance lamp in vac. UV, new developments 79−32017

spectroscopy
see also beam-foil spectroscopy; computerised spectroscopy; electron spectroscopy; Fourier transform spectroscopy; interference spectroscopy; magnetic resonance spectroscopy; mass spectroscopy; matrix isolation spectroscopy; microwave spectroscopy; modulation spectroscopy; optical double resonance; photoacoustic spectroscopy; quantum beat spectroscopy; radiofrequency spectroscopy; Raman spectroscopy; spectroscopy computing; time resolved spectroscopy; tunnelling spectroscopy; two-photon spectroscopy; X-ray spectroscopy
Abel inversion applied to plasma spectroscopy, interactive method 79−23447
absorption coefficients at 632.8 nm intracavity laser meas. 78−8454
absorption spectra, collision-broadened lines, information anal. 80−22433
absorption spectra in 100-900 Å region, device design 79−54202
absorption spectroscopic technique using waveguide loss meas. 78−45729
absorption spectroscopy for temp. meas., principle 78−54375
acoustic spectroscopy, H bonds investigation, N-butyl acetamide association in solns. 80−5891
active polarisation spectroscopy by combinational light scatt. *(Russian)* 78−78006
advances in electron physics, book 80−8742
Aerosil, diffusion coeffs. and characterisation by photon correl. spectrosc. *(German)* 79−29418
alkali halide pelleting technique for solid sampling in IR spectroscopy 78−87171
alkali metals, vapour states, laser spectroscopy and applic., review 80−68260
analytical and quality control techniques, review 80−98989
anion exchange, in tablet pressure for IR spectroscopy *(Russian)* 78−95927
anticrossing spectroscopy appls. 80−23379

spectroscopy continued
applied IR spectroscopy, instrumentation, sampling techniques and appl., book 80−46745
astronomical, high-resolution Michelson interferometer for Isaac Newton Telescope 78−4105
astronomical spectrogram calibration by multiple exposure 77−22107
astronomical spectroscopy, review 79−12408
astronomical spectroscopy, symposium (Victoria, Canada, 20-22 October, 1976) 77−78645
astronomical submillimetre line, detector-telescope systems 77−49305
astronomy, appl. of SIT vidicon detector system for Palomar 1.5 metre telescope 79−92674
astronomy, rotating body obs. via high-resolution spectroscopy, appl. to Sun 78−96403
astronomy, spectrograph with echelle-type grating *(Polish)* 80−26745
atmosphere, submillimetre wave spectroscopy 78−7796
atmospheric spectroscopy and pollution monitoring by tunable dual CO_2 laser 78−3977
atom, narrowed optical lines, laser and accel. beam method 78−37770
atomic, in university science course for talented high-school students 78−89282
atomic absorpt. spectroscopy, absorpt. max. in analytical curves 80−86442
atomic beams, high-resolution spectroscopy 78−89557
atomic hyperfine structure, long isotopic chains, on-line spectroscopy 80−37903
atomic spectroscopy using synchrotron radiation, book contrib. 80−4779
atomic transition cross section meas. by saturation flux with laser oscill. 79−27114
atomic-and-molecular beam, two-freq. separated oscillating fields technique 79−21715
atoms, absorpt. spectra, flame and discharge laser irrad., opto-galvanic spectroscopy 80−42272
atoms, laser excited, reactive collisions 80−66793
atoms near a wall *(Dutch)* 78−70972
ATR, for, film absorpt. coeffs. meas. 78−37073
ATR spectroscopy, Goos-Hanchen shift and effective sample thickness 77−49791
axisymmetric medium, at. reson. level population meas., emission method *(Russian)* 77−68140
baseline variations, elimination by ultra-low freq. filtering 80−90901
beam maser spectroscopy, appl. to Zeeman effect determ. in H_2O_2 78−90152
beam spectroscopy, Hadamard transform appl. 80−62741
biomolecules, Fe-containing, appl. of spectroscopy 79−24956
biophysics, laser techniques, reviews 77−90975
boride coatings on C and alloy steel, spectroscopic thickness determ. 80−85099
Brillouin scattering frequency high-precision meas., rel. to hypersound velocity meas. 80−27349
Brillouin spectra, interferential spectrometry 77−178
calibration, using Edser-Butler bands, for teachers 79−21504
calorimetric detection of excited electronic states 77−41692
capillary waves, active four-photon spectroscopy 79−41699
CARS, pulsed dye laser system, computer controlled 78−62241
cathodoluminescence high-resolution anal. system 77−13806
chemical spectroscopy and dynamics, higher-order susceptibility effects, laser appls. 79−40625
chemistry, laser applications, review 80−45535
chemistry and spectroscopy 78−89556
ciliary activity obs. by laser light-scatt. spectroscopy 78−36076
circular dichroism, sum rules, SCF mol. orbital theory 78−58059
circular dichroism in presence of birefr. and linear dichroism, meas. method 78−27178
COCHISE: laboratory spectroscopic studies of atmospheric phenomena with high sensitivity cryogenic instrumentation 80−95166
coherent and nonlinear optics, conf., Leningrad, USSR (Jun. 1978) 80−98753
coherent forward scattering atomic spectroscopy for multielement anal. 80−57389
coherent optical spectroscopy, transient effects, theory 77−49780
coherent optical spectroscopy of molecules and molecular beams 78−82054
coherent optical transient spectroscopy in flames 79−39147
coherent optical transients, atom, mol. and solid spectroscopy using lasers 77−53986
coherent pulse, using dye laser oscillator-amplifier system 77−83892
collision effects on nonreson. interactions, nonlinear spectrosc. obs. 80−23496
colour film spectral sensitivity meas. by Hadamard spectrosensitometry 77−26414
complex spectrum, band parameters determ., minimisation algorithms operation *(Russian)* 78−74074
complex spectrum, computer separation, optimisation *(Russian)* 78−82051
composite transducer for longitudinal strain modulation for ESR and optical spectroscopy 79−12791
computer-assisted learning methods 79−84906
computer-simulated laboratory experiments, teaching 79−40339
condensed phases, polarisation spectroscopy 78−89559
conference, Grenoble, France (Sept. 1975) 78−3424
conference, group theory and application to spectroscopy, Nova Scotia, Canada (Aug. 1978) 80−41947
consecutive reactions, reaction rate constants, absorbance meas. using isosbectic points 77−73433
cooling and trapping of atoms and mols., by reson. laser field 77−3321
correlation method for light beating spectra, entropy fluctuations of crit. mixture 77−10119
correlation spectrometry meas. of air pollution, 2nd CEC remote sensing campaign, report 78−88908
correlation spectroscopy, rotational and vibrational relaxation autocorrelation functions 80−32856
correlation spectroscopy appl. to dispersion from tall stacks 78−3932
cryogenic spectrometry for airglow and aurora studies 77−70886
crystal field theory, finite symmetry adaptation in spectroscopy 80−43032
cyclohexylcyclohexanes, substituted, anisotropic liq. cryst. solvent for optical absorption spectroscopy 78−45724
data conditioning by digital averaging 79−12867
data sampling and smoothing, review 77−34031
spectroscopy continued
decay time meas., photomultiplier wavelength depend. errors, correction method 79−30558
deconvolution and background subtraction by least-squares fitting with prefiltering 78−31718
depolarised light scatt. spectrom. double scatt. effects 79−42978
depolarised multispectral laser scatt., target classification 78−50846
derivative, fundamentals and practical examples *(French)* 78−58055
derivative, understanding its appl. 80−77875
derivative spectra, anal., reconstruction *(Russian)* 78−82050
derivative spectroscopy, spectra differentiation with digital computer 80−77878
diatomic molecules, sub-Doppler laser spectrosc. 80−52320
difference frequency generation with intracavity absorption 77−42567
differential spectroscopy of charged particle beams, cylindrical mirror 77−50600
diffuse reflect. spect., standards and calibration rel. to chromatography 77−56278
diffuse reflectance spectroscopy, applics., standards and calibration 78−32848
diffuse scattering spectroscopy, quantitative processing of dynamic curves 78−54470
diffuse scattering systems 78−62229
diffuse spectral reflectance, calibration of standards 77−53983
digital deconvolution of spectra, noise amplification and resolution improvement 78−86339
digital lock-in detection technique and appls. 79−49303
diode laser spectroscopy with simultaneous freq. calibration 78−89566
dispersion correlation spectroscopy, mask optimisation procedures 77−73857
dispersion induced circular dichroism, spectroscopic appls. 77−27101
dispersion vs. absorption curve method for distinguishing peak position distrib. from linewidth distrib. 80−4775
distorted spectra, numerical image correction technique *(Russian)* 79−13921
distortion elimination by eigenfunction method 79−7087
Doppler free intermodulated optogalvanic spectroscopy, technique description and sensitivity 80−52333
Doppler line convolution by Gaussian instrument function, appl. to diode laser 80−82830
Doppler method for dispersion analysis of cryosols and suspended microadmixtures in cryogenic liquids 79−75535
Doppler-free, feats and fancies 80−43001
Doppler-free intracavity polarization spectroscopy using elliptically polarized light 80−5537
Doppler-free many-photon spectroscopy 79−35845
Doppler-free polarisation spectroscopy, using linear polarised light 79−3440
Doppler-free stimulated-emission technique, using optically pumped laser 78−93765
double collision spectroscopy 80−58378
double-quantum saturation spectroscopy, laser and RF, appl. to H 80−77880
doubly resonant three-photon spectroscopy, appls. 79−71534
dye laser applications 79−55130
dye laser spectroscopy of biomols. 77−86444
dye lasers, spectroscopic appls., soln. chem. effects 77−40568
Ebert plates, wavelength determ. using microphotometer with micrometer attachment 78−16853
echelle spectrograms reduction, single procedure 80−56713
echelle spectroscopy, astronomical applications 77−25951
education, blackbody radiation and Planck function, derivative spectroscopy expt. 80−77563
electric dichroism spectroscopy 78−1013
electrical engineering material structure research, spectroscopy appln. *(Rumanian)* 80−4774
electro-optic laser technique for probing coherent and incoherent decay processes 77−75338
electro-optics, conference, Utrecht, Netherlands (Oct. 1978) 80−31420
electrochemical reactions, visible region internal refl. method investig. 77−60069
electrochromism, apparatus for gas phase studies in vacuum UV 77−50562
electrographic instrumentation for ultraviolet imaging and spectrography 80−46399
electronic absorption spectra, digital anal. appls. 78−8448
electronic emission spectroscopy, instrumentation, review 78−29166
electrothermal atomisation, atom form. and dissipation 80−57388
environmental samples, spectrometric method for meas. of hard β-emitters 80−94135
ethane, diode laser spectra, baseline variations, elimination by ultra-low freq. filtering 80−90901
EUV and soft X-ray spectroscopy techniques *(Japanese)* 77−65058
exciton spectroscopy, polariton dispersion 80−54613
exponential clipped photon autocorrel. spectra, data anal. 79−2837
extremum position and confidence limits, determ. of absorpt. max. in wide bands 80−22188
faint light detection and spectrometry, book 77−25950
far IR, appl. of far IR lasers in semiconductor research 80−31914
far IR Josephson junction voltage-tunable differential heterodyne spectroscopy 79−30578
far IR laser spectroscopy in liquid and solid states 77−38041
far IR laser thermal spectroscopy of superconductors 80−60144
far IR Michelson interferometry based on fast plasma scanning 77−31513
far IR research, grating era (1925-60) 78−4455
far IR research, Rubens era (1892-1925) 78−4454
far IR transmission and reflection spectroscopy in layer crystals 80−76019
far IR transmission meas., using optically pumped methyl alcohol laser 77−5932
far IR-submillimetre range, Fourier and laser spectroscopy comparison, meas. in V_3Si film 79−93237
far IR-submm spectroscopy using tunable laser 78−4713
far UV spectroscopy using synchrotron radiation 77−67513
fast atomic beams, collinear laser spectroscopy 78−37078
flame spectroscopy, free atom fractions and equilib. comp. calcs. 80−22438
flames, laminar, rise velocity meas., spectroscopic method 78−74064
flash desorption, thermocouple-controlled temp. programmer 79−49224
fluctuation spectroscopy, at. spontaneous emission 77−434

spectroscopy continued
fluctuation spectroscopy, determ. of chemical reaction rates based on optical density fluctuation 78−27730
fluorescence, appl. to airborne monitoring of surface water pollutants 79−2397
fluorescence, moment index displacement theory 77−57395
fluorescence, of subpicosecond states in liquids 79−45758
fluorescence correlation, clip-correlator *(Russian)* 80−42270
fluorescence correlation spectroscopy, effect of clipping 78−55198
fluorescence correlation spectroscopy, profile of focused collimated laser beam near focal minimum 80−43386
fluorescence decay signal analysis by photon time-correlated counting 78−49910
fluorescence intensity correlation, photon counting using clip-correlator *(Russian)* 80−42271
fluorescence polarisation measurements, correction for finite apertures 78−21224
fluorescence spectrometry, beam splitter and cell window errors 80−31897
fluorescence spectroscopy, advantages at low quantum efficiency 77−52684
fluorescence spectroscopy, in study of biochem. processes, review 78−11784
fluorescence spectroscopy, rapid scanning of photochemical anthracene in polychlorinated alkanes 80−86440
fluorescence spectroscopy applied to biopolymer dynamics and struct. 77−60329
four-wave mixing spectroscopy, coherent cancellation of background 80−91842
free exciton reflection spectroscopy for study of deep traps in GaAs and InP 79−60761
frequency metrology for Raman lasers, spectroscopy in 5.3 μm region 77−10935
frequency metrology in 5.3 μm region, freq. synthesis of Raman laser 77−19277
fundamental techniques, spectrographs and spectrochem. anal. *(Japanese)* 78−8452
gain probing by intracavity dye laser spectroscopy 77−7092
galvanic detection of optical absorpt. in gas discharge 77−15251
gas chromatography-IR spectroscopy interface, optimised sampling techniques 77−77831
Gaussian-Lorentzian light, photon counting distrib. factorial moment, spatial coherence 80−83571
generating function techniques 80−44162
geological materials, spectrographic thermometry and manometry using DC arc 78−16796
group theory, space and point group factorization, appl. to crystallography and spectroscopy 79−60295
high power resolution using photon statistics *(Spanish)* 79−21818
high resolution laser spectroscopy, review *(German)* 79−26138
high resolution spectroscopy of atoms and mols., without Doppler broadening, laser techniques 77−54631
high resolution tunable laser spectroscopy, review 77−74515
high temperature gas and vapour characterisation, conf., Gaithersburg, USA (Sept. 1978) 80−53910
high temperature techniques, achievement of high-temp. and material selection *(Japanese)* 78−45726
high-degree ionized spectra excited by spark source and its application *(Chinese)* 79−80695
high-pressure techniques and lab. equipment availability 77−57399
high-resolution, appl. of photon echo method 77−23720
high-resolution, use of $Pb_{1-x}Sn_xTe$ injection laser 79−76714
high-resolution, with tunable dye laser, appl. to SO_2 77−22601
high-resolution laser spectroscopy, techniques and applications 77−57403
high-resolution laser spectroscopy with minute samples 78−17822
high-sensitivity, high-resolution spectroscopy techniques 79−40626
high-speed processes, spectral characts. investig. method 79−93227
high-speed processes, spectrometric investig. method *(Russian)* 78−74076
hole-burning spectroscopy, electron phototransfer in reaction centres of Chlorella photosystem I 80−81561
hook spectra, evaluation limitations 80−90905
hot gases, tunable diode laser spectrometry, noise reduction 80−31909
hypsorhodopsin, squid, form., picosec. spectrosc. obs. 79−39183
ICP background emission, highly structured 80−73467
image, dissector tubes, echelle spectrographs, design considerations 80−91918
image spectrograms of three-dimensional objects, thickness meas. appl. 79−7228
imaged intracavity laser absorpt. spectroscopy 77−41703
inductively coupled plasma emission spectroscopy, sample introduction method *(Japanese)* 78−82045
infrared heterodyne spectroscopy in astronomy 78−85859
inner level spectroscopy with synchrotron radiation, theoretical aspects, book contrib. 80−4778
instrument developments, overview *(French)* 78−293
integrating sphere accessory, spectrosc. meas. of horizontal surface from above 80−86443
intensity correl. spectroscopy, spherical particle continuous distrib. meas. 78−21228
internal reflectance appl. to surface fluorination effects in polyethylene and polypropylene 78−86340
internal reflection, IR characterisation of surfaces and coatings 78−71161
internal-reflection spectroscopy 80−18019
intracavity, quantitative information acquisition on absorpt. line parameters 78−49911
intracavity absorpt. spectroscopy, short pumping pulses and restricted mode competition, numerical anal. 77−82607
intracavity absorption, CW dye laser, Ba at. beam line shape obs. 80−47120
intracavity absorption, using optical parametric oscillator source 77−10976
intracavity absorption model in CW multimode dye laser 80−47119
intracavity absorption spectroscopy, using semicond. injection laser 79−7157
intracavity absorption spectroscopy at reduced pressures, using dye laser 80−47118
intracavity absorption spectroscopy theory, mode competition 78−32890
intracavity absorption spectroscopy theory with singly resonant optical parametric oscillator 80−23742
spectroscopy continued
intracavity absorption spectroscopy utilizing sweep dye lasers 79−89015
intracavity dye laser technique for spectroscopic and kinetic meas. of transients 78−62239
intracavity enhancement of absorpt. in nanosecond regime 78−78839
intracavity inverted Lamb dip, of laser with nonlinear absorpt. cell 77−14765
intracavity laser spectroscopy, absorpt. line profiles determ. 78−12776
intracavity laser spectroscopy, appl. of OH-stabilised F_2^+-centre laser 80−32999
intracavity laser spectroscopy, CH_3CHO decomposition reaction obs. 79−61858
intracavity laser spectroscopy, spectral distrib. kinetics 78−1293
intracavity laser spectroscopy, with continuous and quasicontinuous operation lasers *(Russian)* 78−37080
intracavity laser spectroscopy sensitivity, saturation absorpt. influence 79−63312
intracavity spectrosc., enhancement calc. for single mode laser 80−69426
intracavity versus extracavity absorpt. cells, fractional absorpt. with single-mode laser 77−23700
intraresonator high-sensitivity meas., using Nd:YAG laser with min. amplitude noise 79−63317
intraresonator spectroscopy, laser stimulation optimisation of gases 80−77881
ion beam, high resolution spectroscopy, laser beam-fast ion beam interaction technique 77−6959
ion scattering spectrometry for surface studies, high-resolution energy analyser 77−36333
ion source, saddle-field type, gas depend. characts., at. spectroscopy appls. 78−78039
IR, capabilities of Pb salt tunable laser diodes 77−82630
IR, gas phase species, in high temp. flow tube 80−52235
IR, heterogeneous catalysis research appl., literature review *(German)* 78−53256
IR, high-temp. measuring cell, appl. to benzene adsorption on γ-alumina *(German)* 79−28757
IR, microsampling techniques 78−16862
IR, of mol. beams 77−46655
IR, of supercooled gases 77−23574
IR, prep. of transparent halogenide sections 77−67514
IR, radiative heat transfer determ. in vacuum-powder insulation 77−13759
IR, simultaneous computer acquisition of IR, microwave and Raman spectral data *(Japanese)* 80−4776
IR, solids at high press., shear-stress-induced phase transitions 77−32368
IR, techniques, detectors, appls. 77−5934
IR, ultra-high resolution, review *(Japanese)* 80−31912
IR, using tunable diode laser, review 78−82061
IR, with tunable diode laser *(German)* 80−43361
IR absorpt. spectra, broad, anal. by nonlinear conversion to optical freq. *(Russian)* 77−49793
IR absorption spectroscopy, ultrahigh-resolution, using tunable PbTe laser diode 79−75628
IR and millimetric waves and applications, conf., Miami Beach, USA (Dec. 1979) 80−57009
IR and Raman spectroscopy, molecular structural anal. appls. 79−35859
IR and sub-MM spectroscopy, conf., Bonn, Germany (Mar. 1977) 78−12778
IR astronomical appl., current developments review 78−61737
IR astronomy, laser heterodyne techniques appl. to interstellar submillimetric lines detect. 79−44377
IR ellipsometric spectroscopy, appl. to study of adsorbed species 80−39434
IR emission spectroscopy, double-beam reflectance measuring device 79−80704
IR gas spectroscopy, appl. of Peltier cooled PbSe DH laser 77−23690
IR heterodyne, of atm. O_3 77−91267
IR heterodyne technique, appl. to NH_3 lines near 11 μm 78−5230
IR high-resolution, using optically pumped continuously tunable mol. lasers 78−13678
IR instrumentation, design study, for stratospheric research 80−17391
IR intensity measurements, by band contour anal. 78−29182
IR internal reflection spectroscopy, appl. of diamonds 78−24871
IR internal reflection spectroscopy, high reliability, simplified theory 80−105722
IR lasers and laser techniques in mol. spectroscopy, book contrib. 78−8455
IR physics, conference, Zurich, Switzerland (Mar. 1979) 80−4783
IR polarisation measurements, resolution of complex band shapes 79−12873
IR radiation, parametric up-conversion to visible range, review 80−64104
IR reference spectra, for GC-IR, presentation specifications 80−31908
IR reference spectra, library retrieval based on intensity data 79−96380
IR spectra calibration using spline functions 77−27050
IR spectra deconvolution in real time 77−38034
IR spectral band transmittance, modelling, Prony's method 78−70202
IR spectrometric method for meas. of slight heavy water enrichment in natural water *(French)* 80−104718
IR spectrometry, review of literature 1976-1977 78−85223
IR spectroscopy appl. to charged part. dose meas. in cellulose triacetate 78−94145
IR spectroscopy at very high press., refr. beam condenser for use with diamond anvil cell 77−71389
IR spectroscopy of gas chromatographic peaks, high resolution 78−20101
IR spectroscopy of minerals, appl. to identification 79−62589
IR spectrum deconvolution beyond the Doppler limit 80−86467
IR transmission spectroscopy, variable temp. UHV cell for surface studies 78−41361
IR tunable diode laser spectroscopy, techniques and calibration with HCN ν_2-lines 79−71542
IR tunable laser for semiconductor multiphoton spectroscopy *(French)* 80−82836
IR vibrational, frequency standard in 17 μm spectral region, use of N_2O ν_2 band 79−63991
IR vibrational spectroscopy, modern trends, book 78−13503
IR-ATR spectroscopy, appl. to struct. investigation of biological material in aq. environment 80−61735
isotopic filtration of radiation of dye laser, in-resonator spectroscopy *(Russian)* 77−54752

spectroscopy continued
isotopic isomers, spectroscopic obs. 80−53009
iterative deconvolution, effects of error on convergence 77−53849
Jahn-Teller, research projects at IROE Institute (Firenze) *(Italian)* 80−56668
kinetic IR spectroscopy IR, appl. to biochem. systems 80−98178
Lamb's laser theory, spectroscopic techniques 79−35847
Lamb-dip spectroscopy, collision broadening theory 77−83659
Lamb-dip spectroscopy, using nonlinear absorption, appls. 78−89560
large molecules, picosecond relax., fluoresc. spectroscopy, solvent effects 78−58737
laser, coherent transient effects 78−1112
laser, Doppler-free, bibliography 78−302
laser, Rabi oscillations, double-pole decay 79−86151
laser, summer school, Les Houches, France (June 1975) 78−301
laser absorption calorimetry, automation 78−74084
laser absorption spectroscopy, sensitivity enhancement using Faraday effect 80−86446
laser applications to chemistry, overview 79−58800
laser bandwidth and wavelength stability measurements using self-scanning linear diode arrays 78−86343
laser beam selective interactions, elementary processes 77−27034
laser beams, high intensity, spectral purity anal. 77−88823
laser broadening technique mode competition 78−29991
laser fluoresc. spectroscopy using pulse hollow cathode lamp 80−27973
laser fluorescence spectroscopy, high resolution, in deep blue spectral region 77−82622
laser heterodyne spectroscopy for stratospheric trace constituents meas. 80−109257
laser induced fluoresc. spectroscopy, using induction heated oven, appl. to U 78−21230
laser induced fluorescence spectroscopy, saturation effects 77−44526
laser interaction with matter, nature of light, nonlinear spectroscopy 77−50712
laser interactions, conf. Tsakhkadzor, USSR (Jan. 1976) 77−23706
laser intracavity spectroscopy, absorpt. coeff. determ. of threshold generation characts. *(Russian)* 79−49302
laser intraresonator spectroscopy, competing-beams method sensitivity *(Russian)* 79−93228
laser magnetic resonance using optically pumped far IR laser 77−54725
laser nonlinear spectroscopy polaris. selective optical heterodyne detection 79−58798
laser polarisation, level crossing in forward scatt. 80−43004
laser polarisation spectroscopy, optical anisotropy, appls. 78−82056
laser saturation spectroscopy with optical pumping, Na, Ba atomic-resonance absorption transitions 80−47121
laser saturation spectroscopy with optical pumping in Na and Ba reson. transitions 80−52334
laser sideband spectroscopy *(German)* 79−26975
laser spatial saturation spectroscopy, appl. to diffusion process, interaction pot. 77−75341
laser spectroscopic methods 80−62739
laser spectroscopy, appls., conf., Graz, Austria, (Jun. 1978) 79−26137
laser spectroscopy, atom and mol. interactions, conf., Zarogoza, Spain (June 1979) 80−27041
laser spectroscopy, conf., Rottach-Egern, Germany (Jun. 1979) 80−51957
laser spectroscopy, conf., San Diego, USA (Aug. 1977) 78−82052
laser spectroscopy, conf., San Diego, USA (Aug. 1978) 80−13153
laser spectroscopy, finite bandwidth laser excitation, line shapes, non-perturbative effects 80−52332
laser spectroscopy, historical perspective 80−52331
laser spectroscopy, multiphoton and multistep methods, review 79−35842
laser spectroscopy, picosecond processes, review 79−54194
laser spectroscopy, present problems and tunable laser status, review 78−24867
laser spectroscopy, prospects and appls. 79−75610
laser spectroscopy, review of new techniques 78−32893
laser spectroscopy, review of progress 78−82867
laser spectroscopy conf., Jackson Lake Lodge, WY, USA, 1977 July 78−82666
laser spectroscopy in intense magnetic fields, appl. to astrophysical spectra and plasma diagnostics 80−62738
laser spectroscopy in mol. beams, review 80−22446
laser spectroscopy measurement technique, high sensitivity 78−37082
laser spectroscopy of atoms and molecules 79−55002
laser spectroscopy of primary energy conversion in photosynthesis 79−66461
laser spectroscopy of solutions, ultra-short time techniques *(German)* 78−82049
laser spectroscopy uses, multiphoton transitions and Doppler effect elimination 77−57398
laser spectroscopy uses and applics. 77−57397
laser spectroscopy using an optothermal receiver 80−37810
laser spectroscopy using atomic and molecular beams *(Japanese)* 79−35841
laser-acoustic diffraction spectroscopy, mol. dephasing and radiationless decay meas. 78−37667
laser-induced absorpt. line narrowing for ions in crysts., appl. to $LaCl_3:Pr^{3+}$ 78−15196
laser-spectroscopic method, for studying solids with nonuniform spectral broadening *(Russian)* 79−40630
lasers and applications, conf., Dresden, Germany (Mar.-Apr. 1977) 77−83881
lasers and their applications, conf., Dresden, East Germany (Mar.-Apr. 1977) 79−7137
lateral waves along interface, used in detecting surface absorption 78−4707
layer surfaces, reflectivity at 3.39 μm, meas. method, relevance to pipelines 80−52340
line position, identification and comparison of two spectra 80−47956
line shape studies, signal to noise improvement by numerical procedure 78−65981
line shift and half-width meas., accuracy, apparatus function effects *(Russian)* 77−13800
line spectrum intensity determination by standard paper density scaling *(Portuguese)* 80−11965
linear dichroism spectroscopy, and its applications 78−1011
linear laser spectroscopy, review of absorption, opto-acoustic and fluorescence techniques 78−29170
linear laser spectroscopy in collimated mol. beams, single mode tunable lasers appl. to small mols. 80−52339
lipid bilayer, planar, light guide effect, bilayer spectrosc. appls. 79−29509
liquid, reflectivity meas. by gas ionisation, vac. UV 78−294
liquid, thermal lens effect meas. by photomixing method, laser system 77−42577
liquid-solid interface transmission IR spectroscopy 80−98985
long-wavelength IR spectroscopy, obs. of intermol. interactions in condensed medium 80−34927
low temperature crystal absorption meas. using system response corrector 78−86347
low temperature luminescence spectroscopy using pulsed dye laser *(Czech)* 80−86445
low-temperature techniques, review *(Japanese)* 78−291
luminescence lifetime determ., using CW laser beat noise as multifreq. modulated source 77−57406
luminescence spectrometry, pulsed and continuous wave excitation sources, signal-noise ratios 77−71381
luminescence spectroscopy, refractive index correction, quantum efficiencies calc. 80−86444
luminescence spectroscopy using Weierstrass sphere geometry 77−49777
magneto-optical, solid-state, IR and visible regions, MG field production and appl. 79−71491
magneto-optical rotatory dispersion, meas. at absorpt. freq., pulsed field technique 77−59557
magnetospectroscopy of semiconductors, stable CW HCN laser source *(German)* 77−10948
MCD, variable-temp. cryostat design and construction 77−22554
measurement theory, anal. function optimisation, appl. to spectrometry 80−62614
mechanical spectroscopy of organometallic complexes, ring rot. meas. 80−74259
metal ions, in complexes and biological systems, preliminary vibr. assignment method 78−62953
metastable atomic or molecular species, multiphoton transition detection 80−58231
microcomputer techniques *(Japanese)* 78−16855
microspectrofluorometry, low temp., design of cold chamber 78−57144
microwave plasma spectrometry, for trace metals determ., using the discharge 79−16052
mixtures, IR spectra, ratio method anal., computer simulation 77−71387
molecular, synchrotron radiation appls. 80−53166
molecular, with coherent radiation sources, review 77−3343
molecular beam technique, adiabatic passage by Zener's theory *(French)* 79−870
molecular beams, IR spectroscopy 78−89570
molecular electro-optical emission, for excited state dipole moment determ. 78−62230
molecular electronic spectra, appl. of composite wall hollow cathode source 77−19376
molecular electronically excited states, small mols., vis. and UV laser techniques, book contrib. 78−9277
molecular fluorescence signal sampling, using ultrafast optical Kerr shutter, book contrib. 77−31140
molecular IR and RF spectroscopy, IR laser cavity techniques, book contrib. 78−9278
molecular isotope spectra, from unseparated natural mixture, spectrosc. technique 79−31736
molecular kinetic spectroscopy 79−94110
molecular luminescence spectroscopy, image devices and photomultiplier detectors, signal-noise calc. 77−81433
molecular optical spectroscopy, by 90° photon echo, during reson. scatt. and radiationless transitions 78−86978
molecular spectroscopy, conf., Columbus, Ohio (June, 1978) 79−35848
molecular spectroscopy, conf. Frankfurt, Germany (Sept. 1979) 80−51948
molecular spectroscopy, conference, Wroclaw, Poland (Sept. 1977) 78−62951
molecular spectroscopy, holographic recording 78−62954
molecular spectroscopy using synchrotron radiation, book contrib. 80−4780
molecule, absorpt. spectra, flame and discharge laser irrad., opto-galvanic spectroscopy 80−42272
monochromatic atmospheric transmission determination, laser heterodyne spectrometry 80−72653
monochromators, single, appl. in modern spectroscopy *(Hungarian)* 80−91905
monochromators 1980 state and selection criteria *(Hungarian)* 80−73469
multichannel picosecond absorpt. spectroscopy, wide-band, bacterial photosynthesis obs. 79−66462
multiphoton, for mol. electronic struct. investigations, appl. to 4-photon NO ionis. 78−70887
multiphoton excited molecules, double reson. spectroscopy 78−82060
multiphoton ionisation spectroscopy, appl. to Ca, Sr and Ba even- and odd-parity states 78−86973
multiphoton ionisation spectroscopy, sequential, appl. to I_2 79−50163
multiple frustrated total internal refl. based on layer model 78−83094
multiple internal reflectance-IR spectroscopy for quantitative study of leucocyte adhesion 77−56562
multiple internal reflection IR spectroscopy, for eye tissue examination 77−9304
multiplex, limiting values of Fellgett advantages 79−75609
multiplex and high throughput spectroscopy 80−95145
myristyltrimethylammonium bromide, micelle size, press. dependence, photon correlation spectrosc. 80−11953
nonlinear, appl. to biexcitions in CuCl by reson. coherent scatt. 79−8156
nonlinear, coherent ellipsometry of absorbing media 79−71511
nonlinear, dye laser design 77−79852
nonlinear, recoil effects on Doppler-free lineshapes 80−82829
nonlinear, resolvent formalism appl. *(Japanese)* 80−82833
nonlinear absorption spectroscopy of gases 79−63315
nonlinear high resolution laser spectroscopy, review of techniques 78−29171
nonlinear high resolution laser spectroscopy using 3.39 μm He-Ne laser 77−88757
nonlinear laser, gas laser tuning using SAW light diffraction grating *(Russian)* 78−33759
nonlinear laser, gravitational effects 79−67391

spectroscopy continued
nonlinear laser spectrosc., multiphoton transitions 80−84433
nonlinear laser spectroscopy, book 77−71894
nonlinear laser spectroscopy, density matrix methods, review 78−74071
nonlinear laser spectroscopy, inside Doppler line *(Russian)* 78−21231
nonlinear molecular systems, identification by spectroscopic methods 78−29168
nonlinear narrow ultrahigh resolution laser spectroscopy *(Russian)* 78−70974
nonlinear optical echo spectroscopy 80−48357
nonlinear optics, conf., Novosibirsk, USSR (June 1977) 79−36953
nonlinear polarisation spectroscopy, appl. to small mols. 80−52339
nonlinear spectrograph, based on IR radiation conversion in $AgGaS_2$ 79−10360
nonlinear spectroscopy, atomic and molecular, nigh resolution, review 77−50564
nonlinear spectroscopy, collision induced resonant four photon parametric generation 77−3627
nonlinear spectroscopy, conf., Varenna, Italy (July 1975) 77−49778
nonlinear spectroscopy, development and theory 77−49779
nonlinear spectroscopy, Rayleigh Brillouin light scatt. by fluids 77−50731
nonlinear spectroscopy of OsO_4, SF_6 mols., using tunable high-press. CO_2 waveguide laser 80−43054
nuclear, in university science course for talented high-school students 78−89282
one-atom detection by reson. photoionisation spectroscopy, demonstration 77−38742
one-atom detection by reson. photoionisation spectroscopy 77−79706
optical, CW intracavity dye laser spectroscopy, enhancement, pumping power depend. 80−13155
optical, one-photon absorpt., theory 77−34651
optical bed, referenceable and vibr. isolated 78−83129
optical double resonance Stark spectroscopy, using modulation sidebands 77−58051
optical emission and X-ray spectrometry developments *(French)* 80−68263
optical mixing spectra, real-time analysis system 79−67392
optical processor, incoherent, for making 'spectrogram' of 1-D function 80−87528
Optical Society of America meeting, Rochester, USA (Oct. 1979) 80−12841
optical spectra meas. using SAW spectrum analyser 79−21819
optical spectroscopy of solids at low temp., appl. of acoustic thermometry *(French)* 77−87840
optical spectroscopy technique, multiple coherent interaction in separated fields 80−52338
optics conference, Los Alamos, NM, USA (May 79) 80−73095
optics laboratory, undergraduate, in American universities, status 80−62411
opto-galvanic, atomic He, Rydberg series 79−54779
opto-galvanic of tunable gas lasers in electric discharges 78−95977
optogalvanic, CW dye laser appl. 80−43383
optogalvanic, line profiles meas. in He-Ne laser plasma 78−62233
optogalvanic spectroscopy, analytical appls., elec. meas. 78−62231
optothermal detector with pyroelec. sensitive elements, absorpt. coeff. meas. of formaldehyde 79−40634
overlapping components of spectral line, numerical method for separation 78−21227
panorama spectroscopy of an extended laser medium *(Russian)* 79−12868
parametric superluminescence, picosec. spectroscopy 79−55187
peak profiles, Gaussian and Lorentzian, uniqueness 79−12856
permittivity measurement, time domain spectroscopy, transmission method 77−43926
perturbed total internal refl. spectroscopy for pigment film props. *(Russian)* 77−52197
perylene crystallite, photophoretic force, action spectrum determ. 79−50841
phenylcyclohexanes, substituted, anisotropic liq. cryst. solvent for optical absorption spectroscopy 78−45724
phonon spectroscopy, spectral, spatial and temporal 78−83892
photo correl. spectroscopy, colloid size distrib. data anal. 79−58801
photo-deep level transient spectroscopy, capacitance transient spectra with lock-in method *(German)* 79−65512
photodiode array spectrometer, for ICP emission spectroscopy, correl. readout system 78−31726
photoelastic modulators, appl. to polarisation spectroscopy 79−93224
photoelectric convertor for automated spectral measurements 80−22449
photoelectric spectrographic detection, direct reading attachment 80−275
photoelectron, coincidence device for meas. of photons and photoelectrons 77−27205
photoelectron statistics rel. to photon correlation spectroscopy, book 78−25842
photoflash units, chemical and electronic, temporal spectral characts., meas. method 80−95171
photographic development of spectral plates, use of gaseous-lowest agitation technique 77−67520
photographic plates blackening intensification *(Bulgarian)* 79−30590
photographic recording device based on oscillographic delayed-coincidence method 77−38025
photographic recording of single-pulse CO_2 laser emission spectrum, by parametric conversion 79−10357
photographic registration optimisation *(Bulgarian)* 79−44956
photographically recorded spectral lines, of nonuniform half-width, microphotometric errors 78−86337
photon activation analysis, low-energy photon and classical γ-ray spectroscopy 79−29428
photon correl. spectroscopy, macromolecular soln. dynamics, review 79−59603
photon correlation, appl. to liq. interfaces, fatty acid monolayer 79−75608
photon correlation, appl. to liq.-air interfaces, capillary waves study 79−75607
photon correlation, appl. to polarised Rayleigh scatt. in polystyrene near glass-rubber relax. 80−40124
photon correlation, digital correlator with blinker facility 80−37092
photon correlation, spurious pulse rejection circuit 79−71540
photon correlation spectroscopy, appl. to particle size distrib. meas. 79−67456
spectroscopy continued
photon correlation spectroscopy, automatic processing device, microprocessor, laboratory appl. *(German)* 77−40938
photon correlation spectroscopy, biomedical appls. 78−3575
photon correlation spectroscopy, description and applications 80−52337
photon correlation spectroscopy, determ. of particle size distribs. in lipid vesicle suspensions 77−86711
photon correlation spectroscopy, liquid surfaces, effect of instrumental broadening 77−87852
photon correlation spectroscopy, using jet stream dye laser 77−10117
photon correlation spectroscopy for spermatozoa motility eval. 79−92440
photon correlation spectroscopy meas. of bacterial translation 78−44738
photon correlation spectroscopy of light scattered from microscopic regions 79−44933
photon echo spectroscopy of crysts., review 80−83648
photon-correlation spectrsocopy in near UV, large flexible macromol. internal modes obs. 79−75621
photophoretic force, action spectrum determ. 79−50841
photophoretic spectroscopy, broadband 80−86469
photothermal deflection technique for absorpt. meas. in optically thin media, thermal lens effect comparison 80−105717
photothermal spectroscopy, thermal diffusion model 80−9045
photothermal spectroscopy 78−32808
picosecond, 400-500 nm, using tunable dye laser 78−82988
picosecond, appls. to obs. of ultrafast events in bacterial photosynthesis 79−39375
picosecond, mol. dynamics and electron localisation in liquids 79−46548
picosecond, of semiconductors 79−93230
picosecond, review 78−37081
picosecond absorption spectroscopy, photochem. and photobiol. appls. 78−82053
picosecond chromodynamics, appl. to electrons in fluids 79−35850
picosecond emission spectroscopy, appls. 78−86350
picosecond emission spectroscopy with an ultraviolet sensitive streak camera 79−35857
picosecond fluorescence spectroscopy, competing events 78−58051
picosecond phenomena, conf., Hilton Head, USA (May 1978) 79−44940
picosecond pulse techniques in spectroscopy, fluoresc. and other research areas 79−17504
picosecond spectroscopy, anal. using polarisation method 80−13152
picosecond spectroscopy, broadly tunable repetitive laser system using parametric oscillator 79−46006
picosecond spectroscopy using continuous analyzing light, electronic relaxation of pinacyanol in ethanol 80−99517
picosecond spectroscopy using ultrashort laser pulses, appls. 79−54195
picosecond techniques, probe for ultrafast biological process inc. vision 79−8507
picosecond vibrational and electronic relaxation processes in molecules 79−45808
Planck constant, upper limit determ. to freq. dispersion by nonlinear spectroscopy 77−79050
plasma, inductively coupled Ar, development, technique and appls. 79−35839
plasma-optical emission spectrometer, inductively coupled, light scatt. effect 80−86455
polarisation labelling, simplification of NO_2 visible spectrum, rot. vibr. spectra obs. 80−32730
polarisation of fluorescence spectrum for enhanced resolution 77−6827
polarisation spectroscopy, Doppler free intracavity 80−52335
polarisation spectroscopy, high resolution, in strong saturation regime 79−55189
polarisation spectroscopy, high-resolution in 10 μm region 79−6196
polarisation spectroscopy and forward scatt., in Na gas 80−52336
polarisation spectroscopy with ultrashort light pulses 79−44948
polarisation-sensitive nonlinear spectroscopy, improved geometry 80−1285
polarised photofluorescence excitation spectroscopy, triatomic mol. photodissociation to diatomic fragments 80−28054
polarised specular reflectance spectra meas., microspecular apparatus for Cary spectrophotometer 77−5926
polarising power corrections in reflectance spectra 77−22603
polarization props. of spectral apparatus, influence on results of luminescence spectral measurements 80−31900
polyatomic molecule triplet-singlet conversion, by laser spectrosc. technique 79−86002
power reflection spectroscopy, analytical techniques 80−62714
pressure cell for IR investigations of gases 80−83522
pressure-scanned Fermi reson. spectroscopy, appl. to SO_4^{2-} vibr. spectra 79−73937
pulse-height anal., multichannel scaling, signal averaging, SAMCS1 80−47112
pulsed laser spectroscopy, review 79−26140
pulsed laser spectroscopy, using microprocessor controlled data acquisition system 78−86341
quantum electronics, conf., New York, USA (Jun. 1980) 80−90614
quantum optics, introductory lecture 78−25843
quasiline shape distortion, anisotropic absorpt., meas. using unpolarised light *(Russian)* 78−94292
radiation power of lines, spectrophotometric appl. *(Japanese)* 78−8453
radiation pressure in gas for possible spectroscopic use 77−79164
radiative and radiationless transition rate meas. using tunable pulsed dye laser 77−24891
Ramsey fringes, saturated optical absorpt., spectroscopic appls. 77−38021
Rayleigh scattered light, photon counting 77−41683
reaction rate measurement using fluorometric instrument 77−79157
recoil effects in nonlinear spectroscopy, quantum representation of mol. motion 77−39000
recoil ion spectroscopy, prod. of soft X-ray emitting slow multiply charged ions 77−50516
reflectance spectra, meas. press. to 70 kbar by micro-optic system 77−61133
reflectance spectroscopy, metal surface oxidation appl. 78−39958
reflection, of optical coatings 79−61448
reflection spectroscopy, causality calcs. optical consts. determ. as function of wavelength 78−32887
reflection spectroscopy, Kramers-Kronig transformation, validity 77−66468
refractive index continuously recording spectrograph for transparent/opaque insulators and semiconds. 79−17467

spectroscopy continued
relaxation spectrometry, injected white noise as soln. of phase problem 78−76830
resonance fluorescence, high resolution technique 78−42244
resonance ionisation spectroscopy appl. to atoms and mols. in chem.-phys. 80−68259
resonance ionization spectroscopy and one-atom detection 80−22441
resonant internal-refl. prism spectroscopy, using surface, guided and Fabry-Perot EM waves 78−41358
resonant Rayleigh type optical mixing, appl. to ultrafast relax. process obs. 78−42373
resonant Rayleigh type optical mixing, appl. to ultrafast relax. in dye solns. 78−42374
resonant Rayleigh-type mixing spectroscopy using picosec. dye laser system 79−44944
resonant Rayleigh-type mixing spectroscopy using ps light pulses, ultrafast relax. study 80−91834
ring gas laser, freq. synchronisation region of colliding waves 80−83620
ring laser nonlinear resonance appl. for frequency stabilisation and spectrometry *(Russian)* 79−94261
Rydberg constant, determ. from Hα line fine struct. meas. 79−54093
saturated absorption spectroscopy, direct optical resolution of recoil effect 77−18937
saturated absorption spectroscopy, optical feedback effects suppression by phase modulation of refl. light 78−21225
saturation, tunable laser induced grating dip for sub-picosecond relax. meas. 77−75623
saturation laser spectroscopy, effects of truncated Gaussian beam variations 77−31119
saturation spectroscopy, developments and applics. *(Japanese)* 80−4777
saturation spectroscopy, hyperfine component intensities 80−31886
saturation spectroscopy, lineshape, vel. changing collisions *(French)* 78−12765
saturation spectroscopy, radiative-decay-induced four-level crossover signals 78−77997
saturation spectroscopy, recoil component intensity, level degeneracy *(French)* 78−12762
saturation spectroscopy, relax. processes using Lamb's laser theory 78−70194
saturation spectroscopy, with delayed pulses, Lamb dip profiles 78−21221
saturation spectroscopy including collisional effects, for three-level atomic system 80−37099
saturation spectroscopy of atomic vapour three level system, collisional effects, appl. to Na 80−78579
scalable tunable IR laser operating characteristics and limitations 77−54713
scattered light spectroscopy, signal processing by add-subtract digital correlator 77−61053
second derivative UV absorpt. spectrometry, improving analysis 78−45731
secondary laser cavity for weak absorptions 78−92551
selective excitation spectroscopy, particle kinetics 78−82046
semiconductors, transient capacitance instrumentation for deep level impurities spectrometry 77−51816
separated fields method in laser spectroscopy 79−35844
shock tube spectroscopy, using tunable diode laser 77−71890
single frequency intra-cavity spectroscopy, anal. *(Russian)* 78−37079
slit width effect on IR band shape spectra 80−86463
slit widths, normalised, for diffraction-limited IR spectroscopy 77−71388
solar spectrometric research, automation system for on-line signal processing *(Russian)* 80−12659
solid, low temp., absorpt. spectra, thermal detection 77−74522
solid sorption systems, use of IR cell with Si windows 78−299
Space Telescope, prospects for spectroscopic and direct work 78−57444
Spacelab launch conditions for absorption spectroscopy *(French)* 79−8791
spatial frequency resonances in nonlinear absorbing cell 79−31977
spatial resolution enhancement in coaxial light scatt. geometries 77−57393
spectral reflectance curves estimation from multispectral image data 78−32886
spectrofluorimetry, effects of bandpass intensity distrib. spectrum 77−29071
spectrum reconstruction using test response 80−77884
spectrum-hologram, prod. and practical possibilities 80−37098
spin-flip Raman laser appl. 79−72571
split-pulse laser method for attenuation coeff. meas. of transparent liquids 79−17505
sputter-induced optical emission, absolute photon yields 79−45667
Stark effect in Gaussian noise field, three-level system 78−41266
Stark spectroscopy, technique for molecular vibration-rotation spectra *(Japanese)* 77−494
stellar high-dispersion spectroscopy, appl. of McMullan 4 cm electronographic camera 78−73644
stellar radial velocities, meas. via HF absorpt. cell 80−12681
stellar spectra, photographic equivalent widths calibration against solar photoelectric equivalent widths, feasibility 78−73658
stratosphere, laser spectroscopy relevant to photochem. 78−88951
stratosphere, radiometry and spectroscopy from aircraft 77−70890
subDoppler spectroscopy, motional Stark effect in high mag. fields 78−947
subDoppler Stark spectroscopy in crossed elec. and mag. field 78−948
submillimetre spectroscopy, appl. to low transparency samples 77−176
submillimetre spectroscopy, recent advances *(Japanese)* 77−87855
submillimetre waves and applications, conf., San Juan, Puerto Rico (Dec. 1976) 78−4712
submillimetre waves and applications, conference, Guildford, England (1978) 79−31916
subnanosecond single photon counting fluorescence spectroscopy using tunable dye laser excitation 78−86355
subpicosecond techniques, chem. meas. appls. 79−35849
superhigh resolution spectroscopy, coherent phenomena 80−22445
superradiance triggering spectroscopy 80−52324
supersonic jet spectroscopy, appls., teaching approach 80−41996
surfaces, absorption band studies using internal reflection spectroscopy, appl. 79−6194
synchrotron orbit radiation spectroscopy *(Japanese)* 79−26142
synchrotron radiation, appls. 78−74825
synchrotron radiation, spectroscopic appls., review 77−58239
synchrotron radiation, techniques and appls., book 80−5668
spectroscopy continued
synchrotron radiation, use in spectroscopic research *(Japanese)* 79−63311
synchrotron radiation appls., characts. and sources 78−74960
synchrotron radiation spectroscopy, vapour absorpt. cells and beam generating ovens 78−66688
synchrotron spectroscopy, normal incidence monochromator and order sorting problems 77−31129
thermal blooming spectroscopy of dopamine 80−86441
thermal lensing spectroscopy in the condensed phase 79−35851
thermo-optical spectroscopy, detection by mirage effect 80−47116
thermoelectric absorption spectroscopy of polycryst. tetracene film 79−61451
thin film Mossbauer spectroscopy with commercially available spectrometer 77−10152
thin sandwich film photovoltaic analyzer for wavelength meas. in 2000-7000 Å range *(French)* 79−95441
time correlation method for measuring fluorescence decays with CW laser 79−50072
transient line narrowing, laser spectroscopic technique yielding resolution beyond natural linewidth 80−82834
transmission spectroscopy, interference fringe 78−16851
trapped cyclotron resonance spectroscopy of Ar ions 80−53140
triatomic molecules, sub-Doppler laser spectrosc. 80−52320
tunable diode laser spectrometry for line profile determination in second derivative spectra 80−86435
tunable diode laser spectrometry for line profile determination of second derivative spectra, expt. results 80−86436
tunable dye laser, isotope shift meas. at Isolde mass separator CERN *(German)* 78−41863
tunable laser spectroscopy, of semiconductors, review 79−93231
tunable lasers and applications, conference, Loen (1976) 77−54720
tunable lasers applications 79−64270
UHF-plasma torch emission spectrometry by metal hydride generation *(Japanese)* 78−92582
ultranarrow resonance, use in spectroscopy and for gas laser freq. stabilisation 79−59775
ultraviolet, materials anal. appl., using ion excited UV lines from noble gas-ion impact 79−5230
unconventional, conf., San Diego, Calif., USA, 24-25 Aug. 76 77−74514
US, algorithm for relaxation spectra 80−79038
US pulse spectroscopy, stress analysis 77−42788
US spectroscopy appl. in NDT 80−79090
UV, synchrotron radiation as intensity reference 79−75619
UV and light absorption spectrometry, review of literature 1975-1977 78−85222
UV spectral radiance calibration using H_2 plasma *(French)* 78−12774
UV spectroscopy with Copernicus satellite 78−16310
UV/visible absorption, derivative anal. of component bands 80−98984
vacuum ultraviolet wavelength comparison of two copper sources using an imaging system 79−35686
vacuum wavenumbers, rapid calc. method 79−75616
vapours and gases, high-temp. characterisation, conf., Gaithersburg, USA (Sept. 1978) 79−40579
very high pressure spectroscopy, appl. of ruby R-lines in press. estimation 77−18106
vibrational laser spectroscopy, using multiphoton or multistep processes, mol. appls. 78−90151
vibrational spectroscopy of single crystals, review 80−55093
visible and UV, liq. crystal matrix optical props. 80−45102
Voigt functions, nonlinear least square algorithm 80−90900
wavenumber calibration of Pb salt tunable diode lasers, using etalons 78−45738
weak absorption lines, detect. by Nd:glass and dye laser system 78−89561
weakly absorbing object, high resolution spectroscopy, competing beam method 77−57402
XUV, grazing incidence spectrograph-monochromator, 5-900 Å region 79−17506
Zeeman laboratory, history and research work under way 79−5961
Ar ICP emission spectroscopy, appl. to OI spectra 80−91473
CaCl, $B^2\Sigma-X^2\Sigma$ transitions, rot. anal. by laser spectroscopy 80−91536
H, Balmer-α line, high resolution spectroscopy techniques 80−52915
H_2SO_4, vapour, foreign gas broadening diode laser spectroscopy in IR 78−36261
I_2 saturation, multiwavelength stabilisation of an Ar-Kr ion laser 80−28282
I_2, use as test mol. in modern spectroscopy, review 78−90317
Na_2, mol. spectroscopy by photodeflection in supersonic nozzle beam 79−54995
SiO_2 hydrosols, diffusion coeffs. and characterisation by photon correl. spectrosc. *(German)* 79−29418

spectroscopy applications of computers *see computerised spectroscopy*

spectroscopy computing
see also computerised spectroscopy
16-channel analog store and multiplexer unit 79−45614
168/E microprocessor for offline data analysis 80−58102
A/D conversion, improved pulse height store 80−14054
ABSORB, absorption of muonic X-rays in P and Se allotropic modifications 80−23577
absorption line profiles, instrumental spectral resolution effects 77−6726
acridine orange dye soln., dimerisation equilib., absorpt. spectra least squares anal. 79−50007
activation analysis, gamma-ray data automatic interpretation, computerised 77−44548
activation analysis, low-energy photon spectra, nonlinear least-squares fitting program 79−1987
activation analysis, photopeak area computation methods 78−11593
activation analysis, photopeak integration, quality assurance of computer programs 79−1986
activation analysis and γ-ray spectroscopy, conference, Mayaguez, Puerto Rico (May 1978) 79−1983
aerosol loaded filters, X-ray fluoresc. anal., absorpt. corrects. calcs. 78−7311
AES, by computer *(French)* 80−7890
alkenes, IR absorpt. curves calc. using standard fragments computer library 80−982
alpha spectrum anal. program 78−29692
analogue-digital function generator, for pulsed AAS *(Russian)* 78−70199

spectroscopy computing continued
analysis code for automated reduction of gamma ray data 78−23978
analytical information processing, television methods appls. 80−89568
anthracene, fluoresc. of cryst., Monte Carlo computer method, refl. and reabsorpt. *(German)* 78−68561
arc intensity distortion by transverse oscills., method of statistical regularisation *(Russian)* 77−48746
artificial intelligence for chem. inference, automatic rule formation in mass spectroscopy, meta-DENDRAL 77−18775
atomic emission spectrometry, blackening transformation parameters and computers use *(German)* 80−30300
atomic K and L X-ray line widths determ. 77−42265
atomic spectra, classification, pattern recognition method, H model appls. 78−41982
atomic spectra, classification, pattern recognition method, appl. to Cm energy levels 78−41983
automated information retrieval system, data bank organisation *(Russian)* 77−1960
average FWHM in background-free spectra 79−31349
AX_3 type spin coupled system, two-position exchange, NMR line shape function 77−90600
background subtract subroutine for spectral data 78−93762
backscattered gamma method, universal, based on computer interpretation of spectra 79−1984
baseline recognition and baseline flattening algorithm 78−262
benzene, doubly degenerate high-resolution rot.-vibr. Raman bands 79−6941
benzenes, monosubstituted, NMR, high resolution, automated anal. by computer program DAVINS appl. 80−63669
2-benzoylpyridine crystals, lowest triplet state, optically detected EPR 80−15827
beta-ray spectra, complex, processing method, 'Betarz' programme 78−41884
binary ^{13}C NMR spectra, ^{1}H noise decoupled, classification 78−27832
binary mixtures, anal. by computer decomposition of mol. fluoresc. spectra 78−15735
bremsstrahlung X-ray spectra stripping up to 300 kVp on desk type computer 79−83846
CESSNA interactive spectrum anal. program on minicomputer 78−94177
chemical anal. by heavy-ion induced X-ray emission, automation 77−77863
chemical analysis, direct interferogram comparison of chromatography/Fourier transform IR spectra data 79−100458
chemical analysis, energy dispersive electron probe X-ray, quantitative, compact procedure 80−40793
chemical identification of substances fixed on silica gel, using Raman spectroscopy *(French)* 78−88664
chloromethane, IR spectrum, evidence for $2\nu_3$ overtone 79−68226
chlorotrifluoremethane, IR rovibr. spectrum *(German)* 80−47998
chromatographic information processing by computer 80−71970
coincidence two-dimens. spectral data, offline treatment 79−97960
combined retrieval system for IR, ^{13}C NMR and mass spectral data 78−31717
complex alpha-spectra evaluation using program ALFUN 78−74552
complex spectrum, band parameters determ., minimisation algorithms operation *(Russian)* 78−74074
complex spectrum, computer separation, optimisation *(Russian)* 78−82051
computing 'square arrays' 79−22625
contour breakdown into two components *(Russian)* 79−49989
cumulative spectrum distortion with random scanning errors, digital processing 77−38028
d^3-configuration in trigonal field, Trees correction *(Russian)* 77−46556
data reduction, computer language 78−85241
data sampling and smoothing, review 77−34031
delayed coincidence spectra anal. without knowledge of resolution curve 79−22566
derivative spectroscopy, spectra differentiation with digital computer 80−77878
diatomic molecules, spectral line collisional broadening, numerical method 78−25622
1,2-dichloroethane, enclathrated, conform., reorientation, PMR line shape anal. 79−91300
digital deconvolution of spectra, noise amplification and resolution improvement 78−86339
digital isotope ratio meas. system, using programmable calculator with double collector mass spectrometer 80−63845
dimethyl sulphoxide, 1:1 and 1:2 complexes with H_2O and D_2O, H-bonding, IR and Raman vibr. spectra 77−34633
dioxane, 1:1 and 1:2 complexes with H_2O and D_2O, H-bonding, IR and Raman vibr. spectra 77−34633
DOMUS, analysis of two-dimensional mol. spectra 80−18890
electric quadrupole oscillator strengths, adaptation of ACRZ program 78−90119
electro-optical multichannel spectrommeter for transient resonance Raman and absorption spectroscopy 80−31890
electron and photon transport, SANDYL program, statistical accuracy, optimisation 77−8675
electron energy-loss spectroscopy, as analytical tool, data handling and processing 80−81407
electron microprobe anal., multielement, energy dispersive, procedure, program 77−56317
electron probe anal., energy dispersive spectroscopy, quantitative, computer program 79−43689
electron probe anal., X-ray energy dispersive spectrometer appl., data collection, review 77−56312
electronic absorption spectra, digital anal. appls. 78−8448
emission spectroscopy signal-to-noise ratio improvement and data processing *(Japanese)* 77−21448
energy dispersive X-ray diffractometery, technique, apparatus, data processing, computer profile fitting 77−68892
energy dispersive X-ray spectra, anal., computer techniques 79−43690
energy response of spectrometer calc., computer program 77−41577
environmental samples anal. for U, Th, neutron activation anal. data resolution for high throughput system 79−11848
EPR, absorption curve, spin concentration, numerical double integration, computer subtraction *(German)* 77−37954
EPR, conc. determ. and resolution of multiple-component spectra 78−259
EPR, spectral simulation program, appl. to NO spin labels 78−78730

spectroscopy computing continued
EPR and saturation transfer EPR, fast computation, master supermatrix eqn. soln. 78−62213
EPR and saturation transfer EPR, fast computation, perturbation approach 78−62212
EPR and ST-EPR spectra, fast computation, perturbation approx. extension for overmodulation 78−82754
EPR concentration dependence in magnetically diluted crystals with strong spin-spin interaction 79−42826
EPR digital data acquisition using microprocessor 80−17975
EPR of free radicals, simulated spectra, compensation for integerisation errors 79−33537
EPR of $S=^{1}/_{2}$, $I=^{3}/_{2}$ system, quadrupole effects 79−42827
EPR powder spectral simulation, paramagnetic ions 78−80194
EPR spectra, significance plots use 80−22409
EPR spectral simulation via finite elements, variational method and stochastic-Liouville eqn. 79−85157
EPR spectroscopy data handling and processing method *(German)* 77−53968
ESR spectroscopy, spectra collection and anal. using KRS-4200 minicomputer *(German)* 78−57998
ESR spectrum simulation, single cryst., Fortran IV computer program 77−59447
far IR atmospheric emission and absorption spectrum calc. program 79−35020
fish stock discrimination, X-ray fluoresc. tissue anal., pattern recognition technique 77−60330
fluorescence spectral files for chem. characterisation, data compression by Fourier transformation 78−35744
Fourier spectroscopy, correcting errors in optical path difference, computational method 78−70192
Fourier transform IR, scatter eliminated spectrometry 78−89564
Fourier transform NMR spectroscopy, clipped free induction decay signal anal. 77−63976
Fourier transform spectroscopy, minicomputer appls., errors 78−92543
fuel element scanning, Ge(Li) gamma spectroscopy, ANGEL computer program 79−9755
gamma ray decay scheme computation on basis of γ-γ coincidence meas. 79−59295
gamma ray spectra goodness of fit anal. with IFOM program 80−27912
gamma spectra, accelerated fitting and nuclide identification by graphical and associative memory methods 79−9945
gamma spectra, automatic evaluation of single full energy peaks, program 78−82571
gamma spectra anal., software system VAT-69 79−9949
gamma spectra from Ge(Li) spectrometers, set of computer programs SPECTRAN for anal. 79−9947
gamma spectrometry in neutron activation anal., data processing system 79−11863
gamma spectrum anal., computer methodology, appl. to geological and environmental samples 79−11867
gamma-ray, instrumental neutron activation anal., improvements to basic advance prediction program 80−14042
gamma-ray peak fitting, fast approx. to complementary error function 79−93903
gamma-ray spectra, automatic analysis, fast program 79−9948
gamma-ray spectra, automatic computer anal. for peak area and position 79−9941
gamma-ray spectra, background subtraction, direct method 79−723
gamma-ray spectra, computer code for qualitative anal. 79−9943
gamma-ray spectra, computer methodology for spectral data reduction and anal. 79−1988
gamma-ray spectra, computer processing code for large numbers of spectra 79−9942
gamma-ray spectra, doublet resolving power and area determ. accuracy, comparison of computer programs 79−9944
gamma-ray spectra, environmental, eval. of standard library spectra for use in least-squares resoln. 79−9915
gamma-ray spectra, environmental, least squares method for computing nuclide conc. 79−9914
gamma-ray spectra, for activation anal., computer programmes for anal. 78−7287
gamma-ray spectra, Ge(Li) detector, IAEA intercomparison of computer processing methods 79−9954
gamma-ray spectra, linear least-squares peak search algorithm 79−754
gamma-ray spectra, microprocessor system 79−9955
gamma-ray spectra, monoenergetic, mathematical model of spectra from Ge(Li) detector 78−13372
gamma-ray spectra analysis of fission products, automatic general-purpose program GSAP *(Chinese)* 80−69013
gamma-ray spectra evaluation, appl. of programmable calculators and minicomputers 79−9956
gamma-ray spectra from Ge(Li) detector, simple computer program (BASIC) for spectra eval. 79−9951
gamma-ray spectra multiplet resolution, semiempirical approach 79−234
gamma-ray spectral anal. using FFT *(Japanese)* 78−90047
gamma-ray spectrometer systems, portable, in situ field meas. applications 79−9958
gamma-ray spectrometry, data analysis, theoretical foundations 79−233
gamma-ray spectrometry, peak areas and detection limits, digital calc. methods 78−50433
gamma-ray spectrum analysis program SAMPO, radioisotope identification subroutine IDENT 79−9953
gas chromatography-mass spectrometry, computer-based library system 77−44523
gas chromatography-mass spectrometry data system, research-oriented, principles and applics. 80−40770
gas chromatography/mass spectrometer detector system, computerised scan anal. 77−77817
gas-phase electron diffraction analysis of molecules, computer generated backgrounds 79−97368
GASP, gamma-ray spectra analysis programme, user guide 79−6810
α-glycine, natural and ^{15}N-substituted, solid, Raman spectra, normal vibrs. 77−63408
graphite, polycryst., EPR meas. rel. to temp., crystallite orientation, paramag. suscept. 78−35023
graphite furnace peak shape study using computer 80−21331
graphite intercalation compounds with Rb, Raman scattering, computer fit of doublet 78−35130
Hadamard beam spectroscopy, computer simulation 79−93254

spectroscopy computing continued
high resolution IR mol. spectroscopy with difference frequency generation, refinements 78−90321
high resolution spectrometers, online polynomial optimisation 79−89563
HISLIB, comparison method for GC/MS profiles of complex mixtures 78−7268
homonuclear coupled spin system, inversion-recovery data anal. 79−33554
homonuclear diatomic molecules, CARS spectral profiles, computer program 79−13723
IFOM, a formula for universal assessment of goodness-of-fit of gamma ray spectra 80−27912
inductively coupled plasma emission spectrometry, with programmable monochromator, intensity meas., data processing 80−62728
information retrieval systems, systems comparison and development 79−49297
infrared intensity reference meas., spectrophotometric data reduction, modular computer programs appl. 80−3471
infrared spectra retrieval system 77−22535
ion microprobe analyser, appl. to cast Fe nodule form. 79−43295
ionisation mass spectrometer, with dedicated minicomputer, biological appls. 78−53586
IR data files, hierarchical preprocessing 78−15731
IR file searching, ASTM, algorithm using peak intensity data 80−30295
IR filter preparation using computer, GaAs-polyethylene mixture appl. 80−2763
IR radiation spectral absorptance and transmittance, accurate modelling technique 78−91062
IR reflection spectrum, dispersion formula fitting, Kramers-Kronig anal. 80−50311
IR spectra, binary coded, feature selection for automated interpretation 80−3428
IR spectra, computer-assisted interpretation, pattern recognition and artificial intelligence methods 78−15732
IR spectra, interference fringe elimination, computer method 79−12872
IR spectra, standard organic compounds, principal component analysis *(Japanese)* 80−69143
IR spectra differentiation using Fourier transforms 79−67397
IR spectral identification 77−4948
IR spectral interpretation, artificial intelligence program 78−300
IR spectroscopy microsampling, computerised data enhancement 77−36821
laboratory-based computer, minis, midis and desk-top calculation 79−9984
laser emission spectrochem. anal., data reduction, KSR 4100 small process control computer 77−48707
light scattering, in macromolecular solutions *(Rumanian)* 79−82990
lineshape fitting, iterative least-squares method, NMRCON program for chem. shifts 77−69715
LINFIT, muonic X-ray spectra analysis, P and Se allotropic modifications 80−23577
linked controllees and index-tabled techniques for data storage and rapid retrieval 79−9983
liquid chromatography, spectrometric detect., computer control of data acquisition, reduction and display 78−27850
Lorentz function convolution with spectral line data, accelerated convolution algorithm 79−81239
low-count radiation spectra, LSF processing 78−50448
Lowtran molecular absorption empirical transmission function analysis 79−76400
lunar surface elemental composition, analytical determ. from Apollo X-ray and γ-ray spectrometer data 79−2495
macromolecular rotational diffusion, ^{13}C spin-lattice relax. data anal., computer program, appls. 79−95664
macromolecules, graphics model building and refinement system 78−75505
magnetic resonance, two-centre integrals involving one-electron dipolar coupling and Slater AOs, computational procedure 80−23291
mass spectra, computer identification systems 78−86966
mass spectra, computer-aided classif., pattern recognition techniques, decision-tree approach 80−40774
mass spectra, continuous scan, time-sharing computer data system 77−18127
mass spectra, elemental compositions, computer assignment from isotopic abundance 78−20085
mass spectra, graphic display, dynamically refreshable controller with vertical line generator 78−314
mass spectra, low capacity codes, based on statistical moments 78−255
mass spectra, low-resolution, identification using combined forward-reverse library search system 80−30296
mass spectra, mol. substructures identification and retrieval, K-nearest neighbour methods 78−20084
mass spectra, pattern recognition, mathematical programming techniques 78−92523
mass spectra data identification, text search system based on Boolean logic 79−20480
mass spectra factor analysis 77−44534
mass spectral analysis by simplex pattern recognition 77−21429
mass spectral data bases, information content of retrieval procedures calc. 80−30297
mass spectral search system of MSDC/EPA/NIH 77−4947
mass spectrometer/computer system for collisional activation spectra 77−23576
mass spectrometric photoplate processing, microcomputer based system 80−62787
mass spectrometry, on-line literature search system 78−15734
mass spectroscopic chem. anal. of mixtures, spectral target transform. factor anal. 77−52679
mass spectroscopy for organic analysis, computer data search system, based on catalogue of compressed mass spectra *(Russian)* 80−30292
mass-analysed ion kinetic energy spectrometer, computer-controlled system 79−35884
MCD spectroscopy, permanent mag. interface, rot. system 78−62232
^{13}C-methane, ν_1 fund., quasi-CW inverse Raman spectra 80−48004
methane, and isotopic forms, ν_4 band, line parameters, Jovian atmosphere transmission, 7.7 micron 78−85894
MHD laser, admixture atom conc., automatic meas. system *(Russian)* 78−73123
microspectrofluorometry of biogenic amines, automatic correction of excitation spectra, on-line system 77−9308
microwave spectrometers, modern aspects, book contrib. 80−52328
spectroscopy computing continued
mixtures, anal. by retrospective computer subtraction of gas phase IR spectra 77−77824
molecular, PUMSM 78−62782
molecular dissociation, collision-induced, high-efficiency, in RF-only quadrupole 79−67419
molecular spectroscopic laboratory strategies, queueing theory and digital simulation use 80−30299
molecular valence force consts., computer program, least squares procedure 78−58656
molecular vibrational force consts., computer program 78−58655
molecular vibrational spectra calculations, mol. fragments effects *(Russian)* 78−5203
molecule symmetry analysis in vibr. and electronic spectroscopy computing *(Russian)* 77−46555
Mossbauer spectra, hyperfine structure parameters program 79−15383
Mossbauer spectroscopy, data acquisition and processing system 80−18061
multicomponent fluorescent mixtures, quantitative anal. of data 78−27833
multicomponent spectra, numerical anal., least squares, optimisation methods 77−56264
multicomponent systems, video fluorometer anal., rank annihilation method appls. 78−92546
multiconfiguration Dirak-Fock program, appl. to Ba X-ray levels and 5p excited spectra 80−47865
multielement atomic emission/fluoresc. spectrometer system, computer-controlled 80−45587
multilayer dielectric microwave reflectance and transmittance, characteristic matrix formalism 80−239
multipass-systems for Raman spectroscopic gas analysis *(German)* 80−81393
multislit spectrometer, data processing *(Japanese)* 78−58053
multiuser minicomputer system for gamma-ray spectroscopy and laboratory programming 79−9952
muonic atom cascade program, X-ray calcs. and cataloguing 78−90323
neutral beam injectors, spectroscopic diagnostics, on-line data acquisition, anal. 77−82643
neutron, using multisphere response meas., iterative method appl. *(Slovak)* 77−83444
neutron activation anal., absolute instrumental, consistent set of nuclear parameters 79−11857
neutron activation anal., computer interpretation of spectrometric information 79−31351
neutron activation anal., computer simulated γ-ray spectra 78−92577
neutron activation anal., computer-simulated gamma-ray spectra 79−1985
neutron activation anal., computerised, correction procedure, detection limit, standardisation 77−44544
neutron activation anal., gamma spectra least squares deconvolution on minicomputer, NAALSQ program 79−11853
neutron activation anal., instrumental large-scale routine, computer aspects 79−11862
neutron activation anal., ion microprobe surface anal., control and data analysis software 79−11860
neutron activation analysis, 14 MeV, nonidentical samples and standards 79−11858
neutron activation analysis, complex spectral peaks, computer anal. 78−53302
neutron activation analysis, for anal. of γ-ray spectra modification and appl. of SPECTRA program 78−20107
neutron activation analysis, gamma-ray spectra prediction, detection limits, computational procedure 78−85242
neutron activation and data reduction, flexibility, MULTELMT program 79−11856
neutron spectra, SAIPS system, algorithms for spectra determ. w.r.t. measured reaction rates *(Russian)* 80−102416
neutron spectra determination program, computer ES 1030, algorithm SAND-II *(Russian)* 78−48723
neutron spectrum unfolding with MATXUF on-line real-time derivative method 78−74553
NMR, Fourier transform, resolution enhancement using double exponential function 79−35804
NMR, high resolution, automated anal., principles and computational strategy 80−58287
NMR, knob-controlled CRT display expansion algorithm 77−22578
NMR, pulsed gradient diffusion meas. with microcomputer 80−17973
NMR analysis system, LAOCOON3-type, reliability efficiency and error estimates 78−258
NMR bandshape, complex exchange-broadened, iterative computer anal. 79−35805
NMR bandshape, exchange-broadened, improved algorithm 78−91963
NMR data bank, ^{13}C, DARC PLURIDATA system 80−30298
NMR high resolution, automated anal. by computer program DAVINS appl. 80−63669
NMR in undergrad. instruction, general purpose microcomputers use for hypothetical spectra synthesis 80−42009
NMR saturated bandshapes of coupled multispin systems, simple line approx. anal. 79−75561
NMR spectra, computer-aided interpretation, minicomputer based file search system 80−62702
NMR spectra, computer-aided interpretation using artificial intelligence system 80−62701
NMR spectra recording processing and accumulation, using mag. tape system *(Russian)* 79−26097
NMR T_1 computation, from pulsed data, least-squares formula 78−24837
nuclear, loss-free counting, real time compensation of dead time and pile up losses 78−17465
nuclear data acquisition real time flexible processing software 79−36495
nuclear detectors, simple algorithm for Gaussian peaks best fit *(Italian)* 78−58538
nuclear instrumentation, standard microprocessor based 80−36822
on-line gamma-ray meas., Ge(Li) spectra anal. 77−23395
online spectroscopic data base system status 80−104475
optical constants of thin films, computational algorithm 78−72617
optical mixing spectra, real-time analysis system 79−67392
optical multichannel anal., data microprocessing of thermally stimulated luminescence 78−54347
optical spectral instrument CAD status and prospects 79−44939
optical system simulation for luminescence spectroscopy 77−34036

spectroscopy computing continued
optical temp. meas. evaluation by computer 78−91150
organic, neutron response functions, Monte Carlo program 80−14047
organic compounds, spectroscopic identification, computer methods 78−88679
organic compounds structure determ. from spectral data by CHEMICS-F computer program 79−36794
organic molecules, struct., computer-assisted interpretation, using fluoresc. spectra 77−36805
overlapping spectral bonds separation by computer, appl. to phthalic anhydride Raman scatt. *(Russian)* 79−51968
overlapping spectral component separation using harmonic analysis *(Russian)* 77−45895
panorama spectroscopy of an extended laser medium *(Russian)* 79−12868
partial discharge amplitude spectra, acquisition and automatic processing system *(Italian)* 79−93108
pattern recognition applications to mass spectra classification 78−48722
peak areas, analytical results calc. 79−11851
photoacoustic spectrometer, single-beam, microcomputer assisted, for solid materials anal. 78−58044
photographic emulsion, for spectrographic anal., calibration curve computer calcs. 78−4706
photographically recorded spark source mass spectra, anal. 79−43658
photographically recorded spectra, semi-automatic interpretation, mass, at. spectra appls. 77−48708
photon correlation spectroscopy, motility evaluation of bull spermatozoa 77−48964
photon correlation spectroscopy, spectral analysis with short data batches 79−41346
photosynthetic systems, computer assisted scanning and kinetic spectrophotometry 78−68963
photosynthetic systems, computer-assisted scanning and kinetic spectrophotometry 78−48950
phthalic anhydride crystal, Raman spectra, overlapping spectral bonds separation by computer *(Russian)* 79−51968
PIXE anal. with REX computer program 77−52714
PIXE spectra, computer code trace 77−52713
planetary surface elemental anal. via orbital gamma-ray spectroscopy 79−12412
plasma, diagnostics, axial symmetry, error estimate of optical methods 77−84500
plasma vibrational spectroscopy, data gathering and processing system 79−31737
polyatomic molecule, vibr. struct. of electronic spectra, FORTRAN programs 80−32699
polyatomic molecules, calc. of spectral absorpt. curves 79−10093
polyatomic molecules, structure recognition, from IR, UV, NMR and mass spectra, computer method 78−25737
polychloroprenes, microstruct., IR digital subtraction method, struct. irregularities effect on copolymer IR bands 79−38543
polychloroprenes, microstruct., IR digital subtraction method, struct. irregularities 79−42965
polyethylene, melt crystallized, amorphous phase, IR spectrum 78−76463
polysaccharides, vibr., conformation, IR spectra, computer anal. *(Russian)* 78−13637
polystyrene solutions, light scatt., mol. parameters, computer anal. assessment 79−1766
position sensitive detectors, pseudostructures in spectra caused by digital data acquisition 79−76320
programmable calculator as alternative to minicomputer-based analyser 79−9985
programs for identification of chem. compounds from mol. spectra *(Russian)* 77−52727
proton induced X-ray emission anal. of aerosols, spectral anal. computer program 77−60167
proton-induced X-ray emission anal. for mass determ., spectrum decomp. code 79−11845
pulse height on-line gain stabilisation 78−74551
pulse-height anal., multichannel scaling, signal averaging, SAMCS1 80−47112
PVC, structural studies by Raman spectroscopy 79−7044
quantometer output data processing, regression anal. *(Russian)* 77−21461
quartz, irrad., optical absorpt. spectra, computer calcs. *(Russian)* 78−92091
quartz, irradiated, fused, crystalline, absorpt. spectra, colour centres 80−7384
radiochemical analysis by coincidence spectrometry, minicomputer system 79−11864
radioisotope identification and mass determination, using SAMPO programme with IDENT subroutine 78−48731
radiolysis, pulse, composite optical spectra, synthesis, anal., computerised 77−12810
radiotelescope RT-22 spectrometry, data reduction and analysis *(Russian)* 77−9674
Raman spectra, curve resolution analysis, minicomputer-computer appl. 77−82610
random search algorithm for 2-D data fitting 80−27915
recorders, transient, 1024-point, circuits, operation 77−53868
reduced tensor matrix elements program, AAKP, adaptation for tensor product evaluation 78−17587
RFSP-JUL, program for unfolding n spectra from activation data 78−82570
rock samples, fused, X-ray fluoresc. anal., fundamental parameter method 77−77820
rocks, activation anal., gamma-ray spectra processing with computer graphics 79−2228
rotational Raman spectroscopy of gases using interferometry 77−73494
secondary ion mass spectra, mass peaks identification using computer program 80−101867
secondary ion mass spectroscopy, image quantitation, by microphotodensitometry and digital processing 78−32914
SIMS ion images, multifeature mass analysis utilising digital image processing, Fe anal. appl. 79−43684
software correction, fully automatic 77−43891
solar emission lines of NeV, MgVII, SiIX, SXI, population levels as function of electron density and temp. 80−21963
solar radioastronomy, spectrograph data processing *(Russian)* 78−49320
spectroscopy computing continued
spark source mass spectra, on photoplate, conversational data processing by computer *(Japanese)* 78−8468
SPECAN, rot. spectra automatic assignments program, speed improvements 79−31499
spectra, multidimensional, identification and comparison 80−47956
spectra search systems, computer-aided, efficiency eval. using information theory *(German)* 80−37003
spectral decomposition, generalised algorithm, appl. to UV, IR, at. emission spectrometry 77−12842
spectral line breadth, analysis, digital computer method 79−83522
spectrofluorometer, scanning photon-counting, construction and data acquisition and manipulation system 77−2698
spectrometer user interface to computer systems 79−9986
spectrophotometric titration, equivalence point determ. by computerised curve fitting 78−7258
SPEKT, a dialog program for eval. multichannel spectra *(German)* 79−63196
spherical top molecules, IR spectra, diagonal $F^{(4)}$ and $F^{(6)}$ coeffs., computer listing 78−17669
spin-orbit interaction, matrix elements, computer program AAKL adapted to spectroscopic notation 78−891
steel, inclusions, rapid microprobe analysis using energy dispersive spectrometer and minicomputer *(German, English)* 79−92038
steel, stainless, quantitative AES with computer evaluation 78−76949
steel, standard, energy dispersive X-ray fluoresc. spectrometry, computer directed optimisation 80−45585
steroids, mass spectra, computer-aided interpretation by pattern recognition, preprocessing effects 78−15733
stopped-flow spectrophotometry, fully automated, with hierarchical computer controlled system 77−21426
strontium halides, absorpt. spectra in air-acetylene flame, using AAS with data processing 78−20102
s-tetrazine($-d_1$), and $^{15}N_2$-substituted, rot. consts., ground and $^1B_{3u}$ excited states geometries 78−82862
thermal-neutron activated samples, CERPL and CEREL codes for γ emitter automatic ident. and determ. 79−11852
trace analysis by IR spectroscopy, preconcentration, separation and computer techniques 78−31730
trace element determination, using DC plasma echelle spectrometer, automated 78−53277
triatomic linear mol., parallel bands, band model parameters 80−43026
s-triazine($-d_3$), gas phase IR band contours obs., computer simulation 77−6774
twelve-program package for activation anal. and gamma spectrometry 79−9950
two-parameter information processing on small computer, optimum method 79−76322
unfolding of spectra with continuum and discrete components 79−9946
unknown spectra identification, computer systems, performance evaluation 78−3398
UPEAK spectral decomposition routine 78−32798
vacuum wavenumbers, rapid calc. method 79−75616
vibrational analysis using Cartesian coords. 77−88442
vibrational spectra separation into individual components 79−93979
Voigt and complex error functions, rapid computation 78−57873
Voigt profile, fast calculational algorithm, line-by-line transmittance 78−7767
wavelength modulation spectrometry, computer modelling 77−63974
X-ray anal., conf., Denver, USA (Aug. 1976) 77−70382
X-ray analysis, appls., conf., Denver, USA (Aug 1975) 77−56307
X-ray and gamma-ray remote sensing spectrometers, data analysis system for planetary mission appl. 79−12411
X-ray emission and critical absorpt. energies calc., evaluation of mathematical expressions 77−29065
X-ray fluoresc. anal., correction procedures, accurate coeff. method 77−56311
X-ray fluoresc. anal., data reduction, anal. using QUAN computer program 77−56267
X-ray fluoresc. anal., energy dispersive, least squares, Monte Carlo methods, mathematical anal. techniques 78−85243
X-ray fluoresc. anal., FORTRAN IV program 78−7313
X-ray fluoresc. anal., resolution recovery by digital processing 77−56313
X-ray fluoresc. anal., self-absorpt. effects, Monte Carlo simulation 77−60165
X-ray fluoresc. anal. line intensities calc., computer program, appls. 78−61107
X-ray fluoresc. element anal. in pulps, conc. calcs., iterative method 78−61109
X-ray fluorescence, energy-dispersive, direct meas. of net peak areas 79−1989
X-ray fluorescence anal., interelement correction, models, computer program, appls. to alloys 77−56315
X-ray fluorescence anal., matrix correction, computer program *(German)* 80−3427
X-ray fluorescence of rock samples, major-element data processing, SORT, REORD and MW programs in FORTRAN 77−86398
X-ray fluorescence spectra, nonlinear least squares anal. 77−48731
X-ray photoelectron spectra, surface chemical analysis through even derivatives 79−100463
X-ray powder diffractometer proportional counter detector system, digital read-out 78−4751
X-ray spectra, energy dispersive, peak separation from background 78−7310
X-ray spectra, energy-dispersive, nongaussian peak overlap problem 78−78050
X-ray spectra, energy-dispersive detector, simplex method for fitting Gaussian profiles 79−722
X-ray spectra analysis, energy-dispersive 80−3433
X-ray spectrometry, data interpretation, online system using multivariate statistical anal. and pattern recognition 80−3461
Zeeman effect, orthorhombic rot. mols., doublet-doublet transitions 78−74698
Al alloys, energy dispersive X-ray fluoresc. spectrometry, computer directed optimisation 80−45585
AlF, hyperfine structure simulated by computer programme 78−50538
Ar plasma, spectral line blending of excited at. levels 77−76038
Ar plasma, wall stabilised arc, spectroscopic temp. and radiation standard 77−76199
AsF, molecular constants determ. from $b^1\Sigma$-$X^3\Sigma$ transition, nonlinear least squares procedure 79−798

spectroscopy computing continued
C_2 resonance fluoresc. technique for transient flame investigs. 77−30894
CN, red spectral system anal., mol. consts. 79−13728
CO, $A^1\pi$-$X^1\Sigma$ system, Franck-Condon factors, r-centroids calc. program 77−27121
CO_2, band model parameters prediction, 4.3 micron, 200-3000K 80−43047
CSFCl, vibr. excited states, microwave spectra *(German)* 78−55167
^{13}C NMR, chem. shift retrieval system 79−18206
^{13}C NMR, data analysis by pattern recognition 77−48059
^{13}C NMR chem. shifts, estimation by computer program based on additivity rules 78−13518
^{13}CH fragment, selective population transfer expts., density matrix formalism appl. to NMR spectroscopy 78−15059
Cs, photoplasma, optical excitation in radiation diffusion conditions 78−55227
Cu complexes, spin-labelled, EPR, electron-electron coupling 79−51858
$CuF_2.2H_2O$, X-band ESR powder spectrum and related magneto-microwave effects 79−24214
^{152}Eu, K-forbidden beta transition, spectral shape anal. 78−74335
F III, IV, beam-foil spectra, mean lives, 2150-3200 angstrom 78−55224
Fe, conversion spectrum anal., outer-shell s-electron density, ACSEMP program 80−7208
Fe II, 3000-12000 Å, forbidden transitions, excitation pot. and transition probability 77−79563
Fe powder, Mossbauer spectra parameter calc. with aid of computer *(Russian)* 78−76361
Ge detectors in space, computer spectral anal. of cosmic ray proton induced radioactivity 79−12413
GeH_4, IR spectra, Jovian atm. absorpt. profile, computer simulation 78−81584
Ge(Li) γ-ray spectra, NUKLID program for automatic line identification *(German)* 78−58536
HO_2 radical, near IR emission bands, vibr. and vibronic transitions 78−37633
H_2O, IR line intenisties and widths, ν_2 rot.-vibr. band 78−9200
H_2O, vap., simulation of depolarised Rayleigh scatt. and Raman spectra 78−33513
H_2O vapour, rovibrational Raman spectrum 78−90174
$^4HeH^+ + He$, 1 keV, collision-induced dissoc., ro-vibr. assignments, proton spectra obs. 79−3556
I_2 filter structure, digital normalisation, in quasielastic light scatt. 77−13805
In, oxidised surface, bonding of Cd arachidate monolayers, XPS 79−15011
$K_5(UO_2)F_9$, optical spectra, vibr. freqs. calcs. *(Russian)* 78−31205
KrF*, bound-free emission spectra, simulation 78−29806
Li^+-ligand complexes, NMR appl. ^7Li chemical shifts, expt. and ab initio studies 80−63670
N_2, liquid, vibrational dephasing, computer simulation, Raman spectra, pair potential effect 80−63863
N_2, rot. excitation by electron impact 1-4 eV 78−55248
N_2^+, first negative spectra, modelling 77−61758
NO, and isotopic forms, $X^2\Pi$ state, IR obs., mol. consts. 78−42045
NO, v=0,1 states, spectroscopic data calc. 78−86851
NO^+, $A^1\Pi$-$X^1\Sigma$ system, Franck-Condon factors, r-centroids calc., program 77−27121
N_2O, absorption spectrum anal. press., temp. quantity and spectral resolution retrieval 79−100462
N_2O, synthetic absorption spectra rel. to quantitative anal. 79−100461
$^{15}NH_3$, T_2/T_1 determ. for inversion transitions, power-broadened line shape 77−38654
NaAr, ground and excited state pot. curves, dispersed fluoresc. spectrum 79−98140
Ni porphin, reson. Raman excitation profiles, simulation, vibronic coupling consts. 77−65471
Rh, oxidised surface, bonding of Cd arachidate monolayers, XPS 79−15011
SeO, molecular constants determ. from $b^1\Sigma$-$X^3\Sigma$ transition, nonlinear least squares procedure 79−798
Si, oxidised surface, bonding of cadmium arachidate monolayers XPS 79−15011
SiH_3 radical, in Ar(Kr)(N_2) matrix, anisotropic ESR spectroscopic parameters 80−63687
SiH_4, ν_3 band assignment in IR and Raman spectra, ν_1-ν_3 vibr.-rot. coupling 77−75124
Sn, oxidised surface, bonding of cadmium arachidate monolayers, XPS 79−15011
XeCl* spectra, for $Xe(6s,^3P_2) + RCl$ vibr. energy disposal assignment 79−100345
XeF, B-X transition vibr. anal., flash photolysis UV absorpt. spectroscopy 78−42088
$^{131}_{54}Xe$, K-Auger transitions 77−18883

spectrum *see spectra*

spectrum analysers *see spectral analysers*

speech
see also hearing
abnormal voice qualities, multidimensional classification 77−86513
acoustic aspects of speech production 78−96056
acoustic invariance in speech production, measurements of spectral charcts. of stop consonants 80−10089
acoustical research into life sciences, review 80−97925
Acoustical Soc. Amer. 96th meeting, Hawaii, 1978 Nov. 78−90545
airflow measurement in speech using mask-type wire screen pneumotachograph 77−52808
anticipatory coarticulation, implications from study of lip rounding 79−72764
aphasia, effect of auditory prestimulation on naming 78−65058
aphasia treatment session recording, momentary and interval sampling 79−96704
articulation development, possible nonlinear time varying control in feedback path 78−35870
articulation status and improvement for /r/ and /s/, delayed judgment speech-sound discrimination 78−65060
articulatory effort, subjective evaluation 78−65056
articulatory movement of tongue mapping, model 79−11949
articulatory movements in VCV sequences 77−77918
articulatory-to-acoustic transformation in vocal tract, inversion by computer sorting 78−69110

speech continued
auditory discrimination of rise and decay times in tone and noise bursts 80−19166
auditory feedback, effect on guitar playing intensity and speech prod. 78−85322
auditory-nerve fibre discharge patterns, representation of speech-like sounds 80−108912
automatic parameterization of vocal cord motion from ultra high speed films 80−85419
automatic speech recognition using psychoacoustic models 79−41529
Bengali vowels in connected speech, format freqs. *(Japanese)* 78−3524
Bengali vowels uttered in isolation, formant freqs. 77−16941
bilabial stop consonants differing in voice onset time, noncategorical perception 78−11676
bimodal cues for speech loudness 80−10090
biofeedback training device for speech therapy, portable, microprocessor-based 80−104808
cephalostat for speech physiology research 78−65140
chest wall movements prior to phonation 80−76768
children's newly acquired phoneme articulation, right-ear auditory feedback control 79−57676
coarticulation, formulation of process in formant freq. terms, appl. to automatic speech recognition *(Japanese)* 78−92660
comfortable effort level, expt. variable 77−2013
computer model to characterize the air volume displaced by the vibrating vocal cords 78−69111
computer simulated patients for teaching students of speech and hearing 79−17162
conference on acoustics, speech and signal processing, Denver, CO, USA (Apr. 1980) 80−83689
consonant duration in American English 77−48817
correlations of duration for nonadjacent segments, aspects of grammatical coding 77−56387
deaf children training to comprehend passive voice 80−33372
deaf speech and hearing aids, vocoders, frequency lowering and lipreading cues 80−12309
deafness effects on generation of voice 80−33361
digital coders, optimization by exploiting human auditory masking 80−33356
distinctive features and acoustic cues, distinction 78−11681
early referential speech, linguistic development rel. to sensorimotor attainments 79−57674
EEG activity comparison in right and left cerebral hemispheres by power spectrum analysis 80−45922
electric potentials, cranial and facial, assoc. with speech prod. 78−11675
electroglottograph application experience 77−78062
EMG motor command extraction by pulse counting method *(Japanese)* 78−53546
encoding, predictive and residual 80−33354
encoding in auditory nerve, effects of nonlinearities 80−108913
encoding using freq. domain techniques 80−33355
evolving ideas about nature of speech and relationship with human communication, review 80−96135
extraction from noise by adaptive digital filtering *(Japanese)* 78−13863
feature detectors for voice onset time, voiceless anal. channel 78−3505
feature processing initial consonants, non-independ. 78−27972
formant based speech code for severely impaired hearing subjects 77−64051
formant frequencies of steady-state and consonant-bound vowels, difference limens 78−53426
frequency changes, physiological adjustments in trained and untrained voices 77−90814
fundamental freq. correl. with speaker's height, weight and body surface area 78−65053
fundamental frequency perturbation observed in sustained phonation 79−100635
fundamental voice freq., correl. anal. of physiological factors 78−40201
Glossynograph system for presenting printed text synchronously with speech for hearing-impaired persons 80−56153
glottal sound source, self-oscillating model *(Japanese)* 78−92654
glottal wave, male and female, vars. 78−11678
hearing aid and speech reading contributions to speech communication 79−25002
hemispheric speech organisation in left- and right-handed, test of models 80−8071
history of acoustics, from Echo to 18th century *(German)* 79−76915
human speech imitation by mynah bird, comment on first formant resonance 79−43939
infant babbling, effect of final-syllable position on vowel duration 78−11679
infants and children, fundamental freqs. 78−57023
intonation correction for hard of hearing children, trainer *(Japanese)* 77−25472
intraoral air pressure, production of /p/ and /b/, children, youths, adults 79−20560
involuntary human-voice tremor, physiological model anal. 79−5301
Japanese, consonant perturbations, and vowel articulation by adjacent segments *(Japanese)* 78−92655
Japanese semivowel /j/ production, EMG study 77−5013
Japanese vowel production, EMG study 77−5012
labial muscle EMG analysis and feature extraction by Hanning Cosine Modulated wave function 77−81605
laryngeal activity in Swedish obstruent clusters 80−108920
laryngeal films, ultra high speed, automated anal. 78−36023
laryngeal muscles, reflex activation by sudden induced subglottal pressure changes 79−74691
laryngeal observation using stereo-fibrescope with magnetic interlens bridge 79−44068
laryngeal prosthesis for fistula speech after laryngectomy 77−78056
larynx, electronic, Polish developed, design and operation 80−46098
laterality effect in isometric and isotonic labial tracking 79−57625
lingual tactile sensory system, automated instrumentation for research 80−8205
lip and jaw motion in midsagittal plane, observation using strain gauge transduction technique 79−44069
lip movements, effects of auditory masking 78−65061
lip-opening area, new fast continuous meas. method 78−3520
local tract area function, estimation by adaptive deconvolution and adaptive speech anal. system *(Japanese)* 78−92658
loudness determ. methods *(French)* 77−34996

speech continued
loudness discomfort level and acoustic reflex threshold for speech stimuli 80−76762
low bit-rate coding, signal models 80−106674
masking effects on articulation in normal speaking adults wearing palatal appliances 80−76766
maturation, anatomical and neuromuscular, evidence from acoustic studies, review 77−5014
misarticulation of /r/, contextual-coarticulatory inconsistency 78−65055
misarticulation of /s/ or /r/, oral sensory and motor behaviours in children 78−65059
motor unit recruitment and discharge patterns during speech prod. 78−65054
motor units in speech musculature, mechanical props. 79−70559
mouth model, normalization and adaptation for speech pattern *(Japanese)* 77−90815
movement-related tonal signal processing, left hemisphere superiority 80−35913
nasal air emission in speech disorders, electrodynamometric evaluation 78−77134
nasal sounds, effects of nasal and paranasal cavities *(Japanese)* 77−86514
nasalisation in normal and hypernasal speakers, effects of feedback filtering 80−35921
neural lateralisation of species-specific vocalisations by Japanese macaques 79−62268
neuromuscular model of laryngeal control for pitch change in Japanese word accentuation *(Japanese)* 78−40205
noise-tolerant continuously variable slope DM to linear predictive coding conversion 80−96141
oesophageal speech, productive voice onset time characts. 78−77070
oesophageal speech, vowel duration characts. 77−25474
oral motor tasks, stutterers' and nonstutterers' neural response times 79−96585
oral port size estimation, consistency of pressure-flow technique 79−8515
oral reading, breath volume and flow modification 79−57672
pathological vocal cord vibration, computer simulation 77−16940
perception, hemispheric specialisation, acoustic change rate, expt. obs. 80−104594
perception, order effect of acoustic segments of VC and CV syllables on stop and vowel identification 78−27967
perception of place and manner of articulation 77−48814
perioral reflex amplitude variation, prior to lip muscle contraction 79−20558
pharyngeal and velar displacement for selected speech sounds 80−108921
phonatory initiation, minimal reaction time obs. 79−96583
phonemes processing, speed-accuracy study 78−20193
phonetic categories, acoustic props. 80−106675
phonetic defects caused by facial gaps, correction using prosthetics *(French)* 80−51298
phrase-level timing patterns in English: effects of emphatic stress location and speaking rate 80−51128
preadolescent children's voices, acoustic correlates of perceived sexual identity 80−10088
processing, amplitude and freq. distribs. of speech signal levels 77−16942
processing by auditory nervous system 80−108911
production, physiology and acoustical props. of vocal system *(Japanese)* 80−26242
real-time speech high-performance processor design 80−96144
reception threshold, reliability in the determ., psychometric function 80−61657
respiratory tracking of dichotically presented tonal amplitudes 78−27973
robotic arm voice command system, 6 degrees of freedom 80−12313
sensorineural hearing loss, freq. selectivity and speech discrimination 80−61593
shimmer in sustained phonation 80−94242
sibilant duration, physiological control, insights afforded by speech compensation to dental prostheses 79−74692
signal modelling and recognition, system identification approach 80−51286
singing voice, acoustics 77−66818
SIRENE, computerized speech training aid 79−70701
speaker height and weight identification 77−2014
speaking rate effect on vowel formant movements 78−40202
speech discrimination in infants, developmental changes 78−65048
speechreading ability, visual-neural correlate 78−64992
stammer inhibition, pocket sized DAF unit, bucket brigade delay lines, PCB 78−31825
stammerer fluency aid using delayed auditory feedback, body-worn aid 80−56283
stapedial reflex thresholds with and without anxiety, fluent and disfluent speakers 79−96584
steady-state vowel representation in temporal aspects of discharge batterns of populations of auditory nerve fibres 80−21479
stop consonant place perception with single-formant stimuli, front-cavity resonance 79−50526
stutterers, central auditory function 79−20550
stutterers, effects of noise and rhythmic stimulation on speech 79−20559
stutterers' central auditory function, synthetic sentence identification test 79−96586
stutterers' disfluency rate effects of verbal stimuli 79−57677
stuttering, articulatory behaviours, cinefluorographic anal. 80−94240
stuttering, articulatory dynamics of fluent utterances 80−94239
stuttering, effects of self-recording of stutter frequency or 'the' occurrence 79−57671
stuttering, fundamental freq., effects of delayed auditory feedback and masking 80−35922
stuttering, laryngeal behaviour 78−65057
stuttering, laryngeal muscular activity obs. 79−57675
stuttering adaptation, effects of whispered and aloud reading practice 79−57669
stuttering model, movement disorder 80−94241
subjective loudness measurement, affecting auditory factors *(Japanese)* 80−85409
syllable duration effects using Melodic Intonation Therapy technique 80−35920
syllable-final position, investigations of place and manner 80−10095
syntactic blocking of phonological rules in speech production 77−64058
speech continued
syntactically ambiguous sentences, role of duration in disambiguation 77−12936
temporal order perception for vowels and consonant-vowel syllables 78−69108
therapy, solid state delayed auditory feedback system 77−13028
throat-wall, human, modelling and vocal tract study from input/output meas. 79−34577
timbre perception, review 78−77068
tongue motion tracking by optical distance sensing 79−57673
tongue movement observation using dynamic palatography 78−44687
tongue placement task performance of articulate and inarticulate children 79−57670
tongue profile, approx. by the quadratic curve model *(Japanese)* 78−92656
tongue shape, factor anal. 78−3522
trainers, with visual display system, systematic use for hard of hearing children *(Japanese)* 79−39596
trainers using visual display system, for hard of hearing children *(Japanese)* 79−39595
training aid system incorporating tri-normalized speech processor 79−70700
training patterns for deaf people, computer generated 80−51290
training system for deaf children *(Japanese)* 77−86515
US/EMG transducer for biodynamic research, speech appl. 78−77164
velopharyngeal orifice area meas. by appl. of aerodynamic forced oscill. principles 77−5017
ventilatory phonetory conflict, investigation using glottiscope 80−51145
vibrotactile speech training deaf aid, frequency analysis system 77−29214
vocal cord vibration, continuous model 80−85418
vocal cord vibration, longitudinal displacement, acoustic properties 77−90812
vocal cords vibratory behaviour in tension and mass imbalance 79−83803
vocal distinctive features used by gelada monkeys 77−1971
vocal fold vibration, viscoelastic theory 77−25471
vocal pitch exercising apparatus, deaf children 79−25001
vocal tract length preservation and vowel production 80−61594
vocal tract losses, influence on damping of reson. freqs. 78−85325
vocal tract wall impedance, discussion *(Japanese)* 78−92657
vocal-tract area functions, estimation from acoustical analysis of speech wave, state-of-the-art 79−68506
vocalised speech, acoustical correlates of emotional content 77−12937
voice frequency meas. using fast freq. meter *(German)* 78−3518
voice onset time discrimination 77−25466
voice onset time for voiceless stop consonants in stutterers' and nonstutterers' fluent reading 77−36960
voice production, analysis synthesis, computer appl. *(Dutch)* 77−12938
voice quality, study by speech noise analysis *(Chinese)* 78−92649
voice timbre types, influence of acoustic props. on voice classification 77−90813
voice tremor EMG correlation, psychological stress evaluators 77−9214
voice-onset time, relationship with vowel duration 79−96582
voiced and whispered speaking conditions, closure and constriction duration for alveolar consonants 77−36961
voicing distinction in initial stop consonants, dissociation of spectral and temporal cues 78−3519
vowel articulation, transmission behaviour of human speech generating system 78−15849
vowel articulation correction using trainer *(Japanese)* 77−25473
vowel duration meas., reliability study 78−65052
vowel feature extraction, by use articulatory model 79−20561
vowel formant freqs., piecewise-planar representation 78−31822
vowel sounds, control of vocal-tract length 78−11680
vowels, voice fundamental freq., explanation by source/tract coupling 79−94410
waveform coding technique developments in Japan, review 80−33353
weak speech amplification device with suppression of respiration noise 80−30929
He speech, translation via segmentation, partial-rejection and expansion 78−31823

speech amplifiers *see audio-frequency amplifiers*

speech analysis
acoustic studies of anatomical and neuromuscular maturation of speech mechanism, review 77−5014
acoustics, speech and signal processing, conf., Tulsa, USA, 1978, April 78−63242
acoustics, speech and signal processing, IEEE international conf., Washington, DC, USA, 1979 Apr. 79−55275
American English, acoustic study of medial /t,d/ as function of phonetic environment 80−10093
articulatory activities measurement, computer-controlled method 77−56391
articulatory characteristics of tongue and jaw point movements in connected sounds of Japanese 80−26243
Attached Processor for Speech 80−96145
automatic speech processing, approaches, models and appls. *(German)* 79−50532
automatic speech recognition, independent of the speaker *(German)* 79−90094
basilar membrane electronic model for evaluation of speech disorders 78−40206
category boundary adaption between speech and nonspeech 79−72763
closed glottis interval identification using epoch extraction from linear prediction residual 79−86301
coding using non-uniform linear prediction in transform domain 79−55277
computer aided signal handling 77−56389
continuous speech segmentation into vowel and nonvowel-like intervals using speaker-independent algorithm 79−86302
CRO synthesis of optical lip shapes from vowel sounds 80−19170
deafness effects on generation of voice 80−33361
dichotic and monotic masking of consonant-vowels by consonant-vowel second formants 80−79069
digital sound spectrograph 78−63251
digital speech processing, book 79−72767
digital speech voltmeter using microprocessor 79−72768
digital voice processing techniques 79−81663
Dutch vowels, anal. using fast Fourier transform 79−3858

speech analysis continued
dysarthria associated with cerebellar disease, acoustic characts. 80−56067
electronic artificial larynx, acoustical and perceptual characts. of produced speech 79−72766
electropalatography, thermo-formed pseudopalates and use of 3D display 80−85511
EMG power spectrum analysis, in neuromotor speech disorders 77−29161
equal-articulation segment determination 80−5880
equalizer in spectral domain for speech processing by autocorrelation function 80−1383
esophageal speakers, vocal roughness and jitter characts. of vowels 79−20555
esophageal speech, long-time spectral and intensity characts. 80−74643
Estonian, statistical data *(Russian)* 80−45923
face-voice synchrony for videotape speech dubbing 79−68503
fast spectral estimation of speech signal in analytic form 80−83715
formant freq. extraction by derived PES methods, adaptability to complicated spectra 79−72761
formant frequencies extraction, PES method 78−11674
formant transitions using interactive speech anal. synthesis system 80−83712
fundamental freq. contours at syntactic boundaries 78−3521
fundamental frequency measurement, comparison of contact microphone and electroglottograph 80−109056
glottal inverse filtering from acoustic speech waveform, least squares approach 79−86304
glottal stops, occurrence in fluent speech 78−92652
glottal-area waveform, estimation via nonlinear inverse filtering technique 77−56390
hearing-impaired children, intelligibility meas. 79−20554
homomorphic filter in ARMA model *(Japanese)* 80−87666
hypernasality quantitative evaluation using acoustic perception computer method 78−27971
instantaneous value, statistical depend. represented as analytic signal *(German)* 79−94409
intonation correction for hard of hearing children, trainer *(Japanese)* 77−25472
Japanese, consonant perturbations, and vowel articulation by adjacent segments *(Japanese)* 78−92655
Japanese kinki dialect, anal. and perception of two-mora word accent types *(Japanese)* 78−92659
Japanese phonemes, quantitative estimate of possibility of auditory confusion 79−68507
Japanese vowels, multivariate anal. of estimated vocal tract area functions *(Japanese)* 79−27469
jaw movement, cineradiographic study of chin marker positioning and implications for strain gauge transduction 80−76764
laryngeal dynamics, effects of Teflon injection 79−70560
laryngeal films, ultra high-speed, automated anal. 79−57746
laryngeal pathology detection by glottal area/volume-velocity comparison 77−77920
laryngeal prosthesis, internally worn, design and construction 80−41318
least squares glottal inverse filtering from acoustic speech waveform, comments 80−83707
linear prediction analysis of speech based on a pole-zero representation 79−10432
linear prediction coding for synthesizing natural sounding speech 79−59879
linear prediction parameter estimation using Kalman filtering *(German)* 80−96134
linear predictive analysis using small anal. segment, error evaluation *(Japanese)* 78−31824
linear predictive coding, accuracy improvement 79−46133
linguistically oriented system for word spotting in conversational speech 79−64424
lip and jaw motion, video-scanning system 77−56388
lip motor control using mechanoreceptor feedback 80−33367
local tract area function, estimation by adaptive deconvolution and adaptive speech anal. system *(Japanese)* 78−92658
long-term spectra, computerised meas. method, English and Finnish data comparative study 80−104688
maxillary lesion evaluation by bone-conducted vowel spectral estimation *(Japanese)* 79−5395
mechanical speech processing, new results *(Hungarian)* 80−69604
minimum and mixed phase speech analysis-synthesis by adaptive homomorphic deconvolution 79−90090
mixed-phase homomorphic vocoder 79−59882
motor unit correlates of syllable stress, preliminary obs. 78−92653
multichannel zero-crossing-interval pitch estimat on 79−64427
natural and synthesized speech differences, pattern recognition approach 79−64430
nonstatistical parameter estimation adaptive algorithms 80−91995
oral constriction port, effects of increased vertical dimension on size 80−76765
PARCOR analysis-synthesis telephony, improvement of speech quality 79−50534
PARCOR system for expression of spectral features 79−50533
parser for segmenting continuous speech into pseudo-syllabic nuclei 80−91985
phase information preservation 80−83713
phonation acoustic qualities in young hearing-impaired children 80−33373
phoniatric diagnostics of speech organ disorders, ogjective acoustic methods 80−104598
pitch, new contour display in connection with sound spectra *(German)* 77−833
pitch contour transfer between utterances with differing lexical content 79−81652
pitch determ. using nonlinear digital filter *(German)* 80−91972
pitch estimation algorithm for speech and music 79−14173
pitch extraction, MOS-LSI circuitry 79−64428
pitch extraction and visual display using computer 77−52807
pitch extraction from corrupted harmonics of the power spectrum 79−43936
pitch extraction method based on peak detection and AMDF *(Korean)* 80−102935
pitch period extraction using nonlinear digital filters 79−64429
pitch-synchronous coding, linear prediction coding, analysis frame position influence 80−14523
speech analysis continued
pole-zero modelling of speech 80−83716
Polish voiced consonant fundamental frequency variations 79−68501
preprocessing filter for enhancing linear predictive analysis/synthesis of noisy speech 79−64447
probability density functions for speech waveforms 78−80890
purported Bigfoot vocalisation record pitch and vocal tract length estimates 79−94418
rank-order speech classification algorithm (RASCAL) 79−64426
reflection coeff. calc. of inverse filter of PARCOR anal. lattice without multiplication *(German)* 80−96114
reflection coefficient estimates based on Markov chain model 80−83710
Russian VCV utterances, formant frequency patterns 80−33362
scalar parameter quantization methods 80−83711
Schlieren photography appl. for speech research 80−64145
sound analyser, undergraduate lab. expts. 80−82600
speaker identification by long-term spectra under normal and distorted speech conditions 78−11677
spectral analysis, review of methods 80−21560
spectral envelope extraction by improved cepstral method 79−81659
spectral noise levels and roughness severity ratings for vowels produced by male children 80−51129
spectral properties of fricative consonants in children 80−33364
spectrographic, identification of vocal diseases *(Japanese)* 80−85455
spectrographic analysis of children's speech 80−94238
speech production model, with digital filters 79−81661
speech trainer for multihandicapped children, display method and control program *(Japanese)* 80−108922
spoken word recognition method using nonlinear spectral matching *(Japanese)* 80−69605
statistical properties of speech and musical signals 79−76919
statistical props. of music and speech signals, modulated random processes 79−64412
stop consonant production errors in developmentally dysphasic children 80−33363
stutterers, effects of noise and rhythmic stimulation on speech 79−20559
stutterers' fluent speech, voice onset time, frication and aspiration 80−51130
subglottal air pressure and vocal-fold tension, indirect assessment of contrib. to changes of fund. freq. in English 78−92650
syntactic methods for speech segmentation and recognition 79−59889
talker similarity, psychological dimensions correls. 79−20557
Telugu vowels, acoustic-phonetic features 79−18666
time-domain algorithms of speech signals, harmonic bandwidth compression 79−46125
tongue movement study using dynamic palatography 77−29160
tongue profile, approx. by the quadratic curve model *(Japanese)* 78−92656
transform coding of speech, examples 79−59886
ventilatory phonetics, analogic 80−51131
vibrotactile frequency discrimination, for speech parameter encoding 78−11772
vibrotactile speech training deaf aid, frequency analysis system 77−29214
visual speech vocoder as teaching aid for deaf 78−36069
vocal frequency prediction, physiological meas. method 79−94413
vocal tract, computer representation of geometrical configuration *(Russian)* 80−46111
vocal tract area functions, sensitivity to perturbations in bandwidths and formants 79−59887
vocal tract cross-sectional area functions, estimated values 80−99900
vocal tract losses, influence on damping of reson. freqs. 78−85325
vocal tract real-time hybrid simulation 77−44692
vocal tract shape generation from formant freqs. 79−5303
vocal-tract area estimation 79−68505
vocal-tract area functions, estimation from acoustical analysis of speech wave, state-of-the-art 79−68506
voice information, processing system, features and appls. *(Japanese)* 79−86310
voice production, analysis synthesis, computer appl. *(Dutch)* 77−12938
voice qualities, multidimensional classification 78−92651
voice quality, study by speech noise analysis *(Chinese)* 78−92649
voice quality registration 77−21539
voice timbre types, influence of acoustic props. on voice classification 77−90813
voicing detection algorithms, automatic thresholding 79−64425
voicing distinction in initial stop consonants, dissociation of spectral and temporal cues 78−3519
vowel articulation correction using trainer *(Japanese)* 77−25473
vowel duration as cue for voicing distinction in following word-final consonant 80−74642
vowel formant freqs., developmental study in imitation task 79−43935
vowel formation by profoundly deaf children, Argentine Spanish appl. *(Spanish)* 80−30734
vowel roughness, waveform and spectral features 79−20556
vowel roughness effect on harmonic levels 80−76767
waveform analyser for teaching, evaluation of Pasco Model 9302 77−9842

speech compression *see bandwidth compression*

speech intelligibility
see also hearing
acoustic feedback's influence on speech intelligibility 80−23859
acoustic noise, nonstationary, reduction using LMS adaptive noise cancellation 79−64414
acoustic noise corruption, enhancement of speech based on spectral noise subtraction method 79−64415
acoustic noise in speech, suppression using spectral subtraction algorithm 79−64413
adaptive noise cancellation by short-time Fourier transform 80−91976
ADPCM coded speech, segmental SNR measure as indicator of quality 80−33359
adult perception, overt and covert aspects 77−52803
amplitude and frequency distribs. of levels of process 77−16942
articulation loss of consonants, computation methods *(Czech)* 80−43557
audiograms and audibility of indistinct sentences with distinct components *(German)* 79−81647
auditoria, intelligibility improvement via receiver sound control 77−68328
auditorium acoustics design index, S/N ratio for speech intelligibility 80−19156

speech intelligibility continued
auditorium syllabic intelligibility, computer evaluation *(French)* 79−37095
auditory backward inhibition and concert halls 79−59892
auditory fatigue effect on masked speech intelligibility 80−67096
auditory-visual perception of speech with reduced optical clarity 80−35919
automatic speech recognition by zero-crossing analysis methods 79−94420
bandwidth compression hearing aids, limitations of voiced portion of speech 79−29668
binaural critical masking bands 80−21475
broadband compression for improved hearing procedures *(German)* 80−104591
children's understanding of monosyllabic nouns in quiet and in noise 79−86305
coarticulatory cue decoding rel. to age 80−51126
communication in high noise, intelligibility and S/N ratio *(Japanese)* 77−73533
conference halls, mathematical model of insonification rel. to speech intelligibility *(French)* 78−13857
consonant confusion patterns, effects of filtering and sensorineural hearing loss 78−73163
context sensitive perception of naturally produced stop and fricative consonants by infants 77−64047
deaf children's speech, effect of timing errors on intelligibility 80−19167
deep-sea diver speech distortion, chemical and physiological stress correlation 80−45924
dereverberation process evaluation by normal and impaired listeners 80−91974
distinctive features and acoustic cues, distinction 78−11681
Dutch vowel lengths production and perception in spoken sentences 80−38185
electronic artificial larynx, acoustical and perceptual characts. of produced speech 79−72766
electronic models to simulate sensory distortions on speech perception by the deaf 78−3507
English consonant dissimilarity ratings by normal and hearing-impaired subjects 80−35914
enhancement by frequency-domain spectral weighting 79−94416
frequency selectivity of the cochlea for formant peaks at high signal levels 80−97936
fricative, effects of increased vertical dimension 80−76765
friction analyzers for [j] 77−77911
frquency compression for moderately hearing impaired subjects, speech intelligibility 78−20188
fundamental freq. declination, perception 79−90091
German, speech intelligibility test, DIN 45621 recommendation, acoustics and phonetics *(German)* 78−35867
hall, improvement of acoustics *(French)* 79−37089
halls, sound amplifying systems, model *(French)* 79−37090
hearing aids, quality judgments of speech signals processed by hearing aids, multidimensional scaling 80−97933
hearing aids, use of speech processing 77−17007
hearing tests, word list formats 80−33370
hearing-impaired, calc. model *(Dutch)* 78−73165
hearing-impaired children, expt. meas. 79−20554
hearing-impaired persons, effect of protective device 79−81658
hypernasal speech, oral/nasal intensity ratio meas. 79−83804
identification and discrimination of relative onset time of component tones 77−64059
improvement for ski-slope hearing impaired person, signal processing 77−11091
intensity discrimination with gated and continuous sinusoids 80−10094
interference level as predictor of face-to-face communication in noise 78−57018
intervocalic consonants, intelligibility in noise 79−68514
Japanese, reverberation effects, speech model and articulation tests *(Japanese)* 79−90092
Japanese phonemes, quantitative estimate of possibility of auditory confusion 79−68507
language development, role of rapid auditory processing in normal and disordered development 77−5016
laryngeal configurations effect on acoustics of phonation 79−86309
lateralization of complex waveforms 80−97931
linear predictive coded speech digitisers, background noise spectral subtraction 80−96140
linear predictive coded speech quality problems and expts. 80−91982
linear predictive coding, performance of vocoders in noisy environment 79−64416
linear predictive coding, voice digitizer with background noise suppression 79−64417
loudness function of artificial speech, for reference equivalent meas. 80−79068
low-frequency hearing loss, filtered speech, psychophysical tuning curves and masking 80−51121
masking noises, influence on Lombard and sidetone amplification effects 77−5015
masking of filtered noise bursts by synthetic vowels 79−94412
maximum likelihood parameter estimation of noisy data 79−64418
narrow-band filtered speech perception 77−36956
natural speech interference separation technique 79−94417
noise effects due to traffic, anechoic chamber meas. 79−18590
noise induced hearing listeners, effects of high-freq. compensation 80−38186
noise suppression filter for narrowband vocoder 80−91977
nonsense-syllable mimicry in prosodic phenomena studies 78−40203
NSMRL tri-word test of intelligibility (TTI) 79−41528
objective measures for speech quality testing 80−33358
parameter estimation of noisy all-pole process using pole-zero modelling 79−64419
perception, rhythmic and segmental, interdependency 79−72765
perception, use of comfortable listening levels, effect of loudness level 79−2078
perceptual invariance and onset spectra for stop consonants in different vowel environments 80−48523
peripheral and central processes in selective adaptation of place of articulation in stop constants 78−3523
phoneme boundaries meas. in four ways 80−96138
phoneme boundary effect and selective adaptation to speech, signal detection theory 79−43926
phonetic features, perceptibility in fluent speech 78−92635
phonetic perception, effect of silence as a cue during word utterance 79−81650
phrase boundary perception, influence of supersegmental variables 79−16218
predictor-coefficient and formant-coded speech, two preliminary studies 77−2012
property detectors for bursts and transitions in speech perception 77−64046
psychophysical pitch biases related to vowel quality, intensity difference, and sequential order 79−5295
quality and intelligibility measures and their correlations 80−91978
quality parametric objective measures correlated with subjective results 80−91980
quality subjective and objective measures and their correlations 80−91979
rank-order speech classification algorithm (RASCAL) 79−64426
rapid connected, threshold of intelligibility/compressibility 79−68502
results interpretation of meas. in noise in anechoic room *(German)* 80−91968
reverberation and noise effects on intelligibility of sentences in cases of presbyacusis 80−96139
saturation diving communications system 80−43558
sentence comprehension, multiplicative effects for combined acoustic disturbances 80−35915
SPAC, speech processing using the autocorrelation function, noise reduction in speech communication *(Japanese)* 80−33371
SPAC speech processing system using autocorrelation function, operation and characts. 79−68510
spectral integration 80−21477
speechreading, use of residual hearing *(Japanese)* 77−81511
SPIN test on children using sentence material with controlled word predictability 79−96581
stimulus dominance in fused dichotic syllables, category goodness hypothesis 80−33368
stimulus-onset asynchrony effect on dichotic performance of children with auditory-processing disorders 80−41044
stop consonant place perception with single-formant stimuli, front-cavity resonance 79−50526
stop consonant voicing, relationship between adaptation of percept and transformations 79−86307
teleconferences, influence of vision on auditory direction when presenting speakers *(German)* 79−72762
temporal modulation transfer functions based upon modulation thresholds 80−21478
temporally interrupted sentences, intelligibility with and without intervening noise 77−32911
test of speech intelligibility in noise 77−64048
time delay effect experiment 80−91996
time-altered speech intelligibility rel. to age 77−52805
time-compressed speech, intonation and intelligibility, English vs. French 80−74644
time-varying noise effects *(Japanese)* 79−23147
time-varying noise effects *(Japanese)* 79−81654
tone/noise combination effect, rel. to aircraft noise 77−50824
tones, discrimination of relative onset time of two-component tones by infants 80−33366
translation system, real-time, for hearing impaired 78−7546
transmission channel quality determining physical method 80−33369
unsteady synthetic vowel perception under various formant conditions 78−40196
visual vowel and diphthong perception from two horizontal viewing angles 80−35923
vocal output and preferred listening level rel. to ambient noise 79−68500
voice babble effects, stochastic aspects 79−81653
voice information, processing system, features and appls. *(Japanese)* 79−86310
voice onset time and fundamental freq. cues in /zi/-/si/ distinction 77−2008
voiceless stop consonants, perception expt. 79−98558
vowel normalization procedures eval. 80−33365
waveform coders, objective quality meas. equipment and method 80−91981
wideband noise reduction by spectral weighting 80−96146
word discrimination scores, effect of marking by noise 80−41047
word perception, prosodic cues 78−40204
word perception, role of medial consonant transitions 79−81651
He speech, translation via segmentation, partial-rejection and expansion 78−31823
He speech distortion correction by vocal tract area function conversion *(Japanese)* 80−19171
He speech investigations, intelligibility and unscrambling *(Japanese)* 79−81657
He speech unscrambling by nonlinear power spectrum conversion 79−46134

speech recognition
acoustic noise suppression in speech using spectral subtraction 79−46124
acoustic processors, experimental, recognition results 79−64421
acoustic-phonetic decoding of continuous speech, experimental system 79−59890
acoustics, speech and signal processing, conf., Tulsa, USA, 1978, April 78−63242
acoustics, speech and signal processing, IEEE international conf., Washington, DC, USA, 1979 Apr. 79−55275
artificial language word boundary detection by pitch contours 80−91991
Attached Processor for Speech 80−96145
auditory cues in a speech signal 78−96057
authentication of voice 79−94423
automatic, review of advances in 1976-7 period 79−50536
automatic, using adaptation methods for speaker normalization 79−68512
automatic, using psychoacoustic models 79−41529
automatic forensic speaker recognition 79−94422
automatic recognition, effect of speaker's mood on acoustic parameters 80−64306
automatic speaker identification, zero crossing anal. of speech in short term method 79−55272
automatic speaker identification for large population 79−68504

speech recognition continued
automatic speaker recognition, cepstral/spectral and linear prediction techniques compared 80−91993
automatic speaker recognition system, performance anal. by linear prediction 79−64431
automatic speaker verification by cepstral analysis 80−91998
automatic speech processing, approaches, models and appls. *(German)* 79−50532
automatic speech recognition, independent of the speaker *(German)* 79−90094
automatic speech recognition, speaker authentication and data entry 79−94419
automatic speech recognition by zero-crossing analysis methods 79−94420
automatic spoken language identification, finite-state models 80−91987
automatic spoken word recognition using linguistic information 79−55274
automatic system, equipment used for experimental purposes *(German)* 79−46129
Bengali vowels format struct., tracking loop formant extraction system 80−106673
biological signals detection, use of voice key *(Czech)* 77−5124
book 80−73118
cat, response of collicular auditory neuron to human speech 78−92646
categorical features in speech perception and production 80−64310
category boundary adaption between speech and nonspeech 79−72763
children, speech-pattern learning in French and English 78−57025
chinchilla, identification functions for synthetic VOT stimuli 78−57022
choral speech, speaker recognition 79−98565
coarticulation, formulation of process in formant freq. terms, appl. to automatic speech recognition *(Japanese)* 78−92660
coarticulatory effect perception, maturational influences 79−94415
computer interpretation of speech patterns based on formant trajectories 79−59877
computer-aided recognition of Polish vowels in continuous speech 80−33380
conference, Leningrad, 1977 Apr. 78−96055
consonant confusions in patients with sensorineural hearing loss 77−25469
consonant phonemes, auditory vs. phonetic accounts of observed confusions 79−86308
continuous, using system controlled by finite state parser 79−64420
continuous speech recognition system for data base consultation 80−91990
continuously-read natural language recognition achievements 80−91984
conversational speech recognition system, acoustic processor 79−46130
conversational speech recognition system, linguistic processor 79−46131
deaf subjects with cochlear implants, elec. stimulation of auditory nerve 80−108915
deleted consonant identification 79−10442
dichotic and monotic masking of consonant-vowels by consonant-vowel second formants 80−79069
dichotic perception of English consonants, role of distinctive features 79−68508
dichotic two-response paradigm, random guessing model 78−61206
digital filter model of basilar membrane for voice features extraction 78−77069
digital speech processing, book 79−72767
discrimination functions for normal-hearing subjects 79−92240
discrimination scores, binomial variable model 79−53161
discrimination tests using programmable hearing aid with multichannel compression, children 80−17202
distorted speech perception, role of training 80−5881
distortion error introduced by signal digitisation 77−27256
distribution of acoustic cues for stop consonant place of articulation in VCV syllables 80−64309
evaluating speech recognisers 77−32905
foreign languages, sound pattern recognition, optical methods 77−68337
formant tracking system toward automatic recognition of speech 80−58872
French, perceptual investigation of F_0 contours 79−14198
French speech understanding system, syntactic-semantic sentence interpretation 80−91989
frequency warping for nonuniform talker normalization 79−59894
HEAR acoustic processor, performance statistics 79−59873
infant perception, constancy for spectrally dissimilar vowel categories 80−33360
infant speech perception paradigms, selective adaptation effects 79−50527
infants, discrimination of voiced stop consonants 78−61207
information from data banks over telephone 80−1384
invariant cues for place of articulation in stop consonants 79−10443
isolated word recognition, interactive clustering techniques for selecting speaker-independ. reference templates 79−46126
isolated word recognition system, speaker-independent, using clustering techniques 79−86303
Japanese, processing strings of phonemic symbols using Chinese characters 79−27470
Japanese, speech recognition and speaker identification based on phonetic spectra *(Japanese)* 79−90093
Japanese kinki dialect, anal. and perception of two-mora word accent types *(Japanese)* 78−92659
lexicon for speech understanding system, structure 79−64422
linguistically oriented computer system for recognition natural continuous speech 80−23845
linguistically oriented system for word spotting in conversational speech 79−64424
lipreading, voice/mouth synthesis and tactual/visual perception of /pa, ba, ma/ 79−5302
MESA, multipoint electrotactile speech aid, reception of connected discourse 79−50529
microprocessor based speaker verification device 80−102936
minicomputer based signal processing facility for speaker recognition 79−18667
mispronunciations listening tests by segmenting speech into words 80−64308
multispeaker phoneme classification by canonical correlation analysis 80−91988
nasal sound detect., articulatory model *(Japanese)* 79−81656
nasals detection in continous speech 77−40683
speech recognition continued
natural and synthesized speech differences, pattern recognition approach 79−64430
NMR spectroscopy, ^1H, automatic PMR spectra interpretation system 78−32840
on-line speaker verification system, structure and performance 79−64433
perception, rhythmic and segmental, interdependency 79−72765
perception, use of comfortable listening levels, effect of loudness level 79−2078
person-machine speech communication systems, speech recognition using dialogue process 79−64423
personnel authentication operational system 79−94424
phoneme boundaries, effects of adaptation 78−80884
phoneme boundaries meas. in four ways 80−96138
phoneme chains, correction of incorrectly recognised samples *(German)* 79−46128
phoneme discriminator for automatic discrimination of fricative consonants based on human audition 79−55286
phoneme recognition system based on human audition, psychophysical expts. 78−69115
phoneme recognition with small room reverberation 79−86306
phoneme selection from equally spaced quasi-phoneme string by entropy principle, automatic 79−59891
phonemes, spectral classification by learning subspaces, pattern recognition scheme 79−59888
phonetic features, perceptibility in fluent speech 78−92635
phonetic word verification 79−68513
pitch period analysis of connected speech using digital computer algorithm 79−59878
power spectrum peaks extraction method for acoustic signals with pitch 79−98563
preadolescent children's voices, sex identification 79−43925
preschool children, imitation of synthesized vowels 78−61205
present and future, study *(Japanese)* 80−87663
probabilistic vector model for identification of intervocalic stop consonants 78−69114
quasistationary processes and universal codes 80−91994
range effect in the perception of voicing 78−65044
rank-order speech classification algorithm (RASCAL) 79−64426
reception-discrimination audiometer, computerised *(Japanese)* 79−74774
reflex theory of speech perception 79−46132
review of speech recognition and anal. *(French)* 79−68509
Russian speech automatic recognition, deductive strategy 80−91997
segmentation of band-limited speech signals using linear prediction 80−91970
selective anchoring and adaptation of phonetic and nonphonetic continua 79−14199
sentence information processing, EEG evoked response and CNV obs. 79−57626
sentence intonation in Danish utterances 80−58870
signal reference construction method *(Russian)* 79−50531
SIRENE, computerized speech training aid 79−70701
speaker identification, effects of selected vocal disguises 80−10091
speaker identification by long-term spectra under normal and distorted speech conditions 78−11677
speaker recognition, multistage decision schemes 79−64435
speaker recognizability, voice rating system 79−64434
speaker verification accuracy, orthogonal parameters for noisy speech 79−64432
speaker verification algorithm for noisy utterances 80−91992
speaker-dependent word recognition system, selection algorithms 79−50535
speaker-independent vowel identification in continuous speech 78−69113
speaker-independent word recognition, application of clustering techniques 79−94411
spectral local peaks, dynamic props. rel. to speech recognition system *(Japanese)* 77−68334
spectral peaks use in recognition of spoken words *(Japanese)* 77−64053
speech formant extraction, tracking loop filters 78−65051
speech production measures of speech perception, rapid shadowing of VCV syllables 80−64311
speech recognition system fast training method 79−81649
speech trainer for multihandicapped children, display method and control program *(Japanese)* 80−108922
spoken word recognition method using nonlinear spectral matching *(Japanese)* 80−69605
stop consonant discrimination based on human audition 79−50528
syllable mispronunciation effects on word recognition 80−64307
syllable perception with alternate formants presented to opposite ears 78−65043
syllable-based recogniser for continuous speech 80−91986
syntactic methods for speech segmentation and recognition 79−59889
synthetic /bdg/ by hearing-impaired listeners under monotic and dichotic formant presentation 80−58871
synthetic stop consonant identification, evaluation and integration of acoustic features 80−58869
systems design *(German)* 79−46127
Tadoma speech reading, untrained observers' discrimination ability, tactile sensitivity 79−96587
Tadoma vibrotactile speechreading, preliminary results 78−28127
telephone handset user identification, PARCOR parameters *(Japanese)* 79−81655
tempo of spectrum change as a cue in speech-sound discrimination by infants 79−98562
temporally segmented vowels and consonant-vowel syllable perception 79−98560
time-domain algorithms of speech signals, harmonic bandwidth compression 79−46125
time-intensity trade, temporal speech-Stenger effect 77−25470
tracking procedures for training and evaluating speech reception 78−61204
transition length, effects on perception of stop consonants 78−92636
vibrotactile recorder, speech sound identification 77−78055
visual and auditory contributions 77−16939
visual perception of syllables and sentences, age effects 80−16943
vocal tract area functions, sensitivity to perturbations in bandwidths and formants 79−59887
voice communication, speech production mechanisms and models *(Spanish)* 80−87665
voice controlled system for the disabled 79−5407

speech recognition continued
voice input and output, implementation and appl. *(Japanese)* 80−87664
voice qualities, multidimensional classification 78−92651
voice synthesis and voice recognition, review *(German)* 79−50530
voicing detection algorithms, automatic thresholding 79−64425
vowel, algorithms using zero crossings *(French)* 80−83708
vowel feature perception in temporally-segmented noise portions of stop-consonant CV syllables 79−98561
vowel identification, excerpted from /l/ and /r/ contexts 77−9210
vowel identification using piecewise separation technique 79−46123
vowel perceived duration, temporal course 78−77065
vowel perception, freq. position of centre of gravity of formants 79−32148
Wigner distribution function, optical production, speech signal analysis 80−48521
word sequences, segmentation for automatic recognition *(German)* 80−91971
zero crossing and FFT speech recognition systems compared 79−76917
He speech, translation via segmentation, partial-rejection and expansion 78−31823

speech synthesis
8-channel digital speech synthesizer based on linear predictive coding techniques 79−64439
32 channel multiplex audio response system based on formant vocoder principle *(German)* 80−96133
acoustics, speech and signal processing, conf., Tulsa, USA, 1978, April 78−63242
acoustics, speech and signal processing, IEEE international conf., Washington, DC, USA, 1979 Apr. 79−55275
automatic speech processing, approaches, models and appls. *(German)* 79−50532
autoregressive system, vowel sound synthesis, adaptive filter method *(Spanish)* 80−43556
bispectral synthesizer for acoustic signals 79−50513
coding using non-uniform linear prediction in transform domain 79−55277
compilation, pre-recorded words and phrases for weather reports, expt. system 80−87667
compression system with vector quantizing, two-step 79−59881
computer driven, personal, portable, and intelligent speech prosthesis 78−92745
computer model to characterize the air volume displaced by the vibrating vocal cords 78−69111
computerised, principle and appl. 79−98564
conference, Leningrad, 1977 Apr. 78−96055
data compression and digitisation of speech signal, devices and techniques *(German)* 80−91969
data reduction of sampled speech signals, methods and results 79−81648
deconvolving speech waveform, maximum peakiness criterion 80−83714
digital filter speech prod. model 79−81661
diphone synthesis for phonetic vocoding 79−64440
dyad boundaries, linear interpolation of spectral parameters 80−19168
dynamic vowels, human auditory system perceptual mechanism, dichotic fusion expts. *(Japanese)* 80−53569
electronic methods currently available 80−106677
encoding voice fundamental freq. into vibrotactile freq. 80−10092
Estonian, statistical data *(Russian)* 80−45923
excitation function for LPC synthesis retaining glottal phase characts. 78−69112
formant frequency and bandwidth conversion to reflection coefficients 80−91975
formant representations of parameters for channel vocoder 80−83709
formant transitions using interactive speech anal. synthesis system 80−83712
fundamental freq. contours at syntactic boundaries 78−3521
glottal area waveform synthetic and natural speech comparison 77−77919
glottal inverse filtering from acoustic speech waveform, least squares approach 79−86304
glottal sound source, self-oscillating model *(Japanese)* 78−92654
human communications, appls. 80−96110
human vocal tract, IC technology appl. to speech synthesisers 80−87661
information from data banks over telephone 80−1384
information system speech output using speech synthesis from concept 79−94414
linear prediction based system 79−90097
linear prediction coding for synthesizing natural sounding speech 79−59879
linear prediction of formants for low bit rate digital speech transmission 79−59880
linear prediction synthetic speech, buzz reduction 78−57024
linear predictive coded speech quality problems and expts. 80−91982
linear predictive vocoder with new pitch extraction and exciting source, experimental model 79−59884
lipreading, voice/mouth synthesis and tactual/visual perception of /pa, ba, ma/ 79−5302
local tract area function, estimation by adaptive deconvolution and adaptive speech anal. system *(Japanese)* 78−92658
log likelihood ratio interpretation as measure of waveform code performance 80−83706
microcomputer-based speech synthesis system 79−94421
microcomputer-based speech synthesizer for Spanish language 79−64445
microprocessor based real-time speech processor 79−64437
microprocessor for programmable speech synthesis 80−91983
microprocessor speech synthesiser terminal 79−81660
microprogrammed intoned speech synthesizer system for computer aided instruction techniques 79−64442
minimum and mixed phase speech analysis-synthesis by adaptive homomorphic deconvolution 79−90090
mixed-source model for speech compression and synthesis 79−14200
motor unit correlates of syllable stress, preliminary obs. 78−92653
multimicroprocessor implementation of all-digital speech synthesizer 80−96143
optical lip shapes from vowel sounds, synthesis using CRO 80−19170
parallel processor for real-time speech signal processing 79−64436
PARCOR analysis-synthesis telephony, improvement of speech quality 79−50534
PARCOR system, description and appl. *(Japanese)* 80−79070
PARCOR system for expression of spectral features 79−50533

speech synthesis continued
partial autocorrelation vowel-consonant-vowel concatenation units 79−46135
phase preservation in speech processing 79−59875
phoneme based speech synthesis 79−90098
pitch contour transfer between utterances with differing lexical content 79−81652
pitch dependent algorithm for speech rate changing 78−53428
portable equipment *(French)* 80−51291
portable speech synthesizer for severely handicapped children 80−56154
preprocessing filter for enhancing linear predictive analysis/synthesis of noisy speech 79−64447
prerecorded voice response system 79−90096
preschool children, imitation of synthesized vowels 78−61205
programmable filter synthesiser *(French)* 80−48524
real-time text processing for Italian text-to-speech synthesis system 79−64438
review, digital electronics technology 79−90095
review of current topics *(Japanese)* 80−91973
software for cascade/parallel formant synthesizer 80−58868
software linear predictive coding k-parameter synthesizer via dynamic programming 79−64443
Spanish phonemes, anal. of formant and pitch 79−64444
speaking machines, historical overview *(Japanese)* 80−23846
speech trainer for multihandicapped children, display method and control program *(Japanese)* 80−108922
subglottal air pressure and vocal-fold tension, indirect assessment of contrib. to changes of fund. freq. in English 78−92650
techniques *(Japanese)* 80−87662
text-to-speech synthesizer for blind and handicapped 80−96142
time-domain speech synthesis by rules using flexible fast signal management system 79−64441
touch-sensitive audio tablet for blind access to digital memory 79−76916
transform coding of speech, examples 79−59886
verbal communication aid for nonvocal patients 79−57816
vocal cord vibration, longitudinal displacement, acoustic properties 77−90812
vocal cords vibratory behaviour in tension and mass imbalance 79−83803
vocal tract area function acoustical meas. 79−64446
vocoder concept using discrete time acoustic tubes 79−59885
voice communication, speech production mechanisms and models *(Spanish)* 80−87665
voice production, analysis synthesis, computer appl. *(Dutch)* 77−12938
voice synthesis and voice recognition, review *(German)* 79−50530
vowel articulation, transmission behaviour of human speech generating system 78−15849

speech transmission *see voice communication*

speed *see velocity*

speed control *see velocity control*

speed indicating instruments *see velocity measurement*

speed measurement *see velocity measurement*

spelter *see zinc*

spherical aberration *see aberrations*

spheroidizing
ceramic powder, thermal stresses during spheroidisation process *(Russian)* 80−40386
graphite, effect on fatigue strength of cast Fe *(Japanese)* 78−64626
modular cast Fe, probability prediction of spheroidisation by parametric diagram of chem. bond *(Chinese)* 80−66543
pearlite spheroidization, quantitative meas. 77−44275
steel, 12% W, eutectic carbides struct. and comp. during heating 80−76283
steel, alloy, type 11Kh18M, eutectic carbide composition change due to heating 80−16353
steel, anisotropic rolled plate, fatigue crack growth, rel. to laminated struct. and inclusions 78−92313
steel, austenitic, supercooled, decomposition by heat treatment, carbide particle morphology *(Russian)* 77−70076
steel, austenitic supercooled, transformation kinetics into spheroidised pearlite *(Russian)* 78−95742
steel, C, spheroidized, type 1090, exam. of reverse flow behaviour 78−80610
steel, C, wire, drawing effect on spheroidization *(Korean)* 77−66656
steel, C (0.2 and 0.45 wt.%), spheroidization at 680 to 690°C, struct. changes *(Russian)* 78−15431
steel, C and alloy, cold formability *(French)* 78−60681
steel, hypereutectoid, austenite dissociation depend. on strain at intercritical temps., pearlite transform. *(Russian)* 80−40362
steel, hypoeutectoid, morphology and stability of Widmanstatten struct. *(Slovak)* 79−70094
steel, KhVG, deformation ht. treatment on carbide precip. in KhVG 77−63700
steel, lightly alloyed, S effect on failure following controlled rolling *(Russian)* 79−57086
steel, pearlite, global microstruct. evolution during spheroidization 80−108482
steel, spheroidized, Bauschinger effect and work hardening 78−64596
steel, spheroidized, shear mode of ductile fracture 79−61714
steel, ultrahigh C, superplastic struct. development by heat treatment 80−11703
Zircaloy, effect of dispersion and spheroidisation treatment of δ ZrH 79−76073
zircon, dissociated, form. in plasma furnace, comp. and microstruct. 77−36429
Al_2O_3, cylindrical voids, exam. of instability 78−79603
Co(Cr.Ni)-TaC fibrous eutectic, deformed, thermal stability of microstruct. *(Russian)* 79−1895
Cu, powders, prep. of spherical starting particles, for suspension electrolysis 78−60689
Fe, cast, graphite nodule form., ion microprobe mass anal. appl. 79−43295
Fe, cast, influence of interfacial energy on shape of graphite 80−16360
Fe, cast, Mg, despheroidising effect of Bi, Sn on graphite in alloy 78−56670
Fe, cast, rare earth-Mg, metallurgical and technological features, appl. in China *(Chinese)* 78−84851
Fe, cast, rare-earth-Mg nodular, fracture toughness and fatigue *(Chinese)* 78−95791

spheroidizing continued
Fe, cast, spheroidizing effect of Mg and Ce modifiers 80−35193
Fe, cast graphite spheroidization, Mg residue effects *(Korean)* 79−43286
Fe-C-Si, spheroidization 77−66665
Fe-Si-Mn-C, cast, Ce additions, nonmetallic inclusions *(Russian)* 78−19710
Ni, powders, prep. of spherical starting particles, for suspension electrolysis 78−60689
Pb, powders, prep. of spherical starting particles, for suspension electrolysis 78−60689
Zircaloy, dispersion and spheroidisation treatment of δ ZrH, effect on corrosion resistance 79−76072
ZrO_2-Y_2O_3 powder, prep. for plasma spheroidisation, sputter drying *(Russian)* 80−55324

spicules *see solar prominences*

spin
see also baryon spin and parity; electron spin; isotopic spin (elementary particles); lepton spin and parity; meson spin and parity; nuclear spin and parity; spin density waves; spin hamiltonians
Bernoulli's principle, spin of balls and coins 80−77592
book, axiomatic QFT, PCT, spin and statistics 78−78102
charged particle spin, theory using fluid basis for matter and energy 79−97542
composite hadrons, spin depend., S-matrix theory, TeV energy range 78−58164
dynamical spin spreading of unstable particles in four models 79−54003
elementary particle spin, reln. to universal props. of matter 78−21329
ferromagnet, magnetoelastic gap in spin wave spectrum *(Russian)* 77−59400
four vector components, eigenvalues and -functions for spin 0 and 1 78−49720
Galileian formulation of spin, Clifford algebras and spin groups 78−57736
Galileian formulation of spin, explicit realisations 80−62505
general relativity and spin via square root procedure, supersymmetry 77−82437
generalized quantum spins, coherent states, and Lieb inequalities 79−67172
hadronic high momentum transfer scatt., spin meas. and polarisation review 79−63498
hadrons, relation between spin, isospin, strangeness and charm 80−37183
half-integral spin particle wave function, 720° rot. effect, teaching models 79−62958
isolated system, supertranslation invariance of spin vectors 79−6030
local quantized superfield, local commutativity from spin and statistics 77−57435
Majorana transitions, spin-flip probability, LZS model calc. 77−57959
massive lepton pair prod. by polarised p, constituent spin prop. test, QCD 79−89201
neutron, dipole moments and spin rot. meas. 79−36080
neutron, electric and magnetic dipole moments 80−4993
neutron spinor rotation and the neutron few-body interaction 79−59113
nucleon-nucleon scatt., spin struct. and polarising power 79−67568
Pauli spin matrices, generalised, commutation rules 79−17597
Poincare covariant particle model with mass and spin mixing 80−32016
proton, outcome of violent collisions 80−434
proton spin struct., from polarised lepton-hadron scatt. 79−67560
quantum dynamical semigroups and spin multipole relaxation in isotropic surroundings 78−86813
quark fragmentation in P conserving jet production reactions, spin observables 79−71658
relativistic spin rotation in elementary particle reactions *(Russian)* 78−54586
spin-1 matrices, props., for teaching 79−67128
spin-1 polarisation, helicity formalism, treatment by extension of spin-$^1/_2$ case 79−63383
strong interactions at very high energy, spin depend. 78−58203
translational gauge theory of gravity: post-Newtonian approximation and spin precession 80−46945
unstable particles, dynamical spin spreading 80−9117
world line conditions for spinning particles, spin orbit forces 80−36844
$e^+e^-\rightarrow\tau^+\tau^-$, τ spin from two body decay energy spectra *(Chinese)* 79−49503
$\gamma^*N\rightarrow\psi N$, gluon momentum, spin, parity and coupling 80−42395
K^+p scatt., $Z_1^*(1800)$ resonance from elastic spin-rotation angle 79−63523
$L^0\rightarrow\nu_L\mu^+\mu^-$, heavy lepton spin, massless spin 3/2 ν four fermion interaction 79−13175
NN elastic scatt., spin struct. interpretation, polarising power 79−85342
NN large angle elastic scatt., spin correlation asymmetries, partons and coloured quarks 79−63411
NN→NN, large momentum transfer, spin effects 80−22577
np, elastic scatt. at large transverse momentum, spin-spin forces 78−78216
pp, elastic scattering, high P_t, spin interactions meas. 79−67608
pp, polarisation data interpretation for high energy elastic scatt., eikonal model, spin parameters 79−3048
pp elastic scatt., 10 MeV, A_{yy} component of spin correlation tensor 79−67592
pp elastic scatt., ISR energies, spin behaviour of ang. distribs. at large momentum transfer *(Russian)* 79−80849
pp elastic scatt. at large transverse momentum, spin-spin forces 78−78216
pp interactions, 6 GeV, spin depend. determ. 78−66139
pp→pX, high p_T, spin-spin asymmetries, polarisation, hard scatt model with QCD 80−13339
pp→pp, medium energies, inelasticity and struct., pure spin total cross section data 78−62439
$pp\rightarrow\pi^0X$, pol.p, 24 GeV/c, high $p_T\pi^0$ prod., spin. depend. 80−105935
$\tau\rightarrow\pi\nu_\tau$, spin 3/2 heavy leptons, decay suppression, weak current *(Chinese)* 78−82192

spin arrangements *see magnetic structure*

spin decoupling (NMR) *see double nuclear magnetic resonance*

spin density waves
alloys, antiferromag., nesting type model, spin fluctuations 78−84435
antiferromagnet, itinerant, effect of imperfect nesting of band struct. 78−31045
antiferromagnet, itinerant, paramag. impurity effects on Neel temp., calc. 80−60257
antiferromagnet, itinerant model, spin density wave transition, impurities effect 77−72986
antiferromagnet, neutron scatt. by magnons, modulated spin amplitudes 80−75722
antiferromagnetic metal, nesting type model, spin fluctuations 78−56329
antiferromagnetism itinerant electron theory, spin susceptibilities 78−6504
antiferromagnets, mag. anisotropy in state 77−69540
band structure, relativistic spin polarised calc., technique and its appl. to Gd 77−85128
coexistence with CDWs, appl. of multicritical point anal. 79−77717
commensurate, nearly, effect of harmonics, Hartree-Fock calcs. 78−88104
conduction-electron polarisation at nucl. sites due to indirect exchange interaction 80−34619
electron gas, dielectric function, dynamical exchange decoupling, plasmon dispersion, SDW and CDW 80−59900
electron gas, one dimensional, dynamic interaction screening, spin and charge density wave instabilities 80−24819
electron gas, one-dimens., with backward scatt., soliton Green's functions 78−10386
electron gas, spin polarised, exchange and correl. energy 77−85163
exciton ferromagnet, incommensurate mag. structs., inhomogeneous magnetisation *(Russian)* 80−29566
exciton ferromagnet, spin-lattice relax., light and US absorption *(Russian)* 79−7960
Fermi gas, one dimensional with backward scatt., gap renormalisation 80−24818
ferromagnet, magnetic susceptibility, spin and charge density waves, Curie temp. *(Russian)* 80−100581
ferromagnetic metal, RKKY oscills. in surface spin density, density functional formalism 77−20512
Hubbard model, one-dimens., extended, $2k_F$ and $4k_F$ correl. functions, computer renormalisation group calcs., appl. to one-dimens. conductors 80−54625
Hubbard model, one-dimensional $2k_F$ and $4k_F$ correl. functions, computer renormalisation-group calcs. 79−78029
hydrocarbons, cyclic, non alternant, nonsingle instabilities of HF solns. 80−58164
interaction between localised moments in system with electron hole pairing *(Russian)* 78−88111
itinerant electron antiferromagnet, effects of paramagnetic impurities on Neel temperature 79−4678
itinerant electron antiferromagnetic matrix, local moments, spin Hamiltonian 80−34626
itinerant-electron ferromagnetism, possible coexistence with itinerant-electron antiferromagnetism 78−39286
linear conductor, interchain coupling role 78−6294
linear conductor role of interchain coupling 77−47751
magnetic order coexistence with charge density waves 80−97096
metal, electron theory *(Japanese)* 77−66102
metallic slab, theory of Larmor waves, Fermi-liquid interactions, Fermi-surface and g-tensor anisotropy 79−69397
one dimensional Fermi gas model in relation to spin and field theoretical models 80−24816
one-dimensional electron gas with backward scatt., scale invariant characteristic energy 77−31927
one-dimensional electron system, generalised susceptibilities in mag. field *(Russian)* 77−80750
one-dimensional Fermi gas with backscattering, coupling between charge and spin degrees of freedom 80−17861
one-dimensional Hubbard model, antiferromag. and Peierls instability 78−23233
one-dimensional Hubbard model, Friedel oscills. around a nonmagnetic impurity 80−25073
one-dimensional systems, impurity effects on ordered phases 80−24905
organic linear chain cpds., diffuse $4k_F$ refls., small intramolecular Coulomb interaction 80−34376
paramagnetic metals, nonphonon mechanism of supercond. and static screening *(Russian)* 79−78258
phase transition to incommensurate excitonic phase 80−75510
quasi one-dimensional spin lattice coupled system, collective modes 80−24896
quasi-one-dimensional electron gas with strong on site interactions 77−4306
quasi-one-dimensional electron systems, effect of interchain electron transfer on phase transition 78−51911
quasi-one-dimensional systems, spin-lattice Peierls instabilities, static and dynamic aspects 80−71052
quasi-one-dimensional systems, three-dimens. ordering in system of weakly coupled chains 78−6295
semiconductors, density waves in one, two and three dimensions 79−95353
$(Sn)_x$ chain, energy band struct., Hartree-Fock and CDW solns. 79−23885
spin-orbit coupling, charge and spin density wave effects 79−91009
spinless fermion systems, Coulomb repulsion, bond alternation, Peierls distortion, HF approx. 80−44524
superconductivity-ferromagnetism coexistence in two-band model *(Russian)* 80−84539
superconductor, magnetic, Fermi surface nesting effect on mag. instability 80−54831
superconductors, magnetic ordering rel. to spin density waves 79−99656
surface, itinerant antiferromagnetism and density waves 79−82743
TCNQ-HMTSeF, nucl. spin relax. obs., diffusive character of response function and interchain coupling 78−10797
$(TMTSF)_2PF_6$ (AsF_6), linear-chain conductor, semicond.-metal transition in small elec. field 80−103730
transverse dynamic susceptibility and spin waves in itinerant electron SPW states 80−97076
TTF-TCNQ, microscopic model for three low temp. phases 79−73303
TTF-TCNQ, neutron and X-ray diffuse scatt., phase transitions, one-dimens. behaviour and interpret. 78−10381
TTF-TCNQ, nucl. spin relax. obs., diffusive character of response function and interchain coupling 78−10797
TTF-TCNQ electronic props., PMR 78−2763
two-dimensional layer, model, electron-correlated density-wave states 78−51919
π^0 condensation in symmetric nuclear matter and pure neutron matter 79−3108

spin density waves continued
Cr alloys, localised magnetic moments in band antiferromagnets, impurity interactions *(Russian)* 80−54888
Cr alloys, Neel temp. of one dimens. electron gas in spin density wave state 80−65884
Cr and alloys, itinerant antiferromagnetism and density waves at surface 79−82743
Cr, Anderson model of 3d virtual states 77−72987
Cr, antiferromag., electron interference oscills. and spin-density-wave energy gaps at Fermi surface 80−49574
Cr, antiferromag., mag. and non-mag. impurities, hyperfine interactions, ^{181}Ta and ^{100}Rh TDPAC meas. 78−43704
Cr, antiferromag., magnetostriction and torque meas. below spin-flip transition 77−63186
Cr, antiferromag., stress depend. of Fermi surface 77−11846
Cr, antiferromag., stress depend. of spin density wave state 77−63257
Cr, antiferromag., transverse magnetoresist., electron interference oscills. 80−65534
Cr, antiferromag., uniaxial anisotropy, itinerant model 78−10640
Cr, antiferromagnetic, mixed state, mag. torque and magnetostriction meas. 77−89909
Cr, antiferromagnetic, polarisation domain effects on US velocity 78−52329
Cr, antiferromagnetic, pressure effect on Fermi surface by de Haas-van Alphen effect *(Russian)* 80−6701
Cr, antiferromagnetic spin-density-wave domain and size and behaviour, X-ray and neutron topography 79−42793
Cr, deformation waves and spin density waves, electron diffr. obs. *(Russian)* 79−19721
Cr, electronic structure model, Invar effect, antiferromagnetic-non mag. transitions 80−20370
Cr film, size effects on spin density waves, struct. and elec. props. 77−80973
Cr, Hall coeff., mag. field depend. at low temp. 77−20296
Cr, hyperfine interactions on ^{111}Cd-probe nuclei, TDPAC meas. 80−75904
Cr, incommensurate antiferromag., inelastic neutron scatt. meas. 80−25088
Cr, inelastic neutron scatt. expts., spin density waves 80−44818
Cr, mag. phase diagram, near, spin-flip temp., US attenuation 80−60267
Cr, magnetic excitations of incommensurate spin density wave 80−11183
Cr, magnetic phase diagram in external mag. field, spin reorientation curve, critical point coordinates *(Russian)* 80−29548
Cr, magnetic torque anal. in thermally activated domain model, near spin-flip temp. 77−63229
Cr, paramagnetic, Hartree band struct., Fermi surface, nesting wave vector 80−49583
Cr, Q-vector locking, press. induced hardening 80−103870
Cr, single cryst., mag. hysteresis, neutron diffr. obs. inertia of domain wall motion 79−15327
Cr, spin density wave, CDW and strain wave, effect of spin polarisation of reservoir and imperfect nesting 78−56284
Cr, spin density wave, Nambu-Eliashberg eqns. for k-state electron-hole pairing 80−97050
Cr, spin density wave, temp. depend. of second and third harmonics 77−12094
Cr, spin density wave phases, domains 80−103871
Cr, spin density wave Q vector, vel. depend. 79−4669
Cr, spin density wave Q-vector, temp. and press. depend. 80−11167
Cr, spin density wave state, appl. of interacting virtual bound state picture 77−69464
Cr, spin density wave state, phenomenological free energy density description 80−75720
Cr, spin density waves detected by Ta mag hyperfine field meas. 78−60364
Cr, spin-flip transition temperature, press. depend. from elastic const. meas. 80−65944
Cr, strain and spin-flip transition, Landau theory 78−39318
Cr, stress and impurity conc. depend. 77−73029
Cr, transverse spin-density-wave phase, absence of neutron diffr. line broadening due to polarisation domains 77−24677
Cr-Al, mag. excitation, neutron spectrometry 79−4654
Cr-Al, spin density wave, neutron diffraction studies 79−1664
Cr-Co, dil., antiferromag., elec. resist. min., press. and impurity effects 80−59970
Cr-Co, spin density wave, neutron diffraction studies 79−1664
Cr-Co (4.0 at.%) alloy, antiferromag., disappearance of resist. min. under press., and press. coeff. of T_N 80−10960
Cr-Co (up to 8 at.%), antiferromagnetic, resist. minimum, Kondo effect by pairs of Co atoms 80−39566
Cr-Co alloys, dil., with local mag. moments, Neel temps. 79−73713
Cr-Fe, dil,, antiferromag., elec. resist. min., press. and impurity effects 80−59970
Cr-Fe, dilute, localised moment cluster model, ferromagnetic exchange coupling 80−39774
Cr-Fe (0.6 at.%), antiferromag., anomalous press. effect on resist. minimum 79−15138
Cr-Fe (14 wt.%), spin density wave and spin glass ordering coexistence at low temps. 79−61059
Cr-Fe alloys, itinerant antiferromag. effect of mag. impurities 77−32186
Cr-Fe-Si, mag. excitation, neutron spectrometry 79−4654
Cr-Fe-Si, spin density wave, neutron diffraction studies 79−1664
Cr-Fe-V, dil., V effect on para- to incommensurate and commensurate transitions 78−68260
Cr-Fe(Co) alloys dil., exchange interactions 77−47986
Cr-Ge, dilute alloy, phase diagram of spin density wave states 79−24158
Cr-Mn, order of mag. transitions in antiferromag. alloys 79−4677
Cr-Mn alloy, strain wave and spin density wave intensities, neutron diffr. 78−60266
Cr-Mo, behaviour of mag. impurities 79−4672
Cr-Mo, electrical resistivity, spin density wave gap, Neel temp. 80−88534
Cr-Mo-Fe (2, 14 wt.%), spin density wave and spin glass ordering coexistence at low temps. 79−61059
Cr-Pt alloys, neutron diffraction study, (100) magnetic peak, magnetic structure transitions 79−56506
Cr-Re, mag. excitation, neutron spectrometry 79−4654
Cr-Re, surface spin-density wave near T_N 79−91238
Cr-Re (0.18 wt.%), mag. excitations in longitudinal and transverse SDW phases 80−70946
Cr-Rh, dil., hyperfine fields meas. 79−47056

spin density waves continued
Cr-Si alloys, first order transition of spin density wave state, thermal expansivities meas. 77−85453
Cr-Si-V, (2, 0.1 at.%), paramag. to commensurate spin density wave transition 80−65875
Cr-Si-V, dil., V effect on para- to incommensurate and commensurate transitions 78−68260
Cr-Ta, mixed SDW and Zeeman hyperfine interactions, TDPAC calc. 79−99797
Cr-V alloy, strain wave and spin density wave intensities, neutron diffr. 78−60266
$Cr_{995}Mn_{005}$, spin density wave Q vector, vel. depend. 79−4669
$(Cr_{98}Mo_2)_{90}Fe_{10}$, spin glass behaviour obs. 79−61157
Cu, fluctuations in nuclear spins, susceptibility, internal energy 80−50115
Fe-Cr, dil., spin density wave under high press., neutron diffr. study 80−65798
Fe_xNbSe_2 (2H), mag. susceptibility meas., 1.3-300K 80−39740
H_3, interrelationships between effective hamiltonians 77−30767
K, Larmor wave spectrum 79−69397
γ-Mn, collinear spin structure stability 80−107984
α-Mn, electronic structure model, Invar effect, antiferromagnetic-non mag. transitions 80−20370
$NbSe_2$:Fe, local moment form., mag. susceptibility meas. 79−82756
$(SN)_x$, quantum chem. calcs. of electronic struct. 78−6257
Si-Cr, dil., spin density wave under high press., neutron diffr. study 80−65798
Si(100) inversion layers, two-dimensional electron fluid, spin density, valley density waves 77−69400
TaS_2:Fe, local moment form., mag. susceptibility meas. 79−82756
$TaSe_2$:Fe, competition between charge and spin density waves, Landau-Ginzburg theory 79−95352
$TaSe_2$:Fe, local moment form., mag. susceptibility meas. 79−82756
$TiBe_2$, neturon diffr. study of mag. ordering 80−44811
V_nO_{2n-1} ($3 \leq 3 \leq 9$), Magneli phases, mag. susceptibilities at low temp. 80−20389

spin disorder resistivity
actinide metals and compounds, nearly magnetic, thermoelec. power 78−84197
actinide non-stoichiometric intermetallic cpds., elec. resist. temp. depend. 79−1597
actinide systems, spin fluctuations effect, model approach 77−28404
alloys, highly resistive, temp. depend. on elec. resist. 78−91657
amorphous Heisenberg ferromagnet, force-force correl. function method 80−24918
antiferromagnet, effect of inelastic scatt. on resistive anomalies at mag. crit. points 77−55675
antiferromagnetic, spin fluctuation resist. near T_N, theory 77−40071
antiferromagnetic alloy, stoichiometric depend. of elec. resist. 77−69312
antiferromagnetic alloys, spin disorder resistivity, coherent potential approx. 78−14722
antiferromagnetic metals, electron scatt. features, s-d exchange model 77−8085
antiferromagnetic metals, two band model for elec. resist. 78−14720
disordered systems, Anderson localisation theory in two dimens., real space scaling method 80−44540
ferromagnet, effect of inelastic scatt. on resistive anomalies at mag. crit. points 77−55675
ferromagnet, itinerant, mag. props., temp. depend., functional integral approach 80−60170
ferromagnetic metal, anisotropic 78−56137
ferromagnetic metal, electron scatt. by fluctuations of mag. moment near Curie temp. 79−73502
ferromagnetic metal, impurity resist., band model calcs. 77−39830
ferromagnetic metal, nearly and weakly ferromag., freq. depend. elec. cond., Drude's formula deviation 79−47091
ferromagnetic metal, resist. anomaly near T_c, itinerant mag. electron theory 78−95292
ferromagnetic metal, uniaxial, anisotropic spin fluctuations and anisotropic band struct. effects on resist. near T_c 80−65543
ferromagnetic metals, resist. anisotropy, crit. behaviour and temp. depend. 80−96858
ferromagnetic ternary alloy, spin-disorder resist. in CPA weak scatt. limit 78−39100
Invar, magnetovolume contrib. to temp. variation of magnetoresist. 77−31999
low-temperature, effect of pot. scatt. in uniformly exchange-enhanced system 77−15840
magnetic metal, impurity resistance 78−84205
magnetic ternary alloys, statistical theory of electrical resistivity 78−87969
metals, spin fluctuation theory, for mag. and elec. props., appl. to actinides 78−91869
metals, uniaxial ferrogmagnetic, influence of anisotropic fluctuations on elec. resist. near T_c 79−91038
rare earth metals, electrical resistivity, high temp., scatt. mechanisms 80−39553
rare earth metals, HCP, point defect production during electron irrad. at low temp. 80−49273
rare earth metals and their alloys, liq., elec. resist. meas. 77−51718
rare-earth, light-heavy alloys, resistivity, mag. contrib. to resist. and Neel temp. 78−51971
spin glasses, elec. resist., thermal resist. and thermopower 80−65542
spin glasses, electrical resistivity calc. 79−78090
steel, C, resistivity, thermal and elec., spin disorder scatt. anal. 78−76063
transition metal alloys, ferromagnetic, low temp. resist. calc. 80−24919
transition metal dilute alloy, spin fluctuation contribution to elec. resist., field depend. 77−1413
Au-Cu-Fe spin glass alloys, impurity mag. resist. meas. 80−59972
Au-Fe(Co)(Mn), residual resistivity conc. depend. 80−2382
AuFe, spin glass, anomalous magnetoresistance 79−78077
α-Ce, exchange-enhanced, elec. resist. T^2 depend., press. effect 80−96845
$Ce_{80}Au_{20}$, metallic glass, mag. ordering and cryst. field effects, speromagnetism 80−80531
CeB_6, resist. anomaly and mag. ordering obs. 79−61110
CeP(As)(Sb), microwave resist. meas. 77−4383
Cr-Mn alloys, elec. resist. near T_N 77−69313
Cr_3SeTe_3, anomalous Hall effect 77−69351

spin disorder resistivity continued
Cu-Ni film, struct. and mag. order effects on electron transport props. 78−6460
Cu_2MnAl Heusler alloy, elec. resistivity 79−91020
$Cu_{2.0}Mn_{0.94}In_{1.0}$, In-Heusler single crystal, elec. resist. 78−60107
Dy-Y alloy, scatt. of cond. electrons by spin disorder 78−47778
$DyAg_{1-x}In_x$, elec. and Hall resist. 80−96844
Er film, vacuum-evaporated, rel. to thickness depend. of resist. 77−76956
Fe based ternary alloys, Coulomb and exchange scatt. amplitudes, spin dependent residual resistivities 78−64033
α-Fe, C drift velocity for electromigration temp. depend. in paramag., ferromag. phases 78−18835
$Fe_{1-x}Cu_xCr_2S_4$, Hall effect and magnetoresist. 79−78119
$Fe_xNi_{80-x}P_{14}B_6$, amorphous ferromag., resistivity, mag. contrib., 1.5-50K 79−56182
$Fe_{29}Ni_{49}P_{14}B_6Si_2$, Metglas 2826B, Hall, elec. resist., magnetisation and heat capacity meas. 78−68019
Gd, cryst., elec. resist. meas., 4.2-600K 78−14706
Gd, liquid, electrical resistivity calc., spin disorder contrib. 80−6803
Gd, magnetoresist., 4.2-220K, temp. depend. anisotropy 77−62903
Gd, spin reorientation transition, crit. behaviour of elec. resist. 79−51787
Gd-Ni, ferromag., elec. resist. temp. depend. 80−96843
$GdAg_{1-x}In_x$, elec. and Hall resist. 80−96844
$Gd(Al_{1-x}Cu_x)_2$, C15 struct., elec. resist., comp. depend. 78−14705
$Gd(Ni,Cu)_2$, spin disorder resist. evaluation, influence of antiferromagnetic order 77−73035
$HgCr_2Se_4$, n-type ferromag. semicond., galvanomagnetic props. 80−70727
LiCr ferrite, elec. resist., thermoelec. power and Nernst-Ettingshausen meas. near compensation point 78−10487
Mg-Yb, dil., Kondo scatt. from Yb, low temp. elec. resist. meas. 80−44578
α-Mn, spin fluctuations, temp. depend. of elec. resist. 77−62913
Mn-Zn ferrospinels, carrier transfer phenomena 80−54727
MnO, Hall mobility of photoelectrons 77−69352
Mo-Permalloy, galvanomag. props. 77−39822
$NbS_2(Se_2)$ intercalation complexes with 3d transition metals, mag. and metallic transport props. 80−44814
Nd, transport props., low temp., effect of mag. field 80−70679
$NdSn_3$, elec. cond., cryst. field effect, spin disorder contrib. 80−65540
Ni based ternary alloys, Coulomb and exchange scatt. amplitudes, spin dependent residual resistivities 78−64033
Ni, ferromagnetic, Hall effect, anomalous, rel. to scatt. processes 80−44572
Ni, resistivity, thermal and elec., spin disorder scatt. anal. 78−76063
Ni-Cu, ferromagnetic, Hall effect, anomalous, rel. to scatt. processes 80−44572
Ni-Cu, hydrogenated, Curie point, cluster magnetism 78−14960
$Ni(As_xS_{1-x})_2$, mag. elec. and structural props. meas. 77−85447
$NiS_{2-x}Se_x$, elec. resistivity temp. depend., pressure depend., paramagnetic-antiferromagnetic transition 78−10690
Pd-Ag-Fe, (0.5, 1.0, 2 at.% Fe), elec. resist. reduction near ferromag. and spin glass ordering 77−69299
Pd-Cr (11-18 at.%), resistivity comparison with canonical spin glass system 78−10432
Pd-Mn (1-10 wt.%), mag. ordering, influence on resistivity 80−75557
Pd-Ni, thermopower and crit. conc., spin fluctuation system 78−30909
$(Pd_{99}Ni)_{1-x}Pt_x$, spin-fluctuation thermopower 79−60802
$Pd_{95}Rh_5$, low-temp. spin-fluctuation resist., effect of pot. scatt., effect of Ni addition 77−15840
Pr, transport props., low temp., effect of mag. field 80−70679
$PrAl_2$, cryst. field interpretations of inelastic neutron scatt. meas. and mag. props. 79−56174
Pt-Cr, disordered, atomic order-disorder transform. effect on resist. min. 80−65911
Pt-Mn dilute alloys, spin glass, low temp. resist. meas., cluster model explanation 78−26851
Pu-Np, elec. resist., reson. scatt. from Np and local spin fluctuations 77−28170
Rh-Fe, dil., anti-Kondo effect, de Haas-van Alphen obs. 79−73427
Sc_3In, itinerant electron ferromagnet, spin fluctuations 77−73096
Sm film, electrical resistivity in 77 to 300K range 77−59339
Sm, magnetoresistivity and elec. resist., 4.2 to 300K *(Russian)* 80−88539
Sm, transport props., low temp., effect of mag. field 80−70679
$Sr_{0.3}La_{0.7}MnO_3$, neutron-irrad. induced phase transition 77−89952
TaS_2 intercalation complexes with 3d transition metals, mag. and metallic transport props. 80−44814
Tb, ferromag., electron-magnon interaction and elec. resist., 1.5 to 50K 79−60790
Tb-Y, residual resist. due to spin disorder, magnon component 77−15827
$TbAg_{1-x}In_x$, elec. and Hall resist. 80−96844
$TbNi_{2-x}Cu_x$, elec. resist. and mag. props. 78−72348
TbSc, crit. scatt. of electrons near antiferromag. transition temp. 79−69505
TbZn, elec. resist., behaviour at mag. crit. points 80−65901
TbZn, ferromag., thermoelec. power, temp. depend. and crit. behaviour 80−96852
Th-Gd(Tb)(Dy)(Ho)(Er)(Tm)(Lu) (1 at.%), Heisenberg exchange, residual resist. meas. 80−75558
Tm magnetic transitions, effect of H_2 in solid solns., elec. resist. meas. 80−100585
U_3As_4, elec. resist. in vicinity of Curie point, influence of mag. field 77−69314
UN, antiferromag., mag. susceptibility, elec. resist. and elastic consts. meas. 77−69510
UN, single crystal, electronic props. 77−77061
U_3P_4, press. effects on elec. resist. and Curie temp. 80−75559
$U_{1-x}Th_xAl_2$, ferromag. spin fluctuation system, sp. ht. and elec. props. 77−20604
V_5S_8, metallic evidence of spin flopping by magnetoresist. meas. 78−6352

spin dynamics
see also spin density waves; spin disorder resistivity
actinide metals and intermetallics, localised versus itinerant character of 5f electron states 77−28138

spin dynamics continued
actinide systems, nearly ferromag., coupled d- and f-band model 77−63211
actinide systems, spin fluctuations effect, model approach 77−28404
alaninium copper tetrahalides, exchange, mag. anisotropy, and spin diffusion contribs. to EPR linewidth 80−80597
alloys, antiferromag. nesting type model, spin fluctuations 78−84435
amorphous magnetic metals and alloys, high temp. thermodynamic props. 77−16078
amorphous magnetic order, review 78−68173
anisotropic critical freq. depend. of spin correlation functions 78−56321
anisotropic Heisenberg chain with infinite radius of interaction, correl. functions 77−59372
anisotropic paramagnet with exchange-bond dilution, sixth freq. moments 80−44789
anisotropic spin-phonon coupling model, exact solutions *(Russian)* 80−100590
antiferromagnet, critical dynamics above crit. temp., dipolar coupling 78−52286
antiferromagnet, impure, Heisenberg model, impurity banding and mag. reson., theory 80−93181
antiferromagnet, intermediate state, stability in HF mag. field *(Russian)* 79−95591
antiferromagnet, interphase boundary dynamics, domain wall motion and scatt. *(Russian)* 80−108032
antiferromagnet, magnetic phases, spin configurations in external field 80−70955
antiferromagnet, magnetisation, crit. spin-flop angle, temp. and field depend. *(Russian)* 80−7111
antiferromagnet, one-dimens., nonlinear dynamics 80−80521
antiferromagnet, quantum critical dynamics with mode coupling 80−108024
antiferromagnet, rhombohedral, spin-reorientation phase transition *(Russian)* 80−93122
antiferromagnet, $s=^1/_2$ linear Heisenberg, zero-temp. dynamics in mag. field 80−65764
antiferromagnet, sound generation by EM wave near orientational phase transform. of first kind *(Russian)* 78−39329
antiferromagnet, uniaxial S=1, effect of cryst. field anisotropy 77−28344
antiferromagnetic, uniaxial, spin flip as first-order phase transition 79−69674
antiferromagnetic insulator, magnetothermal resist. 77−35767
antiferromagnetic metal, nesting type model, spin fluctuations 78−56329
antiferromagnets, disordered spin flop, bicritical behaviour, critical experiments 80−65899
antiferromagnets, uniaxial, near bicrit. points 77−16090
Bethe lattice, random ordered phase and glasslike phase 78−29060
biaxial antiferromagnet, spin configuration in longitudinal mag. field *(Russian)* 79−7998
biological macromolecule, truncated driven nucl. Overhauser effect in presence of spin diffusion 80−1095
α-bis(N-methylsalicylaldiminato) copper II, dynamic behaviour of antiferro- to ferromagnetic transition 79−73715
α-bis (N-methylsalicylaldiminato) copper II, one-dimens. spin-$^1/_2$ Heisenberg antiferromag., high-field spin dynamics 80−71224
chemically induced dynamic spin polarisation, orientation depend. 80−63656
chromium phosphinate polymer, one-dimensional antiferromagnet, spin-flop 80−50131
classical dynamics, for particles with spin, Hamiltonian and Lagrangian formulation 80−86079
classical Heisenberg chains, low temp. spin dynamics 78−68243
classical particle spin dynamics and supersymmetry 77−82690
classical planar spin chain, dynamic props., Monte Carlo calc. 79−61144
classical planar spin chain, dynamics calc. 78−80165
classical spin glass, propagating modes in 3 dimensional planar model, dynamic struct. factors 79−99703
classical XY spin dynamics far from equilibrium 78−68136
continuum spin system, as exactly solvable dynamical system 77−47960
continuum spin system dynamics, spin-wave and solitary wave solns. 77−8263
copper benzoate, antiferromag., spin dynamics at low temp. 77−32278
copper benzoate, antiferromag. reson. below 1K, Neel temp. determ. 78−39407
copper benzoate, spin 1/2 system, one-dimensional nucl. relax. 78−39427
Coulomb gas in strong mag. field analogy with electron gas with backward scatt. 80−24817
cubic Ising ferromagnet, three spin interaction effect on mag. props. 80−54910
cumulant approach to spin echo 77−85614
demagnetised cubic magnetic crystals, irreversibility of spontaneous spin-orientation effects 79−73761
density matrix formalism for coupled dynamical systems 78−95522
diammonium layer compounds $(CH_2)_n(NH_3)_2MnCl_4$, quasi-two-dimens. antiferromag., magnetis., spin-flop and crit. exponents 77−66311
1,8-dichlorooctane, quadrupolar relax. centres, limited spin diffusion 80−100649
diethylammonium manganese chloride, 20 spin diffusion, EPR linewidth meas. 79−47289
diethylammonium manganese chloride, Heisenberg magnet, spin diffusion, EPR study 80−66019
diethylammonium manganese chloride, planar Heisenberg magnet, spin diffusion, EPR study 80−15793
diethylammonium-manganese chloride, spin diffusion, quasi-two-dimensional Heisenberg paramagnet 78−88129
differential equations, asymptotic expansion of quantum averages near classical limit *(Russian)* 77−53831
diffusion, effect of spin-photon and spin-phonon interactions 80−44849
dilute and concentrated alloys, magnetism *(Rumanian)* 78−91843
diluted Heisenberg magnet, spin diffusion const., conc. depend. 78−88089
dimethyl ammonium copper chloride, spin dynamics near crit. pt. 80−7112
dimethylammonium manganese tetrachloride, antiferromag. and spin-flop resonance obs., 70 to 100 GHz 80−71190
dipolar system, spin correlation function for free induction decay appl. to CaF_2 77−8421
disordered magnet, spatial correl. of spins 78−23276

spin dynamics continued
disordered magnets, spin glass phase, spatial spin correlation function 78−10691
disordered media, ferro- and antiferromag., and spin glasses, dynamic props. *(Russian)* 78−39350
disordered spin systems, dynamic crit. behaviour 77−66343
doped semiconductor plasma, inelastic light scatt., spin diffusion 77−36241
dynamical correlation functions and scattering from spin fluctuations near magnetic phase transitions 79−73747
dynamical plane rotator model, dynamical correl. functions in mol. field approx. 80−88758
electron spin density functional gradient expansion, local approx. calcs. 80−44792
electron-nuclear spin system in solids, nucl. spin-spin flips *(Russian)* 77−24763
Fe_3O_4, tetrahedral-site Fe^{3+} ion, spin-transfer due to covalency 79−15285
Fermi liquid theory of effect of spin fluctuations 77−62853
fermion system, nearly ferromag. absence of $T^2 \ln T$ term 78−10692
ferrimagnet, magnetisation curves, spin reorientational phase transitions 79−82785
ferroelectric antiferromagnetics, spin wave fluctuations in strong mag. fields *(Russian)* 79−82773
ferromagnet, anisotropic, crit. line shape anomalies 78−10698
ferromagnet, anisotropic Landau-Lifshitz, quasiclassical spectra *(Russian)* 80−15678
ferromagnet, critical dynamics above crit. temp., dipolar coupling 78−52286
ferromagnet, critical dynamics above Curie pt. 79−87262
ferromagnet, critical spin dynamics, appl. of 3-D neutron polarimeter 79−18098
ferromagnet, exact integration of nonlinear Landau-Lifschitz equation 80−80495
ferromagnet, high freq. crit. dynamics above T_c *(Russian)* 78−10718
ferromagnet, isotropic, dynamical spin-spin correl. function at Curie temp. in 6ε dimensions 77−4481
ferromagnet, Landau-Lifshitz eqn., two soliton solns. for nonlinear dynamics *(Russian)* 78−43646
ferromagnet, magnetisation curves, spin reorientational phase transitions 79−82785
ferromagnet, mean spherical model, Langevin approach 78−72350
ferromagnet, planar, with small basal plane anisotropy, crit. dynamics anal. 77−12116
ferromagnet, spin reorientation and magnon-phonon hybridization 78−19233
ferromagnet, substitutionally disordered. spin dynamics, linear spin-wave approx. 77−40067
ferromagnet, three-dimens., crossover in dynamic exponent, hyperfine interaction vs. neutron scatt. expts. 78−84437
ferromagnet, triple dynamic magnetisation fluctuation correl. and feasibility of polarised neutron exam. *(Russian)* 78−88133
ferromagnet, weakly bound impurity spin and rapid relaxation host spin *(Russian)* 77−51960
ferromagnet, with anisotropic exchange, homogeneous relax., time const. calc. 77−16149
ferromagnet with random anisotropy, spin correlation 79−73722
ferromagnet with single ion anisotropy, collective modes 77−28354
ferromagnetic, uniaxial, dynamical behaviour near mag. transition point *(Russian)* 78−84431
ferromagnetic alloys, conc., spin fluctuations, SCR theory and CPA calcs. 78−64290
ferromagnetic conducting cryst., dynamics of s-d model in alternating mag. field *(Russian)* 80−65825
ferromagnetic crystal, spin subsystem thermodynamics, spin-phonon interactions, mag. order parameter 80−103848
ferromagnetic Heisenberg chain, weakly bound magnon states *(Russian)* 80−100591
ferromagnetic insulators at parallel pumping, nonlinear magnetisation dynamics 77−8288
ferromagnetic medium, Landau-Lifshitz nonlinear equation, N-soliton solutions *(Russian)* 79−24184
ferromagnetic metals, spin fluctuation theory, Curie temp., mag. susceptibility 80−65937
ferromagnetic phase transitions, nucl. spin dynamics in anisotropic systems 80−11205
ferromagnetic phase transitions, nucl. spin dynamics in isotropic systems 80−11204
ferromagnetic plane rotors, crit. temp. and correl. functions 78−14974
ferromagnetic plate, domain struct. during spin reorientation, phase diagram *(Russian)* 78−52320
ferromagnetic semiconductor, Raman scatt. due to magnon-spin flip of cond. electrons 77−20839
ferromagnetic slab, finite thickness, spin correl. functions 80−80522
ferromagnetic spin system, under quenched random mag. field, phase transition crit. dynamics 79−82798
ferromagnetic systems, relation between quenched and annealed random systems 79−82794
ferromagnetic systems, singlet-triplet, excitation spectrum, double-time Green's functions 80−84603
ferromagnets, exchange and dipolar coupled, spin wave renormalisation, Damon-Eshbach surface spin waves 80−2564
ferromagnets, quantum critical dynamics with mode coupling 80−108023
ferromagnets, uniaxial, US attenuation and kinetic coeffs. near crit. point, renormalisation group theory 79−4715
ferrous rubredoxin, high spin, spin fluctuation rates from Mossbauer spectra 79−29506
finite disordered Hubbard cluster, thermodynamic and mag. props. 77−85409
frustrated two-dimensional planar model, spin-spin correl. 80−11212
Heisenberg, paramagnetic with bond dilution, freq. moments of spin correlation function 79−15272
Heisenberg antiferromagnet, anisotropic, spectrum and correl. functions in spin-flop phase in generalized HF approx. 78−39283
Heisenberg antiferromagnet, excitations at finite temp. using CPA 79−56554
Heisenberg antiferromagnet, magnon renormalisation, two-magnon Raman scatt., kinematic interaction 78−23228
Heisenberg antiferromagnet, one dimens., spin-flop transition 79−73723
Heisenberg antiferromagnet, one-dimens., autocorrelation function, low freq., temp. and field depend. 80−65929

spin dynamics continued
Heisenberg antiferromagnetic chain, spin dynamics, quantum effects 80−34651
Heisenberg bicritical points in antiferromagnets, universality tests 80−84604
Heisenberg chain, classical, higher moments and spectral shape 80−11147
Heisenberg chain, classical, nearest-neighbour, low temp. dynamics 80−80524
Heisenberg chain, dimerised, spin dynamics 77−20528
Heisenberg chain, ferromag., with biquadratic exchange, spin correl. length, susceptibility and spin diffusion *(Russian)* 77−69568
Heisenberg chain, impure classical, dynamics near T=0 for low impurity conc. 80−71055
Heisenberg chain, theory vs. computer simulation 78−80155
Heisenberg classical nearest-neighbour chain, dynamics, exact perturbative results 78−10700
Heisenberg FCC ferromagnet, surface spin instabilities 77−69475
Heisenberg ferromagnet, correlation functions in ferromagnetic and paramagnetic regions, RPA 80−71075
Heisenberg ferromagnet, crit. dynamics in $2+\varepsilon$ dimens., low temp. phase 78−76262
Heisenberg ferromagnet, critical dynamics of impurity spin below T_c 80−71076
Heisenberg ferromagnet, linear, spin diffusion coeff. and static spin correlators *(Russian)* 77−80942
Heisenberg ferromagnet, spin configurations near singularities in micromagnetism 80−54908
Heisenberg ferromagnet, spin wave excitations at finite temp., CPA calc. 77−32142
Heisenberg ferromagnet, two-dimens., spin dynamics, renormalisation group calc. 78−47966
Heisenberg linear chain, diffusion coeff. at infinite temp. *(French)* 78−10636
Heisenberg linear chain, dynamical correl. functions 77−63221
Heisenberg linear chain, spectral density approach to correlation functions 79−24124
Heisenberg linear spin systems, dynamical spin correlation functions 78−31035
Heisenberg magnet, correlation theory of static and dynamic properties 80−65765
Heisenberg magnet, diluted, spin dynamics at elevated temp. 78−84433
Heisenberg magnet, random one-dimens., classical, spin dynamics, neutron scatt. cross section 80−60312
Heisenberg model, classical, infinite, nonlinear dynamics, quantum time evolution 80−100576
Heisenberg model, classical antiferromag. chain, low temp. dynamics 80−39803
Heisenberg model, classical low temp. spin wave dynamics 78−6501
Heisenberg model, correlation functions long time behaviour 77−89919
Heisenberg model, helical spin chains, static and dynamic props. 79−73661
Heisenberg model, nearest-neighbour spin-spin correl. functions calc. 80−80537
Heisenberg model, spin diffusion coeffs. at finite temp. 77−69592
Heisenberg model with one-ion anisotropy, closing relns. for Green's functions 78−2642
Heisenberg one-dimensional magnet, classical, nonlinear dynamics 80−71056
Heisenberg paramagnet, 2-spin dynamic autocorrels. and energy diffusion 77−47959
Heisenberg paramagnet, electronic spin dynamics, NMR 78−76266
Heisenberg paramagnet, exchange bond dilution, freq. moments of spin correl. function 80−50030
Heisenberg paramagnet, high temp., dynamical 4-spin 2-time correl. functions 77−40026
Heisenberg paramagnet, sixth frequency function of relaxation shape function 78−39348
Heisenberg paramagnets, low freq. props., nonlinear Langevin eqn. 78−31038
Heisenberg spin glass, crit. dynamics, renormalisation group approach 79−91237
Heisenberg spin glass, spin diffusion 78−6538
Heisenberg spin glass, spin wave stiffness, computer simulation 79−78405
Heisenberg system, self-consistent approach at high temps. 77−20531
Heisenberg system, with single-ion anisotropy, longit. correl. functions 78−76214
heteronuclear spin coupling and decoupling dynamics 77−48066
heteronuclear system, spin diffusion, NMR 78−88213
high speed rot., spin diffusion, NMR spin lattice relax. obs. of D 80−66056
high spin/low spin transition, model including lattice dynamics 77−63202
Hubbard chain, strong coupling, electron dynamics 78−39342
Hubbard Hamiltonian, coupled spin and charge fields 77−32147
Hubbard model, one-dimensional, elementary excitation with complex wave vector 80−75783
impurity relaxation in nonresonance field, phonon amplification *(Russian)* 80−100310
induced moment systems, effect of spin fluctuations 80−2585
inhomogeneous itinerant electron ferromagnet, mag. and thermal props. 79−7964
Ising 2D regular model, frustration effects 80−39784
Ising chain, time-dependent correl. functions in high-temp. limit 79−73727
Ising ferromagnet, one-dimens., with phase transition, thermodynamic props. calc. 80−80536
Ising ferromagnet, SO(n)-symm., correls. decay 77−47956
Ising model, effective field theory 79−4684
Ising model, one dimensional in skew mag. field, zero-temp. dynamical props. 78−80153
Ising model, one-dimensional transverse, time-depend. longit. correl. function 77−66332
Ising model, relax. dynamics, cluster approx. *(Russian)* 78−10635
Ising model, spatially nonhomogeneous, correl. functions 80−60314
Ising model, spin-spin correl. function, high temp. expansion and equipartition theorem 78−31089
Ising model, square-lattice, four-spin correl. function 78−39345
Ising model, two dimens., n-spin correl. functions 78−52296
Ising model, with long-range interactions, dynamical props. 80−100593

spin dynamics continued
Ising model in transverse field, spin dynamics, mode coupling 78−56332
Ising models with pair interactions, extremal Λ-inequalities 79−56485
Ising O(2), O(3) and O(4) spin systems, Hamiltonian string-coupling expansions 80−20426
Ising spin glasses, Edwards-Anderson model, autocorrelation function logarithmic decay account 79−78406
Ising spin system, ROP type random magnet 79−15269
Ising square frustration model, numerical study of ground state correl. 80−34638
Ising system on triangular lattice, critical dynamics, time dependent real-space renormalisation group 78−60289
isothermal magnetic system in alternating mag. field, dynamic behaviour 79−82786
itinerant electron ferro- and antiferromagnetism, spin fluctuations 79−7961
itinerant electron ferromag., spin fluctuation *(Japanese)* 78−47936
itinerant electron ferromagnetism, spin fluctuation theory 78−80151
itinerant electron ferromagnets, magnetisation fluctuations, Landau-Lifshitz eqn. 79−73729
itinerant electron magnets, effect of spin fluctuations on elec. field gradient 78−39078
itinerant electron magnets, spin fluctuations 77−72990
itinerant electron magnets, spin fluctuations and thermodynamic props. 79−65687
itinerant electron magnets, theory of spin fluctuations 77−63064
itinerant electron system, mag. excitations, neutron scatt. studies 80−44838
itinerant ferromagnet with helical spin struct., US attenuation 79−78497
itinerant ferromagnetism, statistical mechanics of spin waves 79−82746
itinerant localised systems, dynamic magnetic response 80−34583
Jeener-Broekaert three-pulse sequence, inhomogeneous lineshapes, second rank spin interactions 80−39891
kinetic Ising chain, renormalisation group transform. for master eqn. 80−11214
kinetic Ising model with quenched relaxing impurities, crit. dynamics 78−10167
linear Heisenberg antiferromagnet, $S=^1/_2$ zero temp. dynamics 79−73741
linear Ising-Heisenberg ferromagnet, spectrum of elementary excitations 79−61091
long wavelength spin susceptibility from particle-particle scattering, logarithmic temp. control 80−7124
magnetic crystal, perfect, spin rot. of forward transmitted beam in neutron diffr. 80−50113
magnetic excitations, polarised neutron inelastic and quasi-elastic scattering 80−50045
magnetic glasses at low freq., impurity spin dynamics *(French)* 78−88126
magnetic materials, symmetry and macroscopic dynamics 80−107973
magnetic metals, crit. transverse US attenuation, spin fluctuations 78−48022
magnetic polymers, spin-spin correlation excluded volume effects 79−42781
magnetic structures, non-periodic, ferromagnetic spin wave propagation, interaction with domain walls 79−99692
magnetic superconductors, spin fluctuation and US attenuation 80−80445
magnetically ordered cryst., indirect nuclear spin interactions 80−103847
magnetically ordered crystals, exchange symm., mag. struct. *(Russian)* 80−65785
magnetically ordered materials, anomalous spin-flip scatt. rate near ordering temp. 79−82802
manganese acetate, crit. slowing down, 180-350 MHz 77−16083
many-spin system, dynamics, group approach *(Russian)* 79−11324
many-spin system, group approach in dynamics *(Russian)* 80−4579
many-spin system, group approach in dynamics *(Russian)* 80−44900
many-spin system dynamics, group approach *(Russian)* 80−50221
mean-field theory of Peierls and spin-Peierls instabilities−commensurability, harmonics and dimerized-state pinning 80−108014
metal, antiferromag., magnetoresistance, two band model 78−79979
metal, conduction electrons, surface scatt. under spin resonance conditions *(Russian)* 79−82857
metals, spin fluctuation theory, for mag. and elec. props., appl. to actinides 78−91869
metals, spin fluctuations, mag. field effect, electronic sp. ht. and elec. resist. 80−108026
metamagnet, two-dimens., tricritical spinodal decomp., Monte Carlo study 80−93117
metastable spin-aligned crysts. decay kinetics 80−34669
^{13}C-methane-d_1:O, annealed, spin conversion and proton 2nd moment time-depends. 80−11283
methyl rotator in isotropic fluid, motional asymm. determ. from ^{13}C spin dynamics 77−69718
α-bis(N-methylsalicylaldiminato)-copper (II), ^{1}H NMR spin-lattice relax. time, spin dynamics 79−99786
mictomagnet, spin correl. functions, computer simulation 77−66365
mixed-spin paramagnet, dynamics 80−60173
molecular crystals, photon echoes *(Dutch)* 78−71156
multiple pulse, spin dynamics *(Russian)* 78−35057
Nambu-Goldstone modes, effect on longit. correl. functions 77−16018
nearly ferromagnetic Fermi systems, temp. depend. of spin susceptibility 79−8008
nearly ferromagnetic semiconductor, spin fluctuation theory 79−65636
Neel mode, ferrimagnetic-helical [hh0] mode coupling vector model *(French)* 80−75770
neutron inelastic magnetic scatt., book contrib. 77−89944
neutron matter, spin zero sound and spin diffusion coeff. 77−57278
neutron scattering studies of one- and two-dimens. mag. systems, review 77−66254
NMR, superspin, appl. to ABX system 80−60426
NMR relaxation processes, macroscopic evolution eqns. and virtual spins importance *(French)* 80−32739
nonlinear dynamics of electron-nuclear spin system 77−66438
nonlinear dynamics of first order phase transitions 79−11322
nonmagnetic-paramagnetic transition in one-dimens. electron system due to spin excitations *(Russian)* 78−43606
nonstationary nutations in heteronuclear double resonance 80−20516
nuclear magnetic double resonance, cross relaxation, theory *(Rumanian)* 79−8072
nuclear spin diffusion under magic angle conditions, calc. 78−19363
spin dynamics continued
nuclear spin relax. by translational diffusion in solids, reciprocal-space formalism, mean-field theory 80−71208
one dimensional magnet with easy plane, solitons and magnons 78−23260
one dimensional model systems, theoretical survey 78−68129
one dimensional randomly dilute Ising ferromagnet, dynamics 80−70922
one-dimensional antiferromagnet, interchain coupling, effect on US attenuation 80−19880
one-dimensional classical planar model in applied magnetic field 80−15729
one-dimensional ferromagnet with long range interaction, correlation weakening 79−95561
one-dimensional Heisenberg antiferromag., dynamic struct. factor 79−28497
one-dimensional Heisenberg magnet, in mag. field, dynamic correlations 80−70926
one-dimensional mag. systems, neutron scatt., review 80−50103
one-dimensional magnetic models, fluctuations in energy-energy correlation function 79−73726
one-dimensional magnetic system, high-temp. dynamics 79−4716
one-dimensional organic semiconductors, resonant states, mag. excitations and impurities 80−24839
one-dimensional random Glauber model, magnetisation relax. 80−80523
one-dimensional spin 1/2 chain, soliton excitation in strong spin-phonon interaction 80−103842
one-dimensional spin system, spin-spin correl. function, dynamical spherical model 79−69683
orbital degeneracy, one dimensional two spin models *(Russian)* 80−54899
orientation transitions, stabilising effect of high freq. fields *(Russian)* 77−89972
paramagnet, anisotropic, effect of bond dilution on dynamics at high temp. 78−39343
paramagnet, anisotropic, site- and bond-diluted, spin dynamics at high temp. 79−61117
paramagnet, anisotropic, spin dynamics, exchange-bond dilution effects 80−88763
paramagnet, nearly-one-dimensional, self-consistent diffusion coeff. 77−80997
paramagnet, spin diffusion at low temp. *(Russian)* 77−32240
paramagnetic impurity induced nucl. flip-flop transitions 79−47348
paramagnetic metal, narrow band electron system, temp.-induced local mag. moment 78−76221
paramagnetic metal with nonmag. impurities, spin-flip scatt. 77−4497
paramagnetic spin system, two-level open system, kinetic theory of resonance and relaxation 80−88859
paramagnetic system, disordered, spin diffusion 77−8392
paramagnetic system, spin waves, classical approach 80−29519
paramagnets, anisotropic, spin dynamics 77−69481
paramagnets, high-temp., quadrupolar exchange effects on spin dynamics 79−61038
paramagnets, itinerant electron, spin wave like modes 77−63067
paramagnets, low-dimens., EPR spectra 80−71154
particle with spin n/2, classical and quantum dynamics *(Russian)* 79−44796
phase transitions, spin-reorientation, crit. behaviour 77−12132
planar ferromagnet hydrodynamic mode microscopic theory 78−39280
planar ferromagnetic chain, soliton dynamic struct. factors 80−7125
planar spin system with annealed bond disorder 80−57212
polyacetylene and polyacetylene: AsF_5, one-dimens. spin diffusion, NMR T_1 and dynamic nuclear polarisation meas. 80−44946
polydimethylsiloxane-bisphenol-A polycarbonate block copolymer, PMR spin diffusion effects 77−66431
polydimethylsiloxanes, partially cryst., spin diffusion rel. to nuclear spin-lattice relax. *(Russian)* 79−51878
praseodymium ethylsulphate:Sm, one-dimens. X-Y system, spin dynamics, electron spin echo meas. 80−66031
praseodymium ethylsulphate:Sm, XY system, mag. relax. and spin dynamics 79−61211
precession effects on bubble stability 77−32226
1,3-propanediammonium $MnCl_4$, 2-dimens. antiferromagnet, with dipolar broadening, spin diffusion, EPR obs. 79−38371
protein, proton magnetic reson. and spin diffusion 77−28470
pseudo one-dimensional kinetic Ising model, dynamic susceptibility 80−50025
quasi-localised spin system, mag. excitations, neutron scatt. studies 80−44838
quenched random spin systems, dynamical replica methods, nonequilib. critical phenomena 78−43602
radical pairs, electron spin motion, diamag.-paramag. exchange, mag. field effect 79−98123
random ferromagnet, with long-range interactions, dynamics 77−89942
random ferromagnetic-antiferromagnetic alloy, elementary excitations 79−8001
random Ising bond interactions, paramag. phase, thermodynamic props. 77−20523
random uniaxial systems with dipolar interactions, crit. dynamics 77−73034
rare earth Co Laves phase cmpds., elastic props. rel. to temp., mag. field 79−51834
rare earth compounds, mag. dynamics of singlet-triplet system in paramag. phase 79−91203
rare earth ferrite garnet single crystals, spin reorientational phase transitions *(Russian)* 78−39349
rare earth intermediate valence systems, neutron scatt., review 80−49674
rare earth metal, anomalous sound attenuation near mag. transition temp. 78−15004
rare earth mixed valence compounds, spin dynamics, mag. neutron scatt., Mossbauer effect, XPS studies 80−39786
rare earth orthoferrite, $RFeO_3$, spin reorientation and magneto-optical effects *(Japanese)* 79−47414
rare earth orthoferrite, second-order reorientation transition, NMR signal relax. 77−90066
rare earth orthoferrite, stripe domain struct. near spin-reorientation points 77−24707
rare earth orthoferrites, hyperfine interaction anisotropy, NMR study *(Russian)* 80−66052
rare earth orthoferrites, slow neutron elastic scattering, domain boundary observation *(Russian)* 79−82811
rare earth systems with singlet ground states, low freq. modes 78−68131

spin dynamics continued
rare earth-Co system, spin reorientation and sp. ht. anomaly *(Japanese)* 79−47287
rare-earth magnets, low-frequency modes 78−88087
redox enzyme, Fe-, Cu-, or Mo-containing, electron transfer peculiarities 80−16896
reorientation and appls. *(Japanese)* 77−36083
RF field effect on spin diffusion 80−93104
RKKY interaction and conduction electron polarisation 78−91859
ruby NMR laser, ^{27}Al nucl. spin system, collective ordering phenomena, instabilities 80−11278
ruby NMR laser, spontaneous nucl. spin system self organisation 79−916
semiconductor, antiferromagnetic, spin-magnetomagnon resonance 80−2566
semiconductor, spin injection, carrier polarisation, luminesc. polarisation 77−15957
semiconductor, violation of σH invariance accompanying optical orientation of spin *(Russian)* 78−35068
semiinfinite, effect of next nearest neighbour coupling 77−73014
sine-Gordon chain, classical, low freq. dynamics 80−108020
solids, disorder of NMR and soft collective lattice modes, spins and pseudospins 78−88208
spectral diffusion at low temp. 77−43861
spin correlations, ordered and disordered phase, $2+\varepsilon$ dimen. 78−76210
spin glass, classical, low temp. behaviour of three-dimens. planar model 79−73725
spin glass, dynamical theory of quenched site model 79−19742
spin glass, dynamics near transition, classical soft-spin models 79−95599
spin glass, Heisenberg model *(French)* 78−39336
spin glass, one dimens. ideal, dynamical susceptibility and relax. behaviour 80−65950
spin glass dynamics, barrier modes and spin waves 80−60293
spin glass free energy, phase transition dynamical instability 79−33493
spin glasses, EPR, NMR, muon precession, Mossbauer, and neutron scatt. results 79−65689
spin glasses phase transition, obs. by DC Josephson effect 80−100594
spin Hamiltonian, constant-coupling, higher-order, statics and dynamics 80−60262
spin relaxation and linear irreversible processes 77−20678
spin-$^1/_2$ system, two-point correlations decay for decreasing pots. 78−19202
spin-flip process, non-increasing free-energy 77−73031
spin-lattice relax., effect on mol. groups in solids of symm.-restricted spin diffusion 78−39431
spin-lattice relaxation of nuclei due to impurity nuclei under magic angle conditions, influence of spin diffusion 78−15061
spin-oscillator coupled system, stochastic model for dynamics 77−22500
spin-oscillator coupled system, stochastic model for dynamics, projection operator approach 78−77813
square lattice Ising system, crit. relax. of temp. 79−82793
Stanley model dynamics in magnetism theory 79−15311
Stoner glass, disordered itinerant-electron system, spin-glass condensation 79−78424
TANOL, free radical, spin flopping transition, temp. depend., mag. anisotropy energy 80−54890
TCNQ salt, 1-methyl-3′-ethyl-2,2′-quinoselenacyanine-[TCNQ]$_2$, two-dimens. ferromag., EPR 77−16148
TCNQ salt, K-TCNQ, EPR linewidth, ang. and freq. depend. 80−80591
TCNQ salts, proton nucl. relax. meas. 80−20484
TCNQ salts, spin density distribs., estimation from EPR fine struct. and cryst. data 79−11347
TCNQ-NMP, nucl. relax. and spin dynamics 78−52370
temperature Green's function for tunnelling model, new contraction method 79−35635
tetramethylammonium manganous chloride:Cu, impure Heisenberg chain paramagnet, EPR sidebands, intensity, linewidths 78−76300
thermodynamic influence of spin-spin energy on cross-relax. and spin diffusion 78−76343
thermomagnetic power generation, appl. of spin reorientation phenomenon 77−4325
time-dependent critical behaviour of weakly random systems, Ginzburg-Landau model 77−40065
TMMC:Cu, EPR lines, dynamic effect of low-symmetric spin distrib. 80−39854
TMMC:Cu, EPR linewidth freq. depend., spin dynamics 80−15794
TMMC:Cu, random one-dimens. Heisenberg antiferromag., spin fluctuations 79−61140
TMMC, Cu-substituted, spin dynamics, neutron scatt. cross section 80−60312
TMMC, EPR lines in one-dimensional mag. systems, dynamic effect of low-symmetric spin distrib. 80−39853
TMMC, exchange-narrowed EPR linewidth, temp. depend. 78−52292
TMMC, field-suppression of spin fluctuations, NMR obs. 78−91971
TMMC, linear antiferromag., 3D ordering and spin correlations, mag. field effect 78−19262
TMMC, linear antiferromag., energy gaps in spin-wave dispersion, neutron inelastic scatt. 79−91223
TMMC, low-symmetry spin distrib. effect on EPR line 80−66018
TMMC, one dimens. Heisenberg system, shift of half-field EPR line 78−23325
TMMC, one-dimensional Heisenberg mag., EPR, spin diffusion of 4-spin correl. functions 77−4549
TMMC, spin dynamic exam., effect of mag. field at low temp. 79−73733
TMMC, symmetry crossover in spin dynamics, proton spin lattice relax. calc. 77−40147
TMNC, quasi one dimensional planar ferromag., low temp. NMR study im mag. field 80−97157
transition metal, chemisorption of H, effect of surface spin fluctuations 80−75613
transition metal compounds, Jahn-Teller induced high spin-low spin transitions 79−69676
transition metal magnetic alloys, dilute, props., review of theory 79−15282
transition metal surface, spin fluctuations 78−95451
TTF-Cu bis-dithiolene, dimer, mol. displacements at 4.2K 80−10539
TTFCuBDT, spin-Peierls transition in spin 1/2 Heisenberg chains, RPA calcs. 80−25150
two-component spin system in alternating mag. field, dynamical behaviour, susceptibility 79−99715
spin dynamics continued
two-dimensional heisenberg ferromagnet, open diffusion effects *(Russian)* 77−32201
two-dimensional nonscalar system, dynamics of symmetry-breaking long-ranged order 77−20613
two-dimensional planar magnet, crit. slowing down in transverse autocorrel. function 78−95448
two-level spin system, mag. moment dynamics in mutually perpendicular mag. fields, of arbitrary freq. 79−3415
two-spin system in FCC cryst. and third-nearest-neighbour jumps on a SC lattice 79−15127
type II superconductor, spin diffusion in inhomogeneous mag. fields 78−2618
uniaxial antiferromagnet, nonuniform spin configurations 80−97109
uniaxial antiferromagnetic, phase diagram, spin flop transition *(Russian)* 80−100587
uniaxial antiferromagnets in transverse mag. field, quantum theory, spin configuration 79−69647
uniaxial dipolar magnet, critical dynamics and statics 77−59422
uniaxial Heisenberg antiferromagnet, phase diagrams 80−15730
Van der Waals systems, time-dependent correls. 79−61130
weak ferromagnet, domain wall dynamics, nonlinear waves, mag. solitons *(Russian)* 80−75793
weak itinerant electron ferromagnet, spin fluctuation curvature of Arrott plot 79−8012
X-Y chain, time-dependent correl. functions in high-temp. limit 79−73727
X-Y model, 3-dimensional, relax. function 77−69666
X-Y model, classical, one and two dimens. 78−34997
X-Y model, classical one-dimens., computer simulations 79−78396
X-Y model, one-dimens., with symmetry-breaking fields, thermodynamics and static props. 79−73742
X-Y model, one-dimensional isotropic, dynamics 80−71057
X-Y model, spin dynamics of one-dimens. system 77−4486
X-Y quasi-one-dimens. system anisotropic, spin-Peierls phase transition, tricritical point 80−25142
^{O}, Heisenberg ferromagnet, spin dynamics, neutron scatt. expts. 77−20619
Al film with Er impurity, spin-flip scatt. and supercond. order parameter dynamics 79−78267
Al-Mn, dilute, NMR investig. of spin density oscills. around Mn impurities 77−4570
$Al_2Mn_3Si_3O_{12}$ amorphous spin glass, spin dynamics, neutron scatt. meas. 80−15741
Al_2O_3, corundum, acoustic enhancement of NMR lines 80−29632
$Al_2O_3:Cr^{3+}$, inhomogeneous spin system, time evolution towards saturated state 80−88869
$Al_2O_3:Cr^{3+}$, solid-state nuclear spin-flip maser pumped by dynamic nuclear polarisation 77−31084
AlP, multiple pulsed double NMR and nucl. spin dynamics 77−16208
Au-Fe, dil., crit. dynamics 80−60325
Au-Fe (14.5 at.%), spin dynamic exam. by diffuse magnetic neutron scatt. 77−8320
Au-V, dil., Kondo alloy, spin dynamics, nuclear spin relax obs. 78−68155
AuFe spin glass, μ^+ zero-field spin relax. probe for spin dynamics 80−97177
$BaCo_{1.5}Fe_{16.5}O_{27}$, type W ferrite, spin reorientation 78−60301
$BaCo_{1.65}Fe_{16.35}O_{27}$, spin reorientation obs. using magneticaloric effect *(Russian)* 77−32195
$BaMnF_4$, ESR linewidth and reson. field for Mn^{2+}, 25 to 300K, spin diffusion 77−69681
$BaMnO_4$, ferroelectrically induced ferromagnetism 77−73067
Bi hole pocket, far-IR magnetospectroscopy, electron-electron interaction effects 77−77211
^{13}C-^1H NMR in organic solids, spin decoupling dynamics 77−4582
$Ca_3Cr_2Ge_3O_{12}$, antiferromag. single crystal garnet, magnetostriction *(Russian)* 79−8027
CaF_2, spin diffusion under magic angle conditions, calc. 78−19363
$CaF_2:Eu^{2+}$, nuclear spin diffusion barrier, ^{19}F NMR Obs. 78−64282
$Ca_3Mn_2Ge_3O_{12}$, antiferromagnetic garnet, neutron diffr. study in mag. field 80−50060
CdS, doped, amorphous antiferromagnet model, susceptibility and spin-flip Raman scatt. meas. 80−97057
CdS, pure spin diffusion without charge transport, spin flip Raman scatt. obs. 80−93329
γ-Ce, lattice and spin dynamics, inelastic neutron scatt. obs. 79−86859
$CeIn_{3-x}Sn_x$, conduction electrons role in valency fluctuations 78−47741
$CeIn_{3-x}Sn_x$ mixed valence system, low-temp. susceptibility, paramagnon study 80−97077
$CeIn_{3-x}Sn_x$, scaling behaviour near valence instability, mag. susceptibility and mag. transitions 80−25111
$(Ce_xLa_{1-x})_2Mg_3(NO_3)_{12}.24H_2O$, adiabatic demagnetisation temp., mag. entropy *(Russian)* 80−65892
$Ce_{0.9-x}La_xTh_{0.1}$, mixed valence state, static and dynamic mag. response 80−103816
$Ce_{0.74}Th_{0.26}$, mixed valence alloy, spin dynamics 78−10708
$Ce_{1-x}Th_x$, mixed valence systems, spin dynamics and mag. ordering 78−68162
Co, internal friction anomalies in spin reorientation temp. range *(Russian)* 80−49299
Co, molten, mag. small-angle scatt., persistent spin fluctuations 79−11288
Co, small-angle crit. neutron scatt. 78−31087
Co, spin fluctuations above Curie temp., diffuse mag. neutron scatt. obs. 80−50102
Co-Fe, internal friction anomalies in spin reorientation temp. range *(Russian)* 80−49299
$Co_{1.8}BaFe_{0.2}Fe_{16}O_{27}$, influence of spin-reorientation on magnetoelastic props. *(Russian)* 79−8028
$CoBr_2$, magnetic excitations, neutron scatt. investigation 80−39761
$CoBr_2(Cl_2).2H_2O$, linear chain metamag. system, phonon and magnon widths 77−36065
$CoBr_2.6(0.48D_2O, 0.52H_2O)$ spin-flop system, intermediate phase existence, sublattice magnetisation reorientation 80−80510
$CoCl_2$, antiferromag., phase diagram, heat capacity meas. 80−93126
$CoCl_2.6H_2O$, antiferromag., spin flop and paramag. resons. at very low temp. 77−66426
CoS_2 and $CoSe_2$, local mag. moments, spin fluctuation theory 79−65687
Cr, mag. phase diagram, near, spin-flip temp., US attenuation 80−60267

spin dynamics continued
Cr, mag. struct., effect of mag. field direction, neutron diffr. obs. 77−63121
Cr, magnetic phase diagram in external mag. field, spin reorientation curve, critical point coordinates *(Russian)* 80−29548
Cr, strain and spin-flip transition, Landau theory 78−39318
CrFe, mag. correls. and onset of ferromag., neutron scatt. study 80−50105
$Cr_{0.98}Mn_{0.02}$, spin dynamics and spin wave form factor, neutron scatt. expt. 77−40047
Cr_2O_3, antiferromag., muon spin rotation *(German)* 80−54877
Cr_2O_3, magnetostriction anomalies near mag. field induced transitions 77−66315
$Cr_{1-x}V_x$, nucl. spin relax., spin fluctuation effect 80−34811
$CsCoCl_3$, Ising like antiferromag., mag. phase transition, ^{133}Cs NMR 80−7184
$CsCoCl_3$, Ising-like antiferromag., instantaneous spin correlations 79−42746
$CsCoCl_3$, Ising-like antiferromag., spin dynamics 79−42747
$Cs_2FeCl_5.H_2O$, cryst. struct., superconducting susceptometer mag. meas. 79−73717
$CsMnBr_3$, EPR linewidth anisotropies 80−103878
$CsMnBr_3.2D_2O$, extended scaling in spin flop system 79−73737
$CsMnCl_3$, electron resonance linewidth anisotropy 79−28588
$CsMnF_3$, spin echo form., parametric mechanism, spin dynamics *(Russian)* 78−23367
$CsNiCl_3$, linear chain antiferromag., mag. props., 1.1 to 7K 79−61076
$CsNiCl_3$, mag. props. 79−73736
$CsNiCl_3(F_3)$, one-dimensional anisotropic paramag., nucl. relax. rate and spin dynamics 77−69723
$CsNiF_3$, ^{19}F NMR, spin fluctuation suppression 78−91970
$CsNiF_3$, 1D ferromag., optical absorption and spin dynamics 80−71417
$CsNiF_3$, double-excitonic optical transition intensity, exchange and dimensionality effects 77−69591
$CsNiF_3$, low frequency dynamics in external mag. field 80−108020
$CsNiF_3$, one-dimens. anisotropic paramagnet, EPR meas. 79−73799
$CsNiF_3$, one-dimens. ferromag., solitons in external mag. field 79−19724
$CsNiF_3$, one-dimens. ferromag., solitons as gas of quasiparticles, inelastic neutron scatt. obs. 79−73679
$CsNiF_3$, one-dimensional magnet, dynamics, mol. field theory approach 80−34614
$CsNiF_3$, quasi one dimensional planar ferromag., low temp. NMR study im mag. field 80−97157
$CsNiF_3$, solitons in one-dimens. ferromag., inelastic neutron scatt. 78−95450
$CsNiF_3$, stochastic motion of Sine-Gordon-solitons, spin-correlation function 80−93105
$(Cu,Zn)Cs_2(SO_4)_2.6(H,D)_2O$ Tutton salt, proton spin-lattice relax. time, proton conc. depend. and spin diffusion role 80−71221
Cu complex, α-CuNSal, one-dimensional $S=^1/_2$ Heisenberg system, nucl. relax. at high temp. 77−85610
Cu complex, $CuCl_2.2NC_5H_5$, spin 1/2 system, one-dimensional nucl. relax. 78−39427
Cu-Co, Kondo system, NMR, spin-lattice relax., impurity spin dynamics 77−69724
Cu-Fe, dil. alloy, spin relaxation rates, neutron scatt. study 79−47235
Cu-Mn, spin glass alloy, magnetic excitations, neutron scatt. 78−10695
Cu-Mn (4.7 at.%), spin glass, spin correlations, neutron scatt. cross section meas. 79−51790
Cu-Mn (8 at.%), spin glass, neutron scatt. and susceptibility investig. of spin dynamics 77−40076
Cu-Mn spin glass, spin freezing and exchange narrowing of mag. reson. 80−60411
Cu-Mn spin glass alloy, spin correl. function, combined neutron spin echo and polarisation anal. 80−50107
Cu-Mn spin glasses, spin dynamics, neutron scatt. meas. 79−8002
$CuCl_2.2NC_5H_5$, antiferromag. spin dynamics at low temp. 77−32278
CuMn, spin glass, mag. correls., neutron scatt. study 80−50105
CuMn spin glass, μ^+ zero-field spin relax. probe for spin dynamics 80−97177
$Cu_{0.95}Mn_{0.05}$, spin glass, low temp. mag. excitation spectrum, inelastic neutron scatt. obs. 80−50109
$Cu(NO_3)_2.2^1/_2H_2O$, ^1H spin-lattice relax. time, 4.2K, 5-60 kOe 79−15371
$Cu(NO_3)_2.2^1/_2H_2O$, singlet ground state system, mag. props. 80−44850
$Cu(NO_3)_2.2.5H_2O$, single cryst., $S=^1/_2$ alternating linear antiferromag. spin dynamics 79−51793
$CuSO_4.5H_2O$, low freq. spin dynamics, proton relax. study 80−71218
$CuSO_4.5H_2O$, $S=^1/_2$ antiferromag. Heisenberg chain, spin dynamics 80−11285
$CuSeO4.5H_2O$, S=1/2 antiferromag. chain, proton relax. near saturation field 79−15370
$CuSeO_4.5H_2O$, antiferromag. chain system, proton spin-lattice relax. near saturation field 79−61256
$DyCo_5$, rotational type spin reorientation, collinear to canted spin struct. change 77−63214
$DyFeO_3$, field induced spin reorientation, Mossbauer spectroscopy 80−65878
$DyFeO_3$, mag. field induced intermediate state, magneto-optical effect meas. 77−55672
$DyFeO_3$, non Heisenberg R-Fe exchange interaction, behaviour in mag. field *(Russian)* 80−2568
$DyFeO_3$, spin reorientation, Faraday rot. meas. 77−8547
$DyFeO_3$, spin reorientation transitions induced by magnetic fields, Mossbauer study 80−71246
$Dy_{0.5}Ho_{0.5}FeO_3$, mag. transitions, influence of Dy^{3+}, Ho^{3+} ground states 77−89955
$Dy_{0.7}La_{0.3}FeO_3$, reorientational phase transitions, influence of La^{3+} ions 80−7108
$Dy_xTb_{1-x}Fe_2$, single cryst., torque meas. 80−65877
$ErCrO_3$, dynamic spin reorientation process, magneto-optical meas. 77−69590
$ErCrO_3$, field-induced spin reorientation relax. 79−78402
$ErCrO_3$, mag. field induced spin reorientation, optical Zeeman absorpt. spectra 79−61398
$ErCrO_3$, magnetisation, NMR freq. temps. depend. weak ferromagnetic-antiferromagnetic spin reorientation transition 80−29631
$ErCrO_3$, spin-reorientation, optical obs. 77−63201
$Er_{0.8}Dy_{0.2}FeO_3$, mixed orthoferrite crystals, ^{57}Fe NMR in spin reorientation range 78−15039
$Er(Fe_{1-x}Co_x)_3$, spin reorientation, easy axis of magnetisation 80−25144
spin dynamics continued
$ErFeO_3$, field induced spin reorientation, Mossbauer spectroscopy 80−65878
$ErFeO_3$, low-temperature spin reorientation 79−65683
$ErFeO_3$, second-order reorientation transition, NMR signal relax. 77−90066
$ErFeO_3$, sound velocity meas. at high press., spin-reorientation transition 78−76254
$ErFeO_3$, spin flip, Faraday effect and absorption spectrum meas. 77−43842
$Er_{0.3}Ho_{0.7}FeO_3$, mixed orthoferrite crystals, ^{57}Fe NMR in spin reorientation range 78−15039
$(ErSm)FeO_3$, spin reorientation, Faraday rot. meas. 77−8547
$Er_{0.5}Tm_{0.5}FeO_3$, mixed orthoferrite crystals, ^{57}Fe NMR in spin reorientation range 78−15039
$Er_xY_{3-x}Fe_5O_{12}$, spin reorientation transitions 78−2686
Eu chalcogenide, spin-disorder Raman scatt., mag. phase depend., theory 78−10887
Eu chalcogenides, magnetic semiconductor, light scatt. exam. 79−61372
EuO, critical EPR spin dynamics, sample shape and temp. depend. 77−32244
EuO, zero-wave vector kinetic coefficient near T_c 79−73714
EuO(S)(Se)(Te), spin order and fluctuations, Raman scatt. study 80−97273
EuS, ferromag. semicond., optical spin orientation, Curie temp. increase 77−20627
EuS, spin relax. in crit. region 78−52270
EuS, thermo- and magnetorefl. spectra, dynamical spin fluctuation effect on exciton state 77−52126
EuSe, first- and second-order Raman scatt. near T_N 79−61374
(Eu_xSr_{1-x}) S dilute, spin-cluster freezing observation by low-freq. mag. absorpt. 79−78404
$Eu_{0.4}Sr_{0.6}S$, spin glass, spin dynamics, neutron scatt. study 80−65907
$(Eu_xSr_{1-x})S$, very dil., magnetisation dynamics 80−65915
EuX, X=chalcogen, antiStokes luminesc. 77−63455
Fe complex, $[Fe(2\text{-pic})_3]Cl_2.EtOH$, struct. changes, spin phase transition mechanism 79−78380
Fe complex, bis[2-(2-pyridylamino)−4-(2-pyridyl)thiazole]Fe(II) complexes, high spin-low spin transitions 77−8456
Fe, ferromag., dynamic susceptibility calc. 80−80488
Fe film, nuclear spin system dynamics Mossbauer study in FMR conditions *(Russian)* 80−80651
Fe, magnetic moments, local short range order, high temp. effects 80−65902
Fe, molten, mag. neutron scatt. at small momentum transfer caused by spin fluctuations 77−47968
Fe, spin fluctuations above Curie temp., diffuse mag. neutron scatt. obs. 80−50102
Fe-Co, 3d ferromagnet nuclear spin-lattice relaxation 80−80627
$FeBO_3$, spin-reorientation phase transition *(Russian)* 80−93122
Fe_3BO_6, MOssbauer spectra in spin reorientation region 77−52002
Fe_3BO_6, spin reorientation by mag. field, Mossbauer meas. 78−35074
Fe_3BO_6, spin-reorientation, elec. resist. and microwave absorption 78−14751
Fe_3BO_6, weak ferromagnetism and spin reorientation, antiferromag. reson. spectra 78−6580
$FeCO_3$, metamagnetic insulator Neel temp. anal. by model including spin fluctuations *(Russian)* 80−15715
$FeCl_2$, metamagnet, optical determ. of thermodynamic phase diagram 78−60285
$FeCl_2.2H_2O$, linear chain metamag. system, phonon and magnon widths 77−36065
$Fe_{1-x}M_xCl_2$, disordered, Mn spin excitations by microwave absorption at high freqs. 80−34759
γ-FeMn, alloys, itinerant antiferromag., spin dynamics, neutron scatt. meas. 77−12105
$Fe_{1-x}Mn_xSn$, spin reorientation, Mossbauer study, 77 to 400K 80−97172
$(Fe_{65}Ni_{35})_{75}P_{16}B_6Al_3$, amorphous ferromag., high temp. spin dynamics 78−47965
α-Fe_2O_3, antiferromag., muon spin rotation *(German)* 80−54877
α-Fe_2O_3:Al, hematite, spin reorientation, Mossbauer spectra obs. 78−72356
β-FeOOH, colloidal suspension, ionic spin relax. theory for Mossbauer spectra 78−19384
$Fe_xPd_{82-x}Si_{18}$, amorphous, magnetisation, magnetoresist., spin glass and ferromag. phases 80−34697
FeSi, nearly ferromag. semicond. mag. and thermal props., spin fluctuation theory 79−65687
η-Fe_5Si_3, thermal and mag. props. 77−36080
Fe_5SiB_2, Mossbauer spectra, 140-784K, spin rotation 78−52409
1T-$Fe_{0.1}Ta_{0.9}S_2$, mag. modulation of lattice electric field gradient 77−85628
Ga_2O_3-Fe_2O_3, anomalous Mossbauer lineshapes, spin fluctuations 77−51998
Gd, magnetoelastic anomaly at 240K, spin reorientation region 77−40105
Gd, optical conductivity, direct interband transitions 80−15488
Gd, temp. variation of absolute thermoelec. power 77−11900
$GdAl_2$, ferromag., spin reorientation 78−39334
$GdAl_2$, spin reorientation, NMR features rel. to preferred magnetisation direction change 77−63213
$GdAl_2$, spin reorientation 78−39335
$GdAlO_3$, magnetoelec. susceptibility, mag. struct., mag. phase diagram and crit. coeffs. 77−66303
$GdAlO_3$, spin-flop bicritical line obs. 77−66306
$GeFeO_3$, field induced spin reorientation temp. depend. 77−63200
^3He, BCC, NMR multiple echoes, soln. of eqn. of motion of magnetisation 79−86961
^3He, liq., hydrodynamic modes, macroscopic dispersion relations, two fluid model 78−10242
^3He, liq., hydrodynamic modes, microscopic dispersion relations, transport coeffs. 78−10243
^3He, liq., spin fluctuation peak obs. by inelastic neutron scatt. 80−49447
^3He, liquid, low-energy spin fluctuation peak, theoretical anal. of neutron obs. 80−6584
^3He, liquid, polarisation potentials, viscosity, thermal cond., spin diffusion 80−88389
^3He, neutron inelastic scattering, zero sound and spin-fluctuation peaks 78−79836
^3He, solid, spin diffusion in BCC and HCP phases *(Russian)* 77−35794

spin dynamics continued
^{3}He, solid, spin diffusion coeff. *(Russian)* 77−80679
^{3}He, solid, spin diffusion at very low temp., multiple echo amplitudes 79−19423
^{3}He, superfluid, A-phase, helical textures, NMR response 80−70496
^{3}He, superfluid, A-phase, orbital dynamics in spin fluctuation feedback approx., out-of-phase mode 80−54457
^{3}He, superfluid, creation of mag. solitons 77−15653
^{3}He, superfluid, spin and orbital dynamics, book contrib. 80−2236
^{3}He, superfluid, spin dynamics equations soln., strong mag. field 78−56010
^{3}He, superfluid, spin relax., transport, spin fluctuation dominance model 77−66052
^{3}He, superfluid A- and A_1-phases, spin dynamics 79−51350
^{3}He, superfluid A-phase, dynamic spin behaviour in presence of textures 79−1536
^{3}He, superfluid A-phase, orbital motion in presence of heat current 79−51349
^{3}He, superfluid A-phase, strong-coupling orbital 79−51346
^{3}He, superfluid A-phase direct obs. of orbital dissipation and superflow collapse 79−51347
^{3}He superfluid B-phase, dynamic magnetism relaxation, wall-pinned mode 78−43201
^{3}He, superfluid B-phase, spin oscills. in the presence of dipole forces 80−6583
^{3}He, superfluid orientational dynamics with relax., two-fluid model 77−69135
^{3}He-^{4}He liquid mixture, conc. ^{3}He spin diffusion expts. 78−34671
^{3}He-^{4}He mixture, spin diffusion in tricritical region along coexistence curve 77−15654
^{3}He-^{4}He solutions, spin diffusion under press. 78−56018
^{3}He-A, superfluid, spin disgyrations 77−89611
^{3}He-A, superfluid, spin dynamics, spin-orbit configurations, spin waves *(Russian)* 80−54462
^{4}He, spin diffusion coeff. of ^{3}He impurities, impuriton model 77−59174
^{4}He-^{3}He, solid spin diffusion coeff. and T_2, impuritons, temp. depend. 78−34675
^{4}He-^{3}He, dil. soln., ^{3}He quasiparticle interaction, conc. depend. 77−15655
HgTe type semiconductors, spin-flip transitions in magneto-optics and magneto-transport 80−50306
$HoAl_2$, Ho moment reorientation, polarized neutron diffr. study 79−42761
$HoAl_2$, spin reorientation, sp. ht. meas. 79−73724
$HoCo_2$, cryst. field induced spin rot., Mossbauer meas. 77−16227
$HoCo_2$: ^{57}Fe, easy magnetisation directions, spin rotation like transitions 77−63168
$HoFeO_3$, field induced spin reorientation, Mossbauer spectroscopy 80−65878
HoIG, spin reorientation from Faraday effect meas. 79−51780
$Ho_xTb_{1-x}Co_2$ lave phase compounds, elastic props., temp. and magnetic field dependence 80−60393
$Ho_xTb_{1-x}Fe_2$, single cryst., spin orientations 78−84425
$Ho_xTb_{1-x}Fe_2$, single crystals, continuous spin orientations, magnetisation easy direction 78−84453
HoZn, mag. excitations near spin rot. temp., neutron scatt. study 79−19731
p-InSb, photoexcited exciton spin-flip scatt. 80−74434
InSb type semiconductor, spin-flip transitions in magneto-optics and magneto-transport 80−50306
K_2CoF_4, two-dimens. Ising antiferromag., nearest neighbour correl. function, birefr. expts. 80−71386
$KCuF_2$, linear chain Heisenberg antiferromag., nearest neighbour correl. function, birefr. expts. 80−71386
K_2CuF_4, spin relax., crit. behaviour, high freq. susceptibility meas. 80−65936
K_2CuF_4, two-dimensional planar ferromagnet, giant fluctuation of spins *(Japanese)* 80−54894
$K_2Cu_cZn_{1-c}F_4$, EPR, spin correlation decay rate 79−19772
$K_2Cu_xZn_{1-x}F_4$, two-dimens. ferromag., spin correls. near percolation limit 80−44840
$KFeF_5$, one dimensional antiferromagnets, field depend. spin reduction temp. variation, spin flopping 79−78586
K_2FeF_5, one dimensional antiferromagnet, Mossbauer effect, mag. and electric field gradient axes 79−78587
K_2FeO_4, crit. slowing down of spin fluctuations, Mossbauer spectra and relax. theory 80−65882
$KMg_{1-x}Mn_xF_3$, disordered paramagnet, ^{19}F NMR study 80−71216
$K_2Mn_{1-x}CoF_4$, mag. and neutron scatt. exam. 79−33466
K_2MnF_4, 2-dimens. antiferromagnet, with dipolar broadening, spin diffusion, EPR obs. 79−38371
$K_3Mn_2F_7$, double-layer antiferromag., mag. ordering, neutron scatt. meas. 79−61062
$K_2Mn_{1-x}Fe_xF_4$, layered antiferromag., anisotropy effects on mag. ordering, neutron diffr. study 79−47254
$K_2Mn_{1-x}Fe_xF_4$, mag. and neutron scatt. exam. 79−33466
$KNiF_3$, and K_2NiF_4, double-excitonic optical transition intensity, exchange and dimensionality effects 77−69591
$LuCoO_3$, spin-state equilib. 77−12087
α-Mn, localised spin fluctuations, Knight shift obs. 80−60181
β-Mn, spin fluctuations effect on sp. ht. 79−82788
Mn-V(Cr)(Fe)(Co)(Ni), spin fluctuations effect on sp. ht. 79−82788
$MnCO_3$, spin echo form., parametric mechanism, spin dynamics *(Russian)* 78−23367
MnF_2, reson. NMR near phase transition 78−76265
MnF_2, spin-flop bicritical point, susceptibility and RF absorpt. meas. 79−87277
MnF_2, spin-flop transition obs. by neutron diffr. 79−73734
$MnO-Al_2O_3-SiO_2$ glass, spin freezing, muon spin depolarisation, superparamag. domain model 78−68272
MnSi, itinerant electron system, neutron scatt. 78−68194
MnSi, itinerant ferromag. spin dynamics field depend. 79−38315
MnSi, μ^+ spin-lattice relax rate, paramag. phase, near T_c, temp. depend. 79−19825
$Mn_{1-x}Zn_xF_2$, randomly diluted uniaxial antiferromagnet, CPA theory 79−78388
$(NH_4)_2ReCl_6(IrCl_6)$, proton relaxation near antiferromagnetic phase transitions 80−80640
$NdCO_2$: ^{57}Fe, easy magnetisation directions, spin rotation like transitions 77−63168
$NdCo_2$, cryst. field induced spin rot., Mossbauer meas. 77−16227
spin dynamics continued
$NdCo_5$, ferromag., thermomag. charact. in mag. field *(Russian)* 78−23273
$NdCo_5$, spin reorientation, magnetisation and torque curves, 77-925K 77−4532
$Nd_{1-x}Dy_xCo_5$, rotational type spin reorientation, appl. to thermomagnetic generator 77−85451
$Nd_{1-x}U_xCo_5$, mag. props. and spin-reorientation phase transitions *(Russian)* 78−60284
Ni, dynamical spin susceptibility, noninteracting spin band model 78−31059
Ni, ferromag., dynamic susceptibility calc. 80−80488
Ni, magnetoelastic effect on longitudinal compression, weak field spin rotation model 79−82851
Ni-Cd, dil., ferromagnetic dynamic crit. exponent, hyperfine interaction vs. neutron scatt. expts. 78−84437
Ni-Pt disordered alloy, off-diagonal, T-matrix itinerant electron ferromagnetism calcs. 80−25067
$Ni_{0.95}$ S Fe, spin glass, spin flop in exchange field 80−34640
$Ni(NH_3)_6X_2$, (X^-=Cl^-, BF_4, ClO_4^-) spin dynamics at struct. phase transition 79−15309
NiO (111) platelets, antiferromag. S domains, optical obs., spin flop 80−54915
NiO (111) platelets, magnetic anisotropy investigation by torque and mag. susceptibility meas. 80−54885
$NiWO_4$, antiferromag., low symmetry exhibited during spin-flop phase transition 80−60263
$NiWO_4$ monoclinic antiferromagnet, orientational phase transition and intermediate state *(Russian)* 80−15725
$Ni_{0.25}Zn_{0.75}Fe_2O_4$, Mossbauer study, spin fluctuations 80−60471
$Ni_{1-x}Zn_xFe_2O_4$, statistical model and phase transform. *(German)* 77−85473
$NpRu_2$, spin fluctuation cpd., sp. ht., 3-25K 77−63212
PbTe, far IR spin flip reson. 79−82979
Pd, phonon mediated interaction for triplet pouring 79−23911
Pd, spin fluctuation model interpretation of mag. susceptibility 80−80477
Pd, triplet pairing, spin fluctuation contrib. 78−10711
Pd-Mn alloy, spin glass, low temp. spin dynamics, numerical studies 79−78385
Pd_3Mn, disordered, mag. correls., neutron scatt. study 80−50105
Pr, central peaks and soft modes, quasi-elastic mag. scatt. obs. 77−66377
$PrAlO_3$, ^{27}Al NMR, electronic spin dynamics at Jahn-Teller phase transition 78−68403
Pt, spin fluctuation model interpretation of mag. susceptibility 80−80477
Pu-Np, elec. resist., reson. scatt. from Np and local spin fluctuations 77−28170
$PuAl_2$, low temp. sp. ht., spin fluctuation phenomena 77−28405
Rb_2CoF_4: ^{57}Fe, Ising antiferromag., Mossbauer spectra, critical dynamics 80−15884
$Rb_2Co_cMg_{1-c}F_4$ mag.-nonmag. two-dimens. antiferromag. Ising system, spin fluctuations 80−80545
$Rb_2Co_cMg_{1-c}F_4$, random two-dimens. Ising antiferromag., unstable mag. long-range order, neutron scatt. obs. 80−44839
$Rb_2Co_{0.5}Mn_{0.5}F_4$, two dimens. random antiferromag., excitations 80−107997
Rb_2CrCl_4, 2D-ferromag., renormalisation of long wavelength spin waves, neutron scatt. 80−60229
$Rb_2CuBr_4.2H_2O$, dynamic props. in paramag. state, spin-lattice relax. time meas. 80−71214
$Rb_2FeCl_5.H_2O$, cryst. struct., superconducting susceptometer mag. meas. 79−73717
$RbFeF_5$, one dimensional antiferromagnets, field depend. spin reduction temp. variation, spin flopping 79−78586
$RbMnBr_3$, EPR linewidth anisotropies 80−103878
$RbMnCl_4$, changes in birefr. due to spin flopping 79−73910
Rb_2MnCl_4 antiferromagnet, spin flopping of sublattice mag. moments in mag. fields 79−69687
$RbMnF_3$, Heisenberg antiferromagnet, paramag. region, NMR, spin pair correl. 78−15032
$RbMnF_3$, Heisenberg antiferromagnet, spin diffusion below T_N 78−34968
$RbMnF_3$, zone-boundary magnon energy and damping, Raman scatt. meas. 78−31202
$Rb_2Mn_cMg_{1-c}F_4$, two-dimens. antiferromag., spin fluctuations, neutron diffr. study 80−44846
$Rb_2Mn_xMg_{1-x}F_4$, random magnetic-nonmagnetic 2-dimens. antiferromag., spin fluctuation dynamics 77−63147
$Rb_2Mn_xMg_{1-x}F_4$, spin dynamics near percolation threshold, EPR study 80−39859
$RbNiCl_3$, mag. props. 79−73736
Sc_3In, itinerant electron ferromagnet, spin fluctuations 77−73096
$Si:P^+$, Zeeman energy transfer at surface layer 80−11247
SiC, laser Raman spin-flip scatt. from excitons, luminesc. 80−80786
SiC, spin-flip scatt. of laser light from photoexcited excitons 80−93330
$Sm_{0.7}Er_{0.3}FeO_3$ spin reorientation photomagnetic motor 78−2695
$SmFeO_3$, HF susceptibility, crit. divergence in spin reorientation temp. region *(Japanese)* 77−43836
$SmFeO_3$, magnetisation direction angle meas. in spin reorientation region 77−26366
$SmFeO_3$, magnetostriction meas. in spin reorientation region 78−2721
$Sm_xNd_{1-x}Co_5$ powders, mag. props. *(Russian)* 79−51812
$Sm_{0.55}Tb_{0.45}FeO_3$, orthoferrite cryst., domain memory effect *(Russian)* 77−55693
$Sm_xTb_{1-x}FeO_3$, gyrotropic props. and birefringence, in spin reorientation range 80−7324
$Sm_xTb_{1-x}FeO_3$, mag. reorientation, temp. *(Russian)* 79−87263
$Sm_xY_{3-x}Fe_5O_{12}$, spin reorientation transitons 78−2686
$SrEuFeO_4$, Neel temp. and spin reorientation, Mossbauer study 80−39934
$SrEu_2Fe_2O_7$, ferrite, Mossbauer effect study of hyperfine interactions, spin reorientation 78−19383
$SrGdFeO_4$, Neel temp. and spin reorientation, Mossbauer study 80−39934
$SrRFeO_4$, (R=La,Pr,Nd), Mossbauer spectra, spin reorientation 80−15880
$SrR_2Fe_2O_7$ series, mag. struct. and spin reorientation, neutron diffr. and Mossbauer meas. 77−69503
$SrTb_2Fe_2O_7$, ferrite, Mossbauer effect study of hyperfine interactions, spin reorientation 78−19383

spin dynamics continued
$TaS_2(NH_3)_x$, NMR spectral densities and two-dimens. diffusion 80−50215
Tb-Gd alloy, spin orientation transition obs. 79−99714
$TbFeO_3$, metamag. phase transitions, mag. struct. instability *(Russian)* 79−61107
$Tb_3Fe_5O_{12}$, mag. phase transition exam. 79−19736
TbIG, Faraday rotation and transition of spin config. at high mag. fields 80−39776
TbP, mag. excitations above antiferromag. ordering temp., inelastic neutron scatt. obs. 80−50112
$Tb_xY_{1-x}Co_{5+0.1x}$, exchange interactions and magnetocrystalline anisotropy 80−34618
$Tb_{0.2}Y_{2.8}Fe_5O_{12}$, Mossbauer investigation of spin-reorientation transition 78−88243
$Tb_xY_{3-x}Fe_5O_{12}$, spin-reorientation phase transitions, neutron depolarisation factor 78−27037
TbZn, mag. excitations meas. 80−70979
$TiS_2(NH_3)_{1.0}$, NMR spectral densities and two-dimens. diffusion 80−50215
$TlCoF_3$ paramagnetic, nonmagnetic atomic nuclei spin density, NMR study 80−29633
$Tl_2SeAs_2Te_3$, amorphous semicond., nuclear spin-lattice relaxation by localised electronic states, modification by spin diffusion 78−52372
$TmCrO_3$, temp. and field-induced spin reorientation, magnetisation meas. 77−69588
$TmFe_2$, amorphous, neutron scatt. at transition, spin diffusion, magnetisation meas. 78−68174
$TmFeO_3$, acoustic vel. and attenuation shifts at spin reorientation phase transition 80−65986
$TmFeO_3$, domain struct. in spin reorientation region, Faraday effect obs. 77−20835
$TmFeO_3$, magnetoelastic props. at spin reorientation region 77−8382
TmSe, mixed valence systems, spin dynamics and mag. ordering 78−68162
TmSe, spin dynamics, neutron scatt. study 79−24178
UAL_2, band magnetism due to f-electrons, T_{sf} 77−73039
UAl_2, low temp. sp. ht., spin fluctuation phenomena 77−28405
UAl_2, spin fluctuations, mag. field effect, electronic sp. ht. and elec. resist. 80−108026
$UC_{1-x}N_x$, NMR of ^{13}C and ^{15}N, 5f electrons nature, mag. susceptibility, spin fluctuations 77−20736
UCo_2, elec. resist. and mag. susceptibility meas., non-stoichiometry influence 77−63088
UGe_3, spin fluctuation phenomena, band struct. calcs. and de Haas-van Alphen meas. 77−20225
$U_{1-x}Th_xAl_2$, ferromag. spin fluctuation system, sp. ht. and elec. props. 77−20604
$(U_xTh_{1-}x)S(Te)$ solid solns., electronic struct., mag. susceptibility and elec. resist. obs. 77−20551
V surface, spin fluctuations, finite temp. mag. props. study 80−107994
V_3Se_4, itinerant antiferromag., spin fluctuations, NMR study 80−75874
V_5Se_8, itinerant antiferromag., spin fluctuations, NMR study 80−75874
$Y(Co_{1-x}Ni_x)_5$, spontaneous magnetisation mag. anisotropy, spin reorientation transformation *(Russian)* 80−7082
$YCrO_3$, antiferromag., exciton absorption lines obs. during field induced spin-reorientation 77−63397
$YCrO_3$, magnetisation, NMR freq. temps. depend. weak ferromagnetic-antiferromagnetic spin reorientation transition 80−29631
YFe_2, amorphous concentrated spin glass, susceptibility, Mossbauer and neutron scatt. meas. 80−39783
$Y_3Fe_{5-x}Co_{x/2}Si_{x/2}O_{12}$, spin reorientation, NMR and ferromag. reson. meas. 80−65890
$YFe_{1-x}Co_{x/2}Ti_{x/2}O_3$, anomalous decrease of spontaneous magnetisation in spin reorientation region 77−36059
$YFe_{1-x}Co_{x/2}Ti_{x/2}O_3$, magnetostriction meas. in spin reorientation region 78−2721
$YFe_{1-x}Mn_xO_3$ orthoferrite, spin reorientation, mag. torque meas. 78−47979
$YFeO_3$, Co^{2+} substituted, reorientational transitions 77−59419
$YFeO_3$, induced spin reorientation near Neel point 78−19267
$YFeO_3$:Co^{2+}, Ti^{4+}, spin reorientation, Faraday rot. meas. 77−8547
$Y_{1-x}GdCo_5$, exchange interactions and magnetocrystalline anisotropy 80−34618
YIG, relax. after spin wave excitation in ferrite *(Russian)* 79−19783
YIG, Si substituted, spin reorientation, Mossbauer spectroscopy obs. 80−44989
$Y_{1-x}Nd_xCo_5$, exchange interactions and magnetocrystalline anisotropy 80−34618
$Y_{1-x}Tb_xCo_5$, spontaneous magnetisation anisotropy, spin reorientation transforms. *(Russian)* 80−7082
YbCuAl, intermediate-valent, nucl. reson. and relax. 79−78550
ZnS:Mn^{2+}, spin-lattice relax. time, continuous saturation expts., spin diffusion 77−36120

spin echo (EPR)
chlorophyll-a radical cations, in disordered systems, electron spin echo envelope modulation, isotope effects 78−61141
diffusion of radical-ion pairs, spatial distrib., electron spin echo obs. 80−29622
diphenylmethylene-d_0,-d_{10}, in benzophenone, ground triplet state, electron spin echo expts. 77−16144
disordered matrix, effect of quadrupole coupling on electron spin echo modulation patterns 77−85571
electron plasma relax. characts., 3-30 eV 80−79612
envelope modulation, 2-dimens. Fourier transform 80−63680
envelope modulation effect, powder pattern behaviour, hyperfine coupling consts. determ. 79−33524
EPR, ns time-resolved, in pulse radiolysis, via spin echo method 80−43075
EPR/ENDOR, modified Ka-band spectrometer, obs. of electron spin echoes at 35 GHz 80−13113
ethanol-$d_1(d_2)(d_3)$, glassy state, solvated electron geometry, electron spin echo modulation obs. 80−66009
excited triplet states, coherent averaging by rotary echoes 79−42823
free radicals in nonviscous soln., electron spin-echo theory 77−3386
frozen acid solutions, aq., irrad., at. H trap struct., spin echo obs. 79−42824
frozen alcohol solutions, aqueous, H atom stabilisation, EPR obs. 79−47325

spin echo continued
frozen salt solutions, aq., irrad., at. H trap struct., spin echo obs. 79−42824
glasses, microwave tunnel echo *(Russian)* 79−65726
glassy material, nuclear modulation 78−2727
hydroxymethyl radicals, adsorption on A-type zeolites, electron spin echo obs. 78−21947
liquid, electron spin echo phase memory decay, generalised cumulant expansions appl. 79−11334
macroradical, electron spin echo spectra, instantaneous and conventional spectral diffusion 79−15355
malonic acid, electron spin echo exam. of mutual flip flop electron spin reversals involving forbidden transitions 79−24216
metal particles, conduction electron spin echo modulation, theory 80−39872
methanol, β-irrad., radical truck struct., electron spin-echo obs. 80−93776
13-methylpentane-d_{14}, glass, γ-irrad., solvated electron struct. obs. 77−9101
2-methyltetrahydrofuran glass, solvated electrons by electron spin echo modulation spectra 79−88991
methyltetrahydrofuran glass, three-pulse echo modulation, phase reversal 77−1584
microwave cavity for ENDOR meas., expt. 78−82013
naphthalene pair ($C_{10}H_8$) in $C_{10}D_8$ host, mini-exciton obs., electron spin echo and ODMR 77−4559
naphthalene-d_0, in naphthalene-d_8 cryst., mol. pair mini-exciton form., electron spin echo and ODMR 77−72822
nitroxide free radicals in liquids, electron spin-echo obs. 80−63685
paired radical-paramag. ion spatial distrib. function determ. 79−61223
pentacene in naphthalene, triplet state, EPR study by electron spin-echo and laser flash excitation 80−58172
plant photosynthesis, signal II, electron spin-echo method 78−96118
polyatomic molecules in solid matrices, ODMR in triplet states, appl. of spin echoes 79−18217
porphin free base, triplet state electron spin echoes, fluoresc. detection 78−70856
praseodymium ethylsulphate:Sm, one-dimens. X-Y system, spin dynamics, electron spin echo meas. 80−66031
praseodymium ethylsulphate:Sm, XY system, mag. relax. and spin dynamics 79−61211
quartz, secondary electron spin echo obs. *(Russian)* 78−80191
quartz , fused and γ-irrad. 79−99770
R. spheroides, triplet state electron spin echoes, fluoresc. detection 78−70856
review, electron spin echo modulation phenomena, paramagnetic species immediate environment struct. 78−88164
spectral-diffusion decay in echo experiments 79−1723
structural transitions in solids, electron spin echo investigations 78−84476
1,2,4,5-tetrachlorobenzene, linear chain triplet excitons, electron spin-echo and ODMR 78−76357
tetracyanoethylene in acetone-d_6, anion solvation, electron spin echo modulation 80−63676
tetracyanoethylene in dimethylsulphoxide-d_6, anion solvation, electron spin echo modulation 80−63676
tetracyanoethylene in methanol-$d_3(d_1)$, anion solvation, electron spin echo modulation 80−63676
TGS X-irradiated, paramag. relax, spin-echo study 80−7168
three-pulse modulation, phase reversal 77−1584
transient radicals, EPR time profiles, CIDEP, electron spin-echo method 79−6953
triphenylmethylphosphonium-TCNQ, paramag. echo from triplet excitons obs. 77−28130
tris-sarcosine calcium chloride:Mn^{2+} ferroelec. dynamics, EPR and ENDOR study 80−75972
trissarcosine calcium chloride:Mn^{2+}, ferroelec., electron spin-lattice relax. 78−80208
Ag, and Ag^+, solvation in deuterated-ice matrices, electron spin echo obs. 80−15780
Ag atom solvation in methanol, geometrical model, electron spin-echo modulation obs. 80−63682
Ag solvation in ice matrix, electron spin echo modulation 78−39396
BaF_2, spectral diffusion, coherent effects in ESR of Gd^{3+} 79−51852
$BaWO_4$:Er^{3+}, spin-lattice and spin-spin relax. times, electron spin echo obs. 79−28609
$CaMoO_4$:Er^{3+}, phase relax., EPR spin echo expts. 79−99767
$CaMoO_4$:Er^{3+}, phase relax. time rel. to g-factor anisotropy, electron spin echo obs. 80−29615
CaO:Mo, spin coherence and Stark modulation effect of F_A-Mo centre excited state 77−69733
CaO-P_2O_5 glass, pulsed EPR study of Cu 78−84479
$CaWO_4$, Yb^{3+}, Nd^{3+} phase relaxation electron spin echo spectra 80−29613
$CaWO_4$:Er^{3+}, phase relaxation, spin echo meas. 78−68375
$CaWO_4$:Yb^{3+}(Nd^{3+}), phase relax. time rel. to g-factor anisotropy, electron spin echo obs. 80−29615
Cs vapour, optically pumped, transverse relax. times and diffusion coeff., spin echo meas. 79−10062
$CsZnCl_4$:Cu^{2+}, electron spin echo, 35 GHz 80−13113
Cs_2ZnCl_4:Cu^{2+}, single cryst. and powdered single cryst., EPR, linear elec. field effect 80−11250
Cs_2ZnCl_4:Cu^{2+} electron spin echo envelope, Fourier transform ^{133}Cs modulation 80−58291
Cu^{2+}-imidazole complex, electron spin echo, nuclear modulation effect 79−18211
H_2SO_4:Fe^{2+}, frozen aq. soln., photolysis, H form., distrib. and diffusion 78−20044
$LaCl_3$:Nd^{3+}, coherent interactions of Kramers doublet system with microwaves in zero static mag. field 77−73078
LaF_3:Nd^{3+}, spin echo envelope modulation exam. 79−61212
$La_2Mg_3(NO_3)_{12}.24H_2O$:$Mn^{2+}$, linear electric field effect on ground state splitting, EPR 78−80198
Li, metallic, obs. of intrinsic spin-lattice relax. of conduction electrons 78−10774
$LiTmF_4$ Van Vleck paramagnet, electron and nuclear spin-lattice relaxation of Er^{3+} ions 79−95643
Na_2-B_2O_3 glass, pulsed EPR study of Cu 78−84479
Na_2O-SiO_2 glass, pulsed EPR study of Cu 78−84479
Nd complex, Nd^{3+}:ATP, electron spin echo decay envelope anal. 79−54871

spin echo continued
β-PbF_2, spectral diffusion, coherent effects in ESR of Gd^{3+} 79−51852
$Pb_5Ge_3O_{11}$, spectral diffusion, coherent effects in ESR of Gd^{3+} 79−51852
SrF_2, spectral diffusion, coherent effects in ESR of Gd^{3+} 79−51852
$SrWO_4:Er^{3+}$, spin-lattice and spin-spin relax. times, electron spin echo obs. 79−28609

spin echo (NMR)
^{13}C NMR, proton-decoupled, spin-echo determ. of short T_2 values, errors, appl. to protein mobility 78−2769
acetic acid, $-d_1(=d_4)$ liquid, molecular motion, proton spin echo study *(Russian)* 80−32745
acetone-d_6, deuteron NMR spin echo, time domain spectrum 78−88223
adamantane, nucl. spin echoes ^{13}C magnetisation and intermol. dipolar coupling 78−35062
alkali metal bromates and chlorates, alkali and ^{17}O NQR, spin echo double reson. method, electronegativity 80−54970
antiferromagnets, EM and acoustic response echoes of nuclear spin system *(Russian)* 79−69747
benzene, diffusion coeff. meas., Fourier transform NMR, pulsed field gradient system 80−57353
benzene-2,5-dibromothiophene, self-association, proton mag. relax. 77−28471
benzene-d_6, deuteron NMR spin echo, time domain spectrum 78−88223
benzyl alcohol, C-C spin coupling, two-dimens. Fourier transformation 78−90194
binary liquid systems with strong chem. interaction, spin echo obs. of self-diffusion *(Russian)* 79−95197
blood flow imaging 78−85330
Brownian motion and NMR spin relax., book 78−15054
Carr-Purcell sequence, chemical exchange and T_2 relax., multiple sites 78−78727
Carr-Purcell-Meiboom Gill pulsed NMR sequence, errors in T_2 values 77−85604
cell structure size determ. from water diffusion meas. by pulsed gradient method 78−77159
chlorotrifluoromethane, self-diffusion coeff. near crit. temp., density depend. obs. 78−95530
cholesterol, proton-coupled ^{13}C NMR spectrum, double Fourier transform 78−78725
coherence transfer echoes, coherence defocusing and refocusing occurring at two freqs. 78−48078
coherent NQR relaxometer, two freq. processes by multichannel analyser 80−20498
coupled AB spin systems, spin echoes modulation 78−80242
cumulant approach 77−85614
cyanomethane-d_3, deuteron NMR spin echo, time domain spectrum 78−88223
α-cyclodextrin and α,β-D-xylose, absorption mode spin-echo spectra appl. 80−78634
cyclododecanone, photolytic biradical anomalous CIDNP enhancement, pulse spin echo NMR obs. 78−46369
cyclohexane, isomerisation, proton spin-echo NMR 77−9053
cyclohexane, liquid, density effect on transport properties 80−65264
cyclopropane, liq., mol. dynamics, self-diffusion, quasielastic neutron scatt. and NMR spin-echo meas. 78−10201
dense gases, mutual diffusion coeff., spin-echo meas. 78−67303
dextran T-10 and α-cyclodextrin, absorption mode spin-echo spectra appl. 80−78634
p-dichlorobenzene, ^{35}Cl NQR line narrowing by nonreson. RF photon dressing 80−63662
dichloromethane-d_2, spectral densities determ. from spin-lattice relax. and spin-echo decay rates 80−75877
diffusion, through permeable barriers, applied to NMR with pulsed field grad. 78−91986
diffusion in bounded heterogeneous media, stochastic Liouville eqn., spin quantum phenomena 80−54992
dimethylammonium copper chloride bromide, mag. props., pulsed NMR expts. 80−11292
dioxane, isomerisation, proton spin-echo NMR 77−9053
dipalmitoyl lecithin-water system, lyotropic liq. cryst., pretransitional effects, PMR second moment meas. 78−91234
dipropylammonium copper chloride, ferromag., low temp. magnetism *(Japanese)* 77−20748
p-dodecanoylbenzylidene-p′-aminoazobenzene, smectic A mesophase, self- and impurity diffusion, NMR spin echo obs. 78−94975
double pulse solid echoes for pairs of spin-1 nuclei 79−61262
flow measurement, difference method, plug and laminar flow, appl. to plant stem 78−14110
fluid flow profiles, convective and press.-driven, meas. using pulsed NMR 78−14109
fluorite lattices, $^{19}F^-$, self-diffusion, spin lattice relax., NMR techniques 80−34801
formic acid, heteronuclear double reson., spin echo modulations 78−1009
Fourier transform spin-echo NMR spectroscopy, multiple pulse technique 80−37063
frequency modulation mechanism model, crystal with freq. pulling 77−69727
garnets, cation site distrib. and valence states 79−99167
Gd-alloy, ferromagnetic, nuclear spins as probe for mag. coupling and crystallographic order 78−10799
Hahn spin systems, mechanism of form. of single-pulse echo *(Russian)* 79−78566
heavy water, compressed, NMR spin echo obs., self-diffusion coeffs. 77−1250
Heusler alloys, hyperfine fields and mag. interactions, NMR spectra 78−88222
Heusler alloys, hyperfine fields at sp sites, spin echo NMR meas. 78−19371
hexafluorobenzene, liq., self-diffusion and denisty as functions of press. and temp. 80−92696
hexafluorobenzene-n-paraffins, binary liquid solns., self diffusion, spin echo meas. 80−65263
hexamethylbenzene, perdeuterated, D nucleus, spin-1, spinor behaviour of double quantum transition 79−47355
hexamethylenetetramine, mol. ultraslow rot. obs. using D probe spin alignment tech. 80−88890
p-hexanoylbenzylidene-p′-aminoazobenzene, smectic A mesophase, self- and impurity diffusion, NMR spin echo obs. 78−94975
high-pressure system 78−58002
high-resolution NMR by double Fourier transform, chem. shift and spin echoes 77−57375
hydrazide derivatives, symm., ^{14}N NQR echo envelope slow beats 80−29643
hydrazine monohydrate, ^{14}N NQR, echo envelope modulation obs. 80−50218
hyperfine field inhomogeneity effects, nuclear spin echo in NMR and FMR overlap region 79−24229
indirectly induced NMR spin echoes in solids 80−71239
input pulse phase depend., statistical tensor method *(Russian)* 78−23368
Invar, mag. inhomogeneity, ^{57}Fe and ^{61}Ni NMR 79−19803
J coupling from Carr-Purcell spin echo techniques 77−10690
J spectroscopy, two-dimensional suppression of spurious signals 78−15057
Jeener-Broekaert three-pulse sequence, inhomogeneous lineshapes, second rank spin interactions 80−39891
liquid, Earth field range, review 80−50206
liquid, self-diffusion meas., automated technique, using NMR spin echo 78−27114
liquid, undergoing inhomogeneous Poiseuille flow, spin echo signal shape *(Russian)* 80−50225
liquid binary mixtures, proton mag. relax. and mol. motion 77−28471
liquid crystal, thermotropic mesophase, DMR chain segments assignment 80−24356
liquid crystals, NMR magic echo by sample reorientation 80−103899
lysozyme, absorption mode spin-echo spectra appl. 80−78634
lysozyme, spin echo and spin lock ^{13}C Fourier transform NMR 79−43824
lysozyme, tryptophan residues, H exchange for D, relax., proton NMR spectra 80−35846
MBBA, ring deuterated, dipolar spin system exam. 77−39533
membrane protein-lipid interactions, ^2H NMR investig. 78−80826
metal-H system, NMR depend. on struct., H diffusion and electronic struct., book contrib. 79−82887
metallic hydrides, solid echo amplitude and phase, skin effect 80−108115
methane-Ar, liq. mixture, self-diffusion and nuclear mag. relaxation *(Russian)* 78−87799
methanol, liq., compressed, self-diffusion, NMR spin-echo meas. 77−77122
methylcyclohexane, dense liq., self-diffusion and viscosity 80−15278
molecular crystals, chem. shielding, spin-lattice, quadrupole interactions, ^2D NMR spin echo spectroscopy 80−34817
molecular crystals, D NMR spin echoes, dipolar interactions effects 78−76350
multicomponent self-diffusion measurement using spin echo expts. on standard Fourier transform NMR spectrometers 80−22401
multiple-quantum transition orders separation, using pulsed field gradients 80−50222
muscle, skeletal, Na relaxation, spin echo study, evidence of Na ion binding inside a biological cell 78−88698
nematic liquid cryst., one-deuteron system, multiple quantum spin-echo spectroscopy 80−31832
neutron spin echo appl. on pulsed neutron sources 79−81115
neutron spin-echo integral transform spectroscopy 80−4748
NMR apparatus for meas. of self-diffusion coeffs. in solids 79−217
NMR spin-lattice relax., periodically-irrad. system, master eqn. predictions 78−43664
nonresonant nuclei effects in liquids and solids 77−28473
NQR, at multiple and combination frequencies 80−20499
NQR signal envelope, automatic detection apparatus 77−13785
NQR spectrometer, programming device for a spin-echo installation 80−17972
NQR-NQR double resonance, double quadrupole spin echo resonance 80−20513
nuclear echo formation in spin systems with dynamic freq. shift to NMR 80−93208
organic free radicals, solid, selective pulse NMR expts. 80−60452
organic liquids, NMR spin energy transfer using zero mag. field, spin echoes 79−95675
PAA, homologous series, isotropic phase, mol. self diffusion by spin echo method 80−44109
perfluorocyclobutane, dense fluid, self-diffusion, shear viscosity, density, and temp. depend., NMR 77−36152
phase-modulated spin echoes, derivation of pure absorpt. spectra 80−22410
polarised neutrons, spin-echo appls. 79−46516
poleythylene, linear, butane diffusion coeff., VP depend. nulc. spin echo obs. 79−38404
polycrystalline materials, effect of mag. field on quadrupole spin echo 77−12245
polyethylene, mol. ultraslow rot. obs. using D probe spin alignment tech. 80−88890
polyethylene cocrystals, partially and fully deuterated, chain folding, ^1H NMR solid echo technique 80−20507
polymers, semicrystalline, partially and fully deuterated, chain folding, ^1H NMR solid echo technique 80−20507
polystyrene, solns., diffusion coeffs. meas., Fourier transform NMR, pulsed field gradient system 80−57353
polystyrene soln., monosubstituted, mol. chain dynamics, NMR meas. 78−56393
potassium palmitate-d_{31}, spin-lattice relax., chain position and temp. depends. 78−68405
powders, rot. spin-echoes and high resolution NMR 77−43901
proteins, globular, in water, proton NMR spin echo decay comparative investigation 80−81541
pulsed field-gradient spin echo diffusion data, interpretation using FORTRAN program 79−65758
pulsed magnetic-field programme for investigating diffusion of adsorbed molecules 79−21794
pulsed-gradient multiple-spin-echo technique for diffusion meas. in presence of background mag. field gradients 79−30517
pyridine, compressed liq., self-diffusion coeffs., viscosity, density, temp. press. depend., NMR spin-echo 79−37862
pyridine, proton-coupled ^{13}C J NMR, strong coupling 78−17691
quadrupole, with two-frequency action, amplification and modulation 80−108116
quadrupole spin echo envelope EFG tensor axisymmetry in mag. field 80−20497

spin echo continued
quadrupole spin-system, and energy levels in interaction representation 80−20492
quasiquadrupolar echoes in solid with dipolar coupled rotating methyl groups 78−23366
radiative detection, single-pulse and spin-echo NMR 78−8428
rare earth dil. alloy, nucl. spin-lattice relax. of ^{165}Ho 78−48069
rare earth orthoferrite, second-order reorientation transition, NMR signal relax. 77−90066
rare earth rhodium borides, RRh_4B_4, NMR and sp. ht. in supercond. and mag. ordered phases 80−7037
rare earth-transition metal intermetallics, struct. and props. review 78−10668
relaxation data anal., superimposed exponentially decaying signals, computer technique 78−23360
rotating frame, effect of nonresonant oscillating field, modification of Zeeman energy 77−28454
rotating solid sample, Fourier transform echo envelope anal. 79−65759
rotational spin echoes in solids, anisotropic interaction recovery 78−68410
secondary echo in ferromagnets and antiferromagnets 79−73852
self-diffusion coeff. meas., improved apparatus 78−80243
signal intensity enhancement by polarisation transfer 79−94013
single-pulse spin echo shaping, system with large dynamic freqs. 77−32290
small molecules in protein solns., spin-lattice relax. times, inversion recovery spin-echo sequence 80−21446
smectic liquid crystal, self-diffusion meas. by multiple pulse NMR 78−76352
sodium valerate, mesophase, self-diffusion and spin-lattice relax. 79−69008
solid, mol. and complex ion intramolecular configs., nucl. quadrupole double reson. obs. intramolecular configs., nucl. quadrupole double reson. obs. 80−34821
solid containing spin-1/2 triads undergoing hindered reorientation, quasi-quadrupolar echoes 79−4744
solids, calcs. of NMR spin echo responses 78−88221
solids, D NMR spin echo theory 80−103898
solids, NMR spin echo responses calcs. 79−15376
solution NMR, enhanced selection of non protonated C resonances, ^{13}C spin echo obs. 80−31835
spectra calculation, general method, 2D spin-echo NMR spectroscopy appl. 78−86842
spin density multiplanar image formation using NMR spin echoes 77−22588
spin-lattice relax. time meas. method 77−71355
spin-one system, NMR response to three-pulse sequences in inhomogeneous B_0 field 79−42861
TBBA, nematic liq. crystal, self diffusion coeffs., NMR spin echo 77−31789
TBBA, smectic-A, self-diffusion, neutron incoherent scatt. law 78−83726
three-level NMR system, coherence-transfer rotary echoes prod. by double RF field irrad. 80−66071
TMMC, field-suppression of spin fluctuations, NMR obs. 78−91971
transition phenomena in region of equal NMR and ferromag. reson. frequencies *(Russian)* 77−32272
1,1,2-trichloroethane, phase-modulated spin echoes, derivation of pure absorpt. spectra 80−22410
trimethyl ammonium cobalt chloride dihydrate, antiferromag., ^{59}Co NMR 77−77124
two frequency spin echo spectroscopy, review 80−20506
two-dimensional, appl. to oriented spin systems 78−80244
two-dimensional NMR spectra, elimination of dispersion-mode contribs. 80−20508
two-dimensional spectra, anomalous spinning sidebands 80−17976
water, diffusion const. in presence of large background gradients, modified pulsed gradient technique 80−31831
water, flow through circular pipe, pulsed NMR study 80−28566
water, H_2O and $H_2{}^{18}O$, self-diffusion, pressure and temp. depend., NMR spin-echo obs. 80−65266
water, self diffusion, high-press., low-temp. spin-echo NMR obs. 77−8446
water, self-diffusion coeff., pressure and temp. depend. meas. by proton spin echo 80−39328
water molecules in biological systems, relax. rel. to vol., pulse NMR obs. 80−40960
$AgClO_3$, structural phase transition, ^{35}Cl NQR meas. 80−15819
Al particles, supercond., Zeeman crit. field, NMR spin echo meas. 79−56453
Al_2O_3 multi-level NMR of ^{27}Al, obs. of two-quantum rotary echoes 77−63316
Al_2O_3, multilevel NMR, spin-locking, spin- ocked echo and rotary saturation associated with two-quantum transition 78−80245
β-Al_2O_3-$(Na,Li)_2O$ solid electrolyte, Li motion and activation obs. using ^{7}Li NMR 80−108100
Au-Yb alloys, dil., nucl. reson. of ^{173}Yb local moments 79−65763
BMn, ferromag., ^{55}Mn magnon-induced pseudoquadrupole processes 79−19802
CSI, of ^{127}I, magnetoacoustic excitation *(Russian)* 77−4578
^{13}C coupled with ^{1}H, spinor character for spin $^1/_2$ nucleus via NMR interferometry 78−17699
^{13}C, improved techniques of spectral analysis using chemical shift 77−48086
^{13}C NMR, high-resoln. allowing spin coupling and mag. field inhomogeneity 77−20740
$CaSO_4.2H_2O$, solid echo effect 77−51988
$Ce_{1-x}Gd_xRu_2$, superconductivity and ferromagnetism coexistence, 60 mK-4.2K, spin echo NMR 78−84349
$CeSn_3$, valence instabilities 79−78546
Co, acoustic nucl. spin echo obs. at 4.2K *(Russian)* 78−6599
Co based amorphous alloy, mag. ordered, hyperfine field distribs., NMR meas. 78−68409
Co based Heusler alloys, ferromag., hyperfine fields meas. by NMR 77−63315
Co complexes, NMR studies *(Japanese)* 79−8068
Co, FCC single-crystals, NMR freq. depend. on interatomic distances 79−69748
Co film, mag. anisotropy study using NMR spin echo method 80−60384
Co, HCP, NMR and nucl. relax. meas. in domain walls 77−36146
Co, NMR enhancement of modulating field due to anisotropic component of hyperfine field 77−55729
spin echo continued
Co thin film, nuclear spin echo excitation on subharmonics, and multiple freq. *(Russian)* 80−60454
Co-3d transition metal alloys, hyperfine field and mag. perturbation distrib., NMR spectra meas. 79−61263
Co-Fe, dil., effective mag. field at ^{59}Co, impurity conc. depend., spin echo expts. 78−48080
Co-Ga alloys, ferromag., local configuration studies, neutron scatt. and spin echo NMR 77−63114
Co-Ni, dil., effective mag. field at ^{59}Co, impurity conc. depend., spin echo expts. 78−48080
Co-V, Co rich, ferromag. behaviour, mag. moments, Curie temp., and NMR spectrum 80−70964
Co-V, ferromag. struct. in nucl. spin echoes 80−60453
Co_3B, glassy and cryst., hyperfine field distrib., ^{59}Co spin echo spectra 80−80635
$CoCl_2.2H_2O$, metamagnetic, ^{55}Mn NMR of impurity spin 77−85613
$Co_2Ga_{2-x}Cr_x$, ferromag., local configurational studies, neutron scatt. and spin echo NMR 77−63114
$Co_2Ga_{2-x}V_x$, ferromag., local configuration studies. neutron scatt. and spin echo NMR 77−63114
$(Co_{1-x}M_x)B$, M=Mn or Fe, paramag., spin echo NMR spectra, ferromag. transition, spin-lattice relax. 80−29645
$(Co_{1-x}M_x)B$, M=Mn or Fe, ferromag., internal fields meas. by NMR spin echo 80−29646
Co_2MnSi, ferromag. Heusler alloy, spin echo NMR meas. 77−63319
Co_2TiAl, ferromag., ^{59}Co NMR 78−2760
CoV alloys, phase dependent MNR spectra 80−108114
Co_2VGa, ferromag. Heusler alloy, spin echo NMR meas. 77−63319
Cr-Te system, NMR meas., effect of heat treatment 78−27112
Cs atoms, nonresonance spin echo, transverse relaxation time *(Russian)* 80−50224
$CsCoCl_3$, antiferromag., ^{59}Co NMR spectrum obs. by spin echo method 79−51881
$CsMgCl_3(Br_3)$, quadrupole interaction meas. by NMR spin-echo modulation 77−85615
$CsMnF_3$, new types of nuclear spin echo, single pulse and parametric echo 77−69726
$CsMnF_3$, spin echo form., parametric mechanism, spin dynamics *(Russian)* 78−23367
$CsNiCl_3(Br_3)$, quadrupole interaction meas. by NMR spin-echo modulation 77−85615
$CsNiF_3$, ^{19}F NMR, spin fluctuation suppression 78−91970
Cu-Ga, high dislocation density alloys and oxide precipitated struct., NMR, spin echo 80−39892
Cu-Mn, dil. alloy, spin glass, host NMR, spin freezing 77−40138
Cu-Mn, dil. alloy, spin glass, host NMR, spin freezing 77−40139
Cu-Mn dilute alloys, local moment fluctuations, NMR meas. 77−63091
Cu-Mn(Fe)(Co), Kondo system, host NMR exam. 78−80246
Cu-Si, high dislocation density alloys and oxide precipitated struct., NMR, spin echo 80−39892
$CuCr_2S_{4-x}Se_x$ spinels, NMR spin echo study 80−71238
$Cu_2Mn_{0.98}Al_{1.02}$, Heusler alloy, hyperfine fields at sp elements, spin echo NMR meas. 78−84496
$Cu_{1-x}Ni_x$, mag. transition, NMR meas. by spin-echo technique 77−32267
D NMR spin echo response in solids 80−25248
D probe spin alignment for obs. ultraslow mol. rot. 80−88890
D_2, solid, ordered cubic phase, NMR spin-echo responses 79−47356
DCl, liq., self-diffusion coeffs., NMR spin-echo meas. 80−50223
Dy, domain wall dynamics, NMR 77−69614
$Dy_{1-x}Gd_xAl_2$, ordered alloys, ^{163}Dy NMR, hyperfine field 78−10801
$Dy_{1-x}Y_xAl_2$, ordered alloys, ^{163}Dy NMR, hyperfine field 78−10801
$Dy_xY_{1-x}Al_2$, domain wall dynamics, NMR 77−69614
$ErFeO_3$, second-order reorientation transition, NMR signal relax. 77−90066
$EuCu_5(Pt_2)(Pd_2)$, indirect exchange, spin echo NMR meas. 80−15822
$EuPd_2$, elec. field gradient, spin echo NMR meas. 80−20509
$EuPt_2$, elec. field gradient, spin echo NMR meas. 80−20509
Fe based amorphous alloy, mag. ordered, hyperfine field distribs., NMR meas. 78−68409
Fe film, enriched, NMR obs. 78−39443
Fe radiative detection of single- and multiple-pulse mag. reson. of oriented ^{60}Co radioactive nuclei 77−66437
Fe, stimulated spin echo obs. of oriented ^{60}Co nuclei 79−65780
Fe, triple pulse reson. studies of ^{60}Co nuclei 78−43675
Fe: ^{95}Nb NMR 77−59482
Fe-Al, dil., film, NMR spin echo, rel. to struct. inhomogeneities *(Russian)* 80−29644
Fe-Co, dil., film, NMR spin echo, rel. to struct. inhomogeneities *(Russian)* 80−29644
Fe-Co-Cr alloys, atomic mag. moment, magnetisation, Mossbauer spectra and NMR spin echo spectra 77−63127
Fe-Co-Mn, BCC, mag. state of Mn, NMR and saturation magnetisation meas. 78−39442
Fe-Co-Mn, dil. alloys, NMR freq. temp. depend., spin echo meas. 78−64296
Fe-Co-Mn alloys, BCC, atomic mag. moment, magnetisation, Mossbauer spectra and NMR spin echo spectra 77−63127
Fe-Cr-Ni, Fe-Co-Mn, Fe-Cr-Co and Fe-Ni-Mn alloys, BCC, atomic mag. moments determ. 77−59396
Fe-Ir, hyperfine field distrib., spin echo NMR meas. 78−76351
Fe-Mo, hyperfine field distrib., spin echo NMR meas. 78−76351
Fe-Ni-Mn, BCC, mag. state of Mn, NMR and saturation magnetisation meas. 78−39442
Fe-Ni-Mn, dil. alloys, NMR freq. temp. depend., spin echo meas. 78−64296
Fe-P(Ga)(As)(Sb), dil., short range order, NMR study 80−71237
Fe-Rh, hyperfine field distrib., spin echo NMR meas. 78−76351
Fe-Sb-Ni(Cr), dil., short range order, NMR study 80−71237
Fe-V, ferromag. struct. in nucl. spin echoes 80−60453
$FeBO_3$, dynamic NMR frequency shift for ^{57}Fe *(Russian)* 78−43677
$FeBO_3$, parametric echo, magnetoelastic NMR excitation *(Russian)* 80−66072
$FeBO_3$, parametric effects in nucl. spin echo *(Russian)* 78−56404
$(Fe_{100-x}Co_x)_{79}P_{13}B_8$, amorphous, hyperfine field distrib., ^{59}Co NMR spin-echo meas. 80−34818
$Fe_{3-x}Co_xSi$, structural, mag. moment, and hyperfine field behaviour, local environment model 79−65762
FeF_3, canted antiferromag., spin echo spectra of ^{57}Fe and ^{19}F nuclei 80−2662

spin echo continued
FeF_3, weak ferromag., NMR of ^{57}Fe nuclei 79−95676
$(Fe_{1-x}Mn_x)_3Al$ alloys, disordered, mag. moments and distrib. on lattice sites, magnetisation and spin echo meas. 77−63112
$(Fe_{1-x}Mn_x)_3Al$, local Mn moment distrib., neutron scatt., nucl. spin echo *(Russian)* 77−12091
$(Fe_{1-x}Mn_x)_3Al$, mag. moments determ. from magnetisation and neutron and electron diffr. expts. 79−56520
$Fe_{3-x}Mn_xSi$, struct., magnetisation, and spin echo expts., rel. to local environment model 77−20518
Fe_3O_4, low temp. phase 77−69751
Fe_3O_4, NMR exam. of low temp. phase 78−56401
Fe_3O_4, NMR of low temp. phase, electron ordering anal. 78−56402
FeP(Ga)(As)(Sb), dil., short-range order, neutron diffuse scatt. and spin echo NMR 80−50106
$Fe_3Si_{1-x}Al_x$, hyperfine interactions and structural disorder, spin echo, X-ray and magnetisation meas. 77−32289
FeV (2 at.%), NMR spin echoes, domain wall effects 80−75883
$Fe_{0.85}V_{0.15}$ film, ^{51}V NMR, 77 and 300K 77−69728
$Fe_{3-x}V_xSi$, struct., magnetisation, and spin echo expts., rel. to local environment model 77−20518
^{57}Fe nuclei, spin-echo signal recording by pulse generator and fast signal averager 78−21188
$(Gd,Dy)Al_2$, spin adjustment, NMR spin echo obs. 78−15058
Gd $[Co_xFe_{1-x}]$, NMR, hyperfine fields, conc. depend. 77−43902
Gd-Dy(Er)(Tb)(Tb), magnetic and electric hyperfine fields at Gd, NMR spin echo 77−77123
Gd-Tb (10 wt.%) film, nuclear echo signals, crystal anisotropy consts. *(Russian)* 79−99790
$GdCo_2$, ^{59}Co hyperfine field, temp. depend. splitting 77−8447
Gd_2Co, amorphous ferromag. obtained by splat cooling, local and bulk mag. props. 79−1685
Gd_2Co_{17}, NMR spin echo meas., dipolar field anisotropy 80−71236
$Gd(Co_{1-x}Ni_x)_2$ compounds, NMR and thermal expansion 80−66070
$Gd_{0.99}Ho_{0.01}(Rh_{1-x}Fe_x)_2$, spin echo meas. on ^{165}Ho, quenching effect of Fe substitution 78−48079
$Gd_{0.9}La_{0.1}Al_2$, ferromag., NMR of ^{139}La 78−52377
$Gd_{0.9}La_{0.1}Ni_2$, Ni contrib. to ordering, ^{139}La NMR spin echo 77−63317
Ge_2FeGa, and Fe_2CoGa, site preference and local environment effects, Mossbauer and NMR expts. 78−43710
H, gaseous, high-resolution mag. reson. study, 1 to 1.3K 80−95560
HCl, liq., self-diffusion coeffs., NMR spin-echo meas. 80−50223
$H_{1.6}MoO_3$ bronzes, proton mobility 78−39426
H_xMoO_3 ($0.3<x<2.0$), H mobility from NMR spin echo 79−1416
H_2O, proton chemical exchange, proton spin-echo NMR 77−9053
^1H spin systems, NMR, two-dimensional Fourier transform. of spin echoes 79−3463
^3He adsorbed on graphite, NMR relax. times below 4.2K 78−38898
^3He, BCC, NMR multiple echoes, soln. of eqn. of motion of magnetisation 79−86961
^3He films adsorbed on Grafoil, NMR relax. times 79−28171
^3He, solid, spin diffusion at very low temp., multiple echo amplitudes 79−19423
^3He, solid, susceptibility along melting curve, 20 mK to nucl. ordering temp. 77−31837
^4He:^3He, solid spin diffusion coeff. and T_2, impuritons, temp. depend. 78−34675
$HfV_2H_{2.1}$, proton NMR relax. time and Knight shifts, diffusional activation energies meas., sorption props. 80−75871
$Ho_{0.01}Gd_{1-x}Y_xNi_2$, spin echo meas. on ^{165}Ho, limited quenching of Ho moment by cryst. field 79−73851
K_2CuF_4, 2-dimens. ferromagnet, low-temp. mag. struct. *(Japanese)* 79−33461
KDF_2, deuteron mag. reson., quadrupole coupling consts., F-D distance 77−63313
KH_2PO_4, NMR spin echoes, indirectly induced 80−71239
$KMnF_3$, acoustic nucl. spin echo *(Russian)* 77−48088
$K_2Mn_{1-x}Ni_xF_4$, antiferromagnets, impurity associated and host magnetizations, NMR exam. 78−10800
$LaF_3:Pr^{3+}$, 2K, optically detected coherent transients in nuclear hyperfine levels 79−19806
$La_{1-x}Gd_xAg$, antiferromagnet, spin echo NMR anal. 80−15821
$LaNi_5H_6$, diffusion const. in presence of large background gradients, modified pulsed gradient technique 80−31831
$LaNi_{1-x}Mn_xO_3$, ^{55}Mn NMR study, magnetisation meas., ferromag. and Pauli paramag. components 80−7191
$La_{1-x}Pb_xMn_{1-y}Fe_yO_3$, magnetically ordered, NMR, spin echoes and relax. 77−48087
Li ferrites, nuclear spin echo excitation on subharmonics, and multiple freq. *(Russian)* 80−60454
β-Mn alloys, weakly antiferromag., hyperfine fields, NMR meas. 78−39441
MnB, NMR of ^{55}Mn 77−28468
$MnCO_3$, new types of nuclear spin echo, single pulse and parametric echo 77−69726
$MnCO_3$, single-pulse nuclear spin echo shaping of ^{55}Mn 77−32290
$MnCO_3$, spin echo form., parametric mechanism, spin dynamics *(Russian)* 78−23367
$MnFeO_3$:^{55}Mn, NMR freq. dynamical shift for nuclei in domain walls *(Russian)* 77−40148
$MnFe_2O_4$, additional spin echo of ^{55}Mn nuclei 80−60455
$MnFe_2O_4$, ferrite, dynamic shift of NMR freq. of nuclei located in domain walls 80−15823
$MnFe_2O_4$, nuclear reson. and relax. from domains and domain walls 77−8448
$MnFe_2O_4$, valency states, NMR 77−51987
$Mn_xFe_{3-x}O_4$ NMR of Mn^{3+} in B-sites 78−35061
$Mn_4N_{0.8-1}$, NMR of ^{55}Mn, reson. curve fine splitting, spin echo meas. 78−2768
MnP, noncubic ferromag., relax. times for domain and wall resonances 77−77119
MnSi-CoSi solid solution, mag. props. 78−56403
$(Mo_{0.5}Ru_{0.5})_{80}P_{20}$, amorphous normal and mixed supercond. state, ^{31}P NMR 79−87193
α-N_2, solid, NQR echo envelope modulation due to intramol. dipole coupling 77−48083
NH_4TaWO_6, rapid ionic motion, spin-lattice and spin-spin relax. times meas. 79−38396
^{14}N pulsed NQR-FFT radiofrequency spectrometer description and operation 80−17982

spin echo continued
NaN_3, NMR, Na nuclear quadrupole moment, phase transition 77−73092
$NaNO_2$, ^{14}N NQR, multiple spin echoes 78−19365
Na_xWO_3, $0.22<x<0.84$, low temp. struct., press. effects, NMR study 80−59443
Na_xWO_3, Knight shift, spin-lattice and spin-spin relax., high press. NMR obs. 80−50211
α-NbH_xD_y, H diffusion, NMR spin echo obs. 80−34228
Ni, ferromag. struct. in nucl. spin echoes 80−60453
Ni-Co-Mn, dil. alloys, NMR freq. temp. depend., spin echo meas. 78−64296
Ni-Cu-Mn, dil. alloys, NMR freq. temp. depend., spin echo meas. 78−64296
Ni-Fe-Mn alloy, NMR signals due to Mn atoms with antiparallel moments 78−27113
Ni-Mn alloy, NMR signals due to Mn atoms with antiparallel moments 78−27113
Ni_2MnSn, Heusler alloy, mag. interactions and cond. electron polarisation, spin echo NMR meas. 77−77125
$(Ni_{1-x}Rh_x)_{99}Mn$, ferromagnetic, NMR study of local environment effect 80−7192
$(Ni_{1-x}Ru_x)_{99}Mn$, ferromagnetic, NMR study of local environment effect 80−7192
$Ni_{1-x}Si_x$, electronic states of Si NMR study 80−50216
$(Ni_{1-x}X_x)_{99}Mn$, X=Rh, Fe, Mn, ferromagnetic, NMR study of local environment effect, relaxation mechanism 80−7193
^{31}P, $Fe_{75}P_{15}C_{10}$, $Fe_{75}P_{15}C_{10}$, amorphous, ferromag. state, ^{31}P NMR 78−2770
$Pb_{1.125}Mo_6Se_{7.5}$, Chevrel phase supercond., NMR study 80−49989
$(Pd_{0.996}Co_{0.004})_{1-x}Mn_x$ alloys, ferromag. and spin glass transition, NMR 79−65761
$Pd_2Mn_{1-x}Nb_xSn$, Heusler alloy, NMR and mag. coupling 78−43676
Pd_2MnSn, Heusler alloy, mag. interactions and cond. electron polarisation, spin echo NMR meas. 77−77125
Pd_2MnSn, Heusler alloy, NMR and mag. coupling 78−43676
$Pd_2Mn_{0.98}Sn_1In_{0.02}$, Heusler alloy, hyperfine fields at sp elements, spin echo NMR meas. 78−84496
PdNb, dilute, NMR obs. of ^{93}Nb 80−71203
Pt cluster, conduction electron density oscills., NMR spin-echo meas., indirect exchange interaction 80−44954
PtV, dil. alloys, NMR obs. of ^{51}V 80−71203
Rb_2CrCl_4, NMR of ^{53}Cr 78−10798
$RbMnF_3$, acoustic nucl. spin echo *(Russian)* 77−48088
$RbMnF_3$, nuclear spin echo of ^{55}Mn, freq. pulling 77−69727
Rh_2CoSn, ferromag. Heusler alloys, hyperfine fields, spin echo meas. 77−63314
Rh_2FeSn, ferromag. Heusler alloy, hyperfine fields, spin echo meas. 77−63314
Rh_2MnSn, ferromag. Heusler alloy, hyperfine fields, spin echo meas. 77−63314
Sm-Al(Fe)(Co)(Pt), hyperfine field exam. by NMR spin echo 78−23365
Tb, nucl. echo signals, cryst. anisotropy *(Russian)* 79−99790
Tb-Al(Ag), hyperfine field exam. by NMR spin echo 78−23365
$V(Ir_{1-x}Pt_x)_3$, NMR study of ferromag. 79−65760
$VO_{1.25}$, ^{51}V NMR studies, microscopic mag. props. 80−108086
V_2O_{3+x}, nonstoichiometric, microscopic mag. props., NMR and inelastic-spin-flip neutron scatt. 79−38323
V_3S_4, antiferromag. order, ^{51}V NMR spectrum 79−56625
V_5S_8, antiferromag., NMR meas. 77−36140
V_3Se_4, antiferromag. order, ^{51}V NMR spectrum 79−56625
Y-Co, hyperfine fields, NMR spin echo 77−63318
YCo_3 amorphous films, ^{59}Co spin echo study 80−80636
YCo_5, NMR enhancement of modulating field due to anisotropic component of hyperfine field 77−55729
Y_2Co_{17}, NMR spin echo meas., dipolar field anisotropy 80−71236
$Y(Fe_{1-x}Co_x)_2$, NMR study 80−75882
$Y_3Fe_{5-x}Co_{x/2}Si_{x/2}O_{12}$, spin reorientation, NMR and ferromag. reson. meas. 80−65890
$YFeO_3$:Co, NMR of ^{57}Fe, spin echo 78−91987
$Y_{1-x}Gd_xCo_2$, NMR of ^{59}Co 78−52376
$(Y_{1-x}Gd_x)Co_2$, spin echo NMR of mag. states 80−7190
YIG, domain boundary nuclear spin echo excitation, NMR domain freq. capture effect *(Russian)* 80−44955
$YbAl_3$, valence instabilities 79−78546
Zn, HCP metal, pulsed ^{67}Zn NMR studies at 4.2K 79−91315
$Zr(Fe_{1-x}Co_x)_2$, NMR study 80−75882
$ZrMn_2H_x$, proton NMR relax. time and Knight shifts, diffusional activation energies meas., sorption props. 80−75871

spin glasses
see also mictomagnetism
alloy,dil., electrical resistivity, Kondo effect vs. spin glass behaviour 78−68269
alloys, dilute, mag., press. effects 79−99676
alloys, magnetic localisation and charge oscillations 80−75781
alloys, magnetoresistance, Boltzmann formalism calcs. 80−88540
aluminosilicate glass:Co (14.3 wt.%), AC susceptibility meas. 80−88771
amorphous ferromagnet, spin-glass and ferromagnetic behaviour induced by random uniaxial anisotropy 78−39338
amorphous Ising antiferromagnetic model, frustration effects 80−103838
amorphous magnet spin glass phase possibility *(Russian)* 78−72362
amorphous magnetism, Curie temperature and mag. excitation spectrum 78−10693
amorphous magnetism, random-axis model, low temp. renormalisation group anal. 79−61137
amorphous magnets, random anisotropy axes, high-temp. expansion for sp. ht. 80−71041
amorphous metals, mag. anisotropy, spin glass like phase 77−66295
amorphous substance, ferromag. or spin glass transitions 78−2690
amorphous systems, mag. props. effect of random anisotropy 79−4686
anisotropic, crossover effects 79−65692
annealing and mag. remanence 80−60308
anomalous Hall effect including Kondo effect in molecular field approx. *(Russian)* 80−34424
antiferromagnetic dilute-bond Ising model, spin-glass phase transition 77−69569
Ashkin Teller model for spin glass in d dimensions 79−65691
Berthollides, chaotic mag. states 78−56330
Bethe lattice, random ordered phase, statistical theory 77−85457
Bethe lattice, statistical theory of random ordered phase 77−80895

spin glasses continued
binary magnetic systems, conc., spin glass behaviour, Monte Carlo study 78−2694
binary mixture at T=0, energy and variational props. 80−39794
Bose glass, marginal fluctuations 80−2586
classical, low temp. behaviour of three-dimens. planar model 79−73725
close packed lattices of ferro- and antiferromag. exchange integrals, glass-like phase 78−10697
cluster mean field theory 77−80949
cluster mean field theory and evidence for spin clusters 79−78382
cluster mean-field model, static props. 79−4689
collective excitations in spin glasses (C211) 78−56322
composition for occurrence, glass analogy 77−66323
computer simulation, for 2- and 3-dimens. Ising systems 77−66370
computer simulation 77−66365
computer simulation 80−60299
computer simulations of mag. model systems 80−65924
concentrated, thermodynamic props., cluster mean-field theory using Ising Hamiltonian 79−33499
conference on magnetism, Munster, Germany (Mar. 1977) 78−10626
CoO-Al_2O_3-SiO_2, new state in very weak mag. field 79−78416
critical behaviour, dynamic scaling theory 77−40063
critical dynamics, renormalisation group methods 77−43844
critical properties, simple soluble model 77−12141
critical temperature, scaling 78−10714
cubic lattices, fully frustrated, overblocking effect 79−69678
cubic lattices, fully frustrated, phase transitions, Gaussian and spherical model, free energy calcs. 80−60281
cusps in magnetic susceptibility, self-consistent theory 77−77066
defect hydrodynamics in nonplanar magnetic media *(Russian)* 80−49445
dilute, conc. expansions at zero temp., Ising model 80−60303
dilute frustrated lattice, spin-glass ordering, triangle and FCC lattices, Monte Carlo simulation 80−15746
dilute magnetic alloy, sp. ht. evaluation role of fluctuations 77−69580
dilute magnetic alloys, electron sound absorpt., disordered mag. impurities, spin glasses *(Russian)* 80−80503
dilute RKKY spin glass, Bethe-Peierls theory 78−39351
diluted Ising and Heisenberg magnets with competing interactions, phase diagrams and mag. props. 80−34672
diluted Ising and Heisenberg systems with competing interactions, mag. ordering, appl. to $Eu_xSr_{1-x}S$ 80−65914
dipolar anisotropy and crit. behaviour in small AC fields 77−32199
dipolar spin glass, anomalous sp. ht. Ising model and Monte Carlo calcs. 78−47989
dipole pseudo-spin glasses, collective excitations 80−59617
dirty, paramagnetic reson. 80−11264
disclinations and solitons 80−75786
disordered magnet, effective field approx., Ising model Hamiltonian 77−8261
disordered magnets, spin glass phase, spatial spin correlation function 78−10691
disordered metamagnets, random field effects 80−60318
disordered spin systems, nonrandom free energy in macroscopic limit 79−40477
disordered system, critical phenomena 78−52269
double transition spin glass-ferromagnetic systems, differential susceptibility 78−88131
dynamic properties, theory *(Russian)* 78−39350
dynamical susceptibility calc. 77−85477
dynamics, barrier modes and spin waves 80−60293
dynamics, partial ferromag. order, antiferromag. spin wave modes 80−93133
dynamics near transition, classical soft-spin models 79−95599
Edwards-Anderson model, 3-dimens., using real space scaling transform. 77−69570
Edwards-Anderson model, absence of ordering 77−51909
Edwards-Anderson model, appl. of Migdal's recursion relations 77−40070
Edwards-Anderson model, quartic operators in Ising, X-Y, and Heisenberg systems 79−33498
Edwards-Anderson spin glass model in two dimensions, numerical results 80−97100
effective field distribution, Ising and Heisenberg models 77−43843
electrical resistivity, thermal resist. and thermopower 80−65542
electrical resistivity calc. 79−78090
electron localisation and mobility edge, spin glass problem 78−52283
EPR frequency *(French)* 79−61198
EPR frequency and mag. transverse susceptibility with remanent magnetisation *(French)* 80−7145
EPR relaxation rates, freezing 79−99713
exchange energy, residual entropy and number of minima *(French)* 77−66322
excitation exam. 79−78419
experimental props. and theories 79−65688
experimental status, introduction 80−60292
FCC alloy, long range mag. order 77−63215
FCC lattice, phase transitions of fully frustrated models 80−29517
FCC lattice with RKKY interaction, numerical calc. 78−52275
ferromagnet, spin glass-like states, metastability and energy barriers 79−19710
ferromagnetism onset, mag. inhomogeneity 80−75774
ferromagnets, random, large exchange interaction, Green function theory 78−6537
ferromagnets and spin glasses, supercond. and mag. order 80−93029
film, quench-condensed, apparatus for measurement of initial paramagnetic susceptibility 79−54160
five-dimensional, Edwards-Anderson ordering possibility 80−60295
fluctuation effects 79−78381
fluctuation theory, mag. susceptibility and sp. ht. 79−24176
fluctuations theory 78−52279
free energy, order parameter expansion, random bond model 80−84609
freezing temperature, conc. and Fermi momentum depend. 78−14970
freezing temperature, fluctuations in nearest neighbour distance and damping effects 77−51913
freezing temperature of dil. spin glass, rel. to spin conc. *(French)* 77−63195
frozen spin state, static susceptibility, piezomag. effect 77−51914
frustrated two-dimensional planar model, spin-spin correl. 80−11212
frustration concept, defn. 79−38328
frustration effect, theory 77−59413
spin glasses continued
frustration model, ground states 80−60294
frustration model, ground states by graph theory matching method 80−100592
frustration model, lifetime of excited states 80−15750
frustration network, phase transitions 80−2596
frustrationless models, rel. to spin glasses 80−29561
generalised mean field theory with spin correls. 78−2691
giant moments and spin glasses, order out of disorder *(Dutch)* 80−97107
Ginzburg-Landau equation, time depend. 79−61161
graphite, neutron-irrad., sp.ht., 0.4-4.5K, rel. to localised spin transition 77−28389
ground state, quantisation of classical model 77−4478
Hall effect anomaly 78−68267
Heisenberg, spin diffusion 78−6538
Heisenberg, spin wave stiffness, computer simulation 79−78405
Heisenberg, two-level systems, evidence for existence 80−15736
Heisenberg classical model, Monte Carlo calc. of internal energy and sp. ht. 77−20612
Heisenberg mode, RPA approx. 80−65904
Heisenberg model, classical, Monte Carlo exam. 77−24698
Heisenberg model, excitation spectra, numerical studies 80−60300
Heisenberg model, isotropic, two-dimens. 77−85455
Heisenberg model, spin dynamics *(French)* 78−39336
Heisenberg model, spin glass state, magnetisation of dil. mag. impurities, molecular field approx. 77−20623
Heisenberg model, spin glasses, recent developments 78−68264
Heisenberg model calc. 80−60301
Heisenberg model for elementary excitations *(Russian)* 79−87280
Heisenberg random classical exactly solvable model 77−63057
Heisenberg $S=^1/_2$ spins 80−2581
Heisenberg spin glass, crit. dynamics, renormalisation group approach 79−91237
Heisenberg spin glass, high temp. series, order parameter susceptibility 79−15312
Heisenberg spin-glass, crit. dynamics 78−60295
Heisenberg-Ising magnets, random, critical temps., binary mixture, amorphous magnet and spin glasses 80−54911
high pressure effects, resist. meas. 78−52277
ill-condensed matter, summer school, Les Houches, France (July-Aug. 1978) 80−82561
impurity spin dynamics in magnetic glasses at low frequencies *(French)* 78−88126
induced-moment spin glass, simple mean-field theory 80−29553
infinite range model, stability and susceptibility in Parisi's soln. 80−88762
infinite ranged models 78−80166
infinite-range spin glass, internal field distrib. hole, analytical treatment 80−29554
infinite-ranged model, mean field theory hypothesis 80−97104
insulating, impurity doped antiferromag. insulator 79−51796
internal field distribution, self-consistent 77−16084
Ising, cryst. field effects 77−85460
Ising, two-dimensional, Monte Carlo evidence for absence of phase transition 78−19260
Ising chain with random bonds, remanence and non-exponential relax. 79−73751
Ising dilute magnetic alloys, local mag. fields and fluctuations 77−40061
Ising ferromagnet and spin glass systems, random, crit. dynamics 80−34666
Ising frustration pots., phase transition 80−52142
Ising long and short ranged bond models in cluster approx. 80−20419
Ising model, dual transformation into ferromagnetic models, critical temp. in frustrated models 79−73763
Ising model, dynamical theory of quenched site model 79−19742
Ising model, existence of phase transition 78−56327
Ising model, frustration and ground-state degeneracy 78−31090
Ising model, internal field distribution 79−73740
Ising model, mean field theory 79−4680
Ising model, n-replica method, crit. behaviour of spin glasses 79−42767
Ising model, nearest-neighbour random exchange bonds, short-range mag. order 79−51791
Ising model, random bond, susceptibility and specific heat of glass like phase, cumulant expansion 78−6533
Ising model, random quenched effective field approx. 78−84432
Ising model, random-bond, with continuous distrib. of exchange interactions, solvable model 77−43837
Ising model, relation with mobility edge problem 78−88138
Ising model, remanent magnetisation using Monte Carlo methods 79−78421
Ising model, Sherrington-Kirkpatrick, white and weighted averages over solns. of Thouless-Anderson-Palmer eqns. 80−108012
Ising model, spin 1/2, real-space renormalisation group calcs. 77−12134
Ising model, spin glass, dil., low temp. phase diagram and crit. props. 78−60291
Ising model, spin glass in Bethe-Peierls-Weiss and other mean-field approximations 79−65682
Ising model, spin glass state, magnetisation of dil. mag. impurites, molecular field approx. 77−20623
Ising model, spin glass state, mixed nearest-neighbour exchange interaction 78−39341
Ising model, spin-glass, renormalisation group calc. for two dimens. models 78−14968
Ising model, Toulouse frustration effect 79−24167
Ising model, two-dimens., ferromagnet-spin glass transition, Monte Carlo calc. 80−60287
Ising model, vanishing of Edwards-Anderson parameter 78−43597
Ising model extended field theory description 77−63205
Ising model long-range Gaussian-random interactions 79−15319
Ising model of bond mixtures, spin glass transition, renormalisation group approach 78−43601
Ising model spin glass, Monte Carlo calc. of mag. suscept. 78−31079
Ising model spin glass, phase transitions 77−8327
Ising model transition temperature in new mean-field theory 79−51785
Ising model with random exchange bonds, phase diagram 78−43604
Ising random bond model, spins distrib. and thermodynamic props. 79−51786
Ising site model, random mixtures, Monte Carlo simulation 78−73935
Ising spin gass, glass, Edwards-Anderson order parameter instability 80−71043

spin glasses continued
Ising spin glass, calc. of wavevector depend. susceptibility 77−63223
Ising spin glass, d-dimensional, frustration effect 80−108019
Ising spin glass, d-dimensional, frustration effect and dilution problems 80−108018
Ising spin glass, dil., at zero temp., (1/2)-state Potts model 79−42768
Ising spin glass, nature of ordering 78−80172
Ising spin glass, remanent magnetisation, Monte Carlo exam. 79−61166
Ising spin glass, replica symm. and massless modes 79−33486
Ising spin glass, Sherrington Kirkpatrick model, entropy calc. 80−20411
Ising spin glass, spherical approx. 77−28392
Ising spin glass, three-dimensional mag. correlations 80−103849
Ising spin glass, with RKKY interaction, props. 79−24177
Ising spin glass near percolation threshold 78−72352
Ising spin glasses, Edwards-Anderson model, autocorrelation function logarithmic decay account 79−78406
Ising spin glasses, in effective interaction approx. 80−60288
Ising spin glasses, Monte Carlo simulation 79−78428
Ising spin glasses, two-, three- and four-dimensional, defect energies 78−39330
Ising spins on square lattice, theory of frustration effect 77−89959
Ising spins randomly located, with oscillatory exchange interactions 79−42778
Ising system with quenched impurities, high temp. expansion methods 79−78422
Ising systems, frustrated, interface entropy, phase transitions, 2-dimens. Ising spin-glasses 79−19711
Ising systems, random mixture, phase boundaries 80−60285
Ising two-dimens. random bond model, evidence against spin-glass order 80−15747
Ising type random bond, scaling, eqn. of state and instability 79−73753
Ising-type, Sherrington-Kirkpatrick model generalisation m-component spins 79−11320
Israel Physical Society 1980 annual meeting, Rehovot, Israel (April 1980) 80−94909
Kondo alloys, mag. interactions 77−59385
Kondo system with spin glass temp. below Kondo temp., impurity interactions 77−66360
Landau-Ginzburg gauge model 79−42772
layered two dimensional Ising lattice, phase transitions, spin glasses *(Russian)* 80−65945
local exchange invariance concept 78−60288
localised degrees of freedom *(Russian)* 79−4691
long time correlations reln. to replica correlations 79−75437
long-range model, evidence for massless modes 79−82790
long-range models, Ising spins and classical m-vector spins 80−15739
Lorenz number, low temp. 79−19567
low concentration series expansion, dilute spin glasses at zero temperature 80−93131
low temp. renormalisation group, critical behaviour 78−10688
low temperature nuclear orientation investigation 80−15825
lower critical dimensionality for spin glass transition 80−60291
Luttinger and Edwards Anderson models, equivalence 77−80951
magnetic alloys, dil., transition metal hosts, props. review 78−84417
magnetic and transport props. *(Czech)* 78−80149
magnetic field dependence of susceptibility peak 80−103840
magnetic properties in mean field theory 80−80514
magnetic properties of Sherrington-Kirkpatrick model, Monte Carlo simulations 80−88774
magnetic properties of spin glasses with short-range interaction in mag. field 79−28539
magnetic resonance props. 80−71153
magnetic susceptibility, temp. depend. 79−61125
magnetisation decay of single spin glass model 80−71073
magnetisation relaxation time near freezing temp., HF calc. 80−34665
magnetism conference, Freudenstadt and Bad Nauheim, Germany (March and April 1978) 79−24121
magnetism of dilute and conc. alloys *(Rumanian)* 78−91843
manganese aluminosilicate glass, insulating spin glass, exchange dipole optical transition 80−40136
Matis model, modified, mag. relax. 80−65947
Mattis model, system with random interactions, spin glass transition 77−8322
mean field theory, broken replica symmetry 80−34659
mean field theory, replica method 80−34658
mean field theory 79−99704
mean field theory and ϵ-expansion 78−10705
metallic, computer simulation 77−32203
metallic, spin wave theory 79−11306
metallic rare earths, conference, St. Pierre-de-Chartreuse, France (Sept. 1978) 80−12844
metastability of spin glass, Onsager theory 79−82796
metastable states, crit. free energy 80−88764
mictomagnet props. review 79−24183
mixed magnets, competing spin glass and mag. order, phase diagrams, crit. points 80−39802
mobility edge, analogy with spin glass problem 77−85164
model, accurately solvable *(Russian)* 77−55685
model, exactly soluble *(Russian)* 77−80944
model Hamiltonians, zero temp. spin dynamics 77−85467
models, with non-random interactions, phase transitions 77−55673
molecular field approx. *(Russian)* 77−80940
monoionic anisotropy, influence on transform. to paramag. state *(Russian)* 79−28529
Monte Carlo simulation appl. 80−20421
Monte Carlo studies, review, book contrib. 79−82809
Mott transition, spin glass description 79−65386
neutron diffraction of disordered structs., book contrib. 79−60228
neutron scattering cross-sections, theory 78−80162
nonmagnetic defects, sp. ht., susceptibility and resist. determ. 79−19738
nonmagnetic defects *(Russian)* 78−60298
nuclear magnetic relaxation calcs. *(French)* 80−34797
numerical simulation, recent progress 79−69689
Ohm's law violation 79−82580
one dimensional, ideal, dynamical susceptibility and relax. behaviour 80−65950
one-dimensional, sp. ht. and mag. susceptibility calcs. 80−7120
one-dimensional, with antiferromag. exchange 80−25231
one-dimensional model, rel. to Ising chain in 3-dimens. phonon field 79−56540
one-dimensional random Glauber model, magnetisation relax. 80−80523
spin glasses continued
order parameter expansion of free energy, random site model 80−88772
order parameter for replica symmetry breaking 80−44835
order parameter relaxation 78−80161
order parameter susceptibility, high-temperature series 79−28534
order parameters, infinite no. in mean-field approx. 80−25146
order-parameter susceptibility, series expansion 77−43839
ordering temperature, beyond mean field value 80−60298
parametric amplification of spin waves by elastic pumping *(Russian)* 80−65895
partly disordered magnetic structures 77−51908
percolation effects on spin glass order 79−56549
phase diagrams and order parameters, Oguchi-Kaneyoshi method 80−15727
phase transition, dynamical instability, effect of external mag. field 79−33493
phase transition, fluctuations of local spins, mean-field theory 80−34661
phase transition, mag. susceptibility, specific heat, Ising model calcs. *(Russian)* 80−34671
phase transition examination, by DC Josephson effect 80−100594
phase transitions, instability for Heisenberg, X-Y and Ising systems 78−23285
phase transitions in strongly random systems, review 79−58647
phenomenological theory, weak singularities of susceptibility, sp. ht., near transition point 78−19263
Poisson brackets, nonlinear hydrodynamics eqns. in condensed matter physics 80−54296
polarisation analysis of diffuse neutron scattering from magnetic systems 80−25098
principle of minimum free energy 80−88773
propagating modes in 3 dimensional planar model, dynamic struct. factors 79−99703
quantum spin glass, frustration, 2-D lattice, functional integration technique *(French)* 80−39789
quantum spin glass theory 80−103839
quenched free energy of mag. systems with random interactions, upper bounds 80−103845
quenched random impurities, dynamics, replicas and frustration approaches 80−34673
quenched random magnets, thermodynamic behaviour from position-space renormalisation group 78−68244
quenched random spin systems, dynamical replica methods, nonequilib. critical phenomena 78−43602
quenched random spin systems, spin glass and related orderings 78−10706
random anisotropy and random field models, textural singularities and frustration 79−24182
random bond Ising model, high temp. series expansion 78−16741
random bond Ising model in 2-D, and 3-D, renormalisation group approach 78−68275
random energy model, disordered models family-limit 80−90794
random exchange interactions, and 'frustration effect' 78−68212
random ferromagnetic-antiferromagnetic alloy, elementary excitations 79−8001
random Glauber chain, relax. of magnetisation, numerical studies 80−60313
random Ising bond interactions, paramag. phase, thermodynamic props. 77−20523
random isotropic dipolar magnet, absence of ferromag. long range order 79−28546
random magnetic alloys, mean field effective medium theory, Ising model appl., phases 78−84438
random mixture of ferro- and antiferromag. exchange interactions, high temp. expansion 78−23280
random molecular fields, Edwards-Anderson theory 78−80164
random site, phase diagrams and dimensionality shift 78−52282
random spherical model, crit. dynamics 80−44844
random spin systems, non-analyticity of entropy and Nernst's law 78−2692
random spin systems, thermodynamic props. and spin glass transition, Bethe-Peierls-Weiss approx. 79−78387
random-bond Ising chain, entropy, depend. on temp. and mag. field 79−1679
rare earth alloys, amorphous, study of hysteresis effects using Monte Carlo technique 79−1686
rare earth alloys, bulk mag. props. in amorphous and cryst. systems 80−20415
rare earth amorphous alloys, antiferromagnetism, mol. field approx. 78−80142
rare earth metal based compounds, spin glasses 80−50132
rare earth metals, indirect exchange between localised moments rel. to spin glass behaviour *(Russian)* 79−87237
rare earth spin glass alloys, low field susceptibilities 78−84446
relax. of magnetisation and order parameter 78−27043
relaxation, mean field approx. 78−52281
relaxation times, influence of spectral distrib. on freq. depend. of freezing temp. 80−44848
remanence magnetisation, slow decay theory 80−11211
remanent magnetisation, theory 77−66371
remanent magnetisation in model spin glass, relax. 78−91873
replica method and solvable spin glass model 79−38327
replica symmetry and massless modes, non-Ising spin system 79−56553
replica theory, Sherrington-Kirkpatrick model, sequence of approximated solutions 80−60284
replica-symmetry breaking in spin-glass theories 78−95449
resistance maximum, press. and conc. depend. 77−69300
resistance maximum across spin glass to Kondo transitions 79−19584
resistance maximum and freezing temps., s-d exchange interaction 77−69586
resistance maximum rel. to Kondo temp. and RKKY interaction 77−20307
resistivity below ordering temp. 78−51980
review, recent developments *(Japanese)* 78−47993
review 77−69578
review of recent expt. and systems 78−52274
RKKY, dil., approach to fully magnetised state 80−60302
RKKY, low temp. susceptibility, spin-depend. curvature, Ising model MRF approx. 77−66366
RKKY interaction exam. 78−52290
RKKY Ising, sp. ht. 1/T behaviour 80−11210
RKKY spin glass, conc. depend. of low temp. sp. ht. 77−12135

spin glasses continued
rock magnetism type behaviour 77−66361
roughening transition in crystal growth theory, rel. to spin glass transition 78−27045
scaling laws in theory, validity and limitations 79−56561
second virial coeff., magnetic field depend. 79−65690
self-consistent mean random field approximation, comparison with n→0 expansion 77−20622
semiconductor, indirect exchange interaction of localised spins 80−88768
semiconductor based, conduction electron produced exchange interaction between localised spins *(Russian)* 79−82799
Sherrington-Kirkpatrick model, finite system, low temp., susceptibility, entropy 78−34993
Sherrington-Kirkpatrick model, Thouless-Anderson-Palmer eqn. solution *(French)* 80−39781
Sherrington-Kirkpatrick soln., stability 78−56319
Sherrington-Kirkpatrick solvable model solution 77−36084
Sherrington-Kirkpatrick spin glass model 79−51797
short range interaction in neighbourhood of percolation threshold *(Russian)* 78−68282
site Ising model, spin glass phase, transition temps. 79−95592
specific heat and susceptibility, random series method 80−44542
specific heat of disordered solid, linearity at low temp. 77−69097
spherical model 77−66364
spin dynamics, EPR, NMR, muon precession, Mossbauer, and neutron scatt. results 79−65689
spin exchange scatt. time calcs. 80−50127
spin freezing, exptl. obs. 77−73032
spin glass-ferromag. alloys, high-field magnetisation 79−33488
spin glass-ferromagnetic phase, mean field theory 80−103841
spin glasses, RKKY free energy, pair approx. 79−56557
spin waves, hydrodynamic theory 78−6524
spin waves, microscopic theory *(Russian)* 79−8011
spin waves in amorphous ferromagnets, asperomagnets and spin-glasses 80−75747
spin-flop multicritical points in systems with random fields and in spin glasses 79−33495
spin-wave spectrum, of systems without long-range mag. order 79−33450
spinels, domain wall formation inhibition, effect on bulk mag. props. 80−11220
stability of Sherrington Kirkpatrick soln. of spin glass method 78−80152
statistical mechanical model at low temps. 79−65686
statistical props. *(Russian)* 78−35000
statistical thermodynamics, short and long range props. 77−27834
statistical thermodynamics 77−66363
steel, austenitic stainless, magnetic susceptibility and magnetisation, low temp. 80−25102
steel, austenitic stainless, Mn alloy, sound vel. anomalies near spin glass transition 79−82795
Stoner glass, disordered itinerant-electron system, spin-glass condensation 79−78424
Stoner spin glass, conditions for freezing of spins with itinerant 3d electrons 80−60309
superconductivity, total compensation of paramag. effect 80−7021
superconductivity 79−28428
superconductivity coexistence with mag. order 78−19177
susceptibility, time dependent, rel. to spin self-correlation, Monte Carlo model simulations 79−47290
susceptibility, wave-vector-depend., theory 80−11209
susceptibility, zero-field, rel. to order parameter 77−48005
symmetry and macroscopic dynamics of mag. materials 80−107973
symmetry and topology concepts for spin glasses and other glasses 79−28541
system with competing ferromag. and antiferromag. interaction, spin glass transition 77−20616
TCNQ salt, $Qn(TCNQ)_2$, one-dimens. spin glass with antiferromag. exchange, Knight shift meas. 80−25231
theory, and third law of thermodynamics 77−89964
theory, review 78−2696
theory, time depend. of system 77−4479
thermodynamic properties, mean field approx. 78−52280
thermodynamics, third law violation in spin glass treatment 77−55674
thermodynamics, virial expansion vs. T^{-1} expansion 77−66362
thermodynamics of quenched random spin systems, phase transitions in spin glasses 77−73024
thermopower, rel. to spin glass freezing temp. 78−79983
three dimensional rotator spin glass model 79−61160
time dependent order parameters, Ising and Heisenberg model 77−43843
time translation, spatial scaling and nonexponential relaxation 80−97110
time-dependent Ginzburg Landau model 78−39340
transition, cumulant expansion of free energy of disordered systems 80−71067
transition, depend. on details of disorder 78−72355
transition, search for, using high-temp. series expansions for nearest-neighbour Ising model 77−89960
transition metal alloys, dilute, mag. ordering, book contrib. 80−75787
transition metal alloys, spin glass behaviour, simple itinerant model 78−84436
transition metal compounds and dil. alloys, mag. ordering phenomena in high mag. fields 80−50075
transition metal magnetic alloys, dilute, props., review of theory 79−15282
transition metal magnetic clusters, neutron inelastic scatt., review 80−50083
transition metal-noble metal spin glass films, mag. props. 80−60306
transition metal-rare earth dil. alloy, hyperfine field of rare earth impurity 79−1588
transition metal-rate earth alloy, dil., hyperfine fields, theory 78−68226
transition temperature, conc. depend. 77−85463
transition temperature and magnetisation curves 80−34628
transition temperature and order parameter 79−42771
transition to Kondo system 78−68266
transitions, field-induced, masking effects 80−65943
tricritical points in systems with random fields 79−33494
two-dimens. XY spin glass 79−42729
two-dimensional Ising frustration model, ground-state correl. 80−15732
two-dimensional Ising model, low temp. dynamic props. 80−20425
two-dimensional Ising spin glass, crit. temp. 80−11206
two-dimensional spin systems, computer expts. 77−80945
two-level system, general formalism and two-dimens. model 78−19257

spin glasses continued
two-level systems in spin-glass model, three-dimensional model and mag. field effect 78−39331
type II magnetism, existence discounted 78−47983
type II magnetism in mixed magnets and spin glasses 78−23281
uniaxial, Gaussian internal mol. field distrib. 77−16016
vector and Ising, lower critical dimensionality 78−43603
X-Y and Heisenberg, below four dimensions, vanishing of Edwards-Anderson order parameter 80−60347
X-Y model, disordered, two-dimens., phase transition 79−82789
Ag-Fe alloy film, mag. susceptibility max. 79−24173
Ag-Mn, conc. spin glasses, thermopower 80−65538
Ag-Mn, dil., spin glass, AC susceptibility 79−33490
Ag-Mn, dil., thin-film spin glass, mag. susceptibility and T_G meas., 1.2-60K 79−38346
Ag-Mn, dil. alloy, transverse magnetoresist. in spin glass regime 80−34417
Ag-Mn, dilute spin glass, AC susceptibility and ESR meas. 79−7968
Ag-Mn, spin glass, anomalous Hall effect 78−30908
Ag-Mn, spin glass, mag. susceptibility hydrostatic press depend., RKKY interaction 80−44845
Ag-Mn, spin glass alloy, elec. resist. 77−8067
Ag-Mn, spin-flip scatt. time, superconductive tunnelling 79−8003
$Al_2Mn_3Si_3O_{12}$, amorphous spin glass, spin relax. 79−65685
$Al_2Mn_3Si_3O_{12}$, amorphous, spin dynamics, neutron scatt. meas. 80−15741
$Al_2Mn_3Si_3O_{12}$, amorphous insulating spin glass, susceptibility and magnetisation meas. 80−88765
$(Al_2O_3)_{0.2}(Ho_2O_3)_{0.2}(SiO_2)_{0.6}$, amorphous low temp., AC susceptibility, freq. depend. of spin freezing temp. 79−82808
$Al_{0.35}V_2O_5$, spin glass phase, low temp. mag. susceptibility meas. 80−29565
Au-Co, electron scatt., spin-orbit effects 80−65533
Au-Cr, dil., spin glass, elec. resist., press. and conc. effects 78−52278
Au-Cr, dil. spin glass elec. resist., press. and conc. depend. 80−24864
Au-Cr(Mn), spin glass alloy, elec. resist. 77−8067
Au-Cu-Fe spin glass alloys, impurity mag. resist. meas. 80−59972
Au-Fe, competing interactions in FCC alloys 78−95453
Au-Fe, dil. alloy, transverse magnetoresist. in spin glass regime 80−34417
Au-Fe, dil. alloys, spin glasses, modified bond model calcs. 79−33489
Au-Fe, finite mag. clusters near percolation conc. 78−72371
Au-Fe, long range mag. order 77−63215
Au-Fe, mag. moment dynamics, neutron diffuse scatt. meas. 77−69584
Au-Fe, quench-condensed film, reduced MFP influence on elec. resist. 77−69306
Au-Fe, spin glass, spin relaxation rates, neutron scatt. study 79−47235
Au-Fe, spin glass in low DC field, mag. viscosity, time decays of remanences 78−64209
Au-Fe, spin glasses, alternating susceptibility 80−65912
Au-Fe, spin-glass, characteristic temps. 79−38348
Au-Fe, transition temp., freq. depend. 80−97113
Au-Fe (Mn)(Co), spin glass transition and anomalous Hall effect 79−61162
Au-Fe (1 at.%), spin glass, specific heat 80−60355
Au-Fe (14.5 at.%), spin dynamic exam. by diffuse magnetic neutron scatt. 77−8320
Au-Fe (15 at.%), small angle neutron scatt. study 79−47293
Au-Fe (16.2 at.%), cluster glass, mag. small angle neutron scatt. 80−50111
Au-Fe (3.1-10.4 at.%) spin glass alloys, high field magnetisation curves 80−11213
Au-Fe (4 at.%), spin glass energy relaxation of remanent magnetisation at low temp. 79−87271
Au-Fe (4 at.%), spin glass, magnetisation and energy relax. below T_g 80−65921
Au-Fe (4.2 at.%), DC magnetisation, field depend. 80−97103
Au-Fe (4.4 and 4.8 at.%), isotropic spin glass behaviour and transverse magnetoresist. 77−15830
Au-Fe alloy, behaviour in low DC field 77−66373
Au-Fe alloy, dil., Mossbauer exam. in spin glass regime 79−61289
Au-Fe alloy, long-time relax. processes, heat capacity expts. 77−66374
Au-Fe alloy, spin glass, neutron scatt. 78−68265
Au-Fe alloy film, mag. susceptibility max. 79−24173
Au-Fe alloys, spin correlations, neutron diffr. meas. 80−80482
Au-Fe film spin glass, low temp. resistivity, mean free path effects 78−80163
Au-Fe solid soln. alloys, reson. and relax. effects 79−82865
Au-Fe spin glass, energy flux associated with remanent magnetization relaxation *(French)* 80−7110
Au-Fe spin glass, susceptibility cusp, influence of Fe clusters 79−61163
Au-Fe spin glass alloy, neutron scatt. study 79−61179
Au-Fe spin glasses in low DC fields, susceptibility and thermoremanence 77−77063
Au-Fe(Co)(Mn), residual resistivity conc. depend. 80−2382
Au-Fe(Mn) dil. spin glass alloy, impurity-impurity interaction press. depend., resistivity meas. 77−20308
Au-Mn alloys, reversible and irreversible DC magnetisation in spin glass regime 80−65908
Au-Mn(Cr)(Fe), conc. spin glasses, thermopower 80−65538
Au-Mn(Cr)(Fe), dil., spin glass state and Kondo effect, nucl. orientation of ^{54}Mn 78−6514
Au-Mn(Fe)(Cr), spin glass, anomalous Hall effect 78−30908
Au-Si-Mn, amorphous spin glass film, mag. susceptibility 79−42775
$Au_{1-x}Cu_x$-Fe, dil., resistance maximum 79−61056
AuFe alloy films, mag. susceptibility, Fe concentration and annealing depend. 79−61119
AuFe, spin glass, anomalous magnetoresistance 79−78077
AuFe spin glass, μ^+ zero-field spin relax. probe for spin dynamics 80−97177
AuFe, spin glass freezing above ferromag. percolation limit 78−52264
$(Au_xPb_{1-x})_{1-c}Fe_c$, ferromag. and spin glass ordering 78−56335
$Be_5(Fe_{1-x}Mn_x)$, mag. and calorimetric props. 77−63083
$Bi_3Sr_{1-x}Eu_x$, supercond. and mag. ordering 78−56252
C, soft, sp. ht., 0.4-4.5K, rel. to localised spin transition 77−28389
Co_xGa_{1-x} alloys, cluster spin glass, host and impurity NMR and AC susceptibility 80−71194
Co_xGa_{1-x}, β-phase, spin glass behaviour 80−44837
Co_xGa_{1-x}, cluster spin glass, AC susceptibility in DC mag. fields, 77 to 500K 80−34670

spin glasses continued
$CoO-Al_2O_3-SiO_2$, amorphous, remanent magnetisation short time depend. 80−65919
$CoO-Al_2O_3-SiO_2$, spin glasses, low-field susceptibility, freq. depend. 78−47981
$CoO-Al_2O_3-SiO_2$, spin glass, magnetic aftereffects 79−61176
Cr-Fe, spin-glass phase, magnetisation curve test for mag. ordering 80−11201
Cr-Fe (14 wt.%), spin density wave and spin glass ordering coexistence at low temps. 79−61059
Cr-Mo-Fe (2, 14 wt.%), spin density wave and spin glass ordering coexistence at low temps. 79−61059
$(Cr_{98}Mo_2)_{90}Fe_{10}$, spin glass behaviour obs. 79−61157
$Cr_xPd_{82-x}Ge_{18}$ amorphous alloys, magnetoresist., mag. susceptibility, magnetisation 78−80148
Cu-Al-Mn spin glass, field depend. suscept. 79−73739
Cu-Co superparamagnetic particles, macrospin glass form. *(Russian)* 80−25165
Cu-Co-Fe, dil. alloy, low temp. resistivity maxima *(Russian)* 79−87091
Cu-Cr, dil., spin glass, elec. resist., press. and conc. effects 78−52278
Cu-Fe alloy film, mag. susceptibility max. 79−24173
Cu-Mn, ^{63}Cu NMR linewidth and relax. meas. 77−69583
Cu-Mn, classical RKKY model, thermodynamic props. 78−39333
Cu-Mn, dil., mag. heat capacity, conc. and temp. depend. 79−61164
Cu-Mn, dil., spin-glass dynamics, NMR meas. 78−31120
Cu-Mn, dil. alloy, spin glass, host NMR, spin freezing 77−40138
Cu-Mn, dil. alloy, spin glass, host NMR, spin freezing 77−40139
Cu-Mn, hysteresis loops, temp. and field depend. 80−15742
Cu-Mn, mag. irreversibility and metastability 78−19279
Cu-Mn, mag. viscosity below freezing temp. 80−65910
Cu-Mn, magnetisation curves 79−24172
Cu-Mn, magnetisation curves, time depend. 80−15743
Cu-Mn, specific heat below 3K, spin glass freezing temp. 79−95600
Cu-Mn, spin glass, anomalous Hall effect 78−30908
Cu-Mn, spin glass, meas. of order parameter 80−34642
Cu-Mn, spin glass, US meas. of crit. exponent α' 79−78384
Cu-Mn, spin glass alloy, elec. resist. 77−8067
Cu-Mn, spin glass alloy, magnetic excitations, neutron scatt. 78−10695
Cu-Mn, spin glasses, alternating susceptibility 80−65912
Cu-Mn, transition temp., freq. depend. 80−97113
Cu-Mn, zero field ESR in spin glass state 80−66017
Cu-Mn (10 at.%), meas. of mag. viscosity below freezing temp. 79−24171
Cu-Mn (16.7 at.%), spin glasses, alternating magnetisation 79−91241
Cu-Mn (3.%), specific heat below 3K 79−61165
Cu-Mn (4.7 at.%), spin correlations, neutron scatt. cross section meas. 79−51790
Cu-Mn (8 at.%), spin glass, neutron scatt. and susceptibility investig. of spin dynamics 77−40076
Cu-Mn (8 to 75 at.%), spin correl., neutron polarisation anal. study 80−65905
Cu-Mn alloy, classical RKKY model, zero temp. dynamic struct. factor 78−68271
Cu-Mn alloy, dil., evidence for Mn clustering from high field magnetisation curves 79−78426
Cu-Mn alloy, macroscopic mag. anisotropy, transverse susceptibility and zero field NMR enhancement 80−80525
Cu-Mn alloy, spin glass, neutron scatt. 78−68265
Cu-Mn alloy, spin-glass, US exam. 78−68351
Cu-Mn dil. spin glass alloy, impurity-impurity interaction press. depend., resistivity meas. 77−20308
Cu-Mn spin glass, magnetisation reversal and macroscopic mag. domain obs. 79−61168
Cu-Mn spin glass, saturated thermoremanent magnetisation, time and temp. evolution 79−61167
Cu-Mn spin glass, spin freezing and exchange narrowing of mag. reson. 80−60411
Cu-Mn spin glass alloy, neutron scatt. meas. of Edwards-Anderson order parameters 79−11323
Cu-Mn spin glass alloy, spin correl. function, combined neutron spin echo and polarisation anal. 80−50107
Cu-Mn spin glass neutron diffr. expts. *(French)* 78−43593
Cu-Mn spin glasses, spin dynamics, neutron scatt. meas. 79−8002
Cu-Mn-Au(Pt), anisotropic exchange interactions, effect of nonmag. impurities 80−80534
Cu-Mn(1%) spin glass, remanent mag., zero-field NMR obs. 79−33492
CuFe solid solns., quenched from vap. phase, mag. props. 80−60307
CuMn, hysteresis, spin orbit scattering effect on anisotropy in spin glass state 80−71095
CuMn, magnetisation processes below freezing temp. 80−15748
CuMn spin glass, AC susceptibility 80−60305
CuMn, spin glass, mag. correls., neutron scatt. study 80−50105
CuMn, spin glass, mag. hysteresis meas. 80−34691
CuMn spin glass, μ^+ zero-field spin relax. probe for spin dynamics 80−97177
CuMn, spin glass, random moments time correl., zero field muon spin relax. meas. 80−60335
CuMn, spin glass, remanence, new approach from zero field NMR 80−34785
CuMn spin glass, specific heat and entropy 80−60354
CuMn, spin glass low DC field mag. susceptibility using SQUID 79−69684
CuMn-like alloys, model calcs. on magnetisation processes in moderate fields below freezing temp. 79−24188
$Cu_{0.95}Mn_{0.05}$, inelastic neutron scatt., time-of-flight and three-axis techniques 80−50108
$Cu_{0.95}Mn_{0.05}$, low temp. mag. excitation spectrum, inelastic neutron scatt. obs. 80−50109
$Cu_{0.98}Mn_{0.02}$, spin glass, Heisenberg mode, RPA approx. 80−65904
$Cu_{75}Mn_{25}$, concentrated spin glass, elec. resist., depend. on hydrostatic press. 79−69685
$Cu_{75}Mn_{25}$, spin glass, EPR line breadth, exchange-narrowed 79−15345
$Dy_xCe_{1-x}Ru$, supercond., mag. order 79−87189
$Er_xY_{1-x}Al_2$, mag. props. meas. and neutron diffr. data 80−7126
Eu_xCa_{1-x}, mag. ordering temp. conc. depend., Eu mag. hyperfine field temp. depend. 78−14971
$Eu_{1-x}Gd_xS$ and $Eu_xSr_{1-x}S$, transition temp., freq. depend. 80−97113
$Eu_{1-x}Gd_xS$, concentrated system with ferromag. and antiferromag. interactions, spin-glass props. 80−34639
$Eu_{0.14}Si_{0.31}O_{0.55}$ glass, optical, magnetic, and magneto-optical props., chemical clustering 79−42951

spin glasses continued
$Eu_7Sn_{1-y}Mo_6S_y$, supercond., mag. props. 77−69447
(Eu_xSr_{1-x}) S dilute, spin-cluster freezing observation by low-freq. mag. absorpt. 79−78404
$Eu_{0.4}Sr_{0.6}S$, spin dynamics, neutron scatt. study 80−65907
$Eu_{1-x}Sr_xS$, non-metallic system, spin glass behaviour 79−24175
$Eu_xSr_{1-x}S$, blocking of pairs and spin glass freezing 79−61174
$Eu_xSr_{1-x}S$, chalcogenide-like system, crit. conc. for ferromagnet-spin glass transition 80−34662
$Eu_xSr_{1-x}S$, dil. insulator spin-glass versus blocking 80−34641
$Eu_xSr_{1-x}S$, dilute Heisenberg magnet, complex susceptibility of blocked spins 80−15740
$Eu_xSr_{1-x}S$, ferromagnet-spin glass transition, mag. ordering, mag. susceptibility and neutron scatt. meas. 80−50135
$Eu_xSr_{1-x}S$, Heisenberg spin glass system, excitations 80−84610
$Eu_xSr_{1-x}S$, insulating spin glass, mag. props. 80−2589
$Eu_xSr_{1-x}S$, insulating spin-glass, sp. ht. near ferromag. onset 80−34667
$Eu_xSr_{1-x}S$, insulating spin glass, sp. ht. near ferromag. onset 80−97106
$Eu_xSr_{1-x}S$, mag. clusters, spinodal decomp. trend 80−65923
$Eu_xSr_{1-x}S$, mag. ordering temp. conc. depend., Eu mag. hyperfine field temp. depend. 78−14971
$Eu_xSr_{1-x}S$, non-metallic spin glass system 79−61175
$Eu_xSr_{1-x}S$, onset of ferromagnetism for x near 0.5 neutron diffr. obs. 79−24181
$Eu_xSr_{1-x}S$, spin glass to ferromag. transition, neutron scatt. and susceptibility meas. 80−60254
$Eu_xSr_{1-x}S$, spin wave modes and low temp. sp. ht. 80−80538
$Eu_xSr_{1-x}S$, spin-glass props. and mag. transition 80−97105
$Eu_xSr_{1-x}SO_4$, mag. ordering temp. conc. depend., Eu mag. hyperfine field temp. depend. 78−14971
Fe-Al, spin glass transition, Monte Carlo study 80−39801
Fe-Al (0.27 to 0.50 at.%), spin glass behaviour, microscopic model, Ising lattice, exchange and superexchange 80−39800
Fe-Ni-Cr, mag. props. in weak mag. fields *(Russian)* 80−75771
γ-Fe-Ni-Mn alloys, spin glass state, short and long range order investigation 80−65808
Fe-Pt-Ir, Mossbauer effect of ^{193}Ir and ^{57}Fe, hyperfine field, isomer shift 78−15072
Fe-Y(Lu) amorphous films, mag. props., Mossbauer effect and magnetisation meas. 79−69701
Fe_xCr_{1-x}, spin-wave evolution crossing from ferromag. to spin-glass regime 80−97080
$Fe_xCu_{1-x}Rh_2S_4$, mag. tetrahedral intrasublattice interaction, spin glass type behaviour 78−52241
FeF_3, amorphous, characterisation by thermal, mag. and Mossbauer study 79−42782
$Fe_5(Fe_{1-y}Co_y)$, mag. and calorimetric props. 77−63083
$FeMgBO_4$ and $FeMg_2BO_5$, mag. props., spin glass behaviour 79−61145
$FeMgBO_4$, and $FeMg_2MO_5$, imperfect 1D mag. systems, Mossbauer expts. 80−60466
FeMn hydrated oxides, ferromanganese freshwater nodules, antiferro- to speromag. order 77−70649
$(Fe_{1-x}Mn_x)_{75}P_{16}B_6Al_3$, amorphous, spin-glass-ferromag. multicritical point, AC susceptibility meas. 80−50117
Fe_xNbSe_2 (2H), mag. susceptibility meas., 1.3-300K 80−39740
Fe_xNbSe_2, transport props. and mag. ordering 80−65527
$Fe_{65}(Ni_{1-x}Mn_x)_{35}$, magnetic struct. and inhomogeneities by neutron scatt. and Mossbauer effect *(Russian)* 77−63122
$Fe_{65}Ni_{28}Mn_1$, disordered, mag. struct. near ferro-antiferromagnetic transition 80−60211
$(Fe_{0.04}Ni_{0.96})_{80}P_{10}B_{10}$, amorphous, mictomagnetic to ferromag. transition 78−34981
$Fe_cNi_{80-c}P_{14}B_6$, amorphous, annealing effects on mag. props. 79−78383
$Fe_xNi_{1-x}P_{14}B_6$, amorphous, spin-glass regime, magnetoresist. meas. 80−34418
$Fe_xNi_{80-x}P_{14}B_6$, amorphous, sp. ht. and susceptibility meas., spin glass and mictomag. props. 78−68274
$Fe_xNi_{80-x}P_{14}B_6$, metallic glass, low temp. sp. ht. for spin-glass and spin-cluster-glass regime 80−71071
$(Fe_yNi_{100-y})_{79}P_{13}B_8$, metallic glass, low temp. sp. ht. for spin-glass and spin-cluster-glass regime 80−71071
Fe_3O_4 ferrofluids, spin glass behaviour 80−71120
$Fe_xPd_{82-x}Si_{18}$, amorphous, magnetisation, magnetoresist., spin glass and ferromag. phases 80−34697
$Fe_xPd_{82-x}Si_{18}$ metallic glass, mag. phase diagram, weak ferromagnet-spin glass transition 80−54893
$Fe_xPd_{82-x}Si_{18}$ metallic glass, long range interaction and spin wave interactions 80−65949
$Fe_xPd_{82-x}Si_{18}$ metallic glass, mag. transitions, weak ferromagnetism 80−100583
Fe_2TiO_5, anisotropic spin glass behaviour 79−99707
Fe_2TiO_5, anisotropic spin glass type behaviour 80−60296
Fe_2TiO_5, spin glass system, cation distrib. Mossbaeur spectra 80−71248
$Fe_{3-x}Ti_xO_4$, spin glass behaviour, susceptibility and hysteresis meas. 80−65917
$Fe_{0.35}V_2O_5$, spin glass phase, low temp. mag. susceptibility meas. 80−29565
θ-$Fe_xV_2O_5$, spin glass and paramag. props., susceptibility, EPR and Mossbauer studies 80−75782
$Fe_xV_2O_5$, spin glass transition range, cluster blocking distrib. function 80−80548
$Ga_{1-x}Co_x$, cluster spin glass system, host and impurity NMR studies 79−65745
$Ga_{0.67}Cr_2S_4$, semiconducting thiospinelide, spin glass type mag. ordering *(Russian)* 80−50123
Gd-Al, amorphous film, microwave mag. reson. 78−91948
Gd-Al, amorphous film, microwave mag. reson. 78−92060
Gd-Al sputtered amorphous films, spin glass state 77−66393
Gd-Al(Cu), amorphous alloy films, mag. phase diagram, spin glass and ferromag. regions 78−68234
$Gd_{0.37}Al_{0.63}$ film, amorphous, spin-glass order parameter meas. 77−28396
$Gd_{0.37}Al_{0.63}$ sputtered film, amorphous, conc. spin glass, microwave reson. spectrum obs. 78−15018
$Gd_{37}Al_{63}$ amorphous film, spin glass, microwave mag. resonance, freq. dependence 80−39798
$Gd_xCe_{1-x}Ru_7$, coexistence of supercond. and spin glass mag. freezing 77−28283
$Gd_xTh_{1-x}Ru_7$, coexistence of supercond. and spin glass mag. freezing 77−28283

spin glasses continued
$(Gd_xY_{1-x})Al_2$, ferromag. and spin glass like behaviour, magnetisation meas. 80−75734
H_2, solid, glass phase, use of NMR *(French)* 80−93190
H_2, solid, quadrupolar glass phases, evidence from NMR study 78−84027
^3He, BCC, mag. ordered phase, complicated spin-glass-like phase 78−22928
$Hg_{1-x}Zn_xCr_2Se_4$, magnetic struct., neutrongraphic and mag. investigation *(Russian)* 80−88726
$(Ho_2O_3)_{0.194}(Al_2O_3)_{0.227}(SiO_2)_{0.579}$, amorphous, low temp. spin glass behaviour 80−60297
(La,Gd)Al_2, mag. props. 78−52299
(La,Gd)Al_2, reversible and irreversible mag. susceptibility 80−15738
(La,Gd)Al_2, spin glass, cluster glass and magnetisation characts. for different comps. 77−69585
(La, Gd)Al_2 spin glass, suscept. and sp. ht., mag. field depend. 79−61173
(La,Gd)Al_2 spin glasses, time depend. mag. props. 80−65909
(La,Gd)B_6, dil. alloy, spin glass behaviour, 4.2 to 200K AC mag. susceptibility, RKKY calcs. 78−47994
(La,Gd)B_6, mag. susceptibility, zero field, 0.04 to 10K 78−10696
La-Ce alloy, press. induced spin glass to Kondo phase transition, resist. meas. 79−24174
La-Gd (8 at.%), FCC, under hydrostatic pressure, resistivity meas., comparison with positive-J spin glasses 80−59958
La-Gd-Au, amorphous, mag. field depend. of resist. minima 77−59275
La-Gd-Au, amorphous spin glasses, mag.-cluster description 79−42776
LaEu, mag. supercond., phase diagram, bulk susceptibility meas. 77−59353
$(La_{1-x}Gd_x)Al_2$, dil., reverse resistance anomaly 78−76054
$(La_{1-x}Gd_x)Al_2$, spin glass, susceptibility maximum freq. depend. 79−61172
$La_{1-x}Gd_xAl_2$, thermoremanent and isothermal remanent magnetisation 79−87276
$La_{80-x}Gd_xAu_{20}$, amorphous dil. alloy, RKKY interaction, magnetisation meas. 77−32207
$La_{80-x}Gd_xAu_{20}$, amorphous, supercond. and spin-glass regime, magnetisation and resist. meas. 77−36011
$LaNi_{1-x}Fe_xO_3$, magnetisation meas. and ^{57}Fe Mossbauer studies 80−93217
$Mn_3Al_2Si_3O_{12}$, amorphous, spin-glass, insulating, Mn^{2+} mag. reson. 80−65918
$Mn_xNi_{1-x}Sb$, spin glass state and synthesis in high temp. and press. atmospheres 78−23277
$MnO-Al_2O_3-SiO_2$, amorphous, spin glass like behaviour at low temp. 79−61177
$MnO-Al_2O_3-SiO_2$, amorphous, remanent magnetisation short time depend. 80−65919
$MnO-Al_2O_3-SiO_2$, amorphous spin glass, AC susceptibility 80−80520
$MnO-Al_2O_3-SiO_2$, spin glasses, low-field susceptibility, freq. depend. 78−47981
MnSi amorphous, conc. spin glass system, temp. effect on susceptibility 79−61142
MnSi, amorphous, sputtered, mag., elec., struct. and thermal props., spin glass behaviour 80−50124
MnSi, amorphous magnetisation meas. 80−34599
MnSi(Ge), amorphous, spin glass transition, AC susceptibility meas. 80−75779
Mo-Fe, spin glass and mictomag. regimes, sp. ht., resist. and susceptibility meas. 77−69581
MoFe, occurrence of spin glass and mictomagnetic regimes, props. meas. 77−16085
$Nb_{50}Ni_{50-x}Fe_x$, magnetically dil. glass, 3d moments, mag. susceptibility and magnetisation meas. 79−95574
Nd-Y alloy, mag. character of stable and metastable phases 79−38329
Ni-Cu, ferromagnetic and spin glass transition, DC magnetisation meas. 79−78369
Ni-Cu, low field magnetisation meas., mag. props. comp. depend. 78−91879
Ni-Cu alloy, nearly ferromag., spin-glass-like distrib. of interaction fields 79−91243
Ni-Mn alloys, ferromagnetism-to-spin glass phase transition and strong mag. field effect 80−75773
$Ni_{0.95}$ S Fe, spin glass, spin flop in exchange field 80−34640
$(Ni_{100-x}Fe_x)_{79}P_{13}B_8$, amorphous dil. alloys, spin glasses, magnetisation meas. 79−61178
$(Ni_{99}Fe_1)_{79}P_{13}B_8$, amorphous, low temp. sp. ht., mag. contribs. 80−80552
$(Ni_{1-x}Fe_x)_{1-\delta}S$, anisotropic spin glass, mag. props. 80−39793
Ni_3Mn, partially ordered, remanence reversal 77−69619
$PbMnFeF_7$ and Pb_2MnFeF_9, vitreous, insulating, evidence of spin-glass transition 80−97112
Pd based 3d metal alloys, mag. phase diagram calc. 78−80144
Pd-Ag-Fe, (0.5, 1.0, 2 at.% Fe), elec. resist. reduction near ferromag. and spin glass ordering 77−69299
Pd-Cr (11-18 at.%), resistivity comparison with canonical spin glass system 78−10432
Pd-Cr spin glass, magnetisation and magnetoresist. meas. 79−69680
Pd-Fe, very dilute, very low temp., spin glass-like behaviour 79−99708
Pd-Fe alloy, dil., cond. electron polarisation studied by positive muons 77−28397
Pd-Fe and Pd, muon$^+$ Knight shift, cond. electron polarisation, RKKY oscill. 77−66450
Pd-Fe-Mn, differential susceptibility, spin glass and ferromag. transition 79−61169
Pd-Fe-Mn, ferromag. and spin-glass props; comment 80−2591
Pd-Fe-Mn, ferromagnet-spin glass, thermal expansion forced, magnetostriction and magnetisation under high press. 80−65255
Pd-Fe-Mn, ferromagnetic-spin glass transition 78−39339
Pd-Mn, dil. alloy, giant moment at very low temp. 78−88094
Pd-Mn, dil. alloy, very temp. magnetisation 80−34692
Pd-Mn, ferromagnetism to spin glass behaviour transition 80−71062
Pd-Mn, spin freezing in spin glass phase, susceptibility meas., sp. ht. analysis 77−69582
Pd-Mn, spin glass-ferromag. alloys, high-field magnetisation 79−33488
Pd-Mn (1-10 wt.%), mag. ordering, influence on resistivity 80−75557
Pd-Mn (10 at.%), spin glass, inelastic neutron scatt. exam. 79−61170
Pd-Mn alloy, low temp. spin dynamics, numerical studies 79−78385
Pd-Mn alloy, spin glass, neutron scatt. 78−68265
Pd-Mn(Fe), mag. ordering phenomena, neutron scatt. obs. 80−44812

spin glasses continued
$(Pd_{0.996}Co_{0.004})_{1-x}Mn_x$ alloys, ferromag. and spin glass transition, NMR 79−65761
$(Pd_{0.9965}Fe_{0.0035})Mn_{0.05}$, ferromag. and spin-glass props. 80−2590
$(Pd_{0.9965}Fe_{0.0035})_{1-x}Mn_x$, mag. behaviour at Fe sites, Mossbauer effect meas. 80−66085
$PdH_{0.97}$:Fe(Cr), supercond. transition temp. depression, coexistent mag. behaviour 80−49976
PdH_x-Fe, dil., Kondo system, local moment hyperfine studies, Mossbauer expt. 80−39908
$PdH_x(\alpha')Fe_{0.003}$, Kondo effect and RKKY coupling, Mossbauer spectra 79−61054
PdMn, giant moment-spin glass high field magnetisation, exchange parameter, saturation moment estimation 79−61143
Pd_3Mn, disordered, mag. correls., neutron scatt. study 80−50105
$Pd_{1-y}Mn_yH_x$ alloy, spin glass, transition temp., susceptibility and EPR meas. 80−65930
$Pd_{80-x}Si_{20}Fe_x$, amorphous, low x, hyperfine interactions and mag. ordering temp. 79−15303
Pr-rare earth dilute alloy, low field magnetic props. 78−84443
Pr-Tb alloy, elec. resist. and magnetisation 77−66367
PrP, nonstoichiometric, with singlet ground state, induced van Vleck ferromag. spin glass 77−66378
Pt-Co system, low temp. susceptibility 80−65920
Pt-Cr, disordered, atomic order-disorder transform. effect on resist. min. 80−65911
Pt-Cr, elec. resist. meas. through percolation limit, mag. order onset 77−69298
Pt-Cr alloy, (13-18 at.% Cr) resistivity and AC susceptibility, temp. 1.4−300K 78−2461
Pt-Fe, competing interactions in FCC alloys 78−95453
Pt-Fe alloy, low field AC susceptibility 79−73698
Pt-Fe(Mn), dil., skew scatt. Hall effect, magnetoresist. and mag. anisotropy, orbital magnetism of impurity 80−70678
Pt-Mn, dil., nuclear orientation exam. 79−61171
Pt-Mn, dil. alloy, mag. sp. ht. 78−14966
Pt-Mn alloy, dil., low temp. susceptibility, spin glass and Kondo behaviour 77−66372
Pt-Mn dilute alloy, cubic foil, Mn spin behaviour, nuclear orientation technique 78−27044
Pt-Mn dilute alloys, spin glass, low temp. resist. meas., cluster model explanation 78−26851
PtCr, AC susceptibility near percolation limit, ordered and disordered alloy 80−65900
PtMn, spin glass, nonlinear susceptibility and sp. ht. 80−60304
PtMn spin glass alloy, cooperative freezing, susceptibility meas. 79−91233
Rh-Fe, competing interactions in FCC alloys 78−95453
Sc, sp. ht. data rel. to electronic props. 78−83971
Sc-Gd, spin glasses, low temp. sp. ht. and magnetisation 80−65913
Sc-Gd spin glass, sp. ht., 0.3-10K 80−25145
Sc-Gd(Tb), spin glasses, low-field susceptibility, role of single-ion anisotropy 77−48000
Sc-Tb, induced-moment spin glass, simple mean-field theory 80−29553
$Sr_{1-x}Eu_xS$, dilute spin glass, mag. props. 79−78386
$TaSe_2$:Fe, competition between charge and spin density waves, Landau-Ginzburg theory 79−95352
Th-Gd spin glass, low temp. sp. ht. 79−51795
$Th_{1-x}Fe_x$, amorphous alloys, mag. props. and Mossbauer spectra 79−91326
$(Ti_{1-x}V_x)_2O_3$ spin glass, mag. props., metallic antiferromagnetism 79−82791
$(Ti_{0.9}V_{0.1})_2O_3$, spin glass, dynamic mag. susceptibility meas. 80−39792
$(Ti_{0.99}V_{0.01})_2O_3$ spin glass, sp. ht. anomaly and entropy change 79−56546
$(Ti_{1-x}V_x)_2O_3$, nonlinear magnetisation at spin glass phase transition temp. 79−78403
$(Ti_{1-x}V_x)_2O_3$, spin glass, nonlinear susceptibility and sp. ht. 80−60304
$(Ti_{1-x}V_x)_2O_3$, spin glass props. and anisotropy, comp. depend. 77−66368
$(Ti_{1-x}V_x)_2O_3$, spin glass to antiferromag. regime 78−52276
$(Ti_{1-x}V_x)_2O_3$, spin glass and metallic antiferromagnetism 78−68268
$(Ti_{1-x}V_x)_2O_3$, spin-glass props., 0.05-300K 80−25149
$(Ti_{1-x}V_x)_2O_3$, susceptibility and ^{51}V NMR expts. 77−66369
W-Fe, dil., spin glass props., DC mag. susceptibility meas. 78−68283
W-Fe, optical props. and electronic states 80−20412
W-Fe alloys, spin glass props., DC susceptibility and remanence meas., 1.6 to 295K 80−29560
Y-Fe, evap. amorphous alloys, thermomag. history effects 77−66389
Y-Gd, spin glasses, low temp. sp. ht. and magnetisation 80−65913
Y-Gd spin glass, sp. ht., 0.3-10K 80−25145
$Y_{0.98}Dy_{0.02}$, spin glass, calorimetric exam. 78−68270
YFe_2 amorphous, spin-glass and mag. blocking transitions, low field DC susceptibility meas. 79−61141
YFe_2, amorphous concentrated spin glass, susceptibility, Mossbauer and neutron scatt. meas. 80−39783
$Y(Fe_xAl_{1-x})_2$, Mossbauer spectra and mag. props. 80−39950
$Y_6(Fe_{1-x}Mn_x)_{23}$, struct. and mag. props. 80−25083
$Y_{1-x}Gd_xRh_4B_4$, mag. supercond., anomalous temp. depend. of upper crit. fields 80−29510
Zr-Mn (up to 0.3%), high-magnetic field magnetisation and magnetoresistance 78−10652
$Zr_{40}Cu_{50}Fe_{10}$, magnetically dil. glass, 3d moments, mag. susceptibility and magnetisation meas. 79−95574
$Zr_{40}Cu_{60-x}Gd_x$, magnetically dil. glass, 4f moments, mag. susceptibility and magnetisation meas. 79−95575
$Zr_{40}Cu_{60-x}M_x$ (M=Fe,Mn,Gd,Tb), amorphous, mag. ordering and local random anisotropy 78−68273
$Zr_{40}Cu_{60-x}Tb_x$, magnetically dil. glass, 4f moments, mag. susceptibility and magnetisation meas. 79−95575
$Zr(Fe_{1-x}Al_x)_x$, transition region, spin glass or long range mag. order 80−44841
$Zr(Fe_{1-x}Co_x)_y$, transition region, spin glass or long range mag. order 80−44841

spin Hamiltonians
δ-functions global operators, identities for scatt. states including spin 79−92985
alkali halide:Eu^{2+}, spin-Hamiltonian parameters, superposition model calcs. 80−96830
alkali halide:Eu^{2+}, spin Hamiltonian, cryst. field consts. calcs. 79−51537

spin Hamiltonians continued
alkali halides, heteronuclear XY^- defects, spin Hamiltonian parameter anal. 80−88509
alkaline earth fluoride:Gd^{3+}, ligand ENDOR, spin Hamiltonian and hyperfine parameters 77−43903
alloy, pseudobinary, ferromag., magnon energy derivation 80−107996
alloy, quenched random, phase diagrams, multicritical points, mixed anisotropies 79−38343
alloy with two ferromagnetic components, surface excitations 80−25179
alloys, dilute mag., local moment formation, nonequivalent orbitals model 80−11164
ammonium oxalate monohydrate: Mn^{2+}, ESR, 77-345K 79−19768
amorphous ferromagnet, metastable states in random anisotropy model 79−19710
amorphous metals, mag. anisotropy, spin glass like phase 77−66295
amorphous systems, excitations and critical phenomena within framework of phenomenological models 78−52267
Anderson Hamiltonian, quantal spin system, classical representation and scaling props. of spin Hamiltonians 78−14919
Anderson-localised states, intrastate and interstate interactions 80−20113
anti-ferromagnetic lattice, ground-state energy calc., Kadanoff cells renormalisation procedure 77−77015
antiferromagnet, induced staggered magnetic fields, microscopic mech. 80−80527
antiferromagnet, linear-chain, sine-Gordon solitons 80−80543
antiferromagnet, two-magnon Raman scatt., temp. effects 77−48178
antiferromagnet chain, anisotropic, spin-wave spectrum 78−60273
antiferromagnet cubic, with exactly-known ground state 78−43540
antiferromagnetic cubic model, one-dimens., ground states and magnetization in mag. field 79−78372
antiferromagnetic with four spin interactions for BCC, lattice, mean field theory 79−1652
antiferromagnetism of strongly correlated electrons in narrow bands 78−76218
antiferromagnets, n=4 type II, phase transitions, Landau Ginzburg Wilson Hamiltonian 80−15735
aromatic radical ion recomb., mag. field modulation, Liouville eqn. soln. 77−28995
Bloch electrons, weak magnetism, spin and spin-orbit interactions *(Russian)* 79−33443
cadmium acetate trihydrate, hyperfine forbidden ESR lines of Mn^{2+}, spin Hamiltonian calc. *(French)* 77−28431
cadmium maleate dihydrate:Cu^{2+}, EPR at 77 and 303K 79−33530
channel model in exchange theory 78−39311
charge transfer allowance in effective Hamiltonian method, technique 78−68001
closed-shell systems, effective Hamiltonian for excitation energies, convergence props. 79−3346
collinear metamagnets, two-sub-lattice Ising model 78−95410
conductivity electrons-localized d(f) electrons, exchange interaction, energy within Hartree-Fock theory *(Russian)* 78−43580
constant-coupling, higher-order, statics and dynamics 80−60262
coupled rotational bands in even-even nuclei, model 80−27529
critical phenomena, use of renormalisation group, review 77−20625
crystal field splitting, parametrisation of temperature dependence 78−91652
de Gennes' model sum rules, decoupling procedure in Green's function method *(Russian)* 78−56434
deoxymyoglobin, single cryst., paramag. anisotropy meas. 77−21469
diagonalisation, quadratic Hamiltonian in N spin variables *(French)* 77−1532
diagonalisation of spin Hamiltonian, theory and appls. of generalised operator transforms 77−4546
diamond type crystals, polarization of μ^+ in muonium atom *(Russian)* 78−39492
diamonds, natural, N3 centre, EPR obs. 79−51842
Dicke Hamiltonian, spin-spin interaction on super-radiant phase transition 78−16762
dipolar interaction in solids, low mag. field, thermodynamic props. 78−76205
dislocation scattering, new Hamiltonian for describing multivalued elastic displacement fields 80−24862
disordered linear chain, exchange probability distrib., Hubbard model 78−10641
disordered one-dimensional system, Hubbard model 78−10642
displacive phase transition, S ion spin Hamiltonian parameter dependence on order parameter 80−70356
double group theory, half-shell and two-level systems, rot. and half integral spin states 78−45447
doublet-triplet mag. system, dipolar and quadrupolar ordering 79−8004
DPPH-benzene complex, ht. capacity, 0.55-20K, mag. susceptibility, 0.4-300K 78−56317
effective Hamiltonian approximation, quenched and annealed random systems 80−93125
elastic magnetic system, one-Fermion-one-Boson model 78−43539
electron exchange matrices calcs., spin function recoupling method 77−47782
electron spin magnetic moment relativistic mass correction, classical reinterpretation 77−57213
EPR, perturbation treatment, M=0 electronic state, HFS of triplet state EPR 80−25185
EPR, quadrupole interaction for nucl. spin=3/2 systems 78−48027
from EPR data by least-squares fitting 77−1585
EPR line shift due to spin-phonon interaction 79−65712
EPR of ions, fast computation of accurate spin-Hamiltonian parameters 77−73072
EPR parameters for orbital singlet of d^1 ion in cryst. 78−10751
EPR parameters for paramagnetic ions in tetragonal symmetry, optimal computation 77−4550
EPR quintet transition, exact axial reson. fields calc., rel. to powder spectra 80−2622
EPR single cryst. data, computation of spin-Hamiltonian consts. 77−90013
EPR transition probability determ., approx. methods 79−78506
EPR transitions for ions with S=3/2, small distortions of cubic cryst. field 77−51941
equivalent nuclei, ENDOR fine struct., exact solns. 77−6811
ESR, magnetic field operator 80−108051
ESR of radicals in doublet states, energy weighted maximum overlap model 78−76315

spin Hamiltonians continued
exchange-coupled pairs of paramag. ions, second-order corrections to spin Hamiltonian formalism 78−68133
ferrimagnet, one-magnon light scatt., linear and quadratic magneto-optical coupling, terms in scatt. Hamiltonian 79−11407
ferromagnet, singlet-triplet, Dyson eqn. derivation 80−107974
ferromagnetic crystal, spin subsystem thermodynamics, spin-phonon interactions, mag. order parameter 80−103848
ferromagnetic linear chain, Heisenberg Hamiltonian, existence of isolated magnon 79−4666
ferromagnetic metal, spin-polarised field emission using Appleburn-Brinkman transfer Hamiltonian 79−74065
ferromagnetic metal, two-site interaction model 79−82744
ferromagnetic semiconductor, autolocalised electron states 78−51924
ferromagnetism, itinerant, effective Hamiltonian 80−11150
ferromagnetism, manyelectron exchange Hamiltonian in theory 78−19199
ferrous-formate dihydrate, mag. system model, mag. sp. ht. *(Japanese)* 78−31091
fluorene:pyrene-d_{10} cryst., magnetic resonance absorpt. of host-guest triplet paired centres 80−34750
fluorite type crystal, Ti^{2+} doped, electronic struct. and EPR of Ti^{2+} 78−76034
g values, higher order spin terms of generalised spin Hamiltonian 77−48044
garnet:Fe^{3+}, spin Hamiltonian parameters, g-factors, temp. depend. EPR obs. 77−48038
garnet:Mn^{2+}, spin Hamiltonian parameters, g-factors, temp. depend. EPR obs. 77−48038
garnet, spin Hamiltonian and mag. anisotropy, appl. to $3d^4$ and $3d^6$ ions 79−99669
general commutator equation in the algebra of spin operators 79−4638
generalisation of exactly soluble models 77−82446
generalised, reduction in no. of consts. by unitary transform. 77−43867
guanidinium aluminium sulphate hexahydrate:Mn^{2+}, NMR 78−91939
Heisenberg chain, ferromag., with biquadratic exchange, spin correl. length, susceptibility and spin diffusion *(Russian)* 77−69568
Heisenberg exchange integral, in nonorthogonal basis, for anti- and ferromag. systems 78−2641
Heisenberg ferromagnet, biquadratic exchange, Green's function method, Hamiltonian and Curie temp. 80−15675
Heisenberg Hamiltonian, generalisation for crystal with allowance for orbital degrees of freedom 79−4644
Heisenberg Hamiltonian generalisation for case of atomic system with variable atomic spin value 78−14669
Heisenberg magnet, correlation theory of static and dynamic properties 80−65765
Heisenberg model, classical, infinite, nonlinear dynamics, quantum time evolution 80−100576
Heisenberg model, spin glass order, isotropic, two-dimens. 77−85455
Heisenberg model, two-dimensional spin 1/2 anisotropic, quantum renormalisation approach 77−66348
Heisenberg $S=^1/_2$ spins 80−2581
Heisenberg-Dzyaloshinsky-Moriya model, high temp. expansions for zero-field susceptibility and specific heat 79−33497
Heisenberg-Mattis model, long-wavelength dynamic response 80−20409
helimagnetic-ferromagnetic transition for two-dimens. spins case 77−66349
helimagnetism, isotropic bilinear spin Hamiltonian on Bravais lattice 77−51866
heme-proteins, general spin Hamiltonian for determ. of ligand nucl. Zeeman and hyperfine interactions 77−85617
hexagonal lattice, mag. subband struct. of electrons 79−95307
high spin d^5 system, isotropic g-tensor 78−10757
higher order hyperfine terms, transition metal ion in octahedral symmetry field 78−79967
Hubbard hamiltonian, correlated motions 77−72982
Hubbard Hamiltonian, coupled spin and charge fields 77−32147
Hubbard Hamiltonian, quantal spin system, classical representation and scaling props. of spin Hamiltonians 78−14919
Hubbard Hamiltonian, two-site, half-filled band, thermodynamic props. 77−24505
Hubbard model, electrostatic interaction Hamiltonian, tensor struct. *(Russian)* 78−76216
Hubbard model, equivalent spin Hamiltonian, for phase transition studies 80−80474
infinite-range, exact solns. 79−78281
inhomogeneous itinerant electron ferromagnet, mag. and thermal props. 79−7964
insulator, interaction between mag. ionis., case of degenerate orbitals 79−11309
ionic crystals incorporating S-state ions, expt. exam. 79−28326
ions in $^6S_{5/2}$ ground state, ESR line with 3.33 isotropic g-factor 80−15787
iron porphin in triphenylene, ESR 78−60329
Ising and Heisenberg model, threshold inequalities for ground state 80−7064
Ising double chain, compressible, mag. susceptibility and thermodynamic props. 79−15320
Ising Hamiltonian, crit. points, behaviour of thermodynamic quantities 78−6532
Ising model, compressible, transform. into continuous spin Hamiltonian, renormalisation group treatment 77−66347
Ising model, finite arrays of coupled chains, exact soln. 77−4485
Ising model, spin-one system, correlation functions with bilinear and biquadratic interactions 78−91876
Ising model, three-dimensional spin 1/2, real space renormalisation group calcs. 77−66345
Ising O(2), O(3) and O(4) model, Hamiltonian string-coupling expansions 80−20426
isotropic antiferromagnets, anal. by equivalent Hamiltonian method 79−82734
itinerant electron antiferromagnet, localised spin coupling 78−68142
itinerant electron antiferromagnetic matrix, local moments, spin Hamiltonian 80−34626
itinerant electron paramagnets, coupled charge and spin fields 77−72991
itinerant ferromagnet, effect of planar defects on electronic struct. and mag. ordering 79−99672
Jahn-Teller effect in EPR spectra, multistate theory for ^2E orbital states 78−56369
Jahn-Teller ions, spin Hamiltonian parameters, temp. depend. 78−30891

spin Hamiltonians continued
Kondo Hamiltonian, quantal spin system, classical representation and scaling props. of spin Hamiltonians 78−14919
Kondo Hamiltonians, rotationally invariant, universality and renormalisability 79−95573
Kondo Hamiltonians, s-d exchange, ground states, renormalisation group calcs. 80−50046
Kondo Hamiltonians diagonalisation, zero-temp. mag. susceptibility 80−93078
Kondo Hamiltonians with non-zero ground-state spin 79−51746
Kondo problem, low-temp., Nozieres-Wilson relation, renormalisable quantum field theory 79−95572
lanthanum ethyl sulphate:Gd^{3+}, spin Hamiltonian, higher-order spin terms 77−48044
lanthanum ethyl sulphate:Gd^{3+}, X-band EPR, near room temp., spin Hamiltonian parameters 77−63275
lattice gas model, double spin 1/2, for mag. annealed binary alloy and nematic mixture 77−66342
least-squares fitting for Hamiltonian parameters from resonance data 80−20448
linear chain of classical spins with arbitrary nearest-neighbour interaction 78−10632
Lorentzian lineshapes and isotropic distrib. of molecules, analytical expressions derived for powder samples 80−60401
magnesium hexahydrate $H_2EDTA:VO^{2+}$, single cryst., ESR spectra and spin Hamiltonian parameters 80−75845
magnetic crystal, order parameter for exactly soluble model 78−76207
magnetic impurity in metal, Wolff model 79−61052
magnetic model with spin-phonon interaction 77−80896
magnetic ordering in spin systems with single-ion anisotropy 77−69466
magnetic-atom cluster, spin Hamiltonian for direct exchange interaction 77−20519
magnetically ordered singlet ground state system, nucl. spin Hamiltonian 79−28496
magnon problem, anisotropic spin chain with exchange interaction 78−6502
many-spin system, group approach in dynamics *(Russian)* 80−4579
many-spin system dynamics, group approach *(Russian)* 80−50221
Melosh transformation, SU_2 symm. 77−87914
memory function for spin relaxation graphical representation 77−24733
metal, indirect coupling between localised mag. moments by narrow band electrons 80−70942
metal ions, exchange coupled, pair hamiltonian, coupled representation matrix 78−48026
metal uncompensated, two-component electron Hamiltonian 79−7994
metamagnetic insulators theory, microscopic model *(Russian)* 77−43798
methylammonium chromium alum, single cryst., Cr^{3+} EPR, g-factor, hyperfine splitting 78−2729
mixed ferromagnetic Heisenberg and Ising bonds, appl. of effective Hamiltonian method 80−50023
nematic liquid crystal, ESR of symmetrical three-spin systems, slow motional spectra 77−36135
$(NH_4)_2SO_4:Mn^{2+}$, ferroelec. phonon driven phase transform., reduction of spin Hamiltonian consts. 78−92033
NMR, multiple pulse, of solids, average Hamiltonian theory and phase adjustment 80−22404
NMR, simultaneous use of rotation and RF fields, selective investigation of interactions *(Russian)* 78−56385
one-dimensional classical planar model in applied magnetic field 80−15729
one-dimensional classical spin chain with random interactions, exact calcs. 79−4687
one-dimensional compressible Ising chain with general spin 80−90791
one-dimensional magnetic compounds, orbital interaction 78−6494
one-dimensional system, strongly interacting, Efetov-Larkin model 78−6288
orbital singlet ions, rotational invariance and phonon-induced contribs. to spin-Hamiltonian parameters 78−10410
paramagnetic susceptibility of axial cryst. systems 79−42730
paramagnetic-antiferromagnetic transitions, vector models with $n \geq 4$, renormalisation group analysis 77−66340
percolation models, spin representation and cluster distribs. 78−34998
periodic perturbation of spin-1 system, analogue of Shirley's eqn. 77−3248
perturbation energies and state vectors calc., diagrammatic technique 78−65810
phase transitions in n-component spin system with coupling to non-ordering parameter 77−51906
planar spin two-dimens. model, mag. correlation function, self-consistent calc. 80−29563
polycrystalline system, additional absorpt., in axially symmetric ESR spectra 77−16151
quadrupolar systems, excitation spectra from Green's function methods 78−56278
quantisation of dissipative systems, exclusion of time dependence 79−92981
quantum chain, mag. impurity reson., Fresnel diffr. pattern 77−63051
quantum spin systems, ground state energies, renormalisation techniques appls. 80−93132
α-quartz:Ag, Ag atom paramagnetic centre, $A_{Ag\text{-}Si}$ 78−76308
α-quartz, dynamic interchange among three states of P, EPR obs. 80−66010
radical pair with axial symmetry, EPR parameters and linewidth components 78−6573
random bond systems, effective Hamiltonian method appl. 80−50023
random site Ising model near percolation threshold 78−23282
rare earth ethyl sulphate:Gd^{3+}, host lattice effects on EPR spectra 77−69684
rare earth systems, Anderson model susceptibility for high mag. impurity conc. 77−63069
rare earth trichloride hexahydrate:Gd^{3+}, EPR meas. 78−15017
rare earth trichloride hexahydratee Gd^{3+}, EPR, linear point charge model predictions 80−25200
rare earth trichloride hexahydrates, Tb to Yb, EPR of Gd^{3+}, spin Hamiltonian parameters 77−36128
rare earth trinitrate hexahydrate:Gd^{3+}, EPR, spectral parameters 79−4720
rare earth-transition metal alloys, amorphous, Hubbard hamiltonian, mag. props. 77−72985
reggeon couplings, analogue quantum-spin model 78−45813

spin Hamiltonians continued
Reggeon field theory, ordered phase, Hamiltonian formulation, scatt. amplitude calc. 78−4807
relativistic Hamiltonian theory, covariant formulation, on light cone, fields with spin *(Russian)* 80−9087
Rochelle salt, VO^{2+}-doped, EPR study 80−34762
S=1 generalised Ising model, stability conditions 80−20427
sandwich complexes, mag. props., effective Hamiltonian method 80−37731
scheelites, zero-field splitting of Mn^{2+} ions 80−75531
Schrodinger eqn., exact soln., spinning particle in helical mag. field, non-relativistic quantum theory 80−77651
single electron state classification on basis of spin space groups 80−93065
singlet-triplet ferromagnet hydrodynamics 80−11142
sodium oxalate:Cu^{2+}, anhydrous spin Hamiltonian and bonding parameters and orbital-reduction factors 80−60408
solids, disorder of NMR and soft collective lattice modes, spins and pseudospins 78−88208
spin 1/2 particles, config. representation, bit patterns appl. 77−43804
spin glass, cluster mean-field model, static props. 79−4689
spin glass, Heisenberg model calc. 80−60301
spin glass model Hamiltonians, zero temp. spin dynamics 77−85467
spin operators, general commutator eqn. 79−4638
spin-1/2 system with dipolar interactions, thermodynamic props. in high field 77−1529
spin-orbit coupled system in mag. field, evolution operator factorisation 77−14376
statistical models, thermodynamic properties, variational calc. 77−85405
strontium acetate hemihydrate:Mn^{2+}(Cu^{2+}), EPR, spin Hamiltonian anal. and unit cell symmetry 80−29603
strontium formate:Mn^{2+}, cryst., e.p.r., spin Hamiltonians 77−4552
strontium formate dihydrate, EPR and optical absorption spect. of VO^{2+} ion 77−40112
symmetry adaptation, operator equivalence, mag. reson., operator equivalent formalism *(French)* 78−84374
symmetry and spin-wave Hamiltonian struct. 78−84373
tetra-ammine cadmium acetate:Cu, EPR dynamical effects 79−61204
tetramer clusters, ESR spectra, spin Hamiltonian analysis 77−28429
tetranuclear cluster, eigenvalues spectrum of spin Hamiltonian calc., thermodynamics props. *(French)* 77−35902
TGSe:Cr^{3+}, polarisation reversal and ageing mechanisms, EPR meas. 79−8044
thermal correlation functions, dynamic SCF approx. 79−7952
thermodynamics of spin system, contrib. of spin-phonon interaction 78−2635
three-spin systems in nematic liq. cryst., EPR 77−14463
$[TMPD^+]_2[Cu_xNi_{1-x}(mnt)_2]$, ESR obs. of triplet excitons and Cu(II) ions, mag. interactions 79−95633
transition density matrices, spin variables separation by Fock coordinate function and spin Hamiltonian methods 80−63513
transition metal, symmetric clusters, Schrodinger exchange Hamiltonian 79−7955
transition metal compound, superexchange interaction, effective spin-orbital Hamiltonian 80−70998
transition metal compound, superexchange interaction, multielectron theory 80−70997
transition metal ions in crysts. two-centre exchange interactions between orbitally degenerate ions, effective Hamiltonians 79−15126
transition metal surface, spin fluctuations 78−95451
triglycine calcium bromide:Cu^{2+}, ESR studies 80−97136
tris sarcosine calcium chloride:VO^{2+}, EPR and absorpt. spectra 78−60330
two-component spin system, first-order transition induced by cubic anisotropy 79−4688
two-dimensional planar magnet, crit. slowing down in transverse autocorrel. function 78−95448
X-Y model, one-dimens., zero temp., transverse time depend. spin correlation functions 78−65876
α-quartz:Ge, Ge^{3+} centres, dynamic interchange, EPR obs. 79−19776
$AgClO_3$, ClO_2 spin Hamiltonian 78−60326
α-Al_2O_3:Cr^{4+}(V^{3+}), ground state spin Hamiltonian parameters and electric field effect 77−15801
$Al_2O_3:V^{3+}$, spin-phonon coupling, rot. mode role 80−70329
β-Al_2O_3-Na_2O, EPR and optical absorpt. studies of X-ray produced defects 78−95517
β-Al_2O_3-Na_2O_3:Ag^{2+}, EPR measurements 78−95515
Al_2SiO_5, EPR of Fe^{3+} at V-band and the pair spectra 78−80204
β-B, rhombohedral, EPR anisotropy 80−25183
$BaCa_{1/2}Ru_{2/3}O_3$, biquadratic exchange interaction between Ru^{5+} ions in (Ru_2O_9) clusters 77−20580
$BaF_2:Tm^{2+}$, EPR meas. of Tm^{2+} ion pair interactions 79−95641
$BaO\text{-}Al_2O_3\text{-}B_2O_3$:Ag, X-ray irrad., atomic centre interactions, EPR spectra 80−25207
$BaO\text{-}P_2O_5$:Mo^{5+} glass, EPR spectra, computer simulation 80−88872
$Bi_{12}GeO_{20}$:Cr^{3+}, level distrib. of Cr^{3+} ion, spectroscopic parameters, spin Hamiltonian, EPR spectrum 78−48030
$CaCo_2$, aragonite, EPR of Mn^{2+} impurities, orthorhombic spin-Hamiltonian parameters 80−2631
$CaF_2:Pr^{2+}$, EPR data interpretation for octahedral Γ_8 state in cubic cryst. field 80−2634
CaF_2:PrF_3, EPR of cubic Pr^{3+} 79−28607
$CaF_2:Tm^{2+}$, EPR meas. of Tm^{2+} ion pair interactions 79−95641
$Ca(OD)_2$:Cu^{2+}, ESR, secondary spectra 78−88174
$Ca_5(PO_4)_3F:Cr^{3+}$, ESR, polymorphic transform., spin Hamiltonians 77−36117
CaSe:Sn^{3+}, EPR study of octahedral Sn^{3+} centres, 4 to 290K *(Russian)* 80−84637
$CaWO_4$:Fe^{3+}, EPR, spin Hamiltonian parameters from anal. of Kramers' doublets 79−28595
$CdF_2:Eu^{2+}$, EPR spectra, hydrostatic press. and temp. effects 80−84648
$CdF_2:Gd^{3+}$, hydrostatic press. and temp. effects on EPR spectrum 78−76304
$Cd_{1-x}Mg_x$, mag. props. and electron spectrum parameters *(Russian)* 79−33453
$Cd(NH_3)_4Cl_2$:Cu, EPR dynamical effects 79−61204
$Cd(NH_4)_2(SeO_4)_2.6H_2O:Mn^{2+}$, EPR of Mn^{2+}, spin-Hamiltonian parameters 79−33528
CdS, amorphous antiferromag., mag. props. of dilute neutral donors 79−78367
$3CdSO_4.8H_2O:Gd^{3+}$, EPR, spin Hamiltonian 79−42833

spin Hamiltonians continued
$Ce_2(SO_4)_3.8H_2O:Gd^{3+}$, single cryst., EPR study, spin Hamiltonians 80−80606
Co complex, triazene-1-oxide complexes, EPR spectra in frozen nematic liq. cryst. glass 80−88871
$CoBr_2$, magnetic excitations, neutron scatt. investigation 80−39761
$CoK_2(SO_4)_2.6H_2O:Mn^{2+}$, EPR spectra, spin-Hamiltonian anal. 77−77088
$CoSiF_6.6H_2O:Co^{2+}$, spin Hamiltonians and pair interactions 77−36119
Cr complex, influence of anisotropy of spin-Hamiltonian parameters on EPR spectra *(Russian)* 77−28432
Cr, phase transition at T_N 79−4676
Cr-V, itinerant electron antiferromag., spin fluctuations, low temp. specific heat 80−107439
Cr_2O_3, magnon energy temp. renormalisation calc. 77−1531
$CsMF_3:Mn^{2+}$, (M=Ca,Cd), zero-field splitting of Mn^{2+}, superposition model *(French)* 79−15267
$Cs_2NaRCl_6:Er^{3+}(Gd^{3+})$, R=lanthanide, EPR parameters and interpret. 77−59456
$Cs_2ZrCl_6:Np^{4+}$, EPR data interpretation for octahedral Γ_8 state in cubic cryst. field 80−2634
Cu complex, Cu-glycine in water, EPR spectral parameters, temp. depend. 80−2623
Cu complex, triazene-1-oxide complexes, EPR spectra in frozen nematic liq. cryst. glass 80−88871
Cu complexes, spin coupled ion pair, singlet-triplet splitting 77−85552
Cu complexes with glycine, in aqueous soln., EPR meas. 77−36115
$CuCl_4^{2-}$ anion, [g] tensor calcs. 77−28343
$DyFeO_3$, non Heisenberg R-Fe exchange interaction, behaviour in mag. field *(Russian)* 80−2568
Eu^{2+}, ground state fourth-order spin-Hamiltonian parameters 77−69278
EuO, Eu rich, insulator-metal transition, model Hamiltonian 78−2422
Fe complex, perchlorato(meso-tetraphenylporphinato) iron (III), mag. props., Mossbauer study 79−99802
Fe^{2+}, singlet ground state high-spin, in complexes with rhombic distortions, spectroscopic props. 77−51861
Fe^{3+}, cubic spin-Hamiltonian parameters in inorganic compounds, superposition model anal. 80−20367
Fe^{3+}, spin-Hamiltonion parameters, superposition model analysis 77−15798
$FeCO_3$, siderite, Fe^{2+} Mossbauer spectrum, ligand field theory 77−16212
$FeCs_2(SO_4)_2.6H_2O:VO^{2+}$, EPR, spin Hamiltonian parameters 79−19771
FeF_2, antiferromagnet, fourth-order spin Hamiltonian terms for Fe^{2+} 78−10628
FeF_2, theory of Raman scattering, coupled phonon-magnon excitations 78−72531
$Fe(H_2O)_6^{3+}$, in frozen aqueous soln., Mossbauer spectrum, hyperfine struct. 77−77130
$Fe(H_2O_6)^{3+}$ ion, amorphous frozen soln., Mossbauer study, hyperfine struct. 80−80644
$FeK_2(SO_4)_2.6H_2O:Mn^{2+}$, EPR spectra, spin-Hamiltonian anal. 77−77088
$Fe_{1-x}M_xCl_2$, disordered, Mn spin excitations by microwave absorption at high freqs. 80−34759
Fe^{3+} (^6S) paramagnetisations, spin lattice relaxation Mossbauer study, dynamic spin Hamiltonian formalism 80−97173
$FeSiF_6.6H_2O$, submillimetre EPR and zero field spectra, spin Hamiltonian 80−29604
$FeSiF_6.6H_2O:Mn^{2+}$, EPR line positions and intensities, spin Hamiltonian 79−65714
$FeTh_2S_5$, mag. struct. and props., neutron diffr. and mag. meas. 80−60201
$GaAs:Cr^{2+}(3d^4)$, Jahn-Teller distortion, photoinduced charge conversion, EPR 78−10758
$GaAs:Cr^{3+}$ ($3d^3$), EPR, 5K, evidence for strong Jahn-Teller effects 77−43875
GaP:Mn, ENDOR of cubic $^{55}Mn^{2+}$ 79−69749
GaSe:Mn, ESR spectra, influence of temp. and antiferromag. inclusions 79−99763
Gd^{3+}, ground state, fourth-order spin-Hamiltonian parameters 77−69278
Ge, μSR, spin Hamiltonian and anomalous muonium states 80−71286
Ge-S, glass, ESR, model of paramag. defects 79−78517
$GeO_2:Sc^{3+}(Y^{3+})(In^{3+})$, trapped-hole centres, ESR meas. 79−77597
^3He, HCP, and adsorbed ^3He with triangular lattice, exchange and mag. order 80−107606
^3He, solid mag., review 78−38906
^3He, superfluid, p-wave spin triplet pairing Hamiltonian, 5-D spin 80−75400
$(HfO_2)_{0.9}(Y_2O_3)_{0.1}:Cu^{2+}$, ESR at room temp., spin Hamiltonian parameter determ. 77−16167
$InP:Fe^{3+}$ (Cr^{2+}), EPR, symm., spin Hamiltonian parameters 78−10759
(K,Na) ($AlSi_3O_8$), feldspar, N^{2-} ESR spectrum parameters *(Ukrainian)* 79−38366
$KBr:Eu^{2+}$, spin Hamiltonian cryst. field consts. calcs. 79−38035
$KBrO_4$, UV- and X-irrad., ESR spectra of trapped O_2 78−84474
$KCN:HCN^-$, structural props. using ESR 80−25205
$KCdF_3:Gd^{3+}$, EPR, spin Hamiltonian parameters 79−65725
KCl, F centre pairs, ODMR, close and distant pairs 78−43691
KCl:Cd, EPR of anisotropic Cd_F^+ centres, similarity to Z-centres 77−77101
KCl:Eu, additively coloured, ESR obs. of $^{2+}$ complex 77−16170
$KCl:Eu^{2+}$, spin Hamiltonian cryst. field consts. calcs. 79−38035
$KF:U^{5+}$ EPR of U^{5+} centre meas. 77−20684
KH_2PO_4 type crystals, low lying ferroelec. modes, cluster dynamical theory 78−80305
KH_2PO_4-type crystal, LF dynamics 80−10602
$KH_3(SeO_3)_2:Cr^{3+}$, ferroelastic material, EPR, 77-300K 78−60331
$KMF_3:Mn^{2+}$, (M=Mg,Zn,Mn,Cd), zero-field splitting of Mn^{2+}, superposition model *(French)* 79−15267
$K_2MF_4:Mn^{2+}$, (M=Mg,Zn,Mn), zero-field splitting of Mn^{2+}, superposition model *(French)* 79−15267
$KMgF_3$, spin Hamiltonian parameters for Fe^{3+} ions, superposition model anal. 80−108053
$KMgF_3:Fe$, EPR temp. depend. 78−80202
$KMgF_3:Fe^{3+}$, superposition-model anal. of second- and fourth-order spin Hamiltonian parameters, EPR study 79−87311
$KMgF_3:V^{2+}$, ^{51}V ENDOR meas., spin Hamiltonian parameters 79−28638
$KMnF_3$, antiferromagnetic resonance in strong mag. field *(Russian)* 79−80054
$K_2O-B_2O_3:Mn^{2+}$ glass, fine struct. parameter distribs., EPR meas. 80−11256
$KTaO_3:Gd^+$, influence of external elec. field on EPR 78−15020
$KZnF_3$, spin Hamiltonian parameters for Fe^{3+} ions, superposition model anal. 80−108053
$KZnF_3:Gd^{3+}$, EPR, spin Hamiltonian parameters 79−65725
$KZnF_3:V^{2+}$, ^{51}V ENDOR meas., spin Hamiltonian parameters 79−28638
$La_2(SO_4)_3.9H_2O:Gd^{3+}$, single cryst., EPR study, spin Hamiltonians 80−80606
$LiAlSiO_4:Cu$, β-eucryptite solid electrolyte, Cu^{2+} EPR obs. of ion exchange props. 80−108056
$LiBaF_3:Cr^{3+}(Mn^{2+})(Fe^{3+})(Co^{2+})(Ti^{3+})$, EPR, spin Hamiltonian parameters 79−65718
LiCl:Cd, EPR of anisotropic Cd_F^+ centres, similarity to Z-centres 77−77101
$LiCl:Ni^{2+}$, EPR meas. of Ni^{2+} vacancy dipoles 79−28594
$LiGa_5O_8:Cr^{3+}$, antisymmetric exchange interaction, EPR study 79−47331
$Li_2O-B_2O_3:Mn^{2+}$ glass, fine struct. parameter distribs., EPR meas. 80−11256
$MgCr_2O_4$, magneto-electric splitting of crystal field Γ_2-level of Cr^{3+} ion, neutron spectroscopic obs. 79−19562
$MgK_2(SO_4)_2.6H_2O:Mn^{2+}$, EPR spectra spin-Hamiltonian anal. 77−77088
$Mg(NH_4)_2(SeO_4)_2.6H_2O:Mn^{2+}$, EPR spectra 80−100608
$MgO:Cr^{3+}$ (Mn^{2+}) spin Hamiltonian parameters, lattice expansion and vibr. effects 80−24851
$MgO:Fe^{3+}$ forbidden $\Delta m_s=2$ transitions in EPR spectrum 78−64267
$MgO:Mn^{2+}$ EPR, X-band freq., powder pattern for cubic symm. anal. *(Spanish)* 78−43636
$MgO:Mn^{2+}(Fe^{3+})$, EPR, 94-600K, temp. depend. of cubic spin Hamiltonian parameter 78−60332
$MgO:Pt^{3+}$, Jahn-Teller effect in EPR spectrum 80−7160
$MgO-Mn^{2+}$, Q band ESR spectrum, spin Hamiltonian calcs. *(French)* 78−64262
$MgRb_2(SeO_4)_2.6H_2O:Mn^{2+}$, EPR spectra 80−100608
$MgSiF_6.6H_2O:Co^{2+}$, spin Hamiltonians and pair interactions 77−36119
$MgTiO_3:Fe^{3+}(Mn^{3+})$, EPR spectra 79−91285
$Mg_2TiO_4:Cu(Ni)$, ESR of Cu^{2+} and Ni^{3+} 80−97131
Mn^{2+}, cubic spin-Hamiltonian parameters in inorganic compounds, superposition model anal. 80−20367
Mn^{2+}, powder pattern analysis in cubic crystalline fields 79−47327
Mn^{2+}, spin-Hamiltonian parameters, superposition model analysis 77−15798
$MnFe_2O_4$, exchange splitting of ionic S-state, neutron spectra 78−52240
Mo complex, influence of anisotropy of spin-Hamiltonian parameters on EPR spectra *(Russian)* 77−28432
$MoO_3:Re$, ESR and optical absorption obs. 77−36127
$NH_4Al(SO_4)_2.12H_2O:Mo^{3+}$, EPR, X-band, ion position and spin-Hamiltonian parameters 77−48042
$NH_4Cl:[MoOCl_5]^{2-}$, single cryst., struct. investigations 77−66524
$NH_4Cl:Ni^{2+}$, EPR spectrum, spin Hamiltonian, zero-field splitting effects 80−97135
$(NH_4)_2Co(SO_4)_2.6H_2O$, sbumillimeter ESR meas., SH^3 term of effective spin Hamiltonian 78−64264
$(NH_4)_2InCl_5:Fe^{3+}$ EPR, site g-tensor, spin Hamiltonian factors 77−63270
$(NH_4)_2SeO_4:VO^{2+}$, EPR spectrum 79−61207
NaCl:Cd, EPR of anisotropic Cd_F^+ centres, similarity to Z-centres 77−77101
$NaCl:Cu^{++}$, EPR spectra anal. spin-Hamiltonian parameters determ. *(Spanish)* 77−69673
$NaCl:Eu^{2+}$, spin Hamiltonian cryst. field consts. calcs. 79−38035
$NaCl:Eu^{2+}(Mn^{2+})$, ESR and elec. field effects 77−28441
$NaF:K^+$, γ-irradiated, $H_A(K)$ centres, EPR obs. 77−69689
NaN_3, X-irrad., EPR of N_2^- 77−66421
$NaNbO_3:Mn^{2+}$, ESR, temp. depend., −269-750°C, fine splitting 77−51948
$Na_2O-B_2O_3:Mn^{2+}$ glass, fine struct. parameter distribs., EPR meas. 80−11256
$Na_2O-SiO_2:Cu^{2+}$ glass ESR and optical absorption 79−77526
$Na_2S:Gd^{3+}$, EPR and ENDOR meas., spin-stress Hamiltonian 77−63278
$Na_2Zn(SO_4)_2.4H_2O:VO^{2+}$, EPR spectra at X-band, spin-Hamiltonian parameters 79−56606
$Na_2Zn(SO_4)_2.4H_2O:Ag^{2+}$, EPR, Ag^{2+} dimeric struct., hyperfine and fine struct. tensors 77−51949
Nd^{3+}:scheelite-type crysts., magnetic, thermal properties, cryst. field calcs. 78−91875
$Nd_3Mg_3(No_3)_{12}.24H_2O:Mn^{2+}(Gd^{3+})$, EPR spectra, spin Hamiltonian anal. 79−33527
$Nd_2(SO_4)_3.8H_2O:Gd^{3+}$, EPR, zero field splittings, spin-Hamiltonian parameters 78−91949
$Ni(BF_4)_2.6H_2O$, EPR, cryst. field symmetry 79−28593
$NiBr_2.6H_2O$, antiferromag. ordering and paramag. behaviour 78−14941
$NiBr_2.6H_2O$, small anisotropy, spin Hamiltonian fit of susceptibility 77−69587
$Ni(NH_4)_2(SO_4)_2.6H_2O$, Mn^{2+} doped, EPR study 80−34763
$Ni(NO_3)_2.4H_2O$, two spin ordered states under mag. field 79−15308
$NiSO_4.7H_2O$, Mn^{2+} doped, EPR study 80−34763
$NiSiF_6.6H_2O$, single cryst., EPR, 77-300K, Debye temp. 77−85551
$Pb_5Ge_3O_{11}:Gd^{3+}$, EPR hyperfine struct. 79−82867
$Pb_3(PO_4)_2:Gd^{3+}(Eu^{2+})$, EPR spectra of α- and β-phases 80−11261
$PbWO_4$, EPR of radiation induced MoO_4^{3-} centres 78−80217
Pr, magnetisation and magnetostriction in pulse fields from 3-78K 79−99747
$PrAlO_3$, tetragonal, mag. props. 77−90052
$PrVO_4$, energy levels, opt. and NMR meas. 78−80226
α-quartz:Ge,Ag^+, Ag-compensated Ge centre, EPR meas. 77−77098
α-quartz:P, X- and γ-irradiated, EPR studies of phosphoric ion 77−63263
$RbAl(SO_4)_2.12H_2O$, ENDOR of $^{57}Fe^{3+}$ in trigonally distorted octahedral sites 79−38405
$RbAl(SO_4)_2.12H_2O$, spin-Hamiltonian with trigonal S^3I terms for describing $^{57}Fe^{3+}$ ENDOR spectra 80−75885
$RbCaF_3$, V_K centres, lattice distortion in tetragonal phase, EPR meas. 77−20699

spin Hamiltonians continued
$RbCaF_3:Gd_2O_3$, Gd^{3+}-O^{2-} pair, EPR study of displacive transform. *(French)* 78−27088
RbCl:Eu^{2+}, EPR of $^{153}Eu^{2+}$ and $^{151}Eu^{2+}$ 80−11259
RbCl:Eu^{2+}, tetragonal sites, spin Hamiltonian parameters, EPR and UV absorpt. spectra obs. 80−50177
RbCl:Mn^{2+}, spin-Hamiltonian parameters anal., superposition model applicability 79−28592
$RbGa(SO_4)_2.12H_2O$, ENDOR of $^{57}Fe^{3+}$ in trigonally distorted octahedral sites 79−38405
$RbGa(SO_4)_2.12H_2O$, spin-Hamiltonian with trigonal S^3I terms for describing $^{57}Fe^{3+}$ ENDOR spectra 80−75885
$RbH_3(SeO_3)_2$: VO^{2+}, EPR spectra, spin Hamiltonian parameters 80−100609
$RbIn(MoO_4)_2:Fe^{3+}$ monocrystals, EPR spectrum in the phase transition neighbourhood 80−2624
$RbMF_3:Mn^{2+}$, (M=Mn,Cd,Ca), zero-field splitting of Mn^{2+}, superposition model *(French)* 79−15267
$RbMgF_3:Mn^{2+}$, EPR obs. and struct. interpret. *(French)* 80−50167
$ReNCl_4^-$, EPR in $Ph_4As[RuNCl_4]$, hyperfine splitting and spin Hamiltonians 78−64272
Si, μSR, spin Hamiltonian and anomalous muonium states 80−71286
Si, paramagnetic defects produced by electron irrad., EPR 79−19779
Si:B, ESR at zero and small external stress, interpreted in spin Hamiltonians 78−43641
$Sm_2(SO_4)_3.8H_2O:Gd^{3+}$, EPR, zero field splittings, spin-Hamiltonian parameters 78−91949
$SrCl_2:Fe^{3+}$, EPR spectra of $Fe^{3+}(^6S_{5/2})$, 4-100K 78−95512
$SrF_2:Tm^{2+}$, EPR meas. of Tm^{2+} ion pair interactions 79−95641
SrO:Mn^{2+}, EPR expts. 77−20691
TGSe:Cu^{2+}, EPR studies, spin Hamiltonian parameters 80−7153
$TiO_2:Fe^{3+}$, rutile, temp. depend. of spin Hamiltonian parameters, ESR meas. 77−32251
$TiO_2:Fe^{3+}$, uniaxial stress method for determ. of spin-lattice coeff. for Fe^{3+} 77−90018
$TiO_2:Mn^{2+}(Mn^{4+})$, anatase single cryst., ESR spectra at 77K, 300K 78−10764
$TlCdF_3:Mn^{2+}$, zero-field splitting of Mn^{2+}, superposition model *(French)* 79−15267
TmSe, mixed valency, field-depend. mag. transitions 78−10657
V^{4+}, cryst. field effect on ESR parameters 77−36116
$V_2O_5:Fe^{3+}$, EPR, 5-300K 77−81002
$mV_2O_5.(100\text{-}m)P_2O_5$, (m=100-2), V(IV) complexes conc., absorpt. and ESR spectra 78−64266
$YAlO_3$:Pr, hyperfine interaction in lowest levels of $^3H_4$ and $^1D_2$ states 79−78065
$YCrO_3$, bubble domain struct. temp. depend. 80−71137
YIG, film, spin wave reson., complex mag. surface energies 77−4561
YIG, magnetocrystalline surface anisotropy energy, one-ion mechanism 79−78362
YIG:Si(Ge), Fe^{2+} spectroscopic props., nontrigonal cryst. field effects 80−44553
YbIG, mean field phase diagrams 78−23269
$Zn(BF_4)_26H_2O$:Ni, phase transition study, EPR of diluted Ni^{2+}, 98-298K 80−75846
$ZnCs_2(SO_4)_2.6H_2O:VO^{2+}$, single cryst., X-band EPR meas. 77−90024
$ZnGa_2O_4:Fe^{3+}(Mn^{2+})$, EPR, spin Hamiltonian parameters 80−25195
$ZnK_2(SO_4)_2.6H_2O:Mn^{2+}$, EPR spectra, spin-Hamiltonian anal. 77−77088
$Zn(NH_4)_2(SeO_4)_2.6H_2O:Mn^{2+}$, EPR spectra 80−100608
$ZnRb_2(SeO_4)_2.6H_2O:Mn^{2+}$, EPR spectra 80−100608
ZnS:Mn^{2+}, cubic, EPR, ENDOR 77−77093
ZnSe, two-photon absorpt. spectra, spin Hamiltonian for Wannier excitons 77−52124
ZnSe:Mn^{2+}, refined spin Hamiltonian parameters *(French)* 77−63268
ZnSe:Ti^{2+}, EPR meas. 80−80594
ZnSe(Te):Cr^{2+}, spin Hamiltonian parameters and wave function coeffs., LCAO theory 77−39804
$ZnSiF_6:Cu^{2+}$, spin-spin interactions of impurity pairs *(Russian)* 78−72397
$ZnSiF_6.6H_2O:Co^{2+}$, spin Hamiltonians and pair interactions 77−36119
$(ZrO_2)_{0.9}(Y_2O_3)_{0.1}:VO^{2+}$, ESR of V^{4+} at room temp., spin Hamiltonian parameter determ. 77−16167

spin-lattice relaxation
see also electron spin-lattice relaxation; nuclear spin-lattice relaxation
acetic acid, $-d_1(=d_4)$ liquid, molecular motion, proton spin echo study *(Russian)* 80−32745
anisotropic spin-phonon coupling model, exact solutions *(Russian)* 80−100590
antiferromagnet, phonon-magnon relaxation times, external mag. field depend. 80−44898
bacteria, photosynthetic, triplet-state EPR spin polaris., intramol. model 78−44469
benzene, liq., mol. motion at high press. 80−103509
benzil crystals, triplet state spin-lattice relaxation, zero field magnetic resonance spectrometer analysis 79−97409
binary mixtures, NMR longit. relax., mole fraction depend. 77−61767
biological cells, classical diffusion to explain 'H spin relax. in NMR obs. 79−83721
blood plasma 'H NMR relax. rates, cancer-induced decrease obs. 80−56075
n-butane, solid, mol. reorientation, PMR 77−8431
cellulose, mobility of adsorbed water, NMR pulse obs. 80−108835
4-cyano-4′-d_{17}-n-octylbiphenyl, D spin-lattice relax. time, partially averaged quadrupole tensors 77−1076
cyanoacetylene, liquid, N and ^1H relax. rates using pulsed NMR *(French)* 79−38394
cyclic carbonates, supercooled liqs., dielec., acoustic, NMR, viscoelastic relax. props. 77−1609
deoxyhaemoglobin, proton NMR, modified DEFT technique for obs. hyperfine shifted line, T_1 values meas. 80−76871
diamond, spin-spin interaction of N_2 and Ni centres, temp. effects 78−88177
4,4′-dichlorobenzophenone, cryst., X-traps, rel. populations, elec. field effect 77−12414
dichloromethane-d_2, spectral densities determ. from spin-lattice relax. and spin-echo decay rates 80−75877
dimethylformamide, intramolecular exchange rate determ. from ^{13}C spin-lattice relax. times 80−69169

spin-lattice relaxation continued
exciton ferromagnet, spin-lattice relax., light and US absorption *(Russian)* 79−7960
ferromagnet in mag. field, spin relax., crit. anomalies 78−43669
first order spin-spin multiplets, $AX \rightleftarrows BY$ system, T_1 spin decoupling and chem. exchange 77−71818
intermolecular mechanics, T_1 and T_2, by microwave meas., zero- and non-zero field 79−45738
intracellular water, effect of paramag. impurities on proton spin-lattice relax. 80−51134
intracellular water, two-fraction fast-exchange model of spin-lattice relax. 77−60192
linear defects, local phonon modes and structural instability *(Russian)* 79−73275
macroradical, electron spin echo spectra, instantaneous and conventional spectral diffusion 79−15355
magnetic susceptibility, AC, depend. on magnitude meas. field 80−241
mathematical formulation for selecting optimal parameter for meas. of relaxation times 80−62703
MBBA, dynamic critical behaviour in NLC above nematic-isotropic transition 80−49096
memory function for spin relaxation graphical representation 77−24733
methyl (CH_3D) group tunnelling in solids, quantum model rel. to two T_1 temp. depend. minima 78−2028
methylammonium bromide, solid, phase transitions, PMR, DTA study 80−107421
1-methylimidazole complexes, with ferriporphyrins, PMR obs. 77−12214
molecular crystals, spin-lattice relax. theory 79−15337
multi-level system, relax., double resonance, resistance network analogues 77−1583
muscle, mouse, NMR multiwindow anal. and proton local fields and magnetisation distrib. 80−21444
muscle, skeletal, Na relaxation, spin echo study, evidence of Na ion binding inside a biological cell 78−88698
muscle, skeletal, water protons NMR relax. times anisotropy obs. 80−85341
muscle water, study of spin-lattice and spin-spin relax. times of ^1H, ^2H, and ^{17}O 80−21443
naphthalene: quinoxaline, anisotropic spin lattice relax. of triplet mols. in high mag. field 77−81141
naphthalene:quinoxaline, spin-lattice relax. of triplet states of high mag. fields 79−19933
nematic liquid crystals, continuum theory of disorder, nuclear magnetic relaxation 77−31592
NMR in coupled spin systems, review 78−48072
nuclear magnetisation, temp. dependence 79−33462
organic solid, exciton motion effect on proton relax. 78−14671
PAA, methyl group rotation in solid and nematic phases, NMR obs. 78−6595
paramagnetic impurities undergoing reorientation 77−16153
phenazine, zero field studies of spin lattice relaxation in excited triplet states 79−18219
phosphatidylcholine-cholesterol vesicles interacting with lucensomycin, PMR obs. 80−40954
phosphorescent triplet state, spin-lattice relax. mechanism *(Russian)* 78−68542
porphyrin, triplet-state EPR spin polaris., intramol. model for photosynthetic bacteria 78−44469
proton relaxation times prolongation, regionally ischemic dog heart tissue 80−101216
pulsed NMR data acquisition system, devel., appl. to polyisobutylene 80−34807
pyrazine, zero field studies of spin lattice relaxation in excited triplet states 79−18219
pyrimidine, zero field studies of spin lattice relaxation in excited triplet states 79−18219
quantum lattice systems, linear response and relaxation functions 80−4659
quinoxaline, zero field studies of spin lattice relaxation in excited triplet states 79−18219
randomly coiled polymer, in solution, models for spin relaxation 77−85607
rare earth compounds, cryst. field effects on EPR and NMR 79−4736
reorientation and spin-lattice relaxation due to a tunnel-controlled mechanism 79−28585
ruby:Ni, cross relaxation 78−39389
ruby, high energy phonon spectroscopy 78−83893
ruby, high mag. field spin-lattice relaxation rate of Cr^{3+} 78−52340
SQUID NMR meas. at low-temp., improved technique 78−54417
Δ^5-steroids, methyl group rot. barriers from ^{13}C relax. data, geometry effect 78−13626
TCNQ salt, Rb-TCNQ, electronic spin-lattice relax. time 77−51939
terpenes, methyl groups internal rotation, ^{13}C spin lattice relaxation times and force field calcs. 80−74255
tetrafluoromethane, liq., mol. reorientation 80−106320
three-level system transition probabilites, molecular motion anisotropy by quadrupole relaxation 80−18867
time measurement using saturation, inversion and fast inversion recovery expts. 80−57356
tissues, normal and malignant, pulsed NMR obs. 80−94171
TMMC, symmetry crossover in spin dynamics, proton spin lattice relax. calc. 77−40147
1,3,5-trichlorobenzene, ^{35}Cl spin-lattice relaxation under press. 79−4738
triplet exciton annihilation rate, magnetic field depend. effect of spin-lattice relaxation 80−65459
TTF-TCNQ, electronic spin-lattice relax. time 77−51939
tumour development kinetics obs. by PMR 79−70578
tumour-bearing animals, proton magnetic resonance study 79−70577
two spin system in molecular medium, time correl. functions 77−32275
ultraslow motion, Slichter and Ailion spin-lattice relaxation times 80−44899
vinyl bromide-d_3, ^{13}CBr bond, coupling consts., correl. with C hybridisation s-character 80−34806
water molecules in biological systems, relax. rel. to vol., pulse NMR obs. 80−40960
$Al_2SiO_5:Fe^{3+}$ 77−73076
$Al_6Si_2O_{13}:Fe^{3+}$, mullite:Fe^{3+}, Mossbauer exam. of relaxation behaviour of Fe^{3+} 77−1620
^9Be, nuclear mag:spin-lattice relaxation times 78−86889
^{13}C-labelled organic radicals, ^{13}C- and proton-ENDOR in soln. 78−55190

spin-lattice relaxation continued
CaD_2, neutron diffr., NMR 77−15378
$CaSO_4.2H_2O$, mol. reorientations and mol. diffusion, PMR 78−43671
CdS pulsed optically detected resonance, time depend. recomb. processor study 79−38411
$CdS:Mn^{2+}$, doped, spin-lattice relax. exam. 77−40120
$CoCs_2(SO_4)_2.6H_2O$, obs. of H^2T^7 Raman spin-lattice relax. process 77−51459
$CoK_2(SO_4)_2.6H_2O$, obs. of H^2T^7 Raman spin-lattice relax. process. 77−51459
$Co(NH_4)_2(SO_4)_2.6H_2O$, obs. of H^2T^7 Raman spin-lattice relax. process 77−51459
Cr, antiferromagnetic, muon diffusion, spin relax. and coherent motion 80−71281
^{133}Cs, nuclear mag:spin-lattice relaxation times 78−86889
Cu-Fe alloy, dil. dynamic susceptibility around T_k, satellite nucl. spin-lattice relax. time meas. 77−4573
D probe spin alignment for obs. ultraslow mol. rot. 80−88890
p-GaSb, interband optical pumping, optical detection of EPR 77−28483
Gd-Al, amorphous film, microwave mag. reson. 78−91948
Gd-Al, amorphous film, microwave mag. reson. 78−92060
H_2-He(Ne), NMR longit. relax., mole fraction depend. 77−61767
H_2O proton relaxation in normal and cataractous cryst. lens 77−60203
He^3-He^4 mixture, relax. of 2^3S_1 metastable atoms 80−102469
^3He, spin relaxation to paramagnetic centres, in surfaces at very low temps. 79−33552
^3He superfluid, A and B phases, pulsed NMR, nucl. susceptibility, spin-lattice relax., freq. shifts 78−47628
^3He, superfluid, transport and relax. processes close to transition temp. 77−55411
^{199}Hg nuclear shielding anisotropies rel. to isotropic chem. shifts in methyl mercury compounds 77−3384
KBr, spin-lattice relaxation time of relaxed excited state of F-centre, MCD meas. 79−61350
KCl:Li, 9.4 GHz pulse paraelec. reson. at zero elec. field 77−81076
KD_2PO_4, dispersion, central mode evidence 78−15108
KD_2PO_4, relaxation rates, temp. depend., field depend. 78−88208
KH_2PO_4, relaxation rates, temp. depend., field depend. 78−88208
KI, spin-lattice relaxation time of relaxed excited state of F-centre, MCD meas. 79−61350
$K_2Pt(CN)_4Br_{0.3}.3H_2O$, quasi one-dimens. conductor, EPR linewidth 80−54938
LaF_3, self diffusion studied with ^{19}F relaxation 78−6180
Li-NH_3 concentrated solution, NMR relaxation of ^7Li 80−108084
$LiScO_2:Fe^{3+}$, Mossbauer exam. of relaxation behaviour of Fe^{3+} 77−1620
^6Li, nuclear mag:spin-lattice relaxation times 78−86889
$MgO:Fe^{3+}$, spin-lattice relax. 77−90037
MnO, paramagnetic, positive muon longit. spin relax., temp. depend. 78−80268
MnSi, μ^+ probe, itinerant electrons spin fluctuations 79−56671
MnSi, μ^+ spin-lattice relax rate, paramag. phase, near T_c, temp. depend. 79−19825
Mo-Co Kondo alloy, Co impurity susceptibilities, Knight shift 80−88721
$NH_3(D_3)$, liq., longitudinal proton and deuteron relaxation rates, press. and temp. depend. 80−44941
$(NH_4)_2MCl_6$, (M=Pd, Pt, Te, Ru, Ti, Ir and Re), proton relaxation and tunnelling 79−4737
$NaH_3(SeO_3)_2$, dispersion, central mode evidence 78−15108
$NiSiF_6.6H_2O$, single cryst., EPR, 77-300K, Debye temp. 77−85551
$(Ni_{1-x}X_x)_{99}Mn$, X=Rh, Fe, Mn, ferromagnetic, NMR study of local environment effect, relaxation mechanism 80−7193
Pd-Fe alloy, NMR of ^{27}Al meas. 77−12215
PdGdH, diagram of state elec. props., indirect exchange interaction, EPR study *(Russian)* 80−50179
Si, Jahn-Teller Mn^0 centre ESR spectrum, depend. on axial press. 80−44911
Si:Cr, spin-lattice relax. of Jahn-Teller Cr^0 centre *(Russian)* 78−72402
$Si:Cr^+$ EPR spectra and spin state population inversion with unpolarised optical lighting *(Russian)* 80−44909
n-Si:P, optical orientation of ^{29}Si and its depend. on pumping light intensity *(Russian)* 77−4581
Te, enriched with ^{125}Te, spin-lattice relaxation and Knight shift, high temp. behaviour 77−1614
$ThO_2:U^{4+}$, spin-lattice relax. time calc., nearest neighbour point charge model 77−16146
$YAlO_3:Yb^{2+}$, mag. relax., Mossbauer expts. 79−8078
$Zn_xCn_{0.1}Fe_{2.9}O_4$, Cu, Zn substituted magnetite, domain wall resonance, mag. props. 80−15756
$ZnS:Co^{2+}$, EPR and spin-lattice relax. of Co^{2+} centres *(Russian)* 79−1706
$ZnSiF_6.6H_2O:Ni^{2+}$, EPR 77−59451

spin-orbit interactions
6d metal superheavy hexafluorides, relativistic mol. calcs. 80−5484
$^{16}O(p,p)$, spin orbital interaction and nucl. matter density distrib. *(Russian)* 79−22176
actinide compounds, neutron scatt. studies 80−75716
actinide ions, electronic props., Dirac-Fock studies 78−60094
actinide oxides, chem. bonding, mol. cluster theory 80−10526
activated crystals, Jahn-Teller effect in optical bands of impurity centres 78−6706
alkali chloride: V^{2+}, phonon induced zero field splitting 78−39073
alkali halide, chalcogen^{2-} vacancy centres, absorpt. and fluoresc. spectra 78−48204
alkali halide phosphors, Tl^+ doped, uniaxial stress effects 78−48202
alkali halides, F-centres, optical pumping, spin-orbit and hyperfine coupling 77−16360
alkali halides, heteronuclear XY^- defects, spin Hamiltonian parameter anal. 80−88509
alkali halides, thermoreflect. spectrum, 5 to 9 eV, electronic struct. 77−81123
alkali metal atom, outer-shell photoelectron ang. distrib. 80−37797
alkali metal atoms, spin-polarised, near-reson. two-photon ionis., light polarisation effects 80−106308
alkali metal halide crystals, g-tensor anal. of S− and Se^- centres, ESR 80−84650
amorphous metals, mag. anisotropy, spin glass like phase 77−66295
anisotropic spin-phonon coupling model, exact solutions *(Russian)* 80−100590

spin-orbit interactions continued
β-F-9,10-anthraquinone, internal heavy atom effect, vibronic phosphoresc. spectrum, intermol. spin-orbit coupling 78−82774
9,10-anthraquinone, Shpolskii quasi-line phosphoresc. spectra, electronic-vibrational interactions 78−55196
antiferromagnetic semiconductor, magnon-plasmon interaction and its effect on Raman scatt., theory 78−56302
antiferromagnets, mag. anisotropy in spin density wave state 77−69540
aromatic compounds, intersystem crossing theory, El-Sayed rule extension, anomalous rate consts. 77−30911
aromatic hydrocarbons, intersystem crossing mechanism, rate consts. 77−65497
asymmetric scattering, spin-1 particle by non-central field 78−55214
asymmetric top molecules, doublet-quartet transitions, rot. selection rules 78−94186
atom, K_α hypersatellite ratio, intermediate coupling 77−3296
atom, transition array and energy level distribs. variance, Mo VX-XIV appl. 80−37767
atom+atom collisions, in laser field, ang. momentum anal., quantum mech. theory 78−74733
atomic data handbook 77−23398
atomic f^5-configurations, sextet states spin-orbit parameters, Gelfand-Harter method 77−50345
atomic structure, spin-other orbit and spin-spin interactions 80−913
atomic structures 79−63896
atomic vapour, f-value determ. method using stimulated electronic Raman scatt., appl. to Cs 78−82693
aza-aromatic molecules, intersystem crossing, quantum interference effects 80−53037
benzaldehyde, $n\pi^*$ and pi pi* triplet states, props., SCF calcs. 77−6695
$^3\pi\pi^*$benzaldehyde, zero field splitting and sublevel decay rates, deuteration and host effect 80−37750
benzaldehydes, in mixed cryst., T_1/T_2 interstate interactions, modulation polaris. phosphoresc. spectra, 4.2K 78−9185
1,2-benzocoronene, phosphoresc. and ODMR meas. 79−18220
benzophenone, triplet, optically detected EPR, ENDOR and ODMR, HFS, isotope and spin-orbit effects 78−86898
benzophenones, triplet state fine struct. parameters and phosphoresc. spectra 79−50065
biaryls, nonplanar, spin-orbit coupling effects, luminesc. quantum yields *(German)* 77−42349
biological systems, containing Fe, electronic and mag. struct., semiempirical MO cluster calcs. 78−62733
Bloch electrons, weak magnetism, spin and spin-orbit interactions *(Russian)* 79−33443
bremsstrahlung by transversely polarised electrons, azimuthal asymmetry due to spin-orbit coupling 80−60705
broadening, inhomogeneous and homogeneous, of optical and ODMR transitions in solids 80−32750
bromobenzene ion fragmentation, photoelectron-photoion coincidence spectra 80−95682
bromoethane, and -d_5, first s-Rydberg transitions 78−42094
N-bromosuccinimide, X-irrad., ESR study of Br and σ^* radical 80−66037
bromotrifluoromethane, photoelectron spectra, spin-orbit splitting, vibr. fine struct. 78−21974
C_{3v}-type mols., double degenerate electronic states, Jahn-Teller and spin-orbit coupling 78−50537
calcium tartrate tetrahydrate:Cu^{2+}, spin-orbit coupling, optical absorpt. spectra 80−45120
camphorquinone, cryst., PMDR and fluoresc., S_2 state, intersystem crossing 77−32296
charge and spin density wave effects 79−91009
charge transfer, resonant, spin depend. *(Russian)* 78−29850
chlorophyll b derivatives, metal substitution effect on triplet state, intersystem crossing 77−88476
chloroquinolines, photophys. behaviour, substituent and solvent effects 80−106342
chromocene, solid, Raman transition assignments, mag. susceptibility, mag. moment 78−43861
combined spin-orbit and Jahn-Teller coupling, method of soln. 79−60773
complex specta, theory, tableau matrix elements, vector coupling approach 77−67996
compressed D_{4h} cluster, g_{zz}-g_0 value 77−80756
copper porphin, Zeeman expt. on phosphoresc. triplet and quartet states 79−33786
copperporphin, metastable quartet state radiative decay 80−23453
coronene, luminesc., spin-orbit coupling perturbation by metal chlorides *(German)* 80−1021
critical molecules, neutron scatt., 'optical activity' 80−23567
cubic complexes, weak-field coupling scheme 80−92866
cyanide radical spin-orbit relax., methyl isocyanide photodissoc. 78−73063
$d^{3,7}$-configurations, weak field energy matrices calcs. with nonzero spin-orbit coupling 78−76029
$d^{4,6}$-configurations, weak field energy matrices calcs., spin-orbit coupling effects 78−76030
d^5-configurations, weak field energy matrices calcs. 78−76031
(d,τ) reactions, 52 MeV, analyzing powers, spins of proton hole states 78−25111
DC Fano effect polarised electron source appl. to electron-atom scatt. 78−66689
dialkylammonium copper chlorides, mag. and struct. transitions, IR absorption 77−52097
diamond:N, spin-lattice relax. of Jahn-Teller N centre 77−66412
diamond, natural, free exciton luminesc. line shape 80−40165
diamond and sphalerite type crystals, energy levels of indirect excitons 80−15457
diamond and sphalerite type crystals, with spin-orbit interaction, indirect exciton energy levels 80−24804
diamond-type crystals, energy levels of Mott excitons 78−6282
diatomic alkaline earth halides, multiplet splitting, extended Huckel approach 80−74127
diatomic molecule, nucl. spin-rot. interaction const., electron spin current contrib. 80−23441
diatomic molecule, singlet-triplet perturbations, spin-orbit interaction, matrix elements 77−10653
diatomic molecules, hydrides, oxides and BeF, spin orbit coupling const., ab initio calcs. 80−63537
diatomic mols., doublet states, spin-orbit and spin-rot. coupling cals., isotope depend. 77−57902

spin-orbit interactions continued
diazanaphthalenes, excited state absorpt. spectra and intersystem crossing kinetics 80−74176
1,2,5,6-dibenzocoronene, phosphoresc. and ODMR meas. 79−18220
1,4-dibromonaphthalene, phosphorescence microwave photoexcitation spectrum (PMPS) 77−32294
dichloronaphthalenes, heavy atom effects on subrates of lowest triplet states, MIDP obs. 80−91594
1,8-dichlorooctane, quadrupolar relax. centres, limited spin diffusion 80−100649
9,10-dichlorophenanthrene, intramol. heavy atom effect, PMDR obs. 79−13745
diethyl cadmium, core d-level high resolution photoelectron spectra, spin-orbit splitting 78−50579
dihalogenoacetylene radical cations, $C_2X_2^+$, emission spectra, $A^2\Pi \rightarrow X^2\Pi$ band systems 78−17679
dimer triplet state line shape, small excitons, appl. to phenazine, naphthalene, tetrachlorobenzene 80−48041
dimethyl cadmium, core d-level high resolution photoelectron spectra, spin-orbit splitting 78−50579
dimethyl cadmium, photoelectron spectra, 4d spin-orbit splitting, crystal field and band-broadening effects, CNDO calcs. 78−76577
dimethyl ether, orbital calc. *(Russian)* 78−66461
dimethyl sulphide, orbital calc. *(Russian)* 78−66461
dimethyl zinc, core level photoelectron spectra, electric field gradient splittings 77−88494
dimethyl zinc, valence band and Zn 3d levels, electric field gradients 77−88495
dimethylbenzaldehydes, in durene single cryst., zero-field splitting, guest and host isotope effects 80−107752
dinaphtho-(2′.3′:1.2);(2″3″:6.7)-pyrene, triplet state, phosphoresc. and ODMR obs. 79−27013
dipolar interaction, reduction by off-resonance phonon avalanche 77−63260
dipole absorption oscillator strengths, simple approx. method for computing radial wave functions 78−62111
direct-gap semiconductors, charged excitons 77−62840
disordered electronic systems, spin interaction effects, loop expansion and exact relations among local gauge invariant modes 80−80221
double folding pot. for inelastic scatt. between nuclei 80−13425
dynamic Jahn-Teller systems, calc. of absorption band shapes, use of Lanczos algorithm 80−45023
electrical resistivity with spin-orbit scatt. 78−64018
electron-photon coincidence expts., interpretation 80−83489
EPR parameters for orbital singlet of d^1 ion in cryst. 78−10751
EPR spectra of stable radicals, slow molecular motion study, review 80−25212
equivalent electrons, J allowed values in jj coupling 80−90624
evolution operator factorisation, S=1/2, arbitrary L, in mag. field 77−14376
exciton dielectric, spin-orbit interaction, effect on electron-hole pairing *(Russian)* 79−7790
exponential transformation, quadratically convergent SCF procedure, appl. to closed shell ground states 80−47875
F-centre, vibronic scheme of relaxed excited state 79−90989
F-centre optical absorption bandshape calc. for transition to state with Jahn-Teller and spin orbit couplings 80−55135
Fano effect in photonuclear reactions? 80−519
Fermi velocity calc., linear muffin-tin orbital method 79−28272
ferromagnet, itinerant electron, magnetoresist. and anomalous Hall effect due to electron-phonon interactions 80−70680
ferromagnet, spin-orbit interaction effects on spin-wave resonance *(Russian)* 77−90039
ferromagnetic 3d metal film, rel. to linear mag. birefr. dispersion interpretation 77−69807
ferromagnetic disordered binary alloy, CPA theory of magnetoabsorption, electron scatt. mechanisms *(Russian)* 77−8549
ferromagnetic metals, resist. anisotropy, crit. behaviour and temp. depend. 80−96858
ferromagnets, phase transformation theory, easy axis anisotropy, quadrupole interaction, renormalisation method calcs. *(Russian)* 79−65671
ferrous porphyrin, intermediate (S=1) spin state, PMR characterisation 80−48014
ferrous tetraphenylporphyrin, Mossbauer effect, mag. hyperfine interaction 79−24236
formaldehyde, $^3A''$ state, zero-field splitting param., ab initio CI calcs. 80−99454
formaldehyde, vibronic and spin-orbit coupling, radiative and non-radiative transitions 77−3414
frozen spin state, static susceptibility, piezomag. effect 77−51914
garnets, mag. props. of V^{4+} ion, effect of covalency 78−64010
group theoretical analysis of origin 79−91008
haloacenaphthenes in n-heptane, quasi-line phosphoresc. spectra, vibronic spin-orbit interaction 80−43096
haloanilines, T_1-states, EPR and zero-field ODMR obs. 78−58725
haloanisoles, T_1-states, EPR and zero-field ODMR obs. 78−58725
halobenzonitriles, T_1-states, EPR and zero-field ODMR obs. 78−58725
halofluorescein dyes, fluoresc. internal conversion, intersystem crossing 77−3405
halogen atom, ^2P state, pot. energy surface complex intersection 77−77736
halogen atom (^2P)+inert gas atom (^1S), coupled channel study, rel. to elastic approx. 79−81255
halogenoacetylene radical cations, C_2HX^+, emission spectra, $A^2\Pi \rightarrow X^2\Pi$ band systems 78−17678
halomethanes, vibronic struct. in electron spectra, Jahn-Teller and spin-orbit coupling 78−50537
1-halonaphthalenes, lowest triplet state, spin sublevels decay, internal heavy atom effects 79−95819
Hartree-Fock calcs. of semi-infinite nuclear matter with complete forces (finite range and spin-orbit term) 78−86499
HCP metals, mag. susceptibility near $2^1/_2$th order electron transition, non-linear magnetisation anal. *(Russian)* 80−44859
heat magnetization in the singlet-triplet model 78−64211
heavy ion collisions, rotational transitions, effect of spin-orbit coupling 78−13573
heavy-ion elastic scatt. pots., spin-orbit terms, appl. to (^{6}Li,^{6}Li) 78−66313
heteroaromatic molecules, planar, orientation and phosphoresc. polarisation in stretched film 80−14169
high angular momenta levels 79−54918

spin-orbit interactions continued
high spin/low spin transition, model including lattice dynamics 77−63202
high-Z elements subshells, photoelectron angular distribution 80−99487
homogeneous linewidths in ODMR and optical transitions, connection 79−91316
hydrogenic atom in weak mag. field, polarisability, ground-state energy 79−3594
hydrogenlike atoms, spin-orbit terms derivation 80−73148
II_3V_2 semiconductors, spin-orbit and cryst. field splittings of valence band 78−63980
II-IV-V_2 semiconductors, heat of formation from spin-orbit splitting in valence bands 77−31985
induced electronic transitions, radiative lifetimes, non-Condon effects 80−53051
inert gas atom, first excited config., intermediate coupling coeff. 80−83450
inert gas dimer ions, $A^2\Sigma_{1/2u}^+ \rightarrow D^2\Sigma_{1/2g}^+$ system, theoretical absorption spectrum 80−32734
iodomethane, first s-Rydberg transitions 78−42094
iodotrifluoromethane, photoelectron spectra, spin-orbit splitting, vibr. fine struct. 78−21974
ion+atom collision, electron spin coupling in rot. frame, X-ray emission 79−36724
irreducible tensor operator methods in strong-field coupling 79−7811
itinerant electron ferromagnet, effective Lorentz force and Landau level 78−80120
Jahn-Teller centre optical band polarisation dichroism, forbidden transitions 80−55062
Jahn-Teller effects, ion-lattice and spin-orbit coupling 77−66143
Jahn-Teller impurity centres, piezo-optics and magneto-optics 78−39579
Jahn-Teller problem, $T \times e_g$, spin-orbit allowed tunnelling splitting, zero-phonon line splitting 78−19006
jj-coupling, one-particle matrix element calculation program 79−13624
Josephson coupled layered supercond., upper critical field *(Russian)* 80−100551
lanthanide atomic vapours, (Sm, Eu, Dy, Ho, Er, Tm, Yb,) photoabsorption spectra 77−88417
lanthanides, doubly ionised, f-d interaction 78−90102
ligand field calculations for arbitrary point groups in strong field coupling, energy diagrams, plotter routines 77−76778
ligand field spin-orbit coupling calcs. for d^1, d^8, d^9 five coordinated complexes 77−18781
liquid metals, spin-orbit coupling and resistivity 77−85189
liquid metals, spin-orbit interactions effect on mag. susceptibility, effective pseudohamiltonian 80−29299
magnetic 3d impurity in non-magnetic metal, effective ion Hamiltonian 78−64016
magnetic ions interaction in insulator, degenerate orbitals 79−91010
magnetic multipole interaction between two nonoverlapping charge distributions 79−89731
magneto-optical rotation, spin-depend., for free radicals and singlet triplet transitions 79−10129
magnon relaxation, spin-orbit interaction, itinerant electron ferromagnets 80−11179
many-electron atoms, self-consistent theory of induction and dispersion forces, HF approx. 79−36725
many-electron molecule, self-consistent theory of induction and dispersion forces, HF approx. 79−36725
matrix elements, computer program AAKL adapted to spectroscopic notation 78−891
matrix isolated metal atoms, matrix influence, theory 78−46290
metal, ferromagnetic reson. damping, one electron model 77−8409
metal, paramagnetic, CESR spin-orbit perturbation, spin-phonon scatt. 77−63285
metal, spin scattering and spin-orbit coupling 80−29369
metal film, CESR line width and shape, surface relax. contrib. *(Russian)* 77−32260
metal hexafluorides, MF_6(M=W,Re,Os,Ir,Pt), ionisation energies and optical spectra in Dirac-Slater model 77−83488
metallic particles, small, effect of spin-orbit interaction on spin susceptibility 77−59433
metals, Kondo effect, Anderson hamiltonian 80−60187
metals, spin-orbit coupling enhancement of 3d ions 79−47069
methanol, mol., nucl. spin-spin coupling const., Hartree-Fock calc. 80−9618
microscopic ion-ion spin-orbit pot., appl. to ^{4}He+^{9}Be, and ^{40}Ca+^{13}C 78−17163
mixed valence state, electronic structure, spin-orbit interaction effects, mag. susceptibility 80−54657
molecular crystal, exciton band spin-orbit coupling 78−39025
molecular fluorescence, mag. field effect 79−3483
molecular vibronic level mixing, under electronic coupling operator 80−52968
molecule, linear triat., $^2\Pi$ state, vibronic-spin-orbit interaction, Renner effect 78−70758
molecules, electronic spin orbit interaction, molecular Aharonov-Bohm effect 80−83303
$^{14}N^{16}O$, 1-0 band at 1900 cm^{-1}, meas., interpret. 78−58651
$n\pi^*$- and $\pi\pi^*$-states, n-electron delocalisation effect 79−63902
1,2-naphthacoronene, phosphoresc. and ODMR meas. 79−18220
naphthalene, radiationless transitions, sharp Doppler-free resons. *(German)* 77−58076
narrow gap semiconductors, two-dimensional electron spectrum, spin splitting 80−24861
noble metal, matrix-isolated, matrix-induced changes in opt. spectra 77−57913
noncentrosymmetric crystal, intraband spin-orbit interaction, influence on photogalvanic effect 79−69558
nonlinear polarisation resonances in a continuum, optical activity, spin-orbit interactions *(Russian)* 80−53391
nuclear, matter, V^8 models, variational calcs. for binding energy and density 80−42571
nuclear Dirac phenomenology and the Λ-nucleus potential, anomalous mag. moment 80−37344
nuclear interactions via (n,n) elastic back angle scatt., Fe,Co,In,Bi targets 77−67746
nuclear mass depend. of spin-orbit splitting in A=176-208 region 78−29405
nuclear matter, variational techniques, review 80−22748
nuclear optical model calcs., tensor spin-orbit interaction 78−13112

spin-orbit interactions continued
nuclear single particle levels, spin orbit splitting, 1 boson exchange pot. contribs. *(Russian)* 78−78243
nuclear Skyrme tensor interaction, HF spin-orbit effects in spherical nuclei 77−61350
nuclear surface energy, spin-orbit interaction effects, Fermi liquid drop vibrs. *(Russian)* 78−86495
nucleon optical pot., spin-orbit term 80−27606
open shell restricted HF eqns., role of coupling operators 79−758
optical model spin-orbit pot. for spin $^1/_2$ particles 79−97686
orbital doublet with weak Jahn-Teller interaction, ESR spectra 77−28427
orthorhombic rotating molecules, doublet-quartet transitions, Zeeman effect calcs. 78−94280
palladium porphin, Zeeman expt. on phosphoresc. triplet and quartet states 79−33786
palladiumporphin in n-octane cryst., lowest triplet state, ESR-optical detect. 77−58050
particle motion in ring shaped potential, spin-orbit coupling 80−101723
particles, quantum size effect obs. by CESR and NMR 77−20700
phenazine, triplet state intersystem crossing, picosec. singlet excitation 77−6824
bis-(phenylethinyl)-mercury, spin-orbit coupling, heavy atom and D isotope effects 79−59372
phosphorescent triplet state, spin-lattice relax. mechanism *(Russian)* 78−68542
polar molecule, Stark effect in electron spin transition in zero-field 77−27099
polarisation, comparison in optics and spin-$^1/_2$ particle assemblies, Stokes vector formalism 77−27181
polyatomic asymmetric top mols., matrix elements for multiplet spin-orbit interaction 77−57905
polyatomic mol. quasi line spectrum in paraffin matrix, electronic-vibr. interaction 79−85971
porphyrins, solid solns., phosphoresc. rel. to solvent heavy ats. *(Russian)* 77−40286
potassium halides, F-centres, optical pumping, spin-orbit and hyperfine coupling 77−16359
potential energy surfaces, of mols., VB diatomics-in-mols. method 79−85919
pseudo pot. model Hamiltonian, spin-orbit splitting, intercombination and relativistic orbital reorganisation 78−25424
pyrazine, vibronic and spin-orbit coupling interaction 80−14126
quantum scattering theory inverse problem, fixed energy Jost functions *(Russian)* 80−68082
quinoxaline, in naphthalene-d_8, sublevel phosphorescence spectra, radiative mechanisms 77−75203
radial reduced Coulomb Green's function 80−31559
random electronic models with spin-dependent hopping 80−70574
random system, 2-D, spin-orbit interaction and magnetoresistance 80−70728
rare earth alloys, dil., ESR linewidth of rare-earth ions 78−68373
rare earth ion energy separation, $4f^N$-$4f^{N-1}$ nl, host depend. 80−49676
rare earth ion spectra, crystal field integral parameters, spin-orbit interaction 80−100447
rare earth metals, excitation energies, 3d electrons, relativistic calcs. 80−20109
rare earth metals, ferromagnetic theory of low-temp. and freq. depend. of extraordinary kinetic effects *(Russian)* 79−91408
rare earth orthovanadites, phase transitions and Jahn-Teller distortions 79−28548
rare earth orthovanadites, RVO_3, magnetic and cryst. struct., 'ahn-Teller effect 77−32169
rare earth superconductors, spin splitting of cond. bands and spin-orbit scatt. 79−56461
rare earth-Co alloy, RCo_5, mag. anisotropy, individual Co site contribution 79−78366
relativistic average of config. wavefunctions, applicability to at. and ionic intermediate coupling props. 78−17574
relativistic electron wave diffraction by cylindrical capacitor 80−5671
relativistic energy band calcs., linear APW method and augmented spherical wave method extensions 79−60679
relativistic quantum field theory of finite nuclei 79−6466
relativistic quark model, origin of spin-orbit and spin-spin coupling forces 79−13046
ruby, spin-strain coupling tensor meas. US modulated EPR obs. 80−50170
sandwich complexes, mag. props., effective Hamiltonian method 80−37731
Schrodinger representation, spin-orbit coupling origin 80−42914
secondary electron emission, theory 78−76564
semiconductor, conduction electron paramag. relax., Coulomb mechanism 78−88191
semiconductor, hole scatt. from impurity pots. in spherical-band approx. 77−76803
semiconductor, mixed, EPR theory 78−39402
semiconductor, spin-orbit splitting, tight binding calc. 77−85184
semiconductor, zincblende struct., phonon attenuation in presence of internal strains and mag. field 78−76118
semiconductor film, spin relaxation due to electric fields 77−62928
semiconductor without inversion centre, conduction electrons spin relaxation *(Russian)* 78−52355
semiconductors, graded mixed, effective mass theory for carriers, spin effects 77−85208
single particle levels, one boson exchange potentials, spin orbit splittings 79−9436
spin-orbit coupling, ball in watchglass, for teachers 78−81775
spin-spin integrals, one- and two-centre, analytical evaluation over Slater-type orbitals *(Russian)* 80−9491
spin-splitting factor for Landau levels from de Haas-van Alphen effect first 3 harmonics 77−20226
spin-unsaturated subshells and the nucleon-nucleus optical-model spin-orbit potential 80−18259
substrate-split localised adsorbate levels, spin polarisation effects in photoemission 79−19971
supercondcutors, surface relax. of conduction electron spins 79−60995
superconducting crystal, spin-orbit interaction effect on paramag. props. 77−15994
superconductors, magnetic ordering, susceptibility calc., weak and strong spin-orbit scattering 79−99656

spin-orbit interactions continued
superconductors, slightly dirty, EPR relaxation time, thermal behaviour 79−47195
superexchange between one-particle states 79−91011
superheavy nuclei stability, spin-orbit symmetry potential 78−50104
superheavy region, spin-orbit pot. effect on single particle levels 79−59000
surface potential barrier, Schrodinger eqn., anal. and numerical soln. incl. spin-orbit interaction 79−58492
tensor operators, reduced matrix elements for L-S coupled, N-electron configurations 79−13625
tetrachlorobenzene, mol. crystal, exciton band spin-orbit coupling 78−39025
1,2,3,4-tetrachloronaphthalene, intramol. heavy atom effect, PMDR obs. 79−13745
tetraethyl lead, core d-level high resolution photoelectron spectra, spin-orbit splitting 78−50579
tetraethyl lead, core level photoelectron spectra, electric field gradient splittings 77−88494
di-(tetraethylammonium)tetrahalomanganate, mag. circular and linear dichroism obs. 80−29725
tetragonal complexes, meas. of covalency 77−47781
thioformaldehyde, $\tilde{a}^3A_2 \leftarrow \tilde{X}^1A_1$ IR absorpt. spectra 80−83362
thiomethoxyl anion, and deuterate, electron photodetachment, affinities, vibr. freq. and spin-orbit splitting 80−53063
transition metal, ferromag., band theory of linear magnetostriction 80−71141
transition metal 3d, spin-orbital interaction effect on NMR, g-factor anisotropy *(Russian)* 77−24752
transition metal $^6S(d^5)$ ions in tetragonal and rhombic symm., zero-field splitting 77−1390
transition metal complexes, ligand field spectroscopy, selection rules, intensity enhancement of forbidden transitions 80−45049
transition metal complexes, tetragonal, d^5 ions, ligand fields and electronic struct., theory 77−6666
transition metal ions in HCP hosts, energy splittings 78−67989
transition metal monosulphides of first-row, XPES and UV PES 80−20760
transition metal oxides, second and third-row, XPES 80−87170
transition metals, theory of ferromagnetism involving spin-orbit and cryst. field interactions 80−2541
transition metals and alloys, 3d, Hall effect, electron scatt. processes 80−34419
trimethyl gallium, core level photoelectron spectra, electric field gradient splittings 77−88494
trimethyl indium, core d-level high resolution photoelectron spectra, spin-orbit splitting 78−50579
triplet-triplet transitions role in spin-orbit interactions 79−63915
two photon exchange, Thomas precession, polarisability corrections to fine structure 77−17842
two-body classical Hamiltonian, EM and gravit. examples 77−68386
two-body spin-orbit interaction matrix elements, shell model *(Chinese)* 80−47356
two-electron systems, spin polarisation processes *(Russian)* 79−94085
two-particle mutual interaction, graphical representation 78−94181
universal variational functionals of electron densities, first-order density matrices, and natural spin-orbitals and solution of the v-representability problem 80−95516
vibronic splitting and Zeeman effect for $^4A_{2g} \rightarrow {}^2E_g$ transition 78−60495
water molecule, nucl. spin-spin coupling consts. geometric approx. 79−59380
X-ray 5p emission bands, valence energy band 80−104016
xanthione, large zero-field splitting of lowest triplet state 80−58171
d breakup effect on spin orbit and tensor pots. 80−32286
Λ-hypernuclei, QCD and spin-orbit splitting, spin-orbit pots. 79−85398
μ^- depolarisation, exotic at. orbital ang. momentum alignment effect 80−18946
(p, p), 1 GeV, polarisation data, Glauber anal. spin-orbit parameters, matter distribs. 80−52655
(p,p) 1 GeV, Glauber theory of spin-orbit interactions 78−37336
(p,p′) inelastic scattering, spin effects, diffractive minima 78−89875
(p,p′) to collective states, medium energies, spin-orbit deformation from DWBA calcs. 79−9565
pp elastic scatt., energy depend. and scaling of spin-correl. and polarisation 77−34173
Σ-hypernuclei, QCD and spin-orbit splitting, spin-orbit pots. 79−85398
Ag foil, or film, conduction electron spin disorientation at surface 80−75855
Ag, spin-orbit projected d density-of-states 78−38999
Ag(111), valence band struct. along Λ, angle resolved photoemission spectra 79−95316
Al film, thermomodulation of Al $L_{2,3}$ absorption edge 79−91533
$AlNH_4(SO_4)_2$:Cr^{3+}, optical spectral, crystal field, spin orbit and exciton interactions 80−34958
α-Al_2O_3:V^{4+}, emission spectrum, Jahn-Teller effect in $^2T_{2g}$ and ^2E_g states 79−83007
AlS, $B^2\Pi$-$X^2\Sigma^+$ transition, assignment of UV bands, vibr. and rot. anal. 80−58278
Ar II, transition probabilities, lifetimes, intermediate coupling semiempirical calcs. 79−789
Ar, ns→εp photoelectrons, spin polarisation 80−37792
Ar^+, mobility in Ar, spin-orbit coupling effect 78−26232
Ar^{2+}, levels of $2p^33p^5$ 78−74574
Ar^{2+}, multiple open shell configs. calcs., modified HF method 77−50356
Ar_2^+, bound-free absorpt. cross section for Π and Σ states 78−5140
Ar_2^+, electronic states, pot. curves, with/without spin-orbit interaction 78−33443
Ar_2^+, photodissoc., pot. curves and photofragment spectra 77−88514
ArF_2, ab initio diatomics in mols. pot. surface, spin-orbit coupling 79−3519
$Ar^+(^2P_J)+H_2(D_2)$, Ar^+ two spin orbit state, reaction cross section, direct determ. 80−93748
As_2Se_3, single crysts., fine struct. of direct gap from electrorefl. spectra 80−93280
Au, ground and excited states, pot. energy curves, relativistic effects calcs. 79−31416
Au I, relativistic oscill. strengths 77−14388
Au, spin-orbit projected d density-of-states 78−38999
Au, spin-polarised LEED from low-index surfaces 78−14556
Au subshell photoelectron branching ratio meas. using synchrotron radiation 80−66397

spin-orbit interactions continued
Au-Co, dil. alloy, crystalline electric field and spin-orbit splitting, NMR results 77−32274
Au-Co, electron scatt., spin-orbit effects 80−65533
Au-Fe, spin-orbit coupling and electron scatt. 80−2370
Au-Fe alloys, spin-orbit electron scatt. near percolation limit, anomalous Hall effect meas. 79−73492
Au-Mn, spin-orbit coupling and electron scatt. 80−2370
B isoelectronic series, dipole oscill. strengths, multiconfigurational Hartree-Fock calcs. 77−83540
^{11}B, low lying negative parity states, α-t spin-orbit force 78−50110
BaClF:Sm^{2+}, energy levels, optical props. 78−84631
$Ba_4NbRu_3O_{12}$ and $Ba_4TaRu_3O_{12}$, $(Ru_3O_{12})^{13-}$ cluster obs. in presence of orbital degeneracy and spin-orbit coupling *(French)* 80−70655
BeF, spin orbit coupling const., ab initio calcs. 80−63537
$^9Be+^4He$, microscopic ion-ion spin-orbit pot. 78−17163
Bi II ion, relativistic effects in hyperfine splitting of second spectrum 80−23344
Bi, photoionisation cross section of d-core level synchrotron radiation study of spin-orbit branching ratio 79−74057
Bi V, relativistic oscill. strengths 77−14388
$Bi_{12}GeO_{20}$, reflectivity spectrum and band struct. 79−47474
$Br+O_2(NO)$, quencher paramagnetism, deactivation rate const., spin-orbit relax. study 80−21263
BrCl, photoelectron spectrum, assignments 78−5284
C_2, $X^1\Sigma^+_g$, $6^3\Sigma^-_g$ states, perturbations, ab initio CI calcs. 77−83490
CO_2, threshold photoelectron and photoionisation spectra 77−14491
CO_2^+, photoionisation reson. spectra and threshold electron-ion coincidence meas. of fragmentation 77−38700
CS, nonexponential decay of $a^3\Pi$-$X^1\Sigma^+$ luminesc., II sublevel radiative lifetimes, matrix isolated spin-orbit 79−89699
CS, perturbation parameters between valence states 77−26975
CS, spin-orbit and spin-spin parameter calcs. 77−27044
CS_2, photoelectron spectrum, spin-orbit splitting, excited state form. 80−43102
CSe_2, photoionis. mass spectrum, Rydberg state props. 77−46604
^{12}C spin-orbit force and deformation, self-consistent HF calc. 79−455
$C(2^1S_0)+H_2(O_2)$(ethylene), collisional behaviour, kinetic study 80−74241
$CaCO_3$:Fe^{2+}, electronic spin relax., effect of second-order spin-orbit coupling 80−10935
CaF_2:Fe^{2+}, electronic props., Mossbauer and far IR spectroscopy 79−99803
CaO, F-centres, $^3T_{1u}$ relaxed excited state, uniaxial stress effect and spin-lattice coupling 78−72405
CaO, neutron irrad., MCD, optical absorpt. lines 77−77255
CaO:Cr^{2+}, APR spectra 79−87313
$CaWO_4$:Er, spectroscopic parameters calcs. 80−50379
^{40}Ca, relativistic Hartree-Fock eqns., 1 boson exchange pot., spin orbit splitting 79−3106
$^{40}Ca+^{12}C$, microscopic ion-ion spin-orbit pot. 78−17163
^{40}Ca(p,2p) 200 MeV polarised p, spin-orbit effects 79−89222
^{40}Ca(p,p), imaginary spin-orbit term in proton optical potential, ang. distribs. 78−58273
Cd alloys, spin and spin-orbit contribs. to mag. susceptibility *(Russian)* 79−11287
Cd, de Haas-van Alphen effect under press., Fermi surface and pseudopot. form factors 77−43475
Cd I, $4d^{10}$ subshell photoelectron ang. distrib. 80−14123
Cd, magnetic susceptibility, temp. depend., electron-phonon interaction effects 79−61046
Cd, photoelectron spectra, 4d spin-orbit splitting, crystal field and band-broadening effects, CNDO calcs. 78−76577
Cd, spin-orbit interac. contrib. to mag. susceptibility of interacting electrons 77−63084
$CdCo_3$:Fe^{2+}, electronic spin relax., effect of second-order spin-orbit coupling 80−10935
$CdGa_2Se_4$, thermoreflectance and visible absorpt. spectra, energy gap, cryst. field splitting 80−34945
$Cd_{1-x}Mg_x$, mag. props. and electron spectrum parameters *(Russian)* 79−33453
$Cd_{1-x}Mn_xTe$, spin-orbit coupled bands, indirect exchange interaction via electrons 80−34407
CdS, surface photovoltage in exciton absorpt. range 78−19119
CdTe, energy bands and optical props. calc., tight-binding model with spin-orbit interaction 80−65448
CdTe:Cr^{2+}, absorpt. and luminesc. of $Cr^{2+}(d^4)$, cryst. field theory interpretation 79−83000
CdTe:Ti^{2+}, Jahn-Teller effect on $^3T_1(^3F)$ state, resonance on $^3T_1(^3P)$ state 78−27271
$CeCoSi_2$ film, Hall effect and magnetoresist. *(Russian)* 80−11109
ClBS, form., photoelectron and microwave spectra 78−90214
ClCN, ground and first excited bending, vibr. state, props., mol. beam elec. reson. 80−37823
ClO, UV spectra of $C^2\Sigma^-\leftarrow X^2\Pi$ system, rot. anal. 80−996
Co (VII), semiempirical investigation of spectra 78−33434
Co, liquid, Hall effect, band struct. and exchange scatt. 80−80250
$Co_3(AsO_4)_2.8H_2O$, optical absorpt. spectra, spin orbit splitting and cryst. field parameters 79−38560
$CoCl_2$, electronic absorpt. spectra and coord. in cryst., soln. and melt 79−38570
Cr oxides, XPS study, electron binding energies, spin orbit splittings, exchange splittings 79−78839
Cr_3 spin-density-wave antiferromagnet, uniaxial anisotropy 78−10640
Cr^{3+} in octahedral fluoride lattice, optical spectrum open shell SCF MO cluster CI calc. 78−19501
CrO_3^- radical in K_2CrO_4 and $KCrO_3Cl$, g-factor anisotropy 78−67994
^{35}Cr, ^{7}P states HFS, level crossing technique, core polarisation, spin orbit interaction, config. mixing 78−78668
Cs, 6s-electron photoionisation, ab initio calcs. 80−91523
Cs, excited np states, fine struct., core electrons effect 77−18807
Cs, fine-struct. of excited nd and nf states, at. core effect 78−58606
Cs, four-photon ionis., strongly interacting resons. theory 80−52955
Cs, photoionis. of 6s electron, spin-orbit interaction, ab initio calc. 79−81191
Cs, relativistic model pseudopot., appl. to elec. resist. calc. in liq. phase 78−51866
Cs, spin relax., effect of optical pumping in high mag. field 77−88430
CsAu, photoelectron spectroscopy and energy bands calc. 78−76581
CsBr, (110) surface, electronic struct. of valence bands calc. *(Russian)* 80−75621
spin-orbit interactions continued
CsCl, (110) surface, electronic struct. of valence bands calc. *(Russian)* 80−75621
$Cs_2Cr_2Cl_9$, Cr (III) trigonal pair, exchange interactions, theory 78−19008
$Cs_3Cr_2Cl_9$, optical absorpt., MCD, exchange interactions 78−10917
CsF, F-centre optical absorption bandshape calc. for transition to state with Jahn-Teller and spin orbit couplings 80−55135
$CsFeCl_3$, linear chain cryst., quadrupole and mag. reson., rel. to $RbFeCl_3$ 79−38403
CsI, (110) surface, electronic struct. of valence bands calc. *(Russian)* 80−75621
Cs_2MX_6(M=Se, Te, X=Cl, Br), $\Gamma_4^-(^3T_{1u})$ state, Jahn-Teller effect, luminesc. obs. 80−60650
Cs_2SiF_6:Mn^{4+}, IR absorpt. band, electron-vibr. effect 80−108238
Cs_2SiF_6:Mn^{4+}, Jahn-Teller effect in $^4T_{2g}$ state, Zeeman meas. 80−29367
Cs_2TiF_6:Mn^{4+}, spin-orbit and field splitting, Jahn-Teller effect, Zeeman meas. 80−80234
CsX,(X=F,Cl,Br,I), ionis. energy, relativistic Dirac-Slater and nonrelativistic HF-Slater calcs. 77−26983
Cs_2ZrCl_6:Os^{4+}, multiple state luminesc. 78−72584
Cu, Auger spectra, comparison with multiplet struct. calc. 78−31287
Cu complexes of amino acids and α-hydroxy acids, bonding effect on spin-orbit coupling 77−1399
Cu foil, rel. to conduction electron spin disorientation at surface 80−75855
Cu halides, reflection spectra, 4.5-7.5 eV, bond struct. scheme 79−61402
Cu-Co heterobinuclear complex, cryst., mag. susceptibility of Cu-Co(fsa)$_2$ en, $3H_2O$ 80−2556
Cu-Mn-Au(Pt) spin glasses, anisotropic exchange interactions, effect of nonmag. impurities 80−80534
Cu-transition metal, alloys, satellite NMR study, lineshifts and splitting 80−34786
$CuAlS_{2x}Se_{2(1-x)}$, excitonic structure, spin-orbit and cryst. field splittings 78−2872
CuBr, direct gap semiconductors, charged excitons 77−62840
CuCl, direct-gap semiconductors, charged excitons 77−62840
CuCl, electronic struct., ab initio HF SCF MO calcs of $CuCl_4^{3-}$ cluster 78−95262
$CuGaS_{2x}Se_{2(1-x)}$, excitonic structure, spin-orbit and cryst. field splittings 78−2872
γ-CuI crystalline film, excitonic spectra, spin-orbit splitting *(French)* 79−78771
CuI, thermoreflectance spectrum, 4-7 eV region 79−19904
CuMn, hysteresis, spin orbit scattering effect on anisotropy in spin glass state 80−71095
Cu_2O, self-consistent energy bands 80−59869
Cu(α,α), A=63 and 65, 48 MeV, I.L. potential depth, optical model anal. 78−50187
D_2, $G(3d)^1\Sigma_g^+$ and $g(3d)^3\Sigma_g^+$ singlet-triplet anticrossing 78−42138
$DyFeO_3$, influence of mag. field on Faraday effect 78−27196
^{166}Er, Skyrme-HF calcs., deformation, electric moments, spin-orbit potentials 78−62480
EuO, mag. semicond., dielec. and optical props. 78−10824
EuO(S)(Se), rel. to spin assisted Raman scatt. theory 78−43866
EuO(S)(Se)(Te), spin-disorder induced phonon Raman scatt. 78−60457
EuP_5O_{14}, 4f-level press. depend., fluorescence exam. 77−72841
EuSe, mag. semicond., dielec. and optical props. 78−10824
F I, and isoelectronic series, Z=10-100, L-shell energy struct. and level classification 78−55129
F, spin-orbit splitting and $^2P_{1/2}$ radiative lifetime, absorpt. spectrosc. meas. 80−87063
FH_2, pot. energy surface, valence states, VB diatomics-in-mols. method 79−85920
^{19}F, electroexcitation of ground state rotational band 78−66191
$^{19}F+^{28}Si$ spin orbit pot., single folding model and cluster model 80−9196
Fe complex, Fe (II) pseudo-tetragonal high-spin cpds., paramag. susceptibility amd Mossbauer quadrupole splitting 78−26834
Fe complex, Fe(5-methylpyrazole)$_4X_2$, X=Cl, Br, I, mag. susceptibility, mag. saturation; Mossbauer and ligand field spectra, single model interpretation 78−23064
Fe complex, Fe(pyrazole)$_4X_2$, X=Cl, Br, I, mag. susceptibility, mag. saturation; Mossbauer and ligand field spectra, single model interpretation 78−23064
Fe complexes, electronic and mag. struct., semiempiricial MO cluster calcs. 78−62733
Fe, fine struct. levels fitting, config. interaction effect, spin-orbit and electrostatic interaction parameters 80−69248
Fe, liquid, Hall effect, band struct. and exchange scatt. 80−80250
Fe XVIII, Zn XXII, Ge XXIV, Se XXVI, spectral line identification 79−72230
Fe^-, electron affinity, nonstatistical fine-struct. detachment intensities at 488 nm, laser electron spectra 79−41144
Fe^{2+}, in octahedral symm., vibronic effects from Zeeman field induced Mossbauer spectra 77−8476
$FeBr_4^-$, circularly polarised Raman spectra, spin-orbit induced vibr. antisymmetry 78−5232
$FeBr_4^-$, in various solvents, $^4A_1$ ^4E d-d band reson. Raman spectra, solvent depend., spin-orbit coupling 80−55085
$FeCO_3$, antiferromag., siderite, Raman spectra obs. 77−85708
$FeCO_3$, mag. neutron scatt., spin orbit coupling effects 77−85419
$FeCO_3$, siderite, Fe^{2+} Mossbauer spectrum, ligand field theory 77−16212
$Fe_{68}Co_{32}$, ferromagnet, magnon heat cond. and lifetimes, 1-2 to 4.5K 77−16066
Fe_3O_4, magnetite, mag. aftereffects, 4.35K 80−80571
$Fe(SO_3F)_2$, Mossbauer and electronic spectra, cryst. field splittings, mag. hyperfine interactions 77−48096
$Fe_xTa_{1-x}S_2$ (1T), rel. to low-spin high-spin equilib. 77−48109
GaAs, k-linear coupling, E_1' transitions 78−91583
GaAs:Co, neutral state of Co impurities, optical absorption and mag. susceptibility 78−39578
GaAs:Cr, site symmetry of Cr ions, ground-state splitting, ballistic phonon expts. 78−95273
$GaAs-Ga_{1-x}Al_xAs$ superlattices, resonance enhanced Umklapp Raman process 78−39547
GaAs-GaSb, threshold energies for impact ionisation by electrons and holes 78−6390
GaKr, low-lying electronic states, PE curves, transition moments, emission coeffs. 79−6894

spin-orbit interactions continued
GaP:Fe^{2+}, absorpt. and luminesc. spectra 77−16388
GaSe, exciton spectra at 4.2K rel. to layer struct. 77−16336
Gd, optical conductivity, direct interband transitions 80−15488
Ge, Auger spectra, comparison with multiplet struct. calc. 78−31287
Ge, electron-hole droplets, luminesc. and absorpt. lineshapes, RPA theory 80−49613
Ge, inter-valence-band absorption in electron-hole droplets 79−4515
GeF, use in chemical lasers 80−64004
H halides, spin-orbit coupling effect on proton mag. shielding 80−23440
H-like atom, spin-orbit interaction and single electron excitations rel. to mag. dielectrics 79−54780
H^++Kr, mol. orbit approach, spin-orbit interaction, adiabatic pot. and projected valence band treatments 77−533
H_2, $c^3\Pi_u$ metastable state, fine struct. lifetimes 79−64050
HBr, photoelectron angular distrib. 80−58318
HD, spin-spin coupling const., convergence of calc. 80−9506
HI, photoelectron angular distrib. 80−58318
H_2O^+, spin and rot. fine struct., orbital angular momentum 80−83247
$^1H(n,n)$, pol. n, 13.5-16.9 MeV, anal. power and spin-orbit phase parameters 80−78269
He, 1s3d config., Zeeman sublevel energies, anticrossing and degeneracy 77−23417
He neutron rich isotopes, reaction matrix calcs., stability 78−66225
He-like ions, P_1^0-$^1S_0$ and $^3P_1^0$-$^1S_0$ intercombination-line transitions 78−70771
$HeCl^+$, interaction potential, HF dissociation energies, LCAO SCF calcs. 77−6880
^{3}He atom forbidden singlet-triplet anticrossings, D levels 80−99491
^{3}He, microscopic spin orbit potential, microscopic formulation inadequacies 79−26355
^{3}He, superfluid, A-phase, coupled spin orbit relaxation theory 78−6192
^{3}He, superfluid, B-phase dynamics, broken spin-orbit symmetry 78−71898
^{3}He, superfluid, linear and point singularities, allowing for spin-orbit interaction *(Russian)* 77−20151
^{3}He-A, superfluid, spin dynamics, spin-orbit configurations, spin waves *(Russian)* 80−54462
^{4}He, singlet-triplet anticrossings, ^1D and ^3D state separation, mixing 77−6738
Hg II, relativistic oscill. strengths 77−14388
Hg, $N_{6,7}O_{4,5}O_{4,5}$ Auger electron spectrum, electron impact excitation 77−57958
Hg-N_2, optical pumping, vibr. excitation, laser theory 78−66517
Hg_2, model calc. of electronic struct. and spectroscopy 79−3352
$Hg_{1-x}Mn_xSe$, spin-orbit coupled bands, indirect exchange interaction via electrons 80−34407
$Hg_{1-x}Mn_xTe$, spin-orbit coupled bands, indirect exchange interaction via electrons 80−34407
HgSe, interband absorpt. and Γ-point band structure parameters 79−47010
HgTe, energy bands and optical props. calcs., tight-bonding model with spin-orbit interaction 80−65448
HgTe type semiconductors, spin-flip transitions in magneto-optics and magneto-transport 80−50306
HgTe-HgSe film, optical spectra in fundamental absorption edge 79−74012
HoF_3, single cryst., Ho^{3+} energy level spectrum calc. 79−1586
I, chemical generation of population inversion between spin-orbit states 78−17767
$I(5^2P_{1/2})$+benzene-d_0(-d_6), fluoresc. quenching, spin-orbit interaction, isotope effect obs. 78−62763
$I(5^2P_{1/2})+H_2O(D_2O)(HX)(DX)$, collisional quenching, isotope effects 77−34583
In film, polycrystalline optical transitions from d core states 77−85827
In, photoionisation cross section of d-core level synchrotron radiation study of spin-orbit branching ratio 79−74057
InAs and solid solutions, recombination mechanisms of excess carriers, luminesc. obs. 80−97337
$In_{0.79}Ga_{0.21}As_{0.54}P_{0.46}$, LPE layer, electroreflectance meas. 79−24290
InSb, (110) surface, core level photoionisation spin-orbit branching ratio, initial and final state effects 79−83094
n-InSb, doping and strain depend. of quantum props. 79−60690
InSb type semiconductor, spin-flip transitions in magneto-optics and magneto-transport 80−50306
InSe, band structure, spin-orbit splitting and electron loss struct. of In 4d core level 77−47727
InSe, reflectivity and low energy absorption 80−34944
InSe, spin orbit split off valence bands, exciton transitions, Hopfield's quasicubic model, visible absorpt. spectrum 80−50370
$IrCl_6^{2-}$, circularly polarised Raman spectra, spin-orbit induced vibr. antisymmetry 78−5232
$(IrCl_6)^{2-}$, electronic Raman spectra, spin-orbit components of ground state, vibr. 78−5231
K, excited np states, fine struct., core electrons effect 77−18807
K, excited states field ionis., p states spin-orbit interaction 79−59592
K, stimulated electronic Raman light scatt. by mag. sublevels 78−50492
KBr, electronic states at (100) surface, accounting for spin-orbit interaction *(Russian)* 78−91750
KBr, F-centre luminesc., MCD effects 78−39598
KBr(Cl)(F), spin-orbit interaction of relaxed excited state of F-centres 77−15808
KBr(F), orbital g-factor and spin-orbit splitting of F-centre excited state, magnetoabsorpt. and MCD 78−2886
KCL:Pb^{3+}, interpretation of optical absorption spectra 79−51993
KCl, electronic states at (100) surface, accounting for spin-orbit interaction *(Russian)* 78−91750
KCl, F_2-centre triplet-triplet transition at 685 nm, MCD obs. *(French)* 77−63433
KCl, F-centre luminesc., MCD effects 78−39598
KCl, MCD, magneto-optical parameters of R-centre in H_3-mol. model 77−77253
KCl, mag. circular dichroism of R-center, point-ion lattice model 79−69814
KCl:Ca(Yb), Z_2 and Z_2^+ centres, excited state, magnetooptical spectra 80−108233
KCl(Br), F-centre emission, mag. circular polarisation 80−108251
$KCoF_3$, magnon-phonon interaction mechanism 77−20019
K_2CoF_4, 2-dimens. Ising antiferromag., mag. excitons, Raman scatt. obs. 80−66181
K_2CuF_4, 2-D ferromagnet, optical and magneto-optical props. 77−52062
spin-orbit interactions continued
K_2CuF_4, optical absorption spectra, correl. with g-shifts, reduced spin-orbit coeff. determ. 78−23485
K_2CuF_4, two-dimens. ferromag., magneto-optical props., absorpt., MCD and MLD 79−87419
KF(Cl)(Br), mag. props. of relaxed excited state of F-centre, vibronic theory 78−60502
$K_3Fe(CN)_6$, electronic struct., electron density, elec. field gradient, mag. susceptibility and g-tensor 79−91006
K_2FeF_4, two-dimensional antiferromag., cryst. field effects, Mossbauer spectroscopy 80−71254
$K_3Fe_2F_7$, two-dimensional antiferromag., cryst. field effects, Mossbauer spectroscopy 80−71254
KH_2PO_4:Tl, UV absorption bands obs. 78−27266
KI, containing F-centres, Raman scatt. calc. 77−16306
KI doped with F-centres, mag. vibr. Raman scatt. 77−4636
KI, electronic states at (100) surface, accounting for spin-orbit interaction *(Russian)* 78−91750
KI, F-centre luminesc., MCD effects 78−39598
KI, MCD of α and β bands 78−27192
$KLu_3F_{10}:Eu^{3+}$, crystal field and spin-orbit parameters 78−30892
$KMgF_3:Fe^{2+}$, US relax. absorpt., acoustic wave-impurity coupling, spin-orbit splitting 79−4375
$KMgF_3:Co^{2+}$, $^4T_1$-$^4T_2$ transition, zero-phonon lines intensities 80−75529
$KMgF_3:Cr^{2+}$, dynamic Jahn-Teller effect 77−66416
$KMgF_3:Fe^{2+}$, Jahn-Teller quenched spin-orbit, splitting of $^5T_{2g}$ state 77−63442
$KMgF_3:Mn^{2+}$, exchange and spin-orbit interactions, optical spectra study 79−95817
$KMgF_3:Ni^{2+}$, EPR meas., g-factor, spin-orbit coupling const. and mag. moment determ. 77−80999
$KMgF_3:V^{2+}$, combined spin-orbit and Jahn-Teller coupling, method of soln. 79−60773
$KMgF_3:V^{2+}$, dynamical Jahn-Teller effect on spin orbit multiplets, intensity quenching 79−95374
$KMgF_3:V^{2+}$, first and second order Jahn-Teller coupling const. calc. 79−65906
$K_2PtCl_6:Os^{4+}$, multiple state luminesc. 78−72584
K_3Sb, optical and dielectric props., energy spectra, density of states calcs. 80−20083
$KY_3F_{10}:Eu^{3+}$, crystal field and spin-orbit parameters 78−30892
$KZnF_3:Mn^{2+}$, exchange and spin-orbit interactions, optical spectra study 79−95817
Kr, ns→εp photoelectrons, spin polarisation 80−37792
Kr_2^+, electronic states, pot. curves, with/without spin-orbit interaction 78−33443
$Kr_2Cl(F)$, ab initio diatomics in mols. pot. surface, spin-orbit coupling 79−3519
KrF, electronic states, ab initio CI calcs., spin-orbit coupling, pot. curves, dissoc. energy, dipole moments 77−38619
$LaCl_3:Ho^{3+}$ parametric energy level anal. 78−18991
Li I, and isoelectronic series, Z=10-100, L-shell energy struct. and level classification 78−55129
Li_2Br_2, UPS of dimeric mol., expt. and Xα calc. 80−9640
Li_2Cl_2, UPS of dimeric mol., expt. and Xα calc. 80−9640
LiF, F-centre, excited state, optical absorption 77−20267
Li_2F_2, UPS of dimeric mol., expt. and Xα calc. 80−9640
Li_2I_2, UPS of dimeric mol., expt. and Xα calc. 80−9640
$LiNbO_3$:Co, optical props. 78−64383
Mg, and isoelectronic sequence, relativistic effects on transition probabilities 77−54532
Mg_9 Auger spectra, CI calcs., spin-orbit interactions 77−14558
Mg^+, beam-foil excited, spin orbit-forbidden X-ray transition obs. 80−23537
$MgCl_2:Co^{2+}$, Zeeman electronic Raman scatt. spectra 79−42962
MgO, neutron irrad., MCD, optical absorpt. lines 77−77255
$MgO:Cr^{2+}$, APR spectra 79−87313
$MgO:Cr^{2+}$, APR under applied stress 80−88865
$MgO:Cr^{2+}$, Jahn-Teller parameters determ. using heat pulses 77−62876
$MgO:Cr^{2+}(Mn^{2+})$, phonon spectroscopy using supercond. tunnel junctions 79−65157
$MgO:Cr^{3+}(V^{2+})$, $^4A_{2g}$→$^4T_{2g}$ spectra, new expt. results 80−11441
$MgO:V^{2+}$, first and second order Jahn-Teller coupling const. calc. 79−65906
$MgO:V^{2+}$, mag. circular dichroism in split zero-phonon line 78−56460
$MgS:Ce^{3+}$ phosphors, emission and excitation spectra *(French)* 80−93380
$Mg_xZn_{1-x}Te$, spin orbit splitting, of electron energy levels, reflectivity meas. 79−69479
Mn, fine struct. levels fitting, config. interaction effect, spin-orbit and electrostatic interaction parameters 80−69248
Mn oxides, XPS study, electron binding energies, spin orbit splittings, exchange splittings 79−78839
$MnSiF_6.6H_2O$, optical absorption spectra, 77-300K, assignments 77−36259
Mo, $N_2N_3N_{45}$ super Coster Kronig processes 80−106303
Mo, X-ray spectra, Kα hypersatellites 80−63576
$(Mo_xV_{1-x})_2O_5$, mag. and spectroscopic investigation 80−25206
N_2, isotopic forms, visible spectra, rovibronic and rot. anal., C′ $^3\Pi_u$ and C $^3\Pi_u$ interaction 77−18933
NH_2, spin and rot. fine struct., orbital angular momentum 80−83247
$NH_4Cl:[MoOCl_5]^{2-}$, single cryst., struct. investigations 77−66524
$(NH_4)_6MnMo_9O_{32}.8H_2O$, mag. susceptibility, rel. to EPR, zero field splitting parameter 77−36122
$(NH_4)_2Zn(SO_4)_2:Ni^{2+}$, optical absorpt. spectrum, room and liq. air temp. 79−15499
NO, and isotopic forms, $X^2\Pi$ state, IR obs., mol. consts. 78−42045
NO, fundamental band spectrum, determ. of rotational, spin-orbit coupling and Λ type doubling consts. *(French)* 77−6768
NO, Zeeman spectrum, mol. beam elec. reson. spectrosc. 80−91621
$^{14}N^{16}O$, overtone bands, determ. mol. consts. 78−58652
NO_2, fluoresc. excited by laser, spin-orbit effects 79−64030
NO_2, matrix elements for multiplet spin-orbit interaction 77−57905
NO_2^-, heavy cation effect on singlet-triplet intercombination 79−85946
NO_2^-, microwave transition probability in zero field, spin-orbit interaction 78−25518
^{15}N 3/2$^-$ state spin alignment and polarisation, 1/2-spin orbit interaction from ^{27}Al, $^{88}Sr(^{16}O,^{15}N)$ 80−27622
Na, Auger spectra, CI calcs., spin-orbit interactions 77−14558
Na, excited np states, fine struct., core electrons effect 77−18807
Na, fine-struct. of excited nd and nf states, at. core effect 78−58606

spin-orbit interactions continued
Na, in Xe matrix, 3s excitation, UV and vis. spectra 78−46291
Na, vap., sum frequency generation, via reson. quadrupole transition, theory 78−42385
NaCl:Cu^{++}, EPR spectra anal. spin-Hamiltonian parameters determ. *(Spanish)* 77−69673
NaCl:Zn^{+}, interpretation of optical absorption spectra 79−51993
NaCl(Br), orbital g-factor and spin-orbit splitting of F-centre excited state, magnetoabsorpt. and MCD 78−2886
$NaNO_2$:Ag^{+}, optical and MODR spectra, anion states spin-orbit perturbation 79−19908
$Na_2Zn(SO_4)_2.4H_2O$:Ag^{2+}, EPR, Ag^{2+} dimeric struct., hyperfine and fine struct. tensors 77−51949
Nb, $N_2N_3N_{45}$ super Coster Kronig processes 80−106303
Nb oxides, XPS study, electron binding energies, spin orbit splittings, exchange splittings 79−78839
Nd_2O_3, A-type, optical absorpt. spectrum and paramag. susceptibility 79−56811
Ne II, transition probabilities, lifetimes, intermediate coupling semiempirical calcs. 79−789
Ne, solid, bulk and surface excitons, transmission and refl. spectra obs. 79−95340
Ne_2F, ab initio diatomics in mols. pot. surface, spin-orbit coupling 79−3519
Ni (VIII), semiempirical investigation of spectra 78−33434
Ni, ferromagnetic, Hall effect, anomalous, rel. to scatt. processes 80−44572
Ni, ferromagnetic state, energy bands, self-consistent calcs. 79−19509
Ni, liquid, Hall effect, band struct. and exchange scatt. 80−80250
Ni, magnetic surface anisotropy of transition metals, model calc. 80−34625
Ni, magnetocrystalline anisotropy energy, temp. and magnetisation depend. 78−6525
Ni, optical consts., influence of temp. and relation to bandstruct. 80−25403
Ni-Cu, ferromagnetic, Hall effect, anomalous, rel. to scatt. processes 80−44572
$Ni_{2-x}Co_xBaFe_{16}O_{27}$, ferromagnetic reson., anisotropy and g-factor, spin-orbit interactions 77−24749
NiFe, magnetic surface anisotropy of transition metals, model calc. 80−34625
$NiSiF_6.6H_2O$, and hexadeuterate, optical absorption spectrum, 300 and 80K 79−73966
Ni(α,α), A=62 and 64, 48 MeV, I.L. potential depth, optical model anal. 78−50187
O_2, $^3\Sigma_u^-$-$^3\Sigma_u^+$ spin-orbit mixing in Schumann-Runge predissoc. 77−6875
O_2 molecule, effect of spin orbit interaction on magnetic dipole transition intensity *(Russian)* 79−6948
O_2, spin-forbidden transition intensities, selective heavy atom effects 80−58240
O_2^+, second negative ($A^2\Pi_u$-$X^2\Pi_g$) band system, rot. anal. 77−18911
$O(^1D)$+Ar(Kr)(Xe), inelastic collisions, spin-orbit coupling 80−5605
^{16}O, relativistic Hartree-Fock eqns., 1 boson exchange pot., spin orbit splitting 79−3106
^{16}O(p,2p), 320 MeV polarised protons, quasifree scatt., spin orbit coupling 78−66272
^{16}O(p,p′), 150 MeV, spin-orbit interaction within collective model and DWBA 79−45128
^{16}O(p,p), imaginary spin-orbit term in proton optical potential, ang. distribs. 78−58273
$^{16}O(p_{pol},2p)$, cross section, analysing power, energy sharing spectra, distorted wave impulse approx. 80−78291
$O(2^1D_2)$+Cl_2, reaction kinetics, vac. UV at. spectra 77−21365
PN, valence state interactions, ab initio and semiempirical estimates 78−74567
Pb film, polycrystalline, optical transitions from d core states 77−85827
Pb IV, relativistic oscill. strengths 77−14388
Pb, photoionisation cross section of d-core level synchrotron radiation study of spin-orbit branching ratio 79−74057
Pb, relativistic model pseudopot., appl. to elec. resist. and phonon spectra calc. 78−51866
Pb subshell photoelectron branching ratio meas., using synchrotron radiation 80−66397
$PbMoO_4$, doped and undoped single crysts., polarisation of luminesc. and assignments 80−76069
$Pb(^3P_1^o)$+H, spin-orbit relax., fluoresc. intensity meas. 78−82681
PbSe, spin-orbit splitting in valence bands, angle-resolved UV photoemission 78−2991
$PbWO_4$, doped and undoped single crysts., polarisation of luminesc. and assignments 80−76069
Pd (111), energy dispersions for valence and conduction bands 79−38719
Pd, spin-orbit projected d density-of-states 78−38999
Pr, soft mode excitation behaviour under press., long range order 80−39838
Pr^{3+} aquo ion spectra, MCD of $^3P_0$←$^3H_4$ transition 80−7331
$PrVO_3$, neutron diffr. exam. of first order mag. transition 78−2685
Pt porphin in n-alkane single cryst. ^3E_u-$^1A_{1g}$ transition, Zeeman expts. at 4.2K 80−78645
Pt, spin-orbit projected d density-of-states 78−38999
Pt, spin-polarised LEED from low-index surfaces 78−14556
Pt subshell photoelectron branching ratio meas. using synchrotron radiation 80−66397
rare earth oxides, XPS 80−87170
Rb, electron scatt. differential spin exchange, differential cross section 77−535
Rb, excited np states, fine struct., core electrons effect 77−18807
RbAu, photoelectron spectroscopy and energy bands calc. 78−76581
RbCl(Br), F-centre emission, mag. circular polarisation 80−108251
$RbCoF_4$, 2-dimens. Ising antiferromag., mag. excitons, Raman scatt. obs. 80−66181
$RbFeCl_3$, linear chain cryst., quadrupole and mag. reson., rel. to $CsFeCl_3$ 79−38403
RbHe(Ne), spin relax., Rb hyperfine interaction in Van der Waals mol. 78−94201
Rh, $N_2N_3N_{45}$ super Coster Kronig processes 80−106303
Ru, $N_2N_3N_{45}$ super Coster Kronig processes 80−106303
$(SNBr_{0.4})_x$, supercond. props., dimensionality 80−20344
SO_2, matrix elements for multiplet spin-orbit interaction 77−57905

spin-orbit interactions continued
$^{32}S(^3He,^3He)^{32}S$, ambiguities in ^3He spin-orbit pot. radius, phenomenological optical-model anal. 79−36250
Sb trihalides, non-empirical valence electron MO calcs., ion states spin-orbit splitting 77−34544
Sc+NO_2, chemiluminesc., nonequilib. product distrib. 80−101014
SeD, ground state, spin-orbit coupling const. vac. UV determ. 78−70847
SeH, ground state, spin-orbit coupling const. vac. UV determ. 78−70847
SeH($X^2\Pi$), IR LMR spectrum, spin-orbit coupling const. direct determ. 79−76429
$SeOCl_2$:Pr^{3+}(Nd^{3+})(Er^{3+}), $SbCl_5$ acidified, Racah and Judd-Ofelt parameters in laser liqs. 80−106516
Si MOSFET, spin orbit interaction and many body effects in surface states 78−64132
n-Si:P, Sb, reson. four wave mixing, valley orbit splitting 79−89960
Si:P,Sb(Te), impurity implantation effect on CESR, spin-orbit interactions 77−36133
SiBr, $B^2\Sigma^+ \rightarrow X^2\Pi$ transition, rot. anal. *(French)* 79−50013
SiC:Al,N (6H), ODMR for effective-mass-like acceptor 80−93213
SiF, use in chemical lasers 80−64004
SiO, low-lying electronic states, vib. assigned perturbations 77−27082
SiO, test of perturbation method for vibr. assignments, low lying electronic states 77−34645
^{28}Si(n,n), 14.1 MeV, elastic and inelastic scatt., wide angular range, spin orbit interaction 78−89867
$^{28,30}Si(^{19}F,^{16}O)^{31,33}P$ 60 MeV, j depend., spin-orbit effects, optical pot. 77−41993
Sm I ^{144}Sm-^{152}Sm isotope shift J depend., in ground term. 77−75101
SmS, semicond. thin film, absorpt. and refl. spectra, fine struct., cond. band extremum 79−69897
^{154}Sm, Skyrme-HF calcs., deformation, electric moments, spin-orbit potentials 78−62480
Sn film, polycrystalline, optical transitions from d core states 77−85827
Sn, photoionisation cross section of d-core level synchrotron radiation study of spin-orbit branching ratio 79−74057
Sn tetrahalides, non-empirical valence electron MO calcs., ion states spin-orbit splitting 77−34544
Sn, white, Fermi surface, dilational strain depend., OPW calcs. 80−84418
SnF, use in chemical lasers 80−64004
SnI_2, single crysts. and film, optical props., spin-orbit splitting of cond. band 77−32437
SnTe-MnTe, degenerate semicond., anomalous Hall effect 80−29420
$SrCl_2$:Fe^{2+}(Co^{2+}) electronic absorption spectra in far and middle infrared 78−68537
SrI, low-lying electronic states, vibr. anal. 80−106315
TaS_2(1T) pure and doped, electrical, structural and mag. props. 79−78141
Tb II, Zeeman patterns, g-factors 79−22651
Te compounds, X-ray photoemission, core level binding energy shifts rel. to Mossbauer isomer shifts 78−2984
Te inversion layers in mag. fields 80−44690
Te, valence band struct. under press., spin-orbit splitting, intraband absorpt. spectra 80−2330
TeF, chemiluminesc. from oxidation in F_2+H_2Te(D_2Te) emission spectrum obs. 80−43058
$ThBr_4$:U^{4+}, single cryst., absorpt. and emission spectra 77−90174
Ti, EXAFS from L edge, 200-1000 eV 79−69903
Ti, fine struct. levels fitting, config. interaction effect, spin-orbit and electrostatic interaction parameters 80−69248
Ti oxides, XPS study, electron binding energies, spin orbit splittings, exchange splittings 79−78839
TiO, rot. anal. of (0,0) (1,0) (0,1) (1,1) bands of $\gamma'(B^3\Pi$-$X^3\Delta)$ 79−22719
Tl atom, two-photon laser spectroscopy and ionisation 78−55153
Tl, relativistic Green's function theory 79−82512
U I, electronic configs., HF relativistic calc., spin-orbit const.-Slater integral relation 77−18793
UCl_5, IR absorpt., ground config. splitting, spin-orbit coupling 77−55778
UF_6, electronic struct., relativistic MS Xα calc. 79−85911
UF_6, relativistic scattered wave calculations 80−63538
UF_6^+ and UF_6^-, electronic struct., ab initio calcs. using relativistic core pots. 79−97987
UO_2^{2+}, electronic struct. theory, applied to solid phase $Cs_2UO_2Cl_4$ and $CsUO_2(NO_3)_3$ 79−73476
UO_2^{2+} luminesc., excited states anal. 79−33766
V, fine struct. levels fitting, config. interaction effect, spin-orbit and electrostatic interaction parameters 80−69248
V oxides, XPS study, electron binding energies, spin orbit splittings, exchange splittings 79−78839
W, Fermi velocity calc., linear muffin-tin orbital method 79−28272
W films, (010), energy band calc. including spin-orbit interactions 80−20274
WV_2O_6, magnetic susceptibility, behaviour in terms of quasi-isolated binuclear units 80−97073
Xe, 5s→ϵp photoelectron ang. distrib., interchannel and spin-orbit coupling 77−3329
Xe, 5s→ϵp photoelectrons, ang. distrib. and spin polarisation 78−58634
Xe, absolute photoionis. cross sections of spin-orbit components of 4d electron 77−38646
Xe, ns→ϵp photoelectrons, spin polarisation 80−37792
Xe, photoelectron studies of 5p branching ratio 80−37793
Xe subshell photoionisation, multichannel k-matrix calc., spin orbit interactions 80−63600
Xe+F, collision in laser field, ang. momentum anal., quantum mech. theory 78−74733
Xe_2^+, electronic states, pot. curves, with/without spin-orbit interaction 78−33443
XeF(Cl)(Br)(I), covalent and ionic states, spectroscopic props., ab initio CI calc. 78−90092
XeH^+, pot. energy curves, VB calcs. 77−61688
Xe_2*, Xe_2^+, Xe_2, pot. energy curves, relativistic ab initio effective core pots. 78−86800
$YAlO_3$:Er^{3+}, free-ion-model cryst.-field calc. 77−43545
$YCrO_3$, antiferromag., exciton absorption lines obs. during field induced spin-reorientation 77−63397
$YFeO_3$, influence of mag. field on Faraday effect 78−27196
Yb, 4f levels, hole lifetime and chemical shift, UHV study 80−20762
YbBr, emission spectra in arc discharge, vibr. anal. 78−74670
YbI, emission spectra in arc discharge, vibr. anal. 78−74670
Zn, Auger spectra, comparison with multiplet struct. calc. 78−31287

spin-orbit interactions continued
Zn, de Haas-van Alphen effect under press., Fermi surface and pseudopot. form factors 77−43475
Zn, spin-orbit contrib. to mag. susceptibility of interacting electrons 77−63084
Zn-Mn(Cr), dil. mag. anisotropy, Hartree-Fock calcs. 80−11162
$Zn_xCd_{1-x}Te$ films, absorpt. spectra in 3.0 to 5.8 eV range 79−52034
$ZnF_2:Co^{2+}$, Raman tensor calcs. of isolated impurity in diamagnetic matrix 80−76025
$ZnO:Co^{2+}$, polarised optical absorpt. spectrum, crystal field transitions 77−48206
Zn_3P_2 bulk and thin film, UV reflectivity spectra, photovoltaic effects, optical consts. 80−25472
$ZnS(Se)(Te):Cr^{2+}$, absorpt. and luminesc. of $Cr^{2+}(d^4)$, cryst. field theory interpretation 79−83000
$Zn(\alpha,\alpha)$, A=64 and 66, 48 MeV, I.L. potential depth, optical model anal. 78−50187
^{A}Zr, A=90, 92 and 94, charge densities and single-particle structure 80−9224
$^{90}Zr(p,p)$, spin orbital interaction and nucl. matter density distrib. *(Russian)* 79−22176

spin-phonon interactions
see also spin-lattice relaxation
acoustic superradiance, quantum theory 78−10128
alkali halides, spin lattice relax. and g-shift 80−15799
ammonium halides, cryst., H bonding, order-disorder phenomena 80−6379
anharmonic Heisenberg ferromagnet, renormalised magnons and phonons 77−59373
anisotropic spin-phonon coupling model, exact solutions *(Russian)* 80−100590
antiferromagnet, nuclear spin oscillations, interaction with lattice vibrs. 80−70996
antiferromagnetic insulator, magnetothermal resist. 77−35767
arsenates, ferroelec. phase, E-mode splitting 78−15163
CESR, relax. times for cond. electrons due to indirect spin-spin interaction via phonon field *(Russian)* 77−90035
cubic lattice, multi-mode Jahn-Teller effect for T⊗e 77−76782
diethylammonium cadmium tetrachloride, first order phase transition, optical phonon line broadening, spin-phonon coupling model 80−7335
diffusion, effect of spin-photon and spin-phonon interactions 80−44849
dipolar interaction, reduction by off-resonance phonon avalanche 77−63260
disordered systems, optical energy transfer 78−92105
elementary excitations damping, theory of many-particle processes *(Russian)* 79−56522
EPR in superlattice, taking into account spin correl. via phonon field *(Russian)* 77−69671
EPR line shift due to spin-phonon interaction 79−65712
ESR dipolar splitting of spin pair in presence of avalanche phonons 79−61203
ferrodistortive spin-phonon systems, crit. props. 80−88315
ferroelectric, H-bonded, parametric reson., influence of lattice vibr. by parallel electric microwave pumping 77−48140
ferroelectric transition, tunnelling concept in general theory 77−63375
ferromagnet, planar, US attenuation, spin-phonon coupling, magnons and magnetostriction contrib., calc. 80−34611
ferromagnet, semi-infinite, surface magnon-phonon interaction processes, scatt. and annihilation *(Russian)* 77−63144
ferromagnet, shape of Mossbauer line 80−71251
ferromagnet in mag. field, spin relax., crit. anomalies 78−43669
ferromagnetic crystal, spin subsystem thermodynamics, spin-phonon interactions, mag. order parameter 80−103848
glass, spectral diffusion, phonon echoes and US saturation recovery 78−10149
Heisenberg ferromagnet, anharmonic, renormalised magnons and phonons 78−91837
ideal Heisenberg ferromagnet, phonon renormalisation and spin waves 80−88754
impure crystal, nuclear quadrupole spin-phonon interaction mechanism 79−95674
impurity centres exchange interaction caused by elementary excitations in solids, temp. depends. 80−25193
Ising chain, with next-nearest neighbour interactions, mag. responses to spin-Peierls transition 80−71054
Ising magnet, compressible, critical temperature shift due to spin-phonon interaction 79−99712
Ising spin system, coupled to acoustic and optic lattice modes, critical behaviour 80−71044
itinerant magnets, anomalous sound attenuation near mag. transition temp. 78−15004
Kramers doublets strong spin-lattice coupling, due to Jahn-Teller effect 77−85181
lattice instabilities in coupled pseudospin-phonon systems 78−10157
linear spin chain in uniform mag. field *(Russian)* 80−2594
magnetic crystal, order parameter for exactly soluble model 78−76207
magnetic crystal, sound velocity temp. depend. anomaly 77−72891
magnetic model with spin-phonon interaction 77−80896
magnon elementary excitations damping *(Russian)* 79−28515
metal, electron mediated nucl. spin-phonon interaction 77−1604
metal, paramagnetic, CESR spin-orbit perturbation, spin-phonon scatt. 77−63285
metals, conduction-electron spin flip by phonons, expt. data anal. 79−61219
metals, electron spin-transverse phonon interaction, spin lifetime perturbation calc. 77−12189
metals, nucl. acoustic reson., quantum theoretical treatment 79−42846
multimode linear chain, strong spin-phonon interaction 78−51623
naphthalene: quinoxaline, isolated triplet mol. direct spin-lattice relax., librational model 79−11444
naphthalene, in durene, photoexcited triplet state spin-lattice relax., local phonons effects 78−6605
$(NH_4)_2SO_4:Mn^{2+}$, ferroelec. phonon driven phase transform., reduction of spin Hamiltonian consts. 78−92033
nonmetallic crystals, ENDOR of impurity centres 80−25249
nuclear spin-lattice relaxation, effects of self consistency 77−55719
one-dimensional spin 1/2 chain, soliton excitation in strong spin-phonon interaction 80−103842
orbital singlet ions, rotational invariance and phonon-induced contribs. to spin-Hamiltonian parameters 78−10410

spin-phonon interactions continued
paramagnet, dilute, under bottleneck conditions, kinetics 77−77029
paramagnet, lifetime of coupled spin-phonon excitations 77−69053
paramagnet, reson. rot. of acoustic polarisation plane under spin-system saturation conditions 77−32245
paramagnet, velocity of sound, temp. depend. modification due to spin-phonon interaction, phonon relax. 78−19303
paramagnetic crystal, mag. ordering, spin-phonon mechanism *(Russian)* 78−60302
paramagnetic crystal, mixed spin-phonon waves *(French)* 77−66400
paramagnetic ion, reson. phonon scatt. 78−18716
paramagnetic ion with S=1 in cryst. field of uniaxial symm. 77−76496
paramagnetic spin system, two-level open system, kinetic theory of resonance and relaxation 80−88859
paramagnets, conc., ESR line shift, phonon relax. influence 78−88171
phonon scattering by paramagnetic ions, Zeeman levels in absence of zero field splitting 77−15508
quadratic magnetostriction, exactly soluble model 79−8030
quantum compressible Ising model, critical behaviour 80−108016
rare earth metal, anomalous sound attenuation near mag. transition temp. 78−15004
rare earth zircons, Jahn-Teller cooperative phase transition, crossover effects 80−88316
rare-earth metals, US attenuation, exchange striction, and spin-phonon interaction 79−33518
Rochelle salt, ferroelec. phase transition, Raman scatt. study 80−97211
Rochelle salt, ferroelectric, Raman and IR study 80−71406
ruby, excited state spin-phonon interaction, time resolved spectroscopic exam. 78−19549
ruby, high mag. field spin-lattice relaxation rate of Cr^{3+} 78−52340
screening, dynamic, by carriers, effect on paramag. relax. times 77−16150
self-trapping transition, spin 1/2 system 80−10606
spin Hamiltonians, infinite-range, exact solns. 79−78281
spin system, thermodynamics, contrib. of spin-phonon interaction 78−2635
spin-Peierls transition in mag. field, phonon freq., Heisenberg model calcs. 80−25151
spin-Peierls transition in magnetic field 78−84441
superconductivity originating from quasi-orbital conduction electrons in non-adiabatic systems 79−33382
supernonradiative phase transition, appl. to paramag. impurities in strong mag. field 79−14898
1,2,4,5-tetrachlorobenzene, multiple-quantum spin-phonon interactions, acoustically-induced phosphoresc. obs. 77−40150
tetramethylaminelithium(0), $Li(CH_3NH_2)_4$, existence, conduction- and localised-electron spin reson. 80−66035
thiourea, ferroelectric, Raman and IR study 80−71406
thiourea, phonon modes near order-disorder transforms., hard-core modes due to pseudospin-phonon coupling 80−44285
three-dimensional crystal, with strong spin-phonon interaction, domain wall quantum mechanics 78−51622
TTF.CuBDt, spin 1/2 Heisenberg chain, spin-Peierls transition 79−61135
TTFCuBDT, spin-Peierls transition in spin 1/2 Heisenberg chains, RPA calcs. 80−25150
Ag:Er(Dy), orbit-lattice coupling, nonuniform strain effects 78−88182
Al:Er(Dy), orbit-lattice coupling, nonuniform strain effects 78−88182
$Al_2O_3:Ni^{3+}$, phonon-spin interaction study by thermal cond. meas. 79−82395
$Al_2O_3:V^{3+}$, Jahn-Teller effects, ground state 80−75528
$Al_2O_3:V^{3+}$, spin-phonon coupling, rot. mode role 80−70329
$BaF_2:Gd^{3+}$, spin-lattice coeffs., EPR study 80−66032
$BiI_3:Cr^{3+}$, ESR, spin-lattice relax., temp. depend. 78−88178
$BiI_3:Mn^{2+}$, ESR, spin-lattice relax., temp. depend. 78−88178
$CaF_2:Ce^{3+}$, Kapitza limited spin-bath relax., paramag. Faraday effect meas. at liq. He temp. 79−95642
$CaF_2:Eu^{2+}$ single cryst., temp. depend. of second-order spin-lattice coeffs. 77−90029
$CdCr_2S_4$, phonon Raman scatt., mag. circular polarization effects 79−8134
$CdCr_2Se_4$, resonant Raman scatt. 79−4802
$CoBr_2(Cl_2).2H_2O$, linear chain metamag. system, phonon and magnon widths 77−36065
$CoCs_2(SO_4)_2.6H_2O$, obs. of H^2T^7 Raman spin-lattice relax. process 77−51459
$CoK_2(SO_4)_2.6H_2O$, obs. of H^2T^7 Raman spin-lattice relax. process. 77−51459
$Co(NH_4)_2(SO_4)_2.6H_2O$, obs. of H^2T^7 Raman spin-lattice relax. process 77−51459
CsH_2AsO_4, and deuterated isomorph, E-mode splitting in ferroelec. phase, Raman scatt. meas. 77−16296
CsI, acoustic NMR, role of incoherent phonons *(Russian)* 78−80230
$CsNiCl_3$, linear-chain antiferromag., low temp. thermal expansion 80−39326
Er film, magnetoelastic excitations, phonon spectroscopy and forbidden transitions 79−82853
Er US attenuation near magnetic transitions at 53.9 and 83.8K 79−55837
$ErVO_4$, phonon resistivity mag. field depend. in paramag. phase 80−2226
Eu chalcogenide, spin-disorder Raman scatt., mag. phase depend., theory 78−10887
Eu chalcogenides, magnetic semiconductor, light scatt. exam. 79−61372
Eu chalcogenides, spin-dependent Raman scatt. from phonons 80−97274
EuO(S)(Se)(Te), spin order and fluctuations, Raman scatt. study 80−97273
EuS(Se)(Te), spin-assisted phonon Raman scatt., mag. phase depend. 80−71413
EuTe, antiferromag. semicond., Raman scatt., spin-phonon interactions 80−66185
EuTe, antiferromagnet, phonon Raman scatt. from spin superstructures 80−16030
EuTe, Raman scatt. exam. 79−61375
Fe film, magnetoelastic excitations, phonon spectroscopy and forbidden transitions 79−82853
Fe, thermal cond., elec. resist., Lorenz number and magnetisation, crit. behaviour 77−4521
$FeCl_2.2H_2O$, linear chain metamag. system, phonon and magnon widths 77−36065

spin-phonon interactions continued
Fe^{3+} (^6S) paramagnetisations, spin lattice relaxation Mossbauer study, dynamic spin Hamiltonian formalism 80−97173
Gd film, magnetoelastic excitations, phonon spectroscopy and forbidden transitions 79−82853
^3He, solid, phenomenological treatment of exchange effects in high-temp. limit 77−35795
InSb, acoustic NMR, role of incoherent phonons *(Russian)* 78−80230
InSb, intraband photocond. in mag. fields 79−47123
n-InSb, magneto-photoconductivity, phonon assisted combined reson. magneto-optical absorpt. reson. 78−47831
n-InSb, spin-magnetophonon resonance 80−96918
KH_2AsO_4, and deuterated isomorph, E-mode splitting in ferroelec. phase, Raman scatt. meas. 77−16296
KH_2AsO_4, ferroelec., temp. broadening of hard mode Raman lines near Tc 78−88296
KH_2PO_4, damping of transverse acoustic and ferroelec. modes 78−14413
KH_2PO_4, E-mode splitting in ferroelec. phase, Raman scatt. meas. 77−16296
KH_2PO_4, ferroelec., Raman internal-mode line broadening by proton jumps 77−43981
KH_2PO_4, ferroelec., temp. broadening of hard mode Raman lines near Tc 78−88296
KH_2PO_4 type ferroelectrics, isotopically disordered, collective modes, CPA 77−7825
$KMgF_3:Ni^{2+}$, acoustic Faraday and Cotton-Mouton effects, theory 80−65987
$La_2Mg_3(NO_3)_{12}.24H_2O$:Ce, bottlenecked Orbach relax. process, phonon lifetime 79−65151
$LaRh_2:Nd^{3+}$ cubic metallic host, spin-lattice relaxation, ESR obs. 79−1710
LiF:Co(Mg), nucl. acoustic reson. 77−8445
$MgO:Cr^{2+}$, critically coupled spin-phonon mode 78−67779
$MgO:Cr^{2+}$, paramag., spin-phonon coupling, inelastic neutron scatt. obs. 79−60441
$MgO:Cr^{2+}$, reson. scatt. of phonons by ions 78−18716
$MgO:Fe^{2+}$, lifetime of coupled spin-phonon excitations 77−69053
NH_4, halides, sound attenuation near lambda point 77−66002
NH_4Br(Cl), anomalous sound attenuation above lambda point 78−51617
NaCl, pure and doped, nucl. acoustic reson. 79−69746
Ni film, magnetoelastic excitations, phonon spectroscopy and forbidden transitions 79−82853
$NiSiF_6.6H_2O$, non-Kramers system, spin-lattice relaxation at strong fields 80−100612
PbI_2-piperidine intercalations rel. to NQR, spin-lattice relax. temp. depend. *(Russian)* 78−27108
Pd, triplet pairing, spin fluctuation contrib. 78−10711
Pd, triplet pairing, spin fluctuation and phonon contribution 79−7929
$RbAg_4I_5$, US attenuation near 208K phase transition 79−33085
RbH_2AsO_4, and deuterated isomorph, E-mode splitting in ferroelec. phase, Raman scatt. meas. 77−16296
Rb_2PtI_6, cryst., role of ordinary and harmonic Raman processes, ^{127}I nucl., spin-lattice relax., obs. 79−8063
Si, Jahn-Teller Mn^0 centre ESR spectrum, depend. on axial press. 80−44911
$Si:Fe^0$, spin relax. rate ang. depend. for pulsed saturation of inhomogeneously broadened ESR line 79−65721
TGS, temp. behaviour of optical phonons near T_c, evidence of non-linear pseudospin-phonon interaction 77−7824
TGSe, temp. behaviour of optical phonons near T_c, evidence of non-linear pseudospin-phonon interaction 77−7824
$TmVO_4$, type crystals with cooperative Jahn-Teller effect, acoustic NMR *(Russian)* 77−28460
$TmVO_4$-type crystals, dipole nuclear spin-phonon coupling and US absorpt., theory 77−24753
UN, sound velocity temp. depend. anomaly 77−72891
VI_2, antiferromag., zone-boundary phonon Raman scattering, modulation of exchange interaction 80−11386
VI_2, antiferromagnet, phonon Raman scatt. from spin superstructures 80−16030
VI_2, spin-dependent Raman scatt. from phonons 80−97274
YAG:rare earth metal, US absorpt. meas., relax. model 80−24539
YFe_2 film, ($x \simeq 2$), magnetoelastic excitations obs. 78−68307
$ZnS:Co^{2+}$, spin-lattice relax., phonon heating effect *(Russian)* 78−19317
ZnS(Se)(Te):Ag^{2+}(Cu^{2+}), absence of EPR spectra due to strong spin-lattice coupling of Kramers doublets 77−85181
$ZnSiF_6.6H_2O$, spin-phonon interaction between Ni^{2+} ions, phonon bottleneck effects, splitting parameters *(Russian)* 80−15796

spin polarised electron emission
alkali metal atom, spin polarisation of photoelectrons, one-quantum photoeffect 80−37790
alkali metal atom, two-photon ionis. with two light beams, photoelectron polaris. 80−43011
aniline, photoemission for mol., polarised photoelectrons 78−66607
atom, outer shell ionisation, ang. distribs. and polaris. of charact. X-rays and Auger electrons 79−10205
atom, unpolarised, spin polarisation of ejected electrons 78−78765
book, advances in electronics and electron phys. 77−78906
book 77−46679
dimethylanilines, photoemission for mol., polarised photoelectrons 78−66607
experimental techniques and apparatus, book contrib. 77−81198
ferromagnet, spin polarisation of emitted photoelectrons 80−45215
ferromagnetic metal, spin-polarised field emission, many-body and spin-dependent surface pot. effects 79−74065
ferromagnetic transition metals, review 78−76591
ferromagnetic transition metals, review 78−76592
3-iodoaniline, photoemission for mol., polarised photoelectrons 78−66607
magnetic order and spin depend. of electron scatt. meas technique using photoemission 80−60748
metal surface, clean, spin polarised electron field emission 80−45221
2-methylaniline, photoemission for mol., polarised photoelectrons 78−66607
nonferromagnetic metals, spontaneously broken parity state 78−48277
photoemission, spin energy analysed, feasibility anal. 80−55271
polarisation effects in penetration of barrier with applied mag. field, relativistic corrections, polarisation effects 79−78852
polarisation effects in penetration of nonrelativistic electrons through potential barrier with appl. mag. field 78−11084

spin polarised electron emission continued
polarized electron emission from solids, book 77−78906
substrate-split localised adsorbate levels, spin polarisation effects in photoemission 79−19971
surface magnetisation, size effect 78−15008
Ar, photoelectron emission, polarisation depend. on incident unpolarised VUV radiation wavelength 80−52952
Ar, plane polarised VUV irrad., emitted photoelectron polarisation, ang. depend. 80−47952
Ar, spin-polarised photoelectrons by circularly polarised synchrotron radiation 80−91516
CO_2, spin polarised photoelectrons, synchrotron excited 80−43101
Cs, polarised photoelectrons produced by circ. polarised synchrotron radiation 80−18830
Cu, surface energy band calc., significance for photoemission 78−95330
$ErFe_2$ surface, effect of H and O adsorption, spin polarised photoemission study 80−29854
Eu chalcogenides, cond. band spin struct. 80−71577
EuO:Gd, 4f-photoelectron spin polarization, temp. depend. 79−78842
EuO:Gd, surface depolarisation of photoelectrons 78−15286
EuS, ferromag., on W, electron field emission 79−8230
EuS, spin polarised tunnelling and mixed spin states in conduction band 79−52085
Fe (100), (111), (110), spin polarised field emitted electrons 78−60553
Fe (111), spin polarised photoemission 80−45221
Fe, field-emitted electron spin polarisation by tunnelling through surface pot. 80−29861
Fe, itinerant model of spin polarised field emission 78−95685
Fe, photoelectron spin polarisation and itinerant magnetism 78−68602
Fe_3O_4, single cryst., surface magnetism, spin polarized photoemission 78−52622
FeTi, surface and mag. props., heat treatment and hydrogenation effects 80−75447
GaAs (100) and (110), photoelectrons spin polarisation 80−11530
GaAs, negative electron affinity, optically pumped, depolarization of emitted photoelectrons 79−8223
GaAs:Zn (110), spin polarised electron production by photoemission from Cs-O overlayer 79−95903
$GaAs_{0.62}P_{0.38}$, negative electron affinity, photoemission of spin polarised electrons 80−2916
Kr, photoelectron emission, polarisation depend. on incident unpolarised VUV radiation wavelength 80−52952
Kr, spin-polarised photoelectrons by circularly polarised synchrotron radiation 80−91516
$La_{1-x}Pb_xMnO_3$, spin polarised XPS and LIPS, electronic struct. 77−8717
N_2O, spin polarised photoelectrons, synchrotron excited 80−43101
Na, reson. two-photon ionis., photoelectron ang. distrib. and polaris., nucl. spin influence 79−10083
Ni (001), spin polarised photoemission theory 79−15584
Ni (100), spin polarised photoemission 80−45221
Ni (110) surface, positive spin polarisation in field emission and demagnetisation in H_2 adsorption 78−52646
Ni (111), electron spin polarised photoemission spectrum 80−25525
Ni (111), Λ_2-symmetry surface state, angle resolved photoelectron spectra 78−80034
Ni (111), single crystal, spin polarisation of emitted photoelectrons 80−45215
Ni, (111) surface, VUV photoyield, electron spin polaris. enhancement 79−74054
Ni, chemisorption of H, surface magnetism 78−95510
Ni, demagnetisation of surface due to absorption of H_2 77−80990
Ni, electronic and magnetic props., spin split energy band dispersions 79−78829
Ni, ferromagnetic, photoemission spectra and band struct., spin polarisation of bulk photoemission 79−78843
Ni, field-emitted electron spin polarisation by tunnelling through surface pot. 80−29861
Ni, field-emitted electrons, spin polarisation, theory 77−44134
Ni, photoemission, spin polarisation of reson. two-hole bound state 79−83099
Ni surface (111), photoyield near theshold negative-positive spin polaris. crossover 80−2922
Tl, photoionis. cross section, spin polaris. and ang. distrib. of photoelectrons, RPA calc. 78−13478
US, electron spin polarisation 79−65978
US(Se)(Te), photoelectron energy distrib. and spin polarisation, electronic and mag. props. 80−16146
US(Se)(Te), spin polarisation and magnetism, photoelectron study 80−40219
USe, ferromag., spin polarisation of photoelectrons 79−78831
UTe, ferromag., negative electron spin polarisation in photoemission 79−19967
UTe_xSb_{1-x}, photoemission, densities of states 80−16147
W (001) adsorbate system, directional photoemission of polarised electrons 77−36374
W (100), optical magnetisation from spin polarised photoemission 79−78830
W field emitter, strong polarisation effect in photoinduced field emission 78−95684
W, optically polarised conduction-band electrons, spin-polarised photoemission obs. 79−74055
W, photoemission of spin polarised electrons 78−35248
W, spin filter effect of EuS 80−45221
W-EuS interface, electron spin polarisation in field emission 78−35265
Xe, plane polarised VUV irrad., emitted photoelectron polarisation, ang. depend. 80−47952
YIG, energy location of mag. Fe levels, spin polarised photoemission 79−24413
$ZnGeAs_2$, photoelectron spin polarisations, electron level struct. 79−87557
$ZnSiAs_2$, photoelectron spin polarisations, electron level struct. 79−87557

spin polarised electron phenomena *see electron spin polarisation*

spin-spin nuclear coupling in molecules *see molecular nuclear coupling*

spin-spin relaxation
adensoine 5′-diphosphate, interactions with kyosin, intermolecular spin diffusion study 80−18951
agarose gels, $H_2{}^{17}O$ enriched, ^{17}O NMR, hydration anal. 77−81426
alcohols, liq. mol. rot., deuteron relax. obs. 77−8432

spin-spin relaxation continued
alkali metal-ammonia solns., spin site exchange mechanism for electron relax. times 78−27077
amniotic fluid, human proton relax. times in low field range, appl. to nucl. magnetography *(French)* 78−3574
anisotropic fluid, diffusion, EPR spin exchange and nuclear spin relax., theory 80−34753
apparent spin-spin relaxation time, super-regenerative NQR spectrometric obs. 80−54963
benzenes, substituted, C-C coupling consts., coupled Hartree-Fock calcs. 77−27091
benzyl alcohol, C-C spin coupling, two-dimens. Fourier transformation 78−90194
biological cells, classical diffusion to explain ^1H spin relax. in NMR obs. 79−83721
blood, magnetic relax. time of H_2O protons 79−11898
blood, normal and pathologic, NMR T_2 relax. time studies 80−81682
bottlenecked EPR, singly, doubly, multiply bottlenecked systems 78−27078
bromobenzenes ^{13}CBr bond, spin-spin coupling consts., correl. with C hybridisation s-character 80−34806
bromoethane, liq., relative mol. orientation appl. of nucl. mag. relax. data 79−41933
Carr-Purcell-Meiboom Gill pulsed NMR sequence, errors in T_2 values 77−85604
Carr-Purcell-Meiboom-Gill pulsed NMR experiment, baseline drift 77−85603
CBOOA:nitroxide, liq. cryst. phase transition study by electron spin relax. *(French)* 79−55874
cellulose, mobility of adsorbed water, NMR pulse obs. 80−108835
CESR, relax. times for cond. electrons due to indirect spin-spin interaction via phonon field *(Russian)* 77−90035
CESR line profile, indirect spin spin interaction 79−28616
chloroform diluted in CS_2, proton transverse relax. time and reorientation of chloroform *(French)* 77−32280
chloroform-hexamethylphosphoramide complex, mol. motion and assoc., PMR obs. *(French)* 78−72429
chloroplast, mag. relax. of water protons and state of water photo-dissociation system 80−51133
cobalt formate dihydrate, ordered state, paramag. cross relax. *(Japanese)* 77−43873
coherent series, T_2 as collision time, dephasing time, or reciprocal line-width, for teaching 80−27075
collagen fibril, ^2H NMR of mol. motion 80−67034
correlation time calc. from nuclear mag. relax. data, computer program 78−88210
coupled spin systems, relax. mechanisms and multiple quantum transitions 78−88211
critical dynamics at phase transitions and nuclear relaxation 78−75805
cross-linked polymer system, influence of chem. cross-link network on spin-spin relaxation *(Russian)* 77−32284
cyclohexane, FCC plastic phase, self-diffusion coefficient, 6 to −40°C, nucl. spin-lattice (spin) relax. 77−36144
cytochrome c_3, haeme-haeme mag. interaction, Mossbauer obs. 80−108836
decacyclene anion, photoexcited quartet state, transient EPR 80−78635
diamagnetic crystal, with non-Kramers mag. impurity, relax. of lattice nucleus 77−32282
diamantane, NMR meas. of mol. motion 79−42858
2,6-dichloroanisole, anisotropic reorientation, nucl. relax. in coupled spin systems 77−40145
diffusion of nuclei, correlated, influence on nucl. spin-spin relax. time *(Russian)* 77−51977
p-dihalobenzenes, apparent NQR spin-spin relax. times obs. 80−54991
dilute gases, nucl. mag. relax., theory 78−25559
dilute paramagnet, mag. reson. linewidth due to two-particle interaction 77−90012
dimethyl ammonium copper chloride, nearly two-dimensional ferromag., nucl. transverse relax. rates meas. 77−81024
dimethyl mercury, indirect coupling constants, vibr. corrections 79−50050
dimethylbenzaldehydes, in durene single cryst., zero-field splitting, guest and host isotope effects 80−107752
N,N-dimethylcarbomoylchloride, chem. exchange rate by NMR method, temp. depend. 79−79243
dipolar solid, multiple-pulse spin locking 77−20742
dynamic magnetoresonance effects in solids 80−20447
elastomer, segmented block, morphology, pulsed proton NMR study 80−33907
electrolyte solution, relax. of spin 1/2 nuclei of heavy atoms 77−24758
epoxy polymers, cured spin-spin and lattice relax., proton coupling, ^{13}C NMR obs. 80−34799
EPR, microwave signal detection, effect of relax. processes 77−66413
EPR and saturation transfer EPR, fast computation, master supermatrix eqn. soln. 78−62213
EPR and saturation transfer EPR, fast computation, perturbation approach 78−62212
EPR dispersion signals, mech. detection 79−30520
EPR linewidth and relax., effect of antisymmetric exchange 77−59448
erythrocytes, bound water in frozen solns., proton mag. relax. 77−28472
ethane, nucl. spin-spin coupling, scanning MO HF LCAO calc. 79−50045
ethylene, nucl. spin-spin coupling, scanning MO HF LCAO calc. 79−50045
ethylene oxide, ^{13}C and D variants, T_2-relax., 2_{20}-2_{11} rot. transition by microwave pulse spectrometer 80−47976
ethylene oxide, gas, EPR rot. transitions, T_1 and T_2 relax. 80−9622
ethylene oxide, rot. relax., double reson. and Stark switching obs. 80−106340
eye cataractous lens, NMR study of state of water *(Hungarian)* 78−64986
eye lens, normal and senile cataractous, PMR study of state of water 78−64987
eye lenses, crystalline, of humans, fish and birds, state of water, NMR meas. 79−48212
ferroelectric, order-disorder, crit. dynamics, NMR data compared with dielec. data 78−76415
fluorite lattices, $^{19}F^-$, self-diffusion, spin lattice relax., NMR techniques 80−34801
formic acid, ^{13}C NMR spectra and relax. under intermediate decoupling power conditions 80−20515
free radicals, spin exchange, anisotropic spin-density distrib. 80−102526
furil + pentachlorophenol, photochem. reduction, cross-relax. and CIDNP, PMR relax. obs. 79−52694
garnet, substituted polycryst., low FMR linewidth, relax. processes 77−20718
gas phase NMR, kinetic theory, single relax. time approx. 77−14451
gas phase nucl. mag. relax., DWBA cross sections from S-matrix formalism 77−27151
haemoglobin in red cell suspensions, T_1 and T_2 meas. 78−80832
haemoglobin solution, proton mag. relax. meas. 77−1975
halloysite, $Al_2O_3(SiO_2)_3(H_2O)_2$, NMR study of adsorbed water, molecular motions 78−95226
heteronuclear double resonance, individual Overhauser effects in coupled AX_2 and AX_3 spectra 79−31554
homonuclear coupled spin system, inversion-recovery data anal. 79−33554
hydrocarbon chain, gauche-trans isomerisation, ^{13}C relax. times and nucl. Overhauser enhancement model 78−33520
II-VI semiconductors, electron-electron spin-flip scatt. and spin relax. 80−44916
III-V semiconductors 80−44916
impurity spin-unpolarised lattice nuclei interaction, dynamic susceptibility 79−69648
inhomogeneous systems, line broadening, spin-spin and spin-lattice relax. rate meas. 80−58292
insulators, mag., interference effects in NMR line shape 77−8435
intermolecular mechanics, T_1 and T_2, by microwave meas., zero- and non-zero field 79−45738
ionic conductors, central component NMR relax. rates 80−29640
Ising square lattice, phase transitions, next nearest neighbour interactions 80−50128
J coupling from Carr-Purcell spin echo techniques 77−10690
KCN, relax. times of F-centres meas. at 83K phase transition 77−59458
lipid bilayers, D relax. rates and mol. dynamics 80−26206
liquid, intermolecular nucl. relax. by translational and rot. diffusion, effect of pair correl. functions *(French)* 79−19794
liquid, polyatomic molecular, intermol. dipolar mag. interactions effect on nucl. relax. *(French)* 77−32277
liquid binary mixtures, proton mag. relax. and mol. motion 77−28471
liquid metal, nucl. quad. relax. rate temp. depend. calcs. 77−12273
liquids, nuclear spin quadrupole relaxation 79−78548
low temperature nuclear relaxation stimulated by paramagnetic impurity 79−33563
lysozyme spin-labelled preps., water-protein layer microstruct. study by mag. relax. 78−76980
metal:D, dynamic quadrupole nuclear spin relax., α or α' phases 77−48085
metal tritides, ^3He NMR and distrib. 78−30661
methane, in alkane soln., ^{13}C nucl. spin-spin relax., for mol. correl. times 79−95661
methanol:chromium acetylacetonate, NMR, degenerate transitions, selective excitation transfer and separated relax. meas. 78−80235
methanol, mol., nucl. spin-spin coupling const., Hartree-Fock calc. 80−9618
methyl group, NMR relax. due to dipolar interactions 77−14455
4-methyl-2,6-t-butylphenol, γ-irrad., electron-methyl group spin-spin interaction 77−85572
1-methylimidazole complexes, with ferriporphyrins, PMR obs. 77−12214
molecular relaxation, statistical treatment, review 77−51284
monovalent ions in aq. metal ion solns., ^{14}N NMR relax. 80−20481
Mossbauer relaxation spectra, breakdown of white noise approx. 78−27141
Mossbauer spectra, complications in theory due to spin-spin relaxation *(Russian)* 78−43757
motion-induced nuclear spin relax., orientation depend., point defect self-diffusion mechanism 77−48078
multiple and combinational freq. NQR, dipole-dipole, spin-spin interactions 80−20499
multipulse NMR, relax. processes anal. 80−34798
muonium, bimol. rate consts., Larmor precession relax., kinetic isotope effect rel. to H 77−38752
muscle, frog, spin-spin relax. times rel. to temp. and water content 78−56952
muscle, mouse, ^{13}C NMR and PMR 77−86463
muscle, mouse, NMR multiwindow anal. and proton local fields and magnetisation distrib. 80−21444
muscle, of barnacle, transverse nucl. mag. reson. relax., bounds on bound water 77−4989
muscle, skeletal, Na relaxation, spin echo study, evidence of Na ion binding inside a biological cell 78−88698
muscle, skeletal, water protons NMR relax. times anisotropy obs. 80−85341
muscle water, study of spin-lattice and spin-spin relax. times of ^1H, ^2H, and ^{17}O 80−21443
muscle water transverse and longit. NMR relax. rates 78−35810
myosin, interaction with adenosine 5′-diphosphate, intermolecular spin diffusion study 80−18951
myosin, interactions with HDO, intermolecular spin diffusion study 80−18951
neopentane adsorbed on graphite, quasi two-dimens. fluid, NMR 80−102525
nitrobenzene, anisotropic mol. reorient., ^{13}C, ^{14}N and ^2H mag. relax. 77−48070
NMR, degenerate transitions, selective excitation transfer and separated relax. meas. 78−80235
NMR, gas phase, spin-spin and spin-rot. relax., IOS calcs. 79−18209
NMR, non-secular spin-spin interactions, in nucl. relax. 78−91976
NMR hybrid relaxation and multiple pulse methods for studying chemical, physical and spin exchange 80−80629
NMR line profile, paramagnetic ion nuclei in magnetically conc. solid, theory 80−25238
NMR linewidth, paramagnetic contribs. calcs. 80−58286
NMR measurement technique for slowly relaxing systems with weak NMR signals 77−49752
NMR spectra, non-Lorentzian, in low density gases 78−94259
NMR spin echo, chemical exchange and T_2 relax., multiple sites 78−78727
NQR pulsed panoramic RF spectrometer 77−10074
NQR-NMR double resonance line intensities, level crossing method, two freq. saturation 80−20514

spin-spin relaxation continued
NQR-NQR double resonance, double quadrupole spin echo resonance 80−20513
nuclear acoustic resonance spectrum, kinetics of spin system for spin quantisation by strong acoustic field 78−15052
nuclear magnetic spin relax. of spin-pair undergoing reorientations by jumping among inequivalent sites 79−42862
nuclear spin relax. by translational diffusion in solids, reciprocal-space formalism, mean-field theory 80−71208
nuclear spin relaxation and molecular rotation, review, book contrib. 79−31557
nucleic acid bases, ^{14}N relax. and N-proton spin coupling, NH-proton spin-lattice relax. 80−26202
one-dimensional planar magnets, low temp. NMR 80−44943
organic paramagnetic systems, multiple internal motions, nucl. spin dipolar relax. obs. 80−28037
oxalic acid dihydrate, PMR, water mols., reorientation 79−42856
paramagnet, cross relax. theory *(Russian)* 77−12187
paramagnet, spin diffusion at low temp. *(Russian)* 77−32240
paramagnetic metal ions as structural probes for NMR investigation of inorganic and bioinorganic compounds 78−62828
paramagnetic nonresonance absorpt., kinetic eqns. 80−7151
paramagnetic substance, single spin cross-relax., temp. depend. of transition probability 80−25184
paramagnetic system with quadrupole splitting, magneto-optical effects, magnetic resonance saturation 80−60404
perdeuterobenzophenone, in 4,4'-dibromodiphenylether, cross-relax., microwave pulse obs. 80−53031
phosphatidylcholine hydration, adsorpt.-desorpt. isotherm and PMR 78−15781
phospholipid bilayer membrane, spin $^1/_2$-nuclei, in chain methylene groups 77−48767
photoexcited molecule, exchange between triplet states with nonparallel eigenvectors 79−59374
photoexcited triplet state molecules, in cryst., cross-relax., variable freq. ODMR obs. 80−53031
physiological fluid, human, identification in situ by proton relax. *(French)* 79−48316
planar molecules, anisotropic reorientation, nucl. relax. in coupled spin systems 77−40145
plastic crystal, anomalous high resoln. of NMR linewidths 77−12218
pleural liquids in weak fields, PMR relaxation times, medical diagnosis appl. *(French)* 78−73187
PMR relaxation times vs. water content for tumour and normal tissue 77−12884
poleythylene, linear, butane diffusion coeff., VP depend. nulc. spin echo obs. 79−38404
poly(γ-benzyl-L-glutamate), soln., rot. diffusion, ^{13}C NMR 77−75350
poly(methacrylic acid)-D_2O soln., proton and deuteron relax. rates, temp. and freq. depends. 77−88472
polyacrylic acid:Fe^{3+}, electron state of Fe^{3+}, Mossbauer and magnetisation obs. 79−73872
polyatomic molecules, intramolecular vibr. relax., restricted quantum exchange theory 80−63610
polydiethylsiloxane, mol. motion, NMR spin relax. data re-interpret. 80−84664
polydimethylsiloxane fluid, irradiated, NMR anal. of cross-linked and entangled networks 77−51980
polydimethylsiloxanes, liq., proton spin relax., mol. motion, network form. 79−15369
polyethylene, ^{13}C NMR rotating frame relaxation 80−7182
polyethylene, linear, melt props. correl. with chain length distribs. *(Russian)* 80−37920
polyethylene, linear, nuclear relaxation, mol. motion *(Russian)* 80−44949
polyethylene, linear, struct. and relax. transitions, pulsed NMR and X-ray diffr. *(Russian)* 77−47357
polyethylene, liq., very high mol. wt., pulsed NMR obs., entanglement, crosslinking, irrad. effects 78−66702
polyethylene, NMR with rotation through magic angle *(German)* 78−76341
polyethylene, pulsed NMR obs., crystallinity effects 78−76342
polyethylene melts, entanglement effects in NMR spin-spin relaxation 79−19795
polyethylene terephthalate, NMR relax. and mol. mobility *(Russian)* 78−88219
polyisobutylene, soln., ^1H NMR relax. 77−24759
cis-polyisoprene, ^1H NMR, T_1 and T_2 meas., −50-170°C 79−69738
cis-polyisoprene, ^1H NMR of γ-induced cross-linked polymer 79−69739
polymer glassy and crystalline, relax. process characterisation, ^{13}C NMR obs. 80−34802
polymers, synthetic, dil. solns., NMR relax., review 79−89693
polynuclear system, ENDOR dynamics of F-centres, cross relax. effect 77−40151
polysaccharide gels and sols, PMR relax. times rel. to temp., pH and conc. 78−56952
polystyrene solution, conc., diffusion and NMR relax. times 77−55725
polyurethanes, cross-linked, mol. mobility and struct., thermomechanical and NMR obs. *(Russian)* 80−69285
Portland cement, absorbed H_2O, pulsed NMR study 80−84665
praseodymium ethylsulphate:Sm, one-dimens. X-Y system, spin dynamics, electron spin echo meas. 80−66031
pulsed NMR data acquisition system, devel., appl. to polyisobutylene 80−34807
pyrene-d_{10}, EPR line shape of photo-excited triplet state, in cryst. and glass 79−24210
pyridazine, liq., nucl. relax. and mol. reorientation, nucl. Overhauser enhancement 78−60351
pyridenes ^{15}N NMR chem. shifts, paramag. relax. reagent effect 78−15042
quantum systems, at. or spin two level, reson. EM wave excitation, free induction decay oscills. 80−63562
rare earth compounds, cryst. field effects on EPR and NMR *(Japanese)* 77−43880
rare earth garnets: $^{154}Gd^{3+}$, hyperfine interactions, PAC 77−43909
rare earth nonmetallic compounds, indirect spin-spin coupling, models 80−80238
rare earth orthoferrite, second-order reorientation transition, NMR signal relax. 77−90066
rare earth systems, NMR, EPR, and Mossbauer effect, book contribs. 80−39883
spin-spin relaxation continued
resonant Rayleigh-type mixing spectroscopy using ps light pulses, ultrafast relax. study 80−91834
rotating coordinate system, phenomenological approach 80−39887
ruby, effect of relax. processes on microwave signal detection 77−66413
saturated bandshapes in high-resolution NMR relax., obs., three and four spin 1/2 systems 77−1611
simple cubic lattice, simple hopping, correlation functions, NMR relaxation rates 79−42864
solid, dipole-dipole ordering in nuclear spin system by acoustic pulse 79−11333
solid, nucl. spin relax. by translational diffusion 77−16195
solid polymers, NMR, review 80−88888
soliton gas, interaction with nucl. spin 79−69736
solution, ^{89}Y spin-spin relax. times, no pH depend. 80−2657
soya protein gels and sols, PMR relax. times rel. to temp., pH and conc. 78−56952
spin systems under multiple pulse NMR conditions, chem. shift relax. 80−34808
spin-1/2 systems, strongly coupled, perturbation response symmetries *(French)* 80−43069
spin-echo Fourier transform NMR spectroscopy, multiple pulse technique 80−37063
SQUID NMR meas. at low-temp., improved technique 78−54417
superconductor, slightly dirty, CESR due to exchange and spin-orbit scatt. 77−28300
superimposed exponentially decaying signals, computer-aided anal. technique 78−23360
superionic conducting materials, nucl. mag. relax. by paramag. impurities 79−42866
superionic conductors, mag. reson., book contrib. 80−25240
TCNQ salt, $(N(CH_3)_3H)(I)(TCNQ)$, proton spin-lattice and spin-spin relax. times 79−8065
tetramethyltin, in liq. cryst., ^1H, ^{115}Sn, ^{117}Sn and ^{119}Sn NMR spin-spin relax. 78−91973
tissue molecular dynamics and freezing phase transition studied by proton spin relax. 78−68983
TMMC, field-suppression of spin fluctuations, NMR obs. 78−91971
TMMC, paramagnetic relax. rates, anisotropic diffusion model 77−69668
TMNC, quasi one dimensional planar ferromag., low temp. NMR study im mag. field 80−97157
transition metal hydrides, proton diffusion mechanisms, NMR determ. 77−90060
s-triazine, mol. cryst., low temp. mol. reorientation, phase transition, ^{14}N NQR 77−36150
1,2,3-trichlorobenzene, anisotropic reorientation, nucl. relax. in coupled spin systems 77−40145
1,1,2-trichloroethane, phase-modulated spin echoes, derivation of pure absorpt. spectra 80−22410
trichlorophosphazenes, ^{35}Cl NQR spectra and reorientational motion of PCl_3 group 78−25567
triple NMR technique for N-containing molecules, ^{13}C-{^1H,^{14}N} triple reson. 79−81219
tristearin irreversible liq.-liq. phase transition, ^{13}C NMR meas. 78−26681
two-dimensional planar magnet, crit. slowing down in transverse autocorrel. function 78−95448
two-level model with diffusional modulation of interacting particles *(Russian)* 77−40143
vinyl bromide-d_3, ^{13}CBr bond, coupling consts., correl. with C hybridisation s-character 80−34806
water, adsorbed on cellulose, NMR relaxation times 79−78552
water mobility in blood plasma, NMR determ., viscosity correl. to $1/T_2$ 80−67176
water molecules in biological systems, relax. rel. to vol., pulse NMR obs. 80−40960
water PMR obs. in obligately halophilic blue-green alga 79−96526
$AgNa(NO_2)_2$, ultraslow crit. dynamics of order parameter, ^{23}Na spin relax. times obs. 78−76410
Al_2Cl_6 molten, nuclear mag. relax., mol. rot. 80−71209
Al_2O_3-Fe_2O_3:Cr^{3+}, dil. paramag. system, Cr^{3+} conc., effect on cross relax. 79−15387
Al_2O_3-Fe_2O_3(:Cr^{3+}) paramag. system, cross relax. temp. and mag. field effects on Mossbauer spectra 79−33576
β-Al_2O_3-H_3O^+, pulsed ^1H NMR study, 77 to 440K 79−87329
β-Al_2O_3-NH_4^+, PMR relax. time obs. of ionic motion 80−71213
β-Al_2O_3-NH_4^+ and β″-Al_2O_3-NH_4^+-H_3O, single cryst. PMR and proton motion 80−108101
β-Al_2O_3-Na_2O, anomalous Na behaviour obs. using pulsed and CW NMR 80−108095
Ar:H_2, nuclear spin relax. of H_2, crystal field meas. 79−51875
Au-Fe solid soln. alloys, reson. and relax. effects 79−82865
Au-V, dil., Kondo alloy, spin dynamics, nuclear spin relax obs. 78−68155
Au-Yb, dil. alloy, high field nuclear relax. of ^{173}Yb, anisotropic cond.-electron exchange 77−8434
Au-Yb alloys, dil., nucl. reson. of ^{173}Yb local moments 79−65763
Au-Yb dilute, NMR investig. of anisotropic cond. electron exchange 77−63309
$AuIn_2$, pulsed NMR expts, rel. to performance as nuclear refrigerant 79−61259
B hydrides, relaxation time meas., ^{11}B NMR spectroscopy 77−32276
BF, mol., nucl. spin-spin coupling, diamag. contrib. 79−36665
BaF_2, NMR relax., ionic cond. and self-diffusion 78−23362
BaF_2, spectral diffusion, coherent effects in ESR of Gd^{3+} 79−51852
BaF_2:K^+(La^{3+}), nuclear spin relax. orientation depend., point defect self-diffusion mechanism 77−48078
$BaFe_{12}O_{19}$, nucl. spin-lattice and spin-spin relax. in domain walls 77−69610
$BaWO_4$:Er^{3+}, spin-lattice and spin-spin relax. times, electron spin echo obs. 79−28609
C_8AsF_5 intercalation compound, NMR and static mag. susceptibility meas. 78−88214
β-CO, ^{13}C NMR, self-diffusion activation parameter, press. depend. 77−69719
CO, mol., nucl. spin-spin coupling, diamag. contrib. 79−36665
^{13}C, 2D NMR spectra, off-resonance decoupling 80−74182
^{13}C, interacting with strongly irradiated proton system, longit. mag. relax., Overhauser enhancement 78−19377

spin-spin relaxation continued
^{13}C NMR, high-resoln. allowing spin coupling and mag. field inhomogeneity 77−20740
^{13}C NMR in solids, high-resolution 80−34802
^{13}C, NMR spectra, transition intensities, off-resonance proton spin decoupling influence 80−74183
^{13}C pulsed NMR, simultaneous T_1 and T_2 meas., Fourier transform. visualization 78−24838
^{13}CH fragment, selective population transfer expts., density matrix formalism appl. to NMR spectroscopy 78−15059
$Ca(NO_3)_2$ hydrous melts, proton spin relax. and mobility 77−77118
n-$CdCr_2Se_4$, single crystal, transport props. near Curie temp. *(Japanese)* 78−6406
CdI_2-Cd(I) mixture, molten, nuclear spin relax. 80−88887
$Cd_{0.8}Ni_{0.2}Fe_2O_4$ ferrite, Fe spin relaxation Mossbauer study, mag. hyperfine struct. *(Russian)* 80−15932
ClF, gas, rot. frame NMR, reorientational and ang. correl. times 78−78721
ClO_xF_y, ^{17}O NMR, chem. shifts, indirect coupling consts. 77−14453
Co complex, $Co(acac)_3$, ^{57}Co labelled, $^{57}Fe(III)$ species prod. by electron capture decay, spin relax. 77−63329
Co complex, tris(ethylenediamine)cobalt(III) ion in complex anion solns., ^{59}Co NMR relax. obs. 80−25234
Co complexes, NMR studies *(Japanese)* 79−8068
Co, HCP, NMR and nucl. relax. meas. in domain walls 77−36146
$Co(N_2H_5)_2(SO_4)_2$:Co, Mossbauer effect and paramag. relax., superparamag. behaviour of correl. spin domains 77−69756
$CrBr_3$ anisotropic ferromagnet. crit. mag. relax., field and temp. depend. 79−1717
$CrBr_3$, crit. anomaly in transverse spin-spin relaxation rate 79−15310
Cs atoms, optically pumped, spin relax. in presence of N_2 79−59420
Cs vapour, optically pumped, transverse relax. times and diffusion coeff., spin echo meas. 79−10062
Cs+Cs, spin destruction, obs. 80−63781
$CsMnCl_3.2H_2O$, paramagnetic relax. rates, anisotropic diffusion model 77−69668
$Cs_2NaYbCl_6$, freq. depend. of spin-spin relax. rate from Mossbauer spectroscopy 78−48095
$Cs_2NaYbCl_6$, Mossbauer spectral lineshape in presence of paramag. relax. effects 77−69755
$Cs_2NaYbCl_6$, Mossbauer relax. spectra, breakdown of white noise approx. 78−27141
$CsNiF_3$, ^{19}F NMR, spin fluctuation suppression 78−91970
$CsNiF_3$, quasi one dimensional planar ferromag., low temp. NMR study im mag. field 80−97157
Cu, NMR at high polarisation and low field, nuclear spin exchange interaction 80−34790
Cu-Mn, spin glass, ^{63}Cu NMR linewidth and relax. meas. 77−69583
$CuCl_2.2H_2O$, EPR linewidth and relax., effect of antisymmetric exchange 77−59448
D_2O, liq., mol. rot., deuteron relax. obs. 77−8432
2,6-dichlorophenol-O-d_1, anisotropic reorientation, nucl. relax. in coupled spin systems 77−40145
DyAG, adiabatic magnetisation, optical obs. 78−88283
$DyAlO_3:Yb^{3+}$, Mossbauer relax. 80−15875
$DyFe_{0.998}Co_{0.002}O_3$, orthoferrite, freq. and relax. of ^{57}Fe NMR signal near Morin spin-reorientation phase transition 79−69744
$ErFeO_3$, second-order reorientation transition, NMR signal relax. 77−90066
EuB_6, low temp. nucl. spin-lattice and spin-spin relax. times meas. 77−90063
EuO, ^{153}Eu spin-spin relax. time and Suhl-Nakamura interaction 77−69722
EuO, critical EPR spin dynamics, sample shape and temp. depend. 77−32244
EuO, quadrupole coupling due to lattice imperfections 78−76347
F_2, nucl. spin-spin coupling, scanning MO HF LCAO calc. 79−50045
$Fe(NO_3)_3.9H_2O$, spin-spin relax., Mossbauer effect studies, 4.2K 78−31128
Fe film, nuclear magnetisation relax. at 77 to 500K 78−60352
Fe, triple pulse reson. studies of ^{60}Co nuclei 78−43675
Fe^{3+} ions, in frozen aq. solns., spin-spin relax., Mossbauer obs. of effect of paramag. impurity ions 79−33573
Fe:^{95}Nb NMR 77−59482
FeF_3, canted antiferromag., spin echo spectra of ^{57}Fe and ^{19}F nuclei 80−2662
$Fe(N_2H_5)_2(SO_4)_2$:Co, Mossbauer effect and paramag. relax., superparamag. behaviour of correl. spin domains 77−69756
$FeSiF_6$, phase transform. and relax., EFG and quadrupole spectra 77−51995
GaIn, liq. alloys quad. relax. rates, 3-particle correls., ^{71}Ga and ^{115}Sn 77−12272
Gd, EPR linewidth and spin-spin relax. near T_c 78−68369
H^+, tranverse relax. time in H_2 gas at 300K 78−42099
o-H_2 dilute impurity in rare gas solids and p-H_2, NMR study 80−25228
o-H_2 molecules in solid nonmagnetic host, nucl. spin lattice relax. times calc. 80−20483
H_2, ortho to para conversion on paramag. and artiferromag surfaces 79−34362
H_2, solid, low ortho conc., transverse and longit. relax. meas. 77−81025
H_2, solid, nuclear spin-lattice relaxation, crystal and mag. field effects 79−42865
HCN, nucl. spin-spin coupling, diamag. contrib. 79−36665
HCl, del. gas, proton longit. relax. time 77−34720
α-$HCrO_2$, H^+ mobility investig. by nuclear relax. meas. 77−48076
HD, nucl. spin-spin coupling, diamag. contrib. 79−36665
HD, spin-dipolar term, spin-spin coupling const. corrections, Fermi contact terms calcs. 80−99448
HDO, interactions with myosin, intermolecular spin diffusion study 80−18951
HF, mol. nucl. spin-spin coupling, diamag. contrib. 79−36665
$H_{0.36}MoO_3$ and $H_{1.71}MoO_3$ bronzes, NMR relax. obs. at 77<T<450K, H diffusion 80−108089
H_xMoO_3 (0.3<x<2.0), H mobility from NMR spin echo 79−1416
HNO_3-graphite intercalation cpd., proton relax. meas., two-dimens. system model 77−51968
H_2O, adsorbed molecule in pores of zeolites, intermed. state of enhanced mobility 78−60027
H_2O proton relaxation in normal and cataractous cryst. lens 77−60203
$HTaWO_6$, and $HTaWO_6.H_2O$ defect pyrochlores, NMR study of proton motion 79−82889

spin-spin relaxation continued
$H(UO_2P(As)O_4)4H_2O$, H motion, PMR obs. 78−80239
$H(UO_2PO_4)4H_2O$, solid, fast hydrogen ion diffusion, NMR relax. time meas. 80−2205
He^3-He^4 mixture, relax. of 2^3S_1 metastable atoms 80−102469
He+o-H_2, NMR, spin-spin and spin-rot. relax., IOS calcs. 79−18209
^3He, adsorbed, on MgO, nucl. mag. relax. props. 80−49457
^3He, adsorbed monolayers, dipolar anisotropy effects in spin relax 77−7940
^3He adsorbed on Grafoil, interlayer exchange 77−72736
^3He adsorbed on graphite, NMR relax. times below 4.2K 78−38898
^3He, BCC, NMR multiple echoes, soln. of eqn. of motion of magnetisation 79−86961
^3He film, submonolayer and multilayer, adsorbed on Grafoil, pulsed NMR study 80−49456
^3He film, theory of motional inhibition of interlayer quantum tunnelling 80−54466
^3He films adsorbed on Grafoil, NMR relax. times 79−28171
^3He, liquid, interface with antiferromagnet, anomalous thermal behaviour and nucl. spin relax. 79−56002
^3He monolayer, quantum tunnelling, NMR linewidth 77−39720
^3He, nucl. relax. in gas discharge at liq. N_2 temp. 80−100114
^3He, superfluid, B-phase, low temp. spin relax. 80−15323
^3He, superfluid A-phase, spin relax. and zero sound attenuation at low temp. 80−107595
^3He-^4He solid mixture, ^3He-^3He and ^3He-^4He tunnelling motions, NMR meas. 78−38908
^4He:^3He, solid spin diffusion coeff. and T_2, impuritons, temp. depend. 78−34675
$HfV_2H_{2.1}$, proton NMR relax. time and Knight shifts, diffusional activation energies meas., sorption props. 80−75871
Hg, liq., quad. relax. of ^{202}Tl impurities 77−16215
$Hg_{3-x}AsF_6$, incommensurate chain compound, anisotropic Knight shift, spin-spin interactions 78−80233
^{199}Hg, atom-surface interaction, nucl. relax., temp. depend. 80−88886
^{199}Hg optically oriented atom interaction with cell wall paramag. centres 80−37762
$HoAlO_3:Yb^{3+}$, Mossbauer relax. 80−15875
In-Sb alloys, liq., spin relax. of ^{117}Sb and ^{115}Sn 77−16216
InSb, electron spin relaxation 80−25187
InSb, electron-electron spin-flip scatt. and spin relax. 80−44916
K_2CuF_4, nearly two-dimensional ferromag. nucl. transverse relax. rates meas. 77−81024
K_2CuF_4, two-dimens. ferromagnet, nuclear spin-spin-relax. *(Japanese)* 77−48082
KD_2PO_4, proton spin-lattice relaxation rate, temp. depend., field depend. 78−88208
KH_2PO_4, proton spin-lattice relaxation rate, temp depend., field depend. 78−88208
$KMnO_4$, ^{55}Mn NMR second-order quadrupole splitting, asymmetry parameter 77−63312
$K_2Pt(CN)_4Br_{0.30}.3H_2O$, dynamic ^{195}Pt NMR meas. below metal-insulator transition 80−34810
$K_2Pt(CN)_4Br_{0.3}.3H_2O$, quasi one-dimens. conductor, EPR linewidth 80−54938
K_2TeO_3, D_2O soln., $^{123,125}Te$ Fourier transform NMR 78−15046
Kr:^{86}Sr, 8^{4+} state, nucl. g-factor and nucl. spin relax. in gas phase 77−22884
^{83}Kr spin dephasing 80−38524
La hydrides, relax. time, temp. depend. meas. by pulse NMR 78−88217
La-P-Ce, dilute, NMR investig. of anisotropic cond. electron exchange 77−63309
LaAg, electronic struct., NMR relax. times meas. 79−51871
$LaBe_{13}$-Er(Dy), dil., ESR, crystalline elec. field splitting, exchange parameters 78−52348
LaF_3, ^{19}F NMR study, relaxation times meas. 80−108093
LaF_3, ionic transport, NMR and cond. studies 80−107555
β-$LaNi_{5-y}Al_y$ hydrides, H diffusion, NMR studies 80−15298
$La_{1-x}Pb_xMn_{1-y}Fe_yO_3$, magnetically ordered, NMR, spin echoes and relax. 77−48087
$La_{3-x}V_xS_4$:Gd^{3+} localised moment-conduction electron interact., ESR obs. 78−88183
Li_2, nucl. spin-spin coupling, scanning MO HF LCAO calc. 79−50045
LiAl, NMR relax. investig. of ^7Li self-diffusion 77−12217
α-$LiAlO_2$, NMR study of Li^+ motion 79−42863
Li_5AlO_4, α and β phases, NMR study of Li^+ motion 79−42863
Li_5AlO_4, NMR relaxation by paramag. impurities 79−42866
$LiBF_4$, $LiHBF_3$, spin-spin coupling and T_1 in non-aq. solns. 77−23512
$LiCuCl_3.2H_2O$, EPR linewidth and relax., effect of antisymmetric exchange 77−59448
LiF, dilute paramagnet, ^8Li-^6Li cross relaxation *(Russian)* 79−4747
LiF, NMR, thermodynamic effects of RF pulse pair on system with two spin species 77−66433
$LiIO_3$, cross relax. in two-spin system, inhomog. broadened line 78−88218
LiOH, NMR study, motional narrowing 79−42863
LiTi ferrite, Mossbauer study, relax. and supertransferred hyperfine fields 80−39941
LiZn ferrite, Mossbauer study, relax. and supertransferred hyperfine fields 80−39941
$MgSiF_6$, phase transform. and relax., EFG and quadrupole spectra 77−51995
Mn II-lecithin lipid-water system, NMR and EPR obs. 80−61168
$Mn(ClO_4)_2/NaClO_4$ in aq. soln., interaction between Mn^{2+} and ClO_4^-, NMR studies 80−71212
MnSi, NMR and susceptibility above T_c 78−43665
$MnSiF_6$, phase transform. and relax., EFG and quadrupole spectra 77−51995
N_2, nucl. spin-spin coupling, scanning MO HF LCAO calc. 79−50045
NH_3, magnetic relaxation rates for microwave spectrum and contributions to linewidth 80−5564
NH_3, transverse relax. time, T_2, of inversion doublets from free induction decay 80−58281
N_2H_2, nucl. spin-spin coupling, scanning MO HF LCAO calc. 79−50045
NH_4TaWO_6, rapid ionic motion, spin-lattice and spin-spin relax. times meas. 79−38396
^{15}N, interacting with strongly irradiated proton system, longit. mag. relax., Overhauser enhancement 78−19377
$NaBF_4$, spin-spin coupling and T_1 in non-aq. solns. 77−23512

spin-spin relaxation continued
$NaClO_4/Mn(ClO_4)_2$ in aq. soln., interaction between Mn^{2+} and ClO_4^-, NMR studies 80−71212
$Na_2Si_3O_{7-x}H_2O$, amorphous, pulsed NMR study 79−78555
Na_2TeO_3, D_2O soln., ^{123,125}Te Fourier transform NMR 78−15046
Na_xWO_3, Knight shift, spin-lattice and spin-spin relax., high press. NMR obs. 80−50211
^{23}Na in heterogeneous system, nuclear mag. relaxation time determ., rel. with dimensions of colloidal particles 80−75876
$(NbCl_nBr_{6-n})^-$, ^{93}Nb nucl. spin relax. and mag. shielding 78−58723
$(NbCl_nBr_{6-n})^-$ complexes in acetonitrile soln., ^{93}Nb spin relax. and mag. shielding 80−44944
Ni complex, hexamethylphosphorotriamide Ni (II), paramagnetic, pulsed NMR, substitution reaction *(French)* 78−10793
Ni_3 critical NMR obs. near mag. transition 77−81026
Ni^{2+} aqueous complex, EPR, PMR and spin-spin relax. 79−69713
Ni-b, hyperfine interactions from 6 to 730K, ^{12}B NMR 80−29372
Ni-benzene, second order two-spin cross-relax. 79−95632
$Ni(BF_4)_2.6H_2O$, EPR, cryst. field symmetry 79−28593
$NiSiF_6$, 6%, second order two-spin cross-relax. 79−95632
^{61}Ni, paramag. solid and liq. phases, nucl. spin relax. and Knight shift 78−76327
^{17}O NMR, proton decoupling 78−2752
P, amorphous, NMR studies 79−69740
PF_3Br_2, spin systems under multiple pulse NMR conditions, chem. shift relax. 80−34808
P_2H_4, nucl. spin-spin coupling, scanning MO HF LCAO calc. 79−50045
Pb, liq., mag. relax. of excited ^{207}Bi 77−16217
PbF_2, NMR relax. and self diffusion 78−80236
β-PbF_2, spectral diffusion, coherent effects in ESR of Gd^{3+} 79−51852
PbF_2:Mn, NMR relaxation by paramag. impurities 79−42866
$Pb_5Ge_3O_{11}$, spectral diffusion, coherent effects in ESR of Gd^{3+} 79−51852
$PbSnF_4$, fast ionic cond. of F^- ions, NMR study *(French)* 80−39345
$Pb_{0.9}Sn_{0.1}F_2$, NMR study of F atom motion *(French)* 80−100622
$PdH_xFe_{0.003}$, Kondo system, local moments, hyperfine fields, Mossbauer study 80−80478
Pd(II)-Gly-Tyr complexes, aq. soln., PMR obs., conform. 77−50450
$PrNi_5$, nucl. cooling agent, relax. and exchange, EPR and NMR study 80−25237
Rb, liq., nuclear spin relax. of 13.9 msec ^{88m}Y 77−12270
Rb+^{131}Xer, spin-exchange cross section, ^{131}Xe nucl. spin relax. obs. 80−37868
RbI, press. depend. of I nucl. relax. press. induced polymorphic transform. study 79−1720
^{87}Rb+^{129}Xe, spin-exchange cross-section meas. 80−78686
$Sb_2O_5{}_nH_2O$, crystalline, ^{1}H NMR study of proton transport 80−60446
ScM (M=Cu, Ag, Pd, Rh, Ir, Ru), electronic struct., NMR relax. times meas. 79−51871
Si amorphous film, saturation meas. on ESR signals 79−33535
Si, heavily irrad., ESR study of annealing charact. 78−10771
Si_2H_6, nucl. spin-spin coupling, scanning MO HF LCAO calc. 79−50045
Sn, liq., quad. relax. of ^{114}Sb impurities 77−16215
^{119}Sn NMR by pulse Fourier transform, T_1, T_2 and chem. shifts 77−55715
SrF_2, spectral diffusion, coherent effects in ESR of Gd^{3+} 79−51852
$TbAlO_3$:Yb^{3+}, Mossbauer relax. 80−15875
Th_4H_{15}, NMR investig. of proton environment and motion 77−48077
β-$TiFeH_{1.03}$, H diffusion, NMR meas. 80−10707
Tl, liq., mag. relax. of excited ^{207}Bi 77−16217
TlBr melts, Tl doped and pure, stoichiometric, nucl. spin relax. 80−25236
TlCl, melts, stoichiometric, nucl. spin relax. 80−25236
^{205}Tl, solvated and adsorbed, NMR studies *(Rumanian)* 79−82888
UF_6, isotope enrichment, ^{19}F NMR in gas, liq. and solid 78−23364
$UO_2(NO_3)_2$, aq. soln., pulsed NMR relax. time, ^{235}U enrichment depend. 80−2658
V_3Si, NMR meas. near struct. transform. *(Russian)* 80−44942
V_3Si, NMR of ^{51}V above and below 21K struct. transition *(Russian)* 80−34796
Xe:^{138}Ba, 6^+ state, nucl. g-factor and nucl. spin relax. in gas phase 77−22884
^{89}Y spin-spin relaxation times, pH depend. 80−66059
$YbAlO_3$, mag. relax., Mossbauer expts., and mag. ordering 79−8078
Zn, HCP metal, pulsed ^{67}Zn NMR studies at 4.2K 79−91315
Zr-H system, low temp. NMR 78−72431
$ZrMn_2H_x$, proton NMR relax. time and Knight shifts, diffusional activation energies meas., sorption props. 80−75871

spin systems
see also magnetic properties of substances; magnetism
absorption of energy under parallel pumping conditions 80−2592
abstract three-level system, group approach in dynamics *(Russian)* 80−4579
adamantane powder, dipolar relaxation, short time behaviour, pulse method meas. 80−84667
alloy between ferromag. and antiferromag. species, competing order parameters, Bethe-Peierls approx. 77−48003
anisotropic exchange interactions, effect on singlet ground state system 80−65852
anisotropic lattice spin systems, phase transitions 78−73930
anisotropic linear spin chain, two-magnon problem with arbitrary interaction radius 78−72320
anisotropic magnet, dil., crit. behaviour near percolation threshold 80−88767
anisotropic magnet mixture, Heisenberg spin system by Monte Carlo simulation 79−78408
anisotropic magnets, dil., scaling representation meas. percolation threshold 80−88766
anisotropic media, simple spin systems, magnetisation modes and evolution matrices 79−4734
anisotropic spin system, field theoretic approach to bi-critical point 79−40518
anisotropic spin-phonon coupling model, exact solutions *(Russian)* 80−100590
antiferromagnet, magnetic phases, spin configurations in external field 80−70955
antiferromagnetic effective spin 1/2 system correlated effective field theory 79−73759
atom spin transition, nonadiabatic, in time-depend. mag. field 80−9576
spin systems continued
AX spin 1/2 system, double reson. interferometry, relax. times 78−6603
Bethe lattice, statistical theory of random ordered phase 77−80895
Bethe-ansatz excitations, observability in Heisenberg-Ising spin systems 79−82738
bicritical points in $2+\epsilon$ dimens. 77−24700
Bose expansion for general spin, exact 80−31662
Bose operator expansions of tensor operators in theory of magnetism 77−63061
boson expansion for general spin operators, coeff. 80−42141
boson series expansion of spin 1/2 operators, coeffs. 79−30358
Boson series expansions of arbitrary spin operators, expressions for coeffs. 79−80507
branching diagram and Serber type spin functions, construction algorithms 79−6828
branching diagram for particles with arbitrary spin 77−30027
Bravais lattice, ferromagnetic ground state conditions in Ising and Heisenberg models 80−50129
Carr-Purcell-Meiboom Gill pulsed NMR sequence, errors in T_2 values 77−85604
Carr-Purcell-Meiboom-Gill pulsed NMR experiment, baseline drift 77−85603
chain with nearest and next nearest neighbour interactions 77−47955
chains of classical spins, weak ferromagnetism 79−15268
classical lattice systems, high-temp. analyticity, continuous spin systems 77−2615
classical n-vector model, spin-dimensionality dependence of critical parameters 79−40479
classical planar spin chain, dynamic props., Monte Carlo calc. 79−61144
classical planar spin model, two-dimens., Monte Carlo study 80−25147
classical spin system with long range interaction, phase transition existence conditions 80−88298
coherent two-photon NMR, standard-basis operators, coherent averaging 80−82798
colouring problem on randomly occupied lattice, critical conc. existence for long range order 80−80519
conference on dynamical critical phenomena, Geneva (Apr. 1979) 80−27040
conservation of ang. momentum and thermal mixing *(French)* 78−6562
continuous spin systems, position-space renormalisation group study 79−38350
continuous spin systems, thermodynamic limit of free energy and correl. functions 77−9962
continuum Heisenberg spin system, stationary spherically and axially symm. spin waves 80−34615
continuum spin system dynamics, spin-wave and solitary wave solns. 77−8263
copolymer model with alternating spins, kinetics 80−9768
correlation inequalities for n-vector spin models 80−54860
coupled system, ABC type, matrix elements of tensor operators calc., transition probability matrix 80−25182
critical, in random mag. field, supersymmetry, neg. dimensions 79−97533
critical behaviour, long-range interactions 79−40515
critical behaviour of isotropic system with long-range interactions 77−89966
critical behaviour of random annealed spin systems at n=−2 78−43600
critical dynamics of disordered spin systems 79−40516
critical phenomena, use of renormalisation group, review 77−20625
cross-relaxation between Zeeman and spin-spin degrees of freedom *(Russian)* 77−32237
crossover, field-induced, in mag. chain, scaling theory 80−54904
cubic crossover, approx. renormalisation group calc. 77−49701
cubic model, Monte Carlo simulation, phase transitions 80−34646
cubic systems, axial and diagonal anisotropy crossover exponents 77−13710
d-dimensional lattice spin model, multicritical pt. 77−36041
1,8-dichlorooctane, quadrupolar relax. centres, limited spin diffusion 80−100649
Dicke maser model-van der Waals spin system thermodynamic equivalence 80−83572
diffusion, effect of spin-photon and spin-phonon interactions 80−44849
dilute random magnet, one-dimens., low temp. behaviour of susceptibility, sp. ht. and correl. length 79−69682
dimensionality dependence of T_c in 1/n expansion 78−32772
dipolar interaction in solids, low mag. field, thermodynamic props. 78−76205
dipolar solid, multiple-pulse spin locking 77−20742
dipolar solids, nuclear spin-lattice relax. from hindered rot. 78−52373
disordered, commutator and anticommutator Green's functions 79−51792
disordered, crit. dynamics, shape functions for $T>T_c$ 77−77069
disordered magnet, effective field approx., Ising model Hamiltonian 77−8261
disordered media, spin wave propagation, nonlinear magnon interactions *(Russian)* 80−80496
disordered spin systems, tricrit. behaviour 80−60319
disordered system, scaling function for two-point correlations 78−80147
displacive phase transitions in discrete cubic model 77−32198
dissipative, oscillations and fluctuations 80−27224
distribution function of spin/isospin saturated system, direct and exchange sum rules 80−27212
DPPH, dil., saturated spin system, spin decoupling effect and variation of dipolar energy reservoir temp. 80−88877
DPPH-benzene, organic radical, pressure induced mag. ordering *(Russian)* 78−88120
dynamic renormalization group, phenomenological fitting 79−75471
elastic magnetic system, one-Fermion-one-Boson model 78−43539
electron spin density functional gradient expansion, local approx. calcs. 80−44792
electron-ion system, multiplicity and pseudomultiplicity 77−1389
elementary excitations in spin systems with three-atom exchange 78−84404
EPR of spin system with weak exchange couplings, temp. depend. 78−64258
EPR spin system saturation charact., acoustic wave excitation *(Russian)* 80−66013
equivalent neighbour model, generalised, derivation of high temp. lattice consts 80−77721
ergodic theorem for interacting particles 77−79027

spin systems continued
exchange coupled spins, in lattice dimens. 1 and 2, 1/n expansion 77−66237
exchange energy near singular points or lines 80−93106
exchange narrowing including spin correlations and local field contribs. 77−40060
Fermi liquid, spin ordering 77−15779
fermion interactions, eigenvalue spectrum 77−8035
ferroelectric ferromagnet, soft modes and ferromag. reson. 80−11275
ferromagnet, anisotropic, spin one, Callen's decoupling approx. 77−8258
ferromagnet, Ising model, nonuniform mag. field method, crit. correlation function approximations, calc. 80−20407
ferromagnet, Ising model, transition point calc. 80−20408
ferromagnet. Bloch electrons, dynamic longit. spin susceptibility 79−19709
ferromagnetic, Migdal's recursion relation, generalisation, appl. to O(n) symmetric spin systems, n>2 78−91834
ferromagnetic, two dimensional, Wilson renormalisation group theory appl. *(Norwegian)* 78−56275
ferromagnetic, variable distrib., convergence to normal Gaussians, Lee-Yang theory 79−69681
ferromagnetic metal, anomalous magnetooptic effects near Curie temp., s-f exchange model 80−2736
ferromagnetic scalar spin systems, wall and boundary free energies 78−155
ferromagnets, random, large exchange interaction, Green function theory 78−6537
ferromagnets, spin wave excitation due to parallel pumping, mag. impurity interactions *(Russian)* 80−80497
first-order transition induced by cubic anisotropy 79−4688
fluids, magnetic relaxation in Bogolyubov hierarchy of relaxation times 78−39383
functional integral method appl. to classical and quantum spin models 80−15676
$Ga_xAl_{1-x}As$, optically oriented electron, nuclei spin instability *(Russian)* 80−70660
Gaussian random field, ferromagnets in $4+\epsilon$ space dimens. 78−73954
geometric formulation of Hamilton's Principle, spin particles 78−45482
Glauber-Ising model, crit. showing-down of energylike perturbation, renormalisation group anal. 79−61133
Griffiths singularity, and upper bounds on cluster distrib. functions 79−7958
Hahn spin systems, mechanism of form. of single-pulse echo *(Russian)* 79−78566
Heisenberg and biquadratic exchange, eigenstates of short chains of spin-1 atoms 77−55652
Heisenberg linear chain, alternating spin quantum numbers, mag. and thermodynamic props. 80−34578
Heisenberg magnets, with two kinds of exchange interactions, surface magnons and surface spin arrangements 77−36043
Heisenberg model, anisotropic spin system, $S=^1/_2$ frustration effects 80−65763
Heisenberg model, classical, compressible spin system, zero temperature phase diagram 78−6536
Heisenberg model, classical, infinite, nonlinear dynamics, quantum time evolution 80−100576
Heisenberg model, long-range interaction, asymptotic behaviour 78−56282
Heisenberg model, two-spin, molecular field approx. 79−65634
Heisenberg spin $^1/_2$ system, recursion relations, Migdal renormalisation group approach 80−20368
Heisenberg spin system, one-dimensional, dynamical behaviour 80−29567
Heisenberg spin systems, absence of mag. phase transitions, Hubbard identity calcs. 78−34992
Heisenberg system, ordered phase, reaction field approx., anisotropy presence 79−61030
helical order 77−24701
helicity modulus at low temperatures 78−70052
heteronuclear spin system, second moments of NMR spectra, calc. 79−73836
high spin d^2 system, isotropic g-tensor 78−10757
Hubbard model, cluster-variation method in two-site approx. at high temp. 80−7071
impurity spin-unpolarised lattice nuclei interaction, dynamic susceptibility 79−69648
inequalities in classical lattice and continuum systems 77−90
intelligent spin states, compact representation, time evolution and radiative props. 77−5690
intermolecular spin relaxation by reorientation of off-center spins 79−42821
Ising and Heisenberg model, threshold inequalities for ground state 80−7064
Ising chain, with next-nearest neighbour interactions, mag. responses to spin-Peierls transition 80−71054
Ising ferromagnet, general, Lee-Yang theorem GHS inequality, spin-$^1/_2$ approx. 77−20524
Ising ferromagnet with two- and four-spin interaction, improved product average decomposition method 80−20406
Ising lattices, finite, series expansion anal. of crit. temp. shifts 79−61134
Ising model, crit. props., appl. of real space renormalisation techniques 79−78420
Ising model, random magnetic system, correlation function, upper and lower bounds 80−25063
Ising model, S=1/2, mol. field theory with correlations 79−82804
Ising model, two-dimens., quantum mech. anal. using decimation method 77−47958
Ising model, two-dimensional, frustration in periodic systems 79−61023
Ising model, two-spin correlation function 79−28533
Ising model, variational approx. for renormalization group transforms. 79−61139
Ising model, Yang-Lee edge singularity, real-space renormalisation group method 80−34643
Ising model ground state orderings, several neighbour interactions, appl. to HCP lattice 77−4483
Ising model in transverse field, double-time Green's functions method 79−15313
Ising models, spin correlation functions, class of inequalities, identities 79−44878
Ising O(2), O(3) and O(4) model, Hamiltonian string-coupling expansions 80−20426
spin systems continued
Ising spin $^1/_2$ model, renormalisation group approach 80−2582
Ising spin system, coupled to acoustic and optic lattice modes, critical behaviour 80−71044
Ising spin systems on Cayley tree-like lattices, spontaneous magnetisation, correlation function far from boundary 78−68137
Ising spin systems on union jack lattice, non-universal behaviour of pair or three-spin interactions 80−57206
Ising system, Lifshitz points, phase diagram transition temp. determ. interface free energy vanishing 79−99716
Ising systems, general, planar, correlation-function identities 78−93616
Ising systems with random bonds, thermodynamic props. at low temp. 79−28532
isotropic N-component spin system, with long- and short-range interactions, crit. behaviour 78−76256
isotropic N-component spin systems, crossover exponent to order ϵ^3 78−34990
isotropic N-component spin systems with long and short range interaction, critical behaviour 80−54907
isotropic spin system, cubic lattice, step model of phase transitions, critical behaviour 78−60290
isotropic spin systems, with long and short-range interactions, crit. exponent η 77−65013
itinerant electron system, weakly ferromagnetic ground state, Fermi liquid theoretical study 79−4646
itinerant localised systems, dynamic magnetic response 80−34583
Jeener-Broekaert three-pulse sequence, inhomogeneous lineshapes, second rank spin interactions 80−39891
Kadanoff renormalisation for s-state Potts model in 3-d 78−21074
kinetic Ising model, physical content, Glauber methods 77−12074
Kondo Hamiltonians, s-d exchange, ground states, renormalisation group calcs. 80−50046
Kondo system, spin 1/2, static susceptibility and relax. rate 79−65646
Kramers-Wannier transformation *(Russian)* 79−95558
Krieger-James approx. of short range order effects, antiferro- and ferromag. 78−56276
lattice gauge theory and spin systems, review 80−22528
lattice model, analyticity and cluster props. of unbounded spin systems 78−45571
lattice nuclear mag. system simulation by classical mag. moments 77−69713
lattice spin systems, matching conditions for crit. props., group struct. of block transforms 80−22305
layered spin systems, phase transitions, partition functions and binary correlation functions 80−50133
linear chain of classical spins with arbitrary nearest-neighbour interaction 78−10632
linear spin chain in nonuniform mag. field, energy spectrum *(Russian)* 77−63048
linear spin chain in uniform mag. field, spin-phonon interactions *(Russian)* 80−2594
localised site cluster expansion, interacting paramagnetic sites, spin symmetry projection 79−7951
longitudinal paramag. suscept., inhomogen. broadening conditions 78−88169
low-dimensional correlated spin systems, exchange narrowing theory 79−11335
magnetic crystal, perfect, spin rot. of forward transmitted beam in neutron diffr. 80−50113
magnetic excitations, polarised neutron inelastic and quasi-elastic scattering 80−50045
magnetic mixture of triangle-bond elements, Ising model 77−69467
magnetic ordering in spin systems with single-ion anisotropy 77−69466
magnetic structure elastic polarised neutron scatt. atomic mag. moments 80−29531
magnetic susceptibility of s=1/2 crystallographic two sublattice system 78−14914
magnetically ordered cryst., indirect nuclear spin interactions 80−103847
magnetism, conference, Munich, Germany (Sep. 1979) 80−56997
magnon kinetic eqns. in parametric ultrasonically excited frromagnets 80−44820
many-spin system, dynamics, group approach *(Russian)* 79−11324
many-spin system, group approach in dynamics *(Russian)* 80−44900
memory function for spin relaxation graphical representation 77−24733
metal, conduction electrons, surface scatt. under spin resonance conditions *(Russian)* 79−82857
metastability in kinetic spherical spin system model, nucleation appl. 78−65873
metastable polarised crystals, decay kinetics, exchange magnon-phonon interactions *(Russian)* 80−7060
metastable spin-aligned crysts. decay kinetics 80−34669
Migdal-like approximation, quantum spin systems 80−34649
minimum uncertainty states of angular momentum system 78−93559
mixture, one-dimens., random, of Ising S=1 and $^1/_2$ spins, mag. props., spin distrib. 78−95407
models and mathematics of quantum dynamics, conf., Bielefeld, Germany (Sept. 1975) 77−10158
molecular field theory, simple derivation, with correlation 80−80547
momentum-shell recursion relations in $2+\epsilon$ dimensions 78−6498
Monte Carlo simulation of quantum spin systems, two dimens. X-Y model 78−27011
multilevel spin systems, selective excitation and detection, single transition operators 78−2771
multipulse NMR, nuclear magnetisation relax. *(Russian)* 79−19799
multispin system, time development of nuclear Overhauser effects 80−34822
n-component spin system, anisotropic Brillouin zone, Wilson-Feynman graph technique, universality 77−5764
n-component spin system, energy-energy correl. function calc. 80−31697
nearly ferromagnetic Fermi systems, spin-conserving approx. spin susceptibility 78−47982
NMR of spin-one system, response to three-pulse sequence in homogeneous B_0 field 79−42860
NMR of spin-one system, response to three-pulse sequences in inhomogeneous B_0 field 79−42861
NMR spectra, non-Lorentzian, in low density gases 78−94259
non-Ising, replica symmetry and massless modes in spin glasser 79−56553
noncollinear, spin waves, hydrodynamic theory 78−6524
nonintegral, nuclear double resonance interference spectroscopy, appl. to ^{23}Na satellites in $NaNO_3$ 79−4745

spin systems continued
nontranslationally invariant spherical model, exact soln., phase transition 77−37833
nuclear, in spherical conductor, free induction decay and skin effect 80−2649
nuclear, ultra low temp., nuclear adiabatic demagnetisation *(Japanese)* 79−12807
nuclear acoustic resonance spectrum, kinetics of spin system for spin quantisation by strong acoustic field 78−15052
nuclear dipolar energy relaxation time 77−24755
nuclear dipolar magnetic ordering, dipole-dipole interactions review 77−85475
nuclear echo formation in spin systems with dynamic freq. shift to NMR 80−93208
nuclear magnetic ordering, domains, neutron diffr. patterns, theory 80−100577
one dimensional, with anisotropic interaction, high freq. props. *(Russian)* 77−80902
one dimensional Fermi gas model in relation to spin and field theoretical models 80−24816
one dimensional magnetic behaviour 79−28495
one dimensional system with phase transform., exact linear renormalisation 78−32769
one-dimensional, disordered, magnetism 80−25152
one-dimensional, free energy series expansion, renormalisation group series 78−31081
one-dimensional, spin-spin correl. function, dynamical spherical model 79−69683
one-dimensional disordered spin system with isotropic antiferromag. interaction, susceptibility and Knight shift *(Russian)* 78−88202
one-dimensional electron system, with attractive interaction in mag. field, paramag. transition 80−7072
one-dimensional magnetic system, spin anisotropy and exchange alternation 80−34644
one-dimensional spin 1/2 chain, soliton excitation in strong spin-phonon interaction 80−103842
optical-acoustic two-phonon relaxation 80−11244
optically polarized spin system, long relaxation time meas. *(Russian)* 78−12737
orbital degeneracy, one dimensional two spin models *(Russian)* 80−54899
order-disorder transitions in gauge and spin systems 78−70072
order-order transitions, spin system with double electron exchange 77−4522
organic charge-transfer salts, neutral-ionic interface, energy states and mag. props., VB anal. 79−4537
oscillator action of transverse fields 78−49873
paramagnet, reson. rot. of acoustic polarisation plane under spin-system saturation conditions 77−32245
paramagnet, solid, in alternating longitudinal field, kinetic eqns. 78−2725
paramagnetic substance, single spin cross-relax., temp. depend. of transition probability 80−25184
periodic perturbation of spin-1 system, analogue of Shirley's eqn. 77−3248
phase transitions in many identical thermodynamic spin-like systems 77−17906
phase transitions in n-component spin system with coupling to non-ordering parameter 77−51906
plane rotator model lattice system, Euclidean Bose field approx. 77−28351
polarisation analysis of diffuse neutron scattering from magnetic systems 80−25098
polarisation and magnetisation of electronic matter 80−75929
polycrystal, struct. parameters determ. from NMR spectra anl. of two-spin system 77−89353
position space renormalisation of spin systems with long-range forces, hyperscaling breakdown 78−24755
Potts s-state model on Cayley tree Bethe-Peierls critical coupling 80−103844
probability estimates for continuous spin systems 77−2614
quantal spin systems, classical representation and scaling props. of spin Hamiltonians 78−14919
quantum, classical limit, phase transitions 77−57294
quantum, exact boson representation and crit. behaviour 79−78423
quantum, frustration effect in s=1/2 XY and Heisenberg models 80−15677
quantum, operator formulation of renormalisation transformation 77−59376
quantum, propagation properties study 78−12642
quantum anisotropic antiferromag. Heisenberg model, Gibbs state limitation 80−50027
quantum chain, mag. impurity reson., Fresnel diffr. pattern 77−63051
quantum Ising chain, in real or complex field, real space renormalisation group method 80−71050
quantum lattice spin theory, Jastrow wave functions 79−25999
quantum model of single spin system, von Neumann algebra 78−45459
quantum spin model with unstable stationary states 77−67382
quantum spin system, two-dimens., frustration, renormalisation group study 80−80535
quantum spin systems, ground state energies, renormalisation techniques appls. 80−93132
quantum spin systems, S=1/2, manifestation of frustration effect 80−65767
quantum systems, two-dimens. Ising model, zero temp. renormalisation group method 79−82801
quasi-low dimensional spin system, 3-D mag. ordering, randomness effects 78−10710
quasi-one-dimensional systems, spin-lattice Peierls instabilities, static and dynamic aspects 80−71052
quasi-two-dimensional planar spin system, mag. transition 80−65951
quenched binary mixture, early stage evolution, kinetic Ising model 77−69468
quenched random impurities, dynamics, replicas and frustration approaches 80−34673
quenched random magnetic fields, $\varepsilon=6-d$ expansion of dynamic crit. exponent 79−38335
random, absence of ordering 77−51909
random, with short range interaction, static crit. behaviour 78−39328
random annealed one-dimensional Ising spin system, site model, specific heat, susceptibility 77−32139
spin systems continued
random band square lattice, frustrated plaquettes distrib. 80−108015
random binary alloy, charge and spin struct. factors, CPA theory 77−28374
random chain of classical spins, statistical mechanics 78−10630
random hierarchical model, crit. props. 80−71072
random Ising ferromagnet, upper bounds 80−34663
random magnetic bonds, phys. props. near crit. point 78−84440
random ordered phase, frustration, phenomenological theory 80−60349
random ordered phase, of Ising model, random quenched effective field approx. 78−84432
random spin models with coupling to nonfluctuating parameter, crit. behaviour 79−47292
random spin system, 1/n expansion 78−62173
random spin systems, non-analyticity of entropy and Nernst's law 78−2692
random thermodynamic props. using Bethe-Peierls-Weiss approx. 79−78387
randomly distributed interaction centres, mol. field distrib. function *(Russian)* 80−44834
randomly located spins with oscillatory interactions 79−42778
rare earth mixed valence compounds, spin dynamics, mag. neutron scatt., Mossbauer effect, XPS studies 80−39786
rare earth orthoferrites, hyperfine interaction anisotropy, NMR study *(Russian)* 80−66052
rare earth ternary compounds, coexistence of superconductivity and long-range magnetic order 79−11264
rare-earth, mag. supercond., appl. of boson theory to mixed state 80−7050
reggeon couplings, analogue quantum-spin model 78−45813
renormalisation transformations in position space, parameters determ. criterion 79−17357
renormalization transformations for quantum spin systems 79−40511
restricted chain, spin complexes *(Russian)* 77−85402
rotating coordinate system with quadrupole splitting, paramag. susceptibility 80−11178
ruby NMR laser, spontaneous nucl. spin system self organisation 79−916
S=1 generalised Ising model, stability conditions 80−20427
semiconductors, many-valley, magnetic electron fluctuon states spin direct interactions 80−29364
Sherrington-Kirkpatrick model, Thouless-Anderson-Palmer eqn. solution *(French)* 80−39781
single-ion anisotropy, magnetic systems, high temp. series expansion 80−34576
site-disordered spin systems, generalised CPA 77−20513
solids, averaging method application to high resolution NMR, Magnus expansion *(Russian)* 80−34793
spectra calculation, general method, 2D spin-echo NMR spectroscopy appl. 78−86842
spherical limit for n-vector correls., spin correl. functions 78−24726
spherical model, accel. of convergence of 1/d expansion for crit. temp. 78−19265
spin 1/2 particles, config. representation, bit patterns appl. 77−43804
spin glass transition in system with competing ferromag. and antiferromag. interaction 77−20616
spin glasses, spin exchange scatt. time calcs. 80−50127
spin lattice models, continuous-integral method 78−93615
spin migration amongst tetrahedral or octahedral interstitials in FCC cryst. symmetric and asymmetric jump model 79−15127
spin reduction in systems with orbital degeneracy 77−51873
spin systems, randomly competing, random ordered phase, frustration, phenomenological theory 80−60349
spin-1/2 system, mag. resonance in arbitrarily oriented fields 77−42263
spin-glass, two-dimensional Ising model, low temp. dynamic props. 80−20425
spin-phonon system, transition to self-trapping 80−10606
supersymmetric, extensions 78−21344
surface magnetisation profile singularities near critical point 80−103843
surface tension and phase transition in lattice systems 80−27226
susceptibility relationship to correlation length, renormalisation group calc., anomalous-dimension crossover function 79−42780
symmetric spin system, calc. of NMR spectra of SYMTRY computer program 77−85587
symmetry, wreath groups 80−88724
tetrahedral four spin $^1/_2$ systems, Zeeman and tunnel system reson., coupled and uncoupled relax. 80−50214
thermodynamic limits, group theory approach 77−74343
thermodynamics, contrib. of spin-phonon interaction 78−2635
thermodynamics of quenched random spin systems, phase transitions in spin glasses 77−73024
transient phenomena, soln. using eigen-coordinate system of magnetisation vector 80−25116
transition metal elements and alloys, spin distribution, neutron diffraction expts. 80−25097
transition metal layer compounds, mag. model, 0K phase diagram, spin wave spectrum 79−87273
transition metal magnetic clusters, neutron inelastic scatt., review 80−50083
transverse dynamic susceptibility and spin waves in itinerant electron SPW states 80−97076
tricritical behavior in a two-dimensional field theory 80−77726
tricritical phase transition, critical exponents, classical N-component spin systems 78−4579
tricritical phase transition, eqn. of state, critical exponents, logarithmic corrections 78−27048
two level system, microwave SHG, at. correlations and line shape 77−19219
two level system, microwave SHG, at. correlations and line shape 77−19220
two spin cross relaxations, temp. depend. statistical theory 78−80190
two-component, bicritical points, eqns. of state, cubic anisotropy and tetracriticality 77−55679
two-component spin system in alternating mag. field, dynamical behaviour, susceptibility 79−99715
two-dimens. isotropic spin system, phase transition 79−42716
two-dimensional spin system on square lattice, exact duality-decimation transform. 80−17890
two-spin system, solid without spin-lattice relax., NMR theory *(German)* 78−88197

spin systems continued
two-spin system with chemical exchange, amplitude-modulated DNMR 79−93194
two-sublattice magnetic system with fourth-order uniaxial anisotropy and strong antisymmetric exchange in transverse mag. field 79−56530
unbounded n-component spin systems on lattice, statistical mech. 77−4477
uniaxial antiferromagnet, nonuniform spin configurations 80−97109
uniaxial antiferromagnetic, phase diagram, spin flop transition *(Russian)* 80−100587
unidimensional xy-chain, impurity zone fine struct. *(Russian)* 80−6787
Union Jack lattices, non-universal Ising spin systems 80−68145
Van der Waals systems, time-dependent correls. 79−61130
Wilson's renormalisation group recursion eqns., critical phenomena 78−4581
X-Y(s=1/2) model, renormalisation group method, triangular lattice 77−26247
X-Y model, one-dimens., zero temp., transverse time depend. spin correlation functions 78−65876
X-Y model, S=1/2, phase transitions at T=0, z-field renormalisation group method 80−71051
X-Y quasi-one-dimens. system anisotropic, spin-Peierls phase transition, tricritical point 80−25142
X-Y spin chain model high power terms, spectral and thermodynamic props. 77−80900
XY one dimensional system containing impurities, static mag. props. *(Russian)* 80−65826
Al_2O_3:Cr_2O_3, paramagnetic, saturation effects by double-quantum transitions 78−80197
Al_2O_3:Cr^{3+}, inhomogeneous spin system, time evolution towards saturated state 80−88869
CaF_2, heteronuclear mag. spin system relaxation in many pulse NMR expts. 80−93203
CaF_2:Eu^{2+}, photoluminesc. mag. circ. polaris. 80−89056
$Ca(OH)_2$, mag. ordering of proton spins 79−73746
$CdCr_2Se_4$, spin system heating by drifting current carriers, magnon-phonon system energy transfer *(Russian)* 80−29541
$Co_{1.8}BaFe_{0.2}^{2+}Fe_{16}^{3+}O_{27}(Co_{1.8}W)$, magnetoelastic props. under spin-reorientation conditions 79−69709
Co_xGa_{100-x}, electrical resistivity anomaly, spin cluster model 79−99531
$CsFeCl_3$, linear chain ferromag., optical absorpt. and dichroism in mag. field 77−77237
Cu-Cs diluted deuterated Tutton salts, electron non-Zeeman system, nuclear relaxation study 80−44951
Dy, critical exponents and amplitude ratios from elec. cond. data, theoretical model 80−50126
EuO, spin system heating by drifting current carriers, magnon-phonon system energy transfer *(Russian)* 80−29541
Fe complexes, high spin ionic with halogen ligands, Mossbauer isomer shift calibration 77−16210
Fe film, nuclear spin system dynamics Mossbauer study in FMR conditions *(Russian)* 80−80651
Fe-Cr, mag. props. of Fe, local coupling with spin modulation of matrix 79−15299
Fe-Cr-Ni, spin system, relaxation props. at low temp. 79−82758
FeAs, Mossbauer spectra of paramag. and ferromag. states, helimagnetic spin ordering 80−7197
$FeBO_3$, parametric echo, magnetoelastic NMR excitation *(Russian)* 80−66072
^{57}Fe Mossbauer spectroscopy with polarised γ-rays, mag. material spin arrangement determ. 79−33568
H_3, interrelationships between effective hamiltonians 77−30767
$(H_2O)_2$, nucl. spin statistics effects on group theoret. classification of tunnelling-rot. energy levels 77−54549
^3He, solid, magnetism *(Japanese)* 79−19425
^3He, superfluid, magnetic relaxation and high amplitude spin waves *(Russian)* 80−92749
$KCrF_3$, mag. struct. and cooperative ordering or orbitals 79−99687
$KCuF_3$, mag. struct. and cooperative ordering or orbitals 79−99687
$KFeCl_3$, linear chain ferromag., optical absorpt. and dichroism in mag. field 77−77237
$(La,Gd)Al_2$, reverse Kondo alloy, transport props. at finite mag. field 80−6812
LiF, heteronuclear mag. spin system relaxation in many pulse NMR expts. 80−93203
$LiIO_3$, cross relax. in two-spin system, inhomog. broadened line 78−88218
γ-Mn, antiferromagnetic, self-consistent bandstructure calcs. 80−88475
MnAs, soft mode, energy and entropy, competition with energy and entropy of spin system 79−10908
$MnCl_2.4H_2O$, single cryst., mag. phases, obs. by ^{54}Mn nucl. polarisation 77−81031
Ni, paramagnetic, temp. depend. of spin susceptibility 79−4651
Ni_3Mn, anal. of irrad. disordering data 79−1466
α-O_2 crystals, spin ordering effect on light absorpt. *(Russian)* 80−89029
$RbFeCl_3$, linear chain ferromag., optical absorpt. and dichroism in mag. field 77−77237
$RbMn_{1-x}Mg_xCl_3$, dilute pair antiferromag., mag. susceptibility and ESR meas. 79−78338
$RbNiCl_3$, cryst., ^{35}Cl and ^{87}Rb NMR down to 1.3K 79−42848
Si:Cr^+ EPR spectra and spin state population inversion with unpolarised optical lighting *(Russian)* 80−44909
Si:P, optical excess charging $D^0 \rightarrow D^-$, photoelectron spin relaxation *(Russian)* 79−78572
Tb compounds, anisotropic magnetoelastic props., noncollinear spin arrangements 77−69660
V_2, formation, spectra, electronic struct. 77−54642
V_3O_5, spin order, one-dimensional, Neel transition 80−39799

spin tickling (NMR) *see double nuclear magnetic resonance*

spin wave resonance *see ferromagnetic resonance*

spin waves
see also magnetostatic waves; magnons
advances in basic magnetism during past twenty-five years 80−36791
alloys, ferromagnetic disordered, spin wave and ferromag. reson. linewidth 80−66045
amorphous antiferromagnet, semiclassical theory 77−36064
amorphous ferromagnet, apparent spin wave stiffness, low temps. 79−82776

spin waves continued
amorphous ferromagnet, excitations, calc. using hard sphere models 77−66289
amorphous ferromagnet, localised spin and phonon excitations, theory 79−7979
amorphous ferromagnet, mag. excitations 78−68204
amorphous ferromagnet, random model spin wave spectrum 77−89918
amorphous ferromagnet, spin wave excitations, similarity to liquid metal electronic struct. 77−12109
amorphous ferromagnet, spin wave spectra *(Chinese)* 79−91219
amorphous ferromagnet, spin wave spectrum 79−24148
amorphous ferromagnet, spin wave spectrum rel. to struct. 77−66290
amorphous ferromagnets, asperomagnets and spin-glasses, spin waves, theory 80−75747
amorphous ferromagnets, dispersion rels. and spin-wave spectroscopy *(Russian)* 79−7983
amorphous ferromagnets, excitations 78−80139
amorphous ferromagnets, hidden excitations, theory 80−75748
amorphous ferromagnets, possibility of low temp. phase below ferromag. phase 79−4674
amorphous ferromagnets with random anisotropy axes, spin waves 80−7096
amorphous Heisenberg ferromagnet, effective medium approx. 78−68203
amorphous Heisenberg ferromagnet, spin wave excitations and magnetization curve 79−15292
amorphous magnetic materials, spectral density functions 79−47269
anisotropic chain, elementary excitations, calcs. 79−33467
anisotropic magnet, low-temperature properties 79−65633
anisotropic magnets, spin wave theory 77−20576
anisotropic medium, randomly inhomogeneous, spin wave damping, dispersion relation *(Russian)* 77−43828
antiferrimagnet, two-sublattice, spin waves, magnetocaloric effect 78−31073
antiferromagnet, amorphous, spin waves, exchange fluctuations, calc. 80−65847
antiferromagnet, chain-like, parallel susceptibility 78−80137
antiferromagnet, dislocation slowing down due to spin waves *(Russian)* 79−95584
antiferromagnet, easy-plane, coupled spin wave branches *(Russian)* 80−93096
antiferromagnet, effect of external stress on AFMR and other spin wave frequencies 79−61230
antiferromagnet, ground states, phase transitions and spin wave spectra 79−87246
antiferromagnet, high frequency properties, spin wave spectra corrections magnon interactions *(Russian)* 80−54876
antiferromagnet, IR absorption on impurity excitations near upper edge of spin-wave band 80−80829
antiferromagnet, itinerant electron, mag. excitations 78−56305
antiferromagnet, itinerant electron, spin wave spectrum calc. 77−36063
antiferromagnet, long-wavelength, surface spin-waves 80−88737
antiferromagnet, low-dimensional susceptibility, effect of kinematical interaction in spin wave theory 79−28513
antiferromagnet, mag. excitations within local exchange approx. 77−69517
antiferromagnet, mechanism for hard excitation of spin waves *(Russian)* 78−19235
antiferromagnet, moving dislocations, interaction with spin waves *(Russian)* 78−56303
antiferromagnet, nonsymmetric distrib. of parametrically excited waves *(Russian)* 78−47967
antiferromagnet, nuclear spin oscillations, interaction with lattice vibrs. 80−70996
antiferromagnet, quadratic, with easy-plane anisotropy, spin wave theory 78−91855
antiferromagnet, randomly dil., excitations 78−23258
antiferromagnet, randomly dil., spin wave excitation exam. 77−24665
antiferromagnet, rel. to theory of relax. 77−24750
antiferromagnet, relax. processes, spin-sound wave coupling 78−60340
antiferromagnet, spin wave parametric instability *(Russian)* 78−34971
antiferromagnet, spin wave relaxation in strong mag. field 78−2747
antiferromagnet, transversely anisotropic, spin-wave theory of paramag. phase boundary 77−69552
antiferromagnet, uniaxial, spin configuration in ferromag. phase, field and temp. depend. 79−38321
antiferromagnet chain, anisotropic, spin-wave spectrum 78−60273
antiferromagnet Heisenberg 1-dimens. chain, external mag. field effect 77−89943
antiferromagnetic, triang., spin wave theory 79−7978
antiferromagnetic metals, two band model for elec. resist. 78−14720
antiferromagnetic resonance, spin waves studied by microwave absorpt. 78−91960
antiferromagnetic semiconductor, spin-wave amplification 80−7099
antiferromagnetism itinerant electron theory, spin susceptibilities 78−6504
antiferromagnets, easy-plane, nucl. spin wave relax. 80−65850
antiferromagnets, low anisotropy, nuclear spin waves spectra, relaxation, parametric excitation, NMR dynamic shift *(Russian)* 80−11180
antiferromagnets, magnon damping due to impurity scatt. 78−68206
antiferromagnets, magnon damping due to magnon-phonon interactions *(Russian)* 79−11305
antiferromagnets, magnon damping in zero external mag. fields, magnon-magnon interactions 80−70988
antiferromagnets, nuclear magnetisation motion under parametric influence of longitudinal RF field *(Russian)* 79−82880
antiferromagnets, weakly linear magnetisation density waves 77−51888
asperomagnetic alloy, amorphous, spin-wave theory including short range order 79−38313
atomically rough surfaces, mag. excitations 77−69664
biaxial Lifshitz point problem in 3-dimens., spin wave theory 80−88759
Bloch wall, narrow, magnetic excitations, pole field effect 78−91853
Bloch wall bound spin waves, equations of motion 80−34612
Bloch wall containing Bloch lines, excitation spectrum 77−4527
bootstrap percolation conductivity on Cayley tree, rel. to spin wave stiffness 80−54743
Bose operator expansions of tensor operators in theory of magnetism 77−63061
classical Heisenberg chains, low temp. spin dynamics 78−68243
classical XY spin dynamics far from equilibrium 78−68136
collective-acoustic resonance in system for parametric spin waves 79−69727

spin waves continued
commensurate-incommensurate phase transition in nearly half-filled band 79−65384
composite semiconductor-ferrite struct., surface magnetostatic spin wave interactions *(Russian)* 80−88739
continuum Heisenberg spin system, stationary spherically and axially symm. spin waves 80−34615
coupled fields in one dimension: cross-over from a continuous symmetry to a discrete one 78−87758
cubic ferr-te garnet, diffracted light polarisation characts., spin and magnetoelastic waves 80−20614
damping, magnetic materials with canted mag. struct., thermodynamic and high freq. props. 80−11184
damping at low temps. *(Russian)* 77−36062
dialkylammonium copper chlorides, rel. to NMR obs. of magnetisation 77−85586
dibutylammonium copper chloride, parallel pumping of two-dimens. spin waves, spin wave bandwidth 77−66425
diethylammonium copper chloride, Heisenberg ferromag., spin wave theory 77−89922
dilute ferromagnet, linear spin-wave theory, effective medium approach 80−20393
dilute ferromagnet, spin wave excitations, multicomponent CPA theory 78−68135
dilute Heisenberg antiferromagnet, mean spin on finite clusters 78−68139
dilute Heisenberg magnet excitations near percolation threshold 79−87270
diluted antiferromagnet, linear spin-wave theory, effective medium approach 80−20393
dimethylammonium manganese tetrachloride, Heisenberg ferromag., spin wave anal. 79−61237
dipole-exchange spin waves in cylindrical ferromag. *(Chinese)* 78−6521
dipropylammonium copper chloride, nearly 2D ferromag., spin wave theory 77−85436
dislocated ferromagnet, inhomogeneous magnetisation near dislocation effect on FMR linewidth 80−25213
disordered, magnet, collective modes, Heisenberg-Mattis model 80−39797
disordered magnetic system, spin waves, Heisenberg model 80−71064
disordered media, ferro- and antiferromag., and spin glasses, dynamic props. *(Russian)* 78−39350
disordered media, spin wave propagation, nonlinear magnon interactions *(Russian)* 80−80496
disordered substitutional alloy, mag. props., Heisenberg model 79−38342
dispersion relations for energy eigenvalues of two magnon bound state 78−47964
domain wall velocity, damping parameter meas. from low field microwave excitations 80−34676
doped semiconductor plasma, inelastic light scatt., spin diffusion 77−36241
elementary excitations in spin systems with three-atom exchange 78−84404
EM wave emission at twice freq. of parametrically excited spin waves, line profile depend. on spin wave distrib. 80−60234
exchange and dipoles coupled ferromags., light scatt. from mag. surfaces, response theory 79−42820
excitation by uniform precession of magnetisation due to two magnon scatt. 78−68207
exciton dielectric type system with doping, low freq. excitations *(Russian)* 80−15459
Fermi fluid with paramagnetic impurities, spin wave spectrum *(Russian)* 79−23915
ferrimagnetic layer, spin wave amplification 79−65668
ferrimagnetic materials propagation, parameters indicating microwave appl. suitability 77−20571
ferrimagnets, effect of ellipticity on direction of spinwave rays 79−1659
ferrite, magnetoacoustic reson. in strong mag. field 80−11309
ferrite, mode spectrum, loss mechanisms 78−88548
ferrite, parametrically excited spin waves, amplitude restriction mechanisms *(Russian)* 77−32182
ferrite, spin wave relaxation processes 79−82771
ferrite rod with domain structure, magnetostatic waves and internal field *(Russian)* 78−76236
n-ferrite-n-GaAs layer struct., boundary spin wave amplification *(Russian)* 77−73016
ferrite-semicond. layer struct. with negative differential conductance, instability 80−25118
ferrites, ferroelec., coupled ferroelec. and spin waves, exchange interactions 80−70995
ferrites, frequency tripling of spin waves due to longitudinal pumping excitation *(Russian)* 80−88740
ferrites, inhomogeneous exchange interaction influence on ferromagnetic resonance line moments 80−75864
ferrites, parametric spin wave excitation *(Russian)* 80−93099
ferrites, parametrically excited spin waves, spectral density *(Russian)* 79−4667
ferrites, soft and microwave, grain-size effects on mag. props., review 78−64222
ferrites, spin wave instability on approaching FMR *(Russian)* 78−76318
ferrites, stability of nonlinear homogeneous magnetisation precession *(Russian)* 78−48001
ferroelectric antiferromagnet, damping of spin waves and 'hard' excitation effect 79−28518
ferroelectric antiferromagnetics, spin wave fluctuations in strong mag. fields *(Russian)* 79−82773
ferroelectric ferro- and antiferromagnet, energy gap in spin wave spectrum 78−91858
ferroelectric-magnetic coupled oscills., excitation by electron beam *(Russian)* 78−23257
ferroelectroantiferromagnetics, spin wave spectrum and exchange amplification of magnetoelectric correlation 79−38311
ferroinsulators, spin waves and uniform transverse magnetization, oscillatory eigenstates *(Russian)* 80−11181
ferromagnet, critical dynamics above Curie pt. 79−87262
ferromagnet, diluted, two-dimens., with anisotropic exchange interaction, excitation spectra 77−43826
ferromagnet, dislocation motion, mag. moments around screw dislocations, spin waves retarding dislocations 78−87670
ferromagnet, disordered itinerant-electron, spin waves 78−95427
spin waves continued
ferromagnet, dispersion relations for energy eigenvalues of two magnon bound state 78−47964
ferromagnet, domain wall retardation by spin waves *(Russian)* 80−25154
ferromagnet, dynamic correlations in condensed matter physics, book 80−86046
ferromagnet, dynamic dislocation deceleration by spin waves *(Russian)* 77−28379
ferromagnet, dynamic struct. factor to order ε=6-d, sloppy spin-wave modes 77−63208
ferromagnet, easy-axis, higher order corrections to spectrum 78−80222
ferromagnet, excitonic, zero-sound excitations, Fermi liq. model 80−93101
ferromagnet, Heisenberg, spin wave relaxation due to dipole interactions, damping temp. depend. 79−69664
ferromagnet, high frequency, kinetic and thermodynamic props. *(Russian)* 78−19340
ferromagnet, inter-atomic interaction effect on dynamic susceptibility, RPA calcs. 79−65662
ferromagnet, itinerant, spin waves, appl. of self consistent many-body theory 79−73702
ferromagnet, itinerant, spin waves, surface effects, RPA calc. 80−60226
ferromagnet, itinerant electron, surface spin waves, tight-binding Hubbard model 80−39763
ferromagnet, itinerant electron model, spin wave stiffness temp. depend. 77−20535
ferromagnet, Landau-Lifshitz eqn., two soliton solns. for nonlinear dynamics *(Russian)* 78−43646
ferromagnet, light scatt. by spin waves 80−45086
ferromagnet, linear Ising-Heisenberg, spin waves vs. bound states, exact soln. 78−68202
ferromagnet, magnetostriction is magnetic field, sound-spin wave coupling 79−15334
ferromagnet, many-domain, indirect interaction of electrons via spin waves 77−85382
ferromagnet, model, spin wave stiffness, temp. renormalisation 77−85435
ferromagnet, noncond., Green function, contrib. of bubble graphs due to dynamic and kinematic spin wave interactions 77−51894
ferromagnet, nonsymmetric distrib. of parametrically excited waves *(Russian)* 78−47967
ferromagnet, nuclear magnetisation ground state 79−73703
ferromagnet, nuclear spin waves, possible detection by inelastic neutron scatt. 77−85438
ferromagnet, one-dimensional planar, in external field, static props. 79−51735
ferromagnet, parametric spin waves distrib. function *(Russian)* 79−87250
ferromagnet, randomly anisotropic, long wavelength mag. excitations 78−84406
ferromagnet, randomly dil., spin wave excitation exam. 77−24665
ferromagnet, spin wave damping, theory, and comparison with expt. for EuO 78−52237
ferromagnet, spin wave stiffness coefficient, spin density functional theory 78−76230
ferromagnet, spin wave system, kinetic eqn. on parametric excitation *(Russian)* 79−87249
ferromagnet, spin waves with moving domain wall 80−39764
ferromagnet, stationary weakly turbulent distrib. *(Russian)* 79−38316
ferromagnet, substitutionally disordered, spin dynamics, linear spin-wave approx. 77−40067
ferromagnet, surface, Brillouin light scatt. by spin waves 80−93359
ferromagnet, surface and bulk nucl. spin waves, Green function formalism 80−70984
ferromagnet, surface magnetoelastic waves in the presence of exchange interactions and pinning of surface spins 78−80186
ferromagnet, surface spin waves and surface spin correlations in presence of mag. surface reconstruction 78−6522
ferromagnet, topological solitons, localised *(Russian)* 79−69661
ferromagnet, two dimensional diluted, spin wave spectrum 77−66287
ferromagnet, two-dimens., spin wave theory, magnetisation, susceptibility *(Japanese)* 77−47954
ferromagnet, two-dimensional magnetisation, spin wave theory *(Japanese)* 77−20578
ferromagnet, uniaxial, quantum anomalies in susceptibility during second order phase tansitions *(Russian)* 78−19226
ferromagnet, uniaxial, with flat-parallel domain struct., classical phenomenological description 78−56316
ferromagnet, uniaxial, with random exchange bonds of different signs, spin waves 78−76233
ferromagnet, uniaxial dipolar, crossover behaviour, theory 80−29559
ferromagnet, with liq.-like disorder, excitations 79−61084
ferromagnet, with moving domain wall *(Russian)* 78−88103
ferromagnet, with weakly bound ferromag. impurity, thermodynamic and dynamic props. *(Russian)* 78−27032
ferromagnet film, spin wave propagation near surface 78−68308
ferromagnet with resonant impurities, Heisenberg model *(Russian)* 79−87280
ferromagnet with single ion anisotropy, collective modes 77−28354
ferromagnetic, electron fluid, polar spin waves *(Russian)* 77−89938
ferromagnetic, mag. excitations within local exchange approx. 77−69517
ferromagnetic alloys, itinerant electron model, spin wave stiffness const. calc. 80−34613
ferromagnetic alloys, narrow band with random hopping, stability and damping, Ward relations 79−56524
ferromagnetic alloys, surface spin waves, cluster Bethe lattice approach 80−70983
ferromagnetic array of pseudospin S=1/2, nearest neighbours anisotropic exchange mag. stability at 0K 77−1547
ferromagnetic binary alloy, electron interactions and spin-wave stiffness const. 77−1548
ferromagnetic binary ordered alloy, dynamic mag. susceptibility, spin wave stiffness const. 79−38307
ferromagnetic chain, anisotropic, kink excitations, nonlinear model 80−54881
ferromagnetic chain, spin wave theory in lower dimens., failure of dynamic scaling hypothesis 79−78284
ferromagnetic conducting cryst., dynamics of s-d model in alternating mag. field *(Russian)* 80−65825
ferromagnetic film, crit. angle of external mag. field for surface spin waves 79−47309

spin waves continued
ferromagnetic film, tangentially magnetised, parallel pump spin wave instability 77−8294
ferromagnetic film, tangentially magnetized, spin wave instability 78−2712
ferromagnetic films, spin wave excitation by microwave antenna field 80−44816
ferromagnetic layer in perpendicular mag. field, ground state, spin wave reson. 77−85512
ferromagnetic metal, two-site interaction model 79−82744
ferromagnetic metallic glass, hyperfine field and spin wave excitations, $T^{3/2}$ depend. 78−10672
ferromagnetic metals, simple theory of spin-wave relax. 78−19231
ferromagnetic nonmetallic film, stand exchange mode determ. 80−2565
ferromagnetic partially ordered alloy, spin wave stiffness const. 79−24150
ferromagnetic plate, with anisotropic surface discontinuities, spectrum and damping of quasi-surface spin waves 80−11185
ferromagnetic semicond., spin-helicon wave parametric amplification 79−69665
ferromagnetic semiconductor, autolocalised electron states 78−51924
ferromagnetic semiconductor, carrier-assisted radiation pumping of spin waves under strong mag. field 77−55667
ferromagnetic semiconductor, energy and mobility of spin polarons 80−70982
ferromagnetic semiconductor, spectrum of quantum spin waves in field of strong EM wave 78−91857
ferromagnetic semiconductor in quantizing mag. field, spin wave spectrum 78−19236
ferromagnetic semiconductors, mag. excitations, light scatt. 77−63161
ferromagnetic semiconductors, parametric excitation of magnetoplasma reson. 79−28623
ferromagnetic semiconductors with hot electrons, instability of coupled spin-helical waves 80−107841
ferromagnetic slab, finite thickness, magnetostatic theory of response functions, appl. to Brillouin scatt. 79−61083
ferromagnetic slab, finite thickness, spin correl. functions 80−80522
ferromagnetic slab, light scattering from bulk and surface spin waves, theory 80−71389
ferromagnetic spin waves above Curie temp., Fisher's droplet model 78−56307
ferromagnetic surface, spin fluctuations and light scatt. 80−84727
ferromagnetic surface spin waves, microscopic theory, mag. field effects 78−35044
ferromagnetic surface-rearranged thin films, spinwave spectrum, derivation from generalisation of Bogoliubov canonical transform. 79−69702
ferromagnetic thin film, with nearest neighbour and next nearest neighbour exchange interactions spin-wave excitations 79−73783
ferromagnetic thin films, Brillouin scattering from spin waves 80−65843
ferromagnetic waves, appl. of surface problem expansion technique 77−4244
ferromagnetism, itinerant, local band theory, spin waves 78−31041
ferromagnetism, itinerant electron model, spin quantization direction fluctuations, short range order. 80−34582
ferromagnets, anisotropic, spin wave interactions *(French)* 77−69524
ferromagnets, dilute, spin waves at surface 79−61089
ferromagnets, domain struct. effects on dynamic props., review 80−34678
ferromagnets, exchange and dipolar coupled, spin wave renormalisation, Damon-Eshbach surface spin waves 80−2564
ferromagnets, Heisenberg and planar, exact results for spin-wave renormalisation 79−69660
ferromagnets, internal energy relationship to moment 77−16028
ferromagnets, metallic, spin wave damping, magnetisation relax. 78−88106
ferromagnets, spin wave excitation due to parallel pumping, mag. impurity interactions *(Russian)* 80−80497
ferromagnets, spin waves in domain struct. 80−70993
ferromagnets, uniaxial, negative magnetocaloric effect 79−82783
ferromagnets, weakly linear magnetisation density waves 77−51888
ferromagnets and antiferromagnets, transverse dynamical susceptibility within the local exchange approx. 78−76229
film, ferromag., dynamics near transition pt. from homogeneous to inhomogeneous magnetis. state 80−108038
film, spin pinning and mag. surface reconstruction, effect on standing spin waves 77−1600
film, surface spin waves and surface anisotropy effects at finite temp. 79−78452
film, with internal isotropically coupled impurity layer, spin wave reson. spectrum 78−80223
finite sample, mag. rearrangements near surface 80−11240
frustrated two-dimensional planar model, spin-spin correl. 80−11212
garnets, magnetic relaxation phenomena 79−99776
garnets magnetic excitations 79−99695
ground state representation of infinite one-dimens. Heisenberg ferromagnet 77−66234
heavy rare earth metals, RKKY theory of magnetism, electron-electron interactions 79−73667
Heisenberg antiferromagnet, anisotropic, excitations at finite temp., CPA calcs. 79−95562
Heisenberg antiferromagnet, dil. two dimensional, mean spin per site in linearised spin-wave theory 78−39304
Heisenberg antiferromagnet, excitations at finite temp. using CPA 79−56554
Heisenberg antiferromagnet, one-dimensional, spin waves in spin-flop phase 80−44817
Heisenberg antiferromagnet, spin waves at finite temp., CPA calc. 79−73728
Heisenberg antiferromagnetic chain, nonsinglet excitations 77−4491
Heisenberg antiferromagnetic chain, spin dynamics, quantum effects 80−34651
Heisenberg chain, classical, nearest-neighbour, low temp. dynamics 80−80524
Heisenberg chain, classical, solitons and magnons 80−60161
Heisenberg chain, explicit Plancherel theorem for ground state representation 77−89921
Heisenberg chain, impure classical, dynamics near T=0 for low impurity conc. 80−71055
Heisenberg continuous ferromagnetic chain, finite amplitude spin wave, stability 80−20395

spin waves continued
Heisenberg dilute systems, computer simulation, mag. conc. of clusters, linearised eqns. of motion 79−78409
Heisenberg exchange interaction Hamiltonian, eigenvalues and eigenvectors 79−78289
Heisenberg FCC ferromagnet, surface spin instabilities 77−69475
Heisenberg ferromag. localised magnons around surface impurity *(Russian)* 78−84376
Heisenberg ferromag. two-dimensional dil., density of states near percolation threshold 77−1533
Heisenberg ferromagnet, anisotropic, quasicollective spin waves in paramag. region 77−43827
Heisenberg ferromagnet, consistent linearised Green's function theory for $s=1/2$ 79−4685
Heisenberg ferromagnet, critical dynamics of impurity spin below T_c 80−71076
Heisenberg ferromagnet, critical dynamics spin wave theory, dynamic scaling hypothesis failure 80−97082
Heisenberg ferromagnet, density of states and heat capacity near percolation threshold 77−77021
Heisenberg ferromagnet, dil., CPA theory, spin-wave stiffness and Curie temp. 78−31080
Heisenberg ferromagnet, dil., localisation of excitations near percolation threshold 79−15271
Heisenberg ferromagnet, dil., mag. excitations, localisation, wavefunctions 78−60275
Heisenberg ferromagnet, dil., spin wave localisation near percolation threshold 80−25120
Heisenberg ferromagnet, disordered, two spin species, spin-wave spectra calc. 77−59375
Heisenberg ferromagnet, local levels arising from spin wave kinematic interactions 77−59374
Heisenberg ferromagnet, randomly diluted, 2-dimens., dynamics calcs. 77−40024
Heisenberg ferromagnet, randomly noncollinear mag. struct. and spin waves *(Russian)* 79−42764
Heisenberg ferromagnet, self-consistent renormalisation of spin waves 77−72966
Heisenberg ferromagnet, spin coherent state representation, spin waves excitation spectrum 78−80117
Heisenberg ferromagnet, spin operator study by small angle mag. neutron scatt. 80−15700
Heisenberg ferromagnet, spin wave excitations at finite temp., CPA calc. 77−32142
Heisenberg ferromagnet, spin waves at low temp., method of variational derivatives 79−24152
Heisenberg ferromagnet, spin-wave renormalisation, $S \geq 1$ 80−71070
Heisenberg ferromagnet, stepped surface, spin-wave modes calc. 77−73015
Heisenberg ferromagnet, surface spin waves theory *(Russian)* 77−89939
Heisenberg ferromagnet, two-dimens., spin dynamics, renormalisation group calc. 78−47966
Heisenberg ferromagnet in critical region, Bloch renormalised spin wave approx. 79−82784
Heisenberg ferromagnet surface, spin behaviour, review 77−20527
Heisenberg ferromagnetic system with biquadratic exchange interactions, spin wave theory *(Chinese)* 80−88755
Heisenberg linear chain, alternating spin quantum numbers, mag. and thermodynamic props. 80−34578
Heisenberg model, classical low temp. spin wave dynamics 78−6501
Heisenberg model, helical spin chains, static and dynamic props. 79−73661
Heisenberg model, magnetic excitations on ideas and atomically rough surfaces 78−14944
Heisenberg model, quasilow dimensional, small dilution perturbation theory at 0K 78−56281
Heisenberg model, spin wave theory, existence of spontaneous magnetization 79−11281
Heisenberg spin glass, spin wave stiffness, computer simulation 79−78405
Heisenberg theory, spin wave exam. *(Dutch)* 79−1663
Heisenberg-Ising chain, bosonisation, spin wave vel. calc. 80−54905
Heisenberg-Mattis model, long-wavelength dynamic response 80−20409
helical magnet, surface spin waves and spin arrangements 78−68198
Heusler alloy, Mn-containing theory of spin waves 79−78354
Hubbard antiferromagnetic semiconductor, collective excitations, weak coupling limit 78−19210
Hubbard model, electrostatic interaction Hamiltonian, tensor struct. *(Russian)* 78−76216
Hubbard model, spin-wave excitations in narrow s-band, including intersite exchange interactions 77−16033
hydrodynamic singularities and the renormalization group 79−54063
hydrodynamic theory for spin glass or noncollinear spin system 78−6524
ideal Heisenberg ferromagnet, phonon renormalisation and spin waves 80−88754
induced moment systems, effect of spin fluctuations 80−2585
instability theory for cubic single cryst. mag. insulators 79−65667
insulator, localised surface impurity modes 77−1545
Ising ferromagnet, high-freq. props. quantum theory, susceptibility tensor calcs. *(Russian)* 80−11143
isotropic antiferromagnets, anal. by equivalent Hamiltonian method 79−82734
isotropic antiferromagnets, crit. dynamics using renormalisation group methods 79− 8006
isotropic Heisenberg ferromagnet, localised spin-wave modes, biquadratic exchange effects 77−51896
isotropic model ferromagnet, longitudinal magnetisation spectrum calc., spin wave interaction 78−10627
itinerant electron ferromagnet with domain struct., spin waves 78−64182
itinerant electron magnetism, thermodynamic aspects 77−72992
itinerant electron magnets, spin fluctuations 77−72990
itinerant electron magnets, theory of spin fluctuations 77−63064
itinerant electron model for ferro- and antiferromag. systems, dynamic susceptibility 77−72988
itinerant electron systems, mag. excitations, study by inelastic neutron scatt. 79−47264
itinerant ferromagnet, sloppy spin waves above T_c 77−72979
itinerant ferromagnet, spin wave stiffness const., electron correl. effects 79−19733
itinerant ferromagnet, surface spin waves 77−69480
itinerant ferromagnet, thermodynamics 79−4645

spin waves continued
itinerant ferromagnetism, of two dimensional systems 77−24666
itinerant ferromagnetism, statistical mechanics of spin waves 79−82746
Jahn-Teller cooperative T−(e+t) systems, pseudo spin thermal cond. 80−34406
kinetic equation for spin waves in a weak alternating magnetic field 79−42750
kinetic exchange interaction, doubly degenerate narrow bands 78−23263
layered struct., interaction of spin waves with hot carriers 79−15291
lecture 78−27026
light scattering lineshape for absorptive mag. material 78−23476
linear Heisenberg antiferromagnet, $S=^1/_2$ zero temp. dynamics 79−73741
linear Ising-Heisenberg ferromagnet, spectrum of elementary excitations 79−61091
localised model for systems with double-exchange coupling 79−38318
localised spin excitations 80−15708
mag. excitations, atomically rough surfaces, isolated cluster of overlayer spin 78−31102
magnetic chains with X-Y symmetry, anharmonic effects and IR singularity 77−32146
magnetic dipoles on a lattice, theory at low temps. 80−50082
magnetic domain walls, motion under static mag. field, energy dissipation 79−95605
magnetic excitations in amorphous ferromagnets 79−78356
magnetic film, complex surface pinning parameter and quasi-localised surface spin wave modes 80−50150
magnetic moment waves, nonlinear, limiting vel. and types *(Russian)* 78−60276
magnetic semiconductor, conduction electron spectrum, influence of nonlinear spin waves 79−28270
magnetic structures, non-periodic, ferromagnetic spin wave propagation, interaction with domain walls 79−99692
magnetic surface states, in spin wave resonance, review 80−84654
magnetic symmetry and spin-wave Hamiltonian struct. 78−84373
magnetically ordered materials, specific heats and spin wave theory, review 79−42763
Mattis random magnet, spin waves 77−20572
metal, EM props., general lecture 78−26901
metal, ferromagnetic, excitations in mag. field, theory *(Russian)* 77−8291
metal, ferromagnetic reson. damping, one electron model 77−8409
metal, ferromagnetic resonance linewidth, interaction of spin waves with conduction electron current 80−25216
metal-magnetodielectric layered delay lines, dispersion eqn. *(Russian)* 80−88736
metallic ferromagnet, antiresonance region, EM wave propag., Maxwells' eqns. soln. 80−66038
metallic film with mag. impurities, electron Fermi liq. theory, collective excitation spectrum *(Russian)* 77−62846
metallic spin glass, spin wave theory 79−11306
metals, narrow-band, magnetism and mag. excitations 77−69478
metals, paramagnetic, conduction electron spin transmission 77−69693
metastable polarised crystals, decay kinetics, exchange magnon-phonon interactions *(Russian)* 80−7060
metastable spin-aligned crysts. decay kinetics 80−34669
microcanonical high-temp. expansion 78−2638
micropolar fluids, thermodynamical aspects, non-linear approach 80−105598
neutron beam channelling and focusing in ferromagnets *(Russian)* 80−107351
neutron inelastic scatt. expts., book contrib. 78−1959
neutron matter, spin zero sound and spin diffusion coeff. 77−57278
neutron scattering, polarisation depend. 79−47255
neutron scattering investigation, review *(Japanese)* 78−52227
neutron studies of magnetic densities and magnetic excitations, book contrib. 80−11170
noncollinear magnetic order and spin wave spectrum in presence of competing exchange interactions 80−65834
nonequilibrium oriented spin system, spin waves *(Russian)* 77−80923
nonexchange surface spin waves at interface between two ferromagnets 80−29544
nontransition metals, spin excitations 79−82770
nucleon systems, spin density wave and π^0 condensation 77−61368
one dimensional anisotropic Heisenberg model, spin 1/2, Ising like antiferromag., dynamic correlation function 80−75704
one dimensional magnetic behaviour 79−28495
one domain ferromagnetic insulators, spin wave and elastic wave interactions 79−73700
one-dimensional anisotropic magnet, in long-wavelength approx., spin excitations 79−61085
one-dimensional antiferromagnet, with antisymmetric exchange, Green's function theory 79−15290
one-dimensional Heisenberg antiferromagnet 79−91222
one-dimensional mag. systems, neutron scatt., review 80−50103
one-dimensional quasiclassical spin wave model in mag. field, static and dynamical props. 77−66284
one-dimensional spin system, microscopic crit. dynamics, spin wave sidebands in approx. soln. 79−69683
ordered Heisenberg ferromagnet/liq. ^{3}He system, mag. Kapitza cond. calc. 79−51415
$P(\phi)_2$ Euclidean field theory, boundary conditions rel. to ferromagnetic spin systems 77−54036
paramagnet and ferromagnet, multiboson spin wave representation 79−4664
paramagnetic crystal, mixed spin-phonon waves *(French)* 77−66400
paramagnetic impurities in conductors, relaxation and indirect exchange interaction 78−2728
paramagnetic regime, spin-wave spectrum, of systems without long-range mag. order 79−33450
paramagnetic system, spin waves, classical approach 80−29519
paramagnets, anisotropic, spin dynamics 77−69481
parametric excitation, stochastic auto-oscills., Kolmogorov entropy *(Russian)* 80−75749
parametric excitation by noise pumping *(Russian)* 80−34617
parametric excitation on spin waves in the induced magnetoelastic crystals *(Russian)* 78−60272
parametric wave excitation by incoherent pumping 80−93103
parametrically excited spin wave system soliton obs. *(Russian)* 77−59401
spin waves continued
parametrically excited waves, interaction with defects exhibiting internal structure 80−7173
Pd_3Fe, ferromag. spin wave meas., inelastic scattering of polarised neutrons 78−2665
Permalloy film, with-small surface anisotropy, ferromag. reson. 77−69701
piezoelectric semiconductor, dissipative, amplification of spin waves 79−24000
planar-rotator model with short range interaction 79−80540
Poisson brackets, nonlinear hydrodynamics eqns. in condensed matter physics 80−54296
propagation on ferromagnetic metal 79−7982
pseudospins, S=1/2, simple cubic array, with anisotropic exchange between nearest neighbours, ground state configs. 78−72340
quasi one-dimensional spin lattice coupled system, collective modes 80−24896
random magnet, LF response function 78−6493
rare earth alloys, amorphous, with random anisotropy axes, spin excitations in paramag. phase 80−80476
rare earth antiferromagnet, magnetic excitation, appl. to DySb 79−78358
rare earth metal, magnetic properties, nonlinear s-f exchange interaction effect 80−15711
rare earth metals, mag. excitations, neutron inelastic scatt., review 79−47265
rare earth metals, magnon dispersions in ferromag. and screw structs., nonlinear s-f exchange interaction effect 80−75746
rare earth metals magnetism, review 77−63123
rare earth orthoferrite, phonon slowing down of domain wall *(Russian)* 79−33503
rare earth-Co alloys, spin wave spectra 78−56304
rare earths, heavy, mag., electronic struct., book 78−60259
rare earths, spin waves and excitations 78−84407
resonance, surface mode magnetisation, inhomogeneities effect 77−69710
resonant light scattering from magnetic excitations, review 80−97290
semi-infinite Heisenberg ferromagnet, macroscopic theory of response functions and appl. to light scatt. 80−20410
semiconductor, ferromag., spin polaron props., effect on carrier scatt. 80−60233
semiconductor layered medium, electron dragging by spin wave *(Russian)* 79−78124
semiconductor-ferrite layer structure, EMF created by spin-wave, effect of current 80−11072
semiconductor-ferrite layer structure, influence of Hall effect on spin wave spectron and amplification by current 79−11308
semiconductor-ferrite layered structs., SHF spin wave interaction with electrons, review 79−95507
semiconductor-ferrite plate contact, electron-stimulated absorption of bulk spin waves 80−70992
semiconductor-ferrite structure, surface spin waves, current-induced amplification, effect of static state inhomogeneity 79−28519
semiconductors, ferromagnetic, parametric amplification of coupled spin, helical and acoustic waves *(Russian)* 80−2621
semiconductors, magnetic, spin wave electron amplification theory 80−97083
semiinfinite, effect of next nearest neighbour coupling 77−73014
single site theories for systems with Goldstone modes 77−63145
space disordered media phenomenological Lagrangian, exchange, relativistic interactions *(Russian)* 80−29537
spin density functional theory, linear response functions 78−67965
spin glass, Heisenberg model *(French)* 78−39336
spin glass, parametric amplification of spin waves by elastic pumping *(Russian)* 80−65895
spin glass, rel. between isotropic X-Y model and mobility edge problem 78−88138
spin glass, spin-wave spectrum, of systems without long-range mag. order 79−33450
spin glass dynamics, barrier modes and spin waves 80−60293
spin glass model Hamiltonians, zero temp. spin dynamics 77−85467
spin glasses, dilute ferromagnets, ferromagnetic modes 80−93133
spin glasses, spin waves, microscopic theory *(Russian)* 79−8011
standing spinwave resonance in film with nearest and next-nearest neighbour exchange 78−68390
strip films, bulk and surface spin oscills., mag. reson. 80−97149
strongly anisotropic magnets, canonical transform. method, spin wave energy determ. 77−85404
strongly anisotropic magnets, canonical transform theory 78−68197
strongly anisotropic magnets, spin wave theory 77−63151
submillimetric spectroscopy appl. to mag. excitations 77−40135
superconducting ferromagnet, magnetic ordering, spin wave dispersion *(Russian)* 80−54818
superconductivity-ferromagnetism coexistence, transition temp., magnon freq., indirect exchange 80−44757
surface magnetic moment, induced, effect on spin-wave spectrum 78−19234
systems far from thermodynamic equilib., dissipative structures, broken symm. equilib. phase transition theory 80−65827
tensorial permeability and conductivity medium, EM wave propag., ferromag. resonance, spin waves *(French)* 78−74820
thin ferromagnetic resonators, intermodulation distortion, spin waves 78−48048
thin films, ferro- and antiferromagnetic, two dimens. spin-wave theory, spontaneous magnetisation parameter depend. 80−34714
TMMC:Cu, dynamic props. using local-moment pair correl. functions 80−15728
TMMC:Cu, random one-dimens. Heisenberg antiferromag., spin fluctuations 79−61140
TMMC, 1-D antiferromag., excitation linewidths, temp. depend. 77−20574
TMMC, antiferromag. reson. below 1K 78−39408
TMMC, classical Heisenberg antiferromagnet, one-dimens., dynamic props., review 80−15737
TMMC, Cu-substituted, spin dynamics, neutron scatt. cross section 80−60312
TMMC, linear antiferromag., energy gaps in spin-wave dispersion, neutron inelastic scatt. 79−91223
TMMC, spin dynamic exam., effect of mag. field at low temp. 79−73733
transition metal, itinerant-localised electron model for magnetism 78−14918

spin waves continued
transition metal, mag. susceptibility, spin wave spectrum for improved itinerant-localised electron model 79−1654
transition metal 3d alloys, neutron spin wave scatt., itinerancy 77−73018
transition metal alloys, dilute ferromagnetic, itinerant d-electron(hole) degenerate, spin stiffness constant 80−70930
transition metal alloys, disordered ferromag., spin wave stability 80−70994
transition metal alloys, ferromag. local ordering effect on spin wave stiffness const. 77−66282
transition metal alloys, ferromagnetic, BCC, spin wave stiffness constant 78−91851
transition metal itinerant magnets, neutron scatt. expts. 77−73002
transition metal layer compounds, mag. model, 0K phase diagram, spin wave spectrum 79−87273
transition metals, 3d, ferromag., itinerant electron magnetism, magnetic excitation props., theory 80−34581
transition metals, 3d, ferromag. props., book contrib. 80−75724
transition metals, role of electron correlation 77−72974
transverse dynamic susceptibility and spin waves in itinerant electron SPW states 80−97076
trimethylammonium cobalt trichloride dihydrate, Ising-like system, nucl. spin-lattice relax. of ^{1}H and ^{35}Cl 80−29638
TTF-TCNQ, spin waves, scatt. at $4k_F$, spin-Peierls fluctuations 78−72093
two-sublattice ferromagnet, biquadratic exchange effects 77−4502
uniaxial ferromagnet, in transverse mag. field, quantum theory *(Russian)* 79−15297
uniaxial magnet, spin excitation spectrum in mag. fields of arbitrary direction 77−24662
uniaxial weak ferromagnet, energetic spectrum *(Russian)* 79−51762
weak antiferromagnetic exchange field system 78−43577
weak exchange field systems 78−43576
weak ferromagnet, collective excitations in transverse mag. field, AFMR spectrum 80−93100
X-Y model, classical, one and two dimens. 78−34997
XY model, spin 1/2, spin wave theory 80−7068
Al, spin wave excitations, CESR expts., 79 GHz 77−40128
Au, resonant and nonresonant conduction-electron-spin transmission 80−75857
$Au_2(Mn,Z)_2$, Heusler alloy, (Z=Al, Cu, Ga, In or Zn), magnetic order and coupling 79−38303
$BaMnF_4$, mag. and structural phase transitions, neutron scatt. obs. 79−87259
$Cd_{1-x}Ag_xCr_2Se_4$, ferromag. semicond., influence of strong elec. field on microwave absorption 77−28207
$CdCr_2S_4(Se_4)$, spontaneous magnetisation temp. depend., nuclear resonance freq. depend. *(French)* 80−80483
$CdCr_2Se_4$, excitation of spin waves by current carriers, magnetisation and elec. cond. reduction *(Russian)* 79−7981
β-Ce, heat capacity redeterm. 77−20617
$CeAl_2$, conf. Kondo system, sp. ht. meas. 78−52210
Co based amorphous alloys, struct. and thermomag. meas. 77−16055
Co complex, $Co(C_5H_5NO)_6(ClO_4)_2$ and $Co(C_5H_5NO)_6(BF_4)_2$, $S=^1/_2$ XY magnet, sp. ht. below 1K 77−55682
Co, small-angle crit. neutron scatt. 78−31087
Co-B alloys, amorphous, mag. moment and exchange stiffness constant 79−1662
Co-B-Si, mag. props. different in amorphous and cryst. phases 77−69617
Co-P film, amorphous, spin wave dispersion law, spin wave reson. obs. *(Russian)* 78−88196
$Co_{1-x}Au_x$, amorphous, elec. resist., temp. depend., spin wave contrib. and resist. minimum 78−51961
$Co_{1-x}B_x$, polycrystalline and amorphous sputtered films, Brillouin spectra 80−2775
$CoBr_2$, magnetic excitations, neutron scatt. investigation 80−39761
$CoCO_3$, Brillouin-Mandelstam light scatt. obs. of spin wave spectra 80−93358
$CoCO_3$, light scatt. expts., review 80−50081
$CoCO_3$ light scattering on spin waves *(Russian)* 77−4650
$CoCO_3$, spin wave excitation by uniform precession of magnetisation due to two magnon scatt. 78−68207
$CoCO_3$, weak ferromagnet, optic study of spin wave spectrum *(Russian)* 79−47263
$CoCO_3$, weakly ferromag., light scatt. on spin waves *(Russian)* 78−72419
$CoCl_2$, antiferromag., elementary excitations 77−69519
$CoCl_2$, antiferromag., mag. excitations, mag. neutron inelastic-scatt. meas. 77−85437
$(Co_{1-x}Fe_xNi_y)_{80}(Si_{1-z}B_z)_{20}$, amorphous films, spin wave spectra 80−34777
CoO, antiferromag. mag. excitations, spin wave model, neutron scatt. study 79−51766
CoO, mag. excitations, neutron scatt. expts., 13K 79−61092
CoP-NiCoP, composite ferromag. film, exchange coupling between soft and hard layers, FMR obs. 79−78448
Co_4P, amorphous, mag. excitations and static struct., neutron scatt. obs. 78−68204
Co_4P, amorphous ferromag., mag. excitations calc. in Heisenberg model 77−1546
Cr, antiferromagnetic structure, mag. field effect, spin density wave model *(Russian)* 80−70953
Cr-Re, mag. excitations in commensurate antiferromag. phase 80−50079
$CrBr_3$, HF spectra, susceptibility, spin waves in domain walls *(Russian)* 80−80909
$Cr_{0.98}Mn_{0.02}$, spin dynamics and spin wave form factor, neutron scatt. expt. 77−40047
Cr_2O_3, exchange parameters including temp. effects 79−24153
$CsCoBr_3$, ID Ising antiferromagnet, spin dependent Raman scattering from phonons and electronic excitations 80−103948
$CsCoCl_3$, anisotropic antiferromag., inelastic neutron scatt. study 78−60274
$CsCoCl_3$, antiferromag., spin wave spectrum 79−28514
$CsCoCl_3$, Ising-like antiferromag., spin dynamics 79−42747
$CsCoCl_3$, mag. excitation spectrum, spin-wave response, neutron scatt. study 80−50080
$CsCoCl_3$, one-dimensional antiferromag., neutron scatt. investig. of spin waves 77−47982
$CsCoCl_3$ spin dynamics, neutron scatt. study 80−80493

spin waves continued
$CsCrCl_3$, mag. structure and excitations, neutron diffr. and susceptibility meas. 80−44806
$CsMnCl_3$, antiferromagnetic resonance, parametric spin wave excitation *(Russian)* 80−93183
$CsMnCl_3.2H_2O$, linear antiferromagnet, specific heat, exchange interactions and anisotropy effects 77−1556
$CsMnCl_3.2H_2O$, spin wave anal. 77−8292
$CsMnF_3$, antiferromag., variation of spin wave spectrum in interaction between magnons 80−65841
$CsMnF_3$, NMR saturation, nuclear spin wave excitation, large freq. shifts *(Russian)* 80−50207
$CsMnF_3$, spin wave propag. 77−63159
$CsMnF_3$, spin wave spectrum obs., review 80−50081
$CsMnF_3$, spin waves excitation 79−82772
$CsMnF_3$, spin-wave dispersion relations, neutron inelastic scatt. obs. 77−51895
$CsNiF_3$, easy-plane ferromagnet, one-dimens., dynamic props., review 80−15737
$CsNiF_3$, in mag. field, spin wave dispersion, inelastic neutron scatt. 77−77046
$CsNiF_3$, NMR and relax. exam. 78−52371
$CsNiF_3$, one dimens. ferromag., spin wave dynamics, inelastic neutron scatt. study 79−47270
$CsNiF_3$, one-dimens. ferromag. far IR investig. of ferromag. reson., temp. and mag. field depend. 77−66427
$CsNiF_3$, one-dimens. ferromag., solitons as gas of quasiparticles, inelastic neutron scatt. obs. 79−73679
$CsNiF_3$, one-dimens. ferromag., collective excitations in mag. field 80−44822
$CsNiF_3$, one-dimensional magnet, dynamics, mol. field theory approach 80−34614
Cu complex, $[C_6H_5(CH_2)_nNH_3]_2CuCl_4$, n=1,2,3, two-dimens. ferromagnet, NMR and mag. susceptibility 77−16058
Cu complex, dichloro-bis-pyridine copper II, one-dimens. antiferromagnet, dynamic props., review 80−15737
Cu, resonant and nonresonant conduction-electron-spin transmission 80−75857
$CuCl.2N(C_5D_5)$, one-dimens. antiferromag., mag. excitation line-shape, field depend., neutron study 79−38314
$CuCr_2S_4$, ferromag., spin wave contrib. to nucl. spin-lattice relax. time meas. 77−36147
Cu_2MnAl, dynamical mag. susceptibility, spin waves, calc. from band struct. 80−54871
Cu_2MnAl, Heusler alloy, spin waves, neutron inelastic scatt. meas. 77−80921
dibutylammonium copper chloride, two-dimens. spin wave spectrum, parallel pumping meas. 77−20715
dimethylammonium manganese tetrachloride, 2D Heisenberg antiferromag., spin wave anal. 80−54879
Dy, parasusceptibility meas., 4.2-130K, spin wave anal. 79−95583
Dy, spin wave exam. 78−56306
DySb, magnetic excitations 79−78358
Er, spin wave exam. 78−56306
$ErCo_2(Fe_2)$, mag. excitations, RPA theory 80−65830
$ErCrO_3$, magnetisation, NMR freq. temps. depend. weak ferromagnetic-antiferromagnetic spin reorientation transition 80−29631
ErCu, cubic antiferromag., mag. excitations inelastic neutron scatt. meas. 78−72341
$ErFe_2$, excited state spin waves inelastic scatt. meas. 78−76234
$ErFe_2$, Laves phase, cryst. field effects on spin wave dispersion relations 78−84408
$ErFe_2$, spin excitations, neutron scatt. obs. 77−63153
$ErFe_2$, spin waves, exchange interaction, neutron scatt. study 79−47267
$ErFeO_3$, weak ferromag., high freq. props. in ordering region of spin system, antiferromag. reson. study *(Russian)* 80−2644
EuO, ferromag. light scatt. from bulk and surface spin waves 79−28778
EuO, Heisenberg ferromagnet, exchange interactions, neutron scatt. expts. 77−20579
EuO, light scatt. by spin waves 80−45086
EuO, light scatt. from bulk and surface spin waves 78−19497
EuO, light scatt. from spin waves and magneto-optic hysteresis meas. 80−97244
EuO, spin wave damping, theory compared with expt. 78−52237
EuO, spin wave lifetime, theory compared with expt. 80−60228
EuS, ferromag. semicond., high field susceptibility, spin waves 80−75735
EuS films, ferromag., optical spectra and light scatt. from spin waves 80−16116
EuS, Heisenberg ferromagnet, exchange interactions, neutron scatt. expts. 77−20579
EuS, light scatt. from spin waves and magneto-optic hysteresis meas. 80−97244
EuS, single cryst., high-field susceptibility meas., temp. range 2.5 to 16.5K 80−84589
EuSe, mag. phase stability, spin wave theory 77−63183
$Eu_xSr_{1-x}S$, spin glass, spin wave modes and low temp. sp. ht. 80−80538
Fe alloys, amorphous, mag. saturation, spin wave stiffness, temp. depend. 80−75741
Fe, band theoretic interpretation of neutron scatt. expts., spin wave modes 80−44791
Fe based amorphous alloys, struct. and thermomag. meas. 77−16055
Fe, electron tunnelling 80−60104
Fe, ferromag., dynamic susceptibility calc. 80−80488
Fe, ferromag., spin wave energies and intensities calc. 77−8293
Fe, ferromagnetic, chemisorption of H, spin-spin interactions, UPS spectra calc. 80−6630
Fe film, nuclear magnetisation relax. at 77 to 500K 78−60352
Fe, itinerant ferromagnet, spin-wave dispersion and linewidth 79−4668
Fe, light scatt. by spin waves 80−45086
Fe, magnetic susceptibility, lineshape and moment analysis, magnon excitations 79−99693
Fe, magnetisation, spin wave and Stoner contribs. 77−73017
Fe, magnetoelastic excitations and ferromagnetic resonance 79−82879
Fe, spontaneous magnetisation data up to 0.98 T_c, reanalysis 78−47959
Fe, temp. depend. of spontaneous magnetisation 77−63141
Fe-Al, low energy Stoner excitations, spin wave obs. in neutron scatt. study 79−51770
Fe-Co, BCC, ferromag., spin wave stiffness constant 78−91851
Fe-Cr, BCC, ferromag., spin wave stiffness constant 78−91851
Fe-Cr, spin waves by neutron spectrometry 80−44819
Fe-Mn, BCC, ferromag., spin wave stiffness constant 78−91851

spin waves continued
Fe-Ni, BCC, ferromag., spin wave stiffness constant 78−91851
Fe-Ni, fcc alloys, spin wave energy calc. 79−87247
Fe-Ni alloy, FCC, high-field susceptibility and spin wave spectrum 79−56493
Fe-Ni based metallic glass, Metglas 2826 MB, Mossbauer study 80−75897
Fe-Ni films, scatt. of homogeneous spin waves by anisomeric oriented plane, ferromag. reson. 78−19336
Fe-Ni Invar, magnetisation and high field susceptibility 79−56518
Fe-Ni Invar anomalies, explanation in terms of itinerant electron magnetism 80−75705
Fe-Ni system, ferro-antiferromag. transition, γ phase mag. struct. 79−91231
Fe-Ni(35.4 at.%) Invar alloys, T^2 term contribution to magnetisation 80−71096
Fe-Pd, FCC, ferromag., spin wave stiffness constant 78−91851
Fe-Rh, ferromag., spin wave stiffness constant calc. 79−38307
Fe-Rh alloys, spin wave spectrum in antiferromag. and ferromag. phases, inelastic neutron spectrometry 77−63158
Fe_3Pt, ordered ferromagnetic alloy, magnetic excitation obs. 80−70978
Fe_3Al, order-disorder transition effect on low energy spin waves 79−47271
Fe_3Al, partly disordered B2 struct., spin wave dispersion relation 78−64201
$Fe_{1-x}Au_x$, amorphous, elec. resist., temp. depend., spin wave contrib. and resist. minimum 78−51961
$Fe_{1-x}B_x$, polycrystalline and amorphous sputtered films, Brillouin spectra 80−2775
$Fe_{100-x}B_x$, crystalline and glassy, low temp. magnetisation study 79−95608
$Fe_{80}B_{20}$, amorphous, Brillouin scatt. from magnons, ferromag. reson. 80−65844
$Fe_{80}B_{20}$, binary amorphous ferromagnet, spin-wave excitation 79−4749
$Fe_{80}B_{20}$ film, amorphous metallic, standing spin waves, Brillouin scatt. obs. 80−97291
$FeBO_3$, magnon dispersion by light scatt. and ferromag. reson. 77−55668
$FeBO_3$, size effect during parametric spin wave excitations *(Russian)* 80−103824
$FeBO_3$, spin wave dispersion at small wavevectors, Brillouin scatt. and ferromag. reson. 78−47962
$FeBO_3$, spin waves, Brillouin scatt. studies 79−99696
$FeBO_3$, weak ferromagnet, spin wave band struct. and microwave props. 79−1661
$Fe_{83}B_{16.5}Si_{0.5}$, amorphous, spin waves, inelastic neutron scatt. meas. 79−73701
$FeBr_2(Cl_2)(I_2)$, far IR antiferromag. reson. 77−36138
Fe_xCr_{1-x}, spin-wave evolution crossing from ferromag. to spin-glass regime 80−97080
FeF_2, antiferromag. spin flop boundary 78−84419
Fe_xGd_{1-x}, $0.5>x>0.65$, amorphous film, FMR, spin wave spectra 77−16181
FeI_2, neutron inelastic scatt. from mag. excitations 80−50078
FeI_2, spin waves and two magnon bound states, mag. field IR absorption meas. 80−65840
$Fe_{1-p}Mg_pCl_2$, magnetic excitations 78−91852
γ-FeMn, alloys, itinerant antiferromag., spin dynamics, neutron scatt. meas. 77−12105
$Fe_{78}Mo_2B_{20}$, amorphous ferromag., $T^{3/2}$ depend. of hyperfine field 78−39474
$(Fe_{93}Mo_7)_{80}B_{10}P_{10}$, amorphous, neutron scatt. investig. of spin waves, magnetisation 77−47984
$Fe_{65}Ni_{35}$, quasi-localised spin system, neutron scatt. 78−68194
$Fe_{40}Ni_{40}B_{20}$, amorphous, high-field magnetisation curve, spin wave spectrum and microstructural inhomogeneities 80−15702
$Fe_{20}Ni_{60}B_{19}P_1$, amorphous, spin waves, inelastic neutron scatt. meas. 79−73701
$Fe_{40}Ni_{38}Mo_4B_{18}$ ribbon, magnetic characterisation 80−34680
$Fe_{40}Ni_{40}P_{14}B_6$, amorphous, high field susceptibility meas., spin wave excitation spectrum 77−69506
$Fe_{40}Ni_{40}P_{14}B_6$, amorphous ferromag., spin wave excitations 80−97079
$Fe_{40}Ni_{40}P_{14}B_6$, high-field suscept. and spin wave spectrum 78−10662
$Fe_{40}Ni_{40}P_{14}B_6$ metallic glass, ferromag. reson., spin waves, thermal ageing and long-range order effects 80−25214
$Fe_xNi_{80-x}P_{14}B_6$ (x=0, 20, 40, 60, 80), metallic glass, low temp. sp. ht. 80−2588
$(Fe_{0.3}Ni_{0.7})_{0.75}P_{0.16}B_{0.06}Al_{0.03}$, amorphous, spin wave spectrum, neutron scatt. 77−16064
$(Fe_{1-x}Ni_x)_{75}P_{16}B_6Al_3$, amorphous, saturation magnetisation, temp. depend., ferromag. reson. meas. 79−73818
$(Fe_{65}Ni_{35})_{75}P_{16}B_6Al_3$, amorphous ferromag., high temp. spin dynamics 78−47965
$(Fe_{65}Ni_{35})_{75}P_{16}B_6Al_3$, amorphous ferromagnet, mag. excitations 79−7984
$(Fe_xNi_{1-x})_{75}P_{16}B_6Al_3$, amorphous, spin wave excitations and low temp. magnetisation 79−33468
$(Fe_xNi_{1-x})_{75}P_{16}B_6Al_3$, magnetisation temp. depend., spin wave theory 80−44927
$Fe_{29}Ni_{49}P_{14}B_6Si_2$, Metglass 2826B, saturation magnetisation, temp. depend., ferromag. reson. meas. 79−73818
$Fe_{1-x}O$, wustite, cryst. dynamics, mag. excitations, neutron scatt. study *(French)* 79−51740
α-Fe_2O_3, exchange parameters including temp. effects 79−24153
Fe_3O_4, mag. crit. scatt., neutron spectroscopy 77−20614
Fe_3O_4, single cryst., surface magnetism, spin polarized photoemission 78−52622
Fe_2P, spin wave excitations meas. 80−65831
$Fe_{0.75}P_{0.15}C_{0.10}$, amorphous, mag. excitations and static struct., neutron scatt. obs. 78−68204
$Fe_{75}P_{15}C_{10}$, amorphous, mag. excitations, inelastic neutron scatt. 78−10674
$FePt_3$, neutron scattering study of spin waves 78−91856
Fe_3Pt, quasi-localised spin system, neutron scatt. 78−68194
$Fe_{0.996}S$, antiferromag., energy dispersion of spin waves, inelastic neutron scatt. meas. 77−69522
$Fe_{95}Si_5$, thermal and elec. cond., heat transport by spin waves 79−38047
Gd, magnetoelastic excitations and ferromagnetic resonance 79−82879
Gd, spin wave exam. 78−56306
Gd, spin wave temp. depend., exchange coupling role 78−68199
$GdAl_2$ amorphous, rel. to temp. depend. of mag. heat capacity 77−89969

spin waves continued
GdIG, spin wave intrinsic relaxation, magnon damping at low temps. 80−29543
$GdVO_4$, antiferromag., US attenuation at 9 GHz 77−24728
He II-^{3}He degenerate soln., spin waves and zero sound possibility *(Russian)* 77−35789
He, superfluid B phase, spin wave breathers, double sine-Gordon equations 80−15329
^{3}He, A_1 phase, broken relative symmetry and dynamics 80−24705
^{3}He, A-phase, superfluid, field-induced I textures and mag. resonance 79−46864
^{3}He, liquid-ordered ferromagnet interface magnetic Kapitza conductance, surface spin wave effects 79−99406
^{3}He, solid, localised defect excitations, superimposition on spin wave spectrum 79−28172
^{3}He, superfluid, A-phase, hydrodynamics and macroscopic dynamics in high mag. field 77−72733
^{3}He, superfluid, A-phase uniform magnetisation precision instability in mag. field *(Russian)* 79−95232
^{3}He, superfluid, hydrodynamic modes interaction, sound propag. and spin waves *(Russian)* 79−37897
^{3}He, superfluid, hydrodynamic parameters and correlation functions 79−82406
^{3}He, superfluid, localised spin wave states in mag. field gradient 77−51563
^{3}He, superfluid, magnetic relaxation and high amplitude spin waves *(Russian)* 80−92749
^{3}He, superfluid, order parameter relaxation and hydrodynamics near A-transition 77−66064
B-^{3}He, superfluid, spin susceptibility in acoustic limit *(Russian)* 77−4236
^{3}He, superfluid, spin wave interactions 79−86957
^{3}He, superfluid, zero sound and spin waves coupling near T_c 79−69309
^{3}He superfluid *(Russian)* 79−7727
^{3}He, superfluid A phase, effect of mag. dipole interaction on collective modes 77−89610
^{3}He, superfluid A-phase, composite soliton in narrow circ. cylinder, satellite freq., thermal fluctuations 80−34266
^{3}He, superfluid A-phase, surface spin waves 79−86955
^{3}He, superfluid B phase, soliton-like spin waves 80−44385
^{3}He, superfluid B phase, spin waves creation 79−82411
^{3}He, superfluid B phase, surface textures and NMR 79−37895
^{3}He, superfluid B phase, textural singularities, NMR analysis 77−89608
^{3}He, superfluid B-phase, bound spin wave states associated with n-solitons 78−67884
^{3}He, superfluid B-phase, standing spin wave mode obs. 77−24463
^{3}He, superfluid B-phase, susceptibility in acoustic limit at nonzero temp. 78−84020
^{3}He, superfluid B-phase, textures and NMR, theory 77−39717
^{3}He, superfluid B-phase, textural spin waves 77−66058
^{3}He-^{4}He, superfluid, spin waves *(Russian)* 79−95240
^{3}He-A, superfluid, spin dynamics, spin-orbit configurations, spin waves *(Russian)* 80−54462
^{3}He-He II degenerate soln., kinetic coefficients, thermodynamic props., hydrodynamic, acoustic and spin wave propag. *(Russian)* 78−18867
^{3}He-Z near A. phase transition, collective oscill. hybridisaiton *(Russian)* 80−80020
$HgCr_2Se_4$, spontaneous magnetisation temp. depend., nuclear resonance freq. depend. *(French)* 80−80483
Ho, single cryst., transverse magnetoresist. 77−66154
$HoCo_2$, ground state spin excitations, inelastic nneutron scatt. study 80−50077
Ho_2Co_{17}, spin wave excitations, 4.8 and 78K 80−60230
$HoFe_2$, spin wave and cryst. field excitations, neutron scatt. 78−68196
HoZn, mag. excitations near spin rot. temp., neutron scatt. study 79−19731
HoZn, spin wave spectrum, Green function analysis 78−2666
K, bound spin-helicon wave excitation, reson. refl. coeff. 79−95435
K, microwave transmission modes at cryogenic temps. 79−42473
K_2CrCl_4, ionic ferromag., temp. depend. intensity in optical absorption 77−12399
$K_2CuCl_4.2H_2O$ structure compounds, exchange anisotropy, renormalised spin wave model 77−55714
$KCuF_3$, chain-like antiferromag., parallel susceptibility 78−80137
$KCuF_3$, nearly 1-D spin-$^1/_2$ antiferromagnet, spin wave energy dispersion 80−2551
$KCuF_3$, one-dimens. antiferromag., spin waves, neutron scatt. study 80−65848
K_2CuF_4, microwave excitation, optical detection of ferromagnetic reson. 80−50197
K_2CuF_4, nearly two-dimens. Heisenberg ferromag., renormalised spin wave theory 77−66285
K_2CuF_4, quasi two-dimens. Heisenberg ferromag., spin wave spectrum lineshape, neutron scatt. obs. 77−66286
K_2CuF_4, spin wave meas. in low energy range, inelastic neutron scatt. 78−88105
K_2CuF_4, spin-wave relaxation, parallel pumping expt. 79−4729
K_2CuF_4, two-dimensional ferromag., spin-wave lineshape, neutron scatt. data 77−16065
$K_2Cu_{1-x}Zn_xF_4$, two-dimens., ferromag., spin wave excitations 78−80140
$KFeF_5$, one dimensional antiferromagnets, field depend. spin reduction temp. variation, spin flopping 79−78586
K_2FeF_4, two dimensional easy plane antiferromag., neutron scatt. expts. 80−65838
K_2MnF_4, two-dimensional antiferromag., NMR, magnetisation field-depend., spin-wave theory 77−63294
$K_3Mn_2F_7$, quadratic double-layer antiferromag., NMR, spin-wave anal. of sublattice magnetisation 77−63293
$K_3Mn_2F_7$, quadratic double-layer Heisenberg antiferromagnet, sublattice magnetis., NMR obs. 77−66270
$K_3Mn_2F_7$, two magnon Raman scatt., magnon dispersion, susceptibility, Green's function methods 80−50340
$KNiF_3$, antiferromag., nonlinear optical effects, spin wave contrib. 77−10987
$KNiF_3$:Mn^{2+}, isotropic Heisenberg ferromagnet, localised spin-wave modes, biquadratic exchange effects 77−51896
$(La,Ce)Al_2$, conf. Kondo system, sp. ht. meas. 78−52210
$Li_{0.13}Fe_{2.87}O_4$, acoustic spin wave dispersion branch, exchange const., neutron scatt. study 79−47266
Mn, antiferromag., spin wave mode, wave function calcs. 80−20098

spin waves continued
Mn, FCC, itinerant antiferromag., spin susceptibilities and collective excitations, many band effects 77−63140
Mn ferrite, monocrystalline epitaxial layers, surface spin-wave modes in ferromag. reson. 78−2743
γ-Mn-Cu (10 at.%), spin wave studies using neutron diffraction 80−70991
Mn-Cu alloys, stressed, diffuse neutron scatt. exam. 78−47950
$MnCO_3$, NMR saturation, nuclear spin wave excitation, large freq. shifts *(Russian)* 80−50207
$MnCO_3$, nuclear spin waves from antiferromag. reson. line temp. depend. *(Russian)* 78−48050
$MnCO_3$, spin wave spectrum obs., review 80−50081
$MnCO_3$, spin waves excitation 79−82772
γ-MnCu, antiferromag., stressed, mag. defects meas. by neutron polarisation anal. 80−50076
MnCu, neutron scatt. near crit. comp., effects of stress and ageing 79−19722
MnF_2, reson. NMR near phase transition 78−76265
MnF_2 spin wave lifetime, theory compared with expt. 80−60228
$MnFe_2O_4$ film, bulk and surface spin waves, spin wave reson. expts. 79−73826
$MnFe_2O_4$, nuclear reson. and relax. from domains and domain walls 77−8448
$Mn_xFe_{3-x}O_4$ film, spin wave reson., exchange const. 77−16183
$Mn_{73}Ni_{27}$, generalised susceptibility, spin wave contrib., inelastic mag. neutron scatt. 79−47262
MnO, magnon lifetime 77−69518
MnO, paramag., neutron scatt., spin-wave-like excitations, obs. 78−68146
MnP, ferro-spiral transition, neutron scatt. studies, spin wave dispersion relations meas. 80−65876
MnP, magnetisation and spin waves temp. depend. 79−91221
Mn_2Sb, spin-wave dispersion relations, exchange interactions, neutron inelastic scatt. 80−65832
MnSi, itinerant electron system, neutron scatt. 78−68194
MnSi, itinerant ferromag. spin dynamics field depend. 79−38315
MnSi, weak itinerant ferromag., mag. excitations, neutron scatt. obs. 78−34969
MnSi, weak itinerant ferromagnet, mag. excitations 79−7985
β_1-MnZn, ferromag., spin wave contrib. to nucl. spin-lattice relax. time meas. 77−36147
Na, bound spin-helicon wave excitation, reson. refl. coeff. 79−95435
Na, microwave transmission modes at cryogenic temps. 79−42473
$NaCa_2Mn_2V_3O_{12}$, antiferromag., spin wave contrib. to sp. ht., λ-anomaly at 25.05K T_N 77−77068
$NdAl_2$, ferromag., cryst. field excitations, neutron inelastic scatt. meas. 77−63154
$NdAl_2$, mag. excitation spectrum, neutron inelastic scatt. 78−10673
NdSb, mag. excitation spectrum, neutron inelastic scatt. 77−63152
Ni alloys, mag. props. of alloys, review 80−44823
Ni, band theoretic interpretation of neutron scatt. expts., spin wave modes 80−44791
Ni complex, hexa(pyridine-N-oxide)$(ClO_4)_2$, field-induced mag. ordering in S=1 singlet ground-state 78−23288
Ni, electron tunnelling 80−60104
Ni, ferromag., dynamic susceptibility calc. 80−80488
Ni, ferromagnetic, chemisorption of H, spin-spin interactions, UPS spectra calc. 80−6630
Ni film, ferromag., light scatt. from surface acoustic spin waves 79−33719
Ni, itinerant ferromagnet, spin-wave dispersion and linewidth 79−4668
Ni, Landau-Lifshitz damping, wave no. and temp. depend. 80−34779
Ni, mag. excitations variation of de Haas-van Alphen frequency 79−8019
Ni, magnetic susceptibility, generalised, neutron scatt. meas. 80−34606
Ni, magnetisation spin wave and Stoner contribs. 77−73017
Ni, magnetisation temp. depend. exam. using ^{61}Ni NMR 77−73089
Ni, magnetoelastic excitations and ferromagnetic resonance 79−82879
Ni plate, thin, helicon-Doppleron effect on spin wave prop. 77−66394
Ni, rel. to deformation in const. mag. field, 4.2K *(Russian)* 80−29591
Ni, single-crystal films, spin wave reson. spectra 79−11350
Ni, spin-elastic wave three freq. interactions, parameters, excited wave amplitudes *(Russian)* 79−91276
Ni, spin-wave exchange stiffness const. 77−4510
Ni, spontaneous magnetisation data up to 0.98 T_c, reanalysis 78−47959
Ni, temp. depend. of spontaneous magnetisation 77−63141
Ni-Co, FCC, spin wave stiffness const., neutron scatt. study 79−51769
Ni-Co, high-field susceptibility, spin-wave spectrum, CPA calc. 80−65818
Ni-Co alloy, stiffness const., interpretation within band model 79−42748
Ni-Co alloys, FCC, spin wave stiffness, inelastic neutron scatt. 77−63156
Ni-Cr(V)(Co)(Mn)(Mo)(Ru)(Fe), spin wave stiffness consts., RPA CPA band model 79−61088
Ni-Cu, high-field susceptibility, spin-wave spectrum, CPA calc. 80−65818
Ni-Fe, FCC, Invar behaviour, spin waves stiffness consts., neutron scatt. study 79−51769
Ni-Fe, high-field susceptibility, spin-wave spectrum, CPA calc. 80−65818
Ni-Fe, influence of atomic ordering on spin waves 79−7987
Ni-Fe(Pd)(Pt)(Cu), ferromag., influence of local ordering on spin wave stiffness const. 77−89937
Ni-Mn, spin wave stiffness const., low temp. neutron scatt. meas. 79−51768
Ni-Mn alloy, disordered FCC, stiffness const., single cryst. neutron inelastic scatt. meas. 77−20558
Ni-Pd(Pt), renormalisation of spin wave stiffness 79−51764
Ni-Pt disordered alloy, off-diagonal, T-matrix itinerant electron ferromagnetism calcs. 80−25067
Ni-V(Mo)(Ru)(Cr), weak ferromag., stiffness const., low-temp. meas., rel. to RPA-CPA theories 78−31063
$Ni_{1-x}Au_x$, amorphous, elec. resist., temp. depend., spin wave contrib. and resist. minimum 78−51961
$NiBr_2$, ^1Eg spin-forbidden transition, temp. depend. and magnetoabsorpt. 78−48151
$NiBr_2.6H_2O$, antiferromag. ordering and paramag. behaviour 78−14941
$NiBr_2.6H_2O$, energy gap in spin wave spectrum 77−69587
$Ni_{50}Co_{40}P_{10}$ amorphous film, spin wave excitation, ferromagnetic resonance study 80−50198
spin waves continued
NiF_2, antiferromag. reson., Lagrange and nonequilib. thermodynamics descriptions 79−15357
NiFe alloys, spin-wave exchange stiffness const. calcs., weak ferromagnetism 77−4510
$Ni_{0.75}Fe_{0.25}$, influence of atomic ordering on spin waves, inelastic neutron scatt. 77−69516
Ni_3Fe alloys, low-temperature specific heat, long and short range order effects 80−100339
$NiFe_2O_4$ epitaxial film on NdGG, structural and ferromagnetic reson. meas. 77−1574
$NiFe_2O_4$, parametric excitation of spin waves in samples with regular domain struct. *(Russian)* 77−32183
Ni_3Mn, partially ordered, spin-wave dispersion relation, inelastic neutron scatt. meas. 80−20394
NiS, high energy spin waves, neutron scatt. study 79−51765
O_2, solid, β-phase, mag. excitations spectrum *(Russian)* 80−7101
$PD_{0.75}Ni_{0.25}$, spin wave excitations, neutron inelastic scatt. meas. 77−47983
Pd-Fe alloys, disordered FCC, exchange stiffness consts., temp. depend. of magnetisation 77−69528
Pd-Fe type dil. ferromag. alloys, spin wave propag. *(Russian)* 77−12110
Pd-Mn alloy, spin glass, low temp. spin dynamics, numerical studies 79−78385
$Pd_{0.5}Fe_{0.5}$, disordered, spin wave dispersion relation, neutron inelastic scatt. 79−61090
Pd_3Fe, ferromag., spin wave spectrum 77−69515
Pd_3Fe, spin wave dispersion relation at 4.2K, neutron inelastic scatt. meas. 77−63157
Pd_3Fe, spin wave dispersion, neutron inelastic scatt. meas. 78−14943
Pd_2MnSn, rel. to interaction between local moments 77−1540
Pr-Nd (5%), impurity modes and mag. ordering 78−84422
Rb, Landau Fermi-liquid-theory parameters, conduction-electron spin wave meas. 79−42472
Rb, microwave transmission modes at cryogenic temps. 79−42473
Rb_2CoF_4, two dimens. Ising like antiferromag., spin wave excitations 78−72342
$Rb_2Co_cMg_{1-c}F_4$, random 2D antiferromag., neutron inelastic scatt. 79−28505
Rb_2CrCl_4, 2D-ferromag., renormalisation of long wavelength spin waves, neutron scatt. 80−60229
Rb_2CrCl_4, planar ferromag., spin waves 80−65835
Rb_2CrCl_4, spin wave temp. depend. 79−4662
$RbFeF_5$, one dimensional antiferromagnets, field depend. spin reduction temp. variation, spin flopping 79−78586
Rb_2FeF_5, 1D antiferromagnetic system, Mossbauer investigation 78−95533
Rb_2MnCl_4, 2D Heisenberg antiferromag. spin wave analysis 80−54879
Rb_2MnCl_4 antiferromagnet, spin flopping phase transition 79−69687
Rb_2MnCl_4, Heisenberg antiferromag., spin wave anal. 79−61237
$RbMnF_3$, antiferromag., spin-wave lifetimes calc. 79−7980
$RbMnF_3$, Heisenberg antiferromagnet, spin diffusion below T_N 78−34968
$RbMnF_3$, nucl. spin waves *(Russian)* 78−34973
$RbMnF_3$, nuclear spin waves spectra, relaxation, parametric excitation, NMR dynamic shift *(Russian)* 80−11180
$RbMnF_3$, pure and Fe, Co or Ni doped, thermal cond., spin wave and mag. impurity contribs. 77−40046
$RbMnF_3$, spin wave lifetime, theory compared with expt. 80−60228
$RbMnF_3$, spin wave widths 80−97081
$Rb_2Mn_xMg_{1-x}F_4$, random magnetic-nonmagnetic 2-dimens. antiferromag., spin fluctuation dynamics 77−63147
Tb, ferromag., spin wave resist., 1.5-50K 79−60813
Tb, high-precision elec. resist. meas., 1-4K 77−15817
Tb, magnetoresist., anisotropic electron spin wave scatt. 77−15831
Tb, single cryst., transverse magnetoresist. 77−66154
Tb, spin wave exam. 78−56306
Tb-Y, spin wave dispersion, spiral mag. struct., neutron scatt. study 79−47268
$Tb_{0.5}Ho_{0.5}$, ferromag. and helical phase, spin wave dispersion relations 79−24149
$Tb_{0.76}Y_{0.24}$, spin waves rel. to cond. electron susceptibility 78−68195
TbZn, mag. excitations meas. 80−70979
UO_2, spin wave spectrum, mag. susceptibility, sp. ht. *(Russian)* 79−33470
UPt, weak ferromag., magnon heat capacity, magnetisation and mag. entropy 77−24685
USb, collective elementary magnetic excitation, neutron inelastic scatt. obs. 79−24141
W, ferromagnetic layer coating, longitudinal conduction electron spin waves, Larmor wave 79−33543
W, resonant and nonresonant conduction-electron-spin transmission 80−75857
W, single cryst., coated with ferromagnetic layer, longit. cond. electron spin waves 79−11307
$(Y,Ca)_3(Fe,Ge)_5O_{12}$ LPE layer, exchange stiffness coeffs., 30-300K 79−78464
$(Y,Lu)_3(Fe,Sc)_5O_{12}$ LPE layer, exchange stiffness coeffs., 30-300K 79−78464
$YCrO_3$, magnetisation, NMR freq. temps. depend. weak ferromagnetic-antiferromagnetic spin reorientation transition 80−29631
$Y_3Fe_{5-t}Ga_tO_{12}$ garnet, spin wave parametric excitation threshold anisotropy in second region 80−29542
$YFeO_3$, domain walls vel. *(Russian)* 79−28553
$YFeO_3$, spin-wave damping of domain walls 79−42795
$YFeO_3$, transit time meas. of domain-wall mobilities, magnetostatic and magnetoacoustic effects 79−42794
$YFeO_3$, weak ferromagnet, domain wall motion and velocity *(Russian)* 80−54917
YIG, anomalous subsidiary absorpt. butterfly curves at 9.16 GHz and 300K 79−82875
YIG bubble films, light scatt. from spin waves, hysteresis meas. by Voigt effect 80−15770
YIG epitaxial film, strong in-plane ang. depend. of spin-wave intensities 77−69521
YIG, ferromag. film on nonmag. substrate, magnetoelastic wave propag. 79−99744
YIG ferromagnetic film, quasi surface spin wave giant oscills. *(Russian)* 80−15767

spin waves continued
YIG film, low field microwave excitations of mag. domain walls 79−78456
YIG film, on GdGaG, mag. excitations, diffusion layer effects 78−31112
YIG, film, photoinduced mag. surface anisotropy spin wave reson. 77−4560
YIG, film, spin wave reson., complex mag. surface energies 77−4561
YIG, film, spin-wave spectra in terms of mag. boundary conditions 79−78532
YIG, Hf response and thermodynamic props. *(Russian)* 78−72338
YIG, LPE and CVD films, boundary effects, spin wave reson. meas. 79−78447
YIG, LPE film, magnetostatic wave to exchange resonance coupling 79−82774
YIG, light scatt. by parametric spin waves with longit. pumping *(Russian)* 78−43648
YIG, open die hot pressing, spin wave and FMR line width 80−89170
YIG, parallel microwave pumping threshold, RF modulation of mag. field 78−88195
YIG, parametrically excited spin waves, spectral density *(Russian)* 79−4667
YIG, parametrically excited reson. magnetostatic modes of spin, elastic and magnetoelastic waves 79−56523
YIG, parametrically excited wave discrete structure obs., light diffr. and modulation *(Russian)* 79−95650
YIG, perpendicular pumping, spin wave instabilities, laser probing 77−43889
YIG, polycrystalline, microwave relax. at low power levels 78−39409
YIG, polycrystalline, microwave relax. at high power levels 79−61231
YIG, porous, parallel-pump spin-wave instability temp. depend. 79−78531
YIG, porous and fine grain polycrystalline, temp. depend. of effective linewidth 77−85574
YIG, rel. to nonreciprocal attenuation of elastic surface waves 77−55696
YIG, relax. after spin wave excitation in ferrite *(Russian)* 79−19783
YIG, second group of spin waves, parametric excitation 79−99694
YIG, single cryst., spin-wave linewidth influence on spin wave propagation direction for parallel pumping 79−1660
YIG, spin wave echo, 9440 MHz, room temp. 77−43887
YIG, spin wave instability, parametrically excited spin waves distribs. *(Russian)* 79−38317
YIG, spin wave instability theory 79−73825
YIG, spin wave parametric excitation threshold at low temp. 80−97084
YIG, spin waves, nonlinear spectroscopy studies 79−99696
YIG, spin-wave and magnetostatic mode attenuation, double-pulse echo method 79−82874
YIG, spinwave dispersion curves 78−19230
YIG, subsidiary absorpt. spin-wave instability threshold, anomalous struct. 80−34776
YIG, surface spin waves, microscopic theory, mag. field effects 78−35044
YIG, thin ferromagnetic film, exchange interaction constant, from paramag. resonance spectra of spin waves 79−42811
YIG:La(Ga) films, ferromagnetic resonance, ion implantation effect 80−97145
YIG:Pr^{3+} influence of Pr^{3+} ions on spin-wave damping 79−28625
YIG-Ge layered struct., anisotropy of EMF under nonlinear ferromag. reson. conditions 77−8417
$Y_{2.85}La_{0.15}Fe_{3.75}Ga_{1.25}O_{12}$, inhomogeneous bubble film, spin wave reson. 77−32265
$Y_{2.85}La_{0.15}Fe_{3.75}Ga_{1.25}O_{12}$ LPE films, ion implantation effect on spin waves 80−71124
$Y_{1.62}Sm_{0.21}Lu_{0.27}Cu_{0.9}Ge_{0.9}Fe_{4.1}O_{12}$, implanted bubble garnet, anisotropy profile, FMR study 80−7103
YiG-Bi layer struct., Landau electron absorpt. mechanism, spin wave amplification 78−72344

spinodal decomposition
acrylamide gel, spinodal line and critical point, light scatt. meas. 79−79315
alkali borate glasses, phase separation 79−41965
alloy, binary, atomic misfit effect on coexistence and spinodal transform. boundary 78−60644
alloy, ordered, spinodal decomposition, theoretical basis 80−60862
alloy, spinodally decomposed, interfacial energy effect on mech. strength, theoretical estimation 79−38790
alloy, struct. transform. during ageing, book contrib. 78−11199
alloys, high resoln. diffr. and imaging characterisation 80−104050
alloys, phase transitions via unstable states, review 80−96657
alloys, X-ray diffraction band profile from exptl. prifle of superimposed bands *(French)* 77−39506
Alnico 5, two-phase separation during ageing, Mossbauer study 80−7533
Alnico 5 and 8, spinodally decomposed magnetic alloy, magnetic flux temp. coeff. *(Japanese)* 78−35006
binary critical fluids, spinodal decomposition 79−77759
binary liquid mixture, phase transitions via unstable states, review 80−96657
binary mixtures, liq. and solid, spinodal decomposition theory 78−71863
β-brass, spinodal decomposition, electron microscope and diffr. study 79−78930
β-brass, spinodally decomposed, morphology and characts. 80−60863
chemical spinodal, estimation 79−8271
cluster coagulation model, similarity law 77−24376
computer coupling of phase diagrams and thermochemistry 77−77460
conference, phase transformations in metallurgy, York, England (Apr. 1979) 80−2994
continuous transformations 77−8817
critical fluid mixtures, spinodal decomposition and fluctuation spectrum 78−22825
decomposing system, double light scatt. 78−52516
disordered and spinodally decomposed alloy, residual elec. resist. 79−19569
dynamics, anomalous fluctuation and mode selection 77−11664
dynamics, generalised diffusion eqn., numerical soln. 78−10193
FCC alloy, hardening by spinodal modulated structure 80−60874
fluid, spinodal curve, exptl. verification 79−55625
fluid binary mixture, theory of late stages of decomposition 79−99320
fluids near int. point, early stage spinodal decomposition 77−55340
glass, decomposition, phase separation processes, diffusion coeffs. determ. *(Germany)* 78−39736

spinodal decomposition continued
glass, undergoing phase separation and homogenisation, light scatt. 79−24326
glasses, phase transitions via unstable states, review 80−96657
interface, continuum mechanics *(German)* 80−45272
interphase boundary structure in solids, investig. 80−15112
Invar, phase stability, spinodal decomposition 80−88327
Ising lattice, thermal relaxation, nonideal behaviour, stochastic theory 80−22312
isobutyric acid-water mixtures, spinodal decomposition, light scatt. 77−72688
isotropic systems, spinodal decomposition 77−44210
Lennard-Jones fluid, microscopic theory 79−99046
Lennard-Jones fluid, phase separation by spinodal decomposition, mol. dynamics computer simulation 79−10766
light scattering, depend. on method of quench 78−18782
light scattering, polarised 78−31380
liquid-vapour interface and stability rel. to spinodal decomposition, Cahn-Hilliard theory departure 79−77752
liquid-vapour interface nature, non uniform classical fluids statistical mechanics 79−77468
liquid-vapour system, microheterophase state, characteristic time and size *(Russian)* 78−18740
2,6-lutidine-water, spinodal decomposition, light scatt. obs. 78−34625
2,6-lutidine-water critical mixture, spinodal decomposition, Rayleigh scatt. 80−70416
mag. props. after isothermal thermomag. treatment *(Russian)* 80−25159
magnesioferrite spinels, noncubic, spinodal decomp. of Fe-rich chromites 78−72763
magnetic alloys, binary, spinodal decomp., computer simulation study of interface behaviour 80−84913
metal-H system, basic props., book 79−82349
metal-hydrogen and other alloys, coherent, surface spinodal decomposition and quasiperiodic β-precip. 77−73257
metal-hydrogen system, 2-dimens., elastic interaction, spinodal temp. and density modes 77−69072
metals, expansion, isentropic, vaporisation and condensation kinetics anal. 77−66623
metals, void lattice form, spinodal decomp. of vacancies 78−92234
metamagnet, two-dimens., tricritical spinodal decomp., Monte Carlo study 80−93117
microstructure characterisation, review 80−50588
Nimonic 80A, rapidly solidified, struct. and initial precipitation, field-ion and TEM study 79−78982
non-uniform fluids, statistical mechs., spinodal decomposition and crit. interface 79−68998
nonclassical nucleation *(Japanese)* 79−20026
optical fibres, fabrication using phase separation and leaching method *(French)* 80−106623
orderable system, influence of heat cond. on spinodal decomp. 80−2169
ordering solid solution, theory *(Russian)* 77−21094
percolation and degree of interconnectivity in isotropic, spinodally decomposed, two-phase morphologies 77−28778
phase separation kinetics, Boltzmann's transport eqn. calcs. 80−79952
phase transformations in metals and alloys, thermodynamic and mechanistic classification, review 80−2995
phase transitions, appl. of TEM 79−68988
poly(vinyl methyl ether)-polystyrene mixture, electric field depend. of cloud point temp., laser scatt. meas. 80−6519
polymer blends, fluctuation dynamics, spinodal decomp. 80−79943
polymer systems, binary, high mol. wt., phase transform. assoc. with spinodal decomposition 79−70062
polymers, solidification, as dissipative process 80−65205
pseudocritical phenomena near the spinodal point 78−65894
quenched critical fluid, time evolution of fluctuation spectrum 78−65893
quenched mixture, spinodal decomposition theory, self-consistent method, structure function 78−68671
scaling equation of state derived from the pseudospinodal, liq.-gas system 80−44286
semiconducting binary alloy, cond. band edge shift near precip. point, order fluctuations 77−24517
statistical mechanical theory of the kinetics of phase transitions, review, book contrib. 80−73270
steel, stainless, ferritic and duplex, Mossbauer effect study of 475°C embrittlement 78−52933
strain energy near a free surface 79−61558
superconductors, nonequilibrium, phase transitions induced by quasiparticle injection 78−91808
swallowtails and spinodals, rel. to phase diagrams 77−7844
thermoplastic-photoconductor hologram recording media, frost suppression 78−17869
titanomagnetite from African rift zones, spinodal decomposition and partial self-reversal of magnetisation 77−81869
tolan-mercury diphenyl, occurrence of spinodal decomp., energy characts. of mol. interaction and short range order 79−14794
ultradisperse particles, conc. profiles, free energy *(Russian)* 79−82340
void lattice formation 79−10845
Ag-Cu (50 at.%), splat-cooled, struct. of γ' extended solid solution 78−3147
Al alloys, continuous precipitation, nucleation, spinodal decomposition 80−3061
Al-Ag, low-conc. alloy, spinodal curve and metastable miscibility gap 77−63680
Al-Ag (16 wt.%) alloy, quenched, early stages of decomposition, small-angle X-ray scatt. meas. 77−59740
Al-Cu, ordered domain formation by spinodal decomp. *(French)* 79−20044
Al-Cu (4 wt.%), naturally aged, early stages of G.P. zone form. 77−90355
Al-Cu (4 wt.%), single cryst., small angle X-ray scatt. map after spinodal decomp. 79−15645
Al-Mg supersaturated solid soln., spinodal decomposition at 20°C *(French)* 77−85987
Al-Zn, Guinier-Preston zone form. kinetics study using linear localisation probe *(French)* 78−15413
Al-Zn, miscibility gap, spinodal region, thermodynamic data transferability *(German)* 79−20027
Al-Zn, spinodally decomposing, main wavelength of conc. fluctuations calc. 80−97459

spinodal decomposition continued
Al-Zn (10 wt.%), ageing at low temp., solute conc. fluctuation effects *(Japanese)* 79−4969
Al-Zn (11.8 at.%), growth and dissolution of metastable precipitates, neutron scatt. study 79−15671
Al-Zn (15,16,18 at.%) alloys, coherency spinoidal curve position determ. 77−52281
Al-Zn (18 at.%), position of coherency spinodal curve 78−23660
Al-Zn (38 at.%), alloy, TEM study of precipitation processes or different microstructures during ageing 80−93561
Al-Zn (40 at.%), resistance of homogenization in micro-segregation 79−100180
Al-Zn (6.8 at.%), decomposition, electron microscope study *(French)* 77−40422
Al-Zn (6.8 at.%), hardening during spinodal decomposition *(French)* 79−66035
Al-Zn (6.8 at.%), neutron small angle scatt., interparticle interference 77−77514
Al-Zn (6.8 at.%) alloy, elec. resist. temp. depend. rel. to ageing processes 77−77486
Al-Zn alloys, spinodally decomposing, resistivity behaviour 80−45271
Al-Zn-Cu (22, 0-3 at.%) alloys, coherent spinodal curve 79−87605
Al_2O_3-SiO_2 glasses, phase decomp., small-angle X-ray and neutron scatt. study 79−14688
Au-Cu (50% at.), pretransitional fluctuations *(French)* 80−2160
Au-Ni alloy, modulated struct. form. by spinodal decomp., lattice imaging electron microscopy obs. 79−95996
Au-Pt (60 at.%), solid soln. neutron small-angle scatt. study of phase decomp. 79−15646
Ca Mg $(CO_3)_2$ (dolomite), modulated struct. 79−100832
Co-Ti-Fe (3, 1 to 2 wt.%), spinodal decomposition 80−100839
Cr-Co-Fe, for telephone receiver mag. use 80−45318
Cr-Co-Fe, low Co, phase separation, TEM and Mossbauer spectra obs. 80−71269
Cu alloys, continuous precipitation, nucleation, spinodal decomposition 80−3061
Cu-Ni-Cr, lattice imaging and optical microanalysis of spinodal decomp. 78−52754
Cu-Ni-Cr, microstruct. behaviour and mechanical hardening 78−47281
Cu-Ni-Cr system, coarsening in the $(\gamma_1+\gamma_2)$ region, metallographic study 78−84762
Cu-Ni-Fe, spinodal alloy, heat treatments for improved mech. props. 79−5024
Cu-Ni-Fe alloys superparamag. early stages of decomp. *(Russian)* 78−6890
Cu-Ni-Sn (10, 6 wt.%), spinodal decomposition, X-ray and electron diffr. study 80−81063
Cu-Ni-Sn (10, 6 wt.%), temp. depend of yield stress and work hardening 80−21026
Cu-Ni-Sn (15, 8 wt.%), prior deform. effect on spinodal age hardening 80−108465
Cu-Ni-Sn (4-15, 4-8 wt.%), strip strengthened by spinodal decomp., stress relax. in bending 80−7616
Cu-Ni-Sn (9, 6 wt.%), decomposition, initial stages, TEM study 80−2992
$Eu_xSr_{1-x}S$, mag. clusters, spinodal decomp. trend 80−65923
Fe alloy, design, fundamental aspects, phase transformation utilization *(Korean)* 79−66058
Fe-Al, equilibria of Fe, Al ordered phase *(Japanese)* 79−70042
Fe-Cr-Co, mechanism of coercive force 80−34674
Fe-Cr-Co, spinodally decomposed magnetic alloy, magnetic flux temp. coeff. *(Japanese)* 78−35006
Fe-Cr-Co alloy, coercive force mechanism 80−71103
Fe-Cr-Co alloy, Mossbauer exam. of spinodal decomposition 77−69742
Fe-Cr-Co alloy, spinodally decomposed, micro-twinning 80−92537
Fe-Cr-Co alloys, (5-9 wt.% Co), obtained by slow cooling under mag. field, permanent magnet props. 80−75797
Fe-Cr(55 wt.%), phase decomp. early stages and clustering *(Japanese)* 80−55403
Fe-Mo (13-20 at.%) binary alloys, spinodal decomp. on ageing, TEM and X-ray diffr. study 80−97503
Fe-Mo alloys, spinodal decomp. and modulated struct. form. on ageing *(Japanese)* 79−100184
Fe-Ni-V, nitrided austenitic alloys, modulated substitutional interstitial solute atom clustering 79−74160
Fe-Si alloys, kinetics of spinodal decomposition in 2-phase region of B_2+DO_3 77−28806
$Fe_{1-x}O$, quenched, decomposition and ordering, electron diffr. and microscopy 77−31635
H in metals, phase separation 79−43211
^3He-^4He, superfluid mixture, early stages of spinodal decomposition, calc. 80−20004
$Li_2B_2O_5$ glass, phase separation 79−41965
MgO-Al_2O_3-SiO_2: ZrO_2, TiO_2, glass, phase separation *(German)* 80−38932
Mn-Cu alloys, spinodal decomp. at 380°C, neutron diffr. anal. *(Russian)* 79−20023
Na-rich plagioclase microstructure and exsolution 80−72501
Na_2O-SiO_2 vitreous system with relaxating structure, spinodal decomposition 78−75553
Na_2O-SiO_2-B_2O_3-Al_2O_3, comp. changes as evidence for spinodal decomposition 79−11549
Nb-H, coherent, surface spinodal decomposition and quasiperiodic β-precip. 77−73257
Nb-H, coherent α-α' phase transition, sample shape depend. 79−34005
Ni-Al, spinodal decomposition, atom probe field ion microscopy study 80−3028
Ni-Cr, ordering by nucleation and growth and by spinodal decomposition *(French)* 78−27471
Ni-Cr film, struct. transforms. induced during annealing, resist. obs. 79−77965
Ni-Cu-Al(Si), spinodal decomposition, morphology of microstructure, elastic strain energy anisotropy effect 78−15354
Ni-Cu-Si (38,5 at.%), changes in modulated struct. during ageing early stages *(Japanese)* 79−100183
Ni-Cu-X (X=Sn, Nb, Ti), spinodal decomp. alloys, linear expansion coeff. influence on morphological anisotropy *(Japanese)* 80−70431
Ni-Mn, ordering by nucleation and growth and by spinodal decomposition *(French)* 78−27471
Ni-Mo, off-stoichiometric, ordering 78−52752
spinodal decomposition continued
Ni-Ti (9.6 wt.%), mag. study on phase decomposition *(Japanese)* 80−15758
PbO-Al_2O_3-B_2O_3 vitreous system with relaxation structure, spinodal decomposition 78−75553
PbO-B_2O_3-Al_2O_3 glass, spinodal decomp. during continuous cooling, theoretical anal. 80−1935
Pd-Ag-Cu (35,25 at.%), determ. of ageing transformations by resist. meas., metallography, TEM and X-ray diffr. 79−4967
Pt-Au, amorphous struct. produced by Au implantation, spinodal decomp. TEM obs. 78−31379
SiO_2-Al_2O_3 (36.6 wt.%) plasma prep. powder, metastable immiscibility and microstruct. during sintering 80−35143
αTi-Fe, plastically deformed, $\alpha \rightarrow \omega$ transform. 78−3095
Ti-Mo, martensitic alloy, decomposition by nucleation and growth and spinodal mechanisms 79−61590
U-Nb-Zr (16.6, 5.6 wt.%), stability of BCC phase 79−66039
Zr-Al (14 wt.%), transformation sequence from Zr-Al martensite to Zr_3Al phase 80−3027

spinor groups *see group theory*

spirality *see elementary particle theory*

splines (mathematics)
see also function approximation; interpolation
anatomy, 3D display for radiotherapy treatment planning 80−3773
appearance potential spectra, deconvolution using cubical spline functions, stability, error propagation 80−25487
astronomical optical surface control, Hartmann method, use of splines 79−35149
atmospheric pollution dispersion modelling using cubic splines and chapeau functions 79−83662
B-splines basis, Galerkin method for soln. of one-dimens. primitive eqns. 78−49650
barotropic primitive equation model using splines for typhoon prediction *(Chinese)* 80−4063
bicubic spline interpolation, quantitative accuracy and efficiency test 80−17405
biomechanical movement data smoothing, use of spline functions 80−3699
boundary layer flow equations, integral spline method 79−32450
Burgers' equation for nonlinear shallow water waves, Galerkin method soln., expansion of B-splines 78−87352
cathodic protection of pipeline systems, spline function method for polarisation effect calc. *(Russian)* 78−31566
cubic, use in solving integral eqn. by Galerkin method 77−26189
cubic and bicubic, representation of water props. for nuclear reactor programs 77−23207
cubic bell spline sum function in least squares sense 79−12583
cubic spline, approx. of inaccurate r.m.s. vel. data 80−17406
cubic spline interpolation of unequally spaced data points 79−30210
data compression, input signal Fourier transform 79−35533
data sets with jump discontinuities, interpolation method 79−30211
differential equations solution, linear multistage formulae *(German)* 80−34
digital image processing by smoothing spline functions 77−50628
distributed parameter system identification using doubly cubic spline, underground aquifer appl. 78−69391
ECG baseline estimation and removal using cubic splines and state-space computation 77−44808
EEG signals, reduced spline representations 77−44803
EEG sleep pattern feature extraction and recognition by real-time anal. *(Japanese)* 78−73271
electrocardiogram baseline noise estimation and removal using cubic splines and state space computation techniques 78−11755
electron optical system, trajectory analysis, cubic spline approx. 77−50603
ferromagnetic material, magnetisation characts. approximation *(Russian)* 78−31094
flames, premixed, laminar, time-depend. soln. determ. 78−67282
fluid flow prlblems, incompressible, free surfaces 80−106774
fluid unsteady flow soln. *(Chinese)* 79−72873
fourier analysis with splines, a FORTRAN program 79−12582
Fredholm integral equation, free-knot spline inversion using nonlinear least squares method 79−2486
free vibration calculation for rotating non-uniform disc using spline interpolation technique 80−43656
Galerkin methods, quadrature rules using B-spline basis functs. 80−30
gas phase electron diffraction analysis, use of spline functions, program description 79−89810
geological data automatic contouring techniques 78−7820
geophysical time series alignment, new statistical approach using least-squares cubic splines 79−92623
geophysical unit vectors, time series interpolation using cubic splines 79−92625
heat conduction, in one-dimens., spline identification method 79−37117
heat conduction moving boundary problems, collocation method using B-splines 77−7288
hysteresis modelling and digital simulation, real dipole element appl. *(German)* 79−4706
image reconstruction, linear and modified cubic spline interpolation 79−83929
image restoration by spline functions 78−42280
interpolation of γ-ray spectrometer response function 78−82561
IR spectra calibration using spline functions 77−27050
magnetisation curves representation by cubic spline functions *(German)* 80−71112
MHD channel flow eqns. between electrode walls, fast parabolic module 77−72423
molecular potential energy data, spline interpolation method 78−46412
monosplines, quadrature formulae, one-sided L^1-approx., appl. of weak Chebyshev systems moment theory 77−67248
neuromuscular reflex excitability curve assess. using cubic spline function 79−79510
neutron radiography, high-speed system, modulation transfer function 78−7158
nonlinear partial differential eqns., Galerkin method error analysis 77−78986
ocean currents, calc. using spline polynomials 79−2284
particle track inverse momentum, error estimation using Wind's quintic spline method 79−22563

splines continued
Petrov-Galerkin finite element method, boundary layer problem 78−69989
photon correlation spectroscopy, determ. of particle size distribs. in lipid vesicle suspension 77−86711
plasma simulation, splines and higher order interpolations 79−64902
plasma simulation spatial grid effects reduction using higher order multipoles and splines 78−91148
polynomial spline interpolation for fluid dynamics 77−58636
potential flow about boundary shape, method of singularity with spline fit distrib. 78−22324
potential surface calcs. using 2D cubic splines 77−57851
radiation integral transfer problems, splines under tension calcs. 77−53419
radiocardiography, equilibrium left ventricular ejection fraction determ., background noise estimation 80−94365
reactor physics expts. anal. using spline fitting methods *(German)* 78−66339
resonators, unstable, Fourier transform spline soln. to deal with sharply cut off fields at mirror edges 79−94263
sea model, 3-D numerical, Galerkin method with polynomial basis set 80−72524
seismic data migration, collocation formulation of wave equation migration 80−4126
simplified cubic spline for gravity and magnetic anomaly direct computation 78−7780
singular integro-differential eqn. soln. 77−13595
skew plate free vibration, B-spline coordinate functions 79−68623
skew plate structures, buckling anal. using B-spline functions 80−28446
Sturm-Liouville boundary-value problem error estimation 78−81818
thin film meas. tool calibration by cubic spline fitting 77−18063
transient piezoelectric wave scatt. from crack 79−52615
turbulent flow over body, Fredholm integral eqn., spline fit approx. 79−37302
viscous flow calcs., polynomial interpolation methods 77−65729
water props. modelling using splines, appl. to nuclear reactors 77−42033
wave equations, finite difference approx. using cubic spline technique 79−49
X-ray small angle scatt. curves, comparison of two smoothing methods *(German)* 77−89346
He-H_2^+, classical trajectories, on 3D cardinal spline fitted surfaces 77−90584
O diffusion with absorption, cubic spline appl. to moving boundary problem 79−75475

sponges *see porous materials*

sponginess *see porosity*

spontaneous fission
^{252}103, SF, $T_{1/2}$ meas. 77−6468
^{253}103, SF, $T_{1/2}$ meas. 77−6468
^{257}105, SF, $T_{1/2}$ meas. 77−6468
^{260}104, detection methods, comparison of reactions ^{246}Cm+^{18}O, ^{248}Cm+^{16}O, ^{249}Bk+^{15}N 77−23106
^{261}107, SF, $T_{1/2}$ meas. 77−6468
^{262}[105] spontaneous fission, fragment mass distrib., total kinetic energy release 78−17256
A=354, Z=126, spontaneous fission, α-decay, β-decay half-lives calc. 77−6469
alpha-decay, fission method study *(French)* 79−93565
barrier penetration theory in more than one dimension *(Russian)* 77−33879
beta delayed, prod. of superheavy nuclei in r-process 77−23012
compound nuclei, Z=98, 100, 102, statistical description of decay widths *(Russian)* 78−86549
dynamic aspects of fission process, nuclear mass parameter, action integral minimisation, ^{252}Fm appl. 78−62586
dynamic calc. of half lives for actinide and transactinide nuclei 77−23124
FFTF fuel, neutron source strength as function of irradiation 80−22929
fissile isomers, search via (n,2n) reaction 77−54222
fission isomers, meas. of extreme nucl. deform. *(German)* 79−40971
fissionable source, size and uniformity determ. 78−86711
fragment KE, viscosity effects for spontaneous and induced fission 77−18639
half lives of odd A nuclei, Z≥96 78−86556
heavy muonic atom, muon capture by fission fragments, statistical model anal. *(Russian)* 79−9523
heavy nuclei, review 79−36289
mass and charge division, asymmetry, order-disorder model 80−22866
mass parameters, cranking and hydrodynamic models, deformation depend. *(Russian)* 80−13511
minerals, radiography of geological specimens for determ. of α- and fission-activity 78−20540
muonic atom fission, distribution of muons among fragments *(Russian)* 78−94040
neutron multiple emission in meteorites, evidence for new fissioning nuclide *(Russian)* 77−87352
new nuclide in Allende meteorite, chemical conc. *(Russian)* 77−87353
radionuclide maximum permissible conc. 77−73598
review of expt. data, equilib. quadrupole deformation parameters *(Russian)* 77−54260
rotating nuclei, from heavy ion collision, high spin states instability against fission *(Rumanian)* 78−50150
shape isomer prod. in nuclear reactions and β-decay 79−6377
shape isomers, static and decay props. and excitations, review, book contrib. 78−82402
slope constant of the exponential prompt-neutron yield formula 80−22806
superheavy element prod. in ^{48}Ca ion+^{248}Cm, spontaneous fission 78−74390
superheavy elements, detection by fission activity detect. *(Russian)* 79−13358
superheavy elements, search for fission decay in Madagascar monazite 77−17105
superheavy elements, search for using solid state nuclear track detectors 80−91200
superheavy elements, search in nature based on spontaneous fission meas. 77−29518
superheavy elements, search via neutron emission due to spontaneous fission 78−50117
superheavy elements, synthesis and identification 78−46239

spontaneous fission continued
superheavy nuclei, evidence from meteorite Xe and Kr isotopes 80−63215
superheavy nuclei, spontaneous fission, natural 78−13172
superheavy nuclei, spontaneous fission props. for 98≤Z≤106 and 150≤N≤164, shell model 78−82401
superheavy nuclei, stability and fission barriers, crit. ang. momentum depend. 80−32262
superheavy nuclei, Z>106, lifetimes >2 ps, search in ^{208}Pb+^{86}Kr expt. 78−46102
superheavy nuclei in Cheleken Peninsula geothermal waters 79−96781
ternar fission rate calcs. in Z=126, even-A nuclei 77−54264
toroidal deformation instability, Coulomb energy of circular torus *(French)* 79−6373
transuranics, (3Z-A) depend. of prompt-neutron yield 79−67799
transuranium isomers, exptl. work review 77−79405
α-decay theory 77−79344
^{248}Cm, spontaneous fission Xe and Kr daughter isotope ratios 80−63215
^{262}105 spontaneous fission half life from Bk(^{18}O,5n) *(Russian)* 79−59101
^{263}106, spontaneous fission half life from ^{249}Cf(^{18}O, 4n) *(Russian)* 79−59101
^{298}114, HF calcs. of fragment KE and neutron multiplicity 77−30635
Am, 240-3, spontaneous fission, conversion electron spectra obs. 77−82864
^{A}Am, A=240,244 actinide spontaneous fission activities from ^{209}Bi(^{56}Fe,X) 80−86937
^{240}Am^{m}, spontaneously fissioning isomer optical shift in pumped $^{8}S_{7/2}\rightarrow{}^{10}P_{7/2}$ transition, nuclear deformation 80−27971
^{242}Am^{m}, from ^{243}Am(γ,n), spontaneously fissioning isomer, searches for long-lived excited states 78−86561
^{8}Be spontaneous fission pot. energy curve, cluster shell model *(Chinese)* 80−22867
Bi_2S_3, superheavy element search using neutron multiplicity counter 80−4011
Cf, fragmentation, HF calcs., neutron multiplicities and fragment KE 77−30635
^{A}Cf, A-234,238, actinide spontaneous fission activities from ^{209}Bi(^{56}Fe, X) 80−86937
^{A}Cf, A=250, 252, 254, spontaneous fission fragment kinetic energy and neutron multiplicity meas. 80−42717
^{232}Cf spontaneous fission neutron spectrum 77−50166
^{250}Cf, spontaneous fission, mass distrib., radiochem. and γ-ray spectrometric meas. 77−67775
^{250}Cf, spontaneous fission Xe and Kr daughter isotope ratios 80−63215
^{252}Cf, average neutron yield, Monte Carlo anal. of a direct meas. 77−50180
^{252}Cf, beta, positron, prompt gamma events, superhigh density nuclei formation *(Russian)* 78−17263
^{252}Cf, charge distrib., determ. of fractional cumulative yields of ^{134}Te and ^{135}I 78−41791
^{252}Cf, determ. of heavy-ion interaction pot. *(Russian)* 78−41765
^{252}Cf, element yields from meas. X-ray multiplicities 77−50179
^{252}Cf, element yields from X-ray multiplicities meas. 77−26812
^{252}Cf, empirical limitations for spontaneous fission energy dissipation, fragment deformation 79−3188
^{252}Cf, far-out asymmetric mass distrib. 80−83132
^{252}Cf fission, neutron deficient fragments, search for positron activity *(Russian)* 80−63218
^{252}Cf fission, search for abnormal energy release reln. to superdense nuclei *(Russian)* 79−89340
^{252}Cf, fission neutron spectra Maxwellian temp. 77−26811
^{252}Cf fission neutron TOF spectrum fine struct. 77−88182
^{252}Cf, fission product charge distrib. 78−13176
^{252}Cf fission products, g-factors of isomeric states 77−22890
^{252}Cf fission products, masses, β decay energies, halflives, He jet TOF mass spectrometer meas. 77−23355
^{252}Cf fission-neutron spectrum unfolding experiment 80−13514
^{252}Cf, independent isomeric yield ratio of ^{90}Rb and ^{138}Cs 79−22342
^{252}Cf, low energy neutron spectrum meas. using ^{6}Li spectrom. 78−17477
^{252}Cf, mass distribution of fragments *(Russian)* 78−29517
^{252}Cf, Maxwellian reference description of fission spectrum shape 77−23129
^{252}Cf, meas. of $\bar{\nu}$ and η, Mn bath systematic effects 77−23132
^{252}Cf, neutron emission 80−37405
^{252}Cf, neutron energy distrib. *(Hungarian)* 77−23116
^{252}Cf, neutron spectrum 79−9654
^{252}Cf, positron activity of fission fragments *(Russian)* 77−6474
^{252}Cf, prompt element yields determ. from X-ray multiplicities 77−30643
^{252}Cf, proton origin 77−38309
^{252}Cf, review of meas. of average number of neutrons emitted per fission 79−9652
^{252}Cf, search for low energy delayed neutrons *(Russian)* 77−34359
^{252}Cf, spontaneous fission, charge distrib. 79−97735
^{252}Cf spontaneous fission, forward-backward anisotropy of prompt neutron emission 78−25254
^{252}Cf, spontaneous fission, fragment ranges and kinetic energies in Al 78−94037
^{252}Cf spontaneous fission, fission product β spectra *(Russian)* 80−91204
^{252}Cf spontaneous fission, meas. of fission neutron spectra 80−22873
^{252}Cf, spontaneous fission, neutron spectra and no. depend. on fragment mass and kinetic energy *(Russian)* 77−46197
^{252}Cf spontaneous fission, neutron yields *(Russian)* 79−80965
^{252}Cf, spontaneous fission, prompt γ-ray multiplicity distribs. 77−50174
^{252}Cf spontaneous fission, prompt γ-ray differential angular distrib. 80−102220
^{252}Cf, spontaneous fission, scission point configuration, evaluation anal. 80−37361
^{252}Cf, spontaneous fission, yields and isomer ratio in A=134 chain 78−41786
^{252}Cf spontaneous fission neutron spectrum meas. 79−9653
^{252}Cf spontaneous fission neutron number absolute meas. 79−9642
^{252}Cf, spontaneous ternary fission, multiplicity distrib. of prompt γ rays 78−21615
^{252}Cf, spontaneous ternary fission scission config. from trajectory calcs., Monte Carlo calcs. 79−6718
^{252}Cf, symm. and asymm., fragment yields, β-decay chain lengths *(Russian)* 77−50181

spontaneous fission continued
^{252}Cf, third IAEA evaluation of 2200 m/s, 20°C Maxwellian neutron data 77−23136
^{252}Cf(sf), energy dissipation in fission, comments 80−42719
^{252}Cf(sf), neutron yield dependence on fragment mass 79−67787
^{252}Cf(sf), scission, energy dissipation magnitude during descent from saddle point 80−42718
^{254}Cf spontaneous fission, neutron-rich fragments, even-even products 80−78342
^{254}Cf(Sf), neutron yield dependence on fragment mass 79−67787
^{256}Cf, spontaneous fission, fission barriers and products 80−18355
^{256}Cf spontaneous fission, mass and kinetic energy distribs. from ^{254}Cf(t,p) 80−47518
^{242}Cm, prompt neutron multiplicity distrib. meas. 80−83131
^{243}Cm, cross-section meas. with hemispherical plate ionisation chamber 77−26810
^{245}Cm, cross-section meas. with hemispherical plate ionisation chamber 77−26810
^{248}Cm, spontaneous fission, mass distrib., radiochem. and γ-spectrometric meas. 77−67775
^{248}Cm, Xe isotopic comp. rel. to carbonaceous chondrite fission Xe 77−37581
Fm, fragmentation, HF calcs., neutron multiplicities and fragment KE 77−30635
Fm isotopes, A=254 and 259, low-energy spontaneous fission systematics 77−23125
^{A}Fm, A=242-246, actinide spontaneous fission activities from ^{209}Bi(^{56}Fe, X) 80−86937
^{A}Fm, A=258, 259, spontaneous fission, fission barriers and products 80−18355
^{A}Fm(sf), A=254, 256, 258, 260, fission mass distrib. transition, liquid drop and shell model calcs. 80−32310
^{248}Fm, fragment detection in on-line system of ionisation chambers 78−46226
^{254}Fm, distrib. of mass, KE and neutron yield 78−17257
^{256}Fm(sf), neutron yield dependence on fragment mass 79−67787
^{257}Fm, spontaneous fission fragment kinetic energy and neutron multiplicity meas. 80−42717
^{258}Fm spontaneous fission, mass and kinetic energy distribs. from ^{258}Md^{m} decay 80−47518
^{259}Fm 1.5 sec activity obs. in ^{257}Fm(t,p) at 16 MeV 77−26795
^{259}Fm, fission mass distrib. and half life 77−26776
^{259}Fm spontaneous fission, $T_{1/2}$ and kinetic energies from ^{257}Fm(t,p) 80−47517
No, fragmentation, HF calcs., neutron multiplicities and fragment KE 77−30635
^{252}No, fragment mass and kinetic energy distribs. 77−46194
^{235}Np, fission lifetime from ^{235}U(d,f) reaction 80−63216
^{237}Np, prediction of fission-product mass yields and related parameters 79−30862
^{237m}Np fission isomer from ^{238}U(p,2n), statistical model anal., fission to γ branching ratio 78−25256
^{231}Pa, prediction of fission-product mass yields and related parameters 79−30862
^{236}Pa, β-delayed fission, search *(Russian)* 78−46033
^{238}Pa, β-delayed fission, search *(Russian)* 78−46033
Pu, A=239, 241, spontaneous fission, conversion electron spectra obs. 77−82864
Pu, determination system by passive neutron counting 79−40985
^{232}Pu, fission barrier determ., from β-delayed fission 78−29518
^{238}Pu, spontaneous fission decay const. meas. 77−23149
^{239}Pu fission isomers produced in ^{240}Pu(n,2n), half lives 77−30641
^{239}Pu, fission rate, absolute meas. 79−63678
^{240}Pu, effect of spontaneous fission on energy release in a nuclear explosive 80−95464
^{240}Pu, mass distribution of fragments *(Russian)* 78−29517
U ores, estimation of ratio of induced to spontaneous fission 78−53234
U spontaneously fissionable isomers, excitation by K shell e^{+} annihilation, shape isomery model *(Russian)* 79−30802
UO_2, burnup determ. in PWR and BWR using NDA of neutron emission rates 80−83148
^{A}U, A=236, 238, strength function of β-transitions, probability of delayed fission 80−22764
^{235}U, spontaneous to induced ratio, B and Li impurity effects 79−45305
^{236}U nuclear instability and fission in strong mag. field energy level deformation *(Russian)* 79−13360
^{238}U, decay const., calibration of fission track dating parameters 77−41207
^{238}U, half life and fragment kinetic energies meas. using cylindrical ionisation chamber 78−86555
^{238}U, muonic fission and electron decay 77−38754
^{238}U, natural spontaneous fission, Xe prod., determ., extraction from granite 78−96216
^{238}U, prediction of fission-product mass yields and related parameters 79−30862
^{238}U, spontaneous fission, conversion electron spectra obs. 77−82864
^{238}U, spontaneous fission, constant of disintegration meas. *(Portuguese)* 79−36282
^{298}Z, triple clustering at fission barrier, Hartree-Fock calc. 77−10454

spontaneous magnetisation
Abelian Higgs-Kibble model on lattice, spontaneous magnetisation 78−57870
actinide intermetallics, $AnFe_2$, (An=U, Np, Pu, Am), magnetisation, neutron diffr. and Mossbauer expts. 77−63137
alloy, surface disorder, source of magnetism 79−56487
amorphous ferromagnet, micromagnetic theory 78−10661
amorphous ferromagnetic alloys, domain struct. and mag. microstruct., review 80−15751
amorphous ferromagnetic alloys, micromagnetic eqns. for case of dipolar and magnetocryst. fluctuations 80−11171
antiferromagnet, chain-like, sublattice magnetisation temp. depend., appl. to $KCuF_3$ 77−51892
antiferromagnetic heavily doped semiconductors, Faraday light depolarisation in mixed mag. states 80−29726
classical and quantum lattice systems critical lengths and critical temp. estimates 79−56556
dialkylammonium copper chlorides nearly two dimens. Heisenberg ferromagnet, NMR study of magnetisation 77−85586
diethylammonium copper chloride, Heisenberg ferromag., spin wave theory 77−89922

spontaneous magnetisation continued
disordered Ising model on Cayley tree, mag. transition above percolation threshold 79−73757
eight-vertex model, corner transfer matrices, low-temp. expansions, spontaneous magnetisation 77−28352
Elinvar, Curie point, magnetisation and susceptibility, heat treatment effects *(Russian)* 78−47973
$Fe_xCo_{1-x}Ti$, ferromag., high-field and high-press. mag. behaviour 78−91919
ferromagnet, inhomogeneous, Landau's theory of second-order phase transition 80−50092
ferromagnet, itinerant electron model, spin wave stiffness temp. depend. 77−20535
ferromagnet, neutron scattering, vector polarisation techniques 77−63117
ferromagnetic alloy, temp. depend. of mag. props. and sp. ht., mag. phase transition region 78−64207
ferromagnetic binary alloys, strictly regular, quasi chemical model 78−39316
ferromagnetic film, depend. of Curie temp. and spontaneous magnetisation on film thickness 77−32222
ferromagnetic films, spin correl. functions, crit. indices 80−7133
ferromagnetic system with quenched random impurities, random spherical model in nonzero mag. field 77−55677
ferromagnets, conducting, magnon spectra and magnetoacoustic reson. singularities *(Russian)* 80−50154
fluctuations and mag. eqn. of state 78−64194
GaAs:Fe, superparamagnetism, spontaneous magnetization 79−11285
Ginzburg-Landau-Wilson model, n-component, derivation of nonlinear σ-model, in low temp. limit 80−44787
heat magnetization in the singlet-triplet model 78−64211
Heisenberg, ferromagnet, nearly two-dimensional and nearly one-dimensional thermodynamic props., Green's function investigation 79−15275
Heisenberg ferromagnet, consistent linearised Green's function theory for $s=1/2$ 79−4685
Heisenberg ferromagnet, nearly one- and nearly two-dimensional, long-range order, upper bound for magnetisation 78−34947
Heisenberg ferromagnet, spin-wave renormalisation, $S\geq1$ 80−71070
Heisenberg model, anisotropic, existence of phase transitions 77−32202
Heisenberg model in $d\geq2$ dimensions 78−72319
Invar, magnetisation curves in high mag. fields above Curie point 77−66386
Ising chain, one-dimens., with generalized molecular field 79−91242
Ising ferromagnet, two-dimensional, with second-neighbour interaction, computer simulation, series-expansion method 77−63052
Ising model, appl. of square lattice variational approxs. 79−56555
Ising model, high temperature expansions at arbitrary magnetisation 77−43800
Ising model, layered, spontaneous magnetisation, spatial variations 77−16029
Ising model in $d\geq2$ dimensions 78−72319
Ising model with random quenched broken bond disorder, bounds on crit. temp. 78−2688
Ising system, 2D fully frustrated, correlation functions, on square lattice 80−103805
itinerant electron system, weakly ferromagnetic ground state, Fermi liquid theoretical study 79−4646
itinerant-electron ferromagnetism, possible coexistence with itinerant-electron antiferromagnetism 78−39286
lattice parameters, mag. and elec. props. 80−100578
magnetization reversal of the two-dimensional Heisenberg ferromagnet with weak Ising anisotropy 80−107977
manganese acetate tetrahydrate, susceptibility and magnetis. meas., crit. exponents and crossover behaviour 77−66309
manganese stearate, mag. two-dimensional system, mag. susceptibility 78−10669
nontranslationally invariant spherical model, exact soln., phase transition 77−37833
oxides, $RCu_3Mn_4O_{12}$, R=La to Lu, Y, synthesis and mag. props. 80−75717
phenyl alkyl ammonium copper chloride, quasi-two-dimens. Heisenberg ferromag., mag. props. 77−66273
quasi-two-dimensional planar spin system, mag. transition 80−65951
rare $earth_{50}Ag_{50}$, amorphous, bulk mag. props., field, time and temp. depends. 77−89932
rare earth alloy, amorphous, ferromag. state, non-axial elec. field gradient effect 80−75728
rare earth alloys, R-3d alloys (3d=Mn,Fe,Co,Ni), magnetic properties 78−52231
SQUID magnetometer with temp. control, spontaneous magnetisation and mag. susceptibility meas. 80−68221
static properties of spin systems with truncated secular dipolar coupling 78−88130
superconductor, magnetic, shape effects 80−103773
surface magnetisation profile, in crit. region by ε-expansion, Wilson perturbation theory calc. 80−50100
thin films, ferro- and antiferromagnetic, two dimens. spin-wave theory, spontaneous magnetisation parameter depend. 80−34714
TMNB, linear S=1 ferromag., easy plane anisotropy, low-temp. mag. props. 78−23250
TMNC, linear S=1 ferromag., easy plane anisotropy, low-temp. mag. props. 78−23250
transition metal, magnetic order at surfaces 78−95439
transition metal alloys, magnetovolume effects near crit. conc. for ferromag. 79−56591
triangular Ising model, anisotropic ferromag., corner transfer matrices, spontaneous magnetisation 78−10629
triaxial ferromagnets, spontaneous magnetisation distrib., plane stress state influence *(Russian)* 79−61071
TRM direction, mag. shape anisotropy effect, appl. to basalts 79−29758
V-Fe (29-35 at%), ferromag., mag. props. near crit. conc. for ferromagnetism 78−19225
vacancy distribution along mag. sublattices in β-brass type ferro and antiferromagnetic alloys *(Russian)* 80−79783
X-Y model, quantum effects and dynamics at low temps., path integral approach 80−84584
X-Y model in $d\geq2$ dimensions 78−72319
XY model, one-dimensional, crossover scaling function at zero temp. 79−15273
$Ba_2Zn_2Fe_{12}O_{22}$, model for low mag. moment, magnetisation meas., 5-1375K 78−2655

spontaneous magnetisation continued
$CdCr_2S_4(Sc_4)$, spontaneous magnetisation temp. depend., nuclear resonance freq. depend. *(French)* 80−80483
$CdCr_2Se_4$, crit. behaviour near Curie point 78−31068
$CdCr_2Se_4$, ferromagnetic low anisotropy semicond., spontaneous magnetisation RF determ. 80−22396
$CeAl_3$, singlet ground state at T=0, mag. ordering 2.5-6K 78−84388
Co, magnetic order at surfaces 78−95439
$CoFe_2Se_4$, low-temp. thermal expansion anomalies and isothermal compressibility, mag. ordering and magnetorestriction 79−38363
$CoMnSi_{1-x}Ge_x$, amg. props. 80−60270
$Co_{2-y}Zn_yTiO_4$, cation distrib. and mag. props. 78−14939
$Co_{2-y}Zn_yTiO_4$, spinel series, exchange integrals, mag. struct. and coercive force, magnetisation meas. 77−69507
CsMnFeF$_6$, neutron scatt. and magnetisation meas. 77−66258
$CsNiF_3$, linear S=1 ferromag., easy plane anisotropy, low-temp. mag. props. 78−23250
Cu-Fe, supersaturated, spontaneous magnetisation region development, Mossbauer obs. *(German)* 78−64306
$CuCr_2Se_4$, crit. behaviour near Curie point 78−31068
$CuFe_2S_3$, cubanite, spontaneous magnetisation, polarised neutron obs. *(French)* 78−23245
CuMn, spin glass, mag. hysteresis meas. 80−34691
$Cu(NH_4)_2Br_4.2H_2O$, uniaxial ferromag. insulator, influence of press. on magnetisation 77−69661
$Cu(NO_3)_2.2^1/_2H_2O$, singlet ground state system, mag. props. 80−44850
$CuSO_4.5H_2O$, $CuSeO_4.5H_2O$ and $CuBeF_4.5H_2O$, mag. ordering in external field, NMR obs. 77−66350
Cu_2SeO_4, ferrimag., spontaneous magnetisation meas. 77−63128
Dy-Co amorphous film, prep. by dual-source evaporation, mag. props. 77−89988
$DyCo_{3.4}$, amorphous, mag. props. 77−32177
DyIG, mag. and magnetooptical props., temp. and field depends. 77−89927
DyM_3, M=Fe, Co, Ni, amorphous, mag. struct. and moments 77−66260
$Dy_xTb_{1-x}FeO_3$ orthoferrites, Dy^{3+} and Tb^{3+} contribs. to anisotropy const. *(Russian)* 77−89946
$Er_2Co_{17-x}M_x$, M=Cr, Ni, effect of substitution on mag. props. 79−78363
$(Er_{65}Fe_{35})_{100-x}B_x$ glasses, mag. props. 79−73693
Fe, data up to 0.98 T_c, reanalysis 78−47959
γ-Fe epitaxial film, ferromagnetism, spontaneous magnetisation and Curie temp. determ. 78−2711
Fe, magnetic order at surfaces 78−95439
Fe, magnetisation curves in high mag. fields above Curie point 77−66386
Fe, temp. depend. of spontaneous magnetisation 77−63141
Fe whiskers, soft mag. material, AC response near Curie temp. 78−64223
Fe-Mn-As, crystal struct. and magnetic props. of intermetallic cmpds. with Cu_2Sb type struct. *(Japanese)* 78−59785
Fe-Nb alloys, mag. and Mossbauer meas. 77−63133
Fe-Pt alloy, ordered, anisotropy of mag. props. *(Russian)* 78−60280
Fe-Pt Invar, magnetovolume effects 79−56597
Fe_2MnSi, antiferro- and ferromag. props. 77−12104
$Fe_{40}Ni_{40}B_{20}$, amorphous, high-field magnetisation curve, spin wave spectrum and microstructural inhomogeneities 80−15702
$Fe_{65}(Ni_{1-x}Mn_x)_{35}$, H solid solutions magnetisation behaviour in pulsed mag. fields 79−65674
$Fe_{40}Ni_{40}P_{14}B_6$, quenched amorphous, high field susceptibility and microstructure 77−69506
Fe_3O_4, inverse spinel ferrite, mag. field theory 80−25104
Fe_3Pt Invar alloy, thermal expansion and spontaneous magnetisation, Invar anomalies, low spin model 80−71001
$Fe_{0.9}S$, ferrimag. transition, mag., thermodynamic props., kinetics 79−47280
Fe_3Se_4, mag. props., 4.2-600K 78−43570
$FeTh_2S_5$, mag. struct. and props., neutron diffr. and mag. meas. 80−60201
$Fe_{3-x}Ti_xO_4$, $0.5 \leq x \leq 1$, mag. props. of antiferromag. phase 80−70960
Gd-Fe amorphous film, prep. by dual-source evaporation, mag. props. 77−89988
$Gd_{56}Ag_{46}$, amorphous, susceptibility and magnetisation, 6-300K *(French)* 77−36060
$(Gd_{65}Fe_{35})_{100-x}B_x$ glasses, mag. props. 79−73693
$HgCr_2Se_4$, crit. behaviour near Curie point 78−31068
$HgCr_2Se_4$, spontaneous magnetisation temp. depend., nuclear resonance freq. depend. *(French)* 80−80483
Ho-Co amorphous film, prep. by dual-source evaporation, mag. props. 77−89988
HoGa garnet, mag. ordering induced by hyperfine interaction, neutron diffr. meas. 77−66265
HoIG, anomalous Faraday behaviour, mag. props. 79−82955
$KCuF_3$, chain-like antiferromag., sublattice magnetisation temp. depend. 77−51892
K_2CuF_4, layered spin system, planar rotator symmetry, phase transition 80−65951
$LaNi_{1-x}Co_xO_3$, mag. props. 77−85411
$La_{0.65}Pb_{0.35}MnO_3$, transport props. near Curie points 78−88100
$LiTbF_4$, ferromag., spontaneous magnetisation at marginal dimensionality 77−24683
$LiTbF_4$, mag. props., crit. behaviour at marginal dimensionality 80−54906
$LiTbF_4$, optical study of spontaneous magnetisation at marginal dimensionality 79−73699
Mn-Sb two layer film, cpd. formation kinetics, ion backscatt., X-ray diffr. and mag. meas. 77−72801
$Mn_{1-x}Cu_xCr_2S_4$, phase relationships and mag. phase diagram 79−78374
$Mn_{3-x}Ni_xB_4$, mag. props. *(Russian)* 77−51923
$Mn_{3-x}Ni_xB_4$, with onset of spontaneous magnetisation below T_N, singularities of mag. props. *(Russian)* 77−59427
$Mn_{1.18}Zn_{0.06}Co_{0.01}Fe_{1.75}O_4$, transport props. near Curie points 78−88100
N_2 complex, $NiC(C_6H_5NO)_6(NO_3)_2$, singlet ground-state systems, field induced mag. long range order 80−60266
$Nd_{1-x}Dy_xCo_5$, rotational type spin reorientation, appl. to thermomagnetic generator 77−85451
$Nd(Mn_{1-x}Cr_x)_2Si_2$, mag. and structural props. 79−78342
Ni, data up to 0.98 T_c, reanalysis 78−47959
Ni foil, critical exponent β determ. by microwave transmission 77−69575
spontaneous magnetisation continued
Ni, magnetic order at surfaces 78−95439
Ni, magnetisation curves in high mag. fields above Curie point 77−66386
Ni, temp. depend. of spontaneous magnetisation 77−63141
Ni-Co-H, solid soln., Curie points and spontaneous magnetisation behaviour 80−50093
Ni-Cu-Mn alloys, mag. and galvanomag. meas. 77−89928
Ni-Fe Invar, thermal expansion and spontaneous magnetisation, Invar anomalies, low spin model 80−71001
Ni-Fe-H, Curie points, mag. props. of H solutions FCC metal sublattice parameter behaviour 79−69671
Ni-H, ferromag. disappearance obs. 77−43824
Ni-I single crystals, mag. and dielectric props. 80−93095
Ni-Pt alloys, mag. props. under hydrostatic press. 78−6556
$Ni_3(Fe,M)$, M=Cu, Cr, Mo, W, kinetic phenomena rel. to ordering and electron struct. *(Russian)* 78−76043
$NiFeO_4$, induced ferrimagnetism, temp. depend. of sublattice magnetisation, Mossbauer study 77−66280
$NiFe_2O_4$, domain wall size and mag. losses in freq. spectra 77−85481
Pd-Mn dilute alloys, mag. ordering, sp. ht. calc. by Monte Carlo method 77−77030
$PrAl_2$, cryst. field interpretations of inelastic neutron scatt. meas. and mag. props. 79−56174
PrP, nonstoichiometric, with singlet ground state, induced van Vleck ferromag. spin glass 77−66378
Pr_3Tl, induced ferromag., mag. props. under hydrostatic press. 78−56315
Pt-Co alloys, crit. neutron scatt. in crit. conc. region for onset of ferromagnetism 78−72347
$Pt_3Mn_xCr_{1-x}$ alloys, mag. props. 80−2562
$Sm_2Co_{17-x}M_x$, M=Cr, Ni, effect of substitution on mag. props. 79−78363
$SmFeO_3$, magnetisation direction angle meas. in spin reorientation region 77−26366
$SmFeO_3$, magnetostriction meas. in spin reorientation region 78−2721
$Sr(Fe_{0.766}W_{0.234})O_3$, cryst. growth, mag. and Mossbauer studies 79−42743
$SrRuO_3$ single cryst., reduced ferromag. moment obs. 77−20564
$SrRuO_3$ single cryst., magnetocryst. anisotropy and reduced ferromag. moment 77−24691
$TbFeO_3$, magnetisation exam. 77−24681
TbG_3, uniaxial ferromagnet, logarithmic corrections to crit. behaviour 78−60294
TbGa garnet, mag. ordering induced by hyperfine interactions, neutron diffr. meas. 77−66265
$ThCo_5$ itinerant electron metamagnetism, polarised neutron study 80−39742
$ThCu_3Mn_4O_{12}$, mag. struct. of new perovskite-type ferrimag. 78−52222
$TiFe_{1-x}Co_x$, mag. props., under high press. and in high mag. fields 78−95423
$TmSe_{0.83}Te_{0.17}$, spontaneous magnetisation, mag. susceptibility, magnetostriction, elec. cond. 79−24146
$TmSe_{1-x}Te_x$, mixed-valent cpd., spontaneous magnetisation 80−20392
UIG, Ga-substituted, computer simulation of temp. and field depend. of sublattice magnetisation and spin-flip transition 79−11300
US, magnetisation temp. and field depend. 77−20565
U_3X_4, (X=P, As, Sb, Bi), molecular field approx. study of mag. ordering, Curie temp., paramagnetic susceptibility 79−78410
V, superconducting, microwave biased RF-SQUID system, appl. to magnetic aftereffect 79−26089
$V(Ir_{1-x}Pt_x)_3$, NMR study of ferromag. 79−65760
W/EuS field emitters, electron emission current depend. on annealing temp., mag. props. 80−16160
Y-Ni amorphous alloy, spontaneous magnetisation, Curie temp. and paramag. susceptibility 78−68189
$Y(Co_{1-x}Ni_x)_5$, spontaneous magnetisation mag. anisotropy, spin reorientation transformation *(Russian)* 80−7082
$Y(Fe_{1-c}Al_c)_2$, local model for mag. behaviour 77−63135
$(Y_{65}Fe_{35})_{100-x}B_x$ glasses, mag. props. 79−73693
$YFe_{1-x}Co_{x/2}Ti_{x/2}O_3$, anomalous decrease of spontaneous magnetisation in spin reorientation region 77−36059
$YFe_{1-x}Co_{x/2}Ti_{x/2}O_3$, magnetostriction meas. in spin reorientation region 78−2721
YIG, domain wall size and mag. losses in freq. spectra 77−85481
$Y_{1-x}Tb_xCo_5$, spontaneous magnetisation anisotropy, spin reorientation transforms. *(Russian)* 80−7082
$Zr(Fe_{1-x}Co_x)_2$, mag. props. and Mossbauer effects 79−91322

spontaneous symmetry breaking
1/N dual unitarisation convergence due to SU(4) breaking, charm and strangeness implications 79−6321
(3,3*)⊕(3,3*) bilinear symmetry breaking in linear σ-model, symmetry breaking Lagrangian 79−300
11-dimensional supergravity, dimensional reduction, masses from extra dimensions 79−71332
$^3P_0$ generalised model, reln. to Melosh transform. 78−12885
$\lambda\phi^4$, spontaneous symmetry breakdown, approx. ground state, variational approach 77−79229
$\lambda\phi^4$ self interaction theory, symmetry breaking and mass generation by space-time topology 80−82892
$\lambda\phi^4$ theory, conformal symmetry breaking, cosmological particle creation 80−90998
$\lambda\phi^4$ theory, dynamical mass generation in $S^1 \times R^3$ 80−99046
$(\lambda|\phi|^4)_2$ quantum field model, soliton mass and surface tension 78−58109
σ model, linear in SU(n), n≥4, renormalisation in one loop approx. 79−97516
σ model, $SU_2 \times SU_2$, modified Goldberger-Treiman relation, pseudoscalar form factor 80−27421
σ model, symmetry restoration through finite temp. phase transformation 77−67587
σ model, vacuum stability, strong dynamical symm. breaking 77−13856
σ model relativistic, finite temp., renormalisation, many body problem, interacting nucleons 77−18178
σ model representation of Yang-Mills theory as a spontaneous violation *(Russian)* 80−13220
Σ models of spontaneously broken symmetries 78−399
σ SU(N) model, spontaneous symmetry breaking, renormalisation 80−42340
ϕ^4 theory, spontaneous symmetry breakdown in finite systems 79−45011
ϕ^4 theory with spontaneous symmetry breaking, kink state 77−30235

spontaneous symmetry breaking continued
$(\bar{\psi}\psi)^2$ model, spontaneous symmetry breaking, renormalisation 80−42340
Abelian gauge model, perturb. anomaly compensation 77−13843
Abelian gauge theories, (1+1) dimens., instanton effects 79−261
Abelian gauge theories with dynamical symmetry breaking, effective pot., scale and chiral invariance *(Russian)* 80−57503
Abelian Higgs and Goldstone models, no-hair theorems for black holes 79−17016
Abelian Higgs model relation to spontaneously broken massless scalar electrodynamics 77−54057
Abelian spontaneously broken gauge model, perturbation expansions *(Chinese)* 78−8500
additive quark model with six flavours 80−27455
asymptotic symm. for charmed mesons, new duality 78−21348
asymptotically free massless field theory, self-consistent β functions 78−16911
atomic and molecular physics, dynamical groups 80−42362
axial current in dimensional regularization 80−13233
baryon mass relations in internal SU(6) symmetry 80−82962
baryon mass splitting by the 'strong hyperfine interaction and SU(3) breaking 78−82184
baryon resonances, hadronic decay, broken SU_3 and total reduced width 78−17017
baryon resonances and broken SU(4) symm. 77−71455
baryons, b-quark, magnetic moments, broken SU(5) symmetry 80−95257
baryons, current status, additional symmetry breaking assumptions 80−4995
baryons, symmetry breaking mechanism, universal confining forces between quarks 78−50013
Bethe-Salpeter eqn. spontaneous symmetry breaking in chain approx. 77−5998
bicritical point crossover, asymptotic behaviour of a field theory with quadratic symmetry breaking 79−1488
bifurcation from rotationally invariant states 78−77671
bilinear symmetry-breaking in σ-model, meson mass and decay const. 77−49877
bilocal fields for study of quantum corrections to dynamically broken symmetries 78−16985
bilocal gauge field theory 80−31986
Bose condensate, bounds in dimensions $\nu \geq 3$ 78−54294
boson fields, massless, spontaneous symmetry breaking, and Goldstone theorem *(Chinese)* 80−62861
boson system, scaling equation of state, renormalisation group transformation 78−12643
bound state spectra in ϕ^4 theory and Gross-Neveu model, temp. depend. 78−4770
bound states from instantons 78−78087
broken chiral $SU_4 \times SU_4$ symmetry at infinite momentum, have quark mass ratios 79−80768
broken colour gauge theories, effective weak vertex, colour contrib. 79−40750
broken SU_3 theory, correlations in multiperipheral resonance prod. model 78−45891
broken SU_3-subsymmetries of SU_4 and magnetic moments of charmed baryons 79−63382
broken $SU(6)_w$ analysis of electroproduction 79−93436
broken supersymmetry, existence of massless colour octet quarks and unstable hadrons 78−89631
broken supersymmetry mass formula, quantum corrections 80−27424
Cabibbo angle, gauge invariant rearrangement and theory, SU(2) symmetry breakdown 79−22027
Cabibbo angle and weak interaction invariant props. in chiral dynamics 79−71660
charge symmetry breaking in nuclear forces, test by np elastic scatt. 78−89798
charge-monopole duality and nonAbelian gauge theory phases 79−71625
charge-monopole duality in spontaneously broken gauge theories 79−267
charmed baryons, semileptonic decays, SU(4) breaking, mag. moments, suppression factors 79−387
charmed meson decay, simple symm. breaking 78−21418
charmed meson decay, SU(4) symm. breaking 77−26518
chiral asymmetry in vectorlike weak SU(3), CP violation, one loop correction 79−287
chiral properties of fermionic determinant in two-colour QCD, symm. breaking 78−25015
chiral quantum field theory, covariant formulation 78−21347
chiral SU_2 symmetry, spontaneously broken, equivalence to current algebra in field theoretic model 77−82688
chiral SU(3)×SU(3), combined models of symmetry breaking *(Russian)* 77−6051
chiral SU(4)×SU(4) breaking scheme, vector mesons radiative decays 79−22099
chiral SU(4)×SU(4) model, scalar meson decays 78−4801
chiral SU(4)×SU(4) symmetry, broken chiral, mass spectrum of D, F and η mesons 79−93312
chiral SU(4)⊗SU(4) symmetry breaking parameter, meson mass 78−12838
chiral SU(4)xSU(4) symm., pseudoscalar mesons as Goldstone bosons 77−30278
chiral symm., anal. of cold matter at super-nuclear densities including pion condensates 78−17128
chiral symmetry, $SU_N \times SU_N$, multiplet fermion field model 79−9299
chiral symmetry, using vacuum stability condition 79−35986
chiral symmetry breaking, current and constituent quarks 79−13033
chiral symmetry breaking, Dashen mass formula, baryon mass differences, $\eta \rightarrow 3\pi$ 79−289
chiral symmetry in Nambu model, linearisation of theory 77−54043
chiral $U_3 \times U_3$ symmetry 79−35957
classical lattice field theory, inequalities and symmetry breaking 79−9131
compact group gauge fields, breaking of symmetry and dual charges *(Chinese)* 79−35918
compactification, spontaneous, of arbitrary space-time dimens., SO(N) gauge group 77−22458
completely integrable theories as theories of spontaneous breakdown 79−49416
conceptual foundations of the unified theory of weak and electromagnetic interactions, review 80−95237
conference, critical phenomena, Sitges, Spain (June 1976) 77−22510
confining theories, chiral symmetry breaking in gauge theories 80−95244

spontaneous symmetry breaking continued
conformal and gauge spontaneous symm. breaking, cosmology quantum effects 80−37185
conformal invariance, Higgs mechanism 79−40687
conformal invariance breaking and quark counting rule for form factors 77−30381
conformal invariance in quantum gravity 77−17896
conformal invariant field theories, new approach 77−2728
conformal symm. breaking, quantisation in curved space-time 78−41434
conformal symmetry, nucleon σ-model 77−2729
continuous symmetry breakdown, absence in more than 2-dimens. 79−6293
cosmological ν sea, EM wave propagation, torsionic background 80−77283
cosmological baryon number domain structure, from symmetry breaking in grand unified field theories 79−84876
cosmological models, spontaneous symmetry breakdown, open and closed Friedmann model 80−51929
coupling constant renormalisation anal. in unified theories, generalised gauge hierarchies 79−97556
covariant n^2-plet mass formulas 79−63460
CP^{n-1} model with quarks, confinement and chiral symmetry breaking 79−54302
CP symmetry spontaneous breaking in nonstationary isotropic metric 79−89079
CP violation, radiative symm.-breaking, fermion and Higgs boson masses 78−41435
CP violation in vector-like model of weak interactions 77−54071
CP violation via Higgs boson exchange, Weinberg-Salam model anal. 79−63384
current quark masses and symmetry-breaking effects 80−4952
currents and continuous symmetry restoration in two dimens., perturbation theory 79−21910
defects and symmetry breaking, review 80−95231
Dicke model with classical spins, phase operator and phase transition 77−82448
Dirac particle in mag. field, symmetry breaking by monopole singularities 78−16977
discrete finite nilpotent Lie analogs: new models for unified gauge field theory 78−66025
distorted gauge invariant theory, renormalisation props. 77−45967
dual electromagnetism and neutral-current interactions 79−71678
dual resonance amplitudes, Regge spectra, symm. breaking effects, decay rates of mesons 77−82715
dual resonance model, conformal invariance, spontaneous symm. breaking 77−6092
dual string model, standard, spontaneous symm. breaking 78−41508
Dual Topological Unitarisation scheme, flavour symmetry breaking 80−102030
dual unitarization scheme with several trajectories, diffractive scatt. predictions 79−89133
duality invariance, simple gauge theories including EM-type fields with sources 80−27440
dynamical, in scalar electrodynamics and Yang-Mills fields, scalar particles 79−97536
dynamical cluster properties in the quantum statistical mechanics of phase transitions 80−77693
dynamical generation of effective degrees of freedom, flavours 79−22026
dynamical groups of completely integrable eqns., nonlinear realisations 80−4885
dynamical quark mass generation and the mean instanton density 79−54305
dynamical symmetry breakdown at the two-dressed-loop level and beyond 79−294
dynamical symmetry breaking, extended structs., generation in field theory 77−6026
dynamical symmetry breaking, improved effective-pot. formalism for composite fields 77−6033
dynamical symmetry breaking and mass generation massless field theory, renormalisation group 77−6027
dynamical symmetry breaking in dual resonance model, Regge meason trajectories total renormalisation *(Russian)* 77−82717
dynamical symmetry breakings in quantum chromodynamics *(Chinese)* 79−22050
dynamically broken chiral symmetry and the gauge technique for Ward identities 80−47211
dynamically broken gauge models, natural mass hierarchy, unification 80−68409
dynamically broken-gauge theories, P and T violation in QCD 80−9093
dynamically spontaneously broken symmetries of gauge theories *(Chinese)* 79−80740
E6 unified gauge model, breaking patterns, quark-lepton symmetry and mass scales 78−86434
E_6 model, basic fermion masses and mixings 78−24972
E(6) gauge theory, dynamical symmetry breaking 80−86580
E(6) grand unified theories, one loop renormalisation effects, stepwise symmetry breaking 80−32058
E based vector-like unified theory, group theoretical anal. of symm. breaking 77−87929
early Universe, horizon problem and the broken-symmetric theory of gravity 80−62344
Earth gravitational field, local vanishing due to left turning motion *(Japanese)* 80−98798
education, gauge symmetry breaking, geometrical approach, superconductivity and spontaneous symmetry breaking 80−57028
effective Lagrangian in spontaneously broken gauge theories 79−17653
effective potential calculation to order $\hbar$ using functional Schrodinger Rayleigh-Ritz approach 77−74257
effective potential for non-Abelian gauge theories and spontaneous symmetry breaking 80−4863
effective potential for spontaneously broken gauge theories and gauge hierarchies 80−18080
electric charge possible nonconservation in spontaneously broken gauge model 79−71620
electric-magnetic charge breaking in local field theories 77−18209
electroweak interactions, dynamically broken gauge theories, CP nonconservation without elementary scalar fields 80−86613
elementary particle classification and quark model, symmetry breaking gauge theories, unified theories 79−346
elementary particle phenomena, rel. to undergraduate physics 78−54118
elementary particle theory appl. 77−22666

spontaneous symmetry breaking continued
Euclidean Higgs fields, topology 78−4759
exceptional groups, patterns of symmetry breaking 80−42356
exotic new quarks and dynamical symmetry breaking 80−73669
extended objects from Goldstone bosons in relativistic quantum field theory 79−285
extended PCAC hypothesis, soft-meson chiral symm. breaking 78−21353
extended relativity, T-violation and new particle 80−37182
extended spontaneously broken supergravity models, properties 80−46924
extended supergravity, gauge internal symmetry 77−38115
Fermi quantisation of EM field, model for quantum field theory 77−79208
Fermi system, perturbation theory, system exhibiting dynamic symmetry breaking 79−143
fermion mass, unified gauge model based on E6 80−32053
fermion masses and hierarchy of symmetry breaking, u and d quarks 80−86618
fermion number conservation and supersymm. spontaneous breakdown 77−30248
fermion number conservation spontaneous breakdown in two dimens. 77−67584
fermions, charge density phase transitions in gauge theories with spontaneous symmetry breaking *(Russian)* 79−2969
Feynman-Wilson fluid, density fluctuations, multiparticle event asymptotic struct. 79−36040
fiber bundle structure of gauge field and reduction by the Higgs mechanism 80−82885
fibre bundle analysis of topological charges in spontaneously broken gauge theories 79−2910
five-dimens. model of scalar bosons, O(N) symm. 78−70307
flavour symmetry breaking and production processes in dual unitarisation, ϕ and ψ prod. 79−45080
fluxon solutions in non-abelian gauge models 79−9287
four-quark model, $SU_{2L}\times SU_{2R}\times U_1$ gauge group, Cabibbo angle and quark masses 78−25002
Friedmann model, spontaneous breaking of symmetry and evolution of Universe *(Russian)* 77−5607
$g\phi^4$ static ultralocal field, path integral anal. of spontaneous breakdown of symmetry 79−54249
gauge field in stability subgroup of vacuum in nonlinear realization 78−390
gauge field theories, Higgs-Kibble effect *(Russian)* 77−6038
gauge fields, chiral fields on loop space, colour-electric flux rings 80−42327
gauge fields, geometrical models from fibre bundles 79−21899
gauge hierarchy through spontaneous symmetry breaking 79−17621
gauge invariance broken model, electron- and muon-number nonconservation 77−65128
gauge invariance of spontaneously broken non-Abelian theories in Bogoliyubov-Parsyuk-Hepp-Zimmermann method 77−49861
gauge models of weak and EM interactions, quantisation and renormalisation of gauge theories, book contrib. 79−30669
gauge supersymmetry, spontaneously broken, quantum loops UV finiteness 79−21919
gauge supersymmetry, supergravity gauge invariance 79−9277
gauge symmetry, dynamical symmetry breakdown, appl. to intermediate vector boson mass relations 79−54269
gauge symmetry, spontaneous breakdown, grand unification of QCD and $SU(2)\times U(1)$ 79−49380
gauge symmetry breakdown, nonsingular cosmology as vacuum effect 79−53947
gauge symmetry breaking in nonstationary isotropic metric 79−21643
gauge symmetry hierarchies, tree approx. 77−2758
gauge sypersymmetry eqns., spherically symm. soln. 78−4532
gauge theories, an introduction for experimental particle physicists 78−82119
gauge theories, exact gauge symm. group, ang. momentum operator, mag. monopole props. 77−2764
gauge theories, facts and prospects, conf., Schladming, Austria (Feb.-Mar. 1978) 79−26203
gauge theories, general struct. and renormalisation 79−17598
gauge theories, quantised, large time behaviour, asymptotic anal. 80−27395
gauge theories, spontaneously broken, 1-loop corrections, 2-point functions and fermion masses 79−17599
gauge theories, spontaneously broken, 3- and 4-point functions and renormalisation consts. 79−17600
gauge theories, statistical mechanics of field theories with broken, global, and local SU(3) gauge symmetries 79−58881
gauge theories, U-gauge Green's functions construction, with spontaneous symmetry breaking and Slavnov identities 79−235
gauge theories 77−34083
gauge theories 77−74574
gauge theories in homogeneous, isotropic, closed universe *(Russian)* 77−45979
gauge theories of weak, EM and strong interactions 77−13835
gauge theories with neutral currents, high-density and high-temp. effects on symmetry breaking 77−22664
gauge theory, renormalisation of ghost and Goldstone fields and ghost symmetries 80−90987
gauge theory for superdense matter, symm. breaking 77−45955
gauge theory hidden global symmetry apparent after local symmetry breakdown 77−57453
gauge theory model, e^+e^- colliding beam data 77−2845
Gell-Mann-Okubo formula, total widths of unstable hadrons 78−45805
general mathematical aspects *(French)* 77−17772
geodesic in gauge supersymm. 78−12634
geometric quantisation and internal symm. in gravit. 77−79022
Gibbs fields, absence of continuous symmetry breaking in two-dimensional models of statistical physics 79−21650
goldstino couplings and neutral currents, mass relation for lepton and quark superpartners 79−75717
Goldstone bosons in two dimens., ground state, IR divergences 78−12815
Goldstone neutrinos avoidance mechanism, spontaneously broken supersymm. theories limits 77−30279
Goldstone particle spin values and symmetry breaking *(Russian)* 77−212
Goldstone theorem in classical statistical mech., correl. function non-vanishing boundary terms as phase transition origin 80−27253

spontaneous symmetry breaking continued
grand unification mass scale, cosmological origin 79−88773
grand unification with exceptional group E_6, symmetry breaking, SU(5) relations, quark masses 80−68407
grand unified schemes and spontaneous compaction 77−87896
grand unified theory from broken SO(8) extended supergravity, SU(5) theory 80−99081
gravitational bubbles, radiative corrections to covariant massless quartically self-interacting meson theory 80−62826
gravitational interaction spontaneous symm. breaking 78−36918
gravitational radiative corrections as the origin of spontaneous symmetry breaking 80−86192
gravitational theory of symmetry breaking of transformation intransitive groups 80−36912
gravity, broken symmetric theory, unified gauge field breaking 79−30343
gravity and spin 1 gauge fields 79−21923
Green's function props. of spontaneously broken supersymmetic model at high temperature 79−26257
Gross-Neveu model, exact S-matrix theory 78−24937
Gross-Neveu model, renormalisation, mass generation 80−27393
Gross-Neveu model, spontaneous mass generation 79−21907
gross-Neveu model as $Z_3=0$ limit of the two-dimensional SU(N) σ model 79−35949
group contractions and spontaneous symmetry breakdown 77−13883
hadron decay, relativistic quark model and SU(4) 78−62366
hadron masses and current algebra quark masses 80−42436
hadron microstructure, de Sitter microuniverse, relativistic Hooke group and nonrelativistic quark model 80−27480
hadron spectroscopy, quark models and SU(5) grand unification scheme 80−4958
hadronic structure theory, derivation of static bag and bag constant estimation 79−58932
hadrons, charmed, SU(4) mass-breaking, mass sum rules 80−62959
harmonic confinement, relativistic approx. to meson spectrum 78−29303
harmonic maps as models for describing broken symmetries 79−26222
Hawking particles produced by black hole evaporation Higgs particles 79−2553
heavy Higgs scalars and the renormalization of spontaneously broken gauge theories 79−71607
heavy lepton model of rare μ and K decay modes 78−45898
hidden gauge symmetry, appl. to elementary particle fundamental interactions 79−30658
hierarchy in asymptotic reconstruction of spontaneously broken isotopic symmetry *(Russian)* 79−2968
Higgs boson, charged and trimuon events in neutrino reaction 78−21413
Higgs boson, mass, upper and lower limits *(Russian)* 78−4795
Higgs boson, spontaneously broken gauge theory phenomenon, possible weak interaction model 78−74200
Higgs boson mass, perturbation constraint 79−67493
Higgs bosons, effects on experimental observables, and fermion mass scale 80−32061
Higgs bosons, masses, gauge hierarchies, SU_5 model 80−47236
Higgs bosons from two-gluon annihilation in pp collisions 78−41501
Higgs effect, supergravity and supersymm. massless QED 78−29268
Higgs lattice abelian model, finite temp. behaviour 80−13260
Higgs mechanism, implementation 78−24921
Higgs mechanism, spontaneous symm. breaking in local gauge quantum field theory 78−396
Higgs mechanism and the inverse Einstein-Infeld-Hoffman problem 79−63100
Higgs mechanism in (1+1) supergravity 78−74199
Higgs meson mass and decay of metastable vac. state. 78−4819
Higgs scalar effects on gravity, Nambu Jona Lasinio type model 78−41467
Higgs-Kibble mechanism, superfield theoretical treatment 78−89616
high temperature symmetry breaking 80−42357
horizontal symmetries dynamical symmetry breaking and neutrino masses 80−105830
hot early universe symmetry breaking and phase transition 77−22661
hydrodynamic model, nonlinear pion+pion chiral Lagrangian, e^++e^- and p+p collisions 78−32966
induced second-class currents from isospin and chiral-symmetry breaking 79−97538
induced spontaneous sypersymmetry breaking in first order 77−211
instanton phenomena, real time approach, multidimens. potential with continuous symmetry 79−2922
instantons and quark-mass generation−the how of spontaneous chiral symmetry breaking 80−4963
instantons and restoration of symmetries 78−66033
interaction of scalar field with nonstationary vector field, spontaneous breaking of gauge invariance 78−8545
internal gauge symmetry theory 79−12958
internal symmetry breaking mechanism from quantisation of nonrelativistic free particle 79−6020
internal symmetry origin 77−45959
invariant renormalisation method for non-linear realisations of dynamical symmetries 79−108
Ising field theory, 2-D, $T<T_c$, three point function string structure 79−270
Ising field theory 2-D, $T<T_c$, Green's function strings in n-point functions 79−271
Ising field theory in mag. field, cut breakup in two point function 79−272
isospin SU(3) symmetry, spontaneous breaking of chiral symmetry in QCD 79−93352
isospin violation, induced by current quark mass 80−32069
isotopic breaking of gauge symmetry 79−97517
isotropic cosmological models, vacuum stress energy tensor and particle creation *(German)* 80−94901
Jones matrix, appl. in symmetry breaking, SU_2 theory and theory of neutrinos 79−17632
large-N chromodynamics, chiral symmetry breakdown 80−91052
lattice fermions, Dirac fields and Thirring fields, spontaneous breaking of chiral symm. 78−24962
lattice gauge theories, chiral symmetry dynamical breaking 80−99061
lattice nonlinear $O(2)_3$ model, phase transition between broken/unbroken symmetries 79−9147
left-right symmetry, spontaneous breakdown, parity violation, leptonic right handed, currents 78−21351
left-right symmetry breaking and fermion masses 80−105810

spontaneous symmetry breaking continued
left-right-symm. unified theory of quarks and leptons 78−41466
lepton models, dynamical symm. breaking 77−5980
Lewis Riesenfeld oscillator, dynamical symmetry breaking 80−47210
Lie admissible forces, non-self adjoint, compatible symmetry schemes 79−75696
Lie group broken symmetry of transformation generating general relativistic theories 80−98836
light quark mass spectrum in QCD 79−63427
light quarks and QCD Boson representation, dynamical symmetry breaking 80−52472
linear baryonic string model, dynamical SU(3) symmetry breaking 79−22036
linear gauge theory algebraic struct., spontaneously broken symmetry, quantisation, massive gauge field 79−2906
linear SU(4) meson σ-model, one-loop approx., spin zero mass spectrum and leptonic-decay 80−47278
local gauge supersymmetry, spontaneously broken, struct., real gravit. interactions 77−49843
local QFT, higher symm. interpretation, spontaneous symm. breaking, quarks and flavours 78−16942
Lorentz type internal symmetry 78−50005
low energy light particle processes in spontaneously broken gauge theories, heavy particle effects 80−22521
magnetic flux metamorphosis in spontaneously broken gauge theories 80−99047
magnetic monopole long range interactions in non-Abelian gauge fields 80−22520
magnetic monopoles, non-Abelian, stability analysis, Yang-Mills equations 80−31987
magnetically extended Lagrangian theory, 0(3) gauge theories with spontaneous symm. breaking, shared photon sector 78−62306
magnon fields, finite temp. effective pot. methods, loop expansions 78−2640
magntic moments and machinery of symmetry breaking 79−63477
many-boson model, spontaneous symmetry breakdown and restoration 80−52123
mass, physical, in ϕ^4-model, renormalisation group and mass generation 80−77948
mass formula in broken supersymmetry 79−97535
mass generation for fermion field in absence of chiral symmetry breaking 80−347
mass generation in a normal product formulation 78−25027
massive gauge fields, complete spontaneous symm. breaking, asymptotic freedom, symplectic and G_2 groups 78−62305
massive Schwinger model, asymptotic completeness and confinement 78−66028
massive supergravity, from spontaneous breaking orthosymplectic gauge symmetry 78−77787
massive supergravity nonlinear realisation of orthosymplectic gauge symm., coupling to spin 1/2 spin 1 multiplet 78−33019
massive vector boson field theory with spontaneous symmetry breaking 80−52443
massless quarks in QCD, dynamical symmetry breakdown 80−52471
massless scalar field, conformal symmetry breaking and quantisation in curved spacetime 79−97523
matter interactions in weak gravit. fields, spontaneous origin of Newtons const., modified Einstein eqns. 78−12853
mechanism of spontaneous symmetry breaking, various appls. 78−45510
meson decay, tensor, current algebra approach, symmetry-breaking Hamiltonian, chiral SU(3)×SU(3) or SU(4)×SU(4) 80−68450
meson dipion cascade decays, current algebra techniques, pole plus remainder model, chiral symmetry breaking and QCD 80−62972
meson radiative decays, higher order effects 79−13131
meson radiative transition, symm. and duality constraints 78−78178
meson spectroscopy, quark mixing and quantum chromodynamics *(Russian)* 79−54329
meson weak and EM decays, relativistic confined quarks, MIT bag model 80−47277
MIT bag model, chiral symmetry breaking 79−63408
MIT bag theory, microscopic derivation with spontaneously broken symmetry 79−264
models of dynamically broken gauge theories 80−77974
monopole bound states, SU(4) spontaneously broken 77−82679
monopole solns. in spontaneously broken SU(n) gauge theory 78−82103
multicomponent $\lambda(\phi^2)^2$ model, symmetry breakdown absence, vacuum uniqueness 79−12926
muon g-factor anomaly, review of theoretical contribs. 77−30384
muon number conservation spontaneous breakdown, off-diagonal neutral currents 77−49889
N=8 spontaneously broken supergravity, mass matrix, gauge couplings 79−97281
N=8 supergravity 79−67212
neutral currents, heavy particle decoupling effects in broken symmetry theory 78−82140
neutral currents and quark charge origin 78−21373
neutral weak current, structure, neutrino and antineutrino scattering experiments *(Russian)* 79−49446
neutron oscillation phenomenology in gauge model with spontaneously broken B-L symmetry 80−90996
non Abelian gauge theories in external electromagnetic fields *(Russian)* 80−57533
non-Abelian group spontaneous violation, gauge models and external currents *(Russian)* 77−207
non-Abelian symmetries, spontaneous breaking in SU(2) and SU(2)×SU(2), observable consequences 79−26252
non-metrical supergravity for a spin-two nonet 79−71333
non-relativistic model, spontaneous supersymmetry breaking and superconductivity 80−32031
nonAbelian gauge theory, Higgs couplings and asymptotic freedom 79−21948
nonAbelian gauge theory, light quarks and instantons, chiral symmetry breaking 79−63332
nonAbelian gauge theory, spontaneous breaking of scale invariance *(Russian)* 77−74604
nonAbelian gauge theory, spontaneous symm. breaking without scalar mesons 77−30250
nonAbelian gauge theory, topological symmetry breakdown and quark confinement 79−71611
nonAbelian gauge theory quantisation, nonclassical field configs., broken symmetries, gauge copies 79−49373
nonAbelian theories with nontrivial gauge transforms., topological tunnelling, Goldstone gluons 78−24956
nonlinear σ-model with quadratically broken symmetry, cross-over behaviour 79−17601
nonlinear field theory, two-loop divergences 78−54529
nonlinear Lagrangians and spontaneous symm. breaking 78−70303
nonlinear O(N) σ-model with gauge interactions, two-dimens., phase transitions 77−6029
nonlinear realisation, unified interaction, spontaneous symmetry breaking 79−13010
nonlinear Yang-Mills pseudoparticle solns., quantisation, conformal group contraction 79−67464
nonrelativistic field theories, functional methods, finite temp. behaviour 79−12952
null-plane charges and Fourier transforms, broken symm. 77−2771
O(10) spontaneous symmetry breaking for Higgs fields 80−105812
O(N), diagram technique for low temp. phase in chiral field model 79−58882
O(N) symmetry in ϕ^6 theory in three dimens., global ground state 77−6015
one-dimens. lattice, phase transitions 79−40489
OSp(1,4) supergroup, Wess-Zumino model classical solns. 80−36928
Oxford Rutherford type model, semianalytic treatment, dual unitarisation scheme, trajectory parameters 78−16996
partially conserved axial vector currents, corrections, light-plane commutators, sum rules, meson decay 79−304
PCAC, chiral anomalies and quark masses 78−8556
phase transition in nonAbelian quantised gauge field theories, permanent quark confinement 78−70322
phase transitions, first-order, in spontaneous broken gauge theory 78−24943
phase transitions, Goldstone bosons, topological superselection rules 77−5977
photino and goldstino, scatt. cross sections on matter 79−97558
physical pion low energy electro- and photoprod., Ward identity, chiral symmetry breaking struct. 80−5003
Poincare supergravity as broken superconformal gravity 78−62348
positive parity excited baryons in quark model with hyperfine interactions 78−82161
projective geometry and group contraction 78−8551
protons, flavour symmetry breaking in antiquark distribs. 79−36006
pseudoparticle, four-dimens., quantum effects calcs., SU(2) gauge theory, chiral symm. breakdown 77−30247
pseudoparticle solutions in gauges with unique pots., physical interpretation 77−79222
pseudoscalar meson decay, symm. breaking in chiral SU(4)×SU(4) model 78−21424
pseudoscalar mesons, sum rule, symm. breaking of chiral SU(4)×SU(4), decay const., masses 78−33000
pseudoscalar-meson decay constants, Goldberger-Treiman relations, and chiral SU(4)×SU(4) symmetry breaking 79−293
q meson mixing and SU(3) breaking 79−282
QCD, 1+1 dimens., dynamical symmetry breakdown 80−82949
QCD, dynamical chiral symmetry breaking and explicit breaking due to current quark masses 79−71717
QCD, quark and gluon propagators 80−52469
QCD, spontaneous breaking of chiral SU(2)×SU(2) symmetry 79−36013
QCD, spontaneous breaking of chiral symmetry 79−71700
QCD and resonance physics, appl. of sum rules to ρ-ω mixing 79−22060
QCD development from classical Yang Mills theory, a qualitative critique 79−80804
QCD phase transitions, chiral symmetry breaking, confinement, as tunnelling through singular barriers 78−82145
QCD spectrum, infinite number of colours at fixed coupling, interacting string model 79−2993
QCD theory for the strong interaction 80−4962
QCD vacuum in strong external gauge fields, spontaneously, broken chiral symmetries 80−57555
QED, effective potential derivation 79−12994
QED, heavy particle effects, factorised local operators, renormalisation group 80−62898
QED, heavy particle effects, factorised local operators, renormalisation group 80−62899
QED, nonlinear approach, conformal invariance and fine-structure constant 80−91023
quantum action method in quantum field theory 79−40659
quantum corrections to effective pot., symmetric vac. stability 79−63379
quantum corrections to the quadratic mass formula of broken supersymmetry 80−46942
quantum flavour dynamics, quark masses and flavour mixing angles in six quark model 78−74211
quantum gravity, topological invariants 77−5729
quantum SU(2) gauge theory, vacuum stability, dynamical symmetry breaking 80−32000
quark and lepton masses, chiral charge space, statistical analysis 80−42428
quark charges, developed by spontaneous breaking of colour symm. 78−21387
quark confining theories, chiral symmetry breaking 79−63423
quark magnetic moment, rel. to quark mass and hadron mass in SU(3) breaking 79−13050
quark mass differences in transition form factor, production by charmed baryons 79−93400
quark mass effects as isospin and SU(3) violations in radiative decays of vector mesons 79−22091
quark models, noninvariance groups, internal symms. and ghost symms. 78−25007
quark strong interactions as weak interaction symmetry breaking mechanism 80−18117
quark theory with internal coords., Dirac eqn., Bethe-Salpeter eqn. 77−18224
quark-diquark model with broken colour symmetry, hadron spectrum 78−12874
quark-mass generation by pseudoparticles, spontaneous breaking of chiral symm. 77−74646
quark-quark interaction, phenomenological, from s-wave baryon spectrum 80−101984
quarks, fermion field, nonlinear, origin of four quark flavours, quantum numbers, isosymmetry breaking 80−62920

spontaneous symmetry breaking continued
quarks, flavour number determination using Higgs scalar particle 80−13288
quasiconfinement in colour gauge symmetry, unconfined quarks and gluons 80−86686
quaternion model, gauge theory for leptons and quarks *(Russian)* 78−62315
quaternionic scalar fields, Sp(1,Q)⊗U(1) group for unified gauge theory 77−61236
radiation gauge calc. of high-energy scatt. amplitudes 77−38111
radiative mass generation in perturbation theory and the renormalization group 80−86611
radiative mass generation model renormalisation, spontaneously broken symmetry, IR breakdown 79−71650
Regge behaviour of spontaneously broken non-Abelian gauge theory 78−70287
relativistic dense matter, statistical mechs. description, spontaneous symm. breaking appl. 78−89814
relativistic QFT, boson transformation, extended objects 78−37140
relativistic QFT, spontaneous symmetry violations 80−52411
relativistic quantum fields, particles and currents, book 78−82117
relativistic quark model for mesons, symm. breaking via quark mass differences 77−79253
relativity groups, symmetry breakdown and bundle representations 80−86610
renormalisation group approach to symm. breaking 79−40517
renormalisation group eqn., spontaneously broken symmetry and heavy scalar particle decoupling 80−47189
renormalisation of Spontaneously broken gauge theories 79−12945
renormalization in a symmetry-broken theory 79−93291
restoration of spontaneously broken symmetry in mag. field, massive charged vector meson effects *(Russian)* 78−74178
restored symmetries, quark system, Pomeron as Josephson current 77−61211
rotating fermion systems, quantum mech. treatment 79−17337
rotating fluid, spontaneous symmetry breaking and bifurcations from the Maclaurin and Jacobi ellipsoids 79−35616
S-wave π-π scattering lengths in the (8,8) symmetry-breaking scheme 79−17759
scalar conformal invariant QED, conformal group spontaneous breaking in Abelian Higgs model 78−49960
scalar field theory with massive scalar field, spontaneous symmetry breaking 77−61214
scalar fields in 1+1 dimensions with spontaneously broken U(1) symmetry 78−54554
scalar Higgs eqn., three-dimens. periodic solns. *(Russian)* 77−6052
Schwinger mechanism for chiral breaking dynamical fermion mass generation 77−41789
Schwinger model, A=0 gauge, breaking of chiral symm. 78−62307
Schwinger model, canonical surface formalism, axial anomaly, chiral symm. breaking 78−12816
Schwinger model, chiral symm. breaking and vac. struct. 78−89615
seven lepton model, quantum flavour dynamics, mixing angle, masses, spontaneous symmetry breaking 78−89652
singular gauge transformations, monopole vortex line systems, Nielsen Olsen SU(2) Higgs model, Nambu model 78−66034
six-quark model, spontaneous CP violation *(Russian)* 79−93379
six-quark model of quantum flavourdynamics, Cabibbo angle and quark masses 78−33017
SL(2n,C)⊗SL(2,C), invariant gravitational model, spontaneous symmetry breakdown 77−46009
SO_{10} hierarchical breaking 80−22550
SO(10) grand unified theories, one loop renormalisation effects, stepwise symmetry breaking 80−32058
SO(10) grand unified theory, breaking scheme and neutrino mass 80−47230
SO(10) unified model, phenomenological group, symmetry breaking chain low energy effects 80−86645
SO(3,2) de Sitter symmetry, spontanously broken, gravitational holonomy group 80−57149
SO(3,2) gauge theory, geom. of Einsten-Cartan theory 79−75425
SO(3) gauge group, monopoles, spontaneously broken gauge theory 77−2753
SO(3) gauge invariant theory, quantisation, spontaneous broken gauge theory, S-matrix gauge independ. 79−269
SO(4n+2) gauge theory, dynamical symmetry breaking 80−86580
solitons in Yukawa and Georgi-Glashow models with dynamical spontaneous symmetry breaking 79−6264
space-dispersion approach to the explanation of the Higgs-mechanism 80−90975
space-time geometry and symm. breaking 78−54533
spherical nuclei, self consistent theory of finite Fermi systems and low lying collective states 79−45130
spontaneously broken chiral SU(3)⊗SU(3) symmetry, quark mass ratios, Goldstone pseudoscalar meson pairs 79−80770
spontaneously broken chiral $U(1)_4$, weak-interaction singlet and strong CP invariance 79−80781
spontaneously broken gauge theories with heavy Higgs bosons 80−13209
stepwise breaking of gauge and discrete symm. 78−29269
string type solns., in classical gauge field theories, broken gauge symmetry 78−62317
strings, vortices, gauge fields 77−71493
strong coupling constants in broken SU(3) 80−27423
strong gravity, supersymmetric theory, f- and g-field mixing term by symmetry breaking 78−62141
strong interaction model with chiral symm., multiple particle prod. *(Russian)* 77−38120
strong interaction spontaneous symmetry breakdown and finite struct. const. calc. 77−22707
strong interaction symmetry, calc. of fine struct. const. α 77−41788
SU_3 symmetry breaking, dynamical 78−21346
SU_3 symmetry breaking schemes for radiative decays of ρ, K^{0*}, ϕ vector mesons 77−6114
SU_3 theorems, baryon octets, semileptonic decays 80−32030
$SU_4 \times U_1$ and the origin of the Cabibbo angle, charged gauge boson mixing 80−73639
$SU_L(2) \times SU_R(2) \times U(1) \times [SU(3) \times SU(3)]_c$ gauge model, chiral colour symmetry breaking 80−47234
SU_N, spontaneous breakdown, self interacting fermion multiplet model 79−9298
spontaneous symmetry breaking continued
SU_N gauge group uniqueness in grand unified model, U_1 color, proton stability 79−316
SU(2|1) electroweak interactions, implications for 6 extra time dimensions 80−77998
$SU(2)_L \times (T_3)_R \times U_V(1)$ gauge group, grand unification, symmetry breaking and Z bosons 80−73641
$SU(2)_L \times SU(2)_R \times U(1)$, CP invariance, global chiral U(1) symmetry, axion-quark coupling 79−22009
$SU(2)_L \times SU(2)_R \times U(1)$ based L-R symmetric gauge theory, spontaneous breakdown of parity 79−75681
$SU(2)_L \times SU(2)_R \times U(1)$ gauge symm., Higgs particles, parity conservation 78−70305
$SU(2)_L \times SU(2)_R \times U(1)$ model, weak and EM interactions, Higgs scalars, vac. instability 79−317
$SU(2)_L \times U(1)$, irreducible gauge theory of a consolidated Salam-Weinberg model 79−40707
$SU(2)_L \times U(1)$, strong CP-violating phase, one-loop corrections, Higgs particles 80−62910
$SU(2)_L \otimes U(1) \otimes U(1)$ gauge-theory model 77−30257
SU(2), unification of isospin and hypercharge, electroweak interactions of leptons 80−27439
SU(2)×SU(2), dynamical rearrangement of symmetry 78−49979
SU(2)×U(1), gauge theory of weak interactions 78−21328
SU(2)×U(1)×U(1) model, neutral current, quark mass reactors, spontaneous broken Lagrangian 79−97563
SU(2)×U(1) gauge model, symmetry breaking pattern with two Higgs doublets 79−12978
SU(2)×U(1) vectorlike model: new leptons, quarks, and the axion question 79−40711
SU(2) gauge field, static spherosymmetric sourceless soln., selfduality and induced charge current *(Chinese)* 79−80755
SU(2) gauge invariance, spontaneously broken, $\Delta I = 1/2$ rule, nonleptonic weak interactions model 77−41786
SU(2) gauge theory, nonexistence of spherically symmetric monopoles with multiple mag. charge 77−6010
SU(2) gauge theory, sypersymm. breaking by pseudoparticles, supergravity implications 78−24959
SU(2) Higgs-Kibble model with spontaneous symmetry breaking, covariant-formulation of Yang-Mills theories 79−54256
SU(2) spontaneously broken gauge theory, canonical quantisation *(Chinese)* 79−49406
$SU(3)_L \times SU(3)_R$ as gauge groups of weak and associated charges, symm. breaking 78−74175
SU(3), partial conservation of axial vector current in constituent quark basis 77−2773
SU(3)×SU(3) chiral renormalisable gauge model, nonleptonic decays 78−24938
SU(3)×SU(3) chiral symmetry breaking, BBS coupling constants, sum rules 79−35959
$SU(3) \times U(1)$ low-energy symmetry within the unifying $SU(4)_F \times SU(4)_C$ gauge group 79−67489
SU(3) Λ-Λ' mixing explanation of broken SU(3) hyperon anomalous magnetic moment sum rules 77−18288
SU(3) colour gauge theory, effective scale depend. quark masses in chiral limit 77−18222
SU(3) gauge model of strong and EM interactions, scatt. lengths, baryon mag. moments 78−74133
SU(3) symmetry breaking in baryon resonance decay 78−89712
SU(3) theory of Yang-Mills-Higgs fermion-monopole system, topologically stable soln. 77−13888
SU(4), symmetry breaking effects on strong coupling const., charmed and uncharmed B BP couplings calc. 80−105802
SU(4)×SU(4) breaking, association with Cabibbo angle 79−12974
SU(4)×SU(4) broken chiral symm. 78−74176
SU(4)×SU(4) broken chiral symmetry, charmed hadron masses and decay consts. 79−40686
SU(4)×SU(4) broken chiral symmetry, decay constants, smoothness, and spin-zero charm particles 79−58900
SU(4)×SU(4) chiral symmetry breaking, axial vector current divergences, kaon PCAC 79−45032
SU(4)×SU(4) symmetry breaking, Cabibbo angle, nonlinear hadronic Lagrangian, PCAC *(Russian)* 80−42360
SU(4)×SU(4) symmetry breaking, quantitative meas. 79−93311
$SU(4) \times U(1)$ gauge theory, Cabibbo mixing, new approach, CP nonconservation calc. 79−71657
$SU(4) \times U(1)$ unified gauge theory, CP nonconservation 79−71656
$SU(4) \times U(1)$ unified gauge theory, muon number conservation 79−71655
SU(4) breaking in semileptonic decays of charmed particles 79−63473
SU(4) breaking mass formulae for $^1/_2{}^+$, $^3/_2{}^+$ baryons and 1^-, 0^- mesons *(Russian)* 78−89692
SU(4) broken lattice gauge theory spectrum 79−49474
SU(4) irreducible tensors and norms, symmetry breaking and energy variation 80−105801
SU(4) mass splitting, group theory and quark model comparison 79−6290
SU(4) symm. breaking, e.m. props. of D mesons calc. 78−8668
SU(4) symmetry breaking in hadronic reactions, urbaryon rearrangement model 77−13932
SU(4) symmetry breaking pattern and baryon masses 78−89690
SU(5), broken, meson mass formulae 80−47267
SU(5), symmetry breaking patterns, Higgs fields 80−101953
SU(5), unification of weak, EM and strong interactions, review 80−105814
SU(5)×SU(5) chiral symm. breaking, Cabibbo angle, meson mass spectrum 77−74614
SU(5) asymptotic symmetry, b quark flavour from Weinberg spectral function sum rules 79−67495
SU(5) electroweak-strong interaction model, broken colour symmetry and gluon mass 80−73650
SU(5) unified gauge theory, non-Abelian electric and mag. flux 80−57545
SU(5) x SU(5) broken chiral symmetry, symmetry breaking parameters, limits 79−45026
$SU(6)_W$ structure of baryonic reson. photocouplings duality constraint 79−71649
$SU(6)_W$ symmetry, ang. constraints and collinearity breaking, free quark model 79−30679
SU(6) breaking, neutral current coupling to ν_μm and ν_e 78−54626

spontaneous symmetry breaking continued
SU(6) breaking of baryon wave functions, chromodynamic spin-spin force 79−340
SU(6) broken symmetry model, baryon mag. moment values 79−49417
SU(6) configuration mixing symmetry breaking, one gluon exchange potentials 79−40739
SU(6) grand unification model, hierarchy of symmetry breakings and neutral currents 80−52446
SU(6) grand unified theories, one loop renormalisation effects, stepwise symmetry breaking 80−32058
SU(6) symmetry breaking in MIT bay model, neutron charge radius anal. 78−70334
SU(8) supergravity supersymmetry breaking 80−46908
SU(N+1) gauge theory, exact monopole solns. with spherical symmetry 79−71626
SU(N)×SU(N) chiral symmetry, spontaneous breaking, instanton role 80−47219
SU(N)×SU(N) symmetry breaking with extremum constraints 80−68385
SU(N) gauge models, symm . of Higgs pot. 78−32980
SU(n) gauge theories, directions of spontaneous symmetry breaking 80−13228
SU(n) gauge theories, spontaneous symmetry breaking pattern 80−95228
SU(N) spontaneously broken to U(1), composite magnetic monopoles 77−2765
SU(N) Thirring model and 1/N expansion, chiral symmetry breaking 79−12977
SU(N) unification of extra strong interactions, no-go theorem 80−32056
SU(S) based grand unified theory, monopoles and vector bosons, symmetry breaking 80−99079
super-dense matter, phase transitions in gauge theories and cosmology, review 79−44654
superalgebra with spinor-vector generator, Goldstone spin 3/2 particle, Higgs effect 77−49876
superconductivity and elementary particles theory, review 80−4911
superconformal symmetry breakdown as guide to supergravity constraints 80−46930
superfluid Fermi systems, binary expansion in microscopic theory 79−51338
supergrand unification in E_8, quark-lepton assignments, symmetry breaking scheme 80−68408
supergraph anal., gauge supersymmetry, S-matrix 80−27422
supergravity, massive vector multiplets, lagrangian construction 80−31645
supergravity, symmetry breaking by instantons 79−21625
supergravity coupled to massive self-interacting scalar multplet, spontaneous symmetry breaking 77−74633
supergravity supergraphs, perturbation theory description from globally-supersymmetric gauge breaking 79−67203
supergravity with general scalar interactions, super Higgs effect, gravitinos, spontaneously broken supersymmetry 79−6037
supergravity without cosmological constant, spontaneous symmetry breaking and Higgs effect 79−17310
superspace affine theory, simple Lagrangian 80−105813
supersymmetric gauge models of weak and EM interactions 78−58106
supersymmetric gauge theories and their possible applications to the weak and electromagnetic interactions 79−49419
supersymmetric models of weak and electromagnetic interactions 79−26276
supersymmetric nonlinear σ model, S-matrix determ. 78−66052
supersymmetric nonlinear σ model, spontaneous breakdown of chiral symmetry 78−54549
supersymmetric spontaneously broken theories of weak, EM and strong interactions 77−79244
supersymmetric vector-like model of lepton interaction 78−412
supersymmetry, algebraic props., applic. to particle physics 77−87918
supersymmetry, expanded, spontaneous violation, Goldstone fields *(Russian)* 80−47218
supersymmetry, massless spinors anal. 77−22658
supersymmetry, OSp(1,4), superfield formulation in anti-de Sitter space 80−57508
supersymmetry, review of principles and historical development 77−18197
supersymmetry, spontaneous breaking, unified gauge models appl. 77−71452
supersymmetry, spontaneous breaking in non-Abelian gauge theories 77−49878
supersymmetry, spontaneous breaking through dimensional reduction 79−40441
supersymmetry, superfield notation for supermultiplets spontaneous breaking, Lagrangians and internal symmetry incorporation *(German)* 78−74167
supersymmetry and gauge theories of weak and electromagnetic interactions 79−26208
supersymmetry and Lagrangian field theory 77−6041
supersymmetry and supergravity 77−61212
supersymmetry breaking and Goldstone fermions 77−22659
supersymmetry breaking in anti de Sitter space 77−87915
supersymmetry in QFT, spontaneously broken 78−54582
supersymmetry spontaneous breakdown inducing IR anomaly 77−38095
supersymmetry theories, parity conservation 77−41785
superweak gauge theory of CP-invariance violation 79−75710
tensor and vector meson decay, relativistic confined quark model anal. 79−13116
tensor meson radiative decay in SU(6)×O(3) broken symmetry quark model 80−73710
tensor operator techniques in symmetry breaking perturbation 79−12975
topological charges for N=4 supersymmetric gauge theories and monopoles of spin 1 79−63364
tumbling gauge theories with chiral fermion fields, symmetry breaking 80−99042
twisted quantum fields in a curved space-time 78−73913
twisted scalar field, vacuum solns. 78−93804
two-body equal-time wave eqn., quark-antiquark system 78−32992
two-dimensional σ-model semiclassical anal. of bound states 77−6028
two-dimensional model, pseudoparticles and massless fermions 78−24974
$U_1(M)\otimes U_2(M)\otimes U_3(M)$ with coloured Higgs particles 77−79209
$U_L(1)\times U_R(1)\times R_R$ group, mass ratio and symmetries of electron and muon, model 79−58917
spontaneous symmetry breaking continued
$U(1)\times U(1)(loc)\times SU_2(loc)$ invariant Weinberg Lagrangian, hypercharge group 79−71680
U(1) chiral symmetry breaking from SU(1) gauge theory 80−86617
U(1) Goldstone boson, anal. of BRS invariance in nonAbelian gauge theories 79−80798
U(1) problem and zero-mass quarks 78−82124
U(N)-symmetric gauge theory in 1/N expansion, dynamical symmetry breaking 77−6006
U gauge in Abelian and non-Abelian gauge theory, Gribov ambiguities 78−45788
ultralocal static field theory with imaginary bare mass 78−8499
unification of EM, weak and strong interactions, SU(5) group and symmetry breakdown 80−73637
unification of fundamental forces in nature, elementary particle constituents $SU(3)_c$ gauge symmetry, review 80−27448
unified field theory, axion, avoidance without massless quarks 79−63403
unified gauge model with a nonlinear chiral hadron Lagrangian, $SU_3\times SU_3$ symmetry-breaking 80−42378
unified gauge theories and Higgs bosons 77−45948
unified scalar-free theory, order-R vacuum functional, with spontaneous scale breaking 80−78003
unified theories of strong+weak+EM interactions, Weinberg angle, dynamical symm. breaking *(Russian)* 78−413
unified theories of weak and electromagnetic interactions 78−81908
unified theories with spontaneously broken colour symmetry, QCD scalar parton effects 79−80783
unified theory of elementary-particle forces 80−105827
unified U_3 gauge theory of weak and EM interactions, six quark flavours and lepton types 77−18215
unified vectorlike gauge theory based on group SU(6) for quarks+leptons 78−4818
unitarity and hadron self-energy, mass shifts, and SU_6 symmetry breaking in meson spectrum 79−17687
unitarity and renormalized 't Hooft identities 80−13205
unitary gauge, ambiguities and breakdown configs. 78−93798
universal confining pot. and symmetry breaking in baryons. SU(8)⊗O(3) symmetry 79−13051
universal CP noninvariant superweak interaction and baryon asymmetry of the universe 78−66072
UV infinity suppression in gravity modified field theories 80−105787
V_3(W) gauge theory, parity violation in atomic physics 77−71476
vacuum spontaneous magnetisation in quantum Yang-Mills theory and magnetostatics 79−6268
vacuum spontaneously broken symmetry of Higgs field and Bose condensation 80−82912
vacuum symmetries of gauge supersymmetry, quantum effects 79−17634
vacuum tunneling in spontaneously broken gauge theory 79−40703
valance quark distribs. in π, K, D, Regge trajectories, SU(3), SU(4) breaking 79−30703
vector meson radiative decay evaluation in spectrum generating SU_4 scheme 79−54342
vector meson radiative decays, vector dominance model in broken SU(3) 80−73711
vector mesons, EM decay in broken SU(3) 80−82976
vector mesons, leptonic and radiative decays, Schwinger model with U(3) symm. breaking 79−379
vector mesons, radiative decay, single parameter scheme 80−86720
wave function choice, effect on predictions, DKP formalism view 80−9120
weak hypercharge embedding in strong gauge groups 79−30692
weak interaction, vector-like theories, CP violation, spontaneous breaking 78−62333
weak interaction orientation to strong interaction, quark mass spectrum, dynamical symm. breaking 77−74640
weak interaction symmetry struct. and $K\to\pi\pi$, $\pi\pi\pi$ *(Russian)* 79−22016
weak interaction theory review, dynamical symmetry breaking 78−78131
weak interactions, spontaneous symm. violation, strong quark interaction mechanism *(Russian)* 79−71659
weak interactions and symmetry breaking 80−27428
weak interactions of quark fields, quark masses, spontaneous parity violation 77−34115
weak quark and lepton chiral symmetries, dynamical breaking gauge interaction 80−47215
Weinberg model, spontaneous CP violation 77−26480
Weinberg-Salam model, fermion and Higgs boson mass constraints 79−49437
Weinberg-Salam model, vacuum instability, cosmology and particle mass constraints 80−78007
Weinberg-Salam model reformulation, for lepton scheme with 4-component ν-effects of Higgs scalar bosons *(Russian)* 79−80784
Weinberg-Salam model with two massless Higgs doublets, particle masses, perturbation constraint 80−57541
Weinberg-Salam theory, extension to left-right symmetry and quark-lepton unification 80−78002
Weinberg-Salam theory, spontaneous symmetry breaking dynamics 80−32060
Wess-Zumino model as linear σ-model of spontaneously broken conformal and OSp(1,4) supersymmetries *(Russian)* 79−93315
Wess-Zumino supersymm. model 78−74170
Wightman functions, decomposition in Euclidean framework 78−54566
Wightman theory, all spontaneously broken symmetries for noncovariant currents 80−31975
X-Y model, gauge theory analogue, 4-D self-dual gauge model, phases and transitions 80−27399
Yang Mills theories, high-energy gauge meson exchange reactions, factorisation, Reggeisation 77−18172
Yang-Mills field propagation, Lagrangian gauge fixing terms 79−40652
Yang-Mills gauge invariance on space of Bose and Fermi coordinates 77−45958
Yang-Mills theory, broken symmetry soln., Higgs fields and Einstein gravity action 80−101746
Yang-Mills theory, gauge symmetries 78−359
Yang-Mills theory, spontaneously broken, reggeon field theory appl. 78−8512
Z_N dynamically broken symmetry, electric quark confinement in 2+1 dimens. 79−85263
Zee's broken symmetric gravity theory 80−62558
zero eigenvalues for quantum fluctuations, instanton, spontaneous breakdown of conformal symm. 78−12821

spontaneous symmetry breaking continued
zero-fermion modes in models with spontaneous symmetry-breaking 80−18105
B-B, B-$\bar{B}$ scattering, models of line reversal symmetry breaking 78−62326
D^+-D^0 mass differences, chiral SU(4)×SU(4) model, broken isospin symm. 77−87917
$\Delta^+ \rightarrow P\gamma$, ground and radially excited states, broken symmetry treatment 80−9174
e-μ-τ spontaneous symmetry breaking and rare τ decays 79−9301
e^+e^- collisions, weak neutral current effects, unified theories of dimension *(Hungarian)* 79−9326
$e^+e^- \rightarrow \mu^+\mu^- X$, search for Higgs boson 80−27496
eN, deep inelastic scatt., quark model, field-theoretic, quark indistinguishability, nucleon structure function 80−62993
$\eta \rightarrow 3\pi^\circ$, chiral SU(4)×SU(4) breaking and tadpole term 80−22532
$\eta(\eta') \rightarrow \gamma\gamma$, quark model tests 80−78067
$\eta' \rightarrow \eta\pi\pi$, current algebra calcs. with symmetry breaking, inconsistency with expt. 79−13114
$\gamma\nu$ weak interaction, spontaneous breakdown of γ and gauge symm. at finite temp. 78−70299
$K \rightarrow \pi e(\mu)\nu$, form factors, SU(3) σ-model one loop calc., chiral symmetry breaking 80−52506
$K^\pm \rightarrow \pi^0 l^\pm \nu_l(\bar{\nu}_l)$, decay form factors in relativistic symmetry SO(4,2)⊗SU(3)⊗SU(3) 79−36068
$K_L \rightarrow \mu\mu$, heavy particle decoupling effects in broken symmetry theory 78−82140
$K^{*0} \rightarrow K^0\gamma$, SU(3) and isospin symmetry breaking effects 80−95272
KN σ-term, uncertainties in determ., K-matrix formalism 80−27522
$lp \rightarrow l'X$, weak reaction, large transverse momenta, field theories at finite temp., symm. breaking and restoration 79−399
$\mu \rightarrow e\gamma$ in Weinberg Salam model, spontaneously broken μ-like charge symm., heavy leptons *(Chinese)* 78−82191
NN charge symmetry breaking, nn and pp scatt. length difference, meson mixing 80−13325
NN elastic scatt. in spontaneously broken gauge field theory 79−36091
NN scattering in nonAbelian gauge theory, π-, ρ-, and ω-exchange, scalar Pade approx. 79−67573
NNπ amplitudes, parity violating, QCD calc. in Weinberg-Salam model and SU(4) flavour symmetry breaking 79−67520
ν, massless, left-right symmetric gauge models, $SU_{2L} \times SU_{2R} \times U_1$ 80−27461
$\nu N \rightarrow \mu$+charmed baryon, SU(4) breaking effects, quark parton model 79−40792
$p+N \rightarrow \mu^-\mu^+ X$, 400 GeV, charged gluon effects, broken colour gauge model study 79−49473
$pp \rightarrow \mu^+\mu^- X$, spontaneously broken colour gauge theory effects in Drell-Yan process 79−26344
ϕ^4 model, free energy, spontaneous symmetry breaking 80−101925
ϕ^4-field model with image mass, spontaneous coherent state transition 80−99057
π decay constant, EM form factor, quark EM self-energy in QCD 80−37242
π struct., gauge model, spontaneously broken chiral symmetry 78−45841
πK scattering amplitude, analytic continuation, chiral symmetry breaking 80−63027
πN σ term in hybrid chiral bag model, PCAC and SU(3)×SU(3) symmetry violation 80−78096
$\pi N\sigma$ commutator, discussion using dynamical theory of πN amplitude 79−22134
$\pi^- p \rightarrow \pi^- \pi^+ n$, 203-357 MeV, integrated cross section, chiral symmetry breaking parameter 80−32125
$\pi^- p \rightarrow \pi^- \pi^+ n$, below 1400 MeV, PS11 contrib. threshold K-matrix, chiral symmetry breaking 80−32126
$\pi\pi$, ρ-meson contrib. in broken chiral symmetry model, phase shifts and lengths *(Russian)* 80−86756
$\psi \rightarrow \eta(\eta')\gamma$, SU_3 violation, symmetry breaking and decay amplitudes 80−52499
$\psi \rightarrow$gravitino+antiphotino, gravitino mass lower limit, light gravitino weak interactions 79−75698
$\psi' \rightarrow \psi\pi^0(\eta)$, SU_2 violation, symmetry breaking and decay amplitudes 80−52499
Q, axial vector mesons, dynamical mixing model 78−24973
ρ chiral SU(3)×SU(3) representation, spontaneous symm. breaking, VDM, PCAC 77−57512
ρ-ω mixing charge symmetry breaking force, nonlocal contribs., ^{3}He-^{3}H mass difference 78−70458
$\Sigma^+ \rightarrow p\gamma$, $1/2^-$ resonance poles to parity-violating amplitude, two-quark weak transitions 80−78062

spooling *see winding (process)*

sporadic-E layer
Amsat-Oscar 7 subhorizon ratio signals beacon, above F2 layer, 30 MHz 77−70937
auroral activity in midnight sector, electrojet and precip. particle characts. 78−12039
auroral zone, short and long term movement 78−16235
behaviour in EM field during oblique irradiation by radio waves 78−73566
blanketing E_s-layer charact. at equatorial stations 77−29554
blanketing E_s-layers, rel. to equatorial electrojet type 1 radar echoes with double-peaked Doppler spectra 80−67458
blanketing E_s-layers in equatorial electrojet, VHF radar obs. of assoc. gradient instabilities 77−29577
blanketing layer type ionisation irregularities, growth and decay 80−101477
blanketing type E_s-layers, north-south movement 79−29923
Brazilian geomagnetic anomaly, E_s-layer phenomena rel. to regular particle ionisation source 77−78558
clouds, peculiar shape and radio focussing 79−8753
conjugation in subauroral and midlatitude zones 77−17279
daytime C-type E_s-layer behaviour over Lindau, wind shear theory 78−40735
daytime satellite radio scintillation rel. to sporadic-E layer near mag. equator 77−45225
disturbances, large scale periodic, Faraday fading of satellite 40 MHz signals 80−101475
drift and anisotropy parameters, meas. from Waltair 77−70920
E_3-activity over Japan, sky-wave backscatter obs. 79−44298
E_s-activity at southern mid-latitudes, rel. to scintillation regions horizontal struct. 79−12339
sporadic-E layer continued
E_s-layer, h-type, at Uppsala, features 78−81497
E_s-layer, Langmuir wave propag. and enhanced plasma line 79−29928
E_s-layer, lossless refls. rel. to global ionospheric absorpt. meas. on board ships 80−98500
E_s-layer, props. at Sodankyla, Finland 77−87183
E_s-layer, temperate zone, maps of $f_0E_s > 7$ MHz 78−73579
E_s-layer, temperate latit., skywave backscatter studies 78−85761
E_s-layer form. and winter anomaly absorpt. events due to metallic ion drifts 77−9599
E_s-layer formation, unified theory, neutral wind and elec. field effects 79−5710
E_s-layer formation and variations at midlatit., wind contrib. 77−29544
E_s-layer in equatorial ionosphere, assoc. with radio scintillations 80−77191
E_s-layer of auroral ionosphere, large-scale inhomogeneities 80−4171
E_s-layer parameters determ. from refl. coeffs. 79−53626
E_s-layer peak occurrences latit. var. during half solar cycle 77−29562
E_s-layer with group delay, occurrence probability depend. on mag. activity 77−29545
E_s-layers, form. by gravity waves generated in region of solar terminator 79−12337
electron density explained by wind shear acting on metallic ions 80−46338
electron temperature gradients in mid-latit. E_s-layers, obs. 78−28397
ELF wave propag. at nighttime, sporadic-E effects 80−77202
enhancements over Brazilian Geomagnetic Anomaly, assoc. magnetic storm 78−28431
equatorial, vars. rel. to interplanetary mag. field vars. 79−84572
equatorial E_{sq}, disappearance rel. to interplanetary mag. field vars. 78−77413
equatorial formation, electric fields and neutral winds effect 78−12045
equatorial sporadic-E, multifreq. HF radar studies of plasma instabilities in Africa 78−36370
Gauhati, India, radiowave absorpt. 77−41261
gravity waves at E-region heights, obs. of Es 80−72657
HF and VHF refl. from E_s-layer on 1050 km path, M factor determ. 77−17281
HF and VHF signals amplitude fluctuations due to ionospheric scatt. and E_s-layer refl. 78−45105
HF reflection and transmission coeffs. for horiz. polarised waves 78−32290
high latitude E_s-ionisation during quiet and disturbed conditions 80−61941
high-latitude types of E_s, occurrence, f_0E_s and $h'E_s$ 80−51595
Huancayo recordings during min. sunspot years 78−16230
inhomogeneous structure influence of RF heating *(Russian)* 78−61653
ionisation, photochemistry of Mg and Mg^+ 77−21954
ionization and H aurorae 79−62659
ionosphere quasiperiodic scintillations, rel. t E_s and spread-F activity 77−91361
'low' E-layer studies, preliminary results and latit. regularities *(Russian)* 79−8749
metallic ions of meteor origin effect in VHF ionospheric forward scattering, contribution to sporadic-E formation 80−67461
meteor activity metallic ions rel. to sporadic-E occurrence 80−46336
meteor ionisation creating E_s, effect of different meteor particle sizes 80−105108
meteors, relation to sporadic-E layer, statistical evidence for class 1 E_m 77−29572
meteors, relation to temperate zone sporadic E-layer 77−25837
mid-latitude, irregular structure from incoherent scatter radar obs. 78−96342
mid-latitude E_s-layer formation, effect of strong radio waves 77−60514
midlatitude, obs. using HF Doppler technique 79−66867
midlatitude E_s-layer, form. 77−13157
nighttime c-type E_s-layer, occurrence rel. to night-sky emission *(Russian)* 77−45223
nighttime E_s, seasonal and solar cycle variations at Ahmedabad, India 79−80071
nighttime occurrence rel. to geomag. storms 79−35032
nocturnal E_s-layer, effect on ELF radio waves propag. 78−36392
oblique sounding, behaviour in EM field of strong decametric waves 78−69569
polar region occurrence 77−17280
radio noise propagation through sporadic-E layer in equatorial region 79−84575
radiowave absorption meas., differences between sporadic-E and normal E-layer refls. 78−40734
radiowave critical freq. integral distrib. patterns 77−60524
radiowave propagation, directional dispersion between 9 and 14 MHz 78−28412
radiowave propagation above 30 MHz, role of sporadic-E layer and troposphere 80−41636
radiowave reflection, full-wave anal. 77−87176
radiowaves, oblique-incidence E_s-layer propag. and ionospheric attenuation 78−73578
reflection coefficient at high latitude 80−61922
reflection coeffs., explanation for cut-off freq. 80−82131
satellite radio signals amplitude scintillations rel. to spread-F and sporadic-E over Brisbane 78−49209
scintillations induced by cloud of sporadic-E layer 77−37477
scintillations obs., at Lunping Observatory, geomagnetic activity influence 79−88545
semidiurnal winds seasonal var. in dynamo region 78−93033
space sciences, conf., Waltair, India (Jan. 1978) 79−101000
sunset effect *(Italian)* 79−100997
temperature latitudes, small and large wind shears effects 77−29556
transparency charact. 78−40759
vertical motion and tidal wind system in upper atmosphere 79−100993
VHF multi-satellite scintillations correl. with spread-F and sporadic-E increase over Brisbane 77−53297
VHF signals from satellite radio beacons, ionospheric scintillations 79−53634
wavelike oscills. due to atm. gravity waves 79−101002
whistlers at low latitude, banded struct. origin on refl. from sporadic E-layers 80−101476
O I 5577 Å line depend. on E_s-layer 77−67006

sports and entertainment
see also personal computing
angular momentum conservation, rel. to springboard divers, gymnasts and trampolinists 79−84884
biomechanics velocity of sports activities meas., stroboscopic photography, teaching appl. 79−44679
club noise control by electronic power reduction 78−51004
hockey, collision theory, teaching approach 77−41435
karate, exertion of physical force using bare hand 79−88792
motor vehicle racing and shooting noise 78−55510
noise related to sports, effects on hearing 77−64057
shooting-range noise annoyance threshold variation 79−70498
snow ski boot load normalised covariance matrix computation 79−96608
tennis, probability and statistics teaching illustration 80−41997
tennis racket physics, teaching approach 79−71173
university sports areas, reverberation and noise levels 78−9497

spray coating techniques
see also electrostatic coating techniques; flame spraying; plasma arc spraying; powder spraying
ion plating by field emission deposition 80−35110
metal spraying methods and appls. 79−66202
plasma industrial utilisation, synthesis, powder, metallurgical and surface treatments, review *(French)* 80−96398
pulsed condensation of matrix mixture for spectroscopic investigations 79−36799
solar cell materials, ternary and quaternary, spray pyrolysis 79−70004
spray pyrolysis, aerodynamics of nozzles 79−68782
thin film prep. for solar energy utilisation 80−84847
$AgInS_2$, and $AgIn_5S_8$, spray pyrolysis, film struct., elec. and optical props. 80−71592
CdS, chem. sprayed film growth using centrifugal disc atomiser 78−92189
CdS film spray fabrication, physical props., Cu_2S-CdS solar cell applications *(French)* 80−60113
CdS sprayed film, prep., optical props., struct. and comp. 79−78875
$Cd_{1-x}Zn_xS$-PbS heterojunctions prepared by spray pyrolysis 79−60917
Cu_2S layer spray preparation and CuCl-thiourea complex formation 78−64471
Cu_2S-CdS sprayed solar cells, chemical spray deposition 80−93979
In_2O_3, transparent electrode deposition on PLZT ceramic 78−74848
In_2O_3:Sn/n-Si heterojunction solar cell, fabrication and charact. 78−15314
Li ferrite, fine particle, for arc plasma spraying mm-wave phase shifter 78−64469
PbSe(Te), low-temp. epitaxial film form., on KCl(Br), laser spraying *(Russian)* 77−73238
SnO_2 gas sensor, fast-detecting, prep. 80−61497
SnO_2, transparent electrode deposition on PLZT ceramic 78−74848
Zn phosphating processes and additives 79−79147
ZnO-CdTe heterojunctions and ZnO films preparation using spray pyrolysis 80−96985

spray coatings
see also electrostatic coatings; flame sprayed coatings; plasma arc sprayed coatings; powder sprayed coatings
detonation-sprayed coatings, bonding 79−29251
lens, water soluble cryst., protective coating to aid polishing 80−33250
metal oxides, on Si, reacts., IR investig. 79−39197
NDT methods and measurable properties 79−83431
oxide thermal-sprayed coating on steel, acoustic emission 80−21247
Polaroid print spray lacquer coating 78−54478
polymeric coatings, wear resist. props. 78−72914
powder metal sprayed coatings, bond strength, influence of surface preparation 78−11150
SEM specimen mounting epoxies, aerosols, and adhesive tapes 79−71580
spectrally selective surfaces for photothermal conversion of solar energy 80−101125
steel, electric arc sprayed coating on wire, elastic and elastic-plastic props. *(German)* 79−34089
temperature measurement of spherical or near-spherical particles in plasma stream 80−21138
thermally sprayed coating adhesive strength testing method 79−83432
thermally sprayed nonfused coating, adhesive bond strength NDT 79−83433
tiO_2 antireflection coatings by a low temperature spray process 78−90537
vacuum furnace fusion requirements for self-fluxing overlays 79−83367
wear resistance, hardfacing, review 78−72937
$AgInS_2$, and $AgIn_5S_8$, spray pyrolysis, film struct., elec. and optical props. 80−71592
Al-PbS selective surfaces for solar photothermal conversion, prep., emissivity, absorptivity 80−12030
CdS, chem. sprayed film, struct. and morphology 78−72020
CdS, chemically sprayed, carrier conc. and mobility, thermoelec. and photothermoelectric meas. 80−2503
CdS, chemically sprayed film, prod. by centrifugal disk atomizer, struct. 79−65343
CdS film spray fabrication, physical props., Cu_2S-CdS solar cell applications *(French)* 80−60113
CdS films, prep. by reactive pulverisation, chemical, crystallographic and electronic props. *(French)* 80−60112
CdS solar photovoltaic panels, deposited by spray pyrolysis, film and junction structure studies 80−45689
CdS spray pyrolysis film prep. and characterisation 78−64492
CdS, spray pyrolysis prep., elec. transport props. 78−2590
CdS sprayed film, prep., optical props., struct. and comp. 79−78875
CdS sprayed films, elect. and optical props. 78−39241
CdS sprayed thin films for CdS-Cu_2S heterojunction solar cells 79−61988
CdS_xSe_{1-x} solid soln. film by spray pyrolysis 77−81214
CdSe, chemically sprayed thin films as photoanode in photoelectrochem. cells, power charact. meas. 80−85293
Cd_2SnO_4, $CdSnO_3$ electrodes, elec. sheet resist. and optical transparency 78−27401
$Cd_xZn_{1-x}S$ films, chem. sprayed, carrier density and mobility 80−60121
Cr_xC_y-(Ni-Cr), for gas cooled reactor heat exchangers, factors affecting performance 80−40609
Cu-PbI_2, thin sprayed layer, glass substrate, hologram recording *(Russian)* 77−71956
$Cu(Ga_xIn_{1-x})(S_ySe_{1-y})_2$, spray pyrolysis 79−70004
$CuGaSe_2$, film, spray pyrolysis prod. 79−95953

spray coatings continued
$CuInS_2$ films prepared by spray pyrolysis, elec., optical and struct. props. 79−73609
$CuInS_2(Se_2)$, film, spray pyrolysis prod. 79−95953
$CuIn(S_xSe_{1-x})_2$, spray pyrolysis 79−70004
$CuInSe_2$, spray pyrolysis 79−70004
$CuInSe_2$ thin films, prep. by spray pyrolysis, struct., elect. and optical props. for solar cell appls. 80−100781
CuO, positron annihilation meas. 77−40300
Cu_2O, positron annihilation meas. 77−40300
Cu_xS-CdS solar cells, cu_xS growth kinetics and composition analysis by absorbance transient and galvanic electrochemical measurements 80−92797
Cu_xS-CdS thin film solar cell using chem. sprayed CdS film 78−43465
Fe, cast, grey, electric arc sprayed coating on wire, elastic and elastic-plastic props. *(German)* 79−34089
Fe_5Ge_3 film, electron diffr. study of struct. and microheterogeneity 77−85108
GaAs-$In_{2-x}Sn_xO_{3-y}$ SIS heterostructure solar cells, spray-deposited 80−101106
In_2O_3 layers, chemically sprayed, prep. and intrinsic absorpt. in band edge 77−81169
In_2O_3, transparent electrode deposition on PLZT ceramic, elec. and opt. props. 78−74848
In_2O_3:Sn films, doping profiles and elec. props., appl. to optoelectronic devices 79−38203
In_2O_3:Sn solar collector selective coating resistivity obs. 79−62034
In_2O_3:Sn transparent cond. films, hydrolysis deposition, elec. and optical props. 79−43144
Mo, electric arc sprayed coating on wire, elastic and elastic-plastic props. *(German)* 79−34089
Si, on glass ceramic, thermosprayed, bonding 78−11367
Si, thermosprayed, bonding to glass ceramic 78−23848
Si-$In_{2-x}Sn_xO_{3-y}$ SIS heterostructure solar cells, spray-deposited 80−101106
SnO_2 chemically sprayed antireflecting films on Si solar cells 79−72639
SnO_2, transparent electrode deposition on PLZT ceramic, elec. and opt. props. 78−74848
SnO_2:Sb, transparent cond. films, hydrolysis deposition, elec. and optical props. 79−43144
SnO_2:Sb sprayed film, growth mechanism and cryst. struct. 80−89143
SnO_2/n-Si spray-deposited solar cells 80−12007
SnO_2-polySi solar cells, fabrication, grain size effects on device parameters 80−94045
SnO_x films, passivation effect on Si solar cells 80−61360
TiO_2 AR coating for Si solar cells by spray deposition, review 80−104511
TiO_2, spray-on antireflection coatings for Si solar cells 80−80963
V_2O_5 electrochromism obs. and mechanism, thin film growth *(Russian)* 77−77249
$Zn_{0.1}Cd_{0.9}S$-CdTe p-n junction, prep. by spray pyrolysis, photovoltaic props. 78−60196
$Zn_xCd_{1-x}S$ films, spray pyrolysis, elec. props. 80−75657
$Zn_xCd_{1-x}S$, prep by soln. spray method, and struct., optical and elec. props. 78−52666
$Zn_xCd_{1-x}S$ solid soln. film by spray pyrolysis 77−81214
$Zn_xCd_{1-x}S/Cu_2S$ heterojunction solar cells, fabrication and performance 79−79397
$Zn_xCd_{1-x}S/Cu_2S$ heterojunction solar cells, junction anal. 79−92080
ZnO, film for solar cell appl. structural, optical and elec. props. 80−2294
ZnO films, texture and grain size rel. to chem. spray deposition parameter 77−31921

sprays
see also aerosols; drops; jets
aerosols, size distrib., effect of dispersed concentration 77−60128
atomisation as nonequilibrium process, doplet disintegration distrib. function 78−38387
automatic sprayer with programmable dose for serial expts. *(Hungarian)* 80−104822
binary solution spray evaporation in gas flow 77−39331
cold liquid spray interaction with hot gas stream in channels 77−15108
collection device for capturing a spray sample 78−57920
condensation-evaporation of multidroplet system, by kinetic theory 80−7873
corona discharge effect on spraying mode of liquid *(Japanese)* 79−5186
cryosprayer improvements for surgery 77−78033
cylinder, spray-cooled, heat transfer 79−23354
disinfection sprays for hospitals 78−7548
drop size distrib. in spray from nozzle 79−32633
drop size in dense fuel sprays, in-line holography meas. 78−37827
drop size measurement, spherical mirror method 79−64806
drop trajectories, aerodynamic drag effects, computing methods 77−72347
droplet size distribution, reduced function, determ. from local meas. 77−68717
electrostatic metallic spray theory 77−25317
electrostatic spraying of liquids, role of Joule heating 77−32837
evaporation of atomised liquid *(Russian)* 78−38828
heat and mass transport in spray drying of highly viscous conc. solns. *(Russian)* 78−83230
hollow cone sprays, induced air flows 80−53846
hot-film anemometer for cylinder wake pattern with spray cooling 78−34238
liquid, electric spraying, drops charge to mass ratio *(Japanese)* 78−17835
liquid, electrostatic spraying 78−67274
liquid sprays, aerodynamic behaviour 77−35212
measurement of dropler velocity, using laser Doppler velocimeter *(German)* 79−50818
melt atomising unit, gasdynamic parameters 77−63576
mixing, effect of sharp-edged orifice type and cavitation 77−51107
nozzle, transfer processes in droplet plume during counterdirectional atomisation in gas flow 77−24014
nuclear power station spray cooling, heat and mass atmospheric transfer 78−94078
ocean spray, effect on energy transfers across air-water interface at high wind speeds 78−85574
oil film transient heat exchange in transverse electric field *(Russian)* 79−94607

sprays continued
photomicrographic anal., droplet size and vel. spectra determ. by Dumant's rotating mirror microscope 77−36800
plasmatron spray, parameters meas. (*French*) 77−35402
spray-freezing unit for prep. of specimens for freeze-etching 77−41581
tall-form spray chamber, residence-time distribution of air 78−96709
unsteady, numerical computation, appl. to engines 79−37378
US atomizer, construction, fatigue strength, elec. characts. 78−81959
water-air, dispersion characts., orifice shape depend. 78−34052

spurions *see elementary particles*

sputter etching
AES, surface topography development during depth profiling, sputter-etching effects 79−46900
aromatic polyamide fibre, surface struct. 80−21147
blazed ion-etched holographic grating, prod. methods, optical props. (*Japanese*) 80−10021
broad beam ion source used for sputtering and etching of Ar, Kr, O_2 and N_2 gases 80−69002
butane RF plasma initial etching prior to deposition of C 79−66224
carbonaceous materials, directional O ion beam etching, compared with reactive ion etching 80−71781
cascade mixing in depth profiling by sputtering 79−78811
cementitious materials, ion beam etching 80−30117
cold-cathode ion gun, discharge characts. and improvements 80−105748
combined ion beam deposition and etching for thin film studies 80−71594
conical ion beams use in thin film technology (*Russian*) 80−76383
corrosion science, surface analytic techniques 80−31929
diamond, cryst. surface layers treatment and study by HF ion-plasma etching (*Russian*) 80−16517
diffraction grating form. on optical waveguide surface, ion-beam etching through photoresist mask 80−14492
discharges for sputter deposition and sputter etching, RFI/EMI 78−77566
discharges in magnetron-type cold cathode ion gun for sputter etching apparatus 79−34170
fluoropolymers, ion beam sputtering 79−83353
fluoropolymers, ion-beam textured, adhesive bonding 79−87752
fused silicon substrate, directional reactive ion etching at oblique angles 80−66428
graphite, highly oriented, pyrolytic surface, polarised reflectivity spectra at near normal incidence, surface prop. effects 79−15481
grating formation, asymm. line profile, on glass waveguide surface, ion etching method 79−10418
grating profile evolution under ion beam erosion 79−94874
holey film preparation by ion-etching method, electron microscopy appls. 80−105751
holographic grating production by ion etching (*Japanese*) 78−46542
inclination and rotation effects during ion-beam etching on ion-etched structs. 79−15831
inert gas ion milling processes, etch-rate ratio of oxides to monoxides, increase using halocarbon gases 80−93663
ion beam, plasma and reactive ion etching, review 80−108621
ion beam etching, for SAW refl. struct. fabrication, role of redeposition 77−56123
ion beam milling, anomalous sputter yield behaviour 80−108624
ion etched surface microstructures 79−83362
ion etching, in-situ, scanning electron microscopy appl. in dentistry 79−30629
ion etching device for SEM samples 80−82847
ion etching facility, in SEM, description and appl. 77−54020
ion etching for selective erosion of thin film surface layers, cathodic sputtering, overview (*Hungarian*) 80−66682
ion-etch profiles, interface position determ., nomographic method 77−89655
Kapton, optical, elec. props., struct., ion textured surface 78−72904
laser mirror manufacture, ion beam/plasma chemical etching mixed batch process (*French, English*) 77−83880
loading effect in plasma etching 77−90475
magnetic bubble device fabrication, appl. of sputter etching in Ar-O plasma 79−83347
masked RF sputtering, deposition and etching profiles 77−69990
metal foils, naturally passivated, ESCA, sputter etching 77−70218
metallographic ion etching, adaption of simple sputtering apparatus 78−56849
metallography, appl. (*Japanese*) 80−93715
metals, dispersion coefficient determ. (*German*) 80−40587
metals, ion-beam textured, adhesive bonding 79−87752
ohmic contacts, sputter-etch plus evaporated film technique for contacts to Si devices 78−22165
optical filters, diffractive, prepared by reactive sputter etching, microfabrication and evaluation 79−90008
optical spectroscopy for diagnostics and process control during glow discharge etching and sputter deposition 79−15606
phosphorus silicate glass, etching characts. by plasma reactive sputter etching 78−27661
photoresists, ion-bombardment-induced improved mask props. for RF sputter-etching 77−77601
plasma chemical etching, model for gas discharge plasma containing halogen (*Russian*) 78−15552
plasma etching, flow rate effects 78−72906
plasma etching, mass spectroscopic exam. 78−72909
plasma etching, MOS processing appl. 80−40577
plasma etching for IC processing, chemically selective anisotropic 78−64755
plasma etching mechanisms, using reactive plasmas 80−71778
plasma etching mechanisms 78−72905
plasma process development and monitoring via mass spectrometry 78−35546
plasma stream transport method 78−52684
polyamide fibre, surface struct. 80−21147
polyester fibre, surface struct. 80−21147
polyethylene films, internal lamellar struct. obs. by ion etching and SEM 79−73076
polypropylene film and fibre, plasma etching 78−95871
quartz, ion-etching of grooves for SAW devices 78−95822
quartz high-transmittance antirefl. film, vacuum-etched 80−74449
Re-sputtering and implanting sputtered atoms during deposition 80−[illegible]37
reactive ion etching of III-V compounds 80−58813

sputter etching continued
reactive ion etching RF discharge plasma deterioration filter 78−41370
reactive plasma etching, mag. field control 80−11796
reactive sputter etching, plasma gas temp. determ. 78−65586
red blood cells, by ion beam sputtering, for SEM 80−85554
refractory carbides, adhesion to metal substrates, improved 80−76481
RF plasma etching, ion energy (*French*) 79−46495
RF plasma etching, ion energy 79−73049
RF plasma etching for IC processing, mechanistic considerations for selective etching 78−64754
RF plasma utilisation in sputtering and surface reactions 78−84714
RF plasmas for semiconductor device processing, spectroscopic anal. 78−63589
sapphire, cryst. surface layers treatment and study by HF ion-plasma etching (*Russian*) 80−16517
secondary ion monitoring during ion etching 79−91551
SEM dynamic study 80−50734
semiconductor device fabrication 78−63602
semiconductor materials, RF plasma etching, optical emission obs. 77−51226
Si, complexing mechanism, effect of ion etch rate 79−70587
silane layers, reactive ion etching and Auger electron spectra 79−24594
silicate glass film, etching characts. in CF_4 plasma 77−90474
silicate glasses, carbon tetrafluoride plasma etching characteristics 77−77602
square wave grating with $\lambda/2n$ dimensions, reactive sputter etching 78−35592
steel, stainless, Cr-Ni-Mo, surface, scraping, mech. (electrolytic) polishing, ion etching, effects on ESCA 78−52037
steel, stainless, ground surface ion bombardment, in DC glow discharge 78−95098
steel, stainless, type 304, sputtering yield of first oxide layers by substrate Auger meas. 79−95889
surface, three-dimens., under ion bombardment 80−104029
surface comp. profiles by Auger spectroscopy and ion etching 77−90225
surface treatment by gas plasma (*Japanese*) 78−92586
Teflon, optical, elec. props., struct., ion textured surface 78−72904
TEM specimen preparation, plasma etching use for foil thinning (*Slovak*) 80−45405
TEM thin specimen preparation by sputter-etching 78−24893
tetrafluoromethane plasma, etching of Si, SiO_2, O_2 addition effects 78−75369
for vapour deposition, improvement of adhesion, line definition, contact resistance and semiconductor properties by sputter-etching 79−43145
Al and its alloys, reactive etching in RF plasma containing halogen species 78−72923
Al films, plasma etching, MOS processing appl. 80−40577
Al, plasma etching in CCl_4, end point determ. by spectroscopy 78−76786
Al sputtered film, effects of sputter etching and process technology on props. 79−83122
Al-Cu alloy layer, photolithographically patterned, separation from substrate using plasma etching (*Slovak*) 80−45405
Al_2O_3, CVD film on III-V semicond. substrate, ion beam etching, defect detection 80−89155
Al_2O_3-based ceramics, high rate reactive ion etching 80−85070
Ar plasma bridge neutraliser operation with 10 cm beam diameter ion etching source 78−74102
Au film, vac. deposited on Cu, sputtering yield by substrate Auger meas. 79−95889
Au-TiC, multilayer struct., microhardness and elec. resist. 80−29501
$BaTiO_3$, surface microrelief revealed by ion irradiation 80−54485
$BaTiO_3$, surface microrelief after ion irrad. 80−59774
C, colloidal layers, sputtering, chem. etching in DC glow discharge 78−27666
C, diamond-like, produced by RF glow discharge of hydrocarbon gases, props. and coating rates 80−21146
Cr, cryst. surface layers treatment and study by HF ion-plasma etching (*Russian*) 80−16517
Cr films, photoresist film on reverse gas plasma etching 80−97624
Cu-Al thin film multistructure, Xe^+ ion beam cratering 80−66706
Fe ore raw material, sintered, ionic etching as new method of struct. investigation 77−52585
Fe-Cr alloy, sputter etching oxide film, comp. profile, quantitative AES 80−81585
Fe-Ni, film, depth profiles, sputter etching obs. 79−83079
Fe-Ni alloy, anodic oxide film formed in H_3BO_3-$Na_2B_4O_7$ soln., exam. of in depth profile by AES and sputter etching 79−2024
Fe-Pd film, depth profiles, sputter etching obs. 79−83079
GaAlAs DH lasers, self-sustained pulsation suppression, effect of SiO_2 facet coating films 80−95894
$Ga_{1-x}Al_xAs$-GaAs, abrupt quantum-well heterostruct. grown by metalorganic chemical vapour deposition 79−56933
$Ga_{0.5}Al_{0.5}Sb$, surface cleaning by sputter-etch technique 77−45550
GaAs, heavy metal migration, ESCA and ion etching study (*French*) 78−75885
GaAs, interference grating blazed by ion-beam erosion 80−1302
GaAs, ion etching, effects on optical props. and lattice disorder 78−83122
n-GaAs MIS structs., native oxide, effect on interface props. and removal by sputter etching 79−11228
Gd-Co alloy film, sputter yield ratio, combined ion deposition and etching 80−71594
Ge, cryst. surface layers treatment and study by HF ion-plasma etching (*Russian*) 80−16517
In, sputtering in Ar-N_2 discharge, mechanism, optical spectra study 80−89107
InP surface preparation for Schottky barrier and ohmic contact formation 80−39677
$LiNbO_3$, ion-bombardment erosion of single cryst., prep. for TEM exam. 79−38996
Nb selective plasma etching 78−39940
P_2O_5-SiO_2 glass, selective etching rel. to Si by plasma reactive sputter etching 80−81221
Pt-Si contact, silicide layer struct. and elec. props. sputter etching and annealing ambient effects 77−62991
PtSi film formation by ion sputtering and annealing, form. and exam. problems 80−100782
Si, amorphous, ion bombard., etch pit and ripple struct. formation mechanisms 80−66366
Si, Ar ion etching, carbide form. 80−81222

sputter etching continued
Si, CF_3^+ ion-surface interactions in plasma etching 77−90473
Si chip backside removal, technique and fixture 80−76384
Si, cryst. surface layers treatment and study by HF ion-plasma etching *(Russian)* 80−16517
Si, dry etching induced surface contamination, SIMS, AES, and XPS obs. 80−11810
Si, etch rate uniformity in CF_4+4% O_2 plasma 80−40568
Si, etching by CF_4 plasma, mechanisms 78−72907
Si, etching charact. using reactive ion etching with tetrafluoromethane-Cl_2 gas mixture 80−104313
Si etching in fluorocarbon glow discharge, chemical aspects 79−86631
Si film, polycryst., thinning using plasma etching *(Slovak)* 80−45405
Si, fine pattern etching by RF sputtering *(Japanese)* 77−70196
Si, fluorocarbon ion beam etching charact. 80−35363
Si, high rate reactive ion etching 80−85070
Si, plasma etching, effect of O_2 additions to CF_4 plasmas 78−72908
Si, plasma etching using CF_4 78−39921
Si, plasma etching using microwave discharge 78−11361
Si, polycryst., anisotropic plasma etching 80−85069
Si polycryst., end point detection in plasma etching by optical emission spectroscopy 80−50733
Si RF sputter-etched surface, cryst. damage, spectroscopic ellipsometry obs. 80−103538
Si, reactive plasma etching with CF_4, mag. field control 80−11796
Si, selective etching rel. to SiO_2 by $CBrF_3$ plasma without undercutting 80−76380
Si single crystal, Ar^+ ion sputter-machined surface, lattice disordering obs. *(Japanese)* 80−3228
Si, substrate, sputtering and sputter etching and thermal history 80−25562
Si, surface, sputter etched, damage, contamination, ion backscatt. obs. 79−33167
Si textured wafer, selective absorber for solar thermal conversion 80−30544
Si wafer, ion etching, secondary ion monitoring 79−91551
Si wafers, microwave plasma etching, role of ions and neutral active species 80−3217
Si:P, polycryst. etching charact. in CF_4 plasma 78−76777
SiC, cryst. surface layers treatment and study by HF ion-plasma etching *(Russian)* 80−16517
Si_3N_4, end point detection in plasma etching by optical emission spectroscopy 80−50733
Si_3N_4, etching charact. by plasma reactive sputter etching 78−27661
Si_3N_4 films, plasma etching, MOS processing appl. 80−40577
Si_3N_4, selective etching rel. to Si by plasma reactive sputter etching 80−81221
SiO_2, dry etching induced surface contamination, SIMS, AES, and XPS obs. 80−11810
SiO_2, etching charact. by plasma reactive sputter etching 78−27661
SiO_2, etching charact. using reactive ion etching with tetrafluoromethane-Cl_2 gas mixture 80−104313
SiO_2 etching in fluorocarbon glow discharge, chemical aspects 79−86631
SiO_2 films, plasma etching, MOS processing appl. 80−40577
SiO_2, fluorocarbon ion beam etching charact. 80−35363
SiO_2, plasma etching, effect of O_2 additions to CF_4 plasmas 78−72908
SiO_2, reactive ion etching damage, electron trapping charact. in MOS struct. 79−90704
SiO_2, selective etching, using reactive ion etching with CF_4-H_2 80−3224
SiO_2, selective etching rel. to Si by plasma reactive sputter etching 80−81221
SiO_2 blazed holographic gratings, fabrication by reactive ion etching 80−53484
$SrTiO_3$, surface microrelief revealed by ion irradiation 80−54485
$SrTiO_3$, surface microrelief after ion irrad. 80−59774
Ti, plasma etching, for appl. to patterning of Ti-Pd-Au metallisation 78−27677
Ti, sputtered film, energetic neutrals rel. to impurities 79−69980
TiO_2, etching charact. by plasma reactive sputter etching 78−27661
V_2O_5, etching charact. by plasma reactive sputter etching 78−27661

sputtered coatings
see also reactively sputtered coatings
ABS polymers, deposited in internal magnet magnetron sputtering system, adhesion of Cu films 79−83121
actinide target preparation by focused ion beam sputtering 80−23219
alumina film, RF sputtered, stability 78−22993
aluminide coatings on superalloys, improvement by sputtering *(French)* 79−29278
amorphous film heterostructure solar cell and laser fabrication 78−64472
aspheric element generation by sputtering techniques 78−59168
beam splitter phase coatings, for producing phase quadrature interferometer outputs 78−77974
boride RF sputtered wear-resistant coatings, XPS study of adherence 79−34191
carbide RF sputtered wear-resistant coatings, XPS study of adherence 79−34191
coated Mo tips characterised by atom probe FIM, atomic clusters, voids 80−33863
columnar boundaries, diffusion and interfacial structure 79−28253
combined ion beam deposition and etching for thin film studies 80−71594
compound films, prep. by magnetron sputtering, and special features 80−11565
cooling by thin film coating on polymer substrate 78−197
diamond-Si heterostructure, Auger spectra electron microscopy study 80−34340
dielectric inhomogeneous coating, produced by high temp. sputtering, spectrophotometric props. *(Russian)* 78−39613
dynamic recoil implantation, two-gun ion beam system 79−14833
electrical and optical props. 79−47181
ferrites, plasma sputtering, struct. props. and phys.-chem. transform. *(Russian)* 79−38739
ferroelectric, textured layered prep. by HF sputtering 77−85947
ferromagnetic alloys, amorphous, sputter-deposited, soft mag. props., magnetostriction 80−34696
film deposition by ion beam methods 78−72728
film on Si substrate, eutectic point displacement on annealing *(Russian)* 80−100850
film sandwich structures Auger anal. 78−72030
glass film, RF sputtered, roughness parameters 77−69202
hard coating deposition 80−40544
high rate film growth, book contrib. 78−11117
high resolution shadowing by sputter deposition for electron microscopy 77−55219
ion nitriding by a DC glow discharge method, surface anal. 78−80672
ion sputtering deposition of coatings for ultrahigh resolution SEM 80−76184
isotopic target preparation by ion beam sputtering 80−23220
Luneburg thin film lenses, formation by sputtering through circular mask 78−87132
magnetic anisotropy rel. to columnar microstruct., calc. 80−39822
manganin thin film microtransducers for elastohydrodynamic lubrication studies 80−37048
metal, pulse biased sputter deposited, Kr entrapment 79−28255
metal coatings, obtained by vacuum evaporation and sputtering, mech. props. rel. to prep. conditions 77−59239
metal film, compressive stress transition 78−10310
metal film, deposition by ion beam sputtering, composition and stress state 77−89674
metal film mirror prep. by ultraclean DC sputtering, optical props. 77−50748
metal mirrors, diamond turned, evaporated and sputtered, surface and optical studies 78−79098
metal-containing plasma polymerised fluorocarbon films, deposition, struct., and polymerisation mechanism 79−78928
metal-dielectric bilayer system, optical, mechanical and corrosion props. 77−32707
metal-dielectric codeposited film, optical, elec., mechanical and corrosion props. 77−32708
metal-metal bilayer system, optical, mechanical and corrosion props. 77−32707
metallic film, sputtered, internal stresses, effect of substrate orientation and rotation 79−77968
metallic film characterisation technique, APFIM, time-of-flight spectroscopy 80−75138
metallic films, deposited by cylindrical magnetron sputtering, internal stresses 80−24773
metallic glass, continuous-biased sputter-deposited Kr entrapment 80−24603
metallurgical characterisation 79−15056
MIM, sandwich sputtered film, interfacial effects characterisation 79−82685
multiphase alloy deposits, microstruct. effects 79−28254
mutual influence of particles *(Russian)* 77−69987
optical, production and props. *(Hungarian)* 80−53483
optical coatings of TiO_2, ZrO_2 and SiO_2, deposition by high freq. cathodic method 79−76900
optical film, production by RF cosputtering of dielectrics, and optical props. 78−6849
optical props. *(Russian)* 77−69924
optical props. and appls. 78−72623
oxidation of metallic coatings, during uncooled cathode sputtering in inert atm., X-ray diffr. obs. 78−3041
Penning gas-discharge chamber for uniform thickness film manufacture 77−44153
Permalloy film preparation by RF sputtering 78−3044
Permalloy films, RF sputtered on Au, coercivity 80−80575
Permalloy sputtered film, bevelling by chemical etching, for this film mag. header 78−92375
Permalloy-type sputtered film, structuring rel. to laser sputtering method *(Russian)* 77−59689
planar magnetron sputtering 78−72725
plasma wall sputtered metal density meas. by atomic fluorescence spectroscopy 78−67422
porous metal thermionic cathode with sputtered metal films, emission operating charact. 80−100740
present state and future prospects *(Russian)* 78−23614
pressure transducers, thin film strain gauges 77−49719
PTFE, sliding charact., friction and wear *(Japanese)* 78−56778
rare earth aluminate, scandate and zironate film coatings, electrophys. props. w.r.t. prep. technology 80−60781
rare earth Fe garnet, difference in comp. between targets and sputtered films, expt. 78−6848
rare earth iron alloy, amorphous, cosputtered, struct. and mag. props. 78−60323
rare earth-transition metal, amorphous, microstruct. and magnetism 78−64230
rare earth-transition metal film, amorphous, microstruct., TEM obs. 78−72018
refractory carbides, adhesion to metal substrates, improved 80−76481
refractory compounds, RF sputtered, comp. by XPS 78−51839
refractory films, stability, high temp. and electron irrad. effects 77−39747
SEM, metallic deposition in specimens presenting cavities using sputter coater 78−77171
SEM specimen preparation thin film coating techniques 80−68308
semiconductors, EPMA of inert gas content 80−3443
a-Si:H, structure, effect of H-Ar plasma contact on elec. props., and optical gap 80−34533
Si:H amorphous layers, ion bombard., AES study, $L_{2,3}L_{2,3}V$ Coster-Kronig transition 79−99992
silicide RF sputtered wear-resistant coatings, XPS study of adherence 79−34191
steel, stainless, alloyed with C, magnetron-sputtered, microstruct., and cryst.-amorphous transition 80−19719
steel, stainless, amorphous film, sputtered, prep. and characterisation 78−43266
steel, stainless types 321-SS and 430-SS, alumina coated, H_2 permeation 80−34244
superconducting film, superconducting props. 79−38215
superlattice thin films, sputtered, ion-bombardment-enhanced diffusion during growth 78−87882
techniques, comparison between electron beam evaporation and high rate with plasmatron 78−11110
TEM specimen preparation, fine grained coatings, sputter source design 80−99015
ternary metal oxides, DC electrolum. 77−77300
thermoregulating plasma coatings, UV irrad. influence on optical parameters *(Russian)* 80−40259

sputtered coatings continued
thickness distribution determ. by electron backscatt., layer on metal collector 78−18927
thin film deposition process, line-edge profile simulation appl. 80−104068
thin-film pressure transducers 77−30139
transition metal-Ge, RF cosputtered system, supercond. props. 77−51835
tribological uses, coatings for wear and lubrication 79−19494
vacuum coating units, conversion, for SEM sample prep. 77−34058
Ag, electron beam plasma sputtered coatings on KCl substrate, islet struct. *(Russian)* 80−39460
Ag films, hillock form. hole growth and agglomeration 80−44455
Ag, hillock growth and agglomeration by annealing, SEM obs. 80−2309
Ag, sliding charact., friction and wear *(Japanese)* 78−56778
Ag thin films, deposited by cathodic sputtering using high-resolution electron microscopy, voids obs. 80−49557
Ag-SiO_2 film, elect. and struct. props., ion beam sputtering 78−80071
Al coating development, porosity, durability temp. depend., electric arc metallisation regime *(Russian)* 80−39402
Al, deposition by cathode sputtering in enriched plasma *(Czech)* 77−63557
Al, electron beam plasma sputtered coating, islet struct. *(Russian)* 80−39460
Al film, getter sputtered at low temp. 78−35305
Al film, sputtered, physical props. 79−77938
Al film, wave front reversal, holography applications *(Russian)* 80−58483
Al metallization of semiconductor devices by high rate magnetron/plasmatron sputtering 79−28919
Al on Al_2O_3 and on ZrO_2 particles, influence of ionic treatment on formation of Al coatings *(Russian)* 80−50552
Al, RF sputtered, TCR, calc. and expt. 77−76960
Al, sputtered and electron gun evaporated films, grain size and orientation obs. 78−10308
Al sputtered film, effects of sputter etching and process technology on props. 79−83122
Al, sputtered film, thermal ageing, thickness dependent effects 78−6462
Al-Ag alloy mirror for use as solar reflector, co-sputtering 80−20789
Al-CdS-Au structure, interfacial phenomena, complex impedance meas. *(French)* 79−42668
Al-Cu films, DC sputtered, Cu distrib. 80−80113
Al-GaAs-Al sandwich-type sputtered film, elec. props. 78−91780
Al-Si, DC magnetron-sputtered, residual gas influence on props. 80−80968
Al-SiO_2 film-substrate interface, obs. of Al_2O_3 and free Si 78−91571
Al-Ta_2O_5-Al, healing of defects in dielec. film by anodisation 80−65406
Al-Zn-Mg plasma sputtered, mech. props. rel. to heat treatment *(Russian)* 80−40387
$Al_xIn_{1-x}Sb$, DC sputtering and struct. 78−52674
AlN encapsulation of GaAs:Si, photolum., annealing effects 80−20681
AlN, encapsulation of preliminary heated GaAs *(French)* 77−32714
Al_2O_3 film, RF sputtered by planar magnetron, phys. props. 77−43448
Al_2O_3 films, static compression to 1.2 Mbars, elec. resist. 79−55822
Al_2O_3, RF sputtered, transient currents 78−23184
Al_2O_3, RF sputtered film, transient current meas. 78−52113
Al_2O_3, sputtered insulating film contouring over substrate topography 77−8752
As, amorphous, photoluminescence, bulk and sputtered thin films 80−25457
As, bulk and sputter-deposited amorphous, vibr. props., Raman spectra meas. 77−63411
Au 79−77938
Au, diode sputtering of biological specimens for SEM 79−5421
Au, electrodeposited and sputtered, hard, reactive softening, X-ray diffr. studies 80−100414
Au film, deposition on NaCl by ion beam sputtering, initial growth features 79−77962
Au film sandwiches, recovery kinetics and early stages of diffusion, DC resist. expts. 79−77971
Au, hardening mechanisms, grain size effect 80−35302
Au, microporosity induced by nucleation and growth processes, TEM expts. 78−10303
Au, on Al, thickness distrib. determ. by electron backscatt. 78−18927
Au overlayer, on GaP photoelectrode 78−14812
Au, polycryst., RF bias-diode and triode sputtered, resist. and microstruct. 78−80072
Au, sliding charact., friction and wear *(Japanese)* 78−56778
Au, thin film, discontinuous, high resist., Hall effect meas. 80−65716
Au-Ag bilayers, conc. profile by AES, interdiffusion coefficient determ. *(French)* 78−84077
Au-Cr, cosputtered films, optical props. 0.2 to 6.1 eV 77−32454
Au-Ni (15 at.%) film, evidence of modulated struct., TEM exam. 78−87887
Au-Pd, diode sputtering of biological specimens for SEM 79−5421
Au-Si, amorphous sputtered film, elec. props. 78−68006
Au-$Ti_{0.3}W_{0.7}$, thermal annealing study of metallisation on Si 80−80134
Au-W-GaAs Schottky barrier, elec. and chem. props., AES 80−96973
Au-WO_3 electrochromic cermets, resist. and optical density meas. 79−8201
Au_3Cd, sputtered epitaxial films, order-disorder reaction obs. 78−84092
BN films, optical and electrophysical props. *(Russian)* 77−20941
$Ba(Pb,Bi)O_3$ perovskites, resputtering effects 80−80969
$BaPb_{1-x}Bi_xO_3$, RF sputtered, T_c as function of comp. and annealing conditions 79−24100
$Ba_{0.60}Sr_{0.40}TiO_3$, sputtered film on Pt, pyro-effect for laser registration *(Russian)* 77−20804
$BaTiO_3$, film, ferroelectricity of vap. deposited coating 79−69781
$BaTiO_3$ film, sputtered, elec. props. 79−42676
$BaTiO_3$, RF sputtered amorphous films, phys. and elec. characterisation 79−83119
$BaTiO_3$ RF sputtered ferroelectic film on Si substrate, ferroelectric props. 80−80697
$BaTiO_3$, RF-sputtered tetragonal films on Si, ferroelec. and insulating props. 79−78888
$BaTiO_3$, refr. index, 0.3-1.0 μm, substrate temp. effects 77−55840
Be, RF sputtered film, props. rel. to deposition conditions 77−39965
Be, thick film, amorphous, RF magnetron sputtering 80−80971
Bi_2O_3 compound films for SAW devices and filters *(Japanese)* 77−73116
$Bi_{1-x}Sb_x$, sputtered thin films, first order Raman scatt. 79−69831
sputtered coatings continued
$Bi_{12}SiO_{20}$ film, photoelectric props. obs., UV illumination effects *(Russian)* 80−80313
$Bi_{12}TiO_{20}$, RF sputtered epitaxial film on $Bi_{12}GeO_{20}$, for optical waveguiding 78−9462
$Bi_4Ti_3O_{12}$ stoichiometric thin film prep. by DC sputtering with powder target 77−90273
Bi_2WO_6, RF sputtering, possible piezoelec., pyroelec. and photolithography appl. 77−15705
C, amorphous, diamond-like 3-fold coord. 80−50323
C, amorphous, elec. transport props. 78−6457
C, amorphous elec., struct. and optical props. 77−20474
C, deposition processes, coating struct., for prosthetic devices 77−40374
C film, sputtered glassy, prep., mech. and struct. props. 77−66588
CaF_2-Ge(Si), cosputtered composite semiconductors, selective solar energy absorbers 79−56876
$Cd_xHg_{1-x}Te$ films, growth by cathodic sputtering in Hg vapour plasma 80−97431
CdO films, electrophysical properties *(Russian)* 77−63008
CdO-SnO_2 film, prep. by RF sputtering, elec. cond. and transparency 80−7492
CdS, in Al-CdS-Au struct., asymm. Poole-Frenkel effect *(French)* 77−76949
CdS monocrystalline sputtered X-ray transducer characteristics *(Russian)* 80−47162
CdS polycrystalline layers, electron trapping depend. on preparation conditions 79−78232
CdS:Cu_2S sputtered solar cells, energy anal. of cell fabrication techniques 80−50966
CdS_xSe_{1-x} photosensitive films, prep., props., and use for photodetectors 80−55298
CdS_xSe_{1-x} triode cathode sputtered films, electrophysical props. *(Russian)* 79−42642
CdS_xSe_{1-x}, triode sputtered films, photoelec. props. *(Russian)* 79−15179
CdSe, photocond. film, plasma reson., IR refl. obs. 80−11037
$CdSe_xTe_{1-x}$, triode sputtered films, photoelec. props. *(Russian)* 79−15179
$CdSe_yTe_{1-y}$ triode cathode sputtered films, electrophysical props. *(Russian)* 79−42642
$CdSn_xO_y$ films, transparent conducting, deposited by RF sputtering from CdO-SnO_2 target 80−76179
Cd_2SnO_4 film, RF sputtered from powder targets, props. 77−43759
CdTe film, cathode sputtered, chemical composition and struct. 78−84100
CdTe film, excitation by H of anomalously high voltage *(Russian)* 78−60235
CdTe sputtered films, deposition conditions effects on struct. and props. 77−43452
CdTe sputtered films, struct., photocond., and trap distrib. 80−29489
$Cd_{1-x}Zn_xS$, electro-optical multilayer film, for data storage and display 78−71176
$Cd_{1-x}Zn_xS$, RF sputtered electro-optical film for data storage and display 78−83047
CeO_2:Y_2O_3, bias sputtering, film growth and characts. 77−40366
CeO_2-Y_2O_3, surface characterisation, XPS, ESCA, and AES expts. 78−72028
Co, on Ni-Cr type alloys, surface pretreatment to attain pore-free aluminised coatings 80−40612
Co, sputtered film, high coercivity and high hysteresis loop squareness 79−91259
Co-Cr recording films, perpendicular mag. anisotropy, hysteresis loop, microstruct., TEM obs. 78−95491
Co-Fe-B and Co-Fe-Cr-P-B sputtered amorphous films, mag. props. and corrosion resist. 79−28567
Co-Fe-B films, amorphous, mag. annealing behaviour 79−73782
Co-Gd-Mo amorphous films, resist. and extraordinary Hall effect, thermal annealing effect 80−70852
Co-Gd-Mo films, sputtered, O effects on mag. props. during annealing 80−89374
Co-Mo-Cr-Si Laves intermetallic alloy, struct. and wear props. 77−40477
Co-Re, sputtered film, high coercivity and high hysteresis loop squareness 79−91259
Co(-Re), mag. props. and microstructures 79−82837
$Co_{67}Er_{33}$ amorphous alloy, local order and amorphous struct. 80−88061
$Co_{79}Fe_{6.5}B_{14.5}$ amorphous thin films, zero magnetostriction, high magnetisation 80−34708
$(CoFeB)_{100-x}Cr_x$ thin films, magnetic props. and corrosion resist. 80−34709
Co_2Ge_3, $CoGe_2$, amorphous film, annealing effects on struct. and elec. resist. 77−85099
Co_5Ge_3 amorphous film, elec. resist., microstruct. and annealing 77−85188
Cr, defects and mechanical stability, different deposition methods *(Bulgarian)* 80−44438
Cr film, obtained by thermo ionic precipitation, phase composition, lattice parameters *(Russian)* 80−96756
Cr, growth struct., influence of substrate surface topography and ang. of adatom incidence 80−20058
Cr, sliding charact., friction and wear *(Japanese)* 78−56778
Cr, sputtered wafer, internal stresses 77−39753
Cr/Au metallisation system, corrosion inhibition using intermediary Pd layer 79−79155
Cr-Si, amorphous sputtered film, material for kilo-ohm sheet resistances, prep. and props 79−78227
Cr-Si, deposition method, for controllable comp. with given elec. props. 80−35087
Cr-SiO, electrical and struct. props. 80−39694
Cr-SiO film, RF sputtered, substrate bias effect obs., on electrical resistivity 78−60573
Cr-SiO_2 cermet film, deposition by RF sputtering of powder target, elec. resist. and TCR 79−78890
CrO_2 amorphous thin films, Mossbauer and magnetisation data 80−34712
Cr_2O_3, RF sputtered coating for wear appls., on Inconel X-750 foil, prep. and props. 80−40605
Cr_2O_3/Cr cermet film, RF sputtered, for selective black absorbers 78−30046
Cr_2O_3-Cr cermet films, for selective black absorbers 79−29483

sputtered coatings continued
$Cr_xPd_{82-x}Ge_{18}$, amorphous, RF sputtered, elec. resist. and magnetoresist., Kondo type behaviour 78−76066
Cs halides, storage layers stability under electron bombardment 78−27355
Cu based materials, sputter deposited at high rate, microstruct. and props. 78−22988
Cu, bias sputter parameters effect, hollow cathode 77−40369
Cu, sliding charact., friction and wear *(Japanese)* 78−56778
Cu, surface morphology influence on sputtered yield angular distribution 80−65338
Cu, thick sputter deposit, microstruct., tensile props. 77−40461
Cu-base alloy formed by high rate sputtering 78−11368
Cu-Fe, explosive plasma sputtered coatings, struct. and props. *(Russian)* 80−100783
Cu-Ni alloy, sputtered altered layers, in-depth profile, model 78−19613
Cu-Ni alloy, sputtered and sputter-deposited surfaces, in-situ AES meas. 77−48296
Cu-plated C fabric, plasma sputtering influence on strength and elec. cond. *(Russian)* 80−21008
Cu-Ti-Fe (0.7, 0.9 wt.%) film, dispersion-strengthened, form. by high rate magnetron/plasmatron sputtering, and props. 80−25715
$CuInS_2$ films, RF sputtered, growth and props. 80−80124
$CuInS_2$ films prod. by RF sputtered Cu-In films exposure to H_2S 79−95926
$Cu_2Mo_6S_8$, normal state and superconducting property measurements 78−91660
$Cu_xMo_6S_8$, sputtered, supercond. crit. currents and scaling laws 78−47923
Cu_xO, sputter deposited on Cu, induced stresses 80−24774
Cu_2S sputtered on CdS substrate for solar cell appl. 78−39692
DyIG, non-cryst., Mossbauer and magnetisation studies 80−44979
EuIG, non-cryst., Mossbauer and magnetisation studies 80−44979
Fe sputtered film, amorphous, Mossbauer study and electron diffr. obs. 80−75897
Fe thin layers, vacuum coated on PMMA, mag. behaviour during mech. stress cycles *(German)* 80−80581
Fe-Al_2O_3 granular films, superparamagnetism and relax. effects 80−71118
Fe-B, amorphous, strong stripe domains, Kerr effect obs. and theory 79−91265
Fe-B ferromag. film, props. 79−4709
Fe-B films, amorphous, mag. annealing behaviour 79−73782
Fe-c, Fe-Si-B, and Fe-Cr-P-C sputtered amorphous films, mag. props. and corrosion resist. 79−28567
Fe-Co-Si-B sputtered amorphous thin film, coercivity, galvanomagnetic props., resistivity 80−29578
Fe-Cr, Fe-Cr-Al(Si) film heaters, lifetimes for 800 to 1000°C temp. range 78−215
Fe-Cr-Si, heat resistive films prepared by sputtering, lifetime meas. 80−80132
Fe-O noncrystalline RF sputtered film, vapour species control 78−60575
Fe-Si amorphous film, Hall const. and magnetoresistive effect 78−52105
Fe-Si amorphous films, mag. and magnetoelastic props. 79−99746
Fe-Si ferromag. film, props. 79−4709
Fe-Si-B amorphous films, mag. props. 80−34710
Fe-Si-Cr magnetic films, corrosion reduction effect of Cr obs. 80−80573
$Fe_{1-x}B_x$ amorphous films, mag. props. and thermal stability 79−78446
$Fe_{80}B_{20}$, sputter deposited amorphous, low field mag. props. 78−68335
FeC_x-CrC_y-NiC_z, stainless steel carbide, graded solar selective surface, magnetron sputtered 80−81485
Fe_xC_{1-x} amorphous sputtered film, mag. props. 78−68311
$FeGe_2$, amorphous film, annealing effects on struct. and elec. resist. 77−85099
Fe_5Ge_3, amorphous film, elec. resist., microstruct. and annealing 77−85188
$Fe_{40}Ni_{40}B_{20}$ glass, ^{10}B self-diffusion, meas. by SIMS 80−49406
Fe_2O_3 amorphous RF sputtered thin films, Mossbauer and mag. study 80−34711
Fe_2O_3 amorphous thin films, Mossbauer and magnetisation data 80−34712
Fe_2O_3 sputtered films, optical transmission and reflection spectra depend. on substrate temp. 79−91517
Ga, on GaAs or Si, anodic oxidation, Ga_2O_3 film prep. 77−81338
GaAs, amorphous sputtered films, hydrogenated, photoinduced optical absorpt. 80−50362
GaAs, RF sputtered, ESCA, surface chemistry suitability for photovolt. appl. 80−7476
GaAs, sputtered film, structuring rel. to laser sputtering method *(Russian)* 77−59689
GaAs:H amorphous sputtered films, high field cond. props. 80−44607
GaAs:Si(Mg), doped and undoped, sputtered epitaxial films, elec. props. 79−78234
GaN/Ga layered films, Ga whisker growth 80−92800
GaP film, struct. and elec. props. obs. *(Czech)* 78−52667
GaP, RF sputtering on glass and Au film substrates, struct. and elec. props. 80−2311
GaS, sputtering conditions effect on film struct. and optical absorption *(Russian)* 77−12525
GaSb films, elemental incorporation probability modification by ion bombard. during growth 80−80118
GaSb, sputtered films, on GaAs, growth, Hall effect, impurity levels 80−20334
$(GaSb)_{1-x}Ge_x$ films, single-cryst. metastable semicond., growth and phase stability 80−80115
GaSe sputtered film microhardness, influence of gas discharge *(Russian)* 80−49560
Gd-Al, amorphous film, microwave mag. reson. 78−91948
Gd-Co, amorphous, Ar sputtered, struct. 78−63946
Gd-Co, amorphous, RF sputtered, prep. and props. 79−1693
Gd-Co, amorphous, selective resputtering-induced anisotropy 78−72376
Gd-Co, amorphous, sputtered very thin film struct. 77−15707
Gd-Co, amorphous film, with cylindrical mag. domains, sputtering prep. *(Russian)* 77−12176
Gd-Co, and Gd-Co-Mo, amorphous, mag. props., annealing effects 78−64235
Gd-Co, and Gd-Co-X (X=Mo, Cu, Au), sputter deposited amorphous alloy, substrate bias, magnetic anisotropy, annealing 78−48006
Gd-Co, bias-sputtered, dipolar mechanisms for mag. anisotropy 78−64233
Gd-Co, evap. amorphous film, mag. props. 77−24720
sputtered coatings continued
Gd-Co, evap. amorphous films, anisotropy, magnetisation and FMR meas. 77−66392
Gd-Co, inert gas incorporation effect on uniaxial anisotropy 78−64232
Gd-Co, LV multitarget sputtered film, substrate bias effect on anisotropy 77−16125
Gd-Co, sputtered film, growth induced anisotropy 77−16123
Gd-Co alloy, sputtered film, mag. props. determ. *(Chinese)* 78−2714
Gd-Co alloy film, sputter yield ratio, combined ion deposition and etching 80−71594
Gd-Co amorphous film, DC or RF sputtered, mag. props., He^+-backscatt. investig. 77−20650
Gd-Co amorphous film, sputtered perpendicular mag. anisotropy 79−56576
Gd-Co amorphous film, sputtered, perpendicular anisotropy exam. 79−73707
Gd-Co amorphous film, sputtered, FMR spectra 79−73822
Gd-Co amorphous films, mag. anisotropy, static and ferromag. reson. expts. 79−33477
Gd-Co amorphous films, model calculations for anisotropy formation induced by resputtering processes 78−64242
Gd-Co amorphous films, RF sputtered, magnetisation ripple effects 80−11232
Gd-Co amorphous films, struct. and mag. anisotropy 80−20438
Gd-Co amorphous films, uniaxial perp. anisotropy induced by resputtering effect, expt. *(Japanese)* 77−55885
Gd-Co amorphous sputtered films, magnetoelastic contrib. to perpendicular anisotropy, internal stress meas. 78−95490
Gd-Co amorphous sputtered film, magnetostriction and anisotropy 80−39821
Gd-Co amorphous thin film, mag. and optical props., conc. depend 79−19748
Gd-Co based amorphous sputtered films, microstruct. variability and mag. anisotropy, implanted ion effects 80−88459
Gd-Co film, amorphous, perpendicular uniaxial anisotropy, dominant contrib. of preferential resputtering effect 77−36103
Gd-Co film, homogeneity of films prepared by bias sputtering 78−72379
Gd-Co film, struct. and mag. anistoropy, electron microscopy 79−56578
Gd-Co films, amorphous, mag. anisotropy from torque meas. 77−47987
Gd-Co sputtered amorphous films, resistivity anomalies, 42 to 300K *(Chinese)* 80−7001
Gd-Co sputtered films, preparation process, props. 77−59688
Gd-Co thin films sputtered from mosaic target, thickness and composition distrib. 80−6676
Gd-Co-Cu film, amorphous, influence of biased magnetron deposition parameters on props. 77−43856
Gd-Co-Mo, amorphous, Ar sputtered, struct. 78−63946
Gd-Co-Mo, amorphous, sputtered very thin film struct. 77−15707
Gd-Fe, amorphous, in-situ ion beam sputtered, microstruct. and Lorentz mag. struct. 78−63947
Gd-Fe, amorphous, mag. props., annealing effects 78−64235
Gd-Fe, DC bias RF sputtered film, mag. props. 77−16124
Gd-Fe, LV multitarget sputtered film, substrate bias effect on anisotropy 77−16125
Gd-Fe, sputter deposited amorphous alloy, substrate bias, magnetic anisotropy, annealing 78−48006
Gd-Fe amorphous sputtered films, magnetoelastic contrib. to perpendicular anisotropy, internal stress meas. 78−95490
GdCo, amorphous, in-plane anisotropy induced by rare gas annealing 78−84458
GdCo amorphous film mag. props. from Mossbauer effect obs. *(Japanese)* 80−15933
GdCo sputtered amorphous film, third elements effect on mag. anisotropy 79−91260
$(Gd_xCo_{1-x})_{1-y}Ar_y$ amorphous films, effective anisotropy field, ferromag. reson. obs. 80−71123
$Gd_{0.27}Co_{0.64}Kr_{0.09}$, amorphous film, thermal release of Kr and H, meas. using UHV mass spectrometric technique 80−3439
$Gd_{6.9}Co_{74.0}Mo_{12.8}Ar_{6.3}$, amorphous film, spin wave reson. 79−73823
Gd_xNi_{1-x} sputtered amorphous films, mag. props. and Hall meas. 78−95488
Ge, amorphous and polycryst. layers, sputtered, elec. cond. and thermoelec. power 78−2586
Ge, amorphous sputtered films, hydrogenated, photoinduced optical absorpt. 80−50362
Ge, black, solar selective absorber characterisation 80−80112
Ge condensation, nucleation, growth and transform. of amorphous and crystalline solids 80−24745
Ge, epitaxial film, ion sputtering, growth mechanism, struct., props. 77−31917
Ge film, amorphous, prepared by evap. or sputtering, AC loss meas. 80−65560
Ge film black, solar selective absorber surface 79−29484
Ge, heterodiffusion due to H atom surface recombination stimulation, Cu, Zn, In coated *(Russian)* 80−59726
Ge:Sb, amorphous, electronic transport props. 80−44589
Ge:Sb(In), film, electronic props. 78−84330
Ge-Se-Fe films, metallic and semicond., amorphous, mag. and elec. props. 78−52319
Ge-Si junction, Si monocryst. and Ge film, elec. props. 79−51660
GeSe amorphouse sputtered film, DC and AC behaviour, effect of contact material 79−95513
$Ge_{20}Se_{40}Te_{40}$ amorphous alloys, thermal crystn. study 78−26789
$Ge_{0.5}Te_{0.5}$, strucutral anal. by neutron diffr., radial distribution functions 80−15010
H_xWO_3 films, proton diffusion coeffs. 80−6548
H_xWO_3 film, effect of struct. on optical and electrical props. 78−84671
$Hg_{0.74}Cd_{0.25}Te$ thin film deposition on Si substrates by RF triode-sputtering, large-area photodetector arrays 80−80965
α-HgS films, sputter-deposited in Hg vapour, growth and props. 80−75467
HgS, on NaCl, growth and struct., electron diffr. and TEM obs. 77−90271
Ho-Co film, struct. and mag. anistoropy, electron microscopy 79−56578
HoCo, amorphous, in-plane anisotropy induced by rare gas annealing 78−84458
IN_2O_3:Sn, RF magnetron sputtered film, elec. and optical props. 80−104065
(In, Ga)Sb, sputter deposited amorphous film, impulse stimulated explosive crystallisation 78−84098

sputtered coatings continued
n-In_2O_3 film, RF sputter grown, substrate bias effect on elec. and optical props. 78−64150
In_2O_3, In_2O_3-SnO_2, transparent thin films for satellite temp. control 79−80187
In_2O_3 thin film on polyester substrate, struct. determ. by TEM 80−6674
In_2O_3, transparent electrode deposition on PLZT ceramic, elec. and opt. props. 78−74848
In_2O_3:Sn, electro-reflectance meas. 80−11496
In_2O_3:Sn, film, HF sputtered, cond., Hall mobility, oxidation, charge carrier density 78−72287
In_2O_3:Sn, sputtered films for selective transparent films, prep., elec. and opt. props. *(Japanese)* 77−68247
In_2O_3:Sn, sputtered film, optical and elec. props. 78−76177
In_2O_3:Sn films, prep. at low deposition temps. by ion-beam sputtering, elec. and optical props. 79−66004
In_2O_3-SnO_2, magnetron RF sputtered electro-optical film for data storage and display 78−83047
In_2O_3-SnO_2, on Si, antireflection props. for photovolt. appl. 80−3513
In_2O_3-SnO_2 electro-optical film, for data storage and display 78−71176
In_2O_3-SnO_2 film, XPS expts., energy band model accounting for phys. props. 77−90241
In_2O_3-SnO_2 sputtered film, appls. in displays, vidicon tube windows, dielec. window surfaces 79−59778
In_2O_3-SnO_2 thin film, effects of heat treatment on resist. and optical absorpt. 78−43495
In_2O_3-SnO_2/InP junction, ion probe analysis of chemical nature 79−73411
In_2O_3-SnO_2-CdTe:P, p-n homojunction solar cell, elec., photovoltaic props., photoluminescence 80−81463
In_2O_3-SnO_2-InP solar cell junctions, efficiency, InP surface props. 80−85288
InSb and $InSb_{1-x}Bi_x$ films, elemental incorporation probability modification by ion bombard. during growth 80−80118
InSb/GaSb superlattice thin films, sputtered, ion-bombardment-enhanced diffusion during growth 78−87882
$InSb_{1-x}Bi_x$ films, single-cryst. metastable semicond., growth and phase stability 80−80115
$InSb_{1-x}Bi_x$, metastable epitaxial film, phase diagram 80−76238
InSe thin film, sputter growth and chem. anal. by XPS/ESCA 80−80976
$In_{2-x}Sn_xO_{3-y}$-insulator-poly-Si solar cells, photovoltaic conversion parameters 80−101093
$In_{2-x}Sn_xO_{3-y}$-poly Si SIS solar cells 80−97787
$In_{2-x}Sn_xO_{3-y}$, deposition with sputter gun 77−44162
$K_3Li_2Nb_5O_{15}$ films for optical waveguides epitaxial growth and characterisation 80−79016
$KTa_{1-x}Nb_xO_3$ film, structural and electrical properties obs. 78−88426
Kr.2SiO_2, props. of vitreous deposits 78−22664
La-Fe alloy, amorphous, sputtered at high rate, mag. props. 80−75753
$LiNbO_3$, heteroepitaxial growth on MgO by RF sputtering, SHG 79−27323
Mg-MgF_2, sputtered films, opt. props. 78−80430
Mg-Zn, amorphous sputtered film, elec. props. 78−68006
MgO-Au cermet film, selective black absorbers 77−1747
MgO-Au cermet films, for selective black absorbers 79−29483
$Mn_xPd_{82-x}Ge_{18}$, amorphous alloys, mag. props. 78−91906
MnPt, disordered film produced by RF sputtering, ferromag. behaviour 78−68310
MnSi, amorphous, mag., elec., struct. and thermal props., spin glass behaviour 80−50124
Mo, elec. resist., annealing and struct. effects 80−60109
Mo film, deposited by cylindrical magnetron sputtering, internal stresses, optical reflectance and elec. resist. 77−43449
Mo film, on Si, X-ray line-shape anal., simplifications using Fourier series 79−82123
Mo film, sputtered on Si, annealing effect on uniform and nonuniform strains 79−82504
Mo, RF sputtered, diffusion barrier props. 78−71887
Mo, thin film deposition by high current ion beam sputtering, struct. and elec. props. 80−59837
Mo_3Ge, supercond. crit. temp. 78−14853
MoS_2 film, non-stoichiometry and sputtering conditions 78−87891
MoS_2, RF sputtered layers with variable stoichiometry, lubrication props. 80−40557
MoS_2, RF sputtered lubricant, wear life, sputtering parameter effects 80−40558
MoS_2, RF sputtering, coating on steel surface as solid lubricant, morphology 78−6239
MoS_2, sliding charact., friction and wear *(Japanese)* 78−56778
MoS_2, solid lubricant, morphological growth 77−35825
$MoSi_2$ film, elastic stiffness and thermal expansion coeffs. 80−107451
$MoSi_2$ sputtered films, protective layer form. on oxidation, Auger anal. and backscatt. meas. 79−15029
$NaTiO_3$/SiO_2 charge storage memory films for IGFETs 80−11566
Nb, analysis by X-ray diffr., electron diffr. and AES *(Czech)* 79−51448
Nb films, ion beam sputtered, supercond., laser annealing effects 80−97024
Nb, magnetron-sputtered, intrinsic stresses and supercond. props. 80−24772
Nb, O contamination, Auger anal. 78−52669
Nb, sputter-deposited on stainless steel, electron microscopy and ESCA 77−52554
Nb sputtered film, tunnelling characts. 79−4621
Nb sputtered film interface with stainless steel, for supercond. AC cables 79−74089
Nb weak link SQUID 79−38258
Nb/Cu, layered ultrathin coherent structs., supercond. props. 80−84525
Nb/Cu layered ultrathin coherent struct. 80−80122
Nb-Ge, supercond., TEM expts., correl. of struct. and elec. props. 78−14628
Nb-Ge film, phase transformations due to annealing, electron diffr. study 80−54551
Nb-NbO_x-Al/Pb supercond. proximity function, production by RF sputtering and photolytographic techniques 77−43787
Nb-Ti films, ion beam sputtered, study by ^4He backscattering and nucl. reaction microanal. 79−42400
Nb-Zr sputtered films on Ta, struct. and supercond. props. *(Japanese)* 78−52138
Nb_3Al, complex refractive index meas. 80−93264

sputtered coatings continued
NbC weak link SQUID 79−38258
$NbGe_2$, superconducting transition temp. meas. 80−7019
Nb_3Ge amorphous films, microstruct. X-ray small angle scatt. study 79−14685
Nb_3Ge amorphous films, X-ray diffr. analysis of microstruct. 78−72035
Nb_3Ge, DC sputtered films, annealing and mech. deform. effects on struct. and supercond. props. 79−38217
Nb_3Ge film, high-temp. supercond. phase stabilisation w.r.t. prep. conditions *(Russian)* 80−70871
Nb_3Ge film, low temp. sputter deposition 78−48315
Nb_3Ge film, nucleation of high-T_c phase in presence of impurities 78−88054
Nb_3Ge film, sputtered, chemical composition versus lattice parameter a_o and supercond. transition temp. relations 77−43771
Nb_3Ge film, superconducting, A-15 type, getter-sputtering with controlled additions of O 78−88427
Nb_3Ge film, superconducting props. 79−38215
Nb_3Ge films, magnetron sputtered preps. and microstruct. 79−38276
Nb_3Ge, high T_c film with impurity expanded lattice, form. and stabilisation 79−56099
Nb_3Ge, high T_c films, electron tunnelling and AES anal. 79−28471
Nb_3Ge, metallic glass, internal friction peak obs. 78−79666
Nb_3Ge, RF and DC sputtered films comparison, O content effect 78−72022
Nb_3Ge, sputter-deposited, superconducting T_c and phase relationship 79−56344
Nb_3Ge sputtered and evaporated, struct.-depend. anisotropy of supercond. crit. currents 79−38292
Nb_3Ge sputtered films, Ge surface segregation exam. by AES 79−56084
Nb_3Ge, sputtered on Cu, film-substrate interface obs. by electron microscopy 80−65398
Nb_3Ge, supercond. sputtered film, ion scatt., AES, depth profiling 77−11806
Nb_3Ge superconducting film, Nb_5Ge_3 and NbO content, X-ray diffr. obs. 80−2515
Nb_3Ge superconducting film, crit. temp. correl. with resist. relations and film struct. *(Russian)* 80−15646
Nb_3Ge superconducting films, quantitative Auger anal. 80−55740
$Nb_3Ge(Si)$, amorphous films, thermally-activated internal friction peaks, structural obs. 80−80147
$Nb_3Ge(Si)$, RF sputtered films, amorphous atomic scale struct. 80−84064
NbN superconducting reactively sputtered film, Auger anal. 78−72297
Nb_2O_5-ZrO_2 sputtered thin layer structure and optical props. 79−28851
$NbSi_2$, superconducting transition temp. meas. 80−7019
Nb_3Sn, high-rate sputter-deposited, effect of oxygen on microstruct. 80−20343
Ni, amorphous film, getter sputtered at 25K, resistivity, Curie temp. 78−52673
Ni film, deposited by cylindrical magnetron sputtering, internal stresses, optical reflectance and elec. resist. 77−43449
Ni film, RF sputtered on $LiNbO_3$, SAW delay variation obs. 79−56102
Ni films, HCP and amorphous, RF sputtered, O_2 incorporation, ESCA obs. 80−10832
Ni films, hexagonal and amorphous, O incorporation, ESCA and electron diffr. meas. 79−11046
Ni, on Si, annealing effects on transmission electron diffr. patterns, silicide form. 78−91562
Ni, sliding charact., friction and wear *(Japanese)* 78−56778
Ni, sputter deposited on Cu, induced stresses 80−24774
Ni sputtered coating microstructure on mechanically activated cathode *(Russian)* 79−91586
Ni, thick sputter deposit, microstruct., tensile props. 77−40461
Ni/ZrO_2-Y_2O_3 multilayered ceramic/metal coatings, props. 80−40620
Ni-Cr film, RF sputtered, Seebeck coeff. 77−63004
Ni-Cr thin film production by HF cathode sputtering *(Bulgarian)* 79−19992
Ni-Cr/ZrO_2-Y_2O_3 multilayered ceramic/metal coatings, props. 80−40620
Ni-Fe-Rh films, mag. and corrosion props. 80−34702
NiCr, sputtered, detection by electron probe microanal., substrate depend. 80−35607
NiFe film, sputtered, physical props. 79−77938
Ni_5Ge_3, amorphous film, elec. resist., microstruct. and annealing 77−85188
Ni_3Si coatings, form. and stability during high temp. irrad. 80−35088
PLZT, epitaxial growth by RF sputtering, and characterisation 77−85937
PLZT ferroelectric thin films, epitaxial growth and optical props. 80−70543
PLZT, transparent ferroelec., RF sputtering and film characterisation 78−72727
β-PbF_2, thin films, cond. mechanisms, struct. 77−84970
$PbMo_6S_8$, normal state and superconducting property measurements 78−91660
$PbMo_6S_8$, sputtered film, critical current density meas. 78−84369
PbO-SiO_2 glass, optical coating for GaAs-$Al_{1-x}Ga_xAS$ laser 78−71113
PbS sputtered film microhardness, influence of gas discharge *(Russian)* 80−49560
$Pb_xSn_{1-x}O_2$ film, optical props. 78−39616
$Pb_xSn_{1-x}O_2$:Sb films, DC sputtered, elec. props. 80−80426
$Pb_{1-x}Sn_xTe$, for IR detector appl. elec. and optical props. 80−35084
$Pb_xSn_{1-x}Te$, RF sputtered films, struct., lattice parameter, stoichiometric comp., RHEED 78−38975
$Pb_xSn_{1-x}Te$, RF sputtered film IR detector, photocond. response speed improvement by annealing 79−58790
$Pb_xSn_{1-x}Te$, RF-sputtered epitaxial single-cryst. films, thermorefl. spectra 77−63476
PbTe, polycryst. film, RF sputtered, time stability 77−43758
PbTe, semiconductor polycrystalline thin films, low-frequency 1/f noise meas. 80−15629
$Pb(Zr,Ti)O_3$, ferroelec. and optical props. 77−85674
$Pb(Zr,Ti)O_3$ films, ion beam sputtering, dielec. and ferroelec. props. 79−78881
$Pb(Zr,Ti)O_3$ films, ferroelec., ion beam deposition sputtered from multicomponent targets 80−80974
$Pb(Zr_xTi_{1-x})O_3$ films, deposition by focused ion beam sputtering 80−76177
$(Pd_{80}Au_7Si_{13})/Fe_{30}$, compositionally modulated amorphous film, diffusion, struct. relax. 80−103518

sputtered coatings continued
Pd_2Si, on Si substrate, thermally induced Si accumulation, AES study 80−24718
$(Pd_{85}Si_{15})_{61}/(Fe_{85}B_{15})_{39}$, compositionally modulated amorphous film, diffusion, struct. relax. 80−103518
Pt, microporosity induced by nucleation and growth processes, TEM expts. 78−10303
Pt, RF diode sputtered, thickness distrib., XPS determ. 77−39743
Pt-Sb, amorphous sputtered film, elec. props. 78−68006
Pt-SiO_2 cermet films, struct. and props. 80−96956
PtO_2, sputtered film, optical props. under H_2 reduction 80−20728
PtO_x films, electronic struct., reduction processes, photoemission, optical absorpt. and resist. meas. 80−80931
PtSi film formation by ion sputtering and annealing, form. and exam. problems 80−100782
Re_5Ge_3, supercond. crit. temp. 78−14853
Sb amorphous film, elect. resist. 78−95390
Sb, amorphous sputter-deposited film, vibr. props., Raman spectra meas. 77−63411
Sb-Au amorphous film, elec. resist. 78−95390
$Sb_2S_3(Se_3)$, IR spectra rel. to bonding, amorphous film and cryst. 77−16410
Se film, trigonal, sputtered and evaporated nucleation and growth processes 77−31920
Si, amorphous, control of dihydride bond density using RF sputtering, dark anal. and photocond. 80−34327
Si, amorphous, dark conductivity and photocond. obs. *(French)* 78−64155
Si, amorphous, hydrogenated, soft H plasma effect, IR absorpt. *(French)* 80−45054
Si, amorphous, hydrogenated, electron drift mobility meas. 80−75565
Si amorphous, ion bombardment, controlled hydrogenation at low temps. 79−69119
Si, amorphous, optical absorption at high press. 78−35216
Si, amorphous, Schottky barrier solar cell, large-area RF sputtered, contact form, scaling and optimisation 80−45679
Si, amorphous, sputter deposited, O_2 incorporation during and after fabrication 80−49541
Si, amorphous, sputtered, resist. control by ion implantation 80−100262
Si, amorphous co-sputtered doped, photovoltaic material appl. 80−93488
Si, amorphous film, IR and Raman spectra of Si-H bonds 78−19482
Si, amorphous sputtered film, elec. cond. and photocond. 79−87097
Si, amorphous sputtered films, hydrogenated, photoinduced optical absorpt. 80−50362
Si, amorphous sputtered thin film, US anomalies, 0.5-300K 80−34145
Si and Si:H amorphous films, porosity and oxidation of evap., sputtered and plasma-deposited films 80−10838
Si film, sputtered, physical props. 79−77938
Si, on quartz and MgO substrates, struct. and elec. resist. *(Japanese)* 77−55889
Si, RF sputtered amorphous film, high temp. metal induced crystn. 77−11825
Si:Au, O(H), film, amorphous, elec. cond. meas. 80−80423
Si:B, elec. props., struct., SEM and TEM obs. 79−95298
Si:F, amorphous, heat resistant, prep., elec. cond., IR absorpt., annealing 80−65719
Si:H, amorphous, Auger surface spectroscopy 80−50472
Si:H, amorphous, sputtered on $Gd_2(MoO_4)_3$, ferroelec. domain wall motion, image scanning 80−83663
Si:H, amorphous sputtered, excitation spectra and photoluminesc. 80−50396
a-Si:H, influence of H on optical props., H conc. and H bonds 80−76098
Si:H,P, amorphous, heavily hydrogenated, high gap state densities 80−49803
a-Si:H alloys, sputter deposited thin film coatings, property-comp. relationships 80−80975
Si:H amorphous film, luminesc. and non-radiative decay 80−50395
Si:H amorphous film, sputtered in Ar-SiH_4 mixtures, props. 79−87023
Si:H amorphous films, IR spectrum and struct. 80−97277
Si:H amorphous sputtered films, optical gap, IR absorpt. meas. 80−50320
a-Si:H sputtered films, ohmic contacts by H depletion, H diffusion 80−34511
Si:Mn(Fe)(Ni) amorphous films, ESR and elec. cond. 80−50171
Si:N, amorphous, DC sputtered, enhanced, photocond. 78−56183
Si:Ne(Ar)(Kr), amorphous, implanted and sputtered, epitaxial regrowth, influence of noble gas atoms 80−2289
Si:O, amorphous, sputtered, influence of O and deposition conditions 80−54693
Si:P, RF sputtered polycryst. film, MOS compatibility 78−6455
Si:P, sputter-deposited polycryst. films, resist. meas. 78−14842
Si:P(B), film, electronic props. 78−84330
Si:Sb, amorphous, electronic transport props. 80−44589
Si-Al C fibre composite technological coatings, liquid phase method preparation *(Russian)* 80−108375
Si-Au films, quenched condensed, elec. resist. and supercond. 80−54669
Si-Au-Si, Auger line intensity, contrib. of backscattered electrons 79−65962
a-Si-H sputtered solar cells, temp. depend. of Schottky barrier characts. 80−45669
p-Si-metal Schottky contact surface state spectra and current transport mechanism *(Russian)* 78−43472
$Si_{100-x}Al_x$, RF sputtered, amorphous, props. 80−34754
SiC, comp. and struct. props., effect of target materials 80−54549
SiC, sputtered amorphous film, struct., elec. and optical props. 79−78236
SiH_x amorphous reactively sputtered films, in Pd Schottky barrier devices, photovoltaic props. 80−49910
$Si_{1-x}H_x$, amorphous, RF sputtered, pure and P(B) doped, optical consts. 79−95866
$Si_{1-x}H_x$ amorphous sputtered films, IR vibr. spectra 79−43051
a-$Si_{1-x}H_x$, oxygenated thin film, sputtered, elec. cond. and optical props. 79−15239
$Si_{1-x}H_x$:Al, amorphous, co-sputtered Al modification, electronic and optical props. 80−100461
Si_3N_4, encapsulant for annealing of GaAs, photolum. and AES evaluation 78−27657
Si_3N_4 encapsulation of GaAs:Si, photolum., annealing effects 80−20681
Si_3N_4, encapsulation of preliminary heated GaAs *(French)* 77−32714
Si_3N_4, preparation, characterisation and appl. 80−40268
sputtered coatings continued
Si_3N_4, RF-sputtered thin-film optical waveguide, effect of deposition parameters on optical loss 79−76881
Si_3N_4, sputtered insulating film contouring over substrate topography 77−8752
SiO_2, and $SiO_{0.7}$, amorphous sputtered thin film, US anomalies, 0.5-300K 80−34145
SiO_2 controlled electrode area ratio sputtering system operation and film props. 77−77382
SiO_2 facet coating film effect on self-sustained pulsation suppression in GaAlAs DH lasers 80−95894
SiO_2, facet protection of (AlGa)As lasers 79−81444
SiO_2 film on thermally oxidised Si substrate, interface props., sputter deposition parameters effects *(German)* 80−40257
SiO_2 films, RF-diode-sputtered, step coverage 80−80117
SiO_2 HF plasma sputtered dielectric layer thickness and refractive index obs. 79−56931
SiO_2, IR spectra and elec. props., influence of prep. conditions 79−87176
SiO_2 magnetron sputtered film, oblique deposition effect on growth rate, etching rate, and struct. *(Japanese)* 80−54555
SiO_2, planarised sputter deposition 78−75959
SiO_2 RF magnetron sputtered coatings for laser fusion targets 80−35089
SiO_2, RF sputtered, stoichiometry and atomic defects obs. 79−60647
SiO_2, RF sputtered, stoichiometry and atomic defects obs. 79−90904
SiO_2, RF sputtered films, anomalous etching phenomenon 80−3226
SiO_2, RF sputtered films, AC conductivity and conduction mechanisms 80−20338
SiO_2, sputtered, reactive ion etching in CF_4 plasma, competitive mech. 79−91816
SiO_2 sputtered film as Zn-diffusion mask for GaInAsP-InP planar stripe lasers 80−48249
SiO_2 sputtered film performance as acoustic antireflection coating at sapphire-H_2O interface 80−106686
SiO_2 sputtered films in thin film transistors, trapping centres 80−7014
SiO_2, sputtered insulator film contouring over substrate topography 77−8752
SiO_2 sputtered layers for semicond. devices, effect of impurities on elec. props. *(German)* 77−16495
SiO_2 thin films, comparison of RI and IR spectra 80−11497
SiO_2 ultrathin layers, refr. index meas. 80−103936
SiO_2:Na film, RF sputtered, low elec. field Poole-Frenkel effects in MIM struct. 79−95536
SiO_2-Ta_2O_5, refr.-index-adjustable, for integrated optical ccts., prep. and props. 78−63203
Sn, sputtered film, exam. of frictional props. 79−15814
Sn-Ni metastable equiatomic alloy, sputter deposition 78−3043
SnO_2, O chemisorption, elec. cond. and EPR meas. correlation 80−84369
SnO_2, sputtered film, thermal ageing, thickness dependent effects 78−6462
SnO_2 thin films, analytical characterisation 80−20053
SnO_2, transparent electrode deposition on PLZT ceramic, elec. and opt. props. 78−74848
SnO_2:Sb film, DC sputtered, correspondence between Sb content and targets 79−23847
SnO_2:Sb thin films DC sputtered, heat treatment effects, expt. 77−28719
SnO_x films, phase composition, Mossbauer spectra 80−20051
$Sr_2Nb_2O_7$, sputtered films, amorphous, dielec. props. 80−54573
$SrTiO_3$, refr. index, 0.3-1.0 μm, substrate temp. effects 77−55840
steel, Hadfield, hollow cathode sputtering 78−11433
Ta, bias ion beam sputter deposited, elec. props. and structures 79−82692
Ta film, deposited by cylindrical magnetron sputtering, internal stresses, optical reflectance and elec. resist. 77−43449
Ta film, nucleation of α or β phase, impurity effects 77−24493
Ta film, RF sputtered, thermoelec. power, Hall coeff. and struct. props. 77−43743
Ta, film, sputtered, physical props. 79−77938
β-Ta film, stabilisation by Ta-Si interlayer, SIMS depth profiling 80−54568
Ta films, difference between α-phase layers and β-phase layers 79−52116
Ta, planar-magnetron-sputtered, props. 79−82474
Ta, planar-magnetron-sputtered, phys. and elec. props. 80−6673
Ta, thermal oxidation, reaction kinetics 78−39959
Ta, thin film deposition by high current ion beam sputtering, struct. and elec. props. 80−59837
Ta:N film, triode sputtered, struct.-related cond. props. 79−78225
Ta-Cr-Si-Al, heat resistive films, prepared by sputtering, lifetime meas. 80−80132
Ta-Ti-N, reactive sputtered film, elec. props. 78−84336
Ta-Ti-O, reactive sputtered film, elec. props. 78−84336
TaB_2-Cr-Si-Al, heat resistive films prepared by sputtering, lifetime meas. 80−80132
$TaGe_2$, superconducting transition temp. meas. 80−7019
TaN, sputtered thin films, cross-sectional composition by SIMS, elec. resist. calcs. 79−77953
TaN_x, triode sputtered, struct. and elec. props. 79−78242
Ta_2N, thermal oxidation, reaction kinetics 78−39959
TaO_5 film, used in making lenses and waveguides in collimator 79−68446
Ta_2O_5, RF-sputtered thin-film optical waveguide, effect of deposition parameters on optical loss 79−76881
Ta_2O_5 sputtered film for integrated optics, refr. index meas. *(Italian)* 79−32088
Ta_2O_5, sputtering conditions rel. to electronic cond. 77−40365
$TaSi_2$ film, elastic stiffness and thermal expansion coeffs. 80−107451
$TaSi_2$, superconducting transition temp. meas. 80−7019
Ta_5Si_3 and $TaSi_2$ form. in thin cosputtered (Ta+Si) films on polycryst. Si and SiO_2 80−70546
(Tb,Dy)-Fe amorphous films prep. by cosputtering, magnetoelastic props. 80−97429
Tb-Fe, amorphous ferrimag. film, thermomag. writing using He-Ne laser 77−12163
Tb-Fe amorphous films, mag. aftereffect due to domain well motion 79−73780
Tb-Fe amorphous thin films, magnetic after-effect, Kerr magneto-optic effect obs. 80−97123
Te-As-Ge, RF sputtering, temp. and bias effects on comp. 77−40367

sputtered coatings continued
Ti, diffusion in $LiNbO_3$ planar and channel optical waveguides 80−19096
Ti film, deposited by cylindrical magnetron sputtering, internal stresses, optical reflectance and elec. resist. 77−43449
Ti, sputtered film, energetic neutrals rel. to impurities 79−69980
Ti/Ag metallisation system, corrosion inhibition using intermediary Pd layer 79−79155
Ti-Si cosputtered films, silicide form., X-ray diffr. and resist. study 80−54546
Ti-W, bias-sputtered, resist. and comp. 80−25023
Ti-W films, bias-sputtered, quantitative anal. 80−80114
Ti-W magnetron sputtered films metallisation 80−45231
TiC, activated reactive evaporation and sputter deposition, friction and wear characts. 77−44394
TiC, activated reactive evaporation and sputter deposition, ancilliary props. 77−44395
TiC, RF sputtered film on steel, transition region 78−39956
TiC, TiVC, on steel, sputter deposited, adhesive quality 77−12531
TiN_x, spectral reflectance, selective solar absorber appl. 77−79954
TiO_2 film, photocond. and TSC meas. 80−15560
TiO_2 film, RF sputtering, dielec. props. and X-ray phase analysis 78−80288
TiO_2-Nb_2O_5 sputtered thin layer structure and optical props. 79−28851
TiO_2-SiO_2, semicond. glass, small polaron hopping cond. 78−60126
TiO_2-ZrO_2 sputtered thin layer structure and optical props. 79−28851
$TiSi_2$, film, elastic stiffness and thermal expansion coeffs. 80−107451
V_2O_3 film, reactively sputtered on sapphire, electron microscopy exam. 78−84106
V_2O_4 films, characterisation using XPS, metal-semiconductor transition 79−28900
V_3Si film, superconducting props. 79−38215
W film, sputtered, physical props. 79−77938
W film sputtered on Si crysts., annealing response, strain distrib. characterisation 77−70140
W-SiO_2 cermet film, deposition by RF sputtering of powder target, elec. resist. and TCR 79−78890
WC, elec. resist., mag. susceptibility and adhesion meas. 77−44395
WC, explosive plasma sputtered coatings, struct. and props. *(Russian)* 80−100783
WC-Co, sputter deposition, friction and wear characts. 77−44394
WC-Co DC and RF sputtered coatings, bias effect, struct., X-ray-Auger study 80−70565
WC-Co sputter deposited film, struct. and comp. 78−72023
WC-Co sputter deposited film, friction and wear 78−72918
$W_9Nb_8O_{47-x}$ polycrystalline film as electrochromic material 79−65949
WSi_2 film, elastic stiffness and thermal expansion coeffs. 80−107451
WSi_2, sputtered, props. for MOS IC appl. 80−70831
WSi_2 sputtered film on Si and SiO_2 substrate, thermal oxidation kinetics 80−3208
WSi_2, steam-oxidized, Auger sputter profiling studies 80−107663
YCo_3, amorphous, DC sputtered, easy axis and easy plane magnetisation 78−64237
YCo_3, amorphous, in-plane anisotropy induced by rare gas annealing 78−84458
YCo_3 amorphous films, ^{59}Co spin echo study 80−80636
YIG target and DC glow discharge sputtered film compositions compared 77−55886
Zn film, RF sputtered, ageing processes 78−84322
Zn, sputtered film, thermal ageing, thickness dependent effects 78−6462
$Zn_{1-x}Cd_xS$, polycryst., reactively sputtered, MSM struct. obs. of dielec. props. and cond. mechanism *(French)* 78−14841
ZnO, DC sputtered, prep. and characterisation 78−3040
ZnO film on Corning 7059 glass and Si, SAW transducer appl. 80−80138
ZnO film on ozidised Si, optical measure of acoustic quality 80−80893
ZnO films, RF sputtered single-cryst., on sapphire, struct. and SAW props. 80−80105
ZnO films for SAW devices and filters *(Japanese)* 77−73116
ZnO high-resist., band and hopping cond., AC cond. and capacitance meas. 77−72928
ZnO piezoelectric films, RF planar-magnetron sputtered, characterisation 80−96751
ZnO, RF sputtered epitaxial film, appl. to integrated optics 77−14821
ZnO sputtered films, undoped and Ga doped, props. rel. to deposition conditions 80−107935
ZnO thin piezoelectric film, SAW devices for HF range *(Japanese)* 80−53598
ZnO triode sputtered film elastic props. rel. to structure and composition 79−46988
ZnO triode-sputtered film crystallite structure, X-ray evaluation 79−46987
ZnO/SOS monolithic SAW amplifier 78−6205
ZnO-SiO_2-Si layered films for SAW devices and filters *(Japanese)* 77−73116
ZnS film on Corning 7059 glass and Si, SAW transducer appl. 80−80138
ZnS, RF sputtered film, stoichiometry, chem. comp. 78−34727
ZnS:Tb^{3+}, sputtered film, DC electroluminesc. and host-excited photoluminesc., Tb^{3+} content depend. 77−85807
ZnSe, RF bias-sputtered CVD films on CaF_2 79−14060
ZnSe sputtered laser window coatings, prep. and evaluation 77−50739
ZnSe/metal, dielectric phonon-metal electron interaction, effect on optical props. *(Russian)* 79−19663
$ZrGe_2$, supercond. crit. temp. 78−14853
ZrN_x spectral reflectance, selective solar absorber appl. 77−79954
ZrO_2, reactive sputtering, O_2 press. depend. 77−12530
ZrO_2, stabilised, coating for turbine components, degradation due to internal stresses 79−24671
ZrO_2:Y_2O_3, bias sputtering, film growth and characts. 77−40366
ZrO_2:Y_2O_3 film, preferential sputtering, Auger and XPS spectra obs. 79−52071
ZrO_2-CaO RF sputtered film, solid electrolyte, comp., struct. and AC cond. 77−39741
ZrO_2-CaO thin film O_2 sensor, ionic transference number, cell design 77−70360
ZrO_2-Y_2O_3, surface characterisation, XPS, ESCA, and AES expts. 78−72028

sputtered layers *see sputtered coatings*

sputtering
see also d.c. sputtering; diode sputtering; radiofrequency sputtering; reactive sputtering; sputter etching; triode sputtering
adsorbed layer sputtering by low energy ions 77−62758
adsorbed layers, gas atom scattering, hard sphere theory *(Russian)* 79−38704
AES composition depth profiling sputtering times, conc. gradient effect *(French)* 80−76116
AES depth profiling with N_2^+ ion sputtering 77−16889
air discharge, sputtered cathode metal atoms, time-resolved light emission 78−71601
alkali halide, under bombard. by multiply charged Ar^+-Ar^{5+} and Kr^+-Kr^{5+} ions 78−11046
alkali halides, electron sputtered atoms, energy distrib., time of flight method 78−48263
alkali halides, exciton mechanisms of electron sputtering process 77−55857
alkali halides, interstitial motion during radiation damage and sputtering processes 80−54230
alkali halides, photon induced sputtering 80−35013
alkali halides, sputtering, thermal effects, review 80−35033
alkali halides, sputtering and cluster formation, mass spectra and SIMS 79−19959
alkali halides, sputtering of molecules, low-energy electron bombardment 80−35026
alloy, binary, surface dehomogenisation during evaporation and ion sputtering 77−73207
alloy, surface composition changes 80−2913
alloy components, in plasma, probe method obs. 79−55564
alloy film, monitoring and controlling techniques, review 78−11113
alloy film codeposition using pure metallic wire mesh 78−39688
alloy sputtering 80−50503
alloy surface, enhanced diffusion effect on preferred sputtering 78−43973
alloy surfaces, sputtering process and sputtered ion emission models 80−35044
alloys, ion-implanted, integral Gaussian profile determ. method 80−107313
alloys, preferential sputtering, surface binding and mass difference effects 79−83077
alloys, with second phase precipitates, transient sputtering characteristics, glow discharge optical spectroscopy meas. 77−44156
alloys and compounds, recoil implantation and ion-beam-induced comp. changes 80−34021
amorphous target, surface sputtering by fast ions 79−69947
angular dependence of sputtering yield 79−100005
angular distributions of sputtered material, anal. by autoradiograph technique 78−27362
angular sputter yield peak position, ion reflection theories 77−59662
atom ejection studies by classical trajectory simulation 80−108311
atomic excitation mechanism 78−43971
atoms in excited states, vel. meas. 80−63561
automation and programming of production plants *(Hungarian)* 77−4736
backscattering technique, Rutherford, study of sputtering process in Au, Al, Si targets 77−8703
ball bearings, surface comp., AES and ion sputter profiling 77−40465
binary alloy, time const. for preferential sputtering 80−2912
binary alloys, preferential sputtering with diffusion, equilib. distrib. 78−68592
binary compounds, partial yields calc. 77−8696
binary solids, preferential sputtering, diffusion enhancement effects on comp. changes 79−47574
binary solids, sputtered, influence of incident flux depend. radiation enhanced diffusion on composition changes 79−52067
binary target, sputtering yield calc. 79−87550
biological implant, ion beam sputter of surface morphology SEM exam. 77−44836
bombarding ion dependence of secondary ion emission and sputtering yield 79−33879
book 77−31691
carbonaceous surface contamination growth on ion bombard. 77−90229
cathode, at low energies, theory 78−19624
cathodic in corona positive discharges, in atmospheric air, investigation by spectrophotometry method *(French)* 77−4015
ceramics, local in depth anal. by neutral beam SIMS 80−89565
circular magnetrons, high rate sputter deposition 78−72665
closed field sputtering equipment 80−50556
cluster emission, mech. 79−28872
coating characterisation 77−31919
coating techniques, comparison between electron beam evaporation and high rate sputtering with plasmatrons 78−11110
coating thickness, effect of process parameters *(Russian)* 78−31340
combined ion beam deposition and etching for thin film studies 80−71594
compositional depth profiling by Auger electron spectroscopy 79−52053
compound, surface composition changes 80−2913
computer simulation of sputtering mechanism for light ions 79−56901
cones on sputtered surfaces, geometry, rel. to ang. depend. of sputtered yields 77−81191
conference, atomic collisions in solids, Hamilton, Canada (Aug. 1979) 80−62375
conference on inelastic ion surface collisions, Hamilton, Ontario, Canada (Aug. 1978) 80−31402
cryogenic thin film ultrahigh-vaccum evaporation/sputtering apparatus 80−20790
crystal surface, in-situ cleaning by ion sputtering, in EM 80−101895
crystal surface morphology development during sputter erosion 80−88414
CTR devices, surface effects related to voltage breakdown 77−35356
CTR first wall design, surface phenomena importance 77−34431
depth profile improvement using two ion guns 80−71964
depth profiles, edge effects, anal. correction 80−80925
depth profiles by sputtering in SIMS and AES 79−56891
depth profiles distortions 80−55249
depth profiles obtained by ion-beam sputtering, edge-effects correction 80−55757
depth profiling, new unit for ion dose, Wehner 77−8753
depth profiling, review 80−40214

sputtering continued
depth profiling techniques for thin film interdiffusion and interfacial reactions, book contrib. 79−1564
depth profiling under ion bombard., sputter broadening Monte Carlo simulation *(Japanese)* 79−83089
depth resolution in profiling of sandwich structures 78−92165
depth resolution in sputter profiling, surface transport effects, calc. 80−97393
depth resolution in sputter profiling 77−44102
detonation sputtering, gas flow parameters calc. *(Russian)* 80−16181
detonation sputtering, interaction between detonation waves and gas and powder flows *(Russian)* 80−16182
dielectric films on semiconductor devices, review of deposition techniques 78−23611
dimer ejection, statistical model for fast ion impact 79−69948
effects due to probing electrons and sputtering 77−90706
electron microscope specimen preparation techniques 78−32947
electron microscopy, specimen deposition and fabrication by ion beam sputtering 80−82855
elements, energy spectra of ions sputtered by O_2^+ 79−61484
elements, sputtering process and sputtered ion emission models 80−35044
energy, and mass distribs. of sputtered particles 80−84822
energy distribution, ion mass and target temp. effects 80−66361
energy efficiency of ion sputtering processes *(Russian)* 80−7457
energy reflection by backscatt. and sputtering, total yields and ang. distrib. 80−89101
equilibrium surface topography, developed by sputtering, stability 79−14988
erosion, symmetric triangular microprofile, apparent growth and equilib., angular ranges 78−23571
evaporation chamber LV electron guns with longitudinal compression *(Russian)* 80−50551
excitation efficiency of atoms during ion-beam sputtering 78−19623
excited atom sputtering, cascade and quasi-thermal processes 78−35239
excited state population distributions, from sputtering sources, methods of determ. 79−52063
excited states amongst sputtered particles, thermal origin 78−35238
faceted cone symm. rel. to ejection patterns 78−64439
ferrite films, influence of heating support on struct. and props. *(Russian)* 79−78445
ferrites, plasma sputtering, struct. props. and phys.-chem. transform. *(Russian)* 79−38739
film, materials engineering, electronics appl. *(Japanese)* 77−73229
film analysis using computer-controlled Auger spectrometer, digital methods 77−56268
film deposition, ion beam techniques 80−11564
film deposition, trend of new techniques *(Japanese)* 80−11563
film deposition method, for controllable comp. with given elec. props. 80−35087
film fabrication techniques *(Czech)* 79−69979
film island coalescence of real cryst. surface, unattenuated sputtered atom source 80−6672
films, preparation using low pressure plasmas 77−40361
films and coatings using conc. energy sources *(Russian)* 79−74090
fissured biological object prep. for SEM, vacuum deposition and cathode sputtering comparison 80−72390
Fluorolon-3, utilisation factor determ. during electron beam sputtering *(Russian)* 79−66008
fly ash, depth composition determ. by XPES 78−68943
focuson model, calc. of combined three-dimensional distribution of probability density 79−43086
fusion neutron induced nuclear recoil emission probabilities 78−15256
fusion reactor, plasma-wall interaction, permissible degree criterion 78−89981
fusion reactor, sputtering erosion of cavity walls, comput. procedure 77−38410
fusion reactor first wall material, by H^+, D^+, T^+, and He^+, 1 keV *(Russian)* 77−8697
fusion reactor first wall materials, light ion sputtering studies 80−18647
fusion reactor first-wall mat., physical sputtering model 78−80445
fusion reactor first-wall materials, sputtering model 78−82514
fusion reactor materials, low energy ion erosion expts., Kaufman source appl. 80−68942
fusion reactor materials, sputtering calc. 78−86689
fusion reactors, blister-induced first wall erosion, alpha incident velocity and poloidal angle distribs. 80−37583
fusion technology, surface studies 80−23149
Galilean satellites, ice sputtering and water products contrib. to Jupiter magnetosphere 78−45268
gas sampling in sputtering system, mass spectroscopy 77−69989
gas turbine airfoils, protective coatings, degradation characts. and methods of application 79−24670
getter sputtering at low temp. 78−35305
glass surface, sputtering with inert gas ions 78−64438
glass-metal seals, use of AES and ion sputtering in interface study 80−76587
glow discharge, E×B type, sputtering characts. *(Japanese)* 77−68889
glow discharge, electric probe diagnostics, sputtering of appl. 78−71537
glow discharge, production and energy distrib. of H atoms present in traces *(French)* 77−24229
glow discharge characts. meas. for sputtering appl. 78−72726
glow discharge sputtering diagnostics, optical spectroscopy 78−72666
graphite, chemical sputtering by H^+ ions 77−36341
graphite, D^+ bombardment, surface damage, sputtering, SEM study 80−32459
graphite, energetic ion sputtering, appl. of AES-SIMS (IMA)-FDS combined systems to physical and chemical processes 78−95636
graphite, low energy ion sputtering, theory 79−28880
graphite, permeable, 0.6, 3.5 MeV He^+ irrad., surface erosion, porosity effects 77−35602
graphite, sputtering, physical and chemical, by H_2 and He, 600 to 7500 eV 77−36340
graphite, sputtering yield, use as first wall material 78−95629
graphite sputtering by low energy H and D 78−95630
heavy ion beam targets, damage, lifetime, uniformity, book contrib. 79−31291
heavy ion bombardment, hydrodynamical approach to non-linear effects in sputtering yields 80−66374
heavy ion generator, 150 keV, for sputtering 79−697
high rate film growth, book contrib. 78−11117
high thermal input sputtering heat transfer process 79−28914
high vacuum cryogenic versus turbomolecular pumping in sputtering appl. 79−80629
high-energy, Monte Carlo calc . 77−40319
ice, sputtering by MeV light ions, erosion rate 78−48268
III-V semiconductor, superlattices and related structures *(Slovak)* 80−88620
implant ion collection with radn. enhanced diffusion and sputtering of implant 80−2055
Inconel, sputtering and blistering from H^+ and He^+ bombardment 78−79649
inhomogeneous rod in complex heat exchange conditions, temp. calcs., film sputtering evaporators *(Russian)* 80−38230
inorganic solids, anal. of H_2 in solids by sputter induced emission spectroscopy 79−5231
inorganic thin layers, two-stage formation 79−27450
insulating film for semicond. devices, props., rel. to deposition conditions 78−23612
insulators, fission fragment sputtering 80−40207
intensity, from half-space, angle of incidence depend., theory 80−100735
intermetallic compounds, significance of negative ion formation in sputtering and SIMS anal. 78−72663
interstellar grain destruction by sputtering 78−54020
interstellar grains, destruction by sputtering 78−45382
interstellar graphite grains, chemical sputtering 79−62880
Invar, photon emission from sputtered atoms, obs. of apparent local thermodynamic equilib. in excitation 78−72672
ion assisted deposition, review *(Japanese)* 77−73227
ion beam, review of technique, appl. 78−68587
ion beam focusing designs for sputter deposition 79−78880
ion beam sources, for sputtering technology, review 78−72719
ion beam sputtering, appl. to surface machining 80−30129
ion beam sputtering, application to high resolution electron microscopy 78−32925
ion beam sputtering, combination with AES, surface anal. 80−50474
ion beam sputtering as microsectioning technique, for small diffusion coeff. meas. 78−47551
ion beam sputtering for surface anal., UV vacuum sample chamber 77−4970
ion beam utilisation for etching and film deposition, review 77−32522
ion bombarded surfaces, energy distrib. of sputtered ions using SIMS 79−4457
ion bombardment, electron microscopical anal. of surface effects and volume defects, review *(Rumanian)* 80−29093
ion bombardment-induced photon emission, spectral features, mechanisms band struct. depend., review 77−44072
ion emission, sputtered, universal model 80−55248
ion impact induced shock processes in solids 80−89104
ion induced, technological appls., review 77−44107
ion irradiated solids, disorder accumulation, saturation and sputter limitation 78−67753
ion knock-on mixing model, and its appl. to Si-SiO_2 interface profiling 79−83081
ion microanalyser, neutral particle beam separation, characts., anal. appl. *(Japanese)* 78−85248
ion microprobe analysis, elemental imaging errors, polarity role 78−20103
ion microprobe analysis using ion-induced AES 80−30305
ion microprobe mass analyzer appl. in metallurgy *(Japanese)* 77−25233
ion plating, evaporation sources, gaseous media, and transport modes 80−80984
ion plating, inert gas handling 79−69994
ion source, appl. to IMA analysis *(Japanese)* 79−54734
ion sputtering process, model 78−88398
ion-enhanced film bonding 79−83126
ion-excited Auger emission from sample trays in Auger-sputter profiling study 78−52607
ionisation of atomic particles sputtered from solids, microscopic anal. 80−97392
ionisation of sputtered atoms, microscopical quantum-mech. model 79−8220
ionised and excited particle production, validity of thermodynamic models 79−52062
ionized-cluster beam deposition and epitaxy 79−83137
iron germanate glass, ion-beam sputtering, excitation efficiency of atoms 78−19623
isotope enrichment in sputter deposits 77−27198
isotopic fractionation, sputter-induced, at solid surfaces 80−55244
Josephson junction, sputtering system for fabrication *(Japanese)* 80−55293
laser method, structuring of GaAs and Permalloy-type alloy coatings *(Russian)* 77−59689
layered materials, in powder form, thickness meas. by XPS and ion sputtering 79−88913
light emission from solid bombarded with atomic particles, review 80−35036
light emission from sputtered particles, chem. effect 77−28672
light ion sputtering in fusion reactors, discrete ordinates method calcs., ANISN code 78−92158
long range focusons existence in single crystal sputtering 79−19960
low energy ion sputtering, theory 79−28880
low-energy ion sputtering, anal. formula and important parameters 80−84818
low-pressure plasma applications to surface treatment 79−94824
lunar rocks, solar wind sputtering rel. to microcrater and accretionary grain populations development 80−94732
lunar samples, preferential sputtering rel. to metallic Fe prod. and element fractionation 77−29666
magnetic film, high rate deposition by cathode sputtering from two facing targets 79−28917
magnetically enhanced cylindrical sputtering system 77−73232
magnetron cathode appl. *(Czech)* 79−52114
magnetron cylindrical sputtering system, end losses 79−47628
magnetron high rate sputtering with coaxial cylindrical electrode config. *(Japanese)* 78−23617
magnetron ion sputtering, thin film layers depositon uniformity investigation *(Russian)* 80−20787
magnetron sputtering, high-rate coaxial cylindrical, self-sputtering phenomena 77−44161
magnetron sputtering features 78−84713

sputtering continued
magnetron sputtering systems, 20K cryopumping cryopumping sputtering 79−80634
magnetron sputtering target/substrate configuration 78−39687
mask synthesis, for diffr. limited waveguide Luneburg lenses 78−38076
mass spectrometer to study secondary and sputtered ions 79−83072
mass spectrometry, sputtered neutral, for surface analysis and depth profiling 77−77833
mass spectroscopic measurements, validity for pressures exceeding 10^{-4} mbar 79−85198
measurement of sputtered ion fractions using matrix isolation spectroscopy 80−60738
mechanisms, review 80−40213
metal, BCC, sputtering processes, due to Ar^+ bombardment, computer modelling 79−19957
metal, FCC, sputtering processes, due to Ar^+ bombardment, computer modelling 79−19957
metal, ion beam texturing 77−44402
metal, photon and ion emission similarities, O_2 adsorpt. effect 77−28674
metal, positive secondary ion and sputtered atom energy distrib. 77−32485
metal, with adsorbed Cs effects on photon and secondary ion emission during sputtering 80−35038
metal alloys containing second-phase precipitates, glow-discharge optical spectra 78−48264
metal atoms from cathode in discharge, excited states emission 78−1939
metal atoms sputtered by light and heavy particles, velocity distrib. meas. by fluorescence spectroscopy 78−95626
metal coating of optical fibres, for strengthening and surface protection 78−30103
metal film, vacuum deposited, sputtering rates by O^+ bombardment 78−88390
metal hydride, computer simulation of H reflection and scattering 79−1806
metal impurity origin in DIVA, ion sputtering, evaporation and arcing 79−656
metal layer growth by sputtering, corpuscular diagnostics of hollow cathode discharge 80−16180
metal oxidation, secondary ion energy spectroscopy 80−71788
metal oxide layers, obtained by cathode and HF sputtering, light scatt. and refr. index reduction 80−29877
metal surface, 14.8 MeV neutrons, radionuclide product ejection range 78−15257
metal surface, excited atom emission, survival probabilities 78−48266
metal surface, ion-bombarded, molecular cluster ejection, model 79−87543
metal vapour production by sputtering in hollow-cathode discharge 80−1868
metal wire plasma sputtering mechanism *(Russian)* 77−52538
metal-adsorbed gas systems, sputtering effects, combined analytical techniques 80−35047
metal-semiconductor interface, atomic mixing and preferential sputtering effect on depth profiles and interfaces 79−78806
metal-semiconductor interfacial reaction, AES study *(Japanese)* 80−96701
metallic sputtered powder, stuct. and phase composition, cooling rate effect *(Russian)* 79−56941
metallisation, particle no. filling spot area, calcs. *(Russian)* 78−52668
metallurgical coatings, vapour deposition processes in vac. 80−35430
metals, atomic laser spectrosc. using cathode sputtering method 79−87917
metals, cone formation during sputtering 77−44389
metals, erosion accompanying simultaneous action of laser emission and ultrasound *(Russian)* 80−7442
metals, FCC and BCC polycrystalline, ang. distribs. of sputtered atoms 77−85879
metals, for matrix isolation spectroscopy apparatus 77−26407
metals and carbides, sputtering, low energy, H, D and He ions 80−100734
mica, alpha-particle tracks, prompt process and post effect 78−43053
microanalysis, thermal ionisation of sputtered products *(French)* 79−61924
microprofile, triangular, ion bombardment at oblique incidence, sputtering erosion and growth 77−73202
minerals, sputtering rates, implications for abundances of solar elements in lunar samples 80−61797
MIS structures, AES depth profiles, factors affecting depth resolution 79−15567
MNOS structure, Auger depth profiling and ion sputtering of interfaces 77−20200
MNOS structures, Auger depth profiling by Ar ion sputtering 77−55613
monocrystalline metals, low yield sputtering 80−66364
Monte Carlo analysis of backscattering and sputtering in vacuum systems 80−235
Monte Carlo study, computer program 78−95627
MOS metallisation via automatic S-gun planetary deposition system 78−72724
negative ion formation, by sputtering, work function depend. 78−39645
negative ion formation on sputtering metals and semiconductors with Cs^+, alkali metal monolayer effect 78−46204
negative ions, sputtered, characteristic electronic and vibrational temp., laser photoelectron spectral meas. 80−66346
negative ions sputtered from surfaces by Cs^+ impact, energy distrib. 77−81189
negative sputtered ion emission by O_2, anomalous enhancement 79−19962
neutral particle flux props., ion bombardment of polycryst. targets, review 77−44110
neutron, meas. 78−95621
neutron sputtering at 14 MeV, models for ejection for micron-sized chunks 77−36318
nitrided steel surface wear-related topography 78−60847
non-elemental solid surface, surface composition, yields, desorption effects review 77−44111
nonmetal, Coulomb explosion sputtering by intermediate energy multiply charged ions 80−35049
nonmetallic materials, epitaxial film growth by sputtering, review 77−32521
optical coating production, vacuum system development, review 77−58493
optical emission, sputter-induced, absolute photon yields 79−45667
sputtering continued
optical emission from low-energy particle-surface collisions 77−36300
optical films production and props. *(Hungarian)* 80−53483
optical spectroscopy for diagnostics and process control during glow discharge etching and sputter deposition 79−15606
organic film, synthesis and characterisation, review 79−91584
overheating influence of sputtered particles and oxidised films on heat processes *(Russian)* 80−40385
oxide glasses, ion-bombarded, optical line intensities 80−35037
oxides, sputtering, thermal effects, review 80−35033
oxides, sputtering effects, combined analytical techniques 80−35047
oxidised Iconel surface, quantitative anal. by XPS and rastered ion bombardment 77−40604
oxidised surfaces, sputtering process and sputtered ion emission models 80−35044
parallel-plate sputtering system deposition rate model 79−87579
Permalloy corrosion resistance enhancement 79−79150
Permalloy film oxidation, microbalance, AES, ESCA and sputter profiling 78−15600
Permalloy films, oxidation effects on atmospheric corrosion, AES, XPS and ion sputtering anal. 80−11829
photon emission from sputtered atoms, obs. of apparent local thermodynamic equilib. in excitation 78−72673
photon yield relation to population distribution and excitation function 80−34989
plasma containment vessels, backscatt. and sputtering from pocket and finned structs. 79−14558
plasma contamination, sputtered particles, energy and mass distribs. 80−84822
plasma diagnostic techniques appl. to glow discharge characterisation 78−71536
plasma enriched thin film deposition *(Czech)* 77−63557
plasma solid interaction, surface erosion 80−38665
plasma sputtering, interaction of particles in liquid phase *(Russian)* 78−35306
plasma-enriched deposition for thin film appls. 79−47629
PMMA, optical damage threshold, alteration methods 80−99814
polymer coatings deposition, choice of type of electrostatic sputter *(Russian)* 80−50553
preferential sputtering of O and Al in CdO, ZnO, $Al_{0.33}Au_{0.67}$, and $Al_{0.67}Au_{0.33}$ 79−4877
preferred, phenomenological model for SIMS and Auger profiling 80−55254
production sputtering systems, design, use of high rate magnetron source 79−66006
profiling, depth resolution 79−33874
PTFE films, sputtering conditions effect on comp. and optical props. 79−52115
pulse plasma sputtering, particle velocity and disperse composition *(Russian)* 80−40258
rare earth aluminate, scandate and zironate film coatings, electrophys. props. w.r.t. prep. technology 80−60781
recoil implantation from thin source, extension to recoil sputtering and moderately thick sources 78−95631
recoil-energy, surface-normal distrib. analysis 80−60733
reflected beam sputter source, output improvement with CS collection techniques 79−702
review on sputtering and SIMS *(French)* 78−80450
ring gap discharges for high rate vac. coating 77−69991
sample contamination, during ion implantation 80−54274
Saturn rings, ice sputtering by radiation belt protons 78−89116
scale-up problems 78−72722
scale-up problems in electron-beam evaporation and sputtering 78−95695
secondary ion and photon emission, energetic particle irrad. surface collision cascade 80−45186
secondary ion emission, Saha-Langmuir eqn. appl. 77−8698
secondary ion emission mechanism, energy spectra of secondary ions 79−100013
secondary ion energy distrib. integration for ion sputtering yield meas. 77−77334
secondary ion mass spectra, substrate matrix effects under O^- and Cs^+ ion bombard. 79−15571
secondary ion yields, depend. on ionisation pot. and matrix sputtering yield 79−8214
secondary ion-ion emission ionisation of solids during sputtering, exam. of mech. *(Russian)* 79−33878
secondary photon emission from sputtered excited neutrals, thermal excitation model anal. 79−4878
secondary photon emission from sputtered excited states, role of transition probability 80−102483
secondary-ion emission probability 79−87548
selective, ion-beam effect, ESCA obs. 78−52612
self-shadowed replicas, controlled sputtering 77−26434
SEM, sputter coating in oil-contamination-free vacuum 79−12784
SEM samples metal coating, heating effect *(German)* 80−73338
semiconductor, multicomponent, preferential sputtering, surface binding and mass difference effects 79−83077
semiconductor, positive secondary ion and sputtered atom energy distrib. 77−32485
semiconductor, surface, effects of ion sputtering, ion implantation 78−88395
semiconductors, cone formation during sputtering 77−44389
SiC (6H) thermal oxide layers, AES, Ar ion sputtering *(Japanese)* 79−96386
single and multiple component materials, theory 80−80924
single crystal, differential yield, surface struct., review 77−44112
slowing down particles, spatial depend. of energy spectrum 79−65129
solar wind sputtering, fractionation on lunar surface 78−61762
solar wind sputtering of lunar surface, comments 78−61763
solid surface analysis, ion beam sputtering 77−12477
spatial distribution of energy, fluctuation, deposited by atomic particles 79−90709
Sputter ion pump *(Japanese)* 78−21152
sputtering induced topography on solids, energetics and kinetics 80−88220
sputtering yield meas. on first wall materials of thermonuclear fusion devices *(Japanese)* 77−85865
statistical model, geometrical considerations, sputtering yields 79−100003
steel, 304 stainless, Tokamak wall, by H_3^+, ang. effects 79−46458

sputtering continued
steel, austenite, He blistering at high irradiation doses 79−51167
steel, Ni-Cr, oxide layer form., SIMS obs. 79−52464
steel, stainless, 316, sputtering by fusion neutrons meas. 77−36321
steel, stainless, He induced blistering, during simultaneous sputtering 79−1808
steel, stainless, low energy H^+ sputtering 80−40198
steel, stainless, oxidised, sputtering yield meas. by atomic fluoresc. spectroscopy 80−80922
steel, stainless, photon emission from sputtered atoms, obs. of apparent local thermodynamic equilib. in excitation 78−72672
steel, stainless, sputtering and chem. attack by H ions of 100 eV energy 78−95635
steel, stainless, sputtering by low energy H and D 78−95630
steel, stainless, sputtering of Cr^+ by 10 keV H_3^+ angular effects 79−52058
steel, stainless, sputtering yield meas. using AES 80−18654
steel, stainless, sputtering yields of 1 to 20 keV light ions 77−36339
steel, stainless 12Kh18N10T, in plasma, probe method obs. 79−55564
steel, stainless 316, ion sputtered, surface anal. by Auguer effect and SEM 78−95632
steel, stainless sheet, texture effect on sputtering erosion by Ar^+, SEM-electron channelling study 79−91856
steel, stainless type 304, surface cleanup and sputtered ion production, AES and SIMS obs. 79−66209
steel target, stainless, deuteron trapping model, of gas sputtering 80−49398
Stewart-Thompson theory, surface topography, glow discharge and ion-microprobe sputtering, obs. 78−43977
substrate heater, for sputtering system 79−69983
substrate heating in high rate coaxial cylindrical magnetron sputtering 78−56579
superlattice thin films, sputtered, ion-bombardment-enhanced diffusion during growth 78−87882
surface, coverage of foreign atoms as function of adsorption, sputtering and diffusion rates 79−69354
surface, ion beam texturing 79−77876
surface analysis, advantages and disadvantages of SIMS rel. to ion scattering spectrometry 79−12883
surface analysis by ion sputtering and thermal ionis. *(French)* 77−63510
surface atoms, sputtering mechanism 79−69945
surface barrier curvature influence on sputtering characts. 80−60739
surface coating technology, conference, London (1978) 79−83358
surface composition changes during Ar^+ ion sputtering of alloys 80−49470
surface composition depth profiles, ion sputtering effects 80−35616
surface composition determ. by ion beam sputtering 77−48701
surface diffusion, influence on surface anal., model calc. 79−15016
surface erosion, nonuniform incident flux effect 79−39003
surface ionisation, elemental anal. of sputtering products *(French)* 80−50905
surface layer composition changes 77−73200
surface layer composition changes in sputtering 78−2343
surface morphology, analytical modelling 77−16445
surface properties of materials, Conf., Missouri, USA (August 1977) 78−87867
surface recoil ejection mechanisms, computer studies 80−66363
surface struct. effect., angular distrib. and yield from faceted surfaces 79−15575
surface texture effects of ion bombardment *(Rumanian)* 77−28673
surface-barrier shape effects on sputtering characts. 80−93447
target cracking, acoustic emission testing 80−81248
Teflon-4, utilisation factor determ. during electron beam sputtering *(Russian)* 79−66008
TEM specimen preparation, fine grained coatings, sputter source design 80−99015
thermal sputtering theory, thermal spike due to energetic ions 77−48293
thin and thick film technology, conference, Augsburg, Germany (1977) *(German)* 78−39685
thin film circuit preferential sputtering process *(German)* 78−39691
thin film deposition technique, review *(Japanese)* 80−35107
thin films, deposition techniques, review 80−80964
thin films, thickness meas. anal. characterisation using proton-induced X-ray emission 80−35618
thin films fabrication techniques 80−76176
thin layer activation, appl. to wear and corrosion meas., surface treatment and sputtering 79−87810
Tokamak, Diva, metal impurities origin, arcing ion sputtering, evap. 78−59691
Tokamak, metal impurity reduction by working gas injection 80−106963
Tokamak, superthermal alpha transport and wall bombardment 79−649
Tokamak devices, blistering and flaking by He atoms 78−86690
Tokamak fusion test reactor, thermal response of first wall limiters 80−79585
Tokamak limiter, surface observation, infrared techniques 80−38693
Tokamak reactor, fusion-product bombardment of first wall 77−38409
Tokamak scrape-off plasma, metal impurity recycling effect 80−10421
torsion vacuum microbalance appl. to sputtering yield meas. *(Japanese)* 78−19622
track radiography of heavy-ion induced sputtering 80−91404
transition metal borides, secondary ion sputtering, ionisation, energy distrib. characts., atom binding energy *(Russian)* 79−69940
transition metal carbides, secondary ion sputtering, ionisation, energy distrib. characts., atom binding energy *(Russian)* 79−69940
transition metal oxide and hydroxide surfaces, chem. changes induced by Ar^+ bombardment, XPS obs. 79−83084
transition metal-O bond energy in O_2 glow discharge, mass spectrometry obs. 80−64808
triangular microprofile containing surfaces, oblique incidence sputtering, topographic changes 80−66372
turbomolecular pumps for high gas flow applications 79−80632
turbulent stream of high temp. gas with particles, modelling *(Russian)* 80−38572
ultra cold neutron container materials, surface conc. of H atoms by ion bombardment 80−9446
ultrahigh depth resolution surface analysis, appls. 78−71917
uniformly thick film sputtering optimisation 79−27451
Uranus rings, ice sputtering by radiation belt protons 78−89116
UV metal ion lasers, discharge sputtering of metals 78−66809
vacuum arc, sputtering from cathode spot region 79−82113
sputtering continued
vacuum deposited film, as first wall material, sputtering yield mea. *(Japanese)* 80−25513
Vacuum Society conf., San Francisco, USA (Nov. 1978) 79−77862
vacuum technology, medium, high and ultrahigh, conf., Oxford, England (Apr. 1978) 79−63242
wear resistant surface, review 78−72938
yield, absolute meas., UHV microbalance, with ion gun *(Japanese)* 80−17951
yield, energy depend., semiempirical formula 80−100736
yield, mass dependence, rel. to boundary effect 79−24398
yield dependence on incident atomic number, surface correction 78−43978
Ag, Cu diffusion, SIMS investigations 80−59717
Ag film, sputtering, photon emission enhancement compared with sputtering rate 79−78815
Ag, film, sputtering mechanism, SEM 80−29839
Ag films, electrodeposited and vac. deposited, AES depth profiling anal. 77−59232
Ag films, on mica, graphite, and Si, early growth by ion-beam sputtering 77−44158
Ag, implanted Li atoms, depth profiles and sputtering anal. by optical spectra 77−35579
Ag, ion bombardment, sputtering, re-emitted kinetic energy ang. distrib. 80−2910
Ag, low energy sputtering by Ar and Xe ion bombardment 78−15269
Ag, low temp. self-diffusion, sectioning using ion beam sputtering 79−19393
Ag, polycryst., sputtering rate on Ar ion bombard. 80−55245
Ag, sputtered, angular distrib. during He^+ and Ar^+ ion bombardment 78−95624
Ag, sputtering by heavy atomic and molecular ion bombard. 80−71532
Ag, sputtering yields for ions over 15-135 keV 79−56899
Ag surfaces, temp. defend. of sputtering based on thermal spike effect 80−50491
Ag, temp. depend. 80−2914
Ag thin films, spike effects of heavy ion sputtering 80−35034
Ag-Au, composition changes under ion bombardment, scanning Auger microprobe obs. 79−83076
Ag-Au, sputtering, ion yield depend. on alloy comp. 77−20976
Ag-Au, sputtering by 6 keV Xe^+ ions, energy distribs. 78−43969
Ag-Au, surface layer, effect of Ar^+ bombardment, AES and SIMS 80−25504
Ag-Au alloy, Auger exam. of preferred sputtering 77−44106
Ag-Au alloy, ion irrad., surface segregation and selective sputtering, AES expts. 79−7740
Ag-Au alloy, surface after sputtering, AES obs. 77−55858
Ag-Au-Cu, sputtering and AES 80−50503
Ag-Au-Cu, surface composition change on sputtering with 2 keV Ar ions 80−66365
Ag-Cu alloy, surface comp. after sputtering, AES obs. 77−55858
Ag-Pd alloys, inert gas ion bombardment, dynamic surface composition changes, AES obs. 80−60745
Ag-Pt interface formed by electrodeposition, depth profile 77−16512
Ag-Pu (0.5 wt.%) deposited profiles, homogeneity, from hexagonal point source array 80−25559
Ag-Pu alloys, metastable, high rate sputter deposition, annealing behaviour of deposits 77−21025
Ag-SiO_2 film, elect. and struct. props., ion beam sputtering 78−80071
AgAu, ion bombardment by alkali-metal sputter ion source *(Japanese)* 79−54734
AgF(Br), sputtering processes during 6 keV Xe ion bombard. 78−68590
Al, annealed and powder sintered (SAP 895), sputtering under D^+ and $^4He^+$ bombardment, microstruct. effects study 80−84821
Al, by He^+ photon emission, dose depend. 77−8695
Al, deform. enhanced photoemission meas., effects of ion sputtering 77−32511
Al film, magnetron sputtered deposition, characts. 79−91587
Al, film and polished bulk specimens, initial stages of oxidation obs. using SIMS 80−81239
Al foil, solar wind ion bombardment, lunar surface modification 80−109325
Al foil, sputtering with ^{252}Cf fission products, desorbed secondary ions 78−68596
Al, implanted Li atoms, depth profiles and sputtering anal. by optical spectra 77−35579
Al, ion bombardment, sputtering, re-emitted kinetic energy ang. distrib. 80−2910
Al, oxide films, metal and O_2 transport, AES and inert marker, techniques 80−97641
Al, oxidised, light emission from sputtered O atoms or ions 80−58199
Al, polycryst., sputtering rate on Ar ion bombard. 80−55245
Al sintered powder coatings, form. and behaviour under particle bombard. 80−35029
Al, sputtered excited Al particles, effect of O during ion bombardment on spectra 79−38703
Al, sputtering and chem. attack by H ions of 100 eV energy 78−95635
Al, sputtering by 15 keV Ar^+ ions, microroughness 79−91556
Al, surface ionisation, elemental anal. of sputtering products *(French)* 80−50905
Al/Cr thin films, interdiffusion meas., AES and ion beam sputtering 79−82391
Al-Ag alloy mirror for use as solar reflector, co-sputtering 80−20789
Al-Cu, surface enrichment of Cu due to Xe sputtering, AES and He ion backscatt. meas. 77−4250
Al-Cu film, magnetron sputtered deposition, characts. 79−91587
Al-Cu-Si, effect of sample conditions on sputtering and intensities, emission spectrochem. anal. using glow discharge *(Japanese)* 80−21349
Al-Li solid soln., decomposition exam. by secondary ion ion emission *(Russian)* 78−68696
Al-Pd, preferred sputtering on surface, mass difference and chemical bonding difference effects, AES obs. 79−83078
Al-Pd(Si) film, preferred sputtering on surface, mass and bonding difference effects, AES obs. 79−87552
Al-Si, preferred sputtering on surface, mass difference and chemical bonding difference effects, AES obs. 79−83078
Al-Si coatings, form. and behaviour under particle bombard. 80−35029
Al-Si film, magnetron sputtered deposition, characts. 79−91587
Al-SiO_2-Si structure, Auger depth profiling and ion sputtering of interfaces 77−20200

sputtering continued
$Al_{0.3}Ga_{0.7}As$-GaAs minimum heterojunction width determ. by sputter Auger techniques, interface broadening 79−69586
Al_2O_3 coatings, form. and behaviour under particle bombard. 80−35029
Ar glow discharge, metastable and reson. states density meas. *(French)* 80−14955
Ar^+, 30-cm multipole sputtering electron-bombardment ion source, design and characts. 77−87870
Ar^+ ion, polycrystal bombardment, sputtering efficiency 77−85869
Au amorphous film, getter sputtering at 25K 79−38741
Au, by point defects, time-of-flight spectra 79−47573
Au cryst., ion bombarded, Ar^+ ions, time-of-flight spectra of sputtered atoms 80−89103
Au, discontinuous film, degradation under MeV heavy ion bombard., Rutherford scatt. and TEM obs. 79−24397
Au, fast neutron sputtering 77−36316
Au film, ion bombarded, surface craters induced by displacement cascades 80−107344
Au film, ionic sputtering and AES anal. *(French)* 78−76959
Au film, on Ni, AES anal., influence of ion bombardment on depth resolution 77−20210
Au film, on Si, early growth by ion-beam sputtering 77−44158
Au film on Si, use of sputtering for layer removal 79−78813
Au films, (111), sputtering in high voltage electron microscope 80−35027
Au foil, radiation damage from sputtering by fission fragments 78−2968
Au foil, sputtering in a high voltage electron microscope 77−36328
Au, low energy H^+ sputtering 80−40198
Au, low energy sputtering by Ar and Xe ion bombardment 78−15269
Au, neutron damage calc., deuteron break-up source, sputtering appl. 77−35593
Au, neutron sputtering yield determ. 77−36319
Au, polycryst., sputtering coeff. depend. on Ar^+ ion dose 77−59661
Au, polycrystalline foil, sputtering yield meas. by UHV microbalance with ion gun *(Japanese)* 80−17951
Au, sputtered with 15 or 30 keV H^+, He^+ and Ar^+ ions, energy and angular distrib. 78−95625
Au sputtered with Xe^+, Xe^{2+}, nonlinear effects 80−20748
Au, sputtering and chem. attack by H ions of 100 eV energy 78−95635
Au, sputtering by fast neutrons 79−61470
Au, sputtering with 30 keV Ar^+ ions *(German)* 79−24407
Au, sputtering yield at low energy for light-ions 78−19620
Au, sputtering yields for ions over 15-135 keV 79−56899
Au, sputtering yields for light ions 79−87537
Au, sputtering yields of D^+ and Ar^+ ions using matrix isolation spectroscopy 79−78809
Au thin films, spike effects of heavy ion sputtering 80−35034
Au, transmission sputtering yield for 6.8 MeV Au^+ bombard. 77−1808
Au transmission sputtering 78−52613
Au, transmission sputtering by $Ag^+(Ar^+)(He^+)$ ions 79−4885
Au/Pt/Cr films, diffusion of Si, depth anal., optical and Rutherford backscatt. meas. 79−10981
Au-Ag, thin film, double layer system electron beam effects during sputter profiling AES obs. 79−65347
Au-Ag single phase alloy, sputter yields 79−87546
Au-Cr alloy, quantitative Auger electron anal., sputter-yield ratio 77−44096
Au-Cu alloy, preferential sputtering 79−83080
Au-Cu-O surface, quantitative Auger analysis using relative sensitivity factors 78−7295
Au-Cy alloy, surface comp. after sputtering, AES obs. 77−55858
Au-Ni alloy, preferential sputtering 79−83080
Au-Ni-O surface, quantitative Auger analysis using relative sensitivity factors 78−7295
Au-O bond energy glow discharge, mass spectrometry obs. 80−64808
Au-Pd alloy, surface comp., polishing, cleaning and Ar sputtering effects 77−72763
Au-Sn alloys, surface comp. by Auger spectroscopy, sputter cleaning 77−59648
B, light ion bombarded, sputtering yields 79−38702
B_4C, sputtering yield, use as first wall material 78−95629
$BaTiO_3$, film deposition by HF cathode sputtering 77−36398
Be, foil, ion bombardment, secondary photon emission, ion energy depend. 80−97346
Be, sputtered atoms, ion bombardment induced line radn. 79−91553
Be, sputtering by H^+, D^+, He^+, weight loss measurements 80−35028
Be surfaces, O and H covered, secondary ion emission, coverage dependence 80−35043
BeO, sputtering by H^+, D^+, He^+, weight loss measurements 80−35028
BeO, sputtering by low energy H and D 78−95630
C coating on Pt temp. depend. of H_2^+ sputtering 78−95634
C film, deposited on Pt, H sputtering 77−69951
C on Pt for radiative heat transfer gauges, prod. technique *(Chinese)* 79−38742
C pyroceramic, sputtering and blistering from H^+ and He^+ bombardment 78−79649
C, pyrolytic, 0.6 to 3.5 MeV He^+ irrad., surface erosion, porosity effects 77−35602
C, sputtering by fast electrons 77−90226
CC $Bi_4Ti_3O_{12}$, coaxial magnetron sputtering technique 79−83123
CH radical, sputtered, rotational and vibrational excitation 80−69224
CH radical, sputtered from acetone chemisorption layer on Si, rot. and vibr. population distrib. 78−64436
CO_2 laser bimetallic mirror coating vacuum sputtering technology 80−35086
$CaCO_3$, calcite, sputtering behaviour, optical and electron microscopy 78−43968
CaF_2, appl. of theory of sputter-induced isotopic fractionation at solid surfaces 80−55244
Cd, ion bombardment, sputtering, re-emitted kinetic energy ang. distrib. 80−2910
$(CdGeAs_2)_{1-x}D_x$ amorphous films, property control in common target sputtering, elec. cond. 80−7494
CdI_2, sputtering processes during 6 keV Xe ion bombard. 78−68590
CdTe foils, prep. for TEM, ion sputtering technique *(Czech)* 80−16619
CdTe, sputtered film, electrode effects in AC characts. from equivalence impedance meas. of metal-CdTe-Al struct. 79−82686
CdTe surface, sputter cleaning and dry oxidation, XPS and LEED study 80−108618
Ce oxidised surface, comparative sputtered neutral mass spectrometry and SIMS studies 79−90856
sputtering continued
Co film, ion beam sputtering prep., struct. and mag. props. 80−35085
Co, neutron sputtering yield determ. 77−36319
Co-Mo, multilayer films, depth resolution determ. in Auger depth profiling meas. 79−78800
Co-Pu alloys, metastable, high rate sputter deposition, annealing behaviour of deposits 77−21025
Cr, deposited by high rate sputtering, mech. props. 77−36630
Cr, film, sputtering yields, proton-induced X-ray meas. 80−50488
Cr, gas-phase, plasma, sputtering and beam-foil excitations 80−32820
Cr, photon emission due to Ar^+ ion bombard., adsorbed and recoil-implanted O effect 80−80872
Cr, secondary negative ion emission, effect of adsorbed O_2 *(Russian)* 79−28881
Cr-Cr_2O_3 composite mixture, preferential sputtering, XPS expts. 79−87544
Cr-Ni alloy, He blistering at high irradiation doses 79−51167
Cr-Si, thin films, deposition method, for controllable comp. with given elec. props. 80−35087
Cr_2O_3 films, black, microstruct. depend. of optical props., SEM, XPS, and sputter depth-profiling 79−43049
Cs, pulsed sputter negative ion source 78−33347
CsI, high mass secondary ion clusters detected by SIMS 78−88400
Cu (001), sputtering of atoms and positive ions along [011] and [101] directions, ang. depend. 77−24917
Cu (110), O adsorption, low-energy ion bombardment investigation 80−34302
Cu, amorphous, sputtering, computer simulation in binary collision approx. 79−56900
Cu, BCC, Ar ion bombardment, collision cascades and disturbed zone, computational model 79−74037
Cu bombarded by Ne^+, Ar^+, Kr^+, average kinetic energy of sputtered atoms *(German)* 78−19619
Cu, by Ar ions, Brinkman cross section, approx. for sputtering yield 78−76571
Cu, by Ar^+, appl. of torsion vacuum microbalance to sputtering yield meas. *(Japanese)* 78−19622
Cu, clean and O-covered surfaces, ion-bombarded, molecular cluster ejection, model 79−87543
Cu, efficiency ang. distrib. meas. using thermal particle detector 77−28671
Cu, film, sputtering mechanism, SEM 80−29839
Cu foil, sputtering with ^{252}Cf fission products, desorbed secondary ions 78−68596
Cu glow discharge sputtering redeposition, in noncond. compound chem. anal. 77−77860
Cu, in Hg plasma, sputtered atom angular distrib., mass effects 79−87538
Cu, ion impact phenomena, computer simulation 78−88396
Cu, ion-bombarded, particle ejection, SIMS obs. 79−78810
Cu low energy ion sputtering, theory 79−28880
Cu matrix, small oxide precipitates, two-phase system, sputtering and secondary ion emission 78−39650
Cu, neutron damage calc., deuteron break-up source, sputtering appl. 77−35593
Cu, polycryst., back sputtering of 100 to 500 eV Ne ions, computer simulation 78−60537
Cu, polycryst., sputtering rate on Ar ion bombard. 80−55245
Cu, polycryst. surface, Ar^+ sputtered, ion to neutral yield ratio, SIMS anal. 78−72659
Cu, polycrystalline target, ion-atom cross-sections for sputtering of inert-gas ion incident at low energy 79−52059
Cu polycrystals, oxidation, secondary ion energy spectra 80−71788
Cu, SIMS depth profiling, surface roughening by low energy ion irrad. 80−60727
Cu, secondary negative ion emission, effect of adsorbed O_2 *(Russian)* 79−28881
Cu, self diffusion at low temp., low energy ion beam sputtering 78−18821
Cu, self-sputtered, secondary ion mass spectra 79−74044
Cu single crystal, ang. depend. of sputtering intensities 77−8709
Cu, sputtered, ionisation probability, energy dependence 80−35041
Cu, sputtered Cu_1^+ ion energies by low energy inert gas ion bombard. 80−71555
Cu, sputtered surfaces, stability of cones and pyramids 79−78812
Cu, sputtered with 15 or 30 keV H^+, He^+ and Ar^+ ions, energy and angular distrib. 78−95625
Cu, sputtering, binding energies 80−108312
Cu, sputtering, surface topography, appl. of thermodynamics of capillarity 80−20749
Cu, sputtering by Ar^+ ions, thickness distrib. and struct. characts. of Wehner's spot 77−59655
Cu, sputtering by Hg ions, isotope enrichment 77−59656
Cu, sputtering coefficient, temp. depend. 78−19625
Cu, sputtering processes, due to Ar^+ bombardment, computer modelling 79−19957
Cu, sputtering with 15 and 30 keV H^+, He^+ and Ar^+ ions *(German)* 79−24407
Cu surface, Ar^+ ion bombardment, O_2 enhancement of sputtered ion yields 79−38705
Cu, surface ionisation, elemental anal. of sputtering products *(French)* 80−50905
Cu, thin film, sputtering yields due to Ar^+ milling, He^+ Rutherford backscattering and AES obs. 79−65969
Cu-Al, surface ionisation, elemental anal. of sputtering products *(French)* 80−50905
Cu-Au-Cu, thin film, sandwich struct., bombarded by 3-15 keV Ar^+ at angle of incidence of 30°, sputtering yield coeff. 79−65968
Cu-Ni, film, preferential sputtering due to altered layer struct., AES meas. 78−76573
Cu-Ni, preferential sputtering Auger electron spectra obs. 79−33880
Cu-Ni, sputter-induced subsurface segregation, Auger electrons obs. 80−10757
Cu-Ni, sputtering yield, surface binding energies 80−50503
Cu-Ni, surface layer, effect of Ar^+ bombardment, AES and SIMS 80−25504
Cu-Ni (50 wt.%), preferential sputtering, thickness and in-depth comp. profile of altered layer, AES 78−39649
Cu-Ni alloy, sputtered and sputter-deposited surfaces, in-situ AES meas. 77−48296

sputtering continued
Cu-Ni film, coevaporated, AES anal. and ion sputtering effects 79−15044
Cu-Ni single phase alloy, sputter yields 79−87546
Cu-Ni; preferential sputtering, Auger meas. 78−27358
Cu-Sn, ε and η phases, surface struct. changes due to sputtering 77−73206
Cu-Zn-Sn-Pb (5, 5, 5 wt.%) alloy, analysis in glow discharge lamp and in ion microprobe, sputtering processes 77−52730
Cu_n^+ ion cluster yield intensity from Cu target bombard. by H^+, Ne^+, Xe^+, Kr^+ 80−100728
$Cu_x Zn_{1-x}$, sputtering, binding energies 80−108312
Cu_3Au, partial sputtering yields 77−8696
Cu_5FeS_4, bornite, AES investig. of surface struct., ion sputter and electron beam effects 77−15669
dielectric track registering media, possible new sputtering mechanism 77−392
Fe alloys, ion-implanted, depth profile, ion sputtering study 80−54277
Fe amorphous film, getter sputtering at 25K 79−38741
Fe and Fe alloys, passive films studied using AES combined with ion sputtering technique 80−35378
Fe, and Fe-Cr, film, sputtering yields, proton-induced X-ray meas. 80−50488
Fe, film, ion beam sputtering prep., struct. and mag. props. 80−35085
Fe, passive films and phosphate layers, sputtering rate evaluation in glow discharge lamp 80−45443
Fe, sputtering by fast electrons 77−90226
Fe, under N_2^+ and O_2^+ bombardment, theory and expt. test 77−85864
Fe-Ar low press. flow discharge, axial density profiles of sputtered cathode atoms 80−49029
Fe-CR alloys, ion-etched, surface comp., effect of adsorbed CO, AES obs. 79−46896
Fe-Cr-Mo, sputtering effect on surface comp., AES obs. 80−6601
Fe-Fe_2O_3 composite mixture, preferential sputtering, XPS expts. 79−87544
Fe-Ni, and Fe-Ni-Cr alloys, preferential sputtering, XPS expts. 79−87544
Fe-Ni, sputtered using Hg^+ and Ar^+ beams, variation as function of ejection angle, AES exam. 77−44105
Fe-Zn intermetallides, initial stages of form. *(Russian)* 80−20889
$Fe_{1-x}O$ powder, wustite, AES study, ion and electron bombard. effects 80−76114
α-Fe_2O_3 powder, hematite, AES study, ion and electron bombard. effects 80−76114
Fe_3O_4, film, quantitative sputter rates, AES, ellipsometry determ. 78−72661
Fe_3O_4 powder, magnetite, AES study, ion and electron bombard. effects 80−76114
$Fe_{1-x}Pd_x$ film, air-exposed, comp. profiles by AES, ESCA and ion sputtering 78−95245
GaAs, (110), correl. of short-range order and sputter dose, using vidicon-based LEED system 79−83082
GaAs anodic oxide film prep. by plasma anodisation of O-sputtered surfaces, MOS device characts. 79−66176
GaAs foil, prep., for TEM obs., by ion sputtering *(Czech)* 80−16619
GaAs, ion bombardment by alkali metal sputter ion source *(Japanese)* 79−54734
GaAs, SIMS, energy distrib. of sputtered ions 79−38706
GaAs, sputtering at elevated temps. 80−7456
GaAs/Au and GaAs/Au-Ge/Ni, Schottky barrier energy var. with interdiffusion 77−20435
GaAs-Au Schottky barriers, PES and depth profiling obs. 79−42641
GaAs-based mixed cryst. form. by ion beam synthesis, vibr. anal. 80−103376
$GaAs_{1-x}P_x$, SIMS, energy distrib. of sputtered ions 79−38706
GaSb, sputtered films, on GaAs, growth, Hall effect, impurity levels 80−20334
GaSb-Au Schottky barriers, PES and depth profiling obs. 79−42641
Gd oxidised surface, comparative sputtered neutral mass spectrometry and SIMS studies 79−90856
Gd, sputtered vapour, neutral ground state population, laser obs., appl. to isotope separation *(Russian)* 78−29759
Gd-Co alloy film, sputter yield ratio, combined ion deposition and etching 80−71594
Gd-Co-Cu film, amorphous, influence of biased magnetron deposition parameters on props. 77−43856
Gd-Fe(Co) film, amorphous, preferential resputtering effect induced anisotropic distrib. of atomic pairs 78−63950
GdCo, amorphous thin film, for thermomagnetic recording *(Japanese)* 80−11562
GdF_3:H films, H, F profiles meas. by sputter-induced optical emission 78−47407
Ge (100), surface structure and chemical state 77−15670
Ge, ion bombardment-induced photon emission as function of target temp. 80−100698
H surface layers anal., influence of ion beam bombardment 79−37731
H^+, D^+, T^+ ions 77−36343
$Hg_{0.8}Cd_{0.2}Te$ surface, sputter cleaning and dry oxidation, XPS and LEED study 80−108618
HgTe surface, sputter cleaning and dry oxidation, XPS and LEED study 80−108618
In_2O_3-SnO_2/GaAs, solar cell, fabrication, characts. and interfacial chemistry 80−21401
In_2O_3-SnO_2/InP, solar cell, fabrication, characts. and interfacial chemistry 80−21401
InP (110) surfaces, cleaved and polished-sputtered-annealed, LEED and AES study 80−103550
$InP/In_xGa_{1-x}As_yP_{1-y}$ interfaces, sputter-profiled, depth resolution degradation by cone form. 80−80094
InP-Au Schottky barriers, PES and depth profiling obs. 79−42641
InSb, micron size Hall probe for precision mag. field mapping 79−75558
InSb/GaSb superlattice thin films, sputtered, ion-bombardment-enhanced diffusion during growth 78−87882
InSb-GaSb, compositionally modulated sputtered superlattice, growth and interlayer diffusion 79−56930
$InSb_{1-x}Bi_x$, film, multitarget sputtering growth technique 78−84711
InSe thin film, sputter growth and chem. anal. by XPS/ESCA 80−80976
$In_xSi_yO_z$, thin film, sputter deposition form., optical and elec. props. 80−60123
sputtering continued
n-$In_{2-x}Sn_xO_{3-y}$/p-Si, semicond.-insulator-semicond. solar cell, performance and spectral response, fabrication 79−83596
KBr(I), sputtering, depend. on beam energy and target temp. 79−1804
KCl, sputtering by Ar ion bombardment, temp. depend. of sputtering rate *(Japanese)* 78−88389
Kr immobilisation by incorporation into metallic matrix by ion implantation and sputtering 80−27794
Kr^+ ion, polycrystal bombardment, sputtering efficiency 77−85869
LaB_6, porous, field emitter cathode sputtering and surface damage 79−11492
LaB_6-SmB_6(YbB_6), exam. of secondary ion-ion emission, due to bombardment with 8 keV Ar ions 79−33882
Li, kinetic energies of sputtered excited atoms 80−66373
LiF, kinetic energies of sputtered excited atoms 80−66373
Mg, energy distrib. of sputtered atoms 79−91549
Mg, polarisation of light emitted from sputtered Mg atoms 77−27008
Mg, sputtering by He^+, isotope fractionation 79−87542
Mo (100), negative ion form., Cs overlayer effect 78−39645
Mo, blistering and surface roughening, room temp. ageing effects Ar^+ ion bombardment 78−34550
Mo, bombardment by 1 to 30 keV ions, emitted radiation spectral comp. *(Russian)* 77−81159
Mo films, sputtered from cylindrical-post magnetron with Ne, Ar, Kr and Xe, compressive stress and presence of inert-gas obs. 80−80140
Mo, fusion neutron induced radioactive emissions from surfaces 77−36321
Mo, in Hg plasma, sputtered atom angular distrib., mass effects 79−87538
Mo, ion impact, radiative spectrum of sputtered particles *(Russian)* 79−91504
Mo, particles sputtered with low energy Ne^+ ions, surface microstructure effect on angular distrib. 79−100004
Mo, polycrystn., 2 keV Ne^+ ion bombard., dose and microstruct. effects on surface topography and sputtering yield 79−65124
Mo, secondary ion emission mechanism, under Hg^+ ion bombardment 79−100013
Mo, sputtered, angular distrib. during He^+ and Ar^+ ion bombardment 78−95624
Mo, sputtering by Hg ions, isotope enrichment 77−59656
Mo, sputtering yield at low energy for light-ions 78−19620
Mo, sputtering yield meas. on first wall materials of thermonuclear fusion devices *(Japanese)* 77−85865
Mo, sputtering yield meas. by AES 78−95633
Mo, sputtering yields for light ions 79−87537
Mo surface, 40 keV Ar^+ bombarded, excited at. emission 80−11481
Mo, TFTR protective plate, sputtering and surface damage by D^+ irrad. 80−18645
Mo, thin film deposition by high current ion beam sputtering, struct. and elec. props. 80−59837
Mo:He, accumulation and distrib., monolayer conc. by sputtering quantitative anal. 80−49253
Mo-Cu nonmiscible system, sputter yields 79−87546
Na, from NaI target, velocity spectrum meas. by Doppler shift laser spectrometer 78−19621
Na, thermal and collisional effects influence on energy spectra 80−66370
NaCl, energy spectra of sputtered Na atoms from 20 keV rare gas ion bombard. 79−52068
NaCl, exciton luminesc., correlation with sputtering of atoms 77−12449
NaCl, kinetic energies of sputtered excited atoms 80−66373
NaCl, sputtering by Ar ion bombardment, temp. depend. of sputtering rate *(Japanese)* 78−88389
NaCl, sputtering of atoms by 540 eV electrons, delay times 80−35025
NaI, Xe^+ ion bombard., sputtering processes, time of flight meas. 78−88392
Na_2O-CaO-SiO_2 glass, leaching studies by sputter-induced photon spectrometry 80−80004
Na_2O-SiO_2 glass waveguides, low loss, new fabrication method, exam. 78−55481
Nb, 14 MeV neutron sputtering, ion microprobe, SEM, He^+ backscatt. anal. 77−36317
Nb, angular depend. of energy spectra of sputtered ions 78−68595
Nb, Ar ion surface erosion 77−36342
Nb, cathodic sputtering by Hg^+ ions, mech. of positive ionisation of atoms 78−27363
Nb, fast neutron sputtering 77−36316
Nb, fast neutron sputtering 78−15255
Nb, fusion neutron induced radioactive emissions from surfaces 77−36321
Nb, ion bombardment, sputtering, re-emitted kinetic energy ang. distrib. 80−2910
Nb, neutron damage and sputter yields 77−57742
Nb, neutron damage calc., deuteron break-up source, sputtering appl. 77−35593
Nb, neutron sputtering yield determ. 77−36319
Nb, secondary ion emission mechanism, under Hg^+ ion bombardment 79−100013
Nb, simulation expts. for sputtering by 14 MeV neutrons 77−36320
Nb, sputtering by energetic neutrons and protons, round robin expt. 78−11052
Nb, sputtering yield, SEM and scanning Auger microprobe obs. 79−87545
Nb superconducting film prod. by electron beam sputtering *(Russian)* 78−15308
Nb, surface, coverage of O atom as function of adsorption, sputtering and diffusion rates 79−69354
Nb, surface behaviour under ion irrad., in fusion reactor 77−57740
Nb thin foils, surface segregation during sputtering at elevated temps., Auger study 80−54386
Nb-Al-(Ge) film, superconductor, high rate sputter deposition and heat treatment 77−36399
Nb-Ge, supercond. film, prep. and props. *(Russian)* 77−66218
Nb-Ge superconducting film, prod. by electron beam sputtering *(Russian)* 78−15308
Nb-N, superconducting layers, sputtering in high vacuum apparatus *(German)* 80−89147
Nb-NbO system, single- and two-phase, sputtering yield, SEM and scanning Auger microprobe obs. 79−87545
Nb_3Ge film, superconducting, A-15 type, getter-sputtering with controlled additions of O 78−88427

sputtering continued
Nb_3Si, superconducting, high transition temp., sputtering 78−15309
Nb_3Sn film, growth by high-rate magnetron sputtering, transition temp. and crit. currents 77−28718
Ne-Cu hollow-cathode laser discharge sputtering obs. 78−66800
Ne-Cu laser, discharge processes, cathode sputtering 78−5463
Ni alloys, dilute, near surface composition, effect of irradiation and sputtering 79−33168
Ni, amorphous film, getter sputtered at 25K, resistivity, Curie temp. 78−52673
Ni, amorphous film, getter sputtering at 25K 79−38741
Ni, ang. distrib. and differential sputtering yields for low-energy light-ion irrad. 80−71527
Ni, chemisorption of O_2 and CO, ion bombard., particle ejection, SIMS obs. 79−78810
Ni film, ion beam sputtering prep., struct. and mag. props. 80−35085
Ni film coating of optical fibres, magnetron sputtering, mechanical props. improvement 79−72723
Ni foil, sputtering with ^{252}Cf fission products, desorbed secondary ions 78−68596
Ni, H and CO adsorbates, ion impact desorption of atoms and molecules by low energy ion scattering 79−4883
Ni low energy H^+ sputtering 80−40198
Ni, Medicus matrix cathode, surface charact. 80−66378
Ni, oxide films, metal and O_2 transport, AES and inert marker, techniques 80−97641
Ni, photon emission due to Ar^+ ion bombard., adsorbed and recoil-implanted O effect 80−80872
Ni, polycryst., sputtering rate on Ar ion bombard. 80−55245
Ni, secondary negative ion emission, effect of adsorbed O_2 *(Russian)* 79−28881
Ni, self-sputtering yields, low energy 78−56553
Ni, sputtered, ionisation probability, energy dependence 80−35041
Ni, sputtering of adsorbed layers 77−36335
Ni, sputtering yield as function of incident ion masss 79−74042
Ni, sputtering yields for light ions 79−87537
Ni, tarnishing in air, 23-200°C, relative humidities from ambient to 95%, monitoring 78−19940
Ni wire plasma sputtering with W particles, coagulation, struct. and particle size *(Russian)* 80−40260
Ni, with chemisorbed CO, ion-bombarded, molecular cluster ejection, model 79−87543
Ni:Mn, radiation-enhanced diffusion, effect of point defect fluxes 77−89588
Ni/Cr multilayers, AES depth profiling by sputtering with N_2^+ ions 79−95881
Ni/Fe layers, interdiffusion, Auger sputter profiling obs. 79−46848
Ni-Cr multilayer structs., sputter profiling, depth resolution and surface roughness effects, AES obs. 77−76694
Ni-Cu, sputtered using Hg^+ and Ar^+ beams, comp. variation as function of ejection angle, AES exam. 77−44105
Ni-Cu, sputtering rate, radiation-induced segregation and preferential sputtering effects, kinetic model 80−40199
Ni-Mo, multilayer films, depth resolution determ. in Auger depth profiling meas. 79−78800
Ni-Mo, sputtering rate, radiation-induced segregation and preferential sputtering effects, kinetic model 80−40199
Ni-NiO composite mixture, preferential sputtering, XPS expts. 79−87544
Ni-Si, Cs ion-bombarded, surface Cs concs., AES meas. 79−83073
β-NiAl, oxide films, metal and O_2 transport, AES and inert marker, techniques 80−97641
NiAl, sputtered in vacuum, struct. *(Russian)* 77−69986
NiFe alloy, ion-beam sputtering, excitation efficiency of atoms 78−19623
NiSi, partial sputtering yields 77−8696
O adsorbed on Ni, sputtering by low energy ions 77−62758
PLZT, coaxial magnetron sputtering technique 79−83123
Pb, efficiency ang. distrib. meas. using thermal particle detector 77−28671
Pb, film, sputtering mechanism, SEM 80−29839
Pb, ion bombardment, sputtering, re-emitted kinetic energy ang. distrib. 80−2910
PbI_2, sputtering processes during 6 keV Xe ion bombard. 78−68590
$Pb(Zr_xTi_{1-x})O_3$ films, ion beam deposition, struct., dielec. and ferroelec. props. 80−20788
Pd_2Si, Cs ion-bombarded, surface Cs concs., AES meas. 79−83073
Pt (100) (5×20) and (1×1) surfaces, stability and reactivity, adsorption of H 80−75434
Pt films, high-purity, sputtered onto Si, PtSi and Pt_2Si form. 77−76676
Pt, sputtering yields for ions over 15-135 keV 79−56899
Pt thin films, spike effects of heavy ion sputtering 80−35034
Pt-Rh alloys, surface behaviour on heating in air, XPS and SIMS *(French)* 77−40327
Pt-Si, Cs ion-bombarded, surface Cs concs., AES meas. 79−83073
PtSi, 10-160 keV Ar ion sputtering, Rutherford backscatt. obs. 79−15574
PtSi, Ar bubble formation after 20 to 160 keV sputtering, TEM and backscatt. spectrometry obs. 78−64435
PtSi film formation by ion sputtering and annealing, form. and exam. problems 80−100782
PtSi, partial sputtering yields 77−8696
PtSi thin film structures, preferential sputtering meas. Rutherford backscatt. 79−43087
RbBr, sputtering of atoms by 540 eV electrons, delay times 80−35025
RbBr(I), sputtering, depend. on beam energy and target temp. 79−1804
RbCl(Br)(I), Xe^+ ion bombard., sputtering processes, time of flight meas. 78−88392
RbI, sputtering of atoms by 540 eV electrons, delay times 80−35025
Se film, trigonal, sputtered and evaporated nucleation and growth processes 77−31920
Si, AES examination of Ar^+ ion retention during Ar sputtering 78−56552
Si, amorphous film, sputtering by 0.5 to 5 keV Ar^+ ions 79−91550
Si, anomalous sputter yields of interfacial species, cascade mixing process for interpretation 80−76122
Si, Ar(Xe) ion bombarded, sputtering yield energy and fluence depend. 79−78805
Si, Cs ion-bombarded, surface Cs concs., AES meas. 79−83073
Si, epitaxial layer deposition by ion beam methods 80−100417
Si, film, focused ion beam designs for sputter deposition 79−89841

sputtering continued
Si film, on graphite, early growth by ion-beam sputtering 77−44158
Si film, on quartz and MgO substrates, using double cathode system *(Japanese)* 77−55889
Si, implanted Li atoms, depth profiles and sputtering anal. by optical spectra 77−35579
Si, ion-excited L-shell Auger spectra, charact. 79−87533
Si, minority carrier lifetime, effect of SiO_2 coating deposited by magnetron sputtering 80−11003
Si, photon emission due to Ar^+ ion bombard., adsorbed and recoil-implanted O effect 80−80872
Si, polycryst. and amorphous, sputtering with keV Ar^+ ion, meas. and Monte Carlo calc. of sputtering yield 79−95886
Si, semi-insulating polycrystalline CVD layers, AES and XPS characterisation 80−16129
Si, single cryst., sputtering rate on Ar ion bombard. 80−55245
Si, sputter cleaning using Ar^+ ions, temp. depend. of residual damage, 25 to 800°C 77−48558
Si, sputtered, cluster formation, influence of HF plasma interaction 78−64441
Si, sputtered atom ang. distribs. for keV Ar^+ bombard. 80−84819
Si, sputtering by Ar^+ ions, energy depend. of excitation 79−56906
Si, sputtering by low energy Ar ions, temp. depend. of sputtering coefficient 79−15578
Si substrates, thermal history 80−25562
Si surface, Ar^+ ion bombardment, O_2 enhancement of sputtered ion yields 79−38705
Si surface, ion bombardment enhanced mixing of Ag layers, Rutherford backscatt. meas. 80−65034
Si wafer surface sputtering, secondary postive ion mass and kinetic energy anal. 78−88391
Si:As, SIMS, energy distrib. of sputtered ions 79−38706
Si:As sputter rate meas. SIMS combination with Rutherford backscatter 80−21334
Si:B, sputtering influence on distrib. profile of ion-implanted impurities 79−42091
Si:B sputtering by Ar^+, computer simulation of sputter broadening in impurity depth profiling 80−2908
Si:H, H^+ sputtered as result of ion bombardment, ionis. mechanism 79−100009
Si-Fe-W, dil. alloy, compositional changes on sputtering, projectile energy depend. 80−66362
Si-Mo Schottky barrier diode, sputtering damage effects on I-V and C-V charact. 77−39940
Si-Pd, preferred sputtering on surface, mass difference and chemical bonding difference effects, AES obs. 79−83078
Si-Pd film, preferred sputtering on surface, mass and bonding difference effects, AES obs. 79−87552
Si-refractory metal structs., interface modification by ion implantation 80−70475
Si-SiO_2 interface, Auger-sputter profiling obs. of P pileup 78−95240
Si-SiO_2 interface, intermediate chem. state of Si during sputter profiling, Auger spectra 79−11230
Si-SiO_2 interface, sputter profiling, ion knock-on mixing model 79−83081
Si-SiO_2 interface morphology, P pileup effect, Auger sputter profiling 78−72006
SiC, 0.6, 3.5 MeV He^+ irrad., surface erosion, porosity effects 77−35602
SiC, amorphisation induced by ion bombardment, Raman spectroscopy 77−80551
SiC, energetic H and Ar ion sputtering, AES-SIMS-FDS combined obs. 78−80444
SiC, energetic ion sputtering, appl. of AES-SIMS (IMA)-FDS combined systems to physical and chemical processes 78−95636
SiC, interaction of H^+ with surface, combined AES-IMA system *(Japanese)* 79−74039
SiC, sputtering, physical and chemical, by H_2 and He, 600 to 7500 eV 77−36340
SiC, sputtering processes by energetic ions, combined SIMS-AES study 80−40201
SiC, sputtering yield, use as first wall material 78−95629
SiC surface, H^+, D^+ and Ar^+ bombardment, 5 to 15 keV, meas. of erosion yield 78−79647
SiC, thermal oxide layers, AES depth-profiling anal. 79−43454
SiC-C, sputtering and blistering from H^+ and He^+ bombardment 78−79649
SiO, film, effect of ion implanted O_2 on optical props. 80−45027
SiO_2 glass, sputter yield peak ang. var. 77−32484
SiO_2, light emission from sputtered O atoms or ions 80−58199
SiO_2 on Si, ion bombarded surface, de-excitation processes 77−16446
SiO_2, sputter deposition onto GaAs, and MIS struct. charact. 77−89864
Sm, thermal and collisional effects influence on energy spectra 80−66370
SmAu, significance of negative ion formation in sputtering and SIMS anal. 78−72663
SnO_2, VUV transparent electrode formation by chemical deposition and vacuum sputtering 79−56929
Ta, bombarded by Cs^+, transient emission of continuous photon spectrum by cathodic sputtering products 79−74046
Ta, deposition by ion beam sputtering 77−73228
Ta films, H^+ and D^+ sputtering in energy range 0.6 to 15 keV 79−78808
Ta, sputtered deposition on Si, Si-SiO_2 interface, induced stress meas., X-ray transmission topography 79−24434
Ta, surface, secondary ion emission mechanism, under Hg^+ ion bombardment 79−100013
Ta, thin film deposition by high current ion beam sputtering, struct. and elec. props. 80−59837
Ta thin films, magnetically enhanced sputtering appl. to Penning cylindrical system 78−3042
Ta-Pu alloys, metastable, high rate sputter deposition, annealing behaviour of deposits 77−21025
TaO_n, combined SIMS, AES and XPS investigation 79−33199
Ta_2O_5, anodic, sputtered, equilib. surface comp., mass and energy depend. 79−19472
Ta_2O_5, ion-bombarded cryst., structural and compositional changes 79−46724
Ta_2O_5, preferential sputtering by Ar^+ ions, XPS obs. 79−83083
Ta_2O_5, sputter deposition onto GaAs, and MIS struct. charact. 77−89864

sputtering continued
Ta_2O_5, sputter depth profiling with low press. HF plasma 79−95041
Ta_2O_5, sputtering by Ar^+ below 1 keV 78−88397
(Tb,Dy)-Fe amorphous films prep. by cosputtering, magnetoelastic props. 80−97429
Ti alloy PT-7M, in plasma, probe method obs. 79−55564
Ti atoms sputtered from Ti, Ti oxides, photon emission, nonradiative transition effects 80−58208
Ti film, depth profiles, of D and T from gas emission during sputtering by Ar ions 77−35581
Ti film on Si, induced interface interaction by ion implantation, AES exam. 79−77625
Ti, photon emission due to Ar^+ ion bombard., adsorbed and recoil-implanted O effect 80−80872
Ti, polycryst., sputtering rate on Ar ion bombard. 80−55245
Ti, sputter-erosion and impurity emission under low energy ion bombardment 78−95628
Ti, sputtered ion fraction meas. using matrix isolation spectroscopy 80−60738
Ti, sputtering yields of D^+ and Ar^+ ions using matrix isolation spectroscopy 79−78809
Ti-Al_2O_3 system mixed films, prep., phase comp., struct. and elec. props. 79−37930
Ti-sapphire interface, solid-state reaction 78−72008
TiC, sputtering yield, use as first wall material 78−95629
TiO_2, (100) surfaces, ionisation of sputtered-atomic particles 80−20750
TiO_2 powder, $SiO_2(Al_2O_3)$ coated, thickness meas. of coating, XPS and ion sputtering 79−88913
TiO_2, sputtering defects, associated surface electron states, UPS, XPS and AES obs. 80−60755
Ti_xO_y film, AES, with and without simultaneous sputtering, beam effects 77−90224
TiW-TiO_2-InP thin refractory MIS struct. deposition 80−75647
U, excited state radiative lifetime, sputtering technique 78−17602
U, in Hg plasma, sputtered atom angular distrib., mass effects 79−87538
U, mol. beam bombardment, aggregate form. *(French)* 79−74047
U, sputtered, absorpt. spectra in hollow cathode glow discharge 80−32643
U, sputtered atoms, laser fluorescence spectroscopy 80−66359
U, sputtering yield meas. by fission track technique 78−39646
U, vapour prod. by sputtering, Ne, Ar, Kr, carrier agents, density meas. *(French)* 78−86967
U, yield meas. by obs. of fission tracks in mica 77−88340
$UAl_2(Co_2)$, surface comp. and electronic struct., photoemission study 80−66382
UO_2 nuclear fuel, sputtering by thermal neutrons, depend. of ejection coeff. on neutron flux 80−83157
UO_2-U_3O_8 thin films under influence of fission fragments at low irrad. doses 77−48282
^{235}U foil, sputtered, energy spectrum, fission track technique 78−68593
V, fusion neutron induced radioactive emissions from surfaces 77−36321
V, implanted Li atoms, depth profiles and sputtering anal. by optical spectra 77−35579
V, oxidation during energetic particle irrad., influence of reactive gases on sputtering and secondary ion emission 78−72656
V, secondary ion emission mechanism, under Hg^+ ion bombardment 79−100013
V, sputter-erosion and impurity emission under low energy ion bombardment 78−95628
V, sputtering under 14.1 MeV neutron impact 77−48281
V surface, particle release by neutrons 80−25493
V_3Ge, superconducting, high transition temp., sputtering 78−15309
W (100), coadsorption of Zr and O_2 at high temp. 80−6653
W, adsorption of N_2, effect of SIMS, sputtering induced recomb. anal. 80−55243
W ang. distrib. and differential sputtering yields for low-energy light-ion irrad. 80−71527
W, bombardment by 1 to 30 keV ions, emitted radiation spectral comp. *(Russian)* 77−81159
W, H and CO adsorbates, ion impact desorption of atoms and molecules by low energy ion scattering 79−4883
W high-current multicavity thermionic cathode, erosion mechanisms, sputtering 79−55570
W, in Hg plasma, sputtered atom angular distrib., mass effects 79−87538
W, ion sputtering yield reduction by special surface microtopography 77−36330
W, low-energy ion bombardment, depth of sputtering damage obs. by FIM 80−60734
W, oxidation during energetic particle irrad., influence of reactive gases on sputtering and secondary ion emission 78−72656
W, polycryst., bombardment with Na and K ions, neutral component of scatt. 78−11047
W, surface structure and topological modification during depth profiling, FIM obs. 79−78816
W, vacancy structure in near surface depleted zone following ion bombard. 80−70267
W^+, relative ion sputtering yield, integration of secondary ion energy distribution, retarding dispersive ion energy analyser 79−33875
W:ThO_2, uncarburized filament activation by sputtering 78−52608
W_6Co_6C cemented carbide, with CVD TiC coating, structure, composition and hardness exam. 78−11425
WSi_2, steam-oxidized, Auger sputter profiling studies 80−107663
Xe^+ ion, polycrystal bombardment, sputtering efficiency 77−85869
Y I, Y II, lifetimes of excited states, rel. to solar abundance determ. 78−86815
Zn, efficiency ang. distrib. meas. using thermal particle detector 77−28671
Zn, film, sputtering mechanism, SEM 80−29839
Zn, gas-phase, plasma, sputtering and beam-foil 80−32820
Zn I, relative populations in arc, sputtering and gas phase collisions 80−934
Zn, radiative emission from sputtered atoms, geometry depend. 77−28669
Zn, sputtering, binding energies 80−108312
Zn-Cu system, sputtering during atomic diffusion, UPS meas. 78−92159
ZnO crystalline films, deposition techniques *(Japanese)* 79−74098
ZnO sputtered films, vertical electrode config. to avoid contamination 79−69982

sputtering continued
ZnS, epitaxial growth, appl. to electronic devices, review *(Japanese)* 80−55281
ZnS, film, vac. sputtering deposition by CW CO_2 laser beam *(Russian)* 77−21024
Zr, excited state radiative lifetime, sputtering technique 78−17602
Zr I, lifetimes of excited states, rel. to solar abundance determ. 78−86815
Zr, photon emission due to Ar^+ ion bombard., adsorbed and recoil-implanted O effect 80−80872
Zr, sputtered ion fraction meas. using matrix isolation spectroscopy 80−60738
ZrO_2-Y_2O_3 powder, prep. for plasma spheroidisation, sputter drying *(Russian)* 80−55324

square-wave generators
automatic resistance thermometer bridge 80−98913
beam splitter using operational amplifier as square wave generator 78−77884
calibrator using band-gap voltage reference, oscilloscope appl. 78−65941
electrophysiological instrument calibrator 77−48970
simulator, ECG and EEG *(French)* 79−57786

SQUIDs *see superconducting junction devices*

squirrel cage motors
magnetic fields, quasi-stationary, finite element anal. 78−94356

stabilisation *see stability*

stabilisers *see controllers*

stability
see also flow instability; frequency stability; limit cycles; Lyapunov methods; plasma instability
6 M⊙ star in post-main sequence evolution, continuous nuclear spectrum and secular stability 77−64745
A^4-phonon theory, free energy instability in ground state of A^4-phonon theory 78−41257
absolute temperature stabilizer, below lambda point, the adritron 79−21757
accelerating two-phase nozzle/diffuser flows, virtual mass effects on numerical stability 80−92204
accelerator cavities, improvement by mutual coupling *(Slovene)* 78−29663
active acoustic suppression systems with finite number of couplings, approximation and stability aspects 78−18111
aerodynamically heated body, stable shape during ablation *(Russian)* 78−75162
aerodynamics, unsteady, modelling, for arbitrary motions 78−14033
aeroelastic, large wind turbines 80−61249
aeroelastic behaviour, large Darrieus rotors derived from behaviour of 5.5 m rotor 80−61251
aeroelastic stability of complete rotors in forward teetering flight 78−5677
aeroplane, deformable control systems, numerical anal. of lateral dynamic stability 78−51057
air-condenser microphone, effects of residual moisture on long-term stability 77−84091
airborne target tracking filter configurations compared 80−96130
aircraft, ballistic descent, stabilisation transient processes 77−53395
alpha spectrometry system, total stabilisation using ^{148}Gd source, multichannel analyser 79−22523
alumina film, RF sputtered, stability 78−22993
amorphous Lennard-Jones solid, edge and screw dislocation, stability, elasticity, simulation 80−15099
ampere current source, dialable, with ovenless construction, stability 77−50320
analytic extrapolations towards interior points from a cut, applic. to elementary particle scatt. theory 80−12952
anharmonic system, superstability, probability estimates for correlation functions 80−82708
anisotropic thin evolving shell stability loss *(Ukrainian)* 78−89340
aqueous film, plane-parallel symmetrical, stability, non-spreading oil droplet effect 80−107620
aquifer parameters, invariant imbedding and identification 79−57992
arches, flat, sandwich-type, elastic equilibrium states 80−48570
area-preserving polynomial mapping, instability 78−77463
artificial satellite, spinning, symmetric, in planar periodic orbit, attitude stability 80−4220
artificial satellite with gravitational attitude control, dynamics 77−25905
artificial satellites, dual-spin, nutation damping and stationary rot. stability *(Russian)* 77−60570
astatic gyroscope with elastic cardan suspension, dynamics *(Russian)* 78−63273
asthenosphere, thermal stability or instability of shear flow 78−20370
astronomy, dynamical, Hill's concept generalisation 79−92656
asymptotic and total stability for generalized dynamical systems 79−17205
asymptotic stability of resonance systems 80−68031
asynchronous cardan mounted gyroscope, stability of stationary motion *(Russian)* 77−62147
atmosphere, Budyko climate model 77−45130
atmosphere, frontal instability, semigeostrophic eqns. appls. 77−45077
atmosphere, pot. stability, determ. using wet-bulb pot. temp. charts 77−91232
atmosphere, stability classification schemes for urban area 77−49127
atmosphere, steady states and stability props. of low-order barotropic system 80−72614
atmosphere hydrostatic stability, influence on wind drag coeffs. for marine regime 79−5494
atmosphere of variable composition, static stability, and thermal wind with appl. to Mars 79−84720
atmosphere with density inversion, Taylor instability 77−9476
atmospheric stability category determ. for airborne radionuclide release assessment 78−73504
atoms and bulk matter, nonrelativistic quantum mechanics, review 77−5696
autonomous Hamiltonian system, gyroscopic forces, effect on stability *(Russian)* 80−17794
autonomous Hamiltonian systems, orbital stability of periodic Lyapunov motions *(Russian)* 78−69664
autonomous system instability, sufficient criteria, Lyapunov instability *(Russian)* 79−17210
autonomous third order systems stability, comments and reply 79−94539

stability continued
autoparametrically coupled systems, stochastic stability of stationary response 78−20961
axisymmetric rigid body in air, stability of unperturbed motion *(Russian)* 78−86146
axisymmetric top filled with liquid, regions of stability of uniform rotation *(Russian)* 77−62148
axisymmetric top filled with liquid, sufficient conditions for stability *(Russian)* 77−62149
bar, dynamic stability, subjected to impulse loading 78−46901
bar, impact vibr., motion and dynamic stability analysis 78−26081
bar, localised damage region effect on parametric excitation 78−30215
bar, stability against self-excited frictional oscillations *(German)* 77−54916
bar optimal design by dynamic programming *(Polish)* 79−64542
barrier island breach morphology and dynamics, study in stability 80−12371
beam, nonuniform, static and dynamic instability analysis 78−13942
beam, periodically varying length, instability of motion 80−69716
beam, simply supported thin elastic, parametric instabilities under stochastic loading 79−68582
beam containing fluid flow, on elastic base, flexural vibration stability 79−46248
beam on elastic foundation subjected to nonconservative load, stability 80−79191
beams, dynamic stability with shearing strains and rot. inertia 80−33498
beams, non-linear vibrations, stability analysis method 80−53686
Beck's column, influence of tip mass offset on stability 79−72842
Beck's column subjected to vertical+follower forces, vibr., stability 78−9583
below-knee amputees with patellar-tendon-bearing prosthesis, load carrying 77−60301
biaxial plastic tension, instability calc. *(Russian)* 80−23920
bicycle stability, teaching approach using unsuccessful nongyroscopic theory 80−42001
bidimensional stellar systems in uniform rot., stability for nonaxisymm. modes 78−85980
bifurcation and nonequilibrium phase transitions of limit cycles and multiperiodic flow 78−24759
bifurcation and nonequilibrium phase transitions of limit cycles and multiperiodic flows in continuous media 78−81937
bifurcations of straight line oscills., rel. to Stormer and spring pendulum problems 78−71278
binary stars, close, non-synchronously rotating component stability 79−40223
binary stars, stability criterion from influence of nonsphericity and radiation press. 78−28658
biochemical systems stability anal., practical guide 78−73135
biological pressure meter, temperature and time stability 79−84059
biped locomotion dynamics, control theoretic study *(Japanese)* 79−11963
bipedal locomotion, inverted pendulums stabilisation algorithm *(Japanese)* 80−81630
bipedal walking, linear stabilisation *(Russian)* 78−51055
black foam films stability, review 80−104463
black hole accretion discs, Lightman-Eardley instabilities rel. to disc thickening 80−31324
black holes, gravit. wave instability of maximally rotating Kerr soln. 80−105271
blanks cogged into conical matrix, stability anal. *(Russian)* 80−43636
bodies disposed from aircraft, dynamic flight characteristics *(Polish)* 78−18311
Bondi accretion, linear stability problem 79−44359
boundary value problems, stability evidence 77−84167
brain waves, limit cycle model, Frohlich's model 77−73520
Brillouin electron beam critical current rel. to vacuum level 79−7068
brittle fracture, precedence of stability loss near crack *(Ukrainian)* 79−77007
brittle solid, crack system propagation, stability conditions 78−51131
buckling, bifurcation and limit point instability of dual eigenvalue third order systems 80−87727
buckling, cylindrical shell and spherical panel, stability, critical loading density 80−53664
buckling, imperfection sensitivity and isoperimetric variational problems 77−42760
buckling of elastic beams, analysis using theory of quadratic operator pencils 80−48607
buckling of nonsymmetrical systems, linearised instability analysis 77−72195
bunched beam stability in storage ring, matched line interaction 78−50424
bunched proton and electron beams, longitudinal instability theory 77−83208
BWR stability monitoring using time series anal. of neutron noise 80−47625
camera, aerial, stabilised mount anal. 80−9059
cantilever (Timoshenko), elastically restrained, with attached masses, follower force stability 78−63347
cantilever beam of periodically varying length, parametric instability investigation 79−81758
cantilever column, elastically restrained, subjected to follower force, instability 78−63299
cantilever column, influence of elastic end support 77−11144
cantilever follower force problem, non-conservative load, boundary conditions and stability 77−46956
cantilever panels, in uniform incompressible flow 80−74781
cantilever plates, with biaxial subtangential loading 78−90762
cantilever under multiple loads, postbuckling and stability anal. 80−48617
cantilevers, flutter load, discontinuity, variational technique 80−58944
caps, thin elastic spherical, stability curves, boundary value problems 79−81745
catalytic reaction rate, influential factors, new definition of catalysis 79−1943
catastrophe theory, stability predictions through a succession of folds 79−76991
catastrophe theory role in applied mechanics 77−67232
Cauchy problem, linear eqns. with const. coeffs., absolute instability, 3-dimens. 79−12622
cell cycle kinetics stability and control, cancer chemotherapy appl. 79−34521
stability continued
Cepheid-type stars, stability against nonradial oscills. 77−91552
chaos, reinjection principle, folded and cut chaotic flows 80−12996
chemical diffusion-reaction equations, semilinear parabolic systems, soln. existence and stability 79−47889
chemical reaction-diffusion system, nonlinear, multiscale propag. phenomena 79−91910
chemical system far from equilibrium, bifurcation and stability 77−73461
chemically reacting system, temporal oscillations 77−25359
chlorophyll a in benzene solns. and monolayers, chem. stability 79−47912
circular arches, lateral-torsional instability with motion-dependent loading 77−89049
circular arches with flexibly supported ends, spatial symmetrical vibrations and stability 79−3953
circular cylinder carrying flow, unsteady fluid dynamic forces rel. to stability anal. 78−13936
circular cylindrical shells under hydrostatic press., influence of boundary conditions on stability *(Chinese)* 79−32306
circular plate on floating central collar, moving load stability theory 77−46863
circular rings, stability obs. *(Russian)* 79−76990
clamped plate, finite element anal. of secondary buckling, comparison with expt. 79−1120
climatic models, stability and extremal props. *(Russian)* 78−53716
clouds, stability anal. of deep streets 79−2335
clusters of galaxies, hot gas stabilisation by massive photons *(Russian)* 79−44614
clusters of galaxies, stabilisation by subclustering 79−44624
cm-wave radiometer, with enhanced long-term stability, for solar radio emission obs. 80−109361
cnoidal waves, linear stability anal. 77−68612
collapsing sphere, shape instability pressure stabilisation 80−8537
collinear N-body problem, homothetic solns. structural stability 79−75086
column, free flying, asymptotic solns. to problem of lateral stability 79−14242
columns, Beck and Leipholz types, stability, shear deformation and rot. inertia effects 80−48610
columns, infinitely long with localised imperfections, dynamic buckling 77−27479
composite, multilayer cylindrical shell, elastic filler, strength and stability under combined loading, mass minimising 77−65699
composite, slab, spatially reinforced, optimisation in stability problem 80−102978
composite cylindrical shells, reinforced, stability loss under isotropic external pressure 78−42554
composite material cylindrical shells, stability during nonsteady heating and transverse flexure 80−40445
composite materials, cylindrical shells, probability anal. of stability, mass minimisation 78−42553
composite materials, tension stability, deformation up to failure *(Russian)* 80−75289
composite rib stiffened constructions, design criteria 80−102977
composite ribbed multilayer cylindrical shells, stability and optimal design 80−58949
composite shell, orthotropic, cylindrical, with elastic core, stability 77−65701
composite superconductors, stability anal. by thermal analyser digital computer program 78−54995
composites, multilayer, stability under inelastic deformations 80−99944
compressed air energy storage in hard rock caverns, stability and design criteria 80−30574
compressed laminar structures *(Russian)* 79−18759
cone cylinder jointed shell, ring stiffened, external hydrostatic pressure, elastic stability *(Chinese)* 80−64412
conical models in shock tunnel, static and dynamical stability derivatives *(Chinese)* 80−58941
conical shell, skew, truncated, external hydrostatic pressure, elastic stability *(Chinese)* 80−64413
conservative elastic continua, stability anal. with adjacent equilibrium method 78−28951
conservative finite dimensional system, stability of equilib. branching points *(Russian)* 78−86143
contact binary stars structure, secular stability of stemp. inversion layer 80−109493
contact stress problems, counterformal, improved numerical method and program 79−41632
continental shelf wave side band instability and long wave resonance 78−16030
continuous elastic systems under multiple loads, postbuckling anal., stability theory 80−48616
continuous systems 77−2537
corrected gyrocompass asympotic stability *(Russian)* 79−10457
coupled bending-torsion flutter in cascades, aeroelastic stability boundaries 80−64424
coupled inverted pendulums, stabilising control *(Japanese)* 79−35545
crack growth stability, in plastic material 80−74810
crack instability, directional criteria 78−90789
critical loads for elastic bodies, lower bounds, stability 80−79185
cryogenic system, thermally driven acoustic oscillation, stability limit 80−8992
cryogenic turbogenerator, study *(Russian)* 77−53919
crystals, monatomic, nonlinearly elastic, twinning 80−58903
cubic crystal under hydrostatic loading, Born and classical stability criteria divergences 80−10595
cylinder, compressible, under uniform compression, stability *(Russian)* 78−55577
cylinder, stable conditions for phase change problem with internal heat generation 80−10130
cylinder, thick walled, stability loss and crack formation in failure *(Russian)* 79−77016
cylinders, noncompressible, under all-round compression *(Ukrainian)* 78−90708
cylinders, stiffened, subjected to pure torsion, min. weight design 78−1582
cylindrical envelope, stability under effect of axial contractive power and cross pressure *(Russian)* 78−42550
cylindrical orthotropic shell stability problems, spectrum singularities 80−99950

stability continued
cylindrical panel, motion stabilisation *(Russian)* 77−68498
cylindrical plasma filament under axisymmetric perturbation, numerical anal. 80−106853
cylindrical shell, nonaxisymmetric press., stability loss, deform. *(Russian)* 77−46951
cylindrical shell, thin, instability rel. to mechanical anal. of geologic structs. *(Chinese)* 78−73364
cylindrical shell, thin walled, stability under external pressure, linearised theory *(Ukrainian)* 79−98645
cylindrical shell, with non-small holes, elastic equilib., integral representations method *(Ukrainian)* 79−32256
cylindrical shell with circumferential notch under axial compression, stability *(Polish)* 78−79239
cylindrical shell with elastic filler, eigenfrequency spectra, dynamic instability regions, nonaxisymmetrical vibrations 78−63367
cylindrical shells, influence of loading behaviour on stability 79−72846
cylindrical shells, orthotropic, noncircular, problem solubility *(Ukrainian)* 79−32255
cylindrical shells containing turbulent flowing fluid, numerical anal. 77−72291
cylindrically symmetric bubbles, static and dynamic props. 80−39835
damage induced structural instability 80−28445
damped linear systems, free and forced vibrations, stability 79−64568
damped Mathieu oscill., parametric random excit., moment stability 77−9869
Dead Sea, mixolimnion deepening and water column overturn 80−61822
Dedekind ellipsoids, dynamical instability in post-Newtonian approximation to general relativity 78−32734
deformable bodies, three-dimens., stability study 80−14596
deformable body three dimensional stability theory, variational principles 80−38300
deformation stability for thin bodies with cracks *(Russian)* 77−35081
delayed differential system, stable state domain of attraction 77−34374
dendritic crystal, growth, stability effects 78−26802
detonation products of condensed explosives elec. stability 79−86635
detonation pulsation struct., periodic instability *(Ukrainian)* 77−65751
di(alkylbenzylthio)ethane, oil additive, thermal stability determ. by chromatography, colorimetry 79−15969
diagonal braces in building frame, inelastic stability 78−75083
difference dynamical systems, determ. of global regions of asymptotic stability 77−67225
difference schemes for multidimensional equations of acoustics 80−105512
differential equations, non-linear third order, stability criterion 78−81801
diffusion-reaction equations systems, existence, stability 79−20365
diffusion-reaction problem, nonlinear, dissipative structs., stability anal. 79−1938
disclike galaxies, numerical expts. 78−89251
disclike galaxies in massive halos, stability, models 78−93403
discs, stationary and rotating, stability under edge load 78−38219
dissipative dynamical system, iterative transitions between periodic and turbulent 78−62159
dissipative steady state, stability 79−9187
dissipative systems, numerical expts. on trajectory instabilities trajectory instabilities 78−41235
distributed parameter system control, conference, Coventry (1977) 79−3897
distributed systems, stability of spatially inhomogeneous states 80−30629
drop, incompressible fluid, equilib. and stability analysis 80−59092
ductile notched fracture toughness specimens, instability prediction, approx. flow stress model 78−34082
dynamic instability region, computation by finite element method 80−23927
dynamic systems, numerical anal. of stable motions *(Russian)* 77−57181
dynamical stability anal. of charged homogeneous model, relativistic soln., rel. to stellar models 79−70949
dynamical system, connectance, increasing no. of degrees of freedom 78−81831
dynamics of systems of solid bodies with combined control *(Russian)* 79−17209
early Earth, dynamical and secular stability rel. to Moon fission origin 78−85867
Earth mantle low-velocity zone, stability from melt/solid segregation theory 79−40144
Earth satellites, stability of periodic and quasi-periodic orbits 77−13214
elastic, of hyperbolic paraboloids, analysis using reduced scale models 79−3910
elastic, shell element computation, triangular facet, linear and nonlinear equilibrium and elastic stability appl. 77−68460
elastic bars in circulatory systems, influence of end supports on stability 78−30224
elastic beams, 1-D, stability in torsional extension *(German)* 78−87270
elastic beams subjected to successive loading, bending, stability eqns. *(German)* 78−26045
elastic body, nonlinear relation between stability and continuous dependence at eqn. 80−92063
elastic body stability under isotropic uniform compression 80−4531
elastic compressible bodies under all-around compression, stability for rods and plates 80−43633
elastic hinged body in supersonic flow 77−39257
elastic incompressible bodies under isotropic compression 80−14597
elastic non-conservative stability, appl. of iterative Ritz procedure 77−22422
elastic plastic spherical body, instability under uniform loading 80−58946
elastic plastic structures, stability condition 78−87284
elastic plate, stability via Lyapunov's Second Method 77−54914
elastic plate stability conditions, variational formulations 80−69701
elastic shells of revolution, postbuckling finite-element analysis 77−62185
elastic solids, stability, response to finite strain 80−79187
elastic stability theory for plates with inhomogeneous precritical states *(Russian)* 78−49665
elastic structs., stability, buckling and postbuckling 80−1454
elastic structural stability anal., num. methods 79−94489
elastic systems with small internal friction *(Russian)* 79−17222
elastic thin plates, nonlinear dynamic stability 77−3759
stability continued
elastic tube conveying compressible flow, 2-dimens. model nonlinear stability anal. 79−64547
elasticity, second order, internal instability 79−60
elasto-plastic continua, quasi-bifurcation in dynamics 78−38223
elasto/visco-plastic finite element analysis, unconditionally stable algorithms 78−34030
elastodynamics, linear, stability theorems for abstract eqn. in Hilbert space 78−36832
elastokinetics and elastostability, equation structure from D'Alemberts principle *(German)* 79−63046
elastoplastic sphere under external press., stability 78−94603
elastoplastic trusses, with unstable bars, collapse anal. 78−90729
electret US transducer performances and prospects 78−59244
electro-optic reflector, controlled, temp. fields, thermal distortions 80−96021
electromechanical force meas. devices, long-term stability tests *(German)* 77−79088
electron beam, high-current, stability in mag. field in waveguide 78−66742
electron beam, magnetised, longitudinal stability in periodic metal-dielectric system 77−65563
electron beam, self-focusing in ferrodielectric channel, nonlinear eqn. anal. 77−61905
electron beam interaction with slow waves over impedance-loaded surface *(Russian)* 77−31055
electron layer, low density, in homogeneous mag. field orbital motion instability 77−65561
electron microscope samples, geometric stability *(Ukrainian)* 77−67536
electron microscopes high-voltage supplies, capacitive meas. of slow fluctuations 77−13826
electrostatic generator terminal voltage on-line feedback stabilisation using digital computer 78−82004
electrostatic high voltage generator for TEM, stability improvement *(French)* 78−62268
elliptic thin cylindrical shells, hydrostability 77−75830
EMF of Nicrosil-Nisil thermocouples, 538°C to 1177°C, production furnaces appl. 80−68198
emission instability, in electron guns using directly heated LaB_6 sources, grid aperture contamination 79−12907
endocardial screw electrode stability enhancement 77−81746
endochronic inelasticity and incremental plasticity, tangential linearisation, material instability 78−87277
energy-balance climate models, stability theorem 80−56594
equilibrium and elastic stability problems, appl. of triangular facet shell element method, TRUMP 77−46946
Euler column Lyapunov stability analysis 78−71285
Euler method application for case of follow-up load preset on part of body surface *(Russian)* 78−28948
eutectic, irregular, branching limited growth 80−81042
evaporation cooling system based on porous heat emitting element, stability anal. *(Russian)* 77−71322
evolution systems and convection-diffusion, stiffness and stability, Gershgorin theory 80−77626
evolved stars, thermal and nuclear modes coupling 79−84785
evolving systems instability, elastic stability theory and catastrophe theory approaches 78−44442
excitable medium, auto-oscillatory, 1-dimens., stability complex regimes 78−15752
extremely metal-poor stars, theoretical evolution and radial mode pulsational stability 78−28677
factorization theorems, stability and repeated bifurcation 78−65751
failure kinetics and stability 77−883
ferrites, stability of nonlinear homogeneous magnetisation precession *(Russian)* 78−48001
ferromagnetic Fermi liquid, stability conditions 79−47224
fibre reinforced composite bodies, structure optimisation in stability problems 80−58947
fibre reinforced cylindrical shells, stress strain state and stability 80−14598
fibre reinforced elastic slab subjected to axial loads, instability and buckling 80−64420
fibre reinforced prestressed elastic circular cylinder, stability 78−79234
field emission instability effects on SEM display, electronic removal device 78−21279
films as two-dimensional continua, dynamics, wave propagation and stability 79−68568
flat plate, simply supported, uniaxial compression, secondary buckling anal. 78−55579
flexible viscoelastic cylindrical shell, dynamic stability 78−5678
flow-induced oscillations, bifurcation to divergence and flutter, infinite dimensional anal. 78−89336
fluid spheres symmetry stability in general relativity, virial theorem consequences 79−21593
fluoroscopy, kVp variable, with automatic brightness stabilisation, X-ray tube pot. var. 78−69202
flutter-unstable dynamical system with gyroscopic (circulatory) forces, nonlinear behaviour 78−63276
force-cooled superconductor design for large fusion magnets 79−31216
forced oscillations, lower bound on forcing amplitude for stability, third order non-linear system 80−52013
forced periodic response stability in third order non-linear systems, comments 79−81763
forced periodic response stability in third order nonlinear systems, comments 79−81762
form stability anal. of explosion-accelerated cylindrical metal liners 78−83425
fracture mechanics, stability conditions 78−13974
frameworks' stability analysis appl., w.r.t. sway excess of columns 78−51098
free circulat plate, stability under non-conservative edge loading 80−23948
free rigid body stabilization by gyrocompass type frame *(Russian)* 77−84136
Freeman's elliptical stellar cylinder model, stability 78−28731
frustrated two-dimensional planar model, spin-spin correl. 80−11212
galaxies, criteria of local gravit. instability of double gaseous discs *(Chinese)* 79−17099
galaxies, instability of gravitating rot. viscous gaseous systems rel. to ring struct. form. 77−17690

stability continued
galaxies, spheroidal, perturbations and stability of interstellar gas disc *(Russian)* 77−91616
galaxies, stability against perturbations rel. to nonflat components mass 80−62291
galaxies, stability anal. of finite uniformly rotating disc 79−88732
galaxies discs, second-harmonic oscills. of Maclaurin spheroids in halos 79−8993
galaxies distribution, hierarchical clustering pattern stability 78−86026
Galerkin's method, non-uniform convergence 78−83304
gamma-ray spectrometer self-stabilising peak detector *(Russian)* 79−26814
garnet, Permalloy-coated film, bubble vel. and stability, influence of planar domains 80−39831
gaseous discs with uniform rot., global stability 77−26000
gaseous rotating masses with mag. fields, stability and existence of bifurcation point 78−53924
Gauss-Seidel convergence criterion for elastic structural stability 77−53781
geophysical prospecting, instability of finite difference schemes due to boundary conditions 77−21912
glass fibre reinforced plastic shell with rubber filler, stability under axial compression 80−7643
glass fibre reinforced shell of rotation, stability 78−13938
glow discharge, transversely inhomogeneous, equiv. cct. theory 78−51373
glow discharges, normal and otherwise with parallel resist., anal. 77−11416
granular bed fluidised by gas stream, stability 79−18946
granular material continuum theory, uniqueness and stability 77−40518
gravity wave critical level flow, viscous stabilization 77−45074
gyro-stabilisation platform, nonlinear loss of stability and trembling *(Chinese)* 80−62457
gyroscope, astatic, with hysteretic type interframe correction *(Russian)* 77−23864
gyroscope, dynamically tuned precision, linear acceleration effect *(Russian)* 78−62193
gyroscope, stability of Staude's permanent rot. with damping 78−21126
gyroscope with contactless suspension under ang. vibr., stability conditions *(Russian)* 79−80420
gyroscopes, stability with gas lubricated spin axis bearings *(Chinese)* 79−63205
gyrostabilized platform, nonlinear response to transient input 78−30219
gyrostat, symmetric satellite, uniaxial stabilisation at libration points 80−14560
H-shaped section cylinder in laminar and turbulent flows, aerodynamic charact. 80−106813
half-space with crack, local loss of stability *(Russian)* 79−18821
Hamiltonian autonomous system with 2 degrees of freedom, stability in 1st order reson. *(Russian)* 77−53776
Hamiltonian system, two-dimensional, stability of equilib. position in case of equal frequencies *(Russian)* 78−36814
Hamiltonian systems instability, examples 79−62732
hard and composite superconductors at critical state, anal. 77−89907
hard superconductor flux jumps under time depend. external conditions 80−7038
heat conduction stability in continuous media with heat/material sources/sinks 79−94455
heat exchanger tube banks, turbulent buffeting and fluid elastic instability 79−3958
heavy gyrostat, steady motion stability for free and restrained dynamical systems 80−46791
heavy particle on rotating surface, stability of equilibrium, including damping 77−13604
helical uniform structures, Hadamard stability *(French)* 77−68385
hemispheres, thin elastic spherical, stability curves, boundary value problems 79−81745
high current density magnet, thermal stability 80−37057
high-perveance electron beams with Brillouin focusing 77−83802
horizon gyrocompass, stability of precessional motion, third order resonance *(Russian)* 79−46173
horizontal axis wind turbine blades, aeroelastic stability and response 80−61250
horizontal flat plate, heat transfer in natural convection flow *(Japanese)* 79−64658
hot degenerate stars in steady-state accretion, thermal stability 78−40929
HV stabilised supplies for 25 kV SEM *(Czech)* 79−21858
hyperelastic bodies, Lyapunov stability sufficient criteria 79−12604
ideal crystals, principles of satbility analysis 77−45697
impact vibration, steady, body with impact hysteresis charact., stability anal. 78−51099
imperfect shells, stability, numerical anal. *(Ukrainian)* 79−94514
imperfection sensitivity of N-degree-of-freedom system with coincident critical points, symm. effects, stability props. 78−79236
imperfection sensitivity of semisymm. branching, rel. to catastrophe theory, stiffened plate appl. 77−84170
implicit finite element algorithm for geometrically nonlinear problems of struct. dynamics, stability anal. 78−86157
implicit finite element algorithms for geometrically nonlinear problems of struct. dynamics, accuracy anal. 78−86158
implicit-explicit finite elements in transient analysis: stability theory 79−17215
infinite classical system, stability, equilib. and KMS 78−21055
infinite dimensions and the fold catastrophe, particle modelling 80−8788
inhomogeneous anisotropic linear thermoviscoelastic medium, asymptotic stability proof 79−21554
insolation stability characterisation by stochastic time series 79−57396
instability, ductile fracture and formability limit diagrams 79−64589
integro-differential coupled-core reactor models, asymptotic stability 80−13531
interconnected dynamical systems on Banach spaces, well posedness, instability, Lagrange stability 78−69976
interfacial stability with heat and mass transfer, appl. to Rayleigh-Taylor and Kelvin-Helmholtz cases 78−67253
interpolation by linear least squares, numerical stability of soln. *(German)* 77−9322
interstellar clouds, rotating, stability against fragmentation from three-dimensional hydrodynamical calcs. 80−62236
interstellar contracting CO clouds, thermal instability and fragmentation 80−67838
interstellar gas, isentropic instabilities 77−17644
stability continued
interstellar gas clouds, non-uniform collapse stability 80−101631
interstellar large globules, struct. rel. to gravit. stability 80−62246
interstellar magnetised gaseous discs, gravitational instability 80−4424
intestinal electrical rhythms model, stability of entrainment conditions for RLC coupled Van der Pol oscillators 77−56361
intrinsic, relative strengths of criteria 78−90738
inverse filter which is optimum in error-distrib. sense, stability charact. 78−81424
inverse problem stability, one-dimens. wave eqn., seismic profiles appl. 79−84490
ion-laser discharges, high-power, stability limits 78−37872
ionic crystal, surface stability 80−20016
irreversible thermodynamics, information-theoretic stability and evolution criteria 77−33965
Ising model, two dimens., metastability, dynamic Monte Carlo method, transfer matrix 78−72354
isoenergetic stability 77−49587
isotropic bodies, stability under all-round compression by dead load *(Russian)* 77−42762
Jupiter-Saturn-Sun systems, long-term numerical solns. 78−24450
Kirkwood Gaps and stability of conservative periodic systems 78−65544
KMS states, stability properties, KMS condition 78−81916
KVI cyclotron, dee voltage and beam RF phase stabilisation 79−54688
Lagrange gyroscopes, system of n, stability of uniform rotation *(Russian)* 78−86136
Lagrange gyroscopes, system of two, stability of regular precessions *(Russian)* 77−62145
laminar blocks with plastic deformations, instability 80−43629
laminar shells, with viscoelastic binder, stability 80−10165
laminated composite panels, flutter instability, shear deformation and damping effects 79−72841
laminated reinforced elastic shells, stability 80−58948
landslides, hydrogeological conditions rel. to stability, rheology *(Russian)* 77−25683
laser, CW, stability of quantum model, Lyapounov function approach, using Scully-Lamb theory 78−5445
laser instability, example from synergenetics 80−9848
laser model, stochastic, entropy and stability 79−50279
laser output power stabilisation using acousto-optical method *(Polish)* 79−13994
laser waves, coherent, stability domain 79−50280
lattice system, stability, equilibrium and metastability 79−54070
law of mass action, first order phase transition, chemical instability 78−80778
layered rod on sagging elastic supports, aeroelastic stability, vibr. modes 78−51115
limit state stability, multicause interaction relationships *(German)* 79−23235
linac cavities, field theoretical approach to stabilisation 78−33309
linear accelerator incompatibility theorem, stability and focusing 77−3195
linear differential eqns. with periodic coefficients, stability conditions, energy expressions *(German)* 77−53746
linear randomly perturbed systems, mean-square stability 77−9870
linear systems, stability of motion rel. to part of variables *(Russian)* 78−86144
linear systems with periodic coeffs., stability determ., numerical method 77−2535
linear systems with time delays, stability analysis 77−62198
linear thermoelasticity, continuous depend. and instability 80−74783
lipid bilayer, saddle splay instability, crit. elastic modulus 78−44462
liquid carrying pipe on elastic foundation, dynamic stability 79−90161
liquid film, thickness and stability, on nonplanar surfaces 80−10755
liquid microlayer form. and stability in pool boiling, dry area growth 79−18683
liquid phases interface, hydrochemical stability 78−22933
liquid scintillation counting sealed standard production 79−68145
liquid zone stability, static or rot. 77−59182
LMFBR steam generator rupture disks, dynamic instability anal. 79−85662
load stability problems, power method modification *(Russian)* 80−28444
logarithmic converter stabilized by a baseline restorer employing gain switching 79−45582
lower atmosphere vertical stability determ. from Rn content, stability indexes statistical anal. *(Spanish)* 79−92561
lunar librational stability, effect of external disturbing torques 77−71021
Lyapunov stability in the presence of several resonances *(Russian)* 77−71203
magnetic bubble, transverse mass in rotating gradient 80−39832
magnetic bubbles as tilted cylindrical magnetic domains 78−64246
magnetic field, winding supply current regulator based on industrial thyristor convertors 77−37921
magnetic fields, twisted, stability 78−45217
magnetic insulators, cubic single cryst., spin-wave instability theory 79−65667
magnetic liquids, long term stability for energy conversion devices 77−29051
magnetic monopoles, non-Abelian, stability analysis, Yang-Mills equations 80−31987
magnetic-binary problem, stationary solns. and stability when primaries are oblate spheroids 80−41697
magneto-modulation sensor, even-harmonic type, anal. *(Russian)* 77−53958
magnetoaeroelastic stability of thin panels, space vehicle re-entry *(French)* 77−65702
mass unit of 1 kg, secondary standards, USSR 78−4595
massive stars, gravity modes vibr. stability during H shell burning stage 77−56933
McLauren cool discs, equil. and stability w.r.t. perturbations, gravitating mass effect *(Russian)* 79−92860
mechanical and chemical, of natural rubber latex, potassium fatty-acid soaps effects 79−96034
mechanical dished supports, oscillation and stability conditions based on mixed finite elements *(German)* 78−87299
mechanical stability in creep conditions *(Russian)* 79−18758
mechanical system, geometry and stability theory 79−27558
mechanical systems, conservative and partially dissipative, equilibrium instability 77−5658

stability continued
mechanical systems, follower load type, time invariant functionals 80−77609
mechanical systems, stability of stationary motion, Lagrangian eqns. and Liapunov's direct method 80−69645
membranes, stability of nonlinear oscillations from Liapunov method 80−96212
meniscus joining vertical rod to liquid bath 77−4247
mesh analysis processes, convergence *(German)* 78−87257
metal structures, creep, stress and stability anal. rules and methods 79−32302
metallic column at elevated temp., parametric response 79−72829
metallic glass, stability, hole theory of liquids appl. 80−100174
MHD, thermally radiative magnetofluiddynamic channel flow 77−15129
MHD generator, combustion stability 79−32827
MHD linear induction pump, instabilities at low flow rates 79−77279
Michaelis Menten mechanism, modified, global asymptotic stability of soln. 79−79456
micropolar viscoelastic fluid motions, universal stability 77−11165
microwavelength instability meter 77−10054
minimal normal modes, existence and bifurcation 79−72837
mixed valence, stabilisation by polaronic effects 79−4520
model conduction problem, MacCormacks time-splitting technique stability anal. 79−55361
modulational instability expt. using nonlinear transmission line 77−82397
molecular ions, negative, polar, thermally stable 79−7033
MOSFET, piezoresistivity effects and use as press. transducers 80−4695
motion, approx. Lyapunov function definition *(Russian)* 78−62068
motion on ring *(Russian)* 80−42052
motion stability in neutral case *(Ukrainian)* 79−41594
moving thin elastic strip subjected to random parametric excitation, dynamic stability 80−48618
multilayer shells with fillers, exam. of stability under axial compression comparison to theory 80−7643
multineuron nets, inhibited and excited, anal. *(Russian)* 77−40658
multiparametric discrete-continual elastic systems, characteristic series coeff. *(Ukrainian)* 79−40368
multiple parameter system vibrations and stability, book 78−93532
muscle, striated, analytical soln. to isometric mechanogram of Hill's model 78−73168
N-body problem, restricted, libration points stability in perturbed potentials case 80−4241
N-degree-of-freedom system, imperfection sensitivity of compound branching 78−13934
N-loop ensemble reference phase control system, stability 77−46794
nematic liquid crystals, nonlinear stability of motion *(French)* 77−84623
nerve, temporal stability of solitary impulse solns. of nerve eqn. 78−35830
nerve impulse theory, Hodgkin-Huxley eqns. appl. 78−48782
neural and cellular control system properties 77−40640
neural populations, simplified model eqns. and envelope eqns. 78−31798
neutron stars, rotating, existence of ergoregion instability 78−24523
neutron stars, slowly rotating, radial perturbations, stability 80−98685
neutron stars, thermal-timing instability rel. to pulsars period jumps 79−35293
neutron stars, thermal/timing instability rel. to pulsar timing obs. and X-ray transients 79−92795
neutron stars anisotropic models, stability against radial and nonradial pulsations 77−13378
neutron stars mass upper limit for stability against black hole form. 78−96498
Newmark's algorithm in nonlinear structural dynamics 77−26166
Newtonian stellar dynamics, maximizing functionals, rel. to thermodynamic and dynamical stability 80−12782
NGC 3686 galaxy quartet, surface photometry, mass distribs. and group stability 80−62297
non-stationary motion, stability anal. by linear approx. *(Russian)* 77−71212
nonconservative autonomous and nonautonomous systems, stability, energy approach 78−51097
nonconservative elastic systems, stability under periodic effects *(Ukrainian)* 79−32309
nonconservative simple frame, nonlinear divergence buckling, critical load 80−14594
nonconservative systems, simplified stability criterion from Lyapunov's method 80−46790
nonequilbrium steady states, irreversible processes, Lyapunov functions 80−95049
nonequilibrium thermodynamics, statistical formulation by general Onsager Machlup formula 79−54089
nongradient systems, classification of critical conditions 77−75827
nongradient systems, nonlinear instability behaviour 79−75331
nonhamiltonian systems with one degree of freedom, forced periodic motion *(Russian)* 78−20959
nonisolated equilibrium with max. pot. stabilised by dissipative forces 80−14599
nonlinear Brownian motion, and formation of macroscopic order, theory of instability 78−89408
nonlinear dispersive wave eqns., modulational instability and envelope solns. 78−54199
nonlinear elastic shells, stability loss *(Ukrainian)* 79−32308
nonlinear elastic stability problems using a finite difference perturbation method 78−83273
nonlinear elastic systems, incremental approach to the solution of snapping and buckling problems 79−76975
nonlinear elasticity, potential wells and stability 79−9111
nonlinear fracture mechanics, stability of partially cracked system 78−79261
nonlinear oscillators, normal modes, uncoupling and stability 80−27115
nonlinear plate and shell theory problems soln. 77−53784
nonlinear plate problems, unconditional stability of finite element scheme, nonlinear vibrs. *(Japanese)* 79−77004
nonlinear stability problem, direct variational method 77−57174
nonlinear structures, progressively changing equilib. eqns. soln. 78−1581
nonlinear sway-buckling of an eccentrically loaded frame of two Timoshenko-bars 79−37204
nonlinear systems, stability analysis method 79−84947
nonlinear systems, third order, forced periodic response stability 78−90763

stability continued
nonlinear systems asymptotic stability, geom. props. of Lyapunov functions *(German)* 78−87286
nonlinear third order systems, pulse response 78−83313
nonlinear wave eqns. soln. *(Russian)* 77−30019
nonliner oscillatory systems with delay, stability props. of differential eqn. solns. *(Russian)* 77−41475
nonuniform states, stability in systems exhibiting continuous bifurcation 79−84972
normal modes of coupled nonlinear oscillators, stability 78−89330
novae, accretion disk stability 77−82244
NQR absorption precision thermometer 77−5841
nuclear power reactor, neutron-field control system, stability anal. 77−3086
nuclear reactor constrained feedback control system design 77−88257
nucleonic and other meas. methods compared 77−38594
numerical stability of complex finite elements 78−32659
ocean, stability of shelf water/slope water front south of New England 79−2260
ocean currents stability in eddy-resolving general circulation models 79−16492
one-dimensional Schrodinger eqn., almost periodic soln. *(Ukrainian)* 78−89360
one-dimensional self-gravitating isothermal systems, stability 80−73008
optical bistability, scatt. light spectrum atomic fluctuations 78−94383
optical image stabilisation, using liq. optical element 78−55462
optically levitated particles, feedback stabilisation 77−27290
optimal motion stability *(Russian)* 78−86145
optimization of practical stability problems 80−5966
orbital motion stability for two free ideal conducting current rings *(Ukrainian)* 79−35102
orientation stability of double spin satellite 77−53398
orthotropic annular plate, stability *(Polish)* 78−18209
orthotropic shell with elastic filler under external press., stability *(Russian)* 77−19528
oscillating control system theory 77−25360
oscillating system, light damping, influence of eigenvalues *(German)* 80−31490
oscillator, linear parametrically excited, random vibration and stability 79−64491
oscillator and tie in relative motion *(Polish)* 77−53789
oscillators, planar, nonlinear, stability of modes 80−74790
panels with openings, stability loss and critical stresses 80−10219
parallel channel of forced convection boiling upflow system, instabilities 77−61494
parametric dynamic systems, combination reson. determ., generalised harmonic balance method 78−90753
parametric excitation system instability region determ. 79−23201
parametric instability, demonstration and discussion 80−57032
pendulum in mag. pot. *(Ukrainian)* 79−75329
pendulum inverted, design and stabilisation control *(Japanese)* 80−73167
pendulum-gyroscopic platform stabilised in inertial space, autonomous determ. of coords. *(Ukrainian)* 78−65760
penetration gas cooling, porous wall with external heat appl., stability determ. 79−64761
periodic density patterns as uniform fluid crystallizes 80−107404
periodic motion and nonlinear oscillation theory *(Russian)* 78−86147
periodic optical waveguides of lenslike media with complex permittivity 77−83997
periodically-supported fluid-conveying pipe parametric instabilities 79−68627
perturbation theory, quasi-periodic motion, asymptotic expansion method 80−17877
perturbed Hamiltonian system, stability criterion 80−17793
perturbed motion stability anal. *(Russian)* 78−16640
phase meter, digital, using delayed pulse train 77−49742
phase transition, 1st order, ageing stage, kinetic instabilities 78−87765
photoelectric inclinometer, sensitivity stabilization by negative feedback *(Russian)* 78−4012
photomultiplier using Pb glass channel type secondary electron multiplier, stability behaviour *(German)* 78−852
physical systems, principle of stability of invariance 77−26164
physical systems instabilities, variational principles for complex eigenvalues 79−21527
piecewise continuous elastic systems, eigenvalue lower bounds, stability and vibrations 79−50604
piezoelectric air-spaced Fabry-Perot etalon, stabilisation 77−82591
pipe mode characteristics determination, pipe flow conditions effects *(French)* 78−79246
pipes carrying fluid flow, oscillation stability *(German)* 78−87298
planetary orbits stability, soln. to Poincare problem in celestial mechanics 78−28492
planetary systems, stability with bifurcation theory 77−53406
plasma disruptive instability in TO-1 Tokamak, feedback stabilisation *(Russian)* 79−55546
plasma flute oscillation suppression, regulator synthesis *(Russian)* 80−24212
plastic deformation in tension, stability concepts and conditions 78−26046
plastic instabilities and uniaxial tensile ductilities 80−79180
plate, annular circular, thin, of variable thickness, thermal buckling 79−32312
plate, circular, laterally loaded, elastic instability initiation 77−50936
plate, multilayer sandwich, stability and buckling analysis by finite strip method 78−26069
plate, orthotropic, with small shift rigidity, stability eqns. construction method *(Ukrainian)* 77−31215
plate, prestressed elastic, homogeneous solns. for bending and stability 80−43610
plate, rectangular, dynamic stability, periodic compressive forces 77−23910
plate, thin, unlimited, with noncircular hole, stability problem soln. *(Russian)* 78−18201
plate, thin stretched, with curvilinear holes, buckling and loss of stability *(Russian)* 79−68607
plate, with internal crack, in tension, instability of plane solution *(Russian)* 79−50616
plate incompressible isotropic, stability under all-round compression *(Ukrainian)* 79−37149
plate stability, numerical anal. *(Russian)* 79−3935

stability continued
plate with crack close to one edge, elastoplastic equilib. 80−14624
plates, annular, dynamic stability numerical soln. *(Polish)* 80−10173
plates, dynamic instability anal. by finite element method 77−3769
plates, flat, stability of postbuckling behaviour 80−1453
plates, loaded, thin elastic shell approx., energy conservation, stability eqns. *(German)* 77−873
plates, periodically varying length, instability of motion 80−69717
plates, rectangular, stability anal. by complementary energy method 80−48611
plates, rectangular, stability and vibrations *(Chinese)* 80−43644
plates and shells, elastoplastic, with hydrostatic press. depend. mech. props., stability problem soln. *(Russian)* 80−53668
plates with cut, stability loss critical stresses for steel, Ti and Al alloys 80−11690
polar orthotropic sector plates, stability 79−18765
polyamide mixtures, thermodynamically incompatible, composition-prop. relationship *(Russian)* 80−7872
polyethylene films, fibres, radiation initiated graft polymerisation of acrylonitrile, initiation rate rel. to props. *(Russian)* 80−7531
polyethylene/ethylene vinyl acetate copolymer mixture, rel. between hypermol. struct. and stability *(German)* 80−64929
polyhedral crystal growth from soln., morphological stability 78−26466
polymer, oriented, under load, crystallite stability, X-ray diffr. and IR spectra meas. 77−70126
polystyrene, rubber-modified, rubber particle morphology influence 79−94925
portable easy-operation long-period seismometer, peripheral stabilising device 78−65399
portable voltage source, ultrastable 79−67351
position control system for plasma column, stability 80−106982
postbuckling behavior of thin-walled open cross-section compression members 80−5963
power reactor with multiple transport lags and nonlinear controller characts., parameter plane method 77−14217
premixed flame regime, Linan's linear stability anal. 79−52666
pressure vessel heads, torispherical, elastic instability and with triangular thin shell finite elements 77−58576
prestressed beam, dynamic response and stability 77−39230
probkotron plasma stabilisation system, automatic, against flute oscills. *(Russian)* 80−24211
projectile, axisymmetrically rotating, stability of nonstationary motions *(Russian)* 78−24659
proton storage ring, NAP-M stability of current in guiding-field magnet supply ccts. 77−65363
pseudoconservative systems, effect of damping on stability 78−81832
PSR 0809+74, pulsar, phase stability in drifting subpulse pattern 78−40980
PVC, chlorinated, fibres, radiation initiated graft polymerisation of acrylonitrile, initiation rate rel. to props. *(Russian)* 80−7531
PWR movable in-core neutron detectors *(Japanese)* 79−26722
PWR power plant steam dump valve stability anal. 78−50289
pyroelectric IR visualisation gauges 79−68432
quantum statistical mechanics, algebraic approach 77−22491
quasars, radiatively driven gas clouds dynamics and stability, plane-parallel slabs theory 80−22107
quasi-linear nonautonomous systems, motion stability condition for periodic oscills. *(Russian)* 77−33855
quasi-static potential oscillations of thin conductor, instability 80−87900
quasiperiodic motions stability in Hamiltonian systems 78−93085
λ 8-cm radioheliograph at Toyokawa, new local oscillator system phase stability 79−101073
radiometer sensitivity, varistor freq. transducer instability effect, anal. *(Russian)* 77−22598
random parametric vibr. of hollow cylindrical shells *(Russian)* 79−27572
random threshold element networks with absolute refractory period 77−29143
randomly rotating rigid body, computation of functionals over sample paths 77−74212
rapidly rotating compressed rods 80−79189
Rayleigh-Taylor instability, method of generalised coords. 78−65771
reacting system, effects of nonequilib. corrections to rate coeffs. 77−25254
reaction-diffusion eqns., stability of solns. 78−16759
reaction-diffusion system with one degree of freedom, stability anal. of dissipative structs. 79−87826
reactor nonlinear control system, relative stability anal. 77−3116
reactors with delayed temp. feedback, linear stability anal. 78−29551
rectangular cylinders in heaving mode, aeroelastic instability 79−3954
rectangular plate, stability, mechanical props. dependent on strained condition *(Russian)* 79−10494
rectangular plate static stability soln. with fully conforming element 77−62184
rectangular plates with perforations *(Russian)* 79−32311
rectangular surface embedded in uniform subsonic flow, stability 77−80178
red giant stars, envelopes dynamic instability and mass loss 78−20824
refractory composites, fibre reinforced, directionally solidified tensile tests, in HVEM, deform. and fracture *(French)* 78−68785
reinforced cylindrical shell, nonuniform thickness, optimisation 77−68465
reinforced open cylindrical shells, bending stability 79−41581
reinforced plastic cylindrical shells, optimal design under dynamic constraints 80−102996
reinforced rectangular plate, compressed in two directions in a manner conducive towards stability 78−22289
reinforced shell under external press., max. stability 78−94597
relativistic electron beam instability, passage through dense gas, energy spectrum *(Russian)* 77−3529
relay systems, bifurcation and stability from third order differential equation *(Russian)* 79−46247
resistance thermometer, Ge, stability at 20K 78−41307
restricted three body problem, stability limits appl. to Sun-Earth-Moon system 79−75084
restricted three-body problem, asymmetric, periodic and asymptotic orbits, stability 79−16807
restricted three-body problem, second generation periodic orbits and regions of stability 78−24453
rheonomic shell, cylindrical, local stability in creep conditions *(Russian)* 80−92069
stability continued
rib-reinforced orthotropic cylindrical shell, structural design effect on stability 78−22288
ribbed plates with large openings, design optimisation, finite element anal. appl. 80−87724
rigid body, regular motions stability in Newtonian gravit. field 77−26165
rigid body attitude control in inertial space *(Russian)* 79−9101
rigid body near Earth's surface, stability of flight *(Russian)* 78−89048
rigid body with fixed point, effect of viscous damping on spin stability 77−78974
rigid shaft in short journal bearings, aperiodic behaviour 78−46905
ring, oscillatory behaviour, influence of Coriolis forces on power transmission belts *(German)* 78−87255
ring optical, resonator with arbitrarily situated medium, axial contour and stability *(Russian)* 79−89939
rocket engine oscills. due to burning instability *(Russian)* 77−14893
rod, short elastic, in viscous liquid axial flow, stability and transverse oscillations 80−33521
rod, thermal conduction, dynamic behaviour of distributed systems *(Dutch)* 80−28407
rod shaped continua, stability of free vibrs. 77−68493
rod with clamped ends, axial and transverse loading, stability, plane elasticity theory *(Russian)* 80−79184
rod with nonlinear curvature, dynamic stability theory, lateral bending problem under torsion *(German)* 78−54
rods, influence of mass distrib. on stability in presence of polygenic forces 79−81744
rods, simple orthotropic elastic, shock waves and wave-type instability 80−48622
rotating asymmetric shaft, unequal pedestal stiffness influence on unstable vibrs. 79−18803
rotating black holes, instabilities of massive scalar perturbations 79−54026
rotating body, stabilisation by passive dampers, asymptotic methods use *(Russian)* 78−20957
rotating cantilever, stability and instability conditions, Lyapunov function method *(Russian)* 80−36840
rotating gaseous masses, adiabatic stability 77−91516
rotating liquid drops, asymmetric shapes and stability 80−87796
rotating neo-Hookean cylinder, stability under large deformation 77−50942
rotating stars, perturbs. and stability, eigenvalues and perturb. theory 80−46538
rotating stars, perturbs. and stability, eigenvectors and variational principle 80−46537
rotating stars secular stability, Lagrangian perturbation theory of nonrelativistic fluids 78−49305
rotating viscoelastic tapered cantilever, circulatory force at free end, influence of angle of attack 80−69686
rotor, elastically supported, automatic balancing *(Polish)* 79−10458
rotor, partially filled with viscous incompressible fluid, stability anal. 80−64359
rotor, passing through crit. speed, with gyroscopic effect, asymptotic calc. 78−63354
rotors, elastic wave stability 78−87297
S=1 generalised Ising model, stability conditions 80−20427
sandwich structure stability, analog method 79−32314
satellite, elastic, gravitationally oriented, spatial oscills. and stability of relative equilib. 78−4068
satellite, gravity oriented, with thermally flexed appendages, librational dynamics 78−7868
satellite attitude control system, gyrodampers appl. 78−96379
satellite eccentricity oscills., compensation with stabilizer 78−69643
satellite gyrostat, optimal stabilisation of relative equilib. positions *(Russian)* 77−39213
satellite in elliptic orbit, stability of cylindrical precession *(Russian)* 77−42729
satellite motion, stability limits 79−21163
satellite movements, aerodynamic effects *(French)* 79−21159
satellite orbit stability in restricted three-body problem 79−21162
satellite stabiliser system with 2-stage suspension, dynamics *(Russian)* 79−32222
satellite with 2-degrees-of-freedom gyroscope, stability *(Russian)* 77−39212
satellites attitude control, stability of inertially fixed pitch stabilisation by solar radiation press. 80−101523
saturable transformer ferroresonance anal. using rectangular hysteresis-free approximation method *(Russian)* 77−55708
scale stabilizer based on ^{40}K photopeak for scintillation detector 79−26823
Schrodinger eqn. explicit method stabilisation difference eqn. *(Italian)* 77−71225
Schrodinger operator regularisation stability with singular repulsive pot. 79−88841
scintillation radiometric path automatic stabilisation 77−23372
second law of thermodynamics and stability in thermoelasticity theory 80−31689
second order linear systems with periodic coeffs., approx. method for stability anal. 80−12892
secondary flow in plane channel *(Russian)* 78−87394
sedimentary bedforms in tidal environment, Bay of Fundy, hydraulic stability relationships 78−88814
sedimentary rocks viscous remanent magnetisation, stability to AF demagnetisation, expt. results 79−79826
self-oscillating system, parametrically excitable, forms of movement, stability conditions *(Russian)* 78−16635
semiconductor, electron-hole droplet nucleation and stability, hydrodynamic approach 78−72080
semiconductors, temp. rise due to nonlinear heat generation 78−87983
semiconductors nonequilibrium phase transitions, stability and dissipation, teaching 80−105479
semisimple Lie superalgebras, deformation eqns. and stability 79−93314
shaft, rotating, with single disc, nonlinear inner damping forces *(German)* 78−1562
shaft, whirling motion, stability analysis 78−13894
shallow arch under multiple loads, postbuckling and stability anal. 80−48617
shell, circular cylindrical, of anisotropic material, plastic stability under axial compression *(German)* 78−1585

stability continued
shell, cylindrical, composite with viscoelastic filler, optimisation w.r.t. long-term stability 79−18760
shell, cylindrical, dynamic instability due to attached mass *(Ukrainian)* 80−38297
shell, cylindrical, dynamic stability under periodic axial load 79−14302
shell, cylindrical, fibre reinforced, fluid conveying, vibr. charcts., flow effects 80−14600
shell, cylindrical, isotropic, elastic stability, critical load analysis 80−83744
shell, cylindrical, nonuniform axial edge load, thermal load, linear buckling 78−63345
shell, cylindrical, ribbed, with rectangular holes, design for stability in moment precritical state *(Ukrainian)* 77−50938
shell, cylindrical, subject to local interaction with nonlinear circular base, stability 77−89050
shell, cylindrical, under axial shock, unsymmetrical bulging and buckling *(Russian)* 80−33492
shell, cylindrical composite, with viscoelastic filler, parametric oscills., dynamic instability *(Russian)* 78−38221
shell, elastic, cylindrical, stability, Liapunov's second method 80−64410
shell, loaded thin walled truncated conical, dynamical stability, nonlinear material damping *(Polish)* 79−64496
shell, multilayer composite, optimisation, buckling under stability and vibr. conditions *(Russian)* 80−53667
shell, nonlinear elastic cylindrical biharmonic excitation, parametric vibrations *(French)* 78−87294
shell, spherical, with reinforced holes, local stability 80−50686
shell, spherical transversally isotropic stability *(Ukrainian)* 80−10171
shell, three-layer orthotropic cylindrical, with stiffening ribs, stability 80−74784
shell and plate, reinforced, viscoelastic and elastic, with transverse shear strain, stability 77−84171
shell and surface rigidity, pseudobending, vibrs. and stability loss *(Russian)* 80−33470
shell buckling, nonlinear isometric bifurcation, lower stability limit 77−68469
shell formed by truncated cones, stability and deformation 80−69691
shell of revolution, stability of nonlinear local axisymmetrical strains 77−35042
shell of revolution with slightly curved generator, stability under complex load *(Polish)* 77−54910
shell of rotation exposed to vibrs., optimum shape and reinforcing struct. 79−18792
shell of variable thickness, inverse nonlinear stability *(Russian)* 77−50884
shell stability anal., finite element representation and pressure stiffness 79−90160
shell stability during axial compression, hardening beyond elastic limit 80−99931
shell stability under heating and loading 79−94518
shells, circular cylindrical, dynamic stability under periodic compressive forces 78−90754
shells, compressed viscoelastic orthotropic, stability 79−7305
shells, cylindrical, containing swirling fluid flow, dynamic stability 77−68510
shells, cylindrical, dynamic stability, in-plane inertia and disturbance effects 80−79181
shells, imperfect long cylindrical, lower critical hydrostatic press., stability 80−33491
shells, Kirchhoff-Love, structural stability, mixed variational principles and non holonomeous constraints *(French)* 80−74779
shells, spatial stability problems in elastic systems, modified energetic procedure *(Russian)* 80−58943
shells, thin circular cylindrical, stability problem soln. method *(Chinese)* 80−5928
shells, thin stiffened reinforced, stability and vibrs. 80−14610
shells of revolution, Ritz-Galerkin method *(Russian)* 77−80062
shells of revolution, stability, dynamic programming 79−32270
shells of revolution *(Russian)* 80−43638
shells under external press., stability 80−23898
shells with curvilinear axis, geometric approach 79−32271
shock wave, implosive spherical, produced by laser pulses, shadowgraphic detection 80−87529
simple frame subject to follower force, divergence buckling, limit point instability 79−18763
simple frame with circulatory load, elastic stability 79−94532
single-rotor corrected gyrocompass motion subject to random parametric disturbance *(Russian)* 79−10456
skew orthotropic plates, stability analysis by finite strip method 78−79235
slamming safety membrane, stability loss in elastoplastic and elastic regions, expt. coeffs. 80−33496
soft mode instability mech. 80−86142
soil, deformation of compressible elastoplastic ground 78−96198
solar coronal loop, plasma physics model and stability 77−45371
solar coronal loops, stability 79−101132
solar evolving force-free magnetic fields, stability of configurations and motion of medium 78−12176
solar quiescent corona, dynamical stability 78−40885
solar system, dynamical stability 77−9679
solidification, stability analysis, interfacial surface entropy effect in heat balance 78−26464
solids, uniqueness and stability under config. depend. loading 78−30194
solitons, Poincare stability, gauge theories, nonlinear Schrodinger equation 80−4881
solitons, theory and applications 78−36811
Space Telescope pointing control fine guidance subsystem design 80−82201
Space Telescope solar array requirements and design 79−96885
spacecraft, flexible, in gravitational field, stability 77−25906
spectrometric channel control using blocks 78−866
spectrometric channel stabilization, with automatic reference peak search 79−26803
spectrophotometer colorimeter, colour measurement repeatability appl. *(Hungarian)* 77−26404
spherical cavity, variational anal. of stability *(Russian)* 77−50885
spherical envelope, two layer, stability under uniformly distributed external press. 78−38222
spherical shell, buckled states, under uniform external pressure, asymptotic methods and Newton's method 80−43635
spherical shell, laminated 77−65700
spherical shells, local stability 78−1587
spherically symmetric accretion flows, stability anal., X-ray sources appl. 80−46387
spinning annular plates reinforced with edge beams, vibration and stability 78−38225
spinning elastic disc with transverse load system, stability anal. 77−19562
spinning polar orthotropic annular plates, edge beam reinforced, vibration and stability 79−94534
spinning shell, Magnus instability 79−18693
spring, complex arch type, movable, snap-through action charcts., appl. to microswitches 78−63339
spring, complex arch type, movable, snap-through action charcts., microswitch appls. 78−63340
springs, helical, under compression and twist, stability, nonlinear Kirchhoff-Clebsch equations *(German)* 80−33443
SQUID magnetometer, AC-biased 80−98948
30 M⊙star, stability towards g^+ modes of high spherical harmonic values 77−9740
star clusters, isotropic relativistic, multi-term trial function stability anal. 78−73742
star in thermal imbalance, pulsational stabilities, comparison of methods 78−45316
star seeker using semidisc light-flux modulator, accuracy anal. 78−73648
stars, distorted, Clairaut coordinates and vibr. stability 80−90408
stars, equilib. and stability of Jeans spheroids with toroidal mag. fields 78−45319
stars, late-type, acoustic modes overstability and obs. implications 77−56932
stars, magnetic, convective stability 80−94781
stars, massive, in slow rot., vibr. instability and oscill. props. 77−5536
stars, rigidly rotating, secular instabilities in general relativity, theoretical formalism 80−4341
stars, rigidly rotating, secular instabilities in general relativity, numerical results 80−4342
stars, rotating, secular instability from thermal cond. 80−21986
stars, rotating Newtonian, secular instability to gravit. radiation and viscosity 78−53922
stars, solar-type, mag. cores stability 79−44472
stars, stability problem for polytropic gas bodies *(Chinese)* 79−16937
stars, young, nonspherical thermal instability 79−48779
stars containing mixed poloidal and toroidal mag. fields, adiabatic stability 80−67706
stars in thermal imbalance, broadened definitions of instability 78−16397
stars in thermal imbalance, vibr. stability 78−24506
stars in thermal imbalance, vibr. stability coeff. energy methods 77−13320
stars in thermal imbalance, vibrational stability 78−40916
stars of about 1 $M_\odot$, semiconvection and vibr. stability 77−22204
stars with given entropy distrib., models dynamical stability criterion 79−66993
statistical couplings stability evaluation, meteorology appl. 77−74204
statistical mechanics, stability, equilib., and metastability 80−31659
statistical mechanics, structural stability 80−8932
statistical thermodynamics, nonlinear, mixing distance, steady state stability, appls. 77−9976
statistical-kinematic analysis and limit equilibrium of systems with unilateral constraints 80−1451
steady-state creep determ. eqns., microscopic stability restrictions *(Russian)* 79−10493
steel, stainless, austenite stability, deform. rel. to $\gamma \rightarrow \alpha$ transform. kinetics 79−24522
steel, stainless, cylindrical shell reinforced with longitudinal separate ribs under external pressure pulse, critical pulse estimate 79−14884
steel cylindrical shells, external static+pulsed press., stability *(Russian)* 77−46952
steepest descent technique and stellar equilibrium statistical mechanics, stability 78−65659
stellar clusters, spherical, stability under spherical perturbations *(French)* 79−35317
stellar cores stability criterion *(Russian)* 78−93214
stellar dynamical instabilities at start of convection 78−89181
stellar magnetic fields, vector-operator algebra technique for stationary states determ. 78−73698
stellar models, secular instability of Maclaurin spheroids due to gravit. radiation and viscosity 77−17538
stellar models, tidally distorted, small oscills. stability using Roche cordinates method 79−44462
stellar systems, prolate, instability 80−101642
stochastic differential eqns., stability and boundedness rel. to generalised norm 80−12993
stochastic differential eqns. *(Russian)* 77−71188
stochastic functional differential eqns. and systems of differential inequalities 78−77801
stochastic input-output stability and instability, second-order, of interconnected systems 80−52133
stochastic metastability and Hamiltonian dynamics, phase space invariant tori 79−40465
storage ring, feedback-stabilised, resonator wall instability caused by ponderomotive forces 80−5418
stratosphere photochemical-radiative damping and instability, numerical results 78−81286
structural dynamics, unconditionally stable explicit algorithm 78−48
structural instability critical behaviour and broken symm., demonstrations 80−105476
structural stability in physics (conference, Tubingen, Germany, May and Dec. 1978) 80−8739
structural stability theory, phase transition models, mean field theories, Ising model appls. *(German)* 78−77822
sunspots, stability of axisymmetric mag. flux tube 77−64734
superconducting coil, buckling, vibr., lateral constraint and damping effects 78−63344
superconducting magnets, pulsed, stability studies, fusion reactor appls. *(Japanese)* 80−106158
superconducting threads of mixed materials containing many filaments, stability and transverse conductivity meas. *(French)* 79−73629
superconducting wire, coil simulation, class and instability meas. 79−71487

stability continued
superconductor, hard, critical state stability and oscillations 80−107959
supergiant stars, atmospheric instability rel. to brightness limits and coronae 80−109432
supermassive stars, general relativistic stability towards non-adiabatic perturbations 77−41376
supersonic flow, nonstationary separation of laminar boundary layer, numerical method *(Russian)* 79−14425
surface transport vehicle, stability in weak gravity field 77−64594
suspensions, crystallisation, aggregate stability and effect on purity of product 80−100769
swinging spring with oscillating support, stability boundaries 77−68384
system with chemical reaction, thermodynamic stability, phase transitions 79−5174
system with nonconserved order parameter, influence of heat cond. on relax. of unstable states 80−10637
system with parametric excitations, instability regions determ. 80−90662
systems of coupled partial differential eqns. with random excitation 77−72218
Teflon FEP, annealed electret, charge stability 80−6943
temperature sensors, Pt-100, calibration, 20-273K range *(German)* 77−79094
temporal pattern generation in coupled oscillators, Tritonia mollusc trigger group model 79−96538
thermal instability of vibr.-excited mol. gas, appl. to surface ignition *(Russian)* 78−56895
thermistor thermostat for low-power semiconductor devices 79−71450
thermodynamics at nonequilib. steady states 79−6068
thermoelastic solids, symmetry and stability 79−44743
thermoelastic stability of first strain gradient solids 77−50893
thermoelasticity, stability of some plane deform. states 80−43634
thermoelectric thermometers, stability of readings 78−93682
thermonuclear device flute plasma oscillation, analogue simulation 78−26336
thermostat, with stability of $\pm 3.5\ \mu K$ 78−21132
thick-walled cylinder, stability loss, three-dimens. form 80−5965
thin orthotropic plates, bending stability and free vibration 79−3961
thin shells, stability theory *(Ukrainian)* 79−76970
thin shells, variational analysis of nonlinear problems 78−5673
thin tubes conveying fluid, hydroelastic stability, in plane boundary conditions, shearing loads 80−64419
thin walled shells, elastic stability theory *(Ukrainian)* 79−94515
third order nonlinear differential eqns., stability criterion, comments and reply 79−94540
three-body problem, stability of interplay motions 77−60583
three-body problem, unrestricted, Lagrangian solns. stability problem *(Russian)* 80−4245
three-body problem, unrestricted, Laplace solns. stability *(Russian)* 80−8529
three-body problem, unrestricted stability of constant Laplace solns. 80−68030
three-layer plates, circular, stability 80−79188
tide-recording equipment, phototransducers emission source light output ratio stabilisation *(Russian)* 78−88949
time varying systems, stability anal. 78−37
toroidal plasma, ion temp. control by neutral injection 79−37514
toroidal shell segment subject to external press., stability and postbuckling deform. 79−41595
toroidal shell with external press., stability 79−41596
toroidal shells, branching solns. to nonlinear eqns. *(Russian)* 79−27557
torsional stability of thin circular cylindrical shells *(Chinese)* 79−72833
train, stability of unperturbed motion *(Russian)* 78−18160
transient laser radiation, stochastic process near an instability point, numerical solution 80−23658
transonic flow, unsteady inviscid, local linearisation soln. for pitching bodies of revolution, $M_\infty = 1$, stability anal. 77−31322
transport problems stability investigation *(Russian)* 78−57880
transportable 1000 pF capacitance standard 77−5870
triangular libration point stability in photogravitational restricted circular three-body problem 79−21164
Trojan asteroids motion, long-period effects and 1/1 resonance stability 80−41755
tropical troposphere, Fourier component eigenvalue anal. of CISK-induced disturbances 77−2199
troposphere, instability following solar corpuscular stream arrivals 80−109416
tube, cylindrical, thick-walled, finite twist and external press., stability, vibrs. 78−83286
tubes, infinitely long cylindrical elastic, collapse under bending, press. and axial loads 78−18204
two coupled conductors, stab. anal. 80−96219
two layered parallelepiped under large elastoplastic deformations, deformation instability 80−33499
two-axes indicating gyrostabiliser, anal. *(Russian)* 78−54360
two-bar frame, eccentrically loaded, nonlinear stability anal. 78−63343
Universe, stability of expansion 79−17148
unstable modes of an equilibrium, number calc. 80−36493
unsteady aerodynamic modelling for arbitrary motions 80−19433
vacuum beam diodes, repetitively pulsed 80−63386
Van Allen radiation belt 80−31177
van der Pol oscillator, functionals over discontinuous sample paths 78−29052
vapour pump, recent developments 79−63250
vibration problems, Zienkiewicz four-time-level scheme for numerical integration 78−1594
VICKSI cyclotron, methods and results of RF system stability meas. 79−54687
viscoelastic, bars with nonlinear characteristics, stability 80−10174
viscoelastic rods and shells under loads that decrease with time 80−69700
viscoelastic structures, strength and stability, a method of solving integral eqns. used 80−10167
viscoelastic Voigt column, influence of elastic end support on stability 79−37238
viscoelasticity, nonlinear, bifurcation and uniqueness, Hadamard stability 80−43621
viscoelasticity, stability problems in mathematical theory 80−27133
viscometer automatic thermo-compensator, improvement method *(Russian)* 77−55114
viscoplastic round heated specimen, stability of extension *(Russian)* 79−68601
viscous axial flow in annulus entry region with rotating inner cylinder 77−23967
viscous plastic lubricant, nonlinear effects on stability of bearing tenon movement *(Russian)* 79−32393
VLBI, improvement of freq. stability of local oscillators *(Japanese)* 80−17504
Volterra eqns., generalised, stability theorem 78−86116
waffle cylindrical shell, technological charact. and bearing capacity 79−3936
water film on Fe surface, stability 80−75408
wavelength multiplexer, single-mode-fibre 80−102816
white dwarfs undergoing spherically symmetric steady-state accretion, stability 80−77402
wind generator oscillation modes in large power systems 79−29446
wind induced oscillations, domains of stability 80−64441
wind loaded structure, deterministic stability anal. 79−7314
wind turbine generator dynamic stability, digital simulation 79−96415
Al-Cu(Si)(Mg) binary and ternary alloys, dimensional changes in heat treatment. 80−89271
Al-Pd_2Si-Si junction thermal stability improvement 79−78186
Al-PtSi-Si junction thermal stability improvement 79−78186
Al-Zn-Mg-Li alloys, effect of Li on thermal props. 79−24515
Ar phase stability boundary, nucleus surface tension rel. to surface radius of curvature 79−60603
Ar^+, Ar^{2+}, relative confinement efficiencies in quadrupole ion storage trap 79−2869
As, inorganic, in freshwater environment, stability and solubility theoretical aspects 79−16553
C, glass tip, field emission current stability 80−11544
CO_2 TEA laser stability 77−38935
Cr plates, for photomasks, prep. by vacuum deposition, mech. stability *(Russian)* 79−33203
CuO-Ag film solar absorbers, mechanism of high-temp. instability 78−22971
$Fe_{40}Ni_{40}P_{20-x(B)}B_{x(B)}$, ferromagnetic metallic glass, thermal and mech. stability 77−66698
$Fe_{83}P_{17-x(B)}B_{x(B)}$, ferromagnetic, metallic glass thermal and mech. stability 77−66698
GaAs-metal junctions, thermal stability improvement, with and without near noble metals 79−7143
Ge resist. thermometers, stability test at 20K 78−81971
Ge resistance thermometers, stability data at 3 temperatures 80−86307
Ge thermometers, stability testing via thermal cycling apparatus 77−61066
H, stabilisation at low temp. 80−44390
^{3}He superfluid A phase, stability of superflow 78−14532
γ-Mn, collinear spin structure stability 80−107984
Mo fibre reinforced Cu with weak interfaces, stability of tensile deform. 80−97533
Nb-Ti-Zr, superconducting wire, coil simulation, class and instability meas. 79−71487
Nb_3Sn filamentary hexapole magnet construction and testing 79−30503
Nb_3Sn high field superconductors, filamentary, manuf. and appl. limits *(German)* 77−55647
Nd:YAG laser, reduction of passive Q-switch output jitter 78−46648
Ni complex, bis-4-dimethylaminodithiabenzyl nickel, tetrachlorethane soln., photochem. and thermal stability 80−16708
Ni perfect crystal, stability under various stresses 80−104208
O_2 sensing electrode stability 77−60268
PtSi, epitaxial film, cryst. perfection and thermal stability, channelling and backscatt. meas. 79−99255
^{125}Sb, in HCl solns., valency states investig., radioanal. tracer preparation, stability 77−63943
Si planar diode temperature sensor, long-term stability for 70 to 420K digital thermometers *(Czech)* 77−67435
Si pressure transducer, miniature, features, biomedical appl. 77−86666
Si-SiO_2 interface, elec. props. and influence on service performance and stability 78−23171
SiO_2 films on Si, mobile Na ion instability 79−82503
Ti alloy 679, thermal stability *(Chinese)* 77−73255
UO_{2+x}-ThO_2-MgO system, in air, phase rel., X-ray diffr., electron probe and metallography anal. 79−74137
Xe short-arc lamp, current modulated, arc forms and instability 80−96399

stability criteria
see also Nyquist criterion
biological macromolecules, Lyapunov method 79−96507
brain injury and instabilities 80−45943
centred finite difference scheme for 3-D eqns. of elastodynamics, stability 78−63294
coaxial autoaccelerator, klystron instability of relativistic electron beam, stability criterion 78−82541
continuous system, sufficient condition for stability in first approximation 77−50883
cylinders, thin necked, thermoplastic deformations, stability analysis *(German)* 78−22281
feedback control of unstable waves 77−5671
flexible damped satellites, Liapunov stability anal., comparative study 79−37148
frame nonlinear postbuckling behaviour, finite element analysis 77−62183
Hill equation, simplified stability criterion, applications 78−36820
loaded thin circular plate stability criterion 78−77700
minimum uncertainty states, conditions on Hamiltonian for stability 78−24683
multiple volterra integral eqns., appl. to gas chromatography 78−62049
numerical soln. oscillations, nonlinearity allowance scheme effect *(Ukrainian)* 78−90625
relativistic plasma code instability due to Lorentz force 79−7482
thermodynamic theory, phase transition, specific heat, stability criteria 77−33548
Tokamak plasma equilibrium, feedback control 78−55738
two-phase flow through porous media, starting algorithm for numerical simulation 78−38388
Nd:YAG acousto-optically mode-locked CW laser performance and stability criteria 77−38934

stability of numerical methods *see convergence of numerical methods*

stacking faults
acoustic emission rel. to stacking fault energy 78−14365

stacking faults continued
afghanite, stacking variation, TEM study 79−99219
Ag-Cu fibre composites, highly deformed, lattice defects, X-ray interference lines anal. 80−10559
β- and β''-Al_2O_3-Na_2O, fast ion conductors, TEM obs. 79−86920
alkali feldspar, deformation, plastic defects, TEM investig. 78−32066
alkali halide doped angle crystals, latent hardening 78−51607
alloys, industrial, stacking fault energy rel. to mech. props. *(French)* 79−43339
amorphous semiconductor, tetrahedrally bonded, random stacking model, X-ray scatt. intensity 78−9953
amorphous semiconductor, tetrahedrally co-ordinated, random stacking model 77−62479
amphiboles, high-resolution electron microscopy 80−75241
anthracene, orientationally disordered cryst., lattice relax. effect 80−107278
anthracene crysts., mol. orientational disorder calc. vacancies, dislocations, photodimerisation 77−4915
austenite solid soln., decomposition, effect of struct. of initial state *(Russian)* 77−48442
austenitic steel, solid solution decomposition at defects, TEM meas. 77−12656
autunite, random layer structure by grinding, X-ray powder patterns 77−78174
BCC crystal, held by pair interactions, asymmetry props. 77−19970
biotite, disordered mica struct. high resolution electron microscopy exam. 78−91344
bis(benzonitrile)trichloromonooxovanadium(V), cryst., stacking faults *(French)* 80−49238
brass, burst acoustic emission during Bauschinger effect 77−48475
α-brass, dislocation struct., deform. *(Polish)* 80−24454
α-brass, quenched, chemical composition in stacking fault tetrahedron 77−21183
α-brass, quenched, secondary defect form. during ageing, TEM obs. 78−88482
α-brass, rolling texture development, dependent on relative stacking fault energy 79−52237
brass 70/30, fatigue crack propagation, effect of stacking fault energy as deduced from dislocation patterns, TEM study 79−61719
β_1 brass containing α-precipitates, reversible shape memory effect *(Japanese)* 78−60711
γ-brass type alloys, faulted defects, nature determ. by image matching technique 78−63777
γ- brass type alloys, superstructures and defect obs. 80−107284
α-brasses, cold worked, atomic diffusion kinetics to stacking faults, Laplace transformation method 80−19977
C GaP on GaAs substrate, heteroepitaxial layers, stuct. defects *(German)* 79−23865
chromites, electron microscopy, high-resolution observations 80−75241
close-packed structures, with faults, anal. soln. for X-ray diffr. integrated intensities 80−100256
CMOS ICs electrically active stacking faults, anomalous leakage currents 79−78191
coherent phase form. at stress concentrators, effect of dislocation splitting, dislocation pile-ups, and phase elastic moduli *(Russian)* 80−49356
covalent semiconductors, electronic interface states in intrinsic stacking-faults 80−75522
crystal diffraction pattern, stacking fault insertion effects 79−86803
crystalline materials, in situ deform. by high voltage electron microscopy 80−103352
crystallite, cylindrical, layer disorder, X-ray diffr. intensity effect 80−39113
crystallites, curved, cluster with layer shift, X-ray diffr. intensities 80−39114
Cu-Al, FCC, study of dipoles using weak-beam electron microscopy 78−22724
deformed crystal, faulted dipoles 78−59814
diamond, natural, rel. to flat bottomed trigonal pits 78−26582
diamond, type I_a, phonon scatt. by platelets, N-decorated stacking fault model 77−4173
1,8-dichloro-9-methylanthracene, structural changes, photodimerisation and stacking fault energy 77−62548
dislocation wall form. in contact with surface active melt, stacking fault energy *(Russian)* 77−72626
disordered crystals, 2H to 6H solid state transformation, deformation mechanism, X-ray diffraction study 80−33921
disordered crystals, 2H to 6H solid state transformation, layer displacement, X-ray diffraction study 80−33920
disordered cylindrical lattices, diffracted X-ray intensities 78−79493
electron microscope diffr. contrast 78−83700
electron microscope resolution improvement for crystal structure imaging and atomic movement dynamic obs. 80−70090
electron microscopy, conf., Nancy, France (May 1978) *(French)* 79−41915
electron microscopy, multi-beam, general extinction criteria for extended defects 77−72532
electron wave function in vicinity of planar defect 'on edge' 80−88002
energies, investig. methods, appls. to FCC metals *(French)* 79−42080
energy calc. from fault pairs, threefold extended nodes *(French)* 79−42081
erionite, cryst. struct. exam., stacking faults 78−2083
extended growth defect characterisation, review 78−30649
fatigue failure mechanisms, thermally activated, activation energy calcs. *(Russian)* 80−16436
faulted dipoles, formation and props. 77−72615
FCC, rolling texture development 79−87657
f.c.c. alloy, rolling texture *(Russian)* 77−1843
FCC crystal, containing extrinsic stacking faults, X-ray scatt. intensity calc. 78−91193
FCC crystal, extrinsic faulting, X-ray diffraction 77−19818
FCC crystal, extrinsic faults, X-ray diffr. matrix intensity eqn. 78−38575
FCC metal, dislocation dissociation 80−107235
FCC metals and alloys, elastic energies of dissociated Frank loops 78−75671
FCC metals and alloys, macroscopic shear band contrib. to rolling texture 77−86056
field ion microscopy, developments, lattice imperfections 79−67445
film defect growth and nucleation, electron microscopy and diffraction exam. *(French)* 80−59824
fine fragmented crystals, complex struct. analysis by electron microscopy 80−104416
fluorite structure, shell model calc. of stacking fault energies 77−35573
franzinite, stacking variation, TEM study 79−99219
graphite, anisotropic elec. cond. rel. to stacking disorder 80−34437
hardened, martensite struct. charcts., Cu and Al additions effect *(Russian)* 78−19709
HEED by stacking faults, semiclassical anal., classical limit 79−46523
heteroepitaxial layers, dislocation structures, problems of formation 80−15100
homogeneous material, 2D defects, interface problems 79−46674
humite, real structs., mixed layer charcts. 78−79567
III-V compounds, stacking fault energy and ionicity 78−30651
III-V epitaxial layers, minority carrier lifetime, correl. with defect props. 77−89835
imperfect crystal, semiclassical anal. of HEED, stacking faults 79−1373
inelastic scattering effect, electron microscopy obs. *(French)* 79−60388
interface energies, appl. to stacking faults 79−19547
interfacial energy of planar defects, symm. variations 77−68983
ion implanted, F influence on oxidation-induced stacking faults 80−65011
ionic crystal, stacking fault computer simulation 78−30652
layer materials, fine structure splitting of ground state excitons 77−51665
layer sequence analysis for crysts. with stacking faults, method of structural models 77−19824
martensite nucleation general concept, general concepts, FCC to HCP transform. 77−36502
martensitic nucleation mechanism, FCC→BCC and other martensitic transforms. 77−36503
martensitic transform. kinetics., strain induced, FCC to HCP 77−44249
metal, BCC, computer simulation of stacking faults 78−30653
metal, BCC, stacking fault and twin boundary energies 77−76420
metal, BCC, twin boundary and stacking fault structs., computer simulation 80−59485
metal, fatigue fracture-stacking fault energy correlation *(Russian)* 78−15499
metal, FCC, climb model of extended dislocations 78−6059
metal, FCC, creep rate, stress depend. *(Russian)* 79−1896
metal, FCC, low stacking fault energy, nucleation phenomena 79−90681
metal, FCC, vacancy migration near twin boundaries and stacking faults 80−39075
metal, hardening due to increased subgrain boundary stability 78−52934
metal, irradiated, triangular Frank loop dissociation 77−11599
metal, near surface microstructure effect, on wear 78−64730
metal, polycrystalline, strain hardening, dislocation link length model 80−84953
metal, recovered dislocation substructure, prod. and utility, review 77−84749
metal, resistomatic studies of lattice defects review *(Japanese)* 78−59799
metals, FCC, slip dislocation reactions at coherent twin boundaries, effect on work-hardening 79−1431
metals, FCC, stacking faults energies in pair potentials calc., appl. to point defect props. 80−19798
metals, stacking fault energy meas. by electron microscopy *(French)* 79−42079
metals and alloys, close-packed, temp. depend. of stacking fault energy 79−19266
metals and alloys, stacking faults in HCP and FCC structures, long-range oscillatory interactions and stability 80−65012
metals and alloys, strength/ductility relation *(Japanese)* 79−29145
micas, synthetic, polytypism and faulting, lattice imaging obs. *(French)* 78−79587
modulated struct. phenomena, survey 79−95033
MOS, capacitors, SEM investigs. using electron beam induced current technique 78−23177
MOS capacitor relaxation time, effect of stacking faults 78−76157
MOS capacitors, pulsed relax. time meas., reln. to oxidation induced stacking faults 77−39943
muskovite, disordered mica struct. high resolution electron microscopy exam. 78−91344
observations by electron microscopy *(Hungarian)* 79−55755
order-disorder groupoid family, parameters, stacking 80−38982
order-disorder structures, layer stacking 80−38981
oxidation process development *(Japanese)* 79−29249
plasticity and transform. kinetics under high press. 78−51560
polytype relative stabilities, entropy contribs. 80−100197
quartz, dissociated a-dislocation, effect on plastic deformation 79−7610
quartz, synthetic, growth boundary between −X and Z sectors 78−59775
quartz, synthetic, growth sector boundary between −X and Z sectors 78−59774
quenched-in vacancies, clustering, stochastic theory, solvable model 79−65074
quenched-in vacancies, stochastic theory for clustering, general mathematical props. 79−65073
rare earth-Co alloy, electron microscopy exam. 78−67722
rare earth-Co phases, fault struct. and shear transform., stacking sequence notation 77−35571
rare earths, light, stacking faults and magnetism, transform. effects 80−75840
rectorite, stacking and ordered interstratification, high-resolution TEM obs. 80−109140
RHEED, Bragg diffraction imaging of cryst. surface defects 78−9920
sapphire, dislocation obs. by weak-beam TEM 77−47461
SEM, crystalline contrasts from defects in thin and thick specimens 78−22611
SEM, fitted with field emission gun, for cryst. defect obs. *(French)* 77−35452
SEM imaging, electron channelling appl. 80−70214
semiconductor, layered, DC hopping cond. due to stacking disorder and electron localisation 77−47819
semiconductor, SEM charge-collection images, contrast formation 80−70087
semiconductor, SEM electron beam induced current images of dislocations and stacking faults, computer simulation 80−70198
semiconductor, tetrahedrally coordinated, dislocation struct. 79−82206
semiconductor defects, spectroscopic techniques to study of electronic props. 80−84446

stacking faults continued
semiconductor substrate surface, low loss electron and Auger images correl. 78−22944
shear band formation models, in rolling and extrusion 80−11666
n-Si:B, ion implanted, rapid identification of faulted loops 79−19254
Si, single cryst. characteris. by SEM using Schottky barrier charge collection microscopy 77−4444
Si, X-ray step scanning section topography, lattice imperfection characterisation, automatic Bragg angle control 79−60221
silicates, layered, optical filtering of faulted areas in electron micrographs 80−84035
snow, epitaxial relationship during three dimensional dendrite form. 79−23875
solid soln., ductility, comp. effect *(Japanese)* 79−43334
spinel ferrimagnets, interaction of stacking faults with domain walls, electron microscopy 78−64214
spinel-type lattice, determ. of stacking faults, diffr. effects 77−55290
steel, α-martensite formation in crossing range of ε-martensite platelets *(German)* 78−3126
steel, austenitic, Cr-Mn, Kh4G18F, microstruct. and mech. props. during tensile deform. *(Russian)* 79−20114
steel, austenitic, creep, low-temp., during dynamic relaxation, effect of dislocation struct. *(Russian)* 77−25103
steel, austenitic, Mn-Cr-C(20, 4, 0.5 wt.%), intrinsic stacking fault energy, temperature variation 77−31679
steel, austenitic, Ni alloy, stacking fault energy of austenite, high resolution electron microscopy *(Russian)* 80−44219
steel, austenitic, Ni-Cr high alloy, N_2, P and Ni effect on stress corrosion cracking and stacking fault energy *(Czech)* 78−60875
steel, austenitic, substructure change in hot deform. process *(Russian)* 77−16617
steel, austenitic stainless, creep, rel. to radiation swelling and stacking fault energy *(Russian)* 78−27562
steel, austenitic stainless, defect structure, N content depend. *(Russian)* 77−59022
steel, austenitic stainless, grain size effect on softening *(Russian)* 78−23731
steel, austenitic stainless, stacking fault effect on martensitic transform. during plastic deform. *(Russian)* 80−25696
steel, austenitic stainless, stacking fault energy, composition depend. 78−38733
steel, austenitic stainless, stacking fault energy, effect of N 80−107279
steel, austenitic stainless, stacking fault energy measurement, by weak beam electron microscopy 78−18661
steel, austenitic stainless, tetrahedra and dihedra 77−84768
steel, austenitic stainless stacking fault energy, effect of C, exam. 78−80553
steel, cast, high speed, solidification, $(Fe,Mo)_6C$ form., struct. 79−24514
steel, Cr-Mn, effect of composition, plastic deformation, and heat treatment on martensitic transformation 79−100141
steel, high C, high alloy, $M_{23}C_6$ type carbides, effect of alloying elements on defect struct. and hardness 80−16481
steel, maraging, investigation with lower Ni and Co contents *(Chinese)* 78−84812
steel, stainless, 304, annealed and 9% prestrained, cyclic hardening and softening, room temp. 77−52483
steel, stainless, ε-martensite, direct obs. of reverse transform. 77−55967
steel, stainless, austenitic, deform. substruct. and annealing, stacking fault tetrahedra form 80−107282
steel, stainless, in-situ obs. of deform. in HVEM 80−103338
steel, stainless, martensite formation, in situ obs. 80−25692
steel, stainless, martensite nucleation mechanisms, HVEM obs. 80−104157
steel, stainless, martensite nuclei obs., role of defects in nucleation 80−25693
steel, stainless, shock loaded, residual martensite obs. 80−104414
steel, stainless, type 304L, neutron irrad., rel. to ferrite formation 79−42112
steel, stainless AISI 304, single phase FCC, stacking fault energy and delamination wear 78−3239
steel, stainless type 03Kh13AG19, deformation temp. influence on dislocation struct *(Russian)* 80−11698
steel, X-ray and microhardness meas. at high strain rates *(German)* 78−3184
steels, 110G13 and 40Kh10G10, hardening and structural transformations during friction *(Russian)* 77−52527
STEM microdiffraction patterns, effect of cryst. defects 78−22610
STEM of cryst. specimens, image contrast *(German)* 77−24251
TEM, stacking fault contrast using weak-beam imaging conditions 78−34401
TEM weak-beam contrast of stacking faults 80−75132
tetrahedra, displacement field construction from angular dislocation segments, electron microscope image simulation 80−6325
tetrahedra, electron microscope image contrast 80−6326
thin films cryst. defects obs. in SEM *(French)* 77−31662
time-defect densities in tilt boundaries of f.c.c., b.c.c., h.c.p., crystals 78−2142
transition metal dichalcogenide, stacking layer study, appl. of convergent beam electron diffr. 80−39116
transition metals, stacking fault and twin energies 79−82244
two- and three-layer faulted defects, two-Shockley unfaulting 77−55292
web dendrites, dislocations, stacking faults, X-ray topographic study *(Chinese)* 80−88148
width determ. from 224 reflections with g.b=0 78−59722
X-ray diffr. line profile analysis, on-line computer routine, SFP determ. 78−79498
X-ray diffraction, by FCC crysts. containing extrinsic stacking faults, derivation from theory 79−33005
X-ray diffraction patterns 77−31552
X-ray imaging in cryst. with Bragg geometry 78−59821
X-ray powder patterns for polytypic struct. with stacking faults anal. 78−38577
X-ray section topography, contrast of stacking fault in Laue-Bragg case 79−77453
X-ray topograph, computer simulation 78−30513
X-ray topography, techniques and interpretations 79−67454
X-ray topography, variation of stacking fault contrast with phase shift value 77−65986
AG, electrodeposited, role of stacking fault energy 77−29016
Ag, annealing twins rel. to stacking fault energy 79−33006
stacking faults continued
Ag, colloidal, lattice defects, X-ray diffr. and electron microscopy exam. 78−51567
Ag expitaxial film, twin boundaries of recrystn. type, electron microscope obs. *(Russian)* 79−4484
Ag, FCC, low stacking fault energy, nucleation phenomena 79−90681
Ag, FCC, polycrystalline, deformation-strain curve description using substruct. parameters *(Russian)* 79−87690
Ag, grain growth in strained {110}<112> low stacking fault FCC crystals after artificial nucleation 79−91722
Ag, high purity, nucleation and twinning during recrystallization, TEM study 79−29082
Ag, multiply twinned particles, internal and surface struct. by electron microscopy 80−84189
Ag particles, lattice defect influence on size effect 78−88329
Ag, polygonisation, impurity effects rel. to stacking fault energy 77−63685
Ag, pure, temp. depend. of stacking fault energy 78−51565
Ag, rolled, dislocation struct. and recovery during annealing *(Russian)* 79−29084
Ag, single crystal, electrochem. grooving, gross linear defect obs. 78−67894
Ag, stacking fault energy meas. by tensile deform. of polycrystalline samples 78−95060
Ag, surfaces, dislocation climbing, etch pit investig. 79−19260
Ag, thin-film bicrystals, planar lattice defects and migrating grain boundaries interaction 80−79835
Ag, vapour-deposited on rotating substrate at oblique angle, X-ray struct. anal. 77−62775
Ag-Cd (45 at.%), morphology and struct. of bainite plates in β′ phase 79−52213
Ag-Cd (47 at.%), crystal struct. and internal defects of thermoelastic martensite 77−48438
α-Ag-Ge, cold-worked, lattice imperfections, X-ray diffr. study 78−38732
Ag-Ge (4.5 at.%), FCC, vapour-deposited, lattice imperfections, X-ray diffr. 78−72032
Ag-Ge alloy, liq.-quenched, metastable phase formation and evolution 77−90338
Ag-In alloys, rapidly quenched from melt, stacking faults, TEM and X-ray diffr. meas. 77−59768
Ag-Mn, annealing twins rel. to stacking fault energy 79−33006
Ag-Sn, splat-quenched, X-ray diffr. study 80−81094
Ag-Sn (6,11 at.%) alloy, splat-quenched, X-ray diffr. study of microstruct. 77−8860
Ag-Sn (6(8.2)(11) wt.%), splat-quenched, X-ray line broadening 80−40397
Ag-Zn (38 at.%), morphological and struct. studies of thermoelastic martensites 77−63669
AgI, mixed-polytype cryst. containing new 12H polytype 77−19911
Ag_3Mg, two different types of long-period ordered alloys, characterisation by high resoln. electron microscopy 80−49181
Al, and Al alloys 6061 and 2024, burst acoustic emission during Bauschinger effect 77−48475
Al, creep, low-temp., during dynamic relaxation, effect of dislocation *(Russian)* 77−25103
Al, creep, rel. to radiation swelling and stacking fault energy *(Russian)* 78−27562
Al, FCC, polycrystalline, deformation-strain curve description using substruct. parameters *(Russian)* 79−87690
Al film, struct. and props., effect of ion implantation 79−77936
Al foil, quenched, anomalous annealing phenomena, quantitative study 78−80565
Al, polycrystalline aggregate, various grain sizes, specimen thickness effect on mech props. 79−61645
Al, single phase FCC, stacking fault energy and delamination wear 78−3239
Al, twin and stacking fault energies 79−38018
Al-Cu (3.93 wt.%), planar defects within theta precipitates 77−16583
Al-Si alloy, compression, effect of press. on lattice defects up to 90 kbar *(Japanese)* 77−72654
β''-Al_2O_3, Mg- and Li-stabilised, high-resoln. electron microscopy images 80−107277
β-Al_2O_3-Na_2O, planar [00.l] disorder, TEM obs. 77−31680
Al_2O_3-SiO_2, sillimanite, lattice defects, crystallo-chemical model, TEM obs. *(French)* 78−26570
Au, atomic arrangements of defects, dynamic obs. of atom movement 80−39108
Au foil, radiation damage, in situ study by HV electron microscopy 78−6101
Au, magnetoresist of quenched and annealed metal, defect scatt. 79−4981
Au, multiply twinned particles, internal and surface struct. by electron microscopy 80−84189
Au, quenched and annealed, cond. electron scatt., de Haas-van Alphen Dingle temp. meas. 77−89688
Au, quenched and annealed, conduction electron scattering 78−47774
Au, stacking fault tetrahedra, critical nucleation temp. 78−26581
Au, stacking fault tetrahedra formation, quenched-in vacancy clustering, continuum model 79−77594
Au, thin foil, growth of stacking fault tetrahedra 80−19815
Au, twinned crystals, epitaxial growth on KCl crystals, electron microscopic study of microstructure 78−91566
Au, vacancy clustering of S 77−4100
Au-Ag alloy, vacuum-deposited monocryst., rel. to internal friction, 200-3000 Hz, 20-850°C *(Russian)* 77−21197
Au-Cd (47.5 at.%), modified 2H and 9R martensites 78−14366
Au(-Cu)(Sn) vacancy cluster form. in quenched pure Au and dil. alloys 77−62546
BN powder, wurtzite sphalerite struct. phase transition, effect on substruct. 80−25690
BN wurtzite-sphalerite phase transition, stacking fault role 80−6418
$BaFeO_{2.79}$, 6H polytype, perovskite related phase, electron microscope obs. 77−51391
BaT:O_3, surface microrelief revealed by ion irradiation 80−54485
$BaTiO_3$, ferroelec. domain boundary struct., TEM 77−24806
$BaTiO_3$:Hf, crystal field distortion by stacking faults, PAC meas. 80−11306
Be, twin and stacking fault energies 79−38018
Be-Si-N system polytypes, struct. obs. using TEM 80−107192
Be-Si-O-N system, polytype periodicities, direct obs. 78−18662

stacking faults continued
Be_3N_2-$BeSiN_2$ system, crystallography and phase relationships, TEM and electron diffr. study 80−92502
BiI_3, layered compound, exciton spectra, surface and stacking fault effects 80−40134
α-brass, solid soln., ductility, comp. effect *(Japanese)* 79−43334
C, partially graphitised, K intercalation-desorpt. cycle rel. to stacking faults 78−47396
CC Si:P, secondary defect generation suppression and diffusivity restraint by HCl oxidation 79−70191
$CaBSi_2O_6$, B=Mg, Fe^{3+}, Al, pyroxenes, order-disorder interpretation 80−38987
$CaMg(CO_3)_2$, dolomite, partial dislocations and stacking faults obs. 78−3761
$Ca_2NaHSi_3O_9$, pectolite, TEM obs., of microtwins and stacking faults 78−75677
Cd films, vacuum deposited, microstruct. exam., X-ray diffr. profile anal. 79−46973
Cd, thin film, vac.-deposited, X-ray diffr. struct. obs., props. 79−37937
CdI_2, 2H to 4H structural change, X-ray diffr. study 78−75614
CdI_2, faulted 4H structure analysis 77−80447
CdI_2, hexagonal to rhombohedral phase transform., SFE 79−91643
CdS, deposited anthraquinone, decoration patters 77−1137
CdS-CdTe double layers on various GaAs surfaces, morphology and crystallography 80−34326
CdSe thin film transistor on Cr substrate, cryst. struct., substrate defect effects 80−70563
CdSe, X-ray topography 77−89441
CdTe, aB glide dislocations, dissociated into two Shockley partials, stacking fault energy 78−43024
Ce, cold working, deform. induced struct. effects 80−25719
Co, HCP-FCC transition, mag. domain behaviour, Lorentz electron microscopy 77−80958
Co-Cr-C alloys, $M_{23}C_6$ precip. mechanism 78−44130
Co-Fe alloys, transformation induced microstructs. extended total dislocations, TEM study 79−42073
Co-Nb alloys, segregation of Nb to stacking faults, field ion microscopy investigation 77−8816
Co-Ni (32 wt.%), FCC, rolling texture development 79−87657
Co-Ni (33 wt.%), FCC deform. twinning kinetics, relationship to stress-strain behaviour 78−52887
Co-Ni alloy, slip charact., and fatigue, FCC twinning and FCC to HCP martensite transform. effect 80−35182
Co-Ni-Cr-C, carbide precipitation 79−29065
Co-Ni-Cr-Nb (40, 18, 1.8 wt.%), precipitation behaviour of NbC, effect of ageing temp. on morphology 80−89227
Co-Ni(Ti)(Cu)(Mn), cryst. struct. and stacking fault influence on mag. props. *(Russian)* 80−25164
Co-P films with various preferred orientations, mag. props. 80−100604
Co_3Pd film, ordered, stacking fault obs. by TEM and interpret. using many-beam theory 80−107680
Cr, twin and stacking fault energies calc. 80−2038
$Cr_{2.8}V_{0.7}Fe_{3.4}C_3$, stacking fault study, morphology, comp. and struct. 80−84190
Cu, ⟨100⟩ oriented single crystal plastic deform. and prominent cross slip 78−19852
Cu, alloy, stacking fault energies, weak beam method of electron microscopy 77−19971
Cu and Cu-Si, deformation and fracture under dynamic loading 78−35442
Cu, creep, low-temp., during dynamic relaxation, effect of dislocation struct. *(Russian)* 77−25103
Cu, deform. of ⟨100⟩ single crystal *(Japanese)* 77−59864
Cu electrolytic form. by electrodeposition, structural defects 77−39749
Cu, FCC, polycrystalline, deformation-strain curve description using substruct. parameters *(Russian)* 79−87690
Cu, foils, faulted defect formation by moving boundaries 80−107281
Cu, grain growth in strained {110}<112> low stacking fault FCC crystals after artificial nucleation 79−91722
Cu, near Σ9 grain boundary properties, boundary dissociation 80−100251
Cu, point and planar defects, computer simulation 80−59455
Cu, polycrystalline aggregate, various grain sizes, specimen thickness effect on mech props. 79−61645
Cu, polygonisation, impurity effects, rel. to stacking fault energy 77−63685
Cu, pure, fatigue crack propagation, effect of stacking fault energy as deduced from dislocation patterns, TEM study 79−61719
Cu, rolled, dislocation struct. and recovery during annealing *(Russian)* 79−29084
Cu, single crystals, effect of stacking fault energy on extrusion and intrusion development 78−72826
Cu solid solutions, single phase FCC metal, stacking fault energy and delamination wear 78−3239
Cu, X-ray and microhardness meas. at high strain rates *(German)* 78−3184
Cu-Al, dislocation core cut-off parameter, estimation from stacking fault nodes 80−103370
Cu-Al, intrinsic temp. depend. of stacking-fault energy 78−51564
α-Cu-Al, single crystal, low cycle fatigue 79−43405
Cu-Al (13 at.%), polycrystalline aggregate, various grain sizes, specimen thickness effect on mech props. 79−61645
Cu-Al (6.4 wt.%), rolled low stacking fault energy alloy, struct. and texture 78−52844
Cu-Al (7.9 wt.%), burst acoustic emission during Bauschinger effect 77−48475
Cu-Al alloy, planar faults, faint electron microscopic image contrast obs. 80−107283
Cu-Al martensite, low temp. hardening, formation of clusters and stacking faults 79−43260
β′Cu-Al martensite, stacking order, disorder anal. by continuous Fourier transformation of diffracted intensities 80−39115
Cu-Al-Ni, long period martensite phases, X-ray diffr obs. 80−7571
Cu-Al-Ni alloys, deformed, fine struct. of martensite *(Russian)* 78−6923
Cu-Ge single cryst. containing heavily faulted regions, X-ray diffr. profiles 80−24462
Cu-Ni (10 at.%), struct. changes during deform. *(Russian)* 78−19818
Cu-Ni-Zn alloy, FCC, cold-worked, X-ray diffr. obs. 78−3143
Cu-Ni(Al), strength and substruct., strain point influence *(Russian)* 79−52233

stacking faults continued
Cu-Si, mech. of formation of martensitic struct. *(Russian)* 78−23702
Cu-Si, stacking fault energy meas. by tensile deform. of polycrystalline samples 78−95060
Cu-SiO_2, in-situ deform. in HVEM 80−103338
α-Cu-Zn (5.3 to 21.8 wt.%), single crystals, effect of stacking fault energy on extrusion and intrusion development 78−72826
Cu-Zn-Al, internally faulted martensite, TEM obs. 78−3124
α-Cu-Zn-Al (18, 7 at.%), deform. and mech. props. 79−29159
Cu-Zn-Sn (24-34, 1.0 wt.%), cold-worked microstruct., X-ray diffr. obs. 80−3088
Cu_3Au, deformation twinning 77−63717
CuCoNi ferrite magnetoacoustic oscills. rel. to microstruct. 77−85536
$CuFeS_2$, explosive-shock deform. 78−95108
$CuFeS_2$, natural chalcopyrite, defect struct., TEM 77−62535
Cu_2NiZn, characterisation of superlattice dislocations by TEM 79−55748
Cu_2NiZn, comparison between different theories predicting stacking fault energy from extended nodes 80−75240
Cu_2NiZn, stacking fault energy determ. from extended nodes 80−107280
Cu_2NiZn, superlattice dislocations 78−83816
Cu_2O polycrysts., dislocation obs. by elecron microscope *(Spanish)* 80−75230
Cu_2Se, VPE on mica, defect struct., temp. depend. 77−35837
$Er(Fe_{1-x}Mn_x)_2$, struct. determ. by X-ray diffr. *(Russian)* 77−76358
α-Fe, alloying additions effect on dislocation mobility, stacking fault energy *(Russian)* 77−31671
Fe, deformation, influence of crystallographic lattice type *(Russian)* 79−34106
Fe, twin and stacking fault energies calc. 80−2038
Fe-Co-Ni-W alloy, 45KKhVN, plastic deform., electron microscope obs. *(Russian)* 78−80584
Fe-Ga (25 at.%), precipitation *(French)* 77−70057
Fe-Mn, stacking fault energy, Mn conc. depend. *(Russian)* 77−1836
Fe-Ni (32.86, 30.65 wt.%), textured sheets, charact. of quenched struct., TEM and optimal microscopy obs. of stacking faults 79−34084
Fe-Ni-Cr alloys, stacking fault energies calc. 79−60387
Fe-Ni-Cr-C, effect of austenite yield strength, stacking fault energy, on martensite morphology 78−80546
Fe-Si, dislocation wall form. in contact with surface active melt, stacking fault energy *(Russian)* 77−72626
Fe-Si (3.72 wt.%) fatigue failure in vacuum and air 78−68789
$Fe^{2+}BSi_2O_6$, B=Mg, Fe^{3+}, Al, pyroxenes, order-disorder interpretation 80−38987
Fe_2O_3/Fe_3O_4 transformation matrices, higher-order orientation relationships 80−100846
FeS_2, dislocations and stacking faults, TEM obs. *(French)* 79−99204
FeS_2, pyrite, stacking fault model *(French)* 80−39117
FeS_2, pyrite, TEM obs. *(French)* 79−28004
FeTi-H system, TEM study 79−58850
$Ga_{0.9}Al_{0.1}As$:Ge(Si) epitaxial layers, defect obs. by TEM 77−51618
$Ga_{1-x}Al_xAs$, degraded DH LED, defect struct. by electrolum. topography and TEM obs. 79−60369
GaAs, dissociation of dislocations 79−46665
GaAs epitaxial layers, non-doped, from Ga-$AsCl_3$-H_2 system, TEM and RHEED study of micromorphology and defects 79−65340
GaAs:Li diffused, lattice imperfections, TEM 77−80521
GaAs:S(Te)(Zn), dislocation-free, TEM study of microdefects 79−82213
GaAs:Si, faulted and prismatic loops, TEM obs. 77−51386
GaAs:Si, stacking fault prod. during heat treatment in As vapour 80−96547
GaAs:Sn(Te), epitaxial film, influence of impurities on stacking fault energy 80−103371
GaAs/AlGaAs DH wafers and lasers, defect struct., X-ray topography 79−50312
GaAs-GaAlAs LPE layers, laser material, shallow growth pits obs. 77−7985
GaAs-GaAlAs LPE layers, DH material, TEM obs. of crystal defects 78−6241
$GaAsGa_{1-x}Al_xAs$ DH laser material, rapid optical degradation obs. 77−75528
GaP crystal, structure defect formation due to annealing and stress, dendrites, slip, dislocations 80−29026
GaP, preferential etching of dislocations and stacking faults 77−39589
GaP:S, defect struct. and tetrahedral precipitates, TEM study 80−107246
GaP:Te, defects formed due to precipitation of Te, metallography and TEM exam. 77−84769
GaSe, layered, DC hopping cond. due to stacking disorder and electron localisation 77−47819
GaSe, photocond., influence of stacking disorder 80−2422
GaSe, stacking disorder effect on Wannier excitons 77−62834
$Gd_{1-x}Dy_xNi$, FeB-CrB type stacking variations, cryst. struct. 80−64952
$GdFe_2$, Mossbauer sample, X-ray diffr. obs. 78−22737
GdNi-YNi, FeB-CrB type stacking variations, cryst. struct. 80−64952
Ge, dislocations, lattice images 79−82215
Ge, dislocations under high stress, stacking fault energies, TEM study 80−70202
Ge, dissociated dislocations, constriction correlation with jogs 80−79801
Ge, electron beam irrad., {113} faults, nature and origin 80−70258
Ge, epitaxial growth from monogermane at 685°C 78−51833
Ge, faulted dipoles, high-resolution TEM study 80−103345
Ge film, radiation damage in electron microscope 77−84794
Ge, motion of partial dislocations 79−82229
Ge, stacking fault energies 79−82205
Ge, stacking faults of dislocations, constrictions obs. using weak-beam electron microscopy 77−35576
InGaAsP, epitaxial layer, defect evaluation by cathodoluminescence 80−2866
InP, damage induced during handling for TEM obs. 80−2024
$K_x(H_2O)_yNbS_2$, cryst. struct. determ. 77−89416
$K_x(H_2O)_yTaS_2$, cryst. struct. determ. 77−89416
$K_6Nb_6Si_4O_{26}$, luminesc. bands, Stokes shift, rel. to crystal struct., stacking faults 80−34974
$K_8Nb_{14}Si_4O_{47}$, luminesc. bands, Stokes shift, rel. to crystal struct., stacking faults 80−34974
$LiFe_5O_8$, microstruct. and magnetic props., electron microscope obs. 79−87290
metal, BCC, multi-layer faults on (112) planes and interatomic pots. 78−51563

stacking faults continued
Mg, burst acoustic emission during Bauschinger effect 77−48475
Mg, deformed single crysts., stacking faults and dislocation dissoc. 77−31681
Mg, twin and stacking fault energies 79−38018
Mg-Al spinel, non-stoichiometric, climb dissociation of network dislocations 80−2031
$Mg_{(x+2)/3}T_{(x-2)/3}O_x$ (T=Si, Mg), 145 Å superstructure 79−99143
$MgAl_2O_4$ crystals, flux grown, artificial spinel twin form. by $BeAl_2O_4$ addition 80−96542
$MgAl_2O_4$ spinel, deform., stacking fault energy 77−28853
$MgBSi_2O_6$, B=Mg, Fe^{3+}, Al, pyroxenes, order-disorder interpretation 80−38987
$Mg(Cu_{0.535}Al_{0.465})_2$, 2D lattice images of Friauf-Laves phase and defect type 80−24324
$Mg_{0.8}Mn_{0.2}Fe_{1.8}Al_{0.2}O_4$, grade 6SChl ferrite, milling conditions effect on fine cryst. struct. and activity 79−24483
$MgNi_2$, four-layer, Friauf-Laves phases, stacking variants 80−96468
$MgZn_2$, struct. exam. using Shaw's model potential calc. 77−19906
$MgZn_2$, two-layer, Friauf-Laves phases, stacking variants 80−96468
$MgZn_2$-$MgAg_2$ system, Friauf-Laves phases, stacking variants 80−96468
Mn-Al alloy, domain struct., cryst. defect effects 77−69609
Mn-steel, cryst. geometry in formation of ε′-, ε-, ϰ′- and α-martensitic phases *(Russian)* 78−76648
Mo deformed single crysts., struct. state and dislocation splitting *(Russian)* 80−29029
Mo, twin and stacking fault energies calc. 80−2038
Mo-Re alloy MR47-VP, dislocation struct. and fatigue damage during room temp. deform. *(Russian)* 79−20111
Mo_2BC, planar intergrowth defects and nonstoichiometry 78−2145
MoS_2, homogeneity size estimation, stacking fault conc. effect 80−96661
$MoSe_2$, single cryst., growth, struct. obs. 79−90607
α-N_2 twinning, electron microscope and diffr. exam. 77−35574
$(NH_4)H_2PO_4$, single cryst., X-ray diffr. contrast at twin boundaries, computer simulation 79−33000
Na, martensitic phase transition energetics 79−99314
$NaBSi_2O_6$, B=Mg, Fe^{3+}, Al, pyroxenes, order-disorder interpretation 80−38987
NbS_3, Peierls distortion, chain polytypism and dislocation coupling 78−79589
$Nb_{0.87}V_{0.13}Se_2$(4Hb), stacking layer study, appl. of convergent beam electron diffr. 80−39116
Ni and Ni-Co, recovery of single crystal after varying amounts of cold work 79−100162
Ni cold worked, annealed, exam. of anelastic relaxation at low temp. 78−84877
Ni, computer simulation of point defects and planar defects 78−43013
Ni, creep, rel. to radiation swelling and stacking fault energy *(Russian)* 78−27562
Ni, electrodeposited, role of stacking fault energy 77−29016
Ni, FCC, polycrystalline, deformation-strain curve description using substruct. parameters *(Russian)* 79−87690
Ni, FCC, rolling texture development 79−87657
Ni film, on (001) Ag, FCC and BCC metal-on-metal epitaxy, geometric factors, electron microscopy 78−22980
Ni film, vac. deposited, hexagonal phase *(French)* 78−63944
Ni, intrinsic stacking fault energy, effect on cyclic hardening 79−11638
Ni, lattice vibrations at (111) surfaces and stacking faults 79−86974
Ni, pure stacking fault energy eval. from twinning stress of Ni-Ge (1 to 9 at.%) *(Japanese)* 78−59820
Ni, rolled, dislocation struct. and recovery during annealing *(Russian)* 79−29084
Ni, rolling texture development, dependent on relative stacking fault energy 79−52237
Ni, single phase FCC stacking fault energy and delamination wear 78−3239
Ni, splat quenched, gaseous impurities effect on struct. 77−4042
Ni, stacking fault energy, by electron microscope obs. of dissoc. edge dislocations and faulted dipoles 77−72627
Ni, thin film, growth on Au (001) substrates *(French)* 80−44446
Ni-Co, rolling texture development, dependent on relative stacking fault energy 79−52237
Ni-Cr, (30 wt.%), collective dislocation movements, in situ study 80−100243
Ni-Cr, partial dislocation, stacking fault TEM study *(Chinese)* 80−84174
Ni-Fe(Co) alloys, fatigued, struct. and cyclic stress strain, influence of stacking fault energy and atomic size-module-interactions *(German)* 79−42082
Ni-Ni_4Mo system, deformation microstruct. 80−93591
Ni-Si (12.7 at.%), heterogeneous precipitation at internal and external surfaces during Ni ion irradiation 79−77647
Ni_3Al, cold-worked, substruct., X-ray diffr. obs. 77−59806
NiCoPd, anodic dissolution, SFE effect *(German)* 80−25924
$Ni_{2/3}Fe_{7/3}O_4$, precipitation of α-Fe_2O_3, optical microscopy, SEM and TEM studies *(French)* 80−11650
Ni_3Ga, form. mech. of superlattice intrinsic stacking faults 77−27897
Ni_3Ga, stacking fault form. in situ obs. by stretching thin foils in electron microscope 77−62547
Ni_3Ga, with $L1_2$ struct., dissociated struct. of superlattice dislocations 79−37706
NiSe film, vac. deposited, phase transformation, electron microscope studies 80−2302
NiTi, stacking faults prod. by martensite transition, lattice imaging electron microscopy obs. 79−96026
Ni_3V, deform. propag., electron microscopy obs. 78−6070
Ni_3V, dissociation of $^1/_2\langle 112\rangle$ perfect dislocations and nature of slip dislocations 78−43022
Pb, estimation of stacking fault and twin boundary energies using phonon dispersion curve 78−43031
PbI_2 crystal, gel-grown AgI impurity effects on struct. transformations during growth 77−76339
PbI_2, hexagonal to rhombohedral phase transform., SFE 79−91643
PbI_2, layered compound, exciton spectra, surface and stacking fault effects 80−40134
PbI_2 polytypes, elec. cond., band gap reduction due to stacking fault levels 77−32015
Pd-Ce alloy, SRO determ. 77−7738
SbI_3, layered compound, exciton spectra, surface and stacking fault effects 80−40134
stacking faults continued
Sb_2S_3 spherolite crysts., direct lattice resolution obs. of defect struct. 80−107255
$Sc_{(x+2)/3}T_{(x-2)/3}O_x$ (T=Si, Mg), 145 Å superstructure 79−99143
Si (001) wafer, pyramidal hillocks, TEM obs. during chemical etching 80−70508
Si (100), oxidation induced stacking fault retrogrowth, O_2 press. depend. 78−64747
n-Si (100), oxidation induced, SiO_2-Si interface excess Si depend. on O_2 partial press. 79−70179
n-Si (100), oxidation-induced stacking faults, O_2 partial press. depend. 78−39922
Si, CCD processing, elimination of stacking faults 78−10065
Si, CVD epitaxial film, nucleation and growth 78−10064
Si, carrier generation in depletion layer, effect of stacking faults 79−23983
Si, containing stacking faults, MeV He ion irrad., TEM obs. of defect clusters 77−89483
Si crystal, high O_2 content, Czochralski growth parameters related to epitaxial stacking faults 79−4314
Si, crystal defects in integrated circuits, review 78−88547
Si crysts., dynamic processes associated with stacking faults and deform. twins, HVEM in-situ obs. 80−103369
Si, Czochralski cryst., hillock etching of microdefects, TEM obs. 78−87678
Si, Czochralski crystal growth and charact., oxidation induced stacking faults 79−47621
Si, Czochralski grown, inhomogeneous O precip. and stacking fault form. 79−14820
Si, Czochralski growth and characterisation *(Japanese)* 79−43125
Si Czochralski wafer oxidation-induced stacking faults correl. with bulk defects 77−76428
Si Czochralski wafers, thermally oxidized, stacking fault distrib., O conc. depend. 80−2042
Si Czochralski wave, oxid. induced stacking fault, oxygen content influence 78−10062
Si, damage in electron bombardment, threshold voltage 77−27910
Si, defect form. during high press. low temp. steam oxidation 79−29238
Si, defects, electrically active, correl. of electrolytic etch and surface photovoltage methods 79−77929
Si, deformed, faulted dipole, TEM obs. 78−38712
Si, dislocation dipole lattice image, stacking fault energy 79−60375
Si, dislocation free, O_2 precipitation, stacking fault form. 78−38731
Si, dislocation-free, O_2 precip., IR and TEM obs. 80−29173
Si, dislocations, stacking faults, swirl defects, production and mechanisms *(Chinese)* 79−46684
Si, dissolved O_2 precipitation, homogeneous nucleation 77−11695
Si, doped, motion of partial dislocations 79−82229
n-Si, edge dislocation and stacking fault defect electrical recombination efficiency 80−15106
Si, effect on minority carrier lifetime of MOS capacitor 77−32088
Si, electron beam irrad., {113} faults, nature and origin 80−70258
Si, electron channelling patterns, contrast mechanisms, lattice-defect images, in SEM 79−27884
Si, epitaxial, elec. activity of stacking faults, determ. using SEM in EBIC mode 77−43445
Si, epitaxial (111) surface, etching observation of stacking faults, dislocations, S-pits, etch pits *(Chinese)* 80−70197
Si, epitaxial film, struct. defects, effects on planar diffused p-n junction elec. props. *(Russian)* 78−60195
Si epitaxial film on sapphire, microtwins, TEM exam. 80−70555
Si epitaxial layers, dechannelling by stacking faults, channelling effect technique using He^+ and D^+ ion backscatt. 79−4361
Si epitaxial layers, development, structure and props. of stacking faults *(Russian)* 80−24461
Si, epitaxial layers, stacking defect distrib. anal. using ion channelling tech. 80−100294
Si, epitaxial stacking faults, nucleation sites 77−20201
Si epitaxial stacking fault nucleation site identification, annihilation, and suppression 77−76705
Si, epitaxial wafer, saucer pit microdefects reduction by intrinsic gettering 80−75450
Si epitaxial wafers, role of metallic contamination in formation of 'saucer' pit defects 77−39588
Si, extrinsic stacking faults, core struct., TEM obs. 78−55878
n-Si film, epitaxial, electrical activity of stacking faults 77−39744
Si film, high electron mobility, grown on sapphire at high growth rate 77−81225
Si film, MBE, cryst. defect props., substrate treatment effects 80−70551
Si foil, computer simulation of high resolution images of defects 80−107208
Si, Frank hexagonal interstitial loop, dissoc. energy 77−35556
Si, HCl oxidation conditions for stacking fault nuclei gettering and undesirable etching 78−68830
Si, HVEM struct. images of extended 60° and screw dislocations 80−59466
Si, heavily damaged ion implanted (100) and (111), development of secondary defects 79−51166
Si, high dose self-irrad., spatial correl. between primary and secondary defect profiles 80−59536
Si homoepitaxy in high vac., stacking fault nucleation, crit. temp. for SiC growth 78−14620
Si, integrational etching composition and method 78−10055
Si, ion implanted, complex annealing behaviour of amorphous layers, TEM obs. of defect struct. 80−107299
Si, ion implanted, defect struct., dislocation loops and elongated defects 80−107300
Si laser annealing of SiO_2 layers 80−97505
Si, matrix O_2 precipitation and stacking fault formation 77−76427
Si, n- and p-type (100) wafers, oxidation induced stacking faults 77−32699
Si, new preferential etch for defects in (100) and (111) oriented n- and p-type cryst. 77−59954
Si, nucleation of stacking faults at oxide precipi tate-dislocation complexes, TEM 77−19967
Si on sapphire, stacking faults and twins, TEM obs. at early stage of epitaxy 79−28233
Si, oxidation induced, wafer orientation and ion implantation effects 78−10063
Si, oxidation induced stacking fault growth, role of point defects 78−10061

stacking faults continued
Si, oxidation stacking faults and microdefects, growth behaviour during high temp. annealing 78−72901
Si, oxidation stacking faults, shrinkage and growth, bulk O_2 effects 80−96546
Si, oxidation with trichloroethylene additive to eliminate oxidation induced stacking faults 80−39118
Si, oxidation without stacking fault form. 78−7062
Si, oxidation-induced stacking faults, refl. X-ray topography 77−84767
Si, oxidation-induced stacking fault form., by high press. steam oxidation 78−83830
Si, oxidation-induced stacking faults, control by Cl implantation 79−46682
Si, oxidation-induced stacking faults, nucleation mechanism 80−15122
Si, oxidation-induced stacking faults, influence of annealing ambient on shrinkage kinetics 80−29035
Si, oxidation-induced stacking faults, distinction between clean and decorated faults by etching 80−79818
Si, oxidised, generation annihilation 77−76419
Si, P diffused sample, stacking faults and dislocations formation from interstitials 78−95059
Si, polycrystalline structure stability, stacking defects, twins grain struct. *(Russian)* 80−100248
Si, rel. to oxidation effects on diffusion of P 79−51309
Si, residual stacking-fault-type contrast after unfaulting reactions 79−82243
Si, ring shaped stacking faults induced by oxide precipitates 78−67723
Si, SEM observation in MOS devices 79−42665
Si, self-implanted, ⟨100⟩ and ⟨111⟩, crystallised layers by laser annealing, struct. 78−47644
Si, single-electron excitations, image contrast from delocalised excitations 79−46529
Si, solid-phase-epitaxial, deposited above 380°C, defects obs. 78−63942
Si, stacking fault annihilation by impurity diffusion 77−19968
Si, stacking fault energies 79−82205
Si, stacking fault energies, intrinsic and extrinsic, by TEM 80−10562
Si, stacking fault form. model during oxidation and ageing, defect clustering 77−24322
Si, stacking fault formation, elimination by preoxidation annealing in $N_2/HCl/O_2$ mixtures 78−88550
Si, stacking fault growth, oxidation-induced, HCl and interstitial effects 80−49241
Si, stacking faults growth by Bardeen-Herring mechanism 79−99222
Si, stacking-fault nuclei gettering by trichloroethylene oxidation 77−43226
Si, substrates, review of defects 77−39597
Si, surface, stacking fault generation due to mech. damage, preoxidation annealing influence 80−54261
Si surface, thermal oxidation induced defects, origin and growth *(Chinese)* 80−66681
Si surface defects, influence on MOS radiation sensitivity 77−20445
Si, surface layer defects, influence of multiple oxidation *(Russian)* 78−47650
Si, thermal oxidation, mechanism of appearance of surface roughness and surface defects 77−7956
Si, thermal oxidation in wet O_2/trichloroethylene mixtures at 1200°C 80−16522
Si wafer, defect studies by ASLEEP, SEM and scanning AES 79−19256
Si wafer, oxidation induced stacking faults; surface vs. bulk nucleatior 77−62545
Si wafer, shrinkage and annihilation of stacking faults 77−39598
Si wafer, stacking faults, preoxidation gettering by reverse side P diffusion-induced misfit dislocations 80−60988
Si, wafer, suppression of oxidation stacking fault generation by preannealing in N_2 atm. 78−30648
Si wafer stacking fault formation model 77−76426
Si wafers, Czochralski grown, crystal defects, photoluminesc. topographic obs. 79−1432
Si wafers, N heat-treatment effects, stacking faults formation 78−85016
Si wafers, n- and p-type (100), oxidation-induced stacking faults 77−39599
Si, X-ray channeling technique anomalous transmission, appl. to microdefects induced by heat treatment 79−19124
Si:$Ar^+(Si^+)$, implantation effect on carrier lifetime, damage obs. by TEM 79−65493
Si:B, diffusion of B atoms and growth kinetics of oxidation induced stacking faults, correlation 79−37720
Si:B, heavily implanted wafers, secondary defect generation suppression by HCl oxidation 78−10069
Si:B, implanted, oxidation-induced stacking faults, EBIC and TEM expts. 78−39923
Si:B, ion implanted, struct. of rod defects, TEM obs. 78−71744
Si:B, near intrinsic ⟨100⟩ and ⟨111⟩ samples, inert and oxidising ambients, diffusion, segregation 78−75882
Si:B, TEM study of stacking fault form. and annealing 78−51566
Si:B(P), dislocations under high stress, stacking fault energies, TEM study 80−70202
n-Si:Cs, ion implanted, minority carrier lifetime and defect struct., annealing effect 78−6395
Si:O, annealed, precipitates, dislocation and stacking fault loops, TEM characterisation 77−4111
Si:O, cryst., annealed, struct. defects 78−75673
Si:O wafer, annealed, surface- and inner-microdefects, TEM obs. 80−54236
Si:P, ion implanted, regrowth of damage structs. by laser annealing 80−107289
Si:P, stacking fault and dislocation growth induced by P predeposition 77−59023
Si-on-sapphire MOS devices, effects of planar defects near Si-SiO_2 interface on elec. props. 79−11231
Si-SiO_2 interface, oxidation stacking faults, growth rel. to self-diffusion 80−49239
Si-SiO_2 interface, stacking fault-free region formation by annealing 78−51561
Si-undoped poly Si interface, in oxidation process, defects generation 80−40571
SiC, 2H disordered single crystal, X-ray diffr. stacking fault exam. 77−89452
SiC (2H), vapour grown, growth and deform. faults, X-ray obs. 78−30650

stacking faults continued
SiC crystals, 2H to 6H solid-state transformation, X-ray diffraction study 80−28943
SiC ion implanted, laser induced ordering and defects 80−84754
SiC polytypes, high-resolution TEM observations 79−23621
n-SiC, single cryst. layers deposition on charact. substrates, morphology *(German)* 79−28943
SiC, spiral growth of polytype struct. from faulted matrix, 15R and 4H struct. 77−4778
SiO_2 film, form. by reactive sputtering, effect of defects in Si wafer 77−89676
$SiTe_2$, dislocations and stacking fault energy 78−47378
$SmCo_5$, mag. domains structure rel. to crystal defects, electron microscopy 80−103856
$SmCo_5$, single cryst., grown-in dislocations and stacking faults, TEM investigation 79−19253
$SrTiO_3$, surface microrelief revealed by ion irradiation 80−54485
$TaSe_2$(6R), stacking layer study, appl. of convergent beam electron diffr. 80−39116
Te, hexagonal film vac.-evaporated at normal incidence, X-ray Fourier line shape anal. 79−99454
Ti and Ti-Al (4,6,9 wt.%), X-ray line profile anal. 77−47459
Ti-Al (27.3 wt.%), arc melted, microstruct. 79−61577
Ti-Al-Sn (5, 2.5 wt.%), electron microscope and X-ray diffr. exam., of basal and near basal hydrides 78−80550
β−Ti-Mo, thermal instability, hardness and tensile deform. *(Japanese)* 80−71703
Ti-S system, nonstoichiometric, containing stacking faults, X-ray diffr. intensity distrib. calc. 80−28872
$TiCo_{2+x}$ ($x = -0.06, 0.0, 0.13$), stacking faults in cubic Laves phase 80−19816
TiO_2-Ga_2O_3, crystallographic shear planes and defect pair splitting, electron microscopy 77−76425
$TiS_{1.7}$, hexagonal polytypes form. mechanism 78−9990
V, coherent twin boundary structure *(French)* 79−60379
V, polycryst., struct. changes during deform. *(Russian)* 78−48447
V, twin and stacking fault energies calc. 80−2038
$V_{1+x}P_{1-x}O_{5-c/2}$, density and struct. from X-ray scatt. meas. 77−89380
W, microstress relax. effects, field ion images 77−89453
W, stacking fault stability determ. 80−96548
W, twin and stacking fault energies calc. 80−2038
WC grain, with grown-in stacking fault, contrast effects in electron micrographs 77−19959
$W_{1-x}Nb_xSe_2$, packing defects, correl. with diffr. pattern changes 77−15429
Y-Co, hyperfine fields, NMR spin echo 77−63318
Y_2O_3, dislocation and plasticity dissociation 80−107247
Y_2O_3, stacking fault energy calc. *(French)* 77−62549
Yb, film, energy-scanning X-ray diffr. technique *(French)* 78−43264
Zn, deformed single crysts., stacking faults and dislocation dissoc. 77−31681
Zn film, vac. deposited, X-ray diffr. study of microstruct. 78−26796
Zn, film, vac. deposited, X-ray diffr. study of microstruct. 78−75966
Zn, single cryst. contribution of basal dislocations to residual elec. resist. *(Russian)* 80−75539
Zn, stacking faults, plastic deformation, due to laser beam irrad. *(Russian)* 80−15121
ZnO, dislocation loop nucleation on prismatic faults in high voltage electron microscope 77−72620
ZnO, irradiation in high voltage electron microscope dislocation loops study 80−88157
ZnS crystal, inhomogeneous, microscopic struct. investig. using synchrotron radiation 77−76424
ZnS, crystals with stacking faults, Laue method study 79−94847
ZnS, dependence of hexagonal layer formation on dopant conc. 79−19265
ZnS, deposited anthraquinone, decoration patterns 77−1137
ZnS, electron irrad., ESR 79−91293
ZnS, glide plane of dislocations 79−46667
ZnS, microregions disorientation degree anal. by birefringence, ESK and decoration methods 79−60389
ZnS, natural and stress induced birefringence dispersion 78−6651
ZnS, work done and heat evolved in plastic deform., stacking fault energy 77−80573
ZnS, Zn(S,Se), large single crystals, vapour growth and defect characterisation 80−25540
ZnS:Ag, struct. and mech. props. 78−22753
ZnS:Cu^{2+}, Jahn-Teller effect, stacking faults and formation of polytypes, absorption and emission spectra 77−4660
ZnS:Mn, dopant conc. effect on stacking fault energy 80−2041
ZnS:Mn^{2+}, spin-lattice coupling coeffs. of Mn^{2+} ions in stacking faults 77−20690
ZnS-ZnSe single cryst. grown from melt, anisotropy of mech. props. and struct. 77−24303
ZnSe, parasitic birefringence dispersion induced by lattice plane defects 77−4617
Zr, crept single crystal, nature of γ-hydride 77−21147
Zr-Al (14 at.%), martensitic, discontinuous precipitation, TEM obs. 79−34040
Zr-Nb, stacking solitons in ω-phase systems and quasielastic scatt. 79−38822
Zr_3Al, deformed and irrad., lattice defects obs., superlattice dislocations and defect clusters 80−107261

staff *see personnel*

stainless steel
see also austenitic stainless steel; martensitic steel
95Kh18, vacuum quenching 78−85047
304, bend test ductility of irrad. specimens for LMFBR appls. 80−104235
304, partially ordered, i.r. absorptance, 0-600°C 77−4632
304L, T grainboundary diffusion and trapping, autoradiographic exam. 78−51738
305, surface composition changes with plasma discharges 77−34434
316, erosion in cavitating venturi 80−108602
316, fatigue behaviour of materials containing significant amounts of irrad.-induced He 80−100917
316, oxidation behaviour in the environment, appl. to GCFR fuel claddings 80−104350
416 type, plastic conical shell buckling under axial compression 77−72197

stainless steel continued
absorption of O ions 79−1547
acoustic emission rel. to stacking fault energy 78−14365
acoustic emission signals in plastic deform., amplitude distrib. *(Japanese)* 78−6978
in acrylic bone cement, interfacial shear strength 77−86706
addition of Kh18N10T to Zr alloys, effect on corrosion stability 77−56162
adhesive energy, meas. techniques, appl. to stainless steel/Al_2O_3 system 80−50803
adsorbed layers, low energy ion scatt. *(Japanese)* 77−1774
AES, expts. and interpretation, for steel EN58E 78−27354
AES with computer evaluation 78−76949
aged 304, twin boundary cavitation during creep 77−86099
AGR fuel cladding, development of high strength, ductile stainless steel alloys 80−45367
AGR nitrided stainless steel alloy fuel cladding, struct. and props. 79−54496
AGR steam generators, materials specifications 80−42772
air contamination effect on compatibility with liquid Li in stainless steel vessels at 600°C 78−25285
alloyed with C, magnetron-sputtered, microstruct., and cryst.-amorphous transition 80−19719
alloying constituents, XES determ. 78−73126
alumina coated, types 321-SS and 430-SS, H_2 permeation 80−34244
amorphous film, sputtered, prep. and characterisation 78−43266
amorphous films, corrosion resist. and ion plating use 80−89423
amorphous metal-metalloid alloys production by ion implantation, TEM study 80−15128
anelastic and nonlinear viscoplastic behaviour relations at low homologous temps. 77−63742
annealed 310, deform. at erosion sites, TEM and SEM studies 78−64725
annealed and 9% prestrained, cyclic hardening and softening, room temp. 77−52483
antiferromagnetic ordering in type 310, press. depend., Mossbauer meas. 79−73861
application techniques, exam. *(Japanese)* 78−85114
atmospheric corrosion, of type 18Cr-2Mo-Ti 80−85078
atomised powder, effect of ultrasonic refining on processing preps. 79−33972
atomized 0Kh18N9 powder, activated sintering, US treatment 77−90291
attack by liquid and vaporised CsOH 78−68840
Auger electron appearance potential spectroscopy *(Japanese)* 80−50473
austenitic, type 316, high velocity tensile test at elevated temp. 80−35194
austenitic-ferritic Ni-Cr, 12Kh21N5T, phase and struct. transform. *(Russian)* 78−95748
autoradiography of thin laminars, resolution improvement *(French)* 80−35438
beam, elastic-plastic response to impulse loads of type 304 79−34118
bending, effect of strain rate on dynamic stress factors 77−56046
biaxial fatigue, initiation and growth of cracks 80−30064
bimetal Nb-steel Kh18N10T with Cu interlayer, cyclic heating effect 77−16687
biological implant, ion beam sputter of surface morphology, SEM exam. 77−44836
biphase struct. changes for steel 0Kh12G14N4Yu2, due to plastic deform. when under elongation with superplasticity 78−44176
blistering, of type 316, by 2 MeV He^+ ions, optical microscopy and SEM obs. 79−42119
blistering and exfoliation by 2 MeV He^+ beam of stainless steel-316 79−46722
blistering on irrad. with He^+ ions annealing, surface struct. damage, in type 0Kh16N15M3B *(Russian)* 80−39170
blistering owing to He^+ bombard., 2 MeV 80−49279
blistering under high He^+ irradiation of type 0Kh16N15M3B 80−29095
boiling water reactor, corrosion and oxidation potentials monitoring 79−20252
bone implant, stress corrosion cracking 77−56519
Bourdon tubes design and production *(Hungarian)* 79−85134
α-brass, Bauschinger AE peak detection of back stress component in flow stress *(Japanese)* 78−6977
brazed joints, strength of Ni base filler metals *(Japanese)* 80−16636
brazed joints used in thermal power plants, corrosion resistance 79−43492
brazing to Mo alloy VM1 of type 1Kh18N10T 79−43551
brightness, vacuum heating effect *(Japanese)* 79−61752
brittle fracture resistance improvement by N content reduction 78−95788
burst rod adaptor, failure anal. in Fast Burst Reactor 77−54307
burst tests of type 316 steel for LMFBR and P1 cladding tubes 78−44210
BWR coolant pipe, critical strength under stress corrosion cracking 80−52743
BWR stainless steel piping, corrosion film charact. 79−54498
candidate current collector for Li-FeS_x battery, anodic corrosion rate in LiCl-KCl eutectic 79−100513
carbide, magnetron-sputtered, solar selective absorbing surfaces 79−92079
carbide and intermetallic phases, quantitative anal. by X-ray diffr. 80−66514
carbide precipitates, and Cr carbides at grain boundaries of type 304, AES study 80−3055
carbide precipitation in ion irradiated alloy *(French)* 77−16585
carbide precipitation rel. to in-reactor deform. 79−8302
carbide reactively sputtered solar selective absorbers for all-glass tubular evacuated collectors, absorptance and emittance 80−101132
carbonisation and carburisation in high press. He environment *(Japanese)* 79−26516
carburisation of crevices of type AISI 316, by impure liquid Na 78−80680
cast high-strength steel, fracture toughness 77−56109
cathodic alloying on surface, for increased passivation and corrosion resist. 80−100940
cavitation, abrasion resistance, effect of unstable austenitic struct. *(Russian)* 77−16695
cavitation erosion in chemically aggressive liquids, acetic acid effects *(German)* 79−39050
cavitation-erosion in fresh water, electron microscope and electrochem. study 80−55580
stainless steel continued
cell boundaries of discontinuous γ′-phase precipitates formed during ageing in highly deformed 36 NKhTYu 79−87641
centrifugal cast tube, creep damage estimation from creep void obs. in types HK40 and HP *(Japanese)* 79−87687
clad Al, sandwich sheet material, forming limits 80−3131
clad oxide fuel pin, thermodynamic model for attack 79−97807
cladding, cracks under stainless steel cladding of pressure vessel, detection, causes, danger 80−52760
cladding, effect of stoichiometry on attack in UO_2-PuO_2 fuel 79−26523
cladding, irradiation enhanced creep 77−42074
cladding, stainless steel, cold-worked Type 316, transient mechanical behaviour 78−86598
cladding, updated temp. integrity limit for FFTF driver fuel pins 77−42089
cladding failure during thermal transients 79−8316
cladding material, deform., failure, rigid loading scheme 79−91765
cladding on mixed oxide nuclear fuel, deform. meas. 77−42088
claddings, mixed oxide rods, high burnup irrad. performance 77−3099
coated with Cr_3C_2 (Cr_7C_3) based coatings, detonation deposited, wear resist., 20-1000°C 80−11843
coated with Pd, interdiffusion at reactor wall temps., Rutherford backscatt. obs. 80−39361
coating with Ni by detonation powder spray deposition 80−61028
cold plastic deform. effect on struct. and props. 80−29113
cold rolling, type 304, description of deformation induced plastic anisotropy 79−43268
cold worked, 316, prior stress history effect on irradiation creep 79−87648
cold worked, pitting corrosion in NaCl soln. 78−44257
cold worked 316, in-reactor stress relaxation in bending 77−42079
cold worked 316, irradiation creep, depend. on temp. and atom displacements 77−42075
cold worked swelling increase due to inreactor temp. reduction 78−34547
cold worked type 316, precipitation response to neutron irrad. 80−34073
cold worked type 316, temp. effects on swelling in nucl. reactor 80−32347
cold-worked, 316, chem. comp. effect on rupture life, tensile props. 77−25152
coloured, X-ray photoelectron spectroscopy of surface film 78−64899
component metal oxidation, reflectance IR study 79−47811
composite, 3 component, brittle zone on fibre surface, deform. and fracture 77−56104
consistent creep and rupture properties for creep-fatigue evaluation of nuclear components 80−35329
constitution changes due to radiation effects 80−34048
contact resistance against metals, for high compressive stress and high current density 77−59324
controlled-porosity, mech. props. 79−96083
corrosion, comparison of powder metallurgy and conventionally produced specimens 79−15863
corrosion, crevice, in chloride solns. 79−52414
corrosion, Cs enhanced, Te influence 78−23866
corrosion, H_2SO_4 vapour corrosion, in general atomic S-I thermochem. water-splitting cycle 80−45449
corrosion, intercrystalline, electrochemical testing method 80−55611
corrosion, intercrystallite, testing using potentiostatic etching method 78−7113
corrosion, local, investigation techniques *(Dutch)* 78−15582
corrosion, localised, in acidic Cl^- solns., exam. of galvanic reactions 79−20250
corrosion, LWR and FBR material *(Japanese)* 77−83033
corrosion, performance for condenser tube 79−39046
corrosion, spectrochem. anal. using luminesc. discharge *(Spanish)* 79−92029
corrosion and grain boundary penetration on exposure to coal gasification environment 80−61003
corrosion behaviour in simulated HTGR He environment 79−54495
corrosion behaviour of borided and nitrided steels in aqueous media 78−95837
corrosion behaviour of composite materials in N_2O_4 oxidising atmospheres *(Russian)* 80−76421
corrosion by hydrazine, electrochemical mechanism for room temp. inhibition 78−44249
corrosion by molten alkali metal hydroxides and liquid Li 77−44414
corrosion crack initiation at growing pits under pulsating load *(Japanese)* 78−11409
corrosion crack initiation in active potential range under pulsating loads *(Japanese)* 78−11408
corrosion due to molten LiF-LiCl-LiBr, fusion reactor appl. 78−53217
corrosion fatigue and stress corrosion cracking, in boiling NaOH, for type 304 steel 80−7719
corrosion fatigue charact. of 1Kh18N10T, soln. annealed, effect of cyclic stresses on corrosion in acid environments *(Russian)* 78−31577
corrosion fatigue cracking in NaCl aqueous solution, fractographic anal. *(Japanese)* 78−53023
corrosion fatigue of Kh18N10T, quinoline salt inhibitors for corrosion in $MgCl_2$ soln. *(Russian)* 78−31579
corrosion in flowing Li 80−35399
corrosion in formic acid at 70°C, effect of Mo additions 78−35551
corrosion in nonisothermal Li flow 79−79177
corrosion in seawater circulation plant, comparison with Ti *(German)* 80−25897
corrosion of bins for storage of high level radioactive wastes 77−6535
corrosion of electrolytic coatings in 40% wt. KOH 80−30175
corrosion products in interaction with (U-Pu)O_2 fuel, electron microprobe anal. 79−26524
corrosion protection by heat treatment method 78−68836
corrosion protection of molten carbonate fuel cell gas seal using $LiAlO_2$ coating 79−39293
corrosion protective films, surface treatment development 80−66699
corrosion rates in molten Li salts 80−35400
corrosion resistance for long-term implants *(German)* 79−8565
corrosion resistance in chlorinated lime slurry and calcium hypochlorite soln. 79−83390
corrosion resistance in sea water 78−85028
corrosion resistance increase by Fe-Cr-Pd electrospark deposition *(Russian)* 78−27669
corrosion resistance when sintered with glass 77−77608
corrosion resistant surface alloys, form. by ion implantation 78−88569

stainless steel continued
corrosion testing, type St. 3PS, suitability for power station chimney flue structural material 80−108681
corrosion-fatigue strength, in type 1Kh16K4N2MVFBA *(Russian)* 79−15856
corrosive environment effect on fatigue crack growth rate 80−55584
corrosive reactions obs. by polarimetric Mossbauer spectroscopy 80−40594
Cr-Ni (18,10 wt.%) Ti stabilised, cavitation failure, relationship of corrosive and erosive factors *(Russian)* 77−16722
Cr-Ni-Mo, phase anal. of carbide phases after isothermal annealing *(Czech)* 80−89224
crack, development under high-temp. single-stage, low cyclic loads 79−43389
crack blunting, role in sustained load crack growth 80−21098
crack initiation obs. in low-cycle fatigue specimens 77−52490
crack propag. at high temp. under low cycle loading 78−60838
crack propag. in low cycle fatigue below 600°C, SEM obs. 78−64631
crack propagation in creep *(Japanese)* 77−8927
crack propagation under fatigue-creep conditions and fractography in type 304 *(Japanese)* 80−104267
crack propagation under intermittent overloading at elevated temperatures, in type 304 *(Japanese)* 79−38947
crack resistance in chloride soln., electrochem. protection, polarization effect 80−55589
cracking, H_2 induced, exam. in type 304 sensitised steel 78−76738
cracking in NH_3 at 600°C 79−70207
creep, high temp. 77−63743
creep, irradiation induced, correlation of theory with expt. evidence 80−88255
creep, massive particle formation, precipitation 77−63679
creep, steady state, microstructural parameters 78−39870
creep 78−64583
creep and fatigue crack propag. at elevated temps., fract. mech. and fractography 77−21279
creep and long term strength tests for type KH18N10T *(Russian)* 80−3123
creep and rupture, 525 to 900°C, creep rate 79−11678
creep and rupture, 525 to 900°C, precipitation 79−8328
creep and rupture, 525 to 900°C, rupture and ductility 79−8327
creep behavior of ribbed cladding in prototypic GCFR coolant environment 80−16480
creep crack extension rates in type 304 steel, as function 80−3160
creep crack growth rate, correlation of tension and bending type specimens *(Japanese)* 79−38944
creep crack propagation, J-integral application to type 304 and 316 80−35331
creep curves, const. load 77−7322
creep deform. of 20% cold worked type 316 77−66688
creep ductility, in type 316, microstruct. changes SEM, TEM, optical microscopy and X-ray diffr. study 79−38927
creep ductility, intergranular particle size and spacing effect 80−40461
creep ductility, sigmal phase influence 80−55478
creep failure time of 20% cold worked type 316 78−19894
creep fatigue interaction failure in type 316 78−80652
creep fracture at elevated temps. vacuum environment effect *(Japanese)* 77−8942
creep fracture in DIN 1.4970, in vacuum at 923 to 1073K 78−72817
creep fracture maps, of type 316 80−30083
creep fracture propag., elongation, tensile strength, yield stress meas. applicability of fracture mechanics parameters 78−35508
creep in steel 316, 20% cold worked, exam. 78−72817
creep life, in service inspection, techniques assessment *(Japanese)* 77−81356
creep limit, cyclic load component effect at high temps. 80−104231
creep resistant, AISI 304, residual lifetime assessment by low cycle fatigue testing *(German)* 78−15485
creep rupture testing between 400 and 700°C const. stress, accel. temp. method 78−31495
creep strain recovery during cyclic stress changes of type Kh18N10T 79−43354
creep surface determ. from multiple integral representations for type 304 79−47761
creep test at evaluated temps., based on state variable theory 79−61687
creep under high stress 78−52892
creep-fatigue interaction at 600°C in type SUS 316 79−34123
creep-fatigue life, strainrange partitioning method 77−77586
creep/fatigue interaction at elevated temps. 77−86174
crevice corrosion, mathematical model 78−95834
crevice corrosion in marine conditions 77−56135
crevice corrosion in NaCl soln. 79−52422
crevice corrosion rate prediction, short duration test method 80−30179
crevice corrosion resistance, S mechanism effect *(French)* 77−77635
critical cooling rate for sensitization and intergranular stress corrosion cracking in high temp. water 79−47807
cryogenic constructing material, far IR spectral refl. 77−24855
CTR research, methane growth in T gas exposed to stainless steel 77−50296
cumulative damage in creep 79−70140
cutting, by turning, smoothing appl. for plastic pre-straining *(Russian)* 80−60911
CVD hardfacing using W, for coal gasification unit components 77−40472
cyclic creep behaviour of type 316, as func. of maximum applied stress 78−48460
cyclic deformation behaviour at elevated temps. of type 304 79−52322
cyclic deformation behaviour under biaxial loading, AISI 316 type 80−16431
cyclic plasticity, exponential stress-strain law 77−25157
cylinder, in thermal aerodynamic tube, nonsteady heat transfer method 79−37147
cylindrical shell reinforced with longitudinal separate ribs under external pressure pulse, critical pulse estimate 79−14884
cylindrical surface protrusions, apparent radiative props. *(French)* 78−94569
damping capacities, cantilever beam tests *(Japanese)* 79−91869
deformation, in-situ obs. in HVEM 80−103338
deformation, rapid dynamic, at −196°C 80−104220
deformation broaching, of type 12Kh1810T bushings 80−108473
deformation twins contribution to yield stress, Hall-Petch law for inter-twin spacing 79−24588
stainless steel continued
deformed, Kh18N10T, ageing under gradually increasing load 77−90383
deformed in torsion, annealed, static recrystallization and restoration after hot deform. 79−47735
degassing, lowering of level in type 304 and 316 *(French)* 79−57159
deoxidation in melting with Si *(Korean)* 78−19947
deuteron bombardment, retention and re-emission of 0.125-1 keV D^+ ions 80−66349
deuteron trapping model, of gas sputtering 80−49398
dewar prod. 78−16801
diffusion and permeation of D_2^+, ion beam meas. 80−59492
diffusion bonding with Zircaloy-4 78−34658
diffusion creep 77−77529
diffusion of Cs study using ion beams 77−20125
diffusion of H_2, effect of heat treatment 77−47627
diffusion of H_2, induced tip deflection of steel beam 80−39360
diffusive crack growth under plastic deform. 79−20182
dimensional instability of CF8 stainless-steel castings at elevated temperatures 78−82448
DIN 1.4948 18Cr-11Ni stainless steel for nuclear reactors, mech. props., neutron effects 77−34383
dislocation struct., adjacent to fatigue crack tips 77−36643
dislocation structure, of $\Sigma=9$ related coincidence boundary 79−27994
dislocation substruct. around fatigue cracks, SEM obs. 78−15516
dislocation substruct. prod. by elev. temp. fatigue crack propag., TEM obs. 78−19863
dissolution of Ti, kinetics, steel component absorpt. *(Russian)* 80−34193
ductile, prestrained, 316 method of J_Q and δ_i determ. 77−36724
ductile erosion, prediction, mechanistic model 77−12709
ductile fracture, in situ obs. of microprocess of failure *(Chinese)* 80−55492
duplex, hot ductility and fracture mechanism 78−60731
duplex, lattice-imaging technique 79−64965
duplex, STEM obs. of localized corrosion 80−104324
duplex 308 steel, intergranular corrosion and pitting corrosion, mech. 79−91846
duplex alloy, Cr diffusion 77−20111
duplex type 304, strain rate effect on stress corrosion cracking, in boiling $MgCl_2$ 80−21180
duplex weld metal, ferrite content effect on SCC at room temp. 79−91834
durability in H_2 up to 500°C 80−30170
EBR-II fuel pin cladding, obs. of in-reactor creep and swelling 80−13600
EBR-II reactor components, creep and swelling 79−54499
EBR-II reflector assembly irrad. induced bowing, implications for core restraint design 80−104234
elastic elements made from spring alloy bands 79−87678
elastic limit of Kh15N9Yu, effect of microstruct. and heat treatment 79−83251
elastoplastic fracture mechanics for reactor piping 78−68777
electrode, electrical breakdown of water in μs region 80−103917
electrode material, annealing temp. cycle which improves emission props. 78−95858
electrohydraulic effect and struct. changes *(Russian)* 78−23783
electron field emission sites on unpolished surface 77−21008
electron induced irradiation creep, dislocation process obs. 77−47483
electron irradiated in HVEM, radiation damage obs. 77−50233
electron irradiation, void spatial regularity, impurity and temp. effects 77−47487
electron-bombardment surface prep. for Princeton Large Torus 77−59957
electroplastic drawing, deformation zone current delivery schemes for steel 18N10T 79−91761
electroplastic drawing 79−20142
electroresistance, low-temp. anomalies *(Ukrainian)* 77−32006
ellipsometric meas. of optical const. and thickness of passive film 77−21326
embrittlement by low energy ionic and atomic H particles 78−95809
embrittlement due to soldering with Cu alloy solder, effect of alloying additions 79−47773
embrittlement of 15Kh25T, 400 to 550 degrees C, grain size and cooling rate effects 78−44203
emissivity, total hemispheric, temp. variation, for steel AISI 304 80−15271
emittance, oxidation and surface roughness effects 80−96673
emittance meas. rel. to surface roughness parameters 80−100342
environment effects on partitioned strain life relations in type SUS 304 *(Japanese)* 79−87753
epoxide butt joints, effect of abraded and Ar ion bombarded surfaces on ultimate tensile strength 80−16638
equilibrium surface bombarded with high dose He^+ ions 78−95091
equivalence, coeff. determ., generalised method, by diffusion couples *(French)* 77−62676
erosion at 975°C in combustion gas atoms., type 310 77−66704
erosion by coal ash particles 79−61745
erosion damage, temp. effects 79−34156
exoelectron emission, effect of gas press. and sample temp. during slow electron excitation 79−61505
exoelectron emission by electron impact *(Japanese)* 79−100029
exoelectron emission centre form. by slow electron impact 79−52088
explosive loading technique for uniform plastic expansion at high strain rates for type 304 80−81273
failure analysis at elevated temps. 80−55499
failure by corrosion fatigue, exam. 78−64787
fast neutron irradiated, solution annealed tubing, residual stress behaviour 80−65054
fast neutron void swelling simulation dose and dose rate effects 77−15457
fast reactor cladding tubes subjected to thermal transients, rupture behaviour 80−37465
fast reactor structural material, integral expts. 80−13612
fast reactor structural materials, energy-averaged neutron cross sections 80−13628
fatigue, high temp. low cycle biaxial 80−30063
fatigue, high temp. under isothermal and thermal cycling conditions 78−60836
fatigue, influence of ageing and plastic deformation *(Russian)* 79−15857
fatigue, low cycle, at 649°C, substructural development 77−32664

stainless steel continued
fatigue, low cycle, elevated temp., heat treatment effects 78−27626
fatigue, low cycle, relation with striation spacing, macroscopic crack growth at 625°C 78−11317
fatigue, low-cycle, gaseous, pure H_2 effects on Kh18N10T *(Russian)* 79−15764
fatigue, low-endurance, in pure bending, substructure of steel Kh18N10T *(Russian)* 77−81311
fatigue and tensile properties, of heat resisting bars, type SUH 660-B and SUH 310-B at elevated temps. 79−38979
fatigue characteristics, low-cycle, theoretical predictions and expt. 78−27641
fatigue crack, low growth rate 78−64701
fatigue crack closure over stress ratio range, stress intensity threshold, in SUS304 78−80619
fatigue crack development, 00Kh12N3D, loading freq. effect 79−87727
fatigue crack development of type 00Kh12N3D *(Russian)* 79−29174
fatigue crack growth, effect of grain size on threshold stress intensity 78−44216
fatigue crack growth at elevated temps. 77−46288
fatigue crack growth at room temp., crack closure and cycle ratio effect in type 304 79−70139
fatigue crack growth behaviour in air and high-C liquid Na, carburization studies 80−40625
fatigue crack growth data, three component model anal. 80−3161
fatigue crack growth in A612 grade B steel, effect of temp. and R-ratio 80−3159
fatigue crack growth rate in high temp., high purity oxygenated water 80−40622
fatigue crack morphology of type 304 cycled at const. stress amplitude at elev. temps. 78−64671
fatigue crack propag. and crystallographic orientation *(Japanese)* 78−7027
fatigue crack propag. in neutron irradiation of type 304 and 308 and weld materials 78−23815
fatigue crack propag. rate and stress intensity factor at varying stress ratio 78−7049
fatigue crack propag. work coeff. of type SUS 304 80−16422
fatigue crack propagation, J-integral application to type 316 80−35332
fatigue cracked double cantilever sample, stress meas., US technique 77−25219
fatigue failure kinetics, effect of water 80−55585
fatigue limit, in bi-freq. loading 80−104289
fatigue properties of low-fluence neutron-irradiated stainless steel DIN 1.4948 80−97585
fatigue props. at elevated temps. 78−27643
fatigue resistance of heat-resistant 12Kh1MF, 15Kh1M1F and 1Kh18N12T at normal and elevated temps. 77−90466
fatigue testing fixture, elev. temp. appl. 79−57185
fatigue tests with axial and diametral extensometers 78−85062
FBR blanket facility, gamma-ray heating rate meas. 80−57912
FBR cladding stress distrib., effect of irradiation-induced swelling 80−19850
FBR fuel cladding alloys, phase instabilities and swelling behaviour 79−54500
FBR fuel pin cladding, burst strength eval. 79−89378
FBR fuel pin cladding, failure stress and strain 811 to 1644K 79−89377
FBR fuel pin cladding, in-reactor endurance and rupture life 80−13599
FBR fuel pin cladding strain under transient testing 80−18425
FBR fuel rod cladding damage correl. for rod perform. predictions 80−18424
FBR materials, correl. between void swelling and thermodynamic stability 80−641
FBR structural materials, design appl. of irrad. creep and swelling data 79−59167
Fecralloy, ferritic with and without Y, oxidation in Ar-H_2O-H_2 atmosphere 78−35584
ferrite, graphite solubility, high temp. vacuum metallography determ., 545 to 750°C *(Russian)* 77−55359
δ-ferrite, isothermal decomposition and transform. of heating at 550 to 950°C *(Chinese)* 79−43239
ferrite, magnetomechanical acoustic emission for residual stress NDT 80−71149
ferrite nucleation, appl. to B hardenability 78−27505
ferrite to austenite decomposition 80−3073
ferritic, 18%Cr, stress/strain curve, H_2 charging influence, room temp. *(Japanese)* 78−39884
ferritic, 430, precipitate study using ion microprobe mass analyser 79−15678
ferritic, 430 Zr, oxidation, forming and mech. props. 80−11680
ferritic, alloyed with Y, high temp. scaling 79−47834
ferritic, anisotropic lamellar fracture mechanism 78−64639
ferritic, BCC cryst., fagigue cracking rel. to cryst. orient. *(French)* 79−20178
ferritic, cleavage fracture toughness, temp. and strain rate depend. 80−85028
ferritic, comp. of passive film, AES obs. 77−48571
ferritic, corrosion *(Japanese)* 79−34194
ferritic, corrosion resistance improvement by Mo and Ti additions 77−90505
ferritic, Cr-Al, corrosion in S vapour and H_2S-H_2 mixtures 78−23875
ferritic, Cr-Mo, corrosion behaviour, review 79−39018
ferritic, Cr-Mo, Mo effect on pitting pot., AES anal. 78−95852
ferritic, Cr-Mo-Nb, intergranular corrosion resistance 80−104319
ferritic, Cr-Mo-Ni (29,4,2 wt.%), mech. props. 77−44276
ferritic, drawability, mech. props., and grain boundaries in 08Kh16AMT and 08Kh18T1 80−35270
ferritic, electron microscope obs. of precipitation hardening *(French)* 79−34049
ferritic, fatigue crack propagation in single crysts., orientation depend. 79−29167
ferritic, Fecralloy, creep-rupture props., 650-800°C 80−97535
ferritic, high Cr, penny-shaped central bursting defect in cold drawing 79−20071
ferritic, mech. props., impurity effects *(Russian)* 77−52403
ferritic, metallic second phases, effect on steel behaviour, review 78−31503
ferritic, Mo addition effect on corrosion resistance, X-ray photoelectron study 79−74285
ferritic, Ni-free, effect of V, Ti addition on ductility 79−79048
stainless steel continued
ferritic, passivation films anal., glow discharge surface emission spectrometry *(French)* 79−87923
ferritic, passivity in 1N HCl, X-ray photo-electron spectroscopic study 80−11817
ferritic, phosphide analysis using nonaqueous electrolyte potentiostatic etching method *(Japanese)* 80−89221
ferritic, roping phenomena and tensile strain direction 77−90406
ferritic, roping phenomena and tensile strain direction 77−90407
ferritic, subjected to 475°C embrittlement, exam. of fracture toughness 78−84982
ferritic, swelling and radiation induced creep, fundamental mechanisms *(Italian)* 80−55457
ferritic, tensile strain direction and roping phenomena 77−36533
ferritic, Ti stabilised, changes in structure and mech. props., after alkali bath etching *(Russian)* 79−29271
ferritic, Ti stabilised, exam. of grain boundary structure *(Russian)* 79−15662
ferritic (26 wt.% Cr) passivation, cathodic reduction and AES anal. 77−90500
ferritic and austenitic, susceptibility of underclad cracking, rel. to chem. comp. 77−21280
ferritic and duplex, Mossbauer effect study of 475°C embrittlement 78−52933
ferritic chloride stress corrosion cracking, effects of alloying and environmental variations 79−96194
ferritic Cr-Mo (12,1wt.%) microstructure influence on localised corrosion behaviour 80−61018
ferritic nuclear pressure vessel, methodology for fracture props. variability evaluation 78−33257
ferritic stainless, embrittlement 80−85041
ferritic steel, low alloy, effect of microstruct. on creep fracture 78−80640
ferritic SUS 410 type, coated with organometallic complexes and Ti alkoxides, neutron irrad. effects on mechanical props. 80−34078
ferritic tests for intergranular corrosion 77−73384
ferritic weldment, US testing of defects, charact. and size 78−7104
ferritic-austenitic, variation of tensile and impact strength with heat treatment 79−34085
ferritic-bainitic welded by electron beam, morphology and struct. of heated zone *(French)* 77−73292
ferritic/pearlitic, Mn-Si-C, exam. of fracture toughness for sheets, using linear elastic fracture mechanics 78−56762
fibre reinforced Al, CC strengthened by lattice transformations, mech. props. study *(Japanese)* 79−43332
fibre reinforced Al alloy, exam. of deformation, fracture and forging behaviour 80−11681
fibre reinforced Al alloy, tensile props., cryogenic cooling effect 79−61623
fibre reinforced Al-Zn-Mg system, resistance to crack propagation 79−43409
fibre reinforced epoxy composite, static tensile behaviour *(Japanese)* 78−15482
fibre reinforced porous coating, isostatically compressed for bone ingrowth 80−35134
fibre reinforced wustite, strength and toughness 78−27602
filament produced by glass coated melt spinning, new metastable tetragonal struct. 79−20072
filament produced by glass-coated melt spinning, tensile strength 78−31488
FIM atom probe microanalytical expts., review 78−35622
fine grained, sputter deposited, oxidation resistance 79−57150
fission reactor material, (n,α) cross sections importance for radiation damage prediction 80−13625
fission reactor piping cracks, metallurgical exam., failure anal. 79−67849
fixing pins for fractured bones, strength, ultrasound effect 80−71710
flaw detection by X-ray television system 79−5120
fluid compositions within fatigue cracks 79−5081
foil, type 316, stress-strain behaviour 79−52327
Fokker-Planck eqn. describing evolution of interstitial loop microstruct. during irradiation 80−107215
fracture, of type 12Cr1MoV joint effects of thermal fatigue and creep 80−104297
fracture and crack tip plastic zones, in situ obs. 80−108686
fracture character under tension, in S-H_2 atmosphere *(Russian)* 79−34198
fracture mech. appl. to crack propag. under creep, in type 304 *(Japanese)* 78−27606
fracture micromechanism when kept isothermally in sulphur pulp 80−76355
fracture toughness, −20 to +22°C, of type UNS-S 15500 79−70145
fracture toughness improvement by applying Pb-Sn-Cd coating to crack tip 79−43416
Frank-Read dislocation source obs. in grain boundary 77−84756
fretting corrosion of surgical implant material, electrochemical investigation in type 316L 79−66197
fretting fatigue 77−86164
fretting wear, role of adhesion and delamination 78−35533
fuel cluster sheath of LMFBR, steel-coolant interaction effect on porosity development 77−71651
fusion blanket structures, NAA 80−23145
fusion reactor, stainless steel first wall, swelling and irradiation creep, FWLTB computer code 80−32446
fusion reactor blanket designs, near term, thermal-hydraulic and mechanical anal. 78−58452
fusion reactor blanket materials for Argonne Experimental Power Reactor 80−32450
fusion reactor first wall, thermal stress and creep fatigue limitations 79−76132
fusion reactor first wall lifetime considerations 78−17419
fusion reactor first wall material, Li compatibility, H_2 influence 80−23149
fusion reactor first wall materials, compatibility with impure He 80−32469
fusion reactor first wall radiation damage, H and He gas prod. from stainless steel 78−82512
fusion reactor first wall structural materials, prediction of life limiting props. 78−62605
fusion reactor first wall/blanket system, thermal-hydraulics and fatigue life modelling 78−58453

stainless steel continued
fusion reactor first-wall structural mats., stress and lifetime limitations 80−32447
fusion reactor He embrittlement simulation, splat cooling in development of B doping 80−30072
fusion reactor material, D trapping, temp. depend. 80−37577
fusion reactor material, long term radioactivity minimisation 78−772
fusion reactor materials, design calculations for A 14-MeV neutron collimator 79−59257
fusion reactor materials, design of materials irradiation experiments utilizing spectral tailoring 80−102305
fusion reactor materials, fracture resistance 78−82515
fusion reactor materials, performance and economics 80−32433
fusion reactor shield, neutron induced activity and γ-ray source investigation 78−54872
fusion reactor wall, microexplosion of pellet, energy deposition 78−54890
fusion reactors, effect of pulsed radiation on swelling 79−31190
FV 535, fatigue crack propag. theory 78−5692
galvanic corrosion, electrochem. characts. rel. to Al alloys 80−21162
gas desorption coeffs., electron- and ion-induced, bakeout temp. effect 79−65329
gas liberation in vac., effect of different methods of surface treatment *(Russian)* 80−45429
gas liberation in vacuum, depend. on oxidation process *(Russian)* 80−25901
GCFR core-catcher crucible, material compatibility for UO_2-316 stainless steel graphite system 79−59171
GCFR ribbed cladding, post-irradiation creep rupture tests 80−18430
GCFR ribbed claddings, tensile props. at 650°C 80−45364
global bending response analysis of elastic and viscoplastic nuclear shipping cask structures subjected to impact loading 80−76301
glow discharge treatment of vac. tube, sputtering and reactive effects 78−70141
grain boundaries, electron microscope obs. *(Russian)* 79−4311
grain boundary behaviour, validity of coincidence site lattice model of grain boundary struct. 79−51120
grain boundary ledges, contrast phenomena identification 78−51555
grain growth after deform. by rolling, C effects on kinetics *(French)* 77−28866
grain growth temp. effect 79−57019
ground surface ion bombardment, in DC glow discharge 78−95098
Harrington rod implant failure analysis 79−79686
He cavitation, rel. to TiC precipitation 80−45399
heat treated, oxide comp. and corrosion susceptibility of grades 410 and 430, AES study 80−66692
heat treating and melting with scanning laser or electron beam 78−11406
heat treatment, evaluating tendency for sensitization using Jominy bar test 80−16337
heat treatment procedures for obtaining low degassing rates in type 316L 78−23730
high strength, influence of corrosive medium on low cycle fatigues, photography obs. *(Russian)* 79−34199
high strength, low C, with N_2, yield strength, Mo effects 77−90410
high strength stainless, types 1Kh15N5AM3 and 1Kh16N4AB, phase transformations 80−20931
high-alloy determination of 0.001 to 0.01% by extraction and photometry 77−56275
high-strength 0Kh11N10M2T, phase transform. 77−70046
highly deformed zone and cyclic strain history near fatigue crack tip *(Japanese)* 79−34145
hot cell manipulator remote decontamination facility and repair station 79−9911
hot ductility, B effect 80−30038
hot rolled sheets, martensite distrib. effect on ridging phenomena 79−1887
hot rolled texture, effect on cold rolled and annealed textures *(Japanese)* 78−48425
hot rolling resist., multistage mode of deform. effects *(Russian)* 78−80583
Hugoniot parameters to 320 GPa, dynamic yield strengths and phase transition press. 80−75331
hydrogen assisted cracking, martensite formation on deformation effects 79−52362
hydrogen embrittled, fractography 78−35503
hydrogen induced ε-HCP martensite, TEM obs. 79−34033
hydrogenation effect with, different stability characts. 78−35383
impact strength and substructure produced by deform. during cold rolling *(Russian)* 79−24535
impact three point bend testing for notched and precracked specimens, testing and data analysis procedures 78−53053
impedance diagram in passive and transpassive state in Na_2SO_4 soln. *(Japanese)* 77−21318
implantation of He ions, TEM exam. of He gas bubble lattice 79−46726
in-pile creep measuring rig 77−42083
in-pile irrad. effect simulation by Ni ion bombardment, dislocation density, swelling 77−347
in-reactor deformation and fracture behaviour of EBR-II driver fuel cladding 80−42769
inelastic deformation, generalised strain rate dependent constitutive eqn., load relaxation tests 79−11655
intercrystalline corrosion, depletion theory *(Czech)* 80−35408
intercrystalline corrosion, effect of alloying elements, thermodynamic anal. 77−90504
intercrystalline corrosion test by nondestructive methods *(Russian)* 78−56827
interface with sputtered Nb film 79−74089
intergranular corrosion, effect on acoustic props. for US inspection 79−11745
intergranular corrosion proneness plasticity change tests 77−73366
intergranular crack growth by diffusion 79−24608
internal pressure creep rupture strength of boiler tubes, anisotropy effect 78−23825
intrinsic stacking fault energy, effect on cyclic hardening 79−11638
Invar related system, high press. Mossbauer spectra 79−56642
ion and electron desorption of neutral molecules from type 304 79−83507
ion bombarded, He effects 80−29076
ion bombardment, depth distrib. of swelling, TEM exam. 80−15165
ion bombardment, primary recoil energy spectra characts. 78−10103
ion implantation, oxidation mechanisms study 77−8980
stainless steel continued
ion implantation produced crystalline phase transitions in 316 stainless steel 80−7558
ion induced release of trapped D 78−95095
ion irradiated with He, fracture behaviour, in-situ HV electron microscopy 80−29089
ion irradiated with heavy ions, type 321 steel, defect cluster obs. 80−107341
ion plated filament, improved strength *(Japanese)* 77−90282
ion plating using alumina 77−40476
ion sputtered, surface anal. by Auger effect and SEM 78−95632
ion-induced photon emission spectroscopy, quantitative analysis appl. 77−48740
IR absorptivity of type 304, surface condition effects 79−56754
IR electro-thermal exam. 77−44428
irradiated, D trapping 78−95069
irradiated, vacancy loop effect on swelling 79−14852
irradiated, void nucleation, numerical evaluation 80−70252
irradiated 316, void swelling incubation period, stress effects 78−6105
irradiated stainless steel tube high-speed slitting machine 79−9210
irradiation creep and swelling, microstructural modelling 77−52407
irradiation creep in bending 77−42078
irradiation creep in deuteron and proton bombarded 316 steel 80−39209
irradiation creep in fast neutron flux, of previously irradiated stainless steel 304 78−80600
irradiation induced creep in BR2 reactor using resonant cavity method 77−42080
irradiation induced nuclear cladding swelling, empirical development of design equation 80−59527
irradiation induced stress relaxation in fast flux environment, previously irradiated 77−25104
irradiation induced swelling, stress effects 78−34545
irradiation-induced creep, proton simulation of fusion reactor first wall environment 79−24707
isochronous relaxation curves after monotonic and cyclic strain 79−87676
joint endoprostheses, long-term stability 78−36059
knife line attack phenomena, addition of rare earth metals 79−20289
laminated with Cu interlayers, mech. props. interlayer orientation effects 77−48506
laser fusion reactor first wall, void growth charact. 80−34042
laser generated stress waves, effect on hardness 79−69192
laser induced damage 80−66335
laser produced plasma, radiation absorpt. and diagnostics of plasma cloud *(Russian)* 78−59632
laser radiation coupling coeffs. for CW CO_2 laser 80−84811
laser surface melting for corrosion protection 80−93698
lattice hardening due to dissolved H_2 in Fe, and ferritic steel 78−76656
liner for TFR 400, D, O, and limiter material spatial and depth implantation distrib. 80−18648
liquid boronizing, wear resistant coating *(Korean)* 79−43475
liquid phase bonding with Ni-P plating *(Japanese)* 78−7082
LMFBR cladding, interaction with molten UO_2 during TOP accident 79−54515
LMFBR fuel cladding, stress free swelling at high neutron fluences 77−42093
long-term strength under in-pile irrad. conditions of Kh18N10T 78−6940
low energy D implanted, microstruct. 78−95073
low permeability meas. at cryogenic temperatures 79−30514
low-angle grain boundary dislocations, periodic clustering, TEM 79−46681
LWR fuel cladding material evaluation 80−99213
machine faceted, low-energy ion erosion studies 80−80923
maraging, Cr-Co, effect of ageing on microstruct., TEM and neutron diffraction exam. 78−84867
maraging, crack growth, environment effects 78−64785
maraging, high strength, exam. of ageing embrittlement *(Japanese)* 78−84972
maraging, high strength, notch toughness, effect of ageing *(Japanese)* 78−11311
maraging, structural recrystallisation, alloying element effects 77−70080
maraging, type 03Kh11N10M2T2, exam. of thermal embrittlement 78−84986
maraging, type 03Kh11N10M2T, exam. of thermal brittleness 78−88526
maraging, VNS-2USh, α to and from γ transformation investigation by thermomagnetic structural anal. *(Russian)* 79−83197
maraging high strength, embrittlement on low temp. ageing *(Japanese)* 79−100155
maraging stainless, phase transformation and mech. props. rel. to heat treatment *(Chinese)* 80−66501
ε-martensite, direct obs. of reverse transform. 77−55967
martensite formation, in situ obs. 80−25692
martensite nucleation, in situ electron microscope obs. 80−7572
martensite nucleation and growth, expt. study 78−3125
martensite nucleation mechanisms, HVEM obs. 80−104157
martensite nuclei obs., role of defects in nucleation 80−25693
martensite to austenite transform. at various heating rates *(Russian)* 78−76649
martensitic, ageing, strength/structural charact. relationship 77−90426
martensitic, crack resistance of type VNS-2, heat treatment effects 79−100196
martensitic, new etchant to reveal prior austenite grain boundaries 78−3290
martensitic, practical fatigue and corrosion fatigue limits *(French)* 77−59993
martensitic, SUS 403-B, temp. and strain rate effect on low cycle fatigue *(Japanese)* 79−87717
martensitic 403, heat treated struct. effect on H_2 diffusion 77−63703
martensitic SUS 403-B, high temp. rotating bending fatigue *(Japanese)* 77−59906
martensitic SUS 403-B high temp. rotating bending fatigue 78−60756
martensitic transformation, low cycle loading effect on substruct. development in Kh18N10T *(Russian)* 79−15664
martensitically ageing, techniques for revealing microstruct. characts. 79−70241
mechanical description between 20 to 1000°C, thermoplastic calc., stress strain relations *(French)* 78−35449
mechanical properties, S, Se, Te and Bi additions effect 79−83312
mechanical property characterisation in support of HTR design 78−29577

stainless steel continued
mesh, herniorrhaphic reinforcing prosthetic, mech. and struct. props., SEM study 79−74789
metallic element depth distribution, in passivation layer, luminescent discharge spectrometry exam. *(French)* 78−31585
metallographic technique for detection of ferromagnetic δ-ferrite to paramagnetic σ-phase 79−61816
microcrystalline, rapidly quenched particulates, appl. 80−84887
microduplex, austenite/ferrite, recrystallisation, annealing and cold work effects 79−47713
microplastic deform. *(Russian)* 77−66681
microstructure evolution in ion-irrad., He effects 80−29078
microwave detection of third-order nonlinearities 80−55594
mirror, acted on by laser radiation, reflectivity meas. 79−10342
Mossbauer absorption line-width reduction, US excitation 78−27148
Mossbauer effect at high press. 80−15858
Mossbauer ferritometer, appl. to determ. of ferrite to austenite ratio 79−17453
Mossbauer radiation modulation by coherent US excitation 79−61277
multicomponent duplex stainless, high temp. precipitation of α′ 80−20939
multielement determ. by computer-controlled X-ray spectrometry 77−56318
multilayer desorption meas. using heat of vaporisation spectrometer 79−82453
N toughened, electron beam welding, fusion reactor component fabrication 80−32472
nervous system electrostimulation, stainless steel electrode corrosion control 78−7464
neutraL molecule desorption from SS(304) and Al(6061) due to particle bombardments 79−76213
neutron dose determ. from isotope abundance ratio, mass spectra obs. 80−61220
neutron effects, atom displacement and He prod. using fusion reactor first wall neutron spectrum 78−46168
neutron group constants, meas. of energy and space distribs. 77−26829
neutron induced charged particle spectra on type 316 steel 78−5024
neutron induced creep of cold worked type 316 effect on burst strength 78−62599
neutron irrad., point defect conc. and void radius change, appl. of model for void growth 78−47436
neutron irrad., pore annealing kinetics 77−72638
neutron irrad. effects on tensile props. and microstruct., for type 316 steel 80−65059
neutron irradiated, microstruct. and mech. props. of type 1Kh18N9T *(Russian)* 80−24503
neutron irradiated, Ni ion bombard. effects of injected interstitials on void volume 80−34092
neutron irradiated, occurrence of ordered FCC phase 77−51411
neutron irradiated, rel. between irradiation induced swelling and shear modulus 80−15157
neutron irradiated, stress effects on microstruct. 77−47490
neutron irradiated, TEM study of ferrite formation, for type 304L 79−42112
neutron irradiated, type 316, diamond-cubic η phase formation, TEM study 79−99249
neutron irradiated, type 316, microstruct. and tensile props. 80−34077
neutron irradiated 304 SS, low-cycle fatigue characteristics 80−97586
neutron irradiation effect on low cycle fatigue and tensile props. at 298K 80−30059
neutron irradiation embrittlement, pre-irradiation treatment and composition modification for type 316 80−3171
neutron irradiation-induced creep, of He pressurised type 304L capsules 79−42111
nickelless, low cycle fatigue 80−35326
nitride phase determination method 78−7276
nitrided, internal attack during oxidation 77−36692
nitrided, type 316, microhardness and N_2 conc. profile 79−96226
nitriding charact. at low atmos. press. of NH_3, thermodynamic calc. *(Russian)* 78−15573
nitriding in glow discharge in crossed electric and magnetic fields 80−16578
Norton-Bailey parameters, from creep rupture data from type 304 80−30098
notched, effect of stress hold time on high temp., low cycle fatigue fracture mode *(Japanese)* 78−52952
nuclear fuel cladding, crack nucleation 78−72864
nuclear fusion reactor materials development trends 77−46401
nuclear reactor, dose rate and cascade collapse effects on swelling 79−23656
nuclear reactor, type 316, subassembly response to simulated accident conditions, finite element anal. 77−3123
nuclear reactor claddings, design fix for vibr. induced wear in fuel pin bundles 77−42094
nuclear reactor fuel cladding tubes, 20/25/Nb stainless steel, biaxial creep meas. 78−82442
nuclear reactor materials development for LMFBR primary and secondary circuits, review 77−46295
nuclear reactor stainless steel and Na shield radiation heating expt. 79−9903
nuclear reactor structural materials assessment, AISI 316 and 9Cr-1Mo, for UK LMFBR 78−86581
optical breakdown threshold, illuminated spot dimension effects 78−68582
optical constant dispersion and emissivity, up to 900K 78−52464
optical elements, US cleaning, deleterious effects 77−42631
orthopaedic fixation devices, failure, SEM exam. of fatigue crack surfaces and microstructure 78−77156
orthopaedic implant material, metallurgical cond. effect on pitting resistance of type 316L 79−70704
oxidation, Auger electron, X-ray fluoresc. spectroscopy appls. 77−44412
oxidation, Cr-depleted zones 77−8992
oxidation, ESCA characterisation 78−15584
oxidation, type 316 80−16606
oxidation in Ar-O_2 and N_2-O_2 mixtures in type Kh18N10 *(Russian)* 79−52451
oxidation in melting *(Korean)* 78−19946
oxidation in N_2O_4, 200-700°C, anal. using Fick's second law *(Russian)* 77−73377
oxidation resistance, effect of C, Zr, Ti and Nb 80−35394
stainless steel continued
oxide dispersed, prod. by spray dispersion method, mech. props. exam. of mech. props. *(Japanese)* 78−48419
oxide film, Cl distrib., SIMS *(French)* 80−108765
oxide scale behaviour in carbonaceous gas atmos. 77−36693
oxidised, absorption of Cs, meas. of contamination using washing test 78−62597
oxidised, adsorption and absorption of Cs 78−84061
oxidised, sputtering yield meas. by atomic fluoresc. spectroscopy 80−80922
oxidised substrate, effect on mechanochem. degradation of thin polymeric coatings 79−79134
passivated 304 film, inhibitive action of bound water against Cl corrosion 80−35372
passivation in H_2SO_4, oxidising agent effects 79−20246
with passive film, depth profiling by quantitative AES 78−19611
passive layers, X-ray photoelectron spectroscopy analysis 77−32715
passive state, electron spectroscopy anal. 80−59765
permeation and diffusion of H and D, 472 to 779K 79−55937
permeation by $^2H(^3H)$ in fusion reactor, oxide film influence 80−34241
phase instability effect on cladding deform. profile of LMFBR fuel elements 77−74921
photoetched profiles, quantitative examination 79−20268
photoetching, props. of liq. photoresists 78−39942
photomachining type 410, evidence for lack of H_2 embrittlement in failure 79−74246
physicomechanical and wear props., influence of ion implantation and overlay coatings 80−40603
pipe, small-diameter ribbed-bore Lamb-wave ultrasonic for defect detection 79−15944
pipes, welded branch, stresses calc. 80−108493
pitting, rotation effects 79−100281
pitting corrosion, stochastic theory 78−7077
pitting corrosion in chloride media, electrochem. aspects 80−61007
pitting potential in 0.1 M NaCl soln. at 280°C 79−61799
pitting potential of single and duplex phase, test method and surface cond. effect 80−16550
plasma chamber material for power generating Tokamak, suitability tests 80−32449
plastic deform., accelerated evolution of H_2 77−36594
plastic deform. of single crystal, contribution of γ→ε transform. 77−52394
plastic working of wires, high-density current appl. 79−57002
plastic zone form. and fatigue crack growth 78−64702
plastic zones around creep and fatigue cracks at 650°C 78−48523
plate, steel core/steel tube duplex reinforced, fatigue crack growth 77−28894
PLT Tokamak vacuum vessel, residual gas and surface comp. changes with H_2 discharge cleaning 79−80631
point defect simultaneous clustering during irrad. of type 316 79−95000
Poisson ratio, prestrain effects in type Kh18N10T 79−70103
polishing for optical appl. 78−5587
polycrystalline, elastic consts., inelastic coherent neutron scatt. meas. 80−34122
porous boronising sintering in BC packing material 78−60594
porous sheet, mech. strength, bend and reverse bend tests *(Russian)* 80−93595
porous sheet, pore dimensions, filtration and permeability *(Russian)* 80−76480
post-shock temp. meas. 79−92527
powder, mean normal contact stress in rolling 77−12571
powder, nonspherical, mean pore size of sheet material 77−28757
precipitate crystallography using electron microscopy 78−83698
precipitate observations using convergent beam electron microscopy 80−108689
precipitate phases in type 321 after ageing 17 years at 600°C 78−27525
preparation of 20Kh13 by diffusion impregnation 80−60803
pressurised tubes under dynamic bending and torsional loading, inelastic deform. 77−77549
prestrained, heat treatment effect on fatigue strength *(Czech)* 78−60747
prosthetic hip joints, fatigue strength 79−48375
proton and photon induced X-ray emission anal., depth sensitivity 78−23988
PWR primary circuit constituent materials, design features verification *(French)* 79−17976
PWR primary corrosion products 80−13578
radiation damage and phase stability simulation 78−86602
radiation damage by 1 MeV electrons, dislocation struct., brittleness *(Russian)* 80−75226
radiation effects on nucl. reactor driver fuel 80−32346
radiation induced outgassing from type 304 steel 80−624
radiation-enhanced H_2 permeation in steel 4301 80−59732
radioactive contamination under applied potential in high temp. water 79−24646
radionuclides prod. cross sections induced by 12-45 MeV protons 77−17310
razor blade, wear by rubber 79−66173
reactor materials, effects of material properties on the dynamic response of pressure-loaded core subassembly wrappers 79−49756
reactor pressure vessel, automatic compound scanning US inspection system 77−1892
recovery by annealing of creep produced dislocations of type 316 80−11702
recrystallisation, effect of dislocation structure 77−32595
recrystallisation of thin bands, heating time investig. 79−38848
recrystallisation texture, effect of Cu, Ti additions on development *(Japanese)* 78−80558
recrystallisation texture, effect of N *(Japanese)* 79−4978
reduction of H by Ar glow discharge, rel. to ultra cold neutron storage 80−104459
reflection of H 77−36336
reflectivity, quantitative meas., undergrad. lab. expt. 78−49624
reinforced glass matrix, vibr. damping anal. rel. to internal friction 80−40413
repassivation ability in 3% NaCl at 80°C, stress effect, testing device *(French)* 77−77693
resulphurated, Cr-Mo (18,2 wt.%), Mo effect on corrosion resistance *(French)* 77−63830
reversibility of plastic strain during fatigue with martensitic transform. 78−31526

stainless steel continued
ring notched samples, charge in fatigue crack growth rate 80−50716
rolling element fatigue life 79−20090
roughness factor measurement, energetic D^+, He^+, Ar^+ irradiation of 304 stainless steel 80−39172
rubbing of cast Fe, surface temperature effect on dry sliding wear 80−60983
secondary electron emission, ion-induced for cluster ions V_n^+, Nb_n^+, and $V_nNb_n^+$ 80−35035
secondary electron emission, on proton and deuteron irrad., 0.5-2.5 MeV 77−63512
secondary ion emission due to H ion bombardment 79−8216
sensitised surface normalisation by laser melting 78−60869
sensitization, C content and ferrite morphology effect 80−89400
sensitization, low temp. in type 304 79−74181
sensitized, crack growth in high-temp. water 80−108636
sensitized, direct evidence of Cr depletion near grain boundaries 77−90358
sensitized, electrochemical polarisation in high temp. water *(Japanese)* 79−15868
shear cracks, electron microscope study of single cryst. 80−40522
sheet, deformation charact. determ. test *(German)* 79−24569
sheet deformation, criteria for determ. of deformation limit G *(German)* 80−21000
sheet metal, deep-drawn, for implant device encapsulation, mech. and metallographic props. *(German)* 79−8564
shell, spherical, with reinforced holes, local stability 80−50686
shock hardening, anomalous residual, at short pulse duration 80−20942
shock loaded, peak press. and press. pulse duration effect on crystallographic transform. 78−67769
shock loaded, residual martensite obs. 80−104414
shock loading parameter effect on substruct. and mech. props. 79−52360
shock loading response, grain size effect 77−36601
short term fatigue of type 07Kh16N6, heat treatment 79−66158
shot peened, stress corrosion cracking, const. strain rate investig., cold work, sensitisation effect 79−20259
sigma phase stability and irrad. effect 78−11200
sintered, prod. methods and props. for machine components, review 79−100082
sintered Kh18N10T, friction and corrosion props. for frictional units of nuclear plants 78−60845
sintered sheet material, stopping power and pore size relationship 78−19693
sintering 77−36419
solar absorber-convertors, reflectance meas. of coloured stainless steel 80−7958
solar collector stainless steel selective absorption surface props. 79−62030
solar energy collector optical props. rel. to heat treatment 78−94455
solubility of MnS in Kh18N11, determ. method 80−84910
solution annealed 304L, in-reactor deform. 77−42076
solution annealed type 316, monotonic and cyclic biaxial loading at room temp. 78−52928
solution treated, cold worked, irradiation creep during 4 MeV proton bombardment 77−43256
solution treated, irradiated to low doses with 22 MeV C^{2+} and 46.5 MeV Ni^{6+} ions, interstitial loops 79−14855
solution treated FV 548, irradiated with 22 MeV C^{2+} and 46.5 MeV Ni^{6+} ions void swelling 78−22771
solution-annealed and thermally aged, correl. of high- and low-cycle fatigue data 78−15532
spatial distribution of limiter material and impurities on the first wall of TFR 400 79−651
specific heat, low temp. 78−83966
specific heat 4 to 30K 79−61115
spring alloy, microstruct. and props. at low temps. 77−44286
sputtered atoms, photon emissions, obs. of apparent local thermodynamic equilib. in excitation 78−72672
sputtered film., internal stresses, effect of substrate orientation and rotation 79−77968
sputtering and chem. attack by H ions of 100 eV energy 78−95635
sputtering by fusion neutrons meas. 77−36321
sputtering by low energy H^+, Rutherford backscattering technique 80−40198
sputtering by low energy H and D 78−95630
sputtering erosion, by Ar^+, texture effect 79−91856
sputtering mechanism for light ions, computer simulation 79−56901
sputtering of Cr^+ by 10 keV H_3^+ angular effects 79−52058
sputtering of type 12Kh18N10T in plasma, probe method obs. 79−55564
sputtering yield meas. using AES 80−18654
sputtering yield of first oxide layers of type 304 by substrate Auger meas. 79−95889
sputtering yields of 1 to 20 keV light ions 77−36339
stabilised, knife line attack phenomenon, dissoln. of carbides in thermal cycles *(Japanese)* 78−68701
stabilised, knife line attack phenomenon, dissoln. of carbide during isothermal heat treatment *(Japanese)* 78−72784
stabilised, pressurised capsules in-pile creep meas. 77−42077
stabilised with Cr-Ni-Nb, reaction with Te vapour 77−8986
stacking fault energy and delamination wear in single phase FCC AISI 304 78−3239
stacking faults, weak-beam contrast in TEM 80−75132
stainless steel:C, surface, obs. at very low accel. voltage (200 V-1 kV) by SEM 80−10764
static yield props., changes during fatigue cycling 78−23790
statistical fatigue props. of heat treated JIS steel SUS 403 78−44222
steam pipes, 12Cr1MoV, selection of allowable stresses based on minimum possible strength data 80−104237
steam turbine casings of susceptibility to brittle struct. and fracture, influence of props. 80−104298
steel, elbow-pipe assembly, high-temp. elastic-plastic creep test 77−77551
steel, ferritic stainless, effect of Cl ions on passive layers 80−59766
steel, high-strength, Cr (1 to 15 wt.%) effect on crack initiation stress *(Russian)* 77−16725
steel, maraging, heated to high temperatures, γ to δ transformations 80−20930
steel, stainless, 1Kh16K4N2MVFBA, corrosion-fatigue strength *(Russian)* 79−15856
stainless steel continued
steel, stainless, AISI 316, irrad. creep in bending at low fluence, LMFBR fuel duct deform. 79−61680
steel, stainless, Cr-Ni, for cryogenic engineering, mech. props. 78−11240
steel, stainless, LMFBR fuel pin cladding long-term in-reactor corrosion by liquid Na 80−16593
steel, stainless, passive state breakdown, and repassivation 79−39031
steel, stainless, type 304, TEM study of dislocation emission from grain boundaries 79−66121
steel, stainless, type 304L, neutron irradiated, in-reactor precipitation and ferritic transformation 79−77644
steel, stainless, type 309, low-cycle fatigue, effects of notches on crack initiation 79−74249
steel, stainless, type EP838 ion irradiated, surface structure changes during post-irradiation heating *(Russian)* 80−75272
steel, stainless 316, soln. annealed, cavity alignment and precipitation during dual ion bombardment 80−70273
steel, stainless AISI 316, biaxial cyclic deformation behaviour 80−21057
steel, stainless casts, creep ductility, Auger spectroscopy study 80−60917
steel, stainless type 304, effects of waveshape on crack initiation in low-cycle fatigue 79−79108
steel, stainless type 316, prediction of transient mech. response using equation of state approach 79−74207
STEM, quantitative chem. anal. using standard and standardless programs 79−17578
strain induced γ to α' transform in 18-8 type polycrystal *(Japanese)* 78−11221
strain induced martensitic transform. effect on low cycle fatigue 77−55965
strain measurement, 298 to 1477K, new optical technique 78−85063
strength, long-term, in He atm. containing impurities 79−24662
strength down to 4.2K; influence of stress raisers 80−71754
strength of type Kh18N10T, ionised gas effects, strength of metals, ionised gas effects 79−70252
strengthening by plastic deformation and cold working of type Kh17N13M2T *(Russian)* 78−52839
stress corrosion, high temp. electrochemical studies 80−30146
stress corrosion cracking, chloride effect, constant strain rate testing in high temp. water 78−35568
stress corrosion cracking, due to boiling $MgCl_2$ solution, SEM exam. *(Japanese)* 78−53025
stress corrosion cracking, in H_2SO_4-NaCl soln *(Japanese)* 77−21315
stress corrosion cracking, intergranular 78−15597
stress corrosion cracking, oxyanions inhibitive effect in type 304 80−35374
stress corrosion cracking, prestrain effect, stress relaxation study 80−35384
stress corrosion cracking, slow strain rate 77−59965
stress corrosion cracking and anodisation during straining in boiling NaOH soln. 80−30140
stress corrosion cracking and microhardness, effect of bombardment by He^+, Ni^+, and Cr^+ 80−85087
stress corrosion cracking avoidance by improved welding in BWR pipes 80−42838
stress corrosion cracking control measures 77−90509
stress corrosion cracking in 5 mol/l H_2SO_4/0.1 mol/l NaCl soln., temp., strain effects 78−31590
stress corrosion cracking in boiling $MgCl_2$, crack growth rate study by SERT method *(Japanese)* 79−100290
stress corrosion cracking in boiling $MgCl_2$ soln. of type 304 *(Japanese)* 79−43476
stress corrosion cracking in elev. temp. aqueous environment 79−43462
stress corrosion cracking in elevated temp. Na environment 79−24666
stress corrosion cracking in H_2SO_4-NaBr aqu. soln. *(Japanese)* 80−108629
stress corrosion cracking in H_2SO_4-NaCl soln., martensite form. *(Japanese)* 78−92396
stress corrosion cracking in H_2SO_4-NaCl soln., strain induced martensite effects *(Japanese)* 77−56152
stress corrosion cracking in H_2SO_4-NaCl soln., stress effect *(Japanese)* 79−43471
stress corrosion cracking in H_2SO_4-NaI aqu. soln. *(Japanese)* 80−108630
stress corrosion cracking in high temp. caustic soln. 77−59964
stress corrosion cracking in high temp. water, constant strain rate meas. of type 304 78−31565
stress corrosion cracking in high temp. water, surface prep. effect, type 430 79−5088
stress corrosion cracking in $MgCl_2$ soln., environment effect on initiation and propag. in type 301 *(Japanese)* 80−104338
stress corrosion cracking inhibition in chloride soln. 78−35558
stress corrosion cracking of BWR cooling system pipes 78−23880
stress corrosion cracking of single crystal in H_2SO_4-NaCl soln. in type 304 *(Japanese)* 79−96202
stress corrosion cracking of type 304, environmental effects in high temp. water *(Japanese)* 77−63827
stress corrosion cracking protection, of 18-8 Ti and 18-8 Nb steels, in polythionic acid solution 78−56824
stress corrosion cracking susceptibility, in water 80−45428
stress corrosion cracking susceptibility and anodic behaviour in phosphate solns. at 100°C 78−7096
stress corrosion cracks initiation, in type 304 steel, in 25% $MgCl_2$ solution at 80°C *(Japanese)* 80−10593
stress corrosion morphology in H_2SO_4/NaCl soln. at room temp., electrochemical potential effect 78−15596
stress corrosion resistance, type XM19 80−16558
stress corrosion susceptibility in high purity water, O_2 and temp. effects 80−61002
stress crack initiation in chloride soln., role of corrosion pits in type 304 *(Japanese)* 78−92397
stress distribution effect on chipping of blanking punch *(Japanese)* 78−31543
stress relaxation, in-reactor enhanced of type AM-350 79−93725
stress relaxation, in-reactor study at low temps. 80−93588
stress relieved, microstruct. transformations resulting from ageing 80−71644
stress-rupture data correlation 77−44346
stress/strain behaviour, exam. with high temp. short time testing facility 78−53051
structure and mechanical props. of Kh18N10T, effect of previous deform. in rolling *(Russian)* 79−29099

stainless steel continued
subgrain structure due to discontinuous precipitation of γ' phase of heavily deformed 36NkhTYu *(Russian)* 79−52218
submerged arc welding, effects of flux on cold cracking resist. 77−21238
substrate, electron microscopy and ESCA of sputter deposited Nb film 77−52554
substrate, for Al_2O_3 layer, leaky wave generation at interface with water 80−75419
substrate, for Si evaporated semicryst. layer growth 79−82482
substrate, HfN activated reactive evaporated coatings, high rate deposition, microhardness 80−25580
substrate, ion plating of hard TiN decorative coatings 78−11441
substrate, photovoltaic effect in $Pb(Zr,Ti)O_3$ evaporated film 79−4580
substructure after high-temp. thermomechanical treatment with high deformation rates *(Russian)* 78−76657
sulphidation kinetics of 310, temp. effect and Cr role 78−64773
sulphide stress corrosion cracking resistance, improvement by heat treatment 78−7076
superplasticity of Kh20N80 alloy during creep resist. testing *(Russian)* 77−44294
surface, 10-30 keV H ion bombardment, energy refl. meas. 78−27359
surface, flow boiling bubble population prediction, from gas bubble nucleation expts. 78−90696
surface, $H^+(H_2^+)(H_3^+)$ impact, backscattered H Balmer-β line intensity 77−23470
surface, $H^+(H_2^+)$ ion impact, energy refl. coeffs. 78−54969
surface, He induced blistering, during simultaneous sputtering 79−1808
surface, heated, water droplet evaporation, heat transfer characts. 78−59269
surface, horiz., min. film boiling temp. of saturated ethanol-water mixture 78−90692
surface, O_2 desorpt. during laser irrad., etching, AES study 80−66338
surface, reduction of oxide layer by H atoms 80−40738
surface, rough, liq. spreading 80−39389
surface, SiC coatings, deposition by RF sputtering 80−25563
surface analysis, quantitative, using ion-induced secondary ion and photon emission 77−86423
surface analysis by SIMS, SEM AND ESCA of type 316 79−52825
surface blister bursting, 20 keV He ion irrad., 700 to 800K 77−36349
surface blistering, SEM and TEM obs., ion energy, dose and target temp. depends., review 77−43261
surface characterisation rel. to adhesive bonding chem. etching, SEM, AES, XPS and electron probe microanal. 80−88416
surface chemistry rel. to metallurgical props., SIMS, XPS and AES *(French)* 80−80045
surface cleaning by H^+ bombard., AES study 78−53022
surface coated with C, damage by D^+ and He^+ ion irrad. 80−23146
surface coated with plasma-sprayed TiC, TiB_2 Be and VBe_{12} coatings, fusion reactor appl. 80−18619
surface colouring processes 77−8981
surface Cu barrier influence on C diffusion in type 1Kh18N9T steel *(Russian)* 80−54434
surface damage and mech. changes after H atom irrad. of AISI 321 80−39182
surface damage under high dose $^4He^+$ ion irradiation 78−95092
surface erosion under ion impact, temp. depend. 77−36350
surface finish effect on low-cycle fatigue at 400°C 79−29277
surface implantation of Y and Ce, effect on oxidation resistance at high temp. 77−8977
surface layer element conc., N_2O_4 medium, fission reactor material *(Russian)* 77−83044
surface layer micro-X-ray spectral anal. after exposure to N_2O_4 *(Russian)* 77−40478
surface morphology of H ion eroded samples 79−86968
surface oxide characterisation by Raman spectroscopy 80−50308
surface prep. for adhesive bonding 77−52546
surface preparation for adhesive bonding, surface characteris. techniques 77−56132
surface roughness influence on boiling heat exchange of light hydrocarbons and N_2 *(Russian)* 79−68562
surface segregation in steel 410, atom-probe FIM 79−77883
surface structure investigation in polarised light 77−28947
surface treatment, X-ray photoelectron spectrosc. study 80−50764
surface treatment by plastic deform. effect on gas evolution and H_2 permeability, in type Kh18N10T *(Russian)* 79−15853
surface treatment effect on protium uptake, type 304 77−59984
surface treatment of plane and hollow components in glow discharges 79−1923
surface W-Ni alloy barrier influence on C diffusion in type 1Kh18N9T steel *(Russian)* 80−54434
surgical implant, SCC and corrosion fatigue in Tyrode's soln. 79−29263
surgical implants, corrosion 79−70706
SUS 316, corrosion behaviour in high temp. impure He gas 80−76402
swelling, effect of free surface 78−10097
swelling, neutron irrad. induced, irrad. temp., neutron flux, and extent of cold working depend. 78−79636
TEM foils, white band contrast 80−75134
tempering after air hardening from rolling heat *(German)* 80−93571
Tenelon, fusion reactor materials, radioactivity minimization by elemental substitution and isotopic tailoring 79−22463
tensile deform. induced α' martensite, morphology, in $\alpha+\gamma$ phase 78−44122
tensile ductility minima, elev. temp., in types 304 and 316 78−60730
tensile properties of type 316 steel irradiated in simulated fusion reactor environment 80−34076
tensile testing, of type SUS 304 diffusion welded joints, sound emission *(German)* 80−61062
thermal ageing effect on high temp. low cycle fatigue life *(Japanese)* 80−29988
thermal conductivity, effect of material on working parameters of cryosurgery instruments 78−36037
thermal conductivity meas., method, precision 79−6121
thermal diffusivity meas. using const. rate heating method *(Japanese)* 77−87759
thermal fatigue and strength estimation, creep fatigue interaction 79−11708
thermal fatigue strength in type 304 *(Japanese)* 79−83306
thermal outgassing properties of type 316L, fusion reactor appl. 80−18649
thermal transfer of C *(Russian)* 78−6174

stainless steel continued
thermally aged, type 316, diamond-cubic η phase formation, TEM study 79−99249
thermally exposed, tensile props. 77−25083
thermocyclic treatment effects, 0Kh13N7, 0Kh13AN7, struct., phase composition and mech. props. exam. 78−44204
thermomechanical treatment, high temperature, effect on props. and struct. *(Czechoslovakian)* 77−32603
thin layer thermal conductivity meas., radiometric method 79−94475
thin sheet, fracture resist., critical opening of crack criterion 80−61048
Ti stabilised, creep props. rel. to B conc. *(French)* 79−20132
tip, exposed to ISX and PLT plasmas, field desorption and field ion surface studies 80−34295
Tokamak blanket design concept 80−13815
Tokamak first wall, angular effects in sputtering by H ions 79−46458
Tokamak fusion reactor first walls, hydrogen profiles 80−37578
Tokamak limiter, plasma interaction, current profile evolution effect 80−10420
trace element anal., implications for decommissioning nucl. reactors 78−54833
transition, cryogenic, 07Kh16Nb, fracture toughness and structural strength 77−59927
trapping and replacement of 1 to 14 keV H and D 78−95070
TRIP, orthopaedic implant material, metallurgical cond. effect on pitting resistance 79−70704
tubing, ultrathin, US equipment for structural inspection 78−72990
tubular 304 L, mech. behaviour under constant stress associated with cyclic strain 80−25767
tufftrided, fatigue strength *(Japanese)* 77−77572
two phase, X-ray stress meas., by monochromator method *(Japanese)* 78−64792
two-phase $(\alpha+\gamma)$, twin-related lath occurrence rel. to fracture elongation 77−90443
type, stainless 310, proton induced radiation damage investigation by Mossbauer effect 79−1735
type 304, attack morphology of stress corrosion cracking, TEM study *(French)* 79−83368
type 304, creep modelling incorporating initial strain and ageing 80−58939
type 304, deformation behaviour for high temp. structural design 77−54287
type 304, effect of cold work on sensitization 79−66071
type 304, electron stimulated desorption rel. to CTR first wall appl. 78−51818
type 304, fast-neutron swelling behaviour 79−67864
type 304, grain boundary sliding in isothermal and thermal fatigue *(Japanese)* 78−84979
type 304, laser surface melted, topographical characts. 79−70200
type 304, neutron irrad., solution-annealed and cold-worked, swelling 78−13229
Type 304, pitting corrosion in Na_2SO_4 soln. *(French)* 80−40581
type 304, plastic buckling of cylindrical shells under axial compression 80−74785
type 304, rate equations for elevated temperature creep 80−65141
type 304, rel. between intergranular stress corrosion cracking and intergranular corrosion in acid solns. *(Japanese)* 79−79156
Type 304, surface analysis by soft X-ray XPS *(Japanese)* 77−70231
type 304, surface cleanup and sputtered ion production, AES and SIMS obs. 79−66209
type 304, thermal fatigue, effect of temp. difference in fatigue tests on fatigue life *(Japanese)* 78−84978
type 304, ultrahigh vacuum behaviour, ISABELLE intersecting storage ring vacuum component performance at 1×10^{-11} Torr operation 79−81105
type 304 forging, weld overlaid with type 308 78−13230
type 304 tubular specimens, biaxial fatigue damage at elevated temps. 77−28939
type 304-L, reactivity worths of fixed neutron absorbers 78−21654
type 304L, irrad. induced creep and swelling 79−93723
type 316, cast, precipitation kinetics of χ phase and $M_{23}C_6$ carbide 78−88469
type 316, corrosion obs. in impure phosphoric acid 79−79179
type 316, ductile crack initiation, detection and toughness characterisation 77−16662
Type 316, electron beam heating effect on extracted intermetallic precipitate 78−35394
type 316, electron irradiated, void swelling 78−55891
type 316, influence of preirrad. thermal-mechanical treatment on phase stability and swelling 79−55792
type 316, irradiated, numerical simulation of void nucleation 79−73208
type 316, neutron irrad. damage simulation using HVEM, surface effect on void swelling 78−29572
type 316, Neutron irradiation using HFIR for evaluation as fusion reactor material 78−13324
type 316, set of master curves for creep ductility 79−66112
type 316, Si and Ti effect in phase stability and swelling behaviour 79−78972
type 316, steel, stainless type 316, effect of damage rate on void growth, point defect conc., microstruct. development 79−73209
type 316, stress-free swelling at high neutron fluence, rel. to LMFBR core environment 78−13239
type 316, struct. life anal. for fusion reactor first-wall appl. 78−13326
type 316 20% cold worked fission reactor fuel cladding, axial stress effects on transient mech. response 80−71743
type 316 and 321, irradiation-induced creep following 4 MeV H^+ bombardment 78−14390
type 316 clad fuel rods for GCFR, high temp. fast flux irrad. tests 77−18666
type 316 cladding, Ti-modified, performance in mixed-oxide fuel pins 79−67865
type 316 irradiated cladding, second-phase precipitation 79−54501
type 316 weld metal with controlled residual elements, creep behaviour 77−8902
type AISI 310, strength differential effect, temp. and strain rate sensitivity in saturation cycling 79−66094
type AISI 316, effect on props. of Zn transfer from galvanised wire at 550°C 78−88527
type DIN 1.4970, tensile creep rupture at cyclic load variation at 700°C 79−66143
types 316 and 304, H and He prod. cross sections for 15 MeV neutrons 77−50291

stainless steel continued
uniaxial damage accumulation law for time depend. loading with creep-fatigue interaction in type 304 79−83324
unipolar arc damage in hot, dense D plasma 79−3235
US inspection of type 12Kh18N10T, for intergranular corrosion 78−60912
US methods for intergranular corrosion inspection 78−95898
US surface wave vel. on plane and cylindrical samples, optical methods 77−46875
vacuum components, pre-vacuum surface finish influence on electron stimulated desorption in ultrahigh vacuum 80−57320
vacuum transfer technique for Tokamak in situ surface anal. 79−2778
viscoplastic model, uniaxial, based on total strain and overstress 80−64387
void characteristics from ultrasonic scattering data 79−79188
void form., effect of sequential and simultaneous He implantation 78−71719
void growth kinetics, effect of surface energy barriers 79−51146
void shrinkage during electron irrad. 78−34540
void swelling, 200 keV C^+ bombardment, dose and temp. depend. 77−55309
void swelling, Si point defect trapping, interstitial loop growth rate temp. depend. obs. 80−49270
void swelling obs. by HV electron microscope, due to neturon irradiation in nuclear reactor *(Japanese)* 79−42108
void swelling obs. under HV electron microscope *(Japanese)* 80−54218
void swelling response after fast reactor irradiation 80−6437
voids, TEM, diffr. contrast 80−75218
volume changes during phase changes, meas. using low temp. differential scanning dilatometer *(Russian)* 79−34224
wall and limiter material for Tokamaks, induced desorption diffusion and gas production by 100 eV electrons and ions 79−675
wear, rubbing on mild steel, mag. field influenee 80−60982
wear against graphite filled rubber sliding material, water lubrication conditions 80−21123
wear against polyethylene in unidirectional motion 79−20212
wear and fatigue, improvement of props. by ion implantation 80−16601
wear at high sliding speed of AISI 304 78−3237
wear by magnetic tape, Auger spectroscopy exam. *(Japanese)* 78−39916
wear in dibenzyl disulphide-containing oil, X-ray photoelectron spectroscopy of surface chemistry 78−64736
wear of steel AF 1410, repetitive impact, microstruct. effect 79−74263
weld metal, segregation, S-TEM obs. 77−48431
weld metal, type 316, $M_{23}C_6$ carbide precipitation, intermetallic phases, X-ray diffr. study 80−7586
weld metal, Type 316, transformation of δ-ferrites, diffusion model 80−40347
weld metal AISI 316, high-temp. mech. props. 80−66601
welded, low temp. sensitization, nucleation of Cr carbide nuclei along grain boundaries TEM, SEM study 79−38851
welding decay, precip. of $M_{23}C_6$ during thermal cycles *(Japanese)* 79−52468
welds, type 316, post weld heat treatments on struct., composition and ferrite amount 80−29992
welds, type 444 stainless steel, ductility loss investigation 80−85002
wetting of UO_2 cracked fuel pellets by molten cladding in LMFBR transient undercooling accident 78−4993
wick, sintered, effective thermal cond. meas. 78−94582
wire, axial texture after electroplastic drawing, X-ray struct. investigation *(Russian)* 80−104177
wire, cold drawing 80−50650
wire, effect of stress on phase transformations 78−44119
wire, mechanical and heat treatment effect on static and cyclical strength *(Russian)* 78−35410
wire for high-speed matrix printers, wear resistivity obs. *(Japanese)* 80−55540
wire reinforced Al sheet, prod. by explosive compaction, and mech. props. 77−32542
working curve sample production for spectrochemical anal. from Fe dilution method *(Japanese)* 78−53050
X-ray diffraction patterns, residual stress meas., use of position sensitive proportional counter *(Japanese)* 80−11853
X-ray fluorescence anal., energy dispersive, of 300 and 400 series 80−3465
X-ray fluorescence anal., matrix corrections, minicomputer program 80−3458
X-ray induced desorption of gases from surface 77−35813
Zircaloy-4/stainless steel, diffusion bonding in presence of Fe intermediate layer 79−10987
Al/stainless steel laminate, sandwich sheet materials, deform. in uniaxial tension 79−57061
Al/stainless steel laminate, sandwich sheet material, plane strain compression and rolling 79−57062
Al-304 stainless steel laminate composite, fatigue crack nucleation and propagation 79−100244
B-Cr-Ni steel, neutron irradiation and N_2O_4 corrosion effects *(Russian)* 80−52741
B_4C-304 stainless steel cermet for nuclear shielding appls. 80−102352
C transfer between structural steels and Na in LMFBR 79−97805
C-Cr-Ni-Mn-V, non mag., aged, struct. and mech. props. *(Russian)* 78−56666
Ca-Ni-Mo (16, 14, 3 wt.%), corrosion resist., vacuum heat treatment effect 79−87754
carbide precipitation during post heat treatment, knife line attack phenomena 79−20288
Co-Cr casting, fatigue at welds, hip replacement appl. 78−44697
Cr (10 to 30 wt.%) ferritic, ductile-brittle transition temp. 80−30095
Cr (13 wt.%), abnormal behaviour of H_2 at low temps. *(Russian)* 77−24434
Cr (16 wt.%), OKh16MK, tempering resistance, mech. props., Cu addition effect 79−79012
Cr (17 wt.%), hot-rolled texture, effect on cold-rolled and annealed textures 80−55425
Cr, ferritic, corrosion morphology, electrochem. pot. and Mo additions effect *(French)* 80−45439
Cr ferritic, meas. of alloy and impurity elemental distrib. using STEM 80−35601
Cr, Mo effects on passivation AES and electrochemical anal. 79−74292
Cr, type 403, backscatter Mossbauer spectroscopy 80−40001
stainless steel continued
25Cr-20Ni stainless steel dendritic solidification, growth morphology and solute redistrib. *(Japanese)* 80−81045
Cr-Al (12, 6 wt.%), ferritic, high temp. treated, strengthening mechanisms 80−3106
Cr-Cu (17, 0.6 to 1.1 wt.%), texture 80−84957
Cr-ferritic, critical strain rate 80−16399
Cr-Mn, N strengthened, anomalous low temp. elastic behaviour 77−77524
Cr-Mn, type 03Kh13AG19, deformation temp. influence on dislocation struct. *(Russian)* 80−11698
Cr-Mn (13, 19 wt.%), elastic const. behaviour, anomalous, low temp. 80−97521
Cr-Mn (21, 14 wt.%), grain boundary precipitation and fracture *(Japanese)* 79−100149
Cr-Mn-C-Si (20, 14, 0.2, 0 to 3 wt.%), high-temp. oxidation *(Russian)* 80−25904
Cr-Mo, constitutive eqn. model for high temp. behaviour of fast reactor structural alloys 78−66343
Cr-Mo, ferritic, problem of stress corrosion cracking *(Czech)* 78−85044
Cr-Mo (18, 2 wt.%), cold work effect on 885°F embrittlement 77−77499
Cr-Mo (2.25, 1 wt.%), duplex LMFBR steam generator tubing, US equipment for NDT 78−11469
Cr-Mo-W-V(12, 1, 1, 0.25), stress relax. data anal. using total strain-time parametric method *(Japanese)* 80−104198
Cr-Ni, for cryogenic engineering, mech. props. 78−11240
Cr-Ni, localized corrosion 78−35555
Cr-Ni, low temp. plastic deformation, in mag. field 79−83256
Cr-Ni, maraging, effect of Mo, Co additions on hardening 78−84835
Cr-Ni, radiation-thermal treatment, N_2O_4 coolant action, intergranular corrosion *(Russian)* 78−58357
Cr-Ni (14, 5 wt.%), 00Kh14N5M, tempering resistance, mech. props., Cu addition effect 79−79012
Cr-Ni (18, 10 wt.%), long-term strength in H at high pressure 80−55485
Cr-Ni (18, 8 wt.%), chemically stabilised, sensitisation and corrosion resist., heat treatment depend., precipitation 79−38827
Cr-Ni (18, 8 wt.%) average inclusion size and contents exam. measurements using optical microscopy and Br-Methanol methods *(Korean)* 79−66080
Cr-Ni (18, 9 wt.%), cold rolled, struct. 79−83214
Cr-Ni (18,10 wt.%)-Ti stabilized, corrosion fatigue strength, inhibitor BA-6 effect *(Russian)* 77−16727
Cr-Ni (20, 18 wt.%), effect of tensile stress on growth of He bubbles 79−55796
Cr-Ni (20, 25 wt.%), TiN dispersion effect on oxidation 79−20279
Cr-Ni (20, 25 wt.%) steel 80−89414
Cr-Ni steel, strengthening by elastic deform. at −196°C 77−55987
Cr-Ni type, low temp. plasticity, effects of deform. rate and cooling conditions 77−70099
Cr-Ni-Co (13, 4.5, 0 to 13.8 wt.%), Co effect on martensite ageing *(Russian)* 77−66660
Cr-Ni-Mn, N strengthened, low-temp. elastic props. 79−70109
Cr-Ni-Mn-Mo-N (22,13,5,2, 0.3 wt.%), influence of recrystn. behaviour on mech. props. 79−83213
Cr-Ni-Mo, surface, scraping, mech. (electrolytic) polishing, ion etching, effects on ESCA 78−53037
Cr-Ni-Mo-Cu-Nb, martensitic precipitation hardenable, corrosion resistant, heat treatment, structure and props. 79−74169
Cr-Ni-Mo-Mn (16.55, 10.23, 2.28, 1.34 wt.%), hardfacing materials, friction characts. in high temp. Na *(Japanese)* 80−89356
Cr-Ni-Mo-Mn-Si (17-20, 8-12, 2.5-3.5, 2, 0.2 wt.%), orthopaedic, type En58J, Mo ion-plating, corrosion fatigue 80−66694
Cr-Ni-Mo-N, phase diagrams 80−35161
Cr-Ni-Mo-W-Nb (19, 9, 1.4, 1.4,), stress relax. data anal. using total strain-time parametric method *(Japanese)* 80−104198
Cr-Ni-Mo(26,5,1.3 wt.%), ferrite to austenite decomp. 80−93554
Cr-Ni-Nb (18, 10, 0.7 wt.%), type SUS 347-B, exam. of thermal fatigue props. 78−60755
Cr-Ni-Nb stabilised, Te vapour effect on creep and tensile props. 79−24583
Cr-Ni-Nb-Ti, effect of I_2 vapour on creep fracture props. 78−72814
Cr-Ni-Ti, metallographic detection of $(Ti,Ni)_6C$ 80−66721
Cr-Ni-Ti (18, 10, 0.4 wt.%), type SUS 321-B exam. of thermal fatigue props. 78−60755
Cr(-Mo)(-Ni), self-weldability in high temp Na *(Japanese)* 80−89392
CrNi, localized corrosion *(Slovak)* 78−19948
10CrNiCuP, suitability for power station chimney flue structural material, corrosion testing 80−108681
Cr_2O_3-stainless steel system under fusion reactor first wall condition, oxide dispersoid stability 80−40374
D implanted, thermal desorption 78−71750
D implanted, thermal desorption and bombardment induced release 78−95072
D transport through membranes at low driving press. and 15 keV D bombardment 78−34552
Fe-Cr (26 wt.%) effect of Ni content and austenite phase, on low temp. toughness and embrittlement 78−60754
Fe-Cr-Al (15, 4 wt.%) Fecralloy, oxidation behaviour, Al and Y surface ion implantation effect 80−71790
Fe-Cr-Mn (11.5, 3 wt.%), microduplex ferritic-martensitic steel, exam. 78−39862
Fe-Cr-Ni alloy, shock loading effect on phase equilib. *(Russian)* 79−29017
Fe-Ni-Cr steel, mag. susceptibility and magnetoresistance, temp. depend. *(Ukrainian)* 77−73004
ferrite, FeC form. kinetics, Monte-Carlo simulation *(German)* 78−39779
ferritic, Cr-Mo (10-14, 2-6 wt.%), heat-resist., creep-rupture strengths 80−104271
H recycle from Tokamak walls using plasma-wall interaction simulator 78−94131
He ion bombard., in situ electron microscope examination 80−34094
He ion irradiation of type 0Kh16N15M3B struct. and mechanical props. 78−19848
He production by neutron effects, cross section determ. 79−22282
He^+ implanted stainless steel, microstructure anal. 78−82516
Li compatibility of types 316 and 304 for fusion reactors, H_2 influence 78−68844

stainless steel continued
Li_2O sintered pellets, reaction with type 316, metallographic and X-ray diffr. study 79−39137
Mn-N, low cycle fatigue 77−36646
Na exposed, corrosion in chloride containing aq. soln. 79−57151
Nb, oxidation in Ar-H_2O-H_2 atmosphere 78−35584
Nb/stainless steel interaction in vacuum percussion welding, Ni interlayer effect 79−29061
Nb-stainless steel bimetallic strip Cu interlayer struct. during thermal fatigue *(Russian)* 78−15498
Ni free acid mixture electrolyte, for polishing 80−25902
Ni-Cr-Mo, two-phase, compositional charge of ferrite and austenite *(Japanese)* 79−4948
Ni-Cr-Mo-Ti-Al, quenching and ageing effects on props. of type 36NkhTYuM8 79−52275
Ni-Cr-Mo-W (29, 13, 3, 2 wt.%), long-term strength in H at high pressure 80−55485
Ni-Cr-Ti+Al-Mn-Si-C, aged by discontinuous precipitation mechanism ultrafine grain and mech. props. *(Russian)* 77−70053
Ni-Mo-Cr steel, elastic-plastic material characterisation 78−72854
Ni^+-implanted type-430 steel, struct., comp. and electrochem. anal. of surface alloy 80−16603
^{210}Po contamination of surfaces, removal coeff. determ. 79−26769
T permeability and ultralow press. 79−19402
Ti modified 316, uniaxial tensile behaviour, Na environment effect 78−52916
Ti stabilised intercrystalline corrosion, repeated cold deform. effect 79−57000
UO_2-graphite interactions, effect of stainless steel, temperature on reaction rate 79−59172
UO_2-Na interaction, thermophysical behaviour of type 304 stainless steel impacted by jet of molten core debris 77−46319
UO_2-stainless steel, interfacial props. 79−65223
W alloy wire reinforced stainless steel, fibre/matrix interaction, fabrication and heat treatment effect 79−91607
W, brittle spiral fibre, densification of particulate materials, general law 78−19692

standard microphones *see microphones*

standard voltage generators *see signal generators*

standardisation
air analyzer, automatic, calibration system, zero and span standardization 79−16107
atmospheric gas concs., phytotoxic admixtures, standardisation and meas. of max. permissible levels 79−8685
atmospheric pollution, systems for observing and checking 79−8684
atmospheric testing instrums., standardisation and determ. of dynamic errors 79−8714
audiometric facility at West Middlesex Hospital, London for standardised hearing tests 80−76858
auditory evoked response research on animals, exptl. design 77−78068
B and W viewpoint of standardisation in licensing 80−23023
battery, primary, IEC activities *(Japanese)* 79−83580
Bausch and Lomb Autoplot tangent screen standardisation, for visual field meas. 78−64976
biomedical engineering component quality control system 77−48884
calibration devices, made more accurate by improved basic standards 77−33980
CERN, software standardisation 79−89553
coercimeters with EM attachments 77−12765
collaborative tests, reference material certification procedures 78−28922
communication/control systems for motor impaired people 80−17198
COMOD, program for standardizing mineral resource commodity data 78−20524
conference on analysis instrumentation, Charleston, West Virginia, USA (May 1977) 79−16100
cost calculation standard procedure proposal 79−57389
crater size-freq. data presentation and analysis, standard techniques 79−44387
dosimetry, international intercomparisons 79−20636
dynamometer, machine calibration method *(French)* 77−53894
EEG montages, math. logic design 77−86685
EEG standardised classification, sequential epoch method 78−57101
electrical engineering dimensional unification *(Italian)* 80−27266
electronic industry, Spain measuring equipment choice, criteria *(Spanish)* 78−36963
EM coating thickness meter, for nondestructive testing, in Soviet Union 77−90561
EM non-ionising radiation standardisation 77−38013
fast neutron therapeutic dosage schedule development 79−20678
fibre optic connection systems standardisation 79−68440
fibre optic connectors, update 80−5830
flow calorimeters standardisation, calibration, thermal config. depend. *(French)* 77−67437
flow rate meas., in open channels, Soviet development 77−80241
fossil fuel fired power plants, standardisation, feasibility, advantages, limitations 80−16775
gamma radiation nationwide calibration system 77−38583
HV instrument transformer calibration system based on LV inductive voltage divider 77−82567
hygrometers, precision salt standard, metrological support suite 79−17430
IAU list for stellar designation 77−78661
IEEE computer standards 79−89544
immunochemical analysis, standardisation of light scattering meas. 77−56548
implantable stimulation electrode, standardisation problems 77−64151
industrial chromatograph dynamic error estimation 77−77853
industrial chromatograph static error determ. and correction 77−81446
industrial ear protectors, standardisation of testing, current developments 78−22225
International Gravity Standardization Net 1971, long range meas. with LaCoste-Romberg gravimeters 77−52957
Israeli coastal plain, weather year standardisation for solar heating simulations 79−84444
laboratory, test results, international acceptance *(Danish)* 80−8952
LAMPF standard data-acquisition system 79−89534
light source development support spectroradiometric system *(Japanese)* 78−45733
LV electromedical equipment and radiological apparatus, standardisation *(French)* 77−73602

standardisation continued
LWR power station construction in France, advantages *(French)* 78−58397
meas. devices dynamic properties 77−5797
measurement theory contribution to measuring process intensification *(German)* 80−36966
measuring current of resistance thermometers, meas. accuracy increase 77−74399
medical elec. equipment, current problems 77−73603
medical equipment standardisation and maintenance, role of Indian Central Scientific Instruments Organisation 79−74778
metal, US quality control standardisation 78−53142
metallurgical analysis by atomic absorption spectrophotometry *(French)* 79−5241
metrological characteristics of meas. methods and systems 78−41273
metrological standardisation with Comecon framework 78−89426
movie projector objective lenses, standardisation of optotechnical parameters and testing methods 80−28301
mullite, quantitative X-ray anal., standardisation, texture *(German)* 78−11176
neutron activation anal., computerised, correction procedure, detection limit, standardisation 77−44544
neutron radiation therapy, cyclotron biological intercomparisons 79−20589
neutron radiometers testing, Soviet method 80−99405
noise measurement, hearing damage prevention appl. *(German)* 78−9496
nuclear installations safety, report on 1977 IAEA conference *(Dutch)* 77−83047
nuclear plant startup, benefits of standardisation 80−13686
nuclear power conf., Chicago, United States, July 1979 80−794
nuclear radiation measurement technology, SINUPERM system 78−50410
nucleonic and other meas. methods compared 77−38594
OCR picture enhancement and stroke-width standardisation algorithm 77−38822
optical fibre communications development and need for standardisation *(Italian)* 79−23066
optical fibre standardisation of components, EIA P-6 committee 80−1352
optical fibres, connectors, military appl. 78−30083
optical instrument manufacture based on unitized components 80−9016
optical system for plasma temperature field determ., asymmetrical *(Czech)* 80−38704
orifice meters, quadrant-edged 77−51138
oxygenator, bubble, blood damage test standardisation *(German)* 79−2158
oxygenator gas transfer performance test standardisation *(German)* 79−2159
pH meter construction, standardisation, and use 77−63995
photochromic glasses, parameter standardisation 80−69476
physically handicapped persons' apparatus standardisation *(Japanese)* 78−44699
plastics, materials testing, application-oriented test standardisation *(French)* 78−85061
powder diffraction data, American Crystallographic Association recommendations *(Czech)* 80−24306
prosthetics and orthotics, standardisation of technical terms *(Japanese)* 78−44700
Q system: an experiment in software standardization for data acquisition 79−89549
quartz, quantitative X-ray anal., standardisation, milling effect on degree of disorder *(German)* 78−11176
quick calibration checks, devices to calibrate commonly used meas. instruments 80−47010
radioactive effluent discharge data intercomparability and EEC harmonisation 79−13546
radioactive effluent monitoring, sampling and measurement principles *(French)* 78−89996
radioactive sources, standardisation using $4\pi\beta$-γ coincidence method *(Rumanian)* 77−46472
rheograph linear-distortion estimation 80−85502
robots and manipulators, symposium, Warsaw (Sept., 1976) 78−53574
rock discontinuities, suggested methods for quantitative description 79−84513
rock materials, strength determ. in triaxial compression, suggested methods 78−81432
rock monitoring test procedures using borehole extensometers 79−84512
rocks, petrographic description, suggested method 78−81431
rocks sound velocity determination, suggested methods 78−81433
SI system, need for periodic recalibration of laboratory equipment 80−31705
sieves, Fourier transform method for verification of wire screens 77−53874
spectrophotometry and luminescence meas., conf., Gaithersburg, USA (Nov. 1975) 78−32846
standard CANDU 600 MWe nuclear plant for Point Lepreau 78−29637
stellar designation organization using bibliography-type data base 77−78658
surface roughness meas., hand-held instrument with in-built data processor *(German)* 80−57255
surface waviness, roughness and shape deviations 77−5805
technical thermometer metrological characteristics, normalisation 78−77908
tensile tests, standardization from metal physics viewpoint *(German)* 80−93711
thread gauges, w.r.t. inner-pitch error 77−79053
time dissemination using TV signals from broadcasting satellite 77−60334
transmission spectrophotometry in visible and UV regions, standardisation 77−53989
US instrumentation standardisation, physician's need 78−69168
US Pulse-echo transducer standardization 78−73181
USSR unified system of seismic obs. 79−39912
vacuum couplings, small bore British system, complementary to ISO recommendations 78−21148
vacuum flanges and couplings, small bore British system, complementary to ISO recommendations 77−26316
variable area flowmeter *(German)* 79−50834
Viking lander radar system mechanical design 78−57427
West German solar energy utilisation programme technologies 79−57366

standardisation continued
Westerbork Synthesis Radio Telescope, standardized data formats 77−78641
X-ray fluorescence anal., quantitative, using fundamental parameter technique 77−56309
X-ray high potential generator, PD150L, standardisation of exposure factors *(Japanese)* 77−73577
^{133}Ba decay data and standardisation 77−88081
^{60}Co teletherapy dosimetry, USA nationwide survey 77−56478
$K_2Cr_2O_7$ acidic solns. as UV absorbance standards 77−53990
$Zn/ZnSO_4/Zn$ system, laser interferometric study of corrosion of coated and uncoated metals, technique standardisation 79−35815

standards
see also CAMAC; constants; measurement standards; television standards; units (measurement)
440 Hz standard A tone generator 78−46863
acoustic noise, activities of ISO *(Japanese)* 80−19154
acoustics, International Standards organisation *(Japanese)* 80−14502
air pollution, administrative aspects *(Dutch)* 78−57311
air pollution, German laws, standards, guidelines and limiting values *(Dutch)* 78−57312
antennas safety, 10MHz to 1GHz, ANSI and EPA recommendations 80−30765
architectural acoustics, review *(Japanese)* 80−64294
astronomical data base standards, management and security 77−82282
atmosphere standard, International and Soviet 80−26612
automated perimetry standards 80−46084
biomedical regulatory standards development, as educational and design review process 78−44647
blood pressure transducers, technical evaluation 79−44002
BWR, boilers and pressure vessels, in-service inspection, General Electric's code 77−3152
cardiac monitor, heart rate meter and alarm eval., proposed standard test tapes 80−89899
CIELAB and CIELUV colour spaces, colour difference evaluation *(Hungarian)* 78−29135
coherent-optics image recognition using contour transparencies *(Russian)* 77−58260
colour-reference-standard fluorescent lamp with colour rendering index of 99 80−78925
condenser microphone, laboratory *(Japanese)* 80−79096
conversion factor for radiometric to photometric data 78−86315
corrosion testing, trends in standards and expt. procedures *(Japanese)* 77−28953
cupping, sheet material, automation of standard testing 79−57172
defibrillators, review of instruments and maintenance 78−69251
demand pacemaker standard test signal proposal 77−81721
dosimetry for radiation-technological apparatus in COMECON countries development of methods and standards 79−93836
ECG, grounded, standardisation of resist. to external cophasal power line interference for isolated patients 78−57085
eddy current meter standards 78−27709
EEG montages, recommendation 77−86686
EHV power transmission lines vibrations damper, Indian standards 77−5660
electric shock, safety curves as function of ambient conditions *(French)* 77−17012
electrical engineering dimensional unification *(Italian)* 80−27266
electrical quantities, units, symbols and definitions *(German)* 80−86248
electro-medical apparatus, guideline for provisional safety standard *(Japanese)* 78−73274
EM fields, range 3-30 MHz, exposure, maximum permissible intensity and duration, physiological effects *(German)* 80−12179
EM non-ionising radiation, influence of quality on bioeffects, exposure standards 78−44558
EM radiation protection, in transmission stations, Polish and international regulations *(Polish)* 78−61263
EMC standard for medical electronic devices 77−81597
emergency medical telemetry, development and implementation 78−3635
environmental analysis reference materials, based on river sediment and urban particulate matter (SRM 1645 and SRM 1648) 80−21831
environmental noise pollution, new housing sites 80−48505
examination marks, reliability, in electronic engineering educational courses 79−75305
FASTBUS−details of addressing and bus mastership 79−89554
fibre optic connector system characteristics, aerospace user's viewpoint 78−46804
fibre optics standards 79−14101
fission reactor pressure vessel surveillance capsule exam., appl. of ASTM standards 79−22436
flow meas. in chemical industry, VDI and DIN specifications *(German)* 77−42946
fluorescent X-ray intensifying screen, efficiency determ., standard method 80−37140
fluorescent X-ray intensifying screen efficiency determ., standard method 78−69198
gas flow meas. standard methods review 78−94864
German standards on image assessment 78−58926
gloss measurement of paints, reference glossmeter 80−82805
gravity survey standards 78−7558
heliotechnics, basic values, symbols, units and definitions *(Rumanian)* 80−57243
high-volume preparation of air to standard quality for zeroing analyzers 80−90829
IEEE computer standards 79−89544
image restoration using maximum information norm 80−106476
industrial compressor sound level meas. *(German)* 80−14520
industrial deafness risk, British Government code of practice 78−55513
International Commission on Radiological Protection, dose limits (1934-77) 80−12266
laboratory equipment, electrically operated, safety standard 77−65046
laser applications for discotheque light effects, safety considerations with respect to output power and exposure time, regulations and recommendations *(German)* 80−101224
laser radiation, calc. of max. permissible exposure levels 79−96666
light source colour rendering, international standards *(Russian)* 80−43423
lighting equipment, classification and terminology, new Soviet standards *(Russian)* 80−31706
mass-produced camera objectives, effects of cosmetic defects 80−47135

standards continued
maximum permissible conc. calc. using absorbed dose data of MIRD pamphlet 11 78−53516
maximum tolerable radiation doses recommended by Israel Advisory Committee on Nucl. Safety 78−53517
medical electrical equipment, safety problems 80−56228
microscope, laboratory standard for hardness impression meas. 79−21808
microwave and RF radiation protection, American and European standards 78−80973
microwave radiation, emission and exposure standards 78−44619
microwave radiation exposure protection and need for field measurements 80−26377
NDT standards 79−11738
neutron activation anal., using standard reference materials as multielement irrad. standards, appls. 78−80815
neutron transport, 2-D benchmark expt. using water shield 78−58318
noise, occupational, hearing hazard obs. on heavy industry workers 77−81512
noise level definitions and building design criteria 78−83174
noise nuisance rating 79−86292
nonionising radiation hazard definition problems 80−3823
nuclear energy, quality assurance, international standardisation, FORATOM 80−58008
nuclear materials safety, IAEA safeguards appl., technical criteria survey 79−85678
nuclear plant pressurized systems reliability, influence of codes, standards and practices 79−22433
nuclear power engineering standards development, current status and long term objectives 77−67908
nuclear power industry, nondestructive testing standards, role of NBS 79−54612
nuclear power plant, quality systems standards comparison 79−22439
nuclear power plant design and operation, new security regulations in United States, impact 80−796
nuclear power plant reliability technology, role of ASTM in providing standards 79−22435
nuclear power plant safety rules and standards 77−65301
nuclear power plants, IAEA's activities in safety codes and nuclear safeguards 77−65347
nuclear power stations, nuclear materials, safeguarding experiences *(German)* 80−611
nuclear power stations safety, leakage tests, Spanish policies *(Spanish)* 80−5247
nuclear reactor electrical equipment, qualification concept 80−57883
nuclear regulatory and safety technology, experience in transfer 77−65300
nuclear safety regulations in USA and Germany 77−65298
nuclear standards in technology transfer 77−65296
nuclear steam supply, emergency core cooling system motor operated valves, failure mode anal. 78−54866
nuclear technology standards in developing countries 77−65346
occupational noise standard, 29 CFR 1910.95, problems in enforcement 80−43528
optical cables, LED- and laser-fed, safety aspects 78−74968
optical cables, LED- and laser-fed, safety aspects 78−74969
optical standard test method development by ASTM 80−74528
orthopaedic implants and biomaterials, mech. testing 78−36057
phase equilibrium studies, publication standards 79−10921
photogrammetry, OTF/MTF standards 77−78471
photometric, facilities at National Measurement Laboratory, Australia 78−82019
piping system anal. to nuclear standard regulations 77−6504
pollution due to vehicle exhaust emissions, meas. and testing procedures survey and criticism *(German)* 77−56299
polystyrene, ref. std. material testing, evaluation, glass transition temps., instrumental effects 79−4404
pressure vessel code, ASME, seismically qualified piping, failure probability 80−78365
pressure vessels weld quality assessment, NDT methods and equipment 78−56871
radiation monitor evaluation, techniques for producing standard EM fields 79−97341
radiation protection, implicit built-in safety factors 77−73596
radiation protection derived standards, Euratom directive and ICRP recommendations 78−35969
radiation protection legislation in West Germany, aspects *(German)* 78−5049
radiation shielding standards in USA, development 77−54374
radiation standards for low dose, low dose-rate exposure 78−80972
radioactive, for environmental monitoring, prep. 78−80816
radioactive materials, IAEA regulations for safe transportation 80−63410
radioactive materials, IAEA transport information collection system, influence on improved safety measures 80−63413
radioactive materials, international regulatory control for safe transportation 80−63411
radioactive materials, package design, construction and testing for safe transportation 80−63412
radioactivity standards for medical use 80−67232
radiographic phantoms for testing X-ray imaging performance 80−51229
radioprotection, medical regulations and standards in France *(French)* 78−48897
reactor physics, code implantation, technology transfer 77−65307
reactor pressure vessel brittle fracture, safeguards, American and German ductility requirements *(German)* 79−41017
regulation of surgical implant devices 79−92917
regulations and methods for noise measurement *(German)* 80−69610
respirators, protection against workplace carcinogens, US review 77−79076
RF and microwave exposure, USA occupational safety and health standards 80−3727
RF instrumentation based on superconducting quantum interference 78−57995
rocks, element determ. in National Institute for Metallurgy (S.Africa) reference samples 79−88356
safety principles underlying IAEA nuclear safety programme 80−95361
safety-system instruments for nuclear plants, impact of IEEE Std. (323-1974) 80−52753
SI units, guidelines for use, US National Bureau of Standards 80−68167

standards continued
simulated neutron tomography for nondestructive assays 80−99218
solar collectors, for heating and cooling appl. 80−7915
solar energy, passive systems, developments and appls. 79−96425
solar system, numerical values of consts. of IAU Commission 4 Working Groups Joint Report 78−40845
solar water-heating collector test procedure 79−62067
specular reflectance standards for visible and infrared region using thin Al film vacuum deposited on optical flats *(Japanese)* 80−102789
speech intelligibility test, DIN 45621 recommendation, acoustics and phonetics, German test *(German)* 78−35867
stars, spectrophotoemtric standards, absolute spectra energy distrib. 79−97040
steel, determ. of saturation mag., for residual austenite and props. of standard *(French)* 79−73766
substrate dielectric constants, standard specimens 80−13038
suspended solids in water, macerated glass fibre filter paper appl. 79−8454
temperature sensors, elec. Japanese and international standards 78−65928
two-lens standard phase inhomogeneity 79−14111
US probes, assessment and specification rel. to standards 79−23175
US therapy device surveys, performance standard drafting 79−79613
USA Environmental Protection Agency activities in radioactive waste management 78−94115
USA nuclear standards index 78−29662
UV hazards and protection standards 77−81588
vacuum technique, technical standardisation *(Czech)* 78−65940
visual system quantitative tolerance specification and standard development 80−48384
X-ray diagnostic system compatible with DHEW standards 78−7445
X-ray diffraction powder patterns, NBS 80−64839
X-ray machines output rating, equivalent DC power *(German)* 78−3650
X-ray production equipment, USA safety standard 78−29223
H_2 stabilised arc as vacuum UV radiation standard for 600 to 900 Å 78−66879
Ni-Cr coatings on steel, standardisation 79−57139
^{244}Pu standard reference material for nuclear materials safeguards appls. 80−78373
Zn radionuclide dosimetry standards and crit. organs 78−35961
standby power supply *see emergency power supply*
standing wave detectors *see standing wave meters*
standing wave indicators *see standing wave meters*
standing wave meters
pipeline leak location by coaxial test cable characteristic impedance variation 77−57317
VSWR indicator, type 6953A, ICs, performance, specification 77−53935
star phase rectifiers *see rectifiers*
Stark broadening *see Stark effect*
Stark effect
see also atomic spectra
acetonitrile, far IR laser gas absorption obs. with and without DC field 79−31870
acetylene-d_2, microwave spectrum, P-branch transitions, Stark shifts 77−27057
aggregates, optical transition freqs., Stark effect 79−4789
air pollutants, determ. by Stark modulated microwave spectroscopy 78−57337
alkali halides, relaxed excited state of F-centre, vibronic theory of Stark effects 77−85691
alkali metal, Stark and photoabsorption spectra, density of oscillator strengths 80−83318
alkali metal atom, Rydberg state Stark struct. 80−37754
alkali metal atom, Stark effect for hyperfine structure sublevels and splitting of $n^2S_{1/2}$ states *(Russian)* 79−3401
alkali metal atoms, excited hyperfine and Stark parameters, meas. and calc. 78−86814
alkali metal like homologous atoms and ions, regularities within Stark widths of reson. lines 78−78662
alkali metal Stark profiles, of reson. lines, model microfield method appl. 79−26931
alkali metals, Rydberg states, Stark ionisation 80−52933
allylamine, anomalous Stark effect for torsional splitting 79−64040
3-aminopropanol, and deuterated forms microwave spectrum, dipole moment, struct. 79−59441
anthracene film, electroabsorption spectra obs. 80−50301
anthracene in naphthalene crystal, second-order Stark shifts in optical spectrum 80−88966
atmospheric pollutants spectra, Stark tuning for laser perturbation spectroscopy 78−69526
atmospheric thermal plasma, continuous emission, ionisation potential lowering and total excitation cross section 80−38705
atom, AC Stark effect, fluoresc., in modulated laser beams, two-photon stepwise excitation 80−42989
atom, AC Stark splitting in doubly reson, three-photon ionisation, nonmonochromatic field 78−94220
atom, bound-continuum decay, AC Stark splitting 80−5502
atom, dilation analyticity in constant electric field, two-body Stark problem 79−26900
atom, modulation light wave vibrations *(Russian)* 79−98027
atom, reson. interaction with laser field, nonperturbative theory 77−442
atom, resonant ionisation under adiabatic level inversion conditions *(Russian)* 80−32691
atom, Rydberg autoionising states, props. in elec. fields, appl. to Fe^{23+} dielectronic recomb. 79−59405
atom, selection rules, EM transitions in strong coherent light field 77−447
atom+charged particle anisotropic collision, spectral line shift and broadening, polarisation depend. 78−82695
atom-strong field interactions, generalised dressed atom approach, laser theory and Bloch-Siegert shift 77−71964
atomic Hamiltonians in DC fields, dilatation transformation 78−41999
atomic level field splitting, resonant cooperative light scatt. *(Russian)* 80−74148
atomic neutral particles, electrostatic trapping 80−102485
atomic resonance fluorescence, laser excitation time-dependent spectrum 80−37770
atomic spectra and radiative transitions, book 80−22159
atomic transition in stochastic field, saturation and Stark splitting 80−9546
Stark effect continued
atomic vapour quantum counter, Stark tuning 80−53242
atoms, AC Stark effect, multiphoton processes 77−71775
atoms, and ions, parity nonconservation effects 79−10086
atoms, dispersion relations and AC Stark effect 78−945
atoms, in const. elec. field, rigorous theory of complex scaling 78−70785
atoms, light absorption, subtractive stimulated emission theory 79−59396
atoms, motional-Stark-effect-induced anticrossings 79−13666
atoms, parity violation in neutral-weak current interactions, meas. method 79−45670
atoms, Raman scatt. in presence of two-photon reson., coherence effects 79−45679
atoms, two-photon photoelectron energy spectra, AC Stark splitting 78−86834
Autler-Townes effect, coupled 1- and 2-photon resons., theory 77−83649
band bending and Stark ladders in finite crysts. 78−56112
p-benzoquinone, second order Stark shift of zero-field transitions, isotope effects 77−24860
bibliography at. energy levels and spectra, (July 1971-June 1975) 77−71764
bis-merocyanine dye, intramol. dimer soln., Stark effect, optical absorption and density 78−50573
blackbody radiation interaction with LF atomic transitions, Zeeman, Stark and stimulated emission 79−41127
Bloch electron in step-like elec. pot. 80−59942
Bloch electron Stark ladders via evolution operator 80−44554
bromoacetylene, microwave spectrum, r_s-struct., dipole moment, quadrupole coupling consts., vibr. excited states 77−79606
t-butyl cyanide-HF, hydrogen bonded heterodimer, spectroscopic consts. from IR and microwave spectra 80−43039
t-butylphosphine, microwave spectrum, meas., determ. 78−58675
CaF_2:Na, Stark effect on Na disturbed F_2-centres 77−69279
channelled ions, reson. coherent excitation 79−51178
p-chlorobenzaldehyde, p-dibromobenzene and p-dimethoxybenzene hosts, dipole moments, lowest electronic states 77−18954
chloroethylene, CO_2 laser absorption, Stark modulation 78−17671
coherent optical spectroscopy 78−1112
complex molecules, fluoresc. quenching by strong radiation due to linear Stark effect 77−58074
complex scaling method, theory 79−18123
crystal impurity centres, quadratic Stark effect, quantum mech. band shape calcs. 77−69863
crystal in static elec. field, true width of electron levels 77−66145
crystal lattice electron energy spectrum depend. on external electric field *(Russian)* 80−34498
crystal localised centres, inversion symmetry, Stark effect in wideband, electronic-vibr. spectra 77−69864
cubic crystals, electrooptic absorption of anisotropic Jahn-Teller centres 78−27188
cyanobutadiyne-d_0,d_1, microwave spectrum, substitution struct., dipole moment 77−3348
2-cyanofurane, rot. consts., dipole moments, nuclear quadrupole coupling, spectral obs. 77−34620
cyanomethane-HF, hydrogen bonded heterodimer, spectroscopic consts. from microwave spectrum 80−43038
2-cyanothiophene, rot. consts., dipole moments, nuclear quadrupole coupling, microwave spectra 77−34620
3-cyanothiophene, rot. spectrum and consts., elec. dipole moment, quadrupole coupling, r_0-struct. 77−79607
1,3-cycloheptadiene, microwave spectrum, conform. 79−98074
degenerate semiconductors, electric field influence on exciton states, Stark effect 80−54617
dense equilibrium plasma, Lyman-α Stark profile, Stark broadening theory 77−84505
dense plasma, Lyman-α line broadening, of H and hydrogenic ions 78−42811
diamond:B, photoconductivity and electroabsorpt. spectra 77−4647
diamond-like crysts., electro-optic effects due to the Stark splitting of energy bands 79−82950
diatomic molecule, Stark effect calcs., rigid rotator rotational levels in asymmetric potential well 80−5580
diatomic polar mol., rot. level Stark effect in strong field 78−25611
diatomic polar molecule in electric field, energy levels 79−18136
diatonic molecules, Stark effect variational and perturbational calcs. 80−1022
dibromonaphthalene, quasilinear chain excitons, Stark effects 80−97239
4,4′-dichlorobenzophenone, cryst., X-traps, rel. populations, elec. field effect 77−12414
difluoroethane, Stark effect, appl. to CO_2 laser modulation and stabilisation 79−59667
1-1 difluoroethane in external Stark cell, CO_2 laser possible freq. stabilisation 79−94266
1,1-difluoroethylene, CO_2 laser Stark spectra of ν_4 and ν_9 bands 79−36694
1,1-difluoroethylene, laser Stark saturation spectroscopy, assignments 79−31864
1,1-difluoroethylene, optically pumped, far IR laser line assignment 79−31865
difluoromethylborane, microwave spectra and struct. obs. 80−43036
dilatation transformation and Stark-Zeeman effect 79−3398
dimers, electronic transitions 80−9639
2-dimethylaminoethanol(-d_1), microwave spectrum, hydrogen bonding, rot. consts., struct., dipole moment 77−6764
disilylmethane, microwave spectrum, struct., dipole moment and internal rot. 79−13699
Doppler-free saturated absorption microwave spectrometer 78−55256
double resonance Stark spectrosc., Doppler-free, using acousto-optic modulator 79−44935
durene, mol. cryst., Stark effect origins, point dipole approx. soln. 77−77252
dynamic Stark effect, absorber theory approach 79−54807
education, plane rotator, degenerate perturbation theory, Zeeman and Stark effects 79−9059
electric field induced radiationless transitions, theory 78−74690
ESR dipolar splitting of spin pair in presence of avalanche phonons 79−61203
ethane, $^{13}CH_3{}^{12}CD_3$, $^{12}CH_3{}^{13}CD_3$, microwave spectra, Stark effect, C-C bond length and mol. consts. 77−50428
ethaneselenol, IR, Raman and microwave spectra, barriers to internal rot. 77−38666

Stark effect continued
ethyl cyanide, isotopic species, rot.-torsion-vibr. interaction in rot. spectra 77−458
ethylene oxide, rot. relax., double reson. and Stark switching obs. 80−106340
ethylidenimine, pyrolysis product, microwave spectra, rot. distortion and electric quadrupole const. and rot. barriers determ. 80−78608
excited atomic and molecular states in strong electromagnetic fields 79−49955
excited atoms, orientation in elec. field *(German)* 78−25472
exponential decay 80−91491
far IR laser, optically pumped, electronic tuning and phase-locking 78−59055
far IR waveguide laser, Stark modulation 77−54744
far IR waveguide laser Stark effect obs. 77−38875
finite crystals, Stark ladders 77−24540
fluoroacetylene, laser Stark and IR-microwave double resonance, E1 moment, vibr. states 77−6813
fluoroacetylene-d, Stark and microwave double reson. laser spectra 80−63690
fluoromethane, ν_3 band Lamb dips, effects of RF elec. field modulation on Stark spectra 80−52989
fluoromethane, -^{12}C (-^{13}C), Doppler-free optical double reson. spectroscopy using single-freq. laser and modulation sidebands 80−68274
fluoromethane, and other optically pumped lasers, dynamic Stark effect 78−17911
fluoromethane, far IR laser FM and stabilisation 78−59056
fluoromethane, optically pumped laser, IR-FIR transferred Lamb dip spectra 80−1193
fluoromethane far IR CW laser, Stark effect, large freq. tuning and resolved structures 79−45931
fluoromethane far IR Stark laser using rectangular metal-dielec. waveguide 79−27245
fluoromethane for IR laser, evidence for Stark induced freq. shift 77−58358
fluoromethane-d_3, laser Stark spectra, ν_6 band, vibr.-rot. consts., dipole moment 78−5277
forbidden M_1 transitions, parity violation, stray static elec. fields 80−87078
formaldehyde, $\nu_5 \rightarrow \nu_6$ difference band, laser Stark spectra 78−5227
formaldehyde, CO laser Stark and IR absorpt. spectra, dipole moment and rot. consts. 77−75150
formaldehyde + He(H_2), collisional relax. times and lineshape distortion, Stark absorpt. linewidth obs. 78−74744
formaldehyde-d_1, ν_3 fundamental band, IR absorpt. and laser Stark spectra 77−34629
formaldehyde-d_2, laser Stark spectra, Coriolis coupled ν_4 and ν_6 fundamentals 77−27065
formic acid, far IR laser gas absorption obs. with and without DC field 79−31870
gas, Stark tunable, mirrorless optical bistability and optical limiting, obs. 80−38056
gas detector appl., all-electric 80−74417
gas-pressure shifts of molecular lines 80−23463
germanate glass:Bi^{3+}, time-resolved spectra, radiative and nonradiative processes 79−47501
glass:Eu^{3+}, spectral line inhomogeneous broadening, electron excitation migration *(Russian)* 77−48200
glass:Eu^{3+}, spectroscopic props. of excited states of ions, laser induced fluorescence line narrowing meas. 79−38641
glass:Nd^{3+}, line narrowed fluorescence spectra and site dependent transition probabilities 79−38640
glass:Nd^{3+}, spectral props. *(Chinese)* 80−60645
glass, rare-earth activated, polarised luminesc. 78−48224
highly excited atoms, blackbody radiation effects 80−58176
highly excited atoms, review of recent expts. 80−23325
homogeneously broadened three level atoms, intense standing wave saturated, spatial inhomogeneity, mode competition 80−23646
homologous ions series, Stark broadening trends 80−105157
homonuclear molecules, vibrs. excitation by IR radiation 80−28068
hydrazine-1,2-d_2, microwave spectra, mol. structural parameters 77−27056
hydrogenic atoms and ions, degenerate state transitions, plasma waves, Stark effect 79−72389
hydrogenic ions of high-Z, expt. and calc. of Lamb shift, review 77−54534
impurity centres, quadratic Stark effect in crysts. with wideband absorption spectra, semiclassical approx. 77−66526
impurity centres in crystals, quadratic Stark effect, Jahn-Teller effect 78−68536
iodomethane, Stark effect modulation of CO_2 laser 78−17992
iodomethane-d_3, ν_2 band, laser Stark and laser-microwave double resonance spectra 77−27067
iodomethane-d_3, ν_2 band, laser Stark saturation spectra 78−42125
iodomethane-d_3, Stark tuned level crossings and saturated absorpt., RF elec. field modulation effects 80−52989
ion channelling, coherent excitation 79−46727
ionic crystals, Stark effect of localised electronic centres 77−66476
ionic lines, isolated, Stark broadening function *(French)* 77−23462
IR laser Stark spectroscopy, RF elec. field modulation effects 80−52989
isopropylphosphine, gauche form, Stark spectra, microwave spectrum, identification 78−58674
Josephson junction, ultrasmall, dynamic Stark splitting 80−103790
Klein-Gordon equation, time-independent, relativistic Stark effect, resonances 80−62890
Kronig-Penney potential, widths and spacing of Stark ladder levels 78−72124
laser, far i.r., with metal-dielectric waveguide, for Stark effect obs. 77−700
laser far IR, high speed freq. modulation 77−72010
laser fields, stochastically fluctuating, saturation and Stark splitting of resonant transitions 80−53245
laser plasma diagnostics using Balmer series transitions Stark broadening 80−64780
laser Stark spectroscopy, isotope separation 77−38693
laser Stark spectroscopy, technique for molecular vibration-rotation spectra *(Japanese)* 77−494
linear atomic susceptibility role 78−55142
liquid, nuclear quadrupole relaxation of non centre symm. mols. *(Russian)* 80−88889

Stark effect continued
mesic and muonic mol. ion formation in liq. He, X-ray intensities, Auger and Stark transitions 78−94338
metal vapour coherent two photon reson. third and fifth harmonic VUV generation 79−72627
metallic surface, dispersion of surface plasmons 80−2440
methane, microwave Q branch distortion moment Stark spectrum, rot. transitions, C isotope shifts 77−455
methane-d_1, dipole moment, rot. depend., IR-IR double reson. obs. 79−81298
methane-d_4, Stark effect, rot. transitions in vibr. ground state, isotope shift 79−27029
methane-d, Doppler-free optical double reson. spectroscopy using single-freq. laser and modulation sidebands 80−68274
methanol, collision-induced rot. energy transfer, M-resolved microwave double reson. 79−6955
methanol, double resonance Stark spectrosc., Doppler-free, using acousto-optic modulator 79−44935
methanol, far IR laser gas absorption obs. with and without DC field 79−31870
methanol, far IR laser transition, dynamic Stark effect obs. 78−22114
methanol, optically pumped laser, IR-FIR transferred Lamb dip spectra 80−1193
methanol far IR CW laser, Stark effect, large freq. tuning and resolved structures 79−45931
methanol far IR laser, optically pumped, Stark effects 79−72552
methanol far IR laser line Stark splitting obs. 80−58313
methanol far IR Stark spectroscopy and 9-P(34) CO_2 laser line 80−69145
methanol optically pumped 118.8 μm laser line, Stark splitting obs. 80−102710
methanol waveguide laser radiation modulation by Stark cell 77−38962
methyl alcohol IR absorption, diode laser obs. 79−31518
methyl alcohol IR transitions, saturated absorption spectroscopy 77−38874
methyl bromide, ν_6 band, CO_2 and N_2O laser Stark spectroscopy 78−78698
methyl chloride-d_3, 9.4 μm region laser Stark spectrum, ν_2 and ν_5 bands 77−27112
methyl fluoride, rot. absorpt., Stark modulation expt. 79−59396
methyl fluoride, second-order Coriolis resonance between ν_2 and ν_5 states, microwave spectra 78−74646
methylacetylene, ν_5 band, microwave and IR laser Stark spectrosc. 80−91558
p-methylbenzaldehyde, p-dimethoxybenzene host, dipole moments, lowest electronic states 77−18954
methyldiborane, microwave spectra, bond lengths, dipole moments, rot. consts. 77−83579
methyldichlorosilane, Stark effect and microwave-microwave double reson., struct. *(German)* 80−47975
methylene fluoride, ν_9 fundamental band, 9.4-μm CO_2 laser Stark spectroscopy 78−9191
methylenimine, ν_4 fundamental band, laser Stark spectroscopic obs. 79−64039
methylimine, double resonance Stark spectrosc., Doppler-free, using acousto-optic modulator 79−44935
methylpropylether, trans-trans isomer, microwave spectra, struct., dipole moment and rot. barriers calcs. 80−83348
microwave 'stripline' absorption cell, for use in microwave Stark spectrosc. 79−81305
microwave spectrometer, with electric molecular modulation *(Russian)* 80−9003
microwave spectroscopy Stark cell, broadband and low insertion loss, performance 79−17460
microwave-optical double resonance, off-reson. optical radiation theory 78−25579
MODOR investigations using open Stark cavity 79−63288
modulator, zero-based half-sine wave, for analytical microwave spectrometer 77−13802
molecular aggregate, Stark spectroscopy, geometry, Heitler-London approx. dipole moments 78−55200
molecular collisions, coherence transfer between collision partner mols. 77−71844
molecular crystal, optical transition freqs., Stark effect 79−4789
molecular crystal, polar guest, stark shift, point-dipole approx. 77−1701
molecular crystal, Stark modulation of Lorentzian line shapes, Fourier anal. 77−1691
molecular crystals, Stark splitting ang. depend. dipole moment and polarisability effects 77−51711
molecular FIR laser design, freq. tunable by Stark effect 80−5750
molecular gas, elec. dipole reson. *(Russian)* 79−22755
molecular gas, Stark-induced three-wave mixing, theory 77−14774
molecular gases, Stark tuning, laser radiation absorpt., rel. to CO_2 laser tuning *(Rumanian)* 79−86157
molecular rotational coherence, reson. collisional exchange, time resolved microwave obs. 80−23525
molecular transition frequencies in reson. optical field, Stark shift 77−14487
molecule, anomalous Stark effect for torsional energy splitting 79−64040
molecule, Rabi frequency transitions in AC Stark effect, dressed-molecule description 78−42124
molecule, reson. interaction with laser field, nonperturbative theory 77−442
molecule, reson. modulation of light, dynamic electrooptical effects *(Russian)* 78−9192
molecules, light absorption, subtractive stimulated emission theory 79−59396
molecules beam selection by quadratic Stark effect *(Russian)* 78−78823
multilevel molecular system, excitation by laser IR field 78−55212
multiquantum resonant interactions, canonical description *(Russian)* 77−10714
N-methylhydroxylamine, microwave spectra, struct., moments, internal rot., HFS and rot. consts. 79−45708
naphthalene, mol. cryst., Stark effect origins, point dipole approx. soln. 77−77252
1,4-naphthoquinone, $T_1 \leftarrow S_0$ transition, elec. and mag. field spectra 78−88322
neodymium ethyl sulphate, electronic spectra Stark pattern, crystal elec. field and mag. props. 77−12084
neutral atom lines, Stark broadening, adiabatic theory, classical trajectories of electrons 80−18936

Stark effect continued
neutral atom reson. lines, Stark widths and shifts, regularities from He to Ca 80−47939
neutral line Stark broadening in plasma 78−46299
nonmonochromatic chaotic field, double optical reson. and reson. fluoresc., AC Stark splitting 80−9547
NQR, electronics appls. 80−63668
one-dimensional Bloch electrons, binding by external fields 77−89681
one-dimensional crystal, electron problem in uniform elec. field 77−20280
one-dimensional model system, Stark effects eigenvalues, Pade approximants calcs. 80−4561
one-electron atom in strong light field 79−63946
optical double resonance Stark spectroscopy, using modulation sidebands 77−58051
optical multistability, light self-modulation in double resonance *(Russian)* 80−106560
optical triple resonance, semiclassical anal. 79−93963
optically pumped for IR lasers 77−38963
optically pumped laser three-photon transition theory 80−102690
optoacoustic detection using Stark modulation 79−94325
orthovanadates, rare earth activated, spectroscopic props. 77−16363
7-oxabicyclo (4.1.0) hept-3-ene, conformation, dipole moment, microwave spectrum 78−66539
paramagnetic crystal, magnetisation change by light pulse 80−70932
paramagnetic ion spectra perturbation by high-intensity nonreson. EM radiation 78−71137
parametric luminescence spectra Stark effect, stimulated processes, strong field 77−10977
pentacene, in p-terphenyl, polarisability calcs., from Stark meas., anisotropic Lorentz approx. breakdown 78−5276
perturbation and variation treatments, appl. to H(1s) reson. 80−14105
phenyl isocyanate, microwave spectrum, rot. consts., dipole moment 77−61739
phosphate glass, Nd^{3+} frequency selection by monochromatic laser excitation at resonant transition *(Russian)* 79−78747
photosynthetic membrane, optical and electrochromic props., chloroplast chlorophyll orientation 77−48763
plasma, atomic absorption spectra, high freq. Stark effect 80−23359
plasma, dense, Stark profile of H-like ions, Lyman lines 79−82048
plasma, Gaunt factor temp. depends., from Ar II and Ca II Stark widths 78−87491
plasma, H line curvilinear trajectories and Stark broadening 78−67324
plasma, H line Stark broadening, role of ion dynamics simulation 80−24144
plasma, laser produced, space depend. shift of spectral lines 80−6268
plasma, line width variation within Stark broadened multiplets 78−91073
plasma, nonthermal, two-temp. electron gas, collective elec. field fluctuations estimation 80−43882
plasma, of theta pinch, $N^{+,2+,3+}$ lines Stark broadening, He(II) line diagnostics 80−24249
plasma, photon escape probabilities for Stark-broadened Lyman series lines 80−24143
plasma, resonant laser emission atomic absorpt. line contours *(Russian)* 77−76195
plasma, Stark effect and four-quantum transitions, very strong stochastic electric fields 78−9760
plasma, Stark shift by inhomogeneous strong E field, X-ray Lyman profile 80−106977
plasma, thermal, Stark broadening 77−47165
plasma, turbulent, Stark broadening 77−47166
plasma anisotropic noise, HF, in turbulent plasma, H Stark profiles 78−1896
plasma electron density, laser plasma, Stark-broadened line wings of H-like ions 78−79462
plasma lines, electron impact width of multiply ionised ats., semiclassical formula 80−43972
plasma reson. lines regularities in Stark widths and shifts, He^{+}-Ca^{+} 80−43881
plasma-broadened He I and He II lines, Stark profiles 79−46489
plasmas, Tormac, Gaussian HeII 4686 Å spectral lines, Doppler and Stark broadening effect, turbulence 80−106980
polar molecule, Stark effect in electron spin transition in zero-field 77−27099
polyatomic mol. gas, laser-induced rate processes, collision-free dynamics 77−30934
polyatomic molecule, multiphoton absorpt. resons., dynamic Stark splitting 80−9670
post-collisionally Stark mixed states, autoionisation electron energy and ang. distrib. 80−18829
propiolamide(-d_2, d_3), microwave spectrum, struct., dipole moment 78−78685
pyridine, in benzene single cryst., electronic spectrum Stark modulation, dipole moment 78−29814
quantum beats under pulsed dye laser excitation 77−42277
quinoxaline in durene (naphthalene) crystal, Stark effect, space charge, local field tensor and dipole moment 77−28601
Raman scattering, Stark quantisation effects on cross section calcs. 77−16314
rare earth ions in crystals, electric dipole transitions intensities 79−78062
rare earth ions in cubic field, anal. of absorption spectra $4f^{N+1}\rightarrow 4f^{N}5d$-6s 80−7382
rare earth oxyhalides: Eu^{3+}, fluorescence spectra obs. *(French)* 80−89042
rare-earth ion spectra, effect of coordination polyhedron struct. 77−55807
resonance fluorescence, in phase freq. modulated laser fields 78−37588
resonance fluorescence in modulated laser field, stochastic model 78−5169
resonance Raman scattering and resonance fluoresc., time and freq. resolved 77−75624
resonances in one-dimensional Stark effect and continued fractions 79−59395
resonant media, two-photon coherent interaction of light pulses, Stark shifts 77−79905
resonant transitions in strong chaotic fields, saturation and Stark splitting 79−72542
resorufin, in PMMA, site selection spectra, hole burning and Stark effect 78−9159
Stark effect continued
rhodamine 6G, aggregation, modulation Stark spectrosc. obs. 79−27030
rigid symmetric top molecules, dynamic Stark effect spectrum 80−63621
ring-type state selector and space focuser for mols. with positive induced dipole moment, appl. to mol. beam maser 78−54503
ruby, coherent transients obs. by Stark switching with narrow optical hole burning 78−37947
ruby, multiple optical hole burning obs. using Stark field sweeping 77−46768
ruby, optical free induction decay modulation and absorpt. line struct. due to superhyperfine interaction 80−33091
ruby, optical hole burning, Stark and pump-probe studies 80−48356
ruby, optical nutation echoes, Stark switching obs. 80−69467
ruby, optical pair spectrum, Stark effect with AC elec. field modulation 78−10911
ruby, photon echoes, optical free induction decay, Stark switching technique 79−7182
ruby, Stark induced optical transients, photon echo 78−33785
Rydberg atoms, expts., metastable states, multiphoton ionisation, spectroscopy, Stark struct., collisions, polarisability *(Dutch)* 78−5160
Rydberg atoms, Stark ang. momentum transfer, hydrogenic model 78−17606
saturation laser spectroscopy, dynamic Stark effect 77−31119
Schottky barrier, excitonic refl. of light 80−10885
semiconductor, current fluctuations in quantizing elec. field *(Russian)* 77−28175
semiconductor, density of Wannier-Stark states, calc. 77−11885
semiconductor, donor-acceptor pair in elec. field, anomalous Stark shift of ground state energy 79−19564
semiconductor, interband absorpt. in strong parallel mag. and elec. fields 80−6799
semiconductor, multilayer, exciton Stark effect 79−19528
semiconductor, phonon induced hopping between Stark levels 80−92900
semiconductor, Stark and photoabsorption spectra, density of oscillator strengths 80−83318
semiconductor, with superlattice, plasma resonant interaction with Stark oscills. 80−107842
semiconductor in quantising mag. field *(Russian)* 77−73126
semiconductor in quantized mag. field, multiphoton Stark effect *(Russian)* 78−72541
semiconductor superlattice, phonon spectrum, effect of strong elec. field, parametric reson. 80−44273
semiconductor with impurities, Stark effect of localized electronic centres 77−66476
semiconductors with superlattices, Stark-cyclotron resonance, Larmour freq. *(Russian)* 80−60421
semirigid molecules, Stark effect, isometric groups, elec. dipole moments theory 78−29815
silica glass:Nd^{3+}, laser-spectroscopic method, for studying solids with nonuniform spectral broadening *(Russian)* 79−40630
silyl acetylene, microwave spectra in ground and ν_{10} vibr. state 80−78610
solar flares, nonthermal plasma wave elec. fields meas. using Stark effect 78−12193
solar flares spectral diagnostics for turbulent elec. fields 77−17493
solar H Balmer emission lines, Skylab obs. of active regions 77−33441
solar H Balmer emission lines, Skylab obs. of quiet Sun and polar coronal hole 77−33440
spark discharge, electron density, determ. from Stark broadening of spectral lines *(Russian)* 80−28859
spectral and scatt. theory of Schrodinger operators, Stark effect 77−22435
spectroscopy technique using CW dye laser, appl. to NO_2 77−38026
spectrum profiles in the presence of Stark, Lorentz and Doppler broadenings 78−86820
Stark ladder states as resonances 77−12360
Stark resonances, stabilisation method calcs., convergence 80−91492
Stark switching, coherent transient monitoring technique in optical pulse Fourier transform spectroscopy 78−86974
subDoppler Stark spectroscopy in crossed elec. and mag. field 78−948
submillimetre laser molecules, Stark and ODR spectroscopy 79−31864
submillimetre Stark shift laser spectrochemical analysis 77−40622
N-sulphinylaniline, microwave rot. spectra, torsional freq., dipole moment and internal rot. barrier 78−973
symmetric-top dipole molecule, Stark effect in strong field *(Russian)* 77−61792
terbium ethyl sulphate, mag. and thermal props. 79−7971
tetracene, in p-terphenyl, polarisability calcs., from Stark meas., anisotropic Lorentz approx. breakdown 78−5276
1,1,2,2-tetrafluorocyclobutane, microwave spectrum, dipole moment, rot. and vibr. modes assignments 77−18914
thioacetaldehyde (-d_1), microwave spectrum, substitution struct. internal rot. barrier, dipole moment 77−6762
thioformaldehyde, double resonance Stark spectrosc., Doppler-free, using acousto-optic modulator 79−44935
thioformaldehyde, elec. dipole moment determ. using elec. field spectroscopy 78−70870
three-level atom in radn. field, resonance processes *(Russian)* 79−45687
three-level equidistant degenerate system, self-induced transparency, dynamic Stark effect 78−50863
three-level medium, coherent transient pulse propag. in two-photon reson. 77−79904
three-level system, coherently driven, collisional contrib. to dynamic Stark effect 79−13765
three-level system, Doppler-broadened, Autler-Townes effect 78−41998
three-level system, Stark effect in high-frequency fields for resonant modulation 79−10274
three-level system, two-photon transition in two pulsed fields 79−68215
three-level system in Gaussian noise field 78−41266
trifluoroiodomethane, double resonance Stark spectrosc., Doppler-free, using acousto-optic modulator 79−44935
trifluoromethyl bromide, microwave spectra, mol. rot., isotopic variation in bond lengths, Stark meas., dipole moments determ. 80−74165
trifluoromethyl iodide, microwave spectra, mol. rot., isotopic variation in bond lengths, Stark meas., dipole moments determ. 80−74165
2,4,5-trimethylbenzaldehyde, durene host, dipole moments in lowest electronic states 77−18954
trinitromethane, microwave and rot. spectra, effect of twist of NO_2 groups, rot. and centrifugal distortion const. determ. 80−95605
two level atoms, reson. fluoresc., cooperative effects, bistability 77−10628

Stark effect continued
two photon absorption spectroscopy, motional Stark effect 80−43126
two-electron ions, ground state, quadratic Stark effect 80−37775
two-level atom, influence of relaxation parameters and laser fluctuations 79−72273
two-level atomic system, discontinuous dynamical Stark shift 79−49981
two-photon double-beam optical bistability 80−64113
two-photon spectroscopy, Doppler-free *(Dutch)* 79−50167
two-photon spectroscopy, using counter-propagating laser beams and AC Stark effect 77−49781
two-photon transition, time domain relax. time meas., by Stark switching technique 77−75248
variation method appl. 79−6909
Wannier-Stark ladders of finite crystal, level shifts 78−30895
width and shift depend. on ionisation potential 80−58211
widths of neutral lines, simple estimating formula 79−3397
Zeeman degeneracy, effects on optical dynamic Stark splitting 80−37774
AgBr, Stark effect on I-bound exciton 79−28719
Al I line profiles, Stark broadening meas. 78−9115
Al I resonance line profiles, influence of boundary layer of Al-seeded shock heated plasma 80−43876
Al II line profiles, Stark broadening meas. 78−9115
Al, reson. line broadening, 3961.5 and 3944 Å 78−58622
Al transitions, Stark broadening and oscillator strengths 78−29761
Al XII, electron density meas. using Stark profiles 79−81181
Al XIII, hot pinched plasma, Lyman series Stark profiles, electron density determ. 78−51348
α-Al_2O_3:V^{3+}(Cr^{3+})(Co^{3+}), optical absorption spectra, DC and AC field effects 78−10925
Ar arc, Lyman-α wings Stark broadening 77−27721
Ar I 3949 Å, Stark width in medium electron density plasma 79−63954
Ar plasma, Ar III and IV lines, Stark broadening, Gaunt factor calcs. 77−51231
Ar, plasma, vac. UV emission profile, temp., spectroscopic meas. 77−51229
Ar, Stark shift and splitting in visible spectra 80−32659
Ar XVIII Lyman-α line Stark broadening, hot dense laser-produced plasma 77−11402
$Ar^{16,17+}$ filled glass shell, symmetric laser compression 80−64759
Ar-acetylene van der Waals molecule, radiofreq. spectroscopy and Stark effect meas., equilib. struct. and props. 80−91543
Ar-O_3 Van der Waals complex, struct. and props., RF and microwave obs. 80−32704
Ar.HBr(DBr), van der Waals complexes, rot. spectra and struct. 80−48055
B II, Stark shift, shock tube meas. 77−50403
$BF(OH)_2$, identification, rot. and centrifugal consts., mol. struct., microwave spectra obs. 80−32705
Ba atomic beam, light-shift induced zero-field level crossing, optical Hanle effect 80−52947
Ba I, light shift induced zero-field level crossing 80−58220
Ba I, quantum beats under pulsed dye laser excitation 77−42277
Ba II, Stark half-widths, line shifts, calcs. *(Russian)* 78−62764
Ba, Stark struct. of Rydberg states 78−25471
Ba^+, electron and ion Stark effects in plasma, widths and shifts 77−46526
BaClF:Sm^{2+}, energy levels, optical props. 78−84631
BaF_2:R^{3+}, far IR Stark and Zeeman splitting 77−48190
BaO, A $^1\Sigma^+$ state, dipole moment, MODR Stark effect 77−46584
Be IV, line broadening and self-absorpt. in laser prod. plasma 78−17615
BeF_2-KF-CaF_2-AlF_3-EuF_3 fluoroberyllate glass, Eu^{3+} fluoresc. linewidth 80−66285
Br^-, nuclear quadrupole interaction , second-order Stark effect 78−21879
BrCl, elec. dipole moment, Stark effect meas. 78−90211
^{79}BrF, (^{81}BrF), hyperfine struct., elec. dipole moment, rot. transitions, microwave spectral obs. 80−32695
C I lines, Stark broadening in ARC plasma 77−10634
C II, UV lines Stark widths 79−6910
C, reson. transitions, Stark widths and shifts of UV and VUV Lines 77−88425
C VI, laser plsma, electron density profile, Stark broadening meas. of vac. UV lines 78−59684
C, vac. UV spectral line broadening parameters meas. 80−23352
CO, $d^3\Delta_i$ state elec. dipole moment, vibr. depend. obs. 79−31548
CO, $d^3\Delta_i$ v=4 state dipole moment, laser-induced transition in mol. beam 78−25513
CO, elec. and mag. props., mol. beam elec. reson. spectroscopy 77−61791
CO, hole burning in single quantum power spectrum due to Autler-Townes splitting 80−9671
CS_2, UV spectra, Stark modulation of a^3A_2-$X^1\Sigma_g^+$ system 79−86003
Ca I, emission spectrum, level struct. 77−79562
Ca, Stark mixing of high-lying calcium levels by laser-produced charges 78−25469
Ca^+, electron and ion Stark effects in plasma, widths and shifts 77−46526
CaF_2:Ce, Stark struct., phototransitions, g-factors 78−67995
CaF_2:Eu^{2+}, second order perturbation in vibronic system 78−30893
CaF_2:Gd^{3+}, ligand ENDOR cubic centres, elec. field effect *(Russian)* 78−60357
CaF_2:R^{3+}, far IR Stark and Zeeman splitting 77−48190
CaF_2:Tm^{3+}, 8.2 keV excited state, mag. props., Schottky ht. capacity, nucl. quadrupole splitting 78−76037
CaF_2+Yb^{3+}, Stark level Zeeman energies, mag. susceptibiltiy, Schottky specific heat, crystal field splitting 78−26831
CaO:Mo, spin coherence and Stark modulation effect of F_A-Mo centre excited state 77−69733
$CaWO_4$:Nd^{3+} $4f^3$ configuration, ground level energy state variation rel. to press. *(Russian)* 77−16358
Cd, 5s5d states, Stark effect *(French)* 80−9543
Cd, absorpt. spectra in nonreson. biharmonic radiation field 79−3400
Cd, Stark interaction in nspz$^3P_1$ levels, optical double resonance obs. 79−63941
CdF_2:Er^{3+}, Tm^{3+}, evidence for $Er^{3+} \rightleftharpoons Tm^{3+}$ energy transfers, fluoresc. expts. 80−60655
CdF_2:R^{3+}, far IR Stark and Zeeman splitting 77−48190
CdSe epitaxial layers, on GaP-CdS substrates, absorption and electroabsorption 80−40178
CdTe, shallow impurity spectral linewidths, 4-10K 77−63443

Stark effect continued
Cl III, Stark broadening of isolated lines by plasma 78−9116
Cl III lines, Stark broadening 77−27024
$ClONO_2$, laboratory microwave spectrum, atm. chem. appl. 77−6760
Cs, 16^2P states, reson., 3-photon ionisation, DC Stark effect 78−42026
Cs, forbidden M1 transitions, parity nonconserving effects 78−21844
Cs I, three-photon 16p reson. ionis. and DC Stark effect 80−14124
Cs polarisability constant, Stark interaction for excited states, laser spectroscopy 77−50404
Cs, three-photon ionisation, reson. and AC Stark effects 77−68020
Cs, vap., two-photon resonant third harmonic generation 77−738
Cs vapour, two-photon induced stimulated Raman scatt., optical Stark shifts 77−46756
CsF, Stark effect, deviations from rigid rotator model 79−18234
Cs_2ZnCl_4:Cu^{2+}, single cryst. and powdered single cryst., EPR, linear elec. field effect 80−11250
Cu_2O, electro-optic effects due to the Stark splitting of energy bands 79−82950
D, electron impact, coherent excitation in longit. elec. field, Balmer-α flux 78−22035
DNO, fundamental vibr. bands, laser Stark spectra 77−38692
Er^{3+} doped phosphors, IR excitation and absorpt. and emission spectra *(Russian)* 79−52021
Er_2SiO_5:Ho^{3+}, single cryst., luminesc. and stimulated emission 77−69895
Eu complex, with benzoylacetone, isotropic solns., Eu^{3+} luminesc. excitation spectra and polaris. spectra 79−87487
$Eu(NO_3)_3.6H_2O$, isotropic solns., Eu^{3+} luminesc. excitation spectra and polaris. spectra 79−87487
$EuTi_{1.5}W_{0.5}O_6$, Stark sublevels in mag. suscept. and luminesc. 77−51876
F II, Stark broadening of isolated lines by plasma 78−9116
F II lines, Stark broadening 77−27024
F spectral lines, neutral, in shock tube plasma, Stark widths and shifts 78−9117
FCN, IR laser Stark spectra, C-F stretching mode, dipole moments, rot. consts. 78−1022
FCN, IR-microwave double reson. and double photon transitions, HF Stark effect 77−14464
FNO, Stark spectroscopy of ν_1 band, rot. consts., dipole moment 79−13710
Fe I 5383 Å line width, Stark broadening 79−31463
Ga, ground-state hyperfine struct., differential Stark effect 80−42990
GaAs, field ionisation speed of shallow impurity levels, quantum-mechanical estimates 80−97412
GaAs, shallow impurity spectral linewidths, 4-10K 77−63443
GaP, Stark effect at H-like impurity centres, forbidden electron transitions *(Russian)* 80−16009
GaP:S, shallow donor states, Stark effect and inversion splitting, electroabsorption spectral obs. 80−50385
GaSe, lamellar crystal, exciton translational mass from magneto-Stark effect *(Russian)* 78−48153
$GdAlO_3$:Er^{3+}, $^4S_{3/2}$ to $^4I_{9/2}$ transition laser action, optical and luminescence spectra 80−16082
$GdBr_3$, frozen aq. soln., fluoresc. and absorpt. spectra 79−43022
$GdCl_3$, frozen aq. soln., fluoresc. and absorpt. spectra 79−43022
$Gd(ClO_4)_3$, frozen aq. soln., fluoresc. and absorpt. spectra 79−43022
$Gd_3Ga_5O_{12}$:Nd^{3+}, growth, stimulated emission, spectral props. 78−95593
$Gd_2(MoO_4)_3$:Nd^{3+}, optical spectrum, free ion wavefunctions, radiative transition probabilities 79−24339
Ge, internal Stark effect on impurity states, low-temp. magnet. absorption meas. 80−60636
GeH_2, centrifugal-distortion dipole moment, CO_2 laser spectroscopy 77−75331
GeH_4, Doppler-free optical double reson. spectroscopy using single-freq. laser and modulation sidebands 80−68274
GeH_4, Stark effect, rot. transitions in vibr. ground state, isotope shift 79−27029
H 1s reson., stabilisation method calcs., convergence 80−91492
H, 2p state alignment, influence of surface electric fields after beam foil excitation 78−29849
H, asymptotic expansion for level width 78−70783
H atom, electric field effect on stability of sublevels 79−89634
H atom, highly excited states in static elec. field 77−61707
H atom, Stark effect, dispersion relations 79−63956
H atom, Stark effect, second order correction for energy *(Rumanian)* 80−74147
H atom, Stark energy shifts, dispersion relations 79−93952
H atoms, Stark and Zeeman effects in parabolic coordinates 79−63957
H, Balmer-α line profiles and polarisations in strong mag. field 77−6729
H, complete separability of Stark problem 79−68209
H, eigenvalue resonances in Stark effect and perturbation theory 78−90118
H, electron impact, coherent excitation in longit. elec. field, Balmer-α flux 78−22035
H, excited states, Rayleigh-Schrodinger perturbation theory, Pade approximants calcs. 79−98024
H, existence and Borel summability of resonances 79−13668
H, fine structure levels, Stark component radiative widths 77−3302
H, four dimensional oscillator, rot. invariance of coordinate transform., appln. to Stark problem 80−99436
H, highly excited resonant states, Stark effect, nonperturbative regime 78−70786
H I (3^1P^0−2^1S) line, Stark broadening parameters, modified adiabatic theory, electron scatt. phase shifts 80−43879
H, ion motion on profile, model microfields 78−13469
H, ionised gas, H_α-, H_β-line Stark broadening, space charge field 77−39409
H, L_β reson. line Stark broadening in equilib. plasma 79−32823
H, line broadening for ionised gas in macroscopic field, direct meas. of current density *(French)* 78−9839
H, line profile, Stark broadening, quantum theory, including short-range interactions 78−9114
H lines, effect of reduced mass in Stark broadening *(Russian)* 77−79578
H lines in plasma, Stark broadening, review 78−42001
H, Lyman α-line wings, Stark effect 79−22648
H, Lyman-α line core, effect of emitter ion dynamics 77−47161
H, Lyman-α line wings, contribution of proton perturbers 78−67325
H, model electronic microfields 78−13468
H, n-α line Stark profiles, large θ-discharge 77−24084
H, perturbation theory and Pade approx. in electric field 80−91493

Stark effect continued
H plasma, spectral intensity near series limit, taking into account sub-barrier ionisation *(Russian)* 77−31436
H plasma, Stark broadening, model microfield methods calcs. 80−92274
H, quasibound states, Stark effect, variational 77−3251
H, resonant pole trajectories in complex scaling, stationarity 79−18126
H, resons. calc. from complex-rotation technique applied to variational principle 78−33549
H, Rydberg levels, selective excitation by three-photon absorpt., AC Stark effect obs. 80−5518
H, Rydberg Stark ionis. threshold scaling laws 77−6721
H, scattering theory methods appl. 80−63586
H spark, laser-triggered, electron densities meas. 80−106975
H, spectra, quasistationary states due to CO_2 laser radiation 77−67997
H, spectral broadening in dense plasma, low-freq. elec. field, Lyman-α line 79−98026
H, Stark and photoabsorption spectrum, density of oscillator strengths, atom c.f. semiconductor spectra 80−83318
H, Stark broadened line shape, unified Franck-Condon-JWKB method 77−10635
H, Stark broadening by ion impact on moving emitter, Doppler H shift, theory 80−47940
H, Stark broadening of spectra lines, classical and quantum treatment *(Russian)* 77−61708
H, Stark effect, complex coords., translation and dilatation transforms 79−18141
H, Stark effect, confinement of resons. 79−49982
H, Stark effect, dispersion relation, asymptotic formulae, ionis. rate, perturbation theory calc. 80−14106
H, Stark effect, high orders of perturbation theory 79−98025
H, Stark effect, high orders of perturbation theory for excited states 80−87079
H, Stark effect, iteration procedure for any field strength 80−69104
H, Stark effect, perturbation theory 79−22652
H, Stark effect, theory, teaching appls. 79−5933
H, Stark effect resons., strongly asymptotic approximants 80−52931
H, Stark spectrum and field ionisation, density of continuum states, normalised wavefunctions 80−83317
H, Stark-Zeeman effect, dilatation transformation 79−3398
H, Stark-induced anticrossings, Lamb shift meas. 78−33467
H, Stark-induced anticrossings, $^2P_{3/2}$-$^2D_{3/2}$ Lamb shift meas. 78−33468
H, Stark-induced quantum beats in H_β 80−9757
H, sublevel excitation cross sections following mol. dissoc., Stark effect determ. 77−14593
H^-, $^1P_0$-reson., DC Stark effect calcs. 78−42000
H^-, DC Stark broadening of $^1P^0$ shape reson. 80−63585
H^- resonances in electric field 80−63607
H^-, shape reson., Stark effect, complex coords., translation and dilatation transforms 79−18141
H:T solid, collision induced IR lines caused by T_2 radioactivity 80−84756
H-like atom, Stark effect on fine struct. 79−26929
H-like atoms, Stark broadening, ion dynamics correction to unified classical path theory 79−76382
H-like atoms, Stark effect and perturbation approxs. 80−52932
H-like atoms, Stark shift, classical adiabatic theory of Stark ionis. threshold 78−82687
H-like ion, relativistic acceleration, quasi-Stark effect *(German)* 78−58621
H-like ions, fluoresc. polarisation of Stark quenched spin-polarised beam 78−66501
H-like ions, radiative level widths in low electric fields 78−37589
H-like ions, Stark ionisation threshold electric field and energy calc. 78−25470
H-like ions in laser-produced plasma, Balmer fine struct. (broadening) 80−48860
H_2, CARS, optical Stark effect on vibr., and rot. transitions 80−99512
H_2, Stark effect resonances, Bender-Wu formula 79−36695
$H_{\alpha,\beta}$ lines, dense plasma Stark broadened central struct., comment 77−23464
$H_{\alpha,\beta}$ lines, dense plasma Stark broadened central struct., reply 77−23465
$H_{\alpha,\beta}$ lines, Stark broadened, central struct., in dense plasma 77−6722
H_α and H_β spectral profiles from neutral beams and plasmas in high mag. fields 80−83999
H_α and H_β Stark profiles in LF turbulent plasma 77−7593
H_α Balmer line emission fine struct., Stark effect *(German)* 78−82673
H_α line Stark profiles in low-density arc, exptl. discrepancies 78−67470
H_β, dynamic Stark effect for elec. field strength meas. in waveguide 80−69103
H_β line Stark broadened spectrum obs. in pulsed relativistic magnetron intense elec. field 79−89635
H_β, Stark broadening, wings calc. 79−31464
HBr(DBr), isotopic forms, Stark hyperfine struct., polarisability anisotropy 77−83645
HCN-HF, elect. dipole moment, Stark effect of linear mols. 78−70818
HCN...HF, hydrogen bonded heterodimer, spectroscopic consts. from microwave spectrum 80−43037
HCO, IR spectra of ν_2 fundamental, laser elec. reson. 78−5226
$H_\alpha(D_\alpha)$ Stark broadening in Ar arc plasma 79−36582
HF, laser field interaction, Floquet theory, dynamic Stark shift, broadening 80−63716
$HNCS_2$ microwave transitions 78−9143
HNO $\tilde{A}\,^1A''$ excited state dipole moment, optical-optical double reson. Stark spectrosc. obs. 80−106337
HNO, fundamental vibr. bands, laser Stark spectra 77−38692
HNO_2, trans and cis, ν_2 fundamental vibrational bands, intracavity CO laser Stark spectroscopy 80−47992
HO_2 free radical, dipole moments and Stark effects from microwave spectra 80−63623
H_2O, laser Stark and IR-RF double reson. at 6 μm 79−45760
$H_2{}^{17}O$, $H_2{}^{18}O$, Stark spectra with CO laser, Lamb dip spectra of ν_2 band 78−62840
$(H_2O)_2$, elec. dipole moments from Stark effect meas. 77−54555
H_2S dipole moments, submillimetric Stark cell meas. 77−38694
Hα and Hβ, Stark profiles, ion-motion effect 80−63592
Hα(Dα) plasma red shift meas. in Ar arc, ion dynamic depend. 80−10364
He, arc plasma Stark profile, heavy-particle temp. 79−46484
He, dynamic Stark effect for elec. field strength meas. in waveguide 80−69103
He, emission line profile, hollow cathode source 77−23469
He, high mag. field spectroscopy 79−72445
He, high-L states, laser driven forbidden transitions, line shapes 79−22638
He I, in shock tube plasma, electron density from Stark widths 77−80374
He I, spectral line shift and Stark broadening in plasma 77−18843
He I, Stark broadening of 3965 Å line in plasma jet 79−98023
He I 447.1 and 492.2 nm lines, ion motion effects on Stark profiles 80−69105
He I line profiles, ion motion effect in low electron density plasma 80−43877
He I overlapping lines, model microfield method Stark profiles, ion dynamics effect 79−82049
He I plasma lines, Stark broadening, quantum mechanical calcs. 80−43880
He II, 4686 Å line, Stark broadening, meas. and calcs. 80−91504
He II, 4686 Å Stark broadened profile 77−23460
He II, Doppler and Stark broadened lines, electron density and ion temp. meas. 78−67407
He II, plasma polaris. red shift, Stark profile, temp. depend. 77−18842
He II, Stark broadening of VUV transitions at 304, 1215, 1640 Å 78−66506
He II 4686 Å line, Stark profile meas. in high density plasma 80−96390
He II plasma reson. line Stark broadening and plasma polarisation shift 77−1020
He metastable state, two- and three-photon ionisation 80−91518
He plasma, electron density, determ. by emission coeff. and Stark broadening *(German)* 77−58903
He plasma, Stark effect in 3-D stochastic elec. fields and static mag. field 78−5855
He plasma, Stark shift and line broadening in 3-D stochastic laser field 78−50502
He plasma He I 4471 Å line profile obs. at high electron density 78−67472
He, shift of 4^3S-2^3P line by CW CO_2 laser beam 77−30829
He, singlet-triplet anticrossing, elec. field induced 77−14404
He, Stark broadened 4121 Å and 4437 Å lines in plasma, electron impact effects 77−27025
He, Stark broadening in plasma, close electron collisions effect 77−23459
He, Stark broadening satellite transitions, in turbulent plasma 77−61759
He, Stark effect, high-freq., mol. lines effects on meas. 80−9544
He, Stark effect on optically excited plasma atoms in static mag. field 78−66505
He, subDoppler lineshape obs., of IR mag. reson. Rydberg transitions, using motional Stark effect 78−947
He, transition probabilities in constant electric field, general perturbation theory 78−13466
He triplet principal series, Stark effect at high field strengths *(German)* 77−83537
He^+, Stark broadening, line shape calcs. 77−10636
He-Ne plasma He I 4471 Å line profile obs. at high electron density 78−67472
^{3}He liquid, electron spectra of localised electrons above surface *(Russian)* 80−29241
^{4}He II, widths of Stark components calc., beam-foil data comparison *(French)* 80−9545
^{4}He, laser mag. reson., 7^1S-9^1P energy separation, motional Stark effect, Zeeman tuning parameters 79−6911
$^4He^+$ II, H-like, fine struct. Stark effect *(French)* 78−943
Hg, 546.1 nm line transition probability and Stark constant determ. 78−67471
Hnα radio recombination lines, profile in static ion field 77−78629
Hnβ radio lines profiles in static ion field 79−62740
I_2, 2-step reson. scattering, subnatural linewidths in vapour 79−76419
I_2, polarisability anisotropy, laser assisted mol. beam spectroscopy 80−78646
IBr, elec. dipole moment, rot. transition Stark shift obs. 77−75207
IF, elec. dipole moment, Stark effect 79−18233
InP:Bi, uniaxial stress effect on free and Bi-bound excitons 79−56854
K, resonance spectral lines, Stark broadening and shift 77−75097
K, stimulated electronic Raman light scatt. by mag. sublevels 78−50492
$K_5Bi_{1-x}Nd_x(MoO_4)_4$ solid soln., growth, spectroscopic and laser props. 78−2901
KBr, Stark effect in F-centre emission 77−63434
$KClO_3$, ^{35}Cl NQR, Stark splitting *(French)* 79−47352
KI, Stark effect in F-centre emission 77−63434
KLu_3F_{10}:Eu^{3+}, crystal field and spin-orbit parameters 78−30892
$KMgF_3$:Cr^{3+}, trigonal centres, EPR lines, pseudo-Stark splitting 78−68367
$KMgF_3$:Yb^{3+}, cryst. field parameters, Stark struct. of optical, EPR spectra 77−51950
KY_3F_{10}:Eu^{3+}, cryst. field parameters and intensity parameters, J-mixing effects 80−59932
KY_3F_{10}:Eu^{3+}, crystal field and spin-orbit parameters 78−30892
$KZnF_3$:Yb^{3+}, cryst. field parameters, Stark struct. of optical, EPR spectra 77−51950
Kr I, Stark broadening in visible spectra 78−37590
Kr(-He) arc, wall-stabilised, atm. press. 79−46503
$La_2Be_2O_5$:Nd^{3+} (Pr^{3+}), cryst. growth, spectral and laser properties in $^4F_{3/2}\rightarrow{}^4I_{11/2}$ and $^4F_{3/2}\rightarrow{}^4I_{13/2}$ transitions 80−80853
$LaCl_2$:U^{3+} ($5f^3$), polarised absorption spectra and energy levels 80−16063
$LaCl_3(Br_3)$:Pr^{3+}, IR absorption, energy values for Stark manifolds 80−34955
LaF_3:Ho^{3+}, laser excited fluorescence, absorption spectra Stark components 78−60514
LaF_3:Nd^{3+}, cryst., $4f^3$ config., ground level energy state var. rel. to press. *(Russian)* 77−16358
LaF_3:Pr^{3+}, pseudo-Stark effect meas. using population hole burning and optical free-induction decay 79−24292
$LaNbO_4$:Tb^{3+} (Ho^{3+}), EPR and spin-lattice relax., Stark levels *(Russian)* 77−85563
Li, motional Stark effect in high mag. field 79−63958
Li, resonance spectral lines, Stark broadening and shift 77−75097
LiF, Stark effect, M-centre absorpt. bands 78−84614
$LiYF_4$:Dy^{3+}, spectrum, Stark struct. 77−85756
$LiYFd_4$:Er^{3+}, optical spectra and multifreq. stimulated emission 79−56818
Lu I, 5d6s(^{3}D)6p$^2D_{3/2}$ state, Stark effect, level crossing obs. 77−75098

Stark effect continued
$LuAlO_3:Er^{3+}$, $^4S_{3/2}$ to $^4I_{9/2}$ transition laser action, optical and luminescence spectra 80−16082
Mg^+, electron and ion Stark effects in plasma, widths and shifts 77−46526
$Mo(CO)_6$, polarised absorption, field effects in condensed media 78−997
N I plasma jet, spectroscopic diagnostics, Stark broadening and shift, study 80−38727
N, plasma, Stark broadening, photoelec. obs. 77−23463
N, Stark broadened VUV lines in wall-stabilised arc, 1100-1800 Å 78−90107
N^+, stark broadening of high orbital ang. momentum states 79−22650
N_2, CARS, optical Stark effect on vibr., and rot. transitions 80−99512
NH_3 CW far IR laser lines, CO_2 laser pumping and Stark tuning 80−69382
NH_3 CW far IR laser lines, CO_2 laser pumping and Stark tuning 80−106508
NH_3, Doppler free coherent two-photon transients, collision induced relax. time, meas., Stark switching 78−90249
NH_3, dynamic Stark effect at microwave freq. in mol. beam maser 77−83648
NH_3, dynamic Stark shift, microwave obs. 79−72352
NH_3, excited vibr. states, transition dipole moments, laser Stark spectrosc. 79−68261
NH_3, far IR emissions from forbidden transitions, using Stark effect with CO_2 laser pumping 79−86168
NH_3 forbidden vibr.-rot. transitions, ν_2 band, IR-microwave two-photon spectra 77−3428
NH_3 inverse level doubling mol., space and combined parity nonconservation *(Russian)* 80−52879
NH_3 Stark cell for wideband modulation of CO_2 laser R(18) line 77−23704
NH_3, Stark effect modulation at 2.2 μm *(French)* 78−50912
NH_3, Stark shift, microwave Σ-transitions in presence of strong elec. fields 78−90213
NH_3, Stark tuned 26 GHz parametric upconversion at 10.8 μm 77−88845
NH_3, stimulated hyper-Raman scatt. via 3-photon process to obtain IR and far IR radiation 80−58633
NH_3, two-photon transition, collisional dephasing time meas. by Stark switching 77−75248
$^{14}NH_3$, $^{15}NH_3$ and $^{14}NH_2D$, IR laser Stark spectroscopy 80−47978
$^{14}NH_3$, CW far IR lasing using Stark tuning 79−81407
$^{14}NH_3$, Doppler free spectroscopy, 16 micron generation applications 79−94049
$^{15}NH_3$, IR-IR double resonance, ν_2 vibr. state, electric dipole moment 77−83626
$^{15}NH_3$, modulated coherent Raman beats 80−23464
NHD radical, dipole moment determ., optical Stark spectroscopy 80−23455
NH_2D, dipole moments effects of RF elec. field modulation on IR stark spectroscopy 80−52989
NH_2D, mixing of CO_2 laser radiation with 4 GHz microwaves, Stark-induced three-wave mixing, expt. 77−10974
NH_2D, mixing of CO_2 laser radiation with 4 GHz microwaves, Stark-induced three-wave mixing, calc. 77−14774
NH_2D Stark active mol., cavity dumping for CO_2 laser pulse generation 77−88800
NH_2D Stark cell noise reduction for CO_2 laser beam 78−59059
NO_2, excited state, DC Stark effect from ODMR signal 79−36670
NO_2, Stark spectroscopy using CW dye laser 77−38026
NO_x, Stark effect investig., using two-way EPR cavity system 80−90872
$^{14}NH_2D$, i.r. absorption coeff., press. broadening 77−464
$^{14}NH_3$, ground state, microwave inversion lines 80−87098
$^{14}NH_3$, laser emission at 16 μm by two-quantum excitation of $2\nu_2(7,5)$ state 79−86165
$^{14}NH_3$, ν_2-band Doppler-free two-photon resons. in Stark field 77−23527
$^{15}NH_3$, Doppler-free optical double reson. spectroscopy using single-freq. laser and modulation sidebands 80−68274
Na, atomic beam, AC Stark splitting of two-photon spectra 77−46551
Na, atomic states highly excited by laser radiation 79−13669
Na gas, polarisation spectroscopy and forward scatt. 80−52336
Na, laser temporal coherence effects in two-photon resonant three-photon ionisation 80−32686
Na, multiphoton ionis., AC Stark effect 77−57948
Na, reson. multiphoton ionisation, broadband laser AC Stark splitting 78−70808
Na, resonance spectral lines, Stark broadening and shift 77−75097
Na, Rydberg levels mm resonances detected by field ionis., quantum defects, Stark shifts 77−42262
Na, Rydberg states, IR Stark spectra, term energy, fine struct. 77−57910
Na, Stark effect study, S and D excited states struct., two-photon spectra 77−54547
Na, Stark shifts, absolute and differential, coherent optical transient meas. 80−37773
Na, three-photon ionisation, laser bandwidth and intensity effects 80−52956
Na, two-photon optical free induction decay, Stark switching obs. 77−68024
Na, two-photon optical free-induction decay 78−90138
Na vapour, transient optical nutations in D_2 line 78−66507
$Na^+ + HCN$, rotational excitation, Stark shifted level transitions, energy transfer calcs. 79−98059
Na_2 optically-pumped three-level dimer lasers, amplification profiles and dynamic Stark effect 79−41367
NaBr, Stark effect of F-centre obs. 77−1707
NaF, F_3^+ centre zero-phonon line, photochem. and population hole burning 79−42997
NaF, Stark effect, M-centre absorpt. bands 78−84614
$NaNO_2$, cryst., Stark shift of visible absorpt. of NO_2^- 78−19499
$NaNO_3$, pure cryst., NO_3^- singlet-triplet absorption, Stark effect obs. 79−8153
Nd:silicate glass, resonance laser excitation, inhomogeneously broadended emission spectra 80−66295
Nd^{3+}:glass, inhomogeneously broadened spectra, struct., selective laser excitation obs. *(Russian)* 78−35181
Nd^{3+}:glass luminesc. band profile deform. under free-oscillation conditions 80−71487
$Nd(BO_2)_3$, single cryst., IR absorpt. spectra 80−34903
$NdCl_3$, aqueous frozen soln., phase transformations, optical absorpt. spectra, Nd^{3+} Stark splitting 79−1777
$Nd(NO_3)_3.6H_2O$, optical absorpt. spectra, 4.2K, single crystal, Stark levels 77−81119
Nd_2O_3, A-type, optical absorpt. spectrum and paramag. susceptibility 79−56811
Ne, Autler-Townes effect 78−41998
Ne, cascade level scheme, optical Autler-Townes splitting 77−3301
Ne II line Stark broadening in pulsed arc, obs. 78−67469
Ne II lines from pulsed arc plasma, Stark broadening 78−66504
Ne X Lyman-α line Stark broadening, hot dense laser-produced plasma 77−11402
O II, O III, Stark, broadening estimates 77−18841
O_3, mol. beam electric resonance, electric and mag. props. determ. 77−27055
O_3, mol. beam Stark, Zeeman effects, polarisability, moments, mag. susceptibility anisotropy 77−79649
OCS, laser Stark spectra, 9.5 micron, band origins, dipole moments 77−18969
OCS, M-resolved rot. Stark levels, four-level microwave-microwave double reson., collision induced 77−10696
OPF_3, mol. beam elec. reson. spectrum, mol. props. 79−94011
P, Stark widths and shifts, visible and UV 77−57927
PF_3, microwave l-type reson. transitions in $v_4=1$ state 77−57988
PH_3, dipole moment in ground and excited states, submm. spectrum obs. 80−28056
PH_3, Doppler-free optical double reson. spectroscopy using single-freq. laser and modulation sidebands 80−68274
$POCl_3$-$SnCl_4(ZrCl_4)(TiCl_4)$, splitting of Sm^{3+} near IR absorpt. bands 80−2750
POF_3, level anticrossing effects, vibr., laser Stark spectra obs. 80−32771
$PO(SCN)_3:Nd^{3+}$ solns., spectroluminesc. props. 77−16362
Pb I and II, transition probabilities, Stark broadening parameters 80−23367
$Pr(BO_2)_3$, single cryst., IR absorpt. spectra 80−34903
Rb, $6^2P_{3/2}$ state, β_J Stark const., level-crossing method 77−88424
Rb, high lying Rydberg states, atomic beam laser spectra 79−94101
Rb, photoionis. cross section, elec. field depend. 80−37796
Rb polarisability constant, Stark interaction for excited states, laser spectroscopy 77−50404
Rb, resonance lines 7800.23 and 7947.6 Å, Stark broadening obs. 78−66508
Rb, resonance spectral lines, Stark broadening and shift 77−75097
Rb, Rydberg levels, Stark patterns, expt. and central pot. calc., positions and intensities 79−93953
Rb, Stark shift of $6^2P_{1/2}$ to $5^2S_{1/2}$ line, mag. scanning meas. 80−27977
Rb vapour, dynamic Stark tuned far IR laser 78−63126
RbBr, Stark effect in F-centre emission 77−63434
RbBr(I), parallel and perpendicular Stark effect of F-centre 77−1703
RbI, Stark effect in F-centre emission 77−63434
^{87}Rb, Stark effect on $5^2P_{3/2}$ state 79−3399
SO_2, mol. beam electric reson. in RF field, dipole moments of vibr. states 79−64116
Si III, IV, Stark line broadening in pulsed arc, plasma diagnostics 78−944
Si^+ lines, from plasma, Stark broadening 79−4189
Si^{++}, Stark broadening, shock tube meas. 78−17614
SiH_4, Doppler-free optical double reson. spectroscopy using single-freq. laser and modulation sidebands 80−68274
SiH_4, second-order stark effects, RF-IR double reson. 78−58739
SiH_4, Stark effect, rot. transitions in vibr. ground state, isotope shift 79−27029
SiH_3NCS, microwave spectrum, struct., dipole moment, ^{14}N quadrupole coupling const. 77−46560
$Sm(BO_2)_3$, single cryst., IR absorpt. spectra 80−34903
$SmTi_{1.5}W_{0.5}O_6$, Stark sublevels in mag. suscept. and luminesc. 77−51876
Sn II, cool plasma, isolated lines, Stark broadening, semi-empirical impact approx. calcs. 80−59186
Sn, Sn^{++}, transition probabilities and Stark-broadening parameters, shock tube meas. 79−93956
Sr^+, electron and ion Stark effects in plasma, widths and shifts 77−46526
$SrF_2:Tb^{3+}$, mag., thermal and hyperfine props. 80−29368
$SrO:Ni^{2+}$, linear Stark effect for zero-phonon optical absorpt. line 80−80830
Tb^{3+} in rare earth ion cryst. field in YF_3 struct., spectra 78−19563
$TbAlO_3:Nd^{3+}$, absorpt. and luminesc. spectra 79−91470
Tl, $6^2P_{1/2}$-$7^2P_{1/2}$ transition, parity nonconservation obs. 79−31446
Tl atomic laser pumped by TlI photodissociation, complex line profiles from dynamic Stark effect 79−18411
Tl, ground-state hyperfine struct. tensor polarisability 77−6708
Xe, AC Stark effect, on saturated absorption line shape in partially Doppler-compensated system 79−45669
Xe, autoionising reson., Stark effect 80−58198
Xe, s-p transitions, Stark consts. and oscill. strengths, shock tube meas. 80−18822
$YA-O_3:Er^{3+}$, pulsed laser action, $^4S_{3/2}$ to $^4I_{9/2}$ transition laser action, optical and luminescence spectra 80−16082
$YAG:Ho^{3+}$, spectroscopy, stimulated emission 80−93374
$YAG:Nd^{3+}$, cryst. field parameters calc., exchange charge model 78−47747
$YAG:Nd^{3+}$ crystal, zero-phonon linewidths, in $^4I_{9/2} \rightleftarrows {}^4F_{3/2}$ luminesc. band calc. 79−28834
$YAlO_3:Er^{3+}$, free-ion-model cryst.-field calc. 77−43545
$YAlO_3:Nd^{3+}$ biaxial laser cryst., anisotropy of spectral characts. 79−50303
$YAlO_3:Yb^{3+}$, absorption and luminescence spectra, electron-phonon resonances, Stark splitting *(Russian)* 80−20674
$Y_3Ga_5O_{12}:Nd^{3+}$, cryst. field parameters calc., exchange charge model 78−47747
$Y_2O_3:Eu^{3+}$, absorpt. spectra, fluoresc., electron beam excitation 78−92093
$Y_2O_3:Eu^{3+}$, cubic, laser-induced polarised fluoresc., Stark levels and cryst. field parameters 79−95838
$Y_3Sc_2Al_3O_{12}:Nd^{3+}$, cryst. field parameters calc., exchange charge model 78−47747
$Y_2SiO_5:Ho^{3+}$, single cryst luminesc. and stimulated emission 77−69895
$YVO_4:Eu^{3+}$, absorpt. spectra, fluoresc., electron beam excitation 78−92093

Stark effect continued
Yb, $4f^{13}6s6p\ ^1P_1$ and $^1P_1$ levels, Stark effect, tensor polarisabilities 80−87080
Yb^{3+} doped phosphors, IR excitation and absorpt. and emission spectra *(Russian)* 79−52021
YbAG, cryst. field parameters calc., exchange charge model 78−47747
Zn, Stark interaction in $nspz\ ^3P_1$ levels, optical double resonance obs. 79−63941

stars
see also stellar .....
see also dwarf stars; giant stars; magnetic stars; multiple stars; neutron stars; novae; Sun; variable stars
0- and B-type, UV obs. of mass loss effects 77−17551
0B-type stars, O VI obs. in stellar winds 80−8630
1-1.5$M_\odot$ stars, semiconvection and vibr. stability 77−22204
30 M⊙ star, stability towards g^+ modes of high spherical harmonic values 77−9740
209 BAC, WN8 star, nonisotropic mass loss rel. to circumstellar H II region (M1-67) internal motions 79−92841
134045+083448, no occultation by Pluto on 1980 April 6, ephemeris 80−62070
134045+083448, probable occultation by Charon (1978 P 1), (1980 April 6) 80−62071
2A 0526−328 optical counterpart, identification and spectrum 80−22118
A to G-type stars, proper motions dispersion represented by vel. ellipsoids 79−8904
A- and B-type, B abundance from B II reson. line obs. 79−21276
A- and F-type, heavy element content influence on colour-temp. relation *(Russian)* 78−93234
A- and F-type main sequence stars, scanner obs. 78−36563
A- and F-type stars, absolute energy distribs. 77−17554
A-type, energy distrib. in main-sequence 78−93220
A-type, near South Galactic Pole, UBV photometry of 51 stars 78−4216
A-type, obs. and calc. spectra, 3600-4200 Å region 78−12217
A-type, spectral variations, abundance peculiarities 79−62821
A-type stars, effect of $C+H^+ \rightleftharpoons C^+ + H$ charge transfer on C I 1101 Å absorpt. edge 80−90423
A-type stars, MI spectral classification based on uvby and β photometry 77−29822
A-type stars, non-LTE anal. of O I lines 77−41378
A-type stars, normal and metallic-line, models pulsational stability 78−16414
A-type stars, predicted and observed spectral energy distribs. 78−4208
A-type stars, quest for differential rot. 77−45409
A-type stars, rot., mixing and variability 77−87397
A-type stars in Selected Areas, photoelectric uvbyβ photometry 78−16412
aberration, classical rel. to relativistic theory 80−67517
absolute proper motion meas. in M31 area *(Russian)* 77−71106
absolute RA determ. precision rel. to geographic latitude *(Russian)* 78−28647
absolute right ascensions catalogue, deduction for whole sky from high latit. obs. *(Russian)* 79−16801
abundance effects in classification, IAU Symposium 72 (Lausanne, Switzerland 8-11 July 1975) 77−29802
accreting gas, thermodynamics and hydrodynamics 80−67696
accreting young stars, ang. dimensions 79−44482
accretion of interstellar gas, stability of Bondi accretion 79−44359
accretion onto compact gravitating object, travelling sound wave behaviour WKB anal. 80−67551
activity of solar type, observational aspects 77−56918
AF-type stars in solar vicinity, photometric survey rel. to low mass interstellar clouds catalogue 80−36512
AGK3+19°599, occultation by 65 Cybele, 1979 October 17, obs. 80−31237
AGK3 +0°1022, occultation by Juno, obs. 80−26773
AGK3 stars, proper motion system in polar region *(Russian)* 80−12647
AGK3 stars, proper motions rel. to determ. of precession and galactic rot. 77−45402
AGK3R declinations improvement using Toepfer meridian circle obs. *(Russian)* 78−28645
AGK+19°0599, occultation by 65 Cybele, 1979 October 18, obs. using photoelectric photometer *(Chinese)* 80−105172
Allegheny parallax program, stars in region of 91 and 92 Tauri, Lalande 20111, 18 Bootis and HD 187399 77−74037
Am type stars in Hyades, Hα and O I 7774 Å photometric obs. 77−22286
o Andromedae, Be star, rapid spectroscopic variations 77−56970
α Andromedae, Mn star, UV spectrophotometry from TD 1-A/S 59 77−29848
σ Andromedae, rapid spectral line variability disproved 80−8625
o Andromedae, shell star, lack of linear polarisation variability 80−62157
angular diameter meas. IR interferometry 77−53576
Ap, Am and A stars, radii from observed energy curves 77−87403
Ap, mag. fields struct., and precession in oblique rotator model 77−2432
Ap and Am stars, Y, Ba and rare earth elements abundances 77−33505
Ap stars, analytical expression for local line profile determ. from observed ones *(Russian)* 77−17588
Ap stars, Balmer lines *(Russian)* 77−17587
Ap stars, HD 27309, 119213, 170000, and 192913, ten colour photometry *(German)* 77−17584
AP stars, kinematic mechanism for oblique rotator model 77−45407
Ap stars, long-term light variations *(German)* 77−17585
Ap stars, magnetic, peculiar anomalies of chemical comp. *(Russian)* 77−22239
AP stars, models with toroidal mag. fields and circulation 77−45406
Ap stars, orientation of mag. and rot. axes, decentred mag. dipole theory 78−4241
Ap stars, photoelectric parameter of peculiarity 77−2433
Ap stars, U/Th ratio, r-process nucleosynthesis 77−33508
Ap stars in open clusters, rot. vels. and mag. braking 77−33500
Ap stars in spectroscopic double systems, BV photometry *(German)* 77−17583
AP type models for rotating mag. stars 77−45405
Ap-type stars, mag. fields rel. to chemical anomalies *(Russian)* 77−17591
Ap-type stars, magnetic fields in atmospheres *(Russian)* 77−17594
Ap-type stars in spectroscopic binaries, orbital characts. *(German)* 77−17590
π Aquarii, Be star, spectrum vars. rel. to orbital changes of gaseous ring 77−26013
π Aquarii, gaseous rings apsidal motion and orbital elements slow drift 78−36572
π Aquarii and other Be stars, light variations 77−45420
Aquila X-1 optical counterpart, spectrum 78−77626
α Aquilae, Copernicus UV spectral obs. 77−33480
θ Aquilae (B9.5 III), abundance anal. from model atmosphere 80−90415
β Arietis, Am star, spectroscopic obs. and curve of growth anal. 77−22237
κ Arietis, double-lined Am star, spectroscopic obs. and curve of growth anal. 77−22237
aspherical gravitational collapse, matter associated perturbations, linear Einstein field and conservation eqns. 79−5843
astrometric analyses of bright nearby stars, from Sproul 61 cm refractor plates 80−61991
astrometry, accuracy of average star positions obtained from overlapping plates 78−20622
astrometry, accuracy of star positions obtained by block adjustment 78−20623
astrometry, first astrolabe catalogue of San Juan 77−13253
astrometry, stellar absolute declinations system construction for entire sky using high-latit. obs 80−67520
astrometry and photometry of stars in vicinity of PSR 1913+16 binary pulsar 78−93219
Astronomical Engelhardt Observatory, latitude obs. *(Russian)* 78−4080
astrophysics, symbiosis with solar and galactic astrophysics 77−9736
θ Aurigae, short period Ap star, discovery of mag. field 77−33511
Australian Astronomical Society, conf. Melbourne, Australia (May-June '77) 78−69655
azimuth determ. method *(Russian)* 77−60579
B5 V-P5 V type stars in Geneva Observatory catalogue, radii, temp. and brightness determ. 80−77396
B5-A0 stars, local density and kinematics 77−56931
B6 to A0 spectral types, UV line blocking factors 77−22216
B9 II to G0V stable stars, quantitative spectral classification *(Russian)* 79−44480
B, A and F stars, spectrophotometry, effective temps. 78−57546
B, A and F stars in selected areas, intrinsic uvby β indices, distances and colour excesses 78−89171
B-, A- and F-type, photoelec. K-line indices 79−16953
B- and A-type stars in Lacerta OB1 association, spectral classification and distances 77−37626
B-type, absolute UV spectrophotometry, continua and absorpt. features 77−22217
B-type, empirical calibration of uvby Hβ photometric system 78−32454
B-type, Hβ indices for model atms. 80−31292
B-type, optical counterparts of X-ray sources, luminosity class from O I 7773 Å triplet absorpt. 79−71031
B-type, seven new stars with Hα emission lines *(French)* 77−49391
B-type, uvby indices, empirical effective temps. and bolometric corrections 77−45429
B-type and Be-type stars, search for binaries 78−57551
B-type at intermediate galactic latitude, space distrib. 77−91535
late B-type main-sequence stars, C I as continuous opacity source 77−87393
B-type stars, at galactic centre, as extended thermal radio emission ionising agent 79−97059
B-type stars, He weak, UV flux distrib. 78−96477
B-type stars, luminosity and effective temp. determ. 80−17582
B-type stars, pole-on, rapidly rot., spectral inconsistencies due to gravity darkening 80−17581
B-type stars, radial vels. determined at Radcliffe Observatory 78−12225
B-type stars, wavelengths of neutral He lines 77−25999
B-type stars, XUV obs. and constraints 78−93232
B-type stars at high southern galactic latitudes, four colour and Hβ obs. 80−82357
B-type stars clouds, distrib. of nearly interstellar mols. *(Russian)* 80−105321
B-type stars embedded in R-associations, free-free emission obs. 80−26851
B-type stars in Norma dark cloud region, photometry rel. to cloud struct. 78−16494
late B-type stars small v sin i values, Ap star determ., visible spectra 80−77409
B-type UV obs. of six rapidly rotating stars 77−56938
Balloon-borne UV Stellar Spectrograph, first obs. results 79−70955
Barnard's star, analysis of photometric data 78−81657
Barnard's star, evidence for planetary companions 78−81656
baryon stars, magnetospheres model *(Russian)* 77−91555
basic properties, rel. to anthropic principle of cosmology and physical world struct. 79−48973
Basle catalogue of 1906 blue objects at high galactic latitudes 78−32360
BD+10°2179, BD−9°4395, extreme He stars, UV spectra 79−16976
BD+10°2179, C rich H deficient star, UBV photometric obs. 80−90437
BD+40°4124, star form. in assoc. mol. clouds 78−32542
BD+66°1066, nucleus of planetary NGC 6543, lightcurve oscills. 79−75223
BD−14°3996, appulse on 1977, March 10 of Miranda (Uranus V), predictions 77−2369
BD−15° 3969, occultation by Uranus rings (1977 December 23), obs. 78−89118
BD +1°4381, H deficient A-type star, effective temp. 79−40195
BD −9°4395, H deficient star, spectral photometry and quantitative anal. 77−56946
Be and Bn stars, 206-287 nm UV spectra 80−51776
Be and shell stars, Balmer line polarisation meas. 77−56995
Be and shell stars, conf. Bass River, Mass., USA, 1975 Sept. 77−56964
Be and shell stars, mass loss from Copernicus UV data 77−56986
Be and shell stars, UV spectra, circumstellar absorpt. lines 79−62832
Be and shell stars, UV spectrophotometry with TD-1 satellite 80−90438
Be shell stars, Bβ high-resolution polarisation struct. meas. by digicon spectropolarimeter 79−44485
Be shell stars, intrinsic and interstellar polarization components separation 79−30079
Be shell stars, intrinsic polarization interpretation 79−30080
Be star, optical counterpart of GX 304−1 X-ray source 78−93471
Be stars, as optical counterparts of transient X-ray sources 78−12425

stars continued
Be stars, correl. between presence of Paschen emission lines and IR excess 77−22234
Be stars, disc struct. in extended atms. 78−93206
Be stars, discoveries in open clusters NGC 3766 and (IC 2581) 80−90445
Be stars, electron scatt. effects on Balmer emission lines 80−17589
Be stars, emission features rel. to luminosity class and spectral type 77−56969
Be stars, emission line profiles from envelopes, elliptical gaseous ring model 80−4373
Be stars, emission line profiles from envelopes, theoretical profiles 80−4374
Be stars, emission shell diameter meas. possibility by lunar occultation method 80−56839
Be stars, gaseous rings apsidal motion and orbital elements slow drift 78−36572
Be stars, Hα survey 77−56967
Be stars, identification as X-ray sources 77−87573
Be stars, intrinsic circumstellar polarisation and apparent rot. speed interpretation 78−96484
Be stars, mag. fields determ. via linear polarisation spectrum *(Russian)* 80−90344
Be stars, orbital changes of gaseous ring 77−26013
Be stars, photometric behaviour, UV excess, emission indices, galactic distrib. 80−36637
Be stars, polarimetry at 1.25 and 2.2 microns 79−44484
Be stars, rapid fluctuations detect. in spectra 77−56954
Be stars, rapid Hα variations 77−56971
Be stars, review of early history of studies 77−56965
Be stars, spectra and photometry 77−56966
Be stars, spectroscopic obs. 77−56957
Be stars, spectroscopic obs. in near IR 77−56972
Be stars, surface gravities 77−56974
Be stars, UV radiation intensity obs. *(French)* 78−81635
Be stars and shell stars, possible interacting binaries 77−57041
Be stars envelopes, observational study 77−13355
Be stars Hα photometry through narrow-band interference filter 77−56838
Be stars in galactic clusters, Hα study 77−56968
Be-star circumstellar envelopes, models 77−60777
Be-star duplicity and mass exchange 77−60780
Be-stars, binary hypothesis 77−56998
Be-stars, classification of faint objects 77−56993
Be-stars, energy distrib. in 0.32 to 1.06 μ range 77−56980
Be-stars, Fe II emission line spectra 77−56978
Be-stars, intrinsic linear polarisation rel. to v sin i 77−60773
Be-stars, magnetic fields rel. to dynamics 77−60778
Be-stars, mass-exchange binary evidence from periodic spectral var. 77−60781
Be-stars, Paschen decrements and emission line formation in envelopes 77−56992
Be-stars, photographic IR spectroscopy and near IR photometry 77−56991
Be-stars, polarisation in extended circumstellar discs 77−56994
Be-stars, radiative accel. in extended atmospheres 77−56996
Be-stars, radio obs. 77−56984
Be-stars, rotation rel. to Hα and Hβ meas. 77−56983
Be-stars, spectra rel. to rotational hypothesis 77−56981
Be-stars, UV obs. 77−56985
Be-stars, UV Si IV/C IV ratio, Skylab obs. 77−56987
Be-stars, visible and UV spectra 77−56989
Be-stars showing poles, far UV spectra 77−56990
Be-type southern stars, photoelec. scanner meas. of Balmer emission line profiles 77−45452
Beals' Type III P Cygni line profiles 80−51771
Becklin-Neugebauer object, pre main sequence star, CO band emission detect. 79−101184
Becklin-Neugebauer source in Orion, 3.3 to 5.5 microns spectrum 80−12796
Becklin-Neugebauer source in Orion, high resolution 1.5 to 5 micron spectroscopy 78−93368
bibliographic file for automatic information retrieval 77−78833
bibliographic star index, information retrieval system *(Japanese)* 79−101086
blue horizontal branch stars search on Schmidt plates 78−4362
blue horizontal-branch, He stratification in model atmosphere 80−90409
blue objects and 5C3 radiosources optical counterparts obs. near M31 77−91526
blue stars, resolution in new dwarf irregular galaxy in Sculptor 77−22311
blue stars in SMC Shapley wing, visual counts rel. to S2/68 UV obs. 79−25717
blue stragglers as long-lived stars 80−46542
γ Bootis, Ap star, chemical element distrib. from spectrophotometry *(Russian)* 77−22238
α Bootis (Arcturus), obs. using image sharpening telescope 77−49295
bright northern stars with interesting Stromgren indices, spectral classifications 80−56817
bright O to G0 stars south of dec. +10°, photoelectric Hβ photometry 77−37600
bright stars catalogue, fourth edition considerations 77−78667
bright zenith star obs., Poltava latit. differences interpretation 78−28488
BV magnitudes and spectral classes, of stars in field centred at $\alpha=2^h17^m.9$, $\delta=+58°59'$ *(Russian)* 78−40841
BV photometric observations for Earth atm. aerosol content determ. 78−92976
BVRI photometry, secondary standards 79−70962
5C3 sources, optical idents., spectroscopic results 80−46689
C- and M-type stars near globular cluster NGC 419 in SMC, cluster membership 80−26921
53 Camelopardalis, Ap star, surface mag. field distrib. 77−26015
α Canis Majoris, Lα obs., interstellar H and D determ. 79−21275
α Canis Majoris (Sirius), B abundance 77−53585
α Canis Majoris (Sirius), Ca II K line high resolution profile obs. 80−56830
α Canis Majoris (Sirius), ghost image on Palomar Sky Survey as hiding place for new star cluster 80−109501
α Canis Majoris (Sirius), obs. using image sharpening telescope 77−49295

stars continued
α Canis Majoris (Sirius), optical image improvement via real-time phase correction system 77−22084
α Canis Minoris, Copernicus UV spectral obs. 77−33480
α^2 Canum Venaticorum, Ap star, surface mag. field distrib. 77−26015
ν Capricorni (B9.5 V), abundance anal. from model atmosphere 80−90415
Carina Nebula association, radial vel. study of WN stars and Of star 79−35261
Carina Nebula stars, interstellar λ4430 band obs. 78−32555
Carina spiral feature, distrib. of stars and interstellar dust along inner side 80−51871
Cassiopeia, photoelectric UBV photometry 77−37598
Cassiopeia-Taurus association stars, interstellar 2200 Å feature anomalous strength 80−77469
γ Cassiopeiae, Be star, coordinated IR and optical obs., (in late 1976) 79−25616
γ Cassiopeiae, Be star, IR excess 78−93257
γ Cassiopeiae, Be star, rapid spectroscopic variations 77−56970
γ Cassiopeiae, circumstellar envelope model 78−40952
3 Cassiopeiae, Flamstead missing star, identification with Cassiopeia A supernova 80−62436
γ Cassiopeiae, Hα linear polarisation in Be star 78−16425
3 Cassiopeiae rel. to supernova remnant Cassiopeiae A 80−72792
catalogue coord. system orientation errors, effect on planetary ephemerides *(Russian)* 80−51640
catalogue in Ptolemy's Syntaxis, position meas. method 80−67586
catalogue of stars observed with Bordeaux tracking photoelectric meridian micrometer 77−37509
catalogue of stellar identifications, CDS data base 77−78659
catalogues, machine-readable, critical data evaluation 77−78830
β Centauri, occultation by Earth, satellite obs., atm. O_3 density meas. 77−53259
α Centauri A and B, model chromospheres 77−13326
central star of planetary nebula NGC 7027, identification 79−67008
central stars of planetary nebulae, kinematics 80−51762
central stars of planetary nebulae, spectrogram analysis 79−97001
central stars of planetary nebulae, UV spectral obs. from TD-1 satellite 80−31300
central stars of planetary nebulae, Zanstra temps. and effective temps. relation 79−88654
λ Cephei, variable outflow in Of star, spectroscopic obs. 79−35263
Cepheus OB2 association stars, interstellar line spectra 80−22052
π Ceti, late B-type star, X-ray emission obs. 79−101160
γ Ceti, occultation by 6 Hebe, obs. rel. to asteroid dimensions 79−92694
Chamaeleon T association, JHKL photometry of stars, reddening 79−58384
charts for amateur astronomers 79−62762
chemically peculiar (CP) stars formation, planetesimal impact hypothesis 78−20834
chemically peculiar stars, nuclear and differentiated abundance patterns 77−17597
Chu's object in Perseus, identification as galactic star with refl. nebula 80−62132
CIT fields, near IR vidicon images 77−33683
CL4 optical counterpart, accurate position 79−17116
CL 4 optical counterpart, detect. and position 79−71138
CL 4 optical counterpart, optical position 79−21453
classification criteria by statistics from co-occurrence matrix *(Italian)* 80−98574
clock stars, R.A. correction, Melbourne obs. reduction *(Russian)* 79 92653
cocoon stars, calculated IR spectra 77−64824
cocoon stars, numerical soln. of radiation transfer eqn. in spherical geometry 80−90329
cocoon stars, radiative overstability in accretion 78−85932
collapsing star, neutrino degeneracy and downscatt. effects on neutrino radiation 79−12463
collapsing stars, enhanced gravit. radiation recoil 77−33336
colours, refr. corrections for atmospheric spectral transmission changes 78−28535
colours influence on β-index meas. 79−21270
14 Comae, A-type shell star, spectroscopic obs. 78−7992
17 Comae A, Ap star, Sr spots distrib. rel. to atmospheric mag. field *(Russian)* 77−17594
17 Comae A, magnetically variable Ap star, spectroscopic obs. 77−17595
compact objects, assoc. with X-ray bursters and soft X-ray transients 79−25755
comparison star sequences in six variable star fields, photometry obs. 80−82433
comparison stars in fields of extragalactic sources, photoelectric UBV sequences 77−5562
conference, stars and star systems, Uppsala, Sweden (1978 August 7 to 12) 80−51959
configurations and fields, anal. by statistical methods 80−82224
convective energy transport, review of theories 78−69785
cool, abundance determ., molecular data uncertainty effects 77−29805
cool C stars, $^{12}C/^{13}C$ ratio calc. 78−4205
cool carbon stars, effective temp. scale 77−2421
cool star spectra, TiO $e^1\Sigma^+$-$d^1\Sigma^+$ transition theory 77−67089
cool stars, alkaline earth and rare earth oxides occurrence 78−85933
cool stars, CaCl bands obs. 77−53593
cool stars, H_2O maser emission, catalogue of 82 objects 79−8909
cool stars, HEAO 1 search for coronal soft X-ray emission 79−101140
cool stars, outer atms. struct., solar-type and non-solar-type stars 79−48791
cool stars, polarisation wavelength depend. 77−2426
cool stars, TiO opacity effects on atm. struct. 78−40925
cool stars outer atmospheres, Mg II flux profiles and chromospheric radiative loss rates 80−36611
coordinate meas. on astrographic plates, reduction model 79−44334
coordinate system error reduction using 51 Nemausa posns. 80−72849
S Coronae Austrinae, protostar, high dispersion spectroscopy, Balmer line profiles 77−64754
B Coronae Borealis, Ap star, chemical element distrib. from spectrophotometry *(Russian)* 77−22238
β Coronae Borealis, Ap star, possible indication of mag. deform. 77−45454
β Coronae Borealis, Ap star, struct. of atmospheric mag. field *(Russian)* 77−17594

stars continued
θ Coronae Borealis, Be star, strong shell line at Hα 79−67022
counts, use in determination of galactic struct. 80−82507
CPD−26°389, central star of NGC 1360, radial vel. obs. 80−4350
CPD−56°8032, emission line object, red and IR spectrum 78−4249
Crab Nebula region, star counts rel. to extinction in and near nebula 77−67118
CRL 3068, dust-enshrouded star 77−91664
CTC right ascensions, synthetic catalogue for Chinese time service *(Chinese)* 78−28540
29 Cygni, λ Bootis type star, photometric variability 77−64765
P Cygni type line profiles, theoretical, atlas 79−80297
Cygnus direction, stars and dust space distrib. *(Russian)* 78−20893
Cygnus X-2 optical candidate, high-speed photometry 77−13494
Cygnus X-3, evidence for He star companion from period derivative and asymmetric X-ray light curve 80−105394
Cygnus-Vulpecula direction, stars and dust cloud space distrib. *(Russian)* 78−20892
in dark nebulae, star counts rel. to visual extinction 78−57612
data base, retrieval techniques and graphics display 77−78652
data compilation, evaluation and distrib., conf. (Strasbourg, France, 19-21 Aug. 1976) 77−78828
data distrib. 77−78673
declination determ. using vertical circle near equator *(Russian)* 79−92681
declination obs. of circumpolar stars with meridean circle *(Japanese)* 78−89044
δ Delphini stars, abundance anal., metallicism and pulsation 77−33506
density wave interaction in differential rotating spiral system 78−69871
designation ambiguities, improvement proposals, IAU list 77−78661
designation organization using bibliography-type data base 77−78658
differential rotation and dynamo presence 77−53582
differentially rotating gaseous polytropes, Eulerian eqns. 80−51739
digital speckle interferometry 77−53641
disc population stars, mass loss rel. to origin of galactic spiral arm instability 77−13456
discrimination from galaxies on astronomical plates, Bayesian approach to optimal classification 80−21920
distance measurement, parallax method, undergraduate expt. 77−60871
distances, max. likelihood regression model 80−51745
distances, parallax and relative magnitude, laboratory model for students 78−16610
distant stars distribution, evolution seen by observer falling freely into nonrotating black hole *(Polish)* 80−26897
distribution above galactic plane 78−12375
distribution in globular clusters M10 and M12 rel. to gravitational disturbance 78−69849
distribution in S. Milky Way 80−85997
distribution perpendicular to galactic plane, fine struct. study *(Russian)* 80−73036
diurnal latitude vars. spectra based on obs. at Gor'kii 79−35100
30 Doradus central object (HD 38268), interstellar and nebular lines obs. 80−51839
double Herbig-Haro object in Orion Nebula 77−26006
double stars, rectilinear trajectories calc., appl. to L 5094, effects of erroneous positions *(French)* 78−20857
φ Draconis, short period Ap star, discovery of mag. field 77−33511
E and F region stars, VRI photometry 78−53991
early B-type stars atmospheres, LTE line blanketing by UV lines using accurate damping consts. 78−16419
early B-type stars in local spiral arm, var. of axial rot. vels. with galactocentric distance 77−56929
early generations in scale covariant cosmology, props. 78−36739
early main sequence star model, periods of high pulsation modes 77−49372
early O-type star in SMC, discovery 79−5820
early type, in core of irregular galaxy NGC 6822, correl. with H I column density 78−20889
early type companions of X-ray sources, stellar parameters 78−36564
early type FK4 stars, uvby Hβ photometry 77−82275
early type stars, 'normal', with anomalous mid UV spectra 80−26857
early type stars, intermediate-band photometry 77−49385
early type stars, mid UV spectra obs. 80−21995
early type stars, normal, near UV line blocking depend. on spectral type and luminosity 80−36619
early type stars complexes in M31 (Andromeda galaxy), assocs. with Cepheid variables *(Russian)* 80−90455
early type stars in galactic plane, discontinuity near 140° longit. 77−9797
early-type, disc struct. in extended atms. 78−93206
early-type, evidence for gap in main sequence between B7 and B8 spectral types 77−13341
early-type, in Monoceros region, interstellar extinction determ. 77−9777
early-type, in N. Milky Way, IR photometry, interstellar extinction determ. 77−78783
early-type, interstellar extinction law correl. with wavelength of max. polarisation 78−61902
early-type, IR photometry, extinction ratio, 2200 Å interstellar absorpt. feature 78−53943
early-type, mass loss from radio obs. of 6 cm 80−82347
early-type, Mg II lines near 2800 Å 78−12229
early-type, northern intermediate galactic latit., Hβ photometry, rel. to glactic struct. 80−36631
early-type, rapidly rotating models with radiation press., struct. parameters calc. 80−67697
early-type, Skylab UV obs., MK spectral types 78−40933
early-type, spectral classification from TD1 satellite low dispersion UV spectra 78−16421
early-type, spectral energy distrib., reduction to Oke-Schild system *(Russian)* 77−64755
early-type, vacuum UV spectrophotometry and effective temps. 79−30060
early-type emission-line, intrinsic and interstellar polarization components separation 79−30079
early-type emission-line, intrinsic polarization interpretation 79−30080
early-type spectral classification, calibration using TV multichannel system 77−67091
early-type star assoc. with galactic nebular S206, wind rel. to nebula struct. 78−12326
early-type star in W49A, mass loss phase from Hnα radio recomb. line obs. 80−26998
stars continued
early-type stars, Balmer lines differential Doppler shifts rel. to atmospheres vel. gradients 78−57538
early-type stars, catalogue of 0.2 Å far UV spectra meas. by Copernicus 77−56843
early-type stars, comoving-frame transfer eqn. soln. in spherically symmetric flows 78−28499
early-type stars, Copernicus UB obs. of He I lines 80−41825
early-type stars, evidence for bimodal star form. 77−49374
early-type stars, H and He^+ synthetic line profiles in stellar winds 80−85926
early-type stars, standard line wavelengths for radial vel. meas. 77−17547
early-type stars, theoretical UBV colours and temperature scale 79−16933
early-type stars and cool stars, UV spectroscopy of outer layers 80−72922
early-type stars around l=140°, b=0°, photometry rel. to galactic struct. 78−24555
early-type stars directions, interstellar H_2O^+ abundance 78−69860
early-type stars in α Persei cluster, OAO 2 obs. 78−93331
early-type stars in LMC open cluster NGC 955, stellar winds rel. to motions in bubble-like nebula N51D 80−105295
faint early-type stars in neighbourhood of H II region RCW 38, UBV photometry 80−4352
early-type stars in northern Milky Way fields, UBVβ photometry 77−2424
early-type stars in open cluster M34, UBV photometry rel. to distance and age 78−12307
early-type stars in Perseus, UV spectrophotometry, energy distrib. 79−88653
early-type stars in southern hemisphere, four colour photometry and spectral types 78−40945
early-type stars in southern hemisphere, IR photometry 80−94786
early-type stars near Sun, space vels. and ages 78−61858
early-type stars photospheric expansion, meas. via. Fourier anal. technique 78−93224
early-type stars with Balmer emission, near UV (2000-3000 Å) spectra 80−94811
early-type stars with large IR excess, OH emission 79−71035
early-type stars with six degrees of galactic anticentre direction, radial vels. 78−7990
early-type with circumstellar clouds, evidence from Mg II 2800 Å data *(Russian, English)* 79−96992
early-type with extended envelopes and mass outflow, radio emission 77−74063
electronographic BVR magnitude sequences, for UK 1.2 m Schmidt plates calibration 79−88703
in elliptical galaxies, form. and mass range 77−33636
emission line objects in LMC *(French)* 78−69875
emission line stars, line form. in expanding spherical media with partial freq. redistrib. 79−88643
emission line stars, Mg II obs. near 2800 Å, absolute flux calibration 77−13350
emission line stars, radiative transfer, reson. line form. in decelerating spherical flow 77−78624
emission line stars in LMC, spectroscopy and IR photometry 77−13348
emission-line stars, far IR obs., cool dust cloud evidence 79−92771
emission-line stars, IR Fe II lines and interpretation of IR excesses 78−32478
emission-line stars in NGC 4755, southern open cluster, Balmer line photoelectric photometry 80−56892
emission-line stars misclassified as H planetary nebulae, catalogue 80−109378
emission-line stars of Sanduleak and Stephenson, classification spectra 78−93273
equatorial and southern bright stars, UVBYβ photometry 77−22205
equatorial photoelectric sequences in UBVRI system 79−62875
Equatorial stars, True Visual Magnitude Photographic Star Atlas 79−70967
equatorial stars declinations, obs. programme of Pulkovo Observatory expedition to Equator *(Russian)* 79−96892
ESO-(B)-survey, characteristics curves from stellar image diameters *(German)* 79−70966
ESO-B and SRC-J sky surveys, limiting magnitude 78−69706
EUV radiation, point source contribs. to EUV background 80−62324
evolved stars, in Population I clusters, effects on cluster integrated colours 77−17637
exchange collisions between binary and single stars 77−91563
exciting star of NGC 2024 (Orion B), results from recomb. line obs. 77−29895
exciting stars in H II regions, mean temp. determ. method 80−73024
exciting stars in LMC H II regions, ANS UV obs. 79−71017
exciting stars of low excitation planetary and diffuse nebulae, effective temps. 77−13427
exciting stars of Orion triple emission nebula, UBV photometry 77−13430
extreme Population II stars, age difference from oldest Population I stars 77−56912
extremely metal-poor stars, theoretical evolution 78−28677
extremely red stars at $l^{II}\approx113°$, $-10°\leq b^{II}\leq+90°$, photometry and spectra 78−57554
F0 to M2-type stars, Ca II H and K lines absolute flux profiles rel. to model chromospheres 80−26842
F, G, K-type stars, electron concs. in photospheres, Fe line obs. *(Russian)* 77−49376
F and G stars, MK spectral types 79−66999
F-, G- and K-type, in solar neighbourhood, absolute magnitudes 78−81632
F- and G-type, mag. accel. of winds and ang. momentum loss 77−13334
F- and G-type main sequence stars, R-I colour as temp. indicator 77−87395
F- and G-type stars, props. determ. by spectral quantification 77−29791
F- or G-type star assoc. with CRL 2688 (Egg Nebula), spectroscopic evidence 77−41400
F-type, absolute luminosity calibration 78−65612
F-type, atm. models including OH opacity, comparison with TD1 satellite flux obs. 78−73700
F-type, energy distrib. in main-sequence 78−93220
F-type stars, MK spectral classification based on uvby and β photometry 77−29822

stars continued
F-type stars in Selected Areas, photoelectric uvbyβ photometry 78−16412
faint blue southern stars, Hβ photometry, metallicity, luminosity 77−41381
faint blue star, optical candidate for 4U 1626−67, optical pulsations discovery 79−9034
faint blue stars, photometry, third list of southern stars 79−71030
faint blue stars, southern, UBV photometry 80−82349
faint blue stars, uvby photometry in northern hemisphere 78−16415
faint blue stars in high galactic latits., search of PSS fields near South Galactic Pole 80−46415
faint blue stars near galactic anticentre, spectral types 79−71021
faint blue stars near galactic anticentre, UBV photometry 78−40932
faint blue stars near North Galactic Pole, catalogue 77−49314
faint blue stars photometry, second list of southern stars 77−45424
faint equatorial standard stars for BVRI photometry 79−62876
faint IR star, discovery in open cluster (NGC 1502) *(Russian)* 77−13250
faint OB stars in Coalsack region 77−74047
faint proper-motion stars, spectra and photometry to very low luminosity degenerates deficiency 80−17575
faint red stars, photoelec. photometry of complete sample, space density 79−71034
faint stars, spectral-type standards for objective prism plates 80−46539
faint stars in globular cluster M2 (NGC 7089), photometry and colour-magnitude diagram 80−101623
faint stellar images, colour-magnitude diagrams and clustering correl. functions rel. to star populations 80−82360
faint UBVRI standard stars, photometric obs. 80−51813
Feige 86, horizontal branch star, chemical comp. 77−9745
field stars of solar neighbourhood, chromospheric Ca II H and K emission survey 80−109423
figure, Clairaut-Laplace-Lyapunov problem 77−25963
first generation stars, form. during fragmentation of cosmic gas clouds 77−33628
FK4, corrections to zero points from minor planet obs. *(Russian)* 80−82228
Fk4 corrections based on photographic posns. of Venus 79−8851
FK4 stars general catalogue of astrolabe obs. (1958-75) *(French)* 78−36468
FK4 supplementary stars, right ascensions obs., definitive results 80−17473
FK5, equinox and equator of new fundamental reference coord. system 80−109341
FKSZ stars, differential catalogue of RA in 20-90° zone, Pulkovo obs. *(Russian)* 78−28644
FKSZ stars, meridian circle obs. at Kiev University Observatory, (1972 to 1975) *(Russian)* 79−44336
formation, in shock-compressed layers 78−40919
formation, observational studies conclusions 79−25592
formation from hot matter with primordial chemical comp., role of H_2^+ mol. ion *(Russian)* 78−40924
formation in blue galaxies, theory 78−12356
fundamental bright southern stars, $\Delta\alpha_3$ cos δ corrections *(Russian)* 77−56817
G133.982+1.14 (BS4), far IR source in W3, near IR obs. and identification as massive pre main sequence star 80−22058
G-type stars, flux distribs. comparison with solar flux distrib. 79−66970
galactic anticentre, space distrib. of stars and dust *(Russian)* 78−73754
galactic centre, distrib. of stars and dust, black hole hypothesis 78−86010
galactic centre, star density rel. to nature of IR source IRS 16 80−46671
galactic centre, tidal disruption of stars and massive black hole evolution *(Russian)* 78−12371
galactic distribution, rel. to integrated starlight synthetic spectrum between 3000 and 10000 Å 80−46536
galactic distribution, statistics rel. to gamma-ray burst sources distrib. 80−22117
galactic halo stars, heavy elements abundance gradient 79−92857
N.Galactic Pole region, stellar polarisation meas. rel. to extinction 79−62814
galactic stars optically misidentified with extragalactic radio sources, photometry and spectra 78−73708
galactic struct., in solar neighbourhood, Aquila direction, RGU photometry 77−91621
galaxy disc stars, nonlinear interaction with spiral wave near corotation radius *(Russian)* 80−62289
Galaxy disc stars, z-distrib., rel. to local galactic force field 80−62271
galaxy evolution and stellar populations, Yale conference (May 1977), report 78−69879
Galaxy inner region, stellar distrib. *(Japanese)* 79−80352
GB2 1400 MHz survey, optical identifications of flat-spectrum sources 79−40281
ε Geminorum, occultation, by Mars, obs. at Princeton 78−57482
ε Geminorum, occultation by Mars, 1976 April 8, atm. temp. *(French)* 77−53449
ε Geminorum, occultation by Mars, obs. from C.E. Kenneth Mees Observatory 78−53853
ε Geminorum, occultation by Mars, planetary atm. temp. struct. determ. 77−87306
ε Geminorum, occultation by Mars, struct. and extinction of Martian upper atm. 78−7898
ε Geminorum, occultation by Mars (1976 April 8), preliminary results 77−37545
ε Geminorum, occultation by Mars on 1976, April 8th, theory of light curve 77−53567
ε Geminorum, occultation by Mars photometric obs. 77−91527
ε Geminorum occultation by Mars, McDonald Observatory obs. 77−60702
general catalogue of 1139 stars obs. with astrolabes, 1957-75 period, FK4 stars position corrections *(French)* 78−32359
general magnitude eqn. between FK4 and southern catalogues 80−67705
in giant ellipsoidal shells around normal elliptical galaxies, origin 80−86000
GL 490, GL 2591, obscured IR objects, K-band spectra anal. 79−92828
GL 490, IR obs. of low-luminosity pre-main sequence stars 79−53808
globular cluster horizontal branch stars, effects of forced mixing on evolution 80−56818
in globular clusters M10, M12, M71, M92, radial vels. 78−41004
Gor'kii latitude observations, half-year nutation wave terms errors 79−62728
gravitational collapse, comp. and eqn. of state of thermally dissociated matter 77−33476
gravitational collapse of magnetized stars, whistler mode radiation 78−28509
gravitational focusing effect, short-wave limit imposed by lens star gravity field asphericity 79−58604
gravitational radiation from collapsing relativistic star with rotation 80−56816
Greenwich Obs., Time Report (1976, Jan.-March) 77−45293
Greenwich Obs. Time and Latitude Service, Time Report (April-June, 1977) 78−69661
Greenwich Obs. Time and Latitude Service, Time Report (January-March 1977) 78−57431
Greenwich Obs. Time and Latitude Service, Time Report (January-March 1978) 79−25453
Greenwich Obs. Time and Latitude Service, Time Report (January to March 1979) 80−72749
Greenwich Obs. Time and Latitude Service, Time Report (July-September 1976) 78−20624
Greenwich Obs. Time and Latitude Service, Time Report (July-September 1977) 78−73619
Greenwich Obs. Time and Latitude Service, Time Report (July-September 1978) 79−62729
Greenwich Obs. Time and Latitude Service, Time Report (October to December, 1977) 78−89046
Greenwich Obs. Time and Latitude Service Time Report (April-June 1979) 80−72750
Greenwich Obs. Time and Latitude Service Time Report (October-December 1976) 78−24443
Greenwich Obs. Time and Latitude Service Time Report (October-December 1978) 79−101053
Greenwich Observatory, 1976 April to June time report 77−70581
GX 17+2 (3U 1813−14) optical candidate, photometry 78−28849
GX 17+2 (3U 1813-14), optical identification with dwarf G-type star 78−45428
H 2155−304 optical candidate, spectrophotometric obs. 79−25761
h 5094, optical double star, rectilinear trajectory calc., effects of erroneous positions *(French)* 78−20857
H-H 28, H-H 29, large proper motion Herbig-Haro objects, astrometric obs. 79−71022
H-H 2, condensation H, spectrophotometric data 79−62826
H-H 7 and 11, spectrophotometry of very low-excitation objects 80−46549
H-R diagram, use as astronomical tool, review of IAU Symposium (No.80) 78−81619
habitable zones about main sequence stars 79−40188
halo population near Sun, intermediate-band photometry 79−44473
halo stars, three colour photometric obs., rel. to Galaxy halo to disc mass ratio 77−45548
Harvard magnitude scale 77−71109
HD 101065, peculiar star, presence of Fe questioned 77−45455
HD 101065, Przybylski's star, element identification 78−4233
HD 108, Of star, spectral vars. due to solar wind 79−35262
HD 120640, spectrophotometry and quantitative anal. of B star 77−60758
HD 137613, C rich H deficient star, UBV photometric obs. 80−90437
HD 152 667 unseen companion, possibly B4 main sequence star 79−48848
HD 15570, Of/WN7 spectral classification problem 80−51786
HD 156385, WC7 star, anomalous 2200 Å absorpt. band 77−64769
HD 161480 in open cluster IC 4665, peculiar star study 77−33530
HD 161733, in open cluster IC 4665, peculiar star study 77−33530
HD 174209 (ADS 11719C), photoelectric radial vel. 78−32517
HD 183143, grating scanner meas., corrections for polarization 78−32355
HD 184905, variable Ap star, radial vels. for Si II and Ca II lines 77−22251
HD 184927, He variable star, spectrum obs. 77−22249
HD 190073, A0ep star, Ca II lines struct., nightly vars. and line profiles interpretation 77−17578
HD 192163, 191765, Wolf-Rayet stars, optical interstellar spectra obs. 80−17640
HD 192163, Wolf-Rayet, IUE obs. of absorption by hot gas in NGC 6888 surrounding nebula 79−53896
HD 192163, Wolf-Rayet star, comp. of dust in assoc. ring nebula (NGC 6888) 77−29905
HD 192163, Wolf-Rayet star, forbidden N II/Hα ratio in circumstellar nebula (NGC 6888) 79−8964
HD 192163, Wolf-Rayet star, radius and temp. from spectra of nebula (NGC 6888) 77−57076
HD 192163, Wolf-Rayet star, spectra of filaments and smooth gas in ring nebulae (NGC 6888) *(Russian)* 80−90515
HD 192273, blue subluminous star, possible identification with EUV source in Pavo region 78−28675
HD 192273, high latitude EUV source, low-mass binary 80−4353
HD 192273, optical spectral obs. of proposed EUV source 79−35256
HD 192641, Wolf-Rayet star, IR light vars. 77−9750
HD 193077, probable single WN 5 star with absorption lines 80−56834
HD 193793, Wolf-Rayet binary, visible and near IR spectra 78−8023
HD 193793, Wolf-Rayet star, IR light vars. 77−9750
HD 193793, Wolf-Rayet star, IR obs., cooling of circumstellar dust shell 79−48823
HD 195592, obs. of interstellar K I 4044 Å line 78−24533
HD 200120, Be star, emission features *(French)* 77−56977
HD 200120, Be-type, UV spectra vars. 77−5534
HD 200775, Be star, optical and UV extinction by dust in (NGC 7023) 80−109515
HD 200775, possible protostar in reflection nebula NGC 7023, optical polarization and IR spectrum 80−85944
HD 200775/NGC 7023 complex, star intrinsic and interstellar reddening 80−51832
HD 215441, Ap star, line spectrum variations 78−4232
HD 216533, Ap star, spectral variation obs. 78−4244
HD 219150, F0 V star with remarkable UV excess, optical and UV photometry and spectrum 80−90429
HD 26676, unusual radio star, not close binary 78−73707
HD 269781, abundance anal. 77−91522

stars continued
HD 36665, B1e star, detect. of interstellar CO absorpt. in direction of supernova remnant (S147) 80−67836
HD 37903, far IR study of nearby refl. nebula (NGC 2023) 80−51831
HD 38268, in 30 Doradus, unique interstellar Ca II K-line profile obs. 80−51850
HD 38268 and 38282, hot stars in LMC, far UV spectral evidence for hot gaseous galactic corona 79−67097
HD 42088, O-type star, rel. to ionisation of nebula S252 (NGC 2175) 77−64828
HD 44179 (CRL 915), IR spectra in 2-8 μ range 78−41080
HD 44179 (Red Rectangle), bipolar nebula, IR polarimetry 78−36658
HD 50138, Be star, model for shell from continuous spectrum obs. in IR 77−56976
HD 50896, atlas of Copernicus UV spectra of Wolf-Rayet star 78−57557
HD 50896, distant unreddened star, Copernicus obs. of UV interstellar lines 77−26036
HD 50896, Wolf-Rayet star, detect. of polarisation struct. across emission lines 79−97008
HD 50896, Wolf-Rayet star, UV spectral energy distrib. 77−22211
HD 50896, Wolf-Rayet star, wind struct. determ. from IR continuum 77−78793
HD 50896 (WN5), variable emission-line spectrum obs. 80−51791
HD 50896 and 151932, WN stars, IR spectra 78−8024
HD 51480, shell star, spectroscopic obs., atmospheric struct. and distance 80−31305
HD 51585, B[e] star, visible and near IR spectrum 77−45445
HD 6884, abundance anal. 77−91522
HD 84903 and 184711, differential anal. of extreme metal deficient stars rel. to halo star HD 122563 79−80302
HD 87643, forbidden line Be star, IR obs. with new photometer 77−26017
HD 90657, Wolf-Rayet spectroscopic binary, spectroscopic obs. 77−13357
HD 92740, atlas of Copernicus UV spectra of Wolf-Rayet star 78−57557
HD 93131, probably single WN7 star, spectroscopy and photoelectric photometry 79−8924
HD 93162, probable single WN7-type star in Trumpler 16 cluster 78−85946
HD 93250, O3 massive star in η Carinae complex, non-LTE analysis 80−77398
HD 93521, high galactic latit. peculiar O-type star, spectrum 77−78784
HD 97048, pre-main-sequence star, spectral changes 77−74055
HDE 245770, Be star, identification with X-ray source Ariel 0535+26 confirmed 79−44635
HDE 245770, near IR photometry of OBe star, A 0535+26 optical counterpart 79−48826
HDE 245770 (Ariel 0535+26), recurrent X-ray transient, further outburst 79−40300
HDE 313846, most extreme Of star, spectroscopic obs. and mass outflow 79−88682
He-3 1863, unusual high latit. Be star, spectral obs. 77−87418
Henize 787 (SAO 251905), five-colour photometry 77−29846
Henize S22, emission line star in LMC, spectrophotometric study 78−69803
Herbig Ae/Be stars, spectrophotometry 78−93258
Herbig Be/Ae stars, star form. in assoc. mol. clouds 78−32542
Herbig-Haro 2, detection of H_2 vibrationally excited 2 μm lines 80−94853
Herbig-Haro object 1 exciting star, identification as T Tauri star 80−17633
Herbig-Haro object 24, emission/reflection nature 80−41829
Herbig-Haro objects, Fe abundance 79−62826
Herbig-Haro objects, H_2O masers evolution, compact clouds ejection 79−35329
Herbig-Haro objects, new, spectroscopic obs. 79−5763
Herbig-Haro objects, new nearby H_2O masers discoveries 79−21369
Herbig-Haro objects, radio obs. and nearby compact H II regions 80−51756
Herbig-Haro objects, stellar wind dynamics 80−56822
Herbig-Haro objects, stellar wind model 79−8912
Herbig-Haro objects, stellar wind model 80−85985
Herbig-Haro objects 7-11, compact H II region and H_2O maser sources 80−73019
Herbig-Haro objects and surrounding dark clouds, NH_3 23 GHz obs. 80−72934
Herbig-Haro objects assoc. with Gum Nebula, star for form. triggering 77−29821
Herbig-Haro objects associated with NGC 2264 young cluster 79−71026
Herbig-Haro objects exciting stars, 2 micron search 80−67720
Herbig-Haro objects in Gum Nebula, spectrophotometry 78−36565
Herbig-Haro objects in molecular clouds, mol. obs. and physical props. 80−36689
Herbig-Haro objects in Orion Nebula 80−77397
Herbig-Haro objects in southern dark clouds, objective prism survey 78−28536
τ Herculis, B-type subgiant star, abundance anal. 78−16416
4 Herculis, shell star, Balmer intensity profiles 77−56973
4 Herculis, shell star, photometric obs. rel. to binary star hypothesis 77−91538
Herschel 36, in M8, rel. to H II region near IR and 24 GHz emission 79−48882
high luminosity stars in SMC, interstellar reddening distrib. functions appl. to total/selective absorption. ratio determ. *(German)* 80−67851
high mass stars, evolution including stellar wind effects 80−21982
high-velocity stars, southern, radial vels. 80−21988
high-velocity stars, southern, UBV colours 80−21989
homogeneous collapsing star, orthogonal vector and tensor harmonics, matter and field asymmetries 79−5841
horizontal branch stars and RR Lyrae variables in globular cluster NGC 6121 (M4), UBV photometry 80−22018
horizontal-branch A-type stars, astrophysical parameters determ. 79−62829
hot horizontal branch stars, theoretical B−V colour indices and bolometric corrections 79−58327
hot stars, as source of emission lines in Tololo galaxies 78−49531
hot stars interactions with interstellar medium, obs. of high excitation nebula (Sh 2-158) 79−40241
stars continued
HR 1614 group of metal-overabundant stars, late-type stars intermediate-band photometry 78−53935
HR 3089, He-rich star, anal. of UV spectrum 77−9751
HR 421, δ Delphini star, abundance anal., uvbyβ photometry 77−29823
HR 8799, model atm. anal. 77−74050
HR 9076 (ε Tucanae), Hα shell profile 78−36583
I-118, probable Norma OB1 assoc. member with anomalous distance modulus 80−62129
IC 1795 (W3), UBV photometry of field stars 77−57082
identification using coded numbering system for open clusters 77−78829
images, automatic CCD measuring machine *(Japanese)* 80−82212
images on Palomar Sky Survey prints, magnitude-diameter relations 77−49310
incompressible stars, in bimetric gravit. theory 77−33329
intenal structure, series soln. of Lane-Emden problem 78−36559
interaction with dense interstellar gas clouds, theoretical aspects *(German)* 80−109500
interferometry, first fringe meas. 80−82215
intermediate Population II stars, Stromgren uvby photometry 77−60757
internal structure of Sun and solar-type stars 77−53565
International Time Bureau obs. for continental drift meas. 77−13072
interstellar dense clouds encounters with stars 77−87497
interstellar gas line accretion theory, gas press. effect 78−32525
interstellar linear polarisation, wavelength depend. at near IR wavelengths 80−51833
interstellar lines towards stars of low reddening 78−57603
interstellar reddening law from normal and Be star energy distribs. 77−74109
interstellar UV absorpt. lines, International Ultraviolet Explorer obs. 78−96524
intrinsic colours of luminous stars in Magellanic Clouds *(German)* 77−17560
intrinsic polarisation, obs. and statistical anal. *(Russian)* 77−13346
ionising source model for Allen's obscured IR source in NGC 2264 viscous disc component 79−21370
IR airborne spectrophotometry, 1.2-5.5 μm, spectra and absolute calibration 80−62117
IR astronomy development progress *(German)* 77−67138
IR astronomy investigation of star interplay with interstellar medium 77−53433
IR field stars at North Galactic Pole, props. 78−81622
IR object assoc. with passage of interstellar shock front, radio identification 78−93369
IR point source, obscured, in M17 SW, spectroscopic anal. 79−48878
IR sources identification in Ophiuchus dark cloud region, spectral types and extinction 77−45522
IR sources in compact H II region G45.5+0.1, 1.25 to 10 μm photometry 78−4396
IR sources of AFGL sky survey, ground-based obs. 79−71150
i.r. stars, 20 μ broadband photometry 77−9807
IR stars, review of observational data *(Russian)* 77−49377
IR stars, role of dust in OH and H_2O masers pumping 78−36716
IR stars, search for 18 cm OH emission 78−8026
IR stars and long-period variables, discovery of new 1665/1667 MHz OH/IR sources 77−64763
IR stars in galactic centre, IR spectrophotometry and props. 78−24551
IR stellar speckle interferometry, modulation transfer function and evidence for log-normal statistic 79−101079
IRC+10216, brightness distrib. at 11 μm 79−67115
IRC+10216, C star, HC_5N and HC_7N detect. 79−17126
IRC+10216, late type C star, circumstellar envelope 78−4189
IRC catalogue, reddest stars at 2 μ 79−62841
K-type stars, spectroscopic investigations in 4500 to 7500 Å region 80−109430
Klemola 23, occultation by Neptune, 1980 August 21, obs. 80−109395
Klemola-Marsden 12, occultation by Uranus, 1980 August 15 to 16, reality of additional occultations questioned 80−109396
Landolt celestial equatorial UBV standard stars, spectral classifications 79−75199
late B-type, spectral class. from TD1 UV obs. 77−91529
late B-type stars, Ca II K-line profiles 78−73722
late B-type stars, rot. and incidence of HgMn stars 78−89199
late type stars, Ca II line widths and Wilson-Bappu effect 79−12464
late type stars, theoretical chromospheres and temp. minima heights 78−20818
late-type, 4-8 μ spectral obs. 77−74054
late-type, ^{24}MgH IR rot.-vibr. bands fine struct., transition probabilities, oscill. strengths 77−18918
late-type, absolute luminosity calibration 77−45421
late-type, acoustic modes overstability and obs. implications 77−56932
late-type, ang. dias. by lunar occultation technique 77−74048
late-type, ang. momentum loss rel. to mag., dynamo 78−45331
late-type, in elliptical galaxies, IR OBS. 77−91639
late-type, intensity effect in Wilson-Bappu relationship 78−85937
late-type, intermediate-band photometry, calibration, standard stars 77−22104
late-type, kinematical data 77−26009
late-type, luminosity criteria 77−5527
late-type, search for C IV reson. doublet, TD1 satellite UV obs. 77−5526
late-type, spectrophotometry, incident and emergent flux calc. 78−4200
late-type catalogue of revised Mk spectral types 80−82226
late-type main-sequence and subgiant stars, HEAO 1 obs. of active coronae 80−72925
late-type stars, Ca II 8542 Å line as chromospheric activity indicator 80−62108
late-type stars, Copernicus survey of Mg II emission 79−80301
late-type stars, intermediate band photometry in Geneva system 78−12231
late-type stars, obs. of emission lines in Ca II H and K wings, line width-luminosity relation 77−78766
late-type stars chromospheres, acoustic energy generation theory 78−7986
late-type stars intermediate-band photometry, calibration of indices 78−49424
latitude, azimuth and longitude, simultaneous determ. via time and horizontal angles meas. 77−60339
48 Librae shell star, emission features 77−56975
Lick proper motions referred to galaxies, precession and galactic rot. determ. 78−65487

stars continued
linear polarisation meas., catalogue for 5070 stars 77−13255
LkHα 101, IR spectra of emission line object, preplanetary disc obs. 78−16423
LkHα 198, star form. in assoc. mol. clouds 78−32542
LMC X-1 optical candidate, spectrum and semi-accurate position 80−67908
LMC X-4, possible OB star optical candidate 77−9820
LMC X-4, possible optical counterpart 77−13502
low galactic latitude stars, mean secular parallax 78−57542
LP 182-44, faint blue star with large proper motion, discovery 78−49439
LS I +61°303, possible optical counterpart for GT 0236+610, variable radiosource 78−32473
LS IV −14°109, H deficient A-type star, effective temp. 79−40195
LSI+61°303, possibly optical counterpart of GT 0236+610, absence of variability 78−49438
luminosity function *(Russian)* 77−82214
luminosity function of high-velocity stars and galactic halo mass 78−4368
luminous C stars in LMC, photometry 78−28670
luminous O-B3 type stars in open clusters, circumstellar shells and mass loss *(German)* 78−53925
luminous stars in Monoceros, photometry rel. to galactic struct. 77−9799
luminous stars in symmetric nebulae, IUE low-dispersion spectra 80−46560
lunar occulation events, 1974 to 1977, photoelectric obs. summary 79−88642
lunar occultation, summary of obs. 78−7982
lunar occultations, new technique for photoelec. obs. of dark limb reappearances 78−4115
lunar occultations, obs. at Cracow in 1974-75 period 77−33363
lunar occultations, obs. at Sydney Observatory during (1974-1976) 78−69658
lunar occultations, photoelec. obs. 78−4079
lunar occultations, photoelec. obs. 79−5819
lunar occultations, photoelectric obs. at Dominion Astrophysical Observatory (DAO) 79−75198
lunar occultations, photoelectric obs. at McDonald Observatory 77−2331
lunar occultations (1943-71), catalogue 79−88606
lunar occultations of stars, 1969-72, Sofia Observatory obs. 79−29979
α Lyrae, absolute energy distrib. from 3295 Å to 9040 Å 78−20828
α Lyrae, continuous UV flux, non-LTE calc. 77−49382
α Lyrae, emission lines in IR spectrum, thin expanding extended atm. 78−53946
α Lyrae, Fourier transform method to determine projected rotational vels. 77−29655
α Lyrae, soft X-rays detect. with imaging X-ray telescope 79−48953
α Lyrae, UV spectrum, line identifications 77−17552
α Lyrae (Vega), B abundance 77−53585
α Lyrae (Vega), Ca II H and K lines high resolution profiles 78−85939
α Lyrae (Vega), mass, chemical comp. and age 77−33495
α Lyrae (Vega), obs. with Solar Thermal Test Facility 80−77301
α Lyrae (Vega), spectral anal. from Copernicus 80−26856
M11, open cluster, stellar proper motions rel. to membership 77−17641
M1-2 central star, possible eclipsing binary in planetary nebula 80−105239
in M31, galaxy population synthesis models, nonuniqueness 80−82489
M32, stellar population spectral synthesis and galaxy age 80−67842
M67, open cluster, stellar proper motions rel. to membership 77−22281
in M6 (NGC 6405), open cluster, stellar strip counts *(German)* 77−13411
in M81, M51, spiral galaxies, phase shifts between gaseous arm and stellar arm *(Chinese)* 79−17098
M- and S-type, detect. of 7 mm SiO maser sources 78−4215
M-type, in north galactic polar region, space motions 78−93235
M-type, in Orion population, CaH and TiO band strengths 78−12227
M-type, in solar neighbourhood, absolute magnitudes 78−81631
in Magellanic Clouds, photoelectric (B, V) magnitude sequences 77−53592
Magellanic Clouds stars, five-channel photometric obs. 78−16398
magnetic Ap stars, empirical atmosphere models *(German)* 77−17589
magnitude simulator, IC device 78−81742
main sequence, diffusion in envelope and abundance anomalies 77−13331
main sequence, element abundance regularities rel. to nucleosynthesis *(Russian)* 77−45431
main sequence, F- and G-type, Be abundances 77−13332
main sequence, turbulent diffusion and Li transport 77−45403
main sequence (MS) stars chemical structure, influence of pre main sequence evolution 79−35247
main sequence star collision with white dwarf, results 77−64758
main sequence stars, chem. comp. effects on position in H-R diagram 77−91521
main sequence stars, chemical comp. rel. to main sequence location 77−71105
main sequence stars, linear series of models, supermassive stars 77−91515
main sequence stars with variable Ca II H and K emission, starspot hypothesis 79−58328
main-sequence, chromospheric vars. 79−16931
main-sequence reddened stars, ANS photometry, UV colours 80−77400
main-sequence star collision with white dwarf in dense galactic nuclei 78−65621
main-sequence stars, Ca II H and K emission flux meas. 78−73646
main-sequence stars, comparison of four-colour photometric obs. with evolutionary models 78−8007
main-sequence stars, equivalent widths of H_2 Lyman band and CO and SiO (A-X) band lines 77−87368
main-sequence stars, F to M-type, comparison of activity cycles to old and young stars 80−105235
main-sequence stars, Population I, luminosity functions in SA 51, SA 57 and (SA 68) 80−98648
main-sequence stars, transformations between UBV and RGU multicolour photometric systems 78−28529
Markarian 374 nucleus, western component identified as foreground star 78−69882
mass flux fluctuation theory 80−72923
mass fluxes, fluctuation theory 79−53804
mass loss from hot stars 78−69786
stars continued
massive main-sequence stars, effects of convective and semiconvective mixing 80−90405
massive O-type stars, as source of carbonaceous material in Galaxy 78−24543
massive protostellar clouds, dynamical evolution 77−17543
massive stars, birth 79−2542
massive stars, evolution with mass loss by stellar wind 78−4197
massive stars, form. and development of compact dust-bounded H II regions 77−26032
massive stars, nonradial pulsational instability 77−56908
massive stars main-sequence evolution, effects of mass loss 78−93200
massive young stars, dust shells rel. to H_2O masers VLBI obs. 79−21368
MD 101065, effective temp. and atm. electron press. 77−45468
mean places within 1° of 1978.0 NCP 77−82281
Merate Observatory, time and latit. results of astrolabe obs. (1977) 79−40061
metal-deficient stars, subdwarf ionization equilibrium 80−90421
metal-poor late-type stars, MK spectral classification 80−4340
metal-poor star distrib. in galactic halo *(German)* 80−94867
metal-poor stars, O abundances from O I IR triplet 80−36610
metal-poor stars, spectra and Al/Fe ratios 78−57549
MHD free convection effects on oscill. flow of viscous incompressible fluid past porous limiting surface 79−81985
Michigan 239, peculiar extragalactic or extreme halo emission-line star, obs. 80−4380
Milky Way stars, five-channel photometric obs. 78−16398
Molonglo radiosource catalogues MC2 and MC3, optical identifications, 11^h28^m to 17^h00^m right ascensions 78−20900
β Monocerotis, Be star, spectrum vars. rel. to orbital changes of gaseous ring 77−26013
β^1 Monocerotis, gaseous rings apsidal motion and orbital elements slow drift 78−36572
V616 Monocerotis (A0620-00) field, BV electronographic sequence and nova light curve 77−64777
MWC 17, emission line star, dense planetary nebula like object 77−45449
MWC 349, IR source optical identification with reddened high-luminosity star 80−56971
MWC 349, IR spectra of emission line object, preplanetary disc obs. 78−16423
MWC 349, planetary system formation *(German)* 79−53832
MWC 349A, near-IR spectrographic obs. 80−94810
MXB 1659−29, identification with faint UV stellar object 78−61936
names register *(Swedish)* 78−4188
near IR photometric obs. of 50 stars 78−69795
nearby low galactic latitude stars, linear polarization meas. 80−46641
nearby objects, space astrometry 80−67518
nearby star data published 1969-1978, catalogue 80−36513
nearby stars, gravitational effects on comet orbits evolution 80−98613
nearby stars, long term effects of space motion, constellation pattern changes 79−66995
nearby stars brighter than tenth mag. 80−56825
nearby stars catalogue, third edition requirements 77−78660
nearby stellar systems, ranking method for exploration 78−81522
nearby systems, astronomical data relevant to BIS Project Daedalus 78−81612
nebulae central stars, temps. determ. from forbidden O III lines 78−41015
newly formed stars in Taurus dark cloud complex, IR study 79−8963
newly formed stars in young cluster IC 5146, evidence from CO obs. 79−48881
NGC 2024, H II region, near IR obs. and multiple exciting stars model 79−58393
in NGC 205, stellar content rel. to UV flux 80−98716
NGC 2071(IRS), IR obs. of low-luminosity pre-main sequence stars 79−53808
NGC 253, spiral galaxy, nucleus, stellar population from gas outflow obs. 78−28776
NGC 3603 stars, interstellar λ4430 band obs. 78−32555
NGC 4565, galaxy, dark halo stars luminosity and mass function 79−62905
NGC 6210, planetary nebula, central star, high dispersion EUV obs. and spectral type 80−77466
NGC 6494 (M23), open star cluster, membership from astrometry with PDS microdensitometer 80−98697
NGC 6543, planetary nebula nucleus, periodicity disclaimed due to telescope periodic drive error 79−92763
NGC 7027 central star, radiation rel. to low excitation emission spectrum 77−64823
night sky model for artificial satellite search systems 77−73923
non-spherical stars, appl. of smoothed particle hydrodynamics theory 78−12203
nonradial oscillation mode splitting, effects of differential rotation 78−4211
nonradial oscillation modes in presence of slow rot., quasiadiabatic anal. 79−12462
nonradial oscillations, theories and obs., review 77−26003
Norma nova-like X-ray source, search for optical candidates 77−82322
north galactic pole, A and F star radial vels. and MK classifications 77−22223
north galactic pole, A and F star uvbyβ photometry 77−22224
north galactic pole stars, radial vels. 77−22207
northern early-type stars at intermediate galactic latits., UBV photometry and MK spectral classification 77−82221
northern FK4 stars, radial vel. meas. 80−26848
northern sky photographic optical IR survey 79−21198
Northern stars, True Visual Magnitude Photographic Star Atlas 80−109376
novae and related stars, conf. (Paris, 7-9 Sept. 1976) 77−82240
numerical statistics, rel. to neutron stars from rate in Galaxy 79−40208
O3 to O5.5-type stars, spectra 77−33481
O9-G0 type stars, Balmer discontinuities and line blocking 77−45419
O and B stars, theory of Si spectra 78−57539
O to F type, Balmer lines and mean electron density for 94 stars 77−17564
O- and B-type, ionization conditions in expanding envelopes 78−28671
O- and B-type, UV P Cygni profiles long-term changes 78−12234
O-B3 stars in southern clusters excess absorpt. 77−78791

stars continued
O-B stars, spectrophotometric and UBV colorimetric parameters *(Russian)* 77−17569
O-type stars, assoc. with nebulosity rel. to galactic struct. 80−105236
O-type, effective temps., far UV photometric obs. 79−88656
O-type, He I 10830 Å to spectral line, rel. to mass loss 79−80304
O-type, in galactic centre, dust grains heating, radiation model 78−36697
O-type, in LMC, uvby photometry 77−60756
O-type, O VI P Cygni profiles hourly vars. 77−37596
O-type errors in distance estimation, galactic distrib. *(French)* 77−22209
O-type mass loss rate from UV spectra 80−82346
O-type planetary nuclei, atmospheric props. 78−4206
O-type planetary nuclei, spectral classification, magnitudes, distances 78−4203
O-type runaway, extreme Population I nature 80−85938
O-type runaway stars, statistical parallax, underluminosity 78−57552
O-type star, ionisation of low-density intercloud medium 77−9782
O-type star in open cluster, interstellar dust ejection rel. to cluster dynamics 80−101622
O-type stars, C III 7901 to 9715 Å emission lines obs. 80−77401
O-type stars, catalogue on mag. tape, third edition 77−2348
O-type stars, prod. of galactic extended low-density H II region and diffuse IR emission 79−17047
O-type stars, rotational vels., V sin i and macroturbulence 77−45411
O-type stars, UV reson. lines anal. rel. to coronae possible existence 79−21293
O-type stars, vector space anal. of photometry rel. to atmospheric extension 78−49338
O-type stars, winds and coronae struct. from Hα line-profile anals. 78−40947
O-type stars and T Tauri objects, Hα, O I photometry 77−67092
O-type stars evolution rel. to Wolf-Rayet stars origin 78−81609
O-type stars in Carina nebula, rel. to nebula struct. 77−87520
O-type stars in giant H II regions IC 1805, 1848, evidence from radio obs. 80−36695
O-type stars in Milky Way, props. and catalogue 79−40183
O-type stars in NGC 4594 (Sombrero Galaxy), evidence from H II regions 78−36685
O-type stars in NGC 7000 (North America Nebula), continuum scatt. rel. to rocket UV imagery 80−82440
O-type stars in open cluster IC 1805, C IV UV reson. line P Cygni profiles 80−31296
O-type stars spectra, radial vels. and K-term 77−56922
O-type stars with mass outflow, IR fluxes calcs. for polysaccharide grain model 78−54008
OB3 type stars in young clusters, circumstellar matter 2200 Å hump interpretation 80−82351
OB associations, stellar winds rel. to H I+molecular/H II shells from 1 to 2000 pc dia. 79−25678
OB star 0.5′ from SMC X-2 source position, possible candidate 78−4411
OB star optical candidate of 2S 0114+650, spectral var. 78−16578
OB stars, distrib. in Galaxy, comp. rel. to age and space motions *(Russian)* 78−93216
OB stars, in LMC, spectroscopic obs., galaxy distance determ. 79−71111
OB stars, in Vela region, list of 166 objects 77−87280
OB stars, intermediate latit., origin 78−81627
OB stars, motion effects on H II regions forbidden line emission spectrum 77−78845
OB stars, newly formed, obs. of assoc. H_2O maser sources 78−12390
OB stars, stellar winds rel. to vel. dispersion in giant extragalactic H II regions 79−44606
OB stars in associations, role in sequential form. of OB sugroups 77−60800
OB stars in associations and young clusters, He abundance vars. *(Russian)* 77−82287
OB stars in Circinus-Norma region, search for faint objects 80−62121
OB stars in LMC nebulae complex N 59, stellar winds rel. to H II shell form. 79−17052
OB stars in M31 77−37601
OB stars Local complex, kinematics 78−16396
OB-type southern stars, UBV, Hβ and polarisation meas. 77−26007
OB-type stars, C III 5696 Å and He II 4686 Å obs., C III transition from absorpt. to emission 79−67006
OB-type stars, colour excesses, rel. to interstellar reddening material distrib. in solar neighbourhood 78−49502
OB-type stars, effective temps., ang. diameters, distances and linear radii 80−17584
OB-type stars, form. in stellar system rel. to mass loss and dynamical evolution 80−51815
OB-type stars, kinematics rel. to Galaxy local struct. determ. *(Russian)* 78−77608
OB-type stars, radial vels. rel. to distance of Sun from galactic centre 80−101584
OB-type stars, radial vels. rel. to force field normal to galactic plane 80−46669
OB-type stars and interstellar medium, cloud formation theory, effect of eqns. of state 80−109506
OB-type stars and supergiants in LMC, deep objective prism survey catalogue 79−40090
OB-type stars assoc. with H II region DR15 radio component, obs. 80−94881
OB-type stars in LMC, energetic stellar winds rel. to giant H II ring 78−77593
OB-type stars in SA 98, UBV photoelectric meas. 80−46535
OB-type stars in vicinity of long period Cepheid VZ Puppis, UBV β photometry 78−45339
objective prism low-dispersion spectra from UK 1.2 m Schmidt telescope 77−45311
observation with Solar Thermal Test Facility 80−77301
observational data, surface distribs. on celestial sphere 77−2423
observational ephemeris for constellations, 1977, September to October *(French)* 77−87241
occultation by Uranus and rings, 1980 August 15 to 16, obs. 80−98610
occultation data, effects of photon noise and initial conditions 78−28530
occultation of 13th magnitude star by Charon (1978 P 1), light curve obs. 80−94754
occultations, by Neptune, predictions for 1978-80 period 78−40868
stars continued
occultations, by rings of Uranus during 1977-1980, predictions 78−16343
occultations by asteroids, satellites discovery 80−4286
occultations by Earth, spacecraft obs., tropopause height determ. 77−2280
occultations by planetary atms., turbulence effects on refr. angles 78−61773
occultations by planets, wave optics of central spot 77−67053
occultations by turbulent planetary atmospheres, effects of inhomogeneous background on radiation propag. 78−69679
occultations by turbulent planetary atms., wave-optical theory 78−61772
occultations by Uranus rings, 1977-1980, stellar colours and magnitudes 78−16277
occultations by Uranus rings, 1977-80 period, S/N ratios 78−32392
Oe- rel. to Be-type stars 77−56982
Of and O stars, reasons for difference in mass loss 80−90413
Of stars, raxial vel. meas. 78−4226
Of-type stars, H and He II spectra, theory 78−40950
Of-type stars, search for 2200 Å absorpt. band anomalies 77−64769
old halo stars, chemical comp. rel. to nucleosynthesis in Galaxy 78−65616
oldest Population I stars, age difference from extreme Population II stars 77−56912
open cluster stars, variable extinction anal. rel. to value of R 77−37627
open cluster stars, zero age main sequence correction for age depend. *(Russian)* 79−48871
open clusters, dynamics of close binaries and single stars *(Russian)* 78−61890
open clusters stars, mag. tape catalogue of HD, HDE and DM identifications 77−13254
ζ Ophiuchi, 1980 March emission episode, Hα and He I line behaviour 80−62151
χ Ophiuchi, Be star, rapid spectroscopic variations 77−56970
ζ Ophiuchi, evidence for interstellar shock wave prod. from OH obs. 79−97052
χ Ophiuchi, foreground interstellar material optical obs. 79−25673
ζ Ophiuchi, identification of interstellar lines in UV spectrum 78−93212
ζ Ophiuchi, interstellar $^{12}CH^+/^{13}CH^+$ abundance ratio meas. 80−67809
ζ Ophiuchi, interstellar C I UV lines obs. 79−35332
ζ Ophiuchi, interstellar CO absorpt. bands and cloud density from Copernicus obs. 78−36656
ρ Ophiuchi, obs. of interstellar K I 4044 Å line 78−24533
70 Ophiuchi, occultation by Comet Kohler (1977m), prediction 78−7930
ζ Ophiuchi, rotationally excited interstellar HD column density 79−25674
ζ Ophiuchi, search for C_2 in interstellar spectrum 77−45423
ζ Ophiuchi, search for interstellar NaH line 78−4325
ζ Ophiuchi, spectral vars. related to rot. 80−22000
ζ Ophiuchi, surrounding shocklike struct., distorted interstellar bubble theory 79−71088
ζ Ophiuchi (HR 6175), O-type star, emission line episode 80−72953
ζ Ophiuchi direction, RF mol. emission spectra obs. 80−26958
optical candidates for SMC X-2 and SMC X-3, photometric and spectral obs. 78−8162
optical counterparts of 5C radiosources and blue objects, spectrographic obs. 79−101212
Orion Nebula stars, wavelength depend. of polarisation, rel. to intracluster dust and circumstellar shells 77−78839
Orion OB1 association, spectral types and peculiar stars 78−32539
Orion OB 1 association, photometric study 77−82128
Orion population stars, OH emission survey 80−67716
Orion region, survey of extremely red stars with Schmidt telescope *(Japanese)* 78−20833
ι Orionis, high-vel. interstellar H I absorpt. features obs. and implications 79−48891
YY Orionis, spectral lines profiles rel. to radially symmetric accreting envelope model *(Russian)* 78−57544
χ^1 Orionis (SAO 077705), ang. dia. from occultation obs. 78−20825
θ^2 Orionis B, long-slit spectroscopy in rocket UV 80−105297
σ Orionis E, He star, radial vels. 77−45443
oscillations, PEPSIOS spectrometer search 78−93203
pairs of stars latit. obs. anal., mean pole position calc. 80−21892
parallax stars with MK spectral classifications 80−56721
parallax techniques, discussion 79−88568
parallaxes, anals. of Sproul 61 cm refractor long-interval plate series 79−71015
parallaxes, need for space-borne and ground-based obs. 79−66992
parallaxes and Astrometric Satellite 79−30051
Paris astrolabe observations, time and latitude (1976) *(French)* 77−78078
Paris astrolabe time and latitude obs. for 1977-8 period *(French)* 79−101051
partial ionisation zones, eqns. of state 78−28653
pattern recognition using CCD star sensors for real time spacecraft attitude determination 78−96380
peculiar A and B stars, Y abundances 77−33503
peculiar bright southern stars, identification and spectral types 77−82225
peculiar central stars of planetary nebulae, spectroscopic characts. 77−87405
peculiar stars, evidence for discrete vel. states 77−22307
peculiar stars, optical and UV line emission of ionised Fe 77−13364
o Pegasi, hot Am star, spectroscopic obs. and curve of growth anal. 77−22237
θ Pegasi, rapid spectral line variability disproved 80−8625
21 Persei, Ap star, chemical element distrib. from spectrophotometry *(Russian)* 77−22238
X Persei, Be star, coordinated IR and optical obs., (in late 1976) 79−25616
φ Persei, Be star, Fe III metastable states and mass loss 79−5832
ξ Persei, exciting star for H II region NGC 1499 (California Nebula) 77−33622
ξ Persei, interstellar $^{12}CH^+/^{13}CH^+$ abundance ratio meas. 80−67809
φ Persei, model for Be-star binary system 77−60782
ξ Persei, time depend. radiation flux rel. to struct. of NGC 1499 ionisation front 78−24537
γ Persei cluster, stellar membership determ. by proper motion meas. 80−56890
perturbed spherically symmetric collapsing star, initial value problem in quasi-Newtonian background 79−5842

stars continued
photographic limiting magnitudes, determ. method for large telescope *(Russian)* 78−28531
photographic zenith tube obs. for time and latit. determ., meas. errors estimation 77−56816
photography, limiting stellar magnitudes *(Russian)* 79−92680
photometric catalogues: present and future 80−105179
photometry in Geneva seven colour system, second catalogue 77−13252
photon helicity detection for matter/antimatter star discrimination 78−12092
Piscis Austrinus, UBVR photoelectric sequence 80−62201
planet detection by astrometry, photoelectric equipment 80−56882
planetary nebula central stars, He II 4686 Å emission evidence for stellar winds 78−57608
planetary nebulae, low excitation, central stars, continuous energy distribs. and temps. 80−17646
planetary nebulae central star, far UV flux determ. from nebula ionisation state 80−72945
planetary nebulae central stars, atmospheric models 80−109434
planetary nebulae central stars, evolutionary tracks rel. to nebulae radio flux density distribs. 80−56913
planetary nebulae central stars, hot wind model for nebulae refractory elements gas-phase abundances 80−109516
planetary nebulae central stars, interpretation of UV continuum radiation 80−109524
planetary nebulae central stars, radiation rel. to nebula spectrum in composite shell models 79−25677
planetary nebulae central stars, spectra, temps., binaries and peculiar stars 80−109435
planetary nebulae central stars, temps. determ. from nebulae ionic abundance ratios 79−2565
planetary nebulae nuclei, far UV fluxes rel. to nebulae ionisation and spectra 80−109529
planetary nebulae nuclei, He shell flashes rel. to nebulae ionisation 80−73021
planetary nebulae nuclei, models rel. to distances determined from ionised mass/radius relation 80−101625
planetary nebulae nuclei, photometry and spectra of (Abell 30 and 78) 77−91602
planetary nebulae nuclei, spectral type evolution *(Russian)* 79−58361
planetary nebulae nuclei, stability anal. and short period oscills. prediction 80−77402
planetary nebulae nuclei, UV spectra rel. to effective temps. and radii 79−92843
Pleiades, Hα and O I photometry 79−35315
polarisation of stars within 25 pc of Sun, obs. 78−12202
polytrope of index three, parameters 79−62819
polytropic star, equilib. poloidal mag. field, finite difference-finite expansion method, Fortran program 77−13322
Population I, chem. and physical props. 77−78782
Population II, role in galactic spiral struct. form. 77−13469
Population II (pregalactic) stars, rel. to distortion of cosmoloical microwave black body radiation spectrum 80−67915
position coordinate meas. error reduction of sky photograph by Gaussian freq. distribution curves *(German)* 77−17384
position determ. on Schmidt plate, standard coord. and Stevenson's method 80−82176
positional catalogue for faint stars from AGK3 78−16311
positions, comprehensive general catalogue construction 80−105178
positions, general catalogue compilation, material evaluation 80−109375
positions on overlapping plates, block adjustment *(German)* 78−45237
pre main sequence stars, fragmentation rel. to form. of binaries with nearly identical components 79−48856
pre main sequence stars, rapidly rotating, evolution in gravit. contraction phase 80−62133
pre-main sequence stars in Cepheus IV association, spectrophotometry 77−13328
pre-main sequence stars rel. to bipolar nebulae, optical, IR and radio studies 78−41026
pre-main-sequence A and F stars in NGC 2264, nature of IR excesses 78−32461
pre-main-sequence stars, early evolution with D burning 80−51736
pre-main-sequence stars in NGC 2264, metallicity and circumstellar dust shells 80−26916
pre-main-sequence stars in Orion cluster, masses and stellar age spread 77−13339
presupernovae, stellar wind as possible cause of supernova remnant filamentary struct. 80−62249
proper motion stars, catalogue of stars with $m_V<15$, annual motion $>1''$ 79−58275
proper motions, anals. of Sproul 61 cm refractor long-interval plate series 79−71015
protostar, rotating, fragmentation, comparison of two three-dimensional computer codes 80−26850
protostar formation, physical and numerical problems 77−29800
protostar in bright-rimmed mol. cloud IC 1848 A, obs. 79−5810
protostars, disc accretion in soft potential well 80−8532
protostars, disc struct. in H_2O maser sources 79−48784
protostars, dust shell models for compact IR sources 77−29948
protostars, dynamical interaction with infalling matter, origin of interstellar grains 77−13327
protostars, form. as result of isentropic instabilities in interstellar gas 77−17644
protostars, hydrostatic models evolution rel. to star form. process simulation *(Polish)* 80−21998
protostars, initial stellar mass function from cosmic gas clouds fragmentation 77−56907
protostars, IR polarisation rel. to nearby interstellar polarisation 80−4347
protostars, magnetic, quasistatic contraction due to mag. flux leekage 80−98662
protostars, mass distrib. law of protocluster fragments systems 79−44571
protostars and planets, conf. (Tucson, Arizona, 1978 January 3-7) 79−58329
protostars in NGC 2264 and Rosette Nebula, far IR emission obs. 77−78841
protostellar wind bubbles in Orion Nebula, optical evidence 79−88724
Pu 60, R.A. corrections for clock (equatorial) stars *(Russian)* 78−28643
Pulkovo Observatory, stellar data and computing facilities 77−78631

stars continued
pulsating stars, g- and p-modes definition for self-gravitating fluid 77−41291
L_2 Puppis, H_2O source, linear polarisation of 22 GHz line emission 78−77612
ζ Puppis, interstellar C I UV lines obs. 79−35332
ζ Puppis, O VI P Cygni profiles hourly vars. 77−37596
RR Puppis, peculiar emission-line star, cm wavelength radio emission detect. 77−17573
ζ Puppis, radio emission obs. at 2 cm 78−40969
ζ Puppis, Reticon obs. of Hα P Cygni profile 80−82365
ζ Puppis, spectral line profiles, mass ejection 77−33507
ζ Puppis, UV spectral energy distrib. 77−22211
Puppis region (l=250°, b=0°), new UBV photoelectric sequences 77−45426
PZT stars, mean posns. and proper motions for 304 stars, obs. at Ondrejov 80−82175
QSO candidates, spectroscopic obs., indentifications 80−31385
quark stars, beta decay 80−82398
quark stars, neutrino cooling 80−56858
quark stars, possibility of existence 77−45471
quark stars, possible existence, 2nd order perturbation theory 80−26889
quark stars nonexistence 79−62855
R50 dusty star in SMC, IR photometry 77−45461
R 136 in 30 Doradus, struct., colour, mass and excitation parameter, photometry obs. *(German)* 80−67825
R-type C stars, origin, H mixing during He flicker 78−4223
radial pulsations excited by nonradial modes *(Russian)* 78−16399
radial velocities, of variable velocity stars previously observed at David Dunlap Observatory 79−101141
radii of nearby stars, appl. of Barnes-Evans relation 78−7984
radio emission monitoring at 10.6 GHz 77−60763
radio sources in globular clusters, stellar optical candidates 79−62923
radio stars, new class, identified with supernovae stellar remnants 79−17117
radio stars, positions for extragalactic reference frame 78−16278
radiosources, optical identifications, spectrophotometric obs. 79−92879
radiostars, polytropic models 79−2544
red and nebulous objects in dark clouds, survey, catalogue of 150 objects 80−56904
red stars and faint OB stars, ultralow dispersion spectroscopy 79−53733
red stars survey in 30 Doradus region of LMC, list of 298 stars 79−48794
reddened stars, JHK photometry rel. to near IR interstellar reddening 80−94857
reddened stars, search for diffuse interstellar bands at far UV wavelengths 78−32554
in reflection nebulae near Gum Nebula Herbig-Haro objects, UBVRI photometry 78−32449
relativistic star, curved space-time, vac. stability, polarisation, phase transition 77−49290
relativistic stars, struct. and stability of polytropic fluid spheres with negative index *(Chinese)* 80−57143
right ascension determ. with Sukharev horizontal meridian circle *(Russian)* 78−28646
right ascensions, uniform whole-sky system *(Russian)* 78−4082
Ross 657, metal deficiency obs. 77−5532
rotating early-type stars, V and i from Copernicus UV obs. 77−33492
rotating main-sequence stars, appl. of strained coordinate methods to struct. 77−56910
rotating stars, meridional circulation in surface layers 78−20820
rotation, thermomagnetic torque 77−53574
rotational line broadening, wavelength depend. rel. to rapidly rotating B stars 77−45416
rotational velocities, determ. via appl. of Bessel transform 77−49369
Rubin-152, possible massive O-type star on galactic fringe, spectroscopic obs. 80−98656
runaway stars, as witnesses to supernova explosions 78−32448
2S0921−630, discovery and optical stellar identification 79−21466
S106 IR, S235 B, obscured IR point sources, spectra rel. to circumstellar compact H II regions model 80−12795
2S 0114+650 optical counterpart, emission-line OB star identification 78−61938
2S 1254−690 optical counterpart, identification, photometry and spectrum 79−12545
S-type, CeO band identification, new s-process mol. 77−33488
S-type, FeH and CeO identification 79−21280
S-type, FeH bands identification in spectra 78−7952
S-type, photometric obs. of unidentified spectral bands 77−22226
S-type, revised spectral classification system in red 80−46541
S-type, secular parallax and mean absolute magnitude 78−81623
S-type stars, Keenan band identification problem, IR obs. 80−72946
S-type stars, M-type dwarfs, proposed identification of FeH 77−45418
SA 133 field near galactic centre, three-colour stellar photometry *(German)* 80−36618
ξSagittarii, lunar grazing occultation, 1974, October 21 obs. 77−33368
San Fernando astrolabe catalogue (CASF 3) *(French)* 77−78653
Santiago astrolabe, time, latit. and radius obs. (1968 to 1971) 78−12077
Santiago astrolabe observations from 1972 to 1976, results 80−46363
SAO 015338 (2A 1052+606), analysis of possible identification 78−32608
SAO 114159, occultation by 18 Melpomene, photoelectric obs. 79−12420
SAO 120836, occultation by Pallas, 1973 February 6, reliability of obs. 80−46460
SAO 158687, occultation by new satellite of Uranus, Kavalur obs. 77−53473
SAO 158687, occultation by Uranus, 1977 March 10, obs. at Tokyo Astron. Obs. 78−61716
SAO 158687, occultation by Uranus, 1977 March 10 77−87322
SAO 158687, occultation by Uranus, estimation of true external errors of Tokyo meridian circle obs. 78−28487
SAO 158687, occultation by Uranus, obs. rel. to Uranian upper atmosphere struct. 80−17547
SAO 158687, occultation by Uranus (1977 Mar. 10) 77−22044
SAO 158687, occultation by Uranus and satellite belt 77−29718
SAO 158687, occultation by Uranus on 1977, March 10, predictions 77−29717
SAO 158687, occultation by Uranus rel. to planet upper atmosphere temp. struct. 79−62791

stars continued
SAO 158687, occultation by Uranus rel. to planet upper atmosphere mean temp. and temp. vars. 80−46477
SAO 158687, occultation by Uranus ring system, obs. at Perth and Mauritius 77−67068
SAO 158687, occultation by Uranus rings, 1977 March 10, photoelec. obs. 79−30007
SAO 158687, occultation by Uranus rings, 1977 March 10 photoelec. obs. and anal. *(Chinese)* 78−69657
SAO 158687, occultation by Uranus rings 1978 April 10, rings, radii and widths calc. 79−8878
SAO 158687, occultation by Uranus satellite rings, KAO obs. 77−53471
SAO 158687, occultation by Uranus satellite rings, Perth obs. 77−53472
SAO 158687, occultation by Uranus satellite rings 77−37568
SAO 158687, occultation of Uranus, 1977 March 10, rings discovery 78−69743
SAO 158687 occultation by Uranian rings (1977 March 10) 78−89117
SAO 158687 occultation by Uranus, results rel. to planetary satellite belt 77−33408
SAO 158687 occultation by Uranus satellite rings, discovery accounts 77−74009
SAO 158687 occultation by Uranus satellite rings 77−45358
SAO 159250 by 16 Psyche on 1978 Feb. 25, details 78−16332
SAO 206553 by 704 Interamnia on 1978 April 28, details 78−16332
SAO 75392, occultation by 78 Diana, 1980 September 4, predicted central path revision 80−101547
SAO 80950, occultation by 9 Metis, Guianan obs. 80−31236
SAO 85009, occultation by Pallas, 1978 May 29, corrected prediction, photoelec. obs. 78−57430
SAO 85009, occultation by Pallas on 1978 May 29, prediction 78−53861
SAO 92603, occultation by 13 Egeria, photoelectric obs. rel. to minor planet possible satellite 80−46460
SAO 97745, occultation by 15 Eunomia, visibility track 78−12081
SAO 99401, occultation by Pallas on 1977, July 8 77−53460
SB 21, extremely He rich subdwarf O-star, spectrum 80−98659
Sc galaxies, nuclear regions stellar content 77−9793
τ Scorpii, Copernicus UV spectral atlas 78−12220
τ Scorpii, deep photospheric flows 79−58326
τ Scorpii, expanding envelope, mass loss rate 78−65613
β Scorpii, occultation by Jupiter and Io, de Sitter theory rel. to Jupiter oblateness 77−29715
τ Scorpii, photospheric vel. fields 78−28672
σ Scorpii, search for interstellar NaH line 78−4325
secondary spectrophotometric standards, obs. in 5840-10800 Å range 79−29995
shell stars, 206-287 nm UV spectra 80−51776
shell stars, H shell spectrum form. and envelope struct. 79−48830
shell stars in cluster near IC 1805, photometry and spectral classes 80−62214
single main sequence stars (A0 V to G2 V), radii compared with radii determined using binary systems 80−51758
SKYMAP: a new catalogue of stellar data 79−35151
SMC, stellar content of NE outer arm and halo 78−86013
SMC probable members and foreground stars, additional tests 79−40091
SMC stars, Herschel catalogue rel. to CPD 79−44337
SMC X-2, colours, spectral type and position of optical candidate 78−12421
SMC X-2, SMC X-3 optical counterparts, spectra 78−93469
SMC X-3, colours, spectral type and position of optical candidate 78−12421
solar neighbourhood F, G and K stars, H-R diagram fine struct. 77−29819
solar neighbourhood stars, integrated UBVRIJKL colours 79−44460
solar type stars, thirteen-colour photometry 77−22230
South Celestial Pole stars, extinction and colour coeffs. UBV photoelec. sequence 80−77456
southern metal-poor stars, UBVRI photometry and UV excesses 80−56828
Southern Milky Way stars, photometry, extinction curves, and R values 77−13443
southern OB stars, MK spectral classifications 78−12221
southern peculiar emission-line stars, observational data rel. to mass ejection 80−41843
southern polar skies, star trails taken at Siding Spring 77−56906
southern standard stars, 320-880 nm energy distrib. 80−62125
southern standard stars, monochromatic flux from 3200 Å to 8800 Å 80−51742
southern stars, IR obs. with near photometer 77−26017
Southern stars, True Visual Magnitude Photographic Star Atlas 79−75122
space density derivation methods, systematic comparison 78−61917
speckle interferometry, lens-atmosphere modulation transfer function meas. 79−101078
speckle patterns and plane scintillation, statistics 79−100948
spectral classification from UV line features, Am and Ap stars appl. 79−21272
spectral classification of early-type stars 78−16401
spectral classification rel. to interstellar extinction and galactic struct. *(Russian)* 78−73701
spectral classification using Copernicus UV data 78−12216
spectral classification using Fe III UV lines 78−16404
spectral classification using satellite UV photometric data 78−16402
spectral classification using Skylab UV objective-prism spectra 78−16403
spectral energy distrib. of eight stars used as spectrophotometric standards 79−35147
spectral energy distribution for 50 stars, 3200-7550 Å region *(Russian)* 78−65620
spectral energy distributions, results from Fourier transform spectrometry 77−82215
spectral energy distributions, synthetic colours in UBV, RGU and uvby photometric systems 78−28528
spectral types in NGC 6633 open cluster 77−74108
spectral types of stars with unusual photometric indices 79−71033
spectrophotometric stadnards, absolute spectral energy distrib. 79−97040
spectrophotometric standards, flux distribs. 77−9737
spherically symmetric accretion of gas with self-gravitation 79−8834
in spiral galaxies, vel. dispersion determ. *(Chinese)* 80−85995
in spiral galaxies nuclei, stellar population 80−56926

stars continued
SS 433, evidence for association with supernova remnant (W50) 80−51851
SS 433, radio and optical positions coincidence 80−56840
standard stars defining near two-colour photometric system for near IR, obs. 79−62759
standard stars for uvby photoelectric photometry south of declination +10°, obs. 77−2347
standard stars for VRI photometry with S25 response photocathodes, obs. 77−2422
standard stars for Washington Photometric System 80−31213
standard stars of intermediate brightness, spectral energy distribs. 78−28651
Star of Bethlehem, astronomical hypotheses *(French)* 79−84923
Star of Bethlehem, identifications rel. to Nativity chronology 79−67136
Star of Bethlehem, possible nova in 5 BC 78−32365
star of Bethlehem, possible triple conjunction of Saturn and Jupiter 77−13256
starfield, appearance from relativistic spaceship, nonexistence of 'starbow' 79−62955
static stars, spherical symmetry in general relativity 77−45397
stellar populations in galaxies, mixing processes in galaxy mergers 80−67860
stellar ring, SR 440 in open cluster NGC 6709, two-colour diagram 77−17643
stellar wind, theory of classical fluid dynamics 80−90412
Stephenson-Sanduleak 433, anomalous emission lines, gas around central massive black hole 79−53831
Stephenson-Sanduleak 433, emission-line star/X-ray source/radiosource assoc. with W50 SNR 79−8930
Stephenson-Sanduleak 433, Hα emission object, hot spot detect., rot. vel. and spectrum vars. 79−8933
Stephenson-Sanduleak 433, Hα emission object, nonthermal radio emission obs. 78−86033
Stephenson-Sanduleak 433, Hα emission object, variable radio emission obs. 78−86034
Stephenson-Sanduleak 433, massive black hole hypothesis 79−71057
Stephenson-Sanduleak 433, unusual optical spectrum changes of Hα-emission object 79−5838
Stephenson-Sanduleak 433, X-ray emission obs. 79−12480
Stephenson-Sanduleak 433 (1909+048), new type of radio star, possibly supernova stellar remnant 79−17117
Stockholm Southern Milky Way Survey, uniform edition on mag. tape 77−78655
Stokes' problem, mass transfer effects of MHD free convective flow 80−62003
Stromgren four colour indices, grid for calc. of log g and effective temp. 80−36507
structure of the universe, book 78−32628
subdwarf stars thirteen-colour photometric obs., sensitivity of indices and evolutionary effects 79−92767
subdwarfs in 47 Tucanae, CN vars. 80−94794
subluminous O-type, non LTE model atmospheres, line profiles 79−101149
super-metal-rich stars, boundary cooling and supermetallicity 80−56821
super-metal-rich stars, Fe abundance problem 77−74060
supermassive stars, D prod. by neutrino-induced nucleosynthesis 77−87582
supermassive stars, general relativistic stability towards non-adiabatic perturbations 77−41376
supermassive stars, possible dynamical stabilization by shadow gravitational potential 77−33338
supernovae stellar remnants, spectroscopic search 80−26890
symbiotic, IR variability and nature 77−49399
symbiotic C star (UKS-Cel), spectrum 77−67094
symbiotic stars, dwarf novae and related objects, IR photometry 78−8015
symbiotic stars, origin and evolutionary stage *(Russian)* 77−17616
symbiotic stars, unidentified emission line obs. at 7090 Å 77−33522
symbiotic stars and classical novae, optically thick winds 77−87450
68 Tauri, Am star, photoelectric UBV obs. of magnetic field *(German)* 77−17586
ζ Tauri, apparent wavelength depend. of v sin i 78−12240
ζ Tauri, high-resolution rocket spectra of λ1920 and λ1720 features 78−4236
20 Tauri, interstellar $^{12}CH^+/^{13}CH^+$ abundance ratio meas. 80−67809
ζ Tauri, shell star, Balmer intensity profiles 77−56973
ζ Tauri, shell star, emission features 77−56975
T Tauri stars, Hα and Na I D lines high-resolution profiles 80−62116
T Tauri stars, props. of assoc. ionized regions 80−36624
tidally distorted configurations, external form and potential, third-order approx. 80−41714
time and latitude, astrolabe obs. at Merate Observatory for (1976) 78−12078
time service, data acquisition and real time processing system *(Italian)* 80−8549
Tokyo Astronomical Obs., Time and Latitude Bulletins (1976 April-June) 77−64619
Tokyo Astronomical Obs., Time and Latitude Bulletins (1976 Jul.-Sept.) 77−70982
Tokyo Astronomical Obs., Time and Latitude Bulletins (Apr.-June 1978) 79−101052
Tokyo Astronomical Obs., Time and Latitude Bulletins (April-June 1977) 78−45203
Tokyo Astronomical Obs., Time and Latitude Bulletins (April/June 1979) 80−72752
Tokyo Astronomical Obs., Time and Latitude Bulletins (December 1975) 77−2335
Tokyo Astronomical Obs., Time and Latitude Bulletins (Jan.-March 1976) 77−70983
Tokyo Astronomical Obs., Time and Latitude Bulletins (Jan-Mch. 1978) 80−17476
Tokyo Astronomical Obs., Time and Latitude Bulletins (January-March 1977) 78−45202
Tokyo Astronomical Obs., Time and Latitude Bulletins (Jul-Sep 1979) 80−82177
Tokyo Astronomical Obs., Time and Latitude Bulletins (July-September 1977) 78−73618
Tokyo Astronomical Obs., Time and Latitude Bulletins (July-Sept. 1978) 80−4239

stars continued
Tokyo Astronomical Obs., Time and Latitude Bulletins (November 1975) 77−2334
Tokyo Astronomical Obs., Time and Latitude Bulletins (Oct.-Dec. 1976) 77−87242
Tokyo Astronomical Obs., Time and Latitude Bulletins (Oct.-Dec. 1978) 79−84646
Tokyo Astronomical Obs., Time and Latitude Bulletins (October 1975) 77−2333
Tokyo Astronomical Obs., Time and Latitude Bulletins (October-December 1977) 79−5736
Tokyo Astronomical Obs., Time and Latitude Bulletins (September 1976) 77−2332
Tokyo Astronomical Observatory Time and Latitude Service, Bulletin (January to March 1979) 80−72751
Tokyo PZT star catalogue, third improvement 77−91446
transit obs., external medium effect on accuracy of time meas. 77−87746
transits, automatic photoelec. recording 77−91435
transits, photoelec. recording, grating inclination effect 77−91436
Trapezium, X-ray obs. 79−35348
trigonometric parallaxes, determ. by Yerkes Observatory 40 inch refractor 78−89168
trigonometric parallaxes, freq. distribs. and systematic effects 80−94785
trigonometric parallaxes, internal and external errors 77−91523
trigonometric parallaxes, proper motions, magnitudes and colours for 44 stars 79−35235
trigonometric parallaxes, statistical anal. 77−64743
trigonometric parallaxes, statistical use 77−45315
trigonometric parallaxes, systematic differences 77−78776
trigonometric parallaxes, systematic errors 77−74042
trigonometric parallaxes for southern hemisphere stars 78−69780
trigonometric parallaxes of 14 stars 79−5808
Trumpler 27 star 28, obs. of WC9-type star with large IR excess 80−67738
47 Tucanae stars, colour-magnitude diagrams for inner regions 78−57598
two-dimensional spectral classes, accuracy of derivation from DDO photometry 78−16395
3U 0042+32 and 1728−16, optical counterparts 77−74163
4U 0115+63, transient X-ray source optical candidate, UBV photometry and spectrum 78−32605
4U 0115+63 optical counterpart, early type star identification from new position 78−93467
4U 1543−62 optical candidate, UB photometry 78−77625
4U 1626−67, X-ray pulsar optical candidate, UBV photometry 78−12418
4U 1626−67 optical counterpart, photometry 79−67120
4U 1636−53 (MXB 1636−53), X-ray burster optical candidate, UBV photometry 78−12418
4U 1658−48 optical counterpart, identification and semi-accurate position 78−69908
4U 1735−44 (MXB 1735−44), X-ray burster optical candidate, UBV photometry 78−12418
4U 1755−33 optical candidate, photometry and spectrum 78−77625
UBV photoelastic photometry, homogeneous data catalogue 78−96409
UBV photoelectric photometry, general catalogue on mag. tape 77−78656
UBV photoelectric sequence for studies of NGC 55 galaxy 80−73007
UBV photoelectric sequences, in fields of eight low-red shift quasars *(French)* 80−51904
UBVRGI photometric measurements of 1297 stars, catalogue on mag. tape 78−40839
UBVRI equatorial extinction star network 79−84827
UBVRIJKLMNH photoelectric photometric catalogue on mag. tape 79−16842
unreddened stars, interstellar lines rel. to two-phase model of interstellar medium 77−74110
upper main sequence stars, evolutionary tracks in H-R diagram 77−49379
upper Scorpius region stars, spectrophotometry 79−88647
γ Ursae Majoris, Ap star, chemical element distrib. from spectrophotometry *(Russian)* 77−22238
ε Ursae Majoris, Ap star, UV spectral scans, line identifications 77−45440
α Ursae Minoris, coherence interferometer obs. for atmospheric modulation transfer function estimation *(Russian)* 79−16715
α Ursae Minoris B (Polaris B), spectral type and interstellar reddening 78−8005
US Naval Observatory data files 77−78670
UV and X-ray sources, objective prism spectrophotometry 78−8150
UV Celescope Catalogue, comparison with IRC, common objects identification 77−9676
UV sources, spectral classification 78−65602
UV spectra, atlas, line features use in spectral classification 78−12215
UV spectra of standard stars, IUE rphotometric calibration 80−77383
UV stars, effect on intergalactic medium temp. and ionisation struct. 77−13455
UV stars assoc. with X-ray sources similar to Scorpius X-1, props. 77−13498
UV stellar astronomy, conference, Erice, Sicily, 1975, May *(Italian)* 78−32436
UV survey of high-latitude regions, balloon-borne obs. 80−41891
Valinhos astrolabe obs. (April 1974-December 1977) *(French)* 79−70944
Vela, spatial distrib. of young stars, UBV obs. 77−37597
γ^2 Velorum, atlas of Copernicus UV spectra of Wolf-Rayet star 78−57557
γ^2 Velorum, radio emission obs. at 2 cm 78−40969
very red stars on Palomar Sky Survey prints 77−26008
VI Cygni (Cygnus OB2) association, interstellar λ4430 band obs. 78−32555
vibrational stability of stars in thermal imbalance, energy methods 77−13320
vibrationally unstable massive stars in slow rot., oscill. props. 77−5536
Vilnius photometric catalogue on mag. tape, description 80−98578
109 Virginis, absolute energy distrib. from 3295 Å to 9040 Å 78−20828
32 Virginis, Am star, spectroscopic obs. and curve of growth anal. 77−22237
CU Virginis, short period Ap star, discovery of mag. field 77−33511
visibility estimate using visual instruments, search coeffs. 79−7089

stars continued
15 Vulpeculae, Am star, photoelectric UBV obs. of magnetic field *(German)* 77−17586
Walker No.67 in NGC 2264, candidate for strong interstellar circular polarisation 78−12223
WC stars, near IR spectrometry 80−94816
winds from OB associations, interaction with interstellar medium to form H I supershells 80−82468
Wolf-Rayer stars, UV obs. 78−40965
Wolf-Rayet, electron density in emission-line region 78−93263
Wolf-Rayet, IR light vars. 77−9750
Wolf-Rayet, single-line Population I stars, space vel. 80−77415
Wolf-Rayet and Of-stars obs. in young galactic open cluster 77−64810
Wolf-Rayet atmospheres, structure and composition 80−98668
Wolf-Rayet objects, search in SMC 79−67014
Wolf-Rayet stars, 2 to 4 μm spectrophotometry of late WC stars 78−96491
Wolf-Rayet stars, ANS UV spectrophotometric obs. 80−22023
Wolf-Rayet stars, atlas of Copernicus UV spectra 78−57557
Wolf-Rayet stars, evolutionary status of high-luminosity (WN7/WN8) stars *(Russian)* 80−109425
Wolf-Rayet stars, faint, photometry and spectrography 79−40200
Wolf-Rayet stars, galactic WN7/WN8 stars as massive O-stars in advanced evolution stage 79−92778
Wolf-Rayet stars, in M33, spectral obs. 77−64779
Wolf-Rayet stars, interstellar N V lines, IUE obs. 80−101634
Wolf-Rayet stars, laser action in distended envelopes 77−13354
Wolf-Rayet stars, near IR spectra emission line characts. 79−53825
Wolf-Rayet stars, rotation rel. to ellipticity of surrounding nebulae *(Russian)* 78−12252
Wolf-Rayet stars, short-lived changes of emission lines *(Russian)* 80−72977
Wolf-Rayet stars, struct. of winds from obs. of IR continua 77−78793
Wolf-Rayet stars, WC9, optical spectropolarimetry and spectrophotometry 77−64778
Wolf-Rayet stars as supernova progenitors *(Italian)* 79−53830
Wolf-Rayet stars discovery in 30 Doradus nebula in LMC 79−16980
Wolf-Rayet stars in galactic-centre field, new discoveries from spectroscopic obs. 80−8674
Wolf-Rayet stars in heavily reddened young open cluster Trumpler 27, spectra and photometry 77−78836
Wolf-Rayet stars in LMC, new discoveries, positions, spectra and magnitudes 80−46569
Wolf-Rayet stars in LMC, new discoveries 79−67018
Wolf-Rayet stars origin, critical mass loss rates from massive stars 79−101138
Wolf-Rayet stars origin rel. to O-type stars evolution 78−81609
Wroclaw FKSZ catalogue reduction to FK4 system *(Polish)* 77−64669
X-ray source fields, transmission grating spectroscopy, optical condidates 79−21283
XUV sources, candidate types review *(German)* 80−109372
Yang-Mills gauge theory of gravity, gravit. field of spherically symm. matter distribs. 78−4773
young OB star in NGC 6334, possible assoc. with new H_2O maser 79−21369
young stars, distrib. rel. to local spiral arm fine struct. 77−57091
young stars, high-freq. radio continuum obs. 80−51766
young stars, nonspherical thermal instability 79−48779
young stars embedded in dark clouds, search for radio continuum radiation 77−33585
young stars in galaxy NGC 4314, distrib. from UBV surface photometry of central region 80−77482
young stars in rejuvenated galaxies, rel. to galaxy form. 77−33645
young stars reddening and polarisation, intracluster and circumstellar dust effects 78−93199
young stellar objects, origin of polarisation 79−8911
zero polarisation standard stars, list 79−40187
A- and B-type stars, radiation forces and B abundance diffusion theory 79−88664
Ba 0 stars, abundance anal. 77−17557
Ba, CH and R-type carbon stars, spectrophotometry 77−17575
Ba stars, spectroscopic, radial vel. and photometric obs. 78−12226
C and S stars, mixing between burned core material and surface layers 78−12213
C star, variable, in open cluster, Stock 8, spectroscopic and photometric obs. 79−84791
C star pairs, search of Westerlund's catalogue 78−12301
C stars, $^{12}C/^{13}C$ abundance ratio 77−33494
C stars, $^{12}C/^{13}C$ ratio determ. 78−73710
C stars, 3 μm absorpt. band obs. 78−28682
C stars, 3 μm band compared with interstellar 'water-ice' 3 μm absorpt. 78−49499
C stars, catalogue of 302 stars in LMC 78−20654
C stars, in LMC, VRI photometry, optical spectroscopy and evolutionary implications 79−71019
C stars, photometry at 1-2.5 μm, circumstellar dust shells 79−88652
C stars, possible assoc. with LMC open clusters 78−49428
C stars, rot. depend. of Franck-Condon factors of C_2 Phillips system 77−27058
C stars, spectral clssification by photoelec. photometry of line strengths 78−73711
C stars, spectrophotometry, C/O and $^{12}C/^{13}C$ ratios calc. 77−91533
CH stars in south galactic cap, radial vels., photometry 77−87396
CNO isotope importance in astrophysics 77−87263
CNO isotopes in astrophysics, conf. Grenoble, France, 1976, Aug. 77−87262
Fe/H abundances, rel. to blanketing parameter Δm_2 78−36555
H II region exciting star, influence on nebula temp. and ionisation struct. 78−61911
H_2O masers, detect. of new sources 78−32466
H_2O masers, time vars., 22 GHz obs. 79−30077
Hα emission line stars in Coalsack direction, finding list 77−22115
Hα emission line stars in nebulae, rel. to galactic spiral struct. in vicinity of Sun *(Russian)* 80−62290
Hα emission stars assoc. with Gum Nebula, star form. triggering 77−29821
Hα emission stars in and near NGC 7000, obs. 77−13363
Hα emission stars in Milky Way, catalogue of new discoveries 77−64665
Hα emission stars in southern dark clouds, objective prism survey 78−28536

stars continued
Hα emission stars in southern dark clouds, UBVR photometry 78−81633
Hα emission stars in young cluster NGC 2264, UBVRI obs., pre-main sequence stars 79−35267
Hα stars in NGC 2264 and NGC 7000/IC 5070 , slitless spectrographic search 80−62120
He stars, in symbiotic star systems, evolution *(Russian)* 77−17616
He stars, supernovae progenitors *(Italian)* 79−53806
OH masers, obs. of new assoc. IR objects 78−12407
OH type I maser sources, model 80−90556
OH type II stars, unidentified, search for H_2O emission 79−75286
Si stars, UVBY photometry, variability obs. 77−22233
SiO maser sources, 43 GHz obs. 79−16942

starters *see starting*

starting
see also actuators; ignition
BWR, Brunswick Unit No.1, startup test experience 80−9353
BWR, Fukushima Daiichi power station, preoperational test, start-up test, operating experience *(Japanese)* 78−29635
BWR, startup control rod programming code system 80−13688
BWR, TVO I, startup principles 80−9372
BWR, Wm. H. Zimmer nuclear power station, startup and testing 80−9373
discharge striking in highly inhomogeneous axisymmetric mag. field 78−75473
electron generator based on diffraction radiation, dynamic and static electron shiftings influence, theory and expt. *(Russian)* 79−3617
FFTF startup, instrument calibration program 80−9337
FFTF startup plan 78−17411
fission reactor, zero-power control rod group reactivity worth, computerized determ. method 78−21702
fission reactor boron thermal regeneration system, operating experience 80−13683
fission reactor Crystal River Unit 3, startup experience 80−13684
fission reactor of Lenin Nuclear Power Station second unit 77−23231
Fort St. Vrain HTGR rise-in-power test programme 79−9864
HTGR, 330 MWe nuclear power station, start-up and operating experience since 1975 80−830
HTGR, Fort St. Vrain, nonlinear subcritical multiplication 78−21701
HTGR, startup test techniques 78−21706
HTGR low power startup model development and use 77−88220
HTR, Fort St. Vrain startup experience 78−17407
laser startup system for magnetic fusion 77−18704
low-pressure discharge striking in axisymmetric elec. and mag. fields 78−75472
LWBR, startup and initial operating experience 80−13682
LWR, initial fuel loading problems 78−21741
nuclear plant startup, benefits of standardisation 80−13686
nuclear power plant, Browns Ferry, startup and operating experience including cable tray fire 77−65284
nuclear power plant, startup planning 80−9371
nuclear power plant, Trojan, operating and startup experience 77−65283
nuclear power plant startup scheduling 80−13687
nuclear power station, modification during plant startup and operation 78−21758
nuclear station, with water-cooled water-moderated reactor cooling system faults, hybrid simulation *(Russian)* 78−5008
pulsed short arc lamps, characteristics of controllability 78−42400
PWR, flux monitoring startup and safety system, ex-core, design and qualification 77−65286
PWR, Salem Unit No.1, startup and operating experience 80−13685
PWR, startup, secondary-side corrosion product transport 80−9377
PWR reactors, commissioning and start-up procedures *(Slovak)* 79−36346
PWR transient anal. methods, qualification with plant startup meas. 80−18508
Tokai reprocessing facility start-up *(Japanese)* 78−74457
Ar loaded K heat pipe performance characteristics 78−89934
He-Ne laser 10kV/1.5kV power supply 79−36906

startup *see starting*

state estimation
adaptive laser beam control process, closed loop considerations 77−88660
adaptive optics aberration coefficient estimation 77−19179
adaptive optics aberration coeffs. adaptive estimation 77−88659
air pollutants spatial conc. estimation, new proposal for those which absorb optical energy 79−57533
continuous-time linear system, varying environment, state estimation methods 79−12581
human motion and force sensory mechanism model 80−8094
hydrologic cycle in Lake Biwa basin, system theoretic study 79−53400
liver disease computer-aided diagnosis using nonlinear stochastic modelling technique 78−36024
multidither adaptive optics, estimation and control 77−50757
nuclear materials accountability enhancement in first solvent extraction cycle, modern techniques 80−83216
nuclear reactor, digital control using linear quadratic Gaussian regulator 80−37554
oil exploration seismic data processing, white noise estimators 78−3973
one dimensional distributed parameter system parameter and state estimation, heat conduction experimental result *(Japanese)* 80−83727
physiological system stochastic anal. and control., cancer detection and therapy 77−90713
process dynamics investigation using time-varying models 77−41099
sonar array paired element delay meas. with sequential state estimation 80−96128
water quality modelling, Kalman filter theory and practice 78−45058

state of the art studies *see reviews*

state-space methods
adaptive optics aberration coeffs. adaptive estimation 77−88659
cell cycle kinetics stability and control, cancer chemotherapy appl. 79−34521
ECG baseline estimation and removal using cubic splines and state-space computation 77−44808
electrocardiogram baseline noise estimation and removal using cubic splines and state space computation techniques 78−11755
geophysical structure estimation from acoustic reflection meas. 78−7818
hydrological system, state space modelling and identification 79−79908
lossless layered media described by wave eqn., time-domain models 77−91065
lossless wave eqn. in layered media, canonical Bremmer series decomposition 77−91064
neutron transport, state-space splitting in Monte Carlo calcs. 77−65264
nuclear reactor noise analysis, irreversible circulation parameter 78−94069
reactor spatial control during nuclear station load cycling, multivariable control algorithm 79−13490
seismic waves, reflection coeffs. identification from noisy data 79−29718
stochastic systems, relay-type scalar, fundamental response properties *(Japanese)* 77−2519
stratospheric O_3 reduction due to pollution, system-theoretic model 77−73848
walking-stick maps, syncope, rel. to chaos 77−63894

static (atmospherics) *see atmospherics*

static electricity *see electrostatics*

static electrification
see also triboelectricity
ACS blendmer and chlorine containing polymers, electrostatic property 80−54764
anisotropic insulators, interaction of point charge and interface 79−69584
atmospheric electricity, or static electrification hazard, review 78−28283
charge neutralisation on moving filament *(Russian)* 79−7876
contact charge density, true meas. using soft rubber 78−43462
DC transmission conductors, corona discharge and elec. charge on water drops, obs. 79−82114
dielectric solids, contact electrification, review 78−26934
electrification by plastic deform., mechanism 78−26935
electrostatic charges meas. and localisation, neutralised during lightning flashes 80−77097
ESCA, insulator charging, line energy corrections 80−50898
gas-solid suspensions flowing in steel and insulating coated pipes 77−77811
insulating film moving over grounded metal rollers, electrostatic behaviour 80−49873
insulating films, PET and SiO_2, charge effects at Al electrodes obs. 80−75625
insulator surface charging with liquid Hg 79−78157
insulators, expts. with solid rare gases 80−70797
insulators, role of surface ions in contact electrification 80−54762
ionic crystal, dislocation mechanism of electrification during cleavage 77−24353
jet droplets from bursting bubbles at air/water interface, electrification and size 77−48700
Jupiter Voyager electrostatic discharge protection 78−89042
material transfer in contact electrification 78−6432
metal, surface charge density 78−14797
metal surface heated, charge separation from electrolyte drops 80−88617
metal-insulator contact, electron tunnelling and its role in contact electrification 80−2453
microsphere removal by SAW displacement field 79−45884
moving fluids, progress up to 1979 80−69292
nylon 6, evidence of electron transfer as mechanism of static charge generation, contact with Hg 79−47153
paper sheets, charge decay and resistance parameters correlation determ. 80−70795
particle charging against conducting wall in DC field 77−10808
patient's virtual earth and electrical interference monitor, electrophysiological signal degradation reduction 79−57800
piezoelectric crystal surface, periodic film form. due to SAW 78−72038
polarisation charge build-up on air/dielectric separation surfaces 80−25288
polyethylene: octadecanol, contact charging and donor impurity conc. relationship 80−20286
polyethylene-metal contact charging, electron transfer mechanism, PES characts. 80−35055
polymer, amorphous, excess charges, band gap levels and elec. props. 78−23053
polymer, contact electrification, extrinsic surface state contrib. 77−11984
polymer, molecular charge states, contact charge exchange 78−14822
polymer surfaces charging injection times obs., with aid of computer 80−70796
polymeric capacitors, injection charging 77−76902
polymers, contract electrification, analogue model 79−51655
polymers, frictional electrification, temp. and friction speed dependence obs. 80−70798
polymers by metals, contact time effect obs. 80−70829
polystyrene-polymer, contact electrification model arising from eigenvalue spectra 78−47846
polyvinylcarbazole-Hg interface, contact electrification, internal photoemission study 78−60191
polyvinylidene fluoride, biaxially stretched film, corona charging and piezoelec. effect 78−88256
polyvinylidine fluoride, corona charging at 12.5 kV, obs. 78−92027
PVC, rubbed, TSC meas. 80−55017
PVC, spontaneous current emission, various metal electrodes 78−43412
rocket nozzle, static electricity form. during ionised gas discharge 79−40060
sapphire, contact electrification 78−88018
semiconductors and insulators in contact with metals, charging of bulk states 80−54781
spark hazard in charged powder handling, identification and contol 80−69291
surface analysis techniques appl. 80−80354
thermionic return currents in contact electrification 78−39189
vacuum oil drop electrification in elec. field 79−86101
Hg-polymer interface, contact potential and charge exchange meas. 80−75642
KBr, single cryst., lattice structure distortion on freshly formed surface, electrification 77−51582
LiF, cleaved cryst., electrification mechanism 78−19126
LiF, dislocation mechanism of electrification during cleavage 77−24353
LiF, electrification by plastic deform. 79−33334
LiF, mech. excitation, luminesc. electron emission, friction, static electrification, meas. method *(German)* 77−24904

static electrification continued
NaCl, single cryst., lattice structure distortion on freshly formed surface, electrification 77−51582
Si-P dust, electrification and cond. 79−82662

statics
see also hydrostatics
analogy to dynamics, related by variational techniques 78−28934
closed cylindrical shell in moment state *(Polish)* 77−53774
cracked elastic body statics, three-dimensional problem *(Russian)* 78−73858
education, knots, topology friction and strength 77−33769
education, relativistic statics, covariant formulation 78−49593
elastostatics, body force integral 77−64947
rod, perturbation methods for soln. of linear eigenvalue problem *(German)* 78−18175
spatial structures of shells and grids 77−19526
two-shell spatial structures with feathering, statics 77−39219
unclosed shells of revolution with inhomogeneous boundary conditions, two-dimensional statics *(Ukrainian)* 78−89341

stations, power *see power stations*

stations, radar *see radar stations*

statistical analysis
see also demography; measurement errors; probability; random processes; statistical theory of nuclear reactions and scattering
Abell and Shane-Wirtanen catalogues, cross-correl. anal. 78−4118
accidents during work, mapping of reasons using error beams by function sensed computations of admission probabilities *(German)* 80−68027
acoustic attenuation coefficient slope for liver tissue, statistical estimation from refl. US signals 80−46000
acoustic emission signals interpretation during tensile testing 77−9030
acoustic forward reflection from rough sea surface statistical anal. 78−50983
acoustic noise on vibrations in digital form *(Japanese)* 77−23805
acoustic normal mode amplitudes in random ocean, statistical theory 78−50981
acoustic reflex threshold, variability of measurements 77−16938
acoustic-emission pulse distrib., statistical investigation 80−87638
acupuncture point location using elec. impedance meas., statistical anal. 78−44628
adsorption, molecular-statistical description, ensemble of excess systems 80−10776
air pollutants, ambient, statistical models with reference to Los Angeles Catalyst Study (LACS) data 80−30620
air pollution, short term oxidant control strategy 79−20995
air pollution, statistical prediction by mixed order multi-variable AR scheme in Japan 79−57537
air pollution analysis results 77−41153
air pollution conc. statistical parameters determ. from truncated data set 77−37414
air pollution data, real-time meas. transformation and statistical processing 78−24365
air pollution data analysis rel. to meteorological conditions 77−70816
air pollution impurity concentration meas. sampling error anal. *(Dutch)* 77−70828
air pollution in planetary boundary layer 77−37379
air pollution levels, stat. prediction by Kalman filtering method 79−57535
air pollution levels, statistical distrib. over urban area 77−37400
air pollution long-term dispersion studies, temporal sampling requirements 79−39325
airborne gamma-ray spectrometry data processing using multivariable statistical analysis 79−35004
alloy steels, microstructure characteristics, statistical processes *(German, English)* 78−95884
alloys, criteria of chemical inhomogeneity 80−59670
alloys, multicomponent, optimal composition determ., mathematical-statistical methods *(Czech)* 79−15624
Am stars in spectroscopic binary systems, evolutionary status, statistical anal. 78−93262
analytic theory of extrema, appl. to nonlinear oscillators 80−73160
annealing twin form., statistical anal. *(French)* 77−81281
antennas and interferometers, troposphere random inhomogeneities, effect on operation 77−13111
apparent movement perception, psychophysical optimum condition analysis expt. 77−81510
apparent movement perception, psychophysical optimum condition analysis applications 77−86504
asteroid concentrations in proper elements space, statistics and mapping 78−96420
astrometry, accuracy of star positions obtained by block adjustment 78−20623
asymptotic theory of statistical estimation, regularity versus nonregularity comparison 80−52003
asymptotic time to failure of a mechanical system of parallel members 78−83240
atmosphere, scatt. coeff. and scatt. directivity coeff. in 0-165° angle range, statistical relations *(Russian)* 77−29433
atmosphere, statistical predictability of long-term processes *(Russian)* 77−49105
atmosphere daily temperatures, statistical forecasting using short records of previous temps. 79−58015
atmosphere radiation attenuation depend. on surface layer turbidity, statistical characts. *(Russian)* 78−44997
atmosphere temperature field, spatial anal. from weather satellite meas. 78−20488
atmosphere temperature field over tropical Atlantic, statistical struct. and objective anal. *(Russian)* 77−64373
atmosphere vertical stability indexes, statistical anal. from Rn concs. *(Spanish)* 79−92561
atmosphere visibility trends, appl. of ridit anal. 80−82051
atmosphere-ocean interactions along North American west coast, 1965-69 period, preliminary anal. 78−61508
atmospheric aerosol attenuation spectral struct. *(Russian)* 80−4104
atmospheric attenuation statistics at 15 and 35 GHz for very low elevation angles 79−8674
atmospheric energy dissipation, statistical props. 78−81267
atmospheric humidity field objective anal. using remote sounding data 78−61524
atmospheric O_3 total content trends, from daily Dobson data 78−92915
statistical analysis continued
atmospheric pressure, long-period fluctuations, statistical analysis *(Russian)* 78−81298
atmospheric worldwide total O_3 trends 77−33138
atmospherics in HF band, statistical characts. of signal and atmospheric noise mixture 78−57276
atom stripping in gaseous targets, equilib. charge state distrib., statistical anal., appl. to Cl, I and Br data 80−5610
atomic inelastic collisions, inner shell vacancy prod. 79−45792
autoregressive analysis, a method for detect. of EEG changes in newborns to tones 80−108982
avalanches, critical condition prediction *(French)* 77−33104
avalanching statistics, strong electric field *(Russian)* 77−66171
averaging, choice of mean 78−16604
bandwidth compression effect on military target observers' detection and recognition performance 80−106484
Barkhausen effect, mag. thin films, statistical anal., instrumentation, computer interfacing 78−82008
beach changes in S.California, statistical prediction 80−98305
beam, brittle fracture, Weibull statistical theory 79−81810
biased roulette, mathematical pendulum, limit distrib. of stopping angles 78−81821
Biblis Nuclear Power Station, meas. and control system, fault statistics evaluation *(German)* 79−97819
Bijvoet difference measurement, in crysts. with heavy atoms, stat. method for selecting reflections 79−50923
binary image correlator in absence of geometric distortion 79−22907
binary image statistical modelling, enhancement and recognition *(Russian)* 80−63929
binary stars, statistical distrib. and evolution *(Chinese)* 80−85975
binary stars in open clusters, statistics 77−53626
Bingham distrib. function in palaeomagnetic studies 80−72649
binormal distribution, standardised, percentiles calc., FORTRAN subroutine 78−34
biological signal time averaging, digital Wiener filtering and detection statistical aspects 78−35979
biological time series concatenation and homogeneity 77−40627
biomedical research, basic statistical data analysis techniques 80−42046
biomembrane conductance fluctuations and ionic pores, review 77−90752
blood cell anal., weighted chi-squared test 80−30925
bone, elastic characts. of compact bone tissue of human tibia, differences and correls. 77−25490
borehole measurements in Miocene sediments, anal. of repeated meas. 78−49146
bottom settling of solid particles in turbulent shear flow, distribution statistical properties *(Japanese)* 80−19344
boundary-value problem, two point, statistical version anal. 79−63154
brittle ceramics, effect of data scatter on apparent thermal stress failure mode 80−60949
brittle fracture, evaluation of a fundamental approach 78−64619
brittle rotating disk, probability theory appl. to rupture strength 80−43662
brittle rupture in solid body, distribution function at threshold *(Russian)* 77−84192
bubble chamber tracks, gamma-particle multiplicity distrib. moments meas. 77−30712
bubbly flow, void fraction meas. by light attenuation technique derivation of transmission rate reln. *(Japanese)* 80−48795
BWR, min. critical power ratio thermal limit 80−18398
BWR, prediction model for shutdown margin reactivity 79−26476
BWR containment struct., appl. of frequency domain anal. 79−93753
BWR void reactivity feedback, statistical weight factor 79−9702
4C radiosources clustering, statistical analysis 79−5761
calorimeter resolution effect on high P_T particle distribs. 79−59323
cancer mortality among A-bomb survivors, 1950 to 1972, additive logit model 77−70504
cantilevers, randomly excited, first passage failure 79−46241
cardiogram arrhythmias detection and classification 77−21644
β-carotene, solubilised in lecithin liposomes, linear dichroism, absorption statistics 78−1014
Caspian Sea, water balance and level vars. statistical forecasting 77−78263
catchment model parameters sensitivity anal. 78−77288
CECG waveform, statistical algorithm and struct. anal. 80−72341
celestial mechanics, disruption of three-body systems, high ang. momentum case 77−13220
ceramic, failure prediction under thermal loading, Weibull eqn. 78−88534
ceramic turbine disc, subjected to centrifugal stresses, failure probability, photoelastic model 79−18816
characteristic fuel element temps. calcs., statistical treatment of defects 79−45351
characteristic functions, monotone decrease 77−33843
chemical anal. methods, statistical evaluation, acceptability criterion 77−63977
chemical data, factor analysis reliability improvement 77−36802
chest radiograph texture anal. model 78−40323
chi squared goodness of fit test at signal plus noise alternatives 79−71231
chloroplast conformational variations study 79−92177
chromatographic curves, machine treatment using statistical moments method 77−63981
chromosome density profiles, description and classification 79−43830
classifier model for multi-observational anal. 77−78533
CLEAN method, iterative beam removal, mathematical-statistical description 78−57464
climatic change and goemag. field reversals, statistical correl. 78−61537
climatic change effects on food production, statistical models limitations 78−57303
climatic temperature changes since 1665, statistical study of causative factors 79−8680
climatology, statistical methods *(French)* 78−32252
clinopyroxenes from deep sea basalts, statistical anal. 78−88828
clinopyroxenes from deep-sea basalts, statistical anal. of chemistry 80−41437
coagulating droplets, statistical distrib. 79−74425
coincidence spectra from three particle reactions, projection on kinematical curve 77−10564
collaborative tests, reference material certification procedures 78−28922
Collinder 140, young open star cluster, membership statistics from spectroscopic study 80−62211

statistical analysis continued
colloidal dispersion, particle size distrib. change kinetics, statistical approach 78−7241
comets, groups and pairs 77−41357
comets, long-period, perihelion points distrib. statistical tests 80−4304
comets capture by Laplace scheme, orbital elements statistical consequences 78−53888
community noise abatement, estimation of L_{eq} using Weibull distribution *(Japanese)* 80−55964
complete computer program in FORTRAN, for analysis of variance and means 80−98792
complete structures, appl. of phase refinement, use of statistical information in tangent-formula refinement 79−7511
complex dynamic system statistical energy analysis 77−75740
complex shaped large scale part, statistical eval. of service life 79−91798
composite exponential decay curve anal. 78−46241
composite material, brittle failure prediction 77−89072
composite materials, stochastic fracture models, and strength test results statistical anal. 80−64470
composite shell, optimization model including statistical parameters 78−22271
computerised tomography, statistical limitations, attenuation coeff. variance derivation 79−8537
concrete, compressive fatigue life, estimate of distrib., statistical method *(Japanese)* 78−11328
concrete, quality control, construction of operating charact. curves *(German)* 77−28960
containment liner seismic reliability under statistical uncertainty, cracking 78−89948
continuous noisy signal analysis by autoregression time-series model 79−3209
cooperative stereo algorithm, empirical approach 79−100615
cooperative stereo algorithm anal. 78−53413
Cornish-Fisher expansions, generalised 80−52004
coronary artery disease diagnosis, exercise ECG, VCG and body surface mapping 79−44046
correlated pulse sequences, mixed spectrum, appl. to linear atom chains 79−84944
correlation functions of zero mean random process 78−5428
correlation TOF technique, real modulation 79−49898
cosmic ray interplanetary scintillations at 250 GV, statistical props. 80−8496
cosmic ray propagation from discrete galactic sources 79−44312
cosmic rays cyclic variations correl. with solar activity, regression series 79−16776
cosmic rays transient intensity vars., anal. rel. to solar source 78−89022
counting rate asymmetry detection 79−26853
counting statistics with variable dead time, generalised expressions for distribs. *(French)* 78−21828
crack, semielliptical, in cast components, relation between axes 78−11326
creep, fatigue and fracture data analysis, statistical methods 80−58936
creep rupture data analysis, development of correlation and extrapolation methods 80−58975
cross-section data adjustment iteration procedure 79−9696
crystal powder statistics, line profiles in diffr. spectra of identical crysts. and Gaussian samples, cryst. size distrib. 79−7508
crystallographic orientation, distribution function generalisation using rotation matrix 80−11665
cumulative sum charts, for background count rate monitoring 78−29718
curve fitting to data with low statistics 80−9471
daily solar total irrad. fluctuations, temporal statistical anal. *(French)* 80−61292
data analysis statistical and computational methods, book 77−5655
data lists, analyze to reduce contradiction, averages and least square approx. methods 79−53966
data volume determ., based on risk for arbitrary volume of a priori data 80−95054
dead time, correction for counting losses in single cryst. X-ray diffractometry *(French)* 79−37587
dead time corrections in coincidence measurements by time-to-pulse-height converters or standard coincidence systems 80−9472
dead time effect on power spectral density estimates of discrete time series 79−18096
dead-time estimation method 79−6807
definitions, normal distrib. and signal detect. for astronomers 80−17500
delayed coincidence expts., precision of half life estimation 80−27908
delayed coincidence spectra anal. without knowledge of resolution curve 79−22566
diffracted amplitude and intensity, inhomogeneous and randomly distributed media *(Spanish)* 80−48151
diffusion from ground-level source in turbulent boundary layer, Lagrangian statistical anal. 80−12517
digital filtration in correlation time-of-flight spectrometry 79−49894
digital system for measuring probabilistic and statistical characteristics of infralow-frequency processes 79−71431
disordered materials, bounds for effective elastic moduli 78−4486
disperse particles concentration and spacings between them in Poisson point field model 78−39963
disperse systems, particle concentration determ. by statistics 79−66370
distribution central moments estimation, lung tidal ventilation appl. 79−88104
distribution function for approx. of series of values or classes *(German)* 77−67234
distribution function parameters determ. in real time, instrument description 80−202
distribution function $y=ax^b \exp[-c(\ln x)^2]$, props. *(German)* 78−77686
dose estimation in personnel, neutron monitoring with albedo dosimeters 79−48344
double galaxies, data anal. and galaxian mass (M/L) determ. 80−4428
double galaxies, observational data on well-defined sample 80−17674
droplet size distribution, least squares method for fitting exptl. data 77−39329
droplets, kinetics of processes controlled by diffusion 79−11828
ductile fracture surfaces, statistical charcts. of microcracks *(Russian)* 78−23807
Earth crust vertical movements, rel. to surface relief in Bulgaria, statistical investig. 78−81126
Earth radiation budget data collection and interpretation model 77−37497

statistical analysis continued
earthquake frequency/magnitude prediction for selected surface regions 79−16415
earthquake prediction, risk forecasts 79−79746
earthquake statistics, truncated exponential frequency-magnitude relationship 78−65191
earthquakes, damaging, and volcanic eruptions in Iceland, 1550 to 1978, statistical anal. 80−89975
earthquakes, frequency-magnitude distributions 79−66648
earthquakes, shallow, statistical study of occurrence relations 78−96155
earthquakes, statistical estimation of largest possible magnitudes in Balkan region 77−21680
earthquakes, suspected periodicities in Sweden 79−66647
earthquakes occurrence times, statistical anal. rel. to forecasting expt. 79−53315
EBR-II driver fuel lifetime, cumulative damage anal. and Weibull statistical anal. 80−13601
ECG classification by linear multiple regression analysis 77−13027
ECG-VCG multivariate classification by linear regression, influence of populations 77−44789
ECG/VCG, rhythm diagnosis using statistical signal anal., identification of transient rhythms 78−77142
ECG/VCG rhythm diagnosis using statistical signal anal., identification of persistent rhythms 78−77141
echoes scattered by random fluctuating surface, statistical model *(French)* 77−11066
education, radioactivity, binomial distrib. and Poisson statistics 77−49525
education, statistical methods for non-Gaussian distribs. 77−33782
EEG, topographical display of epileptiform transients based on a statistical approach 80−108833
EEG 80−85504
EEG automatic classification, parametric ARMA time series models 77−90944
EEG-like data, Guassian amplitude distrib., new test 80−30915
effluent sampling programme data statistical evaluation 79−13547
elastomer, relaxation processes, statistical description *(Russian)* 79−23229
electric breakdown, solid dielectrics, Weibull distribution, parameter estimation 77−77149
electromagnetic interference, classification 77−83789
electron beam dose profiles, cumulative normal distrib. model 79−88199
electron ionisation energy loss, approx. to Landau's distrib. functions 79−23664
electron microprobe, automated, evolution of quantitative elementary point anal. in geosciences *(French)* 78−78046
electron microscopy, correlation analysis of radiation damage 80−100282
electron probe analysis, precision and optimisation of thin specimens *(French)* 77−77849
electronic meas. systems error anal. *(Polish)* 79−88902
electrosensory afferent, dogfish, adaptation, neuron discharge regression anal. 78−35833
elliptical galaxies, three-dimensional figures anal. 80−36704
EM induction in thin sheets, statistical theory 77−86769
EM irradiance distribution function in turbulent media, theoretical review 79−64155
EM propagation in turbulent medium, joint Gaussian statistical props. 78−42265
EM wave propagation, in one-dimensional, randomly inhomogeneous medium, with specularly reflecting walls 80−105514
EM waves backscattering, multiple, from randomly fluctuating media 77−50593
EM waves in medium with ellipsoidal inhomogeneities and regular refr., ray statistics 78−25773
EM waves scattering, in nonlinear medium with one-dimensional random nonuniformities 80−106421
empirical standard deviation exactness *(German)* 78−28921
endogenous and exogenous activity in molluscan neurone, identification by spike train anal. 80−89735
energy spectra, deconvolution, modified method of statistical regularisation 78−54164
enthalpy-entropy compensation effect, separation of chemical from statistical effects 77−21412
enthalpy-entropy compensation effect, statistical analysis, van't Hoff and Arrhenius data 77−21411
entropy characterisation by generalised probability distribution 78−6163
environmental noise, exposed population size determ. 79−3851
enzyme dynamics, statistical phys. 80−21439
epidemiology, causality, and public policy 79−97177
equations of state, search procedure, based on step-wise least-squares technique 80−19900
equilibrium characteristics in the condensed state with the nearest-neighbours interaction *(Russian)* 79−12726
error definition for data acquisition systems, in steady and unsteady states 80−95056
erythrocyte osmotic fragility curve, statistical synthesis 78−65070
essential hypertension, empirical data 78−89309
European air temperature band-pass filtered series, correls. and phases 80−26579
evoked responses, statistical detect., evaluation of Woody's adaptive filter 77−81757
examination marks, reliability, in electronic engineering educational courses 79−75305
experiment planning for metrological reliability *(Rumanian)* 79−6075
experimental data, book 78−77834
experimental data, comparison between two sources, anal. 79−97186
experimental design and statistical analysis of data, measurement of period of simple pendulum 80−42017
exponential distribution MTBF confidence limits determ. using Epstein and Harters methods 80−98790
expt. data analysis, normal distribution verification algorithm *(Bulgarian)* 80−27261
extragalactic objects catalogues statistical anal., QSOs and Lick galaxy counts correl. 79−25700
extragalactic objects clustering in Universe *(Polish)* 78−96580
extragalactic radiosources, statistical tests on angular size-flux density relation 77−82315
extreme wind speed probability, mixed wind climates 78−28295
falling liquid film, thickness meas., statistical props. 79−12708
falling snow, occurrence over United Kingdom 77−41124

statistical analysis continued
fast reactor safety, TREAT experiments, fuel pin failure, statistical analysis 79−97840
fast reactor safety, TREAT tests, statistical model to identify boiling inception 79−93779
fatigue, fracture, statistical treatment, maintenance procedures 79−43538
fatigue crack growth data, three component model anal. 80−3161
fatigue crack growth data 77−24351
fatigue life dispersion in rolling contact, new model 78−59349
fatigue life distrib., estimation of three parameters of Weibull distrib. *(Japanese)* 79−59943
fatigue spectral method of rating life under action of random loads 77−19570
fatigue test data, statistical anal. *(Japanese)* 80−62452
fatigue testing, bearings, Weibull distrib. statistical interference 79−52473
fatigue testing, nonstationary loading, stat. analysis methods comparison 79−52488
fibre, oriented, nonisothermal deform., thermomech. curves, statistical interpretation 77−32651
fibre reinforced composite, deform. diagram construction method, based on statistical distrib. of strength of fibres 77−52437
fibre reinforced composite, oriented, statistical theory of fracture and scale factor effect in reliability 77−70171
fibre reinforced composites, failure, probability bounds 79−87716
fibre reinforced laminated composite, reliability anal. approach to fatigue life dispersion *(Japanese)* 79−61704
field problem inference-finite element model 78−81923
film absorptive laser damage analysis by Weibull distrib. 80−33061
first-order kinetic model, optimal design of experiments to estimate parameters 78−15650
fission reactor coated fuel particles, failure statistics 77−74945
fission reactor fuel element/critical assembly power ratio, semistatistical determ. *(Russian)* 77−67815
fission reactor transient analysis, appl. of statistical methods to sensitivity anal. of Problem 2 79−31058
fitting data to dimensionless groups 79−40545
flat galaxies dynamical struct., statistical charact. 80−62269
flaw detection methods, planning statistical acceptance monitoring 79−91901
floating optoacoustic antenna, statistical characteristics 79−27485
flood frequency analysis, Pearson type 3 and log Pearson type 3 distribs. 77−78285
flood statistics comparison in real and log space 79−84319
flow at high Reynolds numbers, real-time statistical laser Doppler velocimeter system 77−3895
flow statistics derived from laser anemometry, retrieval via photon correl. 77−3896
fluctuating signal, detector threshold and saturation effects on statistics 79−31803
fracture, arbitrary criterion, weakest link theory reformulated 78−90786
fracture, extensions of a statistical approach 80−1487
fracture, multiaxial, general approach to statistical anal. 78−90785
fracture, statistics in brittle materials with surface shear-sensitive cracks 79−41616
fracture, transform. of observed crack traces on section to true crack density for fracture calcs. 79−10533
fracture of brittle solids, under multiaxial stresses *(Japanese)* 78−90788
fracture theory, Weibull statistical anal. 78−51132
fragile materials, mech. props. and fracture mech. *(French)* 80−104274
frequency-domain numerical analysis 77−9292
fused xerographic images, optical density model 79−17550
fusion reactor ceramics, Weibull probabilistic design approach 79−93822
galactic background radio emission fine struct. correl. with discrete radiosources 79−21457
galaxies, dispersion relation of gravitating spiral system 77−87538
galaxies, four-point correlation function for Lick and Zwicky catalogues 78−45413
galaxies, masses and ang. momenta anal. rel. to morphological types *(Chinese)* 79−17097
galaxies, redshift-distance square law statistical scrutiny 78−81683
galaxies compact groups, anal. of red shifts and galaxy chains 77−22320
galaxy catalogues, statistical anal. 80−46417
galaxy clustering, statistical test, covariance 80−56955
galaxy clustering 80−105363
galaxy clustering models, discrimination of statistical measures 79−35404
galaxy clusters, N-body simulations, density profiles 79−35398
galaxy clusters, vel. dispersion profiles 79−35397
galaxy distribution, angular covariance function estimation 79−62920
galaxy groups classification technique, appl. to nearby groups quantitative membership probabilities 79−62919
galaxy quintets, statistical anal. of discrepant redshifts 78−65701
gamma camera transfer function study 77−70541
gamma photopeaks in complex spectra from very low activity samples, statistical evaluation 79−76254
gamma-ray counting, Poisson and Brockwell-Moyal freq. distribs., χ-square test 80−5430
gamma-ray spectrometer self-stabilising peak detector *(Russian)* 79−26814
Gaussian distrib. anal. for air pollution rate calc. *(Dutch)* 78−61611
Gaussian distrib. for air pollution conc. calc. *(Dutch)* 78−61546
Gaussian distribution, unconventional calc. of moments 78−49647
Gaussian function approximation using Weibull's distribution function *(Czech)* 80−57083
Gaussian integrals, evaluation by backwards recursion or Taylor expansion 80−31488
gel permeation chromatography of interacting multicomponent systems, protein isomerisation study 78−68950
gel permeation chromatography of interacting multicomponent systems, protein isomerisation kinetic consts. determ. 78−68951
Geminid meteor shower radar obs., statistical modelling 78−61816
generalised Gram-Charlier series with application to the sum of log-normal variates 77−37736
generalized mean of two numbers, simple examples 78−16609
geodesy, props. of Gauss-Helmert least-squares adjustment model *(German)* 78−61309
geodetic measurements for crustal movements monitoring 79−79726
geodetic observations goodness, factor anal. determ. rel. to recent crustal movements estimation 79−57840

statistical analysis continued
geological appl. of G-mode central method, using FORTRAN V program 77−86879
geomagnetic activity depend. on solar wind parameters, statistical anal. 79−48402
geomagnetic activity indices, anal. of 100-year series *(French)* 77−32981
geomagnetic anomalies, Atlantic Ocean, statistical anal. 79−44101
geomagnetic array data, empirical transfer functions for tectonomagnetic event detect. 79−16374
geomagnetic field quiet time var. rel. to interplanetary mag. field, autocorrel. effects 78−61697
geomagnetic Pc3 pulsations at synchronous orbit, statistical anal. of ATS 6 obs. 77−45256
geomagnetic Pc 1 pulsations, statistical study at synchronous orbit 77−25875
geomagnetic reversal sequences, statistics time var. and assym. 77−32994
geomagnetic storms, largest, per solar cycle, statistics 77−2306
geophysical anomaly detection, FORTRAN IV programs for statistical method appl. *(Rumanian)* 77−41214
geophysical data series, linear trend analysis 77−49151
geophysical fluid dynamical systems, statistical anal. and prediction 78−11901
geophysical global potential fields correl. analysis *(German)* 77−29466
geophysical interference fields separation, statistical algorithms *(German)* 77−29462
geophysical interpretation problems, soln., correl. theory of homogeneous random fields appl. 79−100986
geophysical modelling techniques, statistical tests for goodness of fit 78−57333
geophysical observations, problems of statistical theory of interpretation 79−84510
geophysical pot. field anomalies, statistical source models for geodynamic interpretation *(German)* 79−34782
geophysical prospecting, analysis of statistical distribs. rel. to seismic exploration for bauxite *(Russian)* 77−9561
geophysical prospecting, electrical sounding methods, applied EM depth sounding 77−45173
geophysical prospecting, electrical sounding methods, statistical evaluation, expt. design 77−45172
geophysical time series, Hurst range of independent normal summands, distribution 78−16081
geophysical time series alignment, new statistical approach 79−92623
geophysics, appl. of two-timing methods 77−73879
geopotential fields interpretation, statistical algorithms *(German)* 77−29461
geostationary satellite, station-keeping activator subsystem reliability 78−4074
glass, co-acting (synergistic) flaws and strength 77−20168
glass, flat, horizontal annealing process, math. model 79−61615
glass, minimum life prediction, uncertainty 77−16665
glass, strength test, biaxial, use of Weibull statistics 78−68798
glass, surface flaw density, statistical determ. 78−11310
glass fibre reinforced epoxy, unidirectional, strength distrib. 78−68735
glass fibre reinforced plastic, strength dispersion, statistical anal. *(Japanese)* 79−61655
glass reinforced plastic, transverse flexural vibration, statistical charact. of logarithmic decrement 77−7334
global solar radiation est. and prediction by stepwise multiple regression anal. for Greece (1961 to 1975) 80−61880
glow discharge cleaning effectiveness rel. to base material atomisation rate *(Russian)* 80−20797
gradation, information approach to recognition problem 79−17203
graphite reinforced epoxy angle ply laminates, statistical fatigue in shear 79−11690
gravel river, grain size var. statistics 79−5513
gravimeter network adjustment, equiprobable interval method of sample classification 79−29889
gravitational detector, anal. of recorded data 78−21047
gravity disturbance, three-dimensional statistical model 77−90991
gravity disturbance, three-dimensional statistical model 78−96125
ground conditions classification of LANDSAT data by anal. of variance procedures 77−78532
hail-prevention operations, cost effectiveness estimation methods anal. 78−93013
hard magnetic material charact. investigation *(Russian)* 77−18054
heart attacks correl. with geomag. activity 79−39424
heart rate on-line statistical anal., using special-purpose computer 78−35984
heavy ions in strong magnetic field, electron binding energy 79−68176
Hertzian fracture of Pyrex glass using Weibull distribution function 80−66623
HF sky-wave received signal level determination for communication link 78−85758
hierarchical systems, calibration errors influence on end item performance 80−98788
homogeneous turbulence, with internal rotations, theory 80−69772
hourly solar radiation amounts in Thailand, statistical distrib. 78−96271
HTGR coated particles, failure rate prediction during neutron irradiation 77−79466
Hubble parameter, test for homogeneity of galaxies sample 77−13506
human whole-body, vibrations, biodynamic response and variability 78−92672
hurricanes temporal variability, rank order statistics appl. 78−92910
hydrologic records analysis and comparison, statistical program suite 77−21819
hydrological processes, computer simulation using super-kurtic probability density function 80−26558
hydrological system statistical modelling *(German)* 78−96246
hydrometeorological fields, probability algorithms for objective anal. *(Russian)* 77−78247
hydrometeorological fields objective analysis, probabilistic models *(Russian)* 77−56697
hydrometeorological series stationary properties study, Oise river basin appl. *(French)* 78−36210
hydrosphere, statistical predictability of long-term processes *(Russian)* 77−49105
image classification and tone reproduction determination, statistical method 77−74535

statistical analysis continued
impact toughness text results, cold brittleness crit. temps. determ. 80−100980
impurity absorption and emission in solids, Poisson distrib. moments 80−25419
infinite particle system with additive interactions 79−80509
instrument signals conversion, optimal, for measurement accuracy increase 77−5795
instrumentation experiments design methods *(Japanese)* 78−41299
interactive program COSTAT, DEMOS-E library *(Japanese)* 79−2614
internal friction, amplitude dependence data 80−3114
interplanetary scintillation, joint Gaussian statistics appl. 77−2316
interstellar polarisation in irregularly fluctuating medium, statistical anal. 80−26926
inverse geophysical problems, statistical soln. methods *(German)* 77−29460
inverse scalar wave scatt., statistical estimation *(Russian)* 78−54200
invert emulsion, aggregation equilibrium 79−66356
inviscid flow on sphere, statistical mech., atm. appl. 80−90152
ionosphere, VHF and L-band scintillation over Huancayo, signal statistics 78−36381
irradiated tumours, dose/cure relationship 80−46052
isomorphous replacement data, new statistical model for describing errors, case of one derivative 79−50920
J_{Ic}-testing, statistical eval. of different techniques 78−56828
Japanese phonetic spectra, anal. for speech recognition and speaker identification *(Japanese)* 79−90093
jets, two-dimensional water, sensitive to sound, behaviour *(Japanese)* 80−79376
Kac and Renyi statistical tests, computer program 77−37735
Kalman filter technique, neutron flux distrib., optimal allocation of in-core detectors 78−54839
kinetic model of thermal fluctuation fracture phenomena 77−15489
kit of instruments for statistical research 78−87215
Kolmogorov's −5/3 power law, statistical derivation by turbulent-viscosity approach 78−90837
Kolmogorov statistical model, monolayer, for cryst. vaporisation kinetics, pt.I 79−95151
Kolmogorov statistical model, monolayer, for cryst. vaporisation kinetics pt.II 79−95152
Kuroshio with and without cold water mass south of Enshunada, characteristic features 79−20859
Lagrangian and Eulerian characteristics of random field, rel. between *(Russian)* 77−5761
lake surface reverberation, statistical props. 79−1020
laminate, strength anal. and distribution, failure prediction 78−88522
land-use map, remote sensing derived, accuracy test method 78−7805
LANDSAT multispectral images clustering scheme 78−32241
laser propagation in turbulent atm., detector nonlinearity effects on statistics of fluctuating signal 78−55301
latent and developed electrophotographic images, stat. correl. 77−71400
layered medium disturbed by internal waves, statistical props. 78−22359
least squares fits, normalisation parameters and linear constraints 77−67405
least-squares adjustment with probabilistic constraints, astronomical appls. 78−32352
Lennard-Jones one-dimensional chain, stochastic transitions, statistical features 79−67233
lifetimes and numbers of groups, predictions from statistical anal. 80−82327
light scattering by random phase screen, higher order statistics 77−27253
lightning, randomised modification expt., statistical anal. 77−2218
linear dynamic system with many fluctuating parameters, single group approx. *(Russian)* 78−62154
linear regression model, pollutant gas analysis, defining conc. relationships 80−61486
linear state estimator design, updating budget, meas. theory 80−95058
linear system with nondelta-correlated parameter fluctuations, statistical anal. 80−95036
linear systems acted upon by Poisson processes 80−57196
linear systems with multiple inputs and outputs, comment 79−17344
linear vibratory system, multivariate joint probability density function 78−59329
Lisbon solar radiation climate, direct, diffuse and global intensities 80−36383
LMFBR, Na fire, statistical parametric anal. 79−30997
LMFBR HCDA analysis, uncertainty in accident consequences calculated by large codes due to uncertainties in input 80−78413
LMFBR subassembly local boiling detection by outlet temp. fluctuation analysis 79−13390
locally stationary time series, spectral analysis *(Japanese)* 77−67238
long-term rain rate distribution estimation, extremal statistical method 77−13096
lumbo-vertebral facet forces and injuries 77−56395
lunar rock classification by multivariate statistical technique 77−41336
LWR, statistical techniques for core thermal hydraulic design 80−18399
machined surface time series modelling 80−36998
macromolecular system, critical branching, a statistical theory 80−3413
magnetic and gravity anomaly interpretation using statistical algorithms 77−70856
magnetic storms prediction by multivariate statistical anal. *(Chinese)* 80−12614
magnetosphere substorms, statistical mag. signature 78−49237
marine atmosphere, lightly polluted, dark smokes and acid pollution statistics 78−81376
marine geophysical surveys, trackline crossover differences as accuracy indication 79−39893
Markov props. of nonstationary optic tract fibre spike trains in cat *(Japanese)* 77−90780
Mars, crater-associated wind streaks in north equatorial zone, statistical study 78−45256
martensitic transformation, nucleation site, variation in number 77−12621
mass produced parts, appl. of statistical algorithms for optimisation of mech. props. 77−68550
mass spectra factor analysis 77−44534
material with heterogeneous struct., fracture mechanism 78−67127
materials testing, planning and evaluation by statistical methods *(German)* 80−93725
matter-antimatter symmetric universe, random geometry 78−86046
statistical analysis continued
maximum entropy method confidence limits 80−22284
maximum likelihood test in estimation of exptl. inaccuracies, applic. to equilib. data 77−9867
mean value test, acceptance charact. with prior knowledge of standard deviation *(German)* 80−77605
meas. fundamentals of mean values and standard deviations, of stochastic processes *(German)* 80−13031
measurement instruments calibration intervals determ., optimal, generalised method *(Rumanian)* 78−49787
measurement of probability densities, statistical error prediction *(French)* 78−57885
measurement results evaluation, aberrant values elimination *(Rumanian)* 80−47008
measurement system noise spectra determ., simultaneous eqns. soln. method 78−57354
mechanical experimental data, statistical treatment techniques 80−53644
mechanical props. inhomogeneity of materials, statistical considerations 78−67033
mechanics, structural steel, type St3S, hardness, random functions 80−76329
megalithic astronomical alignments, significance tests 79−96928
megalithic sites, statistical significance of astronomical orientations 78−36475
melting/diffusion, linear correlation 77−20108
membrane thickness, statistical distrib. determ. by lineal analysis, biomembrane appls. 79−5253
metal, brittle fracture, low temp. statistical strength criterion 77−73318
metal powders, particle profiles, morphological charact. derived from Walsh coeffs. 80−50816
metals, creep limit and long-term strength, parametric eval. method 80−100996
metastable state relaxation, critical point region nucleation in thermodynamic systems *(Russian)* 80−13026
meteorite chondrules, mass distrib. and Rosin and Weibull statistical functions 79−35201
meteorological data reduction, statistical heresies 78−57291
meteorology, macroprocess classification, statistical methods 78−16132
meteorology, maximum likelihood estimates for parameters of mth extreme value distrib. 77−78332
meteorology, spatial variability of daily temps. and sunshine over uniform terrain 78−3887
meteors, visual shower radiants statistical study 78−96442
micro plastic strain energy criterion applied to reversed biaxial fatigue 78−63391
microdrop, two-dimensional, on solid body surface, stability dynamics 78−51790
microgeometry of stylus roughness tested surfaces, influence of stylus tip geometry on meas. *(German)* 80−68182
micrometeoroid detection, acoustic method reliability 79−80232
microscopy, quantitative, appls. review 79−17484
microwave background radiation spectrum, statistical anal. of data 78−86039
Mira variables, statistical anal. of galactic concentration *(German)* 80−4390
miscible fluids, concentration fluctuations, statistical theory 77−42810
missing values in time series, effect on autocorrelation analysis 79−17197
mixed crystals, 1D and 2D, ion distrib. statistics 80−49167
mixing of multicomponent solids, mixing index and contact number estimation by spot sampling 80−16214
mixing of solids, appl. of multivariate statistical anal. 79−61529
mixtures of compounds, statistical analysis 77−52697
model, with distributed parameters, inverse problem 79−75322
monochromatic speckle patterns, statistical props. 80−53215
Monte Capellino, ice formation, meteorological conditions statistical analysis *(Italian)* 80−12471
motor units charact. determ. from low freq. EMG power spectra 80−3626
multi-input nonlinear system statistical anal. by optimal linearisation *(German)* 78−64918
multicomponent exponential decay data anal. by graphical method 78−41138
multicomponent random media, central momentum functions of material characteristics *(Russian)* 79−9188
multidimensional Gaussian max. likelihood classifiers error probability estimation 77−78540
multifactor experiments, algorithm library 77−61051
multimodal probability density functions fitting, FORTRAN program 77−37748
multipath neural systems method 80−101162
multiphoton detectors of laser radiation, statistical charact. 80−86408
multiple binning analysis, appl. to clusters of galaxies and radio sources space distribs. *(Chinese)* 79−17111
multiple comparisons for Poisson rates 80−98789
multiple measuring systems 79−26049
multiple radiography overexposures anal. 79−49877
multiplicity measurements, statistical algorithm 78−29721
multivariate and conventional ECG analysis programs compared 78−7492
multivariate autoregressive processes for diagnostic anal. of nuclear reactors 77−23220
multivariate data analysis methods, book 77−37741
multivariate joint probability expression of general random processes, finite expansion terms 80−69592
MWPC, missing data reconstruction in principal component anal. 78−17537
N complex random variables, sum, statistical anal., atm. laser beam propag. appl. *(Italian)* 77−45796
N coupled resonant oscillators, statistical energy anal. 78−59191
nerve impulse interspike interval changes during propagation, quantitative description 77−64023
neural multiunit signals, educable waveform recognition system for sorting unit discharges 80−51312
neural response evaluation and statistical judgement to sinusoidal stimulation with superimposed drift and noise 79−88068
neural spike trains, relationship of post-stimulus time and interval histograms to time charact. 78−69032
neuronal activity model, Ornstein-Uhlenbeck process 80−51030
neuronal spike-train statistical anal. methods 78−73149
neuronal waveforms, optimal recognition 80−56003

statistical analysis continued
neurotransmitter release statistics, applicability of binomial distrib. 77−70450
neutron detection, pulse separation spectrum for fission neutrons and single neutron events 77−6651
neutron group cross sections fitting integral meas., adjustment 79−93679
NMR spin-lattice relax. time 77−20739
noise, environmental, urban, computer aided evaluation and control *(Japanese)* 79−88033
noise and vibration control systems, probabilistic evaluation and appl. to single-wall *(Japanese)* 79−18582
noise field scatt. by large cylinder of finite length *(Russian)* 78−55284
noise poly-freq. spectral anal. based on filtered Poisson process model 79−52998
noise reduction, acoustic paths between two rooms connected by ventilation duct 80−10074
non-axially symmetric nuclear ensemble, gamma-ray emission, statistical tensors 79−95694
nonlinear autoregressive processes 78−24642
nonlinear detector effects on statistics of fluctuating signal 78−24735
nonlinear media containing chaotic inhomogeneities, equation closure for average field 79−81601
nonlinear statistical theories, fluctuation effects, truncation schemes of cumulant hierarchies 80−68133
nonlinear system random vibr., Gaussian closure technique, bilinear hysteretic system 79−18802
nonlinear transforms, quantitative universality, recursive mechanism 79−2604
nonstationary radiative transfer in variable scatt. medium, statistical theory *(Russian)* 77−75368
nonstationary random noise, probability distribution function *(Japanese)* 77−84074
North Sea, wave height statistics using hindcast wave data 80−17273
notch toughness data 79−61818
nozzle fluid concentrations, probability density functions in free-diffusion flames, laser-light technique 80−10235
nuclear counting equipment, statistical behaviour described by goodness-of-fit tests 77−54476
nuclear counting equipment statistics, choosing goodness-of-fit test 78−46238
nuclear gauge, with digital response, statistical method for stability testing *(Rumanian)* 80−9459
nuclear imaging of tumour, optimum detector spatial resolution performance study 78−73223
nuclear materials safeguarding, diverse forms of fissile material, large stocks verification 80−73932
nuclear materials safeguarding, optimal estimates of inventory and losses using nuclear material accountancy data 80−68818
nuclear materials safeguarding, statistical anal. of materials accountability, computer simulation 80−73933
nuclear plant design, seismic response spectrum normalisation 78−50415
nuclear plant risks assessment 78−50281
nuclear power, probabilistic risk assessment techniques in Japan 80−18515
nuclear power plants, operator performance and response time, stress degradation, Poisson model 80−63415
nuclear power station forced outages, statistical data anal. 80−13776
nuclear power station security, sabotage and terrorist attack, statistical anal. of threat reality and consequences 80−13727
nuclear pulse spectroscopy, loss free counting performance 79−76312
nuclear reactor, core thermal performance assessment, acceptance of statistical techniques 80−18394
nuclear reactor behaviour unattended surveillance system 78−29621
nuclear reactor identification, test inputs review 78−41819
nuclear reactor model, statistical anal. of neutron density fluctuations 77−26818
nuclear reactor noise analysis, irreversible circulation parameter 78−94069
nuclear reactor noise analysis by multivariate statistical pattern recognition system 77−14228
nuclear reactor noise theory, fluctuation coarse-graining and normality preservation 78−94068
nuclear reactor surveillance, pattern recognition techniques appl. 80−63351
nuclear reactors, statistical aspects of uncertainty anal. 80−18395
nuclear symmetry breaking in ground state region, statistical meas. 78−8737
ocean acoustic propag., long range, statistical anal. of signal intensity 78−90569
ocean high-frequency internal waves, anal. of energy partition among wave modes 80−98330
ocean intermittent turbulence, statistical anal. *(Russian)* 77−29310
ocean internal waves, Gaussianity 77−60386
ocean LF acoustic multipath fluctuations, statistical anal. 78−90571
ocean quarter-diurnal tides loading effects by Ligurian Sea 78−61308
ocean salinity field 79−16510
ocean small-scale turbulence, horizontal struct. statistical charact. *(Russian)* 80−4020
ocean temp. anomalies, 1966-74 period, NE. Pacific, gridded by objective anal. 78−92830
ocean thermodynamic fields fine struct. *(Russian)* 77−33091
ocean transparency field, statistical relationships with hydrological and biological charact. *(Russian)* 79−88361
ocean wave height and period charact. off Mangalore, India 78−36185
ocean waves, statistical distrib. of periods and heights 77−45006
ocean waves, statistical relations between successive wave heights 78−73396
optical experiments, autocovariance functions and power spectra 78−63018
optical fibre signal polarisation statistical meas. 80−99877
optical fibre strength, statistical data, graphical and analytic statistical model depiction 77−83975
optical fibres, multimode, irregular *(Russian)* 77−88913
optical fibres, propagation modes in uniform and imperfect guides *(French)* 77−79914
optical fibres, tensile strength and static fatigue, analysis using Weibull distribution for optimum design 80−85011
optical image quality enhancement, adaptive methods *(Russian)* 80−28163
optical instrument control life test design 80−87572
statistical analysis continued
optical PCM communication system, Poisson probability density, Gaussian distribution *(Italian)* 77−50759
orientation data fitting to von Mises distribution, in FORTRAN 77−5201
OTF, random amplitude and random phase effects 79−72503
pacemaker, battery longevity estimation using statistical methods 78−57131
palaeomagnetic directional data sets, shape 79−39881
palaeotemperature series from last 700000 years, statistical study 79−5598
paper sheet, elastic props., inhomogeneity with reference to basis wt. depend. of elastic moduli *(Japanese)* 80−2110
parameter estimation in X-ray astronomy using max. likelihood 79−62752
parameter estimation methods, application to physical measurements 77−67237
parametric interactions in EEG period analysis 79−29675
particle and pore size distrib. curves quantitative evaluation, Fortran program *(Czech)* 78−80795
particle population statistical inference from scattered light 80−37950
particle slowing down, anisotropic scatt., statistical fluctuations of collision energy losses 77−62572
particle-in-cell method for num. investig. of rarefied gas flows 77−55043
partitioned sub-optimal linear estimator, separate channel implementation 80−94949
Pb airborn particulate concentration variation at two stations in Perth, 1974-76 period 80−94127
peak energy and target thickness in backscatt. data 78−70719
percolation theory, review, appl. and polychromatic percolation 79−58626
period analysis at high noise level 80−73263
phase transitions in semiflexible long-chain molecular crystals 78−91439
phase-frequency signal intensity characteristics *(Russian)* 79−94176
photocounting distributions statistical props. for intensity modulated sources 79−72541
photogrammetric system 'Zenit', scanning spot intensity distribution *(Russian)* 78−21104
photon counter, statistical deviation due to dead time, calc. *(Japanese)* 77−10105
photon counting apparatus, with dead time, waiting times distribution analysis *(Japanese)* 77−10104
pitting corrosion, stochastic theory 78−7077
planet surfaces, appl. of statistical methods 80−101540
planetarynebulae, statistical props., graphical presentation 78−77589
planetesimals in primitive solar system, statistical behaviour 78−93130
plasma probe, digitised random signal analysis method, power spectrum, phase vel. 77−84509
plasmatron channel, spatial-temporal pulsations of arc plasma pinch 80−24210
plastic deformation at elevated temp. 78−27584
plastic slip concept, statistical approach *(Russian)* 78−18196
Poisson distributions of lymphocyte radiation induced chromosome aberrations 79−100675
polarimeter error quadratic mean value determ. *(Russian)* 77−41668
polarity correlations in nuclear reactor anal. using noise techniques 77−14219
pollutions test results evaluation, due to vehicle exhaust emissions *(German)* 77−56299
polyatomic molecule reacting with heat bath molecules, collisional energy transfer 78−60983
polyaxial stress states, fracture statistics 79−41625
polycarbonate, crazes, statistical aspects optical microscopic obs. *(Japanese)* 79−29247
polycrystalline materials, deformed, use of statistical regularisation material in X-ray diffr. study of structs. 79−46511
polyethylene melt, applicability of statistical rubber elasticity theory 78−42579
polymer, star-shaped molecules with branched nuclei, statistics 77−89383
polymer, statistical interpretation of temp. and stress shift factor 77−65999
polymer mechanics, use of statistical methods, review 78−67031
polymer sedimentation coefficient, diffusive broadening of distrib. function, from single record using model functions *(Russian)* 77−63970
polymer solutions light scatt. rel. to mol. wt. distrib. function type *(German)* 79−1767
polymers, atmospheric resistance, distrib. function determ. and anal. *(German)* 80−81225
polymers, mol. wt. distrib., generalised exponential distrib. description 78−94346
polynomials, smoothing, averaging method 80−31
polytypic crystal structs., appl. of self-consistent field method to statistical model 79−37639
positive corona pulses, on conductors of different dia. *(Russian)* 77−7610
positive Poisson distribution characterisation and statistical application 78−93517
positron annihilation, pulsed distrib. from expt. data, parameter reconstruction 78−41290
potential fields due to vertical circular cylinder and dike, statistical anal. 79−34972
power curve regression equations for Ohio River, statistical computer program 78−61472
power flow between linearly coupled oscillators, statistical energy anal. 77−84022
power law fluid, rheology, data treatment from cylindrical viscometer 77−3893
power plants, operational danger levels, mathematical model determ. *(German)* 80−13633
power spectral density and coherence functions, leakage and reduction, resolution increase 79−18097
power spectral density signature analysis, statistical algorithm 79−624
primary auditory neurons, preferred intervals in spontaneous activity 80−45921
probabilistic model for the reflection of waves from a rough surface 79−40380
probabilities of error in research statistical interpretation 80−90658
projector, narrow-beam intensity distribution curve prediction 78−59105
proper functions of two-dimens. field, air pollution appl. 79−21002
pseudo-random number generators, statistical test 78−86125

statistical analysis continued
psychoacoustics, signal detect. theory, statistical nature of response 78−3514
pulsar radiation, signal statistics in polarised shot noise model 77−13374
pulsating flow of turbulent boundary layer on wall of subsonic wind tunnel *(French)* 77−27517
pulse meas. systems, relative variance of distrib. function of events 79−63880
pulse meas. systems, self checking of count losses 79−63879
pulse meas. systems, self checking technique based on waiting file theory 79−36492
pulse sequence with correl. between shape and separation time, power spectrum 78−4556
PVC, crazes, statistical aspects optical microscopic obs. *(Japanese)* 79−29247
PWR, effects of probabilistic design methods on operating characteristics 80−18397
PWR core support barrel motion monitoring using excore detectors 78−25320
PWR load factor statistical analysis 79−9789
PWR operation *(French)* 78−58374
QSO redshift data 78−32598
QSO redshift distribution, selection effects 78−57674
quality control, distribution law for normal production processes of known standard deviation *(German)* 79−52554
quantum chemistry, matching model calcs. with experiment through linear regression 80−58243
quantum system, nonintegrable, irregular part of discrete energy spectrum, statistical theory 80−82667
quasar red shift parameter ln (1+z), statistical anal. rel. to periodicity 80−17687
quasar red shifts, anal. for randomness 78−12400
quasar redshifts, evidence for random distrib. 78−54070
quasar-galaxy assocs. 79−9024
quasars, emission spectra and radio struct. relations 79−40290
quasars brightnesses, correl. anal. of depend. on parameter ln (1+z) 80−105382
quasars red shifts, anal. for randomness rel. to Earth-centred universe 78−16563
radiation, of SO_2, emissivity and absorption coeff. calc. 77−55126
radiation attenuation in atmospheric surface layer, statistical characts. of spectral struct. *(Russian)* 78−24371
radiation induced cancer, statistical method for testing epidemiological results 79−70591
radiation quanta, comparison of least-squares and maximum likelihood estimates for counts which follow a Poisson distrib. 79−23487
radio sources, statistical props. of compact features as function of flux density 78−41071
radio sources in directions of Zwicky clusters of galaxies, statistical investigation 78−4378
radioactive material transport, statistical anal. of low-radiation packages 77−88286
radioactive materials, risk anal. of transport using Monte Carlo and probability methods *(Norwegian)* 79−13437
radioactive waste geologic disposal, safety anal., functional relations of risk to input data uncertainties 80−83189
radioactivity measurement of low levels, interpretation of counting data 77−23387
radiocarbon dates calibration, bristlecone pine and ancient Egypt 78−70234
radioimmunoassay, statistical evaluation of normal range data 77−90885
radiological assessment of inactive nuclear sites, statistical design and anal. 80−95473
radiometeors characts. assessment, weak, w.r.t. seasonal variations *(Russian)* 80−56777
radiometric data from airborne survey, statistical noise reduction 77−17220
radionuclide migration from repository sites, stochastic anal. 80−37486
radionuclides, short-lived, meas., counting statistics 80−58098
radioscopic inspection data of pore defects, statistical anal. 78−48606
radiosource clustering, statistical analysis of surveys 78−28818
radiosource population, statistical anal. of isotropy at 1400 MHz from GB sky survey 77−45584
radiosources, background, Westerbork survey, angular size distrib. and source count 78−96553
radiosources, statistical test on complete sample of identified sources 78−89269
radiosources isotropy in B2 catalogue 78−73766
radiosources of intermediate strength, statistical props. 80−62303
radiosources optical identifications, statistical anal., data selection 78−61928
radiowaves, troposcatter channels and appls. of adaptive equalization techniques, statistical anal. 79−29841
rain attenuation estimation in UK at freqs. 10 to 100 GHz on microwave links 78−73426
rain depolarization statistical distribution for microwave signal propag. *(French)* 78−53673
rain intensity distribution, conversion to shorter or longer integration times 78−61520
rain rate distrib. by theory of extreme value statistics 78−77293
rainfall cumulative periods statistical distrib. rel. to crop planning, Haryana, India 79−96792
rainfall in South Africa, statistical modelling rel. to precipitation forecasting 77−45109
rainfall network analysis, optimal estimation of total areal storm depth 78−49059
rainfall relationship with occurrence of traffic accidents, St. Louis area 79−16604
rainfall statistics over paths from 1 to 50 km 79−70827
random freq. modulation wave propagation in dispersive medium, statistical props. 80−32889
random heterogeneous materials, statistical theory of effective elec. thermal and mag. props. 77−48118
random noise, in imaging systems, characterisation, measurement 77−86562
random noise and vibratory system, multivariate state probability expression using unified statistical treatment *(Japanese)* 79−18584
random process, non-Gaussian, average number of trajectory overshoots over given level calc. 79−71234
random processes, statistics of, use of stochastic occupation densities and local times *(French)* 80−46972
statistical analysis continued
random vibrations, statistical data digital processing method *(Japanese)* 80−64430
random-phase screens, deep, interferometric anal. 80−101834
random-variable probability density approximation by convex function *(Russian)* 77−9865
randomly diffusing surface, laser beam scatt., simplified statistical model *(Chinese)* 79−50217
rare earth chalcogenides, compositions, props., computer prediction 79−42429
reacting reversible small bimolecular systems, numerical anal. of statistical functions 78−64831
reaction, topochem., input mechanism, statistical approach applicability, using model process 78−92446
reaction kinetics, heterogeneous, statistical interpret. 78−60987
reactor cooling channels, flow anomaly diagnosis, autoregressive model appl. *(Japanese)* 80−83146
reactor fuel cell temp. distrib., statistical variance 77−83021
recursive multichannel max. entropy spectral estimation 78−53735
redshift distribution of extragalactic objects, rel. to evolution of galaxies 80−90527
redshift-magnitude-ang. dia. data statistical anal. 78−86016
reduced model theory, hydrodynamical approach for vel. autocorrelation functions 80−27135
reflecting surface roughness evaluation, statistical approach 78−90367
reflexion weak intensities, simple statistical method for estimating, appl. to organic substances 79−50937
refractory metals, group V, diffusions of O and N, statistical calculations on Arrhenius lines 80−59722
regional resource appraisal, statistical methods 78−28326
regression line analysis, teaching 80−73144
regression program in FORTRAN 79−84495
regularisation, finite part prescriptions and products of distributions 79−5976
reinforced polymer, strength, statistical struct. parameter effects *(German)* 77−56095
reliability aspects in metrology, appl. to Weibull distrib. *(Rumanian)* 79−40524
reliability failure rate 77−60918
reliability in metrology *(Russian)* 80−22317
remote sensing, thematic map accuracy, statistical testing 78−77372
remote sensing of environment, automated digital data handling 78−3960
repetitive firing mechanism excitation parameters, nerve impulse trains statistical evaluation 80−40986
reservoir storage size sampling error 78−61466
respiratory control system, time series cluster anal. 78−56959
response surface, pointwise-unbiased models 78−4470
reticulocyte blood count data analysis by maximum entropy spectral estimate 77−78017
reverberant enclosure, impulsive sound-level response statistics 77−84082
review of less well known statistical tests 77−67239
RF energy coupling into cylindrical enclosure 78−87000
River Po low water flow characteristics *(Italian)* 79−84306
river runoff travel time curve, approximation using statistical distribs. *(Russian)* 77−53089
river water quality monitoring, sampling freq. 79−53380
rivers annual average discharge processes, long-range intraseries couplings 77−78260
rivers annual discharge variations, long-range intraseries couplings for ultralong range forecasting 77−78261
road traffic noise, prediction of time pattern of fluctuating sound levels *(Japanese)* 80−55965
road traffic noise studies based on traffic flow models 79−52999
rolled stock, stat. quality control w.r.t. mech. props. 79−43510
Rome road traffic noise, 24-hour obs. and statistical analysis *(Italian)* 80−87651
rotating components, design to probabilistic criteria 77−3716
roughness profile description, separation of random and periodic components 80−36997
rubber elasticity, Gaussian statistical and Mooney-Rivlin theories 77−46935
rubber-epoxy resins, heterogeneity analysis, light scatt. and statistical methods 78−2024
rubbers, swollen, low-freq. dynamics, optical and mech. props. 80−43626
safety factor and Bayesian anal. in reliability engng. *(Japanese)* 79−61837
sample sizes for comparing two proportions 80−98791
sampling theorems in polar coordinates 80−28169
sand grain size distrib. functions 77−29999
satellite-to-satellite statistical orbit determ. error analysis 78−65486
sea level pressure anomalies predictability over N.Pacific Ocean 78−92905
seabed flatness, high resolution bathymetry using resobath system 77−21921
sedimentary rocks, sieve size statistics from grain meas. 77−70645
seismic activity analysis appls. 77−41201
seismic reflection profiles of marine sediments, multivariate statistics tech. and cluster anal. 79−2385
seismic risk anal., renewal process model *(Japanese)* 79−84159
seismic waves, kinematics and dynamics, statistical analysis determ. *(Russian)* 79−84533
seismic waves travel-time anomalies, statistical anal., rel. to earthquake prediction 79−57868
seismoacoustic activity distrib. near coal bed face 78−73320
seismology, statistical algorithm for interfering seismic wave correl. *(German)* 77−25787
semiclassical fluid, with square-well plus hard core potential, equilib. props. 80−10479
semiconductor, statistical theory of multiple-phonon scattering 78−67794
semiconductors, ternary and quaternary solid solutions with nearly perfect sublattices, stoichiometry invariants 79−51270
shadow optical method for turbulent flow microstruct. investig., stat. analysis problems 80−19534
Shane-Wirtanen galaxies, two- and three-point correl. functions 78−8132
shell carrying capacity, statistical eval. 77−89075
siesmic three-component registrations, interpretation via orthogonal regression *(German)* 78−32017
sign test and Wald's sequential analysis, appl. to expt. investigations 80−57082

statistical analysis continued
signal detection, random phase modulated signals, nonlinear medium *(Russian)* 77−75606
signal detection characteristics, evolution of influence of destabilising factors 80−9825
signals, LPM, detection with estimation of their vel. and arrival time 78−90604
single interrelation equation on arbitrary number of factors subjected to meas. errors, statistical estimation 77−53848
single-phase structure, nonuniform, grain size quantitative rating, exam. of system used 78−85072
sintering, 1958 to 1973 77−73245
sky noise at telescope focus, photometry of atmospheric IR emission, statistical props. *(French)* 78−53731
Skylab conical multispectral scanner IR data statistics 80−90223
slope forms in Al(1) clay of Frankische Alb, statistical investigation of deform. *(German)* 78−57211
snow cover at Munich, October 1887 to April 1977, anal. *(German)* 78−69421
SO_2 air pollution levels modelling and forecasting, statistical approach 78−81398
solar 146 MHz C-type bursts correl. with mag. storms *(Chinese)* 80−4321
solar activity cycle during classical antiquity, rel. to auroral cycle 79−92736
solar air conditioning systems simulation, using stochastic weather models 79−57415
solar chromosphere, statistical study of spicule inclinations 77−91508
solar chromosphere line brightness fluctuations *(Russian)* 79−21259
solar coronal line profiles above active regions, statistical anal. 78−7968
solar diameter pulsations, phase coherence simulation rel. to significance 79−92747
solar flare energetics depend. on flare volumes 79−25566
solar granulation morphology and granule spatial distrib. 80−26830
solar insolation, daily irrad., ARIMA modelling with constant and seasonal parameters 80−55821
solar microwave burst spectra, source inhomogeneities 80−41805
solar noise storms and radio bursts during cycle 20, statistical anal. 80−56794
solar point focusing concentrators, effects of tracking errors on performance, statistical anal. of intercept factor 80−61302
solar radiation data, statistical correl. between daily and monthly averages 80−8409
solar radiation data base using bright sunshine data approach 77−25763
solar radiation estimate, in equatorial region (Singapore), power utilisation appl. 79−87972
solar radiation in Peru, two-parameter statistical model of daily irradiation *(French)* 79−29812
solar radio emission S-component, statistical anal. 79−40172
solar soft X-ray bursts 80−26839
solar spectrum, statistics of intensities 77−53537
solar sympathetic flares occurrence, negative result 77−22189
solar wind, very low electron and proton temps., statistical anal., origin 78−65477
solar wind velocity, dispersion anal. 78−7852
solar wind velocity recurrence period, depend. on heliographic latit. 80−62106
solar-radiation regime, energy structure distribution laws analytic representation 80−98378
sound radiation and reflection from duct 79−81585
space time correlations for microearthquakes anal. 78−65184
space vehicle motion in vicinity of collinear libration point, statistical estimates in control problem 78−4067
spacecraft, analysis of weight and cost parameters with reference to Aryabhata satellite 79−84635
speaker identification, telephone voice patterns *(Japanese)* 79−81655
speckle, statistical props. of sum of partially developed patterns 78−1162
speckle, statistics from mixture of moving and stationary scatterers 78−66765
speckle pattern intensity and phase, second-order conditional statistics 80−37951
speckle patterns, partially developed correlated, statistical props. 79−3629
speckle statistical props. and coherence aspects 80−78773
spectroscopic binaries, orbital elements statistical anal. 80−82422
spectroscopic binary stars orbits, test of circularity 78−93321
spectroscopy of high power resolution by means of photon statistics *(Spanish)* 79−21818
speech and musical signals statistical props. 79−76919
spherical indentation mechanics, appl. to reversible and irreversible contact between rough surfaces 78−13976
spoken Estonian, statistical data *(Russian)* 80−45923
spring water, quantitative index of physio-chemical characteristics, appl. to Central Apennines 77−66931
standard deviation of obs. in meas., statistical estimation 78−16770
standard reference materials 78−41268
star fields and configurations 80−82224
star positions obtained from overlapping plates, accuracy of average 78−20622
stars space densities derivation, new method 80−85932
stationary random fields, statistical inference 77−64930
statistical evaluation and measuring strategy for extremely small line shifts 78−86234
statistical prediction of vibr. distrib. and random noise in higher level region *(Japanese)* 79−1023
steel, 20A, melt, tube blanks, mech. props., statistical determ. 79−29316
steel, alloy X8CrNiNb1613, creep limit and long-term strength, parametric eval. method 80−100996
steel, austenitic, weld, with natural flaws, US test techniques *(German)* 78−27713
steel, C, fatigue life, reliability analysis, reliability-based design safe lives *(Japanese)* 77−8939
steel, C and alloyed, cast props. *(Bulgarian)* 79−83192
steel, carburised, alloying effect on props., mathematical-statistical determ. 78−19794
steel, Cr-Mo, notched specimens, statistical eval. of fatigue life and fatigue limit and life distrib. *(Japanese)* 79−61702
steel, fatigue cracking, statistical theories of scale effect, expt. verification *(Russian)* 77−28884
steel, fatigue reliability under random loads 79−79066
statistical analysis continued
steel, fracture toughness dynamic, interlaboratory data, statistical analysis 77−36717
steel, heat treated rimmed, statistical study on fatigue life distrib. in long life region *(Japanese)* 77−12755
steel, heat-treated, toughness factor statistics *(Russian)* 77−44418
steel, low C, increased damping capacity, mathematical planning method *(Russian)* 80−45332
steel, medium C, tempered, normalised or quenched, statistical property of fatigue limit, press-fitted axles *(Japanese)* 77−12693
steel, statistical distrib. of mech. props., and life characts. exam. 78−64606
steel 18 Gps, chemical composition effect on strength, statistical treatment of test data 79−57081
steel defects, US analysis of real defects 78−72976
steels, low C S25C, medium C S45C, Cr-Mo SMC3, statistical fatigue props. eval., heat-to-heat variations 78−7048
stellar dynamics, escape of stars from isolated clusters *(Polish)* 78−16466
stellar spectrograms, relative Zeeman and Doppler shifts determ. via statistical approach 78−36467
stellar trigonometric parallaxes, freq. distribs. and systematic effects 80−94785
stereological estimation of particle number or density by wedge sections 79−2605
Stieltjes functions and approximate solutions of an inverse problem 79−49094
stochastic systems, time evolution in two-phase flow, mathematical model 79−64739
stratified acreage estimates in Illinois crop-acreage expt. using LANDSAT data 77−78501
stratospheric upper winds, tropics, data clustering technique 77−91225
streamflow data, empirical, fitting of multivariate gamma distribution 79−34878
streamflow synthesis, two- and three-parameter log normal distribs. 78−81255
strength parameter dispersion/inhomogeneity of microscopic damage relation 77−86122
striated rough surface, applicability of modified Reynolds eqn., math. verification 78−11347
strong-motion accelerograph records, statistical anal. 79−62459
strongly anisotropic rough surfaces, statistics 79−91805
structural noise and vibration problem solution by statistical methods 79−23126
structural reliability under time varying multi-parameter loading 77−3715
structural-vibr. related noise, anal. via statistical correl. theory 77−84077
structure reliability under random loading 78−38196
structure-factor residuals 78−1948
student physics laboratory courses, university level, mathematical statistics of measurement 78−24601
Sturm-Liouville discrete inverse problem, algorithms *(French)* 79−49022
subjective experiments (e.g. aircraft noise anal.), use of changeover designs 77−82380
summer rainshowers statistical models from fine-scale radar obs. 78−85650
sunshine, differences between morning and afternoon, in New Zealand, statistical anal. 77−29401
sunspot size and facular areas per solar cycle 80−41796
sunspots, largest number per solar cycle 77−22159
sunspots and volcanic dust effects on climate, statistical evidence from long-term temp. records 78−69439
superconducting magnet epoxy fracture after low-temp. irradiation 79−34147
supernova rate in Sc galaxies, max. likelihood estimate 78−45402
superposed processes, serial correlation coefficients of inter-point intervals *(Japanese)* 78−88704
surface irregularities, deformation under static loads 80−58985
surface profiles, reference line selection and fitting, based on random process analysis 78−45594
surface roughness meas., by amplitude density distribution and autocorrelation function of surface profile *(Hungarian)* 78−12668
surface roughness of technical surfaces, characts. of profile angles *(German)* 77−17944
surges, switching, long distance discharge probability calc. *(French)* 77−39493
Sutlej catchment annual rainfall and Bhakra dam site annual runoff statistics 77−53082
symmetric ordered nuclear spin struct., gamma-ray emission at low temps. 79−95695
Syton, determination of size distribution of submicron particles in colloidal suspension, FODA, mean and standard deviation 78−61057
tectonic fracture system, statistical anal. *(Chinese)* 80−41417
temperature pulsation balance in turbulent streams 79−14385
tensile strength, using small number of data *(Japanese)* 77−32736
ternary system compound formation, comp. and props. w.r.t. component electron struct., computer prediction 80−103444
testing procedure for optical fibres, for tensile strength determining, extrapolation of short length test results 78−9456
texture study, use of crystallographic orientation distrib. function 79−52228
thermometer temperature regimes evaluation *(Czech)* 79−63208
thin island films, statistical theory for dielectric props. 80−80699
three-body system disruption. statistical theory for three-dimens. motion 78−77475
thunderstorm wind gusts in Australia, statistical study 77−86996
thyroid functional state, interdependence of symptoms and signs 79−8560
tile, resistance to fracture, Weibull statistics *(German)* 77−7338
time correlation functions of one dimens. infinite system, ergodic props. 78−65862
TOF spectra, parameter estimation and gain of correlation method 79−49895
tolerance limits for censored Weibull data 77−74202
toughness data, fitting curves 80−40511
town air basin pollution levels prediction by empirical statistical regression anal. *(Ukrainian)* 79−34887
trace element measurement, statistical evaluation 79−87921

statistical analysis continued
transducer array with interacting elements, statistical parameters 77−34993
transformation of nonlinear variables in construction of statistical models, review 80−57081
transient electrical transport, general and unified treatment 80−59977
transionospheric propagation from a satellite, observations on the beyond-the-horizon statistics 77−25825
transmission loss estimation of sound absorbent panels, statistical energy analysis 80−64278
triple scanning search statistics 78−94172
tropical cylones, guest speeds along N.Australian coast 77−86997
troposphere, standing planetary waves induced by Sun, comment, statistics reanal. 79−74935
troposphere response to solar mag. field daily changes 78−88888
tsunami risk, estimation via stochastic model 77−21685
turbulence, axisymmetirc homogeneous, direct spectral simulations compared with direct interaction approx. 77−3813
turbulence, non Gaussian variation models, 1-D distributions 80−6032
turbulence, non-Gaussian aspects, num. model approach 77−51037
turbulence, two-dimens., ergodic behaviour 80−28494
turbulent air/water wavy interfaces, using computer 77−924
turbulent diffusion, of passive scalar magnitude *(French)* 80−69778
turbulent dispersion, approach to normality of distance-neighbour function 77−15005
two instruments precision error estimation methods 78−89424
two-dimensional Hermite function expansion for solar tower concentrator flux density calc. 77−75647
two-dimensional optical system MTF meas. by second-order speckle statistics computation 80−74304
typhoon track prediction, appl. of multiple-category discriminant anal. *(Chinese)* 77−66967
underground lens line, coupled to atmosphere, turbulence struct. 77−7008
underwater ambient noise, statistical anal. 77−79996
undisturbed meas., Monte Carlo study of rejection of outliers on estimated mean value and standard deviation 79−26856
upward lightning stroke parameters *(German)* 78−57237
urban runoff pollution analysis, continuous and single event simulations compared 77−37271
urban visibility degradation, multivariate statistical anal. 79−62579
US Geological Survey RASS-STATPAC system for mangement and statistical reduction of geochemical data 78−20522
V_d ratio specification atmospheric noise models 77−81992
Van der Waals equation, statistical anal. of RT_c/P_cV_c *(Spanish)* 80−74213
variable sampling-time technique for improving count rate performance of scintillation detectors 79−22565
vectorcardiographic discrimination of left bundle branch block, descriptive statistical methods 79−44026
vehicular queue acoustic noise anal. 77−80015
vibratory system, nonstationary, nonlinear, with arbit. random input, effect of feedback operation on probability distrib. 79−14316
Visible and Infrared Radiometer evaluation from SeaSat-A surface temp. obs. 80−46325
visual double stars, period-eccentricity relation *(French)* 78−28721
visual processor, human colour-vision discrimination, statistical-communications approach 79−5288
VLF signal propagation, multi-mode *(Russian)* 79−5702
VLF/RLF atmospheric noise, amplitude-probability distribution model 78−32288
volcanic eruptions and damaging earthquakes in Iceland, 1550 to 1978, statistical anal. 80−89975
water, annual flow regulation, appl. of probability and statistical methods *(Chinese)* 79−96778
water, compressed, thermodynamic props., evaluation by statistical error anal. 80−92685
water, statistical anal. of cavitation strength 77−11227
water moderated water cooled reactors, rod bundle burnout characteristics 77−74969
water quality surveillance, optimal sampling frequency selection, autocorrel. techniques 79−53001
water quality trends, statistical tests for dependent obs. 77−29513
water resources, model construction for Box-Jenkins modelling 77−87632
water surface, optical pulse refl., probability characts. *(Russian)* 78−22081
wave field statistical moments in medium with large-scale inhomogeneities 80−37953
wave propagation in random stratified media *(Russian)* 78−1157
wave propagation in randomly inhomogeneous media, quasi-optical parabolic approx., validity analysis 80−106422
wave reflected from randomly inhomogeneous layer description, by series satisfying causality condition 80−106420
weakest link model, for prediction of crack growth rate 78−90797
weakly coupled geophysical systems, statistical anal. techniques 79−80428
weather modification, covariance anal. technique based on bivariate log-normal distrib. 77−70767
weather prediction, probabilistic model 79−39835
weather-forecasting, statistical model 78−92941
weather-solar activity relationships, possible mechanisms 80−17341
Weibull law parameters estimation, of cable insulation dielectric breakdown *(French)* 77−24794
Weibull modulus estimation for brittle materials 79−55344
Weibull statistics use to characterize wind speed distribs. 78−92928
Weibull wind speed distrib. parameters, estimation using Weibull prob. paper and percentile estimators 80−50931
Weibull wind speed distrib. parameters, vertical extrapolation formulae, errors 78−92916
Weibull wind speed freq. distrib. estimation method 78−92908
Weiner-Einstein processes, Markov, maxima and first-passage-time statistics 80−68134
width of Lorentzian convoluted with Gaussian 77−79528
Wiener processes, analogue, existence and uniqueness theories for canonical processes 78−57856
Wiener-filtering, a posteriori, statistical properties 79−88045
wind fields, mesoscale, satellite-derived, covariance anals. 80−82013
wind power, optimum power plant siting evaluation 79−70422
wind time series statistical structure 77−78370
wind velocity magnitude and persistence, probability models 79−5583
wind waves in shallow water, statistical model *(Polish)* 79−25260
statistical analysis continued
wood, fracture toughness variations with specimen size, statistical approach 80−100889
X-ray data anal. 77−70395
X-ray fluoresc. anal., statistics. appls. 77−56310
X-ray intensity meas., statistical control and optimisation 77−33948
X-ray sources, weak, variability analysis, method of time histograms 78−20652
X-ray spectrometry, data interpretation, online system using multivariate statistical anal. and pattern recognition 80−3461
X-ray spectrometry, quantitative, comparison of mathematical models 79−17587
X-ray stress meas., improvement in precision by fixed time method 78−90801
xerographic image, measurability of structure fluctuations 77−18119
ZPR noise anal., interpretation of quadratic approx. 79−76082
Al alloys A5083 and A7075, statistical fatigue props. 79−5060
Al-Mg-Si, brittleness and heat treatment, statistical design of expts. 77−73349
Al_2O_3, high-purity, modulus of rupture, expt. test of Weibull scaling theory 77−21258
Al_2O_3 strength-size relation 77−21255
C fibre reinforced plastic, specimen size effect, statistical anal. 78−68724
CO_2 gas flow impinging on heating surface, heat transfer radiation 80−43710
Cu, high purity, creep cavitation topology, high temperature region *(Czech)* 80−65138
Cu Laue X-ray back reflection pattern solving, algorithm and statistical error analysis 79−99030
Fe, carbonyl powder, particle size distrib. anal. by microscopy with statistical anal. of results 78−19691
Ge(Li) detectors, anal. of monochromatic γ-ray and annihilation spectra 78−50429
H I in Nilson dwarf galaxies, statistical props. 79−92851
H II regions density fluctuatons, statistical approach 80−77468
$H+H_2$, reaction probability, max. entropy derivation, statistical theories 80−66781
H_2, statistical fluctuations in ionisation yield, rel. to electron degradation spectrum 80−99581
NaI(Tl) scintillator, electron detection efficiency for electrons and gamma-rays > few keV 79−36461
$NbSe_x$, x=1.48-2.0, defect. struct. anal. using statistical thermodynamics 79−74139
O_2, singlet, energy transfer in quenching, statistical theory of vibr. energy distrib. 77−68073
Pu dose to lung and bone from contaminated soils, statistical uncertainties 80−109028
Pu in waste, anal. of enhanced variance and twin gate methods 80−5454
^{222}Rn scintillation counting, standard deviation estimation 77−79519
SO_2 concentration distributions in Paris region (1962-72) *(French)* 77−37402
Si solar cells, production process effect on fracture strength 80−93656
SiO_2, fused optical fibre, strength, appl. of Weibull type analysis 77−19418
SiO_2, optical fibre, tensile strength distrib. and gauge length extrapolation 78−9434
SiO_2-K_2O, thermodynamic approach to ionic conds., statistical model of chem. potential 79−46833
SiO_2-Na_2O, thermodynamic approach to ionic conds., statistical model of chem. potential 79−46833
UO_2 reactor material, contact conductivity between core and cladding, statistical processing of experimental data 80−5238
$^{238}U(n,\gamma)$, statistical anal. of intermediate struct. in cross-section 77−23057
WC-Co cemented carbide, bending strength, surface roughness effects *(German)* 77−8947

statistical distributions *see statistical analysis; statistics*

statistical linguistics *see computational linguistics*

statistical mechanics
see also classical theories of fluid structure; lattice theory and statistics; Liouville equation; liquid theory; master equation; quantum statistical mechanics; renormalisation
abstract equipartition of energy theorems 79−71273
acetonitrile, mol. pair correl. functions, scatt. intensities, statistical mechs. calcs. 79−1382
adsorbed phase, virial expansion, eqn. of state and isotherms *(German)* 78−95235
adsorption, gas on solid substrate, Van der Waals model 80−29271
adsorption, grand partition function and adsorption isotherm, statistical mech. calcs. 77−69162
adsorption, molecular dumbbells with distinguishable ends, 1-D neighbour pair degeneracies 78−34735
adsorption, virial expns. in 3D model 79−77891
adsorption and wetting, unified theory using Percus-Yevick eqn. for hard spheres with surface adhesion 77−31879
adsorption density profile, improved calc. 77−31876
adsorption on homogeneous surfaces, statistical mech. of collisions which lower desorption rate *(German)* 78−84072
alkali halides, molten, statistical mechanics 80−19683
anharmonic oscillator, classical, variational method test, sp. ht., elec. susceptibility and oscillation freq. *(Portuguese)* 80−77611
anharmonic oscillator, statistical thermodynamics 77−13724
anharmonic system, superstability, probability estimates for correlation functions 80−82708
anisotropic paramagnet, statistical mechanics using second order Green's function theory 80−25074
antiferromagnet, linear-chain, sine-Gordon solitons 80−80543
arbitrarily slow irreversibility 78−70083
attractors in the non Morse-Smale dissipative dynamical systems 79−75447
axioms and GL-spaces 78−29042
BBGKY hierarchy, first eqn. exact linearisation, Ornstein-Zernicke phase instability 79−75461
BBGKY hierarchy, scaling method of kinetic eqn. derivation 78−54286
BBGKY hierarchy for hard spheres in one dimens., uniqueness 78−29041
BBGKY system, irreversibility, velocity correlations and non-Hamiltonian dynamics 80−77686

statistical mechanics continued
bibliography, probabilistic ideas in field theory and statistical mechanics 78−8230
bifurcation of crystalline solutions and freezing 78−67814
bimolecular reactions, complex and direct reaction mechanisms, unified statistical model 77−1914
binary alloys, concentration derivatives and correlation functions of intrinsic variables 77−17937
binary gas phase collisions, rates, translational energy depend., statistical mech. theory 79−44844
binary liquid mixtures, viscosity, Panchenkov model calcs. *(German)* 77−31797
binary microcluster, struct. and thermodynamics, Monte Carlo simulation 79−7736
biocenoses, Volterra eqns. and Gibbs statistics 77−21467
biodynamics, Hamiltonian content 80−89704
biological, ensemble methods 79−66437
biological multiparticle systems, stat.-thermodynamic treatment, phase transitions *(German)* 79−16119
biological systems, simulation study of nonequilib. ensembles of self organising systems 79−24933
biomechanics, regularity 77−25483
biophysical systems, ensemble theory and Hamiltonian formulation 79−96502
Birkhoff's pointwise ergodic theorem on operator algebras, extension to quantum mech. 78−86218
Block equation, standard form, Markovian relaxation 79−58621
Bogoliubov hierarchy eqns., stationary solns. 77−49665
Bogoliubov hierarchy equations in classical statistical mechs., stationary solns. 78−8335
Bogolyubov chain equations, solution 77−74311
Bogolyubov equation chain, Cauchy problem 77−13689
Bogolyubov hierarchy, translationally invariant solns., local perturbations 79−21651
Boltzmann eqn. for fluctuations in μ-space 77−17929
Boltzmann-Enskog equation, nonlinear, acoustical approx. for elastic sphere system 78−41252
Boltzmann-Enskog equation and asympotic behaviour of the time autocorrelation functions 78−70079
Boltzmann-Gibbs-Shannon generalised entropy, unique characterisation 77−5747
book, statistical mechanics and foundations of thermodynamics 79−97294
book 77−61007
Boolean systems, atomicity and determinism 79−35518
Born-Green-Yvon eqn., two-dimensional, with anisotropic interac. 78−79882
Brownian motion, generalised Einstein theory for nonequilibrium fluctuations 80−31672
Brownian sphere, long time fluctuations 79−85077
Brusselator, dynamic correl. functions, Mori-Zwanzig formalism 80−25988
C* approach to math. foundations of statistical mechanics 77−26226
C*-algebra, *-automorphisms, inner dynamical one-parameter groups, trace and KMS states 77−41526
canonical density matrix, gradient expansion, partial summation 78−16719
canonical description, breakdown of van Hove's theorem 79−71356
canonical formalism in distribution spaces 79−67219
canonical system with periodic coeffs., stability, practical determ. program *(French)* 79−9174
chaotic behaviour in simple system, continuous Euclidean dynamics 77−60046
chaotic processes, time correl. functions, in one-dimens. 79−25985
charge exchange, atomic scattering, many-particle theory 77−10715
charge fluctuations in classical Coulomb systems 80−95027
charged hard sphere fluid mixture, mean spherical approx., analytic soln., multicomponent plasma case 79−85057
charged hard spheres, distrib. function, mean spherical approx. 79−4222
charged hard spheres, pair correlation function, mean spherical approx. 79−4223
charged particle in box, nonlinear integrodifferential eqns. with delay, soln. existence 79−27124
chemical equilibrium, demonstration machine for teachers 79−40337
chemical instability, mol. dynamics model, computer soln. 77−4892
chemical master eqns., Poisson representation 78−35638
chemical mixture in closed vessel, equilib. distrib. 77−21413
chemical reaction statistical models 80−27208
chemical reaction with spatial and temporal structures, stochastic analysis 78−35639
chemical reactions, nascent products, vibr. state distrib., statistical thermodynamics calcs. 77−5782
chemical system, equilibrium fluctuations, deviations from Poisson behaviour, molecular dynamics 80−86211
cholesteric liquid crystal, piezoelectric coeffs., Onsager theory, interparticle pot. and first moment vector 77−24264
cholesteric liquid crystal, statistical hydrodynamics, microscopic theory 77−39540
classical 1-D systems, exact statistical mechanics 78−36924
classical and quantum statistical mech., common Liouville space 78−32758
classical electrodynamics, Boltzmann distrib. for relativistic free particles and Rayleigh-Jeans thermal radiation law, inconsistency 79−49036
classical equilibrium statistical mechanics, mathematical struct., book 79−26017
classical hard sphere system, statistical theory of freezing 80−33868
classical KMS systems, dispersive props. and observables 77−71264
classical lattice system group analysis 77−67385
classical liquids, in equilib., mol. theory, integral eqns. 77−39522
classical one component Coulomb gas, collective coords., thermodynamic props. 77−5777
classical particles in box, continuous system, phase transform. 77−82444
classical system with long-range forces, eqn. props., BBGKY eqn., neutrality, screening, sum rules 80−62569
cluster expansion in statistical mechanics, S-matrix formulation *(German)* 78−41256
cluster identification, computer expts. on systems of particles 78−59725
cluster operator bound states 80−8899
cluster property in classical canonical ensemble 78−49752
cluster size, pair connectedness for fluid and lattice systems, percolation and condensation 77−61019

statistical mechanics continued
coarsened classical distribution function, time evolution *(Russian)* 78−49782
coherence and randomness in quantum theory, uncertainty relations 80−22231
collisional systems, statistical mechanics of Keplerian orbits 78−20625
collisionless stellar systems, statistical mechanics of violent relaxation 79−5864
colloid, electrostatically stabilised, very dilute, struct. and ordering, Monte Carlo method 77−36795
colloidal soln. phase transitions 80−40749
colloidal systems, ordering, statistical mech., theory 78−23968
combustion, turbulent, implications of probability eqns. 78−14098
commensurability in one dimension at nonzero T 79−35655
competitive adsorption, Percus-Yevick approx. 77−31878
completely integrable Hamiltonian systems of N particles on real line 77−9949
complex systems, linkages from fundamental particles to cosmology 79−25964
compressed gas, radial distrib. function hard sphere model 80−69961
condensing systems, generalised theory 79−35653
conditional equilibrium and the equivalence of microcanonical and grand-canonical ensembles in the thermodynamic limit 78−93596
conference, critical phenomena, Sitges, Spain (June 1976) 77−22510
conference, Haifa, Israel, 1977 79−30353
conference, statistical physics, Budapest, Hungary (Aug. 1975) 77−49664
conference on nonlinear nonequilibrium statistical mechanics, Kyoto, Japan, (Jul. 78) 79−75441
conference on solitons and condensed matter physics, Oxford, England (June 1978) 79−75364
conformational dynamics and the rotational isomeric state model 78−90315
conservative, nonlinear oscillators, connection between dissipative and resonant types 79−58619
constrained systems, Hamiltonian construction and diffusion eqns. derivation 80−73258
constrained systems, statistical mechanics, generalized canonical approach 78−48743
constraint on the compound depolarization factor of aligned ellipsoids 79−17328
constraints, flexible vs. rigid 80−31658
continued fraction error bounds, for complex transport coeffs. and spectral functions 79−12744
continuity of the temperature and derivation of the Gibbs canonical distribution in classical statistical mechanics 79−25965
continuous systems, correl. inequalities and thermodynamic limit 78−57848
converse of dominated ergodic theorem 79−71349
converse to Koopman's lemma 80−98851
convex-envelope formulation for separable interactions 79−71355
correlation function, long time asymptotic behaviour, influence of waves on relax. processes *(Chinese)* 80−59195
correlation function, theory 77−49666
correlation function of statistical functional of system of interacting particles *(Ukrainian)* 78−54285
correlation function perturbation theory for non-ideal system 77−30087
correlation functions, 2-dimens., long-time expansion calcs. 77−45784
correlation functions, asymptotic time behaviour, kinetic and pot. terms. 77−5737
correlation functions, asymptotic time behaviour, local equil. and mode coupling theory 77−5738
correlation inequalities and equilib. states 77−74305
correlations decay in lattice models at high temp. 79−80534
Coulomb gas, 2-D, equilibrium props. and phase transition, hard core, neutral dipolar pairs 80−62567
Coulomb gas 2-D, interaction potential, screening length, critical temp. 80−62571
Coulomb lattice, high-temp. expansion 78−143
Coulomb system, Debye screening 80−73256
Coulomb systems, statistical mechanics, review 80−52119
Coulombic fluid, correlation function critical behaviour Ornstein-Zernike theory 79−1957
Coulombic system, statistical mechs., eqn. of state in restricted primitive model 77−7644
Coulombic systems, HNC and RHNC eqns. for restricted primitive model 78−67630
Coulombic systems, restricted primitive model, Monte Carlo simulations, ergodic problems 78−36923
coupled nonlinear oscillators, Brownian motion, thermalised solitons and nonlinear response 78−29053
coupled oscillator system, stochastic transition, Toda criterion reliability 77−74308
coupled oscillators, quasiperiodic to stochastic transition 78−54307
coupled oscillatory-reaction system exhibiting bifurcation scheme leading to a chaos 79−80517
covariance estimation, of stationary, ergodic processes, with non zero mean value *(French)* 79−80513
covariance operators, reflection positivity using Dirichlet or Neumann boundary data 80−131
covariant, determ. and transform. of relativistic temps. *(Russian)* 77−74312
CP violation, statistical theory, K^0 decay 77−41784
creep discharge at dielectric surface, statistical anal., independ. discharges model 78−1938
critical dynamics, classical systems, Fokker-Planck description 78−21057
critical exponents in three dimensions, derivation from ϕ^4 field theory with Gaussian propagator 80−4686
critical point behaviour, probability theory 79−44889
critical scattering theory, book 79−25913
crystal, statistical thermodynamics with collective vibrations 78−54289
crystal orientational disordering, thermodynamic props., stat. mech. model 80−96453
crystal thermodynamics in statistical theory, density Fourier coeffs., stress tenser, internal energy 80−13025
crystal-liquid phase boundary, pair distrib. functions and free energy functionals 80−24734
crystal-vapour interface, thermodynamic props. calc. using canonical and grand canonical ensembles 77−20180
crystallisation, chain folding, statistical mechanical calc. 78−2020

statistical mechanics continued
cyanoacetylene, and isotopic forms, $^{13}C/^{12}C$ effects on partition function 79−29352
Debye screening in dilute classical Coulomb systems 78−41170
decay of local correlations and absence of phase transitions 79−88866
delocalisation, statistical and stochastic aspects 77−30759
delocalisation, statistical and stochastic aspects 77−30760
dense fluid, statistical mechanics of mol. motion 78−38603
dense fluids, equilib. props. semiclassical limit 77−49667
dense fluids, rot. and translational motion, Fokker-Planck eqn. calcs. 77−5736
dense ionised plasma, thermodynamic props., electron screening corrections 77−972
dense Lennard-Jones fluids, solvent struct. and solvation forces between rigid particles 80−30287
deterministic dynamics to probabilistic descriptions 80−68029
deterministic eqn. of motion, master eqn. and steady-state probability distrib. 78−36925
deterministic mechanical systems, statistical concepts 80−22271
deterministic orbits, chaotic behaviour, turbulent phase problems 79−80518
diagram expansions for systems with Coulomb interaction, removal of divergences 78−73056
diatomic molecule, bulk rot. or vibr. relax. processes, information theoretic approach 77−58132
dielectric fluid near critical point, effect of elec. field *(Russian)* 77−62647
diffusion equation, derivation from Fokker Planck equation using perturbation methods 78−54117
diffusion model, statistical distribution of particles over given volume 77−82467
dilute linear Heisenberg chain, partition function and irreducible representation of permutation groups by HLISP 78−34945
dilute solute-binary solvent activity coeffs., statistical mech. theory 80−59663
dimer and Ising models on the Lobacheveskii plane 79−21677
dipeptides, bend form., conformational space, statistical mech. anal. 77−68146
dipolar hard spheres, adsorpt. onto smooth hard wall in elec. field, density profile 79−67221
discrete process, one-dimens., invariant distribs. and stationary correlation functions 78−21059
discrete systems with random excitations, random excitations 77−41537
discs and spheres with dipole, orientational autocorrel. functions 78−4557
disequilibrium system, potential work, statistical mech. calcs. 77−5782
disequilibrium theory applied to two-spin Glauber model 80−31669
dislocations, thermodynamics and thermal activation, book contrib. 80−107241
disordered multicomponent solid solutions conc. fluctuation waves, microscopic theory 80−44327
disordered systems, long time correlations reln. to replica correlations 79−75437
disordered systems, mode softened unified theory 79−55637
dispersions, thixotropic, mech. props., structural hysteresis, statistical thermodynamic anal. 77−46978
dissipative dynamical systems, ergodic problem, numerical approach 79−88878
dissipative dynamical systems of macroscopic phys., common formal struct. of kinetic theory, fluid mechs., nonequilibrium thermodynamics 79−140
dissipative operators for infinite classical systems and equilibrium 80−12982
dissipative system, chaotic flow, fractal dimensions, vortex stretching, cascade model 80−73176
dissipative systems with multiple steady states, trajectory instabilities, stochastic behaviour 79−80519
distribution of zeros, eqn. of state, fundamental relations, Cauchy type integral 78−4577
distributions, Boltzmann, Fermi-Dirac, Bose-Einstein derivation 77−5
DLR invariant measures, one dimens., regularity 79−67220
DNA double helix, supercoils and torsional stiffness 79−83702
double quadratic chain, statistical mech., nonreflectionless solitary wave 80−22518
droplet model for quark confinement phase transition, reduction to string statistical mechanics 79−2991
dynamical fluctuation theory basic eqn. physical anal. 80−36946
dynamical relation 78−49748
dynamical stochastic system, statistical mechanics 79−30349
dynamical systems, first integral 77−60926
dynamical systems, kinetic theory, ergodic props. 77−82
dynamical systems with many degrees-of-freedom, deterministic problem stochastic anal. 79−75455
education, molecular dissociation model, dynamics and time averaged behaviour 78−61968
education, renormalisation group theory, second order phase transitions, undergraduate statistical physics 78−62012
education, Sturm-Liouville problem, eigenfunctions normalization 77−78910
Einstein's nonrelativistic work *(Czech)* 80−27095
elastic phase transitions, crit. dynamics 80−2146
electrical conductivity, quantum theory, appls. 78−84181
electrochemical electrode, ideally polarisable 79−96330
electrolyte, solutions, 1-1 and 1-2, extended mean spherical approxs. 79−4216
electrolyte solutions, interionic radial distrib. function approx. scheme 77−32796
electrolyte solutions, thermodynamics, transport props., semi-phenomenological approach including short range forces 80−3353
electron fluid turbulence, one-dimens., statistical formulation 78−49751
electron gas, radiative interaction, with mag. field, distrib. function 79−60116
electron in random pot., partition function 78−29040
electron liquid, 2-dimens., cluster expansion 79−55461
electron scattering by Coulomb potential in Born approx., bremsstrahlung statistics 80−5665
electron surface layer, dynamic struct. factor 79−40443
electron transport eqn., with random impurities 78−33654
ensemble theory, allowing for variable numbers and species of particles 79−75448
ensembles subjected to singular noncommutative constraints, earlier paper correction 77−33931
statistical mechanics continued
Enskog quasiparticle, non-Hamiltonian dynamics 80−101750
entropy, information theory *(French)* 79−63178
entropy, nonequilib., Lyapunov variables, ergodic props. of classical systems 79−2739
entropy definition for arbitrary phase space densities 79−63185
entropy function representation for grand canonical ensemble 77−74306
entropy general props. review of implications in statistical mechanics 78−73955
entropy max. ensemble, formula derivation 77−33930
equilib. systems, rigorous results 77−22486
equilibrium distribution functions, thermodynamic derivation 79−71175
equilibrium states of continuous transforms on compact metric spaces 79−26000
equilibrium statistical mechanics of a one-dimensional self-gravitational system 79−92810
equipartition theorem generalisation, for teaching 78−49603
ergodic adiabatic invariants, goodness 79−71352
ergodic measures, equivalence singularity dichotomies 77−53754
ergodic processes, moving averages 77−37805
ergodic properties of stopping-time transformations 78−89396
ergodic state with least mean recurrence time in Markovian kinetics 77−49668
ergodic theorem and strong law of large numbers for uncertain ensembles *(French)* 79−58618
ergodic theorem for interacting particles 77−79027
ergodicity, classical, quantum mech. implications 80−8898
Euler flow in two dimensions, periodic, construction of stationary measures 79−93085
exactly solvable statistical mechanical models with nonpolynomial interactions, free energy density calcs. 79−63124
ferromagnetic Heisenberg chains with easy plane, validity of classical statistical mechanics 80−44786
few-body methods, stat. mechanics, atomic and molecular physics, nuclear N-body problem 79−85379
Feynman path integrals, white noise approx., inertialess Brownian system 78−57859
finite closed systems, relaxation, algebraic approach 77−29985
fluctuation-dissipation theorem for classical systems 78−49764
fluctuations, dynamical theory, nonequilib. statistical operator method *(Russian)* 77−67378
fluctuations in nonequilib. state eqn. of motion 77−41538
fluctuations in nonequilibrium state, eqns. of motion, variance eqn. 77−5762
fluid, hard dumbbell mols., reference pot., perturbation theories, spherical reference systems 80−28898
fluid, hard polyat. mols., virial press., Monte Carlo method 77−89357
fluid, one phase, bulk distribution functions and fluctuation theorems for one phase fluid 78−8346
fluid mixtures, unified mol. theory, statistical thermodynamics 77−31570
fluid phase, statistical thermodynamics, review 78−83703
fluid semiclassical statistical mech., quantum effects nonperturbative incorporation 79−64819
fluid struct., variational optimization of truncated approximations 80−44097
fluids, classical, linear irreversible thermodynamics, derivation 79−2740
fluids, equations of motion, stochastic eqn. *(Russian)* 78−21054
fluids, semiclassical statistical mechanics, mean field effective pair pot. 80−54087
fluids with dipolar interactions, boundary conditions for numerical simulation, book contrib. 79−60247
Fokker-Planck dynamics, perturbative expansion of correlation and response functions 78−45566
Fokker-Planck dynamics, response and correlation in stationary state 78−45567
Fokker-Planck equation, manifolds of equivalent path integral solns. 80−4687
Fokker-Planck equation for N one-dimensional free particles 79−97305
Fokker-Planck equation with spatial coordinate-dependent moments, path integral soln. 80−77688
foundation of theory based on thermodynamic theory of measurement 79−85075
free asymmetric rotors, classical system, second rank tensors, ang. correl. functions 80−64865
freezing, mol. theory, bifurcation, density depend. 77−1213
freezing, statistical mechanical theory, appl. to Lennard-Jones fluid 78−47499
freezing transition, statistical mechs. theory 77−7846
fully developed turbulence and statistical mechanics, review 78−51150
functional formalism of classical statistical dynamics 77−45783
functional random walk model, asymptotic steady state soln. 78−62143
gas, monatomic, time average problem, statistical entropy change over constant energy path 80−68123
gas governed by Boltzmann eqn., approach to Maxwellian distrib. 79−58622
gas mixture, Boltzmann collision operator matrix elements 79−86545
gas mixture, modified rough sphere model, rel. to sound absorpt. 78−93597
Gaussian method, attempt to separate long and short range forces 79−63180
general relativistic statistical mechanics, BBGKY hierarchy and Boltzmann eqn. 79−63127
generalised, basic props. 77−5746
generalised (non-Markovian) Langevin eqns., correl. functions and master equations 79−21653
generalised collision integral *(Russian)* 79−48
generalised Langevin eqn. with Gaussian fluctuations 78−32760
generalized Liouville equation, entropy, and dynamic systems containing limit cycles 79−21648
generating functionals in nonequilibrium statistical mechanics *(German)* 80−12981
geometrical aspects of statistical physics, scaling and fractals 79−58625
Gibbs (1839-1903), biography *(Czech)* 80−22180
Gibbs ensemble, approach to equilibrium 77−41553
Gibbs ensembles equivalence, phase transitions 80−134
Gibbs method, validation *(Russian)* 78−73918
Gibbs phase rule, heuristic theory applied to lattice spin system 77−45811
Gibbs phase rule equivalence to ensembles for classical lattice systems 79−75467

statistical mechanics continued
Gibbs random field, integral central limit theorem, equivalence of ensembles 77−53826
Gibbs random fields described by generating functional method 80−31698
Gibbs states, classical approximations 80−132
Ginzburg-Landau model system, quenched, fluctuations growth 78−41260
globular proteins, bend form., conformational space, statistical mech. anal. 77−68146
Goldstone theorem in classical statistical mech., correl. function non-vanishing boundary terms as phase transition origin 80−27253
grand canonical partition function, zeros on unit circle in complex plane, sufficiency condition 77−22498
granular materials, random packing, statistical mech. considerations 80−104088
granular materials, shear deformation, entropy model 80−84233
gravitating systems, statistical correlations 79−35311
H-theorem, time reversible formulation, ergodic theory method 79−30350
H-theorem for hard sphere gas 77−7498
Hamiltonians, nonlinear, continuum-field, universal features 78−93543
hard core particles, Bogolyubov eqns., class of solns. 77−13688
hard disc system, 4-point vel. correls., long time behaviour 78−93598
hard discs, triplet distrib. functions, BGY2 theory 79−44847
hard disks, radial distrib. function, BGY2 theory 79−44846
hard dumbbells, eqn. of state 77−30119
hard heteronuclear dumb-bell fluid, thermodynamic props., eqn. of state 78−38599
hard oblate spherocylinders, Monte Carlo virial coeffs. 78−26400
hard rod fluid in external field, equilib. state 77−27801
hard rods, attractive interactions, scaled particle theory 80−82735
hard sphere fluid, elastic modulus and viscosity coeff. 77−30086
hard sphere fluid, generalised mean spherical approx. 77−11290
hard sphere fluid, locally inhomogeneous, Percus-Yevick eqn. soln. 80−10474
hard sphere fluid, thermodynamic props., quantum corrections 79−4219
hard sphere gas, density expansion of correlation function 79−44843
hard sphere gas, H-theorem for Enskog kinetic eqn. 77−68905
hard sphere gas mixture, vel. autocorrelation function calc. 80−75019
hard sphere mixture, Ornstein-Zernike eqn. with Yukawa closure 78−18513
hard sphere relativistic gas transport coeffs. 78−30401
hard sphere-spherocylinder equimolecular mixture, Monte Carlo simulation of fluids 80−44088
hard spheres, triplet distrib. functions, BGY2 theory 79−44847
hard spheres in thermal eqn., time correlation functions in low-density limit 80−64859
hard-rod clusters, one-dimens. diffusion, stochastic calcs. 77−9948
hard-rod one-dimens. system, ζ-function 77−17901
hard-sphere fluid, interacting with wall, virial coeffs., in surface tension 79−23808
hard-sphere fluid, modified nonlinear Enskog eqn., entropy function 78−63526
hard-sphere fluid, reduced density, radial distrib. function calcs. 77−3903
hard-sphere fluid/soft wall interface, nonuniform fluid in external field 78−34413
hard-sphere fluids, dipolar and quadrupolar, radial distrib. functions, perturbation theory 78−59727
hard-sphere homogeneous gas, Enskog eqn., microscopic interpretation 77−9947
hard-sphere liquid, glass transition, computer mol. dynamics simulation 77−11674
hard-sphere system, with square well attraction, Percus-Yevick theory 77−43123
hard-sphere systems, statistical geometry 80−95028
hard-sphere-like mixtures, soln. of Ornstein-Zernike eqn. 77−4028
harmonic chain with random masses, transmission coeff. and heat conduction 79−80547
harmonic oscillator in random EM field radiative corrections stochastic electrodynamic treatment 77−45736
harmonic oscillators, flexible and rigid constraints 80−90773
heat transfer in linear harmonic chain, nonequilib. steady states, information theoretic approach 80−19214
Heisenberg model, nonlinear excitations 79−78286
helical wormlike chain, dipole moment, elec. birefringence, elec. dichroism, statistical mech. calcs. 80−14262
helical wormlike chain, statistical mech., continuous limits of discrete chains 78−66697
helical wormlike chains, statistical mech., distrib. function calcs. 77−75353
helical wormlike chains, statistical mechanics, operational method 77−560
Henon mapping, topological horseshoe, chaotic behaviour 80−73257
hepatic elimination 79−96503
heterogeneous solid media, statistical continuum theory, information theory approach, static field theory 80−22198
heteronuclear hard dumbbells, eqn. of state derivation 77−30085
heterophase fluctuations in two component systems, distrib. function 79−80563
heteropolymer in random mag. field, Ising chains, statistical mechanics, free energy, numerical calcs. 78−77803
hierarchical model ε-expansion, numerical test of Borel summability 78−12650
high pressure vapour-liquid equilibrium, quantitative description 79−1486
higher monotonicity properties of certain Sturm-Liouville functions 78−57750
homogeneous perturbed classical states and equilibrium conditions 78−93595
hydrodynamic diffusion tensors, translation-rot. coupling effects 78−29038
hydrodynamical fluctuation theory far from equilibrium 80−98856
hydrodynamics, equations of motion and transport coefficients, using discrete formulation 79−90504
hypernetted chained equation, series soln., simple chain recursion method 78−65861
ideal gas in a box, time evolution, thermalisation 77−22481
ideal gas thermalisation in one-dimens. box 79−93034

statistical mechanics continued
identical Newtonian particle system, continuum model with three-point interactions 78−49749
identical particles, theory, classical configuration space 77−26203
impurity states theory, appl. to phase transitions and mixed-valence 78−64004
infinite 1-D hard core system, selfadjointness of Liouville operator 78−29037
infinite classical system, stability, equilib. and KMS 78−21055
infinite crystal, classical statistical mechanics 80−107067
infinite harmonic crystal, dynamics and ergodicity 77−39653
infinite harmonic crystal, dynamics and ergodicity 78−59919
infinite harmonic crystal, dynamics and ergodicity 80−10598
infinite noninteracting particle systems, new observable algebra 77−57268
infinite particle systems, Markov processes existence *(French)* 78−16733
information, irreversibility and statistical equilib. 77−2603
information theoretic approach, exptl. and inherent uncertainties 80−82733
information theory, obs. prob. for stochastic variables *(Norwegian)* 79−80497
information theory role in physics 78−28933
information-theoretic, system in contact with heat reservoir, for teachers 78−36770
inhomogeneous system, nonlinear response theory 77−37806
instanton applications in statistical mechanics 79−75450
integral estimation w.r.t. density of states 78−41224
integro-differential eqns. for partial distrib. functions, BBGKY hierarchy 77−61006
interionic force pot. in ideal dipolar gas 80−96330
intermolecular energy transfer, ergodic collision theory 78−9224
interparticle percolation, statistical mech. anal. 79−96281
intramolecular energy transfer, crit. energy calcs. 77−9046
intramolecular energy transfer and stability of mol. motion 79−45779
inverse problem for random sources 79−97214
inversion problems, information theoretical approach 80−27210
ion beam as drifting gas, cf. optical approach 79−31788
ion solvation in electrolyte solutions, stat. theory 79−91966
ionic recombination in ambient gas, quasiequilibrium statistical method extended to nonlinearity 78−22027
ionic solution in molecular polar solvent 78−30527
ionic systems, hard spheres, mean spherical approx. radial distrib. function 80−62570
ionised mixture, dense, binary, dynamical props., statistical mechs. 80−43895
irreversibility, evolution, process of local conc. 77−26257
irreversibility in strongly coupled system, Boltzmann H-functional 77−74342
irreversible processes, microscopic theory 78−49784
irreversible processes, nonlinear, memory function calc. 77−26265
irreversible thermodynamics, corrections to linear transport laws, Onsager reciprocal relations 77−17938
Ising and Potts models with exponential one-dimens. interaction, comparison 78−21079
Ising lattice, collective excitations in 1-D systems with extended interactions 77−65006
Ising model, finite, statistical mechanics 77−36081
isolated diatomic molecules, in inert gas matrix, cage size anal. 78−47397
isolating integrals in Hamiltonian systems, stochastic and ordered regions 79−2713
isomerisation dynamics, in liquid solutions, statistical mechanics, transition state approx. 78−60999
isostructural phase transitions due to core collapse, one-dimens. model 77−2599
isostructural phase transitions due to core collapse, solid mixtures model 77−84884
isostructural phase transitions due to core collapse, three dimensional model 77−2600
Jacobi polynomials, props. of zeros of polynomial combinations 78−57773
Kac ring model, effect of irreversible microscopic dynamics on macroscopic behaviour of large system 79−49153
Keplerian orbits, statistical mechanics with perturbations 77−49269
kinetic equation derivation in nonequilib. statistical mechanics, approx. results 79−2712
kinetic equation for weakly relativistic system with gravitational interaction 77−49671
kinetic equations for system with weak interaction *(Russian)* 77−64992
kinetic equations from Hamiltonian dynamics: Markovian limits 80−95029
kinetic theory, formal struct. 77−13683
Kirkwood-Salsburg eqns. for bounded stable Kac pot., instability and phase transitions 78−4553
Kirkwood-Salsburg eqns. for bounded stable Kac pot. 78−4552
Kirkwood-Salsburg equation and virial expansion for many-body pots. 77−5744
Kirkwood-Salsburg operator, spectral props., connection with Mayer-Montroll eqns. 77−74307
KMS and equilib. state equivalence for classical systems 77−45782
KMS condition for stable states of infinite classical systems 78−29039
KMS states, stability properties, KMS condition 78−81916
KMS states and ang. momentum, extension 79−75439
KMS states and chem. pot. 77−41525
Kolmogoroff's −5/3 power law, statistical approach 78−1644
Kolmogorov entropy, dynamical system phase space trajectory divergence, numerical anal. 77−26149
Kubo-Martin-Schwinger boundary condition in Neumann algebras 79−75443
Laguerre polynomials, props. of zeros of polynomial combinations 78−57772
Landau equation, non-Markovian terms 80−79432
Landau model with several order parameters 78−41244
Landeu model, critical multiple correlations 79−75440
Langevin eqns., generalised action principle 79−40444
large symmetric matrices, ensemble averaged eigenvalue spectrum 78−132
lattice Coulomb gas representations of two-dimensional problems 78−70068

statistical mechanics continued
lattice fluids, continuous time random walks, non-equilib. Ornstein-Zernike eqn. 77−13687
lattice gas model, press. by Monte Carlo computer simulation 78−4564
lattice gases, strong cluster props. of connected correlations, potential analyticity 78−70062
lattice gauge theory and spin systems, review 80−22528
lattice model, analyticity and cluster props. of unbounded spin systems 78−45571
lattice of randomly placed sites, diffusion, appl. to AC conductivity 77−8097
lattice system, stability, equilibrium and metastability 79−54070
lattice system equilib. states, semi-quantum, AF algebra 78−45576
lattice systems, metric space of interactions, grand canonical pressure, thermodynamic limit 78−12652
Lennard Jones system, nonphysical sampling distribs., Monte Carlo free energy estimation, umbrella sampling 77−26229
Lennard-Jones pot. liquid, high-temperature vapour line using Monte Carlo methods 79−37826
LF current fluctuations in stationary states *(Japanese)* 80−15658
limit cycles and Hamiltonian systems 79−63131
limit relations for model system in case of degenerate state of statistical equilib. 78−8337
linear chain, with arbitrary masses and force consts., correl. functions 77−13685
linear chain, with arbitrary masses and force consts., ergodic props. 77−13686
linear fermion systems, molecular field models, and the KMS condition *(German)* 79−9178
linear interacting processes in nonequilibrium statistical mechanics, thermodynamic Lagrangian formulation 78−21087
linear molecule liquids, computer simulation and theory, review 78−38604
linear relaxation theories, equations of motion, Green's functions, and thermodynamics relations 79−30352
linear response, approx. method of calc. *(Russian)* 80−77685
linear response theory, appl. to itinerant electron ferromagnetism 77−72989
lipid monolayer, statistical mech. theory 78−73141
Lippmann eqn., statistical mech. deriv., dielec. const. 77−20404
liquid, under high press., refr. index vs. density 79−28712
liquid, X-ray and neutron diffraction data interpret using statistical mech. models 77−31551
liquid crystals, stability of mol. orientational distrib. 79−94880
liquid metal, bulk modulus, calc. using press. fluctuation in microcanonical ensemble 80−2106
liquid metal, eqn. of state and triplet and higher correlations in long wavelength limit 77−11453
liquid mixtures, phase separation, umbrella sampling, Monte Carlo calcs. 77−35698
liquid surface, atomic processes, book contrib. 79−60605
liquid surface tension, statistical mechanical theory 79−82414
liquid theory, review 77−7653
liquid-vapour coexistence and correlations in interface 80−65212
liquid-vapour interface, surface tension-compressibility relation 80−44397
liquid-vapour interface and stability rel. to spinodal decomposition, Cahn-Hilliard theory departure 79−77752
liquid-vapour interface nature, non uniform classical fluids statistical mechanics 79−77468
liquid-vapour system in gravit. field, interface correlations 77−1275
liquid-vapour transformations, statistical kinetic theory 77−20044
liquids, kinetic theory, equilib. and non-equilib. props., book contrib. 79−60246
liquids and mixtures, statistical thermodynamics, book 80−90616
local limit theorem for Lennard-Jones type potential 77−49670
locally perturbed 1-D system of elastic spheres 80−4631
Lorentz gas, Fourier's law of heat cond. 79−58620
Lorentz gas, two-dimensional, evidence for slowly decaying tails in velocity autocorrelation function 78−70046
Lorentz invariance of fine-grained one-particle distribution function 79−80433
Lorentz model, statistical dynamics 77−26231
Lorentz process, convergence to random flight process 78−73941
Lorentzian shape, deduction from maximum entropy principle 78−21056
Lorenz surface, wandering motion 77−87687
low-temperature series expansions, algebraic techniques 79−17352
luminescence 79−33756
macromolecular helical wormlike chain statistical mechanics, persistence vectors, comparison rot. isomeric state model 77−50573
macromolecular helical wormlike chain statistical mechanics, scatt. function 77−54637
macromolecular liquids and solutions, statistical thermodynamics 78−18528
macromolecular membrane, statistical mechanics 79−66456
macromolecular systems, statistical thermodynamic analysis, heat capacity function 80−61514
macromolecule, helical to coiled relax., statistical mech. approach, appl. to DNA denaturation by formaldehyde 78−3443
macroscopic cell representation by density matrix eqn. 79−63130
macroscopic non-Markovian systems, microdynamics, time evolution 77−41541
macroscopic non-Markovian systems, microdynamics, time evolution 78−41236
macroscopic system, unstable state decay, deterministic description 79−17347
macroscopic theory, dynamical basis 77−5739
macroscopic theory of statistical thermodynamics 80−105567
magnon elementary excitations damping *(Russian)* 79−28515
many particle spectra, statistical props., two point correlations and fluctuations 78−86216
many particle systems with $1/r^2$ pot., Riccatti eqn. and completely integrable systems *(French)* 79−12711
many-body distrib. function, dilute system generalised Boltzmann equation 79−30351
many-body kinetic eqn., mol. chaos, generalised hypothesis 77−30088
many-particle spectra, ergodicity in random matrix ensembles 79−85056
Markov process generated by Langevin equations, WKB-type expansion 80−86212
martingales, set function processes, vector lattices, Riesz decomposition and characts. *(French)* 80−8908

statistical mechanics continued
master equation, validity for finite closed systems 78−65864
master equation for probability density of vel. distrib. function 77−33935
master operators, with extremal entropy prod. 79−2714
matrix products with application to classical statistical mechanics 79−71351
maximum entropy principle anal., relative freq. reln. and appls. 78−73948
Maxwell vel. distrib. determ., Cenco kinetic theory appl. 77−78916
Maxwell-Boltzmann eqn., exact soln. generation 79−94760
Maxwell-Boltzmann statistical distrib. function of ideal gaseous assembly 80−17858
Maxwellian distrib., four pole approx. 77−82445
Maxwellian distribution, numerical aspects 79−54034
Mayer expansion coeff. 79−141
Mayer function, delta-function expansion, virial coeffs. appls. 79−4221
Mayer graphs with n-root points, improved estimates with appl. 79−67222
mean free flight time of molecules, soln. of apparent concept inconsistency 78−63525
mean spherical approx. for arbitrary hard ions and dipoles, soln. for electrolytes 79−1380
melting curve maxima simple model 77−43313
membrane, passive transport through open membrane, multicomponent system, statistical-mech. theory 78−67261
membranes, excitable, statistical theory, nonlinear force-flux reln. and fluctuation 77−9179
memory alloy, pseudoelastic, model for first-order phase transition 80−92642
metals, chemisorption of gases, book 79−69370
metals, zero-temperature equation of state, statistical model with density gradient correction 80−15215
metastability in kinetic spherical spin system model, nucleation appl. 78−65873
metastability in macrosystems, eigenvalue problem 77−9977
metastable states, relax. and fluctuation theory 78−49769
methane, transport coeffs., statistical mech. calcs. 77−7494
methyl iodide, liquid, rough sphere rot.-diff. model, relax. times 77−15294
micelles, distrib. of solubilised mols., for teaching 79−58497
microcanonical sampling method, simulation appls. 78−73917
microcanonically distributed plasma, reduced distrib. functions 80−28604
microemulsion phase equilibria, statistical thermodynamics 79−5183
microemulsions, statistical mechanics 77−52677
microscopic and macroscopic models correspondence *(French)* 77−45786
microscopic free energy zero fluctuation 77−5740
minimal specific energy 79−90364
mixing and entropy 79−71348
mixing distance of set theory 78−77662
molecular dissociation, RRKM formula correction by non Boltzmann character factors, Markov eqns. 80−71891
molecular dynamics, angular velocity autocorrelation function of fluid of rough spheres, long time behaviour 77−6879
molecular dynamics method in statistical physics, review 80−18895
molecular dynamics of rough sphere fluid, specific kinetic models 77−58936
molecular dynamics simulations at constant pressure and/or temperature 80−64852
molecular dynamics studies of the role of diffusion in chemical models with absorbing boundary states 79−8424
molecular energy distribution in quasiperiodic and ergodic regimes 79−41227
molecular interaction pot., extended law of corresponding states 79−81251
moleculear liquids and liq. crysts., theory of irreversible processes 80−54125
molten salt, possibility of plasmon mode obs., struct. dynamics 80−10477
moment and Fokker-Planck eqns. for growth and decay of small objects 80−82709
moments of multiple distrib. functions 78−49750
momentum autocorrelation functions from classical Green's functions. [Teaching] 78−61976
monolayer, anomalous thermal effects, statistical mechanics 80−15367
Monte Carlo and molecular dynamics, calcs., review, book contrib. 77−37807
Monte Carlo methods, quantum mechanical corrections to classical equilibrium statistical-mechanical results 80−135
multicomponent mixtures, vapour-liquid equilibria predictions, statistical thermodynamic approach 77−55335
multidimensional wave radiation from source with Gaussian time variation and Gaussian approx. distrib. about spherical sheet 78−45487
multiply charged periodic classical systems and random EM radiation, statistical equilib. 79−2621
multipolar continuum mech. eqns. derivation 77−45
multipole approximations, Hilbert-Pade method, appl. to Gaussian function 80−82707
multistate trapping model, rel. to continuous-time random walk model 78−93624
N interacting particle canonical distrib. from kinetic theory 80−105569
N-particles connected by exponential springs, solns. by inverse method 80−46955
negative Kelvin temp., discontinuous transitions 77−98
negative Kelvin temp. connections between regions of opposite temp. sign 77−97
negative Kelvin temperatures, anomalous behaviour anal. 77−99
negative Kelvin temperatures 77−100
negative specific heat paradox, astronomical and physical appls. 78−9557
Nelson's stochastic mechanics on Riemannian manifolds, classical dynamical system 78−57860
nematic liquid crystal, cluster variational const.-coupling theory, thermodynamic props., nematic-isotropic transition 77−24265
nematic liquid crystal, piezoelectric coeffs., Onsager theory, interparticle pot. and first moment vector 77−24264
nematic solution, hard rigid/flexible mols. mixture, unathermal, lattice model *(Russian)* 80−54129
Newtonian system statistical mechanics, Lie-admissible struct. 80−42136

statistical mechanics continued
non-equilibrium phase transitions in cooperative atomic systems 79−80559
non-equilibrium systems, statistical mechanics of steady states 79−54038
non-equilibrium systems near instability, systematic scaling expansion 77−49669
non-Gaussian probability distribs. for vortex fluid 77−47023
non-Hamiltonian perturbations, reduced distrib. functions and entropy prod. 77−9950
non-spherical molecule ensemble, background correl. in statistical thermodynamic calcs. 80−36958
non-uniform fluids, statistical mechs., spinodal decomposition and crit. interface 79−68998
nonadditive hard spheres, mixtures, scaled particle theory 79−44848
nonequilibrium, continued fraction formalism 78−47475
nonequilibrium, perturbation theory, memory function formalism 77−26234
nonequilibrium, perturbation theory, time-displacement operator 77−26233
nonequilibrium entropy and symmetry principle of transport coefficients 79−21683
nonequilibrium expressions for entropy, thermodynamic quantities, using density series expansion 78−8371
nonequilibrium fluctuations in driven systems 80−86210
nonequilibrium phase transitions, synergetics study, recent trends and developments 79−75480
nonequilibrium states, by Kubo and Callen-Welton formulae *(Russian)* 79−17351
nonequilibrium states, Langevin type eqns. from projection operator method 79−97293
nonequilibrium stationary states, light scatt., broken time reversal symm. 79−28776
nonequilibrium statistical mechanics, kinetic eqns. derived 77−57269
nonequilibrium statistical mechanics, path integral formalism based on Onsager's principle 77−67373
nonequilibrium statistical mechanics, review 80−12983
nonequilibrium statistical mechanics, scaling for space-time coarse graining 79−40521
nonequilibrium statistical mechanics, space-time coarse graining scaling, kinetic eqns. 79−75445
nonequilibrium statistical mechanics, validity of exact results 79−75444
nonequilibrium statistical thermodynamics, covariant formulation 77−41542
nonequilibrium thermodynamic Hamiltonian, contact transformations 79−17371
nonequilibrium thermodynamics, statistical formulation by general Onsager Machlup formula 79−54089
noninteracting particles, infinite number, solns. of KMS eqn. 77−33934
nonlinear Brownian motion, and formation of macroscopic order, theory of instability 78−89408
nonlinear dispersive systems, classical mechanics 79−75449
nonlinear evolution eqns., soliton solns. 80−12919
nonlinear excitations by numerical determination 79−71372
nonlinear Kirkwood-Salsburg equation, derivation and low-density soln. 79−9177
nonlinear nonequilibrium statistical mechanics, Oji Seminar opening address 79−75442
nonlinear relaxation and fluctuation 79−30373
nonlinear relaxation processes governed by rotational Smoluchowski eqn. 79−71365
nonlinear stochastic differential eqns., integral representation soln. 77−13730
nonlinear stochastic model 79−2724
nonlinear system, thermal fluctuations, general theory *(Russian)* 77−22484
nonlinear systems, dynamics, heavy damping limit 80−86199
nonlinear thermodynamics, mixing distance, steady state stability, appls. 77−9976
nonlinear transport equations from statistical mechanics 79−75478
nonlinear wave in turbulent medium, with random inhomogeneities *(Russian)* 79−27134
nonrigid polyatomic fluid, chem. equilib., struct., statistical mech. calcs. 77−9111
nonstationary generalised Langevin eqns., methods of multiplicative stochastic processes 77−57270
nonuniform simple hard-sphere fluid, interface props., statistical mech., perturbation theory 77−84607
nuclear and molecular collisions 79−30821
nucleation, microscopic theory *(Russian)* 78−67801
nucleation, microscopic theory *(Russian)* 78−67802
nucleation of liq. droplet, stat. mech. treatment trans.-rot. paradox 77−62625
one component plasma, dynamical struct. factor, collective modes 80−28607
one dimensional infinite particle systems with hard core interaction, nonequilibrium dynamics 77−82443
one-component plasma, internal energy, mean spherical approx., asymptotic form 80−1742
one-dimens. hard rods, linear Boltzmann eqn. exact soln., vel.- and Van Hove self-correl. function *(French)* 78−38441
one-dimens. Ising model in external field 77−57284
one-dimensional complex scalar fields with phase anisotropy, statistical mech. 80−22517
one-dimensional self-gravitational system, equilib. statistical mechanics 78−36922
one-dimensional system, with exponentially repulsive interactions, statistical mechanics 79−55629
Onsager Machlup formula for 1-D nonlinear diffusion processes 78−77816
Onsager relations from Markov system master eqn., symmetry props. 77−22482
Onsager-Machlup function, Lagrangian for diffusion process most probable path 78−73940
Onsager-Machlup Lagrangian for general diffusion processes, Fourier series anal. 79−6060
Onsager-Machlup Lagrangian in theory of stationary diffusion processes 80−128
open binary mixtures, fluctuation theory, entropy prod. and energy dissipation *(German)* 78−64879
open dynamical systems, macroscopic description, Markovisation method 78−62146
statistical mechanics continued
open electron-phonon system, statistical electron transport theory 79−11096
open system, new classical Hamiltonian-Lagrange mechanics 80−36900
open systems, eqns. of motion in nonequilib. statistical mechanics 80−82710
ordered continuously degenerate systems, props. 79−93040
ordered nonsingular systems, topology appls. 78−10166
orientational time correlation functions for J and M diffusion models 78−73939
orthogonal circular ensemble, variables elimination from probability density function 79−17327
oscillations by matrix theory, for teachers 78−61986
oscillator, linear, excitation by stationary random force *(Russian)* 80−27116
oscillators, coupled, stochasticity thresholds 80−46977
oscillators, two-mode self-excited, synchronisation and stochastisation by external field 79−80524
Pade approximants via continued fraction approach 78−61972
paracrystal theory, thermodynamic stability, statistical mechanics 78−75592
parametric amplifier, damping theory anal. 80−52118
parastatistics, Boltzmann, Gibbs and Darwin-Fowler approaches 77−57272
particle growth, mathematical modelling, continuity eqns. for particle distribs. 78−65863
particle in a one-dimensional box, momentum correl. function calcs. 77−33740
particle motion through matter, fluctuations in cascade processes 80−5456
particle penetration statistics, energy loss and multiple scatt. 79−42124
particle transport phenomena, theory, book 79−63176
partition function, variational, phase transition singularities 77−79026
partition functions, series expansion problems 77−33753
percolation concept *(Czech)* 80−127
percolation system, square network diffusion, numerical expts. *(French)* 77−41550
percolation theory, review, appl. and polychromatic percolation 79−58626
Percus-Yevick eqn., existence and local uniqueness of solutions 80−36936
Percus-Yevick eqn., orthonormal series expansion soln. 80−49065
Percus-Yevick equation, series soln., simple chain recursion method 78−65861
Percus-Yevick integral eqn. perturbative soln. for of intermolecular pot. 79−30348
perfect gas, with finite particle number, metric entropy as function of energy 79−17326
periodic density patterns as uniform fluid crystallizes 80−107404
Perron-Frobenius theorem for positive symm. matrices 77−71263
phase space and Liouville theorem of classical statistics, relativistic analoga 80−27184
phase transitions, Gaussian core classical system, low temp., density limit 77−15538
phase transitions 78−71830
phase transitions and critical phenomena, recent developments 77−87713
phase transitions in many identical thermodynamic spin-like systems 77−17906
phase transitions in tree like percolation 79−75473
phenomenological thermodynamics to canonical ensemble 80−22269
phospholipid bilayer melting transition, thermodynamic fluctuations, ion permeability, statistical mechanics model 78−73140
physical adsorption in condensed phases statistical mechanics 80−84365
physical growth laws, equations for the growth of a distribution of small physical objects 80−4630
pion gas, thermodynamical functions 77−64995
plane rotators, equilibrium state uniqueness 78−8369
plasma, MHD turbulence, three-dimens. soln. in cylindrical geometry 78−67351
plasma, one-component, virial pressure 80−38536
plasma, weakly ionised, ion interaction through phonon exchange in neutral gas 79−27775
plasma, weakly ionised, ion interactions through acoustic field, plasmoid existence 79−27776
Poincare group representations on phase space 79−88827
point mass in plane convex region, stochastic transition and entropy 78−54288
polar fluids in elec. fields, statistical mechanics 80−54085
poly-m-phenylene isophthalamide, soln. and cryst., conform. props. calcs. *(Russian)* 79−65009
polyatomic chemical reactions, statistical phase space theory 77−48630
polydisperse hard-disc systems, equations of state, particle size effects 78−73947
polydisperse hard-sphere systems, equations of state, particle size effects 78−73947
polymer, crystallisation, chain folding, statistical mechanical calc. 78−2020
polymer, excluded vol. component, physical bound 78−66698
polymer, orientational ordering rel. to mech. props. *(Russian)* 78−59766
polymer, single ring, Lennard-Jones model, eqn. of state calcs. 78−5379
polymer and fibre systems, entanglement density, statistical theory 78−5381
polymer chain, amorphous state, configs. 77−80427
polymer chain, flexible, angular correlation ranges 77−34790
polymer chains, helical wormlike, statistical mechanics, anisotropic light scatt. near the rod limit 80−93346
polymer chains, self-avoiding random walks, eigenvalues, Monte Carlo determ. 78−57849
polymer chains, with volume interaction, statistical physics problems, coils and globules, review 78−94347
polymer confined to wedge of interior ang. α, config. statistics 79−45875
polymer crystals, chain-folded, statistical mechs. in lattice model 78−47247
polymer linear chains, excluded vol. problem 80−5650
polymer melts, thermal conductivity, statistical mech. calcs. 78−34661
polymer solns., corresponding states theory, appl. to gas solubilities 78−71859
polymer solns., phase diagrams, pulse-induced critical scatt. 79−1490
polymer solution, osmotic pressure, correlation functions, in grand canonical formalism 80−100159

statistical mechanics continued
polymer solution, Rayleigh scattering, intermolecular correlations effect 80−75146
polymers, adsorbed, excluded vol. effects, Monte Carlo investigation 79−95259
polymers, self-consistent field approximation, BBGY and Kirkwood calcs. *(Russian)* 79−64981
polymers, simulation by self-avoiding nonintersecting random chains, conc. effect 78−12639
polymers in poor solvent, loop expansion of irreducible diagrams 80−100160
polymethylene, intramol. scatt. function calc. 77−38761
polymolecular adsorption on heterogeneous surfaces, statistical thermodynamical eqns. *(German)* 78−30830
polyvinylidene fluoride, structural phase transitions, statistical mech. theory 79−82331
positivity conditions on correlation functions that imply Debye screening 79−71350
potential fields, nonstationary, nonlinear distrib. function, hydrodynamic eqns. *(Russian)* 80−52033
Potts model, hierarchical, three-state, high temp. susceptibilities 80−77723
principle of maximum entropy and irreversible processes, review 80−86198
probability, theoretical structure, measuring techniques, ensemble concept 77−9868
probability derivation in statistical mechanics, distribution function coarsening evolution 80−36937
probability foundations, modal frequency interpretation 80−12885
projective limits 80−27209
protein conformation, statistical mechanical theory, appl. to homopolymers 78−64931
protein conformation, statistical mechanical theory, folding pathway 78−64932
protein synthesis, stochastic eqns., ribosome translation along mRNA and tRNA selection processes 79−66440
pseudo-first-order phase transitions in one dimension 80−22270
pseudocritical phenomena near the spinodal point 78−65894
quantal master equation for any time scale, Brownian motion 78−24725
quark matter, one dimens., Abelian approx. 78−41491
quasifree completely positive semi-group generator for nonequilibrium statistical mechanics 79−25963
quaternary alloy, order-disorder transition using classical fluctuation theory and correl. functions 79−73288
quenched magnetic system, statistical thermodynamics 77−66363
quenched random system 79−63155
radiant cavity, one dimens., nonlinear field mode interaction, statistical props. 78−16668
radiation problems transport eqns., using Wigner distribution 80−168
radiative transfer, Eddington tensor, maximum entropy soln. 79−23190
random chain of classical spins, statistical mechanics 78−10630
random matrix ensembles, joint eigenvalue distrib. 80−101748
random walks, self-avoiding and limited order, distrib., orthogonal vector anal. 78−65874
random-walk theory and correl. functions in classical statistical mechanics 77−5768
random-walk theory and ordered phases in lattice-gas systems 77−5769
randomly driven system, strong coupling expansion for classical statistical dynamics 80−105568
randomly-packed spherical particle bed, coord.-no. distrib., effective thermal cond., stat. thermodynamic theory 78−75028
rarefied gas flow with chemical reaction, Monte Carlo simulation of homogeneous dissociating diatomic gas 77−51128
rate processes in condensed media, master eqns. 80−77687
Rayleigh problem, exact transform soln. 77−53844
reaction-diffusion systems, periodic solns. and multiple steady states 79−54082
real fluids, short range repulsions and long range attractions, simple pair pot. model 80−64850
reduction of variables and processes in macrodynamics 77−5786
relation to fluid mechanics, book contrib. 80−94959
relativistic, state indicator or negative probabilities 79−63128
relativistic formulation, appl. of bootstrap theory to thermodynamics and cosmology 79−40452
relativistic gas in thermal equilibrium 77−58830
relativistic gas of interacting particles, phase vol. approx. 78−41225
relativistic Gibbs ensembles 79−63126
relativistic Lagrangians for classical interacting point particles 78−70048
relativistic Lorentz gas of hard spheres, diffusion coeff. 77−5743
relativistic plasmas, binary correlation function 79−82039
relaxation process as contraction of Markovian type multidimensional one 80−31671
renormalised theory of time-depend. pair distrib. function 77−2601
replica method and solvable spin glass model 79−38327
replica method for amorphous materials 80−86197
resonance fluorescence, detailed balance, Lyapunov stability and entropy 79−13941
response theory for systems nonlinearly displaced from equilibrium, graphical approach 80−22285
rigid particle fluid, general zero-separation theorem 79−46533
rigid polyatomic molecules, classical statistical mechanics 78−16718
rigid-rod fluid, thermodynamic props., crit. points and transitions 78−73919
rigorous mean field theory derivation from many body interaction 77−26260
role of statistical mechanics in classical physics 78−8334
rubber containing entanglements, mechanical model 79−81315
Saha equation, elementary derivation, rel. to mol. dissoc. 80−82599
scalar quantum electrodynamics on lattice as classical statistical mechanics 78−16956
scaling function for eqn. of state in $1/n$ and ϵ expansions 77−87718
scaling method for obtaining kinetic eqns. from BBGKY hierarchy 77−45785
scaling theory of transient phenomena near instability point 77−33945
scattering and dynamics, classical and quantum statistical mechs., unified treatment 78−45522
scattering theory, continued fraction expansions and statistical nonequilib. mechanics 78−45523
second virial coeff. from scatt. operator in classical mechanics 77−64993
selection game, fluctuation theory 77−26241
statistical mechanics continued
self-avoiding random walk, external spatial constraints, 'slithering snake' calcs. 77 89
self-avoiding random walk, real-space renormalisation group approach 79−63167
self-avoiding random walks, eigenvalues Monte Carlo determ. 78−57849
self-avoiding random walks, excluded vol. effect 79−44845
self-avoiding walks with span limitations, cubic lattice, mean square end-to-end distance 80−62568
self-oscillating system close to harmonic, width of spectrum *(Russian)* 77−82462
semiconductor, hot electron fluctuations with displaced Maxwellian distrib. 80−29418
separable many-particle interactions, free energy per particle, convex-envelope formulation 78−32781
simple classical, liquids, Bogolyubov method, equilibrium system many body correlation function contracted description *(Russian)* 80−38888
simple fluid, one-component, liquid-vapour phase coexistance, surface tension determ. from many body pot. 80−49465
simple liquid, dynamical structure factor and Green's functions 79−4228
simplified hydrodynamic theory of nonlocal stationary state fluctuations 80−98857
simulation of system with charge-charge interaction, boundary condition 78−62144
sine-Gordon chain, effect of external field 78−62145
sine-Gordon chain, transfer integral techniques 78−57850
sine-Gordon field theory Coulomb gas equivalence, classical gas with logarithmic pot. 80−4850
single-particle density matrix kinetic eqns., linked cluster expansions in eqns. of motion method 77−33933
singular interaction potentials in classical statistical mechanics 79−71354
Smoluchowski equation derivation with corrections for Fokker-Planck and BGK collision models 79−80499
soft rods, one-dimensional, exact partition and thermodynamic functions 80−46953
solar system, distrib. of mean motions of planets and satellites rel. to development 77−91451
solid solution, statistical treatment by first order approx. *(French)* 77−9117
solid state physics, contrib. of Conyers Herring in 1930s 80−57056
solitons in condensed matter: a paradigm, review 80−77632
solitons in condensed matter physics, theory 80−50122
solvent struct. around ions as hard spheres, mean spherical approx. 79−70335
sound wave propagation in two-phase random media, coarse grained eqns. 79−86280
spectral entropy method for distinguishing regular and irregular motion of Hamiltonian systems 80−4629
spectral props. of composition operators 79−80496
spherical and mean spherical models, correlation phenomena 77−74327
spherical limit for n-vector correls., spin correl. functions 78−24726
spin glass, statistical thermodynamics 77−66363
spin systems, crit. behaviour at $n=-2$ 78−43600
spin systems in phase transition to superradiant state, dynamics and thermodynamics 79−22925
square well fuild, elastic modulus and viscosity coeff. 77−30086
stability, equilib., and metastability 80−31659
star clusters, spherical, frozen in pot. waves 79−67070
stationary states, dense fluid fluctuations, appl. to light scatt. 79−54035
stationary states, dynamical variable nonequilib. average, microscopic theory 79−58623
stationary states far from equilib., regression of fluctuations 80−42138
stationary states theory, appl. to low-density systems 79−58624
statistical crystal model, small amplitude acoustic perturbations and Debye-Waller factors 78−55930
statistical equality connecting zero Fourier harmonics with average quantities 80−133
statistical information, information extent and information distance 78−77824
statistical thermodynamics from statistical theory of estimation 78−54328
steady state of stiff linear kinetic systems, Markov matrix method 77−52613
stellar atmosphere in statistical equilib., effects of deviations from LTE 80−31290
stellar equilibrium statistical mechanics, steepest-descent techniques for Newtonian clusters 77−45496
stellar equilibrium statistical mechanics of gravitating systems with energy cutoff 78−93326
stellar equilibrium statistical mechanics of relativistic systems with energy cutoff 78−93327
stellar relativisitc clusters, steepest descent technique and stellar equilib. statistical mechanics 77−49444
stellar turbulent convection equations, ensemble averaging 80−67698
sticky hard sphere potential, Percus-Yevick eqn., and soln. 77−2602
stochastic Hamiltonian classical and quantum, systems, Volta Memorial Conf. 80−8738
stochastic Liouville equation, generalised, nonMarkovian and memoryless master eqns. 78−24737
stochastic systems, finite dimens., ergodic and quasideterministic props. 78−32762
stochastic systems, infinite dimens., ergodic props. 78−32770
stretched dipoles, in applied elec. field, distrib. function 78−64851
structural stability, phase transitions 80−8932
sufficiency and its role in the macroscopic description 80−57171
superionic conductors, lattice gas models, book contrib. 80−24661
surface tension, Fowkes' hypothesis, statistical mechanics basis 80−2249
surface tension, review of theory 79−77866
surface tension, statistical theory 79−51392
surface tension and phase transition in lattice systems 80−27226
symmetry breaking, kinetic model 80−129
synergetics approach 78−16717
tautomeric transform., quantum-statistical model 77−38739
teaching demonstration for 3rd form of secondary school *(Hungarian)* 77−49528
temp. states, von Neumann algebras, asymptotic ratio set 78−12640
thermal equilibrium statistics, by fluctuation in thermodynamic theory of meas. 79−85074
thermal fluctuations, driven nonlinear resistive system 79−25981
thermal radiation of nonlinear material, generalised Kirchhoff law, fluctuation-dissipation theorem 80−4679

statistical mechanics continued
thermodynamic limit for a classical system of particles with hard cores 79−71353
thermodynamic limit in equilibrium and non-equilibrium systems 77−53827
thermodynamic properties, of interacting particle ensemble, by simulation of stochastic disordering 77−87697
thermodynamics, second law, classical derivation 79−21682
thermodynamics and decoding of long molecules 79−31757
Thomas-Fermi-Dirac eqn. nonlinear problem 77−22483
three particle bound states and contribution of three particle unitarity, dispersion method *(Russian)* 78−8336
three-particle scatt. operator, correl. pattern representation 77−13684
time correlation functions of one dimens. infinite system, ergodic props. 78−65862
time evolving system, markovian density operator, generalised H-theorem 79−49184
time-dependent Ising model and Cayley trees 79−75472
time-dependent pair distribution in the mean-field approximation 80−77689
time-local gaussian processes, path integrals and nonequilib. nonlinear diffusion 77−13726
Tolubinskij's stochastic theory of nonequil. processes and rel. to kinetic eqns. *(Russian)* 78−21053
topological excitations in U(1)-invariant theories 77−67383
transfer collision frequencies for inelastic collision 79−71357
transient nonlinear fluctuations, scaling theory, macroscopic order formation 79−80520
transition matrices for Markov chain sampling, model systems, convergence rate comparisons 77−57165
transport coeff., elimination of t-explicit divergence 79−26008
triad interaction flows, isotropic and ergodic motion 79−50712
triatomic molecules, C_{2v} symm., vector statistical distrib., mol. dynamics computer simulation 80−63734
turbulence, Lorenz model, statistical dynamics study using stochastic differential equations 79−92949
turbulence, statistical theory, review of present trends, book contrib. 77−84234
turbulence problem, one dimens., equivalence to one dimens. Coulomb gas 78−5735
turbulence theory, review 80−4536
turbulent diffusion, nonlinear integrodifferential eqn., numerical soln. 78−38306
two component classical Coulomb gas, equilib. props. 79−12709
two time correlation functions for Poisson representation, nonequilib. and equilib. chemical reactions 79−1936
two-component ionic mixture, eqn. of state and phase separation in uniform background 78−21058
two-dimens. neutral Coulomb gas, bounds for classical canonical partition function 77−26227
two-dimensional fluid, adsorption isotherm, summation of virial expansion for eqn. of state 79−15007
two-phase system with interface, derivation of dynamical eqns. 79−49155
unbounded accummulation instability *(Russian)* 79−88867
unbounded n-component spin systems on lattice, statistical mech. 77−4477
unitary group representations, appl., book 79−30198
universality hypothesis in classical mechanics 79−12712
unstable states, relax. and fluctuation theory 78−49769
unstable systems, anomalous fluctuation and relax., multimacrovariables 77−79033
unstable systems, fluctuation dynamics in Ginzburg-Landau models 77−49685
Ursell functions, group functions and derivatives 78−70049
Ursell functions and cluster estimates, representations 80−8900
van der Waal's crystal P-V-T diagram, Holmholtz free energy, mean-field model, for teaching 77−33784
Van der Waals fluid near critical pt., transport props. 79−46537
Van der Waalsian theory of freezing 78−22821
vapour pressure, rel. to liq. internal press. 79−33094
variational principle for Z_+^N action on compact space 77−53825
variational principle in nonequilibrium nonlinear statistical thermodynamics *(Russian)* 79−85058
velocity correlation functions for finite one-dimensional systems 79−25966
vinyl polymers with flexible side chains, configurational statistics, dipole moments 77−38760
virial coefficients for hard rectangular parallelepipeds and cubes on simple cubic lattice 79−97308
virial theorem 77−30089
virial theorem and scale transformations, for teaching 80−17763
virial theorem for open systems, ideal gas law 77−37804
virial theorems, generalised and pointwise 79−30354
Vlasov dynamics and fluctuations in 1/N limit of interacting classical particles 78−130
Vlasov eqn. and entropy, collective, nonHamiltonian model 77−5745
volatile liquid, statistical thermodynamics of new phase form. *(Russian)* 78−18739
Volterra soliton, collapse into weak monotone shock wave 78−49673
Volterra systems of $N \geq 2$ interacting species, evaluation of phase integrals 77−33932
vortex-acoustic ion wave turbulence, statistical mechanics 80−92326
vortices, two dimensional, statistical mechanics 78−30304
vortices, two-dimens., in bounded container, statistical mechanics 77−3831
wall-particle distribution function, soln. of Ornstein-Zernike eqn. 77−26230
water, boundary conditions for numerical simulation, book contrib. 79−60247
water and dil. aq. solns., statistical mech., book contrib. 79−60250
water transport through unsaturated soil, Buckingham-Darcy flux law, statistical mechanical theory 79−16541
water transport through unsaturated soil, conservation laws derived from statistical mechanical methods 79−16540
waves in thermal equilib. 79−9175
weak second law of thermodynamics, classical gas in rectangular box 77−82442
weakly dissipative system, physical props. 77−74309
weakly relativistic gas, equilib. distrib. and eqn. of state 79−21649
statistical mechanics continued
weakly relativistic statistical mechanics, choice of measure and Liouvilles eqn. 80−46956
weakly-coupled classical fluid, kinetic eqn. for test particle 77−74310
wetting, of rigid solid, by simple fluid, work of adhesion 77−89618
Wick's theorem and Fokker-Planck dynamics 79−40504
Wiener-Khinchin theorem 78−57851
Wigner representation, gauge invariant, electrodynamics of scalar particles 78−29251
X-ray structure amplitude phases, statistical-thermodynamic determ. 80−84028
XY_4, tetrahedral, SU $(2s+1)\times\zeta_r$ and spin statistical weights 78−50463
XY_6, octahedral, SU $(2s+1)\times\zeta_r$ and spin statistical weights 78−50463
Yvon-Born-Green and Kirkwood eqns. for hard spheres at very high densities, multiple solns. 77−33929
zero-component classical field, electron localisation and statistical mechanics 78−30855
zero-component field theories, high order behaviour without $n\rightarrow 0$ limit 79−75438
Zwanzig's classical projection operator formalism and coarse graining 77−26232
Al, liquid, bulk modulus, calc. using press. fluctuation in microcanonical ensemble 80−2106
BN, adsorpt. of Ar, thermodynamic values calc. from pot. parameters *(German)* 79−95268
Br_2+Ar, ergodic deactivation, anharmonic effects on transfer rate 78−82818
Cr binary substitutional solutions, thermodynamics 80−54410
Fe-bearing binary, substitutional liq. and solid solns., statistical thermodynamics 80−11630
H plasma, pair correlations down to r=0 80−14883
H_2, many electron systems, chem. binding, local stresses and force densities 80−27920
HCl+H_2, translational and pot. relax., statistical calcs. 77−3435
^{4}He, superfluid, hard-sphere model, crit. anal. 78−51769
Li_xTiS_2, Li ordering in intercalation battery, theory 79−77580
Mn-bearing binary substitutional alloy systems, props., applicability of statistical thermodynamic approach 80−88336
Ni-bearing substitutional binary solutions, thermodynamics 80−44336
Ni-S, phase diagram calc. and thermodynamic props. of liq. phase 80−108401
Rb, liq., pair interaction pot., thermodynamic, neutron diffr. calcs. 77−11463
SF_6, collisionless multiphoton dissoc., statistical theory 78−62862
SF_6, collisionless multiphoton dissoc., statistical thermodynamic process 78−82799
ThC_x, $0 \leq x \leq 2.0$, nonstoichiometric, statistical mechanical model for C activity 79−71892
XY_5, trigonal bipyramidal, SU $(2s+1)\times\zeta_r$ and spin statistical weights 78−50463
Zn-bearing binary substitutional solutions, thermodynamics 80−44337

statistical methods *see statistical analysis*

statistical models
(2+1) dimensional Georgi-Glashow model, critical Higgs mass, clustering, monopoles 80−52441
$\pi^-\pi^+\pi^-$ semi-inclusive distrib. anal. using Kopylov-Podgoretsky-Cocconi formulation, fireball 78−89761
$(\phi^3)_6$, theory, inclusive annihilation processes, jet evolution 79−71640
additive quark model and multiparticle production off emulsion nuclei at 50 GeV 80−68491
anisotropic superfluidity of hadronic matter 79−13090
asymptotic props. of strong interactions, probability interpretation, Veneziano description *(Russian)* 79−93389
atmospheric radio noise statistical models for reception in VLF band 80−72611
axes and scalar measures of two-jet and three-jet events 79−45069
bag model, isobaric ensemble and multiplicity distrib. *(Russian)* 80−82952
bag model, string like solns., baryon-antibaryon states mass formulae *(Russian)* 79−93369
baryonium muliquark system model of fireball, high energy pion production 79−97603
bootstrap duality in inelastic scatt. 77−18239
bootstrap model, π cumulative prod. probability in high energy nuclear collisions *(Russian)* 77−46028
bootstrap model, hadronic mass spectrum, pion condensation, boson gas 78−70345
bootstrap model, statistical, for hadronic matter and multiparticle reactions 77−57502
Bose-Einstein statistics, wave packet formulation of multiparticle production at high energies 80−13338
bottom meson nonleptonic decay, many body final states, isospin-statistical models 80−62975
branching process study from parton distrib. evolution eqn., jet processes 79−89111
cascade models, transverse momentum depend. of quark fragmentation functions 79−45068
causal model of quark fragmentation, charge retention in hadronic jet 78−29313
Chao-Yang statistics, particle ratios and quarks 80−27486
chaotic isospin zero state of one mode isovector field 78−12883
charmed meson, non-leptonic decay in SU(3) Bose quark model 79−85278
charmonium states, multimesonic decays, statistical quark model 78−82171
cluster concept in multiple hadron prod. 78−66177
cluster decomposition of many dimens. phase space, appl. to high energy collisions 80−102027
cluster decomposition soln. of statistical bootstrap with Bose statistics 77−82714
cluster identification from secondary particle speed ranges 77−46026
cluster model, concepts and appls., review 79−357
cluster model, transverse momentum correls. of pions 77−38134
cluster model in lepton prod. in hadron collisions, e/π ratios 77−2886
cluster models, convolution rules, exclusive, semi-inclusive and inclusive processes 77−26497
Cluster problem in physics of high energy particles *(Russian)* 79−93384
cluster production, multi-Regge model with threshold factor, multiplicity distribs. in pp collisions, 50-400 GeV/c 77−18256

statistical models continued
cluster production for high energy pp reactions, field theoretic model 77−6091
clustering in multiparticle production in (2 to 1000) GeV/$\hbar$ hadron interactions 79−101037
clusterisation, role of rapidity interval distrib. *(Russian)* 77−10220
clusters in hadron multiple production processes 79−49545
coherent quark-gluon jets in coherent state formalism 79−97580
collective reson. in hadronic matter, hydrodynamic model 77−71491
collective tube model, credibility of criticism by Azimov et al., effects of target fragmentation 78−93982
composite particles, nonrelativistic many-body theory, foundations and statistical mechanics 80−82947
correlational anal. of inelastic hadronic processes, multicluster mechanism *(Russian)* 78−89684
cosmic ray morphology, one-dimensional diffusion eqn. integration, one-fireball model 78−57416
cosmic ray nuclear event, ~42 TeV, high multiplicity, large transverse momenta, giant fireball 78−33105
cosmic ray showers, ang. distrib. and multiplicity 78−36412
cosmic rays, 10^{13}-10^{16} eV, multiple meson production, longitudinal behaviour of γ air family 77−33309
coupled dynamical systems and the transition from weak to strong coupling 79−50500
covariant parton model, jets, quark confinement large p_T and leptonic inclusive processes 77−30317
CP violation, statistical theory, K^0 decay 77−41784
crossing relations derivation using substitution rule 79−67483
cumulative hadron production, statistical bootstrap model with strangeness *(Russian)* 80−62948
diffractive hadronic reactions, statistical description of multipion prod. 80−95260
dihadron high mass continuum, phenomenological anal. of Fermilab data 80−42511
dimensionality in the statistical bootstrap model 79−97606
diquark and quark jet fragmentation model, meson and baryon production 79−2979
diquark jets in leptoprod. and large p_T reactions, fragmentation functions 78−82149
direct photon emission from excited bosons and e^+e^- collisions, relativistic oscillator model 78−37208
discrete cluster mass spectrum, cosmic ray data anal. 78−33104
double-logarithmic quark and form factors and the evolution of parton jets 80−68421
dual quark pattern for multiplicities, inclusive distribs., in hadron or lepton induced reactions, quark jet universality 78−41476
electron mean free paths and stopping powers in solids calc. 77−19996
energy profile of proton jet 78−50018
equipartitioned jets, new tests of QCD 79−71697
exotic meson ($Q^2\bar{Q}^2$) spectroscopy, instanton effects 79−89140
exotic NN resonances, joined spring model, Bose quark model anal. 79−89120
expanding bag model, effective quark mass 79−97604
explosive quark matter, hypothesis for Centauro event 80−22648
ferroelectric hysteresis cycle computing from a statistical model *(French)* 79−11393
Feynman gas model with Bose statistics, phase transition and multiplicity distrib. *(Russian)* 78−89683
Feynman scaling, multihadron prod. through intermediate reson. 78−78152
Feynman-gas model for semi-inclusive processes, πp appl., multiperipheral model predictions *(Russian)* 78−435
Feynman-Wilson fluid, density fluctuations, multiparticle event asymptotic struct. 79−36040
Feynman-Wilson gas, statistical model for multiparticle physics 79−22071
fireball, single and ideal gas, partition function 77−38133
Fireball behaviour in hadron macroscopic gas 77−22702
fireball characteristics in 400 GeV/c πN collisions 78−58173
fireball decay, internal symmetry structure of statistical bootstrap models 77−57501
fireball decay in statistical-bootstrap theory 78−436
fireball dimension determ. in hadron collisions, Bose-Einstein correlations 79−22069
fireball emission, slope of overlap function 77−67637
fireball mass spectrum, bootstrap condition, J-depend. 77−67626
fireball model, Feynman scaling cosmic γ-ray spectrum from pp collisions 77−18364
fireball model anal. of small and large P_t pion distribs., ISR energies 77−38211
fireball model three component, appl. to $\bar{p}p$ interactions above 9 GeV 80−62946
fireballs, discrete mass spectrum 77−57499
fireballs, quantum-statistical chain decay, pion clusters 78−430
fluid droplet model of tachyons in framework of two centres particles 80−105868
fragmentation model and minimal rule 78−25019
gluon fragmentation, polarised, in e^+e^-, e^-q and hadron scattering 80−82988
gluon fragmentation functions from quark jets 79−49453
hadron, fragmentation from heavy quark partons 78−8603
hadron+hadron, cluster model, field theoretic, multiperipheral production, Feynman scaling violation 80−57576
hadron+hadron, high-energy, inclusive spectra of secondary pions, Feynman scaling and statistical model 80−42502
hadron+hadron, jet production, large transverse momentum 80−42503
hadron+nucleus, spatial temporal development, nuclear hadronic cascades 80−63040
hadron condensation before Hagedorn temp. 78−50016
hadron decay from jet, transverse momentum 78−74268
hadron distributions in quark jets, pion and proton form factors 79−54317
hadron dynamics, multiparticle prod., intermol. pot. in Feynman-Wilson gas 78−477
hadron induced multiparticle reactions, S-1500 GeV, resonance prod. correlations, jet model *(German)* 80−91118
hadron inelastic scatt., secondary hadron multiplicity distribution, Regge like parton model *(Russian)* 80−78100
hadron interactions, inclusive, large momentum transfer, quark counting, EM form factors 80−68498
statistical models continued
hadron interactions, inclusive processes, multiplicity and scaling, resonance production, additive quark model, SU(6) theory, review 80−63043
hadron interactions, local thermodynamic equilibrium *(Russian)* 80−9155
hadron jet in inclusive large transverse momentum prod., covariant parton model *(Russian)* 77−34131
hadron jets, correlating quark rearrangement model 79−2997
hadron mean charged multiplicities, universality in particle and nuclear collisions 77−54086
hadron multiple prod. *(Russian)* 77−67625
hadron plasma theory *(Russian)* 78−37148
hadron production, inclusive, quark fragmentation and triple Regge models, quark decay functions 80−62921
hadron scatt. mediated by qg→qg and gg→gg 80−82988
hadron-hadron interactions at high energy, generalised hydrodynamical models 79−89131
hadron-induced and e^+e^- annihilation, multiplicity ratio 80−105877
hadron-nucleus reactions, 20-400 GeV, multiplicity of relativistic charged particles *(Russian)* 80−5191
hadronic bremsstrahlung, grand partition function determ. 78−33041
hadronic collisions, jet structure, two-jet events, glueball-Pomeron identity, dual field theory 80−63051
hadronic collisions violation of Feynman scaling, central region, fragmentation, mixed two component model 77−26551
hadronic eqn. of state in statistical bootstrap model and linear graph theory 77−22704
hadronic events, inelastic, non-diffractive, charge correlations in jets, quantum number effects 80−86764
hadronic jet, space time evolution, transverse momentum struct. 78−50017
hadronic jets, sequential decay models, nonscaling inclusive distribs. and long range correlations 79−49552
hadronic lepton pair production, QCD jets 80−62994
hadronic matter, anisotropic superfluidity, analytic formulation 80−105869
hadronic matter, critical point exponents 79−58944
hadronic matter, eqn. of state for relativistic quantum gas model 79−9349
hadronic matter, phase transition of second band, anal. in one-loop theory in renormalisable field theory 80−4930
hadronic matter, statistical bootstrap model and critical behaviour 80−42430
hadronic matter, thermodynamic props. of class of solvable statistical models 79−63452
hadronic matter governed by statistical bootstrap eqn. of state, hydrodynamical flow 77−22705
hadronic matter of finite no. of fireballs, phase transition struct. 79−36180
hadronic reactions, trajectory slopes in gauge-dual-topological approach, jet multiplicity 80−18142
hadronic system. solvable thermodynamical models 79−63456
hadronic total cross sections, soft and hard components, model anal. 79−49546
hadrons, extended, stochastic description 78−431
hadrons, parton distribs. calc. 78−421
Hagedorn Frautschi statistical bootstrap model, modification for baryon charge and strangeness conservation *(Russian)* 80−27489
Hagedorn model, topological cross sections in multiplicity asymptotics *(Russian)* 80−9154
hard scattering processes, hadronic jets and QCD 79−71727
heavy 1^{--}-onia, two-jet cross section in perturbative QCD 79−93357
heavy quark and gluon two jet prod. in e^+e^- annihilation *(Russian)* 78−89696
heavy quark states, weak decays and prod., jet like distrib. in SU(2)×U(1) model 79−75746
Heisenberg's approach, modified, meam charged hadron multiplicity in πp and Kp collisions 78−45988
high energy charged current neutrino interactions, spherocity and thrust distribs., jets 79−85293
high energy inelastic hadron reactions, π prod., scaling law, fireball model 78−74287
high energy nuclear collisions, pion multiplicity calc., target at. no. depend., statistical model anal. *(Russian)* 79−9425
higher order QCD jets in photoproduction 80−99087
hydrodynamic model, nonlinear pion+pion chiral Lagrangian, $e^+ + e^-$ and p+p collisions 78−32966
hydrodynamic model, scaling and logarithmic multiplicity of secondary hadrons *(Russian)* 77−10221
hydrodynamic theory of high energy interactions *(German)* 80−406
hydrodynamic theory of multiple hadron production, new approach *(Russian)* 79−6332
hydrodynamical approach, large p_T distrib. in pp interactions 79−49490
hydrodynamical description of the missing-mass clusters 79−71728
hydrodynamical model, resonance prod. *(Russian)* 80−62947
hydrodynamical model of multiparticle prod., scaling solns. 78−8616
hydrodynamical models anal. 78−8617
hydrodynamics and the bag model, multiparticle production, finite geometry effects 79−22044
inclusive distribution, transverse momentum correlations for secondaries, rapidity cluster, stat. model 80−73754
inclusive distributions, statistical model model formulation and mean field approx. 79−36041
inclusive electroproduction of forward protons in fireball model 78−41554
inclusive hadron and lepton prod. for violent collisions 77−18353
inclusive high energy particle-nucleus interactions, A depend. of multiplicity, cross section, rapidity, momenta distrib. 77−79291
inelastic processes, cluster model with repulsion and correlation anal. *(Russian)* 80−102026
information theory application to multiplicity distrib., clusters 77−38131
instantons and the 1/N expansion 80−400
interacting instanton-antiinstanton system under external colour mag. fields in SU(2) gauge 80−101920
intermediate vector boson decay, QED and QCD radiative corrections, hadronic jets 80−73759
J-dependence of statistical bootstrap mass spectrum, S-matrix and semi-classical formalism comparison 78−86448
jet analysis, QCD calcs. and phenomenological models 80−52523
jet decay models, group-theoretical and four-momentum variables 80−73684

statistical models continued
jet fragmentation axis 79−93350
jet model, uncorrelated, implications of Bose-Einstein statistics 79−22070
jet model with quantum statistics, Touschek invariant meas. 79−22068
jet phenomenon and Lorentz deformation 80−105806
jet processes in QCD 78−82104
jet production in e^+e^- collisions to order α^3 and α^4 and including QCD corrections 80−13322
jet production on nuclei, strong A depend. *(Russian)* 80−102084
jet quantum number identification event by event, original parton and gluon jets 80−52466
jet struct. in hadronic lepton pair prod. ang. energy cross section, QCD 79−75806
jet struct. of hadronic final states, Bose-Einstein effect 78−16994
jet structure in e^+e^- annihilation, deviation variable, QCD calc. 79−9388
jet structure in high p_T events, importance of parton transverse momentum 78−432
jet structures of leptons, quarks and gluons, perturbative QCD, process dependence 80−68470
jet studies and large transverse momentum collisions, review 79−22143
jet time development in perturbative QCD 79−93356
jet-enhancement coeffs., diffr. scatt. *(Russian)* 78−29316
jet-mass effects and high-p_T jet production 80−52473
jets, angular distrib. of energy, QCD transverse ang. momentum distrib. 79−71726
jets, appl. of quark parton model 79−30715
jets, rel. to ψ particle expts. (1975, 1976) *(Czech)* 79−26288
jets in high energy collisions 79−45114
jets in neutrino deep inelastic scattering 79−75762
jets of quarks and gluons, leading logarithmic approx., parton interpretation 80−68433
kinematics in strong interaction theory 77−79246
KNO scaling and multicomponent cluster models 77−49918
KNO scaling for high-energy multiplicity distribs., distrib. functions 77−18237
Kopylov-Podgoretsky-Cocconi formulation modification for hadron-hadron collisions 80−78044
Landau's hydrodynamic model, further aspects 78−82173
Landau hydrodynamical model of multiparticle prod. due to viscosity 78−4836
large momentum transfer interactions, jet struct., from rapidity correlations and associated multiplicities 77−49919
large p_T jet prod. in hadronic collisions, QCD calc. for inclusive cross section 78−86439
large p_t processes, parton-parton cross sections constraints from angular correls. 77−71540
large p_T processes, two particle distrib. and associated multiplicity, jet fragmentation 77−82782
large p_T production and hard rearrangement of quarks 79−63454
large transverse momentum hadronic reactions, hard scatt. model of urbaryons with two-jet struct. 77−41813
large transverse momentum particle and jet prod., QCD approach 79−17761
large transverse momentum trigger, multiplicities and rapidity distribs. 78−62376
lepton+hadron, deep inelastic scatt., QCD event states, 3-jet events 80−52515
lepton+nucleon, jet structure, cascade model and jet model 80−42471
lepton+nucleon, quark and gluon jets, Breit frame, QCD 80−62995
lepton pair prod., thermal parton model 79−13075
level density formula in hadron physics 77−13938
linear chain decay, pion coherence, Bose-Einstein symm. 77−49921
local number fluctuation in multiparticle production 80−57574
longitudinal phase space integral with leading particles 78−17058
M_2 baryonium state decays, baryonium assignment scheme 79−71691
many-hadron production at low $P_\perp$, basic concepts and models, review 79−6331
massive lepton pair production at large q_T, large p_T jet props. 79−54326
master equation for parton distributions 79−80792
mean multiplicity dependence on transverse momentum *(Russian)* 77−46027
mesic atom, Fermi-Teller fuzzy model, atomic capture and cascade 77−58209
mesic atoms, Fermi-Teller model, formation and de-excitation 77−58208
meson+proton→3 mesons+proton, partial wave anal., Ascoli anal., fireball dimens. 78−17054
meson jet generated by fast outgoing quark, parametrisation of props. 78−58168
meson jets from quark fragmentation, flavour, power counting rules at $x\rightarrow 1$ 78−37185
meson resonance and pion simultaneous production, correl. jet model 78−86456
meson-proton multiplicity data, two-component fireball model applications 79−63453
mixed two-ion component model, charge transfer 77−22701
Monte Carlo event generation with limited tranverse momentum 79−3001
multi π systems, mass distrib. using information theory method 78−82250
multi-jet dynamics in lepton induced reactions, granular struct. calorimeter anal. 79−9350
multi-jet structure of hadronic final states and trajectory slope 78−93843
multicluster production, multiplicity distribs., group-theoretical approach 77−2800
multihadron production processes, high energy, strong correls., RPA scheme 78−41506
multiparticle prod. long range correls. and parton model 77−82712
multiparticle production, large transverse momenta, momentum conservation, independ. emission model 78−50055
multiparticle production, sequential decay model with cluster formation, cluster mass 78−16993
multiparticle production description by Chapman-Kolmogorov eqns. 78−12882
multiparticle production meson ratios, statistical quark model *(Chinese)* 79−49558
multiparticle production processes, cluster formation model, math. formulation 78−478

statistical models continued
multiparticle production processes, correls. due to energy-momentum conservation, uncorrel. jet model 78−41601
multiperipheral cluster model based on Bethe-Salpeter eqn., comparison with pp and π^-p data *(Russian)* 77−10230
multiperipheral cluster model study of expt. distribs. of rapidity intervals in π^-p interactions at 60 GeV *(Russian)* 77−34189
multiperipheral production of large and small fireballs at very high energies 80−47264
multiple formation process, parton model and statistical equilib., parton fluctuations *(Russian)* 79−13062
multiplicative processes, ρ^0 meson formation cross section, pion prod., multiperipheral cluster model *(Russian)* 78−17067
multiplicity distrib. scaling law at high energies 77−54083
multiplicity distribs. and correls. at high energies, statistical treatment 78−89682
multiquark baryons and the MIT bag model in SU(6), coupling const. and decay modes 79−97600
multitemperature thermodynamical model of large P_T and large mass production 79−3004
n-body decay distribution function, approx. formula 80−27488
neutral-cluster model, charge-transfer distribs. in high-energy hadron collisions 77−82713
nonperturbative gluon jet model, gluon fragments, meson prod. 80−68420
nucleus+hadron, cluster model of hadronic interactions, intermediate energy secondary nucleons prod. *(Russian)* 78−17062
Ochs-Stodolsky jet profile in iterative quark cascade models and low $p_\perp$ meson fragmentation 79−75733
optical-fibre route bandwidth prediction 77−62046
perturbative QCD, jets, inelastic distribs., colourless clusters, scaling, multiplicity and tree evolution 80−52459
perturbative QCD, large p_T hadronic collision jet struct. 79−75721
photon production by gluon jets in QCD 79−75732
pi-ball configurations in high-energy multiparticle production 79−13086
pion gas, relativistic, kinetic props., non-equilib. statistical operator method 79−30718
pion relativistic quantum gas, crit. temps., Bose-Einstein clustering 77−54084
pion-pion interactions, short range correlations, effect of cluster transverse momenta 78−37237
Pomeranchuk trajectory in multiperipheral cluster emission model 77−54089
pomeron and critical temperature 79−3003
pp collisions, high energy, fireball mass, rapidity, spin distribs. 80−57645
prompt neutrino production in beam dump expt., cluster anal. 79−49556
QCD, asymptotic precictions for exclusive processes, form factors, struct. functions, and low-mass jets 79−71701
QCD, generalized Lipatov-Altarelli-Parisi equations and jet calculus rules 79−71704
QCD, jet invariant mass in e^+e^- annihilation 79−85307
QCD, parton jet and shower model 80−86663
QCD, three gluon vertex 79−49454
QCD, two jet process noncollinearity in first order perturbation theory 80−22567
QCD and hadron dynamics 79−97593
QCD calc. of three-jet processes in leptoprod. and hadronic μ-pair prod. 78−21338
QCD Compton effects, quark and gluon jets 80−32101
QCD hadron jets, branching processes, multiplicity distrib., KNO scaling *(Russian)* 80−101998
QCD jet calculus, inclusive p_T distrib. with exclusive form factors consistency 80−391
QCD jet calculus, simple algorithm for quark and gluon jets 79−93346
QCD jet calculus and tests 79−67516
QCD jet fragmentation functions in leading log approx. 80−101981
QCD jets, algorithm to determ. multiparton distribs. 79−45064
QCD jets, hadron prod. dynamical ansatz 79−71702
QCD jets, Markov branching processes 80−27463
QCD jets, resolution algorithm 79−63455
QCD jets from coherent states 80−13266
QCD model for gluon jet fragmentation, oblate transverse momentum struct. 79−9340
QCD multijet model, universal quark-jet fragmentation in soft hadronic reactions 80−13285
QCD multiplicity generating functions, quark and gluon jets 79−71720
QCD perturbation theory, high energy behaviour of jet and lepton-pair prod. 79−2932
QCD predictions for e^+e^- annihilation jets, ang. correlations and asymmetries 79−9389
qCD scattering processes with hard gluon emission, jet prod. 80−62939
QCD three jet prod. in large P_T processes, two particle inclusive distribs. 79−9342
$Q\bar{Q}$ states, P wave decays, jet ang. distrib. and kinematics 79−75737
quantum cluster decomposition of hadronic final state, stochastic theory of multiple hadron prod. 78−41507
quantum number correlations at large transverse momentum and QCD 79−9337
quantum particles in a stochastic linear potential and the temperature of hadrons 80−32087
quantum-chromodynamic phenomenology of gluon jets 80−4941
quark and gluon jet longitudinal momenta, QCD anal. 80−22571
quark and lepton masses, chiral charge space, statistical analysis 80−42428
quark and string interacting system, gauge theory for 2-D statistical mechanics 79−30713
quark form factor and jet cross sections, high energy asymptotics 80−32112
quark fragmentation functions for inclusive hadron production, Regge formalism 80−68462
quark fragmentation functions in Monte Carlo quark parton model of e^+e^- annihilation 79−80791
quark fragmentation into mesons, statistical model, vector meson contrib. 78−54639
quark fragmentation jets in QCD, cascade model 80−78045
quark fragmentation products parity-odd correls., longit. polarisation 78−433
quark jet, $q\bar{q}$ pair production mechanism, average transverse momenta 80−18118

statistical models continued
quark jet fragmentation, large momentum transfer reactions, implication of large vector meson prod. 79−345
quark jet fragmentation 79−45063
quark jet fragmentation universality in lepton processes 78−434
quark jets in e^+e^- annihilation, forward-backward asymmetries 79−97605
quarkonia, S- and P-wave, gluon jets, perturbative QCD anal. 80−32070
rapidity distrib. of large p_T particles and realistic jets 77−30334
relativistic four dimensional field theoretical model of strong interactions based on statistical bootstrap 78−29315
resonance vertex functions and scatt. amplitudes resonance-nucleon scatt. ρ rescatt. *(Russian)* 80−105918
rest-mass level density, statistical model of hadrons, non-interacting pions 78−62353
road traffic noise, relationships between multidimens. correlation props. of intensity and higher order information, Stratonovich's stochastic theory for random points system 80−87645
sequential decay model for hadron-hadron multiparticle prod., appl. to nuclear matter 78−46021
sequential jet decay described by an Inonu-Wigner contraction of the Lorentz group 79−17695
small p_T hadronic collisions, jets, quark, fragmentation universality and rising rapidity plateaus 79−40734
spin ang. momentum effects on clusters and large transverse momentum phenomena 77−22703
stationary random fields, statistical inference 77−64930
statistical bootstrap model with spin, large transverse momenta distribs. 77−65141
statistical concepts in hadron physics, Fermi and Hagedorn models 79−58945
Sterman-Weinberg jet formula corrections for e^+e^- annihilation from QCD perturbation theory 79−36086
string-junction model, hair pin line rule and baryonium decay 80−27487
strings from field theory, statistical approach 78−25023
strong interactions, analytic extrapolations, statistical approach, review *(Russian)* 79−3000
superconductive fireball at large p_T, mass, temp. and multiplicity 77−49922
temperature origin in high energy strong interactions, large transverse accel. 78−37186
thermodynamic model, appl. to hadron-hadron inclusive interactions 77−30453
thermodynamic model for ϕ inclusive and semi-inclusive prod. 77−18238
thermodynamical quark bootstrap, hadron prod. 77−30336
thermodynamical two-fireball model, rich yield of high momentum hadrons in e^+e^- annihilation 77−30335
three-jet prod. in large momentum transfer reactions, perturbative QCD theory 79−93373
topological expansion asymptotic planarity 77−41821
transfer coefficients, behaviour at relativistic temps., dissipative effects *(Russian)* 79−6062
transverse momentum distribution of particles, hydrodynamical model calcs. 78−93865
transverse momentum properties of high energy collisions, cluster model anal. of data 79−3002
triple jet production in hadronic collisions at large transverse momentum 78−93919
two jet model, large p_T hadronic multiplicity, colour octet exchange 78−62377
uncorrelated cluster emission model, diffr. dissoc. and multiplicity distrib. 77−13949
uncorrelated cluster emission models 77−2801
uncorrelated jet model, Bose-Einstein and Boltzmann statistics calc. for rapidity spectrum 80−4969
uncorrelated jet model, diffractive dissociation 77−6099
uncorrelated jet model, evaluation of phase-space vols. and inclusive spectra 77−26496
uncorrelated jet model, isospin conservation 77−49920
uncorrelated jet model, quantum statistical correls., Bose-Einstein statistics, pion prod. 78−16992
uncorrelated jet model at high energy, quantum statistics, soft pion prod. 78−16995
uncorrelated jet model with Bose-Einstein statistics, statistical bootstrap model 78−86445
uncorrelated jet model with Bose-Einstein statistics for π prod. anal. 78−82172
uncorrelated-jet model at large-p_T, momentum conservation role 77−54082
universal multihadron jets, quark interactions 77−38132
urn model, modified, dimens. counting rule, pp elastic scatt. appl. 80−27485
urn model, production parameters, statistical interpretation 79−63451
valence quark clusters in nucleon structure functions from neutrino scatt. 80−95252
velocity of sound in hadronic matter evidence from very large transverse momenta interactions 79−71725
$e\bar{e}\rightarrow\gamma\gamma\rightarrow q\bar{q}$ 79−49531
e^+e^- 80−63010
$e^+e^-\rightarrow$ hadrons, two-fireball model, jet problem 77−65165
e^+e^- annihilation, 10 to 40 GeV, hadron multiplicity 80−63007
e^+e^- annihilation, hadron multiplicity distribution, Regge like parton model *(Russian)* 80−78100
e^+e^- annihilation, jet struct., test of QCD and quark-confining string 78−33040
e^+e^- annihilation, jets, colour-singlet subsystems, large rapidity gaps 80−68469
e^+e^- annihilation, multiperipheral fireball model, momentum distribs. 77−67665
e^+e^- annihilation, quark fragmentation in field-theoretic model of composite hadrons 80−82986
e^+e^- annihilation, single cluster description of jets 77−67666
e^+e^- annihilation, zero mass limit for class of jet-related cross sections 79−71736
e^+e^- annihilation and hadron-induced events, multiplicity ratio 80−105877
e^+e^- final states, $q\bar{q}$ decay, semiclassical model, vacuum polarisation by colour field 80−63011
$e^+e^-\rightarrow$hadron jet, 3 to 17 GeV, including charm threshold and upsilon resonances, review 80−47321
$e^+e^-\rightarrow$hadron jets, QCD, Monte Carlo model 80−27514
statistical models continued
$e^+e^-\rightarrow$hadron jets, two fireball model anal., Monte Carlo method *(Russian)* 80−37288
e^+e^- hadron production at 13, 17 GeV CMS, first observation with PLUTO detector 79−36088
$e^+e^-\rightarrow$hadrons, high energies, two-fireball model, jet problem *(Russian)* 77−82756
$e^+e^-\rightarrow$hadrons, jet struct., three-hadron-ball model 78−82224
$e^+e^-\rightarrow$hadrons, jet struct. and statistical model 78−21440
$e^+e^-\rightarrow$hadrons, jet struct. in the energy range 3.1-9.5 GeV 78−89725
$e^+e^-\rightarrow$hadrons, multiplicity, scaling, inclusive spectrum, simple hadron cascade model 78−66135
e^+e^- inclusive annihilation, scaling and cluster decay phenomena 77−2854
e^+e^- inclusive annihilation, scaling function in multiperipheral fireball model 77−87985
$e^+e^-\rightarrow$jets, particle ratios from quark statistical model 80−73724
$e^+e^-\rightarrow$jets, two photon four jet anal. 80−27513
e^+e^- jets, two-particle distribs. from single-particle fragmentation functions, effects of heavy quark flavours 80−68468
$e^+e^-\rightarrow K(\pi)+$anything anal., two-parameter fit 77−6138
$e^+e^-\rightarrow n\pi$, jet struct., lightlike (zero mass) quarks anal. 79−63496
$e^+e^-\rightarrow q\bar{q}g$, (3g), jet-mass spectra, perturbative QCD 80−63006
$e^+e^-\rightarrow q\bar{q}g$, gluon fragmentation, polarised 80−82988
$e^+e^-\rightarrow q\bar{q}gg$, 4-jet prod. in lowest order QCD perturbation theory 79−49459
$e^+e^-\rightarrow q\bar{q}q\bar{q}$, 4-jet prod. in lowest order QCD perturbation theory 79−49459
e^-p, π multiplicity and asymmetric fireballs 79−93474
$eq\rightarrow eqg$, gluon fragmentation, polarised 80−82988
γe collisions, jet production, QCD study 79−89142
$\gamma\gamma$, jet and single particle prod. at large p_T 79−49565
$\gamma\gamma$, jet production, QCD study 79−89151
$\gamma\gamma\rightarrow$hadrons, energy pattern for two and three jets, colour corrections, calorimetric expts. 79−71774
$\gamma N\rightarrow$jet+X, QCD cross sections 80−73715
γp, π multiplicity and asymmetric fireballs 79−93474
$\gamma p\rightarrow\pi^+\pi^-\pi^+\pi^-\pi^+\pi^-p$, diffractive production, jet-like structure 80−57606
$hh\rightarrow\mu^+\mu^-+$jet+X, QCD anal. of recoiling jets and angular effects in large q_T pair prod. 79−45078
$hN\rightarrow\gamma(\mu^+\mu^-)+$jet+hadrons, gluonic jets, prod. mechanism *(Russian)* 79−58986
in deep inelastic scattering, quark jet as trigger for gluon jet 80−62996
$K\rightarrow 2\pi$, comment of appl. of current algebra and bag model 79−97622
$K^0\bar{K}^0$ pair detection, interference correlations, struct. function behaviour, statistical model *(Russian)* 79−93421
K^-p, 110 GeV/c, prod. of large $p_\perp$ single and multiparticle systems (jets) 79−85345
K^-p, π multiplicity and asymmetric fireballs 79−93474
$K^-p\rightarrow\Lambda^0+$pions, 8.25 GeV/c, resonance prod., fluctuations cluster emission model 78−93904
$K^-p\rightarrow pK^0\pi^-\pi^{+0}$, 10 GeV/c, dynamical mechanism from cluster anal. *(Russian)* 80−42499
K^+p, π multiplicity and asymmetric fireballs 79−93474
$K^+p\rightarrow K^+p2\pi^+2\pi^-$, 16 GeV/c, azimuthal correls., Bose Einstein symmetrization effects 78−37239
$K^+p\rightarrow\pi^-\pi^-X$, 32 GeV/c, two-pion correlations, Monte Carlo model 80−83008
$K^+p\rightarrow\pi^-\pi^-X$, inclusive distribs. in statistical model, correl. function 77−18354
$K^\pm p$, 200 GeV/c, high p_T jet prod., QCD expt. test 79−89200
$K^\pm p$, fireball model, universal scaling function 80−57646
$\mu^-N\rightarrow$hadron shower, charm-pair production effects 80−73748
NN, 10^{12} eV, rapidity gap distrib., Snider multiperipheral cluster model 80−73757
$N\bar{N}\rightarrow(\pi,\rho,\omega,f)$, statistical model 80−102028
$N\bar{N}$ annihilation, even-odd ratio in multipion prod. 77−22755
$N\bar{N}$ annihilations, statistical bootstrap model anal. 78−37224
$N\bar{N}$ cluster prod., pion inclusive cross section 77−71545
NN inelastic interactions, $\sim 10^{12}$ eV, depend. of cluster size and clustering on inelasticity 79−63566
NN interactions, inclusive pion production, low transverse momentum distrib., cluster model 77−67684
$N\bar{N}\rightarrow$pions, direct channel scheme based on statistical bootstrap, low-energy region 78−12924
$NN\rightarrow X$, nuclear size dependence of particle prod., hydrodynamical model 80−22593
$\nu N\rightarrow$hadron shower, charm-pair production effects 80−73748
$\bar{p}$ annihilation in nucl. emulsion, statistical theory of multiple prod. *(Spanish)* 77−67669
p+emulsion 400 GeV, inelastic scatt., secondary charged particle multiplicities *(Russian)* 78−89880
$\bar{p}D$ annihilation, pion rescatt. effect at intermediate energies 80−5010
pN, 22.8 GeV, cluster production, two-particle correlations 79−63550
pN, 400 GeV, azimuthal asymmetry, cluster model anal. 79−63547
$pN\rightarrow$hadron shower, charm-pair production effects 80−73748
pp, 24, 70 GeV/c, transverse momentum distrib. anal. 77−82781
pp, 27 GeV/c, resonant prod. of high $p_\perp$ back-to-back gluon jets 79−93470
$p\bar{p}$, hadronic jets, possible intermediate bosons 80−18149
pp, jet thrust spectrum, 3-jet structure, QCD calc. 80−47333
pp, large p_T two-particle correlation, hadron composite struct. 77−54085
pp, $p\bar{p}$, 200 GeV/c, high p_T jet prod., QCD expt. test 79−89200
pp, $p\bar{p}$, fireball mass and pion multiplicity 78−45974
pp, probabilistic quark-model approach to p fragmentation 80−63049
pp, two component fireball model 78−45965
pp, unitary impact-parameter model for multicluster prod. 78−33091
$pp,p\bar{p}$, Z^0 high p_T bremsstrahlung, Higgs versus quark or gluon jets 80−32063
$\bar{p}p$ annihilation, 0 to 100 GeV/c, statistical and multiperipheral models, π^0 prod. 79−63507
$p\bar{p}$ annihilation channel as a prototype for the central fireball in pp production processes 79−75802
$\bar{p}p$ annihilation cross sections, corrected differences, fireball model, diffraction cross sections 80−91108
$p\bar{p}$ annihilations, multipion distrib., statistical bootstrap model 80−68472
$pp\rightarrow CX,C=\pi^\pm, K^\pm, \bar{p}$, scaling-in-the-mean hypothesis 80−68497
pp collisions, large transverse momentum pions prod., correls., fireball model 78−66174

statistical models continued
pp collisions, meson large p_T distrib. formula, from pre-equilib. fireball state and fireball spin 79−13170
pp collisions, thermodynamical approach to few body hadronic interactions, pion prod. 77−74704
pp collisions at ISR energies, charged particle correlations between forward/backward hemispheres 78−29366
pp→hadrons, phase transition in Feynman-Wilson analogue fluid, multiplicities, plateaux, cross-sections 80−73744
pp high-energy collision multiplicity distribution, Markov and log-normal models 78−89753
pp inclusive interactions, multiplicity distribs. of negative particles, energy depend. of KNO scaling parameter *(Russian)* 79−80860
pp interactions, cluster mass spectrum 80−37307
pp→jets, 400 GeV, p_T plots, Monte Carlo and parton model predictions 78−89747
pp→mesons, multimeson inclusive spectra and recombination model, multiquark structure functions 80−73751
pp multipion production, charge correl. cluster effect *(Chinese)* 77−57500
pp multiple hadron prod. up to 1500 GeV, hadronic matter eqn. of state *(Russian)* 80−32085
pp multiplicities, viscosity effect in Landaus hydrodynamical model 80−63055
pp→NN+nπ, kinematical constraints on particle correls., independent emission model 77−18344
pp nondiffractive collisions, 52.5 GeV, density, charge and transverse momentum correls. 79−80853
pp→pX, 205 GeV/c, leading p spectrum, random walk hypothesis, geometric bremsstrahlung model 80−68493
pp→pp, large momentum transfer, multiple-scattering model, three-quark proton 80−63031
$\bar{p}p \rightarrow \pi^{\pm} K_s^0 X^{\mp}$, low energy, thermodynamical anal. of charged pion momentum spectra 77−65169
$p\bar{p}$ rapidity distrib., rising plateau from longit. phase-space 77−88017
π^+ structure from two jet events, parton scatt. anal. of $\pi^+ p$ and pp 79−49491
π^-d, charge multiplicity distribs., parity tests 79−97602
π^-d, multiplicity distrib. data, simple non-interacting fireball model 79−3178
π^-n, 40 GeV/c, semi-inclusive $\pi^{\pm}$ transverse momentum distributions, statistical model anal. *(Russian)* 79−13174
πp, real photon prod. at large p_T, QCD and CIM anals., jets 79−89185
$\pi p \rightarrow \pi p$, large momentum transfer, multiple-scattering model, three-quark proton 80−63031
π^- p, 40 GeV/c, semi-inclusive $\pi^{\pm}$ transverse momentum distributions, statistical model anal. *(Russian)* 79−13174
π^-p forward scattering amplitude zeros and low energy parameters 79−9400
π^-p inelastic interactions at 205 GeV/c, three-fireball model, computer simulation 78−474
π^+p, π multiplicity and asymmetric fireballs 79−93474
π^+p forward scatt. amplitude, analytic parametrisation of high energy crossing 77−57568
$\pi^{\pm}$p, 200 GeV/c, high p_T jet prod., QCD expt. test 79−89200
$\pi^{\pm}$p, fireball model, universal scaling function 80−57646
$\pi^{\pm}$p elastic scatt., 1.9-9.5 GeV, test of parton and statistical bootstrap models 78−89728
$\pi^{\pm} p \rightarrow p\pi^+\pi^{\pm}\pi^-$, 16 GeV/c, clustering, multidimens. study using Yang variables 80−5020
$\pi^{\pm} p \rightarrow p\pi^{\pm}\pi^+\pi^-$, 16 GeV/c, dynamical mechanism from cluster anal. *(Russian)* 80−42499
$\pi\pi$ interactions, dominant resonances, pole positions, partial waves 80−63020
$\pi\pi$ P-wave anal., ρ pole parameters 77−46079
$\psi\psi$ prod., correl. effects in large p_T pion events 77−26549
Υ(9.46), prod. in e^+e^- interaction at DORIS, quark parton model agreement 79−93443
Υ(9.46) decay into charged hadrons, jet anal. 79−49519
Υ(9.46) orthoquarkonium decay, jet profiles, three gluon structure 80−73698
$\Upsilon \rightarrow$photons+gluons, QCD perturbation theory 78−33028
Υ'(10.02), prod. in e^+e^- interaction at DORIS, quark parton model agreement 79−93443
e^+e^- annihilation, quark jets, transverse momentum profile 80−57621
e^+e^-, high energy interactions *(Chinese)* 80−78074
O_3 formation dynamics in cities 80−31112
ϕ^3, six-dimens., struct. of high-energy jets 78−29248
(π^-,π^-) 40 GeV/c, secondary particle multiplicities as function of number of π^-p collisions *(Russian)* 78−89922
Sm(n,n), (n,n'), (n,n'γ), A+148,150,2, E=2.47 MeV collective excitations obs. 78−33187
$\Upsilon \rightarrow$3g, angular patterns and front-back moments, QCD 80−73702

statistical tests *see statistical analysis*

statistical theory *see statistical analysis*

statistical theory of nuclear reactions and scattering
α-clustering in heavy nuclei, pre-equil. model, nuclear matter NN, Nα interactions 80−63111
Γ_n/Γ_f determ., 12 to 20 MeV excitation, from evaporation-residue cross sections 77−61451
(π,π'), inelastic scatt. in Fermi liquid, nucleon-nucleon interaction effects 80−22862
A=24-108, level widths in charged particle induced reactions, stat. anal. 80−68535
actinide fission, statistical anal. of gamma emission 78−17255
actinide nuclei, statistical aspects in fission mechanism 77−14097
actinides, fission through double-humped barrier excitation energy 10-35 MeV 78−583
analytic hydrodynamic model for expanding fireballs 78−41745
ang. momentum depend. statistical fission parameters from statistical/rotating liquid drop model 78−89846
astrophysics, nuclear reactions in dense plasmas, simple classical fluids theory 80−75141
average fluctuation cross section from unitary analytic K-matrix 80−102172
average resonance parameter eval. and calcs., statistical model for capture process 80−18271
baryonic inclusive spectra in hadron-, photon- and HI-nucleus collisions, fireball model 80−86892
beta-decay, shell effects in gross theory 77−38251

statistical theory of nuclear reactions and scattering continued
beta-decay and electron capture rates of nuclear excited states, gross theory 77−41927
bound state poles, effect on N-body scatt. amplitudes *(Chinese)* 80−5111
cascade evaporation model of 70 MeV pion reactions on s-d shell nuclei 77−10444
cascade evaporation model of high energy nucleus-nucleus reacts. *(Russian)* 78−46107
central nuclear collisions, standard deviation of π multiplicity *(Russian)* 80−73864
channel averages and energy averaged cross section relation 80−68634
classical probability calculus relation to Glauber model 77−50095
cluster cascade model, single particle distributions and two-particle correlations 80−18300
cluster recoil mechanism for inclusive nuclear reactions, appl. to ^{6}Li(p,p')X, ^{181}Ta(p,p')X 78−93998
clustering aspects in nuclei and their microscopic description, review 80−487
coherence energies in pre-equilibrium emission 79−63652
cold nuclear matter, hydrodynamical approximations 79−22219
cold nuclear matter, stationary finite amplitude motions, quantum shock waves and solitons 80−42573
collective eigenstates of ensemble of random particle-hole matrices 77−61388
collective modes in fission and deep inelastic scatt., ang. momenta equilib. statistical treatment 80−42688
collective tube model, multiparticle prod. off hadrons and nuclei 80−5112
collision duration in presence of strong overlapping resonance levels 78−17169
collision expts. with final state partial resolution, maximal entropy procedure and surprisal anal. 80−18279
complex nuclei, α-clusters, preequilibrium model approach 79−6457
complex particle emission, pre-equilibrium exciton model anal. 78−66280
complex particle emission in pre-equilibrium exciton model, comments 79−59046
composite particle emission in relativistic heavy ion collisions, firestreak, and coalescence model 79−80952
compound cross sections, consistency relns. 78−41688
compound nuclei, Z=98, 100, 102, statistical description of decay widths *(Russian)* 78−86549
compound nuclei prod. in (HI, xn), lifetimes with account of fission process *(Russian)* 78−25233
compound nuclei with high angular momenta, de-excitation calcs. 78−50146
compound nucleus decay, failure of statistical theory, discussion of (n, γ) reactions 77−54213
compound nucleus reactions, consequences of isospin mixing 78−25168
compound nucleus reactions, mirror channel and isospin mixing correlations 79−9488
compound nucleus theory, recent developments, review, book contrib. 80−68636
compressed nuclear matter, blast wave production in fireball explosions 79−49592
compressible nuclei, surface energy 80−83031
conservative force between heavy ions, temp. depend. 77−30624
correlated cluster model for energetic proton inclusive spectra is p-nucleus collisions 77−71600
cosmic ray nucleus-nucleus interactions, search for hydrodynamic effects 79−80176
cross-section probability tables generation in unresolved resonance energy range 79−80986
Csikai-Peto effect, reevaluated by statistical model calc. method 78−25180
deep inelastic, ang. distrib. statistical fluctuation effect 77−14093
deep inelastic heavy ion collisions, mass and charge distribs., statistical model 80−18332
deep inelastic heavy ion collisions, quantal theory of Brownian motion, collective vibrs. 79−67774
deep inelastic heavy ion collisions, statistical fluctuations, quantal effects, l-window 78−89895
deep inelastic heavy ion collisions, unified model, collectivity and statistics, coupled channel eqns. 78−66320
deep inelastic scattering, fragment nuclides distribs., neutron rich nuclei prod., diffusion model 78−58297
deeply inelastic heavy-ion reactions, statistical model 78−50192
deformed and superdeformed nuclei from heavy ion reactions, α-decay amplification 80−102156
delayed fission neutron emission probabilities, simple statistical model calcs. 77−50103
delayed neutron theoretical pulse height spectra 78−78328
density isomer formation in high energy heavy ion collisions, 3-dimens. fluid dynamical calcs. 79−49578
density isomers in high energy heavy ion collisions, hydrodynamical model anal. 79−36138
dissipative heavy ion collisions, dynamical description in adiabatic representation, statistical theory 80−5161
dissipative heavy ion collisions, nuclear dynamics 80−42696
dissipative heavy ion collisions, transport equation for microscopic Wigner functions 79−13329
dominant partition method 80−47455
doorway states spreading width, statistical significance, isobaric analogue states 79−93588
Doppler effect calcs., resonance data set choice in unresolved resonance region, sensitivity study 80−52651
doubly even nuclei, yrast band B(E2) values, hydrodynamical model and CAP effect 80−86793
droplet-model theory of the neutron skin 80−47416
duration of reactions for strongly overlapped resonance levels *(Russian)* 78−46044
dynamical interpretation of the statistical theory of fission 79−45311
electric multipole modes in the fluid-dynamical approximation 80−106029
electron capture in nuclear statistical equilibrium 79−92663
electron-nucleus nonintegrated sum rules and projection operator method 77−2967
energy ave. and ensemble ave. equality 78−17170
energy dissipation in heavy-ion collisions 80−106038
entropy approach to statistical nuclear reactions 80−102173
equilibration process, master eqn. and closed form approaches 80−99166

statistical theory of nuclear reactions and scattering continued
ergodic behavior in the statistical theory of nuclear reactions 79−17888
Ericson fluctuations in polarised (p,p) reactions *(Rumanian)* 80−5113
evaporation model, (n,2n) cross section A=45 to 209, threshold to 20 MeV 79−30842
excited nuclei, self-consistent theory of giant dipole resonance, thermodynamic RPA *(Russian)* 80−5106
exciton model, $\Delta n=0$ transitions 79−63651
exciton model, ang. and energy distribs., of nucl. reaction products *(Russian)* 78−54736
exciton model, comparison to statistical approach starting at Neuman eqn. *(Chinese)* 79−93600
exciton model, density of final states determ. 77−14091
exciton model, master eqn. conversion for mean lifetime algebraic eqns. for nuclear reactions 79−518
exciton model, preequilibrium reactions, angular distribs. 80−52652
exciton model of pre-equil. emission 78−13049
exciton model of pre-equilibrium theory for nuclear reactions, master eqn. soln. 78−13050
expanding fireball in high energy heavy ion reactions, pion radiation 80−5155
fast neutron scatt., reaction mechanisms and nucl. struct. 77−26696
fast rotating heated nuclei, collective excitation microscopic description, statistical characts. *(Russian)* 79−97649
Fermi liquid theory and giant resonances in nuclei 79−3095
Fermi model for high multiplicity compound nucleus decay 80−22799
fireball cascade model analysis of multiparticle production on nuclei 79−89283
fireball coplanar decay, 24 GeV/c proton-nucleus interaction 78−50157
fireball model, low energy bremsstrahlung cross sections in relativistic heavy-ion collisions 77−54253
fireball model, pion and nucleon total differential cross-sections 78−17241
fireball model and coalescence model, anal. of nuclear fragmentation 79−93642
fireball model for heavy ion collisions, statistical theory 79−6556
fireball model for proton inclusive spectra, heavy-ion collisions 77−6339
fireball model of relativistic heavy ion reactions, chemical equilibrium relations 79−22262
fireballs, protons as secondary particles, cumulative effect, ang. depend. *(Russian)* 78−50147
fireballs in high energy heavy ion collisions, hydrodynamical description 78−58294
fission, critical evaluation of statistical theory 78−70508
fission, inertia matrix elements of highly deformed nuclei *(French)* 79−71838
fission, isobaric widths, frozen quantal fluctuations, charge equilibration 80−37365
fission, neutron induced, thermal to 14.7 MeV, mass yields, kinetic energies, prompt neutrons 77−23137
fission, saddle point, statistical fluctuations, Suzuki's scaling limit 80−86946
fission, statistical parameters mass depend. 77−57696
fission and neutron evaporation widths, statistical formula correction *(Russian)* 79−13281
fission barrier props., expt. studies and statistical anals. review 80−102216
fission cross section trend, 3-5 MeV 77−23126
fission fragment deexcitation, statistical model anal. of spin influence 79−17941
fission neutron distribution, pre-equilib. *(Russian)* 77−26658
fission of transuranics, neutron yields, estimation by compound nucleus formation 77−50108
fission product charge distrib., statistical calc. 77−18632
fission product nuclear data evaluation, cross sections up to 15 MeV, resonance parameters 77−23044
fission product spin distrib., statistical theory predictions, asymmetric fission explanation 78−70509
fission rate analysis from point of view of Brownian motion *(Chinese)* 80−52657
fission reactions, fragment excitation, prompt neutron distrib., renormalised gas model calcs. 80−99169
fission width distribution, statistical properties, effect on cross-section calcs. *(Russian)* 80−518
fissionability, target mass depend. for π, γ, α, p, cascade-evaporation and liquid drop calcs. *(Russian)* 80−106089
fixed angular momentum moments and level densities, statistical spectroscopic methods 80−467
flucton model of coherent fluctuations of nuclear density 79−75959
fluctuating cross section, direct reaction contrib. 77−50102
fluctuation enhancements of compound cross-sections for elastic, directly coupled and weakly absorbed channels 77−26653
fluctuation of nucleon density, application to scattering 79−517
fluid-dynamical approximation for finite Fermi systems 79−89259
frictional effects in nuclear reactions with large scale collective motion, review 78−78336
generalised exciton model, pre-equilibrium components of the fluctuation cross section 80−18278
giant resonances, electric monopole and dipole vibrations, TDHF equations, fluid dynamical Lagrangian 80−47447
Glauber approx. anal. of high energy heavy ion collisions 80−106039
ground-state correlations observable in hard heavy-ion reactions 78−78406
hadron+nucleus, spatial temporal development, nuclear hadronic cascades 80−63040
hadron chemistry, heavy ion collisions 78−82389
hadron induced fission, low energy evaporative particle emission from emulsion nuclei *(Russian)* 80−86943
hadron-nuclei collisions, statistical mechanism of multiparticle prod. 77−46155
hadron-nucleus collision, cascade model, space-time model 80−68633
hadron-nucleus high energy collisions, two-particle correlations, cluster cascade model 79−49615
hadron-nucleus inelastic interactions, high energy, mean normalised multiplicity target depend. 80−47454
hadronic matter chemical equilibrium, statistical model for heavy ion collisions, nuclear fireball 79−40948
Hauser-Feshbach, (n,α), (α,n) calcs. for Fe group elements, He prod. in fusion reactors 77−23100
Hauser-Feshbach anal. of $^{12}C+^{14}N$ reactions, 53 MeV, reaction mechanisms 77−14166
statistical theory of nuclear reactions and scattering continued
Hauser-Feshbach anal. of elastic and inelastic scatt. of protons on ^{24}Mg, ^{25}Mg, ^{26}Mg 77−316
Hauser-Feshbach calcs. of (n,t) and (n,^{3}He) activation cross sections 77−26721
Hauser-Feshbach calculation of the fission neutron spectrum 80−22801
Hauser-Feshbach improved formulae, surprisal approach 79−67736
Hauser-Feshbach two step code with precompound decays and γ-ray cascades 77−23045
head on heavy ion collisions, compression and temp. extremes, nuclear matter phase changes *(Russian)* 80−83121
heavy ion+nucleus reactions, friction force, gas kinetic model 77−30621
heavy ion collisions, composite particle formation, direct, classical thermodynamic and quantum statistical theories 80−32297
heavy ion collisions, continuous γ-ray spectra anal. 78−41747
heavy ion collisions, dynamics of statistical fluctuations, collective approach 77−14092
heavy ion collisions, energy dissipation and the stochastic process 80−106040
heavy ion collisions, energy loss and ang. distribs., dissipation mechanism, hydrodynamic model 79−3175
heavy ion collisions, fluid dynamical and TDHF models, abnormal nuclear matter, density isomers 80−47502
heavy ion collisions, generalised master eqn., drift and diffusion coeffs. 80−106075
heavy ion collisions, mass transfer, kinetic energy, comparison with hydrodynamic and microscopic calcs. 80−57787
heavy ion collisions, relativistic hydrodynamical approach, shock compression effects *(Russian)* 79−30851
heavy ion collisions, statistical model for mass and charge distrib. 79−17929
heavy ion compound reactions, critical ang. momentum effects on high spin selectivity 79−36272
heavy ion deep inelastic collision processes, optical model description, statistical considerations 80−68687
heavy ion deep inelastic reactions, as probes of nuclear matter, review 78−46083
heavy ion deep inelastic reactions, Coulomb and nuclear forces effects on double differential cross section pattern 78−70560
heavy ion deeply inelastic collisions, simple model calcs. in microscopic transport theory 79−71870
heavy ion energetic reactions, relativistic hydrodynamical description 80−37362
heavy ion fusion reactions, statistical model calcs. 80−42726
heavy ion fusion reactions, statistical yrast line 80−86948
heavy ion inclusive cross sections, collective and statistical effects, fluctuations for complex collisions 79−36258
heavy ion induced reactions, information from γ-spectroscopy *(Rumanian)* 78−58300
heavy ion interaction pot. calc. by Ericson statistical model and ^{252}Cf fission data *(Russian)* 78−41765
heavy ion reactions, 10-200 MeV/N, Markovian and non-Markovian effects in transition probabilities 80−102175
heavy ion reactions, coherence angle and cross section fluctuations correlation function, resonances 80−57790
heavy ion reactions, energy depend. struct., review, book contrib. 80−27671
heavy ion reactions, Hartree-Fock approx., statistical aspects 78−50193
heavy ion reactions, multiple collision model anal., at high and relativistic energies 78−86542
heavy ion reactions, nucleon emission from localised hot zone, fireball model 80−42686
heavy ion reactions, precompound emission inference ambiguities from excitation function anal. 79−22319
heavy ion reactions, statistical γ-rays and ang. momentum alignment 79−67761
heavy ion reacts., coherent and statistical features 78−41771
heavy ion transfer reactions, energy disposal, information theoretic anal., surprisal approach 80−18326
heavy ion-light particle angular correlation, forward peaked, light particle emission from l-windows 80−63142
heavy ions in low energy region, expt. and theoretical range comparison 80−32257
heavy nuclei meson induced fission, statistical relaxation process 79−59098
heavy particles, reson. scatt., pseudocrossing problem 79−49412
heavy-ion collisions, form. and disintegration of high-density nucl. matter 77−10423
heavy-ion compound nucleus reaction 77−14173
heavy-ion deep inelastic reactions, probabilistic model 77−71623
heavy-ion deeply inelastic collisions, form factors determ. within statistical model 78−50205
heavy-ion high energy inelastic collisions, cascade evaporation model of shock waves *(Russian)* 78−41766
heavy-ion induced fusion reaction products, statistical and liquid drop model anal. 78−66312
(HI,X), inclusive one- and two proton spectra by statistical model 79−93624
high energy π(p)+nucleus reactions, secondary particle multiplicity 79−93597
high energy heavy ion collisions, comparison of models, appl. to U+Ne→p+X 78−46088
high energy interactions of nuclei, single particle inclusive spectra 78−46087
high energy nuclear collisions, isobaric-gas model, shock waves, temp., density, pionisation 78−94022
high spin state population, compound nucleus reaction, computer code CARLA 78−89843
high spin states, identification method at high excitation energies 79−17788
highly excited nearly spherical nuclei, ang. momentum effects, backbending, yrast states 79−49566
hydrodynamic tube model for relativistic nucleon-nucleus collisions *(Russian)* 78−606
inelastic collisions, heavy ion-light particle angular correlations, sequential three-body reaction 80−42677
intranuclear cascade model, anal. of 39 MeV reacts with ^{209}Bi and ^{56}Fe 78−33185
ion-ion interaction pot., real part energy depend., antisymmetrization effects, Fermi gas model 80−83120

statistical theory of nuclear reactions and scattering continued
isovector pairing vibrations, in two nucleon transfer ion-nucleus reactions 78−21487
kinetic energy distrib. of fission fragments, thermal fluctuation influence 80−22865
large momentum transfer reactions, density fluctuations, quark-parton mechanism *(Russian)* 79−80868
leading proton spectrum at high energies in (p,X) reactions, intranuclear cascade model anal. 80−5139
lepton-nucleus collision, cascade model, space-time model 80−68633
level density in large spectroscopic spaces, statistical spectroscopic methods 80−86814
linear response approach to heavy ion deep inelastic collisions, dissipation, quantal fluctuations 78−46043
Lipkin Meshkov Glick model multilevel extensions, ground state energy phase transitions 79−85404
many-body problem, classical hydrodynamics and collective motion approx. 80−83027
many-boson absorption, nonreson. maximum 78−8343
mass distribution widths in statistical theory of fission, nucleon tunnelling *(Russian)* 80−5121
maximum entropy approach, analyticity and ergodicity 80−68635
Maxwellian distribs. in nuclear reactions, volume versus surface sampling 78−78355
medium nuclei, photoproton spectra and preequilib. decay, microscopic theory 80−47464
Mehta-Dyson statistics, appl. to sequences of neutron resonances 77−30543
multi-chance high-spin fission, fragment anisotropy, stat. model anals. 80−57812
multispecies Tani transorm., kinematical props. 79−17333
multistep compound cross section from Markovian processes 80−83090
multistep compound processes, autocorrelation function, average fluctuation cross section, different theoretical approaches 80−78234
muon capture, total rates, gross theory 77−41928
neutron capture, total radiative width and degree of freedom, statistical model calcs. 80−57732
neutron cross section representation in unresolved resonance region 77−23051
neutron cross sections at 24 keV 79−26430
neutron cross sections for ^{232}Th, ^{233}Th, ^{233}U and appl. to reactor design 77−54227
neutron cross sections up to 20 MeV, updated THRESH code 77−23046
neutron emission spectra from 14 MeV neutron reaction, precompound model calc. 79−36235
neutron induced cascade reactions 77−26699
neutron induced fission cross sections, parameter testing *(Russian)* 80−52653
neutron induced reactions on $36 \leq Z \leq 83$ targets, tables of cross sections and reaction rate factors 77−46162
neutron resonance data, statistical anal. method 80−102174
neutron resonances, reaction mechanisms and nuclear struct. 77−26564
neutron s-wave strength functions, odd-even fluctuations 77−22856
neutron scatt., width fluctuation correction to reacts. involving continuum level excitations 78−46124
neutron scatt. from parity violating pot. 78−25167
neutron scattering cross sections for ^{48}Ti, ^{54}Fe, ^{56}Fe, ^{209}Bi *(Russian)* 77−26688
neutron scattering theory, parity violating interaction 78−25166
neutron strength function fluctuations 77−22858
nonresonant, possible relax.-time comparisons failure for local thermodynamic equilib. 78−81935
nonstrange baryonic matter, thermodynamic behaviour for rel. mean-field theory 79−75887
nuclear dynamics, TDHF and ATDHF, nuclear vibrs., heavy ion collisions and Fermi hydrodynamics 79−67696
nuclear dynamics and renormalisation group relations, bulk props. 79−6469
nuclear fireballs, break-up densities 78−8790
nuclear fissility at intermediate energy cascade-evaporation and liquid drop model anal. 78−70579
nuclear fission, stopped pion induced, two-step model anal. 79−59097
nuclear fluid dynamics, extended TDHF for approach to thermal equilibrium 80−13448
nuclear pion prod. with heavy ions, statistical approach, pion interferometry 79−85487
nuclear size dependence of particle prod., hydrodynamical model 80−22593
nucleon induced reactions, pre-equilibrium calc. of nuclear spectra 77−22991
nucleon interations with n-quasiparticle excited nucleus, pre-compound and compound systems decay 77−26654
nucleon transfer in light+heavy ion reactions, classical statistical model 78−58304
nucleon-induced preequilibrium reactions, ang. distrib. in exciton and hybrid models 79−40899
nucleon-nucleus collisions, cumulative pion prod., inelastic rescatt. contrib., statistical bootstrap model *(Russian)* 78−54766
nucleus-nucleus collisions, high energy, microscopic study 79−93598
parastitistics with continuous order, nuclear appls. 77−71572
particle-particle collision probability, vol. integral using preequilibrium exciton model 78−70477
phase transitions and shock waves in nuclear matter 79−49594
photo-nucleon spectra, shell and pre-equilibrium decay model of giant reson. decay *(Russian)* 78−579
photon backscattered ang. distrib. for oblique incidence *(Rumanian)* 80−47456
photon induced spallation reactions, intermediate energies, isomeric cross-section ratios 77−41954
photon-nucleus collision, cascade model, space-time model 80−68633
pre-equilibrium anal. of ^{51}V(n,n′) and ^{197}Au(n,n′) 14.1 MeV 77−6366
pre-equilibrium decay, microscopic theory 79−75958
pre-equilibrium decay, time dependence of soft and hard parts of particle spectrum 80−22800
pre-equilibrium decay into complex particle channels−analysis of double differential cross sections 79−93599
pre-equilibrium decay of nuclei of mass ≃90 in 10-100 MeV reactions 78−17171
pre-equilibrium exciton model, mean lifetimes 79−93601
pre-equilibrium particle decay in photonuclear reactions 78−25173
precompound emission, (n,2n) cross sections *(Russian)* 77−34304
precompound nuclear emission models, Feshbach theory, multistep direct and compound emission 79−71829
preequilibrium decay, exciton model formulation, reply to comments 78−78354
preequilibrium decay models *(Rumanian)* 80−47457
preequilibrium decay models and quantum Green's functions 79−9542
preequilibrium Griffin model, complex particles and direct nuclear reactions 77−88098
preequilibrium model anal. of isomer ratios in ^{110,112}Cd(p,n)^{110,112m,g}In 77−6361
preequilibrium processes in atomic nuclei, statistical description 78−13048
preequilibrium reactions, angular distrib. theoretical models *(Russian)* 80−86890
preequilibrium spectrum analysis, computer code ASPIS 79−68174
prequilibrium decay, differences of alternate formulations, possible exciton formulation errors 78−70507
prompt fission neutron spectra calc., nucl. evaporation theory 80−22870
proton+nucleus collisions, hydrodynamical model calcs. at E>200 GeV 79−550
quantal fluctuation squeezing, Schrodinger eqn., deep inelastic reactions 80−47444
quantum fluctuations and quantum mechanical distribs., heavy ion physics appl. 80−78264
quasiclassical stochastic models, analytic extensions of Monte Carlo calcs. 79−13277
radiation widths for 75<A<130 78−33161
reduced partial neutron widths, statistical distrib. using microscopic theory 79−6555
relativistic central heavy ion collisions, spherical and linear fluid dynamical models 80−86926
relativistic continuum mechanics for heavy ion high energy collision calcs. 79−45299
relativistic heavy ion collisions, central and peripheral, p emission patterns 80−73860
relativistic heavy ion collisions, charge multiplicity fireball and statistical model anal. 80−537
relativistic heavy ion collisions, charged particle emission multiplicities and ang. correlations, firestreak models 80−18328
relativistic heavy ion collisions, d prod. mechanism, three models, fireball rate eqns. 80−63198
relativistic heavy ion collisions, statistical thermodynamics 79−17887
relativistic heavy ion collisions, viscous hydrodynamical model 80−5163
relativistic heavy ion fragmentation reactions, abrasion-ablation model 79−97695
relativistic heavy ion reaction large fragment yields, abrasion-ablation calcs. 79−45295
relativistic heavy ion reactions, 1.05-7.52 GeV, π prod., statistical interpretation 79−570
relativistic heavy ion reactions, fireball model, review 78−50195
relativistic heavy-ion collisions, thermodynamic model for composite particle emission spectra 77−30632
relativistic light ion collisions, two-fireball model improvements, p and π spectra 80−5158
relativistic nuclear collisions, pulsating blobs of quark matter in hydrodynamical model 80−83122
relativistic nuclear matter, shock waves, heavy ion collision hydrodynamics 80−52602
relativistic nuclei collisions, multi-hadron prod. mechanism 80−57763
resonance reactions, strong absorption and the distribution of zeros of the S-matrix 79−36214
S-matrix pole expansion examination of energy averaged reaction cross sections 78−58259
scalar and configuration traces of operators in large spectroscopic spaces 78−25165
scattering function energy average, differential equation approach 77−18514
scission mechanism, statistical model, partial equilib. model 77−18631
shell model level densities in evaporation calculations 79−45241
shock waves in a hydrodynamic model of central heavy ion collisions 79−40946
single particle Schrodinger fluid, nuclear fluid dynamics, shell model basis, shape distortions 79−93484
soft nuclear matter eqn. of state, from heavy nuclei central collision fireballs 80−13395
spectroscopic information from nuclear reactions 79−6455
spherical nuclei, giant monopole resonance transition densities, dynamical Thomas-Fermi theory 80−9278
spin-alignment attenuation factors in mass 61-67 nuclei populated by (α, n) and (α, p) reactions 79−26390
spontaneous fission mass parameters, cranking and hydrodynamic models, deformation depend. *(Russian)* 80−13511
stainless steel, type 316, neutron induced charged particle spectra 78−5024
statically deformed nuclei, level spacing by statistical methods 79−45165
statistical compound modulus model, fission and evaporated residue excitation functions 78−86523
statistical evaporation model anal. of ^{51}V(n,n′) and ^{197}Au(n,n′) 14.1 MeV 77−6366
statistical mechanics of nuclear and molecular collisions 79−30821
statistical significance of spreading widths for doorway states, comments 80−27611
stellar environment, nucl. struct. and reactions 80−72765
stellar interiors, thermonuclear reaction rate enhancement due to strong screening, ionic mixtures case 80−36613
strong compression effects in high energy heavy ion reactions, nuclear fluid dynamics anal. 80−18341
Sturm-Liouville expansion method, one- and two-particle transfer form *(Russian)* 78−89844
supercharged nucleus screening, relativistic Thomas-Fermi model, comments 80−91170
thermonuclear reaction rate data for intermediate mass nuclei 80−31427
Thomas-Fermi kinetic-energy density with gradient corrections 80−91169
time delay and correlation length of cross section fluctuations 80−517
time delay of resonance wave packets, stat. model anal. 80−22802
two-step direct reactions through doorways, fluctuation effects 80−13445
unitarity role in statistical theories 77−18513
variational principle based statistical theory of nuclear reactors, optical S̄ matrix 79−36221

statistical theory of nuclear reactions and scattering continued
volume and surface vibr. relations, quantum hydrodynamics 80−9227
width fluctuation correction for compound nuclear reactions, cross sections *(Chinese)* 79−49616
Wigner's random matrix model, time reversal violation 77−30542
X-particles and their backgrounds in 400 GeV/c proton interactions, emulsion chamber anal. 79−63548
Z=103, 105, 107 element prod. from heavy ion fusion, cross sections from statistical model 80−32313
α-preequilibrium decay, emission rate, α-preformation factor 78−41676
β-decay of fictional nuclide, Pandemonium, statistical model 78−8779
β-delayed neutron decay, statistical model, Monte Carlo techniques, fictional pandemonium nucleus calcs. 78−89830
(d,X), 70, 80 MeV, charged light particle spectra and ang distribs. excition model anal. 79−40935
(e,α), Z=29-79, direct and statistical effects, cross sections and ang. distribs. 79−530
(γ,n), preequilibrium exciton model with evaporative component, photoneutron spectra, giant resonances 80−57762
(γ,Π) in nuclear matter, optical pot. and Fermi gas model, Li, Be appl. 79−36230
(n,2n), 14 MeV cross-section calcs. 77−30601
(n,2n), 14.7 eV, isomeric cross-section ratios, statistical theory, moment of inertia 79−97701
(n,2n) cross sections 77−26699
(n,2n) cross sections around 14.5 MeV, integrated preequilibrium-cum-statistical model approach 79−6609
(n,2n) reactions on ^{12}C and ^{238}U, excitation functions 77−23082
(n,2n) reacts. on ^{45}Sc, ^{58}Ni, ^{59}Co, ^{93}Nb, ^{175}Lu, and ^{197}Au, statistical model anal. 77−26655
(n,2n)reaction mechanisms, threshold to 15 MeV, statistical model 77−26729
(n,3n) reacts. on ^{45}Sc, ^{58}Ni, ^{59}Co, ^{93}Nb, ^{175}Lu, and ^{197}Au, statistical model anal. 77−26655
(n,α), 14 MeV, total cross sections, pre-equilibrium model anal. 78−58272
(n,α) cross sections, 14 MeV, empirical formulae 79−63662
(n,α) resonance neutron reactions, α-widths from statistical relationships, deviations 78−33173
(n, α) with resonance neutrons, properties of highly-excited states of nuclei *(Russian)* 80−106053
(n,f) nuclear constants eval. for heavy fissile nuclei *(Russian)* 79−59100
(n,γ), A=75 to 103, γ-strength functions and stat. model cross section calcs. 80−52612
(n,γ), A=94-190, resonance capture, low lying level population fluctuations, γ-rays 80−52619
(n,γ), mechanism in 3s size resonance, s-wave radiative width partition 80−37387
(n,γ), mechanism in 3s size resonance, radiative width statistical and valence effects 80−37388
(n,γ) capture cross section, statistical theory anal., radiative strength functions *(Russian)* 78−17212
(n,γ) total 14 MeV cross sections, meas. and anal. with statistical and direct reaction models 77−54226
(n,γ) total cross sections of 14 MeV neutrons, from activated nuclei β-ray counting 79−3156
(n,$\gamma\alpha$), (n,γf), low energy γ-transitions between compound states, statistical theory 80−57737
(n,n), A=90 region, elastic, inelastic and total cross section, statistical model calcs. 80−68674
(n,n), elastic and inelastic scatt. on various isotopes, cross sections meas. and calcs. 78−13081
(n,n) 2.9 MeV, elastic differential cross section and polarisation ang. depend., statistical anal. 79−45264
(n,n′), 14 MeV, cross-sections calc. using Blanns geom. depend. hybrid model 77−26749
(n,n′), 14 MeV, pre-equilibrium anal., geom. depend. effects and direct component 77−23026
(n,n′), 14.6 MeV, ang. distribs., preequilib. and equilib. neutron emission, unified model 80−86891
(n,n′), 9-14 MeV, anal. of twice differential cross-sections 77−30590
(n,n′), odd mass nuclei, 2-4.5 MeV, level excitation functions, Hauser-Feshbach-Moldauer model test 79−36238
(n,n′) cross sections for nuclei of A=77 to 197, Hauser-Feshbach calcs. 77−14119
(n,n′γ), A=28-152, spherically doubly even nuclei, level excitation cross sections, statistical anal. *(Russian)* 79−67707
(n,np), 14 MeV cross-section calcs. 77−30601
(n,p), 14 MeV, total cross sections pre-equilibrium model anal. 78−58272
(n,p), 14 MeV cross sections, empirical formulas 78−70517
(n,pn), 14 MeV cross-section calcs. 77−30601
(n,t), 14 MeV, cross sections, fast neutron reaction excitation function calc. 79−45267
(n,x) reactions on medium and heavy nuclei, models 77−26698
(n,X) X=p,2n,3n, precompound and compound emission mechanisms 80−102176
n inelastic scattering by Ru, Pd, first 2^+ levels excitation, statistical model test 77−61408
ν capture, statistical theory, inclusion of first forbidden transitions, cross sections 78−93990
(p, α) reaction, statistical direct reaction model 79−80913
(p,γ) capture by A=50 to 100 nuclei, stat. anal. of differential cross sections 79−9555
(p,n), A=90 region, reaction cross section, statistical model calcs. 80−68674
(p,n) and (α,n) data for statistical model parameters 79−9602
(p,p′), compound nucleus lifetimes from X-ray method, statistical properties 80−78295
(p,p′γ), low energy scatt. by medium weight nuclei, statistical theory *(Russian)* 77−319
(p,pπx) reaction, pion production, flucton mechanism anal. 79−6590
(p,X), 200 GeV/c in emulsion, fireball parameters and π emission 80−95317
(p,X), hydrodynamic model 80−68671
(p,X), inclusive one- and two proton spectra by statistical model 79−93624
(p,x), total reaction cross sections, microscopic description 80−95318
p-nucleus multiparticle production data anal. using charged particles created as variable 79−3155

statistical theory of nuclear reactions and scattering continued
p+emulsion nuclei, 23 GeV, probability of proton emission *(Spanish)* 77−30564
p+nucleus collision at very high energies, secondary energy distrib., hydrodynamical model 77−88136
(π^+, 2p) quasi two particle scaling, momentum distrib. from statistical model *(Russian)* 79−40968
(π,γ), cross sections from Boltzmann eqn. 79−89330
(π,π), microscopic theory, review 80−47511
(π,π) near (3,3) region, statistical theory transport eqn. 79−85552
(π^+,π^{+or0}) inelastic reactions, cross sections from Boltzmann eqn. 79−89330
(π,π′), microscopic Fermi liquid approach 79−26459
(π^+,π^+p) quasi two particle scaling, momentum distrib. from statistical model *(Russian)* 79−40968
Ag+^{84,86}Kr, 7.2 MeV/nucleon, nuclear relaxation phenomena, diffusion, orbiting 77−34338
Ag+p, 200 GeV, data anal. hydrodynamical model 79−551
AgBr(^{40}Ar,X), 1.8 GeV, central collisions, Maxwell-Boltzmann distrib. anal. 78−66315
AgBr(^{4}He,X), 2.1 GeV, central collisions, Maxwell-Boltzmann distrib. anal. 78−66315
AgBr(^{16}O,X), 2.1 GeV, central collisions, Maxwell-Boltzmann distrib. anal. 78−66315
^{A}Ag(p,n), A=107,109, 2.0-6.7 MeV, cross sections, Hauser-Feshbach optical calcs. for p absorption systematics 80−47483
^{107}Ag(n,n), 0.25-4.5 MeV, total, elastic and inelastic cross sections, optical-statistical anal. 80−27639
^{107}Ag(p,αX), 20-45 MeV, α spectra, exciton model anal. 80−18306
Ag(α,X), 720 MeV, nuclear fragment prod. thermodynamic evaporation and firestreak description, pre-equilibrium emission 79−54426
Ag(α,X) X=p,d,t,^{3}He,^{4}He, 720 MeV, back-angle prod. of light ions, model calcs. 79−45280
Ag(n,n′), 14.1 MeV, precompound processes 78−13093
Ag(p,^{3}He), 210-480 MeV, implications of statistical theories of fragmentation 78−82347
Ag(p,^{4}He), 210-480 MeV, implications of statistical theories of fragmentation 78−82347
Al+p, 200 GeV, data anal. hydrodynamical model 79−551
^{26}Al compound nucleus, isospin impurity from fluctuations in mirror reactions ^{12}C(^{14}N,t)^{23}Mg, ^{12}C(^{14}N,^{3}He)^{23}Na 78−33157
^{27}Al (e,α), 120 MeV, preequilibrium α-emission, α energy spectra 79−85459
^{27}Al+^{14}N, 100 MeV, α preequilibrium decay 79−6666
^{27}Al+^{16}O fusion, 30-70 MeV, statistical model calcs., yrast states and continuum feeding times 79−579
^{27}Al+p, 62 MeV, complex particle emission, pre-equilibrium exciton model anal. 78−66280
^{27}Al(^{3}He,p) 9-14 MeV, stat. multistep compound emission, residual two-body interaction 80−47493
^{27}Al(α,x), 140 MeV, mass fragment meas., reaction mechanism models 79−63683
^{27}Al(n,α), 14.8 MeV, expt. and statistical model determ. of α-prod. in fusion reactors 80−95397
^{27}Al(n,α)^{24}Na, recoil escape efficiency, evaporation model, Monte Carlo calc. 79−45271
^{27}Al(p,X), 90 MeV, charged light particle energy spectra exciton and evaporation model anal. 79−40923
^{27}Al(p,n)^{27}Si, cross sections and thermonuclear reaction rates 80−73852
Al(α,X) 720 MeV, nuclear fragment prod. thermodynamic evaporation and firestreak description, pre-equilibrium emission 79−54426
Al(α,X) X=p,d,t,^{3}He,^{4}He, 720 MeV, back-angle prod. of light ions, model calcs. 79−45280
Am, A=241,3, neutron capture cross-sections 77−61469
^{243}Am(α,f), fragment mass distrib., and yield, statistical anal. *(Russian)* 80−5183
(Ar, π^-X), 800 MeV/A, π^- energy and ang. distribs., firestreak and hard scatt. model anal. 80−13498
Ar+Th, 388 MeV, deep inelastic reactions, double differential cross section calc. 78−8856
^{40}Ar+^{58}Ni, triple differential cross-section, dynamical model calcs. 78−50212
^{76}As, level structure, transitions and J$^\pi$, from ^{76}Ge(p,nγ) 80−47379
^{85}As, β-decay delayed n emission, simple statistical model description 79−67714
As(n,n′), 14.1 MeV, precompound processes 78−13093
Au(^{86}Kr,X), 724 MeV, deeply inelastic, ^{4}He, ^{1}H emission, fragment spin, semiempirical method 80−47366
^{197}Au, 62 MeV, complex particle emission, pre-equilibrium exciton model anal. 78−66280
^{197}Au (e,α), 120 MeV, preequilibrium α-emission, α energy spectra 79−85459
^{197}Au(^{132}Xe,X), damped collisions, charge distrib. second moments and giant E1 quantal fluctuations 80−27547
^{197}Au(^{16}O,p)X, 315 MeV, high energy p emission, fireball and preequilibrium anals. 80−91194
^{197}Au(^{20}Ne,X), exactly central heavy-ion collisions by nuclear hydrodynamics 80−68690
^{197}Au(d,X), E$_d$=13.6 MeV, d breakup anal. with neutron elastic scatt. 79−9540
^{197}Au(n,γ) standard reaction, Monte Carlo simulation of cross section fluctuations 77−61461
^{197}Au(p,^{3}He x), 72 MeV, pre-equilibrium emission *(German)* 80−68657
^{197}Au(p,αx), 72 MeV, pre-equilibrium emission *(German)* 80−68657
(α,γ), excitation function competition cusps, Mauser-Feshbach calcs. 80−13404
^{10}B(^{14}N,X), 2.9-7.5 MeV, evaporation residue and total fusion cross section 79−22348
^{11}B(d,α_0)^{9}Be, Hauser-Feshbach statistical theory *(Spanish)* 77−67753
Ba, A=134-138, average neutron cross sections, statistical and optical model calcs. 78−29458
Be+p, 150 GeV, inclusive muon pair prod. parameters, statistical interpretation 79−30820
Be+π^+, 150 GeV, inclusive muon pair prod. parameters, statistical interpretation 79−30820
^{209}Be(^{136}Xe,X), statistical fluctuations in dissipative collisions, multidifferential cross sections 80−37399
Be(p,2π^-X), 28.5 GeV, fireball model comparison 79−59059
^{209}Bi, 62 MeV, complex particle emission, pre-equilibrium exciton model anal. 78−66280

statistical theory of nuclear reactions and scattering continued
^{209}Bi+^{136}Xe, 1130 MeV, differential cross section calc., statistical model 78−50192
^{209}Bi+^{14}N, 85 and 95 MeV, preequilibrium α spectra, statistical treatment 78−41750
^{209}Bi+^{84}Kr, 600 MeV, differential cross section calc., statistical model 78−50192
^{209}Bi(^{136}Xe,X), deeply inelastic collisions, mass transport, shell effects 80−99188
^{209}Bi(^{48}Ca, X), fusion reactions from Cf and Fm integral yields, statistical model anal. *(Russian)* 79−97740
^{209}Bi(n,2n), 14.1 MeV, pre-equilib. contributions, neutron yields and energy spectra, statistical model calcs. 77−50126
^{209}Bi(p,X), 90 MeV, charged light particle energy spectra exciton and evaporation model anal. 79−40923
^{A}Br(p,pxn) A=79,80, 10 to 85 MeV, excitation function meas. 79−63673
^{A}Br(p,xn) A=79,80, 10 to 85 MeV, excitation function meas. 79−63673
^{87}Br, β-decay delayed n emission, simple statistical model description 79−67714
(C, π^-X), 800 MeV/A, π^- energy and ang. distribs., firestreak and hard scatt. model anal. 80−13498
^{A}C(^{16}O,X), A=12, 13 exit channel competition for some residual nucleus 80−47499
^{12}C to ^{22}Ne induced nucleon transfer reactions 78−41768
^{12}C+^{12}C, 800 MeV, p and π inclusive cross sections, non-equilibrium processes 79−40947
^{12}C+^{12}C, 800 MeV/nucleon, two-fireball model for p and π inclusive spectra 79−13323
^{12}C+^{16}O complete fusion, partial prod. cross section for nuclides, evaporation model calcs. 79−36294
^{12}C+^{20}Ne elastic scatt., strength of absorpt. 77−3028
^{12}C(^{12}C,X), 27-60 MeV, evaporation residue cross sections from complete fusion, statistical anal. 79−13369
^{12}C(^{12}C,X), two fireball model, pp correlations and inclusive pion spectrum 80−68694
^{12}C(^{12}C,α), 7-15 MeV, excitation function statistical anal., nonstatistical features 80−99167
^{12}C(^{12}C,α)^{20}Ne, resonance anomaly anal. in fluctuation theory 78−25215
^{12}C(^{12}C,α)^{20}Ne, statistical methods for resonance detection, nonstatistical struct. 79−45238
^{12}C(^{12}C,p)X, 800 MeV/N, fireball and preequilibrium cross sections, π condensation proximity influence 80−27659
^{12}C(^{14}N, α), Hauser-Feshbach calcs. and ^{26}Al coherence widths 78−37360
^{12}C(^{14}N,X), 27-60 MeV, evaporation residue cross sections from complete fusion, statistical anal. 79−13369
^{12}C(^{14}N,α)^{22}Na, statistical methods for resonance detection, nonstatistical struct. 79−45238
^{12}C(^{15}N,X), 27-60 MeV, evaporation residue cross sections from complete fusion, statistical anal. 79−13369
^{12}C(^{15}N,α), 21-39 MeV, coherence widths in ^{27}Al 78−41619
^{12}C(^{15}N,α), 36-39 MeV, population of ^{23}Na levels 78−50070
^{12}C(^{15}N,α)^{23}Na, statistical methods for resonance detection, nonstatistical struct. 79−45238
^{12}C(^{16}O,^{12}C^{12}C)α, 68-80 MeV, double differential cross section, Hauser-Feshbach anal. 79−63690
^{12}C(^{16}O,^{16}O*)^{12}C*, 33-54 MeV, intermediate struct. resonances, ang. distribs., statistical anal. 78−82330
^{12}C(^{16}O,^{20}Ne), 10-15.5 MeV, cross sections and ang. distribs., resonances, direct and stat. anal. 79−67730
^{12}C(^{28}Si,αX), 87-91.5 MeV, α-HI angular correlations, excitation functions, statistical anal. 80−86915
^{12}C(^{9}Be, ^{9}Be)^{12}C(g.s.), 39.68, 43.75 MeV, back angle cross section enhancement, Hauser Feshbach anal. 79−89324
^{12}C(p, p), 1.7-1.89 MeV, bremsstrahlung spectra, soft photon and Feshback-Yennie approx. 79−80937
^{12}C(p,p'), 122 MeV, precritical phenomena 80−83089
^{13}C(^{7}Be,X), 11.6 MeV, p,t,d,α, ^{8}Be ang. distribs., Hauser-Feshbach and DWBA anals. 80−91193
^{14}C(^{12}C,α)^{22}Ne, 6.1 to 9.7 MeV, excitation functions, statistical fluctuations 77−23103
^{40}Ca(^{6}Li,^{6}Li)^{40}Ca, 30 MeV, ang. distribs. for elastic and inelastic scatt. at backward angles 79−13343
^{40}Ca(d,d), 4.5-5.4 MeV, excited states, excitation functions and ang. distribs., statistical anal. 80−57686
^{41}Ca damped reaction fragment, energy spectra struct., evaporation processes from ^{40}Ca(^{40}Ca,X) 79−93591
^{41}Ca excited states, excitation functions and ang. distribs., statistical anal. from ^{40}Ca(d,p) 80−57686
^{44}Ca(^{6}Li,^{6}Li)^{44}Ca, 30 MeV, ang. distribs. for elastic and inelastic scatt. at backward angles 79−13343
^{48}Ca(p, γ)^{49}Sc, 0.6-2.7 MeV, cross sections and thermonuclear reaction rates, Hauser-Feshbach calcs. 79−36239
^{48}Ca(p, n)^{48}Sc, 0.95-2.7 MeV, cross sections and thermonuclear reaction rates, Hauser-Feshbach calcs. 79−36239
^{48}Ca(p,γ), 0.76-2.20 MeV, absolute cross sections and yields, statistical model anal. 79−26432
^{48}Ca(p,n)^{48}Sc, 0.76-2.20 MeV, absolute cross sections and yields, statistical model anal. 79−26432
Cd(p,nγ), ^{111,113}In energy levels, spins, lifetimes, Hauser-Feshbach anal. 77−320
^{252}Cf, spontaneous fission, scission point configuration, evaluation anal. 80−37361
^{35}Cl induced reactions, targets A=27-124, 70-170 MeV, fusion and interaction barrier parameters, critical angular momenta 77−10428
^{37}Cl(ν,e$^-$)^{37}Ar, statistical theory calc. of total capture cross section 77−88113
C(n,n), total cross sections below 2 MeV, R-matrix fits to data 80−13466
^{59}Co+n, 16-22 MeV, cross sections for prompt γ, compound statistical model calcs. 79−543
^{59}Co+n, calc. using pre-equil. statistical model code GNASH 78−4946
^{59}Co(^{3}He,α), 34.8±0.3 MeV, α-particle energy spectra distrib., c.f. preequilibrium decay calcs. 79−9598
^{59}Co(n,n'), exciton model, ang. and energy distribs. of nucl. reaction products *(Russian)* 78−54736
^{59}Co(n,n'), exciton neutron inelastic scatt. model *(Russian)* 78−33189
Co(p,^{3}He x), 72 MeV, pre-equilibrium emission *(German)* 80−68657
Co(p,αx), 72 MeV, pre-equilibrium emission *(German)* 80−68657

statistical theory of nuclear reactions and scattering continued
Cr isotopes, A=50-54, n-particle cross-sections from threshold −20 MeV 77−30541
^{A}Cr(n,X), A=50,52, 14.8 MeV, charged particle emission, cross section, Hauser-Feshbach anal. 79−67750
^{A}Cr(p,p), A=50, 52, 6 MeV, elastic and inelastic differential cross sections, spin flip probability *(Russian)* 80−91187
^{54}Cr(p,γ), 1.0-3.8 MeV, γ-yields, cross sections, predicted (p,n) cross section, Stat. anal. 80−5136
Cr(n,n), A=50, 52, 54, 1.5-3.0 MeV elast. and inelast. scatt., differential cross section *(Russian)* 78−25199
^{133}Cs(n,γ)^{134}Cs, E_n=14.1 MeV, γ emission exciton model *(Russian)* 79−13302
^{133}Cs(p,pxn), 550 MeV, cross-sections meas. and Monte Carlo calcs. 77−41969
^{133}Cs(p,xn) 550 MeV, cross-sections meas. and Monte Carlo calcs. 77−41969
^{A}Cu(n,X), A=63,65, 14.8 MeV, charged particle emission, cross section, Hauser-Feshbach anal. 79−67750
^{A}Cu(n,α), A=63,65, 14.8 MeV, expt. and statistical model determ. of α-prod. in fusion reactors 80−95397
^{61}Cu γ-cascade multiplicities, entry state depend. on excitation energy from ^{58}Ni (α,pγ), 17 and 19.5 MeV 78−82311
^{63}Cu+^{147}Au, triple differential cross-section, dynamical model calcs. 78−50212
^{64}Cu levels and transitions, stat. anal. of ^{64}Ni(p, nγ) *(Russian)* 80−5104
^{65}Cu analogue resonance direct n decay, stat. anal. from ^{64}Ni(p,nγ) *(Russian)* 80−5104
^{65}Cu(p,α_0)^{62}Ni, 1.1-3.6 MeV, Wigner cusps 78−41719
^{65}Cu(p,γ)^{66}Zn, 1.1-3.6 MeV, Wigner cusps 78−41719
Cu(n,n'), 14.1 MeV, precompound processes 78−13093
Dy equilibrium and pre-equilibrium decay, α-multiplicities, energies and entry lines from ^{160}Gd(α,xn) 79−93549
^{A}Dy(α,xnγ), A=162,164, Er yrast levels, spin alignment 80−52557
^{158}Dy band side feeding pattern and γ-multiplicities, statistical model from ^{26}Mg(^{136}Xe, 4n) 79−75821
^{162}Dy(p, α), statistical direct reaction model calc. 79−80913
^{164}Dy(α,xnγ), x=6-11, 120 MeV, pre-equilibrium n emission, deexcitation mechanism 79−93641
^{A}Er(p, α), A=166,168, statistical direct reaction model calc. 79−80913
^{166}Er+^{86}Kr, deep inelastic strongly damped collision, fragment isobaric distrib. statistical equilib. 79−40949
^{166}Er(^{86}K,X), deep inelastic collision, charge drift and dispersion calc., thermal eqn. model based on shell model 80−57798
^{166}Er(^{86}Kr,X), 5.1-7.9 MeV/N, deep inelastic neutron emission, preequilibrium effects search 80−63200
^{166}Er(^{86}Kr,X), statistical fluctuations in dissipative collisions, multidifferential cross sections 80−37399
^{151}Eu(n,α)^{148}Pm, α spectra and ang. distribs. calc., statistical knock-on-model 77−79371
^{9}F+n, 16-22 MeV, cross sections for prompt γ, compound statistical model calcs. 79−543
^{19}F(n,α)^{16}N, 13.9, 15.6 MeV, differential cross-sections meas., statistical model calc. 77−41972
^{A}Fe(n,X), A=54,56, 14.8 MeV, charged particle emission, cross section, Hauser-Feshbach anal. 79−67750
^{A}Fe(p,p'), A=54, 56, 6 MeV, resonances, spin flip and cross section depends., Hauser Feshbach anal. *(Russian)* 80−83084
^{19}Fe(p,α_0)^{16}O, 1.5 to 3.8 MeV, Hauser-Feshbach anal., level density of ^{20}Ne *(Spanish)* 77−30562
^{54}Fe+p, 62 MeV, complex particle emission, pre-equilibrium exciton model anal. 78−66280
^{54}Fe(α,γ)^{58}Ni, 7.6 to 12.8 MeV, giant electric resonances in ^{58}Ni 78−41739
^{54}Fe(p,p), 5.5-6.2 MeV, resonance effects, deformation, spectroscopic factors, statistical, optical and DWBA anal. 79−6593
^{55}Fe(^{52}Cr, X), entrance channel mass asymmetry effects on reaction mechanism, fission and fusion 80−106077
(^{56}Fe,x), isobaric charge distrib., energy loss depend. in damped collisions 80−99182
^{56}Fe+n, 16-22 MeV, cross sections for prompt γ, compound statistical model calcs. 79−543
^{56}Fe(α,γ), 4.2-7.1 MeV, reaction cross section, statistical model anal. 79−45278
^{56}Fe(p,p), 6 MeV, elastic and inelastic, quadrupole deformation, IAR excitation, optical pots. *(Russian)* 80−63149
^{252}Fm, pot. energy surface, liquid model, deformation energy formulae *(Chinese)* 80−102106
^{67}Ga, isobaric analogue reson., statistical reaction model anal. 79−13267
^{69}Ga(n,n'γ), fast n, levels, J$^{\pi}$, transitions and mixing ratios, statistical anal. *(Russian)* 80−13382
^{156}Gd(n,γ), up to 2.24 keV, n resonances, spectra fluctuation, statistical theory test 79−36188
^{158}Gd(p,n)^{158}Tb, 7.4 MeV, equilib. and nonequilib. contribs. 78−21565
^{70}Ge+^{32}S, 110, 132 MeV fusion evaporation residues, Monte Carlo simulation 78−41799
^{71}Ge, levels, studied via ^{68}Zn(α,nγ), 8 to 10 MeV, comparison with coupling model calcs. 78−8742
^{72}Ge(p,nγ), 5.0-6.3 MeV, ^{72}As level scheme determ. 77−14032
^{76}Ge(^{86}Kr,xn), 314-376 MeV, γ-multiplicity meas., Er compound nucleus formation 79−89320
H+p, 200 GeV, data anal. hydrodynamical model 79−551
^{1}H(d,d), anal. power ang. distrib., d D-state asymptotic normalisation 79−36247
^{2}H+π^-, multiplicity distrib. data, simple non-interacting fireball model 79−3178
(^{4}He,2nf), statistical model anal. of fission isomer production Pu, A=235, 237 78−66326
(^{4}He,xnf)^{239}Am, statistical model anal. of fission isomer production 78−66326
^{4}He+U, relativistic ions, product spectra, statistical models 78−638
^{4}He(p,p)^{4}He, 0-18 MeV, statistical anal., data fluctuations, error estimation 78−25196
^{A}Hf(p, α), A=176,178,180, statistical direct reaction model calc. 79−80913
Hf(n,α), 14.8 MeV, energy spectra, preequilibrium statistical model anal. 77−10396
^{194}Hg, α evaporation spectrum 80−68715
^{165}Ho(p,αX), 20-45 MeV, α spectra, exciton model anal. 80−18306
^{127}I(p,5n)^{123}Xe→^{123}I statistical model based computation 79−26416

statistical theory of nuclear reactions and scattering continued
^{127}I(p,n)^{127}Xe statistical model based computation 79−26416
^{137}I, β-decay delayed n emission, simple statistical model description 79−67714
^{115}In(p,n), 2.0-6.7 MeV, cross sections, Hauser-Feshbach optical calcs. for p absorption systematics 80−47483
^{37}K(d,α)^{37}Ar, 1.83-2.53 MeV, fluctuations analysis and spin values deduced 77−23095
^{74}Kr, charged particle evaporation following form. from ^{58}Ni+^{16}O 80−47453
^{139}La(n,μ), 14.1 MeV, gamma emission from pre-equilibrium exciton model 79−75960
^{170}Lu→^{170}Hf, beta decay, reduced transition probabilities 77−22945
^{24}Mg high spin states from selective compound reactions, stat. anal. from ^{10}B(^{16}O,d) 80−18180
^{24}Mg(α,α')^{24}Mg, 16.7-20 MeV, quasimol. intermediate resons., statistical anal. 78−41741
^{24}Mg(α,p)^{27}Al, 25-26 MeV, high spin selectivity 77−23097
^{24}Mg(d, pγ)^{25}Mg, differential and double differential cross sections, Hauser Feshbach anal., compound nucleus 79−89282
^{24}Mg(d,p), 1.5-2.5 MeV, fluctuation anal., ^{25}Mg highly excited states 78−46071
^{24}Mg(p,p), 15 Mev, excitation functions, Ericson theory for fluctuations 80−22825
^{25}Mg(^{3}He,p)^{27}Al, 13 MeV, statistical multistep compound emission, proton spectrum fluctuations 78−37357
^{25}Mg(p,n)^{25}Al, cross sections and thermonuclear reaction rates 80−73852
^{26}Mg(p,n)^{26g}Al(7.3×10^{5} yr), ground state cross section, statistical compound model 79−30827
^{27}Mg energy levels, spectroscopic factors, DWBA, Hauser-Feshbach anals. from ^{26}Mg(d,p) 80−52581
^{55}Mn(p,p), (p,p'), cross section fluctuations anal. 78−21551
Mo stable isotope eval., 5 keV-5 meV neutrons, rel. to reactor structural steel 80−13620
^{A}Mo (e,α), A=92, 94, 120 MeV, preequilibrium α-emission, α energy spectra 79−85459
^{A}Mo+^{86}Kr, A=92, 98, deep inelastic reactions, fast collective mode, quantal fluctations 79−67636
^{92}Mo(^{16}O,X), entrance channel mass asymmetry effects on reaction mechanism, fission and fusion 80−106077
Mo(n,X), 2 keV-20 MeV cross sections, coherent optical and statistical model calcs. 80−18318
(N,X), disintegration by high energy nucleons, α-prod. mechanism from pre-equilibrium fluctuations *(Russian)* 80−106059
^{14}N-induced reactions energy relax. during fusion determ. by preequilib. α emission 79−26446
^{14}N+^{12}C, 34.1-178.1 MeV, fusion and peripheral reaction cross sections, direct yield 79−67771
^{14}N(^{14}N,α)^{24}Mg, 10.1 MeV, Hauser-Feshbach calcs. 79−63696
^{14}N(d,d'), 10-17 MeV, isospin non-conservation, direct DWBA and Hauser Feshbach anal. 79−67757
^{15}N(d,α), E$_{d}$<3 MeV, intermediate structure 77−10412
NaF+Ne, 800 MeV/N, p and π inclusive cross sections, non-equilibrium processes 79−40947
^{23}Na high spin states, excitation functions, nonstatistical effects, Hauser-Feshbach anal. of ^{12}C(^{15}N,α) 80−106041
^{23}Na(n,n'γ), 0.52-4.23 MeV, cross-sections, ang. distribs., mag. substate populations meas. 78−13100
^{93}Nb B(Eλ) transitions, quasiparticle-phonon multiplet, nuclear field theory for superfluid nuclei 80−47427
^{93}Nb(n,γ), 14.1 MeV, gamma emission from pre-equilibrium exciton model 79−75960
^{93}Nb(n,γ), cross-section below 3 MeV, coherent optical and statistical model calcs. 77−26713
^{93}Nb(n,γ)^{94}Nb, E$_{n}$=14.1 MeV, γ emission exciton model *(Russian)* 79−13302
^{93}Nb(n,n'), exciton, neutron inelastic scatt. model *(Russian)* 78−33189
^{93}Nb(p,αX), 20-45 MeV, α spectra, exciton model anal. 80−18306
^{93}Nb(p,n)^{93}Mo, direct neutron decay of analogue resonances of ^{94}Mo 80−22824
Nb(n,n'), 14.1 MeV, precompound processes 78−13093
(Ne, π^{-}X), 800 MeV/A, π^{-} energy and ang. distribs., firestreak and hard scatt. model anal. 80−13498
^{20}Ne+Al, relativistic ions, product spectra, statistical models 78−638
^{20}Ne+U, relativistic ions, product spectra, statisical models 78−638
^{20}Ne(^{12}C,X), 66.5 MeV, evaporation residue ang. and energy distribs. from statistical model anal. 80−83110
^{20}Ne(d,d), pol. d, 10-12 MeV, cross section, coupled channel and fluctuations anal. 80−27617
^{21}Ne states cross section, coupled channel and fluctuations anal. from ^{20}Ne(d,p) 80−27617
Ni (e,α), 120 MeV, preequilibrium α-emission, α energy spectra 79−85459
Ni isotopes, (n, particle) cross section data base construction, MeV range 77−26728
^{A}Ni, A=58,60,62, elastic and inelastic neutron scatt., 1.5-3 MeV *(Russian)* 77−26689
^{A}Ni(^{3}He, p), 8, 10 MeV, A=58, 60, 62, p spectra compound nucleus contrib., odd-even effect 80−106061
^{A}Ni(n,X), A=58,60, 14.8 MeV, charged particle emission, cross section, Hauser-Feshbach anal. 79−67750
^{A}Ni(n,n), A=58,60,62,64, 5 MeV, differential cross sections, optical, statistical and coupled channel anals. *(Russian)* 80−37377
^{56}Ni from HI reactions, superdeformed nucleus decay, α-decay amplification 80−68608
^{58}Ni+^{16}O, deep-inelastic collisions, light particle pre-equilibrium emission 78−54786
^{58}Ni+^{16}O fusion, 30-70 MeV, statistical model calcs., yrast states and continuum feeding times 79−579
^{58}Ni+^{32}S, 110, 132 MeV, fusion evaporation residues, Monte Carlo simulation 78−41799
^{58}Ni(^{16}O, X), 70 MeV, compound nuclei charged particle evaporation, moment of inertia 80−57785
^{58}Ni(^{40}Ar,X), 280 MeV, deep inelastic, light fragments, thermal equilib., ang. momentum transfer 80−63203
^{58}Ni(p,X), 90 MeV, charged light particle energy spectra exciton and evaporation model anal. 79−40923
^{58}Ni(p,p'), 5.65 to 6.13 MeV, resonance and statistical mechanisms *(Russian)* 79−80911
statistical theory of nuclear reactions and scattering continued
^{58}Ni(p,p), inelastic and elastic scatt., 17.1-20.6 MeV, cross section fluctuations 78−58286
^{60}Ni+n, total and differential cross-sections, optical-statistical and coupled-channel models 80−13472
^{60}Ni(α,nγ)^{63}Zn, 8-16 MeV, low-lying negative parity states of ^{63}Zn anal. 78−21521
^{60}Ni(e,α)e'X, alpha particle spectra, statistical model calc., direct reaction component 78−41704
^{60}Ni(p,p'), near 6 MeV, spin-flip probabilities distorted wave and statistical anal. *(Russian)* 79−80939
^{64}Ni, elastic and inelastic scatt. of 1.5-3.0 MeV neutrons *(Russian)* 77−61428
^{237}Np(α,f), fragment mass distrib., and yield, statistical anal. *(Russian)* 80−5183
^{A}O(π^{+},π^{-}), A=16,18, cross section and ang. distribs., Glauber and coherent fluctuation models *(Chinese)* 80−102211
^{16}O fragmentation at intermediate energies, statistical fluctuation, fragment momentum distribs. 80−78263
^{16}O level excitation functions, resonances from ^{12}C(^{16}O,^{12}C) 80−63146
^{16}O levels and ang. distribs., ^{3}He spectroscopic strengths, Hauser-Feshbach/DWBA anals. of ^{13}C(^{6}Li,t) 80−47390
^{16}O+^{12}C, 15-72 MeV, gross struct. in γ-ray yields 78−78405
^{16}O+^{16}O, total fusion cross section and excitation function, statistical model anal. 79−13371
^{16}O+p, 62 MeV, complex particle emission, pre-equilibrium exciton model anal. 78−66280
^{16}O(^{12}C,α)^{24}Mg, 12.8-14.5 MeV, energy averaged ang. distribs., Hauser-Feshbach calcs. 79−22318
^{16}O(^{16}O, X), fusion limiting ang. momenta, from evaporation, mass distrib. stat. model fit 80−68714
^{16}O(^{16}O,X), 55 MeV 80−83110
^{18}O+^{12,13}C fusion evaporation reactions, 100 MeV, comparison of residues with statistical calcs. 78−66311
^{18}O($\pi^{\pm}$,$\pi^{\pm}$) inelastic scatt., core polarisation effects from Glauber theory 79−75962
^{30}P level width isospin depend., excitation functions, statistical anal. of ^{29}Si(p,α) 80−78152
^{31}P(d,p), (d,α), cross-section fluctuations at 150° 78−29476
^{206}Pb(n,p), energy dependence, 13.4-20.3 MeV rel. to exciton model calc. 79−75989
^{208}Pb (n,p), energy dependence, 13.4-20.3 MeV rel. to exciton model calc. 79−75989
^{208}Pb+^{40}Ar, deeply inelastic collisions, form factors determ. within statistical model 78−50205
^{208}Pb+^{84}Kr, 500 and 700 MeV, differential cross section calc., statistical model 78−50192
^{208}Pb+Ar, 1.8 GeV/nucleon, fireball model calc. of π-multiplicity distribs. 78−37366
^{208}Pb(^{208}Pb,X), exactly central heavy-ion collisions by nuclear hydrodynamics 80−68690
^{208}Pb(^{20}Ne,X), 400 MeV/N, inclusive p, d, t, ^{3}He cross sections from sequential scatt. model 80−57792
^{208}Pb(^{40}Ar,X), deeply inelastic collisions, form factors, microscopic calcs. 80−18339
^{208}Pb(^{48}Ca, X), fusion reactions from Cf and Fm integral yields, statistical model anal. *(Russian)* 79−97740
^{208}Pb(n,n'γ), 5.2-8.5 MeV, E1 excitations, collective states and spin assignments, statistical model anal. 79−54405
^{237}Pu fission isomers, half lives and yield ratio, statistical model anal. from ^{239}Pu(γ,Zn) 79−40885
^{239}Pu(n,X), nuclear reaction statistical model parameters *(Russian)* 80−18280
^{239}Pu(n,f), statistical model anal. of mass yield 77−26797
^{241}Pu, statistical anal. of reson. neutron fission cross section 77−38305
^{242}Pu(α,f), fragment mass distrib., and yield, statistical anal. *(Russian)* 80−5183
Pu(n,f), 0-18 MeV, prompt neutron spectrum, evaporation model *(Chinese)* 80−42721
^{A}Rb(n,n'γ), 550-2100 keV, A=85,87, levels, excitation functions, J$^{\pi}$, Hauser-Feshbach anal. 80−105982
(^{32}S,X), A=59-89, double differential cross section, mass asymmetry, transport model 80−102203
^{32}S resonances and excitation functions, Hauser Feshbach anal. of ^{20}Ne(^{12}C,X), X=p,d,α 80−78249
^{32}S(d,α)^{30}P, 2 to 2.5 MeV, fluctuation anal., ^{24}Cl compound nucleus 78−46070
^{32}S(d,α)^{30}P, statistical fluctuations at 135°, 2.0-2.5 MeV 78−89882
^{32}S(d,p)^{33}S, statistical fluctuations, at 135°, 2.0-2.5 MeV 78−89882
^{32}S(γ,d), below 30 MeV, photodeuteron yield and cross section, meas. and statistical calcs. 80−63171
^{135}Sb, β-decay delayed n emission, simple statistical model description 79−67714
^{45}Sc(p,γ), 0.7-4.2 MeV, cross section, statistical model anal., stellar interaction rate 79−17897
^{A}Se(p,γ), A=74, 77, 0.6 to 3 MeV, captive cross section, statistical theory anal. 79−9557
^{28}Si (p,p'), 14-40 MeV, low lying states, optical and statistical model anals., giant resonances 79−40894
^{28}Si(^{12}C,^{12}C), 27.8-31.5 MeV, elastic and inelastic excitation functions, fine struct., statistical anal. 80−18269
^{28}Si(^{16}O,^{16}O), 30-32.7 MeV, elastic and inelastic excitation functions, fine struct., statistical anal. 80−18269
^{28}Si(α,α), elastic and inelastic scatt., compound nucleus contrib. anal. 78−37356
^{28}Si(α,n)^{31}S, cross sections and thermonuclear reaction rates 80−73852
^{28}Si(d,d') 6 to 10.46 MeV polarised d, study of Ericson fluctuations 78−54735
^{28}Si(p,p), pol. p, 12-18 MeV, cross section, anal. power and states, ^{29}P resonance coherence widths 80−32258
^{29}Si(d,p), 1.1-2.1 MeV, excitation functions, statistical fluctuations anal. 80−95322
^{30}Si(p,p), polarised proton fluctuation expt., compound elastic enhancement factor determ. 79−519
Sm equilibrium and pre-equilibrium decay, α-multiplicities, energies and entry lines from ^{150}Nd(α,xn) 79−93549
^{147}Sm(n, α)^{144}Nd, 12 to 18 MeV, energy and angular distribution of α-particles, statistical, pre-equilibrium and knock-on models 80−13477
^{147}Sm(n,α)^{144}Nd, 12.4 to 18.2 MeV, energy spectra, ang. distrib., statistical, preequilib., knock-on models anal. 77−26731
^{147}Sm(n,α)^{144}Nd, 2 keV, statistical model anal. 80−102186

statistical theory of nuclear reactions and scattering continued
^{149}Sm(n,γ)^{150}Sm, neutron capture γ-ray spectra calcs. 78−94006
^{152}Sm (n,n), 2.4-7.2 MeV, inelastic and elastic optical model and deformation parameter depend. *(Russian)* 80−13481
^{152}Sm(n,n′γ), 1.0-2.75 MeV, statistical model deviations *(Russian)* 77−26690
^{A}Sn(^{40}Ar, xn), (A=116, 120, 122, 124), 161-236 MeV, γ-multiplicity meas., Er compound nucleus formation 79−89320
^{118}Sn(p,αX), 20-45 MeV, α spectra, exciton model anal. 80−18306
^{120}Sn, 62 MeV, complex particle emission, pre-equilibrium exciton model anal. 78−66280
^{120}Sn+^{40}Ar, deeply inelastic collisions, form factors determ. within statistical model 78−50205
^{120}Sn(^{120}Sn,^{118}Sn), semiclassical description of two nucleon transfer in superfluid nuclei, nuclear Josephson effect 79−45296
^{120}Sn(^{40}Ar,X), deeply inelastic collisions, form factors, microscopic calcs. 80−18339
^{120}Sn(p,n), statistical multistep direct emission, p-h and DWBA calcs. 80−106035
^{124}Sn(^{86}Kr,X), deep inelastic, final and primary yields and dispersions, statistical anal. 79−54452
Sn(p,n)^{116,118}Sb, threshold region, thick-target cross sections, statistical theory, Q values 77−54218
Ta(A,X), 720 MeV, nuclear fragment prod. thermodynamic evaporation and firestreak description, pre-equilibrium emission 79−54426
^{181}Ta(p,n)^{181}W, multi-step compound and direct reactions, statistical theory 80−57761
Ta(α,X) X=p,d,t,^{3}He,^{4}He, 720 MeV, back-angle prod. of light ions, model calcs. 79−45280
^{149}Tb compound nucleus, statistical model de-excitation calcs. 78−50146
^{149}Tb from HI reactions, superdeformed nucleus decay, α-decay amplification 80−68608
^{159}Tb(n,γ)^{160}Tb, E_n=14.1 MeV, γ emission exciton model *(Russian)* 79−13302
^{A}Tc, A=93-96, excitation functions and isomer ratios from ^{93}Nb(α,xn) (x=1 to 4) 80−492
^{124}Te(p,2n)^{123}I statistical model based computation 79−26416
^{232}Th+^{40}Ar, 388 MeV, differential cross section calc., statistical model 78−50192
^{232}Th(n,2n), 13-18 MeV, cross sections, pre-equilibrium contrib. 79−45258
^{232}Th(p,p′f), 52.5 MeV, fission probability 80−99195
^{44}Ti* band crossing search, Hauser-Feshbach calcs. for ^{28}Si(^{16}O,α) 79−22174
^{46}Ti(d,d), 7,10 MeV, ang. distribs., DWBA and Hauser Feshbach anal. 80−47377
^{47}Ti levels, DWBA and Hauser Feshbach anal., compound nucleus cross sections from ^{46}Ti(d,p) 80−47377
^{47}Ti(α,α′), (α,p), level density parameters, α and p energy distribs. 78−13130
Ti(n,n), 1-4.5 MeV, elastic inelastic, total cross sections, optical-statistical, coupled-channels models 79−539
Ti(p,2π^{-}X), 28.5 GeV, fireball model comparison 79−59059
Ti(p,x), 13 to 45 MeV ^{48}V $^{43-48}$Sc, ^{43}K, production excitation functions, statistical equilib. calcs. 79−36220
^{A}Tl, A=199, 200 cross section and excitation function statistical anal. from ^{197}Au(α,xn) *(Rumanian)* 80−22846
^{A}Tl(^{48}Ca, X), A=203, 205, fusion reactions from Cf and Fm integral yields, statistical model anal. *(Russian)* 79−97740
^{169}Tm(n,γ), capture cross section from 10^{-5} eV to 2×10^{7} eV, statistical model 80−63189
^{169}Tm(p,αX), 20-45 MeV, α spectra, exciton model anal. 80−18306
U, A=233, 5, statistical anal. of reson. neutron fission cross section 77−38305
U+^{20}Ne, nuclear fireballs, break-up densities 78−8790
U+^{20}Ne, quark matter, signature in nuclear fireball model 80−37395
U(Ne,X), 250, 400, 800 MeV/N, nuclear matter collective sideward flow, nuclear fluid dynamics 80−57715
^{A}U(^{4}He,xn) A=233-235, x=1-4, cross sections, fission evaporation competition in Pu isotopes 78−66325
^{233}U(n,f), statistical model anal. of mass yield 77−26797
^{235}U, pot. energy surface, liquid model, deformation energy formulae *(Chinese)* 80−102106
^{235}U, thermal-neutron-induced microscopic approach to statistical theory *(Chinese)* 78−86559
^{235}U(n,f), thermal, fragment ionisation, charge distribs., stat. and instant perturbation theory *(Russian)* 80−63219
^{235}U(n,f) standard reaction, Monte Carlo simulation of cross section fluctuations 77−61461
^{235}U(n,f) up to 36 keV, statistical anal., cross sections, intermediate struct. 78−653
^{235}U(n,t), statistical model anal. of mass yield 77−26797
^{236}U fission as multi-dimensional Brownian motion, Fokker-Planck soln. *(Chinese)* 80−99197
^{236}U isomeric and prompt fission, nuclear superfluidity evidence from ^{235}U(d,pf) 80−68711
^{236}U* fission fragment charge distrib. in statistical model *(Russian)* 79−59102
^{238}U, statistical reson. parameters determ. from computer code ADDJA 77−26650
^{238}U, anal. of Rb and Cs isotopic distrib. in ^{11}B and ^{22}Ne-induced fission 77−18634
^{238}U, stat. model calcs. of neutron capture gamma-ray spectra 77−67742
^{238}U(^{238}U,X), 7.42 MeV/N, mass transport, shell effects, anharmonic pots. 80−99187
^{238}U(^{238}U,X) deeply inelastic collisions, mass transport, shell effects 80−99188
^{238}U(α,f), fragment mass distrib., and yield, statistical anal. *(Russian)* 80−5183
^{238}U(n,2n), 13-18 MeV, cross sections, pre-equilibrium contrib. 79−45258
^{238}U(n,γ) cross section, 5-100 keV, doorway state detection, statistical tests 79−93590
U(n,f), 0-18 MeV, prompt neutron spectrum, evaporation model *(Chinese)* 80−42721
^{50}V(p,α), level density parameters, α energy distrib. 78−13130
^{51}V(p,X), X=γ or n, 0.93-4.47 MeV, cross sections, competition effects, Hauser-Feshbach calcs. 80−91184
^{A}W(e,f), A=182,184,186, 35-55 MeV, fission barriers, pairing strength deformation depend., stat. anal. 80−57810

statistical theory of nuclear reactions and scattering continued
^{181}W, level absolute density from n spectra, statistical anal. of ^{181}Ta (p, n) *(Russian)* 79−97657
W(p,2π^{-}X), 28.5 GeV, fireball model comparison 79−59059
^{A}Xe, A=113,5, β-delayed p and α branch ratio, fluctuation function role 79−71820
^{136}Xe+^{209}Bi, 1130 MeV, very heavy-ion collision mechanisms 78−89905
Y isotopes, Hauser Feshbach calcs., of neutron cross sections 80−22839
^{88}Y(n,2n)^{87}Y cross sections, spin dependence and preequilibrium emission 77−30598
^{89}Y+p, 62 MeV, complex particle emission, pre-equilibrium exciton model anal. 78−66280
^{89}Y(n,2n)^{88}Y, preequilibrium emission effects 77−30598
^{89}Y(n,n′), calc. of fluctuation compound nucleus cross sections 77−23029
^{170}Yb(p,α)^{167}Tm, α spectra and ang. distribs. calc., statistical knock-on model 77−79371
^{176}Yb(^{12}C,8n)^{180}Os, 120 MeV, continuous γ-ray spectra anal. 78−41747
Zn even isotopes, fast neutron elastic and inelastic scatt. cross sections, Hauser-Feshbach theory *(Russian)* 77−74853
^{A}Zn, A=64, 66 levels and primary E1 transition strength functions from Cu(p,γ) 80−91149
^{66}Zn* composite particle emission, ang.-distribs., exciton-coalescence model from (d,X), (^{3}He,X), (α,X) 80−78265
Zr isotopes, Hauser Feshbach calcs., of neutron cross sections 80−22839
^{A}Zr(p,p′), A=94,96, 11.2-13.4 MeV, anal. power and excitation function $T_{>}$ fluctuations 80−42626
^{90}Zr(γ,α) statistical and pre-equilibrium cross sections and multipolarities from (e,α) 80−68646
^{90}Zr(p,X), 90 MeV, charged light particle energy spectra exciton and evaporation model anal. 79−40923

statistical thermodynamics *see statistical mechanics*

statistics
see also error statistics; game theory; Monte Carlo methods; probability; queueing theory; time series
15 GHz atmospheric propagation losses on long-range air-to-ground transmission 77−17218
acoustic noise control limits statistical representation 77−54842
acoustic power flow, band-limited, into enclosures 78−9485
arithmetic and geometric mean inequality, thermodynamic proof 78−73952
atmosphere, aerosol optical attenuation statistics, spring and autumn 79−84484
atmosphere, anisotropic homogeneous turbulence statistical description 79−79917
atmospheric precipitations, statistics of spatial distrib. on Experimental meteorological test range, Ukraine 80−101414
atmospheric surface layer turbulent vel. components characts. under convective conditions 79−66754
balloon born cosmic ray electron detectors, curious random counting statistics, electric circuit 78−17540
binomial and Pascal distributions moments of mth order 77−37739
causal relns., statistical models 77−78948
cloud field over Transcaucasia, statistical struct. 78−92942
cloud seeding experimental results analysis 80−8389
cloud seeding experiments, statistics appl. 80−8438
communication structures description *(German)* 77−12869
commutation superoperator of state, appl. to noncommutative statistics 78−28997
concepts for teaching 79−35501
conference, statistical physics, Budapest, Hungary (Aug. 1975) 77−49664
convergence to stable distribution laws in limiting theorem *(Russian)* 78−28920
converse of dominated ergodic theorem 79−71349
correlations construction, use of quantiles 77−91291
counting statistics with uniform dead time distrib. *(French)* 78−58560
course-graining, statistical inference from partial meas. 77−26148
courses in statistics, classification of 77−29970
cross-correlation functions, statistical significance 78−69971
cumulus cloud statistics, satellite-derived, for W.Kansas 79−79955
dead-time effects in photon counting statistics 79−3665
definitions, normal distrib. and signal detect. for astronomers 80−17500
density perturbations in expanding universe, three-point correl. function and higher order functions prediction 78−65730
differential signal channel pulse stream statistics for γ spectrometer *(Russian)* 78−17474
diffusion with strong drift 78−87808
distributions, Boltzmann, Fermi-Dirac, Bose-Einstein derivation 77−5
earthquake frequency-magnitude relation, statistical parameters rel. to seismic zoning problems 79−44112
earthquakes in and near Japan, energy release statistics (1915 to 1978) 80−94471
ECG prototype waveforms generation by piecewise correlational averaging 80−109053
eclipsing binary stars, period statistics rel. to form. and evolution 80−36662
education, Poisson distribution, expectation value and variance 78−69943
education, Poisson statistics demonstration using X-ray tube, electronic 'shot noise' 80−73129
elementary particle quantum characts. 78−70297
EM wave propag. in inhomogeneous medium with large-scale random inhomogeneities *(Russian)* 79−882
entropy, information and statistical, and law of large numbers, opacity of statistics *(French)* 80−73288
Escoufier's operator, construction and appl. to principal components anal. 77−26146
explicativity, mathematical theory of explanation with statistical applications 77−45682
exponential random variables sum, probability density function 78−12537
extremum position and confidence limits, determ. of absorpt. max. in wide bands 80−22188
flood sequences, apparent regional skew 77−64355
galaxies, faint, number magnitude counts 80−26976
geodesy, mathematical struct. and appls. 79−29696
geometric objects with fractional dimension, seacoasts, galaxy clusters, turbulence and soap, book contrib. 77−87640
geophysical anomaly source models, statistical parameters rel. to pot. fields obtained by superposition *(German)* 79−34783

statistics continued
geophysical data analysis, random values separation soln. statistical charcts. *(Russian)* 79−74983
geophysical fields, props. of linear transform. charcts. *(Russian)* 79−35007
HF sea-echo Doppler spectra, statistics 77−17231
Hubble diagram statistics, form of luminosity function and density vars. with appl. to quasars 79−97093
hydrologic data set distribution functions, extremes and confidence intervals 78−24313
image segmentation based on second-order grey level statistics 80−99663
independent random sine waves in additive Gaussian noise 79−68497
inductive statistical explanation, Hempel's conception of inductive interference 77−78945
ionosphere reflected radio signals, effect of travelling disturbances on statistical charcts. 78−45092
ionosphere reflected signal, sum phase random props. investigation 79−53615
K-distributed noise, statistics 80−27220
laser beam propagation in atmosphere, detection effects on statistics of intensity fluctuations 79−16672
laser speckle pattern obs. through finite-size scanning apertures, extreme-value statistics 78−66759
light statistics, influence of multiphoton absorbers with intermediate reson. 79−86208
linear least squares parameters, stat. significance, student guide 80−17770
material test point, statistics of distant perturbs. 78−28494
mathematics courses, effect of class evaluation method on learning 78−57719
Mediterranean earthquake catastrophes, statistics 80−3955
microwave attenuation statistics influenced by rain cell orientation 77−5278
Muller statistics for counting systems for non-extending dead time, exptl. test 78−94173
multiple quadratic regressions, programmable desk calculators in the laboratory 80−42048
multisensor image pattern recognition, statistical and deterministic aspects 80−99647
neutron counting statistics in subcritical cyclo stationary multiplying system 80−32323
Neyman-Pearson theory of testing 78−57728
nuclear medicine, understanding and using statistics 80−12233
ocean internal waves, acoustically relevant statistics for stochastic models 77−46854
ocean storm wave heights, statistical distrib. 78−73390
ocean upper layer, small-scale temp. fluctuations statistical regularities *(Russian)* 80−94528
parastatistics, concept, phys. significance *(German)* 77−49577
particle identification statistics using ionisation 79−36491
particle size calculation simplification 80−90814
particle size distributions, statistical reliability 77−53858
particle tracks, search statistics, Monte Carlo study of random scatt. problem 78−58561
Penning mixtures, statistics of gas gain 79−45535
periodic nonstationary Gaussian process, high level crossings *(Russian)* 80−94948
phase statistics in coherently superposed Gaussian speckle patterns 80−102626
planetary nebulae, spatial and vel. distrib. statistics 80−109518
Poincare Bertrand formula, proof by Fourier transform of distribution 77−82366
Poisson-sampled random process, moments estimation 77−37738
quasar Hubble diagrams, nonparametric statistics 79−40289
radiation counting statistics, with extended variable dead time *(French)* 77−57842
radiation therapy, dose/cure relationships study 80−56218
radiative association reactions in dense interstellar clouds, statistical theory 80−82441
radio sources, double, statistical props., asymmetry and components flux ratio 80−67892
radio sources, extended, statistical evidence on dynamical evolution 79−88757
radio sources, faint, interpretation of interplanetary scintillation meas. at 81.5 MHz 80−90554
radio sources, faint, statistical study of mean ang. size and sky density at 81.5 MHz 80−51893
radioactive contamination in aquatic organisms, evaluation by statistical and information theory 78−53535
radioactivity counting statistics with non-extended variable dead time *(French)* 77−30735
radioactivity meas., statistical distribs. accumulation in real time 78−94178
Rand-condition form generalisation in theory of chaotic movements, appl. reverberation 77−26147
random variables, independent identically distributed, asymptotic sufficiency in non-regular cases 77−41462
ripples slope statistics, effects of long waves 77−45005
road traffic total noise exposure and time average statistics *(Japanese)* 79−70499
science statistics, inequality indices and skewed frequency distribs. 79−58523
sea surface slope distrib. function determ. from Sun glitter, accuracy *(Russian)* 80−94611
seismicity, global, statistical props. from earthquake catalogue 79−53320
seismology, Gutenberg-Richter relation appls. problems in earthquake statistics 77−44923
simulation of statistical systems, homogeneous nucleation *(Russian)* 78−83934
simulation of statistical systems, two level system *(Russian)* 78−77690
simulation of statistical systems *(Russian)* 78−69970
Smoluchowski process, number fluctuation anal. of random locomotion 78−54318
stability evaluation of statistical couplings, meteorology appl. 77−74204
stellar, speckle patterns and plane scintillation, statistics 79−100948
stellar statistics, rel. to neutron stars form. rate in Galaxy 79−40208
stellar trigonometric parallaxes, statistical anal. and systematic errors 77−64743
strip rolling, kinetostatics *(Russian)* 80−38348
sub-poissonian statistics of an anharmonic oscillator in thermal equilibrium 80−82669
statistics continued
subcritical cyclostationary nuclear reactor, neutron counting statistics, sinusoidally modulated neutron source 80−99203
superposition of epochs, statistical method, anal. and appl. 80−4267
teaching, general applied maths and statistics development for appl. to all sciences secondary level 78−57716
teaching approach for non-specialists 78−57715
tennis, probability and statistics teaching illustration 80−41997
textures, discriminable, with identical Buffon needle statistics 79−34568
truncated Kullback statistic, objective function for fitting partially known probability vectors 77−37737
turbulence, statistical theory, review of present trends, book contrib. 77−84234
visual analyser space-frequency filter harmonisation with statistics of images 80−30726
visual response, expected waiting time 80−51091
weather experimentation, statistical issues 80−8439
Westerly granite, stress-volumetric strain behaviour statistical var. 78−96196
white light image speckle statistical props. 80−106461
Wilks matrix comparison, scalar variables *(French)* 77−67233
wind speed, freq. distribs. of hourly meas. 80−94554

stators
axial flow compressor blade wake guidevane mean velocity and decay charcts. anal. 80−95085
bar insulation in stator winding of large turbogenerator, inspection using microwave defectoscope 80−35474
quality control using thermovision flaw detector 'Stator-1', meas. channel 80−76449
turbogenerator, short circuits, stator end windings deformation *(Japanese)* 78−11465
turbogenerator, water/oil cooled type TVM-300, winding vibration tests *(Russian)* 77−9886
turbogenerator stator core losses simulation, expt. 80−88798
turbogenerators type TVV-800-2, endwinding vibration tests *(Russian)* 77−9885
windings, failure mechanisms under thermal cycling *(Japanese)* 80−104189

steady-state theory *see cosmology*

steam
air-steam mixtures, heat transfer to moving droplets 78−90997
annular flow condensation, of steam inside tubes, heat transfer 78−14003
boiling in steam generating pipe with Fe oxide deposits on wall, steam bubble growth 79−76947
bubble, nonspherical, collapse in suddenly pressurised water *(French)* 78−33997
bubbles, condensation, influence of noncondensable gases *(French)* 79−23717
bubbles direct contact condensation in water at high press. 77−39202
BWR steam condensation pressure variations 78−46134
channel two phase flows, threshold steam qualities and cutoff heat fluxes 79−90242
condensation, dropwise, on electroplated Au layer, thickness depend. 79−46791
condensation heat transfer on below-freezing pt. surface 78−75042
condensation in annular duct flow, heat transfer to condensate film 78−94709
condensation in capillaries 79−1066
condensation in tubes, augmented internal geom., and press. drop 78−94556
condensation inside vertical straight and coiled pipes, heat transfer 79−90244
condensation on bundle of tubes, heat transfer effects 78−30164
condensation on external entrance length of cooled rot. tube 77−75906
condensation on plate condenser with grid pattern slotlike channels, low-press., heat transfer 78−75040
condensation on PTFE coated surface, heat transfer 77−89012
condensation on turbulent water surface 79−64748
condenser, supersonic nozzle discharge, heat transfer and gas dynamics 78−55671
condensing, method for calculating expansion 77−27573
contact angle hysteresis, dropwise condensation heat transfer 78−71273
critical behaviour of thermodynamic potential 80−42175
critical region, universality, revisions and corrections to scaling 78−38810
desublimation under vacuum, rate of ice form. 77−24402
droplets growth in Laval nozzle 79−32648
dropwise condensation, effect of condenser tube material on heat transfer 78−75059
dropwise condensation, heat transfer coeff., surface shape, orientation, coolant flow rate 77−27528
electrolysis, high temperature, H_2 production, fusion reactors, synfuel production 80−72099
electrolysis at high temp. for H_2 production 80−61440
equation of state, between 350 and 1000°C (0 to 10 GPa) and between 100 to 350°C (200 MPa to melting curve) 80−15214
film condensation in tube, heat transfer, vibr. effect 78−51044
film condensation of steam in vertical Cu tube, heat transfer coeff. 78−94553
fission reactor ECCS, flooding phenomena with condensation 79−89429
fission reactor LOCA containment anal., new condensation mass removal model 79−89423
flow, nonequilib., two-phase, relation between thermal and flow charcts. 78−55694
flow, steam-generating tubes, rough (smooth), post-dryout, heat transfer 78−55678
flowing wet steam, condensation, heat transfer 77−62297
generating channels, boiling crisis, critical heat loads 79−90247
generating channels, heat exchange intensification by surface roughness in transcritical region 79−55371
generator, accumulation type, using NaOH as thermal storage material *(French)* 80−40914
high pressure steam/water mixture flow through cylindrical channels, obs. 80−79404
horizontal flow on cylinder, condensation 78−94550
ice-water-steam system, two-dimens. triangular lattice model, matrix calc., props. 77−27975
Incoloy 800, corrosion resist. props. in high temp. steam, review 79−47839

steam continued
Incoloy 800, thin wall tubing, creep-rupture testing in steam under constant and cyclic load 79−47774
inert gas steam uncondensable gas content effect on steam condensation heat transfer in vert. tube 78−75041
jet condensation, dynamical pressure pulse effects 78−94549
Lanzarote (Canary Islands) geothermal area, isotopic comp. of steam samples 77−49048
liquid-steam, annular dispersed flow, hydrodynamic characts. 78−94806
LMFBR steam generator leak, meas. of sound produced during steam injection into Na 79−93782
LMFBR steam generators, leak detection of steam or water into sodium 79−13434
low and moderate density, compressibility factor and viscosity coeff. eqn. 80−33722
LWR steam explosion pressure buildup estimation 79−13473
LWR steam explosion triggering expts. with oxidised Corium-E simulants 79−13472
mass-transfer measurements on steam-generating pipe containing porous defects 78−38398
measuring instrument, steam fraction determ. in flowing air/stream mixtures by meas. of IR rad. attenuation 80−75010
MHD generator, production of short bursts of power 80−64789
mixed 2-D flows of supersaturated and two-phase medium with nonequilib. phase transitions 79−77224
mixture of bubble struct., sound velocity, damping decrement 79−55444
nuclear and coal heating, steam generation for industry 78−37455
radiative transfer, Curtis-Godson approx. 78−67019
relative velocity in steam-water two-phase mixture, determ. of void fraction 78−5791
saturated and superheated, up to 800°C, equation of state 79−14908
saturated steam parameters in reactor containments with escape of coolant, simplified calc. 80−68764
shock wave induced condensation 80−34177
sorption effect on cross-linked polyester film struct. *(Russian)* 80−59405
steam-air mixture, condensation, transport and thermodynamic props. *(Japanese)* 78−34251
steam-water annular dispersed flow, liq. distrib. between core and film 77−75971
steam-water mixture, upward flow in tube, liq. film-core mass transfer, liq. distrib. 78−75189
steam-water systems, two-phase press. drop correlations 77−82995
steel, superheated-steam oxidation, exam. of catalyst influence 78−85030
submerged steam jet into unbounded space, temp. field 79−72920
supercooled, thermodynamic props., virial eqn. of state 80−14872
supercritical, compressed, proton spin-lattice, relax. time meas. 80−22403
supercritical, isotopic separation of metals 77−63922
superheated, AFCRL atm. absorpt. line parameters in 2900-3000 cm^{-1} atm. window 80−36396
superheated, dispersion in saturated water, bubble form., heat transfer 77−47068
superheated, dispersion in saturated water, bubble form., heat transfer 77−47069
superheated steam, control system using an adaptive regulator, synthesis *(Polish)* 79−75518
thermal cond. in large Knudsen range, theory and expt. 78−94888
thermal conductivity equation, 0 to 800°C, triple pt. press. to 1000 bars, crit. region 80−39364
thermal reactor, steam explosion propagation phenomena, multidimensional aspects 79−89420
thermodynamic parameters, approximation formulae in binary polynomial form *(German)* 78−59532
thermodynamic props., numerical calc. program *(French)* 77−69101
total emissivity, press. depend. 78−90673
treatment of SiO_2 gel, struct. changes 80−35579
two-phase countercurrent flow, turbulent steam condensation in a horizontal channel 80−106800
two-phase flow, nonequil., true mass steam content meas. by diffusion indicator method 79−86538
viscosity calculation, applicability of effective spherically symmetric pots. 78−1779
volumetric steam content determ. by noncontact neutron sensor 79−30904
volumetric steam content determ. of steam generating channels by slow neutron method 79−30903
water-steam, flow characts. at high press. 78−94805
water-steam mixture, upflow in heated tubes, void fraction 77−62296
water-steam mixture, with high vap. content, annular flow, heat transfer, press. loss 78−75193
water/steam systems, thermodynamic data tables 78−26679
wet, supersonic flow, total- and static-press. probe characts. 77−84353
wet steam, high speed flows, drop dimensions meas. method 80−90817
wet-steam flow, critical pressure ratio 77−84300
Zircaloy, breakaway mechanism, corrosion kinetics in steam 80−61030
Zircaloy-2 claddings, oxidation reaction kinetics in steam environment in temp. range 1273-1673K 80−35401
Zircaloy-4, oxidation at 900 and 1100°C in high pressure steam 79−66208
^{252}Cf neutron source for water-steam mixture void fraction meas. 79−26762
D_2O, gaseous, viscosity, 200-400°C, up to 300 bar 78−63527
D_2O, saturated and superheated steam, eqn. of state up to 500°C 78−79401
H production from H_2O by two-stage plasmochemical cycle 80−45772
H, thermochemical production by steam reforming of methane, kinetic anal. 80−35788
H, thermochemical production by coal gasification using steam 80−35789
SiO_2, vaporisation in steam atmosphere 80−44306
ZrO_2, cell electrolysis of H_2O at 800° to 1000°C *(French)* 80−26024

steam boilers *see boilers*

steam generators *see boilers*

steam plants
see also boilers; condensers (steam plant)
1300 MW cross compound turbine unit IP rotor coupling, fatigue crack due to combined corrosion and low alternating stresses, report 80−16611
1300 MW nuclear reactor steam isolating valve blowdown tests *(German)* 80−22967
centralised heat source, energy distribution and storage 79−48184
chemical washing, aqueous effluent neutralisation by use of ash 80−89486
dynamic simulation of the Gentilly-1 reboiler system 78−82439
flaw detection in steam generator tubes, EM acoustic transducer 80−76464
flow dynamics stability in once-through steam generator *(Czech)* 77−38386
fluidised bed evaporator, liq.-solid wall to liq. heat transfer 79−1245
fossil-fired, with geothermal preheating 79−48084
generator, Na heated, dynamic instabilities 78−17281
geothermal, using fossil superheating, thermodynamic analysis 79−48088
heat pump for steam generation from industrial waste heat 80−35732
heat pump system for process steam generation 80−35729
heat pumps, absorpt. and compression, energy conversion by alternative working fluids, book contrib. 79−43783
heat transfer in vertical steam generating tube, at low pressures and moderate mass velocities of flow, post-dryout coeff. calc. 78−67257
HTGR 900-MW(e) steam cycle plant design 80−592
liquid/vapour flow visualisation and localised fast meas., instrumentation 79−46404
main steam isolating valves, back pressure light, PWR appl. 78−29602
material consideration for large sodium-heated steam generators 78−82503
material selection for a sodium-heated steam generator 78−82504
MHD, coal-fired, economic optimisation using computer-based model 79−52942
MHD combined, single-load, performance and efficiency obs. *(Italian)* 80−26148
MHD generator, diagonal-type, nonequilib. plasma, steam plant appl. 78−67443
MHD/steam combined-cycle plant, combustion air temperature variations reduction, computer simulation appl. 79−52943
nuclear, globe main steam isolation valve unbalanced forces and novel actuator design 78−50288
nuclear plants, heat extraction from steam generators 78−37465
nuclear power steam mains, Gentilly-I generating station, inertial analysis of hydrodynamic oscills. 78−89944
nuclear process steam for coal gasification 78−78488
nuclear reactor components, weld seam inspection, steam supply system, quality assurance *(German, English)* 77−83052
pressure vessels and steel pipes structures anal. under creep conditions, acoustic emission method 77−25237
primary and secondary water chemistry of PWR power stations, European experience 80−106110
PWR power plant steam dump valve stability anal. 78−50289
PWR steam generator corrosion problems and design implications 79−93812
solar steam generation system for industrial appls. 80−55825
steel, Cr-Mo-V, steamline bends, restorative heat treatment effects 78−68716
steel, steam pipes, 12Cr1MoV, selection of allowable stresses based on minimum possible strength data 80−104237
thermionic energy convertors appl., conceptual design using advanced boiler concept 79−48156
true volume steam content in thin channels at high pressures meas., spectrometric method 79−13585
water in critical region, thermal cond. results analysis 77−89599

steam power stations
antiscale forming effectiveness of seeding crystals in thermal power plant 80−89527
boiler feedwater redox potential meas. by Pt thin-layer electrodes 80−89578
boiler plate restriction two-phase flow hydraulic resistance calc. 78−1734
boiler tube corrosion investigation using gamma-ray transmission meas. technique 77−9011
boiler tubes in service inspection, creep testing techniques assessment *(Japanese)* 77−81356
chemical water treatment pH value calc. for district heating power station, computer-aided analysis *(Russian)* 79−43572
coal, fluidised bed firing, technological state and economic chances *(German)* 79−92050
coal, gamma-ray activity rel. to power station choice 78−11746
coal fired, gas-particle conversion obs. in plumes 80−81502
coal fired power plant, downwind elemental deposition 79−20838
coal fired steam power plants, metallurgical problems and opportunities to improve reliability 79−52089
coal gasification/combined cycle power generation test facility, preview 80−16773
coal-fired, elemental particle-size emissions, inertial cascade impactor appl. 79−12278
coal-fired, financial impact of air pollution control costs 80−3497
coal-fired power plants, minor and trace elements emissions and particle size distribs. 79−92108
dryout, premature in conventional and nuclear power station evaporators, model 78−94120
environmental dispatch simulation and emission dispersion modelling 78−32221
fossil fuel fired power plants, standardisation, feasibility, advantages, limitations 80−16775
fossil plant efficiency, and heat rate improvement program 79−67829
heat transfer with steam condensation, theory, problems of interest 78−30161
Homer City power plant plume, aerosols and ice nuclei meas. 79−74570
hybrid geothermal/coal fired power plant, site specific economic anal. 79−24887
KILnGAS coal conversion system for low BTU gas production, electricity generation appls. 80−16776
LWR and coal power stations, effects on ambient media from mining to waste disposal *(Spanish)* 77−75005
MHD/steam power generation systems, commercial viability 80−35701
noise control design concepts 77−75738
nuclear and fossil power plants effluent environmental impact comparison 78−96290
performance evaluation by thermal hydraulic anal. 79−67831
phase distribution in two-phase steam flows, effects of probe position 80−87799

steam power stations continued
plant, chemical washing, aqueous effluent neutralisation by use of ash 80−89486
plumes visual impact model 79−16664
river/atmosphere time dependent, single dimensional heat exchange, aspects *(Bulgarian)* 78−57221
steam-gas power station with multi-stage high-sulphur residual fuel oil combustion 77−9487
steel, stainless type 10CrNiCuP and St. 3PS, suitability for power station chimney flue structural material, corrosion testing 80−108681
supplementary steam generation using H_2/O_2 combustors, a viable H power generation concept 80−30330
thermal efficiency, CO_2 fund. condensation cycles, performance characts. 80−63368
thermal power stations, achievement of environmental harmony *(French)* 79−92094
unconventional power generation systems, economic aspects *(German)* 79−87981
H_3PO_4 fuel cell power plant with high temp. steam reforming and autothermal reforming 80−30466
SO_2 removal from waste gases, citrate process demonstration at 60 MW power plant 79−100553

steam turbines
see also turbogenerators
200 MW, with accessories, noise reduction research and development 80−91958
440 MW, type KhTZ K-220-44 description 77−18691
1300 MW cross compound turbine unit IP rotor coupling, fatigue crack due to combined corrosion and low alternating stresses, report 80−16611
axial flow compressor stator blade boundary layer development 79−4002
blade vibration measurements, radio link telemetry appl. 77−68538
blading overspeed vibrations meas. optical methods 77−74387
BWR turbine trip, RELAP/RETRAN steam line models, accuracy considerations 79−59197
BWR turbine valve closure, pressure transients 79−89441
cascade, two phase flows, mixed and discontinuous, calc. 80−79391
cascades, transonic flow computation 80−96276
concentrator/photovoltaic/Rankine cycle steam turbogenerator system efficiency 79−62002
corrosion protective coatings for reliable operation 78−11424
district heating plant, condensing and regenerating equipment 80−92029
drop coagulation in cross-over pipe flows of wet steam 80−74982
droplet size distribution in liquid phase of two-phase flow effect on characts. 80−103070
flow dynamic stability in once-through steam generator channel, influence of press. loss components *(Czech)* 77−3148
flow holographic interferogram processing by minicomputer 77−19656
flow-through clearance measurement transducer test equipment 77−53881
fusion augmented steam turbine high efficiency power cycles 79−22475
geothermal plant optimum design conditions, Geysers Unit 16, Northern California (USA) 79−52877
heat transfer in tubular condenser apparatus *(Russian)* 80−1411
heat trasnfer in channels, convective, unsteady 78−67198
high-capacity, supersonic cascades flow calc. 78−87360
LMFBR, BOR 60, modular Na heated steam generators, performance, specifications *(Czech)* 77−3147
nozzle cascades, local heat transfer, approach flow turbulence effects 80−38381
nozzle steam flow under periodic perturbation, anal. by streak photography 77−80249
nuclear power plants, district heating 78−37437
nuclear power stations, turbogenerator overspeed protection, reliability study, design *(French)* 77−3156
nuclear steam turbines for power prod., district heating, desalination 78−37438
rotor boundary layer turbulence anal. 79−32490
rotor steel type EI-415, low-cycle fatigue and short term creep investigation 77−25238
solar thermal power plant turbine sizing, performance and economic anal. 80−30403
spontaneously condensing and wet steam discontinuous flows, subsonic, transonic and supersonic, numerical investigation *(Russian)* 80−87800
steam-gas power stations using multi-stage high-sulphur residual fuel oil combustion 77−9487
steam-water annular dispersed flow, liq. distrib. between core and film 77−75971
steel casings, 15Cr1Mo1VL, susceptibility to brittle struct. and fracture, influence of props. 80−104298
steel turbine casings, residual life determ. 80−93585
structural stresses, experimental anal. 80−93727
subsonic/transonic flow, one-dimensional, isentropic, calc. 77−23986
three-dimension transonic flow prediction, characteristic method appl. 80−96277
titanium low pressure turbine blades, metallurgical opportunities to improve reliability 79−52089
turbulent flat jet condenser, nozzle hydraulic and heat transfer characts. 78−94793
vapour turbine plants using combined thermal-power convertor and photoelectric convertor, thermodynamic efficiency for solar energy conversion 80−89614
vibration and noise review, central power station large turbomachinery 80−23835
welds, with the 25000 R/min Linac 80−97656
wet stream, water drops deformational breakup, differential eqns. 79−14462
Cr-Mo-V steel thermal fatigue tests 78−39912

steel
see also alloy steel; austenitic steel; carbon steel; stainless steel
40Kh, heat-treated, wear during friction under extreme conditions 78−85007
ablation and fuel-steel mixing phenomena following LMFBR accident 80−47649
abrasive wear resistance, effects of microstruct. 78−92367
acoustic emission anal. during fatigue crack growth 77−56090
acoustic emission and ductile crack growth 78−11320
acoustic emission associated with phase conversions 79−70275
acoustic emission during extension, of HF-1, frequency content variation 77−81301
acoustic emission fatigue monitoring, new technique 77−28938
acoustic emission in deformation, at various strain rates and sign change 78−44188
acoustic emission parameters, brittle fracture, crack propagation in types St3+0Kh13 *(Russian)* 80−93633
acoustic emission sources and dislocation patterns 80−61040
acoustic hardness testing 79−39088
acoustical method of studying steel microstructure 80−76469
acoustoelastic stress field imaging technique, stress field contour plots 79−77033
adherence, friction, and wear improvement of type 440-C using RF sputtered TiC coatings 79−47823
adhesion of epoxy resins to surface 77−4888
adhesive wear, heat treated load effect 78−11344
adiabatic shear explanation 77−14924
AE use for mech. tests 80−35467
against Al_2O_3, elastohydrodynamic contact, lubricated by naphthenic hydrocarbon, IR meas. of surface temp. 79−15807
age hardened, dynamics of cyclic plasticity *(Czech)* 80−108464
age-hardenable, relation between fatigue S-N and P-N charact., definite fatigue limit *(Japanese)* 77−8938
AGR boilers, gas side corrosion, breakaway oxidisation treatment 78−48558
alloy, 0Kh16N15M3B, irradiation effects on resistance to cyclic elastoplastic deformation 79−91767
alloys, continuously cast, numerical study of optimal solidification conditions 79−83188
alpha-particle bombardment, He liberation during tempering 77−46290
aluminising, thermodynamic anal. of phase transforms. 80−76413
aluminising by circulation method, thermodynamics 80−30163
aluminized, atmospheric corrosion kinetics 79−47808
analysis, C and C conc. determ. by nuclear methods *(French)* 77−60160
analysis by ion microprobe, quantitative, using matrix ion species ratios 78−61070
anisotropic rolled plate, fatigue crack growth, rel. to laminated struct. and inclusions 78−92313
anisotropic rolled plate, torsional fatigue in middle and high cycle fatigue ranges *(Japanese)* 77−12691
anisotropic sheet, strain hardening, stress state depend. 80−55421
anisotropy of strength and ductility, elevated temp. effect 77−4825
annealed, 4130, fretting, material removal mechanism 79−20217
annealed, limit stress, effect of specimen length 77−44357
annealing effect on texture, microstruct., and mech. props. 78−44138
antioxidation protective glass enamel cladding exam. of development 78−85031
anvil, truncated, compressive strength, high press. apparatus appl. 78−84906
arc cathode craters, oxide film thickness effects, meas. using SEM *(German)* 78−38558
austenite to martensite transformation, orientation relationships 79−78964
austenitic weld in LMFBR, US testing 77−1903
austenitic-martensitic, yield strength rel. to struct. and phase comp. 79−66127
austenito-martensitic, struct. changes during plastic deform., mutual influence of phases *(Russian)* 80−30015
austenization heat treatment effect on microstuct. and mech. prpps. 80−29993
automatic visual inspection of moving steel surface 77−81349
Babbitt-steel bimetal, exam. of structure of transition layer 79−100293
backing plate, hot pressing with powder layer, joint form. kinetics 80−100961
bainite, ^{57}Fe Mossbauer spectra 80−15051
bainite formation mechanism 80−108431
bainite transform. kinetics and mech. props. of 35KhN3MFA and 25KhN3MFA *(Russian)* 78−80539
bainitic, habit plane determ., austenite orientation determ. 79−1926
bainitic, low C and alloy, quenched microstruct. effect on mech. props. *(French)* 79−79003
ball, fatigue life prediction, fully automatic X-ray diffr. apparatus *(Japanese)* 79−39076
ball bearing, fatigued, phase changes, nomenclature 80−89198
ball bearing, heat treated, fatigue crack propag. 79−20188
ball bearing, martensitic decay during rolling contact fatigue 77−32682
ball bearing rods, inspection installation 80−81268
ball bearing with modified chem. comp., improved rolling contact fatigue 78−64732
ball-bearing, ESR, martensitic, size effect during rotating beam fatigue tests 80−7674
bar, and wire rod, small sample prep. and spectrometric anal. *(German)* 80−93704
bar, axially symmetrical residual stresses, with longitudinally nonuniform stress distrib. 78−51070
bar, Hall probe meas. of residual and active leakage fields round artificial flaw 78−88595
bar deformation meas. by holographic interferometry using four point bending machine 78−60721
bar with inhomogeneous props. of lagging creep, deform. 79−15731
bars, deform. meas. by holographic interferometry, four-point bending machine assessment 79−34266
bars after drawing, mechanical characts. *(French)* 79−91662
base composite, sintering, mech. props. 77−21061
Bauschinger effect minimization by dynamic strain ageing 78−48469
bearing and frictional material, current state of prod. and development trends review 78−19902
bearing materials, rolling, effects of high temperature operation 80−21124
bearing parts, mag. inspection of heat treatment quality 78−73007
bearing rings, optimisation of thermomechanical working parameters *(Russian)* 80−93579
bearings, for gas turbines brittle fracture due to stress combination 78−56771
belt grinding, struct. transformations in type 12Kh2N4A 80−30169
billet, high speed automatic surface inspection, MIDAS 79−83420
bimetal, high-speed steel + machine steel, chem. comp. influence on magnitude of residual stresses in cooling *(Russian)* 79−74183
bimetal rolled plate, low-cycle fatigue in bending 79−91794
bimetallic tube with internal Cu coating segmental specimens, tensile testing 79−70255

steel continued
boiler steel fatigue crack propagation test results *(Hungarian)* 79−83293
bonded with epoxy resin, effect of adhesive bond thickness on mech. resist. *(French)* 77−63882
boride coatings, form. mechanism and struct. during crystn. of castings 80−35412
boride coatings, formed by B diffusion, pack cementation process, microstruct. and mech. props. 78−15592
boride coatings, technology, props., book contrib. 78−48574
boride coatings, under elec. heating conditions, hydroabrasion wear resist. 80−55543
boride coatings on steel effect of Cu impurities in reaction mixture on brittleness, acoustic emission meas. 80−16581
boride diffusion coatings on steel, fractographic exam. of struct. 78−44270
boride films, produced by ion bombardment on Fe and plain steel, X-ray struct. anal. *(French)* 79−73413
borided, 45, 20Kh, 30KhGSNA and Kh12F1, relative wear resistance 77−73351
boriding, electrolytic, effect of iron oxides 79−39042
boriding by ion bombardment with B_2H_6 *(French)* 78−60876
boriding with B_4C based paste 80−16583
boronised, corrosion resistivity *(Japanese)* 77−52544
boundary lubrication with Zn dithiophosphate 79−79120
brass diffused coating on steel from vapour-gas phase *(Russian)* 79−5080
brass/steel, explosively bonded and roll bonded clad plate, fatigue crack growth *(Japanese)* 79−61706
brass/steel couple, wear results from talysurf traces 79−52392
bright strip, light oil annealing, mathematical simulation 77−77512
brittle and tough fracture depend. on C content, heat treatment *(Russian)* 80−40500
brittle cracks, propagation velocity determ., expt. eval. 79−70236
brittle failure of Fe in 15G2AFDps, quantitative electron fractography 77−63804
brittle fracture, grain boundary P segregation, effect after quenching and tempering *(Russian)* 80−81145
brittle fracture, J-integral fracture criterion *(Japanese)* 77−48597
brittle fracture, type 4340, effect of H_2 and impurities, review 78−60765
brittle fracture criteria for nuclear reactor press. vessel steels, neutron effects *(German)* 77−34389
brittle fracture in ductile material, model and applic. to H embrittlement 78−23814
brittle fracture mech., review *(Russian)* 79−34139
brittle fracture of compressor materials under impact loading 77−25137
brittle fracture of plate for pressure vessels 77−3115
brittle fracture resist., fractography and grain refinement 77−60024
brittle fracture resistance, welding and heat treatment effects 80−50723
brittle fracture susceptibility rel. to grain size of 10Kh11N20T3R *(Russian)* 77−59901
brittle rupture, (n,α) radiography method with B doping *(Russian)* 78−48491
brittle transition temp. comparison of arc, gas-pressure and friction-pressure welded alloy by hardness measurements *(Japanese)* 79−11691
brittle transition temp. determs. from impact ductility tests, comparative evaluation 79−15888
brittleness dependence, high temp. deform. in 3Kh2V8F steel at high stress. temp. *(Russian)* 80−50698
brittleness of nitrided case 77−21418
bronze-on-steel contact, lubricated, effect of zinc di-n-butyl dithiophosphate on wear 79−20219
bronze-steel, phase composition and struct. of diffusional interlayer in fusion zone, X-ray analysis 78−56821
buckling under axial compression on circ. integrally stringer-stiffened shell 78−63346
burnishing, formation of hardened layer in steel 55SM5FA 78−85046
butadiene coatings, delamination by corrosion 78−64765
butt weld structure and mech. props., explosive treatment effects 79−24541
C content effect on annealing texture, plastic anisotropy and mechanical props. 80−29976
cam-roller pair, wear resistance after strengthening treatment *(Russian)* 78−31542
cantilever bend specimen, side grooving effect on compliance relationships 78−35472
carbide and nitride phases dissolution *(Russian)* 80−20888
carbide cracking as source of acoustic emission 78−19872
carbide formation, microscopic exam. aided by rating charts *(German)* 79−61805
carbide layer form. in fused borax bath containing metals and metal chlorides or oxide powders *(Japanese)* 77−48684
carbide layer form. in fused borax bath with electrolytically dissolved V, Nb, Cr and Ta *(Japanese)* 77−52671
carbide particle size and pearlite grain size changes during deform. and hot working of ShKh15 *(Russian)* 78−6946
carbide particles, fine microstructural details, characterisation, using EM400 electron microscope 80−24328
carbide phases formation during annealing *(Russian)* 78−6930
carbide structure quantitative analysis using Epiquant analyser quantitative analysis using Epiquant analyser *(German)* 80−3284
carbon steel water tubes in alkali loaded solvents, corrosion speed investigation *(Hungarian)* 78−48559
carbonitrided, case struct. investigation by warm electrolytic etching 80−35414
carbonitrided, nature of dark component, metallographic exam. 78−19978
carbonitriding, gas, N, saturation 79−57152
carbonitriding high-speed, struct. and props. 79−57155
carburisation, calc. of mass transfer in diffusional saturation 80−24676
carburisation by polymer paste, exam. of saturation 80−16582
carburisation process, diffusion modelling 80−108632
carburised, alloying effect on props., mathematical-statistical determ. 78−19794
carburised, fracture resistance 79−24612
carburised, microstruct. and fracture 79−24658
carburised, with non martensitic microstruct. at surface, fatigue *(Japanese)* 77−48535
carburized, fatigue, non-martensitic struct. effect, rel. to mean stress and residual stress *(Japanese)* 78−7024
carburized, fractography of fatigue fractures 77−86137
steel continued
carburized, wear exam. 79−87738
carburized and quenched, residual stresses *(Japanese)* 80−89262
carburizing, composition effect 80−35432
carburizing, vacuum, case depth 80−100956
carburizing in fluidized bed 78−19951
carburizing in glow discharge methane plasma 79−11724
case carburised, residual stress effect in mech. performance 79−24659
case depth after quench hardening, inspection using coercimeters 80−104377
case hardened cylinders, heat treated, residual stress fields 80−3102
case hardening quality control by ferromagnetic coercive force transducer probes in alloy 45 78−53151
casecarburized and hardened, relationship between fatigue strength and case hardness distrib. *(Japanese)* 79−61782
cast, ductility near melting pt., hot tearing 79−83314
cast, effect of non-uniform struct. on props. 78−84850
cast, equipment for thermal shock resistance determ. 80−55614
cast, fatigue from cast-to-shape notches 77−16679
cast, fractographic features of coarse grained intercrystalline fractures *(Czechoslovakian)* 77−36627
cast, high tensile strength, heat treatment 80−16358
cast, mech. props., fatigue behaviour, influence of microdiscontinuities, review 78−35512
cast, nonmetallic inclusion size frequency distrib. determ. 78−39989
cast, tendency to brittle fracture *(Russian)* 78−56735
cast, thermal fatigue crack propag. *(Japanese)* 79−83305
cast, type 20, exam. of strain characts. in premelting temp. range *(Russian)* 79−29140
cast 20KhML, deform. resistance and low cycle fatigue in pure shear creep effect 78−3192
cast automatic couplings, yield strength, crack propag. resistance and ductile-brittle transition temp. 80−104281
cast billets, influence of hot working on internal cracks 79−83242
cast continously, segregation at halfway cracks 80−60869
cast high-strength, local integranular fractures, formation mechanism *(Russian)* 78−95795
cast iron-steel mixture, interaction of Zr, formation reaction thermodynamics *(Russian)* 80−55645
cast slabs, formation of longitudinal midface cracks 79−83315
cast steel, heat treatment, effects of explosive loads, radiographic anal. 77−25072
cast steel shot, impact fracture *(Japanese)* 78−92338
cast struct. form. in continuous casting *(German)* 78−92256
cast structural, 20KhGSL, 30KhNML and 40KhL types, heat treatment and mech. working influence on mech. props. *(Russian)* 80−40392
casting, C-scan method of US inspection, developments 79−29294
casting, calc. method of thermal and thermo-visco-elasto-plastic processes *(German)* 80−79859
casting, meas. and significance of residual stresses 80−21253
casting defects, NDT 78−27690
casting surface alloying feasibility trials 79−83395
castings, type 27KhGSNL, exam. of cracks due to heat treatment 78−44205
castings for use at high temp., correlation between US and radiographic inspection *(German)* 78−88599
cathodes, phosphate pickled mild steel, behaviour during deep electrolytical water enrichment, T meas. 80−93764
cementite coarsening in type 1080 in a temp. gradient 78−88486
cementite migration in temp. gradient 78−44151
cementite phase evolution during annealing *(Russian)* 77−32836
cementite precipitation from binary alloys, hardness and Mossbauer effects 77−70054
centrifugal casting method, and high frequency induction melting, sample prep., emission spectral anal. 77−48367
CERN Super Proton Synchrotron beam-splitting steel septum magnets 79−31295
Charpy V-notch toughness test, computer simulation 79−70138
chemical microinhomogeneity recovery during thermal working *(Russian)* 78−15442
chemicothermal treatment quality control by fractographic method 79−39080
chevron fracture in tube reduction by spinning in alloys 7178 and M580 78−64664
chromoaluminosiliconising with electroheating, for oxidation resistant coatings 79−52457
circular hot rolled stock, magnetic inspection of external surface, zond automated installation 79−79210
cladding, proposed mechanism for internal cladding corrosion in LMFBR mixed oxide fuel pins 79−8384
clean steel, review 80−84839
cleaning corroded surfaces for electron microscope exam. by cathodic polarisation 79−70242
cleavage fracture model at low temperatures *(German)* 80−35293
coated with Al and Cr, structural transformations, oxidation effect in Kh25N20S2 steel 79−57154
coated with plasma-sprayed Ni-Cr (80, 20 wt.%) alloy, coating struct. and mech. props. 79−96222
coating, Al, on steel by thermal decomposition of alkyls 78−15590
coating, CVD of Cr_7C_3 79−83393
coating, TiC_x refractory layers by CVD 80−39471
coating applied by explosive energy, adhesive strength 77−70235
coating by boronising, sliding and abrasive wear, corrosion resist. 78−11428
coating with Al_2O_3 and Al_2O_3-TiO_2 by detonation technique, wear resist., antifriction 78−60877
coating with Ta by CVD 78−15594
coatings for corrosion protection, data sheet 79−70211
coatings of Zn and Sn, X-ray fluorescence thickness meas. 77−55884
coercimeters with attached electromagnets used for quality control 80−108672
coercive force, differential meas., appl. to ELA steel 77−71351
coercive force measurement method of quality inspection of heat and thermomechanically treated parts 79−5113
cold crack formation following laser welding *(Russian)* 79−38938
cold cracking resistance under continuous multipass welding 78−39911
cold drawn prestressing tendon, rational test for stress corrosion cracking 78−44246
cold drawn wire, anisotropic fracture *(Russian)* 77−1867
cold formed tubes, residual stresses 79−61605

steel continued
cold plastically deformed, exam. of structure of diffusion layers after borating *(Russian)* 79−34054
cold resistance determination, quick method 80−100997
cold rolled, deep drawing, continuous annealing effect on mech. props. *(German)* 77−90362
cold rolled, high strength, mech. props. 77−36527
cold rolled high strength sheet, with high drawability, fabrication process 77−73288
cold rolled strip, surface defects, online automatic system, design study 79−34231
cold strained, defects interaction with carbide strengthening phases, carbide decomp. degree *(Russian)* 80−84955
cold worked, alloying additions effect on 200°C internal friction peak *(Russian)* 77−8867
cold worked, cementite state, gamma-reson. study, plastic deform. *(Russian)* 78−68706
cold worked, heat treated, electromagnetomech. props. NDT 79−4980
cold worked FV548, electron irradiated, void swelling after 10 ppm He preinjection 77−19989
cold worked layer of used railroad rail, Rayleigh wave dispersion 79−1014
cold-formed, NDT of mech. props., coercimeter results 79−34240
cold-rolled, corrosion resistance in 1M $LiAsF_6$/THF, suitability for organic electrolyte Li secondary batteries 79−100387
cold-rolled, isotropic, specific magnetic loss meas. at high frequency 80−101808
cold-rolled sheet, St10 kp, St10 sp, mag. inspection by ferroprobe coercimeters 80−21234
cold-worked, alloying elements effect on cementite decomp. during plastic deform., Mossbauer study 79−82900
column design, I-section, braced multi-storey, torsional buckling at limit state of collapse 78−1586
combined saturation with C, N and O by chemicothermal, surface treatments, oxidation carburisation 78−95856
commercial, type In-787, for use in Arctic, low temp. effects on mech. props. 80−76310
compact specimens, finite element analyses of dynamic stress intensity factors, and crack arrest stress intensity factors 79−61732
compliance correction for determining load-line energies for compact fracture toughness specimens 79−57186
components, dimensional stabilisation, thermoplastic treatment *(Russian)* 80−20960
components, safety anal. for loading conditions 78−39979
composite, bronze surface, water lubricated bearing material, manufacture, friction, corrosion and erosion 78−11341
compressive strain induced austenite transform. 77−86027
in concrete, cathodic protection 79−70216
concrete, prestressed, low-temp. tensile strength and linear expansion coeff. of reinforcing steel 80−30051
concrete bearing with steel inserts in precast column to beam connections, load capacity determ. 77−73427
concrete-steel composite T-beam, third point loading tests, ultimated flexural strength determ. 77−86252
cone, phase velocity of longit. impact wave *(Japanese)* 78−9600
construction type, spectrochem. determ. of Ca 78−7275
constructional, EI736, creep, viscosity, resist. to inelastic deform. 80−89309
constructional, EM field distribution, wave impedance, power loss derived 77−23595
constructional, fracture toughness in cyclic loading 78−72860
constructional, fracture toughness testing, cracks critical opening determ. *(Russian)* 79−52479
constructional, nitriding process in glow discharge *(Russian)* 80−55560
constructional, struct., props., isothermal thermomechanical working *(Russian)* 77−25076
constructional 15Kh2NMFA, fatigue crack development *(Russian)* 79−29174
constructional material, K_{1c} determ. from mech. props. and struct. parameters *(Russian)* 77−60010
constructional materials, brittle failure resistance, calc. charact., expt. methods 77−77662
contact, rapid meas. tech. for electrical contact resistance applied to lubricant additive studies 77−16698
contact fatigue life of S-P type extreme pressure additive lubricated surfaces 79−47780
contact resist. in working media in static, dynamic loading, testing unit 79−15900
continuous casting, thermal, thermo-visco-elasto-plastic processes *(German)* 80−81044
continuously cast, macrosegregation, effect of electromagnetically induced fluid flow 77−73256
continuously cast, optimum conditions for annealing castings during dynamic working *(Russian)* 78−44134
continuously cast, tensile strength and ductility above 800°C 80−55476
continuously cast slab, liquid-solid interface obs. by Pb additions to mould 77−21128
core/sheath tube system, non-fracturing core, stress transfer mechanism 77−52454
corroded, Mossbauer effect anal. of corrosion products 78−19943
corrosion, Na loop system, analysis of radioactive corrosion product transfer 78−78464
corrosion, nature of iron sulphides in H_2S-O_2 environment 79−96195
corrosion and organic coatings, possible Mossbauer studies 80−39988
corrosion and polarization and electrocapillary behaviour in H_2SO_4, radioactive n-dibutyl sulphide effect 79−70215
corrosion by seawater, cathode protection using Si solar cells 80−40859
corrosion cracking of 20GS2 and 20KhGS2 high-strength reinforcing bar steels 80−55578
corrosion cracking of spherical liquid NH_3 storage tanks *(Japanese)* 77−21316
corrosion cracking resist. of ferrite-austenite welded joints *(Russian)* 79−52437
corrosion cracking susceptibility, C and Cr effects in 23Kh2G2T 78−19952
corrosion fatigue, steady-state electrode pot. in sea water under cycle loading *(Russian)* 78−56802
corrosion fatigue and crack growth in salt water, of HY130 78−72929
corrosion fatigue crack growth, compliance tests and metallographic exam. 78−53027
corrosion fatigue crack growth in HY80 and HY130 79−79174
steel continued
corrosion fatigue during anodic polarisation after thermomech. treatment *(Russian)* 77−59976
corrosion fatigue inhibitor for $MnCl_2$ soln., use of quaternary pyridine salts *(Russian)* 77−59973
corrosion fatigue kinetics of 45 and 10KhN4MDF, low cycle loading by pulse extension *(Russian)* 78−31578
corrosion fatigue of offshore structures 79−79170
corrosion fatigue strength, 40KhNMA, effect of polishing and diamond smoothing *(Russian)* 78−31575
corrosion fatigue strength, influence of magnetite films and environment *(Russian)* 79−52433
corrosion fatigue strength of St-3 and 45G17Yu3 effect of paint coatings on strength in seawater *(Russian)* 78−31572
corrosion in NH_3 and NH_3-N_2-H_2 mixture at high press. and temp., testing unit 77−56174
corrosion in Pb bath up to 1400K, corrosion prevention *(German)* 77−90482
corrosion inhibitor action ellipsometric obs., of propargyl alcohol, film growth on steel surfaces *(Rumanian)* 80−60996
corrosion of off-shore structure in splash zone 77−59996
corrosion of radioactive waste form containers 80−18493
corrosion potential/time, and potentiostatic polarisation curves as a method of predicting corrosion 80−45419
corrosion protection, NAA obs. 78−53038
corrosion protection by coating, economics *(German)* 79−39054
corrosion protective coating, phosphate binder based 79−79151
corrosion protective organic coating failure by contamination 77−90486
corrosion protective props. of diammonium salt-based inhibitors *(Russian)* 78−56808
corrosion protective props. of N-containing inhibitors *(Russian)* 78−56809
corrosion resistance, effect of diffusion Fe plating *(Russian)* 77−70208
corrosion resistance in geoethermal brine environments 78−85032
corrosion resistance rel. to electroerosion treatment conditions *(Russian)* 79−15848
corrosion resistant coatings 77−56141
corrosion stability to double iodate-iodide salt melt in H prod. *(Russian)* 80−55593
crack branching, in A533B 78−64705
crack detectability by radiography 79−91857
crack detection, single probe US technique, NDT 77−66732
crack detection using image quality indicators, comparison 77−25232
crack electrochemistry model in active state 80−21192
crack form. during continuous casting 78−7038
crack growth velocity in gaseous H_2 embrittlement, rel. to chemisorption 80−11831
crack initiation, impurity effects, dynamical loading *(Czech)* 80−60955
crack initiation detection by AC potential method *(Chinese)* 80−21196
crack movement rate during cyclic deform., internal microstress effects 78−3225
crack opening displacement appl. to fracture toughness eval. *(Italian)* 79−52378
crack opening displacement in deeply notched specimens 78−27617
crack propag. in ductile struct. 78−68805
crack propagation, struct. effects 79−52370
crack propagation properties in rotating bending fatigue tests 77−32669
crack propagation stress wave obs. of brittle fracture *(German)* 77−56110
crack resistance, −196 to 500°C 80−71750
crack resistance, J-integral approach, crack line wedge loaded specimen 78−35513
crack resistance, J-integral approach 77−66699
crack resistance, reduction in surface-active media *(Russian)* 79−52441
crack tip opening displacement and J-integral criteria 77−3777
crack tip studies, stretched zone and COD 78−68812
crack-resistance limit and stress analysis in the ductile state 80−81188
cracking due to H_2S, exam. of fracture surface by SEM *(Japanese)* 78−53024
cracking resistance of high-strength 40Kh and 35KhGSA, tempering temp. influence *(Russian)* 79−52252
cracking resistance under impact loading *(Russian)* 77−25138
cracks, steady diffusion-migration eqns., representing mass conc. of dissolved species 80−30108
cratered overheating facets 77−52482
creep, and plasticity charact., stress state influence rel. to cyclic stress intensity change 79−87694
creep, rupture of structures subjected to variable loading and temp. 77−3786
creep and creep fatigue *(Czech)* 77−86089
creep and fatigue fracture prevention 78−60837
creep curve prediction, force factor and Dom relationship *(Russian)* 78−18185
creep fracture, temp. effect on data scattering 79−74258
creep rate mismatch interaction in stress relief cracking 80−97578
creep resistant, fine grained, structural, welded-joints, cause of cracking during stress relieving *(German)* 77−70141
creep resistant, rare earth metal effect on inclusion charact. *(Czech)* 77−86134
creep strength under high H_2 press. *(Russian)* 78−35423
creep-resistant, creep rupture under variable stress and temp. *(German)* 79−24597
creep-resistant influence of temp., holding time, cooling rate on formability *(German)* 78−84901
creep-respective strength and fracture mode of 12 MKh in H_2 *(Russian)* 77−52461
critical strain rate in type 20 steel 80−16399
cryogenic, creep, review 80−104222
crystal growth from melt based on Czochralski method, for material with high phase transform. temp. 78−23599
current pulse effects on structure at crack tip *(Russian)* 77−44332
cutting, high-speed, hardened by quenching, nondestructive testing 77−90559
cutting and grinding, surface adsorption effects 78−39938
cutting cemented carbide grade, HfN coating 79−24667
CVD coating temp. effect on hardness and dimens. stability 77−40470
CVD coating with Ti(CN) for abrasion resist., deposition parameter depend. 77−40471
cyclic crack opening displacement behaviour during high-amplitude block loading 80−45375

steel continued
cyclic creep and mean stress influence on fatigue life *(Czech)* 79−43403
cyclic fatigue loading, effect of plastic zone size, −196°C to room temp. *(German)* 79−1915
cyclic stress-strain and failure testing, effect of meas. stress and mean strain *(German)* 77−21338
cylinder, quenched without transform., residual stresses *(German)* 80−25725
cylinder impact on rock half-space 80−85649
cylindrical bar loaded by longitudinal impact, dislocation struct. and plastic deform. *(Czech)* 78−60713
cylindrical ingot, continuous casting, elastic-plastic temp. stresses and deformation *(Russian)* 79−61576
cylindrical parts, hardness inspection by EM method with higher harmonics 78−23891
cylindrical shells, external static+pulsed press., stability *(Russian)* 77−46952
cylindrically layered conductors, electromagnetic NDT 79−74318
damping capacity of VNS-5 77−1849
damping props., effect of plastic deform. by torsion 77−70095
decarburised layer effects on fracture toughness of 60S2 77−59930
defective zones in cold rolling, activation analysis method 78−7278
defects, microdefect behaviour in steel 12X18H10T *(Russian)* 80−19793
deform. resist., softening effects, analytical depend. calcs. *(Russian)* 80−49293
deformability, H_2 absorption effects *(Russian)* 77−77561
deformability characts. in surface-active medium at decreasing temp., mech. working effect *(Russian)* 77−59851
deformation, under conditions of superplasticity of type 0Kh12G14N4Yu2, struct. 80−21031
deformation ageing of 40Kh, effect on impact resistance and tensile strength *(Russian)* 78−31427
deformation and fracture resistance due to low-cycle fatigue in plane bending 79−66166
deformation and stresses during elongation, application of Ludwig eqn. *(German)* 80−40475
deformation anisotropy in yield point, precompression effects *(Russian)* 78−11268
deformation at large plastic strains, work hardening rate 79−20065
deformation ht. treatment as carbonite precip. 77−63700
deformation microheterogeneity and ductility in 45 and U7 77−73309
deformation process, stage-by-stage nature investigation using acoustic emission *(Russian)* 80−40434
deformation strengthening, of bayanite phase in type KVK *(Russian)* 80−100851
deformation under mutual indentation in contact with Li melt *(Russian)* 77−59853
deformed, potential distrib. meas. technique, appl. to corrosion study, apparatus *(Japanese)* 78−53049
deformed 20Kh type, austenite grain size, inheritance effect with quenching and tempering 80−60881
deformed strain-aged St.3 and 09G2S, stress conc. susceptibility, H_2 effect 78−95774
delayed fracture, hydrogen and impurities 78−84988
deoxidation by Ca-Si alloy, thermodynamics *(Russian)* 80−16268
deoxidation effect on fatigue and endurance limit in wear tests varying P and S content *(Russian)* 78−35523
deoxidised, AlN and V carbonitrides precip. effect on mech. props. *(French)* 80−45311
detector designed to meas. retained austenite 78−35602
determination of C, Si, Cr, Mn, Ni by spectrographic method using combined discharge 79−57327
die steels with high heat resist. and toughness 78−84989
die type, vacuum quenching parameters 79−38861
die type 5KhNM, stressed state effect on softening 79−66168
dies, durability improvement using isothermal hardening in salt bath 80−35198
diffusion and distribution of S in St3 and 12Kh18N9 78−2306
diffusion chromizing of sintered steel 77−66607
diffusion coating for protection against H_2 effect on mech. props. 78−31589
diffusion coatings, carbide and boride, props. *(Russian)* 79−52443
diffusion phenomena determ. between coated metal carbide and steel *(German)* 78−15623
dimple fracture, relation between inclusions and morphology *(Chinese)* 79−74231
disintegrated stream, simplified model of oxidation 77−73373
dislocation density, problems of X-ray determ. from one diffraction line *(German)* 78−2129
dispersion hardening type 0Kh12NDL, cast, resistance to cold crack formation during welding 79−87731
dispersion strengthened with Al_2O_3 or ZrO_2, by spray method into molten stream, exam. of mech. props. 79−11636
dissolution in HNO_3, thermometric method of rate estimation, a limitation 77−56138
distribution of H_2 in 12Kh18N10 and 12Kh18N10T after 12 days in the H_2-T_2 mixture *(Russian)* 77−7752
double lapped composite joints, efficiency in bending, with B reinforced Al and epoxy 78−68870
double martensitic transformation, distribution of austenite orientation in N31 and N26khT *(Russian)* 78−64540
double-layer, adhesion strength determ. method 77−63857
drill tubing, exam. of cyclic cracking resistance *(Russian)* 79−15767
dual phase, C1020, mech. behaviours and structs. *(Korean)* 80−25779
dual phase, improved etching technique for percent martensitic determ. 80−16624
dual-phase, notched, fatigue 79−100253
ductile, PWR pressure components, mechanical factors affecting reliability *(French)* 79−20198
ductile fracture, rel. between plastic deform. in fracture zone and fracture characts. *(Russian)* 77−52457
ductile fracture in presence of elongated sulphides *(French)* 80−45394
ductile structural, crack resistance and cohesive strength 80−50722
ductile structural, fatigue crack propag. rate and striation spacing 80−93635
ductility anisotropy in 14Kh17N2 77−70119
duplex reinforced metal sheet, fatigue crack growth 77−28894
duplex reinforcing member behaviour under cyclic loading, core element geometry effects 77−28894
steel continued
dynamic fracture initiation in types 4340 and 1018 80−35333
dynamic fracture toughness meas. by instrumented impact bend and compact K testing 77−36718
dynamic fracture toughness testing 77−77650
dynamic testing, wave propag. effects on dynamic loading of pressure vessels 77−3090
dynamic testing by resonant flexion, energy consumption for degradation *(French)* 78−19961
eddy current losses, estimation method, in large steel plate having one-phase excitation *(Polish)* 80−93145
eddy current surface crack detection *(French)* 79−61831
elastic constants, meas. app. 77−33739
elastic moduli, temp. depend., −196 to 1000°C 80−6451
elastic moduli, temp. depend. *(Japanese)* 77−59840
elastic moduli, temp. depend. *(Japanese)* 80−25750
elastic-plastic fracture, plastic zone correction application 79−70147
elastic-plastic plane-strain crack growth, comparison of theory and experiment 80−108560
elastoplastic bending of beams of various cross section 78−3196
elastoplastic props. in explosive loading 78−6999
electric, EO-100 and E-11, surface cleansing with ML-51 combined with monoethanolamine, corrosive action study 79−39052
electric arc sprayed coating on wire, elastic and elastic-plastic props. *(German)* 79−34089
electric field effect on strength, hardness 80−50714
electric generator type, anisotropic mag. props. obs. using NDT 80−21212
electric sheet, hot-rolled, recrystallization and texture formation during ht. treatment 77−44271
electric steel, induction above magnetisation curve knee from pole density texture 77−12151
electrical, crystal orientation and dimension determ. by magnetic method 79−70278
electrical, mag. props. determ. with Epstein hysteresis tester 80−60364
electrical sheet, wattmeter unit for measuring specific losses, system errors 79−91893
electrical steel sheet, magnetostriction meas. using Hall effect transducer *(German)* 80−13111
electrical steel sheet, systematic and random errors, in wattmeter apparatus for measuring unit losses 80−71858
electrical steel sheets, specific core loss meas. using analogue wattmeter *(German)* 80−13099
electrical steel strips, grain-oriented, effect on stress-relief annealing treatments on permeability and ageing 78−23832
electrical steel strips, grain-oriented, effects of ageing on mag. AC permeability 78−23833
electrode for discharge sintering of metal powders, effect of diffusion coatings 77−63598
electrode for electric discharge sintering, metal powder+punch electrode reactions 78−11148
electrode material, influence on electric breakdown in dielectric liquids *(Russian)* 80−50265
electrodeposition stress meas., X-ray methods 79−29298
electrodes, pitting corrosion currents rel. to conc. of inhibitive and corrosive anions under corrosion conditions 80−85181
electrodes, polymer film coated, prep., characterisation, electrochem. stability 78−76866
electroless Ni plated, fatigue strength, effect of P content of Ni film *(Japanese)* 77−52478
electrolytic Zn coatings on steel, adhesion strength determination by centrifugal method 77−56149
electrolytically notched, in direct evidence of active path formation in stress corrosion cracking in Al-alloys 80−85077
electron bombardment effects, gas evolution obs. *(Russian)* 79−1460
electron emission depend. on surface mechanical treatment *(Russian)* 80−100945
electron microdiffr. determ. of orientational correls. between ferrite and cementite 77−52584
electron microscopy, conf., Nancy, France (May 1978) *(French)* 79−41915
electron microscopy on etched thin foils, comparative SEM, STEM and TEM analysis 80−100144
electroplastic drawing, type of Kh13N13M2, magnetically hard wire *(Russian)* 80−20967
electroplated with chromated Zn, corrosion rel. to chromate content 79−20286
electroplated with Cr, laser treatment 80−21191
electroslag refining, O_2 removal *(Russian)* 77−55903
electroslag welded sheet, impact strength and toughness, welding effect *(German)* 77−86139
electrospark alloying to Ag, residual stresses obs. *(Russian)* 77−56145
electrospark machining, appl. of W_2B_5- and Mo_2B_5-based alloys as electrodes 80−21174
electrotechnical, single strips, mag. props. meas. using AC compensated permeameter 80−86352
electrotechnical steel, quality significance on energy and materials savings in magnetic circuits *(Czech)* 80−20947
elemental distribution measurement, using STEM 80−35601
embrittlement by impurity segregation 79−8367
embrittlement mechanism, microcrack formation, dislocation model *(Russian)* 80−65143
emission spectrochemical analysis, use of quantitatively coupled plasma quantometer *(Japanese)* 78−83624
emission spectrometric, determ. of Al *(Japanese)* 80−16750
emulsion, magnetic and dielectric, prep., as rubbing sludge *(German)* 78−3376
endurance, effect of surface diffusion alloying 77−81344
endurance limit, effect of residual stresses caused by Cr plating and cyaniding 77−86184
energy absorption during uniaxial tension and axial compression, geometric and heat treatment effects 77−73312
energy dispersive X-ray fluoresc. spectrometry, computer directed optimisation 80−45585
enhancement of delayed failure resistance by partial unloading method, environment effects 79−79146
epoxy-steel system, friction and wear 78−44229
erosion by high-press., high-temp., short gas pulse 78−7092
eutectic, fatigue life improvement by thermomech. processing 80−25732
eutectoid, activation energy of oxidation in wear 77−52507

steel continued
eutectoid, fatigue crack tip props. in rotary bending and cyclic torsion 77−32668
eutectoid, superplasticity parameters 77−56042
eutectoid and hypoeutectoid, time-temp.-austenization diagram *(Japanese)* 78−6900
eutectoid and hypoeutectoid viscoelasticity under transformational superplasticity *(Japanese)* 77−52416
explosive welding to $Ni_{40}Fe_{40}B_{20}$ glass alloy, rapidly quenched 78−39954
extrusion effects on struct. and mech. props. *(Russian)* 77−56022
faceted Mn sulphides in 45, 17G2AF, 55S2 and 60S2, formation on crystn. dendrites *(Russian)* 80−50621
failure assessment method and fracture mechanics 78−48488
fast fracture and crack arrest, finite difference anal. 78−1607
fast fracture toughness 77−44362
fast reactor irradiated, solution treated, type AISI 316, struct. 77−69008
fast reactor structural materials, meas. and calcs. of integral capture cross-sections 80−13613
fatigue, effect of active liquid media on struct. and stress condition *(Russian)* 77−28929
fatigue, impact loading, friction, wear in surface active media *(Russian)* 79−29268
fatigue, low cycle, hysteresis loops, cyclic strain curves, fatigue diagrams *(Polish)* 80−66638
fatigue, low cycle, in type 20 exam. of damage accumulation rule, for loading in air and H impregnating medium 78−64649
fatigue, low cycle, test results, least square deviation method 77−63796
fatigue, low cycle *(French)* 77−28903
fatigue, low-cycle, of SW7M at high hardness levels *(Polish)* 80−89323
fatigue, total life estimation of notched and cracked members 79−77015
fatigue, variable and constant amplitude 79−61711
fatigue analysis, random, of structural bars subjected to plastic bending *(Japanese)* 78−27619
fatigue and cyclic plasticity rel. to struct. inhomogeneity 80−81184
fatigue crack, decrease in growth rate after thermal treatment and reduced load *(Russian)* 77−25142
fatigue crack depth meas. by US technique 77−9006
fatigue crack detection, potential-drop meas. system 79−34225
fatigue crack development, 15Kh2NMFA, loading freq. effect 79−87727
fatigue crack growth, delayed retardation phenomena, stress ratio at baseline loading effect 79−79065
fatigue crack growth, delayed retardation phenomenon, from single overload in SNCM8, HT80, A553 78−92317
fatigue crack growth, exam. of some aspects 78−56772
fatigue crack growth delay in 4140 steel, yield strength, neg. stress ratio depend. 78−3210
fatigue crack growth eqn., correlation of threshold stress intensity factor, review 79−34127
fatigue crack growth prediction, under variable amplitude loading history 78−18233
fatigue crack growth rate, intensity of random fluctuation in type CSN 12060 *(Czech)* 80−30079
fatigue crack growth rate in air and saltwater, stress ratio effect 80−100952
fatigue crack growth rate of A516-60 press. vessel steel 77−77585
fatigue crack growth testing, 1045, decreasing stress intensity technique, computer-controlled 78−72949
fatigue crack init. at notch tip, early stage propag. *(Japanese)* 78−7021
fatigue crack initiation and microcrack growth 79−24617
fatigue crack length determ. in fracture mechanics by electric potential technique of RSt 37-2 *(German)* 78−15486
fatigue crack propag., metallographic and fractographic anal. in type A533B 79−83325
fatigue crack propag., single overload effect 77−86170
fatigue crack propag. and crack closure behaviour, under various loading conditions for steel WT 80C 78−68795
fatigue crack propag. data, Weibull anal. 80−16416
fatigue crack propag. data anal., new method 77−73321
fatigue crack propag. in weld 77−81324
fatigue crack propag. kinetics *(Russian)* 77−70146
fatigue crack propag. near to threshold stress intensity 80−100898
fatigue crack propag. rate and stress intensity factor at varying stress ratio 78−7049
fatigue crack propag. under random loading 78−76726
fatigue crack propagation, kinetics 78−68804
fatigue crack propagation, quantifying the parameters 80−100891
fatigue crack tip plastic deform., X-ray diffr. investigation *(Russian)* 80−104251
fatigue cracking, statistical theories of scale effect, expt. verification *(Russian)* 77−28884
fatigue cracking diagrams *(Russian)* 79−29301
fatigue cracking kinetics in drilling soln. *(Russian)* 77−25183
fatigue cracking under cyclic bending of 17KhG2SAFR, 45, and 40Kh *(Russian)* 78−31506
fatigue damage and crack propagation, classification zone approach 77−56106
fatigue damage in 12Kh18N10T and 03Kh13AG19, possibilities of inspection on basis of change of natural oscillations freq. 79−57116
fatigue damaged, fracture toughness 80−89353
fatigue endurance tests in moist H_2S *(Russian)* 78−31510
fatigue failure, temp. effect *(Russian)* 78−88517
fatigue failure of 1Kh17N2Sh, surface finishing influencing 80−60972
fatigue fracture near slot shaped stress concentrators 77−1870
fatigue in gaseous H_2 of Kh16N6 *(Russian)* 78−31509
fatigue in surface active media, adsorption facilitation mech. 80−55586
fatigue life, influence of cyclic loading conditions 80−76350
fatigue life, load sequence effects *(Polish)* 79−34135
fatigue life, structural parameters and chem. comp. effects, rel. to test parameters 77−59928
fatigue life enhancement by ion implantation 79−1910
fatigue life estimates, of bluntly notched members 80−100999
fatigue life prediction for fillet welded attachments, under service loadings 78−64683
fatigue life scatter and loading conditions reproduction methods 77−70262
fatigue limit, static and cyclic loading 80−71755
fatigue limit assessment, progressive load methods *(German)* 80−61058
fatigue limit estimation when subject to bending loads 77−21281
fatigue limit in inhibited H_2SO_4 soln., halide anion effects *(Russian)* 78−11399
fatigue reliability under multiple-amplitude loads 79−79072
fatigue reliability under random loads 79−79066
fatigue resistance, of type 1018 in sea water, specimen size and freq. effect 80−93678
fatigue resistance of heat-resistant 12Kh1MF, 15Kh1M1F and 1Kh18N12T at normal and elevated temps. 77−90466
fatigue strength, effect of residual stresses and cold working 77−56101
fatigue strength, effect of tensile and rolling prestrains 77−52455
fatigue strength, low cycle overload effect 80−60967
fatigue strength, low cycle steels and welds, relationship to static tensile props. 78−64684
fatigue strength, low-cycle, under severe loading, friction-strengthening treatment effect *(Russian)* 79−52435
fatigue strength, short cycle, stress concentration effect 78−95859
fatigue strength, statistical prop. *(Japanese)* 79−20169
fatigue strength, tempering effect 80−60891
fatigue strength and residual stress distrib., machining method effects in ShKh15 78−31528
fatigue strength determ. apparatus, in corrosive environmental under complex stress *(Russian)* 77−77657
fatigue strength during two-freq. loading, stress conc. effect 79−52347
fatigue strength of 30 KhGSNA, 12 KhN3A, effect of friction in abrasive medium, after hardening 78−35507
fatigue strength on combined surface strain-hardening and tempering *(Russian)* 77−59900
fatigue strength testing of steel shafts up to 280 mm diameter 80−3184
fatigue strength under fretting corrosion, effect of plasma-sprayed coatings on 30KhGSA *(Russian)* 78−11394
fatigue strength with stress concentrator, mean compressive stress effect 77−21264
fatigue substructures after high cycle vibrs. of plates 77−8945
fatigue testing, exam. of scale relationship of endurance limit 78−60914
fatigue testing, low cycle, effect of testing method on fatigue 79−52515
fatigue tests, low cycle, material variance distrib. law, type 15Kh2NMFA 79−91799
fatigue under in-plane combined axial loading and torsion in type JIS-SNCM8 79−96147
fatigue with programmed loading, damage accumulation, nomogram 79−38964
fatigued steel brittle transition temp. meas. by hardness testing *(Japanese)* 79−87797
FBR developments, low swelling and creep at high neutron fluences 79−22374
ferrite, 15Kh1M1F, microstruct. changes rel. to creep and fracture *(Russian)* 79−24572
ferrite, transform. kinetics, grain size, alloying element effect, carbide precip. 80−93560
ferrite and dual phase, mech. props., effect of Si and P 79−57063
ferrite grain size, and comp. influence on Ludwik eqn. constants *(German)* 80−81107
ferrite-austenite transition, diffusion const. of C and carburisation rate consts., thermopower meas. 80−89216
ferrite-austenite welded joints, corrosion cracking resist. *(Russian)* 79−52437
ferrite-cementite mixtures, austenite form., HVEM obs. 77−66639
ferrite-pearlite, fatigue crack growth rates, stress ratio dependence 79−70148
ferrite/steel composite bar magnet, large size, for mobile appls. 78−93740
ferritic, base material for powder flame spraying process, intercrystn. corrosion *(Czech)* 80−30158
ferritic, C and N migration at low temps., monograph 80−22149
ferritic, Charpy impact testing criteria 79−47855
ferritic, clad with austenitic steel 309, US detection of undercladding microcracks *(Italian)* 80−108683
ferritic, corrosion resistant, review of heat treatment, mech. and corrosion resist. charact. *(Korean)* 79−24653
ferritic, Cr-Mo, less than 12 wt.% Cr, sensitisation dring welding to intergranular corrosion 78−88566
ferritic, crack extension, cleavage micromechanisms, review 80−108562
ferritic, creep resist., high-temp. props. residuals effect 80−66600
ferritic, criteria for Charpy impact testing 80−7752
ferritic, FV607, void swelling, theory 78−71763
ferritic, FV607, void swelling in 1 MeV electron irradiation 78−71762
ferritic, impurity defect interaction influence on radiation hardening and embrittlement 80−35199
ferritic, low to intermediate strength, fracture toughness, upper shelf temp. depend. 77−73330
ferritic, MA 956, oxide dispersion strengthened, mech. props. and damping behaviour 79−47702
ferritic, underclad cracking mechanism, effects of residual strain and heat affected zone ductility 77−25158
ferritic, with interstitial N, continuous precipitation and clustering 80−7585
ferritic and austenitic, corrosion in NaOH contaminated Na *(French)* 77−52541
ferritic disc, biaxial fatigue testing under changing temps. *(German)* 80−71759
ferritic weldments, characterisation of non-planar defects by ultrasonic testing 79−87812
ferritic-pearlitic, X-ray elasticity constants *(German)* 80−30004
ferritic-peralitic, fatigue crack development load-cycle asymmetry coeff. effect 79−87710
ferrography of polymer form. under lubricated nibbing contact 77−21292
ferromagnetic, transduction efficiency using magnetostrictively coupled meander-coil EM transducers 79−46144
ferromagnetic 2Kh13, rod, coupled flexural and torsional vibrs., energy dissipation 80−89281
ferromagnetic materials, coercive force determ. *(Russian)* 79−73764
ferromagnetic round bar, eddy current crack detection *(German)* 79−91880
fibre reinforced Al_2O_3-Al, production and mech. props. 80−11619
fibre reinforced Al, fibre orientation effect on strength *(Korean)* 80−30027
fibre reinforced Al, fracture mechanics under fatigue *(Czech)* 78−64629
fibre reinforced Al, thermophys. props. 80−59745
fibre reinforced Al, vacuum hot pressing, strength *(Czechoslovakian)* 77−32543

steel continued
fibre reinforced Al alloy, corrosion resistance, electrochemical characts. 80−11806
fibre reinforced Al alloy, stressed state nondestructive testing method *(Russian)* 80−40631
fibre reinforced Al alloy D16T, sheet reinforced by Ti alloy butt straps, fatigue 79−100262
fibre reinforced Al composite, role of brittle layers at elevated temps. 79−96135
fibre reinforced cement based beams, flexural strength, fibre pull-out 77−56020
fibre reinforced cementitious material, radiographic anal. of fibre distribs. 78−52747
fibre reinforced concrete, strength problems 77−4844
fibre reinforced concrete, tensile strength and ultimate strain *(Polish)* 80−21027
fibre reinforced concrete, vibr. compaction, pressure compaction and curing *(Japanese)* 80−89179
fibre reinforced concrete *(Japanese)* 77−4762
fibre reinforced Cu, exam. of creep behaviour *(German)* 78−52931
fibre reinforced Cu, fatigue 79−29221
fibre reinforced Mg, fibre-matrix interfacial reactions 80−20043
fibre reinforced Pb, fabrication, mech. props. *(Korean)* 77−12579
fibre reinforced silicon rubber composites, interfacial slip and damping 79−5010
fibres, polycrystalline, Mossbauer spectroscopy 80−44959
fibrous composite, short steel wire reinforced (polymer impregnated) concretes, cracking and toughening 78−80626
fibrous crack extension, micromechanisms 80−108563
fibrous cracking, COD and initiation, replication technique on HY 100 and 130 77−56069
fillet weldment of ASTM A588, fatigue test, practical aspects of analysis 78−64682
FIM atom probe microanalytical expts., review 78−35622
fine structure, effect of isothermal transform. temp. 77−21137
fine structure after heat treatment, X-ray diffr. exam. 80−60890
finite life characteristics, notch effects *(German)* 77−90434
finite life characteristics, temperature change effects, torsion cycle tests *(German)* 78−7004
fire simulation, determ. method of critical value in case ofnonstationary heating *(German)* 77−86268
first order phase transformations, in non-isothermal conditions, exam. of kinetic parameters *(Russian)* 79−34028
fission reactor, choice based on high energy neutron irradiation *(French)* 78−8902
fission reactor material, defect development in contact area with coolant *(Russian)* 80−57859
fission reactor pressure vessel, reliability 79−22430
fission reactor pressure vessel surveillance capsule exam., appl. of ASTM standards 79−22436
flaws, detection in macrostruct. of large specimens 79−87777
flocculation detectability factor in US inspection in quality control 78−3268
foil, microanalysis by energy dispersive X-ray spectrometry *(French)* 80−85250
forgings, expt.-calc. model of quenching 80−16345
forgings, untreated surface, US monitoring, sensitivity comparison 80−66751
formability sheet, rapid test for props. assessment 80−40650
fractographic features of rupture, rel. to struct. changes 77−63801
fracture, environmental, metallurgical variables effects, review 77−28887
fracture, intergranular, and solute segregation 80−60957
fracture characterization, implications for reactor pressure component reliability 79−20199
fracture initiation moment, I-integrals critical value determ., ultrasonic method 80−61049
fracture mech. during creep, interference microscopy exam. of 12Kh18N9, 08Kh18N10T 78−56756
fracture mechanics and surface chemistry in water and hydrogen, subcritical crack growth 79−8392
fracture mechanics appl. to H_2 embrittlement under press. *(French)* 78−23821
fracture mechanics parameters, influence of specimen thickness on types RSt 37-2, st52-3, StE70 and 30CrNiMo8 *(German)* 80−66614
fracture micromechanisms, fracture toughness, exam. 78−56766
fracture mode, determ. from shear lip width 80−60968
fracture mode, tearing topography surface fracture 80−7670
fracture of Kh18N10T in low-cycle fatigue tests in H_2 *(Russian)* 80−76332
fracture resistance, delayed, test-piece dimensions influence *(Russian)* 79−52478
fracture resistance, from impact bending tests and oscillograms 80−61047
fracture resistance, low cycle, stress conc. effect on types 4Kh5MFS, 5KhNM, 5KhNMFS 79−87697
fracture toughness, dynamic, interlaboratory data, statistical analysis 77−36717
fracture toughness, fatigue precracking and grain size effect in low alloy St 52-3 78−60782
fracture toughness, influence of low-cycle damage 78−72873
fracture toughness, temp. and loading rate effect 77−36663
fracture toughness and impact strength, correl. breakdown 80−55523
fracture toughness charact. in fatigue 79−15790
fracture toughness data review for pressure vessel steel at upper shelf temp. 79−15797
fracture toughness determ., rel. to mech. props. 77−21277
fracture toughness determ. from fatigue test results in circular bending 78−15526
fracture toughness determ. under developed plastic deform. conditions, construct. steels 77−77664
fracture toughness determination, from crack propagation measurements *(German)* 79−43421
fracture toughness eval. by equivalent energy method *(Slovak)* 79−43402
fracture toughness eval. of small specimens 78−60762
fracture toughness evaluation using oscillograms, optimum heat treatment 79−57169
fracture toughness of nuclear reactor pressure vessels 80−81172
fracture toughness testing, obs. of crack initiation and stable growth processes *(Japanese)* 78−52954
fracture toughness testing at low temps. *(Russian)* 77−25206

steel continued
fracture under low-cycle fatigue in seawater of 15KhN3DMA *(Russian)* 77−52535
fracture viewing under optical microscope by use of impressions 77−56185
FRC, reinforcement parameter 78−79223
free plate elastoplastic stress condition, during phase transformation 78−95781
free-cutting type, inclusion investigs. using EPIQUANT automatic structure analyser 80−55609
fretting, selected fretting resistant surface treatments 79−29223
fretting fatigue resistant coating for steel/Ti-Al-V mating surfaces 78−64721
fretting on polycarbonate, influence of experimental conditions on wear 78−44228
friction, lubrication and wear studies, Mossbauer spectroscopy appl. 80−40547
friction and wear against C and glass fibre reinforced PTFE and polyacetal 78−56783
friction and wear during hot forging 80−89358
friction between steel ball and ice single cryst., load, velocity and temp. depend. *(Japanese)* 78−88537
friction measuring test for use under conditions of high normal interfacial force 80−76454
friction of rubber containing $CuSO_4$ paired with steel, selective transfer mechanism 80−55544
friction pair with polymer, temp. calc. under severe friction 80−40550
friction pairs C steel-antifrictional alloys, electrochem.-mech. investigation *(Russian)* 80−76367
friction stress method for cyclic inelastic behaviour of metals 77−4855
friction with P bronze, lubricant at friction boundary behaviour *(German)* 77−86190
frictional fatigue, microcrank formation in surface layers 77−86193
galvanic corrosion, electrochem. characts. rel. to Al alloys 80−21162
galvanic couple with Al alloys, velocity effect on corrosion 78−35566
galvanised, identification of grains with (0001) orientation, chem. test 79−47853
galvanised, interface struct., scanning Auger microprobe study 80−34322
galvanised, pipe carrying potable water, corrosion 78−92409
galvanised, prepassivation, chem. nature of film and corrosion resist. *(French)* 79−43480
galvanised, with paint coating, adhesion failure, XPS study 80−40671
galvanised coatings, thickness meas. using X-ray fluorescence radiation, apparatus design 80−21202
galvanising process, digital control system for Zn coating distrib. 78−19960
galvanized, thermal oxidation affect on adhesion of polyethylene coating *(German)* 80−35419
gas boronized, sliding wear charact. 80−16499
gas nitrosulphurizing, temp. range 813-903K, wear props., surface and cross-sectional hardness, X-ray diffr. and SEM study *(Japanese)* 79−29224
gas pipe, H_2 press. tests appl. to H_2 transmission 79−74550
glass fibre reinforced plastics, laminated ring with extra steel pin radial reinforcement, mech. props. 80−11714
glass-enamel coatings, effect of firing method on adhesion 79−24647
glued overlapped sheets, strength tests with nonuniform epoxy adhesive layer *(German)* 78−15647
grain boundary failure model for intergranular fracture modes 80−25825
grain boundary migration rate during secondary recrystallisation, N_2 effect *(Czech)* 77−59812
grain boundary segregation of C, atom probe FIM study 80−37134
grain boundary strengthening mechanism 80−35207
grain size dependence of low yield point *(German)* 78−56689
grain size meas., NDT, deep-drawing steel sheet and band, method and instrum. *(German)* 78−85059
grain size spread, quantitative rating method 78−85073
granular model material, equipment for shear deform. investigation *(German)* 80−35449
graphite reinforced epoxy steel scarf joint, adhesively bonded, exam. of failure 78−92350
grinding, effect of hardness, texture, and bond of grinding wheel, temp. effect *(German)* 79−43459
grinding effect with Elbor wheel 78−48540
Gruneisen parameter and thermal diffusivity, thermoelastic meas. method 80−107581
H effect on weldability 80−50720
H-beams, tensile samples shape influence on results of mech. props. determ. 77−52569
hardened, exoelectron emission from torsion fatigue damage 77−86142
hardened, stress determ. from X-ray meas., by fixed time method 78−90801
hardened, twelve-sided polygon prod. 79−81573
hardened, X-ray elasticity constants *(German)* 80−30004
hardened and casecarburized, fatigue crack initiation, propag. and termination, notch depth effects *(Japanese)* 78−7022
hardened layers, struct. and composition, after electrospark doping *(Russian)* 77−70213
hardening, mathematical model including phase changes 79−4950
hardening and cyaniding, by heating in electrolytic plasma *(Russian)* 78−11390
hardening and structural transformations during friction of steels 110G13 and 40Kh10G10 *(Russian)* 77−52527
hardening by focused laser beam *(Russian)* 78−27670
hardening by loading in 45KhN 77−86050
hardening of surface, using linear-contour laser beam *(Russian)* 77−12731
hardness, effect of laser irrad. in inert gas atm. *(Russian)* 79−38935
hardness, rel. to tensile and impact strength 77−90428
hardness, tensile and impact props. correlation, at low temps. *(Japanese)* 77−52413
hardness and ductility variations and micrographs rel. to heat treatment and phase diagram obs. 79−87609
hardness determination method 78−53114
hardness testing, depth of impression meas., automated 79−15892
hardness testing of crankshaft forgings, by type NChG instrument 78−53133
heat conduction, transient temp. distortion due to thermocouple cavity 77−10016
heat exchanger, liquid-fluidised bed, scale control and corrosion tests, geothermal power plant appl. 79−48090

steel continued
heat resist., crack growth resist. on long-term loading 79−29178
heat resistance, thermal stability, stress-rupture strength, and creep 80−81194
heat resistant, cyclic determ. at elev. temps. 79−66125
heat resistant, explosive loading effects on struct. and mech. props. *(Russian)* 78−39787
heat resistant, tensile strain and endurance, normal and radiation conditions, linear load variation 80−81189
heat resistant cast and wrought for petrochemical industry, creep rupture *(German)* 77−36618
heat resistant charact. extrapolation by temp.-time methods, creep data 78−15477
heat treated, deform. due to thermal gradient *(French)* 79−61631
heat treated, electromagnetic device for quality inspection 78−53104
heat treated, residual stress calc. with finite element program *(German)* 79−66075
heat treated, test specifications changes *(German)* 77−9019
heat treated high strength, X-ray diffr. anal. of residual stress 80−3200
heat treated rimmed, statistical study on fatigue life distrib. in long life region *(Japanese)* 77−12755
heat treated SCM3, SNCM8 and SUS403, statistical fatigue props. *(Japanese)* 77−48532
heat treated small parts, electromagnetic hardness inspection 79−34241
heat treatment, computer based interpretation of heat and cooling *(German)* 79−78995
heat treatment, high-temp. isothermic, and mech. working influence on struct. and mech. props. of 60S2 *(Russian)* 80−20969
heat treatment, specification 79−52247
heat treatment achievements and prospects in USSR 78−95765
heat treatment quality inspection by magnetic method 79−52574
heat treatment with induction heating, 78−92285
heat-exchanger alloys for use in nuclear steam coal gasification plant 78−15589
heat-treated, toughness factor statistics *(Russian)* 77−44418
heat-treatment furnace trays, in service embrittlement, microstruct. and prop. changes 77−63784
heating effect on phase composition, microstruct. and mech. props. 80−100859
heavy gauge, rolled, mechanical props. using type KIFM-1 coercimeter 78−72973
hereditary transfer of lattice defects at γ-α-γ transform. 79−96020
high hardenability carburising, accelerated annealing 78−84857
high heat resistant, industrial appl. and comp. *(Korean)* 79−24716
high permeability grain oriented elec. steels and instrument current transformers 80−88824
high purity, low S content, for tough semi-finished products in nuclear power plant *(German)* 80−45393
high speed, annealed, carbide determ. by anodic oxidation technique *(Japanese)* 78−85040
high speed, eutectic carbide structure, SEM exam. 78−85075
high speed, matt-facet fractures *(Chinese)* 78−95793
high speed, props. after electroslag remelting 80−104139
high speed steels, vacuum hardening *(German)* 79−100175
high strength, anodic polarization and corrosion cracking in liquid NH_3 *(Japanese)* 77−21317
high strength, Cd plated, effect of composition and thermal treatment, a hydrogen embrittlement susceptibility *(Russian)* 79−15769
high strength, compliance technique appl. for side grooving effect study on stress corrosion crack kinetics 79−74312
high strength, corrosion cracking in liquid NH_3, preventive methods *(Japanese)* 77−48578
high strength, corrosion fatigue in low press. H_2 gas 79−79172
high strength, crack propagation behaviour, stress, temp. and fracture toughness effects *(German)* 78−31494
high strength, deformation, tension, torsion compression test exam. *(Russian)* 78−31455
high strength, dislocation sweeping model for hydrogen assisted subcritical crack growth 80−97577
high strength, failure stress, structural relationships 80−81190
high strength, fatigue crack growth 78−64697
high strength, fatigue crack growth anal., variable amplitude block loading effects 77−8953
high strength, fatigue crack initiation and early growth 78−7009
high strength, fatigue crack propag., stress intensity threshold levels 77−73324
high strength, fatigue crack propag. and fractography under periodic overstressing, exam. *(Japanese)* 78−52958
high strength, fatigue of V-bent specimens 77−16681
high strength, fine grained, quenched and tempered, residual welding stresses, stress relieving temp. *(German)* 78−72793
high strength, H_2 embrittlement due to cathodic charging during specimen prep. for SEM *(German, English)* 80−11760
high strength, heat resistant, fracture resistance at low temps. 80−104284
high strength, low cycle fractures, electron microscope exam. of 33Kh35NMVFA *(Russian)* 78−31512
high strength, Nb(C, N) precipitation in austenite, effect on mech. props. *(Japanese)* 77−21186
high strength, plastic deform. and fracture under tensile stress *(Russian)* 77−70100
high strength, press. depend. yield and plastic vol. change 78−19810
high strength, sensitivity to stress concentration with various H content *(Russian)* 79−15724
high strength, shell, stress distrib. around notch, beyond fatigue limit 78−13928
high strength, slow crack growth in H_2-H_2S mixture 79−43461
high strength, state of stress effects on ductile failure initiation 77−56070
high strength, strain concentration and occurrence of fatigue cracks in welded joint *(Japanese)* 77−90452
high strength, stress corrosion cracking in liquid NH_3, effect of air and water *(Japanese)* 77−48579
high strength, stress corrosion cracking mechanism 77−28925
high strength, stress corrosion cracking susceptibility in liquid NH_3 at low temps. 79−47809
high strength, subcritical crack growth, role of time delayed H_2 assisted plastic zone growth 80−97576
high strength, sulphide stress cracking props., density and distrib. of intergranular sulphide effects 79−74291
steel continued
high strength, thermally strengthened by rolling heat, H_2 embrittlement *(Russian)* 77−77562
high strength, weld cold cracking, anal. of fracture morphology, using SEM *(Japanese)* 78−52960
high strength, weld zone resistance to welding induced cold cracking, preliminary heat treatment effects 79−91720
high strength 300-M, slow fatigue crack growth, threshold behaviour, temper embrittlement, impurity segregation effects 77−86152
high strength 4340, fatigue crack growth resistance, fracture mechanism effect *(Japanese)* 80−104265
high strength dual phase, martensite/bainite differentation using improved etching technique 80−100951
high strength sheet, absorbed energy during compression and crushing 77−36593
high strength weld metal, fractography, microstructure and reheated zone toughness effects *(Japanese)* 80−108543
high temperature strength, corrosion-erosion effect of gas metal mixture stream *(Russian)* 78−35576
high temperature strength, influence of preferred dislocation orientation, in 12Kh1MF *(Russian)* 79−4999
high tensile strength, base plate and welded joints, exam. of fatigue crack growth rate *(Japanese)* 78−52956
high-speed, 30Kh2N2SMKt, deform. effects on physicomech. props. 78−23741
high-speed, fracture toughness, carbides influence *(French)* 80−108559
high-speed, fracture toughness of powder metallurgy vs. conventionally produced steels 78−64647
high-speed, grain size effect on wear charact. 77−59944
high-speed, powder, atomised, microdefects in particles 77−28753
high-speed, shiny nonfusion rings in friction welding, origin 78−23872
high-speed, sintered, refractory carbide additions effect on hardness and cutting performance 77−66608
high-speed, solidification cycle, thermal anal. 80−29945
high-speed cutting, struct. and props., Co addition effects *(Russian)* 77−21177
high-strength, 80 kg/mm^2 class, effects of metallurgical factors on susceptibility of stress relief testing *(Japanese)* 79−43458
high-strength, brittle fracture in calcium hydroxide environment *(Russian)* 79−52439
high-strength, corrosion cracking under antiplane strain *(Russian)* 77−52531
high-strength, criteria for determining struct. strength and reliability 77−60021
high-strength, gun barrel, fracture mechanics 77−77569
high-strength, H distrib. and delayed brittle fracture 80−108577
high-strength, specific energy of fracture, adsorption lowering by H_2, H_2S, HCl and CH_4 gases *(Russian)* 79−52440
high-strength, strain relax., model *(Spanish)* 77−73296
high-strength, subcritical crack growth depend. on effective stress intensities 78−56726
high-strength 12KhN3A, anode and cathode processes in corrosive environment, fatigue *(Russian)* 78−35573
high-strength castings, AE study of intercrystalline crack form. 80−104403
high-strength plate with soft cladding layer, failure resistance during repeated static banding 77−44406
high-strength reinforcing, 20GS2, local microstresses on creep strength in hydrogenating media *(Russian)* 77−52462
high-strength tool steel D7KhFN, remelting effect on mech. props. 80−76284
high-temperature materials, technological requirements, R and D, report 80−45222
high-temperature thermomechanical treatment, holding after deform. effect on strengthening 79−38868
high-temperature thermomechanically heat treated, fatigue strength improvement by cathodic polarisation *(Russian)* 77−25188
high-tension, effect of side-grooving on K_{IC} meas. by bending *(Japanese)* 78−35614
hollow cylinders, thick walled, effect of thermomech. treatment 80−11674
holographic, nondestructive testing of brazed, and epoxy bonded honeycomb panels 78−40017
holographic interferometry study of chemical bond of concrete to smooth steel rods 78−88593
hot, US inspection 78−88586
hot blooms, US inspection to detect internal pipe 80−97655
hot deformed austenite, transition from discontinuous to continuous formation of pearlite *(German)* 80−35214
hot forging die type, fractography *(Japanese)* 80−108547
hot forming property and struct. *(German)* 80−25730
hot plastic strain, stress- strain-time dependences *(Russian)* 80−40430
hot rolled strip and plate shape meas. device 80−35498
hot rolled strip formability, mech. testing and mech. props. *(German)* 79−66089
hot rolling, effects on struct. of deformed 45G17Yu3 *(Russian)* 77−25073
hot rolling, simulation while preserving criteria of similarity *(Russian)* 79−52266
hot shortness, high-temp. embrittlement, residual and trace elements influence 80−66644
HSLA, crack properties 78−52943
HSLA control-rolled, surface residual stress meas., X-ray diffractometer 78−5716
hybrid bodies, propagation of multiple ended fatigue crack 78−68801
hydroextrusion, effect of longitudinal US oscills. *(Russian)* 79−34071
hydrogen, embrittlement prevent, H_2 transport appl. 79−74260
hydrogen absorption, anilines surfactants effectiveness, HCl conc. effect 80−108638
hydrogen blister-crack array extension 79−24613
hydrogen cracking mechanism *(Russian)* 77−25130
hydrogen embrittlement, book contrib. 79−66172
hydrogen embrittlement, effect of S content in H_2 80−97562
hydrogen embrittlement, effect on band strength 80−104293
hydrogen embrittlement, experimental test of Petch-Stables theory 78−60738
hydrogen embrittlement, method of fixing reversible to irreversible transition 80−25840
hydrogen embrittlement, model including reversible and irreversible processes 77−25155
hydrogen embrittlement, role of gaseous impurities 77−59904

steel continued
hydrogen embrittlement, SEM obs. *(German)* 78−19858
hydrogen embrittlement, standard qualification tests 79−74259
hydrogen embrittlement *(French)* 80−16460
hydrogen embrittlement *(French)* 80−16462
hydrogen embrittlement and selective adsorption 77−36645
hydrogen embrittlement of high tensile steel, estimation from viscous failure 77−73335
hydrogen embrittlement of U8, diffusion coating protection *(Russian)* 78−31513
hydrogen embrittlement resist., selection of test conditions *(Russian)* 79−15883
hydrogen embrittlement susceptibility, fracture toughness *(Czech)* 77−59915
hydrogen induced cracking under wet H_2S environment 77−32721
hydrogen traps, classification 80−19792
hydrogenation and cracking in H_2S, cathodic polarization and surface layer effects *(Russian)* 77−52528
hydrogenation by cathode polarisation, controlling factors 77−52645
hydrogenation during acid corrosion under stress, laboratory apparatus for study *(Russian)* 77−77656
hydrogenation in HCl, influence of conc. depend. of anilines additives on time to fracture, principle of linearity of free energy *(Russian)* 79−15854
hypoeutectoid, singularities of cryst. geometry of pearlite *(Russian)* 77−21093
impact abrasive wear improvement by TiC coating 77−70187
impact of small steel spheres on glass surfaces 77−73338
impact specimen fractures, stress concentrator sharpness effect on size of tough component 78−7015
impact strength, exam. with pulsed drop impact loading 78−84944
impact strength/brittle fracture relationship in ductile-brittle transition zone 78−56740
impact welding to Cu, fundamental parameters 80−97679
impact welding to Cu, wavy interface characts. and formation 80−97680
impurity element determ. by spark sources mass spectrometry using powdered salt 78−7304
impurity spectral lines, intensity, temp. and conc. effects 80−64774
inclusion, grain boundaries, and H_2 attack, fracture analysis 77−32695
inclusion behaviour investigations using SEM 78−23916
inclusion chemistry control for machinability enhancement 80−85067
inclusion cleanliness, US meas. 80−25978
inclusion content, sampling in quantitative image analysis *(French)* 77−28961
inclusion content, ultrasonic method of determination *(French)* 79−52555
inclusion effect on cold formability 80−29975
inclusions, rapid microprobe analysis using energy dispersive spectrometer and minicomputer *(German, English)* 79−92038
inclusions, SiO_2, Al_2O_3, FeS, effect of high temp. heating on size, number and distrib. 78−44145
inclusions and plasticity, crystn. conditions influence *(Russian)* 80−20923
inclusions effect on distrib. of local microheterogeneous deform. *(Russian)* 78−80586
induced anisotropy influence on mag. props., thermomagnetic working *(Russian)* 80−55549
induction hardened, static bending strength and correlation between static strength and endurance limit *(Japanese)* 77−70108
induction hardened sheet, inhomogeneity and distrib. of residual stresses, effect on fatigue *(Japanese)* 78−31518
industrial tests for determining lamellar testing susceptibility *(French)* 80−21250
inelastic cyclic deform. and fatigue 77−63795
inelastic deformation mechanism, fatigue testing in air and corrosive environments *(Russian)* 79−52432
ingot, state of viscoelasticoplastic stress deformation, in process of solidification *(Russian)* 80−45295
ingots, cooling regime in conditions of minimal thermal stress, modelling *(Russian)* 80−65194
interface with TiC RF sputtered film, chem. and microstruct. 78−39956
interface with water drop, contact angle meas. technique 77−55421
interfacial tension in phase boundary with $MnO\text{-}TiO_2\text{-}SiO_2(Al_2O_3)$ *(Czech)* 78−63907
intergranular failure, role of grain boundary composition 79−20155
intergranular fracture, impurity effects 77−8842
intermediate class Kh16N6, structural aspects of work hardening 77−90369
internal cavities in objects, exam. by scanning with ionising radiation beams, from radioactive sources 78−40003
internal oxidation during carburizing and heat treating 79−24660
ion bombardment induced secondary ion and photon emission based quantitative anal. method 79−19963
ion irradiated ST M316, numerical evaluation of combined self-ion injection and vacancy loop prod. 79−7635
ion nitrided, rolling wear props. *(Japanese)* 77−48554
ion nitriding, case depth vs process time 78−72922
ion plated Pb film covered, Hertzian contact expt. 77−52511
ion plated Ti coatings 77−70217
ion-nitrided steel surface structure and hardness, heat treatment effects *(Japanese)* 79−87718
ionic nitriding, procedure and equipment, nitrided layer hardness obs. 80−45414
ionic nitriding thermochemical process, equipment, process details and advantages and prospects *(French)* 80−108641
irradiated in FRJ-1 research reactor, neutron flux densities, temp. fields meas. 77−83029
irradiation by neutrons, damage function for mech. props. 78−13228
isothermal and pearlitic transform. of XC80, mech. prop. meas. using dilatometer *(French)* 78−31598
J_c data, indirect elec. determ., specimen config. effects 78−7011
J-integral fracture toughness, specimen size effect, extension to elastoplastic region 78−68808
jig brushes, wear resist. *(Russian)* 80−60977
joints glued with reaction resinous mortar, photoelastic exam. *(German)* 78−76825
killed, microsegregation and macrosegregation, relevance of processes in front of solidification front *(German)* 77−90342
knife blade, wear by rubber 79−66173
Kossel patterns with SEM on small area 79−1375

steel continued
lamellar pearlite, containing proeutectoid ferrite, brittle fracture *(Japanese)* 79−66152
lamellar pearlite, containing proeutectoid ferrite, prestrain effect on brittle fracture *(Japanese)* 80−45388
lamellar tearing susceptibility, US testing 77−25231
laminar, high hardness, ballistically damaged, fracture mech. approach to residual strength 77−56050
laminar composite, crack extension, rising tensile load effect 77−36642
laminate, Co-Ni/steel/Co-Ni, high strength with increased damping capacity 77−1850
laminated, tensile props. 77−52441
large forging, mech. props. 77−4797
laser beam melting kinetics *(Russian)* 77−56121
laser erosion value depend. on metallic props. anisotropy during plastic deform. *(Russian)* 78−31452
laser impact, multiple crater refl., effect on refl. props. 78−52596
laser transformation hardening, fatigue and wear rates, for AISI 1045 79−70198
laser-irradiation surface treatment *(Russian)* 77−59978
lattice defects during $\Gamma \rightarrow \alpha \rightarrow \gamma$ transform. in 120Kh3G3, electron microscopy obs. *(Russian)* 79−47681
lattice hardening and anomalous softening caused by electrolytic H_2 charging *(Japanese)* 79−43398
lattice hardening due to dissolved H_2 77−8952
lattice hardening/softening due to dissolved H_2 77−77581
leaded, resulphurised, deform. index of MnS inclusions 77−66683
light gauge steel diaphragms, buckling, bending anal. under concentrated loads 79−23233
linepipe, S content influence on H_2 induced fracture 80−30088
liquid, nonmetallic inclusion behaviour simulation by multiple phase medium eqn. *(Russian)* 78−94965
liquid, Stokes coagulation model, particle motion according to Boltzmann eqn. *(German)* 80−40357
LMFBR, fuel-steel mixtures, basic collapse criteria for HCDA 77−3107
locally deformed, Fry's reagent action 79−87806
long-term strength prediction, nature of temperature-time parameter 77−21275
low alloy, bainite, transform. behaviour, struct., toughness 78−27513
low alloy, hot deform. and modified ausforming *(Japanese)* 78−11244
low alloy, ion microprobe anal., sampling error 78−7264
low alloy, metallurgical factors and toughness in structural steel welds *(Japanese)* 79−52377
low alloy, photometric anal. by time resolution of radiation *(Russian)* 78−23995
low C, γ-α transform. kinetic rel. with self-diffusion characts. *(Russian)* 78−67850
low C, effect of grain size on transition behaviour and bending speed correl. *(Japanese)* 79−8345
low C, S 35 C, annealed, crack initiation life, anal. of smooth and notched specimens *(Japanese)* 79−8347
low C-Cu composite plates, vol. fraction and residual stress, effect on fatigue strength *(Japanese)* 79−8349
low cycle corrosion fatigue, protective effect of inhibitor HOSP-10 *(Russian)* 77−16721
low cycle fatigue in Kh12M high strength steel 79−87724
low cycle loading of 10KhSND deform. diagram *(Russian)* 78−52908
low S, ESR, overheating effect on toughness 78−52860
low S, ESR and electric arc, notch toughness, interaction between overheating and tempering temp. effects 78−52970
low strength, blunting effects on fracture toughness 78−68814
low strength, fracture toughness value determination by compact testing 80−45451
low strength, impact tests with oscillography, exam. of fracture toughness using new method 80−21215
low strength notched specimens, preloading effects on brittle fracture 78−27642
for low temperature applications, comp. and processing, research 77−52365
low-alloy, impurities, segregation and creep embrittlement 80−66653
low-temperature materials, mechanical, electrical and magnetic props. *(German)* 80−3081
lower bainite, struct. changes during tempering *(Russian)* 77−21178
macrosegregation of S and form. of equiaxed crystals, autoradiographic study, cast struct. effect 77−63658
magnetic, technology, development *(Polish)* 77−89973
magnetic anisotropy, magnetostatic fields, numerical simulation 77−27220
magnetic anisotropy of electrical steel sheet, determ. method and laboratory tests *(Polish)* 80−97071
magnetic fundamental and harmonic flux, sinusoidal applied mag. field, steel plate 78−2708
magnetic inspection, of hardness and struct. of type KhVG annealed 80−7750
magnetic method of mech. prop. determ. of thick sheet of 17G1S 78−48600
magnetic stray fields, optical detection 78−31602
magnetic susceptibility, 4.2 to 300K, and magnetoelasticity of Kh18N(10-25) *(Russian)* 80−65812
magnetically-soft materials, mag. characts. determ. methods, review 79−40593
magnetisation, low frequency magnetic field, oscillations in envelope of harmonic levels, struct.-mech. characts. determ. 78−60940
magnetisation transitions, Barkhausen noise 78−91894
magnetite film formation at metal scale interface, during cooling 78−88575
magnetoelastic effect, differential and susceptibility consts. *(Russian)* 79−42817
magnetoresistance, grain-oriented mag. steel sheet *(German)* 78−68020
magnetostriction, dynamic, meas. using induction method *(Russian)* 77−56171
magnetostriction effect, depend. on magnetising field intensity *(Russian)* 79−51831
manometer reference free-piston oxidation process for trimming mass of weights 78−93715
maraging, 18% Ni content, exam. of age hardening-grain size relationships 78−84833
maraging, ductility and resist. to deform., −196-1000°C 80−89313
maraging, precipitation hardening, struct. and fracture *(German)* 79−61696

steel continued
martensite form., hardening cracks, acoustic emission investig. possibility 79−29177
martensitic, Gruneisen parameter determ. using thermoelastic effect 79−28068
martensitic ferritic struct., fracture toughness *(Russian)* 77−77560
martensitic growth 80−108439
martensitic transform., inverse, plastic deform. effect, 200 to 550°C *(Russian)* 77−73274
martensitic transform, stress calcs. using statistical model *(Russian)* 80−93557
martensitic transformation, lattice deform. 78−27511
martensitic transformation kinetics, mag. field effects 79−87630
martensitic-bainitic, lath morphology effect on yield stress, martensitic and ductile-brittle transition temps. 79−100215
Martin steel, thermoelectric determination of C content during melting 77−56276
mass spectrometric analysis of S content by remote meas. technique 78−23994
mass transfer of C between parallel steel St3 plates under influence of shock waves *(Russian)* 78−91380
massive object inspection, coercimeter with attached electromagnetic appl. 79−70277
material scale length as a measure of fracture toughness in fracture mechanics of plastic materials 78−68763
mechanical ageing susceptibility, assessment method for 5 to 7 mm thick steel 77−63850
mechanical props., temp. effects *(French)* 77−56017
mechanical strength, effect of H_2 sorption and Al and N_2 surface treatment *(Russian)* 78−31570
medium C, isothermally quenched, high-temp. deform. effects on struct. and props. *(Russian)* 80−25760
medium C, structural changes and elastic-plastic stresses during quenching *(Japanese)* 79−38858
medium C resulphurised, compressive strength at high strain rates, short load cells 79−29305
medium strength, fracture toughness eval. by J-integral and equivalent energy method *(French)* 77−77578
medium strength plate, quenched and tempered, fracture toughness in ductile-brittle range 78−7036
melt, interaction with Al_2O_3:Zr ceramic 80−104305
melting, effects of laser light focusing conditions *(Russian)* 77−59823
melting and solidification *(French)* 77−66635
melting of finite steel slabs in flowing nuclear reactor fuel 79−54494
metallic coated, sliding wear resistance 77−12708
metallography of worn surfaces, exptl. difficulties, delamination theory implications 79−34253
metallurgical stability and corrosion in impure He atmospheres, HTR appl. 79−36329
microalloyed with Ce, La, Nd, effect on crystal structure and thermal fatigue and resistance *(Russian)* 79−34136
microhardness changes under high-press. and laser irrad. *(Russian)* 77−59903
microhole working by laser irrad., accuracy increase *(Russian)* 80−55434
microplastic deformation measurement in grains of polycryst substances, construct. steel 77−77665
microstructure control in flash butt welding 79−91715
microstructure determ., transmission type electron microscope appl. *(German)* 80−15089
microstructure of 0Kh16N15M3B after creep tests in BR-10 reactor, electron microscope invest. *(Russian)* 80−92531
migration of C during shock compression of steel clad glassy C 80−24679
mild, acid dissolution inhibition by aniline and thiourea, iodide effect 79−79181
mild, acoustic emission during magnetisation, stress effects 79−82854
mild, adhesion of Al plasma sprayed coating, substrate pretreatment effect 79−83391
mild, bar stress wave propagation, finite element analysis *(Japanese)* 79−79030
mild, corrosion and passivation in benzoate solutions 79−79180
mild, cyclic creep reversal 80−25766
mild, fatigue crack initiation, fractographic exam. *(Japanese)* 78−52957
mild, implantation of Cu(Cr), annealing and rolling behaviour of conc. profiles 78−75684
mild, inhomogeneous yielding, slip plane intersection with stress free boundary 78−5667
mild, materials specifications for AGR steam generators 80−42772
mild, plates, fatigue crack propag. estimation method in pre-strained and mean stressed samples 80−21067
mild, rotational hysteresis 78−91889
mild, rubbing on brass, magnetic field effect on diffusive wear of cutting tools 80−60985
mild, S determ., flame chemiluminesc. method 78−48711
mild, sheet, C depth distrib., glow discharge spectrometry anal. *(French)* 79−87923
mild, Ta coating at atm. press. using CVD method 80−55591
mild, tensile deformation, behaviour under high pressure *(Japanese)* 80−16381
mild, with small flaws elastic-plastic anal. of fatigue limit 80−21069
mild rimming, thin sheet, grain growth in the recrystallisation *(French)* 79−70074
mild steel, diamond tools wear due to clean surface reactions 78−85008
model magnet, for reson. spectrometer, reproducibility of fields, field heights and magnetisation props. of materials *(German)* 78−24832
molten, addition of VO_xC_y 78−40049
molten, deoxidised, reaction with oxidising gas bubbles 78−88438
molten, heat loss during solidification hydrodynamic eqns., hardening front kinetics *(Russian)* 80−55385
molten, wettability of aluminosilicate refractories 79−82415
molten deoxidised, reaction with oxidising gas bubbles 78−84739
molten interfacial tension in phase boundary molten CaO-SiO_2-Al_2O_3-CaF_w2 slag *(Czech)* 78−63908
monitoring, with pulsed magnetic analyser, IMA-5 80−104399
morphology of inclusions changes obs., due to heating, influence on ductile fracture *(Spanish)* 80−25744
moulds for die-casting Al alloys, thermal fatigue 79−24619
moving target in N_2-Ar-He, action of laser beam at high pressures, surface hardening *(Russian)* 78−94925
multimaterial impact, dynamic yield point 77−32731

steel continued
NDT, automatic combined inspection line for type 3102 bright steel bars 77−77714
NDT, magnetic inductive method appl. *(German)* 78−48581
NDT, mech. props., KF-1 coercimeter 79−87769
NDT instrument for grain size and anisotropy meas. 79−11753
NDT of billets, bars, tubes 77−12759
NDT of steel structures from anal. of Barkhausen noise statistics 77−77647
NDT thick rolled sheet with unfinished surface, US defect assessment expt. 77−77720
NDT with electromag. coercimeter, exam. of current amplitude effect 78−39997
neutron activation anal. in VVER reactor *(Czech)* 80−5234
neutron effects, mass spectrometer system for He assay 77−34397
neutron effects at high temp., simulation by HV electron microscope 77−1153
neutron irradiated, additivity deviations in thermal and radiation induced embrittlement 77−73348
neutron irradiated, kinetics of nucleation and growth of vacancy pores and dislocation loops *(Russian)* 77−51408
neutron irradiated, liberation of He in uniform heating 77−50248
neutron irradiated 15KhMFA, H_2 induced delayed fracture *(Russian)* 78−35476
neutron irradiated press. vessel material, small angle neutron scatt. meas. 79−13428
neutron irradiation induced swelling, empirical relationship with dose and temp. 77−50247
neutron quasialbedo thickness meas. of single layer product, optimization 80−105611
Ni-rich, tetragonality anomalies of martensite 77−77478
nil ductility transition temp., and Charpy V-notch fracture appear transition temp. relationship between them, determ. *(Czech)* 79−91783
nitridation process, ionic, in glow discharge *(Russian)* 77−11412
nitride coated, brittleness eval. by AE *(Chinese)* 78−11453
nitride form. by implantation, wear rate reduction 78−27149
nitride inclusions, identification by differential thermal anal. and evolved gas anal. 78−48721
nitrided EN41B, effect of residual stresses on fatigue failure 78−64698
nitrided layer depth, electroinduction meas. method 80−104379
nitrided steel surface wear-related topography 78−60847
nitriding, diffusion layer hardening calc. 79−52456
nitriding, distortion prediction, appl. 79−24663
nitriding, mag. field effect 79−57153
nitriding in molten nitrates 80−35417
nitriding processes, controlled 79−100294
non metallic inclusion eval. using Quantinet systems 79−15923
non-alloy, work hardening due to shearing *(French)* 78−15423
non-irradiated and irradiated specimens, autoclaves for fatigue crack growth tests *(German)* 80−45467
nonmagnetic, carbide-intermetallic strengthening 79−83208
nonmetallic inclusion effect on hot ductility 80−29999
nonmetallic inclusion effect on plasticity and impact strength in 12X2H4A *(Ukrainian)* 78−92296
nonmetallic inclusions effect on ductility 80−30042
nonmetallic inclusions effects on low-temp. fracture *(Russian)* 77−59895
nonpropagating fatigue cracks, in steel component strengthened by surface plastic deformation anal. 78−88529
nonstationary temperature fields due to moving heat sources, heat capacity, thermal cond. *(Russian)* 80−107448
normalised and strained Ck45, length charges under cyclic load *(German)* 80−100869
North Sea oil production platforms, use of steel and concrete in construction 79−78985
notch sensitivity, in mains water, SCC at EI643 and 30KhGSNA *(Russian)* 77−77624
notch sensitivity in fatigue 78−60757
notch sensitivity under cyclic impact loads 78−3220
notched, cyclic stress/strain behaviour, random fatigue life *(German)* 80−100907
notched 1018, air fatigue in endurance limit range 77−36631
notched bar, plastic zone determ. near rupture *(French)* 78−88515
notched bar impact bending test, Robertson test, and drop-weight test relationship 77−81364
notched bar impact test specimens, strain hardening distrib. *(German)* 77−60004
notched rods in tension, 20-700°C, yield and conditions *(Polish)* 78−80604
nozzle erosion, ion implantation effects, ion beam anal. 79−48011
nuclear bolts, heat treatment for structural retraction prevention *(French)* 79−91713
nuclear containment vessel response to impact using PISCES finite difference codes 77−3097
nuclear fuel rods steel-coated, effect of impurities on clad-corrosion *(German)* 79−49693
nuclear pressure vessel, type A533B-1, three point bending, yield stress, exam., Charpy V-notch and precracked specimens 78−92310
nuclear pressure vessel steels, transient finite element crack propag. model 77−3106
nuclear pressure vessel time A533 grade B class 1, thermal shock fracture toughness at elev. temp. *(Japanese)* 79−83304
nuclear reactor, role of ASTM in providing standards 79−22435
nuclear reactor pressure vessel, neutron radiation effects on material props., review *(German)* 77−34382
nuclear reactor pressure vessel materials, AE assessment 79−83422
nuclear reactor pressure vessel steel irradiation, neutron flux densities neutron spectra and temp. fields in large specimens 77−74924
nuclear reactor pressure vessel steels, neutron irrad. embrittlement, temp. effects, annealing *(German)* 77−34384
nuclear reactor pressure vessels, irrad. and post-irrad. examination equip. and techniques *(German)* 77−36696
nuclear reactor structural material, irrad. effects, neutron energy depend., damage model *(German)* 77−34385
nuclear reactor vessel, neutron irrad. effect on brittle fracture characts. *(Slovak)* 78−50254
organic corrosion protective coatings, adhesion and permeability 78−64764
oxidation by Fe-Si-Ca-V complex alloy, nonmetallic inclusions *(Russian)* 80−93685

steel continued
oxidation-reduction processes on surface during heating in vacuum *(Russian)* 78−11403
oxide inclusions 78−23648
oxide insulation layers meas., of magnetic laminations, by X-ray and electron microscopy *(Polish)* 77−12743
oxide layer removal, Cr depletion, ion-beam effects obs. by ESCA 78−52612
paint coatings, corrosion fatigue resistance *(Russian)* 77−59979
paramagnetic matrix with ferromagnetic inclusions, magnetic susceptibility determ. 79−97407
passivation by sulphochromic soln. *(French)* 78−23869
passivation treatment, of galvanised strip 80−61146
pearlite, annealed, hot fatigued, eutectoid spheroidization 77−52374
pearlite, interlamellar spacing effect on yield stress *(Czech)* 79−43341
pearlite, SEM obs. of tensile deform. and fracture 78−84897
pearlitic, atom probe microanal., computer controlled 77−66781
pearlitic, brittle fracture of structures 78−72869
pearlitic, fatigue, metallographic aspects 78−60828
pearlitic, heat treatment effect on fracture resistance, microstruct. and mech. props. 80−104191
pearlitic, heat treatment effects on mech. props. and microstruct. *(German)* 77−8857
pearlitic, P internal friction peak *(Russian)* 78−38774
pearlitic, partitioning, atom probe microanal. 80−3079
pearlitic, statistical anal. of joint effect of Ni, Cu, P on irradiation embrittlement 78−71770
pearlitic, strength, fracture, microstructure effect 77−40449
pearlitic, temp. relationship of failure charact. 78−3158
pearlitic, wear behaviour rel. to basic material props. 80−108592
pearlitic constructional, K_{IIIc} expt. determ. 80−100985
pearlitic eutectoid, crack initiation and effective grain size for cleavage fracture 80−30085
pearlitic structural, austenite grains, growth rate during heating 80−100860
pearlitic/ferritic, pearlite interlamellar spacing and grain size effect on US attenuation 79−34230
perforated bent sections, microstruct. near holes 78−23725
perlite, with Ni-Cr steel anticorrosion coatings, viscous-failure charact. from dynamic failure energy 79−43391
perlitic, ferritoperlitic and bainitic, stress state influence on fracture *(French)* 79−79093
permeability of hydrogen in inhibited H_2SO_4 corrosion, stress level effects *(Russian)* 77−52530
phase boundary decarburization of pouring jets and droplets *(German)* 77−90318
phase conversion kinetics, exam. using ultrasonic method, apparatus design 80−21203
phase separation, effect of plastic deform. and heat treatment *(Polish)* 78−92295
phase transform., α to γ, during rapid resistance heating, apparatus for investigation *(Slovak)* 78−19742
phase transformations and props. 77−12614
Phosphate conversion coatings on steel 78−3251
photometric determ. of Ce *(German)* 78−68955
physicomechanical props., hydroextrusion effects 77−21287
pipe, creep-resistant, influence of chem. comp. on formability *(German)* 78−84900
pipe, flaw detection by US pulse-echo method 80−66756
pipe with axial surface crack, resistance of failure in plastic deform., type 12Kh1M1F 79−100235
pipes, flow of gas-solid suspensions, electrification 77−77811
piping components, incremental collapse tests, structural behaviour 77−6526
plane strain fracture mode criterion based on plastic zone size-thickness correlation 80−43670
plasma coatings, elastic properties, acoustic meas. *(Russian)* 80−97519
plasma magnetic confinement system, surface problems caused by dissolved H_2 80−57946
plasma thermochemical treatment 79−94823
plastic, anisotropic hardening pot., stress/strain relation under combined axial load/torsion 78−52896
plastic, thermally strengthened, not prone to H_2 embrittlement, prod. *(Russian)* 79−52267
plastic anisotropy coeff., effect of strain rate 77−25097
plastic deform., density changes *(German)* 80−60908
plastic deform. and fracture of pearlitic or spheroidal steel *(French)* 78−35448
plastic deform. effect on third-order elastic moduli, dislocation anharmonism *(Russian)* 80−50786
plastic deform. resist. during continuous hot rolling *(Russian)* 80−55462
plastic deformation, C distrib. *(Ukrainian)* 80−50668
plastic deformation, cyclic stress anal. within hysteresis loop of type 11423 *(Czech)* 80−30031
plastic deformation mechanism, meas. of microplasticity 78−60720
plastic deformation resist., three-cam plastometer meas. 79−87792
plastic deformation zone, caused by crack, extent determ. with microhardness, surface roughness, measurements *(French)* 80−7682
plastic flow area, determ. of relative elongation and rel. to yield point 78−23769
plastic props., room temp. to recrystallisation temp., stress-strain relations, computer program 77−1865
plastic working of wires, high-density current appl. 79−57002
plastic working with vibr., US hardness tester 78−53044
plastic zone growth, quantitative evaluation of acoustic emission, book contrib. 79−100328
plastically deformed, force and speed criteria interactions during hot rolling *(Russian)* 80−55463
plastically deformed, magnetoelastic props. of types 45 and U8 *(Russian)* 80−44893
plastically deformed or hardened, moment method anal. of X-ray diffr. data *(Czech)* 78−31593
plasticity, simplex planning method for temp. rate determination 77−56025
plasticity, temp. and rate dependence for different rigidities of stressed state *(Russian)* 79−29139
plasticity depend. on hydrostatic press. in low-angle fatigue, Manson-Coffin coeff. *(Russian)* 79−61651
plasticity indices in anisothermal extension *(Russian)* 80−16378

steel continued
plasticity of grooved specimens at high temp., rel. to hot forming 78−23902
plasticity of two-phase, coarse microstruct.-material *(German)* 77−59882
plate, alloying, normalising, controlled rolling 77−48459
plate, high tensile strength, fatigue props of butt welded joint 78−80649
plate, Pb-Sn soldered joint strength study *(Japanese)* 78−7166
plate, rolling direction determ. with notched bend test specimen *(German)* 77−60003
plate, thick high stregth, for press. vessels, low cycle fatigue and notch sensitivity *(French)* 80−66670
plate, thin, in compression, initial deflection and postbuckling behaviour analysis 80−50666
plate, type SM50A for weld struct., statistical fatigue props. 79−96146
plate collapse, anal. by live energy minimisation 78−52910
plate manufacture, on-line US inspection appl. 78−80702
platelike parts, quenching, temp. field calc. 80−60889
plates, hot rolled, anisotropic texture, exam. of elastic deformation behaviour *(Japanese)* 78−64586
plates, plastic coated, RF welded, quality and strength *(German)* 79−34185
plates, thin, welding residual stresses calc., elastoplastic thermal stress anal. 78−83262
plates,explosively clad, fatigue crack propagation behaviour *(Japanese)* 80−104262
plates with cut, stability loss critical stresses for 20, 08 kp and 65G steels 80−11690
polishing in H_2SO_4 + methanol, polarisation curves 78−56851
polyamide coating on steel roller, experimental exam. of contact parameters 78−68842
polyethylene, high density, adhesion strength to St. 3 steel 78−23920
polyethylene-steel adhesive bond strength, rel. to ultrathin layer of polymer remaining on metal 77−70279
polymer coated, electrolyte permeation and elect. permittivity rel. to metal substrate corrosion 79−96175
polyvinylbutyral, high density, adhesion strength to St. 3 steel 78−23920
porous, permeability, deform. effects 79−100229
porous gauze materials, struct. and hydraulic charact. 80−11729
powder, prealloyed, struct. formed by atomisation, props. *(French)* 77−70020
powder, rotary forging, porosity and deform. 78−23646
powder forged, impact strength and fatigue strength, slag inclusion effects 77−21271
powder forged for carburizing appl., core props., mech. props. 78−15339
powder metallurgy, recent developments, Sweden 80−93514
powder metallurgy technology innovations, 1978 status 79−47646
powder-forged, fracture toughness 79−66155
power plant pipelines under creep conditions, allowable thermal stresses *(Russian)* 78−13930
precipitation of AlN *(French)* 78−23711
precompression cracking method, for fracture toughness testing *(Japanese)* 78−15612
preferred orientation investigation by pole figures and mathematical technique 79−34227
pressure vessel, A533B, ductile, plane strain crack growth 78−80621
pressure vessel, acoustic emission during loading by pulsating internal press. *(German)* 78−19973
pressure vessel, ASME SA-387 grade D, fatigue crack growth, liquid Na environment effects 77−8997
pressure vessel, multilayer, without longitudinal seam, model investigation *(German)* 79−34276
pressure vessel, notched, acoustic emission meas. during pressurisation 78−21638
pressure vessel, nuclear, fracture toughness at elevated temps. 79−20193
pressure vessel, RT_{NDT} shift of ductile-temp. curve, correl. with neutron dose *(German)* 77−34388
pressure vessel for light water reactors, corrosion fatigue, data review 79−79169
pressure vessel rupture tests, heavy section steel technology programme 78−44212
pressure vessel type, H_2 effect on corrosion, fatigue strength and embrittlement *(French)* 79−47770
pressure vessels, internal pulsed loads, effect of scale, geometry and filler on strength 78−21659
pressure vessels, testing by pendulum impact machines, energy meas. using optical system 80−69746
pressure vessels and steel pipes structures anal. under creep conditions, acoustic emission method 77−25237
prestrained pressure vessel, correl. between dynamical toughness characteristics 78−68816
prestrained pressure vessel, dynamic toughness charact., expt. correlations 79−15783
prestressed cast segments for HTR with 3000 MW thermal power, thermodynamic calc. and design *(German)* 78−4982
prestressed concrete wire, strain tempering by rapid heating *(Japanese)* 79−70088
prestressed steel pressure vessels for nuclear reactors *(German)* 79−3196
process induced matrix inclusion separation 77−28818
products, production line X-ray fluoresc. anal., coating thickness meas. 77−54029
products for nuclear power stations, research and development *(Russian)* 79−34080
proeutectoid reaction, review 77−4777
protective coating on steel, US testing 78−23908
protective coatings of Fe-Ni-Cr 78−48572
prow formation processes, sliding against mild steel *(Japanese)* 80−35336
purity, nonmetallic inclusions, quantity and origin, isotope methods 77−56201
quasi-cleavage fracture *(Chinese)* 80−21060
quench-hardened, exam. of anomalous plasticity when deformed *(Russian)* 79−11663
quenched, corrosion cracking in NaCl soln. *(Russian)* 78−56801
quenched, exam. of phenomena taking place during tempering by positron annihilation *(Russian)* 79−24543
quenched, local H distrib. and internal microstresses *(Russian)* 80−50654
quenched, Mossbauer study of surface martensite 77−32578
quenched, notch sensitivity, effect of tempering temp. 77−1846

steel continued
quenched, surface layer hardness rel. to adsorption contact fatigue *(Ukrainian)* 80−40478
quenched, tempered, intergranular failure during fatigue crack growth 79−8357
quenched, tempered and austempered 4340 effect of plastic strain followed by ageing on elastic limit 78−31446
quenched, tempering treatment, ultimate tensile strength and yield point *(Russian)* 77−32599
quenched, verification of change of props. in mag. field 78−52985
quenched and low-annealed steel, X-ray determ. of macroscopic stresses 77−77660
quenched and tempered, environmentally assisted fatigue crack propag. 77−44403
quenched and tempered, localised corrosion sensitivity *(German)* 78−19949
quenched and tempered, microstructure effect on cleavage fracture toughness 79−74252
quenched and tempered 52100 bearing steel, plastic deform. in compression 77−40437
quenched and tempered sheet, first operation cupping *(German)* 78−72788
quenched KhVG, change in structure under influence of cyclic loads 78−56676
quenched-tempered, relationship between half value breadth and hardness *(Japanese)* 77−52366
quenching, computer anal. of thermal processes 77−70085
quenching, temp. field, exact calc. in large pieces, computer use 77−70086
quenching, thermal processes 77−63699
radiation induced embrittlement of nuclear reactor steel, slow neutron small angle scatt. study *(German)* 77−34390
radiation swelling, type X16H15M3B, predictions for conditions in fast reactors *(Russian)* 79−67870
radioactivation of shielding materials Fe, Benelex by fast neutrons, γ-ray spectra, decay rates 79−682
radiographic inspection method, productivity 80−71861
radiography, with the 25000 R/min Linac 80−97656
radiography with gamma rays, using Se electroradiographic plates, comparison with X-ray plates 78−72978
rail and structural, fatigue crack growth 78−64695
rail steel NDT, residual stresses meas. using magnetoelastic effect 77−81379
railway bridge, expt. determ. of coeff. of excess dynamic fatigue stress *(French)* 79−34151
railway line, acoustoelectric and third-order elastic constants meas. 77−4798
railway rail steel NDT, residual stresses meas. using magnetoelastic effect 77−81379
rapid, contrib. to assimilation of new labels *(Rumanian)* 80−35216
rapid, surface modification by ZrB_2 treatment 79−66203
rapid electrothermal treatment of wire 78−84871
rare earth additions, effect on physicomechanical props. 77−12639
rare earth metal additions effects on mech. props. 78−52829
reactor containment sealing layer, use of steel lining *(Russian)* 79−30962
reactor pressure vessel failure and radiation damage *(Czech)* 80−619
reactor pressure vessel material, radiation embrittlement, current regulation assessment 78−52966
reactor pressure vessels, positron annihilation as nondestructive monitor of radiation damage 77−4130
reactor shielding material, 6 MeV γ penetration, bremsstrahlung 78−58350
recrystallisation, structural inheritance characts., X-ray and internal friction obs. 79−57017
recrystallisation kinetics, of unkilled deep drawing sheets, N-content influence *(German)* 80−40376
reflectivity at 10.6 μm, calorimeter meas. 78−55393
reheat cracking in weld zone, method for evaluating sensitivity to cracking 78−72855
reinforced composite pull-out forces, effect of matrix stresses 77−21334
reinforced concrete, local bond-stress/slip relationships under repeated loading 79−20123
reinforced concrete slabs, connected via shear connectors, exam. of fatigue in shear connectors, exam. of method 79−43539
reinforced Cu and Al based composites, fatigue strength, surface layer effects 77−12697
reinforcement, low, high temp. static strength testing 79−15902
reinforcement in concrete, fatigue crack growth 80−30060
reinforcement of concrete slabs, subjected to biaxial moments, optimum design using analytical and graphical methods 80−50664
reinforcing, 20GS2, brittle fracture resistance in corrosive environments, tempering effects *(Russian)* 77−59974
reinforcing, in concrete, corrosion *(Japanese)* 79−39038
reinforcing wires, high strength, microstruct. obs. *(Czech)* 79−43342
residual quenching stress determ. in cylinder, consideration of transform. *(German)* 80−35213
residual stress change in conc. zone in cyclic loading of 22K and 09G2S 78−3224
residual stress determ. by X-ray integration *(German)* 79−52551
residual stress influence on mech. props. *(German)* 78−27587
residual stress meas. by centre hole method 77−54941
residual stresses, X-ray apparatus for meas. 77−60016
residual stresses meas., using position sensitive X-ray detector 77−56211
restorational carbonisation in one and two phase states *(Russian)* 80−65225
resulphurised, fractography and X-ray photoelectron spectroscopy 80−7673
rhomboidal steel panel, elastoplastic stress and strain diffusion 79−20128
rimmed, metallographic method of cleanliness eval. 77−52562
rimming, continuous casting and solidification *(French)* 80−25685
rimming, continuously cast, nonmetallic inclusion distrib. *(Russian)* 78−80534
rimming, continuously cast ingot, honeycomb blowhole depth, absorption-scattering method 78−53148
rimming, shape change and pore form. during multiple polymorphic transform. *(Russian)* 77−25044
rimming, teeming and solidification *(French)* 80−16296
rimming type, high temp. oxidation studies using $^{18}O(p,\alpha)^{15}N$, ^{18}O distrib. determ. 79−87912
steel continued
ring against Cu pin, dry sliding wear, role of dynamic recrystallisation 80−108599
rod, dynamic bending and residual deformation *(Russian)* 80−75293
rod, transverse vibrations, energy dissipation, static longitudinal load effect 80−81099
rolled, anisotropic, fatigue fracture surface obs. *(Japanese)* 80−108546
rolled, fisheyes produced by exposure to H_2 at room temp. 77−90455
rolled, low-cycle torsional and push-pull fatigue anisotropy 78−27589
rolled, used of statistically justified methods in determining heterogeneity and mech. props. 79−52516
rolled plates, anisotropic, fatigue behaviour under cyclic torsion 77−44326
rolled repetitive sections, ultrasonic quality inspection 79−87770
rolled sections, continuous rolling process considerations *(Rumanian)* 79−29097
rolled sheet, effect of inclusions on torsional fatigue 78−92314
rolled sheet, mag. testing of mech. props. 78−72972
rolled sheet, thick, metrological peculiarities when inspecting with US shadow flaw detectors 80−81263
rollers, case-hardened, nitrided, surface failure, durability 78−84959
rolling, controlled, correlation links between mech. props. 80−35234
rolling discs, coeff. of friction 79−14360
rolling texture, neutron diffr. analysis, steels with micro-duplex structure 80−16327
rotating bending fatigue tests in hydrostatic environment 77−21343
round bar used for seamless tube manufacture, US testing 77−40479
ruled shell exposed to internal load pulses, compact strength 79−3929
ruled steel grating system for length meas. 80−13039
rusted, exam. of tannin treatment action mode 78−88564
SAE 1045, creep and relaxation curves for torsion-tension members at elevated temps. 78−83260
saturated, equivalent permeability calc., Stefan's equation with small parameter *(French)* 77−28409
saturation magnetisation, for residual austenite, and props. of standard *(French)* 79−73766
scale and spalling resistance determination, appl. of cyclic oxidation method 77−77695
scoring and scuffing on lubricated sliding surfaces, Mossbauer study 80−7690
second phases, appl. of DTA-evolved gas anal. 77−55971
segregation, solute, and intergranular fracture 80−60957
segregation and adsorption of S, influence on carburisation and nitrogenation 80−66701
seizure, effect of polymer-containing metal-filled lubricant 80−104301
self-consistent junctions and spatial relative organisation in type 50N29 80−19750
self-lubricating Ni coating 80−21189
shaft, residual tangential stress determ. after elastoplastic twisting 78−60902
shear stress distribution caused by transverse force, rails of DIN 15087E *(German)* 79−61647
shear-band temp. meas. of type 4340 80−48655
shear-spun tubes, texture inhomogeneity 79−91691
sheet, apparatus for mag. props. meas. in freq. range 50 to 10000 Hz 79−30497
sheet, carbonaceous residues, chemical characterisation from C Auger spectra, appl. of pattern recognition and factor anal. 79−79347
sheet, cold-rolled, surface chemistry 80−61146
sheet, cold-rolled, US inspection for mech. prop. anisotropy 78−23750
sheet, effects of strain rate and deformation heating in tensile testing 78−85089
sheet, in-plane stretching, limit strain meas. 78−80573
sheet, strain-induced changes in mech. props. and press formabilities 78−19781
sheet, thermomechanical bending, induction heating calc. 79−52280
sheet, type 08Kp, blackness degree rel. to heat treatment in controlled atms. 79−57165
sheet, Zn and Al-Zn coated, chromate passivation protection against wet-storage stain 78−95854
sheet galling, development of quantitative test 78−92433
sheet steel, mechanical anal. of internal friction meas. apparatus 77−32752
sheet structural changes during rolling influence of lubricants on friction and wear 78−95815
sheets bonded with low density polyethylene, static fatigue *(French)* 80−108522
shelf energy rel. to fracture surface dimensions *(Czech)* 77−59917
shell, explosive expansion, deform. and rupture modes and mechanisms 80−85064
shell, explosive expansion, rupture behaviour 80−85063
shell, mech. behaviour during solidification 80−81043
shells, spinning, aerodynamic ablation, side force 79−37347
Shiva mechanical systems 78−63135
shock transition rise-time meas., limiting viscosity coeffs. 79−77680
shock waves meas., dielectric and magnetic pickup signals comparison 78−5707
shot-peened, type JAE 1144, fatigue damage, development rate by exoelectron meas. 80−25835
signature response, for friction and wear 80−40541
silchrome, thermomech. hardening 78−23736
silicide coatings, on steel, exam. of fracture processes 78−44206
siliconised, alloy formation kinetics at solid cathodes, metal electrodeposition from molten salt electrolytes 80−26028
sintered, boronizing 79−96210
sintered, diffusion treatment with B, Si, Cr and C, corrosion and wear improvement 77−77642
sintered, fracture of residual pores 80−76352
sintered, mech. props., effect of small cold reduction 79−39048
sintered, mech. props. 77−40439
sintered, oxidation in superheated steam, corrosion protection 79−39049
sintered bearing material, standardisation, wear and friction props. 78−19901
sintered constructional, resistance to cyclic impact loads 77−77583
sintered ductile fracture, microvoid effects *(Japanese)* 80−108542
slab, scattered radiation intensity of ^{192}Ir gamma rays 77−30673
sleeve, type St 37, deformation behaviour contrib. in rod drawing *(German)* 80−11684
sliding wear reduction by metallic coatings 77−21331
small diameter pipe weld, gamma radiography using enriched ^{169}Yb source 79−83399

steel continued
soft, EM wave propagation, penetration depth calc. *(Bulgarian)* 78−50679
soft, explosive deform. and destruction of tubes 78−6995
solidification of castings in mould *(Russian)* 78−27502
solidification of melting, fixed boundary condition modal, phase interface velocity *(Russian)* 78−15390
solification during continuous casting, cooling regime comparison *(Russian)* 80−93548
solubility of O_2 in steel Kh18-Ti-Al alloy *(Russian)* 80−92676
sorbitic, yield point rel. to average carbide particle size *(Russian)* 78−6967
spall investigations, pressures up to 100 kbar, failure and strength *(Ukrainian)* 77−73317
spalling prod. by sheet charge explosion and collision of plate 78−44198
spectrochemical analysis of molten steel 79−16096
spectrochemical analysis with glow-discharge lamp *(Japanese)* 78−85262
spectrophotometric determ. of Nb and Ta, Zr in mixed ligand complex 77−16878
sphere, dissolution in H_2SO_4 in elec. field *(Russian)* 77−4867
spheres, impact on glass surface, damage 78−52994
spheroidised AISI 1095, U-notched bend specimens, hydrogen effect on fracture 79−52363
spheroidised type AISI 1090, hot rolled H_2 promotion of plastic instability 78−60725
spheroidization of pearlite, global microstruct. evolution 80−108482
spheroidized, Bauschinger effect and work hardening 78−64596
spheroidized AISI 1095, ductile fracture of U-notched bend specimens 79−24616
spot welding process, acoustic emission signals, anal. *(German)* 78−44296
spring wire and springs, type 60S2A and 50KhFA, stress tempering effect on mech. props. 79−66085
sputter deposited carbide coating, adhesion 77−12531
square parts, surface inspection, defect depth meas., eddy current method 79−29307
statistical distrib. of mech. props., and life characts. exam. 78−64606
statistical fatigue props. of SM50A for welded structures *(Japanese)* 79−20168
steady state unidirectionally solidified, dendrite morphology 77−16569
steam turbine, rotor steel type EI-415, low-cycle fatigue and short term creep investigation 77−25238
steam turbogenerator rotors, fatigue crack initiation and growth, from macroscopic slag inclusions 78−64681
steel, carburising, carbide-austenite layers, form. and development 80−35413
steel, Ck 45, cylindrical bodies rolling over one another, plastic deformations caused by frictional forces 80−11735
steel, corrosion fatigue crack growth, compliance tests and metallographic exam. 78−53027
steel, forged axle spindle, fractographic anal. of shear fracture 78−68821
steel, fracture ductility, determ. in bending tests and US emission 78−23899
steel, fretting against polymers, composition effect on metal surface wear 78−60848
steel, heat-resist., C replica method of investigating creep damage in TEM 80−21012
steel, impact strength, effect of surface decarburization and carburization of faces and core struct. 78−23811
steel, long-term strength, H effect 80−55581
steel, Mn, stacking fault energy rel. to mech. props. *(French)* 79−43339
steel, plastic deformation and cryst. texture in equibiaxial expsn. 80−7653
steel, rails of DIN 15087E, shear stress distribution caused by transverse force *(German)* 79−61647
steel, static bend testing of cracked samples until failure, −60 to 20°C 78−23893
steel, structural, grain size depend. of yield stress in homogeneous deformation range *(German)* 80−30013
steel, type 1045, hydrogen enhanced nucleation of microvoid as function of local plastic strain 79−79053
steel, type 12X18H10T, strengthening based on intensifying heat exchange processes in martensitic transformation region *(Russian)* 79−70065
steel fibre reinforced Al, fatigue strength *(Czech)* 78−60748
steel sheet, surface anal. by ion etching and atomic absorpt. spectroscopy *(German)* 80−81377
steel tubes, ferromag., complex of devices for automatic nondestructive testing 78−53092
steel tubing, cold rolled, nondestructive mag. method for determ. of mech. props. 78−23903
steel-Al-steel plate, fatigue damage analysis and life predictor 77−25120
steel-aluminium plates, exam. of adhesion strength by impulse loading 78−84943
steel-bronze bimetal mech. props., diffusional interlayer effects 79−29169
steel-Cu (steel) channel with parallel flat walls, ice growth in laminar flow 79−3908
steel-Cu M3 bimetal, eutectic alloy, crack development, failure energy capacity *(Russian)* 80−40480
steels, 2Kh13 and 20Kh1M1FTR, sulphide cracking resistance, strengthening method influence 80−55577
steels, spring, 60S2A and 50KhFA, heat treatment and mech. working effect on mech. props. *(Russian)* 80−20962
strain hardening, weakening factor 1273-1473K *(Russian)* 79−78990
strain-hardened subsurface layer, residual stress change in fatigue 80−81185
strength, acoustic monitoring 80−35479
strength, chemical composition effect statistical treatment of test data 79−57081
strength, ductility rel. to H_2 corrosion at 1000 kg/cm^2 press., 450°C, type 12 MKh *(Russian)* 79−15723
strength, effect of H_2 78−3197
strength reduction by adsorpt., stress-corrosion *(Russian)* 79−29265
strength tests, hydrogen cracking 77−86243
strength variation under influence of shock waves for steels St3 and KhVG *(Russian)* 78−92299
strengthened, high temp. deform. line charact. *(Russian)* 77−25099
strengthened by surface plastic deform., tempering effect on physicomech. props. *(Russian)* 78−35409
strengthening by rapid electrothermal treatment 78−84870
steel continued
strengthening type Kh18N9T by vibrational stirring effect 80−40405
stress and strain intensity, determ. after plastic deform. using microhardness meas. 80−40641
stress corrosion cracking, in liquid NH_3, electrochemical exam. *(Japanese)* 78−39945
stress corrosion cracking, intercrystalline, in $Ca(NO_3)_2$ soln. *(German)* 80−30130
stress corrosion cracking, modelling and kinetics *(Russian)* 77−77623
stress corrosion cracking, optical detection of acoustic emission 77−90510
stress corrosion cracking of 20, 17GS, 65C, and 40, simulated field trials of inhibitor KXO in H_2S cracking *(Russian)* 78−31573
stress corrosion in inhibited H_2SO_4, surface macrogeometry and endurance *(Russian)* 77−25184
stress cracking, of pressure vessels in chem. plants 78−85027
stress distribution, calcs., during cooling, program system THEPLA *(German)* 80−35237
stress meas. and calc. around drilled hole, with hole-gage-rosettes aid *(German)* 80−25757
stress measurement, US method, calibration expt. results *(German)* 80−53725
stress relaxation, long-time, in 19-9 DL *(Japanese)* 77−59841
stress relaxation, short-term, creep and strain hardening *(Russian)* 80−30005
stress relaxation characts., reinforcing steel 23Kh2G2T 78−44159
stress relaxation in cyclic deformation 80−3119
stress/deformation response meas. device *(German)* 78−3261
stress/strain diagrams of structures 79−87703
stretch-bend test strain distribution obs. 77−70243
strip, coating by high rate electron bean evaporating of Al 79−24440
strip, US inspection by differential method using binary comparative probes 79−70285
strip, Zn coated, plastic deform. of coating 77−90368
strip components, automatic US macrostruct. monitoring 79−79203
strip inspection for cracks, magnetic instrument 79−52584
struct. type 05KhGM 80−35313
structural, 34KhN3M, heat treatment effect on magnetostriction 80−104306
structural, 35KhN1M2F, forgings, struct. inheritance during ht. treatment 78−23735
structural, arrested brittle cracks in Robertson test with temp. gradient 77−56052
structural, austenite form. during heating *(Russian)* 77−32572
structural, Bauschinger effect *(French)* 78−23787
structural, brittle fracture, conditions for prediction in welded structures *(French)* 80−25867
structural, brittle fracture, intermediate fracture stress, fracture initiation mode transition 78−60802
structural, brittleness susceptibility rel. to heat treatment 79−24620
structural, classification according to ductile-brittle transition temp. 78−11298
structural, corrosion fatigue strength, effect of medium temp. 80−55583
structural, ductile-brittle transition, anal. soln. by deadweight tensile test method *(Slovak)* 79−79095
structural, elastic limit determ. by acoustic emission 80−66716
structural, fatigue crack propagation in ductile-brittle transition temp. range 77−59929
structural, fracture initiation, exam. 78−60778
structural, fracture toughness 77−59923
structural, fracture toughness dynamic meas. 77−56167
structural, high strength type StE47, specimen geometry and plastic deform. effect on fracture mechanics *(German)* 80−66613
structural, indentation testing, mech. characts. calcs. inc. elastic strains *(Russian)* 78−95863
structural, influence of deform. heat on the mech. props. *(German)* 78−84904
structural, lateral notches rel. to ductile fracture characts. 79−43392
structural, low temp. fatigue strength 77−21273
structural, naturally and artificially weathered, SEM characteris. 78−23882
structural, nondestructive method of struct. damage investig. using cyclic loading effects and mag. characts. 78−3275
structural, notched, cathodic polarisation effect on fatigue in seawater 79−47805
structural, rate of damage detection by fatigue testing of instrumentation *(German)* 78−19972
structural, rel. between static and dynamic fracture toughness 78−68815
structural, resistance to low endurance fatigue fracture, in biaxial stress 78−15531
structural, second phase particle effects on impact strength 80−108581
structural, sharp notched bending specimens, fracture stress, temp. depend. anal. 77−56062
structural, slow stable crack growth, exam. of crack profile 78−84965
structural, strained in tension after tempering, compression effects on struct. changes *(Russian)* 80−66577
structural, subject to low temp. low cycle fatigue, failure charact. 77−70174
structural, supercooled austenite, structural characts. of decomposition 80−60870
structural, susceptibility to brittle fracture criteria, comparison of notch impact and fracture toughness testing *(German)* 77−70237
structural, temp. increase during plastic deform. *(German)* 78−84903
structural, thermal etching displaying hardening structure 77−40487
structural, type St 37, microstruct. rel. to fracture toughness and fracture load of bending specimens *(German)* 80−89352
structural, wide plate tensile testing eval. *(German)* 80−100969
structural, with elevated and high strength, damping capacity 77−21205
structural, with yield pt. of about 420 to 720 N/mm^2, correlation between yield pt./tensile strength ratio and toughness *(German)* 80−66615
structural 15Kh2NMFA, use of linear and nonlinear fracture mech. for crack propagation resist. determ. 79−5056
structural 15KhNMFA, resist. to weakening during tempering, high purity effect 80−76279
structural changes in types 60 G, ShKh15 near holes and inclusions due to pulsed currents *(Russian)* 80−108459
structural fatigue life distrib., statistical anal., mixed Weibull distrib. *(Japanese)* 78−72841
structural heterogenities, detection by mag. aerosol method 78−44314
structural mechanism of recrystallisation during ht. treatment 78−84847

steel continued
structural recrystallisation, phase and struct. transformations during heating 77−55990
structural St 37-2, cleavage fracture, report 80−25868
structural steel, effect of stressed state nature on ductility and failure 79−57078
structural steel cracking, plastic deform. and fracture toughness obs. *(German)* 77−59936
structural ties, NDT by eddy current transducer, optimum parameters and capabilities 80−108669
structure after high-speed cold plastic deformation steels 60, 18Kh2N4MA, 17GSND, and 12Kh21N5T 80−76316
structure and strength, conf., Kiev, USSR (Sep. 1976) 77−59921
structures, appl. of risk analysis to brittle fracture and fatigue 78−56768
substrate, acoustic emission of thermal-sprayed oxide coating 80−21247
substrate, plasma-sprayed Al coating, microstruct., TEM and SEM obs. 78−11426
substrate, Sn autocatalytic deposition 80−100965
substrate for Cr_7C_3 electrophoretic coatings, sintering 80−66707
substrate for Cv vacuum coatings, influence of precipitation conditions on porosity *(Russian)* 80−54578
substrate for W_2C and W_3C wear resistant coatings formed at low temp. by CVD 78−92404
substrate limiting temp. during vaporisation and condensation coating in vacuum *(Russian)* 80−100787
subsurface defects in metals, detection using gamma rays 78−85104
sulphide stress corrosion cracking, threshold stress and crack initiation stress intensity comparison 80−21158
sulphide stress cracking of big-inch live pipes 77−12730
superheated-steam oxidation, exam. of catalyst influence 78−85030
superplasticity under compression of U8A, 5KhNM and 12KhNZA 77−86086
surface, chem. characterisation by SIMS, glow discharge spectrometry and other techniques 80−66907
surface, contact angs. meas., aq. ethanol (glycerine) solns., 20-70°C 78−56025
surface, in contact with polycarbonate, surface morphology changes in polymer induced by fretting 78−15538
surface, nitrided, chem. state anal. by conversion electron Mossbauer spectrometry 80−7718
surface, saturation with Sb and As under glass fusion treatment *(Russian)* 78−35585
surface, supersonic plasma inpact effect, boundary layer role 79−32780
surface cleaning in glow discharge, ion bombardment effect *(Russian)* 78−95848
surface cold work, residual stress distrib. *(Russian)* 77−59975
surface composition, degreasing and batch annealing effects 80−66700
surface decarburation, luminescent discharge spectrometry exam. *(French)* 78−31585
surface defect detection by magnetographic method 78−44332
surface deformation by oblique impact of square plates 77−66701
surface hardened, luminescent-discharge optical emission spectrometry appl. to surface anal. *(French)* 79−79164
surface hardening, ion-carbo-nitriding in CO-N_2-H_2 gas mixtures, expt. *(Japanese)* 80−71670
surface hardening by US treatment *(Russian)* 77−73364
surface hardening during electrospark alloying with transition metals IV-VI *(Russian)* 78−95849
surface hardening using CO_2 laser beam 77−90490
surface HF inductive pulse hardening *(German)* 78−27687
surface layers, cross-sectional struct., appl. of cryogenic fracturing technique 77−30219
surface layers of NbC and VC formed by immersion in hot bath containing Fe-V or Fe-Nb and carbonate *(Japanese)* 77−52672
surface machined, morphology, struct., SEM, topographic investigs. *(German)* 77−73372
surface metrology using peak counting, quality control 80−95065
surface pretreatment effect on joint bond strength by cyanoacrylate adhesive Kanokonlit-E of type A St 3 *(German)* 79−57202
surface Si reinforced type U8, metastable phase, composition, struct. *(Russian)* 80−92599
surface state influence on etching effect 80−81235
surface stress measurement using US goniometer 79−15947
surface structural changes on exposure to plasma, etch resistance *(Russian)* 79−83234
surface treatment, protective coatings for scuffing and adhesive wear resistance 77−86217
surface treatment process in nontoxic salt bath 79−83398
surface wearing ability, finished surface direction effect on wearing ability 80−11793
surface work hardening effect on life 77−70234
surfaces, machined, X-ray diffr. residual stress meas. methods, comparison 77−56212
surfaces, O and N profiles, Rutherford backscatt. and (d,p) reaction anal. 79−5216
surgical implant materials, corrosion fatigue props. 79−39604
surgical implant materials, corrosion props. 79−39605
tape, US inspection for segregate type defects, exam. of method 79−15943
tapered beam, collapse behaviour 78−87287
tearing rate determ. by elec. resist. meas. method *(German)* 78−15619
temper brittleness and intercrystalline segregation in type 20 CND 10-10 *(French)* 77−81316
temper embrittlement, effect of sp-3d impurity interactions on resistivity 79−46696
temper embrittlement, fracture mech. of grain boundary segregated phases 78−48531
tempered, kinetics of solution of Mn in precipitated cementite *(Russian)* 78−6891
tempered, low-temperature, shock wave loading effects on mech. props. *(Russian)* 77−59857
tempered, notched, impact bending tests, cold brittleness curves 80−71758
tempered or quenched, exam. of fracture toughness tests, for C shaped specimens 79−29215
tempered StE70, water quenched, residual stress field in centrally welded plates *(German)* 78−72794
tensile prestrained strength of anisotropy rolled steel, rot.-bending fatigue tests, slip bands 78−27590
tensile strength, and ductility of 45, Kh18N10T, and 30KhGSA, relative elongation 79−15927
steel continued
tensile test pieces, comparison of micro and standardised size *(German)* 79−83414
tensile testing, effect of specimen form, specimen prep., testing velocity, straining amount *(German)* 77−16764
tensile testing, fastening method for wire rope 79−87779
tensile testing of ultra high tensile roping wire 77−44426
testing in moist H_2S 78−23901
texture sheet, mechanical anisotropy estimation using quantitative metallography *(German, English)* 77−77696
textured, X-ray stress meas. 77−46975
thermal conductivity temp. depend. *(Russian)* 77−55514
thermal cycling and cyclic stress effects on strength and creep resist. of type 15Kh1M1F *(Russian)* 79−52341
thermal cycling fracture 78−60839
thermal fatigue, effects of inclusions 80−81183
thermal fatigue resistance, nuclear power plant materials, relation with strain and time for various steels, at temp. 350-900°C 78−31534
thermal fatigue strength in presence of stress conc. 77−70180
thermal hardening stress determ. by thermoplasticity theory 79−29076
thermal props. meas. *(French)* 80−25977
thermal shock cracking, fracture mechanics and fractographic exam. *(Japanese)* 78−52964
thermally strengthened rolled, 35GS and 20GS, H_2 embrittlement and cracking resistance *(Russian)* 78−35479
thermoelastic problem for Griffith crack, temp. dependent props. under linear temp distrib. 80−48579
thermomechanical hardening *(Czechoslovakian)* 77−32602
thermomechanical treatment, sulphide inclusion behaviour 79−11647
thermomechanical treatment 77−4796
thermomechanical treatment effect on mech. props. and microstruct. *(French, German)* 79−66090
thick articles, thickness and continuity monitoring by neutron radiometry 79−93100
thin sheet flaw detector, magnetisation system 77−12751
thin sheets, C and N contents determ. by internal friction *(German)* 78−27715
thin steel plate, anal. of longit. stresses and strains due to moving heat source 79−81723
thin walled shell, failure of model when loaded by internal press. 77−11147
thread rolled, Moire fringe method for examining local deform. zones 80−21220
time and spatially resolved at. absorpt. anal. 80−40760
tin plate, passivation treatment 80−61146
tinplate surfaces, Auger depth profiling and anal. 80−59768
tool, type NC6, cementite network separation, kinetics *(Polish)* 80−25698
tool and high-speed, high freq. induction melting and centrifugal casting in instrumental anal. 80−84886
tool steel, US vel. meas., 20-900°C 80−70318
torsion tests 79−61690
toughness, effect of Sn, SEM exam. 80−97569
toughness, review of joint tests *(German)* 80−65142
trace element analysis, spectra of laser plasma, nuclear reactor steels 78−88691
trace element UV emission, spectrochem. anal. *(French)* 80−71997
track autoradiography for N detect. 80−100979
tranforms CC types M6 and M3N, elastoplastic bending, insulating coating influence on magnetic losses *(Russian)* 79−100284
transformation microtwins formation in ferrite, types 10G2 and 18G2F *(Russian)* 79−1866
transformations, influence of type of cold plastic strain *(Russian)* 79−52232
transformer, anisotropy of temp. depend. of mag. props. *(Russian)* 78−39362
transformer, domain structure, triaxial ferromagnets, spontaneous magnetisation distrib., plane stress state influence *(Russian)* 79−61071
transformer, EM losses, effect of degree of perfection of crystallographic texture *(Russian)* 78−60309
transformer, EM losses, influence of charact. of substruct. distrib. *(Russian)* 78−7058
transformer, inhibitory phase *(Russian)* 78−3139
transformer, oriented, coated stresses determ. by bending experiments *(German)* 79−28569
transformer, texture formation tendency *(Russian)* 77−59803
transformer steel, cold-rolled effect of uniaxial elastic stress on dynamic magnetostriction *(Russian)* 77−69651
transition element depth profile meas. using (p,γ) react. 80−50910
transition temp. determ. from fibrous structure in fracture, exam. of method 78−85080
TRIP, fatigue crack propagation 78−64696
TRIP, powder processing, tensile strength, ductility 78−64499
TRIP steels, strength and plasticity rel. to thermomech. treatments 77−44281
TRIP steels, strengthened struct., and mechanical props. *(Russian)* 78−76647
tube, mech. prop. testing by harmonic method using instrument type KAP with feedthrough transducer 78−53154
tube eversion, effect of material and geometrical parameters 79−15690
tubes, 12 Kh1MF, cross-section shape change, during creep of bent tubes loaded with internal pressure 78−31485
tubes, helical welded, computerised US quality control 78−35601
tubes, square section, collapse in bending 80−25792
tubing, NDT method comparison, optimum combination determ. 78−44308
tubing, viscoplastic bending 78−35464
tubular, type 0Kh16N15M3B, reactor irradiated, creep resist. *(Russian)* 80−25762
tufftrided, fatigue strength estimation from heat generation in specimen *(Japanese)* 77−52476
tufftrided, fatigue strength under reversed torsion *(Japanese)* 79−61707
tufftrided, hardened, fatigue life, effect of programmed load history *(Japanese)* 79−20160
tufftrided, observation of fatigue fracture surface *(Japanese)* 78−52951
tufftrided, residual stress and fatigue crack propag. *(Japanese)* 77−48536
tufftrided, S15CK smooth specimens, fatigue strength, strengthening mechanisms *(Japanese)* 78−27609
type 33Kh3SNMVFA, high-strength, failure accompanying cyclical elastoplastic straining *(Russian)* 79−70152

steel continued
type 35L, heat treated, exam. of surface defects using fluorescent liquids 79−5101
type 35L, heat treated, exam. of surface defects using fluorescent liquids 79−15933
type ASTM A36, Cl embrittling effect on fatigue crack growth rate 79−74254
type CW316, void-swelling, response to temp. changes 79−65116
type HT80, delayed retardation phenomena of fatigue crack growth, exam. 78−56745
U8, hydrogenation effects on fatigue crack propag. *(Russian)* 78−56800
ultra high strength, P induced 350°C embrittlement 79−57099
ultra-high strength, H induced delayed plasticity and cracking 80−21100
ultra-high strength, strengthening, props. and charact. *(Korean)* 79−24607
ultrahigh strength, effects of strength and grain size on near-threshold fatigue crack growth 78−64704
ultrahigh strength, historical case study 80−7609
ultrahigh strength, monotonic and cyclic stress strain curves 80−35268
ultrahigh strength, near-threshold fatigue crack propagation, load cycle and cyclic strength effects 78−11331
ultrasonic inspection through fluid gap of square ingots 78−56855
ultrasonic investigation of casting 79−66252
ultrasonic testing, sensitivity adjustment for focusing probes, testing of planar and curves surfaces *(German)* 78−7152
unalloyed, brittle fracture, effect of prestrain and ageing *(German)* 78−19857
unalloyed, electric metallisation, corrosion resistance tests *(Russian)* 78−19935
unalloyed, high temp. short term fatigue tests 79−66233
undirectionally solidifying melt, horizontal macrosegregation during solidification with heterogeneous layer *(German)* 78−19733
unhardened, grinding by Si_3N_4-based abrasive material 78−35529
unlubricated sliding wear, effect of N ion implantation 79−74261
unnotched C-35, cumulative damage rule based on knee point of S-N curve 77−25156
unnotched samples, fatigue limit, estimation of scale relationship, error anal. 79−15793
upper bainite, relation between cementite and ferrite lattice orientations in steel U15 and 130 Gz *(Russian)* 78−23663
US analysis, real defects, statistical methods appl. 78−72976
US attenuation, defect effects in US inspection *(Italian)* 78−48609
US attenuation, precrack damage and crack propag. study 80−40656
US attenuation at large strain amplitudes 77−1182
US attenuation sorting of normally and partially annealed sheet *(German)* 77−77692
US charact., change with stress appl., exam. 78−48579
US cleaning incorporation in continuous annealing plants 77−1884
US critical angle reflectivity, near-surface metallic prop. gradient effect 80−70516
US defectometry, reliability for welds in 22K steel 78−56858
US grain size determ. 78−40015
US immersion testing, effects of curved entry surfaces on calibration, steel sample expts. 80−71849
US inspection of hot thick steel products 80−40661
US inspection to 1000°C, hot-metal defectoscopy 80−66750
US internal flaw detection system 77−66717
US plate testing, dynamic evaluation of flaw size 79−15949
US strengthening treatment effect on fatigue resistance 80−81193
US testing, possibilities and limitations 78−19979
US testing of strength 79−39104
US tube expansion force reduction expts. 78−59186
US velocity, meas. method for isotropic nondispersive solids 80−69616
vacuum furnace developments, heat treatment, high speed steels *(German)* 79−100174
vibrating stressed plate, anal. by combined holographic interferometry and finite element anal. *(German)* 78−90806
voids and swelling following $^{56}Fe^{3+}$ bombardment, fast neutron effects simulation 77−30651
volatile products from reaction with H_2O-CO_2, high temp. 80−81233
water accleratred fatigue, lubricant additive effects 78−64710
water soluble polymer quenchants 79−100190
wear, cyclic, or brass 79−52380
wear at high sliding speed of AISI 1020 78−3237
wear at PTFE, high density polyethylene, and polyoxymethylene sliding surface 78−64727
wear charact. of burnished machined surfaces 80−108595
wear due to paper and printer ribbon exam. 79−15812
wear loss, using $^{56}Fe(p,n)^{56}Co$ and loss of activity meas. 77−4881
wear meas. by ^{56}Co activity reduction 79−57166
wear mechanism during fretting corrosion on polymers 78−35522
wear mechanism review 78−72891
wear mechanisms, metallographic obs. 77−59942
wear of single abrasive grains, using pin on disc wear test *(Japanese)* 78−44230
wear produced by polyisoprene, polybutadiene, rubber 79−15810
wear resist., effect of rolling friction strengthening, oil abrasive environment *(Russian)* 79−15799
wear resistance, determ. using MI-1M machine 80−25943
wear resistance, effect of compressive stress, methods of investigation 77−25208
wear resistance during abrasive wear, comp. and struct. effects 80−35337
wear resistance fo 30 KhGSA and 40 KhNMA after thermal and thermomech. treatment 77−70087
wear resistance in oil abrasive environment, various grinding methods *(Russian)* 77−70184
wear resistance of broaching bits in relation to boriding and heat treatment 78−85051
wear resistance of low temp. nitriding treatment 80−89357
wear resistant coatings on steel, vapour deposition 79−56935
wear resistant silicide coating 78−72936
wear testing in oils containing organosulphur epds., XPS obs. of surface comp. rel. to wear 77−36668
wedged crack propagation, in type AISI 1018 80−2115
weld, flaw-size meas. by US frequency anal. 77−44429
weld fatigue life estimation, multichannel NDT monitor 78−56846
weld radiograph interpretation 79−91861
weldable, C and alloy, brittle fracture, metallurgical factor effects, NDT data, impact tests *(French)* 79−5128
steel continued
weldable, fatigue data, low and high cycle compatibility *(Czech)* 80−89343
welded joint, standardization of radiographic flaw detection 79−91900
welded joint brittle fracture susceptibility test 79−29168
welded joint impact strength, preheating and tempering effects 79−24542
welded joints, bead-on-plate, H2 diffusion and trapping 80−96697
welded joints, durability in repeated impact loading, low temp. effects 77−63800
welded joints, resistance to cold cracking obs., C and H_2 content influence 77−21283
welded joints of tube 10G2SD, corrosion fatigue *(Russian)* 78−35574
welded specimen AE testing by external static loading of cold cracking susceptibility 78−40013
welded steels, types D36, D50, secondary ion anal. of segregation 80−7580
welding, development and results of an instrumented restrained cracking (IRC) test *(German)* 78−85060
welding residual stresses, sources, X-ray meas. *(German)* 77−86265
welds in plates, flaw classification using microprocessor controlled flaw detector 80−100992
welds obs. at high temperature, by moire photography 79−74336
whisker, polycryst., FIM obs. of struct. 78−84111
white layers forming at high rates of friction, struct. props. *(Russian)* 79−15800
white phases structure after heat treatment, steels ShKh15 and 12KhN3A 80−76281
white zone formation, in type 1Kh17N2, and props. during friction in vac. *(Russian)* 80−40542
wide plate tests, and V-notch bending tests evaluation on basis of materials mechanics *(German)* 80−66571
wire, brass coated, surface composition, oxidation, sulphidation, study by XPS 78−11423
wire, drawn, age hardening props. obs., mechanical and electrical props. relationship 80−50662
wire, drawn, quantitative texture anal., neutron diffr. studies 80−81078
wire, dynamic moduli of elasticity meas. by travelling normal wave method 78−53110
wire, reinforced prestressed concrete, strain-tempering conditions and mech. props. *(Japanese)* 78−39816
wire, US inspection, immersion method 80−66757
wire reinforced Al-Zn-Mg, tensile strength depend. on angle of reinforcement *(Russian)* 78−15452
wire reinforced Portland cement mortar, wire pull out, inelastic behaviour 78−56681
wires reinforced Pb, deform. behaviour and effect of volume fraction and surface treatments *(Japanese)* 79−66118
wooden fracture pattern obs. *(Chinese)* 79−43376
work hardening modulus and malleability in static tension 77−77496
work hardening of 40Kh specimens, plastic-strain mechanism 78−42530
work hardening parameter determ. 77−77495
work hardening under nonisothermal loading 79−57005
work-hardenable, N26T low magnetic phase, fatigue strength effect of surface treatment 77−48546
X-ray and microhardness meas. at high strain rates *(German)* 78−3184
X-ray spectral anal., theoretical correction parameters rel. to chem. composition 78−61108
yield, H_2 effect 78−15474
yield point, research of Cottrell and Bilby, (1945-55) 80−62444
yield point charact., of C15, grain size effect *(German)* 78−72810
yield point suppression by H_2 in A-106 79−8368
yield strength, influence of deform. rate on type 10G2SAF *(Bulgarian)* 80−89315
yield strength, statistical treatment of experimental data 80−53644
yielded pipeline, fracture resistance changes, impact tests 77−16667
Young's modulus of Fe_3C phase *(Russian)* 80−76297
Ag/steel sliding system, tribological behaviour, effect of temp., atmos., load and geometry *(German)* 79−34158
Al coated, porosity evaluation, micro X-ray spectral anal. *(Russian)* 80−35389
Al killed, cold rolled and recrystallised grain shape anisotropy 79−34064
Al-steel bimetalic wire for overhead lines, manufacturing methods 80−16247
Al-steel mixture, wear resistant, produced by compaction by discrete shock waves 80−84882
Al-steel profiled composite, pulling from melt, mech. props. 78−3075
Al-steel radiation shields, build-up factors for 6.2 MeV photons 79−81093
B coating on steel 45, effect of abrasive particle size on wear 78−44225
B-Cu(Al) coating on steel 45, effect of abrasive particle size on wear 78−44225
C, brazed joints, corrosion mechanical strength 79−43491
C-C interaction energy, thermodynamics of steels 80−93793
Cd, protective coating, on 30KhGSA steel, in Black Sea 78−19956
Cr deposited cylinder X-ray meas. of internal stresses in electrodeposition stress 78−27693
Cr plated, factors influencing durability 80−108643
Cr plated, high strength, with and without surface strengthening prior to plating 79−39051
Cr, stress relaxation, superplasticity and thermal cycling *(Russian)* 80−21019
Cr-Cu-Mn, fatigue crack propag. rate eval. by J integral method *(Japanese)* 79−8346
Cr-Mo-V, brittle failure resistance obs. influence of cold plastic deform. 78−72858
Cr-Ni-Mn, adiabatic shear band determ. by surface obs. 80−97579
Cr-Ni-Ti alloy and steel, emissitivty and reflectivity, oxide film thickness effect 79−82364
Cu alloys, cavitation during superplastic flow, affecting factors 78−60728
Cu clad, bond strength through intermediate Zn layer *(Korean)* 79−66213
Cu clad pipe, determ. of yield, tensile strength 80−25771
Cu-graphite brushes, friction and wear under severe sliding conditions against steel 79−38991
Cu-Ni, effect of alloying and residual elements 78−85033
Cu-steel, system, realisation of selective transport mode with friction, effects of normal stresses 79−87735
Fe, Armco, boride coatings, under elec. heating conditions, hydroabrasion wear resist. 80−55543

steel continued
Fe_2O_3, transformation to Fe_3O_4 in oxide scales on steel, conversion kinetics 80−7561
H assisted cracking, mechanisms, review 80−50721
H discharging phenomena, effect of ϵ-Cu precipitates *(Japanese)* 80−7583
H embrittlement detection by US velocity 79−52613
H-dislocation, interactions rel. to H_2 embrittlement 79−42097
H_2 absorption, effect of organic inhibitors *(Russian)* 78−35570
H_2 assisted cracking equilibrium and kinetic studies 78−3201
H_2, effect on phys. and mech. props. 80−101657
I_2 adsorption on steel in HTGR He environment 80−44233
LiO_2-Na_2O-CaO-SiO_2 glass-ceramic coating, high temp. effects on steel substrate 79−61776
Mn-C-Si-Cu (0.95, 0.85, 0.25, 0.16 wt.%), fibrous-banded fracture mechanism 80−104280
MnCr (16, 5 wt.%), bending fatigue behaviour improvement by surface treatment *(German)* 78−84957
$Mn_3(PO_4)_2$ coating on steel, wear resistant appl. 80−16609
Mo^+ ion bombardment, phase composition and struct. change of surface layers *(Russian)* 80−24506
Mo-bearing, intercritically annealed dual-phase strip, props. and appl. 78−84858
Na-cooled fast reactor, structural steel properties 80−22942
Ni/steel, roll bonded clad plate, fatigue crack growth *(Japanese)* 79−61706
Ni-Co-Cr-Mo-C (10,14,2,1,0.16 wt.%), stress corrosion cracking at 22°C in 3.5% NaCl 79−8390
Ni-Cr coatings on steel, standardisation 79−57139
Ni-Cr-Ti-C (2.8, 0.9, 0.2, 0.73 wt.%) *(Russian)* 80−81072
O and Al content determ. by neutron activation *(Hungarian)* 78−92586
O_2 adsorption in ultra-high vacuum system at room temp. 77−20188
P, deep-drawing, spatial orientation distrib. of crystallites in cold-rolled and in annealed sheets 80−81079
S segregation problematics of additive segregation *(Czech)* 78−84818
Si determination by at. emission spectroscopy using steeloscope 79−57330
Si, mag., developments in technologically important materials, review 79−33509
Si, nonoriented sheet prod. with texture of {100} ⟨ovw⟩ 80−89246
Si-Al electrical steel, surface oxidation during annealing 78−68838
SiO_2, sitall coating, control of phase composition, microstruct. and props. 77−32545
SiO_2-Al_2O_3 glaze, adhesive behaviour of metallic cation glaze exchanged on acid site struct. *(Japanese)* 79−66216
TiC-steel cermet with Cu additions, precip. hardening and ht. treatment temp. 77−40414
Ti_3N_4 plasma condensation on steel and carbide *(Russian)* 80−20796
UO_2 molten, interactions with steel and graphite 79−49700
W-Mo-Co high-speed cutting steels, Co determ. 78−3416
WC-Co hard alloy-steel welds, effect of intermediate layer composition on structural changes and mechanical properties 78−60616
Zn coated, cold rolling influence on struct. and deform. of diffusional layer *(Russian)* 80−55465
Zn coated, fast reactions in hot galvanising rel. to props. 79−43486
Zn coated strips, plastic deform. influence on struct. and quality *(Russian)* 80−40377
Zn coating *(Dutch)* 78−48571

steel industry
air pollution control technology 77−21891
Burnpur-Jamshadpur mills (India), effects on rainfall within 200 km 77−56714
cooling water flow control in continuous casting process, vortex flowmeters 80−64655
EPIQUANT automatic structure analyser for inclusion investigs. in free-cutting steel 80−55609
furnace control, UNITROL Σ series using microcomputer, Japan 77−53877
heat treatment digital process control systems *(German)* 79−74166
high-temperature contactless testing by EM acoustics 78−85095
high-temperature ultrasonic testing *(Italian)* 79−96242
central Hungary, precipitation amounts, steelworks effects 79−20943
induction heating of slabs 80−71672
induction heating steel sheets, calc. 79−52280
laser-surface purification of ferrous metals 78−92392
metal flame spray coating acceptance factors and tests 79−83397
NDT, ferroprobe monitoring of rolled steel products with local transverse alternating magnetisation 77−73420
plasma melting furnace, development in GDR *(German)* 78−22522
sinter plant air pollution control system options 77−66982
US internal flaw detection system for blooms, billets and slabs 77−66717
X-ray energy spectrometers for anal. of ferrous metals, report *(French)* 78−85281
Zn thin metal primer systems for steelwork 79−79148

steel manufacture
basic oxygen furnace, process monitoring, use of X-ray spectrometer 79−17586
computerised spectrometric analysis and management information system 80−89574
condensation fume, nature and origin of particles 79−39221
continuous casting machine design, based on heat flow analysis, review 77−21048
hardening, secondary, of hot worked and rapidly worked steels *(German)* 80−3083
high-temperature working, effects on products props. *(German)* 80−3108
killed ingot, freezing process liq. core movement *(Russian)* 80−20921
liquid bath, shooting methods for projecting buoyant alloy additions, expt. and mathematical eval. 77−21047
low C, Al killed, improvement in Al control using rings 77−21049
for low temperature applications, comp. and processing research 77−52365
Martin bath, blowing with oxygen, smelting dust phase comp. determ. 77−52705
MHD industrial smelting, techniques, economics *(Russian)* 77−24980
nuclear energy steel making process, high temperature heat exchanger test plant *(Japanese)* 79−67817
oxidation processes in jet refining unit, activation anal. 79−87898
phase diagrams, use in production 79−11572

steel manufacture continued
refractory oxide electrolytes, elec. props. at steelmaking temps. *(German)* 77−90605
respirable airborne crystalline silica, silicosis in steelmaking environments 80−45832
rolling mill forces meas., using semiconductor strain gauge based extensometer 78−41296
semi-killed and rimmed, O_2 probe meas. 77−21050
slag, F determ. by 14 MeV neutron activation anal. *(Japanese)* 79−20484
smelting using MHD generator 79−70453
thermodynamics of rare earths 77−4782
C content in Fe_3C melt, measurement using automatic device 79−39252

stellar atmospheres
see also solar atmosphere
0B-type stars, O VI obs. in stellar winds 80−8630
209 BAC, WN8 star, nonisotropic mass loss rel. to circumstellar H II region (M1-67) internal motions 79−92841
A- and F-type stars, absolute energy distribs., temps. and surface gravities 77−17554
A- and F-type stars, heavy element content influence on colour-temp. relation *(Russian)* 78−93234
A-type stars, effect of $C+H^+ \rightleftharpoons C^+ + H$ charge transfer on C I 1101 Å absorpt. edge 80−90423
A-type stars, Lyman α effect on non-LTE model atmospheres 80−90422
A-type stars, mag. field generation by Coriolis EMF 78−8027
A-type stars, non-LTE anal. of O I lines 77−41378
A-type supergiant stars, mass loss rates from UV reson. line profiles 80−90424
absorption line formation depth *(Russian)* 77−64749
abundance effects in classification, IAU Symposium 72 (Lausanne, Switzerland 8-11 July 1975) 77−29802
abundance effects on atmosphere calcs. 77−29803
accreting compact object in binary system, magnetosphere theory, X-ray sources 80−46394
accreting stars, model IR spectra for dusty circumstellar shells 78−85934
accretion, spherical, buoyancy effect 80−109349
accretion disc of magnetised compact object, theory *(Russian)* 79−44467
accretion disc stability 77−29796
accretion discs, ang. momentum transfer 78−65609
accretion discs, fluid, orbiting Kerr black hole, analytic theory 78−36631
accretion discs, steady, optically thick, convective vertical energy transport 80−62112
accretion discs, turbulent energy transport 78−28661
accretion discs, viscosity determ. for Hercules X-1 and (SS 433) 80−62110
accretion discs *(Polish)* 78−89175
accretion discs in close binary systems, tidal torques 78−12296
accretion discs in X-ray binaries, structured coronae, model 79−48852
accretion disks, optically thick, pulsational instability to axially symm. oscills. 80−82190
accretion disks, theoretical review *(Polish)* 80−26739
accretion flows, in binary X-ray systems 78−12432
accretion magnetosphere stability, adiabatic gas model 77−49368
accretion magnetospheres, general solns. 77−45400
adiabatic gradient calc. using fast algorithm 77−74043
AFGL/CRL IR sources, spectroscopic obs. rel. to circumstellar extinction 78−32599
Algol, eclipsing binary, X-ray spectra interpretation, corona model 80−105283
Algol type systems, secondaries with active chromospheres, possible RS Canum Venaticorum system 80−105276
Am stars, model of extended atmosphere by nongravitational forces criticism 77−53597
Am-type, binary stars, tidal interaction producing stable atm., evolution 80−67752
o Andromedae, Be star, radial vels. obs. rel. to atmosphere stratification 79−58355
o Andromedae, Be star, spectrographic obs. and shell behaviour (1967 to 1976) 77−71116
o Andromedae, Be star, spectroscopic evidence for new shell episode 80−90444
λ Andromedae, spectroscopic binary, UV and optical obs. of chromospheric lines 79−30087
Z Andromedae, symbiotic star, atmospheric struct. from IUE obs. 80−109450
Ap and Bp stars, radiation forces and B abundance diffusion theory 79−88664
Ap stars, Barnes-Evans relation appl. as clue to atmospheric struct. and evolutionary status 79−67011
Ap stars, flows and mag. fields in surface layers 79−62854
Ap stars, heavy element abundances from Copernicus UV data, reference stars α Lyrae and α Canis Majoris A 78−28688
Ap stars, line blanketed model atmospheres 79−44495
Ap stars, line blanketed model atms. 79−21304
Ap stars, mag. latit. of metals 79−58341
Ap stars, magnetic, chemical comp. anomalies and atmospheres struct. *(Russian)* 77−22239
Ap stars, obs. evidence for pulsational stability 79−21303
Ap stars, thickness estimation of anomalous chem. comp. layer in atm. *(Russian)* 78−93279
Ap-type stars, magnetic fields in atmospheres *(Russian)* 77−17594
Ap-type stars, nonuniform surface chemical comp. rel. to mag. fields generation *(Russian)* 77−17591
α and β Aquari, G-type supergiants, evidence for hybrid atmospheres and winds from UV spectra 80−72948
α Aquarii, chromospheric event detect. from UV spectrum obs. 80−31299
R Aquarii, Mira variable, 14.9 GHz obs. rel. to chromosphere/corona radio emission 79−75210
σ Aquarii (A0 IVs), hot metallic-line star, abundance anal. from model atmosphere 80−90415
R Aquarii (M7+pec), late type variable star, IUE obs. of circumstellar emission 80−82370
R Aquilae, Mira variable, 14.9 GHz obs. rel. to chromosphere/corona radio emission 79−75210
V923 Aquilae, motion in shell and atmosphere 77−60776
θ Aquilae (B9.5 III), abundance anal. from model atmosphere 80−90415

stellar atmospheres continued
V603 Aquilae (Nova 1918), accretion disc eclipse model for periodic light vars. 80−82391
Ariel 0620−00, transient X-ray source, spherical model 78−12415
56 Arietis, spectrophotometry of Ap star, continuum features vars. 80−36638
UX Arietis (H0324+28), RS Canum Venaticorum system as coronal X-ray source 79−16979
α Arionis (Betelgeuse), UV flux and model atmosphere 77−22231
atomic line broadening by neutral H, simple formula 79−92665
ζ Aurigae, eclipsing binary, Ca I 6752 Å obs. rel. to circumstellar matter 77−17619
ζ Aurigae, eclipsing binary, UV obs. of supergiant atmos. 80−94836
ε Aurigae, extinction by circumstellar matter rel. to wavelength-depend. fluctuations 80−62190
ϵ Aurigae, fine analysis of atmosphere of primary F-type supergiant 78−85976
θ Aurigae, short period Ap star, mag. field rel. to atmospheric circulation currents 77−33511
α Aurigae (Capella), coronal line emission in soft X-ray spectrum 78−93228
α Aurigae (Capella), extra-atmospheric obs. analysis 79−25647
α Aurigae (Capella), model chromosphere 78−40931
α Aurigae (Capella), theoretical stellar chromosphere model 80−67718
α Aurigae (Capella), X-ray line emission obs., corona models 80−26905
axisymmetric accretion discs and flows, thickening 78−40989
axisymmetric moving envelopes, spectral line form. numerical method and appl. to YY Orionis stars 80−41813
B 1 Ia-0 supergiants, mass loss meas. 79−16948
late B dwarf in circumstellar dust cloud, IR source coincident with OH 205.1−14.1 80−101630
B-stars of early type, atm. LTE model using opacity sampling technique 80−90414
late B-type main-sequence stars, C I as continuous opacity source 77−87393
B-type stars, pole-on, rapidly rot., spectral inconsistencies due to gravity darkening 80−17581
B-type stars hot circumstellar plasma, constraints from XUV obs. 78−93232
baryon star magnetospheres, inclined rotator case 80−26887
baryon stars, magnetospheres model *(Russian)* 77−91555
BD −9°4395, H deficient star, spectral photometry and quantitative anal. 77−56946
Be and shell stars, UV radiation deficiency correl. with shell existence 80−90438
Be shell stars, Hβ high-resolution polarisation struct. rel. to circumstellar envelope scatt. 79−44485
Be stars, electron scatt. effects on Balmer emission lines 80−17589
Be stars, envelope struct. rel. to Paschen line emission and IR excess 77−22234
Be stars, equatorial disc model rel. to 1.25 and 2.2 microns polarimetry 79−44484
Be stars, intrinsic circumstellar polarisation and apparent rot. speed interpretation 78−96484
Be stars, orbital changes of gaseous ring 77−26013
Be stars, surface gravities 77−56974
Be stars envelopes, observational study 77−13355
Be stars review, circumstellar shells physical props 79−84809
Be-star circumstellar envelopes, models 77−60777
Be-stars, Paschen decrements and emission line formation in envelopes 77−56992
Be-stars, polarisation in extended circumstellar discs 77−56994
Be-stars, radiative accel. in extended atmospheres 77−56996
binary and multiple stars, polarisation by Thomson scatt. in optically thin stellar envelopes 78−81655
binary component, photospheric circulation, nonuniformly heated surface 79−96993
binary star giants, chromospheric activity due to tidal interactions 80−82420
binary stars, coronae above turbulent accretion discs 77−57038
binary stars, interpretation of circumstellar matter obs. 77−57042
binary stars, reflection effects evaluation, generalised approach 79−25631
binary stars with mass transfer, circumstellar discs form., particle motion calcs. 77−5545
close binary systems, atmospheric gas streams effects on radial vel. curves 80−94829
black hole, charged rotating, accretion disc mag. torque effects 79−17010
black hole, rotating, in mag. field, particle creation 77−2452
black hole accretion discs, boundary-layer behaviour of flow at disc inner edge 80−46598
black hole accretion discs, rapid X-ray variability and dying pulse trains 80−56872
black hole magnetospheres existence, theory 77−64792
black holes, relativistic accreting discs hydrodynamic struct. 78−36632
black holes, spin-up by thick accretion discs 80−105273
black holes, supercritical accretion discs models 80−105272
black holes, thick accretion discs models rel. to supercritical luminosities 80−101614
blue supergiant with neutron star immersed in envelope 80−98689
η Bootis, coronal emission model for soft X-rays obs. with imaging X-ray telescope 79−48953
44=i Bootis, eclipsing binary, variable lightcurve obs. rel. to circumstellar gas stream 78−61887
α Bootis, He I 10830 Å emission obs., high-temp. chromosphere 79−48792
α Bootis, K giant, surface gravity and mass 77−53587
α Bootis, non-thermal vels. height variation 77−13344
α Bootis (Arcturus), anal. of chromospheric O I spectrum 77−56923
A Bootis (Arcturus), atmospheric parameters determ. 78−20826
α Bootis (Arcturus), chromospheric Ca II K-line rel. to variable mass loss and convection 77−22213
α Bootis (Arcturus), CO fundamental bands, inhomogeneous chromosphere 78−36561
α Bootis (Arcturus), far UV spectrum, coronal temp. determ. 78−16407
α Bootis (Arcturus), line blanketing and atm. struct. 77−33483
α Bootis (Arcturus), model-atmos. analysis of spectrum 77−29827
α Bootis (Arcturus), UV obs. of chromospheric emission line profiles 78−81620

stellar atmospheres continued
α Bootis (Arcturus) (K2 IIIp), theoretical temp. minima and explanation of Wilson-Bappu effect 79−62825
ξ Bootis A, active dwarf star, chromospheric emission lines obs. 80−12762
boundary conditions with mass conditions with mass loss 78−12209
Z Camelopardalis, dwarf nova, accretion disc models at standstill and in eruption 80−82366
α Camelopardalis, O-type supergiant, spectroscopic study, model atm. anal. 78−28681
α Camelopardalis (O9.5 Ia), expanding envelope rot. rel. to variable Hα P Cygni profile 80−41818
α Camelopardalis (O9.5 Ia), stellar wind terminal vel. short time changes from UV spectrum 80−36625
κ Cancri, Hg-Mn star, diffusion processes and abundance amometers 77−87407
49 Cancri, spectrophotometry of Ap star, continuum features vars. 80−36638
WY Caneri, eclipsing binary, scatt. in cool component atmosphere 79−92799
VY Canis Majoris, circumstellar disc struct. from OH masers very long baseline interferometry 78−36712
VY Canis Majoris, circumstellar shell dia. upper limits 79−16974
VY Canis Majoris, circumstellar shell heterodyne interferometry 78−8000
UW Canis Majoris, eclipsing binary, mass flow anal. from UV spectrum 80−109429
UW Canis Majoris, eclipsing binary, UV photometry and primary component shape and atmospheric struct. 78−40992
α Canis Majoris, EUV obs., Sirius B model atm. 77−33489
UW Canis Majoris, O7f supergiant, mass loss rate meas. 80−67736
VY Canis Majoris, OH and H_2O microwave maser emission obs. 78−53949
α Canis Majoris (Sirius), Ca II K line profile rel. to atmospheric rel. fields 80−56830
α Canis Majoris (Sirius), Debye screening, no evidence for Hγ red shift 79−31369
α Canis Majoris (Sirius B), EUV obs., evidence against photospheric origin of 0.25 keV flux 78−49481
α Canis Majoris B, acoustically heated corona rel. to X-rays 77−60755
α Canis Majoris B (Sirius B), corona model constraints 79−2543
α Canis Minoris (Procyon), theoretical stellar chromosphere model 80−67718
Y Canum Venaticorum, C star, $^6Li/^7Li$ atmospheric abundance 77−33523
Y Canum Venaticorum, C star, IR spectrum rel. to photosphere and circumstellar shell 80−46544
TX Canum Venaticorum, cataclysmic variable shell and dust emission, visible spectra obs. 80−105249
α^2 CAnum Venaticorum, line blanketed model atmospheres of Ap-star 80−90440
α^2 Canum Venaticorum, magnetic field gradient in Ap-star atmosphere, Zeeman spectra 78−85953
RS Canum Venaticorum binary stars, mag. starspot model for photometric and spectroscopic behaviour 80−109488
α^2v Canum Venaticorum magnetic variable, H I lines and atmospheric parameters 79−97011
RS Canum Venaticorum systems, X-ray obs. and coronal model development 80−56873
RS Canum Venaticorum type binaries, Hγ line vars., chromospheric diagnostics 80−62181
δ Capricorni, eclipsing binary, Am primary component metallicism var. 77−67115
ν Capricorni (B9.5 V), abundance anal. from model atmosphere 80−90415
η Carinae, Fe II dielectronic recomb. rel. to IR excess 78−32478
η Carinae, IR ang. diameter 78−93271
η Carinae, spherical circumstellar dust shell model, radiative transfer 78−36577
α Carinae (Canopus), chromospheric scattering and generalised Compton effect in spectrum 78−53938
QZ Carinae (HD 93206), O-type quadruple eclipsing system, evidence for mass loss from supergiant 80−105275
γ Cassiopeiae, Be star, circumstellar shell expansion vel. from new UV shell lines 79−84802
γ Cassiopeiae, Be star, coordinated IR and optical obs. rel. to mass loss rate 79−25616
γ Cassiopeiae, Be star, IR excess 78−93257
γ Cassiopeiae, Be star, polarisation rapid vars. rel. to rot. circumstellar envelope inhomogeneities 80−22022
γ Cassiopeiae, Be star, possible identification with MX0053+60 transient X-ray source 77−49401
γ Cassiopeiae, circumstellar envelope model 78−40952
VX Cassiopeiae, circumstellar shell rel. to photometric variability *(Russian)* 80−72973
AO Cassiopeiae, eclipsing binary, intrinsic linear polarization, rel. to circumstellar envelope 77−17618
RZ Cassiopeiae, eclipsing binary, spectroscopic orbit and evidence for circumstellar matter 80−22040
κ Cassiopeiae, effective temp. radius, mass loss and luminosity 80−51748
R Cassiopeiae, late-type giant, circumstellar H_2O thermal emission 78−81628
κ Cassiopeiae, spectral obs., coarse atm. anal. 77−33487
6 Cassiopeiae, spectroscopic obs. of supergiant star, equivalent widths, microturbulence and radial vel. 80−22006
γ Cassiopeiae, UV and optical spectral var. rel. to coronal emission 78−93251
o Cassiopeiae (HD 4180), Be star circumstellar ionised gas rel. to IR and optical vars. 79−58353
cataclysmic binaries, circumstellar material geometrical and photometric parameters 80−109492
cataclysmic binaries accretion discs, convection as viscosity source 78−93307
cataclysmic binary formation through common envelope evolution 80−8651
cataclysmic variables, emission lines from accretion discs 80−51774
cellular convection in a stratified atmosphere 80−98652
proxima=V645 Centauri, dMe flare star, quiescent corona, transition region, and chromosphere obs. 80−56850
α Centauri A and B, IUE spectra and transition region models 80−46543

stellar atmospheres continued
α Centauri A and B, model chromospheres 77−13326
α Centauri binary system, sealed solar model atmospheres for spectroscopic anal. 80−62128
Centaurus X-3, neutron star accretion disc rel. to spin-up and X-ray luminosity 80−101648
Centaurus X-3, stellar wind vel. change during transition 80−12829
U Cephei, accretion discs obs. 80−82412
δ Cephei, atmospheric vel. field 79−25611
9 Cephei, B2-type supergiant, circumstellar CO lines discovery 79−84793
U Cephei, eclipsing binary, gas stream effects in UV spectrum, IUE obs. 80−26898
U Cephei, eclipsing binary, hot/cool spots obs. in UV light curves 78−57577
EM Cephei, eclipsing binary, spectroscopic obs. of shell *(Russian)* 78−57587
VV Cephei, eclipsing binary, UV spectrum 80−82415
VW Cephei, evidence for circumstellar matter 77−33563
δ Cephei, Hα radial vel. curve rel. to form. in stellar outer atmosphere 80−51788
μ Cephei, late-type supergiant, circumstellar H_2O thermal emission 78−81628
μ Cephei, M supergiant, circumstellar shell and mass loss rate 77−45415
U Cephei, mass transfer from light vars. outside primary eclipse, obs. and anal. 78−36636
19 Cephei, O-type supergiant, spectroscopic study, model atm. anal. 78−28681
U Cephei, recent eclipses obs. rel. to circumstellar luminous matter 79−67061
VV Cephei, spectroscopic obs. during eclipse rel. to rot. ring-shaped envelope 78−45359
λ Cephei, variable outflow in Of star, spectroscopic obs. 79−35263
9 Cephei (B2 Ib), circumstellar CO obs. 80−94795
IV Cephei (Nova 1971), shell physical conditions and ejecta He abundance 79−40203
β Cephei stars, effects of mass loss on instability strip 80−90436
Cepheid variables, He enrichment effects in atm., models 80−26884
Cepheid variables, stellar winds rel. to masses 78−57556
Cepheid-type stars, stability against nonradial oscills. 77−91552
Cepheids, model atmospheres rel. to intrinsic colours and physical props. 78−28696
Cepheids, relation between UV excess and superficial gravity 77−53604
o Ceti, atmosphere expansion vel. from IUE obs. 80−22027
π Ceti, late B-type star, X-ray emission obs. rel. to atmosphere mass motions 79−101160
o Ceti (Mira), TiO-related dia. vars. rel. to atmosphere optical thickness 78−16429
o Ceti (Mira) of 1978 max., light scatt. in atm., spectropolarimetry 80−94799
o Ceti circumstellar dust, 11 micron radiation vars. 79−5828
Z Chamaeleontis, eruptive binary, accretion disc struct. rel. to photometric behaviour 80−72961
chemical composition peculiarities rel. to stellar evolution 78−12207
chemically peculiar A-type stars, magnetosphere/grains interaction rel. to grains accretion 79−67017
chemically peculiar stars, nuclear and differentiated abundance patterns 77−17597
chromosphere Ca II emission in main sequence stars, comparison of activity cycles to old and young stars 80−105235
chromosphere Ca II H and K emission in field stars of solar neighbourhood, survey 80−109423
chromosphere models, Ca II H and K lines absolute flux profiles in F0 to M2-type stars 80−26842
chromosphere models, high-press. transition regions theory 80−26847
chromospheres, catalogue of stars with Ca II H and K emission lines *(Polish)* 80−82227
chromospheres, observational indicators, empirical models 80−12755
chromospheres, review *(German)* 80−109421
chromospheres, semi-empirical models *(Italian)* 78−32447
chromospheres, time dependent ionisation obs. 80−98651
chromospheres 77−91517
chromospheres and convection theory, H-R diagram boundary line 80−56823
chromospheres of F, G and K-type stars, radiative losses in continuum 80−72924
chromospheres of late type stars, temp. minima heights 78−20818
chromospheres of late-type stars, acoustic energy generation 78−7986
chromospheres of late-type stars, empirical estimates of radiative losses 78−40915
chromospheric activity in F- and G-stars 77−53594
chromospheric and coronal activity of solar type, observational aspects 77−56918
chromospheric scaling laws, width-luminosity correls., Wilson-Bappu effect 79−40177
chromospheric supersonic turbulence, Wilson-Bappu effect 77−17541
chromospheric var. in main sequence stars, Ca II line obs. 77−56936
chromospheric variations in main-sequence stars 79−16931
circumstellar bubble origin of solar O VI gas 78−57528
circumstellar clouds, evidence from Mg II 2800 Å data for early-type stars *(Russian, English)* 79−96992
circumstellar clouds, implications for existence of interstellar Mg lines obs. 80−94782
circumstellar clouds, scattered stellar radiation circular polarisation theory 78−96428
circumstellar disks and planetary formation 79−58321
circumstellar dust clouds, IR astronomy appls., review *(French)* 78−12352
circumstellar dust envelopes, calc. of eclipse light curves and fringe visibilities 79−35234
circumstellar dust grains formation, influence of Fe condensation 80−26927
circumstellar dust shells, among brightest IR sources of AFCRL Survey 77−87283
circumstellar dust shells, emission and absorption spectra 77−87376
circumstellar dust shells, IR obs. 77−41404
circumstellar dust shells, Monte Carlo simulation of polarised light transfer 78−81608
circumstellar dust shells, photoelectric yield of insulating dust grains 80−90507
stellar atmospheres continued
circumstellar dust shells, polarisation by Mie scatt., Monte Carlo anal. 80−98650
circumstellar dust shells, radiative transfer 77−13318
circumstellar envelopes, Monte Carlo analysis of polarization by Thomson scattering 80−85931
circumstellar envelopes scatt., radiation linear polarisation spectrum rel. to mag. field determ. *(Russian)* 80−90344
circumstellar gaseous ring around Be-stars, emission lines V/R var. 77−37604
circumstellar grains, evaporation and growth 79−35240
circumstellar radiating dust clouds 77−78863
circumstellar ring systems, SiO and H_2O maser line evidence 78−89195
circumstellar shell model for H_2O maser emission 77−60765
circumstellar shells, constraints on props. from thermal CO and SiO millimetre line emission obs. 78−49423
circumstellar shells angular diameter meas. IR interferometry 77−53576
circumstellar shells of long-period variables, weak maser emission pedestal assoc. with SiO maser 78−93256
circumstellar shock waves, H_2O masers collisional pumping 77−53675
circumstellar unbound particles, luminosity changes rel. to stochastic scatt., accretion and ejection 79−44338
CIT 6 (IRC+30219), IR C star, CO obs. of mass outflow 80−12761
classical novae, optically thin winds struct. 80−36643
classical novae, photospheric props. of optically thick winds 78−24516
classification dispersion spectra synthesis from atmos. theory 77−29804
close binaries, energy release, flares and particle acceleration *(Russian)* 80−73005
close binaries, light scattering in extrastellar gaseous material, emission line profiles spectropolarimetry obs. 80−109471
close binaries, narrow-band photometry and differential effects 80−67780
close binary components, model atms. 79−62869
close binary stars, gaseous circumstellar discs obs. 77−57043
close binary stars, nonradial radiative transfer 77−91567
close binary stars linear polarisation 77−49435
close binary systems, atmospheric gas motions rel. to radial vel. curves anal. 80−90470
cocoon stars, radiative transfer in envelope and IR spectra 77−64824
collapsed stars, accretion magnetosphere stability, polar cap dripping motion 78−4194
colliding stellar winds, X-ray emission upper limits 78−65607
collisionless subsonic accretion, stellar appl. 80−46380
17 Comae A, Ap star, Sr spots distrib. rel. to atmospheric mag. field *(Russian)* 77−17594
17 Comae A, magnetically variable Ap star, atmospheric struct. 77−17595
compact objects, nonrelativistic electrons interaction with radiation in mag. field 80−109354
compressible convection onset in model atmospheres 78−65605
Compton scattering opacity in partially degenerate electron plasma at high temp. 77−11322
contact binaries, common convective envelope 77−57048
contact binaries, envelope energy transfer model 80−90478
contact binaries, transport processes in envelopes 78−4279
contact binary stars, gas circulation 77−57017
contact binary stars, possibility of convective energy transfer between components *(Russian)* 77−17615
contact binary stars, unstable mass outflow 77−57018
convection parameters, meas. technique 79−21273
convection theory, choice of characteristic length 77−13317
convection zone, thermal equilib. in presence of mag. flux tube 77−53581
convective energy flux in atm. with gravit. field changes *(Russian)* 78−49422
convective energy transport in non-grey atmosphere 78−73703
convectively unstable atmospheres in shear flow, hydrodynamic instability 77−87253
cool C stars, $^{12}C/^{13}C$ ratio calc. 78−4205
cool C stars, distances and radii rel. to mass ejection 78−49434
cool DA white dwarf and subdwarf discrimination by spectroscopy and photometry 78−7999
cool giant stars, chromosphere mass loss determ. from Mg II UV line obs. 80−85935
cool giant stars, model depend. of detailed anal. 77−53590
cool Mira variables, shock waves accel. in photosphere 77−13352
cool stars, HEAO 1 search for coronal soft X-ray emission 79−101140
cool stars, IUE UV spectra obs. rel. to atmospheres struct. 78−96475
cool stars, model atmospheres rel. to effective temps., ang. dias. and reddening 79−44458
cool stars, model atmospheres rel. to neutron-ion spectral anomaly 78−7985
cool stars, narrow-band polarisation obs. rel. to extended atmospheres characts. 78−16427
cool stars, outer atms. struct., solar-type and non-solar-type stars 79−48791
cool stars, polarization across TiO bands and scattering envelopes 79−97005
cool stars, supersonic stellar winds and rapid mass loss 79−21268
cool stars, TiO opacity effects on atm. struct. 78−40925
cool stars, wavelength depend. of polarisation rel. to atmospheres struct. 77−2426
cool stars outer atmospheres, Mg II flux profiles and chromospheric radiative loss rates 80−36611
cool stellar atmospheres, rare-earth elements atomic partition functions 80−67544
cool stellar wind models for late type stars 80−51733
cool supergiant stars, near IR excesses 78−16406
coronae, energy balance 79−44466
coronae, evidence for existence from X-ray and UV obs. 80−12756
coronae, IUE search 80−4233
coronae, low-temperature, contrib. to EUV background 80−62324
coronae, min. flux concept rel. to energy balance and mass loss 78−81611
coronae, two-parameter models 80−8619
S Coronae Austrinae, bright southern YY Orionis star, spectroscopic obs. rel. to envelope struct. 77−29818
S Coronae Austrinae, T Tauri star, red-displaced absorpt. features rel. to atmospheric motions 78−4221
R, S, T Coronae Austrinae, T Tauri stars, circumstallar shells rel. to long period light vars. 80−82350

stellar atmospheres continued
β Coronae Borealis, Ap star, struct. of atmospheric mag. field *(Russian)* 77−17594
θ Coronae Borealis, Be star, strong shell line at Hα 79−67022
θ Coronae Borealis, Be-type star, shell line profile and radial vel. obs. 80−77426
R Coronae Borealis, dust shell pulsation rel. to 1100 day periodicity in IR excess 77−45462
R Coronae Borealis, He I λ10830 line obs. rel. to circumstellar gas cloud 79−16975
β Coronae Borealis, magnetic field gradient in Ap-star atmosphere, Zeeman spectra 78−85953
R Coronae Borealis, UBVRIHKLMN photometry, interpretation 80−67756
σ Coronae Borealis (HD 46361) spectroscopic binary, coronal X-ray emission obs. 80−56886
R Coronae Borealis stars, opaque material ejection rel. to long-term IR behaviour 78−96490
coronae of He-rich white dwarfs 78−85940
coronae of late-type main-sequence and subgiant stars, HEAO-1 X-ray obs. 80−72925
coronae of nearby main sequence and subgiant stars, XUV radiation upper limits 79−12471
coronal regions, effect on winds of OB supergiants and Of-type stars 79−48783
Crab pulsar, momentum distrib. of high energy particles 78−73727
Crab pulsar magnetosphere, nonlinear space charge waves rel. to coherent radio emission 77−41386
Crab pulsar magnetosphere, relativistic particles injection into Crab Nebula 78−36678
CRL 2104, CRL 2179, late WC stars, 2 to 4 μm spectrophotometry and circumstellar dust 78−96491
CRL 3068, dust-enshrouded star 77−91664
V1500 Cygni, (Nova 1975), emission line profiles during early nebular stage 79−53826
V Cygni, C star, 1-4 mm continuum emission obs. 79−88670
X Cygni, Cepheid, radial vels. rel. to atmosphere pulsation 78−73723
V460 Cygni, cool C star, atmospheric $^{12}C/^{13}C$ ratio 78−93223
CH Cygni, dust grains form. in circumstellar shell from linear polarisation vars. 78−69808
SS Cygni, dwarf nova, spectrophotometry rel. to accretion disc models in erruption and at min. light 80−36635
31 and 32 Cygni, eclipsing binaries, supergiant components atmospheres from UV spectra 80−109499
31 Cygni, eclipsing binary, Ca I 6752 Å line obs. rel. to circumstellar matter 77−17619
V367 Cygni, eclipsing binary, spectroscopic obs. rel. to circumstellar shell 78−53984
P Cygni, effective temp. radius, mass loss and luminosity 80−51748
P Cygni, electron scattering in expanding atmosphere 79−21311
P Cygni, extreme B-type supergiant, UV spectroscopy rel. to low-vel. stellar wind 80−22004
V1016 Cygni, forbidden Fe VI emission rel. to electron density 79−8970
V1057 Cygni, FU Orionis star, IR spectroscopy rel. to expanding envelope 80−17587
P Cygni, H Balmer line profiles, accel.-decel. envelope, mass loss 79−40205
P Cygni, H Paschen α equivalent width rel. to circumstellar envelope struct. 80−62156
V1057 Cygni, hydromag. model of peculiar activity *(Russian)* 78−49442
V1016 Cygni, IR spectrum and circumstellar dust shell 78−93266
32 Cygni, IUE obs. and effects of B-type star within late-type supergiant upper chromosphere 80−22036
V832=59 Cygni, mass-losing Be star, changes in UV spectrum 80−46561
32 Cygni, opacity wavelength depend. in atm. of K-type supergiant component 78−73741
χ Cygni, P Cygni profiles obs. in Na I and K I reson. lines 77−13362
V1016 Cygni, peculiar emission object, M star model 77−53598
CH Cygni, red giant, mag. field interpretation for outburst 78−4250
CH Cygni, symbiotic star, 1977 outburst, radial vel. and atm. struct. determ. 80−72969
CH Cygni, symbiotic star, binary model and hot companion circumstellar envelope struct. 80−62158
CH Cygni, symbiotic star, coronal model rel. to IUE obs. during active phase 79−62846
CI Cygni, symbiotic star, emission lines source regions from UV and optical obs. during eclipse 80−105258
CH Cygni, symbiotic star, spectroscopic obs. during outburst rel. to circumstellar envelope 79−75211
P Cygni, UV spectrum rel. to expanding circumstellar shell struct. 80−26873
59=V832 Cygni, variable mass flux from spectroscopic obs. 80−41840
V444 Cygni, Wolf-Rayet star mass loss rel. to orbital period var. *(Russian)* 79−101178
α Cygni (Deneb), variable line profiles interpretation 77−64761
V1500 Cygni (Nova 1975), anisotropically radiating condensations rel. to Balmer line emission profiles evolution 80−82371
V1500 Cygni (Nova 1975), distance and temp., visible spectral obs. *(Chinese)* 80−85955
V1500 Cygni (Nova 1975), mechanism of quasieclipses after outburst *(Russian)* 78−93280
V1500 Cygni (Nova 1975), radio emission from expanding shell 80−26868
V1500 Cygni (Nova 1975), shell electron temps., densities and other props. 79−30068
V1500 Cygni (Nova 1975), shell radius and mass from wide-band IR photometry 78−36615
V1500 Cygni (Nova 1975), spatial and kinematic envelope model 78−36600
V1500 Cygni (Nova 1975), spectroscopic studies, models for 3 hour profile vars. 79−8920
V1500 Cygni (Nova 1975), stellar wind rel. to 3 hour photometric period stabilisation 79−92776
V1668 Cygni (Nova 1978), dust form. phase time from linear polarisation obs. 80−26875
V 1668 Cygni (Nova 1978) ejecta shell, dust form. rel. to spectral development 80−51789
V1668 Cygni (Nova 1978) envelope, dust form. rel. to multifilter photometry and polarimetry 80−90454
stellar atmospheres continued
P Cygni envelope mass loss, equivalent two-level atom approach 78−93255
Cygnus OB2 number 12, spectrum rel. to mass loss and possible duplicity 80−51760
Cygnus X-1, accretion disc corona 78−16569
Cygnus X-1, gas accretion rel. to line blending and black hole candidacy 77−64878
Cygnus X-1, photospheric scatt. model for optical polarisation orbital vars. 78−54077
Cygnus X-3, cocooned X-ray binary pulsar model 78−36723
Cygnus X-3, gamma-ray emission from mag. accretion disc 77−78894
DA white dwarfs, atmospheric parameters and mass distrib. 79−88655
degenerate dwarf stars, props. of low temp. pure He surface layers 78−7994
degenerate stars with H atmospheres, props. rel. to theoretical models 80−17576
degenerate stars with He atmospheres 77−13335
HR Delphini, UV spectrum, stellar wind 80−26880
HR Delphini (Nova 1967), C and N overabundances in stellar wind from UV spectra 80−109440
HR Delphini (Nova 1967), envelope, photoionization models in nebula stage, 1969 June-July 79−62835
HR Delphini (Nova 1967), models of envelope ionization 77−87439
HR Delphini (Nova 1967), photoionisation models, binary system evolution 80−17590
HR Delphini (Nova 1967), photoionisation models of envelope in nebular stage, obs. data 78−61864
HR Delphini (Nova 1967), physical conditions of different regions of envelope 80−4369
HR Delphini (Nova 1967), physical props. and element abundances in nebular state 78−36573
HR Delphini (Nova 1967), premax. envelope conditions 78−24518
HR Delphini (Nova 1967), radio emission from expanding shell 80−26868
HR Delphini (Nova 1967), spectra, line identification, radial vels. 80−17594
dense stars atmospheres, atomic spectra in intense mag. fields 80−105160
diffusion and turbulence rel. to abundance anomalies in main-sequence stars 78−89198
disc formation in stellar wind accretion *(Russian)* 79−88648
DO white dwarfs, model atmospheres rel. to effective temps. and He abundances 79−35249
S Doradus, LMC star, evidence for circumstellar envelope and mass loss from IUE and optical obs. 80−101595
73 Draconis, CH lines in spectrum of Ap star *(Russian)* 77−56958
BY Draconis, flare star, BVRI obs. rel. to spot model 77−53595
BY Draconis, flare star, coronal soft X-ray emission obs. by (HEAO 1) 79−101140
ϕ Draconis, short period Ap star, mag. field rel. to atmospheric circulation currents 77−33511
73 Draconis, spectral variability of Ap star *(Russian)* 78−65624
73 Draconis, spectroscopic study and model atm. anal. of Ap star 77−33531
BY Draconis stars, luminosity vars. and light curve period changes 79−71039
BY Draconis type variables, photometry, amplitudes and phases 79−67038
BY Draconis-type stars, Hα emission line profiles, rapidly rot. gaseous envelopes *(Russian)* 78−65625
dust grains, IR spectra and props 80−26943
dust shell contracting around expanding supermassive star, Einstein's theory of gravit., black hole formation 78−12088
dwarf Me-type stars, cyclical photometric vars. interpretation 77−74059
dwarf novae, accretion disc struct. rel. to soft X-ray emission 77−45457
dwarf novae, nature, H accretion, mag. field, radiation mechanisms *(Russian)* 78−93277
dwarf novae, outbursts, accretion model 79−88680
dwarf stars, degenerate accreting, thermonuclear bursts assoc. with chromosphere flares 80−98684
dwarf stars, model chromospheres and chromospheric activity 79−48773
early B-type stars, radial shock effects 79−53807
early B-type stars atmospheres, LTE line blanketing by UV lines using accurate damping consts. 78−16419
early Be stars, macroscopic radial atmospheric motions, UV obs. 78−8009
early type stars, line blanketed model atmospheres rel. to mid UV spectra 80−21995
early type stars, line driven sound waves 79−71023
early-type emission-line stars, intrinsic and interstellar polarization components separation 79−30079
early-type emission-line stars, intrinsic polarization interpretation 79−30080
early-type star Lyman α and β profiles 77−87391
early-type stars, blanketed model atmospheres rel. to UBV colours and temp. scale 79−16933
early-type stars, disc struct. in extended atms. 78−93206
early-type stars, effect of gas-dust envelopes on IR spectral energy distrib. 80−67732
early-type stars, winds and expanding envelopes 79−21288
early-type stars and cool stars, UV spectroscopy of outer layers 80−72922
early-type stars in LMC open cluster NGC 955, stellar winds rel. to motions in bubble-like nebula N51D 80−105295
early-type stars in Perseus, UV spectrophotometry, energy distrib. 79−88653
early-type stars photospheric expansion, meas. via. Fourier anal. technique 78−93224
early-type stars with Balmer emission, outer atmospheres props. from near UV spectra 80−94811
early-type stars with extended envelopes and mass outflow, radio emission 77−74063
early-type stellar winds, H and He^+ synthetic line profiles 80−85926
eclipsing binaries, linearised limb-darkening coeffs. for light curves anal. 78−49480
eclipsing binaries with extended atmospheres, light curve anal. techniques and appl. to V444 Cygni 80−82417
eclipsing binary stars, near IR photometry rel. to mass transfer rates 80−67784

stellar atmospheres continued
eclipsing binary systems with disclike envelopes, light curve interpretation, appl. to HZ Herculis 78−65658
eclipsing variable stars with extended atmospheres, Fourier anal. of light curves 80−46604
Eddington approx., radiative transfer for spherically symmetric atmospheres 78−77484
effective optical depth for absorption line formation 77−53578
ejected envelope ^{26}Mg, interaction with collapsed core prod. neutrinos, ^{26}Al prod. *(Russian)* 80−77285
electron excitation of H and hydrogenic ions, cross-sections and rates 78−50649
electron gas, relativistic degenerate in strong mag. field, transport props., covariant relaxation-time model 77−41531
envelopes, competition between diffusion processes and hydrodynamical instabilities 78−12212
envelopes, light element decay 78−12214
ν Eridani, β Cephei variable atm. parameters from H and He spectral obs. 80−67739
ϵ Eridani, model chromosphere of K-type dwarf 78−65610
ϵ Eridani, UV line spectrum of active chromosphere star, models 80−77394
40 Eridani A(=o^2 Eridani), evidence of corona on X-ray image 80−105282
EUV spectroscopic method for electron density determ. in stellar atms. 79−16836
evolved stars expanding envelopes, CO thermal and maser emission 80−82334
excited cosmic plasmas, review 78−69671
expanding and rotating atmospheres, curves of growth and line profiles 80−31295
expanding envelopes, form. and nature of carbonaceous material 78−24543
expanding envelopes, line profiles 79−44464
expanding envelopes, Lyman α quanta scattering *(Russian)* 80−67556
expanding envelopes, radiative forces 78−28659
expanding media, opacity, effect of spectral lines 77−49283
expanding molecular envelopes around evolved stars, CO emission line obs. 77−22219
expanding spherical atmosphere, line form. with partial freq. redistrib. function R_I 79−88643
expansion and rotation, combined effects on spectral line shapes 78−53920
extended, atmospheres, anisotropy of radiation field *(French)* 79−48776
extended, distorted atmospheres, wavelength depend. of linear polarisation in early type stars 77−60779
extrastellar electron cloud around spherical limb-darkened star, Thomson scatt. rel. to light polarisation 79−58324
F8-K1 stars, recalibration and anal. of quantitative three-dimensional spectral classification 77−78768
F, G, K-type stars, electron concs. in photospheres, Fe line obs. *(Russian)* 77−49376
F, G, K-type stars, giants and dwarfs chromospheres, wave dissipation of mechanical energy 80−82340
F- and G-type main sequence stars, R-I colour as temp. indicator 77−87395
F- and G-type stars, mag. accel. of winds and ang. momentum loss 77−13334
F- and G-type stars, model atmospheres rel. to C and N abundances 77−91530
F-type star, main sequence, convection and photospheric granulation 80−90417
F-type stars, models including OH opacity, comparison with TD1 satellite flux obs. 78−73700
fast nova model evolution from pre-explosion to decline 79−35273
Feige 24, hot white dwarf, model atmosphere rel. to intense EUV emission 77−9746
Feige 24, hot white dwarf, UV photometry and model atmosphere 77−9747
Feige 86, horizontal branch star, chemical comp. 77−9745
finite extent, effect on colour indices 78−32450
finite plane parallel atmos., polarisation studies, F_N method 79−40070
flare star 2329−03, spectra, chromospheric emission 77−74070
flare stars, chromosphere theory, fast electrons hypothesis 78−24514
flare stars, model chromospheres, Balmer-line profiles 80−46558
flare stars, nonmonotonic optical light curve model 77−29842
flare stars, theory of flare mechanism *(Russian)* 78−49444
flare stars, X-rays influence on optical light curve 77−29843
flare stars chromospheres, electron heating rel. to nature of flares optical continuum *(Russian)* 80−109445
flare stars physical characts. 77−41383
force-free magnetic fields toroidal component upper limit rel. to flares 77−33479
free convection effects on MHD accel. flow past vertical porous limiting surface 80−23996
free convection in Stokes' problem for infinite vertical limiting surface, mass transfer effects 80−28501
fundamental definition interpretation, book contrib. *(French)* 77−87380
G128-7, cool DA white dwarf, atmospheric parameters and evolutionary consequences 80−62126
G200-39, hot hybrid white dwarf, spectroscopic obs. and atmospheric props. 80−26852
G, F, A, B and O stars, model atmospheres 79−80298
G 165−7, metallic line white dwarf, model atm. code anal. of spectrum 80−85940
G- and K-type giants, theoretical colours, model atms. 79−12474
G- and K-type giants, theoretical colours from synthetic spectra 79−62827
G-type dwarfs, macroturbulence and age anticorrel. 78−93226
GD 40, He white dwarf, spectrum anal., CA abundance determ. 77−87385
γ Geminorum, differential abundance anal. rel. to α Lyrae standard 80−82362
β Geminorum (Pollux), chromosphere model 78−40931
β Germinorum (Pollux), theoretical stellar chromosphere model 80−67718
giant and supergiant stars, nonradial oscills. excitation 77−74049
giant stars, late-type, O I 7773 Å and theory 79−35250
giant stars, microturbulence rel. to evolution 78−81625
giant stars, model envelopes, physical props. *(Portuguese)* 80−22014
stellar atmospheres continued
giant stars in globular clusters M5, M13, M3, model atmospheres rel. to chemical comp. 80−67695
giant stars in M3, M13, M92 and M67, IR photometry comparison with model atmospheres 78−57595
giant stars with IR excesses, gas-dust shells rel. to optical emission linear polarisation 78−96481
giants and supergiants, atm. $^{12}C/^{13}C$ ratio 77−13337
globular cluster giant stars, blanketing differences meas. 80−4345
grain formation in cool stellar envelopes 80−56814
gravity stratification, perturbation propag. *(Chinese)* 80−85934
gray atmosphere, absorpt. lines form. *(Russian)* 79−21177
H1-36 (3U 1746-37), emission line object, radio spectrum rel. to mass outflow 77−82239
h 4636, binary star in young cluster NGC 5367, IR photometry rel. to circumstellar shell 77−82294
HBV 475 (V1329 Cygni), electron densities from high-excitation emission lines 78−40955
HC 105056, ON supergiant, spectroscopic evidence for variable stellar wind 80−90427
HD 102567, optical counterpart to 4U 1145−61, atm. model from UV obs. 80−105396
HD 10783, Ap star, model atmospheres rel. to spectrophotometric obs. 80−98663
HD 108, Of star, spectral vars. due to solar wind 79−35262
HD 116745, Population II F giant, extended static stellar atmosphere 77−60759
HD 120640, spectrophotometry and quantitative anal. of B star 77−60758
HD 122563, metal-deficient giant, atm. $^{12}C/^{13}C$ ratio, mixing 78−4201
HD 128279, cool halo star, abundances, reduction procedure and equiv. widths 77−49384
HD 151932, single WN 7 type star with var. He I envelope 79−44493
HD 153919(3U 1700−37), coronal emission line search 79−35302
HD 153919 (3U 1700−37), forbidden Fe XIV emission rel. to extended atmosphere struct. 78−16571
HD 153919 (3U 1700−37), spectroscopic obs. rel. to mass loss rate and corona 80−4358
HD 153919 (3U 1700-37), binary X-ray source, stellar wind effects on radial vels. meas. 78−49556
HD 153919 (3U 1700-37), X-ray binary, photometry rel. to circumstellar matter 77−29877
HD 161698, Hg-Mn star, curve of growth anal. 79−30070
HD 184905, magnetic variable, H I lines and atmospheric parameters 79−97011
HD 190073, a0ep star, reson. scatt. rel. to struct. and vars. of Ca II lines 77−17578
HD 190603, effective temp. radius, mass loss and luminosity 80−51748
HD 192163, Wolf-Rayet star in ring nebula HGC 6888, SHF obs. 80−82386
HD 193793, radio emitting Wolf-Rayet binary star, variable mass flow model 77−45469
HD 193793, shell condensation around W-R binary, IR obs. 79−12495
HD 193793, Wolf-Rayet star, circumstellar dust form. episode 80−31301
HD 193793, Wolf-Rayet star, graphite grains form. rel. to C rich dust cloud 80−26861
HD 193793, Wolf-Rayet star, IR obs., cooling of circumstellar dust shell 79−48823
HD 200120, Be star, UV spectra vars. 77−5534
HD 206267, exciting star in H II region IC 1396, stellar wind, role in cloud struct. 80−105316
HD 214419, Wolf-Rayet spectroscopic binary, light and vel. changes, common envelope model 79−53856
HD 30466, Si star, double wave photometric var. rel. to chemical comp. patches 77−87410
HD 34452, Si Ap star, spectrum rel. to enhanced element abundance spots 78−65634
HD 4174, symbiotic star, circumstellar envelope model rel. to spectroscopic obs. 80−85945
HD 44179, binary with surrounding dusty nebula, 3.3 micron feature 80−82466
HD 45166, dwarf in Wolf-Rayet clothing, spectrum, radius and envelope struct. 79−5826
HD 45677, peculiar Be-star 0.12-12.6 μm obs. of circumstellar dust shell 80−72957
HD 45677 or 50138, hot Bep stars with circumstellar dust IR excesses, UV obs. 78−93250
HD 49798, H-deficient subdwarf O-type binary, non-LTE model atmosphere anal. 79−16978
HD 50896, Wolf-Rayet star, emission lines polarisation rel. to extended atmosphere struct. 79−97008
HD 50896, Wolf-Rayet star, UV spectral energy distrib. and interstellar extinction 77−22211
HD 50896, Wolf-Rayet star, wind struct. determ. from IR continuum 77−78793
HD 51480, shell star, spectroscopic obs., atmospheric struct. and distance 80−31305
HD 76932, subgiant halo star, chem. comp. rel. to nucleosynthesis 78−81626
HD 77581 (=Vela X-1), supergiant+neutron star, stellar wind mass transfer, spectral obs. 80−94892
HD 77581 (Vela X-1), X-ray binary, photometric obs. circumstellar gas rel. to photometric obs. 77−41392
HD 80077, superluminous supergiant, evidence for circumstellar dust shell 77−17555
HD 90657, Wolf-Rayet spectroscopic binary, spectrum and atmosphere struct. 77−13357
HD 93250, O3 massive star in η Carinae complex, non-LTE analysis 80−77398
HD 97048, pre-main-sequence star, spectral changes rel. to shell vars. 77−74055
HD 97048 (=HM 18), pre-main sequence star, unidentified IR features obs. 80−85943
HDE 226868 (Cygnus X-1), extendend secondary envelope with eclipsing region, V-polarization obs. 79−35433
HDE 245770, near IR photometry of OBe star, A 0535+26 optical counterpart 79−48826
HDE 313846, most extreme Of star, spectroscopic obs. and mass outflow 79−88682

stellar atmospheres continued
Henize 715 (4U 1145−61), Be star, circumstellar envelope disappearance (1979-80) 80−72979
Herbig-Haro objects, stellar wind model 80−85985
Hercules X-1, coronal contrib. to X-ray continuum and Fe line emission during X-ray low state 80−105393
Hercules X-1/HZ Herculis, evaporative winds 77−78888
68=μ Herculis, ^{3}He identification in atmosphere of primary component 77−57045
ϕ Herculis, Ap star, X-ray emission obs. rel. to atmosphere mass motions 79−101160
τ Herculis, B-type subgiant star, abundance anal. 78−16416
DY Herculis, dwarf Cepheid, model atmosphere from uvbyβ photometry 79−58357
α^1 Herculis, He I 10830 Å emission obs., high-temp. chromosphere 79−48792
ϕ Herculis, Hg-Mn star, corona search, UV obs. 80−72986
α Herculis, line form. in circumstellar shell rel. to α^2 Herculis location along line of sight 78−73739
α Herculis, M supergiant, circumstellar shell and mass loss rate 77−45415
α Herculis, M-type supergiant, Mg II h and k emission rel. to overlying absorpt. 78−53945
HZ Herculis (Hercules X-1), pulsed optical radiation from X-ray exposed stellar atmosphere 78−57580
V446 Herculis (Nova 1960), ejecta He abundance 79−92775
high mass stars, stellar wind effects on evolution 80−21982
high velocity giant stars, model atmospheres rel. to detailed chemical anal. 80−82352
hot coronae, possible detection from XUV emission *(German)* 80−109372
hot horizontal branch stars, model atmospheres, B−V colour indices and bolometric corrections 79−58327
hot massive stars, stellar wind mass loss, evolution study 80−17578
hot stars, effect of winds and coronae on IR and radio continua 77−29817
hot stars, line-driven Rayleigh-Taylor-type instability 78−53927
hot stars with circumstellar clouds, synthetic UV spectra calcs. 80−77382
hot white dwarfs as thermal soft X-ray sources 78−57553
HR 1099, H and Ca II emission obs. and surface distrib. during February 1978 radio outburst 79−21340
HR 1099, RS Canum Venaticorum binary, Hα profile rel. to rot. circumstellar envelope 79−21343
HR 3089, He-rich star, model atmosphere rel. to anal. of UV spectrum 77−9751
HR 5999 (V856 Scopii), multicolour photometry, circumstellar dust shell 79−48828
HR 6127, chemically peculiar star, spectral lines and equivalent width lists, visible obs. 80−82387
HR 8752, binary supergiant, photosphere, emission feature variability, visible obs. 80−109463
HR 8752 (HD 217476), superluminous superiant, line spectrum changes rel. to expanding shell 79−80308
HR 8799, model atm. anal. 77−74050
HR 96, Ap-type star, atm. parameters and stellar comp., visible obs. 80−67740
W Hydrae, circumstellar envelope mag. field rel. to OH masers suspected Zeeman splitting 80−36632
EX Hydrae, dwarf nova, accretion disc dimensions from IR and optical light curves 80−67747
W Hydrae, form. of carbyne and cyanoacetylenes in stellar atm. 80−67708
W Hydrae, long-period variable star, cyanodiacetylene in expanding envelope 77−82238
VW Hydri, dwarf nova, accretion disc dimensions from IR light curves 80−67747
hydromagnetic flow, near oscillating porous limiting surface 78−12200
hydromagnetic free convection flow in Stokes problem, for porous vertical limiting surface with const. suction 80−90328
HZ 43, hot white dwarf, self-consistent model atm. anal. 77−22220
HZ 43, white dwarf, He abundance and stellar struct. from soft X-ray spectra 80−72944
IC 1318, giant H II region, stellar winds rel. to large-scale line splitting 78−96521
ϵ Indi, late type dwarf star, model atmosphere 80−90425
ϵ Indi moving group, detailed anal. of members HD 40409, HD 102365 and λ Aurigae 78−85982
ionisation fronts, weak D-type, departures from equilibrium 77−49288
ionising source model for Allen's obscured IR source in NGC 2264 viscous disc component 79−21370
ionization front propag. in inhomogeneous medium 80−46379
IR limb-darkening coeffs. for late-type giant model atmospheres 79−71029
IR stars, H_2O maser source in circumstellar envelope 78−73724
IR stars, OH maser emission obs. rel. to expanding spherical shell model 77−53699
IRC+10216, C star, circumstellar shell temp. vars. rel. to new near IR mol. feature 79−92762
IRC+10216, C star, HC_5N and HC_7N detect. in mol. envelope 79−17126
IRC+10216, C star, NH_3 obs. in circumstellar envelope 79−48793
IRC+10216, C star, possibility of detecting cyanoacetylene-d_1 (DC_3N) 78−69901
IRC+10216, circumstellar dust shell model rel. to IR energy distrib. 80−56972
IRC+10216, late type C star, circumstellar envelope 78−4189
IRC+10420, supergiant star, new OH maser feature struct. and circumstellar shell dia. 79−48946
IRC+10°216, circumstellar acetylene in IR spectrum 77−5591
IRC+30219, extreme C star, circumstellar envelope optical emission-line phase 80−90569
IRC +10216, C star, circumstellar dust cloud size from far IR obs. 80−82539
irradiated stars in active galactic nuclei, mass loss and evolution 80−56949
K giants and G and K supergiants, observational evidence for mass loss 77−56928
K-type giant stars, evidence of circumstellar shells 80−90420
K-type giants, $^{12}C/^{13}C$ ratio correl. with Fe/H ratio 79−48798
stellar atmospheres continued
K-type giants, multivariate anal. of spectrophotometry rel. to atmospheric characts. 77−78772
K-type giants, turbulence in normal and super-metal-rich stars 79−92756
K-type giants, upper photospheric temp. models, super-metal-rich and normal giants 79−21278
K-type subdwarfs, model atmospheres 79−25595
EV Lacertae, evidence for photospheric starspots from photometric and spectroscopic obs. 80−98665
EV Lacertae, flare star, hot-plasma model of strongest flares 78−20838
EW Lacertae, motion in shell and atmosphere 77−60776
10 Lacertae, spectral line studies using LTE-method *(Russian)* 79−92769
CP Lacertae (Nova 1936), ejecta He abundance 79−92775
Lamb freqs. of spherical gaseous star 79−66997
laser action in distended envelopes, appl. to He II 4686 Å 77−13354
laser line emission detection in spatially inhomogeneous broadening 77−41312
late B horizontal branch stars, effects of CNO abundances on Balmer jump 78−4192
late type dwarf stars, temp. minima, chromosphere models 80−67717
late type giants, departures from LTE ionization equilib. 78−4204
late type giants, pulsation-convection nonlinear coupling rel. to mass loss 77−13356
late type stars, chromospheric mass column densities rel. to Ca II line widths 79−12464
late type stars chromospheres, struct. from Ca II H and K lines photoelectric calibration 80−36617
late-type, stars, sphericity effects in extended atms., models 78−81617
late-type chromospheres, shock heating theory observational tests 78−28663
late-type field stars in S.hemisphere, evidence for chromospheric activity 80−98686
late-type giant model atmospheres, limb darkening coeffs. 78−20821
late-type giant stars, CO emission lines obs. from expanding molecular envelopes 77−22219
late-type giants, position on Hertzsprung-Russell diagram 77−78792
late-type stars, 4-8 μ spectral obs. 77−74054
late-type stars, ^{24}MgH IR rot.-vibr. bands fine struct., transition probabilities, oscill. strengths 77−18918
late-type stars, acoustic modes overstability and obs. implications 77−56932
late-type stars, Ca II 8542 Å line as chromospheric activity indicator 80−62108
late-type stars, Ca II emission V/R ratio rel. to mass loss 78−93208
late-type stars, Copernicus survey of Mg II emission 79−80301
late-type stars, emission lines in Ca II H and K lines wings rel. to atmosphere struct. 77−78766
late-type stars, extended atmospheres, sphericity effects in red giants, model study 80−22012
late-type stars, FeH column densities 78−24507
late-type stars, He abundance effects on spectrum appearance 80−46540
late-type stars, intensity effect in Wilson-Bappu relationship 78−85937
late-type stars, O-rich, 16 to 39 micron spectroscopy rel. to circumstellar silicate dust 80−22002
late-type stars, sensitivity of internal struct. to surface boundary condition 78−12208
late-type supergiants, atmospheric struct. from freq. depend. diam. 77−56924
late-type supergiants, spectra rel. to atmospheric struct. and luminosity 77−60753
late-type young stars in ρ Ophiuchi dark cloud, photometry obs. 80−72942
R Leonis, circumstellar shell heterodyne interferometry 78−8000
ρ Leonis, effective temp. radius, mass loss and luminosity 80−51748
AS Leonis, flare star, chromospheric emission lines in nonflare red spectrum 79−21294
R Leonis, IR spectroscopy of Mira variable, H_2O vibr. rot. bands 79−35258
R Leonis, Mira variable, atmospheric struct. from CO and OH IR vibr.-rot. overtone bands 78−36574
R Leonis, TiO-related dia. vars. rel. to atmosphere optical thickness 78−16429
CW Leonis (IRC+10216), IR C star, circumstellar dust orientation by paramag. relaxation rel. to intrinsic polarisation 80−67730
48 Librae (FX Librae), shell star, spectroscopic study and shell struct. 78−96486
line accretion theory, gas pressure effect, stagnation point 78−53932
line blanketed model atmospheres, limb darkening coeffs. determ. 79−35243
line formation, non-isotropic redistrib. theory in chromospheric-type stellar atmosphere 77−5522
line formation in expanding atmospheres 77−56919
line photons, equality of mean escape probability and mean net radiative bracket 78−40815
line scattering intensity radiative transfer, exact soln. using Wiener-Hopf technique 79−84784
line transfer, non-LTE, with convective transport of excited atoms 79−88584
line transfer in spherical media with partial freq. redistrib., soln. 79−16932
linear acoustic waves in radiating scatt. grey medium, effect of transverse mag. field 77−56911
linear transport equation, degenerate case, full range theory, appl. to Milne problem 78−57874
linear transport equation, degenerate case, half-range theory, appl. to Milne problem 78−57875
long period variable stars atmospheres shock wave periodicity rel. to mass loss 79−44487
long-period variable stars, photospheric absorpt. and scatt. rel. to narrow-band polarimetry 80−98666
long-period variables, H emission line form., models 78−28709
LP 131-66, new cool red degenerate star 79−48780
LTE/non-LTE boundary, determ. from wide-band colour index and bolometric correction comparison 79−35236
luminous cool stars, atm. $^{12}C/^{13}C$ ratio 77−13336
luminous O-B3 type stars in open clusters, circumstellar shells and mass loss *(German)* 78−53925
luminous stars in symmetric nebulae, IUE spectra rel. to stellar wind props. 80−46560

stellar atmospheres continued
RU Lupi, T Tauri star, chromosphere and corona parameters and expected X-ray fluxes *(Russian)* 80−51770
Lyman continuum in atmosphere in statistical equilib., effects of deviations from LTE 80−31290
α Lyrae, continuous UV flux, non-LTE calc. 77−49382
α Lyrae, coronal emission model for soft X-rays obs. with imaging X-ray telescope 79−48953
α Lyrae, emission lines in IR spectrum, thin expanding extended atm. 78−53946
β Lyrae, H emission profiles rel. to pattern of gaseous flow in system 78−57576
β Lyrae, high time-resolution Hα spectroscopy rel. to gas flow 77−13388
β Lyrae, nature of disc around secondary component 78−16458
RR Lyrae, UV light curve rel. to hydrodynamic atmospheric models 77−45435
α Lyrae (Vega), Ca II H and K lines high resolution profiles 78−85939
α Lyrae (Vega), LTE blanketed models rel. to visible and UV continuous energy distribs. 80−26856
RR Lyrae stars, Ca and Fe decoupling 79−30069
M92, globular cluster, C and N abundance variations in horizontal branch 77−87495
M- and S-type stars, detect. of 7 mm SiO maser sources 78−4215
M-type dwarf stars in galaxy cluster Abell 2029, coronal X-ray emission rel. to SAS 3 obs. 80−82519
M-type dwarfs, radii from Barnes-Evans relation, effects of atmospheric opacity sources 78−7984
M-type giant stars, atm. physical conditions 78−24512
M-type giants, atmosphere mass estimate *(Russian)* 79−21292
M-type giants, circumstellar envelopes, high-dispersion spectra 79−92755
M-type giants and supergiants, circumstellar gas and dust shells, optical and IR obs. 79−21281
M-type semiregular variables, atmospheric anal., chem. comp. *(Russian)* 78−65623
M-type subdwarfs, press. effects on line strengths 77−13330
M-type supergiants in reddened Ara cluster, IR photometry rel. to thermospheres 77−41395
macroturbulence rel. to luminosity in early K-type stars 79−96997
magnetic Ap stars, empirical atmosphere models *(German)* 77−17589
magnetic DA white dwarfs, model atmospheres and line profiles 80−62123
magnetic field horizontal stability in stably stratified atmosphere 79−75200
magnetic neutron stars, accretion flow, magnetospheric struct. and stability 78−4269
magnetic stars, magnetodynamic mechanism 77−87404
magnetic stars, model atmospheres 79−16973
magnetoatmospheric instabilities, max. growth rates 77−53573
magnetogasdynamics, axially symmetric explosion 80−62007
magnetogravity waves, propag. in isothermal conductive atmosphere 79−92670
magnetoplasma stability against EM perturbations in presence of gravit. field 77−41295
magnetospheres and radio emissions, conf. Snowmass, Colorado, USA (Aug. 1978) 80−41939
magnetospheres of accreting compact stars possessing multipole magnetic fields 79−97020
magnetospheric explosions, role of gravitational instabilities 78−28655
main sequence stars, diffusion in envelope and abundance anomalies 77−13331
main sequence stars, F- and G-type, Be abundances 77−13332
main sequence stars with variable Ca II H and K emission, starspot hypothesis 79−58328
main-sequence stars, comparison of four-colour photometric obs. with evolutionary models 78−8007
maser emission by nebular regions and stellar atmospheres 78−89242
maser stars, late supergiants and long period variables 80−77410
maser stars, search for water vapour absorpt. lines 77−78804
mass flux fluctuation theory 80−72923
mass flux from stars, fluctuation theory 79−53804
massive eclipsing binary stars, spectrophotometry and search for circumstellar matter 80−26900
massive luminous stars, stellar winds effect on evolution 79−12467
massive single stars, main sequence evolution with and without stellar wind 79−16936
massive stars, mass loss and convective overshooting influence on evolution 79−84789
massive stars, mass loss by stellar wind rel. to evolution 78−4197
massive stars, single and binaries, evolution review 80−82343
massive white dwarfs, mass accretion, rel. to thermonuclear runaways 80−41822
massive young stars, dust shells rel. to H_2O masers VLBI obs. 79−21368
MD 101065, effective temp. and atm. electron press. 77−45468
metal-deficient stars, subdwarf ionization equilibrium and model atmospheres 80−90421
metal-poor late-type stars, model atmospheres rel. to MK spectral classification 80−4340
MHD, Brinkley-Kirkwood method, appl. to shock waves in stellar atm. *(Russian)* 78−93102
MHD, unsteady thermal boundary layer problem, numerical treatment 80−92227
MHD thermal boundary layer flow near oscill. limiting surface, stellar atm. appl. 78−94831
MHD unsteady thermal boundary layer flow with zero heat transfer 77−87250
MHD waves, propag. in mag. flux tube 78−69789
microturbulence, spectral line broadening 78−45321
microturbulence behaviour with evolution 78−12206
Milne's integral eqn., general variational method 79−8828
Milne problem, invariance principles and integral eqns. for radiation fields in plane atmosphere 80−67559
Milne problem for inhomogeneous atm. 79−21179
minimum flux corona theory 80−26844
Mira envelopes, OH maser luminosity and expansion vel. gradient 79−71043
Mira type variables atm., OH maser, IR line overlap pumping mechanism 80−72764
Mira variables, polarisation variation detect. in absorption features 77−33496
stellar atmospheres continued
Mira variables, supersonic mass ejection 77−53605
Mira variables, supersonic mass flow theory 79−35270
model atmosphere analyses of solar-type stars, metal abundances and microturbulence 79−67002
model atmospheres, temps. determ. for uvbyβ photometric system 77−64740
models, thermodynamics, review *(Italian)* 78−81614
models application to determ. of effective temp., bolometric corrections, Balmer discontinuity and distrib. functions *(Rumanian)* 78−36557
R Monocerotis, model for assoc. cometary nebula NGC 2261 79−21372
R Monocerotis, T Tauri star, circumstellar shell changes rel. to long period light vars. 80−82350
moving envelopes, radiation field and statistical equilib. eqns. rel. to spectral line form. 77−87374
multicomponent nonequilibrium plasma atmospheres, higher order fluid eqns. 80−105156
multidimensional radiative transfer in stratified atmosphere, grey radiative equilib. 80−26845
θ Muscae, Wolf-Rayet binary, envelope struct. 77−22235
MWC 342, emission line spectrum in 1974-75 period 78−57558
neutrino pair emission, stellar plasma in strong mag. field, photon-neutrino coupling theory 77−17548
neutron star, accreting, magnetopause struct. 78−65647
neutron star, interaction between accretion disc and mag. field *(Russian)* 80−51799
neutron star, magnetised, atmosphere, cyclotron line form. 79−48839
neutron star, rot. with magnetosphere, effect of elec. field. 80−109453
neutron star, rotating, with strong mag. field, electron cap shape 78−12265
neutron star magnetosphere, plasma dynamics and accretion, fate of sinking filaments 80−51798
neutron star magnetospheres, charged particle distribs. 77−13379
neutron star magnetospheres, laboratory modelling 79−75240
neutron star magnetospheres, struct. rel. to fate of matter and ang. momentum in disc accretion 78−28715
neutron star magnetospheres, Thomson scatt. rel. to hard X-ray spectra of Centaurus sources 77−2493
neutron star X-ray emission models 80−62175
neutron stars, accreting, normal mode anal. of interchange instability at magnetopause 77−13376
neutron stars, accreting, thermonuclear bursts assoc. with chromosphere flares 80−98684
neutron stars, accretion disc interaction with rot. mag. field 80−62173
neutron stars, accretion disc torques rel. to pulsating X-ray sources period changes 80−31320
neutron stars, extended atmosphere form during supercritical time-dependent accretion 80−85967
neutron stars, pair annihilation in superstrong magnetic fields 80−85847
neutron stars, radiative effects in supersonic accretion 78−40978
neutron stars, rotating, magnetic, accretion flow inside magnetosphere rel. to rot. rate 78−8037
neutron stars, X-ray refl. from surfaces 78−28716
neutron stars accretion discs and spheres, plasma accretion theory 80−109452
neutron stars with mag. fields, radiative heat transfer in surface layers 80−94826
NGC 2264, young open cluster, circumstellar shells, IR excess obs. 77−45410
non-LTE line formation in mag. field, two-level atom with freq. independent source function 78−61726
non-LTE radiative transfer, asymptotic expansion for small ε 78−16287
non-LTE radiative transfer, multi-dimensional, new approach to soln. 77−22057
non-LTE radiative transfer, rapidly convergent iterative method for Wiener-Hopf integral eqns. 78−12089
nonequilibrium plasmas, density diagnostics via C III EUV lines 78−53899
nova, H-rich envelope mass 77−87451
Nova Cephei 1971, chemical comp. and mass of ejected shell 78−12244
Nova Cygni 1975, diffuse enhanced spectrum rel. to envelope struct. 77−29850
Nova Cygni 1975, rapid vars. in ejected material emission line profiles 77−45434
Nova Cygni 1975, stellar wind and light vars. 77−82237
Nova Cygni 1978, P Cygni lines widths and atmosphere expansion vel. 78−89213
Nova Cygni 1978, photometric obs., light vars., IR obs. showing dust form. phase 78−96494
Nova Delphini 1967, central star props. and envelope ionisation conditions *(French)* 77−53603
Nova Delphini 1967, envelope struct. from He I triplet lines *(French)* 77−56939
Nova Delphini 1967 (HR Delphini), circumstellar envelope props. *(Russian)* 78−77564
nova ejecta, dust grains sudden nucleation and growth 80−26941
nova envelope, grain formation 77−82254
nova envelope C enrichment on surface accretion at white dwarf 80−85936
nova envelope model and total energy considerations 77−82250
nova envelopes, CNO composition 77−87453
nova envelopes, dust form. and ionisation theory 80−98678
nova expansion before light max. and principal envelope formation 77−87436
nova model evolution with Z=0.03 envelope 77−82265
Nova Sagittarii 1977, IR obs., high temp. dust shell form 77−60766
Nova Serpentis 1978, evolution of dust shell 80−90430
Nova Serpentis 1978, IR photometry rel. to dust shell condensation 80−4365
nova shell ionisation, time-depend. model 79−53816
nova shells, radio emission obs. 80−26868
novae, coronal line emission origin 79−16965
novae, dusty circumstellar envelopes *(French)* 77−56940
novae, effect of expanding envelope interaction with binary companion on outburst 80−82394
novae, expanding shells, matter-bound or radiation-bound 77−64780
novae, grain formation in ejected envelopes 77−91548
novae, nonuniform stellar wind manifested in light curves 80−62160
novae, photospheric collapse rel. to transition zone oscills. inception 77−87402

stellar atmospheres continued
novae, transient thermal X-ray emission from shocked circumstellar gas 77−45437
novae flare-ups theory, exact analytic self-similar solns. 79−35269
novae in nebular stage, collisional spectrum development 77−87441
novae shells, structural development theory 77−64746
NP 0532 magnetosphere, cyclotron instability rel. to origin of radiation *(Russian)* 80−8645
NQ Vulpeculae (Nova 1976), spectroscopic obs. and radial vels. 79−21316
O3 to O5.5 type stars, spectra and atmospheric struct. 77−33481
O and B stars, model atmospheres grid rel. to Si spectra 78−57539
O- and B-type stars, ionization conditions in expanding envelopes 78−28671
O-B3 stars in southern clusters excess absorpt by circumstellar envelopes 77−78791
O-type planetary nuclei, atmospheric props. 78−4206
O-type star, wind, effect on H II region evolution in mol. clouds 80−94846
O-type stars, coronae existence from UV reson. lines anal. 79−21293
O-type stars, extended atmospheres rel. to C III 9701 to 9715 Å lines 80−77401
O-type stars, O VI P Cygni profiles hourly vars. 77−37596
O-type stars, photospheric vel. fields 79−25597
O-type stars, vector space anal. of photometry rel. to atmospheric extension 78−49338
O-type stars, winds and coronae struct. from Hα line-profile anals. 78−40947
O-type stars in open cluster IC 1805, C IV line P Cygni profiles and mass loss indices 80−31296
O-type stars with mass outflow, IR fluxes calcs. for polysaccharide grain model 78−54008
O-type subluminous stars, non LTE model atmospheres, line profiles 79−101149
OB3 type stars in young clusters, circumstellar matter 2200 Å hump interpretation 80−82351
OB associations, stellar winds rel. to H I+molecular/H II shells from 1 to 2000 pc dia. 79−25678
OB stars, newly formed, H_2O emission from circumstellar shells 78−12390
OB stars, stellar wind mass loss determ., UV spectra obs. 80−94789
OB stars, stellar winds rel. to vel. dispersion in giant extragalactic H II regions 79−44606
OB stars in associations and young clusters, He abundance vars. *(Russian)* 77−82287
OB stars in LMC nebulae complex N 59, stellar winds rel. to H II shell form. 79−17052
OB supergiants, radiation-driven density waves rel. to mass transfer to X-ray binaries 77−9809
OB-type stars in LMC, energetic stellar winds rel. to giant H II ring 78−77593
OB-type stars in LMC, stellar winds rel. to super-giant H II shells form. 78−86012
observational evidence relevant to stellar evolution 78−12205
Of and O stars, stochastic accel. in photospheres rel. to difference in mass loss 80−90413
Of stars, radial vels. and K-term rel. to stellar winds 77−56922
Of stars, raxial vel. meas. 78−4226
Of stars in LMC, spectra rel. to low-excitation envelopes 77−78777
Of-type stars, expanding envelope models rel. to H and He II spectra 78−40950
opaque envelope clearing and sudden appearance of star 79−35238
ζ Ophiuchi, spectral vars. related to rot. 80−22000
70 Ophiuchi A, model chromosphere of K-type dwarf 78−65610
70 Ophiuchi A, theoretical stellar chromosphere model 80−67718
ρ Ophiuchi cloud, cosmic ray accel. by stellar winds 80−77512
optically thick winds in classical novae and symbiotic stars 77−87450
Orion Nebula stars, circumstellar shells, intracluster dust and wavelength depend. of polarisation 77−78839
α Orionis, 14.9 GHz obs. rel. to chromosphere/corona radio emission 79−75210
α Orionis, circumstellar shell heterodyne interferometry 78−8000
α Orionis, CO circumstellar absorpt. obs. in 4.6 micron spectrum 80−26858
α Orionis, M supergiant, circumstellar shell and mass loss rate 77−45415
U Orionis, Mira variable, atmospheric perturbation rel. to 1612 MHz flare and light curve 80−56844
ζ Orionis, Reticon obs. of Hα P Cygni profile rel. to stellar wind vel. law 80−82365
α Orionis, speckle interferometry diameter, limb darkening 77−91525
α Orionis, supergiant variable, mass loss, visible spectra obs. 80−67755
α Orionis, vel. fields in shell from Fe II emission line obs. 79−101144
α Orionis (Betelgeuse), circumstellar gas shell spatial extent 78−28673
α Orionis (Betelgeuse), K I 7699 å emission from circumstellar shell 77−22210
α Orionis (Betelgeuse), model atm., effective temp. 77−56935
α Orionis (Betelgeuse), optically thin dust shells 80−22011
λ Orionis A, far UV flux, emission line obs. of surrounding H II region 78−93303
σ Orionis E, mag. field discovery rel. to atmosphere struct. 78−93268
U Orionis OH maser flare detect. 79−40197
oscillatory flow past infinite porous vertical limiting surface with constant suction, free convection effects 79−92751
outflowing atmospheres across HR diagram, review 79−66996
partial ionisation zones, eqns. of state 78−28653
partially redistributed resonance radiation, ang. depend. 77−42285
particle discs, infrequently colliding, in binary system, tidal torques and appl. to asteroid belt truncation 80−98596
γ Pegasi, β Cephei star, dynamics of photosphere and shells 78−49447
EQ Pegasi, active dwarf binary star, chromospheric emission lines obs. 80−12762
RU Pegasi, dwarf nova, accretion disc instability rel. to rapid light vars. 77−53596
β Pegasi, M-type giant star, Mg II h and k emission rel. to expanding chromosphere 78−53945
AG Pegasi, symbiotic binary star, circumstellar cloud and stellar winds rel. to spectrum 80−109449
AG Pegasi, symbiotic nova, radio emission rel. to circumstellar nebula 77−22232
penetrative atmosphere, instabilities 79−84783

stellar atmospheres continued
X Persei, Be star, coordinated IR and optical obs. rel. to mass loss rate 79−25616
φ Persei, Be star, Fe III metastable states and mass loss 79−5832
X Persei, eclipsing binary, gaseous ring struct., H I alpha obs. 80−109482
β Persei, eclipsing binary, Mg II 280 nm line profile, calcs. and UV obs. 80−82421
RY Persei, eclipsing binary, spectroscopy and physical parameters of atmospheres 80−101618
S Persei, M-type supergiant, OH emission rel. to circumstellar envelope struct. 77−22218
21 Persei, spectrophotometry of Ap star, continuum features vars. 80−36638
X Persei (A 0535+26), stellar wind parameters from Prognoz-6 X-ray obs. *(Russian)* 80−109562
α Persei cluster stars spectral types, Be and shell stars obs. 79−58385
SX Phoenicis, simultaneous photometric and polarimetric obs. rel. to shock wave 78−49451
photosphere line profiles, thick circumstellar dust shell effect 79−30058
photosphere oscillations, PEPSIOS spectrometer search 78−93203
photospheres, mag. structs., models *(Italian)* 78−81603
photospheric vel. structure of long-period variable stars 79−53815
TX Piscium, disc brightness distrib. and envelope obs. from lunar occultation meas. 80−67725
SZ Piscium, RS Canum Venaticorum star, starspots surface distrib. from photometric obs. 80−109490
piston problem, one-dimensional, in non-ideal gas, time-dependent soln. 80−82185
planetary nebula central stars, He II 4686 Å emission evidence for stellar winds 78−57608
planetary nebulae central stars, atmospheric models 80−109434
planetary nebulae central stars, hot wind model for nebulae refractory elements gas-phase abundances 80−109516
planetary nebulae central stars, model atmospheres from UV radiation meas. 78−28679
plasma, highly ionized, ionization equilib. validity 80−21906
plasma laser star model of QSOs 78−96558
plasma-neutral gas interaction in cosmic physics 78−69669
Pleione (28 Tauri), envelope behaviour in 1976, spectroscopic obs. 80−8636
Pleione (28 Tauri), metallic-line shell spectrum anal., (1973-1976) 80−8637
polarisation by Thomson scatt. in optically thin axisymmetric envelopes 77−56914
polarisation of light in atmospheres and circumstellar envelopes *(Russian)* 80−17573
polarised radiation field, statistical equil. eqns., density matrix technique 77−5425
polytropic envelopes, thermal wave propag. *(Russian)* 77−82213
pre-main-sequence A and F stars in NGC 2264, circumstellar dust rel. to IR excesses 78−32461
pre-main-sequence stars in NGC 2264, metallicity and circumstellar dust shells 80−26916
pre-supernovae, stellar winds rel. to H abundances in supernovae and remnants 78−53969
presupernovae, stellar wind as possible cause of supernova remnant filamentary struct. 80−62249
propeller spindown of rotating magnets, torque calc., neutron stars appl. 79−8831
protostars, dynamical interaction with infalling matter, origin of interstellar grains 77−13327
protostars, H II regions development rel. to IR objects and maser sources 77−26032
protostellar wind bubbles in Orion Nebula, optical evidence 79−88724
pulsar, force-free aligned atmosphere, response to perturbations 78−53974
pulsar, radio emission mechanism model, by electron/positron-magnetosphere EM interaction 78−8036
pulsar atmosphere with arbitrary mag. and rot. axes, qualitative features 78−57569
pulsar atmospheres, beam-plasma interaction mechanism for radio emission 78−20847
pulsar atmospheres, numerical solns. of trans-relativistic shock relations 80−31202
pulsar constrained atmosphere, min. energy state 79−25622
pulsar electron cap, electrons accel. in internal zone 80−46592
pulsar emission, mag. bremsstrahlung of ultrarelativistic particle beam in relativistic plasma 80−46390
pulsar force-free magnetospheres, temp. stabilisation of instabilities 77−49413
pulsar magnetosphere, behaviour of mag. lines of rot. system 78−20848
pulsar magnetosphere, Cherenkov radiation of charged particle moving in mag. cold plasma 79−62736
pulsar magnetosphere, curvature radiation-pair prod. model for gamma-ray emission 79−5852
pulsar magnetosphere, electron absorpt. rel. to spectra low-freq. dropoff 80−17602
pulsar magnetosphere, EM wave dispersion relations for charge-separated plasma 77−7549
pulsar magnetosphere, generalised Ohm law 77−37610
pulsar magnetosphere, instability 78−53976
pulsar magnetosphere, mag. energy density rel. to curvature radiation absorpt. 79−75090
pulsar magnetosphere, magnetoactive plasma equilib. in gravit. field *(Russian)* 80−26895
pulsar magnetosphere, natural wave modes, rel. to radio emission polarization 78−69822
pulsar magnetosphere, nonaxisymm., relativistic plasma streaming, particle inertia 79−21320
pulsar magnetosphere, plasma waves propag. along mag. field in strongly anisotropic relativistic plasma 80−67542
pulsar magnetosphere, quasi-transverse propag. theory rel. to individual pulse-polarisation patterns 80−46591
pulsar magnetosphere, radio propag. effects on pulsar emission polarisation 79−75235
pulsar magnetosphere, radio wave generation at plasma frequency 80−109451
pulsar magnetosphere, relativistic particle curvature radiation 80−77434
pulsar magnetosphere, relativistically streaming plasma, flux conservation, MHD and force-free approxs. 79−19081

stellar atmospheres continued
pulsar magnetosphere, vibrations generation by klystron mechanism 78−53971
pulsar magnetosphere models, interior and exterior struct., pair prod. 80−46594
pulsar magnetosphere pair prod. 79−44515
pulsar magnetosphere radio emission, plasma supply and elec. forces, review 80−46595
pulsar magnetospheres, axisymmetric, finite inertia and resistivity effects 78−24521
pulsar magnetospheres, axisymmetric, self-consistent description 80−31318
pulsar magnetospheres, basic props., models *(Polish)* 77−17608
pulsar magnetospheres, consequences of polar cap model *(Russian)* 79−101169
pulsar magnetospheres, cosmic ray acceleration mechanisms *(Russian)* 78−16448
pulsar magnetospheres, gamma ray emission model 78−65641
pulsar magnetospheres, narrowband versus broadband emission processes rel. to luminosities 80−51797
pulsar magnetospheres, plasma co-rotation 78−12258
pulsar magnetospheres, probing via signal mcirostruct. periodicities and polarisation 79−75232
pulsar magnetospheres, propag. effects in shearing field-free plasma rel. to microstruct. 80−17483
pulsar magnetospheres, quasi-steady, Vlasov-Maxwell eqns. 77−13375
pulsar magnetospheres, relativistic MHD wind or plasma wave 80−31317
pulsar magnetospheres, stellar-wind model for plasma-EM fields 80−22031
pulsar magnetospheres physics, limitations on force-free approximation 77−5541
pulsar magnetospheres with arbitrary geometry, force-free approx. 77−64788
pulsar magnetospheres with parallel electric fields 78−65643
pulsar open magnetosphere, plasma instabilities as source of coherent radio emission 80−82403
pulsar polar cap, inhomogeneous struct. and radiation processes 79−25623
pulsar polar caps, pair form. and struct. of low altitude accel. zone 79−92790
pulsar polar caps, pair prod. discharges 77−53618
pulsar polar caps, pot. drops and ultrarelativistic particle accel. along curved mag. field 78−53970
pulsar rotating magnetosphere, charge bunching mechanism for coherent curvature radiation 77−33538
pulsars, axisymmetric magnetosphere model 79−84813
pulsars, axisymmetric magnetosphere models 79−92794
pulsars, charge-separated magnetospheres props. 78−40981
pulsars, finite force face cold plasma atm. models, plasma differential rot. 80−77378
pulsars, pulse width and period relations for various models 78−28714
pulsars, stellar wind rel. to radiation model 78−40979
pulsars, ultrarelativistic electron-positron beams rel. to radio emission 78−12257
pulsars axiosymmetric magnetospheres, method of soln. of self-consistent description 80−94825
pulsars force-free wind zone, stability 78−49468
pulsars plasma oscillations in polar caps 77−60784
pulsating star, atm. expansion due to periodic shock waves *(Russian)* 78−93244
pulsating stars, two-time asymptotic method appl. to one-zone atm. 77−53570
pulsating stars asymptotic theory, boundary layer method 80−82389
ζ Puppis, 2 cm radio emission obs. rel. to stellar wind and mass loss rate 78−40969
ρ Puppis, chromospheric activity and atm. dynamics of δ Scuti star 77−17581
V Puppis, eclipsing binary, circumstellar matter obs. 77−13385
ζ Puppis, of supergiant, mass flow var., visible and UV obs. 80−90431
ζ Puppis, Of type star, stellar wind model from UV line fit 80−72965
ζ Puppis, Reticon obs. of Hα P Cygni profile rel. to stellar wind vel. law 80−82365
ζ Puppis, spectral line profiles, mass ejection 77−33507
ζ Puppis, UV spectral energy distrib. rel. to atmosphere struct. 77−22211
ζ Puppis, visible and UV spectroscopy of stellar wind var. 79−16949
R50, peculiar emission-line star in SMC, circumstellar dust shell IR emission 77−45461
radially symmetric accreting envelopes, spectral lines form. and profiles *(Russian)* 78−57544
radiation field, in plane parallel atmosphere involving energy sources *(Russian)* 77−91417
radiation field in deep layers of semiinfinite atmosphere 79−58325
radiation field in semi-infinite atmosphere containing energy sources 80−21907
radiation integral transfer problems, splines under tension calcs. 77−53419
radiation pressure in spectral lines in gaseous systems with axisymm. motions, kinematics 79−88579
radiation redistrib., diffuses reflection effects 78−53819
radiation scattering, approx. soln. *(Russian)* 80−36621
radiation transfer eqn. in spherical geometry, numerical soln. 80−90329
radiation transfer in infinite atmosphere, interrelations between angular distribs. of intensity *(Russian)* 77−49281
radiation transfer in plane atmospheres, nonlinear eqns. in linear transfer problems 79−62741
radiative acceleration of gas above luminous disc, QSOs matter ejection mechanism 77−49373
radiative equilibrium departures, grey absorpt. 78−81531
radiative equilibrium mediumcool non-LTE models, effective temp. 10000-15000K, gravity 10^4 78−40921
radiative heat transfer in presence of mag. field *(Russian)* 77−87247
radiative shock dynamics, H continua 78−40918
radiative transfer, Banach space anal. of Chandrasekhar H-equation 77−13224
radiative transfer, brightness coeffs. for two-layer atmosphere with anisotropic scatt. *(Russian)* 77−17349
radiative transfer, calc. methods for line broadening by electron scatt. *(Russian)* 77−17347
stellar atmospheres continued
radiative transfer, charact. lengths for moving media *(Russian)* 77−82117
radiative transfer, coherent scattering 78−28667
radiative transfer, comoving frame eqn. in spherically symmetric flows, scatt. source functions 77−22056
radiative transfer, comoving-frame transfer eqn. soln. in spherically symmetric relativistic flows 80−82181
radiative transfer, departure from LTE 79−48777
radiative transfer, exact soln. of diffuse refl. and transmission problem in Rayleigh scatt. 79−35116
radiative transfer, generalised Eddington approximation in envelopes 79−80214
radiative transfer, in expanding atmos., Feautrier method 79−25593
radiative transfer, in lines of reson. multiplet 78−24460
radiative transfer, integral eqn. spectrum calc. for semi-infinite medium 80−67540
radiative transfer, key eqn. exact soln., Laplace transform and linear singular operators method 80−72762
radiative transfer, light diffusion problem in optically finite shell *(Russian)* 77−13236
radiative transfer, LTE problems, numerical techniques 77−71108
radiative transfer, non-conservative problem 80−36492
radiative transfer, non-LTE diagnostics *(Italian)* 78−81615
radiative transfer, non-LTE line form. in presence of mag. field 78−7871
radiative transfer, noncoherent renormalisation group approach 78−65495
radiative transfer, one-dimensional transport problem soln. *(Russian)* 77−13235
radiative transfer, polarisation of scattered radiation in presence of internal energy sources 80−67541
radiative transfer, quasiasymptotic solns. for nonconservative scatt. in optically thin layer *(Russian)* 77−17348
radiative transfer, reson. line form. in decelerating spherical flow 77−78624
radiative transfer, response functions for mag. lines 77−45304
radiative transfer, Sobolev method generalisation for flows with nonlocal radiative coupling 78−28500
radiative transfer, soln. of equation for Rayleigh's phase function by principle of invariance 79−84660
radiative transfer, synthetic scattering phase function 80−98541
radiative transfer, time-dependent, exact soln. of integro-differential eqn. via Laplace transform 80−94703
radiative transfer, Unno-Kondo generalized Eddington approx. in extended atmospheres 80−21997
radiative transfer, Voigt function, partial differential equations 78−28507
radiative transfer equation, quadratic integrals for monochromatic isotropic scatt. 77−33332
radiative transfer equation geometric solns., diagnostic anal. 77−5423
radiative transfer equation perturbation soln. 77−45404
radiative transfer in atmospheres with spherical symmetry, conservative Milne problem 78−49312
radiative transfer in dynamic atmospheres 77−60752
radiative transfer in expanding envelopes, two-level atom model 78−61849
radiative transfer in finite atmosphere, exact soln. of basic eqn. via Laplace transform 80−94702
radiative transfer in geometries other than plane-parallel layers *(Italian)* 78−81616
radiative transfer in magnetic atmospheres, analytical soln. 80−36494
radiative transfer in noncoherent anisotropically scatt. plane-parallel slab, Green's function method *(Russian)* 78−61723
radiative transfer in nongray extended dust shell models, Eddington approx. generalization 78−73627
radiative transfer in plane-parallel atmosphere with polynomial emission source distrib. 80−94700
radiative transfer in semi-infinite Rayleigh scattering atmosphere, exact soln. 79−35112
radiative transfer in spherical dust shells, generalised two-stream Eddington approx. 79−35120
radiative transfer in spherically symmetric flows, comoving-frame eqn. soln. for multilevel atoms 78−28499
radiative transfer multiple nonstationary scatt. with curved surfaces 77−29641
radiative transfer transport equation with scattering albedo $\omega_0<1$, exact soln. 79−35111
radiative transfer with discontinuous source function in spherical extended envelope 77−53417
radio pulsars, rot. magnetised neutron star model with H or He envelope *(Russian)* 78−40982
radiostars, polytropic models rel. to envelope dynamics and mass loss rate 79−2544
radiowave generation by gyrosynchrotron and Langmuir-wave processes, solar and stellar appl. 79−21172
red giant envelope composition rel. to evolution 80−105237
red giant model atmospheres, opacity sampled models grid 80−82348
red giant stars, circumstellar shells chem. struct. 80−105242
red giant stars in globular clusters M92 and NGC 6397, model atmospheres and C abundances 79−48785
red giants, absolute mass loss scale determ. from obs. of α Herculis 78−7997
red giants, ejection of ^{13}C enriched matter rel. to interstellar $^{12}C/^{13}C$ ratio 77−9788
red giants, grain-gas interaction in envelopes 77−60760
red giants, mass loss from dynamically unstable envelopes 78−20824
red giants, model atmospheres rel. to TiO absorpt. bands 78−96480
red giants and supergiants, circumstellar envelopes and mass loss 77−9743
red giants in M13, Na abundance var., protocluster gas inhomogeneities 80−82439
red supergiant stars, detect. of surrounding refl. nebulae from polarisation obs. 77−13340
red supergiants, model atm. based on band-model opacity 77−56934
red variable stars, mol. absorpt. rel. to amplitude extension and amplitudes limit 79−62836
redistribution effect in expanding atmospheres, angle averaged in comoving frame 77−17545
relativistic and nonrelativistic gas flows, general symm. soln., low press. limit 77−9655

stellar atmospheres continued
relativistic centrifugal winds, appl. to pulsars 78−96473
relativistic star, rotating shell model 79−88650
resonance radiation transfer in extended envelopes with differential rot. and expansion *(Russian)* 77−64747
resonance radiation transfer in infinite isotropically expanding medium *(Russian)* 78−61721
resonance radiation transfer in moving media with large-scale radiative coupling *(Russian)* 78−93088
Ross 640, H-poor white-dwarf, H abundance determ. 77−87388
rotating star, surface darkening or brightening 77−60750
rotating star, vibr. buildup in surrounding plasma *(Russian)* 77−3946
S-type stars, molecular spectra and model atmospheres 80−51764
FG Sagittae, anomalous planetary nebula, photometry rel. to optically thick shell effective temp. 79−88687
HM Sagittae, emission-line star, polarimetry rel. to circumstellar dust shell *(Russian)* 80−36649
WZ Sagittae, eruptive binary, accretion disc radius from hot spot eclipses anal. 80−72962
HM Sagittae, eruptive BQ emission-line star, emitting nebula props. 78−20835
HM Sagittae, IR spectrum and circumstellar dust shell 78−93266
WZ Sagittae, recurrent nova, accretion disc models comparison with IUE obs. during outburst 80−109448
WZ Sagittae, recurrent nova, circumbinary gaseous disc model for super-hump phenomena 80−82368
HM Sagittae, young planetary nebula, interacting stellar winds model rel. to 2.8 cm flux density increase 79−67025
XZ Sagittarii, Algol system, UBV photometry rel. to circumstellar matter 80−22041
V356 Sagittarii, eclipsing binary, opaque circumstellar ring model 78−49477
MV Sagittarii, H deficient variable, nature of circumstellar envelope 77−9756
RY Sagittarii, pulsating R Coronae Borealis star, circumstellar dust shell rel. to IR vars. 77−45462
RY Sagittarii, spectra near min. light 80−36642
Schwarzchild black hole, gas accretion 80−56871
ζ^1 Scorpii, B1 supergiant, UV reson. lines rel. to expanding envelope struct. 80−4349
α Scorpii, circumstellar absorption lines in UV spectrum 80−51804
α Scorpii, circumstellar shell heterodyne interferometry 78−8000
τ Scorpii, deep photospheric flows 79−58326
τ Scorpii, expanding envelope, mass loss rate 78−65613
ζ^1 Scorpii, extreme B1 supergiant, IUE obs. rel. to mass loss mechanism 80−17583
ζ^1 Scorpii, extreme B-type supergiant, UV spectroscopy rel. to low-vel. stellar wind 80−22004
α Scorpii, line form. in circumstellar shell rel. to α^2 Scorpii location along line of sight 78−73739
α Scorpii, M supergiant, circumstellar shell and mass loss rate 77−45415
AH Scorpii, M-type supergiant, OH emission rel. to circumstellar envelopes struct. 77−22218
τ Scorpii, photospheric vel. fields 78−28672
V861 Scorpii (HD 152667), X-ray binary, Hα obs. rel. to mass transfer and mass loss 79−101171
V818 Scorpii (Scorpius X-1), atmosphereic ionisation vars. rel. to UV, visible, IR and X-ray obs. 80−82541
Scorpius X-1, linear X-ray polarisation upper limit rel. to accretion-disc model 78−49557
RY Scuti, silicate grains IR emission from early-type supergiant binary system 80−41827
δ Scuti-type stars, chromospheric activity and atom. dynamics 77−17581
self-gravitating rotating masses, book contrib., review 80−21915
self-gravitating rotating plasma, gyroviscosity effects 78−5860
RT Serpentis (Nova 1909), ionised envelope props. from spectrum in 1964, 1975 and (1978) 80−46566
FH Serpentis (Nova 1970), radio emission from expanding shell 80−26868
FH Serpentis (Nova 1970), thick inhomogeneous shell model for radio emission 78−12236
shell ejection timing in nova outbursts 77−82252
shell stars, H shell spectrum form. and envelope struct. 79−48830
shock heated atmospheres, methodological discussion, appl. to solar atmospheres 77−29745
SN 1973r in NGC 3627, expansion vel. of type II supernova 77−49407
solar neighbourhood F, G and K stars, H-R diagram fine struct. 77−29819
source function surface value derivation in non-LTE radiative transfer 79−35122
spectral line formation depth in mag. field, theory *(Chinese)* 80−105159
spectral line formation in microturbulent magnetic fields 80−31201
spectral line formation in YY Orionis envelopes 77−64741
spectral lines form. depths calc., rel. to curve of growth method *(Russian)* 78−65604
spectroscopic binaries, Ca II H and K line emissions in late-type giants and supergiants 77−91566
spectrum line contours in incoherent scatt. 79−88590
spherical accretion onto compact X-ray sources, luminosity thermal limit 80−82546
spherical dust shell around central star, two-shell moment method for radiative transfer 80−62001
spherical envelopes, line profile computation by three methods 80−85868
spherical transonic flow, reson. line radiative transfer 80−94698
SS 433, accretion disc model for beam accel., radiation and precession 80−72971
SS 433, circumstellar ring model rel. to weak lines pair wavelength vars. 79−67023
Stein 2051B, temp. and radius of cool white dwarf 77−13338
Stokes' problem, mass transfer effects of MHD free convective flow 80−62003
stratification of elements in quiet atmosphere, diffusion process 78−12211
Stromgren four colour indices, grid for calc. of log g and effective temp. 80−36507
strong internal mag. field diffusion through radiative envelope of 2.25 M$\odot$ star 78−85931
structure, mol. effects 80−21999
stellar atmospheres continued
subatmospheric nonthermal storage modes vs. radiation pressure for stellar wind origin 77−33468
subgiant stars, F-, G- and K-type, Be abundance rel. to post-main sequence evolution 77−13333
super-metal-rich stars, boundary cooling and supermetallicity 80−56821
super-metal-rich stars, Fe abundance problem 77−74060
superadiabatic charged particle accel. and flares 79−21251
supercritical accretion discs winds struct. and appearance, numerical models 80−21984
supergiant OH maser sources, optical radial vels. rel. to outflow vels. 77−49378
supergiant stars with stellar winds LMC, luminosity and extinction values, UV obs. 80−77477
supergiants, model atmospheres rel. to metal abundances in G- and K-type Ib stars 77−33482
supergiants instability effects, brightness limits and coronae 80−109432
supergiants of O- and B-type in Magellanic Clouds, stellar winds 80−51863
supernova ejecta, dust grains sudden nucleation and growth 80−26941
supernova expanding envelope, grain condensation 78−24520
supernova shell expansion, cooling wave props. 77−9760
supernova shock waves structure 77−17603
supernovae, atmospheric struct. rel. to radiation dynamics, envelope ejection and light curves 77−64783
supernovae, distance determ. by Baade's generalised method, appl. to H_0 and q_0 80−73082
supernovae, expanding atmospheres rel. to light curves and spectra 77−87455
supernovae, expanding gas shell external excitation rel. to outburst light 78−40976
supernovae, type I, conservative scatt. theory for effects of line overlapping on spectra *(Russian)* 80−105266
supernovae, Type I, ejected envelope struct. 78−65636
supernovae, type I, envelope expansion vel. as function of brightness decline rate 78−96495
supernovae, Type I, envelope model, Hubble constant determ. 77−53617
supernovae, Type I, envelopes, radioactive excitation source model for late time spectra 80−105264
supernovae, type II, nonequilib. processes in evolution 80−46586
supernovae envelopes, Thomson scattering and emission line profiles *(Russian)* 78−16445
symbiotic stars, stellar wind and accretion rates rel. to subclasses 80−62144
symbiotic stars, super-critical accretion model with stellar wind 77−45458
ζ Tauri, apparent wavelength depend. of v sin i 78−12240
RW Tauri, eclipsing binary, gaseous ring struct., H I alpha obs. 80−109482
V471 Tauri, eclipsing binary, K-type star chromospheric Mg II emission obs. 80−26912
DL Tauri, Hα profile in T Tauri type star *(French)* 78−8003
ζ Tauri, high-resolution spectra of λ1920 and λ1720 features rel. to extended atmosphere 78−4236
SU Tauri, R Coronae Borealis star, circumstellar dust shell discovery from optical and IR photometry 80−101601
α Tauri, semiempirical model photosphere from Fe I lines obs. 78−4202
ζ Tauri, Si II lines in shell 77−60774
DR Tauri, T Tauri star, mass flow var. in envelope, visible spectra 80−85939
α Tauri (Aldebaran), chromosphere model 78−40931
BU=28 Tauri (Pleione), envelope during shell phase, 1972-75 period 78−28707
BU Tauri (Pleione), polarisation rel. to circumstellar disc 77−45500
28=BU Tauri (Pleione) Be shell star, 3167 to 4924 Å spectrum atlas 80−98673
RV Tauri and yellow semiregular variables, circumstellar dust prod. rel. to metallicity 80−26865
T Tauri stars, Hα emission line core formation in chromosphere 80−94792
T Tauri stars, H envelopes radiation rel. to location in (J-H), (H-K) diagram 77−78790
T Tauri stars, outflowing envelopes models 78−96482
T Tauri stars, photometric and spectral props. 79−21282
T Tauri stars, props. of assoc. ionized regions 80−36624
T Tauri stars atmospheres, sphere and low chromosphere model 80−36623
T Tauri stars in dust cloud Lynds 134, mass loss causing cloud turbulence 80−94845
T Tauri stars in Orion Nebula (M42), possible coronal X-ray emission obs. 78−28852
T Tauri type stars, hydromag. model of peculiar activity *(Russian)* 78−49442
RR Telescopii, nova-like variable, spectrophotometry and expanding shell model 77−45460
temperature minima in chromospheres 77−74041
temperatures and gravities, calibration of uvbyβ photometric system 78−4198
thermal conductivity, without mag. field 77−87375
thermal convection approximations 79−35127
thermal radio emission from explosive energy release 77−53580
thermal-convective instability, finite Larmor radius effect 78−32438
thermal-convective instability, radiative transfer effects 78−53929
thermal-convective instability of partially ionized plasma, radiative transfer, medium porosity and collisional effects 80−67538
thermal-convective instability through porous medium 80−53769
Thomson scatt. in thick layer 77−82216
transfer equation, in semi-infinite atmosphere with albedo (ω>1) 80−82184
Trumpler 27 star 28, WC9-star with thermal dust shell 80−67738
turbulence, conference, London, Ontario, Canada (1979 August 27 to 30) 80−73102
turbulence, effect on spectral line form., finite correl. length 80−77387
turbulence, review 79−30056
two-dimensional radiative transfer, planar geometry theory 78−40810
4U 1626−67, X-ray pulsar, X-ray and optical obs. rel. to accretion disc optical emission 80−51914
3U 1700-37, Copernicus X-ray obs. rel. to circumstellar matter distrib. 78−96568
unsteady laminar boundary-layer flow past porous limiting surface, free convection effects 79−35237

stellar atmospheres continued
upper main-sequence peculiar stars, atmospheric stability rel. to radiatively driven diffusion theory 80−82374
r Ursae Majoris, Am star, microturbulence and metal content determ. 80−82377
XY Ursae Majoris, eclipsing binary, light curve changes, starspot activity 77−57044
XY Ursae Majoris, eclipsing binary, observational evidence for large-scale spot activity on primary component 80−109491
α Ursae Majoris and close companion star, spectrum synthesis 77−49436
W Ursae Majoris stars, nonradial radiative transfer, appl. to bolometric refl. effect 77−91567
W Ursae Majoris stars, role of photospheric convection 78−49478
UV 1758+36, He deficient hot subdwarf B star, atm. parameters, radial vel. 78−53944
uvby photometry, theoretical analysis 78−85930
velocity gradients, determ. from differential Doppler shifts in spectral lines 78−57538
γ^2 Velorum, 2 cm radio emission rel. to stellar wind and mass loss rate 78−40969
λ Velorum, K-type supergiant, UV spectrum rel. to chromosphere and wind struct. 80−72948
γ_2 Velorum, Wolf-Rayet binary, spectral obs. 80−85950
β Virginis, chemical composition and age 78−61855
EQ Virginis, dK5e star, new absorpt. line obs., possible infalling gas 77−37602
AH Virginis, eclipsing binary, circumstellar gas rel. to light curve vars. 77−78822
ε Virginis, Fe spectrum, differential model atmosphere analysis 79−25604
78 Virginis, magnetic field gradient in Ap-star atmosphere, Zeeman spectra 78−85953
CU Virginis, short period Ap star, mag. field rel. to atmospheric circulation currents 77−33511
CU Virginis (HD 124224), Ap star, model atmospheres rel. to spectrophotometric obs. 80−98663
Voigt function computation, path lengths of integration 80−105234
Voigt lines, random array, curve-of-growth function 78−89055
NQ Vulpeculae (1976), Hα emission line profiles rel. to primary envelope expansion vel. *(Russian)* 78−40971
NQ Vulpeculae (Nova 1976), CO emission and η Carinae stage 79−25609
NQ Vulpeculae (Nova 1976), spectra evolution and ejection vels. 78−89205
wave propag. with high radiation pressure 80−26729
wave propagation in medium with high radiation press., basic eqns. for homogeneous media 79−88581
wave propagation with magnetic field, Lagrangian procedure 80−8620
waves, effect on spectral line anal. 79−44465
weak G-band stars, CH and NH band strengths, atm. material from CNO cycle 79−8917
white dwarf magnetospheres, polarised synchrotron radiation emission 77−2428
white dwarf stars, model atmospheres rel. to two-colour diagram, masses and radii 80−46547
white dwarfs, abundance effects on spectra of very cool objects, model atmospheres 77−29829
white dwarfs, atmosphere structure rel. to composition in hot stars 80−98658
white dwarfs, conf., Rome, Italy (Sep. 1976) *(Italian)* 78−93239
white dwarfs, convective mixing and accretion 77−5529
white dwarfs, cool, IR photometry, atm. comp. 79−16950
white dwarfs, DB-type, model atmospheres 80−51761
white dwarfs, highly magnetised, accretion, role of electron conduction 80−82358
white dwarfs, hot, model atmospheres and effective temps. 79−25602
white dwarfs, magnetic, model atmospheres calc. of cyclotron absorpt. spectra 80−4351
white dwarfs, minimum-flux coronal models for H and He atmospheres 80−8626
white dwarfs, mixing processes and elements separation in envelopes 78−12222
white dwarfs, model atmospheres and synthetic spectra, effective temps. 5000-7000K *(Italian)* 78−93240
white dwarfs, southern, model atmospheres calcs. rel. to Stromgren photometry 78−32456
white dwarfs chem. evolution, diffusion and accretion 80−36628
white dwarfs model atmospheres, masses and radii 77−33485
white dwarfs rejuvenation due to interstellar accretion 77−17550
white dwarfs superflares, model for cosmic gamma-ray bursts *(Chinese)* 77−22021
wind, ejection of matter into space, mechanisms 79−5811
wind, radiatively ionised, in emission nebula NGC 6302, direct evidence 80−67835
wind driven circumstellar shells, struct. and evolution 78−16400
wind flow, axisymm. ideal MHD eqns. 78−89174
wind flow past compact object, X-ray intensities 80−22116
wind from early-type star, rel. to struct. in galactic nebula (206) 78−12326
wind from massive close binaries, mass loss 80−90474
winds, influence on cosmic systems charge polarisation 79−48771
winds, interaction with interstellar medium, cosmic ray origin and accel. 80−77512
winds, nonequilibrium ionisation 79−48751
winds, rapidly diverging flow, heat and momentum addition effects 77−29755
winds, relativistic modes of tearing instability in background plasma 80−62012
winds, steady state transonic wind model, radiative cooling effects 80−77391
winds, theory of classical fluid dynamics 80−90412
winds, turbulent mixing with interstellar gas 80−67701
winds in massive binary stars, effects on heavy elements prod. 80−46534
Wolf Rayet stars, late type with circumstellar dust shell, 8-13 micron spectral obs. 80−101599
Wolf-Rayet atmospheres, structure and composition 80−98668
Wolf-Rayet binaries, eclipses at emission-line freqs. rel. to envelope struct. determ. 77−17596
Wolf-Rayet stars, electron density in emission-line region 78−93263
stellar atmospheres continued
Wolf-Rayet stars, He rich-expanding atmosphere model rel. to UV energy distribs. obs. 80−22023
Wolf-Rayet stars, IR light vars. 77−9750
Wolf-Rayet stars, Roche lobe overflow and stellar wind mass loss 80−105250
Wolf-Rayet stars, struct. of winds from obs. of IR continua 77−78793
Wray 977, optical counterpart to X-ray binary pulsar, 4U 1223−62, optical spectra 80−72984
X-ray binaries, matter supply mechanisms 77−9813
X-ray binaries, stellar winds rel. to anomalous periastron positions 79−25756
X-ray binary sources, pulsating, accretion from Keplerian disc rel. to spin-up 80−67904
X-ray binary stars, primary stars stellar winds rel. to evolution 78−12431
X-ray binary system, Fe fluoresc. line struct. 77−78889
X-ray binary systems, evaporative winds 77−78888
X-ray burst sources, model, substorm process at accreting neutron star 79−17132
X-ray flux from stellar winds, rel. to H II regions narrow recomb. lines 79−8972
X-ray induced shocks in stellar winds of massive binaries 80−94784
X-ray pulsars, role of Alven surface in X-ray pulses form. 77−78899
X-ray pulsars, vacuum polarisation effect rel. to radiative transfer and X-ray spectra 80−27015
X-ray sources, accretion disc plasma oscills. rel. to radio emission 80−62317
X-ray sources, compact, optically thick radiative transfer rel. to X-ray spectra form. 80−22115
X-ray sources, IUE UV spectra rel. to circumstellar matter 78−96569
X-ray sources, pulsating, accretion disc interaction with stellar mag. field 78−93461
X-ray sources, pulsating, accretion disc mag. field calc. for oblique mag. dipole configuration 80−94895
X-ray sources, stellar wind heating and bow shock form. *(Russian)* 77−60855
X-ray sources, strongly magnetised plasma collisional relax. of ion beam 80−33785
X-ray sources with repeating bursts, magnetospheric accretion model 77−5597
yellow semiregular and RV Tauri variables, circumstellar dust prod. rel. to metallicity 80−26865
young stars, circumstellar dust rel. to interstellar gas and EHF continuum emission 80−51766
young stars, circumstellar mols. 80−22013
young stars circumstellar shells, contrib. to reddening and polarisation 78−93199
young stars in Chamaeleon T1, photometry and spectral obs. 80−72943
young stellar objects, polarisation prod. by scatt. in circumstellar shell 79−8911
A- and B-type stars, radiation forces and B abundance diffusion theory 79−88664
C isotope ratio 79−57656
C overabundances in C star atmospheres 79−21284
C stars, $^{12}C/^{13}C$ ratio determ. 78−73710
C stars, circumstellar envelopes and evolution 79−40178
C stars, determination of $^{12}C/^{13}C$ and N/C ratios in atm. 80−17580
C stars, enhanced C abundances in long-period variables 77−33501
C stars, form. of carbyne and cyanoacetylenes in stellar atm. 80−67708
C stars, Li line formation 78−65615
C stars, low-energy spallation rel. to $^6Li/^7Li$ ratio 78−40927
C stars, photometry at 1-2.5 μm, circumstellar dust shells 79−88652
C^-, free-free transitions, continuous absorpt. estimation 78−9098
CNO abundances in red giant envelopes 77−29825
CO, $X^1\Sigma^+$ state elec. dipole moment function, transitions, vibr.-rot. band calcs. 77−14410
Ca II emission from stellar chromospheres of late-type stars 79−30061
Ca II K line emission widths 77−41373
Fe curve of growth split as function of atmospheric pressure 77−29794
Fe I 3719.94 Å line broadening by He, line width and shift meas., lab. expt. 77−73942
Fe/H determ. catalogue, comments 77−29806
H^-, bound-free photodetachment cross section, rel. to opacity in cool stellar atms. 79−49996
H_2^- and N_2^- free free absorpt. rel. to opacity 78−81610
H_2-He plasma interface in strong gravit. field, bremsstrahlung, neutron stars and pulsars appl. *(Russian)* 79−67048
H_2D^+, interstellar and circumstellar search, upper limit determ. 79−2562
H_2O masers, time vars., 22 GHz obs. 79−30077
Hβ indices for model atms., B-type stars appl. 80−31292
He abundance in stellar atmospheres in O-associations and young clusters *(Russian)* 77−64815
He I $2^3S \rightarrow 2^3P$ transition, rate coeff. for electron impact excitation 79−48664
He rich atmospheres, elec. fields influence on accretion and stellar winds 79−48772
He stratification in model atmosphere of blue horizontal-branch star 80−90409
He variable stars, IR excesses rel. to circumstellar matter 80−67733
He-proton diffusion coeff. in stars 79−16811
He-rich white dwarfs, convective mixing 79−71018
^3He stars, spectroscopic search, diffusion hypothesis 79−35264
Hg-Mn binary stars, inhibition of atmos. diffusion 80−62153
HgMn stars, diffusion and line asymmetries 78−40948
HgMn stars, evidence for Hg in thin atmospheric layer rel. to diffusion model 80−105243
HgMn stars, line blanketed model atmospheres rel. to spectrophotometry 80−26867
Li abundances *(Russian)* 77−64748
Li, Be, B, isoelectronic sequences, ionization equilib. balance, solar and stellar atms. appl. 79−36587
OH 26.5+0.6, late-type variable star, 2 to 40 micron spectrophotometry rel. to dust shell 78−24568
OH maser sources, envelope struct. from interferometric obs. 77−53583
OH/IR stars, OH main lines masers inversion 78−28664
τ Scorpii, spectral line studies using LTE-method *(Russian)* 79−92769
Si^- opacity source 78−53930
SiO circumstellar maser 78−16511

stellar atmospheres continued
SiO maser stars, J=1→0 ν=1 and 2 masers obs. and spatial coincidence 80−4339
SiO mass loss and grain formation in expanding envelopes around evolved stars 79−48782
SiO, nonmaser emission lines from expanding envelopes around evolved stars 78−28650
TiO blanketing effect *(Russian)* 79−30065

stellar binaries *see binary stars*

stellar clusters and associations
see also globular star clusters
07021−1940, cluster hidden in ghost image of Sirius on Palomar Sky Survey, discovery 80−109501
abnormal stars in open clusters, freq. of occurrence 79−71038
absolute magnitudes of stars in the same seven colour photometric box 78−28662
active galaxy nuclei energy sources, choice between, magnetoid, black hole and compact star cluster *(Russian)* 77−78885
AFGL 437, optical and IR obs., young star cluster embedded in nebulosity 78−4394
ages of open clusters from comparison of four-colour photometry with evolutionary models 78−8007
AM-3, SMC faint outlying open cluster, description 79−25651
Ara, IR photometry of highly reddened cluster 77−41395
Ara OB1, NGC 6193 and Ara R1, young southern complex, UBVRI obs. 78−16473
associations, rel. to origin of galaxy structural features *(Russian)* 77−17691
axisymmetric star cluster model, with discrete stellar mass distrib. 77−13418
axisymmetrical stellar systems, periodic orbits of stars 80−17619
Be 94, UBV photometric obs. of young distant open cluster in Cepheus 78−61892
Be 94, young cluster, early-type stars photometry and distance 77−2424
Be stars in galactic clusters, Hα study 77−56968
Berkeley 11, compact open cluster, UBV obs. 80−94840
Berkeley 19, anticentre open cluster, age determ. from colour magnitude diagram, BV photometry 80−90486
Berkeley 21, UBV photometry of faint anticentre cluster 79−40229
Berkeley 58 in Cassiopeid, membership of an open cluster *(Russian)* 79−92812
bidimensional stellar systems in uniform rot., stability for nonaxisymm. modes 78−85980
binary stars formation by three-body encounters, probability and effects on cluster evolution 77−13396
binary stars on main sequence, freqs. among cluster and field stars 80−26901
binary stellar systems, tidal disruption and coalescence 78−93330
binding energy distrib. of binaries in cluster, homogeneous cluster model 80−62209
Bochum 15 stellar aggregate, photoelectric and spectroscopic obs. 77−87490
Byurakan 2, open cluster, photometric obs. 77−2345
Canis Major OB1, luminous C star obs. 78−12312
Canis Major OB1, uvbyβ obs. of young assoc. 78−85985
Canis Major OB1 association, probable membership of shell star (HD 51480) 80−31305
Canis Major R1, anomalous diffuse bands 80−51820
Canis Major R1, optical and IR props. of newly formed stars 78−93332
Canis Major R1, supernova-induced star formation region 77−87494
Canis Major R1, uvbyβ obs. of Canis Major OB1 members and foreground stars 78−85985
Canis Major R1 and OB1, Fabry-Perot obs. of assoc. expanding gas shells 78−93336
Canis Major R1 association, supernova induced star formation 78−8063
Carina Nebula association, radial vel. study of WN stars and Of star 79−35261
Carina OB1, association, probable membership of near VV Cephei star (LSS 1916) 79−35299
Carina OB 1 association, membership and absolute magnitude of cepheid VY Carinae 77−64764
Carina OB 1 association, RI photometry, reddening law determ. 79−8957
Carina spiral feature inner side, star groups and interstellar dust distrib. 80−51871
Cassiopeia-Taurus association stars, interstellar 2200 Å feature anomalous strength 80−77469
III Cephei association, distance of eclipsing binary CW Cephei 79−21326
Cepheids, period-age relation 79−21317
Cepheus IV association, spectrophotometry of young stars 77−13328
Cepheus IV star formation region, continuum and recomb. lines, SHF obs. 80−90501
Cepheus OB2 association stars, interstellar line spectra 80−22052
Cepheus OB3 association, near main line OH maser with Zeeman pattern in assoc. mol. cloud 80−56908
Cepheus OB3 association, star form. in mol. cloud complex 78−28750
Cepheus OB3 association, supernova-induced star form. 78−12306
Cepheus OB3 association and Sharpless 155 nebula, thermal radio emission obs. 78−96514
Cepheus OB3 association molecular cloud, mol. obs. rel. to star form. 80−12798
Cepheus OB3 molecular cloud, obs. of new IR sources 79−67072
Chamaeleon T1, young stars, photometry and spectral obs. 80−72943
Chamaeleon T association, JHKL photometry of stars, reddening 79−58384
Chamaeleon T-assoc., YY Orionis stars 79−30064
chemical composition determ. method using evolved members 77−29889
classification criteria by statistics from co-occurrence matrix *(Italian)* 80−98574
cluster around massive black hole, stationary state *(Russian)* 80−67806
cluster membership probabilities, problems in interpretation 78−28736
clusters containing massive central black holes, Monte Carlo simulations in two-dimensional phase space 79−8955
Collinder 132a, b, UBVβ photometry of two sparse open clusters 78−32540
Collinder 135, nearby field of view, wide and narrow band photometry obs. 80−109504
Collinder 140, nearby open cluster, UBV photoelectric photometry 78−53994

stellar clusters and associations continued
Collinder 140, photoelectric UBV photometry, age and distance 78−49489
Collinder 140, young open cluster, spectroscopic and statistical study 80−62211
Collinder 228, in great Carina Nebula, obs. of massive multiple system HD 93206 (QZ Carinae) 79−97027
Collinder 228 and 232 in Carina Nebula, extinction determ. from UBV photometry obs. 80−90513
collinder 228 in Carina Nebula, open clusters distance determ., photometry obs. 80−85977
collisionless spherical stellar system in steady state 79−5865
Coma Berenices open cluster, spectral types 77−29886
Coma cluster, HD 108102 (T111), possible RS Canum Venaticorum system 79−67020
Coma cluster, proper motion and membership of W Ursae Majoris star CC Comae 77−74099
Coma cluster, reddening 80−62222
complexes of stars in Galaxy, star form. regions *(Russian)* 78−69851
complexes rel. to gas complexes *(Russian)* 79−35391
core collapse in isolated clusters, eqns. 79−30097
core collapse of spherical cluster, approx. theory 78−49486
Corona Austrina T1 association, UBV photometry of member stars *(Russian)* 79−17035
Cygnus OB2, spectral type and membership of star number 12 80−51760
Cygnus OB2 (VI Cygni), soft X-ray emission sources discovery 80−26918
Cygnus OB2 association, connection with Cygnus X-ray superbubble 80−90575
Cygnus OB2 association, interstellar C_2 detect. in spectrum of star (No.12) 78−12332
Cygnus OB2 association, possible membership of IR source (MWC 349) 80−56971
Cygnus OB2 association, wavelength depend. of polarisation and interstellar birefringence 77−33577
Cygnus OB2 No.12, high resolution 2μ spectroscopy rel. to interstellar and stellar features 78−57613
Cygnus OB 2 association, H content, radio continuum emission search 77−64809
Czernik 29 in Puppis open cluster pair, UBV obs. 80−109503
dense clusters, evolutionary tracks *(Russian)* 78−69852
dense stellar systems, fates 79−25652
dense system, high-density gaseous disc formation and evolution 77−5549
30 Doradus cluster, relation to foreground unique interstellar Ca II K-line profile 80−51850
30 Doradus complex, in LMC, UV reddening law 78−96516
30 Doradus region, in LMC, interstellar extinction and stellar population 78−96517
30 Doradus region, interstellar extinction and stellar population 77−13413
dynamical evolution, analytical approximations for effect of mass loss 80−51815
dynamical evolution, effects of time-varying gravity 78−24459
dynamical evolution of cluster models with continuous stellar mass loss 80−82438
dynamical evolution of clusters with two stellar groups 77−82289
dynamical evolution of Keplerian systems, numerical simulations of collisions 80−109342
dynamical evolution of large clusters with stellar mass loss 77−64807
dynamical evolution of multiple stars, from small clusters 79−44568
dynamical evolution of star cluster models, early stages 79−8958
dynamical evolution with multi-mass populations *(Italian)* 77−91584
dynamics, collision integral determ. *(Polish)* 80−67799
dynamics, evolution and statistical methods *(French)* 77−71133
dynamics, higher order fluid eqns. for multicomponent nonequilib. systems 80−105156
dynamics, nonexistence of additional integral of motion of star 78−65663
dynamics, purely discontinuous random processes in field of irregular forces *(Polish)* 78−16465
dynamics, stability of one-dimensional self-gravitating isothermal systems 80−73008
dynamics and shapes of stellar clusters 77−17635
dynamics of cluster binaries 78−12295
energy sources in quasars and nuclei of galaxies 77−60849
escape velocities and mean velocities, in open and globular clusters *(German)* 78−53995
ESO/Uppsala survey of ESO(B) Atlas of southern sky, fifth list containing 2395 objects 78−20653
ESO/Uppsala survey of ESO(b) Atlas of southern sky, fourth list, 2920 objects 77−26059
ESO/Uppsala survey of ESO (B) Atlas of S. sky, pt.VII 80−56722
ESO/Uppsala survey of ESO (B) Atlas of southern sky, sixth list containing 3162 objects 79−8850
exchange collisions between binary and single stars 77−91563
faint blue stars in young cluster fields 79−21291
faint clusters in LMC, colour magnitude diagrams, BV photometry 80−94841
flares in stellar aggregates, freq. function *(Russian)* 79−8918
flat systems, stellar kinetics, relaxation times 77−13405
Fokker-Planck eqn. numerical integration, stellar dynamics in fixed inhomogeneous gravit. background 78−32526
formation rel. to universal expansion and big-bang theory *(Dutch)* 80−62212
G133.8+1.4 (W3N), far IR source, near IR obs. and identification as OB stars cluster 80−22058
galactic centre, IR obs. of compact clusters 78−24551
galactic centre region, sources and obscuration 80−77487
galactic clusters, Basle catalogues data rel. to interstellar reddening in solar neighbourhood 80−62239
galactic clusters in Cassiopeia, stellar photometry and proper motions obs. *(Russian)* 79−97042
galactic clusters observed in three colours, catalogue and distances 79−40089
galactic density wave, molecular clouds and star formation 78−8088
galactic stellar subsystems, kinematical model 77−13402
Galaxy, young and old clusters 79−25723
globular cluster classification, physical mechanism for Oosterhoff dichotomy 77−78837

stellar clusters and associations continued
globular cluster luminosity as extragalactic distance indicators 77−91641
globular cluster on WLM galaxy (A2359), BV photometry and absolute magnitude 77−82302
globular cluster populations uniformity 77−53654
globular clusters, (V-K) colour rel. to metal abundance 77−87485
globular clusters, ANS UV obs. in 1550-3300 Å range 77−91598
globular clusters, appl. of QSO black tide model to X-ray sources 77−78884
globular clusters, CN strengths and UV excesses of evolved stars from DDO photometry 77−64753
globular clusters, dynamics during gravit. encounters between Local Group galaxies 77−57098
globular clusters, element abundance survey 77−87489
globular clusters, ellipticities of RR Lyrae star systems 77−60805
globular clusters, evolutionary model sequences, ages 77−87487
globular clusters, integrated UBV photometry 77−67116
globular clusters, number correl. with spheroidal system luminosity for external galaxies 77−91594
globular clusters, obs. of assoc. radiosources 77−87484
globular clusters, parametric approach to slope of giant branch 77−53649
globular clusters, radial distrib. and total number in M104 galaxy 77−74140
globular clusters, structure and content 77−91597
globular clusters, test computations on dynamical evolution 77−49445
globular clusters, transitional period-luminosity depend. for RR Lyrae stars 77−53614
globular clusters in Virgo cluster of galaxies, distance modulus 77−74149
globular clusters rel. to Magellanic Stream origin 77−91648
globular clusters space distrib. 77−87481
Gould's Belt, structure 79−35368
gravitational radiation from orbiting point masses, post-Newtonian theory 77−13226
Gurzadyan's clustering in Auriga, spectral types 79−21366
Gurzadyan UV stellar group in Auriga, UBV and uvby photometry 78−45373
H-R diagrams, use as astronomical tool 78−81619
Haffner 10 in Puppis open cluster pair, UBV obs. 80−109503
Haffner 19, 18ab, assoc. with expanding H II complex NGC 2467, Hα obs. 77−22304
Hodge 11, in LMC, electronographic photometry and colour-magnitude diagram 79−40230
HR 1614 group of metal-overabundant stars, late-type stars intermediate-band photometry 78−53935
Hyades, abundances of HD 28068 and 28344 dwarfs 77−29890
Hyades, Allegheny astrometric studies contd. 78−69779
Hyades, BVRI photometry of new possible cluster members 78−32533
Hyades, CNO abundances in main-sequence stars HD 27561 and 45 Tauri 78−93222
Hyades, convèrgent point method for kinematic parallaxes determ. 77−91596
Hyades, distance from proper motion data 77−87486
Hyades, distance from speckle interferometry of binary star 51 Tauri 77−71011
Hyades, distance from speckle interferometry of spectroscopic binary 51 Tauri 77−29876
Hyades, distance modulus from stellar models 77−57067
Hyades, distance rel. to extragalactic distance scale 78−8121
Hyades, estimation of freq. of binary stars, comparison of methods 77−49441
Hyades, late-type stars intermediate-band photometry 80−31289
Hyades, lunar occultations, 1978 September 22 reappearance events 79−40185
Hyades, lunar occultations and α and θ^1 Tauri diameters 79−75253
Hyades, lunar occultations in 1979 March, stellar angular diameters 80−72921
Hyades, photometric survey for δ Scuti variable stars 80−36677
Hyades, reddening, polarimetry and field star photometry 80−62222
Hyades, shape and luminosity distrib. 80−17622
Hyades, spectroscopic orbits of dwarf stars van Bueren 62, 117, 121 79−5862
Hyades, UV spectra of white dwarf eclipsing binary V471 Tauri 80−26912
Hyades cluster, possible members BVRI photometry 80−51821
Hyades giants, identification of δ and θ^1 Tauri as spectroscopic binaries 77−64794
Hyades metal content and distance rel. to solar colour 80−101569
Hyades stars, Hα and O I 7774 Å photometric obs. 77−22286
Hyades trigonometric parallax, statistical anal. and correction 77−64743
IC 1613, star formation regions and star clusters in dwarf irregular galaxy 79−62900
IC 1805, 1848, OB-associations and giant H II regions, physical anal. from radio obs. 80−36695
IC 1805, open cluster, O-type stars C IV UV reson. line P Cygni profiles 80−31296
IC 1805 (W4), nearby cluster, spectral classes and photometry 80−62214
IC 2391, relative proper motions of stars, ident. of member stars 80−51818
IC 2581, open cluster, discovery of two Be stars 80−90445
IC 2581, young open cluster, ratio of total to selective extinction determ. 79−5870
IC 2944, open cluster, photometry of BH Centauri, early-type contact system 77−33552
IC 2944, stellar aggregate surrounding HD 101205, spectrographic and photometric obs. 77−17636
IC 361, open cluster, preliminary photometry 78−89228
IC 4665, open cluster, spectroscopic study of peculiar stars HD 161480 and 161733 77−33530
IC 4665, open clusters, chemical elements in spectrum of Hg-Mn star (HD 161698) 79−58354
IC 4756, open cluster, uvby β photometry, distance modulus 78−53997
IC 5146, young open cluster, CO obs. of assoc. dark cloud 79−48881
IC 5146, young star cluster, polarisation of starlight 77−5550
IC 5146 dark cloud complex and cluster, IR obs. 78−89234
ε Indi moving group, detailed anal. of members HD 40409, HD 102365 and λ Aurigae 78−85982
initial stellar mass function, theory of cosmic gas clouds fragmentation 77−56907
stellar clusters and associations continued
interferometry of star cluster with prominent variable 79−84680
interstellar radiating dust clouds, review 77−78863
IR emission from dust in stellar aggregates *(Italian)* 79−48869
IRC-10442 (GL5268S), possibly two star clusters, near IR and radio obs. 80−4412
isolated clusters, classical theory of star escape *(Polish)* 77−71134
isolated clusters, star escape, Fokker-Planck eqn. generalization *(Polish)* 78−36645
isolated star clusters statistical theory of stellar escapes *(Polish)* 78−16466
isotropic relativistic star clusters, multi-term trial function stability anal. 78−73742
kinetic theory for finite inhomogeneous gravit. systems 77−9775
An King 13, open cluster, UBV obs. *(German)* 80−77459
Lacerta OB1 association, spectral classification and distances 77−37626
Lacerta OB1 association, uvby photometry 77−22285
large N-body systems, two-body tidal dissipation effects 78−93329
late-type stars in stellar groups, intermediate band photometry 78−4300
LMC, instrumental colour-magnitude diagrams for 24 stellar clusters 77−22279
in LMC, survey, visible obs. 80−73011
Lo 807, open cluster, two-colour photographic photometry 78−96512
Loden cluster candidates in S. Milky Way, colour excess, distance and spectral types 80−85997
loose clustering in S. Milky Way, UBV and uvby β photometry 79−44572
loose clusterings in southern Milky Way, continued photometric studies 80−36679
loose open cluster search in southern Milky Way, UBV photometry 77−64814
loose stellar clusters in southern Milky Way, spectral type and UBV obs. 80−94839
Lyngå 6, age of galactic open cluster *(Italian)* 77−91591
Lynga 6, open cluster, reality and membership of Cepheid TW Normae 77−87491
Lynga 6, open cluster, relation of long period Cepheid TW Normae 77−17639
M11, galactic open cluster, age and distance, colour diagram, photometric obs. 80−73012
M11, open cluster, internal motions 77−22280
M11, open cluster, membership 77−17641
M25, He abundance rel. to stellar pulsation 78−28690
M25, young open cluster, UBV obs., photoelec. calibration, distance, reddening 79−8956
M25 (IC 4725), open cluster, stars four colour and Hβ photometry 78−8067
in M31, open star clusters obs. rel. to spiral struct. 79−75270
in M31, studies of luminous stars in associations in Baade's Field IV 80−36622
M31, UBV photometry of star clusters *(Russian)* 79−17034
M33, identification of star clusters, list of 58 candidates 79−9002
M34, open cluster, spectral types of brightest stars 78−12311
M34, open cluster, UBV photoelectric photometry 78−12307
M36, photographic obs., mass, radius, central density, stellar vels. of open cluster *(German)* 80−31333
M37, open cluster, luminosity function 77−13419
M38, photographic obs., mass, radius, central density, stellar vels. of open cluster *(German)* 80−31333
M39, open cluster proper motion membership 77−91588
M3, M13, M92, M67, giant stars IR photometry, bolometric magnitudes and effective temps. 78−57595
M4, RR Lyrae type variable star discovery, possible cluster member *(Chinese)* 78−69804
M67, curve of growth anal. of T626 red giant star 79−48797
M67, gap in Hertzsprung-Russell diagram, comparison with evolutionary models 78−24530
M67, main-sequence stars differential blanketing rel. to Hyades and Coma 78−57597
M67, obs. of contact binary AH Cancri 79−40222
M67, old open cluster, H-R diagram compared with southern high-velocity stars 79−25600
M67, open cluster, spectroscopic obs. of faint blue objects in field 77−22329
M67, open cluster, stellar membership 77−22281
M67, open cluster, upper limit to mass and vel. dispersion 78−28735
M67, radial distrib. of evolved stars 77−13408
M67, reddening 80−62222
M6, open cluster, supergiants in field and interstellar matter towards galactic centre 78−16405
M6 (NGC 6405), open cluster, strip counts investigations *(German)* 77−13411
M92, globular cluster, age difference from old open cluster (NGC 188) 77−56912
M 67, abundances of F 170 and F 244 giants 77−29890
Magellanic Cloud clusters, spectral types of red supergiants 79−40190
Markarian 38, galactic open star cluster, photometric obs. *(German)* 80−73015
massive star formation in open clusters 78−28660
master list of non-stellar objects 77−78668
material test point, statistics of distant perturbs. 78−28494
Melotte 66, oldest open cluster, colour-magnitude diagram rel. to age 80−17621
Melotte 66, very old open cluster, BV photometry rel. to broad giant branch 78−32538
membership probabilities, photographic meas. of relative proper motions of stars 80−51817
Monoceros OB1 and OB2, interstellar extinction determ. 77−9777
Monoceros OB2 association, evidence for supernova-induced star form. 80−31334
Monoceros R1 molecular clouds ring struct., CO obs. 80−12784
Monoceros R2, far IR obs. of young assoc. 80−73010
Monoceros R2, IR obs. of CO line 79−25654
Monoceros R2, obs. in 40-400 μm range 78−69853
Monoceros R2 association, stellar UBV photometry and spectra 77−13409
moving groups, calibration of intermediate band photometric indices for late-type stars 78−49424
moving groups, kinematic age, focusing phenomenon 77−60801
multiple star formation by dynamical interaction in clusters 79−44567
N-body calculations, statistical results depend. on N 79−80339

stellar clusters and associations continued
N-body calculations, statistical results validity 78−12084
Newtonian clusters, steepest-descent technique for stellar equilib. statistical mechanics 77−45496
NGC 1039, NGC 2281, NGC 6475, rot. vels. of Ap stars rel. to mag. braking 77−33500
NGC 1039 (M34), uvbyβ photometry 79−84831
NGC 1245, luminosity functions for open cluster nucleus and halo 79−5872
NGC 129, He abundance rel. to stellar pulsation 78−28690
NGC 129, open cluster membership from four colour and Hβ photometry 80−90485
NGC 1502, open cluster, IR photographs processing, discovery of faint source *(Russian)* 77−13250
NGC 1778, H-R diagram, gap in evolving main sequence 79−30096
NGC 1817, UVB photometry of open cluster, distance, age 77−91587
NGC 188, ER Cephei membership rel. to open cluster H-R diagram gap theory 78−77580
NGC 188, old open cluster, age difference from globular cluster (M92) 77−56912
NGC 188, old open cluster, photographic photometry 77−53430
NGC 188, open cluster, anomalous giant branch 78−41001
NGC 188, open cluster, BV photographic photometry with PDS microdensitometer 79−88600
NGC 1955, open cluster in LMC, early-type stars stellar winds rel. to motions in bubble-like nebula N51D 80−105295
NGC 1960, radial vels. of early type stars 78−7990
NGC 2050, NGC 2055, in LMC, Apollo 16 for UV spectra and absolute intensities 77−33634
NGC 2169, H-R diagram, gap in evolving main sequence 79−30096
NGC 2169, open cluster, spectral types of brightest stars 78−12310
NGC 2169, photometric and spectroscopic study of open cluster 78−45371
NGC 2175, galactic cluster, obs. of dense H II condensation 78−20883
NGC 2231, in LMC, electronographic photometry and colour-magnitude diagram 79−92813
NGC 2243, metal abundance of old open cluster 78−93333
NGC 2243, old open cluster, UBV photometry 77−78835
NGC 2244, young open cluster, uvby Hβ photometry, colour excess, distance, age 78−32532
NGC 2264, Allen's obscured IR source spectrophotometric anal. 79−21370
NGC 2264, DNC detection, difficulties of chemical equilibrium hypothesis for D enrichment 77−82298
NGC 2264, Herbig-Haro objects assoc. with young cluster 79−71026
NGC 2264, nature of IR excesses in pre-main-sequence A and F stars 78−32461
NGC 2264, nature of member star W92, possible gravit. contracting binary system 78−32462
NGC 2264, open cluster, CH radio obs. 78−28751
NGC 2264, open cluster, CO obs. of mol. cloud 79−21363
NGC 2264, open cluster, HD 47732 spectroscopic orbit 78−57574
NGC 2264, open cluster, reddening, blanketing and metallicity from spectroscopic obs. 80−26916
NGC 2264, photometry and struct. of HD 47732, young close binary 78−57575
NGC 2264, rotation of pre-main sequence stars rel. to solar angular momentum problem 79−58332
NGC 2264, UBVRI photometry of 70 field stars in young cluster 80−51819
NGC 2264, Walker No.67 as candidate for strong interstellar circular polarisation 78−12223
NGC 2264, young cluster, UBVRI obs. of Hα emission stars, pre-main sequence stars 79−35267
NGC 2264, young open cluster, circumstellar shells, IR excess obs. 77−45410
NGC 2264, young open cluster, differential reddening due to intracluster dust clouds 78−53996
NGC 2264, young star cluster, interstellar OH and NH_3 obs., SHF and UHF 80−94847
NGC 2264 and 7000/IC 5070, new Hα stars, slitless spectrographic search 80−62120
NGC 2264 and Rosette Nebula, far IR emission from compact sources 77−78841
NGC 2264 formaldehyde kinematics and distrib. near IR source 80−4418
NGC 2281, open cluster, UBV photometry, binary star freq., luminosity function 78−81663
NGC 2287, open cluster, spectral classification of brightest stars 80−26919
NGC 2287, open cluster, UBVRI photometry, distance, age, metal content 79−12498
NGC 2353 rel. to Canis Major OB1, uvbyβ obs. 78−85985
NGC 2362, very young open star cluster, photographic star counts *(German)* 78−16472
NGC 2420, chemical composition determ. using evolved members 77−29889
NGC 2420, comparison rel. to galactic evolution 77−45499
NGC 2420, old disc cluster, chemical comps. of stars 80−46620
NGC 2420, PDS photometry of old open cluster, colour-magnitude diagram 78−57600
NGC 2423, 2482, Hyades-like clusters, late-type stars intermediate-band photometry 80−31289
NGC 2439 association, photometric and spectroscopic study 78−16470
NGC 2477, photographic obs., mass, radius, central density, stellar vels. of open cluster *(German)* 80−31333
NGC 2516, presence of some thirty Ap stars 79−16972
NGC 2516, proper motions in the region 79−88706
NGC 2516, spectroscopic binaries, radial vels. from objective prism plates *(German)* 78−45360
NGC 2527, galactic cluster, UBV photometry 78−16479
NGC 2527, UBV photographic photometry of open cluster 78−89231
NGC 2547, open cluster in Vela star cloud, photometric survey 80−90482
NGC 2571, open clusters, UBV anal. 79−58386
NGC 2669, relative proper motions of stars, ident. of member stars 80−51818
NGC 2818, open cluster, photoelec. sequence 77−91595
NGC 3105, young open cluster, photoelectric UBV obs. 77−64811
NGC 3114, open cluster, objective prism radial velocities *(French)* 79−48868

stellar clusters and associations continued
NGC 3247, RGU photometry of open cluster, catalogue of 129 stars *(German)* 77−82290
NGC 3293, galactic cluster, photometry of β Canis Majoris stars 78−12243
NGC 3293, open cluster, UBVRI photometry and relation to OB complex in Carina 80−90490
NGC 3293, uvby β photometry rel. to other young clusters 80−101621
NGC 330, in SMC, radial vels. of individual stars 80−67803
NGC 3324, very young open cluster in Carina spiral feature 77−22282
NGC 3532, relative proper motions, membership 79−35318
NGC 3532, southern galactic cluster, stellar photoelectric sequences 77−45502
NGC 3532, southern open cluster, UBV photometric study 80−46621
NGC 3603, compact galactic cluster central star HD 97950, interstellar features, visible obs. 80−101586
NGC 3603, luminous young cluster, UBV photometry 78−36643
NGC 371 OB association, red variable star content 78−53961
NGC 3766, open cluster, discovery of twelve Be stars 80−90445
NGC 4103, open cluster, membership determ. from proper motions, visible obs. 80−67802
NGC 4755, open cluster, search for β Cephei stars 79−8921
NGC 4755, southern open cluster, Balmer line photoelectric photometry 80−56892
NGC 4833, southern globular cluster, BV photometry of variable stars 78−4304
in NGC 5128, young associations discovery by multicolour photography 79−53913
NGC 5367, young open cluster, relation to X-ray source (Ariel 1353-40) 77−82294
NGC 559, open cluster with possible supernova remnant (G127.3+0.7) 77−64826
NGC 5617, open cluster, photoelec. and photographic photometry of member stars 79−17032
NGC 5662, open cluster, photoelec. and photographic photometry of member stars 79−17032
NGC 581 (M103), UBV photoelectric photometry of galactic cluster 78−89230
NGC 5823, open cluster, photoelec. UBV sequences for north and south regions 77−82293
NGC 6025, open cluster, nonmember identification from proper motions 77−53653
NGC 604, 5471, giant extragalactic H II regions, UV spectra rel. to exciting clusters comp. 80−77467
NGC 6067, galactic cluster, assoc. with Cepheid variable GU Normae 77−45464
NGC 6067, open cluster, photographic, obs. *(German)* 77−53650
NGC 6087, galactic cluster, four-colour and Hβ photometry 80−62208
NGC 6200, loose young open cluster in Sagittarius arm extension 77−87493
NGC 6231, open cluster, spectral types 80−90492
NGC 6231, young open cluster, main sequence stars photometry and spectra 79−88709
NGC 6231, young open cluster, new β Canis Majoris star (HDE 326333) discovery and photometry 80−17595
NGC 6235, globular cluster, obs. of variable stars 78−4305
NGC 6250, young southern cluster, extinction law and high R-values in dust clouds 78−16490
NGC 6383, photometry and spectral classifications, age and distance of open cluster 78−93342
NGC 6383, young open cluster, central core stars obs. 78−41003
NGC 6475, open cluster, spectroscopic binaries obs. 77−87488
NGC 6494 (M23), open star cluster, membership from astrometry with PDS microdensitometer 80−98697
NGC 6530, open cluster, broadband photometry 77−45504
NGC 6530, UBV photometry of variable stars in open cluster 77−74106
NGC 6530, young open cluster, UBV photometry, magnitudes, reddening, distance, age 78−93341
NGC 6530 in M8 (Lagoon Nebula), rel. to nebula far IR emission 80−4413
NGC 6546, open cluster, assoc. with Cepheid AV Sagittarii disproved 79−58387
NGC 654, young open cluster, membership obs. 77−29885
NGC 654, young open cluster, UBV photometric study 80−109502
NGC 654, young star cluster, polarisation of starlight 77−5550
NGC 6604 and 6704, UBV photometry of open clusters 78−53993
NGC 6611, young open cluster, UBV magnitudes and colours, reddening, distance, luminosity 80−31332
NGC 6633, open cluster, stellar spectral types 77−74108
NGC 663, galactic cluster, emission line stars spectroscopic obs. 80−4363
NGC 663, UBV photometry of open cluster, distance 79−5869
NGC 6649, anomalous open cluster and V367 Scuti 79−5866
NGC 6649, UBV photometry of double-mode Cepheid V367 Scuti in open cluster 78−49460
NGC 6709, open cluster, anal. of assoc. stellar ring (SR 440) 77−17643
NGC 6811, UBV photographic photometry of open cluster 79−5871
NGC 6823, UBV photometry and spectra, extinction study of young open cluster 80−4407
NGC 6871, galactic cluster, distance of eclipsing binary V453 Cygni 79−21326
NGC 6910, uvby Hβ photometry of open cluster 77−91586
NGC 6913, photoelec. photometry of brighter stars, variability obs. 80−46625
NGC 6913, uvby Hβ photometry of open clusters 77−91586
NGC 7380, young cluster, interstellar polarization obs. 77−17649
NGC 741, 1316, 7626, radio galaxies, central dense star clusters luminosities rel. to accreting black holes 80−94871
NGC 752, DDO astrophysical study 79−48864
NGC 7654 (M52), open cluster, stars four colour and Hβ photometry 78−8067
NGC 7788 and 7790 in Cassiopeid, membership of open clusters *(Russian)* 79−92812
NGC 7789, metal abundance and He content of open cluster, mass loss 80−31335
NGC 7789, open cluster, blue straggler K1211, photometry and polarimetry obs. 80−109433
NGC 7789, open cluster, DDO and UBV photometry 77−53648
NGC 957, young open cluster, distance and reddening, RGU photometry 80−85976

stellar clusters and associations continued
O-associations and young clusters, He abundance in stellar atmospheres *(Russian)* 77−64815
OB and T associations, membership in star form. regions rel. to population categories 80−17645
OB association form. around galactic longitude 111°, H II regions aperture synthesis obs. 77−64827
OB association in direction of long period Cepheid VZ Puppis, UBV β photometry 78−45339
OB association in LMC nebulae complex N 59, stellar winds rel. to H II shell form. 79−17052
OB association in M33, distrib. rel. to spiral struct. and star form. 79−21437
OB association integrated luminosity as extragalactic distance indicators 77−91641
OB associations, 22 GHz obs. of nearby H_2O masers 79−25649
OB associations, births induced by interstellar shock waves 79−2542
OB associations, CNO abundances in B-type stars 80−67702
OB associations, in Galaxy and spiral galaxies, ring-like distrib. *(Russian)* 78−93424
OB associations, initial mass function in young objects 80−98695
OB associations, interstellar medium interactions, H I supershell form. 80−82468
OB associations, mag. fields influence on subgroups sequential form. 80−4408
OB associations, membership of long period Cepheids RZ Velorum, SW Velorum, KQ Scorpii 79−88666
OB associations, sequential form. of subgroups 77−60800
OB associations, sequential form. of subgroups 80−98696
OB associations and gamma-ray sources 79−92887
OB associations and young clusters, He abundance vars. *(Russian)* 77−82287
OB associations in Carina-Crux-Centaurus region of Milky Way, UBV photometry obs. 79−40242
OB associations in giant extragalactic H II regions, props. from vel. dispersion meas. 79−44606
OB associations in H I+molecular/H II shells from 1 to 2000 pc dia., in LMC, obs. 79−25678
OB associations in LMC, assoc. with super-giant H II shells 78−86012
OB associations in LMC, energetic stellar winds rel. to giant H II ring 78−77593
OB associations in M31, correl. with spiral struct. in UV image 80−98716
OB associations in M 31, distrib. rel. to spiral struct. morphology 78−65690
OB stars, newly-formed, struct. and kinematics of assoc. H_2O vapour sources 78−61901
OB stars compact groups, obs. of assoc. superluminous supergiants 77−17555
OB type stars, Gould belt, local cosmic ray origin 80−77512
observational tests on star formation, upper mass spectrum variation with cluster size 77−57066
Ocl 352, open cluster, excitation of W4 H II region and form. 80−94843
old galactic clusters, interpretation rel. to evolution of super-metal-rich stars 77−49370
old open clusters, abundance determ. in sequences 77−29888
old open clusters, theoretical isochrones with decreasing gravit. const., Dirac's multiplicative cosmology 78−16586
oldest open clusters, galactic distrib. in disk 80−101620
open, places of form 78−8064
open cluster, proper motions rel. to solar motion and apex determ. 80−46418
open cluster assoc. with Cepheid variable CV Monocerotis 79−58349
open cluster containing Wolf-Rayet and Of-stars 77−64810
open cluster distrib. in Galactic plane *(Russian)* 78−32541
open clusters, age determ. 78−61893
open clusters, age determ. methods *(Italian)* 80−90489
open clusters, binary stars frequency and mass ratios, stellar rot. effects 78−36639
open clusters, blue stragglers as long-lived stars 80−46542
open clusters, determ. of R from variable extinction anal. 77−37627
open clusters, diam. and luminosity functions from starcounts 77−91589
open clusters, dynamics of close binaries and single stars *(Russian)* 78−61890
open clusters, energy distrib. of Be-stars 78−85944
open clusters, energy distributions in main-sequence A and F stars 78−93220
open clusters, evaporation of stars rel. to coronas and moving groups development 79−92814
open clusters, formation positions rel. to galactic spiral arms 77−2457
open clusters, H I upper limits 79−30095
open clusters, H-R diagram, gap in evolving main sequence 79−30096
open clusters, H-R diagrams anal. rel. to Galaxy chemical abundance gradient 80−56938
open clusters, late evolutionary stages *(Russian)* 78−49485
open clusters, luminous O-B3 stars colours rel. to circumstellar shells and mass loss *(German)* 78−53925
open clusters, southern, kinematics and dynamics from radial vel. obs. *(German)* 80−94724
open clusters, spectrophotometric identification of late type binaries 79−44548
open clusters, spectroscopic differences between solar-type stars and Sun 78−36560
open clusters, spectroscopic obs., search for Ap stars 78−45367
open clusters, statistics of binary stars 77−53626
open clusters, transit tables for star numbering, magnetic tape 79−44573
open clusters, white dwarf members obs. rel. to progenitor stars upper mass limit 80−51738
open clusters assoc. with interstellar gas-dust clouds, dynamics 80−101622
open clusters in LMC, possibly assoc. C stars 78−49428
open clusters membership determ., maximum-likelihood method for proper motions 78−16471
open clusters near η Carinae, RGU photometry 77−37631
open clusters rel. to multiple stars *(French)* 79−44547
open clusters stars, mag. tape catalogue of HD, HDE and DM identifications 77−13254
open clusters with circular orbits, galactic rot. calc. 78−8068
open star clusters, space distrib. and age *(Russian)* 79−48871
ρ Ophiuchi cloud, cosmic ray accel. by stellar winds 80−77512
stellar clusters and associations continued
ρ Ophiuchi dark cloud complex, embedded cluster, anisotropic scatt. and formaldehyde lifetimes 78−8080
origin of stars and gas from superdense protostellar matter *(Russian)* 77−82286
Orion, contraction of star cluster-molecular cloud complex 78−12313
Orion, intracluster dust, circumstellar shells and wavelength depend. of polarisation 77−78839
Orion association stars, five-channel photometric obs. 78−16398
Orion cluster, intracluster and circumstellar reddening and polarisation of young stars 78−93199
Orion cluster, pre-main-sequence stars masses and age spread 77−13339
Orion I OB assoc. and evidence for associated expanding shell 79−53866
Orion Nebula cluster, MK spectral types 77−22283
Orion Nebula cluster, search for expansion 77−74102
Orion Nebula cluster, variable stellar polarisation *(Russian)* 77−60807
Orion OB1 (Belt), photometric studies 80−46618
Orion OB1 assoc., expanding gas shell, UV obs. 79−71086
Orion OB1 association, stellar spectral types 78−32539
Orion OB 1, subgroup analysis of uvbyβ data 78−77582
Orion OB 1 association, anal. of photometric study 77−82288
Orion OB 1 association, photometric study 77−82128
Orion region, radiocontinuum struct. of associations 78−49549
θ^1 Orionis (Trapezium), photographic photometric obs. 79−58380
λ Orionis association, photometric props. of young cluster 78−16478
particle dynamics in spheroidal mass distribs., third integral of motion 77−74101
h and χ Persei, B2 to G0 supergiant stars small amplitude light vars. 78−32469
γ Persei, cluster membership determ. by proper motion meas. 80−56890
h and χ Persei, SIT camera sensitivity expt. *(Japanese)* 78−89085
ζ Persei association, bright star subsystem dynamical evolution 77−53655
II Persei association, distance of eclipsing binary AG Persei 79−21326
h and χ Persei association, membership of Cepheid star UY Persei 77−74069
α Persei cluster, OAO 2 photometric obs. 78−93331
α Persei cluster, photometric survey for δ Scuti variables 78−93246
α Persei cluster, stellar spectral types 79−58385
α Persei star cluster, polarisation wavelength depend. 79−48865
Perseus II complex, ζ Persei direction, Copernicus obs. 78−4301
Perseus OB1 assoc., new Hα-emission stars 80−56855
Perseus OB2 association, spectroscopic survey of B- and A-type stars 77−91585
Perseus OB2 association molecular cloud, mol. obs. rel. to star form. 80−12798
Perseus OB2 dark cloud, CO obs. 77−64836
perturbations of spherical cluster in general relativity, variational principle 79−53860
Pismis 13, open cluster, colour magnitude diagram, UBV obs. 80−67805
Pismis 6 and 8, open clusters, photometry and spectra rel. to proximity to (Wat 6) 79−88712
Pleiades, contracting stars, UBVR photometry 79−96996
Pleiades, Hα and O I photometry 79−35315
Pleiades, interstellar dust and gas obs. near 20 Tauri (Maia) 78−28734
Pleiades, kinematic age of moving groups 77−60802
Pleiades, new flare stars *(Russian)* 77−13366
Pleiades, photometric obs. of flare stars. *(Russian)* 77−91536
Pleiades, possible cyclic recurrence of flare activity in flare stars *(Russian)* 78−49443
Pleiades, reddening-face colours, photometric zero age main sequence definition 80−26920
Pleiades, spectral classification of brightest stars, Ap, Am and shell stars 78−57601
Pleiades, UV and photographic obs. of flare stars *(Russian)* 77−13367
Pleiades, wide binary stars number and distrib. 79−88710
Pleiades central field, internal motions 79−88711
Pleiades reflection nebulosity, model for filamentary struct. 78−8082
Pleiades stars, lunar occultation obs. 78−7982
Pleiades stars, wavelength depend. of polarisation 77−45500
Population I clusters, integrated colour synthesis 77−17637
Population I stars He abundance rel. to stellar pulsation 78−28690
Praesege radial and nonradial pulsation periods in δ Scuti star BT Cancri (38 Cancri) 80−85948
Praesepe, estimation of freq. of binary stars, comparison of methods 77−49441
Praesepe, passages of Mars through open cluster (1950-2000 period) 77−91460
Praesepe, photometry in BVRI colours 80−26917
Praesepe, stellar metal abundance rel. to Hyades 77−57064
Praesepe field, flare stars, plate records and cluster membership 77−53652
protocluster cloud rotation, mag. braking of aligned rotator during star form., exact time-depend. soln. 80−90493
protocluster fragments systems, mass distrib. law 79−44571
protosolar OB association supernovae, rel. to Allende isotopic anomalies and cosmochronology 80−4462
Puppis open cluster pair Czernik 29 and Haffner 10, UBV obs. 80−109503
quasar energy sources, choice between, magnetoid, black hole and compact star cluster *(Russian)* 77−78885
quasars, star cluster models of collapsed objects with large central gravit. redshifts 77−5588
R associations, early-type stars in CMa R1 and Vel R2, JHKL photometry 77−45505
R associations in southern dust clouds study of stars and bright nebulosities 80−56893
R-associations, obs. of free-free emission from embedded B-type stars 80−26851
radial vels. in LMC, catalogue 79−101089
relativistic, with high central redshift 80−105293
relativistic clusters, steepest descent technique and stellar equilib. statistical mechanics 77−49444
relativistic spherical systems, binding energy criterion for dynamical stability 80−94837
relativistic star clusters, unphysical distrib. functions 78−8066
relaxation of inhomogeneous gravit. systems, delocalisation effect 79−62877
relaxation with close encounters in stellar systems 79−48862
relict circumstellar matter in young clusters 80−41865

stellar clusters and associations continued
rotating stellar systems, two-dimensional, nonlinear nonradial oscills. stability 78−53992
rotation, ang. moments mass depend. rel. to self-similarity 80−36490
scale-covariant dynamics of stellar systems 80−26913
Upper Scorpius, rot. vels. of Ap stars rel. to mag. braking 77−33500
ζ Sculptoris (Blanco 1) open cluster, multicolour photometry 78−45372
Scorpius-Centaurus association, evidence for membership of α^1 Crucis from improved spectroscopic orbit 80−67792
Sirius moving group, evidence for existence from chromospheric Ca II H and K emission in field stars of solar neighbourhood 80−109423
SMC, star formation regions and star clusters 79−62900
SMC, UBV photometry of open, intermediate and globular clusters 79−17033
SMC star cluster colour magnitude diagrams and stellar identification charts 80−73014
SMC star clusters catalogues, identifications and coordinates 78−89086
southern clusters, excess absorpt. in O-B3 stars 77−78791
southern open clusters, anal. of MK classification of 176 stars 79−88644
southern open clusters, DDO photometry of giant stars 79−12468
southern open clusters, search for interstellar H I 80−46619
speckle interferometry, high resolution imaging, simulation 78−77492
spherical clusters, stability under spherical perturbations *(French)* 79−35317
spherical gravitating systems, radial vel. dispersion at outer regions *(Russian)* 78−61720
spherical self-gravitating systems, energy transfer 79−40226
spherical stellar systems, analytical models 78−12302
spherical stellar systems, dynamical relaxation, tidal perturbations by external systems 77−49443
spherical stellar systems, marginal mode to second order *(French)* 78−32527
spherically symmetric accretion with self-gravitation, criteria for enhanced accretion 79−71098
spherically symmetric model cluster with stars of uniform mass, struct. and dynamics 80−62215
star distribution in vicinity of massive black hole *(Russian)* 77−74083
star escape from isolated clusters, numerical methods *(Polish)* 80−26922
star formation evidence from bright star clusters round NGC 5253, visible obs. 80−77489
star formation in galactic cluster 79−62878
star formation in open clusters and associations 79−21365
star identification using coded numbering system for open clusters 77−78829
star swarms, as cosmic calibrators 78−57599
stellar systems nonradial-oscillations, homogeneous models *(Russian)* 77−57063
stochastic tidal disruption 78−12303
Stock 16, Basel 18, 19, Cr 272 and NGC 5168, open clusters, RGU photometry 78−16474
Stock 8, new C star obs. 79−84791
subsystem space distrib. and population in Galaxy 77−53689
supergiants and O-type stars in clusters and associations, catalogue 79−40183
T association in Chamaeleon dark cloud, embedded Be-star, IR obs. 80−85943
T Tauri star groups enveloped by small dense molecular clouds 79−58400
theoretical isochrones for stellar evolution with variable G, Brans-Dicke theory 79−67125
tidal disruption by massive black hole in dense star cluster, fate of debris 79−67069
tidal distribution by spiral density waves *(German)* 79−17086
Tr 14, O-type cluster, rel. to Carina I and II H II regions far IR sources 79−25657
Tr 18, open cluster, location of supernova remnant G291.0−0.1 78−20875
Tr 22, open cluster, photoelec. and photographic photometry of member stars 79−17032
Trapezium, X-ray emission from colliding stellar winds rel. to source (4 V 0531−05) 78−65607
Trapezium type multiple systems, connection with associations, galactic clusters and emission nebulae 80−67781
Trapezium-like multiple systems in molecular clouds 79−101180
Trumpler 10, open cluster in Vela star cloud, photometric survey 80−90482
Trumpler 14, 15, 16 in Carina Nebula, extinction determ. from UBV photometry obs. 80−90513
Trumpler 14, 15 and 16 in Carina Nebula, open clusters distance determ., photometry obs. 80−85977
Trumpler 14, relation to Carina nebula struct. 77−87520
Trumpler 15 in η Carina, open cluster, age and reddening from UBVRI obs. 80−90487
Trumpler 16, interstellar absorpt. and assoc. with η Carinae 77−64744
Trumpler 16, obs. of HD 93162 probable single WN7-type star 78−85946
Trumpler 1, H-R diagram, gap in evolving main sequence 79−30096
Trumpler 1, open cluster, UBV photometry 77−74105
Trumpler 27, heavily reddened young open cluster with blue and red supergiants 77−78836
Trumpler 27, obs. of possible long-period Cepheid Tr 27-102 (HD 159378) 78−45336
Trumpler 37, young open cluster, stellar UBV magnitudes and MK classifications 77−22284
UBV and DDO photometry of stars and open clusters rel. to metallicity gradient across galactic disk 79−48905
UBV photoelectric photometry of M31 clusters *(Russian)* 80−36680
upper Scorpius region stars, spectrophotometry 79−88647
Ursa Major group, new members 79−84830
Ursa Major stream, spectral types 78−85984
Ursa Major stream eclipsing binaries, ages and absolute dimensions 79−92800
Vela star cloud, large scale photometric survey 80−90482
velocity dispersions, Doppler broadening parameters meas. technique without spectrograph 78−20646
VI Cygni (Cygnus OB2) association, interstellar λ4430 band obs. 78−32555
Vulpecula OB2, case for membership of 67 day Cepheid S Vulpeculae 80−41831

stellar clusters and associations continued
Wat 6, open cluster, photometry and spectra rel. to proximity to (Pismis 6 and 8) 79−88712
William Herschel's early investigations of nebulae 80−12876
X-ray emission energy sources 79−44574
young associations in LMC, stars embedded in ring-shaped nebulae 80−77457
young clusters, circumstellar matter round OB3 type stars, 2200 Å hump interpretation 80−82351
young open clusters, evidence for gap in main sequence between B7 and B8 spectral types 77−13341
young open clusters, uvbyβ photometry rel. to bimodal star form. 77−49374
young Orion stars, scanner K-line photometry 77−33579
young stellar groups towards galactic anticentre, photometry and spectra rel. to outer Galaxy struct. 80−22079
zero age main sequence stars in open clusters, rot. vel. anal. 78−93213
He/H ratio of B-type stars in young clusters and associations 77−29887
OH 18 cm line obs. of young clusters 79−25655

stellar composition
see also element origin; solar composition
A0-G2 stars, abundance effects in Geneva system 77−29830
A- and B-type stars, B abundance from B II reson. line obs. 79−21276
A- and F-type stars, heavy element content influence on colour-temp. relation *(Russian)* 78−93234
A-type stars, comp. rel. to rot., mixing and variability 77−87397
A-type stars, O abundances from non-LTE anal. of O I lines 77−41378
A-type stars, spectral variations, abundance peculiarities 79−62821
early A-type stars, V/H abundance ratio 79−21314
abundance anomalies in main-sequence stars, diffusion and turbulence 78−89198
abundance determ. by photometric and spectroscopic methods 77−29807
abundance determ. in sequences of old open star clusters 77−29888
abundance effects in classification, IAU Symposium 72 (Lausanne, Switzerland 8-11 July 1975) 77−29802
abundance effects in spectral classification of peculiar stars 77−29859
abundance effects on uvby photometry 77−29808
abundances in stellar populations 77−29812
actinides in stellar spectra 77−78769
age-abundance relation 77−29813
Algol type star, accretion and chem. struct., evolutionary calcs. 80−109481
Am stars, model of extended atmosphere by nongravitational forces criticism 77−53597
Am stars in main sequence, rotational vel. effect on metallicity 79−48814
Am stars in spectroscopic binary systems, evolutionary status, statistical anal. 78−93262
Am-stars, abundance indices problem *(French)* 77−29863
Am-type stars, mol. weight gradient effect on envelope meridional circulation 80−4370
AC Andromedae, pulsating variable, mass, comp. and evolution 77−29845
Ap, Am stars, chemical differentiation and abundance spots prod. by diffusion 80−77381
Ap and Am stars, numerical taxonomy 80−22015
Ap and Am stars, possible nuclear origin of comp. anomalies 79−35277
Ap and Am stars, Y, Ba and rare earth elements abundances 77−33505
Ap and Bp stars, radiation forces and B abundance diffusion theory 79−88664
Ap stars, CN lines identification 77−91551
Ap stars, flows and mag. fields in surface layers 79−62854
Ap stars, heavy element abundances from Copernicus UV data, reference stars α Lyrae and α Canis Majoris A 78−28688
Ap stars, line blanketed model atmospheres rel. to element abundances 79−44495
Ap stars, mag. latit. of metals 79−58341
Ap stars, magnetic, peculiar anomalies of chemical comp. *(Russian)* 77−22239
Ap stars, magnetic field generation and chemical anomalies 77−13359
Ap stars, Pt in magnetic sequence 77−45436
Ap stars, review of obs. and possible nucl. reactions *(Russian)* 78−20843
Ap stars, thickness estimation of anomalous chem. comp. layer in atm. *(Russian)* 78−93279
Ap stars, U/Th ratio, r-process nucleosynthesis 77−33508
Ap stars abundance anomalies, correl. with fission mass distribs. in astrophysical r-process 78−93204
Ap stars in spectroscopic binary systems, chemical anomalies surface distrib. 80−62140
Ap variable stars, comp. rel. to rot. period 77−87426
Ap-type stars, mag. fields rel. to chemical anomalies *(Russian)* 77−17591
U Aquarii, R Coronae Borealis star, extraordinary comp. rel. to unusual s-processing event 80−17588
R Aquarii, symbiotic long-period variable, spectrum and comp. of assoc. nebulosity 80−90450
σ Aquarii (A0 IVs), hot metallic-line star, abundance anal. from model atmosphere 80−90415
θ Aquilae (B9.5 III), abundance anal. from model atmosphere 80−90415
V539 Arae, photometric analysis of B-type double lined eclipsing binary 79−44535
β Arietis, Am star, spectroscopic obs. and curve of growth anal. 77−22237
κ Arietis, double-lined Am star, spectroscopic obs. and curve of growth anal. 77−22237
asymptotic giant branch evolution of intermediate-mass stars, post-second dredge-up phase 80−72936
atmospheric chemical composition peculiarities rel. to stellar evolution 78−12207
atmospheric structure, mol. effects 80−21999
B-type stars, CNO abundances in associations and general field 80−67702
BCD classification for different chemical constitution 77−29811
BCD system of stellar classification and chemical composition *(French)* 77−29797
BD+0°2989, late-type dwarf star, metal abundances 77−78779
BD+10°2179, BD−9°4395, extreme He stars, UV spectra 79−16976
BD+12° 1919 (IV-202 in M 67), curve-of-growth analysis of red giant 77−29841

stellar composition continued
BD +1°4381, H deficient A-type star, effective temp. 79−40195
BDS 1269, visual binary, metal abundances and characts. of components 80−4397
Becklin-Neugebauer object, CO band emission detect. 79−101184
binary stars, close detached, Ap components, chem. anomalies surface distrib. 80−109475
binary stars, He abundances from speckle interferometric obs. 80−90475
binary stars on main sequence, freq. depend. on metallicity 80−26901
γ Bootis, Ap star, chemical element distrib. from spectrophotometry *(Russian)* 77−22238
α Bootis (Arcturus), comp. and atmospheric parameters 78−20826
α Bootis (Arcturus), effects of mag. mixing on C/N and $^{12}C/^{13}C$ ratios 80−105229
α Bootis (Arcturus), line identifications in UV spectrum 79−25598
α Bootis (Arcturus), model-atmos. analysis of spectrum 77−29827
α Bootis (Arcturus), O and C abundances *(Russian)* 78−16420
BPM 4729, cool DA white dwarf with self-broadened Balmer lines 79−35255
α Camelopardalis, O-type supergiant, spectroscopic study, model atm. anal. 78−28681
κ Cancri, Hg-Mn star, diffusion processes and abundance amometers 77−87407
α Canis Majoris (Sirius), B abundance 77−53585
α Canis Majoris (Sirius), rot. vel. and Ba abundance 78−12218
α Canis Minoris (Procyon), CNO abundances from near IR spectrum 78−93222
Y Canum Venaticorum, C_3 and IR spectrophotometry of C star 78−65619
Y Canum Venaticorum, C star, $^6Li/^7Li$ atmospheric abundance 77−33523
α^2 Canum Venaticorum, UV flux distrib. 79−80313
δ Capricorni, eclipsing binary, Am primary component metallicism var. 77−67115
ν Capricorni (B9.5 V), abundance anal. from model atmosphere 80−90415
Cassiopeia A, Fe group elements absence rel. to black hole form. 79−75244
R Cassiopeiae, late-type giant, possible H_2O thermal emission identification 78−81628
WZ Cassiopeiae, semiregular variable star, variable CaCl absorpt. bands 79−88683
κ Cassiopeiae, spectral obs., coarse atm. anal. 77−33487
CD −31°622 as metal-deficient subdwarf 78−65618
CD-38°245, metal-deficient halo red giant, spectrum, photometry and Ca/H ratio 78−69797
ω Centauri, anomalous giant branch rel. to abundance vars. in dwarf spheroidal galaxies 79−5904
V553 Centauri, C rich Cepheid, C and N abundances 80−4378
V553 Centauri, CH-type Cepheid, chemical comp. and luminosity 79−62849
SZ Centauri, eclipsing binary, four-colour photometry, photometric elements, dimensions and He content 77−41391
ω Centauri, main sequence stars photometry rel. to He abundance 80−90491
α Centauri A, Be abundance and constraints on Be form. 77−41379
α Centauri binary system, spectroscopic chemical anal. 80−62128
ω Centauri giant branch, mixing versus primordial abundance vars. 77−17640
9 Cephei, B2-type supergiant, circumstellar CO lines discovery 79−84793
U Cephei, chem. comp. of secondary component of close binary system 79−35308
μ Cephei, late-type supergiant, possible H_2O thermal emission identification 78−81628
T Cephei, Me variable, Tc discovery 78−32483
19 Cephei, O-type supergiant, spectroscopic study, model atm. anal. 78−28681
9 Cephei (B2 Ib), circumstellar CO obs. 80−94795
IV Cephei (Nova 1971), ejecta He abundance 79−40203
Cepheid instability strip 80−56833
Cepheid variables, He enrichment effects in atm., models 80−26884
Cepheid variables, He-enriched convection zones rel. to masses and stellar winds 78−57556
Cepheids, double-mode, surface He enhancement, linear theory period ratios 79−67021
Cepheids metal abundances rel. to period-amplitude diagrams characts. in different galaxies 78−53956
TV Ceti, light curves, photometric elements and He content 79−44526
T Ceti, semiregular variable, Tc I absorpt. line obs. 78−28689
RS Chamaeleontis, eclipsing binary, four-colour photometry rel. to photmetric elements, absolute dimensions and He abundance 80−67783
chemically peculiar (CP) stars formation, planetesimal impact hypothesis 78−20834
chemically peculiar A-type stars, grains accretion rel. to comp. 79−67017
chemically peculiar stars, nuclear and differentiated abundance patterns 77−17597
CIT 6 (IRC+30219), IR C star, $^{12}C/^{13}C$ lower limit from CO obs. 80−12761
cluster composition determ. method using evolved members 77−29889
CoD−38°10980, white dwarf, gravit. redshift mass-radius relation and interior comp. 78−24511
cold degenerate stars, immiscibilities rel. to luminosities and comps. 78−69798
17 Comae A, Ap star, Sr spots distrib. rel. to atmospheric mag. field *(Russian)* 77−17594
17 Comae A, magnetically variable Ap star, spectroscopic obs. 77−17595
cool C stars, $^{12}C/^{13}C$ ratio calc. 78−4205
cool giant stars, model depend. of detailed anal. 77−53590
cool giant stars, obs. and anal. of CO at 5 μm 78−36569
cool stars, abundance determ., molecular data uncertainty effects 77−29805
cool stars, alkaline earth and rare earth oxides occurrence 78−85933
cool stars, CaCl bands obs. 77−53593
core He burning stars, H profile, previous mixing and loops in H-R diagram 77−29792
core molecular weight gradient, penetration by meridional currents 77−33474
stellar composition continued
S Coronae Austrinae, identification of absorpt. lines, irradiated amethyst 79−25601
B Coronae Borealis, Ap star, chemical element distrib. from spectrophotometry *(Russian)* 77−22238
R Coronae Borealis, He I λ10830 line obs. at 1978 pre-maximum phase 79−16975
β Coronae Borealis, mag. star, spectral peculiarities *(Russian)* 77−64773
R Coronae Borealis, search for graphite feature at 2200 Å 77−87419
R Coronae Borealis stars, comp. and rel. to Type I supernovae, appl. to Crab Nebula 79−5845
cyanogen distrib. in 47 Tucanae red giants 79−71025
V460 Cygni, cool C star, atmospheric $^{12}C/^{13}C$ ratio 78−93223
XX Cygni, dwarf Cepheid, composition and motion, visible photometric and spectrographic obs. 80−77424
V1057 Cygni, FU Orionis star, IR spectroscopy with contact-type image tube 80−17587
R Cygni, pure S star, new molecules identification 78−28700
V645 Cygni (AFGL 2789), broad absorpt. band obs. and identification 80−73066
V1500 Cygni (Nova 1975), heavy element abundances 79−21295
61 Cygni A, B, late-type dwarfs, metal abundances 77−78779
degenerate stars with H atmospheres, spectra rel. to comp. and theoretical models 80−17576
degenerate stars with He atmospheres 77−13335
δ Delphini, spectroscopic binary fine anal. 77−17620
Delphini 1967 (HR Delphini), physical conditions in envelope at max. light 78−24519
HR Delphini (Nova 1967), C and N overabundances in stellar wind from UV spectra 80−109440
HR Delphini (Nova 1967), physical props. and element abundances in nebular state 78−36573
HR Delphini (Nova 1967), premax. envelope conditions 78−24518
δ Delphini stars, abundance anal., metallicism and pulsation 77−33506
dense stellar cores, chemical comp. oscills. rel. to time-dependent neutrino transport 80−94783
disk stars, metal abundance rel. to orbital elements *(Russian)* 79−25733
DO white dwarfs, effective temps. and He abundances 79−35249
73 Draconis, CH lines in spectrum of Ap star *(Russian)* 77−56958
BC Draconis, double-mode Cepheid, mass, comp. and evolution 77−29845
BY Draconis, late-type flare star, metal abundances 77−78779
ζ Draconis, line identifications in UV spectra 77−87384
CM Draconis, low dispersion spectrum, metal abundance of eclipsing binary 79−25636
φ Draconis, Si Ap-star, UV vars. rel. to patchy stellar surface model 77−49389
73 Draconis, spectroscopic study and model atm. anal. of Ap star 77−33531
dust grains composition, evidence from IR spectra 80−26943
dwarf Cepheids, double-mode, theoretical periods and masses 79−44488
dwarf Cepheids, metal abundances rel. to evolutionary stage 80−46562
early type peculiar stars, Cr, Mn and Fe abundances 77−78803
early-type stars, envelope mixing of elements, shear flow instability 80−109424
early-type stars, He abundance effect on H and He^+ line profiles in stellar winds 80−85926
eclipsing binaries, late-type, mass-luminosity and radius relations, chem. composition 78−28728
eclipsing binary stars, masses, radii and absolute magnitudes 79−44520
element abundance, atomic and mol. f-values 78−20792
elliptical galaxies, chemical evolution 80−67843
γ Equulei, peculiar A-type star, line identification study, 3086 to 3807 Å 79−88659
evolutionary models from zero age main sequence to red giant branch 80−21987
evolved stars, chemical abundances perturbations rel. to thermal and nuclear modes coupling 79−84785
evolving 6 M⊙ star, chemical abundances perturbation rel. to continuous nuclear spectrum 77−64745
extreme Population II stars, comp. rel. to age difference from oldest Population I stars 77−56912
extreme subdwarf stars, metal abundances from mol. band strengths, theoretical approach 78−93221
F- and G-type dwarf stars, Mn/Fe abundance ratios 78−45325
F- and G-type stars, C and N abundances 77−91530
F- and G-type stars, metallicity determ. by spectral quantification 77−29791
F- and G-type supergiants, enhanced He abundance effects on visible spectra 80−12759
F-type supergiants in Magellanic Clouds, Ca abundances 80−98655
faint blue southern stars, Hβ photometry, metallicity, luminosity 77−41381
Feige 86, $^3He/^4He$ from He I 6678 Å obs. of He deficient blue horizontal-branch star 79−92774
Feige 86, horizontal branch star, chemical comp. 77−9745
first generation stars form., heavy element abundances rel. to cosmic gas clouds fragmentation 77−33628
Fornax dwarf elliptical galaxy, abundance range from giant branch photometry 80−4431
G128-7, cool DA white dwarf, atmospheric metal abundance and evolutionary consequences 80−62126
G200-39, hot hybrid white dwarf, He/H ratio 80−26852
G35-26, high velocity mag. degenerate, H/He ratio 78−73709
G, F, A, B and O stars, metal abundances rel. to model atmospheres 79−80298
G 165−7, metallic line white dwarf, abundances, model atm. code anal. of spectrum 80−85940
G and K-type giant stars, Li abundances 80−41819
G- and K-type giants, CNO abundances 77−5530
G- and K-type stars, correl. between motions and CN anomalies 77−17566
G-K giants, low $^{12}C/^{13}C$ ratio explanation constraints 79−5817
G-K giants and C stars, origin of $^{12}C/^{13}C$ ratios freq. distrib. 77−78780
G-type giants, heavy-element abundance effect on classification 77−29834
galactic chemical evolution, He enrichment 77−22208
galactic clusters, abundances from weak lines 77−29890

stellar composition continued
galactic disc chemical evolution and radial metallicity gradient 77−29937
galactic disc dwarf stars, evolutionary effects on metal abundance distrib. 79−88733
galactic disc stars metallicity distrib. rel. to origin of galactic subsystems *(Russian)* 79−21441
galactic halo stars, heavy elements abundance gradient 79−92857
galactic populations, metals distrib. rel. to Galaxy chemical evolution 78−96545
GD 40, He white dwarf, spectrum anal., CA abundance determ. 77−87385
GD 428, variable star, metal abundance and nature of dwarf Cepheids 78−73720
γ Geminorum, differential abundance anal. rel. to α Lyrae standard 80−82362
giant stars, G- and K-type, CNO abundances 78−7993
giant stars, late-type, O abundances rel. to O I 7773 Å triplet 79−35250
giant stars, mixing during He shell flashes 77−56909
giant stars, Population I, theoretical surface abundances 80−94796
giant stars in globular cluster M71, IR colours, CO band strengths and physical parameters 79−25650
giant stars in globular clusters, near IR photometric props. rel. to metal content 77−45503
giant stars in globular star clusters, Ca II H and K-lines and abundance 80−72940
giant stars in M13, M92, NGC 6397 and M15, weak-G-band effect obs. 77−78778
giant stars in M3, M13 and M92, metal abundances from IR CO indices 78−57595
giant stars in open cluster NGC 7789, metal abundance, He content and mass loss 80−31335
giants and supergiants, atm. $^{12}C/^{13}C$ ratio 77−13337
GK giants, CN strengths, mixing and supermetallicity 77−56930
GK-type dwarf stars, Mg isotopic abundances 80−51757
globular cluster giant stars, metal abundance parameter determ. from blanketing differences 80−4345
globular cluster stars, He settling and effect on inferred ages 80−73013
globular clusters, (V-K) colour rel. to metal abundance 77−87485
globular clusters, age and chemical comp. determ., review *(Polish)* 78−61751
globular clusters, ages and comp. rel. to fundamental knowledge about galaxies evolution 80−90488
globular clusters, evolutionary model sequences, ages 77−87487
globular clusters, He content from RR Lyrae stars evolution 80−51778
globular clusters, metal-rich, TiO band strengths, reddening and metallicity determ. 79−40227
globular clusters, metallicity rel. to RR Lyrae stars transition period-luminosity depend. 77−53614
globular clusters, metallicity rel. to spatial struct. of cluster system 77−37625
globular clusters evolved stars, CN strengths and UV excesses from DDO photometry 77−64753
globular clusters in Galaxy, Fornax and M31, integrated colours and metallicity 78−16469
globular clusters red giants, metal abundances in M92 and (M15) 79−92759
halo stars, cool, Al abundance implications for galaxy abundance 80−105232
HD 101065, peculiar star, presence of Fe questioned 77−45455
HD 101065, Przybylski's star, element identification 78−4233
HD 101065 (Przybylski's star), spectral type and classification 77−29861
HD 10380, Population I giant, chemical anal. and comparison with high vel. stars 80−82352
HD 122563, metal-deficient giant, atm. $^{12}C/^{13}C$ ratio, mixing 78−4201
HD 128279, cool halo star, abundances, reduction procedure and equiv. widths 77−49384
HD 149499B, hot white dwarf, continuous spectrum, H deficient 79−48795
HD 161698, Hg-Mn star, chemical elements identification in spectrum 79−58354
HD 161698, Hg-Mn star, curve of growth anal. 79−30070
HD 175305, red horizontal branch star in general field, metal deficiency 79−40189
HD 18474, G-type giant, rare earth's abundance *(Spanish)* 79−25605
HD 186205, He star, fine abundance anal. 77−87408
HD 187473, rare earths in Si star 80−98671
HD 192163, WN-type star, evidence for graphite in assoc. ring nebula (NGC 6888) 77−29905
HD 192913, Si Ap-star, lanthanide abundances, spectral identifications 78−45345
HD 215038, Ap star, line identification list 78−32484
HD 25329, subdwarf, metal deficiency from spectroscopic anal. 80−62122
HD 269781, abundance anal. 77−91522
HD 27561, Hyades cluster star, CNO abundances from near IR spectrum 78−93222
HD 30466, Si star, double wave photometric var. rel. to chemical comp. patches 77−87410
HD 34452, Si Ap star, spectrum rel. to enhanced element abundance spots 78−65634
HD 3473, A2p star, spectrograms, Si and rare earth elements overabundance 77−74071
HD 36619, Am-type star previously misclassified as O7 type 79−84805
HD 49798, H-deficient subdwarf O-type binary, He abundance from non-LTE anal. 79−16978
HD 6884, abundance anal. 77−91522
HD 76932, subgiant halo star, chem. comp. rel. to nucleosynthesis 78−81626
HD 84903 and 184711, differential anal. of extreme metal deficient stars rel. to halo star HD 122563 79−80302
HD 91805, spectrum anal. rel. to nature of Bidelman-MacConnell weak G-band stars 78−49432
HD 94028, subdwarf, Mn abundance and Mn/Fe ratio 78−45328
HD 94033 ultra short period cepheid, metal deficiency 80−22024
HD stars with peculiar abundances, statistics and notation 77−29860
HDE 232078, variable mass loss in metal deficient red giant 79−67010
heavy element abundance, effects on evolution of stars, struct. of models 80−105231
heavy element abundance effect on evolution 78−89167
heavy-element excess in late spectral class stars 80−26854
Henize 2-38, symbiotic star, steam and CO absorpt. obs. 78−40970
Herbig-Haro objects, Fe abundance 79−62826
68=μ Herculis, ^{3}He identification in atmosphere of primary component 77−57045
φ Herculis, Ap star, X-ray emission obs. rel. to abundance anomalies 79−101160
τ Herculis, B-type subgiant star, abundance anal. 78−16416
14 Herculis, C/Fe ratio of K-type dwarf 78−93227
DY Herculis, dwarf Gepheid, metallicity and evolutionary status from uvbyβ photometry 79−58357
OP Herculis, irregular variable, Tc I absorpt. lines obs. 78−28689
τ Herculis, line identifications in UV spectra 77−87384
BL Herculis, short-period Population II variable, chem. comp. determ. 79−8923
V446 Herculis (Nova 1960), ejecta He abundance 79−92775
α Herculis A, M-type supergiant, Li abundance in atmosphere *(Russian)* 80−72950
high velocity giant stars, detailed chemical anal. 80−82352
high-luminosity thermally pulsing stars, surface comp. rel. to interstellar medium element enrichment 78−40917
Hodge 11, in LMC, colour-magnitude diagram, metal abundances 78−69850
Hodge 11 star cluster in LMC, electronographic photometry rel. to metal deficiency 79−40230
horizontal-branch A-type stars, He abundances 79−62829
hot horizontal branch stars, comp. rel. to B−V colour indices and bolometric corrections 79−58327
HR 1614 group of metal-overabundant stars, intermediate-band photometry and comps. 78−53935
HR 2172, double-lined binary, radial vels. equivalent widths and comp. *(French)* 77−17625
HR 3089, He-rich star, anal. of UV spectrum 77−9751
HR 421, δ Delphini star, abundance anal., uvbyβ photometry 77−29823
HR 6127, chemically peculiar star, spectral lines and equivalent width lists, visible obs. 80−82387
HR 6766, weak G-band star, detect. of Li 77−49386
HR 6766, weak G-band star, light-element abundances 78−57548
HR 774, Mg isotopes and s-process elements in Ba star 79−25594
HR 8799, model atm. anal. 77−74050
HR 96, Ap-type star, atm. parameters and stellar comp., visible obs. 80−67740
Hyades metal content and distance rel. to solar colour 80−101569
Hyades stars, Be abundances 77−53584
Hyades stars, models. rel. to comp. and cluster distance modulus 77−57067
χ^2 Hydrae, eclipsing binary, four-colour photometry, orbital elements, dimensions and He abundance 78−65653
W Hydrae, form. of carbyne and cyanoacetylenes in stellar atm. 80−67708
HZ 43, hot white dwarf, self-consistent model atm. anal. 77−22220
HZ 43, white dwarf, He abundance and stellar struct. from soft X-ray spectra 80−72944
III-106, CH star in globular cluster M22, CO in IR spectra 80−62131
ε Indi, late type dwarf star, model atmosphere and abundance anomalies 80−90425
ε Indi moving group, detailed anal. of members HD 40409, HD 102365 and λ Aurigae 78−85982
initial chemical comp. discontinuity and non-radial oscills. of 1 M⊙ star 80−82341
intermediate-mass stars asymptotic giant branch evolution as function of mass and comp. 80−12749
internal composition, effect of interstellar grain motions during star form. 78−69788
IRC+10216, C star, HC_5N and HC_7N detect. 79−17126
IRC+10216, C star, near IR obs. of new mol. feature 79−92762
IRC+10216, C star, NH_3 obs. in circumstellar envelope 79−48793
IRC+10216, C star, possibility of detecting cyanoacetylene-d_1 (DC_3N) 78−69901
IRC+10216, circumstellar graphite dust shell model 80−56972
IRC+10216, isotope abundance anomalies in C star 79−5814
IRC+10216, molecular abundances in cool C star 80−4354
IRC+10°216, circumstellar acetylene in IR spectrum 77−5591
K-dwarfs, chemical composition and mass 77−29837
K-type giant stars, Population I, CN strengths and $^{12}C/^{13}C$ ratios 78−93229
K-type giant stars polulation at South Galactic Pole, CN anomalies and distances 80−8622
K-type giants, $^{12}C/^{13}C$ ratio correl. with Fe/H ratio 79−48798
K-type giants, comp. rel. to multivariate anal. of spectrophotometry 77−78772
K-type stars, abundance effects in classification 77−29833
Kapteyn's star and M subdwarfs, comp. 77−13330
L973, red giant in globular cluster M13, curve of growth anal. 79−48796
AR Lacertae, double-subgiant eclipsing binary, spectra, abundances 78−8044
CP Lacertae (Nova 1936), ejecta He abundance 79−92775
late M-type giants in elliptical galaxies, comp. rel. to stellar population synthesis 78−57626
late-type dwarfs, accretion and abundance distrib. 77−2425
late-type dwarfs, photometric metal abundance index and appl. to galactic evolution 77−60754
late-type main-sequence stars near Sun, photometry and metal abundances 78−53934
late-type stars, Ba oxide and halide identification in near IR 77−56926
late-type stars, H_2 abundance rel. to acoustic energy generation and chromospheres 78−7986
late-type stars, He abundance effects on spectrum appearance 80−46540
late-type stars, O-rich, 16 to 39 micron spectroscopy rel. to circumstellar silicate dust 80−22002
late-type supergiants, C, N and O abundances for G and K Ib stars 78−24509
LDS 678B (EG 131), white dwarf, spectrum and He/H ratio 78−40946
LDS 785A (EG 153), DB white dwarf, discovery of H 77−45425
AQ Leonis, homogeneous model of Population II double-mode RR Lyrae star 80−62134
R Leonis, IR spectroscopy of Mira variable, H_2O vibr. rot. bands 79−35258

stellar composition continued
LMC disc stars, photometry rel. to population struct. and metal abundance 77−33633
long-period variables, SiO in 4 μ spectrum 77−13360
LP 145-141, C_2 white dwarf, CO, C_2 and O_2 abundences rel. to strong UV absorpt. 80−67715
LP 701-29, heavily blanketed white dwarf, spectrum synthesis and metal abundance 78−32455
LP 790-29, southern mag. white dwarf, C_2 identification from spectrophotometric obs. 79−92765
LS II+33°5, new H deficient B-type star, spectrum 78−93265
LS IV −14°109, H deficient A-type star, effective temp. 79−40195
LTT 2437, most metal-deficient subdwarf, spectrum, photometry and Ca/H ratio 78−69797
luminous cool stars, atm. $^{12}C/^{13}C$ ratio 77−13336
RR Lyncis, Am eclipsing binary, photometry and spectroscopy, abundances 77−33558
β Lyrae, CNO abundances in atmosphere, IR spectra *(Russian)* 80−67794
R Lyrae, M-type supergiant, Li abundance in atmosphere *(Russian)* 80−72950
α Lyrae (Vega), B abundance 77−53585
α Lyrae (Vega), mass, chemical comp. and age 77−33495
α Lyrae (Vega), spectral anal. from Copernicus 80−26856
RRab Lyrae field stars, metallicity rel. to luminosity 78−77561
RR Lyrae stars, Ca and Fe decoupling 79−30069
RR Lyrae stars, effective temp. and colour, metallicity effects 80−56841
RR Lyrae stars, in 47 Tucanae, membership and metallicity 80−62206
RR Lyrae stars, in Baade's window region, metal abundances 77−9749
RR Lyrae stars, instability strip red edge depend. on luminosity and comp. 77−53600
RR Lyrae stars, line blanketing and metallicity from VBLUW photometry 79−48806
RR Lyrae stars, multiperiodic vars. rel. to metal abundances 77−87430
RR Lyrae stars, period-luminosity-colour relations, metallicity effects 80−56842
RR Lyrae stars in ω Centauri, UBV photometry rel. to comps. 78−73719
RR Lyrae stars in galactic bulge, spectra and comp. 77−26012
RR Lyrae stars in globular cluster M4, metal abundances 79−58351
RR Lyrae stars in globular clusters, heavy element abundance rel. to Oosterhoff dichotomy 77−78837
RR Lyrae stars in M22 and ω Centauri globular clusters 79−16962
RR Lyrae stars in M4, metallicity from UBV photometry 77−78802
RR Lyrae variables, metallicity rel. to three-dimensional motion 80−12754
RR Lyrae variables in globular cluster NGC 6121 (M4), metal and He abundances 80−22018
RR Lyrae variables in N.Galactic pole fields, metal abundances 79−88660
M15 faint stars, He abundance distrib. from main-sequence intrinsic width 77−78834
M22, globular cluster, membership, spectra and comps. 78−32537
M31, M32 nuclei, luminosity-sensitive spectral features rel. to metallicities 78−49431
M32, metallicity and galaxy age from spectral synthesis 80−67842
M5, M13, M3, globular clusters, giant stars chemical comp. 80−67695
M67, cluster comp. from contact binary AH Cancri obs. 79−40222
M67, main-sequence stars differential blanketing and metallicity rel. to Hyades and Coma 78−57597
M87 halo globular clusters, metallicity meas. 78−89244
M92, globular cluster, C and N abundance variations in horizontal branch 77−87495
M92, globular cluster, giant star C and N abundances 77−87496
M-type dwarf stars, IR Fourier transform spectroscopy, abundance anal. 79−21279
M-type dwarfs, proposed identification of FeH 77−45418
M-type dwarfs and S-type stars, FeH bands identification in spectra 78−7952
M-type semiregular variables, atmospheric anal., chem. comp. *(Russian)* 78−65623
M-type supergiants in SMC rel. to low metallicities 79−96995
magnetic star model, circulation within nuclear burning shell rel. to latit. depend. chem. comp. *(Russian)* 79−16940
magnetic stars, equatorially symmetric rotator model, inhomogeneous element distrib. 80−4371
main sequence (MS) stars chemical structure, influence of pre main sequence evolution 79−35247
main sequence galactic disk stars, chem. comp., implications for galaxy 80−109553
main sequence stars, chem. comp. effects on position in H-R diagram 77−91521
main sequence stars, chemical comp. rel. to main sequence location 77−71105
main sequence stars, diffusion in envelope and abundance anomalies 77−13331
main sequence stars, element abundance regularities rel. to nucleosynthesis *(Russian)* 77−45431
main sequence stars, F- and G-type, Be abundances 77−13332
main-sequence massive stars, mass loss effects on evolution and surface comp. 78−93200
main-sequence stars, Li, Be and B abundances rel. to envelopes hydrodynamical instabilities 78−93202
marginal metallic line (Am) stars, metallicism and pulsation 78−49448
massive star core collapse, eqn. of state and composition near β equilib. 80−82335
massive stars, element abundances rel. to evolution 80−90416
massive stars, mass loss effects on ^{14}N abundances and C/O ratios 79−101138
massive stars, protostellar cloud evolution rel. to photosphere chemistry 77−17543
Melotte 66, oldest open cluster, metallicity from colour-magnitude diagram 80−17621
α Mensae, chemical composition of cool southern dwarf 77−22225
metal abundance and MK class. for F5-K4 stars, relationships 77−29809
metal abundance determ. in late-type stars, new method 79−12405
metal abundance in Draco dwarf spheroidal galaxy 77−91638
metal abundances, three-level models of chemical evolution 79−48873
metal abundances and microturbulence from model atmosphere analyses of solar-type stars 79−67002
stellar composition continued
metal abundances in galactic disc stars, rel. to gas inflow problem and disc chemical evolution 80−62279
metal abundances of F- and G-dwarfs from CORAVEL radial vel. scanner 80−94791
metal rich globular cluster NGC 5927, colour-magnitude diagram 80−36678
metal rich stars, zero age main sequence position 80−109426
metal-deficient stars, CO obs. at 2.2 and 2.4 μm 79−58336
metal-poor binaries, He abundance determ. 78−81660
metal-poor dwarf stars, abundance anals. of yellow spectra 79−92760
metal-poor late-type stars, metal content effects on spectral classification 80−4340
metal-poor stars, abundance anals. of high-vel. dwarfs blue spectra 78−53933
metal-poor stars, O abundances from O I IR triplet 80−36610
metal-poor stars relative abundances, Al/Fe ratio 78−57549
metal-poor-stars, spectral energy distrib. and Fe/H ratio 78−53937
metallic-line stars, He depletion rel. to theoretical pulsation 79−97004
metallicity distribution, rel. to Galaxy form. and chem. evolution 77−91520
metallicity distribution in old stars and effect of dust accretion 77−29795
metallicity effects on integrated colours, calibration of globular clusters and early-type galaxies 78−89227
metallicity gradients in galaxies, weakening during galaxy mergers 80−67860
metals in stellar populations in bright galaxy nuclei 80−98708
neutron star matter, comp. during decompression 77−33544
neutron star matter expansion and its final nuclear composition 80−67769
neutron stars, hadronic matter components, leptons and baryons *(Polish)* 79−88587
neutron stars, inner crust nuclear compositions 80−31322
neutron stars, structure and physics 79−67046
NGC 1261, globular cluster, metallicity rel. to colour-magnitude diagram 80−17623
NGC 1851, 6624, globular cluster, abundance gradients spectroscopic investigation 80−82437
NGC 188, open cluster, He and CNO abundances rel. to anomalous giant branch 78−41001
NGC 1904, globular cluster, BV photometry rel. to metallicity 77−13415
NGC 2209, LMC cluster, metal abundance 78−8122
NGC 2231, star cluster in LMC, age and metal abundance from colour-magnitude diagram 79−92813
NGC 2243, metal abundance of old open cluster 78−93333
NGC 2243, old open cluster, metallicity of UBV photometry 77−78835
NGC 2264, open cluster, reddening, blanketing and metallicity from spectroscopic obs. 80−26916
NGC 2420, old disc cluster, chemical comps. of stars 80−46620
NGC 2423, 2482, Hyades-like clusters, metal abundance from intermediate-band photometry 80−31289
NGC 362, globular cluster, BV photometry rel. to metallicity, anomalous characts. 77−13416
NGC 4565, galaxy, dark halo stars metal content rel. to mass function 79−62905
NGC 5053, halo globular cluster, metal abundance from photometric study 77−74103
NGC 6121 (M4), near IR photometry of metal-poor globular clusters 77−41398
NGC 6144, globular cluster, photometric obs. rel. to metal deficiency 80−51816
NGC 6265, highly reddened metal rich globular cluster 78−77583
NGC 6266, globular cluster, colour magnitude diagram, distance and metallicity 78−61894
NGC 6528, globular cluster, colour-magnitude diagram rel. to metallicity 80−4406
NGC 6530 open cluster, broadband photometry rel. to ^3He burning 77−45504
NGC 6541, globular cluster, UBV photometry, metallicity and distance 79−35316
NGC 6717, globular cluster, colour-magnitude diagram, distance and metallicity 80−46624
NGC 6752, globular cluster, main sequence stars metallicity from UBV photometry 79−71079
NGC 7099, metal-poor globular cluster, UBV photoelectric photometry 78−77584
NGC 752 red giants, metallicity from DDO astrophysical study 79−48864
NGC 7789, open cluster, giant stars photometry and metal abundances 77−53648
nova, H-rich envelope mass 77−87451
Nova Cephei 1971, chemical comp. of ejecta 78−12244
Nova Cygni 1975 (V1500 Cygni), Ne/N ratio rel. to fine-struct. lines and 10 micron excess 78−93269
nova envelopes, CNO composition 77−87453
nova outburst, CNO abundances and hydrodynamics, 1 M⊙ models with small mass envelopes 79−12475
Nova Serpentis 1978, enhanced C abundance in dust shell 80−90430
novae, ^7Li prod. 78−57555
novae, explosive hot CNO-Ne cycle H burning rel. to abundances 79−44489
novae, Li/Na ratio upper limit 79−101156
novae, nebular stage, abundance determ. methods 77−87279
nucleosynthesis at explosive Ne burning in supernovae 80−94780
O and B0 supergiants in Magellanic Clouds, spectral classification and comps. 77−78777
O and B stars, Si spectra theory rel. to Si abundances 78−57539
O-type stars, metal-deficient, in SMC, spectroscopic obs. 79−5820
OB stars, CNO anomalies in spectra 77−29835
OB stars, distrib. in Galaxy, comp. rel. to age and space motions *(Russian)* 78−93216
OB stars in associations and young clusters, He abundance vars. *(Russian)* 77−82287
OBN star origin, mass loss calcs. 77−45412
old halo stars, chemical comp. rel. to nucleosynthesis in Galaxy 78−65616
oldest Population I stars, comp. rel. to age difference from extreme Population II stars 77−56912

stellar composition continued
open cluster, galactic chemical abundance gradient from H-R diagrams 80−56938
Orion population stars, OH emission survey 80−67716
β Orionis, B8 Ia star, UV spectrum and line identifications 77−22221
α Orionis, CO circumstellar absorpt. obs. in 4.6 micron spectrum 80−26858
FU Orionis, IR spectroscopy with contact-type image tube 80−17587
α Orionis (Betelgeuse), UV flux rel. to C and O underabundances 77−22231
Pal 12, metal-rich globular cluster in outer galactic halo, optical and IR obs. 80−105290
Palomar 5, remote globular cluster in galactic halo, chem. comp. 77−87482
γ Pavonis, C and N abundances 77−91531
peculiar A and B stars, Y abundances 77−33503
o Pegasi, hot Am star, spectroscopic obs. and curve of growth anal. 77−22237
21 Persei, Ap star, chemical element distrib. from spectrophotometry *(Russian)* 77−22238
IW Persei, metallic-line close binary, local metallicity surface distrib. 80−62186
β Persei-type eclipsing binaries, red spectra, element abundances and neutrinos 77−57041
photospheric abundances of Fe and Cr 78−69793
19 Piscium, C star, violet spectrum line identification and radial vel. 80−82361
planetary nebula central star evolutionary scenario towards white dwarf stage 80−109427
planetary nebulae, C abundances from C IV 1550 Å lines fluxes 79−17051
planetary nebulae, CNO abundances rel. to central stars masses and Population II planetaries origin 78−85992
planetary nebulae, spectrophotometry and chemical abundances 78−36663
planetary nebulae central star abundances corrections from UV flux determ. 80−72945
planetary nebulae central stars, C abundance rel. to nebulae refractory elements gas-phase abundances 80−109516
polyatomic molecules in C star 3 μ band 79−5807
Population I stars, chem. and physical props. 77−78782
Praesepe A-type stars, metal abundances rel. to Hyades 77−57064
pre-main-sequence stars, D abundance and D burning rel. to early evolution 80−51736
pulsar outer crust composition, influence of mag. field 80−101610
ζ Puppis, Of-star, UV spectrum, line identifications 77−45441
L_2 Puppis, semiregular variable, Ca I uneven distrib. from narrowband polarimetry 80−98666
rare earth elements, atomic partition functions, Chebyshev approximations 80−67544
red giant of 6 M$\odot$, envelope composition rel. to evolution 80−105237
red giant stars, circumstellar shells chem. struct. 80−105242
red giant stars, meridional circulation and CNO anomalies 79−48786
red giant stars, s-process abundance evolution in galactic disc 77−13449
red giant stars evolutionary sequences, effects of mass and comp. 78−65611
red giant stars in globular clusters M92 and NGC 6397, C abundances 79−48785
red giants, abundances in M3 and 13 globular clusters 78−93334
red giants, CNO isotopes 77−87399
red giants, CNO isotopes rel. to main-sequence mixing 77−33475
red giants, convective He shells, s-branch nucleosynthesis during thermal pulses 80−90410
red giants, in Draco dwarf galaxy, metal abundance determ. 79−17078
red giants, Li synthesis by spallation reactions 77−49366
red giants, O/C abundance ratio from TiO absorpt. bands 78−96480
red giants, prod. and observability of ^{14}C and ^{17}O 77−26005
red giants, s-process element prod. in deeply mixed convective envelopes 77−33470
red giants, spectra and comp. *(Norwegian)* 77−71111
red giants in 47 Tucanae, C and N abundances 79−97000
red giants in Draco dwarf spheroidal galaxy, metal abundance 80−73030
red giants in globular cluster NGC 6752, DDO photometry and spectra 79−71079
red giants in halo globular clusters, abundances 79−5898
red giants in M13, Na abundance var., protocluster gas inhomogenleities 80−82439
red variable stars, mol. absorpt. rel. to amplitude extension and amplitudes limit 79−62836
Ross 640, H-poor white-dwarf, H abundance determ. 77−87388
Ross 640, He-rich white dwarf, Ca, Mg, S and Fe abundances from UV spectra 80−94790
Ross 657, metal deficiency obs. 77−5532
rotating stars, chemical mixing and ang. momentum redistrib. rel. to evolution 78−36553
rotating stars, meridional circulation rel. to comp. anomalies 79−62818
S-type stars, CeO band identification, new s-process mol. 77−33488
S-type stars, FeH and CeO identification 79−21280
S-type stars, Keenan and Wing bands, IR obs. 80−67722
S-type stars, M-type dwarfs, proposed identification of FeH 77−45418
S-type stars, possible presence of ZrO IR spectrum 80−62124
S-type stars, R Cygni and V Cancri, Zr isotope abundances 78−53957
S-type stars, revised spectral classification system in red 80−46541
FG Sagittae, 1975-8 spectral obs. of peculiar variable 80−72959
FG Sagittae, Fe-peak and s-process elements abundance *(Russian)* 78−12253
U Sagittae, photometric study of eclipsing binary 77−22270
FG Sagittae, spectral type and element abundances *(Russian)* 78−93281
SB 21, extremely He rich subdwarf O-star, spectrum 80−98659
3 Scorpii, He weak star, He surface distrib. rel. to mag. field geometry 79−88676
Sculptor dwarf galaxy, colour-magnitude diagram and metal deficiency 77−53429
Sculptor dwarf spheroidal galaxy, abundance vars. on giant branch rel. to ω Centauri anomaly 79−5904
δ Scuti and related stars, rot. and metallicism rel. to pulsation 79−62847
δ Scuti and RRs variable stars, role of He diffusion and heavy elements abundances 77−87433
semi-Ba and Ba stars, heavy element abundance effect on spectroscopic luminosities 77−53586
stellar composition continued
slow nova, envelope CNO abundance rel. to hydrodynamics 78−40954
SMC Cepheids, five colour photometry, and metal abundances, comparison with galactic Cepheids 77−29923
SN 1972e in NGC 5253, Type I, spectrum after 365 and 435 days 78−4255
solar neighbourhood C and M-type stars 79−16946
solar neighbourhood crossing times effect on observed stellar age and metallicity distribs. 78−12362
solar type stars, relation between metallicity and multiplicity 77−78788
solar type stars, thirteen-colour photometry, metallicity effects 77−22230
solar-type stars, metal abundances, microturbulence, spectroscopic data 78−40943
southern metal-poor stars, UBVRI photometry and UV excesses 80−56828
southern peculiar A-type stars, spectra and atmospheric anals. 78−24517
spectroscopic binary stars, He and metal abundances rel. to apsidal motion 80−82413
spiral galaxies nuclei, stellar population and metal abundance 80−56926
stars with given entropy distrib., influence of comp. changes on struct. 79−66993
static models with varying He core mass, linear series of 7 M$\odot$ star 78−65603
stratification of elements in the envelopes ejected by type I supernovae 79−16997
strong CN stars, correl. with super-metallicity 78−53921
subdwarf stars, metallicity rel. to thirteen-colour photometry indices 79−92767
subdwarf stars, odd-Z and r-process elements abundances from spectroscopic anals. 80−62122
subdwarfs, 37−45 excess calibration using Fe/H abundances 80−82363
subdwarfs, He abundance and galactic halo 80−22003
subdwarfs, old disc population, comp. from CaH and TiO band strengths 78−40930
subdwarfs, photometry rel. to compositions and kinematics 80−82364
subdwarfs, UV excesses and metal abundances 80−17574
subgiant stars, F-, G- and K-type, Be abundance rel. to post-main sequence evolution 77−13333
super-metal-rich stars, boundary cooling and supermetallicity 80−56821
super-metal-rich stars, Fe abundance problem 77−74060
super-metal-rich stars, influence of initial He content on evolution 77−49370
supergiant stars, southern, late-type, chem. comp., solar neighbourhood metallicity distrib. 80−12758
supergiants, metal abundances of G- and K-type Ib stars 77−33482
supermetallicity and the strong-lined binary systems 79−75204
supernovae, comps. of Types I and II 77−87455
supernovae, Type I, and supernova remnants, H abundances 78−53969
supernovae, Type I, envelopes, comp. rel. to radioactive excitation source model for late time spectra 80−105264
surface composition, effects of interaction with dense interstellar gas glouds *(German)* 80−109500
T626, red giant in open cluster M67, curve of growth anal. 79−48797
V471 Tauri, eclipsing binary, UV spectra rel. to white dwarf atmospheric comp. 80−26912
ζ Tauri, high-resolution spectra and identification of λ1920 and λ1720 features 78−4236
45 Tauri, Hyades cluster star, CNO abundances from near IR spectrum 78−93222
α Tauri (Aldebaran), Ti isotopic abundance ratios 77−22212
RV Tauri and yellow semiregular variables, metallicity and mass from photometric investigations 80−26865
RR Telescopii, symbiotic star, steam and CO absorpt. obs. 78−40970
thermally dissociated matter, comp. and eqn. of state 77−33476
U Trianguli Australis, double-mode Cepheid, mass, comp. and evolution 77−29845
47 Tucanae, globular cluster, chemical comps. of stars 80−46620
47 Tucanae, spectral inhomogeneities in faint globular cluster stars 78−93340
47 Tucanae cluster, abundance gradients from spectroscopic obs. 79−40228
47 Tucanae stars, N anomaly anal. 79−48867
turbulent diffusion and $^{12}C/^{13}C$ abundance ratio 80−21993
unevolved stars, abundances rel. to interstellar gas mixing *(Russian)* 79−40192
upper main-sequence peculiar stars, chemical and physical props. rel. to radiatively driven diffusion theory 80−82374
Ursa Minor dwarf spheroidal galaxy, abundance vars. on giant branch rel. to ω Centauri anomaly 79−5904
τ Ursae Majoris, Am star, microturbulence and metal content determ. 80−82377
γ Ursae Majoris, Ap star, chemical element distrib. from spectrophotometry *(Russian)* 77−22238
ε Ursae Majoris, Ap star, UV spectral scans, line identifications 77−45440
UV5, in globular cluster NGC 1851, He abundance determ. 78−49441
UV 1758+36, He deficient hot subdwarf B star, atm. parameters, radial vel. 78−53944
32 Virginis, Am star, spectroscopic obs. and curve of growth anal. 77−22237
β Virginis, chemical composition and age 78−61855
ε Virginis, Fe spectrum, differential model atmosphere analysis 79−25604
EQ Virginis, late-type flare star, metal abundances 77−78779
CU Virginis, short period Ap star, mag. field rel. to abundance anomalies 77−33511
Voigt lines, random array, curve-of-growth function 78−89055
NQ Vulpeculae (Nova 1976), CO emission and η Carinae stage 79−25609
weak G-band stars, CH and NH band strengths, atm. material from CNO cycle 79−8917
weak-G band giant stars, Li abundance determ. 78−53948
white dwarf in binary system, outer layer C and O enrichment from companion 80−109465
white dwarfs, atm. chem. evolution, diffusion and accretion 80−36628
white dwarfs, atmosphere structure rel. to composition in hot stars 80−98658
white dwarfs, cool, IR photometry, atm. comp. 79−16950
white dwarfs, diffusion time scales rel. to element abundances 79−92761
white dwarfs, hot, effective temps. and He/H ratios 79−25602
white dwarfs, spectra and atmospheric comps. 80−82356

stellar composition continued
white dwarfs external layers, comp. rel. to interpretation of spectra 79−62824
Wolf-Rayet atmospheres, structure and composition 80−98668
Wolf-Rayet binaries, evolution of mass losing massive He burning stars rel. to comp. 80−36615
Wolf-Rayet stars, binary freq. distrib. and chemical comp. 80−105250
Wolf-Rayet stars, CNO abundance var. in massive binaries 80−94802
Wolf-Rayet stars, He, C and N abundances from UV obs. 78−40965
Wolf-Rayet stars, He/H ratios rel. to UV energy distribs. obs. 80−22023
yellow semiregular and RV Tauri variables, metallicity and mass from, photometric investigation 80−26865
young stars, chemical inhomogeneity rel. to nonspherical thermal instability 79−48779
young stars, metallicity rel. to extragalactic distance scale determ. 78−8121
young variable stars, absorpt. and emission features, IR spectrophotometry obs. 80−72954
A- and B-type stars, radiation forces and B abundance diffusion theory 79−88664
Ba 0 stars, abundance anal. 77−17557
Ba II metal rich stars, Ba abundance implications 79−71024
Ba II stars, uvby photometry rel. to s-process element enrichment 79−58337
Ba II stars and s-process calcs. 80−56824
Ba stars, spectroscopic, radial vel. and photometric obs. 78−12226
C and S stars, mixing between burned core material and surface layers 78−12213
C enhancement in nova envelope on surface accretion at white dwarf 80−85936
C overabundances in C star atmospheres 79−21284
C stars, $^{12}C/^{13}C$ abundance ratio 77−33494
C stars, $^{12}C/^{13}C$ ratio determ. 78−73710
C stars, $^{12}C/^{13}C$ ratios 79−35257
C stars, 3.9 micron absorpt. band identification 78−93231
C stars, absorption by SiC and IR excess 78−16413
C stars, C and N isotope ratios from spectral analysis 79−30057
C stars, determination of $^{12}C/^{13}C$ and N/C ratios in atm. 80−17580
C stars, enhanced C abundances in long-period variables 77−33501
C stars, form. of carbyne and cyanoacetylenes in stellar atm. 80−67708
C stars, N-type, luminosity and C enhancement 78−93247
C stars, spectrophotometry, C/O and $^{12}C/^{13}C$ ratios calc. 77−91533
C stars and G-K giants, origin of $^{12}C/^{13}C$ ratios freq. distrib. 77−78780
C/Fe ratio in metal-poor stars from CH features 79−16945
C/N abundances on first giant branch of NGC 6752 globular cluster 80−67719
C/O ratio in massive stars, core convection effects 80−17579
C-O white dwarfs, C-O eutectic model 80−77405
C_2 white dwarfs, evolutionary status 80−4355
C_2^-, $A^2\Pi_u$-$X^2\Sigma_g^+$ lines, obs. in carbon stars 80−98661
CN variations among main-sequence 47 Tucanae stars 80−94794
CNO abundances in red giant envelopes 77−29825
CNO nuclei enhancement in nova progenitors 77−33484
CO in evolved stars expanding envelopes, thermal and maser emission lines profiles 80−82334
CO in giants in globular cluster, IR obs. 78−93339
Cr stars, classification criteria, Cr II lines with blending 78−85951
Fe abundances in F8-K1 stars, recalibration of three-dimensional spectral classification 77−78768
Fe I in Ap stars, photoionisation spectrum causing UV absorpt. 80−109437
Fe/H abundance, catalogue for 628 stars 80−98579
Fe/H abundance determ., catalogue for 515 stars 77−29815
Fe/H abundances, rel. to blanketing parameter Δm_2 78−36555
Fe/H abundances of extreme Population II stars in globular and dwarf galaxies 78−40939
Fe-O 2 $M_\odot$ rotating star, gravitational collapse *(Russian)* 78−4199
FeH in stellar atmospheres, column density calcs. 78−24507
H burning stars, comps. rel. to Hertzsprung-Russell diagram age and mass calibrations 80−51744
He abundance anomalies, radiative forces calcs. in stellar envelopes 80−31291
He abundance in stellar atmospheres in O-associations and young clusters *(Russian)* 77−64815
He abundance rel. to pulsation 78−28690
He rich stars, elec. fields influence on accretion and stellar winds 79−48772
He stratification in model atmosphere of blue horizontal-branch star 80−90409
He/H ratio of B-type stars in young clusters and associations 77−29887
He-rich stars 77−37608
He-rich white dwarfs, convective mixing 79−71018
He-weak stars, photoelectric meas. of H Balmer lines 79−16994
^{3}He stars, spectroscopic search, diffusion hypothesis 79−35264
Hg-Mn binary stars, inhibition of atmos. diffusion 80−62153
Hg-Mn stars, chemical abundances 80−56838
HgMn stars, evidence for Hg in thin atmospheric layer rel. to diffusion model 80−105243
Li abundances for G- and K-type supergiants 78−28676
Li in C stars, abundance rel. to Li I line form. 78−65615
Li in stellar atmospheres *(Russian)* 77−64748
Li in weak G-band stars, spallative origin 80−51752
$^6Li/^7Li$ ratio in C stars, low-energy spallation model 78−40927
Mg index in old galaxy populations 78−41033
Mn-Hg stars, differential curve-of-growth analyses 79−16971
N deficient supergiants in loose assoc., LTE and non LTE abundance anals. 79−44478
Si overabundance in chemically peculiar stars and oblique rotator model 79−30067
Tc in late-type stars, spectral analysis 80−8623
Tc stars, search for TcO spectral bands 78−40935
Ti, isotopic abundance ratios in cool stars 80−26840
U stars and related objects, spectroscopic study 78−49465

stellar dimensions
accreting young stars, ang. dimensions 79−44482
AGK3+19°599, ang. dia. from occultation by 65 Cybele 80−31237
angular diameter determ. using IR flux method 80−62030
angular diameter from lunar occultations, photoelec. obs. 80−72920
stellar dimensions continued
angular diameter meas. with large altazimuth telescope *(Ukrainian)* 79−96925
angular diameters from lunar occultations of Hyades photoelec. obs. 80−72921
angular diameters rel. to visual surface brightness, improved definition 78−53931
Ap and Am stars, radii 79−16970
Ap stars, angular diameters, radii, and effective temps. 80−26870
Ap stars, Barnes-Evans relation rel. to radii, atmospheric struct. and evolutionary status 79−67011
KO Aquilae, eclipsing binary, mass ratio and secondary component fractional radius from photoelectric study 80−62198
V535 Arae, absolute characts. of W Ursae Majoris system 79−58373
V539 Arae, photometric analysis of B-type double lined eclipsing binary 79−44535
atmospheres, effect of finite extent on colour indices and temp. and radius determ. 78−32450
SX Aurigae, early-type semidetached binary, absolute dimensions from UBV photometry 79−44521
ζ Aurigae, eclipse data rel. to radius change of K-type supergiant component 79−84820
SX Aurigae, eclipsing binary, light curves anal. by automated Fourier techniques 79−92798
LY Aurigae, eclipsing binary, photometric elements, masses, radii, luminosities 78−28723
EO Aurigae, eclipsing binary star, revised elements from light curve anal. 80−90471
KW Aurigae (14 Aurigae A), pulsating ellipsoidal variable, masses, radius and luminosity from tidal modes 79−97028
α Aurigae (Capella) AB, angular diams. by two telescope interferometry 78−8055
B5 V-P5 V type stars in Geneva Observatory catalogue, radii, temp. and brightness determ. 80−77396
B-type semidetached systems, photoelectric obs. 79−44522
Be stars, emission shell diameter meas. possibility by lunar occultation method 80−56839
beat Cepheids, model constraints 79−5831
binary stars, distances, masses and dias. from speckle interferometric obs. 80−90475
binary stars, main sequence, absolute dimens. determ., errors requirement review 80−109473
binary stars with single optical component, ellipsoidality effect on light vars. 79−92806
binary systems, stars distortion rel. to gravit. radiation effect on evolution and spins 78−12292
α Bootis, ang. dia. and mass from predicted and observed spectral energy distrib. 80−46546
AH Cancri, contact binary in M67, masses, radii, effective temp. and luminosity 79−40222
BT Cancri (38 Cancri), δ Scuti star, multiple periods rel. to radial and nonradial pulsation periods 80−85948
β Canis Majoris, β Cephei star, pulsations periods from Fourier anal. of radial vel. changes 80−105246
UW Canis Majoris, absolute dimensions and evolution 79−12496
VY Canis Majoris, diameter upper limits 79−16974
UW Canis Majoris, eclipsing binary, UV photometry and primary component shape and atmospheric struct. 78−40992
VY Canis Majoris, OH/IR star, 1612 MHz OH maser multibaseline VLBI obs. 80−12766
α Canis Majoris (Sirius), components masses and radii from astrometric study 79−5858
β Capricorni, 1977 October 20 lunar occultation results 79−44523
η Carinae, IR ang. diameter 78−93271
OY Carinae, white dwarf cataclysmic, eclipsing binary, parameter determ. 80−82385
QZ Carinae (HD 93206), massive multiple system in great Carina Nebula, masses and radii 79−97027
V523 Cassiopeiae, BV photometry of W UMa type system *(Russian)* 79−92807
SU Cassiopeiae, Cepheid variable, temp. and radius determ. rel. to luminosity and mass 80−90435
OX Cassiopeiae, eclipsing binary, photometric radii and luminosities 80−56877
κ Cassiopeiae, effective temp. radius, mass loss and luminosity 80−51748
AZ Cassiopeiae, long-period eclipsing system, stellar radii ratio from photoelectric obs. 80−46608
TU Cassiopeiae, periods and amplitudes from radial vels. 79−101159
TV Cassiopeiae, revised photoelectric elements *(Russian)* 79−92808
SU and TU Cassiopeiae, short-period Cepheids, photometry and spectra rel. to radius anomalies 80−26864
cataclysmic binaries, circumstellar material geometrical and photometric parameters 80−109492
BV Centauri, dwarf nova and spectroscopic binary, masses and absolute dimensions 80−51775
CW Cephei, eclipsing binary in III Cephei association, absolute dimensions and distance 79−21326
β Cephei, non-radial pulsations detect. attempt 79−40198
VW Cephei, W Ursae Majoris star, rot. line broadening rel. to shape and mass ratio 80−109494
Cepheid masses from observations and pulsation theory 79−48802
Cepheid variables, double-mode, Wesselink radii 80−31311
Cepheid variables, short-period, radial vels., BVRI photometry, radii 80−31309
Cepheids, classical, radii and temps. 78−49446
Cepheids, stellar pulsation problem, time dependent convection local theories 80−72964
XY Ceti, eclipsing binary, masses, radii and luminosities from revised photometric elements 80−109458
o Ceti, vars. in spatial distrib. of 11 micron radiation 79−5828
o Ceti (Mira), diameter apparent var. at 10.2 μm 78−93267
o Ceti (Mira), strong TiO-related dia. vars. 78−16429
ZZ Ceti stars and pulsations, physical props. 79−48781
Z Chamaeleontis, cataclysmic binary, masses radii, and mass exchange rel. to gravit. radiation 80−4386
RS Chamaeleontis, eclipsing binary, four-colour photometry rel. to photmetric elements, absolute dimensions and He abundance 80−67783
Z Chamaeleontis, eruptive binary, model from photoelectric data anal. 80−72961
classical Cepheids, check on light and radial vel. curves phase shift for distance determ. 78−16439

stellar dimensions continued
classical Cepheids, surface brightness and radii *(Polish)* 79−58359
close binary systems, components dimensions and distortion rel. to radial vel. curves anal. 80−90470
close binary systems, mass-radius relation 78−12290
close binary systems with elliptical orbits, components shape, ellipsoid-ellipsoid approx. 79−80338
CoD−38°10980, white dwarf, gravit. redshift rel. to mass-radius relation 78−24511
cool C stars, nearby, distances, luminosities and radii 78−49434
cool stars, effective temps; ang. dias. and reddening determ. from 1 to 5 μm flux curves 79−44458
ε Coronae Austrinae, W Ursae Majoris type star, spectra, radii, masses 79−71069
AI Crucis, eclipsing binary, photometric mass and radius ratios and configuration 80−109459
X Cygni, Cepheid, radial vels. rel. to atmosphere pulsation 78−73723
32 Cygni, eclipsing binary, λ6575 and λ4870 light curves anals. and components radii 79−88700
V380 Cygni, eclipsing binary, masses, radii and luminosities from revised photometric elements 80−109458
V453 Cygni, eclipsing binary in cluster NGC 6871, absolute dimensions and distance 79−21326
P Cygni, effective temp. radius, mass loss and luminosity 80−51748
NML=V1489 Cygni, OH/IR star, 1612 MHz OH maser multibaseline VLBI obs. 80−12766
NML Cygni, power spectrum and dia. from IR speckle interferometry 80−31216
CG Cygni, spectroscopic study of close eclipsing binary 79−97031
V 1668 Cygni (Nova 1978), photospheric radius at max. brightness 80−51789
V1668 Cygni (Nova 1978), temps. and radii from UBV light curve 80−46565
detached double-lined eclipsing binaries, revised photometric elements 78−61886
diameters from photoelec. obs. of lunar occultations 78−7866
distorted stars, Clairaut coordinates and vibr. stability 80−90408
double mode pulsation as resonance phenomenon 79−67015
BS Draconis, BV photometry of eclipsing binary 79−44536
WW Draconis, eclipsing binary, masses, radii and luminosities from photoelectric lightcurves 80−46606
CM Draconis, spotted dM4e eclipsing binary flare star, absolute dimensions and masses 78−12289
BY Draconis, spotted flare star, primary rot. vel. and radius rel. to pre-main-sequence nature 80−36633
BY Draconis stars, photometric radii compared with luminosity class V stars *(Russian)* 78−57564
dwarf Cepheids, masses and radii from obs. of (GD 428) 78−73720
dwarf novae, quasi-periodic oscills. and nonradial pulsations of accretion disks 80−46568
early type companions of X-ray sources, stellar parameters 78−36564
eclipsing binaries, sd-d and R Canis Majoris type, struct. and dimens. 80−82423
eclipsing binary stars, V−R photometry rel. to distances, masses, radii and absolute magnitudes 79−44520
eclipsing double-lined binaries, masses and radii from photometric elements 78−69834
eclipsing variable stars, distortion and light curves photometric perturbations, Fourier anal. 78−12291
eclipsing variable stars, light curves Fourier analysis, appls. to eccentric orbits 79−25630
ν Eridani, β Cephei star, pulsations periods from Fourier anal. of radial vel. changes 80−105246
AS Eridani, eclipsing binary, photometric elements, masses, radii, luminosities 78−28723
flare stars, physical characts. 78−12242
flare stars in solar neighbourhood, physical parameters 80−51777
YY Geminorum, VRI photoelectric photometry and absolute dimensions 78−69827
giant stars, ang. diameters determ. from lunar occultation obs. 79−30054
gravitational radius, equilib. of gravity and elec. forces 80−57152
RS Gruis, dwarf Cepheid in binary system 78−77559
HD 165052, O-type binary, spectroscopic obs., masses and radii 78−93308
HD 167771, O-type binary, spectroscopic obs., masses and radii 78−93308
HD 190603, effective temp. radius, mass loss and luminosity 80−51748
HD 45166, dwarf in Wolf-Rayet clothing, spectrum, radius and envelope struct. 79−5826
HD 49798, H-deficient subdwarf O-type binary, mass, radius and luminosity from non-LTE anal. 79−16978
HD 87892B, nucleus of NGC 3132, luminosity and radius 78−20859
HD 93250, O3 massive star in η Carinae complex, non-LTE analysis 80−77398
HDE 245770, optical counterpart to A 0535+26, dimens. spectral type and luminosity visible obs. 80−72976
u Herculis, BVR lightcurves interpreted 80−41856
DY Herculis, dwarf Cepheid, radial vel. and radius 79−58358
HZ Herculis, eclipsing binary, accretion disc size from optical light curve 78−65658
LT Herculis, eclipsing binary, photometric elements 80−31328
ι Herculis, nonradial pulsations (1975-77) 79−5823
HR 1099, RS Canum Venaticorum binary, radio flaring volume dimensions 79−21330
TT Hydrae, absolute dimensions of β Persei type eclipsing binary 80−62184
EX Hydrae, dwarf nova, accretion disc dimensions from IR and optical light curves 80−67747
χ² Hydrae, eclipsing binary, four-colour photometry, orbital elements, dimensions and He abundance 78−65653
VW Hydri, dwarf nova, accretion disc dimensions from IR light curves 80−67747
IRC+10216, spatial spectra from 2.2 to 20 microns, deviations from spherical symmetry 80−41911
IRC+10420, supergiant star, new OH maser feature struct. and circumstellar shell dia. 79−48946
IRC +10216, C star, far IR size 80−82539
Jeans spheroids with toroidal mag. fields, equilib. and stability 78−45319
10 Lacertae, nonradial pulsations (1975-77) 79−5823
late-type stars, angular diameters from lunar occultations 79−44475
LB 3459, O-type subdwarf plus hot white dwarf eclipsing binary, photometry, anal. 79−48859
ρ Leonis, effective temp. radius, mass loss and luminosity 80−51748
87 Leonis, lunar occultation ang. diameter 79−25599
R Leonis, strong TiO-related dia. vars. 78−16429
υ Leonis (SAO 138298), angular diameter from lunar occultation obs. 78−45332
β Lyrae, radii and masses from light curve, peculiarities of system *(Russian)* 79−97036
RR Lyrae stars, effects of hydromagnetic cycle on photospheric radius and pulsation period 80−105261
magnetic stars, model atmospheres and shapes 79−16973
main-sequence binary stars, Roche consts. and components dimensions 79−35297
ZZ Microscopii, radius of dwarf Cepheid from BV photometry 78−77560
VV Monocerotis, eclipsing binary, orbital elements and dimensions *(French)* 78−89225
Mira variables and IR sources, angular dia. in near IR, 2-5 μm speckle interferometry 80−27010
1 Monocerotis, δ Scuti star, oscill. modes and radius 80−51787
VV Monocerotis, RS Canum Venaticorum eclipsing binary, photometry and geometric elements 79−40218
MXB 1728−34, emission region apparent radius from type I X-ray burst obs. 80−17692
neutron stars, mass and radius with neutrino retention 79−62817
neutron stars, mass-radius relation, obs. constraints, dense matter eqn. of state 80−46597
neutron stars, mass-radius relation 80−77444
neutron stars, radius from superdense neutron matter theory 78−45349
neutron stars, review of nuclear physics 79−92797
non-radial oscillations, linear eigenvalue problem props. study, model 80−17571
nonradial oscills., eigenvalue multiplicity 80−51740
nonradial oscills., modal analysis by asymptotic method 80−21996
nonradial pulsation hypothesis with simulated line profile vars. 80−8618
NP 0532, Crab pulsar, mass and radius from supernova remnant physical theory 80−51834
OB-type stars, effective temps., ang. diameters, distances and linear radii 80−17584
UV Octantis, VBRI obs. of RRab star, radius determ. 79−8928
ζ Ophiuchi, rot.-related spectral vars. rel. to stellar radius 80−22000
optical interferometry with two telescopes *(French)* 80−46403
optical lunar occultation meas., statistically rigorous reduction 78−73650
α Orionis, ang. diameter, speckle interferometry *(Russian)* 78−40922
α Orionis, IR speckle images, two-dimens. obs. *(French)* 80−46553
oscillations of main sequence stars, observability by photometry and spectra 80−51724
AW Pegasi, eclipsing binary, photometric elements, masses, radii, luminosities 78−28723
AG Persei, eclipsing binary in II Persei association, absolute dimensions and distance 79−21326
IW Persei, metallic-line close binary, primary component fractional radius and local metallicity distrib. 80−62186
53 Persei, nonradical pulsator, light var. rel. to line profile changes 80−4362
AI Phoenicis, orbital elements and dimensions of eclipsing binary *(French)* 79−71074
photospheric expansion and macroturbulence, line broadening effects 80−56813
planetary nebulae central stars, temp. and and radius evolution and relaxation, process 80−67724
planetary nebulae central stars, temps., luminosities and radii from UV radiation meas. 78−28679
planetary nebulae nuclei, UV spectra rel. to effective temps. and radii 79−92843
pulsars, size limit for uniformly pulsating EM radiation sources 79−84656
pulsational stability, magnetic field influence 79−53800
pulsations, period determination using phase dispersion minimisation 79−5756
radial and nonradial stellar oscills. effect on light, colour and vel. vars. 80−31310
radial oscills. of magnetic cylinder, matched asymptotic expansions method appl. 79−16817
rigidly rotating star, influence of nonsphericity and radiation press. on moment of inertia 78−28658
rotating, variable stars, period-radius-rot. vel. relation 79−2546
WZ Sagittae, eruptive binary, accretion disc radius from hot spot eclipses anal. 80−72962
FG Sagittae, photometric radius and pulsation mass 78−36576
AQ Sagittarii, C star, ang. dia. from lunar occultation meas. 80−22008
σ Scorpii, β Cephei star, pulsations periods from Fourier anal. of radial vel. changes 80−105246
V701 Scorpii, dimensions and evolution of early-type contact binary 80−62188
ζ¹ Scorpii, extreme B1 supergiant, IUE obs. rel. to mass, radius and bolometric luminosity 80−17583
semi-detached eclipsing binaries, revised photometric masses, radii and luminosities 78−20858
single main sequence stars (A0 V to G2 V), radii compared with radii determined using binary systems 80−51758
speckle interferometry for size and shape determ. 78−77491
speckle interferometry for stellar diameter meas. *(Russian)* 78−40922
SS 433, emitting region dia. and electron density from IR energy distrib. 80−31312
stellar angular diameters and effective temperatures determination, IR flux method appl. 79−92682
surface large-scale pulsations, nonlinear coupling to small-scale deep-seated instabilities 80−62115
γ Tauri, ang. diameter determ. from lunar occultation obs. 80−62119
V471 Tauri, BV photometry of white dwarf eclipsing binary, light curve vars. 78−96508
α and θ¹ Tauri, diameters from Hyades lunar occultations 79−75253
λ Tauri, eclipsing binary, photometric elements, masses, radii, luminosities 78−28723
α Tauri (Aldebaran), angular diameter from lunar occultation 79−40185
α Tauri (Aldebaran), radius from 1978 Aug. 26 occultation fast photometry 79−67005

stellar dimensions continued
RW Trianguli, nova-like eclipsing binary radial vels., dimens. from visible spectra 80−82418
U Trianguli Australis, UBVRI obs. of beat Cepheid, pulsation energy changes 80−4360
3U 1538−52, binary X-ray pulsar, mass and radius of companion 78−16573
Ursa Major stream eclipsing binaries, ages and absolute dimensions 79−92800
W Ursae Majoris stars, A-type, radii and evolutionary state 79−8943
W Ursae Majoris stars, rot. line broadening functions rel. to stellar shapes 80−109494
variable star radius determ. by Wesselink method, appl. to nonradially oscill. star 79−48824
AI Velorum, oscills., pulsation models 79−48813
AH Velorum, radius, delta luminosity and pulsation mode of δ Cepheid 80−46572
AI Velorum, radius and mass from BVRI photometry and photoelectric radial vels. 80−94815
very close binary systems, struct. eqns. including rot. and tidal distortions for ZAMS stars 80−22037
vibrating white dwarfs, ultra-short var. 79−21287
θ Virginis A, pulsating star of unknown type 79−44555
ER Vulpeculae, W Ursae Majoris star, rot. line broadening rel. to shape and mass ratio 80−109494
white dwarf stars, masses and radii from two-colour diagram 80−46547
white dwarfs, mass and radius with neutrino retention 79−62817
white dwarfs, masses and radii of H-rich and He-rich stars 79−35245
white dwarfs, rapid mass accretion and extended envelope form. 80−67723
white dwarfs, virial theorem, energy content and mass-radius relation 78−45327
white dwarfs, visual surface brightness relation appl. 78−81624
white dwarfs mass-radius relation, constraints on gravit. const. 79−25464
X-ray bursters, radius and mass, general relativistic effects 80−8712
OH/IR Type II sources, radial diameters from 1612 MHz OH line obs. 78−36713

stellar evolution
2 to 10 M⊙ stars, effect of heavy element abundance on evolution, struct. of models 80−105231
6 M⊙ star thermal post-main sequence evolution, importance of continuous nuclear spectrum 77−64745
30 M⊙ star, evolution rel. to g^+ modes of high spherical harmonic values 77−9740
A- and F-type stars, absolute energy distribs. and masses rel. to evolutionary tracks 77−17554
accreting main sequence stars, radii 77−17623
accreting neutron stars, He burning shell evolution 80−85968
accreting stars, model IR spectra 78−85934
advanced evolution of massive stars, Si burning 78−28652
AFGL 333, far IR obs., evidence for star form. at ionization front 79−53932
age-abundance relation 77−29813
Algol type star, accretion and chem. struct., evolutionary calcs. 80−109481
Am stars, time scale 77−29849
Am stars in spectroscopic binary systems, evolutionary status, statistical anal. 78−93262
Am-type, binary stars, tidal interaction producing stable atm., evolution 80−67752
AC Andromedae, mass determ. of triple-mode Cepheid 78−93261
AC Andromedae, pulsating variable, mass, luminosity and evolution 77−29845
anisotropic spheres, adiabatic contraction in general relativity 80−36489
anomalous mass stars, evolution on main sequence 80−72929
Ap stars, Barnes-Evans relation appl. as clue to atmospheric struct. and evolutionary status 79−67011
Ap stars in open clusters, rot. vels. rel. to loss of ang. momentum 77−33500
KO Aquilae, eclipsing binary system, evolutionary phase from UBV photoelectric study 80−62198
asymptotic giant branch evolution of intermediate-mass stars, post-second dredge-up phase 80−72936
asymptotic giant branch evolution with steady mass loss 80−26846
atmospheric chemical composition peculiarities rel. to stellar evolution 78−12207
atmospheric physical characts., observational evidence relevant to stellar evolution 78−12205
EO Aurigae, eclipsing binary star, revised elements and evolutionary stages of components 80−90471
axially symmetric star, general relativistic collapse, initial data 80−85960
axion production, astrophys. implications of new light Higgs boson 79−22007
B7 to G4 stars, ages rel. to distrib. perpendicular to galactic plane *(Russian)* 80−73036
B 1 Ia-0 supergiants, mass loss rel. to evolution 79−16948
B-type stars, evidence for form, in R-associations 80−26851
B-type stars formation is interstellar clouds, effects on distrib. of molecules *(Russian)* 80−105321
BD-3°5357, eclipsing binary with hot subdwarf component, evolutionary history 77−91574
Be stars, evidence for evolutionary stage from presence in two open clusters 80−90445
Be stars review, evolutionary status 79−84809
Berkeley 19, anticentre open cluster, age determ. from colour magnitude diagram, BV photometry 80−90486
beta transition rates in hot dense stellar matter 78−73699
bimodal formation, evidence from nearest early-type stars 77−49374
bimodal formation rel. to early main sequence 77−29826
binaries, wide visual, spectral type, age and uvbyβ photometry 80−94833
binary and multiple systems 77−91571
binary fission in damped rotating polytropes 78−93209
binary fission in damped rotating polytropes 79−71016
binary formation, statistical model for the initial stellar mass function 79−48851
binary neutron stars, evolution, gravit. radiation and mass transfer 77−78821

stellar evolution continued
binary star, close low-mass, evolution with mass exchange and gravit. radiation losses 77−53631
binary star orbital elements and run-away vels. caused by symmetric explosion 77−91570
binary stars, binding energy distrib. in cluster, homogeneous cluster model 80−62209
binary stars, close low-mass systems, evolution into contact 77−33557
binary stars, detached, evolution to contact binaries involving mass flow 80−109477
binary stars, low mass, gravit. radiation and evolution 77−57030
binary stars, statistical distrib. and evolution *(Chinese)* 80−85975
binary stars 78−73733
binary stars formation, evidence from q(α), mass ratio distrib. 79−21356
binary stars with mass transfer, particle motion rel. to binary evolution 77−5545
binary system evolution, Roche problem for polytropes in central orbits problem for polytropes in central orbits 80−82179
binary systems, effect of gravit. radiation on evolution and spins 78−12292
binary X-ray sources, spin up as indicator of normal component evolution *(Russian)* 77−74100
bipolar nebulae, photometry and spectra rel. to evolutionary status 78−41026
birth rate rel. to galactic chemical evolution at initial rapid-collapse phase 78−69870
birthrate and nucleosynthetic yields of metals 80−51741
birthrate constraints in solar neighbourhood based on kinematics and star counts 77−29930
blue stragglers, evolution on main sequence 80−72929
blue stragglers as long-lived stars 80−46542
blue supergiant with neutron star immersed in envelope 80−98689
Bok globules rel. to star formation 77−78860
ZZ Bootis, double spectrum eclipsing binary, revised orbital elements and age 78−61885
Brookhaven experiment sensitivity to solar neutrinos, collapsing stars and cosmic neutrinos, ^{37}Cl neutrino absorpt. cross-sections 78−4929
brown and black dwarfs, structure, evolution and missing mass contrib. 79−48800
calculation programme and standard solar model 80−67703
Canis Major R1, optical and IR props. of newly formed stars 78−93332
Canis Major R1, supernova-induced star formation region 77−87494
Canis Major R1 association, supernova induced star formation 78−8063
UW Canis Majoris, absolute dimensions and evolution 79−12496
VY Canis Majoris, mass, luminosity and evolutionary state from relation to mol. cloud complex 78−24536
α Canis Majoris B (Sirius B), coronal model constraints from historical pseudo red giant phase 79−2543
α Canis Majoris B (Sirius B), search for surrounding nebulosity rel. to historical mass loss 78−93242
β Canis Majoris variables, β photometry of early B-type stars 78−77562
β Canis Majoris variables, luminosity calibration and evolution 78−96488
TX Canum Venaticorum, evolution from cataclysmic to stationary P Cygni stage 79−12479
RS Canum Venaticorum binaries, observational selection and evolution 78−89208
RS Canum Venaticorum binaries, possible origins 77−57060
RS Canum Venaticorum binary stars, evolutionary status and orbital parameters rel. to starspot phenomena 80−109488
RS Canum Venaticorum type binaries, evolutionary status 79−67029
RS Canum Venaticorum-type binaries, evolutionary status 77−33570
Carina spiral arm, galactic struct. and star formation, spectrographic and photometric obs. *(French)* 78−89256
QZ Carinae (HD 93206), massive multiple system in great Carina Nebula, case-B mass transfer 79−97027
Cassiopeia A supernova, progenitor, consistent evolutionary picture involving supergiant mass loss 78−36623
TU Cassiopeiae, mass determ. of triple-mode Cepheid 78−93261
AO Cassiopeiae, O-type evolved contact system 78−93302
SU and TU Cassiopeiae, short-period Cepheids, radius anomalies investigations rel. to evolution 80−26864
cataclysmic binaries, evolution and origin 80−56885
cataclysmic binaries, masses and evolution 77−57031
cataclysmic binaries evolution, ang. momentum loss 77−57032
cataclysmic binary formation through common envelope evolution 80−8651
cataclysmic variables, apsidal motion and evolution 79−62834
catastrophe theory of nonlinear dynamical stability 79−8906
V553 Centauri, C rich Cepheid, C and N abundances rel. to nuclear processes and evolutionary status 80−4378
SV Centauri, early-type contact binary, evolutionary models 80−4403
SZ Centauri, eclipsing binary, photometric elements and evolutionary stage 77−41391
ω Centauri, near IR photometry, giant branch struct. 77−41397
ω Centauri giant branch, mixing versus primordial abundance vars. 77−17640
α Centauri triple system 78−45356
Centaurus X-3 and related binary X-ray sources, origin 77−29954
β Cephei stars, effects of mass loss on instability strip 80−90436
β Cephei stars, pulsations and evolutionary status 80−85959
β Cephei stars, radiation pressure and pulsational instability 79−84806
β Cephei stars, search in open cluster NGC 4755, evolutionary stage determ. 79−8921
β Cephei stars, theoretical models, evolution and pulsation 77−13347
Cepheid instability strip 80−56833
Cepheid variables, intrinsic colours rel. to amplitudes, periods and evolution 79−84797
Cepheid variables, rot. and convection effects rel. to evolutionary and pulsation masses 78−93249
Cepheids, anomalous, in dwarf spheroidal galaxies, binary system model 77−45451
Cepheids, double-mode, surface He enhancement, linear theory period ratios 79−67021
Cepheids, evolution of normal and double mode variables 77−87428
Cepheids, freq.-period distribs. in Local Group galaxies 78−28694
Cepheids, membership in open clusters from star and cluster age determ. *(Italian)* 80−90489
Cepheids, period-age relation 79−21317
Cepheus A mol. cloud, OH maser lines obs., star form. region 80−36691
chemical evolution, stellar lifetimes and abundance ratios 79−53801

stellar evolution continued
chemical evolution rel. to galactic evolution and nucleosynthesis 80−67847
chemical history in solar neighbourhood 77−91635
chromospheric K-line emission on H-R diagram, absolute fluxes 77−56937
circular binaries, effect of instantaneous mass ejection on orbital elements 77−57026
circumstellar disks and planetary formation 79−58321
close binaries, form. by two-body tidal capture 77−33556
close binaries, intermediate mass, mass transfer for different stars within evolutionary scheme 80−109476
close binaries, orbital angular momentum loss during evolution 79−97033
close binaries, struct. and evolution 77−57019
close binaries, synchronous systems devel. from tidal are rot. interactions 80−109468
close binaries, unsteady mass loss 77−57049
close binaries and the evolution of star clusters 79−5863
close binaries formation, fission hypothesis 78−32334
close binary stars, low mass, evolution, gravitational wave emission influence 80−82425
close binary stars evolution, mass transfer effects on props., obs. and theory comparison 80−62187
close binary systems, neutron stars tidal disruption by black holes 77−13387
close binary systems with neutron star components, evolution *(Italian)* 79−21354
close low-mass binary systems, evolution, unsteady mass loss, contracting secondary star 77−17617
cluster core collapse, theory 79−84829
cluster dynamics, evolution and statistical methods *(French)* 77−71133
cluster models with continuous stellar mass loss, dynamical evolution 80−82438
clusters, dynamical evolution with multi-mass populations *(Italian)* 77−91584
clusters of stars, common origin of stars and gas from superdense protostellar matter *(Russian)* 77−82286
cocoon stars, evolution and IR spectra 77−64824
cocoon stars, radiative overstability in accretion 78−85932
CoD −35°C 10525, bright YY Orionis star, spectrum and evolutionary age 78−36566
cold white dwarf, gravitation collapse 77−17568
collapse, adiabatic hydrodynamics and shock wave propag. 80−56861
collapse, gravit. radiation burst 77−53571
collapse, rate in Galaxy 77−71122
collapse, triggering by thermonuclear burning in degenerate C core 78−65608
collapse and black hole limit, dynamical view 79−30081
collapse and explosion, massive star core hydrodynamics 79−16995
collapse and transport supernovae with neutrino degeneracy 78−40977
collapse generating gravitational radiation, strength estimate 80−46584
collapse of hot dense matter 79−16996
collapse of massive star cores, supernova explosion from shock heating 80−56863
collapse under gravitation, equation of state 79−97014
collapsed core, neutrino prod. of bypassed isotopes, neutrinos role in nucleosynthesis 79−40182
collapsed stars, mass loss during form. rel. to slow rot. 78−49426
collapsing core, shock struct. and neutrino radiation, rel. to supernova explosions 78−49427
collapsing cores and supernovae 79−62815
collapsing relativistic stars, radiation, linearized even-parity EM and gravit. radiation 79−75228
collapsing rotating gaseous ellipsoid, gravit. radiation 77−53572
collapsing star, neutrino degeneracy and downscatt. effects on neutrino radiation 79−12463
Collinder 140, young open cluster, age from spectroscopic study rel. to membership statistics 80−62211
common envelope binaries 77−57025
compact far IR source in W31 region assoc. with G10.6−0.4, early stage of stellar evolution 78−49504
compression into disc, gravit. radiation *(Russian)* 77−13325
condensation formation of primary gas, HD cooling effects *(Russian)* 77−33623
contact binaries, cyclic thermal instability 77−57050
contact binaries, evolution rel. to light curve and period changes 77−57054
contact binaries, evolutionary tracks 77−57053
contact binaries, mass and energy flow 79−48850
contact binaries, solar type, ang. momentum controlled evolution 80−36670
contact binaries, solar type, mass ratio evolution function rel. to initial mass ratio distrib. function 80−109496
contact binaries, transport processes in envelopes 78−4279
contact binaries of low mass, evolutionary fate 77−2453
contact binaries with age-zero components, secular stability 80−67786
contact binary star, idealised dynamical evolution *(French)* 80−62199
contact systems, massive zero-age binaries 77−57058
convection and stellar models and evolution computation 78−89194
convection phenomena numerical simulations 77−29789
convective envelope stars, value of mixing length rel. to stellar evolution sequences 80−77379
convective regions, proton-proton chain 77−29799
convective stars, forced mixing effects on evolution 80−56818
convective zone boundaries 78−89187
cool C stars, nearby, distances and evolutionary status 78−49434
cool giant stars, nuclear processes and mixing from obs. and anal. of CO at 5 μm 78−36569
cool stars, mass loss, review *(German)* 79−16957
cool stars, supersonic stellar winds and rapid mass loss rel. to evolution 79−21268
core collapse, effects of nuclear forces, partition function and dissoc. 79−48833
core collapse, ellipsoidal model calcs., gravitational and neutrino radiation 79−53802
core collapse, limits on nuclei excitation energies in hot matter 80−56703
core collapse, neutral currents and neutrino Comptonisation in high-temp. nuclear matter 80−21905
stellar evolution continued
core collapse, neutrino prod. and inelastic scatt. by nuclei at extreme temps. 80−36488
core collapse, role of neutrino dissipation 79−101166
core collapse, Thomas-Fermi model of warm nuclei 80−51648
core collapse, time-dependent neutrino transport theory 80−94783
core collapse, vacuum neutrino oscills, inhibition by high matter density 80−36496
core collapse and overturn with Rayleigh-Taylor unstable gradient 80−94819
core collapse outcome, effects of core eqn. of state 80−85928
core collapse to neutron star, electron neutrino and antineutrino emission, spectral calcs. 80−109454
core He burning stars, H profile, previous mixing and loops in H-R diagram 77−29792
core He flash and C and CH star origins 78−4190
core He-burning and convective shells of massive stars 78−93207
core-mantle mixing rel. to evolution, currents penetration of mol.-weight barrier 77−33474
S Coronae Austrinae, bright southern YY Orionis star, spectroscopic obs. rel. to evolution 77−29818
β Coronae Borealis, mag. deform. ot evolved stellar model, hypothesis 79−30076
cosmic masers and star formation *(German)* 79−58410
CRL 3099, highly evolved C star, IR photometry and spectrum 78−49436
cycle of star formulation and death 79−58318
V460 Cygni, cool C star, 3α process rel. to C prod. and $^{12}C/^{13}C$ ratio 78−93223
V1016 Cygni, proto-planetary nebula mass ejection rel. to photometric and spectroscopic evolution 78−85947
CH Cygni, red giant, He shell flash rel. to mag. field interpretation for outburst 78−4250
V1016 Cygni, single star model, possible forming planetary nebula 77−60762
V1500 Cygni (Nova 1975), spectral evolution 77−87447
DA white dwarfs, atmospheric parameters and mass distrib. 79−88655
dark clouds and cocoons, rel. to star form. *(French)* 79−67087
dark nebulae and globules, star form. regions 78−12347
degenerate C core, thermonuclear explosion problem 78−28669
degenerate C cores, microstruct. of detonation waves 79−62810
degenerate C ignition, burning front propag. rel. to core implosion or disruption 80−77390
degenerate star, propagating slow deflagration front struct. and evolution 79−84790
degenerate stars, photometry and spectra rel. to evolution 78−12224
degenerate stars with H atmospheres, cooling law from space freq. 80−17576
HR Delphini (Nova 1967), photoionisation models, binary system evolution 80−17590
HR Delphini (Nova 1967), spectral evolution during decline 77−87440
dense clusters, evolutionary tracks *(Russian)* 78−69852
dense stars, ang. momentum loss by neutrino emission 77−49371
dense stellar matter, diffusion approx. to neutrino transport 78−93096
detached double-lined eclipsing binaries, photometric elements and evolutionary stages 78−61886
disrupted the star in close binary containing neutron star, model for Crab Nebula 79−25696
S Doradus, Hubble-Sandage variable in LMC, effect of mass loss on evolution 80−101595
double core evolution, of 16 M⊙ star with 1 M⊙ neutron star companion 78−53980
double mode Cepheids, masses and radii 77−82236
double shell source stars, evolution through second loop in Hertzsprung-Russell diagram 78−36556
BC Draconis, double-mode Cepheid, mass, luminosity and evolution 77−29845
BY Draconis, prototype spotted flare star, pre-main-sequence nature 80−36633
BY Draconis stars, angular momentum initial distrib. and evolution 80−85954
BY Draconis stars, photometric radii rel. to ages *(Russian)* 78−57564
dust cloud in Corona Austrina, mm wavelength obs., nonhomologous collapse, rel. to star form. 79−30102
dust-embedded protostar in Sharpless 140, compact source, strong far IR emission obs. 78−36649
dwarf Cepheids, double-mode, theoretical periods masses and evolutionary stage 79−44488
dwarf Cepheids, mass and evolutionary stage from obs. of (GD 428) 78−73720
dwarf Cepheids evolutionary stage, anal. and conclusions 80−46562
dwarf stars, evolution rel. to chromospheric models and activity 79−48773
dwarf stars, K- and M-type, space motions rel. to stellar age 78−69846
dynamical r-process, nuclei far from β-stability 77−26004
early type stars, mass loss 78−69796
early-type stars near Sun, space vels. and ages 78−61858
eclipsing binary stars, period statistics rel. to form. and evolution 80−36662
Einstein's field equations, solns. for static fluid spheres, relativistic polytrope anal. 79−12669
in elliptical galaxies, evolutionary synthesis of late M giants stellar population, comp. effects 78−57626
in elliptical galaxies, form. and mass range 77−33636
elliptical galaxies formation model, stellar population explosions 79−35388
energy loss rate due to electron capture in highly evolved stars 77−64752
envelopes, light element decay 78−12214
exploding or collapsing magnetized rotating spheroid, mag. dipole radiation 79−35106
explosion models, new solns. 80−12751
explosions, radial gas oscills. after shock wave passage *(Russian)* 79−8903
explosions, Rayleigh-Taylor instability 78−36551
explosive nucleosynthesis, massive star evolution preceding and during supernova, element abundances *(German)* 79−44469
explosive r process cooling process 78−69791
extreme Population II stars, H-R diagram and age difference from oldest Population I stars 77−56912
extremely metal-poor stars, theoretical evolution 78−28677

stellar evolution continued
fast nova model evolution from pre-explosion to decline 79−35273
final evolution of stars *(Italian)* 79−53805
final phases, rel. to supernova phenomenon *(Italian)* 79−88646
first generation stars, form. during fragmentation of cosmic gas clouds 77−33628
flare stars in Pleiades, possible cyclic recurrence of flare activity *(Russian)* 78−49443
fluid drops as cosmological models, stellar evolution, solar system origin, planetary geology 80−73086
formation, angular momentum considerations 78−69781
formation, brightening of star associated with variable cometary nebula 78−4333
formation, collapse dynamics and models 78−32566
formation, cosmic gas clouds fragmentation rel. to initial stellar mass function 77−56907
formation, dark cloud evolution, role of magnetic fields 77−67117
formation, early stages 78−32452
formation, gravit. instability of interstellar magnetised gaseous discs 80−4424
formation, H_2O maser phase and galactic distrib. 79−35343
formation, Hα emission line star obs. 79−58333
formation, hydrodynamic model reviews *(Polish)* 80−67709
formation, IAU Symposium 75 (Geneva, 1976 September 6-10) 78−32561
formation, implication of blister model for H II regions and CO clouds 79−25681
formation, in M104 (Sombrero galaxy), peculiar mass spectrum 77−17675
formation, in shock-compressed layers 78−40919
formation, in spiral galaxies, rel. to density wave theory 77−2468
formation, IR obs., review 78−7988
formation, magnetic braking 79−58319
formation, magnetic braking 79−58320
formation, maintenance of spiral structure in galaxies *(Chinese)* 77−60830
formation, observational studies 78−93215
formation, of binaries with nearly identical components 79−48856
formation, predictability limit for collapsing isothermal spheres 79−75088
formation, protostar interaction with infalling matter, interstellar grains origin 77−13327
formation, protostellar cloud ang. momentum problem, mag. breaking 80−82342
formation, radio obs. 78−32565
formation, rel. to ambipolar diffusion in interstellar clouds 79−40237
formation, rel. to var. of rot. vels. of early B-type stars with galactocentric distance 77−56929
formation, role of grain motions 78−69788
formation, role of interstellar gas, dust and molecules 78−54006
formation, role of ionisation-coupled acoustic instability 79−97044
formation, role of supernovae 80−82232
formation, shock-induced in H II region NGC 281, obs. of shock 79−25688
formation, stable shapes for axisymm. gravitating incompressible fluid body 77−53414
formation, supernova trigger 80−26891
formation, theoretical processes 78−32453
formation, thermal instability in nonstationary medium 79−21178
formation, two dimensional collapse calcs. for cylindrical interstellar clouds 79−40247
formation, unified theory for objects from meteors to stars 77−9739
formation activity in irregular galaxies 79−9001
formation and dark globules 79−58398
formation and early evolution in NGC 1333, colliding molecular clouds 80−12757
formation and evolution, role of UV obs. *(Italian)* 78−32446
formation and interstellar gas density in Galaxy 78−86008
formation and interstellar matter *(German)* 79−84787
formation and large-scale phenomena in Galaxy 78−32583
formation and protostellar clouds, review 80−101589
formation around galactic longitude 111°, H II regions aperture synthesis obs. 77−64827
formation at galactic centre, rel. to extended thermal radio emission ionisation 79−97059
formation before galaxies, missing mass soln. 78−57654
formation by interstellar grain clouds gravit. contraction 77−53575
formation by spherical gravit. collapse of interstellar clouds, unsteady hydrodynamics 78−45212
formation by spiral density wave in disc of Galaxy 80−12812
formation evidence from bright star clusters round NGC 5253, visible obs. 80−77489
formation from collapsing gas sphere, nonlinear development of gravitational instability 80−62114
formation from gas cloud, three-dimens. collapse and fragmentation 78−77552
formation from globules, evidence from microwave spectral lines obs. 78−57609
formation from hot matter with primordial chemical comp., role of H_2^+ mol. ion *(Russian)* 78−40924
formation from mol. and at. cloud-cloud collisions 80−94844
formation from rotating gas clouds, gravit. axisymm. adiabatic collapse 78−7875
formation from rotating interstellar cloud collapse, isothermal rings fragmentation 78−93205
formation in barred galaxies rel. to nucleus activity 80−105341
formation in blue galaxies, theory 78−12356
formation in bright galaxy nuclei, spectra anal. 80−98708
formation in Cepheus IV region, continuum and recomb. lines, SHF obs. 80−90501
formation in Cepheus OB3 and Perseus OB2 mol. clouds, evidence from mol. obs. 80−12798
formation in Cepheus OB3 association induced by supernova 78−12306
formation in Cepheus OB3 mol. cloud complex 78−28750
formation in clusters, mass distrib. law of protoclusters fragments systems 79−44571
formation in disk galaxies 80−82483
formation in dust clouds with bright nebulosities 80−56893
formation in early Galaxy, evidence for active phases *(Russian)* 77−74141
stellar evolution continued
formation in expanding molecular shell surrounding Pelican Nebula H II region, evidence from CO obs. 80−105296
formation in faint galaxies, spectrsocopy and photometry rel. to evolution 80−105353
formation in galactic cluster 79−62878
formation in gas clouds in elliptical galaxies 80−67868
formation in gas complexes *(Russian)* 79−35391
formation in Gum Nebula, Herbig-Haro and Hα emission objects obs. 77−29821
formation in H II region NGC 7538, results from IR study 79−84842
formation in II Zw 70, optical and radio data 79−16935
formation in inner Milky Way, evidence from CO obs. of interstellar mol. clouds 80−4425
formation in M17 region, rel. to struct. of assoc. extended mol. cloud 77−37635
formation in M82, implications for exploding galaxy model 79−75279
formation in M82 and NGC 253 nuclei, model constraints 80−82485
formation in M8 (Lagoon Nebula), evidence from far IR obs. 80−4413
formation in mol. clouds assoc. with Herbig Be/Ae stars, LkHα 198, BD+40°4124, NGC 7129 78−32542
formation in NGC 6649, anomalous open cluster 79−5866
formation in NGC 7129 region, CO mol. line and far IR obs. 79−17043
formation in non-elliptical galaxies, galaxy two colour diagram 80−67875
formation in open clusters and associations 79−21365
formation in photometry of remote clusters 80−105364
formation in primaeval galaxies, high luminosity epoch 80−105354
formation in Taurus dark cloud complex, IR photometry results 79−8963
formation in Taurus Molecular Cloud 1 in Heiles' cloud 2, molecular radio obs. 78−69858
formation in young cluster IC 5146; evidence from CO obs. 79−48881
formation induced by galactic density wave 80−17649
formation mechanisms and galactic evolution 80−12811
formation near ESO 210-6A southern globule 79−21399
formation of massive stars in Local Group galaxies 79−30053
formation of solar-type stars in spherical symmetry, accretion shock effects 80−62107
formation rate, rel. to galactic extended low-density H II region and diffuse IR emission 79−17047
formation rate and ionising Lyman continuum photon flux 80−67711
formation rate in case of irregular galaxy NGC 6822, correl. with surface density 78−20889
formation rate in galaxies and extragalactic background light 78−36687
formation rate in inner Galaxy, IR obs. 80−67704
formation rate in M83 and Milky Way 80−51870
formation rates and IR radiation in galaxies 78−49526
formation rates calc. in Galaxy 78−61919
formation regions, IR obs. 78−32564
formation regions, IR spectroscopy of assoc. lineless objects 79−44586
formation regions, southern H II regions and assoc. mol. clouds 79−35353
formation regions near SNR W44, IR obs. 79−58399
formation regions structure, population categories and mol. clouds evolution 80−17645
formation rel. to spiral galaxies irregular struct. 77−13450
formation rel. to spiral galaxy types Sab to Scd luminosity freq. distrib. 80−82482
formation through accretion shock, model for H II blisters 80−21994
G128-7, cool DA white dwarf, atmospheric parameters and evolutionary consequences 80−62126
G-K giants and C stars, origin of $^{12}C/^{13}C$ ratios freq. distrib. 77−78780
G-type dwarfs, macroturbulence and age anticorrel. 78−93226
galactic centre, energy balance, star formation 78−81684
galactic density wave, molecular clouds and star formation 78−8088
galactic density waves influence on star form. rate 79−88743
galactic disc chemical evolution and radial metallicity gradient 77−29937
galactic disc dwarf stars, evolutionary effects on metal abundance distrib. 79−88733
galactic neutrino sources, expt. neutrino astronomy, test of stellar evolution theories 77−70964
in galaxies, review 80−77486
gas cloud collapse, fluid-in-cell method 77−5523
gaseous nebulae, radiospectroscopy 79−58408
gaseous sphere contraction vel., virial-based soln. 79−48665
general relativistic stellar evolution code 79−58317
giant stars, ages determ. via photoelectric MgH+Mgb index 80−12753
giant stars, internal mixing rel. to strong CN phenomenon 78−53921
giant stars, mass loss before envelope ejection due to pulsational instability 80−72935
giant stars, microturbulence rel. to evolution 78−81625
giant stars, Population I, evolution from ZAMS rel. to theoretical surface abundances 80−94796
giant stars as progenitors of planetary nebulae, struct. anal. form. 80−109537
giant stars in M13, M92, NGC 6397 and M15, evolution rel. to weak-G-band effect 77−78778
giant stars in M3, M13, M92 and M67, IR photometry comparison with evolutionary tracks 78−57595
giant stars in open cluster NGC 7789, metal abundance, He content and mass loss 80−31335
giants of late-type, molecular envelopes and planetary nebula origin 78−40940
GL 2591, protostellar source, 3 μm ice absorpt. band, linear polarisation obs. 80−105303
GL 2636, star form. region in Cygnus-X, IR obs. 80−105302
globular cluster age differences rel. to chemical evolution 79−80340
globular cluster stars inferred ages, effects of He settling 80−73013
globular cluster X-ray source, evolution of 100 M$\odot$ black hole in binary 78−61932
globular clusters, ages and comp. rel. to fundamental knowledge about galaxies evolution 80−90488
globular clusters, evolutionary model sequences, ages 77−87487
globular clusters, formation and evolution 77−26031
globular clusters, models, props. based on stellar evolution and cluster structure 80−62210
globular clusters, theoretical isochrones, tables 79−71081
globular star cluster, relax. degree and evolution, appl. of N-body system numerical integration 80−67808

stellar evolution continued
globular star cluster age and distance determ. using subdwarf photometry results 80−82435
globular star clusters, dynamic evolution, review of obs. and numerical theories 78−77585
gravitational collapse, comp. and eqn. of state of thermally dissociated matter 77−33476
gravitational collapse, ellipsoidal models and gravit. radiation 78−45317
gravitational collapse, hydrodynamics 78−45318
gravitational collapse, maximal time slicing condition 80−67554
gravitational collapse, neutrino ang. momentum losses 77−56916
gravitational collapse, neutrino trapping effect on nucl. dissoc. 80−90407
gravitational collapse, neutronisation and lepton escape rel. to hydrodynamics 80−77388
gravitational collapse, theory 80−77389
gravitational collapse, weak interactions and supernova outbursts 77−87464
gravitational collapse criteria for mass ejection 77−33534
gravitational collapse of core of massive star, neutrino trapping 78−32437
gravitational collapse of rot. gas cloud, binary systems form. 78−65494
gravitational collapse of spherical star without rotation *(French)* 79−93016
gravitational collapse to neutron stars and black holes, computer generation of spherical spacetimes 80−46385
gravitational construction phase, mass outflow mechanisms 77−53579
gravitational contraction of protosun and Laplacian gas ring shedding 79−62765
gravitational instability role in galaxy and star form. theories *(Czech)* 80−41718
gravitational radiation detection from stellar collapse 78−24707
gravitationally unstable isothermal spheres, collapse, star form. appl. 78−32332
H-H 2, condensation H, spectrophotometric data 79−62826
H-R diagram, IAU Symposium 80 review 78−96511
H-R diagram, stellar evolutionary tracks 78−81619
H-R diagram boundary for chromospheres and convection theory 80−56823
halo star origin and globular cluster evolution 79−58388
HD 128220, peculiar spectroscopic binary, photometric separation rel. to evolution *(French)* 77−57014
HD 166734, Of binary system, evolutionary state, visible obs. 80−82414
HD 47732, young close binary in NGC 2264, photometry struct. and evolution 78−57575
HD 49798, H-deficient subdwarf O-type binary, non-LTE anal. and evolutionary state 79−16978
HD 49798, strange composite sdO star, evolution and nature of companion 78−49435
HD 92740, spectroscopic binary WN7 star, obs. rel. to evolution 79−8924
HD 93250, O3 massive star in η Carinae complex, non-LTE analysis 80−77398
heavy and neutron-rich elements synthesis by rapid neutron capture process 78−77488
heavy element, origin in star development supernovae and galactic matter *(German)* 79−44468
heavy element abundance effect on evolution 78−89167
Henyey-type evolution code, appl. to stars with shell energy sources 78−61848
Herachel 2621, multiple star, intermediate-band photometry rel. to advanced stellar evolution 78−53934
Herbig-Haro objects, Fe abundance 79−62826
Herbig-Haro objects, shock wave interpretation of individual condensations 78−45324
Herbig-Haro objects associated with NGC 2264 young cluster 79−71026
Herbig-Haro objects in Gum Nebula, spectrophotometry 78−36565
Hercules X-1 (HZ Herculis) binary system, pre-supernova parameters 80−62318
α^1 Herculis, absolute magnitude, evolutionary state and mass loss 78−7997
DY Herculis, dwarf Cepheid, uvbyβ photometry and evolutionary status 79−58357
Hertzsprung-Russell diagram, discovery, meaning, development appl. 78−45322
high mass stars, evolution including stellar wind effects 80−21982
homogeneous ellipsoidal figures evolution 77−33333
horizontal and asymptotic branches in globular clusters 78−81613
horizontal branch stars, evolution with semiconvection, models 77−17540
hot massive stars, stellar wind mass loss, evolution study 80−17578
hot neutron star formation, neutrino radiation rel. to envelope outburst problem. 78−45350
hot white dwarfs with masses over Chandrasekhar limit 77−17567
HR 1099, RS Canum Venaticorum variable, visual companion rel. to evolution 77−9754
HR 3126, peculiar M giant in reflection nebula, mass loss 77−17558
HR 3153, young cluster M giant, mass loss 77−17558
HR 6392, very high-luminosity binary star, evolution 77−45493
Hyades stars, models rel. to cluster distance modulus, turnoff mass and age 77−57067
χ^2 Hydrae, eclipsing binary, four-colour photometry, dimensions, He abundance and age 78−65653
AI Hydrae, light curves and photometric elements of eclipsing binary 78−65652
HZ 22 (UX Canum Venaticorum), hot subdwarf binary, evolution and mass 79−12472
IC 361, open cluster, preliminary photometry, distance and age 78−89228
ideal Fermi gas, thermodynamics and eqn. of state 77−30117
ε Indi moving group, detailed anal. of members HD 40409, HD 102365 and λ Aurigae 78−85982
initial mass function nonmonotonous *(Russian)* 79−40181
instability due to local mixing length approx. 77−53569
intermediate-mass stars asymptotic giant-branch evolution as function of mass and comp. 80−12749
interstellar clouds, rotation rate, connection with binary star periods 77−33584
interstellar clouds angular momentum problem and mag. braking, time independent soln. 79−62884
interstellar cold gas clouds with mag. field gravit. contraction, star form. 78−8102
stellar evolution continued
interstellar dark clouds with assoc. young stellar objects, radio obs. of mol. lines 79−58390
interstellar magnetic clouds fragmentation by ambipolar diffusion, star formation 77−91608
irradiated stars in active galactic nuclei, mass loss and evolution 80−56949
in irregular and blue compact galaxies, evolutionary models rel. to galaxies chemical comp. 80−36711
K1211, blue straggler in NGC 7789, evolution status and mass, photometry obs. 80−109433
L 183 (L 134 N) dust cloud, evolution of condensations 80−105307
late B-type stars, early evolution rel. to rot. and HgMn stars duplicity 78−89199
late B-type stars with low-mass companions, previous mass-transfer stage 78−57547
late-type stars, gravit. phase transitions 77−49380
late-type stars of solar neighbour emission with age 80−109423
late-type supergiants, evolution rel. to CNO abundances 78−24509
LB 3459, subdwarf eclipsing binary, evolutionary model 80−51808
δ Librae, Algol-type eclipsing binary, main-sequence primary and evolved secondary 78−49475
lifetime of binary stars 79−44563
lifetimes, effects of interaction with dense interstellar gas glouds *(German)* 80−109500
LMC, blue to red supergiant star ratio across face, rel. to star form. 80−26984
LMC central regions, stellar count-brightness ratios rel. to population struct. 78−89245
long-period variables, mass loss and circumnebular shells form. 78−8014
low mass close binary evolution, catastrophic mass loss 77−33554
low-mass stars formation, evidence from NC_5N and NH_3 obs. in Taurus 80−26957
lower main-sequence stars, age-rot. vel. rotation 80−51767
luminous stars in M31, evolution from studies in Baade's Field IV 80−36622
α Lyrae (Vega), mass, chemical comp. and age 77−33495
β Lyrae evolution, accretion onto ZAMS secondary and contact binary stage 79−66994
M11, galactic open cluster, age and distance, colour diagram, photometric obs. 80−73012
M33, density wave motion obs. evidence from star form. and evolution 77−45552
M51, spiral arm struct. and star form. 78−73762
M67, evolved stars distrib., evidence for mass loss 77−13408
M67, open cluster, gap in Hertzsprung-Russell diagram, comparison with evolutionary models 78−24530
M67 main sequence stars, effects of evolution on differential blanketing rel. to Hyades and Coma 78−57597
magnetic variable Ap stars, light vars., rot. and evolution 77−87426
magnetic white dwarf in binary system, collapse, mass ejection, nova mechanism 78−32485
main sequence stars, element abundance regularities rel. to nucleosynthesis *(Russian)* 77−45431
main sequence stars, single, (A0 V to G2 V), evolutionary effects on radii 80−51758
main sequence stars in close binary systems, rapid mass accretion effect 77−91578
main-sequence binary stars, evolutionary models rel. to Roche consts. 79−35297
main-sequence stars, comparison of four-colour photometric obs. with evolutionary models 78−8007
main-sequence stars, effects of mixing on CNO isotopes in red giants 77−33475
Markarian galaxies origin of radio and optical radiation 77−17682
mass loss, fate of loss material in galactic nuclei 80−67858
mass loss, rel. to white dwarfs form. 80−77281
mass loss by hot stars, review *(German)* 79−16958
mass loss by stellar wind, effect on Galaxy chemical enrichment 80−41814
mass loss effects on dynamical evolution of large star clusters 77−64807
mass loss in stars of moderate mass by stellar wind 78−12210
mass loss rates, constraints from white dwarf data 80−46548
massive accreting white dwarfs in close binary systems, H shell flashes 79−75203
massive Algol-type systems, evolutionary status 77−57047
massive close binaries, evolution of systems with primaries of 10-15 M$\odot$ 77−87473
massive close binaries, post-supernova stage, tidal instability 77−57024
massive close binaries evolution, final considerations for conservative case 78−49479
massive close binaries inc. wind mass loss, evolution 79−44527
massive close binaries with OB components, evolutionary calcs. comparison with obs. 80−90474
massive close binary stars, effect of stellar evolution on components synchronous rot. 80−62192
massive close binary systems, late evolutionary stages 77−57023
massive close binary systems 77−57022
massive clusters, dynamical evolution 79−48866
massive He burning stars losing mass by stellar wind, evolution rel. to Wolf-Rayet binaries 80−36615
massive luminous stars, stellar winds effect on evolution 79−12467
massive main-sequence star, early evolution 80−62113
massive protostellar clouds, dynamical evolution 77−17543
massive single stars, main sequence evolution with and without stellar wind 79−16936
massive star evolution rel. to Hubble Sequence 77−91651
massive star formation in open clusters 78−28660
massive stars, 10^3-10^4 M$\odot$ range, final evolution 77−87371
massive stars, birth 79−2542
massive stars, bulk yields of nucleosynthesis 78−36552
massive stars, early mass loss and transition WR star evolution 79−48775
massive stars, effect of convective and semiconvective mixing on evolution 80−90405
massive stars, effects of binary evolution on heavy elements prod. 80−46534
massive stars, evolution in Galaxy and LMC 79−101191
massive stars, evolution with mass loss by stellar wind 78−4197
massive stars, gravity modes vibr. stability during H shell burning stage 77−56933

stellar evolution continued
massive stars, mass loss and convective overshooting influence on evolution 79−84789
massive stars, single and binaries, review 80−82343
massive stars (20-100 M⊙) with mass loss 78−36554
massive stars (M≳50 M⊙), evolutionary status, mass transfer model *(Russian)* 80−109425
massive stars evolution, critical mass loss rates for Wolf-Rayet stars prod. 79−101138
massive stars evolution, observational review 80−90416
massive stars formation in dense molecular clouds, radio and IR appearance of dusty H II blisters 80−85979
massive stars losing mass and ang. momentum, evolution 79−25591
massive stars main-sequence evolution, effects of mass loss 78−93200
massive stars nucleosynthesis, effect of mass loss on chemical yields 80−36614
massive stars presupernova evolution 79−16930
massive X-ray binaries, evolution of optical components 80−41857
massive X-ray binaries, OB stars, evolutionary influence of stellar wind 79−101172
matter distribution in nuclei far from β stability valley, charact. features 77−64635
Melotte 66, oldest open cluster, colour-magnitude diagram rel. to age 80−17621
TY Mensae, contact eclipsing binary, evolutionary stage from UBV light curve anal. 80−105278
metal rich stars, zero age main sequence position 80−109426
metal-poor binaries, He abundance determ. 78−81660
metal-rich horizontal branch stars 77−45466
metallic line (Am) stars, evolution and pulsation rel. to metallicism 78−49448
metallicity distribution in old stars and effect of dust accretion 77−29795
microturbulence behaviour with evolution 78−12206
Mira variables, envelope pulsational instability rel. to planetary nebula form. 80−26928
Mira variables, mass loss and red giant stars evolution 77−17571
Mira variables rel. to Wood-Cahn model of late stellar evolution 78−45333
model computations for mass and age determ. *(French)* 79−2541
models, effect of gravitational const. var. 80−82186
molecular clouds, critical mass rel. to supernova phase 77−78770
Monoceros OB2 association, evidence for supernova-induced star form. 80−31334
multiple star formation by dynamical interaction in clusters 79−44567
multiple star formation from N-body system decay 79−44569
multiple star system formation from rotating interstellar clouds 78−93366
multiple stars, dynamical evolution from small galactic clusters 79−44568
multiple stars, IAU Colloquium 33, proceedings (Oaxtepec, Mexico, 13-16 October 1975) 79−44539
multiple stars, origin by condensation in dense nebulae 79−44565
MWC 349, planetary system formation *(German)* 79−53832
neutrino angular momentum loss by Poynting-Robertson effect 79−16928
neutrino bremsstrahlung by degenerate electron gas, neutral current effects 77−13225
neutrino bremsstrahlung in an intense magnetic field 79−30055
neutrino chemical potential and heat cond. with allowance for scatt., collapsing stars appl. 79−84657
neutrino opacity, pure neutral vector boson contrib. 78−53928
neutrino transport calcs. using neutron transport methods 77−87377
neutrino transport in supernova models, multigroup diffusion scheme 79−25590
neutron gas interactions at high density and temp., supernova models appl. 77−33330
neutron star, episodic accretion of gas and cosmic Γ-ray bursts 78−69824
neutron star binaries formation rel. to gravit. radiation 79−35291
neutron star X-ray emission models 80−62175
neutron stars, cooling 80−77443
neutron stars, form. rate in Galaxy, estimated from stellar statistics 79−40208
neutron stars, form. rel. to mass constraints 77−5543
neutron stars, general relativistic eqns. 77−33471
neutron stars, in close binary systems, X-ray source model *(German)* 79−84814
neutron stars, neutrino cooling in pion-condensed phase 78−45351
neutron stars, nuclear energy release and X-ray emission 77−78814
neutron stars, quark beta decay and cooling 80−82406
neutron stars, role of neutrinos and antineutrinos in formation and cooling 78−8038
neutron stars, structure, stability, and normal-abnormal transition 79−71063
neutron stars cooling, calcs. 79−101170
neutron stars formation, neutrinos and gravit. waves emission 78−12266
neutron stars formation rate in Galaxy, upper limit 78−49471
neutron-proton electron mixture with zero charge density, eqn. of state, rel. to supernova explosions 77−53416
neutron-rich Si burning, nucleosynthesis equilib. processes 79−62816
newly formed stars, location in molecular clouds 79−58330
NGC 188, open cluster, stellar evolution and mass loss rel. to anomalous giant branch 78−41001
NGC 188 giant stars, evolution rel. to colour magnitude diagram 77−53430
NGC 1904, globular cluster, BV photometry and colour magnitude diagram 77−13415
NGC 2209, LMC cluster, colour-magnitude diagram rel. to metal abundance 78−8122
NGC 2231, star cluster in LMC, age and metal abundance from colour-magnitude diagram 79−92813
NGC 2264, young open cluster, circumstellar shells, IR excess obs. 77−45410
NGC 2571, open cluster, UBV anal. and cluster age 79−58386
NGC 3293, open cluster in Carina, UBVRI photometry and age 80−90490
NGC 362, globular cluster, BV photometry and colour-magnitude diagram 77−13416
NGC 604, giant H II region in M33, SNRs rel. to content of high mass stars 80−31340
stellar evolution continued
NGC 6052, complex galaxy, star form. burst rel. to late-type spirals collision 80−8681
NGC 6397, globular star cluster, age from main sequence turnoff, BV photometry 80−90484
NGC 6752, blue horizontal branch stars evolutionary state 78−49488
NGC 752, age from DDO astrophysical study 79−48864
nonradial oscillations, avoided level crossing 80−31294
nova model evolution with Z=0.03 envelope 77−82265
nova outburst, CNO abundances and hydrodynamics, 1 M⊙ models with small mass envelopes 79−12475
novalike object in Vulpecula, UV decline and expanding cooling photosphere 80−67741
nuclear reactions during late evolutionary phases, possible non-thermal processes 78−20816
nucleosynthesis, heavy elements origin and evolution 78−32619
nucleosynthesis, reaction rates of (p,n) and (α,n) 79−45253
nucleosynthesis and structure evolution rel. to CNO isotopes origin and abundance ratios 78−93201
nucleosynthesis explosions, accelerator expts. and theory 77−71110
nucleosynthesis rel. to galaxy chemical evolution, He enrichment 77−22208
numerical modelling, use of collocation methods 77−87370
O3 to O5.5 type stars, spectra, mass loss and evolution 77−33481
O- and Of-type stars, masses and mass loss 80−94793
O-type main sequence stars, rotational vel. evolution 80−51759
O-type star formation, different mechanisms 79−58331
O-type stars, kinematics, close binary evolution and ages 79−101145
O-type stars evolution rel. to Wolf-Rayet stars origin 78−81609
OB associations, mag. fields influence on subgroups sequential form. 80−4408
OB associations, sequential form. of subgroups 77−60800
OB binary stars, evolutionary sequence to X-ray stars and pulsars, tugboat model 77−56915
OB stars, distrib. in Galaxy, comp. rel. to age and space motions *(Russian)* 78−93216
OB stars, intermediate latit., origin 78−81627
OB stars, newly-formed, struct. and kinematics of assoc. H_2O vapour sources 78−61901
OB stars formation, obs. of assoc. H_2O maser sources 78−12390
OB supergiants, mass loss and massive binary evolution 77−57020
OBN, OBC stars, binary frequencies rel. to origins 78−53951
OBN star origin, mass loss calcs. 77−45412
observational tests on star formation, upper mass spectrum variation with cluster size 77−57066
Of-type stars as evolved O-type stars, rel. to difference in mass loss 80−90413
old clusters, theoretical isochrones with decreasing gravit. const., Dirac's multiplicative cosmology 78−16586
oldest Population I stars, H-R diagram and age difference from extreme Population II stars 77−56912
opacity limited star formation, fragmentation of cosmic gas clouds 77−49365
opaque core in early phase of star formation 79−58322
opaque envelope clearing and sudden appearance of star 79−35238
open, places of form 78−8064
open cluster H-R diagram gap theory rel. to NGC 188 and ER Cephei membership 78−77580
open clusters, age determ. methods *(Italian)* 80−90489
open clusters, formation positions rel. to galactic spiral arms 77−2457
open clusters, H-R diagram, gap in evolving main sequence 79−30096
open clusters, H-R diagrams anal. rel. to Galaxy chemical abundance gradient 80−56938
open clusters, late evolutionary stages *(Russian)* 78−49485
open star clusters, space distrib. and dias. rel. to ages *(Russian)* 79−48871
V566 Ophiuchi, evolutionary stage of eclipsing binary 77−71130
origin and early evolution of planetary nebulae 79−62893
Orion H_2O masers, matter outflow in star formation last stages 78−8091
Orion Nebula, low-luminosity X-ray sources obs., assoc. with star form. 80−26959
Orion OB 1 association, subgroup analysis of uvbyβ data 78−77582
FU Orionis type stars, eruptive phenomena in early stellar evolution 78−12233
p-process isotopes nucleosynthetic origin in supernova explosions 78−57541
parity nonconservation and stellar collapse 79−92789
MW Pavonis, W Ursae Majoris system, evolutionary stage from UBV light curve anal. 80−105278
β Persei (Algol) eclipsing binaries, mass loss and mass transfer theory 80−62191
β Persei type systems, orbital period changes and evolutionary status 80−4396
PG 1413+01, white dwarf-red dwarf eclipsing binary, masses and evolutionary state 79−8944
SX Phoenicis, evolutionary stage of RRs star 80−46583
Pismis 6 and 8, open clusters, common distance and age with (Wat 6) 79−88712
planetary nebula central star evolutionary scenario towards white dwarf stage 80−109427
planetary nebula formation and C detonation supernova models, mass limits 79−17053
planetary nebulae, 10 micron props. rel. to evolutionary development 79−48879
planetary nebulae, birthrate in solar neighbourhood 77−13423
planetary nebulae, central stars of solar mass, evolution 80−109428
planetary nebulae, Population II, origin rel. to CNO abundances and central stars masses 78−85992
planetary nebulae 78−32560
planetary nebulae central stars, evolution 78−12325
planetary nebulae central stars, evolutionary tracks rel. to nebulae radio flux density distribs. 80−56913
planetary nebulae central stars, protoplanetary stage of evolution rel. to cool stars 80−109435
planetary nebulae central stars, temp. and and radius evolution and relaxation, process 80−67724
planetary nebulae central stars, two-wind model for nebulae refractory elements gas-phase abundances 80−109516
planetary nebulae ejection by He shell flashes, appl. to planetary distance scale 78−24540

stellar evolution continued
planetary nebulae formation models, implications for Fe condensation 79−40238
planetary nebulae formation with close binary nuclei 79−71097
planetary nebulae in M31, form. rate rel. to interstellar matter distrib. 78−28737
planetary nebulae nuclei, evolutionary tracks rel. to halo white dwarf masses 80−82344
planetary nebulae nuclei, He shell flashes rel. to nebulae ionisation 80−73021
planetary nebulae nuclei, spectral type evolution *(Russian)* 79−58361
planetary nebulae of overall field and galactic centre, physical charact. and evolution 78−54029
Pleiades, contracting stars, UBVR photometry 79−96996
Population I 15 M⊙ star, effect of mass loss and semiconvection 78−45320
Population I evolutionary tracks for open cluster age determ. 78−61893
Population I stars, chem. and physical props. 77−78782
Population I stars in clusters, evolution rel. to cluster integrated colour synthesis 77−17637
Population II star formation 77−17562
potential novae and kinds of objects 77−82241
pre main sequence evolution, influence on main sequence (MS) stars chemical struct. 79−35247
pre-horizontal branch and Oosterhoff dichotomy in globular clusters 78−69784
pre-main sequence, observational studies for Hα emission stars 80−56827
pre-main sequence stars in Cepheus IV association, spectrophotometry rel. to evolution 77−13328
pre-main-sequence mass loss constraint 79−58335
pre-main-sequence stars, early evolution with D burning 80−51736
pre-supernova behaviour of 15 M⊙ star 79−35282
pregalactic H-He stars formation and nucleosynthesis 77−71157
prestellar gas, element separation by gravitational diffusion 79−21386
presupernova models and supernovae 80−56864
primordial matter cooling by H_2, rel. to star form. 79−35440
primordial star formation in cold early universe 77−87578
primordial star generation and missing dark mass 78−61946
progenitor stars for Type I supernovae, moderate He stars *(Italian)* 79−53806
protogalaxies, rot. and star form. rate 79−35374
protosolar nebula, dust grain motion time evolution 80−82234
protostar, rotating, fragmentation, comparison of two three-dimensional computer codes 80−26850
protostar formation, physical and numerical problems 77−29800
protostars, Barnard globules evolution 80−82462
protostars, form. as result of isentropic instabilities in interstellar gas 77−17644
protostars, H II regions development rel. to IR objects and maser sources 77−26032
protostars, magnetic, quasistatic contraction due to mag. flux leekage 80−98662
protostellar cloud, rotating isothermal axisymm. collapse 79−62737
protostellar cloud, solar-type star form. with spherical symmetry 80−85930
protostellar cloud fragmentation processes, evidence from solar neighbourhood mass distrib. 80−98649
protostellar clouds evolution, three dimens. dynamics 79−16929
protostellar clouds fragmentation, three-dimensional hydrodynamical calcs. 80−62236
protostellar envelope evolution, radiative transfer and spectrum 80−77384
protostellar envelopes of masses 3 M⊙ and 10 M⊙, struct. and hydrodynamic evolution 80−36616
protostellar evolution *(Russian)* 79−40180
protostellar formation in rotating interstellar clouds, axially symmetric collapse 80−77380
protostellar formation in rotating interstellar clouds, nonaxisymmetric collapse 80−85927
protostellar rotating gas clouds, fragmentation 80−51827
pseudoscalar bosons rule *(French)* 79−44361
pulsar age, correl. with P_3 period 80−90461
pulsar/supernova remnant associations, possible origin in close binary systems 78−85965
pulsars, characteristic and kinematic ages rel. to mag. monopoles creation 79−35287
pulsars, classification method from period change and radio luminosity *(Chinese)* 80−85963
pulsars, distribution, birthrate and flux density distrib. 80−98681
pulsars, evolution rel. to torques, magnetic moment and pair production 80−62169
pulsars, galactic distrib. and birth rate 79−75231
pulsars, initial magnetic moments rel. to decay times 79−62861
pulsars, mag. monopoles creation rel. to evolution 79−44516
pulsars, magnetogyro ratios and evolution 79−8937
pulsars, space velocities rel. to evolution 78−4264
pulsars, spatial distrib. and birth-rate 79−25624
pulsars formation frequency, results from search for galactic supernova remnants 79−29998
pulsars galactic distribution and evolution 78−4260
pulsating stars, two-time asymptotic method appl. to one-zone atm. 77−53570
pulsational stability, magnetic field influence 79−53800
pulsational stability of very low mass stars on H and D main sequences 77−17544
pycnonuclear reactions, pair correlation function in dense plasma 79−67001
quark stars, beta decay 80−82398
r-process seed nuclei prod. at low densities and temps. 77−64742
R-type C stars, origin, H mixing during He flicker 78−4223
radio emission from immediate postoutburst supernovae, origin and evolution 78−40973
rapidly rotating pre main sequence stars, evolution in gravit. contraction phase 80−62133
red dwarf stars, origin, evolution and variability 79−16954
red giant envelope composition rel. to evolution 80−105237
red giant stage 80−12752
red giant stars, evolution rel. to meridional circulation and CNO anomalies 79−48786
red giant stars, evolutionary sequences 78−65611
stellar evolution continued
red giant stellar wind/circumstellar nebula interaction model of planetary nebula origin 78−36674
red giants, ^{14}C and neutrons prod. during He shell flashes 77−26005
red giants, IR radiation emission in final stages 80−72931
red giants, mass loss from dynamically unstable envelopes 78−20824
red giants, peculiar, constraints on evolution from masses and space densities 80−22001
red giants 77−26010
red giants and supergiants, mass loss rates 77−91534
red giants in M13, Na abundance var., protocluster gas inhomogeneities 80−82439
red supergiants, lower mass limit for C detonation supernovae, influence of envelope dynamical instability 77−17553
Reissner-Norstrom black hole, interior final state evolution 80−8648
Roberts 22, bipolar nebula with OH emission, obs. rel. to evolutionary status 80−94859
Roche and Darwin problems for polytropic stars, numerical study 79−75202
rotating $2M_{\odot}$ Fe-O star, gravitational collapse *(Russian)* 78−4199
rotating collapsing stars, low freq. gravit. radiation 79−71314
rotating stars, 7 and 10 M⊙ stars evolution with time-depend. redistrib. of ang. momentum 78−36553
rotating stars, angular momentum conservation, surface rotation vels. prediction 79−96991
rotating stars, method and exploratory calcs. for 7 M⊙ star 77−13316
rotating stars, secular instability from thermal cond. 80−21986
rotation and Kelvin-Helmholtz instability 79−46287
RRs type variable stars, periods rel. to evolutionary status 77−87432
Rubin-152, possible massive O-type star on galactic fringe, evolutionary stage 80−98656
runaway stars, as witnesses to supernova explosions 78−32448
FG Sagittae, 1975-8 spectral obs. of peculiar variable 80−72959
HM Sagittae, eruptive BQ forbidden line star, evolution to planetary nebula 78−20835
HM Sagittae, proto-planetary nebula mass ejection rel. to photometric and spectroscopic evolution 78−85947
WZ Sagittae, recurrent nova, physical parameters, present state, past and future evolution 78−85948
HM Sagittae as young planetary nebula 79−48801
V356 Sagittarii, eclipsing binary, model and evolutionary stage 78−49477
V701 Scorpii, dimensions and evolution of early-type contact binary 80−62188
V 701 Scorpii, early type eclipsing binary, contact props. 78−8051
KQ Scorpii, long-period Cepheid evidence for membership of OB association 79−88666
α Scorpii AB, mass loss and circumstellar absorption lines 79−8916
δ Scuti and RRs variables, periods rel. to evolutionary status 77−87433
self similar collapse of isothermal spheres and star formation 77−53568
semiconvection as occasional breaking of weakly amplified internal waves 79−48778
shell ejection in nova outbursts, time before max. 77−2441
slowly rotating stars, gravit. collapse, supernova explosion, neutron star or pulsar remnant 78−96472
small mass stars, strong He flash *(Russian)* 77−26001
in SMC, distrib. and evolution of stellar populations 80−94868
SMC, star formation regions and star clusters 79−62900
SMC, stellar populations and ages in NE outer arm and halo 78−86013
solar nebula, primordial, struct. and evolution 80−62042
solar neighbourhood, initial mass function and stellar birthrate 80−62259
solar neighbourhood crossing times effect on observed stellar age and metallicity distribs. 78−12362
solar neighbourhood F, G and K stars, H-R diagram fine struct. 77−29819
solar neighbourhood initial mass function determ. from upper H-R diagram study 80−36626
solar type protostars, late stages 79−58334
solar type stars, relation between metallicity and multiplicity 77−78788
spectroscopic binaries, evolution rel. to primary mass, mass ratio and orbital semiaxis distribs. 80−46616
spiral galaxies, star form. bursts rel. to radio continuum flux from discs 77−13460
sporadic mass ejection in red supergiants 79−40186
SS 433, early-type binary model and evolutionary state 80−56843
SS 433, lifetime against gravit. radiation in ultra-close binary system model 80−4384
SS 433, mass loss rates and lifetime from W50 optical filaments 80−12804
SS 433, nature and evolutionary state *(Russian)* 80−36647
star formation, CO obs. of compact H II regions assoc. with OH masers 77−57078
star formation, in galactic dust/molecular clouds 80−26925
star formation, in giant ellipsoidal shells around normal elliptical galaxies 80−86000
star formation, influence of initial vel. fields in interstellar medium 80−21985
star formation, mag. braking of aligned rotator, cloud rotation, mag. braking of aligned rotator during star form., exact time-depend. soln. 80−90493
star formation, numerical calcs. of collapse of nonrotating magnetic gas clouds 80−105299
star formation, observational studies conclusions 79−25592
star formation, recent, in lenticular galaxy (NGC 5102) 79−44609
star formation, rel. to density waves accretion-induced overstability in self-gravitating galactic disc 78−73752
star formation, rel. to galactic populations, metals abundances and Galaxy chemical evolution 78−96545
star formation, ring form. in rotating protostellar clouds 80−56820
star formation, role of interstellar cloud formation induced by OB-type stars 80−109506
star formation, stochastic model rel. to spiral galaxies props. 80−12818
star formation and interstellar clouds, impact of cosmic plasma physics 78−73744
star formation associated with shock front passage, radio obs. of IR object 78−93369
star formation bursts in galaxies of Magellanic type, effects on struct. and colour *(German)* 80−105348
star formation bursts in Markarian galaxies, evidence from radio continuum obs. 80−46668

stellar evolution continued
star formation bursts in S0 galaxies, rel. to radio continuum and H I obs. 77−87549
star formation from collapsing turbulent interstellar clouds, three-dimensional numerical models 80−56910
star formation in barred spiral galaxy NGC 925, correl. with H I distrib. 80−105329
star formation in binary galaxies, rel. to galaxies peculiar luminosity function and colours 80−41900
star formation in bright-rimmed mol. cloud IC 1848 A, obs. 79−5810
star formation in central regions of galaxy IC 342, evidence from IR emission 80−62256
star formation in dark clouds, radio continuum interferometric search for newly formed H II regions 80−98699
star formation in galactic centre, rate 80−36713
star formation in galaxies, dating from N/O ratio 79−25728
star formation in galaxies, suppression rel. to delayed star form. problem 80−105349
star formation in galaxy NGC 4314, distrib. from UBV surface photometry of central region 80−77482
star formation in H II region NGC 281, evidence from CO and H_2O obs. 78−28740
star formation in interstellar dark clouds, implications of radio continuum obs. of young H II regions 80−105301
star formation in M31 (Andromeda galaxy), depend on interstellar gas density rel. to Cepheid periods radial var. *(Russian)* 80−90455
star formation in M32, duration from galaxy spectral synthesis 80−67842
star formation in M33 rel. to spiral struct. evidence from supergiants distrib. 79−21437
star formation in merging galaxies, influence on population gradients 80−67860
star formation in NGC 6334, rel. to H_2 O masers 80−73025
star formation in OB associations, sequential form. of association subgroups 80−98696
star formation in W3, near IR obs. of two far IR sources 80−22058
star formation in W3, struct. of OH maser source W3(OH) from VLBI synthesis obs. 80−105368
star formation in W58, evidence from CO obs. 80−67810
star formation laws, implication of bright stars luminosity function 80−82499
star formation process simulation, hydrostatic models evolution *(Polish)* 80−21998
star formation rate in anaemic spiral galaxy NGC 4378, meas. 79−8990
star formation rate in external galaxies, numerical simulation 77−45555
star formation rates, in normal and peculiar galaxies 78−24550
star formation regions, H_2O maser sources evolutionary sequence from VLBI obs 80−26954
star formation regions, rel. to galactic spiral struct. in vicinity of Sun *(Russian)* 80−62290
star formation rel. to solar system origin, reviews in book 78−85865
star formation sites in W3/W4/W5 direction, correl. with heavy optical obscuration 80−62301
star swarms, formation and evolution 78−57599
star-forming complex in S252 (NGC 2175), mol. line obs. 80−4411
stars in thermal imbalance, vibrational stability 78−40916
steady disc accretion, ang. momentum transfer 78−65609
stochastic self-propagating star formation rel. to evolution of galaxies 80−12810
stochastic star formation, rel. to galaxies spiral struct. 78−93395
stochastic stellar evolution, fluctuations due to convection 80−31293
strong internal mag. field diffusion through radiative envelope of 2.25 M⊙ star 78−85931
strong lined elliptical galaxies, overabundances of Na and Mg heavy isotopes 77−13464
subdwarf stars, age and evolution effects on thirteen-colour photometry indices 79−92767
subgiant stars, F-, G- and K-type, Be abundance rel. to post-main sequence evolution 77−13333
successive He shell flashes, anal. rel. to stationary shell burning 80−51737
Sun, early evolution rel. to origin of life 78−69923
Sun, evolutionary luminosity increase rel. to Earth climate and biosphere 78−32435
Sun, implications for Earth's early atmosphere 78−36285
Sun, implications of solar neutrino expts. 79−16918
Sun, neutrino problem and evolution *(French)* 80−72933
Sun, solar system origin rel. to transneptunian planets and long-period comets 79−8856
super-metal-rich stars, evolution rel. to interpretation of old galactic clusters 77−49370
supergiants, early-type, with mass loss, two-core model and evolutionary status *(Russian)* 80−109425
supergiants in Magellanic Clouds, birthrate and mass function 80−67699
supermassive star, expanding, and contracting dust shell, Einstein's theory of gravit., black hole formation 78−12088
supermassive star collapse to black hole, Einstein eqns., numerical soln. 80−41851
supermassive star in dense stellar systems 79−12465
supernova explosion mechanisms 77−87465
supernova mass ejection and core hydrodynamics *(Italian)* 79−53842
supernova model, neutrino degeneracy effects 77−2447
supernova models, Fermi statistics effects on neutrino transport 77−26019
supernova off-centre explosions, rel. to high vel. pulsars form. 80−46587
supernova precursors, mass loss by stellar winds *(Italian)* 79−53841
supernova progenitors evolution 77−87462
supernova progenitors masses 77−87461
supernova remnants, galactic, birth rate from new catalogue 79−75120
supernova remnants, galactic, radio evolution and population characts. 79−75254
supernovae, Type I, models 78−65636
supernovae, Type I, origin from short-lived stars 79−88692
supernovae, types I and II, evolution rel. to radial distrib. in spiral and elliptical galaxies 80−62163
supernovae ^{26}Al prod. from stellar evolutionary sequence 79−5809
supernovae in binary systems, rel. to HD 108 possible collapsed companion 77−13369
supernovae in molecular clouds, spectra and luminosity, evolution 80−82399
supernovae influence 80−31315

stellar evolution continued
symbiotic stars, evolutionary considerations 80−62144
symbiotic stars, origin and evolutionary stage *(Russian)* 77−17616
DR Tauri, highly variable young star, spectrum, photometry and evolutionary stage 78−20829
DR Tauri, pre-main-sequence star, brightening, 1970 to 1979, and historical light curve 80−31297
V471 Tauri (BD+16°516), eclipsing binary white dwarf, spectroscopy and photometry rel. to evolution 77−57028
T Tauri star, extremely young, and assoc. nebula, fading 78−93236
T Tauri star formation, regulatory force in dark mol. cloud evolution 80−85980
T Tauri stars, subgroups on two colour diagram 79−71041
T Tauri stars and Herbig Ae-Be stars, broad-band IR photometry 78−4217
terminal stages in quantum chromodynamics 77−78773
theoretical isochrones for stellar evolution with variable G, Brans-Dicke theory 79−67125
thermal and nuclear modes coupling, in highly evolved stars 79−84785
thermal pulse and interpulse props. of intermediate-mass models with C-O cores 78−12199
thermal pulses in high-luminosity stars, effects on surface comp. and interstellar medium enrichment 78−40917
thermonuclear combustion of C, neutrino mechanism, form. of neutrino stars and supernova outbursts *(Russian)* 77−87379
thermonuclear explosion of degenerate C core, numerical calcs. 78−36558
thermonuclear explosions 80−72766
transformations from theoretical H-R diagrams to C-M diagrams 77−13321
Trapezium type multiple systems, evidence for youth from connection with association and nebulae 80−67781
U Trianguli Australis, double-mode Cepheid, mass, luminosity and evolution 77−29845
47 Tucanae, metal-rich globular cluster, photometric study rel. to evolution 77−57065
turbulent diffusion and $^{12}C/^{13}C$ abundance ratio 80−21993
Type I supernovae, theory, light curve anal., evolutionary sequence 79−62858
unevolved stars, abundances rel. to interstellar gas mixing *(Russian)* 79−40192
upper main sequence stars, evolutionary tracks in H-R diagram 77−49379
Ursa Major stream eclipsing binaries, ages and absolute dimensions 79−92800
W Ursae Majoris metal-poor systems, evolution models 79−25628
W Ursae Majoris stars, A-type, radii and evolutionary state 79−8943
W Ursae Majoris systems, struct. and evolution 77−45488
W Ursae Majoris type binaries, evolutionary models 77−53644
variable gravitational constant, Universe age effects 79−30052
AI Velorum, dwarf Cepheid, mass and evolutionary state from uvbyβ photometry 77−78801
SW Velorum, long-period Cepheid evidence for membership of OB association 79−88666
γ^2 Velorum, WC+O binary, evolutionary model for mass-losing massive He star 80−36615
very close binary systems, struct. eqns. including rot. and tidal distortions for ZAMS stars 80−22037
vibrational stability of stars in thermal imbalance, energy methods 77−13320
β Virginis, chemical composition and age 78−61855
SV Vulpeculae, Cepheid, period change meas. rel. to evolution 79−92777
W51 Main as expanding bubble around young massive O-star 80−8701
W92, possible gravit. contracting binary system in NGC 2264 young cluster 78−32462
Wat 6, open cluster, common distance and age with (Pismis 6 and 8) 79−88712
weak G-band stras, nature and evolution from spectrum anal. of (HD 91805) 78−49432
weak interactions in astrophysics and cosmology 77−25934
weak neutral current, effects in stellar collapse, review, book contrib. 78−85964
white dwarf creation rate from planetary nebulae space density 77−17652
white dwarf formation in binary systems 79−44483
white dwarf formation rate, luminosity function determ. 80−90418
white dwarf formation rate in globular clusters 80−4346
white dwarf in binary system, outer layer C and O enrichment from companion 80−109465
white dwarf luminosity in scale covariant theory of gravity 79−80303
white dwarf remnants production, progenitor stars upper mass limit determ. 80−51738
white dwarf with mass accretion, H shell flashes rel. to symbiotic stars vars. 78−57550
white dwarfs, ages and cooling rel. to very low luminosity degenerates deficiency 80−17575
white dwarfs, birth rate rel. to planetary nebulae distance scale 78−20867
white dwarfs, convective mixing and accretion 77−5529
white dwarfs, evolution rel. to external layers models and spectra interpretation 79−62824
white dwarfs, formation and evolution 79−48799
white dwarfs, H burning shells, thermal stability 78−4212
white dwarfs, He flash and nova evolution 80−72938
white dwarfs, mass loss 77−74044
white dwarfs, mixing processes and elements separation in envelopes 78−12222
white dwarfs, physics of structure and evolution 79−25606
white dwarfs, rapid mass accretion and extended envelope form. 80−67723
white dwarfs, spectral evolution and accretion from intersteller clouds 79−35252
white dwarfs, struct. and evolution theory rel. to EUV obs. and spectra 80−82356
white dwarfs formation rate in stellar systems 78−28674
white dwarfs mass-radius relation, constraints on gravit. const. 79−25464
white dwarfs rejuvenation due to interstellar accretion 77−17550
white holes, nonexistence, anal. of star bursting Schwarzschild barrier 78−32506

stellar evolution continued
wind interaction with surrounding disc nebula 79−58323
Wolf-Rayet stars, binary freq. distrib. 80−105250
Wolf-Rayet stars, CNO abundance var. in massive binaries 80−94802
Wolf-Rayet stars, evolutionary status of high-luminosity (WN7/WN8) stars *(Russian)* 80−109425
Wolf-Rayet stars, galactic WN7/WN8 stars as massive O-stars in advanced evolution stage 79−92778
Wolf-Rayet stars, UV obs. rel. to evolutionary status 78−40965
Wolf-Rayet stars as supernova progenitors *(Italian)* 79−53830
X-ray binaries, double core evolution 79−84816
X-ray binaries, evolutionary history 78−12431
X-ray binaries, lifetimes 77−9812
X-ray binaries, limitations on nature and evolution 77−82273
X-ray binaries, Roche lobe overflow and evolution 78−32601
X-ray binaries evolution, accretion onto ZAMS stars and contact binary stage 79−66994
X-ray binary sources, highly compact, evolutionary history and observational props. 79−35430
X-ray bursters, form. of neutron star and low mass main sequence star binary system 80−109455
X-ray sources, galactic, creation rate rel. to large-scale distrib. 79−48954
young stars in Chamaeleon T1, photometry and spectral obs. 80−72943
young stars with mass accretion 80−101592
zero age horizontal branch stars, expected location 78−77551
zero age main sequence to red giant branch, evolutionary sequences 80−21987
(n,γ) for A=138-181, stellar nucleosynthesis and s-process neutron flux 80−42663
Ba II metal rich stars, Ba abundance implications 79−71024
Ba stars, Ba line strengths rel. to ages and luminosities 78−12226
C burning, products at const. temp. *(Russian)* 78−61722
C burning in degenerate core, convection effects 80−41810
C cores evolution, nuclear energy generation rates and energy dissipation 80−82339
C ignition, effects of thermonuclear ion-electron screening, static soln. 77−29793
C ignition, effects of URCA process in convective degenerate cores 77−22203
C shell burning to Fe core collapse, evolution of 15 M⊙ star 80−72937
C shell flash in 9 M⊙ star 78−89170
C stars, $^{12}C/^{13}C$ ratio determ. 78−73710
C stars, circumstellar envelopes and evolution 79−40178
C stars, in LMC, VRI photometry, optical spectroscopy and evolutionary implications 79−71019
C stars and G-K giants, origin of $^{12}C/^{13}C$ ratios freq. distrib. 77−78780
C-burning flash in degenerate C-O stellare core, thermal phase 77−78774
C-O white dwarf freezing, C-O eutectic model 80−77405
C_2 white dwarfs, evolutionary status 80−4355
CNO burning and zero age horizontal branch stars location 78−12201
^{12}C prod., He burning stars, 3α system forming O_2^+ resonance 78−50108
Fe-O stars collapse, physical and mathematical formulation and computational method 77−87369
Fe-O stars with masses of 2M⊙ and 10 M⊙, gravit. collapse 78−20815
H burning evolutionary stages, Hertzsprung-Russell diagram age and mass calibrations 80−51744
H burning of $^{29,30}Si$ in explosive C burning 79−22289
H II regions, IR obs., 1-1000 μm wavelength, star form. regions 79−67084
He core flash onset and $^{14}C(\alpha,\gamma)^{18}O$ in low-mass stars 80−51735
He diffusion rel. to evolution, appl. to Sun 77−56888
He flash and convection in stellar cores 78−89191
He flash in stars with shell energy sources 78−89169
He shell burning stages, core mass-luminosity relations 80−21983
He shell flash quenching conditions 77−29790
He shell flashes in red supergiants, convective penetrations and observable effects 80−51755
He shell flashes rel. to galactic He enrichment 77−45428
He stars, evolution using Carson's radiative opacities 78−4191
He stars, post-giant evolution 77−56947
He white dwarfs rejuvenation by mass accretion 78−73712
Hg-Mn stars, absolute magnitude and evolutionary status 80−46564
N deficient supergiants in loose association, comps., masses and evolutionary stage 79−44478
$^{15}N(p,\alpha_0)^{12}C$, 93 to 418 keV, remeas. of low energy cross section, astrophys. S-factor determ. 79−63665
$^{18}O(\alpha,\gamma)$, 0.6 to 2.3 MeV, props. of ^{22}Ne compound states, astrophys. reaction rate 78−57545
$^{18}O(p,\alpha)$, 661 to 223 keV cm, cross section meas. and S-function extrapolation using R-matrix theory 78−82341
$^{A}Os(n,\gamma)$, A=186-188, 2.6-800 keV, capture Maxwellian cross sections, galactic nucleosynthesis 80−42664
$^{45}Sc(p,\gamma)$, 0.7-4.2 MeV, cross section, statistical model anal., stellar interaction rate 79−17897

stellar interiors *see stellar internal processes*

stellar internal processes
see also solar interior; stellar evolution
α^2-dynamos, finite amplitude, with large scale in compressible circulation, theory 78−81534
A-type stars, rot. and internal mixing rel. to variability 77−87397
adiabatic collapse of core, general relativistic hydrodynamics 79−96903
Am-type stars, envelopes circulation 80−4370
angular momentum loss from star with rapidly rot. core in close binary system *(Russian)* 78−93196
Ap stars, radiative forces in stellar envelopes rel. to He abundance anomalies 80−31291
U Aquarii, R Coronae Borealis star, extraordinary comp. rel. to unusual s-processing event 80−17588
asymptotic giant branch evolution of intermediate-mass stars, post-second dredge-up phase 80−72936
axions, very low mass, astrophysical bounds and stellar-energy loss 80−109353
beta transition rates in hot dense stellar matter 78−73699
beta-decay and electron capture rates of nuclear excited states, gross theory 77−41927
α Bootis (Arcturus), giant convective elements hypothesis rel. to variable mass loss 77−22213

stellar internal processes continued
Boussinesq turbulence, statistical theory, appl. to stellar convection 80−48713
Cassiopeia A supernova, O burning rel. to remnant abundance inhomogeneities 80−12797
SU Cassiopeiae, Cepheid, distance and pulsation mode 78−89204
V553 Centauri, C rich Cepheid, C and N abundances rel. to nuclear processes and evolutionary status 80−4378
β Cephei stars, core convection rel. to pulsation excitation 77−87425
β Cephei stars, models, He^+ ionization driving 79−8922
Cepheid model, transitory R-type ionisation front 79−75209
Cepheid pulsation period variability and convective efficiency 80−26885
Cepheids, stellar pulsation problem, time dependent convection local theories 80−72964
close binaries, angular vel. distrib. in one component with fast rotating core *(Russian)* 78−28648
close binary stars, tidal friction theory 77−57013
CN cycle, rel. to CN strengths and $^{12}C/^{13}C$ ratios in K-type giants 78−93229
CN cycle, role in N abundance anomaly in globular cluster 47 Tucanae 79−48867
cold degenerate stars, immiscibilities as energy source rel. to luminosities 78−69798
cold dense star with frozen-in mag. field, degeneracy removal, ideal electron gas approx. *(Russian)* 77−87365
cold relativistic neutron gas, study of massive neutron cores 79−35292
collapse of massive star cores, supernova explosion from shock heating 80−56863
collapsed core, neutrino prod. of bypassed isotopes, neutrinos role in nucleosynthesis 79−40182
collapsed stars, neutrino flux from quark matter 80−22028
collapsing core, shock struct. and neutrino radiation, rel. to supernova explosions 78−49427
collapsing cores and supernovae 79−62815
collapsing star, neutrino degeneracy and downscatt. effects on neutrino radiation 79−12463
collapsing stellar cores, light element production by emitted neutrinos 79−21173
compressible convection in stellar interiors 78−89183
Compton scattering opacity in partially degenerate electron plasma at high temp. 77−11322
connection, random fluctuations rel. to stochastic evolution and oscill. props. 80−31293
contact binaries, objection to model of Shu, Lubow and Anderson 78−28720
contact binary stars, temp. discontinuity maintenance 80−8655
convection, energy transport 78−89180
convection, fundamental hit correctable inconsistency of local mixing-length theory 80−26841
convection, hydrodynamics rel. to solar obs. 78−89182
convection, mixing length parameter rel. to Hertzsprung-Russell diagram age and mass calibrations 80−51744
convection, mixing-length theory 78−89178
convection, mixing-length theory rel. to physical models 78−89179
convection, modal eqns. in spheres and spherical shells 79−101137
convection, turbulent, in Boussinesq fluids, viscosity, conductivity and power spectra 80−98543
convection and magnetic fields 78−89185
convection and stellar models and evolution computations 78−89194
convection equations, ensemble averaging 80−67698
convection in massive star cores, effect on C/O ratio 80−17579
convection in rotating magnetic star, toroidal field effect 80−41816
convection in rotating spheres and spherical shells 78−89184
convection onset in radially pulsating star 80−41809
convection phenomena numerical simulations 77−29789
convection theory, choice of characteristic length 77−13317
convection theory, numerical methods 78−89058
convection theory (1930-1945) 78−89177
convection theory including turbulent kinetic energy flux, appl. to main sequence star models 78−57543
convection zones dynamics, effect of rot. on turbulent viscosity and cond. 80−36612
convection zones in λ4670 white dwarfs 77−17559
convective and semiconvective mixing in massive stars, effects on struct. and evolution 80−90405
convective energy transport, review of theories 78−69785
convective envelopes, non-local convection, statistical theory *(Chinese)* 80−85933
convective instability, mag. fields and g^- modes 78−93211
convective instability of ga s sphere *(Russian)* 77−87378
convective modes and convective stability, of rotating fluids 79−16818
convective regions, proton-proton chain 77−29799
convective zone boundaries 78−89187
convective zones, wave generation and pulsation 78−89193
cool giant stars, nuclear processes and mixing from obs. and anal. of CO at 5 μm 78−36569
core collapse, effects of nuclear forces, partition function and dissoc. 79−48833
core collapse, limits on nuclei excitation energies in hot matter 80−56703
core collapse, neutral currents and neutrino Comptonisation in high-temp. nuclear matter 80−21905
core collapse, neutrino prod. and inelastic scatt. by nuclei at extreme temps. 80−36488
core collapse, neutrino prod. and interaction with ejected envelope ^{26}Mg, ^{26}Al prod. *(Russian)* 80−77285
core collapse, shape instability pressure stabilisation 80−8537
core collapse, Thomas-Fermi model of warm nuclei 80−51648
core collapse, vacuum neutrino oscills, inhibition by high matter density 80−36496
core collapse and overturn with Rayleigh-Taylor unstable gradient 80−94819
core collapse outcome, effects of core eqn. of state 80−85928
core collapse to neutron star, electron neutrino and antineutrino emission, spectral calcs. 80−109454
core gravitational collapse, shockwave prod., neutrino transport effects 80−94818
core He burning in extremely metal-poor stars, theory 78−28677
core He flash, models with two-dimensional convection 80−105230
core He flash and C and CH star origins 78−4190
core He-burning and convective shells of massive stars 78−93207

stellar internal processes continued
core homologous collapse, perturbations effects 80−94779
V460 Cygni, cool C star, 3α process rel. to C prod. and $^{12}C/^{13}C$ ratio 78−93223
CH Cygni, red giant, mag. field generation rel. to symbiotic outburst 78−4250
V1329 Cygni (HBV 475), symbiotic variable, shell flash assoc. with optical outburst 80−62148
V1500 Cygni (Nova 1975) as thermonuclear runaway event 77−82261
degenerate C core, thermonuclear explosion problem 78−28669
degenerate C cores, microstruct. of detonation waves 79−62810
degenerate C ignition, burning front propag. rel. to core implosion or disruption 80−77390
degenerate C/O cores, detonation formation 77−45398
degenerate dwarfs, internal struct. rel. to nonradial oscills. 77−87398
degenerate star, propagating slow deflagration front struct. and evolution 79−84790
degenerate stars, slow deflagration mechanism for mass ablation 79−35248
dense ionised plasma, thermodynamic props., electron screening corrections 77−972
dense matter, transport props., neutron stars appl. 79−67236
dense stars, ang. momentum loss by neutrino emission 77−49371
dense stellar matter, diffusion approx. to neutrino transport 78−93096
dense stellar matter in asymptotically free gauge theories, high density limit 77−53421
differential rotation, due to latitude depend. convective heat transport 80−90411
diffusion, radiatively driven, in upper main-sequence peculiar stars, rel. to chemical and physical props. 80−82374
diffusion in stars, astrophysical context 80−77381
double shell source stars, evolution through second loop in Hertzsprung-Russell diagram 78−36556
BC Draconis, radial pulsation period indicating Population II Cepheid 78−32491
dwarfs, degenerate accreting, thermonuclear bursts assoc. with chromosphere flares 80−98684
dynamical instabilities at start of convection 78−89181
dynamical r-process, nuclei far from β-stability 77−26004
early-type stars, envelope mixing of elements, shear flow instability 80−109424
electron capture, screening effects at high density 77−33478
ellipsoidal potentials of polynomial distributions of matter 80−46532
energy loss rate due to electron capture in highly evolved stars 77−64752
evolutionary models from zero age main sequence to red giant branch 80−21987
evolved stars, thermal and nuclear modes coupling 79−84785
experimental nuclear astrophysics, review 79−25471
explosions in radiating stars, similarity solns. 78−32443
explosive C burning, ^{26}Al production 78−20814
explosive H burning, ^{26}Al synthesis 80−85929
explosive nucleosynthesis, massive star evolution preceding and during supernova, element abundances *(German)* 79−44469
explosive nucleosynthesis, rel. to Al/Fe ratio in metal-poor-stars 78−57549
explosive nucleosynthesis, rel. to meteoritic isotopic anomalies 79−62795
explosive nucleosynthesis 80−72766
explosive r process cooling process 78−69791
F-type star, main sequence, convection and photospheric granulation 80−90417
fast nova model evolution from pre-explosion to decline 79−35273
final evolutionary phases, internal processes rel. to supernova phenomenon *(Italian)* 79−88646
final evolutionary phases, struct. rel. to supernova phenomenon *(Italian)* 79−88646
forced mixing in convective stars, theory and effects on evolution 80−56818
fusion, power prod. in reactors, and astrophys. appl. *(Norwegian)* 79−30872
g- and p-modes of non-adiabatic self-gravitating fluid, perturbational-variational expansion 78−32337
G-K giants and C stars, $^{12}C/^{13}C$ ratios freq. distrib. rel. to nuclear processes 77−78780
galactic ^4He and heavy elements enrichment by stellar nucleosynthesis 78−28657
giant stars in M13, M92, NGC 6397 and M15, mixing rel. to weak-G-band effect 77−78778
GK giants, CN strengths rel. to internal mixing and supermetallicity 77−56930
globular cluster stars, He settling and effect on inferred ages 80−73013
gravitational collapse, comp. and eqn. of state of thermally dissociated matter 77−33476
gravitational collapse, hydrodynamics 78−45318
gravitational collapse, neutronisation and lepton escape rel. to hydrodynamics 80−77388
gravitational collapse, theory 80−77389
gravitational collapse, weak interactions and supernova outbursts 77−87464
gravitational collapse of core of massive star, neutrino trapping 78−32437
gravitational collapse of stellar core, secondary indications 80−62177
gravitational waves generated by collapse, wave strength estimate 80−46584
gravitationally collapsing stars, neutrino processes rel. to mass ejection 77−33534
heavy and neutron-rich elements synthesis by rapid neutron capture process 78−77488
heavy element, origin in star development supernovae and galactic matter *(German)* 79−44468
heavy element nucleosynthesis, current astrophysical theory review 77−29644
heavy element synthesis and β-strength function shape 79−66918
heavy elements production in massive stars, effects of binary evolution 80−46534
Henyey-type evolution code, appl. to stars with shell energy sources 78−61848
high Coulomb barrier secondary nucl. reaction rate, ion distrib. effects *(Russian)* 80−64684
high mass stars, semiconvection and convection rel. to evolutionary effects of stellar wind 80−21982
stellar internal processes continued
horizontal branch stars, evolution with semiconvection, models 77−17540
hot CNO nucleosynthesis, $^{18}O/^{17}O$ abundance ratio 77−78767
hot degenerate stars in steady-state accretion, H burning shells thermal stability 78−40929
hot dense stellar matter, adiabatic index with full nuclear interaction 80−36620
hot neutron star matter, neutrino transport, opacity 79−75238
HR 6766, weak G-band star, light-element abundances rel. to CNO cycle 78−57548
Hyades giants, dilution and mass loss rel. to Be abundance 77−53584
Hyades giants, evidence for CNO processing from main-sequence stars CNO abundances 78−93222
hydrostatic and thermal equilib. eqns., soln. in Eulerian coords. 77−17546
hydrostatic C burning, estimates using $^{12}C(^{12}C,n)^{23}Mg$ neutron branching meas. 77−34336
ideal Fermi gas, thermodynamics and eqn. of state 77−30117
instability due to local mixing length approx. 77−53569
interacting neutron matter model at postsupernova temps. 77−45399
intermediate-mass stars asymptotic giant branch evolution as function of mass and comp. 80−12749
isotopic anomalies from neutron reactions during stellar explosive C burning 80−12651
late-type stars, ang. momentum loss rel. to mag. dynamo 78−45331
late-type stars, sensitivity of internal struct. to surface boundary condition 78−12208
low energy neutrino elastic scattering and supernova explosions 78−89056
RR Lyrae stars, convection depend. on pulsation phase, theoretical red edge of instability strip 77−17572
RR Lyrae stars, convective steady-state models, theoretical red edge of instability strip 78−4229
RR Lyrae stars, hydromagnetic processes as cause of period changes 80−105261
RR Lyrae stars, instability strip red edge depend. on luminosity and comp. 77−53600
RR Lyrae stars, theoretical red edge of instability gap, overtone pulsation 77−78794
magnetic dynamo α-effect, determ. for slow and fast rot. 79−40069
magnetic flux tube, buoyancy and equilib. 80−109420
magnetic star model, circulation within nuclear burning shell rel. to latit. depend. chem. comp. *(Russian)* 79−16940
magnetic stars, kinematic mechanism for oblique rotator model 77−45407
magnetic stars, perpendicular rotator model with meridional circulation 78−16438
main sequence, turbulent diffusion and Li transport 77−45403
main sequence star, results of collision with white dwarf 77−64758
main sequence stars, diffusion in envelope and abundance anomalies 77−13331
main sequence stars, element abundance regularities rel. to nucleosynthesis *(Russian)* 77−45431
main-sequence mixing, effects on CNO isotopes 77−33475
main-sequence stars, mag. mixing rel. to CNO isotope abundances and α Bootis (Arcturus) problem 80−105229
main-sequence stars envelopes, hydrodynamical instabilities constraints from Li, Be and B obs. 78−93202
massive accreting white dwarfs in close binary systems, H shell flashes 79−75203
massive star core collapse, eqn. of state and composition near β equilib. 80−82335
massive stars, 10^3-10^4 M⊙ range, final evolution 77−87371
massive stars, bulk yields of nucleosynthesis 78−36552
massive stars, mass loss and convective overshooting influence on evolution 79−84789
massive stars, nonradial pulsational instability 77−56908
massive stars presupernova evolution 79−16930
matter distribution in nuclei far from β stability valley, charact. features 77−64635
meridional circulation, in surface layers of rot. stars 78−20820
meridional circulation caused by stellar rot., general vel. eqn. 79−62818
meridional currents, pentration of core mol.-weight barrier 77−33474
metallic-line stars, He gravit. settling rel. to theoretical pulsation 79−97004
Mira variables, nuclear shell flashes rel. to planetary nebula form. 80−26928
mixing, rel. to strong CN phenomenon 78−53921
mixing between burned core material and surface layers 78−12213
n-process nucleosynthesis, alternative to r-process 77−2336
neutrino bremsstrahlung by degenerate electron gas, neutral current effects 77−13225
neutrino capture rate problem, role of phion in composite neutron mode 80−41808
neutrino chemical potential and heat cond. with allowance for scatt., collapsing stars appl. 79−84657
neutrino opacity, pure neutral vector boson contrib. 78−53928
neutrino processes, reaction rates 78−45215
neutrino prod. by neutral currents, energy loss rates 77−53577
neutrino thermalisation, contribs. of conservative scatt. and electron scatt. 79−92659
neutrino transport, direct simulation and aspects of equilibration 78−89050
neutrino transport, time-dependent, out of dense stellar cores, theory 80−94783
neutrino transport, weak neutral currents; supernova model 78−62391
neutrino transport calcs. using neutron transport methods 77−87377
neutrino transport in supernova models, multigroup diffusion scheme 79−25590
neutrino trapping at stellar collapse, effect on nucl. dissoc. 80−90407
neutrino viscosity in collapsing stellar cores 78−61875
neutron capture nucleosynthesis in He burning cores of massive stars 78−4195
neutron gas interactions at high density and temp., supernova models appl. 77−33330
neutron star, accreting, thermonuclear burning in degenerate envelope 80−109455
neutron star, eqn. of state of ideal neutrons in intense mag. field 78−89401
neutron star, plasma interface, physical processes in strong gravit. field, electron-positron pair prod., γ-ray emission *(Russian)* 79−80333

stellar internal processes continued
neutron star, relativistic quantum mechanical model for solid core 77−33546
neutron star, thermonuclear flashes in degenerate envelope *(Russian)* 79−35294
neutron star cores, AC Josephson effect rel. to pulsars emission 80−82404
neutron star envelopes, nuclear energy release and X-ray emission 77−78814
neutron star interior plasma, mag. field rel. to pulsar periods long-term changes 80−22029
neutron star interiors, presence of force-free mag. fields 78−40983
neutron star matter, abnormal phase 78−20849
neutron star matter, neutrino scatt. by phonons 79−12488
neutron star X-ray emission models 80−62175
neutron stars, β-decay of π condensates as cooling mechanism 78−4271
neutron stars, accreting, nuclear burning and X-ray bursts 78−36724
neutron stars, accreting, thermonuclear bursts assoc. with chromosphere flares 80−98684
neutron stars, eqn. of state for dense hadronic matter, asymptotic freedom 78−36627
neutron stars, heating and cooling processes rel. to thermal props. and detectability 80−31323
neutron stars, inner crust nuclear compositions 80−31322
neutron stars, luminosity enhancement following X-ray bursts 78−32502
neutron stars, MHD eqns. 79−35288
neutron stars, neutrino emissivities 79−97016
neutron stars, neutrino retention rel. to mass and radius 79−62817
neutron stars, nuclear fusion and C flashes 78−93293
neutron stars, pion condensate form. rel. to cooling 80−77443
neutron stars, postglitch behaviour of quantum plasma 79−35289
neutron stars, review of nuclear physics 79−92797
neutron stars, thermal-timing instability rel. to pulsars period jumps 79−35293
neutron stars, thermonuclear flahses model for X-ray bursts 78−12417
neutron stars, thermonuclear runaways rel. to X-ray bursts 80−22032
neutron stars ν transport in π condensed matter 78−4270
neutron stars cooling, calcs. 79−101170
neutron stars superfluid interiors, relax. processes between superfluid and crust 78−65645
neutron-proton electron mixture with zero charge density, eqn. of state, rel. to supernova explosions 77−53416
neutron-rich Si burning, nucleosynthesis equilib. processes 79−62816
NGC 6530 open cluster, broadband photometry rel. to ^{3}He burning 77−45504
NGC 7027, planetary nebula, evidence for CNO and 3 α processing of nebular material 80−82459
normal modes of self-gravitating fluids in perturbed configurations, perturbational-variation procedure 78−32336
Nova Cephei 1971, CNO thermonuclear runaway rel. to ejecta chemical comp. 78−12244
nova outburst, review of thermonuclear runaway model 77−82262
novae, ^{7}Li prod. 78−57555
novae, CNO nucleosynthesis 77−87452
novae, explosive hot CNO-Ne cycle H burning rel. to abundances 79−44489
novae, low-temp. photonuclear p-nuclei nucleosynthesis in degenerate H burning zones 78−57540
novae thermonuclear runaways, effect of binary companion on outburst 80−82394
nucelosynthesis in massive stars, mass loss effects on ^{14}N abundances and C/O ratios 79−101138
nuclear fissions in r and r-cooling processes 79−16816
nuclear reaction rate enhancement in dense stellar matter 79−21168
nuclear reactions, possible non-thermal processes 78−20816
nuclear reactions, struct. and strong interactions 80−72765
nuclear reactions associated with nucleosynthesis problem 80−101585
nuclear reactions in dense plasmas, theory rel. to stellar evolution 80−77281
nucleosynthesis, effect of mass loss by stellar wind on Galaxy chemical enrichment 80−41814
nucleosynthesis, element abundances evaluation in long neutron capture chains 78−45216
nucleosynthesis, heavy elements origin and evolution 78−32619
nucleosynthesis, history in Galaxy rel. to old halo stars chemical comp. 78−65616
nucleosynthesis, possible explanation for isotopically anomalous Xe and normal Os in Allende meteorite 77−45368
nucleosynthesis, reaction rates of (p,n) and (α,n) 79−45253
nucleosynthesis, review of recent exptl. research 78−4100
nucleosynthesis, Si burning, ^{45}Sc,(p,p') and ^{45}Sc(p,α) rates meas. 77−88134
nucleosynthesis due to explosive alpha-capturing reactions 79−44470
nucleosynthesis explosions, accelerator expts. and theory 77−71110
nucleosynthesis in exploding supernova inner shells 79−62860
nucleosynthesis in massive stars, effect of mass loss on chemical yields 80−36614
nucleosynthesis in massive stars, rel. to origin of cosmic rays and solar system elements 77−70952
nucleosynthesis induced during nova outburst 77−82263
nucleosynthesis rel. to element origin, review 80−62359
oscillations, adiabatic nonradial, freq. splitting by slow differential rot. 80−105233
p-process elements, neutrino induced prod. in collapsing star 77−45408
p-process isotopes nucleosynthetic origin in supernova explosions 78−57541
penetrative convection 78−89186
photoconvection 78−89190
photon-electron scattering, opacity due to electron correls. 77−64634
photoneutrino reactions in superstrong magnetoactive plasma, neutron stars appl. 79−35105
planetary nebulae central stars, CNO processing rel. to nebulae chemical abundances 78−36663
planetary nebulae nuclei, He shell flashes rel. to nebulae ionisation 80−73021
plasma diffusion rates, automatic computation, stellar interiors appl. 78−57434
Poisson's eqn. numerical soln. for flattened centrally condensed objects, stellar models 79−35110
polytropic models and early main sequence star periods of higher pulsation modes 77−49372

stellar internal processes continued
pre main sequence evolution, influence on main sequence (MS) stars chemical struct. 79−35247
pre-main-sequence stars, early evolution with D burning 80−51736
pre-supernova collapse, nuclear partition functions at high temperature 79−101059
pulsar crust superfluid, pinning and threading of quantized vortices 77−45475
pulsar radio emission, generation in neutron star mantle *(Russian)* 79−101168
pulsars, mag. field generation and possible radio emission mechanism 79−84812
pulsars, magnetogyro ratios rel. to core-crust decoupling and evolution 79−8937
pulsating stars, mixing length theory of convection 77−49367
pulsating stars asymptotic theory, boundary layer method 80−82389
pulsation damping due to interior weak interaction processes 80−77439
pulsation periods of stars with convection zones 77−33499
pulsations, nonlinear coupling 80−62115
pycno-nuclear reaction rate 78−61724
pycnonuclear reactions, and pair correl. function in dense plasma 78−32445
pycnonuclear reactions, pair correlation function in dense plasma 79−67001
quark stars, neutrino cooling 80−56858
r-nuclei production sites 80−72932
r-process abundance peak, A≈252, due to subshell effect of N≈164 77−2993
r-process nucleosynthesis, implications of fission mass distrib. 78−93204
r-process nucleosynthesis, required conditions 79−44459
R-type C stars, origin, H mixing during He flicker 78−4223
radiation pressure, Thomas-Fermi eqn. of state, high temp., coupling to high-density electron plasma 77−3925
radiative transfer in atmosphere, departure from LTE 79−48777
Rayleigh-Taylor convective overturn in stellar collapse 80−41815
reactions producing D, T, and ^{3}He in advanced stellar evolution, cross sections 80−56815
red giant stars, evolutionary sequences and He flash 78−65611
red giant stars, meridional circulation and CNO anomalies 79−48786
red giant stars, s-process abundance evolution in galactic disc 77−13449
red giants, ^{14}C and neutrons prod. 77−26005
red giants, mass loss from dynamically unstable envelopes 78−20824
red giants, peculiar, constraints on evolution from masses and space densities 80−22001
red giants, s-process element prod. in deeply mixed convective envelopes 77−33470
red giants with neutron cores, energy sources *(Russian)* 78−93197
red supergiants, envelope dynamical instability and lower mass limit for C detonation supernovae 77−17553
resonant thermonuclear reaction rate integrals, closed-form evaluation and approximation considerations 80−8535
rotating relativistic neutron star, interior MHD struct. 79−71062
rotating stars, 7 and 10 M⊙ stars evolution with time-depend. redistrib. of ang. momentum 78−36553
rotating stars, core instabilities rel. to evolution 77−13316
s-process, pulsed neutron flux effects 78−20812
s-process calcs. and Ba II stars 80−56824
s-process isotopes, nonthermal isomeric branching, importance of long-lived states 78−7983
s-process neutron capture by ^{208}Pb at stellar temps. 78−4196
s-process nucleosynthesis, effects of unthermalised isomeric states and time-varying neutron flux on branching ratios 80−90410
s-process nucleosynthesis, neutron capture time scale from s-process Kr in meteorite 80−73080
s-process nucleosynthesis, possible relics in Murchison meteorite inert gases 79−21243
s-process nucleosynthesis, thermally pulsing stars 78−4193
s-process nucleosynthesis and stellar mixing 77−33466
s-process nucleosynthesis during thermal pulses of He shell burning 78−28668
s-process nucleosynthesis in giant stars, implications of Ti isotopic abundance ratios 80−26840
s-process studies, exact soln. for unbranched network 78−28649
S-type stars, CeO band identification, new s-process mol. 77−33488
self-gravitating gas, self-similar adiabatic movements *(Russian)* 78−32451
semiconvection, semitheory 78−69787
semiconvection as occasional breaking of weakly amplified internal waves 79−48778
shell flashes, difficulty with ^{22}Ne as neutron source for solar system s-process 80−72926
slow nova, evolution of model with Z=0.03 envelope from pre-explosion to extinction 78−32468
slow nova, hydrodynamic study of outburst 78−40954
slow novae and symbiotic stars, role of white dwarf H shell flashes 80−94813
small mass stars, strong He flash *(Russian)* 77−26001
solar-type stars, mag. cores stability 79−44472
spallative origin of Li in weak G-band stars 80−51752
stability criterion for stellar cores *(Russian)* 78−93214
stable method heavy leptons, astrophysical mass constraint, condensation in stars and galaxies *(Russian)* 80−72768
stars of about 1 $M_\odot$, semiconvection and vibr. stability 77−22204
static models with varying He core mass, linear series of 7 M⊙ star 78−65603
stellar collapse, adiabatic hydrodynamics and shock wave propag. 80−56861
stellar collapsing core, role of neutrino dissipation 79−101166
stellar convection, value of mixing length 80−77379
successive He shell flashes, anal. rel. to stationary shell burning 80−51737
Sun and solar-type stars 77−53565
superdense configuration, internal struct., effect of nucl. interactions *(Russian)* 77−13324
superdense magnetised astrophysical objects, interiors physical conditions 80−17603
superdense matter, hydrodynamic model, nonlinear pion+pion chiral Lagrangian, $e^+ + e^-$ and p+p collisions 78−32966
superdense matter and stellar collapse, eqn. of state 79−16996
superdense matter eqn. of state, nuclear size correction to relativistic Thomas-Fermi model 78−29413

stellar internal processes continued
superdense stars in quantum limit of ultrastrong frozen-in mag. fields 77−53620
supergiant stars with degenerate neutron cores, equilib. models struct. 77−33472
supermassive stars, D prod. by neutrino-induced nucleosynthesis 77−87582
supernora collapse, high temp. matter comp. and adiabatic index 79−44354
supernova collapse, eqn. of state at subnuclear densities 80−77278
supernova core, Rayleigh-Taylor convective overturn rel. to explosion 80−77429
supernova explosion mechanisms 77−87465
supernova mass ejection and core hydrodynamics *(Italian)* 79−53842
supernova model, neutrino degeneracy effects 77−2447
supernova models, Fermi statistics effects on neutrino transport 77−26019
supernova models with slow energy pumping, appl. to galactic supernova remnants 78−73726
supernova nucleosynthesis, evidence from O/H ratios in LMC remnant N132D 78−93345
supernova nucleosynthesis mechanisms 77−87463
supernova off-centre explosions, rel. to high vel. pulsars form. 80−46587
supernovae, explosive core overturn and mass ejection 80−72988
supernovae, Fe group elements prod. through e-process nucleosynthesis, relative abundances *(Russian)* 80−62167
supernovae, He-driven r-process, rel. to solar system isotopic anomalies 78−57567
supernovae, lepton-driven convection 79−84811
supernovae, magnetorotational explosion in cylindrical model 80−101605
supernovae, mass range for r-process nucleosynthesis 79−5844
supernovae, Mg and Al isotopic yields from C and Ne shells of massive star 80−90406
supernovae, MHD model 80−46588
supernovae, models with gradual energy release 77−78807
supernovae, neutrino transport in collapsing stellar core model 78−8029
supernovae, Type I, radioactive excitation source rel. to interpretation of spectra 78−49467
supernovae, Type I, slow energy injection model rel. to envelope ejection and light curve 78−65636
supernovae, type I and II, neutrino mechanism of thermonuclear explosion of degenerate C-O cores 80−62162
supernovae core collapse, neutrino energy equilibration models 80−105265
symbiotic stars, H shell burning rates and evolutionary considerations 80−62144
symbiotic stars and slow novae, role of white dwarf H shell flashes 80−94813
thermal convection, mag. field effect on onset under const. flux boundary conditions 78−69676
thermal props. of self-gravit. plane-symm. gas 77−13323
thermal pulse and interpulse props. of intermediate-mass models with C-O cores 78−12199
thermal pulses in high-luminosity stars, effects on surface comp. and interstellar medium enrichment 78−40917
thermal pulses in nuclear shell burnings, finite amplitude, general theory 79−80299
thermal relaxation oscills. in two-zone model 79−96990
thermodynamics of hot stellar mass, appl. of stability predictions through a succession of folds 79−76991
thermonuclear astrophysics, element abundances rel. to nucleosynthesis *(Italian)* 79−53715
thermonuclear burning in degenerate C core, triggering of stellar collapse 78−65608
thermonuclear combustion of C, neutrino mechanism, form. of neutrino stars and supernova outbursts *(Russian)* 77−87379
thermonuclear explosion of degenerate C core, numerical calcs. 78−36558
thermonuclear flashes in envelopes of accreting neutron stars 80−67772
thermonuclear flashes on accreting neutron stars 80−31321
thermonuclear ion-electron screening at all densities, static soln. 77−29793
thermonuclear reaction rate, parameter-depend. integral evaluation 79−29985
thermonuclear reaction rate enhancement due to strong screening 78−13186
thermonuclear reactions, high energy particle excess, effect on secondary reaction rates *(Russian)* 80−77393
thermonuclear reactions, quantum theory of screening effect in relativistic electron plasma *(Russian)* 77−17350
thermonuclear reactions, rate enhancement due to strong screening, ionic mixtures case 80−36613
thermonuclear runaways in white dwarf envelopes 77−56961
thermosolutal convection 78−89188
turbulence, conference, London, Ontario, Canada (1979 August 27 to 30) 80−73102
turbulent convection, spectral model 77−33465
turbulent diffusion and $^{12}C/^{13}C$ abundance ratio 80−21993
turbulent thermal convection in presence of rot. and mag. field, stellar and planetary dynamos appl. 80−6042
turbulent transport coefficient for rot. fluid 78−36452
Type I supernovae, theory, light curve anal., evolutionary sequence 79−62858
URCA convection 78−89189
URCA process, in convective degenerate C cores 77−22203
SU Ursae Majoris stars, g-mode oscills. rel. to periodicity of supermaxima 80−101596
wave transport in stratified, rotating fluids 78−89192
weak G-band stars, origin through CN process and meridional mixing 78−49432
weak interaction rates for sd-shell nuclei, appl. to supernovae 80−82336
white dwarf degenerate cores, thermomagnetic instability conditions 80−77395
white dwarf envelopes, heavy ion diffusion 80−51754
white dwarf interiors, nuclear crystals form. *(Polish)* 77−17355
white dwarf with mass accretion, H shell flashes rel. to symbiotic stars vars. 78−57550
white dwarfs, accreting, instability of steady state nuclear burning 80−77402
white dwarfs, diffusion time scales 79−92761
white dwarfs, H burning shells, thermal stability 78−4212
white dwarfs, He flash and nova evolution 80−72938
white dwarfs, neutrino retention rel. to mass and radius 79−62817
white dwarfs, rapid mass accretion rel. to H shell burning and extended envelope form. 80−67723
white dwarfs, thermonuclear runaways 78−40937
white dwarfs, virial theorem, energy content and mass-radius relation 78−45327
white dwarfs external layers, convection and sedimentation, rel. to interpretation of spectra 79−62824
Wolf-Rayet stars, CNO abundance var. in massive binaries 80−94802
Wolf-Rayet stars, mixing before shell ejection, evidence from ring nebula (NGC 6888) 79−8964
young stars, nonspherical thermal instability 79−48779
(n,γ) for A=138-181, stellar nucleosynthesis and s-process neutron flux 80−42663
pp→de$^+\nu$, effect of vac. polarisation on solar reaction rate 77−57555
pp reaction, exchange current corrections π and ρ exchange 80−26733
π^- condensation, nonrelativisitc treatment, mean field method 77−30500
^{26}Al nucleosynthesis, long lived nucl. isomeric states, thermlaization 80−85846
^{26}Al, prod. from stellar evolutionary sequence 79−5809
^{26}Al production during C burning, stellar rates, calc. 79−70948
^{11}B, neutrino-induced prod. in stellar C layer 80−82337
C burning, products at const. temp. *(Russian)* 78−61722
C burning in degenerate core, convection effects 80−41810
C burning in electron-degenerate stellar core, thermal oscills. 79−21269
C cores, evolved, nuclear energy generation rates and energy dissipation 80−82339
C degenerate core thermonuclear reaction propag., neutrino mech. *(Russian)* 79−5812
C detonation supernova models, lower mass limit 79−17053
C shell burning to Fe core collapse, evolution of 15 M⊙ star 80−72937
C shell flash in 9 M⊙ star 78−89170
C-burning flash in degenerate C-O stellare core, thermal phase 77−78774
C-O cores of intermediate mass stars, Urca neutrino loss rates 78−20813
C-O dwarf, H and He burning in degenerate envelope *(Russian)* 80−17585
C-O white dwarfs, C-O eutectic model 80−77405
CNO burning and zero age horizontal branch stars location 78−12201
CNO cycles in stellar nucleosynthesis 77−87381
CNO isotope nucleosynthesis 77−87383
CNO nuclei enhancement in nova progenitors 77−33484
CNO nucleosynthesis, cross section meas. 77−87382
CNO processing in stellar envelopes, isotopes origin and isotopic ratios evolution 78−93201
CNO tri-cycle, nucleosynthesis rel. to galactic obs. of CNO isotopes 78−4356
^{12}C, internal pair emission branch of 7.65 MeV, stellar triple-α reaction 77−54183
^{12}C prod., He burning stars, 3α system forming O_2^+ resonance 78−50108
^{12}C(α, α'), 40.2 MeV branching ratio of 7.654 MeV state, rate of stellar He burning 77−2941
^{13}C(α,n)^{16}O, 0.60-1.15 MeV, astrophysical appls. 77−13230
^{13}C(α,n)^{16}O process, 0.60 to 1.15 MeV, reaction rate 77−45300
^{14}C(α,γ)^{18}O and onset of core He flash in low-mass stars 80−51735
^{40}Ca(α,γ)^{44}Ti, 2.75-4.00 MeV, γ-ray ang. distrib. of reson. for spin parity values 77−65230
^{42}Ca(p,γ), 0.7-5.5 MeV, cross section and stellar nucleosynthesis reaction rates 79−13294
^{42,44}Ca nucl. reaction rates, reactions involving proton and α-particle absorpt. 80−82183
Fe-O stars collapse, effects of neutrino radiation and absorpt. 77−87369
Fe-O stars with masses of 2M⊙ and 10 M⊙, gravit. collapse 78−20815
H and He, thermodynamic props. and eqns. of state in stellar conditions thermodynamic props. and eqns. of state in stellar conditions 79−35241
H burning, intermediate nuclei behaviour 78−45218
H burning of ^{29,30}Si in explosive C burning 79−22289
H burning thermonuclear reactions, pp chain and CNO cycle 77−22202
^{1}H(p,eν^+)^{2}H, bounds on rate, impulse approx. 77−3000
^{2}H, superdense, cold, nuclear reaction energy output in mag. field *(Russian)* 77−29801
He burning information from ^{12}C(^{6}Li,d) and ^{16}O(^{6}Li,d) studies 78−89897
He burning shells, explosive neutron processing rel. to metoeritic abundance anomalies 79−58302
He core flash, convection efficiency and mixing possibilities 79−48774
He flash and convection in stellar cores 78−89191
He flash in stars with shell energy sources 78−89169
He fusion information from ^{12}C(^{7}Li,t)^{16}O, α spectroscopic factors and reduced widths 78−89896
He shell burning, thermal pulses in accreting white dwarf 80−22009
He shell burning stages, core mass-luminosity relations 80−21983
He shell flash quenching conditions 77−29790
He shell flashes, rel. to planetary nebulae ejection and planetary distance scale 78−24540
He shell flashes, theory 77−56909
He shell flashes in red supergiants, convective penetrations and observable effects 80−51755
He star evolution using Carson's radiative opacities 78−4191
He-burning flashes on accreting neutron star, X-ray burst source model 79−17008
He-rich white dwarfs, convective mixing 79−71018
^{4}He(α,n)^{7}Be, ^{4}He(α,p)^{7}Li, α-α scatt. phase shifts, cross sections near threshold 79−3163
HgMn stars, diffusion model rel. to obs. of Hg in thin atmospheric layer 80−105243
Li nucleosynthesis from $\alpha+\alpha$ 61.5-158.2 MeV 79−17886
Li production by weak G-band stars, results from abundance meas. 80−41819
^{6}Li(d,n)^{7}Be, low energy cross section, 100-180 keV 78−4949
^{7}Li nucleosynthesis in UV Ceti flares 79−30073
^{25}Mg(p,γ) reaction, relative yields of ^{26}Al^g and ^{26}Al^m 79−101058
^{26}Mg(p,γ)^{27}Al, isotopic anomaly, stellar reaction rate, astrophysical aspects 80−99132
Mg(p,γ), 0.3-2.1 MeV, stellar H burning in explosive C burning 80−86875
N, stellar nucleosynthesis rel. to galaxies ages determ. 79−25728

stellar internal processes continued
$^{15}N(p,\alpha_0)^{12}C$, 93 to 418 keV, remeas. of low energy cross section, astrophys. S-factor determ. 79−63665
Ne explosive burning in supernovae isotope production 80−94780
^{20}Ne, form. in $^{19}F(p,\gamma)$ reaction, 668 keV, γ-ray transitions to ground state, rel. to stellar nucleosynthesis 78−17191
$^{20}Ne(p,\gamma)^{21}Na$, 1.7 MeV, DSA lifetime 2425 keV state 77−82860
^{22}Ne neutron source effects on Mg and Ne abundances in red giants 78−49430
$^{18}O(\alpha,\gamma)$, 0.6 to 2.3 MeV, props. of ^{22}Ne compound states, astrophys. reaction rate 78−57545
$^{18}O(p,\alpha)$, 661 to 223 keV cm, cross section meas. and S-function extrapolation using R-matrix theory 78−82341
$^{18}O(p,\alpha)$ 72 to 935 keV, astrophysical reaction rate, ^{19}F resonances 79−26439
$^{A}Os(n,\gamma)$, A=186-188, 2.6-800 keV, capture Maxwellian cross sections, galactic nucleosynthesis 80−42664
$^{32}S(n,X)$, 2.5-1100 keV, resonance struct. from total and capture cross sections 80−42620
$^{45}Sc(p,\gamma)$, 0.7-4.2 MeV, cross section, statistical model anal., stellar interaction rate 79−17897
$^{45}Sc(p,\gamma)^{56}Ti$, stellar reaction rates 78−93090
Si burning, during advanced evolution of massive stars 78−28652
Si burning models, influence on $^{16}O(p,\alpha)$, $^{20}Ne(p,\alpha)$, $^{24}Mg(p,\alpha)$ reactions 77−82929
Si explosive burning, Ca reactions in approach to equilib. phase 80−82183
$^{49}Ti(p,\gamma)$, 0.74-3.25 MeV, cross section and thermonuclear reaction rates, nucleosynthesis, IAR effects 80−102187
$^{49}Ti(p,n)$, 0.74-3.25 MeV, cross section and thermonuclear reaction rates, nucleosynthesis 80−102187
^{50}V, ^{138}La and ^{180}Ta, low temp. photonuclear nucleosynthesis in H-CNO burning zones 77−13319

stellar light curves *see stellar photometry*

stellar magnetism
see also solar magnetism
α^2-dynamos, finite amplitude, with large scale in compressible circulation, theory 78−81534
α-effect dynamo, determ. for slow and fast rot. 79−40069
2A 0311−227, high-speed photometry of AM Herculis-type binary 80−41912
A-type stars, mag. field generation by Coriolis EMF 78−8027
accreting compact object in binary system, magnetosphere theory, X-ray sources 80−46394
accreting magnetic degenerate dwarfs, X-ray and UV emission 80−41826
accretion magnetospheres for dipole-magnetised stars, general solns. 77−45400
adiabatic stability of toroidal magnetic fields in differentially rotating stars 79−66998
angular momentum and magnetic moment from superheavy hadrons 80−26843
Ap, Am stars, mag. fields rel. to chemical differentiation by diffusion 80−77381
Ap and Bp stars, surface mag. field intensity rel. to Geneva photometry 80−105248
Ap stars, decentred dipole and dipole quadrupole magnetic field models, anharmonic analysis 79−101154
Ap stars, flows and mag. fields in surface layers 79−62854
Ap stars, mag. fields meas. techniques and field geometries 80−82213
Ap stars, mag. fields struct., and precession in oblique rotator model 77−2432
Ap stars, magnetic field generation and chemical anomalies 77−13359
Ap stars, magnetodynamic mechanism 77−87404
Ap stars, model atmospheres 79−16973
Ap stars, orientation of mag. and rot. axes, decentred mag. dipole theory 78−4241
Ap stars, review of obs. and possible nucl. reactions *(Russian)* 78−20843
Ap stars in open clusters, rot. vels. and mag. braking 77−33500
Ap variable stars, mag. fields rel. to light vars. and evolution 77−87426
Ap-stars, mag. field obs. using photoelec. method, visible spectra obs. 80−82373
Ap-stars, magnetic intensification of spectral lines *(Russian)* 78−4254
Ap-stars, photometry and surface magnetic fields 80−56847
Ap-type stars, mag. fields rel. to chemical anomalies *(Russian)* 77−17591
Ap-type stars, magnetic fields in atmospheres *(Russian)* 77−17594
Ap-type stars in spectroscopic binaries, orbital characts. rel. to mag. field generation *(German)* 77−17590
R Aquarii, symbiotic long-period variable, magnetically active single star model rel. to nebula spectrum 80−90450
UX Arietis, binary star, synchrotron radio emission obs. 77−64793
atmospheres, non-LTE line form. in presence of mag. field 78−7871
atmospheres, radiative heat transfer in presence of mag. field *(Russian)* 77−87247
atom motion in very strong mag. fields, mass anisotropy effect *(Russian)* 80−67557
θ Aurigae, short period Ap star, discovery of mag. field 77−33511
baryon star magnetospheres, inclined rotator case 80−26887
baryon stars, magnetospheres model *(Russian)* 77−91555
Be stars, mag. fields determ. via linear polarisation spectrum *(Russian)* 80−90344
Be-stars, magnetic fields rel. to dynamics 77−60778
binary stars, short period, X- and γ-ray bursts from mag. reconnection 78−81654
binary stars, surface nucl. reactions and origin of mag. fields 80−101616
black hole, charged rotating, mag. torque effects 79−17010
black hole, rotating, in mag. field, particle creation 77−2452
ξ Bootis A, late-type dwarf star, mag. field obs. 80−72949
BPM 25114, hot magnetic white dwarf, image tube spectrophotometry 77−74051
BPM 25114, peculiar white dwarf, light vars., oblique rotator model *(Italian)* 78−93241
BPM 25114, southern mag. white dwarf, spectrophotometric obs. 79−92765
53 Camelopardalis, Ap star, surface mag. field distrib. 77−26015
53 Camelopardalis, binary Ap star, evidence for mag. period var. 79−80320

stellar magnetism continued
53 Camelopardalis, mag. field meas. using circular polarization analyzer *(Russian)* 78−40923
α^2 Canum Venaticorum, Ap star, surface mag. field distrib. 77−26015
α^2 Canum Venaticorum, mag. Ap star high-resolution polarisation obs. inside spectral line 78−40951
α^2 Canum Venaticorum, mag. field meas. using circular polarization analyzer *(Russian)* 78−40923
RS Canum Venaticorum binaries, effects of tides and flares 79−71068
RS Canum Venaticorum binary stars, mag. starspot model for photometric and spectroscopic behaviour 80−109488
α Carinae (Canopus), periodic variable mag. field detect. 77−49381
β Cephei stars, magnetic fields in nine variables 78−65631
Cepheid variables, mag. fields effects on pulsational behaviour 80−31302
charged particle motion in an electromagnetic field on Kerr background geometry 79−9167
chemically peculiar A-type stars, magnetosphere/grains interaction rel. to grains accretion 79−67017
circumstellar clouds, mag. fields rel. to scattered stellar radiation circular polarisation 78−96428
cold dense star with frozen-in mag. field, degeneracy removal, ideal electron gas approx. *(Russian)* 77−87365
collapsed stars, accretion magnetosphere stability, polar cap dripping motion 78−4194
collapsed stars, mag. braking rel. to slow rot. 78−49426
17 Comae A, Ap star, mag. field meas. and rot. period *(Russian)* 80−90457
17 Comae A, variable Ap star, mag. field struct. 77−17595
compact objects, mag. field struct. rel. to disc accretion *(Russian)* 79−44467
conducting sphere rotating in time independ. homogeneous mag. field, unipolar induction *(German)* 78−17836
convection and magnetic fields 78−89185
convection in rotating magnetic star, toroidal field effect 80−41816
convection zone, thermal equilib. in presence of mag. flux tube 77−53581
convective instability, mag. fields and g^- modes 78−93211
convective stability in magnetic stars, theory 80−94781
corona, open mag. structures 78−4158
β Coronae Borealis, Ap star, high resolution polarization obs. 78−8011
β Coronae Borealis, Ap star, possible indication of mag. deform. 77−45454
β Coronae Borealis, Ap star, struct. of atmospheric mag. field *(Russian)* 77−17594
β Coronae Borealis, Ap star, transverse Zeeman effect, oblique rotator model 77−13361
β Coronae Borealis, mag. deform. 77−49400
β Coronae Borealis, mag. deform. ot evolved stellar model, hypothesis 79−30076
β Coronae Borealis, mag. field meas. using circular polarization analyzer *(Russian)* 78−40923
β Coronae Borealis, mag. star, spectral peculiarities *(Russian)* 77−64773
β Coronae Borealis, magnetic deformation and precession model 78−53963
β Coronae Borealis, magnetic field of Ap-star 79−5822
β Coronae Borealis, obs. with Zeeman analyzer system on McDonald 2.7 m telescope 80−62021
cosmic betatron model, general relativistic induction accelerator 77−37793
cosmological interpretation 80−46714
Crab Nebula, central mag. dipole rot. neutron star theory for supernova remnant 80−51834
Crab pulsar, electron-positron flux at neutron star surface 77−64789
Crab pulsar, magnetized cracks in crust rel. to matter flow, radio, X-ray and optical emissions 80−72990
Crab pulsar magnetosphere, relativistic particles injection into Crab Nebula 78−36678
cyclotron self-absorption in accretion columns of magnetic degenerate stars, X-ray sources appl. 80−12760
ss Cygni, hard X-ray source, obs., accretion onto white dwarf 79−30078
V1057 Cygni, OH line Zeeman splitting and stellar mag. field 80−36629
CH Cygni, red giant, mag. field interpretation for outburst 78−4250
Cygnus X-3, gamma-ray emission from mag. accretion disc 77−78894
DA white dwarfs, calc. and obs. spectra 79−71032
DA white dwarfs, mag. field geometries rel. to spectral line profiles 80−62123
degenerate stars, force-free mag. fields stability 78−49425
dense neutron matter, ferromag. transition, pure hard core gas model 78−70478
dense stars, atomic spectra in intense mag. fields 80−105160
differential rotation effect on velocity and magnetic fields, superposition of poloidal and toroidal field 80−72928
73 Draconis, CH lines in spectrum of Ap star *(Russian)* 77−56958
ϕ Draconis, short period Ap star, discovery of mag. field 77−33511
73 Draconis, spectral variability of Ap star *(Russian)* 78−65624
BY Draconis syndrome among dMe stars, rotating spotted star model 78−16428
dwarf nova brightening, magnetic fields and outburst phenomena *(Afrikaans)* 78−32481
dwarf novae, nature, H accretion, mag. field, radiation mechanisms *(Russian)* 78−93277
dwarf stars, mag. fields rel. to chromospheric models and activity 79−48773
dwarfs, degenerate accreting, thermonuclear bursts effects on mag. field 80−98684
dynamo model of magnetic field, self-consistent treatment 80−81808
dynamo theorems 80−81810
dynamo theory, spherical dynamo with anisotropic α-effect 80−81809
electric field, around rot. mag. dipole 78−45141
electrically conducting rot. sphere behaviour in time-independ. homogeneous external mag. field 78−49309
electron-positron pair annihilation in strong mag. field *(Russian)* 79−17705
equilibrium structures, of self-gravitating gas masses containing axisymmetric mag. fields 80−94708
γ Equulei, magnetic field obs. of Ap-star 80−51782
eruptive variables, magnetic field effects 79−62845
exploding or collapsing magnetized rotating spheroid, mag. dipole radiation 79−35106

stellar magnetism continued
F- and G-type stars, mag. accel. of winds and ang. momentum loss 77−13334
Feige 7, hot rotating magnetic white dwarf discovery 77−53589
Feige 7, mag. white dwarf, spectroscopic studies 79−25603
field generation by close binary interaction 80−26903
field line reconnection, relativistic modes of tearing instability in background plasma 80−62012
flare stars physical charcts. 77−41383
flux tube in star interior, buoyancy and equilib. 80−109420
force-free magnetic fields toroidal component upper limit rel. to flares 77−33479
G35-26, high-velocity mag. degenerate, obs. 78−73709
GD229, cyclotron absorpt. in white dwarf 79−53813
GD 229, mag. white dwarf, spectroscopic studies 79−25603
GD 90, magnetic white dwarf, circular polarisation obs. 78−16409
giant stars with IR excesses, mag. fields rel. to optical emission linear polarisation 78−96481
gravitating magnetised cylinders equilib. struct. 78−96471
HD 116458, mag. Ap star, photometry, spectrum and orbit 77−64767
HD 153882, obs. with Zeeman analyzer system on McDonald 2.7 m telescope 80−62021
HD 215441, mag. field geometry 78−53950
HD 215441 (Babcock's star), magnetic vars., non-axisymmetric eccentric dipole model 80−51779
HD 3980, late Ap star, photometric and mag. variability obs. 80−56845
HD 4174, peculiar M-giant, magnetic field 80−8631
HD 4174 (=EG Andromedae), peculiar M giant, mag. field existence, UV spectra obs. 80−94798
HD 9996, Ap star, spectrsocopic obs. 78−77558
helical velocity and magnetic fields, stability 78−73624
Hercules X-1, cyclotron self-absorpt. in accretion column of mag. degenerate star 80−12760
Hercules X-1, mag. field rel. to prod. of cyclotron features in X-ray spectrum 80−86015
Hercules X-1, struct. and higher harmonics of cyclotron lines in strong mag. field 78−20912
Hercules X-1, X-ray lines and magnetic field 78−24574
AM Herculis, accretion onto highly magnetised white dwarf 79−92764
AM Herculis, high-speed circular polarimetry 79−25629
AM Herculis, highly magnetised, accreting white dwarf 77−49396
AM Herculis, X-ray binary, polarization obs., mag. compact star discovery 77−33569
AM Herculis (3U 1809+50), polarimetry and spectrophotometry rel. to mag. field 80−94835
AM Herculis (4U 1814+50), mag. white dwarf models for X-ray source 80−105403
AM Herculis objects, accreting mag. white dwarf model for linear polarisation 78−16460
AM Herculis type binaries, cyclotron self-absorption in accretion columns of magnetic degenerate stars 80−12760
AM Herculis/3U 1809+50 X-ray binary, rot. mag. white dwarf model 77−33571
horizontal magnetic field stability in stably stratified atmosphere 79−75200
HR 1099, binary star, synchrotron radio emission obs. 77−64793
HR 1099, rapidly variable circular radio polarisation obs. rel. to mag. field 79−21336
HR 1099, RS Canum Venaticorum binary, VLA obs. rel. to large-scale mag. field 79−21334
HR 5597, irregularly variable magnetic star 77−74061
HR 7129, He variable, oblique rotator model 79−62838
W Hydrae, long-period variable, suspected Zeeman splitting in OH masers 80−36632
VW Hydri, dwarf nova, almost corotating mag. white dwarf model 79−16977
hydromagnetic phenomena described by elec. currents 80−36495
inhomogeneous field, spectral line circular polarisation 79−5804
internal flux range, effects of toroidal fields 77−45406
IRC+10420, stellar OH maser VLBI obs. rel. to mag. field 79−25742
Jeans spheroids with toroidal mag. fields, equilib. and stability 78−45319
Kerr black hole, elec. and mag. cond. 79−25625
Kerr black hole with tilted accretion disc, mag. alignment 77−60789
EV Lacertae, flare star, mag. fields in flares hot-plasma model 78−20838
late-type stars, ang. momentum loss rel. to mag. dynamo 78−45331
CW Leonis (IRC+10216), IR C star, circumstellar dust orientation by paramag. relaxation rel. to intrinsic polarisation 80−67730
linear acoustic waves in radiating scatt. grey medium, effect of transverse mag. field 77−56911
linear oscillations of mag. configurations, unrestricted second-order tensor virial eqns. 79−44461
linked poloidal-toroidal magnetic fields and pulsation freqs. 78−96470
LP 790-29, southern mag. white dwarf, spectrophotometric obs. 79−92765
LP 790-29 mag. degenerate with heavily blanketed energy distrib., obs. 79−5815
α Lyrae, mag. field activity rel. to soft X-rays obs. 79−48953
RR Lyrae, multiperiodic behaviour rel. to mag. field 77−87430
RR Lyrae stars, hydromagnetic processes as cause of period changes 80−105261
magnetic binary problem, charged particle motion stationary solns. for oblate spheroid primaries 80−41697
magnetic field calculation of cosmological bodies 79−12399
magnetic pole model for pulsar emission 79−48838
magnetic star phenomena *(German)* 77−67103
magnetic star polarity reversal, appl. of skin effect approx. 80−62010
magnetic stars, equatorially symmetric rotator model, inhomogeneous element distrib. 80−4371
magnetic white dwarfs, line and continuum spectra 78−4207
magnetoatmospheric instabilities, max. growth rates 77−53573
magnetospheres of accreting compact stars possessing multipole magnetic fields 79−97020
main-sequence stars, mag. mixing rel. to CNO isotope abundances and α Bootis (Arcturus) problem 80−105229
MHD, Brinkley-Kirkwood method, appl. to shock waves in stellar atm. *(Russian)* 78−93102
MHD dynamo theory of mag. field *(French)* 79−35161
MHD equilibrium figures with magnetic field 77−45303
stellar magnetism continued
MHD oscillations in convectively neutral fluids, pure perturbation spectra 77−41292
MHD processes near compact superdense objects 79−40206
MHD waves, propag. in mag. flux tube 78−69789
model for magnetic stars, equatorially symmetric rotator 78−8020
models with small-scale magnetic fields *(Russian)* 79−92754
MXB 1730−333, rapid X-ray burster, accreting rot. magnetised neutron star model 79−84866
n-vertex loop diagrams in superstrong calc. field, calc. method 77−71472
neutron star, accreting, magnetopause struct. 78−65647
neutron star, eqn. of state of ideal neutrons in intense mag. field 78−89401
neutron star, interaction between accretion disc and mag. field *(Russian)* 80−51799
neutron star, magnetic, disc accretion effects on rot. 78−93294
neutron star, magnetised, cyclotron line form. in atmosphere 79−48839
neutron star, neutrino-pair bremsstrahlung in hot plasma, strong mag. field 78−61878
neutron star, particle acceleration at magnetic poles 78−93295
neutron star, rotating, with strong mag. field, electron cap shape 78−12265
neutron star crust, correl. between speeds of fast and slow magnetoelastic modes 79−8942
neutron star interior plasma, mag. field rel. to pulsar periods long-term changes 80−22029
neutron star interiors, presence of force-free mag. fields 78−40983
neutron star magnetosphere, plasma dynamics and accretion, fate of sinking filaments 80−51798
neutron star magnetospheres, laboratory modelling 79−75240
neutron stars, accreting, mag. fields rel. to cyclotron emissivity 80−90463
neutron stars, accreting, normal mode anal. of interchange instability at magnetopause 77−13376
neutron stars, accreting, thermonuclear bursts effects on mag. field 80−98684
neutron stars, accretion flow, magnetospheric struct. and stability 78−4269
neutron stars, effects of rot. and mag. fields on superfluidity 80−77441
neutron stars, electrodynamics in curved space 80−90465
neutron stars, electrodynamics of disk acrretion, magnetic field structure 80−85973
neutron stars, electron solids in superstrong mag. fields, bifurcation-theory approach 80−4640
neutron stars, EM multipole fields 80−26896
neutron stars, H transition probabilities and expectation values, in intense mag. field 79−10066
neutron stars, mag. field effects on plasma accretion 80−109452
neutron stars, mag. field effects on thermal radiation 80−56869
neutron stars, mag. fields and related effects 80−72991
neutron stars, mag. fields rel. to radiative heat transfer in surface layers 80−94826
neutron stars, mag. fields rel. to X-ray refl. from surface 78−28716
neutron stars, magnetospheres rel. to fate of matter and ang. momentum in disc accretion 78−28715
neutron stars, pair annihilation in superstrong magnetic fields 80−85847
neutron stars, pair formation and electric field boundary conditions at magnetic poles 80−101613
neutron stars, positronium annihilation in strong magnetic fields 79−17007
neutron stars, positronium decay in strong mag. fields, 10^{12} Gauss 79−88578
neutron stars, props. of condensed matter in huge mag. fields 80−82187
neutron stars, radiation source form. mechanism, mag. annihilation *(Chinese)* 80−77440
neutron stars, rot. and magnetism rel. to possible accretion instabilities 77−13377
neutron stars, rot. mag. field interaction with accretion disc 80−62173
neutron stars, rotating, magnetic, accretion flow inside magnetosphere rel. to rot. rate 78−8037
neutron stars, superdense quark core, spontaneous magnetisation possibilities 80−8646
neutron stars, torques rel. to pulsating X-ray sources period changes 80−31320
neutron stars, vacuum birefringence effects on X-ray polarisation 79−40209
neutron stars, X-ray emission lines Zeeman splitting by mag. field 78−4275
neutron stars in close binary systems, mag. fields rel. to spindown rates 79−40210
non-LTE line formation in mag. field, two-level atom with freq. independent source function 78−61726
non-spherical magnetic polytropes struct., appl. of smoothed particle hydrodynamics theory 78−12203
nonlinear dynamo models, multiple-period dynamo wave oscills. solns. 79−16813
nonlinear magnetic dynamos, bifurcation of steady dynamos from oscillating dynamos 78−49306
nonrelativistic para-Fermi gas, thermodynamic and mag. props. 79−25974
NP 0532, Crab pulsar, mag. field rel. to Crab Nebula small-scale polarisation 79−25656
NP 0532 magnetosphere, cyclotron instability rel. to origin of radiation *(Russian)* 80−8645
oblique rotator model, kinematic mechanism 77−45407
oblique rotator with irrotational axisymmetric mag. field surface distrib., effective mag. field 80−26872
70 Ophiuchi A, late-type dwarf star, mag. field obs. 80−72949
U Orionis, stellar OH maser VLBI obs. rel. to mag. field 79−25742
σ Orionis E, mag. field discovery 78−93268
oscillation freqs. of magnetic stellar models 78−69783
perpendicular rotator model with meridional circulation, surface and internal mag. fluxes 78−16438
photoneutrino reactions in superstrong magnetoactive plasma, neutron stars appl. 79−35105
photospheres, mag. structs., models *(Italian)* 78−81603
plasma mechanisms, mag. field modifications theories, review 77−73946
polytrope n=3, poloidal mag. field effect on linear and adiabatic oscills. 78−24505
polytropic star, equilib. poloidal mag. field, finite difference-finite expansion method, Fortran program 77−13322

stellar magnetism continued
polytropic stars with toroidal magnetic fields, hydromagnetic instabilities 79−8905
propeller spindown of rotating magnets, torque calc., neutron stars appl. 79−8831
protostars, quasistatic contraction due to mag. flux leekage 80−98662
protostellar sources, IR polarisation rel. to nearby interstellar polarisation 80−4347
pulsar, magnetism rel. to constrained atmosphere min. energy state 79−25622
pulsar atmosphere with arbitrary mag. and rot. axes, qualitative features 78−57569
pulsar crust, crust, infinitely magnetised H atom theory 80−77282
pulsar electron cap, electrons accel. in internal zone 80−46592
pulsar magnetosphere, behaviour of mag. lines of rot. system 78−20848
pulsar magnetosphere, curvature radiation-pair prod. model for gamma-ray emission 79−5852
pulsar magnetosphere, electron absorpt. rel. to spectra low-freq. dropoff 80−17602
pulsar magnetosphere, instability 78−53976
pulsar magnetosphere, mag. energy density rel. to curvature radiation absorpt. 79−75090
pulsar magnetosphere, magnetoactive plasma equilib. in gravit. field *(Russian)* 80−26895
pulsar magnetosphere, plasma waves propag. along mag. field in strongly anisotropic relativistic plasma 80−67542
pulsar magnetosphere, quasi-transverse propag. theory rel. to individual pulse-polarisation patterns 80−46591
pulsar magnetosphere, radio propag. effects on pulsar emission polarisation 79−75235
pulsar magnetosphere, vibrations generation by klystron mechanism 78−53971
pulsar magnetosphere models, interior and exterior struct., pair prod. 80−46594
pulsar magnetosphere pair prod. 79−44515
pulsar magnetospheres, consequences of polar cap model *(Russian)* 79−101169
pulsar magnetospheres, gamma ray emission model 78−65641
pulsar magnetospheres, narrowband versus broadband emission processes rel. to luminosities 80−51797
pulsar magnetospheres, plasma co-rotation 78−12258
pulsar magnetospheres, probing via signal microstruct. periodicities and polarisation 79−75232
pulsar magnetospheres, stellar-wind model for plasma-EM fields 80−22031
pulsar magnetospheres physics, limitations on force-free approximation 77−5541
pulsar open magnetosphere, plasma instabilities as source of coherent radio emission 80−82403
pulsar polar cap, inhomogeneous struct. and radiation processes 79−25623
pulsar polar caps, pair form. and struct. of low altitude accel. zone 79−92790
pulsar polar caps, pot. drops and ultrarelativistic particle accel. along curved mag. field 78−53970
pulsars, axisymmetric magnetosphere model 79−84813
pulsars, axisymmetric magnetosphere models 79−92794
pulsars, charge-separated magnetospheres props. 78−40981
pulsars, charged particle accel. to extremely high energies in far field 77−29868
pulsars, field lines curvature rel. to amplified linear accel. radio emission 79−8936
pulsars, gamma-ray emission by electrons moving in curved mag. field 78−53975
pulsars, inertial mechanism of mag. field generation *(Russian)* 77−82268
pulsars, influence of mag. field on comp. of outer crust 80−101610
pulsars, initial magnetic moments rel. to decay times 79−62861
pulsars, mag. dipole axis orientation rel. to relation between braking and beaming 79−92793
pulsars, mag. dipole moments secular var. 77−9764
pulsars, mag. field correl. with P_3 period 80−90461
pulsars, mag. field generation and possible radio emission mechanism 79−84812
pulsars, mag. fields evolution 77−78808
pulsars, mag. fields rel. to radio emission mechanism 78−20847
pulsars, mag. geometry and hollow-cone radiation model 77−9761
pulsars, mag. monopoles creation 79−44516
pulsars, mag. monopoles creation rel. to mag. field decay 79−35287
pulsars, magnetic field similarities with Jupiter, radio emissions *(Russian)* 80−77333
pulsars, magnetogyro ratios and evolution 79−8937
pulsars, single mag. pole model for main pulse and interpulse emission 78−16449
pulsars axiosymmetric magnetospheres, method of soln. of self-consistent description 80−94825
pulsars force-free wind zone, stability 78−49468
pulsars magnetic alignment, classification system 77−45476
pulsating star, hydromagnetic flow near oscillating porous limiting surface with transverse mag. field 78−12200
pulsational stability, magnetic field influence 79−53800
VV Puppis, accretion column absorpt. spectrum rel. to mag field 79−101176
VV Puppis, AM Herculis type binary, mag. pole accretion model 79−5860
VV Puppis, AM Herculis type binary, optical absorpt. spectrum, cyclotron intepretation and models 80−73003
VV Puppis, spectrum broad absorpt. bands rel. to mag. field 79−44502
radial oscills. of magnetic cylinder, matched asymptotic expansions method appl. 79−16817
radiative transfer in magnetic atmospheres, analytical soln. 80−36494
radio pulsars, rot. magnetised neutron star model with H or He envelope *(Russian)* 78−40982
red dwarf stars, mag. field instability rel. to flares 79−16954
red dwarfs, starspot magnetic fields 79−92758
relativistic centrifugal winds, appl. to pulsars 78−96473
rotating gaseous stars, effects of mag. field on adiabatic stability 77−91516
rotating magnetic stars, existence of bifurcation point 78−53924
rotating magnetic stars, nonradial oscill. mode splitting 80−77414
rotating magnetic stars, steady-state models 77−45405
stellar magnetism continued
rotating neutron star, mag. configuration of plasma-sphere 79−75241
rotating polytropic star, equilib. struct. and oscill. with large mag. field 77−87366
rotating polytropic star with large toroidal mag. field, equilib. struct. 77−87367
W Sagittarii, magnetic field from Zeeman meas. 78−4240
3 Scorpii, He weak star, mag. field discovery 79−88676
Scorpius X-1, mag. field determ. via linear polarisation spectrum *(Russian)* 80−90344
self-gravitating magnetic sphere, exact soln. for differential rotation 79−84665
solar-type stars, mag. cores stability 79−44472
spectra, response functions for mag. lines 77−45304
spectral line formation depth in mag. field, theory *(Chinese)* 80−105159
spectral line formation in microturbulent magnetic fields 80−31201
spectral synthesis in mag. field 77−17459
SS 433, accreting mag. neutron star model *(Russian)* 80−36647
SS 433, dipole mag. field rel. to mass accel. and collimation mechanisms 80−4368
SS 433, magnetic X-ray binary model 80−109447
stars containing mixed poloidal and toroidal mag. fields, adiabatic stability 80−67706
stationary states of stellar mag. fields, vector-operator algebra technique 78−73698
steady accretion disk, with magnetic field, basic equations 79−40179
stellar structure, effects of mag. fields on models calc. *(German)* 77−17592
Stokes' problem, mass transfer effects of MHD free convective flow 80−62003
Stokes parameters and mag. field vector profiles *(Chinese)* 80−77386
strong internal mag. field diffusion through radiative envelope of 2.25 $M_\odot$ star 78−85931
Sun as magnetic star 77−53566
superdense magnetised astrophysical objects, interiors physical conditions 80−17603
superdense stars, high mag. fields, cyclotron reson. emission 79−75207
superdense stars, quantum theory of magnetism 79−92753
superdense stars in quantum limit of ultrastrong frozen-in mag. fields 77−53620
supermassive rapidly rotating stars, mag. field effect on pulsational stability *(Russian)* 77−82220
supernovae, magnetorotational explosion in cylindrical model 80−101605
supernovae, MHD model 80−46588
68 Tauri, Am star, photoelectric UBV obs. of magnetic field *(German)* 77−17586
thermal convection, mag. field effect on onset under const. flux boundary conditions 78−69676
toroidal magnetic field effects on nonradial oscills. of n=3 polytrope 77−9738
toroidal magnetic field instability and differential rotation 79−16939
transverse magnetic field, effect on hydromag. free convection flow in Stokes problem 80−90328
turbulence, intermittency and magnetic fields 78−89059
turbulent diffusion of magnetic fields, stochastic phenomena 80−105161
upper main-sequence peculiar stars, chemical and physical props. rel. to radiatively driven diffusion theory 80−82374
AN Ursae Majoris, nova-like variable, circular polarisation rel. to white dwarf mag. field 78−8018
78 Virginis, Ap star, mag. field geometry, oblique rotator model 80−51773
78 Virginis, magnetic Ap star, high resolution polarisation obs. inside spectral lines 80−51772
CU Virginis, short period Ap star, discovery of mag. field 77−33511
15 Vulpeculae, Am star, photoelectric UBV obs. of magnetic field *(German)* 77−17586
white dwarf in binary system, collapse, mass ejection, nova mechanism 78−32485
white dwarfs, degenerate, mag. flux conservation rel. to critical parameters estimation 78−65622
white dwarfs, equilib. configs. with frozen-in mag. field 78−8008
white dwarfs, Faraday effect and depolarization of optical emission 79−97002
white dwarfs, Hα polarisation and line profiles in strong mag. fields 77−2427
white dwarfs, highly magnetised, accretion, role of electron conduction 80−82358
white dwarfs, highly magnetised, accretion theory 79−92764
white dwarfs, integrated polarisation of H lines in strong magnetic field 77−17563
white dwarfs, mag. fields rel. to cyclotron absorpt. spectra 80−4351
white dwarfs, mag. fields rel. to polarised radiation 77−2428
white dwarfs, mag. fields rel. to unexplained spectral features theory 80−82187
white dwarfs, magnetic flux distrib., radiative/conductive equilib. models 79−53811
white dwarfs, magnetobremsstrahlung and optical polarisation 77−45417
white dwarfs, relative freqs. of mag. fields among cool stars and hot stars 79−84788
white dwarfs, rotating magnetic, equilib. struct. 78−49433
X-ray binaries, synchronous rotation appl. to AM Herculis 79−62867
X-ray binaries and pulsars, effect of vacuum birefringence on polarisation 78−4408
X-ray bindary systems, X-rays polarisation from mag. accretion disc *(Russian)* 77−87575
X-ray burst sources, model, substorm process at accreting neutron star 79−17132
X-ray pulsars, mag. fields rel. to vacuum signature in spectra 80−27015
X-ray sources, pulsating, accretion disc interaction with stellar mag. field 78−93461
X-ray sources, pulsating, accretion disc mag. field calc. for oblique mag. dipole configuration 80−94895
X-ray sources, steady accretion discs general struct. with mag. field 80−8714
Zeeman and Doppler shifts in spectrograms, statistical determ. technique 78−36467
Zeeman effect in magnetic stars 77−45442
H_b line profiles for white dwarfs with dipole and quadrupole magnetic fields 78−8004

stellar magnetism continued
²H, superdense, cold, nuclear reaction energy output in mag. field *(Russian)* 77−29801
He strong stars, mag. fields meas. 79−44486

stellar mass
adiabatic mass loss, spin evolution 79−75201
ADS 4299, 8048 and 9352, parallaxes and masses for visual binaries 80−4402
ADS 8887, photographically unresolved visual binary, parallax and orbit 78−57593
AC Andromedae, mass determ. of triple-mode Cepheid 78−93261
anomalous mass stars, evolution on main sequence 80−72929
AE Aquarii, cataclysmic variable, rapid light oscills. obs. rel. to masses 80−36634
KO Aquilae, eclipsing binary, mass ratio and secondary component fractional radius from photoelectric study 80−62198
asymptotic giant branch evolution of intermediate-mass stars, post-second dredge-up phase 80−72936
LY Aurigae, eclipsing binary, photometric elements, masses, radii, luminosities 78−28723
KW Aurigae (14 Aurigae A), pulsating ellipsoidal variable, masses, radius and luminosity from tidal modes 79−97028
T Aurigae (Nova 1891), old nova, primary star mass from photometric and spectroscopic obs. 80−90446
B-type semidetached systems, photoelectric obs. 79−44522
binary formation, statistical model for the initial stellar mass function 79−48851
binary stars, distances, masses and dias. from speckle interferometric obs. 80−90475
binary stars, mass ratio rel. to tidally-distorted models small oscills. 79−44462
binary stars, spectroscopic, statistical investigation 80−109466
binary stars in open clusters, rot. effects on determ. of freq. and mass ratio 78−36639
binary stars mass ratios, significance of binaries with nearly identical components 79−48856
binary stars on main sequence, secondary masses freq. distribs. 80−26901
black holes, mass rel. to time-scale of rapid X-ray variability and dying pulse trains 80−56872
blue stragglers as long-lived stars 80−46542
α Bootis, ang. dia. and mass from predicted and observed spectral energy distrib. 80−46546
TZ Bootis, mass ratio of W Ursae Majoris system 78−69832
α Bootis (Arcturus), atmospheric parameters and mass 78−20826
brown and black dwarfs, structure, evolution and missing mass contrib. 79−48800
bump Cepheids, mass anomaly as opacity effect 79−16964
CC 1299 (BD+27°4120), unresolved astrometric binary, orbital anal., mass and parallax 80−109464
AH Cancri, contact binary in M67, masses, radii, effective temp. and luminosity 79−40222
VY Canis Majoris, mass, luminosity and evolutionary state from relation to mol. cloud complex 78−24536
UW Canis Majoris, O-type massive evolved contact system 78−65651
α Canis Majoris (Sirius), astrometric study rel. to distance and components masses 79−5858
α^2 Canum Venaticorum type stars, dynamical parallax, absolute magnitudes and masses *(Russian)* 79−88690
β Capricorni, triple star, fundamental parameters from occultation astrometry and spectroscopy 79−40216
η Carinae, mass loss from IUE UV obs. 79−30071
OY Carinae, white dwarf cataclysmic binary 80−82385
QZ Carinae (HD 93206), massive multiple system in great Carina Nebula, spectral types and orbits 79−97027
Cassiopeia A, presupernova star mass rel. to black hole form. 79−75244
V523 Cassiopeiae, BV photometry of W UMa type system *(Russian)* 79−92807
SU Cassiopeiae, Cepheid variable, pulsation and evolutionary masses from temp. determ. 80−90435
OX Cassiopeiae, eclipsing binary, masses and photometric elements 80−56877
AB Cassiopeiae, eclipsing binary, masses from light vars. preliminary anal. 80−94831
RZ Cassiopeiae, eclipsing binary, spectroscopic orbit and mass 80−22040
AZ Cassiopeiae, interacting eclipsing binary, mass loss of cool supergiant component 78−32522
TU Cassiopeiae, mass determ. of triple-mode Cepheid 78−93261
TV Cassiopeiae, revised photoelectric elements *(Russian)* 79−92808
cataclysmic binaries, evolution and origin rel. to period/secondary mass relation 80−56885
BV Centauri, dwarf nova and spectroscopic binary, masses and absolute dimensions 80−51775
α Centauri and Proxima Centauri, space motions, masses 79−21348
Centaurus X-3, neutron star lower mass limit from spin-up and X-ray luminosity meas. 80−101648
NY Cephei, eclipsing binary, UBV photometry and masses 80−67789
VW Cephei, transportation of masses in close binary *(German)* 79−58383
VW Cephei, W Ursae Majoris star, rot. line broadening rel. to shape and mass ratio 80−109494
17=ξ Cephei A, speckle interferometry, mass-luminosity relation 80−56874
Cepheid masses from observations and pulsation theory 79−48802
Cepheid variables, mag. fields rel. to pulsational and evolutionary masses discrepancy 80−31302
Cepheid variables, rot. and convection effects rel. to evolutionary and pulsation masses 78−93249
Cepheid variables masses, implication of mass and ang. momentum losing stars evolution 79−25591
Cepheids, double-mode, masses 79−35278
Cepheids, mass calc. methods, anomalies 78−49466
Cepheids in M31 (Andromeda galaxy), masses radial var. rel. to interstellar gas density *(Russian)* 80−90455
Cepheids masses, effects of He deficient stellar winds 78−57556
XY Ceti, eclipsing binary, masses, radii and luminosities from revised photometric elements 80−109458
Z Chamaeleontis, cataclysmic binary, masses radii, and mass exchange rel. to gravit. radiation 80−4386

stellar mass continued
Z Chamaeleontis, eruptive binary, secondary component relative mass from photometric data anal. 80−72961
Ci 182354 unseen companion, astrometric anal. from 61 cm Sproul refractor plates 78−16459
classical Cepheids, mass-luminosity relationship 79−35278
close binaries, intermediate mass, mass transfer for different stars within evolutionary scheme 80−109476
close binaries with OB components, evolution of massive systems 80−90474
close binary stars, masses and mass ratios distribs. before and after mass transfer 80−62187
close binary stars, masses and mass ratios rel. to evolution 78−49479
close binary systems, mass-radius relation 78−12290
CoD−38°10980, white dwarf, gravit. redshift rel. to mass-radius relation 78−24511
35 Comae Berenicis, masses and K-line absolute magnitudes 80−8649
contact binaries, mass and energy flow 79−48850
contact binaries, solar type, initial mass ratio distrib. function 80−109496
contact binary star, fractional mass var. during dynamical evolution *(French)* 80−62199
contact binary stars, mass of third component responsible for sudden period changes 80−109497
continuous loss from cluster models, dynamicl evolution 80−82438
core mass-luminosity relations, for He shell burning stars 80−21983
ε Coronae Austrinae, W Ursae Majoris type star, spectra, radii, masses 79−71069
σ Coronae Borealis (=ADS 9979), binary, mass and orbital elements *(French)* 80−77449
R Coronae Borealis stars, mass and rel. to Type I supernovae, appl. to Crab Nebula 79−5845
AI Crucis, eclipsing binary, photometric mass and radius ratios and configuration 80−109459
SS Cygni, dwarf nova, white dwarf mass from rapid optical oscills. obs. 80−85947
V380 Cygni, eclipsing binary, masses, radii and luminosities from revised photometric elements 80−109458
P Cygni, mass loss, Balmer line profiles 78−45334
V729 Cygni, O-type evolved contact system, masses 78−93309
CG Cygni, spectroscopic study of close eclipsing binary 79−97031
V1329 Cygni (HBV 475), symbiotic variable, masses from eclipsing binary model 80−62148
DA white dwarfs, atmospheric parameters and mass distrib. 79−88655
DA white dwarfs, H I Balmer γ line profiles and masses 80−77399
degenerate mass in bimetric theory of gravitation *(Russian)* 79−12466
dense matter star, limiting mass 80−101611
detached double-lined eclipsing binaries, revised photometric elements 78−61886
distribution in solar neighbourhood, Weibull statistical function 80−98649
BY Draconis, binary spotted flare star, mass and luminosity ratios rel. to pre-main-sequence nature 80−36633
WW Draconis, eclipsing binary, masses, radii and luminosities from photoelectric lightcurves 80−46606
AI Draconis, masses of components of eclipsing binary 78−89221
CM Draconis, spotted dM4e eclipsing binary flare star, absolute dimensions and masses 78−12289
dwarf Cepheids, double-mode, theoretical periods and masses 79−44488
dwarf Cepheids, mass and evolutionary stage 80−46562
dwarf Cepheids, mass and evolutionary stage from obs. of (GD 428) 78−73720
dwarf stars, scaling hypothesis, relativistic statistics and critical mass 79−16960
early type companions of X-ray sources, stellar parameters 78−36564
early type stars, mass loss 78−69796
early-type stars near Sun, space vels., masses and ages 78−61858
eclipsing binaries, with periods <5 days, period-mass ratio relations 78−57585
eclipsing binary stars, V−R photometry rel. to distances, masses, radii and absolute magnitudes 79−44520
eclipsing double-lined binaries, masses and radii from photometric elements 78−69834
AS Eridani, eclipsing binary, photometric elements, masses, radii, luminosities 78−28723
evolution in large star clusters, mass loss 79−48866
evolution of massive stars (20-100 M$\odot$) with mass loss 78−36554
evolutionary models from zero age main sequence to red giant branch 80−21987
Feige 24, spectroscopy of EUV source, binary orbit, mass 78−93218
final evolution of stars *(Italian)* 79−53805
flare stars, dynamical parallax, absolute magnitudes and masses *(Russian)* 79−88690
G128-7, cool DA white dwarf, mass rel. to atmospheric parameters and evolution 80−62126
G and K-type giant stars, mass correl. with Li abundance 80−41819
giant stars in open cluster NGC 7789, metal abundance, He content and mass loss 80−31335
globular clusters in Magellanic Clouds, masses determ. 79−5867
globular clusters stellar mass spectrum, necessary condition for equilib. 78−93328
h 3556, triple star, binary orbit and masses and third component relative motion 79−88701
HD 152667=OAO 1653−40, unseen companion mass 79−17021
HD 159176, spectroscopic binary, radial, vel. obs., orbit and masses 79−25644
HD 165052, O-type binary, spectroscopic obs., masses and radii 78−93308
HD 165590 triple system, spectroscopic obs., total mass 79−84825
HD 167771, O-type binary, spectroscopic obs., masses and radii 78−93308
HD 199892, spectrographic binary, spectrograms, orbital elements and mass function 79−21359
HD 214686, double-lined spectroscopic binary, orbital elements and masses 79−58376
HD 34664 (S 22) in LMC, peculiar emission line supergiant 80−77416
HD 45088, dK3 spectroscopic binary, mass ratio from double red lines 80−67778
HD 49798, H-deficient subdwarf O-type binary, mass, radius and luminosity from non-LTE anal. 79−16978

stellar mass continued
HD 50896, Wolf-Rayet binary, secondary component mass from linear polarisation periodic vars. 80−72972
HD 698, massive spectroscopic binary, spectral obs., evolutionary state, mass loss 78−57590
HD 92740, spectroscopic binary WN7 star, mess ratio and evolution 79−8924
HD 93250, O3 massive star in η Carinae complex, non-LTE analysis 80−77398
HD 96953, spectroscopic binary, secondary component mass from photoelectric radial vels. 80−56887
Hercules X-1 (HZ Herculis), mass from optical pulsation calcs. 78−57580
Hercules X-1 (HZ Herculis) system, non-degenerate star pre-supernova mass 80−62318
LT Herculis, eclipsing binary, photometric elements 80−31328
AD Herculis, eclipsing binary, spectroscopic obs., orbital elements and mass 78−73738
AM Herculis, IR spectroscopy, period, mass function 79−71066
DQ Herculis, red and white dwarf eclipsing binary, component mass determ. 80−94800
DQ Herculis (Nova 1934), masses of interactive binary 79−97029
DQ Herculis (Nova 1934), spectrophotometry rel. to red dwarf companion nature and mass 80−22017
DQ Herculis (Nova 1934), UBV photometry of visual binary 80−8661
high-mass stars ($M \gtrsim 50\ M\odot$) masses and space vels. rel. to evolutionary status *(Russian)* 80−109425
horizontal-branch A-type stars, effective temps., bolometric magnitudes and masses 79−62829
hot main-sequence, eclipsing binaries 78−32514
hot massive stars, stellar wind mass loss, evolution study 80−17578
HR 1225, δ Scuti star, absolute magnitude, effective temp. and mass from photoelectric study 80−109436
HR 2081, double-lined spectroscopic binary, radial vel. orbit and min. masses 80−51811
HZ 22 (UX Canum Venaticorum), hot subdwarf binary, evolution and mass 79−12472
ϵ Indi moving group, detailed anal. of members HD 40409, HD 102365 and λ Aurigae 78−85982
initial mass function nonmonotonous *(Russian)* 79−40181
interferometry appl. to mass meas., gravit. starlight deflection in close visual doubles *(French)* 79−62753
intermediate-mass stars asymptotic giant branch evolution as function of mass and comp. 80−12749
IRC+10216, C star, NH_3 obs. and circumstellar envelope mass 79−48793
K1211, blue straggler in NGC 7789, evolution status and mass, photometry obs. 80−109433
Kuiper 41, orbit and flare activity of visual red dwarf pair 79−97032
5 Lacertae, obs. of second max. for long period spectroscopic binary 78−57591
LDS 720BC (CD−32° 16135), visual binary, orbit and mass 78−32515
γ Leonis, masses and K-line absolute magnitudes 80−8649
19 Leonis Minoris, spectroscopic binary, orbital elements and mass ratio 80−62197
δ Librae, Algol-type eclipsing binary, masses derived from vel. curves 78−49475
LMC X-4, spectroscopic obs., orbit and components masses 79−9028
β Lyrae, radii and masses from light curve, peculiarities of system *(Russian)* 79−97036
RR Lyrae variables in globular cluster NGC 6121 (M4), masses from UBV photometry 80−22018
M36, photographic obs., mass, radius, central density, stellar vels. of open cluster *(German)* 80−31333
M38, photographic obs., mass, radius, central density, stellar vels. of open cluster *(German)* 80−31333
M3, mass function and cluster dynamics from individual stars photoelectric radial vels. 79−75251
magnetic variables, intrinsic rot. rels. correl. with colour index and masses 78−40967
main sequence B-type stars, physical parameter determ. from uvbyβ photometry obs. 80−72952
main sequence star, max. mass for white dwarf evolutionary stage 80−105237
main-sequence binary stars, mass ratios rel. to Roche consts. 79−35297
massive close binaries inc. wind mass loss, evolution 79−44527
massive star core collapse, eqn. of state and composition near β equilib. 80−82335
massive star formation in Local Group galaxies 79−30053
massive stars, core convection, effect on C/O ratio 80−17579
massive stars, early mass loss and transition WR star evolution 79−48775
massive stars, masses rel. to evolution 80−90416
massive stars, single and binaries, evolution review 80−82343
massive white dwarfs, mass accretion, rel. to thermonuclear runaways 80−41822
Mira variables, mass from observational data 78−45333
Mira variables, mass loss and OH maser emission 79−16969
model computations for mass and age determ. *(French)* 79−2541
VV Monocerotis, eclipsing binary, orbital elements, masses and dimensions *(French)* 78−89225
multimode Cepheid variables, masses and radii from period ratio diagrams 78−28698
neutron star, model within general relativity, mass evaluation 80−101612
neutron star formation through stellar core collapse, effects of eqn. of state on mass 80−85928
neutron star mass, determ. from theory for cold spherical stars 80−56859
neutron stars, mass and radius with neutrino retention 79−62817
neutron stars, mass-radius relation, obs. constraints, dense matter eqn. of state 80−46597
neutron stars, mass-radius relation 80−77444
neutron stars, max. mass and moment of inertia from superdense neutron matter theory 78−45349
neutron stars, max. mass determ. from pulsars and compact X-ray sources 80−77442
neutron stars, nonrotating, mass and moment of inertia bounds 79−2551
neutron stars, review of nuclear physics 79−92797
neutron stars, rotating, masses in bi-metric theory of gravitation 80−90466
stellar mass continued
neutron stars, slowly rotating, masses rel. to inertial props. in bimetric gravitation theory 79−85042
neutron stars mass upper limit for stability against black hole form. 78−96498
NGC 2362, very young open star cluster star counts and cluster mass *(German)* 78−16472
NGC 2477, photographic obs., mass, radius, central density, stellar vels. of open cluster *(German)* 80−31333
NGC 4565, galaxy, dark halo stars luminosity and mass function 79−62905
NGC 752 red giants, masses from DDO astrophysical study 79−48864
nova envelopes, mass rel. to dust grains form. 80−98678
NP 0532, Crab pulsar, mass and radius from supernova remnant physical theory 80−51834
O- and Of-type stars, masses and mass loss 80−94793
O-type binaries, binary freq. and anomalous mass ratios 80−109478
OB associations, initial mass function in young objects 80−98695
open clusters, age and mass of stars using Population I evolutionary tracks 78−61893
YY Orionis, mass from spectral line profiles, in radially symmetric accreting envelope *(Russian)* 78−57544
χ^1 Orioniz, new solar-type astrometric binary, companion mass 78−73740
AU Pegasi, binary Type II cepheid, companion mass and nature 80−26866
AW Pegasi, eclipsing binary, photometric elements, masses, radii, luminosities 78−28723
κ Pegasi, low total mass quadruple system 79−44550
ϕ Persei, binary Be star, He II emission obs. rel. to components masses 80−12768
12 Persei, masses and luminosities from speckle interferometric obs. 78−93305
β Persei (Algol), detection of B component, mass determ. 78−65654
β Persei (Algol), orbital inclination and masses determ. from speckle interferometry 80−36668
β Persei (Algol) eclipsing binaries, masses rel. to mass loss and mass transfer theory 80−62191
PG 1413+01, white dwarf-red dwarf eclipsing binary, masses and evolutionary state 79−8944
planetary nebula formation and C detonation supernova models, mass limits 79−17053
planetary nebulae central stars, masses rel. to CNO abundances 78−85992
planetary nebulae central stars mass rel. to evolution 78−12325
planetary nebulae nuclei, core masses rel. to He shell flashes, nebula ejection and distance scale 78−24540
planetary nebulae nuclei, masses rel. to nebulae evolution 80−82344
Population I 15 M⊙ star, effect of mass loss and semiconvection 78−45320
pre-main-sequence mass-loss constraint 79−58335
protocluster fragments systems, mass distrib. law 79−44571
PSR 0820+02, long-period binary pulsar, orbital period and mass function 80−56867
red giant mean initial mass from visual binary data 78−49429
red giant stars evolutionary sequences, effects of mass and comp. 78−65611
red giants, peculiar, constraints on evolution from masses and space densities 80−22001
Rst 4036, red-dwarf binary star, orbital period and total mass 80−12780
runaway stars, masses rel. to supernovae, duplicity and binary star mass loss 78−32448
WZ Sagittae, binary components masses rel. to past and future evolution 78−85948
WZ Sagittae, eruptive binary, masses from hot spot eclipses anal. 80−72962
FG Sagittae, photometric radius and pulsation mass 78−36576
WZ Sagittae, physical parameters from eclipse anal. 79−80336
U Sagittae, secondary mass from vel. curve 79−97025
ψ Sagittarii, evolved spectroscopic triple system 79−44551
V861 Scorpii=OAO 1653−40, unseen companion mass 79−17021
ζ^1 Scorpii, extreme B1 supergiant, IUE obs. rel. to mass, radius and bolometric luminosity 80−17583
V701 Scorpii, masses and mass exchange rates of early-type contact binary 80−62188
V861 Scorpii (=OAO 1653−40), X-ray emitting component mass 78−69838
δ Scuti type stars, dynamical parallax, absolute magnitudes and masses *(Russian)* 79−88690
semi-detached eclipsing binaries, revised photometric masses, radii and luminosities 78−20858
solar neighbourhood initial mass function determ. from upper H-R diagram study 80−36626
spectroscopic binaries, models for distrib. with respect to primary mass, mass ratio and orbital semiaxis 80−46616
spectroscopic binaries, properties of 826 stars 79−97037
spectroscopic binary member of visual double, mass determ. method *(French)* 79−44549
spectroscopic binary stars, mass ratio distrib., q(α) redeterm. 79−21356
stars with given entropy distrib., influence of mass changes on struct. 79−66993
Stepanyan's star, eclipsing binary, relative orbit radius and collapsed component mass 80−67788
subdwarf stars, no evidence for low spectroscopic masses 80−62122
Sun, mass/gravit. const. relation rel. to solar luminosity cosmological var. 80−82182
Sun possible compact companion, mass, vel., and luminosity 79−2490
supergiant stars, pulsation mass calcs. 80−46556
supergiant stars, sporadic mass ejection 79−40186
supergiants in Magellanic Clouds, birthrate and mass function 80−67699
supernova that produced N63A, lower mass limit 80−62165
supernovae, envelope mass and energy pumping rel. to galactic supernova remnants 78−73726
supernovae, mass range for r-process nucleosynthesis 79−5844
supernovae, type II, mass of ejected matter from light curves analytic solns. 80−77427
λ Tauri, eclipsing binary, photometric elements, masses, radii, luminosities 78−28723
RV Tauri and yellow semiregular variables, metallicity and mass from photometric investigations 80−26865

stellar mass continued
RW Trianguli, nova-like eclipsing binary radial vels., dimens. from visible spectra 80−82418
4U 0115+63, hard X-ray transient, orbital elements and mass function 78−93470
3U 1538−52, binary X-ray pulsar, mass and radius of companion 78−16573
4U 1538-52, optical counterpart spectroscopy and system parameters 79−5924
3U 1700−37, compact component mass from Copernicus X-ray obs. 78−96568
unresolved visual binaries, reexamination and companion stars masses 78−40993
W Ursae Majoris stars, A-type, evolved models rel. to mass ratios 79−8943
W Ursae Majoris stars, rot. line broadening functions rel. to mass ratio 80−109494
W Ursae Majoris type binaries, mass ratio function 79−8947
AI Velorum, radius and mass from BVRI photometry and photoelectric radial vels. 80−94815
γ_2 Velorum, Wolf-Rayet binary, minimum mass from spectra obs. 80−85950
visual binaries, orbital elements and masses for 18 pairs 80−62180
visual binaries, southern orbits and masses 78−96502
ER Vulpeculae, W Ursae Majoris star, rot. line broadening rel. to shape and mass ratio 80−109494
white dwarf progenitors, upper mass limit determ. 80−51738
white dwarf stars, masses and radii from two-colour diagram 80−46547
white dwarfs, degenerate magnetic, limiting mass and central density estimation 78−65622
white dwarfs, luminosity function depend. on progenitor masses 78−65614
white dwarfs, mass and radius with neutrino retention 79−62817
white dwarfs, mass distrib. rel. to stellar mass loss rates and galactic evolution models 80−46548
white dwarfs, masses and radii of H-rich and He-rich stars 79−35245
white dwarfs, rotating magnetic, equilib. struct. and critical mass 78−49433
white dwarfs, virial theorem, energy content and mass-radius relation 78−45327
white dwarfs, visual surface brightness relation appl. 78−81624
white dwarfs mass-radius relation, constraints on gravit. const. 79−25464
Wolf 1062 unseen companion, astrometric anal. from 61 cm Sproul refractor plates 78−16459
Wolf 922, nearby red dwarf, evidence for low-mass unseen companion 80−51809
Wolf Rayet binary, binary freq., mass ratio, low mass companion evidence 80−109479
Wolf-Rayet stars as supernova progenitors *(Italian)* 79−53830
Wray 977, optical counterpart to X-ray binary pulsar, 4U 1223−62, optical spectra 80−72984
X-ray binaries, anomalous periastron positions rel. to neutron star masses 79−25756
X-ray binaries, masses rel. to hard and soft X-ray spectra 80−62316
X-ray bursters, radius and mass, general relativistic effects 80−8712
X-ray sources in globular clusters, locations rel. to masses 79−97102
yellow semiregular and RV Tauri variables, metallicity and mass from, photometric investigation 80−26865
1228, nearby red dwarf, evidence for low-mass unseen companion 80−51809
20,986, new unresolved astrometric binary 78−57594
H burning stars, Hertzsprung-Russell diagram age and mass calibrations 80−51744
N deficient supergiants in loose association, comps., masses and evolutionary stage 79−44478
SiO mass loss and grain formation in expanding envelopes around evolved stars 79−48782

stellar models
2 to 10 M⊙ stars, effect of heavy element abundance on evolution, struct. of models 80−105231
6 M⊙ star thermal post-main sequence evolution, importance of continuous nuclear spectrum 77−64745
10-day Cepheids, theoretical models 78−49449
30 M⊙ star, stability towards g^+ modes of high spherical harmonic values 77−9740
A-type stars, Lyman α effect on non-LTE model atmospheres 80−90422
A-type stars, model atmospheres rel. to non-LTE anal. of O I lines 77−41378
A-type stars, normal and metallic-line, models pulsational stability 78−16414
accretion disc, polarisation effects in emission 79−35128
accretion disc models and cataclysmic variables, H line blocking of UBV colours 79−101155
accretion discs in X-ray binaries, structured coronae, model 79−48852
accretion disk model, gas flow above alpha disk 80−62161
adiabatic linear oscillations of spherically symm. star in terms of potential fields 77−74038
adiabatic non-radial oscillations with moderate or large l, theory 80−56819
Am-type, binary stars, tidal interaction producing stable atm., evolution 80−67752
FF Andromedae, BY Draconis variable, spectroscopic binary, orbit and active region model 77−33527
AC Andromedae, multiperiodic RR Lyrae star, pulsation theory and models 77−87431
AC Andromedae, triple mode variable, oscillating c-type RR Lyrae star 78−57560
Ap stars, decentred dipole and dipole quadrupole magnetic field models, anharmonic analysis 79−101154
Ap stars, line blanketed model atmospheres 79−44495
Ap stars, line blanketed model atms. 79−21304
Ap-stars, decentred magnetic dipole models for 17 objects 79−67013
Ap-stars, oblique rotator model, Deutsch and Khoklova methods 79−35271
AE Aquarii, cataclysmic variable, rapid light oscills. rel. to white dwarf oblique rotator model 80−36634
R Aquarii, symbiotic long-period variable, magnetically active single star model rel. to nebula spectrum 80−90450

stellar models continued
σ Aquarii (A0 IVs), hot metallic-line star, abundance anal. from model atmosphere 80−90415
Aquila X-1, binary and triple star models for X-ray outbursts 78−20909
θ Aquilae (B9.5 III), abundance anal. from model atmosphere 80−90415
V1301 Aquilae (Nova Aquilae 1975), dust grain IR emission model 80−105254
V539 Arae, photometric analysis of B-type double lined eclipsing binary 79−44535
Ariel 0620−00, transient X-ray source, spherical model 78−12415
atmosphere analyses of solar-type stars, metal abundances and microturbulence 79−67002
atmosphere models application to determ. of effective temp., bolometric corrections, Balmer discontinuity and distrib. functions *(Rumanian)* 78−36557
atmospheres, colour index and bolometric correction rel. to LTE/non-LTE boundary 79−35236
atmospheres, expanding, comoving frame radiative transfer eqn. soln. 77−22056
atmospheres, microturbulent broadening of spectral lines 78−45321
atmospheres, temps. determ. from uvbyβ photometric system 77−64740
ε Aurigae, peculiar binary system, circumstellar dust and gas disc model 77−9771
LY Aurigae, tidal effects in O-type eclipsing binary system 79−25638
α Aurigae (Capella), model chromosphere 78−40931
α Aurigae (Capella), theoretical stellar chromosphere model 80−67718
T Aurigae (Nova 1891), old nova, cataclysmic binary model from photometric and spectroscopic obs. 80−90446
axisymmetric rotating fluid, asymptotic estimates 80−98542
B-stars of early type, atm. LTE model using opacity sampling technique 80−90414
B-type stars, pole-on, rapidly rot., spectral inconsistencies due to gravity darkening 80−17581
baryon stars, magnetospheres model *(Russian)* 77−91555
baryon system, strong interacting, finite temp. many body theory, phase transition 77−65210
Be stars, emission line profiles from envelopes, elliptical gaseous ring model 80−4373
Be stars, emission line profiles from envelopes, theoretical profiles 80−4374
Be stars, envelope models 77−13355
Be stars, equatorial disc model rel. to 1.25 and 2.2 microns polarimetry 79−44484
Be stars, review of early history of studies 77−56965
Be stars in binary systems, apsidal motion of gaseous rings 78−32521
Be stars review, rot. and envelope models 79−84809
Be-star circumstellar envelopes 77−60777
Be-stars, model parameters, observable effects 79−35266
beat Cepheids, model constraints 79−5831
binary fission in damped rotating polytropes 78−93209
binary fission in damped rotating polytropes 79−71016
binary stars, accretion disc inner region model *(Russian)* 78−69843
binary stars, ang. momentum loss and mass exchange instability 77−49433
binary stars, close low-mass systems, evolution into contact 77−33557
binary stars, mass transfer and accretion disc flow, numerical simulation 77−57035
binary X-ray sources, properties and models 77−41419
black hole in radiation-dominated non-relativistic gas, Bondi accretion problem 78−77575
black hole magnetospheres existence, theory 77−64792
black holes, supercritical accretion discs models 80−105272
black holes, thick accretion discs models rel. to supercritical luminosities 80−101614
black holes, X-ray polarisation features for geometrically thick clouds and accretion disc model 80−46700
bloated dwarf model of nova light curves 77−82251
α Bootis, comparison of predicted and observed spectral energy distrib. 80−46546
α Bootis, K giant, surface gravity and mass 77−53587
α Bootis (Arcturus), line blanketing and atm. struct. 77−33483
α Bootis (Arcturus), model-atmos. analysis of spectrum 77−29827
Z Camelopardalis, dwarf nova, accretion disc models at standstill and in eruption 80−82366
VY Canis Majoris, apparent orbit, rotating holey dust cloud hypothesis 79−40191
UW Canis Majoris, O7f supergiant, warm wind model for mass loss 80−67736
α Canis Majoris B (Sirius B), corona model constraints 79−2543
α Canis Majoris B (Sirius B), degenerate stars models rel. to astrometric study 79−5858
α Canis Minoris (Procyon), theoretical stellar chromosphere model 80−67718
RS Canum Venaticorum, explanation of observations 79−84826
α^2 CAnum Venaticorum, line blanketed model atmospheres of Ap-star 80−90440
RS Canum Venaticorum binaries, starspot model rel. to light and spectrum vars. 77−87479
RS Canum Venaticorum binary stars, mag. starspot model for photometric and spectroscopic behaviour 80−109488
RS Canum Venaticorum stars, intrinsic light vars. due to starspots, model 79−35295
RS Canum Venaticorum systems, X-ray obs. and coronal model development 80−56873
ν Capricorni (B9.5 V), abundance anal. from model atmosphere 80−90415
γ Cassiopeiae, circumstellar envelope model 78−40952
γ Cassiopeiae, UV and optical spectral var. rel. to coronal emission model 78−93251
cataclysmic variables, accretion discs models rel. to emission line spectra 80−51774
SV Centauri, early-type contact binary, evolutionary models 80−4403
α Centauri A and B, IUE spectra and transition region models 80−46543
α Centauri A and B, model chromospheres 77−13326
α Centauri binary system, sealed solar model atmospheres for spectroscopic anal. 80−62128
VW Cephei, evidence for circumstellar matter 77−33563
U Cephei, mass transfer models rel. to light vars. outside primary eclipse 78−36636
β Cephei stars, line profile variables, pulsational modes 80−85951

stellar models continued
β Cephei stars, line profiles and oscill. modes 77−33521
β Cephei stars, models, He^+ ionization driving 79−8922
β Cephei stars, models nonradial stability 77−49390
β Cephei stars, radial and non-radial models 77−82235
β Cephei stars, theoretical models with new radiative opacities 77−13347
Cepheid model, transitory R-type ionisation front 79−75209
Cepheid variables, double mode, anal. of modal selection pulsating stars 80−82372
Cepheid variables, double-mode and bump, rot. and convection effects on period ratios 78−93249
Cepheid variables, He enrichment effects in atm., models 80−26884
Cepheids, anomalous, in dwarf spheroidal galaxies, binary system model 77−45451
Cepheids, double-mode, masses 79−35278
Cepheids, double-mode, period ratios from linear and nonlinear theory 78−40953
Cepheids, double-mode, surface He enhancement, linear theory period ratios 79−67021
Cepheids, double-mode and bump, revised masses 77−56949
Cepheids, freq.-period distribs. in Local Group galaxies 78−28694
Cepheids, multimode, two-zone models, resonances 80−36641
Cepheids, stellar pulsation problem, time dependent convection local theories 80−72964
multimode Cepheids, two zone rel. to classical models 80−72967
Cepheids in Magellanic Clouds, extrinsic model of anomalies 80−4361
Cepheids pulsating envelopes models, mag. field effects 80−31302
Z Chamaeleontis, eruptive binary, model from photoelectric data anal. 80−72961
chromosphere models, Ca II H and K lines absolute flux profiles in F0 to M2-type stars 80−26842
chromosphere models, high-press. transition regions theory 80−26847
chromospheres, observational indicators, empirical models 80−12755
chromospheres of late type stars, theoretical models and temp. minima heights 78−20818
chromospheric-type atmospheres models, non-isotropic redistrib. theory rel. to spectral line form. 77−5522
Circinus X-1, binary model, orbital eccentricity from X-ray and radio obs. 80−98735
Circinus X-1, binary model, radio emission 80−98736
Circinus X-1, nature and binary star model 79−75296
Circinus X-1 as gamma-ray source, eccentric orbit binary model 79−97100
circumstellar dust envelopes, calc. of eclipse light curves and fringe visibilities 79−35234
classical and dwarf novae, energy sources and systematics 79−67041
classical and dwarf novae explosions, review 79−67042
close binaries, distortion effects on struct. 78−57584
close binary components, model atms. 79−62869
close binary stars, accretion disc model 78−4282
close binary system, matter flow around one component, period changes 79−62870
close binary systems, neutron stars tidal disruption by black holes 77−13387
close low-mass binary systems, evolution, unsteady mass loss, contracting secondary star 77−17617
cluster models with continuous stellar mass loss, dynamical evolution 80−82438
cold dense star with frozen-in mag. field, degeneracy removal, ideal electron gas approx. *(Russian)* 77−87365
compact binary systems, tidal interactions 77−57027
compact star, radiation, anisotropic fluid in spherical spacetime 77−56821
complete polytrope, linearised theory invalidity 78−77553
complete viscous polytropes, linearized theory validity 79−35244
composite rotating plasma, gravitational instability, including Larmor radius, Hall currents, collisions 77−60591
compressible convection onset in model atmospheres 78−65605
contact binaries, cyclic thermal instability 77−57050
contact binaries, energy transfer problem 77−57052
contact binaries, envelope energy transfer model 80−90478
contact binaries, objection to model of Shu, Lubow and Anderson 78−28720
contact binaries, structure, zero-age models 78−8045
contact binary, model for horizontal energy transfer 77−57051
contact binary stars, discontinuity model internal inconsistencies 80−46613
contact binary stars, gas circulation 77−57017
contact binary stars, struct. of high-mass models 79−48855
convection, mixing-length theory rel. to physical models 78−89179
convection and stellar models and evolution computation 78−89194
convection theory, choice of characteristic length 77−13317
convection theory including turbulent kinetic energy flux, appl. to main sequence star models 78−57543
convective cores with overhsooting and abundance determ. in sequences of old open star clusters 77−29888
convective instability, mag. fields and g^- modes 78−93211
convective instability of ga s sphere *(Russian)* 77−87378
convective models, fundamental hit correctable inconsistency of local mixing-length theory 80−26841
cool, luminous stars, mass flow models 79−5813
cool giant stars, model depend. of detailed anal. 77−53590
cool stellar wind models for late type stars 80−51733
core collapse, ellipsoidal model calcs., gravitational and neutrino radiation 79−53802
core He burning stars, H profile, previous mixing and loops in H-R diagram 77−29792
core He flash, models with two-dimensional convection 80−105230
coronae, energy balance 79−44466
coronae, two-parameter models 80−8619
S Coronae Austrinae, YY Orionis star, satellite UV spectrum and low mass protostar model 79−67016
β Coronae Borealis, mag. deform. of evolved stellar model, hypothesis 79−30076
β Coronae Borealis, magnetic deformation and precession model 78−53963
β Coronae Borealis, magnetic field of Ap-star 79−5822
coronae of He-rich white dwarfs 78−85940
coronae of late-type main-sequence and subgiant stars, loop model rel. to HEAO 1 obs. 80−72925
stellar models continued
coronal-type ionisation model rel. to galactic cosmic ray sources 78−49240
Crab pulsar, electron-positron flux at neutron star surface 77−64789
Crab pulsar, magnetized cracks in crust rel. to matter flow, radio, X-ray and optical emissions 80−72990
Crab pulsar (NP 0532), model for unpulsed light 79−44518
SS Cygni, dwarf nova, spectrophotometry rel. to accretion disc models in erruption and at min. light 80−36635
P Cygni, envelope model and mass loss 78−45334
V1057 Cygni, hydromag. model of peculiar activity *(Russian)* 78−49442
CH Cygni, new active period, model, double system with accretion disc *(Russian)* 78−69813
V1016 Cygni, peculiar emission object, M star model 77−53598
V1016 Cygni, single star model, possible forming planetary nebula 77−60762
CH Cygni, symbiotic star, binary model 80−62158
CH Cygni, symbiotic star, spectroscopic obs. and long-lived hot spot model 79−75211
V1329 Cygni (HBV 475), symbiotic variable, accreting binary star model 80−62148
V1500 Cygni (Nova 1975), anisotropically radiating condensations rel. to Balmer line emission profiles evolution 80−82371
V1500 Cygni (Nova 1975), emission line vars. rel. to central object radiation model 80−82367
V1500 Cygni (Nova 1975), meas. and nova outburst model 77−87448
V1500 Cygni (Nova 1975), model for spectrographic obs. 77−87444
V1500 Cygni (Nova 1975), spatial and kinematic envelope model 78−36600
V1500 Cygni (Nova 1975), spectroscopic studies, models for 3 hour profile vars. 79−8920
V1500 Cygni (Nova 1975) as thermonuclear runaway event 77−82261
Cygnus X-1, black hole candidate, accretion disc models 78−16577
Cygnus X-1, inverse Compton model 80−51918
Cygnus X-1, model of neutron star surrounded by massive disc 80−36736
Cygnus X-3, cocooned X-ray binary pulsar model 78−36723
Cygnus X-3, observational constraints, on models 78−16567
DA white dwarfs, atmospheric parameters and mass distrib. 79−88655
degenerate dwarf models, thermodynamic inconsistency of modified Saha eqn. at high press. 78−36450
degenerate dwarf stars, props. of low temp. pure He surface layers 78−7994
degenerate star-red giant interacting binary stars, compressible fluid flow, accretion 80−67779
degenerate stars with H atmospheres, props. rel. to theoretical models 80−17576
HR Delphini (Nova 1967), envelope, photoionization models in nebula stage, 1969 June-July 79−62835
HR Delphini (Nova 1967), models of envelope ionization 77−87439
HR Delphini (Nova 1967), photoionisation models, binary system evolution 80−17590
HR Delphini (Nova 1967), photoionisation models of envelope in nebular stage, obs. data 78−61864
dense stellar matter in asymptotically free gauge theories, high density limit 77−53421
differentially rotating gaseous polytropes, second-order perturb. theory 80−21990
DO white dwarfs, model atmospheres rel. to effective temps. and He abundances 79−35249
double shell source models, s-process enhancements 78−49430
double shell source stars, evolution through second loop in Hertzsprung-Russell diagram 78−36556
double star system, energy and distrib. *(Chinese)* 79−75249
BY Draconis, flare star, BVRI obs. rel. to spot model 77−53595
BY Draconis stars, luminosity vars. and light curve period changes 79−71039
dwarf Cepheids, double-mode, theoretical periods and masses 79−44488
dwarf Cepheids, linear survey of models, pulsation 79−35259
dwarf stars, model chromospheres and chromospheric activity 79−48773
dynamical stability anal. of charged homogeneous model, relativistic soln., rel. to stellar models 79−70949
dynamo model of magnetic field, self-consistent treatment 80−81808
early B-type stars, atm. radial shock effects 79−53807
early B-type stars atmospheres, influence of LTE line blanketing by UV lines 78−16419
early main sequence star model, periods of high pulsation modes 77−49372
early-type stars, blanketed model atmospheres rel. to UBV colours and temp. scale 79−16933
early-type stars, model atmospheres rel. to H and He^+ line profiles in stellar winds 80−85926
Earthlike planets, prevalence in Universe 80−41735
eclipsing binaries, late-type, mass-luminosity and radius relations, chem. composition 78−28728
Emden-Chandrasekhar axisymmetric solid-body rotating polytropes, exact solns. for (n=0, 1 and 5) 80−109419
energy method in stellar stability problem 79−35239
equilibrium equations soln. for rapidly rot. stars 78−65601
ε Eridani, UV line spectrum of active chromosphere star, models 80−77394
evolution, numerical modelling, use of collocation methods 77−87370
evolution calc. programme and standard solar model 80−67703
evolutionary models from zero age main sequence to red giant branch 80−21987
evolutionary tracks, effect of gravitational const. var. 80−82186
exploding shell, relativistic dynamics, spherically symmetric model 79−21271
explosions, radial gas oscills. after shock wave passage *(Russian)* 79−8903
F- and G-type supergiants, enhanced He abundance effects on visible spectra 80−12759
F-type stars, atm. models including OH opacity, comparison with TD1 satellite flux obs. 78−73700
fast nova model evolution from pre-explosion to decline 79−35273
Feige 24, hot white dwarf, model atmosphere rel. to intense EUV emission 77−9746
Feige 24, hot white dwarf, UV photometry and model atmosphere 77−9747
flare stars, nonmonotonic optical light curve model 77−29842

stellar models continued
flare stars, physical characts. 78−12242
fluid bodies, rapidly rotating, struct. and stability in general relativity beyond ang. vel. peak 79−101139
G, F, A, B and O stars, model atmospheres 79−80298
G- and K-type giants, theoretical colours from synthetic spectra 79−62827
galactic bulge X-ray sources, models, binary systems 78−81706
gamma-ray pulsars, curvature radiation-pair prod. model 79−5852
gaseous discs with uniform rot., global stability 77−26000
gaseous rotating cylinders, thermodynamic stability anal. by linear series 78−81618
GD229, cyclotron absorpt. in white dwarf 79−53813
γ Geminorum, differential abundance anal. rel. to α Lyrae standard 80−82362
U Geminorum, model of disk and accreting stream 77−82246
U Geminorum, radial vel. meas., rot. accretion disc and hot spot model 77−33561
β Geminorum (Pollux), chromosphere model 78−40931
general relativistic stellar evolution code 79−58317
β Germinorum (Pollux), theoretical stellar chromosphere model 80−67718
giant and supergiant stars, nonradial oscills. excitation 77−74049
giant stars in globular clusters M5, M13, M3, model atmospheres rel. to chemical comp. 80−67695
giant stars in M3, M13, M92 and M67, IR photometry comparison with model atmospheres 78−57595
globular cluster X-ray source, evolution of 100 M⊙ black hole in binary 78−61932
gravitational collapse, ellipsoidal models and gravit. radiation 78−45317
gravitational construction phase, mass outflow mechanisms 77−53579
gravitational radiation detection from stellar collapse 78−24707
gravothermal catastrophe 78−81536
gravothermal instability in two dimensions 78−89395
HD 101065 (Przybylski's star), Ap-star model rel. to light vars. and temp. 79−101151
HD 10783, Ap star, model atmospheres rel. to spectrophotometric obs. 80−98663
HD 152667 (V861 Scorpii), phys. props. and orbital parameters, super-giant star with black hole companion model 79−71067
HD 184927, He variable star; oblique rotator model rel. to spectroscopic props. 80−51790
HD 192163, Wolf-Rayet star, radius and temp. from spectra of nebula (NGC 6888) 77−57076
HD 193793, radio emitting Wolf-Rayet binary star, variable mass flow model 77−45469
HD 215441, mag. field geometry 78−53950
HD 215441 (Babcock's star), magnetic vars., non-axisymmetric eccentric dipole model 80−51779
HD 216533, Ap star, spectroscopic binary oblique rotator model, spectral var. study 79−101153
HD 44179 (Red Rectangle), precessing jets model 80−4422
HD 49798, H-deficient subdwarf O-type binary, non-LTE model atmosphere anal. 79−16978
HD 50138, Be star, model for shell from continuous spectrum obs. in IR 77−56976
HD 93250, O3 massive star in η Carinae complex, non-LTE analysis 80−77398
heavy element abundance effect on evolution 78−89167
Herbig-Haro objects, shocked cloudlet model 78−89196
Herbig-Haro objects, stellar wind model 80−85985
HZ Hercules, energy transport by circulation from illuminated region 79−71070
Hercules X-1, accretion disc viscosity determ. using slaved disc model 80−62110
Hercules X-1, precessing accretion disc with 70 day period 77−33693
Hercules X-1 (HZ Herculis), 35 day cycle investigation 78−32509
Hercules X-1 binary system, possible third star existence 77−33572
AM Herculis, 1.2 and 2.2 μm light curves interpretation, model parameters 79−8949
AM Herculis, accretion onto highly magnetised white dwarf 79−92764
AM Herculis, highly magnetised, accreting white dwarf 77−49396
AM Herculis, X-ray binary model 77−33568
AM Herculis (3U 1809+50), binary star model 77−71155
AM Herculis (3U 1809+50), multicolour linear and circular polarisation obs. and geometrical model 78−8053
AM Herculis (3U 1809+50), single accretion column model 78−57578
AM Herculis (4U 1814+50), mag. white dwarf models for X-ray source 80−105403
HZ Herculis (Hercules X-1), Sonneberg photographic obs. rel. to physical model 77−37618
AM Herculis objects, accreting mag. white dwarf model for linear polarisation 78−16460
AM Herculis/3U 1809+50 X-ray binary, rot. mag. white dwarf model 77−33571
high velocity giant stars, model atmospheres rel. to detailed chemical anal. 80−82352
high-luminosity degenerate stars with He burning near surface, pulsational props. 77−5519
horizontal branch stars, evolution with semiconvection, models 77−17540
hot horizontal branch stars, model atmospheres, B−V colour indices and bolometric corrections 79−58327
hot white dwarfs as thermal soft X-ray sources 78−57553
HR 3089, He-rich star, model atmosphere rel. to anal. of UV spectrum 77−9751
HR 7129, He variable, oblique rotator model 79−62838
HR 8799, model atm. anal. 77−74050
Hyades binary stars, models and distance modulus 77−57067
VW Hydri, cataclysmic variable, light curve superhumps model 80−4381
VW Hydri, dwarf nova, model 79−16977
hydromagnetic instabilities in polytropic stars containing toroidal magnetic fields 79−8905
HZ 43, hot white dwarf, self-consistent model atm. anal. 77−22220
ε Indi, late type dwarf star, model atmosphere 80−90425
instability due to local mixing length approx. 77−53569
interacting neutron matter model at postsupernova temps. 77−45399
interacting stellar wind model of planetary nebular formation 79−48801
interior Kerr metrics, tests 78−28666
intermediate-mass stars asymptotic giant branch evolution as function of mass and comp. 80−12749
stellar models continued
interstellar He abundance, rel to stellar models and cosmological models 78−16518
ion viscosity in hot accretion disc around black hole 79−62813
ionising source model for Allen's obscured IR source in NGC 2264 viscous disc component 79−21370
IR limb-darkening coeffs. for late-type giant model atmospheres 79−71029
IR stars, OH maser emission obs. rel. to expanding spherical shell model 77−53699
IRC+10216, circumstellar dust shell model rel. to IR energy distrib. 80−56972
Jacobi's virial eqn. soln. for celestial bodies 79−8832
Jupiter, D-burning star hypothesis 77−13282
K-type giants, upper photospheric temp. models, super-metal-rich and normal giants 79−21278
K-type subdwarfs, model atmospheres 79−25595
EV Lacertae, flare star, hot-plasma model of strongest flares 78−20838
late type dwarf stars, temp. minima, chromosphere models 80−67717
late-type, stars, sphericity effects in extended atms., models 78−81617
late-type giants, nonlinear model for coupling between pulsation and convection 77−13356
late-type stars, Ca II 8542 Å line as chromospheric activity indicator 80−62108
late-type stars, extended atmospheres, sphericity effects in red giants, model study 80−22012
LB 3459, subdwarf eclipsing binary, evolutionary model 80−51808
AQ Leonis, homogeneous model of Population II double-mode RR Lyrae star 80−62134
R Leonis, Mira variable, pulsation-shock model from CO and OH IR bands obs. 78−36574
line blanketed model atmospheres, limb darkening coeffs. determ. 79−35243
linear stability anal. by inverse iteration method 77−33469
α Lyrae, continuous UV flux, non-LTE calc. 77−49382
β Lyrae, high time-resolution Hα spectroscopy and model of system 77−13388
β Lyrae, secondary star spectral type and struct. of system *(Russian)* 79−97036
RR Lyrae, UV light curve rel. to hydrodynamic atmospheric models 77−45435
α Lyrae (Vega), LTE blanketed models rel. to visible and UV continuous energy distribs. 80−26856
RR Lyrae stars, convection depend. on pulsation phase, theoretical red edge of instability strip 77−17572
RR Lyrae stars, convective steady-state models, theoretical red edge of instability strip 78−4229
RR Lyrae stars, instability strip red edge depend. on luminosity and comp. 77−53600
RR Lyrae stars, theoretical red edge of instability gap, overtone pulsation 77−78794
RR Lyrae stars models, radial pulsations 80−26863
Maclaurin spheroids, secular instability due to gravit. radiation and viscosity 77−17538
magnetic Ap stars, empirical atmosphere models *(German)* 77−17589
magnetic cylinder, radial oscills., matched asymptotic expansions method appl. 79−16817
magnetic DA white dwarfs, calc. and obs. spectra 79−71032
magnetic DA white dwarfs, model atmospheres and line profiles 80−62123
magnetic field, dynamo theorems 80−81810
magnetic field, spherical dynamo with anisotropic-α effect 80−81809
magnetic neutron stars, accretion flow, magnetospheric struct. and stability 78−4269
magnetic pole model for pulsar emission 79−48838
magnetic small-scale fields, inner structure models *(Russian)* 79−92754
magnetic star model, circulation within nuclear burning shell rel. to latit. depend. chem. comp. *(Russian)* 79−16940
magnetic stars, equatorially symmetric rotator model, inhomogeneous element distrib. 80−4371
magnetic stars, equatorially symmetric rotator model 78−8020
magnetic stars, kinematic mechanism for oblique rotator model 77−45407
magnetic stars, magnetodynamic mechanism 77−87404
magnetic stars, model atmospheres 79−16973
magnetic stars, models with toroidal fields and circulation 77−45406
magnetic stars, perpendicular rotator model with meridional circulation 78−16438
magnetic stars structure, calc. of models *(German)* 77−17592
magnetic white dwarfs, gamma ray burst model *(Chinese)* 80−12831
magnetised gravitating cylinders equilib. struct. 78−96471
main sequence intermediate and late type stars, differential rot. models 80−105238
main sequence stars, chem. comp. effects on position in H-R diagram 77−91521
main sequence stars, linear series of models, supermassive stars 77−91515
main-sequence binary stars, evolutionary models rel. to Roche consts. 79−35297
Mass and age computations *(French)* 79−2541
mass-radius relations for cold spherical body, relativistic effects 80−26730
massive accreting white dwarfs in close binary systems, H shell flashes 79−75203
massive He burning stars losing mass by stellar wind, evolution rel. to Wolf-Rayet binaries 80−36615
massive luminous stars, stellar winds effect on evolution 79−12467
massive main-sequence star, early evolution 80−62113
massive stars, 10^3-10^4 M⊙ range, final evolution 77−87371
massive stars, gravity modes vibr. stability during H shell burning stage 77−56933
massive stars, single and binaries, evolution review 80−82343
massive stars (20-100 M⊙) with mass loss, evolution 78−36554
massive stars (M≳50 M⊙), binary star mass transfer model rel. to evolutionary status *(Russian)* 80−109425
massive stars losing mass and ang. momentum, evolution of 15 M⊙ model 79−25591
massive stars presupernova evolution 79−16930
massive X-ray binaries, OB stars, evolutionary influence of stellar wind 79−101172

stellar models continued
metal-deficient stars, subdwarf ionization equilibrium and model atmospheres 80−90421
metal-poor late-type stars, model atmospheres rel. to MK spectral classification 80−4340
metallic-line stars, theoretical pulsation models 79−97004
MHD unsteady thermal boundary layer flow with zero heat transfer 77−87250
Mira variables, envelope pulsational instability rel. to planetary nebula form. 80−26928
Mira variables rel. to Wood-Cahn model of late stellar evolution 78−45333
mixed-up models, CNO isotopes abundances 77−33475
MWC 349, possible model of emission line star *(Italian)* 79−48829
MXB 1730−333, rapid X-ray burster, accreting rot. magnetised neutron star model 79−84866
MXB 1730−335, accreting neutron star model of rapid burster 79−30145
MXB 1730−335, rapid X-ray burster, long-term behaviour rel. to burster models 78−32602
MXB 1730−335, X-ray bursts obs. rel. to source models 79−17139
neutrino transport, weak neutral currents; supernova model 78−62391
neutrino transport in supernova models, multigroup diffusion scheme 79−25590
neutron star, cold, binding energy and stability 79−17006
neutron star, magnetic, disc accretion model 78−93294
neutron star, model within general relativity, mass evaluation 80−101612
neutron star, quantum statistical mechanics treatment 77−49418
neutron star, relativistic quantum mechanical model for solid core 77−33546
neutron star models, theory for cold spherical stars 80−56859
neutron stars, models from microscopic interpretation of struct. 77−64790
neutron stars, postglitch behaviour of quantum plasma 79−35289
neutron stars, relativistic fluid spheres appl. 79−5855
neutron stars, slowly rotating, models and stability against radial perturbations 80−98685
neutron stars, transformation between two kinds *(Chinese)* 79−80332
neutron stars anisotropic models, stability against radial and nonradial pulsations 77−13378
neutron-proton electron mixture with zero charge density, eqn. of state, rel. to supernova explosions 77−53416
Newtonian stars with stratified flows, mirror planes 78−32444
non-radial oscillations, linear eigenvalue problem props. study, model 80−17571
non-spherical stars, appl. of smoothed particle hydrodynamics theory 78−12203
nonevolutionary sequences of models in thermal equilib., appl. to mass loss from close binary systems 78−24508
nonlinear running density waves in homogeneous model *(Russian)* 78−49421
nonradial oscillations, avoided level crossing 80−31294
nonradial oscillations of generalized Roche series models 80−21992
nonradially oscillating star, light and radial vel. vars. 77−91514
nova envelope model and total energy considerations 77−82250
nova model evolution with Z=0.03 envelope 77−82265
nova outburst, CNO abundances and hydrodynamics, 1 M⊙ models with small mass envelopes 79−12475
nova outburst, induced nucleosynthesis 77−82263
nova outburst, optically thick time-dependent wind model for postmax phase 79−12476
nova outburst, review of thermonuclear runaway model 77−82262
nova outburst models 77−82248
nova shell expansion and IR brightening 79−97007
nova shell ionisation, time-depend. model 79−53816
novae, white dwarfs, accretion belts model 78−36582
novae flare-ups theory, exact analytic self-similar solns. 79−35269
O and B stars, model atmospheres grid rel. to Si spectra 78−57539
O-type stars evolution rel. to Wolf-Rayet stars origin 78−81609
O-type subluminous stars, non LTE model atmospheres, line profiles 79−101149
oblique rotator model and Si overabundance by diffusion in chemically peculiar stars 79−30067
oblique rotator with irrotational axisymmetric mag. field surface distrib., effective mag. field 80−26872
Of-type stars, expanding envelope models rel. to H and He II spectra 78−40950
70 Ophiuchi A, theoretical stellar chromosphere model 80−67718
α Orionis (Betelgeuse), model atm., effective temp. 77−56935
σ Orionis E, mag. field discovery and oblique rotator model 78−93268
FU Orionis mechanism 80−51763
FU Orionis stars, composite spectra rel. to three models 78−65617
oscillation freqs. of magnetic stellar models 78−69783
outflowing atmospheres across HR diagram, modelling 79−66996
partial ionisation zones, eqns. of state 78−28653
β Persei, eclipsing binary, Mg II 280 nm line profile, calcs. and UV obs. 80−82421
RY Persei, eclipsing binary, visible spectral obs., model 80−67795
φ Persei, model for Be-star binary system 77−60782
X Persei (3U 0352+30), eccentric close binary model 77−29879
X Persei (4U 0352+30), absence of ellipsoidal light vars. 79−80337
SX Phoenicis, evolutionary stage of RRs star 80−46583
SZ Piscium, RS Canum Venaticorum star, photometric obs. rel to starspot model 80−109490
planetary nebulae, truncated composite shell models 79−25677
planetary nebulae central stars, atmospheric models 80−109434
planetary nebulae central stars, envelope models and rapid variability 77−45439
planetary nebulae formation models, implications for Fe condensation 79−40238
planetary nebulae formation with close binary nuclei 79−71097
planetary nebulae nuclei, models rel. to distances determined from ionised mass/radius relation 80−101625
plasma laser star model of QSOs 78−96558
plasma-laser star model for quasars, rel. to Wu states and absorption spectra 79−48950
Poisson's eqn. numerical soln. for flattened centrally condensed objects, stellar models 79−35110
polytrope n=3, poloidal mag. field effect on linear and adiabatic oscills. 78−24505
polytrope n=3, with toroidal mag. field, nonradial oscills. and stability 77−9738
polytrope of index 5, proof of its finiteness 78−40920
polytropes, Lane-Emden eqn. solns. 79−96994
polytropes, uniformly rotating, equilib. struct. investig. using iterative method 78−32441
polytropic envelopes, thermal wave propag. *(Russian)* 77−82213
polytropic models, g and p modes 77−60751
polytropic models, periods of high pulsation modes 77−49372
polytropic star, equilib. poloidal mag. field, finite difference-finite expansion method, Fortran program 77−13322
presupernova, models rel. to radiation dynamics, envelope ejection and supernova light curve 77−64783
presupernova models and supernovae 80−56864
presupernova stars rel. to gas dynamics of supernovae and their remnants 77−17605
protostars, hydrostatic models evolution rel. to star form. process simulation *(Polish)* 80−21998
protostellar H_2O maser sources, disc struct. 79−48784
PSR 0809+74, pulsar, subpulse pattern phase stability rel. to emission models 78−40980
pulsar emission models, implications of drifting subpulses obs. in CPS 80−67763
pulsar emission models and plasma collective effects 79−25461
pulsar interpulses, two-pole and one-pole models 78−16449
pulsar magnetosphere models, interior and exterior struct., pair prod. 80−46594
pulsar magnetospheres, basic props., models *(Polish)* 77−17608
pulsar magnetospheres, consequences of polar cap model *(Russian)* 79−101169
pulsar magnetospheres, stellar-wind model for plasma-EM fields 80−22031
pulsar plasma, MHD, Lorentz covariant eikonal method 77−27663
pulsars, axisymmetric magnetosphere model 79−84813
pulsars, axisymmetric magnetosphere models 79−92794
pulsars, finite force face cold plasma atm. models, plasma differential rot. 80−77378
pulsars, gamma ray emission model 78−65641
pulsars, gamma-ray production mechanism 80−77433
pulsars, model of radio emission mechanism 78−12257
pulsars, pair creation model rel. to source of coherent radio emission 80−82403
pulsars, particle acceleration by DC electric fields 80−31316
pulsars, phenomenological model 78−40979
pulsars, possible radio emission mechanism 79−84812
pulsars, pulse width and period relations for various models 78−28714
pulsars, Ruderman-Sutherland model, emission zone limits 80−51795
pulsars axiosymmetric magnetospheres, method of soln. of self-consistent description 80−94825
pulsars charge-separated magnetospheres, aligned rotator model 78−40981
pulsars radio emission models, relativistic clock error effects 77−64786
pulsating stars, two-time asymptotic method appl. to one-zone atm. 77−53570
pulsating X-ray sources, secular period changes 77−45613
pulsation freqs., linked poloidal-toroidal magnetic fields 78−96470
pulsation modes, simple props. 79−35260
pulsational stability of very low mass stars on H and D main sequences 77−17544
VV Puppis, AM Herculis type binary, mag. pole accretion model 79−5860
VV Puppis, AM Herculis type binary, optical absorpt. spectrum, cyclotron intepretation and models 80−73003
V Puppis, eclipsing binary, as main sequence contact binary 78−4293
ρ Puppis, line profile variable, pulsational mode-typing 80−90432
ζ Puppis, Of type star, stellar wind model from UV line fit 80−72965
RX Puppis, peculiar emission-line object, physical model 78−61871
quark stars, eqn. of state and possibility of existence 77−45471
quark stars nonexistence 79−62855
quark stars with 'realistic' equations of state 78−73725
radial pulsations excited by nonradial modes *(Russian)* 78−16399
radially symmetric accreting envelope model, spectral lines profiles rel. to YY Orionis *(Russian)* 78−57544
radiative equilibrium mediumcool non-LTE models, effective temp. 10000-15000K, gravity 10^4 78−40921
radio binary systems, X-ray emission model 77−33700
radio pulsars, model *(Russian)* 78−40982
radiostars, polytropic models 79−2544
rapidly rotating models with radiation press., struct. parameters calc. 80−67697
rapidly rotating spheroids of n=1 polytropic index 77−17539
rapidly rotating stars, equilibr. and secular stability 79−62811
red giant model atmospheres, opacity sampled models grid 80−82348
red giant of 6 M⊙, envelope composition rel. to evolution 80−105237
red giant stars in globular clusters M92 and NGC 6397, model atmospheres and C abundances 79−48785
red giants, model atmospheres rel. to TiO absorpt. bands 78−96480
red supergiants, model atm. based on band-model opacity 77−56934
relativistic star, curved space-time, vac. stability, polarisation, phase transition 77−49290
relativistic star, rotating shell model 79−88650
response functions and secular modes 80−17572
Roche and Darwin problems for polytropic stars, numerical study 79−75202
rotating magnetic stars, steady-state models 77−45405
rotating main-sequence stars, strained coordinate methods for Cowling model 77−56910
rotating neutron stars, general relativity, exact solns. for slow rot. 79−75239
rotating polytropes, hydrostatic equilibria 79−80300
rotating stars, ang. momentum distrib. rel. to evolution 77−13316
rotating stars, perturbs. and stability, eigenvalues and perturb. theory 80−46538
rotating stars, perturbs. and stability, eigenvectors and variational principle 80−46537
rotating stars, with circulation free rot. laws 77−67088
rotational distortion of polytropes by analytic approx. 77−74039
rotationally distorted star, small oscills., Roche coords. appl. 78−69782
S-type stars, molecular spectra and model atmospheres 80−51764

stellar models continued
WZ Sagittae, cataclysmic variable, light curve superhumps model 80−4381
HM Sagittae, continuum spectrum, model, dense nebular around hot star *(Russian)* 78−69814
WZ Sagittae, eruptive binary, model from hot spot eclipses anal. 80−72962
HM Sagittae, eruptive variable, IR variability rel. to symbiotic binary model 79−25614
WZ Sagittae, recurrent nova, accretion disc models comparison with IUE obs. during outburst 80−109448
WZ Sagittae, recurrent nova, model for superhump phenomena 80−82368
WZ Sagittae, recurrent nova, photometric study and mass transfer model 78−24513
HM Sagittae, young planetary nebula, interacting stellar winds model rel. to 2.8 cm flux density increase 79−67025
V356 Sagittarii, unusual eclipsing binary, model 78−49477
Scorpius X-1, linear X-ray polarisation upper limit rel. to accretion-disc model 78−49557
Scorpius X-1, semiopaque plasma model of X-ray source 77−13501
V367 Scuti, double-mode Cepheid, pulsation mass calc. 77−67102
δ Scuti, line profile variable, pulsational mode-typing 80−90432
S Scuti stars, linear survey of models, pulsation 79−35259
δ Scuti subgiants, possible model 79−48809
self-gravitating systems, fluctuating hydrodynamics and thermodynamics 78−77485
selfgravitating accretion disc with hot corona, black hole 79−62812
semiconvection and vibrational stability of stars of about $1M_{\odot}$ 77−22204
FH Serpentis (Nova 1970), outburst model test 77−82253
FH Serpentis (Nova 1970), thick inhomogeneous shell model for radio emission 78−12236
FH Serpentis (Nova Serpentis 1970), dust grain IR emission model 80−105254
slow nova, evolution of model with Z=0.03 envelope from pre-explosion to extinction 78−32468
slow nova with 1.25 M⊙ white dwarf model 77−82264
slow novae and symbiotic stars, binary star model from obs. of late-type components 80−94813
solar model, constant mass, differentially rotating gaseous polytropes configurations 80−82338
spectroscopic binaries, models for distrib. with respect to primary mass, mass ratio and orbital semiaxis 80−46616
spectroscopic binary systems, main-sequence homogeneous stellar models rel. to apsidal motion 80−82413
spherical, general relativistic models, stability and normal modes 79−29983
spherical gravitating systems, radial vel. dispersion at outer regions *(Russian)* 78−61720
spherical star emitting neutrinos, relativistic model 78−73705
spherical stars, reformulations of Einstein eqn. solns. 78−49731
spherical stellar systems, dynamical relaxation, tidal perturbations by external systems 77−49443
spherically symmetric model in gravitational gauge theory *(Chinese)* 77−67086
SS 433, accreting black hole model 80−85958
SS 433, accreting mag. neutron star model *(Russian)* 80−36647
SS 433, accretion disc viscosity determ. using slaved disc model 80−62110
SS 433, beam models, energetics anal., possible triple system 80−90433
SS 433, binary star model including mag. white dwarf 80−4385
SS 433, circumstellar ring model rel. to weak lines pair wavelength vars. 79−67023
SS 433, deviations from standard model 80−98669
SS 433, dissipative infall model 80−67749
SS 433, early-type binary model 80−56843
SS 433, general spectral features 80−77421
SS 433, kinematic model for line wavelengths vars. 79−75226
SS 433, magnetic X-ray binary model 80−109447
SS 433, massive black hole and pulsar models rel. to precessional motion origin of 164^{d} period 80−62138
SS 433, Of star orbited by neutron star, model 80−22025
SS 433, precessing ring model, test by spectral line obs. 79−101152
SS 433 model, precessing jets in ultra-close binary system 80−4384
stability criterion for stellar cores *(Russian)* 78−93214
stars with given entropy distrib., models dynamical stability criterion 79−66993
static models with varying He core mass, linear series of 7 M⊙ star 78−65603
static spherically symmetric stellar models, admissible coord. system 78−28665
static stars, mathematical curiosities in Newtonian and general relativistic aspects 77−74045
static stellar models with He cores 77−17542
steady accretion disk, with magnetic field, basic equations 79−40179
Stephenson-Sanduleak 433, massive black hole hypothesis 79−71057
Stromgren four colour indices, grid for calc. of log g and effective temp. 80−36507
Sun, convection zone and angular vel., Boussinesq model 77−56898
Sun, model of solar cycle driven by dynamo action 77−56903
Sun, simple model for educational purposes 78−36756
Sun, two-dimens. model of nearly flux constant atmosphere 79−25571
Sun 1968 nonstandard model, nonradial oscills. 79−35218
super-metal-rich stars, evolution rel. to interpretation of old galactic clusters 77−49370
supercritical accretion discs winds struct. and appearance, numerical models 80−21984
superdense stars in quantum limit of ultrastrong frozen-in mag. fields 77−53620
supergiant stars with degenerate neutron cores, equilib. models struct. 77−33472
supergiants, early-type, with mass loss, two-core model and evolutionary status *(Russian)* 80−109425
supernova model of heavy element origin, r- and s-processes 77−56825
supernova models with slow energy pumping, appl. to galactic supernova remnants 78−73726
supernova nucleosynthesis mechanisms 77−87463
supernova progenitors masses 77−87461
supernovae, magnetorotational explosion in cylindrical model 80−101605
supernovae, MHD model 80−46588
supernovae, models with gradual energy release 77−78807
stellar models continued
supernovae, neutrino degeneracy effects 77−2447
supernovae, neutrino transport in collapsing stellar core model 78−8029
supernovae, self-similar oscillations of gas *(Russian)* 79−17001
supernovae, Type I, early part of light curve, modelling, H abundance effects 77−87458
supernovae, Type I, models 78−65636
supernovae and black holes analytic models, Einstein eqn. solns. 78−4258
supernovae core collapse, neutrino energy equilibration models 80−105265
supernovae in binary systems, rel. to HD 108 possible collapsed companion 77−13369
symbiotic stars, binary model with super-critical accretion 77−45458
symbiotic stars, H shell flashes in white dwarf with mass accretion 78−57550
symbiotic stars, models, spectral characts. *(Polish)* 79−88689
symbiotic stars, models of two subclasses 80−62144
symbiotic stars and classical novae, optically thick winds 77−87450
symbiotic stars and slow novae, binary star model from obs. of late-type components 80−94813
α Tauri, semiempirical model photosphere from Fe I lines obs. 78−4202
α Tauri (Aldebaran), chromosphere model 78−40931
T Tauri Nebula, stellar wind model 79−8912
T Tauri stars, infall model 77−13329
T Tauri stars, outflowing envelopes models 78−96482
T Tauri stars atmospheres, sphere and low chromosphere model 80−36623
T Tauri type stars, hydromag. model of peculiar activity *(Russian)* 78−49442
RR Telescopii, nova-like variable, spectrophotometry and expanding shell model 77−45460
temperature models derived from multiplet line-centre fluxes, rotation and macroturbulence effects 79−5806
thermal pulse and interpulse props. of intermediate-mass models with C-O cores 78−12199
thermal relaxation oscills. in two-zone model 79−96990
tidally distorted star, oscill. freq., perturb. method 77−22206
tidally distorted stars, form factor method for struct. determ. 80−21991
tidally distorted stars, Roche coords. appl. to small oscills. 78−77577
tidally-distorted stellar models small oscills., Roche coordinates appl., second-order terms effect 79−44462
twisted accretion discs in binary systems 77−53632
4U 2129+47, X-ray light curve and binary model 80−46704
unhomogeneous spheroid, Stokes dynamic constants 77−49442
uniformly rotating polytropes, boundary eqn. 77−74040
unstable models, solns. for dynamical rupture of equilib. 77−56913
unstable modes of equilibrium, topological props. 78−65606
upper main-sequence stars, models and evolutionary tracks in H-R diagram 77−49379
W Ursae Majoris metal-poor systems, evolution models 79−25628
W Ursae Majoris stars, A-type, radii and evolutionary state 79−8943
W Ursae Majoris systems, models, struct. and evolution 77−45488
W Ursae Majoris type binaries, evolutionary models 77−53644
Vela pulsar (PSR 0833−45), radiation model 80−94824
AI Velorum, oscills., pulsation models 79−48813
very close binary systems, struct. eqns. including rot. and tidal distortions for ZAMS stars 80−22037
vibrational stability of stars in thermal imbalance 78−24506
α Virginis, β Cephei type pulsation characts. 80−56835
78 Virginis, Ap star, mag. field geometry, oblique rotator model 80−51773
ε Virginis, Fe spectrum, differential model atmosphere analysis 79−25604
CU Virginis (HD 124224), Ap star, model atmospheres rel. to spectrophotometric obs. 80−98663
visual surface brightness depend. on colour, model stellar atm. calcs. 80−67707
wave propagation in prestressed nonlinear elastic solids, relativistic theory, dense stellar objects 79−1124
white dwarf stars, model atmospheres rel. to two-colour diagram, masses and radii 80−46547
white dwarf surface accretion, thermal runaway, nova phenomenon 77−82222
white dwarfs, abundance effects on spectra of very cool objects, model atmospheres 77−29829
white dwarfs, conf., Rome, Italy (Sep. 1976) *(Italian)* 78−93239
white dwarfs, DB-type, model atmospheres 80−51761
white dwarfs, hot, model atmospheres and effective temps. 79−25602
white dwarfs, magnetic flux distrib., radiative/conductive equilib. models 79−53811
white dwarfs, minimum-flux coronal models for H and He atmospheres 80−8626
white dwarfs, model atmospheres and synthetic spectra, effective temps. 5000-7000K *(Italian)* 78−93240
white dwarfs, nonradial nonadiabatic oscillations 77−56925
white dwarfs, rapidly rotating, oscills., numerical calc. 80−46554
white dwarfs, rigidly rotating, critical ang. vel. and equilib. configurations 77−5525
white dwarfs, slowly rotating, nonradial oscills. 80−4348
white dwarfs, thermonuclear runaways models 78−40937
white dwarfs accretion of rotating fluids by barytropes 77−33486
white dwarfs external layers, ingerpretation of spectra 79−62824
white dwarfs seismological theory for 1 $M_{\odot}$ model with crystalline core 80−17577
Wolf-Rayet atmosphere, wavelength depend. of linear polarisation 77−60779
Wolf-Rayet stars, He rich-expanding atmosphere model rel. to UV energy distribs. obs. 80−22023
X-ray binaries, matter supply mechanisms 77−9813
X-ray binaries, recurrent transients model 80−109565
X-ray binaries in dense stellar clusters, dynamical effects 79−97098
X-ray binary source in stellar wind, variable spectral features interpretation 77−17716
X-ray binary stars, Roche-lobe overflow model 78−32601
X-ray binary systems, massive, gas streams and accretion discs 78−93464
X-ray binary systems, models, X-ray transfer, Monte Carlo study 78−93463
X-ray burst sources, magnetised accretion disc model 77−53702

stellar models continued
X-ray burst sources, model, substorm process at accreting neutron star 79−17132
X-ray burst sources, models 78−49566
X-ray burst sources, simple physical model 77−29960
X-ray burst sources and convective accretion discs 78−16568
X-ray bursters, props. and model 77−71154
X-ray bursters 80−4460
X-ray pulsars, accretion torques 77−49505
X-ray pulsars, radiating accretion column model 77−53710
X-ray source, intensities from stellar wind flow past compact object 80−22116
X-ray sources, pulsating, oblique mag. dipole configuration model 80−94895
X-ray sources and induced surrounding clouds 79−67117
X-ray sources in globular clusters, binary star and black hole models 78−12428
X-ray sources of galactic bulge, highly compact binary model 79−35430
X-ray sources with repeating bursts, magnetospheric accretion model 77−5597
X-ray transient sources, close binary star model 77−33695
zero age horizontal branch stars, expected location 78−77551
C detonation supernova models, lower mass limit 79−17053
C-O white dwarfs, C-O eutectic model 80−77405
H burning stars, Hertzsprung-Russell diagram age and mass calibrations 80−51744
Hβ indices for model atms., B-type stars appl. 80−31292
He stratification in model atmosphere of blue horizontal-branch star 80−90409
He-rich white dwarfs, convective mixing 79−71018
HgMn stars, diffusion model rel. to obs. of Hg in thin atmospheric layer 80−105243
HgMn stars, line blanketed model atmospheres rel. to spectrophotometry 80−26867
Mn stars, diffusion model, implications of Hg II line oscillator strength 80−72966

stellar motion
see also celestial mechanics
2A 0311−27 optical counterpart, spectroscopic binary, radial vels. 79−25762
61 Cygni A, wobble obs. possible massive planet partner 77−71131
2A 0311−227, AM Herculis type X-ray binary, optical counterpart, radial vel. obs. 80−94890
2A 0311−227 optical counterpart, radial vel. meas. 79−101222
2A 0526−328 optical counterpart, radial vel. meas. and orbital period 80−90579
2A 0526−328 optical counterpat, radial vel. var. 80−77515
3A 2252−035, optical counterpart, proper motion and radial vel. determ. 80−82395
A and F stars near N.Galactic Pole, local mass density determ. 79−40267
A-type central stars of planetary nebulae, radial vel. study 78−81629
absolute proper motion compiled catalogue, composition method *(Russian)* 80−51747
absolute proper motion meas. of stars in M31 area *(Russian)* 77−71106
ADS 11871 (β 648), visual binary star, orbital elements, determ. using two methods 80−51805
ADS 1538=Σ 168=BDS 1015, orbit of visual double *(French)* 78−8056
ADS 1833 and 6871 AB, visual binaries, orbital calc. *(French)* 80−98690
ADS 7251, photographic obs. in 1962-73 period, orbital motion *(Russian)* 78−28726
ADS 7390 (ω Leonis), visual binary, orbital elements and removal of nodal ambiguity 77−13399
ADS 9476 (Aitken 14), possible astrometric companion *(French)* 79−44553
AGK3 stars, proper motions rel. to determ. of precession and galactic rot. 77−45402
Algol, orbit, lightcurve and struct. review 80−109460
algorithms for numerical orbit computation in galaxy models 80−67797
Allegheny Observatory parallax program, astrometric constants for 47 stars 78−53923
o Andromedae, Be star, radial vels. obs. 79−58355
o Andromedae, Be star, spectra and radial vels. from (1967 to 1976) 77−71116
CG Andromedae, Si binary star, spectrum variable, short period radial vel. variability determ. 80−72968
angular motion of trapped stars near spiral galaxies corotation circle *(French)* 79−88705
Ap stars in spectroscopic binary systems, orbital inclinations rel. to chemical anomalies surface distrib. 80−62140
AE Aquarii, spectroscopic binary variable, X-ray source, orbital element determ. 80−105288
U Aquilae, Cepheid variable, detect. as long-period binary by radial vel. spectrometer 80−51667
V342 Aquilae, eclipsing binary, period and light curve changes, (1966 to 1976) 80−67791
KO Aquilae, eclipsing binary system, period increase from UBV photoelectric study 80−62198
V923 Aquilae, motion in shell and atmosphere 77−60776
α Aquilae (Altair), 1941-77 astrometric obs. 79−12470
V539 Arae, photometric analysis of B-type double lined eclipsing binary 79−44535
Astrographic (Carte du ciel) Catalogues, variable star positions 77−49393
astrometric detection of planets, photoelectric detection equipment 80−56882
asymmetrical drift, influence of spiral struct., peculiar solar motion and G giants kinematics 77−13403
SX Aurigae, early-type semidetached binary, orbital elements from UBV photometry 79−44521
SX Aurigae, eclipsing binary, light curves anal. by automated Fourier techniques 79−92798
ε Aurigae, eclipsing binary, orbital elements and parallax from astrometric study 78−89219
IU Aurigae, eclipsing binary, two-colour photometry and third component orbit 80−36669
IU Aurigae, massive triple system, spectra and orbits 77−64798
IU Aurigae, revised photometric elements 79−101175

stellar motion continued
ε Aurigae, spectrum and radial vels. outside eclipse 77−71129
KW Aurigae (14 Aurigae A), pulsating ellipsoidal variable, orbital inclination from tidal l=1 p_5-modes 79−97028
α Aurigae (Capella), orbital motion determ. using phase effect detect. at CERGA stellar interferometer *(French)* 80−36508
T Aurigae (Nova 1891), old nova, orbital elements from photometric and spectroscopic obs. 80−90446
axisymmetric nucleus stellar system, stellar motion anal. 77−17687
axisymmetrical stellar systems, periodic orbits of stars 80−17619
B5-A0 stars, local density and kinematics 77−56931
B supergiants, kinematical parameters from UBV photometry 77−26011
B-star kinematics and local compression 79−8954
B-type stars, radial vels. determined at Radcliffe Observatory 78−12225
B-type stars, space vel. field rel. to differential galactic rotation 79−58340
B-type supergiant stars, radial vel. vars. 79−21285
Barnard's star, parallax and proper motion obs. 1916-1976, sexagintennial report 77−45432
BD+29°3805, K-type giant, spectroscopic binary orbit 80−67790
BD+57° 1942, faint short-period binary, influence of Schwarzschild effect on orbital and system elements *(German)* 80−8653
BD+61° 1211 (2A 1052+606), RS Canum Venaticorum binary star, spectroscopic obs. 80−36663
Be-stars, apsidal motion of gaseous ring rel. to emission lines V/R var. 77−37604
binaries, orbital inclination, polarimetric determ. for five systems 78−45358
binary central star in planetary nebula NGC 6853 from proper motion obs. 77−49434
binary pulsar, orbital characts. rel. to pulsar period change 77−5542
binary star light and velocity curves simultaneous solution, eccentric orbit generalisation 80−36664
binary star orbits solution, Fourier transform method 80−26899
binary stars, inclinations determ. from Thomson scatt. polarisation in optically thin envelopes 78−81655
binary stars, minimum projected distance in eccentric orbits 80−26904
binary stars, Newtonian attraction of two adjacent round ellipsoidal segments *(Italian)* 80−8531
binary stars, orbital eccentricity effect on polarimetric obs. 80−109472
binary stars, unresolved, epochs of speckle interferometric obs. rel. to orbital parameters 78−73735
binary system, close, with mass and ang. momentum loss, period changes 80−72998
binary systems, effect of gravit. radiation on evolution and spins 78−12292
binary systems, speckle interferometric obs. with Haute-Provence 1.93 m telescope 80−90475
binary X-ray sources, constraints on apsidal motion 77−87571
ZZ Bootis, double spectrum eclipsing binary, revised spectrographic and photometric elements 78−61885
BV 845, contact binary, improved photometric soln. 78−45365
CC 1299 (BD+27°4120), unresolved astrometric binary, orbital anal., mass and parallax 80−109464
53 Camelopardalis, Ap star, radial vels. and binary nature 79−80320
AH Cancri, contact binary in M67, radial vel. obs. 79−40222
WY Cancri, eclipsing binary, radial vels. rel. to absolute information derivation at lower end of main sequence 79−92799
β Canis Majoris, β Cephei star, Fourier anal. of radial vel. changes 80−105246
VY Canis Majoris, apparent orbit, rotating holey dust cloud hypothesis 79−40191
α Canis Majoris (Sirius), possible orbits for third star 78−93312
R Canis Majoris eclipsing binary, multiband photoelectric photometry and orbital elements 77−53633
TX Canum Venaticorum, cataclysmic variable, orbit from visible spectra obs. 80−105249
RS Canum Venaticorum, explanation of observations 79−84826
Carina Nebula association, radial vel. study of WN stars and Of star 79−35261
θ Carinae, radial vel. of chemically-peculiar B-type star 80−8635
OY Carinae, white dwarf cataclysmic, eclipsing binary, parameter determ. 80−82385
α Carinae (Canopus) spectrum, generalised Compton effect and radial vel. 78−53938
QZ Carinae (HD 93206), massive multiple system in great Carina Nebula, spectral types and orbits 79−97027
QZ Carinae (HD 93206), O-type quadruple eclipsing system, spectroscopic and radial vel. study 80−105275
RZ Cassiopeiae, Algol-type binary, period vars. 77−13394
V523 Cassiopeiae, BV photometry of W UMa type system *(Russian)* 79−92807
TV Cassiopeiae, eclipsing binary, orbital period vars. rel. to mass transfer 79−84818
RZ Cassiopeiae, eclipsing binary, spectroscopic orbit 80−22040
DO Cassiopeiae, eclipsing binary, stellar structure 78−16462
DO Cassiopeiae, eclipsing star, as contact binary, three-colour photoelectric investigation 78−16462
TV Cassiopeiae, light curve, long period var. interpretation 79−101174
TV Cassiopeiae, light curve and orbital elements of eclipsing binary 77−49430
μ Cassiopeiae, subdwarf binary, spectroscopic orbit 78−8046
o Cassiopeiae (HD 4180), Be star, radial vels. and IR and optical vars. 79−58353
cataclysmic binaries, radial vel. data rel. to circumstellar material geometrical and photometric parameters 80−109492
cataclysmic binary stars (CBS), critique of polarimetric evidence on physical parameters and orbital inclination 80−109486
cataclysmic variables, apsidal motion and evolution 79−62834
BV Centauri, dwarf nova and spectroscopic binary, radial vel. orbits 80−51775
V346 Centauri, eclipsing binary, spectroscopic orbit 79−58378
α and Proxima Centauri, radial vels. and bound state 80−41859
V78 in ω Centauri, radial vels. and circular orbit of eclipsing binary 79−97030
α Centauri and Proxima Centauri, space motions, masses 79−21348
central stars of planetary nebulae, kinematics 80−51762
EM Cephei, eclipsing, binary, UBV photometry rel. to constancy or variability of period 80−105286
U Cephei, eclipsing binary, anal. of radial velocity curve of B9 component 80−94829

stellar motion continued
T Cephei, long-period variable, radial-vel. obs. 79−88684
NY Cephei, massive eclipsing binary, orbital period and inclination from UBV photometry 80−67789
U Cephei, three colour light curve perturbations and orbital element determ. *(French)* 80−67787
U Cephei, UBV photometry, light curve solns. 79−67054
VW Cephei, W Ursae Majoris star, orbital period decrease and B-V colours rel. to physical status 80−109495
17=ξ Cephei A, speckle interferometry, visual orbital elements 80−56874
Cepheid variables, distance determ. method 77−45467
Cepheid variables, double-mode, freq. anal. 80−31308
Cepheid variables, short-period, radial vels., BVRI photometry, radii 80−31309
Cepheid variables between l∼294° and 331°, kinematics rel. to galactic rot. model 79−48910
Cepheids, double-mode, photoelectric radial vels. and BVRI photometry 79−88675
δ Ceti, β Cephei variable, spectroscopic binary, radial vels. and period var. 80−82376
TV Ceti, light curves, photometric elements and He content 79−44526
o Ceti (Mira), enhanced activity of B-type component at 1976 light minimum 78−81636
o Ceti (Mira), long-period variable, radial-vel. obs. 79−88684
RS Chamaeleontis, eclipsing binary, four-colour photometry and photometric orbital elements 80−67783
RS and RZ Chamaeleontis, photometric elements of detached eclipsing biuaries 80−90473
Chu's object in Perseus, radial vel. rel. to identification as galactic star 80−62132
Ci 182354, astrometric anal. of unseen companion from 61 cm Sproul refractor plates 78−16459
Circinus X-1, binary model, orbital eccentricity from X-ray and radio obs. 80−98735
Circinus X-1, Hα emission mean radial vel. rel. to runaway origin 80−67910
Circinus X-1 as gamma-ray source, eccentric orbit binary model 79−97100
classical Cepheids, light and radial vel. curves phase matching 77−17574
close binaries, form. by two-body tidal capture 77−33556
close binaries, orbital angular momentum loss during evolution 79−97033
close binaries, synchronism between axial rotation and orbital motion 79−97034
close binary stars, effects of tidal friction on orbital eccentricities 77−57013
close binary stars, orbital periods distribs. before and after mass transfer 80−62187
close binary systems, precession and nutation 77−13392
close binary systems, radial vel. curves anal. 80−90470
close binary systems with neutron star components, evolution *(Italian)* 79−21354
cluster, spherically symmetric with stars of uniform mass, struct. and dynamics 80−62215
cluster binaries, dynamics 78−12295
cluster dynamics, higher order fluid eqns. for multicomponent nonequilib. systems 80−105156
cluster stars, proper motions rel. to cluster membership probabilities 78−28736
clusters, dynamical evolution with changing gravit. const. 79−17030
clusters, dynamical evolution with multi-mass populations *(Italian)* 77−91584
clusters, dynamics and shapes 77−17635
clusters, isolated, numerical methods of star escape rate determ. *(Polish)* 80−26922
clusters, kinetic theory for finite inhomogeneous gravit. systems 77−9775
clusters, nonexistence of additional integral of motion of star 78−65663
clusters, ratio of escape rel. to mean vel. *(German)* 78−53995
clusters, tidal disturbances by spiral density waves *(German)* 79−17086
clusters, vel. distrib. relaxation with close encounters 79−48862
clusters containing massive central black holes, dynamical simulations with self-consistent potentials 80−26915
clusters containing massive central black holes, Monte Carlo simulations in two-dimensional phase space 79−8955
collapsing stars, enhanced gravit. radiation recoil 77−33336
collision between white dwarf and main sequence star, results 77−64758
collisionless systems, statistical mechanics of violent relaxation 79−5864
collisions, by oscill. orbits of second kind 79−35312
collisions near Kerr black hole, compact extragalactic source model 79−12490
contact binaries, orbital periods sudden changes due to third component 80−109497
contact binary star, idealised dynamical evolution *(French)* 80−62199
cool C stars, nearby, distances rel. to space vels. and proper motions 78−49434
Cor 197, deviation of residuals in motion 79−44552
σ Coronae Borealis (=ADS 9979), binary, mass and orbital elements *(French)* 80−77449
CPD−26°389, central star of NGC 1360, radial vel. obs. 80−4350
Crab pulsar, proper motion 77−82269
α^1 Crucis, improved spectroscopic orbit 80−67792
25 G Crucis (HD 108250), orbital elements from spectrograms 80−82432
31=o^2 Cygni, astrometric studies 78−69779
EM Cygni, cataclysmic variable, red and white dwarf binary, period change, B photometry 80−90434
XX Cygni, dwarf Cepheid, composition and motion, visible photometric and spectrographic obs. 80−77424
CG Cygni, eclipsing binary, light curve and orbital period vars. 79−48857
32 Cygni, eclipsing binary, orbital elements from λ6575 and λ4870 light curves anals. 79−88700
GO Cygni, eclipsing binary, orbital period changes 80−72999
V367 Cygni, eclipsing binary, spectrum and radial vels. 78−53984
χ Cygni, long-period variable, radial-vel. obs. 79−88684
V444 Cygni, orbital period var. rel. to Wolf-Rayet star mass loss *(Russian)* 79−101178
V389 Cygni, peculiar (Ap-type) binary, spectroscopic obs. 78−85975
SS Cygni, radial vel. of dwarf nova 79−62833
stellar motion continued
57 Cygni, spectroscopic binary, search for systematic radial vel. anomalies 80−17617
SS Cygni, spectroscopic binary variable, X-ray source, orbital element determ. 80−105288
CH Cygni, symbiotic star, radial vels. and binary model 80−62158
V1329 Cygni (HBV 475), symbiotic variable, radial vel. vars. rel. to eclipsing binary model 80−62148
Cygnus OB2 No.12, radial vel. from high-resolution 2μ spectroscopy 78−57613
Cygnus X-1, critique of polarimetric evidence on physical parameters and orbital inclination 80−109486
Cygnus X-3, period derivative and asymmetric X-ray light curve from HEAO 2 obs. 80−105394
HR Delphini (Nova 1967), He I radial vel. var. 77−82249
HR Delphini (Nova 1967), revised orbital ephemeris from simultaneous X-ray, UV and optical obs. 80−109440
HR Delphini (Nova 1967), spectroscopic orbit 79−44510
dense stellar systems, fates 79−25652
detached double-lined eclipsing binaries, revised photometric elements 78−61886
detached systems, revised photometric elements for 8 double-line biuaries 80−46610
diffusion of stellar orbits from age depend. of vel. dispersion 77−82283
disc galaxies, stellar and gas responses to oval distortions, effects of dissipation 78−12355
disc galaxies, stellar motion following massive objects ejection in plane of stellar disc 80−82495
disc galaxies, stellar motion following massive objects ejection out of stellar disc plane 80−82496
disk stars, metal abundance rel. to orbital elements *(Russian)* 79−25733
double stars, rectilinear trajectories calc., appl. to h 5094, effects of erroneous positions *(French)* 78−20857
Draco dwarf spheroidal galaxy, stellar colour magnitude diagram and proper motion 80−73029
BY Draconis, binary spotted flare star, orbital elements and pre-main-sequence nature 80−36633
AR Draconis, BV light curves and orbital elements 79−101173
RZ Draconis, eclipsing binary, photoelectric light curve and orbital period study 80−109461
AI Draconis, period and spectroscopic orbit of eclipsing binary 78−89221
dwarf Cepheids, space motions rel. to evolutionary stage 80−46562
dwarf stars, K- and M-type, space motions rel. to stellar age 78−69846
dwarf stars, three-dimensional motion 80−12754
dynamical astronomy, integrable and stochastic behaviour 80−12650
dynamical evolution of cluster models with continuous stellar mass loss 80−82438
dynamical evolution of Keplerian systems, numerical simulations of collisions 80−109342
dynamical evolution of stellar systems, anal. rel. to hidden masses *(Russian)* 77−91583
dynamical systems, evolution with time-varying gravity 78−24459
dynamics, collision integral determ. *(Polish)* 80−67799
dynamics, global particular solution to initial value problem 79−35314
dynamics, stability of one-dimensional self-gravitating isothermal systems 80−73008
dynamics in galaxies, stability rel. to galaxies nonflat components mass 80−62291
dynamics in thin disk galaxies, hydrodynamic eqns. 79−92809
dynamics of colliding bodies in gravitational field, numerical simulation of standard model 77−29634
dynamics of stellar bar, computer model 79−30093
early-type stars near Sun, space vels. and ages 78−61858
early-type stars with six degrees of galactic anticentre direction, radial vels. 78−7990
eclipsing binaries, photoelectric lightcurves of possible sd-d systems, revised elements 80−56879
eclipsing binaries, sd/d nature from radial vels. 80−82423
eclipsing binaries orbits, appl. of Kalman filter to light curves 77−5546
eclipsing binary runaway, orbital data, UV obs. 80−85952
Eggen's moving groups, high-dispersion analysis check 77−29838
ellipsoidal distrib. of vels. in spiral galaxies *(Chinese)* 80−77484
elliptical galaxies, anisotropic vel. distribs. generation 80−36715
encounters with field stars, statistical effect on wide binaries 79−44562
equilibrium in stellar systems with continuous mass spectrum, necessary condition 78−93328
equilibrium statistical mechanics, steepest-descent techniques for Newtonian clusters 77−45496
equilibrium statistical mechanics of a one-dimensional self-gravitational system 79−92810
δ Equulei, improved orbit for visual binary 78−45364
α Equulei, radial vel. vars. from microphotometer scans 78−77581
δ Equulei, three-dimens. orbit 79−53852
ν Eridani, β Cephei star, Fourier anal. of radial vel. changes 80−105246
escape from isolated clusters, classical theory of close encounters *(Polish)* 77−71134
experimental stellar dynamics with axial symmetry 77−13404
extratidal variables and dynamics of Sculptor dwarf galaxy 79−67088
faint blue stars proper motions near galactic anticentre 77−87386
faint short-period spectroscopic binaries, influence of Schwarzschild effect on orbital and system elements *(German)* 80−8653
FK4/FK4 Sup stars, three-dim. kinetics anal. 78−8060
flat galaxies, stellar orbits rel. to galaxy dynamics, integral eqn. for normal modes 77−33637
flat galaxies dynamical struct., statistical characts. 80−62269
flat spiral galaxies, scattering of trapped star orbits, bananas 78−16464
flat systems, stellar kinetics, relaxation times 77−13405
Fokker-Planck eqn. numerical integration, stellar dynamics in fixed inhomogeneous gravit. background 78−32526
formal third integral of motion, construction in reson. cases 77−53647
formal third integral of motion for resonance *(Russian)* 77−57062
Freeman's elliptical stellar cylinder model, stability 78−28731
G139-29, perturb. from rectilinear motion, astrometric red dwarf binary system with subluminous component 79−8910
G24-16, parallax and astrometric orbit from Sproul plate series 78−53983
G35-26, high-velocity mag. degenerate, obs. 78−73709
G77-61, dwarf C star, proper motion 78−4209

stellar motion continued
G- and K-type stars, correl. between motions and CN anomalies 77−17566
G- and K-type stars, space motions 77−45430
galactic clusters, membership probabilities, photographic meas. of relative proper motions of stars 80−51817
galactic clusters in Cassiopeia, stellar photometry and proper motions obs. *(Russian)* 79−97042
galactic density wave, molecular clouds and star formation 78−8088
galactic density waves, excitation at Lindblad and corotation resons. by external potential 80−22072
galactic density waves, maintenance and phase shifts between stellar and gaseous arms 79−44618
galactic dynamics, trapping of particles in time-depend. Hamiltonian 77−13217
galactic globular clusters, orbital evolution due to dynamical friction 78−24529
galactic models with variable spiral structure, computer simulations 78−32574
galactic motion, Hamilton-Jacobi eqn., velocity field gradient coeffs. *(Russian)* 79−88707
galactic nucleus, stellar dynamics rel. to black hole sustenance 78−57632
S.Galactic Pole, astrometry of B<14 stars, UK Schmidt results 79−66929
galactic populations, kinematic parameters correl. with metal abundances 78−96545
galactic spiral structure persistence and stellar orbits 78−41046
galactic stellar subsystems, kinematical model 77−13402
galaxies, cool stellar discs equilib. 78−54037
galaxies, density waves and discrete spiral modes rel. to stellar dynamic theory 77−33638
galaxies, early-type, rot. curves meas. 78−54034
galaxies, flat disc, retrograde stars effect on global bar-forming mode 79−21411
galaxies, gravit. N-body models rel. to form. and evolution 79−17100
galaxies, gravitational instability of loosely wound spiral density wave 80−85998
galaxies, radial oscill. modes of cool stellar discs 78−57628
galaxies, stellar spiral density wave caused by orbiting retrograde companion 78−96533
galaxies active nuclei, irradiated stars motion rel. to emission line broadening 80−56949
galaxies dynamics, criteria of local gravit. instability of double gaseous discs *(Chinese)* 79−17099
galaxies dynamics, numerical models and spiral struct. variability 79−25725
galaxies inner Lindblad resonance, nonlinear theory including bars 78−20863
galaxies material arms, tidal disturbances by spiral density waves *(German)* 79−17086
galaxies structuring mechanism 79−48924
Galaxy, hydrostatic equilib. for three unequal stellar vel. dispersions 77−57094
galaxy disc stars, nonlinear interaction with spiral wave near corotation radius *(Russian)* 80−62289
Galaxy dynamics, appl. of generalised twice restricted three-body problem *(Russian)* 80−51643
galaxy dynamics, appl. of problem of four fixed centres 78−28493
galaxy formation, dynamical development and struct. of six collapsing models 79−25710
Galaxy kinematical-local struct. relation, appl. to OB-stars and variables *(Russian)* 78−77608
galaxy mergers, stellar populations mixing processes 80−67860
galaxy models, numerical orbit computation algorithms comparison 79−12497
galaxy nuclei, distrib. and consumption rate of stars around massive collapsed object 77−45497
galaxy stellar disc, axisymmetric disturbances growth rates 79−21410
Galaxy stellar orbits, applicability of approximate third integral of motion 80−67798
Galaxy-escaping stars, dynamics during gravit. encounters between Local Group galaxies 77−57098
GCl 0422−213, distant globular cluster in Eridanus, heliocentric radial vel. 80−17624
YY Geminorum, eclipsing binary, photometry and orbital period study 80−105287
1 Geminorum B, spectroscopic binary, orbit from photoelectric radial vels. 77−22269
general catalogue for southern stars, proper motions in α, corrections *(Russian)* 79−92685
glaxy collisions, numerical expts. 80−51864
globular cluster cores evolution, life and death matters 79−25653
globular clusters, distrib. and consumption rate of stars around massive collapsed object 77−45497
globular clusters, ellipticities of RR Lyrae star systems 77−60805
globular clusters, late core collapse in gravitating systems 80−22048
globular clusters, stellar dynamics rel. to present and past death rates 78−28733
globular clusters, test computations on dynamical evolution 77−49445
globular clusters, two body capture processes for close binary systems form. 79−44530
globular clusters in Galaxy, tidal disruption 80−105294
globular clusters near galactic centre, dynamics rel. to expected number density 78−32535
globular clusters stellar dynamics and evolution of ellipticities 77−13406
globular clusters with massive black holes, dynamical evolution 78−4302
globular star clusters, dynamic evolution, review of obs. and numerical theories 78−77585
Gould Belt, kinematics of Lesh's OB stars 79−67089
gradient of field of directions normal to trajectory, and forms of potential 78−65662
gravitating discs, models, phase description *(Russian)* 78−69887
gravitating systems, energy transfer 79−40226
gravitational instability, non-linear effect for adiabatically deformed case 78−20864
gravitational potentials of spheroidal stellar systems, appl. to the Galaxy 77−53645
gravitational radiation damping of binary stars calc. 79−97272
RS Gruis, dwarf Cepheid in binary system 78−77559
RS Gruis, RRs variable, photoelectric radial vels. 77−5533

stellar motion continued
GX 304−1 (3U 1258−61), 272 second periodic var. rel. to orbital motion 78−8152
H 2252−035, cataclysmic variable, photometry and spectrum rel. to orbital and rot. periods 80−101651
h 3556, triple star, binary orbit and masses and third component relative motion 79−88701
h 4866 B, vars. in spectral type and radial vel. 78−32518
H-H 28, H-H 29, large proper motion Herbig-Haro objects, astrometric obs. 79−71022
halo stars and old disc population, orbits and kinematics, active phases in Galaxy evolutions 79−35394
HD 102567 (4U 1145−61), X-ray periodicity and orbital motion 78−8160
HD 105056, ON supergiant, radial vel. study 80−90427
HD 108078, spectroscopic binary orbit from photoelec. radial vel. meas. 80−77451
HD 11579, spectroscopic binary orbit from photoelectric radial vels. 80−41862
HD 116458, binary Ap star, spectrum and orbit 77−64767
HD 127617 (Bidelman's high latitude Be star), photometric and visible spectra obs. 80−77420
HD 134439/40, high vel. stars, parallaxes, proper motions and positions 77−71128
HD 137126 spectroscopic binary orbit from photoelectric radial velocities 79−84824
HD 13738, spectroscopic orbit from photoelec. radial vels. 78−12297
HD 143313, orbit for double-lined spectroscopic binary from radial vels. 79−62873
HD 147508, spectroscopic binary, orbit from photoelectric radial vels. 78−69839
HD 14969, IAU radial-velocity standard star, orbit from photoelectric radial vels. 80−56884
HD 153919 (3U 1700−37), binary X-ray source, radial vel. data in blue spectral region 78−61888
HD 153919 (3U 1700-37), binary X-ray source, radial vels. in blue spectral region 78−49556
HD 155989, spectroscopic binary, orbit from photoelectric radial vels. 79−21355
HD 159176, spectroscopic binary radial vel. obs., orbit and masses 79−25644
HD 165590 triple system, spectroscopic obs., orbital elements 79−84825
HD 166734, Of star, spectroscopic binary orbit determ. from visible obs. 80−82414
HD 174209 (ADS 11719C), photoelectric radial vel. 78−32517
HD 175742, spectroscopic binary, orbit determ. with CORAVEL photoelectric radial vel. spectrometer *(French)* 80−36671
HD 179558, spectroscopic binary, orbit from photoelectric radial vels. 79−101177
HD 181330, spectroscopic binary, orbit from photoelectric radial vels. 78−93320
HD 187299, spectroscopic binary orbit from photoelectric radial vels. 77−91575
HD 193857, metallic-line binary star, orbital elements 79−75250
HD 197406, Wolf-Rayet spectroscopic binary, radial vels. and orbital elements 80−51812
HD 199892, spectrographic binary, spectrograms and orbital elements 79−21359
HD 200925 radial vels. of new short period δ Scuti star *(French)* 80−90441
HD 203631, spectroscopic binary orbit from photoelectric radial vels. 80−105285
HD 214686, double-lined spectroscopic binary, orbital elements and masses 79−58376
HD 216533, Ap star, spectroscopic binary oblique rotator model, spectral var. study 79−101153
HD 218154, spectroscopic binary, orbital elements 77−87476
HD 219150, F0 V star with remarkable UV excess, unsuccessful search for radial vel. var. 80−90429
HD 22007 (primary of ADS 16681), spectroscopic binary, radial vel., orbit elements 80−67793
HD 223969, spectroscopic binary orbit from photoelec. radial vels. 77−82279
HD 22403, spectroscopic binary with Ca II emission, orbital elements *(French)* 79−53854
HD 2343, spectroscopic binary, orbit from photoelectric radial vels. 80−8656
HD 26676 unusual radio star, radial vel. and search for duplicity 78−73707
HD 27507, proper motion determ. of A-type high-vel. horizontal branch star 80−77407
HD 27507 and escape vel. from Galaxy 78−85935
HD 39937, 101379, 155555, 174429, southern RS Canum Venaticorum stars candidates, radial vel. study 80−98686
HD 4174, symbiotic star, radial vels. vars. and binary star model 80−85945
HD 43930, photoelec. radial vels. and spectroscopic binary orbit 77−33574
HD 47732, double-lined binary, spectroscopic orbit 78−57574
HD 50896, Wolf-Rayet binary, orbital period and inclination from linear polarisation periodic vars. 80−72972
HD 50896 (WN5), emission-line spectrum and radial vel. vars. 80−51791
HD 56925 in NGC 2359, radial vel. of exciting WNS star 78−81678
HD 77581 (4U 0900−40), apsidal motion test of eclipsing binary 80−51908
HD 84903 and 184711, differential anal. of extreme metal deficient stars rel. to halo star HD 122563 79−80302
HD 90657, Wolf-Rayet spectroscopic binary, orbital elements 77−13357
HD 92740, spectroscopic binary WN7 star, spectroscopy and photoelectric photometry 79−8924
HD 94033 ultra short period cepheid, radial vel. and galactic orbit 80−22024
HD 96953, spectroscopic binary orbit from photoelectric radial vels. 80−56887
HDE 226868 (Cygnus X-1), line blending rel. to radial vels. and black hole candidacy 77−64878
HDE 226868 (Cygnus X-1), orbital period and Hβ light curve 79−48952
HDE 226868 (Cygnus X-1), orbital period and inclination 78−16579

stellar motion continued
HDE 226868 (Cygnus X-1), radial vels. rel. to existence of third star 77−45606
HDE 245770 (A0535+26), spectroscopy and orbital periods 78−93306
Hercules X-1 (HZ Herculis) system, pre-supernova binary period 80−62318
DY Herculis, dwarf Cepheid, radial vel. and radius 79−58358
AK Herculis, eclipsing binary, light freq.-domain anal. and orbital elements 77−53635
DI Herculis, eclipsing binary, relativistic motion of periastron 80−94830
AD Herculis, eclipsing binary, spectroscopic obs. and orbital elements 78−73738
AM Herculis, low-mass X-ray binary, radial vels. and line intensities 77−78826
AM Herculis, X-ray binary, vel. curves for emission lines broad and sharp components 78−32513
HZ Herculis (Hercules X-1), optical pulsations calcs. rel. to inferred optical vel. 78−57580
HZ Herculis (Hercules X-1), orbital precession 78−65718
HZ Herculis (Hercules X-1), Sonneberg photographic obs. and orbital motion change 77−37618
high galactic latitude stars, division into giants and dwarfs by proper motion *(Russian)* 80−109431
high-mass stars (M≳50 M⊙) masses and space vels. rel. to evolutionary status *(Russian)* 80−109425
high-velocity stars, southern, radial vels. 80−21988
Hipparcos satellite, proposed space-astrometry mission 80−82164
HR 1300 spectroscopic binary Am star, orbital elements 77−49438
HR 1614 group of metal-overabundant stars, intermediate-band photometry and space motion 78−53935
HR 2081, double-lined spectroscopic binary, radial vel. orbit and min. masses 80−51811
HR 2172, double-lined binary, radial vels. and equivalent widths *(French)* 77−17625
HR 2317, spectroscopic binary orbit from photoelectric radial vels. 79−40225
HR 5161, spectroscopic binary star, radial vel. orbit 80−12781
HR 6392, double star with very high luminosities, radial vel. 77−45493
HR 6659, spectroscopic binary, radial vel. obs. 80−82430
HR 6684, β Cephei-type star, radial vel. vars. from microphotometer scans 78−77581
HR 6684, β Cephei-type variable, radial vel. var. 78−45344
HR 6940, spectroscopic binary orbit from photoelectric radial vels. 78−4294
HR 7083, spectroscopic binary, orbit from photoelectric radial vels. 78−32517
HR 7331, δ Scuti star, relation between radial vel. and light vars. 77−9752
HR 9049, (HD 224113), eclipsing spectroscopic binary star, period and orbital elements 80−46609
Hussey 1399, relative motion of AC components rel. to invisible companion 79−44552
Hyades, convergent point method for kinematic parallaxes determ. 77−91596
Hyades, distance from proper motion data 77−87486
χ^2 Hydrae, eclipsing binary, four-colour photometry, orbital elements, dimensions and He abundance 78−65653
HS Hydrae, photometric elements of detached eclipsing binary 80−90473
VW Hydri, cataclysmic variable, orbital eccentricity rel. to light curve superhumps model 80−4381
hydrodynamic equations, rel. to radius depend. of elliptical galaxies vel. dispersion 80−51876
IAU Radial Velocity Standard stars, radial vels. meas. *(French)* 80−51743
IC 2391, relative proper motions of stars, ident. of member stars 80−51818
IC 2944, stellar aggregate surrounding HD 101205, radial vels. meas. 77−17636
inhomogeneous spherical gravitating systems dynamics, simplest hydrodynamic models 80−17620
intermediate Population II stars, Stromgren uvby photometry 77−60757
isolated clusters, star escape, Fokker-Planck eqn. generalization *(Polish)* 78−36645
isolated star clusters statistical theory of stellar escapes *(Polish)* 78−16466
isotropic relativistic star clusters, multi-term trial function stability anal. 78−73742
K-effect, linearised local vel. field in presence of density waves 77−33576
K-giants, z-motions in polar zones 77−17565
kinematics, appl. to galactic spiral structure parameters derviation 80−17665
kinematics and galactic spiral structure *(Russian)* 79−21362
kinematics and interstellar turbulence 79−35313
Kolmogorov entropy, of dynamical system with increasing number of degrees of freedom 79−80562
Kuiper 41, orbit and flare activity of visual red dwarf pair 79−97032
AR Lacertae, eclipsing binary, period vars. 77−37616
EW Lacertae, motion in shell and atmosphere 77−60776
large proper-motion stars, luminosity and motions for stars with annual motion >1″ 79−71020
large-amplitude red variables, luminosities and space motions 77−22244
late B-type stars, spectroscopic obs. rel. to duplicity 78−57547
late-type dwarfs, radial vels. rel. to photometric metal abundance index 77−60754
late-type field stars in S.hemisphere, radial vel. study rel. to possible duplicity 80−98686
late-type stars, kinematical data 77−26009
LB 3479, subdwarf eclipsing binary, evolutionary model comment 80−90426
LDS 720BC (CD−32° 16135), visual binary, orbit 78−32515
R Leonis, Mira variable, radial vel. from CO and OH IR vibr.-rot. overtone bands 78−36574
20 Leonis, triple system with a δ Scuti variable, orbits 77−49440
19 Leonis Minoris, spectroscopic binary, orbital elements and mass ratio 80−62197
δ Librae, Algol-type eclipsing binary, masses derived from vel. curves 78−49475
δ Librae, revised photometric elements 79−101175

stellar motion continued
48 Librae (FX Librae), shell star, spectroscopic study and radial vels. 78−96486
Lick proper motions referred to galaxies, precession and galactic rot. determ. 78−65487
LMC X-4, spectroscopic obs. and orbit 79−9028
LMC X-4 optical candidate, radial vels. and binary nature 77−64879
long-period variable stars, radial vel. obs. 79−88684
low galactic latitude stars, relative proper motions and mean secular parallax 78−57542
LP182-44, faint high-vel. degenerate star with probable C features, photometry and spectrum 79−67007
LP 182-44, faint blue star with large proper motion, discovery 78−49439
LSI+61°303, supergiant Be star, radio emission and radial vel. periodic vars. 80−62149
luminous C stars in LMC, radial vels., photometry and spectra 78−28670
β Lyrae, orbital period variability 80−72997
β Lyrae, UV spectrum and radial vels. 78−8048
α Lyrae (Vega), evidence for light and vel. vars. 79−75208
RR Lyrae stars, absolute proper motions for 64 stars *(Chinese)* 79−80319
RR Lyrae stars, vel. ellipsoid 78−77563
RR Lyrae stars in galactic bulge, spectra, comp. and radial vels. 77−26012
RR Lyrae stars in Palomar-Groningen fields, luminosities, distances and kinematics 78−93276
RR Lyrae variables, three-dimensional motion 80−12754
M11, open cluster, internal motions 77−22280
M11, open cluster, stellar proper motions rel. to membership 77−17641
M13, globular cluster, new stellar proper motions and membership probabilities 79−75252
M13, globular cluster, old proper motions rel. to astrometric cluster membership probabilities 79−88708
M15, globular cluster, dynamical models without black hole 78−32536
M15-K1082, two-hour variable UV-bright star in NGC 7078 (M15), radial vel. 79−88681
M22, globular cluster, stellar radial vels. rel. to membership 78−32537
M31, inertial frames of reference determ. from rot. vels. 79−21433
M31, vel. dispersions in nucleus and bulge 77−26049
M31 nuclear bulge, rotational vels. meas. 80−41888
M36, photographic obs., mass, radius, central density, stellar vels. of open cluster *(German)* 80−31333
M38, photographic obs., mass, radius, central density, stellar vels. of open cluster *(German)* 80−31333
M39, open cluster proper motion membership 77−91588
M3, photoelectric radial vels. of individual stars rel. to cluster dynamics 79−75251
M67, open cluster, stellar proper motions rel. to membership 77−22281
M67, open cluster, upper limit to mass and vel. dispersion 78−28735
M81, spiral galaxy dynamics, axisymmetric models and stellar density wave 80−105335
M87 (NGC 4486), vel. dispersion from a population model 80−77490
M87 core dynamics, anisotropic vel. distribs. rel. to supermassive black hole model 80−82500
M92, globular cluster, membership and internal motions 77−17634
M-type dwarf stars near north galactic pole, MgH band strength rel. to space vel. 77−78789
M-type stars, in north galactic polar region, space motions 78−93235
M-type stars in direction of N galactic pole, distances and tangential motions 77−37594
Magellanic Clouds, Wolf Rayet binaries, spectroscpic orbits 80−109479
material test point, statistics of distant perturbs. 78−28494
Me, globular cluster, stellar proper motions, membership and cluster internal motions 80−8665
Milky Way dynamics, work of Johann Georg Soldner (1776-1834) 78−81787
Mira variables, radial vel. meas. 77−56951
Mira variables kinematics towards galactic centre 80−46578
1 Monocerotis, δ Scuti star, oscillation modes from photoelectric radial vels. and BVRI photometry 80−51787
VV Monocerotis, eclipsing binary, orbital elements and dimensions *(French)* 78−89225
moving groups, kinematic age, focusing phenomenon 77−60801
multiple stars, parallaxes and proper motions, Sproul 61 cm refractor astrometric meas. 77−9768
θ Muscae, Wolf-Rayet binary radial vel. meas. 77−22235
N-body calculations, statistical results depend. on N 79−80339
N-body systems, existence of families of periodic orbits 78−24449
N-body systems, two-body tidal dissipation effects 78−93329
nearby stars, long term effects of space motion, constellation pattern changes 79−66995
nearest stars, vel. components rel. to galactic plane 79−97088
neutron stars space velocities, role of EM multipole fields 80−26896
Newtonian stellar dynamics, maximizing functionals, rel. to thermodynamic and dynamical stability 80−12782
NGC 2362, very young open star cluster star counts rel. to cluster struct. and dynamics *(German)* 78−16472
NGC 2477, photographic obs., mass, radius, central density, stellar vels. of open cluster *(German)* 80−31333
NGC 2516, proper motions in the region 79−88706
NGC 2669, relative proper motions of stars, ident. of member stars 80−51818
NGC 3114, open cluster, objective prism radial velocities *(French)* 79−48868
NGC 330, young cluster in SMC, radial vels. of individual stars 80−67803
NGC 3532, relative proper motions, cluster membership 79−35318
NGC 4103, open cluster, membership determ. from proper motions, visible obs. 80−67802
NGC 6025, open cluster, nonmember identification from proper motions 77−53653
NGC 6397, globular cluster, metal poor late-type stars and early A-stars, radial vels. 77−17638
NGC 6397, globular cluster, vel. dispersion meas. using TV detector and cross-correl. techniques 78−16305
NGC 6494 (M23), open cluster, proper motions and membership from astrometry with PDS microdensitometer 80−98697
NGC 6546, open cluster, assoc. with Cepheid AV Sagittarii disproved 79−58387

steilar motion continued
NGC 741, 1316, 7626, radio galaxies, dynamics 80−94871
nonlinear orbital behaviour near corotation in spiral systems 80−98694
north galactic pole, A and F star radial vels. and MK classifications 77−22223
north galactic pole stars, radial vels. 77−22207
northern FK4 stars, radial vel. meas. 80−26848
Nova Persei 1974 (V400 Persei), spectral evolution and radial vels. 78−73715
Nova Scuti 1975 (V373 Scuti), spectral evolution and radial vels. 78−73715
Nova Vulpeculae 1976 (NQ Vulpeculae), light, colour and vel. curves 78−28708
numerical integration of stellar orbits 79−21361
O-type runaway stars, statistical parallax, underluminosity 78−57552
O-type stars, galactic rotation parameters from radial vels. 79−12523
O-type stars, kinematics, close binary evolution and ages 79−101145
O-type stars, radial vels. and K-term 77−56922
O-type stars, relation between peculiar vels., assoc. with nebulosity and z-distances 80−105236
OB associations subgroups, motion towards parent cloud rel. to sequential form. 80−98696
OB stars, distrib. in Galaxy, comp. rel. to age and space motions *(Russian)* 78−93216
OB stars, motion effects on H II regions forbidden line emission spectrum 77−78845
OB stars Local complex, kinematics 78−16396
OB-type stars, radial vels. rel. to distance of Sun from galactic centre 80−101584
OB-type stars, radial vels. rel. to force field normal to galactic plane 80−46669
OBN, OBC stars, radial vels. and short period binaries frequency 78−53951
UZ Octantis, W Ursae Majoris system, UBV light curves and orbital elements 80−22042
OH/IR sources, microwave spectra, galactic distrib., radial velocity 78−16432
old stars, kinematics rel. to Galaxy initial contraction 80−62204
open cluster, proper motions rel. to solar motion and apex determ. 80−46418
open clusters, dynamics of close binaries and single stars *(Russian)* 78−61890
open clusters, evaporation of stars rel. to coronas and moving groups development 79−92814
open clusters, orbits in Galaxy and places of form. 78−8064
open clusters, southern, kinematics and dynamics from radial vel. obs. *(German)* 80−94724
open clusters assoc. with interstellar gas-dust clouds, dynamics 80−101622
open star cluster models dynamical evolution, early stages 79−8958
RZ Ophiuchi, orbital elements for eclipsing binary from new obs. 79−21327
optical doubles, proper motions from rectilinear trajectories and SAO catalogue *(French)* 79−30089
orbit segregation in nonhomologously changing nonlinear gravitational field 78−4351
orbital inclinations of spatially close spectroscopic doubles *(German)* 79−44532
orbits, near particle resonance of galaxy, numerical study 79−88746
orbits, semi-major axes of binary systems 77−57059
orbits in galaxies, warping of galactic plane and ellipticity changes 78−69847
orbits in growing spiral field in galaxy near corotation resonance 78−61891
orbits in region of inner Lindblad resonance, numerical studies for spiral galaxies 78−45396
orbits in rotating galactic bar, isolating integrals of motion 80−4404
orbits near galaxy particle resonance, theoretical study 80−26914
Orion OB 1 association stars, proper motions and radial vels. compilation 77−82128
δ Orionis, apsidal motion of spectroscopic binary 79−8952
χ^1 Orionis, new solar-type astrometric binary, parallax and orbital elements 78−73740
RU Pagasi, radial vel. of dwarf nova 79−62833
parallax and proper motion meas. for seven stars 80−62109
parallax stars in Herstmonceux programme, second list 78−77498
parallax stars with MK spectral classifications 80−56721
parallaxes, need for space-borne and ground-based obs. 79−66992
particle dynamics in spheroidal mass distribs., third integral of motion 77−74101
MW Pavonis, eclipsing binary, UBV light var. and orbital elements 77−49429
AU Pegasi, binary Type II cepheid, photometric and spectroscopic study 80−26866
periodic orbits near particle reson. in galaxies, theory 78−49484
periodic stellar orbits, superposition for spiral density waves illustration 79−84828
AW Persei, binary cepheid variable, radial vel. meas. 77−74072
IW Persei, metallic-line close binary system, spectroscopic orbital elements 80−62186
AG Persei, two-colour photometry of eclipsing binary system, apsidal motion 78−96504
20 Persei, visual binary, radial vel. obs. 78−73736
X Persei (3U 0352+30), Balmer line vels. rel. to reality of massive companion 77−13495
β Persei (Algol), orbital period (1964 to 1978) 79−58377
β Persei (Algol), triple system, long term apsidal motion study 77−87478
ζ Persei association, bright star subsystem dynamical evolution 77−53655
γ Persei cluster, stellar membership determ. by proper motion meas. 80−56890
AI Phoenicis, orbital elements and dimensions of eclipsing binary *(French)* 79−71074
AE Phoenicis, W Ursae Majoris type system, orbit 78−85970
19 Piscium, C star, violet spectrum line identification and radial vel. 80−82361
64 Piscium, double line spectroscopic binary, orbital elements *(French)* 79−35305
UV Piscium, short period eclipsing binary, light and colour curve obs. and orbital elements 79−88697

stellar motion continued
PK 181+1.1, new weak planetary nebula near galactic anticentre, spectrum and radial rel. 79−17049
planar orbits in spiral galactic potential 78−69845
planar stellar orbits, in spiral galaxy with extensive inner Lindblad reson. 79−88704
plane galactic orbits, epicyclic approx. 80−36674
planetary nebulae, kinematic distances rel. to synthetic distance scale 78−89240
planetary nebulae, spatial and vel. distrib. statistics 80−109518
Pleiades central field, internal motions 79−88711
polytropes in central orbits, Roche problem 80−82179
Population I O-type runaway stars 80−85938
Population I objects in vicinity of long period Cepheid VZ Puppis, evidence for kinematic groups 78−45339
Population I stars, kinematical trend of vel. residuals 79−48863
Population II stars, role in galactic spiral struct. form. 77−13469
post Newtonian relativistic stellar dynamics, tensor-virial eqns. 78−4298
prolate stellar systems, instability 80−101642
proper motion, radial vel. and parallax, perspective secular changes 77−91524
proper motion, role in luminosity and density function determ. 78−12204
proper motion errors rel. to nonpolar latitude vars. *(Russian)* 78−20637
proper motion of circumpolar stars, precessional corrections and solar motion consts. rel. to AGK3 system *(Russian)* 80−12647
proper motion programmes, importance of star coords. determ. *(Russian)* 78−12079
proper motion star catalogues, comparison, systematic errors *(Russian)* 78−93126
proper motion stars, catalogue of stars with $m_V<15$, annual motion $>1''$ 79−58275
proper motion stars in direction of galactic centre *(French)* 80−77404
proper motions, anals. of Sproul 61 cm refractor long-interval plate series 79−71015
proper motions, determs. by Yerkes Observatory 40 inch refractor 78−89168
proper motions, effect of new adopted value of precession constant 79−25459
proper motions, evidence for expansion of Galaxy 77−5574
proper motions, extrasolar planetary systems, dynamical instability and detection 80−82429
proper motions, formal values for solar motion and galactic rot. consts. 78−32440
proper motions, maximum-likelihood method for open clusters membership determ. 78−16471
proper motions, meas. by space astrometry project 78−12082
proper motions, membership and internal motions in M5 globular cluster 80−41864
proper motions and parallaxes, meas. at Van Vleck Observatory 77−37595
proper motions catalogue, via celestial photography with wide-angle astrographs *(Russian)* 78−40800
proper motions from reduction and repetition of Astrographic Catalogue 80−105178
proper motions measurement, sky photography programme with wide-angle astrographs *(Russian)* 80−72747
proper motions of bright nearby stars, astrometric anals. from Sproul 61 cm refractor plates 80−61991
proper motions rel. to galaxies, systematic errors in photographic obs. *(Russian)* 79−16941
PSR 0820+02, long-period binary pulsar, orbital period and mass function 80−56867
PSR 1913+16, binary pulsar, gravit. radiation and period changes in alternative metric theories 77−60589
PSR 1913+16, binary pulsar, orbit rel. to general relativity testing, progress report 79−75234
PSR 1913+16, binary pulsar, orbital period vars. in bimetric gravit. theory 78−45347
pulsar acceleration by asymmetric radiation, observational evidence 77−60783
pulsar proper motions, velocities and lifetimes 79−35284
pulsar proper motions from timing obs. 77−33540
pulsars, critical review of vels. 77−78811
pulsars, low-velocity, tugboat model for evolution from OB binaries and X-ray stars 77−56915
pulsars, periods, positions and proper motion determ. from pulse arrival times, UHF, obs. 80−77431
pulsars, proper motions from timing obs. 79−17003
pulsars, space vel. vector orientation rel. to spin axis 77−53619
pulsars, space velocities rel. to evolution 78−4264
V Puppis, main sequence contact binary, photometric orbital elements 78−4293
VV Puppis, proper motion meas., distance and luminosity 78−96510
PZT stars, mean posns. and proper motions for 304 stars, obs. at Ondrejov 80−82175
radial and nonradial stellar oscills. effect on light, colour and vel. vars. 80−31310
radial vel. determ., survey of different methods 80−73006
radial vel. determ. methods 78−96406
radial vel. determ. with CORAVEL, Cassegrain spectrophotometer 80−82210
radial vel. dispersion rel. to galactic longitude and distance 79−101142
radial vel. meas. using telluric A-band on objective prism spectra *(Japanese)* 78−89083
radial velocities, barycentric, computation with classical perturbation theories 77−45291
radial velocities, correl. meas. in stellar field at galactic latitude $b^{II}=-30°$ *(French)* 78−89173
radial velocities, determ. of relative Zeeman and Doppler shifts in spectrograms 78−36467
radial velocities, Doppler shifts meas. technique without spectrograph 78−20646
radial velocities, influence in Balmer-index photometry 78−96404
radial velocities, meas. via HF absorpt. cell 80−12681
radial velocities, of variable velocity stars previously observed at David Dunlap Observatory 79−101141
radial velocities measurement, Radcliffe Cassegrain d-camera vel. system 78−73645
radial velocities of long-period variables from SiO line obs. 78−40956
radial velocity curves of close binary systems, anal. 80−94829
radial velocity data, surface distribs. on celestial sphere 77−2423

stellar motion continued
radial velocity measurement, standard wavelengths and vels. for twelve stars 77−17547
radial velocity measurement via slitless fieldspectroscopy, focal-reducer system appl. 80−36504
radial velocity measurement with objective prism 79−84681
radial velocity photoelectric spectrometry, use of echelle grating *(French)* 77−91438
radial vels. of luminous composite stars in the Large Magellanic Cloud 79−58375
radial-velocity standard stars, list of 200 stars 80−26849
red dwarf stars near north galactic pole, vel. dispersion 78−7989
red stars at north galactic pole, proper motions 78−4214
relativistic stellar dynamics, energy integral 78−4299
relaxation of inhomogeneous gravit. systems, delocalisation effect 79−62877
resonances of discrete symmetric dynamical systems, appl. to axisymmetric galaxies 79−67066
resonant 2/1 orbits stellar reson. orbits comparison, 2/1 reson. 80−67796
resonant orbits comparison, theoretical results 80−56889
resonant orbits in spiral galaxies, disc equilib. for Lindblad resonances 78−49524
resonant stellar systems, formal third integral of motion *(Russian)* 77−82284
response of disk population to spiral perturbation near corotation resonance 79−71077
response to spiral density waves in galaxies, individual orbits 79−44570
in rotating galaxy gravitational field *(Russian)* 80−94838
rotating sphere of stars, free collapse 78−93325
rotating stellar systems, two-dimensional, nonlinear nonradial oscills. stability 78−53992
rotation, evidence for discrete vel. states 77−22307
Rst 4036, red-dwarf binary star, orbital period and total mass 80−12780
Rubin-152, possible massive O-type star on galactic fringe, radial vel. and galactic orbit 80−98656
runaway planetary nebula ejection from M32 80−46626
runaway stars, as witnesses to supernova explosions 78−32448
runaway stars and supernovae *(Italian)* 79−53812
S-type stars, secular parallax and mean absolute magnitude 78−81623
WZ Sagittae, cataclysmic variable, orbital eccentricity rel. to light curve superhumps model 80−4381
HM Sagittae, eruptive BQ forbidden line star, spectrum and radial vel. 78−20835
WZ Sagittae, orbital parameter determ. for recurrent nova 78−93317
FG Sagittae, planetary nebula central star, radial vel. meas. rel. to binary star model 80−98664
WZ Sagittae, recurrent nova, radial vels. obs. and model for superhump phenomena 80−82368
U Sagittae, secondary mass from vel. curve 79−97025
WZ Sagittae, spectroscopic obs. and photoelectric V-magnitudes 79−16984
AV Sagittarii, Cepheid, assoc. with open cluster NGC 6546 disproved 79−58387
ψ Sagittarii, evolved spectroscopic triple system 79−44551
RY Sagittarii, pulsating R Coronae Borealis star, IR photometry and radial vels. 77−45462
scale-covariant stellar dynamics, theory 80−26913
σ Scorpii, β Cephei star, Fourier anal. of radial vel. changes 80−105246
V861 Scorpii, near IR meas. rel. to orbital phase 78−93324
V701 Scorpii, radial vels. of early-type contact binary 80−62188
V703 Scorpii, RRs variable, photoelectric radial vels. 77−5533
β Scorpii A, spectroscopic orbit 79−67059
self-gravitating star system dynamics, time depend. soln. 80−4405
semi-detached systems, revised photometric elements for 8 single-line binaries 80−46611
semi-detached systems, revised photometric elements for 9 binaries 80−46612
semidetached systems, revised photometric elements 80−62193
RT Serpentis, symbiotic star/nova, H_2O maser obs. and radial vel. 79−8932
SMC X-1, X-ray vel. curve rel. to mass 77−29957
SMC X-1 (Sanduleak 160), binary system, orbital elements and masses 77−9815
solar apex, correl. with long-period comets perihelion points distrib. 80−4304
solar motion, vel. and apex determ. from open clusters proper motions 80−46418
solar neighbourhood, star density 79−21447
solar neighbourhood crossing times effect on observed stellar age and metallicity distribs. 78−12362
solar system, impending encounter with interstellar cloud 78−93352
solar system, motion rel. to extragalactic redshifts interpretation 80−4427
South Galactic Cap stars, search for common-proper-motion pairs 78−73734
southern high-velocity stars, kinematical and orbital props. 79−25600
southern peculiar A-type stars, radial vels. and atmospheric anals. 78−24517
spectroscopic binaries, Barr effect anal. 80−8650
spectroscopic binaries, catalogue of orbital elements *(French)* 77−22112
spectroscopic binaries, massive, anal. rel. to low eccentricity orbits detect. 79−67060
spectroscopic binaries, orbital elements statistical anal. 80−82422
spectroscopic binaries, test of circularity of orbits 78−93321
spectroscopic binaries with Ap star components, characts. *(German)* 77−17590
spectroscopic binary systems, apsidal motion 80−82413
spectroscopic binary systems orbital elements, seventh catalogue 79−16843
spherical clusters, stability under spherical perturbations *(French)* 79−35317
spherical stellar system, distrib. of stars around massive central black hole 78−65660
spherical stellar systems, dynamical relaxation, tidal perturbations by external systems 77−49443
spherical stellar systems, marginal mode to second order *(French)* 78−32527
spherical stellar systems submitted to aspherical perturbations, second variation of energy *(French)* 77−53646
stellar motion continued
spiral galaxies, density wave theory in finite spiral arm inclination regime 78−49534
spiral galaxies, reson. stellar orbits rel. to hydrodynamic flows near Lindblad resons. 78−96527
spiral modes in disc galaxies, density wave theory 78−54053
SS 433, period and evidence for eccentric orbit from IR light curves 80−8642
SS 433, radial vel. curve low amplitude section, visible spectra anal. 80−67737
star catalogue data presentation in galactic coordinates 77−78657
star clusters, evolution, Fokker-Planck eqn. numerical integration 80−36675
star systems, purely discontinuous random processes in field of irregular forces *(Polish)* 78−16465
stars in fields of globular clusters M10, M12, M71, M92, radial vels. 78−41004
statistical mechanics of gravitating systems 79−35311
stellar system dynamics, field of directions of motion in Contopoulos potential *(Russian)* 80−62205
stellar systems dynamical evolution, analytical approximations for effect of mass loss 80−51815
stellar systems dynamics, limiting radii of direct and retrograde satellite orbits 79−88572
stellar systems nonradial-oscillations, homogeneous models *(Russian)* 77−57063
Stepanyan's star, eclipsing binary, eclipses obs. and orbital period refinement 80−62195
Stepanyan's star, eclipsing binary, relative orbit radius and collapsed component mass 80−67788
streaming motions and obs. determ. of structural consts. in Galaxy 78−96528
subdwarfs, kinematics rel. to galactic halo rot., also He abundance 80−22003
subdwarfs, photometry rel. to compositions and kinematics 80−82364
Sun, absolute motion and discrete redshift 78−49530
Sun, basic solar motion components calcs. *(Italian)* 79−12414
Sun, motion rel. to centroid of Local Group 78−12376
Sun, motion rel. to kinematics of Galaxy and Andromeda nebula (M31) 77−91518
Sun, motion rel. to Local Group galaxies, possible new members discoveries 77−22321
Sun, motion relative to neighbouring galaxies *(Russian)* 78−24553
Sun, proper motion rel. to cometary orbits perihelion distrib. asymmetry 78−96429
Sun possible compact companion, mass, vel., and luminosity 79−2490
supergiant OH maser sources, optical radial vels. 77−49378
supergiant radial vel. meas., expanding dust cloud effects on maser source 79−5816
supergiant stars, in SMC, radial vels. 78−93237
supergiants in SMC, radial vel. determ. by spectrographic and photometric data study 79−101147
supergiants in SMC 79−101192
45, 97 and 102=ι Tauri, astrometric studies 78−69779
CD Tauri, eclipsing binary, orbital element determ., BV photometer obs. 80−73000
θ^1 Tauri, Hyades giant, identification as spectroscopic binary from photoelectric radial vels. 77−64794
α Tauri, Hyades giant, photoelectric radial vels. and spectroscopic binary orbit 77−64794
51 Tauri, Hyades spectroscopic binary, speckle interferometry 77−29876
T Tauri stars, radial vels. and spectral types 77−56921
T Tauri stars assoc. with Taurus-Auriga dark clouds, proper motions 80−41821
BL Telescopii, eclipsing binary, light curves and radial vels. of supergiant companion 77−64797
thin disc galaxies, stellar dynamics, hydrodynamic and orbit theories 78−8059
thin disc galaxies, stellar hydrodynamics 79−25706
three-body encounters, probability of binary form. 77−13396
three-body systems disruption, statistical theory for high ang. momentum 77−13220
Trapezium member stars, space motions *(Chinese)* 80−8654
Trapezium type multiple systems, relative proper motions *(Russian)* 78−93314
trapped orbits in time-dependent potential 80−8664
RW Trianguli, nova-like binary star, eclipse timings 79−21357
RW Trianguli, nova-like eclipsing binary radial vels., dimens. from visible spectra 80−82418
trigonometric parallaxes for luminosity calibrations, practical improvement method 79−40083
trigonometric parallaxes of 14 stars 79−5808
triple stars, stability of interplay motions 77−60583
triple stellar system staiblity, Hill's concept generalisation 79−92656
triple system decay, numerical expts. 79−44561
triple systems, dynamics, review 79−44559
triple systems, non-rotating, exact mean time of decay *(Russian)* 78−32523
triple systems and close approaches, dynamics, review 79−44560
tube orbits, three-dimensional, around intermediate axis in triaxial galaxy model, nonexistence 80−22046
two point-masses bound system, influence of weak gravit. wave 80−21903
4U 0115+63, orbital elements and nature of hard X-ray transients 78−93470
4U 0115+63, pulsating X-ray transient, orbital period 78−61939
3U 0900-40 (HD 77581), binary X-ray source, spectroscopic orbit and masses of components 78−16461
3U 0900-40 (HD 77581), X-ray to binary, orbital elements and pulsational period increase 77−64877
3U 1538−52, binary X-ray pulsar, orbital elements 78−16573
4 U 1538−52, eclipsing X-ray source, corrections to ephemeris and revised period 79−25760
4U 1538-52, optical counterpart spectroscopy and system parameters 79−5924
Ursa Major group, new members 79−84830
CQ Ursae Majoris, line identification list and radial vel. of Ap-star 80−41841
α Ursae Minoris (Pole Star), stellar parallax meas. by Flamsteed and aberration 79−88786

stellar motion continued
variable DA white dwarfs, kinematics rel. to nonvariable DA stars 78−53947
variables, OH radial vel. pattern rel. to period 79−35427
velocity dispersion, age depend. in scale covariant gravit. 78−65661
velocity dispersion determ. in spiral galaxies *(Chinese)* 80−85995
velocity dispersion inhomogeneities in local spiral arm 80−98653
velocity field multiplicity, ergodicity of motion *(Russian)* 77−37623
AH Velorum, Cepheid, radial vel. study, possible binary, coude spectrograms 77−49394
AI Velorum, nature from BVRI photometry and photoelectric radial vels. 80−94815
AI Velorum, RRs variable, photoelectric radial vels. 77−5533
γ_2 Velorum, Wolf-Rayet binary, orbital element determ. from spectral obs. 80−85950
visual binaries, orbital elements for 15 pairs 78−85969
visual binaries, orbits for 24 objects *(Russian)* 79−25646
visual binaries, radial velocities for objects with astrometric orbits 79−67057
visual binaries, southern orbits and masses 78−96502
visual binaries orbital eccentricities, observational selection 77−74098
visual binaries with variable components, orbital elements, visible obs. *(Russian)* 80−77455
visual binary star orbit, computation method for any eccentricity *(French)* 78−85974
visual binary stars, orbital elements 80−46607
visual binary stars, parallaxes, orbits, mass ratios and masses for six pairs 77−64795
visual double stars, period-eccentricity relation *(French)* 78−28721
visual double stars, relative motion meas. in 17 pairs *(French)* 78−57586
15 Vulpeculae, radial vel. from spectrograms 77−56952
W851, high-velocity subdwarf, parallax and tangential vel. 77−49387
white dwarf space motions and luminosity function 77−45413
white dwarfs, proper motions and search extension 79−8914
Wolf 1062, astrometric anal. of unseen companion from 61 cm Sproul refractor plates 78−16459
Wolf 1062, red dwarf, orbital elements from astrometric perturbation 77−49439
Wolf 922, nearby red dwarf, evidence for low-mass unseen companion 80−51809
Wolf-Rayet, single-line Population I stars, space vel. 80−77415
WRA 977 (4U 1223−62, GX 301−2), binary star orbit determ., X-ray obs. 80−90570
X-ray binaries, anomalous periastron positions 79−25756
X-ray binaries, distortion of absorpt. line vel. curves due to X-ray heating 77−29878
X-ray binaries in dense stellar clusters, dynamical effects 79−97098
X-ray sources, optical and X-ray vel. curves rel. to masses 78−12430
X-ray sources as runaway systems, effect on large-scale distrib. 79−48954
zone stars, proper motions dispersion represented by vel. ellipsoids 79−8904
μ Draconis (ADS 10345), radial vel. var. from spectra in visible 80−17612
1228, nearby red dwarf, evidence for low-mass unseen companion 80−51809
Ba II giant stars binary nature from visible radial vel. obs. 80−82355
Ba stars, absolute magnitudes determ. from Yale proper motions 78−8006
Ba stars, spectroscopic, radial vel. and photometric obs. 78−12226
CH stars in south galactic cap, radial vels., photometry 77−87396
OH/IR unidentified Type II stars, galactic distrib. and kinematics from 1612 MHz survey 78−49450

stellar multicolour photometry *see stellar photometry*

stellar origin *see stellar evolution*

stellar photometry
see also stellar radiation; stellar spectra
HR 1099, RS Canum Venaticorum type binary, light and colour curve meas. 80−73004
25 1702−363, IR candidate in error box, JHKL photometry 78−61934
A0535+26, transient slow X-ray pulsar, spectrophotometric survey 78−4263
A0620−00, transient X-ray source, spectrophotometry 78−4400
A0-G2 stars, abundance effects in Geneva system 77−29830
A1742−28, transient X-ray source, optical counterpart, visible and IR obs. 80−101653
2A 0042+323 (3U 0042+32) optical candidate, photometry and spectrum 78−54088
2A 0311−227, AM Herculis type binary star, IR photometry and polarimetry 80−77517
2A 0311−227, high-speed photometry of AM Herculis-type binary 80−41912
2 A 0311−227, IR flickering obs. 79−40298
2A 0311−227, optical counterpart, AM Herculis type eclipsing binary, V-band obs. 80−101617
2A 0311−227 optical counterpart, binary star, light curve Fourier anal. 80−82549
2A 0311−227 optical counterpart, high speed photometry 80−82547
2A 0311−227 optical counterpart, simultaneous photometric and spectroscopic obs. 80−90572
2A 0311-227 optical counterpart, spectroscopic and photometric obs. 79−101222
2A 0526−328 optical candidate, high speed optical photometry 80−51917
2A 0526-328, optical photometry of assoc. star 80−22120
2 A 1052+606, X-ray and optical variability of RS CVn star 80−31331
A and F stars near N.Galactic Pole, local mass density determ. 79−40267
A- and F-type main sequence stars, scanner obs. 78−36563
A- and F-type stars, absolute energy distribs. 77−17554
A- and F-type stars, narrow-band α and λ photometry 77−29832
A- and F-type stars in Selected Areas, photoelectric uvbyβ photometry 78−16412
A- and F-type visual binaries, uvbyβ photometry 79−21346
A-type stars, MI spectral classification based on uvby and β photometry 77−29822
A-type stars, uvbyβ calibrations 80−41820
absolute magnitudes of stars in the same seven colour photometric box 78−28662
absolute spectrophotometry, spectral energy standard *(Russian)* 79−44372
absolute spectrophotometry and UBV photometry, comparison of results 78−96476
abundance determ. by photometric and spectroscopic methods 77−29807
accretion disc models and cataclysmic variables, H line blocking of UBV colours 79−101155
accretion discs theoretical photometric and spectroscopic props., cataclysmic variables appl. 79−80312
AE 1, He-rich variable, spectroscopy and photometry 80−41836
AFCRL IR sources, optical, IR and radio studies 78−4393
AFCRL Sky Survey objects, 2-14 μ spectrophotometry 77−22331
AFCRL sources, identification of southern objects 77−33682
Am and Ap stars, photometric parameters 78−96483
Am stars, evolved, search for photometric variability on lower part of Cepheid instability strip 80−62145
Am stars, multicolour photometry Hα and O I obs. 77−67101
Am stars, photometric stability 77−56953
Am stars, UBVRI photometry of 225 objects 78−69799
Am-stars, α,λ photometry 78−81638
Am-stars, ANS UV photometry of 26 objects 78−61869
Am-stars, photometric study of three objects 79−40204
RT Andromedae, eclipsing binary, three-colour photoelectric obs. and improved ephemeris 80−22043
RT Andromedae, light curve anal. of short period eclipsing binary 80−46603
AN Andromedae, light curve of Am binary systems, possible third body 79−58374
α Andromedae, Mn star, UV spectrophotometry from TD 1-A/S 59 77−29848
GP Andromedae, photoelectric photometry of RRs variable *(German)* 79−71044
SW Andromedae, RR Lyrae variable, uvbyβ photometry 78−12249
o Andromedae, shell star, UBV photometry 77−82227
BM Andromedae, spectroscopic and photometric obs. of T Tauri-type star 80−62130
ζ Andromedae, spectroscopic binary, photometric and spectroscopic obs. *(Russian)* 78−57588
o Andromedae, UBV photoelectric obs. of shell star 79−71046
AC Andromedae, UBV photometry of triple mode variable star 78−93260
RT Andromedae, V photoelectric obs. and lightcurve 79−71073
λ Andromedae, V photometric obs. during 1976-77 period 78−40994
ET Andromedae (HR 8861), Ap star, light vars. and period 80−46571
ET Andromedae (HR 8861), spectrum variable, period from photometric measures *(French)* 77−17579
angular diam. determ. from IR photometry, appl. to Arcturus 77−64760
anomalous Cepheids in Draco dwarf galaxy, masses 77−2434
anomalous nova-like object in M31 79−80316
Ap, Bp stars catalogue of photometric data rel. to surface mag. fields 80−85873
Ap and Bp stars, surface mag. field intensity rel. to Geneva photometry 80−105248
Ap and Hg-Mn stars, spectrophotometric scans, search for broad continuum features 78−12247
Ap stars, HD 27309, 119213, 170000, and 192913, ten colour photometry *(German)* 77−17584
Ap stars, narrow band photometry of broad absorpts. 77−67095
Ap stars, new Δa-photometry and evidence for two-component struct. of 5200 Å feature 80−67734
Ap stars, obs. evidence for pulsational stability 79−21303
Ap stars, photoelec. obs. of light vars. *(German)* 78−20841
Ap stars, photometric peculiarity index 77−91550
Ap stars, photometry, photoelectric parameter of peculiarity 77−2433
Ap stars, recognition in Vilnius photometric system 78−65635
Ap stars, spectrophotometry of broad flux depressions and comparison with synthetic spectra 80−67735
Ap stars, test results of photometric twin reflector *(German)* 77−17365
Ap stars, UBV photometry, light curves, periods 78−32472
Ap stars in spectroscopic double systems, BV photometry *(German)* 77−17583
δ_{1400}-Ap type stars, excess UV index, photometry obs. 80−72963
Ap-stars, ANS UV photometry of 79 hot and cool objects 78−61869
Ap-stars, Hα and O I photometry of 23 objects 78−81640
Ap-stars, photometry and surface magnetic fields 80−56847
Ap-stars, Stromgren photometry of 341 objects 79−71047
CY Aquarii, RRs type star, BV photometric obs. *(Italian)* 80−90449
EE Aquarii, UBV photometry of β Lyrae-type eclipsing binary 79−84817
π Aquarii and other Be stars, light variations 77−45420
Aquila X-1, photometry and spectroscopy of optical counterpart, model 78−32614
Aquila X-1, UBV photometry during 1978 X-ray outburst *(Russian)* 79−101224
η Aquilae, Cepheid variable, absolute energy distrib. in radiation spectrum *(Russian)* 80−72974
KO Aquilae, eclipsing binary system, UBV photoelectric study 80−62198
V889 Aquilae, photometric obs. of eclipsing binary, apsidal motion 79−25640
TW V586 and V1079 Aquilae, photometry, photographic obs. *(Russian)* 78−20842
β Aquilae, single G-type subgiant, UVB photometry 79−62823
V1301 Aquilae (Nova 1975), VBLUW photometry, absolute magnitude, distance and reddening 79−58342
Ara OB1, NGC 6193 and Ara R1, young southern complex, UBVRI obs. 78−16473
V535 Arae, absolute characts. of W Ursae Majoris system 79−58373
V539 Arae, photometric analysis of B-type double lined eclipsing binary 79−44535
Arakelyan 120, Seyfert galaxy nuclei, optical variability, UBV obs. 80−73049
SX Arietis, He spectrum variable, UV photometry with ANS 78−36585
TT Arietis, nova-like cataclysmic variable, photoelectric photometry 80−82382
UX Arietis, RS Canum Venaticorum type binary, UBV photometry, 1974-5 period 77−91569
UX Arietis, RS Canum Venaticorum type star, UV excess, spectrophotometric obs. 78−8043

stellar photometry continued
56 Arietis, spectrophotometry of Ap star, continuum features vars. 80−36638
UX Arietis, V photometric obs. during 1976-77 period 78−40994
γ Arietis, visual binary Ap-system, photometry 78−85950
astrometric and photometric system appl., automatic *(Russian)* 78−24467
astrophotometric scale definition by N.R. Pogson 77−49306
atlas of stellar spectra 78−20657
atlas of stellar spectra 79−88649
atmospheric extinction reduction, anal. of Rufener's method 77−22083
ζ Aurigae, 1973 to 1978, photoelectric obs. 79−84819
59 Aurigae, δ Scuti star, light curves periodogram anal. 80−62141
SX Aurigae, early-type semidetached binary, UBV photometric anal. 79−44521
ζ Aurigae, eclipse data rel. to radius change of K-type supergiant component 79−84820
SX Aurigae, eclipsing binary, light curves anal. by automated Fourier techniques 79−92798
NW Aurigae, eclipsing binary, photoelectric photometry 78−8052
LY Aurigae, eclipsing binary, photometric elements, masses, radii, luminosities 78−28723
IU Aurigae, eclipsing binary, two-colour photometry rel. to presence of third body 80−36669
T Aurigae, eclipsing binary nova, times of minima 77−22267
KR Aurigae, optical spectrum, variability *(Russian)* 78−36597
ε Aurigae, photometry during 1955-57 eclipse rel. to wavelength-depend. fluctuations 80−62190
CQ Aurigae, RS Canum Venaticorum type eclipsing binary, photoelectric obs. 79−40218
SX Aurigae, semidetached massive binary system, period changes 79−25637
KW Aurigae (14 Aurigae A), pulsating ellipsoidal variable, blue light photometry rel. to tidal modes 79−97028
T Aurigae (Nova 1891), old nova, photometric and spectroscopic obs. 80−90446
AA Aurigae field, UBV photoelectric magnitude sequence 77−74073
automatic image processing, 'Zenit' photogrammetric system *(Russian)* 78−24466
B, A and F stars, spectrophotometry, effective temps. 78−57546
late B dwarf in circumstellar dust cloud, IR source coincident with OH 205.1−14.1 80−101630
B supergiants, kinematical parameters from UBV photometry 77−26011
B-, A- and F-type stars, photoelec. K-line indices 79−16953
B-type stars, He weak, UV flux distrib. 78−96477
B-type stars, luminosity and effective temp. determ. 80−17582
B-type stars, uvby indices, empirical effective temps. and bolometric corrections 77−45429
B-type stars absolute UV spectrophotometry, continua and absorpt. features 77−22217
B-type stars at high southern galactic latitudes, four colour and Hβ obs. 80−82357
B-type stars at intermediate galactic latitude, space distrib. 77−91535
(B-V), (V-I_{KC}) diagram, intrinsic lines 78−73704
Ba II stars, spectral energy distribs. from DDO photometry 79−92757
Balmer-index photometry, quantitative anal. of influencing factors 78−96404
Barnard's star, analysis of photometric data 78−81657
Barnard's star, spectrophotometry with Carnegie image tube 78−57466
Basle catalogue of 1906 blue objects at high galactic latitudes 78−32360
BD+10°2179, C rich H deficient star, UBV photometric obs. 80−90437
BD+61°1211, optical counterpart of 2A 1052+606, RS Canum Venaticorum binary system 79−92803
BD+66°1066, nucleus of planetary NGC 6543, lightcurve oscills. 79−75223
BD−7°3007, nova-like variable, simultaneous spectroscopy and photometry 78−12250
BD +1°4381, H deficient A-type star, effective temp. 79−40195
BD −9°4395, H deficient star, spectral photometry and quantitative anal. 77−56946
BDS 1269, visual binary, metal abundances and characts. of components 80−4397
BDS 1269 A, metal-poor δ Scuti star, pulsation periods from b-band photometry 80−105247
Be 94, UBV photometric obs. of young distant open cluster in Cepheus 78−61892
Be stars, photometric behaviour, UV excess, emission indices, galactic distrib. 80−36637
Be stars, spectra and photometry 77−56966
Be stars, UV radiation intensity obs. *(French)* 78−81635
Be stars, variability search, 1971-8 photometric obs. 80−36650
Berkeley 11, compact open cluster, UBV obs. 80−94840
Berkeley 19, anticentre open cluster, age determ. from colour magnitude diagram, BV photometry 80−90486
Berkeley 21, UBV photometry of faint anticentre cluster 79−40229
binaries, wide visual, spectral type, age and uvbyβ photometry 80−94833
binary stars, JHKLM photometry of close systems 80−46614
blanketing parameter Δm_2, rel. to [Fe/H] abundances 78−36555
blue star in SNR 1006, spectral features and UBV photoelectric meas. 80−41830
blue star-like objects in field of M31, photometric obs. 77−9744
Bochum 15 stellar aggregate, photoelectric and spectroscopic obs. 77−87490
γ Bootis, Ap star, chemical element distrib. from spectrophotometry *(Russian)* 77−22238
AC Bootis, eclipsing binary, detailed photometric study 78−36637
i Bootis, light curve and period vars. of W Ursae Majoris type star 80−4398
XY Bootis, photometric obs. of contact binary, light curves, mass ratio 78−4286
SS Bootis, UBV obs. and Fourier anal., eclipsing RS Canum Venaticorum binary 80−17613
TZ Bootis, W Ursae Majoris system, spectroscopic and photoelectric obs. 78−69832
AC Bootis, W Ursae Majoris system, V photoelectric photometry 77−64800
TZ Bootis, W Ursae Majoris type system, eclipsing binary, photoelec. obs. 80−73001
BPM 25114, hot magnetic white dwarf, image tube spectrophotometry 77−74051
stellar photometry continued
BPM 25114, peculiar white dwarf, light vars., oblique rotator model *(Italian)* 78−93241
BPM 30551, ZZ Ceti type white dwarf, high-freq. oscills. 77−2445
BPM 31594, new southern hemisphere variable white dwarf 77−5531
bright O to G0 stars south of dec. +10°, photoelectric Hβ photometry 77−37600
broadband 20 μ photometry of 50 stars 77−9807
broadband filter photometry, TiO band absorption effect 80−41811
broadband linear polarimetry, zero polarisation standards list 79−40187
BV photometric observations for Earth atm. aerosol content determ. 78−92976
BV photometry in dwarf spheroidal galaxy in Draco 79−97076
BVRI photometry, faint equatorial standard stars 79−62876
BVRI photometry, secondary standards 79−70962
BVRI photometry, with photometer using Si diodes as light detectors 78−20651
Byurakan 2, open cluster, UBV photometry 77−2345
3C 120, Seyfert galaxy nuclei, optical variability, UBV obs. 80−73049
C- and M-type stars near globular cluster NGC 419 in SMC, cluster membership 80−26921
Z Camelopardalis, dwarf nova, spectrophotometry at standstill and in eruption 80−82366
SZ Camelopardalis, early type close eclipsing binary, UBV light curve anal. 77−45486
SV Camelopardalis, eclipsing binary containing BY Draconis variable, motion round third component 79−67055
53 Camelopardalis, photometric vars. 80−4367
XX Camelopardalis, R Coronae Borealis star, photometry in optical and IR ranges 80−101601
SZ Camelopardalis, semi-detached eclipsing binary, UBV lightcurves 80−85974
SS Camelopardalis, UBV photometry and light curve soln. for eclipsing RS Canum Venaticorum binary 80−41854
AX Camelopardalis (53 Camelopardalis), Ap star, UBV photoelectric photometry and period of var. *(Italian)* 80−90448
38 Cancri, δ Scuti star, UBV photometric obs. of variability 80−22021
S Cancri, close eclipsing system, freq. domain anal. of light changes 77−53638
AH Cancri, contact binary in M67, spectrum and photometry 79−40222
WY Cancri, eclipsing binary, obs. rel. to absolute information derivation at lower end of main sequence 79−92799
WY Cancri, light curve of eclipsing system, UBV photometry 77−37619
RU Cancri, RS Canum Venaticorum type eclipsing binary, photoelectric obs. 79−40218
49 Cancri, spectrophotometry of Ap star, continuum features vars. 80−36638
BT Cancri (38 Cancri) δ Scuti star, photometry rel. to radial and nonradial pulsation periods 80−85948
38 Cancri in Praesepe cluster, δ Scuti variable, pulsation anal. from light curves 80−77419
Canis Major R1, optical and IR props. of newly formed stars 78−93332
UW Canis Majoris, BV light curves of close binary 79−12496
R Canis Majoris, eclipsing binary, multiband photoelectric photometry 77−53633
CW Canis Majoris, eclipsing binary, UBV photometry 77−37615
UW Canis Majoris, eclipsing binary, UV photometry and primary component shape and atmospheric struct. 78−40992
VY Canis Majoris, IR obs. with new photometer 77−26017
α Canis Majoris B, photoelectric obs. 78−4220
W Canis Majoris rel. to assocs. Canis Major OB1 and R1 and NGC 2353 cluster, uvbyβ obs. 78−85985
β Canis Majoris stars, ANS UV photometry 80−26871
β Canis Majoris stars in southern hemisphere, photometric search 78−12243
β Canis Majoris variables, β photometry of early B-type stars 78−77562
YZ Canis Minoris, negative flares and dips of UV Ceti-type star 79−80317
R Canis sMajoris stars, photometric elements 79−58371
4 Canum Venaticorum, δ Scuti variable, photoelectric photometry 77−53601
4 Canum Venaticorum, BV photometry of δ Scuti star 79−35268
VZ Canum Venaticorum, eclipsing binary star, photometric elements and intrinsic variability 77−45487
AM Canum Venaticorum, orbital period increase 80−12765
RS Canum Venaticorum, spectrophotometric obs. of light curve wave distortion 77−33562
RS Canum Venaticorum, UV excess, spectrophotometric obs. 78−8043
Cape BVRI system, intrinsic lines 79−44481
Carina OB 1 association, RI photometry, reddening law determ. 79−8957
Carina spiral arm, galactic struct. and star formation, spectrographic and photometric obs. *(French)* 78−89256
Carina spiral feature, photometry and spectra rel. to stars and interstellar dust distrib. 80−51871
Carina-Crux-Centaurus region of Milky Way, interstellar extinction investigation 79−40242
VY Carinae, Cepheid, luminosity and membership of assoc., visible obs. 80−94797
l Carinae, search for comparison stars, uvbyβ photometry, colour excess 80−62136
β Carinae, UV spectra, comparison of synthetic and observed spectra 77−29820
VY Carinae field stars, spectra and photometry rel. to cepheid absolute magnitude 77−64764
Cassiopeia, photoelectric UBV photometry 77−37598
SX Cassiopeiae, Algol type binary, spectrophotometry 77−2454
TV Cassiopeiae, Algol variable, UBV photometric obs. 79−35306
γ Cassiopeiae, Be star, coordinated IR and optical obs., (in late 1976) 79−25616
γ Cassiopeiae, Be star, IR excess 78−93257
V523 Cassiopeiae, BV photometry of W UMa type system *(Russian)* 79−92807
SU Cassiopeiae, Cepheid variable, spectrophotometric determ. of effective temp. 80−90435
VX Cassiopeiae, early-type star, UBV obs. rel. to photometric variability *(Russian)* 80−72973
CW Cassiopeiae, eclipsing, binary, anal. of V light curve 77−57009
TV Cassiopeiae, eclipsing binary, period and UBV light curves 78−4287
OX Cassiopeiae, eclipsing binary, photometric elements from UBV light curves 80−56877

stellar photometry continued
DO Cassiopeiae, eclipsing binary, three-colour photoelectric investigation 78−16462
MN Cassiopeiae, eclipsing binary orbital elements 77−71127
AB Cassiopeiae, eclipsing binary with δ Scuti primary, light vars. preliminary anal. 80−94831
TV Cassiopeiae, light curve, long period var. interpretation 79−101174
AZ Cassiopeiae, long-period eclipsing system, photoelectric obs. 80−46608
UV Cassiopeiae, R Coronae Borealis star, photometry in optical and IR ranges 80−101601
TV Cassiopeiae, revised photoelectric elements *(Russian)* 79−92808
SU and TU Cassiopeiae, short-period Cepheids, photometry and spectra rel. to radius anomalies 80−26864
TU Cassiopeiae, third period in beat Cepheid 78−16424
TU Cassiopeiae, UBV photoelectric obs. of double-mode Cepheid 78−77556
SU Cassiopeiae region, field stars photometry rel. to Cepheid distance and pulsation mode 78−89204
cataclysmic variables, visual continuum flux distribs. 80−36636
catalogue of photometric sequences, second supplement considerations 77−78664
CD −33°12119, 3U 1727−33 candidate, UBV photometry 78−12251
CD-38°245, metal-deficient halo red giant, spectrum, photometry and Ca/H ratio 78−69797
V553 Centauri, C rich Cepheid, VRI photometry rel. to C and N abundances 80−4378
V553 Centauri, CH-type Cepheid, BVRI photometery rel. to chemical comp. and luminosity 79−62849
V436 Centauri, dwarf nova, photometry during superoutburst (May 1978) 80−46570
BV Centauri, dwarf nova and spectroscopic binary, UBV photometry, spectral types and orbit 80−51775
BH Centauri, early-type contact system in IC 2944 open cluster 77−33552
SZ Centauri, eclipsing binary, four-colour photometry, photometric elements, dimensions and He content 77−41391
ω Centauri, globular cluster, search for new variables 78−61895
ω Centauri, JHK photometry of globular cluster, giant branch spread 78−16476
ω Centauri, near IR photometry, giant branch struct. 77−41397
ω Centauri, near IR photometry anomalous giant branch 78−16477
ω Centauri, SEC Vidicon photometry of main sequence 80−90491
UW Centauri, visual magnitude estimates, UBV photometry 78−40962
V748 Centauri (Centaurus X-4?), high-latit. eclipsing system, VBLUW photometry 79−44529
V810 Centauri (HD 101947), yellow variable supergiant near Cepheid instability strip, VBLUW photometry 80−98672
ω Centauri giant branch, mixing versus primordial abundance vars. 77−17640
central star of Abell 46, eclipsing binary 80−73027
VV Cephei, 1976 November obs. in UBV rel. to eclipse start 77−9774
U Cephei, Algol type binary, spectrophotometry 77−2454
EI Cephei, Am eclipsing binary, light curve anal. 77−33560
ε Cephei, B photometry of δ Scuti-type star 79−44500
ER Cephei, contact binary in open cluster NGC 188, BV light curves 78−77580
VW Cephei, contact eclipsing binary, polarisation obs. 77−45489
U Cephei, eclipsing binary, light curve, perturbations and orbital element determ. *(French)* 80−67787
CQ Cephei, eclipsing binary, narrowband photoelectric obs. *(Russian)* 77−22278
EI Cephei, eclipsing binary, occultation at primary minimum 77−9770
VV Cephei, eclipsing binary, UBV obs. 77−2456
CW Cephei, eclipsing binary in III Cephei association, photometry and distance 79−21326
U Cephei, excess light obs. rel. to accretion discs 80−82412
δ Cephei, interstellar reddening 77−22243
EM Cephei, light curve from UBV photometry *(Russian)* 77−64803
U Cephei, mass transfer from light vars. outside primary eclipse, obs. and anal. 78−36636
NY Cephei, massive eclipsing binary star, progress report from UBV photometry 80−67789
VV Cephei, narrow band photometry during 1976-78 eclipse ingress 78−4296
EE Cephei, obs. of long period eclipsing binary *(Italian)* 78−93319
U Cephei, outbursts in 1969 and 1974, period change 77−87475
U Cephei, period changes in 1972-7 interval 80−8657
VW Cephei, periodic vars. in light curve of W Ursae Majoris system 80−36667
XY Cephei, photoelec. elements of semidetached binary system 80−31327
U Cephei, photoelectric obs. of recent eclipses 79−67061
U Cephei, primary eclipses obs., recent period behaviour 77−74087
VV Cephei, UB photoelec. obs. 77−17633
EM Cephei, UBV, photometry rel. to constancy or variability of period 80−105286
VV Cephei, UBV obs. of eclipsing binary, 1976-8 eclipse 80−17611
VV Cephei, UBV photometry during ingress phase of 1976-78 eclipse 78−20862
U Cephei, UV excess, mass transfer in eclipsing binary system 77−33555
β Cephei star search, northern photometric and spectroscopic obs. 77−74057
β Cephei stars, search in open cluster NGC 4755, evolutionary stage determ. 79−8921
β Cephei stars, search south of declination −20°, B-type giants and subgiants 78−61863
VV Cephei system, distant, in Puppis, spectral classification, UBV photometry and polarimetry 80−51810
VW Cephei W Ursae Majoris system, period and colour change mass transfer model 80−77453
Cepheid binary detection from U-V curve obs. 80−98667
Cepheid variables, distance determ. method 77−45467
Cepheid variables, short-period, radial vels., BVRI photometry, radii 80−31309
Cepheids, binary star frequency from UBV photometry 77−45465
Cepheids, BVI photometric determ. of reddening 78−65630
Cepheids, double-mode, photoelectric radial vels. and BVRI photometry 79−88675
Cepheids, in LMC, BV photometric obs., galaxy tilt determ. 79−53912

stellar photometry continued
Cepheids, in LMC, BVI obs., period-luminosity-colour relation 79−71055
Cepheids, in Magellanic Clouds, UBV photometry, evidence for interstellar reddening 77−2435
Cepheids, in southern hemisphere, VBI photometry 77−53612
Cepheids, short period, in N.hemisphere, UBV photometry rel. to search for double mode Cepheids 80−94814
Cepheids, southern, BVI photometry 77−60772
Cepheids, ultrashort period, classification from photometric and astrometric data 80−62135
Cepheids between l=294° and 331°, UBV and 21 cm obs. 79−12478
Cepheids in Dunsink LMC II region, BV photographic photometry 78−45340
sinusoidal Cepheids in LMC, first overtone pulsations, photometry obs. 80−77422
Cepheids in LMC and SMC, UBVRI obs. 77−71113
Cepheus IV association, spectrophotometry of young stars 77−13328
XY Ceti, eclipsing binary, masses, radii and luminosities from revised photometric elements 80−109458
TV Ceti, F-type eclipsing binary, four-colour photometric obs. 79−40217
TX Ceti, UBV obs., photometric elements of eclipsing binary star 79−8950
o Ceti (Mira), rapid light vars. of companion star during 1977 light min. 78−96492
UV Ceti stars, photometric features near flare initial phase 80−105252
ZZ Ceti stars and pulsations, physical props. 79−48781
ZZ Ceti stars search, photometric obs. of apparently quiescent stars 80−22005
Chamaeleon T1, young stars, photometry and spectral obs. 80−72943
Chamaeleon T association, JHKL photometry of stars, reddening 79−58384
RS Chamaeleontis, eclipsing binary, four-colour photometry rel. to photmetric elements, absolute dimensions and He abundance 80−67783
RS and RZ Chamaeleontis, photometric elements of detached eclipsing biuaries 80−90473
Z Chamaeleontis, photometry of dwarf nova 79−67028
RS Chamaeleontis, uvby photometry of bright double-lined A-type eclipsing binary 78−69833
chopping photometer to eliminate auroral sky background 80−72776
Chu's object in Perseus, UBV photometry and spectrum rel. to identification as galactic star 80−62132
Circinus, UBV photometry rel. to props. of large new galaxy 77−41409
Circinus galactic window, early type star obs. 77−13342
Circinus X-1, JHKLM photometry and light curve 78−54086
classical Cepheids, light and radial vel. curves phase matching 77−17574
classical Cepheids colour excesses 77−22242
classification in intermediate multiband photometry, photometric star box 77−87373
close binaries, narrow-band photometry and differential effects 80−67780
close binary stars, H I α and β line photometry 80−109470
close visual double stars, electronographic UBV magnitudes and separations 79−67056
cluster composition determ. method using DDO photometry of evolved members 77−29889
cluster stars near IC 1805 (W4), spectral classes and photometry 80−62214
clusterings in S. Milky Way, UBV and uvby β photometry 79−44572
clusters in LMC, instrumental colour-magnitude diagrams 77−22279
CMT_1T_2 system, southern standard stars 77−37507
CoD−38°10980, white dwarf, photometry and spectroscopy rel. to gravit. redshift 78−24511
CoD −35° 10525, bright YY Orionis star, spectrum and UBV photometry 78−36566
Collinder 132a, b, UBVβ photometry of two sparse open clusters 78−32540
Collinder 135, nearby field of view, wide and narrow band photometry obs. 80−109504
Collinder 140, nearby open cluster, UBV photoelectric photometry 78−53994
Collinder 140, photoelectric UBV photometry, age and distance of open cluster 78−49489
colour excess ratios versus interstellar grain size 79−17040
Coma cluster, new stellar standard sequence 78−93436
CC Comae, W Ursae Majoris type binary, photometry and geom. elements 77−22272
CC Comae Berenicis, UBV photometry of shortest period contact binary 77−57055
comparison star sequences, BV photoelectric photometry and reliability 79−97039
comparison star sequences in six variable star fields, photometry obs. 80−82433
comparison stars in fields of extragalactic sources, photoelectric UBV sequences 77−5562
comparison stars near OJ287 and ON325, variability, period determ. 80−26882
cool stars in E and S0 galaxies, H_2O absorption at 2 μ 78−41034
cool supergiant stars, near IR excesses 78−16406
cool white dwarfs, spectrophotometric obs. 77−45422
Corona Austrina dark cloud stars, BV polarimetry and interstellar reddening law 79−17050
Corona Austrina T1 association, UBV photometry of member stars *(Russian)* 79−17035
S Coronae Austrinae, spectroscopic and photometric vars. of YY Orionis star 79−48812
ε Coronae Austrinae, W Ursae Majoris type star, spectra, radii, masses 79−71069
B Coronae Borealis, Ap star, chemical element distrib. from spectrophotometry *(Russian)* 77−22238
R Coronae Borealis, UBVRIHKLMN photometry, interpretation 80−67756
R Coronae Borealis stars, JHKLM photometry and long-term IR behaviour 78−96490
R Coronae Borealis type variables and related objects, UBV photometric obs. 80−90437
Cousins VRI system, temp. and absolute flux calibration, appls. 80−26750
CPD −62° 1837 (HDE 308122), long-period variable member of triple 80−105260
CRL 3068, dust-enshrouded star 77−91664

stellar photometry continued
CRL 3099, highly evolved C star, IR photometry and spectrum 78−49436
β Crucis, β Canis Majoris star, photometric obs. 80−17595
AI Crucis, revised photometric elements 80−109459
29 Cygni, λ Bootis type star, photometric variability 77−64765
V1500 Cygni, (Nova 1975), photoelec. obs., period decrease, visual magnitude estimates 77−22252
V389 Cygni, BV photometry of peculiar variable 79−44534
EM Cygni, cataclysmic variable, red and white dwarf binary, period change, B photometry 80−90434
SU Cygni, classical Cepheid and spectroscopic binary, UBVRI photometry 79−62852
XX Cygni, dwarf Cepheid, composition and motion, visible photometric and spectrographic obs. 80−77424
SS Cygni, dwarf nova, outburst, visual magnitudes (1978 June 14 and 15) 78−65628
SS Cygni, dwarf nova, spectrophotometry rel. to accretion disc models in erruption and at min. light 80−36635
V380 Cygni, eclipsing binary, masses, radii and luminosities from revised photometric elements 80−109458
MR Cygni, eclipsing binary, photoelec. photometry and computer soln. *(Chinese)* 78−28724
V388 Cygni, eclipsing binary, photoelectric obs. 77−37617
MR Cygni, eclipsing binary, photometric elements, period changes 78−61884
GO Cygni, eclipsing binary, UBV photometry rel. to period changes 80−72999
V453 Cygni, eclipsing binary in cluster NGC 6871, photometry and distance 79−21326
V1515 Cygni, FU Orionis type, UBVR photometry 78−12230
NML Cygni, IR speckle interferometry 80−31216
CH Cygni, linear polarisation vars. rel. to circumstellar dust grains form. 78−69808
V1057 Cygni, mean B-band magnitude (1978 July 30 ± 2^{d}) 79−84792
γ Cygni, nearby nebula exciting star, UBV photometry 79−97003
CH Cygni, new active period, model, double system with accretion disc *(Russian)* 78−69813
V729 Cygni, O-type evolved contact system, masses 78−93309
V1016 Cygni, photometric and spectroscopic obs. rel. to proto-planetary nebula mass ejection 78−85947
CC Cygni, photometric obs. of RS Canum Venaticorum type binary, interpretation 80−62182
V1500 Cygni, post-nova light curve development, UBV and Hβ obs. 77−71115
1500 Cygni, spectrophotometry of early phase with objective prism plates 77−17576
V1016 Cygni, symbiotic star, IR variability obs. from VJHKL photometry *(Russian)* 80−105263
CH Cygni, symbiotic variable, flickering obs. during outburst, binary model 79−8929
UZ and VW Cygni, UBV light curve solns. for Algol-like systems 80−41855
V1500 Cygni, UV photometry 77−64766
V645 Cygni (AFGL 2789), spectroscopic and photometric obs. 80−73066
V645 Cygni (CRL 2789), bipolar nebula, O-type exciting star 78−4392
V1357 Cygni (Cygnus X-1), UBVR obs. and accreting disk radiation *(Russian)* 79−25645
V1341 Cygni (Cygnus X-2), UBV photometry and light vars. 79−5833
V1341 Cygni (Cygnus X-2), UBV photometry and possible 82-minute quasi-periodic bursts obs. *(Russian)* 79−17140
V1500 Cygni (Nova 1975), BV photometric obs. 78−36613
V1500 Cygni (Nova 1975), BV photometry 78−36619
V1500 Cygni (Nova 1975), light curve for 1975 Aug.-1977 July period 80−4372
V1500 Cygni (Nova 1975), linear polarization obs. 78−36601
V1500 Cygni (Nova 1975), multiband photometry 77−87445
V1500 Cygni (Nova 1975), photoelectric obs. 78−36620
V1500 Cygni (Nova 1975), photometric and spectroscopic obs. 78−36604
V1500 Cygni (Nova 1975), photometric obs. 78−36616
V1500 Cygni (Nova 1975), photometry, light curves, magnitude estimates 78−85960
V1500 Cygni (Nova 1975), photometry rel. to 3.3 hour var. and flickering 78−36591
V1500 Cygni (Nova 1975), polarimetric and photometric obs. 78−36612
V1500 Cygni (Nova 1975), short-term light vars. 78−36609
V1500 Cygni (Nova 1975), small amplitude light var. 78−36608
V1500 Cygni (Nova 1975), thirteen-colour photometry and anal. of short period variability 79−92788
V1500 Cygni (Nova 1975), three hour light var. 79−80314
V1500 Cygni (Nova 1975), TV photometry 78−36602
V1500 Cygni (Nova 1975), UBV photometry, short period variability 78−61862
V1500 Cygni (Nova 1975), UBVR Hα photometry and polarimetry 78−36611
V1500 Cygni (Nova 1975), UBVRI photometry and polarimetry 78−36614
V1500 Cygni (Nova 1975), UV photometry after visual max. 77−82260
V1500 Cygni (Nova 1975), visible and near UV photoelec. photometry 78−36610
V1500 Cygni (Nova 1975), visible and near UV spectrophotometric obs. 78−32492
V1500 Cygni (Nova 1975), visible and near UV spectrophotometry 78−32494
V1500 Cygni (Nova 1975), wide-band IR photometry 78−36615
V1500 Cygni (Nova 1975) photometric obs. at Skalnate Pleso Observatory 78−36617
V1668 Cygni (Nova 1978), JHKLM photometry 79−53828
V1668 Cygni (Nova 1978), multifilter photometry and polarimetry 80−90454
V1668 Cygni (Nova 1978), optical light curve, uvby photometry 80−62154
V1668 Cygni (Nova 1978), photoelec. photometry, rapid flickering 80−36640
V1668 Cygni (Nova 1978), spectroscopic and photometric obs., (1978 to 1979) *(Russian)* 80−109444
V1668 Cygni (Nova 1978), UBV light curve 80−46565
V1500 Cygni (Nova Cygni 1974), periodicities and rapid line variability 77−33524
stellar photometry continued
V1500 Cygni (Nova Cygni 1975), interstellar reddening and distance 78−4230
V1500 Cygni (Nova Cygni 1975), IR photometry and spectroscopy 77−53599
V1500 Cygni (Nova Cygni 1975), low resolution spectrophotometry 77−49403
V1500 Cygni (Nova Cygni 1975), shell phase obs. 77−49392
V1500 Cygni (Nova Cygni 1975), spectrophotometric obs. 77−49402
V1500 Cygni (Nova Cygni 1975), UBV photometry 77−33525
V1500 Cygni (Nova Cygni 1975), UBVRI photometry 77−33509
V1668 Cygni (Nova Cygni 1978), post-max. short period oscills., photoelectric photometry 80−82380
Cygnus X-1 (HDE 226868), optical photometry, (1972-1976) 78−32609
Cygnus X-1 (V1357 Cygni), optical photometry (1980 May 25 to July 7) 80−90578
Cygnus X-2, TV photometer obs. of optical counterpart *(Russian)* 78−57697
Cygnus X-2, X-ray binary, optical variability in UBV 77−26027
Cygnus X-2 optical candidate, high-speed photometry 77−13494
data, critical evaluation 77−78831
David Dunlap Observatory photometry, derivation of two-dimensional spectral classes 78−16395
David Dunlap Observatory test of late-type star spectral classifications 77−29831
degenerate star candidates, photoelectric and spectroscopic obs. 80−12763
degenerate stars, multichannel spectrophotometry 78−12224
degenerate stars, UV spectrophotometry, IUE obs. 79−53810
HR Delphini (Nova 1967), short period light vars. from UBV photometry 80−67744
δ Delphini stars in Michigan Spectral Catalogue, uvbyβ photometry rel. to spectral types 80−4377
detached systems, revised photometric elements for 8 double-line biuaries 80−46610
differential photometer, 6800 microprocessor control, astronomical appl. *(French)* 79−58253
β Doradus, Cepheid, reddening determ. from nearby star UBV obs. 80−101598
β Doradus, UV photometry of Cepheid by ANS 79−35272
S Doradus (HD 35343), luminous LMC supergiant, long time baseline VBLUW photometry 80−22007
S Doradus (HD 35343), luminous LMC supergiant, long time baseline VBLUW photometry 80−36630
double star photometry and variability 79−44554
double stars, focal grating photometer for magnitude difference determ. 80−67567
double-mode Cepheids, UBV photometry of four suspected stars 79−48825
BY Draconis, binary, slow light variability anal. 77−53629
CX Draconis, binary Be star, UBV obs. 80−82388
AR Draconis, BV light curves and orbital elements 79−101173
BS Draconis, BV photometry of eclipsing binary 79−44536
RZ Draconis, eclipsing binary, photoelectric light curve and orbital period study 80−109461
BY Draconis, flare star, Ca II emission variability 77−33528
BY Draconis, magnitudes, colours and photometric period changes *(Russian)* 77−64771
TW Draconis, photometric study of Algol-type system 78−45361
WW Draconis, RS Canum Venaticorum type star, two-colour photoelectric lightcurves and elements 80−46606
ϕ Draconis, Si Ap-star, UV vars. rel. to patchy stellar surface model 77−49389
BY Draconis, spectroscopic binary flare star, BVRI obs. 77−53595
BY Draconis, spotted flare star, spectra and photometry rel. to pre-main-sequence nature 80−36633
BV Draconis (ADS 9537A), W Ursae Majoris type star, photoelectric photometric obs. 79−35296
BW Draconis (ADS 9537B), W Ursae Majoris type star, photoelectric photometric obs. 79−35296
BY Draconis stars, photometric radii compared with luminosity class V stars *(Russian)* 78−57564
BY Draconis type variables, flare activity and quiescent variability 78−45338
BY Draconis type variables, photometry, amplitudes and phases 79−67038
BY Draconis-type stars of 1 M⊙, photoelectric obs. *(Russian)* 77−64772
dwarf nova outbursts, colour vars. 80−46576
dwarf novae, cataclysmic variables, review of spectroscopic and photometric obs. 77−56959
dwarf novae, photometry of rise to max. and decline 77−9753
dwarf novae, spectrophotometry, 1250-7500 Å region 80−46577
dwarf novae and possibly related objects, IR photometry 78−8015
dwarf stars, late-type, broad-band IR colours, CO and H_2O absorpt. indices 78−4218
dwarfs and subdwarfs, UBVRIJHK photometry and bolometric corrections 79−75205
E3 (ESO-037-SC 01) dying globular cluster, photometry and stellar content rel. to tidal truncation 80−105291
E and F region stars, VRI photometry 78−53991
early type stars, intermediate-band photometry 77−49385
early type stars, photoelectric Hα line photometry 77−91528
early type stars, UBV photometry rel. to galactic plane discontinuity near (l=140°) 77−9797
early type stars in H II regions NGC 6334 and 6357, distances 78−85998
early type stars in Hauck-Mermilliod catalogue of four colour data, astrophysical parameter determ. 80−72951
early-type contact binaries, uvby beta photometry 78−53981
early-type stars, absolute magnitude calibration test 78−61857
early-type stars, intrinsic colour indices 79−84794
early-type stars, IR photometry, extinction ratio, 2200 Å interstellar absorpt. feature 78−53943
early-type stars, northern intermediate galactic latit., Hβ photometry, rel. to glactic struct. 80−36631
early-type stars, UV spectrophotometry 77−29836
early-type stars in N. Milky Way, IR photometry, interstellar extinction determ. 77−78783
faint early-type stars in neighbourhood of H II region RCW 38, UBV photometry 80−4352

stellar photometry continued
early-type stars in northern Milky Way fields, UBVβ photometry 77−2424
early-type stars in S. Milky Way, ubvyβ photometry 80−85942
early-type stars in S.Milky Way 79−62822
early-type stars in southern hemisphere, four colour photometry and spectral types 78−40945
early-type stars in southern hemisphere, IR photometry 80−94786
early-type supergiants, Balmer discontinuity from uvby photometry 77−53591
early-type ultra-short-period variable stars, new class identification and photometry 79−88662
eclipsing binaries, Fourier anal. of light curves 78−69830
eclipsing binaries, UBV photometric programme at Palomar and Kitt Peak 77−64796
SW eclipsing binary, period study, photometry and spectra obs. 80−82424
eclipsing binary distance determ. using Barnes-Evans relation 77−45482
eclipsing binary stars, near IR photometry rel. to mass transfer rates 80−67784
eclipsing binary stars, V−R photometry rel. to distances, masses, radii and absolute magnitudes 79−44520
eclipsing double-lined binaries, photometric elements of 14 detached systems 78−69834
eclipsing variables, Fourier anal. of light curves, photometric perturbs. 78−96507
electronographic BVR magnitude sequences, for UK 1.2 m Schmidt plates calibration 79−88703
emission line stars in LMC, spectroscopy and IR photometry 77−13348
emission line stars in southern hemisphere, IR obs. 80−90496
emission variable in Sagitta, photographic magnitudes from Harvard patrol plates 77−2431
emission-line variable (No.86) in core of M 15, UBV photometry, probably W Virginis star 80−77458
equatorial and southern bright stars, UVBYβ photometry 77−22205
AS Eridani, eclipsing binary, photometric elements, masses, radii, luminosities 78−28723
CD Eridani, photometric soln. for eclipsing binary system 80−62185
RX Eridani, RR Lyrae variable, BVI photometry and radius 77−2436
66 Eridani, spectroscopic binary, search for light var. 78−32524
WX Eridani light curves, period, orbital elements of eclipsing binary 80−26902
exciting stars of Orion triple emission nebula, UBV photometry 77−13430
extinction, oscills. caused by atmospheric disturbances, obs. 80−56606
extinction towards South Galactic Pole from A and F star reddening 77−60812
extreme galactic B and A supergiants, light vars. 77−56927
extremely red stars at $l^{II}\approx113°$, $-10°\leq b^{II}\leq+90°$, photometry and spectra 78−57554
F-type stars, MK spectral classification based on uvby and β photometry 77−29822
faint blue southern stars, Hβ photometry, metallicity, luminosity 77−41381
faint blue stars, photometry, third list of southern stars 79−71030
faint blue stars, southern, UBV photometry 80−82349
faint blue stars, uvby photometry in northern hemisphere 78−16415
faint blue stars near galactic anticentre, UBV photometry 78−40932
faint blue stars photometry, second list of southern stars 77−45424
faint clusters in LMC, colour magnitude diagrams, BV photometry 80−94841
faint proper-motion stars, spectra and photometry to very low luminosity degenerates deficiency 80−17575
faint red stars, photoelec. photometry of complete sample, space density 79−71034
faint red stars at intermediate galactic latit., UBVR photometric obs. 78−32457
faint stellar images, colour-magnitude diagrams and clustering correl. functions rel. to star populations 80−82360
faint UBVRI standard stars, photometric obs. 80−51813
fast irregular variables, UBV and JHKL photometry *(Russian)* 78−28684
Feige 24, EUV star, spectrophotometry in 3800-8200 Å region 78−4280
Feige 24, hot white dwarf, OAO-2 UV photometry 77−9747
FJM 3, 100 micron source, IR obs. of reddened stars 77−26082
FJM 6 region, reddened stars near IR photometry 80−26929
flare star search in Cassiopeia region near W3 77−37603
flare stars, photoelectric monitoring (1974 to 1976) 79−44509
flare stars, photographic photometry, discovery of five new stars 77−56943
flare stars, photographic photometry of four new objects 78−89207
flare stars in Pleiades, photometric obs. *(Russian)* 77−91536
flare stars in Pleiades, UV and photographic obs. of flares *(Russian)* 77−13367
flux distributions, comparison with solar flux distrib. and solar B−V and U−B colours determ. 79−66970
fundamental quasimonochromatic photoelectric photometry, accuracy *(Russian)* 78−65505
G139-29, perturb. from rectilinear motion, astrometric red dwarf binary system with subluminous component 79−8910
G35-26, high-velocity mag. degenerate, obs. 78−73709
G- and K-type giants, theoretical colours, model atms. 79−12474
galactic anticentre, space distrib. of stars and dust *(Russian)* 78−73754
galactic anticentre direction, young stars photometry and spectra rel. to outer Galaxy struct. 80−22079
galactic clusters in Cassiopeia, stellar photometry and proper motions obs. *(Russian)* 79−97042
galactic clusters observed in three colours, catalogue and distances 79−40089
galactic distrib. of interstellar absorpt. from Celescope catalogue, UBV and Hβ obs. 77−60810
galactic G-type supergiants, UBV photometry 80−41824
galactic globular clusters colour excess ratio, rel. to interstellar absorpt. law 78−28797
galactic halo, density gradients in SA 82 and SA 107 fields *(German)* 77−60825
galactic North Pole, NGC 4147 direction, halo density distrib., RGU photometry 77−37599
galactic struct., in solar neighbourhood, Aquila direction, RGU photometry 77−91621
galactic supernovae, colour curves and visual light curves 79−58368

stellar photometry continued
in galaxy IC 1613, colour-magnitude diagram and luminosity function for brightest stars 77−5561
Galaxy nuclear bulge, stellar UBV photometry 78−53926
GCl 0422−213, distant globular cluster in Eridanus, preliminary photometry and spectroscopy 80−17624
GD 428, extreme dwarf Cepheid, photometry and spectrum 77−78798
Gd 428, variable star, photometry and spectrum rel. to nature of dwarf Cepheids 78−73720
U Geminorum, dwarf nova, spectrophotometric parallax 79−67012
YY Geminorum, eclipsing binary, photometry and orbital period study 80−105287
U Geminorum, eclipsing binary dwarf nova, times of minima 77−22267
ε Geminorum, occultation by Mars (1976 April 8), preliminary results 77−37545
ε Geminorum, occultation by Mars on 1976, April 8th, theory of light curve 77−53567
YY Geminorum, VRI photoelectric photometry and absolute dimensions 78−69827
Geneva Observatory system, catalogue of stellar photometric parameters 77−73974
Geneva photometric boxes as absolute magnitude indicators, comparison with MK spectral types through trigonometric parallaxes 80−77385
Geneva seven colour photometry, second catalogue of obs. 77−13252
Geneva seven colour system, computerized differential photometer 79−48682
Geneva seven-colour photometry using electronic camera *(French)* 9−84682
giant branch of Fornax dwarf elliptical galaxy, colour-magnitude diagram 80−4431
giant stars, late-type, O I 7773 Å triplet obs. 79−35250
giant stars in Draco dwarf galaxy, effective temp. from photometry and spectral obs. 80−72941
giant stars in globular cluster M71, IR colours, CO band strengths and physical parameters 79−25650
giant stars in M13, M92, NGC 6397 and M15, photometry rel. to weak-G-band effect 77−78778
giant stars in M3, M13, M92 and M67, IR photometry, bolometric magnitudes and effective temps. 78−57595
giant stars in open cluster NGC 7789, metal abundance, He content and mass loss 80−31335
giant stars in Ursa Minor dwarf spheroidal galaxy, abundance vars. and ω Centauri anomaly 79−5904
giants in globular cluster ω Centauri, CO absorption and effective temp. 80−51749
giants in southern open clusters, DDO photometry 79−12468
GK giants, photometry rel. to CN strengths, mixing and supermetallicity 77−56930
Gleise 490 AB (BD+36°2322), red dwarf binary, flares and starspots, rot. period determ. 80−77423
Gliese 867, flares obs. on both components of visual binary 79−48861
globular cluster giants, intermediate-band photometry rel. to blanketing differences 80−4345
globular clusters, (V-K) colour rel. to metal abundance 77−87485
globular clusters, ANS far UV photometry of blue horizontal branches 79−71080
globular clusters, axial ratio and major axis position angle, UBVR obs. 77−17642
globular clusters, in M31, luminosity distrib. 80−36708
globular clusters, integrated IR photometry and wide field techniques 80−67574
globular clusters, integrated IR photometry using wide field photometer 80−62029
globular clusters, integrated UBV photometry 77−67116
globular clusters, metal-rich, TiO band strengths, reddening and metallicity determ. 79−40227
globular clusters, southern, surface-brightness profiles rel. to struct. and stellar content 79−71078
globular clusters, UBVI colour excesses 77−13417
globular clusters evolved stars, CN strengths and UV excesses from DDO photometry 77−64753
globular clusters integrated colours, radial distribs. obs. 79−25648
globular star cluster age and distance determ. using subdwarf photometry results 80−82435
globular star clusters, metal abundance and reddening from photometry obs. 80−67800
X Gruis, Algol variable, mean light curve and photometric solution 77−64799
RS Gruis, dwarf Cepheid in binary system 78−77559
Gurzadyan UV stellar group in Auriga, UBV and uvby photometry 78−45373
GX 17+2 (3U 1813−14), photometry of optical candidate 78−28849
GX 1+4 optical counterpart, symbiotic star, spectrophotometry 77−33498
GX 339−4 (4U 1658−48), possible black hole binary, optical studies 79−101220
H 2155−304 optical candidate, spectrophotometric obs. 79−25761
H 2252−035, optical counterpart photometry and spectrum 80−101651
H-H 2, condensation H, spectrophotometric data 79−62826
halo giant in north galactic cap, photometry and spectra 78−85942
halo population near Sun, intermediate-band photometry 79−44473
halo stars, three colour photometric obs., rel. to Galaxy halo to disc mass ratio 77−45548
HD 01891, subdwarf, photometry and spectrum rel. to UV excess and metal abundance 80−17574
HD 101065 light variations, comparison stars UBV photometry 78−69812
HD 101205 region, spectrographic and photometric obs. of stars and interstellar medium 77−49383
HD 101799, W Ursae Majoris star, contact system anal. 77−22274
HD 101947, yellow supergiant star, Cepheid with 125 day period 79−88671
HD 105902 (ADS 8448), Ba star in visual binary, spectra and photometry 77−78805
HD 10783, Ap star, spectrophotometric obs. 80−98663
HD 108078, spectroscopic binary orbit from photoelec. radial vel. meas. 80−77451
HD 113001, photometric separation of visual binary *(French)* 80−105281
HD 116458, Ap star, search for light variability 77−64767

stellar photometry continued
HD 116890, Ap star, 5200 Å depression index and light variability 77−64767
HD 116890, Si Ap star, UBV photometry, periodicity 79−80318
HD 116994, uvby photometry, var. period determ. 77−13358
HD 118246, new Be star at high galactic latit., photometry and spectrum 78−73721
HD 120640, spectrophotometry and quantitative anal. of B star 77−60758
HD 127617 (Bidelman's high latitude Be star), photometric and visible spectra obs. 80−77420
HD 129708, new bright short-period Cepheid variable with unusual spectrum, photometric obs. 80−67751
HD 133461, spectroscopic binary orbit from photoelec. radial vel. 77−57016
HD 137613, C rich H deficient star, UBV photometric obs. 80−90437
HD 139216, unusual Balmer lines in M-type giant 79−80310
HD 13970, photometry of probable close binary component 79−8948
HD 149499B, hot white dwarf, continuous spectrum, H deficient 79−48795
HD 152667, =OAO 1653−40, photometry, spectrum and physical parameters 79−17021
HD 152667 (V861 Scorpii), eclipsing binary X-ray source, possible black hole 79−53858
HD 152667 (V861 Scorpii), phys. props. and orbital parameters, supergiant star with black hole companion model 79−71067
HD 153747, freq. anal. of early-type δ Scuti star 79−71053
HD 153919, Of supergiant, X-ray binary 3U 1700−37 optical counterpart, light curve anal. 78−32470
HD 153919, Of X-ray binary, narrow band photoelectric photometry 77−60761
HD 153919 (3U 1700−37), X-ray binary, UV photometric obs. 77−45490
HD 153919 (3U 1700−37), X-ray binary uvby photometry 77−17624
HD 153919 (3U 1700−37), X-ray eclipsing binary, VBLUW photometric obs. 79−17135
HD 153919 (3U 1700-37), X-ray binary, five colour photometry 77−29877
HD 153919 (=4U 1700−37), eclipsing binary, supergiant-neutron star, optical variability 80−82419
HD 159378 (Tr 27-102), yellow variable supergiant near Cepheid instability strip, VBLUW photometry 80−98672
HD 170899, possible halo population giant star 80−26859
HD 175305, red horizontal branch star in general field, spectroscopic and photometric anal. 79−40189
HD 17576, UV subdwarf companion discovery from uvbyβ photometry 78−96479
HD 184279, B-type subgiant, variability 79−84804
HD 185332, new δ Scuti star, photometric and spectroscopic obs. 80−90451
HD 186205, He star, fine abundance anal. 77−87408
HD 187299, spectroscopic binary orbit from photoelectric radial vels. 77−91575
HD 188753, close visual binary with spectroscopic binary component 77−57015
HD 191639, B-type main sequence star, variability 79−84804
HD 192273, EUV flux upper limit, Voyager 1 obs. 80−77406
HD 193793, Wolf-Rayet star, photometric evidence for C-rich dust cloud 80−26861
HD 200120, Be star, UV spectra vars. 77−5534
HD 206860, G0 V star, UBV and IUE obs. of active region 79−92766
HD 21479, brightness microvariability and non-radial pulsations *(Russian)* 80−67754
HD 219150, F0 V star with remarkable UV excess, optical and UV photometry and spectrum 80−90429
HD 223969, spectroscopic binary orbit from photoelec. radial vels. 77−82279
HD 224085, spot-covered red dwarf, light curves 77−74093
HD 226868 (Cygnus X-1), periodicity in optical light curve during X-ray flare 78−81652
HD 30466, double wave photometric variable Si star 77−87410
HD 30849, periodic variability photometric obs. *(French)* 79−101157
HD 31908, freq. analysis of δ Delphini star 80−46581
HD 33579, 35343, HDE 286757, 269006, most luminous LMC supergiants, long time baseline VBLUW photometry 80−22007
HD 33579, HD 35343 (S Doradus), HDE 268757, HDE 269006, most luminous LMC supergiants, long time baseline VBLUW photometry 80−36630
HD 3580, 187473, 212432, Si stars, uvby photometry and periods 78−96487
HD 36619, Am-type star previously misclassified as O7 type 79−84805
HD 3765, variability due to eclipsing star or planetary system, BV photometry 80−17615
HD 3980, late Ap star, photometric and mag. variability obs. 80−56845
HD 47732, young close binary in NGC 2264, photometry and struct. 78−57575
HD 50169, Ap star, uvby photometric obs. 77−22236
HD 50896, Wolf-Rayet star, UV spectral energy distrib. 77−22211
HD 52788, freq. anal. of δ Delphini star 79−35276
HD 5980, eclipsing W-R binary in SMC, photoelectric light curve 78−45366
HD 63791, probable metal-poor halo G-type giant field star 80−26859
HD 65750, photometric vars. of red giant, obs. of surrounding refl. nebula IC 2220 78−36567
HD 72968, low amplitude photometric double wave Ap star, light curve 78−28697
HD 77581 (=Vela X-1), supergiant+neutron star, visible obs. 80−94892
HD 77581 (Vela X-1), four colour photometric obs. and light curve anal. 77−17621
HD 77581 (Vela X-1), X-ray binary, photometric obs. 77−41392
HD 77581 (Vela X-1), X-ray obs. and UBV photometry 78−65722
HD 77581 and 153919, polarimetric obs. of massive X-ray binaries 80−98688
HD 80383, UBV photometry of β Cephei type star 80−36644
HD 8781, freq. anal. of low-amplitude δ Scuti star 80−46575
HD 87892, central star of NGC 3132, obs. of visual companion 78−20859
HD 88230, dM0 star, high-dispersion photometric atlas from 3900 to 6000 Å 78−7996
HD 88661, Be star, photometry and light vars. *(French)* 78−57562

stellar photometry continued
HD 91619, 96919, B-supergiants, peculiar H_α profile variations 77−17577
HD 92664, Ap star, photometric variability and period from uvby photometry 79−40199
HD 92740, spectroscopic binary WN7 star, spectroscopy and photoelectric photometry 79−8924
HD 94033 ultra short period cepheid, UBV and uvbyβ photometry 80−22024
HDE 226868 (Cygnus X-1), orbital period and inclination 78−16579
HDE 245770, near IR photometry of OBe star, A 0535+26 optical counterpart 79−48826
HDE 245770 (A0535+26), UBV photometry during X-ray outburst 79−67024
HDE 245770 (Ariel 0535+26), photoelectric UBV photometry 78−36592
HDE 245770 (Ariel 0535+26), UBV photometry during X-ray flare-up 78−28705
HDE 326333, new β Canis Majoris star, photometric obs. 80−17595
He2-442, UVRK photometry and spectroscopic obs. *(Russian)* 80−94817
Henize 715 (4U 1145−61), Be-type star, colour and luminosity vars. (1976-1980) 80−72979
Henize 787 (SAO 251905), five-colour photometry 77−29846
Henize 788 (Wray 977), counterpart of 3U 1223-62, five colour photometry 77−29846
Herbig Ae/Be stars, spectrophotometry 78−93258
Herbig-Haro objects in Gum Nebula, spectrophotometry 78−36565
HZ Herculis, 1978 UBV photometry of active state 80−62189
AK Herculis, atypical W Ursae Majoris type, BV light curves 78−28719
u Herculis, BVR lightcurves interpreted 80−41856
DY Herculis, dwarf Cepheid, uvbyβ photometry and evolutionary status 79−58357
AH Herculis, dwarf nova outburst, rapid oscills. evolution 80−94805
u Herculis, eclipsing binary, photometric elements, period changes 78−61884
LT Herculis, eclipsing binary, photometric elements 80−31328
DI Herculis, eclipsing binary, photometric obs. anal. rel. to relativistic motion of periastron 80−94830
u Herculis, eclipsing variable, two new light curves 80−90472
AM Herculis, high speed photometric obs., 186 min. var., dwarf nova model 77−64806
88 Herculis, light and colour vars. of shell star 79−53817
AM Herculis, light curves and Fourier analysis 78−49483
52 Herculis, magnetic, spectral and photometric vars. of Ap-star 78−85952
AM Herculis, multicolour photometry, slow optical pulsar 78−28693
AK Herculis, photoelec. obs. and period study, possible visual companion 79−67065
DQ Herculis, photometric study of light curve 71 s oscill. 78−93259
AM Herculis, polar, IR photometric obs. 80−98687
AM Herculis, possible cataclysmic variable of Z Camelopardalis type 77−33497
AK Herculis, R and I light curves, B and V light curves comparison, starspot 79−67064
AC Herculis, RV Tauri star, UBV obs. 80−56857
4 Herculis, shell star, photometric obs. rel. to binary star hypothesis 77−91538
BL Herculis, short-period Population II variable, chem. comp. determ. 79−8923
AM Herculis, spectrophotometric obs. at min. light min. light 80−98692
BL Herculis, Stromgren uvbyβ photometry 78−85954
AM Herculis, UBVRI light curves 78−85972
AM Herculis, UBVRI photometric and polarimetric obs. 79−5861
AM Herculis, X-ray binary, optical light curve 77−33566
AM Herculis, X-ray binary, spectroscopy and photometry, model 77−33568
AM Herculis (3U 1809+50), simultaneous three-channel photometry rel. to optical flickering mechanism 80−82411
AM Herculis (3U 1809+50), X-ray eclipsing binary, multicolour photometry 77−78887
HZ Herculis (Hercules X-1), optical and UV obs. 80−109487
HZ Herculis (Hercules X-1), UBVR photometry during 1977 Jul.-Aug. *(Russian)* 79−17028
DQ Herculis (Nova 1934), high time resolution spectrophotometry 80−22017
DQ Herculis (Nova 1934), UBV photometry of visual binary 80−8661
V533 Herculis (Nova 1963), 63 sec. oscill., UBV photometry 80−17592
HFE 2, 100 micron source, IR obs. of reddened stars 77−26082
high-velocity stars, southern, UBV colours 80−21989
Hodge 11 star cluster in LMC, electronographic photometry and colour-magnitude diagram 79−40230
horizontal-branch A-type stars, UV by photometry rel. to astrophysical parameters 79−62829
TU Horologii, ellipsoidal variable, UBV photometry 78−4292
TU Horologii, period and spectroscopic orbit of ellipsoidal binary system 79−58372
hot stars, IR photometry *(Italian)* 79−53829
HR 1099, Hα region spectrophotometry during February 1978 radio flare 79−21344
HR 1099, optical ephemeris and photometric wave minimum phase 78−36641
HR 1099, photometric and spectroscopic obs. 1978 Feb. 78−40998
HR 1099, RS Canum Venaticorum binary, optical spectrophotometry during major flare outburst 79−21342
HR 1099, RS Canum Venaticorum variable, photoelectric photometry 77−53602
HR 1099, V photometric obs. during 1976-77 period 78−40994
HR 1099 (V711 Tauri), JHK photometry of noneclipsing RS Canum Venaticorum type star 80−72995
HR 1170, δ Scuti-type star, light and colour curves 77−74058
HR 1170, HR 7331, nonradial δ Scuti pulsators, photometry multiperiod anal. 79−88663
HR 1225, δ Scuti star, photoelectric study and periodogram anal. 80−109436
HR 1614 group of metal-overabundant stars, late-type stars intermediate-band photometry 78−53935
HR 2557, light vars., luminous δ Scuti-type star 78−32490
HR 3413, Ap star, photometric vars. and period *(French)* 78−32471
HR 421, δ Delphini star, abundance anal., uvbyβ photometry 77−29823

stellar photometry continued
HR 5110, Algol type RS Canum Venaticorum star, Hα, yu photometry obs. 80−105276
HR 5110, RS Canam Venaticorum binary, V photometry near radio outburst time 80−90469
HR 5999, circumstellar dust around variable shell star 79−8926
HR 5999, lightcurves for irregular variable shell star 78−77557
HR 5999, variable shell star, VBLUW photometry 78−28701
HR 5999 (V856 Scopii), multicolour photometry, circumstellar dust shell 79−48828
HR 6388, spectroscopic binary, orbit determ. from photoelec. radial vels. 78−49482
HR 6392, supergiant double star, UBV photometry and luminosities 77−45493
HR 6766, weak G-band star, photometry and spectrum rel. to light-element abundances 78−57548
HR 6940, spectroscopic binary orbit from photoelectric radial vels. 78−4294
HR 8102, uvby anal. of δ Scuti type star 78−53965
HR 9049, (HD 224113), eclipsing spectroscopic binary star, period determ. 80−46609
Hyades, BVRI photometry of new possible cluster members 78−32533
Hyades, late-type stars intermediate-band photometry 80−31289
Hyades cluster, possible members BVRI photometry 80−51821
Hyades cluster, shape and luminosity distrib. 80−17622
Hyades stars, Hα and O I 7774 Å photometric obs. 77−22286
TT Hydrae, absolute dimensions of β Persei type eclipsing binary 80−62184
VX Hydrae, dwarf Cepheid, uvbyβ photometry 77−29856
χ² Hydrae, eclipsing binary, four-colour photometry, orbital elements, dimensions and He abundance 78−65653
EZ Hydrae, eclipsing binary, photometric obs. and primary min. ephemeris 78−73737
VZ Hydrae, eclipsing binary, transit or occultation at primary minimum 77−9770
EX Hydrae, eclipsing binary dwarf nova, times of minima 77−22267
AI Hydrae, light curves and photometric elements of eclipsing binary 78−65652
HS Hydrae, photometric elements of detached eclipsing binary 80−90473
TT Hydrae, UBV photometry, improved light elements 78−69837
χ² Hydrae, uvby light curves of double-lined eclipsing binary 78−40996
AI Hydrae, uvby photometric obs. of eclipsing F-type binary 78−69835
VW Hydri, outbursts of dwarf nova, long and short eruptions comparison 79−88669
IC 2581, young open cluster, ratio of total to selective extinction determ. 79−5870
IC 2944, stellar aggregate surrounding HD 101205, spectrographic and photometric obs. 77−17636
IC 361, open cluster, preliminary photometry 78−89228
IC 4756, open cluster, uvby β photometry, distance modulus 78−53997
IKA-65 UV stellar photometric equipment on Cosmos 215 satellite *(Russian)* 77−64642
instrumentation, voltage-frequency convertor for photomultipliers 78−45233
integrated IR photometry, of globular clusters, colours and interstellar reddening 80−67575
intermediate brightness stars, for UV photometry from ASTP 79−71027
intermediate Population II stars, Stromgren uvby photometry 77−60757
intermediate-band photometry of late-type stars, calibration, standards 77−22104
interstellar extinction law correl. with wavelength of max. polarisation 78−61902
interstellar reddening in clouds near Sun from SA colour excesses 79−30111
interstellar reddening in high-latit. field around ω Bootis 79−101185
interstellar reddening in solar neighbourhood, anal. 80−62239
intrinsic colours of luminous stars in Magellanic Clouds *(German)* 77−17560
IR bright stars in region of galactic centre, catalogue and photometry 80−77299
IR colours, meas. rel. to diffuse interstellar bands strengths 78−93198
IR photometer, wide field for extended stellar sources 77−82582
IR photometry of late type stars 80−41823
IR sources in compact H II region G45.5+0.1, 1.25 to 10 μm photometry 78−4396
IR sources near Herbig-Haro objects, obs. during search for exciting stars 80−67720
IR sources of AFGL sky survey, ground-based obs. 79−71150
IR stars in galactic centre, IR spectrophotometry and props. 78−24551
IRC +10216, C star, far IR photometry and circumstellar dust cloud size 80−82539
K1211, blue straggler in NGC 7789, evolution status and mass, photometry obs. 80−109433
K-type giant stars, David Dunlap Observatory (DDO) photometry rel. to interstellar reddening determ. 78−4222
K-type giant stars, evidence for circumstellar shells from 0.4 to 20 μm photometry 80−90420
K-type giant stars at South Galactic Pole, DDO photometry rel. to CN anomalies and distances 80−8622
K-type giants, colour excesses, interstellar dust grains distrib. determ. 79−40251
K-type giants, multivariate anal. of spectrophotometry rel. to atmospheric characts. 77−78772
An King 13, open cluster, UBV obs. *(German)* 80−77459
Kottamia Observatory site, seasonal atm. extinction due to aerosol 80−46253
KP 790-29, mag. degenerate with heavily blanketed energy distrib. spectrophotometry and polarimetry 79−5815
KUV09313+4052, variable UV excess object, UGR photographic photometry 80−62159
L19-2, low-amplitude ZZ Ceti type variable, UBV colours, period determ. 78−4242
Lacerta OB1 association, uvby photometry 77−22285
12 and 16 Lacertae, β Cephei stars, light var. anal. and photoelec. photometry 80−77412
SW Lacertae, contact eclipsing binary, polarisation obs. 77−45489
AR Lacertae, eclipsing binary, photometric obs., intrinsic variation 77−22271
CM Lacertae, eclipsing binary, transit or occultation at primary minimum 77−9770

stellar photometry continued
EV Lacertae, flare star, photometry and spectrum rel. to starspots and rot. period 80−98665
EV Lacertae, flare star, polarimetric and photometric obs. *(Russian)* 77−13368
EV Lacertae, high-speed five-colour photometry of flare star 77−56956
AR Lacertae, RS Canum Venaticorum type star, UV excess, spectrophotometric obs. 78−8043
SW Lacertae, W Ursae Majoris star, photoelectric obs. and epochs of min. light 80−62196
large-amplitude red variables, luminosities and space motions 77−22244
late-type (K0 to M6) giant stars, IR photometry and effective temps. 80−46545
late-type dwarfs, photometric metal abundance index and appl. to galactic evolution 77−60754
late-type giant and supergiant stars, 1.25-3.25 μ airborne photometric obs. 78−40934
late-type giant model atmospheres, limb darkening coeffs. 78−20821
late-type main-sequence stars near Sun, intermediate-band photometry 78−53934
late-type stars, anal. of balloon-borne near IR multicolour photometry 80−98654
late-type stars, balloon-borne near IR multicolour photometry 80−4356
late-type stars, balloon-borne near IR photometry 77−13345
late-type stars, intermediate band photometry 78−81558
late-type stars, intermediate band photometry in Geneva system 78−12231
late-type stars, near IR multicolour photometry from BAT *(Japanese)* 80−31298
late-type stars, near IR photometry with balloon-borne telescope 78−73713
late-type stars, near IR photometry with balloon-borne telescope 80−4357
late-type stars, search for C IV reson. doublet, TD1 satellite UV obs. 77−5526
late-type stars, spectrophotometry, incident and emergent flux calc. 78−4200
late-type stars in stellar groups, intermediate band photometry 78−4300
late-type stars intermediate-band photometry, calibration of indices 78−49424
late-type stars photometry, photoelectric MgH+Mgb index meas. 80−12753
late-type young stars in ρ Ophiuchi dark cloud, photometry obs. 80−72942
LB 3459, O-type subdwarf plus hot white dwarf eclipsing binary, photometry, anal. 79−48859
LB 3459, short period eclipsing binary system containing two O-type subdwarfs, uvby photometry 78−53987
AD Leonis, flare conditions from photometry and spectra 79−92773
AQ Leonis, light var. anal. of RR Lyrae star 77−56941
87 Leonis, lunar occultation ang. diameter 79−25599
20 Leonis, possible eclipse obs. in triple system 78−12298
EH Librae, BV photoelectric photometry of dwarf Cepheid 79−44498
EH Librae, dwarf Cepheid, BV photometry 77−82226
LMC, main sequence luminosity function 78−8111
LMC, stellar photoelectric UBV photometry *(German)* 80−21932
LMC, yellow stars UBV photometry and LMC members number 78−93417
LMC central regions, stellar count-brightness ratios rel. to population struct. 78−89245
LMC disc, underlying stellar component photometry rel. to population struct. 77−33633
LMC giants and supergiants, photometric luminosity calibration, visible obs. 80−94797
LMC nova, UBV photometric meas. (1977, March-April) 77−53608
LMC supergiants, BVI photometry 77−33490
LMC X-2 optical candidate, UBV photometry and variability 79−17136
LMC X-4 optical candidate, UBV photometry rel. to binary nature 77−64879
Lo 807, open cluster, two-colour photographic photometry 78−96512
long period Cepheids, UBVRI photometry and classification 77−71112
long-period close binaries, general relativistic periastron advances 77−91564
long-period variables, pulsation from near IR photometry 78−4248
loose clusterings in southern Milky Way, continued photometric studies 80−36679
loose open cluster search in southern Milky Way, UBV photometry 77−64814
loose stellar clusters in southern Milky Way, spectral type and UBV obs. 80−94839
low amplitude variables in Cepheid instability strip, photoelectric photometry 77−17580
low galactic latitude stars, photoelectric photometry rel. to mean secular parlallax 78−57542
LP182-44, faint high-vel. degenerate star with probable C features, photometry and spectrum 79−67007
LP 131-66, new cool red degenerate star 79−48780
LP 701-29, lowest luminosity degenerate star with heavily blanketed spectrum 78−36562
LS55° −8, high-speed photometric obs. of new nova-like variable 78−57565
LS IV −14°109, H deficient A-type star, effective temp. 79−40195
LSI+61°303, possibly optical counterpart of GT 0236+610, absence of variability 78−49438
LSS 1916, 3371, new VV Cephei stars, spectra and colours 79−35299
LTT 2437, most metal-deficient subdwarf, spectrum, photometry and Ca/H ratio 78−69797
luminous C stars in LMC, photometry 78−28670
luminous stars in M31 80−36622
luminous stars in Monoceros, photometry rel. to galactic struct. 77−9799
luminous stars in NGC 6822 and IC 1613, visible spectra and photometry 80−82345
luminous variable stars in M31 and M33, spectra and photometry 78−28686
lunar occultation, summary of obs. 78−7982
α,τ Lupi, β Canis Majoris stars, photometric obs. 80−17595
α Lupi, UV light curve of β Cephei-type star 78−36570
RR Lyncis, Am eclipsing binary, photometry and spectroscopy, abundances 77−33558
SZ Lyncis, BV photoelectric photometry of dwarf Cepheid 79−44498

stellar photometry continued
SW Lyncis, close binary, orbital elements 77−74090
Lynga 6, open cluster, photometry rel. to reality and membership of Cepheid TW Normae 77−87491
Lynga 6, open cluster, relation of long period Cepheid TW Normae 77−17639
β Lyrae, narrow-band photometry in (1971) 80−46605
β Lyrae, optical and IR photometry, gaseous disc electron density distrib. 78−28722
β Lyrae, photoelectric photometry (in 1971) 78−12294
β Lyrae, photoelectric photometry rel. to orbital period variability 80−72997
RR Lyrae, UV photometry from Orbiting Astronomical Observatory, light curve interpretation 77−45435
RR Lyrae star in globular cluster NGC 6717, photometric investigation 80−46624
RR Lyrae stars, atlas of light and colour curves 77−82228
RR Lyrae stars, cycle area in two colour diagram 79−21297
RR Lyrae stars, in southern hemisphere, VBI photometry 77−53612
RR Lyrae stars, photoelectric UBV obs., second list 78−81639
RR Lyrae stars, VBLUW photometry rel. to reddening and blanketing 79−48806
RR Lyrae stars in ω Centauri, UBV photometry rel. to comps. 78−73719
RR Lyrae stars in M4, UBV photometry 77−78802
RR Lyrae stars in Microscopium, VBLUW photometry and proposed intergalactic dust cloud 80−56851
RR Lyrae variables in globular cluster NGC 6121 (M4), UBV photometry 80−22018
RR Lyrae variables in N.Galactic Pole fields, revised periods and light curves 79−88660
M11, galactic open cluster, age and distance, colour diagram, photometric obs. 80−73012
M13, central region, colour-magnitude diagram 77−53656
M13, globular cluster, two colour photographic photometry of variable stars 77−87492
M15, BVR area photometry of globular cluster 78−85983
M15, faint stars photometry rel. to main sequence intrinsic width and luminosity function 77−78834
M15, globular cluster, core, Hα and continuum obs. 79−17031
M15, globular cluster, photovisual magnitudes of central stars 77−13412
M17, dusty H II region, stellar UBVRI photometry and optical polarisation meas. 78−45379
M22, globular cluster, BVI$_K$ photometry rel. to membership and other problems 78−32537
M25, young open cluster, UBV obs., photoelec. calibration, distance, reddening 79−8956
M25 (IC 4725), open cluster, stars four colour and Hβ photometry 78−8067
M2 (NGC 7089), globular cluster, faint stars photometry and colour-magnitude diagram 80−101623
M31, globular clusters colour indices, rel. to interstellar absorpt. law 78−28796
M31, UBV photometry of star clusters *(Russian)* 79−17034
M31, UBV photometry of star clusters 79−62879
M34, open cluster, UBV photoelectric photometry 78−12307
M3, globular cluster, luminosity function 77−57069
M4, globular cluster, colour-magnitude diag. 77−37629
M55, globular cluster, colour-magnitude diagram 77−64812
M67, main-sequence stars differential blanketing rel. to Hyades and Coma 78−57597
M69, metal-rich globular cluster, photometric calibration 77−91592
M6 field, supergiant IR photometry and interstellar matter towards galactic centre 78−16405
M92, globular clusters, luminosity function 77−57068
M-stars at l^{II}=138°, photographic photometry 77−9748
M-type dwarf stars, spectrophotometry with Carnegie image tube 78−57466
M-type stars in direction of N galactic pole, BVRI photometry and spectra 77−37594
M-type supergiants, highly reddened IRC objects, IR photometry and near IR spectra 79−84796
M-type supergiants, photoelectric two-dimensional spectral classification 78−53936
M-type variable stars, obs. in DDO photoelec. system, spectral classification 78−32463
Magellanic Clouds stars, five-channel photometric obs. 78−16398
Magellanic Clouds stars, photoelectric (B, V) magnitude sequences 77−53592
magnitude, colour index and position meas. from astronomical photographs, automated technique 79−21194
main sequence B-type stars, physical parameter determ. from uvbyβ photometry obs. 80−72952
main sequence stars, effective temp. from U−B and B−V indices *(Italian)* 79−21286
main sequence stars, oscills., observability by photometry and spectra 80−51724
main sequence stars with variable Ca II H and K emission, starspot hypothesis 79−58328
main-sequence reddened stars, ANS photometry, UV colours 80−77400
Markarian 38, galactic open star cluster, photometric obs. *(German)* 80−73015
Mauna Kea Observatory 33 μ photometry, calibration 77−67044
MD 101065, effective temp. and atm. electron press. 77−45468
dMe stars, survey of BY Draconis syndrome 78−16428
Medium-Amplitude Red Variables, UBVRI photometry 77−45438
Melotte 66, oldest open cluster, colour-magnitude diagram rel. to age 80−17621
Melotte 66, very old open cluster, BV photometry rel. to broad giant branch 78−32538
TY Mensae, contact eclipsing binary, evolutionary stage from UBV light curve anal. 80−105278
Michigan 239, peculiar extragalactic or extreme halo emission-line star, IR photometry 80−4380
ZZ Microscopii, radius of dwarf Cepheid from BV photometry 78−77560
Milky Way stars, five-channel photometric obs. 78−16398
Mira type variables, Me and Se types, UBV photometry 80−82375
Mira variables, airborne IR spectrophotometry, H_2O and CO absorpt. bands 78−32465
Mira variables, IR Photometry and OH maser pumping efficiency 80−82379
Mira variables, light and colour variations 77−64770
Mira variables, polarisation variation detect. in absorption features 77−33496
MK spectral types for 67 early type stars 77−33473
Monoceros R2 association, stellar UBV photometry and spectra 77−13409
N Monoceros region, two-micron IR objects survey 80−8555
19 Monocerotis, β Canis Majoris variable, photometric obs. 80−4379
1 Monocerotis, δ Scuti star, oscillation modes from photoelectric radial vels. and BVRI photometry 80−51787
1 Monocerotis, δ Scuti star, photometry and anal. 78−32495
21 Monocerotis, δ Scuti type star, freq. anal. 77−49398
V616 Monocerotis, A0620−00, transient X-ray source, spectrophotometry 77−33684
CV Monocerotis, Cepheid variable in anon. open cluster 79−58349
AU Monocerotis, eclipsing binary, cyclic variation in period 77−33565
AU Monocerotis, eclipsing binary, photoelec. obs. 80−73002
VV Monocerotis, RS Canum Venaticorum type eclipsing binary, photoelectric obs. 79−40218
V616 Monocerotis (A0620-00) field, BV electronographic sequence and nova light curve 77−64777
V616 Monocerotis (A 0620−00), UBV photometry 80−56846
R Monocerotis (NGC 2261 cometary nebula), spectrophotometry *(Russian)* 77−49446
V616 Monocerotis (Nova 1975=A0620−00), 8-day modulation from photoelec. photometry 77−87442
V616 Monocerotis (Nova 1975=A 0620−00), UBV photometry *(Russian)* 79−58360
V616 Monocerotis (Nova 1975), photographic photometric obs. 78−36587
multicolour photometric data, comparison with Moscow and Alma-Ata stellar spectrophotometry 80−101590
multicolour stellar photometric systems, investigation of UBV, RGU and uvby systems 78−28528
multicolour stellar photometric systems, transforms. between UBV and RGU systems 78−28529
θ Muscae, Wolf-Rayet binary, spectrum and photometry 77−22235
MXB 1730−335, X-ray rapid burster, IHKL photometry rel. to search for IR bursts 80−98740
narrow-band photometry in O6 to G2 stars 80−8621
near IR obs. of 50 stars 78−69795
near IR photometry, effects of atmospheric extinction 80−51539
near IR photometry, new two-colour system 79−62759
nearby stars, spectroscopic and photometric data published (1969-1978) 80−36513
NGC 1039 (M34), uvbyβ photometry of galactic cluster 79−84831
NGC 1261, globular cluster, colour-magnitude diagram 80−17623
NGC 129, open cluster membership from four colour and Hβ photometry 80−90485
NGC 1817, UVB photometry of open cluster, distance, age 77−91587
NGC 1854, LMC blue globular cluster, photographic photometry 77−74107
NGC 1868 in LMC, BV photometry of metal-poor intermediate-age cluster 80−51814
NGC 188, old open cluster, photographic photometry 77−53430
NGC 188, open cluster, BV photographic photometry with PDS microdensitometer 79−88600
NGC 1904, globular cluster, BV photometry 77−13415
NGC 1904 (M79), UBV photometry, colour-magnitude diagram of halo globular clusters 78−32528
NGC 2169, photometric and spectroscopic study of open cluster 78−45371
NGC 2175, photometry and spectral types of stars in H II condensation 78−20883
NGC 2231, star cluster in LMC, electronographic photometry and colour-magnitude diagram 79−92813
NGC 2243, metal abundance of old open cluster 78−93333
NGC 2243, old open cluster, UBV photometry 77−78835
NGC 2244, young open cluster, uvby Hβ photometry, colour excess, distance, age 78−32532
NGC 2264, far IR emission from compact sources 77−78841
NGC 2264, UBVRI photometry of 70 field stars in young cluster 80−51819
NGC 2264, young open cluster, circumstellar shells, IR excess obs. 77−45410
NGC 2264, young open cluster, differential reddening due to intracluster dust clouds 78−53996
NGC 2281, open cluster, UBV photometry, binary star freq., luminosity function 78−81663
NGC 2287, open cluster, UBVRI photometry, distance, age, metal content 79−12498
NGC 2419, globular cluster, variable star obs. 77−60804
NGC 2420, old disc cluster, photometry and spectra rel. to stars chemical comp. 80−46620
NGC 2420, PDS photometry of old open cluster, colour-magnitude diagram 78−57600
NGC 2423, 2482, Hyades-like clusters, late-type stars intermediate-band photometry 80−31289
NGC 2439 association, photometric and spectroscopic study 78−16470
NGC 2516, UBV and uvby photometry rel. to presence of some thirty Ap stars 79−16972
NGC 2527, galactic cluster, UBV photometry 78−16479
NGC 2527, UBV photographic photometry of open cluster 78−89231
NGC 2571, open clusters, UBV anal. 79−58386
NGC 2808, anomalous globular cluster, photoelectric UBV and DDO photometry 78−45369
NGC 2818, open cluster, photoelec. sequence 77−91595
NGC 3105, young open cluster, photoelectric UBV obs. 77−64811
NGC 3201, globular cluster, BV photometry 77−2458
NGC 3201, globular cluster, UBV photometry of bright stars 77−60803
NGC 3247, RGU photometry of open cluster, catalogue of 129 stars *(German)* 77−82290
NGC 3293, open cluster, UBVRI photometry and relation to OB complex in Carina 80−90490
NGC 3293, uvby β photometry rel. to other young clusters 80−101621
NGC 3324, very young open cluster in Carina spiral feature UBV β photometry 77−22282

stellar photometry continued
NGC 3532, southern galactic cluster, stellar photoelectric sequences 77−45502
NGC 3532, southern open cluster, UBV photometric study 80−46621
NGC 3603, luminous young cluster, UBV photometry 78−36643
NGC 362, globular cluster, BV photometry 77−13416
NGC 4590, metal poor globular cluster, BV photometry 77−64813
NGC 4755, southern open cluster, Balmer line photoelectric photometry 80−56892
NGC 4833, southern globular cluster, BV photometry of variable stars 78−4304
NGC 5053, haloglobular cluster, photometric study 77−74103
NGC 5367, field stars of cometary globule (reflection nebula) 78−93364
NGC 5367, young open cluster, UBV and IR photometry 77−82294
NGC 5617, open cluster, photoelec. and photographic photometry of member stars 79−17032
NGC 5662, open cluster, photoelec. and photographic photometry of member stars 79−17032
NGC 581 (M103), UBV photoelectric photometry of galactic cluster 78−89230
NGC 5823, open cluster, photoelec. UBV sequences for north and south regions 77−82293
NGC 6087, galactic cluster, four-colour and Hβ photometry 80−62208
NGC 6121 (M4), near IR photometry of metal-poor globular clusters 77−41398
NGC 6144, globular cluster, and neighbouring region, photometric obs. 80−51816
NGC 6200, loose young open cluster in Sagittarius arm extension 77−87493
NGC 6224, X-ray globular cluster, photometry of nucleus 77−37628
NGC 6231, young open cluster, main sequence stars photometry and spectra 79−88709
NGC 6250, young southern cluster, UBVRI photometry and spectra rel. to high R-values 78−16490
NGC 6256, probable galactic globular cluster, BV photometry 78−77583
NGC 6266, globular cluster, colour magnitude diagram, distance and metallicity 78−61894
NGC 6356, photometric obs. of Mira variables in globular cluster 78−32530
NGC 6366, metal-rich globular cluster, colour magnitude diagram 77−5462
NGC 6383, photometry and spectral classifications, age and distance of open cluster 78−93342
NGC 6383, young open cluster, central core stars UBV photometry 78−41003
NGC 6397, globular star cluster, age from main sequence turnoff, BV photometry 80−90484
NGC 6397, metal-poor globular cluster, BV photometry of 399 stars 77−82292
NGC 6440, globular cluster, cluster core surface photometry and colour-magnitude diagram 80−82436
NGC 6528, globular cluster, colour-magnitude diagram for field stars 77−87483
NGC 6528, metal-rich globular cluster, colour-magnitude diagram from UBV photometry 80−4406
NGC 6530, open cluster, photographic UBV photometry 77−45504
NGC 6530, UBV photometry of variable stars in open cluster 77−74106
NGC 6530, young open cluster, UBV photometry, magnitudes, reddening, distance, age 78−93341
NGC 6535, photometric study of variable stars in globular cluster 78−32529
NGC 6541, globular cluster, UBV photometry, metallicity and distance 79−35316
NGC 6546, open cluster, assoc. with Cepheid AV Sagittarii disproved 79−58387
NGC 654, young open cluster, UBV photometric study 80−109502
NGC 6604 and 6704, UBV photometry of open clusters 78−53993
NGC 6611, young open cluster, UBV magnitudes and colours, reddening, distance, luminosity 80−31332
NGC 6624, optical counterparts of X-ray burster in core of globular cluster 80−67801
NGC 6624, UBV photometry of X-ray globular cluster 78−93337
NGC 6635, globular cluster, colour magnitude diagram, BV photometry 80−90483
NGC 663, UBV photometry of open cluster, distance 79−5869
NGC 6656, metal-poor globular cluster, BV photometry of 374 stars 77−82291
NGC 6717, globular cluster, colour-magnitude diagram, distance and metallicity 80−46624
NGC 6752, globular cluster, blue horizontal-branch stars photometry 78−49488
NGC 6752, globular cluster, main sequence from UBV photometry 79−71079
NGC 6811, UBV photographic photometry of open cluster 79−5871
NGC 6823, UBV photometry and spectra, extinction study of young open cluster 80−4407
NGC 6910, uvby Hβ photometry of open cluster 77−91586
NGC 6913, uvby Hβ photometry of open clusters 77−91586
NGC 6913 galactic cluster, photoelec. photometry of brighter stars, variability obs. 80−46625
NGC 7099, metal-poor globular cluster, UBV photoelectric photometry 78−77584
NGC 752, DDO astrophysical study 79−48864
NGC 7654 (M52), open cluster, stars four colour and Hβ photometry 78−8067
NGC 7789, open cluster, DDO and UBV photometry 77−53648
NGC 957, young open cluster, distance and reddening, RGU photometry 80−85976
Norma dark cloud stars, UBVβ photometry rel. to cloud struct. 78−16494
GU Normae, Cepheid, BVI photometry and assoc. with (NGC 6067) 77−45464
S Normae, Cepheid, luminosity and membership of NGC 6087 visible obs. 80−94797
north galactic pole, A and F star uvbyβ photometry 77−22224
northern early-type stars at intermediate galactic latits., UBV photometry and MK spectral classification 77−82221
Nova, Aquilae 1975 (V1301 Aquilae), IR development 77−17570
Nova, Sagittarri 1977, UBV photoelec. obs. (1977, March-April) 77−53607

stellar photometry continued
Nova Centauri 1979, UBV photometry and spectrum, identification with X-ray transient 79−62842
Nova Cigni 1978, BV and IR photometry and visual magnitude estimates 78−89211
Nova Cygni 1975, spectrophotometric exam. *(French)* 77−22240
Nova Cygni 1975 (V1500 Cygni), light curve 77−2437
Nova Cygni 1978, photometric obs., light vars., IR obs. showing dust form. phase 78−96494
Nova Cygni 1978, rapid flickering and UBV photometry (1978 Sept.) 79−16985
Nova Cygni 1978, spectra, polarisation, photometry and visual magnitude estimates 78−93283
Nova Cygni 1978, UBV photometry, brightnesses and distance 78−93284
Nova Cygni 1978 79−67035
Nova Delphini 1967, spectrophotometry in 3400 to 6500 A range 78−16430
Nova Delphini (1967), photoelectric and spectrographic obs. 78−20844
nova in LMC, discovery confirmation, magnitude, photometric obs., pre-max. spectra 78−49456
nova in LMC, IR obs. with HJKL filters 77−33518
nova in LMC, photometric obs. 77−60769
nova in NGC 5272 (=M3), discovery, V mags. and spectrum 79−71050
Nova LMC 1977b, photometry, light curves, distance modulus 78−8019
Nova LMC 1977b, VBLUW photometry, absolute magnitude, distance and reddening 79−58342
Nova Sagittae 1977, visual magnitude estimates (1977 November 6 to 1978 January 7) 78−36593
Nova Sagittarii 1977, visual magnitude, UBV and Hα obs. (1977, March) 77−33517
Nova Scuti 1975, UBVRI photometry 77−33520
Nova Serpentis 1978, IR magnitudes and BVR photometry 78−65629
Nova Serpentis 1978, IR photometry 80−4365
Nova Serpentis 1978, UBV photometry, visual magnitude estimates, spectrographic obs. 78−40963
Nova Serpentis 1978, UBV photometry and magnitude estimates 78−40959
Nova Serpentis 1978, VBLUW photometry, absolute magnitude, distance and reddening 79−58342
Nova Serpentis 1978, visible and IR photometry rel. to dust shell evolution 80−90430
Nova V3888 Sagittarii (1974), UBV and uvby photometry during decline stage 78−20836
Nova Vulpeculae 1976, magnitudes and photoelectric obs. (1976 October-November) 77−5538
Nova Vulpeculae 1976, spectrograms and photoelectric V obs. 1976, Oct. and Nov. 77−2443
Nova Vulpeculae 1976 (NQ Vulpeculae), light, colour and vel. curves 78−28708
Nova Vulpeculae 1979, posn., magnitudes, spectrum and photometry 79−48818
Nova Vulpeculae 1979, spectroscopic and photometric obs., possible exceptionally slow nova 79−48820
novae, UBV obs. and two-colour method appls. 79−71042
novalike object in Vulpecula, light curve, photometric and spectroscopic obs. 80−67758
novalike object in Vulpecula, photoelectric UVB obs. (1979 June 9 to 15) 79−80323
novalike object in Vulpecula, photometry, June 1980, and spectral classification 80−94807
novalike object in Vulpecula, UBV photometry (1979 August 6 to September 20) 80−8644
novalike variable in Virgo, discovery, approximate positions and magnitudes, (1980 July and August) 80−98674
O-B stars, spectrophotometric and UBV colorimetric parameters *(Russian)* 77−17569
O-type stars, effective temps., far UV photometric obs. 79−88656
O-type stars, in LMC, uvby photometry 77−60756
O-type stars and T Tauri objects, Hα, O I photometry 77−67092
O-type stars towards Carina Nebula, extinction law 80−105240
OB stars in Puppis, UBVβ photometry 80−85937
OB stars near Carina arm, UBVβ photometry 80−85941
OB-type southern stars, UBV, Hβ and polarisation meas. 77−26007
OB-type stars, spectrophotometry rel. to effective temps., ang. diameters, distances and linear radii 80−17584
OB-type stars in SA 98, UBV photoelectric meas. 80−46535
OB-type stars in vicinity of long period Cepheid VZ Puppis, UBV β photometry 78−45339
OBA supergiants and Of stars, IR photometry and mass loss rates 77−45414
UV Octantis, VBRI obs. of RRab star, radius determ. 79−8928
UZ Octantis, W Ursae Majoris system, UBV light curves 80−22042
old novae, search for rapid photometric oscills. 78−4251
open cluster containing Wolf-Rayet and Of-stars 77−64810
open cluster reddening, polarimetry and field star photometry of M67, Hyades and Coma cluster 80−62222
open clusters, scatter in colour-magnitude diagrams rel. to duplicity 77−53626
open clusters in Carina Nebula, extinction determ. from UBV photometry obs. 80−90513
open clusters near η Carinae, RGU photometry 77−37631
open clusters NGC 2547 and Trumpler 10 in Vela star cloud 80−90482
open clusters Tr 14, 15, 16 and Cr 228 in Carina Nebula, dist. determ. 80−85977
V1010 Ophiuchi, early-type contact system, two-colour light curves 77−33553
V566 Ophiuchi, eclipsing binary, period change, UBV photometry 77−29883
U Ophiuchi, eclipsing binary, photometric anal. 77−53628
U Ophiuchi, massive eclipsing binary star, spectrophotometry 80−26900
ω Ophiuchi, UBV photometry of Ap star, periodicity in luminosity vars. *(French)* 78−57559
Ophiuchus region, interstellar extinction and stellar space density 77−64839
Orion Nebula stars, wavelength depend. of polarisation, rel. to intracluster dust and circumstellar shells 77−78839
Orion OB1 (Belt), photometric studies 80−46618
Orion OB 1 association, anal. of photometric study 77−82288
Orion OB 1 association, photometric study 77−82128
Orion OB 1 association, subgroup analysis of uvbyβ data 78−77582

stellar photometry continued
Orion region, survey of extremely red stars with Schmidt telescope *(Japanese)* 78−20833
ζ Orionis, C III line obs. 77−87387
42 Orionis, Copernicus UV spectra and IR photometry 77−49437
YY Orionis, spectroscopic and photometric obs. 78−93225
δ Orionis, spectroscopic binary, spectrophotometry *(Russian)* 77−64802
θ Orionis A, eclippsing binary, photographic photometric obs. 79−58380
θ^1 Orionis A, UBV photoelec. obs. of primary eclipse 77−91576
λ Orionis association, photometric props. of young cluster 78−16478
σ Orionis E, period and luminosity stability from uvby β photometry 78−8017
θ^1 Orionis E, suspected variable, photographic photometric obs. 79−58380
YY Orionis stars in Orion population, UBV photometry of young emission-line objects 80−46552
Pal 12, metal-rich globular cluster in outer galactic halo, optical and IR obs. 80−105290
Palomar 2, distance and structural props. of globular cluster 80−62213
Palomar 5, remote globular cluster in galactic halo, chem. comp. 77−87482
MW Pavonis, eclipsing binary, UBV light var. and orbital elements 77−49429
MW Pavonis, W Ursae Majoris system, evolutionary stage from UBV light curve anal. 80−105278
AU Pegasi, binary Type II cepheid, photometric and spectroscopic study 80−26866
BB Pegasi, BV photoelectric lightcurve analysis of eclipsing binary 80−62194
DY Pegasi, dwarf Cepheid, revised ephemeris, period decrease 79−67040
AW Pegasi, eclipsing binary, photometric elements, masses, radii, luminosities 78−28723
57 Pegasi, long-period pulsating variable, spectrographic and photometric obs. 79−21305
BB Pegasi, photoelectric photometry of totally eclipsing W Ursae Majoris systems, 1978 Oct. to Nov. *(Chinese)* 80−31330
AQ Pegasi, UBV light curve solns. for Algol-like system 80−41855
β Persei, 4.8 μ photometry 77−74092
X Persei, 580 day and other periodicities 78−16435
21 Persei, Ap star, chemical element distrib. from spectrophotometry *(Russian)* 77−22238
X Persei, Be star, coordinated IR and optical obs., (in late 1976) 79−25616
X Persei, distance determ., 3U 0352+30 optical counterpart *(Chinese)* 78−69836
β Persei, eclipsing binary, study of light curve at 3428 Å 77−53634
RT Persei, eclipsing binary, V light curve 77−53636
AG Persei, eclipsing binary in H Persei association, photometry and distance 79−21326
21 Persei, magnetic variable, Fe, H_γ and H_δ obs. *(Russian)* 77−49388
AG Persei, massive eclipsing binary star, spectrophotometry 80−26900
IW Persei, metallic-line close binary star, photometric and spectroscopic obs. 80−62186
53 Persei, nonradial mode identification 80−8632
β Persei, partially eclipsing binary, freq. domain light curve anal. 77−53639
1 Persei, photometric variability, possible eclipsing binary 78−32489
21 Persei, spectrophotometry of Ap star, continuum features vars. 80−36638
AG Persei, two-colour photometry of eclipsing binary system, apsidal motion 78−96504
b Persei, UBV photometry and spectroscopic study of ellipsoidal variable 80−36666
RW Persei, UBV photometry of semidetached binary system 79−25639
X Persei (2U 0352+30), photoelec. obs., light vars. 78−40999
X Persei (3U 0352+30), photometry, search for optical 13.9 minute period 78−16426
X Persei (3U 0352+30), simultaneous X-ray and ground-based optical obs. 80−17591
X Persei (3U 0352+30), UBVRI photometry 78−8049
X Persei (4U 0352+30), Be star, photoelectric photometry rel. to 6-year periodicity 80−109446
X Persei (4U 0352+30), light vars., tidal distortion by massive unseen companion 78−36640
β Persei (Algol), anal. of red and IR wide-band photometry 78−20853
β Persei (Algol), minimum light obs. rel. to orbital period (1964 to 1978) 79−58377
β Persei (Algol), UV photometry and spectrum rel. to primary component rot. 80−72996
V400 Persei (Nova Persei 1974), photoelectric obs. 78−4252
α Persei cluster, OAO 2 photometry 78−93331
α Persei star cluster, polarisation wavelength depend. 79−48865
PG 1413+01, white dwarf-red dwarf eclipsing binary, photometry and spectral types 79−8944
ξ Phoenicis, periodic variability photometric obs. *(French)* 79−101157
SX Phoenicis, short period dwarf Cepheid, UBV photometric obs. 78−57561
ρ Phoenicis, temp. vars. of δ Scuti type star 78−53960
photoelectric meas., continuously acting luminous solid for 300-800 nm range 79−3757
photoelectric photometry, fundamental problems *(Russian)* 77−64656
photoelectric photometry, UBV obs. method and reduction 80−72784
photoelectric photometry at Hvar Observatory, colour systems, and extinction meas. 77−78643
photoelectric photometry at Trieste, data acquisition and processing software *(Italian)* 79−58258
photoelectric photometry at Trieste, real time data acquisition and processing *(Italian)* 79−62757
photoelectric photometry at Trieste, real time spectral analysis *(Italian)* 79−62756
photoelectric photometry at Wise Observatory, performance assessment 78−73657
photographic, digitalised image processing, reduction procedures *(Italian)* 80−98569
photographic method optimisation, review *(Russian)* 79−35144
photographic photometry, PDS microdensitometer technique 79−88600
photographic photometry around l=140°, b=0°, rel. to galactic struct. 78−24555
photometer for rapid stellar light variation, microprocessor controlled *(Spanish)* 80−82222

stellar photometry continued
photon counting, dead time correction for bright star photometry 77−22106
53 Piscium, confirmed β Canis Majoris type variable 79−44492
SS Piscium, RRc variable uvbyβ photometry 77−33526
UV Piscium, short period eclipsing binary, light and colour curve obs. 79−88697
RZ Piscium, UBV photometry, light minima *(Russian)* 78−93323
Pismis 13, open cluster, colour magnitude diagram, UBV obs. 80−67805
Pismis 6 and 8, open clusters, photometry and spectra rel. to proximity to (Wat 6) 79−88712
planetary nebulae central stars, intermediate band UV photometry 78−28679
planetary nebulae central stars, variability from UV obs. 78−36668
planetary nebulae nuclei, photometry and spectra of (Abell 30 and 78) 77−91602
Pleiades, contracting stars, UBVR photometry 79−96996
Pleiades, Hα and O I photometry 79−35315
Pleiades cluster, reddening-face colours, photometric zero age main sequence definition 80−26920
Pleiades stars, wavelength depend. of polarisation 77−45500
polarisation of stars within 25 pc of Sun, obs. 78−12202
Praesepe, photometry in BVRI colours 80−26917
Praesepe stars, Ca II K-line photometry and metal abundance rel. to Hyades 77−57064
pre-main-sequence A and F stars in NGC 2264, nature of IR excesses 78−32461
pre-main-sequence stars in Orion cluster, photometry and spectra rel. to masses and ages 77−13339
proper motion stars, catalogue of stars with $m_V<15$, annual motion $>1''$ 79−58275
Przybylski's star (HD 101065), β photometry and period determ. 80−41835
PSR 1913+16, optical candidate, astrometry and high-speed photometry 80−101609
ρ Puppis, chromospheric activity and atm. dynamics of δ Scuti star 77−17581
VV Puppis, obs. in faint state 79−25643
RX Puppis, peculiar emission-line object, spectrum and UBV photometry 79−44497
VV Puppis, photometric activity, flickering 77−67112
VV Puppis, polar, IR photometric obs. 80−98687
ζ Puppis, UV spectral energy distrib. 77−22211
R Puppis (HD 62058), G-type supergiant, UBV photometry and variability confirmation 80−41824
Puppis open cluster pair Czernik 29 and Haffner 10, UBV obs. 80−109503
Puppis region (l=250°, b=0°), new UBV photoelectric sequences 77−45426
T Pyxidis, recurrent nova, photoelectric obs. 78−4252
PZT stars including suspected variables, photoelec. UBV photometry obs. 80−77392
R50 dusty star in SMC, IR photometry 77−45461
R548, pulsating white dwarf, photometric obs., light curve anal. 78−32488
R548, pulsating white dwarf, photometric props. 77−9742
R 136, central star in 30 Doradus, nebula, variability *(German)* 77−45448
R 136 in 30 Doradus, struct., colour, mass and excitation parameter, photometry obs. *(German)* 80−67825
R associations, early-type stars in CMa R1 and Vel R2, JHKL photometry 77−45505
red dwarf stars, photometric errors rel. to space density 77−5524
red dwarf stars near north galactic pole, vel. dispersion 78−7989
red dwarfs in southern hemisphere, absolute magnitude and distance, BVRI photometry 80−90419
very red giant stars in Fornax galaxy, discovery and BV photometry 80−51768
red giants, in metal-rich globular clusters, near IR photometry 77−45503
red giants in Draco dwarf spheroidal galaxy, metal abundance 80−73030
red giants in globular cluster NGC 6752, DDO photometry and spectra 79−71079
red giants in globular clusters, parametric approach to slope of giant branch 77−53649
red giants in M5 (NGC 5094), intermediate band electronography 78−49490
red stars, RSO 1 catalogue cross correl. with IRC, AFGL and EIC catalogues 80−77511
red variable stars in globular cluster M22, light curves 77−64808
red variable stars in M13, photometric investigation 77−74104
red variables, medium-amplitude, UBVRI obs. 77−82224
reddened star cluster in Ara, IR photometry 77−41395
reddened stars, JHK photometry rel. to near IR interstellar reddening 80−94857
reddening relations in UBV, uvby and Geneva systems 77−22303
RI photometry, response functions from observed and computed (V−R) and (V−I) colour indices 80−56715
Roberts 22, bipolar nebula with OH emission, IR photometry of assoc. A2 Ie star 80−94859
Rosette Nebula, far IR emission from compact sources 77−78841
2S1728−337 vicinity, 5 IR sources detected by K-band photometry 78−54076
2S 1254−690 optical counterpart, identification, photometry and spectrum 79−12545
2S 1702−363 optical counterpart, BV photometry and spectrum 78−54082
2S 1822-371, optical photometry of assoc. star 79−92894
S stars, photometric obs. of unidentified spectral bands 77−22226
S-type stars in Southern Milky Way, objective prism survey and BVI photometry 78−61754
SA 133 field near galactic centre, three-colour stellar photometry *(German)* 80−36618
HM Sagitaae, emission-line star, UBV photometry and spectral obs. in (1978) *(Russian)* 80−36648
U Sagittae, Algol type binary, spectrophotometry 77−2454
FG Sagittae, anomalous planetary nebula, spectrophotometry and UBV photometry (1968 to 1977) 79−88687
WZ Sagittae, B mags. and total visual magnitude estimates 79−21308
UU Sagittae, eclipsing binary, central star of Abell 63 planetary nebula 78−93304

stellar photometry continued
U Sagittae, eclipsing binary, elements determ. from light changes anal. in freq. domain 77−53637
HM Sagittae, emission-line star, polarimetry, (1977 to 1978) *(Russian)* 80−36649
HM Sagittae, eruptive BQ forbidden line star, BVE photometry 78−20835
V Sagittae, light curve coherent oscills. 78−8022
HM Sagittae, near emission-line object, optical and IR obs. 78−36575
FG Sagittae, nonstable star, spectrophotometric obs. 78−28683
HM Sagittae, photometric and spectroscopic obs. rel. to proto-planetary nebula mass ejection 78−85947
U Sagittae, photometric study of eclipsing binary 77−22270
WZ Sagittae, recurrent nova, photometric study at minimum light 78−24513
HM Sagittae, symbiotic star, IR variability obs. from VJHKL photometry *(Russian)* 80−105263
WZ Sagittae, time of minimum light, period, magnitudes 79−21353
HM Sagittae, UBV changes and planetary nebula emission lines 77−71120
HM Sagittae, UBV photometry and spectral obs. (1977) *(Russian)* 79−16991
FG Sagittae, UBV photometry and spectroscopic obs. 77−71119
WZ Sagittae, UBV photometry and spectroscopy of 1978 Dec. outburst 79−12483
HM Sagittae, variable emission object, spectrophotometry 80−17599
WZ Sagittae, visual magnitude 1979 April 8 79−44508
XZ Sagittarii, Algol system, UBV photometric investigation 80−22041
AQ Sagittarii, C star, visible and IR photometry rel. to ang. dia. 80−22008
AV Sagittarii, Cepheid, assoc. with open cluster NGC 6546 disproved 79−58387
V1647 Sagittarii, light curves, photometric elements and apsidal motion 77−60795
V356 Sagittarii, massive eclipsing binary star, spectrophotometry 80−26900
V1437Sagittarii, Population II Cepheid, identification and dist. 80−82396
RY Sagittarii, pulsating R Coronae Borealis star, IR variability 77−45462
MV Sagittarii, R Coronae Borealis variable, brightness decline obs. and UBV photometry 80−8641
KQ Scorpii, long-period Cepheid evidence for membership of OB association 79−88666
U Scorpii, magnitudes and UBVRI photoelectric obs. of 1979 June outburst 79−71049
V861 Scorpii, near IR meas. rel. to orbital phase 78−93324
V861 Scorpii =OAO 1653−40, photometry, spectrum and physical parameters 79−17021
ζ^1 Scorpii (HD 152236), UV spectroscopic and photometric vars. 80−101594
V818 Scorpii (Scorpius X-1), UV, visible, IR and X-ray obs. 80−82541
Scorpius X-1, light and colour curve of periodic variation 77−49497
Sculptor dwarf galaxy, BV photometry and preliminary colour-magnitude diagram 77−53429
RT Sculptoris, close eclipsing binary, uvby light curves 77−60798
AI, WZ and XX Sculptoris, southern δ Scuti stars, photoelectric study 80−90452
ζ Sculptoris (Blanco 1) open cluster, multicolour photometry 78−45372
RY Scuti, eclipsing binary, ephemeris and UBV obs. 80−94832
RZ Scuti, JKL IR obs., light curves for eclipsing binary 80−101615
V373 Scuti (Nova 1975), VBLUW photometry, absolute magnitude, distance and reddening 79−58342
V367 Scuti in open cluster NGC 6649, double-mode Cepheid nature 78−49460
δ Scuti variables, photometric search of Hyades cluster 80−36677
δ Scuti variables, photometric survey of α Persei cluster 78−93246
δ Scuti variables, southern survey 78−96489
δ Scuti-type stars, chromospheric activity and atom. dynamics 77−17581
Scutum Cloud direction field, RGU photometry 79−35242
secondary spectrophotometric standards, obs. in 5840-10800 Å range 79−29995
secondary standards, spectrophotometric obs. rel. to Ap stars HD 10783 and CU Virginis 80−98663
Selected Areas 82 and 107, electrographic extension of UBV magnitude sequences 79−44610
semi-detached systems, revised photometric elements for 8 single-line binaries 80−46611
semi-detached systems, revised photometric elements for 9 binaries 80−46612
semidetached systems, revised photometric elements 80−62193
Serpens X-1 (4U 1837+04), burster optical binary counterpart visible spectra and photometry 80−94891
CV Serpentis, BVRI photoelectric obs., but no eclipse 78−85971
CV Serpentis, IR photometry and CRL 2120 identification 77−78825
Y Sextantis, W Ursae Majoris system, UBV obs., light curve soln. by computer program 80−77454
simultaneous UBV photometry, by fast double head photometer 80−72775
Sk 160, optical counterpart of SMC X-1, VBLUW photometry 77−82277
Skibotn Observatory, in northern light zone, stellar obs. with chopping photometer *(Norwegian)* 78−69699
Skibotn Observatory, in northern light zone, stellar photometric obs. *(Norwegian)* 78−69698
SMC, BV photometry and stellar content of NE outer arm and halo 78−86013
SMC, photoelec. UBV and RI sequences 77−82307
SMC, UBV photometry of open, intermediate and globular clusters 79−17033
SMC Cepheids, five-colour obs. and comparison with galactic Cepheids 77−29923
SMC probable members and foreground stars, spectral types and UBV, photometry 79−40091
SMC Shapley wing, UV obs. from S2/68 sky-survey telescope 79−25717
SMC star cluster colour magnitude diagrams and stellar identification charts 80−73014
SMC wing, photoelectric UBV sequence 78−69874
SMC X-1, VBLUW photometry, evidence for accretion disc 78−12409
SMC X-1, X-ray binary, 5 colour photometry 77−17622
stellar photometry continued
SMC X-2, UBV photometry of proposed optical counterpart 79−67116
SN 1969l in NGC 1058, obs. and theoretical light curves comparisons 77−13370
SN 1973f in NGC 4944, photometric obs. 79−21318
SN 1973r in NGC 3627 BV light curves of type II supernova 77−49407
SN in NGC 4321, JHKL mags., 1980 Jan. obs. 80−41847
solar neighbourhood stars, integrated UBVRIJKL colours 79−44460
solar type stars, thirteen-colour photometry 77−22230
solar vicinity stars, photometric survey rel. to low mass interstellar clouds catalogue 80−36512
solar-type stars, photoelec. scanner obs., search for solar spectral analogues 78−40938
South Celestial Pole stars, extinction and colour coeffs. UBV photoelec. sequence 80−77456
southern Ap stars, photometric vars. *(French)* 79−16981
southern B-type stars, radial vels., spectral types and H β indices 78−12225
southern double stars, magnitude differences, focal grating photometer obs. 80−67785
southern metal-poor stars, UBVRI photometry and UV excesses 80−56828
Southern Milky Way stars, photometry, extinction curves, and R values 77−13443
southern peculiar A-type stars, photometry and atmospheric anals. 78−24517
southern standard stars, monochromatic flux from 3200 Å to 8800 Å 80−51742
southern stars, IR obs. with near photometer 77−26017
southern subdwarfs, UBV photometry, UV excesses 79−5818
speckle interferometry, fringe visibility recovery from recorded images quantised to two levels 78−12104
Spectracon image tubes, operation and results in stellar spectroscopy 77−5451
spectral classification using satellite UV photometric data 78−16402
spectral energy distrib. of eight stars used as spectrophotometric standards 79−35147
spectral energy distributions, results from Fourier transform spectrometry 77−82215
spectral types of stars with unusual photometric indices 79−71033
spectrograph-photometer, four-channel, on Danish 50 cm reflector at ESO, photometric system stability 77−60622
spectrophotometric accuracy, anal. 79−21193
spectrophotometric atlas 78−20657
spectrophotometric scans, catalogue 77−5520
spectrophotometric scans, evaluation 77−9737
spectrophotometric standards, obs. rel. to extinction monochromatic coeffs. on Terksol Peak *(Russian)* 79−44246
spectrophotometric survey of stars along Milky Way in Perseus 78−45403
spectrophotometry with TV-type detectors 77−78646
spectrum variables, He weak and He strong stars 78−4243
SS 433, B V photometry and short-term light vars. (1979 July 23 to September 17) 79−101165
SS 433, IR and visible obs., IR excess and emission processes 80−4387
SS 433, IR light curves from BVIJHK photometry, period and ephemeris 80−8642
SS 433, IR photometry, and search for short period variability 79−58346
SS 433, JHK photometry rel. to IR variability 80−98676
SS 433, light curves, double peak and binary-like period, photometry 80−94804
SS 433, V band photometry and broad min. prediction (1980 April-May) 80−82390
SS 433, visible and JHKL photometry and light vars. periodicity 79−53821
standard stars, IUE photometric calibration, UV spectra 80−77383
standard stars, polarisation obs. by Hatfield near IR polarimeter 79−2482
standard stars for uvby photoelectric photometry south of declination +10°, obs. 77−2347
standard stars for VRI photometry with S25 response photocathodes, obs. 77−2422
stars in field centred at $\alpha=2^h17^m.9$, $\delta=+58°59'$, BV magnitudes and spectral classes *(Russian)* 78−40841
stars in reflection nebulae near Gum Nebula Herbig-Haro objects, UBVRI photometry 78−32449
stars in vicinity of PSR 1913+16 binary pulsar, astrometry and photometry 78−93219
stars near South Galactic Pole, UBV photometry of 51 stars 78−4216
stars occulted by rings of Uranus, 1977-1980, colours and magnitudes 78−16277
stars optically misidentified with extragalactic radio sources, photometry and spectra 78−73708
Stein 2051B, temp. and radius of cool white dwarf 77−13338
Stepanyan's star, spectrophotometric and photometric obs., 228-min period 80−56883
Stephenson-Sanduleak 433, 1.2-2.5 μm spectroscopy, photometry and polarimetry 80−41838
Stock 16, Basel 18, 19, Cr 272 and NGC 5168, open clusters, RGU photometry 78−16474
Stromgren four colour indices, grid for calc. of log g and effective temp. 80−36507
Stromgren photometry of bright southern stars, appl. to spectral classification 79−88645
Stromgren uvby four-colour system bibliography 78−96407
Stromgren uvby photoelectric obs. of stars in dust clouds with bright nebulosities 80−56893
subdwarf stars thirteen-colour photometric obs., sensitivity of indices and evolutionary effects 79−92767
subdwarfs, 37−45 excess calibration using Fe/H abundances 80−82363
subdwarfs, photometry rel. to compositions and kinematics 80−82364
supergiant stars, B2 to G0, small amplitude light vars. 78−32469
supergiant stars, in LMC, long-term light vars. 78−45326
supergiant stars, late-type, in Magellanic Clouds, IR photometry 79−35254
supergiant stars in LMC, spectral types and magnitudes, catalogue of 1882 objects 78−32361
supergiant stars in the SMC 78−16411
supergiants, photometric histories of three highly reddened blue objects 79−5916

stellar photometry continued
supergiants, semi-period of variation for B2 to G0 type stars 78−61854
supergiants assoc. with groups of luminous OB stars, photometry and spectra 77−17555
supergiants in SMC, radial vel. determ. by spectrographic and photometric data study 79−101147
supergiants in SMC 79−101192
supermetallicity and the strong-lined binary systems 79−75204
supernova in anonymous galaxy in Cygnus, photometric and spectrophotometric obs. 79−5847
supernova in anonymous galaxy in Cygnus, UBV photometry and spectrum 79−5846
supernova in IC 5201, UBV photoelectric meas. 79−17000
supernova in NGC 3733, spectrophotometry (1980 March 22) 80−62164
supernova in NGC 4321, type II characts. and 1979 April UBV and visual obs. 79−58364
supernova in NGC 4321, UBV photometry, light curve and type 79−67045
supernova in NGC 4321, UBV photometry 79−53835
supernova in NGC 4321, UBVR photometry 80−77428
supernova in NGC 4321, UBVRI photometry and visual mag. estimates 79−80330
supernovae, BV magnitudes, spectroscopic obs., brightness, distance 79−16999
supernovae, photometric classification *(Russian)* 78−12255
supernovae, Type I, photometric data appl. to Hubble const. determ. 79−40304
supernovae, Type II, photometric classification and observed characts. 79−25621
supernovae, Type II and peculiar, photometric props. *(Italian)* 79−53840
supernovae, type II objects, photometric props. 79−44511
supernovae in NGC 488 and NGC 977, UBV photometry 79−62857
supernovae in NGC 7723, NGC 1325, NGC 4402, UBV photometric obs. 78−16444
symbiotic star candidates in LMC, optical spectroscopy and IR photometry 80−62139
symbiotic stars, IR variability and nature 77−49399
symbiotic stars and recurrent novae, high speed photometry 77−60799
68 Tauri, Am star, photoelectric UBV obs. of magnetic field *(German)* 77−17586
V471 Tauri, BV photometry of white dwarf eclipsing binary, light curve vars. 78−96508
RW Tauri, eclipsing binary, elements determ. from light changes anal. in freq. domain 77−53637
CD Tauri, eclipsing binary, orbital element determ., BV photometer obs. 80−73000
λ Tauri, eclipsing binary, photometric elements, masses, radii, luminosities 78−28723
CD Tauri, eclipsing binary star, intermediate-band photometric anal. 77−13389
SU Tauri, emission lines at min. and BV photoelectric photometry 80−8640
DR Tauri, highly variable young star, spectrometric and photometric obs. 78−20829
T Tauri, integral brightness and Hα emission vars., 1971-77 period *(Russian)* 78−61852
λ Tauri, massive eclipsing binary star, spectrophotometry 80−26900
44 Tauri, periodogram analysis of light curves of δ Scuti star 79−84799
SU Tauri, R Coronae Borealis star, photometry in optical and IR ranges 80−101601
RR Tauri, rapid periodicity, photometric investigations 80−26853
V471 Tauri, U photometry of eclipses and flares 79−71072
RW Tauri, UBVRI light curves of Algol-type eclipsing binary 77−91577
SU Tauri, visible and IR photometry and polarimetry *(Russian)* 78−61860
α Tauri (Aldebaran), radius from 1978 Aug. 26 occultation fast photometry 79−67005
V471 Tauri (Bd+16°516), Ca II H and K and Hα line vars. 79−67063
V471 Tauri (BD+16°516), eclipsing binary white dwarf, spectroscopy and photometry rel. to evolution 77−57028
V711 Tauri (HR 1099), 1977-1978 photometry before radio outburst 79−21337
V711 Tauri (HR 1099), 1978 photometry during radio outburst 79−21338
V711 Tauri (HR 1099), RS Canum Venaticorum star, BV light curve during (1978-79) 80−105279
20 Tauri (Maia) and related stars, photometric constancy 79−58338
BU = 28 Tauri (Pleione), UBV obs. and light curve 77−56979
BU Tauri (Pleione), UV photometry during shell phase 77−64768
RV Tauri and yellow semiregular variables, photometric investigations 80−26865
T Tauri like stars, far UV photometry 78−20827
T Tauri star, extremely young, and assoc. nebula, fading 78−93236
T Tauri stars, photometric and spectral props. 79−21282
T Tauri stars, photometric vars. 77−9741
T Tauri stars, seven-colour TV photometry, obs. methods *(Russian)* 77−64756
T Tauri stars, seven-colour TV photometry, variability *(Russian)* 77−64757
T Tauri stars and Herbig Ae-Be stars, broad-band IR photometry 78−4217
T Tauri stars and related objects, UBV photometry 79−44499
T Tauri stars in Orion population, UBV photometry of young emission-line objects 80−46552
RR Telescopii, nova-like variable, spectrophotometry 77−45460
BL Telescopii A, yellow variable supergiant near Cepheid instability strip, VBLUW photometry 80−98672
Tr 22, open cluster, photoelec. and photographic photometry of member stars 79−17032
Trapezium type systems, UBVRI photometry 79−44558
Trapezium-like objects, visual and IR photometric obs. 79−92805
Trapezium-type systems, UBVRI photometry 80−82431
RW Trianguli, short-period close binary, circumstellar material size and brightness vars. 78−32512
EK Trianguli Australis, peaks in lightcurve during 1979 June outburst 79−75222
EK Trianguli Australis, SU Ursae Majoris dwarf nova, superhumps, light curve UBV obs. 80−105255
U Trianguli Australis, UBVRI obs. of beat Cepheid, pulsation energy changes 80−4360
stellar photometry continued
U Trianguli Australis, UBVRI obs. of beat Cepheid 79−53833
Trumpler 15 in η Carina, open cluster, age and reddening from UBVRI obs. 80−90487
Trumpler 27, heavily-reddened young open cluster, spectra and photometry 77−78836
Trumpler 27 star 28, obs. of WC9-type star with large IR excess 80−67738
Trumpler 37, young open cluster, stellar UBV magnitudes and MK classifications 77−22284
47 Tucanae, colour-magnitude diagrams for inner regions 78−57598
AQ Tucanae, eclipsing binary, UBV photometry, light curves 79−8951
47 Tucanae, globular cluster, photometry and spectra rel. to stars chemical comp. 80−46620
47 Tucanae, globular cluster, UBV photometry 77−37630
47 Tucanae, metal-rich globular cluster, UBV photometric study 77−57065
47 Tucanae stars, spectra and photometry rel. to N anomaly 79−48867
4U 0115+634, X-ray binary, 1980 Aug. photometry and spectroscopy 80−101650
4U 0115+63, transient X-ray source optical candidate, UBV photometry and spectrum 78−32605
3U 1538-52 field, photometric search for optical candidates 78−12412
4U 1543−62 optical candidate, UB photometry 78−77625
4U 1626−67, UBV photometry of X-ray pulsar candidate 79−17130
4U 1626−67, X-ray pulsar optical candidate, UBV photometry 78−12418
4U 1626−67 optical counterpart, photometry 79−67120
4U 1636−53 (MXB 1636−53), X-ray burster optical candidate, UBV photometry 78−12418
4U 1735−44 (MXB 1735−44), X-ray burster optical candidate, UBV photometry 78−12418
4U 1755−33 optical candidate, photometry and spectrum 78−77625
3U 1956+11 optical counterpart, photometry and spectrum 78−49554
4 U 2129+47 optical counterpart, spectrum and photometry rel. to 80−17693
UBV and DDO photometry of stars and open clusters rel. to metallicity gradient across galactic disk 79−48905
UBV for S. Milky Way, stellar distrib. and colour excess obs. 80−85997
UBV obs. of faint blue stars in young cluster fields 79−21291
UBV photoelastic photometry, homogeneous data catalogue 78−96409
UBV photoelec. obs. of Cepheids in Magellanic Clouds, Wesenheit function, reddening corrections 77−91553
UBV photoelectric photometry, general catalogue on mag. tape 77−78656
UBV photoelectric photometry of M31 clusters *(Russian)* 80−36680
UBV photoelectric sequence for studies of NGC 55 galaxy 80−73007
UBV photoelectric sequences, in fields of eight low-red shift quasars *(French)* 80−51904
UBV photoelectric standards in SA 1-115, final catalogue 80−41733
UBV photometric colour indices, rel. to LTE/non LTE atmospheres boundary 79−35236
UBV photometric data, surface distribs. on celestial sphere 77−2423
UBV photometric standards *(Polish)* 78−89082
UBV photometry for N.Norway during auroral activity, technique and results 79−40084
UBV photometry of stars in field of IC 1795 (W3) 77−57082
UBV photometry of stars in open clusters in Cassiopeid *(Russian)* 79−92812
UBV reductions, influence of Balmer discontinuity 77−74046
UBV system, uniform transitions for extinction coeffs. 80−67408
UBVR photoelectric sequence in Piscis Austrinus 80−62201
UBVR photometric sequences around globular clusters (NGC 5946, 6440 and 6624) 79−88702
UBVRGI photometric measurements of 1297 stars, catalogue on mag. tape 78−40839
UBVRI equatorial extinction star network 79−84827
UBVRI equatorial photoelectric sequences 79−62875
UBVRIJKLMNH photoelectric photometric catalogue on mag. tape 79−16842
RU Urase Minoris, photometric obs. of contact binary 77−74088
γ Ursae Majoris, Ap star, chemical element distrib. from spectrophotometry *(Russian)* 77−22238
CQ Ursae Majoris, Ap star, UBV photometry, light curves, colour indices 78−49454
CQ Ursae Majoris, Ap star, UBV photometry, light vars., period determ. 79−88667
VV Ursae Majoris, BV photometry and elements of eclipsing binary 77−26026
TX Ursae Majoris, close eclipsing system, freq. domain anal. of light changes 77−53638
AW Ursae Majoris, contact eclipsing binary, polarisation obs. 77−45489
XY Ursae Majoris, eclipsing binary, light curve changes, starspot activity 77−57044
XY Ursae Majoris, eclipsing binary, photometry and spectrum rel. to spot activity on primary component 80−109491
UX Ursae Majoris, eclipsing binary, time series photometry 80−77446
AN Ursae Majoris, nova-like variable, light curve and circular polarisation obs. 78−8018
W Ursae Majoris, OAO-2 UV photometry 77−13393
AN Ursae Majoris, polar, IR photometric obs. 80−98687
AN Ursae Majoris, steady low luminosity state 79−40219
W Ursae Majoris, uvby obs. 79−44533
W Ursae Majoris, vars. of period and light curve of eclipsing binary *(Italian)* 78−93318
W Ursae Majoris type systems, UVBY photometry 77−57056
RT Ursae Minoris, photoelectric obs. of eclipsing binary 77−82276
α Ursae Minoris region, field stars uvbyβ photometry rel. to reddening of Polaris 79−58356
US Naval Observatory data associated with stellar parallax determ. 80−72788
Utrecht photometric system and adopted standard stars 80−62202
UV 1758+36, He deficient hot subdwarf B star, atm. parameters, radial vel. 78−53944
UV and X-ray sources, objective prism spectrophotometry 78−8150
UV flux measurements, comparison of S2/68 and OAO-2 calibrations 77−87372
UV photographic photometry from Skylab 77−60608
UV photometry from Cosmos 215 satellite *(Russian)* 77−64750
UV photometry from S2/68 obs. on TD1 satellite 77−78775

stellar photometry continued
uvbyβ and prediction of MK spectral classification, general case 80−82216
uvbyβ photoelectric photometric catalogue 80−62036
uvbyβ photometry appl. spectral classification prediction with assumed luminosity class 80−67700
uvbyβ system, absolute luminosity calibrations check by means of small trigonometric parallaxes 78−57463
uvby Hβ photometry of spectroscopic binaries, G-type dwarfs and early type FK4 stars 77−82275
uvby Hβ system, empirical calibration for B-type stars 78−32454
uvby photometry, theoretical analysis 78−85930
uvby photometry of bright northern stars with interesting Stromgren indices 80−56817
uvby system, abundance effects 77−29808
uvby system, reddening determ. method 78−73655
variable emission-line star in core of M15, spectrum, photometry and position 79−5840
variable stars, 3-colour photoelectric obs. at Mt. Kobau (1970-3) 77−56955
variable stars, reduction of obs. to standard photometric system *(Russian)* 77−64657
variable stars, UBV photometry at geographic latitude 69°22′ north 79−44376
variable stars in globular cluster NGC 1261, Oosterhoff type I system 77−53651
variable stars in globular cluster NGC 5286, B photometry, cluster membership 78−32534
variable stars in globular cluster NGC 6934, photometry 80−56891
VB10, spectrophotometry rel. to low luminosity M-type dwarfs optical spectral classification 79−58339
VBLUW photoelectric photometric catalogue on mag. tape 80−36515
vector space methods of photometric anal., appls. to O stars and interstellar reddening 78−49338
Vela, spatial distrib. of young stars, UBV obs. 77−37597
Vela X-1 (HD 77581), X-ray binary, uvby obs. 77−37668
γ^2 Velorum, bright Wolf-Rayet binary, optical light curve 77−56945
AH Velorum, classical cepheid, binary detect., UBV obs. 80−109443
AI Velorum, dwarf Cepheid, nature from uvbyβ photometry 77−78801
CV Velorum, light curves, photometric elements and absolute dimensions 77−60796
RZ Velorum, long-period Cepheid evidence for membership of OB association 79−88666
γ Velorum, multiple system, photometric obs. 80−90482
AI Velorum, nature from BVRI photometry and photoelectric radial vels. 80−94815
AH Velorum, radius, delta luminosity and pulsation mode of δ Cepheid 80−46572
δ Velorum, UV spectra, comparison of synthetic and observed spectra 77−29820
γ^2 Velorum, WR binary, photometry and polarimetry 77−29847
Vilnius photometric catalogue on mag. tape, description 80−98578
BF Virginis, β Lyrae-type eclipsing binary, light curves 77−13395
AH Virginis, eclipsing binary, photometry rel. to period and light curve vars. 77−78822
DL Virginis, eclipsing binary in triple system, UBV photometry 78−8050
CU Virginis, He spectrum variable, UV photometry with ANS 78−36585
XX Virginis, Stromgren uvbyβ photometry of field BL Herculis star 78−85954
CU Virginis (HD 124224), Ap star, spectrophotometric obs. 80−98663
W Virginis stars, in southern hemisphere, VBI photometry 77−53612
visual double stars, spectral classification and UBV photometry 77−74084
visual surface brightness depend. on colour, model stellar atm. calcs. 80−67707
Vulpecula OB2 stars, photometry and spectra rel. to membership of 67 day Cepheid S Vulpeculae 80−41831
15 Vulpeculae, Am star, photoelectric UBV obs. of magnetic field *(German)* 77−17586
SV Vulpeculae, Cepheid, period change meas. rel. to evolution 79−92777
21 Vulpeculae, new luminous long period δ Scuti star, photometry 80−31306
BS Vulpeculae, photoelec. photometry of eclipsing binary, light curve, period 79−21351
BW Vulpeculae, UV light curve of β Cephei-type star 78−36570
BW Vulpeculae, V photometry, light curve, quadratic ephemeris 80−26881
NQ Vulpeculae (Nova 1976), IR photometry, dust form. in exploded shell 79−48832
NQ Vulpeculae (Nova 1976), isothermal dust condensation phase, broad-band photometry 78−36586
NQ Vulpeculae (Nova Vulpeculae 1976), photoelectric obs. 78−4252
NQ Vulpeculae (Nova Vulpeculae 1976), photometric obs., visual magnitudes 77−60767
W3, dusty H II region, stellar UBVRI photometry and optical polarisation meas. 78−45379
W92, possible gravit. contracting binary system in NGC 2264 young cluster 78−32462
Walraven VBLUW photometric system, props. 77−17377
Washington Photometric System, props. and standard stars 80−31213
Wat 6, open cluster, photometry and spectra rel. to proximity to (Pismis 6 and 8) 79−88712
weak G-band stars, photometry and spectra 77−49386
weak G-band stars, photometry rel. to nature and evolution 78−49432
weak-G-band stars, CO 2.3 μ band strength 78−12228
wedge-sensitometer for photographic photometry *(Japanese)* 79−44373
white dwarf C_2 stars, spectrophotometry 77−29824
white dwarf stars, two-colour diagram rel. to masses and radii 80−46547
white dwarfs, calibration of photometry 78−85938
white dwarfs, cool, IR photometry, atm. comp. 79−16950
white dwarfs, HR-diagram and luminosity function determ. *(Chinese)* 80−77403
white dwarfs, search at south galactic pole 79−21274
white dwarfs, southern, Stromgren photometry 78−32456
white dwarfs, spectrophotometry with Carnegie image tube 78−57466
white dwarfs, uvby photometry of 112 southern objects 80−8624
white dwarfs, visual surface brightness relation appl. 78−81624

stellar photometry continued
white dwarfs in open clusters, obs. rel. to progenitor stars upper mass limit 80−51738
white dwarfs with He lines 77−53588
wide visual double stars, B, A and F type, uvbyβ photometry 79−17025
Wolf-Rayet stars, 2 to 4 μm spectrophotometry of late WC stars 78−96491
Wolf-Rayet stars, ANS UV spectrophotometric obs. 80−22023
Wolf-Rayet stars, faint, photometry and spectrography 79−40200
Wolf-Rayet stars, IR light vars. 77−9750
Wolf-Rayet stars, WC9, optical spectropolarimetry and spectrophotometry 77−64778
X-ray binary stars, optical photometry and spectra 78−12429
yellow semiregular and RV Tauri variables, photometric investigations 80−26865
young Orion stars, scanner K-line photometry 77−33579
II Zw 136, Seyfert galaxy nuclei, optical variability, UBV obs. 80−73049
Ba, CH and R-type carbon stars, spectrophotometry 77−17575
Ba II stars, JHK photometry 77−74053
Ba II stars, uvby photometry rel. to s-process element enrichment 79−58337
Ba stars, DDO system photometry, luminosity anomaly 79−35246
Ba stars, spectroscopic, radial vel. and photometric obs. 78−12226
C and M-type giant stars distrib. in galactic nucleus and Magellanic Clouds 78−32460
C star, variable, in open cluster, Stock 8, spectroscopic and photometric obs. 79−84791
C stars, 3 μm absorpt. band obs. 78−28682
C stars, catalogue of 302 stars in LMC 78−20654
C stars, in LMC, VRI photometry, optical spectroscopy and evolutionary implications 79−71019
C stars, JHKL photometry 80−46555
C stars, photometry at 1-2.5 μm, circumstellar dust shells 79−88652
C stars, spectral clssification by photoelec. photometry of line strengths 78−73711
C stars, spectrophotometry, C/O and $^{12}C/^{13}C$ ratios calc. 77−91533
C stars, variable, IJHKL photometry obs. 80−98657
C stars in Cygnus, new discoveries and BV photometry 80−46551
C stars in NGC 419, SMC globular cluster, photographic photometry 78−53962
CH stars in south galactic cap, radial vels., photometry 77−87396
Ca II H and K emission, flux meas. by four-channel photon-counting spectrophotometer 78−73646
H deficient and He weak stars, uvby photometry, variability 80−46579
Hα emission line star near Gum nebula, UBVRI photometry and variability 78−32449
Hα emission stars in and near NGC 7000, search for variability 77−13363
Hα emission stars in southern dark clouds, UBVR photometry 78−81633
Hα emission stars in young cluster NGC 2264, UBVRI obs., pre-main sequence stars 79−35267
Hα photometry through narrow-band interference filter 77−56838
Hβ indices, calibration and instrumental considerations 79−96923
Hβ indices for model atms., B-type stars appl. 80−31292
Hβ system, bibliography 78−96407
He I 4026 Å narrow-band index for B-type stars in young clusters and associations 77−29887
He variable stars, IR photometry and IR excesses 80−67733
He-weak stars, photoelectric meas. of H Balmer lines 79−16994
HgMn stars, spectrophotometry 80−26867
Hγ equivalent width computation method for objective-prism astrograph, for SMC stars 78−57462
RR Lyrae stars in Sonneberg fields near north galactic pole, distances, density distrib. 77−82229
OH 26.5+0.6, late-type variable star, spectrophotometry from 2 to 40 microns 78−24568
OH/IR stars, IR search and photometry 78−24510
Si stars, UVBY photometry, variability obs. 77−22233

stellar positions *see astrometry*

stellar radiation
see also solar radiation; stellar photometry
10-day Cepheids, theoretical models and light curves, comparison with obs. 78−49449
1732−303, 1745−248, new X-ray burst sources, discovery and identifications with globular clusters (Terzan 1, 5) 80−98739
2A 0042+323 (3U 0042+32), periodic behaviour rel. to binary nature 78−54089
2 A 0311−227, IR flickering obs. 79−40298
2A 0311−227, optical counterpart, AM Herculis type eclipsing binary, V-band obs. 80−101617
2A 0311−227, optical counterpart identification and X-ray meas. 79−30149
2A 0311−227, soft X-ray emission from AM Herculis-type system 79−101219
2A 0311−227, variable soft X-ray source discovery 79−35434
2A 0311−227, X-ray flux modulation period from HEAO obs. 80−77516
2A 0526−328, optical counterpart position and spectrum 79−5925
2A 0526−328 optical candidate, rapid brightness vars. obs. 80−51917
2A 0526−328 optical counterpart, X-ray emitting cataclysmic variable, spectrum and photometry 79−97103
A 0535+26, transient X-ray source, flare obs. by (Prognoz 6) *(Russian)* 80−51920
A-type stars, Lyman α effect on non-LTE model atmospheres 80−90422
A-type stars, uvbyβ calibrations 80−41820
Abell 46, planetary nebula, eclipsing binary nucleus, hot component UV continuum obs. by IUE 80−98693
aberration of light rel. to spectral type *(German)* 78−73702
absolute luminosity calibrations, consistency 80−62111
absolute magnitude determ. methods 78−96405
absolute magnitudes determination, comparison between Geneva photometric boxes and MK spectral types 80−77385
absolute magnitudes of stars in the same seven colour photometric box 78−28662
accreting magnetic degenerate dwarfs, X-ray and UV emission 80−41826
accreting magnetic white dwarfs, cyclotron emission 77−45427

stellar radiation continued
accreting nonmagnetic degenerate dwarfs, X-ray and UV radiation 79 40184
accreting white dwarfs, pulsed UV radiation from hot spots 77−13343
accretion discs, secondary winds and evaporation 77−64751
accretion disks round neutron stars and white dwarfs, flux distrib. and colours 80−94778
Algol, orbit, lightcurve and struct. review 80−109460
Am stars, τ Ursae Majoris and 15 Vulpeculae, energy distrib. from spectral obs. 80−85949
amplification by turbulent atm. 80−72782
RT Andromedae, light curve anal. of short period eclipsing binary 80−46603
BX Andromedae, period increase *(Chinese)* 78−36642
λ Andromedae, radio emission detect. from giant binary 77−22248
o Andromedae, shell star, lack of linear polarisation variability 80−62157
Z Andromedae, symbiotic star, hot stellar UV contiuum identification from IUEobs. 80−109450
Z Andromedae, UV spectra, 1979 Feb. 17, quiescent phase 79−40202
RT Andromedae, V photoelectric obs. and lightcurve 79−71073
AB Andromedae, W Ursae Majoris type star, 1.2 and 2.2 micron light curves 79−84822
Ap and Am stars, bolometric magnitudes 79−16970
Ap stars, Barnes-Evans relation appl. as clue to atmospheric struct. and evolutionary status 79−67011
Ap stars, line blanketed model atmospheres rel. to photometric props. 79−44495
Ap stars, long-term light variations *(German)* 77−17585
Ap stars, photoelec. obs. of light vars. *(German)* 78−20841
Ap stars, photoelectric parameter of peculiarity 77−2433
Ap stars, radiative forces in stellar envelopes rel. to He abundance anomalies 80−31291
Ap stars, reddening-free parameters rel. to recognition in Vilnius photometric system 78−65635
Ap stars broad flux depressions, comparison between synthetic spectra and spectrophotometry 80−67735
S Apodis, R Coronae Borealis variable, visual magnitude estimates 77−53611
AE Aquarii, cataclysmic variable, rapid light oscills. rel. to white dwarf oblique rotator model 80−36634
R Aquarii, Mira variable, 14.9 GHz obs. 79−75210
EE Aquarii, UBV photometry of β Lyrae-type eclipsing binary 79−84817
R Aquarii, UBVRI polarimetric obs., orbital motion effect *(Russian)* 80−36646
R Aquarii, UV, visible and 85 GHz continuum obs. 80−85946
R Aquarii (M7+pec), late type variable star, IUE obs. of circumstellar emission 80−82370
π Aquarii and other Be stars, light variations 77−45420
Aquila X-1, nature of X-ray outbursts 78−20909
Aquila X-1, X-ray outburst obs. (1978 June 14 to 22) 78−65721
Aquila X-1 (4U 1908+00), optical outburst, obs. 78−69911
Aquila X-1 (4U 1908+00), optical outburst obs. 80−67909
Aquila X-1 (4U 1908+00), X-ray outburst obs. 80−77514
V603 Aquilae, accretion disc radiation of cataclysmic binary 77−91537
V794 Aquilae, AM Herculis-like brightness vars. 79−92804
η Aquilae, Cepheid variable, absolute energy distrib. in radiation spectrum *(Russian)* 80−72974
η Aquilae, classical Cepheid, UV obs. and companion star detect. 80−90443
V342 Aquilae, eclipsing binary, period and light curve changes, (1966 to 1976) 80−67791
β Aquilae, single G-type subgiant, UVB photometry 79−62823
V603 Aquilae (Nova 1918), IUE obs. of periodic light vars. 80−105251
V603 Aquilae (Nova 1918), old nova, eclipses obs. 80−90476
V603 Aquilae (Nova 1918), periodic light vars. detect. 80−82391
V1301 Aquilae (Nova Aquilae 1975), dust grain IR emission model 80−105254
R Aquilae Mira variable, 14.9 GHz obs. 79−75210
Ariel 0327+43 new X-ray source near Nova Persei 1901, discovery 78−69910
Ariel 0535+26, flaring X-ray source, 2 cm obs. 78−54081
Ariel 0535+26, transient X-ray source, new pulse period data 79−44635
Ariel 0535+26 (HDE 245770), recurrent X-ray transient, further outburst 79−40300
Ariel 1524-61 optical counterpart, identification and light curve 77−45611
Ariel 1540−53, eclipsing X-ray binary pulsator 78−8151
UX Arietis, binary star, radio obs. 77−64793
UX Arietis, RS Canum Venaticorum binary, two-freq. radio polarimetry 79−21335
β Arietis, var. of highly eccentric spectroscopic binary 79−17026
atmosphere in statistical equilib., effects of deviations from LTE on emergent spectrum 80−31290
atmospheric extinction, allowance for IR absorpt. by H_2O mols. *(Russian)* 78−40832
atmospheric scatt., approx. soln. *(Russian)* 80−36621
59 Aurigae, δ Scuti star, absolute magnitude, effective temp. and mass from light curves periodogram anal. 80−62141
KR Aurigae, brightness history from 1890 AD 80−105245
ε Aurigae, dual aspect of wavelength depend. fluctuations 80−62190
ε Aurigae, eclipsing binary, distance and absolute visual magnitude 79−53859
ε Aurigae, eclipsing binary, parallax and absolute magnitude from astrometric study 78−89219
IU Aurigae, eclipsing binary, variable light curve 77−17627
EO Aurigae, eclipsing binary star, revised elements from light curve anal. 80−90471
IU Aurigae, light curve study of early-type close binaries in triple systems 78−89222
IU Aurigae, massive triple system, component stars luminosities 77−64798
LY Aurigae, tidal effects in O-type eclipsing binary system 79−25638
KR Aurigae, X-ray source nearby, X-ray, IR and visible obs. 80−67742
KW Aurigae (14 Aurigae A), pulsating ellipsoidal variable, masses, radius and luminosity from tidal modes 79−97028
α Aurigae (Capella), intense line emission in soft X-ray spectrum 78−93228
B5 V-P5 V type stars in Geneva Observatory catalogue, radii, temp. and brightness determ. 80−77396

stellar radiation continued
B, A and F stars in selected areas, intrinsic uvby β indices, distances and colour excesses 78−89171
B 1900+14, soft gamma-ray bursts obs. *(Russian)* 80−36742
B stars, empirical effective temp. determ. 80−101587
B stars, seven new stars with Hα emission lines *(French)* 77−49391
late B-type main-sequence stars, C I as continuous opacity source 77−87393
B-type stars, He weak, UV flux distrib. 78−96477
B-type stars, luminosity and effective temp. determ. 80−17582
B-type stars, optical counterparts of X-ray sources, luminosity class from O I 7773 Å triplet absorpt. 79−71031
B-type stars, XUV obs. and constraints 78−93232
B-type stars at high southern galactic latitudes, four colour and Hβ obs. 80−82357
B-type stars embedded in R-associations, free-free emission obs. 80−26851
(B-V), $(V-I_{KC})$ diagram, intrinsic lines 78−73704
Balmer discontinuities, effects of line blocking 77−45419
Barnes-Evans brightness/colour relation, appl. to radii determ. for nearby stars 78−7984
BD-3°5357, eclipsing binary with hot subdwarf component 77−91574
Be and shell stars, UV radiation deficiency, TD-1 satellite obs. 80−90438
Be stars, correl. between presence of Paschen emission lines and IR excess 77−22234
Be stars, identification as X-ray sources 77−87573
Be stars, intrinsic circumstellar polarisation and apparent rot. speed interpretation 78−96484
Be stars, polarimetry at 1.25 and 2.2 microns 79−44484
Be stars, UV radiation intensity obs. *(French)* 78−81635
Be stress, bright, Hα emission variability 79−67027
Be-stars, energy distrib. in 0.32 to 1.06 μ range 77−56980
Be-stars, intrinsic linear polarisation rel. to v sin i 77−60773
Be-stars, intrinsic polarisation 79−75213
Be-stars, photographic IR spectroscopy and near IR photometry 77−56991
Be-stars, polarisation in extended circumstellar discs 77−56994
Be-stars, radiative accel. in extended atmospheres 77−56996
Be-stars, radio obs. 77−56984
Be-stars, UV fluxes 78−61870
binary and multiple stars, polarisation by Thomson scatt. in optically thin stellar envelopes 78−81655
binary star gravitational radiation, limits on finite size effect 77−33337
binary star light and velocity curves simultaneous solution, eccentric orbit generalisation 80−36664
binary stars, reflection effects evaluation, generalised approach 79−25631
binary stars, review of X-ray emission 80−109564
binary stars with single optical component, ellipsoidality effect on light vars. 79−92806
binary system gravitational radiation, relativistic corrections and spectrum fine structure 80−90479
binary systems, radiation pressure force influence on critical surfaces 78−96505
black hole, disc accretion at subcritical luminosity 77−64791
black hole, spherical, with thin accretion disc, image 79−67049
black hole explosions, theory of optical and radio detect. 77−53622
black hole radiance, Planck spectrum, local calc. 78−45354
black holes, accreting, gamma rays emission spectrum 78−32504
black holes, rotating, neutrino fluxes resulting from macroscopic parity violation 80−22034
black holes, supercritical accretion discs luminosities 80−105272
black holes, theory, of rapid X-ray variability and dying pulse trains 80−56872
black holes, thick accretion discs models rel. to supercritical luminosities 80−101614
black holes, X-ray radiation polarisation features 80−46700
black holes in binary stellar systems, gamma emission during spherically symmetric accretion 80−17608
blanketing effect by TiO absorption *(Russian)* 79−30065
UZ Bootis, cataclysmic variable similar to WZ Sagittae, outburst charcts. 80−17596
α Bootis, comparison of predicted and observed spectral energy distrib. 80−46546
ZZ Bootis, double spectrum eclipsing binary, revised spectrographic and photometric elements 78−61885
44=i Bootis, eclipsing binary, variable light curve obs. and implications 78−61887
η Bootis, soft X-rays detect. with imaging X-ray telescope 79−48953
SS Bootis, UBV obs. and Fourier anal., eclipsing RS Canum Venaticorum binary 80−17613
44 i Bootis, W Ursae Majoris type star, 1.2 and 2.2 micron light curves 79−84822
α Bootis (Arcturus), UV search for flux variability 78−81620
α Bootis (Arcturus) (K2 IIIp), Wilson-Bappu effect, explanation from theoretical temp. minima 79−62825
BPM 30551, ZZ Ceti type white dwarf, high-freq. oscills. 77−2445
brightness distrib. of stellar disc, determ. from photoelec. obs. of lunar occultations 79−35146
Z Camelopardalis, dwarf nova, photometric obs. and light curve (1973-77) 80−56853
AY Camelopardalis, eclipsing variable, element determ. by Fourier anal. of light curve 77−45484
RU Camelopardalis, photometric behaviour, (1966 to 1977) 78−89206
RS Cancri, late-type variable star, spectral energy distrib. and spectral types *(Russian)* 78−40958
WY Cancri, light curve of eclipsing system, UBV photometry 77−37619
BT Cancri (38 Cancri), δ Scuti star, multiple periods rel. to radial and nonradial pulsation periods 80−85948
α Canis Majoris, EUV obs., Sirius B model atm. 77−33489
YZ Canis Majoris, flare star, coordinated X-ray, optical and radio obs. 78−8012
W Canis Majoris, luminous C star in Canis Major OB1 78−12312
VY Canis Majoris, mass, luminosity and evolutionary state from relation to mol. cloud complex 78−24536
VY Canis Majoris, OH and H_2O microwave maser emission obs. 78−53949
VY Canis Majoris, OH/IR star, 1612 MHz OH maser multibaseline VLBI obs. 80−12766

stellar radiation continued
α Canis Majoris (Sirius B), EUV obs., evidence against photospheric origin of 0.25 keV flux 78−49481
α Canis Majoris B, acoustically heated corona rel. to X-rays 77−60755
α Canis Majoris B (Sirius B), minimum flux H coronal model rel. to X-ray emission 80−8626
α Canis Majoris B (Sirius B), search for far UV emission 79−5821
α Canis Majoris B (Sirius B) corona model constraints rel. to X-ray emission 79−2543
β Canis Majoris stars, observational aspects of multiperiodic light vars. 77−87424
β Canis Majoris stars, UV flux obs., basic data obtained with TD-1A satellite 80−51783
β Canis Majoris variables, luminosity calibration and evolution 78−96488
YZ Canis Minoris, red dwarf star, weak radio flares interferometric obs. 78−65633
Y Canum Venaticorum, C star, IR spectrum between 1.2 and 30 microns 80−46544
RS Canum Venaticorum, intrinsic linear polarization of eclipsing binary 80−4394
α^2 Canum Venaticorum, mag. Ap star high-resolution polarisation obs. inside spectral line 78−40951
RS Canum Venaticorum, out of eclipse light var. and comparison with similar stars 80−109489
RS Canum Venaticorum, quiescent X-ray emission obs. 78−81659
RS Canum Venaticorum, radio flare obs., (1979, February 6) 79−40220
α^2 Canum Venaticorum, UV flux distrib. 79−80313
RS Canum Venaticorum binaries, effects of tides and flares 79−71068
RS Canum Venaticorum binaries, multiperiodic light and spectrum vars. 77−87479
RS Canum Venaticorum binary stars, mag. starspot model for photometric and spectroscopic behaviour 80−109488
RS Canum Venaticorum binary stars, radio luminosities and spectra 79−21333
RS Canum Venaticorum stars, intrinsic light vars. due to starspots, model 79−35295
RS Canum Venaticorum systems, X-ray emission progress report 79−21345
RS Canum Venaticorum type binaries, Hγ line vars., chromospheric diagnostics 80−62181
α^2 Canum Venaticorum type stars, dynamical parallax, absolute magnitudes and masses *(Russian)* 79−88690
RS Canum Venaticorum-type binaries, light curve distortions rel. to emission line vars. 78−24527
Carina spiral arm, starlight as S.Celestial Pole nebulosity illumination source 79−92839
χ Carinae, β Canis Majoris type variability discovery from UBV photometry 79−80326
VY Carinae, Cepheid, luminosity and membership of assoc., visible obs. 80−94797
VY Carinae, cepheid variable, absolute magnitude 77−64764
l Carinae, Cepheid variable, Fourier anal. of light var. 80−90442
OY Carinae, eclipsing ultrashort periodic dwarf nova discovery 79−53823
η Carinae, high-resolution IR radiation maps of homunculus, spectral and spatial distrib. 80−12767
η Carinae, interstellar colour excess rel. to distance 77−64744
R Carinae, intrinsic linear polarisation narrow-band struct. 77−49397
η Carinae, ionising photons emission rel. to spectral obs. at 4 microns 78−4237
η Carinae, light and spectrum vars. and interaction with Carina Nebula 77−45433
η Carinae, possible assoc. with X-ray source 77−2492
η Carinae, reddening of optical radiation 77−41385
η Carinae, soft X-ray results from OSO-8 Wisconsin Expt. 78−36722
ν Carinae, X-ray emission obs. from star and surrounding nebula 80−26876
η Carinae and Carina Nebula, polarimetric study 79−67043
Cassiopeia A supernova, low luminosity rel. to identification as black hole 79−75244
SX Cassiopeiae, Algol type binary, spectrophotometry, u.v. excess 77−2454
γ Cassiopeiae, Be star, polarisation rapid vars. 80−22022
γ Cassiopeiae, Be star, rapid linear polarisation variability *(Russian)* 80−77417
SU Cassiopeiae, Cepheid variable, spectrophotometric determ. of temp. and luminosity 80−90435
TU Cassiopeiae, double-mode Cepheid, periods and amplitudes 79−48804
VX Cassiopeiae, early-type irregular variable, photometric variability *(Russian)* 80−72973
TV Cassiopeiae, eclipsing binary, period and UBV light curves 78−4287
OX Cassiopeiae, eclipsing binary, photometric radii and luminosities 80−56877
κ Cassiopeiae, effective temp. radius, mass loss and luminosity 80−51748
YZ Cassiopeiae, Fourier analysis of light curves for transit eclipses 78−96506
γ Cassiopeiae, Hα linear polarisation in Be star 78−16425
TV Cassiopeiae, light curve, long period var. interpretation 79−101174
TV Cassiopeiae, light curve and orbital elements of eclipsing binary 77−49430
γ Cassiopeiae, polarisation obs. rel. to circumstellar envelope model 78−40952
TU Cassiopeiae, UBV photoelectric obs. of double-mode Cepheid, light curve 78−77556
o Cassiopeiae (HD 4180) Be star, IR photometric vars. rel. to optical spectrum vars. 79−58353
V509 Cassioperae (HR 8752), light vars. during period of spectrum vars. 79−101161
cataclysmic binaries, accretion disk radiation emission 77−82247
cataclysmic binaries, circumstellar material geometrical and photometric parameters 80−109492
cataclysmic binary stars (CBS), critique of polarimetric evidence on physical parameters and orbital inclination 80−109486
cataclysmic variable stars, multiple periodicities 77−87434
cataclysmic variables, emission lines from accretion discs 80−51774
cataclysmic variables, pulse timing meas., accretion disc models 79−62831
cataclysmic variables, short-period light oscills. rel. to non-radial oscills. of rot. stars 78−32477
stellar radiation continued
cataclysmic variables, theoretical UBV colours of accretion discs 78−61865
CD−42°14462 (V3885 Sagittarii), dwarf nova in permanent outburst 78−53966
ω Centauri, anomalous giant branch rel. to abundance vars. in dwarf spheroidal galaxies 79−5904
V553 Centauri, CH-type Cepheid, chemical comp. and luminosity 79−62849
Proxima=V645 Centauri, coordinated X-ray, optical and microwave study 79−5830
proxima=V645 Centauri, dMe flare star, quiescent corona, transition region, and chromosphere obs. 80−56850
V436 Centauri, dwarf nova, no periodic modulation in quiescent state light curve 79−88677
SV Centauri, early-type contact binary, evolutionary models, luninosities and effective temps. 80−4403
V78 in ω Centauri, light curve anal. in freq. domain by automatized Fourier technique 80−22039
SV Centauri, period changes of β Lyrae-type eclipsing binary 77−33575
α Centauri, soft X-ray emission 79−16951
UW Centauri, visual magnitude estimates, UBV photometry 78−40962
V743 Centauri (HD 116994), light variability 79−97006
α Centauri A and B, UV line fluxes from IUE spectra, and transition region models 80−46543
α Centauri C (Proxima Centauri), EUV flare obs. rel. to flare star scaling theory 77−45453
V645=Proxima Centauri optical flares during 1977 May, S.African obs. 78−32480
Centaurus X-3, neutron star charact. from correlated spin-up and X-ray luminosity meas. 80−101648
central star of Abell 46, eclipsing binary 80−73027
central stars of planetary nebulae, Zanstra temps. and effective temps. relation 79−88654
VV Cephei, absolute visual magnitude Mg II reson. lines widths 80−109498
U Cephei, Algol type binary, spectrophotometry, u.v. excess 77−2454
EI Cephei, Am eclipsing binary, light curve anal. 77−33560
EM Cephei, B-type eclipsing binary system, investigation of period and min. 80−17614
U Cephei, circumstellar luminous matter rel. to eclipse light curves 79−67061
VV Cephei, complex close binary, linear polarisation during 1977 elcipse 78−40995
VV Cephei, eclipsing binary, distance and absolute visual magnitudes 79−53859
U Cephei, eclipsing binary, hot/cool spots obs. in UV light curves 78−57577
EI Cephei, eclipsing binary, occultation at primary minimum 77−9770
U Cephei, excess light obs. rel. to accretion discs 80−82412
EM Cephei, light curve from UBV photometry *(Russian)* 77−64803
β Cephei, linear polarisation obs. rel. to non-radial pulsations 79−40198
λ Cephei, linear polarization variability in emission line O star 78−36571
EE Cephei, obs. of long period eclipsing binary *(Italian)* 78−93319
VW Cephei, periodic vars. in light curve of W Ursae Majoris system 80−36667
RZ Cephei, RRc-type star, period var. *(Italian)* 77−91546
μ Cephei, semi-regular, supergiant, narrow-band polarimetry 79−25617
VW Cephei, W Ursae Majoris star, identification with faint X-ray source 80−51913
VW Cephei, W Ursae Majoris star, orbital period decrease and B-V colours rel. to physical status 80−109495
17=ξ Cephei A, speckle interferometry, mass-luminosity relation 80−56874
β Cephei stars, photometric search of southern B-type stars 79−71040
β Cephei stars, possible polarization effects 79−84807
β Cephei stars, pulsation effect on period-luminosity relation 80−72970
β Cephei stars, radiation pressure and pulsational instability 79−84806
β Cephei stars, vel./light curves for six objects 79−75214
Cepheid variables, amplitudes in instability strip 79−44491
Cepheid variables, double-mode, freq. anal. 80−31308
Cepheid variables, intrinsic colours 79−84797
Cepheid variables, period-luminosity-colour relation, numerical simulations 80−82393
Cepheid variables, phase shift technique for determining incidence of duplicity 80−90453
Cepheid variables determ. of colour term in period-luminosity colour relation 80−94812
Cepheids, BVI photometric determ. of reddening 78−65630
Cepheids, in different galaxies, progression in period-amplitude diagrams charact. 78−53956
Cepheids, in Magellanic Clouds, evidence for interstellar reddening 77−2435
Cepheids, in NGC 2403, period-luminosity-colour calibration and galaxy distance 77−2471
Cepheids, intrinsic colours and physical props. from Walraven VBLUW photometry 78−28696
Cepheids, long period, colour excess scale and intrinsic colour props. 77−29858
dwarf Cepheids, period changes 80−62142
Cepheids, reddenings from mean UBV colours 79−71056
Cepheids, relation between UV excess and superficial gravity 77−53604
Cepheids, vars. of normal and double mode variables 77−87428
Cepheids in Magellanic Clouds, colour luminosity-amplitude relations 77−91554
δ Ceti, β Canis Majoris variable, period meas. and detect. of period decrease 80−105257
UV Ceti, anomalous flare activity obs. 78−89202
WX Ceti, cataclysmic variable similar to WZ Sagittae, outburst charcts. 80−17596
UV Ceti, continuum and Hβ emission vars. during large flare 77−45456
XY Ceti, eclipsing binary, masses, radii and luminosities from revised photometric elements 80−109458
UV Ceti, IR obs. of flares *(Russian)* 78−93278
π Ceti, late B-type star, X-ray emission obs. 79−101160
TV Ceti, light curves, photometric elements and He content 79−44526
XY Ceti, light vars. of eclipsing binary with Am spectra 78−93310
o Ceti, SiO maser variability at 86 GHz 80−41839
o Ceti, vars. in spatial distrib. of 11 micron radiation 79−5828

stellar radiation continued
o Ceti (Mira), effects of luminosity vars. on CO 2.6 mm emission 78−12241
o Ceti (Mira), enhanced activity of B-type component at 1976 light minimum 78−81636
o Ceti (Mira), rapid light vars. of companion star during 1977 light min. 78−96492
o Ceti (Mira)-type stars, colour curves for Me and Se types 77−29857
o Ceti AB, IUE obs. of UV spectrum 80−22027
ZZ Ceti stars, constraints on possible long-term variability 80−90428
UV Ceti stars, photometric features near flare initial phase 80−105252
Z Chamaeleontis, cataclysmic binary, possible gravit. radiation emission 80−4386
Z Chamaeleontis, eruptive binary, photometric data anal. 80−72961
Z Chamaeleontis, gravitational waves from eclipsing cataclysmic binary 80−90439
Z Chamaeleontis, monitoring of southern dwarf nova, 1954-76 period 78−93272
RS Chamaeleontis, uvby photometry of bright double-lined A-type eclipsing binary 78−69833
Cherenkov radiation of charged particle moving in mag. cold plasma, pulsars appl. 79−62736
chromosphere Ca II H and K line radiation, absolute flux profiles in F0 to M2-type stars 80−26842
chromosphere radiative loss rates in cool stars, rel. to Mg II flux profiles 80−36611
chromospheres of F, G and K-type stars, radiative losses in continuum 80−72924
chromospheric K-line emission on H-R diagram, absolute fluxes 77−56937
chromospheric radiative losses of late-type stars, empirical estimates 78−40915
chromospheric scaling laws, width-luminosity correls., Wilson-Bappu effect 79−40177
chromospheric variations in main-sequence stars 79−16931
Circinus X-1, binary model, radio emission 80−98736
Circinus X-1, changes in optical, IR and radio emission 80−67910
Circinus X-1, continuation of anomalous X-ray behaviour 78−32606
Circinus X-1, nature of radio, X-ray and optical radiation 79−75296
circular polarisation by magnetite grains, two-cloud model 77−78838
circular polarisation of stellar radiation scattered on circumstellar clouds 78−96428
circumstellar dust shells, radiative transfer and radiation emission 77−13318
CIT 6 (IRC+30219), IR C star, CO obs. of mass outflow 80−12761
classical Cepheids, check on light and radial vel. curves phase shift for distance determ. 78−16439
classical Cepheids, light and radial vel. curves phase matching 77−17574
classical Cepheids, light curves, optimal curve fitting procedure appl. 77−78795
classical Cepheids, mass-luminosity relationship 79−35278
classical Cepheids, surface brightness and radii *(Polish)* 79−58359
classical Cepheids colour excesses 77−22242
classical novae, optical vars. rel. to props. of optically thick winds 78−24516
close binary stars linear polarisation 77−49435
close binary systems, convergence of Kopal's iteration method for light curve soln. *(Chinese)* 79−62872
close binary systems, effects of libration on light curves 78−57579
close eclipsing binaries, J-integrals numerical evaluation 77−9668
close eclipsing binaries, recursion formulae for J-integrals 77−9666
close X-ray binary stars, ellipsoidality effects and linear polarisation in optical component 77−78898
clusters in LMC, instrumental colour-magnitude diagrams 77−22279
cocoon stars, calculated IR spectra 77−64824
cocoon stars, numerical soln. of radiation transfer eqn. in spherical geometry 80−90329
collapsed object, in globular cluster NGC 6624, X-ray emission 77−45498
collapsed stars, neutrino flux from quark matter 80−22028
collapsing core, ang. momentum losses through neutrino radiation 77−56916
collapsing relativistic stars, linearised odd-parity radiation 78−93297
collapsing relativistic stars, radiation, linearized even-parity EM and gravit. radiation 79−75228
collapsing stars, enhanced gravit. radiation recoil 77−33336
collapsing stars, nonradial pulsations damping by neutrino radiation 77−56999
colour excesses, rel. to interstellar reddening material distrib. in solar neighbourhood 78−49502
colour indices, effect of stellar atmospheres finite extent 78−32450
colours influence on β-index meas. 79−21270
35 Comae Berenicis, masses and K-line absolute magnitudes 80−8649
compact star, radiation, anisotropic fluid in spherical spacetime 77−56821
comparison stars near OJ287 and ON325, variability, period determ. 80−26882
contact binaries, evolution rel. to light curve and period changes 77−57054
contact binaries, synthetic light curves 78−24528
contact binaries, theoretical atlas of light curves and rot. broadening functions 80−17610
contact binary stars, convective energy transfer rel. to deviation from mass-luminosity relation *(Russian)* 77−17615
cool C stars, nearby, distances, luminosities and radii 78−49434
cool carbon stars, effective temp. scale 77−2421
cool stars, 1 to 5 μm flux curves rel. to effective temps., ang. dias. reddening 79−44458
cool stars, HEAO 1 search for coronal soft X-ray emission 79−101140
cool stars, narrow-band polarisation effects 78−16427
cool stars, polarisation wavelength depend. 77−2426
cool stars, UV spectra obs. by International Ultraviolet Explorer (IUE) 78−96475
core collapse, ellipsoidal model calcs., gravitational and neutrino radiation 79−53802
core He burning stars, H profile, previous mixing and loops in H-R diagram 77−29792
coronae, min. flux concept rel. to energy balance and mass loss 78−81611
ε Coronae Austrinae, polarimetric obs. of eclipsing binary 80−56888
R, S, T Coronae Austrinae, T Tauri stars, long period vars. 80−82350
stellar radiation continued
S Coronae Austrinae, YY Orionis star, satellite UV spectrum and continuum energy distrib. 79−67016
R Coronae Borealis, 1977, February 17-26 magnitude fading 77−29854
R Coronae Borealis, light curve, Poisson statistics 77−56942
R Coronae Borealis, origin of 1100 day periodicity in IR excess 77−45462
σ Coronae Borealis (HD 146361), spectroscopic binary, soft, X-ray obs. with (HEAO-1) 80−56886
R Coronae Borealis stars, long-term IR behaviour 78−96490
R Coronae Borealis-type variables, B mag. and visual estimates 77−53609
Crab pulsar, high-energy photon spectrum rel. to energetic particles momentum distrib. 78−73727
Crab pulsar, magnetized cracks in crust rel. to matter flow, radio, X-ray and optical emissions 80−72990
Crab pulsar, model for pulsed γ-ray and X-ray emission 80−62230
Crab pulsar, nonlinear space charge waves rel. to coherent radio emission 77−41386
Crab pulsar, upper limit for gravit. radiation energy flux 78−73730
Crab pulsar (NP 0532), model for unpulsed light 79−44518
cyclotron self-absorption in accretion columns of magnetic degenerate stars, X-ray sources appl. 80−12760
CH Cygni, 1977 April surge before September outburst 77−87412
V1500 Cygni, (Nova 1975), photoelec. obs., period decrease, visual magnitude estimates 77−22252
SS Cygni, accretion disc radiation during dwarf nova outburst 77−91537
V Cygni, C star, 1-4 mm continuum emission obs. 79−88670
SS Cygni, dwarf nova, accretion disc radiation models in eruption and at min. light 80−36635
SS Cygni, dwarf nova, ANS detection of both soft and hard X-ray emission 78−36579
SS Cygni, dwarf nova, identification as hard X-ray source by HEAO 1 scanning modulation collimator 79−2548
SS Cygni, dwarf nova, rapid optical oscills. phase variability 80−85947
SS Cygni, dwarf nova, soft X-ray pulsation obs. 80−46563
SS Cygni, dwarf nova, X-ray polarisations discovery 78−65628
CG Cygni, eclipsing binary, changing light curve obs. 79−48857
V380 Cygni, eclipsing binary, masses, radii and luminosities from revised photometric elements 80−109458
P Cygni, effective temp. radius, mass loss and luminosity 80−51748
V1057 Cygni, FU Orionis-type star, flare up in 1720 MHz OH line 79−62843
V1500 Cygni, ionising source UV flux rel. to Balmer-line emission profiles evolution 80−82371
SS Cygni, light curve periodicity 79−21300
V1057 Cygni, mean B-band magnitude (1978 July 30 ± 2^d) 79−84792
χ Cygni, Mira variable, effects of luminosity vars. on CO 2.6 mm emission 78−12241
V1057 Cygni, OH obs. 80−36629
NML=V1489 Cygni, OH/IR star, 1612 MHz OH maser multibaseline VLBI obs. 80−12766
CH Cygni, outburst and spectral changes, 1977 August 31 obs. 77−82231
γ Cygni, radio emission upper limits rel. to nature of Cygnus X radio source 78−28809
32 Cygni, supergiant eclipsing binary, λ6575 and λ4870 light curves anals. 79−88700
CH Cygni, symbiotic star, binary model rel. to blue continuum and emission and absorpt. lines 80−62158
V1016 Cygni, symbiotic star, IR variability obs. from VJHKL photometry *(Russian)* 80−105263
CH Cygni, symbiotic star, IUE obs. during active phase 79−62846
CH Cygni, symbiotic star, rapid and slow light vars. 80−51792
CI Cygni, symbiotic star, UV continuum fading during eclipse 80−105258
CH Cygni, symbiotic variable, flickering obs. during outburst, binary model 79−8929
V1500 Cygni, visual magnitude estimates 1976, Nov. and Dec. 77−9758
V1357 Cygni (Cygnus X-1), brightness var. rel. to disk accretion subphotospheric layers *(Russian)* 79−25764
V1357 Cygni (Cygnus X-1), no long-term light vars. (1928-77) 80−41861
V1341 Cygni (Cygnus X-2), possible 82-minute quasi-periodic bursts obs. *(Russian)* 79−17140
V1341 Cygni (Cygnus X-2), shortest optical variability *(Russian)* 80−17695
V1329 Cygni (HBV 475), symbiotic variable, photometric and spectroscopic history 80−62148
V1500 Cygni (Nova 1975), 3.35 hour 1978 light curve, rel. to possible double period 79−67039
V1500Cygni (Nova 1975), 3 hour photometric period stabilisation 79−92776
V1500 Cygni (Nova 1975), 3 hour var. 79−16966
V1500 Cygni (Nova 1975), brightness meas., (1917 to 1976) 78−36618
V1500 Cygni (Nova 1975), continuous energy distrib., IR obs., thermal bremsstrahlung 79−80315
V1500 Cygni (Nova 1975), emission line vars. rel. to central object radiation model 80−82367
V1500 Cygni (Nova 1975), fine-struct. lines rel. to 10 micron excess 78−93269
V1500 Cygni (Nova 1975), flux distribs. rel. to shell electron temps. and densities 79−30068
V1500 Cygni (Nova 1975), light curve for 1975 Aug.-1977 July period 80−4372
V1500 Cygni (Nova 1975), light fluctuation period var. 79−97012
V1500 Cygni (Nova 1975), linear polarization obs. 78−36601
V1500 Cygni (Nova 1975), luminosity and distance, light curve obs. 80−72981
V1500 Cygni (Nova 1975), meas. and nova outburst model 77−87448
V1500 Cygni (Nova 1975), mechanism of quasieclipses after outburst *(Russian)* 78−93280
V1500 Cygni (Nova 1975), obs. of magnitude and spectrum changes *(French)* 77−82258
V1500 Cygni (Nova 1975), optical polarisation obs. 78−36622
V1500 Cygni (Nova 1975), photometry, light curves, magnitude estimates 78−85960
V1500 Cygni (Nova 1975), polarimetric and photometric obs. 78−36612
V1500 Cygni (Nova 1975), radio emission from expanding shell 80−26868
V1500 Cygni (Nova 1975), short-term light vars. 78−36609

stellar radiation continued
V1500 Cygni (Nova 1975), small amplitude light var. 78−36608
V1500 Cygni (Nova 1975), spectral energy distrib. 78−36605
V1500 Cygni (Nova 1975), spectrum, visual magnitudes and absolute luminosity *(Chinese)* 79−16982
V1500 Cygni (Nova 1975), UBVR Hα photometry and polarimetry 78−36611
V1500 Cygni (Nova 1975), UBVRI photometry and polarimetry 78−36614
V1500 Cygni (Nova 1975), visible and UV spectra and light curve 80−12771
V1500 Cygni (Nova 1975), visible-band linear polarimetry 78−36621
V1500 Cygni (Nova 1975), visual magnitude estimates (1977 May-Aug.) 77−82230
V1668 Cygni (Nova 1978), BV photometry rel. to absolute magnitude and distance 79−67035
V1668Cygni (Nova 1978), linear polarisation obs. 80−26875
V1668 Cygni (Nova 1978), optical light curve, uvby photometry 80−62154
V1668 Cygni (Nova 1978), UBV photometric search for short term light vars. *(Russian)* 80−109444
V 1668 Cygni (Nova 1978), visual light curve correl. with spectral development 80−51789
V1668 Cygni (Nova 1978), visual mag. estimate (1979 April 25) 79−53824
V1668 Cygni (Nova 1978), visual magnitude estimates, 1978 Nov.-1979 Apr. 79−48819
V1668 Cygni (Nova 1978), visual magnitude estimates, 1979 June 79−80324
V1668 Cygni (Nova Cygni 1978), post-max. short period oscills., photoelectric photometry 80−82380
Cygnus OB2 association, wavelength depend. of polarisation and interstellar birefringence 77−33577
Cygnus X-1, black hole candidate, X-ray and optical radiation 78−16577
Cygnus X-1, critique of polarimetric evidence on physical parameters and orbital inclination 80−109486
Cygnus X-1, discovery of synchronous binary polarization 78−41087
Cygnus X-1, evidence for new variabilty in hard X-ray emission 80−27011
Cygnus X-1, extended-bandwidth X-ray obs. 80−17689
Cygnus X-1, mean blue light curve feature 77−17718
Cygnus X-1, neutron star plus massive disc model rel. to light curve 80−36736
Cygnus X-1, obs. during high state (1980 June 11 to 27) 80−86017
Cygnus X-1, optical and X-ray evidence for 78/39-day period 78−89274
Cygnus X-1, optical polarisation orbital vars. rel. to binary system inclination 78−54077
Cygnus X-1, physical reality of millisecond bursts questioned, shot noise effects 78−45429
Cygnus X-1, short-term time variability 78−93466
Cygnus X-1, short-term variability in hard X-ray region *(Japanese)* 79−80369
Cygnus X-1, transition from high X-ray state to low X-ray state, 1980 June to July 80−98738
Cygnus X-1, UV shot noise upper limit 80−4458
Cygnus X-1, X-2 and X-3, long-term-studies with Ariel 5 All-Sky Monitor (ASM) 80−17688
Cygnus X-1, X-ray flux time variability struct. *(Russian)* 80−51921
Cygnus X-1 (HDE 226868), 78.4 day period search in X-rays and optical polarisation 79−75297
Cygnus X-1 (V1357 Cygni), optical light curve vars. rel. to X-ray vars. 80−109560
Cygnus X-1 (X-2, X-3), X-ray polarisation obs. from OSO 8 80−90571
Cygnus X-2, optical variability upper limits 78−96564
Cygnus X-2, rapid UV flux vars., IUE obs. 80−12833
Cygnus X-2, X-ray and optical obs., (1973 to 1977) 79−30148
Cygnus X-3, 100 MeV gamma-ray source, very high energy gamma-ray emission search 79−40293
Cygnus X-3, 34.1 day period, 2-12 keV obs. by COS-B 80−94897
Cygnus X-3, 4.8 hour modulation period change disproved 80−8713
Cygnus X-3, 4.8 hour periodicity in spectra 79−5920
Cygnus X-3, gamma-ray emission from mag. accretion disc 77−78894
Cygnus X-3, hard X-ray spectrum obs. 80−31388
Cygnus X-3, model for quiescent radio emission 77−33689
Cygnus X-3, period derivative and asymmetric X-ray light curve from HEAO 2 obs. 80−105394
Cygnus X-3, X-ray and gamma-ray emission rel. to cocooned X-ray binary pulsar model 78−36723
degenerate star, radiative luminosity from propagating slow deflagration front 79−84790
degenerate stars with H atmospheres, props. rel. to theoretical models 80−17576
HR Delphini (Nova 1967), continuum fluxes, temp. and luminosity from simultaneous X-ray, UV and optical obs. 80−109440
HR Delphini (Nova 1967), radio emission from expanding shell 80−26868
HR Delphini (Nova 1967), short period light vars. from UBV photometry 80−67744
HR Delphini (Nova 1967), short period photometric vars. obs. 79−44503
dense stars, continuum spectrum polarisation in intense mag. fields, atomic physics theory 80−105160
detached double-lined eclipsing binaries, revised photometric elements 78−61886
diffuse galactic light interpretation, models 78−8118
disc population stars, luminosity functions in SA 51, SA 57 and (SA 68) 80−98648
DO white dwarfs, spectrophotometry rel. to effective temps. and He abundances 79−35249
S Doradus, LMC Hubble-Sandage variable, IUE and ground based spectroscopic obs. 80−101595
BY Draconis, binary spotted flare star, mass and luminosity ratios rel. to pre-main-sequence nature 80−36633
AR Draconis, BV light curves and orbital elements 79−101173
WW Draconis, eclipsing binary, masses, radii and luminosities from photoelectric lightcurves 80−46606
BY Draconis, flare star, Ca II emission variability 77−33528
BY Draconis, flare star, coronal soft X-ray emission obs. by (HEAO 1) 79−101140

stellar radiation continued
BY Draconis, magnitudes, colours and photometric period changes *(Russian)* 77−64771
AI Draconis, period and spectroscopic orbit of eclipsing binary 78−89221
CR Draconis, UV Ceti variable, flares colour behaviour 80−22020
BY Draconis stars, luminosity vars. and light curve period changes 79−71039
BY Draconis stars, out of eclipse light var. and comparison with RS Canum Venaticorum stars 80−109489
dwarf nova brightening, magnetic fields and outburst phenomena *(Afrikaans)* 78−32481
dwarf nova outbursts, colour vars. 80−46576
dwarf novae, eruption types and superhumps, obs. 79−75212
dwarf novae, HEAO-A2 soft X-ray survey during optical outburst 80−46574
dwarf novae, nature, H accretion, mag. field, radiation mechanisms *(Russian)* 78−93277
dwarf novae, period-amplitude relationships 77−91545
dwarf novae, quasiperiodic luminosity vars. 79−80311
dwarf novae, rapid brightness oscills. obs. 78−40968
dwarf novae, rise to maximum and decline rel. to radiation sources 77−9753
dwarf novae, satellite UV obs., temp. calc. 77−57033
dwarf novae, search for light oscills. during outbursts 78−40966
dwarf novae, soft X-ray emission 77−45457
dwarf novae, X-ray emission 79−67031
dwarf stars, metal-poor, effective temps. and abundance anals. from yellow spectra 79−92760
Dyson spheres, stellar energy requirements and IR emission 78−69710
early A stars, empirical effective temp. determ. 80−101587
early type companions of X-ray sources, luminosities, rot. and other parameters 78−36564
early type stars, luminosity determ. X-ray obs. 80−105241
early type stars, mid UV spectra obs. 80−21995
early type stars, normal, near UV line blocking depend. on spectral type and luminosity 80−36619
early-type stars, 0.2 Å far UV spectra catalogue and absolute fluxes 77−56843
early-type stars, absolute magnitude calibration test 78−61857
early-type stars, mass loss rel. to luminosity from radio obs. at 6 cm 80−82347
early-type stars, rapid rot. and suspected variability rel. to line emission 79−67036
early-type stars, suspected variability and line emission, Hα obs. 79−67036
early-type stars, terminal wind vels. 79−16943
early-type stars, theoretical UBV colours and temperature scale 79−16933
early-type stars, wavelength depend. of linear polarisation 77−60779
early-type stars near Sun, photometric distances, space vels. and ages 78−61858
early-type stars with Balmer emission, luminosity classes from near UV spectra 80−94811
early-type stars with extended envelopes and mass outflow, radio emission 77−74063
early-type stars with gas-dust envelopes, IR spectral energy distrib. 80−67732
eclipsing and spectroscopic binaries, period distrib. 78−69829
eclipsing binaries, average absolute brightness of components *(Polish)* 77−17630
eclipsing binaries, corrected light elements for nine objects 77−37620
eclipsing binaries, Fourier anal. of light curves 78−69830
eclipsing binaries, light curves, Fourier analysis, integral evaluation 78−45236
eclipsing binaries, photoelectric lightcurves of possible sd-d systems, revised elements 80−56879
eclipsing binaries in Scutum-Vulpecula regions, visual minima obs., 1920-1950 period 77−33564
eclipsing binaries light curve analysis, new techniques and appl. to V444 Cygni 80−82417
eclipsing binary light curve analysis, Fourier techniques 79−58261
eclipsing binary light curves, Fourier analysis techniques, series expansions 79−75248
eclipsing binary light curves, Fourier analysis techniques and light changes 79−75247
eclipsing binary light curves anal., linearised limb-darkening coefficients 78−49480
eclipsing binary light curves soln. using LIGHT computer program 80−77454
eclipsing binary light loss analysis, Fourier techniques 79−58262
eclipsing binary stars, Fourier anal. of light curves, reduction of integrals 78−20856
eclipsing binary stars, Fourier anal. of light curves 77−87474
eclipsing binary stars, Fourier anal. of light curves 78−24525
eclipsing binary stars, light curve analysis by Fourier techniques 80−72993
eclipsing binary stars, light curve analysis by Fourier techniques 80−72994
eclipsing binary stars, light curves Fourier anal. 77−9769
eclipsing binary stars, soln. of light curve by Kopal's iterative process 79−35310
eclipsing binary stars, V−R photometry rel. to distances, masses, radii and absolute magnitudes 79−44520
eclipsing binary systems with disclike envelopes, light curve interpretation, appl. to HZ Herculis 78−65658
eclipsing variable light curves, Fourier analysis for partial phases 79−21350
eclipsing variable stars, Fourier anal. of light curves, photometric perturbations for total and transit eclipses 78−12291
eclipsing variable stars, Fourier anal. of light curves 77−49428
eclipsing variable stars, Fourier anal. of light curves 78−93311
eclipsing variable stars, Fourier analysis of light curves, error anal. in freq. domain 80−31214
eclipsing variable stars, light curves Fourier analysis, appls. to eccentric orbits 79−25630
eclipsing variable stars with extended atmospheres, Fourier anal. of light curves 80−46604
eclipsing variables, Fourier anal. of light curves, geometric elements soln. 79−25634

stellar radiation continued
eclipsing variables, Fourier anal. of light curves, photometric perturbs. 78–96807
eclipsing variables, Fourier anal. of light curves, photometric perturbs. for partial eclipses 79–25635
eclipsing variables, Fourier anal. of light curves 78–20854
eclipsing variables, Fourier anal. of light curves 79–25633
eclipsing variables, Fourier anal. of light curves 79–25632
eclipsing variables, Fourier anal. of light curves 79–30088
eclipsing variables, Fourier analysis of light curves 79–8945
eclipsing variables, Fourier analysis of light curves 79–8946
eclipsing variables, light curve Fourier analysis, eclipse parameters, geometric determinacy 78–96503
eclipsing variables, light curves linear analysis, fractional light loss anal. 80–82416
eclipsing variables, photometric perturbations for partial eclipses, Fourier anal. 78–28717
eclipsing variables in Magellanic Clouds, tabulated light curves 78–16536
eclipsing variables light curves, $B_{n,m}{}^{q}$ integrals in Fourier anal., explicit expression 79–35298
elliptical galaxies, late M giants population synthesis rel. to colours and spectra, comp. effects 78–57626
in elliptical galaxies, UV radiation field rel. to star form. 77–33636
energy distrib. in Hayes-Latham calibration from spectrophotometric data 80–72790
energy distrib. of southern standard stars (320-880 nm) 80–62125
energy distribution, absolute spectrophotometry results comparison with UBV photometry 78–96476
energy distributions in main-sequence A and F stars 78–93220
energy distributions of Be stars in clusters 78–85944
energy loss rate through ν-prod. by second class weak neutral current 79–35997
ergoregion instability of rotating stars, eigenfrequency calc. 79–8835
CC Eridani, BY Draconis variable, Hα variations 77–87406
RX Eridani, RR Lyrae variable, radius, mass and absolute magnitude 77–2436
40 Eridani, triple star, X-ray emission discovery 79–97035
eruptive blue variables at high galactic latit., spectrophotometry 78–32482
EUV radiation, point source contribs. to EUV background 80–62324
evolved stars expanding envelopes, CO thermal and maser emission 80–82334
exciting stars of planetary and diffuse nebulae, effective temps. and flux distribs. 77–13427
EXP 0520–66, flaring X-ray pulsar, recurrent gamma-ray bursts obs. *(Russian)* 80–36741
expanding envelopes, Lyman α quanta scattering *(Russian)* 80–67556
expanding envelopes, radiative forces 78–28659
extreme Population II stars, H-R diagram and age difference from oldest Population I stars 77–56912
F8-K1 stars absolute magnitudes, recalibration of three-dimensional spectral classification 77–78768
F and G-type supergiants, search for light vars. 79–88657
F-, G- and K-type stars, in solar neighbourhood, absolute magnitudes 78–81632
F- and G-type stars, luminosity and temp. determ. by spectral quantification 77–29791
F- and G-type supergiants, luminosity calibration using O I 7774 Å line equivalent width 78–53942
F-type main-sequence stars, effects of granulation on spectral energy distrib. 80–90417
F-type stars, absolute luminosity calibration 78–65612
F-type stars, atm. models including OH opacity, comparison with TD1 satellite flux obs. 78–73700
far UV radiation background at high galactic latits., D2B-Aura satellite obs. 79–17143
Faraday effect and depolarization of optical emission from magnetic white dwarfs 79–97002
fast nova model evolution from pre-explosion to decline 79–35273
Feige 24, EUV obs. of hot white dwarf, temp. determ., interstellar H I density calc. 78–16422
Feige 24, hot white dwarf, intense EUV emission 77–9746
Feige 4, hot white dwarf, identified with bright EUV source 78–89200
Feige 7, mag. white dwarf, spectroscopic studies 79–25603
flare star, near Orion Nebula, UBV obs. *(Russian)* 77–82223
flare star outbursts in Praesepe field, plate records and cluster membership 77–53652
flare stars, combined optical and radio obs., long-duration events 79–53827
flare stars, dynamical parallax, absolute magnitudes and masses *(Russian)* 79–88690
flare stars, fast electron hypothesis 77–78796
flare stars, flare emission spectrum rel. to fast electron hypothesis 80–67731
flare stars, mean colours of flare continuum 77–13349
flare stars, nature of flares optical continuum *(Russian)* 80–109445
flare stars, nonmonotonic optical light curve model 77–29842
flare stars, X-rays influence on optical light curve 77–29843
flare stars as candidates for new class of transient soft X-ray sources 78–45337
flare stars discovery in Ophiuchus-Scorpius region *(Chinese)* 78–69804
flare stars in Orion Nebula region, new objects and repeated outbursts 80–56852
flare stars in Pleiades, new discoveries *(Russian)* 77–13366
flare stars in Pleiades, possible cyclic recurrence of flare activity *(Russian)* 78–49443
flare stars in Scorpius-Ophiuchus region, discoveries *(Chinese)* 80–77418
flare stars in solar neighbourhood, physical parameters 80–51777
flare stars physical charcts. 77–41383
flares, data acquisition and processing at Italian observatories *(Italian)* 79–62751
flares, IR obs. *(Russian, English)* 79–75216
flares caused by tidal action of massive black hole *(Russian)* 79–30086
flares in stellar aggregates, freq. function *(Russian)* 79–8918
Fourier analysis of light curves of eclipsing binaries for transit eclipses 78–96506
G127.1+0.5, very compact radio source as supernova stellar remnant 78–16555
stellar radiation continued
G, F, A, B and O stars, fluxes and UBV, uvby colours from model atmospheres 79–80298
G- and K-type giants, theoretical colours from synthetic spectra 79–62827
G- and K-type stars, correls. between luminosities, motions and CN anomalies 77–17566
galactic 2 μm radiation, mean intensity in solar neighbourhood 80–36744
galactic centre, B-type stars as extended thermal radio emission ionising agent 79–97059
Galactic Centre, polarisation obs. at 2.2 microns 77–64850
galactic centre region, 2.2 μm spectroscopy rel. to giant stars IR flux 78–36686
galactic interstellar extinction law, vars. 78–85990
galactic photometric disc model, direct starlight intensities and interstellar dust clumping effects 80–22077
galactic supernovae, colour curves and visual light curves 79–58368
galactic UV background, TD-1 satellite obs. 77–13504
galaxies, E and S0 types, CO and JHK photometry rel. to stellar populations 78–36684
galaxies young massive halos, spectral energy distribs. at large redshifts 77–78866
gamma-ray emission, observational and physical review 79–80373
gamma-ray pulsars, curvature radiation-pair prod. model 79–5852
GC 17353, Ap star with large photometric var., period *(French)* 79–2545
GD 154, new pulsating white dwarf, obs. 78–40928
GD 229, mag. white dwarf, spectroscopic studies 79–25603
U Geminorum, 1978 February magnitude estimates 78–36589
U Geminorum, dwarf nova, spectrophotometric parallax and absolute visual magnitude 79–67012
U Geminorum, dwarf nova, visual magnitude estimates, (1979, March 23 to 24) 79–44501
U Geminorum, dwarf nova, visual magnitudes during outburst, (1980 May 6 to 9) 80–72978
RW Geminorum, eclipsing variable, element determ. by Fourier anal. of light curve 77–45484
U Geminorum, HEAO 1 obs. of hard X-rays 79–21299
U Geminorum, HEAO obs. of low-energy X-ray emission 79–21298
U Geminorum, magnitude estimates for 1978 Oct. 78–96493
U Geminorum, soft X-ray emission and visual magnitude estimates 77–91544
U Geminorum, V mag., primary eclipse and visual mag. estimates 79–44505
U Geminorum, visual magnitude estimates during outburst (1980 Oct.) 80–109439
U Geminorum, visual magnitudes for 1978 Jun. 78–65627
giant stars in AFCRL IR Sky Survey, 4-20 μm emission 77–87283
giant stars in M3, M13, M92 and M67, IR photometry, bolometric magnitudes and effective temps. 78–57595
giant stars with IR excesses, optical emission intrinsic linear polarisation origin 78–96481
globular cluster stars, He settling rel. to main sequence turnoff luminosity and inferred ages 80–73013
globular clusters, (V-K) colour rel. to metal abundance 77–87485
globular clusters, UBV photometry 78–16468
globular clusters, UV energy distribs. from Orbiting Astronomical Observatory photometry 80–73009
globular clusters in Galaxy, Fornax and M31, integrated colours and metallicity 78–16469
grating scanner meas. of stellar energy distrib., polarization effects 78–32355
gravitation radiation from homologous oscill. of compressible Newtonian spheroid 80–46533
gravitational diffraction of plane wave by large star 77–5724
gravitational radiation, from neutron stars and white dwarfs 78–65646
gravitational radiation damping of binary stars calc. 79–97272
gravitational radiation energy loss from binary stars, free-fall sources model 80–51647
gravitational radiation from Crab and Vela pulsars, revised estimate 78–32501
gravitational radiation from stellar collapse, ellipsoidal models 78–45317
gravitational waves, correl. with neutrino bursts and experimental appls. 78–77567
gravitational waves from binary stars, detection opportunities 79–5746
gravitational waves generated by collapse, wave strength estimate 80–46584
gravitationlly collapsing stars, neutrino luminosity rel. to mass ejection 77–33534
GX 1+4, search for Hα pulsations from candidate star 78–86037
GX 304–1 (3U 1258–61), discovery of 272 second period var. 78–8152
GX 3+1, X-ray bursts obs., (1980 July 19 to August 18) 80–98739
H-R diagram, use as astronomical tool, review of IAU Symposium (No.80) 78–81619
halo population stars, luminosity functions in SA 51, SA 57 and (SA 68) 80–98648
halo stars, luminosity function rel. to Galaxy halo to disc mass. ratio 77–45548
Harvard magnitude scale rel. to B mag. for Sa 183 stars 77–71109
HBV 475 (V1329 Cygni), exciting star temp. increase from high-excitation emission lines 78–40955
HD 101065, Przybylski's star, light variability freq. anal. 80–62152
HD 101065, search for light vars. 78–69812
HD 102567, optical counterpart to 4U 1145–61, atm. model from UV obs. 80–105396
HD 102567 (4U 1145–61), X-ray periodicity and orbital motion 78–8160
HD 105902 (ADS 8448), Ba star in visual binary, absolute magnitude and mass 77–78805
HD 111133, Ap star, 5200 Å flux depression variability *(German)* 79–44496
HD 113001, visual binary absolute magnitude determ. *(French)* 80–105281
HD 127617 (Bidelman's high latitude Be star), photometric and visible spectra obs. 80–77420
HD 128220, peculiar spectroscopic binary, photometric separation and spectral types *(French)* 77–57014
HD 129041, new δ Scuti star, period and amplitude 79–2547

stellar radiation continued
HD 129494, new pulsating δ Delphini star, luminosity from period-luminosity-colour relation 80−67750
HD 129494, new pulsating δ Delphini star, photometric obs. and luminosity 80−67750
HD 142373 (χ Herculis), var. intrinsic polarisation obs. 78−12202
HD 147889, B2 star, radiation rel. to ρ Ophiuchi dark cloud radio emission 77−33585
HD 153919, Of supergiant, X-ray binary 3U 1700−37 optical counterpart, light curve anal. 78−32470
HD 153919 (3U 1700−37), X-ray luminosity rel. to forbidden Fe XIV and Fe X emission 80−4358
HD 153919 (4U 1700−37), optical oscills. obs. 78−96572
HD 190603, effective temp. radius, mass loss and luminosity 80−51748
HD 192163, Wolf-Rayet star, excess UV extinction rel. to comp. of dust in (NGC 6888) 77−29905
HD 192163, Wolf-Rayet star, radius and temp. from spectra of nebula (NGC 6888) 77−57076
HD 192273, EUV flux upper limit, Voyager 1 obs. 80−77406
HD 192641, Wolf-Rayet star, IR light vars. 77−9750
HD 193793, Wolf-Rayet star, IR brightening rel. to circumstellar dust form. 80−31301
HD 193793, Wolf-Rayet star, IR light vars. 77−9750
HD 193793(=BD+43°3571), near IR magnitude increase 77−87413
HD 196517, new δ Scuti type variable star 78−49462
HD 200775, possible protostar in reflection nebula NGC 7023, optical polarization and IR spectrum 80−85944
HD 200775/NGC 7023 complex, intrinsic and interstellar reddening components 80−51832
HD 21479, brightness microvariability and non-radial pulsations *(Russian)* 80−67754
HD 219150, F0 V star with remarkable UV excess, optical and UV photometry and spectrum 80−90429
HD 221568, Ap star, light var. period 80−56856
HD 224085, K2e star, long-term variability 79−48849
HD 226868 (Cygnus X-1), periodicity in optical light curve during X-ray flare 78−81652
HD 26676, radio emission at 6 and 21 cm wavelengths 77−91532
HD 31908, freq. analysis of δ Delphini star 80−46581
HD 3765, variability due to eclipsing star or planetary system, BV photometry 80−17615
HD 47129 (Plaskett's star), massive O-star binary system, variable linear polarisation obs. 78−53989
HD 49798, H-deficient subdwarf O-type binary, mass, radius and luminosity from non-LTE anal. 79−16978
HD 50896, UV radiation effects on interstellar medium, Copernicus obs. 77−26036
HD 50896, Wolf-Rayet star, detect. of polarisation struct. across emission lines 79−97008
HD 50896, Wolf-Rayet star, linear polarisation periodic vars. rel. to binary star nature 80−72972
HD 50896, Wolf-Rayet star, wind struct. determ. from IR continuum 77−78793
HD 52788, freq. anal. of δ Delphini star 79−35276
HD 5980, eclipsing W-R binary in SMC, photoelectric light curve 78−45366
HD 77581 (4U 0900−40), optical pulsations from eclipsing binary 79−48951
HD 77581 (Vela X-1), discovery of optical pulsations 77−82327
HD 77581 (Vela X-1), optical pulsations discovery 78−20911
HD 87643, forbidden line Be star, IR flux distrib., 2 to 12 μm obs. 77−26017
HD 8781, freq. anal. of low-amplitude δ Scuti star 80−46575
HD 93250, O3 massive star in η Carinae complex, non-LTE analysis 80−77398
HDE 226868 (Cygnus X-1), anomalous light curve during X-ray increase of 1975 April-May 78−28850
HDE 226868 (Cygnus X-1), extendend secondary envelope with eclipsing region, V-polarization obs. 79−35433
HDE 226868 (Cygnus X-1), long-term circular polarisation variability 79−9031
HDE 226868 (Cygnus X-1), orbital period and Hβ light curve 79−48952
HDE 226868 (Cygnus X-1), variable linear polarisation, 1974-1975 obs. 77−9810
HDE 226868 (Cygnus X-1), variable UV polarisation 77−37622
HDE 245770, optical counterpart to A 0535+26, dimens. spectral type and luminosity visible obs. 80−72976
HDE 245770, possible counterpart of variable X-ray source A 0535+26, line and continuum vars. 80−17600
Henize 715 (4U 1145−61), Be-type star, colour and luminosity vars. (1976-1980) 80−72979
Herbig Ae/Be stars, multicolour linear polarization meas. 79−25607
Herbig Ae/Be stars, multicolour polarimetry 78−49445
Herbig-Haro object 1, far UV continuum obs. rel. to nature of object 80−67714
Herbig-Haro objects, spectrophotometry and radiating shock waves 78−85936
Herbig-Haro objects in southern dark clouds, objective prism survey 78−28536
HZ Hercules, 23 day lo state, Uhuru obs. 77−5594
HZ Hercules (Hercules X-1), 70 day period refuted 80−56975
Hercules X-1, cyclotron line form. by reson. Compton cyclotron scatt. 80−8711
Hercules X-1, cyclotron self-absorpt. in accretion column of mag. degenerate star 80−12760
Hercules X-1, Fe line emission discovery in low-state spectrum by (HEAO-1) 79−5922
Hercules X-1, high-energy pulsed X-ray spectrum from OSO 8 obs. 79−92888
Hercules X-1, mag. neutron star, cyclotron emission and beaming mechanisms 78−36726
Hercules X-1, pulse profile in hard X-rays 77−9811
Hercules X-1, X-ray spectrum of pulse 78−8154
Hercules X-1 (HZ Herculis), Bowen fluorescence mechanism evidence 78−53985
Hercules X-1 (HZ Herculis), hard X-ray obs. 78−36728
Hercules X-1 (HZ Herculis), mass from optical pulsations 77−78891
Hercules X-1 (HZ Herculis), periodic mass transfer rel. to X-ray light curve 80−51911
stellar radiation continued
Hercules X-1 (HZ Herculis), soft X-ray results from OSO-8 Wisconsin Expt. 78−36722
Hercules X-1 (HZ Herculis), X-ray continuum and Fe line emission during X-ray low state 80−105393
AM Herculis, 1.2 and 2.2 μm light curves interpretation, model parameters 79−8949
α^1 Herculis, absolute magnitude, evolutionary state and mass loss 78−7997
AM Herculis, accretion onto highly magnetised white dwarf 79−92764
φ Herculis, Ap star, X-ray emission obs. 79−101160
u Herculis, BVR lightcurves interpreted 80−41856
AH Herculis, dwarf nova, changes in rapid oscills. during outburst 79−88686
LT Herculis, eclipsing binary, photometric elements 80−31328
AK Herculis, eclipsing system, anal. of light changes in freq. domain 77−53635
u Herculis, eclipsing variable, two new light curves 80−90472
AM Herculis, high-speed circular polarimetry 79−25629
OP Herculis, late-type variable star, spectral energy distrib. and spectral types *(Russian)* 78−40958
HZ Herculis, light curve, radiation pressure effects 80−105280
α Herculis, M-type supergiant, Mg II emission linewidth/luminosity relation 78−53945
AM Herculis, narrow-band photoelectric obs. *(Russian)* 78−77565
AM Herculis, photometric and polarimetric obs. 78−65657
AM Herculis, photometric and spectrographic obs. 77−45492
AK Herculis, R and I light curves, B and V light curves comparison, starspot 79−67064
YY Herculis, symbiotic star, radio continuum detect. 79−25615
YY Herculis, symbiotic star, radio emission report refuted 79−35274
u Herculis, synthetic light curve soln. of OAO-2 UV light curves 80−4399
AM Herculis, visual magnitude estimates (1977, April-May) 77−53642
AM Herculis, visual magnitude estimates (1980 March-June) 80−82428
AM Herculis, X-ray binary, optical light curve 77−33566
AM Herculis, X-ray binary, optical variability 78−53952
AM Herculis, X-ray binary, polarization obs., mag. compact star discovery 77−33569
AM Herculis, X-ray light curve 77−45491
AM Herculis (3U 1809+50), IR light curves 78−28727
AM Herculis (3U 1809+50), multicolour linear and circular polarisation obs. and geometrical model 78−8053
AM Herculis (3U 1809+50), polarimetry and spectrophotometry rel. to mag. field 80−94835
AM Herculis (3U 1809+50), single accretion column model rel. to X-ray and optical radiation 78−57578
AM Herculis (3U 1809+50), soft X-ray results from OSO-8 Wisconsin Expt. 78−36722
AM Herculis (3U 1809+50), UV continuum radiation and spectrum obs. 80−67782
AM Herculis (4U 1813+50), rapid light variability obs. *(Russian)* 80−8662
AM Herculis (4U 1814+50), radiation modulation with orbital period 80−105403
AM Herculis (=3U 1809+50), near IR and violet mag. obs. 77−53643
HZ Herculis (Hercules X-1), hard X-ray spectrum, strong cyclotron line emission 78−41085
HZ Herculis (Hercules X-1), IUE obs. spectrum and light var. 80−73069
HZ Herculis (Hercules X-1), optical behaviour, 1976 Aug.-1977 Nov. 79−53855
HZ Herculis (Hercules X-1), optical behaviour in (1976) 78−32603
HZ Herculis (Hercules X-1), optical pulsation theoretical calcs. 78−57580
DQ Herculis (Nova 1934), light curve and double maxima 77−82255
DQ Herculis (Nova 1934), short-period oscills. modulation and pulsed emission lines asymmetry interpretation 80−22044
V533 Herculis (Nova 1963), periodic light oscills. obs. 78−93285
AM Herculis objects, linear polarisation model 78−16460
AM Herculis type binaries, cyclotron self-absorption in accretion columns of magnetic degenerate stars 80−12760
AM Herculis/3U 1809+50 X-ray binary, rot. mag. white dwarf model 77−33571
Hertzsprung-Russell diagram, discovery, meaning, development appl. 78−45322
high luminosity stars in Galaxy and Magellanic Clouds, UBV intrinsic colours 80−26855
high luminosity stars in SMC, interstellar reddening distrib. functions appl. to total/selective absorption. ratio determ. *(German)* 80−67851
high-luminosity stars in nearby galaxies, interstellar reddenings distrib. function rel. to reddening law determ. *(German)* 80−67850
horizontal-branch A-type stars, effective temps., bolometric magnitudes and masses 79−62829
hot horizontal branch stars, theoretical B−V colour indices and bolometric corrections 79−58327
hot plasma, X-ray emission and radiative transfer effect 78−36451
hot stars, prod. of isentropic instabilities in interstellar gas 77−17644
hot stars, UV spectra obs. by International Ultraviolet Explorer (IUE) 78−96474
hot white dwarfs, EUV flux interstellar absorpt., local clumpiness factor determ. 80−36627
hot white dwarfs, luminosity function, spectral type anal. 80−90418
hot white dwarfs as thermal soft X-ray sources 78−57553
HR 1099, binary stars, radio obs. 77−64793
HR 1099, Ca II H and K emission enhancement during February 1978 radio flare 79−21341
HR 1099, flare activity observed at 2.8 cm wavelength 78−36590
HR 1099, H and Ca II, emission during February 1978 radio outburst 79−21340
HR 1099, optical linear polarisation meas. 78−53958
HR 1099, quiescent X-ray emission obs. from RS Canum Venaticorum star 78−81659
HR 1099, radio flux vars. obs. and optical ephemeris 78−36641
HR 1099, RS Canum Venaticorum binary, February 1978 radio flare obs. 80−26911
HR 1099, RS Canum Venaticorum binary, Hα profile obs. 79−21343
HR 1099, RS Canum Venaticorum binary, nonthermal flare emission during February 1978 outburst 79−21332
HR 1099, RS Canum Venaticorum binary, rapidly variable polarisation obs. at radio freqs. 79−21336

stellar radiation continued
HR 1099, RS Canum Venaticorum binary, strong radio flaring discovery 79−21330
HR 1099, RS Canum Venaticorum binary, two-freq. radio polarimetry 79−21335
HR 1099, RS Canum Venaticorum binary, VLA radio obs. during 1977 international campaign 79−21334
HR 1099, RS Canum Venaticorum binary star, radio obs. at 8.0 GHz 79−21331
HR 1099, RS Canum Venaticorum type binary, radio emission detect. 77−9772
HR 1099, RS Canum Venaticorum type binary, strong radio flaring obs. 79−84821
HR 1099, X-ray outburst obs. from RS Canum Venaticorum star 78−81658
HR 1170, δ Scuti-type star, light and colour curves 77−74058
HR 1217, Ap star, spectrum and light vars. relationship 80−26878
HR 1225, δ Scuti star, absolute magnitude, effective temp. and mass from photoelectric study 80−109436
HR 2557, light vars., luminous δ Scuti-type star 78−32490
HR 3413, Ap star, photometric vars. and period *(French)* 78−32471
HR 4594, freq. anal. of low-amplitude δ Scuti star 79−35275
HR 4594, pulsating marginal metallic line (Am) star, obs. 78−49448
HR 4665, spectroscopy of bright long-period RS Canum Venaticorum system 80−36665
HR 5110 (HD 118216), RS Canum Venaticorum binary, radio flaring obs. 79−67053
HR 5153, Ap star, rot. vel. and light vars. period 77−17593
HR 5999, lightcurves for irregular variable shell star 78−77557
HR 7331, δ Scuti star, relation between radial vel. and light vars. 77−9752
HR 8210, freq. anal. of low-amplitude δ Scuti star 79−35275
HR 8210, pulsating marginal metallic line (Am) star, obs. 78−49448
Hyades, mass-luminosity relation from speckle interferometry of binary star 51 Tauri 77−71011
Hyades binary stars, mass-luminosity relations and cluster distance modulus 77−57067
EX Hydrae, 2:3 period ratio in light curve 80−46580
EX Hydrae, dwarf nova, IR and optical light curves 80−67747
EX Hydrae, dwarf nova lightcurve, periodic and secular vars. 80−77413
VZ Hydrae, eclipsing binary, transit or occultation at primary minimum 77−9770
W Hydrae, long-period variable, suspected Zeeman splitting in OH masers 80−36632
VW Hydri, cataclysmic variable, light curve superhumps model 80−4381
VW Hydri, dwarf nova, IR light curves 80−67747
VW Hydri, dwarf nova, light curve superhump model 79−16977
WX Hydri, dwarf nova, obs. of superhumps during supermaximum 79−88677
VW Hydri, dwarf nova, short period light oscills. 78−20837
VW Hydri, light curves of dwarf nova 78−12245
HZ 43, EUV obs. of hot white dwarf. temp. determ., interstellar H I density calc. 78−16422
IC 1795/1805, exciting star total luminosity compared with H II regions IR luminosity 78−96519
IC 4997, compact planetary nebula, central star, UV radiation changes rel. to rapid emission-line vars. 79−92838
IC 5146, young star cluster, polarisation of starlight 77−5550
illumination of ring-shaped nebulae in LMC by embedded stars 80−77457
integrated starlight, synthetic spectrum between 3000 and 10000 Å, discussion 80−62200
integrated starlight synthetic spectrum between 3000 and 10000 Å, calc. method and results 80−46536
intensity statistical distrib. resulting from star random distrib. 80−98700
interferometry, long baseline, S/N ratio 80−26749
interstellar absorption effects in visible and UV *(Italian)* 77−87517
interstellar dark clouds, anisotropic scatt. and formaldehyde lifetimes 78−8080
interstellar diffuse starlight, inverse Compton interactions with relativistic electrons rel. to gamma-ray prod. 80−17448
interstellar linear polarisation, wavelength depend. at near IR wavelengths 80−51833
interstellar linear polarisation in 1-2.2 μ wavelength range 78−77588
interstellar polarisation, fluctuation theory 80−82442
interstellar polarisation anomalies, props. of nearby interstellar medium 77−53659
interstellar polarisation in irregularly fluctuating medium, statistical anal. 80−26926
interstellar radiation field, predicted far UV brightness distrib. 77−64739
interstellar radiation field, rel. to Fe grains temps. 77−71135
interstellar reddening, vector space methods of photometric anal. 78−49338
interstellar reddening in clouds near Sun from SA colour excesses 79−30111
interstellar reddening law in Corona Austrina dark cloud polarimetric meas. 79−17050
interstellar UV radiation, role in interstellar gas heating 80−67839
interstellar UV radiation field, in clouds cooled by C atoms and ions *(Russian)* 80−12801
interstellar UV radiation field, obs. from S2/68 sky-survey telescope 80−77523
intrinsic polarisation, obs. and statistical anal. *(Russian)* 77−13346
inverse Compton effect of electrons on starlight 80−26702
ionising Lyman continuum photon flux and galactic star formation rate 80−67711
ionising source model for Allen's obscured IR source in NGC 2264 viscous disc component 79−21370
ionising star in interstellar density gradient, radio and IR appearance of dusty H II blisters 80−85979
IR and radio continua of hot stars, effects of winds and coronae 77−29817
IR colours, rel. to diffuse interstellar bands strengths 78−93198
IR flux method for stellar temps. and diameter determ. 80−62030
IR fluxes, method for stellar ang. dias. and effective temps. determ. 79−92682
IR fluxes of single main sequence stars (A0 V to G2 V), rel. to radii determ. 80−51758
IR object assoc. with passage of interstellar shock front, radio identification 78−93369
stellar radiation continued
IR point source, obscured, in M17 SW, spectroscopic anal. 79−48878
IR radiometer data, image processing technique appls. 77−49312
IR source in 2S 1702−363 field, IR brightening, probably Mira variable 78−81705
IR sources in compact H II region G45.5+0.1, IR photometry rel. to extinction 78−4396
IR star in open cluster NGC 1502, magnitude *(Russian)* 77−13250
IR stars, search for OH 18 cm emission 78−40949
IR stars, survey for circumstellar OH emission 79−48787
IR stars, very long baseline interferometric obs. of assoc. OH masers 77−53699
IRC+10216, circumstellar dust shell model rel. to IR energy distrib. 80−56972
IRC+10216, far IR obs. 77−29949
IRC+10374, IRC+10523, IR stars, H_2O maser emission detect. 80−62298
IRC+10420, stellar OH maser VLBI obs. rel. to mag. field 79−25742
IRC+10420, supergiant star, new OH maser feature spatial struct. 79−48946
IRC-10442 (GL5268S), possibly two star clusters, near IR and radio obs. 80−4412
K1082, in globular cluster M15, suspected ultrashort period variable star 80−26883
K-type giant stars, IR excesses rel. to presence of circumstellar shells 80−90420
K-type giant stars, reddening determ. from David Dunlap Observatory (DDO) photometry 78−4222
K-type giants, colour excesses, interstellar dust grains distrib. determ. 79−40251
Kerr black hole, elec. and mag. cond. rel. to energy extraction rate 79−25625
Kerr black hole, low-freq. radiation from infalling particle 80−62176
Kuwano's novalike object in Vulpecula, IR photometric obs. 80−62147
12 and 16 Lacertae, β Cephei stars, light var. anal. and photoelec. photometry 80−77412
AR Lacertae, eclipsing binary, light curve distortion rel. to period vars. 77−37616
CM Lacertae, eclipsing binary, transit or occultation at primary minimum 77−9770
RT Lacertae, eclipsing double-lined spectroscopic binary, light curve soln. 78−32511
EV Lacertae, flare star, hot-plasma model rel. to flare radiation 78−20838
AR Lacertae, Fourier anal. of light curves, gas stream effects 78−20855
EV Lacertae, IR obs. of flares *(Russian)* 78−93278
12 Lacertae, nonradial oscills. of β Cephei type star 80−4366
DD=12 Lacertae, obs. study of secular var. and pulsational stability 80−41833
RT Lacertae, RS Canum Venaticorum binary, radio emission obs. 79−58379
AR Lacertae, RS Canum Venaticorum type variable, soft X-rays detect. 78−45362
AR Lacertae, times of minima, photoelec. obs. 77−57012
EV Lacertae, UV Ceti variable, flares colour behaviour 80−22020
SW Lacertae, W Ursae Majoris star, photoelectric obs. and epochs of min. light 80−62196
SW Lacertae, W Ursae Majoris type star, 1.2 and 2.2 micron light curves 79−84822
large proper-motion stars, luminosity and motions for stars with annual motion >1″ 79−71020
large-amplitude red variables, luminosities and space motions 77−22244
laser line emission detection in spatially inhomogeneous broadening 77−41312
late B-type stars, rapidly rotating, observed and calculated photometric indices 78−89199
late type stars, Ca II H and K lines and nearby continuum photoelectric calibration 80−36617
late-type giants, position on Hertzsprung-Russell diagram 77−78792
late-type main-sequence and subgiant stars, X-ray obs. of active coronae 80−72925
late-type stars, absolute luminosity calibration 77−45421
late-type stars, intensity effect in Wilson-Bappu relationship 78−85937
late-type stars, IR spectral observations *(Japanese)* 79−80307
late-type stars, kinematical data 77−26009
late-type stars, line width-luminosity relation for Ca II H and K wing emission lines 77−78766
late-type stars, luminosity criteria 77−5527
late-type stars, spectrophotometry, incident and emergent flux calc. 78−4200
late-type supergiants, luminosity effects in spectra 77−60753
late-type supergiants, radio emission search 77−87392
LDS 678B, null circular polarisation meas. of white dwarf 78−96478
CW Leonis, (IRC+10216), IR C star, intrinsic polarisation origin 80−67730
ρ Leonis, effective temp. radius, mass loss and luminosity 80−51748
AS Leonis, flare star, chromospheric emission lines in nonflare red spectrum 79−21294
AD Leonis, flare star, Hα emission short-period variability limits 79−48807
XY Leonis, light curve synthesis for contact binary 79−12494
AQ Leonis, light var. anal. of RR Lyrae star 77−56941
γ Leonis, masses and K-line absolute magnitudes 80−8649
AQ Leonis, Population II double-mode RR Lyrae star, theoretical period ratio 80−62134
R Leonis, SiO maser variability at 86 GHz 80−41839
AD Leonis, UV Ceti variable, flares colour behaviour 80−22020
T Leonis Minoris, Algol-type semi-detached binary system 77−91580
limb darkening, coeffs. from line blanketed model atmospheres 79−35243
line photons, equality of mean escape probability and mean net radiative bracket 78−40815
linear polarisation meas., catalogue for 5070 stars 77−13255
linear polarisation spectrum of compact thermal sources, appl. to mag. fields determ. *(Russian)* 80−90344
linear polarization of 313 nearby low galactic latitude 80−46641
LMC, 30000K star model for far UV spectrum 77−13461
LMC bright stars, luminosity function and comparison with galactic luminosity function 80−82499
LMC giants and supergiants, photometric luminosity calibration, visible obs. 80−94797

stellar radiation continued
LMC OB and supergiant stars, B-band magnitudes and spectral types catalogue 79−40090
LMC OB associations, Apollo 16 for UV spectra 77−33634
LMC X-2 optical candidate, X-ray/optical luminosity ratio 79−17136
LMC X-4 optical counterpart, photometric and spectroscopic obs. 77−49431
long-period variable stars, maser activity rel. to Hδ emission, obs. 79−88685
long-period variable stars, OH maser lines struct. and saturation 78−93264
long-period variable stars in S.hemisphere, narrowband polarimetry 80−98666
long-period variables, discovery of new 1665/1667 MHz OH/IR sources 77−64763
long-period variables, SiO maser pump mechanism and luminosity 79−92772
long-term luminosity variations and flares, evidence and appl. to Sun 78−32435
LP 182-44, faint blue star with large proper motion, discovery 78−49439
LP 701-29, lowest luminosity degenerate star with heavily blanketed spectrum 78−36562
LS 630, subdwarf O star, spectrum and absolute magnitude 77−17561
LS I+61°303, variable binary radio star (B1 Ib), X-ray emission detect. 80−105400
LSI+61°303, radio, optical, X-ray, gamma-ray Be star, long term light vars. 79−88755
LSI+61°303, supergiant Be star, radio emission and radial vel. periodic vars. 80−62149
luminosity calibrations from trigonometric parallaxes, practical improvement method 79−40083
luminosity classification of ADH objective prism spectra, procedure 80−72930
luminosity function, implications of mass distrib. law of protocluster fragments systems 79−44571
luminosity function *(Russian)* 77−82214
luminosity rel. to macroturbulence in early K-type stars 79−96997
luminosity systems calibration, trigonometric parallaxes appl. 80−4343
luminous blue variable stars in M31 and M33, IR detect. 78−49437
luminous O-B3 type stars in open clusters, colours rel. to circumstellar shells and mass loss *(German)* 78−53925
luminous stars in Milky Way, absolute magnitudes of supergiants and O-type stars 79−40183
luminous stars in NGC 6822 and IC 1613, visible spectra and photometry 80−82345
RU Lupi, T Tauri star, chromosphere and corona parameters and expected X-ray fluxes *(Russian)* 80−51770
α Lupi, UV light curve of β Cephei-type star 78−36570
Luyten proper motion stars, use of Luyten's magnitude estimates of red nearby star suspects selection 80−82353
Lyman α radiation in planetary nebulae, rel. to recomb. and level populations of ions 77−45529
α Lyrae, absolute energy distrib. from 3295 Å to 9040 Å 78−20828
ι Lyrae, Be star, Hα emission disappearance 79−5834
α Lyrae, continuous UV flux, non-LTE calc. 77−49382
XY Lyrae, late-type variable star, spectral energy distrib. and spectral types *(Russian)* 78−40958
β Lyrae, light curve rel. to struct. of system *(Russian)* 79−97036
β Lyrae, nature of disc around secondary component 78−16458
MV Lyrae, polarisation and spectrum obs., polar class candidate *(Russian)* 78−93322
AY Lyrae, soft X-ray emission detect. from dwarf nova, H1839+37 79−75227
MV Lyrae, soft X-ray emission form nova-like object 79−92787
α Lyrae, soft X-rays detect. with imaging X-ray telescope 79−48953
β Lyrae, UV spectrum and light curves 78−8048
α Lyrae (Vega), absolute calibration 79−40193
α Lyrae (Vega), continuous energy distrib. rel. to LTE blanketed models predictions 80−26856
α Lyrae (Vega), evidence for light and vel. vars. 79−75208
RR Lyrae blue variables in M22, photometry 78−85945
RRab Lyrae field stars, metallicity rel. to luminosity 78−77561
RR Lyrae stars, cycle area in two colour diagram 79−21297
RR Lyrae stars, multiperiodic, pulsation modes rel. to H-R diagram 77−87431
RR Lyrae stars, observational review of multiperiodic behaviour 77−87430
RR Lyrae stars, period-luminosity-colour relations, metallicity effects 80−56842
RR Lyrae stars, semiconvection and period changes 79−30072
RR Lyrae stars, theoretical period ratios 80−62134
RR Lyrae stars in globular clsuters, period-amplitude relation and ω Centauri anomalous horizontal branch 79−67019
RR Lyrae stars in globular clusters, transitional period-luminosity depend. 77−53614
RR Lyrae stars in IC 4499 globular cluster, periods and light curves 79−44490
RR Lyrae stars in Palomar-Groningen fields, luminosities, distances and kinematics 78−93276
RR Lyrae stars light variations, hydromagnetic processes as cause of period changes 80−105261
RR Lyrae type variable discovery near M4 *(Chinese)* 78−69804
RR Lyrae variables, δ(0.6) UV excess rel. to metallicity and three-dimensional motion 80−12754
RR Lyrae variables in NGC 1851, periods and light curves 78−73714
M13, globular cluster, colour-magnitude diagram using astrometric membership probabilities 79−75252
M13, globular cluster, stellar luminosity function rel. to calculated and observed integral magnitudes 79−97043
M15 faint stars, main sequence intrinsic width and luminosity function 77−78834
M17, exciting stars radiation rel. to far IR obs. and H II region/mol. cloud interaction 80−22053
M1-2 central star, possible eclipsing binary in planetary nebula 80−105239
M31, M32 nuclei, luminosity-sensitive spectral features rel. to stellar luminosity function 78−49431
M37, open cluster, luminosity function 77−13419
M67, main-sequence stars differential blanketing rel. to Hyades and Coma 78−57597

stellar radiation continued
M-type dwarf stars in galaxy cluster Abell 2029, coronal X-ray emission rel. to SAS 3 obs. 80−82519
M-type giant stars, spectral energy distribs. and effective temp. scale 78−28678
M-type stars, in solar neighbourhood, absolute magnitudes 78−81631
M-type stars, spectral type and luminosity classification from near IR spectrograms 79−16952
M-type supergiants, in LMC, MK spectral types, luminosities 79−62820
magnetic DA white dwarfs, spectral line and circular polarisation profiles 80−62123
magnetic neutron stars, vacuum birefringence effects on X-ray polarisation 79−40209
magnetic pole model for pulsar emission 79−48838
magnetic variable Ap stars, light vars., rot. and evolution 77−87426
magnetic variables, intrinsic rot. rels. correl. with colour index and masses 78−40967
magnetic white dwarfs, gamma ray burst model *(Chinese)* 80−12831
magnetic white dwarfs, source of polarised radiation 77−2428
magnetobremsstrahlung and optical polarisation in white dwarfs 77−45417
magnitude-diameter relations for star images on Palomar Sky Survey prints 77−49310
main sequence location as function of chemical comp. 77−71105
main sequence stars, chem. comp. effects on position in H-R diagram 77−91521
main-sequence reddened stars, ANS photometry, UV colours 80−77400
main-sequence stars, comparison of four-colour photometric obs. with evolutionary models 78−8007
maser emission, role of dust in pumping 78−36716
mass flux from stars, fluctuation theory 79−53804
mass loss in stars of moderate mass by stellar wind 78−12210
massive black holes, X-ray spectrum from disc accretion 78−40985
massive close binaries, conservative evolution rel. to optical and X-ray luminosities 78−49479
massive stars, effects of convective and semiconvective mixing on main-sequence luminosity 80−90405
massive stars, evolution with mass loss by stellar wind, tracks in HR-diagram 78−4197
massive stars, luminosities and temps. rel. to evolution 80−90416
Me-type dwarf stars, interpret. of cyclic photometric variations 77−74059
Me-type dwarf stars, long-term variability 78−93254
Melotte 66, oldest open cluster, giant branch clump luminosity rel. to age 80−17621
metal-poor stars, effective temps. and element abundances of high-vel. dwarfs 78−53933
metallic line stars, spectral energy distrib. *(Russian)* 80−72975
Mira and semiregular variables, microwave and IR obs. of H_2O vapour maser emission 79−67037
Mira envelopes, OH maser luminosity and expansion vel. gradient 79−71043
Mira type stars, luminosity props. from spectra and light curve elements 80−105253
Mira type variables, mass outflow vel. rel. to luminosity 78−93270
Mira variables, H_2O emission characts. 77−45447
Mira variables, intrinsic amplitude and TiO absorption 78−36580
Mira variables, luminosity from observational data 78−45333
Mira variables, mass loss and OH maser emission 79−16969
Mira variables, OH emission high-sensitivity search 78−89203
Mira variables, SiO maser luminosity and spectral type correl. 77−33512
21 Monocerotis, δ Scuti type star, freq. anal. 77−49398
AU Monocerotis, mathematical anal. of photometric peculiarities 80−77448
R Monocerotis, T Tauri star, long period vars. 80−82350
V616 Monocerotis (A0620-00), light curve 77−64777
V616 Monocerotis (Ariel 0620-00), colour excess rel. to distance 77−64744
V616 Monocerotis (Nova 1975=A0620−00), 8-day modulation 77−87442
V616 Monocerotis (Nova 1975=A0620−00), X-ray and visible light curves 77−82331
moving envelopes, radiation field and statistical equilib. eqns. rel. to spectral line form. 77−87374
multiple periodic variable stars, IAU Colloquium, Budapest, Hungary (1-5 Sep., 1975) 77−87422
α Muscae, β Canis Majoris type variability discovery from UBV photometry 79−80326
MWC 349, IR source optical identification with reddened high-luminosity star 80−56971
MWC 349, possible model of emission line star *(Italian)* 79−48829
MXB 1636−53, X-ray burst source, simultaneous X-ray and optical bursts obs. 79−92893
MXB 1728−34, type I X-ray burst obs. by (HEAO-1) 80−17692
MXB 1730−333, Rapid Burster, possible X-ray emission 79−84868
MXB 1730−335, HEAO obs. of X-ray burst 79−17139
MXB 1730−335, Rapid Burster, IR bursts detect. confirmation 80−27020
MXB 1730−335, rapid burster, SAS-3 obs., (1979, March 3 to 4) 79−40299
MXB 1730−335, rapid X-ray burster, SAS-3 obs. 79−9037
MXB 1730−335, X-ray rapid burster, unsuccessful search for IR bursts 80−98740
MXB 1730−335 (Rapid Burster), microwave bursts obs. 80−62320
MXB 1730−335 (Rapid Burster), steady X-ray emission obs. 80−22119
MXB 1735−44, optical bursts obs. 78−61937
MXB 1735−44, X-ray burst sources, 3 s delay in optical burst 79−58442
MXB 1837+05 (Serpens X-1), detect. of optical burst coincident with X-ray burst 80−27013
nearby supernova, climatic and biological impact on Earth 78−28297
nebulae central stars, temps. determ. from forbidden O III lines 78−41015
negative bursts of flare star radiation, mechanism *(Russian)* 77−64776
neutrino bursts, correl. with gravit. waves and experimental appls. 78−77567
neutrino emission and pre-supernova behaviour of 15 M⊙ star 79−35282
neutrino emission by collapsing stellar cores, light element production 79−21173

stellar radiation continued
neutrino emission from dense stellar cores, time-dependent neutrino transport theory 80−94783
neutrino emission from spherical star, relativistic model 78−73705
neutrino pair emission, stellar plasma in strong mag. field, photon-neutrino coupling theory 77−17548
neutrino radiation for hot neutron star form., rel. to envelope outburst problem 78−45350
neutrinos, high energy, emission from point sources and detect. techniques 79−2484
neutrinos and cosmic rays from pulsars 80−31319
neutron star, accreting, X-ray bursts rel. to thermonuclear flashes in degenerate envelope 80−109455
neutron star, magnetised, X-ray radiation and cyclotron line form. 79−48839
neutron star, neutrino-pair bremsstrahlung in hot plasma, strong mag. field 78−61878
neutron star crust, contribution to neutrino luminosity 79−97018
neutron star formation, competition between neutrino and gravitational radiation 77−49421
neutron star progenitors, galactic luminosity and neutron stars form. rate upper limit 78−49471
neutron stars, accreting, nuclear burning and X-ray bursts 78−36724
neutron stars, accreting magnetic, cyclotron line form. 80−90463
neutron stars, electrodynamics and radiated power in curved space 80−90465
neutron stars, electron-positron annihilation in mag. field 77−10236
neutron stars, gamma-ray bursts from accretion instabilities 77−13377
neutron stars, highly magnetised, thermal radiation 80−56869
neutron stars, luminosity and spectrum from supercritical time-dependent accretion 80−85967
neutron stars, luminosity enhancement following X-ray bursts 78−32502
neutron stars, neutrino emissivities 79−97016
neutron stars, neutrino energy loss rel. to cooling 80−77443
neutron stars, nuclear energy release and X-ray emission 77−78814
neutron stars, radiation source form. mechanism mag. annihilation *(Chinese)* 80−77440
neutron stars, radiative effects in supersonic accretion 78−40978
neutron stars, thermal/timing instability rel. to X-ray transients 79−92795
neutron stars, thermonuclear runaways rel. to X-ray bursts 80−22032
neutron stars, X-ray bursts prod. by thermonuclear flashes 78−12417
neutron stars, X-ray bursts radiation spectrum rel. to mass-radius relation 80−77444
neutron stars cooling, calcs. 79−101170
neutron stars EM recoil radiation, role of EM multipole fields 80−26896
neutron stars formation, neutrinos and gravit. waves emission 78−12266
neutron stars surface radiation, detectability rel. to cooling and heating processes 80−31323
neutron stars X-ray bursts, radiative heat transfer in surface layers 80−94826
newly formed stars in Taurus dark cloud complex, IR study 79−8963
NGC 188, open cluster, anomalous giant branch 78−41001
NGC 2024, H II region, near IR obs. and multiple exciting stars model 79−58393
NGC 2024 (Orion B), exciting star props. from recomb. line obs. 77−29895
NGC 205, stellar content rel. to UV flux 80−98716
NGC 253, Sc-type galaxy, stellar content determ. from two-micron spectrophotometry 80−4442
NGC 4565, galaxy, dark halo stars luminosity and mass function 79−62905
NGC 4565, spiral galaxy, late-type stars in optical halo 78−12364
NGC 654, young star cluster, polarisation of starlight 77−5550
NGC 6611, young open cluster, UBV magnitudes and colours, reddening, distance, luminosity 80−31332
NGC 6752, globular cluster, blue horizontal-branch stars photometry and temps. 78−49488
NGC 7027 central star, radiation rel. to low excitation emission spectrum 77−64823
NGC 741, 1316, 7626, radio galaxies, central dense star clusters luminosities rel. to accreting black holes 80−94871
NGC 7822 (W 1), supernova remnant, exciting stars radiation rel. to 2.8 and 6 cm obs. 78−4383
Nilson dwarf galaxies, H I survey rel. to photometric props. 79−92851
S Normae, Cepheid, luminosity and membership of NGC 6087 visible obs. 80−94797
non-LTE radiative transfer, asymptotic expansion for small ε 78−16287
non-LTE transfer, rapidly convergent iterative method for Wiener-Hopf integral eqns. 78−12089
nonradially oscillating star, light and radial vel. vars. 77−91514
S Normae, Cepheid in NGC 6087, distance and luminosity from cluster four-colour and Hβ photometry 80−62208
Nova Centauri 1979, radio detect. of novalike object 79−67026
Nova Cygni 1975, continuum periodic variability 77−13365
Nova Cygni 1975, energy distrib. in 3100-5100 Å range *(French)* 77−22240
Nova Cygni 1975, polarisation obs. *(Chinese)* 77−67097
Nova Cygni 1975, stellar wind and light vars. 77−82237
Nova Cygni 1975 (V1500 Cygni), light curve 77−2437
Nova Cygni 1975 (V1500 Cygni), minute time scale flickering and 6.6 hour light period 77−17582
Nova Cygni 1978, discovery report and visual magnitude estimates 78−85962
Nova Cygni 1978, photoelectric obs. and visual magnitude estimates 78−89214
Nova Cygni 1978, photometric obs., light vars., IR obs. showing dust form. phase 78−96494
Nova Cygni 1978, polarisation obs. and visual magnitude estimates 78−89213
Nova Cygni 1978, prediscovery mags. and 1978 September spectral features 78−93282
Nova Cygni 1978, rapid flickering and UBV photometry (1978 Sept.) 79−16985
Nova Cygni 1978, spectra, polarisation, photometry and visual magnitude estimates 78−93283
Nova Cygni 1978, spectrum, distance and absolute magnitude 78−89212
Nova Cygni 1978, UBV photometry, brightnesses and distance 78−93284
Nova Cygni 1978, UBV photometry and short-period vars. 79−5835
stellar radiation continued
Nova Cygni 1978, V photoelectric and visual magnitudes (1978 Sept.-Nov.) 79−5837
Nova Cygni 1978, visual magnitude estimates, (1978 September 13 and 14) 78−89210
Nova Cygni 1978, visual magnitude estimates (1978 September 10 to 12) 78−85963
Nova Cygni 1978, visual magnitude estimates for 1978 Oct. 78−93286
Nova Delphini 1967, forbidden lines flux rel. to envelope ionisation and central star props. *(French)* 77−53603
nova in Magellanic Clouds (LMC), premaximum spectrum 79−62853
probable nova in Sagittarius (1978), magnitudes (1978 June 30 to October 3) 79−101164
nova light curves, as manifestation of nonuniform stellar wind 80−62160
nova light curves, bloated dwarf model 77−82251
Nova Monocerotis 1975 (Ariel 0620−00), linear polarisation obs. 77−13351
Nova Monocerotis 1976 (Ariel 0620−00), Ariel 5 obs. of decay 77−29950
Nova Ophiuchi 1977 (H1705−25), X-ray light curve 78−49453
Nova Ophiuchi 1977 (H1705−25), X-ray nova, HEAO 1 obs. 78−49452
nova outburst, induced nucleosynthesis 77−82263
nova outburst, review of thermonuclear runaway model 77−82262
nova outburst models 77−82248
nova outbursts, shell ejection timing 77−82252
Nova Persei 1974 (V400 Persei), light curve and spectral evolution 78−73715
Nova Sagittaè 1977, spectral obs., visual magnitude estimates 77−22253
Nova Sagittae 1977, visual magnitude estimates 77−60768
Nova Sagittae 1977, visual magnitude estimates (1977 Aug.-Oct.) 78−8021
Nova Sagittarii 1977, early spectrum and spectrophotometry 78−32496
Nova Sagittarii 1977, photometry, spectrum, absolute magnitude and distance 78−53955
Nova Sagittarii 1977, visual magnitude, UBV and Hα obs. (1977, March) 77−33517
Nova Sagittarii 1977, visual magnitude estimates 77−60766
Nova Sagittarii 1977, visual magnitude estimates (1977, Aug.-Oct.) 78−4246
Nova Sagittarii 1978, identified with IRC *7a C−$_{\rightarrow}$C −20494=V3876 Sagittarii, IR obs. 78−49459
Nova Sagittarii 1978, precise position, visual magnitude estimates 1978 Apr. 78−49458
Nova Scuti 1975 (V373 Scuti), light curve and spectral evolution 78−73715
Nova Serpentis 1978, distance and luminosity from dust shell ang. expansion rate 80−90430
Nova Serpentis 1978, precise position, spectra, visual magnitude estimates 78−36596
Nova Serpentis 1978, UBV photometry and magnitude estimates 78−40959
Nova Serpentis 1978, visual magnitudè estimates 1978 Mar.-Apr. 78−49457
Nova Serpentis 1978, visual magnitude estimates (1978 April) 78−53959
Nova Serpentis 1978, visual magnitude estimates (1978 April-June) 78−61873
nova shell expansion and IR brightening 79−97007
nova shells, radio emission obs. 80−26868
Nova Vulpeculae 1976, IR energy distrib. 1976, Nov./Dec. 77−9757
Nova Vulpeculae 1976, magnitudes and photoelectric obs. (1976 October-November) 77−5538
Nova Vulpeculae 1976, photoelec. obs., visual magnitude estimates 77−33533
Nova Vulpeculae 1976, photoelectric V measures and visual magnitude estimates 1976, Dec. 77−17600
Nova Vulpeculae 1976, polarisation meas., reddening and distance 77−29855
Nova Vulpeculae 1976, visual magnitude estimates 1976 Nov.-Dec. 77−17598
Nova Vulpeculae 1976, X-ray emission upper limits, Ariel V data 77−64781
Nova Vulpeculae 1979, photoelectric obs., (1979 April 21 and 25) 79−53822
Nova Vulpeculae 1979, photometric history (1898 to 1978) 79−53819
Nova Vulpeculae 1979, posn., magnitudes, spectrum and photometry 79−48818
Nova Vulpeculae 1979, prediscovery obs. and visual magnitude estimates 79−48817
Nova Vulpeculae 1979, slow nova, pre-maximum light curve 80−4364
Nova Vulpeculae 1979, spectroscopic and photometric obs., (1958 and 1968) 79−58344
Nova Vulpeculae 1979, visual magnitude estimate, (1979, May 2) 79−58348
Nova Vulpeculae 1979, visual magnitude estimates, 1979 Jun. 79−75221
nova-like variables, photometric obs. 77−82245
novae, effect of binary companion on outburst 80−82394
novae, radiation press. effects on shells structural development 77−64746
novae, reddening by dusty circumstellar envelopes *(French)* 77−56940
novae, shell ionisation and remnant Lyman continuum output from time-depend. model 79−53816
novae, transient thermal X-ray emission from shocked circumstellar gas 77−45437
novae, transition zone oscills. inception 77−87402
novae, UV radiation rel. to dust form. and ionisation in envelope 80−98678
novae, visual magnitude estimates (1977, April-May) 77−53610
novae, visual magnitude estimates (1977, June-Aug.) 77−74064
novae, visual magnitude estimates (1977 January-February) 77−29853
novalike object in NGC 5272, photometry and identification as W Virginis variable 79−75224
novalike object in Vulpecula, 1980 May-June spectra and magnitudes 80−82392
novalike object in Vulpecula, UBV photometry (1979 August 6 to September 20) 80−8644
novalike object in Vulpecula, UV decline and expanding cooling photosphere 80−67741
novalike object in Vulpecula, visual and red photographic magnitudes 79−92784
novalike object in Vulpecula, visual magnitude estimates 79−88673

stellar radiation continued
novalike object is Vulpecula, visual magnitude estimates (1980 February 2 to May 9) 80−72980
NP 0532, Crab pulsar, model, X-ray, optical and radio emission 78−4265
NP 0532, Crab pulsar, optical and X-ray pulses, Compton effect 79−53849
NP 0532, Crab pulsar, radiation, role of magnetosphere cyclotron instability *(Russian)* 80−8645
NP 0532, Crab pulsar, search for X-ray polarisation 79−5851
NP 0532, Crab pulsar, transient structure of high-energy X-ray emission 77−33541
NP 0532, Crab pulser, gravitational radiation obs., energy flux upper limit 80−36655
O-B3 stars in southern clusters excess visual extinction 77−78791
O-type runaway stars, statistical parallax, underluminosity 78−57552
O-type star, ionisation of low-density intercloud medium 77−9782
O-type stars, coronal emission rel. to UV reson. lines 79−21293
O-type stars, dispersal of massive molecular clouds 79−25693
O-type stars, effective temps., far UV photometric obs. 79−88656
O-type stars, photometric catalogue on mag. tape, third edition 77−2348
O-type stars, prod. of galactic extended low-density H II region and diffuse IR emission 79−17047
O-type stars, vector space anal. of photometry rel. to atmospheric extension 78−49338
O-type stars in NGC 7000 (North America Nebula), continuum scatt. rel. to rocket UV imagery 80−82440
O-type stars in open cluster IC 1805, luminosities rel. to C IV line P Cygni profiles 80−31296
O-type stars towards Carina Nebula, extinction law 80−105240
OB3 type stars in young clusters, circumstellar matter 2200 Å hump interpretation 80−82351
OB star winds, radiative amplification of sound waves 79−96999
OB stars, newly formed, H_2O emission from circumstellar shells 78−12390
OB supergiants, radiation-driven density waves rel. to mass transfer to X-ray binaries 77−9809
OB supergiants, X-ray flux and ionization in wind, corona effects 79−48783
OB-type southern stars, UBV, Hβ and polarisation meas. 77−26007
OB-type stars, effective temps., ang. diameters, distances and linear radii 80−17584
OB-type stars, luminosity depend. of C III 5696 Å transition from absorpt. to emission 79−67006
Of-type stars, X-ray flux and ionization in wind, corona effects 79−48783
OH maser emission from late-type stars, UHF obs. 80−56826
old stars, UV excesses rel. to kinematics and Galaxy initial contraction 80−62204
oldest Population I stars, H-R diagram and age difference from extrême Population II stars 77−56912
opacity in dense plasma 80−26731
open cluster stars, variable extinction anal. rel. to value of R 77−37627
open cluster stars, zero age main sequence correction for age depend. *(Russian)* 79−48871
open clusters, binary stars freq. estimation from colour-magnitude diagrams 77−49441
open clusters, H-R diagram, gap in evolving main sequence 79−30096
open clusters, H-R diagrams anal. rel. to Galaxy chemical abundance gradient 80−56938
Y Ophiuchi, anomalous Cepheid, evidence for duplicity 78−53990
V566 Ophiuchi, eclipsing binary light curve 77−71130
ω Ophiuchi, UBV photometry of Ap star, periodicity in luminosity vars. *(French)* 78−57559
ζ Ophiuchi, UV radiation rel. to rotationally excited interstellar HD obs. 79−25674
V566 Ophiuchi, W Ursae Majoris binary, synthetic light curve calc. 77−74097
Orion Nebula cluster, variable stellar polarisation *(Russian)* 77−60807
Orion Nebula stars, wavelength depend. of polarisation, rel. to intracluster dust and circumstellar shells 77−78839
Orion OB 1 association stars, absolute magnitudes from photometric study 77−82288
Orion population stars, OH emission survey 80−67716
Orion stars, far UV radiation scatt. in Barnard Loop Nebula region 77−29911
α Orionis, 14.9 GHz obs. 79−75210
β Orionis, line blocking, reddening empirical effective temp. determ. 77−87389
U Orionis, Mira variable, relation between 1612 MHz flare and light curve 80−56844
λ Orionis, obs. of UV radiation scattered by interstellar dust 80−56918
α Orionis, polarized light scattered by dust shell 79−12473
U Orionis, stellar OH maser VLBI obs. rel. to mag. field 79−25742
α Orionis (Betelgeuse), radio emission 79−48788
α Orionis (Betelgeuse), UV flux meas. 77−22231
χ^1 Orionis (SAO 077705), ang. dia. and visual surface brightness meas. 78−20825
λ Orionis A, far UV flux, emission line obs. of surrounding H II region 78−93303
θ^2 Orionis A, stellar wind driving of high-vel. features in Orion Nebula 79−8978
δ Orionis A, UV spectrophotometry and optical polarimetry, stellar wind variability 79−21277
σ Orionis E, peculiar eclipsing binary, linear polarization obs. 78−32508
U Orionis OH maser flare detect. 79−40197
γ Pavonis, uvby β colours rel. to C and N abundances 77−91531
RU Pegasi, dwarf nova, rapid and ultrarapid light vars. 77−53596
B Pegasi, M-type giants Mg II emission linewidth/luminosity relation 78−53945
AG Pegasi, symbiotic nova, radio emission obs. 77−22232
EQ Pegasi (BD+19°5116), flare active binary system 78−61868
period-luminosity relation for Cepheids in Magellanic Clouds, Wesenheit function, reddening correction 77−91553
AX Persei, 1978 Jan.-Feb. outburst of Z Andromedae-type object 78−36588
β Persei, 3428 Å light curve rel. to components luminosities and temps. 77−53634
KT Persei, dwarf nova, brightness oscills. during two outbursts 77−2438
UV Persei, dwarf nova, characts. of outbursts 79−71052
X Persei, energy distrib., light vars. 1972-76 period 78−16437

stellar radiation continued
RT Persei, light curve analysis by automated Fourier technique 79−17020
S Persei, M-type supergiant, OH emission rel. to circumstellar envelope struct. 77−22218
12 Persei, masses and luminosities from speckle interferometric obs. 78−93305
53 Persei, nonradical pulsator, light var. rel. to line profile changes 80−4362
S Persei, periodic nature of semiregular variable 77−67099
X Persei, photometric behaviour, 1964 to 1979, and binary star model 79−53820
S Persei, supergiant 22 GHz H_2O maser emission temporal var. 78−49461
ξ Persei, time depend. radiation flux rel. to struct. of NGC 1499 ionisation front 78−24537
RW Persei, UBV photometry of semidetached binary system 79−25639
X Persei, V-band polarization variability 78−49455
Gk Persei, visual magnitude estimates (1978 July) 78−69809
X Persei (4U 0352+30), Be star, evidence for 6-year photometric periodicity 80−109446
X Persei (A 0535+26), Prognoz-6 obs. of X-ray fluxes and energy spectra *(Russian)* 80−109562
β Persei (Algol), hard X-ray obs. 77−13493
β Persei (Algol), light curve at 10 μm near scondary min. 78−93315
β Persei (Algol), radio outbursts and possible period change 80−26907
β Persei (Algol), X-rays detect. 77−9773
β Persei (Algol) system, gravity darkening 79−44525
GK Persei (Nova 1901), visual magnitude estimate for 1978 July 78−69807
GK Persei (Nova 1901), visual magnitude estimates for 1978 Jul. 78−73718
β Persei type systems, orbital period changes and evolutionary status 80−4396
SX Phoenicis, dwarf Cepheid, light and radial vel. vars. 79−25612
SX Phoenicis, simultaneous photometric and polarimetric obs. 78−49451
SX Phoenicis light curve, colour effect obs. 78−93248
photon emission from gravitationally intense cylindrical bodies 78−57840
photon helicity detection for matter/antimatter star discrimination 78−12092
δ Pictoris, β Lyrae-type eclipsing binary, satellite UV obs. 77−57033
RR Pictoris, accretion disc radiation of cataclysmic binary 77−91537
64 Piscium, double line spectroscopic binary, orbital elements and absolute magnitude *(French)* 79−35305
SZ Piscium, RS Canum Venaticorum star, photometric obs. rel to starspot model 80−109490
RZ Piscium, UBV photometry, light minima *(Russian)* 78−93323
planetary nebulae, low excitation, central stars, continuous energy distribs. and temps. 80−17646
planetary nebulae central star, far UV flux determ. from nebula ionisation state 80−72945
planetary nebulae central stars, colour temps. and spectral classifications 80−109435
planetary nebulae central stars, interpretation of UV continuum radiation 80−109524
planetary nebulae central stars, radiation rel. to nebula spectrum in composite shell models 79−25677
planetary nebulae central stars, rapid variability theory 77−45439
planetary nebulae central stars, temps. and EUV radiation rel. to nebulae H and He II spectra 80−67724
planetary nebulae central stars, UV radiation meas. 78−28679
planetary nebulae central stars, visual spectra comparison with Zanstra temps. 80−109434
planetary nebulae nuclei, far UV fluxes rel. to nebulae ionisation and spectra 80−109529
planetary nebulae nuclei, luminosity rel. to He shell flashes, nebula ejection and distance scale 78−24540
planetary nebulae nuclei, radiation during He shell flashes rel. to nebulae ionisation 80−73021
planetary nebulae nuclei, temps. rel. to masses and nebulae evolution 80−82344
planetary nebulae nuclei, UV spectra rel. to effective temps. and radii 79−92843
planetary nebulae of overall field and galactic centre, nuclei temp. differences 78−54029
plasma laser star model of QSOs 78−96558
Pleiades, radiation press. rel. to filamentary struct. of refl. nebulosity 78−8082
Pleiades cluster, reddening-face colours, photometric zero age main sequence definition 80−26920
Pleiades region stars, radio and optical obs. of flares *(Russian)* 78−93245
point source orbiting Schwarzschild black hole, polarised radiation props. 77−67109
polarisation, from Thomson scatt. of light of spherical limb darkened star 79−58324
polarisation, meas. of stars near N.Galactic Pole rel. to interstellar extinction 79−62814
polarisation by Thomson scatt. in optically thin axisymmetric envelopes 77−56914
polarisation of scattered radiation, in medium with internal energy sources 80−67541
polarised radiation, from point source orbiting Schwarzschild black hole 77−67109
polarised radiation from stars with nonuniform surface brightness distrib. 77−17549
polarization by Thomson scattering in circumstellar envelopes, Monte Carlo analysis 80−85931
Population I star clusters, integrated colour synthesis 77−17637
Population II (pregalactic) stars, rel. to distortion of cosmoloical microwave black body radiation spectrum 80−67915
pre main sequence stars, rapidly rotating, evolution in gravit. contraction phase 80−62133
pre-main sequence stars, H-R diagram from star form. observational study 79−25592
prenovae and outburst amplitudes, physical parameters 77−87437
pressure in spectral lines in gaseous systems with axisymm. motions, kinematics 79−88579
primordial black hole explosions, search for optical pulses 77−57006
propagation in stellar atmosphere, vibr. buildup in surrounding plasma *(Russian)* 77−3946

stellar radiation continued
protostar, radiation rel. to interaction with infalling matter and interstellar grains origin 77−13327
protostar in bright-rimmed mol. cloud IC 1848 A, luminosity rel. to CO emission 79−5810
protostars, radiation rel. to cosmic gas clouds fragmentation and initial stellar mass function 77−56907
protostellar envelopes of masses 3 M⊙ and 10 M⊙, coupled radiative transfer/hydrodynamics eqns. and IR appearance 80−36616
protostellar H_2O maser sources, disc struct. rel. to maser emission 79−48784
protostellar sources, IR polarisation rel. to nearby interstellar polarisation 80−4347
PSR 0031−07, drifting subpulses obs. and implications for pulsar models 80−67763
PSR 0239+54, four-freq. study of single-pulse structure 78−53972
PSR 0525+21, pulsar, radio polarisation rel. to assoc. with supernova remnant 78−85965
PSR 0531+21, Crab pulsar, optical light curve changes in 1970-7 period 80−36654
PSR 0531+21, radiation generation mechanisms *(Russian)* 79−58370
PSR 0611+22, short time scale integrated pulse shape vars. 80−105267
PSR 0809+74, pulsar, phase stability in drifting subpulse pattern 78−40980
PSR 0820+02, period vars. rel. to membership of long-period binary system 80−56867
PSR 0833−45, Veal pulsar, optical pulses detect. 77−49417
PSR 0833−45, Vela pulsar, optical pulse profile 80−46593
PSR 0833-45, Vela pulsar, pulsed high energy gamma rays 80−41848
PSR 0950+08, pulsar, micropulses freq. struct. 80−22030
PSR 1133+16, high time resolution obs. of high freq. radio emission microstruct. 78−45348
PSR 1133+16, pulse microstruct. direct. obs. at timescales down to 6 μs 78−28711
PSR 1913+16, binary pulsar, gravit. radiation in alternative metric theories 77−60589
PSR 1913+16, binary pulsar, radio emission props. progress report 79−75234
PSR 1919+21, interpulse radio emission at freqs. 16.7-38 MHz 78−16447
PSR 1919+21, pulsed radiation at 16.7, 20 and 25 MHz 77−87466
PSR 2020+28, pulsar, orthogonal polarisation modes obs. 78−93291
pulsar, mag. bremsstrahlung of ultrarelativistic particle beam in relativistic plasma 80−46390
pulsar coherent radiation, relativistic soliton model *(Russian)* 78−77568
pulsar gamma-ray emission, production and beaming 78−4266
pulsar interpulses, two-pole and one-pole models 78−16449
pulsar magnetosphere, magnetoactive plasma equilib. in gravit. field *(Russian)* 80−26895
pulsar magnetosphere, relativistic particle curvature radiation 80−77434
pulsar magnetospheres, radiation rel. to limitations on force-free approximation 77−5541
pulsar microstructure, periodicities, polarisation and pulsar magnetospheres probing 79−75232
pulsar microstructure, propag. effects in shearing field-free plasma 80−17483
pulsar produced radiation accelerates supernova envelope 79−62859
pulsar radiation, plasma waves propag. along mag. field in strongly anisotropic relativistic plasma 80−67542
pulsar radiation 79−97015
pulsar radiation patterns, obs. of objects with synchronised drift across window 77−57005
pulsar radio emission, generation in neutron star mantle *(Russian)* 79−101168
pulsar radio emission, magnetosphere vibrs. generation by klystron mechanism 78−53971
pulsar radio emission, propagation effects on polarisation 79−75235
pulsar radio emission pulses, dispersion rel. to interstellar mag. charges dispersion 79−75704
pulsar radio signals spectra and microstruct., relativistic electron beam model 78−65639
pulsar relativistic beaming process rel. to pulses 77−29870
pulsar repetition rate, effects of neutron star thermal-timing instability 79−35293
pulsar rotating magnetosphere, charge bunching mechanism for coherent curvature radiation 77−33538
pulsar scintillations, freq. cross-correl. and finite bandwidth effects 80−4392
pulsar signals interstellar scintillation, analytic soln. of second-order moment eqn. 80−26726
pulsar spectra, nature of low-freq. dropoff 80−17602
pulsar synchro-Compton radiation damping of linearly polarised plasma waves 78−61877
pulsars, amplified linear accel. emission 79−8936
pulsars, average pulse width-period relation rel. to polar cap model for magnetosphere *(Russian)* 79−101169
pulsars, average wave forms, anal. rel. to hollow-cone beam models 77−2449
pulsars, binary, neutrino emission 79−2550
pulsars, charged particle accel. to extremely high energies in far field 77−29868
pulsars, coherent amplification mechanism 77−78809
pulsars, coherent radiation mechanism 79−53848
pulsars, contrib. to gamma-rays from galactic disc 77−67143
pulsars, distribution, birthrate and flux density distrib. 80−98681
pulsars, EM radiation source pulsation characts. rel. to size limit 79−84656
pulsars, emission regions location, obs. limits 78−65637
pulsars, emission regions rel. to ang. momentum and energy loss 77−91557
pulsars, energy spectra and pulse shapes at metre wavelengths 79−75233
pulsars, force-free wind zone stability rel. to coherent radiation spectrum 78−49468
pulsars, fundamental luminosity 79−5850
pulsars, gamma ray emission model 78−65641
pulsars, gamma-ray emission theory 78−53975
pulsars, high-energy pulsed gamma rays obs. 78−45346
pulsars, hollow-cone model of radiation geometry 77−9761
pulsars, individual pulse-polarisation patterns and quasi-transverse propag. theory 80−46591

stellar radiation continued
pulsars, integrated pulse profiles and mean fluxes at 2.388 GHz 79−92791
pulsars, interpulse emission struct. 80−36652
pulsars, interpulses and other off-pulse emission 77−87467
pulsars, magnetosphere instability rel. radiation modulation and 'glitches' 78−53976
pulsars, model of radio emission mechanism 78−12257
pulsars, modulation instability of relativistic plasma rel. to radio radiation *(Russian)* 77−22258
pulsars, narrowband versus broadband emission processes rel. to luminosities 80−51797
pulsars, obs. at 14.8 and 22.7 GHz 78−81645
pulsars, pair form. above polar caps rel. to X-ray and gamma-ray emission 79−92790
pulsars, polarisation characts. at 640 MHz for 43 southern pulsars objects 78−65642
pulsars, polarised shot noise model 77−13374
pulsars, possible radio emission mechanism 79−84812
pulsars, pulse width and period relations for various models 78−28714
pulsars, radiation patterns, observational results rel. to physical mechanism 78−53973
pulsars, radio emission beaming possible relation with rot. braking 79−92793
pulsars, radio emission in axisymmetric magnetosphere model 79−84813
pulsars, radio emission processes rel. to inhomogeneous polar cap struct. 79−25623
pulsars, radio emission rapid var., mechanism *(Russian)* 80−77437
pulsars, radio flux density and pulse profile at 102.5 and 61 MHz 80−17601
pulsars, relativistic beam-plasma system, electrostatic excitation level 77−9762
pulsars, search for thermal EUV radiation 77−22259
pulsars, source of coherent radio emission 80−82403
pulsars, subpulse and micropulse emissions rel. to neutron star crusts torsional oscills. 80−90464
pulsars, timing measurements appl. to search for gravit. waves 80−36743
pulsars emission mechanism, AC Josephson effect hypothesis 80−82404
pulsars in compact supernova remnants, possible γ-ray emission 78−45435
pulsars in S.Hemisphere, obs. of optical pulsations 78−77569
pulsars polarisation, rot. induced by non-Minkowskian spacetime 79−35115
pulsars radio emission, curvature radiation absorpt. theory 79−75090
pulsars radio emission, phenomenological model 78−40979
pulsars radio emission, possible mechanism 78−20847
pulsars radio emission microstruct., qualitative model 77−49415
pulsars radio emission models, relativistic clock error effects 77−64786
pulsars scintillation, mathematical anal. of physically thin screen 78−28501
pulsating X-ray sources, radiation polarisation and beaming, vacuum birefringence effect in mag. field *(Russian)* 78−93476
pulsed and impulsed light from the Vela and Crab pulsars 79−17005
VV Puppis, AM Herculis type binary spectrophotometric obs. 79−5860
VV Puppis, brightening of magnetic variable (1978 March) 78−36595
VV Puppis, circular polarimetry in active state and evidence for two accreting poles 79−48854
V Puppis, eclipsing binary star, radiation rel. to shell spectrum 77−13385
V Puppis, light curve study of early-type close binaries in triple systems 78−89222
VV Puppis, linear and circular polarisation during active phase 77−37621
VV Puppis, linear polarisation obs. in faint state 79−25643
ζ Puppis, of supergiant, mass flow var., visible and UV obs. 80−90431
VV Puppis, proper motion meas., distance and luminosity 78−96510
ζ Puppis, radio emission obs. at 2 cm 78−40969
CP Puppis (Nova 1942), soft X-ray emission detect. 79−80325
TY Pyxidis, light curve of RS Canum Venaticorum type binary 79−25641
QSOs 1548+056, 1721+343, 1722+33, historical light curves 78−32594
radial and nonradial stellar oscills. effect on light, colour and vel. vars. 80−31310
radiative transfer, Sobolev method generalisation for flows with nonlocal radiative coupling 78−28500
radio binary systems, X-ray emission model 77−33700
radio emission from immediate postoutburst supernovae, origin and evolution 78−40973
radio pulsars, subpulse polarization pattern theory 79−48837
radio star obs. at 3.3 mm 77−74065
radiostars, polytropic models rel. to radio emission spectra 79−2544
radiowave generation by gyrosynchrotron and Langmuir-wave processes, solar and stellar appl. 79−21172
rapid var., double telescope system for cross correl. detection 77−82127
recurrent novae, magnitude-frequency relation 78−28699
red dwarf stars, flares characts. 79−16954
red dwarf stars, X-ray flares rel. to galactic X-ray background 77−9755
red dwarfs in southern hemisphere, absolute magnitude and distance, BVRI photometry 80−90419
red giant stars, neutrino emission rel. to evolutionary sequences 78−65611
red giant stars in globular clusters M92 and NGC 6397, C abundances effects on DDO colours 79−48785
red giant variable stars, multiple periodic vars. 77−87427
red giants, in globular cluster NGC 6624, optical and IR obs. 77−45498
red variable stars, amplitude extension and amplitudes limit 79−62836
red variable stars in SMC OB association NGC 371, periods 78−53961
reflection nebulae, radiation effects rel. to CO obs. 77−53658
rigidly rotating star, influence of nonsphericity and radiation press. on moment of inertia 78−28658
rotating Newtonian stars, secular instability to gravit. radiation and viscosity 78−53922
rotating stars, luminosities and radii of models with circulation-free rot. laws 77−67088
rotating stars, surface layers meridional circulation rel. to gravity darkening law 78−20820
Rubin-152, possible massive O-type star on galactic fringe, spectrum rel. to luminosity and distance 80−98656
S-type stars, absolute magnitudes rel. to galactic distrib. and population-type characts. 79−88651

stellar radiation continued
S-type stars, list of brightest stars in IR 77−41382
U Sagittae, Algol type binary, spectrophotometry, u.v. excess 77−2454
WZ Sagittae, B mags. and total visual magnitude estimates 79−21308
WZ Sagittae, BV photometry and magnitudes (1978 Nov.-Dec. outburst) 79−12484
WZ Sagittae, cataclysmic variable, light curve superhumps model 80−4381
WZ Sagittae, eruptive binary, hot spot eclipses rel. to model of system 80−72962
Hm Sagittae, eruptive variable, IR variability 79−25614
HM Sagittae, fast flares UBV photometry and spectra *(Russian)* 79−16991
FG Sagittae, light vars. rel. to photometric radius and pulsation mass 78−36576
U Sagittae, photometric study of eclipsing binary 77−22270
WZ Sagittae, physical parameters from eclipse anal. 79−80336
HM Sagittae, radio emission flux density 77−60770
WZ Sagittae, recurrent nova, IUE obs. in outburst 80−109448
WZ Sagittae, recurrent nova, model for superhump phenomena 80−82368
WZ Sagittae, spectroscopic obs. (1978 December 1 and 2) 79−16983
WZ Sagittae, spectroscopic obs. and photoelectric V-magnitudes 79−16984
HM Sagittae, symbiotic star, IR variability obs. from VJHKL photometry *(Russian)* 80−105263
U Sagittae, theoretical light curve of contact system 78−77578
WZ Sagittae, time of minimum light, period, magnitudes 79−21353
WZ Sagittae, time-resolved broadband obs., optical pulsations, period 79−92781
WZ Sagittae, visual magnitude estimate 1979 June 20 for recurrent nova 79−84800
WZ Sagittae, visual magnitude estimates, 1978 Nov., 1979 Jan.-Feb. 79−30075
WZ Sagittae, visual magnitude estimates, (1978, November 28 to December 11) 79−12481
HM Sagittae, young planetary nebula, 2.8 cm flux density secular increase 79−67025
HS Sagittae (Nova 1977), visual magnitude estimates, (1978, August 5 to September 3) 78−89209
HS Sagittae (Nova 1977), visual magnitude estimates 78−61872
HS Sagittae (Nova 1977), visual magnitude estimates 1978 June 78−85961
μ Sagittarii, binary star, obs. of eclipse of unseen companion 80−4401
AQ Sagittarii, C star, ang. dia. and effective temp. 80−22008
RY Sagittarii, decline and magnitudes (1977 September-August) 77−87414
RY Sagittarii, light-curve at minimum 78−61874
RY Sagittarii, magnitude estimates for R Coronae Borealis-type star 77−78800
MV Sagittarii, R Coronae Borealis variable, brightness decline obs. and UBV photometry 80−8641
RY Sagittarii, visual magnitude estimates (1977 Oct.) 77−91543
RY Sagittarii, visual obs. of 1977 Sept.-Oct. minimum 78−49463
V4021 Sagittarii (Nova 1977), visual magnitude estimates for 1978 May and July 78−69806
μ Sagittarii primary eclipse prediction (for 1979 March 10) 79−35307
Schwarzschild black hole, tachyons from free falling body 77−53625
scintillation, aperture averaging effects, photon counting meas. 77−91519
scintillation in Earth's atmosphere 78−53726
U Scorpii, 1979 March outburst, visual magnitude estimates 79−44504
ζ^1 Scorpii, extreme B1 supergiant, IUE obs. of line spectrum and continuum energy distrib. 80−17583
V866 Scorpii, linear polarization obs., wavelength depend., circumstellar dust envelopes 79−53809
V701 Scorpii, luminosity ratio of early-type contact binary 80−62188
β Scorpii, lunar occultation obs., magnitudes for five components 77−87471
β Scorpii, lunar occultation obs., magnitudes for three components 77−87472
AH Scorpii, M-type supergiant, OH emission rel. to circumstellar envelopes struct. 77−22218
U Scorpii, recurrent nova, 1979 March outburst unconfirmed 79−44506
U Scorpii, recurrent nova, visual magnitude obs. during outburst 79−75225
V861 Scorpii, upper limit on X-ray emission, and non-coincidence with (OAO 1653−40) 80−73072
V861 Scorpii, X-ray emission from unseen companion 78−89226
V861 Scorpii (=OAO 1653−40), X-ray eclipses obs. 78−69838
V818 Scorpii (Scorpius X-1), bremsstrahlung, model for UV continuum energy distrib. 80−82541
Scorpius X−1, interstellar extinction and UV flux distrib. 79−25754
Scorpius X-1, linear X-ray polarisation obs. 79−101221
Scorpius X-1, linear X-ray polarisation upper limit 78−49557
Scorpius X-1, Prognoz-6 obs. of X-ray fluxes and energy spectra *(Russian)* 80−109562
Scorpius X-1, rapid variability simultaneous X-ray and optical obs. 80−62322
Scorpius X-1, review of X-ray, optical and radio emission 78−16576
Scorpius X-1, X-rays effect on equatorial lower mesosphere ionisation 78−36233
Sculptor dwarf spheroidal galaxy, abundance vars. on giant branch rel. to ω Centauri anomaly 79−5904
VY Sculptoris, novalike variable, faint state occurrence and spectrum 80−98675
RZ Scuti, JKL IR obs., light curves for eclipsing binary 80−101615
δ Scuti and RRs stars, observational view of multiperiodicity 77−87432
δ Scuti stars, empirical period-luminosity-colour relations 79−25610
δ Scuti stars, period computation from complex signals *(French)* 78−85949
δ Scuti type stars, dynamical parallax, absolute magnitudes and masses *(Russian)* 79−88690
semi-detached eclipsing binaries, revised photometric masses, radii and luminosities 78−20858
semi-regular variables in stellar groups, absolute magnitudes 77−5537
semiinfinite atmosphere, radiation field in deep layers 79−58325
RT Serpentis, symbiotic star/nova, possible H_2O maser obs. 79−8932
FH Serpentis (Nova 1970), outburst model test 77−82253
FH Serpentis (Nova 1970), radio emission from expanding shell '80−26868

stellar radiation continued
FH Serpentis (Nova Serpentis 1970), dust grain IR emission model 80−105254
Seyfert galaxies, stellar component of IR energy distrib. 78−57645
Seyfert galaxies nuclei, UBV and Hα photometry rel. to variability and stellar contrib. 78−96543
short-period Cepheid blue variable in M22, photometry 78−85945
slow nova, hydrodynamic study of outburst rel. to light vars. and mass ejection 78−40954
SMC, stellar contents and luminosity functions of NE outer arm and halo 78−86013
SMC wing, stellar luminosity function and population 78−86011
SMC X-1, soft X-ray emission detection, 2-day flaring period 79−35432
SMC X-1 (Sanduleak 160) binary source, X-ray pulsations, orbital elements and masses 77−9815
SN 1181 (3C 58), absolute magnitude and type classification 80−56862
SN 1969l in NGC 1058, obs. and theoretical light curves comparisons 77−13370
SN 1973f in NGC 4944, photometry and absolute magnitude 79−21318
SN 1979c in NGC 4321 (M100), detect. at 60 nm wavelength 80−82402
solar neighbourhood stars, integrated UBVRIJKL colours 79−44460
solar type stars, thirteen-colour photometry, luminosity effects 77−22230
southern high-velocity stars, UBV colours rel. to kinematical and orbital props. 79−25600
southern open clusters, stars MK classifications and absolute magnitudes estimation 79−88644
spectral energy distribution of 16 stars in 3500 to 7500 Å region, absolute calibration 80−67710
spectral energy distributions, synthetic colours in UBV, RGU and uvby photometric systems 78−28528
spectrophotometry, Moscow and Alma-Ata data comparison with multicolour photometric systems 80−101590
spectroscopic and eclipsing binaries, survey for intrinsic linear polarization 78−4288
spectroscopic binaries, single-line, nature of secondary stars from X-ray obs. 80−31329
SS 433, assoc. radio jet flux density vars. 80−31381
SS 433, B V photometry and short-term light vars. (1979 July 23 to September 17) 79−101165
SS 433, beam acceleration, radiation and precession theory 80−72971
SS 433, beam models, energetics anal., possible triple system 80−90433
SS 433, emission regions and black hole accretion disk 80−67746
SS 433, Hα emission object, 21.6 and 43 GHz obs. 79−92783
SS 433, implications of 13-day variation for mag. X-ray binary model 80−109447
SS 433, IR energy distrib. obs. 80−31312
SS 433, IR variability obs. 80−98676
SS 433, light curves, double peak and binary-like period, photometry 80−94804
SS 433, light minimum epoch and period 80−26886
SS 433, photometric and astrometric obs. 79−84801
SS 433, photometry, 1979 July to October, and 6.5 day period identification 80−8643
SS 433, radiation press. rel. to mass accel. and collimation mechanisms 80−4368
SS 433, radio and optical obs. 79−88661
SS 433, short term Hα central intensity increases 80−4375
SS 433, spectral features interpreted a precessing neutron star with jets, possible binary 80−90447
SS 433, V band photometry and broad min. prediction (1980 April-May) 80−82390
standard zero polarisation stars, list 79−40187
star image at telescope focus, quality, rel. to photoelectric obs. efficiency 80−62034
starlight aberration and gyroscopic precession, calcs. in stationary metrics 78−54284
stellar collapsing core, role of neutrino dissipation 79−101166
stellar ring, SR 440 in open cluster NGC 6709, two-colour diagram 77−17643
Stepanyan's star, eclipsing binary, eclipses obs. and orbital period refinement 80−62195
Stephenson-Sanduleak 433, Hα emission object, nonthermal radio emission obs. 78−86033
Stephenson-Sanduleak 433, Hα emission object, variable radio emission obs. 78−86034
Stephenson-Sanduleak 433, X-ray emission obs. 79−12480
Stephenson-Sanduleak 433 (1909+048), new type of radio star, possibly supernova stellar remnant 79−17117
strong shock with radiation near stellar surface 78−32442
subatmospheric nonthermal storage modes vs. radiation pressure for stellar wind origin 77−33468
subdwarf bolometric corrections 79−75205
subdwarfs, luminosity-temp. diagram locus rel. to He abundance 80−22003
subdwarfs, UV excesses and metal abundances 80−17574
Sun possible compact companion, mass, vel., and luminosity 79−2490
super-metal-rich stars, evolution rel. to H-R diagrams of old galactic clusters 77−49370
supercritical accretion discs winds struct. and appearance, numerical models 80−21984
superdense stars, high mag. fields, cyclotron reson. emission 79−75207
superflares, model for cosmic gamma-ray bursts *(Chinese)* 77−22021
supergiant stars, B2 to G0, small amplitude light vars. 78−32469
supergiant stars, brightness limits set by atmospheric instabilities 80−109432
supergiant stars, in LMC, long-term light vars. 78−45326
supergiants, atmospheric struct. from limb-darkening and freq. depend. diam. meas. 77−56924
supergiants, semi-period-luminosity-colour relation 78−61853
supergiants in LMC, IUE obs. of UV spectra and flux distribs. 80−101593
supernova, light curve for very distant (z=0.5) object 80−94821
supernova, nearby, UV and gamma radiation effects on terrestrial atmosphere 80−94584
supernova discovery in anonymous galaxy in Camelopardalis, photographic magnitude 79−5849
supernova explosions early stages, relativistic particles total energy upper limit, rel. to galactic nuclei and quasars 79−71059
supernova in anonymous galaxy, photovisual magnitude 79−2549

stellar radiation continued
supernova in anonymous galaxy in Centaurus, magnitude (1980 June 30) 80−85962
supernova in anonymous galaxy in Grus, discovery and magnitudes (1980 May 23 to July 12) 80−94820
supernova in anonymous galaxy near k Centauri, discovery and magnitudes 80−85962
supernova in ESO 153-G27, discovery and magnitudes (1979 August 19 to October 15) 80−26892
supernova in galaxy MCG-5-9-22, blue magnitude 78−81643
supernova in IC 5201, discovery, magnitude and spectrum 79−44514
supernova in MCG 10-16-117, H Balmer emission lines obs. 78−69818
supernova in MCG-4-32-23, discovery and magnitude 78−53968
supernova in MCG-5-9-22, spectrum and absolute magnitude 78−81644
supernova in NGC 4321, spectrum, lightcurve and magnitude of type II object 79−71061
supernova in NGC 4647, classification and time since maximum 79−25620
supernova light curves, pulsar theory, dynamical effect and thermalisation of strong waves 78−8028
supernova light curves rel. to existence of central pulsar 78−4256
supernova outburst light, expanding gas shell external excitation 78−40976
supernova radio pulses, searches and possible sensitivity improvements 78−40975
supernova shock-accelerated cosmic rays, early radiation spectrum, cooling and escape 79−48626
supernovae, gravit. radiation generation by escaping neutrinos 78−93092
supernovae, light and colour index curves in models with slow energy pumping 78−73726
supernovae, light curves and spectra obs. at Asiago Astrophys. Observatory 77−87457
supernovae, light curves and spectra of Types I and II 77−87455
supernovae, light curves of models with gradual energy release 77−78807
supernovae, neutrino emission 78−77486
supernovae, photometric classification *(Russian)* 78−12255
supernovae, radiation dynamics, envelope ejection and light curves 77−64783
supernovae, shock steepening and prompt thermal emission 79−16998
supernovae, soft X-ray flux prediction method 79−71060
supernovae, Type I, early part of light curve, modelling, H abundance effects 77−87458
supernovae, Type I, interpretation of spectra 78−49467
supernovae, Type I, light curve postmax. stages, model *(Russian)* 78−36624
supernovae, type I, light curves, colour curves and expansion vel. rel. to brightness decline rate 78−96495
supernovae, Type I, light curves from slow energy injection model 78−65636
supernovae, Type I, luminosity *(Italian)* 79−53843
supernovae, Type I, luminosity calcs. 80−82400
supernovae, Type I, photometric props. *(Italian)* 79−53839
supernovae, Type I, use as cosmological clocks 77−2446
supernovae, type II, comparison of theoretical and obs. light curves *(Russian)* 77−57003
supernovae, type II, light curves analytic solns. 80−77427
supernovae, Type II and peculiar, photometric props. *(Italian)* 79−53840
supernovae in Coma cluster of galaxies, light curves anal. 78−32497
supernovae in molecular clouds, spectra and luminosity, evolution 80−82399
supernovae stellar remnants, identified with new class of radio star 79−17117
surface brightness rel. to angular diameters, improved definition 78−53931
symbiotic stars, 2 cm emission obs. 78−93274
symbiotic stars, evolutionary considerations and origin of brightness vars. 80−62144
symbiotic stars, super-critical accretion model rel. to light vars. 77−45458
symbiotic stars, survey at 1612 MHz 80−12774
synchrotron neutrino emission, charge collision emission, star neutrino luminosity 80−41719
44 Tauri, δ Scuti star, light curves and periods, least squares determ. 79−62850
ζ Tauri, Be star, rapid linear polarisation variability *(Russian)* 80−77417
SU Tauri, brightness increase, visual magnitude estimates 77−29852
V471 Tauri, BV photometry of white dwarf eclipsing binary, light curve vars. 78−96508
V711 Tauri, change in nature of light curve, and flare, 1979 October to December 80−26906
T Tauri, flare obs. in U-band *(Russian)* 77−22228
T Tauri, integral brightness and Hα emission vars., 1971-77 period *(Russian)* 78−61852
SU Tauri, light curve, Poisson statistics 77−56942
T Tauri, linear polarization obs., wavelength depend., circumstellar dust envelopes 79−53809
V471 Tauri, period var. and light curves of eclipsing binary system 80−22038
44 Tauri, periodogram analysis of light curves of δ Scuti star 79−84799
DR Tauri, pre-main-sequence star, brightening, 1970 to 1979, and historical light curve 80−31297
SU Tauri, R Coronae Borealis star, IR excess discovery from optical and IR photometry 80−101601
SU Tauri, R Coronae Borealis variable, brightening after long minimum, 1980 August to September 80−109438
SU Tauri, R Coronae Borealis variable, fading, visual magnitude obs. 79−92785
T Tauri, rapid Hα vars. nonconfirmation 78−73706
RR Tauri, rapid periodicity, photometric investigations 80−26853
V471 Tauri (Bd+16°516), Ca II H and K and Hα line vars. 79−67063
V711 Tauri (HR 1099) and related Ca II emission binaries, Hα emission survey 79−21339
20 Tauri (Maia) and related stars, photometric constancy 79−58338
V471 Tauri (Nova 396 AD), identification of possible outburst *(Russian)* 79−101162
BU = 28 Tauri (Pleione), UBV obs. and light curve 77−56979
T Tauri star formation, stellar wind as dynamic input into dark mol. clouds 80−85980
stellar radiation continued
T Tauri stars, continuum emission synthesis from photosphere and low chromosphere model 80−36623
T Tauri stars, for UV radiation *(Russian, English)* 79−75217
T Tauri stars, H_2 emission obs. 78−93230
T Tauri stars, location in (J-H), (H-K) diagram 77−78790
T Tauri stars, optical luminosity mechanism and FU Orionis type flares *(Russian)* 77−22229
T Tauri stars, outflowing envelopes models rel. to line and continuum radiation 78−96482
T Tauri stars and related objects, IR meas. 78−8002
T Tauri stars in Orion Nebula (M42), possible coronal X-ray emission obs. 78−28852
BL Telescopii, eclipsing binary, unusual variability of bright supergiant companion 77−64797
thermal X-ray emission 80−41849
Tr 27-102 (HD 159378), possible long-period Cepheid, light vars. obs. 78−45336
transformations from theoretical H-R diagrams to C-M diagrams 77−13321
R Trianguli, Mira variable, narrow-band polarimetry 79−25617
RW Trianguli, nova-like binary star, eclipse timings 79−21357
RW Trianguli, nova-like eclipsing binary radial vels., dimens. from visible spectra 80−82418
EK Trianguli Australis, peaks in lightcurve during 1979 June outburst 79−75222
EK Trianguli Australis, SU Ursae Majoris dwarf nova, superhumps, light curve UBV obs. 80−105255
47 Tucanae, metal-rich globular cluster, colour-magnitude diagrams and luminosity functions 77−57065
Tycho's supernova, distance and luminosity from fast shock wave model for remnant 80−46631
Tycho's supernova (SN 1572), unsuccessful search for optical stellar remnant 80−101603
Tycho supernova, He II Lyman α radiation rel. to search for fossil Stromgren sphere 78−36661
4U 0115+63, transient X-ray source, 3.61 s pulsations and X-ray spectrum obs. 78−61939
4U 0115+63, transient X-ray source, obs. 79−92890
4U 0115+63, X-ray transient, position and pulse profile 78−93467
3U 0614+09, case for X-ray burst 78−32610
4U 1626−67, 7.7-second X-ray pulsar, simultaneous X-ray and optical obs. 80−51914
4U 1626−67, light pulses from optical counterpart 80−51916
4U 1626−67, X-ray pulsar, HEAO 1 obs. 79−92889
4U 1626-67 optical candidate, optical pulsations discovery 78−65720
4U 1658−48, optical counterpart identification and X-ray flare obs. 78−69908
4U 1700−37, 97 minute periodicity discovery 79−5921
3U 1700−37, further Copernicus X-ray obs. 78−96568
4U 1700−37 (HD 153919), X-ray binary, high-energy X-ray obs. 80−86014
4U 1735−44 (MXB 1735−44), optical identification, X-ray and optical luminosities 78−93468
4U 1822−37, 2129+42, X-ray fluxes modulation periods from HEAO obs. 80−77516
4U 1907+09, X-ray spectrum and variability, position and optical identification 80−82542
4U 2129+47, X-ray light curve and binary model 80−46704
upper main sequence stars, evolutionary tracks in H-R diagram 77−49379
upper Scorpius region stars, spectrophotometry 79−88647
Ursa Minor dwarf spheroidal galaxy, abundance vars. on giant branch rel. to ω Centauri anomaly 79−5904
UX Ursae Majoris, anomalous 1977 period change for nova-like eclipsing binary 78−85956
XY Ursae Majoris, eclipsing binary, light curve changes, starspot activity 77−57044
XY Ursae Majoris, eclipsing binary, variable light curve 77−91568
AW Ursae Majoris, light curve anal. of contact binary 80−56875
AN Ursae Majoris, nova-like variable, extremely high circular polarisation obs. 78−8018
AN Ursae Majoris, polarisation meas. of nova-like object 77−29851
AN Ursae Majoris, polarisation of AM Herculis-type nova-like binary 78−85958
SU Ursae Majoris, probable 1980 March super outburst 80−51785
AN Ursae Majoris, steady low luminosity state 79−40219
AW Ursae Majoris, theoretical light curve of contact system 78−77578
W Ursae Majoris, vars. of period and light curve of eclipsing binary *(Italian)* 78−93318
W Ursae Majoris binary stars, synthetic light curves calc., appl. to V566 Ophiuchi 77−74097
W Ursae Majoris stars, atm. parameters of A-type systems 80−36672
W Ursae Majoris stars, effects of photospheric convection on limb darkening 78−49478
W Ursae Majoris stars, Fourier analysis of light curves 79−21349
SU Ursae Majoris stars, important sub-group of dwarf novae, photometric props. 80−101596
W Ursae Majoris stars, rot. line broadening functions rel. to gravity brightening and limb darkening 80−109494
W Ursae Majoris stars, theory of light curves 77−57008
α Ursae Minoris (Polaris), interstellar reddening from field stars uvbyβ photometry 79−58356
α Ursae Minoris B (Polaris B), spectral type and interstellar reddening 78−8005
UV 1758+36, He deficient hot subdwarf B star, atm. parameters, radial vel. 78−53944
UV chromospheric and transition-layer emission 80−56823
UV flux measurements, comparison of S2/68 and OAO-2 calibrations 77−87372
UV fluxes, S2/68 obs. of 31215 objects 79−8852
UV interstellar radiation field, galactic latit. depend. of 1530 Å radiation 77−33704
UV observations by Earth-orbiting satellites of hot components and extended coronas 80−109379
UV photometry from Cosmos 215 satellite *(Russian)* 77−64750
UV radiation, extinction in dark clouds rel. to CO isotopic abundances 77−29912
UV radiation, interstellar grains scatt. props. rel. to particle size distrib. 80−26932

stellar radiation continued
UV radiation field in interstellar clouds, attenuation theory *(Russian)* 80−73026
UV stars, effect on intergalactic medium temp. and ionisation struct. 77−13455
uvbyβ photometric indices, cluster anal. for spectral classification errors detect. 78−20819
uvbyβ photometric system, calibration in terms of temp. and gravity 78−4198
uvbyβ photometric system, determ. of stellar absolute fluxes and temps. 77−64740
V444 Cygni, eclipsing binary, light curve anal. 80−109374
variable and peculiar stars, search for radio emission 77−22248
variable star, luminosity changes rel. to orbiting particle motion, accretion and ejection 79−44338
variable star discovery in M33, light curve, magnitude 78−73717
variable stars, 3-colour photoelectric obs. at Mt. Kobau (1970-3) 77−56955
variable stars, BAV results for 1973-5 period *(German)* 77−71118
variable stars, double periodicity in light vars. 77−87423
variable stars, Scorpius-Ophiuchus region, discoveries *(Chinese)* 80−77418
variable stars, short-period, max. entropy spectral anal. appl. 78−16436
variable stars in globular cluster NGC 5986, periods and light curves 79−5868
variable stars period determination, maximum entropy method accuracy 80−56712
Vela pulsar (PSR 0833−45), radiation model 80−94824
Vela X-1, X-ray spectrum obs. by OSO 8 78−49555
γ^2 Velorum, bright Wolf-Rayet binary, optical light curve 77−56945
γ^2 Velorum, radio emission obs. at 2 cm 78−40969
AH Velorum, radius, delta luminosity and pulsation mode of δ Cepheid 80−46572
very red stars on Palomar Sky Survey prints 77−26008
109 Virginis, absolute energy distrib. from 3295 Å to 9040 Å 78−20828
α Virginis, decline of β Canis Majoris pulsation 79−12482
XX Virginis, field Population II Cepheid, absolute mag. 80−41832
78 Virginis, magnetic Ap star, high resolution polarisation obs. inside spectral lines 80−51772
AR Virginis, RR Lyrae variable, photographic photometry and mean light curve *(Russian)* 80−12769
CG Virginis, soln. of photoelect. light curve of eclipsing binary *(Chinese)* 79−53857
ψ Virginis (SAO 139033), ang. dia. and visual surface brightness meas. 78−20825
visual surface brightness depend. on colour, model stellar atm. calcs. 80−67707
S Vulpeculae, 67 day Cepheid, luminosity from membership in (Vulpecula OB2) 80−41831
BW Vulpeculae, UV light curve of β Cephei-type star 78−36570
Vulpeculae 1976, polarization and magnitude obs. 1976, Nov. 77−2442
NQ Vulpeculae (Nova 1976), spectral evolution, distance and absolute magnitude 78−89205
NQ Vulpeculae (Nova 1976), visual magnitude estimates 77−22254
NQ Vulpeculae (Nova 1976), visual magnitude estimates for 1978 Aug.-Oct. 79−5839
NQ Vulpeculae (Nova 1976), visual magnitudes, 1977 Nov.-1978 Jun. 78−65626
NQ Vulpeculae (Nova 1976), visual magnitudes (1978 June 29 to July 13) 78−85959
NQ Vulpeculae (Nova Vulpeculae 1976), photometric obs., visual magnitudes 77−60767
NQ Vulpeculae (Nova Vulpeculae 1976), visual magnitudes (1977 Aug.-Nov) 78−16434
W851, high-velocity star, subdwarf main-sequence calibration rel. to parallax 77−49387
Walker No.67 in NGC 2264, candidate for strong interstellar circular polarisation 78−12223
WC stars H−K colours, effects of near IR emission lines 80−94816
white dwarf binary systems, hard X-ray obs. 78−36732
white dwarf luminosity in scale covariant theory of gravity 79−80303
white dwarf space motions and luminosity function 77−45413
white dwarf variable stars, multiple periodicities 77−87434
white dwarf with mass accretion, H shell flashes and luminosity vars. 78−57550
white dwarfs, comparison between observed and theoretical luminosity functions 77−5528
white dwarfs, DB-type, model atmospheres rel. to emerging fluxes and colours 80−51761
white dwarfs, EUV and neutrino emission rel. to cooling theory 80−82356
white dwarfs, excess luminosity due to meridional circulation caused by stellar rot. 79−62818
white dwarfs, hot, effective temps. 79−25602
white dwarfs, HR-diagram and luminosity function determ. *(Chinese)* 80−77403
white dwarfs, integrated polarisation of H lines in strong magnetic field 77−17563
white dwarfs, luminosity function depend. on progenitor masses 78−65614
white dwarfs, multiperiodic light curves, g-mode rotation 78−4210
white dwarfs, visual surface brightness relation appl. 78−81624
white dwarfs in globular cluster NGC 6752, UB photometry 78−93233
wide-band colour index and bolometric correction, appl. to LTE/non LTE atmospheres boundary 79−35236
wind bubbles effects on density gradients in H II regions 77−74112
wind interaction with surrounding disc nebula 79−58323
winds, polytropic fluid flow in central gravitational field 77−45301
Wolf-Rayet close binaries, X-ray production 77−13401
Wolf-Rayet stars, ANS obs. of UV variability 78−65632
Wolf-Rayet stars, IR light vars. 77−9750
Wolf-Rayet stars, struct. of winds from obs. of IR continua 77−78793
Wolf-Rayet stars, UV obs. and temps. 78−40965
Wolf-Rayet stars in LMC, new discoveries, positions, spectra and magnitudes 80−46569
Wolf-Rayet stars in LMC, new discoveries absolute magnitudes 79−67018
WRA 977, high-speed UV photometry of periodic modulation 78−16442
WRA 977 (4U 1223−62), lightcurve and radial vel. curve 79−21307
X-ray and soft X-ray radiation mechanism of accreting neutron stars 77−87468

stellar radiation continued
X-ray binaries, optical radiation polarization *(Russian)* 79−58450
X-ray binaries, recurrent transients model 80−109565
X-ray binaries, X-ray refl. from neutron star surfaces 78−28716
X-ray binaries and pulsars, effect of vacuum birefringence on polarisation 78−4408
X-ray binary stars, X-ray heating effects on absorpt. line vel. curves 77−29878
X-ray burst sources, obs. of assoc. optical flashes 77−41420
X-ray burst sources, persistent emission rel. to nature of galactic bulge X-ray sources 79−84871
X-ray burst sources, search for correlated X-ray and radio emission 78−57695
X-ray burster phenomenon, mathematical simulacrum 77−87570
X-ray bursters and soft X-ray transients, different phenomena from same objects 79−25755
X-ray bursts, simple physical model 77−29960
X-ray emission from colliding stellar winds, upper limits 78−65607
X-ray flux from stellar winds, rel. to H II regions narrow recomb. lines 79−8972
X-ray pulsar binary, X-ray reflection effects on timing obs. of pulses 79−53935
X-ray pulsars, role of Alven surface in X-ray pulses form. 77−78899
X-ray pulsator, 38.22 second period, in vicinity of OAO 1653−40, very hard spectrum 80−27014
X-ray source, intensities from stellar wind flow past compact object 80−22116
X-ray source counts, spectral anal. rel. to binarity detect. via Doppler effect *(Russian)* 78−77623
X-ray sources, compact, radio emission origin 80−62317
X-ray sources, evidence for Population I distrib. in Milky Way 78−28851
X-ray sources, galactic, hard and soft X-ray spectra rel. to physical nature 80−62316
X-ray sources, galactic, luminosity function rel. to large-scale distrib. 79−48954
X-ray sources, light and X-ray vars. rel. to masses 78−12430
X-ray sources, time-dependent Comptonisation and X-ray reverberations rel. to rapid time variability 80−86013
X-ray sources in SMC, max. luminosities from deep survey 79−25702
X-ray stars in globular clusters 78−20916
X-ray transient sources, hard and soft transients parameters 79−84867
XUV emission, possibility of detect. *(German)* 80−109372
XUV radiation from nearby main sequence and subgiant stars, upper limits 79−12471
young stars, high-freq. radio continuum obs. 80−51766
young stars reddening and polarisation, intracluster and circumstellar dust effects 78−93199
ZB 33, RR Lyrae type star, light curve study *(Chinese)* 80−8633
$\nu(\bar{\nu})$ emission from supernovae, form. and cooling of neutron stars 78−8038
Ba stars, absolute magnitudes redeterm. 78−8006
Ba stars, DDO system photometry, luminosity anomaly 79−35246
C stars, absorption by SiC and IR excess 78−16413
C stars, N-type, luminosity and C enhancement 78−93247
C stars, search for HCN and CH maser emissions 80−51856
C stars, violet opacity 78−53940
Ca II H and K emission, chromospheric, in main-sequence stars, comparison of activity cycles to old and young stars 80−105235
Ca II H and K emission, chromospheric, in field stars of solar neighbourhood, survey 80−109423
Ca II H-line emission from Sun observed as star *(Russian)* 77−64727
SS Cygni, soft X-ray emission detect. during optical outburst 80−46574
Fe-O stars with masses of 2 M$\odot$ and 10 M$\odot$, neutrino radiation during gravit. collapse 78−20815
U Geminorum, soft X-ray emission detect. during optical outburst 80−46574
H burning stars, Hertzsprung-Russell diagram age and mass calibrations 80−51744
H continua from radiative shock, theory 78−40918
H II region exciting star, influence on nebula temp. and ionisation struct. 78−61911
H II regions in Perseus Arm, exciting stars radiation rel. to nebulae dynamics 78−32549
Hα emission stars in southern dark clouds, objective prism survey 78−28536
He shell burning stars, core mass-luminosity relations 80−21983
He variable stars, IR excesses obs. 80−67733
Hg-Mn stars, absolute magnitude 80−46564
RR Lyrae stars in Sonneberg fields near north galactic pole, distances, density distrib. 77−82229
Mn-Hg stars, surface gravity and stellar temp. derivation from uvbyβ data, statistical anal. 80−82397
O-rich late-type stars, 16 to 39 micron spectroscopy 80−22002
OH main line emission from globular clusters, high sensitivity search 80−62207
OH masers, interferometry and source struct. 77−53583
OH Mira variables, light curve shapes rel. to mass loss 77−56944
OH type II stars, unidentified, search for H_2O emission 79−75286
OH/IR stars, OH main lines masers inversion 78−28664
OH-IR stars, time var., correl. with visual magnitude 77−60764
SiO 86.2 GHz maser sources, polarisation props. 80−4449
SiO maser obs. in late-type stars at 43 GHz 77−74067
SiO masers, J=1→0 ν=1 and 2 masers relative intensity and vel. 80−4339

stellar rotation
see also solar rotation
accretion disc, thin, surrounding spherical black hole, rot. rel. to optical image 79−67049
adiabatic pulsations of tidally perturbed rotating stars 78−89172
adiabatic stability of toroidal magnetic fields in differentially rotating stars 79−66998
Am stars in main sequence, rotational vel. effect on metallicity 79−48814
Am stars in spectroscopic binary systems, evolutionary status, statistical anal. 78−93262
Am-type stars, rot. vels. and spectral types catalogue 80−36514
Am-type stars, rotationally driven envelope circulation 80−4370
ET Andromedae (HR 8861), Ap star, light vars. and period 80−46571

stellar rotation continued
angular momentum and magnetic moment from superheavy hadrons 80−26843
angular momentum conservation, surface rotation vels. prediction 79−96991
angular momentum loss from star with rapidly rot. core in close binary system *(Russian)* 78−93196
angular velocity determ. for rotating liquid figures in equilib. *(Russian)* 79−10572
Ap, Am stars, slow rot. rel. to chemical differentiation by diffusion 80−77381
Ap stars, rot. periods rel. to mag. latit. of metals 79−58341
Ap stars, surface heterogeneities 78−12254
Ap-stars, mag. field rel. to rot. period, visible spectra obs. 80−82373
Ap-stars, oblique rotator model, Deutsch and Khoklova methods 79−35271
AE Aquarii, cataclysmic variable, rapid light oscills. rel. to white dwarf oblique rotator model 80−36634
Ariel 0535+26, transient X-ray source, new pulse period data 79−44635
axisymmetric rotating fluid, asymptotic estimates 80−98542
B-type stars, pole-on, rapidly rot., spectral inconsistencies due to gravity darkening 80−17581
late B-type stars small v sin i values, Ap star determ., visible spectra 80−77409
Balmer-index photometry, rot. vel. influence quantitative anal. 78−96404
Be stars, intrinsic circumstellar polarisation and apparent rot. speed interpretation 78−96484
Be stars review, rot. and envelope models 79−84809
binary fission in damped rotating polytropes 78−93209
binary fission in damped rotating polytropes 79−71016
binary stars, nonsynchronous rot. generalisation of light and vel. curves simultaneous soln. technique 80−36664
binary stars in open clusters, rot. effects on determ. of freq. and mass ratio 78−36639
binary stars on main sequence, freq. depend. on mean rot. vel. 80−26901
binary systems, effect of gravit. radiation on evolution and spins 78−12292
binary X-ray pulsars, rot. history 79−62871
black hole, charged rotating, mag. torque effects 79−17010
black holes, neutrino emission ang. depend. 79−88696
black holes, rot. rel. to free oscills. reson. freqs. and gravit. waves 80−105271
black holes, rotating, neutrino fluxes resulting from macroscopic parity violation 80−22034
black holes, spin-up by thick accretion discs 80−105273
BPM 25114, peculiar white dwarf, light vars., oblique rotator model *(Italian)* 78−93241
53 Camelopardalis, Ap star, Ca II K and Hδ lines vars. in rot. period *(Russian)* 80−90458
53 Camelopardalis, binary Ap star, evidence for mag. period var. 79−80320
AX Camelopardalis (53 Camelopardalis), Ap star, UBV photoelectric photometry and period of var. *(Italian)* 80−90448
α Camelopardalis (O9.5 Ia), expanding envelope rot. rel. to variable Hα P Cygni profile 80−41818
α Canis Majoris (Sirius), rot. vel. and Ba abundance 78−12218
RS Canum Venaticorum binaries, effects of tides and flares 79−71068
RS Canum Venaticorum binary stars, rot. rel. to mag. dynamo and starspot model 80−109488
γ Cassiopeiae, Be star, polarisation rapid vars. rel. to rot. circumstellar envelope inhomogeneities 80−22022
γ Cassiopeiae, UV and Hα spectrophotometric variability obs. rel. to rot. 79−5829
cataclysmic variables, short-period light oscills. rel. to non-radial oscills. of rot. stars 78−32477
Centaurus X-3, neutron star characts. from correlated spin-up and X-ray luminosity meas. 80−101648
VV Cephei, spectroscopic obs. during eclipse rel. to rot. ring-shaped envelope 78−45359
Cepheid variables, double-mode and bump, rot. and convection effects on period ratios 78−93249
charged particle motion in an electromagnetic field on Kerr background geometry 79−9167
close binaries, angular vel. distrib. in one component with fast rotating core *(Russian)* 78−28648
close binaries, synchronism between axial rotation and orbital motion 79−97034
close binaries, synchronous systems devel. from tidal are rot. interactions 80−109468
close binary systems, problem of components oblique rot. axes 78−96509
collapsed stars, reason for slow rot. 78−49426
collapsing core, neutrino dissipation rel. to differential rot. and oscills. damping 79−101166
17 Comae A, Ap star, mag. field meas. and rot. period *(Russian)* 80−90457
concave hamburger equilibrium of rotating bodies 80−109422
contact binaries, solar type, ang. momentum controlled evolution 80−36670
contact binaries, theoretical atlas of light curves and rot. broadening functions 80−17610
convection in rotating magnetic star, toroidal field effect 80−41816
convection in rotating spheres and spherical shells 78−89184
convection in spheres and spherical shells, model eqns. and rot. symmetries 79−101137
convection zones dynamics, effect of rot. on turbulent viscosity and cond. 80−36612
convective modes and convective stability, of rotating fluids 79−16818
θ Coronae Borealis, Be-type star, shell line profile and radial vel. obs. 80−77426
β Coronoae Borealis, Ap star, Ca II K and Hδ lines vars. in rot. period *(Russian)* 80−90458
Crab Nebula, central mag. dipole rot. neutron star theory for supernova remnant 80−51834
Crab pulsar, rot. axis alignment rel. to gravit. radiation 78−32501
curved space-time of rotating star, instability of quantum field, particle creation 78−69790
Cygnus X-1, rapidly rotating neutron star plus massive disc model 80−36736
differential rotation, due to latitude depend. convective heat transport 80−90411
stellar rotation continued
differential rotation effect on velocity and magnetic fields, superposition of poloidal and toroidal field 80−72928
differentially rotating gaseous polytropes, Eulerian eqns. 80−51739
differentially rotating gaseous polytropes, second-order perturb. theory 80−21990
differentially rotating gaseous polytropes construction of const. mass solar model 80−82338
distorted star, small oscills., Roche coords. appl. 78−69782
distorted stars, vibr. stability anal. using Clairaut coordinates 80−90408
Doppler broadening parameters, meas. technique without spectrograph 78−20646
BY Draconis, spotted flare star, primary rot. vel. and radius rel. to pre-main-sequence nature 80−36633
BY Draconis stars, angular momentum initial distrib. and evolution 80−85954
BY Draconis syndrome among dMe stars, rotating spotted star model 78−16428
BY Draconis type variables, photometry, amplitudes and phases 79−67038
BY Draconis-type stars, Hα emission line profiles, rapidly rot. gaseous envelopes *(Russian)* 78−65625
early type companions of X-ray sources, luminosities, rot. and other parameters 78−36564
early type stars, rotation effects, TD-1A obs. 79−44476
early-type rotating stars, meridional circulation in surface layers 78−20820
early-type stars, envelope mixing of elements, shear flow instability 80−109424
effects on temp. models derived from multiplet line-centre fluxes 79−5806
electrically conducting rot. sphere behaviour in time-independ. homogeneous external mag. field 78−49309
ellipsoidal potentials of polynomial distributions of matter 80−46532
Emden-Chandrasekhar polytropes, exact solns. for axisymmetric solid-body rotators with (n=0, 1 and 5) 80−109419
equilibrium equations soln. for rapidly rot. stars 78−65601
equilibrium states of nonsynchronous stars in detached binaries 79−53853
ergoregion instability of rotating stars, eigenfrequency calc. 79−8835
evolution, of 7 and 10 M⊙ rot. stars with time-depend. redistrib. of ang. momentum 78−36553
exploding or collapsing magnetized rotating spheroid, mag. dipole radiation 79−35106
Fourier method for stellar rot. vel. determ. using stellar spectrum *(Russian)* 79−80240
G200-39, hot hybrid white dwarf, rot. rel. to atmospheric mixing 80−26852
G-type dwarfs, macroturbulence and age anticorrel. 78−93226
gamma-ray pulsars, rot. rel. to magnetosphere optical depths 79−5852
gaseous rotating cylinders, thermodynamic stability anal. by linear series 78−81618
GC 17353, Ap star with large photometric var., period *(French)* 79−2545
Gleise 490 AB (BD+36°2322), red dwarf binary, flares and starspots, rot. period determ. 80−77423
gravitational radiation and stability of rotating stars 78−93210
H 2252−035, X-ray flux modulation, compact star rotation 80−101652
H 2252−035 cataclysmic variable, white dwarf rot. period from photometry and spectrum 80−101651
HD 101065, Przybylski's star, rot. vel. from light variability freq. anal. 80−62152
HD 118246, new Be star at high galactic latit., rot. vel. 78−73721
HD 124224, He Si variable, spectroscopic obs., starspots, oblique rotator model 78−12239
HD 127617 (Bidelman's high latitude Be star), photometric and visible spectra obs. 80−77420
HD 184927, He variable star; oblique rotator model rel. to spectroscopic props. 80−51790
HD 206860, G0 V star, IUE obs. of active region rel. to rot. period 79−92766
HD 216533, Ap star, spectroscopic binary oblique rotator model, spectral var. study 79−101153
HD 221568, Ap star, light var. period 80−56856
HD 26676, unusual radio star, rot. vel. and search for duplicity 78−73707
HD 34452, Si Ap star, spectrum and line profiles vars. 78−65634
HD 3580, 187473, 212432, Si stars, uvby photometry and periods 78−96487
HD 3980, late Ap star, photometric and mag. variability obs. 80−56845
HD 45088, BY Draconis binary, surface activity from high rot. vel., visible obs. 80−77425
HD 64740, He rich star, UV spectral vars. 80−22016
HD 92664, Ap star, photometric variability and period 79−40199
HD 9996, Ap star, spectrsocopic obs. 78−77558
AM Herculis, multicolour photometry, slow optical pulsar 78−28693
AM Herculis, X-ray binary, obs., slow rotator model 78−12408
HZ Herculis (Hercules X-1), accretion disk precession period 80−73070
HZ Herculis (Hercules X-1), precessing twisted accretion disks 80−56973
DQ Herculis (Nova 1934), white dwarf rot. period rel. to nova remnant shape 80−105244
HR 1170, HR 7331, nonradial δ Scuti pulsators, rot. vel./period ratio relationship 79−88663
HR 7129, He variable, oblique rotator model 79−62838
VW Hydri, dwarf nova, almost corotating mag. white dwarf model 79−16977
interior Kerr metrics, tests 78−28666
ion viscosity in hot accretion disc around black hole 79−62813
JP 1953+29, timing data anal., spinup/spindown 78−24522
K-type giants, turbulence in normal and super-metal-rich stars 79−92756
Kerr black hole, elec. and mag. cond. 79−25625
EV Lacertae, flare star, rot. period from photometric and spectroscopic obs. 80−98665
AR Lacertae-type stars, starspots 78−16443
late B-type stars, binary, rot vels. rel. to orbital periods 78−57547
late B-type stars, rot. and incidence of HgMn stars 78−89199
late-type stars, ang. momentum loss rel. to mag. dynamo 78−45331
lower main-sequence stars, rot. studies 80−51767

stellar rotation continued
α Lyrae (Vega) rot. rate determ. from line profile photoelec. obs., Fourier transforms 80−77408
magnetic dynamo α-effect, determ. for slow and fast rot. 79−40069
magnetic sphere, self-gravitating, exact soln. for differential rotation 79−84665
magnetic stars, elec. field around rot. mag. dipole 78−45141
magnetic stars, equatorially symmetric rotator model, inhomogeneous element distrib. 80−4371
magnetic stars, exact MHD solns. 78−69800
magnetic stars, existence of bifurcation point 78−53924
magnetic stars, perpendicular rotator model with meridional circulation 78−16438
magnetic variables, intrinsic rot. vels. 78−40967
magnetic white dwarfs, rotating, equilib. struct. 78−49433
magnetic X-ray binaries, synchronous rotation appl. to AM Herculis 79−62867
main sequence intermediate and late type stars, differential rot. models 80−105238
mass-gaining star, ang. momentum transfer during steady disc accretion 78−65609
massive close binary stars, effect of stellar evolution on components synchronous rot. 80−62192
massive stars, single and binaries, evolution review 80−82343
massive stars losing mass and ang. momentum, evolution and rot. loss 79−25591
meridional circulation caused by stellar rot., general rel. eqn. 79−62818
metallic line (Am) stars, temp., age, rot. and pulsation rel. to metallicism 78−49448
moment of inertia of rigidly rotating star, influence of nonsphericity and radiation press. force 78−28658
1 Monocerotis, δ Scuti star, evidence for dipole mode oscills. split by stellar rot. 80−51787
MXB 1730−333, rapid X-ray burster, accreting rot. magnetised neutron star model 79−84866
neutrino angular momentum loss by Poynting-Robertson effect 79−16928
neutron star, accretion disc/mag. field interaction rel. to spin-up and spin-down *(Russian)* 80−51799
neutron star, laboratory modelling of magnetospheres of aligned and oblique rotators 79−75240
neutron star, mag. configuration of plasma-sphere 79−75241
neutron star, magnetic, disc accretion effects on rot. 78−93294
neutron star elec. field anal., effect on accretion and radio pulsar model 80−109453
neutron star spin down rel. to X-ray sources in binary stars *(Chinese)* 78−28857
neutron star with strong mag. field, electron cap shape 78−12265
neutron stars, effects of rot. and mag. fields on superfluidity 80−77441
neutron stars, effects of rot. on form of quantum vortex filaments 80−67770
neutron stars, effects of slow rotation on stability against radial perturbations 80−98685
neutron stars, EM multipole fields rot. rel. to vel. 80−26896
neutron stars, general relativity, exact solns. for slow rot. 79−75239
neutron stars, lab. expts. of superfluid dynamics 78−49469
neutron stars, magnetic, accretion torques rel. to pulsating X-ray sources period changes 80−31320
neutron stars, magnetised, fate of matter and ang. momentum in disc accretion 78−28715
neutron stars, postglitch behaviour of quantum plasma 79−35289
neutron stars, rapidly rotating, gravit. radiation 78−65646
neutron stars, relativistic slowly rotating stars 79−21321
neutron stars, rot. mag. field interaction with accretion disc 80−62173
neutron stars, rotating, magnetic, accretion flow inside magnetosphere rel. to rot. rate 78−8037
neutron stars, rotating, moments of inertia in bi-metric theory of gravitation 80−90466
neutron stars, slowly rotating, appl. of bimetric theory of gravit. 79−85042
neutron stars, thermal-timing instability rel. to pulsars period jumps 79−35293
neutron stars in close binary systems, spindown rates 79−40210
Newtonian spheroid, homologous oscill., gravit. radiation 80−46533
Newtonian stars, secular instability to gravit. radiation and viscosity 78−53922
Newtonian stars with stratified flows, mirror planes 78−32444
non-spherical rotating polytropes struct., appl. of smoothed particle hydrodynamics theory 78−12203
non-synchronous stars in close binary systems, stability 79−40223
nonradial oscillation modes in presence of slow rot., quasiadiabatic anal. 79−12462
normal modes of rotating stars, general variational principle 80−12750
novae, effects of white dwarf rot. on remnants shapes 80−105244
NP 0532, Crab pulsar, random walk timing noise anal. 80−77432
NP 0532, Crab pulsar, rot. axis orientation rel. to Crab Nebula small-scale polarisation 79−25656
NP 0532, rotation parameters, temporal var. 80−62170
O-type main sequence stars, rotational vel. evolution 80−51759
OB stars, Copernicus UV spectral data 79−84795
oblique rotator model and Si overabundance by diffusion in chemically peculiar stars 79−30067
oblique rotator with irrotational axisymmetric mag. field surface distrib., effective mag. field 80−26872
ζ Ophiuchi, spectral vars. related to rot. 80−22000
σ Orionis E, mag. field discovery and oblique rotator model 78−93268
YY Orionis stars, rot. rel. to spectral line form. in axisymmetric moving envelopes 80−41813
oscillations, adiabatic nonradial, freq. splitting by slow differential rot. 80−105233
II Pegasi (HD 224085), surface active binary star, Hα emission vars. rel. to rot. 80−90480
periodic polarization variations in rotating astrophysical systems 79−88585
β Persei, eclipsing binary, Mg II 280 nm line profile, calcs. and UV obs. 80−82421
β Persei (Algol), primary component rot. 80−72996
β Persei (Algol) type semi-detached binaries, rotational vels. 78−89220
α Persei cluster stars, OAO 2 UV photometry and rot. effects 78−93331
perturbations and stability of rot. stars, eigenvalues and perturb. theory 80−46538
perturbations and stability of rot. stars, eigenvectors and variational principle 80−46537
Poisson's eqn. numerical soln. for flattened centrally condensed objects, stellar models 79−35110
polytropes, hydrostatic equilibria 79−80300
pre main sequence stars, rapid rot. effect on evolution in gravit. contraction phase 80−62133
pre main sequence stars rotation, theory of rotating interstellar clouds nonaxisymmetric collapse 80−85927
pre-main sequence stars in NGC 2264 rel. to solar angular momentum problem 79−58332
propeller spindown of rotating magnets, torque calc., neutron stars appl. 79−8831
protostar, rotating, fragmentation, comparison of two three-dimensional computer codes 80−26850
protostars, rot. fission rel. to origin of close binary and planetary systems 79−5859
PSR 0329+54, binary motion to explain freq. variations 80−26894
PSR 0611+22, short time scale integrated pulse shape vars. 80−105267
PSR 1913+16, binary pulsar, nature from observational data 80−77435
pulsar, rot. rel. to constrained atmosphere min. energy state 79−25622
pulsar atmosphere with arbitrary mag. and rot. axes, qualitative features 78−57569
pulsar electron cap, electrons accel. in internal zone 80−46592
pulsar magnetosphere, behaviour of mag. lines of rot. system 78−20848
pulsar magnetosphere models, interior and exterior struct., pair prod. 80−46594
pulsar magnetospheres, plasma co-rotation 78−12258
pulsar NP 0531, distrib. model of press., density, ang. vel., matter rot.,, grav. field *(Ukrainian)* 80−12775
pulsar polar caps as foil-less diodes, nonneutral relativistic beam accel. 80−17604
pulsars, axisymmetric magnetosphere model rel. to rot. braking 79−84813
pulsars, characteristic and kinematic ages rel. to mag. monopoles creation 79−35287
pulsars, classification method from period change and radio luminosity *(Chinese)* 80−85963
pulsars, evolution rel. to torques, magnetic moment and pair production 80−62169
pulsars, finite force face cold plasma atm. models, plasma differential rot. 80−77378
pulsars, gamma-ray luminosity rel. to rot. vel. 78−53975
pulsars, long-period, absence rel. to force-free mag. fields instabilities 78−49425
pulsars, long-term changes in periods and neutron star interior plasma 80−22029
pulsars, magnetogyro ratios and evolution 79−8937
pulsars, magnetosphere instability rel. to 'glitches' 78−53976
pulsars, period derivatives rel. to existence of solar companion star 78−12198
pulsars, periods, positions and proper motion determ. from pulse arrival times, UHF, obs. 80−77431
pulsars, periods correl. with galactic distrib. 79−75231
pulsars, rot. and slowdown rel. to short-lived Crab-type supernova remnants (plerions) 79−12504
pulsars, rot. braking possible relation with radio emission beaming 79−92793
pulsars, rotational behaviour rel. to superfluidity 80−98683
pulsars, rotational energy loss, slowing down index and time derivs. 80−67762
pulsars, self-consistent description of axisymmetric magnetosphere of parallel rotator 80−94825
pulsars, superfluid liquid rotation, theory, relativistic effects in vortices *(Russian)* 78−61876
pulsars, timing obs. rel. to neutron stars thermal/timing instability 79−92795
pulsars axisymmetric magnetosphere models, co-rotating ions zone props. 79−92794
pulsars charge-separated magnetospheres, aligned rotator model 78−40981
pulsars spin-down rates, distrib. in sky rel. to reality of Sun companion star 78−57475
pulsating stars, rot. effect on low-freq. gravity modes 79−16934
pulsating X-ray binaries, spindown by EM friction with stellar wind 78−12431
pulsating X-ray sources period vars., torque vars. and stellar response 79−9029
VV Puppis, AM Herculis type binary, oblique mag. rotator accretion model 79−5860
VV Puppis, AM Herculis type binary, optical absorpt. spectrum, cyclotron intepretation and models 80−73003
radio pulsars, rot. magnetised neutron star model with H or He envelope *(Russian)* 78−40982
rapidly rotating fluid bodies, struct. and stability in general relativity beyond ang. vel. peak 79−101139
rapidly rotating models with radiation press., struct. parameters calc. 80−67697
rapidly rotating stars, criterion for secular instability 78−7987
rapidly rotating stars, equilibr. and secular stability 79−62811
red giant stars, internal rot. vel. to meridional circulation and CNO anomalies 79−48786
relativistic neutron star, interior MHD struct. 79−71062
relativistic spherical mass, effects of rot. on gravit. focusing of light 80−105155
relativistic stars, generic instability 78−93567
rigidly rotating stars, secular instabilities in general relativity, theoretical formalism 80−4341
rigidly rotating stars, secular instabilities in general relativity, numerical results 80−4342
rotation and Kelvin-Helmholtz instability 79−46287
3 Scorpii, He weak star, mag. field obs. and rot. period 79−88676
δ Scuti and related stars, rot. and metallicism rel. to pulsation 79−62847
secular instability in rotating stars, resulting from thermal cond. 80−21986
secular stability of rotating stars, Lagrangian perturbation theory of non-relativistic fluids 78−49305
self-gravitating rotating masses, book contrib., review 80−21915
slowly rotating stars, gravit. collapse, supernova explosion, neutron star or pulsar remnant 78−96472

stellar rotation continued
SMC X-1, spin-up rate meas. 78−41083
solar-type stars, mag. core rot. and stability 79−44472
spectral line broadening effects of macroturbulence and rotation 80−56813
spectral line shapes, combined effects of atmosphere expansion and rot. 78−53920
spin evolution during adiabatic mass loss 79−75201
SS 433, 164^d period as precessional motion, massive black hole and pulsar models 80−62138
SS 433, beam acceleration, radiation and precession theory 80−72971
SS 433, black hole rot. rel. to precessing jets model in ultra-close binary system 80−4384
SS 433, disk-driven precession 80−94803
SS 433, kinematic model for line wavelengths vars. 79−75226
SS 433, spectral features interpreted a precessing neutron star with jets, possible binary 80−90447
stability and perturbations, normal mode completeness 80−4344
Stephenson-Sanduleak 433, Hα emission object, hot spot detect., rot. vel. and spectrum vars. 79−8933
supernovae, magnetorotational explosion in cylindrical model 80−101605
41 Tauri, Ap star, Ca II K and Hδ lines vars. in rot. period *(Russian)* 80−90458
ζ Tauri, apparent wavelength depend. of v sin i 78−12240
V711 Tauri (HR 1099), RS Canum Venaticorum star, rot. rel. to BV light curve during (1978-79) 80−105279
tidally distorted stars, form factor method for struct. determ. 80−21991
toroidal magnetic field instability and differential rotation 79−16939
RW Trianguli, nova-like eclipsing binary radial vels., dimens. from visible spectra 80−82418
4U 0115+63, pulsating X-ray transient, pulse period obs. 79−92890
4U 1626−67, X-ray pulsar, pulse period from HEAO 1 obs. 79−92889
4U 1700−37, 97 minute periodicity discovery 79−5921
upper main-sequence peculiar stars, chemical and physical props. rel. to radiatively driven diffusion theory 80−82374
CQ Ursae Majoris, Ap star, UBV photometry, light vars., period determ. 79−88667
W Ursae Majoris stars, rot. line broadening functions rel. to stellar shapes 80−109494
variability due to rotation, period-radius-rot. vel. relation 79−2546
Vela pulsar, rot. axis alignment rel. to gravit. radiation 78−32501
Vela X-1, pulse period vars. from OSO-8 obs. 78−49555
very close binary systems, struct. eqns. including rot. and tidal distortions for ZAMS stars 80−22037
very compact rotating stars, existence of ergoregions 78−24523
78 Virginis, Ap star, mag. field geometry, oblique rotator model 80−51773
visual binaries, correl. between rot. vels. of components 78−20861
white dwarfs, Balmer line formation 79−30059
white dwarfs, mixing processes and elements separation in envelopes 78−12222
white dwarfs, multiperiodic light curves, g-mode rotation 78−4210
white dwarfs, rapidly rotating, gravit. 78−65646
white dwarfs, rapidly rotating, oscills., numerical calc. 80−46554
white dwarfs, slowly rotating, nonradial oscills. 80−4348
Wolf-Rayet stars, rotation rel. to ellipticity of surrounding nebulae *(Russian)* 78−12252
X-ray binaries, recurrent transients model rel. to spin-up and spin-down timescales 80−109565
X-ray binaries, rot. law rel. to double core evolution 79−84816
X-ray binary sources, pulsating, spin-up due to accretion from Keplerian disc 80−67904
X-ray sources, pulsating, accretion disc/mag. field interaction rel. to spin-up rate 78−93461
zero age main sequence stars in open clusters, rot. vel. anal. 78−93213
ν angular momentum loss in rotating stars 78−20822
He strong stars, mag. fields and mass loss rel. to rot. 79−44486

stellar size *see stellar dimensions*

stellar spectra
see also solar spectra; stellar photometry
O and B stars, UV obs. of mass loss effects 77−17551
OB-type stars, O VI obs. in stellar winds 80−8630
2A 0311−27 optical counterpart, identification and spectroscopic obs. 79−25762
HR 1099, RS Canum Venaticorum type binary, light and colour curve meas. 80−73004
χ Cygni, Hα emission line profile obs. of long-period variable 79−25618
A$_p$ stars, Fe I photoionisation spectrum causing UV absorpt. 80−109437
2A 0042+323 (3U 0042+32) optical candidate, photometry and spectrum 78−54088
2A 0311−227, AM Herculis type X-ray binary, optical counterpart, radial vel. obs. 80−94890
2A 0311−227, new AM Herculis-type system, optical identification 79−101211
2A 0311−227 optical counterpart, identification as AM Herculis type star 79−30149
2A 0311−227 optical counterpart, simultaneous photometric and spectroscopic obs. 80−90572
2A 0311-227 optical counterpart, spectroscopic and photometric obs. 79−101222
2A 0526−328, optical counterpart, eclipsing binary, visible emission line variability 80−73075
2A 0526−328, optical counterpart position and spectrum 79−5925
2A 0526−328 optical counterpart, identification and spectrum 80−22118
2A 0526−328 optical counterpart, radial vel. meas. and orbital period 80−90579
2A 0526−328 optical counterpart, spectroscopic obs. 80−77515
2A 0526−328 optical counterpart, X-ray emitting cataclysmic variable, spectrum and photometry 79−97103
A 0535+26, transient X-ray source, flare energy spectra obs. by (Prognoz 6) *(Russian)* 80−51920
2 A 1052+606, X-ray and optical variability of RS CVn star 80−31331
2A 1822−3"1 optical counterpart, identification, photometry and spectrum 79−12545
3A 2252−035, optical counterpart, proper motion and radial vel. determ. 80−82395
A- and B-type stars, B abundance from B II reson. line obs. 79−21276
A- and F-type main sequence stars, scanner obs. 78−36563

stellar spectra continued
A- and F-type stars, heavy element content influence on colour-temp. relation *(Russian)* 78−93234
A-type central stars of three planetary nebulae 79−17064
A-type stars, Ca II K line obs. 78−20830
A-type stars, effect of $C+H^+ \rightleftharpoons C^+ + H$ charge transfer on C I 1101 Å absorpt. edge 80−90423
A-type stars, obs. and calc. spectra, 3600-4200 Å region 78−12217
A-type stars, predicted and observed spectral energy distribs. 78−4208
A-type stars, spectral variations, abundance peculiarities 79−62821
early A-type stars, V/H abundance ratio from V II lines 79−21314
A-type supergiant stars, reson. line profiles from IUE and Copernicus spectra 80−90424
Abell 46, planetary nebula, eclipsing binary nucleus, hot component UV continuum obs. by IUE 80−98693
absolute spectrophotometric gradients interstellar reddening effects *(Russian)* 79−92752
absorpt. and emission features, IR spectrophotometry obs. 80−72954
absorption bands on O, B and A stars, polarized intensities 79−8915
absorption line formation depth in atmospheres *(Russian)* 77−64749
accreting stars, model IR spectra for dusty circumstellar shells 78−85934
accretion disc models and cataclysmic variables, H line blocking of UBV colours 79−101155
accretion discs theoretical photometric and spectroscopic props., cataclysmic variables appl. 79−80312
accretion disks around massive black holes: persistent emission spectra 78−93296
actinides, search and future work 77−78769
AE 1, He-rich variable, spectroscopy and photometry 80−41836
AFCRL IR sources, optical, IR and radio studies 78−4393
AFGL/CRL IR sources, spectroscopic obs. 78−32599
AGK2+81°266, hot subdwarf, spectral type 78−45323
Algol, eclipsing binary, spectral obs., description and interpretation 80−105283
Algol type stars, H I α obs. 80−109484
Am stars, τ Ursae Majoris and 15 Vulpeculae, energy distrib. from spectral obs. 80−85949
Am-stars, scanner obs. 79−5827
Am-type stars with known spectral types, second catalogue 80−36514
o Andromedae, Be star, radial vels. obs. 79−58355
o Andromedae, Be star, rapid spectroscopic variations 77−56970
o Andromedae, Be star, spectrographic obs. from (1967 to 1976) 77−71116
o Andromedae, Be star, spectroscopic evidence for new shell episode 80−90444
o Andromedae, Be-star shell spectrum changes, spectrograms 78−4245
σ Andromedae, rapid spectral line variability disproved 80−8625
CG Andromedae, Si binary star, spectrum variable, short period radial vel. variability determ. 80−72968
BM Andromedae, spectroscopic and photometric obs. of T Tauri-type star 80−62130
ζ Andromedae, spectroscopic binary, photometric and spectroscopic obs. *(Russian)* 78−57588
λ Andromedae, spectroscopic binary, UV and optical obs. of chromospheric lines 79−30087
Z Andromedae, UV spectra, 1979 Feb. 17, quiescent phase 79−40202
α Andromedae, UV spectrum of Mn star 78−69802
anomalous nova-like object in M31 79−80316
Ap and Am stars, numerical taxonomy 80−22015
Ap and Hg-Mn stars, spectrophotometric scans, search for broad continuum features 78−12247
Ap Si stars, UV spectral vars. 79−8927
Ap star, spectral line profiles *(Russian)* 77−87421
Ap stars, CN lines identification 77−91551
Ap stars, heavy element abundances from Copernicus UV data, reference stars α Lyrae and α Canis Majoris A 78−28688
Ap stars, line blanketed model atmospheres rel. to line spectra 79−44495
Ap stars, line blanketing rel. to Barnes-Evans relation and stellar radii determ. 79−67011
Ap stars, line identifications, new wavelength lists 79−16967
Ap stars, mag. fields meas. techniques and field geometries 80−82213
Ap stars, spectrum vars. rel. to mag. latit. of metals 79−58341
Ap stars, summary of physical and chemical props. from UV obs. *(Italian)* 78−32479
Ap stars, thickness estimation of anomalous chem. comp. layer in atm. *(Russian)* 78−93279
Ap stars 5200 Å feature, evidence for two component struct. from new Δa-photometry 80−67734
Ap stars broad absorptions, narrow band photometry 77−67095
Ap stars broad flux depressions, comparison between synthetic spectra and spectrophotometry 80−67735
δ_{1400}-Ap type stars, excess UV index, photometry obs. 80−72963
Ap-stars, detection of 4200 and 5200 Å, continuum features 79−75215
Ap-stars, mag. field obs. using photoelec. method, visible spectra obs. 80−82373
Ap-stars, magnetic intensification of spectral lines *(Russian)* 78−4254
Ap-stars, spectral energy distrib., spectrophotometry in 3300 to 7100 Å region 80−85953
Ap-stars, UV spectra in 1350-2550 Å range, TD1 satellite obs. 78−36581
α and β Aquari, G-type supergiants, evidence for hybrid atmospheres and winds from UV spectra 80−72948
AE Aquarii, cataclysmic variable, IUE satellite UV obs. 80−72985
α Aquarii, chromospheric event detect. from UV spectrum obs. 80−31299
U Aquarii, R Coronae Borealis star, extraordinary comp. rel. to unusual s-processing event 80−17588
R Aquarii, symbiotic long-period variable, spectrum of assoc. nebulosity 80−90450
R Aquarii, UV, visible and 85 GHz continuum obs. 80−85946
R Aquarii, UV obs. of hot component 80−56854
σ Aquarii (A0 IVs), hot metallic-line star, spectrum and abundance anal. 80−90415
R Aquarii (M7+pec), late type variable star, IUE obs. of circumstellar emission 80−82370
Aquila X-1, photometry and spectroscopy of optical counterpart, model 78−32614
Aquila X-1, X-ray spectra during outbursts 78−20909

stellar spectra continued
Aquila X-1 (4U 1908+00), emission line spectrum obs. during optical outburst 80−67909
Aquila X-1 (4U 1908+00), optical outburst, emission line spectrum obs. 78−69911
Aquila X-1 optical counterpart, spectrum 78−77626
V923 Aquilae, atmospheric motions from spectrum analysis 77−60776
η Aquilae, classical Cepheid, UV obs. and companion star detect. 80−90443
θ Aquilae (B9.5 III), spectrum and abundance anal. 80−90415
T Aquilae (Nova 1891), spectrophotometry of shell 80−72955
V535 Arae, absolute characts. of W Ursae Majoris system 79−58373
γ Arae, line of sight interstellar cloud, model from spectra anal. 80−105312
Ariel 0620−00, transient X-ray source, continuum spectrum rel. to spherical model 78−12415
Ariel 0620−00, transient X-ray source, obs. using OSO-8 Bragg cryst. spectrometer 78−12426
UX Arietis, binary star, radio spectrum from 430 to 8085 MHz 77−64793
UX Arietis, Copernicus UV obs. of Lyman α and Mg II emission 78−81651
56 Arietis, spectrophotometry of Ap star, continuum features vars. 80−36638
asymptotic giant branch stars in globular clusters 79−8913
atlas of stellar spectra 79−88649
atlas of UV spectra from OAO 2 spectrometer flux data 79−48691
atmosphere models application to determ. of effective temp., bolometric corrections, Balmer discontinuity and distrib. functions *(Rumanian)* 78−36557
atmospheric structure, mol. effects 80−21999
atom, laboratory hyperfine struct. for astrophysical interest 78−17818
atomic line broadening by neutral H, simple formula 79−92665
atomic line profile calc., method *(Russian)* 79−92684
atomic spectral survey for analysis of stellar spectra *(Spanish)* 79−75099
ε Aurigae, ^{7}Li I 6708 Å line and Li interstellar abundance 78−49494
ε Aurigae, eclipsing binary, International UV Explorer obs. 79−17027
ζ Aurigae, eclipsing binary, UV obs. of supergiant atmos. 80−94836
AR Aurigae, eclipsing binary Hg star, peculiar spectral var. during eclipse 80−98679
ϵ Aurigae, fine analysis of atmosphere of primary F-type supergiant 78−85976
RW Aurigae, IR spectroscopy with contact-type image tube 79−92768
IU Aurigae, massive triple system, spectra and orbits 77−64798
KR Aurigae, optical spectrum, variability *(Russian)* 78−36597
KR Aurigae, peculiar variable star, possible black hole *(Russian)* 77−87420
ε Aurigae, spectrum outside eclipse 77−71129
RW Aurigae, T Tauri star, far UV spectra, emission measure obs. 80−94788
ε Aurigae, UV spectrum using IUE 79−71071
α Aurigae (Capella), Ca II and Mg II lines rel. to chromosphere model 78−40931
α Aurigae (Capella), intense line emission in soft X-ray spectrum 78−93228
α Aurigae (Capella), X-ray line emission obs., corona models 80−26905
T Aurigae (Nova 1891), old nova, photometric and spectroscopic obs. 80−90446
B7 to G4 stars, spectral type depend. of distrib. perpendicular to galactic plane *(Russian)* 80−73036
B9 II to G0V stable stars, quantitative spectral classification *(Russian)* 79−44480
B, A and F stars, spectrophotometry, effective temps. 78−57546
B 1 Ia-0 supergiants, spectra and mass loss 79−16948
B-, A- and F-type stars, photoelec. K-line indices 79−16953
B-type and Be-type stars, search for binaries 78−57551
B-type stars, nonradial pulsations, line profile variations 78−4228
B-type stars, pole-on, rapidly rot., spectral inconsistencies due to gravity darkening 80−17581
B-type stars, search for weak interstellar lines in spectra 77−74124
late B-type stars small v sin i values, Ap star determ., visible spectra 80−77409
B-type supergiant assoc. with GL 2636, IR obs. 80−105302
B-type variable star in LMC, possible identification with LMC X-3, spectral type 79−5923
Ba II stars, spectral energy distribs. from DDO photometry 79−92757
Balloon-borne UV Stellar Spectrograph, first obs. results 79−70955
Balloon-borne UV Stellar Spectrograph, instrumentation and obs. 79−70954
Balmer discontinuity, influence on UBV photometry reductions 77−74046
Balmer line formation in rotating white dwarfs 79−30059
Balmer-index photometry, quantitative anal. of influencing factors 78−96404
Barnard's star, spectrophotometry with Carnegie image tube 78−57466
BD+0°2989, late-type dwarf star, metal abundances 77−78779
BD+10°2179, BD−9°4395, extreme He stars, UV spectra 79−16976
BD+33°2642, galactic halo blue star, mass loss determ. from IUE obs. 80−72947
BD+39°3226, BD+34°1543, hot subdwarfs, spectral types 78−45323
BD+61° 1211 (2A 1052+606), RS Canum Venaticorum binary star, spectroscopic obs. 80−36663
BD−7°3007, nova-like variable, simultaneous spectroscopy and photometry 78−12250
BD +1°4381, H deficient A-type star, effective temp. 79−40195
BD −9°4395, H deficient star, spectral photometry and quantitative anal. 77−56946
BD-3°5357, eclipsing binary with hot subdwarf component 77−91574
Be and shell stars, Balmer line polarisation meas. 77−56995
Be and shell stars, conf. Bass River, Mass., USA, 1975 Sept. 77−56964
Be and shell stars, UV spectra, circumstellar absorpt. lines 79−62832
Be and shell stars, UV spectrophotometry with TD-1 satellite 80−90438
Be shell stars, Bβ high-resolution polarisation struct. meas. by digicon spectropolarimeter 79−44485
Be stars, discoveries in open clusters NGC 3766 and (IC 2581) 80−90445
Be stars, electron scatt. effects on Balmer emission lines 80−17589
Be stars, emission features rel. to luminosity class and spectral type 77−56969
stellar spectra continued
Be stars, emission line profiles from envelopes, elliptical gaseous ring model 80−4373
Be stars, emission line profiles from envelopes, theoretical profiles 80−4374
Be stars, evidence for mass loss in mid-UV spectra 78−8010
Be stars, Hα survey 77−56967
Be stars, rapid fluctuations detect. in spectra 77−56954
Be stars, rapid Hα variations 77−56971
Be stars, spectra and photometry 77−56966
Be stars, spectroscopic obs. 77−56957
Be stars, spectroscopic obs. in near IR 77−56972
Be stars in galactic clusters, Hα study 77−56968
Be stress, bright, Hα emission variability 79−67027
Be-stars, classification of faint objects 77−56993
Be-stars, emission-line profile computations 77−56920
Be-stars, Hα vars. in spectra of bright northern objects 79−35265
Be-stars, IUE obs. 80−82383
Be-stars, mass-exchange binary evidence from periodic spectral var. 77−60781
Be-stars, Paschen decrements and emission line formation in envelopes 77−56992
Be-stars, photographic IR spectroscopy and near IR photometry 77−56991
Be-stars, rotation rel. to Hα and Hβ meas. 77−56983
Be-stars, spectra rel. to rotational hypothesis 77−56981
Be-stars, TV obs. of Hα and Hβ line profile rapid vars. *(Russian)* 79−16992
Be-stars, UV fluxes 78−61870
Be-stars, UV Si IV/C IV ratio, Skylab obs. 77−56987
Beals' Type III P Cygni line profiles 80−51771
Becklin-Neugebauer source in Orion, 3.3 to 5.5 microns spectrum 80−12796
binaries, wide visual, spectral type, age and uvbyβ photometry 80−94833
binary stars, G and K-type giants Ca II H and K lines emission intensity 80−82420
binary stars, spectroscopic, spectral obs. with solid state detector 80−109469
binary system gravitational radiation, relativistic corrections and spectrum fine structure 80−90479
binary X-ray sources, cyclotron line feature identification 80−90577
black holes in binary stellar systems, gamma emission during spherically symmetric accretion 80−17608
blue star in SNR 1006, spectral features and UBV photoelectric meas. 80−41830
Bochum 15 stellar aggregate, photoelectric and spectroscopic obs. 77−87490
γ Bootis, classical evolved δ Scuti star 79−75219
ZZ Bootis, double spectrum eclipsing binary, revised spectrographic and photometric elements 78−61885
α Bootis, He I 10830 Å emission obs., high-temp. chromosphere 79−48792
α Bootis, search for Ti II 3080 Å multiplet emission 80−51769
α Bootis, spectrophotometric profile, 3200-3600 Å 80−62118
α Bootis, stellar gravity from metallic line profiles and effective temp. 77−64759
TZ Bootis, W Ursae Majoris system, spectroscopic and photoelectric obs. 78−69832
α Bootis (Arcturus), anal. of chromospheric O I spectrum 77−56923
α Bootis (Arcturus), CO fundamental bands, inhomogeneous chromosphere 78−36561
α Bootis (Arcturus), far UV spectrum, coronal temp. determ. 78−16407
α Bootis (Arcturus), line identifications in UV spectrum 79−25598
α Bootis (Arcturus), O and C abundances *(Russian)* 78−16420
α Bootis (Arcturus), spectral line asymmetry meas. rel. to Sun 80−51753
α Bootis (Arcturus), spectrum and atmospheric parameters 78−20826
α Bootis (Arcturus), UV obs. of chromospheric emission line profiles 78−81620
α Bootis (Arcturus) (K2 IIIp), Wilson-Bappu effect, explanation from theoretical temp. minima 79−62825
ξ Bootis A, active dwarf star, chromospheric emission lines obs. 80−12762
ξ Bootis A, late-type dwarf star, mag. field obs. 80−72949
BPM 25114, peculiar white dwarf, light vars., oblique rotator model *(Italian)* 78−93241
BPM 25114, southern mag. white dwarf, spectrophotometric obs. 79−92765
BPM 4729, cool DA white dwarf with self-broadened Balmer lines 79−35255
bright IR star monitoring at 2.7 μm 78−16433
bright southern stars with interesting Stromgren indices, spectral classifications estimation 79−88645
53 Camelopardalis, Ap star, Ca II K and Hδ lines rapid vars. *(Russian)* 80−90458
53 Camelopardalis, Ap star, radial vels. and binary nature 79−80320
α Camelopardalis, O-type supergiant, spectroscopic study, model atm. anal. 78−28681
XX Camelopardalis, R Coronae Borealis star, spectral type from optical and IR photometry 80−101601
α Camelopardalis (O9.5 Ia), stellar wind terminal vel. short time changes from UV spectrum 80−36625
α Camelopardalis (O9.5 Ia), variable Hα P Cygni profile 80−41818
AH Cancri, contact binary in M67, spectrum and photometry 79−40222
WY Cancri, eclipsing binary, obs. rel. to absolute information derivation at lower end of main sequence 79−92799
RS Cancri, late-type variable star, spectral energy distrib. and spectral types *(Russian)* 78−40958
UU Cancri, long-period eclipsing binary, radial vel. meas. 77−74096
49 Cancri, spectrophotometry of Ap star, continuum features vars. 80−36638
Canis Major R1, anomalous diffuse bands 80−51820
Canis Major R1, optical and IR props. of newly formed stars 78−93332
UW Canis Majoris, eclipsing binary, mass flow anal. from UV spectrum 80−109429
R Canis Majoris, eclipsing binary, multiband photoelectric photometry and spectral types 77−53633
VY Canis Majoris, expanding circumstellar cloud, SiO 8 μm band obs. 79−62840
α Canis Majoris, Lα obs., interstellar H and D determ. 79−21275

stellar spectra continued
29 Canis Majoris, massive hot binary star, spectrograms, mass loss 78−12299
UW Canis Majoris, O7f supergiant, UV lines P Cygni profiles rel. to mass loss rate 80−67736
VY Canis Majoris, OH and H_2O microwave maser emission obs. 78−53949
VY Canis Majoris, OH masers very long baseline interferometric obs. 78−36712
VY Canis Majoris, OH/IR star, 1612 MHz OH maser multibaseline VLBI obs. 80−12766
27 Canis Majoris, spectroscopic obs. in 0.14-4.7 μ range 78−85957
α Canis Majoris (Sirius), B abundance 77−53585
α Canis Majoris (Sirius), Ca II K line high resolution profile obs. 80−56830
α Canis Majoris (Sirius), Ca II K-line asymmetry unconfirmed 79−30062
α Canis Majoris (Sirius), Ca II Kline asymmetry, comments 79−30063
α Canis Majoris (Sirius B), spectral energy distrib. 80−8629
β Canis Majoris stars, spectral vars. rel. to multiperiodicity 77−87424
α Canis Minoris, flux spectrogram, UV line blending and wavelengths, spectral resolution influence 80−56811
YZ Canis Minoris, spectroscopic flare obs. 79−92780
α Canis Minoris, Utrecht UV spectrophotometer obs. 78−69793
α Canis Minoris (Procyon), CNO abundances from near IR spectrum 78−93222
Y Canum Venaticorum, C_3 and IR spectrophotometry of C star 78−65619
Y Canum Venaticorum, C star, IR spectrum between 1.2 and 30 microns 80−46544
TX Canum Venaticorum, cataclysmic variable, P Cygni type, visible spectral obs. 80−105249
TX Canum Venaticorum, evolution from cataclysmic to stationary P Cygni stage 79−12479
RS Canum Venaticorum, explanation of observations 79−84826
α^2 Canum Venaticorum, mag. Ap star high-resolution polarisation obs. inside spectral line 78−40951
α^2 Canum Venaticorum, magnetic field gradient in Ap-star atmosphere, Zeeman spectra 78−85953
α^2 Canum Venaticorum, UV flux distrib. 79−80313
RS Canum Venaticorum binaries, multiperiodic light and spectrum vars. 77−87479
RS Canum Venaticorum binary stars, mag. starspot model for photometric and spectroscopic behaviour 80−109488
RS Canum Venaticorum binary stars, radio luminosities and spectra 79−21333
α^2v Canum Venaticorum magnetic variable, H I lines and atmospheric parameters 79−97011
RS Canum Venaticorum stars, spotted component spectral type rel. to amplitude of out of eclipse light var. 80−109489
RS Canum Venaticorum type binaries, Hγ line vars., chromospheric diagnostics 80−62181
RS Canum Venaticorum-type binaries, emission line vars. 78−24527
ζ Capricorni, Ba star, white dwarf+giant, UV spectra obs. 80−105284
δ Capricorni, eclipsing binary, Am primary component metallicism var. 77−67115
β Capricorni, triple star, fundamental parameters from occultation astrometry and spectroscopy 79−40216
ν Capricorni (B9.5 V), spectrum and abundance anal. 80−90415
Carina Nebula association, radial vel. study of WN stars and Of star 79−35261
Carina Nebula stars, interstellar λ4430 band obs. 78−32555
Carina spiral arm, galactic struct. and star formation, spectrographic and photometric obs. *(French)* 78−89256
Carina spiral feature, photometry and spectra rel. to stars and interstellar dust distrib. 80−51871
η Carinae, high-resolution IR radiation maps of homunculus, spectral and spatial distrib. 80−12767
η Carinae, IR Fe II lines and interpretation of IR excesses 78−32478
η Carinae, IUE spectral obs. 79−71051
AG Carinae, luminous star in symmetric nebulae; IUE low-dispersion spectrum 80−46560
AG Carinae, P Cygni supergiant, spectrum of ring nebula 77−67100
θ Carinae, radial vel. of chemically-peculiar B-type star 80−8635
η Carinae, spectral obs. at 4 microns 78−4237
η Carinae, UV spectrum and expansion vel., IUE obs. 79−30071
α Carinae (Canopus), echelle spectrogram 78−96396
α Carinae (Canopus), generalised Compton effect in spectrum 78−53938
QZ Carinae (HD 93206), massive multiple system in great Carina Nebula, spectral types and orbits 79−97027
QZ Carinae (HD 93206), O-type quadruple eclipsing system, spectroscopic and radial vel. study 80−105275
VY Carinae field stars, spectra and photometry rel. to cepheid absolute magnitude 77−64764
Cassiopeia-Taurus association stars, interstellar 2200 Å feature anomalous strength 80−77469
ρ Cassiopeiae, absolute energy distrib. in 3400-7100 Å range 78−49440
γ Cassiopeiae, Balmer lines obs. rel. to circumstellar envelope model 78−40952
γ Cassiopeiae, Be star, IR excess 78−93257
γ Cassiopeiae, Be star, new UV C IV and Si IV shell lines 79−84802
γ Cassiopeiae, Be star, rapid spectroscopic variations 77−56970
γ Cassiopeiae, Be star, spectrophotometric variability from UV and Hα obs. 79−5829
γ Cassiopeiae, Be-star, visible spectra 77−56989
RZ Cassiopeiae, eclipsing binary, spectroscopic orbit 80−22040
VX Cassiopeiae, fast irregular variable, H_α and H_β lines obs. *(Russian)* 77−87400
R Cassiopeiae, late-type giant, possible H_2O thermal emission identification 78−81628
BM Cassiopeiae, long-period eclipsing binary, radial vel. meas. 77−74096
R Cassiopeiae, Mira variable, vel. struct. in SiO maser spectrum 78−12248
γ Cassiopeiae, N I interstellar absorption, UV obs. 80−51823
κ Cassiopeiae, OBC star, spectrophotometry, 3300-7100 Å region 79−67009
UV Cassiopeiae, R Coronae Borealis star, spectral type from optical and IR photometry 80−101601
WZ Cassiopeiae, semiregular variable star, variable CaCl absorpt. bands 79−88683
stellar spectra continued
SU and TU Cassiopeiae, short-period Cepheids, photometry and spectra rel. to radius anomalies 80−26864
HT Cassiopeiae, spectroscopic obs. of dwarf nova 79−88668
6 Cassiopeiae, spectroscopic obs. of supergiant star, equivalent widths, microturbulence and radial vel. 80−22006
γ Cassiopeiae, UV and optical spectral var. rel. to coronal emission 78−93251
o Cassiopeiae (HD 4180), Be star, Balmer emission lines vars. rel. to IR photometric vars. 79−58353
V509 Cassiopeiae (HR 8752), no emission at Hβ (1979 July 31) 79−92782
V509 Cassiopeiae (HR 8752), spectrum variable supergiant, Hα emission obs. 79−88672
cataclysmic variables, emission lines from accretion discs 80−51774
CD−42° 14462, binary nature of nova-like variable 77−87435
CD-31°622, spectroscopic obs. of DC white dwarf candidate 77−67090
CD-38°245, metal-deficient halo red giant, spectrum, photometry and Ca/H ratio 78−69797
V553 Centauri, C rich Cepheid, C and N abundances 80−4378
V553 Centauri, CH-type Cepheid, spectrum, chemical comp. and luminosity 79−62849
proxima=V645 Centauri, dMe flare star, quiescent corona, transition region, and chromosphere obs. 80−56850
BV Centauri, dwarf nova and spectroscopic binary, UBV photometry, spectral types and orbit 80−51775
V346 Centauri, eclipsing binary, spectroscopic orbit 79−58378
μ Centauri, far UV spectra analysis of pole-on Be-star 79−48805
μ Centauri, pole-on Be-star, far UV spectra 77−56990
ζ Centauri, shell star, Copernicus UV obs. 77−56989
ν Centauri, single-lined spectroscopic binary, β Cephei-type star 79−48821
μ Centauri (B2 IVe), new circumstellar shell development, spectroscopic obs. (1980 June 10 to 12) 80−94808
α Centauri A, Utrecht UV spectrophotometer obs. 78−69793
α Centauri A and B, IUE spectra and transition region models 80−46543
α Centauri binary system, spectroscopic chemical anal. 80−62128
Centaurus X-3, spectroscopic obs. of Krzeminski's star 79−53934
Centaurus X-4, SIT Vidicon spectra 79−80370
Centaurus X-4, spectroscopic obs. of visual counterpart, companion type 80−82545
central stars of planetary nebulae, spectrogram analysis 79−97001
central stars of planetary nebulae, UV spectral obs. from TD-1 satellite 80−31300
EM Cephei, 3600-4900 Å spectrophotometric observations *(Russian)* 77−64803
9 Cephei, B2-type supergiant, circumstellar CO lines discovery 79−84793
U Cephei, chem. comp. of secondary component of close binary system 79−35308
U Cephei, eclipsing binary, gas stream effects in UV spectrum, IUE obs. 80−26898
EM Cephei, eclipsing binary, spectroscopic obs. of shell *(Russian)* 78−57587
δ Cephei, Hα radial vel. behaviour 80−51788
VV Cephei, Hα region spectra and system analysis 77−78823
μ Cephei, late-type supergiant, possible H_2O thermal emission identification 78−81628
T Cephei, Me variable, Tc discovery 78−32483
19 Cephei, O-type supergiant, spectroscopic study, model atm. anal. 78−28681
VV Cephei, spectroscopic obs. during 1976/77 eclipse ingress phase 78−45359
DI Cephei, spectrum vars. in T Tauri star 80−8628
VV Cephei, supergiant eclipsing binary UV spectrum 80−82415
VV Cephei, UV spectrum in 1978, flux distrib. 79−88698
VV Cephei, UV spectrum obs. during chromospheric eclipse phase 80−109498
λ Cephei, variable outflow in Of star, spectroscopic obs. 79−35263
IV Cephei (Nova 1971), spectrum and ejecta He abundance 79−40203
β Cephei star search, northern photometric and spectroscopic obs. 77−74057
β Cephei stars, non-radial oscillators, single period variables 79−25613
VV Cephei system, distant, in Puppis, spectral classification, UBV photometry and polarimetry 80−51810
Cepheid variables, He enrichment effects in atm., models 80−26884
Cepheids, Hα emission in southern beating objects 79−21301
classical Cepheids, nonvariable supergiants and bright giants, spectrophotometric comparison 80−56837
δ Ceti, β Cephei variable, spectroscopic binary, radial vels. and period var. 80−82376
τ Ceti, Ca II 866.2 nm emission event 80−26860
κ Ceti, IUE obs. of far UV spectra of G-type dwarf 80−56831
δ Ceti, period changes of β Cephei type star 78−32487
T Ceti, semiregular variable, Tc I absorpt. line obs. 78−28689
o Ceti (Mira), enhanced activity of B-type component at 1976 light minimum 78−81636
o Ceti (Mira), H I emission line profiles *(Russian)* 79−16990
o Ceti (Mira), mass loss rate determ. 79−48831
o Ceti (Mira), polarized Balmer emission lines, spectropolarimetry 79−21302
o Ceti (Mira), spectrum of companion star 78−4253
o Ceti (Mira), strong TiO-related dia. vars. 78−16429
o Ceti (Mira), variable 2.6 mm CO emission obs. 78−12241
o Ceti (Mira) at 1978 max., visible spectropolarimetry 80−94799
o Ceti AB, IUE obs. of UV spectrum 80−22027
UV Ceti type stars, weak Ca II triplet absorpt. lines *(Russian)* 79−88691
chromosphere lines, high-press. transition regions rel. to Ca II and Mg II reson. lines profiles 80−26847
chromospheric K-line emission on H-R diagram, absolute fluxes 77−56937
chromospheric scaling laws, width-luminosity correls., Wilson-Bappu effect 79−40177
chromospheric spectral lines, primary and secondary indicators of hot envelopes *(German)* 80−109421
chromospheric var. in main sequence stars, Ca II line obs. 77−56936
Chu's object in Perseus, UBV photometry and spectrum rel. to identification as galactic star 80−62132
Circinus X-1, Hα emission vars. 80−67910

stellar spectra continued
Circinus X-1, H I radio absorpt. obs. and distance 78−12413
Circinus X-1 (3U 1516−56), spectra of optical and radio counterpart 78−12414
circumstellar dust shells, emission and absorption spectra 77−87376
CIT 6 (IRC+30219), IR C star, CO obs. of mass outflow 80−12761
classification errors, detect. by cluster anal. 78−20819
classification from UV line features, Am and Ap stars appl. 79−21272
classification in intermediate multiband photometry, photometric star box 77−87373
classification of ADH objective prism spectra, procedure 80−72930
classification of early-type stars 78−16401
classification rel. to interstellar extinction and galactic struct. *(Russian)* 78−73701
classification using Copernicus UV data 78−12216
classification using Fe III UV lines 78−16404
classification using satellite UV photometric data 78−16402
classification using Skylab UV objective-prism spectra 78−16403
classifications for bright northern stars with interesting Stromgren indices 80−56817
close binaries, light scattering in extrastellar gaseous material, emission line profiles spectropolarimetry obs. 80−109471
cluster stars near IC 1805 (W4), spectral classes and photometry 80−62214
cocoon stars, calculated IR spectra 77−64824
CoD−38°10980, white dwarf, gravit. redshift meas. 78−24511
CoD −35° 10525, bright YY Orionis star, spectrum and UBV photometry 78−36566
Collinder 140, young open cluster, spectroscopic and statistical study 80−62211
α Columbae, rapid spectral vars., cross correlation analysis 79−48808
14 Comae, A-type shell star, spectroscopic obs. 78−7992
CC Comae, W Ursae Majoris type, spectroscopic orbit 78−12300
17 Comae A, Ap star, mag. field meas. and rot. period *(Russian)* 80−90457
composite spectra stars, new classification scheme for bright stars of Hynek's (1938) list *(French)* 80−56876
continuous spectrum, electron scattering effect *(Russian)* 79−12461
cool C stars, $^{12}C/^{13}C$ ratio calc. 78−4205
cool giant stars, obs. and anal. of CO at 5 μm 78−36569
cool standard stars spectra, Fe lines equivalent widths for spectral anal. 77−78771
cool star spectra, TiO $e^1\Sigma^+$-$d^1\Sigma^+$ transition theory 77−67089
cool stars, alkaline earth and rare earth oxides occurrence 78−85933
cool stars, CaCl bands obs. 77−53593
cool stars, local interstellar H and D Lyman α towards four objects 79−5886
cool stars, neutral-ion anomaly 78−7985
cool stars, outer atms. struct., solar-type and non-solar-type stars 79−48791
cool stars, polarization across TiO bands 79−97005
cool stars, prediction of EUV H_2 lines 78−12184
cool stars, Ti isotopic abundance ratios 80−26840
cool stars, UV spectra obs. by International Ultraviolet Explorer (IUE) 78−96475
cool supergiant stars, near IR excesses 78−16406
S Coronae Austrinae, identification of absorpt. lines, irradiated amethyst 79−25601
S Coronae Austrinae, line profiles in YY Orionis star 79−84808
S Coronae Austrinae, protostar, high dispersion spectroscopy, Balmer line profiles 77−64754
S Coronae Austrinae, spectroscopic and photometric vars. of YY Orionis star 79−48812
S Coronae Austrinae, T Tauri star, red-displaced absorpt. features obs. 78−4221
ε Coronae Austrinae, W Ursae Majoris type star, spectra, radii, masses 79−71069
S Coronae Austrinae, YY Orionis star, satellite UV spectrum 79−67016
R Coronae Austrinae dark cloud stars, interstellar absorpt. spectra rel. to dust grain growth 80−67834
β Coronae Borealis, Ap star, Ca II K and Hδ lines rapid vars. *(Russian)* 80−90458
θ Coronae Borealis, Be star, strong shell line at Hα 79−67022
θ Coronae Borealis, Be-type star, shell line profile and radial vel. obs. 80−77426
β Coronae Borealis, Hα line variability *(Russian)* 78−69815
β Coronae Borealis, H I Paschen lines and Ca II triplet study 80−26869
R Coronae Borealis, He I λ10830 line obs. at 1978 pre-maximum phase 79−16975
ιCoronae Borealis, Hg-Mn star, spectroscopic binary, visible spectra obs. 80−72983
β Coronae Borealis, mag. star, spectral peculiarities *(Russian)* 77−64773
β Coronae Borealis, magnetic field gradient in Ap-star atmosphere, Zeeman spectra 78−85953
β Coronae Borealis, magnetic field of Ap-star 79−5822
R Coronae Borealis, search for graphite feature at 2200 Å 77−87419
σ Coronae Borealis (HD 146361), spectroscopic binary, soft, X-ray obs. with (HEAO-1) 80−56886
R Coronae Borealis in quiet state, spectral energy distrib. *(Russian)* 80−51781
coronal plasma, EUV spectra and contribs. to diffuse EUV background 80−62324
Coude spectrograms, effects of stellar rotation 77−82219
coude spectrograms of stars in dust clouds with bright nebulosities 80−56893
CPD−56°8032, emission line object, red and IR spectrum 78−4249
CPD −62° 1837 (HDE 308122), long-period variable member of triple 80−105260
CRL 2688 (Egg Nebula), IR polarimetry and central source spectrum 78−36658
CRL 3099, highly evolved C star, IR photometry and spectrum 78−49436
CRL 618 and 915 (HD 44179), IR spectra in 2-8 μ range 78−41080
BI Crucis, new symbiotic star, spectrum 80−109442
25 G Crucis (HD 108250), orbital elements from spectrograms 80−82432
cyanogen distrib. in 47 Tucanae red giants 79−71025
CH Cygni, 5700-8700 A spectrograms 77−87415
31 and 32 Cygni, ζ Aurigae stars, UV spectroscopic obs. 80−109499

stellar spectra continued
V1500 Cygni, (Nova 1975), emission line profiles during early nebular stage 79−53826
α Cygni, anomalous spectral line contours of Fe II multiplet *(Russian)* 78−93243
X Cygni, Cepheid, radial vels. 78−73723
SU Cygni, classical Cepheid, binary companion spectral type from UBVRI photometry 79−62852
V460 Cygni, cool C star, atmospheric $^{12}C/^{13}C$ ratio 78−93223
XX Cygni, dwarf Cepheid, composition and motion, visible photometric and spectrographic obs. 80−77424
V367 Cygni, eclipsing binary, spectroscopic study 78−53984
P Cygni, extreme B-type supergiant, UV spectroscopy 80−22004
θ Cygni, F-type dwarf star, spectral type of faint distant companion 80−90481
υ Cygni, far UV spectra analysis of pole-on Be-star 79−48805
V1016 Cygni, forbidden Fe VI emission rel. to electron density 79−8970
V1057 Cygni, FU Orionis star, IR spectroscopy with contact-type image tube 80−17587
P Cygni, H Balmer line profiles, accel.-decel. envelope, mass loss 79−40205
P Cygni, H Paschen α obs. 80−62156
P Cygni, high resolution UV spectrum obs. 80−26873
V1016 Cygni, image-tube spectrograms 80−8639
59=V832 Cygni, IR emission increase, spectrum scanner obs. 80−94809
V1016 Cygni, IR spectrum 78−93266
32 Cygni, IUE obs. and effects of B-type star within late-type supergiant upper chromosphere 80−22036
V382 Cygni, IUE spectra of massive close binary 80−8659
P Cygni, mass loss, Balmer line profiles 78−45334
α Cygni, mass loss from mid UV spectrum obs. 78−93217
V832=59 Cygni, mass-losing Be star, changes in UV spectrum 80−46561
χ Cygni, Mira variable star, variable 2.6 mm CO emission obs. 78−12241
V1016 Cygni, near-IR spectrographic obs. 80−94810
CH Cygni, new active period, model, double system with accretion disc *(Russian)* 78−69813
V1016 Cygni, new spectroscopic obs., simultaneous presence of increasing excitation and cool features 80−26874
V1057 Cygni, OH obs. 80−36629
NML=V1489 Cygni, OH/IR star, 1612 MHz OH maser multibaseline VLBI obs. 80−12766
CH Cygni, outburst and spectral changes, 1977 August 31 obs. 77−82231
V389 Cygni, peculiar (Ap-type) binary, spectroscopic obs. 78−85975
V1016 Cygni, photometric and spectroscopic obs. rel. to proto-planetary nebula mass ejection 78−85947
υ Cygni, pole-on Be star, far UV spectra 77−56990
R Cygni, pure S star, new molecules identification 78−28700
α Cygni, radial vel. and line profile vars. in supergiant 80−22010
V1331 Cygni, radial vels. of spectra lines in unusual T Tauri star 79−71045
V1500 Cygni, spectral development, visible and near IR obs. 78−4231
57 Cygni, spectroscopic binary, search for systematic radial vel. anomalies 80−17617
CI Cygni, spectroscopic obs. using multichannel analogue detector system 78−36461
CG Cygni, spectroscopic study of close eclipsing binary 79−97031
α Cygni, supergiant, near UV spectrum 78−7991
CH Cygni, symbiotic star, 1977 outburst, radial vel. and atm. struct. determ. 80−72969
CH Cygni, symbiotic star, binary model rel. to blue continuum and emission and absorpt. lines 80−62158
CH Cygni, symbiotic star, IUE obs. during active phase 79−62846
CH Cygni, symbiotic star, spectroscopic obs. during 1977 to 1978 outburst 79−75211
59=V832 Cygni, variable mass flux from spectroscopic obs. 80−41840
CH Cygni, visible and near IR spectra 77−82232
V645 Cygni (AFGL 2789), Ae star, perplexing spectrum 80−73066
V645 Cygni (CRL 2789), bipolar nebula, O-type exciting star 78−4392
V1341 Cygni (Cygnus X-2), halo population binary 79−97099
α Cygni (Deneb), Ca II K line high-resolution obs. 78−16408
α Cygni (Deneb), Ca II K-line core asymmetry 80−85981
α Cygni (Deneb), Copernicus obs. of UV spectrum 78−45330
α Cygni (Deneb), variable line profiles interpretation 77−64761
V645 Cygni (GL 2789), IR and EHF spectroscopy 80−72956
V1329 Cygni (HBV 475), symbiotic variable, photometric and spectroscopic history 80−62148
V1500 Cygni (Nova 1975), Balmer line emission profiles evolution in early decline phase 80−82371
V1500 Cygni (Nova 1975), binary nature, spectral meas. 77−87446
V1500 Cygni (Nova 1975), distance and temp., visible spectral obs. *(Chinese)* 80−85955
V1500 Cygni (Nova 1975), emission line vars. rel. to struct. of central object 80−82367
V1500 Cygni (Nova 1975), fine-struct. lines rel. to 10 micron excess 78−93269
V1500 Cygni (Nova 1975), flux distribs. rel. to shell electron temps. and densities 79−30068
V1500 Cygni (Nova 1975), Hα and Hβ emission line vars. 80−4389
V1500 Cygni (Nova 1975), H I emission line profiles vars., envelope ejection vels. determ. 79−35281
V1500 Cygni (Nova 1975), He abundance of ejecta 78−28691
V1500 Cygni (Nova 1975), heavy element abundances 79−21295
V1500 Cygni (Nova 1975), IR spectra and photometry 78−36615
V1500 Cygni (Nova 1975), line spectrum evolution 78−32493
V1500 Cygni (Nova 1975), model for spectrographic obs. 77−87444
V1500 Cygni (Nova 1975), near IR spectroscopy 78−36599
V1500 Cygni (Nova 1975), near IR spectrum 78−36606
V1500 Cygni (Nova 1975), nebular stage spectrum rel. to linear polarisation 78−36621
V1500 Cygni (Nova 1975), obs. of magnitude and spectrum changes *(French)* 77−82258
V1500 Cygni (Nova 1975), photometric and spectroscopic obs. 78−36604
V1500 Cygni (Nova 1975), pre-maximum spectra 77−87449
V1500 Cygni (Nova 1975), spectral energy distrib. 78−36605
V1500 Cygni (Nova 1975), spectral evolution 77−87447
V1500 Cygni (Nova 1975), spectral features time evolution from thirteen-colour photometry 79−92788

stellar spectra continued
V1500 Cygni (Nova 1975), spectrographic obs. *(Chinese)* 79−16982
V1500 Cygni (Nova 1975), spectrophotometric study *(French)* 77−82259
V1500 Cygni (Nova 1975), spectroscopic data 79−16988
V1500 Cygni (nova 1975), spectroscopic obs., three hour periodicity, nebular model 78−12235
V1500 Cygni (Nova 1975), spectroscopic studies, models for 3 hour profile vars. 79−8920
V1500 Cygni (Nova 1975), spectroscopic studies, nebular and central binary system 79−62830
V1500 Cygni (Nova 1975), spectrum variations 78−36607
V1500 Cygni (Nova 1975), visible and near UV spectrophotometric obs. 78−32492
V1500 Cygni (Nova 1975), visible and near UV spectrophotometry 78−32494
V1500 Cygni (Nova 1975), visible and UV spectra and light curve 80−12771
V1500 Cygni (Nova 1975), visible spectroscopy 78−36598
V 1668 Cygni (Nova 1978), spectral development 80−51789
V1668 Cygni (Nova 1978), spectrographic obs. around max. brightness *(French)* 79−58343
V1668 Cygni (Nova 1978), spectroscopic and photometric obs., (1978 to 1979) *(Russian)* 80−109444
V1668 Cygni (Nova 1978), UV spectrum, emission lines 79−62837
V1500 Cygni (Nova Cygni 1975), IR photometry and spectroscopy 77−53599
V1500 Cygni (Nova Cygni 1975), spectrum around max. light 77−87411
61 Cygni A, B, late-type dwarfs, metal abundances 77−78779
P Cygni Balmer line spectrum, equivalent two-level-atom approach rel. to mass loss 78−93255
P Cygni in far UV *(Russian)* 79−8919
CI Cygni symbiotic star, UV and optical spectrum changes during eclipse 80−105258
P Cygni type line profiles, theoretical, atlas 79−80297
Cygnus OB2 No.12, interstellar and stellar features from high resolution 2μ spectroscopy 78−57613
Cygnus OB2 No.12 (VI Cygni No.12), C_2 detect. in interstellar spectrum 78−12332
Cygnus OB2 number 12, spectral classification and membership of association 80−51760
Cygnus X-1, X-ray binary, variable star, SHF obs. 80−73071
Cygnus X-2, binary, radial vel. and orbital elements from visible spectra obs. 80−77519
Cygnus X-2, X-ray and optical obs., (1973 to 1977) 79−30148
Cygnus X-3, 4.8 hour periodicity in spectra 79−5920
Cygnus X-3, evidence for X-ray Fe line emission obtained with cryst. spectrometer 78−8153
Cygnus X-3, hard X-ray spectrum obs. 80−31388
DA white dwarfs, H I Balmer γ line profiles and masses 80−77399
degenerate star candidates, photoelectric and spectroscopic obs. 80−12763
degenerate stars, H lines meas. 78−12224
degenerate stars, UV spectrophotometry, IUE obs. 79−53810
degenerate stars with H atmospheres, spectra rel. to comp. and theoretical models 80−17576
HR Delphini, UV spectrum, stellar wind 80−26880
HR Delphini (Nova 1967), cataclysmic binary spectrum 80−4359
HR Delphini (Nova 1967), emission line spectrum peculiarities 79−35280
HR Delphini (Nova 1967), emission lines at nebular stage *(Russian)* 80−17597
HR Delphini (Nova 1967), He I radial vel. var. 77−82249
HR Delphini (Nova 1967), nebular stage spectra rel. to envelope regions physical conditions 80−4369
HR Delphini (Nova 1967), photoionisation models of envelope in nebular stage, obs. data 78−61864
HR Delphini (Nova 1967), physical props. and element abundances in nebular state 78−36573
HR Delphini (Nova 1967), premax. and principal absorpt. line systems in spectrum 79−35279
HR Delphini (Nova 1967), premaximum mass loss rate, H line anal. 80−82378
HR Delphini (Nova 1967), simultaneous X-ray, UV and optical obs. 80−109440
HR Delphini (Nova 1967), spectra, line identification, radial vels. 80−17594
HR Delphini (Nova 1967), spectral evolution during decline 77−87440
Hr Delphini (Nova 1967), spectral evolution during decline period 78−40957
HR Delphini (Nova 1967), spectroscopic orbit 79−44510
δ Delphini stars in Michigan Spectral Catalogue, uvbyβ photometry rel. to spectral types 80−4377
dense stars, atomic spectra in intense mag. fields 80−105160
differential Doppler shifts, appl. to atmospheres vel. gradients determ. 78−57538
diffuse interstellar absorpt. bands origin, Ti depletion, accretion onto oxide grains 79−53879
diffuse interstellar band at 5780 Å, photoelectric meas. 78−93350
diffuse interstellar bands, strengths rel. to stars IR colour excesses 78−93198
diffuse interstellar bands at far UV wavelengths, obs. 78−32554
diffuse interstellar bands in 6500-8900 Å region 79−21373
diffuse interstellar line at 6284 Å, obs. and relation to interstellar reddening 80−51843
diffuse interstellar lines rel. to long chain C molecules 79−53897
digitized spectrogram processing using microdensitometer, ELSPEC/1 procedure *(Italian)* 79−62758
DO white dwarfs, spectrophotometry rel. to effective temps. and He abundances 79−35249
S Doradus, LMC Hubble-Sandage variable, IUE and ground based spectroscopic obs. 80−101595
β Doradus, Mg II h- and k-lines in UV spectra of Cepheid 79−40196
30 Doradus central object (HD 38268), interstellar and nebular lines obs. 80−51839
double stars, visual, new spectral classification on MK system 80−109462
K Draconis, Be star, search for short time scale vars. in Hα emission 80−109441
73 Draconis, CH lines in spectrum of Ap star *(Russian)* 77−56958

stellar spectra continued
BY Draconis, late-type flare star, metal abundances 77−78779
ζ Draconis, line identifications in UV spectra 77−87384
CM Draconis, low dispersion spectrum, metal abundance of eclipsing binary 79−25636
ϕ Draconis, Si Ap-star, UV vars. rel. to patchy stellar surface model 77−49389
73 Draconis, spectral variability of Ap star *(Russian)* 78−65624
BY Draconis, spotted flare star, spectra and photometry rel. to pre-main-sequence nature 80−36633
BY Draconis-stars, ages from spectra *(Russian)* 77−64774
BY Draconis-type stars, Hα emission line profiles, rapidly rot. gaseous envelopes *(Russian)* 78−65625
BY Draconis-type stars, spectroscopic binary incidence 77−87401
dwarf novae, cataclysmic variables, review of spectroscopic and photometric obs. 77−56959
dwarf novae, spectra *(Russian)* 80−8638
dwarf novae, spectrophotometry, 1250-7500 Å region 80−46577
dwarf stars, Ca II K and Hα profiles rel. to chromospheric models and activity 79−48773
dwarf stars, M-type, in South Galactic Pole direction, catalogue of 282 objects 79−5762
early A-type UV spectral classification 78−69794
early B-type stars atmospheres, LTE line blanketing by UV lines using accurate damping consts. 78−16419
early O-type star in SMC, discovery 79−5820
early type peculiar stars, Cr, Mn and Fe abundances 77−78803
early type stars, 206-287 nm UV spectra of Ap, Bp, Be, Bn and shell stars 80−51776
early type stars, 'normal', with anomalous mid UV spectra 80−26857
early type stars, line driven sound waves 79−71023
early type stars, luminosity determ. X-ray obs. 80−105241
early type stars, Mg II lines near 2800 Å 78−12229
early type stars, mid UV spectra obs. 80−21995
early type stars, normal, near UV line blocking depend. on spectral type and luminosity 80−36619
early type stars, photoelectric Hα line photometry 77−91528
early type stars, spectral classification from UV line features 80−72927
early-type star Lyman α and β profiles 77−87391
early-type stars, line profiles Fourier anal. for photospheric expansion meas. 78−93224
early-type stars, near UV obs. of line blocking factors 78−45329
early-type stars, Skylab UV obs., MK spectral types 78−40933
early-type stars, spectral classification, calibration using TV multichannel system 77−67091
early-type stars, spectral classification from TD1 satellite low dispersion UV spectra 78−16421
early-type stars, spectral energy distrib., reduction to Oke-Schild system *(Russian)* 77−64755
early-type stars, suspected variability and line emission, Hα obs. 79−67036
early-type stars, vacuum UV spectrophotometry and effective temps. 79−30060
early-type stars and cool stars, UV spectroscopy of outer layers 80−72922
early-type stars in galactic anticentre direction, spectral types and radial vels. 78−7990
early-type stars in Perseus, UV spectrophotometry, energy distrib. 79−88653
early-type stars in southern hemisphere, four colour photometry and spectral types 78−40945
early-type stars with Balmer emission, near UV (2000-3000 Å) spectra 80−94811
early-type stellar winds, H and He^+ synthetic line profiles 80−85926
early-type supergiants, spectrum variability, UV obs. *(Italian)* 78−32458
SW eclipsing binary, period study, photometry and spectra obs. 80−82424
eclipsing binary runaway, orbital data, UV obs. 80−85952
eclipsing binary stars, period distrib. rel. to components spectral types 80−36662
effective optical depth for absorption line formation 77−53578
element abundance, atomic and mol. f-values 78−20792
emission line asymmetry in novae 79−101214
emission line stars, spectrographic obs., 5650 to 11000 Å *(French)* 79−48815
emission lines, broadening and displacement during nonlinear transfer in turbulent plasma *(Russian)* 77−91418
emission lines near Ca II H and K, obs. of spatial intensity vars. on solar limb 80−51720
emission-line spectra, rel. to ouflowing atmospheres across HR diagram 79−66996
emission-line stars in galactic cluster NGC 663, spectroscopic obs. 80−4363
emission-line stars of Sanduleak and Stephenson, classification spectra 78−93273
energy distribution for 50 stars, 3200-7550 Å region *(Russian)* 78−65620
energy distributions in main-sequence A and F stars 78−93220
equivalent widths, photographic, calibration against solar photoelectric equivalent widths, feasibility 78−73658
γ Equulei, peculiar A-type star, line identification study, 3086 to 3807 Å 79−88659
ν Eridani, β Cephei variable atm. parameters from H and He spectral obs. 80−67739
ε Eridani, UV line spectrum of active chromosphere star, models 80−77394
eruptive blue variables at high galactic latit., spectrophotometry 78−32482
eruptive variable stars, IR spectra rel. to grains props. 80−26943
EUV spectroscopic method for electron density determ. in stellar atms. 79−16836
evolved stars expanding envelopes, CO thermal and maser emission 80−82334
expanding and rotating atmospheres, curves of growth and line profiles 80−31295
extragalactic supernovae spectra, comp. and kinematics of ejected material *(Italian)* 79−53844
extreme subdwarfs molecular band strengths, theoretical approach 78−93221

stellar spectra continued
extremely red stars at $l^{II} \approx 113°$, $-10° \leq b^{II} \leq +90°$, photometry and spectra 78−57554
F8-K1 stars, recalibration and anal. of Spite's quantitative three-dimensional classification 77−78768
F and G stars, MK spectral types 79−66999
F- and G-type dwarf stars, Mn/Fe abundance ratios 78−45325
F- and G-type stars, CH, CN and NH bands rel. to C and N abundances 77−91530
F- and G-type supergiants, enhanced He abundance effects on visible spectra 80−12759
F- and G-type supergiants, luminosity calibration using O I 7774 Å line equivalent width 78−53942
F-type supergiants, southern, visible spectra obs. 80−98660
F-type supergiants in Magellanic Clouds, spectra and Ca abundances 80−98655
faint blue stars in high galactic latits., search of PSS fields near South Galactic Pole 80−46415
faint blue stars near galactic anticentre, spectral types 79−71021
faint proper-motion stars, spectra and photometry to very low luminosity degenerates deficiency 80−17575
faint short-period spectroscopic binaries, influence of Schwarzschild effect on orbital and system elements *(German)* 80−8653
faint stars, spectral-type standards for objective prism plates 80−46539
far UV spectra at 0.2 Å resolution, catalogue of Copernicus obs. 77−56843
Feige 24, spectroscopy of EUV source, binary orbit, mass 78−93218
Feige 7, mag. white dwarf, spectroscopic studies 79−25603
Feige 86, $^3He/^4He$ from He I 6678 Å obs. of He deficient blue horizontal-branch star 79−92774
Feige 86, UV high-resolution spectrum 80−41834
Feige 86, UV spectrum of peculiar hot halo stars 79−48811
fine structure lines, dust UV opacity effects 80−90505
flare star 2329−03, spectra, chromospheric emission 77−74070
flare stars, model chromospheres, Balmer-line profiles 80−46558
flare stars, multichannel spectrophotometry 80−105256
flare stars identified with transient soft X-ray sources, spectroscopic evidence against flaring 78−96485
Fourier method for stellar rot. vel. determ. using stellar spectrum *(Russian)* 79−80240
G128-7, cool DA white dwarf, spectrophotometry rel. to atmospheric parameters and evolution 80−62126
G200-39, hot hybrid white dwarf, spectroscopic obs. 80−26852
G35-26, high-velocity mag. degenerate, obs. 78−73709
G, F, A, B and O stars, Balmer line profiles from model atmospheres 79−80298
G 165−7, metallic line white dwarf, model atm. code anal. of spectrum 80−85940
G and K-type giant stars, Li abundances 80−41819
G- and K-type giants, theoretical colours, model atms. 79−12474
G- and K-type giants, theoretical colours from synthetic spectra 79−62827
G- and K-type giants in short period binaries 77−87394
G-type dwarf stars, far UV Si emission line analysis 80−56829
G-type dwarf stars, Mg II and Ca II emission line intensities 79−80306
G-type dwarfs, macroturbulence and age anticorrel. 78−93226
galactic anticentre direction, young stars photometry and spectra rel. to outer Galaxy struct. 80−22079
galactic halo C star possible association with Magellanic Stream, visible obs. 80−77411
ingalaxies assoc. with QSOs, spectroscopic search 80−105355
GCl 0422−213, distant globular cluster in Eridanus, preliminary photometry and spectroscopy 80−17624
GD229, cyclotron absorpt. in white dwarf 79−53813
GD 229, mag. white dwarf, spectroscopic studies 79−25603
GD 40, He white dwarf, spectrum anal., CA abundance determ. 77−87385
GD 428, extreme dwarf Cepheid, photometry and spectrum 77−78798
Gd 428, variable star, photometry and spectrum rel. to nature of dwarf Cepheids 78−73720
GD 552, emission-line proper-motion star 78−85943
U Geminorum, dwarf nova, M-type dwarf companion spectral type 79−62851
U Geminorum, dwarf nova, radial vels. from emission line obs. 77−57029
β Geminorum (Pollux), CA II and Mg II lines rel. to chromosphere model 78−40931
giant branch of M5, spectroscopic survey 78−16467
giant stars, late-type, O I 7773 Å triplet obs. 79−35250
giant stars in Draco dwarf galaxy, effective temp. from photometry and spectral obs. 80−72941
giant stars in globular cluster M71, IR colours, CO band strengths and physical parameters 79−25650
giant stars in globular clusters M5, M13, M3, spectra and chemical comp. 80−67695
giant stars in M13, M92, NGC 6397 and M15, weak-G-band effect obs. 77−78778
giant stars in Sculptor dwarf spheroidal galaxy, abundance vars. and ω Centauri anomaly 79−5904
giants, CN strength differences in disk and halo 80−51750
giants, emission lines in UV spectra of α Bootis and α Tauri 79−71028
giants in distant satellites of Galaxy 78−40926
giants in globular cluster ω Centauri, CO absorption and effective temp. 80−51749
giants of G and K type, Fe abundances 79−16944
GK-type dwarf stars, Mg H lines obs. rel. to Mg isotopic abundances 80−51757
GL 3068, IR spectrum of C star 79−12469
GL 490, GL 2591, obscured IR objects, K-band spectra anal. 79−92828
Gliese 815, dMe spectroscopic-visual triple 79−12493
globular cluster giant stars, blanketing differences meas. 80−4345
globular clusters, element abundance survey 77−87489
globular clusters, metal-rich, TiO band strengths, reddening and metallicity determ. 79−40227
globular clusters, UV spectroscopic meas., central surface brightness distribs. 79−67067
globular clusters red giants, metal abundances in M92 and (M15) 79−92759
β Gruis (M2 II), S I emission obs. in EUV spectrum 80−82359
Gurzadyan's clustering in Auriga, spectral types 79−21366

stellar spectra continued
GX304−1 (4U 1258−61), shell spectrum of optical counterpart 80−46582
GX 339−4 (4U 1658−48), possible black hole binary, optical studies 79−101220
H1-36 (3U 1746-37), emission line object, radio spectrum 77−82239
H 2155−304 optical candidate, spectrophotometric obs. 79−25761
H 2252−035, optical counterpart photometry and spectrum 80−101651
H 2252−035, spectrophotometry, no periodic linear polarization (1980 Sept.) 80−105401
h 4636, visual binary in young cluster NGC 5367, relation to Ariel 1353-40 77−82294
h 4866 B, vars. in spectral type and radial vel. 78−32518
H-H 7 and 11, spectrophotometry of very low-excitation objects 80−46549
H-R diagram, use as astronomical tool, review of IAU Symposium (No.80) 78−81619
halo giant in north galactic cap, photometry and spectra 78−85942
halo stars in galaxy NGC 4565, spectral types radial gradient 80−62261
HBV 475 (V1329 Cygni), high-excitation emission lines obs. 78−40955
HD 01891, subdwarf, photometry and spectrum rel. to UV excess and metal abundance 80−17574
HD 101205 region, spectrographic and photometric obs. of stars and interstellar medium 77−49383
HD 101947, yellow supergiant star, Cepheid with 125 day period 79−88671
HD 102567, optical counterpart to 4U 1145−61, atm. model from UV obs. 80−105396
HD 105056, ON supergiant, radial vel. study 80−90427
HD 105902 (ADS 8448), Ba star in visual binary, spectra and photometry 77−78805
HD 10783, Ap star, spectrophotometric obs. 80−98663
HD 108078, spectroscopic binary orbit from photoelec. radial vel. meas. 80−77451
HD 108, Of star, spectral vars. due to solar wind 79−35262
HD 111133, Ap star, 5200 Å flux depression variability *(German)* 79−44496
HD 116458, binary Ap star, spectrum and orbit 77−64767
HD 118246, new Be star at high galactic latit., photometry and spectrum 78−73721
HD 120640, spectrophotometry and quantitative anal. of B star 77−60758
HD 122563, metal-deficient giant, atm. $^{12}C/^{13}C$ ratio, mixing 78−4201
HD 124224, He Si variable, spectroscopic obs., starspots, oblique rotator model 78−12239
HD 127617 (Bidelman's high latitude Be star), photometric and visible spectra obs. 80−77420
HD 128220, peculiar spectroscopic binary, photometric separation and spectral types *(French)* 77−57014
HD 128279, cool halo star, abundances, reduction procedure and equiv. widths 77−49384
HD 129708, new bright short-period Cepheid variable with unusual spectrum, photometric obs. 80−67751
HD 13738, spectroscopic orbit from photoelec. radial vels. 78−12297
HD 139216, unusual Balmer lines in M-type giant 79−80310
HD 147508, spectroscopic binary, photoelectric radial vels., orbit and spectral type 78−69839
HD 149499 B, IUE obs. of hottest white dwarf 80−41828
HD 149499B, hot white dwarf, continuous spectrum, H deficient 79−48795
HD 151932, single WN 7 type star with var. He I envelope 79−44493
HD 152667, =OAO 1653−40, photometry, spectrum and physical parameters 79−17021
HD 152667 (V861 Scorpii), eclipsing binary X-ray source, possible black hole 79−53858
HD 152667 (V861 Scorpii), phys. props. and orbital parameters, supergiant star with black hole companion model 79−71067
HD 153919, HDE 226868, X-ray sources, IUE UV spectrum obs. 78−96569
HD 153919(3U 1700−37), coronal emission line search 79−35302
HD 153919 (3U 1700−37), binary X-ray source, radial vel. data in blue spectral region 78−61888
HD 153919 (3U 1700−37), forbidden Fe XIV emission detect. 78−16571
HD 153919 (3U 1700−37), further spectroscopic obs. 80−4358
HD 153919 (3U 1700−37), X-ray binary, spectrum variations 78−8158
HD 153919 (3U 1700-37), binary X-ray source, radial vels. in blue spectral region 78−49556
HD 154368, interstellar species, excitation temps. and column densities in direction of supergiant 79−8981
HD 15570, Of/WN7 spectral classification problem 80−51786
HD 155989, spectroscopic binary photoelectric radial vels., orbit and spectral type 79−21355
HD 156385, WC7 star, anomalous 2200 Å absorpt. band 77−64769
HD 161698, Hg-Mn star, chemical elements identification in spectrum 79−58354
HD 165052, O-type binary, spectroscopic obs., masses and radii 78−93308
HD 165590, visual binary with spectroscopic binary component 78−32519
HD 165590 triple system, spectroscopic obs. 79−84825
HD 166734, Of star, spectroscopic binary orbit determ. from visible obs. 80−82414
HD 167771, O-type binary, spectroscopic obs., masses and radii 78−93308
HD 168607 (B9 Ia^+), S Doradus type star candidate, spectral line profiles *(Russian)* 80−90456
HD 174237, periodic radial vel. changes, interacting binary with var. mass transfer 79−53818
HD 175305, red horizontal branch star in general field, spectroscopic and photometric anal. 79−40189
HD 175742, spectroscopic binary, orbit and components spectral types *(French)* 80−36671
HD 17576, spectrum rel. to luminosity class and UV subdwarf companion 78−96479
HD 18474, G-type giant, rare earth's abundance *(Spanish)* 79−25605
HD 184905, H I line strength var. in Ap-star 79−16987
HD 184905, magnetic variable, H I lines and atmospheric parameters 79−97011
HD 184927, He variable star, spectroscopic props. 80−51790

stellar spectra continued
HD 185332, new δ Scuti star, photometric and spectroscopic obs. 80−90451
HD 186205, He star, fine abundance anal. 77−87408
HD 187299 B, spectroscopic detect., late B-type main sequence star 79−48860
HD 187399, spectroscopic binary, spectral obs. *(Russian)* 77−49427
HD 187473, rare earths in Si star 80−98671
HD 188209, O-type supergiant, spectrophotometry, 3300-7100 Å region 79−67009
HD 190073, Ca II H- and K-line complex structure 77−60775
HD 192163, 191765, Wolf-Rayet stars, optical interstellar spectra obs. 80−17640
HD 192163, WR star in filamentary nebula NGC 6888, optical spectra calc. 80−105304
HD 192273, EUV flux upper limit, Voyager 1 obs. 80−77406
HD 192273, optical spectral obs. of proposed EUV source 79−35256
HD 192913, Si Ap-star, lanthanide abundances, spectral identifications 78−45345
HD 193077, probable single WN 5 star with absorption lines 80−56834
HD 193793, Wolf-Rayet binary, visible and near IR spectra 78−8023
HD 193857, metallic-line binary star, orbital elements 79−75250
HD 195592, obs. of interstellar K I 4044 Å line 78−24533
HD 197406, Wolf-Rayet spectroscopic binary, radial vels. and orbital elements 80−51812
HD 199892, spectrographic binary, spectrograms and orbital elements 79−21359
HD 200120, Be star, emission features *(French)* 77−56977
HD 200775, Be star, optical and UV extinction spectrum due to dust in (NGC 7023) 80−109515
HD 200775, possible protostar in reflection nebula NGC 7023, optical polarization and IR spectrum 80−85944
HD 200775/NGC 7023 complex, interstellar reddening and 2200 Å feature strength 80−51832
HD 206860, G0 V star, IUE obs. of active region Mg II lines 79−92766
HD 214419, Wolf-Rayet spectroscopic binary, light and vel. changes, common envelope model 79−53856
HD 215038, Ap star, line identification list 78−32484
HD 215441, Ap star, line spectrum variations 78−4232
HD 215441, effective mag. field meas. and field geometry 78−53950
HD 216533, Ap star, spectral variation obs. 78−4244
HD 216533, Ap star, spectroscopic binary oblique rotator model, spectral var. study 79−101153
HD 219150, F0 V star with remarkable UV excess, optical and UV photometry and spectrum 80−90429
HD 22403, spectroscopic binary with Ca II emission, orbital elements *(French)* 79−53854
HD 25329, subdwarf, metal deficiency from spectroscopic anal. 80−62122
HD 26676, unusual radio star, spectral type and search for duplicity 78−73707
HD 26676 (HR 1307), UV spectrum, possible radio star 79−101150
HD 27561, Hyades cluster star, CNO abundances from near IR spectrum 78−93222
HD 34452, Si Ap star, spectroscopic study 78−65634
HD 34664 (S 22) in LMC, peculiar emission line supergiant 80−77416
HD 3473, A2p star, spectrograms, Si and rare earth elements overabundance 77−74071
HD 36619, Am-type star previously misclassified as O7 type 79−84805
HD 36665, B1e star, detect. of interstellar CO absorpt. in direction of supernova remnant (S147) 80−67836
HD 38268, in 30 Doradus, unique interstellar Ca II K-line profile obs. 80−51850
HD 39937, 101379, 155555, 174429, southern RS Canum Venaticorum stars candidates, radial vel. study 80−98686
HD 4174, peculiar M-giant, magnetic field 80−8631
HD 4174, symbiotic star, spectroscopic obs. 80−85945
HD 4174 (=EG Andromedae), peculiar M giant, UV spectra obs. 80−94798
HD 44179, 3.3 micron unidentified feature, high resolution spectra 80−82466
HD 45088, BY Draconis binary, surface activity from high rot. vel., visible obs. 80−77425
HD 45088, reticon obs. in red of dK3 spectroscopic binary 80−67778
HD 45166, dwarf in Wolf-Rayet clothing, spectrum anal. 79−5826
HD 45677, peculiar Be-star, 0.12-12.6 μm obs. 80−72957
HD 45677 or 50138, hot Bep stars with circumstellar dust IR excesses, UV obs. 78−93250
HD 47732, double-lined binary, spectroscopic orbit 78−57574
HD 49798, H-deficient subdwarf O-type binary, non-LTE spectral anal. 79−16978
HD 50138, Be star, model for shell from continuous spectrum obs. in IR 77−56976
HD 50896, Wolf-Rayet star, detect. of polarisation struct. across emission lines 79−97008
HD 50896 (WN5), variable emission-line spectrum obs. 80−51791
HD 50896 and 151932, WN stars, IR spectra 78−8024
HD 51480, shell star, spectroscopic obs., atmospheric struct. and distance 80−31305
HD 64740, He rich star, UV spectral vars. 80−22016
HD 64740, He variable star, X-ray source 4U 0750−49 optical candidate 78−36584
HD 67084, new southern spectroscopic binary, radial vels., orbital elements 78−57592
HD 67198, new southern spectroscopic binary, radial vels. 78−57592
HD 698, massive spectroscopic binary, spectral obs., evolutionary state, mass loss 78−57590
HD 76932, subgiant halo star, chem. comp. rel. to nucleosynthesis 78−81626
HD 77581 (3U 0900-40), X-ray binary, spectroscopic orbit and masses of components 78−16461
HD 77581 (=Vela X-1), supergiant+neutron star, X-ray, UV and visible obs. 80−94892
HD 84903 and 184711, differential anal. of extreme metal deficient stars rel. to halo star HD 122563 79−80302
HD 88230, dM0 star, high-dispersion photometric atlas from 3900 to 6000 Å 78−7996
HD 91805, spectrum anal. rel. to nature of Bidelman-MacConnell weak G-band stars 78−49432
HD 93131, probably single WN7 star, spectroscopy and photoelectric photometry 79−8924
stellar spectra continued
HD 93162, probable single WN7-type star in Trumpler 16 cluster 78−85946
HD 93521, high galactic latit. peculiar O-type star, spectrum 77−78784
HD 93521, Population II O-type star, spectroscopic obs. 79−16961
HD 94028, subdwarf, Mn abundance and Mn/Fe ratio 78−45328
HD 97048, pre-main-sequence star, spectral changes 77−74055
HD 97048 (=HM 18), pre-main sequence star, unidentified IR features obs. 80−85943
HD 97950, central star in NGC 3603, interstellar spectral lines, visible obs. 80−101586
HD 9996, Ap star, spectrsocopic obs. 78−77558
HDE 226868 (Cygnus X-1), Hα emission in (1977) 80−51919
HDE 226868 (Cygnus X-1), He II 4686 Å emission in spectrum 79−21328
HDE 226868 (Cygnus X-1), line blending effects rel. to black hole candidacy 77−64878
HDE 226868 (Cygnus X-1), temporal and spectral var., X-ray rocket obs. 78−8163
HDE 226868 (Cygnus X-1), X-ray and UV spectra from HEAO 2 and IUE 80−82543
HDE 228766, evolved Of system, spectroscopic obs. 78−12237
HDE 232078, variable mass loss in metal deficient red giant 79−67010
HDE 245770, optical counterpart to A 0535+26, dimens. spectral type and luminosity visible obs. 80−72976
HDE 245770, possible counterpart of variable X-ray source A 0535+26, line and continuum vars. 80−17600
HDE 245770 (A0535+26), Hβ var., general props., spectral obs. 78−4247
HDE 245770 (A0535+26), spectroscopy and orbital periods 78−93306
HDE 245770 (Ariel 0535+26), 1977 spectrum, objective prism study 78−61866
HDE 245770 (Ariel 0535+26), optical spectrum of Be star 78−4227
HDE 283048, hot subluminous star, spectrum 78−20823
HDE 313846, most extreme Of star, spectroscopic obs. and mass outflow 79−88682
He2-442, UVRK photometry and spectroscopic obs. *(Russian)* 80−94817
He 2-467, yellow symbiotic star, emission lines and continuum 80−62155
He-3 1863, unusual high latit. Be star, spectral obs. 77−87418
HeH^{2+}, photodissoc., rel. to UV flux deficiency of stellar spectra 80−9654
Henize 2-38, symbiotic star, steam and CO absorpt. obs. 78−40970
Henize S22, emission line star in LMC, spectrophotometric study 78−69803
Herbig Ae/Be stars, Hα profiles 78−16410
Herbig Ae/Be stars, spectrophotometry 78−93258
Herbig-Haro object, far UV spectrum obs. rel. to nature of object 80−67714
Herbig-Haro object 1 exciting star, identification as T Tauri star 80−17633
Herbig-Haro object 24, emission/reflection nature 80−41829
Herbig-Haro objects, emission lines and stellar wind whocks 78−89196
Herbig-Haro objects, Fe abundance 79−62826
Herbig-Haro objects, nearby IR sources optical spectra 80−67720
Herbig-Haro objects, new, spectroscopic obs. 79−5763
Herbig-Haro objects, spectrophotometry and radiating shock waves 78−85936
Herbig-Haro objects in Gum Nebula, spectrophotometry 78−36565
Herbig-Haro objects in southern dark clouds, objective prism survey 78−28536
HZ Hercules, (Hercules X-1), X-ray spectra, pulse phase depend. on high-energy continuum 79−17128
Hercules X-1, cyclotron line form. by reson. Compton cyclotron scatt. 80−8711
Hercules X-1, Fe line emission discovery in low-state spectrum by (HEAO-1) 79−5922
Hercules X-1, hard X-ray spectrum, strong cyclotron line emission 78−41085
Hercules X-1, high-energy pulsed X-ray spectrum from OSO 8 obs. 79−92888
Hercules X-1, implications of cyclotron features in X-ray spectrum 80−86015
Hercules X-1, struct. and higher harmonics of cyclotron lines 78−20912
Hercules X-1, X-ray lines and magnetic field 78−24574
Hercules X-1, X-ray spectra near turn-on in 35 day cycle 77−60794
Hercules X-1, X-ray spectrum of pulse 78−8154
Hercules X-1 (HZ Herculis), X-ray continuum and Fe line emission during X-ray low state 80−105393
HZ Herculis, 0.8 day periodicity in line emission 77−74089
68=μ Herculis, ^{3}He identification in atmosphere of primary component 77−57045
HZ Herculis, abnormal N III emission lines in 1978 Aug. spectrum 78−81661
ι Herculis, B3 IV type star, Copernicus, UV spectral atlas 80−67583
14 Herculis, C/Fe ratio of K-type dwarf 78−93227
α^2 Herculis, circumstellar absorpt. lines rel. to absolute mass loss scale for red giants 78−7997
α^2 Herculis, circumstellar lines form. rel. to location along line of sight 78−73739
AC Herculis, curve-of-growth analysis of RV Tauri variable 80−22026
DY Herculis, dwarf Cepheid, radial vel. and radius 79−58358
LT Herculis, eclipsing binary, photometric elements and spectral types 80−31328
AD Herculis, eclipsing binary, spectroscopic obs. and orbital elements 78−73738
DQ Herculis, eclipsing binary emission line eclipse phenomena, visible spectra obs. 80−94800
DQ Herculis, emission lines phase depend. in accretion disc 77−74095
AM Herculis, hard X-ray spectrum 79−17022
α^1 Herculis, He I 10830 Å emission obs., high-temp. chromosphere 79−48792
DQ Herculis, He II 4686 Å line phase shift from spectrophotometry 79−21296
52 Herculis, instrumental profile for spectra *(Russian)* 78−28704
AM Herculis, IR spectroscopy, period, mass function 79−71066
OP Herculis, irregular variable, Tc I absorpt. lines obs. 78−28689
OP Herculis, late-type variable star, spectral energy distrib. and spectral types *(Russian)* 78−40958
τ Herculis, line identifications in UV spectra 77−87384

stellar spectra continued
AM Herculis, low-mass X-ray binary, radial vels. and line intensities 77−78826
α Herculis, M-type supergiant, Mg II h and k emission obs. 78−53945
52 Herculis, magnetic, spectral and photometric vars. of Ap-star 78−85952
AM Herculis, narrow-band photoelectric obs. *(Russian)* 78−77565
ι Herculis, nonradial pulsations (1975-77) 79−5823
4 Herculis, shell star, Balmer intensity profiles 77−56973
BL Herculis, short-period Population II variable, chem. comp. determ. 79−8923
HZ Herculis, spectrograms, radial vels. and equivalent width meas. 77−74094
AM Herculis, spectrophotometric obs. at min. light min. light 80−98692
AM Herculis, spectroscopic obs., H lines and He II 4686 Å line intensities 78−57589
AM Herculis, white dwarf binary system, hard X-ray spectrum 78−36732
AM Herculis, X-ray binary, obs., slow rotator model 78−12408
AM Herculis, X-ray binary, vel. curves for emission lines broad and sharp components 78−32513
AM Herculis, X-ray eclipsing binary, UV and visible spectra anal. 80−109563
AM Herculis (3U 1809+50), He II 4686 Å photometry vel. to optical flickering mechanism 80−82411
AM Herculis (3U 1809+50), polarimetry and spectrophotometry rel. to mag. field 80−94835
AM Herculis (3U 1809+50), UV spectrum obs. 80−67782
HZ Herculis (Hercules X-1), Ariel V X-ray spectra 80−90580
HZ Herculis (Hercules X-1), IUE obs. spectrum and light var. 80−73069
HZ Herculis (Hercules X-1), IUE UV spectrum obs. 78−96569
HZ Herculis (Hercules X-1), optical and UV obs. 80−109487
HZ Herculis (Hercules X-1), pulse phase spectroscopy, 6-60 keV 79−84870
DQ Herculis (Nova 1934), extended nova shell spectra 78−93253
DQ Herculis (Nova 1934), high time resolution spectrophotometry 80−22017
DQ Herculis (Nova 1934), masses of interactive binary from spectroscopic data 79−97029
DQ Herculis (Nova 1934), short-period oscills. modulation and pulsed emission lines asymmetry interpretation 80−22044
V446 Herculis (Nova 1960), recomb. line spectrum rel. to ejecta He abundance 79−92775
α Herculis A, M-type supergiant, Li abundance in atmosphere *(Russian)* 80−72950
high dispersion spectra, numerical fitting accuracy *(Italian)* 79−21192
high dispersion studies using anamorphic camera 80−41727
high resolution UV spectrography appl. 79−25520
high velocity giant stars, detailed chemical anal. 80−82352
high-latitude blue variables, slit spectra 79−21312
high-velocity stars, southern, radial vels. 80−21988
horizontal-branch A-type stars, spectral scans rel. to astrophysical parameters 79−62829
TU Horologii, period and spectroscopic orbit of ellipsoidal binary system 79−58372
hot stars, evidence for mass loss 78−69786
hot stars, UV spectra obs. by International Ultraviolet Explorer (IUE) 78−96474
hot stars in LMC, far UV spectral evidence for hot gaseous galactic corona 79−67097
hot stars in Magellanic Clouds, UV spectra, evidence for galactic hot gaseous corona 80−82490
hot stars with circumstellar clouds, synthetic UV spectra calcs. 80−77382
hot subdwarfs in Carnochan and Wilson catalogue, UV spectra 80−82354
hot white dwarfs, luminosity function, spectral type anal. 80−90418
HR7922, B-type spectroscopic binary, orbital soln. 80−26910
HR8891, B-type spectroscopic binary, orbital soln. 80−26910
HR 1099, binary star, radio spectrum from 1400 to 8085 MHz 77−64793
HR 1099, Ca II H and K emission enhancement during February 1978 radio flare 79−21341
HR 1099, Copernicus obs. of UV interstellar absorption lines 78−93358
HR 1099, Hα region spectrophotometry during February 1978 radio flare 79−21344
HR 1099, H and Ca II, emission during February 1978 radio outburst 79−21340
HR 1099, photometric and spectroscopic obs. 1978 Feb. 78−40998
HR 1099, radio flare spectrum during February 1978 rel. to nonthermal nature 79−21332
HR 1099, RS Canum Venaticorum binary, Hα profile obs. 79−21343
HR 1099, RS Canum Venaticorum binary, optical spectrophotometry during major flare outburst 79−21342
HR 1099, RS Canum Venaticorum binary, VLA radio obs. during 1977 international campaign 79−21334
HR 1099 (V711 Tauri), Copernicus UV obs. of Lyman α and Mg II emission 78−81651
HR 1099 (V711 Tauri), RS Canum Venaticorum star, Hα line variability, visible spectra obs. 80−105277
HR 1105, He I 10830 Å line obs. of cold giant *(Russian)* 80−17586
HR 1217, Ap star, spectrum and light vars. relationship 80−26878
HR 1300, spectroscopic binary Am star, classification and orbital elements 77−49438
HR 2142 and 7084, mass loss from UV spectra obs. 80−109485
HR 432, 515 and 8006, δ Scuti stars, spectrographic obs. 80−36639
HR 4665, spectroscopy of bright long-period RS Canum Venaticorum system 80−36665
HR 5049, Co II in spectrum of southern magnetic Ap-star 80−82384
HR 5049, spectrogram meas. with digital microdensitometer 77−64655
HR 6127, chemically peculiar star, spectral lines and equivalent width lists, visible obs. 80−82387
HR 6659, spectroscopic binary, radial vel. obs. 80−82430
HR 6766, weak G-band star, light-element abundances 78−57548
HR 7083, photoelectric radial vels., spectroscopic binary orbit and improved spectral type 78−32517
HR 7129, He variable, oblique rotator model 79−62838
HR 774, Mg isotopes and s-process elements in Ba star 79−25594
HR 8752, binary supergiant, emission feature variability, visible obs. 80−109463
stellar spectra continued
HR 8752, spectrum var. of G-type supergiant 79−62828
HR 8752, spectrum var. of superluminous supergiant, near IR obs. 78−81630
HR 8752, superluminous star, hot companion discovery by IUE 79−16947
HR 8752 (HD 217476), superluminous superiant, line spectrum changes rel. to expanding shell 79−80308
HR 8752 (V509 Cassiopeiae), emission-line spectrum rapid changes 80−36645
HR 8799, model atm. anal. 77−74050
HR 9070, Be star, spectral vars. obs. 80−12773
HR 9076 (ε Tucanae), Hα shell profile 78−36583
HR 96, Ap-type star, atm. parameters and stellar comp., visible obs. 80−67740
Hyades stars, Be abundances 77−53584
TT Hydrae, absolute dimensions of β Persei type eclipsing binary 80−62184
W Hydrae, long-period variable, suspected Zeeman splitting in OH masers 80−36632
W Hydrae, long-period variable star, cyanodiacetylene detect. 77−82238
EX Hydrae, spectra of dwarf nova 80−98670
HZ 43, ultra soft X-ray spectrum of hot white dwarf 78−85941
HZ 43, white dwarf, He abundance and stellar struct. from soft X-ray spectra 80−72944
IAU Radial Velocity Standard stars, radial vels. meas. *(French)* 80−51743
III-106, CH star in globular cluster M22, CO in IR spectra 80−62131
ε Indi, late type dwarf star, spectrum rel. to model atmosphere and comp. 80−90425
integrated starlight, synthetic spectrum between 3000 and 10000 Å, discussion 80−62200
interstellar absorption feature at 2200 Å, identification 78−12346
interstellar absorption lines of Na I, K I, Ca II, in stellar spectra rel. to galactic gas distrib. 80−26963
interstellar CH^+ line obs., $^{12}CH^+/^{13}CH^+$ abundance ratio meas. 80−67809
interstellar diffuse bands, 2175 Å band correl. with other features 77−60813
interstellar extinction feature at 220 nm and diffuse 443 nm band, ANS obs. 80−62244
interstellar H I lines, implications of high-vel. absorpt. features 79−48891
interstellar lines towards Cepheus OB2 association, anal. 80−22052
interstellar lines towards stars of low reddening 78−57603
interstellar Mg lines, obs. rel. to existence of circumstellar clouds 80−94782
interstellar Na I and/or Ca II lines, obs. towards 47 stars 79−25676
interstellar Na I lines hyperfine struct. in α Cygni direction 78−24542
interstellar O VI absorption lines, statistical anal. rel. to coronal gas in Galaxy 78−36653
interstellar Ti II 3384 Å line, obs. rel. to Ti abundance 78−57611
interstellar UV absorpt. lines, International Ultraviolet Explorer obs. 78−96524
interstellar UV absorption features, in two stars in 30 Doradus 80−85978
interstellar UV absorption lines, intermediate-vel. gas obs. 78−36655
interstellar UV and optical absorpt. lines, comparison with H I 21 cm obs. 78−24532
interstellar UV lines, S 59 obs. rel. to Fe, Mn and Mg depletion 79−2563
IR airborne spectrophotometry, 1.2-5.5 μm, spectra and absolute calibration 80−62117
IR sources embedded in molecular clouds, optical spectrophotometry 78−96520
IR sources of AFGL sky survey, ground-based obs. 79−71150
IR spectral obs. *(Japanese)* 77−82218
IR spectral obs. in 1-2.5 μ range from balloon-borne telescope *(Japanese)* 78−61850
IR stars, unidentified spectral features 80−26936
IRC+10216, C star, HC_5N and HC_7N detect. 79−17126
IRC+10216, C star, near IR obs. of new mol. feature 79−92762
IRC+10216, C star, NH_3 obs. in circumstellar envelope 79−48793
IRC+10216, C star, possibility of detecting cyanoacetylene-d_1 (DC_3N) 78−69901
IRC+10216, circumstellar dust shell model rel. to IR energy distrib. 80−56972
IRC+10216, variable C star, IR spectra obs. 80−90568
IRC+10374, IRC+10523, IR stars, H_2O maser emission detect. 80−62298
IRC+10420, high-resolution OH maser obs. at 1612 MHz 79−44471
IRC+10420, IR emission lines from F-type supergiant star 78−4395
IRC+10420, stellar OH maser VLBI obs. rel. to mag. field 79−25742
IRC+10420, supergiant star, new OH maser feature spatial struct. 79−48946
IRC+30219, variable C star, optical emission-line phase obs. 80−90569
IRC +10216, detection of vibrationally excited CO at 114 GHz from C star 78−40941
IRC +10°216, circumstellar methane in IR spectrum 78−57694
JL 76, spectroscopic obs. of DC white dwarf candidate 77−67090
K dwarfs assoc. with X-ray transients A060−00 to A1742−28, visible and IR obs. 80−101653
K giants and GK supergiants, circumstellar Ca II lines rel. to mass loss 77−56928
K-type giant stars, Population I, CN strengths and $^{12}C/^{13}C$ ratios 78−93229
K-type giant stars at South Galactic Pole, spectral types from DDO photometry 80−8622
K-type giants, metallicity determ. problems 79−44474
K-type stars, spectral profiles, macroturbulence rel. to luminosity 79−96997
K-type stars, spectroscopic investigations in 4500 to 7500 Å region 80−109430
L973, red giant in globular cluster M13, curve of growth anal. 79−48796
EW Lacertae, atmospheric motions from spectrum analysis 77−60776
AR Lacertae, double-subgiant eclipsing binary, spectra, abundances 78−8044
EV Lacertae, flare star, photometry and spectrum rel. to starspots and rot. period 80−98665

stellar spectra continued
AR Lacertae, Hα spectrogram following radio outburst, results 77−49432
10 Lacertae, nonradial pulsations (1975-77) 79−5823
5 Lacertae, obs. of second max. for long period spectroscopic binary 78−57591
12=DD Lacertae, radial vel. and line profile var. 77−78797
EW Lacertae, shell spectrum change, 1978 Dec. radial vels. 79−21306
10 Lacertae, spectal line studies using LTE-method *(Russian)* 79−92769
12 Lacertae (DD Lac), spectral variations 77−71114
CP Lacertae (Nova 1936), recomb. line spectra rel. to ejecta He abundance 79−92775
Landolt celestial equatorial UBV standard stars, spectral classifications 79−75199
late B-type stars, Ca II K-line profiles 78−73722
late B-type stars, rot. and incidence of HgMn stars 78−89199
late B-type stars, spectral class. from TD1 UV obs. 77−91529
late B-type stars, spectroscopic obs. rel. to duplicity 78−57547
late type binaries in open clusters, spectrophotometric identification 79−44548
late type stars, Ca II H and K lines and nearby continuum photoelectric calibration 80−36617
late type stars, Ca II line widths and Wilson-Bappu effect 79−12464
late-type catalogue of revised Mk spectral types 80−82226
late-type field stars in S.hemisphere, radial vel. study rel. to possible duplicity 80−98686
late-type giant stars, H_2O band absorpt. effect on balloon-borne near IR multicolour photometry 80−98654
late-type giants, position on Hertzsprung-Russell diagram 77−78792
late-type stars, 4-8 μ spectral obs. 77−74054
late-type stars, Ba oxide and halide identification in near IR 77−56926
late-type stars, Ca II 8542 Å line as chromospheric activity indicator 80−62108
late-type stars, Copernicus survey of Mg II emission 79−80301
late-type stars, He abundance effects on spectrum appearance 80−46540
late-type stars, intensity effect in Wilson-Bappu relationship 78−85937
late-type stars, IR spectral observations *(Japanese)* 79−80307
late-type stars, Mg II reson. line fluxes rel. to chromospheric radiative losses 78−40915
late-type stars, S I emission in EUV spectra 80−82359
late-type stars, search for Ti II 3080 Å multiplet emission 80−51769
late-type supergiants, luminosity effects in spectra 77−60753
late-type supergiants, spectra and CNO abundances in G and K Ib stars 78−24509
late-type young stars in ρ Ophiuchi dark cloud, photometry obs. 80−72942
LDS 678B (EG 131), white dwarf, spectrum 78−40946
ρ Leonis, expanding envelope OAO-3 spectra *(Russian)* 78−4224
AD Leonis, flare conditions from photometry and spectra 79−92773
AS Leonis, flare star, chromospheric emission lines in nonflare red spectrum 79−21294
AD Leonis, flare star, Hα emission short-period variability limits 79−48807
R Leonis, IR atomic line spectrum of Mira variable 80−46557
R Leonis, IR spectroscopy of Mira variable, H_2O vibr. rot. bands 79−35258
η Leonis, mass loss from mid UV spectrum obs. 78−93217
R Leonis, Mira variable, CO and OH IR vibr.-rot. overtone bands 78−36574
α Leonis, nearby star, Mg II interstellar resonance doublet absorption 78−45391
ρ Leonis, non-anomalous diffuse interstellar absorpt. features 78−16418
R Leonis, strong TiO-related dia. vars. 78−16429
20 Leonis, triple system with a δ Scuti variable, spectral types 77−49440
AD Leonis, X-ray emission from flares, HEAO 1 obs. 80−41837
T Leonis Minoris, Algol-type semi-detached binary system 77−91580
19 Leonis Minoris, spectroscopic binary, orbital elements and mass ratio 80−62197
δ Librae, Algol-type eclipsing binary, detection of secondary 78−49475
48 Librae, Be star, shell spectrum line profiles 80−62146
β Librae, nearby star, Mg II interstellar resonance doublet absorption 78−45391
48 Librae (FX Librae), Be star, search for short time scale vars. in Hα emission 80−109441
48 Librae (FX Librae), shell star, spectroscopic study 78−96486
48 Librae shell star, emission features 77−56975
light ion lines sensitive to LTE departure in early type stars *(Russian)* 79−92770
line asymmetry, appl. to stellar convection parameters meas. 79−21273
line blanketed model atmospheres, limb darkening coeffs. determ. 79−35243
line broadening effects of macroturbulence and rotation 80−56813
line contours in incoherent scatt. 79−88590
line formation, in expanding spherical media with partial freq. redistrib. function R_I 79−88643
line formation depth in mag. field, theory *(Chinese)* 80−105159
line formation in axisymmetric moving envelopes, numerical method and appl. to YY Orionis stars 80−41813
line formation in expanding atmospheres 77−56919
line formation in microturbulent magnetic fields 80−31201
line formation in moving stellar envelopes, radiation field and statistical equilib. eq. 77−87374
line formation in turbulent media 80−77387
line formation in YY Orionis envelopes 77−64741
line formation with complete freq. redistrib. 77−53422
line photons, equality of mean escape probability and mean net radiative bracket 78−40815
line polarisation due to magnetic and vel. field inhomogeneities 79−5804
line profile calc. for close systems with mass transfer 80−41860
line profile measurements, accuracy 80−26751
line profiles, anal. using linear filtering theory *(Italian)* 80−90340
line profiles, effects of waves on spectrum anal. 79−44465
line profiles in expanding envelopes 79−44464
line profiles in spherical envelopes, three computation methods 80−85868
line scattering intensity radiative transfer, exact soln. using Wiener-Hopf technique 79−84784
line shapes, combined effects of atmosphere expansion and rot. 78−53920

stellar spectra continued
line transfer in spherical media with partial freq. redistrib., soln. 79−16932
lines form. depths calc., rel. to curve of growth method *(Russian)* 78−65604
Lk Hα 120, T Tauri star, spectrum 77−74052
LMC OB and supergiant stars, deep objective prism survey catalogue 79−40090
LMC X-1 optical candidate, spectrum and semi-accurate position 80−67908
LMC X-2, spectrogram confirms optical counterpart 79−21463
LMC X-4, spectroscopic obs. and orbit 79−9028
LMC X-4 optical candidate, spectral type, radial vels. and binary nature 77−64879
LMC X-4 optical counterpart, photometric and spectroscopic obs. 77−49431
long period variable stars, emission lines rel. to periodic shock waves and mass loss 79−44487
long-period variable stars, maser activity rel. to Hδ emission, obs. 79−88685
long-period variable stars, OH maser lines struct. and saturation 78−93264
long-period variable stars, polarisation vars. across TiO bands and Ca I line 80−98666
long-period variable stars, radial vel. obs. 79−88684
long-period variables, CO and SiO millimetre line emission obs. rel. to circumstellar shell props. 78−49423
long-period variables, H emission line form., models 78−28709
loose stellar clusters in southern Milky Way, spectral type and UBV obs. 80−94839
low dispersion objective prism spectra, automatic reduction *(Italian)* 80−98567
low-temperature star automatic recognition by two-channel IR systems 79−75118
lower main-sequence stars, spectral lines Fourier anal. rel. to rot. vels. 80−51767
LP182-44, faint high-vel. degenerate star with probable C features, photometry and spectrum 79−67007
LP 145-141, C_2 white dwarf, spectrum, strong UV absorpt. obs. by IUE 80−67715
LP 701-29, heavily blanketed white dwarf, spectrum synthesis 78−32455
LP 701-29, lowest luminosity degenerate star with heavily blanketed spectrum 78−36562
LP 790-29, mag. degenerate star, surface field strength and broad absorpt. trough identification 79−5815
LP 790-29, southern mag. white dwarf, spectrophotometric obs. 79−92765
LS I+61°303, radio, optical, X-ray, gamma-ray Be star, optical and radio obs. 79−88755
LS I +61°303, radio variable Be star, UV spectrum, stellar models 80−26879
LS I +61°303 as optical counterpart for GT 0236+610 source 78−36568
LS II+33°5, new H deficient B-type star, spectrum 78−93265
LS IV −14°109, H deficient A-type star, effective temp. 79−40195
LSS 1916, 3371, new VV Cephei stars, spectra and colours 79−35299
LTT 2437, most metal-deficient subdwarf, spectrum, photometry and Ca/H ratio 78−69797
luminous C stars in LMC, photometry 78−28670
luminous composite stars in the Large Magellanic Cloud 79−58375
luminous early type stars in giant extragalactic H II regions, IUE UV spectra 80−77467
luminous stars in M31 80−36622
luminous stars in NGC 6822 and IC 1613, visible spectra and photometry 80−82345
luminous stars in symmetric nebulae, IUE low-dispersion spectra 80−46560
luminous variable stars in M31 and M33, spectra and photometry 78−28686
RU Lupi, far UV spectrum of T Tauri type star 79−44494
RU Lupi T Tauri star, far UV spectra, emission measure obs. 80−94788
SW Lyncis, close binary, orbital elements 77−74090
ι Lyrae, Be star, Hα emission disappearance 79−5834
β Lyrae, CNO abundances in atmosphere, IR spectra *(Russian)* 80−67794
β Lyrae, eclipsing binary, intrinsic linear polarisation in Hα, Hβ emission lines 77−41390
β Lyrae, emission sources and gas streams *(Russian)* 79−92802
R Lyrae, M-type supergiant, Li abundance in atmosphere *(Russian)* 80−72950
β Lyrae, narrow-band photometric index of emission line strength 80−46605
β Lyrae, secondary star spectral type and struct. of system *(Russian)* 79−97036
α Lyrae (Vega), B abundance 77−53585
α Lyrae, emission lines in IR spectrum, thin expanding extended atm. 78−53946
β Lyrae, H emission profiles rel. to pattern of gaseous flow in system 78−57576
XY Lyrae, late-type variable star, spectral energy distrib. and spectral types *(Russian)* 78−40958
MV Lyrae, polarisation and spectrum obs., polar class candidate *(Russian)* 78−93322
β Lyrae, secondary component spectral type from radio emission 78−36638
β Lyrae, UV spectrum 78−8048
α Lyrae (Vega), Ca II H and K lines high resolution profiles 78−85939
α Lyrae (Vega), Copernicus UV obs. of C II and Si II lines 80−8627
α Lyrae (Vega), Coude spectroscopy of emission lines 79−21290
α Lyrae (Vega), evidence for spectrum and vel. vars. 79−75208
α Lyrae (Vega), O I and Ca II emission in near IR spectrum 79−21289
α Lyrae (Vega), spectral anal. from Copernicus 80−26856
α Lyrae (Vega) rot. rate determ. from line profile photoelec. obs., Fourier transforms 80−77408
β Lyrae primary and secondary, catalogue of absorption lines *(Russian)* 78−28725
RR Lyrae stars, Ca and Fe decoupling 79−30069
RR Lyrae stars, in 47 Tucanae, membership and metallicity 80−62206
RR Lyrae stars, line blanketing and metallicity from VBLUW photometry 79−48806

stellar spectra continued
RR Lyrae stars in Palomar-Groningen fields, [Ca/H] index rel. to luminosities and distances 78−93276
RR Lyrae variables in ω Centauri cluster, spectroscopic obs. 79−5824
RR Lyrae variables in N.Galactic pole fields, metal abundances 79−88660
M15-K1082, two-hour variable UV-bright star in NGC 7078 (M15), spectra 79−88681
M1-76, possible forbidden line BQ star rather than planetary nebula 79−84847
M22, comparison with ω Centauri, spectroscopic evidence 80−46617
M22, globular cluster, stellar spectra rel. to membership and other problems 78−32537
M34, open cluster, spectral types of brightest stars 78−12311
M-type dwarf stars, IR Fourier transform spectroscopy, abundance anal. 79−21279
M-type dwarf stars, spectrophotometry with Carnegie image tube 78−57466
M-type dwarf stars near north galactic pole, scanner obs. of MgH band 77−78789
M-type dwarfs, Hα emission line var., stellar surface phenomena 79−21313
M-type dwarfs, low-luminosity, optical spectral classification from spectrophotometry of (VB10) 79−58339
M-type dwarfs and giants, near IR luminosity-sensitive features rel. to M31 and (M32) 78−49431
M-type dwarfs and S-type stars, FeH bands identification in spectra 78−7952
M-type giant stars, atm. physical conditions 78−24512
M-type giant stars, spectral energy distribs. and effective temp. scale 78−28678
M-type giants, circumstellar envelopes, high-dispersion spectra 79−92755
M-type giants, temp. sequence based on TiO spectra *(Russian)* 78−20831
M-type giants and supergiants, circumstellar envelopes, observational study 78−53939
M-type semiregular variables, atmospheric anal., chem. comp. *(Russian)* 78−65623
M-type stars, classification from spectral scans 80−62127
M-type stars, in Orion population, CaH and TiO band strengths 78−12227
M-type stars, rotational excitation temp. from TiO band 79−48790
M-type stars, spectral type and luminosity classification from near IR spectrograms 79−16952
M-type supergiants, highly reddened IRC objects, IR photometry and near IR spectra 79−84796
M-type supergiants, in LMC, MK spectral types, luminosities 79−62820
M-type supergiants, photoelectric two-dimensional spectral classification 78−53936
M-type supergiants in SMC rel. to low metallicities 79−96995
M-type supergiants in southern hemisphere, search for OH 1612 MHz emission 78−69792
magnetic DA white dwarfs, calc. and obs. spectra 79−71032
magnetic DA white dwarfs, spectral line and circular polarisation profiles 80−62123
magnetic stars, model atmospheres and line. form. 79−16973
magnetic stars measurement with improved Abbe comparator 77−67043
magnetic white dwarfs, line and continuum spectra 78−4207
main sequence B-type stars, physical parameter determ. from uvbyβ photometry obs. 80−72952
main sequence stars, oscills., observability by photometry and spectra 80−51724
Markarian II, 180 and 421, spectra of stellar population 78−54047
maser stars, late supergiants and long period variables 80−77410
maser stars, search for water vapour absorpt. lines 77−78804
metal abundance determ. in late-type stars, new method 79−12405
metal-poor dwarf stars, abundance anals. of yellow spectra 79−92760
metal-poor dwarfs, Fe/H abundances from red spectra of nine objects 80−51751
metal-poor late-type stars, MK spectral classification 80−4340
metal-poor stars, abundance anals. of high-vel. dwarfs blue spectra 78−53933
metal-poor stars, C/Fe ratio from CH features 79−16945
metal-poor stars, O abundances from O I IR triplet 80−36610
metal-poor stars, spectra and Al/Fe ratios 78−57549
metal-poor-stars, spectral energy distrib. and Fe/H ratio 78−53937
Michelson Fourier transform spectrophotometer for stellar obs. 78−81550
Michelson Fourier transform stellar spectrometer 80−98552
Michigan 239, peculiar extragalactic or extreme halo emission-line star, obs. 80−4380
AT Microscopii, X-ray emission from flares, HEAO 1 obs. 80−41837
microturbulent broadening of spectral lines in late-type atms. 78−45321
Mira envelopes, OH maser luminosity and expansion vel. gradient 79−71043
Mira type stars, luminosity props. from spectra and light curve elements 80−105253
Mira type variables atm., OH maser, IR line overlap pumping mechanism 80−72764
Mira variables, airborne IR spectrophotometry, H_2O and CO absorpt. bands 78−32465
Mira variables, intrinsic amplitude and TiO absorption 78−36580
Mira variables, OH emission high-sensitivity search 78−89203
MK classification, rel. to temp. and gravity calibration of uvbyβ photometric system 78−4198
MK classification of 176 stars in 37 southern open clusters, anal. 79−88644
MK spectral classification from photometric obs., appl. to uvbyβ photometry with assumed luminosity class 80−67700
MK spectral classification from uvbyβ photometry, general case 80−82216
MK spectral classifications, third general catalogue 77−78671
MK spectral types as absolute magnitude indicators, comparison with Geneva photometric boxes through trigonometric parallaxes 80−77385
molecular lines, equivalent widths of H_2 Lyman band and CO and SiO (A-X) band lines 77−87368
molecular spectra of pure S stars 78−77554
N Monoceros region, two-micron IR objects survey 80−8555
CV Monocerotis, Cepheid variable in anon. open cluster 79−58349
VV Monocerotis, eclipsing binary, orbital elements, dimensions and spectral types *(French)* 78−89225

stellar spectra continued
R Monocerotis, Fe II forbidden line intensity changes *(Russian)* 79−8907
15=S Monocerotis, interstellar lines, UV obs. 80−90494
VV Monocerotis, RS Canum Venaticorum eclipsing binary, cool component spectral type 79−40218
V616 Monocerotis (Nova 1975=A0620−00), spectral characts. 77−87443
V616 Monocerotis (Nova 1975=A0620−00), spectroscopic obs. 77−82257
MS-stars, near-IR spectrophotometry *(Russian)* 78−20832
multilevel atoms spectra, comoving-frame transfer eqn. soln. in spherically symmetric flows 78−28499
multiplet line-centre fluxes, effects on temp. models 79−5806
MWC 342, emission line spectrum in 1974-75 period 78−57558
MWC 349, Be star, radiosource, spectral EHF obs. 80−105262
MWC 349, separate spectra of components of visual binary 79−48858
MWC 349A, near-IR spectrographic obs. 80−94810
MXB 1728−34, type I X-ray burst spectral evolution, HEAO-1 obs. 80−17692
MXB 1730−335, X-ray bursts spectra 79−17139
near IR low dispersion spectra, ground based obs. *(Italian)* 79−48689
nearby stars, Mg II interstellar resonance doublet absorption 78−45391
nearby stars, spectroscopic and photometric data published (1969-1978) 80−36513
neutron star, magnetised, cyclotron line form. in atmosphere 79−48839
neutron stars, accreting magnetic, cyclotron line form. 80−90463
neutron stars, highly magnetised, thermal radiation spectrum 80−56869
neutron stars, rotating, max. surface redshifts in bi-metric theory of gravitation 80−90466
neutron stars, X-ray bursts radiation spectrum rel. to mass-radius relation 80−77444
neutron stars, X-ray emission lines Zeeman splitting by mag. field 78−4275
neutron stars, X-ray spectra from accretion column, optically thick region inc. 80−67767
NGC 1851, Hα absorption of UV5 and core of globular cluster 78−61896
NGC 2169, open cluster, spectral types of brightest stars 78−12310
NGC 2169, photometric and spectroscopic study of open cluster 78−45371
NGC 2175, photometry and spectral types of stars in H II condensation 78−20883
NGC 2264, open cluster, reddening, blanketing and metallicity from spectroscopic obs. 80−26916
NGC 2264, young open cluster, differential reddening due to intracluster dust clouds 78−53996
NGC 2287, open cluster, spectral classification of brightest stars 80−26919
NGC 2420, old disc cluster, photometry and spectra rel. to stars chemical comp. 80−46620
NGC 2439 association, photometric and spectroscopic study 78−16470
NGC 3105, young open cluster, UBV photometry and spectral types 77−64811
NGC 3603 stars, interstellar λ4430 band obs. 78−32555
NGC 6200, loose young open cluster in Sagittarius arm extension 77−87493
NGC 6210, planetary nebula, central star, high dispersion EUV obs. and spectral type 80−77466
NGC 6231, open cluster, spectral types 80−90492
NGC 6231, young open cluster, main sequence stars photometry and spectra 79−88709
NGC 6250, young southern cluster, UBVRI photometry and spectra rel. to high R-values 78−16490
NGC 6383, photometry and spectral classifications, age and distance of open cluster 78−93342
NGC 6383, young open cluster, central core stars spectral types 78−41003
NGC 6546, open cluster, assoc. with Cepheid AV Sagittarii disproved 79−58387
NGC 6633, open cluster, stellar spectral types 77−74108
NGC 6823, UBV photometry and spectra, extinction study of young open cluster 80−4407
NGC 7789, open cluster, giant stars photometry rel. to CN strengths and metallicities 77−53648
non-LTE line formation in mag. field, two-level atom with freq. independent source function 78−61726
non-LTE transfer in lines, asymptotic expansion for small ε 78−16287
nonradial pulsation hypothesis with simulated line profile vars. 80−8618
IM Normae (Nova 1920), recovery, spectral obs. of faint candidate stars 79−71058
northern early-type stars at intermediate galactic latits., UBV photometry and MK spectral classification 77−82221
nova, probable, in LMC, discovery and spectrum 79−8931
Nova Centauri 1979, UBV photometry and spectrum, identification with X-ray transient 79−62842
Nova Cephei 1971, emission lines rel. to ejecta chemical comp. 78−12244
Nova Cygni 1975, diminishing of emission line widths in postmax. spectrum *(Russian)* 77−74075
Nova Cygni 1975, spectrum obtained with small image-intensifier spectrograph 78−73647
Nova Cygni 1978, distance and interstellar reddening 79−21310
Nova Cygni 1978, prediscovery mags. and 1978 September spectral features 78−93282
Nova Cygni 1978, spectra, polarisation, photometry and visual magnitude estimates 78−93283
Nova Cygni 1978, spectrum, distance and absolute magnitude 78−89212
Nova Cygni 1978, spectrum, polarisation and visual magnitude estimates 78−89213
Nova Cygni 1978, spectrum, precise position and photometry 78−89211
Nova Cygni 1978, spectrum and visual magnitude estimates 78−89210
Nova Delphini 1967, emission line spectrum *(Russian)* 78−16440
Nova Delphini 1967, forbidden lines flux rel. to envelope ionisation and central star props. *(French)* 77−53603
Nova Delphini 1967, He I triplet lines *(French)* 77−56939
Nova Delphini 1967 (HR Delphini), emission lines widths var. rel. to circumstellar envelope *(Russian)* 78−77564
nova in LMC, discovery confirmation, magnitude, photometric obs., premax. spectra 78−49456
nova in Magellanic Clouds (LMC), premaximum spectrum 79−62853

stellar spectra continued
nova in NGC 5272 (=M3), discovery, V mags. and spectrum 79−71050
nova in Sagittarius, discovery of probable declining nova (1978 March) 80−4376
Nova Persei 1974 (V400 Persei), spectral evolution 78−73715
Nova Sagittarii 1977, early spectrum 78−32496
Nova Sagittarii 1977, photometry, spectrum, absolute magnitude and distance 78−53955
Nova Sagittarii 1978, discovery on 1978 April 7, position, Balmer emission lines 78−45342
Nova Scuti 1975, spectrum, line identifications 78−45335
Nova Scuti 1975 (V373 Scuti), spectral evolution 78−73715
Nova Serpentis 1978, image tube spectrograms, emission lines 78−40964
Nova Serpentis 1978, precise position, spectra, visual magnitude estimates 78−36596
Nova Serpentis 1978, UBV photometry, visual magnitude estimates, spectrographic obs. 78−40963
Nova V3888 Sagittarii (1974), spectrum and photometry during decline stage 78−20836
Nova Vulpeculae 1976, Hα emission line profile variations *(Russian)* 77−74074
Nova Vulpeculae 1976, IR spectrum *(Russian)* 78−16441
Nova Vulpeculae 1976, spectra in range .38 to 1.12 microns *(French)* 77−53606
Nova Vulpeculae 1976 (NQ Vulpeculae), light, colour and vel. curves 78−28708
Nova Vulpeculae 1979, posn., magnitudes, spectrum and photometry 79−48818
Nova Vulpeculae 1979, spectroscopic and photometric obs., (1958 and 1968) 79−58344
Nova Vulpeculae 1979, spectroscopic and photometric obs., possible exceptionally slow nova 79−48820
nova-like stars, cyclotron line search in optical spectra *(Russian)* 80−67753
novae, coronal line emission origin 79−16965
novae, effects of dusty circumstellar envelopes on line fluxes *(French)* 77−56940
novae, envelope collisions model, dynamics of transition from premax. to principal spectrum 78−8025
novae, Li/Na ratio upper limit 79−101156
novae in nebular stage, collisional spectrum development 77−87441
novalike object in Vulpecula, 1980 May-June spectra and magnitudes 80−82392
novalike object in Vulpecula, light curve, photometric and spectroscopic obs. 80−67758
novalike object in Vulpecula, photometry, June 1980, and spectral classification 80−94807
NQ Vulpeculae (Nova 1976) spectroscopic obs. 79−21316
nuclear waste spectrum, means of detecting extraterrestrial civilisations 80−82230
O and B0 supergiants in Magellanic Clouds, spectral classification 77−78777
O-B3 stars in southern clusters, spectral classification rel. to excess absorpt. 77−78791
O-B stars, Fourier transform spectroscopy in 4800-10200 Å range 79−16993
O-stars, He II 10124 Å and H Paschen 7 line obs. 79−67003
O-type planetary nuclei, spectral classification, magnitudes, distances 78−4203
O-type stars, C III 7901 to 9715 Å emission lines obs. 80−77401
O-type stars, gravity and effective temp. determ. by automatic procedure 80−98557
O-type stars, Hα line-profile anals. rel. to winds and coronae struct. 78−40947
O-type stars, He I 10830 Å to spectral line, rel. to mass loss 79−80304
O-type stars, mass loss rate from UV spectra 80−82346
O-type stars, photospheric vel. fields 79−25597
O-type stars, radial vels. and K-term 77−56922
O-type stars, UV reson. lines anal. rel. to coronae possible existence 79−21293
O-type stars in open cluster IC 1805, C IV UV reson. line P Cygni profiles 80−31296
O-type subluminous stars, non LTE model atmospheres, line profiles 79−101149
OAO 1653-40, 38 s X-ray pulsar, optical counterpart, spectroscopic search 80−73072
OB3 type stars in young clusters, circumstellar matter 2200 Å hump interpretation 80−82351
OB star optical candidate of 2S 0114+650, spectral var. 78−16578
OB stars, Copernicus UV spectral data of rotation 79−84795
OB stars, in LMC, spectroscopic obs., galaxy distance determ. 79−71111
OB stars, in Vela region, list of 166 objects 77−87280
OB stars, stellar wind mass loss determ., UV spectra obs. 80−94789
OB stars, UV P Cygni profiles long-term changes 78−12234
OB stars in Circinus-Norma region, search for faint objects 80−62121
OB supergiant X-ray binaries, line distortion effects 78−7995
OB-type stars, C III 5696 Å and He II 4686 Å obs., C III transition from absorpt. to emission 79−67006
OB-type stars, search for H Paschen α 80−62156
objective prism spectra, radial vel. meas. using telluric A-band *(Japanese)* 78−89083
objective prism spectra of stars, computer classification *(German)* 77−49304
OBN, OBC stars, radial vels. and short period binaries frequency 78−53951
Oe- rel. to Be-type stars 77−56982
Of stars, raxial vel. meas. 78−4226
Of-type stars, H and He II spectra, theory 78−40950
Of-type stars, HD 150958, 152386 and 163758 in blue region 79−5825
Of-type stars, search for 2200 Å absorpt. band anomalies 77−64769
OH 205.1−14.1 in Lynds 1630 dark cloud, coincident IR source obs. 80−101630
OH/IR sources, microwave spectra, galactic distrib., radial velocity 78−16432
open cluster containing Wolf-Rayet and Of-stars 77−64810
open cluster stars, southern, radial vel. obs. *(German)* 80−94724
open clusters, spectroscopic obs., search for Ap stars 78−45367
ζ Ophiuchi, 1980 March emission episode, Hα and He I line behaviour 80−62151
Y Ophiuchi, anomalous Cepheid, evidence for duplicity 78−53990

stellar spectra continued
χ Ophiuchi, Be star, rapid spectroscopic variations 77−56970
χ and 66 Ophiuchi, Be stars, search for short time scale vars. in Hα emission 80−109441
XX Ophiuchi, emission-line star, near IR spectrum 77−49404
χ Ophiuchi, foreground interstellar material optical obs. 79−25673
ζ Ophiuchi, identification of interstellar lines in UV spectrum 78−93212
ζ Ophiuchi, interstellar C I UV lines obs. 79−35332
ζ Ophiuchi, interstellar CO absorpt. bands and cloud density from Copernicus obs. 78−36656
ζ Ophiuchi, interstellar O abundance from O I line profile 79−44583
ζ Ophiuchi, obs. of interstellar K I 4044 Å line 78−24533
RS Ophiuchi, recurrent nova, spectrum obs. 79−62848
ζ Ophiuchi, rotationally excited interstellar HD column density 79−25674
ζ Ophiuchi, search for interstellar NaH line 78−4325
ζ Ophiuchi, search for interstellar Sc II 80−82445
ζ Ophiuchi, spectral vars. related to rot. 80−22000
ζ Ophiuchi (HR 6175), O-type star, emission line episode 80−72953
70 Ophiuchi A, late-type dwarf star, mag. field obs. 80−72949
ζ Ophiuchi cloud, Copernicus UV obs. of interstellar C_2 78−41022
ρ Ophiuchi dark cloud stars, interstellar absorpt. spectra rel. to dust grain growth 80−67834
Ophiuchus region, interstellar extinction and stellar space density 77−64839
Orion, far-UV rocket survey 77−64762
Orion OB1 association, stellar spectral types 78−32539
Orion OB 1 association stars, spectral types compilation 77−82128
Orion population stars, variables light curve characts. and emission line intensities 80−67721
δ Orionis, apsidal motion of spectroscopic binary 79−8952
κ Orionis, B0.5 Ia star, Hα profile variable 79−101146
ζ Orionis, C III line obs. 77−87387
α Orionis, CO and SiO millimetre line emission search rel. to circumstellar shell props. 78−49423
α Orionis, CO circumstellar absorpt. obs. in 4.6 micron spectrum 80−26858
42 Orionis, Copernicus UV spectra and IR photometry 77−49437
κ Orionis, expanding envelope OAO-3 spectra *(Russian)* 78−4224
UX Orionis, fast irregular variable, H_α and H_β lines obs. *(Russian)* 77−87400
U Orionis, H I emission lines rapid variability *(Russian)* 79−16989
κ Orionis, interstellar B II 1362 Å detect. 80−51841
δ, ε and ι Orionis, interstellar D/H ratio from D absorption features 79−53865
ε Orionis, interstellar K-line, photographic obs. 79−16956
ζ Orionis, interstellar MgI line structure, balloon UV obs. 79−35251
FU Orionis, IR spectroscopy with contact-type image tube 80−17587
β Orionis, mass loss and shell, IUE and balloon UV obs. 80−51765
β Orionis, mass loss from mid UV spectrum obs. 78−93217
U Orionis, Mira variable, relation between 1612 MHz flare and light curve 80−56844
V380 Orionis, near IR spectrum line identifications, equiv. widths *(Russian)* 78−61861
π^5 Orionis, Orion OB1 association star, interstellar lines obs. by Copernicus 80−22050
U Orionis, outbursts in main line OH emission 79−101158
ζ Orionis, Reticon obs. of Hα P Cygni profile 80−82365
YY Orionis, spectroscopic and photometric obs. 78−93225
δ Orionis, spectroscopic binary, spectrophotometry *(Russian)* 77−64802
U Orionis, stellar OH maser VLBI obs. rel. to mag. field 79−25742
α Orionis, supergiant variable, mass loss, visible spectra obs. 80−67755
α Orionis, vel. fields in shell from Fe II emission line obs. 79−101144
β Orionis, visible spectrum of supergiant 79−44479
α Orionis (Betelgeuse), model atm., effective temp. 77−56935
λ Orionis A, far UV flux, emission line obs. of surrounding H II region 78−93303
δ Orionis A, UV spectrophotometry and optical polarimetry, stellar wind variability 79−21277
θ^2 Orionis B, long-slit spectroscopy in rocket UV 80−105297
θ^1 Orionis C and θ^2 Orionis A, UV spectra 80−90499
FU Orionis stars, composite spectra rel. to three models 78−65617
YY Orionis stars in Chamaeleon T-assoc. 79−30064
oscillator strengths of astrophysical interest 80−12656
Pal 12, metal-rich globular cluster in outer galactic halo, optical and IR obs. 80−105290
parallax stars with MK spectral classifications 80−56721
γ Pavonis, CH, CN and NH bands rel. to C and N abundances 77−91531
peculiar bright southern stars, identification and spectral types 77−82225
peculiar central stars of planetary nebulae, spectroscopic characts. 77−87405
γ Pegasi, β Cephei star, dynamics of photosphere and shells 78−49447
EQ Pegasi, active dwarf binary star, chromospheric emission lines obs. 80−12762
AU Pegasi, binary Type II cepheid, photometric and spectroscopic study 80−26866
57 Pegasi, long-period pulsating variable, spectrographic and photometric obs. 79−21305
β Pegasi, M-type giant star, Mg II h and k emission obs. 78−53945
κ Pegasi, radial vel. meas., visual binary with spectroscopic binary component 78−32520
θ Pegasi, rapid spectral line variability disproved 80−8625
AG Pegasi, symbiotic binary system, UV and optical spectrum rel. to nature of components 80−109449
γ Pegasi, UV spectrum of early B-type star, Copernicus obs. 78−81621
II Pegasi (HD 224085), surface-active binary star, spectroscopic obs. 80−90480
X Persei, 580 day and other periodicities 78−16435
ζ Persei, ^{7}Li I 6708 Å line and Li interstellar abundance 78−49494
φ Persei, Be star, Fe III metastable states and mass loss 79−5832
φ Persei, Be-star, visible spectra 77−56989
φ Persei, binary Be star, He II emission obs. rel. to components masses 80−12768
X Persei, eclipsing binary, gaseous ring struct., H I alpha obs. 80−109482
β Persei, eclipsing binary, Mg II 280 nm line profile, calcs. and UV obs. 80−82421
RY Persei, eclipsing binary, spectroscopy and physical parameters of atmospheres 80−101618

stellar spectra continued
β Persei, eclipsing binary, UV obs. from TD-1A satellite 80−77447
RY Persei, eclipsing binary, visible spectral obs., model 80−67795
ζ Persei, interstellar C_2 rot. fine-struct. lines obs. 80−67811
ε Persei, interstellar N_2 band, Copernicus search, upper limits 79−25661
21 Persei, magnetic variable, Fe, H_γ and H_δ obs. *(Russian)* 77−49388
IW Persei, metallic-line close binary star, photometric and spectroscopic obs. 80−62186
53 Persei, nonradical pulsator, light var. rel. to line profile changes 80−4362
ζ Persei, obs. of weak interstellar lines below 3400 Å 77−45509
A-type bright supergiants in LMC, spectra, line intensities 77−22215
A-type stars, line profiles rel. to differential rot. 77−45409
A-type stars, MI spectral classification based on uvby and β photometry 77−29822
A-type stars, non-LTE anal. of O I lines 77−41378
abundance change effects on spectra of very cool white dwarfs 77−29829
abundance determ. by photometric and spectroscopic methods 77−29807
abundance effects in classification, IAU Symposium 72 (Lausanne, Switzerland 8-11 July 1975) 77−29802
abundance effects in spectral classification of peculiar stars 77−29859
ADS 7390 (ω Leonis), visual binary, spectroscopic obs. and removal of nodal ambiguity 77−13399
AFCRL Sky Survey objects, 2-14 μ spectrophotometry 77−22331
AFCRL sources, identification of southern objects 77−33682
o Andromedae, binary star, UV spectrum 77−45485
α Andromedae, Mn star, UV spectrophotometry from TD 1-A/S 59 77−29848
Ap and Am stars, Y, Ba and rare earth elements abundances 77−33505
Ap stars, analytical expression for local line profile determ. from observed ones *(Russian)* 77−17588
Ap stars, Balmer lines *(Russian)* 77−17587
Ap stars, Pt in magnetic sequence 77−45436
Ap stars in open clusters, rot. vels. and mag. braking 77−33500
π Aquarii, Be star, spectrum var. rel. to orbital changes of gaseous ring 77−26013
α Aquarii, supergiant, Ca II H and K line variation 77−22227
α Aquilae, Copernicus UV spectral obs. 77−33480
β Arietis, Am star, spectroscopic obs. and curve of growth anal. 77−22237
56 Arietis, Ap star, spectrum vars. rel. to mag. field, precession and rot. 77−2432
κ Arietis, double-lined Am star, spectroscopic obs. and curve of growth anal. 77−22237
WW Aurigae, Am eclipsing binary, spectrographic obs., radial vel. curves 77−33559
ζ Aurigae, eclipsing binary, Ca I 6752 Å circumstellar line obs. 77−17619
θ Aurigae, short period Ap star, discovery of mag. field 77−33511
B6 to A0 spectral types, UV line blocking factors 77−22216
B- and A-stars, spectral class. from S2/S68 UV expt. 77−29839
B-type stars, wavelengths of neutral He lines 77−25999
B-type stars absolute UV spectrophotometry, continua and absorpt. features 77−22217
Balmer discontinuities, effects of line blocking 77−45419
BCD classification, relation between spectral type and effective temp. 77−29798
BCD system of stellar classification and chemical composition *(French)* 77−29797
BD+12° 1919 (IV-202 in M 67), curve-of-growth analysis of red giant 77−29841
Be stars, correl. between presence of Paschen emission lines and IR excess 77−22234
Be stars, spectra rel. to envelope props. 77−13355
Be-type southern stars, photoelec. scanner meas. of Balmer emission line profiles 77−45452
Bonner Spectral Atlas for peculiar stars 77−29810
α Bootis, non-thermal vels. height variation 77−13344
α Bootis (Arcturus), Ca II K-line rel. to variable mass loss and giant convective elements 77−22213
α Bootis (Arcturus), model-atmos. analysis of spectrum 77−29827
53 Camelopardalis, Ap star, Balmer line meas. of surface mag. field distrib. 77−26015
α Canis Minoris, Copernicus UV spectral obs. 77−33480
α^2 Canum Venaticorum, Balmer line meas. of surface mag. field distrib. 77−26015
η Carinae, earliest spectroscopic obs. and interaction of star with Carina Nebula 77−45433
η Carinae, new Fe II identification, IR spectrum 77−45463
η Carinae, reddening of optical radiation 77−41385
β Carinae, UV spectra, comparison of synthetic and observed spectra 77−29820
SX Cassiopeiae, Algol type binary, spectrophotometry, Balmer emission obs. 77−2454
γ Cassiopeiae, Be star, spectroscopic variations rel. to assoc. with X-ray source MX0053+60 77−22250
AO Cassiopeiae, eclipsing binary, intrinsic linear polarization, rel. to circumstellar envelope 77−17618
γ Cassiopeiae, Hα and Hβ emission lines equivalent widths, scanner obs. 77−2430
κ Cassiopeiae, spectral obs., coarse atm. anal. 77−33487
α Centauri A, Be abundance and constraints on Be form. 77−41379
α Centauri A and B, Ca II k-line rel. to model chromospheres 77−13326
ω Centauri giant branch, mixing versus primordial abundance vars. 77−17640
U Cephei, Algol type binary, photometry, Balmer emission obs. 77−2454
β Cephei, Copernicus UV obs. 77−33502
ξ Cephei, triple system, spectroscopic study 77−22275
U Cephei, UV excess, mass transfer in eclipsing binary system 77−33555
β Cephei stars, line profiles and oscill. modes 77−33521
UV Ceti, variations of Hβ emission line during large flare 77−45456
chemically peculiar stars, nuclear and differentiated abundance patterns 77−17597
classical Cepheids, light and radial vel. curves phase matching 77−17574
classification, via Walraven VBLUW photometry 77−17377
classification dispersion spectra synthesis from atmos. theory and high-dispersion spectra 77−29804

stellar spectra continued
collision damping consts. rel. to stellar atmospheres 77−42279
μ Colombae, distant unreddened star, Copernicus UV obs. 77−33591
Coma Berenices open cluster, spectral types 77−29886
17 Comae A, Ap star, Sr spots distrib. rel. to atmospheric mag. field *(Russian)* 77−17594
17 Comae A, magnetically variable Ap star, spectroscopic obs. 77−17595
cool stars, abundance determ., molecular data uncertainty effects 77−29805
cool white dwarfs, spectral classification 77−29828
cool white dwarfs, spectrophotometric obs. 77−45422
S Coronae Austrinae, a bright southern YY Orionis star, spectroscopic obs. 77−29818
β Coronae Borealis, Ap star, Fe I spectrum rel. to atmospheric mag. field struct. *(Russian)* 77−17594
α Coronae Borealis, binary star, UV spectrum 77−45485
CPD-26°389, hot subdwarf, spectroscopic binary within planetary nebula (NGC 1360) 77−45494
31 Cygni, eclipsing binary, Ca I 6752 Å circumstellar line obs. 77−17619
χ Cygni, P Cygni profiles obs. in Na I and K I reson. lines 77−13362
V1500 Cygni (Nova Cygni 1975), spectroscopic obs. of coronal line phase 77−33504
61 Cygni B, ^{24}MgH IR rot. band equivalent width calc. 77−18918
Cygnus OB2 association, wavelength depend. of polarisation and interstellar birefringence 77−33577
Cygnus X-1, accretion disc temp. rel. to spectrum 77−45479
Cygnus X-1, distortion of absorpt. line vel. curves due to X-ray heating 77−29878
Cygnus X-1, submillisecond meas. of X-ray spectrum during low state 77−45607
δ Delphini, spectroscopic binary fine anal. 77−17620
δ Delphini stars, abundance anal., metallicism and pulsation 77−33506
diffuse interstellar absorpt. bands origin, evidence for interstellar MgO and CaO grains 77−9785
φ Draconis, short period Ap star, discovery of mag. field 77−33511
73 Draconis, spectroscopic study and model atm. anal. of Ap star 77−33531
early-type stars, in Monoceros region, interstellar extinction determ. 77−9777
early-type stars, main sequence gap between B7 and B8, effects on Balmer jump 77−13341
early-type stars, UV spectrophotometry 77−29836
element abundance distrib. and origin, reln. to evolution of universe 77−26099
emission line stars, Mg II obs. near 2800 Å, absolute flux calibration 77−13350
emission line stars in LMC, spectroscopy and IR photometry 77−13348
emission lines in Be-stars, V/R var. rel. to gaseous ring 77−37604
RX Eridani, RR Lyrae variable, radial vels., light curve and radius 77−2436
F-type stars, MK spectral classification based on uvby and β photometry 77−29822
faint blue stars, spectral classification from UVBY photometry 77−45424
Feige 86, horizontal branch star, chemical comp. 77−9745
flare stars in Pleiades, spectral types *(Russian)* 77−13366
fluorescent molecular lines originating in or around stellar objects, catalogue 77−23514
Fourier analysis of spectral line profiles 77−22105
G262−21/22, subluminous stars in common proper motion binary 77−33491
G- and K-type giants, spectra and CNO abundances 77−5530
G- and K-type stars, space motions 77−45430
U Geminorum, radial vel. meas., rot. accretion disc and hot spot model 77−33561
1 Geminorum B, spectroscopic binary, orbit from photoelectric radial vels. 77−22269
giants and supergiants, atm. $^{12}C/^{13}C$ ratio 77−13337
RS Gruis, RRs variable, photoelectric radial vels. 77−5533
GX 1+4 optical counterpart, symbiotic star, spectrophotometry 77−33498
HD 101065, peculiar star, presence of Fe questioned 77−45455
HD 101065 (Przybylski's star), spectral type and classification 77−29861
HD 184905, variable Ap star, radial vels. for Si II and Ca II lines 77−22251
HD 184927, He variable star, spectrum obs. 77−22249
HD 190073, A0ep star, Ca II lines struct., nightly vars. and line profiles interpretation 77−17578
HD 192163, Wolf-Rayet star, excess UV extinction rel. to comp. of dust in (NGC 6888) 77−29905
HD 200120, Be star, UV spectra vars. 77−5534
HD 28497, distant unreddened star, Copernicus UV obs. 77−33591
HD 50896, distant unreddened star, Copernicus obs. of UV interstellar lines 77−26036
HD 51585, B[e] star, visible and near IR spectrum 71−45445
HD 6497, high-dispersion analysis of giant in Eggen's Arcturus group 77−29838
HD 90657, Wolf-Rayet spectroscopic binary, spectroscopic obs. 77−13357
HD 9996, Ap star, mag. field and precession rel. to spectrum vars. 77−2432
HD stars with peculiar abundances, statistics and notation 77−29860
HDE 245770, spectroscopic obs. of X-ray nova Ariel 0535+26 optical counterpart 77−45450
AM Herculis, photometric and spectrographic obs. 77−45492
AM Herculis, X-ray binary, emission lines, radial vel. var. 77−33567
AM Herculis, X-ray binary, spectroscopy and photometry, model 77−33568
HR 1099, new bright RS Canum Venaticorum variable, spectrum 77−9754
HR 2172, double-lined binary, radial vels. and equivalent widths *(French)* 77−17625
HR 3089, He-rich star, anal. of UV spectrum 77−9751
HR 5153, Ap star, line profiles, rot. vel. and light vars. period 77−17593
HR 6392B, Wolf-Rayet star, spectral classification and luminosity of (HR 6392) 77−45493

stellar spectra continued
IC 2944, stellar aggregate surrounding HD 101205, spectrographic and photometric obs. 77−17636
interstellar absorpt. in five stars, Copernicus obs. 77−33598
interstellar UV absorption lines assoc. with Vela SNR 77−33604
IR sources identification in Ophiuchus dark cloud region, spectral types and extinction 77−45522
IRC+10°216, circumstellar acetylene in IR spectrum 77−5591
Kapteyn's star, M-type subdwarf, IR spectrum and comp. 77−13330
Lacerta OB1 association stars, spectral classification and distances 77−37626
12=DD Lacertae, vel. curves and period charge, spectrograms 77−26016
laser action in distended envelopes, appl. to He II 4686 Å 77−13354
laser line emission detection in spatially inhomogeneous broadening 77−41312
late-type spectroscopic binary stars, search for Ca II H and K lines 77−33551
late-type stars, ^{24}MgH IR rot.-vibr. bands fine struct., transition probabilities, oscill. strengths 77−18918
late-type stars, search for C IV reson. doublet, TD1 satellite UV obs. 77−5526
late-type stars, spectral class. accuracy test using DDO photometry 77−29831
LDS 785A (EG 153), DB white dwarf, discovery of H 77−45425
line broadening by collisions with atomic H, theory 77−13237
line formation, non-isotropic redistrib. theory in chromospheric-type stellar atmosphere 77−5522
line profiles, in spherically symmetric expanding atmospheres, scatt. source functions 77−22056
LkHα101, 1-4 μ spectra, aircraft and ground-based obs. 77−5590
LMC OB associations, Apollo 16 for UV spectra 77−33634
long-period variables, SiO in 4 μ spectrum 77−13360
LS 630, subdwarf O star, spectrum and absolute magnitude 77−17561
luminous cool stars, atm. $^{12}C/^{13}C$ ratio 77−13336
RR Lyncis, Am eclipsing binary, photometry and spectroscopy, abundances 77−33558
β Lyrae, eclipsing binary, random vars. in UV spectrum 77−22273
β Lyrae, high time-resolution spectroscopy at Hα 77−13388
α Lyrae, UV spectrum, line identifications 77−17552
RR Lyrae stars in galactic bulge, spectra and comp. 77−26012
M-stars at $l^{II}=138°$, space density from objective prism spectral studies 77−9748
M-type dwarfs, population discriminant 77−29840
M-type dwarfs, proposed identification of FeH 77−45418
M-type stars in direction of N galactic pole, photometry and spectroscopy 77−37594
magnetic stars, spectral synthesis technique 77−17459
magnetic stars, Zeeman effect 77−45442
magnetoactive spectral lines, response functions for polarised light 77−45304
main sequence stars, F- and G-type, Be abundances 77−13332
MD 101065, effective temp. and atm. electron press. 77−45468
metal abundance and MK class. for F5-K4 stars, relationships 77−29809
Michelson stellar interferometer, seeing effects removal 77−29659
Mira variables, SiO maser luminosity and spectral type correl. 77−33512
MK classification, remarks 77−29814
MK classification data, surface distribs. on celestial sphere 77−2423
MK spectral types for 67 early type stars 77−33473
Monoceros R2 association, stellar MK spectra and UBV photometry 77−13409
β Monocerotis, Be star, spectrum vars. rel. to orbital changes of gaseous ring 77−26013
V616 Monocerotis, spectroscopic obs. of X-ray nova, Ariel 0620−00 optical counterpart 77−45450
θ Muscae, Wolf-Rayet binary, spectrum and photometry 77−22235
MWC 17, emission line star, dense planetary nebula like object 77−45449
non-LTE radiative transfer, multi-dimensional, core-saturation method 77−22057
north galactic pole, A and F star radial vels. and MK classifications 77−22223
Nova, Aquilae 1975 (V1301 Aquilae), IR development 77−17570
Nova Cygni 1975, Copernicus near UV spectral obs. 77−29844
Nova Cygni 1975, Hα, Hβ emission lines equivalent widths, scanner obs. 77−2430
Nova Cygni 1975, rapid vars. of emission line profiles 77−45434
Nova Cygni 1975, spectroscopic obs., detect. of diffuse enhanced spectrum 77−29850
Nova Cygni 1975 (V1500 Cygni), spectral features during early decline phase 77−22245
Nova Cygni 1975 (V1500 Cygni), spectroscopic developments and kinematics 77−45446
Nova Sagittae 1977, spectral obs., visual magnitude estimates 77−22253
Nova Sagittarii 1974 (V3888 Sagittarii), line identifications and radial vels. 77−22246
Nova Sagittarii 1977, image-tube spectra (April 1977) 77−41384
Nova Sagittarii 1977, visual magnitude, UBV and Hα obs. (1977, March) 77−33517
Nova Vulpeculae 1976, spectra and light 77−33510
Nova Vulpeculae 1976, spectrograms and photoelectric V obs. 1976, Oct. and Nov. 77−2443
O3 to O5.5-type stars, spectra 77−33481
O to F type, Balmer lines and mean electron density for 94 stars 77−17564
O-B stars, Balmer jump rel. to U-B colour *(Russian)* 77−17569
O-type stars, O VI P Cygni profiles hourly vars. 77−37596
O-type stars, spectroscopic catalogue on mag. tape, third edition 77−2348
OB stars, CNO anomalies 77−29835
objective prism low-dispersion spectra from UK 1.2 m Schmidt telescope 77−45311
V2051 Ophiuchi, AM Herculis-type variable, spectrum scans 77−45492
ζ Ophiuchi, search for C_2 in interstellar spectrum 77−45423
Orion Nebula cluster, MK spectral types 77−22283
β Orionis, B8 Ia star, UV spectrum 77−22221
α Orionis (Betelgeuse), K I 7699 å emission from circumstellar shell 77−22210
α Orionis (Betelgeuse), UV spectrum rel. to model atmosphere and comp. 77−22231

stellar spectra continued
η Orionis A, binary star, UV spectrum 77−45485
peculiar A and B stars, Y abundances 77−33503
peculiar emission-line stars, IR lines 77−29862
peculiar stars, optical and UV line emission of ionised Fe 77−13364
o Pegasi, hot Am star, spectroscopic obs. and curve of growth anal. 77−22237
X Persei, 13.9 minute periodicity, 3U 0352+30 optical counterpart 77−22247
S Persei, M-type supergiant, OH emission rel. to circumstellar envelope struct. 77−22218
21 Persei, spectrophotometry of Ap star, continuum features vars. 80−36638
b Persei, UBV photometry and spectroscopic study of ellipsoidal variable 80−36666
53 Persei, undulations of B-type star 78−89201
20 Persei, visual binary, radial vel. obs. 78−73736
X Persei (2U 0352+30), spectral line variations *(Russian)* 78−65655
X Persei (3U 0352+30), Balmer line vels. rel. to reality of massive companion 77−13495
X Persei (3U 0352+30), simultaneous X-ray and ground-based optical obs. 80−17591
X Persei (A 0535+26), Prognoz-6 obs. of X-ray fluxes and energy spectra *(Russian)* 80−109562
β Persei (Algol), detection of B component, mass determ. 78−65654
β Persei (Algol), gas stream producing absorpt. features in red wings of Mg II reson. lines 78−24524
β Persei (Algol), UV line profiles obs. rel. to primary component rot. 80−72996
β Persei (Algol), X-ray spectrum 77−9773
α Persei cluster, stellar spectral types 79−58385
β Persei-type eclipsing binaries, red spectra, element abundances and neutrinos 77−57041
Perseus OB2 association, spectroscopic survey of B- and A-type stars 77−91585
PG 1413+01, white dwarf-red dwarf eclipsing binary, photometry and spectral types 79−8944
SX Phoenicis, dwarf cepheid, spectrum 77−49405
AE Phoenicis, W Ursae Majoris-type star with elliptical orbit 77−57010
photosphere lines, search for stellar oscills. 78−93203
19 Piscium, C star, violet spectrum line identification and radial vel. 80−82361
53 Piscium, confirmed β Canis Majoris type variable 79−44492
64 Piscium, double line spectroscopic binary, orbital elements *(French)* 79−35305
UV Piscium, short period eclipsing binary, light and colour curve obs. and spectral types 79−88697
Pismis 6 and 8, open clusters, photometry and spectra rel. to proximity to (Wat 6) 79−88712
planetary nebula central stars, spectral types and absolute magnitudes 77−87504
planetary nebulae central stars, Cassegrain image-tube scanner obs. 77−22214
planetary nebulae central stars, UV spectral lines intensities vars. 78−36668
planetary nebulae central stars, visible and near IR spectra 77−78785
planetary nebulae central stars, visual spectra comparison with Zanstra temps. 80−109434
planetary nebulae nuclei, photometry and spectra of (Abell 30 and 78) 77−91602
planetary nebulae nuclei, spectral type evolution *(Russian)* 79−58361
Pleiades, spectral classification of brightest stars, Ap, Am and shell stars 78−57601
Pleione (28 Tauri), envelope behaviour in 1976, spectroscopic obs. 80−8636
Pleione (28 Tauri), metallic-line shell spectrum anal., (1973-1976) 80−8637
polyatomic molecules in C star 3 μ band 79−5807
Praesepe stars, Ca II K-line photometry and metal abundance rel. to Hyades 77−57064
pre-main-sequence stars in Orion cluster, photometry and spectra rel. to masses and ages 77−13339
protostar in sharpless 140, compact source, strong far IR emission obs. 78−36649
protostars, dust shell models for compact IR sources 77−29948
protostellar envelope evolution, radiative transfer and spectrum 80−77384
PSR 0531+21 (Crab pulsar), pulsed Γ-ray emission, energy spectrum COS-B obs. 78−8033
PSR 0833-45 (Vela pulsar), pulsed γ-ray emission energy spectrum, COS-B obs. 78−8033
PSR 0950+08, pulsar, micropulses freq. struct. 80−22030
PSR 1133+16, 14.8 and 22.7 GHz obs. rel. to pulse components and whole pulse spectra 78−81645
PSR 1919+21, spectral indices of pulsed radiation at 16.7, 20 and 25 MHz 77−87466
pulsar spectra, nature of low-freq. dropoff 80−17602
pulsar spectrum, charact. freqs. rel. to pulsar models *(Russian)* 79−58369
pulsars, charact. feature interpretation 80−109451
pulsars, energy spectra and pulse shapes at metre wavelengths 79−75233
pulsars, infinitely magnetised H atom spectrum 80−77282
pulsars, low-latit., H I absorpt. spectra meas. 80−101606
pulsars, narrowband versus broadband emission processes rel. to luminosities and spectra 80−51797
pulsars, phenomenological model for spectra 78−40979
pulsars, radio emission mechanism rel. to spectra 78−12257
pulsars, radio flux density and spectral index from obs. at 102.5 and 61 MHz 80−17601
RX Puppis, 2 μm spectroscopy, H_2O and CO absorpt., symbiotic binary model 79−67032
VV Puppis, AM Herculis type binary, accretion column absorpt. spectrum obs. 79−101176
VV Puppis, AM Herculis type binary, optical absorpt. spectrum, cyclotron intepretation and models 80−73003
VV Puppis, AM Herculis type binary spectrophotometric obs. 79−5860
VV Puppis, AM Herculis-type variable, spectrum scans 77−45492
VV Puppis, brightening, emission line spectrum 78−40960
ρ Puppis, chromospheric activity and atm. dynamics of δ Scuti star 77−17581

stellar spectra continued
VV Puppis, dwarf nova, spectroscopic obs. during active phase 79−80322
V Puppis, eclipsing binary, circumstellar matter obs. 77−13385
ζ Puppis, interstellar absorpt. lines in far UV spectrum 78−65665
ζ Puppis, interstellar C I UV lines obs. 79−35332
ρ Puppis, line profile variable, pulsational mode-typing 80−90432
ζ Puppis, of supergiant, mass flow var., visible and UV obs. 80−90431
ζ Puppis, Of type star, stellar wind model from UV line fit 80−72965
ζ Puppis, Of-star, UV spectrum, line identifications 77−45441
RX Puppis, peculiar emission-line object, spectrum and UBV photometry 79−44497
ζ Puppis, Reticon obs. of Hα P Cygni profile 80−82365
ζ Puppis, spectral line profiles, mass ejection 77−33507
VV Puppis, spectroscopic obs., broad absorpt. features discovery 79−44502
ζ Puppis, visible and UV spectroscopy of stellar wind var. 79−16949
CP Puppis (Nova 1942) soft X-ray emission detect. and evidence for steep spectrum 79−80325
quasar plasma-laser star model, O VI and He II emission lines 77−45597
R 136, central star in 30 Doradus, nebula, variability *(German)* 77−45448
radial vel. determ., survey of different methods 80−73006
radial vel. determ. with CORAVEL, Cassegrain spectrophotometer 80−82210
radial velocity measurement, standard wavelengths and vels. for twelve stars 77−17547
radial velocity measurement with objective prism 79−84681
radially symmetric accreting envelopes, spectral lines form. and profiles *(Russian)* 78−57544
radiation pressure in spectral lines in gaseous systems with axisymm. motions, kinematics 79−88579
radiative transfer equation geometric solns., diagnostic anal. 77−5423
radio star obs. at 3.3 mm 77−74065
radiostars, polytropic models rel. to radio emission spectra 79−2544
red and nebulous objects in dark clouds, survey, catalogue of 150 objects 80−56904
red giant stars in globular clusters M92 and NGC 6397, C abundances 79−48785
red giants, in Draco dwarf galaxy, metal abundance determ. 79−17078
red giants, spectra, TiO bands obs. and theory 78−96480
red giants, spectra and comp. *(Norwegian)* 77−71111
red giants and supergiants, circumstellar spectra and mass loss 77−9743
red giants in Draco dwarf spheroidal galaxy, metal abundance 80−73030
red giants in Galactic nuclear bulge, spectroscopy 77−26058
red giants in globular cluster NGC 6752, DDO photometry and spectra 79−71079
red giants in globular clusters, mass loss 78−93238
red giants in M13, Na abundance var., protocluster gas inhomogeneities 80−82439
red stars and faint OB stars, ultralow dispersion spectroscopy 79−53733
red stars survey in 30 Doradus region of LMC, list of 298 stars 79−48794
red supergiants, model atm. based on band-model opacity 77−56934
red supergiants in Magellanic Cloud clusters, spectral types 79−40190
red variable star, possible optical candidate of 2S 1702−363, spectroscopic obs. 78−77566
rel. to props. of optically thick winds 78−24516
relative Zeeman and Doppler shifts, determ. via statistical approach 78−36467
resonance lines polarisation, theory for line core 77−29744
resonance multiplet lines, radiative transfer theory 78−24460
Ross 640, H-poor white-dwarf, H abundance determ. 77−87388
Ross 640, He-rich white dwarf, Ca, Mg, S and Fe abundances from UV spectra 80−94790
rotating early-type stars, V and i from Copernicus UV obs. 77−33492
rotational line broadening, Bessel transform appl. to rot. vel. determ. 77−49369
rotational line broadening, wavelength depend. rel. to rapidly rotating B stars 77−45416
Rubin-152, possible massive O-type star on galactic fringe, spectroscopic obs. 80−98656
S106 IR, S235 B, obscured IR point sources, ZAMS spectral types from Bγ fluxes 80−12795
2S 1702−363 optical counterpart, BV photometry and spectrum 78−54082
S stars, photometric obs. of unidentified spectral bands 77−22226
S-type stars, CeO band identification, new s-process mol. 77−33488
S-type stars, FeH and CeO identification 79−21280
S-type stars, Keenan and Wing bands, IR obs. 80−67722
S-type stars, Keenan band identification problem, IR obs. 80−72946
S-type stars, M-type dwarfs, proposed identification of FeH 77−45418
S-type stars, molecular spectra and model atmospheres 80−51764
S-type stars, possible presence of ZrO IR spectrum 80−62124
S-type stars, revised spectral classification system in red 80−46541
S-type stars in Southern Milky Way, objective prism survey and BVI photometry 78−61754
HM Sagitaae, emission-line star, UBV photometry and spectral obs. in (1978) *(Russian)* 80−36648
FG Sagittae, 1975-8 spectral obs. of peculiar variable 80−72959
WZ Sagittae, 1978-9 outburst of dwarf nova, spectra 80−94801
HM Sagittae, continuum spectrum, model, dense nebular around hot star *(Russian)* 78−69814
HM Sagittae, emission line variable, near IR spectrum *(Russian)* 78−81637
HM Sagittae, emission variable, optical spectrograms and IR magnitudes 77−67098
HM Sagittae, emission-line star, spectrum vars. (1978 to 1979) 79−58347
HM Sagittae, eruptive BQ forbidden line star, spectrum and radial vel. 78−20835
WZ Sagittae, image-tube spectroscopic obs. of 1978 Dec. outburst 80−72958
HM Sagittae, IR spectrum 78−93266
HM Sagittae, near emission-line object, optical and IR obs. 78−36575
HM Sagittae, new spectroscopic obs., simultaneous presence of increasing excitation and cool features 80−26874
HM Sagittae, photometric and spectroscopic obs. rel. to proto-planetary nebula mass ejection 78−85947
stellar spectra continued
FG Sagittae, planetary nebula central star, radial vel. meas. rel. to binary star model 80−98664
HM Sagittae, planetary nebula excited by Wolf-Rayet star, spectrum 78−54003
WZ Sagittae, recurrent nova, eclipsing binary, outburst of December 1978, UV obs. 80−72982
WZ Sagittae, recurrent nova, IUE obs. in outburst 80−109448
WZ Sagittae, recurrent nova, spectroscopic obs. and model for superhump phenomena 80−82368
WZ Sagittae, recurrent nova, spectroscopic obs. during 1978 outburst 80−26862
WZ Sagittae, recurrent nova, spectroscopic study during 1978 outburst 80−56849
FG Sagittae, spectral type and element abundances *(Russian)* 78−93281
WZ Sagittae, spectroscopic obs. (1978 December 1 and 2) 79−16983
WZ Sagittae, spectroscopic obs. and photoelectric V-magnitudes 79−16984
HM Sagittae, UBV photometry and spectral obs. (1977) *(Russian)* 79−16991
WZ Sagittae, UBV photometry and spectroscopy of 1978 Dec. outburst 79−12483
HM Sagittae, variable emission object, spectrophotometry 80−17599
υ Sagittarii, absorpt. lines identification as Fe II high level transitions 78−93316
AV Sagittarii, Cepheid, assoc. with open cluster NGC 6546 disproved 79−58387
μ Sagittarii, eclipsing binary star, unseen companion spectral type 80−4401
V3955 Sagittarii, field RV Tauri/SRd variable 79−88665
MV Sagittarii, H deficient variable, emission line spectrum and circumstellar envelope 77−9756
RY Sagittarii, spectra near min. light 80−36642
υ Sagittarii, UV spectrum 79−35300
SAO 015338, optical counterpart of 2A 1052+606, RS Canum Venaticorum type binary 79−21352
SAO 015338, possible RS Canum Venaticorum star and counterpart of 2A 1052+606, spectrum 80−22118
SAO 015338 (2A 1052+606), Hα emission and analysis of possible identification 78−32608
SB 21, extremely He rich subdwarf O-star, spectrum 80−98659
α Scorpii, circumstellar absorption lines in UV spectrum 80−51804
α^2 Scorpii, circumstellar lines form. rel. to location along line of sight 78−73739
τ Scorpii, Copernicus UV spectral atlas 78−12220
τ Scorpii, deep photospheric flows 79−58326
μ′ Scorpii, eclipsing binary, UV obs. from TD-1A satellite 80−77447
τ Scorpii, expanding envelope, mass loss rate 78−65613
ζ^1 Scorpii, extreme B1 supergiant, IUE obs. of line spectrum and continuum energy distrib. 80−17583
ζ^1 Scorpii, extreme B1 supergiant, UV reson. lines obs. 80−4349
ζ^1 Scorpii, extreme B-type supergiant, UV spectroscopy 80−22004
δ Scorpii, interstellar N_2 band, Copernicus search, upper limits 79−25661
KQ Scorpii, long-period Cepheid evidence for membership of OB association 79−88666
AH Scorpii, M-type supergiant, OH emission rel. to circumstellar envelopes struct. 77−22218
U Scorpii, recurrent nova, spectroscopic obs. during outburst 79−75225
V703 Scorpii, RRs variable, photoelectric radial vels. 77−5533
σ Scorpii, search for interstellar NaH line 78−4325
V861 Scorpii, X-ray emission and UV spectra rel. to unseen companion 78−89226
V861 Scorpii =OAO 1653−40, photometry, spectrum and physical parameters 79−17021
V861 Scorpii (=OAO 1653−40), UV and visible spectra 78−69838
ζ^1 Scorpii (HD 152236), UV spectroscopic and photometric vars. 80−101594
V861 Scorpii (HD 152667), X-ray binary, behaviour of Hα 79−101171
V861 Scorpii (HD 152677), Hα emission features vars. 78−77579
V818 Scorpii (Scorpius X-1), UV, visible, IR and X-ray obs. 80−82541
β Scorpii A, spectroscopic orbit 79−67059
α Scorpii B circumstellar absorption lines 79−8916
Scorpius X−1, 2200Å absorpt. rel. to interstellar extinction and UV flux distrib. 79−25754
Scorpius X-1, binary star, X-ray spectrum 20-75 keV, high sensitivity determ. 80−98741
Scorpius X-1, binary star X-ray obs. from 20 to 250 keV 80−94893
Scorpius X-1, high energy X-ray obs. with Ariel V 80−17694
Scorpius X-1, Prognoz-6 obs. of X-ray fluxes and energy spectra *(Russian)* 80−109562
Scorpius X-1, review of X-ray, optical and radio emission 78−16576
Scorpius X-1, X-ray binary, spectrum calc. 77−29881
Scorpius X-1, X-ray energy spectrum in 0.2-50 keV range, rocket obs. 78−57696
VY Sculptoris, novalike variable, spectrum during faint state 80−98675
RY Scuti, β Lyrae system, optical and radio spectra 79−30090
δ Scuti, line profile variable, pulsational mode-typing 80−90432
δ Scuti variables, spectrographic obs. of σ Andromedae, θ Pegasi and 2 Lyncis 78−61867
δ Scuti-type stars, chromospheric activity and atom. dynamics 77−17581
semi-Ba and Ba stars, heavy element abundance effect on spectroscopic luminosities 77−53586
Serpens X-1 (4U 1837+04), burster optical binary counterpart visible spectra and photometry 80−94891
RT Serpentis (Nova 1909), spectrum in 1964, 1975 and (1978) 80−46566
W Serpentis stars, long period eclipsing binaries, new class, spectral charcts. 80−109483
41 Sextantis A, new metallic line spectroscopic binary 78−53982
shell stars, H shell spectrum form. and envelope struct. 79−48830
SIMS, C and SC stars, new discoveries on southern, red-sensitive objective-prism plates 80−36511
simulation using optical filters G- and F-type stars 77−37505
slitless fieldspectroscopy, focal-reducer system appl. 80−36504
slow novae and symbiotic stars, late-type components spectral classifications 80−94813
SMC probable members and foreground stars, spectral types and UBV, photometry 79−40091

stellar spectra continued
SMC X-1, distortion of absorpt. line vel. curves due to X-ray heating 77−29878
SMC X-2, colours, spectral type and position of optical candidate 78−12421
SMC X-2, optical identification with main sequence Be-star 79−40301
SMC X-2, SMC X-3 optical counterparts, spectra 78−93469
SMC X-3, colours, spectral type and position of optical candidate 78−12421
SN 1970g, in M101, spectra of type II supernova 78−8030
SN 1970j, 1971l and 1971u, spectra and type identifications 77−22255
SN 1972e in NGC 5253, spectrum 80−41844
SN 1972e in NGC 5253, Type I, spectrum after 365 and 435 days 78−4255
SN 1973r in NGC 3627, spectrum of type II supernova 77−49407
SN 1974g, type I, in NGC 4414, post-maximum spectral obs. 77−78806
SN 1979c in M100, coordinated obs. (1979 April-June) 80−101604
SN 1979c in M100 (NGC 4321), spectrophotometry 80−62166
SN in MCG −3-34-61, Type I spectrum revealed (1980 June) 80−82401
SN in NGC 3913, B magnitude and spectrophotometry 79−44513
SN in NGC 4321 (M100), interstellar Na I and Ca II absorption 80−51847
solar-type stars, in open clusters, spectroscopic differences from Sun 78−36560
solar-type stars, metal abundances, microturbulence, spectroscopic data 78−40943
southern B-type stars, radial vels., spectral types and H β indices 78−12225
southern dwarf novae, image tube spectra 77−56960
southern OB stars, MK spectral classifications 78−12221
southern peculiar A-type stars, spectra and atmospheric anals. 78−24517
southern peculiar emission-line stars, observational data rel. to mass ejection 80−41843
speckle interferometry data processing method 80−17498
spectral energy distrib. of eight stars used as spectrophotometric standards 79−35147
spectral energy distributions, results from Fourier transform spectrometry 77−82215
spectral quantification technique 77−29791
spectral types of stars with unusual photometric indices 79−71033
spectrophotometric data processing by large scale interactive one dimens. array processing system 80−82220
spectrophotometric stadnards, absolute spectral energy distrib. 79−97040
spectrophotometric standards calibration against α Lyrae 79−62760
spectrophotometry at Moscow and Alma-Ata, comparison 79−58273
spectroscopic binaries, Ca II H and K line emissions in late-type giants and supergiants 77−91566
spectroscopic binaries, precession period determ. from spectroscopic data 79−67062
spectroscopic binaries discovered from composite spectra 78−69826
spectroscopic binaries in open cluster NGC 6475, radial vels. 77−87488
spectroscopic binaries near southern open clusters, radial vel. obs. near southern open clusters *(German)* 80−94724
spectroscopic binary orbits, catalogue improvements 77−78665
spectrum variables, He weak and He strong stars 78−4243
SS 433, 1978 spectrograms reanalyzed and emission spectral feature ephemeris 79−58345
SS 433, 6.55 day periodicity in emission line wavelengths 80−51784
SS 433, emission line wavelength changes 79−48816
SS 433, enormous periodic Doppler shifts obs. 80−17593
SS 433, general spectral features 80−77421
SS 433, Hα blue component wavelength obs. and weak lines interpretations 79−67023
SS 433, Hα emission object, spectral index from 21.6 and 43 GHz obs. 79−92783
SS 433, Hα radial vel. obs. (1979 July) 79−88674
SS 433, implications of 13-day variation for mag. X-ray binary model 80−109447
SS 433, IR spectral obs., reddening and emission 80−4388
SS 433, kinematic model for line wavelengths vars. 79−75226
SS 433, line posn. vars. interpretation 79−75218
SS 433, near IR (600 to 1100 nm) spectra, 1979 June and September 79−97009
SS 433, near IR spectrum obs. 79−84803
SS 433, no 6-day periodicity in 1978 June-1980 Feb. obs. period 80−62150
SS 433, optical spectroscopic obs. 79−88661
SS 433, precessing jets in ultra-close binary system rel. to spectrum 80−4384
SS 433, precessing ring model, test by spectral line obs. 79−101152
SS 433, radial vel. curve low amplitude section, visible spectra anal. 80−67737
SS 433, reality of 6-day periodicity in spectral lines wavelengths var. 80−67743
SS 433, search for radio spectral lines in UHF 80−109556
SS 433, short term Hα central intensity increases 80−4375
SS 433, spectral features interpreted a precessing neutron star with jets, possible binary 80−90447
SS 433, spectroscopic obs. and probable binary nature 80−51780
SS 433, wavelength shifts 164^d period as precessional motion, massive black hole and pulsar models 80−62138
SS 433 inside SNR, unique spectrum 80−82381
SS 433 region of SNR W50, visible obs. relativistic jets interaction with interstellar medium 80−101629
standard stars, IUE photometric calibration, UV spectra 80−77383
standard stars of intermediate brightness, spectral energy distribs. 78−28651
star associated with variable cometary nebula, spectrum and brightening 78−4333
stars in field centred at $\alpha = 2^h17^m.9$, $\delta = +58°59'$, BV magnitudes and spectral classes *(Russian)* 78−40841
stars in X-ray source fields, transmission grating spectroscopy, optical condidates 79−21283
stars optically misidentified with extragalactic radio sources, photometry and spectra 78−73708
stars with peculiar interstellar polarisations, interstellar lines and grains props. 77−53659
Stepanyan's star, obs. of G8 V absorpt. spectrum and emission spectrum 80−67788
stellar spectra continued
Stepanyan's star, spectrophotometric and photometric obs., 228-min period 80−56883
Stepanyan's star found to be eclipsing binary, possibly cataclysmic 80−51806
Stephenson-Sanduleak 433, 1.2-2.5 μm spectroscopy, photometry and polarimetry 80−41838
Stephenson-Sanduleak 433, emission-line star/X-ray source/radiosource assoc. with W50 SNR 79−8930
Stephenson-Sanduleak 433, Hα emission object, hot spot detect., rot. vel. and spectrum vars. 79−8933
Stephenson-Sanduleak 433, moving emission features, dynamical models 79−67034
Stephenson-Sanduleak 433, spectral variability 79−62839
Stephenson-Sanduleak 433, unusual optical spectrum changes of Hα-emission object 79−5838
Stokes parameters and mag. field vector profiles *(Chinese)* 80−77386
strong CN phenomenon, effects of internal mixing 78−53921
subdwarfs, masses and metal abundances from spectroscopic anals. 80−62122
subdwarfs, old disc population, CaH and TiO band strengths 78−40930
subgiant stars, F-, G- and K-type, Be abundance rel. to post-main sequence evolution 77−13333
Sunlike stars, planetary systems, spectrographic search 77−78827
supergiant OH maser sources, optical radial vels. 77−49378
supergiant stars in LMC, spectral types and magnitudes, catalogue of 1882 objects 78−32361
supergiant stars in the SMC 78−16411
supergiant stars with stellar winds LMC, luminosity and extinction values, UV obs. 80−77477
supergiants, C IV resonance lines in B- and early A-type objects 80−46550
supergiants, emission lines in UV spectra of α Orionis and α Scorpii 79−71028
supergiants, metal abundances of G- and K-type Ib stars 77−33482
supergiants, spectral classification of 26 objects in SMC 77−29936
supergiants, thick circumstellar dust shell effect on photospheric line profiles 79−30058
supergiants assoc. with groups of luminous OB stars, photometry and spectra 77−17555
supergiants in LMC, diffuse interstellar 4430 Å feature 80−73033
supergiants in LMC, IUE obs. and 2200 Å feature detection 79−16959
supergiants in LMC, IUE obs. of UV spectra and flux distribs. 80−101593
supergiants in SMC, MK classifications 77−87390
supergiants in SMC, radial vel. determ. by spectrographic and photometric data study 79−101147
supergiants in SMC 79−101192
supergiants of O- and B-type in Magellanic Clouds, stellar winds 80−51863
supernova, possible, in Virgo galaxy cluster, discovery, position and spectrum 80−90460
supernova, type I, in ESO 290-G50, spectral obs. 78−96496
supernova, Type V, in galaxy MCG 43223, spectrum obs. 78−93288
supernova in anonymous galaxy in Cygnus, UBV photometry and spectrum 79−5846
supernova in IC 5201, discovery, magnitude and spectrum 79−44514
supernova in M100 (NGC 4321), discovery of possible type II object before max. 79−48835
supernova in MCG 10-16-117, classification and spectrum 78−69818
supernova in MCG-5-9-22, spectrum and absolute magnitude 78−81644
supernova in NGC 3733, spectrophotometry (1980 March 22) 80−62164
supernova in NGC 3780, spectrophotometry of type II object 79−17000
supernova in NGC 4321, spectrograms (1979 April) 79−48836
supernova in NGC 4321, spectrophotometry, type II characts. 79−67044
supernova in NGC 4321, spectrum, lightcurve and magnitude of type II object 79−71061
supernovae, BV magnitudes, spectroscopic obs., brightness, distance 79−16999
supernovae, distance determ. by Baade's generalised method, appl. to H_0 and q_0 80−73082
supernovae, expanding gas shell external excitation rel. to spectral lines evolution 78−40976
supernovae, gamma-ray emission, continuum intensity and spectrum 80−101602
supernovae, light curves and spectra obs. at Asiago Astrophys. Observatory 77−87457
supernovae, light curves and spectra of Types I and II 77−87455
supernovae, spectrum before max. luminosity in Type I objects 80−41845
supernovae, type I, effects of line overlapping on spectra in conservative scatt. case *(Russian)* 80−105266
supernovae, Type I, interpretation of spectra 78−49467
supernovae, Type I, prior stellar wind envelope detect. via absorpt. lines 78−53969
supernovae, Type I, radioactive excitation source model for late time spectra 80−105264
supernovae, Type I, spectroscopic data appl. to Hubble const. determ. 79−40304
supernovae, Type II, O I absorpt. lines obs. in spectra *(Russian)* 77−45474
supernovae, Type II, spectral analysis from 8 to 15 months after explosion 78−40974
supernovae in molecular clouds, spectra and luminosity, evolution 80−82399
supernovae stellar remnants, spectroscopic search 80−26890
symbiotic C star (UKS-Cel), spectrum 77−67094
symbiotic star candidates in LMC, optical spectroscopy and IR photometry 80−62139
symbiotic stars, models, spectral characts. *(Polish)* 79−88689
symbiotic stars, obs. of unidentified bands at 6830 and 7088 Å 80−46573
symbiotic stars, radio mol. maser line obs. 80−72960
symbiotic stars, unidentified emission line obs. at 7090 Å 77−33522
symbiotic stars and slow novae, late-type components spectral classifications 80−94813
T626, red giant in open cluster M67, curve of growth anal. 79−48797
41 Tauri, Ap star, Ca II K and Hδ lines rapid vars. *(Russian)* 80−90458
ζ Tauri, apparent wavelength depend. of v sin i 78−12240

stellar spectra continued
RW Tauri, eclipsing binary, gaseous ring struct., H I alpha obs. 80−109482
λ Tauri, eclipsing binary star, mass loss from UV spectra obs. 80−109485
SU Tauri, emission lines at min. and BV photoelectric photometry 80−8640
T Tauri, H_α line profile, fast variations obs. *(French)* 78−61859
T Tauri, Hα line profile vars. 78−40944
DL Tauri, Hα profile in T Tauri type star *(French)* 78−8003
ζ Tauri, high-resolution rocket spectra of λ1920 and λ1720 features 78−4236
DR Tauri, highly variable young star, spectrometric and photometric obs. 78−20829
45 Tauri, Hyades cluster star, CNO abundances from near IR spectrum 78−93222
ζ Tauri, near UV spectrum, TD-1A satellite obs. 77−56988
ζ Tauri, near UV spectrum of shell star 78−81653
DR Tauri, pre-main-sequence star, brightening, 1970 to 1979, and spectrum 80−31297
SU Tauri, R Coronae Borealis star, spectral type from optical and IR photometry 80−101601
α Tauri, search for Ti II 3080 Å multiplet emission 80−51769
ζ Tauri, shell star, Balmer intensity profiles 77−56973
ζ Tauri, shell star, emission features 77−56975
ζ Tauri, Si II lines in shell 77−60774
DR Tauri, T Tauri star, Balmer line profile changes and inverse P Cygni profiles 80−101591
DF Tauri, T Tauri star, He I triplet-to-singlet ratio 78−28680
DR Tauri, T Tauri star, mass flow var. in envelope, visible spectra 80−85939
β Tauri, UV spectrum of Mn star 78−69802
V471 Tauri, white dwarf eclipsing binary, IUE UV spectra 80−26912
α Tauri (Aldebaran), Ca II and Mg II lines rel. to chromosphere model 78−40931
α Tauri (Aldebaran), Ca II K line high-resolution obs. 78−16408
α Tauri (Aldebaran), TiO spectrum and Ti isotopic abundances 77−22212
V471 Tauri (Bd+16°516), Ca II H and K and Hα line vars. 79−67063
V471 Tauri (BD+16°516), eclipsing binary white dwarf, spectroscopy and photometry rel. to evolution 77−57028
V711 Tauri (HR 1099) and related Ca II emission binaries, Hα emission survey 79−21339
α Tauri (K5 III), S I emission obs. in EUV spectrum 80−82359
BU=28 Tauri (Pleione), envelope during shell phase, 1972-75 period 78−28707
BU=28Tauri (Pleione), spectral var. during 1969-1975 period 77−33532
BU=28 Tauri (Pleione), spectrum vars., 1938-75 period 78−36578
BU Tauri (Pleione), UV photometry and UV absorpt. during shell phase 77−64768
28=BU Tauri (Pleione) Be shell star, 3167 to 4924 Å spectrum atlas 80−98673
T Tauri star, extremely young, and assoc. nebula, fading 78−93236
T Tauri stars, gas flow from line profiles 79−67004
T Tauri stars, H_2 emission obs. 78−93230
T Tauri stars, Hα and Na I D lines high-resolution profiles 80−62116
T Tauri stars, H line emission rel. to location in (J-H), (H-K) diagram 77−78790
T Tauri stars, line profiles rel. to infall model 77−13329
T Tauri stars, OH and NH_3 emission line obs. 79−25662
T Tauri stars, outflowing envelopes models rel. to line and continuum radiation 78−96482
T Tauri stars, photometric and spectral props. 79−21282
T Tauri stars, radial vels. and spectral types 77−56921
T Tauri stars, spectral features synthesis from photosphere and low chromosphere model 80−36623
RR Telescopii, nova-like variable, spectrophotometry 77−45460
RR Telescopii, slow nova, evolution of nebular spectrum 77−60771
RR Telescopii, symbiotic star, steam and CO absorpt. obs. 78−40970
RR Telscopic, spectra, rel. to term anal. of Fe IV 78−82677
Trapezium-like objects, spectral types rel. to visual and IR photometric obs. 79−92805
α Trianguli, radial vel. vars. from microdensitometer scans of photographic spectra 79−25642
Trumpler 27, heavily-reddened young open cluster, spectra and photometry 77−78836
Trumpler 37, young open cluster, stellar UBV magnitudes and MK classifications 77−22284
47 Tucanae, globular cluster, photometry and spectra rel. to stars chemical comp. 80−46620
47 Tucanae, spectral inhomogeneities in faint globular cluster stars 78−93340
47 Tucanae cluster, abundance gradients from spectroscopic obs. 79−40228
47 Tucanae stars, spectra and photometry rel. to N anomaly 79−48867
two-dimensional spectral classes, accuracy of derivation from DDO photometry 78−16395
type I supernovae, photographic and spectroscopic obs. 77−57000
4U 0115+634, X-ray binary, 1980 Aug. photometry and spectroscopy 80−101650
4 U 0115+63, absorption line in pulsed hard X-ray spectrum, HEAO 1 obs. 80−27017
4U 0115+63, transient X-ray binary, 20 keV absorpt. feature in pulsed spectrum 78−69909
4U 0115+63, transient X-ray source, 3.61 s pulsations and X-ray spectrum obs. 78−61939
4U 0115+63, transient X-ray source, obs. 79−92890
4U 0115+63, transient X-ray source optical candidate, UBV photometry and spectrum 78−32605
3U 0614+09, X-ray burst spectrum 78−32610
3U 1118−60 (Centaurus X-3), hard X-ray obs. 77−2493
3U 1223-62 (GX 301-2), hard X-ray obs. 77−2493
3U 1254−69, hard X-ray obs. 77−2493
4U 1258−61, spectrum change in optical counterpart 79−71154
4U 1538−52, spectrograms of optical candidate, confirmation of identification 78−41094
4U 1538-52, optical counterpart spectroscopy and system parameters 79−5924
4U 1538-52 optical counterpart, discovery of reddened Be-type star 78−36727
4U 1626−67, X-ray pulsar, HEAO 1 obs. 79−92889
stellar spectra continued
4U 1700−37 (=HD 153919), eclipsing binary, X-ray obs. 80−86016
4U 1700−37 (HD 153919), high-energy obs. rel. to thermal bremsstrahlung X-ray spectrum 80−86014
4U 1702-36, Scorpius X-1 like source, high energy X-ray obs. with Ariel V 80−17694
3U 1735−44, spectral obs. of optical counterpart 77−64882
4U 1735−44 (MXB 1735−44) optical counterpart, spectrum, similarity to (Scorpius X-1) 78−93468
4U 1755−33 optical candidate, photometry and spectrum 78−77625
4U 1837+04 (Serpentis X-1), absorption spectrum of counterpart 78−69912
4U 1907+09, optical identification and OB supergiant binary hypothesis 80−82542
3U 1956+11 optical counterpart, photometry and spectrum 78−49554
4 U 2129+47 optical counterpart, spectrum and photometry rel. to 80−17693
unreddened stars, interstellar lines rel. to two-phase model of interstellar medium 77−74110
upper main sequence, rotational effects in spectra 77−71104
upper Scorpius region stars, spectrophotometry and Balmer lines equivalent widths 79−88647
Ursa Major stream, spectral types 78−85984
τ Ursae Majoris, Am star, microturbulence and metal content determ. 80−82377
ε Ursae Majoris, Ap star, UV spectral scans, line identifications 77−45440
XY Ursae Majoris, eclipsing binary, photometry and spectrum rel. to spot activity on primary component 80−109491
AN Ursae Majoris, emission lines and radial vel. curve 77−33514
CQ Ursae Majoris, line identification list and radial vel. of Ap-star 80−41841
α Ursae Majoris and close companion star, spectrum synthesis 77−49436
W Ursae Majoris stars, rot. line broadening functions rel. to stellar shapes 80−109494
γ Ursae Minoris, high dispersion spectroscopy 80−41853
α Ursae Minoris B (Polaris B), spectral type and interstellar reddening 78−8005
UV5, in globular cluster NGC 1851, He abundance determ. 78−49441
UV, atlas, line features use in spectral classification 78−12215
UV 1758+36, He deficient hot subdwarf B star, atm. parameters, radial vel. 78−53944
UV absorpt. at 2175 Å, correl. with interstellar features 77−45401
UV catalogue of stellar spectra from Skylab S-019 expt. 77−78662
UV chromospheric and transition-layer emission 80−56823
UV high-resolution obs. by balloon-borne echelle spectrograph 78−49318
UV lines in O, B and A-type spectra 77−78787
UV objective-prism spectrography from Skylab 77−60609
UV obs. of Cl lines towards 10 stars, interstellar Cl and P abundances 78−36646
UV sources, spectral classification 78−65602
UV spectra, IUE preliminary results, workshop, Udine, Italy (1978 October 12) *(Italian)* 80−86033
UV spectra, second OAO atlas 80−72786
UV spectroscopy, spaceborne instrumentation 79−25518
UV spectroscopy from balloon using echelle and SEC-vidicon system 79−25482
UV spectrum of early type stars, rotation effects, TD-1A obs. 79−44476
V 65 in ω Centauri, cluster membership determ. 78−73743
V 78 in ω Centauri, cluster membership determ. 78−73743
van Bueren 62, 117, 121, dwarf stars in Hyades, spectroscopic orbits 79−5862
variable emission-line star in core of M15, spectrum, photometry and position 79−5840
variables with long periods, radial and expansion vels. from SiO line 78−40956
AH Velorum, Cepheid, radial vel. study, possible binary, coude spectrograms 77−49394
γ Velorum, interstellar absorption lines in UV spectrum 79−35324
λ Velorum, K-type supergiant, UV spectrum rel. to chromosphere and wind struct. 80−72948
RZ Velorum, long-period Cepheid evidence for membership of OB association 79−88666
AH Velorum, radius, delta luminosity and pulsation mode of δ Cepheid 80−46572
AI Velorum, RRs variable, photoelectric radial vels. 77−5533
δ Velorum, UV spectra, comparison of synthetic and observed spectra 77−29820
γ_2 Velorum, Wolf-Rayet binary, orbital element determ. from spectral obs. 80−85950
γ_2 Velorum, Wolf-Rayet binary star, UV obs. from TD-1A satellite 80−77447
VI Cygni (Cygnus OB2) association, interstellar λ4430 band obs. 78−32555
32 Virginis, A-type main-sequence and Am-type star components 79−30091
32 Virginis, Am star, spectroscopic obs. and curve of growth anal. 77−22237
78 Virginis, Ap star, lines circular polarisation profiles rel. to mag. field geometry 80−51773
α Virginis, binary star, UV spectrum 77−45485
α Virginis, Copernicus UV obs. 77−33502
EQ Virginis, dK5e star, new absorpt. line obs., possible infalling gas 77−37602
AH Virginis, eclipsing binary, Ca II emission and light curve vars. 77−78822
ε Virginis, equivalent widths of Fe lines for spectral anal. 77−78771
ε Virginis, Fe spectrum, differential model atmosphere analysis 79−25604
CU Virginis, He I 4026 Å line var., photoelectric meas. 78−77555
EQ Virginis, late-type flare star, metal abundances 77−78779
78 Virginis, magnetic Ap star, high resolution polarisation obs. inside spectral lines 80−51772
78 Virginis, magnetic field gradient in Ap-star atmosphere, Zeeman spectra 78−85953
CU Virginis, short period Ap star, discovery of mag. field 77−33511
α Virginis, UV interstellar lines in 935-2960 Å range 79−35323
CU Virginis (HD 124224), Ap star, spectrophotometric obs. 80−98663
visual binaries, spectra, statistical props. 79−97038

stellar spectra continued
visual double stars, spectral classification and UBV photometry 77−74084
Voigt lines, random array, curve-of-growth function 78−89055
Vulpecula OB2 stars, photometry and spectra rel. to membership of 67 day Cepheid S Vulpeculae 80−41831
WW Vulpeculae, fast irregular variable, H_α and H_β lines obs. *(Russian)* 77−87400
15 Vulpeculae, radial vel. from spectrograms 77−56952
LV Vulpeculae (Nova 1968 No.1), spectroscopy 77−87438
NQ Vulpeculae (Nova 1976), CO emission and η Carinae stage 79−25609
NQ Vulpeculae (Nova 1976), Hα emission line profiles in 1976 November to December *(Russian)* 78−40971
NQ Vulpeculae (Nova 1976), Hα var. 79−58352
NQ Vulpeculae (Nova 1976), spectral evolution 78−89205
NQ Vulpeculae (Nova 1976), UV and visual spectra analysis *(Chinese)* 80−12770
NQ Vulpeculae (Nova Vulpeculae 1976), spectroscopic obs. of slow nova 78−85955
VV Puppis, 3470 Å emission as cyclotron line 80−36673
Wat 6, open cluster, photometry and spectra rel. to proximity to (Pismis 6 and 8) 79−88712
wave-broadened spectral line profiles, anal. of Fourier transforms 79−80229
WC stars, near IR spectrometry 80−94816
weak G-band stars, CH and NH band strengths, atm. material from CNO cycle 79−8917
weak G-band stars, photometry and spectra 77−49386
weak lines profiles, macro- and microturbulent filter functions 79−53803
weak-G band giant stars, Li abundance determ. 78−53948
weak-G-band stars, CO 2.3 μ band strength 78−12228
white dwarf spectra obtained with low-dispersion Fehrenbach prism, computer simulation 78−57468
white dwarfs, classification of 47 southern stars 78−16417
white dwarfs, DB-type, model atmospheres rel. to line profiles and equivalent widths 80−51761
white dwarfs, external layers models rel. to spectra interpretation 79−62824
white dwarfs, Hα polarisation and line profiles in strong mag. fields 77−2427
white dwarfs, H I Balmer line strengths, profiles and equivalent widths 79−96998
white dwarfs, magnetic, cyclotron absorpt. spectra theory 80−4351
white dwarfs, magnetic, unexplained spectral features theory 80−82187
white dwarfs, model atmospheres and synthetic spectra, effective temps. 5000-7000K *(Italian)* 78−93240
white dwarfs, review 77−50383
white dwarfs, rot. and gravit. redshift 77−29816
white dwarfs, spectra and atmospheric comps. 80−82356
white dwarfs, spectral evolution and accretion from interstellar clouds 79−35252
white dwarfs, spectrophotometry with Carnegie image tube 78−57466
white dwarfs, spectroscopic survey using Luyten catalogues 78−7998
white dwarfs H line asymmetries and gravitational redshifts 77−17556
wide visual double stars, B, A and F type, uvbyβ photometry 79−17025
Wing-Ford 9910 Å molecular band as mass function constraint in old galaxy populations 77−17673
Wolf Rayet stars, late type, 8-13 micron spectral obs. 80−101599
Wolf-Rayer stars, UV obs. 78−40965
Wolf-Rayet binaries, interpretation of eclipses at emission-line freqs. 77−17596
Wolf-Rayet stars, 2 to 4 μm spectrophotometry of late WC stars 78−96491
Wolf-Rayet stars, atlas of Copernicus UV spectra 78−57557
Wolf-Rayet stars, calc. of oscillator strengths of transitions for ion spectra C III, N IV, and O V *(Russian)* 78−57566
Wolf-Rayet stars, evolution and binary freq. distrib., spectra anal. 80−105250
Wolf-Rayet stars, faint, photometry and spectrography 79−40200
Wolf-Rayet stars, in M33, spectral obs. 77−64779
Wolf-Rayet stars, interstellar N V lines, IUE obs. 80−101634
Wolf-Rayet stars, near IR spectra emission line characts. 79−53825
Wolf-Rayet stars, short-lived changes of emission lines *(Russian)* 80−72977
Wolf-Rayet stars, Si IV and C IV, absorpt. lines, IUE obs. 80−67748
Wolf-Rayet stars discovery in 30 Doradus nebula in LMC 79−16980
Wolf-Rayet stars in galactic-centre field, new discoveries from spectroscopic obs. 80−8674
Wolf-Rayet stars in LMC, new discoveries, positions, spectra and magnitudes 80−46569
Wolf-Rayet stars in LMC, new discoveries spectral classifications 79−67018
Wolf-Rayet stars in SMC, spectral classification 78−73716
WRA 977, B-type supergiant, spectroscopic obs., X-ray source identification 79−101148
Wray 977, optical counterpart to X-ray binary pulsar, 4U 1223−62, optical spectra 80−72984
Wray 977 (4U 1223−62), B-type supergiant, spectral classification 79−80305
X-ray binaries, distortion of absorpt. line vel. curves due to X-ray heating 77−29878
X-ray binaries, Fe line emission from Alfven shell 80−98737
X-ray binaries, spectra of X-rays refl. from neutron star surfaces 78−28716
X-ray binaries, test of quark bags and interacting neutrons models 77−78812
X-ray binary stars, optical photometry and spectra 78−12429
X-ray binary system, Fe fluoresc. line struct. 77−78889
X-ray burst sources, spectrum vars. during bursts 78−12427
X-ray novae, spectroscopic obs. in 3800-10900 Å range 77−87577
X-ray pulsars spectra, possible vacuum signature 80−27015
X-ray pulsator, 38.22 second period, in vicinity of OAO 1653−40, very hard spectrum 80−27014
X-ray sources, compact, spectra form. 80−22115
X-ray sources, galactic, hard and soft X-ray spectra rel. to physical nature 80−62316
X-ray transient sources, hard and soft transients parameters 79−84867
young emission line objects in S Hemisphere, image tube spectrograms 78−8016
young stars in Chamaeleon T1, photometry and spectral obs. 80−72943

stellar spectra continued
I Zw 18, dwarf blue compact galaxy, blue star emission spectra 77−37593
II Zw 40, dwarf blue compact galaxy, blue star emission spectra 77−37593
μ Draconis (ADS 10345), radial vel. var. from spectra in visible 80−17612
AlO IR bands rel. to Mira phenomena 78−69801
Ba II giant stars binary nature from visible radial vel. obs. 80−82355
Ba stars, spectroscopic, radial vel. and photometric obs. 78−12226
C III, photoionization cross sections calc. 78−17625
C IV in stars hotter than B 1, Copernicus obs. 79−44463
C star, variable, in open cluster, Stock 8, spectroscopic and photometric obs. 79−84791
C stars, $^{12}C/^{13}C$ abundance ratio 77−33494
C stars, 3 μm absorpt. band obs. 78−28682
C stars, 3 μm band compared with interstellar 'water-ice' 3 μm absorpt. 78−49499
C stars, 3.9 micron absorpt. band identification 78−93231
C stars, C and N isotope ratios from spectral analysis 79−30057
C stars, circumstellar envelopes and evolution 79−40178
C stars, enhanced C abundances in long-period variables 77−33501
C stars, IR CN spectra rel. to $^{12}C/^{13}C$ ratios 79−35257
C stars, in LMC, VRI photometry, optical spectroscopy and evolutionary implications 79−71019
C stars, Li line formation 78−65615
C stars, polyatomic molecular line search in photographic IR 77−78786
C stars, search for HCN and CH maser emissions 80−51856
C stars, spectral clssification by photoelec. photometry of line strengths 78−73711
C stars, spectrophotometry, C/O and $^{12}C/^{13}C$ ratios calc. 77−91533
C stars, spectroscopic problems 80−56832
C stars, violet opacity 78−53940
C stars in Cygnus, new spectroscopic discoveries 80−46551
C stars in red globular clusters in Magellanic Clouds 79−101143
C_2 (4670 Å band) stars, evolutionary status 80−4355
C_2 absorption bands in stellar spectra, 876 nm obs. 80−12805
C_2, Phillips system, rot. depend. of Franck-Condon factors 77−27058
C_2 Swann band strengths calc. 77−61810
C_2^-, $A^3\Pi_u$-$X^2\Sigma_g^+$ lines, obs. in carbon stars 80−98661
CH star in M22 globular cluster, CH and CN anomalies 78−8001
CN (0,0) 3883 Å band strengths of subdwarfs in 47 Tucanae 80−94794
CN, spectral absorpt. coeffs. for fundamental and first overtone vibr.-rot. bands 77−14405
CO in giant stars in globular clusters, IR obs. 78−93339
CO in metal-deficient stars 2.2 and 2.4 μm obs. 79−58336
Ca II emission from stellar chromospheres 79−30061
Ca II emission line, V/R ratio rel. to mass loss 78−93208
Ca II H and K emission, chromospheric, in main-sequence stars, comparison of activity cycles to old and young stars 80−105235
Ca II H and K emission, chromospheric, in field stars of solar neighbourhood, survey 80−109423
Ca II H and K emission, flux meas. by four-channel photon-counting spectrophotometer 78−73646
Ca II H and K emission lines, catalogue *(Polish)* 80−82227
Ca II H and K lines, emission lines in wings, line width-luminosity relation 77−78766
Ca II H and K lines in F0 to M2-type stars, high resolution absolute flux profiles 80−26842
Ca II H and K-line, and abundance in globular star cluster giant stars 80−72940
Ca II H-line emission from Sun observed as star *(Russian)* 77−64727
Ca II K line emission widths 77−41373
CaO, J=4-3 106 GHz undetected transition in stars and molecular clouds 79−71090
CeO, gas, electronic spectrum 79−41178
Cr stars, classification criteria, Cr II lines with blending 78−85951
CuH, vibr.-rot. interaction influence on band intensity parameters 79−49999
Dy III lines in spectra of Ap and Bp stars 80−12764
Fe curve of growth split as function of atmospheric pressure 77−29794
Fe I 3719.94 Å line broadening by He, line width and shift meas., lab. expt. 77−73942
Fe II emission line spectra in Be-stars 77−56978
Fe II resonance line UV obs. toward early-type stars, interstellar gaseous Fe depletion 79−44584
FeH in stellar atmospheres, Wing-Ford band strengths calc. 78−24507
H I Balmer α and β lines in O6 to G2 stars, equivalent widths and narrow-band photometry 80−8621
H I Balmer α emission line core formation in chromosphere of T Tauri-type variables 80−94792
H I survey from Lyman α absorption meas. towards 100 stars 78−93357
H spectra, consequences of departures of electron energy distrib. from Maxwellian 77−80274
H_b line profiles for white dwarfs with dipole and quadrupole magnetic fields 78−8004
H_2O absorption and coolest stellar component of E and S0 galaxies at 2 μ 78−41034
H_2O maser line evidence for circumstellar ring systems in supergiant stars 78−89195
Hα emission line stars in Coalsack direction, finding list 77−22115
Hα emission stars, suspected, in and near NGC 7000, spectroscopic obs. 77−13363
Hα emission stars in southern dark clouds, objective prism survey 78−28536
Hα, Hβ rapid line variability in Be, Of and Wolf-Rayet stars 77−26014
Hα stars in NGC 2264 and NGC 7000/IC 5070 , slitless spectrographic search 80−62120
Hα-emission stars in Perseus OB1 assoc. region 80−56855
Hβ index, correction of uvby photometry for Hδ, appl. to stellar temps. determ. 77−64740
He I 4026 Å narrow-band index for B-type stars in young clusters and associations 77−29887
He I lines in early-type stars, Copernicus UV obs. 80−41825
He rich stars, intermediate and extreme, spectral atlas in 3700 to 4600 Å range 80−94806
He weak and He strong stars, spectrum variability 79−40201
He-rich stars 77−37608
He-weak stars, photoelectric meas. of H Balmer lines 79−16994
^{3}He stars, spectroscopic search, diffusion hypothesis 79−35264

stellar spectra continued
Hg II line oscillator strength determ. in Ap-type stars, diffusion model implications 80−72966
Hg-Mn spectroscopic binaries, high-dispersion spectrograms 77−17629
HgMn stars, line asymmetries rel. to diffusion 78−40948
HgMn stars, spectrophotometry 80−26867
HgMn stars, UV spectra rel. to thin Hg layers and diffusion model 80−105243
Hγ energy levels and Debye screening, no evidence for red shift 79−31369
Hγ equivalent width computation method for objective-prism astrograph, for SMC stars 78−57462
Li abundances for G- and K-type supergiants 78−28676
Li, Be, B, isoelectronic sequences, ionization equilib. balance, solar and stellar atms. appl. 79−36587
Mg I 2852A line obs. towards moderately reddened stars 78−20874
Mg I b2 5175 Å index in old galaxy populations 78−41033
Mg II, interstellar column density towards nearby stars 78−41023
Mg II 2800 Å data for early-type stars, circumstellar clouds *(Russian, English)* 79−96992
Mg II flux profiles in cool stars, obs. rel. to chromospheric radiative loss rates 80−36611
Mg II h and k lines in cool giant star chromospheres, mass loss determ. 80−85935
Mn-Hg stars, differential curve-of-growth analyses 79−16971
N deficient supergiants in loose assoc., LTE and non LTE abundance anals. 79−44478
O I 7774 Å line in O6 to G2 stars, equivalent widths and narrow-band photometry 80−8621
O VI interstellar survey, UV spectra of OB stars 78−36679
O-rich late-type stars, 16 to 39 micron spectroscopy 80−22002
OH emission from early-type stars with large IR excess 79−71035
OH main line emission from globular clusters, high sensitivity search 80−62207
OH type II stars, unidentified, H_2O emission profiles 79−75286
OH/IR stars, new SiO transition detect. 78−53954
OH/IR stars, OH main lines masers inversion 78−28664
SI II, Stark broadened linewidths, plasma diagnostics and stellar spectra appls. 77−84496
τ Scorpii, spectral line studies using LTE-method *(Russian)* 79−92769
Si spectra in O and B stars 78−57539
SiO 86.2 GHz maser sources, polarisation props. 80−4449
SiO maser line evidence for circumstellar ring systems in supergiant stars 78−89195
SiO masers, $J=1\rightarrow0$ $v=1$ and 2 masers relative intensity and vel. 80−4339
SiO masers in late-type stars, VLBI obs. at 43 GHz 79−92779
SiO, nonmaser emission lines from expanding envelopes around evolved stars 78−28650
T 79−48789
Tc in late-type stars, spectral analysis 80−8623
Tc stars, search for TcO spectral bands 78−40935
Ti II 3384 Å line obs. towards ζ Persei, interstellar Ti vel. distrib. 79−53877
TiO band absorption effect on stellar photometry with broadband filters 80−41811
TiO band strengths in metal-rich globular clusters 78−49487
U stars and related objects, spectroscopic study 78−49465
ZrO, band identifications in $^1\pi$-$X^1\Sigma^+$ system 77−18931
ZrO, γ system anal., isotopic band shifts in stellar spectra calc. 79−50029
ZrO, vibr.-rot. interaction influence on band intensity parameters 79−49999

stellar spectrophotometry *see stellar photometry*

stellar structure
see also solar interior
2 to 10 M⊙ stars, effect of heavy element abundance on evolution, struct. of models 80−105231
6 M⊙ star thermal post-main sequence evolution, importance of continuous nuclear spectrum 77−64745
10-day Cepheids, theoretical models of internal struct. 78−49449
16 M⊙ supergiant with 1 M⊙ neutron star companion, double core evolution 78−53980
30 M⊙ star, stability towards g^+ modes of high spherical harmonic values 77−9740
$\varepsilon XY(dY/dX)=X-Y(Y+1)$, exact perturbation soln., stellar struct. theory 78−32439
accreting neutron stars, He burning shell evolution 80−85968
accretion disc of magnetised compact object, theory *(Russian)* 79−44467
accretion disc stability, viscosity and cooling mechanism effects 78−49476
accretion disc stability 77−29796
accretion discs, secondary winds and evaporation 77−64751
accretion discs *(Polish)* 78−89175
accretion magnetospheres, general solns. 77−45400
adiabatic non-radial oscillations with moderate or large l, theory 80−56819
adiabatic pulsations of tidally perturbed rotating stars 78−89172
adiabatic stability of rotating gaseous masses 77−91516
Algol, orbit, lightcurve and struct. review 80−109460
AC Andromedae, pulsating variable, mass, luminosity and evolution 77−29845
AC Andromedae, triple mode variable, oscillating c-type RR Lyrae star 78−57560
anisotropic spheres, adiabatic contraction in general relativity 80−36489
Ap stars, orientation of mag. and rot. axes, decentred mag. dipole theory 78−4241
AE Aquarii, cataclysmic variable, IUE satellite UV obs. 80−72985
atmosphere in statistical equilib., effects of deviations from LTE on struct. 80−31290
59 Aurigae, δ Scuti star, pulsation modes from light curves periodogram anal. 80−62141
B-type semidetached systems, photoelectric obs. 79−44522
BDS 1269 A, metal-poor δ Scuti star, pulsation periods from b-band photometry 80−105247
binary component, photospheric circulation, nonuniformly heated surface 79−96993
binary star giants, chromospheric activity due to tidal interactions 80−82420

stellar structure continued
binary stars, critical surface, influence of radiation pressure, X-rays and asynchronisation 77−29880
black hole, accretion disc struct. at subcritical luminosity 77−64791
black hole accretion discs, Lightman-Eardley instabilities rel. to disc thickening 80−31324
black holes, Kerr naked singularities, accretion disks 79−30084
black holes, theory and observational methods *(Hungarian)* 78−77574
blast waves, isothermal self-similar, one-dimensional flow and its stability 78−45214
blast waves, isothermal self-similar, two-dimensional flow and its stability 78−49307
AC Bootis, eclipsing binary, photometric study rel. to struct. 78−36637
boundary conditions with mass conditions with mass loss 78−12209
brown and black dwarfs, structure, evolution and missing mass contrib. 79−48800
RU Camelopardalis, outer layers, modification rel. to photometric behaviour, (1966 to 1977) 78−89206
38 Cancri, δ Scuti star, UBV photometry and possible non-radial pulsation 80−22021
38 Cancri in Praesepe cluster, δ Scuti variable, pulsation anal. from light curves 80−77419
β Canis Majoris, β Cephei star, pulsations periods from Fourier anal. of radial vel. changes 80−105246
UW Canis Majoris, eclipsing binary, UV photometry and primary component shape and atmospheric struct. 78−40992
α Canis Majoris B (Sirius B), coronal model constraints from historical pseudo red giant phase 79−2543
TU Cassiopeiae, double-mode Cepheid, periods and amplitudes 79−48804
cataclysmic binaries accretion discs, convection as viscosity source 78−93307
cataclysmic variables, review 77−26018
cellular convection in a stratified atmosphere 80−98652
Centaurus X-3, accretion disk evidence from month-long X-ray obs. 79−44636
U Cephei, eclipsing binary, G-type star g-mode oscills. rel. to gas stream effects 80−26898
β Cephei, non-radial pulsations detect. attempt 79−40198
VW Cephei, W Ursae Majoris star, orbital period decrease and B-V colours rel. to physical status 80−109495
β Cephei stars, effects of mass loss on instability strip and pulsation 80−90436
β Cephei stars, line profile variables, pulsational modes 80−85951
β Cephei stars, nonradial oscills., linear nonadiabatic analysis 80−56836
β Cephei stars, pulsation effect on period-luminosity relation 80−72970
β Cephei stars, pulsation excitation mechanisms 77−87425
β Cephei stars, pulsations and evolutionary status 80−85959
Cepheid instability strip, behaviour of light vars. amplitude 79−44491
Cepheid variables, He-enriched convection zones rel. to masses and stellar winds 78−57556
Cepheid variables, radii determ. via method of max. likelihood 77−45459
Cepheids, double mode pulsation, iterative treatment 80−82369
Cepheids, double-mode, period ratios from linear and nonlinear theory 78−40953
Cepheids, double-mode and bump, rot. and convection effects on period ratios 78−93249
Cepheids, mass calc. methods, anomalies 78−49466
Cepheids, multimode, two-zone models, resonances 80−36641
cepheids, northern hemisphere, double mode excitation search using existing obs. 80−8634
Cepheids, pulsation theory and multiperiodic variables 77−87429
Cepheids, pulsation theory for normal and double mode variables 77−87428
multimode Cepheids, two zone rel. to classical models 80−72967
sinusoidal Cepheids in LMC, first overtone pulsations, photometry obs. 80−77422
Cepheids pulsating envelopes models, mag. field effects 80−31302
Cepheids with He enriched inhomogeneous outer layers, three mode reson. 80−101600
δ Ceti, β Canis Majoris variable, period meas. and detect. of period decrease 80−105257
close binaries, distortion effects on struct. 78−57584
close binaries, energy release, flares and particle acceleration *(Russian)* 80−73005
close binaries, review 77−33573
close binaries, struct. and evolution 77−57019
close binary components, model atms. 79−62869
close binary stars, radiative interiors rel. to orbital precession and nutation 77−13392
close binary systems, components dimensions and distortion rel. to radial vel. curves anal. 80−90470
close binary systems, mass transfer and accretion disk flow 77−82280
cocoon stars, envelope struct. and spectra 77−64824
CoD−38°10980, white dwarf, gravit. redshift rel. to mass-radius relation 78−24511
cold degenerate stars, immiscibilities rel. to luminosities and comps. 78−69798
cold matter in Einstein-Cartan gravitation theory, static spherical configurations 78−49308
cold relativistic neutron gas, study of massive neutron cores 79−35292
collapse and transport supernovae with neutrino degeneracy 78−40977
collapsed stars, limits on nuclei excitation energies in hot matter 80−56703
collapsed stars, neutrino flux from quark matter 80−22028
collapsed stars with huge magnetic fields, astrophysical problems 80−82187
collapsing core, effects of nuclear forces, partition function and dissoc. 79−48833
collapsing core, shape instability pressure stabilisation 80−8537
collapsing stars, neutrino damping of nonradial pulsations 77−56999
compact binary systems, tidal interactions 77−57027
complete viscous polytropes, linearized theory validity 79−35244
concave hamburger equilibrium of rotating bodies 80−109422
contact binaries, objection to model of Shu, Lubow and Anderson 78−28720
contact binaries, solar type, initial mass ratio distrib. function 80−109496
contact binaries, structure, zero-age models 78−8045
contact binaries, theories of struct. 80−109493

stellar structure continued
contact binaries of low mass, struct. rel. to evolutionary fate 77−2453
contact binary stars, struct. of high-mass models 79−48855
contact binary stars, temp. discontinuity maintenance 80−8655
contact binary systems, possibility of convective energy transfer between components *(Russian)* 77−17615
contact discontinuities, perturbed, junction conditions 80−94787
convection, IAU Colloquium 38 (Nice, France, 1976 August 16-20) 78−89176
convection equations, ensemble averaging 80−67698
convection in massive star cores, effect on C/O ratio 80−17579
convection onset in radially pulsating star 80−41809
convection theory including turbulent kinetic energy flux, appl. to main sequence star models 78−57543
convection zones dynamics, effect of rot. on turbulent viscosity and cond. 80−36612
convective cores extent in massive stars, role of convective and semiconvective mixing 80−90405
convective degenerate cores, effects of URCA process 77−22203
convective elements, fluctuations rel. to stochastic evolution and oscill. props. 80−31293
convective envelope stars, value of mixing length 80−77379
convective envelopes, non-local convection, statistical theory *(Chinese)* 80−85933
convective instability, mag. fields and g^- modes 78−93211
convective models, fundamental hit correctable inconsistency of local mixing-length theory 80−26841
convective shells are core He-burning in massive stars 78−93207
core collapse, effects of neutrino ang. momentum losses 77−56916
core gravitational collapse, shockwave prod., neutrino transport effects 80−94818
core He burning stars, H profile, previous mixing and loops in H-R diagram 77−29792
core homologous collapse, perturbations effects 80−94779
core hydrodynamics for massive star, collapse and explosion 79−16995
core mass-luminosity relations, for He shell burning stars 80−21983
β Coronae Borealis, Ap star, struct. of atmospheric mag. field *(Russian)* 77−17594
θ Coronae Borealis, Be-type star, shell line profile and radial vel. obs. 80−77426
β Coronae Borealis, mag. deform. 77−49400
Crab pulsar, magnetized cracks in crust rel. to matter flow, radio, X-ray and optical emissions 80−72990
Al Crucis, eclipsing binary, photometric mass and radius ratios and configuration 80−109459
V444 Cygni, IR eclipse obs. and Wolf-Rayet wind structure 78−45357
CH Cygni, red giant, core convection rel. to mag. field interpretation for outburst 78−4250
CH Cygni, symbiotic star, 1977 outburst, radial vel. and atm. struct. determ. 80−72969
Cygnus X-1 (HDE 226868), accretion disc struct. rel. to long-term circular polarisation vars. 79−9031
degenerate C core, collapse triggering by thermonuclear burning 78−65608
degenerate C core, struct. during thermonuclear explosion 78−36558
degenerate C-O cores, degenerate C ignition afterclap 80−77390
degenerate C-O stellar core, struct. during C burning flash thermal phase 77−78774
degenerate dwarfs nonradial oscills., theoretical review 77−87398
degenerate matter, pionisation *(Russian)* 77−91558
degenerate star, propagating slow deflagration front struct. and evolution 79−84790
degenerate stars, force-free mag. fields stability 78−49425
dense matter star, limiting mass 80−101611
dense plasma, form. during stellar evolution 80−77281
dense stellar cores, time-dependent neutrino transport dependent neutrino transport 80−94783
differentially rotating gaseous polytropes, second-order perturb. theory 80−21990
differentially rotating gaseous polytropes construction of const. mass solar model 80−82338
distorted stars, Clairaut coordinates and vibr. stability 80−90408
double shell source star, successive He shell flashes anal. rel. to stationary shell burning 80−51737
double shell source stars, He shell flashes 77−56909
BY Draconis, area and temp. of surface spots *(Russian)* 77−64775
BC Draconis, double-mode Cepheid, mass, luminosity and evolution 77−29845
BY Draconis syndrome among dMe stars, rotating spotted star model 78−16428
dwarf Cepheids, double-mode, theoretical periods and masses 79−44488
dwarf novae, accretion disc struct. rel. to soft X-ray emission 77−45457
dwarf novae, mass transfer instabilities and accretion disk structure 77−82243
dwarf novae, quasi-periodic oscills. and nonradial pulsations of accretion disks 80−46568
early-type stars, winds and expanding envelopes 79−21288
eclipsing binaries, sd-d and R Canis Majoris type, struct. and dimens. 80−82423
eclipsing binary stars, masses, radii and absolute magnitudes, comparison with theory 79−44520
eclipsing binary systems with disclike envelopes, light curve interpretation, appl. to HZ Herculis 78−65658
Einstein's field equations for charged static spheres of fluid, exact interior solns. 78−73892
ellipsoidal potentials of polynomial distributions of matter 80−46532
Emden-Chandrasekhar axisymmetric solid-body rotating polytropes, exact solns. for (n=0, 1 and 5) 80−109419
envelope meridional currents, penetration of core mol.-weight barrier 77−33474
equilibrium equations soln. for rapidly rot. stars 78−65601
equilibrium structures, of self-gravitating gas masses containing axisymmetric mag. fields 80−94708
ergoregion instability of rotating stars, eigenfrequency calc. 79−8835
ν Eridani, β Cephei star, pulsations periods from Fourier anal. of radial vel. changes 80−105246
evolved stars, thermal and nuclear modes coupling 79−84785
exploding shell, relativistic dynamics, spherically symmetric model 79−21271
extremely metal-poor stars, theoretical evolution and radial mode pulsational stability 78−28677
F-type star, main sequence, convection and photospheric granulation 80−90417
figure, Clairaut-Laplace-Lyapunov problem 77−25963
fluid bodies, rapidly rotating, struct. and stability in general relativity beyond ang. vel. peak 79−101139
gaseous configuration of star under convective equilibrium, generalised integrals involving elliptic functions 77−71107
gaseous discs with uniform rot., global stability 77−26000
gaseous rotating cylinders, thermodynamic stability anal. by linear series 78−81618
GD 154, variable white dwarf, pulsation modes 78−40928
general relativistic stellar evolution code 79−58317
general relativistic stellar stability towards non-adiabatic perturbations 77−41376
giant stars, mass loss before envelope ejection due to pulsational instability 80−72935
giant stars as progenitors of planetary nebulae, struct. anal. form. 80−109537
giant stars in M13, M92, NGC 6397 and M15, mass loss rel. to weak-G-band effect 77−78778
Gleise 490 AB (BD+36°2322), red dwarf binary, flares and starspots, rot. period determ. 80−77423
gravitational collapse, hydrodynamics 78−45318
gravitationally collapsing stars, core bounce rel. to mass ejection 77−33534
gravothermal instability in two dimensions 78−89395
HD 101065, Przybylski's star, pulsation mode identification from light variability freq. anal. 80−62152
HD 101584, effective viscosity in accretion disc 77−64804
HD 153919 (3U 1700−37), forbidden Fe XIV emission rel. to extended atmosphere struct. 78−16571
HD 21479, brightness microvariability and non-radial pulsations *(Russian)* 80−67754
HD 45088, BY Draconis binary, surface activity from high rot. vel., visible obs. 80−77425
HD 47732, young close binary in NGC 2264, photometry and struct. 78−57575
Henyey-type evolution code, appl. to stars with shell energy sources 78−61848
AD Herculis, eclipsing binary, spectroscopic obs. rel. to binary system struct. 78−73738
HZ Herculis (Hercules X-1), accretion disk precession period 80−73070
HZ Herculis (Hercules X-1), precessing twisted accretion disks 80−56973
DQ Herculis (Nova 1934), short-period oscills. modulation and pulsed emission lines asymmetry interpretation 80−22044
homogeneous ellipsoidal figures evolution 77−33333
hot degenerate stars in steady-state accretion, thermal stability 78−40929
hot neutron star, form. and neutrino radiation rel. to envelope outburst 78−45350
hot stars, line-driven Rayleigh-Taylor-type instability 78−53927
hot white dwarf, radial oscill. mode nonlinear calc. 80−67713
HR 1225, δ Scuti star, pulsation freqs. meas. rel. to absolute magnitude, effective temp. and mass 80−109436
hydromagnetic instabilities in polytropic stars containing toroidal magnetic fields 79−8905
hydrostatic and thermal equilib. eqns., soln. in Eulerian coords. 77−17546
HZ 43, He abundance and stellar struct. from soft X-ray spectra 80−72944
incompressible stars, in bimetric gravit. theory 77−33329
instability, broadened definitions for stars in thermal imbalance 78−16397
interacting binary stars, book 79−8953
IRC+10216, spatial spectra from 2.2 to 20 microns, deviations from spherical symmetry 80−41911
Lamb freqs. of spherical gaseous star 79−66997
Lane-Emden eqn. of index 5, geometric technique for M-solns. 78−61851
Lane-Emden eqn. soln. using Pade approximants 77−82217
Lane-Emden equation for index 5, non-elliptic soln. 77−41377
Lane-Emden functions, concise approximation formulae 77−33467
Lane-Emden problem, series soln. 78−36559
late type giants, nonlinear coupling between pulsation and convection 77−13356
late-type stars, gravit. phase transitions 77−49380
late-type supergiants, atmospheric struct. from freq. depend. diam. 77−56924
linear stability anal. by inverse iteration method 77−33469
linear stellar structure model in general relativity 80−94709
local stellar stability, general nonradial adiabatic case 78−28654
local stellar stability, theory 77−5521
β Lyrae, emission sources and gas streams *(Russian)* 79−92802
RR Lyrae stars, instability strip red edge depend. on luminosity and comp. 77−53600
RR Lyrae stars, light vars. double periodicity rel. to internal struct. changes 77−87423
RR Lyrae stars, multiperiodic, pulsation theory 77−87431
RR Lyrae stars, pulsation theory and multiperiodic variables 77−87429
RR Lyrae stars, semiconvection and period changes 79−30072
RR Lyrae stars models, radial pulsations 80−26863
magnetic configurations linear oscills., unrestricted second-order tensor virial eqns. 79−44461
magnetic star model, circulation within nuclear burning shell rel. to latit. depend. chem. comp. *(Russian)* 79−16940
magnetic stars, convective stability 80−94781
magnetic stars, models with toroidal fields and circulation 77−45406
magnetic stars containing mixed poloidal and toroidal mag. fields, adiabatic stability 80−67706
magnetic stars structure, calc. of models *(German)* 77−17592
magnetised gravitating cylinders equilib. struct. 78−96471
main sequence (MS) stars chemical structure, influence of pre main sequence evolution 79−35247
main sequence stars, linear series of models, supermassive stars 77−91515
main-sequence binary stars, Roche consts. 79−35297
main-sequence massive stars, mass loss effects on struct., appl. to Wolf-Rayet stars 78−93200

stellar structure continued
main-sequence stars envelopes, hydrodynamical instabilities constraints from Li, Be and B obs. 78−93202
massive cold spherical stars, rest-mass density and redshift 80−56859
massive highly evolved star, Ne-rich layers, explosive burning and nucleosynthesis 80−94780
massive main-sequence star, early evolution 80−62113
massive neutron star, fermionic matter, coupled Dirac-Einstein eqns., self consistent soln. 78−73731
massive star core collapse, eqn. of state and composition near β equilib. 80−82335
massive star Ne and C zones, supernova explosion producing Mg and Al 80−90406
massive stars, nonradial pulsational instability 77−56908
massive stars, single and binaries, evolution review 80−82343
massive stars ($M \gtrsim 50$ M⊙), binary star mass transfer model rel. to evolutionary status *(Russian)* 80−109425
massive stars advanced evolution, struct. during Si burning 78−28652
massive stars losing mass and ang. momentum, evolution 79−25591
meridional circulation caused by stellar rot., general vel. eqn. 79−62818
metallic line (Am) stars, temp., age, rot. and pulsation rel. to metallicism 78−49448
metallic-line stars, theoretical pulsation models 79−97004
MHD equilibrium figures with magnetic field 77−45303
Mira variables, envelope pulsational instability rel. to planetary nebula form. 80−26928
Mira variables, pulsation and mass loss 79−25608
models with small-scale magnetic fields *(Russian)* 79−92754
moment of inertia of rigidly rotating star, influence of nonsphericity and radiation press. force 78−28658
1 Monocerotis, δ Scuti star, oscillation modes from photoelectric radial vels. and BVRI photometry 80−51787
multiple periodic variable stars, IAU Colloquium, Budapest, Hungary (1-5 Sep., 1975) 77−87422
neutrino opacity, pure neutral vector boson contrib. 78−53928
neutron star, accreting, magnetopause struct. 78−65647
neutron star crusts, nuclear crystals form. *(Polish)* 77−17355
neutron star envelopes, nuclear energy release and X-ray emission 77−78814
neutron star interior plasma, mag. field rel. to pulsar periods long-term changes 80−22029
neutron star interiors, presence of force-free mag. fields 78−40983
neutron star matter, abnormal phase 78−20849
neutron star structure, microscopic interpretation 77−64790
neutron star structure from X-ray timing obs. of pulsating X-ray sources 79−5917
neutron star torsional oscills., period determ. 80−90464
neutron stars, disk accretion, transition zone radial and vertical structure 80−4393
neutron stars, dynamics and structure 79−97017
neutron stars, electrodynamics of disk acrretion, magnetic field structure 80−85973
neutron stars, eqn. of state for dense hadronic matter, asymptotic freedom 78−36627
neutron stars, general relativistic eqns. 77−33471
neutron stars, hadronic matter components, leptons and baryons *(Polish)* 79−88587
neutron stars, implications of dense neutron matter physics 80−77277
neutron stars, mass and radius with neutrino retention 79−62817
neutron stars, mass-radius relation 80−77444
neutron stars, max. mass and moment of inertia from superdense neutron matter theory 78−45349
neutron stars, maximum mass, Brans-Dicke theory 77−33543
neutron stars, nonradial oscills. and micropulses 80−67766
neutron stars, nonrotating, eqn. of state and bounds on mass 77−45477
neutron stars, nonrotating, mass and moment of inertia bounds 79−2551
neutron stars, nonuniform rotating struct. and mass *(Russian)* 77−91559
neutron stars, nuclear fusion and C flashes 78−93293
neutron stars, pion condensate form. rel. to cooling 80−77443
neutron stars, props. of condensed matter in huge mag. fields 80−82187
neutron stars, pulsation damping due to interior weak interaction processes 80−77439
neutron stars, rapidly rotating, pulsations and gravit. radiation 78−65646
neutron stars, relativistic fluid spheres appl. 79−5855
neutron stars, review of nuclear physics 79−92797
neutron stars, rotating, form of quantum vortex filaments 80−67770
neutron stars, rotating, moments of inertia in bi-metric theory of gravitation 80−90466
neutron stars, slowly rotating, radial perturbations, stability 80−98685
neutron stars, structure and physics 79−67046
neutron stars, test of quark bags and interacting neutrons models 77−78812
neutron stars, thermal-timing instability rel. to pulsars period jumps 79−35293
neutron stars, thermal/timing instability rel. to pulsar timing obs. and X-ray transients 79−92795
neutron stars, transformation between two kinds *(Chinese)* 79−80332
neutron stars outer crust, theory of electron solids in superstrong mag. fields 80−4640
neutron stars structure, determ. from pulsars and compact X-ray sources 80−77442
neutron stars thermal properties and detectability, cooling and heating processes 80−31323
Newtonian spheroid, homologous oscill., gravit. radiation 80−46533
non-radial oscills. of 1 M⊙ star with initial chemical discontinuity 80−82341
non-spherical stars, appl. of smoothed particle hydrodynamics theory 78−12203
non-synchronous stars in close binary systems, stability 79−40223
nonlinear running density waves in homogeneous model *(Russian)* 78−49421
nonradial oscillations, theories and obs., review 77−26003
nonradial oscills., eigenvalue multiplicity 80−51740
nonradial oscills., modal analysis by asymptotic method 80−21996
nonradial stellar oscillations, avoided crossing of modes 77−60748
nonradially oscillating star, light and radial vel. vars. 77−91514
nonspherical thermal instability *(Russian)* 79−67000
Nova Delphini 1967, envelope struct. from He I triplet lines *(French)* 77−56939
stellar structure continued
nova envelope model and total energy considerations 77−82250
novae, accretion disk stability 77−82244
novae, temp.-density profiles rel. to explosive hot CNO-Ne cycle H burning 79−44489
novae, transition zone oscills. inception 77−87402
novae flare-ups theory, exact analytic self-similar solns. 79−35269
novalike object in Vulpecula, UV decline and expanding cooling photosphere 80−67741
O-type stars, winds and coronae struct. from Hα line-profile anals. 78−40947
opacity, electron correl. effects in photon-electron scatt. 77−64634
opacity, review 77−26002
22 Orionis, nonradial m-mode changes in 53 Persei variable 80−72939
oscillations, pure perturbation spectra of convectively neutral fluids 77−41292
partial ionisation zones, eqns. of state 78−28653
β Persei (Algol), red and IR wide-band photometry rel. to struct. 78−20853
β Persei (Algol) system, gravity darkening rel. to struct. 79−44525
photosphere oscillations, PEPSIOS spectrometer search 78−93203
photospheric vel. structure of long-period variable stars 79−53815
planetary nebulae central stars, pulsational instability and rapid variability 77−45439
planetary nebulae central stars, struct. and evolution 78−12325
planetary nebulae nuclei, core masses rel. to He shell flashes, nebula ejection and distance scale 78−24540
Poisson's eqn. numerical soln. for flattened centrally condensed objects, stellar models 79−35110
polytopes, Lane-Emden eqn. solns. 79−96994
polytrope n=3, with toroidal mag. field, nonradial oscills. and stability 77−9738
polytrope of index 5, proof of its finiteness 78−40920
polytrope of index three, parameters 79−62819
polytropes, hydrostatic equilibria in rotating objects 79−80300
polytropes, uniformly rotating, equilib. struct. investig. using iterative method 78−32441
polytropes in central orbits, Roche problem 80−82179
polytropic gas bodies, stability problem *(Chinese)* 79−16937
polytropic star, equilib. poloidal mag. field, finite difference-finite expansion method, Fortran program 77−13322
Population I 15 M⊙ star, effect of mass loss and semiconvection 78−45320
Population I stars, chem. and physical props. 77−78782
protostars, hydrostatic models evolution rel. to star form. process simulation *(Polish)* 80−21998
protostars, magnetic, struct. and quasistatic contraction due to mag. flux leekage 80−98662
protostellar envelopes of masses 3 M⊙ and 10 M⊙, struct. and hydrodynamic evolution 80−36616
protostellar H_2O maser sources, disc struct. 79−48784
pulsar crust, crust, infinitely magnetised H atom theory 80−77282
pulsar nucleus, superconducting vortex systems *(Russian)* 79−8935
pulsar polar cap, inhomogeneous struct. and radiation processes 79−25623
pulsar polar caps, pair form. and struct. of low altitude accel. zone 79−92790
pulsars, interpulse emission struct. 80−36652
pulsars, magnetogyro ratios rel. to core-crust decoupling and evolution 79−8937
pulsars, neutron crystal theory *(Polish)* 77−61369
pulsars outer crust, influence of mag. field on comp. 80−101610
pulsating stars, modal selection theory rel. to double-mode Cepheids 80−82372
pulsating stars asymptotic theory, boundary layer method 80−82389
pulsating variables, statistical theory of turbulent convection *(Chinese)* 78−28703
pulsation g-modes and p-modes, definition for self-gravitating fluid 77−41291
pulsation theory, recent developments 79−84786
pulsational instability of accretion disks to axially symmetric oscillations 79−16938
pulsational stabilities of star in thermal imbalance, comparison between methods 78−45316
pulsational stability, magnetic field influence 79−53800
pulsational stability of very low mass stars on H and D main sequences 77−17544
pulsations, nonlinear coupling 80−62115
ρ Puppis, line profile variable, pulsational mode-typing 80−90432
quark stars, eqn. of state and possibility of existence 77−45471
quark stars nonexistence 79−62855
radial gas oscills. after explosion shock wave passage *(Russian)* 79−8903
radiostars, polytropic models 79−2544
rapidly rotating models with radiation press., struct. parameters calc. 80−67697
rapidly rotating pre main sequence stars, struct. and evolution in gravit. contraction phase 80−62133
red giant stars, evolutionary sequences and struct. 78−65611
red giant stars, meridional circulation and CNO anomalies 79−48786
red giant variable stars, pulsation mechanisms rel. to multiple periods 77−87427
red giants, convective He shells, s-branch nucleosynthesis during thermal pulses 80−90410
red supergiants, envelope dynamical instability and lower mass limit for C detonation supernovae 77−17553
relativistic star, rotating shell model 79−88650
relativistic stars, struct. and stability of polytropic fluid spheres with negative index *(Chinese)* 80−57143
response function to energy and mass transfer 77−60749
response functions and secular modes 80−17572
rigidly rotating stars, secular instabilities in general relativity, theoretical formalism 80−4341
rigidly rotating stars, secular instabilities in general relativity, numerical results 80−4342
Roche and Darwin problems for polytropic stars, numerical study 79−75202
Roche lobe formation in highly eccentric X-ray binary systems 80−41858
Roche-lobe overflow and massive X-ray binary systems 79−35301
rotating fluids, convective modes and convective stability 79−16818

stellar structure continued
rotating magnetic polytrope, equilib. struct. and oscill. with large mag. field 77−87366
rotating magnetic polytrope, equilib. struct. with large toroidal mag. field 77−87367
rotating magnetic stars, existence of bifurcation point 78−53924
rotating magnetic stars, internal circulation and mag. field struct. 77−45405
rotating magnetic stars, nonradial oscill. mode splitting 80−77414
rotating main-sequence stars, appl. of strained coordinate methods to struct. 77−56910
rotating Newtonian stars, secular instability to gravit. radiation and viscosity 78−53922
rotating relativistic polytropes, integral characts. and internal struct. *(Russian)* 77−91513
rotating star oscillations, low-freq. gravity modes 79−16934
rotating stars, 7 and 10 M⊙ stars evolution with time-depend. redistrib. of ang. momentum 78−36553
rotating stars, core struct. and evolution 77−13316
rotating stars, luminosities and radii of models with circulation-free rot. laws 77−67088
rotating stars, meridional circulation in surface layers 78−20820
rotating stars, non-radial oscills. rel. to cataclysic variables short-period light oscills. 78−32477
rotating stars, secular instability from thermal cond. 80−21986
rotating stars secular stability, Lagrangian perturbation theory of nonrelativistic fluids 78−49305
rotating variable stars, surface features and period-radius-rot. vel. relation 79−2546
σ Scorpii, β Cephei star, pulsations periods from Fourier anal. of radial vel. changes 80−105246
V367 Scuti, double-mode Cepheid, pulsation mass calc. 77−67102
δ Scuti, line profile variable, pulsational mode-typing 80−90432
δ Scuti and RRs stars, observational view of multiperiodicity 77−87432
δ Scuti and RRs type variables, theoretical aspects 77−87433
δ Scuti stars, empirical period-luminosity-colour relations 79−25610
self accreting stellar winds 80−101588
self-gravitating fluids in perturbed configurations, perturbational-variation procedure for normal modes 78−32336
self-gravitating fluids normal modes, expansion of g- and p-modes of non-adiabatic fluid 78−32337
self-gravitating rotating masses, book contrib., review 80−21915
semiconvection and vibrational stability of stars of about $1M_{\odot}$ 77−22204
semiconvection as occasional breaking of weakly amplified internal waves 79−48778
shell ejection in nova outbursts, time before max. 77−2441
shell flashing stars, core masses rel. to ^{22}Ne as neutron source for s-process 80−72926
slow nova, hydrodynamic study of outburst 78−40954
solar-type stars, mag. cores stability 79−44472
spherical gravitating systems, radial vel. dispersion at outer regions *(Russian)* 78−61720
spotted stars, spot sizes 80−41812
stars in thermal imbalance, vibrational stability 78−40916
stars with given entropy distrib., struct. eqns. 79−66993
static models with varying He core mass, linear series of 7 M⊙ star 78−65603
static stars, mathematical curiosities in Newtonian and general relativistic aspects 77−74045
static stars, spherical symmetry in general relativity 77−45397
static stellar models with He cores 77−17542
stationary accretion disk surrounding black hole, structure assuming vertical distribution given by polytrope 78−20851
strong internal mag. field diffusion through radiative envelope of 2.25 M⊙ star 78−85931
Sun, nonradial oscills. of 1968 nonstandard solar model 79−35218
superdense celestial bodies, theory 80−67773
superdense configuration, internal struct., effect of nucl. interactions *(Russian)* 77−13324
superdense magnetised astrophysical objects, interiors physical conditions 80−17603
superdense matter eqn. of state, nuclear size correction to relativistic Thomas-Fermi model 78−29413
superdense stars, internal density distrib. rel. to mag. dipole moment, quantum theory 79−92753
superdense stars, state of matter *(Japanese)* 77−29643
supergiant photospheres, large turbulent elements 79−75206
supergiant stars with degenerate neutron cores, equilib. models struct. 77−33472
supergiants, early-type, with mass loss, two-core model and evolutionary status *(Russian)* 80−109425
supermassive star, expanding, and contracting dust shell, Einstein's theory of gravit., black hole formation 78−12088
supernova core, Rayleigh-Taylor convective overturn rel. to explosion 80−77429
supernova envelope, temp. struct. rel to ^{11}B neutrino-induced prod. in C layer 80−82337
supernova interior, eqn. of state at subnuclear densities 80−77278
supernovae, anisotropic explosion of rotating, self-gravitating uniform spheroids 79−8822
supernovae, effects of core eqn. of state on outcome of stellar collapse 80−85928
supernovae, high temp. matter comp. and adiabatic index rel. to collapse 79−44354
supernovae, lepton-driven convection in collapsing cores 79−84811
supernovae, radiation dynamics, envelope ejection and light curves 77−64783
supernovae, self-similar oscillations of gas *(Russian)* 79−17001
supernovae, shell struct. in models with gradual energy release 77−78807
supernovae, Type I, ejected envelope struct. 78−65636
44 Tauri δ Scuti star, periods, least-squares determ. 79−62850
thermal props. of self-gravit. plane-symm. gas 77−13323
thermally dissociated matter, comp. and eqn. of state 77−33476
tidal torques on accretion discs in binary systems with extreme mass ratios 79−40224
tidally distorted configurations, external form and potential, third-order approx. 80−41714
tidally distorted stars, form factor method for struct. determ. 80−21991
tidally-distorted stellar models small oscills., Roche coordinates appl., second-order terms effect 79−44462
stellar structure continued
U Trianguli Australis, double-mode Cepheid, mass, luminosity and evolution 77−29845
turbulent convection, spectral model 77−33465
Universe, high density matter, many body treatment, pulsars 80−26738
unstable gravity modes, asymptotic representation 78−28656
unstable models, solns. for dynamical rupture of equilib. 77−56913
unstable modes of an equilibrium, number calc. 80−36493
unstable modes of equilibrium, topological props. 78−65606
upper main-sequence stars, envelope opacity rel. to tracks in H-R diagram 77−49379
W Ursae Majoris stars, convective envelope struct. rel. to light curves 77−57008
W Ursae Majoris systems, struct. and evolution 77−45488
W Ursae Majoris type contact binaries, theories, observational tests 79−97026
very close binary systems, struct. eqns. including rot. and tidal distortions for ZAMS stars 80−22037
very compact rotating stars, existence of ergoregions 78−24523
vibrational stability of stars in thermal imbalance, energy methods 77−13320
α Virginis, β Cephei type pulsation characts. 80−56835
weak G-band stras, nature and evolution from spectrum anal. of (HD 91805) 78−49432
white dwarf in binary system, outer layer C and O enrichment from companion 80−109465
white dwarfs, atmosphere structure rel. to composition in hot stars 80−98658
white dwarfs, degenerate magnetic, limiting mass and central density estimation 78−65622
white dwarfs, equilib. configs. with frozen-in mag. field 78−8008
white dwarfs, mass and radius with neutrino retention 79−62817
white dwarfs, physics of structure and evolution 79−25606
white dwarfs, rapid mass accretion and extended envelope form. 80−67723
white dwarfs, rapidly rotating, pulsations and gravit. radiation 78−65646
white dwarfs, rigidly rotating, critical ang. vel. and equilib. configurations 77−5525
white dwarfs, rotating magnetic, equilib. struct. 78−49433
white dwarfs, struct. and evolution theory rel. to EUV obs. and spectra 80−82356
white dwarfs, virial theorem, energy content and mass-radius relation 78−45327
white dwarfs and giant planets 79−16955
white dwarfs external layers, ingerpretation of spectra 79−62824
white dwarfs mass-radius relation, constraints on gravit. const. 79−25464
white dwarfs seismological theory for 1 $M_{\odot}$ model with crystalline core 80−17577
white dwarfs undergoing spherically symmetric steady-state accretion, stability 80−77402
Wolf-Rayet atmospheres, structure and composition 80−98668
X-ray binaries, double core evolution 79−84816
X-ray sources, pulsating, torque vars. and stellar response rel. to period vars. 79−9029
X-ray sources, steady accretion discs general struct. with mag. field 80−8714
Yang-Mills gauge theory of gravity, gravit. field of spherically symm. matter distribs. 78−4773
young stars, nonspherical thermal instability 79−48779
C cores, evolved, nuclear energy generation rates and energy dissipation 80−82339
C-O white dwarfs, C-O eutectic model 80−77405
Ca II H- and K-line complex structure in HD 190073 (A0ep-type) 77−60775
H and He, thermodynamic props. and eqns. of state in stellar conditions thermodynamic props. and eqns. of state in stellar conditions 79−35241
H_2O masers assoc. with late-type variable stars, structure 79−71037
He stars, struct. and post-giant evolution 77−56947
Mn-Hg stars, surface gravity and stellar temp. derivation from uvbyβ data, statistical anal. 80−82397
OH maser sources, envelope struct. from interferometric obs. 77−53583

stellar variables *see variable stars*

stellarators
AC Tokamak, design criterion 80−38726
Asperator NP-3, nonplanar helical mag. axis system, line of force, toroidal effect 80−70020
Asperator NP-3, toroidal device with nonplanar mag. axis, current equilib. 80−48932
Asperator NP-L stellarator, mag. field config. meas. 80−92367
CLEO, helical winding, design, construction and installation 80−43958
CLEO stellarator, heating, confinement and fluctuations 80−24225
CLEO stellarator, low and zero current plasma confinement 80−83983
Cleo stellarator, neutral beam injection heating 80−28714
coil systems, modular, for stellarator fields 80−6274
current turbulent ion heating, modulation instability 80−79525
current-free stellarators, RF and neutral beam heating 80−28853
cyclotron self-absorption in two-temp. plasma, temp. and density meas. 80−48987
divertor fluxes in stellarators and torsatrons, azimuthal distrib. 80−6216
drift instability, stabilisation by AC elec. field *(Russian)* 79−7459
electron cyclotron plasma radiation, in L-2 stellarator *(Russian)* 79−4178
energy confinement comparison of ohmically heated stellarators to Tokamaks 80−92360
enhanced plasma loss due to secondary currents, Tokamaks and non-Ohmic stellarators 77−65884
equations of motion calcs. 80−103198
equilibrium and stability calcs. 80−83982
ferromak, ferromag. wall shaping for linked min-B config. 80−24233
Ferromak, helical mag. configuration produced by ferromagnetic materials 80−48936
fields, m=2 tearing mode, linear growth rate 80−75037
helical stellarator, Asperator NP-3, toroidal discharge forbidden region 80−79592
helical winding, stress analysis of supporting tube 77−19776
helical winding geometry modulation and optimisation 80−79549
high beta MHD theory, stellarator equilibrium and stability, mirror traps and reverse field machines 80−28778
high beta stellarator, l=2,3 helical fields, stabilisation effects 80−28779

stellarators continued
high beta stellarator stability theory 80−28797
high-β, with low compression ratio, wall stabilisation 77−27697
ion temp. and parametric decay development in RF-generated stellarator plasma 80−79436
JIPP T-II, neutral beam injection system, design and expt. test 80−106226
Josephson junctions, applications in plasma physics 80−103194
Kharkov stellarators, plasma-wall interactions 80−79552
L-2 stellarator, current equilibrium and effective ion charge 80−24228
L-2 stellarator, ohmic heating discharges with gas puffing 80−79593
L-2 stellarator, ohmic heating ion component characts. and particle lifetimes *(Russian)* 78−59547
L-2 stellarator, solid H_2 pellet injection parameters and effects 80−28775
linear theta pinch Isar II, low compressed high-β stellarator, surface effects 77−76161
low frequency parametric processes in magnetically confined plasmas 80−28827
magnetic hill effects on equilibrium 80−79558
magnetic surfaces, destruction near separatrix, attributed to perturbations of mag. fields 78−38554
MHD equilibrium and stability of plasma in toroidal geometry, 3-D computer code 80−70041
MHD instabilities, stabilisation in current-carrying stellarator 79−86582
MHD instabilities in current carrying stellarator, stabilisation 79−64848
modular coil design for 2.1 m radius device 80−79548
neutral injection heating of CLEO stellarator−theory and experiment 80−28755
particle orbits and toroidal vacuum fields 80−79450
plasma energy balance, in L-2 stellarator, with ohmic heating *(Russian)* 79−4179
plasma equilibrium currents, effect on separatrix characts. in l=3 stellarator 80−64706
plasma losses, quasi-neoclassical law 80−79544
positional stability of a current-carrying plasma in an l=2 stellarator field 80−106906
pressure effects, plasma equilib. evolution *(Russian)* 80−10418
R-OM stellarator, MHD resonant HF heating 80−79518
research status 80−74013
review 77−47239
review 78−30467
Saturn, drift oscills. characts., high shear stabilisation *(Russian)* 79−98887
Saturn stellarator-torsatron, collisionless plasma diffusion 77−1011
Scyllac, theta pinch implosion, gross plasma motion model and feedback stabilisation 77−24141
stationary RF discharges of stellarator configuration, meas. with ion sensitive probe 79−60194
high-β stellarator with l=3, stability 77−7529
superbanana diffusion of plasma, effect of fluctuating elec. fields 77−62330
toroidal field production by modular systems 80−10441
toroidal vacuum fields, particle orbits 80−79445
torsatron, superconducting mag. engineering design 80−99297
torsatrons, neutral beam injection calcs. 80−48949
Uragan-2, microwave radiation, energy transfer and transmission coeffs. meas. *(Russian)* 79−98915
Uragan-2, ohmic heating, charged particle anomalous diffusion, turbulence, gravitational drift instability *(Russian)* 77−47150
Uragan-2, ohmic heating, hard X-ray emission from electron-wall interaction *(Russian)* 77−47215
Uragan-2 helical winding, metal-GRP struct. form. 80−6289
W VII-A, neutral injection 80−83960
W VII-A (2,1) tearing mode depend. on stellarator field 80−79550
W VII-A stellarator, m=2 mode at q=2 80−24227
W VII-A stellarator, neutral injection, heating efficiencies, deposition profiles 80−79524
W VII-A stellarator, Ohmic heating, energy and particle confinement 80−24226
W VII-A stellarator, particle and energy transport 80−83222
W VII-A stellerator, line emission, poloidal and toroidal asymmetry 80−79578
WEGA stellarator, lower hybrid heating 80−79515
Wendelstein VII, neutral beam injectors, HV power supply system, thyristor control 80−99332
Wendelstein VII-A, neutral beam injectors, performance 80−99389
Wendelstein-VII A, charge exchange atoms yield, elliptic cross-section effect *(Russian)* 79−98950

STEM *see scanning-transmission electron microscopy*

step motors *see stepping motors*

step-recovery diodes *see charge storage diodes*

step response
see also transient response
accelerometer, induction generator type transient characts. and Law-Novotny expression development *(Japanese)* 79−88921
eye, vergence movements, heuristic feedback system model 77−21517
linear stable structure maximax response estimates compared 79−68626
piezoelectric plate, infinite, on elastic medium, transient response to pot. pulse 78−52442
saccadic and vergence eye movements, reciprocal innervation model 78−31811

Stepanov method *see crystal growth from melt*

stepped motors *see stepping motors*

stepping motors
chart recorder and plotter assimilation 79−93128
differential ball screw actuator driven deformable mirror design and performance 80−33137
digital control system for repetitive scanning of a monochromator 78−54355
drive, gamma-ray transmission meas. instrument for boiler tube corrosion investigation 77−9011
drives for use in synchronous interlock systems for cinematographic special effects 80−98991
fast beam scraper, stepping motor control 79−71562
film camera construction impact of electronics *(German)* 77−79170
graphics plotter using linear step motors 79−93127
laser grating mount drive unit modification 80−87402
lenslet-array optical device for paginal information reproduction 79−27194
stepping motors continued
mechanical actuator, stepper motor, appl. to control of scientific apparatus 78−62683
microcomputer mechanical proportional control for solar energy appls. 80−50987
microprocessor controlled for 100 kJ CO_2 laser beam alignment system 77−54035
multiaxis neutron diffractometer automation 80−102417
observatory scanning spectrophotometer *(French)* 78−20638
pneumatic amplifier pump, for supercritical fluid chromatography, control and programming 78−88665
presettable digital control for neurophysiological microelectrode drive 78−36079
'shutter' drive, using monostables 78−35860
timber volumetric meter angular displacement control *(Russian)* 80−57253
translation motors for position with micron precision *(German)* 80−86271

stereo amplifiers *see audio-frequency amplifiers*

stereoisomerism *see isomerism*

stereoscopy *see vision*

stiffness constants *see elastic constants*

stimulated Brillouin scattering
acetone, wave front reversal for depolarised light 79−3743
amplitude and phase time oscills. noise *(Russian)* 80−87435
anisotropic medium, stress induced, stimulated backscatt. 78−1304
atmospheric turbulence, phase distortions, correction via nonlinear optical techniques 77−88855
backscattering, Brillouin mirror theory, specified field approx. 77−62010
backward stimulated scattering, comments 80−9953
backward stimulated scattering, reply to comments 80−9954
benzaldehyde, wavefront reprod. obs. by stimulated Brillouin, Raman scatt. 80−53369
benzene, stimulated diffusion induced by two photon absorption *(French)* 78−90455
carbon tetrachloride, Stokes wave phase fluctuations in stimulated light scatt. *(Russian)* 80−87436
chloronaphtalene, stimulated diffusion induced by two photon absorption *(French)* 78−90455
complex conjugation of fields, vol. hologram analogy 77−58388
coupled Stokes-antiStokes processes 80−9943
depolarised radiation, stimulated scattering, wave front reversal effect 79−86217
dynamic holograms for light stimulated scatt. 79−89964
EBBA, self-focusing, stimulated Brillouin scatt. 77−75625
electrolytic solution, stimulated Brillouin scatt. gain 77−75618
EM wave, stimulated Brillouin scatt., transverse static mag. field effect 80−50355
expanding laser plasma, stimulated Mandelstam-Brillouin scattering *(Russian)* 78−38502
extended media, pulse form., intensity modulation 77−50727
Faraday effect on stimulated backward scatt., theory 77−34910
fibre Raman and Brillouin laser gains, polarisation effects 80−9887
fluids, Rayleigh-Brillouin scatt., nonlinear spectroscopy 77−50731
high efficiency Brillouin laser analysis, wavefront reversal influence on operation 79−23026
induced scatt. amplifier with wide band pumping, information signal transmission 78−83035
internal transverse resonator, stimulated Mandelstam Brillouin scatt. component self-synchronisation *(Russian)* 80−48345
ionosphere, possible generation by Eiscat radar 77−37478
ionosphere, stimulated Brillouin scatt. and incoherent backscatter 77−78552
ionosphere, stimulated Brillouin scatt. detect. by Jicamarca radar 78−77412
kinematics and dispersion relation for Brillouin scatt. process, wave vector surfaces representation *(German)* 78−19492
laser beam, diverging, conversion into plane wave by dynamic vol. hologram 79−18376
laser beam intensity ratio increase by possible use of stimulated Brillouin and Raman scatt. 80−5796
laser heated solenoid, Faraday rot. effect 78−71511
laser induced, asymptotic residual pump transmission characts. anal. 77−38988
laser Q-switching mechanism by intracavity stimulated Brillouin scatt. 80−106552
laser resonator, stimulated Mandelstam-Brillouin scatt. component synchronisation *(Russian)* 80−48346
laser system with phase conjugation, stimulated Mandelstam-Brillouin scatt. 80−5786
laser-plasma interaction, stimulated Brillouin to stimulated ion Compton scatt. evolution 78−42762
laser-target self-adjusting system, wavefront reversal by stimulated Brillouin scatt. mirror 79−14024
lattice vibration nonlinear interaction with powerful light beam 78−46711
mirror, selective props. improvement using wide band pumping 77−88863
mirror, short high-power pulses obtained by wavefront reversal 80−99801
mirror, wave-front inversion of laser output 79−14038
molecular crystal, Mandelshtam-Brillouin scatt., dipole-plasma oscills. 80−1278
N two-level atoms, quantum theory of nonlinear optical phenomena 80−5790
nonlinear optical phase conjugation for laser systems 78−79072
nonlinear optical phase conjugation for pulsed laser systems 78−59092
nonlinear optical resonator filled with Raman or Brillouin active medium, theory 77−50722
nonlinear selection of optical radiation on refl. from stimulated Mandelstam-Brillouin scatt. mirror *(Russian)* 80−28280
nonmonochromatic radiation stimulated scatt., efficiency depend. on pump radiation statistics 80−95950
optical cavity plasma, stimulated Raman and Brillouin scatt., electrostatic and EM waves 78−34324
optical fibre, high power narrow band laser radiation transmission, nonlinear optical processes 80−53443
optical fibre, nonlinear effects, appl. to active and passive device fabrication 80−58638
optical fibres, single-mode, Brillouin spectrum 79−46032

stimulated Brillouin scattering continued
optical fibres, single-mode, normal acoustic modes and Brillouin scatt. 79−76760
optical glass, laser bulk damage, stimulated Brillouin scatt. influence 79−59762
parametric oscillator, Brillouin, mode-locked optical fibre, bandwidth-limited operation 78−50851
phase aberration correction via stimulated Brillouin scatt. 78−37944
phase conjugated wavefronts by stimulated Brillouin and Raman scatt. 80−5791
phase conjugation by stimulated scatt. in waveguide, theory 79−3742
piezoelectric semiconductor, n-type, magnetoactive, Brillouin instability in magnetostatic field 80−78909
piezoelectric semiconductor, stimulated Brillouin scatt. of helicon waves 79−99571
piezoelectric semiconductor, stimulated Brillouin scatt. of laser radiation 79−95793
plasma, Brillouin and dielec. side-scatt. of 10 μm laser light 80−103156
plasma, Brillouin backscatt. depend. on density scale lengths near crit. density 80−43888
plasma, dense, nonlinear intense CO_2 laser beam interaction 78−22562
plasma, efficient saturation due to nonlinear ion wave decay 79−86585
plasma, enhanced Brillouin scatt. of Gaussian laser beam 79−94799
plasma, H_2, underdense, CO_2-laser radiation filamentation 80−14941
plasma, inhomogeneous, Brillouin backscatt. 79−19046
plasma, ion temp. meas. using stimulated Brillouin and Compton scatt. 77−58892
plasma, laesr beam self-focusing 78−30447
plasma, laser light scatt. 78−51312
plasma, laser light stimulated Brillouin scatt. 78−47129
plasma, laser prod., z-depend. absorpt. and stimulated backscatter processes 80−43944
plasma, mag. confined, stimulated Brillouin backscattering 78−51307
plasma, magnetised, relativistically strong circ. polarised pump wave scatt. 78−34330
plasma, parametric decay and Brillouin backscatt. instabilities, IR laser induced 77−47187
plasma, parametric instability saturation by electrostatic daughter wave nonlinear decay 80−53945
plasma, scatt. from resonance layer 77−19713
plasma, self-focusing effect on parametric back-scatt. 78−22510
plasma, stimulated Brillouin scatt. in laser plasma expts., review 79−10706
plasma, stimulated Brillouin scattering initiated by ponderomotive force density fluctuations 80−103129
plasma, stimulated Raman and Brillouin backscattering along mag. field 80−69983
plasma, weakly inhomogeneous laser-produced, stimulated Brillouin back-scatt. losses 80−19561
plasma critical surface, enhanced stimulated Brillouin scatt. due to light refl. 80−1750
plasma jet form. by focusing laser beam on plane target, investigation using wavefront method 80−75103
PMMA, threshold energy, stress effect 78−1304
pre-ionised plasma, side- and backscattering 80−92267
pump beam spatial amplitude and phase distrib. reproduction 77−75617
pump wave reproduction in stimulated scattering radiation *(Russian)* 78−83031
pump wave wavefront reversal in Brillouin mirror, influence of certain radiation parameters 80−9961
pumping wave reproduction 79−64280
quartz, molten, stimulated Mandel'shtam-Brillouin scattering in a magnetic field 79−76762
quartz, stimulated Brillouin scatt. correlation with laser induced damage 77−38984
quartz-liquid ^{4}He interface, saturation effects in phonon reflection 80−92736
quasisoliton pulses, head-on stimulated scatt. 79−27332
Raman laser, CW fibre, bandwidth reduction using prisms, gratings and etalons 80−53366
rescattering in plasma 80−87896
ruby laser, with stimulated Brillouin scatt. complex conjugate mirror 80−87438
self-focusing, limiting diameter mechanism 77−19371
self-focusing by Raman or Brillouin dispersion 77−23721
semiconductor plasma, magnetised, stimulated Brillouin scatt. 80−33085
SHG, parametric amplification and stimulated scatt. phenomena 77−38994
Stokes component wavefront, complex conjugacy with wavefront 77−88862
Stokes radiation, spatial struct. 77−50726
Stokes signal amplified under stimulated scatt. conditions, influence of pump field changes 79−59763
three dimensional, for focused Gaussian beam 80−69456
wavefront inversion in Stokes wave Raman conversion in oppositely directed pump beams 80−5797
wavefront reconstruction of complex signal in stimulated back scatt. 79−31996
wavefront restoration, ruby laser beam with multi-mode modulation *(Russian)* 77−38989
wavefront reversal, Mandelstam-Brillouin stimulated scatt. inertia *(Russian)* 79−98445
wavefront reversal, small-signal, during stimulated Brillouin scatt. in optical waveguides 79−94298
wavefront reversal, transverse enhancement of coherence of scatt. field 80−95952
wavefront reversal and short pulse generation using steady-state stimulated Brillouin scatt. 80−53381
wavefront reversal by stimulated Brillouin scatt., four-wave process 80−53382
wavefront reversal effect 79−41417
wavefront reversal limits of existence 79−10356
wavefront reversal of beam with incomplete spatial modulation, small-scale distortions 80−95953
wavefront reversal phenomenon appl. to induced Mandelstam-Brillouin scatt. *(Russian)* 79−59769
CF_4 Nd laser excited stimulated Mendelstam-Brillouin scatt. phase fluctuations *(Russian)* 80−89014
CO_2 laser-plasma interaction, stimulated Brillouin backscatter saturation 80−24175

stimulated Brillouin scattering continued
CS_2, coherent Brillouin spectrum, Raman induced Kerr effect, acoustic phonon excitation study 79−59754
CS_2, liq., wavefront restoration during stimulated Brillouin scatt. 78−18013
CS_2, wavefront reprod. obs. by stimulated Brillouin, Raman scatt. 80−53369
CdS, coherent interaction of externally generated 35 GHz of sound with light 77−43964
CdS, stimulated Mandelstam-Brillouin scatt. on acoustic phonon amplification *(Russian)* 80−71437
Ge reflectivity changes due to illumination by beams of unequal frequency 79−76749
H_2 gas target, stimulated Brillouin scatt., press. depend. 78−42764
n-InSb, Brillouin instability in magnetostatic field 80−78909
n-InSb, SBS of laser radiation in presence of mag. field, ion acoustic wave nonlinearity 80−45091
Te, CO_2 laser irrad. 79−47469

stimulated dielectric relaxation currents *see thermally stimulated currents*

stimulated emission
see also laser theory; lasers; population inversion
alkali halides, coloured, light amplification at activator centres 80−2795
alkali phosphate glass:Nd^{3+}, laser material evaluation 77−54715
anharmonic quantum oscillator stimulates EM radiation *(Russian)* 77−46715
anthracene crystal, stimulated emission and Raman scatt. 78−1303
anthracene-perylene energy transfer dye laser, gain meas. 79−59695
atomic spectra ionisation broadening under action of intense pumping wave *(Russian)* 77−42283
atoms, multiphoton rate equations, generalised 80−91525
atoms, spontaneous and stimulated emission 77−79788
atoms, transitions between highly excited levels, rel. to anomalous Balmer decrement 78−5176
biphenyl doped molecular crystals, stimulated emission at 4.2K 79−28790
blackbody radiation interaction with LF atomic transitions, Zeeman, Stark and stimulated emission 79−41127
bremsstrahlung, resonator consideration *(Japanese)* 80−5721
carbon tetrafluoride laser, emission spectrum in 16 micron range, CO_2 laser stimulation 80−9870
channelled electrons and positrons, quantum theory of spontaneous and stimulated emission *(Russian)* 78−49999
chlorophyll, fluorescence quenching, exciton annihilation excited state absorption and stimulated emission 79−98137
chlorophyll and Mg-free derivatives, lasing and stimulated emission 77−52742
chlorophyll-a, laser action and excited singlet state absorpt. 77−27288
chromophores, $^1O_2$, annihilation luminesc., in polymer matrices 77−88488
classical system, stimulated emission and absorpt., appl. to free electron laser 78−63047
coherent emission, caused by pulsed laser in low-density gas 79−18389
coherent spontaneous and stimulated emission, quantum theory 77−3557
complex molecule solutions, stimulated emission, light quenching *(Russian)* 78−33735
complex molecules, solns., stimulated emission by simultaneous 2-freq. excitation *(Russian)* 78−13701
complex organic vapor lasers, new active media, buffering gas influence 79−94213
complex solutions, stimulated radiation anisotropy, spectral depend. *(Russian)* 77−68085
cooperative emission of excited mol. monolayer into surface plasmons of metallic substrate 80−20666
cryogenic active media as Raman lasers, stray transverse stimulated emission 78−25927
cumarine derivatives, stimulated emission by laser and lamp excitation 79−72563
cyclotron resonance, gyrotron, review 77−34865
1,4-di-[2-(5-n-tolyloxazolyl)] benzene vapour, generation power, dependence on extraneous gas pressure *(Russian)* 77−50660
dibenzyl doped molecular crystals, stimulated emission at 4.2K 79−28790
Dicke state N two level atom assembly, radiation emission theory 80−69350
3,3-diethyl thiadicarbocyanine iodide dye, stimulated fluoresc. and stimulated reson. Raman scatt. relationship 80−91853
7-diethylamino-4-methylcoumarin acriflavine binary soln., laser pulse pumped 77−50670
diffracted stimulated emission induced by coherent crossed laser beams for conc. meas. 80−35585
diphenyl:naphthacene, relax. times of ground electronic state vibrational levels 79−19907
diphenyl:pyrene, self induced transparency under nonreson. excitation, luminesc. and stimulated emission 80−11436
diphenyl:pyrene, stimulated emission at 0-0 transition, 4.2K 80−11437
diphenyl with pyrene cryst., self induced transparency self stimulated excitation *(Russian)* 80−14403
dispersion of opt. characts. in amplification range, freq. spectrum of stimulated emission, calcs. *(Russian)* 77−54757
dye laser, CW, pumped, stable multifreq. picosecond pulse emission, phase-locked radiation pumping 80−91789
dye laser tuning range extension using electrochem. reaction products 79−31895
dye molecules, excited state lifetimes and lasing conditions, time-resolved spectroscopy 77−71983
dye solns., alcoholic, stimulated emission in blue and violet regions *(Russian)* 78−25874
dye solution, amplitude-spectral asymmetry of stimulated emission 79−10299
dye solution, polarisation of stimulated emission *(Russian)* 78−25872
dye solutions, light-induced quenching of spontaneous and stimulated emission *(Russian)* 78−27290
dye solutions, short-wavelength stimulated emission limit, induced absorpt. spectra 79−59696
dye solutions, simultaneous 2 or 3 band tunable emission, band competition 77−7082
Einstein theory of stimulated emission of radiation *(Hungarian)* 79−89880
electron-ion collisions, stimulated multiphoton bremsstrahlung 79−19007

stimulated emission continued
EM scatt. from active objects, negative and zero extinction cross-sections 79−13874
emission intensity, depend. on radiation field 79−3662
exciton systems, dense, laser action 77−75531
external transverse resonator, spectral and time characts. of stimulated scatt. *(Russian)* 77−85738
extragalactic radio sources, stimulated emission origin of radio recomb. lines 78−45418
extrinsic molecular crystal, luminesc. spectra, relax. of vibr. levels 79−87484
ferroelectric with impurity atoms, stimulated emission, effect of phase transition 79−15490
fluorene doped molecular crystals, stimulated emission at 4.2K 79−28790
fluorinated alkyl iodides, stimulated emission, laser appls. 77−27285
four level laser, Q-switched, dynamics and lifetime of terminal energy level *(Chinese)* 78−66832
free electron laser, classical, semiclassical and quantum field theories 77−14684
Fresnel formulas and law of stimulated emission 80−58489
glass:Nd laser materials, intensities of optical transitions 77−689
glass-Yb^{3+},Er^{3+}, laser pumped, 1.54 μm emission 77−50675
halide vapour, discharge, potential fusion laser systems 78−63074
highly excited atoms, blackbody radiation effects 80−58176
impure molecular crystals, ground electron state, vibr. levels, relax. time determ. *(Russian)* 78−15195
laser induced molecular predissociation, by stimulated emission or absorpt. of IR photons 79−54925
linear acceleration bremsstrahlung 79−92658
liquid intermolecular relaxation spectroscopy 79−95844
metal pure vapours, apparatus for stimulated emission obs. from transverse discharges 79−13954
metal vapour, explosively formed, apparatus for stimulated emission obs. 78−50764
metal vapour lasers excited by pulse trains 79−13955
Mossbauer coherent γ-radiation generation, collective and stimulated processes *(Russian)* 78−9356
multilevel molecular system, light pulse interaction 77−38699
multiphoton processes, equilibrium between radiation and matter 77−50713
N two-level atoms, interaction with radiation field in restricted rotating wave approx. 80−5713
N-two level atoms, interaction with radiation field in restricted rotating wave approx., numerical anal. 80−5714
naphthalene:$\beta\beta'$-dinaphthylethylene, phonons role 77−8606
naphthalene:$\beta\beta'$-dinaphthylethylene, stimulated emission suppression in phonon wing 78−2881
naphthalene:β-naphthyl-n-biphenyl-n-biphenylyl ethylene, relax. times of ground electronic state vibrational levels 79−19907
naphthalene:β-naphthyl-n-biphenylylethylene, cryst., ground electron state, vibr. levels, relax. time determ. *(Russian)* 78−15195
naphthalene, doped, role of nonequilibrium phonons in stimulated radiation emission 80−103971
naphthalene doped molecular crystals, stimulated emission at 4.2K 79−28790
naphthalene in various crystals, luminesc. and stimulated emission on laser irrad. *(Russian)* 77−48236
napthalene:pentacene, zero-phonon transition bottlenecks, photon echo detect. 80−33092
narrow gap semiconductors, stimulated emission characts. 79−31903
narrow gap semiconductors, stimulated plasmon emission 79−73461
negative light absorption by medium with selective freq. modulation of quantum oscillators 80−106501
neutral radiant gas, kinetic eqns. with allowance for radiation polarisation 79−23399
nonlinear active medium in Gaussian random optical field, stimulated emission statistics 80−58488
optical parametric oscillator, theory in CW and pulsed stimulated emission regimes 79−10359
optically pumped lasers utilizing self-terminating transitions, CW stimulated emission possibility 80−14329
organic compounds, complex, nuclear relaxation influence on stimulated emission 80−48019
organic dyes, stimulated fluoresc., four-photon parametric interaction 79−13748
organic dyes, stimulated fluorescence, energy level scheme, photoisomerisation effect 77−70310
organic laser dyes, nonlinear transmission including stimulated emission influence 80−99720
organic molecules, polyatomic, stimulated emission, laser spectral kinetics 79−55132
oxide glasses:Sm^{3+}, optical transitions 79−61430
pendulum effect influence on optical modulation of diffr. electron beam in cryst. *(Russian)* 80−55219
2-phenyl-5(4-difluoromethyl-sulfonylphenyl)oxazole, stimulated emission, laser pumped 77−75504
photoelectric counting photon correls. and stimulated emission, comment 77−23639
photoelectric counting photon correls. and stimulated emission, reply 77−23640
photon fluctuations and interaction with solids 77−748
phthalimides, spectrum luminesc. props., laser generating capacity and generation features *(Russian)* 79−31897
phthalimides, stimulated radn. with lamp pumping *(Russian)* 79−51987
plasma, expanding, laser produced, radiative transfer line intensities and stimulated emission 77−3988
plasma turbulence simulation, phase space granulation due to mode-mode coupling 80−38651
polyatomic molecules excited by CO_2 laser pulses, stimulated emission *(Russian)* 79−94214
polymethine dye solns., phonon-free electron-vibration transitions *(Russian)* 77−79660
polymethine dye unstable photoisomers, superluminesc. and stimulated emission 79−31896
POPOP, polarisation of spontaneous and stimulated radiation 79−31583
quadratic quantum systems that are periodic in time, stimulated emission 78−82937
quantum beat high-resolution polarisation spectroscopy in transmission, technique 78−58640
quantum statistics of light, evolution 78−58964
p-quaterphenyl, polarisation of spontaneous and stimulated radiation 79−31583
radio recombination lines from galactic centre direction, evidence for stimulated emission 78−32589
rare earth doped $Bi_4Ge_3O_{12}$, cryst. growth, spectral and laser props. 80−45115
rare earth ion containing inorg. materials, 3μm band stimulated radiation 80−97306
recoilless γ-rays, observation of stimulated emission, possibilities *(Russian)* 79−18383
recombination lasers using elemental vap., metal ion transitions 78−17923
recombination lasers using elemental vap., stimulated emission conditions 78−17922
rhodamine 6G, superluminesc. band structureless spectra 79−7124
rhodamine 6G solution, stimulated emission under internal refl. conditions 77−58327
Rhodamine-dye double-pulse method stimulated emission 77−90172
ring laser with spontaneous emission in generation channel, semiclassical eqns. of motion 80−1240
rotating anharmonic oscillator, stimulated emission power 78−50744
rotating anharmonic oscillators in resonator, stimulated emission power 80−99689
ruby, phonons, at 29 cm^{-1}, stimulated emission 80−45114
semiconductor, highly excited, excitation induced optical absorption 77−44025
semiconductor, nonequilibrium optical phonons generated by electrons in laser radiation field 78−71802
semiconductor, radiative and nonradiative recomb., spontaneous and stimulated emission *(Polish)* 80−53293
semiconductor electron beam-pumped laser, stimulated emission, effect of variable-gap struct. 79−31902
semiconductor laser, asymmetric waveguide structure, anomalous stimulated emission, theory 79−64228
semiconductor laser, asymmetric waveguide structure using external resonator, anomalous stimulated emission 79−64227
semiconductor laser, stimulated emission threshold, surface recombination influence 79−10311
semiconductors, exciton condensation and electron hole liquids, state-of-the-art 80−49625
semiconductors, photocarrier distrib. and photomagnetoelectric effect near stimulated emission threshold 80−80320
shock radiation in freq. dispersive media 77−83796
spectrally inhomogeneous active medium, giant external pulse 78−17897
stimulated versus spontaneous emission as cause of photon correlation 77−34862
superradiance from extended systems, propag. in ab initio theory 77−642
superradiance waveguide laser, stimulated emission spectrum, leaky modes *(Russian)* 80−87400
thermally excited quantum oscillators and second law of thermodynamics 77−34863
three-level atom, multilevel laser excitation dynamics 77−57941
TOPOT, polarisation of spontaneous and stimulated radiation 79−31583
bis-trifluoromethyl phosphine iodide, stimulated emission, photodissoc. laser appls. 79−10295
two-(three-)level systems, steady and transient behaviour 78−1200
two-level atom, radiation by intense laser beam, resonance fluorescence, photon antibunching, Doppler shift 80−74146
UV molecular lasers with transverse electronic pumping, review *(French)* 79−31880
viscous media with induced absorption at stimulated emission wavelength, laser threshold 77−58326
water-ice transition, production of stimulated coherent radiation 78−83920
xanthene dyes, effect of pH on laser output power 77−38881
γ-rays from pair recombination in travelling wave struct., stimulated emission 78−37863
$Al_xGa_{1-x}As$, DH, defect generation in active regions at high optical excitation rates 79−23845
$Al_xGa_{1-x}As$-GaAs, p-n heterojunction laser, low temp. operation 80−1204
$Al_xGa_{1-x}As$-GaAs, p-n heterostruct. laser, tunnel injection and phonon-assisted recomb. 80−5733
$Al_xGa_{1-x}As$-GaAs heterostructures, MO-CVD, phonon assisted recomb. and stimulated emission 80−1205
$Al_2O_3:V^{4+}$, dil. solution, stimulated phonon emission 78−63817
$As_{50}Te_{50}$, amorphous films, metal and semicond. contacts, threshold switching, IR emission 80−49831
Au vapour, discharge excitation, pulse stimulated emission in visible and UV 77−79810
Bi atom, pulse stimulated emission of 472.2 nm line 78−17920
CN photodissociation laser, IR stimulated emission due to BrCN photolysis 79−31888
CO cooled electron-beam-controlled laser, two-quantum transitions 79−45935
CO electron beam controlled laser, stimulated emission characts. 78−1221
CO in *o* Ceti, evidence for 2.6 mm stimulated emission 78−12241
CO_2 electric discharge laser, free oscill. stimulated emission, nanosecond pulse duration 79−31860
CO_2 laser light pulse amplification calc. Fortran program PULSAMP 77−58312
CO_2 photoionisation laser, elec. and stimulated emission characts. 77−71971
Ca, Stark mixing of high-lying calcium levels by laser-produced charges 78−25469
CaF_2:Na, γ-irrad. cryst., spontaneous and induced colour centre emission 79−7131
CaF_2-YF_3:Er^{3+}, stimulated emission 77−52135
$CaLa_4(SiO_4)_3O:Nd^{3+}$, spectra, stimulated emission 77−85755
CaO, tunable optical gain at 3600 Å using F^+ centres 79−45947
CaO-Li_2O-B_2O_3:Dy^{3+} glass, optical excitation energy transfer from $Dy^{3+}\rightarrow Nd^{3+}$ 79−15515
Cd II, A factors of ^{111}Cd and ^{113}Cd isotopes by hyperfine level crossing, stimulated emission 80−9564
CdS active surface, exciton stimulated emission and superradiance refl. spectra, props. 80−25411
CdS crystals, one-photon pumping, active layer structure, light amplification 80−78858
CdS, doped laser mechanism and output study 80−43340

stimulated emission continued
CdS, excitonic mol. transitions, optical gain and induced absorpt. spectra 80−11438
CdS, highly excited, stimulated emission process at 80K 80−97307
CdS, laser action in dense exciton systems 77−75531
CdS, laser thresholds and stimulated emission, intrinsic recomb. processes 79−15489
CdS platelet lasers, optically pumped, spatial and spectral distribution of laser emission 80−64032
CdS, pure and Cl doped, stimulated emission due to indirect band-band transitions 80−7376
CdS screen for laser CRT, stimulated emission with TV type operation 78−59028
CdS single crystal, laser emission at one-photon excitation *(Russian)* 77−79835
CdS, single crystal, subnanosecond light pulse generation by laser radiation pumping 79−64234
CdS single crystals, depend. of radiative props. on equilib. carrier density 79−19932
CdS, size effect of dense electron hole systems 80−7413
CdS, spontaneous and stimulated emission from electron-hole plasmas 77−69241
CdS, stimulated and spontaneous emission from degenerate electron-hole plasma at 300K 80−29762
CdS, stimulated emission under N_2 laser excitation 77−14723
CdS, stimulated emission and optical gain in dense exciton system 79−33731
CdS, two-photon-excitation, tunable laser emission, luminesc. processes 80−55127
CdS type direct semiconductor, high excitation 77−48202
CdS(Se), ps. spectra, high density exciton system 78−19553
CdS_xSe_{1-x}, strongly excited by electron beam, determ. of nonequilibrium carrier lifetime 80−39603
CdSe crystal, stimulated emission from electron-hole plasma, temp. depend. 78−88331
CdSe, excitonic mol. transitions, optical gain and induced absorpt. spectra 80−11438
n-CdSe, laser excited stimulated emission, optical gain spectrum 80−76050
Ce^{3+}:$LiYF_4$, UV laser at 325 nm, stimulated emission obs. 79−72574
$ClF_3(F_5)+H_2$ chemical laser, stimulated emission rel. to reaction mechanism 77−50667
Cr^{3+}:$BeAl_2O_4$, alexandrite, potential laser material, stimulated emission and absorpt. spectrum 79−33734
Cu atom pulse stimulated emission, discharge excitation in $CuBr_2$, $CuCl_2$ 77−23663
Cu atoms in halide vap. transverse discharge 77−88716
Cu, in radial transverse discharge 77−50658
Cu vapour, explosively formed, apparatus for stimulated emission obs. 78−50764
Cu, vapour laser emission, pulse characteristics rel. to plasma parameters 78−71090
Cu vapour pulsed laser, stimulated emission mechanism 79−64213
CuCl, excitonic mols., ps time resolved luminesc. spectra 77−16383
CuCl, luminesc. spectra, excitonic mol. reson. two phonon excitation 78−19514
CuCl, ps. luminesc. spectra, resonantly excited excitonic mols. 78−19555
CuCl, resonantly excited excitonic molecules, time resolved spectroscopy 78−92109
DF laser, refr. index changes during stimulated emission 78−17929
D_2O, far IR superradiant laser action 77−663
D_2O vapour, stimulated Raman emission obs. 77−38998
Dy^{3+}:oxide glass, intensity parameters and laser transitions 79−50300
Er^{3+}:$Gd_3Ga_5O_{12}$, stimulated emission 79−91466
Er^{3+}:$KGd(WO_4)_2$, stimulated emission by subsidiary transitions 79−3696
Er^{3+}:$KLu(WO_4)_2$, room temp. stimulated emission obs. 80−106527
Er^{3+}:$Lu_3Al_5O_{12}$, 3-μm crystal laser functional scheme, stimulated emission 80−43339
ErAG:Er^{3+}, 3 μm stimulated emission at room temp. 77−42541
Er_2SiO_5:Ho^{3+}, single cryst., luminesc. and stimulated emission 77−69895
Eu^+ metastable states in discharge plasma, anomalously high speed deexcitation, modulation of induced radiation obs. 80−44014
$F+H_2(Cl_2)$(HCl)(methane), delay and decay times of stimulated emission 78−3317
F_2-Ne(He) mixtures, VUV emissions, mol. F_2 laser at 1575 Å 77−75487
GaAs excited by HV pulses, stimulated emission and luminesc. obs. 79−59704
GaAs injection laser, active region effect on single-freq. stimulated emission conditions 80−9884
GaAs laser diodes, junction temp. meas. method 79−36895
GaAs, N_2 laser pumped under appl. elec. field, gain anisotropy 77−61958
GaAs, stimulated and spontaneous emission from degenerate electron-hole plasma at 300K 80−29762
$GaAs_xSb_{1-x}$, spontaneous and stimulated emission, electron beam excitation 77−58333
$Ga_xIn_{1-x}As$, spontaneous and stimulated emission, electron beam excitation 77−58333
$Ga_xIn_{1-x}As_{1-y}P_y$, spontaneous and stimulated emission, electron beam excitation 77−58333
$Ga_xIn_{1-x}As_ySb_{1-y}$, epitaxial film and DH, efficiency 77−686
$Ga_{1-x}In_xSb$:Zn(Te), photolum. and stimulated emission obs. 78−72595
GaN, stimulated emission under high one and two quantum excitation 78−35171
GaS, luminescence excited by high-intensity two-photon pumping 77−44038
GaSe, highly excited photoluminesc. exciton-exciton and exciton-carrier scatt. 77−48244
GaSe, luminescence excited by high-intensity two-photon pumping 77−44038
GaSe, optical excitation, excitonic spectra, stimulated luminesc. 80−40132
GaSe, spontaneous and stimulated emissions due to exciton-electron and exciton-exciton collisions 77−32421
GaSe, stimulated eimission due to electron-hole plasma recomb. 80−50374
$GaSe_{1-x}S_x$, stimulated photoluminesc. excitons role 77−48201
$GdAlO_3$:Er^{3+}, $^4S_{3/2}$ to $^4I_{9/2}$ transition laser action, optical and luminescence spectra 80−16082
stimulated emission continued
Ge, far IR radiation amplification on hot hole population inversion *(Russian)* 80−16060
H I radio recombination lines, in interstellar H II regions, quasiclassical anal. 78−28511
H II region, H137β/109α intensity ratio interpretation 80−31344
$H+ClF^- \rightarrow HCl^*+F$, reaction rate const. meas. 77−71980
$H+H^+$, vibr. excited H_2^+ form. by stimulated radiative association 79−100346
H_2, metastable $c^3\Pi_u$ state, population densities and quenching times meas. 78−94296
HF, chem. laser, spectral and time characts. 77−75499
HF, vibr.-rot. emission, from highly rot. excited states, in ClF_x-H_2 chem. laser 78−17926
HF*, interaction with ClFx, relax. consts., stimulated emission delay 77−7077
He-Cd, energy characts., longit. mag. field *(Russian)* 77−50661
He_2 dimer, electron-beam pumped, anal. of feasibility of stimulated vacuum UV radiation 80−9857
HgI_2, cooperative fluoresc. by excitonic reson. pumping 79−33732
HgI_2, stimulated emission at high exciton density, temp. depend. 78−84608
HgI_2, stimulated photoluminesc. excitons role 77−48201
Ho^{3+} in oxygen-containing crysts., stimulated emission at low temps. 80−106526
Ho^{3+}:$BaYb_2F_8$ 80−95902
Ho^{3+}:$Gd_3Ga_5O_{12}$, stimulated emission and Ho^{3+} cascade laser action 79−91466
Ho^{3+}:$LiYF_4$, 1.392, 1.673 and 3.914 μm stimulated emission, laser cascades 80−9886
Ho^{3+}:$LiYbF_4$, active medium for Nd laser freq. convertor, cascade stimulated emission 80−102727
$Ho_3Ga_5O_{12}$:Ho^{3+}, stimulated emission 77−52135
$Ho^{3+}KGd(WO_4)_2$, stimulated emission by subsidiary transitions 79−3696
$Ho_3Sc_3Al_3O_{12}$:Ho^{3+}, stimulated emission 77−52135
I, $^2P_{1/2}(F=3) \rightarrow {}^2P_{3/2}(F'=4)$ transition, stimulated emission cross section determ. 79−13961
I_2 molecule pumped by Cu vapour laser, pulsed stimulated emission due to electronic transitions 80−14330
InAs, electron beam excitation, luminesc. and stimulated emission 77−16339
InAs, epitaxial, laser action mechanisms with electron beam excitation 80−28240
$In_{1-x}Ga_xP_{1-z}As_z$, stimulated yellow-green emission under electron excitation, 80K 79−33846
$KB_5O_8.4H_2O$, tunable UV generation at 1966 Å 77−68238
$K_5Bi_{1-x}Nd_x(MoO_4)_4$ solid soln., growth, spectroscopic and laser props. 78−2901
KCl:Eu^{2+}, γ-irrad., photostimulated low temp. recomb. luminesc. 80−11435
$KEr(WO_4)_2$, crystallisation cond., stimulated emission in 2.8 μm band 80−53301
$KGd(WO_4)_2$:R^{3+} 78−23496
$KNdP_4O_{12}$, determ. of fluoresc. quantum efficiency and laser emission cross sections 80−48264
$KNdP_4O_{12}$, laser emission cross sections, fluorescence spectra, radiative lifetimes, quantum efficiency 80−23694
$KY(WO_4)_2$:Er^{3+}, stimulated emission at 300K 80−34951
$KY(WO_4)_2$:Ho^{3+}, 3 μ stimulated emission at 300K 80−20667
$KY(WO_4)_2$:R^{3+} 78−23496
$La_2Be_2O_5$:Nd^{3+} (Pr^{3+}), cryst. growth, spectral and laser properties in $^4F_{3/2} \rightarrow {}^4I_{11/2}$ and $^4F_{3/2} \rightarrow {}^4I_{13/2}$ transitions 80−80853
$LaNbO_4$:Ho^{3+} crystal, 3 μm stimulated emission by Ho^{3+} ions 79−99910
Li-$La_{1-x}Nd_x$ phosphate glasses, stimulated emission spectroscopy of $^4F_{3/2}$ to $^4I_{11/2}$ and $^4F_{3/2}$ to $^4I_{13/2}$ transitions 79−38573
Li_2, $^3\Sigma_g^+ - {}^3\Sigma_u^+$ excimer emission, ab initio calcs. 80−91608
LiNd phosphate glass, spectral and generation props. 77−1700
$LiNdP_4O_{12}$, laser emission cross sections, fluorescence spectra, radiative lifetimes, quantum efficiency 80−23694
$LiRF_4$, R=rare earth, laser matrices prep. and characterisation 77−24945
$LiYFd_4$:Er^{3+}, optical spectra and multifreq. stimulated emission 79−56818
$(Lu,Er)_3Al_5O_{12}$:Er^{3+}, stimulated emission 77−52135
$(Lu,Yb)_3Al_5O_{12}$:Yb^{3+}, stimulated emission 77−52135
$LuAlO_3$:Er^{3+}, $^4S_{3/2}$ to $^4I_{9/2}$ transition laser action, optical and luminescence spectra 80−16082
$Lu_3Al_5O_{12}$:Er^{3+}, 3 μm stimulated emission at room temp. 77−42541
$Lu_3Al_5O_{12}$:Er^{3+}, absorpt., luminesc., stimulated emission 77−32402
$Lu_3Al_5O_{12}$:Er^{3+}(Ho^{3+}), stimulated radn., electron-phonon interaction *(Russian)* 77−8605
$Lu_3Al_5O_{12}$:Ho^{3+}(Er^{3+}), sensitized stimulated emission at 3 microns 80−53302
Mn-He laser, stimulated emission mechanism, energy characts. 77−3571
N_2, active solid, surface excitation prod. by at. beam deposition, stimulated emission 79−99911
N_2 laser, stimulated emission kinetics under pulse-periodic conditions 79−64212
N_2 laser discharge emission model and meas. 78−71093
NH_3 J=K=1 line mol. beam maser emission, ring-type focusing 80−28119
$^{14}NH_3$, laser emission at 16 μm by two-quantum excitation of $2\nu^-{}_2(7,5)$ state 79−86165
Na beam deflection by reson. standing wave radiation 79−98056
Na:CaF_2, tunable room temp. laser action of M-centres, luminesc. and absorpt. spectra 79−31907
Na:SrF_2, tunable room temp. laser action of M-centres, luminesc. and absorpt. spectra 79−31907
Na_2, $^3\Sigma_g^+ - {}^3\Sigma_u^+$ excimer emission, ab initio calcs. 80−91608
NaF, gamma irrad., colour centre stimulated emission, threshold pump power, tuning range 79−73971
$NaNdP_4O_{12}$, laser emission cross sections, fluorescence spectra, radiative lifetimes, quantum efficiency 80−23694
Nd crystals, determ. of fluoresc. quantum efficiency and laser emission cross sections 80−48264
Nd^{3+} in $Nd(NO_3)_3$(tributylphosphate-d_{27})$_3$, soln. luminesc., stimulated emission *(Russian)* 78−33734
Nd:$CaY_2Ge_3O_{12}$, energy levels and laser action, fluoresc. meas. 79−81438

stimulated emission continued
Nd:glass, stimulated emission cross sections and absorpt. coeffs. at 1.06 μm, calorimetric meas. 77−71987
Nd:glass, stimulated emission cross section by absorpt. meas. from thermally populated $^4I_{11/2}$ levels 78−71107
Nd:glass laser, gain coeff. for fusion laser amplifier 77−19261
$Nd:La_2Be_2O_5$, laser crystal properties 77−19260
Nd^{3+}: glass, spectral props. *(Chinese)* 80−60645
$Nd^{3+}:Ca_3Ga_2Ge_3O_{12}$, stimulated emission at 300K 80−38019
$Nd^{3+}:Gd_3Ga_5O_{12}$, growth, stimulated emission, spectral props. 78−95593
Nd^{3+}:glass based on alkali metal metaphosphates, luminesc. and lasing *(Russian)* 77−46724
Nd^{3+}:Li-Nd-La phosphate glass, nonradiative losses, pulse periodic stimulated emission and luminesc. 77−83878
Nd^{3+}:NdAlCl vapour complex, optical gain meas. 77−88708
Nd^{3+}:quartz fibre, stimulated radiation generation and amplification 77−88729
$Nd^{3+}:YAlO_3$ biaxial laser cryst., anisotropy of spectral characts. 79−50303
$Nd^{3+}:YAlO_3$ laser, $^4F_{3/2}\rightarrow{}^4I_{13/2}$ transition, stimulated emission wavelength, continuous tuning 77−58334
NdP_5O_{14} and $Nd_xLa_{1-x}P_5O_{14}$, large single crystal growth from H_3PO_4 and oxide, props. *(French)* 77−4723
NdP_5O_{14} laser, flashlamp excited, emission cross section at 1.32 μm 79−59701
Ne like multiply charged ion transitions, stimulated emission possibility in far UV 79−10292
Ni^{2+}:MgO laser system, optical parameters 80−48260
O I 6300 Å in type A aurora rays, emission intensification 80−4163
OCS, vibr. excitation and stimulated emission, CO_2 laser pulse pumping 77−23662
P_2O_5 glasses for laser amplifiers and optical isolators 78−25885
PbI_2, cooperative fluoresc. by excitonic reson. pumping 79−33732
PbI_2, luminescence excited by high-intensity two photon pumping 77−44038
PbI_2, photoluminesc. spectra, generation of stimulated radiation 77−8647
PbI_2, stimulated photoluminesc. excitons role 77−48201
$PbS_{1-x}Se_x$ thin film, stimulated emission, temp. depend. 80−66232
PbSe, photoluminesc. spectra and stimulated emission, effect of temp. 77−8638
PbTe epitaxial film, absorption spectra and recombination 78−80409
PbTe-$Pb_{1-x}Sn_xTe$-PbTe DH, LPE and VPE, stimulated emission 77−75526
Pr^{3+}:oxide glass, intensity parameters and laser transitions 79−50300
PrF_3, laser action of Pr^{3+} 80−95901
Rb, $5^2D_{3/2,5/2}$ and $7^2S_{1/2}$ two-photon excitation stimulated and parametric emission 77−10651
Te, opt. props. under high press., band struct. transform. 80−55112
Tl atomic vapour, obs. of Dicke superradiance at 1.30 μm 77−441
Tl I, photodissociative pumping effect 80−58182
Tl, inverted atomic populations, obs. of stimulated level shifting 80−58218
XeF, from photodissoc. of XeF_2, $B(^1/_2)$-$X^2\Sigma^+$ transition, stimulated emission 78−71097
XeF*, in enhanced quenching of Xe+F by intense laser light, computer modelling 78−55232
$(Y,Yb)_3Al_5O_{12}:Yb^{3+}$, stimulated emission 77−52135
YA-$O_3:Er^{3+}$, pulsed laser action, $^4S_{3/2}$ to $^4I_{9/2}$ transition laser action, optical and luminescence spectra 80−16082
YAG:Er^{3+}, 3 μm stimulated emission at room temp. 77−42541
YAG:Er^{3+}(Ho^{3+}), stimulated radn., electron-phonon interaction *(Russian)* 77−8605
YAG:Ge^{3+}, excited state absorpt. loss, 5d→4f rare earth lasers 78−90417
YAG:Ho^{3+}, spectroscopy 80−93374
$Y_3Al_5O_{12}:Er^{3+}$, stimulated emission 77−52135
$Y_3Al_5O_{12}:Tb^{3+}$, mechanism of $^5D_3$-$^5D_4$ cross-relax. 77−4656
$(Y_{0.8}Gd_{0.2})AlO_3:Er^{3+}$, spectroscopic props. 77−85791
$Y_{1-x}Gd_xAl(Sc)O_3:Ho^{3+}$, stimulated emission of Ho^{3+} ions 77−81126
$Y_{1-x-c}Gd_xNd_cScO_3$, crystal, absorption, luminescence, stimulated emission spectra 78−15220
$Y_{1-x}La_xAl(Sc)O_3:Ho^{3+}$, stimulated emission of Ho^{3+} ions 77−81126
$Y_{1-x-y}R_xEr_yAlO_3$, $Y_{1-x-y}R_xEr_yScO_3$, stimulated emission of Er^{3+} ions 78−6705
$Y_2SiO_5:Ho^{3+}$, single cryst luminesc. and stimulated emission 77−69895
$Y_2SiO_5:Nd^{3+}$, stimulated emission 77−52135
YVO_4:Nd, stimulated emission cross-sections at 1064 and 1342 nm 78−39575
$Zn_xCd_{1-x}S$, graded single crysts., laser or electron beam excited, luminesc. 77−85792
$Zn_xCd_{1-x}S$ monocrystal, optical and nonlinear optical characts. *(Russian)* 79−98442
$Zn_xCd_{1-x}S$, platelet single cryst. one-photon optical excitation, spatial distrib. and mode struct. of laser emission 79−31912
ZnHg excimer, optical pumping of Zn reson. line, optical and kinetic props. 78−58991
ZnO epitaxial film, UV luminesc. due to one-, two-photon excitation, laser possibility 79−11468
ZnO, excitonic mol. transitions, optical gain and induced absorpt. spectra 80−11438
ZnO, laser thresholds and stimulated emission, intrinsic recomb. processes 79−15489
ZnO, two-photon-excitation, tunable laser emission, luminesc. processes 80−55127
ZnS:Mn, electroluminescent film, stimulated emission *(Russian)* 77−19255
ZnSe film, grown on sapphire substrate, stimulated emission 79−78708
ZnSe, optically pumped stimulated emission at 4580 Å, near band edge luminesc. 78−71105
ZnTe film, grown on sapphire substrate, stimulated emission 79−78708
ZnTe, laser thresholds and stimulated emission, intrinsic recomb. processes 79−15489

stimulated Raman scattering
see also coherent antiStokes Raman scattering
absorbing media, ultrashort laser pulse excited, fluctuation-dissipation theory *(Russian)* 80−23753
acetone, scatt. excited by picosecond light pulses 79−14034
acetone, vibr. dephasing theories, test using selective coherent ps. Stokes scatt. 80−59609

stimulated Raman scattering continued
active Raman and Rayleigh scatt. spectroscopy, nonlinear optical methods, review 79−991
angular structure of anti-Stokes and second Stokes components 78−18014
anthracene crystal, stimulated emission and Raman scatt. 78−1303
anthracene crystals, pre-reson. Raman scatt., 4.2-30K 80−60571
anti-Stokes radiation by Gaussian noise pump *(Russian)* 78−30015
anti-Stokes radiation spatial distrib., expt. and four-photon model 80−28270
antiStokes wave, excitation and amplification, with broad-freq. spectrum pump radiation *(Russian)* 79−50346
applications *(German)* 79−27320
atomic gas, Raman transitions, active reson. spectroscopy 77−27003
atomic oscillator strength, meas. using stimulated electronic Raman scatt. polarisation flip method 79−31471
atomic system, superradiant Raman scatt. of light *(Russian)* 79−36964
atomic vapour, f-value determ. method using stimulated electronic Raman scatt., appl. to Cs 78−82693
atomic vapours, stimulated electronic Raman scatt., saturation of tunable IR lasers 78−37941
backscattering from relativistic unmagnetised electron beams, book contrib. 79−27334
backward Raman amplifier, technique for parasitic superfluoresc. suppression 80−38073
backward stimulated scattering, comments 80−9953
backward stimulated scattering, reply to comments 80−9954
beat wave imaging props., in stimulated Raman scatt. medium, holographic appl. 80−5709
benzaldehyde, wavefront reprod. obs. by stimulated Brillouin, Raman scatt. 80−53369
benzene, anti-Stokes components, class II radiation cones 80−28276
benzene, high order stimulated Raman scatt. *(Chinese)* 79−81206
benzene, high-order stimulated Raman scatt. obs. *(Chinese)* 80−45053
benzene, laser wavefront reconstruction by stimulated scatts. in picosecond range 79−986
benzene, liq., spectroscopy using low power CW lasers 78−29172
benzene, Raman nonlinearity characterisation by two-beam interferometry 77−38986
benzene, stimulated diffusion induced by two photon absorption *(French)* 78−90455
benzene, ultrahigh sensitivity stimulated Raman gain spectroscopy 80−48337
benzene, UV two-photon absorpt. relative to known Raman cross section 79−81487
benzene filled capillary fibres, spectra 78−66869
benzene-nitrobenzene, liq., stimulated Raman scatt., intensity changes, selective excitation 78−13753
broad-band pumping, action on stimulated Raman scatt. excitations near reson. *(Russian)* 77−34913
carbon tetrachloride, neat and cyclohexane mixture, nonlinear susceptibility, $\chi^{(3)}$, reson. and non-reson. contribs. 79−987
carbon tetrachloride intense ps pulse excitation, time evolution of multiple spectra 78−66867
chemical reaction wave, propag. of coherent probe light pulse 80−61190
Cherenkov type parametric optical oscillator, optical saturation 80−102771
chloromethane, liq., transient stimulated vibr. Raman scatt. 78−71144
chloronaphtalene, stimulated diffusion induced by two photon absorption *(French)* 78−90455
coherent antiStokes Raman scattering, reson. excitation, lineshape 78−9415
coherent backward Raman propag. effect analysis 77−79894
coherent polarisation spectroscopy of Raman scatt. 78−13758
coherent radiation novel sources, book 79−27231
coherent Raman gain spectroscopy using CW laser sources 78−37076
coherent Raman scattering with three lasers 79−23016
coherent Raman spectroscopy techniques, review 80−22440
coherent Raman spectroscopy using powerful tunable lasers 77−53985
colliding particle system, two-photon transition, stimulated Raman scatt. 80−9663
combined stimulated Raman scattering and continuum self-phase modulation 80−69460
condensed phase fluoresc., double reson. excitation spectroscopy 80−86438
cooperative combination scattering, light pulse propag. effects 79−81485
coupled waves, dispersion functions, rel. to dielec. dispersion *(German)* 80−1281
crystalline transparent and absorbing matrices, using Raman laser excitation sources 79−18480
CW coherent Raman gain spectroscopy 78−58057
CW Raman gain spectroscopy, coherent detect. of Raman modes 77−87845
CW spectroscopy, sensitivity limitations 77−87848
cyclohexane, laser wavefront reconstruction by stimulated scatts. in picosecond range 79−986
cyclohexane, neat and CCl_4-C_6H_{12} mixture, nonlinear susceptibility, $\chi^{(3)}$, reson. and non-reson. contribs. 79−987
density operator, diagrammatic evaluation 78−5523
diamond, coherent nonlinear two-phonon Raman spectra 79−19878
3,3-diethyl thiadicarbocyanine iodide dye, stimulated fluoresc. and stimulated reson. Raman scatt. relationship 80−91853
difference frequency generation by stimulated Raman scatt. using inhomogeneous electrostatic field 80−95954
dimethyl sulphoxide, high efficiency stimulated Raman scatt. source *(Chinese)* 80−87433
dispersive medium, incoherent, coherent stimulated Raman scatt. with multimode pump *(Russian)* 80−38063
dispersive medium, Stokes, anti-Stokes scatt. of ultrashort pulses, phase modulation effect 78−50857
Doppler broadening at electronic resonance 80−38065
dopplertrons and gyrotrons, coherent radiation from magneto-resonant relativistic electron beams, book contrib. 79−27227
double resonance Raman amplifier, theory 80−87434
dye laser frequency locking by intracavity stimulated Raman scatt. 78−79050
dyes, secondary fluoresc. under very powerful pumping, fine struct. spectra 77−58383
dynamic holograms for light stimulated scatt. 79−89964
electromagnetic-mechanical model experiment *(German)* 78−86077

stimulated Raman scattering continued
electron beam, intense, relativistic, stimulated Raman radiation spectral props. 79−64163
electron beam, relativistic, intense, subjected to rippled elec. field 79−98439
electron-positron annihilation 77−57519
enhanced SRS, theory, alleged nonexistence 78−46722
ethanol, picosecond stimulated Raman effect, time-resolved spectra 77−3369
ethyl alcohol, dynamics of psec. pulse train scatt. 79−64286
ethylene glycol, vibrational dephasing time of subgroup, transient stimulated Raman scatt. 78−37718
excimer laser Raman pulse compression for appl. to laser fusion 79−59756
excimer laser Raman pulse compressor systems for laser fusion 79−59757
femtosecond pulse generation possibility in optical resonator 77−23717
fibre optical CW Raman oscillator, using two-mirror resonator config. 79−7152
fibre Raman lasers 80−102767
fibres, cascade effects *(Russian)* 77−23714
first Stokes component amplification in pump field 79−98443
first Stokes component in substances with different Raman cross-section, self-focusing *(Russian)* 77−10984
fluorescent organic molecules, excited state intramol. vibrs. 80−32717
fluoromethane, liq., transient stimulated vibr. Raman scatt. 78−71144
forbidden rotational and vibr.-rot. transitions in strong optical field, spontaneous and stimulated Raman scatt. 80−74174
four-photon spectroscopy of condensed media, nonlinear spectroscopy developments 80−91860
free electron laser based on stimulated Raman scatt. by relativistic electron beam, oscill. characts. 80−99688
free electron laser basic mechanisms, stimulated Raman and Compton backscattering 79−7106
free-electron laser, sub m.m. wavelength, stimulated Raman backscatt. regime 79−7107
frequency conversion of inert gas halide lasers in atomic or mol. media 79−36965
frequency shifts, nonreson. contribs. to nonlinear susceptibility 80−53373
frequency-modulated shot noise limited stimulated Raman gain laser system for monolayer vibr. spectroscopy 80−62744
gain, bounds, quantum theory 79−94290
gain, influence of polarisation degree 79−89965
gases, coherent Raman scatt., quantum theory of line shapes 79−64049
gases, effects on optical radiation propagation *(Russian)* 79−3740
gases, second Stokes component, dispersion effects 80−91857
glass fibere, 1-1.3 μm source 77−42568
glass fibre, quasicompensated losses 77−14811
group velocities of light, meas. of relative dispersion by stimulated Raman scatt. 77−65608
heptafluoroiodopropane, Raman spectum, cross-sections, implications for large-scale atomic I laser 79−23022
hexafluoride molecule selective excitation via Doppler free multiphoton process 78−55178
high intensity Raman interactions, review 79−76759
hyper-Raman scattering, degenerate, quantum statistical props. of photon and phonon fields 79−89873
hyper-Raman scattering, non-degenerate, quantum statistical props. of photon and phonon fields 79−89872
image reconstruction in three-dimens. using stimulated Raman scatt. 78−83038
induced scatt. amplifier with wide band pumping, information signal transmission 78−83035
inhomogeneous plasma stimulated Raman scatt. spectrum 79−7449
inhomogeneous stationary laser plasma, stimulated Raman spectra 78−83578
n-InSb, intraband processes exam. by stimulated spin-flip Raman scatt. 77−19362
interaction of light with phonon excitations in medium, coherent effects 79−15103
intracavity polariton parametric oscill., stimulated Raman emission 78−30026
IR and far IR source, powerful and tunable 80−5787
IR generation, book 77−46761
IR generation, difference freq. mixing, parametric oscill. and stimulated Raman scatt., book contrib. 77−46762
IR generation, optical mixing, SHG and parametric oscills., book contrib. 77−46764
isotropic medium, angular distribs. *(Russian)* 77−34911
Kerr effect, Raman induced, with nonmonochromatic waves 80−48359
laser and Stokes pulses, coherent propag. in Raman active medium 77−7157
laser bandwidth effects, using broad-band lasers 79−81486
laser beam, ps, spatial struct. in a non-linear medium 79−94287
laser beam intensity ratio increase by possible use of stimulated Brillouin and Raman scatt. 80−5796
laser fusion target chamber, stimulated Raman scatt. 79−9873
laser intraresonator forced Raman radiation with polariton excitation *(Russian)* 79−94286
laser plasma, stimulated Raman light scatt. spectrum *(Russian)* 80−106926
laser resonator, stationary amplification using stimulated Raman scatt. *(Russian)* 79−27333
laser resonator, stimulated combined scattering of light, effect of generation of 'hot' vibrs. 80−58601
laser source creation, near IR to submillimetric waves *(French)* 79−31993
laser sources frequency conversion 80−69451
lasers application in Raman spectroscopy, review 78−65979
lasing and non-lasing systems, resonance scatt., review 77−79897
lineshape, coherent resonant Raman scatt. 3rd order nonlinear optical susceptibility 78−42378
liquid, induced Raman scatt., anomalous line broadening 78−56490
liquid, optical Kerr const., electronic and orientational contribs., obs. by coherent Raman techniques 77−88874
liquid, photoacoustic Raman gain spectroscopy 79−75606
liquid core hollow quartz fibre, stimulated Raman scatt. 78−30087
liquid media, comparison of inverse Raman scatt. and CARS 79−7178
liquid polyatomic molecule vibrational mode obs. with picosecond laser pulses 77−58007
stimulated Raman scattering continued
liquid solution, nonlinear reson. processes, influence of spectral line broadening mechanism 79−7181
liquids, coherent Raman scatt., quantum theory of line shapes 79−64049
liquids and binary liquid mixtures, stimulated Raman scatt., intensity changes 78−13753
locking of Raman emission components, in optical resonator with dispersive medium 78−50858
magneto-optic Raman scattering of Raman-inactive phonon polaritons 80−91843
MBBA, dye activated, isotropic phase, induced Raman emission *(Russian)* 78−13766
MBBA, nematic liq. cryst., nonlinear optical suscept. using light combination scatt. *(Russian)* 80−38064
medium with varying energy level populations, evolution of coherent radn. probing pulse 79−76755
megawatt sub-mm pulse production by stimulated magneto-Raman scatt. 77−50719
metal vapour, tunable IR generation by optical mixing, book contrib. 77−46766
metal-halide arc, laser Raman scatt. determ. of local density 77−11424
methane, ν_1 fundamental, CW stimulated Raman gain spectroscopy 79−6943
methane, backward Raman amplifier, large-signal gain and intensity enhancement 78−90450
methane, backward Raman gain meas. for KrF laser radiation 78−66863
methane, excimer laser Raman pulse compression for appl. to laser fusion 79−59756
methane, high-resolution coherent Stokes Raman scattering, of ν_1 and ν_3 bands 79−31981
methane, scaled Raman pulse compression experiments at 248 nm, KrF pump laser 80−38071
methane, shifting of ArF and KrF wavelengths 77−75539
methane, stimulated Raman scatt. of excimer laser wavelengths for new lines in UV 79−59755
methanol, vibr. dephasing theories, test using selective coherent ps. Stokes scatt. 80−59609
methanol, vibrational dephasing time of subgroup, transient stimulated Raman scatt. 78−37718
methyl thionine chloride, intramol. vibr. spectra 80−977
molecular, vibrational dephasing time of subgroup, transient stimulated Raman scatt. 78−37718
molecular system, superradiant Raman scatt. of light *(Russian)* 79−36964
molecules, excited and ground states, stimulated resonance Raman scatt. theory, review *(German)* 77−58013
molecules, optically active, coherent Raman scatt., quantum theory 80−69150
molecules, stimulated Raman and two-photon absorpt. 80−52999
multimegawatt tunable IR source up to 7.7 μm, using dye laser and H_2 78−1301
multimode laser steady-state stimulated Raman scatt. 80−99796
multimode pumping, theoretical study *(Russian)* 78−13768
multiple-pass Raman gain cell 80−48334
multiplicative stochastic processes in statistical physics appl. 80−22289
mutual quenching of modes 79−36960
N two-level atoms, quantum theory of nonlinear optical phenomena 80−5790
(near) two-photon-resonant freq. up-convertors, limitations and optimisation 79−31985
near-IR stimulated Raman emission in single-mode fibres by Nd-YAG laser pumping in low-dispersion region at 1.3 μm 80−64100
nitrobenzene, liq., induced Raman scatt., anomalous line broadening 78−56490
nitrobenzene, spectral splitting 78−50860
nitrobenzene-in-benzene optical fibre amplifier performance estimation 79−7217
nonlinear optical phase conjugation for pulsed laser systems 78−59092
nonlinear optical resonator filled with Raman or Brillouin active medium, theory 77−50722
nonlinear Raman active media, third-order light mixing at polariton reson. frequencies 77−19364
nonlinear susceptibility, $\chi^{(3)}$, reson. and non-reson. contribs., time resolved obs. 79−987
nonmonochromatic pumping amplification, expt. *(Russian)* 77−88864
nonmonochromatic radiation stimulated scatt., efficiency depend. on pump radiation statistics 80−95950
nonstationary Raman scattering, by polaritons, correlation spectroscopy *(Russian)* 78−23450
nonstationary Raman scattering, of light, by vibration and polariton excitations *(Russian)* 78−23449
optical cavity plasma, stimulated Raman and Brillouin scatt., electrostatic and EM waves 78−34324
optical fibre, backscatter of stimulated Raman scatt. 80−64109
optical fibre, multimode step-index, forward and backward stimulated Raman scatt. 80−58639
optical fibre, nonlinear effects, appl. to active and passive device fabrication 80−58638
optical fibre, pulse delay meas. in zero material dispersion region 78−33822
optical fibre, Raman oscillators and nonlinear effects 77−88854
optical fibre, three-wave stimulated Raman scatt. *(French)* 80−78902
optical fibre guide, stimulated Raman scatt. dynamics by Stokes component detect. 80−14394
optical fibres, low loss, Raman scatt., model 78−55410
optical fibres, Raman scatt., guiding structs. effects on spontaneous and stimulated emission 80−58636
optical fibres, wideband near IR continuum generation (0.7-2.1 μm) 79−23064
optical multimode fibres, backward stimulated scattering 78−87128
optical waveguide, freq. scanning *(Russian)* 77−10983
optical waveguide, stimulated Raman scatt. excitation by wideband pump 80−64108
optical waveguide, Stokes components recording opposite to pump wave 80−106569
organic dyes, absorption ege struct. in stimulated fluorescence spectra, Raman scatt. 78−55350
organic dyes, reson. SRS at transverse pumping, mol. vibrs. 77−88453
organic molecule solns., stimulated Raman scatt., self-focusing, rel. to Kerr const. *(German)* 79−61355

stimulated Raman scattering continued
ortho-para mixtures, vibr. coherence decay 80−78903
oscillations, spatial and temporal, in saturated optical phonon generation 78−87099
parametric amplification based on four-wave parametric processes in two-photon reson. 79−94296
parametric and Raman processes in second axial Stokes component generation 78−30025
parametric effects on nonmonochromatic pump radiation stimulated scatt. 79−64284
parametric excitation of Stokes waves, spatially inhomogeneous pumping *(Russian)* 78−18012
parametric Raman scatt. in crystals *(Russian)* 79−18476
phase conjugated wavefronts by stimulated Brillouin and Raman scatt. 80−5791
phase conjugation by stimulated scatt. in waveguide, theory 79−3742
phosphate glass laser, statistical props. and stabilisation 80−48266
picosecond interactions in liquids and solids, book contrib. 77−65057
picosecond laser techniques for obs. of vibr. modes in liqs. 80−5800
picosecond light pulse excitation, scatt. characts. 79−14034
picosecond nonlinear optics, book contrib. 77−65609
picosecond Raman gain technique for vibr. spectra of mol. monolayers 80−91859
picosecond Raman techniques, vibr. dynamics in liqs. 80−52325
piezoelectric cubic crystals, stimulated Raman effect 79−73927
piezoelectric cubic single crystal stimulated Raman effect, coupled waves dispersion *(German)* 79−36963
plasma, backscattering of circ. polarised EM waves propagating along mag. field 79−37465
plasma, EM wave, finite-wavelength, dielectric tensor determination 79−64876
plasma, EM wave parametric decay 78−34323
plasma, laesr beam self-focusing 78−30447
plasma, laser light scatt. 78−51312
plasma, parametric instability saturation by electrostatic daughter wave nonlinear decay 80−53945
plasma, Raman and Thomson scatt., beat-wave electron trapping 78−51308
plasma, scatt. of circ. polarised EM wave 78−91113
plasma, self-focusing effect on parametric back-scatt. 78−22510
plasma, stimulated Raman and Brillouin backscattering along mag. field 80−69983
plasma, stimulated Raman and induced Compton scatt., nonlinear kinetics 77−35328
plasma, stimulated Raman scattering, of finite length EM waves *(Russian)* 78−83571
plasma, wave excitation by Gaussian laser beam and stimulated Raman scatt. 77−27680
polarisation state evolution near self-focusing or stimulated Raman threshold 78−50867
polaritons, two-photon absorption and stimulated Raman effect 77−50729
polaritons in transversely bounded layer 77−75621
polyatomic molecule, ultrafast vibr. using laser light pulses 80−9699
polymethine dyes, secondary luminesc. 79−99934
pulse generation amplified by dye amplifier, for laser-matter interaction diagnostics 79−41414
pump beam, spatially inhomogeneous, enhanced gain of stimulated Raman scatt. 80−28279
pump radiation, non-monochromatic, power transform. inversion *(Russian)* 79−3741
pump spectrum reproduction, dispersion-free medium 79−31995
pump wave reproduction in stimulated scattering radiation *(Russian)* 78−83031
pumping wave reproduction 79−64280
pyridine, in carboxylic acid soln., stimulated Raman scatt., H-bonded complex effects *(Russian)* 77−3625
pyridine in aliphatic alcohol solns., relationship between stimulated Raman scatt. and complex formation *(Russian)* 77−48174
pyridine solutions, degree of depolarisation 79−55184
quantum theory 80−106565
quartz fibre, Stokes components recording opposite to pump wave 80−106569
quasisoliton pulses, head-on stimulated scatt. 79−27332
radiation self-synchronisation during stimulated Raman scatt. in external resonator *(Russian)* 80−102772
radiation with broad freq. spectrum, theory *(Russian)* 79−45997
random structure of lines 78−18019
randomly modulated pump, stimulated Raman scatt., method of successive approxs. 80−95951
reconstruction of wavefront and real volume image 78−30018
reflection symmetry violation for crysts. and mols. 78−48184
relativistic electron beam, submillimetric pulse production by stimulated magnetoresonant Raman scatt. 77−38846
relaxation oscills. in gases with focused laser pulse, time depend. 78−18011
resonance illumination conditions 80−64105
resonance-stimulated Raman scatt., susceptibility *(Russian)* 77−88840
resonant, intense optical waves, quantum mechanical theory 79−89958
resonant scatt. in noise pump field 80−9944
resonant scattering excitation at various freqs. 77−83931
rhodamine 6G, resonant interference of nonlinear optical suscept. *(Russian)* 77−7160
rhodamine 6G soln., stimulated reson. Raman scatt., first excited and ground electronic states contrib. 79−89968
rhodamine solutions, quenching of two-photon fluoresc. and stimulated anti-Stokes emission 79−72619
saturation effects in hyper-Raman scatt., resonant three photon processes 80−38069
scaled Raman pulse compression experiments at 248 nm, KrF pump laser 80−38071
self-focusing by Raman or Brillouin dispersion 77−23721
semiconductor, zinc-blende struct., shallow acceptor contribution to near-resonance spin-flip Raman scatt. 79−95754
semiconductors, nonlinear effects, induced by lasers 79−94300
sensitivity enhancement by quasi CW laser scheme 80−53003
SHG, parametric amplification and stimulated scatt. phenomena 77−38994
sideband amplification, in self-focused laser beam in atomic vapour 79−76767
silica fibre, high efficiency tunable CW Raman oscillator 77−14773
silica multimode fibre waveguide, cascade stimulated Raman scatt. 77−62008
soliton regimes *(Russian)* 77−3634
solitons, laser physics appls. 80−48333
solitons in SRS, semiclassical eqns., two level mol. *(German)* 77−79889
source with dye amplifier, development 78−87095
spatial structure of first Stokes component 80−14398
spatial- and temporal-intensity distrib. of stimulated Raman emission 79−86213
spontaneous anti-Stokes scatt., ultra-short pulse biharmonic vibr. excitation 78−33715
stationary mode, scatt. inside laser cavity *(Russian)* 80−38067
statistical effects in reson. nonlinear optics 77−50718
stimulated hyper-Raman scattering in a molecular gas via a three-photon process to obtain IR and far IR radiation 80−58633
Stokes and anti-Stokes components correl. 78−18017
Stokes component amplification, influence of field polarisations 78−13761
Stokes components, ang. distrib. calcs. 77−65607
Stokes pump wave capture in stimulated Raman scatt. amplifier 80−23749
Stokes radiation amplified in pump field of stimulated-Raman scatt. amplifier, spatial characts. change 79−89971
Stokes radiation freq. diffr. shift 79−72625
Stokes signal amplification in nonmonochromatic pump field, theory 79−31994
Stokes signal amplified under stimulated scatt. conditions, influence of pump field changes 79−59763
Stokes signal spectral width and statistics, influence on scatt. efficiency of pump radiation 78−18018
subnatural linewidth spectra by optical double reson. with two-photon pumping 80−74200
superradiance in Raman light scatt., pump depletion effect 80−9957
surface polaritons, excitation by stimulated Raman scatt., theory 78−9413
surface polaritons, stimulated Raman scatt., amplification coeff. *(Russian)* 77−38993
surface vibrational spectroscopy using stimulated Raman scatt. 80−38062
synchronously pumped stimulated Raman oscillator, for liq. group refr. index meas. 80−55059
temporal pump stochasticity for scatt. in dispersionless media 79−98441
three level system, optically pumped, reson. Raman scatt. and laser emission 77−50716
three-level atoms, SRS line-shaped nonlinear reson. 79−72624
three-level system, stimulated Raman scatt. and stimulated collision induced fluoresc. 78−87103
thresholds for ultra-short excitation 80−33078
time-dispersion-tuned fibre Raman oscillator 77−42562
time-reversal symmetry in light scatt. theory, Stokes-anti-Stokes connection formula 78−56479
transient regime theory in scattering with saturation *(Russian)* 78−22174
transient resonance Raman scatt., quantum theory, appl. to strongly coupled localised electron-phonon system 78−94412
transient stimulated Raman scatt., saturation effects 79−23021
transient stimulated Raman scattering in lossy media 80−102768
transversely excited stimulated reson. Raman scatt., gain 77−14779
triethylenediamine, aq. soln., stimulated Raman scatt., struct. enhancing solute 78−27222
trifluoroiodomethane, molecular vibration energy stochastization in intense IR laser field by Raman spectroscopy *(Russian)* 80−14149
tunable Raman freq. generation from dye laser 78−33772
two-photon absorption calibration via stimulated Raman gain 78−87098
ultrahigh sensitivity stimulated Raman gain spectroscopy 80−48337
vibration relaxation time measurement, by coherent Raman-induced IR fluoresc. 79−7038
vibrational dynamics of liquids and solids, Raman scatt. of picosecond light pulses 78−94414
vibrational relaxation of molecules in condensed media, survey, book contrib. 77−36295
water, dynamics of psec. pulse train scatt. 79−64286
wavefront inversion of ruby laser radiation *(Russian)* 77−34912
wavefront reconstruction and self-focusing of light 80−23752
wavefront reconstruction in stimulated light scatt. 80−64107
wavefront reconstruction of light beams 79−41419
wavefront registration and volume object image reconstruction *(German)* 80−53367
wavefront reproduction, laser action 78−1305
wavefront reproduction and reversal phenomena 78−13760
wavefront reversal effect 79−41417
wavefront reversal with freq. shift, based on anti-Stokes stimulated Raman scatt. 80−74440
p-xylene, stimulated Raman scatt., intensity changes 78−13753
Ba atom, laser excited, ionisation studies 80−83330
Ba, Raman conversion of XeCl-laser radiation in metal vapours, up to 40% efficient 79−23025
Ba vapour, efficient Raman conversion of XeF laser output, 351 to 585 nm 77−58377
Ba vapour, efficient Raman conversion of XeCl excimer laser radiation 78−79069
$Ba(NO_3)_2$, Nd laser second harmonic stimulated Raman scatt., efficiency in calcite, nitrate crysts. 80−95949
$Ba(NO_2)_2.H_2O$, nonlinear optical props. and polariton scatt. spectra 77−75616
$BaTiO_3$, coherent excitation of soft polariton mode 79−15464
Bi, Raman conversion of XeCl-laser radiation in metal vapours, up to 40% efficient 79−23025
Br_2, condensed phases, spontaneous and stimulated Raman scatt., weak and strong radiation fields 79−3450
CN, monolayer on Ag surface, vibr. spectra, picosec. Raman gain technique 80−91859
CO_2, liq., transient stimulated vibr. Raman scatt. 78−71144
CO_2, optical pumping in stimulated Raman scatt., tunable laser emitting at 14,16 μm, theory 78−46568
CO_2, pure rotational stimulated Raman photoacoustic spectroscopy 80−32724
CS_2, ang. distrib. of stimulated Raman scatt. 78−83039
CS_2, anti-Stokes stimulated Raman scatt., anomalous behaviour 77−50723

stimulated Raman scattering continued
CS_2, spectral splitting 78−50860
CS_2, vibrational dephasing meas. with CW mode-locked dye lasers 79−65846
CS_2, wavefront inversion of ruby laser radiation *(Russian)* 77−34912
CS_2, wavefront reprod. obs. by stimulated Brillouin, Raman scatt. 80−53369
Ca atom, laser excited, ionisation studies 80−83330
$CaCO_3$, calcite, random structure of lines 78−18019
$CaCO_3$, calcite, single-crystal, wave front reconstruction of light 80−93323
$CaCO_3$, calcite, spectral splitting 78−50860
CdS electronic two- and one-photon Raman scatt. via biexcitons, stimulated config. obs. mag. field shift 80−103963
CdS, resonance hyper-Raman light scatt. on optical photons *(Russian)* 80−14396
CdS, two photon absorption relative to Raman cross sections 78−87098
CdS, two-photon absorpt. effect on hyper-Raman scatt. 80−74441
Cl_2, liq., transient stimulated vibr. Raman scatt. 78−71144
Cs, $6s^2S_{1/2}$ to $5d^2D_{5/2}$ transition, stimulated electronic Raman scatt. 79−41411
Cs, vap., stimulated electronic Raman scatt., 2.7-3.5 μm 78−1300
Cs vapour, IR picosecond pulse generation 80−53371
Cs, vapour, optical frequency down conversion and stimulated electronic Raman scatt. 79−50350
Cs vapour, threshold for stimulated electronic Raman scatt. determ. using picosecond laser pulses 80−102768
Cs vapour, tunable IR generation using 6s-5d Raman transition 80−53365
Cs vapour, two-photon induced stimulated Raman scatt., optical Stark shifts 77−46756
Cs vapour, visible laser radiation down conversion to tunable IR laser radiation 77−10973
Cs vapour tunable IR source using stimulated electronic Raman scatt., appl. to HCN (001) relax. obs. 80−9696
D_2 shifting of ArF and KrF laser wavelengths 77−75539
D_2, stimulated Raman scatt. of excimer laser wavelengths for new lines in UV 79−59755
D_2O, excited by CO_2 laser, far IR emission 77−54755
D_2O vapour, stimulated Raman emission obs. 77−38998
GaAs, tunable stimulated Raman scatt. in far IR, laser feasibility 79−50344
GaP, gain in stimulated Raman scatt. by coupled phonon-plasmon modes from spontaneous Raman spectra 79−68418
GaP, single cryst., Raman scatt., effective cross-section rel. to nonlinear coeffs. *(Russian)* 78−71152
GaP, two photon absorption relative to Raman cross sections 78−87098
H_2, coherent source tunable down to 16 μm 77−65605
p-H_2 cooled gas, 16 μm source using four-wave mixing and stimulated Raman scatt. 78−1298
H_2, freq. shifting of tunable dye laser radiation 80−9963
p-H_2 gas, 16 μm generation by CO_2, pumped rot. Raman scatt. 78−94410
H_2 gas, efficient higher-Stokes-order Raman conversion 80−33082
H_2 gas, stimulated Raman scatt. obs. between $v=1$ and $v=2$ levels 77−46757
p-H_2 gas, stimulated rot. Raman scatt., pumped by CO_2 TEA laser 78−94411
H_2 gas, tunable coherent Raman mixing, 4.3-13 μm 77−88850
H_2 gas, tunable coherent radiation source, 185 to 880 nm 79−31980
H_2 gas in multiple-pass Raman gain cell 80−48334
p-H_2, generation of 16 μm radiation by four-wave mixing 77−50720
H_2, improvement using up to 10 m path length 77−72033
H_2 laser, stimulated Raman scatt., appl. to holography 80−91782
H_2 laser, tunable IR waveguide Raman type pumped by dye laser, 0.7-7 μm range 79−45959
H_2 molecule, high resolution CW stimulated Raman spectroscopy 78−70973
H_2, Raman pulse propag., 30 atm., self-induced gain/loss modulation 77−10980
H_2, refractive props. due to SRS *(Russian)* 77−88865
H_2, shifting of ArF and KrF laser wavelengths 77−75539
H_2, solid, stimulated Raman scatt. and CARS 78−13752
H_2, stimulated Raman scatt. of excimer laser wavelengths for new lines in UV 79−59755
H_2, stimulated Raman scatt. gain of Nd laser radiation by rot. levels 80−69464
H_2, tunable efficient VUV generation using ArF pumped stimulated Raman scatt. 80−38072
H_2, tunable IR generation, by coherent Raman mixing 77−42561
H_2, tunable UV radiation obs. 78−55408
H_2, two-photon enhanced third harmonic generation and Raman scatt. 77−88843
H_2+A, vibr.-vibr. energy transfer, stimulated Raman excitation obs. 79−64086
H_2+HCl(DCl)(CO),(NO_2)(HBr)(DBr)(NO)(CO)(^{13}CO), vibr. relax. rate, stimulated Raman scatt. obs. 77−75269
HBr, liq., transient stimulated vibr. Raman scatt. 78−71144
HCl, liq., transient stimulated vibr. Raman scatt. 78−71144
HCl, tunable far IR generation 79−31983
HCl, tunable far IR Raman generation 78−5525
HF resonantly enhanced stimulated Raman scatt. for tunable IR generation 77−54759
HF, tunable far IR generation using resonantly enhanced stimulated Raman scatt. 79−14031
H_2O, interstellar, maser lines very-high-velocity satellite features generation 78−73746
H_3PO_4, broad-band picosecond light generation by mode-locked ruby laser 79−31989
$^nH_2$, vibr. relax. at low temps., gas, liq. and solid phases 77−83691
He II rotating, geostrophic and Tkachenko wave threshold intensity *(Russian)* 78−43192
^{3}He-^{4}He, superfluid solns., nonlinear sound interaction 80−34267
$Hg_{1-x}Cd_xTe$, CESR meas., four-photon mixing via spin-flip Raman scatt. 79−82873
$Hg_{1-x}Cd_xTe$, shallow acceptor contribution to near-resonance spin-flip Raman scatt. 79−95754
n-InSb, electron spin-flip relax. time meas. 77−3631
n-InSb, optically pumped stimulated recomb. radn. in mag. fields 79−94284
p-InSb, photoexcited exciton spin-flip scatt. 80−74434
stimulated Raman scattering continued
n-InSb, semicond. plasma, Raman scatt. of waves of fluctuations *(Russian)* 79−94299
n-InSb, spin flip Raman scatt. from electrons in localised donor states 77−3630
InSb, spin flip Raman scattering, gain, linewidth, effective g-value 78−22167
p-InSb, stimulated magneto-Raman scatt. obs. 77−83924
InSb, stimulated spin-flip Raman scatt. and stimulated recomb. radn. 79−72623
K atom, stimulated multipole Raman scatt. between opposite-parity states 79−76753
K, atomic vapour, resonant interaction with laser, Vavilov-Cherenkov effect *(Russian)* 80−106573
K, stimulated electronic Raman light scatt. by mag. sublevels 78−50492
K vapour, 16 μm and 8.5 μm generated via stimulated Raman process 77−19361
K vapour, mag. sublevels, stimulated electron Raman scatt. *(Russian)* 78−50861
KBr(I), UV two-photon absorpt. relative to known Raman cross section 79−81487
KrF laser beam, Raman pulse compression, for fusion expts. 78−59086
$LiIO_3$ crystal, noncollinear stimulated Raman scatt. using parallel pump beam 80−78912
$LiIO_3$, crystal inside Nd:$YAlO_3$ pumping laser, 0.9 W Raman oscillator operation 77−62004
$LiIO_3$, high power Raman oscillator, shared resonator config. 77−88853
$LiIO_3$, parametric oscillator, stimulated Raman scatt. competition 78−18016
$LiIO_3$, Raman induced Kerr effect with elliptical polarisation 78−42392
$LiIO_3$ Raman oscillator, high-average-power, employing shared resonator config. 78−30013
$LiIO_3$, simultaneous stimulated Ramam scatt. and optical freq. mixing 79−86210
$LiIO_3$, simultaneous stimulated Raman scatt. and optical freq. mixing using three-mirror config. 80−48342
$LiNbO_3$, hyper-Raman scatt. *(Russian)* 78−87102
$LiNbO_3$, non-centrosymm. crystal, hyper-Raman scatt. obs. 78−94409
$LiNbO_3$, nonstationary intracavity stimulated Raman scatt. by polaritons 79−18473
$LiNbO_3$, optical consts. determ. by background stimulated Raman scatt. 80−48336
$LiNbO_3$, polariton excitation for tunable coherent far IR generation 79−31982
$LiNbO_3$, tunable parametric Raman laser utilizing polaritons 79−41418
N_2, compressed, multimode radiation conversion to coherent Stokes wave 79−89971
N_2, constituent in propane-O_2-air flame, laser Raman spectrum for temp. meas. 77−5833
N_2 gas, stimulated Raman scatt. on rotational and vibrational transitions 79−27330
N_2, liq., ang. distrib. of stimulated Raman scatt. following excitation by two coherent beams 80−106571
N_2, liq., delay of broadband-pumped stimulated Raman gain 79−50351
N_2, liq., gain under spatially inhomogeneous pumping 77−58389
N_2, liq., high repetition rate stimulated Raman scatt., thermal blooming 80−91865
N_2, liq., parametric generation 77−741
N_2, liq., Raman lineshape 80−11384
N_2, liq., spectral splitting 78−50860
N_2, liq., stimulated Raman scatt. of excimer laser wavelengths for new lines in UV 79−59755
N_2, liq., tunable anti-Stokes Raman scatt. by light mixing 78−18007
N_2, liq., tunable millijoule radiation output 15 to 18 μm 77−88859
N_2, liq., wavefront restoration during stimulated Raman scatt. 78−18013
N_2, liquid, scatt. excited by picosecond light pulses 79−14034
N_2 liquid Raman laser, output radiation divergence, optical inhomogeneities formation 79−98352
N_2, solid, stimulated Raman scatt. and CARS 78−13752
N_2 stimulated scattering investigation, 1-4 atm press. range 80−91568
N_2, vibration stimulated Raman scatt., four photon parametric effects 80−33087
NH_3, far IR CW Raman lasing 80−83595
NH_3, stimulated hyper-Raman scatt. via 3-photon process to obtain IR and far IR radiation 80−58633
N_2O, liq., transient stimulated vibr. Raman scatt. 78−71144
N_2O, pure rotational stimulated Raman photoacoustic spectroscopy 80−32724
Na vapour, stimulated hyper-Raman emission obs. 77−79892
Na vapour, two-photon reson. four-wave mixing 78−46716
$NaNO_3$, Nd laser second harmonic stimulated Raman scatt., efficiency in calcite, nitrate crysts. 80−95949
$NaYF_4$:Ho, Yb, two photon anti-Stokes effect, excited by 2 μm radiation 78−50852
Nd:glass composite tunable laser at 1.89, 3.39 and 16 μm 79−72596
Nd:YAG pumped tunable sources, appl. to spectroscopy 80−58576
O_2 A band differential absorpt. lidar meas., using ruby lidar and stimulated Raman scatt. 79−39904
O_2, liq., stimulated Raman scatt., vibr.-translational relax. rate, schlieren technique meas. 80−9955
Pb, Raman conversion of XeCl-laser radiation in metal vapours, up to 40% efficient 79−23025
Pb vapour, XeCl laser pulse backward Raman compression 80−19068
$Pb(NO_3)_2$, Nd laser second harmonic stimulated Raman scatt., efficiency in calcite, nitrate crysts. 80−95949
n-$Pb_{0.88}Sn_{0.12}Te$, stimulated spin-flip Raman scatt. 79−72621
Rb vapour, IR stimulated Raman scatt. 79−27325
Rb vapour, stimulated electronic Raman scatt. for tunable IR output 79−76754
RbBr, UV two-photon absorpt. relative to known Raman cross section 79−81487
SF_6, liq., transient stimulated vibr. Raman scatt. 78−71144
SF_6, molecular vibration energy stochastization in intense IR laser field by Raman spectroscopy *(Russian)* 80−14149
SF_6, Stokes signal amplification, effect of pump radiation incoherence 78−18015
Si, efficient stimulated Raman scattering using Q-switched single mode Nd:YAG laser 79−94289
SiO_2 glass fibres, spectra 78−66869
SiO_2 multimode fibre stimulated Raman scatt. obs. 78−1396

stimulated Raman scattering continued
SiO_2 optical fibre, three-wave stimulated Raman scatt. obs. *(French)* 80−78902
SiO_2, silica fibre, transmission of high power laser radiation, role of stimulated Raman scatt. 79−37011
SiO_2:P_2O_5, optical fibre, stimulated Raman scattering *(French)* 79−27324
Sn vapour, Raman emission at 285 nm 79−3748
Sr vapour, generation of tunable 16 μm radiation by stimulated hyper-Raman effect 78−46715
TeO_2, paratellurite cryst., polariton Raman scatt. 78−25928
Tl, Raman conversion of XeCl-laser radiation in metal vapours, up to 40% efficient 79−23025
Tl, stimulated Raman scatt. and stimulated collision induced fluoresc. 78−87103
Tl+Ar, stimulated collision-induced fluoresc. and stimulated Raman scatt., simultaneous obs. 78−13463
Y_2O_2S:Ho, Yb, two photon anti-Stokes effect excited by 2 μm radiation 78−50852
ZnSe, two photon absorption relative to Raman cross sections 78−87098

stimulated scattering
see also stimulated Brillouin scattering; stimulated Raman scattering
absorbing liquid, coherent light transient self-diffr., simulated thermal scatt. laser expt. 80−48361
atom scatt. by stimulated light press., appl. to isotope separation 78−66526
backscattering from relativistic unmagnetised electron beams, book contrib. 79−27334
backscattering in bounded dissipative plasma, nonlinear theory 77−7547
benzene, laser wavefront reconstruction by stimulated scatts. in picosecond range 79−986
charged particle beam interaction with monochromatic radiation in inhomogeneous medium *(Russian)* 77−31114
coherent radiation novel sources, book 79−27231
collective EM scatt. from magnetised relativistic electron beam 77−38791
Compton laser, scatt. stimulation by decelerated EM waves, semiclassical theory 78−29926
cyclohexane, laser wavefront reconstruction by stimulated scatts. in picosecond range 79−986
dense optically transparent media, third-order optical susceptibilities 77−38981
dye active solution, conical scatt. of laser beams 79−94294
electrocaloric effect in stimulated scatt. of ultrashort pulses 79−10358
electron, slow EM wave stimulation, laser radiation scatt. *(Russian)* 77−46674
electron beam, relativistic, unmagnetised, stimulated scatt. anal. of HF incident pump wave 79−77345
EM shock radiation for far IR and submillimetric wave generation 77−38997
EM shock radiation with frequency up-conversion 77−38996
EM wave scattering by relativistic electron beam, nonlinear theory *(Russian)* 80−102601
Faraday effect on stimulated backward scatt., theory 77−34910
fluids, Rayleigh-Brillouin scatt., nonlinear spectroscopy 77−50731
free electron laser, enhanced gain 78−63050
frequency conversion and amplification by stimulated EM shock radiation 77−42475
gases induced scattering and self-action, effect on optical radiation propagation 79−72628
intense relativistic electron beam and zero frequency pump 77−38995
laser, solid-state, two-standing mode operation with stationary ats., saturation effects and stimulated scatt. 79−68398
laser beam, spatially inhomogeneous, induced scatt. 80−28274
laser-plasma, interaction, stimulated scatt., constant mismatch effect 77−31477
laser-plasma interaction, stimulated Brillouin to stimulated ion Compton scatt. evolution 78−42762
light concentration using inversion of wave front technique *(Russian)* 78−63154
light field reconstruction accuracy after stimulated scatt. 80−78911
molecular crystals, uniaxial, light scatt. on light phase synchronism *(Russian)* 77−38992
multimode light beams, threshold expt. study, pumping wave reproduction *(Russian)* 77−75609
non-steady state theory, soln. in convolution integrals 77−10978
nonlinear theory of stimulated scattering *(Russian)* 77−75610
nonmonochromatic radiation stimulated scatt., efficiency depend. on pump radiation statistics 80−95950
nonmonochromatic spatially inhomogeneous radiation, wavefront reconstruction and reversal 80−9952
parametric amplification, oscillation and interaction processes, induced scattering by polaritons 79−72629
parametric effects on nonmonochromatic pump radiation stimulated scatt. 79−64284
parametric luminescence spectra Stark effect, stimulated processes, strong field 77−10977
phase conjugation, reprod. of light field weak components at stimulated scatt. 80−5792
phase locking in transient stimulated scattering 80−53378
picosecond nonlinear optics, book contrib. 77−65609
picosecond spectroscopy of parametric superluminesc. 79−55187
plasma, ion temp. meas. using stimulated Brillouin and Compton scatt. 77−58892
plasma, magnetised, relativistically strong circ. polarised pump wave scatt. 78−34330
plasma, polarisation effects *(Russian)* 78−79440
plasma, Raman and Thomson scatt., beat-wave electron trapping 78−51308
pump spectrum reproduction under stimulated scatt. conditions, group velocity mismatch influence 79−89966
quartz, fused, photoelastic light scatt. from surface Rayleigh waves 80−97235
rate equations 79−94291
Rayleigh scattering, principle techniques and expts., review 80−34938
Rayleigh wing stimulated scatt. line, anomalous shift in external transverse resonator containing CS_2, CS_2-ethanol, o-xylene 78−13763
reflection coefficient in stimulated parametric backscatt. 77−62005
relativistic electron beam, stimulated Compton scatt. *(Russian)* 79−86122
relativistic free-electron wave generators, electrically pumped 80−91742
resonance stimulated four-photon parametric scatt. in three-level medium, spectral ang. distrib. *(Russian)* 78−71145
semiconductors, scatt. from free carriers created by light absorption 78−88330
semiconductors, transient light scatt. by free carriers 80−102766
spatial interference influence on amplification 78−71149
stationary turbulence spectrum evolution on scatt. of waves by particles *(Russian)* 77−31118
Stokes radiation spatial charact., saturation conditions 80−53379
surface wave scattering, total internal refl. conditions 77−742
Thomson scattering, rel. to plasma 79−94801
transparent dielectric, nondirectional glow under laser irrad. 78−52575
wave front reversal, reproduction, during stimulated scatt. *(Russian)* 78−87100
wavefront reconstruction of complex signal in stimulated back scatt. 79−31996
wavefront reproduction, laser action 78−1305
wavefront reproduction, rel. to dynamic holography 79−10361
wavefront reversal effect 79−41417
wavefront reversal in stimulated light scatt., focused spatially inhomogeneous pump beam 79−27331
wavefront reversal limits of existence 79−10356
wavefront reversal of two-freq. pump radiation 79−41420
weak beam wavefront inversion in stimulated light scatt. 80−5798
Ar, collision induced light scatt. spectra, pair polarisability 78−55135
CS_2, radiation self synchronisation on Rayleigh edge time stimulated scatt. in external resonator *(Russian)* 80−69461
Ge, picosecond optical response, effects of parametric scatt., energy-gap narrowing and state filling 80−11424
n-InSb, stimulated recomb. radiation 78−90456
K, vapour, stimulated four-photon parametric scatt. *(Russian)* 78−71145
$LiIO_3$, parametric scatt. at interface between two media *(Russian)* 79−59767
$Na(3S_{1/2}, 3P_{1/2})$ + He, total cross section, stimulated photon echo obs. 79−76503

STO calculations
$3d^N$ ions, free and in crystals, Slater parameters, 3d-4s excitation energy 78−33433
10-electron systems, minimal basis set localised orbitals, conjugate gradients method calcs. 79−6849
AB system, molecular calcs., electric dipole moments and electronic valence population, CNDO study 80−37742
acetaldehyde, proton affinity, geom. and basis set depend., MO calcs. 78−50461
acetylene, Verdet consts., ab initio calcs. 77−3390
acetylene, vibr. fine struct. accompanying core ionis., STO calcs. 78−62844
actinide ions, tetrapositive, nucl. hexadecapole antishielding factors 79−26909
addition theorems of spatial functions, multicentre integrals of arbitrary atomic functions, symmetry and analytical struct. *(German)* 80−37729
AH system, molecular calcs., electric dipole moments and electronic valence population, CNDO study 80−37742
alkanes, tritiated, fragmentation by β-decay, dissoc. of daughter species 78−31669
alkyl chlorides, proton affinity correl., ab initio SCF calc., MINDO/3, STO and G basis sets 78−33421
alkyl fluorides, geometries, props. and protonation, ab initio mol. orbital study 79−22588
allene, transition state for internal rot., HF/STO-3G calcs. with correlation energy corrections 78−25430
analytic radial orbitals, optimisation on variational parameters 80−42941
analytical calculation of two-centre Coulomb and hybrid integrals 77−83479
analytical calculation of two-centre Coulomb and hybrid integrals with correlation factor 77−83481
anions, struct. and energetic predictions, modified HF procedure evaluation 78−62720
18-annulene, geometrical parameters, STO-3G ab initio calc. 80−52867
approximate Hartree-Fock methods using density approximations and Coulomb field corrections, testing 80−91422
at. quadrupole shielding factor 79−10222
atom, energy levels and oscill. strengths 79−63896
atomic basis sets, orbital exponents for $3<Z<18$ 78−29738
atomic electron binding energies, determ. from relaxed-orbital relativistic Hartree-Fock-Slater calcs. 77−42255
atomic excited terms generator program 79−54759
atomic ionisation potential, X_α eigenvalues and Slater transition state 79−31394
atomic one-electron model hamiltonians with STO eigenfunctions 77−3269
atomic orbital translation in j-j coupling scheme *(French)* 78−41922
atomic orbital X_α optimised STO exponents 78−62721
atomic three parameter pseudopots., Li to Kr, PSIMBOL algorithm 77−26963
atoms, $5f^N$ and $5f^N7s$ config., parametric study 80−91444
atoms, $70\leq Z\leq 82$, Kα X-ray linewidths and relative intensities, energy dispersive meas. 80−99483
atoms, first row, real STOS, parameter optimisation method 78−41929
atoms, near threshold struct. in K-shell spectra, photoionisation or fast charged particle ionisation 80−87064
atoms of first row, min. basis sets of Slater-transform-Preuss functions 79−59343
cis-azo group, ionisation and excitation energies depend. on bond angle, ab initio MO calc. 79−72236
benzene, ground, singlet and triplet states, ab initio VB STO, GTO calcs. 77−75060
benzene, monosubstituted, ring protonation and C_{1s} binding energies, STO-3G calc. 79−29336
benzene radical anion, ab initio MO calcs., struct. 79−18113
benzothiazole, and homologues electronic struct., photoelectron spectra and MO calcs. *(French)* 79−31598
bonds, AH and AB (A, B=Li-F), linear momentum operator expectation values calcs. in molecules 79−7566
Born-Oppenheimer adiabatic pot. energy hypersurface gradient, exact formula 79−9992

STO calculations continued
t-butyl radicals, ab initio geometry calc., ^{13}C hyperfine coupling 77−10580
chemical shift, two-centre integrals calculation method including ang. momentum *(French)* 80−32601
closed-shell atoms, approximate relativistic Hartree-Fock eqns., soln. using Slater-type functions 80−58168
closed-shell configurations of isoelectronic ions and atom, SCF and STO energies 79−89598
$Co_4Sb_4(CO)_{12}$, electronic struct. calc. *(Russian)* 80−58136
Compton profiles using Gaussian expansion of at. orbitals, appl. to He, Ne, Ar, Kr, Na, and Al 80−945
configuration interaction calc., atoms and atomic complexes confined in spherical boxes, Hartree-Fock-Slater potential 80−47898
copper (II) complex, bis(dithiocarbamate), HF-Slater-LCAO calcs., mag. coupling parameters and optical spectrum 80−99447
correlation energy for closed and open shells, approx. calcs. 80−42942
Coulomb exchange integrals, correlation factor r_{12}^k, kinetic energy 78−62699
Coulomb exchange integrals, correlation factor r_{12}^k 78−62698
Coulomb integrals, one and two-centre, anal. evaluation 78−13432
cyanoacetylene, IR absorpt. bands, integrated intensities, ab initio and LMO calcs. 79−72234
cyclobutadiene, π face bonding with CO, HCN, benzene 79−98180
cyclobutane derivs., nucleophilic substitution, mechanism 77−9057
cyclopentadienyl radical, vibronic valence isomerisation, Jahn-Teller effect, D_{5h} symmetry 79−97986
diagrammatic perturbation theory, appl. to N_2, CO_2, BF 80−58131
diatomic molecule, electron static interaction potl., computation 77−3255
diatomic molecules, LCAO Hartree-Fock-Slater method calcs. 79−31374
diatomic mols., 2nd row, STO and HF calcs., bond length, dipole moment 77−23431
diazomethane, electronic struct., least energy dissoc. path to CH_2 and N_2 products 78−5131
dicyanoketene, and isomeric forms, heat of form., ab initio STO-3G calcs. 80−58190
dihydroxycarbene, singlet and triplet state rot. pot. surfaces 80−32627
dipeptide, struct. and bonding, ab initio calcs. 79−53039
electric field variant orbitals, STO field gradient depend., atomic quadrupole polarisability 80−23295
electric-field-variant orbitals, at. and mol. elec. props. 78−37543
electron repulsion integrals, three and four centre for Slater type orbitals, spherical harmonic expansion 79−18108
electron-repulsion integrals evaluation, expansion of Slater-type orbitals 80−99451
electrostatic isopotential maps for large biomolecules, STO transferable bond calc. 80−3571
ethylene, dipole moment derivatives, IR vibr. intensities, STO-3G, 4-31G, calcs. 77−6750
ethylene+H⇌ethyl radical, pot. energy surface, analytic function 79−11779
exact Slater integrals determ. for H wave functions, computer method 78−90074
exchange integral, three-centre nuclear attraction integrals, STAO anal. 77−18787
exchange integral, two centre, analytical evaluation 77−18788
film, HF formalism for calc. of total energies and charge densities 80−49850
first row atoms, utility of spd-type orbital 77−38617
first-row elements, model pots., STO calcs. 77−408
1-fluoro-2-propanol, conformational energies and rot. barrier, ab initio calc. 79−31390
fluorobenzene radical anion, ab initio MO calcs., struct. 79−18113
fluoromethane, total energy, MOs nonempirical minimum STO-4LGF calcs. 78−9074
formaldehyde, proton affinity, geom. and basis set depend., MO calcs. 78−50461
formaldehyde-water, heuristic intermol. pot. function, ab initio MO calcs. 78−33566
formamide, low-lying triplet states, relative energies and conformational preferences 77−3266
formic acid, proton affinity, geom. and basis set depend., MO calcs. 78−50461
generalised X-ray scattering factors, two-centre case with Slater type orbitals 78−79491
generator coordinate method 78−29731
glyoxal, $^3n\pi^*$ states, ab initio STO-3G CI calcs., ΔE_{SCF} transition energies 78−94194
graphite, electronic struct. exact exchange HF calcs. 80−65438
guanidinium ion, rot. barriers, ab initio calcs. 78−41923
heavy ion+atom collisions, mol. M-X-rays, self-consistent relativistic HF-Slater many electron correl. diagrams 77−14567
heavy ion+nucleus, RPA theory, time dependent, quasi-boson approx. 80−57800
trans-1,3,5-hexatriene, low-lying $\pi\pi^*$ excited states, ab initio STO method 77−3284
HF frozen core calc., Lagrangian multipliers in terms of Slater integrals 78−17554
hybrid integrals, two-centre, anal. evaluation 78−13432
hydrides, third row, electron binding energies, one-centre expansion method 77−6677
hydrides of 1st three row elements, pseudopotential calcs., PSIBMOL algorithm 77−26963
hydrocarbon radicals, ab initio calc. of spin densities 79−93938
hydrocarbons proximity and conform. effects, ^{13}C chem. shifts at γ position, INDO computations 77−50451
meta-hydroxyaniline, mol. complex., electronic struct., basis set and correlation effects 80−91436
integral expression, for $(nl|n'l')$ with n, n′=3, 4 77−30769
integrals involving continuum orbitals, numerically oriented evaluation method 77−61673
interconversion pot. energy surfaces, geometries, electronic structs. 78−35660
internal conversion calc., Hartree-Fock-Slater and Hartree-Fock models 80−18238
inverse Gaussian transforms, general props., Slater type orbitals appl., coord. and momentum representation 78−37549
lactam-lactim tautomeric equilibria, quantum chem. calcs. 80−50833
lanthanide ions, tripositive nucl. hexadecapole antishielding factors 79−26909
STO calculations continued
lanthanides, 4f-screening, ionisation pots. by modified Slater method *(Chinese)* 79−97977
LCAO Hartree-Fock-Slater method, evaluation 79−31374
LCAO Slater-type orbital band structure calcs., computable expressions, derivation 80−24776
lone pair orbital explicit representation, augmented contracted Gaussian basis set 78−25423
magnetic dipole-dipole hyperfine integrals for Slater-type orbitals 79−11095
magnetic multipole moment integrals, mols., Slater-type orbitals 77−88384
magnetic multipole moment integrals for Slater-type orbitals, analytic evaluation 80−58110
magnetic resonance, two-centre integrals involving one-electron dipolar coupling and Slater AOs, computational procedure 80−23291
many-body perturbation theory, modified pots., 3- and 4-body contribs. 77−88376
methane, coord. bond calcs. 80−58129
methane, excited states, photochem., ab initio calcs. 77−14371
methane, localisability in MO calcs., measured by absolute overlap and 2nd moment dispersions 78−74557
methane, VB calc. using minimal Slater basis set, $^1A_1$ ground state 78−62729
methane derivatives, stabilisation of planar tetracoordinate C, substituent effects, RHF/STO-3G calcs. 77−6671
methanol, coord. bond calcs. 80−58129
methanol, total energy, MOs nonempirical minimum STO-4LGF calcs. 78−9074
methanol dimer, intermol. function from ab initio calcs. 80−32629
methyl cyanides and isocyanides, isomerisation, ab initio (STO-3G) geometry optimised calc. 78−46265
methyl fluoride, coord. bond calcs. 80−58129
methyl fluoroformate, isomer conformation, CNDO and ab initio STO calcs. 80−58151
methyl glyoxal, $^3n\pi^*$ states, ab initio STO-3G CI calcs., ΔE_{SCF} transition energies 78−94194
methyl group, conform. problems, correlation effects 79−97999
methyl ion, electrostatic force theory appl. to mol. geometry ab initio verification 79−98002
methylamine, coord. bond. calcs. 80−58129
methylamine, total energy, MOs nonempirical minimum STO-4LGF calcs. 78−9074
methylene, singlet-triplet separation, configuration interaction study 78−13438
3-methyleneoxetane, electron structure, orbital-O interaction, MO calcs., UV photoelectron spectra 80−28058
methylsilylene, closed shell states, isomerisation, config. calcs. 78−35652
modulated perturbation theory, mol. interactions, STO expansions non-linear parameter minimisation 77−57871
molecular electric multipole moment integrals, STO orbitals 77−50557
molecular electrostatic potentials influence of polarisation functions 79−839
molecular geometry optimisation in mols. with second row atoms 77−42232
molecular ionisation potential, quark influence, ab initio SCF calcs., appl. to H_2O and SO_2 79−10058
molecular multicentre integrals calc. 79−22590
molecular orbital methods, speed and accuracy, comparison of methods 79−41106
molecular orbital theory, relativistic, in Dirac Slater model *(Japanese)* 78−66480
molecular Z-centre 1-electron integrals and Coulomb integrals over STOs 78−82608
molecule, electronic struct. and physicochem. props., modified partial neglect of differential overlap 78−82645
molecule, model pot. 77−408
molecule, modified Sharma formula for STO Lowdin alpha functions, coeff. matrix recurrence relations 79−31364
molecule, overlap integrals for AO NSTO basis set 79−31379
molecule with d-orbitals, automatic geometry optimisation, Slater orbital derivatives 79−6831
molecules, bond contributions to electronic energies, ab initio STO 3G calcs. 77−6669
molecules, optimum minimal basis of exponential atomic orbitals, STO basis 78−41921
monothioformate anion, protonation site, ab initio SCF calc. 79−47894
naphthalene, triplet excimer conformation, σ-π interaction transitions 77−6701
NMR spin-spin coupling consts. calcs. 77−68060
noninteger Slater orbital calcs., two-centre mol. integrals 77−26969
nonrelativistic atomic orbital calc. program using Slater functions 79−49930
nonrelativistic atomic states matrix element generator program 79−54758
one centre pot. energy functions and two electron integrals for STO's 80−14070
orbital interaction and chemical bonds. Exchange repulsion and rehybridization in chemical reactions 78−85142
3- oxetanone, electron structure, orbital-O interaction, MO calcs., UV photoelectron spectra 80−28058
partial at. charges calc. from ab initio mol. electrostatic pots., appls. 78−70739
particle energy loss, individual atomic orbital contrib., Hartree-Fock-Slater orbital 78−43060
perturbation theory, many-body, algebraic approx. 77−18776
phenyl cation, singlet, triplet state mol. geometries, energies, ab initio UHF STO calcs. 77−6672
polyacetylene, band struct. valence Hamiltonian minimal STO-3G basis calc., nonempirical model pot. 80−54596
polyethylene, band struct. valence Hamiltonian minimal STO-3G basis calc., nonempirical model pot. 80−54596
population optimised basis function in semiempirical atomic state energy calcs. 78−914
β-propiolactone, electron structure, orbital-O interaction, MO calcs., UV photoelectron spectra 80−28058
pyridinium salts, hydrogen-bonded systems, deuteron quadrupole coupling 79−78563
pyrrole-acetonitrile, H-bonded complex, ab initio MO calcs. 80−102440
radical, small, isotropic hyperfine coupling consts., MINDO/3 calcs. 80−52894

STO calculations continued
rare earth compound, crystal field and Slater parameters and coordination 78−6771
rare earth metal ions, 3d and 4f energy level parametrisation, Slater parameters and correl. corrections 80−87041
Rayleigh-Ritz method, convergence of Slater, Gauss and two-electron functions 77−65419
semiempirical theory for ground and excited states, Fock operator expansion, STO-3G and CNDO/S calcs. 80−58154
Slater 1s orbital four centre mol. integrals, Fourier transforms 80−74104
Slater-Koster integrals, general expressions in two-centre approx. 80−70585
Slater-Koster LCAO integrals, general expressions for reduction to two-centre approx. 79−68187
Slater-transform-Preuss functions, one centre integral calculation program 79−13626
spin-spin integrals, one- and two-centre, analytical evaluation over Slater-type orbitals *(Russian)* 80−9491
spirohydrocarbons, strained, bond angles, interatomic distances, semiempirical and ab initio calcs. 80−95533
subtilisin charge-relay system, electrostatic pot. map, STO transferable bond calc. 80−3571
TCNQ, and anions, PRDDO method using Slater orbital basis 79−764
3,3,4,4-tetramethyldiazetine, photoelectron spectra, ring size effects on azo group ionis. pots. 77−61793
thiocarbonates, mol. struct., S-substitution effect *(French)* 80−23335
thionitrates, mol. struct., S-substitution effect *(French)* 80−23335
three-centre one-electron integral calc. in Slater orbitals with different exponents 79−26876
three-electron bonds, strengths, ab initio LCAO MO CI calcs. 80−87046
transition metal, Racah parameters, atomic screening parameter Slater and Clementi-Raimondi values 80−69071
transition metal complex, LCAO-HFS-STO calc., basis set effects 80−52882
transition metal complexes, LCAO Hartree-Fock-Slater method calcs. 79−31374
transition metal ions, 3d and 4f energy level parametrisation, Slater parameters and correl. corrections 80−87041
transition state determination and characterisation ab initio calcs. 77−28975
trifluoromethyl cyanides and isocyanides, isomerisation, ab initio (STO-3G) geometry optimised calc. 78−46265
two centre and three centre integrals for attraction of Slater type orbitals to nucleus, coord. systems 80−14068
two centre integrals for attraction of STO to nucleus 80−14069
two-centre case, generalized X-ray scattering factors and Fourier transforms 79−99020
two-centre charge distrib., Fourier transform, STO general expression derivation 80−58119
two-centre Coulomb and hybrid integral coeffs., analytical evaluation formulae 77−67958
universal atomic basis sets, light atom HF ground state energies 78−78605
universal basis set, for atoms and mols. 79−36502
universal basis sets 79−10021
unsaturated hydrocarbons, dipole polarisabilities, STO-4G calcs. 80−83255
vinyl fluoride, geometries, props. and protonation, ab initio mol. orbital study 79−22588
vinyl isocyanate, and vinylcyano ether, geometry and conform., ab initio minimal STO-3G MO calcs. 80−23337
vinylcyano ether, and vinyl isocyanate, geometry and conform., ab initio minimal STO-3G MO calcs. 80−23337
virtual orbitals calc. method, in extended basis function space 77−46491
water, liq., structure and props., minimal basis set description 80−6347
water dimers, stability, CNDO/2 and STO-3G calcs. 79−760
water-imidazole, H bond interrupted chain, cooperative effects, STO-3G ab initio calcs. 80−63535
X-ray photoionisation cross section calcs., at. and mol. levels, HF rel. to OPW method 77−42353
Al, Raffenetti-type atomic basis set calcs. 79−97974
Al_2, repulsive region ground state pot. curves, SCF with STO basis set calc. 80−14188
Al_2^{6+}, repulsive region ground state pot. curves, SCF with STO basis set calc. 80−14188
$Al_2(Al_2^-)(Al_2^+)$ configurations, ab initio study, LCAO, STO, MO-SCF and CI calcs., binding energy *(French)* 80−91447
α-Al_2O_3, charge distribution determ., SCF calc., Slater-type orbitals, Madelung type const. 80−107100
Ar, electron binding energies, one-centre expansion method 77−6677
Ar, inner shell alignment calc. in electron impact ionisation 77−14586
AsF_3, inversion barrier, STO SCF calc. 80−63567
AsH_3, inversion barrier calc. 78−9271
BF, $X^1\Sigma^+$ state, many-body effects, HF STO calcs., diagrammatic perturbation theory 77−50355
BH, electron density, basis set, electron correl. effects 78−74581
BH, localisability in MO calcs., measured by absolute overlap and 2nd moment dispersions 78−74557
BH_3, localisability in MO calcs., measured by absolute overlap and 2nd moment dispersions 78−74557
B_2H_6, APSG method as a localised process 78−33415
B_4H_4, B_4H_{10}, APSG method as a localised process 78−33415
B_5H_9, B_5H_{11}, APSG method as a localised process 78−33415
B_6H_{10}, APSG method as a localised process 78−33415
BN, electronic struct., exact exchange HF calcs. 80−65438
$BaTiO_3$ crystals, octahedral TiO_6^{8-} cluster atomic population, ionisation energy, SCF MS Xα calcs. 79−72244
Be, atom, ground state, accurate CI wavefunction 77−42245
Be compounds, electronic structure, configs., energy, bonding, of small mols. and complexes 78−13420
Be, total nonrelativistic ground state energy, CI STO calc. 77−18800
BeH_2, localisability in MO calcs., measured by absolute overlap and 2nd moment dispersions 78−74557
C, electron excitation cross section calc., Born approx. with Slater wave functions 80−69243
C_2, $X^1\Sigma^+_g$, $6^3\Sigma^-_g$ states, perturbations, ab initio CI calcs. 77−83490
CH_3CO', low lying states, struct., energetics, ab initio STO calcs. 77−61682
CH_3NN', low-lying states, struct., energetics, ab initio STO calcs. 77−61682
STO calculations continued
CO, CO^+, MO correlation diagrams 77−61689
CO, core pseudopot. valence electron calc., orbital energy and bond length 79−72233
CO^+, ab initio pot. energy curves, full valence CI with minimal STO 79−72361
CO_2, anomalous energy minima surfaces 78−86791
CO_2+Ne, intermol. pot. in repulsive short-range region, ab initio 80−69204
CS, core pseudopot. valence electron calc., orbital energy and bond length 79−72233
CS, perturbation parameters between valence states 77−26975
CaH, spin doubling, SCF calcs. 80−95649
CaO, electronic structure 80−2332
Cl, Raffenetti-type atomic basis set calcs. 79−97974
Cl-containing systems, core Auger and core electron binding energy shifts, ab initio LCAO SCF MO UHF calcs. 77−30777
ClF, total energy, MOs nonempirical minimum STO-4LGF calcs. 78−9074
$Cr(CO)_6$, LCAO-HFS-STO calc., basis set effects 80−52882
F, Raffenetti-type atomic basis set calcs. 79−97974
FBO, electronic struct. calcs. 77−30772
F_2CS, pot. surfaces, X^1A_1, a^3A_2 and $a^3A_2(b_1)$ states, ab initio SCF calcs. 78−86795
Fe X (XI), energy levels and oscill. strengths, Slater radial integrals 77−79583
Fe(100), chemisorption of O, molecular orbital theory of bonding 77−85059
H, He atmosphere, hyperfine press. shift, MCSCF-variational procedure 77−6735
H, quasibound states, Stark effect, variational 77−3251
H^--positron bound states, CI-Hylleraas calcs. 77−10603
$H+NH_2 \rightarrow NH_3$ react., force, density anal. 78−60997
H_2 $^1\Sigma_g^+$ ground state, hybrid Slater-Gaussian-type 1s orbitals calc. 77−38605
H_2, electron wave function calc. with Weinbaum function supplemented by floating function 79−26882
H_2, nonempirical calc. for molecules in electric field 78−25459
H_2, octapole magnetisability, multiple SCF perturbation calc. with STO basis set 77−34550
H_2, STP basis sets, energies calc. 77−3262
H_2, Verdet consts., ab initio calcs. 77−3390
HCN, electronically excited states, SCF CI calc. using Slater type orbitals 78−78645
HCN, vibr. fine struct. accompanying core ionis., STO calcs. 78−62844
HCO′, low lying states, struct., energetics, ab initio STO calcs. 77−61682
HCl, electric field gradient at Cl, two- and one-centre wavefunction expsn. 78−17561
HF, ab initio HF-STO perturbation Auger transition rate calc. 79−72368
HF chain, ab initio cryst. orbital calcs., basis set depend. 78−34746
HF, geometries, props. and protonation, ab initio mol. orbital study 79−22588
HF, nuclear spin-spin coupling const., finite perturbation calcs. 78−78616
HF, STP basis sets, energies calc. 77−3262
HF, $X^1\Sigma^+$ state, many-body effects, HF STO calcs., diagrammatic perturbation theory 77−50355
HF, $X^2\Sigma^+$ state, 3- and 4-body perturbation theory modified pots. 77−88376
HNC→HCN, transition state determination and characterisation ab initio calcs. 77−28975
HNN′, low-lying states, struct., energetics, ab initio STO calcs. 77−61682
HNO_2, isomers, protonation mechanism, electrostatic pot. prediction limits 78−11506
H_2O, ab initio SCF CI calcs., ground state energy, config. and force consts. 77−18782
H_2O CI, high-order many-body perturbation theory 77−88397
H_2O dimer, intermolecular pot. functions from ab initio calcs. 80−5473
H_2O, electron density, basis set, electron correl. effects 78−74581
H_2O, localisability in MO calcs., measured by absolute overlap and 2nd moment dispersions 78−74557
H_2O, minimal Slater basis set VB calcs. 78−46272
H_2O, pot. energy surface, many-body methods using STO 79−85921
H_2O, SCF energy optimisation with regard to Slater's exponents *(French)* 79−49936
H_2O, VB minimal Slater basis set calcs., comparison with H_2S, MO calcs. 79−36536
H_2PNH_2, inversion-rot. mechanism, basis set and geometry optimisation effects 80−83273
HS_n^-, n=1-4, electronic struct., ab initio Hartree-Fock-Slater calcs. 80−74107
HS_n^{2-}, n=1-4, electronic struct., ab initio Hartree-Fock-Slater calcs. 80−74107
H_2S, electron density, basis set, electron correl. effects 78−74581
H_2S, SCF energy optimisation with regard to Slater's exponents *(French)* 79−49936
H_2S, VB minimal Slater basis set calcs., comparison with H_2O, MO calcs. 79−36536
H_2S_n, n=1-4, electronic struct., ab initio Hartree-Fock-Slater calcs. 80−74107
H_2SO hypothetical molecule, nonempirical STO calc. of chem. bonds 80−23307
He, He^--positron bound states, CI-Hylleraas calcs. 77−10603
He, orbitals calculations, using extended STO basis sets 79−6844
He, quantum-mechanical calculations 77−14350
He to Ne, STP basis sets 77−3262
He-CH_3^+ interaction energy, nonempirical calc. 78−86799
He-like ions, ground-state electron impact excitation strengths, close-coupling calcs. 80−23561
He_2, He_2^+, MO correlation diagrams 77−61689
He_2, pair polarisability correl. effects, SCF-CI-GTO-SO calc. 78−82651
He_2^+ $^1\Sigma_g^+$ ground state, hybrid Slater-Gaussian-type 1s orbitals calc. 77−38605
He_2^{2+}, autoionising states, adiabatic pot. energy curves calcs. 78−42140
$^4He^{2+}$, slowing down in solids, 0.4 to 4 MeV range, calcs. 77−7776
K, electronic excitation cross-section determ. method 77−540
KCl:$In^+(Tl^+)$, HF calc. for ground and excited states of impurity centre 77−72835

STO calculations continued
KOH, MHD plasma mol., pot. energy curves and dipole moment, bond lengths 78−71462
Kr, inner shell alignment calc. in electron impact ionisation 77−14586
Li, adsorption of methyl groups, complex form., STO calcs. 77−9124
Li chain, disordered system, ab initio cryst. orbital calcs. 77−47715
Li clusters, dissociative chemisorption of H_2, ab initio SCF-MO calcs. 79−77918
Li compounds, electronic structure, configs., energy, bonding, of small mols. and complexes 78−13420
Li, electron excitation cross section calc., Born approx. with Slater wave functions 80−69243
Li, electronic excitation cross-section determ. method 77−540
Li, multipole polarisabilities, shielding factors calc., hydrodynamic analogy to quantum mechs. 77−68134
Li, positron bound states, CI-Hylleraas calcs. 77−10603
Li_2, mol. struct. 2-electron integral evaluation by Multipole Expansion of Diatomic Overlap 78−908
Li_5B_4, molecular and electronic struct. 80−20107
LiCl, aqueous soln., self consistent wavefunctions, HFS Xα pot. in cluster model, Compton profile calc. 79−78783
LiF, $X^1\Sigma^+$ state, many-body effects, HF STO calcs., diagrammatic perturbation theory 77−50355
LiH, dipole moments and transition moments, semi-rigorous bounds, error limits 78−78635
LiH, mol. struct. 2-electron integral evaluation by Multipole Expansion of Diatomic Overlap 78−908
LiH, SCF ab initio calcs. with noninteger Slater orbitals 77−26969
LiH, STO calcs. 79−6847
LiH, STP basis sets, energies calc. 77−3262
LiH^-, mol. orbital calcs., diffuse functions for basis sets, electron affinity 78−25436
$LiNH_3^+$, $LiNH_2$, Li_2NH, localised orbital anal., bond props. 77−6676
Mg_2, Mg_2^+, electronic struct., pot. energy curves, multiconfig. SCF calcs. 78−5124
MnO_4^-, valence mol. orbital energy, nonempirical pseudopot. 79−22592
N_2, energy band calc. by linear combination of muffin tin orbitals method 77−4283
N_2, mol. struct. 2-electron integral evaluation by Multipole Expansion of Diatomic Overlap 78−908
N_2, N_2^+, MO correlation diagrams 77−61689
NH, fine struct. in $X^3\Sigma^-$ and $A^3\pi$ states, STO and GTO calcs. 77−6679
NH_3, IR absorption band integrated intensities, ab initio and LMO studies 80−23458
NH_3, localisability in MO calcs., measured by absolute overlap and 2nd moment dispersions 78−74557
NH_3, NH_3^+ ion, electrostatic force theory appl. to mol. geometry ab initio verification 79−98002
NH_2CO', low-lying states, struct., energetics, ab initio STO calcs. 77−61682
Na, electronic excitation cross-section determ. method 77−540
Na_2 $A^1\Sigma_u^+ \rightarrow X^1\Sigma_g^+$ system, transition moments and radiative lifetimes calcs. 77−34697
$NaCl^-$, mol. orbital calcs., diffuse functions for basis sets, electron affinity 78−25436
NaH^-, mol. orbital calcs., diffuse functions for basis sets, electron affinity 78−25436
Ne, at. struct. by many-body perturbation method, algebraic approx. 77−18776
Ne, triply-excited states contributing to correl. energy, diagrammatic perturbation theory 79−81161
NpF_6, energy levels and bonding, relativistic SCF Dirac-Slater calcs. 77−6691
O_2^+, ab initio CI STO calc. 78−74585
O_3, conformation, ab initio HFS method calc. 79−36526
OH^+, fine struct. in $X^3\Sigma^-$ and $A^3\pi$ states, GTO and STO calcs. 77−6679
P, excited config., Hulthen and Slater type 2d functions 78−41972
PH, fine struct. in $X^3\Sigma^-$ and $A^3\pi$ states, GTO and STO calcs. 77−6679
PH_2F, total energy, MOs nonempirical minimum STO-4LGF calcs. 78−9074
$Pd(CO_4)_4$, valence mol. orbital energy, nonempirical pseudopot. 79−22592
Pr ion in free state and in crystal, change of spectra 79−33271
PuF_6, energy levels and bonding, relativistic SCF Dirac-Slater calcs. 77−6691
S, excited config., Hulthen and Slater type 2d functions 78−41972
S_3, conformation, ab initio HFS method calc. 79−36526
SBr_2, transient species, He(I) photoelectron spectroscopy, discrete variational HFS calc. 79−31594
SF_6, ionisation pot., discrete variational Xα calc., Slater-type orbitals in Hartree-Fock basis 78−78837
SH^+, fine struct. in $X^3\Sigma^-$ and $A^3\pi$ states, GTO and STO calcs. 77−6679
SH_3^+, struct., ab initio HF calcs. 79−31371
SHF, total energy, MOs nonempirical minimum STO-4LGF calcs. 78−9074
S_2N_2, $(SN)_x$, (x=2 or 3), minimal STO-3G basis HF ab initio LCAO SCF MOC, geometry 78−903
ScH_3, valence mol. orbital energy, nonempirical pseudopot. 79−22592
SeH_3^+, inversion barrier calc. 78−9271
Si, lattice energy, pseudopotential calc. 78−23002
SiH_3F, total energy, MOs nonempirical minimum STO-4LGF calcs. 78−9074
SiH_3NCO, geometric struct., ab initio MO calc. 79−13834
SiH_3NH_2, total energy, MOs nonempirical minimum STO-4LGF calcs. 78−9074
Si_2H_6O, geom. and electronic struct., ab initio MO calc. 79−97972
SiH_3OH, total energy, MOs nonempirical minimum STO-4LGF calcs. 78−9074
SiH_3X (X=H, F, NH_2, OH), coord. bond calcs. 80−58129
SiO, core pseudopot. valence electron calc., orbital energy and bond length 79−72233
SiO, $X^1\Sigma^+$, $A^1\Pi$, $C^1\Sigma^-$ and $E^1\Sigma^+$ states, SCF CI calcs. 79−45641
SiS, core pseudopot. valence electron calc., orbital energy and bond length 79−72233
Ti:C, molecular cluster approach to electronic struct. and bonding mech. for impurity C 77−20270
TiH_3F, valence mol. orbital energy, nonempirical pseudopot. 79−22592
STO calculations continued
U I, electronic configs., HF relativistic calc., spin-orbit const.-Slater integral relation 77−18793
UF_6, energy levels and bonding, relativistic SCF Dirac-Slater calcs. 77−6691
UO_2^{2+}, electronic struct., secondary ligands effects, Dirac-Slater model 77−411
$Zn(CH_3)_2$, valence mol. orbital energy, nonempirical pseudopot. 79−22592

stochastic automata
SO_2 density prediction for Tokyo, adaptive transformation network method 79−5609

stochastic processes
see also random processes
1/f current noise, random walk model 77−8162
Abraham-Lorentz eqn. 78−20985
acceleration of particle in random pot., renormalised canonical perturbation theory 77−27233
acoustic emission signals, transient, stochastic model 79−72749
additive and cancellative interacting particle systems, book 80−41960
aerosol cylindrical particles, overall drift angle in sedimentation 79−50777
aerosol particle motion, stochastic nature, analytical approach 77−86385
agargel electrophoresis, protein transport, stochastic model 77−77769
air pollution episodes in Venetian region, real-time forecasting via advection-diffusion model 80−77096
air pollution episodes in Venetian region, real-time forecasting via Kalman predictor 80−82046
air pollution modelling and dosage area product forecast 79−5601
Alfven waves, in stochastic mag. field, Khasminskii's theorem 80−59198
amorphous solids, stochastic geometry, review, book contrib. 80−73269
angular correls. random perturbations, asymptotic attenuation coeffs. 77−30507
anharmonic molecules, stochastic multiphoton absorpt. processes, classical model 79−45778
antiseismic calc., stochastic model appl. 78−96139
astrophysics, stochastic phenomena 80−105161
asymmetric random walk with exponential transition probabilities, exact analytic results 79−44875
asymmetric top, rotational Brownian motion 78−8349
atmosphere, turbulent, conditional fading statistics of scintillation 78−66757
atmosphere daily temperatures, statistical forecasting using short records of previous temps. 79−58015
atmospheric hourly temperatures generation, stochastic model 78−61502
atom+diatom, collinear collision, vibr. energy transfer, stochastic theory, nonmarkovian effects 79−81262
atom+diatom, stochastic one-dimens. model 78−42159
atom+diatom trajectories, collinear, pattern recognition appl. to H_2+F(I), He+H_2^+ 80−45481
atomic motion in resont fluctuating laser radiation 80−43310
atomic transition in stochastic field, saturation and Stark splitting 80−9546
autocatalytic reaction system, sustained oscills., deterministic and stochastic theories 78−95922
autoregressive stochastic stationary processes, effect of missing values on autocorrel. anal. 79−17197
Backward stochastic partial differential eqns. and diffusion processes with noisy observations *(French)* 79−54052
bars, cylindrical and prismatic, stochastic, holonomic, elastoplastic torsion *(German)* 79−37192
beam propagation in focusing media with random-axis misalignments: Second- and higher-order moments 79−17236
beam volume scattering coefficient inadequacy 77−27251
betatron oscillation reduction, low-noise wide-band power amplifier system 80−58011
bifurcations inducing attractor in Oboukhov's turbulence system 80−1536
binomial redistribution process, Ehrenfest urn problem 80−52144
biological compartmental models, parameter estimation 78−40109
biological n-compartment model, identification by filtering techniques 79−34507
biradical magnetic field dependent ^{13}C and ^1H CIDNP, hyperfine coupling 79−3460
bistable optical system, phase transitions induced by white noise 79−18388
bistable reaction system, stochastic dynamics investig. of discrete trimolecular chemical model 80−16645
bistable system, catastrophe prediction using externally applied force 78−77823
Boltzmann equation, stochastic, hydrodynamic fluctuations 80−68158
Boltzmann kinetic eqn., influence of stochastic sources 77−2627
boundary-value problem, two-point, statistical variant using Einstein-Fokker-Planck eqn. *(Russian)* 78−81924
boundary-value problems, solns. using digital simulation of space-random fields 79−41510
Brownian distorted paths, energy forms, Hamiltonians 77−57279
Brownian fluid affected by potential, Maxwell-Boltzmann distrib. in infinite-time limit 80−105573
Brownian motion, fast variables elimination using time-convolutionless projection operator formalism 80−8913
Brownian motion, renormalisation theory 79−54060
Brownian motion, stochastic calculus, derivation from path integral expansion of conditional probability density 79−67227
Brownian motion, stochastic integral approximation by Stieltjes-Lebesque integrals *(French)* 79−49162
Brownian motion and NMR spin relax., book 78−15054
Brusselator, dynamic correl. functions, Mori-Zwanzig formalism 80−25988
Burgers equation, relationship to differential stochastic eqn. 80−36869
BWR stochastic neutron flux fluctuation obs. and modelling, thermohydraulic parameters 78−94065
carcinogenesis, time and dose factors 79−70590
catalytic processes and stochastic processes of chem. kinetics, historical review 80−105483
Cebysev mixing transformations, use in random process digital simulation 79−80510
cell kinetics stochastic model using DNA microfluorometric data 79−83723
charged particle trapped in mag. field, bounce motion 79−67150

stochastic processes continued
charged particles in single wave fields, adiabatic and stochastic motion 80−9795
chemical 'birth' and 'death' processes, absorbing zero boundary problem 78−95911
chemical instabilities, fluctuations in multiple steady state systems 79−11813
chemical instabilities, stochastic approach, anomalous fluctuation and transient behaviour 80−89465
chemical kinetics, validity of stochastic approach anal. 77−60044
chemical Langevin equations, stochastic source term 77−28982
chemical master eqns., Poisson representation 78−35638
chemical reaction diffusion systems, Chapman-Enskog development of multivariable master eqn. 80−81283
chemical reaction scheme, with autocatalysis and saturation law, stochastic model 79−52623
chemical reaction system, nonequilib. coexistence of three phases *(German)* 77−21351
chemical reaction system, nonequilibrium thermodynamics, stochastic approach 79−52749
chemical reaction with complex form., stochastic reduction for dynamics 78−3315
chemical reaction with spatial and temporal structures, stochastic analysis 78−35639
chemical reactions, macroscopic equivalence of fluctuation descriptions 77−77734
chemical reactions, reversible, asymptotic expectation and variance of stationary probability distribution 79−11789
chemical reactions, second-order, stochastic theory 78−73015
chemical reactions and reactive collision phenomena, props. of stochastic process description 78−60991
chemical system, multiple steady state, phase transform. stochastic theory, nucleation 78−53187
chemical system far from equilibrium, stochastic simulation 80−3339
chemical systems, single variable, master eqn. approximation by Fokker-Planck type eqns. 80−77702
chemically induced spin polarisation, finite element method, stochastic-Liouville eqn. 79−64018
Chirikov criterion for stochastic instability, illustrative example 78−93607
CIDN(E)P, infinite elements, in variational soln. of stochastic-Liouville eqn. 79−94014
classical dynamics systems, stochastic props., numerical methods reliability, time averages 78−41151
classical stochastic electrodynamics, positive temp. random EM field 79−40382
climate models, appl. to zonally averaged energy models 78−20502
climate var. model, theory 77−37347
cloud droplets, collisional problem in turbulent environment 77−5293
cloud droplets, stochastic collection eqn., computational instability in numerical soln. 77−2211
cloud drops stochastic coagulation, kinetic eqn. 78−92944
coherent states and stochastic formulation of quantum mechanics 78−57810
collisional drift waves, nonlinear evolution, bifurcations to chaotic state 80−14666
colloidal systems, stochastic transport eqns. 78−93609
column, stochastically imperfect finite, on nonlinear elastic foundation, buckling 80−48619
compartmental analysis, stochastic contributions 80−27215
complex molecular systems, collision phenomena by stochastic model, observables distribs. and information entropy 78−25640
complex nonlinear oscillation regimes 80−8919
composite materials, stochastic fracture models, and strength test results statistical anal. 80−64470
composite stochastic processes 79−80514
computer simulation in science teaching 77−17739
condensation, homogeneous, cluster size distrib., stochastic model 80−22311
condensation, kinetic theory, stochastic approach *(Russian)* 77−72676
condensed matter physics, dynamic correlations, book 80−86046
conditional expectations and Brownian motion, stochastic integration *(French)* 77−13585
conference proceedings, nonlinear dynamics, tribute to Sir Edward Bullard 78−93603
construction by Dirichlet forms 80−8921
continuous time stochastic approx. procedures 78−69969
contracted description of fluctuating systems 80−90781
convective cells, stochastic oscill. spatial-time spectra *(Russian)* 80−103029
convolutionless master equation, perturbation expansion 78−70047
cooperative cascade emission, linear stochastic theory 80−74326
core operating limit supervisory system stochastic simulation 79−630
correlation functions, finite-time averaging, statistical error 78−20946
cosmic ray particles propag. in interplanetary region, transport eqn. 79−44315
cosmic ray scatt. in stochastic mag. field, solar wind fluctuations, above 1 GeV 78−61689
coupled chemical reactions, stochastic time evolution, Monte Carlo simulation procedure 77−9047
coupled oscillater systems, stochasticity thresholds for chain of particles 79−80465
coupled oscillators, quasiperiodic to stochastic transition 78−54307
coupled random walk process, spatial structure, regression to steady states 79−25986
covariance estimation, of stationary, ergodic processes, with non zero mean value *(French)* 79−80513
critical points, relaxation phenomena, stochastic and deterministic theory 80−182
crystal growth, anal. treatment, comparison of two interface dynamics 77−89397
crystal growth, stochastic models, diffusion and relax. kinetics 79−37642
crystalline surface, atomic cluster diffusion, stochastic model 77−28077
crystallisation from melt, nucleation on supercooling, inter-nuclear separation distrib. function *(German)* 77−19885
crystallographic structures, non-linear physics anal. 80−10631
cumulative damage model 79−44736
cumulative damage stochastic model, fatigue and wear life test data anal. 79−18823
cumulative damage stochastic model 79−18822

stochastic processes continued
curve crossing problem for Gaussian stochastic processes, neural modelling appl. 78−85299
curved space, operator ordering schemes and covariant path integrals of quantum and stochastic processes 78−81812
curved space-time quantum stochastic processes, covariant Kolmogorov-Klein-Fock eqn. 80−18083
cyclic, normalisation according to period, algorithm *(Russian)* 79−75117
daily precipitation stochastic models, estimation of Fourier coeffs. to describe parameters seasonal vars. 79−53481
damped harmonic oscillator, quantum friction in c-number picture 80−94980
Davidson's generalization of the Fenyes-Nelson stochastic model of quantum mechanics 80−62531
dead-time effects in photon counting statistics 79−3665
defective crystals, diffusion processes and multistate diffusion 79−19389
delocalisation, statistical and stochastic aspects 77−30759
delocalisation, statistical and stochastic aspects 77−30760
desorption kinetics, Kramers-Langevin stochastic eqn., heavy-adatom limit, adatom-phonon coupling 78−84065
desorption rates, stochastic description 77−20184
deterministic eqn. of motion, master eqn. and steady-state probability distrib. 78−36925
deterministic motion of macrovariables inequality 80−42147
detonation waves, stochastic phenomena 79−77180
dhnamical systems, weak interaction of a small system with a large one *(Russian)* 79−12718
dielectric charge carrier drift simulation using stochastic graphs 80−15539
dielectric liquid in electric field, two-dimensional vel. field stochastic charact. *(Russian)* 78−75208
differential eqns. with non-Markov processes 79−25989
differential equations, diffusion approx. corrections 79−40466
differential equations, solns., splitting correls. 78−49770
diffusion process modelling, equivalence of different methods 78−57818
diffusion processes, stochastic description 78−41253
diffusion processes with two-point boundary conditions, probability distribs. 80−42144
dilations as propagators of Hilbertian varieties 79−9189
Dirichlet stochastic problem *(French)* 78−89406
disc dynamo, pseudo-stochastic behaviour in circuits with shunt, couple and series resistance 78−93608
discontinuous processes, weak solutions *(French)* 80−62579
discontinuous transitions into chaos after single bifurcation, hysteresis existence 80−73264
discrete process, one-dimens., invariant distribs. and stationary correlation functions 78−21059
dissipative structures, origins and perspectives *(French)* 80−151
dissipative system instabilities; nonlinear fluctuations 77−87696
dissipative systems, dynamical description 80−17867
dissipative systems with multiple steady states, trajectory instabilities, stochastic behaviour 79−80519
droplets, laser light scatt., multiplicative and additive stochastic processes 78−84596
Duffing oscillator, statistical linearisation approx. method for nonlinear stochastic processes 77−17790
dynamic system, classical quantisation conditions with stochastic behaviour anal. 80−8922
dynamical astronomy, integrable and stochastic behaviour 80−12650
dynamical stochastic system, statistical mechanics 79−30349
dynamical system, connectance, increasing no. of degrees of freedom 78−81831
dynamical systems, critical transition to stochasticity 80−73265
dynamical systems, kinetic eqn. derivation based on cumulant function props. 80−12995
dynamical systems with many degrees-of-freedom, deterministic problem stochastic anal. 79−75455
earthquake frequencies, stochastic modelling *(Japanese)* 80−94480
earthquake occurrence as stochastic event, theoretical models 78−40491
earthquakes, risk prediction as stochastic process 77−49029
earthquakes, shallow, statistical study of occurrence relations 78−96155
earthquakes characterization through response spectrum 79−20758
education, stochastic model, radioactive decay, difference-differential eqns. 80−51992
EEG analysis by all-pole model 80−41287
eigenvalue problem, stochastic, limit distribution *(German)* 80−52134
eigenvalues of stochastic differential operator, approx. soln. of mean problem *(German)* 78−12540
Einstein symposium, Berlin, Germany (Mar. 1979) 80−90596
elastic phase transitions, crit. dynamics 80−2146
elastomer, relaxation processes, statistical description *(Russian)* 79−23229
electrochemical noise generated by anodic dissolution or diffusion 77 - 25277
electrodynamics, derivation of quantum mechanics 78−36801
electrodynamics, derivative of Schrodinger eqn. 77−82411
electrodynamics and quantum mechanics *(French)* 77−50
electromagnetic wave propagation, local energy density distribution using Wigner distribution functions 80−9781
electron avalanches, stochastic approach 77−89338
electron gas, ground state, stochastic method calcs. 80−95031
electron microscopy, correlation analysis of radiation damage 80−100282
EM wave multiple scatt. effects from stochastic medium 78−44941
EM wave propagation in stochastically stratified medium, transmission coeff. 80−32887
EMG signal nonstationary model 77−86481
EMG spectra, factors affecting interpretation, stochastic process model 77−44825
entropy production in stochastic model of open system 78−4574
epidemic models for malaria progress 77−22397
EPR, rat liver and hepatoma mitochondrial lipids, stochastic anal. 78−76984
ergodic meas. instrument technology, student laboratory experiments *(German)* 77−49705
exciton line shapes and migration with stochastic exciton lattice coupling 79−11070
excitonic molecules, reson. Raman scatt. and luminesc. 79−95763
excitons, diffusive and percolative lattice migration 80−59879
extrema, asymptotic analytic theory for Fokker-Planck processes 80−12992

stochastic processes continued
eye movements of African chameleons, spontaneous saccade timing 78−69053
fast charged particle, dechannelling from planar channel, stochastic theory 80−96579
fatigue crack growth, in diffusion model 79−72860
fatigue crack propag., stochastic model 80−53701
Fatigue lives of metals up to crack initiation 78−7050
fatigue loadings, random signal analysis applic. 77−44453
FBR, thermal-hydraulic flow fields, stochastic processes 79−30991
fermion system, tight-binding spinless, many particle quantum diffusion in stochastic medium 80−42143
ferromagnet, critical dynamics under quenched random magnetic fields 79−4681
ferromagnetic crystal with defects, domain boundary displacement and magnetisation discontinuities, statistical theory *(Russian)* 79−51800
few-body quantum system stochastic variational method for all conventional N-N pots. 77−53799
Feynman path integrals, white noise approx., inertialess Brownian system 78−57859
filtering, nonlinear, conditional laws, smoothness, stochastic calculus of variations *(French)* 80−68128
filtering, nonlinear, some stochastic differential eqns. *(French)* 77−17787
finite dimensional stochastic systems, ergodic and quasideterministic props. 78−32762
fission, spontaneous, mass and charge division, asymmetry, order-disorder model 80−22866
fission reactor fuel-coolant interactions, temperature noise in one-phase heat transfer: stochastic models 80−68726
flicker noises in astronomy, stochastic prop. 78−57473
flood event real-time predictors, stochastic model 80−67383
floods, analysis using stochastic models 79−5528
fluctuating Boltzmann gas, stochastic theory of hydrodynamic systems 79−75476
fluctuation-dissipation theorem derivation for linear anelasticity 78−43066
fluctuation-dissipation theorems from the generalised Langevin equation 79−49167
fluctuations, random, moment behaviour of soln. processes for nonlinear stochastic differential eqns. *(Japanese)* 80−95039
fluctuations and nonlinear irreversible processes. II 80−82724
fluid mechanics, successive bifurcation of nonlinear dissipative system 77−14975
fluid model of quantum statistics with irregular stochastic fluctuations, derivation of Nelson equations 79−40450
fluids, equations of motion, stochastic eqn. *(Russian)* 78−21054
Fokker Planck eqn., steepest descent approx. 79−80516
Fokker Planck equations, exact time dependent soln. 79−63125
Fokker-Planck dynamics, perturbative expansion of correlation and response functions 78−45566
Fokker-Planck dynamics, stochastic quantisation and detailed balance 80−4645
Fokker-Planck eqn. soln. by path integral method 77−2628
Fokker-Planck equation, stochastic quantisation, path integral formulation 78−86228
forced oscillators, transition to stochasticity 79−84997
four-photon parametric oscillator theory 79−86216
four-vortex integrable and chaotic motions 80−103035
Fourier transform NMR spectroscopy, clipped free induction decay signal anal. 77−63976
fracture models, appl. to composites and polymers 80−10198
friction, stochastic quantisation, nonlinear Schrodinger equation 80−27164
friction, stochastic quantisation, nonlinear wave eqn. 80−98825
friction in quantised Langevin systems, Schrodinger eqn., damped harmonic oscill. solns. 79−21570
functional equations, random, stochastic approx. in Banach space *(Japanese)* 80−95038
functional integral methods for stochastic fields 79−25973
galaxies fields stochastic simulation 80−62295
gamma-ray imaging stochastic distributed filtering approach 77−13026
gases, weakly ionised, electron motion, stochastic theory of homogeneous systems, review 80−77735
gauge invariant QED construction in stochastic space 79−21998
Gaussian process testing method 79−1993
Gaussian quantum stochastic processes on the CCR algebra 80−12985
Gaussian random fields 78−36934
Gaussian stochastic processes, renormalisation group limits for Wick polynomials 78−54565
Gaussian stochastic processes, unified treatment of fluctuation theories 78−32761
Gaussian stochastic processes in physics, review 79−25982
general stochastic differential eqn., existence, unicity of soln. *(French)* 78−36800
generalised Langevin eqn. with Gaussian fluctuations 78−32760
generalised representation, of physical situation, appl. to hydrodynamics *(Russian)* 80−69760
geological materials and processes, models 77−81890
geomagnetic storms, largest, per solar cycle, statistics 77−2306
geophysical potential fields on sphere, stochastic props. study 80−56338
gradient problems, error of estimation of direction 80−22282
gravitational fluctuations in self-consistent mean field theory, review 80−90734
great earthquakes, chaotic behaviour, coupled relax. oscillator model, billiard model and electronic circuit model 80−94462
great earthquakes, stress drops, wave spectra and recurrence intervals 79−44116
gross variables, microdynamics and nonlinear stochastic processes 80−101754
ground water, stochastic analysis of one- and three-dimens. subsurface flows 79−5520
groundwater flow, stochastic anal. of spatial variability 79−84321
hadrons, extended, stochastic description 78−431
Hamilton function, conditionally periodic movement presentation 80−8915
Hamiltonian, classical with two degrees of freedom near an equilibrium point 80−8916
Hamiltonian, Henon-Heiles, survey and applications to related examples 80−8917
Hamiltonian, resonance and stochastic behaviour 78−93604
stochastic processes continued
Hamiltonian, thermodynamic, stochastic props. central limit theorem soln. 79−6069
Hamiltonian classical and quantum systems, Volta Memorial Conf. 80−8738
Hamiltonian system, ergodic components in the stochastic region 80−8918
Hamiltonians, stochastic character effect on particle accelerator design 78−93606
hard-rod clusters, one-dimens. diffusion, stochastic calcs. 77−9948
hard-sphere fluid, translational correl. functions, stochastic theory 77−84608
harmonic oscillations of single degree of freedom systems 80−33516
harmonic oscillator in random EM field radiative corrections stochastic electrodynamic treatment 77−45736
heat and mass transfer, mathematical model, stochastic perturbation effect 78−94546
heat transfer in fixed and fluidised beds, stochastic model 78−51234
Henon's map truncation, role of dissipation 79−85081
Holder continuity of sample paths in Euclidean field theory 80−9085
homogeneous condensation, from supersaturated vapour, stochastic simulation 78−51657
hot-atom collisional energy density function, stochastic calc. 79−29342
hydrodynamics, stochastic formulation, instability at onset of convection 77−19590
hydrology, normal distribution approx. by three-parameter log normal distrib. 79−53389
hydrology, reservoirs, asymptotic distrib. of functions of partial sums of stationary processes 77−41091
hydrometeorological processes measurement, information optimum conversion to digital form 79−29903
hyperfine spectra in presence of relax. 78−43743
hyperfine spectra lineshapes, stochastic model for classical bath variables 77−85631
impulse automatic control for 3D crystallographic lattice 77−22499
induced consecutive transitions, stochastic models 78−46429
inert gas exchange in living organs 80−81520
infinite dimensional stochastic systems, ergodic props. 78−32770
infinite harmonic crystal, dynamics and ergodicity 80−10598
infinite nonlinear lattice, localised mode due to a light impurity 80−10624
infinite particle two-dimens. systems, stochastic dynamics 79−80512
information contained in open systems by example of chemical reaction systems 79−91915
information theoretical aspects of gravit. field, space-time fluctuations 77−57266
inhomogeneous structures, macroscopic third-order elastic moduli 80−69672
inhomogeneous systems, stochastic version of Boltzmann eqn. 79−55442
insolation stability characterisation by stochastic time series 79−57396
instability theory applics. to nonlinear plasma systems, review *(Czech)* 80−38580
integro-differential stochastic operator, optimal non-anticipative policy *(French)* 77−17786
intermicellar kinetics theory, stochastic approach, master equation for, irreversible reactions 80−76561
internal stress, stochastic model for dip test in steady-state creep 80−58915
intramolecular energy transfer, crit. energy calcs. 77−9046
intramolecular energy transfer, stochastic, crit. point anal. of Hamiltonian system instabilities 79−98005
intramolecular energy transfer, stochastic theory 79−22618
introduction for physicists 79−25988
inverse problem in noise radiation 79−49168
ion beam stochastic heating by lower hybrid waves 78−83586
ion heating, by lower hybrid waves in Tokamak plasma 78−91126
ion heating by a perpendicularly propagating electrostatic wave 80−10410
ions confined by quadrupole RF field, free transit time, Poisson process appl. 77−62392
IR ν_5 absorption band profile of isotopically diluted OH group in crysts. 79−69821
IR staring mosaic sensor performance, effect of spacecraft-induced line-of-sight jitter 80−86416
irreversible entropy change, detailed imbalance of stochastic process 77−49700
Ising lattice, thermal relaxation, nonideal behaviour, stochastic theory 80−22312
Ising lattices critical behaviour, stochastic model simulation method 77−45804
Ising model, magnetisation probabilities and metastability 80−29516
Ising model, stationary measure as Gibbs state 77−71274
Ising models, stochastic dynamics 77−49690
isolating integrals in Hamiltonian systems, stochastic and ordered regions 79−2713
isotropic turbulence, conditional flow struct., anal. 80−19335
iterated logarithm, stochastic approx. processes *(Russian)* 77−37746
iterative maximisation of system of differential eqns., stochastic constraints 78−57757
itinerant oscillator model, anal. for dielectric relax. and incoherent neutron scatt. 79−90509
joint distributions and tachyons 79−58541
Josephson junctions, Fokker-Planck solution for thermal noise 77−89906
kinetic theory of gases, stochastic approach 78−9744
Klein-Gordon eqn., two dimensional model anomalously slow stochastisation *(Russian)* 79−89068
Kolmogorov direct equation, solution, Galerkin measures *(Russian)* 80−46981
Kolmogorov entropy, dynamical system phase space trajectory divergence, numerical anal. 77−26149
Lagrangian for non dimensional non constant diffusion processes 80−31688
Langevin equation solution, using Wiener's method *(Korean)* 78−49766
Langevin equation with multi-Poissonian noise, appl. to birth and death process, Boltzmann-Langevin equation 79−25978
Langevin equations, Fokker Planck Dynamics approach 80−57194
Langevin equations, stochastic integrals, removal of ambiguity, invariance postulate 78−70061
Langevin-equation approach, generalised phase space method for stochastic kinetic eqn. 78−54303
laser, single mode, nonlinear stochastic eqn. of motion calcs. 77−648

stochastic processes continued
laser fields, stochastically fluctuating, saturation and Stark splitting of resonant transitions 80−53245
laser fluctuations, semiclassical stochastic master eqn. theory, and Scully-Lamb theory 79−27236
laser generated plasma, stochastic (white noise) anal. of resonant absorption 79−50874
laser instability, example from synergenetics 80−9848
laser speckle, time-differentiated, first order statistics, vel. meas. 80−82750
laser theory, statistical mechanics of open systems *(Japanese)* 79−76658
laser theory, statistical mechanics of open systems *(Japanese)* 79−76659
lattice of randomly placed sites, diffusion, appl. to AC conductivity 77−8097
Lennard-Jones chain, stochastic transition in classical nonlinear dynamical system 78−142
Lennard-Jones one-dimensional chain, stochastic transitions, statistical features 79−67233
linear oscillator, nonstationary narrow band response and first passage probability, stochastic process 80−62465
linear polar molecule, rotational Brownian motion, spherical harmonics 79−30368
linear response theory, master eqn. approach 80−31663
linear stochastic differential equations in Hilbert spaces 79−63148
linear stochastic diffusion equations, two-dimens. system, asymptotic behaviour of functional for distribs. from argument of soln. *(Russian)* 78−21083
linear systems with nonwhite parameter fluctuations, differential anal. 79−85082
linear transport relaxation equations, matrices, variational principle 80−17785
Liouville equation, generalised, nonMarkovian and memoryless master eqns. 78−24737
Lithuanian river groundwater discharge long-term fluctuations *(Russian)* 79−92554
LMFBR, probabilistic accident anal. with deterministic codes 78−37420
LMFBR probabilistic accident anal., stochastically variable parameters 79−31021
loading, random, laminated plates, dynamic response 80−58902
loose medium, discontinuity of displacements, interpretation 80−12990
Lorentz process, convergence to random flight process 78−73941
Lorenz surface, wandering motion 77−87687
Lotka-Volterra eqns. with stochastic approx., numerical soln. 80−8912
Lyapunov characteristic numbers and Kolmogorov entropy of a four-dimensional mapping 80−46978
macromolecules, interacting, spherical, light scatt., conc. fluctuations, transport eqn. 79−1775
macroscopic non-Markovian systems, microdynamics, time evolution 77−41541
macroscopic non-Markovian systems, microdynamics, time evolution 78−41236
magnetic anomaly field vertical intensity, autocovariance function analytic derivation for sources statistical distrib. *(German)* 79−34746
magnetic flux annihilation in a large Josephson junction 80−11139
many-dimensional oscillator problems, 'Arnold diffusion' instability 79−75334
many-particle systems, stochastic var. method 77−41891
martingales, set function processes, vector lattices, Riesz decomposition and characts. *(French)* 80−8908
martingales, stochastic integral representation 77−67379
master kinetic equation for a particle in the field of randomly varying scatterers 79−58634
mathematical theory survey, book 78−21072
Maxwell field, stochastic mechanics in Euclidean formulation 80−42081
meas. fundamentals of mean values and standard deviations *(German)* 80−13031
measure preserving mapping, stochastic transition, approx. determ. 80−95035
mechanical system, with stochastic loading, first crossing probability *(German)* 80−86219
metal, stochastic model for fatigue under repeated stress or strain 77−56107
metal-composite shell, three-layer, stochastic formulation of optimisation using heuristic methods 80−38268
metallic one component systems, normal cryst. growth fluctuations theory 80−15025
metallisation by sputtering, particle no. filling spot area, calcs. *(Russian)* 78−52668
metals, heavy ion implantation, stochastic formulation of site populations 79−19271
metastability in macrosystems, eigenvalue problem 77−9977
meteorology 79−16621
methanol-$d_3(d_1)$ in freon 11, self-associated, OH frequency temp. depend. 80−37809
methods and techniques for quantum mechanics, book 80−4584
MHD equilibria, stochastic stability 79−77414
micellar phase dissoc.-recombination kinetics, stochastic model 80−55628
micelle dissociation-recombination kinetics, stochastic model 80−30291
microinhomogeneous media, appl. of random functions theory *(Russian)* 78−63280
micromechanics of discrete systems forming macroscopic body, stochastic deformations 77−40
microphysics, stochastic basis for quantum mechanics 79−53997
mixed boundary conditions in half-space, stochastic resolution *(French)* 77−9866
modelling of solar systems, for space and water heating 79−57459
molecular collisions, stochastic reductions, projection operator formalism forced oscill. model 77−65521
molecular collisions, stochastic theory in perturbation limit 78−1042
molecular dynamics, semiclassical study of bound states 80−9693
molecular emission spectra, in presence of strong driving field, stochastic Liouville eqn. 79−59503
molecular energy transfer collisions, master eqn. transition probabilities and moments, stochastic theory 79−3533
molecular pair, fluoresc. depolarisation, using stochastic Liouville eqn. with radiative terms 80−16074
molecular spectra, fluctuations effect on emission spectra 77−58055
molecules, Fokker-Planck eqns., stochastic modeling 80−43128
stochastic processes continued
monthly rainfall forecasting and synthetic generation, stochastic models 79−70861
motion of particle in velocity-dependent random force 77−22493
moving thin elastic strip subjected to random parametric excitation, dynamic stability 80−48618
multi-droplet system in vapour flow, time-evolution, mathematical formulation 79−41733
multifrequency *n*th order coherence function, path integral approach 79−89836
multigroup diffusion process in a fixed or variable set *(French)* 79−93678
multiphoton resonance interaction with matter 80−33073
multiple integrals, evaluation, correl. functions of Legendre ensembles 77−22396
multiple nonequilib. steady states, Maxwell-type constructions 79−88877
multiplicative stochastic anal. of nonstationary generalised Langevin eqns. 77−57270
multiplicative stochastic processes, exact solns. 79−40464
multiplicative stochastic processes in statistical physics, appls. 80−22289
multiplicative stochastic processes in statistical physics 79−25980
multistate diffusion in perfect and defective system, stochastic theory 79−93066
multistationary behaviour systems, stochastic approaches 80−98854
multivariate, MacDonald's and Milatz's theorems 77−33950
multivariate master eqn. diffusion operator, reaction diffusion system eigenfunctions 78−29077
multivariate stationary stochastic process, bilateral prediction error matrix 79−71369
muon, diffusion in presence of traps, spin depolarisation, stochastic theory 79−28666
muscle control system Ia feedback pathway correlations, origin and nature 79−24977
muslce mass potential, stochastic model, NMV activity *(Japanese)* 78−24056
n-photon resonance phenomena, finite laser bandwidth effect 80−58230
n-vector model, dynamic crit. props. 77−45805
n-vector model, stochastic, dynamic critical props. 77−24362
narrow sound bundle reflected from irregular surface, amplitude and phase var. 77−46825
Nelson's stochastic mechanics on Riemannian manifolds, classical dynamical system 78−57860
nematic liquid crystal, Maier-Saupe lattice model, stochastic model method simulation 77−43129
network design for estimation of areal mean of rainfall events 77−41082
network design for runoff prediction 77−41083
neuron, stochastic electronic model 77−48775
neuron populations as information processing system, stochastic properties 78−80860
neuron with shunting inhibition, stochastic modelling 77−9183
neuronal activity and the time dependent threshold problem, diffusion approximations 79−74639
neuronal activity model, Ornstein-Uhlenbeck process 80−51030
neuronal spike-train statistical anal. methods 78−73149
neurone stochastic activity models, book 77−44632
neurone susceptibility to changes in synaptic inflow, evaluation using stochastic model 78−24059
neutron stochastic transport, functional theory 80−37413
neutron transport, Bell-Pal fundamental eqn. for n stochastic behaviour in Boltzmann continuum model 78−78436
NMR spectroscopy, Ito and Stratonovich calculus calcs. 77−13787
non equilibrium systems, stochastic model, master eqns. *(Chinese)* 80−68126
non-Markov processes, time evolution, correls., linear response 77−13587
non-Markovian, memory 78−93612
non-Markovian equilibrium dynamics and fluctuation-dissipation theorem 78−62157
non-Markovian Langevin equations, new approach 80−27222
nonadiabatic losses of particles in a dipole trap *(Russian)* 78−87002
nonequilibrium chemical systems, transitions, fluctuations, stochastic simulation approach 79−24722
nonequilibrium phase transition, exact results, stochastic anal. 78−29076
nonequilibrium steady states of open systems, 2nd order type transitions and fluctuations 77−49680
nonequilibrium systems, conf., Sitges, Spain (June 1978) 79−25987
nonequilibrium thermodynamics, stochastic measures 80−86240
nonequilibrium thermodynamics inequality conditions, stochastic laws 79−75482
nonequilibrium transitions and stationary probability distribs. 79−12720
nonequilibrium transitions induced by external noise 80−152
nonlinear, comparison of statistical linearisation, diagrammatic expansion, and projection operator methods 78−54306
nonlinear, validity of Onsager-Machlup postulate 79−67226
nonlinear birth and death models, controlled truncation global bounds 80−52130
nonlinear birth and death processes, relaxation mode anal. 77−49681
nonlinear chemical rate processes with multiple stationary states, stochastic theory 77−90582
nonlinear differential equations 78−93516
nonlinear diffusion-process, appl. of Onsager-Machlup function 79−44888
nonlinear dispersive system with small dissipation, statistical theory 78−70058
nonlinear filtering equations for two parameter doubly stochastic Poisson processes *(French)* 80−17870
nonlinear medium nondegenerated wave interaction with amplification, stochasticity occurrence *(Russian)* 78−83027
nonlinear oscillator interaction with discrete system of oscillators 78−70050
nonlinear oscillators, limit cycle, chaotic response 80−148
nonlinear stochastic differential eqns. excited by Gaussian noise and harmonic disturbances 77−87631
nonlinear stochastic differential equations, approx. soln. by statistical linearization method, variational procedure 77−17789
nonlinear stochastic functional, correlation depend. *(Russian)* 77−67235
nonlinear stochastic model, statistical mechanics 79−2724
nonlinear stochastic systems, asymptotic state estimation 79−12580
nonlinear systems, vibrations under space-time stochastic loads 80−33524
nonlocal stochastic equation of motion with damping in electrodynamics 80−17872

stochastic processes continued
nonMarkovian stochastic model of non-relativistic wave mechanics *(French)* 77−82450
nonmonotone stochastic integrals and stochastic differential calculus *(French)* 80−90779
nonstationary, probability characts. of mass flow rate meas. 80−73302
nonstationary stochastic process, computer programme for statistical characts. 80−22283
nuclear reactor, point reactor without delayed neutrons, moments of probability distrib. calc. 77−57705
nuclear reactor system, parameter identification applying stochastic approx. 78−17279
nuclear spin-lattice relax., effects of hindered rotation of NH_4^+ 77−8433
nucleation in early stage, stochastic process 79−80521
nucleus growth, spatial kinetic systems, multi-stationary state transitions, Langevin stochastic approach 78−73136
ocean internal waves, acoustically relevant statistics for stochastic models 77−46854
ocean oil spill trajectory, modelling advancements 79−5509
ocean wind waves growth stochastic form. 79−16499
Of and O stars, stochastic accel. in photospheres rel. to difference in mass loss 80−90413
Onsager-Machlup function, Lagrangian for diffusion process most probable path 78−73940
Onsager-Machlup Lagrangian in theory of stationary diffusion processes 80−128
open dynamic subsystem, nonlinear eqn. with fluctuating parameters derivation 80−94991
open dynamical system, equations with fluctuating parameters 80−62584
operator orderings rel. to functional formulations, quantum and stochastic dynamics 77−45740
optical, statistics and multichannel time analyzers for luminescence spectroscopy 79−85185
optical Bloch equation, stochastic incoherences 79−68373
optical frequency up-conversion with stochastic pumping, exactly soluble model 80−23744
optical phase tracking, Fourier series and estimation appl. 78−25812
optical processes, second order, stochastic models of intermediate state interaction, stationary response 77−85769
optical processes, second order, stochastic models of intermediate state interaction, stationary response 77−85770
optimal filter design for beta gauge 77−1904
optimal stopping times, existence and characterisation results *(French)* 77−13586
orthoses for lower extremities, adaptive control principle study 78−48932
oscillator with bilinear hysteresis, response to stationary random excitation, stochastic averaging 79−46179
oscillators, coupled, stochasticity thresholds 80−46977
oscillators, nonlinear stochastic, triangular wave, optimally controlled, Weiner process and Poisson process, numerical studies 80−52128
oscillators, two-mode self-excited, synchronisation and stochastisation by external field 79−80524
overlapping avoided crossings, rel. to quantum stochasticity 80−90694
oviductal egg transport, stochastic model 80−51059
Pal-Bell stochastic equations for particle transport scattering theory 79−45319
papillary muscle in rat, dynamic behaviour stochastic model 78−35821
parametric frequency up-conversion with stochastic pumping, canonical model 80−53368
parametric resonance, wave intensity fluctuations in one- dimensional randomly inhomogeneous medium 80−18970
parametrically excited nonlinear chain, stochastic oscills. *(Russian)* 79−55363
Parkinson tremor, long-term recording and evaluation 77−21639
particle accel. by MHD turbulence 80−31203
particle beam, stochastic cooling, review 80−37675
particle kinetics on one-dimensional lattice with inequivalent sites, stochastic model 77−41546
particle mobility in Gaussian pot. at high temp. *(Russian)* 79−30364
particle motion in stochastic force fields 78−73928
particle motion in stochastic space, relativistic dynamics 80−82639
particle motion in two waves, numerical study 80−8914
particle motion round variable luminosity source, stochastic scatt. accretion and ejection 79−44338
particle size-shape distribs., general spheroid problem, model 78−62055
particle transport, stochastic theory, appl. to radiation damage cascades 78−153
particle transport, stochastic theory, appl. to radiation damage cascades 80−54291
passive tracking acoustic array evaluation, nonlinear filtering lower bound algorithms 80−96088
path integrals for inertial classical particles, rapid stochastic processes 78−57858
peak-detection probability for line spectra, stochastic model 78−78597
pendulum, double with varying length, probabilistic characteristics of solns. *(Polish)* 80−8781
percolation problem, Hausdorff dimension of largest cluster and backbone, numerical estimates 79−97316
periodic potential, stochastic diffusion 80−12994
perturbation theory, quasi-periodic motion, asymptotic expansion method 80−17877
phase transition probability, system size depend., consequences for stochastic eqns. 78−41258
phase transitions, nonequilib., soluble stochastic model 79−12748
phenol(d_1)-dioxan(-acetonitrile), in carbon tetrachloride ($CDCl_3$) solns., H-bonds vibr. relax. bands anal. 78−84560
photon, stochastic phase space kinematics 79−2649
photon counting system, with dead time, waiting times distribution analysis *(Japanese)* 77−10104
photon echo spectroscopy of crysts., review 80−83648
piston engines, elastically suspended, nonlinear vibr. under kinematic stochastic excitations *(Polish)* 78−18221
plane orbit estimation using discrete timing of range measurements, Hermite polynominals appl. 80−21890
planetary regolith dissipation during cratering, stochastic model 79−70974
plasma, electrostatic large amplitude standing wave, particle stochastic motion 79−77406
plasma, magnetised, unstable, turbulent, stochastic photon diffusion 79−48662
stochastic processes continued
plasma, renormalised Vlasov turbulence 80−19579
plasma, SS 80−14927
plasma test electron transport in stochastic mag. field, principles and problems 79−77341
plasmas, stochastic ion heating by lower hybrid wave 80−28707
plastic structures, dynamic adaptation to stochastic excitation 79−1116
plastic structures, stochastically loaded, reliability estimate, kinematic approach 79−27546
point mass in plane convex region, stochastic transition and entropy 78−54288
point process with continuous probability measure, non-parametric test *(French)* 80−57184
point processes, physical background and mathematical model *(Chinese)* 80−62577
point reactor kinetics eqn. soln. 79−63719
pollution modelling, numerical estimation of unknown parameters *(Japanese)* 80−89702
polyatomic molecules, vibronic spectra, stochastic model 79−50004
polymer, cross-linked, on basis of oligodienedihydrazides and diepoxides, characts. *(Russian)* 80−58431
polymer chains, Edwards' model, stochastic model 80−68140
polymer dynamics simulation, general theory 78−91210
polymer dynamics simulation, relax. rates and dynamic viscosity 78−91211
polymer growth models 77−72567
polymer solutions, dilute, regularly alternant, thermodynamic props. self avoiding random walk calcs. *(French)* 80−59369
polystyrene, glassy state, relax., free vol. fluctuations effect 80−19722
polytypic crystals, stochastic model of layer distrib. 77−80435
probability density, time dependent, for nonlinear non-Markovian stochastic process, coloured noise effect 80−22281
Proca's eqn. stochastic derivation, Weyssenhoff top fluid considerations, velocity of light random fluctuations 79−97247
propane-O_2 mixture, combustion to detonation transition, stochastic aspects 79−100381
protein synthesis, stochastic eqns., ribosome translation along mRNA and tRNA selection processes 79−66440
proton (antiproton) beam in storage ring, stochastic cooling anal. 80−5420
quantification of stochastic process, principles of quantification noise *(Spanish)* 80−57190
quantisation, semiclassical, periodic orbit role for the quantal bound state 80−8831
quantisation of wave fields, appl. to dissipatively interacting fields 78−86184
quantum, thermodynamic limit, master eqn. 77−37814
quantum dynamics with dissipative forces as stochastic dynamics 77−33891
quantum electrodynamics, derivation of quantum mechanics 77−74252
quantum field theory, review of probabilistic concepts 77−5975
quantum harmonic oscillator, stochastic electrodynamics approach 79−49077
quantum Heisenberg ferromagnets and stochastic exclusion processes 80−88712
quantum intramolecular dynamics: criteria for stochastic and nonstochastic flow 80−53082
quantum K-systems, kinetic description, stochasticity condition 79−85080
quantum mechanical transformation function, stochastic action integral interpretation 80−77644
quantum mechanics, canonical commutation relns., and stochastic regularity 77−33939
quantum mechanics, equivalence to classical stochastic theory 79−80468
quantum mechanics, stochastic formulation, quantum operator algebra origin 80−88
quantum mechanics, stochastic foundations, harmonic oscill. in stochastic electrodynamics 77−9910
quantum mechanics, stochastic interpretation, review 78−70056
quantum mechanics, stochastic interpretation 79−40399
quantum mechanics as stochastic process in phase space 77−64964
quantum nonequilib. statistical mech., classical Markov stochastic process 77−33938
quantum pendulum under periodic perturbation, stochastic behaviour 80−8834
quantum statistical mechanics, K-flow, K-entropy 77−5749
quantum statistical mechanics, stochastic phase spaces and master Liouville spaces 79−85076
quantum system under stochastic perturbation, time correlation functions 79−49154
quantum theory, physical foundations, stochastic formulation, proposed expt. test 80−52049
quantum theory, stochastic electrodynamics formulation *(Spanish)* 80−82925
quantum-mechanical scatt. for particle in field of variable scatterers, soln. of stochastic Liouville eqn. 78−140
quasilinear reactor system subject to white Gaussian multiplicative noise, moment stability anal. 79−22373
quenched in vacancies, clustering, stochastic theory, continuum model 79−77593
radiation effects after partial body irrad. in radiography 78−69152
radiation field, mean specific emission intensity, fluctuation effects *(Italian)* 79−18346
radioactive contamination in aquatic organisms, evaluation by statistical and information theory 78−53535
radionuclide migration from repository sites, stochastic anal. 80−37486
rainfall, annual, stochastic anal. rel. to effects of urbanisation 80−98407
random excitation of harmonic oscillations of single degree of freedom systems 78−54175
random moires processes, densities of Minkowski measures *(German)* 77−64932
random noise, in imaging systems, statistical anal. characterisation, measurement 77−86562
random processes, statistics of, use of stochastic occupation densities and local times *(French)* 80−46972
random walks, spatial structure and stability 79−49169
random walks and generalized master eqns. for system with internal degrees of freedom 77−82461
randomly inhomogeneous medium with reflecting boundary, wave intensity fluctuations 80−42075

stochastic processes continued
rapid reaction of two chemical species in the presence of weak random advection and molecular diffusion 79−66261
ray paths in refractive scattering medium 77−68175
Rayleigh-Benard system, turbulence near onset of convection 80−48686
reactor neutron noise anal. techniques, unified theory 79−30886
reactor noise, neutron multigroup theory, calc. of second order correl. functions *(German)* 79−89390
relativistic Brownian motion, space-time approach to quantum mechanics 80−31567
relativistic Brownian motion and the foundations of quantum mechanics 79−63084
relativistic harmonic oscillator imbedded in random stochastic thermostat, stable states 79−49033
relativistic quantum kinematics on stochastic phase spaces for massive particles 79−2648
relativistic wave equations derivation, elementary domains theory, stochastic quantisation procedures 77−41502
relativistic wave mechanics, hypothesis on origin of quantum potential *(French)* 78−86405
relativistic wave mechanics, stochastic model, Newton's second law *(French)* 79−30226
relativistic wave mechanics, stochastic model *(French)* 78−86404
remote sensing, error anal. of ill-conditioned data, inversion technique 77−66992
reproducing-kernel Hilbert spaces of distributions and generalized stochastic processes 79−54059
reservoir optimisation, discrete representation of storage 77−64354
reservoir storage capacity, small sample expectation of population and adjusted ranges 78−61468
reservoir storage capacity, small sample expectation of rescaled population and adjusted ranges 78−61469
review, book contrib. 80−73268
RF plasma heating, stochasticity role 80−28752
rigid sphere embedded in elastic medium, response to incident stochastic waves 80−64451
risks of maximum likelihood estimators of parameters of Ito-like process 77−49576
rocks modal analysis, error assoc. with point-counting 78−32232
rotating liquid layer heated from below, form. and interaction of three-dimens. convective cells 79−14397
rotational Brownian motion, graphical study 77−13702
rotational Brownian motion of a symmetrical top 79−54061
rotational Brownian motion of an asymmetric body 79−54062
rotational Brownian motion of nonspherical top, Smoluchowski equation 78−24738
rough sphere fluid, computer simulation comp. to stochastic models 79−82138
Rutherford 180° backscatt. anomaly in solid, Monte Carlo simulation 80−45189
Rydberg angular momentum transfer, stochastic model for induced consecutive transitions 78−46429
Schrodinger's variational quantisation method in stochastic framework 80−105532
Schrodinger eqn., model of stochastic origins 80−81
Schrodinger equation, Brownian motion interpretation challenged 80−94974
Schrodinger equation, quantum mechs. as generalised stochastic theory in phase space 78−45505
Schrodinger equation, stochastic resolution, analyticity and integrability, existence and uniqueness of soln. *(French)* 80−73195
Schrodinger equation, stochastic solution, asymptotic behaviour *(French)* 80−46844
Schrodinger equation derivation from Newtonian mechanics, Nelson's method, discussion 77−33908
Schrodinger equation nonseparable potentials, vibr. energy level semiclassical calc. 80−8832
scintillation counting, liq., unified approach to counting process, stochastic model 77−3240
scintillation counting, liq., unified approach to counting process, optimising optical design 77−3241
sea ice deformation, viscous law as stochastic average of plasticity 78−16028
second order stochastic processes and the dilation theory in Banach spaces 80−90778
seismic events, non-linear stochastic models with appls. in event identification 79−16396
seismic waves, reflection coeffs. identification from noisy data 79−29718
self-consistent analysis for two-dimensional hydrodynamics 80−4533
semiclassical laser theory in the stochastic and thermodynamic frameworks 80−1178
semiclassical stochastic radiation theory 78−21010
separated hypotheses for stochastic processes, tests *(French)* 80−17871
short-time stochastic electron, modified Brownian particle, Schrodinger eqn. 78−36853
shot noise, extended class, inverse problems 79−17199
simple dynamics, systems, stochastic behaviour 79−25991
slightly dissipative systems, stochastic behaviour 80−22290
SO_2 air pollution levels modelling and forecasting, statistical approach 78−81398
solar air conditioning systems simulation 79−57415
solar convective zone, two-dimensional stochastic motions rel. to differential rot. problem 77−53518
solar cooling performance predictions via stochastic weather algorithms 80−35642
solar cooling system performance predictions using stochastic weather data 80−85269
solar flare protons, stochastic accel. 80−21953
solar photosphere, stochastic mag. pumping model rel. to mag. fields fine struct. 80−98646
solar radiation, convection efficiency and time variation of solar const. 79−21262
solar radiation data, stochastic modelling and forecasting appl. 78−36243
solar radiation geometric Brownian distribution, implications for economical solar heating system 79−83571
solar water heating models comparison 80−30387
soliton lattices, dynamic and stochastic oscills. *(Russian)* 77−74324
soluble-model Boltzmann equations for spatially uniform systems, written in form of stochastic equation 80−95046
sonar output fluctuation modelling 78−66981
stochastic processes continued
space dependent stochastic neutron kinetics with Gaussian parametric excitation 80−63223
space independent low power model, multigroup energy formalism for reactor stochastic eqns. 80−63224
spectral analysis of randomly sampled signals 77−9961
spectral estimates, randomly sampled signals, variability reduction by filtering out parts of spectral energy 80−57193
spectral simulation via finite elements, variational method and stochastic-Liouville eqn. 79−85157
spin states in stochastic dynamics model 77−30039
spin system, critical, in random mag. field, supersymmetry, neg. dimensions 79−97533
spin-oscillator coupled system, stochastic model for dynamics 77−22500
stability, input-output, of continuous time and discrete time interconnected stochastic systems 80−52133
stability of stochastic differential eqns. *(Russian)* 77−71188
star formation, stochastic model rel. to spiral galaxies props. 80−12818
stars, stochastic marginal forced mixing rel. to evolution 80−56818
stationary Gaussian processes, rarefied gas theory *(Russian)* 77−35173
stationary point processes, estimation procedures 77−2517
statistical mechanics, obs. prob. for stochastic variables *(Norwegian)* 79−80497
statistical mechanics, stochastic master eqn. representation 77−33935
steady state stochastic nonlinear vibrs., covariance anal. *(German)* 79−88880
steel, low C, high cycle fatigue, crack initiation model *(Japanese)* 80−104258
stellar evolution, fluctuations due to convection 80−31293
stochastic control, regularity of weak solns. of variational irregularities *(French)* 79−54053
stochastic differential eqns., Green's function soln. by hierarchy method, closure approx. error 80−149
stochastic differential eqns., stability and boundedness rel. to generalised norm 80−12993
stochastic electrodynamics, alternative to quantum mechs., path integrals 78−9307
stochastic fields from stochastic mechanics 80−95033
stochastic functional differential eqns. and systems of differential inequalities 78−77801
stochastic mag. field fluctuations, self-consistent model 80−100074
stochastic metastability and Hamiltonian dynamics, phase space invariant tori 79−40465
stochastic physics, quark bag model 79−54000
stochastic quantisation processes, review, Markov processes, Martingales, quantum dynamics 80−94969
stochastic quantum mechanics, dissipative forces, operator algebra 80−98826
stochastic transition, determination method 79−71366
Stokes' formula, stochastic integrals and path independence *(French)* 80−27216
storage ring, stochastic cooling tests on proton beams, initial cooling expt. 78−90006
strange attractor type motion, simplest case 79−17345
Stratonovich calculus, superiority over Ito for stochastic processes with non-additive fluctuations 79−85078
Stratonovich calculus, superiority over Ito for stochastic processes with non-additive fluctuations 79−85079
streamflow, small sample estimation of Hurst coeff. 78−61467
string, stochastic vibr., mean displacement determ. by successive approx. 79−27523
suboptimal adaptive control of stochastic object 79−30371
Sun, differential rotation for unrestricted rot. rates, 2-dimens. stochastic motions 77−56899
sunspots Wolf numbers, rhythmic struct. amplitude-phase disturbances anal. 79−62806
superfluorescence, two-level atoms system, quantum theory, incl. propag. effects 80−58491
superionic conductors, continuous stochastic models, book contrib. 80−24663
superionic conductors, theoretical models, review 80−107465
surface patterns in theoretical geography 78−57156
surface transport and reaction, stochastic calcs. 80−108736
suspension, random behaviour simulation, interval of quiescence method 78−31708
symmetric or asymmetric many degrees of freedom nonlinear systems, stochastic linearisation 80−77708
system influenced by time dependent electric field, fourth order variation perturbation theory 80−22230
temperature fields in solid spheric cone *(Ukrainian)* 79−50566
temperature spikes stochastic analysis, contribution towards component damage exposed to nuclear radiation environment 79−7627
tensors, geodesic connection to stochastic parallel displacement 80−8920
terrestrial catastrophism, theory incorporating galactic modulation 80−31043
thermal conduction of solids, temperature stochastic field in cylinder computing, digital simulation algorithm *(Polish)* 79−71370
thermal conduction of solids, temperature stochastic field in cylinder computing, digital simulation algorithm *(Polish)* 80−17879
thermal mechanics: a quantum mechanical analogue of nonequilibrium statistical thermodynamics 80−52125
thermodynamic limit in stochastic systems 78−73938
thermodynamic properties, of interacting particle ensemble, by simulation of stochastic disordering 77−87697
thermodynamics, irreversible, extended, hydrodynamical fluctuations 80−86235
time average identification in stochastic process numerical studies 79−54056
time convolution Master equation and generalised Langevin equation equivalence 78−93610
time ordered operator cumulants, statistical independence and noncommutativity 80−31670
time-dependent statistical props., recording method *(German)* 80−101706
time-evolution of non-Markov processes 78−54305
Tolubinskij's stochastic theory of nonequil. processes and rel. to kinetic eqns. *(Russian)* 78−21053
transfer function with several inputs, model, math. methods of investigation identification 80−62451
transient laser radiation, stochastic process near an instability point, numerical solution 80−23658

stochastic processes continued
transmission image reconstruction from projections, max. likelihood meth. 77−86690
triatomic molecules, motion, regular and irregular spectra, theory 80−9590
tsunamis, stochastic model for risk estimation 77−21685
turbulence analysis, recurrence rate techniques 79−50831
turbulence in the motion of a free particle and de Broglie waves 80−57189
turbulent diffusion, stochastic model 79−18880
turbulent mixing with react. of miscible reactant streams, simulation 80−64651
two component Boltzmann gas, fluctuating kinetic eqn. 80−171
two-level atoms, saturation in chaotic field 80−37982
two-person nonzero sum stochastic differential game with stopping time 77−53755
two-phase flows, high-intensity X-ray system for stochastic measurements 79−93791
underwater sound, stochastic internal-wave model for deep moving ocean 80−64267
unimolecular reaction theory mean first passage time and reaction rates 78−60986
unstable state decay, trajectory time spread, laser photon statistics 80−83585
unstable systems, anomalous fluctuation and relax., multimacrovariables 77−79033
unstable systems, evolution eqns. of long wavelength fluctuation spectra 77−87695
unsteady state age distrib. of particles in flow systems 80−12991
Van der Pol oscillator, renormalised perturbation theory 80−27225
van Hove master equation, derivation 78−89397
vibrational compaction, of bulk materials 78−52701
viscoelasticity, stress/strain relationships, fluctuations 80−17802
volcanic activity dust veil index, stochastic simulation rel. to apparent periodicity 79−92514
Volterra eqn., existence and uniqueness of soln. 78−89405
Volterra stochastic integral eqns. of second order, anal. of dynamic system of variable inertia 77−57166
Volterra stochastic nonlinear integral eqns., interconnected systems stability 79−71368
vortex system, stochastic properties *(Russian)* 79−4022
vortex systems stochastisation, configurational temp. range in which quasiperiodicity is absent *(Russian)* 79−77132
water pollution, internalization in stochastic model 78−61455
water quality surveillance, optimal sampling frequency selection, autocorrel. techniques 79−53001
water waves, nonlinear, dynamic properties stochastic modelling 79−23332
wave field statistical moments in medium with large-scale inhomogeneities 80−37953
wave propagation, ambiguity function 78−69993
wave propagation in random media, temporal moments 78−20979
weather forecasting, stochastic dynamic prediction appl. to real data 77−56669
weather stochastic prediction, stochastic dynamic method, perturb. approx. 79−58060
white noise direct product, noncausal stochastic integral *(French)* 79−44858
Wick's theorem, relation between canonical and Fokker-Planck dynamics 79−17329
Wicks theorem and Fokker Planck dynamics 77−87715
Wigner representation, semi-classical ergodicity of quantum eigenstates 80−8833
wind, stochastic predictors, AR and ARMA models 80−67400
zero power reactor neutron power spectral density with injection of air bubbles *(French)* 77−10463
Al, vacancy loop formation, quenched-in vacancy clustering, continuum model 79−77594
Au, stacking fault tetrahedra formation, quenched-in vacancy clustering, continuum model 79−77594
CO+He, vibr.-rot. energy transfer, stochastic theory 79−54944
$CsNiF_3$, stochastic motion of Sine-Gordon-solitons, spin-correlation function 80−93105
H-bonded species, in soln., vibr. relax. model 78−84559
H-bonding, strong, stochastic model and IR spectra temp. effects 78−62805
H_2-O_2 mixture, explosion limits as stochastic phenomenon 77−21387
H_2O-H_2SO_4, mixtures, transient nucleation, stochastic theory 77−1221
He+p-H_2, vibr.-rot. inelasticity, stochastic theory 77−71848
$K_2Mg_xTi_{8-x}O_{16}$, stochastic Langevin dynamics study of correlated ionic motion in 1-D solid electrolytes 80−65279
N_2+Ar, rot. relax., approx. treatments 79−76494
Ni-Cr-Fe (15.7, 7.63 wt.%), Inconel 600, anal. of pit generation by 3.5% NaCl, by stochastic theory *(Japanese)* 78−85038
OHO H-bond, IR spectra, stochastic model 77−27060
SF_6, breakdown voltages dispersion, anal. 80−38772
SO_2 concentrations of Venice air, time series anal. 79−57540

stochastic programming
ocean radio location appl. *(Russian)* 78−65419
reservoir design and management, SESLP model 79−2314
river water quality management model stochastic programming model 79−57507
torsion appl. *(German)* 79−37192

stochastic systems
see also random processes
algebraic structure and finite dimensional nonlinear estimation 79−5975
atomic, stochastic destruction of bound states in interaction with radiation field *(Russian)* 77−10644
autogenerator displaying stochastic behaviour 79−17198
Bedford Ouse River, systems model of stream flow and water quality 80−81956
Benard problem, R^2 class of mappings, invariant Cantor sets and strange attractors 80−59037
betatron cooling, slot type pick-up and kicker 78−33332
bifurcation and transition toward stochasticity for dissipative dynamical systems 80−57201
boundary-value problem, two point, statistical version anal. 79−63154
Box-Jenkins modelling advances, appls. 77−87633
Bubnov-Galerkin method appl. *(Russian)* 77−49578

stochastic systems continued
BWR void effects, stochastic point model and zero-power reactor simulation 78−94061
catastrophe and stochasticity in semiclassical quantum mechanics 80−8861
cellular systems, probability model *(German)* 80−90661
closed loop control systems, appl. to blood pressure control 80−81522
compartments, general time-depend. reversible systems 78−64916
conference on plasma intrinsic stochasticity, Cargese, France (June 1979) 80−59174
conservative, nonlinear oscillators, connection between dissipative and resonant types 79−58619
continuous time stochastic approx. procedures 78−69969
control system, integral inequalities 79−17341
coupled oscillator system, stochastic transition, Toda criterion reliability 77−74308
critical transition to stochasticity 80−57202
deformable solids with rough surface, stochastic problem of heat conduction and thermoelasticity *(Russian)* 78−38169
differential eqns. and differential inequalities 77−5641
discrete stochastic electric double layer, electrostatic props. 79−96318
dislocation movement, in volume dispersion of obstacles, stochastic model, low temp. anomalies rel. to yield stress 79−60367
dissipative non-Hamiltonian dynamical system, stochastic props. and strange attractors 80−57200
dissipative systems, canonical quantisation, von Neumann equation 80−52132
distributed parameter system control, conference, Coventry (1977) 79−3897
dynamic multi-nonlinearity systems, action of white noise 80−68135
Dyson eqn., exact soln. for mean value of Green's function 78−4559
eight-vertex model, universality in critical dynamics, Ising model appl. 78−41246
ergodic components in stochastic region, stability of isolating integrals 78−73924
evolution eqns. with general white noise disturbance 78−16734
field problem inference-finite element model 78−81923
flow boundary layer, stochastic model of fluctuations 78−90818
Fokker-Planck dynamics, response and correlation in stationary state 78−45567
galaxy fields, stochastic simulation 80−90530
gastro-duodenal zone spike activity, stochastic activity 79−79496
Gaussian lattice model, kinetic, formulation from master eqn., diffusive and relax. behaviour 77−9966
gravitational field stochastic fluctuations 79−44837
gravitational waves stochastic background, energy density upper limit from pulsar timing meas. 80−36743
Green's function mean value, Dyson eqn. higher approximations, anal. *(Russian)* 77−74201
Hamiltonian with stochastic trajectories, spectrum and eigenfunctions 79−54013
intermittancy in turbulence onset 80−59013
Klein-Gordon eqn., stochastic derivation 77−61185
Kolmogorov Arnold Moser theorems, appl. to struct. problems in condensed matter 80−59878
lattice columns with stochastic imperfections, buckling, Ritz method 79−18757
linear, moment and cumulant functions *(Russian)* 78−32759
linear dynamic system, optimal transfer impulse function calc. *(Polish)* 77−53753
linear dynamics, field quantum theory, using Green's functions *(Russian)* 78−16722
linear randomly perturbed systems, mean-square stability 77−9870
linear systems with nonwhite parameter fluctuations, differential anal. 79−85082
liver disease computer-aided diagnosis using nonlinear stochastic modelling technique 78−36024
Lyapunov characteristic exponents and stochasticity 80−59177
Lyapunov characteristic numbers and Kolmogorov entropy, stochasticity of dynamical systems 80−59178
Mathieu damped oscill., parametric random excit., moment stability 77−9869
measurement data processing system error expressions 78−41287
models for density meter characteristics *(Russian)* 77−9987
moment equation methods for nonlinear stochastic systems 79−21666
moment method in stochastic perturbation of angular correlations 77−3268
multi-component system, mean stress *(Polish)* 77−54874
multivariate joint probability function of state variables with quantized levels for environmental system with discrete data 80−36836
n-vector model below T_c, critical dynamics 78−36959
n-vector model below T_c, hydrodynamic excit. spectra, crit. dynamics 77−74326
Navier-Stokes random forced flow ensemble mechanics 77−7363
neutron adjoint Boltzmann eqn., stochastic models for Monte Carlo integration 78−21618
non-Gaussian, operators method of anal. *(Russian)* 78−16627
nonequilibrium systems, existence of thermodynamic limit 79−54084
nonlinear, stochastic differential eqn., perturbation theory, projection operator method, statistical linearisation 78−41229
nonlinear differential eqns., integral representation soln. 77−13730
nonlinear mixed stochastic integral equations existence, uniqueness and stability of solutions 80−68131
nonlinear oscillator systems, primary resonances do not overlap 80−59176
nonlinear rate processes with multiple stationary states, stochastic theory, metastable state relax. time 79−2725
nonlinear relaxation and fluctuation 79−30373
nonlinear vibrating system, combination reson. response amplitude calcs. *(German)* 79−10527
nonordinary Poisson flows, moment dynamics 80−22280
nonwhite fluctuations of parameters, differential eqn. description of system *(Russian)* 79−145
one-variable system, growth of fluctuations from marginal eqn. 80−86213
optimal control, measurer containing unknown variable parameters *(Russian)* 80−86218
oscillating irregular field, effective potential 79−75457
oscillator systems, nonlinear stochastic models 79−80525
pendulum, bounce resonance and Kolmogorov entropy 80−57199

stochastic systems continued
physiological system stochastic anal. and control., cancer detection and therapy 77−90713
physiology, martingale model for estimation in nonlinear stochastic systems 77−77865
plasma, coupled three wave system, instability saturation, bifurcations and strange attractor 80−59233
plasma, discrete unstable modes, transition to turbulence, theory and expt. 80−59240
plasma, electrostatic wave, magnetised plasma charged particle stochastic accel. 80−59230
plasma, electrostatic wave, stochastic ion motion, mag. field config. depend. 80−59229
plasma, linearly unstable mode stabilisation by reson. nonlinear coupling to damped modes 80−59234
plasma, particle stochastic motion in mirror machines 80−59264
plasma, pulsed RF-trapped particle interaction stochastic effects in tokamak 80−59245
plasma, self-consistent kinetic theory of stochasticity 80−59179
plasma, stochastic heating of plasmas in inhomogeneous magnetic fields 80−59231
plasma, stochastic orbits in Tokamak, statistical description, low freq. fluctuations 80−59265
plasma, toroidal, overlapping and stochasticity, critical limits 80−59268
plasma adiabatic to stochastic motion transition, Kolmogorov Arnold Moser surface 80−59175
plasma magnetic field line trajectory calc., Kolmogorov Arnold Moser surface 80−59263
plasma particle motion, regular and stochastic, Hamiltonian formalism 80−59167
plasma wave, electrostatic, perpendicularly propag., vel.-space diffusion 80−59228
plastic yielding, bounding theorems of stochastic limit anal. 77−89037
probabilistic anal. of unification of quantum theory and relativity 78−86176
PWR components, using correlation techniques *(German)* 80−79247
quantum harmonic oscillator, driven and stochastically modulated, reduced eq. of motion 78−77764
quantum nonlinear systems, stochasticity condition 78−49760
quantum system, nonintegrable, irregular part of discrete energy spectrum, statistical theory 80−82667
quantum two-level system, damped and stochastically modulated, reduced eq. of motion 78−77764
quenched critical fluid, time evolution of fluctuation spectrum 78−65893
radiant cavity, one dimens., nonlinear field mode interaction, statistical props. 78−16668
ray and wave optics of integrable and stochastic systems, WKB method 80−59244
regional wastewater management systems, chance constrained approach 79−57513
river basin water resource, Pareto region, stochastic multicriterial problem in control 80−4055
scalar relay type, fundamental response properties *(Japanese)* 77−2519
soliton gas, turbulence due to weak dispersion, stochastisation of soliton motion 78−41169
stability, input-output, of continuous time and discrete time interconnected stochastic systems 80−52133
steady state Universe using stochastic electrodynamics, cosmic background radiation and red shift 78−77631
stochastic excitation systems, identification of damping and stiffness parameters *(Polish)* 78−69973
stochastic phase space, generalised functions 78−77796
structural model, of radiation effects in living cells 77−37016
surface roughness analyser, using amplitude density distribution and autocorrelation function of surface profile *(Hungarian)* 78−12668
systems theoretic representation of mechanical systems, stochastic interpretation 79−17343
temporal pump stochasticity in stimulated Raman scatt. in dispersionless media 79−98441
time evolution in two-phase flow, mathematical model 79−64739
turbulence, Lorenz model, statistical dynamics study using stochastic differential equations 79−92949
turbulence and stochastic self oscillations, review 80−4537
underwater sound ray theory relations, exptl. agreement 77−84051
van der Pol oscillator, functionals over discontinuous sample paths 78−29052
water resource management, gaming-simulation appl. in Hunter River Valley, New South Wales 79−57517
water resources, model construction for Box-Jenkins modelling 77−87632
AuFe spin glass, μ^+ zero-field spin relax. probe for spin dynamics 80−97177
CuMn spin glass, μ^+ zero-field spin relax. probe for spin dynamics 80−97177

stock control
see also production control
dynamic materials accounting for LWR fuel cycle 79−36325
nuclear fuel drum storage capacity computation via inventory model 79−9776
on-line nuclear materials accounting and control 78−29629

stock control data processing
see also computerised materials handling
nuclear material computer assisted accountancy and control system *(German)* 79−13415
nuclear materials accounting and control system 79−13507
Pu computerised inventory control system 79−36386

Stockbarger method *see crystal growth from melt*

Stokes flow *see flow*

Stokes law (fluid mechanics) *see flow*

Stokes law (optical) *see luminescence*

Stokes lines *see spectra*

Stokes optical law *see luminescence*

stopping of particles *see energy loss of particles*

storage, analogue *see analogue storage*

storage, digital *see digital storage*

storage devices
see also energy storage devices; magnetic storage devices; optical storage devices; semiconductor storage devices
AI-128-2 pulse height analyser, in multichannel counting mode, operational organisation of storage 79−26843
electron beam bombard. target temp. profile, evaluation of suitable materials 77−68998
electronic system for leg prostheses axial load meas. *(German)* 79−84006
Harris data memory, operation and educational uses 80−17779
memistor, solid electrolytes appl. *(Czech)* 77−77779
SAW devices based on interaction of SAW with electrons in semicond. 77−80025
p^+n SAW memory correlators, modified theory 80−43563
$CuO\text{-}CaO\text{-}P_2O_5$ glass devices, memory switching 78−56192

storage organisation *see file organisation*

storage rings
18 GeV electron-positron storage main ring magnet system 79−31267
28 GeV proton synchrotron and intersectig storage rings, interconnected vacuum system 78−86706
acceleration of ions in electron storage rings 79−18064
ACO storage ring, design of undulator, use as free electron laser 80−91334
Adone e^+e^- ring, beam-beam effects 80−37649
Adone storage ring transverse wiggler magnet design 79−41054
Adone wiggler magnet, status report 79−68081
ALA, high luminosity e^+e^- storage ring, 1.2 GeV, design study 79−72066
Aladdin, status of the Synchrotron Radiation Center of the University of Wisconsin, Madison 80−91326
ALFA, electron pulse stretcher to increase Frascati Linac duty factor, feasibility study 80−23237
bakable Al vacuum chamber and bellows with flange and seal for ultrahigh vacuum 79−30486
beam energy loss to vacuum components, particle bunch simulation meas. at PETRA 77−83258
beam position stabilization system for electron storage ring 79−68079
beam-beam interaction, radical diffusion simulation 80−37653
beam-beam interactions, perturbation method solns. 80−37667
beam-beam interactions in e-p storage rings 78−78889
beam-beam interactions in p-p storage rings 78−78900
beam-beam simulation for modest Fermilab proton colliding beam expt. 77−83337
BESSY, 800 MeV dedicated light sources, choice of principal parameters and light source 80−91333
BESSY, a 800 MeV storage ring dedicated to synchrotron radiation, review 79−68021
BNL National Synchrotron Light Source, 100 to 700 MeV booster synchrotron 79−67973
BNL National Synchrotron Light Source, 2.5 GeV X-ray ring, design status 79−68023
BNL National Synchrotron Light Source, 700 MeV VUV storage ring 79−68031
brightness of synchrotron radiation from electron storage rings 80−91330
bunch lengthening and energy spread in electron storage rings, SPEAR II data 77−83210
bunch lengthening and microwave instability 77−83370
bunch lengthening in electron storage rings, resistive theory 77−83209
bunched beam stability, matched line interaction 78−50424
CERN, 25 years history and equipment *(French)* 80−98778
CERN, 25 years of physics, review 80−82626
CERN, comparison of characteristics of X-ray and γ-ray sources 80−14030
CERN, international scientific cooperation *(Dutch)* 77−45669
CERN 60 GeV ISR collider for 400 GeV SPS 78−58513
CERN accelerators, radiation protection *(Dutch)* 77−46434
CERN antiproton accumulator, dispersion suppression with missing magnets in FODO struct. 79−72162
CERN intersecting, flexible cryogenic system for testing superconducting quadrupole magnets 79−58706
CERN ISR, 120 GeV superconducting conversion study 78−58509
CERN ISR, 50 MHz transverse feedback system 77−83319
CERN ISR, at 31.4 GeV, phase displacement acceleration, operating techniques and beam diagnostics 79−68003
CERN ISR, cold bore expt. 79−76212
CERN ISR, control system, addition of local intelligence to CAMAC 79−72212
CERN ISR, facility and hadron physics program review 80−873
CERN ISR, on-line Q meas. during phase displacement acceleration 79−72076
CERN ISR, overlap knockout resonances with colliding bunched beams 79−76195
CERN ISR, phase displacement accel. of high intensity stacks 77−83254
CERN ISR, revised skew quadrupole system for coupling compensation 79−72097
CERN ISR, supercond. quadrupole magnets, wire dimension meas. and short circuit detection 79−31255
CERN ISR, superconducting high luminosity insertion 79−72049
CERN ISR, transition energy variation with momentum aperture 79−76194
CERN ISR, transparent vac. chambers for interaction areas 79−76211
CERN ISR, vac. cold bore test section 77−83248
CERN ISR clearing current monitoring system 77−83249
CERN ISR collimator system 79−72119
CERN ISR control scheme for acceleration by phase displacement 79−72213
CERN ISR operation with antiprotons, project description 79−72064
CERN muon storage ring, calib. of NMR magnetometers and mag. field meas. system 77−57780
CERN muon storage ring, NMR mag. field meas./stabilisation system 77−57779
CERN proton synchrotron, electron ring addition, proposal for weak interaction study 78−55062
CERN proton-antiproton colliding beam facilities 79−67996
CERN SPS, acceleration and storage of dense single bunch 79−72094
CERN superconducting proton storage rings, 400 GeV, feasibility study for e-p, p-p and p-$\bar{p}$ facilities 78−58510
CESR, characts., points of interest 79−72038
CESR, e^+e^- storage ring, vac. system 77−83247
CESR, status 80−74047
CESR, synchrotron radiation exit ports, thermal design 79−68035
CESR computer control system, description 79−72210

storage rings continued
CESR control system, distributed microprocessors appls. 79−72217
CESR control system, interface hardware 79−72069
CESR electron storage ring, ultra fast pulsed magnets for beam manipulation 77−83239
CESR injection linac, electron beam modulator, design, performance 77−83374
CESR magnet power supply system 79−76210
charge bunch radiation losses in pill-box resonator, time domain numerical computations of EM fields 79−31781
CHESS − the Cornell high energy synchrotron source 80−91328
CHESS synchrotron radiation facility, high energy tunable X-ray source 80−68984
CHESS synchrotron source, photon position sensitive monitors 80−91336
chromatic corrections for large storage rings 79−72106
chromaticity correction in large storage rings 77−83206
circular beam tube, longitudinal coupling impedance of step discontinuities 79−72115
circular electron accelerators, beam stability calc. 79−72099
clearing electrode control system for CERN ISR 77−38514
colliding beam facilities, overview 80−37642
comparison apparatus for bunch excited fields and energy loss meas. 79−72164
computer model, system anal. of accelerators for inertial fusion 77−83474
conference, LEP summer school, Les Houches, France (Sep. 1978) 79−97916
conference, storage ring beam-beam interactions and nonlinear dynamics, Upton, NY, USA (March 1979) 80−36758
conference, theoretical aspects of beam behaviour, Erice, Sicily (1976) 78−78878
conference on cosmic rays and particle physics, Newark, USA, Oct. 1976 79−58987
Cornell electron ring, high resolution digital time base 79−76215
Coulomb shift of betatron freqs., stability of coherent oscills. of circulating bunch 77−46436
DCI double ring facility, status report 77−83326
D.C.I. storage rings, double frequency RF system 77−88299
DCI storage rings, status report, space charge compensation, and 3- and 4-beam behaviour 79−76190
depolarisation during acceleration and storage of polarised protons and deuterons 78−58519
depolarisation in large electron rings 77−3197
design considerations for parasitic use of synchrotron radiation in the infrared 80−91340
DESY e^+e^- experiments, QED checks, τ and Υ studies 80−18111
detector systems for LEP 79−97952
distributed sputter-ion pumps for use in low magnetic fields, electron storage ring appl. 79−67325
DORIS, as vacuum UV radiation source, high resolution monochromator 77−7165
DORIS, Damping antennas for spurious RF-modes in electron-positron storage rings 78−70659
DORIS, e^+e^- storage ring, superconducting accelerating cavities 79−72140
DORIS, luminosity limitations 80−37648
DORIS, satellite reson. due to beam-beam interactions 77−83252
DORIS current supplies, equipment design and performance *(German)* 78−21797
DORIS double storage ring, synchrotron radiation source in X-ray and UV regions 78−62668
DORIS e^+e^- storage rings, modifications to 2×5 GeV, magnet struct. and RF system 79−68000
Doubler-Tevatron, characts., points of interest 79−72038
drift chamber vertex detector for intersecting storage rings 79−3310
electron, coherent microwave emission fine struct. 78−78875
electron, synchrotron radiation focusing on single point 77−10991
electron, syncyrotron orbital radiation appl., vacuum ultraviolet and soft X-ray radiation sources *(Japanese)* 78−25941
electron, vacuum system for synchrotron radiation source 79−63830
electron, VEPP-2M, -3 and -4 as synchrotron radiation sources, beam characts. 78−62667
electron, VEPP-3, proposal to install supercond. wiggler magnet, synchrotron radiation prod. 78−62671
electron, weak-strong instability as diffusion process 79−72111
electron and positron depolarisation suppression in storage rings and cyclic accelerators 80−42882
electron beam polarisation in storage ring by laser beam interaction 79−93860
electron bunch, relativistic, instability in reson. storage chamber 77−54381
electron bunch lengthening in storage rings due to fast longitudinal instability 77−83340
electron bunch widening as due to self-bunching, computer simulation 77−83333
electron combined-function storage rings 77−83331
electron cooling and new possibilities in elementary particle physics, review 79−68118
electron cooling method, proton-antiproton colliding beam appl. 79−18067
electron cooling of beams in heavy particle storage rings, kinetics 77−67922
electron cooling of proton beam in storage ring 77−14281
electron polarisation by circularly polarised EM waves 80−14020
electron ring and accelerator lattices, linear and nonlinear, interactive computer program 77−83332
electron rings, quantum lifetime 77−83334
electron storage ring, beam distrib. parameters using transport matrices 79−54725
electron storage ring, SRS, press. meas. 79−63264
electron storage ring for Daresbury 2 GeV synchrotron radiation source 78−62666
electron storage rings, meas. of detector losses of synchrotron X-rays 78−86752
electron synchrotron storage ring RF power supply *(German)* 78−17453
electron-positron rings, design and appl., review 79−80833
electron-positron storage ring, elementary particle physics *(Polish)* 79−76218
electron-positron VEPP-2M, radiative polarisation of beams 77−18719
electron-proton facility in CERN SPS 77−83203

storage rings continued
electron-proton project TRISTAN, design features 77−83204
electrons, SHF radiation, coherent synchrotron vibrs. effect *(Russian)* 78−66438
enhanced resistive wall instability for off-centred beams 79−72091
ESCAR bending magnets, design, construction and operation 79−36444
ESCAR superconducting fully cryogenic accelerator 77−83236
EUV photodiodes for high accuracy location of orbital plane 80−91335
Fermilab, 100 GeV beam storage, improved chromaticity control 79−76187
Fermilab antiproton cooling ring, initial operation 79−68004
Fermilab antiproton cooling ring, injection, magnet and vacuum systems 79−72139
fermilab doubler magnet design and fabrication techniques 79−36443
Fermilab electron-proton colliding beams, design study 79−72067
Fermilab energy doubler construction progress 79−36441
filamentation instability of electron and positron colliding beams in storage rings 80−872
FODO struct., dispersion suppression with missing magnets, appl. to CERN antiproton accumulator 79−72162
free electron laser amplifier, storage ring appl. 80−871
free electron laser amplifier operation in storage ring 79−68399
free electron laser sensitivity to electron energy reduction 79−94246
free electron laser-electron storage ring system, review of basic characteristics and possible developments 79−68019
free electron storage ring laser, Boltzmann simulation 79−72547
free-electron storage-ring laser, synchrotron motion 79−55103
future technologies in high-energy physics, collective accelerators, laser accelerators, single-pass collecters 80−78466
hadronic and nuclear EM probe system using electron accelerator and storage ring 80−23200
heavy ion storage supercond. coil radial sector guiding field calc. 79−31262
high energy physics program at BNL, equipment, experiments, future research 77−18716
high-perveance electron optic system with electron-energy recuperation 77−23322
horizontal wiggler, modelling of effect on beam parameters 79−68029
IHEP accelerator storage complex USSR, design 77−83338
impact of elementary particle physics 79−72121
impact on elementary particle physics 79−72120
injection technique, mol. ion photodissoc. 77−83134
interacting beam models, summary 80−37644
interaction effects of EM fields on particle beams 80−37643
internal electron scatt., polarisation effects 79−85843
intersecting, electromagnet power supplies, types 77−42197
intersecting storage accelerator supercond. magnet construction and performance 79−31263
intersecting storage ring supercond. solenoid installation and performance 79−31270
ion storage in electron ring, ion-ion interaction effects 80−52796
ISABELLE, beam transfer from AGS, momentum stacking method 79−76188
ISABELLE, beam tube material and vacuum chamber design 79−76199
ISABELLE, beam-beam interaction, transfer map approach 80−37651
ISABELLE, bunched beams, instability threshold 80−37652
ISABELLE, characts., points of interest 79−72038
ISABELLE, enhanced resistive wall instability for off-centred beams 79−72091
ISABELLE, high frequency beam bunches 79−72112
ISABELLE, impact of changing computer technology 79−89539
ISABELLE, lattice status 79−76189
ISABELLE, linear and nonlinear beam-beam effects 80−37656
ISABELLE, nonlinear beam-beam interaction, computer model 80−37654
ISABELLE, pp intersecting storage accelerator facility at BNL 77−83344
ISABELLE, superconducting dipole prototypes, operational parameters 77−83215
ISABELLE, superconducting magnet power supply and quench protection 79−76209
ISABELLE, superconducting magnet quench protection system 77−83233
ISABELLE, two superconducting storage rings 79−36440
ISABELLE closed orbit correction system 77−83336
ISABELLE facility, Brookhaven, design features and project status 79−63825
ISABELLE field convection and tuning system 79−72105
ISABELLE full cell, ultrahigh vacuum system 80−77798
ISABELLE half-cell control system 77−88303
ISABELLE half-cell prototype, magnet power supply system 77−83244
ISABELLE insertion quadrupoles 79−76197
ISABELLE ISR, computer based control and monitoring system 78−46191
ISABELLE ISR, supercond. magnet update 79−36442
ISABELLE magnet support and adjustment system 79−76198
ISABELLE quadrupoles 77−83227
ISABELLE ring magnets, design, construction, operational update 79−68088
ISABELLE ring magnets, operating characts. 77−26900
ISABELLE storage ring magnets, mag. field meas. 79−68089
ISABELLE storage rings magnet cryostats, mech. design 77−83218
ISABELLE superconducting dipole magnets, forced flow cooling 77−26907
ISABELLE ultrahigh vacuum system, self-modulating ion gauge 80−82786
ISABELLE vacuum component performance at 1×10^{-11} Torr operation 79−81105
ISABELLE vacuum system, design characts. 77−83224
ISR, beam-beam investigations, review 80−37645
ISR, CERN, excitation of coupling reson. 77−83257
ISR, CERN, overlap knock-out effects 77−83251
ISR, CERN, stochastic cooling of vertical betatron oscills. 77−83373
ISR, longitudinal bunch dilution due to RF noise 77−83260
ISR, phase displacement accel. in presence of RF noise, efficiency 79−76231
ISR, stochastic cooling in initial cooling expt. 79−72089
ISR absorber blocks for high intensity beams 79−68060
ISR at CERN, beam stability, coupling impedance, meas. by RF excitation 77−83269

storage rings continued
ISR at CERN, high luminosity operation, 26 GeV/c proton beams, loss rates, background control 77−83276
ISR at CERN, longitudinal instabilities of bunched beams, microwave instabilities 77−83270
ISR performance for pedestrians 78−29676
ISR RF cavities, beam load compensation, feedback system 77−83294
KEK, sextupole magnets with nonlinear lattice, computational methods for dispersion, betatron functions, closed orbit distortion 79−68028
KEK photon factory storage ring lattice, design principle 79−68033
large electron-positron colliding beam machine, design study, CERN 79−67999
laser, isochronous storage ring type 80−48204
LEDA-F storage ring dedicated to free electron laser operation, preliminary design 79−68030
LEP, 15 GeV injector alternatives, storage ring and synchrotron 79−72052
LEP, and CERN SPS, luminosity optimisation for e-p collisions 79−76230
LEP, design, tests of unified field theories and quark properties, search for new quarks and leptons 80−74048
LEP, design constraints, basic principles 79−97917
LEP, e^+e^- experiment 79−97613
LEP, electron positron storage ring, vac. chamber, glow discharge surface cleaning 80−58010
LEP, scenarios for high energy physics 79−93848
LEP, use in weak-EM interference effects studies 79−97614
LEP 100 GeV e^+e^- storage ring, synchrotron injector design 77−67913
LEP C-shaped laminated magnets, implication of low field levels 79−72051
LEP colliding beam machine, data handling and standard practices 80−58009
LEP control system design 79−72050
LEP storage ring, polarised $e^{\pm}$ beams, Siberian Snake scheme 79−63827
magnet of third muon (g−2) expt. at CERN 79−22504
magnetic beam position detector 77−88307
magnets in the PEP injection lines 79−68103
modular drift-chamber vertex detector at the CERN ISR 79−3302
multiwire drift chambers for the CERN intersecting storage rings 79−3301
MWPC, appl. as energy loss detector for the ISR 79−3331
N-100 storage ring, vacuum ultraviolet-radiation extraction channels 78−5071
NAP-M, meas. of momentum cooling rates with electron cooling 79−72095
NAP-M proton storage ring, equilib. beam orbit meas. 78−831
National Synchrotron Light Source, vac. system 79−81106
National Synchrotron Light Source basic design and project status 80−91329
National Synchrotron light source magnetic component system 79−68038
neutraL molecule desorption from SS(304) and Al(6061) due to particle bombardments 79−76213
neutral molecule desorption from vac. chamber walls by ion and electron bombard. 79−83507
neutrons, torroidal superconducting magnet ring 78−21795
next generation of accelerators 79−72122
NUMATRON project, high energy heavy ion facility, design, performance 78−62665
NUMATRON project test accumulation ring, vacuum system *(Japanese)* 80−18724
Orsay, e^+e^- interactions, beam-beam effect observations, review 80−37650
PAMPUS storage ring synchrotron radiation, physical applications *(Dutch)* 77−61639
particle distribution parameter in electron storage ring 77−3196
pellet fusion reactor appl. 79−678
PEP, 4-18 GeV storage ring, single wavelength standard wiggler 79−68080
PEP, characteristics and experimental program 79−97919
PEP, charact., points of interest 79−72038
PEP, comparison of characteristics of X-ray and γ-ray sources 80−14030
PEP, estimate of spin polarisation 79−72093
PEP, high-speed data acquisition and analysis system 80−23194
PEP, polarisation expts., review 77−34487
PEP, proposed orbit and vertical dispersion correction system 79−72098
PEP, semi-automatic precision surveying system 77−83246
PEP, superconducting proton storage ring, for electron-proton collisions 79−72068
PEP, vacuum system, synchrotron-radiation-induced heating effects 79−81107
PEP accelerating cavities, longit. feedback system 79−72144
PEP at SLAC, high efficiency high power UHF klystron, performance 77−83296
PEP beams line components, bench meas. of loss impedance 79−68055
PEP chopper magnet power supply system 79−76208
PEP II RF system 79−72113
PEP injection line, sensitivity to perturbations 79−72096
PEP insertion quadrupole design features 79−68105
PEP interaction region quadrupole magnets, meas. and corrections 79−68104
PEP RF reference line 79−68050
PEP storage ring, computer control systems, design and performance 79−72208
PEP storage ring, Laser Surveying System for automatic data acquisition and anal. 79−68061
PEP storage ring, RF system 77−88298
PETRA, 19 GeV e^+e^- storage ring 79−72037
PETRA, comparison of characteristics of X-ray and γ-ray sources 80−14030
PETRA, control system 77−83315
PETRA, history, current expts. 79−97918
PETRA, intensity monitor, design, operation and performance charact. 79−72081
PETRA, luminosity limitations 80−37648
PETRA, obs. of beam-beam effects 79−72123
PETRA, physical plant 77−83335
PETRA, recent results 80−74044
PETRA, single beam instabilities 79−72092
storage rings continued
PETRA electron-positron storage ring, vacuum system techniques and problems 78−17452
PETRA magnets, results of field meas. 79−68040
PETRA storage ring, RF power supply and cooling systems 79−68054
PETRA storage ring, serial data acquisition system 79−72085
PETRA storage ring control system, applications and future developments 79−72083
PETRA storage ring control system, control console for man machine communication 79−72084
PETRA vacuum system, RF parasitic mode losses, fabrication cost, new techniques 77−83217
phase space cooling for $p\bar{p}$ colliders at CERN and Fermilab 80−99360
photon, electron and positron prod. from primary proton beams, Monte Carlo calcs. 80−32555
photon dose rate from induced activity in the beam stop of a 400 GeV proton accelerator 78−94144
PIA, positron intensity accumulator for PETRA injection 79−71984
polarised beams, acceleration and storage 78−58518
polarised high energy particle production in cyclic accel. and storage rings, possibilities 79−63843
polarised positron, electron production by colliding photon beams 80−5426
POPAE, cold-bore vacuum system design 77−83226
positron-electron 18 GeV facility at SLAC, design and status 77−83320
positron-electron colliding beam at Cornell, design status 77−83323
positron-electron storage ring PETRA, plans and status 77−83321
$p\bar{p}$ storage rings, Fermilab/CERN, progress report, phase space cooling and high luminosity 79−63824
proton, cooling effect of electrons 77−23334
proton, operation of Fermilab accelerator 77−83330
proton, selection of formulae 77−83348
proton, very high energy, synchrotron radiation in non-uniform mag. fields 77−79736
proton (antiproton) beam in storage ring, stochastic cooling anal. 80−5420
proton (antiproton) storage ring, incoherent motion damping by dissipative elements 80−5419
proton accelerator ISABELLE, review 80−32545
proton beam, bunched, interaction with ion wake in storage ring 77−83345
proton beam in storage ring or synchrotron, monitoring by narrow band synchrotron radiation 77−83293
proton high-energy rings, low energy current accumulator 77−83329
proton storage ring, NAP-M, accelerating system and beam parameters monitoring 77−65364
proton storage ring, NAP-M, current stabilisation in guiding-field magnet supply ccts. 77−65363
proton storage ring, NAP-M, mag. and vacuum system 77−65362
proton storage ring, NAP-M, supervising system 77−65365
proton storage ring, neutral beam injection, LASL 79−76156
proton storage ring 400 GeV facility, CERN design 77−83202
proton storage ring lattice design 77−83190
proton storage ring vacuum systems, in situ conditioning 78−74519
proton synchrotrons, future expts. 78−78528
Proton-Electron Tandem Ring Accelerator 'transparent' solenoid superconductor 79−31274
proton-proton, high frequency beam bunches 79−72112
proton-proton 1000 GeV on 1000 GeV facility, Fermilab proposal 77−83201
proton-proton colliding beam facility at Brookhaven, ISABELLE, design status 77−83322
prototype supercond. quadrupole magnet for CERN intersecting storage rings 79−31265
pulsed RF systems for large storage rings 79−72141
radiative polarisation, review 78−33335
radiative polarization at ultra-high energies for e^- and e^+ beams in storage rings 79−72127
relativistic charged particle beams, soliton solns. phase-locked bunch prod. 78−50425
resonant, relativistic electron bunch phase distrib. 77−380
resonator wall instability caused by ponderomotive forces, feedback-stabilised system 80−5418
review of ISR projects situation (1979) *(Czech)* 80−870
secondary electron amplification in high energy accelerators 78−46193
Sendai 1.5 GeV linac electron accelerator with pulse-beam stretcher ring 80−23188
Serpukhov, two stage synchrotron and IHEP storage complex, status report *(Russian)* 79−63829
sextupole magnets with nonlinear lattice, computational methods for dispersion, betatron functions, closed orbit distortion 79−68028
single beam collective phenomena 78−78893
single feedback systems for simultaneous damping of horizontal and longitudinal coherent oscillations 79−72075
SLAC accelerator, automatic phasing using microprocessor controller 77−88305
soft X-ray microscopy/lithography branch line at SSRL 80−91344
SOR-RING, electron storage ring as synchrotron radiation source 77−6584
SPEAR, backscatt. laser polarimeter for transverse beam polarisation meas. 80−14019
SPEAR, beam-beam functional dependencies of machine parameters 80−37647
SPEAR, crystal ball detector, recent results 80−74046
SPEAR, estimate of spin polarisation 79−72093
SPEAR, flip-flop beam-beam effect 79−72101
SPEAR, initial operation of mag. wiggler 79−68025
SPEAR, Mark II detector, recent results 80−74045
SPEAR, Stanford Synchrotron Radiation Laboratory, status report 80−91327
SPEAR, synchrotron radiation beam ports, installation and thermal design 79−68034
SPEAR, synchrotron radiation source 77−83186
SPEAR, use of wiggler magnets as synchrotron radiation source 80−91332
SPEAR beam-beam effects expts. 80−37646
SPEAR I, beam-beam limit simulation 80−37655
SPEAR II ring, parasitic mode losses in cylindrical cavities with beam ports 77−83271
SPEAR storage ring, as synchrotron radiation source for X-ray spectroscopic studies 77−41745

storage rings continued
SPEAR storage ring and synchrotron radiation research 79−41052
SPEAR transport line toroids, intensity monitors calib. system 77−88295
SRS, shielding design 80−37659
stable and unstable beam motions, mathematical statements 80−37663
Stanford Synchrotron Radiation Laboratory, operation and development, review 79−68020
stochastic cooling tests on proton beams, initial cooling expt. 78−90006
storage rings, linear and nonlinear orbit motion 79−72109
strong focusing colliding beams for electric power generation 79−18032
superconducting accelerating cavities for high-energy e^+e^- storage rings 79−97924
superconducting bar-loaded resonator for electron accelerator application 79−36434
superconducting dipole magnet design for POPAE 77−26898
superconducting dipole models for accelerator-storage ring complex 79−31259
superconducting dipole window-frame type high precision magnets at BNL 77−83228
superconducting magnet system, PLUTO, large 77−46435
superconducting proton storage rings, 400 GeV, feasibility study 79−6780
superconducting quadrupole magnet construction for CERN ISR 77−10507
superconducting solenoid, Al stabilised design and construction, for CERN intersecting storage rings 77−46428
superconducting solenoid, large high current density, for use in high energy physics expts. 77−23326
superconducting storage ring for very slow neutrons 79−72043
SURF II, 250 MeV storage ring for UV synchrotron radiation, progress report 79−68032
SURF II, large spectrometer calibration chamber 80−91339
SURF II, synchrotron flux meas. using Si radiometer 80−90895
SURF II storage ring, status report 80−91325
SURF storage ring calibrations for NASA stratosphere and climate programs 80−94721
synchrobetatron oscillation driving mechanism 79−72108
synchrotron radiation, acoustic delay line efficiency in view of beam lines 79−88965
synchrotron radiation, appls., review 78−9010
synchrotron radiation, enhancement by storage ring beam modulation 78−82550
synchrotron radiation, expt. enclosures and beam line safety components 80−91341
synchrotron radiation, IR, from Orsay storage ring, photometric anal. 77−34922
synchrotron radiation, review of props., facilities, and source parameters and optimisation 79−68018
synchrotron radiation, sources, properties, and research appl. 77−75403
synchrotron radiation, spectroscopic appls., review 77−58239
synchrotron radiation facility 240 MeV electron storage ring 77−58243
synchrotron radiation facility at Orsay's ACO storage ring 77−10505
synchrotron radiation far IR source 79−30577
synchrotron radiation filtering for Mossbauer source production 78−25374
synchrotron radiation for storage rings for X-ray laser holography 78−55322
synchrotron radiation from electron storage ring, focusing condition 77−42584
synchrotron radiation research, developments 78−78051
synchrotron radiation research, review 79−22505
synchrotron radiation source, 2 GeV at Daresbury, supercond. wiggler magnet design 78−62672
synchrotron radiation source, Daresbury 2 GeV storage ring with 600 MeV booster synchrotron, review 79−68022
Synchrotron Radiation Source booster magnet power supply 79−31272
Synchrotron Radiation Source booster synchrotron combined-function magnets 79−31269
Synchrotron Radiation Source storage ring multipole magnet prototype 79−31268
synchrotron radiation sources, nuclear physics appls., review 80−106216
synchrotron radiation sources and utilisation, review 78−41390
targets, molecular beam apparatus 77−6586
Test Accumulation Ring for NUMATRON project 79−72117
thin window gas absorption apparatus suitable for storage ring synchrotron radiation sources 78−62955
time resolved spectroscopy with synchrotron radiation 80−31902
transposal ring intersecting storage accelerator, TRISTAN project *(Japanese)* 77−83341
ultra high vac. system, Ti sublimation and sputter ion pumps 77−57336
ultracold neutron storage ring supercond. magnet design 79−31266
ultrahigh vacuum technology for electron and proton storage rings 77−83213
ultrathin-coil supercond. solenoids for high-energy accelerators and storage rings 79−31260
undulator for the 700 MeV VUV-Ring of the National Synchrotron Light Source 80−91337
undulator radiation, hard, in dispersive medium, in dipole approx. 80−23608
UV beamlines for National Synchrotron Light Source 80−91342
vacuum control system for synchrotron radiation beam lines 79−68027
vacuum techniques for small aperture proton storage rings 77−83250
vacuum technology, medium, high and ultrahigh, conf., Oxford, England (Apr. 1978) 79−63242
VEPP-2, apparatus for investigating electron scattering by atomic nuclei 79−97473
VEPP-2M storage ring, synchrotron radiation use to test VUV detectors absolute efficiency 80−82824
vertical beam size due to orbit and alignment errors 77−83207
VUV beam line instrumentation for National Synchrotron Light Source storage ring 80−91343
wiggler, helical synchrotron radiation source, orbits and fields 77−79203
wiggler magnets, control of low-energy characteristics, appl. to CERN LSR 77−6585
wiggler magnets, standard, effects on synchrotron radiation spectrum and storage ring operation 78−62670
wiggler with short period helical path as synchrotron radiation source 77−79202
wigglers and undulators, interaction with stored electron beam 80−91331
X-ray synchrotron source, design status 79−68024

storage rings continued
X-ray/γ-ray region source characteristics 80−14030
d acceleration in CERN PS and ISR 77−83283
e^+,e^-, polarisation asymm. prod. by imperfection resonance methods 77−38512
e^+-e^- storage ring, 100 GeV facility, design concept 77−83325
e^+e^-, high duty factor structures 77−38469
e^+e^- 100 GeV storage ring, LEP, at CERN, design concept 77−83349
e^+e^- CERN 100 GeV ring design, LEP injection 77−83135
e^+e^- PETRA storage ring, beam polarisation, backscattered Ar^+ laser meas. 79−63839
e^+e^- SPEAR storage rings, beam polarisation meas., backscattered laser method 79−63838
e^+e^- storage ring, PETRA 78−78530
e^+e^- storage ring, parallel coupled RF cavity struct. 77−83295
e^+e^- storage rings, beam-beam interactions 78−78894
e^+e^- storage rings, expt. review of beam polarisation 79−63837
e^+e^- storage rings, insertion design 79−72100
e^+e^- very high energy beams, exptl. physics 77−38516
$\mu^\pm$, at CERN, device description and operation 79−45088
$\bar{p}p$ colliding beams at Fermilab, phase space cooling 77−83324
ψ particles and charm, 1975 and 1976 expts. *(Czech)* 79−26288
Al storage ring vacuum chambers, glow discharge processing versus bakeout 78−70658
Al strips used in accelerator coils instead of Cu 79−72126
Be windows for synchrotron radiation beam lines 79−68026
Nb TM_{010} superconducting RF cavities for high energy storage rings, 700 MHz meas. 79−68059
Nb_3Sn, superconducting accelerating struct., high field exam. 79−36439
Pb-scintillation counter, modular EM shower detector for CERN ISR 79−76275
Si radiometer for storage ring synchrotron radiation 80−86411

storage tubes
see also image storage tubes
tera-bit electron beam memory realization 80−53198
vacuum-deposited layers formation, use of borosilicate glass intermediate layer 80−80979

stored program control *see electronic switching systems*

stores (computer) *see digital storage*

storms
see also magnetic storms; thunderstorms
S.Africa, unusual deep depression (1974, Feb.-March) 77−91247
air-sea heat and moisture exchange during stormy weather 77−78375
Alberta hailstorm, gravity wave patterns 77−21827
Arabian Gulf, 1977 June severe cyclone 78−69429
Arabian Sea storms and depressions, 1961-74 period 77−53168
N.Atlantic, statistical distrib. of wave periods and heights during September 1961 storm 77−45006
N.Atlantic easterly gales, 1881-1970 period 80−77101
Atlantic seaboard, East Coast, winter-storms, aerial reconnaissance 77−70731
atmosphere fronts dynamics, numerical modelling and cyclogenesis *(Russian)* 77−64370
atmospheric sources location, via triangulation direction finding network 79−100981
Baltic beach scouring and detritus accumulation in short-term disturbance *(Russian)* 80−36288
SE.Baltic coast transit section, suspended load composition in calm and storm *(Russian)* 80−67360
SE.Baltic storm surge peculiarities of water level *(Russian)* 78−36189
baroclinic spatially growing waves finite amplitude dynamics on f-plane 79−79985
Bay of Bengal, forecasting tropical storm movements 80−41531
Bay of Bengal, storms rel. to wave characts. off Paradip Port 80−41450
Bay of Bengal and Arabian Sea, cyclones and depressions during 1975 78−32148
Bay of Bengal cyclone, 1972 September 20-25, radar tracking 77−53126
blizzard, 1978 February 18 to 19, in SW.England and S.Wales 80−12507
Bombay High area swells due to storms in Arabian Sea 79−100845
Brahmaputra river, flood of Aug. 1962, synoptic aspects 80−81939
S.California, 1978 February 10, forecasting, satellite imagery rel. to model initial conditions 80−31084
Caspian Sea, spatial struct. of storm waves *(Russian)* 79−29790
N.Caspian Sea, storm surge simulation using bottom friction *(Russian)* 77−21810
climate, soil and vegetation, annual precip. distrib. from storm sequences 79−84314
climate, soil and vegetation, annual water balance dynamics 79−79896
climate, soil and vegetation, storm surface runoff distrib. 79−84315
cold front of midlatitude cyclone, cloud and precipitation struct. 80−109192
NE.Colorado convective storm, Doppler radar meas. of turbulent kinetic energy dissipation 77−29388
NE.Colorado hailstorms and radar reflectivity of ground-level hail 79−53470
Colorado winter storms snowcrystals and natural ice nuclei 77−9475
convection currents in axisymmetric cyclone 80−77084
convective, warm-based, evolution of raindrop spectra 79−88417
convective dynamics, simulation of three-dimens. cloud model 79−16590
convective storm, triple-Doppler radar obs. 79−39886
convective storm environment, large aerosol particles meas. 80−41512
convective storms over St. Louis, rainwater pH var. 77−37333
cumulonimbus convection, numerical modelling 79−84414
cumulonimbus motion and splitting, role of downdraught, numerical simulation 79−44227
cyclogenesis, asymmetric jets instability theory 80−56537
cyclone centre location using kinematical determinant 80−56535
cyclone development along weak thermal fronts, model soln. 80−81994
cyclone forecasting applications to typhoons 77−25801
cyclone formation, kinetic energy budget 78−16127
cyclone genesis in Mediterranean and Ligurian Sea *(French)* 79−48534
Cyclone Joan 1975, wind and rain meas. over W.Australia by satellite microwave sensing 80−98485
cyclone waves and front development, surface friction effects 77−86966
cyclone-anticylcone couplets, quasi-Lagrangian kinetic energy budgets 77−66958
cyclones, anticyclones and depressions (France, 1832-1956) *(French)* 77−45063
cyclones, dynamics, two-arm struct. and tracking 78−77299

storms continued
cyclones, extratropical, with northerly component, rel. to poor summers in British Isles 80−109241
cyclones, in Antarctica, effect on O isotopic comp. of fallen snow 78−36237
cyclones, investigation of atmospheric front motion employing two-layer model *(Russian)* 77−53109
cyclones, midlatitude, satellite-derived mesoscale wind fields covariance anals. 80−82013
cyclones, pressure drop reduction using deswirler 79−12176
cyclones, unstable baroclinic waves downstream and upstream development 80−56540
cyclones evolution, study by astronauts *(Russian)* 78−40795
cyclonic, over Cascade Mountains, ice particle concs. 77−2210
cyclonic storm, 1974 Aug. 14-16, Calcutta, rainfall estimate using S-band radar 78−32157
cyclonic storm, Arabian Sea, 1976 June, diurnal var. and secondary vortices form. 79−20915
cyclonic storm, Porbandar, India, 1975 Oct., features 79−48538
cyclonic storm, rainbands, precip. cores and generating cells 78−81307
cyclonic storms, mesoscale and microscale organization and struct. of clouds and precip. 79−74946
cyclonic storms, theory of vortices in rot. stratified flow 79−39814
cyclonic storms and depressions during 1974, Bay of Bengal and Arabian Sea 77−53110
dangerous weather phenomena prediction, research prospects 79−34932
Darling River system floods, chronological evolution, Nimbus-5 radiometry obs. 80−94543
design storm selection for stormwater management simulation 77−37278
detection, National Weather Service's training programme 80−8382
detection and prediction by ionospheric Doppler sounding 79−2326
diagnostic analysis in weather forecasting, appl. to storms *(Chinese)* 80−12467
dust cyclone, 1975 obs. at Ashkhabad *(Russian)* 77−29396
dust impairment of flat plate solar collector performance 79−62054
dust storm in Israel, dust property obs. 80−90162
dust storms, aerosol and momentum mixing, fast-response meas. 78−65364
dust storms, freq. and diurnal var. in contiguous United States 77−29353
dust storms, types, locations and mechanisms 77−9481
easterly waves and tropical storm formation, development 78−7703
electric field observations of storm clouds *(French)* 80−85712
energy production and control of atmospheric vortices 78−61510
S.England, 1968, September 14-16, mesoscale and small scale motions revealed by hourly rainfall maps 77−45122
SE.England, 8-9 July 54 BC, effect on Julius Caesar invasion 77−49149
E England coast, storm surge (1978 January 11 to 12) 80−12419
English Channel, 1974 September 2, storm surge 78−88895
Europe, exceptional weather in (1975) 77−25756
evaporating downdraught model comparison with obs. behind squall lines 78−92913
exceptional weather in 1976 over Europe 78−36251
extratropical cyclone, enhancement after separation from polar front *(French)* 80−56517
extratropical cyclones, mesoscale rainbands, assoc. cloud microphysics and dynamics 80−82030
extratropical cyclones, real-time wind meas. by Doppler radar, colour display system 78−61594
extratropical severe storms, contrib. to stratospheric water vapour budget 77−87029
flash floods, American National Weather Service (NWS) warning and disaster preparedness program 79−25289
flash floods, synoptic and mesoscale mechanisms for heavy rainfalls 80−8385
flood freq., analysis of storm prediction techniques 78−11976
flood inundation of agricultural land, LANDSAT digital image anal. 80−61913
formation, instability of low-level jet 79−88415
France, meteorological events at the end of the 14th century and the beginning of the 15th *(French)* 77−86960
frontal systems, passage correl. with Ligurian Sea free oscill. 79−34826
frontogenesis, Eady wave evolution in basic flows 79−88426
funnel clouds, characts. from obs. during sailplane flights 78−69396
gale damage, 1976 January 2-3, Lincolnshire, England 77−2207
NW.Georgia, prevailing storm tracks rel. to monthly rainfall spatial correls. 80−51479
SW.Germany, heavy rainfall from May 22 to 24 (1978) *(German)* 80−61869
glaze storms and wire icing in Ukraine 78−81329
Great Britain, northerly gales of (1978 January 11 to 12) 80−12508
W.Gulf of Maine, storms rel. to gulf winter circulation 80−51430
hail reports rel. to 45 dBZ contour level 77−56688
hail showers in Rumania *(French)* 80−4061
hail suppression seeding, Ag analysis 78−65367
hailstone formation within cloud, microphys. recycling 80−90146
hailstorm, finger radar echoes, form. mechanism *(Chinese)* 80−109234
hailstorm damage to vegetation, LANDSAT remote sensing epxt. *(Italian)* 77−81986
hailstorms, numerical simulation using cloud model 78−28269
hailstorms, Switzerland, time-resolved hailstone size distrib. and radar struct. 78−49109
hailstorms in Transvaal, 1972 November 29, radar obs. 78−20482
hailstorms of S.Saskatchewan, Canada, climatological characts. 80−109204
hailstorms variability on South African plateau 78−92911
heavy rainstorms in Britain, diurnal var. in occurrence 77−64402
Himalaya, wind and storms during summer 80−72620
hurricane, barotropic ocean response 78−36191
hurricane, estimation of eddy viscosity and H_2O vap. flux 80−51503
hurricane, probable maximum and assoc. flooding potential 79−20941
Hurricane Agnes storm and flood, geomorphic effects, SE.Pennsylvania 78−77280
hurricane and typhoon forecasting appl. of Kalman filter 77−64409
Hurricane Anita, assoc. longshore currents, Gulf of Mexico 79−34837
hurricane Ava, Skylab scatterometer meas., anomalous data correction 79−29881
hurricane boundary layer response to sea surface temp. changes, model 79−53439
Hurricane Camille, evolution, Nimbus 3/ATS 3 obs. 78−92921
storms continued
hurricane Camille, wind speed and direction, ocean wave height and barometric press. meas. 78−36254
hurricane cloud system, model of cloud-group activity 80−26601
hurricane Debbie, 1969 August 13-19, cloud distrib. and development 78−20493
hurricane dection by Doppler radar for coast of U.S.A. 80−67414
Hurricane Eloise, ionospheric obs. of assoc. gravity waves 79−66872
Hurricane Eloise (1975), ocean data buoy meas. 78−77302
hurricane forcing of longshore currents in Gulf of Mexico 80−76998
hurricane formation, tropical storm control by cloud seeding *(German)* 80−90207
hurricane formation near Cape Verde Islands, general circulation from Meteosat 80−105042
Hurricane Gladys (1975), subcloud layer energy transformations 80−77089
Hurricane Gloria, ocean wave patterns, obs. with airborne synthetic-aperture radar 78−44873
hurricane modification expts. by cloud seeding, evaluation 78−85654
hurricane motion forecasting using nested grids 79−44240
hurricane over Arabian Sea, surface wind and sea waves 77−53159
hurricane rainbands, possible form. mechanism 79−8658
hurricane rainbands, vertical struct., interaction with mean vortex 79−8659
hurricane reconnaissance, data transmission, via aircraft satellite data link 78−96299
hurricane sea surface wind speed, L-band radar backscatt. obs. 80−56561
hurricane season activity analysis, N.Atlantic (1886-1974) 80−101427
hurricane surge potentials over SE.Louisiana, forecast model 80−46216
hurricane-intensity extratropical storms, satellite forecasting, comments and reply 77−17249
hurricanes, forced secondary circulations 79−84387
hurricanes, formation and structure rel. to tropical circulation 79−88462
hurricanes, inertia-buoyancy waves 78−7705
hurricanes, moving, baroclinic nonlinear response of ocean, model 79−16497
hurricanes, spiral bands excitation by interaction between symmetric mean vortex and shearing steering current 80−56538
hurricanes and tropical meteorology 79−39785
hurricanes in the USA, speed determ. by Monte Carlo method 80−90209
hurricanes temporal variability, rank order statistics appl. 78−92910
ice phase formation in natural and seeded storms 78−61509
immature cyclonic storm struct. in Bay of Bengal revealed by radar 78−85628
India, N.E. monsoon rainfall pattern rel. to solar activity in Tamil Nadu 77−70749
India, N.E. monsoon rainfall singularities over Tamil Nadu 77−70746
India, November 1977 Andhra Pradesh cyclone and associated storm surge 80−51499
Indian region, primitive eqn. barotropic model for storm tracks prediction 78−85625
Indian sea areas, 1976 cyclonic storms and depressions 80−56533
Indian summer monsoon, intensity rel. to ocean surface temp. 80−90121
Iraq, duststorms, climatological and meterological study 77−73794
ITCZ over W. central Bay of Bengal, disturbances during 1974, October 77−45115
jet stream, fronts and wave disturbances compared with Gulf Stream 79−2268
Kansas City flash flood (1977, September 12), events and causes 79−25291
Kouchibouguac Bay, New Brunswick, storms rel. to barrier island breach morphology and dynamics 80−12371
Lake Constance, heavy storms and wind strength and direction *(German)* 77−56695
Lake Ontario, north shore coastal boundary layer response to storm 78−24322
lakes, circulation, seiches, tides and storm surges, finite element methods, book contrib. 79−34876
Leningrad storm surges, shallow water eqn. soln., hydrodynamic method *(Russian)* 77−29318
local severe storms in summer, anal. and forecasting method *(Chinese)* 79−84450
London, August 1975, urban effects on precip. 78−81339
London area rainstorm of 16-17th Aug. 1977 80−77093
Masirah Oman, September monsoon depression 79−8669
maximum precipitation, 1900-1977, Great Britain 78−85672
mesoscale convective system, momentum budget and temporal evolution 77−70757
mesoscale intense convective storm, Oklahoma, objective anal. 78−32168
microseism generation mechanism from sea floor obs. off Shikotan Island 78−73319
monsoon circulation over Bay of Bengal, 1976, winter to spring 80−82038
monsoon depression, Bay of Bengal, intensifying into cyclonic storm over land 79−20916
monsoon depression, composite structure 77−45117
monsoon depression, vorticity budget and vertical vel. distrib. 77−78321
monsoon depressions growth, combined CISK-barotropic-baroclinic instability 79−2337
monsoon depressions in Bay of Bengal, freq. of first occurrence, 10-day epochs, 1891-1970 period 78−81303
monsoon disturbances, growth studies 79−16611
SW monsoon on W.India coast, aerosol and rain trace constituents 80−81967
monsoon over Calcutta, rel. to VLF atmospherics anomalies 80−82127
monsoon over Indian region, energy anal. by baroclinic model 80−77073
monsoonal mid-tropospheric cyclone formation mechanism 79−34913
monsoons, symposium (New Delhi, 1977 March 7-12) 79−88410
motion in three dimensions, detection by conventional weather radar 78−57360
moving atmospheric pressure disturbance, energy generation in ocean *(Russian)* 77−33087
multicellular severe storm simulations, three-dimens. cloud model 80−77049
Nagapattinam cyclone, India, 12 Nov. 1977, radar-synoptic study 80−82026
Nile valley, synoptic disturbances north of ITCZ 77−45116
NMC forecasting of record-breaking Feb. 1978 winter storm 79−16564
North Sea, wave height statistics using hindcast wave data 80−17273

storms continued
North Sea, wind fields during gales 78−96272
North Sea and River Thames, surge and tide interaction 78−96219
northern hemisphere climate vars. rel. to N.Atlantic tropical cyclones characts. 79−39843
W.Norway coast, long barotropic waves and storm surges, model 80−81907
ocean, storm-induced catastrophic mixing in surface mixed layer 79−16503
ocean depths disturbed by surface storm, persistant nature of disturbance *(Russian)* 80−81921
ocean storm surge simulation expts. 78−16052
ocean storm wave heights, statistical distrib. 78−73390
ocean storm waves, rel. between heights and periods *(French)* 77−2157
ocean surges prediction on east coast of India 78−85566
ocean thermal response to strong atm. forcing, events characts. 78−92827
ocean thermal response to strong atm. forcing, one-dimens. mixing processes 78−92828
ocean-atmosphere interaction parametrisation for storm conditions, atm. circulation models appl. *(Russian)* 78−65359
oceanic mixed-layer deepening, obs. and simulation 79−20843
N.Pacific, finestructure and microstructure during passage of mild storm 77−2167
NW Pacific, wind-wave tropical cyclone model, parametrisation characts. 78−24301
Port of Leba, Poland, reconstructed entrance, storm tides prediction, math. modelling *(Polish)* 78−40568
precipitation, depth-area relations from digitised radar returns 77−91249
precipitation in small mountain watershed, storm type effect, theoretical study 80−8355
precipitation scavenging of urban pollutants, inorganic nonmetallic species 80−12039
precipitation-forced circulations in winter orographic storms 79−34912
prediction, overview and recommendations 79−8703
principal component anal., hail index *(French)* 78−96267
radar estimation of precipitation, using dual-wavelength radar 80−46220
radar remote sensing, optimal positions of multiple-Doppler system 80−31140
rain, in Sydney, Australia, quality characts. of storm water runoff 77−64357
rain throughfall under a forest, estimation methods 79−2307
rainfall, maximum possible in Great Britain−time limited, determ. methods 80−4091
rainfall, spatial distrib. in small catchment, influence on storm runoff 80−8357
rainfall intensity effect on storm flow and peak discharge from forest land 77−78271
rainfall network analysis, optimal estimation of total areal storm depth 78−49059
rainfall prediction for attenuation prediction in Earth-space paths *(French)* 78−49062
rainstorms, radar study of attenuation on terrestrial terrestrial microwave links 77−41130
Red River Valley, June-July 1975 record storms and flood 77−91193
river floods, wind effects on flood routeing 77−21808
runoff, flow component separation, solute conc. and contact time study 80−8358
sandstorm dust fallout, Kuwait, summer 1978 obs. 80−81966
sandstorms effect on microwave propagation 79−70834
sea foam microwave emission, remote monitoring of storm intensity 80−41528
Sea of Azov, storm surges calc. 78−96231
sea surface temp. anomaly generation rel. to atm. storms 79−39721
sea surge produced by storm, theory for stratified sea 80−51437
secular variation in tropical N.Atlantic and E.Pacific Oceans 79−100929
SESAME '77 experiments and data availability 78−65355
severe cyclonic storm, 1975 October, over India 78−85626
Severe Local Storm Warning and Disaster Preparedness Programs at NWS 77−86959
severe local storms, automated 12 to 36 hour probability forecasts 80−77062
severe-storm identification, multimoment Doppler display 77−56756
shallow sea thermal structure, during heating and storms *(Russian)* 80−56480
Shikotan Island, storm microseisms form., conditions 1974 Feb. 8-11 period 77−53004
snowfall systems induced by Lake Ontario, objective forecast method 80−51484
snowstorm avalanche forecasting in Khibins, model *(Russian)* 77−21812
splitting and simulation of right- and left-moving storms 79−16591
splitting leading to long-lived storms, numerical model 79−58032
squall forecasting from synoptic and thermodynamic condition anal. 77−78360
squall line, formation from boundary layer forcing and temp. gradient, model 80−8396
squall line formation, nonlinear process 78−81323
St. Louis urban precip. anomaly rel. to synoptic weather factors 79−39806
stationary tropical cyclone, energetics of stratified ocean below *(Russian)* 80−61808
steady convection, two-dimens., in const. vertical shear, dynamical struct. 79−12209
Storm Water Management Model for runoff prediction 77−37275
strong gales in E.Atlantic region, jet stream effects in subtropical latits. *(Spanish)* 78−44966
subsoil behaviour in Potsdam rel. to storms and atmospheric pressure *(German)* 79−62425
subwatershed storm response timing, runoff model 77−37274
Sunray tornado, photographs showing evolution 77−25731
supercell hailstorms, airflow and hail growth rel. to hail suppression 77−21856
surge prediction at Milford Haven, wind-induced motion models 79−66743
surge prediction using vertical pendulums 80−36764
swell waves at St. Helena related to distant storms 78−20432
Switzerland, 1975 August rainfall at Vitznau on Lake Lucerne 78−7743
thermosphere storms, and related ionospheric effects 77−9583
thunderstorm, precipitation obs. immediately after lightning stroke 80−77055
storms continued
thunderstorm gust front, wind shear meas. using pulsed lidar 80−67415
thunderstorm top, ascent rate obs. 80−61861
tides and storm surges, three-dimens. non-linear numerical model 77−37240
tornadic storm research, implications for dual-Doppler radar spacing of effective coverage area anal. 80−82093
tornadic storms and hurricanes warning system, gravity waves ray tracing 78−73448
tornadic storms on 1976 January 13, assoc. gravity waves 80−41515
tornado, contrib. of vortex-stabilised arc to energy 78−53711
tornado, simulated, feasibility of flow meas. via three-dimensional anemometers 77−17244
tornado activity rel. to precipitation, assessment 80−61882
tornado and models of atmospheric random vortices 78−28265
tornado flowfield struct., laboratory expts. 80−56566
tornado funnel formation, simulation expt. 77−21853
tornado life cycle, photographic sequence 80−41537
tornado outbreak (1974, April 3), upper atmosphere gravity waves obs. 78−85753
tornado over Delhi, of 1978 March 17, sodar obs. 80−109188
tornado over Punjab, 1975 March 10, synoptic situation and meteorological conditions 79−96793
tornado simulation, core radii and peak vels. in modeled vortices 80−90130
tornado threat in United States, distrib. 78−69397
tornado vortex, barotropic instability theory 80−51458
tornado vortex model, appl. to nuclear plant design 78−17444
tornado vortex simulation at Purdue University 78−40677
tornado warnings, Indiana alerting systems 79−5549
tornado watches compared to observed tornadoes, rel. to weather modification 80−12505
tornado wind speeds required to drive splinters into wood 77−17174
tornado-like vortex, laboratory expt. of swirl ratio effect 80−61862
tornado-like vortex dynamics, calculations 79−86440
tornado-like vortices, lab. simulation 77−55003
tornado-parent storm relationship from dual-Doppler radar anal. 77−21830
tornado-producing cumulonimbus, 1973 June 4, Oklahoma, USA 77−17202
tornadoes, Huntsville, AL, luminous electrical phenomena 77−45060
tornadoes, nearby magnetometer data 77−9467
tornadoes, stochastic vorticity-augmentation, theory 77−45100
tornadoes in UK, rel. to solar mag. sector crossing, 1957-77 period 80−77094
tornadoes probing with pulse Doppler radar 78−20558
tornadogenesis, numerical model of vortex growth 78−49114
tornadogenesis, precipitation and rotating wind, comments and reply 77−66963
tornadogenesis, vertical stability effects 79−53442
tornados, vorticity and divergence fields from dual-Doppler radar obs. 77−17172
tropical atmosphere, Taifun-75 data from equatorial Pacific area, typhoons 79−58052
tropical cloud cluster, struct. and evolution 80−12488
tropical cyclone, model of ocean-atmos. boundary layer interaction 80−109231
tropical cyclone, nested grid for 3-dimens. 3-level model 78−28342
tropical cyclone, three-dimens. dynamic models and track prediction 80−56508
tropical cyclone development, latent heat release, numerical simulation 78−81309
tropical cyclone generated surges in Bay of Bengal, numerical model 80−81923
tropical cyclone intensity measurement from tropospheric aircraft 80−67416
tropical cyclone model vortex motion with and without current 78−28266
tropical cyclone motion 77−53146
tropical cyclone nested grid model, noise control 78−11957
tropical cyclone recurvature forecast from temperature wind-height data 77−64380
tropical cyclone statistical prediction models, Monte Carlo significance testing 78−44943
tropical cyclone surge model, finite difference method 79−12132
tropical cyclones, convective fluxes 78−28267
tropical cyclones, features of boundary and surface layers 79−58053
tropical cyclones, landfall numerical simulation 78−81308
tropical cyclones, movement prediction using primitive eqn. barotropic model 77−17167
tropical cyclones, photometric method for estimating cloud cover from satellite data 78−4007
tropical cyclones, preferred mode of Ekman conditional instability of second kind (CISK) 80−72617
tropical cyclones, radius and frequency of 15 m s^{-1} (30 kt) winds 80−105025
tropical cyclones in Bay of Bengal and Arabian Sea, max. wind speed calc. 77−53124
tropical cyclones simultaneous occurrence on either side of equator, Indian Ocean area 78−81301
tropical cylones, guest speeds along N.Australian coast 77−86997
tropical depression, synoptic scale kinetic energy source, cumulus cloud convection 80−77088
tropical hurricane, main ocean waves calcs. *(Russian)* 78−16021
tropical large scale disturbances instability theory 77−5302
tropical meteorology, review 77−64365
tropical rainstorm over Queensland, 6-min. intensity data 79−100937
tropical regions, atm. noise data 80−61875
tropical storm Becky, B concs. in coastal N. Florida rainfall 77−21838
Tropical Storm Delia, ocean surface gravity waves directional spectra and kinematics 79−48506
tropical storm Delia, prod. of ocean currents on continental shelf 78−7655
tropical storm freqs. rel. to sea surface temps. 77−91226
tropical storm motion statistical prediction for Bay of Bengal and Arabian Sea 79−96789
troposphere-ionosphere coupling during 1973 November 20 isolated tornadoes 79−70851
turbulent zones in troposphere prediction 77−70789
typhoon and hurricane areas, distrib. models of press. and wind over sea surface 79−62570

storms continued
typhoon characteristics over South China Sea 79−25309
Typhoon Della, weather conditions in eye of storm 79−29828
typhoon havens research program at the Naval Environmental Prediction Research Facility 79−5616
typhoon June, 55 GHz meas. of winds 79−100906
Typhoon June (1975), obs. by scanning microwave spectrometer 78−73436
typhoon movement affected by equatorial anticyclone, Pacific and S.China Sea *(Chinese)* 80−46236
typhoon movements expt. simulation *(Chinese)* 79−84449
typhoon Ora, form. in intertropical convergence zone under influence of midlevel jets 80−12527
typhoon prediction by barotropic primitive equation model using splines *(Chinese)* 80−4063
Typhoon Tess (1975), transformation of ocean temp. field *(Russian)* 77−53069
typhoon Tess wake vertical struct. in upper layer of Pacific Ocean 80−26538
typhoon track prediction, appl. of multiple-category discriminant anal. *(Chinese)* 77−66967
typhoon tracks near Taiwan, forecasting using simulations 80−90200
typhoon trajectories seasonal activity rel. to subarctic frontal zone position over NW.Pacific 78−61526
typhoons, detection and appl. of associated acoustic waves *(Chinese)* 79−34996
typhoons, intensity change with cloud-plume outflow aloft 77−45107
typhoons, transform in northern latits. 78−92947
typhoons anomalous tracks, over East China Sea, mechanism *(Chinese)* 80−82043
typhoons structure over Soviet Far East during transformation of decay 77−78378
typhoons transformation, effects of extratropical circulation 78−3908
United States E. coast, storm rel. to narrow warm water tongue intrusion in Sargasso Sea 78−73382
upper atmosphere disturbances, seasonal vars. in latit. struct. 78−32264
urban flooding rel. to land use change, stormwater management model 77−37280
urban runoff, effects of storm freq. on pollution 78−53667
urban storm water drainage system design, rainfall criteria 77−64336
urban storm water management, flood vol. distrib. 80−8361
urban stormwater management, basinwide planning programme 77−37268
USA, National Severe Storms Forecast Centre, 1970-9, predictive success 80−46214
VLF sferics from Union City, Oklahoma tornadic storm 78−85639
central Wales, large, summer storm 1971, June 77−56717
S.Wales floods of late December 1979, meteorological anal. 80−98429
warm core cyclone over North Sea, conditional instability *(German)* 78−16118
warning of ocean storms using meteorological satellites 78−69423
water runoff from various land cover types, characterisation and impact 78−88852
waterspout frequencies along USA East and Gulf Coasts 77−78329
waterspout in association with large cumulus congestus 80−41473
waterspout statistics for Nassau, Bahamas 78−92919
wave and swell forecasting for North Sea 78−7658
wave forecasting service, pot. benefits case study anal. 78−77357
wave height prediction during gales in North Sea 80−98346
western disturbances development over India, role of westerly upper air troughs 80−90173
wind meas. in severe storms using airborne pulsed Doppler lidar system 79−66812
wind turbulence, characts. near top of spruce forest 80−17349
wind-wave height max. in storm, determ. 79−12125
windstorm downslope from mountain 80−56551
winter cloud systems over Sierra Nevada, liquid water content meas. 77−2213
zone location methods using radiothermal remote meas. of ocean *(Russian)* 78−16189
AgI particles in seeded storms, detection 78−3884
D areal distribution in California and Nevada precipitation, 1968-1969 period 79−100918

strain ageing
αbrass, single cryst., yielding behaviour rel. to low temp. annealing treatment *(Japanese)* 80−93582
α-brass, single crystal, deform. and ductility at elev. temps. *(Japanese)* 79−5012
dynamic strain ageing, and serrated yielding, mechanism 80−88245
Inconel 600, mechanisms of dynamic strain ageing and jerky flow 79−79024
plastically prestrained materials and components, high cycle fatigue *(Czechoslovakian)* 77−32680
steel, 35Kh3MFS, strengthening involving austenite fine grain processing *(Russian)* 77−52358
steel, alloy, 08kp, denitriding annealing, affect on mech. props. 79−52461
steel, alloy, strain ageing anomalies, plastic strain mechanisms *(Russian)* 79−52300
steel, austenitic, Cr-Ni-Mn-V, X-ray anal. of carbide phases formed during ageing *(Russian)* 80−20936
steel, austenitic stainless recrystallisation *(Japanese)* 77−52346
steel, Bauschinger effect minimization by dynamic strain ageing 78−48469
steel, C. cold strained, effect of rapid heating on strain ageing *(Russian)* 79−11642
steel, C, fatigue life prediction under programmed loading *(Japanese)* 79−20167
steel, C, strain ageing and fatigue limit 80−40378
steel, C, strain ageing contribution to fatigue hardening 78−23817
steel, C and Co, carbide transitions during post-strain ageing and tempering *(Russian)* 78−95741
steel, C-Mn, pressure vessel usage, elevated temp. mech. beahviour 78−35462
steel, CC Cr-Mo (2.25, 1 wt.%) effect of heat treatment on tensile props. 78−23745
steel, Cr-Mo (2.25, 1.00 wt.%), bainitic, strain rate effects on elevated temp. tensile behaviour 78−35461
steel, Cr-Mo (2.25, 1 wt.%), annealed, heat treatment effect on tensile props. 78−11243
strain ageing continued
steel, creep resistant, fine grained, structural, welded-joints, cause of cracking during stress relieving *(German)* 77−70141
steel, deformed strain-aged St.3 and 09G2S, stress conc. susceptibility, H_2 effect 78−95774
steel, H_2 effect on yield 78−15474
steel, hot rolled Al killed sheet, strain ageing control 79−61628
steel, impact and tensile props., Si effects 79−24614
steel, low, C, rimmed and killed, exam. of impact fatigue behaviour *(Japanese)* 78−88528
steel, low alloy, type 4340, quenched and tempered, effect of plastic strain followed by ageing, on torsion fatigue resistance 78−92360
steel, low C, cyclic strain ageing effect on crit. stress for crack propag. 79−34124
steel, low C, fatigue crack propagation in smooth specimen, strain ageing effect *(Japanese)* 79−20163
steel, low C, fatigue limit, strain ageing effect *(Japanese)* 77−8933
steel, low C, fatigue strength under rotating bending and torsion, under-stressing effects *(Japanese)* 78−44201
steel, low C, grain size effect on fatigue strength, high temps. 78−68759
steel, low C, P, plastic anisotropy and mech. prop. dynamic strain ageing effect 78−64608
steel, low C, rephosphorised static strain ageing 77−70079
steel, low C, strain ageing, effect of prestrain *(Korean)* 77−8865
steel, low C, strain ageing, essential work of plane stress ductile fracture 79−29187
steel, low C, stress ageing embrittlement under short term thermally stressed cycle *(Russian)* 80−60885
steel, low C, with various strain ageing potentials, tension compression fatigue *(Japanese)* 79−20162
steel, low C, yield point, effect of ageing stress 79−96091
steel, low C and alloy, serrated flow and thermomechanical treatment *(Korean)* 80−30026
steel, maraging Ni-Co-Mo, strengthening by repeated strain ageing *(Japanese)* 79−100157
steel, medium and high C, deformation ageing, entropy, free energy, dislocations *(Russian)* 80−66581
steel, medium C, fatigue behaviour of NiAl precipitation hardening 78−84983
steel, Mg effect on precipitation of C and or N, and mech. props., during strain ageing *(German)* 78−35387
steel, mild, activation energy for strain ageing 78−56677
steel, mild, annealed, fatigue crack init., microstructure and strain ageing effect 77−86162
steel, mild, with different sensitivities to strain ageing, cyclic plastic strain amplitude *(Japanese)* 77−8932
steel, mild, work hardening and strain ageing during fatigue *(Japanese)* 77−8931
steel, Mn-V reinforcing type, strain ageing characts. rel. to mech. props. 80−84969
steel, plane C, nonstrain-ageing state 77−52349
steel, structural martensitic, corrosion resist. under stress effect of strain ageing with hydroextrusion *(Russian)* 79−38853
steel, type 15Kh2NMFA, strain ageing effect on strength and toughness, susceptibility to strain hardening 79−57028
steel, V and V-N , high strength, mech. props. and strain ageing, processing variables effects 77−59819
steel, V containing dual-phase, yielding and strain ageing, early stages 80−25794
steel austenitic stainless, fatigue, low cycle, temp. and strain rate effects *(Japanese)* 79−29198
steel C, types AISI 1008, 1020, 1035, renitrogenized 1010 and 1522, dynamic strain ageing, tensile notch impact and fatigue props. 79−43288
steel pressure vessel, nuclear, fracture toughness at elevated temps. 79−20193
steels, spring, 60S2A and 50KhFA, heat treatment and mech. working effect on mech. props. *(Russian)* 80−20962
Zircaloy-4, β-transformed, flow stress and dynamic strain ageing 80−3101
Zircaloy-4, load relaxation and tensile tests 79−20093
Zircaloy-4, quenched, strain ageing behaviour, ageing time and temp. effects 78−56657
Zircaloy-4, quenched and annealed 77−25071
Zircaloy-4 cold worked, strain ageing behaviour with varying O_2 content 77−48455
Al alloy 7075, serrated flow and thermomechanical treatment *(Korean)* 80−30026
Al-alloys, precipitation hardening, effect on dynamic strain ageing and jerky flow 80−20945
Al-Cu alloys, Guinier-Preston zones study by stress ageing 79−100152
Al-Mg (1 wt.%), mechanisms of dynamic strain ageing and jerky flow 79−79024
Al-Mg (2.4 wt.%) alloy, solution-treated, grain size effects on fatigue strength 77−4839
Al-Mg (4 wt.%), enhanced ductility at elevated temps. 77−63740
Al-Mg (5 wt.%), serrated flow 79−43343
Al-Mg (5 wt.%), static strain ageing at low temp. 79−29116
Al-Mg-Si (0.7, 0.4 at.%), effect of precipitation hardening on strain rate behaviour and yield behaviour 79−29075
Cu, cold work, P effect on annealing 79−47707
Cu-Be, dynamic strain age hardening 77−52375
Cu-Cd (1.0 wt.%), yield stress and flow stress 80−97524
Cu-Cr (0.55 wt.%), crystallography of precipitates, strain field study 80−25699
Cu-Cr(-SiO_2), single crysts., yield and pre-yield behaviour rel. to aging time 80−81103
Fe, Armco, deform. strengthening during low-cycle fatigue in H gas *(Russian)* 77−52460
Fe, Armco, stress relaxation expt., significance under strain ageing cond. 79−57039
Fe, cast, ductile, strain rate and temp., influence on strength, elongation and deformation *(Japanese)* 80−45356
Fe, H_2 effect on yield 78−15474
Fe, pure, strain ageing and fatigue *(Japanese)* 79−20161
Fe-C-N, annealing in dry H_2, below 1180K, to purify to low C and N concs. 78−3072
Fe-C-N, BCC, Snoek type reordering during strain ageing *(French)* 79−8312
Fe-Cu alloy, effect of ε-Cu phase on strain ageing *(Japanese)* 80−7582
Fe-Mn (1 at.%), strain age hardening 80−108472

strain ageing continued
Fe-N, single cryst., solid soln. softening, effect of interstitial N 80−97496
Fe-Ni-C, martensitic delayed fracture *(Slovak)* 79−43401
α-Fe-P, static strain ageing 77−70079
Fe-Si (3 wt.%), strain aged polycrystalline samples, AE study of deform. 77−63696
NaCl, strain ageing exam. 78−56661
Nb-O, cyclic creep, effect of O_2 conc. and temp. 78−48466
Nb-O, Snoek mechanism and long distance diffusion under strain ageing *(French)* 77−81279
Nb-Zr-C, (1, 0.1 wt.%) alloy, mech. characts. structral sensitivity in strained state *(Russian)* 79−52301
Nb-Zr-C alloy, strengthening phase, struct. and morphology after stress ageing *(Russian)* 78−31454
NbN_x, solid soln, strain ageing, internal friction, elec. cond. kinetics *(Russian)* 78−76667
NbN_xO_y, solid soln, strain ageing, internal friction, elec. cond. kinetics *(Russian)* 78−76667
NbO_x, solid soln, strain ageing, internal friction, elec. cond. kinetics *(Russian)* 78−76667
Ni 200, C interstitial effect of yield point develop. during static strain ageing, model 78−88498
Ni 200, static strain ageing, 373 to 473K 77−36558
Ni-alloys, precipitation hardening, effect on dynamic strain ageing and jerky flow 80−20945
Ni-Be alloy, annealed under load, spatial distrib. of precips., electron microscopy *(Russian)* 77−59790
Ta wire, strain ageing by return of elastic limit method *(French)* 78−68713
Ta-O, relaxation anal. after ageing under stress *(French)* 80−16365
α-Ti, commercial purity, static strain ageing 77−86061
Ti, dynamic annealing, effect on dynamic strain ageing phenomena 80−7594
α-Ti, initial stage of strain ageing *(Russian)* 77−81278
α-Ti, solid soln., strain ageing *(Japanese)* 78−6953
α-Ti-O system, exam. of static strain ageing 78−76675
TiO_2 rutile single crystals, stoichiometric, dynamic strain ageing 80−50661
V-Nb, mech. props., −196-1000°C, comp. depend. 78−39847
V-Ta, mech. props. 79−61682
Y, plastic deformation props., deformation ageing, plastic flow, dislocation-impurity interactions *(Russian)* 80−66582
α-Zircaloy, strain ageing at 1000K 79−47725
α-Zr, strain ageing at 1000K 79−47725
Zr-Nb (1 wt.%), static strain ageing between 295 to 773K, TEM obs. of plastic strain 79−38855
Zr-Nb (1 wt.%), stress drop expt. during creep 79−29152
Zr-Nb (1 wt.%), tensile props., 295 to 773K 79−8318
Zr-Nb (1 wt.%) exam. of creep behaviour, 373 to 773K 78−80599
Zr-Nb (2.5 wt.%), strain ageing 77−77511

strain control
biaxial tensile strain field from conventional load-splitting tree 77−84203
composite transducer for longitudinal strain modulation for ESR and optical spectroscopy 79−12791
epoxy resin, heat generated by fatigue *(Spanish)* 80−11736
plastic extension control during fatigue tests 77−25220
resonant electromagnetic fatigue tester, appl. *(French)* 78−56870

strain gauges
see also strain measurement
antishunting screened resistance type 77−17973
application on compact bone 80−3883
application techniques 77−41591
applications of strain gauge rosettes *(German)* 79−67294
atomic resistance transducers (wire), effect of loops 80−22346
automated strain-gauge plethysmograph 79−29648
automatic multirange calibrator of strain-gauge bridges 79−67285
biaxial laser-based displacement transducer 78−73967
biaxial transducer type, to 1033K, use of 1366K resist. strain gauge 79−30465
blood pressure transducer, chopper preamplifier cct. 78−3659
bonded, thermally compensated, fabrication method 79−40551
bonded resistance foil, used in determination of dynamometer time ageing 79−35726
borehole instrument for stress meas. in coal 77−9415
Bourdon tubes, stainless, design and production *(Hungarian)* 79−85134
calibration machine construction and parameters *(German)* 80−36970
capacitance type, design 78−4609
capacitive, static meas. at high temp. *(German)* 79−30455
capacitive strain measuring circuit 79−17416
ceramic, electrical transducers for automatic recording of mechanisms occurring during drying 77−52561
clamp and strain gauge, for shear characts. determ. of glass reinforced plastic 80−85114
compact fracture mechanics specimens, crack and load monitoring using strain gauges 79−83411
compensation for temp. effects, cable capacitance and hysteresis in strain gauge meas. *(German)* 80−31734
composite transducer for longitudinal strain modulation for ESR and optical spectroscopy 79−12791
concrete, elastic modulus variations, gauge meas. by embeddable-strain-units 78−84878
Constantan single wire, thermal expansion +20 to −60°C, strain gauge use 77−67427
coordimeter, two-dimens. for displacement meas. in rock masses 79−35016
creep meas., high temp., use of capacitance type strain gauges 80−21256
critical gap meas. and adjustment instrument 78−62177
cylindrical tensoresistive pressure transducer 80−8978
data logger, for educational purposes 80−73353
DC resistance strain gauge using integrated operational amplifier 79−75522
deformation meas. at increased temp., using UMEh-10T test machine 78−57927
description, and appl. to buildings and public works *(French)* 77−5828
design formulae 80−22354
diaphragm pressure sensors using wire strain gauges *(German)* 79−80569
diffused Si pressure transducer, stress conc. at transverse gauges 78−12711

strain gauges continued
diffusion rate determination, metallic materials in Al melts 79−86913
digital output obtained from a transducer, using counter and logic ccts. 79−67281
discontinuous metal films, resist. and strain gauge factors expressions, quantitative formulation 79−95521
ductile fracture initiation, strain gauge method for detecting 78−85085
dynamic signals treatment *(French)* 80−22352
dynamometer system, body of rotation form, non axially symm. load 80−73350
dynamometers, effect of temp. on characts. 78−93677
electrical foil strain gauges, appl. to meas. of linear thermal expansion of plastics 77−41598
electrical resistance type, for mortar and concrete internal meas. 77−44446
electromechanical, for testpiece deform. meas. during low-temp. tensile testing 78−7118
embedment strain gauges for prestressed concrete pressure vessels 78−41873
error compensation 77−84198
error estimation for strain-gauge measurements in heat-resistance tests 80−4703
extensometer, rolling mill performance monitoring appl. 77−41590
fibre optic strain gauge, arbitrarily shaped path length meas. 78−70112
fibre optics 78−94426
film strain resistor for temp. up to 1000°C 77−37920
fluidic strain gauge load cell 80−37024
foil, use on materials with heat constraints during heat treatment 80−25938
foil resistance type, fatigue crack dimensions recording appl. 77−63856
force distribution under human foot, online meas. system 78−96110
force meas. rod bending moment compensation by parallel resistors *(German)* 77−79078
force transducer transformation analysis *(German)* 77−74380
force transducer with screw tenso-resistor, linearity anal. *(Russian)* 78−89475
force transducers, normalization of AC characts. 79−35705
fracture mechanics specimens monitoring during environmental testing, strain gauging technique 78−31606
gamma-ray thermometer and strain gauge for remote meas. 78−12694
glass fibre reinforced plastics mechanical properties measurement, use of electrical resistance strain gauges, effects on props. 79−43541
hand function, normal finger functional strength meas. 79−92276
high-temperature without base, manufacture 80−37018
holographic optical strain gauge 80−52182
hydrostatic press. effects *(German)* 79−30456
hydrostatic pressure cells producing anisotropic strain, calibration 79−17410
implantable biomedical pressure transducer 77−73606
internal strain meas. by built-in gauges *(French)* 78−32806
intestinal mechanical and electrical activity recording transducer 77−44862
Langmuir film balance meas. system 80−62659
laser microstrain gauge principle and technique 77−68541
load cell, for water table level sensing 77−21802
load cell transducers, shear force, mathematical modelling and design 79−35722
load cells, automatically controlled, method for digitizing measured values *(German)* 79−35721
load cells, characterisation of creep response 79−35718
load cells, small dead weight machines with compensators and computerized data processing 79−37266
load cells, stabilisation and compensation of temp. dependent errors *(German)* 79−35717
load cells, testing for suitability in electromechanical weighing machines *(German)* 79−35682
load cells and force transducers 80−86276
load cells and indicators for weighing machines, permissible number of digits *(German)* 79−35681
low temperature, search for standard resist. Al alloys 77−17997
magnetoelastic load cell and performance of force transducers *(German)* 79−35714
manganin foil like gauge calibration in planar shock wave expts. 80−95091
manometer, strain gauge type, for press. up to 14 Kbar *(German)* 77−26322
mass comparator, high precision, using bonded strain gauge load cell 80−57261
measurement error reduced, by connection in Wheatstone bridge manner 77−10004
measurement of high temperature deformations during welding, new device characteristics 77−67417
measuring transducer strain gauges, principles, appls., and new designs *(German)* 79−30449
mechanical quantities meas., by electrical methods 77−33981
mechanical strain indicators and recorders 80−13054
mechanicochemical testing of metals, electrochemical cell for mechanicochem. behaviour determ. 78−60905
mechanics testing, lateral deform. gauge 79−57163
metal foil, performance under large cyclic strains 77−77651
metal foil gauge, long-term stability of strain meas. 79−17417
metal thermoelastic coeff. meas. by strain gauges 78−56853
metallic foil vs. thin film, manufacturing techniques and performance 79−30464
miniature drag force anemometer 78−14117
myopotential controlled elec. operated hand with sensory feedback 79−57815
noncontact strain meter, exam. of design 80−7740
nuclear fuel cladding strain meas., microprocessor-controlled microwave extensometer 78−33240
operating amplifiers with strain gauge bridge networks, ccts., features *(German)* 77−71311
optoelectronic meas. methods appl., with twin diodes *(German)* 80−13064
optoelectronic strain gauge, force and strain measurements giving high accuracy and resolution *(German)* 79−98673
orthopaedic load meas. using strain gauges 80−56262
pasted semiconductor, amplitude-freq. characts. calc. *(Russian)* 79−97379
performance in pressurised water at 50°C, reactor pressure vessels testing 79−35713

strain gauges continued
photoelastic strain gauge, concrete structure boundary stress meas. appls. *(Chinese)* 79−72867
physiological miniature strain-gauge pressure transducers 79−100778
pickup for soil compressibility investig. under static loadings 79−88345
piezoelectric diffused MOS strain transducer 77−5825
piezoelectric transducer, for clinical recording of ocular microtremor 78−96109
piezoresistive strain gauge transducers for millinewton force meas. with millisecond response time 79−12793
piezoresistive strain gauges, biaxial gauge factors 80−52185
plane shearing stress meas. with wired strain gauges *(German)* 78−89471
plastic model meas. use of strain gauges, instrumentation, accuracy 80−21255
plethysmograph, calibration-free Hg strain-gauge device 80−17161
plethysmography using Hg strain gauge, in evaluation of efficacy of nitroglycerine paste 77−40905
polyimide adhesive based, effect of cyclic heat exchanges, 20 to 300°C 77−16775
polymer material bending strain, strain gauge to meas. reliably 80−25948
pressure cells, operating ranges and principles *(Hungarian)* 78−54335
pressure measurement in industrial environments *(Hungarian)* 80−86278
pressure pick-up with Si column strain-gauge convertor 80−31732
pressure transducer, signal simulator, for physiological monitoring applic. 77−40804
pressure transducer performance, effect of zero offset changes 80−56255
principles, types and instrumentation 77−41589
protection, sealants suitability determ. 78−4610
protection for long-term stability 79−17418
reactor experiments 79−49648
remote transducer for magnetostriction meas. at high temps. 77−26365
residual stresses, meas., with hole-drilling strain gauge method 79−39108
resistance, adaptive amplifier convertor using sensitivity stabilisation *(Russian)* 77−41593
resistance, bonded 79−93122
resistance, device for calibration of low temps. 79−17413
resistance, high-temp., appl. in study of thermal stresses 77−44442
resistance, in alternating sign deform., calibration 79−15901
resistance, metrological characteristics 79−75521
resistance bridge amplifier, high measurement accuracy 77−5826
resistance gauges, effectiveness in liquids from 100 to 150°C 77−53887
resistance strain gauges bonded to bone surface in vivo, post-mortem calibration 78−28135
resistance type, developments and appls. *(French)* 78−12686
resistance type, to 1366K, and use in biaxial strain transducer to 1033K 79−30465
resistance type, use in long-term dimensional stability meas. 77−49711
resistance type, use up to 320°C *(German)* 79−30454
resistance wire, strain meas. in optical fibres and cables 80−23804
resistance wire type, metrological charact., effect of formaldehyde resin 77−120
resonant electromagnetic fatigue tester, appl. *(French)* 78−56870
respiratory pattern monitor for premature infants, computerised, apnoea detection 77−81635
rod, strain meas. with capacitive strain gauge 77−16774
rotating part deformations, strain gauge for measuring, exam. of design 78−76820
Sapfir semicond. transducers, development and appls. 80−13059
SAW device 77−79091
selection, applications and technical specifications, output signals 80−101790
self-conditioning transducers for long cable runs, operation 77−5827
semiconductor, acoustic power meas. of US medical probes 80−87679
semiconductor, linearisation measurement transducers *(German)* 77−37942
semiconductor, method to improve temp. stability 80−87826
semiconductor, rolling mill forces meas. appl. 78−41296
semiconductor pressure transducers, temp. compensation, strain gauge appls. *(Polish)* 80−31726
semiconductor sensors, props. and appls. *(German)* 78−36991
semiconductor strain gauge resistors, exam. of charact. in elastic waves 78−85097
semiconductor strain gauge with elastic coating 79−7350
semiconductor strain gauges, strain indicator 77−71313
sensitivity, K factor 78−77900
shrinkage measurement during hot pressing strain gauge device 78−11146
Si, for cryostatic temp. 78−24782
silastic strain gauge as in vivo muscle force transducer 79−29680
single shunt calibration to simulate bridge unbalances 77−22542
slip ring circuits 79−67291
small high-elongation foil strain gauges as fatigue damage indicators 79−32417
space shuttle insulation coating, combined load testing at 1100°C 79−34261
speech production anal. using transducer for observation of lip and jaw motion in midsagittal plane 79−44069
spinal deformities correction, force meas. 80−76861
split Hopkinson pressure bar test on C fibre composites, opt. and strain gauge methods comparison 80−85132
spreading pressure of adsorbed film, direct reading strain gauge 77−15692
sputter-deposited thin-film pressure transducers 77−30139
sputtered thin films for press. transducers 77−49719
Statham strain gauge, fission reactor safety-related sensor, comparison with pressure transducer 78−13253
steel, with brass inserts, Whittemore gauge length meas., reliability 77−36669
steel weld fatigue life estimation, multichannel NDT monitor 78−56846
strain measurement with resistance strain gauges subject to high press. *(German)* 79−49245
strain measuring instrument, low stiffness, three component, for tubular specimens 77−32749
stress distribution meas. of patient sitting immobile, instrumented wheelchair 77−90930
stress intensity factors estimation, tensometric methods 79−32424
strain gauges continued
stress/strain distrib. meas. inside plastic zone of notched sheet, fatigue crack propag. *(Japanese)* 78−6981
temp. and dissipation effects investigation, interference method appl. *(German)* 77−53892
temperature compensating gauges, param. discussion *(German)* 77−53893
temperature compensation methods 77−22541
tenso-resistive type, output error anal. *(Russian)* 78−89474
tensoresistors, measuring force 80−17930
tensoresistors, protection methods from phenol formaldehyde resin medium 79−54121
testing, four-point bending machine assessment by holographic interferometry of steel bar deform. 79−34266
thermal expansion charact. determ. using strain gauges, appl. to metals and alloys 78−81942
thermal expansion meas. technique 78−53059
thermoelastic, design, appl. of thermoelastic response of engineering materials 79−35724
thick-film strain gauges and pressure transducers 80−57285
thin film, construction and appls. *(French)* 79−93130
transcriptor F595 control unit for measurement and recording of strain parameters *(Russian)* 79−88945
transducer compensation linearisation by shunt resistors 78−12688
transducer for jaw force meas. 77−86669
transducer for myocardial stimulation and local tension meas. 79−48357
transducer sensitivity to directional thermal gradient error 77−74382
transducer with one-piece strain sensitive element design 78−1617
transducers in testing machine and as force standards 80−42215
transient response determ. 79−93132
transverse sensitivity correction of strain-gauge readings by a method of Mohr's circles 79−90203
triaxial strain cell for rock stress meas. 77−9574
vacuum deposited constantan alloy-film/ceramic steel system, electromech. behaviour 78−6634
vibrating wire nine-gauge devices, use in meas. internal strain in concrete 77−51008
vibrating wire strain gauges, temp. effect 80−73354
vulcanized-rubber protection and waterproofing in seawater environment 78−16787
weldable, high-temp., meas. of static operation stresses up to 530°C *(German)* 77−13745
Whitney (Hg-in-rubber), for plethysmography error due to temperature drift, compensation 77−52900
wind tunnel dynamometer, five component 78−54361
wire systematic error estimation *(Russian)* 78−65916
YYB1-1 telemetering strain gauge, design and meas. accuracy *(Chinese)* 79−35699
zero-stiffness, use with low modulus structural modes 77−68543
Au film, discontinuous, substrate radiation damage effect on resist. and strain gauge stability 79−95520
Bi, film, evaporated, elect. and elastoresistance props. 79−33367
C fibre reinforced plastic, fatigue failure mechanism identification, AE detection using piezoelectric strain gauge 79−96239
Cu, electrical resistivity, linear strain effect at elevated temps., strain gauge factor 79−91022
Cu-Mn alloy, manganin, hysteresis-corrected calibration under shock loading 80−74818
Cu-Ni/Au-Ni multilayer films, ohmic behaviour, use as strain gauge 80−65713
Fe-Cr-Co, heat treatment effect on strain gauge factor *(Japanese)* 78−6954
Ge:Au film strain gauges, press. sensor *(Japanese)* 80−105631
Ni-Cr, high temp. wire resistance strain gauges 77−53896
Ni-Cr foldfoil strain gauge, for cryogenic anal. of supercond. structs. in high mag. fields, fusion reactors 78−54947
$Pb_{1-x}Sn_xTe$ film, possible applic. as mechanical stress transducers 77−58621
Si, for in vivo bone deformation telemetering in monkey 77−86720
Si force transducer, extraluminal meas. of oviduct contractile activity 77−40805
Si integrated bridge strain gauges with diffusion piezoresistors, strain sensitivity *(Polish)* 80−73341
Si strain-gauge device, two-component, for aerodynamic tests on thin assemblies 78−3263
Si whisker, sensitivity to elastic pulses in −50 to 110°C range 79−17409
Si whiskers as basis for strain resistors 79−5094
Si:B(P) implanted layers as strain sensors 77−35098
Ta thin film, elec. cond., strain gauge factor, ion bombardment effects 80−80417

strain hardening *see work hardening*

strain measurement
see also strain gauges
absolute retardation accurate meas. using holography 79−27201
accelerometer base strain sensitivity test device 80−52173
accuracy improvement in impact tests 80−81259
alloy, cold-worked, particle size and strain determ. from X-ray diffr. profiles 78−88588
anisotropic reinforced resin laminate, cyclically reversing load, strain behaviour determ., approx. method *(German)* 79−5096
arbitrarily deformed objects, principle surface strain determ. using tandem speckle photography 79−32408
assessment of methods of investigation *(Russian)* 79−52539
automated method of strain state determination, dividing nets appl. 80−100982
bending, in plates, direct determ. using projected gratings 79−32420
biaxial strain transducer for appl. up to 1033K 79−80600
biaxial tensile strain field from conventional load-splitting tree 77−84203
birefringent materials, meas. of time-depend. principal strain directions 77−2647
bone, in-vivo *(French)* 79−34695
bone strain in-vivo telemetry in monkeys, method 78−3697
brittle lacquer technique, book contrib. 79−20332
capacitance-torsion balance for measuring small stresses and strains 78−73988
ceramic composition rheological meas. device for 20° to 90°C and constant moisture content 78−85079
coatings, brittle, strain sensitive, for stress, strain testing of surfaces of loaded structs. 79−29311

strain measurement continued
composite structure 10 μm spots, using X-ray microdiffractometer, rel. to IC failure 78−86262
concrete, meas. of internal strains by nine-gauge devices 77−51008
contactless, laser beam and photoresist grating method *(German)* 80−68195
crack tip strain meas. by electron micrograph stereoscopy 80−69752
cyclic microstrain meas. in tension and compression 77−74389
cylinder distortion measurement, holographic obs. *(German)* 79−34273
cylindrical rod, linearly elastic, elastic waves anal. from two-point strain meas. 77−72211
deformation, cyclic, static, meas., recording, automatic system 79−15893
deformation anal. with additional degrees of freedom during reconstruction by holographic interferometry 79−32411
deformation strength props., simultaneous meas. of several samples, polymer films appl. 79−15896
displacement components and derivatives, holographic-moire technique 78−51140
ductility meas. technique at high strain rates 78−80694
dynamic errors in spring-mass-damping system *(German)* 79−12794
Earth, laser interferometer appl. *(Japanese)* 77−81783
Earth, laser interferometer methods *(Japanese)* 79−25346
Earth crust, strain meas. in Ancona (Italy) area 77−86742
Earth strain measurements by bore-hole strainmeter at Matsushiro, seismic waves response *(Japanese)* 79−96745
Earth strain obs. with Cambridge laser strainmeter 77−44895
Earth tidal strain, topography, geology and cavity effects 77−44896
elasto-plastic strain eval. by strain gauge 80−28473
elastoplastic strain meas., elastic and residual components, single plate hologram interferometry 80−32932
electric resistance strain gauge principles, types and instrumentation 77−41589
electron inertial effect, shock loaded rod 78−51139
electronic potentiometer, attachment for measuring deform. 77−17974
engineering materials, thermoelastic response, appl. to dynamic response of engineering structures 79−35724
error due to communication lines, elimination, 20-550°C 80−64499
extensometer, rolling mill performance monitoring appl. 77−41590
extensometric method, for inside nuclear reactor channels 80−100998
extensometry, diffracting gauge principle 79−85119
extremely soft material, embedded marker method 79−57162
ferroconcrete, cracked, strain meas. *(German)* 79−34275
fibre reinforced composites, intralaminar-shear charact., 10 deg off axis test 78−35422
film strain resistor for temp. up to 1000°C 77−37920
floor reaction, medical appl. *(Japanese)* 80−12291
fluidic strain gauge load cell 80−37024
fracture mech. techniques, review 79−41635
fracture mechanics specimens monitoring during environmental testing, strain gauging technique 78−31606
fracture strain measurement at high strain rates, radial expansion technique 80−85134
fragile materials, at high temperatures, improved clamp for transducer attachment 80−73351
full field optical method having postrecording sensitivity and directional selectivity 78−57892
fusion reactor coil, multilayer structs., laminated beam theory anal. 78−55011
galvanomagnetic transducers, steady pressure effects 77−79129
gas gun expts. for two-dim. strain meas. 78−5709
general object deformation decomposition by speckle displacement 80−106486
geophysical wire strainmeter 77−41178
gravitational radiation detection method, elastooptical antenna, photoelastic effect 80−46947
Hall effect extensometer for simple shear meas. in polymers 79−23286
high temperature, 298 to 3000K, new optical technique 78−85063
high temperature deformations during welding, new strain gauge characteristics 77−67417
hip joint prosthesis, internal meas. by built-in gauge, calibration and error sources *(French)* 78−44705
holographic combined with two-beam interferometry for small inhomogen. strains 79−3650
holographic interference, fringe contrasts, displacement gradient determ. *(French)* 77−61928
holographic interferometric meas. of strain and material props. using single view 77−31073
holographic interferometry, deform. anal., reconstruction 77−38829
holographic interferometry, high-freq. moire technique, and speckle correlation, on flat metal plates 79−32421
holographic interferometry, strain components from fringe contrast 77−88665
holographic interferometry appls. *(German)* 80−78815
holographic interferometry for quantitative strain meas. 78−32794
holographic interferometry with continuously scanning reconstruction beam 78−71055
holographic moire pattern differentiation 79−59951
holographic strain analysis, expt. implementation of fringe-vector theory 79−18839
image-shearing camera for surface strain direct meas. 79−58773
impact force vs. displacement curves, expt. determ. 78−83344
in-plane strain meas. by holographic modulated diffr. grating 79−90202
inclusion spherical strain fields, S-matrix theory calcs. 80−100133
instrumentation for impact, erosion and fracture studies 77−81383
interferometric method, appl. to sheet metal and transparent plastic sheets 78−75108
interferometric method for shear strain and rot. meas., diffr. beams of diffr. beams 79−32397
interior displacement and strain measurement using white light speckles 80−95064
internal strain meas. by built-in gauges *(French)* 78−32806
irradiation-induced creep strain measurement, design and construction of apparatus 78−15634
laser grating method appl., strain distrib. meas. in plane, opaque surface 79−32407
laser microstrain gauge principle and technique 77−68541
laser speckle interferometry, anal. of double aperture speckle and shearing camera techniques 79−6169
laser speckle photographic technique *(German)* 78−1616
lasers in metrology and testing, review 77−5817
living cells, stress-strain meas. using cell poker 80−76880
strain measurement continued
lumbar vertebra cortical surface strain distribution tests 78−11692
magnetostrictive SAW generation efficiency meas. of residual stress 77−28972
metal, cold-worked, particle size and strain determ. from X-ray diffr. profiles 78−88588
metal, plastic strain graph plotting at high strain rates by cutting method 77−90521
metal, strong, compressive stress/strain props. meas. at very high strain rates, modified Hopkinson bar system 80−85128
metal, surface strain meas. by intensity of reflected light flux 77−17972
metal, torsional creep under accelerator irradiation, meas. instrument 78−3262
metal contact, strain in microrelief ridge 77−44443
metal fibre stress/strain curves determ. using X-ray goniometer *(German)* 78−92413
metals, deformed, US charact., meas. apparatus 78−60898
methods, survey, state or art *(German)* 77−11152
minerals, thermal expansion, characterisation technique 79−70795
moire band displacement strain determination, use of FTM type phototransformer 79−52519
Moire band maps, processing automation peculiarities 79−50681
Moire effect and deformation meas. in structural components *(German)* 78−88587
moire fringe method, strain anal. by multipurpose optical moire processor 80−9028
moire fringe methods 80−28476
moire fringe technique, book contrib. 79−20333
moire gratings strain meas., long time high temperature appl. 80−38361
moire interferometry strain meas. in elastic thin membranes, appl. to human skin 80−30828
Moire method, raster manufacture and copying for exptl. strain anal. *(German)* 77−121
moire method combined with photoelastic coating method *(Japanese)* 79−32400
Moire method effects modelling using finite element method 78−38259
Moire method using diffraction beams, compensation of errors 80−13068
Moire Rosette method for determ. of principal strain and direction 78−27695
Moire rosette method for principal strain analysis, mismatch changeable equipment 79−32396
moire strain analysis in cryogenic environments 79−77029
Moire strain measurement method, sensitivity and accuracy 77−17971
mortar and concrete internal meas. using elect. resist. strain gauge 77−44446
multiaperture method, strain analysis by one-beam laser speckle interferometry 79−81821
nuclear fuel cladding, internally pressurised, instrument for strain meas. 77−65271
nuclear fuel cladding tube deformation monitoring, photodiode image scanning technique 79−30938
nuclear reactor pressure vessels, strain measurements 80−79865
opposed-anvil high-press. devices, material strength effect 80−47068
optical fibre cable vibration characteristics, fibre strain and optical loss meas. 80−99870
optical fibre cables, modular, composite strain analysis 79−64351
optical fibres and cables using resist. wire 80−23804
optical methods for determining strain and displacement, book 79−20331
optical windows at high-press. chamber, strain determ. by holographic interferometry and finite element anal. 77−26323
optoelectronic strain gauge, force and strain measurements giving high accuracy and resolution *(German)* 79−98673
photoelastic coating method of meas. stress and strain 78−1614
photoelasticity, monograph 78−19988
piezoelectric transducer distortion measurement 77−10006
plate, cantilever, strain meas. from holographic data 79−20303
pneumatic measuring/calibration system, for meas. at up to 300°C 78−45610
polymer, volume stress/strain state 78−23896
polymeric, liq., spike-strain test relevance for network connectivity destruction by deformation 80−6001
polymers, between −60 and +50°C 78−19974
polypropylene, transparent film, strain anal. by scattered-light speckle photography 79−32399
pressure meas. at solid-lubricant interface, strain and deform. meas. techniques with diaphragms, comparison *(French)* 79−30453
pressure transducer, operating temperature range extension using semicond. tensoresistors 78−4608
pressure vessel, defect detection, strain evaluation laser holographic and speckle photography methods 77−81365
pressure vessel, stress concentrations around multiple windows photoelastic anal., strain gauge tests 77−72254
pressure vessel stud bolt, high temp. *(German)* 79−30937
prosthesis mechanical efficacy determ. by holographic strain meas. *(German)* 79−8573
prosthetic deformation measurements using holographic interferometry *(German)* 78−35911
quantum acoustic strain detector 77−51009
relaxometer, low temp. testing modification 79−43517
residual strains in components, determ. by holographic interferometry 80−99980
residual stress determ. by mechanical method, recommendations for strain meas. 77−23921
resistance bridge amplifier, high measurement accuracy 77−5826
resistance strain gauge-meas. techniques in biomech. expts. *(German)* 80−104819
resistance strain gauges subject to high press. *(German)* 79−49245
rheological property meas. apparatus *(French)* 80−14644
ring under diametral compression, strain meas. using surface grid distortion 79−43529
rock, algebraic method for strain estimation from deformed ellipsoidal objects 77−21766
rocks, deform. under uniaxial compression 77−53043
rocks, finite strain anal. using lines with initial random orientation 78−20568
rocks, polygonal strain markers adaption 78−20567
rocks elastic properties determination, modified borehole jack method 78−81448
rod, strain meas. with capacitive strain gauge 77−16774

strain measurement continued
rubber tube, inflation and extension, biaxial strain studies 78−83251
sediments, Skrino anticline strain var. determ. from deformed reduction spots 77−37184
seismic, differential capacitance displacement transducer appl. 77−49710
SEM, combined deformation/heating stage, acoustic emission rate meas. 80−101892
semiconductor strain gauge with elastic coating 79−7350
shear-band temp. meas., appl. to 4340 steel and 2014-T6 Al 80−48655
sheet materials, attachment for testing during sign alternating loading 77−52579
shell reinforced around hole, deformability meas. 80−16371
skin, living, in plane method for determ. of 2-dimens. stress-strain behaviour 77−37120
soft materials, reinforcement effect of strain gauge, numerical anal. 79−72864
solids and granular materials, stress and strain cells 79−32416
specimen-grating photograph electro-optical processing 77−39266
speckle hologram, strain meas. near stress conc. in life size specimen 77−119
speckle interferometry, decorrel. effects, machine induced strain obs. 77−45887
speckle pattern interferometer for total plane strain field meas. 77−26388
speckle photographic technique, hybrid optical and electronic image processing 80−99976
speckle photography technique, accuracy assessment 79−86389
speckle photography with hybrid optical/electronic image processing 80−106768
speckle shearing interferometry, fringe parameters 79−220
speckling application, for stress-strain state of parts 80−19300
Spherical shell, shallow, on elastic subgrade, under ring load along the edge 79−41644
steam turbine blades, vibration meas. via radio link telemetry 77−68538
steel, austenitic stainless, microdeform. meas. using method of grids 80−55615
steel, mild, bolt thread strain meas. 78−60972
steel, stainless 304, stress corrosion cracking in high temp. water, constant strain rate meas. 78−31565
steel penstock, large diameter, embedded in rock, strain measurements, using strain gauges 79−43544
strain gauge array, triangular, temp. field effect *(German)* 77−53892
strain gauge meas. in cyclic elastoplastic tests, automatic processing on portable computer 77−5829
strain gauges, temp. effects and compensation *(German)* 77−53893
strain measuring instrument, low stiffness, three component, for tubular specimens 77−32749
strain tide spectroscopy, 30 m laser system, Earth structure study appl. 79−5440
stress analysis in elasto-plastic media using birefringent coatings *(French)* 79−18846
stress intensity factors estimation, tensometric methods 79−32424
stress-intensity factor determ. by strain-gauge method 80−76445
structural deformation meas. by holographic speckle interferometry *(French)* 78−30249
superconducting strain transducer 77−37877
surface displacement and strain anal. by speckle interferometry 80−14635
surface strain field meas. on rubber structures, optical method 77−34017
surfaces, curved, strain anal., grid-transferring technique 79−18845
tensile specimen, normal mech. anisotropy meas. by Moire technique 78−16788
tensile testing, low-temp. strain gauge for testpiece deform. meas. 78−7118
tensile testing, strain meas., device 79−43515
tensile testing at const. true strain rates, test machine 79−34262
tensoresistors, measuring force 80−17930
thermal expansion characts. determ. using strain gauges, appl. to metals and alloys 78−81942
thin-walled tubes accelerated rate test system for two-dimensional stress states 79−43514
three dimensional deformation measurement, Moire and light slicing methods 78−8382
tip of propagating fatigue crack, strain distrib. meas. by Moire fringe multiplication method 77−80124
transmission replica system for strain measurement 79−74323
transparent materials, low-modulus, mech. props. determ. method 78−5704
transparent plates, light interferometry 77−75865
truss joint strain meas. by modified Michelson interferometer 80−74821
two-dimensional structure in-plane vibr., stress analysis by laser speckle method 80−103006
vibrating plate like struct., displacement and strain meas. using time average holography 79−46272
vibrating wire strain gauges, temp. effect 80−73354
viscoelastic plastic components, using Moire method *(German)* 78−22309
viscoelastometer, dynamic, direct reading, automation, appls. to polymer films, fibres 79−3980
welded joints, strain concentration zone detection by holographic interferometry 77−40512
whisker crystals uniaxial deformation, at He temperatures in magnetic field, mechanical displacement transformers design 80−50788
white light speckle method of experimental strain analysis 79−37255
X-ray differential photometry, appl. to meas. of piezoelec. coeff. in $LiNbO_3$ 77−8511
X-ray diffraction non-destructive testing method *(French)* 78−15626
X-ray diffraction profile, microstrain correction 78−59852
YYB1-1 telemetering strain gauge, design and meas. accuracy *(Chinese)* 79−35699
zircaloy calandria tubes in CIRENE PWR, stress evaluation using strain data *(Italian)* 77−50204
Al plate, thermal strain meas. by one-beam laser speckle interferometry 80−103005
Al, plates, exam. of stress conc. around conical cutouts, using strain gauges 79−41639
Fe-Cr-Co, effect of heat treatment on strain gauge factor 78−72802
Fe-Ni-Ti, preaged martensite, shear strain magnitude, X-ray diffr. method 80−93592
Li_2O-Al_2O_3-SiO_2 glass, crystallised, grain size and internal strain 80−103259

strain measurement continued
Mg alloys, strain rate effects during reverse torsional shear 77−4143
Si, elastically bent, strain canc. determ. by microfluorescent densitometry of X-ray topography 80−79245
Si impurity-doped cryst. plate, as an X-ray monochromator, strain distribs. for 220 reflection 80−100126
Si, strain meas. by Pendellosung effect after P ion bombard. 78−55773

strange particles
see also hyperons; kaons
1/N dual unitarisation convergence due to SU(4) breaking, charm and strangeness implications 79−6321
$\Delta S=\Delta Q$ isolation, charmed particle at SU_3 27-plet effect 77−26501
associated strange and charm prod. in dual unitary approach 77−41824
axial vector meson non-diffracture prod. in Kp and πp interactions 80−32122
baryonium, spectrum, decay, production 78−93854
Cabibbo angle physical interpretation, weak interactions nonleptonic $\Delta I=1/2$ rule, four-quark scheme 77−22679
charmed baryon nonleptonic decays, sum rules for $\Delta C=\Delta S=1$ S-wave decays 79−58957
charmed baryons, $\Delta C=\Delta S=1$ nonleptonic decays, amplitude relations 79−54339
coalescence analogy with ferromagnetism, prod. of ψ-mesons 77−13951
condensation in dense nucleonic matter *(Russian)* 80−5086
flavour changing weak radiative decays, short and long distance effects 80−73712
flavour symmetry breaking and production processes in dual unitarisation, φ and ψ prod. 79−45080
four-quark scheme, $\delta I=1/2$ rule, existence of K_L^0, K_S^0 77−22688
hadronic multiparticle reactions, models, prod. of strangeness, baryon number, charm 78−74286
hadrons, relation between spin, isospin, strangeness and charm 80−37183
Hagedorn Frautschi statistical bootstrap model, modification for baryon charge and strangeness conservation *(Russian)* 80−27489
heavy neutral strange lepton predicted by mag. quark model 79−75738
inclusive strangeness changing neutral current interactions 78−8652
long lived hyperstrange multiquark droplets in MIT bag model 80−9137
nonleptonic decay, asymptotic freedom, light quarks and $\Delta T=1/2$ rule 77−38164
nonleptonic decays of ordinary and charmed hadrons, vector-like model 78−41545
PCAC and weak nonleptonic strangeness changing Hamiltonian 77−71460
production by $\nu(\bar{\nu})$ in quark model 79−13103
pseudovector prod. in SLAC $Q(K\pi\pi)$ data anal. 77−54100
QCD, 2-dimens., nonleptonic weak decays of charmed and storage mesons 79−40773
quark fusion model, strange and charmed quark numbers, vector meson description 78−58158
Regge exchange building by strange quarks, K^-p data anal. 79−2995
semi-leptonic weak interactions, book contrib., strangeness-conserving current, strangeness-changing decays 78−78162
semilocal duality constraints for mesons, on-shell particles, masses, couplings 78−58174
$SU(2)\otimes U(1)$ gauge model, strange baryon weak radiative decays and CP violation 79−6260
F-meson production suppresion relative to D-meson 79−36100
$F^+(2030)$, lifetime estimates, free quark model anal. 79−67544
γn to 5.3 GeV, multipion and strange particle prod., reson. 77−10261
K^0-$\bar{K}^0$ system, flavour-changing neutral currents 80−22553
$K^*\pi\rightarrow K^*\pi$, analytic quasi-unitary isobar model anal. 79−36099
$K_S^0K_S^0$ pair rapidity correlations, quark level strangeness compensation in multiparticle production 79−36024
K^-p interactions, 8.25 GeV/c, flow of strangeness and baryon number 78−74277
$K^\pm p\rightarrow p\bar{\Lambda}p(\Lambda\bar{p})$, 50 GeV/c, strange bosons decaying into baryon-antibaryon pairs 80−37306
$K_L^0p\rightarrow Q^0(\bar{Q}^0)p$, differential cross section slope, further Deck model anal. 80−73737
ν, charmonium and strangeonium, linear+Coulomb pot. study, high α_s regime 80−62935
$\nu,\bar{\nu}$ experiments at Gargamelle, strange particle production by neutral currents 78−37200
$\nu,\bar{\nu}$ reactions at Gargamelle, strange particle prod. by neutral currents 78−37201
νN, charm and strangeness production, role of gluons 79−13104
νN interactions in Gargamelle, μ^-e^+ pair prod., associated strange particles 77−61275
$\nu N\rightarrow\mu eV^0$, Gargamelle results, charm search 77−26509
$\nu N\rightarrow\mu\mu X$, neutral strange particle prod. in opposite sign dimuon events 80−57584
$\nu_\mu N\rightarrow\mu^-e^+$ hadrons, Gargamelle picture anal., strange particles and charm prod. 77−54097
$\nu p\rightarrow\mu^-\Lambda 3\pi^+\pi^-$, E>10 GeV, inclusive 79−376
$P\rightarrow\gamma\gamma$, relativistic quark pair creation model for reduced decays and enhanced EM tadpoles 79−67555
$\bar{p}p$, 100 GeV/c, inclusive meson and strange particle prod., energy partition 80−95289
$pp\rightarrow(K_s^0,\Lambda,\text{or }\bar{\Lambda})\pi^\pm+X$, 405 GeV/c cross section determ., vector meson dominance 79−89207
$pp\rightarrow K_3^0K_3^0X^{++}$ 19 GeV, strong dynamic correlations 79−93468
$\bar{p}p\rightarrow K^0X$ or ΛX or $\bar{\Lambda}X$ at 12 GeV/c 78−4885
$pp\rightarrow\Delta^0X$, small-angle production from nuclear and nucleon targets, collective tube model and triple-Regge picture 80−52538
$pp\rightarrow\Lambda K_3^0X^{++}$, 19 GeV, strong dynamic correlations 79−93468
π double recharging in nuclei with change of strangeness *(Russian)* 79−89332
π^+d interactions, 4 GeV/c, cross sections for strange particle prod. 79−17753
π^+d interactions, strange-particle cross-sections at 4 GeV/c 78−89734
π^-p, 100 GeV/c, inclusive meson and strange particle prod., energy partition 80−95289
π^-p, 21 GeV, prompt e^- associated with strange particle in strong interaction, direct evidence 79−419
π^-p, 4.85 GeV/c, strange particle prod., absolute and topological cross-sections *(Russian)* 77−254
π^-p, charged multiplicity with strange particle prod., 4.9 to 205 GeV/c 77−18334
π^-p, strange particle production data, 5 GeV *(Russian)* 79−3040
$\pi^-p\rightarrow V^0X$, 5 GeV/c, cross-section meas. *(Russian)* 77−61331

strange particles continued
π^+ p, strange-particle cross-sections at 10.3 GeV/c 77−87999
π^+ p reactions, 16 GeV/c, strange particle prod. in 3 and 4 body final states 78−475
$Q_1(1280)$, mass formulas and selection rules in large SU(3) mixing 80−86700
$Q_1(1290)$, $Q_2(1400)$ vector-pseudoscalar decay rates and SU(3) implications 77−61283
$Q_2(1400)$, mass formulas and selection rules in large SU(3) mixing 80−86700
Q_A-Q_B mixing angle, axial vector meson decay, A_1 and C obs., SU(3) implications 79−89148
$V \rightarrow P\gamma$, relativistic quark pair creation model for reduced decays and enhanced EM tadpoles 79−67555

strangeness *see strange particles*

stratified flow
accelerating shear flow, internal gravity waves 79−32628
acoustic field in stratified media of variable viscosity, Green's functions 80−4545
air turbulent flow in heated channel, effect of gravitational field 80−64533
air-H_2O turbulent-turbulent stratified flow in circular tube 79−90307
air-Hg flow, stratified, co-current, in rectangular channel, interfacial wave structure 80−74955
air-water flow in Y-junctions 78−51218
Alfven-acoustic-gravity wave propag. and reflection, compressible, inviscid, perfectly conducting isothermal fluid 77−51124
algebraic disturbances in stratified shear flows 79−50766
annuli, spherical rot., stratified convection of viscous Boussinesq fluid 79−27635
asymptotic stability of unsteady inviscid stratified flows 80−83832
atmosphere, buoyancy driven mixed layers modelling 77−33150
atmosphere, finite amplitude Kelvin-Helmholtz billows, evolution 78−81293
atmosphere, flow of stratified fluid over obstacle *(Russian)* 78−24291
atmosphere, numerical method for stratified shear flows over long obstacle, numerical method 77−33157
atmosphere, turbulence and internal waves spectra in stably stratified boundary layer *(Russian)* 78−81297
atmosphere, turbulent shearing layers, dominant eddy scale, growth, limiting thickness 77−87022
atmosphere, turbulent shearing layers, growth, limiting thickness, dominant eddy scale 78−92955
atmosphere and oceans, wave disturbances 78−32209
atmosphere-ocean system, equilib. Langmuir circulation model for ocean 80−101381
axisymmetrical filtration of two liquids differing in viscosity and density 77−11234
baroclinic instability in three-layer fluid 78−16099
Benjamin-Ono equation, Backlund transform. and conservation laws 80−4540
Benjamin-Ono equation, internal wave solitons, linear stability 80−53802
Benjamin-Ono equations, two-parameter Miura transform. 80−14720
body in stratified medium with free surface, near field disturbance 78−59443
bottom waves in rotating stratified fluid 79−2274
boundary layer flow over hills, stratification effects 78−53707
boundary layer flows in tilted square cavity, finite difference method 77−7385
boundary layer in stratified medium, shear flow 79−64736
boundary layers, stratified, stability calc., numerical integration *(German)* 80−53834
boundary-value problems in stratified shear flows with a nonlinear critical layer 78−79357
Boussinesq differentially heated fluid, struct. 80−109190
Boussinesq equation for infinite wall in stratified fluid 78−30336
Boussinesq fluid, in rotating spherical annuli, small Reynolds number convection 80−6047
buoyancy effects in entraining turbulent boundary layers: a second-order closure study 80−21815
buoyancy-induced flow stratification in cylindrical plenum 77−46366
buoyant surface jet, 2-D flow props. *(Japanese)* 80−48762
buoyant surface jet, entrainment intermittancy props. at stratified interface *(Japanese)* 79−81940
capillary-gravity waves in two-layer fluid *(Russian)* 79−39733
cellular convection in stratified sugar soln., effect of inclination of heated wall 77−39323
centrifugally stratified helical Couette flow, stability 77−89183
channel, open, critical flow conditions for two stably stratified fluids 80−74956
chemically reactive flow characts., simultaneous heat-mass transfer *(Japanese)* 78−22431
coastal trapped waves at low latitudes in a stratified ocean 80−90097
cocurrent gas-liq. stratified flow, mass transfer obs. 79−18931
cocurrent or countercurrent, of two fluids between vertical planes, interface stability *(French)* 78−38382
cold gas, noninteracting particles, nonlinear periodic motion *(Russian)* 80−14868
composite mixture, flow through porous medium, Rayleigh-Taylor instability 80−69912
compressible flow, inhomogeneous acoustic-gravity wave eqn. 77−80174
concentration interface in turbulent mixing layer, visual growth 80−38392
contaminant lateral dispersion in open-channel flow, buoyancy effects 79−50775
continuously-stratified fluid of finite depth, nonstationary wave development *(Russian)* 77−39322
control of stratification in almost-enclosed regions 79−46358
convection, free, from sphere in slightly thermally stratified fluid, streamlines 78−5781
convection, penetrative, boundary conditions imposed by stratified flow 79−55404
convective flow, free, over point heat source 80−79323
convective flow of incompressible stratified fluid, Euler-Poisson eqns. *(Russian)* 77−31300
convective flow structure in stratified liquid after lateral heating *(Russian)* 77−11232
convective free flow struct. above heated cylinder 80−79322
convective heat transfer from a confined jet in a centrifugal force field 79−98720

stratified flow continued
convective layers, form. and merging in differentially heated slot 79−59982
Coriolis force blocking attenuation, wakes, baroclinic vorticity and boundary layers 80−6129
critical flow regime in a stratified medium 80−92200
Czochralski bulk flow in the growth of garnet crystals 80−38979
decaying turbulence in neutral and stratified fluids 80−96247
density interface, wind-wave interaction 77−62291
density stratification as catalyst for instability 80−48676
density stratified reservoir, selective withdrawal from line sink 77−14980
density stratified turbulent liquid flows, refractive index variation elimination 79−77215
density-stratified fluid flow along heated inclined wall, double diffusive instability 79−55405
diffusers, curved, performance, separation in subsonic, transonic channels *(French)* 78−94818
disc rotating in fluid with surfactant surface layer 80−10284
double-diffuse convection, diffuse interface model, high Rayleigh nos. 78−90963
duct, equilibrium breakdown, thermosiphon work *(French)* 80−59114
ducts, one-dimensional models for transient gas-liquid flows 80−64614
dynamo action associated with random waves in a rotating stratified fluid 80−33687
energy stability of the Eulerian-mean motion in the upper ocean to three-dimensional perturbations 80−92149
entrainment at interface of two-layer flow *(Japanese)* 79−14454
entrainment interface in a stratified fluid 78−55672
entrainment process, laboratory expts. reinterpretation for stratified fluid 80−51405
environmental, finite element analysis, book contrib. 79−34875
estuaries, two dimensional, approx. solution to obtain the streamfunction 78−81187
estuaries of variable breadth and depth, tidally induced two-layer residual currents 80−72544
FFTF upper-plenum mixing and stratification, comparative studies 80−583
finite depth stratified flow over topography on a beta-plane 80−6128
finite depth stratified fluids, internal wave solitons, infinite depth limit 80−64574
flame 79−64795
flat plate boundary layer in porous medium, free convection, similarity solns. 78−75199
flow-through reservoir, vel. and temp. fields, num. simulation 77−17152
fluid-fluid interface, rotlet or sphere rot., torque values 79−86494
fluids of finite depth, exact one- and two-periodic wave solns. 80−53797
fluids of finite depth, N-soliton soln. of higher order wave eqn. 80−48724
forced oscillations in rotating stratified liquid 78−63478
forced standing wave instability in viscous stratified fluid, stratosphere quasibiennial oscill. simulation 79−55396
free convection between horizontal concentric cylinders in a slightly-thermally stratified fluid 79−59972
gas and non-Newtonian liquid, stratified flow in horizontal pipes 80−48787
gas bubble plumes in stratified environments, vertical fluid transport, double plume model 78−47019
gas-liquid film flow, stratified, eqns. of motion 79−37376
gas-liquid mixtures, stratified cocurrent flow in horizontal pipes 79−77214
gas-liquid moving interface diffusion 78−22404
gas-liquid pipe flow, influence of return bends on velocity ratio 80−74962
gas/liquid, hydrodynamic eqns. formulation 77−68682
gas/liquid flow, heat trnsfer, local Nusselt number prediction 80−38393
generalised Benard problem for stratified fluid, rotation effects 80−24031
geophysical fluid dynamics theory, book 80−105443
geostrophic motion of stratified fluid above uneven bottom *(Russian)* 77−91140
gravity wave propag., dispersion relations in sheared, stably stratified flow 77−27577
gravity waves, buoyant-parcel motion 78−55655
gravity waves, internal, resonant over-reflection from Helmholtz velocity profile 79−50740
gravity waves, shape and breaking in stratified shear flow 78−34147
gravity waves, weakly nonlinear, long, on two-layer fluid 78−83419
Hartmann boundary layer control of spin-up of stratified, conducting fluid 77−42923
heated pounds, turbulent boundary layer of stratified airflow, surface waves 80−92133
hemisphere in MHD rotating stratified fluid 80−100039
holographic interferometry obs. of stratified flow, isopycnic contours 78−1713
horizontal jet penetration in stratified fluid, unsteady laminar flow 77−7430
Howard's semicircle theorem 79−60047
hydromagnetic generalised Benard problem, mag. field character, stratified layer stability 79−77267
hydrostatic mountain waves, terrain shape effects for stratified fluid 80−21804
immiscible liquids, flow in helix, high press. boiler analogue 77−58763
inclined fluid layer, double diffusive instability, linear stability anal. 80−92113
inclined fluid layer, double diffusive instability, secondary convecting layers 80−92112
incompressible stably stratified fluid, internal waves, Brunt-Vaisala freq. 80−79343
incompressible viscoelastic fluid, Rayleigh-Taylor instability 80−79363
inertial and frictional effects on flow over topography 77−45106
instability and convection in fluid layers: a report on Euromech 106 79−68783
insulated water layer, combined heat transfer, stratified layer, energy eqn., boundary value problem 80−79290
internal gravity wave break on slope *(Japanese)* 79−81909
internal gravity wave instability 77−68663
internal gravity waves, long, large amplitude, propagation in stratified fluid 79−37333
internal linearized waves propagating in a stably stratified system, props. 78−34149
internal nonlinear waves in closed basin 78−75159

stratified flow continued
internal solitary waves 77−75963
internal solitary waves in linearly stratified fluid 78−79332
internal solitary waves in stratified flows, cubic and quadratic nonlinearity 80−69856
internal solitary waves prod. by tidal flow over three-dimens. ridge, ocean appl. 79−46332
internal wave eqn. governing long gravity waves 79−97217
internal wave generation in stratified fluid collapse *(Russian)* 80−74942
internal wave motion in a periodic stratification 80−1672
internal wave solitons, numerical computation 78−59410
internal waves, radiation by sources in exponentially stratified flow *(Russian)* 77−64300
internal waves caused by a system of sources and drains in flow of stratified liquid *(Ukrainian)* 79−41732
internal waves in pipe 77−23971
internal waves in stratified Boussinesq fluid, turning-level dynamics 77−15092
internal waves in stratified flow around source run off system *(Ukrainian)* 77−68658
internal waves in stratified fluid, tank wall effect 80−53799
internal waves with finite fluid depth, inverse scatt. problem, Backlund transformation 80−31517
jet, horizontal five-layer, instability 78−79348
jet entrainment at density interface in thermally stratified vessel 80−6119
Jupiter atmosphere zonal flow, baroclinic instabilities 80−31245
Kelvin-Helmholtz instability, nonlinear wave packets, amplitude eqn., formulation and soln. 79−46289
Lake Baikal, ice covered, statistical props. of velocity and temp. profiles *(Russian)* 77−78269
lakes, stagnant, thermal stratification 80−36340
laminar flow in rot. annulus, stable stratification effect 78−94797
layer formation in double-diffusive system with sloping boundary 77−72342
layered medium disturbed by internal waves, statistical props. 78−22359
linear wave theory, internal wave operator solution 80−43759
linearly stratified fluid, gravitational collapse of mixed region 80−33653
linearly-stratified horizontal layer, onset of thermohaline convection 77−42897
liquid, plane internal waves during flow around a source-sink system *(Russian)* 77−68659
liquid, stratified, internal waves generated by local disturbances 79−86485
liquid-metal-H_2O stratified flow, horizontal co-current, interface heat transfer, turbulence model 80−92131
lorenz attractor behaviour in a continuously stratified baroclinic fluid 80−83806
LWR safety, condensation heat transfer in stably stratified systems 80−63311
MHD of fluid rotating between two discs, Boussinesq. approx. of linearised eqns. 78−79387
MHD pulsating viscous flow superposed on steady laminar motion 80−92228
MHD stratified flow between oscillating disks, boundary layers 80−28570
MHD-gravity waves, over-reflection in stratified flow 77−11207
mixed fluid, nonlinear internal wave formation from gravitational collapse 80−33619
mixed layer, deepening rate model *(Russian)* 78−24292
mixed layer growth, penetrative convection in stratified fluid 78−44908
mixed-region collapse model, inertia buoyancy balance 77−936
mixing layers, 2-dimens., statistical model of turbulence 79−68680
moving surface layer, flow structure in front *(German)* 78−1712
multilayered stratified flow investigation using water tunnel *(Russian)* 80−1703
natural convection, in slightly inclined rectangular box heated from above 79−59976
natural convection from spheres and cylinders immersed in a thermally stratified fluid 80−6059
natural convection from vertical surface in thermally stratified fluid 77−15021
natural convection heating of liqs. in closed containers 77−15006
natural convection in vertical fluid layer, anal. by linear stability theory 78−34180
natural convective transfer at low temp., thermal stratification effect 80−6039
Newtonian stars with stratified flows, mirror planes 78−32444
non-isothermal flow, turbulence measurement, laser Doppler velocimetry appl. 79−41776
nondiffusive fluid confined between horizontal planes, flow due to object motion 77−51097
nonlinear internal wave solitons, Calogero-Moser-Sutherland N-body problem 79−27679
obstacle in weakly stratified flow, upstream influence, theory 80−56527
ocean, density-stratified, perturbation method appl. to internal waves theory 77−49070
ocean, eddy diffusion effects on western coast boundary layer struct. 77−17142
ocean, influence of rot. on surface gravity and internal waves 79−2281
ocean, influence of stratified currents with vel. shear on forced wave motion *(Russian)* 78−77255
ocean, realistically stratified, nonlinear energy and enstrophy transfers 80−101370
ocean, spread of mixing in stratified fluid and analogue in rot. fluids 79−57949
ocean, stably stratified, convective instability 77−86913
ocean, wave-induced mass transport in stratified bottom boundary layer 79−2282
ocean, wind-driven flow in zonal channel with stratification and bottom topography 80−51402
ocean bottom, flow of stratified fluid over obstacle *(Russian)* 78−24291
ocean coastal zone, stratified water circulation forecasting for water quality management planning 79−5543
ocean multi-layer fluid flow, effect of shifting press. on internal ship waves *(Russian)* 78−77256
ocean small-scale stratification, study via towed instruments carrier 80−36423
oceanic warm front propag., rotating stratified fluid theory 80−94538
open channel thermally stratified flow, eddy diffusivity buoyancy effects, obs. 78−90904
stratified flow continued
parallel flow, role of negative energy waves in some instabilities 79−59967
parallel flow normal modes in inviscid stratified fluid with propagation at infinity 80−24071
parallel or swirling stratified shear flow, internal gravity and axisymmetric waves 79−86446
penetrative convection model, appls. to atmopshere, ocean and laboratory expts. *(Russian)* 78−24335
permanent wave structs. on an open two layer fluid 78−59411
permanent wave structures and resonant triads in a layered fluid 79−37377
pipes, two-phase stream, stratified flow, condensation calc. 79−23349
plane two-layer flows, effect of fluid microstructure on stability 79−77212
planetary atmosphere, convective instability of fluid layers 80−56754
planetary boundary layer flow with neutral stratification over gentle topography 78−3851
planetary boundary layer model with variable eddy viscosity coeff. 77−9482
plates, flat, rotating stratified flow, boundary layers 80−53793
plume, buoyant, turbulent, issuing vertically into stratified or uniform ambients 77−58756
point force in a stratified fluid in a cylinder under a magnetic field 80−14776
Poiseulle flow, thermally stratified plane, linear differential eqn., asymptotic fundamental system construct. *(German)* 77−902
polyethylene, melts, stratified two-phase flow, interface deform. 77−11158
polymer melts, stratified two-phase flow, interface deform. 77−11158
polymeric liquids in pipes, non-steady two-phase stratified laminar flow 79−81832
polystyrene, melts, stratified two-phase flow, interface deform. 77−11158
propagative thermal excitations, Rayleigh scatt. meas. *(French)* 80−33590
rectangular enclosures, stabilising thermal gradient effects on natural convection 79−81889
reflectionless shock wave in stratified medium 78−51193
reservoir, stratified layer config. *(Japanese)* 78−20454
reservoir, stratified layer turbidity *(Japanese)* 78−20455
rotating, small oscillations, internal waves 77−68664
rotating annulus, expt. 77−31357
rotating fluid, parallel shear flow, baroclinic and barotropic instability 80−98328
rotating fluid, vortex created by mass transfer between layers 80−12401
rotating stratified channel, low-freq. waves 77−47030
rotating stratified flow, in horizontal mag. field, stability 78−67246
rotating stratified fluid, appl. of radiation condition for a source 79−64676
rotating stratified fluid, hydromagnetic stability 78−55692
rotating stratified fluid, internal and inertial waves 78−67245
rotating stratified liquid, waves energy relations *(Russian)* 77−27575
rotating superposed fluids, MHD instability, flow through porous medium 78−14089
rotating two-layer fluid, barotropic and baroclinic Rossby waves interactions and instabilities 79−57955
round buoyant jets in stratified flows, integral eqns. 79−27680
salt fingers, rot. effects 79−50767
selective withdrawal of layered fluid from reservoir 77−11233
separated flow models, stratified flow, averaged formulation, high order dispersion effects 80−74960
shear flow, over-reflection instability 79−60048
shear flow, stratified, free-turbulent, buoyancy effects on large scale struct. 78−90849
shear flow, stratified, turbulence and entrainment *(Japanese)* 78−55674
shear flow, wave breakdown 77−31358
shear flow, weakly nonlinear stability theory 78−18331
shear flow past three-dimens. obstacles 78−71383
shear layer, thermally stratified, turbulence structure and stability *(Japanese)* 79−41731
shear-induced instabilities in stratified fluids, modal struct. 77−68662
shear-induced turbulence spectrum in stratified fluids 77−68661
slug formation, horizontal and inclined pipes, gas-liq. flow model 78−14083
small inviscid disturbance, evolution to marginally unstable stratified shear flow 78−83453
spectral theory of stratified turbulent shear flow, interactions between motion fields 80−90114
stability of aligned, stratified, compressible magnetoatmospheric shear flow 78−26197
stable salinity gradient heated from below, convection and layers 80−24016
stably and neutrally stratified flow over three dimens. hill 80−48770
stably stratified medium, plane free convection from local heat source 80−96253
stably stratified shear flow in channel, internal gravity wave packet mean flow 79−98740
stationary nonlinear waves in stratified rot. fluid, periodic solns., solitary waves *(Russian)* 79−7378
stationary obstacle ion channel, stratified fluid flow expt. 78−79321
steady stratified flows over a long obstacle 79−90306
Stewartson vertical layers 80−48772
stratified and rotating fluids, review of selected aspects 77−68660
stratified fluid with shear, instability and turbulence 79−77216
stress-driven entrainment expts. scaling 79−50768
superposed flow, interfacial instability 79−4057
Taylor columns on β-phase 78−42639
thermal energy storage tank, thermal stratification during charging 79−3890
thermal instability of layer heated from below 78−63476
thermal layer plane shock interaction flow props. and temp. profiles 77−58735
thermally forced stratified rot. fluids, axisymmetric steady motion 80−69844
thermally stratified enclosures with localised heating from below, natural convection 80−24017
thermally stratified rot. fluid, secular spin-up, expt. and numerical study 79−77217
thermoconvective waves in stratified compressible fluid, stability criterion contradiction 80−19414
three-dimensional barrier in flow-field 80−48769

stratified flow continued
topographic planetary waves, resonant interactions, continuously stratified fluid 78−36186
transient solutions, initial value problem for buoyant fluid 77−35196
tropical atmosphere, thermally driven motion, influence of stable stratification 77−2201
tube, horizontal, laminar combined convection, circumferentially nonuniform heating effect 78−71331
turbulence, mixing 78−22400
turbulence, normal and abormal turbulent transport in stratified medium *(French)* 80−59095
turbulence and mixing in stably stratified waters, book contrib. 78−59444
turbulent boundary layer, vel. profile *(Russian)* 79−10601
turbulent boundary layer development *(Russian)* 78−63477
turbulent boundary layers near separation point, numerical prediction, heat transfer *(French)* 78−94657
turbulent entrainment at stable density interface 77−35197
turbulent flow, finite element method appl. 78−90964
turbulent shear flow, stable stratification expts. 77−27576
turbulent spot in stably stratified fluid, dynamics *(Russian)* 78−40558
turbulent stably stratified fluid, mixed layer growth 79−55358
two layer shear flow, radiation field and baroclinic eddy development in β-plane 79−81897
two layer system with baroclinic mean shear flow, solitary Rossby waves theory 80−17293
two-dimensional obstacle, upstream influence and Long's model 77−75962
two-fluid stratified layers in trapezoidal channel, nonuniform steady flow *(Rumanian)* 79−14452
two-layer, entrainment at interface *(Japanese)* 78−9671
two-layer quasi-geostrophic turbulence, simple special case 78−81186
two-layer shallow water flow, internal and surface waves, numerical anal. 80−19472
two-layer stratified fluid, internal waves generated by local disturbances *(Russian)* 79−16480
two-layered, at outlet of open channel, dynamical singularities analysis *(Japanese)* 80−10285
two-layered flow, internal waves at interface, statistical props. *(Japanese)* 80−1673
two-layered fluid, wave motion due to periodic pressure, uniform asymptotic anal. 78−55673
two-phase pressure driven stratified laminar pipe flow 80−64609
two-phase stratified flow through fractures in porous media 78−5792
two-phase stratified horizontal flow, averaged and local instantaneous formulations, stability 80−64613
Uchinskii reservoir, ice covered, statistical props. of velocity and temp. profiles *(Russian)* 77−78269
unstable displacement problem for porous media with different permeability layers, developed stage anal. 80−14813
valley ventilation by cross winds 80−48771
vertical coplanar Y-junctions, two-phase steam-water flow 80−38478
vertical turbulent diffusion in a stably stratified fluid 79−16585
viscoelastic fluids, stratified two-phase flow through rectangular duct, interfacial instability 77−31359
viscosity distribution effect on flow stream parameters along bottom surface, model *(Russian)* 78−22401
viscosity stratified fluid layer, heated from below, thermal instability 77−58762
viscous flow of stably stratified fluid over barrier 77−75961
viscous flow of variable viscosity between porous bed and moving impermeable plate 78−90962
viscous incompressible liquid, heat conductivity problem *(Russian)* 80−69897
viscous nondiffusive flow, over horizontal flat plate, boundary layers and wakes 77−47058
viscous plane Couette flow, stability, const. buoyancy freq. 77−47059
viscous plane Couette flow, stability, variable buoyancy freq. 77−47060
viscous stratified flow in an oscillating cylinder 79−98782
viscous stratified shear flow, stability eqns., completeness obs. 80−64519
viscous two-layer flow, stability to small perturbations, neutral stability curve 80−33652
vortex ring evolution in stratified and shearing environment 78−30303
vortex rings in stratified fluid, unsteady motions and distorted ring obs. 77−15091
vortex struct. in wake of sphere drawn-through stratified fluid 77−42896
vortices in rotating stratified fluids, theory and atmospheric appls. 79−39814
wake collapse in the thermocline and internal solitary waves in stratified fluid in channel 80−53787
wakes in stratified flow, book contrib., review 80−19473
water, thermally-stratified, cooled from above, free convection 79−46315
wave interactions, explosive, reson., in three-layer fluid flow 79−64680
wave interactions in stratified media *(Russian)* 77−11231
wave motion during flow around submerged body *(Russian)* 79−14453
wave motion in continuously stratified fluid during flow around submerged body 79−77213
wave propagation, modified finite depth fluid eqn., exact N-soliton soln. 80−28517
wave transport in stratified, rotating fluids 78−89192
wave/mean flow interaction, mean motion induced by transient inertio-gravity waves 80−105029
waves, miscible (immiscible) fluids, in closed horizontal (vertical) ducts 77−62263
waves in stratified fluid, nonlinear reson. interactions 78−83418
waves in stratified heavy incompressible fluid, variational principle 78−59495
whirlwind, ring-shaped, onset caused by rising air in stratified atmosphere *(Russian)* 78−77298

stratosphere
see also ozonosphere
10 mbar geopot. height vars. rel. to solar activity 79−29824
10 mbar surface geopotential and geomag. disturbance fields characts. 77−13055
acetylene, tropospheric and lower stratospheric vertical profiles 80−4073
acidic Cl vapour, midlatit. seasonal meas. 78−32142
acoustic sounding with balloonborne instrument, scatt. structs. vertical profile 78−57353
aerosol global distribution, 162-238 millibar altitude 80−56591
aerosol, determ. of characteristic parameters *(French)* 80−8387

stratosphere continued
aerosol, interaction of Cl and Cl_2 with H_2SO_4 and water, surface reactions at low temps. 79−79288
aerosol, laser radar meas. *(Japanese)* 80−21810
aerosol, lidar obs. at Menlo Park, California 77−21865
aerosol, microstruct. from sounding by multifrequency lidar *(Russian)* 77−64374
aerosol, modification by supersonic transport and space shuttle operations, climatic implications 80−98408
aerosol, remote sensing techniques 80−109269
aerosol, sulphate, contrib. of OCS emissions rel. to climate 80−41524
aerosol and gaseous constituents from spacecraft solar extinction data, inversion retrieval 79−74961
aerosol collected at 34°S, change in nature 78−28286
aerosol conc. at Mildura, Australia following 1974 Fuego eruption in Guatemala 77−5276
aerosol conc. using iterative method from twilight polarization meas. 78−20464
aerosol content, satellite monitoring systems, SAM II and SAGE 80−82082
aerosol content var., rel. to atm. transparency and direct solar radiation 80−82035
aerosol content vars. rel. to fluctuations of solar radiation and temp. in troposphere 78−81327
aerosol detection, ground based techniques, laser usage 80−17390
aerosol event, 1974-1975, balloon obs. of time development 77−45084
aerosol formation and evolution model, SO_4^{2-} particles 80−17327
aerosol layer, climatic effects, review 78−81331
aerosol layer, Earth zonal radiation balance perturbation 80−56602
aerosol layer, simulated lidar return from one-dimensional model 79−44247
aerosol meas., southern hemisphere, time vars., rel. to 1974-75 volcanic eruptions 79−48551
aerosol meas. by solar occultation method 77−45090
aerosol meas. using two-colour lidar 77−25752
aerosol measurement problems 79−66839
aerosol measurements in S hemisphere, impactor and in situ single-particle detect. 78−73437
aerosol microstructure, lower stratosphere, sounding with multifreq. lidar 80−56645
aerosol model, steady-state 79−53445
aerosol optical thickness meas. at Adelaide (35°S) 79−44248
aerosol particle size distrib. meas. 80−51578
aerosol particles, collection and analysis techniques 80−17306
aerosol particles, concentration rel. to error in satellite retrieved atmospheric temp. profiles 80−98449
aerosol particles, microphysical processes 78−7709
aerosol particles, optical props., instrumentation and techniques for meas. 80−17389
aerosol pollution, albedo and radiative equilib. temp. changes 77−45092
aerosol size distribution, lidar obs. at 0.6943 μm and 1.06 μm 77−41120
aerosol vertical distribution, meas. by Skylab photographic coronagraph 77−60568
aerosols, airborne lidar meas. during winter (1973) 77−33159
aerosols, from Agung eruption, solar radiation absorpt. estimation 77−87072
aerosols, global time vars. and source consideration 77−25739
aerosols, long term vars. after Fuego volcano eruption, lidar obs. 79−16597
aerosols, physical state and nature of undissolved granules 78−28275
aerosols, post-Fuego layer, lidar meas., radiative and thermal implications 77−56679
aerosols, remote anal. by differential scatter lidar system 78−69524
aerosols, visible and IR optical props. influence on global climate 77−2240
aerosols latit. vars. 79−58040
aerosols optical props. and size distrib. effects on heating rates 79−12222
air collection and analysis techniques, troposphere and stratosphere 80−26566
aircraft engine emission surveillance 79−74562
Aitken nuclei meas. with aircraft-borne instrument 77−64399
Aitken particles, nature and sources 77−87050
anisotropic multiple scatt. effects on solar radiation 79−80016
annual and semi-annual waves, obs. using Nimbus 5 selective chopper radiometer data 78−81315
Antarctica, winter, Nimbus-5 atmospheric temp. fields deviation from radiosonde data 78−32138
Antarctica and equatorial India, atm. struct. during southern summer 77−53121
anthropogenic effects on UV radiation and climate 78−28289
atomic processes, O_3 formation and destruction, book contrib. 77−37339
auroral zone neutral wind vels. near tropopause using Chatanika UHF Doppler radar 77−5274
balloon, tethered system, feasibility study *(Italian)* 79−44251
balloon trajectory analysis for long-term missions *(Italian)* 77−82055
balloon two-dimensional sounding method for stratospheric shallow layer 78−3985
balloon-borne ion sampling package 78−69497
balloons, buoyancy control expts. 77−87113
balloons flight behaviour 77−13138
Baltic Sea region, aerological climatology rel. to atmospheric heat and moisture balance 77−87057
baroclinic instability, model with realistic tropopause 77−78307
baroclinic instability at long wavelengths on β-plane 77−66953
baroclinic instability in summer circulation 77−45111
baroclinic models, growth rate and vertical propag. of initial error 79−16620
barotropic 3-dimens. instability in upper stratosphere 80−41498
chemical composition, importance of energetic particle precip. 80−109213
chemical-diffusive model 77−21873
chemistry, concise model 78−85634
chemistry, model, Monte Carlo anal. of imprecisions due to reaction rates 78−85635
chemistry, multiple solns. 79−58008
chemistry, N_x^+, O_x^+ and NO^+ reactions with various mols., reaction rate coeffs. and product distribs. 78−81305
chemistry, ozone layer, environmental hazards 77−17267
chemistry, recent advances, review 79−12204

stratosphere continued
chlorofluorocarbons, stratospheric photodissoc., residence times 78−53703
chlorofluoromethanes in lower stratosphere, latitudinal profiles 78−44989
chlorofluoromethanes in stratosphere, vertical distrib. 78−73476
chlorofluoromethanes in upper troposphere and lower stratosphere, vertical distrib. 78−73477
circulation, seasonal and interhemispheric vars. 77−49118
circulation and total O_3 trends over Australia 77−21866
circulation change dates determ. from limited-area data 79−58054
circulation in circumpolar vortex, model 80−77082
circulation in lower stratosphere, appl. in five-day average air temp. forecasting technique 79−29817
circulation over Antarctica, seasonal vars. 77−21829
circulation response to solar activity oscills. 77−45118
cirrostratus cloud, obs. over Scotland 79−16627
cirrus clouds, influence on IR cooling rate 78−73455
classification of pollutants and pathways in atmosphere 79−70489
climatic var. induced by magnetic field screening of cosmic rays 77−78398
ClO remote meas. from IT solar spectrum obs. 79−58005
cloud microphysics anal. 79−16853
clouds, thin persistent very high, in stratosphere over Antarctica, nature determ. 78−36247
composition, at. and mol. fluoresc. as species monitor, review 77−9472
composition, atmospheric constituents mass spectrometric obs. *(Japanese)* 79−79920
composition, chemical response to changes in UV solar flux 77−33167
composition, chemical studies using air sampling equipment on Concorde aircraft 79−80058
composition, IR meas. radiometer, H_2O vapour profile 79−8718
composition investigation using gas expansion and mass spectrometer beam system 80−31934
composition of middle atm., in situ meas. 80−17339
composition perturbations and temp. feedback, climatic effects 80−41525
cosmic ray albedo determ. from meas. in stratosphere 79−80134
cosmic ray and pressure oscills., balloon obs. *(Japanese)* 80−31182
cosmic ray electrons and protons quasiperiodic pulsations in stratosphere 79−80133
cosmic ray electrons in stratosphere, spectrum above 3 GeV 77−53374
cosmic ray intenstiy variations in midlatit. stratosphere, total solar mag. field effect 79−62696
cosmic ray ion-pair production rate above 18 km altitude, parametrisation 78−65469
cosmic ray variations, evidence for interplanetary modulation processes 80−101508
cosmic rays, eleven-year cycle 80−4212
cosmic rays height-intensity distrib., meson decay effects 79−12364
cosmogenic radioisotope production estimates, flux magnitude and time variation 78−61634
coupling with troposphere and variability rel. to vacillations in general circulation model 79−79926
cumulonimbus anvils, protrusion into stratosphere, lifting of tropopause *(French)* 77−29357
daily average solar heating or photolysis, exponential approx. 77−5285
data compatibility used in meteorological analysis, empirical study 80−17308
daytime, HNO_3/NO_2 conc. ratio 78−73460
decametric radiowaves emitted by dipole, propag. problem 78−69399
density inhomogeneity struct. determ. from Salyut obs. of astronomical scintillation *(Russian)* 80−109186
density vars. during northern hemisphere winter 77−78372
dichlorodifluoromethane, height profile meas. at several latits. 80−72601
dichlorodifluoromethane, total ionis. and electron attachment cross sections by electron impact 79−59586
dichlorodifluoromethane, UV absorpt. cross sections temp. depend., stratospheric appls. 77−64423
dichlorodifluoromethane and N_2O conc. meas., mixing ratios 78−81281
dust, response of hemispheric mean temp. 77−29419
dust collected from interplanetary space, optical absorpt. spectra 80−101554
dust from St. Augustine Volcano, ruby lidar meas. 77−29431
dust loading index, 1923-54, pyrheliometric and circumsolar sky radiation obs. 80−46240
dust measurements, (1970-1977) 78−73445
dynamical climatology during late winter 1973 in southern hemisphere 77−25769
dynamics of middle atmosphere, review 80−17338
eddy and turbulent diffusion at 0-65 km altitude, model simulation 79−84438
eddy kinetic energy budget for winters with and without warmings 77−37297
electric field, balloon meas., SAMBO-1 expt. 79−66738
electric field in mag. storm negative phase, 1975 March 20-21, balloon obs. 79−79921
electric fields, solar flare modification, direct evidence 79−48553
electric fields and currents at Syowa Station, Antarctica, vertical components meas. 77−53142
electrical conductivity, solar modulation rel. to atmospheric electricity supply current 80−17329
electrical conductivity and aerosols, simultaneous balloon meas. 77−73813
electrical conductivity meas. in lower stratosphere over Poona 77−70750
electrical parameters and aerosols, meas. *(Japanese)* 80−31087
electron precipitation at high latitude, X-ray bremsstrahlung obs. 80−77205
emission model, spectral lineshape calc. 79−62586
emission spectrum, balloon-borne far IR Michelson interferometer meas. 79−39870
energetic O atoms distrib. functions 77−41127
energy dissipation within intermittent clear air turbulence patches 77−56676
environment monitoring system, benefit assessment 78−73507
environmental decisions in context of large observational uncertainties 80−104535
equatorial, effect of waves on SW monsoon 79−8664
equatorial, vertical vel. determ. from Diurnal Experiment 80−77047
equatorial planetary waves, Eliassen-Palm relation and mean zonal accel. 77−49111
equatorial planetary waves in horizontal and vertical shear 77−49112

stratosphere continued
equatorial quasi-biennial oscill. strength rel. to max. temp. at Oxford 77−81975
equatorial stratopause, planetary wave disturbances 79−5557
equatorial wave mean-flow interaction, role of latitudinal shear 80−51461
equatorial waves in upper stratosphere and mesosphere, rel. to zonal wind semiannual oscill. 79−5575
equatorial westerlies rel. to Indian monsoon 77−29370
ethane, tropospheric and lower stratospheric vertical profiles 80−4073
W.Europe, atmos. temp. 20-110 km altitude, 1975/6 winter anomaly 80−36356
fallout residence time, 1965-1971 obs. made in India 80−41526
far IR emission, balloon-borne obs. 79−34896
fission products, removal rate seasonal vars. 80−55957
fluorocarbon-O_3 theory, one-dimens. modelling of atm. 79−70831
fluorocarbon-ozone theory, atm. modelling, diurnal steady state calc. 79−88390
fluorocarbons, world production and release, 1975, rel. to stratospheric O_3 78−3919
fluorotrichloromethane in N.American troposphere and stratosphere 79−79430
forced standing wave instability in viscous stratified fluid, stratosphere quasibiennial oscill. simulation 79−55396
formaldehyde, chem. of stratosphere, UV absorpt. spectra implications 80−109209
formaldehyde, meas. by high resolution IR absorpt. spectroscopy 79−84371
formaldehyde, meas. in atm. by ground based IR absorpt. obs. *(French)* 79−66764
formaldehyde+ClO radical, expt. showing no reactivity, stratospheric implications 80−90119
Fourier transform IR absorpt. spectroscopy, airborne, for atm. comp. meas. 78−61604
Fourier transform spectroscopy appl., far IR 78−58069
free radicals, meas. by matrix isolation EPR 78−46374
frost point meas. systematic error using Meteorological Office Mk3 hygrometer 78−73538
gamma-ray lines observed in balloon flights at high rigidity, extraterrestrial line flux upper limit 80−21882
gamma-rays, quasi-periodic intensity variations *(Russian)* 80−90177
gas composition, comparison of one-, two- and three-dimens. models 79−70870
gas concentrations from limb sounding radiometry, inversion algorithm 80−82000
gas monitoring, two-photon spectroscopy, Doppler-free technique 77−9514
gaseous halogens in the atmosphere during 1975 77−56681
general circulation, anal. of rocket soundings on Kerguelen Island (February-May, 1973) 78−20489
general circulation, radiative transfer, transport processes, review 78−49105
general circulation model, space-time spectral anal. of midlatit. disturbance 77−66951
global scale waves with zonal wave number zero 78−61515
gravity wave-meanflow interaction, indication in upper atmosphere radar obs. 78−81282
H_2, CO, N_2O, methane, chlorofluoromethanes, vertical profiles meas. 79−84384
halocarbon meas. in Alaska troposphere and lower stratosphere 77−70719
halocarbon sinks, photooxidation, $O(^1D)$ atom and OH radical reactions 77−17165
halocarbons, hydrocarbons and SF_6, global distrib., sources and sinks, rel. to 0_3 depletion 80−4088
halocarbons, identification and meas. 78−32186
halocarbons, SF_6 and N_2O concs., rel. to tropospheric OH conc. 77−45069
halogen compounds global monitoring by satellite borne spectrometer 77−45162
HAPP wind study, high-altitude platform operation feasibility 80−17369
heating and cooling due to aerosol IR radiation scatt., calc. 80−72630
heating due to 9.6 μm O_3 band in inhomogeneous atm. 78−88918
heating due to solar radiation absorpt. by NO_2 77−17199
heating rate parameterization, 15-120 km altitude, due to O_2 and O_3 absorpt. of solar radiation 79−39798
horizontal eddy diffusivity in northern hemisphere 79−84439
inclinations of atmospheric layers, determ. from sounding data *(Russian)* 80−72569
inertial waves, obs. 79−12216
infrasound observations of circulation vars. during stratospheric warmings 79−2339
intense ionisation events, effects on NO_2, O_3 and climate, rel. to life extinction 78−96273
internal inertia-gravity waves in tropics 80−41497
internal waves interaction with mean flow, rel. to quasi-biennial oscill. 78−69404
intrusion into troposphere, explanation for ^{7}Be var. 80−98525
ion composition and ionisation rates 80−61885
ion concentration, elec. parameters and space charge density correls. 77−13104
ion mobility and conc. and ionic conductivity, rocket and balloon obs. 80−72605
ion mobility and concentration, and conductivity, 10-70 km altitude 80−36358
ionosphere-magnetosphere-stratosphere coupling at midlatitudes, 1969-74, southern hemisphere 77−9471
IR airborne astronomy, fluctuating sky emission meas. and interpretation 78−81552
IR cooling during stratospheric warming of 1971 Jan. 77−87020
IR emission obs. at balloon altitudes 79−16669
IR heterodyne spectroscopy, stratospheric sounding 79−100971
IR high resolution spectra, ground based obs. 77−41167
IR high resolution spectra, numerical simulation 77−41166
IR laser heterodyne spectroscopy for trace gases remote detect. 78−61606
IR optoacoustic spectroscopy of atmospheric gases 77−41243
IR spectroscopy instrumentation, design study 80−17391
isentropic coordinate models, boundary problems soln. 77−29372
jet stream, different, theory 80−46242
Kelvin waves, struct. and behaviour from Nimbus 5 IR meas. 80−8394

stratosphere continued
laser photochemistry of O_3 and distant spectroscopy *(Russian)* 78−28314
laser spectroscopy relevant to stratospheric photochemistry 78−88951
LF radio wave absorpt. variations, press. and temp. depend. 79−44282
LF sound waves relax. absorpt. *(Russian)* 78−65356
light attenuation, experimental profiles in visible and near IR regions up to 30 km *(Russian)* 78−61558
Limb Infrared Monitor of Stratosphere, radiometer spatial frequency response 79−101048
Limb Infrared Monitor of Stratosphere (LIMS) radiometer, design and performance, expt. goals 78−61601
linear lee waves reson. characts. in three-layer atm. 79−44228
long waves, comparison of thermal struct. in N. and S.Hemispheres 77−5296
lower, aircraft meas. of humidity, S.England, 1972-76 period 78−73488
lower, frost-point hygrometer for horizontal soundings 79−21048
lower, high resolution IR spectra, airborne obs. 100 to 140 cm^{-1} 77−49164
lower, obs. of unusually high humidity 79−79980
lower, power spectral anal. of meteorological data 78−40616
lower, trajectory slopes, countergradient heat fluxes and mixing by waves 79−2340
major warming, 1976-77, dynamical development 79−79968
mass motions, mean meridional 79−88419
mass spectrometer beam system, stratospheric comp. meas. appls. 78−7808
mass spectrometry for in situ meas. 80−17388
mean meridional circulations of stratosphere and mesosphere, monthly mean planetary wave fluxes 80−109219
meridional shear and spherical geometry effects on long waves 79−12212
mesosphere at Thumba from in situ UV absorpt. photometry obs. 80−105051
meteor trail metal ions, chem. reactions 80−72580
methane, stratosphere content at mid-latitude, simultaneous N and S hemisphere obs. 80−77052
methane+$O^+_4(O_2^+)$, products, rate consts., rel. to stratosphere 77−9040
methane at several latitudes in 0-35 km altitudes 79−34894
methane meas. and predictions 79−84432
methanol (dimethyl ether)+Cl, absolute rate consts., 200-500K, stratospheric chem. appl. 79−66271
methyl chloride conc. profile up to 32 km. altitude 80−36368
methyl chloroform, impact on stratospheric O_3 78−53722
methylchloroform, vapour phase, UV absorpt. spectrum, photodissoc., stratospheric appls. 79−81208
Michelson interferometer, use as selective filter for stratospheric trace gas concs. meas. 80−17408
Michelson interferometer on Canberra aircraft for stratospheric studies 77−87132
micrometeorite particles, detect. of ^4He 77−56878
microwave limb sounding for composition and temp. determ. 77−21940
middle atmosphere, obs. from balloons, rockets and satellites, conference, London, England, (1978 December 12 to 13) 80−77540
minor constituent chemistry, volcanic eruption effects 79−84437
minor constituent meas. 77−21874
minor constituents, chemistry and transport, conf., Seattle, USA (Aug. 1977) 79−84428
minor constituents, concs., chemiluminescence in situ instrums. and techniques 80−16886
minor constituents concentration profiles, Spacelab obs. 77−21967
minor constituents detection using tunable spin flip Raman laser, review 80−55762
minor constituents transport between troposphere and stratosphere 80−105034
minor gases determ. using occultation technique *(Russian)* 79−25342
minor gases in middle atm., optical meas. 79−84480
minor species and temp. meas. using cryogenic etalon-spectrometer on Space Shuttle 79−58232
minor species meteorological control of lower stratosphere 79−12171
model, temp. feedback effect on O_3 conc. 78−28277
models of physical and chemical processes 77−21875
movements, Lagrangian motion of air parcels in presence of planetary waves 80−109215
multi-ion complexes, implications for aerosols and trace gases 80−61872
natural structure rel. to chlorofluoromethanes effect on O_3 layer 79−84436
negative ion hydration in stratosphere and lower ionosphere 79−100909
negative ions, mass spectrometric meas. 78−96274
nightglow intensity fluctuations during stratospheric warmings 80−4162
northern hemisphere, temp., contour height and wind at 30 mbar level 78−24350
northern summer, long-range circulation var. rel. to solar activity *(German)* 77−56694
odd N mixing ratio 77−70744
ozonometer, using chemiluminescent reaction of ozone and olefins *(French)* 79−48574
ozonosphere, chemical-kinetic criteria of effect of substances of natural and anthropogenic origin *(Russian)* 78−53699
particle layer injected by aircraft at 23 km, balloon obs. 78−81283
particulate transport, downward to aerosol layers 77−78348
periodic temp. and wind fluctuations 77−78361
peroxynitrates, UV absorpt., spectra, photodissoc. lifetime meas. 80−83386
photochemical model, input sensitivity study 79−84434
photochemical-radiative damping and instability in the stratosphere 78−28259
photochemistry, computer simulation 79−21481
photochemistry, orbital simulator using superpress. balloon 79−29966
photochemistry and kinetics, modelling 79−53495
photochemistry interpretations 79−74943
photochemistry model, O_3 calcs. uncertainty 79−16567
photodissociation fluxes, tropospheric and stratospheric, Mie scatt. contrib. improved model 80−77103
planetary wave, radiatively damped, in middle atmosphere, interaction with zonally averaged circulation 80−109217
planetary wave forcing, quasigeostrophic theory 78−73482
planetary wave secondary circulation, vertical air exchange implication 80−72584
stratosphere continued
planetary waves at 20-80 km altitude rel. to ionospheric absorpt. winter anomaly 80−36359
planetary waves in stratosphere global propag. in spherical atmos. 80−90139
planetary-scale temperature waves seasonal var., Nimbus 5 obs. 77−21868
planetary-scale waves, vertical energy flux, obs. results 77−2193
polar-night jet rel. to clear air turbulence effect on general circulation model 77−86968
pollution, chemistry of ozone depletion 77−91256
pollution, review of Climatic Impact Assessment Programme (CIAP) 78−16153
pollution measurement using balloon-borne grab-sampling system 77−29504
positive ion chemistry of formaldehyde and methanol 78−57251
positive ion composition, balloon-borne mass spectrometric meas. 78−32194
positive ion density meas. by rocket-borne Gerdien condenser, 23-39.5 km altitude 79−84378
positive ions, comp. meas. 78−88877
positive ions, mass spectrometric meas. 77−49133
post-volcanic aerosol decay, lidar meas. 79−53444
potential vorticity and transport 77−87009
pressure fluctuations, time spectra 77−78367
radar echo mechanisms, returns from clear air 80−90181
radar facility, MST radar at Poker Flat, Alaska 80−90254
radar for observing middle and upper atmosphere, Yaggi antenna array design 80−90255
radar observation of fine struct., pulsed VHF radar method 80−51566
radar signal reflection and scatt. from refr. index structs. 80−90182
radar studies at VHF and UHF freqs., review of obs. 80−90180
radar techniques (VHF and UHF) for dynamic struct. 80−105078
radiance variation seen by horizon sensors 79−100957
radiation budget affected by N_2O and methane 80−90211
radiative equilibrium temperatures, comparison for stellar occultation and BUV O_3 data 78−81280
radiative transfer, simplified radiative-convective model 77−5320
radiative transfer in CO_2 4.3 μm band with non-LTE *(Russian)* 78−88914
radiative transfer in Doppler broadening atmospheres, stratosphere, mesosphere and thermosphere 77−78418
radiative-dynamic coupling, 3-dimens. circulation model 77−86965
radicals, atomic and diatomic, meas. 80−17307
radioactive pollution evolution, influence of jet stream *(Spanish)* 79−100549
radiometric measurements made in situ with superpressure balloon 80−85763
radiometry and spectroscopy from aircraft 77−70890
radiowave backscattering, depolarisation obs. at 50 MHz 80−85729
radiowaves, medium and short, seasonal absorpt. courses, rel. to strato-mesosphere dynamics 79−58149
reactive N in unpolluted troposphere, stratospheric source 80−94561
remote monitoring using discretely-tunable IR gas lasers and heterodyne detect. techniques 78−61605
remote sensing by two satellites, radio illumination method 80−51550
residence times from β activity of Antarctic and Greenland snows 79−79421
response to solar eclipse, sunrise and sunset 79−100907
rotational electric field of auroral origin 78−45102
satellite observations, instrum. description 80−26713
satellite observations of middle atmosphere processes 80−21803
satellite solar occultation sounding of the middle atmosphere 80−105079
satellite-borne IR scanning radiometer obs. of stratosphere, optimum field view and spacing 78−16201
scattered solar radiation field meas. *(Russian)* 79−16667
Schumann resonances, elec. vertical component obs. by stratosphere balloon 79−44221
seasonal climate, numerical simulation, energetics 79−5567
seasonal climate, numerical simulation, zonal temp. and wind 79−5566
semiannual oscillation in tropical middle atmosphere, review of observational evidence 80−109216
solar eclipse effect on NO_2 and O_3 conc. and atm. temp. 80−105017
solar MUV photometer, rocket borne, stratospheric ozone concentration measurement 80−52292
solar occultation sounding, appl. to press. and temp. profiles meas. 80−98452
solar radiation absorption by water vapour, thermotidal exciting function 78−28310
solar radiation absorption in O_2 Herzberg continuum, influence of O_4 and O_2N_2 dimers 78−87429
solar radiation budget in cloudy atm., modified two-stream approx. 79−58090
solar UV radiation, absorpt. in mesosphere and stratosphere 80−109248
solar UV radiation effects, rel. to solar cycle signal in tropospheric winds 80−72604
solar UV transmission calc. down to 28.7 altitude 79−62575
sonic booms from Concorde aircraft flight, atm. struct. information 79−66742
southern hemisphere stratosphere, temp. and press. field spring transformation anal. 80−98420
space sciences, conf., Waltair, India (Jan. 1978) 79−101000
stable layers obs. by vertical pointing VHF radar 80−90189
stationary planetary waves and zonal wind, southern hemisphere 78−28276
strato-mesosphere, seasonal relation between winds and LF radiowave absorpt. 79−62645
stratopause, double, thermal struct. features over Thumba 79−100901
stratosphere-troposphere exchange at polar latits. in summer, from O_3 concs. meas. 80−72599
stratospheric sudden warming, planetary-scale forcing of USA Jan. 77 weather 78−57279
structure, composition, temperature and motion, general review 79−39997
structure, southern hemisphere, winter 1973, from satellite obs. 77−5282
structure in presence of noctilucent clouds 80−8412
submillimetre spectrum meas. with high resolution Fourier spectroscopy 77−87133
submillimetric-wave interferometric spectrometry 79−34979
sudden stratospheric warming initiated by planetary wave, model 80−90150

stratosphere continued
sudden warming, 1973 January-February, energetics and dynamics 79−79973
sudden warmings, wave-mean flow interactions numerical model 77−5297
sulphate aerosol, kinetics of growth by condensation in homogeneous medium *(Russian)* 80−94566
sulphate aerosol layer, processes, models, obs. and simulations 80−109212
summertime temps. during solar cycle 20 (1965-77) 79−79936
SURF storage ring calibrations for NASA stratosphere and climate programs 80−94721
temperature, aerosols from Mount Agung eruption as test of global climatic perturbation 78−69440
temperature, obs. by satellite IR limb scanning method 80−105086
temperature, recent trends 79−29845
temperature and pressure determ. from OH fluoresc. lidar instrument 79−80033
temperature and wind correl. with mesospheric electron densities and drifts 77−9470
temperature at 30 mb level, coherence with ionospheric absorpt., five-day wave 77−33275
temperature corrections for Menaka-II meteorological rocket payload 79−5558
temperature correl. with ionospheric f-min at southern midlatitudes 77−9469
temperature diurnal variation, 25-65 km altitude equator region 80−82022
temperature fluctuations, latitudinal-wavenumber power spectra 80−41499
temperature remote sensing by O_2 60 GHz absorpt. 80−77172
temperature trends and O_3 conc. rel. to 11-yr. solar cycle 79−84443
temperature variations in lower stratosphere rel. to atmosphere total O_3 content natural fluctuations 79−29819
temperature wave in polar winter upper stratosphere 80−72597
temperature waves, ultralong, during 1973 austral winter 78−92901
temperature/O_3/water vapour trends in N. temperate latitude 79−53474
temperatures and geostrophic winds during 1973-74, Nimbus 5 radiance meas. 79−79976
tetrafluoromethane, v_3 vibr.-rot. band identification in balloon-borne IR solar spectra 79−100894
thermal relaxation rate 79−79940
thermal response to O_3 fluctuations 79−39797
thermal structure and total O_3 obs., Nimbus 4 Iris expt. 77−21839
thermal structure and trace constituents, effects of solar UV variability 78−61492
tidal energy distrib. with altitude, wind field influence *(Russian)* 78−69402
tide in temperature due to Moon, NIMBUS 5 obs. 80−101405
tides, thermal exciting energy, numerical anal. 79−70833
trace constituents, in situ meas. 79−8676
trace constituents, laser heterodyne spectroscopy 80−109257
trace constituents correlated seasonal and climatic vars. 79−84433
trace gas analysis method based on in situ ion composition obs. 80−105077
trace gas concentration determ. by Spacelab passive sounding expt. 77−21950
trace gas concs. during 1976 in N.Hemisphere 80−67016
trace gas sampling, chemical absorption filter techniques 80−17305
trace gases, temporal and latitudinal vars. 78−40619
trace gases detection *(German)* 79−53003
trace molecule Fourier transform spectrometer optical design 80−82099
trace species vars. during solar eclipse, theoretical study 79−58013
tracers, use of cosmogenic isotopes 77−41237
transient eddy statistics of northern hemisphere winter circulation 79−58027
transport, diffusive, one-dimensional parametrisation using ^{95}Zr data from Chinese thermonuclear explosions 79−2342
transport and chemical processes 77−25761
travelling planetary waves, theory and obs. 80−105030
trichlorofluoromethane, 8-12 μm band model calcs. 80−43112
trichlorofluoromethane, 8-12 μm bands intensities, temp. depend. 80−43048
trichlorofluoromethane, height profile meas. at several latits. 80−72601
trichlorofluoromethane, UV absorpt. cross sections temp. depend. stratospheric 77−64423
tropic winds meas. by Arecibo 430 Mhz radar 79−100975
tropical atmosphere, influence of stratospheric aerosols on solar and longwave radiative fluxes 77−25743
tropical O_3 spatial variations, influence of meridional transport and planetary waves 78−20463
tropical stratopause, 2-day oscill. of meridional wind 80−56557
tropical stratospheric waves 79−92585
tropopause, detect. by partial specular refl. with VHF radar 80−8411
tropospheric-stratospheric polar vortex breakdown 1977 January 77−53107
turbulence, optical remote sensing and comparison with simultaneous thermal meas. 79−34965
turbulence and mean flow study by tracer balloons 79−8661
turbulence from IR astronomy data 80−12475
turbulence in buoyancy subrange of stably stratified shear flow, theory 79−5568
turbulence struct., 10-30 km altitude, high resolution 430 MHz radar obs. 80−90258
turbulence struct. near tropopause, review of radar obs. 80−90179
turbulent layer struct., 2380 MHz radar obs. 80−90191
two-layer atmosphere, orographic perturbations *(Russian)* 78−16136
UHF radar echoes, Arecibo expt., for wind and turbulence obs. 77−33135
upper, radiative damping, obs. evidence 79−84368
upper winds, tropics, data clustering technique 77−91225
UV solar radiation effects on upper atmosphere, review of Saha's work 79−53599
vacillation cycles, quasigeostrophic β-plane channel model 77−49119
vacillations in general circulation model, large-scale energy cycle 79−53430
Van der Waals molecules comp. of lower atmos. 80−85699
vertical sounder radiances rel. to midlatit. 300 mb flow patterns 78−92983
vertical wind shear from Lagrangian wind field obs. 80−82032
stratosphere continued
VHF coherent radar sounding, wind and refractivity turbulence struct. 78−28281
VHF radar obs., specular reflection 79−39822
VHF radar obs. of struct. and dynamics 80−105032
vibrationally excited hydroxyl radicals, instantaneous rate model 77−5273
volcanic eruption cloud dispersion in stratosphere, lidar and numerical models for Vulgan Fuego and Augustine 77−56682
volcanic plume contributing sulphur and halogen to atmos. 80−51474
warming, Eulerian and Lagrangian mean meridional circulations 80−21799
warming, Jan-Feb 1979, troposheric-stratospheric interaction 80−4074
warming, simultaneous increase of electron density in lower ionosphere 77−91356
warming and circulation effect on polar surface energy budget 77−66957
warming forced by mountain 80−72583
warming of 1976-77, temp. and wind fields 77−56699
warmings, influence on lower thermosphere natural infrasound refl. 79−21089
warmings, interactions with troposphere, thermal and kinetic 80−105031
warmings, O I 5577 Å, Na and OH nightglow emissions var. 77−53270
warmings, obs. and theory 79−74944
warmings, rel. to wind field disturbances at 90-100 km altitude *(German)* 77−70894
water, vertical transport rel. to atmospheric HT and HTO 79−2347
water vapour, in situ meas. with new moisture sensor 79−74930
water vapour, mixing ratio from solar brightness temp. balloon-borne obs. 78−85921
water vapour 0.94 μ absorption cross-section obs. *(Japanese)* 80−17427
water vapour budget, contrib. of extratropical severe storms 77−87029
water vapour changes, effects on O_3 reduction estimates 78−73444
water vapour conc. meas. using aircraft-borne UV fluorescence instrument 80−82100
water vapour vertical profile in stratosphere *(French)* 80−77033
wave motion, balloon obs. using data storage system on balloon 80−46263
wave motions and daily neon winds, 52-110 km altitude, at midlatits. 79−5565
wave processes rel. to wind vel. fluctuations in 95-100 km altitude region *(Russian)* 77−29523
wave spectra resembling turbulence, implications for turbulent transport estimates 79−79981
wave transience and dissipation role in mean flow vacillations 79−5577
wave/mean flow interaction, introduction to generalised Lagrangian-mean distribution 80−109214
wave/mean flow interaction, mean motion induced by transient inertio-gravity waves 80−105029
waves in lower stratosphere, radar meas. 78−44917
waves in lower stratosphere, radar meas. 78−81292
waves of short-period, 13-25 km altitude, Doppler radar obs. 80−90192
western hemisphere, rocketsonde-derived temperature vars. 79−58018
wind and temp. diurnal and semidiurnal oscills., rocket meas. 79−5556
wind and thermal structure, W.Europe 1975/6 winter anomaly obs. 80−36438
wind diurnal variation, 25-65 km altitude equator region 80−82022
wind meas. with clear air Doppler radar, vertical component 80−72642
wind measurement by radar, method for reducing backscatt. data 80−90257
wind measurements by radar in Arctic region 78−49172
wind monitoring using Concorde-generated infrasound 80−51492
wind phenomena affecting troposphere circulation pattern 80−82021
wind profile in troposphere and stratosphere, using Poker Flat MST radar 80−72579
wind structure over Antarctica 80−81992
wind vel. components, power spectra *(Russian)* 79−88403
winds and turbulence continuous meas. using VHF Doppler radar, preliminary results 80−8444
winds in lower stratosphere over Jicamarca, full-day radar meas. 79−25308
winds in troposphere and stratosphere, connections with dynamical processes in lower thermosphere *(Russian)* 78−24401
winds in upper troposphere/lower stratosphere rel. to satellite-derived radiance gradient 80−98447
winter processes, rel. to wind regime of lower thermosphere 78−4019
winter warmings, ionospheric characts. vars. 77−29550
winter warmings in N.Hemisphere 80−26591
zonal mean circulation of middle atmosphere, numerical model 80−109218
zonal mean winds, vars. rel. to planetary wave props. and links with troposphere 80−109225
zonal wind cycle in southern hemisphere 79−79977
zonal wind speed oscills., solar cycle influence 80−94562
zonal winds effect on Earth rot. 80−81804
zonal winds variation, correl. with 27-day solar rot. 78−88878
zonally averaged circulation, 15-125 km altitude region 79−5564
^7Be, stratospheric tracer, distrib. within high-press. systems in E.United States 80−4072
Br chemistry and depletion of O_3 layer 80−98391
$Br+H_2O_2$, rate constant upper limit, stratospheric chemistry implication 80−30216
$BrONO_2$, stratospheric photolysis, UV and IR spectra 78−53227
$CCl_2FO_2+NO(NO_2)$, reaction, photolysis obs. 79−74931
$CCl_2FO_2NO_2$, thermal dissoc., rel. to photodissoc. and stratospheric Cl budget 79−74931
$CCl_3O_2NO_2$, thermal decomposition, form. and lifetime in stratosphere 79−57256
CO, content observed on circumpolar airliner flight 80−51475
CO, stratosphere content at mid-latitude, simultaneous N and S hemisphere obs. 80−77052
CO-OH-CH_4 cycle, implications of anthropogenic CO emissions 77−49160
CO_2 conc. meas., comparability 78−20495
CO_2 increase effects on stratospheric O_3, photochem. and radiative transfer model 78−65370
CO_2, stratosphere content at mid-latitude, simultaneous N and S hemisphere obs. 80−77052
COS detect. 79−58014
CS_2 and COS oxidation rel. to S budget 79−84423
Cl and ClO radical in situ obs., rel. to O_3 depletion 78−36241

stratosphere continued
Cl effects on O_3 layer, zonally averaged two-dimens. model 79−84435
Cl-ClO-Cl cycle, possible roles of ClO*, $ClNO_3$ and HOCl 77−17185
$Cl+C_2H_2$, reaction kinetics, stratospheric implication 78−31618
Cl + formaldehyde, rate const., 200-500K 79−39133
Cl + formaldehyde→HCl + HCO, stratospheric O_3 decreased sensitivity to Cl perturbations 79−12190
$Cl+HNO(H_2O_2)(HO_2)$, rate consts., stratospheric appl. 78−85125
Cl + methane, reaction rate const., stratospheric modelling appl. 79−20345
$Cl+NO+N_2 \rightarrow NOCl+N_2$, rate const. temp. depend. 78−76828
$Cl+SO_2$, rate const. rel. to stratospheric Cl chemistry and Venus atm. 79−84353
^{38}Cl + ethane (methane)(vinyl bromide), rate consts., stratospheric temps., radiotracer meas. 77−48632
Cl_2-O_3 system photochemistry rel. to stratospheric composition 77−16849
ClO, aircraft search for 3 mm emission 80−41510
ClO composition balloon borne in situ reson. fluoresc. obs. 80−90167
ClO, conc. vars. at twilight rel. to interpetation of solar occultation meas. 80−85756
ClO, predissociation cross sections and rate consts. 77−70763
ClO radical, IR vibr.-rot. spectra, background data for atm. meas. 78−58679
ClO, UV absorpt., lab. spectra rel. to atmos. identifications 77−34653
$ClO+HO_2$, free radical reaction rate consts. and products at 298K, discharge flow mass spectra 80−67391
$ClO+NO_2 \rightarrow ClNO_3$, reaction rate consts., stratospheric appl. 77−78306
$ClO+NO_2 \rightarrow ClONO_2$, fall-off curves, N inclusion effects 77−63910
$ClO+O \rightarrow Cl+O_2$, rate consts. calc. 220-1000K 79−79233
ClONO, near UV absorpt. spectrum, rel. to atm. chem. 77−30881
$ClONO_2$, chem. degradation in stratosphere 77−33134
$ClONO_2$ collection using impregnated filters, simulation 79−12257
$ClONO_2$, form., photolysis in stratosphere, photochem. absorpt. cross sections, UV spectra 77−33154
$ClONO_2$, high resolution IR absorptivity 77−33184
$ClONO_2$, mechanism of UV photolysis at 302.5 nm 78−20031
$ClONO_2$, relative abundance among stratospheric Cl compounds 77−33155
$ClONO_2$, solar photodissoc. rates, current levels in stratosphere 79−53496
$ClONO_2$, stratospheric distrib. at sunset, balloon borne IR solar spectra obs. 80−41487
$ClONO_2$ upper limits from balloon borne IR meas. 77−70743
$ClONO_2+OH$, reaction kinetics, stratospheric conditions 77−86303
$ClONO_2+O(^3P)$, fast flow reaction, rate const. 77−12777
$ClONO_2+O(^3P)$, rate consts. 77−77796
ClOO, stratospheric chem., formation and loss reactions 78−16138
ClO_2O_2 possible existence and chemistry 80−77066
$Cl(^2P)+ClONO_2$, reactive channels, stratospheric altitudes 77−60038
$Cl(^2P)$ + methane, absolute rate and temp. depend. 78−80731
$Cl(^2P_{3/2})+O_3(H_2O_2)$(methane) reaction kinetics, temp. depend., reson. fluoresc. obs. 77−4903
^{38}Cl and ^{39}Cl radioisotopes, chemical form 78−44913
Cs_2, precursor for atm. COS 79−53490
F chemistry, comparison between theory and meas. 79−16568
F mass mixing ratio, direct meas. 77−53106
H_2 mixing ratio vertical profiles 78−32181
$HBr+OH \rightarrow H_2O+Br$, absolute rate const., 249-416K 79−70303
HCl, HF, volume mixing ratios simultaneous meas. 80−72587
HCl mixing ratio, radiometric meas. 77−25745
HCl, stratosphere content at mid-latitude, simultaneous N and S hemisphere obs. 80−77052
HCl, vertical distrib. in stratosphere 78−20470
HCl + O(OH), reaction rate const. temp. depend., stratospheric implications 78−31616
HF meas. in upper stratosphere 77−45070
HF, stratosphere content at mid-latitude, simultaneous N and S hemisphere obs. 80−77052
HF/HCl, ratio in 14-38 km region of stratosphere 78−20469
HNO_2+O_3 reaction kinetics under stratospheric conditions 78−11499
HNO_3 channel spectral meas., fluorocarbons 11 and 12, contamination effects 77−87054
HNO_3 composition, in situ obs. 80−105077
HNO_3 concentrations, obs. in N.hemisphere for three seasons 78−81288
HNO_3, IR spectra rel. to abundance 80−12464
HO_2 and HOCl, struct., vibr. freqs., IR intensities, ab initio calcs. 79−98007
HO_2 radical, atmospheric reactions studied by laser mag. reson. spectroscopy 80−12511
$HO_2+HO \rightarrow H_2O+O_2$, rate coeff. meas. by laser mag. reson., atm. chem. appl. 77−52614
$HO_2+O_3 \rightarrow OH+2O_2$, rate coeff., effects on stratospheric O_3 78−96275
$HO_2+O \rightarrow HO+O_2$, rate coeff. meas. by laser mag. reson., atm. chem. appl. 77−52614
H_2O and O_3 conc., far IR spectroscopy, quantitative anal. 79−39790
H_2O, composition, in situ obs. 80−105077
H_2O mixing ratio, in-situ obs. using NOAA UV fluoresc. instrument 80−90137
H_2O, stratosphere content at mid-latitude, simultaneous N and S hemisphere obs. 80−77052
H_2O structure, maintenance of extreme aridity 80−105028
H_2O, thunderstorms as micrometeorological sink 79−84385
H_2O vapour burden areal distrib. and jet stream 77−5275
H_2O vapour distribution, temporal and spatial vars. 77−45112
H_2O vapour latit. distrib. in lower stratosphere, aircraft meas. 78−32173
H_2O vapour meas. using UV fluoresc. hygrometer *(French)* 78−65401
H_2O vapour mixing ratio, Australia, 1973-76 period 78−49116
H_2O vertical distrib., UV fluorescence meas. 79−34891
H_2O-H_2SO_4-ion aerosol particles, ultrafine, stratospheric form., ion-induced nucleation 80−72608
HOCl, ab initio MRD CI calc., electronic spectrum, dissoc., heat of reaction, formation 78−21857
HOCl abundance 79−84427
HOCl as inert atmospheric Cl reservoir, prospects 79−12207
HOCl, HOOCl, stratospheric chem., formation and loss reactions 78−16138
$H_3O^+(H_2O)_n$, photodissoc. meas. and calc., rel. to atmospheric stability 79−86017
HO_2NO, unimol. dissoc., rate consts., temp. depend., atmospheric implications 78−7175
HO_2NO_2, gas phase, UV and IR absorpt. cross sections 79−13733
H_2SO_4 gas phase meas. 80−36366
H_2SO_4-H_2O solution aerosol particles nucleation 77−56678
HT and HTO, stratospheric vertical transport of water 77−9463
Hf acid, presence confirmed by solar spectrum obs. *(French)* 77−53105
N fixation in instantaneous linear discharges, variable energy input effect 79−20952
N_2, collision-induced absorpt., temp. depend., rel. to atm. far IR transmission 79−62584
NH_4^+, mutual neutralisation, with simple and clustered positive (negative) ions 78−44372
NO and NO_2 mixing ratio profiles from IR sunset spectra 80−94563
NO and O_3 meas., mixing ratio 78−44915
NO, conc. vars. at twilight rel. to interpetation of solar occultation meas. 80−85756
NO concentrations, obs. in N.hemisphere for three seasons 78−81288
NO concentrations in lower stratosphere, geographical vars. 78−73438
NO, far IR spectral lines and absorptance calcs. 77−46564
NO meas. to 45 km altitude using balloon-borne chemiluminesc. detector 77−29397
NO mixing ratios near stratopause, chemiluminescent meas. 79−34893
NO, NO_2, simultaneous IR meas. 79−8671
NO, photodissoc. in mesosphere and stratosphere, theory 80−41580
NO, photodissoc. rate, calc. 80−51498
NO predissociation, photochemistry 80−21802
NO, self-N_2- and O_2-broadened linewidths 5.4 micron band, quadrupole moment 77−30930
NO, stratospheric growth before sunrise by photolysis 77−29356
NO + BrO, controlling [BrO]/[Br] and [BrO]/[HBr] ratios in stratosphere 80−50866
NO + BrO, temp. depend. kinetic study, stratospheric Br photochemistry implication 80−50866
$NO+O_3 \rightarrow NO_2+O_2$, rate const., 203-361K, fast flow method 77−33143
NO_2 and H_2O, mixing ratio profiles from IR solar spectra obs. 80−105015
NO_2 and HNO_3 concentration, simultaneous meas. *(French)* 78−16107
NO_2, at latitude 45°S at midsummer, ground based meas. 79−96784
NO_2 content during stratospheric warming, 1979 obs. 80−51476
NO_2 determination, observational method and behaviour at mid.-latit. 80−17414
NO_2, global behaviour 80−17334
NO_2 in Antarctic winter 79−34892
NO_2, minor atm. components, visible absorpt. spectra, temp. depend. *(French)* 80−36355
NO_2, stratospheric, ground based obs. 80−85697
NO_2, tangent ray meas. technique, effect of NO_2 conc. vars. at twilight 78−32141
NO_2 transport, production in thunderstorms 80−8376
NO_2 vertical distrib. at night, NO_3 layer effect *(French)* 77−66947
NO_2 vertical profile, balloon obs. *(Japanese)* 80−31086
NO_3, detect. and column abundance 78−88880
NO_3 in nighttime stratosphere, composition change following sunset 80−31097
NO_x catalytic O_3 destruction, sensitivity to rate coeffs. 77−37472
NO_x chemistry, significance of HO_2NO_2 78−11971
NO_y mixing ratios, effect of NO photolysis 77−29399
N_2O altitude profiles at five latitudes 77−78318
N_2O conc. in northern hemisphere during 1975, July 77−78304
N_2O, conc. meas. using electron capture-gas chromatography technique 77−9531
N_2O, distrib., mixing ratio 78−32175
N_2O, global atmos. composition and residence time 80−51519
N_2O, greenhouse effect and climatic implications 77−9460
N_2O in lower stratosphere, latitudinal profiles 78−44989
N_2O in N.American troposphere and stratosphere 79−79430
N_2O, instantaneous global photochemical reaction rates 80−17335
N_2O mixing ratio, height profile meas. at several latits. 80−72601
N_2O, sources and sinks, review 77−37374
N_2O, stratosphere content at mid-latitude, simultaneous N and S hemisphere obs. 80−77052
N_2O, three-dimens. distrib. and variability, numerical simulation three-dimens. distrib. and variability, numerical simulation 79−58006
N_2O, trichlorofluoromethane and dichlorodifluoromethane conc. meas. 78−32171
N_2O UV absorpt. spectrum at stratospheric temps. 78−28260
N_2O vertical distrib., from balloon meas. of solar spectra 78−61493
N_2O_5 abundance, upper limit 77−5299
N_2O_5 gaseous, integrated band intensity data, stratospheric detection implications 80−58250
N_2O_5, thermal dissoc. in N_2 79−96294
N_2O_5+O, rate const., 220K, 300K, discharge-flow method 78−44352
$NOHSO_4$ and $NOHS_2O_7$ identification in aerosols, rel. to N oxides pollutants removal 79−39795
Na and minor constituents, meteoric origin 79−70835
$NaOH_2^+(H_2O)_n(NaOH)_m$ cluster ions 79−34895
No_2 concentrations, experimental estimation *(Russian)* 77−49109
O I 5577 A emission rel. to lower thermosphere interaction with stratosphere 77−70899
O_2, mag. dipole transitions, line positions and strengths from stratospheric emission spectra 80−78604
O_2, photodissoc. and spectral absorpt. in stratosphere and mesosphere 80−51497
O_2-O_2 and O_2-N_2 dimers from O_2+N_2 collisions, solar radiation absorpt. 78−9167
O_3 10 μ absorption line obs. with IR heterodyne spectrometer 78−61494
O_3, 9.6 μm band radiance calc., excitation processes 78−36350
O_3 affecting ground-level oxidant concs. at Santa Rosa 78−16112
O_3 and aerosol monitoring using orbiting photodetectors 77−78445
O_3 and Aitken nuclei conc. correl. over Americas 77−49141
O_3 and mass transport, stratosphere to troposphere, Project Dustorm, tropopause folding 78−32177
O_3 and NO meas., mixing ratio 78−44915
O_3 and temps., satellite obs. for 1970-71 period 77−9466
O_3 and tracer particles creation and destruction, probability distribs. 78−20496
O_3 behaviour and thermal structure during S. Hemisphere spring 80−105014
O_3 budget, zonal mean circulation model and linearized photochem. 77−70780

stratosphere continued
O_3 column, increase rel. to NO_x emission from SST and subsonic aircraft 78−11979
O_3 composition, effect of chlorofluoromethane photolysis 80−109197
O_3, composition observed on circumpolar flight 80−51475
O_3 conc., effects of NO_x emissions of high-altitude aircraft 78−32176
O_3 conc. meas. at high latit. during twilight 77−41128
O_3 concentration meas. at sunrise and sunset *(French)* 79−48535
O_3 concentrations, obs. in N.hemisphere for three seasons 78−81288
O_3, concentrations in lower stratosphere, geographical vars. 78−73438
O_3 concs., increased CO_2 effect 78−57250
O_3 concs., seasonal vars., Umkehr and Nimbus 4 BUV obs. 79−100911
O_3 content, CO_2 cooling affecting chem. production and loss rates 80−36369
O_3 content, influence of 1972 August 4 solar proton event 78−7732
O_3 content affected by N_2O from fertilisers, latitudinal effects 80−36370
O_3 content in tropics, during March-April 1976 stratospheric warming 80−12494
O_3 density meas. using lidar, feasibility 77−60493
O_3 density perturbations, photochemical-radiative damping rel. to instability, numerical results 78−81286
O_3 density reductions, zonally averaged circulation response 79−53461
O_3 depletion, ClO influence 77−75052
O_3 depletion, rel. to N_2O emission from soils during nitrification of fertilizer N 78−57313
O_3 depletion by chlorofluoromethanes, two-dimens. time-depend. model 78−24341
O_3 depletion by chlorofluoromethanes, contradiction of theory 78−49099
O_3 depletion by halomethanes 80−16866
O_3 depletion chemistry 79−70872
O_3 depletion in stratosphere, space-time distrib. and UV radiation changes at Earth surface 80−94577
O_3 depletion thermal effects at 85°N latit., airborne particles influence 78−81279
O_3 destruction by fluorocarbons 77−9459
O_3 destruction by NO_x catalysis, comment 77−73812
O_3, distrib. and circulation in meridional plane *(French)* 77−49100
O_3 distribution in winter polar low region 77−78371
O_3 diurnal var. and scattering rel. to Cl concs. 78−7710
O_3, effect of CH_4, HCl and ClO 77−87032
O_3, effect of increased N fixation 78−28288
O_3, effects of agriculture 78−16123
O_3 global distrib. Ogo obs. 77−73809
O_3, heterogeneous decomposition, lab. study 79−70850
O_3, highly excited metastable forms rel. to photochemistry and heat balance 79−44225
O_3, influences on and effects of changes *(French)* 77−5271
O_3, instantaneous global balance including observed NO_2 80−109211
O_3, latitude-dependent depletion due to supersonic transports, model predictions 77−45051
O_3 layer, changes in chemical balance 78−92933
O_3 layer, depletion by nearby supernova explosion 78−32499
O_3 layer, fluorocarbon hazard assessment 79−79963
O_3 layer depletion by chlorofluorocarbons, calc. using two-dimensional model 80−109221
O_3 levels in stratosphere, solar activity, cosmic rays effects 77−53362
O_3, long-term vars. global distrib. during 1957-75 period 79−84429
O_3 meas. during Aladdin 74 program above Wallops Island 78−57247
O_3 measurement by satellite IR limb scanning method 80−105086
O_3 monitoring, satellite benefit assessment 77−78613
O_3 monitoring with airborne laser absorpt. spectrometer 77−91303
O_3 monitoring with IR heterodyne radiometer 78−16216
O_3, natural depletion mechanism, energetic radiation belt electron precip. 77−41134
O_3 net vertical flux from circulation model, implication for troposphere O_3 budget 80−101402
O_3, nighttime concentration (15-68 km), Nimbus 6 obs. comparison with OAO-3 obs. 80−105016
O_3, numerical model of effect of N oxides 77−53269
O_3 obs. and atm. physics research at Belsk, Poland *(Polish)* 77−21825
O_3, obs. of meridional flux by transient eddies in 0 to 30 km height range 80−109224
O_3, partial press. profile over Uccle, Belgium, April-June 1979 obs. *(French, Flemish)* 80−98385
O_3, partial pressure profile over Uccle, Belgium, 1979 obs. *(French, Flemish)* 80−94571
O_3 perturbation by N fertilisers, independent variables anal. 77−53134
O_3, perturbation by N fertilisers, independent variables anal. 78−73505
O_3 photodissoc., $O(^1S)$ yield at 1700-2000 Å 80−97714
O_3 problem, reassessment of stratospheric models 79−5553
O_3 profiles and chemical loss rates in tropics, BUV meas. 78−49091
O_3 profiles rel. to solar mag. activity 78−65373
O_3 reduction by natural NO_x and man-made pollution, model 77−60461
O_3 reduction due to industrial fixed N fertilizers 77−78383
O_3 reduction due to pollution, system-theoretic model 77−73848
O_3 response to nuclear bomb tests 77−81966
O_3 seasonal var. from rocket-borne UV obs. 77−29402
O_3, simultaneous effects of CO_2 and chlorofluoromethanes on column density 79−74940
O_3, spectroscopy with CO_2 waveguide laser 77−13117
O_3 stability and depletion scares 77−70722
O_3, stratosphere content at mid-latitude, simultaneous N and S hemisphere obs. 80−77052
O_3, stratospheric determ. at ground level using $^7Be/O_3$ ratios 79−58011
O_3 total amount at Belsk, Poland, harmonic anal. 78−92883
O_3 total content determ. using remote spectroscopy 78−65437
O_3 total content estimation from UV radiance meas., aerosol effects 79−8662
O_3 total content vars. correl. with ionospheric f_0F_2 vars. 78−45098
O_3 transport from stratosphere to troposphere 78−7687
O_3, two dimens. behaviour model *(French)* 78−49104
O_3, UV absorption bands, new vib. quantum no. assignments, based on isotope effect 79−94008
O_3, Umkehr vertical profile errors caused by presence of stratospheric aerosols 79−70849
O_3, variations rel. to general atmospheric circulation over Middle East in summer *(Russian)* 77−53156
O_3 vars. correl. with cloudiness vars. rel. to UV radiation protection 78−73456
O_3 vertical distrib. during polar front passage over Uccle 80−94582

stratosphere continued
O_3 vertical distrib. in upper stratosphere, satellite and surface-based obs. 78−40620
O_3 vertical distrib. over Aspendale, Australia, climatology 78−20475
O_3, vertical profile determ. by lidar sounding from ground 78−11972
OCS, stratosphere content, solar spectra meas. by 12 km attitude aircraft 80−41486
$O(^1D)$, chemical reactions of stratospheric importance, temp. depend. 79−53494
$O(^1D)$ quantum yield from O_3 photolysis 79−53492
$O(^1D)+H_2O$, rate coeff., atm. OH prod. 79−58009
OH radical, in Earth's atmosphere, pure rot. lines 79−92593
OH radical calculated densities in troposphere and stratosphere, uncertainties 79−53426
OH, vibr. energy distrib., atm. chem. modification 77−25735
$OH+ClO(Cl_2)(Cl_2O)$, rate const. at 298K, rel. to stratospheric O_3 depletion 79−87831
$OH+CO$, rate consts. 77−16781
$O(^3P)$ translationally hot, energy distrib. function 80−21811
$^{18}O^{16}O$, photodissociation as source of atmospheric O_3 80−94559
$O(2^1D_2)+N_2(O_2)(N_2O)(CO_2)(H_2O)$(methane), collisional deactivation meas., 295K, rel. to atmospheric processes 80−16663
$O(2^3P,2^1D)+N_2O(CO_2)$, diabatic correlations 77−25256
$O_2^+.O_2$, reactions with CO_2, O_3 and methane rel. to stratospheric ion chemistry 79−2343
$O_2^+.O_3$, reactions with H_2O and methane rel. to stratospheric ion chemistry 79−2343
$O_2(b^1\Sigma_g^+)$ quenching by $O(^3P)$ and O_3, rate coeffs. 79−70309
Pu distribution in Ohio soils, local and stratospheric sources 78−16015
S compounds, large-scale spatial and temporal distrib. 79−20981
S content, contrib. from OCS transported from troposphere 78−20466
SO_2, balloon-borne mass spectrometric obs. 77−33200
SO_2 detection, analytical technique 77−5314
SO_2, minor atm. components, near UV absorpt. spectra, temp. depend. *(French)* 80−36355
SO_2 oxidation chemiluminesc., appl. to atm. chem. *(German)* 79−52670
SO_{2_3} oxidation role for HSO_3 layer, reaction rate consts. 78−32202
SO_4^{2-} aerosol form. and growth 79−5604
SO_4^{2-} aerosol layer, form. and evolution model 80−21801
SO_4^{2-}, concs. at high altitudes 78−20468

strays (atmospherics) *see atmospherics*

streak photography
Agat, streak image camera with picosecond time resolution used in plasma investig. 80−38717
arc, high current, rotating, hot wake investigation by streak photography and schlieren systems 80−1862
arc, pulsed, high-current, initial anode heat flux meas. and modelling 79−50903
arc motion in narrow chamber, photography with optical waveguides and rotating mirror *(German)* 77−74542
betatron beam structure study via synchrotron radiation 77−65368
camera, direct readout devices 78−38037
camera, wide dynamic range, proximity focusing, visible and X-ray recording 77−89304
camera for subpicosecond chronoscopy 78−38030
camera synchronisation using picosecond laser pulse activated Si switch, jitter reduction 80−53440
compressed laser fusion targets, time resolved X-ray pinhole photography 78−38548
dye laser, actively mode-locked, flashlamp pumped, streak camera obs. of pulses 78−22158
electro-optical deflector streak camera system, for picosecond laser pulse diagnostics 78−33909
electron beam fusion compression targets, fuel preconditioning studies 79−81076
electron beam produced plasma, fast photography, emission spectroscopy 77−39458
electron optical photochronography, photoemission limit of time resolution 77−18103
electron optical picosecond chronoscopy, 140 MHz repetition rate, fluoresc. lifetime meas. 78−78019
electron-optical Feniks streak camera, quick change dyanamic processes application 79−50391
electron-optical photography, pico-femtosecond 78−82064
electron-optical streak camera for picosecond pulse detect., book contrib. 77−61138
electrooptic beam deflectors as streak cameras, theory 79−58809
filament velocity measurement, during spinning, streak photography 78−41367
flashover of solid insulator surface in vacuum 78−59700
flow of gas, two dimens., laser streak photography of 77−42937
glass microballoons, laser imploded dynamics, X-ray streak camera study 79−68937
high energy CO_2-laser pulse, interaction with liquid and solid targets, optical investigations 78−42829
high speed optical techniques, conf., San Diego, USA (Aug. 1976) 77−79182
high-speed, pulsed image convertor exposure time meas. using N_2 laser 77−30205
high-speed photography and photonic recording 78−86367
holographic interferometry, high-speed, real-time 78−37839
Homalite-100 plates, modified compact-tension specimens, dynamic anal. 80−97561
image convertor camera, for laser and laser-plasma diagnostics 78−38550
image convertor camera, with microchannel intensifier, modular design 78−42427
image convertor streak camera 78−54484
image convertor tubes, high speed, for laser pulse recording 78−33903
image convertor tubes for nanosecond, subnanosecond photography, dynamic range 78−38034
image convertor tubes for streak cameras, operating characts. comparison 78−38031
image-convertor camera, high-speed, computer treatment of images 78−42295
indigo derivatives, fluorescence decay times, meas. by synchroscan streak camera 80−84759
laser driven subnanosecond blast shutter, opening time 77−79842
laser fusion, image convertor camera optical measurement 78−38549

streak photography continued
laser impulses, 10^{-12} sec, anal. using Kerr cell and streak camera *(Italian)* 78−54477
laser material nonlinear refractive index meas. by time-resolved interferometry 77−18088
laser picosecond pulse meas., Nd:YAG mode-locked laser 77−19271
laser picosecond pulse meas. using streak camera 78−33902
laser temporal pulse shape meas. by streak camera 77−79799
lightning, photographs, daylight time-resolved 79−20954
low jitter streak camera picosecond measuring systems 77−87864
magneto-optical meas. in ultrahigh mag. field using image convertor camera *(Japanese)* 77−67505
microchannel plate technology and applications 79−23075
nanosecond hydrodynamic diagnostics, streaking camera, fibre optic probes 78−37096
optoelectronic framing camera tube for <100 ps range 78−70207
perylene, excimer form. process, ps laser fluoresc. obs. 79−11448
photochron picosec. streak cameras for linear photoelec. recording 80−86365
Photochron picosecond streak cameras, intensity dependent time resolution and dynamic range 78−45745
photoelectronic streak camera tube, magnetically focused 78−33907
photoelectronic streak-tube technology, review 77−79184
picosecond camera, nearly online, for diagnostics of CW mode-locked Nd:YAG laser radiation 79−49314
picosecond chronoscopy of repetitive weak light sources 78−38033
picosecond emission spectroscopy with an ultraviolet sensitive streak camera 79−35857
picosecond exposure scanning camera, and associated recording system *(French)* 78−42429
picosecond framing camera using a passive microchannel plate 79−49307
picosecond image convertor streak cameras, dynamic range 78−38032
picosecond laser, appl. to study of photosynthesis 77−81480
picosecond light pulse, meas. techniques *(Japanese)* 80−52291
picosecond light pulse techniques, historical overview of rapid phenomena meas., book contrib. 77−65026
picosecond photochronoscopy, generation and meas. of pulses from mode-locked lasers 79−76734
picosecond pulse measurement techniques, book contrib. 77−61139
picosecond pulses generation and meas. 79−41401
picosecond spectroscopy, appl. to chem. and biological reactions 79−80697
picosecond streak camera, dynamic range and spatial resolution 78−42428
picosecond X-ray chronoscopy 78−38546
picosecond X-ray spectral studies 78−38547
planar streak camera, picosec. recording appls. 79−44943
plasma diagnostics, of subnsec. laser fusion implosion, streak photo. FFT technique 79−71945
plastic plate velocity measurement, as continuum, by streak camera technique 78−37095
plastic scintillator props. meas., streak camera technique 78−66450
polycarbonate plates, modified compact-tension specimens, dynamic anal. 80−97561
proton pulse ang. divergence meas., 0.2TW pulse 77−22618
pulsed laser real-time holographic interferometry 80−74319
remote profilemeter, commented streak camera 77−79058
Shuttle Orbiter re-entry, remote IR imagery and tracking 80−82171
space charge field, spatio-temporal distrib. determ. in breakdown 80−38771
spectral and time-based anal. using streak camera in XUV region *(Italian)* 78−54513
streak camera, picosecond jitter 80−73486
subnanosecond X-ray framing camera, fibre array technique 78−41394
subpicosecond camera, proximity-focused, for laser fusion experiments 77−5938
subpicosecond proximity-focused streak camera, for X-ray and visible light 77−79183
subpicosecond proximity-focused visible streak camera, evaluation and appl. 78−59155
subpicosecond X-ray streak camera, for laser-fusion diagnostics 78−42822
superradiance development observed by streak camera 79−18384
surface irradiation shielding time with CO_2 laser beam, appl. to Al and graphite 79−55530
synchro-streak technique *(German)* 78−41368
synchronized ultra-short pulse generation and streak-camera measurement with CW mode-locked lasers 79−44951
theta-pinch, high-energy, linear, quartz end plug effects 77−76184
three dimensional imager, using mode-locked laser, beam splitter and streak camera 77−42597
three-dimensional measurement technique combining streak camera with modelocked laser 77−83832
time resolved spectroscopy, high-sensitivity streak camera, design *(Japanese)* 80−52327
time resolved spectroscopy system, vidicon and image intensifier, picosec. operation 79−44945
time-resolved X-ray spectroscopy of laser-produced plasmas 80−84004
trigger system, picosec., for mode locked laser pulse meas. 77−26406
turbine nozzle steam flow anal. under periodic perturbations 77−80249
ultrafast scintillators, response 78−41393
ultrashort pulse operations using flat lenses 78−66883
velocity-time history recording, by laser interferometer system 78−45602
X-ray and visible streak camera for subpicosecond laser fusion diagnostics 77−18122
X-ray streak camera, for obs. of tightly pinched relativistic electron beams 77−49818
X-ray streak camera, high time resolution, with X-ray microscope *(French)* 78−42823
X-ray streak camera electrode design using a plasma simulation code 79−30632
X-ray stream camera, ultrafast X-ray diagnostics for laser fusion experiments 77−79185
Al, shock-waves, ultrahigh-press., laser-driven 79−55823
CO_2-N_2-He system, CO_2 TEA laser discharge development, high-speed-camera investigation 79−55109
GaAs:Se cathodoluminescence decay obs. with SEM and streak camera, 90 to 300K 80−97348
KrF, 0.8 J multi-atm. laser, glow discharge characts. 78−58992

streak photography continued
Li wire high energy density exploding plasma, holographic interferometry, self pinching, charge density 79−77436
$LiNbO_3$ deflector, use in streak camera of approx. 100 ps resolution 79−18533
$LiNbO_3$ electro-optic deflector based streak camera, 20 ps resolution 79−85189
Nd:glass laser irradiated fusion targets, time and space resolved harmonic emission 79−82095
$(Y, Gd, Yb, Bi)_3(Fe, Al)_5O_{12}$ epitaxial film, domain wall motion and oscill. 80−2616
$(YGdYbBi)_3$ $(FeAl)_5O_{12}$ epitaxial film, diffuse domain wall, bubble domain expansion 80−25170
Zn, deform. twin form. kinetics, Rose channel form. and interactions, twin growth rate *(Russian)* 79−60378
Zn, dislocation mechanism of Rose channel formation under impact loading conditions *(Russian)* 79−79073

streamer chambers
2 m chamber in mag. field for α-particle spectrometer installation, SKM-200 80−23241
C-CD camera for streamer chamber appl. 78−37513
C-CDs for recording streamer chamber tracks 78−37515
charge-coupled devices recording streamer chamber tracks 77−88336
cryogenic targets for streamer chambers and cryofluid target supply *(Russian)* 78−13381
electron induced cascade shower, 350 MeV, angular distrib. 79−6802
electron track reconstruction in small volume self shunted streamer chamber 77−57821
filling by scavenging technique 78−9026
flash tube discharge mechanism determ. from digitisation pulse output 78−17504
four electrode streamer chamber construct. 79−68135
heavy ion track reconstruction program 79−31348
high resolution streamer chambers, design, operating parameters, appls. 79−744
high-energy particles detection by electronic method, principles of spark, streamer, proportional, drift and hybrid chambers *(Czech)* 77−42213
hodoscope, automatic system for meas. of transmission channels 77−3219
HV circuit for two-pulse supply 77−6619
ionization of streamer tracks, automatic meas. 79−68136
JINR high press. streamer chamber, selection criteria for $^{3,4}He(\pi,\pi)$ elastic interactions 80−102401
JINR high press. streamer chamber, triggering system efficiency for $^{3}He(\pi,\pi)$ elastic interactions 80−102400
large, for study of pion and proton induced nuclear breakup 77−10532
laser registration method for nuclear reactor detection *(Russian)* 80−18765
limited streamer tube operation 79−81123
low energy heavy ion reaction study appl. 80−58035
memory time control using filmless method 79−97940
nuclear physics appl. 79−72194
particle identification in large chamber with reduced memory time 77−57814
particle tracks recording technique using TV 80−69023
particle-nuclei interaction studies at high energy 77−30706
photography, rapid-cycling cameras, stereo images 78−37484
pulse transformer-based HV system 78−5095
RISK 5 m magnetic spectrometer streamer chamber, bipolar nanosec. pulse shaper 79−68166
RISK 5 m magnetic spectrometer streamer chamber, bipolar voltage pulse generator 79−68131
self-quenching streamer discharge in a wire chamber 79−63869
self-shunted, particle trace and event reconstruction *(Italian)* 77−42212
self-shunted hydrogen streamer chamber, localising admixtures 77−6624
sensitivity comparison of Kodak SO-143 film and CCD for streamer chamber appl. 78−21820
track digitisation using standard 625 line TV camera 77−30715
track integral brightness, measurement using installation incorporating multiplier 80−27882
ZGS streamer chamber and kaon physics 80−91308
K^+ decays, branching ratio meas. by mag. spectrometer with streamer chambers 77−18275
ν detector based on combined operation of streamer chamber and Converse hodoscopic tubes 80−63455
H_2, up to atmospheric pressure, cosmic ray tracks 77−38553
Ne-He high press. flash tubes, digitisation pulse characteristics 80−9455

streamers *see discharges (electric)*

streaming, acoustic *see acoustic streaming*

street lighting
two-cell mesopic photometer 77−37966
urban, large orbiting mirrors for night illumination 80−45632
urban lighting, effects on night sky brightness 77−73853

strength (mechanical) *see mechanical strength*

stress *see internal stresses; stress effects; stress/strain relations; yield stress*

stress analysis
see also bending; crack-edge stress field analysis; photoelasticity; photoplasticity; strain gauges; thermal stresses; torsion; yield strength; yield stress
acoustic reflection at interface of two highly stressed elastic half-spaces 78−63213
acoustoelasticity, appl. to nondestructive stress anal. 79−34259
acoustoelasticity, general stress-velocity expressions 79−81722
adhesive bonded lap joints, elastic stresses theory 78−55563
adhesive bonded tubular lap jont, stress anal. 78−18253
adhesive joints, effect of structural parameters on stressed state 79−41630
African plate, stress system rel. to mantle convection pattern 77−81859
Airy functions, stress problem solns., teaching appl. 78−86063
Airy stress function, anisotropic plates with mixed boundary conditions *(German)* 79−86345
central Aleutians lithosphere, unbending stresses rel. to double Benioff zone 78−32047
Alpine fault, New Zealand, frictional metamorphism, Ar depletion and tectonic stress 80−41440
angle-ply laminate, edge effects 78−19803
anisotropic axisymmetric solids, asymmetric stress anal. 78−26033
anisotropic cantilever plate with variable rigidity, stress and deflection anal. 79−59927

stress analysis continued
anisotropic composite cantilever, bending and torsion, mathematical formulation 79−18708
anisotropic cone, axisymmetrically loaded, stress state *(Russian)* 77−68413
anisotropic linear-elastic medium, self-force on planar dislocation loop 77−35557
anisotropic nonhmogeneous elastic media, radial deform. and stresses 78−51079
anisotropic plate, method of caustics 77−7344
anisotropic plate with closed rod pressed into curvilinear hole, state of stress 77−72173
anisotropic plate with curvilinear holes, plane elasticity problem, soln. approach *(Russian)* 80−33457
anisotropic plate with curvilinear holes, plane elasticity problem, comment *(Russian)* 80−38260
anisotropic plate with curvilinear holes, plane elasticity problem, basis of soln. *(Russian)* 80−38261
anisotropic reinforced plate, stress distrib. near recesses, variational anal. *(Russian)* 79−27521
anisotropic shells symmetry considerations 77−11123
anisotropic solids with magnetic symm., unified dynamic theory 78−77713
anisotropic strip under tension, stresses round hole or annular inclusion 77−3726
annular elastic membranes, large deflections, theoretical and expt. exam. 78−30186
annular plates, buckling under uniform external pressure, Timoshenko's conjecture 77−31226
annular plates, variable rigidity, post critical stressed and strained state 77−46942
anti-median elastic problem, N-harmonic solutions 80−99928
antiphase problems in linear elasticity theory *(French)* 78−87268
antisymmetric stresses in plane elastostatics, rel. to displacements and stress functions *(German)* 77−35038
aortic valve, human, finite element analysis 77−44699
aortic valve mechanics, anal. in diastole 80−35928
arched roof with curved longitudinal edges *(German)* 79−23217
artery wall, stress state estimation from vascular murmurs 77−56398
artificial hip joint construction compatible with femoral natural stress distrib. *(German)* 79−8576
asymptotic techniques for stress conc. regions in plane problems 78−28953
AT-cut quartz plate vibration anal. using light modulated oscillator 78−71255
automotive struct. analysis using hybrid stress finite elements 78−30176
axisymmetric butt joints, stress anal. in torsion and tension, response of adhesives 78−63397
axisymmetric cylinder, experimental numerical hybrid method 80−48657
axisymmetric elastic problems, stress function solns. *(Japanese)* 80−64371
axisymmetric solid of revolution elements based on assumed stress hybrid model 79−3917
axisymmetric solids with rectangularly orthotropic props., asymmetric stress anal. 77−35031
axisymmetric thermoelasticity problem for two-temperature hollow cylinder 80−5941
bar, axially symmetrical residual stresses, with longitudinally nonuniform stress distrib. 78−51070
bar, elastic, prismatic, with rigid ends, lower and upper bounds for torsional rigidity 80−48568
bar, round, subject to combined static and repeated bending and torsion, fatigue strength criterion 80−40496
bar, stress changes and warping during heating *(Russian)* 79−59920
bar, thin-walled, effective torsional rigidity optimisation *(Russian)* 80−19245
bar (tube), compressible, combined loading, elastic-plastic problem 78−63311
bar on elastic foundation, buckling strength *(German)* 79−64546
bar with various bends, dynamic stress conc. due to flexural wave propag. 77−23904
bars and tubes, anal. of axially symmetrical residual stresses 79−18734
bars with central circular holes, dynamic response to longit. impact 77−65703
beam, elastic, on elastic half-space support, forced flexural vibr. 78−63353
beam, impulsively loaded, clamped end bending moment, Bessel function eval. 79−92937
beam, Timoshenko, non-stationary loaded, use of Laplace transformation and classical method 80−14564
beam anal., finite difference formulae for boundary value problems 78−73856
beam on elastic medium, force distrib. change effects 79−55326
beam-truss gridworks, design formulae for exact elastic analysis 77−50870
beams, curved, shear stress formulas and shear centre 79−18726
beams, finite, curved, stress anal. under general equilib. loading 79−14258
beams, pure elastic-plastic bending diagram, general relationships 80−14588
beams flexural-torsional problem by series expansion in eigenfunctions 80−83732
Beltrami-Michell and Beltrami-Michell type eqns. in static and dynamic elasticity 77−53782
bending, finite elastic, existence-uniqueness results 77−75811
bending circular plates nonuniform, finite element analysis 77−7316
bending wave propag. in transversely struck plate, birefringence obs. *(German)* 78−48582
bending-free torsion condition to define centre of twist 80−79140
biaxial flexure test, exam. of loading factors 78−80695
biaxial residual stress, acoustic method of anal. *(Russian)* 77−19560
biaxial residual stress distrib., meas. method for determ. throughout workpiece height *(German)* 78−35596
biaxially fibre reinforced composites, two dimens. mixture theory, dynamic crack appl. 78−87301
bimaterial full-plane with crack at any angle to interface 77−14965
bimodulus sphere, nonstationary thermal stresses 77−50902
biwedge, stress singularities under various boundary conditions 79−12601
block-type fuel elements, stress calc. with finite element code *(German)* 77−71654

stress analysis continued
body with array of fine elastic inclusions, elongation and stress concentration 80−33466
body with period system of cracks laminar plastic zone development during longitudinal shear *(Russian)* 77−68442
bolted joints in wood, photomech. stress determ. 79−32406
bonded composite hollow circular cylinder, asymmetrical transient thermoelastic problems 78−30181
bonded composite hollow circular cylinder, transient thermal stresses under symm. temp. distrib. 77−54887
bonded sector plates, stress anal., soln. of elastostatic boundary value problems 80−1425
bonded wedge shaped stamp apex singularity, Green's functions for elastic half space 80−64489
bone, osteonic lamellae, evidence for state of initial stress 78−3536
bone, stress distrib. in long bone due to prosthesis positioning 77−36984
bone, stress estimation, analytical 79−92250
bone stress wave detection using piezoelec. effect, non-invasive technique 78−31948
boundary integral eqn. method, anisotropic 3-D stress anal. 78−90714
boundary integral eqn. method, resolution of tension discontinuity problem *(French)* 77−71215
boundary integral eqn. methods, advanced appl. 78−42531
boundary stresses, anal. by displacement of known element processes *(German)* 79−23203
boundary-integral equation method, stress anal. fracture mechs., computer calcs. 77−80111
Boussinesq-Papkovich displacement functions, generalisation to anisotropic medium 78−12570
Boussinesq-Papkovich stress functions for linear elasticity 79−68579
box beams subject to torsion, stress anal., strain energy 79−30245
Bridgeman anvils, optimal distrib. of stresses 79−23679
brittle coating analysis of orthotropic materials 79−27606
brittle material, optimal structural design 78−79207
brittle material, phase transform., plane stress anal. 77−86024
butadiene-styrene gum elastomers, compounds, viscoelastic props., stress relaxation meas. 77−7321
CANDU, stress anal. of fuel channel interaction with end shields 79−59161
cantilever beam, with unequal breadth/depth tapers, transverse vibrations 78−63373
cantilever curved beam, stress singularity anal. 79−23214
cantilever cylindrical shells, seismic design, appl. to nuclear steam system 78−58339
cantilever of material with deform. anisotropy max. stress determ. 77−65689
caustics equations for crack and dynamic plane elasticity problems 80−43669
ceramic, stress intensity factor estimates for a peripherally cracked spherical void and a hemispherical surface pit 79−29196
ceramics, toughened, stress corrosion charact., exam. 78−71295
chain of pores near free surface, stress conc. coeffs. *(Russian)* 77−75799
chemical apparatus, expt. strength anal. *(German)* 79−32427
chemically hardening material cast in elastic cylindrical mold, transient thermal stresses 80−7589
chemostress effect in ionic crysts. and metals 79−28193
circular bar of rate sensitive material, elastic-plastic tension-torsion 80−48602
circular cylinder under intermittently sudden heat generation, transient thermal stresses 77−3728
circular discontinuity in elastic plate dynamic stress conc. during passage of cylindrical wave 77−62191
circular hole, normal surface displacement, reflection holographic interferometry 78−57893
circular notches and loaded ends, interference effects 80−64365
circular plate, thin, with single eccentric circular holes, bending stresses 77−3721
circular plates, thermoviscoelastic anal. of a thermorheologically simple material 80−10161
circular ribbed cylindrical shell, of glass-like material, design external hydrostatic press. loading 77−84151
circular sliding contact on transversely isotropic spheres, stress field 79−18833
circumferentially notched tension specimens, stress distrib. and plastic strain 77−50919
cladding, thermal stress analysis *(Russian)* 77−59952
clamped heterogeneous circular cylinder, torsion problem, stresses and displacement 79−32278
clamped hyperbolic paraboloid shell, bending analysis 77−11129
coated fibre and cable unit structure optimisation 80−53466
coatings on plates, determ. of residual stresses using curvature gauging method *(Russian)* 79−98674
cohesive strength of constructional components with crack-type defects, stress intensity coeff. *(Russian)* 78−30234
coiled multilayer shell, stress anal. of elastic and elastoplastic work 80−79156
cold rolling of laminated composite sheet, finite element anal. 78−39797
colliding cylinders, resulting stress field for linearly elastic material *(Russian)* 80−79237
columns and plates, lower bounds to fund. freq. and buckling loads 79−10469
compact tension specimen, J-integral eval. *(Japanese)* 78−9607
complementary energy principle, finite elasticity solns., hybrid finite element anal. 79−32274
complex loading of materials, plastic deform. 80−99939
complex part stress anal., photoelasticity and finite element methods 78−71279
complex-stress criterion governing creep fracture 77−3783
composite, biaxial analogs of triaxial stresses 79−55345
composite, constrained zones at singular pts. of inclusion contours, method of caustics 77−51003
composite, laminate, crack normal to interface, impact response 80−14628
composite, steady creep bending stresses 78−71280
composite beam, multilayered, anisotropic, exam. of shear stress distrib. under transverse loading 79−18731
composite beams, exam. of contact problem, using boundary value problem soln. 78−42532
composite cylinder, mechanical loading, photoelastic stress anal. 78−26031

stress analysis continued
composite inhomogeneous anisotropic body, stress singularity near rib *(Russian)* 80−19243
composite laminates, stress field, theory based on Reissner's variational principle 78−67038
composite materials, stretching, stress distribs. 80−58931
composite plates with smooth or rough interfaces, stress singularities at vertices 77−7348
composite shell, orthotropic, cylindrical, with elastic core, stability 77−65701
composite wedge, stress state anal. near vertex *(Russian)* 80−19242
composites, dynamic anal., review and computer programmes 77−50946
composites, strength criteria, stress anal. *(Russian)* 80−1482
composites, stretching, zone of disturbed stress state calc. 80−39206
composites transient hygrothermal stresses, coupled diffusion of heat and moisture 80−33451
compound arbitrary anisotropic body, stress singularity, composites appl. *(Russian)* 80−33455
computer simulation of stress field, use in photoelasticity technique 79−41637
computer-aided analytic element analysis and similarities of tetrahedron 77−37749
concentration around plane slit-shaped cavities *(Russian)* 80−28417
concrete, endochronic model for nonlinear triaxial behaviour 78−51095
concrete, reactor shielding thermal stress cracking anal. *(German)* 80−5232
concrete, unreinforced pavement slabs, environmentally induced stresses, computer experiments 78−35435
concrete creep under nonuniform temp. distrib., linear viscoelastic analysis 77−62172
concrete slab, reinforcement optimisation by linear programming 77−89022
concrete splitting test, nonlinear numerical analysis 77−7339
concrete structs., steady-state stresses under sustained and cyclic temp. 77−83024
conference, computational methods in nonlinear problems in mechanics and engineering, Austin, Texas, USA (March 1979) 80−51945
conference, reliability and stress anal., San Francisco, CA, USA, 1975 80−8740
conical bar, transients propag. treated by Rayleigh's correction 79−81749
conical inclusions, singularity values for ranges of elastic constants 78−51071
conical shell, anisotropic, stress conc. new hole *(Ukrainian)* 78−83247
connector choice in finite element anal. 78−45
constained plates, Rayleigh-Ritz method using Lagrange multipliers 77−68502
constant strain triangle elements, efficient use 79−72798
constant-stress surfaces and stress conc. minimisation 77−869
contact friction stress problems, soln. using superposition principle 79−32394
contact of deformable bodies, influence of adhesive forces 77−70281
contact problem, circular cylindrical shell and open circular rod 78−38195
contact problem, non-axisymmetric cylindrical 77−19574
contact stress anal. involving fretting fatigue loadings, computer soln. 78−34096
contact stress minimisation by contour design 78−63396
contact stress of cylindrical insertion in plate *(French)* 79−72862
contact stress problems, counterformal, improved numerical method and program 79−41632
container wall, quasistatic stress distrib. due to internal press. and external temp. changing 77−84113
continuous stress and displacement fields, algorithm, finite element anal. 78−30178
continuum mechanics, introduction, book 79−30234
cooling bodies, thermal stresses and temps. determ. by finite elements 77−14881
corrugated tubes, semi-circular, slender ring shell theory *(Chinese)* 80−19234
cortical bone, anisotropic anal. of strain rosette information 79−16237
Cosserat composite elastic cylinders, thermal stresses 80−5937
Cosserat strip under tension, effect of couple-stresses on stress conc. around rigid circular inclusion 78−13898
couple stress effect on stress conc. near inhomogeneity, photoelasticity meas. 77−89076
couple stresses on infinite strip with periodic edge loads 77−72160
crack, elastoplastic range 78−67144
crack growth in concrete, computer simulation using Monte Carlo method 78−76764
crack in anisotropic elastic slab 77−50908
crack propagation in metals, model rel. to appl. of stress wave emission anal. 77−63837
cracked elastic surface layer bonded to half-space, fracture anal. 79−27586
cracks, model deduced from thermodynamics *(French)* 78−63386
creep, diffusive, particle inhibited, threshold stress 79−38922
creep analysis of rotating orthotropic disks 80−33476
creep fracture, Dugdale model for crack opening and growth 78−5699
creep fracture strength of precracked round bars under torsion, expt. and anal. investigation *(Japanese)* 77−59908
creep of spherical thick walled vessels under internal press. 78−30190
creeping struct. approaching rupture, upper and lower bounds on damage 79−50612
critical resolved shear stress, from misfitting particles 78−79613
crystal, residual stresses with gradient, determ. by X-ray diffr. 77−28944
crystal with island film, dislocations and stresses 79−87015
cubic boxes subjected to pressure, exptl. stress and strain anal. 78−59307
cubic crystal, ⟨111⟩ line force, anisotropic elasticity theory 79−55741
cubic crystal, application of integrated photoelasticity *(Russian)* 78−47465
cubic crystals, dislocation theory, soln. of eqns. *(German)* 78−38701
cubic crystals, elastic strip, moving stress sources, boundary-value problem soln. *(German)* 78−38702
cuboid surrounded by infinite elastic space, stress field due to initial strains 78−55565
cup wall ironing, stress calc. 80−29989
curved plate assemblies under biaxial loading, finite strip buckling anal. 78−18203

stress analysis continued
curved plates, subject to arbitrary temp. distrib., stresses and displacements 80−5938
curved sandwich beam, finite elements for linear static elastic anal. 77−62153
curvilinear aeolotropic solids, 3-D thermoelasticity 80−56
cyclic heating and loading, recovery-creep theory 77−19551
cyclic strain hysteresis loop, width and area determ. 78−26056
cyclic stress amplitude meas. by time-averaged photoelasticity 78−18261
cylinder, circular, thermal stress conc. determ. by integrated photoelasticity *(Russian)* 77−46925
cylinder, circular, transversely isotropic, concentrated loads, 3-D anisotropic elasticity theory 80−83734
cylinder, circular embedded in resisting medium, twisting, stress anal. 80−53637
cylinder, clamped heterogeneous, stresses and displacement anal. 80−14571
cylinder, composite circular, transient thermal stresses 78−79217
cylinder, dynamic thermal stresses due to heating *(Polish)* 78−18183
cylinder, elastoplastic, necking under uniaxial tension 78−63335
cylinder, finite, of anisotropic material, thermal stresses due to thermal crack 77−39233
cylinder, hollow, nonlinear viscoelastic material, dynamic pressure loading 80−38289
cylinder, hollow infinite, with temp. depend. thermal cond., thermal stress anal. 80−14575
cylinder, hollow thick-walled, having axial holes and varying section thickness, stress state anal. 80−100879
cylinder, hollow with internal circular crack, axially symmetric torsion determ., numerical results for boundary value anal. 80−64456
cylinder, infinite, solid, diametrically opposite conc. load deform. and stress 78−63287
cylinder, infinite circular elastic inhomogeneous, stressed state calc. body containing foreign components 77−89035
cylinder, orthotropic materals design for stress optimisation 78−63291
cylinder, subjected to heating and cooling, thermoelastoplastic soln. 79−72816
cylinder, transient thermal stresses due to arbitrary heat supply, 3-D anal. 79−46215
cylinder, transversely isotropic brittle elastic, stress and failure probability analysis for internal press. and thermal loading 77−50990
cylinder, transversely isotropic with circumferential edge crack, singular stresses 80−19284
cylinder elastic orthotropic brittle, under axisymmetric thermal and press. loading failure probability anal. 78−34078
cylinder of short length, thermal stresses *(Russian)* 77−75798
cylinder under uniform pressure, transition functions 80−10158
cylinder-to-cylinder shell models, expt. anal. comp. with theory 77−42748
cylinder-to-cylinder structure, analytical and exptl. stress anal. 78−59308
cylinders, approx. of buckling stresses 77−19553
cylinders, constrained, elastic stress analysis by special finite element method 80−106718
cylinders, deform. anal. in modified Bessel functions *(Russian)* 79−10478
cylinders, fibre-reinforced, singular stress layers 79−14268
cylinders and plates, dynamic deform. at high frequencies *(Russian)* 78−18223
cylindrical bar in tension, necking, num. anal. 79−90147
cylindrical cavity in elastic half-space, Rayleigh wave loading, stress spectral representation 80−64453
cylindrical curved surfaces, X-ray diffraction meas. of axial stress, geometrical effect anal. 78−63403
cylindrical punch, three-dimensional stress field, photoelastic studies 80−93272
cylindrical shell, design for minimum wt. 78−9560
cylindrical shell, dynamic response to concentrated impact load, radial displacement, stresses 78−67072
cylindrical shell, dynamic stress response to conc. periodic force 77−84172
cylindrical shell, loaded by concentrated force acting along the generator, load carrying ability 77−89044
cylindrical shell, pressurized, containing long part-through notch plane strain general yielding 78−18199
cylindrical shell, radial loading through plate brackets 77−89032
cylindrical shell, stress and strain in elastically distinct layer 77−872
cylindrical shell, stress concentration near inclined holes 80−33460
cylindrical shell, stress intensity factor soln. for crotch corner cracks of tee intersections 79−23279
cylindrical shell, three layer, with strap reinforcement under internal pressure, stress-strain state calc. 78−30184
cylindrical shell and belt, interaction contact stresses, elastic layer model 80−33543
cylindrical shell stresses by local heating, optimisation *(Russian)* 77−39225
cylindrical shell under axial tension, crack tip stress anal. using caustics 77−3775
cylindrical shell under torsion, stress conc. around elliptic hole 77−68422
cylindrical shell with circular cut out, uniform bending, strength and flexural rigidity 78−87282
cylindrical shell with small circular cutout subject to asymmetric bending, stress anal. 77−46920
cylindrical shell with strain depend. permeability, torsional response in radial and axial mag. fields 79−19754
cylindrical shell with wind load, membrane/bending forces ratio anal. *(German)* 77−31211
cylindrical shells, calc. of stresses *(German)* 80−33454
cylindrical shells, dynamic behaviour under transient inner pressures 79−23215
cylindrical shells, dynamic response to concentrated impulse loads 78−22259
cylindrical shells, finite element anal. of stress deform. states *(Russian)* 79−14256
cylindrical shells, stress conc. anal. by integral eqn. method 77−75806
cylindrical shells under internal pressure, approx. anal. 80−5943
cylindrical specimen with external crack reaching surface of annular stress concentrator, tension and bending 79−14349
cylindrical tank, stresses due to uneven circumferential settlement 79−68588
cylindrical testpieces, axial residual stresses determ. problem 78−7115

stress analysis continued
cylindrical tube, isotropic elastic, holographically meas. surface displacement, stress/strain extrapolation 80−64374
cylindrical tubes, compressible, wire-layer reinforced, inflation and extension 79−3922
cylindrical vessels, contact stress anal. 78−63395
cylindrically orthotropic rings subject to conc. loads., state of stress anal. 77−65688
damping, internal, in 2 and 3 dimens. continua 78−13970
defect geometry, stress intensity factors, photoelastic meas. correlation *(German)* 80−53727
defects in continuum 79−69104
deflection of cables, cylindrical suspended roofs with complex loading, incremental algorithm 78−9558
deformable solid, stress calc., finite element basis *(German)* 79−50602
deformation, stress distribution of frictional bonds, computer model *(Hungarian)* 79−14275
deformation condition, modelling *(Russian)* 79−27515
deformation procedures, stress, strain calcs., approximation method *(German)* 79−76978
deformed boundary determ. by method of caustics 77−89077
dental implants, stress anal; effect of elastic parameters and geometry 80−30930
dental implants, stress anal., effect of root-length and pseudo periodontal ligament incorporation 80−30931
design fatigue analysis, use of fracture mechanics, exam. 78−90794
design optimization of structures, discrete models for continuous-type problems 77−89034
dielectric, elastic, containing 2 rigid spherical conductors, electrostrictive stress conc. 77−23883
dielectric bodies stress determ. using EM waves 80−38370
dielectric const. depend. on strain tensor, stress determ. by EM waves *(Ukrainian)* 79−32254
dielectric elastic half space with point charge, stress and polarisation anal. 77−83776
dielectric parts, stress patterns and deformation charact., computer anal. 80−17787
dielectrics, elastic, stress tensor, polarisation vector, electric tensor 80−55018
diffusion coating of plate, residual stresses, with allowance for phase transform. *(Russian)* 78−11357
dilute suspension of spheres in power model fluid, apparent stress deform. behaviour 78−42578
direct and variational principles rel. to approx. techniques 80−28420
disc, constant stress, quasi-isotropic laminate, longitudinal and transverse stresses *(Italian)* 79−41573
disc, nonhomogeneous, accelerating, with varying thickness and density with radial loading, yielding 78−63322
disc, rigid, circular, in infinite plate, tensile, compressive stress 79−37164
disc test measurement of combined mode fracture toughness stress analysis 78−92432
disc with regular system of holes, stress concentration, computer computation 77−3723
disc with variable thickness, cross-section warping and corres. stress quantities *(German)* 78−18206
discoidal agglomerate, stress pattern, distributed loading effect during diametral compression test 80−60934
discontinuous boundary traction, connection between finite element and integral equation methods *(French)* 77−87649
discs, impact stresses, photoelastic investigation 79−37182
displacement anal., three-dimensional from image plane hologram 79−17385
displacement stress reln. evaluation *(German)* 79−12603
displacements, strain and stress error nodal lines in finite elements 79−2606
dissipative media, nonlinear, one-dimensional waves, theory 77−58592
dolomite, ramp wave compression studies 77−78161
double cantilever beam, dynamic stress intensity factors computation and crack arrest stress intensity factors 78−34088
double torsion specimen, stress analysis 78−9567
drawing, of continuous round ultrasonically perturbed profiles, stressed states at centre of deformation *(Russian)* 80−59557
duct with initial shape irregularities, stresses calc. 79−32273
ductile wire-through-glass seal, stress anal. 77−84161
duralumin, elastic-plastic stress anal. by photoelasto-plastic method and X-ray method *(Japanese)* 78−13978
dynamic props. of impulsive-type loading 79−70106
dynamic stress-optical coeffs. of transparent media, simple interferometric instrum. 80−86394
dynamic thermoelasticity of body with crack, two- and three-dimensional *(Russian)* 77−68400
Earth, Precambrian global stress field from dykes intrusion preferred orientation 78−88829
Earth crust, aseismic geodynamics in Urals rel. to geomag. secular var. anomalies 80−26447
Earth crust, effect of craton on distrib. of seismicity and stress in N.America 80−98248
Earth crust, energy changes due to mining 77−64236
Earth crust, foreland folding model 78−81141
Earth crust, plume generated radial stress fields rel. to Hawaiian rifts and recent Icelandic volcanism 80−90051
Earth crust, regional stresses determ. from seismic b-value space-time scanning *(Chinese)* 79−12072
Earth crust, shear deform. zones along major transform faults and subducting slabs 78−73330
Earth crust, stress field rel. to dilatancy-fluid diffusion theory and aftershock sequences 80−85604
Earth crust, stress meas. in Michigan Basin 79−39681
Earth crust, stress state and fault patterns assoc. with continental rifts, analytical model 79−79805
Earth crust convection-generated stress concentration and Tangshan earthquake seismogenic models 79−92507
Earth mantle, convection and subcrustal stresses under Australia 80−72484
Earth mantle, stresses due to phase changes in subduction zones 77−73718
Earth mantle peridotites, stress estimates from structural studies 78−69330
Earth upper mantle, nonlinear stress propag. 79−16422
stress analysis continued
Earth uppermost mantle, lateral var. of differential stress across SW.Japan island arc 80−98275
earthquake modelled by centrifuge, seismic signal and stress change 78−81429
edge cracked sheets with mixed boundary conditions, stress intensity factors, displacements, stresses 80−64477
edge problem of fracture mechanics, plasticity theory inadequacy 79−3978
edge-dislocation displacements in elastic strip, Fourier transform method 79−21553
edge-dislocation lying in plate, stress field 79−23603
elastic, with aid of computer, axisymmetric pressure vessels with structural discontinuities *(Japanese)* 80−38265
elastic anisotropic media, stress anal. by integral eqn. method 77−72176
elastic body, slip plane intersection with stress free boundary, inhomogeneous yielding 78−5667
elastic body containing fine inclusion system in single plane *(Russian)* 78−34017
elastic circular cone, thermal stresses 78−90715
elastic circular cylinder with prolate spheroidal cavity under tension, stress distribs. 80−19236
elastic contact problem, half-space indented by truncated conical stamp 79−98672
elastic contact problem of semi-infinite strip and half plane, plane soln. 77−46924
elastic contact problem with friction, solution using nodal parameters *(French)* 78−63401
elastic continuum, two-diemsional, side effects of discrete methods 79−58
elastic continuum penetrated by elastic tube, biaxial stress field, appl. to concrete pressure vessel 77−46921
elastic crack mechanics influence function method computer program 77−75859
elastic dissimilar semiinfinite strips, different widths, plane symmetric contact problem 78−55615
elastic elbow, in-plane bending behaviour, finite element anal., pipeline design 78−18166
elastic eqns. of uniform systems, general integral solns., appl. *(Russian)* 79−14272
elastic field outside ellipsoidal inclusion 78−55566
elastic fracture mechanics, boundary integral eqn. anal. 80−14622
elastic fracture mechanics, of bondline cracking and crack branching, power type singularities analysis, using finite elements 77−80106
elastic half space, rectangular cylinder penetration, contact problem, stress fields 80−64490
elastic half space, ring shaped punch contact stress determ. 80−38356
elastic half space containing embedded rigid block 80−23890
elastic half-space, coupled thermoelastic problems 78−59300
elastic half-space, stress distrib., nonlocal effects 77−80070
elastic half-space containing axially loaded rigid cylindrical rod 80−1423
elastic half-space with cavity, SH wave excitation, dynamic stress conc. 77−62194
elastic half-space with spherical inclusion, eigenstresses 77−11131
elastic inclusions in anisotropic solids, generalised plane problems 77−17823
elastic infinite thick plate, axially symmetric loading, numerical method *(Japanese)* 78−9568
elastic inhomogeneous medium, high freq. Reissner-Sogocci problem, exam. of stress singularity 78−83239
elastic isotropic micropolar continuum, stress and couple stress fields prod. by circular dislocations 79−97209
elastic layer containing penny shaped crack, bonded to dissimilar half-spaces 77−58603
elastic liner in cylindrical tunnel subjected to SH waves, dynamic stresses 80−79201
elastic longitudinal waves, diffr. at elastic circular inclusions (fibres) *(Russian)* 78−63368
elastic materials, nonlinear, stress tensor, Kauderer's postulates *(German)* 80−64364
elastic plane with const. tangential stress at free boundary, expt. stress anal. of subdomains 80−99978
elastic plate, infinite, concentrated load, stress. anal., numerical method *(Japanese)* 78−22273
elastic plate with unsymmetrical cruciform crack, stress distrib. 77−31256
elastic porous media, acoustic phenomena 78−25997
elastic rings under essentially nonaxisymmetric load, large deform. 79−98637
elastic stress analysis of an anisotropic compound rotating disc under thermal loading 78−67036
elastic stress-deformation relns. inversion, associated inequalities 77−50904
elastic structures, computer automated synthesis for minimum struct. weight 78−34015
elastic thin strip, transversally loaded, elastic waves propagation solution, by physical discretisation 77−50943
elastic three-dimensional bodies with rigid inclusion or periodically spaced holes, macroscopic behaviour *(French)* 78−87260
elastic transient waves in medium with axisymmetric cavities, stress anal. *(Ukrainian)* 80−33503
elastic viscoplastic disk, uniformly rotating, axially symmetric stress state *(Russian)* 79−50611
elastic waves, scattering by elastic sphere embedded in isotropic elastic medium 80−96214
elastic wedge or notch loaded by localised internal source 77−42741
elastic-perfectly plastic solid, stress field via min. principle 77−878
elastic-plastic body, min. principles and strain uniqueness, stress fields 77−3734
elastic-plastic body, strain and stress fields, min. principles 77−3735
elastic-plastic deformation stress-strain anal., parametric linear programming method 79−37194
elastic-plastic fracture mechanics for structure design 77−14961
elastic-plastic materials, K_{Ic}-value determination, fracture mechanics method 80−45376
elastic-plastic plane stress, direct soln. vs. quadratic programming 77−42740
elastic-plastic solids, min. principles for stress and strain fields 77−879
elastic-viscoplastic boundary value problem, stress anal. variational method 77−35051

stress analysis continued
elastic-viscoplastic materials, stress concentrations determ. by integral eqn. methods *(French)* 77−72194
elastic-viscoplastic structures, accommodation to periodic loading, stress and strain fields *(French)* 77−46928
elastically nonlinear medium, field of dislocation shifts, integral eqn. *(Russian)* 78−47374
elasticity, fundamental theory, and applications, book 80−22158
elasticity equations for cubic cavities in elastic space *(Russian)* 80−1430
elasto-plastic buckling of curved webs, Gauss-Seidel iterative procedure 78−34043
elasto-plastic problems, error anal. 78−1578
elastodynamic stress states rel. to photoviscoelastic model *(Russian)* 78−75080
elastodynamics, vel. pots., stress functions 78−93534
elastoplastic array weakened by biperiodic system of holes *(Russian)* 79−46228
elastoplastic concentration factors, determination by deformation theory of plasticity 77−31225
elastoplastic kinematically hardened structures, accommodation *(French)* 77−27475
elastoplastic medium with cylindrical cavity, stress distrib., photoelastic investigations, successive elastic solns. *(Polish)* 80−64391
elastoplastic shell constitutive eqns. 78−18188
elastoplastic strip or half-plane under moving load, residual stresses and plastic zones 80−53645
elastoplastic torsion stress distribs. 77−50922
elementary elasticity 79−81721
ellipsoidal inclusion elastic field, appl. to martensite formation 77−48436
ellipsoidal inclusion in anisotropic material, stress and strain concs. factors 77−50900
ellipsoidal inclusions in anisotropic material, numerical evaluation of stresses and strains 77−68410
elliptic hole, under uniform tangential force in homogeneous isotropic compressible medium, in second order elasticity 77−31216
elliptic infinite bar, impulsive loads, three dimens. elastic stress-strain anal. 78−87259
elliptic plate, heated, deflection under uniform load 77−35040
embedded foundations, soil-structure interaction problem, spring method 78−79216
energy methods, book 78−1571
engineering design, numerical, vital role of expt. stress anal. 79−32418
epoxy models, thermoelastic strains and stresses using strain gauges *(Polish)* 79−64609
epoxy resin, exam. of stress conc. around conical cutouts, using photoelastic method 79−41639
epoxy resin reinforced by multilayer systems, exam. of stress states, using photoelastic method 79−41638
epoxy resins, strain anal. by fluoresc. meas. *(French)* 79−47846
equilibrium method using finite element displacement models 77−23875
Eulerian computation technique for domains with moving boundaries 77−53779
experimental, conf., Bradford, England (Sept. 1978) 80−17718
experimental numerical hybrid technique 79−32419
experimental stress anal., methods and recent developments *(French)* 79−59953
expt., conf., Munich, Germany (Sept. 1978) 79−34256
extensional stress pulses, energy transmission from bar to helix of small pitch 77−19564
extrapolation of strain and stress from holographically measured surface displacement 79−32410
Eyring creep model, effective stress 79−90722
F-E approximation validity for polygonal flanged plate *(German)* 79−86344
fast burst reactor, WSMR, thermal shock stress anal. for enlarged irradiation cavity 78−33242
fastener details, stress analysis hybrid finite element 77−54879
fastener hole, cold worked, residual strain 79−29088
fatigue crack, propagation rate, mechanical property effects of materials 78−90776
fatigue crack growth, Paris eqn., C and m parameters 78−18243
fatigue cracks, dislocation model, threshold stress intensity 78−18244
fatigue fracture analysis of rotating disks under torque 80−43668
fatigue life, prediction of Miner damage distribution by Bayesian method *(Japanese)* 79−59942
fatigue limits and curves, sloping branches, correlation relationships *(Russian)* 79−77018
fatigue strength, notched plates 78−9601
femoral stress and strain calc., finite element method *(German)* 79−2089
femur, human, with implanted Charnley prosthesis, stress anal. 78−20314
femur with proximal prosthesis, 3-dimens. anisotropic stress anal. and failure prediction 78−40424
Fermilab Doubler warm Fe supercond. dipole, stress anal. 80−58012
fibre reinforced composite, nonlinearly elastic in transverse direction, programmed winding of articles 79−86339
fibre reinforced composite, plane stress state anal. in macroscopic model *(Russian)* 77−80069
fibre reinforced composite annular discs surrounding circular hole in flat plate 77−46912
fibre reinforced composite with viscous matrix, random stresses in components, laws of distrib. 79−23226
fibre reinforced composites, bond stresses of isotropic body with elastic inclusions 78−30180
fibre reinforced composites calculation of stress distrib. and X-ray elastic consts. *(German)* 78−52883
fibre reinforced cylindrical shells, stress strain state and stability 80−14598
fibre reinforced plastics, exam. of strength criteria 78−75105
fibre reinforced plastics, stress distributions along short fibre 80−60913
fibrous composites, dynamically induced interfacial stresses 79−18727
fibrous heat treated composites, thermal stress anal. 77−46943
field emitter, field-induced stresses, numerical analysis 78−35274
film, stability and rupture using perturbation analysis 78−79911
film edge induced stress in substrates 79−94492
finite antiplane shear field near crack tip in elastic solid 78−18245
finite elastic cylinders, Ritz solns. for axisymm. temp. and stress fields 78−38190
finite element anal., three dimensional computer code 77−49586
stress analysis continued
finite element method, discretisation of stress fields 77−50879
finite element program 79−64522
finite element thermal loading calcs., automatic mesh generation 77−3740
finite elements method, iterative algorithm for continuous stress field anal. 77−72179
finite plate with circular hole, summary of SIF design graphs for cracks 79−23278
first wall model, mechanical anal. using state variable approach 80−32452
fission reactor, FEM anal. of pellet-clad bonding 80−42765
fission reactor grid plenum assembly stress anal. 77−54288
flat elliptic paraboloid shells subjected to uniformly distrib. horizontal load at edges *(German)* 79−27518
flat ring subject to internal pressure, elastic-plastic anal. 78−13913
flat shells, bending stresses, parametric study *(German)* 79−86365
flexed plate, slope and curvature contours meas. using interferometer 77−87810
flexure of composite laminates using thick finite strip method 77−42739
floating ice plate, time depend. deflections, linear viscoelasticity theory 77−17107
flow localisation in tensile samples, containing geometric and metallurgical defects 78−79233
fluid-structure coupling problem soln. using boundary-integral eqn. method 77−54920
fracture, stress intensity factor criterion for combined loading *(Chinese)* 79−32372
fracture *(Chinese)* 79−32371
fracture mirrors, fracture mechanics, stress intensity factor calcs. 79−79082
fracture problems, conic-section simulation anal. using finite elements 77−3773
fracture zone analysis of fission reactor elastoplastic materials *(Spanish)* 79−66139
frame corner plane stress distrib. and local buckling *(German)* 78−13940
Frank disclinations in isotropic elastic micropolar continuum, stress and couple-stress fields 77−72245
free edge stress fields, in composite laminates 78−67039
fusion reactor, compact toroidal ignition experiment, support struct. anal. by numerical code 80−106167
fusion reactor, PDX, toroidal field coil and frame struct., anal., finite element anal. 80−106165
fusion reactor, PDX Tokamak, struct. anal. by finite element method 80−106166
fusion reactor, SLPX TF coil, stress anal. using COSMIC-NASTRAN 80−106168
fusion reactor, TEXT toroidal field coil stress anal. 78−50381
fusion reactor, three-dimens. solid finite element anal. for simulating composite windings 78−55003
fusion reactor, toroidal field coil in-plane bending stress, struct. support design 80−106164
fusion reactor anisotropic B_T-coil two-dimens. finite element anal. of laminate sliding 78−50382
fusion reactor B_T-coil stress anal., constraint finite element anal. for contact problem 78−55004
fusion reactor blanket, thermal stresses and cyclic creep-fatigue 78−62655
fusion reactor blanket first wall time-depend. thermal stress model 78−787
fusion reactor cavity wall loads and stresses, scaling 78−58446
fusion reactor first wall/blanket system, thermal-hydraulics and fatigue life modelling 78−58453
fusion reactor first-wall structural mats., stress and lifetime limitations 80−32447
fusion reactor materials, stress distrib. from He ion irrad., vol. expansion, calcs. 77−35599
fusion reactor solenoid, orthotropic, finite element stress anal. 78−55010
fusion reactor superconductor strain and mag. system design parameters, closed-form anal. 78−50377
fusion reactor toroidal field coil finite element stress anal. 80−91256
fusion reactor toroidal field coil stress anal., cost effective procedures for TFTR 78−50379
fusion reactor toroidal field coils, stress anal. by finite element method 80−13926
fusion reactor vacuum vessel, magnetic stress induced by plasma motion, 3-dimens. anal. 78−66370
fusion reactor vacuum vessel, stress anal. 78−66371
general shell finite elements development 78−87274
generalised stress intensity factors, numerical determ. method, crack problem appl. 79−72851
generalised stress intensity factors, numerical eval. using Lobatto-Jacobi numerical integration rule 79−3921
genesis problem, approx. soln. of initial states and properties 77−14927
geological structures, structural fracture and stress fields, review *(Chinese)* 79−53343
girder webs, epoxy resin models, flange thickness, stress effects, photoelasticity study 79−41640
glass, fracture mechanics studies, specimen *(French)* 77−73401
glass, ion-exchanged, anomalous stress profile, photoelastic meas. 78−90803
glass, tempered, stress analysis, oblique incidence light scattering, birefringence *(Polish)* 80−71374
glass, tempered plate, stress state model and heat transfer rate determ. 78−60684
glass fibre composite, shell, carrying capacity, heating effects 77−4865
glass fibre reinforced, thin walled cylinder, tangential stress charact. during twisting 78−13911
glass fibre reinforced composite, semifinished product nonlinearity model, force anal. of winding 78−63325
glass fibre reinforced epoxy, exam. of interlaminar shear stress distribution 79−43308
glass fibre reinforced plastic, dynamic stress conc. around defects, discrete model 80−30024
glass fibre reinforced plastic, laminate, stress anal. finite element modelling 79−59924
glass fibre reinforced plastic, optimal reinforcement for cylindrical shell subject to temp. field. 77−84148
glass fibre reinforced plastic dome, anal. and expt. stress anal. 78−72813

stress analysis continued
glass fibre reinforced plastic pipe, thin walled, finned, stress anal. and load bearing capacity 80−81100
glass fibre tube, two layer, stressed state 79−64513
glass fibres, stresses induced by draw force 79−47737
glass narrow sandwich seal, correction factor for thermal expansion mismatch 78−75110
glass plate, stress analysis of large deflection by finite element method 77−7307
glass reinforced plastic laminates, stress, strain anisotropy, tensor calculus *(Polish)* 77−12678
glass reinforced plastic shell, cylindrical laminated mech. behaviour 77−58567
glass segment, resting on elastic ring, structural strength 80−14630
glass toughened, stress corrosion charact., exam. 78−71295
glass-metal seal, finite element anal. of stresses, photoelastic meas. 79−29197
glued joint, axially symmetric, stress determ. for torque loading *(Polish)* 78−79287
grain boundary sliding, stresses and deform. 78−68739
granite, weathered, bearing capacity determined by graphical soln. of pole trail method *(Japanese)* 78−56706
granular elastic layer underlain by smooth rigid base, surface load 77−14905
granular half-space axisymmetric contact problem, stress and normal displacement 77−57196
granular layer, axisymmetric contact problem, stress singularity under stamp 77−57195
granular materials, intergrain slip in flowable zone, stress distrib., internal friction 79−99261
graphite, failure in lab. tests, fracture mech. approach, finite element stress anal. 77−4149
graphite fibre reinforced epoxy, epoxy matrix, effect of material variability on predicted environmental behaviour, numerical anal. 78−90733
graphite materials, isotropic, resist. to deformation and fracture under complex stress conditions 80−16479
graphite reflectors in PBR with OTTO fueling, neutron effects, stress anal., cooling measures *(German)* 77−34368
graphite reinforced epoxy laminate, edge effects 78−19803
graphite structures in PBR, neutron radiation damage, mech. props., stress fields *(German)* 77−34387
graphite-epoxy laminates, AS/3501-5, compressive fracture strength 79−43396
Griffith cracks, stresses due to rigid inclusions 79−32373
Griffith cracks in infinite elastic strip, stress distrib. 79−40370
grillage with free edge, optimal beam layout 78−63332
half space, elastic field due to ellipsoidal inclusions with uniform dilational eigenstrains 80−58913
half-planes, distributed load end values by optical caustics technique 79−18851
half-space, axisymmetric body force problems 77−42738
harmonic extensions of body under variable traction and no body force 80−8792
harmonic holes for nonconstant stress fields, deloids and cardeloids 80−64373
heart left ventricle, computerised finite element procedure 77−86518
intact heart stress and strain three dimensional finite element anal. 77−66821
hemitropic micropolar thermoelastic continuum, static and dynamic problems 78−22293
heterogeneous materials, linear analysis 78−5664
heteromodular materials, stress strain correls. 80−87716
high temperature plant design methods, reference stresses and bounding theorems 80−58937
high-temp. behaviour of inelastic metals 77−4830
hip, total prosthesis, 3D stress anal. of femoral stem 80−98176
hip bone stress analysis using finite element model 78−44518
hip prostheses femoral component biomechanics, bone cement stress 80−56285
hip prosthesis, analytical approaches to femoral stem stresses 77−44849
holed plates, stress and deformation, finite quadrilateral elements technique *(Rumanian)* 79−18707
hollow cylinder with heat flux on inside surface, nonstationary thermal stresses 77−7308
hollow shaft with longitudinal slots, torsional stress state 78−30183
hollow sphere with stamps on external surface, creep stresses 77−84152
hollow thick-walled cylinders, stress-deformation, limiting state anal. *(Russian)* 79−27538
Holmalite-100, dynamic photoelastic and dynamic finite-element analyses of dynamic-tear-test specimens 79−55348
holographic interferometry and speckle photography combined technique 78−70095
homogeneous elastic matrix containing short fibre, stress state *(Russian)* 77−68412
homogeneous isotropic compressible elastic media, circular concentric ring, second-order torsion problem 79−32276
hoop stresses at tee intersections of cylindrical shells, approx. prediction 80−5942
HTGR fuel and graphite structure stress analysis methods and programs *(Japanese)* 78−74434
human femur, three-dimensional finite element analysis 78−7379
human left ventricular wall finite element stress analysis 77−64079
hybrid composite material beams, exam. of shear stress correction factors 78−46899
hydrostatic pressure loaded membrane of revolution 80−64363
hyperboloid, elastic parted, mixed axisymmetrical problem *(Russian)* 78−36831
hypercircle method in the problem of a case-bonded cylinder in the gravity field 78−45484
hyperelastic isotropic behaviour laws for large deform. *(French)* 78−77715
hypoelastic materials undergoing uniform rectilinear shear, rotation and stress rate anal. 79−98604
impact, high velocity, three dimens. finite element anal. 77−65674
impact test, finite element analysis 78−68806
impulse loaded plates, exam. of stress distribution, using Mach-Zehnder interferometer *(German)* 79−41643
incompatible quadrilateral basis functions 78−41146
incompressible flow, elasticity techniques, stream function-stress function approach 79−1146
indentation of elastic half-space by rigid rectangular punch 78−18167

stress analysis continued
indeterminate beams, variable cross section, stress anal. using repeated integration 79−64510
inelastic material stress-strain stiffness matrix calc. 78−34032
infinite cylindrical shell containing filler, reinforced by ring, influence of arbitrary load 78−42533
infinite elastic body, with two intersecting cylindrical holes, stress conc. factors 77−89033
infinite elastic solic containing spherical cavities, stress distrib. 79−98616
infinite elastic solid with spherical inclusions, linear elasticity eqns., stresses, displacements 78−65773
infinite elastic strip, circular inclusion undergoing dimensional changes, stress components 80−48590
infinite linearly-elastic circular cylinder, wrinkling induced by surface stress 78−26070
infinite medium, thermal stress problem for ribbon-like inclusion 77−58554
infinite medium with cavities, response to impact load 77−50945
infinite plate, axisymmetric interaction with elastic halfspace, influence of Mindlin force 78−38193
infinite plate, with cut along arc of circle, limiting equilibrium state 77−84195
infinite plate containing plane curved polygonal defects and cusps, stress anal. *(Chinese)* 79−72793
infinite plate with doubly periodic hole array, transverse bending, Poisson-Kirchhoff theory 80−58920
infinite plate with two holes, stress concentration reduction by interference fits 79−37158
infinite strip, with elliptical hole, definition of stress *(Russian)* 78−55562
infinite wedge, first boundary value problem *(French)* 77−35041
inhomogeneous materials, elastic deform. under multiaxial stress, analytical relations 80−44247
inhomogeneous strips, elastic equilibrium, stress *(Russian)* 80−19244
inhomogeneous viscoelastic Voigt-Kelvin rod, stress propag. and harmonic vibrs. 79−94543
initial stress problems, stress function appl. 79−18722
integrated load increment method for finite elasto-plastic stress analysis 80−92072
intensity factor for mode I loaded cracks, exam. using shadow spot method *(German)* 79−41642
intensity factor K_{III}, photoelastic determ. method *(Chinese)* 79−64602
intensity factors calc. by finite element methods, 3-D 77−27491
interfacial stresses in viscoelastic adhesive-layers due to moisture sorption 79−90145
interference fits in cylinders with concentric and eccentric holes, stress anal. 77−50916
internal, macrostress in deposits, spontaneous, calcs. 77−36710
internal struct. tensor 78−79227
isoparametric elements, stiffness matrix, stress intensity factors *(Chinese)* 79−92943
isoparametric linear bending element and one-point integration 79−3919
isoparametric nine-noded finite elements, accuracy 78−26039
isoparametric shell element moment balance 77−14903
isoparametric shell elements study *(Japanese)* 78−34016
isotropic body containing rigid plate-like inclusions, antiplane deform. *(Russian)* 77−27476
isotropic body with sharp elastic inclusion, longitudinal shear *(Ukrainian)* 77−68401
isotropic elastic body, displacement tensor representation by Piola stress tensor *(Russian)* 77−42743
isotropic material, modified stress deviator for plastic compressibility *(German)* 78−13914
isotropic plate, stresses under concentrated forces 80−48572
isotropic semiinfinite plate heated by moving point source of heat, temperature stresses 80−43628
isotropic thick plates, review of problems of plates with geometric, and load discontinuities 79−46218
isotropic thin shells with circular hole, stress state, numerical investigation 80−48586
JET Tokamak inner poloidal field coil design 79−31209
JET vacuum vessel, mechanical reliability in disruptive instability 80−18643
joints, double adhesive bonded, loaded in shear tension *(French)* 80−23968
joints, stress concentrations, Modeltech method, full scale models and photoelastic coatings *(Polish)* 80−64369
justification of the von Karman equations *(French)* 79−49047
Kirchhoff plates and shells, conforming approx. 79−90129
knee osteo-arthritis, evolution of max. stress 77−48825
Lamb's problem, generalisation to class of inhomogeneous elastic half-spaces 78−32023
Lamb's problem, line load suddenly applied on micropolar elastic half-space 80−12907
laminate, calculation of stress distrib. and X-ray elastic consts. *(German)* 78−52883
laminate, multilayer, stress-strain state 78−18177
laminate, simple shear charact., comparison of test methods 78−44283
laminate, stress anal. finite element modelling 79−59924
laminated anisotropic plates, transverse shear deformation effect 80−19237
laminated anisotropic shells, thermal stresses *(Ukrainian)* 77−68399
laminated anisotropic shells, transverse shear stiffness calc. 78−42526
laminated composite shells, mixed isoparametric finite element models 77−78979
laminated cylindrical shell, coupling effect under internal press. *(Japanese)* 80−55449
laminated plates subjected to transverse dynamic loading, stress anal. for transient response 77−31245
laminates, angle ply, 3D finite difference soln. of free edge effect 80−79152
laminates, cross-ply, edge effects, traction-free-edge condition satisfaction 80−79151
laminates, damage zone failure analysis 80−85059
laminates, interlaminar stresses 79−10472
laminates, multilayer, thick, hybrid-stress finite element formulation 80−92043
laminates, piecewise continuous eigenfunction solns. 78−18178
laminates, symmetric, new results on edge effects 77−46971

stress analysis continued
large strain applications of modified const. strain finite elements 79−2632
laser speckle interferometry for nondestructive evaluation 78−60976
lateral stresses in beams, existence of lateral tensile and compressive stresses 79−98638
lateral tibial plateau, axisymm. finite element anal. 78−69127
lattice strain distrib. obtained by X-rays, linear and nonlinear *(German)* 78−91200
layered beams, interlaminar thermoelastic stresses 80−1432
layered composite containing a crack, impact response and dynamic intensity factors 77−50991
layered cylindrical shell, with transversely isotropic core stability in axial compression 77−3722
layered shells, stress states, asymptotic approach *(Italian)* 79−10461
layered system, thermal stresses and displacements 80−23891
leg-foot, complex, in conditions of lesion and reconstruction, holography 80−67142
limit analysis, complete static solns., appl. to vertical cut *(French)* 79−18702
limit state stability, multicause interaction relationships *(German)* 79−23235
limiting diagrams, construction considering defectiveness of material 79−81730
limiting lines theorem in perfectly plastic material 77−62159
linear Cauchy and Piola-Kirchhoff constitutive theories for stress in solids 79−37173
linear elastic fracture mechanics, stress singularities interfaces 78−34079
linear elastic half-space, frictional unloading problem, variational soln. for stress analysis 78−59350
linear elastic solid with mass addition, stresses and displacement eqns. 77−55955
linear elastostatics, uniqueness theorems for displacement fields with locally finite energy 79−97201
linear reinforced composite material with anisotropic structural components *(Russian)* 79−30250
lithosphere, isostatic disturbances rel. to elastic stresses 77−81842
lithospheric slab at Kurile-northern Honshu arcs junction, stress from mantle earthquakes mechanism 77−81805
LMFBR claddings with axial fins, stress anal. including creep effects 77−88224
LMFBR modular steam generator tube plates, stress anal. 79−71883
load carrying flat bar with hole, Poisson ratio influence on stress distrib. *(Polish)* 77−9032
load distribution under contact area 77−84146
load increment analysis, elastic-plastic analysis of anisotropic materials by variable stiffness finite element method 77−7319
loaded construction, randomly loaded, crossing probabilities, numerical anal. *(German)* 80−96186
loaded projection, photoelastic anal. of stresses 78−87275
Love waves, propagation in elastic iostropic incompressible medium 80−23929
machine parts, safety factor determ. during cyclic loading taking account of initial stresses 80−43675
magnetic tape, coil, determ. of stressed-strained state 79−14283
magneto-elasticity, stresses in plate with holes 77−866
martensite, microstresses associated with tempering 80−3111
material elastic anisotropy, analysis, by acoustic ellipsometry 79−47864
material fatigue under random complex state of stress, hybrid simulation 77−42786
materials and structures testing 78−3298
matrix analysis of composed bar of open cross section 80−83736
Maxwells stress function representation, completeness 80−36851
mean stress calc., equivalence of stress and energy 78−1565
mechanical test methods and strength of structures, review 79−43507
mechanics of materials, book 77−68425
medullary implants with porous coating, stress distrib. 78−69256
medullary shaft implant, finite element anal. 77−44850
membrane, slack circular, under point load 77−46911
membrane shells written in cylindrical coordinates 77−31208
mesh analysis processes, convergence *(German)* 78−87257
metal, BCC, polycrystalline aggregate, prediction of plastic props., deformation by ⟨111⟩ pencil glide 80−11731
metal, porous, stresses in deform. region during cold rolling 78−11241
metal, secondary creep rate, comparison of sinh and effective stress creep 79−52321
metal, stress concentration sensitivity, scale factor effect on fatigue strength 79−39064
metal constructions, stress analysis and longevity curve, using computer simulated random loads 79−43545
metal creep, deform. struct. modeling, compatibility conditions *(Russian)* 78−13924
metal extrusion process, stress and deform. distribs., elastic-plastic anal. 77−48364
metal fatigue analysis, inversion of strain-life and strain-stress anal. 80−19289
metal specimen, ultrasonic technique for stress anal. 78−64790
metal structures, creep, stress and stability anal. rules and methods 79−32302
metal-to-metal bonds, stress analysis in hostile environments 79−20338
metal/glass fibre reinforced plastic vessel, with damaged reinforcing layer, carrying capacity 78−39876
metallic composite materials, stress redistrib. upon breakage of brittle fibres 78−48527
metallic materials, fatigue life distrib. theoretical obs. near fatigue limit 80−59569
metallic nuclear fuel rod heat conduction and thermal stress anal. 77−7295
metals, BCC, under elastic stress, Snoek peak height determ. 80−65153
metals, engineering, multi-axial creep characts. 80−64398
metals, high temp. stress anal. by finite element method 80−96203
metals, residual stress and deformation, due to quenching, elastic-plastic anal. *(Japanese)* 78−83268
micropolar continua, generalisation of Saint-Venant's principle 77−68395
micropolar continuum, isotropic, elastic fields of dislocations and disclinations 77−68971
micropolar elastic half space with suddenly applied line load, Lamb's problem 79−98614
micropolar elastic half-space, body-force and couple effects 77−50896
micropolar elastic thick-walled tube under forces and moments 77−865
micropolar elasticity, stress concentration around elliptic hole 78−5658
stress analysis continued
micropolar plate bending, stress concentration around hole 77−3731
micropolar semispace, effect of heated boundary on normal stress distrib. 80−1433
microscopic for sintered carbide tips 78−5663
microstructure with finite deformations, reciprocity theorem, stored energy function *(Italian)* 78−81836
Mindlin plate, transient and pseudotransient anal. 80−36850
mixed boundary-value problems, orthogonal polynomial solns. 78−54193
mode I crack, non-steady growth 78−18241
modified crack closure integral, finite element calc. of stress intensity factors 78−18235
Mohr-Coulomb material, axisymmetric compression around circular hole, stress and strain fields 79−57914
Moine thrust zone, differential stress determ. from deformation-induced microstructs. 80−85652
moire fringe and laser speckles, optical stress anal. 80−10217
moire stress analysis interferometer with microprocessor 80−31858
Moon, tidal stress functions calc. rel. to deep moonquakes triggering 79−66938
mountain massif, pre-face zone, stressed state, finite difference method *(Ukrainian)* 80−74735
multicircuit shells of revolution, computer anal. by field method 77−3729
multicomponent-medium, macroscopic stresses *(Polish)* 79−63040
multiconnected shell, closure conditions for surface deformations *(French)* 77−23887
multilayer cylinder, exam. of stresses, considering layer contact characts. 78−63399
multilayer cylindrical shell, with elastic core, bending under local radial load 77−27474
multilayer stress displacement calc. by double layer method *(Chinese)* 79−37162
multilayer wall of cylindrical vessel, calc. 77−19540
multilayered composite soft interlayer, limiting stressed state and carrying capacity 78−30201
multilayered inhomogeneous packet of elastic strips on elastic half-plane, contact stresses *(Russian)* 77−75796
multilayered laminated disc, orthogonality reln. for stress anal. 79−98621
multiphase materials, props. determ. from computer simulation 77−3717
multiply connected orthotropic body, plane thermoelastic problem 78−38199
myocardium of human left ventricle, stiffness distrib. rel. to shape change in diastole 80−41095
natural factor iterative approach to accurate stress calc. 79−94490
natural stress rate, three-dimens. defn. 77−67291
neck, stress distribs., Bridgman anal. 79−81737
necked cylindrical bar, elastic-plastic, residual stresses after unloading 80−38284
necking, dynamic analysis based on stress wave propagation 80−1440
necking, loading history depend. 80−5957
negative selection, for production of uniform intensity of light 77−2685
non-homogeneous elastic shells transient displacement and stress 77−65684
non-homogeneous stratum under long rigid rectangular body 77−868
non-linear elastic thermal stress analysis with phase changes 78−79218
non-piezoelectric crystals, consts. determ. by method of homogeneous deformation 77−80570
non-piezoelectric crystals, elastic constants anal. 77−84827
noncircular cross section, elastic torsion anal., simplified general method 79−90133
nonhomogeneous elastic layer bonded to nonhomogeneous half-space, torsion by circular die 78−87263
nonlinear analysis, natural force approach 79−2631
nonlinear elastic half-space, dynamic contact stresses due to axisymmetrical projectile impact 78−42573
nonlinear finite element anal. ADINA program for stress anal. 78−41148
nonlinear photomechanics, birefringence in polymers, stress anal. appl. 80−33545
nonlinear stress wave propagation, in perfectly flexible string 78−5670
nonlinear theory of hereditary media, functional relationship between stress, strain and temp. 78−26054
nonlinear viscoelastic materials, stress formulation relations *(German)* 79−76987
nonsteady inelastic deform., stress anal. by photoviscoplasticity 79−94563
normal stress difference, estimation from shear stress data in polymer rheology 79−64506
notch analysis, Neuber-based method verification by companion-specimen technique 77−50985
notch analysis using conformal mapping, book contrib. 78−94620
notch problems, body force method of soln., book contrib. 78−94619
notch stress anal. in elastic bodies, energy variations 80−64378
notch tip stress distrib. in strain hardening material 79−3927
notched bars, creep stress redistrib., finite element anal. 77−62164
notched bars, elastic plastic stress and strain conc. factor *(Japanese)* 78−26052
notched plate, stress anal., body force method *(Japanese)* 77−23868
notched rectangular bars, stresses at plastic deflection *(German)* 78−34025
notches in plane bodies, asymptotic character of stress field 77−19569
nozzle-to-cylinder structures subjected to internal pressure, finite plate method 78−34007
nuclear fuel, coated HTR particles, failure statistics calc., effect of SiC fracture stress and kernel porosity 80−73920
nuclear fuel can designs for Safety Test Facility, structural analysis 77−46310
nuclear fuel cladding, slightly oval cylindrical shells, creep anal. 78−78468
nuclear fuel pin inelastic modelling and stress analysis using FULMOD code 77−46233
nuclear fuel-cladding interaction between cracked surfaces, mechanical and temp. contact 78−66341
nuclear reactor, dynamic response of ducts to press. pulses, expts., finite element calcs. 77−3124
nuclear reactor, LMFBR, HCDA, structural response calcs., methods, codes development 77−3126
nuclear reactor components, design by analysis 77−3095

stress analysis continued
nuclear reactor fuel pin behaviour, computer code FRUMP, stress, strain, temp. distribs., displacements 77−14235
nuclear reactor pressure vessels, stress analysis program, STANSAS *(Japanese)* 80−22969
nuclear steam generator life evaluation, safety features in stress anal. for some accidents 79−54560
numerical stability of complex finite elements 78−32659
numerical-experimental hybrid technique for 3-D stress anal. 78−22265
nylon 6 fibres, dynamic mech. props., interpretive nonlinear viscoelasticity 79−4994
oceanic trench outer rise, stresses and dynamic support 78−81116
one-dimens. problems, diagonal mass matrices and finite element eqns. 78−73857
optical fibre cable stress during manufacture and installation 79−37024
optical fibre cables, structure design, compressive loads and internal stress determination 79−59829
optical material, photoelastic investigation of freezing and defreezing of temperature stresses 77−66733
optically-sensitive materials with disc-shaped macrosplits, determination of tension distrib. using photoelastic method *(German)* 79−37267
optimisation of photoelastic stress separation procedures 79−32402
optimization of geometric discontinuities in stress fields [and reply] 80−14569
optimum safety factors 78−38197
optimum strength shape, axisymmetric body, finite element technique 78−51060
orthodontic direct bonding systems 77−56513
orthotropic annular plates, general nonsymmetric postbuckling anal. 79−7307
orthotropic bridge decks with closed stiffeners, anal., behaviour 78−18164
orthotropic cylinder, nonuniform, thermoelastic stresses 77−7312
orthotropic cylindrical shell acted upon by local load 80−43617
orthotropic cylindrical shells, periodic problems, computer anal. *(Russian)* 80−23889
orthotropic laminate composite, broken layer 78−38254
orthotropic materials design for stress optimisation 78−63291
orthotropic parallelepiped, weakened by double periodic plane cracks, theory of elasticity 79−86340
orthotropic plate, plastic flow, effect of shear stress and geometrical changes *(Russian)* 78−13925
orthotropic rotating discs, flexure, stresses and deflection 80−5927
orthotropic shell of revolution, plastic flow, effect of shear stress and geometrical changes *(Russian)* 78−13925
orthotropic shell with tangential and normal strain, engineering theory eqn. 78−63303
othortropic medium in presence of symmetrical body forces, stress intensity factor 79−7337
overstrained spring strip, effect of Bauschinger effect 77−7320
paints and varnishes, stress anal. during drying 79−34183
panels, stiffened, eight-stringer, with rectangular cut-out, stresses and deformations, eccentric tensile load *(Japanese)* 80−64467
panels with openings, stability loss and critical stresses 80−10219
parallelogram plate, thermal deflection 77−3724
patella stress analysis, rel. to patellar articular cartilage lesions 80−35942
pencil point breaking, stress anal., size and shape of points 79−84901
penny-shaped crack in sphere embedded in infinite medium, stress intensity factor 79−27585
perforated plate, global stress strain behaviour 80−10169
perforated plate with cracks, stress intensity factor 79−14263
perforated plates, finite element elasto-plastic anal. 80−10168
perforated plates numerical limit analysis 77−27471
photo-orthotropic elasticity, numerical method 78−59296
photoelastic, isochromatic fringes, comparison of stress intensity factor determ. methods 77−84197
photoelastic, superposition of data 79−59952
photoelastic coatings, stress anal. technique 77−84201
photoelastic determination of stress intensity factors *(Chinese)* 79−32395
photoelastic frozen stress slices, fractional fringe order lines obtained by controlled density techniques, self-calibration 77−51001
photoelastic investigation of thermal stress fields due to travelling heat source *(Japanese)* 77−42747
photoelastic isodynes, new type of stress modulated light intensity distrib. 78−26092
photoelastic load meas. and testing *(German)* 80−19297
photoelasticity, 3-d, matrix method for determination 79−41636
photoelasticity, frozen stress model repeated use 77−7309
photoelasticity, holographic determination of absolute retardation fringes by vectorial reconstruction 78−87315
photoelasticity, matrix theory, matrix theory, book 79−64612
photoelasticity, photographic recording and sharpening of isoclinics 77−51002
photoelasticity, three dimensional, non-destructive method for stress-state determ. using scattered light 78−90805
photoelasticity for stress analysis under hydrostatic press. up to 700 MPa 78−18260
photomechanical information, acquisition and processing 79−32403
photothermoelastic technique, appraisal for transient 2D thermal stress analysis 80−79244
photoviscoelastic data, two procedures for recording and analysing on a μs time scale 79−37188
piecewise homogeneous bodies, two-dimens. elasticity theory stress problems 80−74749
piecewise linear elastic-plastic analysis 79−55331
piezoceramic benders, circular, bond stresses 78−21124
piezoelectric thin plate, electroelastic equilib. anal. *(Russian)* 78−19417
pinched rigid-plastic cylindrical shell, mode of collapse, geometrical parameters 79−10492
pipe, curved, in creep, flexibility 78−34039
pipe, layered, support layer thickness effect on stress-strain state *(Russian)* 80−43614
pipe bend in-plane bending, shell theory anal. 77−6516
pipe bends, flexibility and stress factors, finite ring method 77−75828
pipe bends, stress anal. by ring elements 79−10483
pipeline, axially compensated, buckling load determ. *(German)* 78−31456
pipes, welded branch, stresses calc. 80−108493

stress analysis continued
plane crack arbitrary shape, soln. of three dimensional problem 78−79265
plane elastic-plastic stress with variational problem in Hilbert space 77−13607
plane elasticity, mixed finite element method, convergence and performance 80−38258
plane elasticity, periodic contact and crack problems, closed form solns. 77−42783
plane elasticity, stress behaviour *(German)* 77−82394
plane field pattern determ. by photo-elastic method and electrical analogy *(Polish)* 77−12768
plane notch and crack problems, appl. of displacement and hybrid stress methods 78−63375
plane plastic flow, hydrostatic press. influence on shear resistance *(Russian)* 77−58562
plane slice optically isolated in three dimens. photoelasticity, plane and circular anal. 77−68540
plane strain, alternative approach 77−50899
plane stress crack geometries, comparison of finite element and expt. studies 77−89069
plane V-notched specimen, elastic-plastic limit load anal. 80−69684
plane weakened by openings, periodic and inverse elastoplastic problems soln. 77−35055
plane with curvilinear cuts, mixed thermoelasticity problem *(Ukrainian)* 78−90709
plane with heat-permeable curvilinear cut, limiting equilib. *(Russian)* 79−50576
plastic, stress-deformation diagram for materials without significant elastic section *(Russian)* 78−13923
plastic bending and torsion of simple geometries, subjected to cyclic loading, stress-strain analysis 78−90734
plastic design of complex machine parts 77−35048
plastic plates, infinitely extended, dynamic response to pressure pulse 77−68516
plastic range stress-strain concentrations for struct. materials 77−31222
plastic slip concept, statistical approach *(Russian)* 78−18196
plastic zone during rolling under plane strain conditioner, Fourier calcs. *(Russian)* 78−80555
plasticity, rate-independ. theory for multimode plastic straining, unifying concepts 78−42545
plasticity with hardening, mixed finite element method appl. 78−9577
plastics, using pseudo-elastic method 78−39868
plate, anisotropic, transcritical strength optimisation 78−30175
plate, anisotropy, theory of sharp stress concentrators *(Russian)* 77−68404
plate, annular, bending anal., closed form solns. 80−38263
plate, annular, uniformly stressed, with variable rigidity, axisymmetric bending problem 79−32295
plate, bounded by curvilinear contour, weakened by cracks, elastic equilibrium *(Russian)* 77−68524
plate, circ., large deflection anal., with nonuniform Jacobi polynomial load 79−37184
plate, circular, nonlinear analysis using Chebyshev polynomials 77−49597
plate, circular, thermally induced vibr. analysis 79−94524
plate, composite layered, loads and stresses 79−94570
plate, containing infinite row of holes, effect of couple-stresses on stress concentration 78−41159
plate, elastic, infinite, thick, fixed, subject to axially symmetric load, numerical stress anal. *(Japanese)* 79−50600
plate, elastic, under tension stress conc. due to surface pit 78−83243
plate, elastic deform. due to axisymmetric punch 78−75065
plate, elastic-plastic, flexed in its plane, stress concentrations, method of small parameter *(Russian)* 80−74759
plate, elastically orthotropic or isotropic, stress around pin loaded holes 77−84143
plate, geometric imperfection meas. appl. 79−81713
plate, heated equilateral triangular, large deflection, uniform load, temp. distrib. 78−83250
plate, homogeneous, circular, prestressing effect evaluation 79−59
plate, impact force meas. method 80−79242
plate, increase of first natural freq. and buckling load by optimal fields of initial stresses 78−13945
plate, inelastic thick, dynamic response, rectangular finite element development 79−94520
plate, infinite, with circular disc, tensile and compressive stress problems 80−38255
plate, infinite, with doubly periodic elliptical hole array, two-dimens. stress anal. 78−46892
plate, infinite row of holes, effect of couple-stresses on stress concentration 78−38192
plate, laminated composite, under tension, interlaminar stresses around circ. cutout 78−34010
plate, medium thickness, stepped holes, stress conc. 78−13912
plate, notched, plane strain general yield due to combined axial force and bending 78−18197
plate, obliquely stiffened, subjected to uniform compression, buckling strength *(Japanese)* 78−67067
plate, perforated, under axial loading, geometric discontinuities, in stress fields, optimization 79−37150
plate, radially stressed annular, elastic-plastic anal. 77−68456
plate, rectangular with stiffening ribs, stress-strain state, elasticity eqns. *(Russian)* 80−1427
plate, rectangular with two opposite edges supported and partially loaded *(Japanese)* 78−34004
plate, relaxed by holes, elastic-plastic deformation, stress state *(Russian)* 79−27545
plate, semi-infinite, joint with strip plate, analytical solution 80−10139
plate, simply supported, stresses, displacements under arbitrary temp. distrib. 79−72814
plate, square with inset circular discs, elastic consts. effect on interference fit *(Russian)* 79−77031
plate, star shaped, soln. of temp. problem by photo-thermo-viscoelastic method *(Russian)* 79−86343
plate, symmetrically notched, plane-strain general yield due to combined axial force and bending 78−18198
plate, temp. bending, generalised eqns. WRT transversal mech. characts., stress conc. problems *(Ukrainian)* 77−54876
plate, thick, containing eccentric spherical cavity, transverse bending stresses 78−63288

stress analysis continued
plate, thick infinite, transversely isotropic, containing circ. hole, end effects 79−27510
plate, thin, under elastic bending, optical method for slope and curvature contours 79−37259
plate, thin, unlimited, with noncircular hole, stability problem soln. *(Russian)* 78−18201
plate, thin elastic, with hypotrochoidal hole, under uniform press., stresses 79−98617
plate, three-layered, weakened with cylindrical cavities, stressed state determ. for bending problem *(Russian)* 78−22263
plate and shell theory, generalised two-dimens. theories generation 78−12569
plate bending elements, quintic triangle 78−77716
plate in tension, single edge V-notched, plate width and notch angle correlation factors 77−50891
plate of variable thickness, defined applied theories construction, asymptotic method *(Russian)* 80−53634
plate tectonics, roles of boundary friction, basal shear stress and deep mantle convection 78−57188
plate theory, high order, stress soln. determ. 78−83248
plate thick, circular hole under axisymm. radial load, stress anal., displacements 78−79201
plate with bend interaction, numerical calc. method for stress and deflection *(Japanese)* 80−23919
plate with central hole, effect of J_3 on creep and relaxation 77−54905
plate with central hole, estimation of plastic zones from elastic stress field 77−19547
plate with circular hole, axisymmetric stress distrib. 78−51066
plate with circular hole, stress distrib. under simple tension in electrostriction 78−10845
plate with curvilinear elasticity, stress distrib. around hole, asymptotic method *(Russian)* 79−81726
plate with hole, contour reinforcement, plane stress state anal. *(Russian)* 80−33447
plate with rectilinear thin walled elastic inclusion, bending stress state *(Russian)* 79−81736
plate with sharp angled holes, bending *(Russian)* 78−34045
plate with two circular holes having tangential stresses, stress anal., electrostatics 80−48571
plate with two unequal circular holes, stress concentrations 80−92047
plate-cylinder intersection, elastic, three-dimensional anal. by boundary-point-least-squares technique 77−58558
plates, annular, clamped edges, asymmetric bending, Ritz method 80−58907
plates, concentrated load effects 77−870
plates, isoparametric finite elements, variational formulation of plate equilib. problem *(French)* 80−43608
plates, laterally loaded, expt. soln. by method of caustics 77−65724
plates, open and loaded holes, exam. of part elliptical cracks 80−10195
plates, rectangular orthotropic, stress anal. and generalised orthogonality relations 80−38252
plates, ring sector, flexure under uniform and concentrated normal loads 79−72802
plates, simply supported, under uniform loading, caustics 78−22277
plates, tapered, circular, with affine imperfections, large deflections, stresses 78−75070
plates, thick, bending anal. *(Russian)* 79−10485
plates, thin, converged stress solns. by extended field method 80−38306
plates, thin, harmonic buckling due to constrained thermal expansion 80−48620
plates, thin and thick circular, subjected to transverse pressure, lower bound limits 79−68565
plates, uniaxially loaded, minimising stress concentrations around circular holes 79−18806
plates, V-notched elastic, symm. loaded, stress intensity factors, caustic method 80−83770
plates and shells, dynamic plastic anal. using stress resultant finite element formulation 79−37191
plates and shells, viscoelastic, flexible, thermomech. behaviour during cyclic loading 80−33478
plates and slabs, perforated *(Russian)* 80−74728
plates under uniaxial load, optimum hole shapes, cracks and fracture appl. 80−64479
plates with cut, stability loss critical stresses for steel, Ti and Al alloys 80−11690
plates with flows or cracks; twisting and bending theory 79−64545
plexiglas shell, orthotropic, cylindrical, interacting under straight angle, manufacture and strength 77−90417
plug formation in plates, cylindrical projectile impact, nonlocal viscous fluid model 78−49653
PMMA, expt. checking of ultimate equilibrium for crack in plane stress field 77−90462
point loaded beam, stress distrib., analysis using symmetric/antisymmetric loading 79−41641
polyaxial stress states, fracture statistics 79−41625
polybutadienes, use of high modulus inclusion gauge, in stress analysis 80−21254
polycarbonate, glassy, fatigue crack initiation in high strain fatigue tests 80−97564
polychromatic X-ray stress meas. *(Japanese)* 78−7143
polycrystalline aggregate, continuous distrib. of dislocations, stress fields, movements in elastic-plastic deform. 78−75709
polycrystals, bond between deformation and stress *(Russian)* 79−33031
polyester, stress-optic law, photoplasticity, RPE transition temp. 78−10120
polymer, toughened glassy, crazing within glassy occlusions in rubber particles, micromech. analysis 79−91824
polymer, viscoelastic-plastic, birefr. relation 77−31266
polymer agglomerates, forces in dispersive mixing 77−29052
polymer composite anisotropic plates, stress conc. around holes with shear strain taken into account 80−43618
polymer granules, compression, stress state 80−10218
polymer matrix, amorphous, stressed, thermodynamics of embedded crystallite deform. *(Polish)* 77−52424
polymer plate, analysis subject to local loads 77−65687
polymer solns., dilute, Hartree self-consistent field analysis 80−5648
polymeric adhesive layer, interlaminar stresses, direct determ. 77−86237
polymeric liquids, nonlinear viscoelasticity, stress-temp. equiv. eqns. 77−80128

stress analysis continued
polymers, stress analysis of circular craze, extension of linear membrane model 78−75081
polypropylene, reasons for disintegration under tension 78−84940
polyurethane, stress plate in contact zone with solid indentor 78−1624
poroelastic cone, inhomogeneous, forced torsional vibrs. 79−32338
poroelastic cylinder, twisted pore effect on fluid flow, solid deformation and stress 80−64377
poroelastic medium, semi-infinite disturbance and stress prod. by surface load 77−19533
porous body of simple shape, internal stress distrib., expt. and calc. *(Russian)* 79−68569
porous ductile media, rupture by void nucleation and growth, criteria and flow rules 77−52492
porous elastic half space, Lamb's line load problem 79−30248
porous elastic half-space, displacements and stresses prod. by impulsive line load 77−23908
pre-stress, influence on imperfection sensitivity 78−67035
precipitate and dislocation loop strain and stress field calcs. using affine transformations 80−106722
pressure vessel, elastic-plastic analysis, computer programs and appls. *(Japanese)* 79−21555
pressure vessel, load bearing segmental walls, stress state anal. 79−64514
pressure vessel, reinforced concrete, stress anal. of cracked shell 78−44213
pressure vessel, stress concentrations around multiple windows photoelastic anal., strain gauge tests 77−72254
pressure vessel, structural representation in stress anal. 80−27703
pressure vessel intersections, review of lower-bound limit anal. 78−34008
pressure vessel with hemispherical head, shell intersection, elastic stress anal., homogeneous eigenfunction method 77−23884
pressure vessels, creep bounds and brittle damage estimates 80−23908
pressure vessels, shearing stress minimisation by automated design optimisation 78−17289
pressurized cylindrical shell with a rigid circular inclusion 79−14267
prestressed pressure vessel, calc. of principal stresses 78−13206
principal stress separation using a computer 79−94496
prismatic body for nonstationary thermal action, stress-state algorithm *(Russian)* 78−13905
prismatic plate assemblies, buckling and vibr. anal. with compact computer program 78−90737
prolate spheroidal inclusion, stress conc. 78−67042
prosthesis, hinged knee, influence of dynamic loading on mech. loosening 78−48938
prosthetic aortic valve, Reul-Ghista optimal tri-leaflet Avcothane design performance 78−44736
prosthetic aortic valve stress analysis using finite element compute program 78−48930
prosthetic stem, stress estimation, analytical 79−92250
prosthetic trileaflet aortic valve, optimum design and in vitro testing 77−56541
pseudoplane equilib. state, stress eqns. 77−50889
PTFE, partly crystalline, viscoelastic props., stressed state estimation 79−66099
punch-elastic body dynamic contact, superseismic stage, exact soln. 78−55614
PVC, glassy, fatigue crack initiation in high strain fatigue tests 80−97564
PWR containment vessel optimisation 80−106137
PWR pressure vessel nozzle, comparison of 3-D and axisymm. finite element anal. 79−13423
pyrocarbon coating of Biso fuel, neutron effects on stress and strain 77−79437
pyrocarbon coating of Biso fuel, neutron effects on stresses and strains 77−79436
quadratic isoparametric elements, calc. of stress intensity coeff. *(Russian)* 77−58548
quarter plate support, planar flexibility depend. on fillet radius 80−5944
quartz, phase transform. in brittle materials, plane stress anal. 77−86024
quartz resonators, anisotropic circular plate initial stress effect calc. 79−55300
quasi-static deflection of thin rectangular plate due to transient heating 77−72199
random heat stresses in elastic space with a cylindrical cavity *(Ukrainian)* 79−76971
reactor cladding tube, effective temp. for expanding tube 77−74931
reactor emergency cooling systems, transient thermal stresses, appl. to circuit integrity 77−6544
reactor fuel pins, internal and external press. effects *(Czech)* 80−5233
reactor fuel rods, cladded, thermo-irradiation induced creep, stress analysis 80−35275
reactor vessel, determ. of stress intensity factor 80−37455
recrystallisation, induced, in thin metal plates *(German)* 78−19783
rectangular orthotropic plates with nonlinear stress-strain relns., large deflections 78−26040
rectangular plate, partially loaded, anal. *(Japanese)* 77−23869
rectangular plate on elastic foundation, uniform loading, computer anal. 77−46915
rectangular plate resting on Pasternak-type elastic foundation, large deflection 78−38215
rectangular plate with central hole, thermal stresses and buckling 77−3755
rectangular plate with fins, stress anal. under bending, approximation theory *(German)* 79−90144
rectangular plates with reactangular inserts, finite element anal. 77−23876
rectangular regions, plane stress problem using functions related to beam flexure 78−59297
reference stress method, creep of struct. with non-uniform temp. distrib. 77−14915
reference theta pinch reactor, first wall thermal-mechanical anal. 77−57750
refractory, thermal stresses produced by temp. gradient, finite element anal. *(Japanese)* 80−33538
reinforced concrete, lower bound anal. for torsion 78−35436
reinforced concrete slabs, generalised yield lines 79−83265
reinforced cylindrical shell, tranverse bending rel. to rigidity of local insertions 79−90154
reinforced panels, variable stiffness, plane stress problem 79−94497

stress analysis continued
reinforced plastic, elastic orthotropic cylindrical shell, axisymmetric contact problems, shell interaction with tires 78−1569
reinforced shell, in plane stressed state, strength characts. 79−14264
reinforced viscoelastic disc, equilibrium 78−9576
reinforcement material distrib. for specified stress field criteria, plane elasticity hybrid problem 80−64376
relativistic initially stressed elastic solids, infinitesimal discontinuities 77−45775
relaxation calculations in strips, errors due to approxs. 80−23909
remaining creep life for components under stress at elevated temperatures 80−59566
residual, US drawing 80−97674
residual stress effects in failure from flaws 79−66228
residual stresses in welded joints of double-wall piping *(Russian)* 78−27541
resin slab, stress response, fluctuating external moisture (temp.) effects 78−55620
retaining walls, conoid, cylindrical shells, numerical methods 78−5655
Reykjanes Ridge, stress directions rel. to ridge crest morphology near 62°N 80−90070
Rhinegraben rift system, Holocene movements and stress state 79−79801
rhomboidal steel panel, elastoplastic stress and strain diffusion 79−20128
ribbed plate, stress distrib. modelling using combined photoelastic-moire method *(German)* 79−32280
rigid circular punch on elastic halfspace, Mindlin force 79−18716
rigid indentor sliding over power law viscoelastic half space 79−27602
rigid plate on elastic-plastic foundation, load-deflection, contact stress distrib. 77−46931
rigid punch bonded to elastic half plane, stress singularities 80−64491
rigid punch problem on non-homogeneous elastic half-space 80−53720
rigid-plastic medium, ideal, surface force strength lower limit under plain strain 80−99937
ring, axially cracked, numerical anal. of residual stress effect on crack closure 79−77012
ring, plane deformation, determ. of stresses and displacements, composite boundary conditions *(Russian)* 80−74738
ring, under diametral compression, geometric discontinuities, in stress fields, optimization 79−37150
ring caps, shallow spherical, transverse twisting 80−79139
ring loaded by distributed forces, stressed state anal. 77−46923
ring subjected to time-depend. fluid pressures, dynamic behaviour 77−65704
rock, discontinuous, photoelastic anal. *(German)* 79−34811
rock, laminar, stress distrib. during sliding failure 79−2225
rock, soft, vibrating wire stress gauge 77−84199
rock bodies, cooling, residual stress development 78−88819
rock joint orientation meas. evaluation in terms of regional stress 77−64487
rocks, cylindrical stress waves generated by moving axisymm. superseismic pressure pulse 77−44979
rocks, metamorphic, stress distrib. in thermomechanical expts. using shear machine *(French)* 79−5474
rocks tensile strength indirect measurements, specimen exact theoretical stress field var. 79−29883
rod, conical, nonlinear viscoelastic materials, soln. using generalised correspondence principle 80−38288
rod, slightly curved, residual stress determ. 78−30185
rod of time hardening (softening) material, thermoelastic stresses 80−92046
rod with helical anisotropy 77−62155
rod-shaped elements, under simultaneous static loads and elevated temps., linear limited stress relax. 80−14590
rods, large curvature, residual stresses determ. 79−41571
rods, round and flat, stress conc. coeff. in sharp circular notch zone, design feature effects 79−14350
rolled-up cylindrical shell, stress-strain state, approx. computation 77−14911
rolling, determ. of stress distrib. in rolled material 80−48651
rolling, stress distrib. during asymmetrical processes, two dimensional strain conditions *(Russian)* 78−94601
rolling, vibratory, contact strains *(Russian)* 77−65722
rolling disc, elastic-plastic anal. of stress distrib., finite element anal. 77−68444
rotating circular disc with time depend. shearing stress on outer edge 77−68415
rotating components, design to probabilistic criteria 77−3716
rotating composite inhomogeneous disc of variable thickness with axial hole, stresses 79−94484
rotating deformable elastic disc, vibr. stress anal. *(Russian)* 80−19265
rotating disc, elastic stress state distrib. calc. 79−37175
rotating disc, orthotropic materials design for stress optimisation 78−63291
rotating discs, variable thickness, transition theory of creep, stress determ. 78−90725
rotating disks, elastic and elasto-plastic, with temp. gradient, stress distrib. determ. *(Italian)* 79−41633
rotating orthotropic disc, stress distrib. 79−90127
rough curved surfaces, elastic contact stresses calc. 80−10213
round plate with radial and circular reinforcing ribs, load bearing capacity 79−98636
round tubes in flexure, critical buckling strains 80−23921
rubber covered rolls, contact and deformation nonlinear elastic problem, stress anal. 80−79239
ruled shell exposed to internal load pulses, compact strength 79−3929
ruled three layer shell, large coefficient of friction between layers, stresses-strained state calc. 79−14354
Saint-Venant's problem for micropolar elastic cylinder 77−3719
San Andreas fault, local mag. field vars. and stress changes near slip discontinuity 80−26448
San Andreas fault, stress changes due to creep episodes rel. to local mag. field meas. 80−85629
sandwich plate, modified Berger method, large thermal bending anal. 78−63297
sandwich plates, simply supported in shear, critical stresses *(Polish)* 79−32247
sandwich plates with thick faces, orthotropic, hybrid stiffness matrix 77−80072
screw dislocation simple model, Peierls stress 77−76401
stress analysis continued
sea ice, relationship between mean stresses and internal forces local values in drifting cover 80−31056
second order beam theory 80−58908
sector problem soln. using Mellin transform technique 79−97204
sector problem with arbitrary loads on edges 79−32263
self stresses, expt. and numerical study *(German)* 79−90142
semi-infinite medium with anisotropic elasticity, 1st and 2nd periodic fundamental problems *(Chinese)* 80−5931
semi-infinite strip under symmetric load, stresses, elastic plane theory 78−59301
semicircular plate of variable thickness, finite element stress anal. 79−37180
semiinfinite elastic solid, frictional shear effect on dynamic stresses 79−10537
shadow-moire principle applied to contact problems *(German)* 79−32281
shaft, circular, with surface traction, perturbation of shear stresses 79−41577
shaft with regular round polygon, stress state 80−35284
shafts, endurance subject to bending and torsion *(Russian)* 79−72831
shafts, non-circular, analogue simulation *(German)* 77−68551
shallow cylinder subject to axial compression, max. stress computation 77−14909
shallow grooves in shaft under torsion, stress conc. factors 77−46919
shallow shell theory, series representation of fundamental solution 79−10468
shallow shells, effect of rapidly varying loads by asymptotic methods *(Italian)* 79−12599
sharp edge in contact problems with friction, stress singularity 77−7313
shear stress bounds in Saint-Venant's theory of flexure 77−13608
shear wall with N-rows of openings, stress anal., weighted residuals method *(Chinese)* 80−64362
sheet, stress changes and warping during heating *(Russian)* 79−59920
shell, circular cylindrical, infinite, dynamic stresses under conc. impulsive loads 77−42765
shell, circular cylindrical under tension, stresses around rib-reinforced elliptic hole 77−58557
shell, conical, quasi cylindrical, with angular discontinuity, stress field 78−67032
shell, conical, stress distrib. near hole, orthotropy effect 80−43630
shell, cylindrical, cantilever, dynamic deforms. and stresses under impulsive loads 79−27504
shell, cylindrical, effect of material orthotropy on stress state around circular hole 78−34023
shell, cylindrical, in vicinity of supporting elements, stress state 80−48585
shell, cylindrical, of a vessel with the bottom, membrane connection, internal pressure effect 79−86341
shell, cylindrical, subject to local interaction with nonlinear circular base, stability 77−89050
shell, geometric imperfection meas. appl. 79−81713
shell, high-shallow, with rib of equal resistance, contact interaction, tangential stress distrib. *(Russian)* 80−87745
shell, load carrying ability, critical concentrated force anal. 79−94499
shell, multilayer, cylindrical, viscoelastic strain equations under axisymmetric load 77−80079
shell, orthotropic cylindrical of reinforced plastic, axisymmetrical contact problems, theory 77−84147
shell, reinforced plastic, optimisation with allowance for geometrically nonlinear factors 80−38270
shell, reinforced with zero Gaussian curvature, momentless stressed state 77−35043
shell, round cylindrical with free edge, anal. under radial load *(Russian)* 79−76973
shell, spherical, glass, with metal insert, design strength parameters 80−14576
shell, spherical, non-shallow, moderately thick, stresses and deform. 79−32241
shell, spherical, with conical nozzle, thermal stress anal. 78−79204
shell, spherical, with elliptical hole, stress state 80−33449
shell, thick, finite element study of large deflections 77−3725
shell, thin spherical, axisymm. thermal stress by method of matched asymptotic expansions 77−72169
shell elements, thick curved, temperature load calc. 77−80066
shell loaded along line of main curvature special features of strained state 79−14290
shell of double curvature, bending in zone of elliptical loading area, stress anal. *(Russian)* 79−50593
shell of revolution, cyclically loaded, elastic-plastic state study 77−46941
shell of revolution high modulus material shape of wound membrane rationalization 77−27473
shell of revolution with internal press. subject to temp. field, optimum shape 78−22272
shell stability under heating and loading 79−94518
shell structure analysis, new stress finite element 78−18165
shell structures, hood-shaped, membrane solution *(German)* 78−46891
shell structures, new high-precision stress finite element 77−62156
shell subjected to centrifugal force, stress anal. *(German)* 80−23900
shell-plate intersection, 3-dimens. stress anal. 77−84144
shells, coiled, stress state under action of internal pressure 79−86342
shells, concentrated load effects 77−870
shells, conoid, parabolic, with vertical director line 78−51058
shells, cylindrical, imperfect, closely-spaced, dynamics and failure criterion for axial impact 78−30207
shells, cylindrical, thermoelastic problem 80−38273
shells, efficient high order finite elements 77−35044
shells, finite cylindrical, of various wall thicknesses, flexural vibrs. 78−1588
shells, paraboloid, elliptic, generalised computer program 78−59294
shells, thin, axial compression, mass reduction, stress anal. 80−106716
shells, thin cylindrical, ring-reinforced, impulsive inner load effects 77−68481
shells, transversely isotropic, elastically deformed, optimal reinforcement of openings 80−38269
shells, truncated conical, thermal buckling, axisymmetric initial deflections 78−79240
shells of resolution, transient dynamic and inelastic anal., survey of programs 77−3767
shells of revolution, computer program for linear and geometrically nonlinear static analysis *(Japanese)* 80−64500

stress analysis continued
shells of revolution, state of stress by min. energy and orthogonal proj. method 80−28415
shells of revolution, thin, numerical anal. thermal stress relief 77−89041
shells of revolution, variable thickness, stress state determ. 80−38275
shells of revolution under axisymmetric and asymmetric loadings, linear elastic dynamic analysis program using finite element analysis *(Japanese)* 80−106719
short fatigue cracks, exam of propagation 80−10196
shrink-fit stress analysis by photoelastic stress-freezing method *(Chinese)* 79−37256
shrinkage, semicircular inclusion in semi infinite plane *(Japanese)* 77−65672
silicon rubber model for design and stress analysis of large parts 77−7350
simple harmonic waves in infinite nonhomogeneous elastic medium, diffr. by Griffith crack, rigid strips 77−54913
simple plate bending theory, approx. stress intensity factors 80−43612
simulated diffusion bonded lap joints, finite element stress analysis 78−18254
sintered two phase material, calculation of stress distrib. and X-ray elastic consts. *(German)* 78−52883
slab, semi-infinte, stress amplitudes and fatigue damage resulting from cyclic Hertzian compression 77−19567
sliding contact, stress conc. on rough surfaces determ. by polarisation-optical method *(Russian)* 78−30244
slip zones along interface, caused by plane horizontally polarised SH stress pulse 80−53648
slit, entrance flow analysis 79−64619
snow, shear stress rel. to strain softening precipitated shear fracture and dry slab avalanche release 80−8338
soft elastic material dynamic elastic modulus determ. *(German)* 78−71297
soft materials, reinforcement effect of strain gauge, numerical anal. 79−72864
soft shells, geometrically nonlinear strain *(Ukrainian)* 79−50589
soil, nonhomogeneous water saturated, plane shock wave propag. 77−56607
soil mechanics, optimal lower bounds 77−72262
solar collectors with multilayer cylinder heat exchangers, heat balance eqn. and thermal stress anal. 80−58977
solid deformable body, residual stresses by creating holes, holographic interferometry appl. *(German)* 80−79243
solid free boundary, slip line initial development, elastic-plastic problem 80−96196
solid with annular crack, bending effect 79−72806
solids of revolution, stressed state 77−14910
sound porous material, stress anal. during stretching *(Russian)* 79−76980
space truss analysis in post-buckling range in dual load method 80−38298
spatial structure stress analysis, continuum treatment method *(Japanese)* 78−22260
spatial structures, mathematial system, Prochnost'-75 79−90140
sphere, approx. calc. of temp. and stress fields *(Russian)* 77−35034
sphere, composite elastic nonhomogeneous, with concentric spherical inclusion, opposite couple stress, displacement 79−94494
spheres, porous, in a linear flow field, motion and rupture 79−64755
spheres at high pressure, contact stresses and spreading resistance 78−71296
spherical cavity in prestressed medium arbitrary orientation, elastic relaxation coeffs. 77−73692
spherical dome, three-dimens. elasticity soln. and edge effects 78−59306
spherical inclusions, stress concentrations between two 77−80077
Spherical shell, shallow, on elastic subgrade, under ring load along the edge 79−41644
spherical shell, shallow radially ribbed, stress state, struct. parameters influence 80−14581
spherical shell with circular elastic inclusion, thermal stresses 77−3727
spherical thick-walled shell with filler thermal stresses 78−13909
spheroplastics, mech. characts. calc. 80−60931
spot weld between elastic plates, near field stress anal. 77−11160
square plate, large deflection, behaviour according to Foeppl and Von Karman 78−63296
static stress fields, L^p estimates 79−58545
statistical theory, fracture of brittle solids, under multiaxial stresses *(Japanese)* 78−90788
statistical treatment of experimental data 80−53644
steam turbines, structural stresses, experimental anal. 80−93727
steel, austenitic stainless, X-ray stress anal. by new position sensitive proportional counter with uniform angular resolution *(Japanese)* 80−30190
steel, C, elastoplastic stress anal. by photoelasto-plastic method and X-ray method *(Japanese)* 78−13978
steel, C, fatigue crack exam. using slip initiation phenomena *(Japanese)* 77−8930
steel, cold worked layer of used railroad rail, Rayleigh wave dispersion 79−1014
steel, Cr-Ni-Mo-V, plate, type HY130, exam. of elastic-plastic R curve 79−29157
steel, crack-resistance limit and stress analysis in the ductile state 80−81188
steel, high strength, shell, stress distrib. around notch, beyond fatigue limit 78−13928
steel, low C, effective stress determ. during the loading cycle 79−38879
steel, parts, stress calcs. during cooling, program system THEPLA *(German)* 80−35237
steel, plates, thin, welding residual stresses calc., elastoplastic thermal stress anal. 78−83262
steel, rails of DIN 15087E, shear stress distribution caused by transverse force *(German)* 79−61647
steel, SA540, fracture toughness props. for nuclear bolting appl. 78−35514
steel, stainless, 316, nuclear fuel cladding, crack nucleation 78−72864
steel, tapered beam, collapse behaviour 78−87287
steel, thin walled shell, failure of model when loaded by internal press. 77−11147
steel case hardened cylinders, heat treated, residual stress fields 80−3102
steel core/sheath tube system, non-fracturing core, stress transfer mechanism 77−52454
stress analysis continued
steel pressure vessel, multilayer, without longitudinal seam, model investigation *(German)* 79−34276
steel tube eversion, effect of material and geometrical parameters 79−15690
steels, thermal hardening stress determ. by thermoplasticity theory 79−29076
stiffened layered structs., dynamic large-deflection inelastic and thermal stress anal. 77−3752
stiffened plate, model studies of elastic buckling 77−7324
stiffened shear webs with skin stabilisation, optimum design 77−892
stiffness matrix softening, artificial 77−80067
stochastic multi-component system, mean stress *(Polish)* 77−54874
stochastically inhomogeneous solid with opening, plane deform. problem 79−86337
straight edge dislocation in nonlocal elasticity, stress field, elastic energy 77−35555
strain energy J-integral correlation *(Chinese)* 77−72167
strain gauges, error compensation 77−84198
strain hardening structures under repeated loading, deflection analysis 78−63313
stranded wire helical spring, general axial response 80−33453
stratified material, compressed, stress determ. *(Rumanian)* 80−28434
stress anal. of viscoelastic bars subjected to impulsive loading 79−32305
stress analysis of aortic valve leaflets 77−52815
stress concentration factors and stress distribution around sharp corner elastic inclusions 77−84164
stress concentrations round cylindrical cavity in half-plane under tension, effect of couple-stresses 77−19524
stress intensity factor determ., accurate finite element method 77−54878
stress intensity factor for a flat elliptical crack in an elastic solid under uniform tension 79−27525
stress intensity factor specimen design, constant factor for crack length range 77−73380
stress intensity factors calc. using special 3-D elements 79−94556
stress relieving notches, expt. and computer aided study, and optimisation 79−59926
stress state of structural elements of vessels under external hydrostatic press. 77−14908
stress wave propagation calcs., effect of material constitutive models 78−90769
stress-concentration factors, intersecting and closely approaching orthogonal coplanar holes 77−50892
stress-cycle asymmetry degree, determ. problem 79−90187
stress-deformation relns. allowing for anisotropic material strengthening *(Russian)* 79−10503
stress-equilibrium membrane elements with holes 77−78980
stress-focusing effect in uniformly heated cylindrical rod 77−19521
stressed state in reactor pressure vessels, model studies by polarised optics 78−78454
stretch components transformation using Mohr's circle 77−82393
stretched plane slab, rational reinforcement round hole 79−3930
stretched plates weakened by inner curvilinear holes 78−55567
strip or beam, state of stress, rectilinear thin walled inclusion effects 80−96187
strip weakened by identical circular transverse openings, stress state 80−43606
strip with semicircular notches, tensile load conditions at end, interf. effects obs. 80−64455
strips, seizure, elastic stresses, extra loading moments *(Russian)* 80−69664
structural components, photoelastic methods of stress distrib. anal. *(Polish)* 77−9031
structural materials for inertial confinement fusion reactors, scaling laws for structural loads and stresses 79−76137
structural materials in complex stress state, criterion for strength at low temp. 78−71292
structural systems, time-varying stresses calc. by variational principle 77−3732
structure reliability under random loading 78−38196
sub-structure analysis for elastic fields with stress singularities, hybrid formulation 77−3730
Super Phenix nuclear reactor containment vessel, stress anal. *(French)* 79−41023
superconducting accelerator and beam-line mags., mech. and thermal stresses 77−83362
superconducting dipole magnets for high energy accelerators, stress and strain distribs. 79−31250
superconducting fusion magnetic systems, struct. anal. methods and standards 80−86972
superconducting magnet, MHD, structural analysis 77−27739
superconducting warm Fe dipoles, stress anal. 79−68041
surface loads, reciprocating dynamic stresses produced in elastic half space 78−9562
surface stress in solids 78−63290
tape twist induced stress estimation and reduction by pretwisting 80−53471
tapered anvil high-pressure apparatus, stress distrib. rel. to max. press. 77−74419
tapered beams, stress trajectories, stress contours 78−63305
telescope, altazimuth mounted, primary mirror deflection and stress anal. 80−58659
temperature data uses 79−12796
temperature stress-state of internal combustion engines finite element study 77−80073
tensile specimen preparation, stress distrib., for TEM 78−73973
tensionless contact without friction between elastic layer and elastic foundation 80−64487
testing machines, contact area for nonuniformly distributed load, calc. 78−67155
thermal diffusion in elastic layer, temp. and concentration fields distrib. 77−59137
thermal elastoplastic stress analysis based on initial strain method *(Japanese)* 80−77620
thermal emission for stress pattern analysis 80−33552
thermal stress anal., finite element variational method 77−7310
thermal stress in bimodulus thin plate 77−19527
thermal stress variational finite element anal. 77−7311
thermal stresses due to moving heat sources *(Polish)* 78−18184
thermal stresses in cylindrical shell with circular hole or rigid inclusion 77−19518

stress analysis continued
thermal stresses in rectangular plates, variational and finite element solns. 78−51082
thermodiffusion in elastic cylinder, quasistatic problem *(Polish)* 80−10150
thermoelastic anal. of finite orthotropic slab 79−1111
thermoelastic coupled field, spherical symmetric problems analysis 77−42737
thermoelastic punch problem for elastic layer overlying elastic half-space 77−42742
thermoelasticity, distribution for stresses in half space, with moving boundary, influence of inertial effects *(Russian)* 79−55327
thermoelasticity problem, plane, for solids with curvilinear hole and cracks, integral eqns. *(Ukrainian)* 77−31257
thermoelastoplastic anal. for hollow sphere, incremental plasticity theory 77−62168
thermoelastoplastic solution for a circular solid cylinder subjected to heating and cooling 80−5952
thermoelectric cooler, single stage, finite element thermal stress anal. 80−108807
thermoplastic beams, constant stress, design 80−38248
thermoplastic rectangular parallelepiped pressure vessel, photoelastic coating anal. 79−59950
thermoviscoelastic laminate beam, stress anal. *(German)* 80−106727
thick cylinder under non-axisymmetric loads, computer stress analysis 77−54880
thick infinite plate with circular hole, axisymmetric stress and displacement boundary value problems 79−27511
thick multiply connected plates, stress state investigation by finite element methods 77−11132
thick plate, containing eccentric spherical cavity, stresses under uniaxial tension 77−23873
thick plate, expt. investigation of stress conc. around conical cutouts 79−41639
thick plate, with elliptical hole, subjected to simple out of plane bending, photoelastic anal. to determ. stress distrib. 79−37187
thick plate, with spherical cavity, stresses under transverse bending 77−23874
thick plate flexure by arbitrary load *(Russian)* 78−22287
thick plate with circular hole resting on smooth rigid bed, stresses, displacements 79−98602
thick plate with circular hole under axisymmetric loading 77−19530
thick plate with oblique hole, stress conc. determ. by photoelasticity 77−84149
thick plate with spherical cavity, three-dimens. stress concs. under uniaxial tension 77−31214
thick rectangular plate bending under own weight *(Japanese)* 78−22284
thick walled composite tube manufactured by polymerisation of inner cylinder 78−46916
thick walled cylinder subject to torsion, stresses at offset oblique holes 79−32404
thick-walled cylinder subject to internal press. and bending, full plastic anal. at collapse stage 78−22275
thick-walled shells of revolution, axisymmetric problems soln. by design and exptl. methods *(Russian)* 78−73853
thick-walled vessel, of brittle material, strength under external press. 78−30182
thin annular plate, inner clamp carrying bending moments 77−89031
thin cylindrical shells subjected to transient inner pressures, dynamic stress anal. 78−89344
thin shell finite element by mixed method formulation 77−9872
thin shell theory, stress boundary conditions 80−79137
thin shells, infinite, elastically vibrating, response to initial stress 77−31236
thin shells of resolution, torsion and Saint-Venant's principle 77−50912
thin steel plate, anal. of longit. stresses and strains due to moving heat source 79−81723
thin-walled structures, elastoplastic analysis by finite strip method *(Japanese)* 77−42753
thinwall framed beam, numerical integration of differential eqns. 77−19520
threaded connections, load transfer modelling using finite elements 79−90195
threaded pieces, stress calc. from US meas. 78−56859
three dimensional, by boundary integral eqn. method 79−58546
three dimensional notch problems, elastic medium, book contrib. 78−94622
three dimensional stress analysis holophotoelastic method appl. *(Chinese)* 79−72866
three dimensional structures, system of mathematical calc. 79−98623
three-bar struct. under variable temp. 77−68389
three-dimensional stress anal., transition finite elements 80−92042
three-phase anisotropic medium, antiplane line force 78−67041
tibial shaft internal fixation, biomech. study 78−20313
Timoshenko beam, shear coeff. *(German)* 80−106729
Tokamak fusion reactor, structural anal. 77−3162
Tokamak reactor, first wall stress anal. 77−83093
Tokamak reactors, supercond. toroidal magnets, mag. and thermal loading 79−36407
Tokamak reactors, supercond. toroidal magnets, max. mag. fields, mech. stress calcs. 79−36405
Tokamak zero moment toroidal field coils, compatibility calcs. 79−93824
toroidal field coils, bending-free, for Tokamak reactor 78−55012
torsion analogue, simplified numerical calc. *(German)* 79−32279
torsional vibrs. of spherical shell, numerical results 78−59322
trajectory determ. in geometrically similar plastic flows, expt. 78−64588
transient thermal stress problems, numerical anal. method 79−72810
transition finite elements for axisymmetric stress analysis 80−92048
transverse flexure of rectangular plate of arbitrary stiffness *(Russian)* 78−51084
transversely isotropic finite cylinders, elastostatic analysis 78−51074
transversely isotropic half space, indentation anal. 80−92090
transversely isotropic medium with closed conical cavity, stressed state *(Russian)* 80−43616
transversely isotropic medium with cylindrical cavity and external crack, stress distrib. 78−79259
transversely isotropic plate with hole, edge supported, shear compliance in bending and torsion 77−2543
transversly isotropic half-space, Boussinesq and Cerruti solns. 78−55568
trigonal monocrystals, classes 3 and $\bar{3}$, elastic potential and yield condition *(Russian)* 80−29108

stress analysis continued
truncated cone, subject to axisymmetric loading, stress-strain state 78−1570
truss struct., accurate nonlinear anal. 79−90159
tube, porous, nonlinear viscoelastic materials, soln. using generalised correspondence principle 80−38288
tube T-joint, stress conc. in elastic region 79−50601
tubes, thick-walled, thermoelastoplastic creep stress anal. 80−58922
tubular joints stress anal., finite element anal., computer programs 78−41808
tubular specimen, torsion stresses 78−63298
turbine-engine component, photoelastic and holographic anal. 79−37257
twisted bar, elliptic, stress and deform. states produced by axisymmetric elastic torsion *(Italian)* 78−22262
twisted circular cylinder with radiating internal cracks stress intensity factor *(Chinese)* 80−5984
twisted elastic prismatic solid, torsion, Gohner-Giovannozzi stress anal. *(Italian)* 79−18766
two component medium, stressed state, method of conditional momenta *(Ukrainian)* 77−68392
two material elastic media, stress computation by best fit strain tensors method 77−46910
two-axis tensile test machine, for static and dynamic tests *(French)* 78−15627
two-dimensional, expt. numerical hybrid technique 77−50910
two-layer transversely isotropic elastic plate, energy-asymptotic method *(Russian)* 78−13906
two-phase nodules, heat treatment, stressed state, connection with nodule size, cooling rate and phase ratio *(Russian)* 80−16334
tyre, photoelastic modelling of stresses 79−34274
underwater acoustical compliance tube for sound projectors, stress and deformation analysis 80−33310
unhomogeneous bars, normal mode response, stress anal. by boundary operator method 80−19239
US nondestructive inspection system, microprocessor utilization 80−71845
vacuum vessel for ASDEX fusion reactor, finite element stress anal. 80−18655
variable-thickness conical shell, transient stresses in clamped section 77−89051
viscoelastic bodies, deformation taking into account influence of accumulated defects 80−19252
viscoelastic cylinder, optimal management of diffusion treatment rel. to conc. depend stresses 79−94510
viscoelastic half-space, stress field in randomly varying temp. field *(Ukrainian)* 80−33467
viscoelastic linear on non-linear bodies, creep and relax. phenomena generalisation 77−876
viscoelastic materials, nonlinear, creep and relax., book 77−11141
viscoelastic response to small deformations superposed on large stretch 77−72187
viscoelasticity, information theory approach, stress predictions from available strain history 77−57191
viscometric flows of general fluids *(Japanese)* 78−87425
viscoplastic model, cyclic load, stress evolution, asymptotic behaviour *(French)* 80−64382
viscoplasticity, min. principle in stress field boundary-value problem 77−46927
waffle cylindrical shell, technological charact. and bearing capacity 79−3936
wall in contact with Rivlin-Ericksen fluid, viscometric flow *(French)* 77−72210
weakly absorbing solid medium, opacity fluctuations, heating by intense radiation and thermoelastic stresses problem 80−38048
web structures between cavities, stress anal., appl. to struct. materials with microcavities 77−874
webs, stress state under uniform partial edge loading 79−77028
webs, thin, under partial edge loading, influence of longitudinal stiffening determ. 80−79857
wedge, 3-dimens., functional equations of static elasticity theory *(Russian)* 79−46203
wedge, composite, plane elasticity stress singularities 80−38262
wedge, infinite, stress distrib. 80−23885
wedge, plane, nonlinear viscoelastic materials, soln. using generalised correspondence principle 80−38288
wedge adhesive joint, nonuniform stress distrib. under combined normal and shear stresses 79−18837
wedge under surface press., elastodynamic response 78−18169
welded joints, low cycle fatigue anal. 77−3789
welded unit of finite shells of different materials 77−68418
wheel temperature in railroad service, effect of brake shoes 80−93660
wind stress coefficient over water surfaces, new evaluation 80−72603
Winkler layer, axisymmetric deform. by internally loaded elastic half-spaces 78−26044
X-ray, recent German activities 77−81359
X-ray *(German)* 79−34269
X-ray diffraction stress analyser, for large structures *(Japanese)* 77−48599
X-ray residual stress anal. theory 77−84200
X-ray stress analyser, field type, applicability *(Japanese)* 77−52591
X-ray tensometry *(Czechoslovakian)* 77−28958
zircaloy calandria tubes in CIRENE PWR, stress evaluation using strain data *(Italian)* 77−50204
Zircaloy cladding, stresses due to pellet cladding interaction 80−42762
Al alloy, yield surface after proportional preloading, Tresca-type strss-strain rel. 77−32628
Al alloy 7075-T6, stress intensity factor specimen design, constant factor for crack length range 77−73380
Al plates, exam. of stress conc. around conical cutouts, using strain gauges 79−41639
Al, powder, nonuniformity of stress and strain distrib. over width of rolled powder strip 77−12577
Al, single cryst., latent hardening *(Japanese)* 78−44135
Al, use in design of composite superconductors in elasto-plastic region 77−28851
Al-Si-Mg (1, 0.6 wt.%), plasticity due to superimposed macrosonic and static strains 78−60719
B fibre reinforced Al, stress redistrib. anal., upon brittle fibre breakage 78−48527
Bi anisotropic crystal, dislocation wall stress field and strain energy 80−100233

stress analysis continued
C fibre reinforced laminate, elastically orthotropic or isotropic, stress around pin loaded holes 77−84143
C fibre reinforced plastic, stress analysis of butt strap joint 79−43300
C fibre-reinforced plastic joints, fatigue life, stress distrib. analysis 80−55497
Fe, cast, rod, torsion, St. Venant's problem 77−70135
$Ga_{1-x}In_xAs$-GaAs epitaxial interface with small misfits, TEM image contrast 80−2275
NaCl, rock salt, progressively mined soln. cavities, struct. behaviour 78−61409
Na_2O-CaO-Si_2O glass, mixed mode fracture 79−79083
Ni, electrical resistivity and stress amplitude change during push-pull fatigue 79−91792
Si_3N_4, hot pressed, flawed plate under combined stresses, failure prediction 78−72884
Ti-6Al-4V, stress distrib. for steady axisymmetric extrusion 80−3103
Ti-Al-V (6, 4 wt.%), temp. distrib. for steady axisymmetric extrusion 80−11670
Ti-Al-V (6, 4 wt.%), temp. distrib. for steady axisymmetric extrusion numerical results 80−11671
W-Al fibrous heat treated composites, thermal stress anal. 77−46943
WC-Co sintered carbide tips, microscopic stress anal. 78−5663

stress birefringence *see mechanical birefringence*

stress control
fatigue testing machine, stress amplitude stabilising system 79−52501
PbF_2-ZnSe multilayer 16 μm dichroic mirror, 16 μm region, mech. stress compensation 80−74465

stress corrosion cracking
1300 MW cross compound turbine unit IP rotor coupling, fatigue crack due to combined corrosion and low alternating stresses, report 80−16611
adhered lap-shear and double cantilevered beam specimens, cyclic stress testing 79−15820
adhesive bonds, stress corrosion testing 80−16514
admiralty brass, stress corrosion cracking, aqueous $CuSO_4$ 77−59961
Admiralty Metal, transgranular stress corrosion crack propag. 80−89402
AK4-1 alloy, sheet mat., fatigue and corrosion fatigue strengths, coatings effects *(Russian)* 78−11397
alloy, high strength, marine corrosion fatigue crack growth rate, bulk soln. chemistry condition effect 79−83373
alloy 01420 fine structure effect on stress corrosion cracking *(Russian)* 78−35571
alloys, high-strength, subcritical crack growth 79−43494
alloys, passivatable, role of oxide films in stress corrosion cracking initiation 80−50762
alloys, susceptibility to SCC in geothermal brine environments 78−85032
alloys testing, for coal gasifiers appl. 80−7726
anodised Al rods, humidity and coating thickness effects on fatigue in reversed torsion 77−25205
austenitic alloys in hot water, low cycle fatigue, appl. to nuclear reactors 77−4871
bending fatigue testing machine, multi-specimen 79−39060
biotite stress corrosion cracking, seen in granodiorite 80−36299
brass, admiralty, in nonammoniacal sulphate solns. 78−27592
α-brass, corrosion fatigue and stress corrosion cracking in ammoniacal soln. 78−64757
α-brass, FCC, fractographic obs. of SCC 78−64786
α-brass, fractographic study of early stage fatigue cracks in vacuum *(Japanese)* 79−61781
brass, intergranular stress corrosion cracking mechanism 78−15597
α-brass, mechanically assisted dezincification during stress corrosion in ammoniacal solns. 80−3243
brass, stress corrosion cracking, effect of strain rate 79−20257
brass, stress corrosion cracking, in ammoniacal atmosphere, surface stress change and crack growth *(Japanese)* 77−59986
α-brass, stress corrosion cracking, initiation and propag. stages 77−73361
brass, stress corrosion cracking at low stress intensity factors 77−73362
brass, stress corrosion cracking at low stress intensity factors 79−29264
brass, stress corrosion cracking constitution of Pourbaix diagrams for ternary systems by digital computer 78−35595
α-brass, stress corrosion cracking in 15 N ammoniacal soln. 79−47802
α-brass, stress corrosion cracking in 15N ammonia solns., fractographic aspects 80−16547
α-brass, stress corrosion cracking in ammoniacal soln., strain rate effect 79−91830
α-brass, stress corrosion cracking in Mattsson's soln., benzotriazole inhibitive effect 80−16554
α-brass, stress corrosion cracking in neutral ammoniacal soln., tarnish film role 79−96183
α-brass, stress corrosion cracking in single and bicrystals 77−4866
α-brass, stress corrosion fracture surface anal. by AES 80−104321
α-brass, X-ray study *(Czech)* 78−85043
α-brass stress corrosion cracking in nontarnishing ammoniacal environment, fractography, chemical anal. 77−40466
Br.AZhNMts 7-2.5-1.5-9 bronze, Mg-Al, type, fatigue and stress corrosion cracking, welding effects 80−3233
brittle materials, thermally activated processes, reaction kinetics theory appl. 79−52429
bronze, low-cycle fatigue, NH_3 effect 80−104348
bubble form. in Al-Zn-Mg at grain boundaries after water vapour embrittlement 78−15564
BWR coolant pipes, integranular stress cracking, in-service inspection influences 80−68887
BWR Dresden-3 fuel rods, pellet/cladding interaction induced stress corrosion cracking 79−67899
cantilever beam method to investigate J_{Ic} and J_{Iscc} *(Chinese)* 78−15488
cell construction for metal SCC obs. in boiling $MgCl_2$ 78−39962
ceramic, growth micromechanism in corrosive environment 80−108616
ceramic, toughened, stress corrosion characts. 78−19912
ceramics, toughened, stress corrosion characts., exam. 78−71295
compliance and K_I calibration of double cantilever beam specimens 78−55598
concrete, cracking in seawater due to embedded metal corrosion 80−30116
conference on electrochem. test methods for stress corrosion cracking, Firminy, France (Sep. 78) 80−94910

stress corrosion cracking continued
control measures review in Cu, Ti, Al and Ni alloy and stainless steeel 77−90509
corrosion fatigue, conf., Newcastle upon Tyne, England (April 1978) 79−79166
corrosion-fatigue crack initiation in metals 77−40468
corrosion-fatigue resistance, specimen with V-shaped stress concentrator and annular cracks *(Russian)* 77−16702
crack propagation, exam. of kinetic control processes 78−60884
creep strength of deformed material, conditions of physico-chemical action *(Russian)* 77−16703
D16 alloy, sheet mat., fatigue and corrosion fatigue strengths, coatings effects *(Russian)* 78−11397
deformation and fracture kinetics 78−56791
dicyano bisphenol polycarbonate, crazing, polar group incorporation 78−85017
diffusion of H_2 towards crack in stressed solid, eigensoln. 77−24446
dissolution controlled cracking mechanism, repassivation effects 78−64772
electrochemical method for detecting threshold stress intensity 79−96189
electrode holder for electrochem. stress corrosion expts. at high temp. and press. 80−61102
electrode pot. distrib. within growing stress corrosion crack 77−90506
energy measurement and significance in acoustic emission testing 78−31594
engineering materials, intergranular fragility index 80−66637
failure, predictive approaches 80−97611
failure in corrosive medium and low cycle loading, meas. equipment 77−77676
fatigue failure, flat specimens and struct. elements in liq. corrosive media, test method 80−40646
Fe, fatigue, effect of active liquid media on struct. and stress condition *(Russian)* 77−28929
feldspar stress corrosion cracking, seen in granodiorite 80−36299
fibre reinforced plastics, creep damage *(Japanese)* 77−32702
fission reactor fuel performance anal. by finite element method 80−42750
fission reactor fuel rod deformation code FEMAXI-II and its application 80−37446
fission reactor pellet-clad interaction modelling 80−37445
fission reactor statistical fuel model, FRP 80−42748
fluid compositions within fatigue cracks 79−5081
fracture analysis of exfoliation 79−43464
fracture analysis of failure in service *(Japanese)* 80−104337
fracture of materials, conf., Waterloo, Canada (June 1977) 78−56763
fretting fatigue mechanism, environment effect 79−61775
geophysical applications of theory 77−62212
glass, annealed and tempered, contact induced static fatigue 79−8376
glass, crack front curvature and slow fracture in liquid decane 79−8375
glass, growth micromechanism in corrosive environment 80−108616
glass, toughened, stress corrosion characts. 78−19912
glass fibre reinforced plastic, NDT of strength after immersion in hot water 77−90530
glass fibre reinforced polyester crack growth micromechanism in corrosive environment 80−108615
glass fibres, crack growth during dynamic fatigue and effect on strength loss for tensile loading 80−89334
glass reinforced plastics, static and fatigue failure, fracture mechanics 78−19898
glass toughened, stress corrosion characts., exam. 78−71295
glass-ceramic, strength, effects of moisture-assisted slow crack growth 78−27593
glass-plastic AG-4c, fatigue resistance under bending in H_2SO_4 *(Russian)* 79−34163
glasses, mech. strength fracture dynamics, behaviour forecasting *(French)* 77−73344
graphite, crack propag., temp. and environment effects 78−56794
graphite fibre reinforced composites, damage by moisture, diffusion anal. 80−81227
growth over extended period, US pulse high difference method of recording 79−70235
Hastelloy C, stress corrosion cracking in high temp. caustic soln. 77−59964
Hastelloy C-276 and G, accelerated H_2 charging in aq. H_2SO_4 at 0.2% yield stress 80−30144
Hastelloy X, crevice corrosion by water vapour and methane in Ar at 1 and 25 atm. 77−25203
heat-resisting alloy, EP199, creep-rupture strength in NH_3 and decomp. products *(Russian)* 77−52534
high strength structural mats., microstruct. influences on fatigue and fracture resist. 78−56728
high temperature fracture under cyclic loading, book contrib. 79−66171
hydrogen effect on stress corrosion cracking, state of art review 80−61017
Incoloy, stress corrosion cracking in high temp. caustic soln. 77−59964
Incoloy 800, corrosion fatigue crack propagation in pure water at 85°C *(Japanese)* 79−43472
Incoloy 800, corrosion resist. props. in high temp. steam, review 79−47839
Incoloy 800, effect of liquid Na on creep and rupture props. 79−47775
Incoloy 800, exam. of caustic stress corrosion cracking, comparison with type 304 stainless steel 79−29261
Incoloy 800, high temp. corrosion and mech. props. in Na environment 79−47840
Incoloy 800, sensitisation and intergranular corrosion 79−47721
Incoloy 800, stress corrosion cracking and anodisation during straining in boiling NaOH soln. 80−30140
Incoloy 800, stress corrosion cracking in contaminated aq. media at high temp. *(French)* 79−20273
Incoloy 800, stress corrosion cracking in NaOH solns., electrochem. aspects, peening treatment 80−97618
Incoloy 800 in 50% NaOH, stress corrosion cracking, slow strain rate method *(Japanese)* 80−55575
Inconel, caustic stress corrosion cracking resistance, processing variables effect 80−71796
Inconel, stress corrosion cracking in high temp. caustic soln. 77−59964
Inconel 600, corrosion fatigue crack propag. at 85°C in 50% NaOH, potential effect *(Japanese)* 80−11834
Inconel 600, corrosion fatigue crack propagation in pure water at 85°C *(Japanese)* 79−43472

stress corrosion cracking continued
Inconel 600, exam. of caustic stress corrosion cracking, comparison with type 304 stainless steel 79−29261
Inconel 600, oxide layer, mechanical impedance meas. method 80−45444
Inconel 600, small bore tubing, crevice corrosion 80−60999
Inconel 600, stress corrosion cracking and anodisation during straining in boiling NaOH soln. 80−30140
Inconel 600, stress corrosion cracking in NaOH soln. 79−66196
Inconel 600, stress corrosion cracking in NaOH solns., electrochem. aspects, peening treatment 80−97618
Inconel 600, stress corrosion cracking in primary water 79−93728
Inconel 600, thermal treatment, grain boundary microstruct. and SCC resistance 80−71675
Inconel 600 alloys, stress corrosion cracking, prediction in 10% NaOH soln. at 315°C 80−97616
Inconel 600 and 718 in liquid Na environment, fatigue crack propag. 80−40624
Inconel 600 in 50% NaOH, stress corrosion cracking, slow strain rate method *(Japanese)* 80−55575
Inconel 625, accelerated H_2 charging in aq. H_2SO_4 at 0.2% yield stress 80−30144
Inconel 625, creep rupture strength and corrosion in HTC in He *(German)* 77−77557
Inconel alloy 600 in 10% NaOH soln. at 315°C, influence of thermal treatment 79−91841
Inconel alloy 600 steam generator tubing, effect of C content and thermal treatment on SCC behaviour 79−91844
inelastic deform. mechanism, fatigue testing in air and corrosive environments *(Russian)* 79−52432
LMFBR materials, exam. of material requirement 78−50256
low-alloy cast steel, high-strength, fracture toughness 77−56109
LWR, reliability of piping 79−18017
LWR, stress conc. in cladding produced by cracked fuel pellets 78−50260
LWR fuel rod failure associated with power changes 80−16525
LWR piping, intergranular stress-corrosion cracking 80−81234
machine for testing materials under biaxial cyclic stress in corrosive medium 79−52537
mechanicochemical testing of metals, electrochemical cell for mechanicochem. behaviour determ. 78−60905
metal, hardening and softening during absorption fatigue in surface active medium, governing laws 77−86230
metal, hydrogenating under continuous static loading, accurate electrolytic method 78−23854
metal, inhomogeneous strain effects on surface props., rel. to fracture model development 77−72907
metal, stress corrosion cracking testing apparatus in rapidly flowing liquid environment *(Russian)* 77−70249
metal, surface layer dissolution, effect of rate on softening during plastic strain 78−39957
metal in atomized NaCl solutions, fatigue strength testing unit 77−77677
metal specimens, threadlike, apparatus for performing kinetic studies on dry stress corrosion 79−83381
metallic systems, liq. metal embrittlement mechanism, Rebinder effect *(Russian)* 79−34186
metals, avoidance, critical potential data appl. 79−74308
metals, corrosion fatigue, electrochemical aspects 79−79167
metals, corrosion fatigue, role of mechanics 79−79168
metals, H effect on mech. props., review 80−50718
metals and alloys, crack resistance, aggressive environment influence *(Russian)* 79−52434
metals and alloys, electrical resistance meas. at increased temp. under stress 77−56147
metals and alloys *(Japanese)* 78−56820
micromechanisms of crack extension, conf., Cambridge, England (March 1980) 80−105421
modelling and kinetics *(Russian)* 77−77623
modelling and load ratio effects 78−90779
Monel 400, stress corrosion cracking in high temp. caustic soln. 77−59964
Monel 400, stress corrosion cracking in NaOH soln. 79−66196
Monel K-500, environmental fatigue crack growth in H_2 79−5084
Monel K-500, fatigue crack growth rates in vacuum and O_2 environment 79−5083
Mossbauer spectroscopy applics. 77−12749
Ni-base alloy 713LC, creep rupture strength and corrosion in HTR in He *(German)* 77−77557
Ni-Co, H_2 embrittlement, heat treatment and impurities effect 80−76331
Nimonic 75, crevice corrosion by water vapour and methane in Ar at 1 and 25 atm. 77−25203
Nimonic 80A, creep rupture strength and corrosion in HTR in He *(German)* 77−77557
nuclear fuel rod pellet clad interaction failures, I stress corrosion cracking tests 78−58351
nuclear fuel rod ramp ext. 78−86590
nuclear power plant, prevention *(Japanese)* 77−26835
nuclear power stations, corrosion damage, influence of water chemistry 79−54517
nuclear power stations, overview of water chemistry 79−54553
nuclear reactor vessel, corrosion fatigue crack growth rate data, appl. to integrity anal. 80−32353
nylon, stress cracking induced by $ZnCl_2$ solns. 78−27594
optical fibre, dynamic fatigue and strength degradation 80−58719
optical fibre fatigue strength, environmental and temp. effects 78−46835
optical fibre high-temperature fatigue strength and OH^- stress-induced corrosion 78−1387
optical fibre moisture effect on fracture strength 79−37019
optical fibres, stress corrosion susceptibility constant meas. 80−66680
optical waveguide fibre cladding composition effect on stress corrosion and fatigue 77−3664
paint coatings on steel, corrosion fatigue resistance *(Russian)* 77−59979
pellet cladding interaction failures, stress corrosion of fission reactor cladding tubes 80−16526
photogrammetric technique, determ. of orientation of stress-corrosion fractures 79−79163
pit propagation rate curves, new method assessing corrosion resistance 77−90514
plane strain fracture mode criterion based on plastic zone size-thickness correlation 80−43670
stress corrosion cracking continued
plastics, stress-cracking test 79−74311
PMMA, glassy, craze and crack growth *(Japanese)* 77−8970
PMMA, glassy rods, craze initiation, kerosene wetting effects 77−25172
PMMA, methanol and ethanol environment effect on stability of cracking 79−100273
PMMA, methanol crazes, craze-strain profile from holographic interferometry meas. 78−72844
PMMA, plate containing 'silver' cracks, arterial crack growth 77−86209
PMMA, stability of cracking, effect of environment 78−95806
PMMA, stability of cracking, effect of environment 78−95807
PMMA, unstable crack propagation in liq. environment, fractographic study 80−30155
polycarbonate, craze morphology, 77 to 375K, gaseous environment effect 77−63819
polycarbonate, environmental stress crazing 78−68832
polycarbonate, glassy, craze and crack growth *(Japanese)* 77−8970
polycarbonate, glassy, rolled, craze initiation *(Japanese)* 77−8969
polycarbonate, stress crazing, liq. environment effects 78−84970
polyethylene, environmental stress cracking, liq. efficiency criteria 80−21134
polyethylene, environmental stress cracking, theory 79−34176
polyethylene, environmental stress cracking at high stress, liquid wetting props. effects 78−92383
polyethylene, environmental stress cracking due to liq. viscosity, kinetic effect 77−4863
polyethylene, high density, durability, in emulsifier soln., effect of mol. mass and polydispersity *(Russian)* 79−66191
polyethylene, high density, environmental stress cracking and morphology 78−68834
polyethylene, high-density, longevity prediction, effect of surface active media 77−12729
polyethylene, ionising radiation effects crosslinking with accelerated electrons, ageing, SCC *(Polish)* 79−52701
polyethylene, low density, SEM exam. of environmental stress cracking 78−53011
polyethylene, low-density, environmental stress cracking, surfactant soln. effect 80−89376
polyethylene, resist. to stress corrosion cracking, ionising radiation effect *(German)* 80−81224
polyethylene, stress cracking in aqueous detergent 77−12727
polyethylene,environmental stress cracking, interlamellar failure 77−90476
polyethylene insulation of HV cables, water-treeing, environmental stress cracking phenomenon of elec. origin 80−40575
polyethylene terephthalate, crazing and shear deformation on stretching in air and liquids *(Russian)* 78−88558
polyethylene terephthalate fibres, chem. stress cracking after exposure to aq. methylamine 79−57131
polymer, creep prediction during random load changes and random stationary temp.-humidity conditions 77−86104
polymer, deform. polarisation effect on interaction with liquid environment, fracture *(Russian)* 77−25166
polymer, high, material behaviour under influence of stress and aggressive media *(German)* 79−39009
polypropylene, oriented, thermooxidative degradation kinetics, durability, influence of mech. initiated processes *(Russian)* 79−24591
polystyrene, fatigue props., effect of environment and surface coatings 79−43455
polystyrene, n-heptane and methanol crazes, micromechanics 77−12680
polystyrene, n-heptane and methanol crazes, structure 77−12681
polystyrene, stress cracking, pressure-induced, mechanism 80−35361
polythene, finite element anal. of crazing and cavitation by dil. aq. detergent 78−53006
potential variations 79−96176
pressure vessels, two cases of stress cracking in chem. plants 78−85027
prevention 79−96160
proportional counter appl., position sensitive *(Japanese)* 80−11853
PVC, glassy, craze and crack growth *(Japanese)* 77−8970
PVC, glassy rods, craze initiation, kerosene wetting effects 77−25172
PVC, rigid plate, simultaneous diffusion and dechlorination in H_2SO_4 *(Japanese)* 77−52521
Rebinder effect in breakdown of dielectrics 77−44328
research, book 79−100303
resistance in materials under long term static loading, evaluation methods 80−45461
review 77−8991
Sanicro 30, stress corrosion cracking in NaOH soln. 79−66196
service failure and prevention *(Japanese)* 77−28921
sheet materials, failure kinetics, method for investigating under long-term static loading in corrosive medium 80−85110
silicate glasses, stress corrosion cracking in N_2, CO_2, Ar, HCl, H_2SO_4 79−34171
specimen configuration effects, tensile and precracked data 80−16413
stainless cast high-strength steel, fracture toughness 77−56109
static and dynamic loading, crack kinetics 80−89334
steel, 15KhN3DMA, fracture under low-cycle fatigue in seawater *(Russian)* 77−52535
steel, 18 Ni-maraging, SCC, subcritical flow growth, comparison of aircraft alloys in NaCl soln. 78−53028
steel, 1Kh18N10T, corrosion fatigue during anodic polarisation after thermomech. treatment *(Russian)* 77−59976
steel, 20, 17GS, 65g and 40, H_2S cracking, KXO inhibitor simulated field trials *(Russian)* 78−31573
steel, 300M, in deionised water, temp. effects 78−53029
steel, 30CrMnSiNi2A, fracture toughness parameter K_{ISCC} 80−21099
steel, 30KhGSA, fatigue strength under fretting corrosion, effect of plasma-sprayed coatings *(Russian)* 78−11394
steel, 40KhNMA, corrosion fatigue strength, effect of polishing and diamond smoothing *(Russian)* 78−31575
steel, 4340, fracture toughness depend. on Cl_2 environment 79−100295
steel, 45 and 10KhN4MDF, corrosion fatigue under low cycle loading *(Russian)* 78−31578
steel, A533 grade B, class 1, in PWR coolant, fatigue crack growth 77−77584
steel, AISI 1020, stress corrosion cracking susceptibility and anodic behaviour in phosphate solns. at 100°C 78−7096
steel, AISI 4340, subcrit. crack growth, fracture mech. and surface chemistry obs. 79−8392
steel, AISI 6150, corrosion fatigue, effect of NaCl and shot peening 79−8391

stress corrosion cracking continued
steel, alloy, corrosion-impact-cyclic strength of boring bars, effective hardening treatment 78−53034
steel, alloy, Fe-Ni, effect of metallurgy on stress corrosion cracking, and hydrogen embrittlement 78−60885
steel, alloy, Fe-Ni-Cr-Mo-V-C, H_2S stress corrosion cracking, effects of overload, exam. 78−60886
steel, alloy, Fe-Ni-Mn-Si-Cr-Ni-Mo, effect of metallurgy on stress corrosion cracking, and hydrogen embrittlement 78−60885
steel, alloy, hardened, electrochem. charact. and stress corrosion cracking, ageing and cold treatment effects 80−108639
steel, alloy, heat-treated, crack resist. in seawater 80−104347
steel, alloy, oxidation resistance at elevated temps., effect of various alloying additions 77−56134
steel, alloy, sheet, crack-propag. resist. in heat-affected zone in presence of H, rolling direction and preliminary plastic tensile strain effects 80−60971
steel, alloy 40Kh, sulphide cracking resistance, strengthening method influence 80−55577
steel, alloy D6AC, fatigue, under const. and variable amplitude loading, air environment effect 80−35386
steel, alloy in NaOH, potentiostatic control limitations in stress corrosion crack growth meas. 78−53031
steel, austenite stainless, mechanisms *(Japanese)* 80−104336
steel, austenitic, Ni-Cr high alloy, N_2, P and Ni effect on stress corrosion cracking and stacking fault energy *(Czech)* 78−60875
steel, austenitic, type 316, in $MgCl_2$, acidity and applied potential effect on stress corrosion cracking 80−85076
steel, austenitic, X6CrNi1811 and X6CrNiMo1713, crack growth under Na cooled fast breeder reactor conditions *(German)* 78−56798
steel, austenitic and austenitic-ferritic Mn-Cr, stress corrosion cracking resistance *(Czech)* 80−45437
steel, austenitic Cr-Ni, SCC and pits in $MgCl_2$ solns. at 40-90°C 80−50748
steel, austenitic stainless, AISI 304, stress corrosion cracking and electrochem. behaviour in $(NH_4)_2SO_4$-Cl^- solns. 80−55666
steel, austenitic stainless, alloying and environmental variation effects on SCC susceptibility 78−31563
steel, austenitic stainless, analysis of fracture surface in stress corrosion cracking *(Japanese)* 80−16573
steel, austenitic stainless, cladding, stress-corrosion cracking in LWR primary circuit 79−20293
steel, austenitic stainless, corrosion product in hot conc. NaOH, effect of container material 77−63834
steel, austenitic stainless, Cr-Ni (18,8 wt.%), induction and propag. periods 78−85057
steel, austenitic stainless, electrochemical behaviour in Ringer's soln., composition effects, SCC 77−90485
steel, austenitic stainless, FCC, fractographic obs. of SCC 78−64786
steel, austenitic stainless, grain boundary segregation studies, intergranular fracturing technique for stress corrosion cracking investigation 79−39057
steel, austenitic stainless, H_2 embrittlement and SCC, austenite stability effect 79−100291
steel, austenitic stainless, high voltage electron metallography 79−52425
steel, austenitic stainless, hydride phases rel. to SCC 80−35385
steel, austenitic stainless, in boiling $MgCl_2$ solns., alloying elements effect on stress corrosion cracking and K_{ISCC} *(Japanese)* 80−93692
steel, austenitic stainless, in concentrated chloride solution 78−56825
steel, austenitic stainless, in $MgCl_2$ soln., temp. effect *(Korean)* 80−93694
steel, austenitic stainless, Kh17N13M3T, corrosion fatigue fracture in carbamide prod. *(Russian)* 78−31574
steel, austenitic stainless, metastable, fatigue endurance rel. to test piece size, corrosive environment effects *(Russian)* 79−29270
steel, austenitic stainless, Mo effect on mech. behaviour in inert medium and hot Cl^- medium *(French)* 79−43482
steel, austenitic stainless, of type 55 23 33, slow strain rate testing under electrochem. control in high temp. water 80−97650
steel, austenitic stainless, piping cracks, JPDR, stress corrosion and fatigue tests 79−66204
steel, austenitic stainless, rel. between polarisation behaviour and susceptibility to stress corrosion cracking *(Japanese)* 80−93693
steel, austenitic stainless, repassivation kinetics study in Ct media 80−97614
steel, austenitic stainless, sensitised factors influencing susceptibility 80−97617
steel, austenitic stainless, sensitized, type 304, intergranular corrosion fatigue crack growth in oxygenated pure water at 85°C 79−47814
steel, austenitic stainless, steam generator tubing, stress corrosion cracking in NaOH soln. 78−60866
steel, austenitic stainless, stress corrosion crack growth, electrochem. aspects 80−97620
steel, austenitic stainless, stress corrosion cracking, comparison with mech. tests in neutral environment *(French)* 77−70222
steel, austenitic stainless, stress corrosion cracking, effect of Cl^- content, pH, test soln. temp. 78−11388
steel, austenitic stainless, stress corrosion cracking, exam. of inhibiting action of Pb^{2+} 79−20249
steel, austenitic stainless, stress corrosion cracking, mixed mode, fractographic evidence in surgical implant 80−30156
steel, austenitic stainless, stress corrosion cracking at low stress intensity factors 79−29264
steel, austenitic stainless, stress corrosion cracking by polythionic acid *(Korean)* 80−21179
steel, austenitic stainless, stress corrosion cracking critical potential, determination *(Czech)* 79−91850
steel, austenitic stainless, stress corrosion cracking in boiling MgCl solution *(Japanese)* 78−92400
steel, austenitic stainless, stress corrosion cracking in H_2SO_4-NaCl soln., Ni and N_2 effects *(Japanese)* 79−100289
steel, austenitic stainless, stress corrosion cracking in high temp. water, heat and cooling rate effects 79−61800
steel, austenitic stainless, stress corrosion cracking problems in chemical plants 79−96190
steel, austenitic stainless, SUS 304, stress corrosion cracking in various environments, fractography *(Japanese)* 80−93690
steel, austenitic stainless, type 18-10, stress corrosion cracking in boiling solutions of $CaCl_2$, $MgCl_2$ and LiCl *(French)* 77−81342
steel, austenitic stainless, type SUS 304, welded joint, polarisation behaviour, boiling $MgCl_2$ soln. *(Japanese)* 80−93695

stress corrosion cracking continued
steel, austenitic stainless 77−90484
steel, austenitic stainless *(German)* 78−19953
steel, austenitic stainless 12Kh18N10T and 15Kh17N2, corrosion cracking in chloride and alkaline solutions 80−55576
steel, austenitic stainless 304, stress corrosion cracking in $MgCl_2$ soln., cold working effect *(Japanese)* 80−104339
steel, austenitic stainless Cl^- SCC, forming process of fan-shaped pattern 79−20287
steel, austenitic stainless SUS 301, stress corrosion cracking susceptibility, effect of strain-induced α'-martensite *(Japanese)* 80−104335
steel, austenitic stainless type-316, fracture mechanics study of stress corrosion cracking 80−16580
steel, austenitic type 304, sensitised, intergranular stress corrosion cracking inhibition study 80−100939
steel, boiler plate, comp. effects on SCC resist. *(Russian)* 78−11400
steel, C, control of SCC in radioactive waste storage tanks 79−70226
steel, C, corrosion carcking by sulphide, effect on props. 80−55587
steel, C, corrosion fatigue resistance in cavitations, bainitic and martensitic structs. *(Russian)* 78−56815
steel, C, diffusion of H_2, SCC via martensite form. cooling rate changes on Mn and Ni addition *(Russian)* 78−56813
steel, C, fatigue crack growth rate in high temp., high purity oxygenated water 80−40622
steel, C, fatigue cracks, in NaCl, oil and water vapour *(Japanese)* 78−11414
steel, C, fretting fatigue tests, effects of environmental H_2O, O_2 78−92407
steel, C, sulphide cracking resistance 80−108640
steel, C(0.2 wt.%), explosively strengthened, cause of anomalous increase in H_2 of low cycle endurance *(Russian)* 77−16729
steel, C and sensitized stainless, crack growth in high-temp. water 80−108636
steel, C-Cr (0.4, 1 wt.%), medium C, stress corrosion cracking, effect of H_2S, aggressive components of gas condensates and moisture *(Russian)* 77−16726
steel, C-Mn, accelerated H_2 charging in aq. H_2SO_4 at 0.2% yield stress 80−30144
steel, C-Mn, corrosion cracking, role of microstresses and crystal lattice stresses *(Russian)* 77−25190
steel, C-Mn, environmentally assisted fatigue crack propag., stress waveform and hold-time effects 79−79175
steel, C-Mn, stress corrosion cracking in PO_4 solns. over range of potentials and PHs 79−39021
steel, CC, rig for S-N data determ. of welded joints in corrosive environment 79−66227
steel, Co-Cr-Mo HY 180M, SCC in NaCl, temp. effect 80−108633
steel, Co-Cr-Mo type HY-180M, mech. props. and SCC, overageing effect 80−108634
steel, cold drawn prestressing tendon, rational test for stress corrosion cracking 78−44246
steel, commercial C, stress corrosion cracking susceptibility in liquid NH_3 *(Japanese)* 78−11411
steel, corrosion cracking of spherical liquid NH_3 storage tanks *(Japanese)* 77−21316
steel, corrosion fatigue, cathodic coatings effects *(Russian)* 77−52532
steel, corrosion fatigue crack growth, compliance tests and metallographic exam. 78−53027
steel, corrosion fatigue crack growth in HY80 and HY130 79−79174
steel, corrosion fatigue of offshore structures 79−79170
steel, corrosion fatigue strength, influence of magnetite films and environment *(Russian)* 79−52433
steel, Cr, cast, fracture toughness and fatigue crack propagation, structural components of hydro-turbines, in water and air 78−68822
steel, Cr (13 wt.%), tempered, quenched, fatigue resistance in corrosive medium *(French)* 78−23870
steel, Cr-Mo, H embrittlement in H_2S environment, Mo effect 80−76415
steel, Cr-Mo, low alloy, effects of stress intensity rate and stress ratio on corrosion fatigue crack growth enhancement 79−39022
steel, Cr-Mo, low alloy, stress corrosion cracking and corrosion fatigue 79−47806
steel, Cr-Mo (2.25,1 wt.%), exposed to H_2-H_2O-H_2S environment, fatigue crack growth 80−40623
steel, Cr-Mo (2.25, 1 wt.%), SCC and temper brittleness, P grain boundary segregation effect 80−55571
steel, Cr-Mo-V, cyclic oxidation and crack growth during high strain fatigue 78−31586
steel, Cr-Mo-V, environmental crack growth during isothermal high strain fatigue and temp. cycling 79−5082
steel, Cr-Mo-V, fatigue crack growth rate and threshold under oxidising conditions 79−20272
steel, Cr-Mo-V (1 wt.%) oxidation assisted crack growth during high cycle fatigue at 550°C 77−16742
steel, Cr-Ni (18,10 wt.%)-Ti stabilized, corrosion fatigue strength, inhibitor BA-6 effect *(Russian)* 77−16727
steel, Cr-Ni-Mo, resist. to corrosion and corrosion-fatigue in seawater 80−104346
steel, crack electrochemistry model in active state 80−21192
steel, crack growth velocity in gaseous H_2 embrittlement, rel. to chemisorption 80−11831
steel, crack resist. reduction in surface-active media *(Russian)* 79−52441
steel, cracking due to H_2S, exam. of fracture surface by SEM *(Japanese)* 78−53024
steel, deformability charact. in surface-active medium at decreasing temp., mech. working effect *(Russian)* 77−59851
steel, EI643 and 30KhGSNA, notch sensitivity, in mains water *(Russian)* 77−77624
steel, electrolytically notched, in direct evidence of active path formation in stress corrosion cracking in Al-alloys 80−85077
steel, environmental fracture, metallurgical variables effects, review 77−28887
steel, fatigue, effect of active liquid media on struct. and stress condition *(Russian)* 77−28929
steel, fatigue, impact loading, friction, wear in surface active media *(Russian)* 79−29268
steel, fatigue cracking kinetics in drilling soln. *(Russian)* 77−25183
steel, fatigue limit in inhibited H_2SO_4 soln., halide anion effects *(Russian)* 78−11399

stress corrosion cracking continued
steel, fatigue strength, low-cycle, under severe loading, friction-strengthening treatment effect *(Russian)* 79−52435
steel, ferrite-austenite welded joints, corrosion cracking resist. *(Russian)* 79−52437
steel, fracture toughness and dynamic strength, surface active agent effects *(Russian)* 78−56812
steel, H_2 permeability in inhibited H_2SO_4 corrosion, stress level effects *(Russian)* 77−52530
steel, high strength, anodic polarization and corrosion cracking in liquid NH_3 *(Japanese)* 77−21317
steel, high strength, corrosion cracking in liquid NH_3, preventive methods *(Japanese)* 77−48578
steel, high strength, corrosion fatigue in low press. H_2 gas 79−79172
steel, high strength, environmental effects on initiation and propag. of fatigue cracks 77−86216
steel, high strength, slow crack growth in H_2-H_2S mixture 79−43461
steel, high strength, stress corrosion cracking in liquid NH_3, effect of air and water *(Japanese)* 77−48579
steel, high strength, stress corrosion cracking mechanism 77−28925
steel, high strength, stress corrosion cracking susceptibility in liquid NH_3 at low temps. 79−47809
steel, high strength, sulphide stress cracking props., density and distrib. of intergranular sulphide effects 79−74291
steel, high strength, type 90 Mn V8, stress corrosion crack velocities in NaCl soln. 80−21161
steel, high strength 0.77%C, surface dissolution effect 77−8883
steel, high strength D6AC, compliance technique appl. for side grooving effect study on stress corrosion crack kinetics 79−74312
steel, high temperature strength, corrosion-erosion effect of gas metal mixtures stream *(Russian)* 78−35576
steel, high-strength, 80 kg/mm^2 class, effects of metallurgical factors on susceptibility of stress relief testing *(Japanese)* 79−43458
steel, high-strength, brittle fracture in calcium hydroxide environment *(Russian)* 79−52439
steel, high-strength, corrosion cracking under antiplane strain *(Russian)* 77−52531
steel, high-strength, Cr (1 to 15 wt.%) effect on crack initiation stress *(Russian)* 77−16725
steel, high-strength, criteria for determining struct. strength and reliability 77−60021
steel, high-strength, endurance in air and NaCl soln., loading freq. effects *(Russian)* 78−56810
steel, high-strength, type 4340, new inhibitors for crack arrestment in corrosion fatigue 80−100941
steel, high-strength 12KhN3A, anode and cathode processes in corrosive environment, fatigue *(Russian)* 78−35573
steel, high-strength low-alloy, stress corrosion cracking in NaCl solution *(Japanese)* 78−92401
steel, high-strength plate with soft cladding layer, failure resistance during repeated static banding 77−44406
steel, high-strength reinforcing, 20GS2, local microstresses on creep strength in hydrogenating media *(Russian)* 77−52462
steel, high-temp. high temperature thermomechanically heat treated, fatigue strength improvement by cathodic polarisation *(Russian)* 77−25188
steel, hollow cylinder, thick walled, effect of thermomech. treatment 80−11674
steel, HY130, corrosion fatigue and crack growth in salt water 78−72929
steel, hydrogen induced cracking under wet H_2S environment 77−32721
steel, hydrogenation and cracking in H_2 S, cathodic polarization and surface layer effects *(Russian)* 77−52528
steel, hydrogenation during acid corrosion under stress, laboratory apparatus for study *(Russian)* 77−77656
steel, hydrogenation in HCl, influence of conc. depend. of anilines additives on time to fracture, principle of linearity of free energy *(Russian)* 79−15854
steel, inelastic deform. mechanism, fatigue testing in air and corrosive environments *(Russian)* 79−52432
steel, low alloy, 18KhMVTCh, corrosion cracking resistance in sulphide environments *(Russian)* 78−31571
steel, low alloy, C, corrosion fatigue crack growth, waveform effect *(Japanese)* 79−29274
steel, low alloy, constructional, fatigue cracking in corrosive media 78−85081
steel, low alloy, exam. of stress corrosion cracking in H_2S environments by const. strain rate method 79−29260
steel, low alloy, fatigue crack growth rate in high temp., high purity oxygenated water 80−40622
steel, low alloy, fatigue crack propag. in deaerated distilled water 77−25177
steel, low alloy, Ni, exam. of stress corrosion cracking in S environment 79−20256
steel, low alloy, SMCM 8, tempered, fractographic study of stress corrosion cracking *(Japanese)* 79−66214
steel, low alloy, SNCM 8, quenched, tempered, prior austenite grain size effect on stress corrosion cracks *(Japanese)* 79−66215
steel, low alloy, sulphide corrosion cracking resistance, test procedure and eval. 77−63842
steel, low alloy and mild, stress corrosion cracking in CO-CO_2-H_2O 77−21308
steel, low alloys, high strength, stress corrosion cracking in saturated $Ca(OH)_2$ solns., due to Cl^- and SO_4^{2-} additions 78−88567
steel, low C, and alloy, corrosion fatigue strength determ. *(Japanese)* 80−25910
steel, low C, C content effects in corrosion fatigue in nitrate solns. *(Russian)* 78−56811
steel, low C, close coiled helical spring, corrosion under axial deflection and const. load 79−52428
steel, low C, corrosion, heat treatment and plastic deform. effects 77−63825
steel, low C, corrosion fatigue strength, soln. pH effects *(Japanese)* 77−52545
steel, low C, fatigue endurance limit, metallurgical technology and mech. treatment effect 80−55536
steel, low C, fatigue strength, influence of mech. stress level in preliminary corrosion 80−55579
steel, low C, high frequency fatigue limit, external factor effects *(Czech)* 77−59988
steel, low C, hot rolling effects on struct. *(Russian)* 78−19793
stress corrosion cracking continued
steel, low C, long life corrosion fatigue strength under continuous and alternate immersion in 1% NaCl *(Japanese)* 77−12736
steel, low C alloy, SNCM2, waveform effect on corrosion fatigue crack growth in NaCl soln. 80−21163
steel, low cycle corrosion fatigue, protective effect of inhibitor HOSP-10 *(Russian)* 77−16721
steel, low-alloy pipe, low-cycle fatigue in H_2-evolving media, S content and sulphide inclusion effects *(Russian)* 78−11398
steel, low-C, corrosion inhibitors, effect on corrosion fatigue *(Russian)* 77−59977
steel, maraging, 18 Ni, welded joints ageing props. obs. *(Japanese)* 80−40401
steel, maraging, Co-Ni-Mo (20,15,5 wt.%), environmentally assisted fracture 77−52547
steel, maraging, Ni, stress corrosion cracking 78−35563
steel, maraging N18K9M5T, crack propag. resistance under stress corrosion 77−70224
steel, martensitic, corrosion cracking mechanism in Cl and sulphide containing environment *(Russian)* 77−59969
steel, martensitic, low C without Ni, for deep-well sucker rods, corrosion fatigue 80−55588
steel, martensitic, low tempered, high strength, fatigue crack, propag. rate *(Czech)* 78−64770
steel, martensitic, Ni-Cr-Mo, fatigue crack initiation and propag. in water 77−9000
steel, martensitic, stainless, CrMoV, stress effect on pitting susceptibility 80−16542
steel, martensitic 07Kh16N4B, corrosion cracking in chloride and alkaline solutions 80−55576
steel, martensitic low C, development and props. *(Russian)* 80−20933
steel, martensitic stainless, in SO_4 solns., activation pH and susceptibility to H_2 assisted stress corrosion cracking 80−97619
steel, martensitic-aged, plastic deformation influence in type N17K12M5T steel on mech. props. *(Russian)* 80−76305
steel, medium C, 45, fatigue strength increase by plasma steel coatings, fretting corrosive cond. 79−15875
steel, medium C, 45, Ti+Al coated, failure during high temp. creep in NH_3 79−11731
steel, medium C, surface burnishing effect on low cycle corrosion fatigue *(Russian)* 77−16730
steel, mild, cathodic protection against corrosion fatigue cracks 79−74281
steel, mild, corrosion in lime water, stress effect 80−11815
steel, mild, cyclic plastic deform. effect on electrode reactions in aq. chloride soln. of varying pH 77−52548
steel, mild, cyclic strain enhanced dissolution in NH_4NO_3, corrosion fatigue props. 80−85083
steel, mild, fatigue life, effect of H_2S and SO_2 gas 79−15871
steel, mild, interface between corrosion fatigue and stress corrosion cracking 77−86172
steel, mild, mild, transgranular stress corrosion cracking in H_2SO_4-KCl soln., XPS obs. 80−16556
steel, mild, stress corrosion cracking in NH_3 vapour above liquid NH_3 77−28926
steel, mild, time dependent plastic relaxation at crack tip, fracture implications 77−63765
steel, mild, transgranular stress corrosion cracking in H_2So_4-KI soln. 80−71797
steel, Mo-Nb (2.5, 0.035 wt.%) Mo content effect on sulphide stress cracking resistance 80−21157
steel, modelling and kinetics *(Russian)* 77−77623
steel, Nb-Mo, Mo effect on sulphide stress cracking resistance 80−16552
steel, Ni, low alloy, low strength, stress corrosion cracking in sulphide environment 79−47812
steel, Ni (5 wt.%), corrosion fatigue 78−27683
steel, Ni-Co-Cr-Mo-C (10,14,2,1,0.16 wt.%), stress corrosion cracking at 22°C in 3.5% NaCl 79−8390
steel, Ni-Cr, exam. of caustic stress corrosion cracking, comparison with type 304 stainless steel 79−29261
steel, Ni-Cr, SCC, grain boundary impurity effect 80−30150
steel, Ni-Cr-Mo, crack growth in different media, test frequency effect *(German)* 79−66194
steel, Ni-Cr-Mo, influence of air temp. and water vapour content on fatigue behaviour 79−43463
steel, Ni-Cr-Mo, surface burnishing effect on low cycle corrosion fatigue *(Russian)* 77−16730
steel, Ni-Cr-Mo, weld, stress corrosion cracking, metallurgical effects 79−43468
steel, Ni-Cr-Mo (11, 5, 3 wt.%), maraging, corrosion cracking in chloride and alkaline solutions 80−55576
steel, Ni-Cr-Mo-V, corrosion fatigue crack growth in NaOH soln., cathodic pot. effect 80−89403
steel, Ni-Cr-Mo-V, fatigue crack growth, effect of aq. and H_2 environment 79−79173
steel, Ni-Cr-Mo-V, in NaOH soln., corrosion fatigue crack growth rate, applied pot. effect 80−60998
steel, Ni-Cr-Mo-V, stress corrosion cracking 77−52542
steel, NiCrMoV, stress corrosion cracking, cold work effects 78−11383
steel, non-irradiated and irradiated specimens, autoclaves for fatigue crack growth tests *(German)* 80−45467
steel, nonsensitized ferritic stainless, effects of alloying and environmental variations on chloride SCC 79−96194
steel, optical detection of acoustic emission 77−90510
steel, pressure vessel, ASME SA-387 grade D, fatigue crack growth, liquid Na environment effects 77−8997
steel, pressure vessel for light water reactors, corrosion fatigue, data review 79−79169
steel, pressure vessels, two cases of stress cracking in chem. plants 78−85027
steel, protective props. of N-containing inhibitors *(Russian)* 78−56809
steel, quaternary pyridine salts as inhibitors of corrosion fatigue in $MnCl_2$ soln. *(Russian)* 77−59973
steel, quenched, corrosion cracking in NaCl soln. *(Russian)* 78−56801
steel, quenched and tempered, environmentally assisted fatigue crack propag. 77−44403
steel, reinforcing, 20GS2, brittle fracture resistance in corrosive environment, tempering effects *(Russian)* 77−59974
steel, reinforcing bar, high-strength 20GS2 and 20KhGS2 80−55578
steel, short-cycle, fatigue, stress concentration effect 78−95859

stress corrosion cracking continued
steel, Si-Mn-Ni-Cr-Mo, acoustic emission during stress corrosion cracking appl. to materials testing 78−53042
steel, Si-Ni and Cr gas turbine blade material, corrosion fatigue testing 79−70247
steel, St-3, and 45G17Yu3, effect of paint coatings on corrosion fatigue strength, for corrosion in seawater *(Russian)* 78−31572
steel, stainless, 18-8, stress corrosion cracking, in H_2SO_4-NaCl soln. *(Japanese)* 77−21315
steel, stainless, 18-8, stress corrosion cracking in H_2SO_4-NaCl soln., strain induced martensite effects *(Japanese)* 77−56152
steel, stainless, 18-8 Ti and 18-8 Nb, in polythionic acid solution, preventive measures determ. 78−56824
steel, stainless, 1Kh16K4N2MVFBA, corrosion-fatigue strength *(Russian)* 79−15856
steel, stainless, 1Kh18N10T, solution annealed effect of cyclic stresses on corrosion rate in acid environments *(Russian)* 78−31577
steel, stainless, 304, shot peened, stress corrosion cracking, const. strain rate investig., cold work, sensitisation effect 79−20259
steel, stainless, 304, stress corrosion cracking in boiling $MgCl_2$ soln. *(Japanese)* 79−43476
steel, stainless, 304, stress corrosion cracking in H_2SO_4-NaBr aqu. soln. *(Japanese)* 80−108629
steel, stainless, 304, stress corrosion cracking in H_2SO_4-NaI aqu. soln. *(Japanese)* 80−108630
steel, stainless, 304, stress corrosion cracking of single crystal in H_2SO_4-NaCl soln. *(Japanese)* 79−96202
steel, stainless, 304 type, cracks initiation in 25% $MgCl_2$ solution at 80°C *(Japanese)* 80−10593
steel, stainless, austenitic, surface films grown in Cl^- solns., ellipsometric investig. 79−20261
steel, stainless, bone implant, stress corrosion cracking 77−56519
steel, stainless, BWR cooling system pipes 78−23880
steel, stainless, cold worked, pitting corrosion in NaCl soln. 78−44257
steel, stainless, corrosion fatigue cracking in NaCl aqueous solution, fractographic anal. *(Japanese)* 78−53023
steel, stainless, corrosive environment effect on fatigue crack growth rate 80−55584
steel, stainless, Cr-Mo, problem of stress corrosion cracking *(Czech)* 78−85044
steel, stainless, crack resistance in chloride soln., electrochem. protection, polarization effect 80−55589
steel, stainless, critical cooling rate for sensitization and intergranular stress corrosion cracking in high temp. water 79−47807
steel, stainless, duplex type 304, strain rate effect on stress corrosion cracking, in boiling $MgCl_2$ 80−21180
steel, stainless, duplex weld metal, ferrite content effect on SCC at room temp. 79−91834
steel, stainless, failure by corrosion fatigue, exam. 78−64787
steel, stainless, fatigue, influence of ageing and plastic deformation *(Russian)* 79−15857
steel, stainless, fatigue crack growth behaviour in air and high-C liquid Na, carburization studies 80−40625
steel, stainless, fatigue crack growth rate in high temp., high purity oxygenated water 80−40622
steel, stainless, fatigue failure kinetics, effect of water 80−55585
steel, stainless, ferritic, Cr-Mo, corrosion behaviour, review 79−39018
steel, stainless, fluid compositions, within fatigue cracks 79−5081
steel, stainless, high strength, influence of corrosive medium on low cycle fatigue, photography obs. *(Russian)* 79−34199
steel, stainless, Kh18N10T, quinoline salt inhibitors for corrosion in $MgCl_2$ soln. *(Russian)* 78−31579
steel, stainless, maraging, crack growth, environment effects 78−64785
steel, stainless, martensitic, practical fatigue and corrosion fatigue limits *(French)* 77−59993
steel, stainless, orthopaedic, type En58J, Mo ion-plating, corrosion fatigue 80−66694
steel, stainless, proneness to intergranular corrosion, plasticity change tests 77−73366
steel, stainless, sensitised type 304, cyclic loading effect of SCC susceptibility in water 80−45428
steel, stainless, stress corrosion cracking, due to boiling $MgCl_2$ solution, SEM exam. *(Japanese)* 78−53025
steel, stainless, stress corrosion cracking, prestrain effect, stress relaxation study 80−35384
steel, stainless, stress corrosion cracking and anodisation during straining in boiling NaOH soln. 80−30140
steel, stainless, stress corrosion cracking and microhardness, effect of bombardment by He^+, Ni^+ and Cr^+ 80−85087
steel, stainless, stress corrosion cracking avoidance by improved welding in BWR pipes 80−42838
steel, stainless, stress corrosion cracking in elev. temp. aqueous environment 79−43462
steel, stainless, stress corrosion cracking in H_2SO_4-NaCl soln., stress effect *(Japanese)* 79−43471
steel, stainless, stress corrosion cracking in high temp. water, surface prep. effect 79−5088
steel, stainless, stress corrosion cracking inhibition in chloride soln. 78−35558
steel, stainless, stress corrosion susceptibility in high purity water, O_2 and temp. effects 80−61002
steel, stainless, stress corrosion testing, slow strain rate, elevated temp. and high press. study 80−97615
steel, stainless, sulphide stress corrosion cracking resistance, improvement by heat treatment 78−7076
steel, stainless, surgical implant, SCC and corrosion fatigue in Tyrode's soln. 79−29263
steel, stainless, SUS 304, environment effects on partitioned strain life relations *(Japanese)* 79−87753
steel, stainless, type 300 and ferritic, stress corrosion cracking in high temp. caustic soln. 77−59964
steel, stainless, type 304, BWR coolant pipe, critical strength under stress corrosion cracking 80−52743
steel, stainless, type 304, corrosion fatigue and stress corrosion cracking, in boiling NaOH 80−7719
steel, stainless, type 304, elastoplastic fracture mechanics for reactor piping 78−68777
steel, stainless, type 304, oxyanions inhibitive effect on stress corrosion cracking 80−35374
steel, stainless, XM19, stress corrosion resistance 80−16558

stress corrosion cracking continued
steel, stainless 18-8, stress corrosion cracking in H_2SO_4-NaCl soln., martensite form. *(Japanese)* 78−92396
steel, stainless 301, stress corrosion cracking in $MgCl_2$ soln., environment effect on initiation and propag. *(Japanese)* 80−104338
steel, stainless 304, corrosion crack initiation at growing pits under pulsating level *(Japanese)* 78−11409
steel, stainless 304, corrosion crack initiation in active potential range under pulsating loads *(Japanese)* 78−11408
steel, stainless 304, intergranular stress corrosion cracking mechanism 78−15597
steel, stainless 304, sensitized electrochemical polarisation in high temp. water *(Japanese)* 79−15868
steel, stainless 304, slow strain rate 77−59965
steel, stainless 304, stress corrosion, high temp. electrochemical studies 80−30146
steel, stainless 304, stress corrosion cracking, chloride effect, constant strain rate testing in high temp. water 78−35568
steel, stainless 304, stress corrosion cracking, classification in various environments *(Japanese)* 80−71805
steel, stainless 304, stress corrosion cracking environmental effects in high temp. water *(Japanese)* 77−63827
steel, stainless 304, stress corrosion cracking in boiling $MgCl_2$, crack growth rate study by SERT method *(Japanese)* 79−100290
steel, stainless 304, stress corrosion cracking in high temp. water, constant strain rate meas. 78−31565
steel, stainless 304, stress corrosion cracking in high temp. water, effect of environmental factors 79−1924
steel, stainless 304, stress crack initiation in chloride soln., role of corrosion pits *(Japanese)* 78−92397
steel, stainless 304L, stress corrosion cracking in 5 mol/l H_2SO_4/0.1 mol/l NaCl soln., temp., strain effects 78−31590
steel, stainless 304L, stress corrosion morphology in H_2SO_4/NaCl soln. at room temp., electrochemical potential effect 78−15596
steel, stainless and C, cracking in NH_3 at 600°C 79−70207
steel, stainless austenitic 316, stress corrosion cracking, environments responsible 79−20242
steel, stainless fracture character under tension, in S-H_2 atmosphere *(Russian)* 79−34198
steel, stainless in elevated temp. Na environment 79−24666
steel, stainless type 304, fission reactor piping cracks, metallurgical exam., failure anal. 79−67849
steel, stainless type 304, rel. between intergranular stress corrosion cracking and intergranular corrosion in acid solns. *(Japanese)* 79−79156
steel, stainless type 304 attack morphology of stress corrosion cracking, TEM study *(French)* 79−83368
steel, steady diffusion-migration eqns., representing mass conc. of dissolved species in cracks 80−30108
steel, steady-state electrode pot. in sea water under cycle loading *(Russian)* 78−56802
steel, stress corrosion cracking, in liquid NH_3, electrochemical exam. *(Japanese)* 78−39945
steel, stress corrosion in inhibited H_2SO_4, surface macrogeometry and endurance *(Russian)* 77−25184
steel, struct., corrosion fatigue strength, effect of medium temp. 80−55583
steel, structural, naturally and artificially weathered, SEM characteris. 78−23882
steel, structural, notched, cathodic polarisation effect on fatigue in seawater 79−47805
steel, sulphide stress corrosion cracking, threshold stress and crack initiation stress intensity comparison 80−21158
steel, sulphide stress cracking of big-inch line pipes 77−12730
steel, testing in moist H_2S 78−23901
steel, TRIP, strength and plasticity rel. to thermomech. treatments 77−44281
steel, tufftrided, observation of fatigue fracture surface *(Japanese)* 78−52951
steel, U8, diffusion coating protection for H_2 embrittlement, SCC and tensile tests *(Russian)* 78−31513
steel, ultrahigh strength, Si addition and retain austenite effect on SCC, quenched and tempered 78−48567
steel, welded joints of tube 10G2SD, corrosion fatigue *(Russian)* 78−35574
steel, white layers effects on stress-corrosion resistance rel. to C content *(Russian)* 78−11393
steel, with anodic coating, corrosion fatigue *(Russian)* 77−70206
steel, X70, fatigue crack growth rate in air and saltwater, stress ratio effect 80−100952
steel 20, protective props. of diammonium salt-based inhibitors *(Russian)* 78−56808
steel 23K2G2T, corrosion cracking susceptibility, C and Cr effects 78−19952
steel 30KhGSNA, strength under combined compound stresses and corrosive environment *(Russian)* 78−56803
steel 40Kh, thermally strengthened, influence of loading rate and sea water on K_{1c} value *(Russian)* 78−56799
steel 45, B-Al coated, creep and long term strength in NH_3 79−91854
steel 45, fatigue strength determ. apparatus, in corrosive environment under complex stress *(Russian)* 77−77657
steel austenitic stainless, stress corrosion cracking at low stress intensity factors 77−73362
steel fracture resistance, delayed, test-piece dimensions influence *(Russian)* 79−52478
steel intercrystalline stress corrosion cracking in a $Ca(NO_3)_2$ soln. *(German)* 80−30130
steel JIS SNCM8, enhancement of delayed failure resistance by partial unloading method, environment effects 79−79146
steel Ni-Cr-Mo-V, and Cr-Ni-Mn type 4340, hydrogen bearing environment effect on K_{Iscc} 80−104325
steel stainless, Ti stabilised, intercrystalline corrosion, repeated cold deform. effect 79−57000
steel U8, hydrogenation effects on fatigue crack propag. *(Russian)* 78−56800
steel/steel bimetal, creep-rupture strength in corrosive environment *(Russian)* 77−52533
steels, austenitic stainless, stress corrosion cracking, correl. between electrochem. and mech. parameters 80−97613
steels, hydrogen cracking under long-term strength tests 77−86243
steels, mechanism of H_2 entry in acid environments 79−39023

stress corrosion cracking continued
steels, stainless, accelerated test for susceptibility to Cl_2 stress corrosion cracking 80−21199
steels, strength reduction by adsorpt., stress corrosion *(Russian)* 79−29265
steels 2Kh13 and 20Kh1M1FTR, sulphide cracking resistance, strengthening method influence 80−55577
strain gauging techique for monitoring fracture mech. specimens during environmental testing 78−31606
stress corrosion cracking, effect of orientation and loading history 77−56143
structural steels and alloys, conf., Kiev, USSR (Sep. 1976) 77−59921
styrene alpha methylstyrene copolymer, microcrack development under atmospheric ageing 77−86210
styrene-acrylonitrile copolymer swelling, glass transition and crazing, polar group incorporation 78−85017
subcritical crack velocity, free energy considerations 79−8374
surgical implant materials, corrosion fatigue props. 79−39604
TEM study *(French)* 77−56153
test equipment, multisection plan for H_2 absorpt. of metals for tests under cathodic polarisation conditions 79−52504
test machine, design and construction, appl. to Fe-Cr-Ni alloys 80−97649
test specimen-fixture interaction for slow crack-growth 77−56166
testing device, lab. and autoclave testing 79−52502
thermocyclic stress effects in corrosive-media, electrochem. polarization applic. *(Russian)* 78−11356
Vitallium, surgical implant, SCC and corrosion fatigue in Tyrode's soln. 79−29263
wedge opening load specimen, side grooved, stress intensity factor soln. and calibration 78−51130
Zircaloy, cladding in fuel rods, stress corrosion fracture on power increase 79−47818
Zircaloy, fatigue crack propag., environmental effects *(French)* 77−66711
Zircaloy, LWR cladding, I_2 stress corrosion cracking 79−89380
Zircaloy, LWR fuel rod cladding, damage accumulation during I_2-induced stress corrosion cracking 80−71810
Zircaloy, textural model for stress corrosion crack susceptibility 79−47825
Zircaloy, unirrad., I_2-induced, effect of test temp., alloy comp. and heat treatment 80−97632
zircaloy 2, annealed, corrosion fatigue in aqueous soln. at 575K 78−64789
Zircaloy 2/I_2 system, stress corrosion crack growth for short cracks 78−80685
Zircaloy clad UO_2 fuel elements, irrad. effects 80−666
Zircaloy cladding, stress corrosion cracking, inner surface texture effect 80−66695
Zircaloy cladding, stress corrosion cracking due to I and Cs redistrib. in LWR fuel rods 80−32343
Zircaloy cladding, stresses due to pellet cladding interaction 80−42762
Zircaloy cladding stress corrosion cracking due to I *(Japanese)* 80−78361
Zircaloy LWR cladding, modeling of deform. and fracture in SPEAR code system 79−93729
Zircaloy tubing, I_2 stress corrosion cracking, pellet cladding interaction mechanism *(German)* 80−16565
Zircaloy-2, Cd metal embrittlement in 300-340°C 77−16747
Zircaloy-2, deformation and fracture behaviour, uniaxial tension test in I_2 environment 80−13580
Zircaloy-2, embrittlement in I_2, environmental purity effect 80−30149
Zircaloy-2, exposed to I_2 vapour, stress corrosion crack initiation sites 78−92324
Zircaloy-2, for nucl. reactor applic., cracking mechanism in iodine containing solns. 77−34402
Zircaloy-2, I_2 stress corrosion cracking, Cs_2O and Cs influence, in- and out-of-pile 80−3252
Zircaloy-2, iodine environment, plane strain tension test 80−22944
Zircaloy-2, mech. props. after exposure to I_2-methanol solutions, SEM study 80−93689
Zircaloy-2, reversible embrittlement in CH_3OH/HCl 79−91833
Zircaloy-2 cladding, fracture in iodine environment 78−31581
Zircaloy-2 cladding, in iodine vapour, 250-450°C 78−17313
Zircaloy-4 clad UO_2 fuel, long term storage in water and stress corrosion cracking 79−93737
Zircaloy-4 cladding rubes, burst strain and stress corrosion cracking, I influence 80−3248
Zircaloy-4 tubes, I stress corrosion cracking *(Korean)* 79−34195
Zircaloy-4 tubing, unirradiated, under internal pressurisation, threshold conditions for I-induced stress corrosion cracking 79−66206
Zircaloys, fractographic distinction between hydride cracking and stress corrosion cracking 78−92363
Zircaloys, I_2 induced stress corrosion cracking 79−8381
Zircaloys 77−63824
Al alloy, 2024-T851 SCC, subcritical flow growth, comparison of aircraft alloys in NaCl soln. 78−53028
Al alloy, 7175 T 651, crack tip opening under cyclic loading, effect of environmental and R-ratio 80−45377
Al alloy, anodised, corrosion fatigue endurance *(Russian)* 77−16724
Al alloy, corrosion fatigue testing, galvanostatic vs. potentiostatic control 77−40467
Al alloy, D16ATV, clad, effect of surface corrosion on fatigue testing *(Russian)* 78−31576
Al alloy, fatigue, mechanoenvironment effects 77−32717
Al alloy, fracture mechanisms review 80−35296
Al alloy, fretting fatigue tests, effects of environmental H_2O, O_2 78−92407
Al alloy, stress corrosion cracking, active path form., electrolytically notched specimens 77−16713
Al alloy, stress corrosion cracking, effect of orientation and loading history 78−95835
Al alloy, surface layer influence on corrosion fatigue strength *(Japanese)* 80−16574
Al alloy, type 7075, hydrogen induced fracture 79−91837
Al alloy 2017, corrosion fatigue strength, tensile prestrain effects *(Japanese)* 78−56819
Al alloy 7075, cyclically deformed, high strength, hydrogen embrittlement 78−31584
Al alloy 7075-T6, embrittlement by cathodic H_2, surface film effect 78−64643
stress corrosion cracking continued
Al alloy fatigue crack growth, stage I, effect of liquid environment 77−86164
Al alloy RR 58, stress corrosion cracking, effect of orientation and loading history 77−56143
Al alloy V95T1 sheets, failure kinetics, method for investigating under long-term static loading in corrosive medium 80−85110
Al alloys, constant strain rate test method evaluation 79−20296
Al alloys, extrusion, purity effect on fracture props. 79−100248
Al alloys, fatigue crack arrest, corrosive environment, at low stress intensities 78−92415
Al alloys, marine atmosphere stress corrosion tests on precracked specimens, corrosion product wedging effect 78−88570
Al alloys, stress corrosion crack growth 78−19930
Al alloys, stress corrosion cracking protection, by $\gamma_1 Al_2O_3$ anodic film 78−95836
Al alloys RR58 and LM30, fatigue crack growth, environment effect 79−79171
Al, bicrystal, liquid metal induced grain boundary fracture, relative orientation effects 77−36690
Al bronze, duplex alloy, corrosion fatigue behaviour 79−70218
Al, commercial purity, mean stress effect on commercial purity 77−86227
Al, fatigue, effect of active media on struct. and stress condition *(Russian)* 77−28929
Al single crystals, effect of environment on liquid-metal embrittlement, stress corrosion cracking and corrosion fatigue 78−64676
Al, sliding wear in NaCl of varying pH 78−3240
Al-Cu (4 wt.%), fatigue crack propag. role of adsorption in H_2S, Hg and moist air *(French)* 78−15580
Al-Cu (4 wt.%), stress corrosion cracking, effect of cold reduction *(Japanese)* 77−48580
Al-Cu-Mg, aged, stress corrosion cracking in NaCl soln. 80−7709
Al-Cu-Mg-Fe-Ni, Hiduminium RR58, crack propag. rates in air and salt soln. 80−21063
Al-Cu-Mn (6.3,0.3 wt.%), alloy Al 2219-T851, crack closure load development for surface microcracks 77−86226
Al-Cu-Mn-Mg alloy D16, sheet, corrosion fatigue strength, with anodised and painted surfaces *(Russian)* 78−35575
Al-Cu-Mn-Mg-Fe-Si, corrosive environment effect on fatigue crack growth rate 80−55584
Al-Cu-Mn-Mg-Fe-Si-Zn alloy D16, surface layers chem. composition rel. to fatigue resist., corrosion-fatigue resist. 79−29275
Al-Mg, alloy 5083, effect of environmental factors on stress corrosion cracking 78−80684
Al-Mg (7 wt.%), corrosion cracking, exam. of slip dissolution and hydrogen embrittlement mechanisms 78−72852
Al-Mg (7wt.%), corrosion fatigue crack propag. 80−30145
Al-Mg alloy Al27-1, corrosion cracking behaviour and fine struct. *(Russian)* 79−52438
Al-Mg-Zn, granulated, degassing atm. effect on mech. props. of semifinished products 80−7720
Al-Mg-Zn alloy 7179-T651, reduced ductility under tensile after exposure to water 80−11835
Al-Mn-Zn, fatigue cracks, in NaCl, oil and water vapour *(Japanese)* 78−11414
Al-Si-Cu, LM30, crack propag. rates in air and salt soln. 80−21063
Al-water vapour reaction, stress corrosion susceptibility STEM study, Mg addition effect 80−3247
Al-Zn alloy, type 7010, die-forged, tensile props. after heat treatment, stress corrosion 79−66103
Al-Zn-Mg, crack-arrest markings on integranular stress corrosion fracture surfaces 80−89405
Al-Zn-Mg, effect of microstruct. and corrosive environments on stress corrosion cracking *(Japanese)* 79−79159
Al-Zn-Mg, stress conversion cracking based on micromech. surface reactions 80−7716
Al-Zn-Mg, welded section stress in rolled plate edges, mechanical surface treatment and environment effects 80−21193
Al-Zn-Mg (4.5, 2 wt.%) alloys, stress corrosion resist., vac. heat treatment effect 79−96203
Al-Zn-Mg (4.5, 2.5 wt.%), composition effect on stress corrosion and mech. behaviour 78−27684
Al-Zn-Mg (5, 1 wt.%), relation between mech. props., SCC and dislocation struct. *(German)* 77−81345
Al-Zn-Mg (5,2.5 wt.%) observation of stress corrosion cracking 78−60868
Al-Zn-Mg (6.27, 2.94 wt.%), single crystals, effect of environment on liquid-metal embrittlement, stress corrosion cracking and corrosion fatigue 78−64676
Al-Zn-Mg alloy, stress corrosion cracking, exam. *(Japanese)* 78−53026
Al-Zn-Mg alloy 1915, stress corrosion cracking, protective anodic film *(Russian)* 78−35572
Al-Zn-Mg alloy AA-7039, stress corrosion cracking, SEM obs. 80−104323
Al-Zn-Mg alloys, grain boundary segregation, implications to stress corrosion cracking 80−84936
Al-Zn-Mg alloys, H_2 bubbles in embrittlement 78−19868
Al-Zn-Mg alloys, stress corrosion cracking *(Japanese)* 77−25194
Al-Zn-Mg alloys 80−35395
Al-Zn-Mg type 7N01-T4, weld, SCC in NaCl-H_2O_2 soln. *(Japanese)* 80−108631
Al-Zn-Mg type 7017 and 7018 alloy plate, fractographic study of stress-corrosion crack propag. 79−57158
Al-Zn-Mg-Cu, age hardened, effect of strain rate, temp. and environment on ductility 80−45368
Al-Zn-Mg-Cu, flaw growth in stress corrosion environment 79−66198
Al-Zn-Mg-Cu, type 7075, microstruct. role in hydrogen assisted fracture 80−30091
Al-Zn-Mg-Cu (6,2, xwt.%) type alloy, fatigue crack propag., Cu content and recryst. effect 80−60960
Al-Zn-Mg-Cu (6.76, 2.37, 1.80 wt.%), cyclic SCC in salt water *(Japanese)* 80−45435
Al-Zn-Mg-Cu age-hardened alloys, fatigue crack propagation rel. to grain size in vac. and NaCl soln. 80−16538
Al-Zn-Mg-Cu alloy, stress corrosion cracking mechanisms, rel. to micrographic obs. *(French)* 77−73376
Al-Zn-Mg-Cu alloy, type 7050 and AZ 74.61, engineering props. 79−70219
Al-Zn-Mg-Cu alloy 7075, SCC from T6 to overaged T7X 77−90487

stress corrosion cracking continued
Al-Zn-Mg-Cu alloy 7075, overaged, precracked stress corrosion specimen, incubation effects 79−91832
Al-Zn-Mg-Cu alloys, effect of alloying elements as stress corrosion failure using regression analysis 78−80669
Al-Zn-Mg-Cu type 7XXX, Cu effect and recrystallisation, low cycle corrosion fatigue 79−91852
Al-Zn-Mg-Zr (6.45, 2.08, 0.11 wt.%), exam. of cyclic stress strain response in corrosion fatigue 78−64788
Al_2O_3 bioceramic synthesis, for orthopedic purposes, props. *(Polish)* 80−66465
Al_2O_3, dense, exposed to steam, influence of Ca migration on strength reduction 80−11797
Al_2O_3, fatigue, static and dynamic in moist air 79−39002
Al_2O_3, porous, sintered, delayed failure, static fatigue in distilled water 78−64750
Al_2O_3 refractories, stability of refractory bond phases in steam-CO atmosphere 79−24634
Al_2O_3, sintered, strength, effects of moisture-assisted slow crack growth 78−27593
AlZnMg, corrosion cracking *(Czech)* 79−43478
Au-Cu (4 wt.%), fatigue crack propag., environmental effects *(French)* 77−66711
α-brass corrosion fatigue in $CuSO_4$-$(NH_4)_2SO$ -NH_4OH *(Japanese)* 77−52543
C fibre reinforced composite, mechanical properties, environmental cycling effects 77−86207
C steel containers for nuclear process liquid waste, stress corrosion 77−46311
Cr-Ni-Mo steel, low-cycle fatigue in sea water, mechanism *(Russian)* 77−59970
Cu and Cu-Al (8 wt.%) single crystal, surface dissolution effect on fatigue damage and crack nucleation 78−39936
Cu, creep rate, effect of surface anodic dissolution in acetate buffer soln. 78−3249
Cu, electrode potential, transient response to elastic straining rel. to reaction kinetics 79−70212
Cu, fatigue, effect of active liquid media on struct. and stress condition *(Russian)* 77−28929
Cu, fatigue crack propag., environmental effects *(French)* 77−66711
Cu, hard drawn wire *(Japanese)* 77−25193
Cu, stress reduction of straining single crystal due to anodic dissolution *(Japanese)* 78−15579
Cu, transgranular cracking in 1M $NaNo_2$ solution 79−100287
α-Cu-Al, FCC, fractographic obs. of SCC 78−64786
Cu-Al (5.5, 7.3, 6.3 and 2.5 wt.%), Hg embrittlement under cyclic loading 77−86225
Cu-Be, SCC in NH_3 80−104326
Cu-Be(2 wt.%), tarnish surface films, formed in ammoniacal Cu(II) solns. 80−97624
Cu-Mn(Ti)(Sn)(Si), dil., oxide film form. in ammoniacal Cu(II) solns., AES obs. 80−45415
Cu-Ni-Fe, corrosion resistant, SCC, crevice corrosion in seawater 79−96177
Cu-Ni-Fe tube, stressed, corrosion failure caused by cooling water, denickelation *(German)* 79−29286
Cu-Ti (4 wt.%), aged, stress corrosion cracking in Cu-NH_3 solutions, effect of pH, Cu and NHz conc. 78−88562
Fe alloy, crevice corrosion by water vapour, CO, methane in HTR coolants, model 77−25202
Fe alloy, ductile, stress corrosion cracking theory based on model for anodic dissolution reactors 77−56133
Fe and Fe_3Si, hardening and softening during adsorption fatigue in surface active medium, governing laws 77−86230
Fe, Armco, cyclic deform. in presence of H_2 *(Russian)* 77−16728
Fe, Armco, SCC in phosphate soln. 79−96184
Fe, Armco, surface dissolution effect 77−8883
Fe, effect of atm. corrosion on fatigue crack nucleation and fracture surface morphology, in air and vacuum *(Japanese)* 79−8387
Fe, fatigue crack propag., environmental effects, in large crystals *(French)* 77−66711
Fe, H_2 embrittlement and H_2 adsorption 80−89401
Fe, in caustic 77−16715
Fe, pitting in Na_2SO_4-NaCl solns. *(Japanese)* 78−85042
Fe-Cr (5, 10 and 20 wt.%), microcrack generation, healing of oxide scale 79−20280
Fe-Cr-Ni, stress corrosion cracking in high temp. caustic soln. 77−59964
Fe-Cr-Ni, test machine, design and construction 80−97649
Fe-Cr-Ni (25, 20 wt.%), single crystal, stress corrosion cracking 78−35553
Fe-Cr-Ni austenitic alloys, environment sensitive cracking, metallurgical variables effect 80−35391
Fe-Cr-Ni-P-C, amorphous, stress corrosion cracking 77−25123
Fe-Cu pseudoalloy, contact corrosion in tropical marine environment 78−11422
Fe-Ni (1 wt.%), machine induced residual stress contrib. to pitting susceptibility 79−61784
Fe-Ni (3 wt.%), influence of temper embrittlement, on stress corrosion susceptibility 78−85023
Fe-Ni-Cr (10, 6 to 14 wt.%), electrochemical polarisation in high temp. water *(Japanese)* 79−15868
Fe-Ni-Cr-Mo, exam. of tapered tensile specimen, for stress corrosion threshold stress testing 78−53055
Fe_3O_4, film formed in caustic electrolyte, deform. 77−25181
I stress corrosion of reactor fuel element cladding tubes 77−3100
Incoloy 800, cracking in NH_3 at 600°C 79−70207
$LaNi_4Fe$, H_2 absorpt. cracking, acoustic emission characts. *(Japanese)* 80−66631
LiF, thermocyclic stress effects in corrosive-media, electrochem. polarization applic. *(Russian)* 78−11356
$Li_2O.2SiO_2$ glass and glass-ceramic, fatigue props. in various environments 79−91820
Mg alloys, fatigue endurance and cyclic fracture toughness in air and vacuum *(Russian)* 79−34188
Mo-Cr, cracking in NH_3 at 600°C 79−70207
Na_2O-CaO_2-SiO_2 glass, stressed, chemical reaction in water vapour 79−91819
Nb-W-Mo-Zr-C(5,2,1,0.02 wt.%) alloy 5 BMTs, short-time tensile strength in liquid Bi and Li *(Russian)* 77−25186
Ni 201, stress corrosion cracking in high temp. caustic soln. 77−59964
stress corrosion cracking continued
Ni alloy, crevice corrosion by water vapour, CO, methane in HTR coolants, model 77−25202
Ni alloy, oxidation resistance at elevated temps., effect of various alloying additions 77−56134
Ni, stress corrosion susceptibility, S segregation effect, Auger spectrosc. study 80−61019
Ni-base alloy, age hardened, stress corrosion cracking resistance, plastic deform. and microstruct. relation 77−63829
Ni-base superalloy IN713LC, hot corrosion, thermal cycling effects 77−70204
Ni-Cr-Al, oxidation at 850°C in air containing HCl gas 79−8396
Ni-Cr-Al-Ti, stress corrosion cracking, factors influencing susceptibility 80−97617
Ni-Cr-Co-Mo alloy MP35N, accelerated H_2 charging in aq. H_2SO_4 at 0.2% yield stress 80−30144
Ni-Cr-Fe, high temp. corrosion and creep in carburizing and oxidising atmos. 79−11727
Ni-Cr-Fe, stress corrosion cracking, factors influencing susceptibility 80−97617
Ni-Cr-Fe Alloy 600, acid intergranular corrosion rel. to caustic stress corrosion cracking stress relieving effect 77−66712
Ni-Cr-Fe Alloy 600, in high purity water, effect of microstruct. 77−66713
Ni-Cr-Fe steam generator tubes, stress corrosion susceptibility, heat treatment effect 79−20258
Ni-Cr-Mo-Mn alloy 02KhN40MB, corrosion-resist, heat-resist., phys. and mech. props. 80−35411
(NiCo)-Cr-Al-Y/ZrO_2-Y_2O_3 plasma sprayed ceramic coating for turbine engine components 80−40616
SiC, subcrit. crack growth, in corrosive environment, 600-850°C 77−56080
SiF_4, thermocyclic stress effects in corrosive-media, electrochem. polarization applic. *(Russian)* 78−11356
Si_3N_4, stress corrosion 77−8917
Si_3N_4-CeO_2, surface stress development during oxidation 80−50736
SiO_2 fibres, reductions in static fatigue by hermetic jacketing with Al 79−43448
SiO_2, fused, polymer coated optical fibre, static and dynamic fatigue 79−29244
Ti alloy, corrosion cracking resist. of type VT3-1 containing artificial defects *(Russian)* 79−52436
Ti alloy, high temp., NaCl-induced accelerated oxidation 77−21322
Ti alloy AT-3, crack development in air, H_2, aq. H_2SO_4, electrochem. charact. *(Russian)* 77−70209
Ti alloy TA6V, stress corrosion cracking in organic solvents, effect of microstruct. *(French)* 77−16745
Ti alloy type TA6V, hot salt stress corrosion cracking *(French)* 80−21185
Ti alloys, corrosion in saline radioactive waste isolation environments 80−104349
Ti alloys, corrosion resistance in H_2S and NaCl, cracking tendency, strength *(Russian)* 78−31568
Ti alloys, develop. of cracks under hot salt corrosion 77−56147
Ti alloys, hot salt stress corrosion cracking, electrochemical model 78−7078
Ti alloys, hot salt stress corrosion cracking 79−47799
Ti alloys, pseudo-α, salt-corrosion effects on long-term strength, vacuum annealing and stress concentrators effects *(Russian)* 78−11392
Ti, cold rolled, transcrystalline SCC in methanol-bromine soln., crystallographic texture effect 79−15872
Ti, commercial, texture depend. stress corrosion cracking 80−104334
Ti commercial purity, stress corrosion cracking at high temps. in caustic soln. 77−59964
Ti, corrosion resist. in marine environments *(French)* 80−50767
Ti, cracking in NH_3 at 600°C 79−70207
Ti, electrochemical behaviour under tensile stress in boiling H_2SO_4 and acidic chloride solns. 78−95851
Ti, high-temp. ductility in vacuum, air and liq. metals *(Russian)* 77−52537
α-Ti sheet, texture dependent stress corrosion cracking in Br_2-methanol soln. 80−71803
Ti-Al age-hardened alloys, fatigue crack propagation rel. to grain size in vac. and NaCl soln. 80−16538
Ti-Al-Mo-V, crack resistance in chloride soln., electrochem. protection, polarization effect 80−55589
Ti-Al-Mo-V (8, 1, 1 wt. %), stress corrosion cracking and slow strain rate H_2 embrittlement 78−48569
Ti-Al-Sn (5, 2.5 wt.%), electron microscope and X-ray diffr. exam., of basal and near basal hydrides 78−80550
Ti-Al-Sn(V), corrosion resist. in marine environments *(French)* 80−50767
Ti-Al-Sn(V)(V-Cr)(Mo-V), electrochemical behaviour under tensile stress in boiling H_2SO_4 and acidic chloride solns. 78−95851
Ti-Al-V (Mo-Sn)(Zr), environmental effects in alloy fretting, effect on fatigue props. 78−56787
Ti-Al-V (6, 4 wt.%), stress corrosion cracking, composition, microstruct. and texture effects 79−11725
Ti-Al-V (6, 4 wt.%), texture depend. stress corrosion cracking 80−104334
Ti-Al-V (6,4 wt.%), corrosion fatigue behaviour, surgical implant material 79−39027
Ti-Al-V-Sn (6,6,2 wt.%), depend. of K_{ISCC} on loading rate and crack orientation 80−45427
Ti-Al-V-(Sn), SCC, subcritical flow growth, comparison of aircraft alloys in NaCl soln. 78−53028
Ti-Al-(V) (6,4 wt.%), hot salt stress corrosion susceptibility, microstruct. effects 77−36688
Ti-Cu, corrosion resist. in marine environments *(French)* 80−50767
β-Ti-Mo-V-Fe-Al(8,8,2,3 wt.%), metastable factors affecting stress corrosion cracking 77−28928
Ti-O, stress corrosion crack propag. in aqueous and methanolic soln. 78−19919
Ti-V-Cr-Al (13, 11, 3 wt.%), stress corrosion cracking in methanolic solutions 80−50752
Ti-V-Fe-Al (10, 2, 3 wt.%), fracture toughness and stress corrosion resistance 80−100904
U-Mo(Ti)(Q^4)(Q^5), Q^4-quad, Q^5-quint, stress corrosion cracking in moist air, salt water, salted moist air 78−35562
U-Nb (4.5 wt.%), correlation between oxidation and stress corrosion cracking 79−20253

stress corrosion cracking continued
U-Nb(2-3, 4.5, 6.0 and 8.0 wt.%), SCC in air 77−73363
W arc welds, fatigue crack growth behaviour in air and high-C liquid Na, carburization studies 80−40625
Zircaloy, I_2 stress corrosion cracking, temp. and stress depend., threshold press. determ. 80−16595
Zn, liquid metal embrittlement 79−83375
Zn, single crystal, crack growth in contact with liq. Hg and Ga 79−87757
Zr base alloy, fatigue crack propag., role of adsorption in H_2S, Hg and moist air *(French)* 78−15580
Zr, embrittlement in I_2, environmental purity effect 80−30149
Zr-Nb (2.5 wt.%), tensile specimen, stress corrosion cracking by stray contamination 77−70215
ZrO_2, anodic films, growth and morphology 77−16717

stress effects
see also cavitation; deformation; elastic waves; heat treatment; high-pressure phenomena and effects; magnetomechanical effects; materials testing; mechanical properties of substances; mechanical testing; piezo-optical effects; piezoelectricity; piezoresistance; shock wave effects; stress analysis; stress measurement; stress/strain relations; tribology
bone, human, acoustic emission in restressing 80−3704
bone, radius remodelling, sheep, rel. to functional stress and strain 80−35939
bone remodelling, quantification of stresses 80−85437
α- brass, effect of mean stress on high temp. fatigue 79−20153
chinaware, vitreous, elimination of crazing by repeating glost firing *(Japanese)* 79−20236
composite wire critical current density rel. to tensile stress at 4.2K, obs. 79−33439
constitutive equations of continuum creep damage mechanics 78−67054
couple stress effects on elastic waves and vibr. 79−14307
couple stress effects on wave prop. in elastic layer immersed in infinite liquid 79−1126
couple stresses effect on crack tip 78−18240
dislocation mobility in inhomogeneous stress field, hardening effects 80−70219
elastic cylinder under stress, biharmonic problem solution 80−4532
glass containers, exam. of fragmentation 79−20148
graphite, cyclic fatigue, influence of stress cycle and neutron irrad. 79−52335
graphite reinforced epoxy laminates, cracked, deformation and failure in biaxial stress fields 79−47763
graphite/epoxy laminates, stress wave damage 80−93611
interface transonic separation due to plane stress pulse 79−68624
irradiation and stress induced mass transport, anal. soln. 79−60401
martensite layers, external stress effects on equilibrium morphology, thermodynamic model *(Russian)* 78−52804
mechanical stress influence on indentation hardness *(German)* 78−95794
metal BCC, divacancy binding energy, appl. stress effect, computer simulation 77−15408
mica, stress-induced K^+ ion migration, X-ray fluoresc. anal. 77−4221
parelastic force on homogeneous cryst. inclusion, theory 80−79777
perspex spheres, internal fractures due to stress wave focusing 78−18239
polyethylene films, lifetime under small loads 79−95301
polyethylene terephthalate, fatigue failure under cyclic loading, overstress in chem. bonds 79−57106
polymer melts, normal stresa and Barus effect 80−64589
polypropylene, shear effect on crystallisation *(German)* 78−75586
poroelastic semi-infinite cylinder, torsional vibr. 79−32334
smectic cylinder, instabilities under mech. tension 77−19868
stainless steel, 304, tensile stress effects on high-cycle fatigue 78−86603
steam turbines, structural stresses, experimental anal. 80−93727
steel, high strength, sensitivity to stress concentration with various H content *(Russian)* 79−15724
steel, spring, 60C2A, tempered under stess, influence of tempering conditions on mech. props. *(Russian)* 79−47724
steel, stainless, cc Cr-Ni (20, 18 wt.%), effect of tensile stress on growth of He bubbles 79−55796
steel, stainless, wire, effect of stress on phase transformations 78−44119
steel US characts., change with stress appl., exam. 78−48579
thick membrane strip, effect of shearing prestress, static case 80−10137
US plane wave reflectivity from water-metal interface, stress effect 79−81586
void growth and incubation, stress effect 79−51147
Al alloy, US characts., change with stress appl., exam. 78−48579
Al alloy 7050-T76, crack propagation rate and crack closure, mean stress effects 79−52336
AuMn alloy, ordered, vacuum deposited epitaxial films, orientation control by external stress 80−100426
$CaF_2:Dy^{3+}$, Γ_8 quartets, orbit-lattice interaction, e.p.r. under stress 77−1591
CaO, $^3T_{1u}$ of F-centre, EPR, unaxial stress effects 78−48040
$CdCr_2Se_4$, modulated piezoreflection spectra 80−97237
Cu-Fe (1 wt.%), stress induced martensitic transformation of spherical Fe particles, exam. 78−52803
Cu-Sn (16.5 wt.%) alloy, stress induced martensite from γ phase 79−70066
Cu-Zn-Al, single cryst., stress induced martensitic transformation 80−45308
CuAu alloy, ordered, vacuum deposited epitaxial films, orientation control by external stress 80−100426
Fe-N single crystals, solid soln. stress assisted nucleation of α'' precipitates 78−52810
Fe-Ni-Al, Mossbauer spectra, strong elastic stress effects 77−90084
Fe-Ni-C (30.59, 0.02 wt.%), effect of loading on transformation of retained austenite to martensite 79−47686
Fe-Ni-C alloy, external stress effects on equilibrium morphology, thermodynamic model *(Russian)* 78−52804
Fe-Si, influence of stress on rotational loss, lamination appl. 78−35384
n-Ge, piezo-thermal cond. calc. 77−15639
n-Ge, piezothermomagnetic analogue of Grabner effect 77−4378
p-Ge, thermal conductivity, effect of uniaxial stress 79−23792
Ge-electrolyte contact, current-voltage characts., effect of mechanical deform. 78−68082
In crystals, twin layer broadening under stresses 79−65098
$MgO:Er^{3+}$, Γ_8 quartets, orbit-lattice interaction, e.p.r. under stress 77−1591

stress effects continued
MnCu, neutron scatt. near crit. comp., effects of stress and ageing 79−19722
Nb_3Sn, multifilamentary conductors, stress-induced enhancement of critical currents 79−69644
Nb_3Sn, multifilamentary supercond., crit. temp. and current 77−32133
Nb_3Sn superconducting multifilamentary wire, stress effects 79−33431
Ni perfect crystal, stability under various stresses 80−104208
$Pb_{0.97}La_{0.02}(Zr_{0.92}Ti_{0.08})O_3$, ferroelec. ceramic, stress effects 80−2119
$Pb_{0.99}Nb_{0.02}(Zr_{0.95}Ti_{0.05})_{0.98}O_3$, ferroelec. ceramic, stress effects 80−2119
Si, neutron irrad., EPR, ⟨100⟩ split di-interstitial, positive charge state 77−20698
Si p-channel MOS structure, stress effects on elec. props., press. transducer props. 80−100526
Si:Fe, ESR, cryst. field under stress, C_{11} and C_{44} meas. 77−12194
Si-electrolyte contact, current-voltage characts., effect of mechanical deform. 78−68082
Ti-Nb-Zr-Ta, superconducting props. comp. depend., stress effects and precipitation behaviour, X-ray scatt. 80−93059
V_3Ga superconducting tape, stress effect on critical current *(Japanese)* 80−50020

stress field analysis at cracks *see crack-edge stress field analysis*

stress measurement
absolute retardation patterns, laser diametrically compressed photoelastic disc 77−27496
acoustic, stress determ. improvement of accuracy 78−15631
acoustoelasticity, appl. to nondestructive stress anal. 79−34259
aqueous polymer solns., shear stress and normal stress meas. using cone-and-plate rheogoniometer 80−1496
automated plating stress monitor 79−24696
bar, stress meas. in dynamic deform. to plastic range 77−84158
bending stress relaxation in complex system, apparatus for investigation 77−23922
biomechanical, of patient sitting immobile, instrumented wheelchair 77−90930
birefringence small retardation meas. using uniform-field Babinet compensator 79−93208
birefringent object, isopachics meas. using immersion method polarisation holography 80−99672
blind hole drilling technique for residual stress measurement: application in NDT 80−40660
bolted joints in wood, photomech. stress determ. 79−32406
bone, in vivo determ. using noncontacting EM device 78−77133
brittle coating analysis of orthotropic materials 79−27606
bulk forces modelling, increasing effectiveness of centrifuging *(Russian)* 78−87314
capacitance-torsion balance for measuring small stresses and strains 78−73988
capacitive stress transducer optimum dielectric selection 77−73428
ceramic materials structural stresses, meas. using X-ray diffr. meas. *(German)* 78−52744
chemical apparatus, expt. strength anal. *(German)* 79−32427
circular ring, inner boundary shapes, optimised, diametral compression 80−38369
coal, stress meas. using borehole instrument 77−9415
coatings, brittle, strain sensitive, for stress, strain testing of surfaces of loaded structs. 79−29311
coatings on plates, determ. of residual stresses using curvature gauging method *(Russian)* 79−98674
composite and nonuniform bodies, stress determ. from gravitational force action *(Russian)* 79−64603
compound optical polarisation materials for stress meas. *(Russian)* 78−87313
concrete, stress determ. by holographic and speckle techniques *(French)* 79−27603
conference on measurement techniques for optical fibre systems, London, England (May 1979) 79−64348
counter method as X-ray microbeam diffraction technique and its application to stress concentration problems *(Japanese)* 79−39077
countersunk hole in flat bar in tension and transverse bending, stress concentration factors 79−46274
crack front, stress intensity factor, three dimens. speckle interferometry 77−84196
crack growth, 3-D geometric effects, implications for composite material structures 80−10204
cutting tools, stress anal., Moire technique 78−64799
cyclic stress amplitude meas. by time-averaged photoelasticity 78−18261
cylinder, solid, residual tangential stress determ. from segment sections, appl. 78−60902
cylindrical curved surfaces, X-ray diffraction meas. of axial stress, geometrical effect anal. 78−63403
cylindrically curved surfaces, tangential stress meas. using X-ray diffractometer 78−87590
deformation, cyclic, static, meas., recording, automatic system 79−15893
deformation strength props., simultaneous meas. of several samples, polymer films appl. 79−15896
dielectric bodies stress determ. using EM waves 80−38370
diffusely reflecting objects, deformation meas. by lasers, appl. of holography and speckle, review *(Japanese)* 80−9832
discontinuous variations of stress, detection by magneto-inductive method *(German)* 79−52547
drill hole method, comprehensive extension to the photo-stress process of investigating surface layers *(German)* 80−33551
dry stress corrosion kinetic studies of threadlike metal specimens 79−83381
Earth crust, diagnostic stress-relief curves in stress meas. by overcoring 79−29886
Earth crust, in situ stress in N. America, compilation 79−29728
Earth crust in situ stress field, determ. via hydrofracturing, fracture mechanics approach 78−81435
Earth crust stress changes, in situ monitoring 79−29884
Earth mantle, applicability limits of grain size geopiezometer 78−85715
elastic contact of two discs, method of caustics study 79−59948
elasto-optical technique for measurement of stress at surfaces 79−7347
elastomeric bearings, high-capacity, laminated, finite-element anal. 80−96197
electrodeposition stress in plate, X-ray methods 79−29298
electroplated coatings internal stresses, effect in Ni and Zn *(German)* 78−56049

stress measurement continued
electroplating method for high-temp. stress meas., fundamentals *(Japanese)* 78−15616
ellipsometry, three-dimens., stress meas. in birefringent medium 80−101821
EM shear stress gauge for large amplitude shear waves 78−70113
embedded interacting defects in transparent model, holographic meas. of magnification factor 79−32413
energy measurement and significance in acoustic emission testing 78−31594
epoxy resin (Araldite B), photothermoelasticity meas. by heating method 80−6000
experimental numerical hybrid technique for stress anal. 79−32419
experimental stress anal., methods and recent developments *(French)* 79−59953
expt., conf., Munich, Germany (Sept. 1978) 79−34256
extruded billets, nondestructive determ. of residual stress from acoustoelastic meas. 80−76467
fatigue cracked sample stress meas. by US phase shift detection 77−28971
ferromagnet, meas. by internal induction 77−62222
ferromagnetic materials, magnetoelastic effect/stress and strain in plane stressed state 77−77718
fibre reinforced composite, by IR spectroscopy 79−52559
fibrous composite models, photoelastic analysis of interlaminar matrix stresses 77−3799
film, stress measurement method using real-time holographic interferometry 78−84099
film, UH vacuum stress meas. via Michelson interferometer 77−2650
film on single cryst. substrate, X-ray method 78−51860
films deposited on semicond. substrates, X-ray topographic meas. method 78−5710
fission reactor irradiated cladding, in-cell facility for mechanical testing 80−21244
fragile materials, at high temperatures, improved clamp for transducer attachment 80−73351
friction machine, residual stresses meas., appl. to wear resist., surface wear 78−60906
gel, appl. to study of viscoelastic props. at small constant shear stresses 79−54123
glass, chem. tempered, surface stress meas. using opt. waveguide effect *(Japanese)* 80−45473
glass, chemically strengthened, stress profile determ. using scatt. light 80−30186
glass, float, optical waveguide effect 80−43681
glass, thermally tempered sheet and plate, surface stress meas. using optical waveguide effect 80−25967
glass fibre reinforced epoxy, brittle coating stress anal. technique 79−43528
glass fibre reinforced Textolite, method of stressed state study during hardening 79−57191
goniometer, for stress measurement in single crysts. and coarse-grained specimens 80−64837
graphite/epoxy laminates, stress meas. by X-ray diffr. from fillers 79−43331
grid method for residual deforms. meas. 77−52572
ground anchor, new apparatus *(German)* 79−34270
heteroepitaxial system, dislocation struct. at stress meas., theory 80−2017
holographic interferometry, variable residual stress meas. 79−29312
holographic interferometry appl. to NDT 79−8420
holographic photoelasticity, using dual-hologram method 77−19198
holographic recording of displacement field inside stressed sample 77−57299
holographic shearing interferometry for plane stress state determ. in models *(German)* 79−32426
holographic techniques used in non-destructive testing, book contrib. 79−18380
hydraulic fracturing for stress meas. in hard and soft earthen material 77−9577
hydrofracturing stress meas. technique, American field results 77−9576
hydrostatic, photoelasticimetry and holographic interferometry appl. 79−7353
impression method for plastic deforms. determ. at apex of stress concentrator, bare choice considerations 77−52571
in-plane stress waves in solids, mapping by laser speckles 79−27608
Inconel X, X-ray study of stress meas., elastic const. *(Japanese)* 79−66092
integrated retardation technique, rotationally symmetrical bodies, thermal stresses 80−38362
intensity factors at arched crack tip, caustics method 80−19298
internal, of sphere by X-ray in depositing method 77−36409
internal friction in solids, direct meas. with continuous variation of freq. 80−99979
internal stress meas., critical assessment 79−59955
internal stress measurement using optical microscope stage polarisation adapter 80−31863
internal stresses, calc. with integration methods, X-ray stress meas. 79−32415
internal stresses, cracking temps., automatic installation 80−55605
isoclinics and isochromatics in birefr. slice, speckle pattern visualization 77−2687
jacketed optical fibre residual stress diagnosis, pulse delay technique 80−53469
laser speckle photography, double-exposure, magnification change effect 79−40607
light ellipticity, azimuth and system parameters linking eqns., 3-dimens. model propag. 78−50695
living cells, stress-strain meas. using cell poker 80−76880
machined surfaces, residual stresses, X-ray diffr. meas. methods 77−56212
macrostress in deposits, spontaneous, dilatometric method 77−36709
macrostress in deposits, spontaneous, improved methods 77−35100
magnetic core multivibrator, tensile stress transducer appl. 78−9615
magnetostrictive SAW generation efficiency meas. of residual stress 77−28972
Manganin stress gauges, technique for calibrating effect of resistive hysteresis on dynamic piezoresistive coeff. 79−54118
mechanical measurement, holographic system for interferogram form., processing and interpretation 77−75449
metal, residual stresses determ. using internal boring technique 80−3263
stress measurement continued
metal, textured cubic, residual stress evaluation 80−89435
metal faced cylinders and discs, residual stresses determ. by combined method of Zaks 77−52568
metal fibre stress/strain curves determ. using X-ray goniometer *(German)* 78−92413
mode I stress intensity factors, method of caustics 80−38364
Moire effect and deformation meas. in structural components *(German)* 78−88587
Moire strip attainment at specified pt. on contour of stress concentrator 77−52573
myocardial activity determ. at surgery using shrinking stress meas. 78−31966
non-Newtonian fluids, capillary and slit methods of normal stress measurements 80−43807
nondestructive X-ray diffr. method 78−68853
opposed-anvil high-press. devices, material strength effect 80−47068
optical fibre cables, measurement of longitudinal internal stress 79−64350
optical glass, thermally tempered, surface stress meas. by crit. ray method 80−106766
optical methods for determining strain and displacement, book 79−20331
optical multifilm manufacturing, large scale, function stress testing 79−81576
optical polarisation method, linear compensator for beams path difference 79−93204
optically isotropic and anisotropic materials, rapid optical method for stress-optical const. determ. 77−5899
oscillating quartz crystal stress distribution meas. by laser probe 77−20803
paints and varnishes, stress anal. during drying 79−34183
photoelastic, isochromatic fringes, comparison of stress intensity factor determ. methods 77−84197
photoelastic birefringent material stress determ. in single hologram exposure 80−106770
photoelastic coating method of meas. stress and strain 78−1614
photoelastic coatings, stress anal. technique 77−84201
photoelastic cylinder with radial temp. gradient, integrated retardation fringe technique 77−62219
photoelastic dynamic studies of fracture 80−38358
photoelastic fringe pattern analyzer, computer aided 80−38359
photoelastic fringes, automatic stress analysis method 80−14639
photoelastic isodynes, new type of stress modulated light intensity distrib. 78−26092
photoelastic isodynes method, integrated plane stress field components 80−14638
photoelastic load meas. and testing *(German)* 80−19297
photoelastic measurement for crysts., appl. to Si 80−48656
photoelastic method, automated system for treating expt. data 79−15929
photoelastic method of thermal stress determ. circumferentially grooved cylinder 80−38363
photoelastic param. from scatt. light meas. 79−18848
photoelastic sensor *(Russian)* 77−11150
photoelastic strain gauge, concrete structure boundary stress meas. appls. *(Chinese)* 79−72867
photoelasticimeter, three-dimensional *(French)* 79−34268
photoelasticity, holographic determination of absolute retardation fringes by vectorial reconstruction 78−87315
photoelasticity, monograph 78−19988
photoelasticity for stress analysis under hydrostatic press. up to 700 MPa 78−18260
pickup for soil compressibility investig. under static loadings 79−88345
piezoelectric convertor appl., advantages *(Russian)* 78−70114
plane shearing stress meas. with wired strain gauges *(German)* 78−89471
plastics, anisotropic reinforced, stress distrib., using mm region of EM waves 80−25968
plate vibrating in water, stress meas. by interferometric holography 79−3653
plating, residual stress meas. by improved ring-core method *(German)* 79−34272
PMMA, critical stress-intensity factor, determ. under mixed mode loading conditions by shadow optics 78−68868
PMMA, shock loaded, lateral compressive stresses meas. using Yb piezoresist. gauges 80−103007
polarisation device application, by compensation method 80−40643
polarisation-optical mechanical-stress meter 77−45879
polariscope interactive control system to evaluate stresses 80−19299
polyacrylamide solns., anomalous effect in first normal stress difference meas. 77−80130
polychromatic X-ray stress meas. *(Japanese)* 78−7143
polycrystals, single phase, stress strain relations by X-ray diffraction *(Russian)* 80−5999
polydiacetylene fibre resonance Raman spectrum meas. 79−17507
polymer, volume stress/strain state 78−23896
polymer materials based on cured synthetic resins, residual stresses meas. equipment 77−77675
polymer solns., constitutive relns. determ. using stiffened Weisenberg rheogoniometer for uniaxial shear flow 77−80188
polymer solution, conc., appl. to study of viscoelastic props. at small constant shear stresses 79−54123
polymer solutions, dilute, normal stress difference and shear rate 80−83776
polymer solutions, normal stress meas. using flight velocity 79−77039
polymeric adhesive layer, interlaminar stresses, direct determ. 77−86237
polymeric materials, stress meas., X-ray diffr. technique, review 78−5713
polymers, stress-enhanced chemiluminesc. 80−40628
porcelain-metal cermet, stress determ., meas. method *(German)* 80−76425
porous materials, stress determ. by X-rays *(German)* 77−44436
position-sensitive detector, employed in diffractometer, geometrical problems, stress measurement use 79−85205
pressed powder bed, bottom pressure distrib., meas. by scattered light photoelasticity *(Japanese)* 79−75543
pressure vessels and steel pipes structures anal. under creep conditions, acoustic emission method 77−25237
proximity method, internal stresses in electroless Ni films on stainless steel, features 79−64611
punch indenting elastic half-plane, stress distrib. 79−64606

stress measurement continued
PVC, calendering, prediction of stress and torque 79−8266
quartz, plate and fibre, internal stress and birefringence microanal. using optical phase microscope interference-polarisation 79−39109
quartz gauges, shorted guard-ring, measurement of current and stress profiles 79−58680
rail steel NDT, residual stresses meas. using magnetoelastic effect 77−81379
reactor vessel, determ. of stress intensity factor 80−37455
reflected caustics method for stress-optical consts. determ. 79−51931
relaxation, by cone-plate instrument 80−28477
residual, butt-weld, moire fringe method 79−86390
residual, use of position sensitive proportional counter *(Japanese)* 80−11853
residual pseudo-macrostress, X-ray meas. errors due to plastic deform. 77−68544
residual stress, X-ray evaluation, treatments for nonlinear distribs., review 80−25966
residual stress determ. by mechanical method, recommendations for strain meas. 77−23921
residual stress meas., Alignment Error of the hole-drilling method 79−81823
residual stress meas. from X-ray peak shift anal., appl. to hexagonal Zn films 77−72807
residual stress measurement, bending deflection and stress source methods *(French)* 79−34265
residual stress measurement, X-ray diffr. equipment, comparison 80−82858
residual stress measurement by magnetic method *(Japanese)* 78−59352
residual stress measurement using holographic interferometry and etching 77−52577
residual stress using elastic punching method 79−34264
residual stresses, review 80−44245
residual stresses, with hole-drilling strain gauge method 79−39108
residual stresses determ., ground and lapped metal surfaces 79−34211
residual stresses determination in rod specimens with stresses varying along rod length 78−38260
residual stresses in non-homogeneous hollow cylinders *(French)* 79−32423
residual stresses in ring-shaped specimens, apparatus for electrochem. etching with rotating cathode 77−25212
residual stresses in thin specimens, layer-by-layer X-ray diffr. analysis, additional strains and corrections 78−39964
residual stresses measurement using X-rays 79−97484
Reynolds stresses in turbulent boundary measurement 77−42807
rheogoniometer, Weissenberg, modification to normal stress meas. unit 80−69750
rheological property meas. apparatus *(French)* 80−14644
ring specimen deformation, stress relax., meas. method, increased accuracy 77−75863
rock, soft, vibrating wire stress gauge 77−84199
rock, trends in relationships between meas. in situ stresses and depth 79−29729
rock stress meas., conference (Sydney, 11-13 August 1976) 77−9573
rock stress meas. using CSIR triaxial strain cell 77−9574
rock stress measurement, hydrofracturing method and recent field results 79−29885
rocks, anelastic strain rel. to virgin stresses, possible meas. method 77−9416
rocks, borehole jack fracturing technique 77−64488
rocks, meas. in bored raise at Mount Isa Mine 77−9414
rocks, meas. methods in Norway 77−9422
rocks, palaeopiezometry using recrystallized grain size 77−91317
rocks, primary stress meas. at Eisenhower Memorial Tunnel, Colorado 79−29727
sandwich composite beams, stress distrib. meas. under four-point bonding, multilayer builtup theory 80−96190
sandwich speckle photography *(German)* 80−10216
SAW resonator as stress sensor, freq./stress sensitivity 77−2645
scattered light three-dimensional photoelasticimeter. Application to a blade of a compressor 79−32405
scattered-light photoelasticity, for meas. of stress distrib. in cubic single crystals *(Russian)* 80−7326
scragged torsion bar, residual shear stress meas. 79−59954
seals, glass-metal and glass-ceramic, annealing effect on internal stresses 80−40389
self-contained stress determination by means of hardness measurements *(German)* 80−21200
self-exciting reflection oscillator US spectrometer 77−32758
servo force-balance instrum. for wall shear stress meas. 79−1273
shear stress of solids, at 120 to 300K and up to 100 kbar 80−50787
shear stress on cohesionless grain, movement on stream bed, relative protrusion effect 77−13094
shell reinforced around hole, deformability meas. 80−16371
shock-loaded solids, wave profile measurement 79−94564
shock-wave environments, use of low-impedance Mn stress gauges in 1.0 to 40.0 GPa range 80−38367
single crystals, internal stresses determ. with multicryst. X-ray spectrometer 80−64832
solid propellant stress transducer evaluation 80−81245
solids and granular materials, stress and strain cells 79−32416
speckling application, for stress-strain state of parts 80−19300
split birefringent coating on birefringent material, determ. of dynamic stress intensity factors 79−50684
steel, acoustoelastic stress field imaging technique, stress field contour plots 79−77033
steel, austenitic, measured internal stress and anelasticity in creep *(Czech)* 79−38909
steel, austenitic, X-ray elasticity constants *(German)* 80−30004
steel, austenitic stainless, X-ray elastic constants, determination by ψ_0 oscillation method *(Japanese)* 78−64575
steel, austenitic stainless, X-ray stress anal. by new position sensitive proportional counter with uniform angular resolution *(Japanese)* 80−30190
steel, austenitic stainless, X-ray stress meas., accuracy and method of data treatment *(Japanese)* 80−104365
steel, C, X-ray diffraction correlation between cyclic loading and residual stress *(German)* 78−48583
steel, C, X-ray stress meas., appl. of position sensitive proportion counter *(Japanese)* 78−64791
stress measurement continued
steel, Cr-Mo-Ni-V, dynamic stress intensity factor meas., possibilities and limits *(German)* 80−93719
steel, ferritic-pearlitic, X-ray elasticity constants *(German)* 80−30004
steel, flat bars, stress meas. and calc. around drilled hole, with hole-gage-rosettes aid *(German)* 80−25757
steel, hardened, stress determ. from X-ray meas. by fixed time method 78−90801
steel, hardened, X-ray elasticity constants *(German)* 80−30004
steel, heat treated high strength, X-ray diffr. anal. of residual stress 80−3200
steel, high C, plate, rolling residual stress meas. by X-ray diffr. *(Japanese)* 79−66081
steel, low C, dynamic stress intensity factor meas., possibilities and limits *(German)* 80−93719
steel, low C, initial stages of plastic deform. *(Japanese)* 80−93618
steel, mild, elastic stress meas. using X-ray diffraction, wavelength effect 77−84202
steel, mild, residual stress meas., acoustoelastic, in a patch-welded disc 79−27604
steel, mild plate, explosive hardening of one end, X-ray back reflection meas. 77−36531
steel, Ni, 11.6%, quenched cylinder residual stresses, boring/turning and X-ray diffr. obs. *(German)* 80−93586
steel, Ni-Co-Mo, dynamic stress intensity factor meas., possibilities and limits *(German)* 80−93719
steel, Ni-Mn-C, austenitic, proof stress change meas. by internal friction with martensitic transform. 78−56638
steel, plain C, type 304 and type 316 stainless, fatigue damage indicators, non-desructive 80−25932
steel, quenched and low-annealed, X-ray determ. of macroscopic stresses 77−77660
steel, residual stress meas. by centre hole method 77−54941
steel, stainless, two phase, X-ray stress meas., by monochromator method *(Japanese)* 78−64792
steel, surface stress measurement using US goniometer 79−15947
steel, textured, X-ray stress meas. 77−46975
steel casting, meas. and significance of residual stresses 80−21253
steel deformation response meas. device *(German)* 78−3261
steel pressure vessel, multilayer, without longitudinal seam, model investigation *(German)* 79−34276
strain gauge meas. in cyclic elastoplastic tests, automatic processing on portable computer 77−5829
strain gauge using integrated operational amplifier 79−75522
stress analysis, experimental, conf., Bradford, England (Sept. 1978) 80−17718
stress intensity factor, of simplified geometries of structural parts, experimental determ. 78−68866
stress intensity factor, simplified three parameter method 79−1138
stress-intensity factor determ. by strain-gauge method 80−76445
structural stress distrib. determ. by remote IR thermometry 80−87749
Stycast-1266, mechanical props. at low temps. 80−57286
subsurface stress meas. 80−21252
surface displacement meas. by holographic interferometry, stress determ. in components *(German)* 79−32425
surface rock stress meas. using new cylindrical jack 77−9575
tempered glass discs, meas. of nonuniform distribution of residual stresses 78−95865
temporary and residual stresses, high-temps. 80−64498
tensile strip with large hole, max. stress 77−31265
tensile testing at const. true strain rates, test machine 79−34262
texture effect, on stress determination by X-rays 79−91701
textures materials, residual stress evaluation by X-rays *(German)* 80−40670
thermoplastic rectangular parallelepiped pressure vessel, photoelastic coating anal. 79−59950
thick walled cylinder subject to torsion, stresses at offset oblique holes 79−32404
three dimensional distribution, scatt. light meas. method using depolarised incident light 79−37254
transmission holographic bench, for qualitative and quantitative analysis *(Rumanian)* 78−46545
transparent bodies small deformation meas. instrument 78−77898
trident seal, thermal expansion differential test 79−61815
turbine blade natural freq. and stress meas. *(German)* 79−34260
two-dimensional structure in-plane vibr., stress analysis by laser speckle method 80−103006
two-layer plane elastic system on rigid base, stress distrib. 77−39263
tyre, photoelastic modelling of stresses 79−34274
underground mine openings design rel. to stress meas. 77−9425
US method, calibration expt. results *(German)* 80−53725
US nondestructive eval. using unipolar transducers 80−76471
US phase technique for stress region meas. 77−25219
US pulse spectroscopy, stress analysis 77−42788
viscoelastic converging pipe flow, vel. vectors and radial stresses, rheological model and laser anemometry 79−60028
viscoelastic plastic components, using Moire method *(German)* 78−22309
viscoelastometer, dynamic, direct reading, automation, appls. to polymer films, fibres 79−3980
wedge with holes 79−94566
welding stresses on component surfaces, semi-automatic measuring device 80−68194
welds, residual stresses, evaluation by Barkhausen noise meas. 80−76436
wind stress on sea ice, meas. techniques and results *(Japanese)* 78−88842
wire, fatigue testing method, error reduction 79−52493
wires in steel cables, tension measuring device and method of use *(Russian)* 80−68196
X-ray anal., conf., Denver, USA (Aug. 1976) 77−70382
X-ray analysis, appls., conf., Denver, USA (Aug 1975) 77−56307
X-ray detector, position sensitive proportional counter, for residual stress meas. 77−56211
X-ray diffr. method calibration, elastic const. meas. technique 78−7164
X-ray diffr. residual strain meas., elastic const. meas., material errors 78−5714
X-ray diffr. residual stress meas. method using parallel beam optics 78−5717
X-ray diffraction method, statistical study, improvement in precision by fixed time method 78−90801
X-ray diffractometer for stress meas. in different ψ-directions 78−5715

stress measurement continued
X-ray dual detector diffractometer for residual stress meas. 78−5716
X-ray elasticity method 79−43506
X-ray integration method, extension of $\sin^2\psi$ method *(German)* 80−92420
X-ray meas. of internal stresses in electrodeposition stress in cylinder 78−27693
X-ray method, three axial stresses of general orientation *(German)* 77−9020
X-ray microbeam meas. of local stress, appl. to fatigue crack growth *(Japanese)* 78−64793
X-ray portable stress analyser using position-sensitive scintillation detector 80−13190
X-ray residual stress anal., computer controlled, software, precision 78−5712
X-ray stress anal., diffractometer line profile location, computation techniques 78−5711
X-ray stress anal. using position-sensitive proportional counter 80−1498
X-ray stress meas., computer-aided system *(Japanese)* 80−104366
X-ray stress meas. by counter method, statistical anal. 78−27694
X-ray stress measurement, error caused by side declining angle of counter scanning plane *(Chinese)* 80−52373
X-ray stress measurement method, appl. to practical materials *(Japanese)* 80−52379
X-ray technique, comparison with three different detectors 80−1499
X-ray technique by side inclination method without $-\eta$ inclining incident angle *(Chinese)* 78−15608
X-ray tensometric measurement, reliability *(Czech)* 80−27382
Zircaloy-4, microstrain and particle size meas. by Warren-Averbach method 80−55420
Ag film, electroplated, using holographic interferometry 80−20806
Al, acoustoelastic stress field imaging technique, stress field contour plots 79−77033
Al alloy, residual stress gradient meas., modified hold-drilling technique 79−29300
Al, initial stages of plastic deform. *(Japanese)* 80−93618
Al plate, explosive hardening of one end, X-ray back reflection meas. 77−36531
Cr electrodeposit on steel, stress meas., X-ray methods 79−29298
Cu electroplating method, sensitization methods *(Japanese)* 80−68197
Cu-W(Fe)(Ag), biphase material X-ray stress determ. *(Russian)* 79−5097
Fe, slip-initiation phenomenon by fatigue, appl. to stress meas. 80−45342
Ge-GaAs heteroepitaxial system, dislocation struct. in stress measurements 80−29030
KCl, stress distrib., meas. by scattered light photoelasticity *(Russian)* 80−7326
NaCl, US deformation, stress anal. by polarised light method *(Russian)* 77−11641
Ni *(Japanese)* 78−15617
Ni, cold-rolled, anomalous effects during X-ray stress meas. *(German)* 80−104184
Ni, electrodeposited in sulphamate bath, cyclic stress, meas. appl. at 125-200°C 80−19295
$Pb(Zr_xTi_{1-x})O_3$, meas. of Hugoniot curve with commercial manganin stress gauges 80−70362
Si-SiO_2, interface, stress meas. technique 80−84395
SiO_2-Na_2O-CaO-MgO, glass, fibre and plate, internal stress and birefringence microanal. using optical phase microscope interference-polarisation 79−39109
Yb stress transducer, piezoresistive effects 77−68539
ZrO_2 films on Zr alloys, model of stress distrib. 79−49694

stress-optical effects *see piezo-optical effects*

stress relaxation
see also anelastic relaxation; creep; viscoelasticity
δ_R criterion for brittle fracture in BCC single crysts. *(Russian)* 78−56732
acryl-melamine resin film, crosslinked, stress relaxation in hot water *(Japanese)* 78−60695
acrylonitrile-styrene copolymer melts, rheological behaviour *(German)* 77−51012
activation energy of logarithmic stress relaxation *(Russian)* 77−68441
activation volume stress depend. 80−54304
alkali silicate glasses, high temp. relax. mechanisms 80−70134
allyl ester polymerizates and copolymerizates, relaxation behaviour, 77 to 170K *(German)* 77−32614
amorphous solids, time-temperature-pressure superposition phenomena, free volume theory 78−26059
arterial wall empirical linear response models 77−90831
articular cartilage, electromechanical props. during compression and stress relaxation 78−92667
articular cartilage in compression, biphasic creep and stress relax., theory and expts. 80−94275
austempered reinforcing wire, tempering under stress, effect on mech. props. and relaxation resistance 80−100861
Bakor 33, refractory, stress relaxation capacity determ. 80−60910
bar, axially symmetrical residual stresses, with longitudinally nonuniform stress distrib. 78−51070
bar, circular, in tension, strain energy release rate for edge crack 79−18815
beam, nonlinear viscoelastic, torsion creep 79−18745
in bending, alternative eqns. 79−7294
bending stress relaxation in complex system, apparatus for investigation 77−23922
biological soft tissue nonlinear viscoelastic behaviour 78−69128
bitumen, rheological model of Maxwell-Norton type *(French)* 79−64614
bitumous mixes, complex modulus calc. *(French)* 79−20092
α-brass, single crystal, obstacle strength variation during stress relaxation 78−68723
brittle fracture kinetics, one-dimensional stress fields and spherical wave reflection 78−9608
brittle materials, intergranular creep crack growth, diffusion controlled theory 78−84950
Burgers vector sign determ. for nearly screw dislocations, X-ray dynamical theory applic. 80−59467
burn-scarred human skin rheological props. in vivo meas. 78−31935
butadiene methylstyrol, exam. of low temp. relaxation processes *(German)* 78−92291

stress relaxation continued
butadiene nitrile, exam. of low temp. relaxation processes *(German)* 78−92291
butadiene styrol base elastomer, relaxation mech. *(German)* 77−36565
butadiene-styrene polymers, relaxation time spectra and mechanical losses *(Russian)* 78−76698
butadienepstyrene, surface phenomena in struct. rearrangement after deform. *(German)* 78−19913
butyl rubber, resin cured, filled, relaxation study *(German)* 80−35243
cable insulation for nuclear power station, deterioration testing *(Japanese)* 80−27743
ceramic, electrical transducers for automatic recording of mechanisms occurring during drying 77−52561
ceramic materials, fine-grained, cyclic plastic deform. as cuase for thermal expansion hysteresis 80−89290
ceramic nuclear fuels, mech. props. at compressive deformation 80−651
ceramics, cracking characterisation by double torsion test *(French)* 80−104369
ceramics, polycrystalline, stress-relaxation technique for deformation studies in four point bending 79−100200
clamped skewed plates, elastic deformations by dynamic relaxation 78−34049
coating, diffusion solution, relaxation of residual stresses *(Russian)* 77−70195
colloids, nonlinear rheological behaviour and shear dependent struct. 79−7358
composite, lamellar, matrix strain hardening mechanism *(Russian)* 77−59801
composite flat belt drive material, tension relaxation under simulated drive conditions 78−56688
concrete, creep, time dependent behaviour under high tensile stress *(Japanese)* 78−31465
concrete, prestressed, low-temp. tensile strength and linear expansion coeff. of reinforcing steel 80−30051
constitutive eqn., stress depend. 79−7298
corundum single crystals, stress relax., cracking during growth 78−47263
creep, grain-boundary sliding controlled, grain rolling, superplasticity 77−90399
creep, transition between dislocation and diffusion 80−88253
creep and relaxation curves for torsion-tension members at elevated temps. 78−83260
creep const. determ. from stress-relaxation meas. in bending and torsion 78−9572
creep dynamics in stress relax. regime, analyt. expressions 77−11627
creep modelling incorporating initial strain and ageing 80−58939
crystal growth from melt, stress form., dislocation density estimation *(German)* 80−15022
crystalline materials, fracture, stress relaxation effect 80−88256
crystals, review 79−73248
curve prediction from creep data *(German)* 77−70097
cyclic loading phenomena simulation in nonlinear hardening model 77−21158
deformation resistance, depend. on hot press. working speed *(Russian)* 80−65126
deforming stress relaxation, non-uniform internal stress field effect 77−21204
discrete structure solids, mathematical models for stress relaxation and deformation 77−14923
rel. to dislocation electron microscope image calc. and Burgers vector sign determ. 77−59017
dislocation motion through random array of point obstacles, vel. load depend. 77−7732
Earth upper mantle, nonlinear stress propag. 79−16422
earthquakes stress relaxation models, finite difference calc. 77−73682
elastic limit relationship *(Japanese)* 79−98632
elastic-plastic torsion, variational inequality concept, finite element anal. 80−23907
elasticity, linear theory, with point Maxwellian sources of stress relax., numerical solns. 79−5982
elastomer, relaxation time spectra calc. from stress relax. data *(Russian)* 77−44288
elastomeric network, finite linear viscoelastic theory, time-depend. deform. behaviour 80−38292
elastomers, rel. between relax. behaviour and tensile strength *(German)* 80−66604
elastomers, relax. transitions from relax. spectrometry and internal friction *(German)* 80−34136
elastomers, viscous flow, strength characteristics, activation energy, fracture behaviour *(German)* 79−57105
electric connector materials, estimation for Cu alloys and plastics, expts. 77−21206
electron micrograph, theoretical, of dislocation, foil surface stress relax. effect 77−31665
endopelvic fascia, human, stress/strain history relations in simple elongation 78−44539
epichlorohydrin/bisphenol A epoxy polymer concrete, viscoelastic props. 80−45340
episulphide network polymers, mech. relaxation 79−96061
Epon 828-Z, acoustical determ. of shear relax. functions 78−76686
epoxide resin cured with aliphatic dicarboxylic acids, fatigue behaviour *(Japanese)* 79−79092
epoxy EDT-10, rigid polymer, thermal stress isothermal relaxation 80−71683
epoxy resin, Cl-containing, relation between static and dynamic deform. characts. 80−3137
epoxy resin systems, synthesis review, phys. and mech. props. at low temps. 80−25650
epoxy structural adhesives, tensile tests, stress/strain relations, stress relaxation 78−60702
epoxy system, rubber-modified and unmodified, sub-T_g annealing expts. 79−11643
equation of state for class of viscoelastic deforms. 78−26060
ethyl acrylate ionomers, stress relax. 80−104200
experimental data, analysis methods 77−84822
fibrous structures, mech. relax. theory 78−13916
filamentary crystals, complex stressed state, method of investigating mech. props. 80−3264
film/substrate, two-layer structs., relaxation of internal stresses 80−34341
finite elasticity theory, research directions 77−68416

stress relaxation continued
fluoropropylmethylsiloxane fluids, viscoelastic behaviour 79−14361
fracture, computational models for one and two dimens. wave propag. 77−11628
fracture, plasticity model, dislocation based, geometrically consistent 78−30242
galena, polycryst. synthetic, stress relax. 500 to 800°C 78−87737
gelatin gels, in water and glycerol/water mixtures, dynamic viscoelastic props. 80−64508
geological materials, stress relaxation testing method for mechanical behaviour studies 78−96309
glass, mechanical destruction role of relaxation processes 80−89282
glass, tempering, stress and structural relaxation 78−64574
glass, thermal stresses, temporary and residual, monitoring by semiautomatic heating polariscope-polarimeter 78−16833
glass, toughened, 200 to 600°C 78−19800
glass, toughened, stress relax. at temp. below annealing range *(Czech)* 79−43305
glass and glass-forming liq., viscoelastic properties, comparison with Lennard-Jones model 80−84983
glass and glass-to-metal seal, meas. device 77−63845
glass-metal sealing, set point of glass 80−108423
glasses, commercial, viscosity and stress relax. in glass transition region 80−93589
glassy state and highly viscous liq., rheology 80−70130
2-hydroxyethyl methacrylate-methacrylonitrile or acrylonitrile copolymer network, mech. response 79−57031
Hypalon 40, chlorosulphonated polyethylene, mech. props., press. effects 77−32618
Inconel X750 springs, in-reactor stress relaxation 78−11256
incubation period following stress reduction during creep 79−7603
injection moulded GFRP distortion meas. by holographic interferometry 79−79020
inorganic solid, stress depend. of activation volumes in creep and stress relaxation 79−19312
ionene polymers, counterions and absorbed water influence on mech. relax. 77−40430
ionene polymers, ion conc. effect on mech. relax. 77−44284
ionised ethylene-acrylic acid copolymer, heterogeneous ionomer, dynamic mech. props. *(Japanese)* 77−59843
Kevler fibre, mech. props. in aq. H_2SO_4 soln. *(Japanese)* 79−47753
lecithin-water system, lamellar phase, rheology 80−89779
linear one-dimensional viscoelastic solid, flow and relaxation distribution 78−36833
linear viscoelastic systems, constant strain rate and stress relax. obs. 78−90727
3-lumped parameter vibrational mdoel, anal. for dynamic characteristics of materials of relaxation type 79−72827
martensitic transformation, internal stress relax. effect on microstruct. and kinetic features 77−44250
Maxwell fluid, diffusion of vortex line in stagnation point flow 80−74892
Maxwell fluid, Rayleigh-Taylor instability 80−33631
Maxwellian materials, nonlinear dissipative, thermodynamics, constitutive eqns., stress relax. function 78−73950
MBBA, shear modulus and viscosity relax. near isotropic-nematic phase transition *(Russian)* 77−39543
measurement by cone-plate instrument 80−28477
metal, cleavage plane prediction, Ayres-Stein method 79−29213
metal, diffusional relaxation of stress conc. at second phase particles 79−1889
metal, FCC, polycrystn., fatigued, behaviour model during plastic deformation *(German)* 80−21023
metallic solid, stress relaxation, pre-exponential factor 79−18748
metals, crack resistance, high temp., during creep due to stress relaxation *(Russian)* 79−52348
metals, strain hardening, creep, stress relaxation correlation with high temp. processes *(Russian)* 79−34053
metals and alloys, creep and stress relaxation curves, phenomenological description 79−100231
metals and alloys, in-reactor, study at low temps. 80−93588
metals and alloys, polycryst., strength differential effect, temp. and strain rate sensitivity in saturation cycling 79−66094
metals and alloys relaxation resistance testing using constantly loaded sample 78−39965
methylstyrene rubber, relaxation time spectra calc. from stress relax. data *(Russian)* 77−44288
model crystal, thermally activated glide in strain rate change and stress relaxation expt. 77−36615
modulus, evaluation from response to constant strain rate followed by constant strain 80−74765
neointimas developing on flocked surfaces of left ventricular assist device, mech. anal. 78−40431
Neoprene WB, polychloroprene rubber, mech. props., press. effects 77−32618
nylon 6, influence of monomer and water diluents on mech. relax. 79−4993
nylon 6, relationship between morphology and dynamic mech. props. 79−4992
nylon 6-Li halide mixtures, viscoelastic behaviour, stress relaxation 80−58995
oligoesteracrylates, three dimensionally linked, dynamic mech. props. *(German)* 78−64577
optical ceramic KO-1 strain, yield limit, and stress relaxation obs. 79−46018
optimal heating of solid body and stress relax. role *(Russian)* 78−22258
Ozhennite, yield point, effect of ageing stress 77−21223
phenolic resin filled and unfilled, mech. relaxation behaviour, effects of temp. and time *(German)* 78−6963
plastic, static relaxation behaviour, test rig design *(German)* 79−39081
plastic, time dependence, at crack tip 77−63765
plastic flow, order-disorder transform. effect on creep, traction and relaxation *(French)* 80−35180
plastic relaxation in shock wave, slip mechanism 79−41605
plastics, high temperature 77−25092
plastics, testing method 77−52576
plate with central hole, effect of J_3 on creep and relaxation 77−54905
PMMA, acoustical determ. of shear relax. functions 78−76686
PMMA, piezobirefringence, optical and mech. relaxations, temp. depend. 80−34885
PMMA, rigid polymer, thermal stress isothermal relaxation 80−71683
stress relaxation continued
PMMA, stress relaxation during crazing, eqn. 79−61762
PMMA, viscoelastic props. in plastic zone, cooling rate effect 80−40418
PMMA melt, stress relax. at large deformations 80−58994
PMMA organic glass, stress relax. calc. from creep curves 80−71709
poly(alkyl methocrylates), US determ. of relax. 77−51449
poly(di-n-heptyl itaconate), alkyl side chain independent relax., double glass transition 80−59636
poly(N-monosubstituted methacrylamides), relaxation 79−57033
polyamide, stress relaxation, eqn. and expt. *(German)* 77−28846
polyamide, viscoelastic behaviour determ. from reln. between creep and relaxation *(German)* 77−62174
polyamide coating on steel roller, experimental exam. of contact parameters 78−68842
polyamide-polyurethane copolymer dispersions, structurisation and relax. props., coating from props. 80−76559
polyanide, thermorheological and mech. props. 79−96067
polybutadiene, dihydroxy-terminated, with unattached styrene-butadiene copolymer, stress relax. 80−104202
polycarbonate, compressive recovery behaviour 79−38919
polycarbonate, stress relaxation during crazing, eqn. 79−61762
polycarbonate, viscoelastic behaviour determ. from relationship between creep and relaxation *(German)* 77−62174
polycarbonate, viscoelastic props. in plastic zone, cooling rate effect 80−40418
polydecamethylene-oxide, dynamic mechanical measurements using a dynamic viscoelastometer *(Spanish)* 79−61636
polyester, unsat., copolymers, molecular mechanism of relaxation, free torsion oscill. study *(Russian)* 79−34093
polyesters, aromatic, structural variation rel. to low temp. relax. 79−66096
polyether-polyester elastomer, fine structure and mech. props. 77−59844
polyethylene, crystalline struct. transitions 77−51496
polyethylene, effect of ketones, temp. depend., environmental stress relax. study 80−45336
polyethylene, hard elastic fibres, deform. and struct., −196 to 80°C 78−51437
polyethylene, high density, effect of strain rate on stress relaxation behaviour 78−72807
polyethylene, high density, time depend. deform. resistance 79−5019
polyethylene, high-density, gaseous environment effect on mech. relaxations, tensile and torsion tests 79−96068
polyethylene, high-density, lamellar sep. during deform. 78−23775
polyethylene, high-density fibres, solid-state extruded, α-relaxation mechanism 79−70035
polyethylene, high-press. charact. by torsional vibration anal. *(German)* 77−59842
polyethylene, highly oriented fibre composite, self-hardening, tensile props. 77−55939
polyethylene, hot drawn, low density, stress relaxation 79−29121
polyethylene, injection moulded high density, internal stress parameter, chemical cross linking effects 79−57035
polyethylene, linear, γ-loss band, stress relax. 77−21201
polyethylene, linear, cold-deformed, texture and molecular chain mobility 78−19805
polyethylene, linear, effect of HNO_3 treatment on γ-loss band 77−36562
polyethylene, low and high density, tensile relaxation changes *(German)* 78−64599
polyethylene, low density, linear viscoelasticity, relaxation func. determ. 79−7359
polyethylene, low-temp. relax., effects of chem.- and electron irrad.-crosslinking 79−4990
polyethylene, sonic frequency vibration effect on stress relaxation 77−86072
polyethylene melt, nonlinear shear behaviour, strain-dependent memory function 78−67161
polyethylene melt, nonlinear shear response during periodic deformation 79−100202
polyethylene rod, high oriented, mech. behaviour 78−15446
polyethylene terephthalate, β relax., dynamic mech. and dielectric loss data 79−15399
polyhydroxyethyl methacrylate swollen network filled with polyhydroxyethyl methacrylate, viscoelastic and ultimate behaviour in rubbery region 79−83247
polyimide, influence of monomer and water diluents on mech. relax. 79−4993
polyisobutylene, in simple extension, nonlinear stress relax., recovery after partial relax. 80−5949
polyisobutylene, low molecular weight, melt, nonlinear shear response during periodic deformation 79−100202
polyisobutylene, relax. of birefringence and stress, extension ratio depend. 77−43962
polyisobutylene, RQP method of inferring a mechanical relaxation spectrum 79−37195
polyisobutylene soln., start-up tests, relaxation meas. of shear and normal stress *(German)* 78−67166
polymer, amorphous, enthalpy relax. rel. to T_g 77−52278
polymer, amorphous, molecular origin of relaxations 78−26058
polymer, crazing limit in creep and stress relax. 79−34177
polymer, deformation, failure, kinetic model *(Russian)* 78−72832
polymer, filled, rheology, steady state shear flow and periodic deform., relaxation time, spectra, viscosity 79−96066
polymer, flowing, relaxation of normal stresses 77−881
polymer, linear viscoleastic creep under arbitrary temp. variations 79−95075
polymer, long-term durability prediction methods 79−20320
polymer, physically nonlinear, stress relaxation during stretching 78−23754
polymer, plane materials stress relax. and creep under biaxial loading, test procedure 78−3279
polymer, relaxation properties investigation method and instrument 78−39967
polymer, relaxation time spectra calc. from stress relax. data *(Russian)* 77−44288
polymer, rubbery state, correl. between strength and relaxation props. 77−28848
polymer, specimen size effect on mech. behaviour associated with crazing 77−73337
polymer, stress relaxation, pre-exponential factor 79−18748
polymer, stress-relaxation apparatus, stress and vibration relaxation in sound frequency range 77−1905

stress relaxation continued
polymer, thermostable oriented, load effect on relax. transitions *(Russian)* 79−52294
polymer, viscoelastic, microrelax. model for moment effects interpret. 79−20098
polymer chain trapped in suddenly deformed gel, relaxation *(French)* 77−62483
polymer dynamics simulation, relax. rates and dynamic viscosity 78−91211
polymer glass, isothermal struct. relax., in high elasticity transition region, mol. model *(Russian)* 78−87629
polymer latex film composite, glass transition temp. determ. using thermomech. curves 80−75342
polymer liquid, entangled, phenomenological consequences of Doi-Edwards viscoelasticity theory 80−79250
polymer melts, isothermal and non-isothermal stress relaxation following steady state shear flow *(German)* 79−77044
polymer melts and soln., flow under const. and periodic deform. 78−64579
polymer melts and solns., deformation, mol. motion under flow 79−41646
polymer melts and solutions, rheological equations, review 79−86391
polymer relaxation phenomena, conference, San Francisco, CA, USA (Aug. 1976) 79−4257
polymer relaxation props., automatic assembly for exam. over wide range of temp., and medium moisture contents 80−7739
polymer solns., constitutive relns. determ. using stiffened Weisenberg rheogoniometer for uniaxial shear flow 77−80188
polymer strength, kinetic nature 78−15524
polymer viscoelasticity and strength characterisation, advanced light scatt. techniques 80−11857
polymer-elastomer mixtures, temp.-time analogy 79−19317
polymeric glasses, non-elastic deformation, thermodynamic and kinetic anal. 78−64604
polymeric material, temperature shear function and temp.-time analogy in linear thermoviscoelasticity region 79−18747
polymeric materials, stress meas., X-ray diffr. technique, review 78−5713
polymers, construction of single relaxation time spectrum 78−44160
polymers, cryst., hard-elastic fibres, morphology mech. props., mechanisms, review 77−32612
polymers, entangled, ternary blends of monodisperse homopolymers, viscoelastic props. 80−19301
polymers, entangled, viscoelastic props., binary blends of monodisperse homopolymers 79−96062
polymers, glassy, amorphous, secondary loss peaks, mol. motions 79−11649
polymers, glassy, viscoelastic relaxation processes role in macrodeformation 79−72825
polymers, nonlinear, under tension and torsion 79−52290
polymers, partially crystalline, nonlinear mech. relax. *(Russian)* 80−40467
polymers, relaxation props., photometric transducer method of meas. 80−3268
polymers, solid-liquid state transitions, state before breakdown 78−63842
polymers, viscoelasticity, calc. using relaxation and retardation spectra *(German)* 78−92290
polymers, yield stress estimation from relaxation data 78−64594
polymethacrylic acid-polyethylene oxide polymer complex, H bond form., thermal behaviour *(Japanese)* 79−15454
polymethyacrylate, swollen, and methacrylate copolymers, secondary relaxation 79−57032
polymethyl acrylate, phosphorescence depolarisation studies of relaxation effects 78−56685
polyoxymethylene, low-strain deform., transmission electron microscope exam. 79−5013
polyoxymethylene, transitions and relaxation spectrograph 80−65204
polyoxymethylene copolymers, solid, mol. motions, 4-315K, dynamic-mech. study 79−4258
polypropylene, glassy state, macrodeformation stresses, anelastic characteristics 79−52289
polypropylene, hard elastic fibres, stress relaxation 77−36564
polypropylene, nonlinear viscoelastic effects 77−90401
polypropylene, oriented, stress relax. process characts., 20-100°C 79−20097
polypropylene, oriented, stress relaxation 77−44285
polypropylene drawn film, rheo-optical studies 78−15440
polypropylene film, double-exposure speckle pattern obs. of tensile deform., displacement, Poisson's ratio and stress relax. 80−84795
polysiloxane dizwitterionomers, mech., dielec. relax., effect of H_2O sorpt., thermal history 80−50261
polystyrene, atactic, isothermal internal friction meas. of glass transition 79−74191
polystyrene, glassy state, macrodeformation stresses, anelastic characteristics 79−52289
polystyrene, nonisothermal rheology 77−32619
polystyrene, oriented high-molecular, physicocomech. props. *(Russian)* 79−33028
polystyrene, stress relaxation during crazing, eqn. 79−61762
polystyrene melt, carbon-black filled, rheological study 80−48665
polystyrene melt, normal and shear stress relax., Rheometrics mech. spectrometer transient response 78−42577
polystyrene polybutadiene polystyrene triblock copolymers, extension of contour plotting method for representing linear viscoelastic loss 77−32620
polystyrenes, rubber modified, mech. props., mol. orientation effects 79−52331
polytheylene, high density, under tension and torsion 79−52290
polytrifluorochloroethylene, moulding press. effect on struct. and props. *(Russian)* 79−52295
polyurethane, filled, relation between static and dynamic deform. charcts. 80−3137
polyurethane, stress relax. meas., effect of cure temp. on network struct. 77−84674
polyvinyl acetate, struct. relax., enthalpy and elec. polarisation obs. 79−41978
polyvinyl difluoride, γ-irrad., low-temp. TSD obs. 77−63358
polyvinyl furfural, CdO, MoS_2 and graphite filled, contact area, filler effect 79−57040
porcelain-metal cermet, stress determ., meas. method *(German)* 80−76425
powder, compacted, stress relaxation pattern, moisture effect 80−20994
power plant pipelines under creep conditions, aspects *(Russian)* 78−13930
PTFE, relaxational props. effect of temp. and hydrostatic press. *(Russian)* 77−44325
PVC, glassy state, macrodeformation stresses, anelastic characteristics 79−52289
PVC, kinetic nature of strength 78−15524
PVC, plasticised, history-independent recovery, creep, stress relaxation 78−80607
PVC, stress relaxation in macrodeformation range 80−16370
PVC, unplasticized, evaluation method for chemical resistance *(Japanese)* 80−25893
PVC plastisol films, thermally hardened, struct. and props. *(German)* 79−70097
PVC-ethoxymethylmelamine blends, dynamic mech. props. *(Japanese)* 79−96063
quartz, ion bombardment, extrusion, evidence for radiation-induced stress relax. of silica network 77−24335
refractory, high-temp. stress relaxation during alternating torsional loading 77−16636
relaxation test method, for plastic deform. *(Hungarian)* 80−97661
relaxation times and dynamical modulus, viscoelasticity theory *(Russian)* 79−52293
repeated, consecutive energy barriers 79−14881
resins, thermoplastic, glass-fibre-reinforced, performance at elevated temperatures obs. 79−95067
rheological analysis of stress change experiments during high temperature creep 79−37193
rigidly plastic media with hardening, shock-loaded, dislocation model and elastoplastic waves 79−86379
ring specimen deformation, stress relax., meas. method, increased accuracy 77−75863
rod-shaped elements, under simultaneous static loads and elevated temps., linear limited stress relax. 80−14590
roving glass cloth fibre reinforced plastic, fracture mech., time depend. *(Japanese)* 80−55508
RQP method of inferring a mechanical relaxation spectrum 79−37195
rubber, irradiation-cured, stress relax. in N_2 78−84884
rubber-like polymer, molecular relaxation process effect on strength *(German)* 78−31440
rubbers, swollen, low-freq. dynamics, optical and mech. props. 80−43626
Rzhanitsyn-Koltunov nucleus, anal. determ., relax. function for shear and stretching 80−58932
sandstone, stress relaxation, water effects 79−16453
sea ice, compressive strength and stress relax. meas. *(Japanese)* 77−81916
second phase particle, diffusional relaxation 80−60898
shells of revolution, thin, numerical anal. thermal stress relief 77−89041
silicate glasses, stabilised, exam. of stress relaxation and deformation 78−92292
skin, living, human, constant strain rate, hysteresis and stress relax. behaviour 78−40237
smectic-A liquid crystal, layer rigidity, stress relax. 78−18545
spherical cavity in prestressed medium arbitrary orientation, elastic relaxation coeffs. 77−73692
steel, 19-9 DL, long-time stress relaxation *(Japanese)* 77−59841
steel, 23Kh2G2T, exam. of stress relaxation charcts. 78−44159
steel, age hardened, dynamics of cyclic plasticity *(Czech)* 80−108464
steel, alloy cyclic strength after strain hardening and tempering, precip. hardened 40FT, and 40 78−52988
steel, austenitic, 0Kh14AG12M, temp. depend. of mech. props. and kinetics of phase transforms. *(Russian)* 78−92297
steel, austenitic, alloyed with N, model of relaxation processes *(Russian)* 79−11650
steel, austenitic, approx. method for high-temp. cracking resistance estimation 78−23914
steel, austenitic, cold worked 10Kh11N23T3MR, structural transformations, aging effect, electron microscope obs. 80−40402
steel, austenitic, Cr-Mn-N, plastic deformation influence on internal friction, relaxation processes *(Russian)* 80−100870
steel, austenitic, creep, low-temp., during dynamic relaxation, effect of dislocation struct. *(Russian)* 77−25103
steel, austenitic, metastable, 0Kh14AG12M, Cr-Mn and Cr-Mn-Ni, phase transform. kinetic effect on mech. props. *(Russian)* 79−34024
steel, austenitic stainless, cold worked, 20%, heat treatment effects on mech. state, load-relaxation expts. 77−52350
steel, austenitic stainless, stress corrosion cracking in H_2SO_4-NaCl soln., Ni and N_2 effects *(Japanese)* 79−100289
steel, austenitic stainless, stress relaxation model, experimental confirmation of model 78−92293
steel, austenitic stainless 316, load relaxation data, comparison with Hart's deform. model 77−70091
steel, C, accelerated deform. by to H_2 absorption *(Japanese)* 79−70121
steel, C, St.3, thermal stresses, spontaneous relaxation 79−1892
steel, C(0.2 wt.%), explosively strengthened, cause of anomalous increase in H_2 of low cycle endurance *(Russian)* 77−16729
steel, CC Cr-Mo-V, stress relief cracking mechanism 78−64669
steel, Cr, stress relaxation, superplasticity and thermal cycling *(Russian)* 80−21019
steel, Cr-C, (2.14, 1.08 at.%) tempered, resistance to small plastic deformation, strain relaxation *(Russian)* 78−56698
steel, Cr-Mo, secondary relaxation, correspondence of steady state creep *(Japanese)* 79−83250
steel, Cr-Mo weld metal, trace element embrittlement suppression by creep strength effects 80−66656
steel, Cr-Mo-V, high temp. main steam pipe, residual stresses in butt welds 80−21059
steel, Cr-Mo-V (1, 0.5, 0.25 wt.%), long-time stress relaxation props. 77−12666
steel, Cr-Mo-V-(W), for bolts, stress relaxation data 78−60699
steel, Cr-Mo-W-V, long time stress relaxation props. *(Japanese)* 77−59841
steel, Cr-Ni-Mo-W-Nb, for bolts, stress relaxation data 78−60699
steel, eutectoid and hypoeutectoid stress relaxation during rapid heating transform. *(Japanese)* 78−11258
steel, fatigue life, structural parameters and chem. comp. effects, rel. to test parameters 77−59928
steel, high-strength, strain relax., model *(Spanish)* 77−73296
steel, low alloy creep resisting, causes of weldment cracking 78−56760

stress relaxation continued
steel, low C, dynamics of cyclic plastic deform. at low temps. *(Czechoslovakian)* 77−32679
steel, low C, effective stress determ. during the loading cycle 79−38879
steel, martensitic, low C wire, strain tempering by rapid heating *(Japanese)* 78−31428
steel, martensitic, quenched, strength variation rel. to H behaviour 77−59924
steel, medium C, deformed, H_2 enhanced load relaxation 79−61635
steel, medium C, fatigue behaviour of NiAl precipitation hardening 78−84983
steel, medium C, S 45 C, influence of mean strain on low-cycle torsional fatigue life *(Japanese)* 79−8348
steel, mild, time dependent plastic relaxation at crack tip, fracture implications 77−63765
steel, Mn-Cr-Ni-N, N effect on relaxation behaviour, internal friction temp. depend. *(Russian)* 78−52872
steel, MnMoNi(Cr), pressure vessel, stress relief cracking 79−43404
steel, Ni-Mn (16, 2 wt.%), 40N16G2, single crystal, stabilisation and destabilisation mechanisms *(Russian)* 78−23732
steel, nuclear bolts, heat treatment for structural retraction prevention *(French)* 79−91713
steel, prestressed concrete wire, strain tempering by rapid heating *(Japanese)* 79−70088
steel, quench-hardened, exam. of anomalous plasticity when deformed *(Russian)* 79−11663
steel, relaxation of residual stress with fatigue loading 77−56051
steel, stainless, 20% cold worked 316, in-reactor stress relaxation in bending 77−42079
steel, stainless, 304, isochronous relaxation curves after monotonic and cyclic strain 79−87676
steel, stainless, AM-350, enhanced in-reactor stress relaxation 79−93725
steel, stainless, stress corrosion cracking, prestrain effect, stress relaxation study 80−35384
steel, stainless, type 304, viscoplastic behaviour, strain rate sensitivity, creep, relaxation, tensile tests 80−66727
steel, stainless, type 304, viscoplastic model, uniaxial, based on total strain and overstress 80−64387
steel, stainless 304, previously irradiated, irradiation induced stress relaxation in fast flux environment 77−25104
steel, stainless ferritic, drawability, mech. props., and grain boundaries in 08Kh16AMT and 08Kh18T1 80−35270
steel, stress relaxation, short-term, creep and strain hardening *(Russian)* 80−30005
steel, stress relaxation in cyclic deformation 80−3119
steel, structural bending moments and tensile creep, relaxation bending test device 79−70245
steel, structural martensitic, corrosion resist. under stress effect of strain ageing with hydroextrusion *(Russian)* 79−38853
steel, type 4052Kh, thermomechanical working influence on mech. props. *(Russian)* 80−93578
steel, type A508, C1 2, microcrack formation during stress-relief annealing of a weldment 78−80629
steel, wire, reinforced prestressed concrete, strain-tempering conductions and mech. props. *(Japanese)* 78−39816
steel 65G, elastic props., effect of additional tempering temp. 77−21192
steel alloys, low and medium C content, relaxation phenomena in volume changes during tempering *(Russian)* 79−100176
steels, alloy, stress relax. data anal. using total strain-time parametric method *(Japanese)* 80−104198
strain tempering by rapid heating and cooling of cold drawn wires *(Japanese)* 78−84863
stress dip technique for effective stress determination in cyclic straining 80−2113
strips, errors occurring due to approx. formula, for radius of curvature 80−23909
styrene butadiene rubber, dicumyl peroxide cured, behaviour in moderately large deform. 78−60692
styrene butadiene rubber, strain energy function, temp. effects 78−56684
styrene-butadiene copolymer, birefringence and stress relaxation 78−44158
styrene-butadiene rubber, vulcanised $CaCO_3$ filled, stress/strain relations *(Japanese)* 80−40443
styrene-butadiene-styrene block copolymer, stress relax. following steady-state flow, residual shear stress development 80−83772
test, appl. to discerning frictional and internal stresses 77−63712
test device, for variable temp. 80−85113
tetrafluoroethylene-vinylidene fluoride mixture, in epoxide-diphenylene propane resin, exam. of temp. depend. of stress relaxation, viscoelasticity 80−11688
textolite glass, stress relax. calc. from creep curves 80−71709
theoretical analysis, as three-stage process 77−84835
theory 77−16632
thermal activation analysis, of plastic deformation and dislocation motion using stress and temp. jumps 80−74771
thermodynamics of internal variables, rel. to absolute reaction rate theory 78−18696
thermoelastic half-space transient response 79−32253
thin plate, behaviour of circular prismatic dislocation loops, using linear theory of elasticity *(Japanese)* 79−4302
time spectrum determ. from components on complex shear modulus, iterative method 77−50965
toughened glass, 200 to 600°C stress relax., anal. *(Czech)* 78−79661
trifluoropropylmethylsiloxane fluids, viscoelastic props., mechanical impedance, viscosity and density meas. 80−79249
two-dimensional lattice, ordered phase form. by elastic stress relax. at antiphase boundaries *(Russian)* 79−14817
Udimet 700, Ni-Co-Cr-Ti, hold time effects on high temp. fatigue crack growth 79−5036
uniaxial stretching curve data anal. using creep with anisotropic hardening theory *(Russian)* 79−76981
visceral smooth muscles in vertebrates, viscoelastic and plastic props. 78−73169
viscoelastic bodies, deformation taking into account influence of accumulated defects 80−19252
viscoelastic fluid, nonlinear stress relax. after steady shear flow 77−51015
viscoelastic fluids, Weissenberg rheogoniometer, R-17, axial compliance reduction 80−106859
viscoelastic linear on non-linear bodies, creep and relax. phenomena generalisation 77−876
viscoelastic liquid, fast and slow relaxation limits 79−47465
viscoelastic material, automatic system for short-time stress relaxation 77−63710
viscoelastic materials, linear, numerical cond. between creep and relaxation *(German)* 77−62174
viscoelastic properties dynamic evaluation for use in cardiac prosthetics 78−40405
viscoelastic response to small deformations superposed on large stretch 77−72187
viscoelastic strip, dynamic crack propagation due to antiplane loading 80−64464
viscoelasticity, nonlinear, stress relaxation, Volterra integral equation, numerical analysis 80−53646
viscoelasticity, time reversal and symmetry relations 80−102970
Viton B, vinylidene fluoride-hexafluoropropylene copolymer, press. effects on mech. props. 77−32618
Zircaloy, unirrad., stress corrosion cracking, I_2-induced, effect of test temp., alloy comp. and heat treatment 80−97632
Zircaloy 4, creep anal. and appl. in prediction of residual stress relaxation 79−43325
Zircaloy 4, stress relaxation in bending 78−68719
Zircaloy 4 tubing, cold-worked and annealed, stress relaxation behaviour 77−57717
Zircaloy-2, recoverable plastic strain 77−63708
Zircaloy-4, load relaxation and tensile tests 79−20093
Zircaloy-4, stress relaxation specimens, thermally induced strain recovery causing microstruct. changes 77−25057
Zircaloy-4, stress-relieved and cold-worked, stress relaxation in bending at 673K 80−93609
Ag film, sputtered, hillock growth and agglomeration by annealing, SEM obs. 80−2309
Ag films, hillock form. hole growth and agglomeration 80−44455
Ag single crystal, dislocation dynamics during stress rate changes 78−19813
Ag-Au thin films, interdiffusion, pore formation, stress effects, adhesive effects *(Russian)* 79−82502
Al alloy, RR58, prior stress history effects on creep rate and fracture 77−4829
Al alloy, residual stress relax. rel. to temp., load cycling, aircraft struct. appl. 78−7053
Al and Al-Mg (5.7 at.%), test, appl. to discerning frictional and internal stresses 77−63712
Al, cold worked, effect of bias stress on US attenuation induced by geometrical kinks mobility *(French)* 77−31728
Al, creep, low-temp., during dynamic relaxation, effect of dislocation *(Russian)* 77−25103
Al, FCC, strain hardening and recovery by pure metal mode, high temp. deform. *(Japanese)* 78−52843
Al foil, internal friction changes during low temp. plastic deform. *(Russian)* 80−100304
Al, load relaxation, plastic deform. theory and plastic eqn. of state 78−27554
Al, plastic deformation thermal activation parameters from creep kinetics and stress relaxation 80−71717
Al, recovery during stress relaxation testing at 298K 77−8872
Al, stress wave propag., transmitted wave profile 77−80578
Al, thermoactivated creep and stress relax. 79−87692
Al-alloy, type 6351 and 6061, stress relaxation in cyclic deformation 80−3119
Al-Cu, Bauschinger effect 79−61646
Al-Cu (5 wt.%) alloy, ageing during relax. of elastic stresses, X-ray diffr. expts. *(Russian)* 77−59821
Al-Cu-Mg, acoustic emission during tensile testing 80−7632
Al-Fe dil. alloy, bamboo struct., grain boundary internal friction peak 79−43306
Al-Mg, acoustic emission during tensile testing 80−7632
Al-Mg, Mg effect on ductility, 25 to 250°C 79−100214
Al-Mg (2.2 at.%), high temp. creep mech. determ. by stress-relaxation 77−12670
Al-Zn (11 wt.%), stress depend. of strain rate at elev. temps. 78−23757
Al_2O_3-epoxy mechanical mixtures, stress-wave propag. model, dynamic response expts. 79−1477
Ar, liq., elastic modulus and stress relaxation 79−19304
$BaTiO_3$, deform. and stress relax. of single crysts. 77−59542
$BaTiO_3$, polycrystalline, X-ray diffraction, Curie temp., lattice defects, phase changes 79−99830
Be, brittle-ductile transition, intergranular embrittlement *(Russian)* 78−3208
Be-Cu alloy stress relaxation in bending, 63° to 343°C 80−50693
Be-Cu mill-hardened strip stress relaxation obs. 78−48485
C, glassy, graphitisation kinetics 79−52246
C steel, prior stress history effects on creep rate and fracture 77−4829
CaF_2, impurity effects on strengthening 77−63682
Cd, electroplastic deform., stress relax. meas. *(Russian)* 79−38894
Cd, polycrystalline, effect of strain rate on stress relaxation behaviour 78−72807
Cd, single cryst., elec. current depend., electron plastic effect 79−79021
CdS, reversible hardening induced by electron-beam irrad. 77−62580
CdTe, crysts., mech. behaviour, yield stress function of temp., stress relaxation 79−60427
CdTe, plastic deformation activation anal. below room temp. 78−84935
Co, deformed, microstruct. singularities in pre-transform. temp. range *(Russian)* 80−45347
Co, single crysts., $\{11\bar{2}1\}$ twins, accommodation and form. 80−96540
Cu, activation vol. and dislocation density determ. from relaxation tests 78−3264
Cu alloys, effect of surrounding medium *(Russian)* 79−100199
Cu alloys, flat spring, mechanical props. in bending, stress relax. test, 23 to 232°C 78−72806
Cu alloys, strain hardened, struct. factor effect on stress relaxation *(Russian)* 80−25748
Cu, condensates of different thicknesses, polycrystalline, mech. props. 79−65350
Cu, creep, low-temp., during dynamic relaxation, effect of dislocation struct. *(Russian)* 77−25103
Cu film, internal stress determ. by stress relaxation method *(Russian)* 77−62787
Cu, internal stress meas. by decremental unloading technique 78−64576
Cu, plastic deformation thermal activation parameters from creep kinetics and stress relaxation 80−71717

stress relaxation continued
Cu, polycrystn., stress relaxation in cyclic deformation 80−3119
Cu, powder, compression and stress relaxation *(Japanese)* 79−96060
Cu, stress component determination during loading cycle *(Czech)* 79−91725
Cu, thermoactivated creep and stress relax. 79−87692
Cu-Al, eutectic composition, exam. of high temp. mechanical behaviour *(French)* 78−72818
Cu-BeCo (1.85, 0.29 wt.%), type CA172 (TH04), strengthened by spinodal decomp., stress relax. in bending 80−7616
Cu-Ni-Sn (4-15, 4-8 wt.%), strip strengthened by spinodal decomp., stress relax. in bending 80−7616
Cu-SiO_2, low-temp. recovery creep, Orowan loop accumulation 80−81126
Cu-Zn, amorphous, viscoelastic behaviour *(Japanese)* 77−86110
Cu-Zn (30 wt.%), single crysts., quantitative anal. of stress relax., obstacle strength and athermal stress variation 80−89277
Cu-Zn (30 wt.%), slip band growth, thermally activated 80−40457
Cu-Zr, amorphous, viscoelastic behaviour *(Japanese)* 77−86110
$Cu_{60}Zr_{40}$, amorphous, ductility and stress relief, low-temp. annealing effects 80−76296
α-Fe, $(\bar{1}\bar{1}2)$ $[\bar{1}\bar{1}\bar{1}]$ anti-twinning slip system, low temp. strengthening, dislocation struct. 77−21164
Fe, Armco, stress relaxation expt., significance under strain ageing cond. 79−57039
Fe, BCC, strain hardening and recovery by pure metal mode, high temp. deform. *(Japanese)* 78−52843
Fe, BCC surface ledge simulation, dislocation-like relaxation 78−30620
Fe, high purity, mag. viscosity mechanism 78−19282
Fe, inelastic deformation, mech. eqn. of state, stress relax. 77−56047
Fe, internal stress meas. by decremental unloading technique 78−64576
Fe, low temperature deform., strain-rate cycling and stress relaxation tests *(Japanese)* 78−52876
Fe, martensitic transformation at high temp., transform. temp., growth rate, stress relaxation 78−56636
Fe, pure, dislocation relaxation peaks under low temp. deform. *(French)* 80−100867
Fe, pure, effect of H_2 on relaxation 77−52391
Fe, relaxation process effect on initial stages of flow *(Russian)* 79−74189
Fe, stress relaxation in high purity single crystal with controlled amounts of C *(French)* 79−70105
Fe-Al (0.069 and 0.158 wt.%), internally oxidised, low temp. deform. *(Japanese)* 78−52876
Fe-B-Si amorphous ribbon, strain induced anisotropy, and toroid diam. effect on mag. props. 80−34623
Fe-Co-Cr (27, 0.5 wt.%), internal stress and brittleness in ordered state *(Russian)* 79−61698
Fe-Co-V, ordered and disordered, dynamic ageing *(French)* 80−16355
Fe-Mn, jump stress relaxation obs. during cooling before martensitic transform. *(Russian)* 79−38884
Fe-Ni alloys props. of materials used in electromechanical filter resonators *(Czech)* 80−76318
Fe-Ni austenitic, effect of Al and Ti on relaxation resist. 80−20993
Fe-P-C, viscoelastic behaviour of amorphous alloys *(Japanese)* 77−86110
Fe-Si (2-8 wt.%), single crysts., growth striations, X-ray studies 80−79774
Fe-Ti (0.056 at.%), mobile dislocations during stress relaxation 78−68721
Fe-Ti (0.056 at.%), mobile dislocations during stress relaxation 78−68722
Fe-Ti (0.056 at.%), stress relaxation curves, anal. interpretation 77−59847
Fe-Ti (0.056 at.%) alloy, mobile dislocations during stress relax. 77−7729
Fe-Ti (0.056 wt.%), mobile dislocations during stress relaxation, comment 79−74193
Fe-Ti (0.056 wt.%), mobile dislocations during relaxation, reply to comment 79−74194
$Fe_{80}B_{20}$, amorphous, deform. and annealing effects on mag. and mech. props. 77−12717
$Fe_{80}B_{20}$ metallic glass, crystn. and struct. relax., Mossbauer effect study 80−75182
Fe_xB_{100-x}, amorphous, stress relax. after annealing 80−55447
$Fe_{40}Ni_{40}B_{20}$, metallic glass, embrittlement kinetics and crystn., quenching influence 78−68766
$Fe_{40}Ni_{40}P_{14}B_6$, amorphous ribbon, cold rolling, annealing mag. props. 77−8958
$Fe_{40}Ni_{40}P_{14}B_6$, amorphous, deform. and annealing effects on mag. and mech. props. 77−12717
$Fe_{40}Ni_{40}P_{14}B_6$, amorphous alloy, structural relaxation kinetics, X-ray diffr. exam. 78−38627
$Fe_xNi_yP_{14}B_6(S_2)$, coiled ribbons, stress relaxation 79−29120
$Fe_{2-x}SiO_4$, fayalite, oxidation kinetics and growth of Fe_2O_3 whiskers 78−84113
KCl, annealed in KBr vapour, crack and pore formation, diffusionally induced stress relaxation *(Russian)* 80−40388
KCl single crystal, dislocation velocity stress exponent estimation by stress relaxation and creep tests *(Japanese)* 78−55875
KCl, strain hardening during relax. of deforming stresses 77−7786
KCl with Al_2O_3 disperse spheres, dislocation mechanism for stress relaxation in cooling crystal *(Russian)* 80−54347
KCl:Ba^{2+}, localised stress relaxation in excess vacancy system, prismatic loops *(Russian)* 80−88160
KI, load relaxation studies 79−79016
LC-440, shear modulus and viscosity relax. near isotropic-nematic phase transition *(Russian)* 77−39543
LiF, kinetics analysis of stress relaxation 80−65136
LiF, load relaxation studies 79−79016
LiF, monitoring of stress relaxing profile using shorted guard-ring quartz gauge 79−58680
LiF, plastic deform. and dielec. losses 78−19410
LiF, shock wave, precursor decay, stress threshold 77−4156
MgO, photoluminesc. during mechanical deform. 80−60665
MgO single cryst., internal stresses and dislocation mobility, stress relaxation method 80−6413
Mo, mag. field effect on mech. props. and dislocation struct. *(Russian)* 79−42818
Mo, mechanical eqn. of state *(Japanese)* 78−91375
stress relaxation continued
Mo, mechanical props. and dislocation struct., mag. field effect 80−54935
Mo, monocrystalline, exam. of microplasticity at ambient temps. *(French)* 78−52888
Mo, single cryst., δ_R criterion for brittle fracture *(Russian)* 78−56732
NaCl, internal stresses and dislocation mobility 78−48440
NaCl, load relaxation studies 79−79016
NaCl, plastic deform. and dielec. losses 78−19410
NaCl, single cryst., crack healing at low temp. 77−36622
NaCl single crystal, plasticity, effect of alternating electric field 78−15481
NaCl, strained in one glide system at 450°C, dislocation struct. 78−22728
NaCl type crystal, dislocations due to high temp. stress relax. 78−2126
NaCl, US deformation, stress anal. by polarised light method *(Russian)* 77−11641
NaF, load relaxation studies 79−79016
Na_2O-CaO-SiO_2 glass, vol. relaxation and thermal history during forming process 80−70130
Nb, deformed, α-peak, internal friction meas. between 90 and 300K 79−100205
Nb film, low temp. thermal stresses *(Russian)* 79−11036
Nb, high purity, dislocation relaxation by internal friction meas. over wide freq. range 79−38876
Nb, mag. field effect on mech. props. and dislocation struct. *(Russian)* 79−42818
Nb, mechanical props. and dislocation struct., mag. field effect 80−54935
Nb, relaxation from room temp. to 114°C, computer optimization of elastic aftereffect curves 77−90390
Nb, relaxation intensity due to interstitial O, temp. effect *(French)* 77−86080
Nb, single crysts., plastic relaxation of internal stresses during mech. twinning at 4.2K, optical and SEM study *(Russian)* 79−66108
Nb-Zr, deformed, α-peak, internal friction meas. between 90 and 300K 79−100205
Nb_3Sn, hot isostatically pressed, plastic deform. 80−108510
Ni evaporated thin films, stress and relaxation effects meas. by Michelson interferometer 77−2650
Ni, magnetised mono- and polycryst., activation vol. var. during low temp. deform. *(Russian)* 78−3178
Ni, superplastic superalloy IN-738 load relaxation testing 77−40507
Ni-Co (25 wt.%), single crysts., mag. annealing effect on magnetostriction and magnetisation *(Japanese)* 80−34744
Ni-Cr base alloy, strain relaxation, effect of grain size, particle size, γ′ vol. fraction 79−47741
Ni-Cr-Co alloys, relax. resist. exam. by bending and tension 79−24564
Ni_3Fe, disordered single crysts., thermo-activated mechanism of plastic deform. *(Russian)* 78−84909
Ni_3Fe, ordered, monocrystals, thermally activated deform. processes 80−50684
Ni_3Fe, single cryst. ordered and quenched, stress relax. *(Russian)* 77−44282
NiO, stress relief and plastic flow in temp. range 1323-1473K 80−89302
NiPt, quenched, ordering kinetics and domain struct. form. during isothermal tempering *(Russian)* 80−66502
Pb, elec. current depend., electron plastic effect 79−79021
Pb, electroplastic deform., stress relax. meas. *(Russian)* 79−38894
Pb, film, deposited on Si substrate, residual strains 78−18915
Pb, film, thermal strain, strain relax. above room temp. 80−59841
Pb, work hardening, and recovery rates during steady state deformation, temp. and stress effect 80−45319
Pb-In-Au alloy, Josephson junction electrode materials, strain relax. 79−38255
Pb-In-Au Josephson tunnel junctions, strain relax. effects 79−65617
Pb-Sn eutectic, superplastic, anelasticity effect on stress relaxation 78−31443
$Pb_{0.94}Sr_{0.06}Ti_{0.47}Zr_{0.53}O_3$, piezoelectric ceramic, stress relax., time depend. deformation 80−60899
$Pb(Zr,Ti)O_3$, fracture and deform. 80−79870
Pd-Si amorphous, viscoelastic behaviour *(Japanese)* 77−86110
PdSi, amorphous, structural relaxation enhancement following stress reduction 80−3118
Se, amorphous, struct. relax. effects, obs. by mech. props. *(French)* 79−51201
Se amorphous film, spherulite formation and role of stresses due to volume changes in crystallisation 77−1083
Se amorphous films, structural relax., viscosity, creep, heat capacitors, and IR spectra meas. 79−42424
Si, analysis of expt. results 77−84835
Si, low temp. relax. of local stresses, dislocation behaviour, X-ray obs. 79−69110
Si, near (III) surface, dislocation movement at annealed scratches, X-ray topography obs. 80−2029
Si_3N_4, cracking characterisation by double torsion test *(French)* 80−104369
SiO_2-Al_2O_3-B_2O_3-CaO-Na_2O-K_2O system glasses, relax. of struct. stresses rel. to forming process 79−34088
Sn-In (50 wt.%), mech. state relations at low and high homologous temps. 77−63707
Sn-Pb alloys, stress relaxation and activation enthalpy 79−74190
Ta-O, relaxation anal. after ageing under stress *(French)* 80−16365
α and α+βTi alloy of different stability, exponential law use for anal. of strain hardening process 79−15697
Ti, commercial purity, stress relaxation expt. 77−48472
Ti, high purity, flow stress relaxation *(French)* 77−86117
Ti, internal stress meas. by decremental unloading technique 78−64576
Ti, martensitic transformation, strain energy minimisation 77−21140
Ti-Al-Mo, type Ti-6242S, irrad. induced creep 80−39163
Ti-Al-Sn, alloy 6242, dynamic effects of flow and fracture during isothermal forging 80−76343
Ti-Al-Sn, type Ti-5621S, irrad. induced creep 80−39163
Ti-Al-V, irrad. induced creep 80−39163
Ti-Al-V(Sn) alloys, plastic deformation and fracture characts. at low temps. *(Russian)* 80−7624
Ti-V (40 wt.%), effects of H on anisotropic elastic props. 79−74192
Ti-V-Cr, type Ti-15-333, irrad. induced creep 80−39163
TiNi, strain recovery, memory effect, in martensite phase *(Russian)* 77−4806

stress relaxation continued
TiO_2 rutile single crystals, stoichiometric, dynamic strain ageing 80−50661
U-alloys, thermal creep and swelling, characterisation 79−74226
V and V-Fe (5.0 at.%), stress relaxation test, appl. to discerning frictional and internal stresses 77−63712
V, zone-refined, deform. behaviour, stress relax. and slip plane patterns 79−29163
W fibre reinforced Cu composites, correl. between thermal cycling-induced microstructural changes at interphase boundaries and tensile behaviour *(Japanese)* 80−71674
W, plasma spray coatings, relaxation phenomena 80−19876
W, stacking faults, microstress relax. effects, field ion images 77−89453
WC, cemented carbide, deformation, high temp., stress relaxation, and strain rate depend. 78−39854
WC-Co, cemented carbide, deformation, high temp., stress relaxation, and strain rate depend. 78−39854
WC-Co-Ta (Ta-Ti-Nb), cemented carbide, deformation, high temp., stress relaxation, and strain rate depend. 78−39854
Zircaloy 2, mechanical equation of state, stress relax. meas. 78−52880
Zn, deforming stress under basal slip, contrib. of forest and primary dislocations 78−3186
Zn, electrodeposited, planar stress relaxation 79−24563
Zn, electroplastic deform., stress relax. meas. *(Russian)* 79−38894
Zn, hydrostatically compressed single crystal, work hardening studied by stress relax. method 79−20069
Zn, plastic deform., effect of hydrostatic press. stress relax. meas. *(Russian)* 79−96102
Zn, single cryst. elec. current depend., electron plastic effect 79−79021
Zn single crystals, fatigue failure at low temp., under low-freq. cyclic loads *(Russian)* 79−61697
Zr alloys, acoustic emission during tensile testing 77−90433
Zr, martensite, furnace cooled and water quenched, strength and deform. 79−20101
Zr, neutron irradiated, yield point phenomenon 79−52304
Zr-Cu (1.6 wt.%), mechanical equation of state, stress relax. meas. 78−52880
Zr-Ti martensites, furnace cooled and water quenched, strengh and deform. 79−20101

stress wave emission testing *see ultrasonic materials testing*

stress/strain curves *see stress/strain relations*

stress/strain diagrams *see stress/strain relations*

stress/strain relations
see also elastic constants; elastic limit; serrated yielding; yield point; yield stress
30th Annual Frequency Control Symposium, Atlantic City (1976) 77−37852
acoustic emission amplitude estimation model 79−68476
acrylic, denture base, tensile testing 80−16621
adhesive tubular lap joint, nonlinear stress-strain anal. 80−16637
alkali halide doped angle crystals, latent hardening 78−51607
p-n-alkoxybenzoates of p-n-alkoxyphenyl, smectic A phases mol. struct. and elastic behaviour 80−59382
alkoxyphosphazene polymer, elastic and thermoelastic props. 77−56014
alloy, space lattice types A_1, A_2 and A_3, strain hardening function *(German)* 80−20955
alloy, strain rate sensitivity rel. to ductility, anomalies 77−36590
alloys, hot plastic strain, stress- strain-time dependences *(Russian)* 80−40430
alloys, industrial, stacking fault energy rel. to mech. props. *(French)* 79−43339
alloys of two ductile phases of unequal strength, deform. *(Japanese)* 78−11284
amino acid block copolymers, morphology and mech. props. 78−91264
amylose, micromech. fracture anal. 78−68784
anelastic deformation, generalised representation by num. sol. of initial boundary value problems *(German)* 79−12610
aneurysm of ascending aorta in patients with and without Marfan's syndrome 77−37001
anisotropic elastic deformation, effective stress law, appl. to saturated porous rocks 80−51385
anisotropic elastic half-space, plane indentation by moving punch 78−18181
anisotropic elliptical layered plates, deflection, interlayer shear effects 79−98622
anisotropic material, different moduli in traction and compression, stress-strain laws in small strain theory *(French)* 78−90704
anisotropic metal blanks, plastically deformable, stress/strain relations *(Russian)* 80−1438
anisotropic plate with closed rod pressed into curvilinear hole, state of stress 77−72173
aorta, human, morphological and functional aspects of study of mech. props. 77−25499
aortic wall stress-strain characts. after sequential enzymolysis 78−3530
Araldite CT200/HT907, 263 to 343K, mechanical, physical and optical props. 78−56682
arterial grafts, synthetic, mech. props. 80−17192
arterial segments, canine, nonlinear anisotropic viscoelastic props. 78−20205
articular cartilage controlled impact test instrum. and procedure 78−28130
articular cartilage in uniaxial tension, nonhomogeneous directional mech. props. meas. 77−29167
aryloxyphosphazene polymer, elastic and thermoelastic props. 77−56014
asbestos cement/glass reinforced plastics hybrid composites, tensile strength *(Italian)* 77−56024
automatic piecewise linear approximation of yield function in ideal plasticity 77−46929
axially loaded butt joints, stress strain behaviour 79−74209
axisymmetric solids with rectangularly orthotropic props., asymmetric stress anal. 77−35031
bar (tube), compressible, combined loading, elastic-plastic problem 78−63311
bar-to-block based testing method for materials characteris. in high-vel. tension 80−85133
Bauschinger effect, grain boundary contrib. 79−47759
beam, thin wall, bending stiffness 80−28425
beam bending, internal damage induced instability 77−7341
beam element in space, geometrical stiffness, virtual work approach 80−14567
stress/strain relations continued
beams, inelastic response, elasto-plastic transition effect 79−32300
beams, straight, finite displacements and small deform., asymptotic anal. *(French)* 78−90716
beams, thin walls, stress-strain state determ., method of segments 80−28424
biological soft tissue, living, stress/strain relationship, mathematical model 77−29170
biological soft tissues, elastic stress/strain relation based on a struct. model 80−101205
block copolymers, morphology rel. to stress/strain props., deform. hardening effect, birefringence meas. 77−48501
blood vessel dynamic strain tolerance at different post mortem conditions 80−16988
blood vessels, exam. of mech. props 80−12175
bodies in plane strain, stress-strain state calcs. 80−14574
bonded bodies, internal stress/strain relations *(German)* 79−90143
borsic fibre reinforced Ti, unidirectional, K-calibration and compliance curves 78−88518
bounded domain undergoing sequential crystallisation, stress and strain investigation 80−100183
Boussinesq problem for material with different moduli in tension and compression 78−55564
Boussinesq-Papkovich displacement functions, generalisation to anisotropic medium 78−12570
brain tissue, nonlinear constitutive relations 77−40707
β-brass, bicrystal and tricrystal stress strain behaviour 77−36607
γ-brass, brittle to ductile transition under high hydrostatic pressure and high temp. *(Japanese)* 80−35305
brass, burst acoustic emission during Bauschinger effect 77−48475
brass, crack initiation at high strain rates, uniaxial and biaxial tests 80−85141
brass, cyclic creep and fracture under stress-controlled cyclic conditions 79−74232
brass, cyclic creep under increasing stress condition, constitutive eqn. 80−93593
brass, cyclic strain induced creep, relation between modes of stress and strain superposition 78−60733
brass, fatigue hardening and high cycle fatigue under reversed bending 79−20180
brass, hot ductility and torsional deform. *(Japanese)* 79−57069
brass, mechanical ratcheting, plastic theory 78−76702
brass, plastic deform., stress-strain relation of integral type 80−74754
brass, plastic deform. under complex loading 79−38890
brass, plastic props., room temp. to recrystallization temp., stress-strain relations, computer program 77−1865
α-β-brass, two phase bicrysts., deform. and fracture at 150K 80−16388
α-β brass, two-phase bicrystals, plastic deform. and fracture mechanism 78−84898
β-brass, uniaxial tension and compression, cyclic stress-strain behaviour 80−97551
α-β-brass two-phase bicrystals, operative slip systems at 150K 79−70119
brittle material, strain rate depend. effect of specimen vol. on strength 78−90726
brittle rod, optimum specimen shape for compression tests, gluing technique effects 80−50797
brittle rod, optimum specimen shape for compression tests, struct. and technological parameters 80−50798
burn-scarred human skin rheological props. in vivo meas. 78−31935
butadiene methylstyrol, exam. of low temp. relaxation processes *(German)* 78−92291
butadiene nitrile, exam. of low temp. relaxation processes *(German)* 78−92291
butadiene-styrene three-block copolymer, rheological props., 60-110°C *(Russian)* 79−23292
cable design and testing, optical fibre 80−69551
calcite rocks, experimentally deformed, texture development 79−83230
carbonate rock, interrelation of flow or fracture and phase transition during deform. 80−51389
cavity growth, by surface diffusion in polycrystn. metals 80−104217
celluloid, mech. props. under proportional load, time lapse, heating and isotropic props. effect *(Japanese)* 79−79043
celluloid, nonlinear viscoelastic deform. under superimposed hydrostatic pressure 79−34116
cellulose acetate membranes, modified, tensile props., desalination performance 79−11818
cement mortar, deform. charact., expt. study *(Japanese)* 78−56704
central-force interatomic pot. construction from whisker deform. data 79−56103
ceramic nuclear fuels, mech. props. at compressive deformation 80−651
ceramics, polycrystalline, stress-relaxation technique for deformation studies in four point bending 79−100200
circular blank, stress-strain state during forging *(Russian)* 79−52231
circular crystal plate thickness-shear resonance frequencies, acceleration effects 77−39136
circular plate, anisotropic and homogeneous, with circular hole at centre, creep behaviour 80−48597
circumferentially notched tensile specimen, finite element anal. 78−67150
compliance determ. of hydraulic tensile testing machine, comparison of methods *(German)* 77−21332
composite, multimodulus material, apparent flexural modulus and strength 77−28845
composite cylindrical shell, stiffened and stable, rational design using elasticity 80−5954
composite discs, fibre-reinforced, rotating strength, stress distrib., failure criterion rel. to mould process 78−76701
composite glass shells, bonded joint efficiency during external hydrostatic pressure cyclic loading 79−57079
composite material, in-plane shear charact. 80−35251
composite materials, stretching, stress distribs. 80−58931
composite media, elastic-plastic phases, constitutive law 77−875
composite polymers, viscoelasticity theory, appl. 80−64397
composite ribbed cylindrical casings, stressed-deformed condition under external hydrostatic press. 78−6996
composite shell structs., stress-strain state, elastic equilib. 80−74748
composite spherical pressure vessels with hardening metal liners 80−7655
compound rotor, exam. of stress state, taking account of interference stresses, contact stresses 78−83342
compressible elastic solids, finite plane-strain problems 77−14900

stress/strain relations continued
compressible hyperelastic solid, failure of ellipticity of eqns. for finite elastostatic plane strain 77−54875
compressible rubberlike materials, determination of elastic potential function 80−10159
compression, high strain rate, 1023 steel 79−34099
compression struts, of nonlinear viscoelastic materal time dependent load bearing capability *(German)* 78−48474
compression test, determ. of accurate flow props. 78−27718
concrete, bamboo-reinforced columns, behaviour when subjected to eccentric loads 79−52320
concrete, creep, time dependent behaviour under high tensile stress *(Japanese)* 78−31465
concrete, damping meas., expanded hysteresis loop method 77−12665
concrete, deformation under complex loading, mathematic description 80−25783
concrete, endochronic model for nonlinear triaxial behaviour 78−51095
concrete, fatigue, load-deform. behaviour *(German)* 79−11693
concrete, plastic-brittle behaviour, hardening and softening constitutive eqns. 77−21270
concrete, reinforced, failed slabs, nonlinear analysis by finite element method *(Japanese)* 77−42785
concrete, reinforced cross-section, reponse to short-term and sustained loads 79−52358
concrete, reinforced slabs, nonlinear statical props. anal. 80−25809
concrete, stress-strain relationships, applicable to biaxial tension and compression 80−65133
concrete, uniaxial compression, finite element failure anal. *(Japanese)* 80−35265
conference, reliability and stress anal., San Francisco, CA, USA, 1975 80−8740
connector choice in finite element anal. 78−45
corundum refractory ceramic deformation curve analysis *(Russian)* 79−90716
crack, stress intensity factor, near doubly riveted stiffeners 78−67152
crack initiation notches, pure strain rate role, finite element computer program 77−70166
crack propag., quasistatic energy anal. 77−46972
crack tip plastic zone, thermal props. calcs. 80−7659
cracked holes and rings, loaded with polynomial crack face pressure distrib., stress intensity factor solution 78−83335
cracked lug, test and analysis 78−67153
cracktip under incipient creep deform., stress field and modified J-integral *(Japanese)* 80−103411
creep, dislocation struct. and stress/strain relations, thermodynamic theory *(Russian)* 79−43319
crook of round plate, calculation, asymmetric strain *(Russian)* 79−10496
crystal inclusion, oblate spheroid, exam. of stress concentration due to inclusion 78−71281
crystal plates, higher-order effects of initial deform. on vibrs. 77−46862
crystalline and amorphous solids, plastic behaviour in terms of defect motions 78−95104
cuboid surrounded by infinite elastic space, stress field due to initial strains 78−55565
curve determination at high strain rate in uniaxial compression *(Japanese)* 80−96238
curved structural members, large displacement theory, applic. to lateral-torsional buckling anal. of circular arches 80−23924
cyclic elastoplastic bending, recording deform. curves and working life 79−52499
cyclic plasticity and masing behaviour in metals and alloys 78−64616
cyclic plasticity for nonproportional paths, comparison with prediction of three incremental plasticity model 78−92308
cyclic strain diagrams recording under nonisothermal conditions, review 80−71830
cylinder, hollow, linear viscoelastic, dynamical loading by internal press. 79−18793
cylinder, hollow, nonlinear viscoelastic material, dynamic pressure loading 80−38289
cylinder, hollow thick-walled, having axial holes and varying section thickness, stress state anal. 80−100879
cylinder, rupture under wave conditions, stress-strain state for explosive loading *(Russian)* 80−79220
cylinder, subjected to heating and cooling, thermoelastoplastic soln. 79−72816
cylinder, thick-walled, creep transition under internal pressure 80−53659
cylinder, thick-walled heteromodular, subjected to underwater waves, numerical calc. 80−74746
cylinder compression at small elastico-plastic deformations *(Russian)* 79−10497
cylinder elastic orthotropic brittle, under axisymmetric thermal and press. loading failure probability anal. 78−34078
cylinder under torsion elastic, spherical cavity effect in stress-strain state 80−101717
cylindrical envelope, stability under effect of axial contractive power and cross pressure *(Russian)* 78−42550
cylindrical ingot, continuous casting, elastic-plastic temp. stresses and deformation *(Russian)* 79−61576
cylindrical notched specimen, four-point bending, crack resist. tests 80−53735
cylindrical shell, contact problem with ribbed cylinder under axisymmetric loads 80−99974
cylindrical shell, radial loading through plate brackets 77−89032
cylindrical shell, stress and strain in elastically distinct layer 77−872
cylindrical shell, three layer, with strap reinforcement under internal pressure, stress-strain state calc. 78−30184
cylindrical shells, orthotropic, dynamics under axial impact 79−59936
cylindrical three layer pipe, stress-strain state, filler compressibility effects *(Russian)* 80−58901
cylindrical tube, isotropic elastic, holographically meas. surface displacement, stress/strain extrapolation 80−64374
damage analysis under nonproportional cycling 80−97556
decohesive carrying capacity in thermal stress problems 77−3741
deformation and fracture of materials in creep range, effects of nonlinear stress-strain rate relations 80−58938
deformation during combined sequential and bulk crystallisation *(Russian)* 77−59771
deformation procedures, stress, strain calcs., approximation method *(German)* 79−76978
stress/strain relations continued
deformation strength props., simultaneous meas. of several samples, polymer films appl. 79−15896
deformation wave processes, corrected nonlinear eqns., stresses and strains 80−102998
deposits, spontaneous mactrostress calc., from substrate deform. 80−15412
design plastic stress concentration factors using Ramberg-Osgood stress-strain parameters 78−63310
diagram, automatic plotting during mech. testing 78−27724
diamond, compressive strength for [111] loading 79−79036
diamond, high press. appl. by spherical diamond indentor, plastic deform. obs. method 78−35619
diamond, sintered compact, stress-strain curves using ultrahigh-pressure apparatus 79−43322
diamond anvil high-press. X-ray camera, effect of uniaxial stress component on lattice strains 78−38584
disc, with crack, stress and strain calcs. *(German)* 80−106760
dislocation gliding, by-passing of hardened particles, coplanar Orowan loops form., stress-strain curves 80−49226
dislocation pile-up formation, by Frank-Read source, emission of sound 79−37705
dislocation theory, nonlinear elastic problems, book contrib. 80−39093
dislocations, elastic theory, book 80−36784
dissipative medium, stress/strain rate relations 80−74736
distribution measurement, inside plastic zone of notched sheet, fatigue crack propag. *(Japanese)* 78−6981
dolomite, strain rate depend. inferred from impact and static compression studies 77−44977
double cantilever beam, dynamic stress intensity factors computation and crack arrest stress intensity factors 78−34088
ductile crack extension, evaluation of resistance in single notch edge specimens 78−68807
Duraluminium rings, stress/strain relations, compression and tension tests, rigid plastic theory 79−34098
dynamic biaxial loading techniques and apparatus 80−85129
dynamic measurements under superimposed high press., torsion bomb machine 80−85130
dynamic recrystallisation model *(German)* 77−4792
Earth interior, shear heating as explanation for lithosphere-mantle decoupling 79−20790
Earth interior, stress/strain relation for anelasticity 80−26471
elastic, linear and nonlinear solids, stress and strain fields at crack tip *(French)* 80−14615
elastic bodies, nonlinear, of different tensile and compression-strengths, stress and strain *(Ukrainian)* 80−69661
elastic body, system of curved cracks under different boundary conditions on their lips 80−53713
elastic contact between sphere and semi-infinite transversely isotropic body 77−31217
elastic contact problem, automatic anal., point-matching method 77−31213
elastic continua discretised stress, strain, eqns. and theorems 77−49596
elastic field outside ellipsoidal inclusion 78−55566
elastic materials, plates and sloping shells, exam. of theory 78−63307
elastic members, thin-walled, displacement theories for straight and circ. curved members *(Japanese)* 80−43615
elastic plane, stress-strain state at brittle crack vertex, geometric nonlinearity effects *(Russian)* 80−79221
elastic springback in beams and plates, bending 80−38256
elastic wave propagation when negative slope region in stress/strain diagram *(Russian)* 78−79255
elastic-perfectly plastic von Mises material, accuracies of numerical soln. constitutive eqns. 78−59315
elastic-plastic body, weakened by double periodic slit system, antiplane strain 80−53657
elastic-plastic materials, uniaxial stress/strain relations 80−83739
elastic-plastic thermal stress problem, soln. 77−3742
elastic-viscoplastic structures, accommodation to periodic loading, stress and strain fields *(French)* 77−46928
elastic/viscoelastic bar interface, impact wave behaviour 78−26075
elastic/viscoplastic media, constitutive eqn. covering wide range of strain rates *(Japanese)* 80−79862
elastically loaded polycrystal, stress state by contact problem theory 80−14573
elasto-plastic stress wave propag. *(Czech)* 80−108507
elastomer, relaxation processes, statistical description *(Russian)* 79−23229
elastomeric block copolymer properties obs. 78−27560
elastomeric network, finite linear viscoelastic theory, time-depend. deform. behaviour 80−38292
elastomers, effect of filler on network behaviour at high elongation 79−79049
elastomers with inert fillers, swollen state, network density determ. from stress/strain meas. 79−34112
elastoplastic bodies with cracks in complex states of stress, limiting equilib. 80−53715
elastoplastic structures, stresses and strains during loading, mathematical programming, pivoting procedure 80−53641
elliptic inclusion in anisotropic medium, antiplane strain problems 78−38200
elongation, dynamic, of material, stress/strain curve up to scabbing, meas. method 79−7348
endopelvic fascia, human, stress/strain history relations in simple elongation 78−44539
epoxide resin, light polarisation exam. of stress 78−68857
epoxy adhesive layers, interlaminar stress distrib. in nonlinear range 79−39117
epoxy resin, deform. rate depend. of mech. props. at cryogenic temps. 80−55456
epoxy resin, exam. of shear stress-strain characts. 78−60691
epoxy resins, crack propag. stability, effects of water, temp., specimen geometry, hardener 78−11324
epoxy resins, fracture props. study at cryogenic temps. 80−25869
epoxy resins, mech. and elec. low temp. props. 80−25814
epoxy structural adhesives, tensile tests, stress/strain relations, stress relaxation 78−60702
epoxy-polyglycol elastomers, fracture strength under compression 79−38929
ethylene-propylene copolymers, mech., photoelastic props. rel. to chain microstruct. 77−48468

stress/strain relations continued
eye, elasticity of sclera and choroid in humans, rel. to scleral rigidity and accommodation 78−80907
fabric reinforced laminates, stress-strain relationship *(Polish)* 79−91750
fatigue, cumulative damage, under random loads algorithm of hysteresis loop counting 80−21064
fatigue crack, macroscopic residual stress at tip, X-ray obs. and finite element anal. *(Slovak)* 78−19885
fatigue crack propag., in deformable media with nonlinear characteristics, model 78−63393
fatigue crack propag., plastic work role 79−79070
fatigue crack propagation, crack closure, effective stress range factors 80−100924
fatigue life predictions using computer modelling, cyclic stress/strain curves 80−19290
fatigue model for elastic materials with freq. independent Q 79−86384
fatigue testing, cyclic stress-strain curve determination *(Czech)* 80−89434
fatigue-life prediction, cumulative damage approach using local stress/strain concepts 77−50984
FCC cryst., theory of response to [110] uniaxial loading 79−19310
FCC crystal, transient effects during tensile tests in model of correlated dislocation motion 78−38715
f.c.c. polycrystals plastic deform. in microstrain region 77−1165
Fe, pure, lattice hardening due to H_2 charging, during tensile testing 79−66156
ferroelectric ceramics, 1-D linear dynamic electromechanical responses 79−47397
fibre cross-reinforced layered composites, moment effects in plane problem 80−64393
fibre reinforced composite, anelastic behaviour using continuum theory of internal separation 77−46907
fibre reinforced composite, fibre pull-out at high loading rate *(Japanese)* 80−45357
fibre reinforced composite, mech. behaviour, axial residual stress effect 77−36573
fibre reinforced composite, nonlinear stress-strain behaviour 78−26035
fibre reinforced composite, response to hydrostatic states of stress 77−36602
fibre reinforced composite, secondary stresses associated with structure, exam. 78−67043
fibre reinforced composite, shear props., test method eval. 77−81353
fibre reinforced composites, deformability characteristics, reinforcement scheme effect 80−58930
fibre reinforced composites, elastic moduli and shrinkage factors, calc. taking account of anisotropy 79−52291
fibre reinforced composites, intralaminar-shear charact., 10 deg off axis test 78−35422
fibre reinforced composites, reinforcement scheme optimisation with respect to deformability at assigned stresses 80−69689
fibre reinforced composites, thermal cycling, elastoplastic strain calc. under action of external stresses *(Russian)* 79−38896
fibre reinforced composites, unidirectional, Saint-Venant effect 79−34121
fibre reinforced composites, viscoelastic thermal shrinkage stresses 80−38287
fibre reinforced composites, weakened by periodic system of cracks, longitudinal shear 80−35323
fibre reinforced concrete beam, load-deflection curves in flexure 78−35437
fibre reinforced laminate, elastic law for materials with different tensile and compressional moduli 80−11713
fibre reinforced plastic, dynamic strain investigation using EM wave method 79−20321
fibre reinforced plastic, fracture mechanism study, cumulative failure model 78−92315
fibre reinforced plastics, optimum reinforcement laydown 80−38267
fibre reinforced silicone rubber composites, interfacial slip and damping 79−5010
filled rubber, stress/strain behaviour at moderate strains 80−38293
filler metal, deformation mechanism at brazed joint 78−80616
finite centre crack specimen, biaxial and nonlinear effects on energy release rate, J-integral 78−18232
finite disc, thermal shock, finite integral transform method 77−3765
fission reactor materials, thermomechanical transient anal., strain-rate dependent plasticity 80−79864
flat cylindrical shell, with infinite series of cracks, stress state 80−53716
flawed elastoplastic structure, method of lines applied to crack problem 79−46259
flow type in hyperbolic theory of plasticity 77−7317
fluid-infiltrated elastic materials, deformation of cavities and inclusions 78−51073
fluid-saturated rocks, elastic dilatancy and earthquake dynamics 77−21683
forced oscillations in large vessels of circulatory system, dog's arterial blood flow anal. 78−85329
fracture initiation site prediction, idealized polycrystalline materials, stress and strain fields 78−34092
fracture strain measurement at high strain rates, radial expansion technique 80−85134
free surface, wrinkling 78−5676
friction stress method for cyclic inelastic behaviour of metals 77−4855
fusion reactor limiters; thermal and stress environment effects 80−32461
gels, non-linear behaviour under strong deform. 78−7240
gels of rodlike macromolecules, nonlinear elasticity in condensed state 80−104199
geological media, hysteresis behavioural effects 80−21712
GFPR, sloping cylindrical shell, reaction during nonstationary coating 77−1857
glass, rupture behaviour, long-term strength, thermofluctuation theory *(Russian)* 80−40536
glass bead reinforced nylon, design parameters, fibre orientation effect 80−81141
glass bead reinforced polycarbonate, design parameters, fibre orientation effect 80−81141
glass fabric reinforced phenol resin, effect of thermal loading on physicomech. props. 79−24622
glass fibre reinforced cement, review of reinforcing theory, ageing, stress/strain relations 78−44165
glass fibre reinforced composite, fatigue failure, role of shear deform. 78−15494
stress/strain relations continued
glass fibre reinforced composite, semifinished product nonlinearity model, force anal. of winding 78−63325
glass fibre reinforced epoxy laminates, exp. determ. of nonlinear shear behaviour 80−66575
glass fibre reinforced epoxy resin, mech. props. 78−64582
glass fibre reinforced epoxy-phenolic, cyclically deformed under shear, energy dissipation, static tensile-compressive stress effect 80−104225
glass fibre reinforced nylon, design parameters, fibre orientation effect 80−81141
glass fibre reinforced plastic, cemented joint of cylindrical shell with cover, stressed state 80−69668
glass fibre reinforced plastic, fracture dynamics 80−100906
glass fibre reinforced plastic, laminate, fatigue strength under normal and interlaminar shear stresses 80−11758
glass fibre reinforced plastic, woven-roving type, high-speed punching, failure mechanisms 80−85143
glass fibre reinforced plastic laminates, strength and deformability, artificial ageing effect 80−60893
glass fibre reinforced plastics, ageing by boiling in water, effect on physicomech. props. 80−60892
glass fibre reinforced plastics, cylindrical shells, compressive and flexural strength *(Japanese)* 80−81115
glass fibre reinforced plastics, stress/strain conc. round hole, Moire fringe study 77−28964
glass fibre reinforced polyamide, GFPA 66, rel. strain meas. during creep in liq. environments 80−30046
glass fibre reinforced polyamide thermoplastic, stiffness and strength 78−27600
glass fibre reinforced polycarbonate, design parameters, fibre orientation effect 80−81141
glass fibre reinforced polyester filament wound pipe, failure 78−44192
glass inorganic, shell, stress/strain state investigation under external hydrostatic press. 77−81370
glass reinforced plastic laminates, stress, strain anisotropy, tensor calculus *(Polish)* 77−12678
glass reinforced plastic orthotropic shell and filler system, compactile performance 78−5659
glass reinforced plastic shell subject to local load, analysis of state of stress and strain 77−4822
glass rod, optimum sample shape for compression testing, failure 80−71756
glass shell, cylindrical, bearing capacity under axial compression 80−76323
glass shells with metallic inserts, structural strength 80−35283
glass-epoxy laminate post failure behaviour, stress concentration 77−48521
glass-fibre reinforced cement, strength study by reliability concept, fibre concept and temp. depend. *(Japanese)* 80−66586
grain boundary cavities, star-shaped unstable growth 79−46679
granular material with no intergrain slip, elastic zone 79−34087
granular materials, intergrain slip in flowable zone, stress distrib., internal friction 79−99261
granular materials shear deformation microscopic and macroscopic exam. *(Japanese)* 80−11691
granular mats., stress-strain relations, intergrain slip 80−16374
graphite, ATJ-S, strain response to mixed tension and compression loading 78−26032
graphite, isotropic, nonlinear stress/strain relationship effect on band strength 79−20119
graphite, nonlinear deformation, theoretical-exptl. correl. of material models 77−32626
graphite, stress/strain behaviour, exam. with high temp. short time testing facility 78−53051
graphite fibre reinforced epoxy, epoxy matrix, effect of material variability on predicted environmental behaviour, numerical anal. 78−90733
graphite-epoxy laminates, AS/3501-5, compressive fracture strength 79−43396
graphite/epoxy composite laminates, splitting process charact. 80−25843
graphite/epoxy laminates, T300/5208, effect of curing stresses on first ply failure 79−43329
graphitic materials deformation, crack and fracture behaviour, SEM exam 80−11706
Griffith-Irwin-Orowan cracks, unification theory 79−10529
hard tension/compression tester developed for high temp. microscope, metallurgical appl., functional features *(Japanese)* 79−70259
Hastelloy X, creep props. and appl. to structural design *(Japanese)* 77−59862
Hastelloy-X, low cycle fatigue crack propagation at 25°C and 760°C 80 104270
HCP metals and alloys, plastically deformed, electron microscopy *(French)* 77−44300
heteromodular materials, stress strain correls. 80−87716
heterophase systems, pressure-induced elastic fields, effective inclusion method 79−10502
heteroplastic material, memory function, stress/strain vel. relations *(French)* 79−10488
high strain rate behaviour, incremental elastic-viscoplastic constitutive eqns. integration 80−85138
high strain rate mechanical properties, conf., Oxford, England (Mar. 79) 80−82575
high-temp. nucl. reactor components, elastic-plastic-creep response, computer program 77−3112
homogeneous simple strain in elastic-plastic media, necessary and sufficient conditions 80−28427
hot twisting, shearing stresses, anal. determ. 78−60900
hydraulic bulge test, use in biaxial tensile testing 80−1493
hydrogels, two-component, elasticity theory and compress. meas. 80−44246
2-hydroxyethyl methacrylate-methacrylonitrile or acrylonitrile copolymer network, mech. response 79−57031
hyperelastic rod dynamics, second-order theory 78−77717
hypoelastic materials with internal variable, work-hardening, hysteresis, fracture law 77−62177
hysteresis properties of nonlinear nonideally elastic materials *(Russian)* 80−90675
ice, Antarctic deep core, mech. tests under hydrostatic pressure *(Japanese)* 79−79890
ice, plastic deformation, ultrasonic wave attenuation by dislocations *(French)* 80−59564

stress/strain relations continued
Incoloy 800H, high temp. low cycle fatigue, ageing and cold working effect 79−43277
Incoloy 800H, high temp.-low cycle fatigue, ageing and cold working effect on initial stress/strain curve 79−47720
Inconel 718, low cycle fatigue at 298 and 823K 77−86151
inelastic deformation, hardness law 78−46896
inelastic deformation, stiff constitutive models, numerical integration 80−96208
infinite cylindrical shell containing filler, reinforced by ring, influence of arbitrary load 78−42533
infinite elastic solid, with two spherical cavities, asymmetric problem 77−31212
infinite plane with crack in nonuniform steady field, stress intensity coeffs. 80−38343
infinite strip, with elliptical hole, definition of stress *(Russian)* 78−55562
inhomogeneous bodies, finitely deformed, effective stress/strain relations 77−75809
initial flaw shape, effect on cracks emanating from fastener holes under combined stress 78−64694
inorganic glass, effect of liq. medium on process of mechanical destruction 80−89283
isotropic materials, infinitesimal isothermal deformations, implicit functional representation 79−32297
isotropic stable media, stress tensors and creep-strain rates correl. 80−87722
kaolin, -flint mixtures, polyethylene oxide additive effect on plastic strength after tempering 79−24568
Kapton (polyimide), insulators for superconducting magnets, effect of low temp. irradiation 80−25817
Kevlav fibre reinforced cement composites, cement boards, exam. of mech. props. 78−48499
kinematic hardening models, use in multi-axial cyclic plasticity 80−25717
laminate, multilayer, stress-strain state 78−18177
laminate, nonlinear stress-strain response 79−91738
laminate, simple shear charact., comparison of test methods 78−44283
laminated anisotropic shells, nonlinear eqns. of Timoshenko-type theory 80−69669
laminated composite, nonlinear transient pulse propag., interface reflection effect 78−63222
laminated composite plates, stress/strain relation, finite element anal. 79−17219
laminates, fracture, effect of adhesive layers 78−90791
laminates, plane strain state with transverse crack 80−38338
laminates, thin, optimal struct. and strength in two-dimens. stress state 80−64395
large strain inelastic anal., dynamic problems 80−38278
large strain inelastic analysis, quasi-static problems, finite element anal. 80−14568
Larson-Miller parameter, rel. to stress rupture and creep 77−72192
layered or reinforced composites, elastic constants and stress-strain parameters *(Russian)* 79−46209
limestone tubes, dynamic torsional failure obs. 80−85648
linear elastic solid with mass addition, stresses and displacement eqns. 77−55955
linear isotropic viscoelastic material, exptl. determ. of relaxation modulus 79−61810
linear one-dimensional viscoelastic solid, flow and relaxation distribution 78−36833
linear viscoelastic systems, constant strain rate and stress relax. obs. 78−90727
LMFBR slow overpower transient, simplified computing method for cladding and fuel strain 79−31005
loaded column, creep and ageing optimisation problems stress-strain state *(Russian)* 79−46226
low deforming materials, classification and anal. of stress-strain diagrams by their behaviour under stress 79−15753
lung structure and elasticity, 3-dimens. modelling 77−36992
lung translation, rot. and strain calc. from roentgen-videographically recorded marker displacements 78−31843
macro-molecules, cross-linked, mech. props. theory *(German)* 77−63752
magnetic tape, coil, determ. of stressed-strained state 79−14283
magnetoviscoelastic initially-stressed conducting medium, plane Lamb's problem 79−37183
materials testing, constant-rate-of-extension instrumentation 77−4883
materials with different moduli in tension and compression 77−42735
Maxwell stress tensor derivation, electrostrictive effects in cryst., for teachers 77−33792
mechanical hysteresis, analytical description 77−3764
mechanical testing machine stiffness, activation volume 77−28966
mechanics of materials, book 77−68425
mechanics testing, lateral deform. gauge 79−57163
metal, ductile, hard inclusion effect on plastic strain distrib., model meas. 77−59062
metal, dynamic and static response to simple compression, tension and torsion 77−28858
metal, electroplastic effect 79−24589
metal, finite elastic-plastic deformation at high temp., work hardening rule 77−4828
metal, friction during working stresses and rheological charact. at high temps. *(Russian)* 77−66702
metal, nonlinear mech. response, Swift effect 78−35433
metal, notched, cyclic stress/strain behaviour, random fatigue life *(German)* 80−100907
metal, plastic anisotropic hardening pot., stress/strain relation under combined axial load/torsion 78−52896
metal, plastic deform. effects from X-ray diffr. data, moment method *(Czech)* 78−31593
metal, polycryst., Bauschinger effect and mutual restriction between grains 78−52895
metal, recovered dislocation substructure, prod. and utility, review 77−84749
metal, single crystal, dislocation loop formation, during deformation in quantising mag. fields *(Russian)* 80−103354
metal, space lattice types A_1, A_2 and A_3, strain hardening function *(German)* 80−20955
metal, stress/strain diagram determ. by spherical punch *(German)* 78−76803
metal, strong, compressive stress/strain props. meas. at very high strain rates, modified Hopkinson bar system 80−85128
metal, Swift effect, in twisted tubes 77−28859
metal, Swift effect, rel. to stress/strain behaviour in simple compression, tension and torsion 77−28860
metal, thin sheet, crack growth, effect of strain rate 77−1869
metal ductile fracture, void growth stress/strain relations *(French)* 80−19280
metal fatigue analysis, inversion of strain-life, and strain-stress relationships 80−16428
metal fatigue analysis, inversion of strain-life and strain-stress anal. 80−19289
metal fibre stress/strain curves determ. using X-ray goniometer *(German)* 78−92413
metal panels, adhesively bonded, cracked, fracture anal., crack tip stress intensity factors 78−90792
metal powders, cold rolling, deform. region stresses 79−61609
metal powders, rolling, contact stresses distrib. 79−66083
metal rods, stress state and fracture in pulsed mag. field 80−81201
metal subjected to intense heat source, plastic deformation 77−86085
metal systems, high voltage electron microscopy of dislocation dynamics *(Japanese)* 77−47458
metal-to-metal bonds, stress analysis in hostile environments 79−20338
metallic glasses, steady state inhomogeneous flow, microscopic mechanism 77−48476
metallic shell, explosive expansion, rupture behaviour 80−85063
metallic structures, elastic/plastic bodies with work hardening, general shakedown theorem 77−3746
metals, and alloys, corrosion testing under stress, unit for producing biaxial tensile stresses 79−57174
metals, aspects of impact testing, propagation of deformation 79−79111
metals, cold forging, upset tests anal., stress-strain law determ. appl. *(French)* 79−20064
metals, determ. of yield strength 80−25937
metals, dynamic compression testing, mech. behaviour 80−40464
metals, hardening response in small deform. 79−47719
metals, hot plastic deform., stress/strain/time relations *(Russian)* 80−20968
metals, inelastic cyclic strain under nonuniform stress state conditions, residual stresses effect 80−81132
metals, mechanical behaviour under impulse loading, model 79−52332
metals, plastic deform., stored energy determ., temp. recording method 79−87775
metals, polycrystn., creep damage and cavity growth, assessment using density meas. 80−104217
metals, single and polycrystn., plateaus in cyclic stress-strain curves 79−79054
metals, stress transients, at changes of electron drag during plastic deformation 79−61677
metals, work-hardening, dislocation multiplication model 79−61608
metals and alloys, polycryst., strength differential effect, temp. and strain rate sensitivity in saturation cycling 79−66094
metals and alloys, strain rate history, endochronic theory of viscoplasticity 80−65122
metals and alloys, strength/ductility relation *(Japanese)* 79−29145
metals and alloys, stress-strain time dependence based on nonlinear heredity, delayed yielding 78−48452
metals during settling, technique using rotation of thin layer *(Russian)* 80−97529
methane, freq.-depend. shear viscosity 79−77798
micro plastic strain energy criterion applied to reversed biaxial fatigue 78−63391
Mn strain hardening at room and low temps. *(German)* 79−38845
model crystal, thermally activated glide in strain rate change and stress relaxation expt. 77−36615
montmorillonite, mech. props. at high press., rel. to fault behaviour 79−84234
multi-axial stress states, elasto-plastic stress-strain relationships 79−1115
multilayer cylinder with monolithic insert, exptl. study of stress/strain state 79−42139
multilayer shells, stress-strain state and stability at high temps. 77−54903
multilayer winding around hollow cylinder, creep and ageing optimisation problems stress-strain state *(Russian)* 79−46226
multiphase materials, props. determ. from computer simulation 77−3717
muscle, human skeletal, mech. simulation 78−35878
muscular organ mechanics 77−90836
Mylar (polyester), insulators for superconducting magnets, effect of low temp. irradiation 80−25817
Mylar film/adhesive/Al foil laminate, mech. interactions 80−81112
Navier-Stokes eqn. derivation without stress tensor linearity assumption 77−13542
neck, stress distribs., Bridgman anal. 79−81737
necking, dynamic analysis based on stress wave propagation 80−1440
necking, loading history depend. 80−5957
necking, strain rate sensitivity under uniaxial tension 77−77525
Nimonic cylinder, stress redistribution obs. 77−4831
Nomex (nylon paper), insulators for superconducting magnets, effect of low temp. irradiation 80−25817
nonisothermal elastic-plastic and elastic-viscoplastic deforms., stress/strain relations 78−22276
nonlinear aftereffect medium, longitudinal one-dimens. wave propagation 80−5974
nonlinear anisotropic medium 80−98800
nonlinear elastic body, stress/strain deviator ratio *(Russian)* 79−25854
nonlinear elasticity, complementary energy principle 77−67289
nonlinear elasticity, continuous dependence of solution on given data 78−18182
nonlinear eqns. of axisymmetric surfaces of revolution, numerical soln. *(Russian)* 78−81838
nonlinear fracture mechanics 78−79261
nonlinear multimodulus orthotropic material, nonsymmetric compliance matrix theory 78−26032
nonlinear stress wave propagation, in perfectly flexible string 78−5670
nonlinear theory of hereditary media, functional relationship between stress, strain and temp. 78−26054
nonsteady cyclic load 77−89073
notch fatigue behaviour, multiaxial stress-strain approx. 77−40446
notch fatigue life predictions, using smooth bar fatigue data 78−63387
notch-tip geometry, influence on stress and strain distrib. 80−33535

stress/strain relations continued
notched and bend specimens with equivalent geometries, cyclic deform. *(German)* 77−86271
notched plates, monotonic and cyclic loaded, exam. of elastic-plastic stress-strain behaviour 78−63390
nuclear reactor core mats., constitutive eqn. 78−80598
nylon 6 fibres, chain rupture during tensile deform. 79−15740
1-nylon polymers, stress-strain curve 80−60938
nylon-1 polymers and copolymers, mech. props. rel. to glass transition 77−11625
4-n-octyloxy-4′-cyanobiphenyl, smectic A liq. cryst., elastic modulus determ., stress/strain relationships 78−91229
one-dimensional plastic material with work hardening constitutive eqns., stress-strain relations 79−32296
organosilicon ladder polymers, struct. and phys. props., book contrib. 79−65012
orthotropic cylindrical shells, periodic problems, computer anal. *(Russian)* 80−23889
orthotropic dilatant bodies, plasticity theory, plane problems *(Russian)* 80−23910
orthotropic laminate composite containing layer with crack, stress intensity factors 78−5694
orthotropic layer weakened by double periodic plane cracks, compound problem of theory of elasticity 79−90139
orthotropic medium, strain localisability function 79−18743
orthotropic plate, twisting in large deflection regime 77−23870
osteons with crossed lamellae, micromech. study 77−25493
paper sheet, elastic props., inhomogeneity with reference to basis wt. depend. of elastic moduli *(Japanese)* 80−2110
particulate material, stress dependent behaviour 77−90398
perforated plate, global stress strain behaviour 80−10169
photopolymer, biaxial stress-strain test 80−40417
piecewise-homogeneous plate with slits on elliptic line separating materials 80−99932
pigment dispersion rheology, kinetic model, expt. results 79−7361
piled bed, deform. character, two-dimens. model calcs. *(Japanese)* 79−34115
plane stress crack geometries, comparison of finite element and expt. studies 77−89069
plane stress crack problems, fully plastic soln. and large scale yielding estimates 77−19573
plane triangular element, stress-strain finite dynamic element, FORTRAN IV program 80−53
plastic, computation for polycrystalline metals 77−22419
plastic anisotropy theory based on yield function of fourth order 78−31457
plastic bending and torsion of simple geometries, subjected to cyclic loading, stress-strain analysis 78−90734
plastic deform., generalised constitutive eqns. 80−104219
plastic deformation, cyclic, exam. of reversible strain, effect on dislocation motion 78−84892
plastic deformation, steady-state straining 78−5669
plastic deformation analysis, metalworking process appl. 78−27586
plastic deformation incompatibilities, resulting from moderate cold drawing, X-ray line broadening determ. *(French)* 79−43265
plastic deformation instability, effects of physical parameters 79−47758
plastic fracturing materials, work inequalities and stress-strain relations 80−103000
plastic range stress-strain concentrations for struct. materials 77−31222
plastic solids, stress and strain fields at crack tip *(French)* 80−14615
plastic strain rate changes, transient functions 77−15480
plastic stress-strain relation anal. using anisotropic hardening plastic pot. 80−19250
plastic wave theory, comparison of predictions with impact expts. 80−83742
plastic/elastic transition, strains and stresses *(German)* 80−28431
plastically prestrained materials and components, high cycle fatigue *(Czechoslovakian)* 77−32680
plasticised cellulose acetate sheet, post-yield fracture 80−25859
plastics, anisotropic reinforced, stress-strain state, theoretical principles of nonvisible exam. 78−68745
plastics, radio and light polarisation stress analysis 78−68857
plate, elastic circular cylindrical, with arbitrary transference, stress-strain state *(Russian)* 80−23895
plate, orthotropic, transient response to uniformly distributed transverse load, computer calcs. 77−68503
plate, rectangular with stiffening ribs, stress-strain state, elasticity eqns. *(Russian)* 80−1427
plates, inelastic response, elasto-plastic transition effect 79−32300
plates, orthotropic laminated, stress-strain state *(Russian)* 79−46189
plates, rectangular cross-ply laminated, with nonlinear stress-strain behaviour, buckling 80−64415
plates, thick, multiply connected, stressed-strain state under nonstationary heat conditions *(Russian)* 80−87714
plates and slabs, perforated *(Russian)* 80−74728
plotting device for stress-strain diagrams in tensile testing 80−3269
PMMA, activation parameters of creep 79−38925
PMMA, crazing, deform. kinetics 80−84990
PMMA, glassy atactic, thermodynamic analysis of plastic deform. modes, 150 to 330K 80−84999
PMMA, large deforms. at tip of running crack, opt. interference obs. 80−85062
PMMA, solid, stress-strain behaviour, strain rate and temp. effects, cryogenic temps. *(Japanese)* 78−11315
poly(butadiene-co-styrene), rubber, radiation cured, dynamic phys. props. 77−69003
polyacetal, stress-strain relations, effect of strain rate and static outer press. *(Japanese)* 77−52418
polyacetylene films, tensile props. and partial alignment 80−104210
polyamide, PA 66, rel. strain meas. during creep in liq. environments 80−30046
polyamide, test pipes, static tensile strength, equipment effect on tension-extension diagram *(German)* 78−35453
polyamide 6 , glass fibre reinforced, response funetion characterization of thermal state in dynamic testing 79−18680
polyamide-polyoxirane copolymers, mechanical properties evaluated 80−11700
polyamides 6 and 66, response function characterization of thermal state in dynamic testing 79−18680
1,2-polybutadiene, crosslinked in states of strain, entanglement networks, swelling anisotropy obs. 80−79666

stress/strain relations continued
1,2-polybutadiene crosslinked in strain states; entanglement networks, stress-birefr. relations 80−66590
polybutadiene networks, cis-trans, thermoelastic obs. 79−74220
polycarbonate, amorphous, yield behaviour in oriented and unoriented condition, effect of temp. 80−97537
polycarbonate, anelastic component of strain *(Japanese)* 77−8870
polycarbonate, effect of mol. weight on craze shape and fracture toughness 80−25858
polycarbonate, glassy state, rel. between thermal pre-treatment and viscoelastic behaviour 79−79038
polycarbonate, insulators for superconducting magnets, effect of low temp. irradiation 80−25817
polycarbonate, rigid plastic, yield behaviour *(Japanese)* 80−93620
polycarbonate, stress-strain relations, effect of strain rate and static outer press. *(Japanese)* 77−52418
polychlorotrifluoroethylene, tensile deform. in He, N_2, Ar, O_2 and CO_2 gaseous environments 77−56040
polycrystalline metal, FCC, plastic stress-strain rels. under proportional loading 77−32627
polycrystalline metals, effect of grain boundary sliding on steady creep 80−96590
polycrystalline metals, stored energy and strain hardening 79−82276
polycrystals, constitutive relns. in elastic-plastic range 78−63801
polycrystals, elastic stress and strain microinhomogeneity, finite element method 80−79155
polycrystals, large elastic-plastic deform. anal. with finite element method 78−26049
polycrystals, single phase, stress strain relations by X-ray diffraction *(Russian)* 80−5999
polycrystals of anisotropic substances under hydrostatic press., microstresses 79−25231
polydimethylsiloxane, crosslinked, stress/strain relations from large compression to high elongation 80−66589
polydimethylsiloxane, end-linked chains, elastomeric properties, dilution effects 79−90570
polydimethylsiloxane, end-linked chains, model elastomeric networks, Gaussian, nonGaussian and ultimate props. 80−103260
polydimethylsiloxane, end-linked model network, elastic modulus and equilib. deg. of swelling 77−35616
polydimethylsiloxane, stress-strain props., cross link functionality 79−46575
polydimethylsiloxane chains, end-linked, swollen model networks, stress/strain isotherms and elastic modulus 80−79668
polydimethylsiloxane chains, with known radiative side chain amounts, model elastomeric networks prep. by sel. crosslinking 79−73106
polydimethylsiloxane networks, stress-strain isotherms at high elongations to rupture point 77−40433
polyester model material, optical response and yield behaviour 78−31453
polyester moulding compounds, cyclic loading and strength 77−81310
polyester resin, creep, uniaxial elongation under variable temperature humidity 77−52434
polyester resin, PN-3, creep, effect of temp. and moisture 77−4820
polyester-polyurethane semi-interpenetrating networks, mech. props., morphology 80−45362
polyethyl acrylate atactic networks, stress-strain isotherms at high elongations to rupture point 77−40433
polyethylene, crysts., subject to fold-surface tensile stress, elastic deform. 78−76712
polyethylene, doubly oriented, low density, deformation and structure, exam. 80−11705
polyethylene, effects of mol. rot. and crosslink on specific draw ratios *(Japanese)* 79−96099
polyethylene, hard elastic fibres, deform. and struct., −196 to 80°C 78−51437
polyethylene, high density, effects of draw rate and temp. on necking stress *(Japanese)* 79−91757
polyethylene, high-density, damage accumulation kinetics under creep during prolonged loading 80−40447
polyethylene, high-density, deform. resistance and flow curve 77−90405
polyethylene, high-density, stress-strain curve shape 77−63754
polyethylene, linear, plastic deform. behaviour 78−84910
polyethylene, linear, strain rate effects on ratio of recoverable to nonrecoverable strain 78−27566
polyethylene, linear role of recovery forces in deformation 78−48459
polyethylene, low density, melt elongation, stress and recovery maxima 79−90209
polyethylene, low-temp. relax., effects of chem.- and electron irrad.-crosslinking 79−4990
polyethylene, mech. and elec. low temp. props. 80−25814
polyethylene, oriented, stress-strain curve, analogy with van der Waals isotherm 77−59869
polyethylene, stress rel. to draw ratio during ultra draw *(Japanese)* 79−91759
polyethylene, ultra-high-strength filaments, soln. spun/drawn, mech. and thermal props. 80−40440
polyethylene, ultra-oriented high density, shrinkage as meas. of deformation efficiency 80−40398
polyethylene, ultradrawing, effects of temp. and drawing rate *(Japanese)* 79−91760
polyethylene, X-ray diffr. at press. up to 14000 kg cm^{-2}, 298K 77−35492
polyethylene films, hard elastic, deform. mechanism 77−32652
polyethylene oxide blends, thermal and mechanical props. 79−11679
polyethylene spherulites, high density, microstruct. and mech. props. 78−42921
polyethylene terephthalate sheeting, storage in aqueous media rel. to props. *(German)* 79−29250
polyhydroxyethyl methacrylate swollen network filled with polyhydroxyethyl methacrylate, viscoelastic and ultimate behaviour in rubbery region 79−83247
polymer, crystalline, necking stress, thermodynamically derived equation *(Japanese)* 79−91758
polymer, glassy, tensile stress/strain curve description 78−67158
polymer, specimen size effect on mech. behaviour associated with crazing 77−73337
polymer film elasto-plastic deformation calc., in re-drawing stretched film, finite element analysis calc. *(Japanese)* 80−7621
polymer films and sheets 78−80590
polymer network, crosslinks and trapped entanglements, two-network model 80−38962

stress/strain relations continued
polymer networks, stress-strain behaviour, nonlocalized junction effects 77−59063
polymer networks, stress-strain behaviour models, multiaxial tension *(German)* 79−69183
polymer plate, analysis subject to local loads 77−65687
polymer science, conf., Pittsburgh, USA, (June, 1975) 77−38756
polymer with spherical inclusions, slope discontinuity prediction in stress/strain behaviour 78−94596
polymeric materials, thin-wall tubes, rupture time determ. 80−64473
polymers, anal. of mechanics of solid phase extrusion 80−39204
polymers, apparatus for determ. of volume stress/strain state 78−23896
polymers, glassy, glass bead filled, crazing characts., slope-discontinuity method 79−11712
polymers, multicomponent, props. and struct., review 78−44076
polymers, torsional shear testing using electromech. high-press. apparatus 77−51005
polymers in nonisothermal strain, thermomechanical coupling effect in viscoelasticity 79−86355
polyoxymethylene copolymers, response function characterization of thermal state in dynamic testing 79−18680
polypropylene, crystalline, yield behaviour in oriented and unoriented condition, effect of temp. 80−97537
polypropylene, insulators for superconducting magnets, effect of low temp. irradiation 80−25817
polypropylene, shear stress/strain behaviour, press. effect 78−84936
polypropylene fibre, melt-spun with twist, helical orientation and mech. props. 78−75569
polypropylene fibrillated film reinforced cement matrix for low cost sheeting 80−80996
polypropylene films, hard elastic, gas permeability, extension effects 80−40412
polypropylene monofilaments, tensile props., orientation degree depend., IR dichroism obs. 78−3163
polysiloxane dizwitterionomers, mech. props., microstruct. 80−49131
polystyrene, coarse shear bands and fracture, SEM study, craze fracture surfaces 79−29191
polystyrene, cyclically deformed under shear, energy dissipation, static tensile-compressive stress effect 80−104225
polystyrene, high impact, under press., mech. behaviour 79−52305
polystyrene, oriented amorphous, supermol. structures rel. to mech. behaviour 78−22673
polystyrene, swollen network in benzene, pendent chains, influence on thermodynamic and viscoelastic props. 80−28481
polystyrene-ethylene propylene copolymer, strength and impact props. 78−52899
polystyrene-poly(styrene-b-butadiene-b-styrene) polyblends, mech. props. 78−52919
polystyrene-polyolefin blends, mech. and swelling properties on heating 79−57053
polystyrol, test pipes, static tensile strength, equipment effect on tension-extension diagram *(German)* 78−35453
polytetramethylene oxide-polytetramethylene terephthalate, block copolymer, props. 78−51438
polythene-polystyrene blends, differential scanning calorimetry and swelling characterisation 79−57053
polyurethane, stress relax. meas., effect of cure temp. on network struct. 77−84674
polyvinyl acetate, torsional stress/strain meas., press. effect 78−84937
polyvinyl butyral, activation parameters of creep 79−38925
polyvinyl-pyrrolidone/polyethylene glycol oligmers, elasticity theory, and compression meas. 80−44246
porous bodies, stresses induced by drying, elastoviscoplastic model, finite element anal. 80−23904
porous deep drawn conical shells, permeability 80−11728
porous materials, plastic deformation, constitutive eqns. 79−61667
porous metals, plasticity, stress-strain curves, yield stresses, strain vectors 80−83738
porous metals, plasticity theory, stress-strain curves determ. 77−17812
Portevin-Le Chatelier effect and inverse strain-rate sensitivity 79−1476
powder metallurgy, fatigue strength significance *(German)* 80−60946
powdered mixture, stress-strain determ. by high press. X-ray diffr. 77−7792
power law fluids, mass transfer into boundary layers 79−32588
precipitate and dislocation loop strain and stress field calcs. using affine transformations 80−106722
pressure vessel, strength analysis, by thermal shock 78−68819
pressure vessel heads, internally pressurized ellipsoidal and torispherical elastic plastic, nonsymmetric buckling 77−58575
pressure vessels, creep bounds and brittle damage estimates 80−23908
prestressed beam, dynamic bending response 77−39230
primary normal stress function from shear viscosity data 77−68548
prismatic beams with circular cracks under tensile loading 80−53714
propylene-butene-1 copolymers, thermal and mech. props. 79−34091
PTFE, partially crystalline, time-temp. superposition 77−4801
PTFE, stress-time analogy under shear and hydrostatic pressure in creep regime 80−104227
PTFE, struct. effects in stress-strain relations at elev. temps. 78−31484
PVC, crazing, deform. kinetics 80−84990
PVC, orientation hardening 78−76662
PVC, plasticised, processing-morphology-mech. props. relation 79−8264
PVC, rigid plastic, yield behaviour *(Japanese)* 80−93620
PVC, solid, stress-strain behaviour, strain rate and temp. effects, cryogenic temps. *(Japanese)* 78−11315
PVC, test pipes, static tensile strength, equipment effect on tension-extension diagram *(German)* 78−35453
PVC, volume stress/strain state using new apparatus 78−23896
PVC block copolymers, physical props. and morphology 79−82166
quasistatic problem of mechanics of deformable body in stresses 79−37179
rate and temp. depend., analytic formulation 80−40466
reactor fuel pin tubes 79−47755
rectangular plate, stability, mechanical props. dependent on strained condition *(Russian)* 79−10494
rectangular plate with fins, stress anal. under bending, approximation theory *(German)* 79−90144
rectangular viscoelastic prism exposed to repeated stretching and contraction, thermomech. anal. 77−54896
reinforced plastics, mech. damage, thermodynamic anal. *(Ukrainian)* 79−37186

stress/strain relations continued
relaxation modulus, evaluation from response to constant strain rate followed by constant strain 80−74765
residual stress meas., Alignment Error of the hole-drilling method 79−81823
ribbed plates with large openings, design optimisation, finite element anal. appl. 80−87724
rigid-plastic medium, ideal, surface force strength lower limit under plain strain 80−99937
ring-stiffened filled cylindrical shell, loaded, stress-strain state 79−41582
rings, circular optimal plastic, stress/strain relations for rigid plastic material 79−34098
rock, dry, quantitative model of dilatancy and appl. to Westerly granite 79−16445
rock, laminar, stress distrib. during sliding failure 79−2225
rock, plastic-brittle behaviour, hardening and softening constitutive eqns. 77−21270
rocks, form and stress state of high-amplitude longit. folds 77−9382
rocks, stress wave attenuation, linear magnetic hysteresis model *(Chinese)* 79−39702
rod in penetrating liquid, exam. of lengthwise bending 80−5955
rolled-up cylindrical shell, stress-strain state, approx. computation 77−14911
rotation of nonhomogeneous composite cylinder, plane strain problem 77−72161
roving glass cloth fibre reinforced plastic, fracture mech., time depend. *(Japanese)* 80−55508
rubber, Mooney-Rivlin constants correl. with polymer chain cross-section 77−11624
rubber, strain-energy density function 80−25773
rubber, uniaxial extension and compression 78−80578
rubber, vulcanized, rheological props., stress-strain rels. 77−32608
rubber balloon bursting under biaxial strain, tear behaviour 80−19287
rubber elasticity, new statistical theory 77−35623
rubber half-cylindrical tube compressed between parallel plates 77−50999
rubber under biaxial strain, non Gaussian theory, mechanical props. 80−16366
rubber under biaxial strain, nonGaussian theory, optical props. 80−16367
rubber-like elastic materials, stress-strain behaviour 78−67049
rubbers, swollen, low-freq. dynamics, optical and mech. props. 80−43626
ruled three layer shell, large coefficient of friction between layers, stresses-strained state calc. 79−14354
running crack tip, effect of strain rate depend. Young's modulus on stress and strain fields 78−75097
salt glaciers, flow 79−84261
scattered light photoelasticity for stress and strain determ. in axisymm. problems 77−72168
sea ice deformation, viscous law as stochastic average of plasticity 78−16028
SEM attachment to record stress-strain diagram 80−25961
shallow shells, arbitrarily oriented cracks, stress intensity factor 79−7341
shape memory effect, criteria for efficiency assessment *(Russian)* 80−21015
shaped charge jet stability 78−13919
shaped strip, tension during rolling 78−84890
sheet metal forming, material behaviour 78−95787
sheet metals, strain-induced changes in mech. props. and press formabilities 78−19781
shell, cylindrical, optimisation of strong loading modes, stress/strain state 80−10136
shell, cylindrical, three-layered, stress-strain state *(Russian)* 80−90677
shell, finite circular cylindrical, rate formulation for elastic-plastic creep anal. 77−58568
shell, rotating, stress-strain state for random loading, numerical soln. *(Russian)* 80−90676
shell of revolution, orthotropic, thick, stress-strained state, finite element method *(Russian)* 80−87713
shell of rotation, existence and uniqueness of soln. for stress-strain state *(Russian)* 78−36830
shells, thin shallow axisymmetric, strain displacement equations, incremental anal. 80−53628
shells, thin walled, elastic, Rayleigh method anal., energy calcs. 77−65677
shells, two-layer cylindrical, stress-strain state, elasticity theory eqns. 80−33462
shells of resolution, ring-stiffened, dynamic nonlinear anal. by finite element program DYNAPLAS 77−3766
shells of revolution with inhomogeneous boundary conditions, deformation 80−33480
short fibre reinforced polymers, expressions governing stress-strain curves 78−80592
simulation appl. to materials, conf., Gaithersburg, USA (April 1976) 78−27387
sitall cylindrical shell reinforced with internal stiffening ribs, stress-strain state under external press. 80−71684
skin, living, in plane method for determ. of 2-dimens. behaviour 77−37120
skin rheological behaviour, expt. results and struct. model 80−16968
soft tissues, tension field theories 78−65064
soil, layered, effective moduli theory appl. *(Polish)* 79−25237
soil, pulverulent, homogeneous, stresses due to vertical local load *(French)* 78−61398
soil, two phase with viscoelastic skeleton, finite element anal. of consolidation 77−11138
soil, viscous nonlinear, stresses and strains 78−73363
soil, wave interaction, stresses and strains 77−86801
solidifying ingot, temp., strain and stress distrib. *(Russian)* 77−25041
solids of revolution, stressed state 77−14910
spherical cavity surrounded by infinite elasto-plastic medium, upper bound on asymptotic pressure 78−38214
spherical shell, shallow radially ribbed, stress state, struct. parameters influence 80−14581
split Hopkinson pressure bar application to fracture dynamics 80−85140
split Hopkinson pressure bar use in obtaining dynamic stress/strain data at const. strain rates *(Japanese)* 80−16630
springs, helical torsion, design for minimum weight 77−54881
stable crack-growth, fracture criteria, numerical approach 78−67104
stacking fault, antiphase boundary energies, investig. methods, review, appls. to FCC metals *(French)* 79−42080

stress/strain relations continued
static flow stress, decrease, by superimposition of ultrasonics 79−7652
steel, AISI 1010, low-cycle fatigue at temps. up to 1200°F 78−35516
steel, Al-killed, sheets, effect of strain path changes on formability 79−43347
steel, Al-killed rolled sheet, plastic anisotropy theory based on yield function of fourth order 78−31458
steel, alloy, Ni-Cr-Mo, exam. of transformation behaviour 78−76718
steel, alloy, rectangular beam, stress-strain anal. of cyclic plastic bending and torsion 78−90734
steel, alloy, tension test, computer simulation of deform. to fracture 79−11667
steel, anisotropic sheet, strain hardening, stress state depend. 80−55421
steel, austenitic, precipitation of $Cr_{23}C_6$ at grain boundaries 78−84846
steel, austenitic, variation coeffs. of permissible stresses, at low temps. 80−16402
steel, austenitic stainless, 304, solution annealed, tensile flow behaviour after exposure to flowing Na, in temp. range 550 to 700°C 78−35463
steel, austenitic stainless, 316, surgical implant ion beam textured, stress/strain relations, fatigue characts. 78−73297
steel, austenitic stainless, AISI 316 L, viscoplastic deformation under hot working conditions, struct. model 79−83278
steel, austenitic stainless, dynamic recrystallization kinetics 79−47731
steel, austenitic stainless, electron beam welding effect, on mech. props. of steels 310L, 316, 21-6-9 78−48498
steel, austenitic stainless, fatigue and cyclic stress-strain characts. austenite-martensite transform. effect 80−21109
steel, austenitic stainless, H_2 induced strain in single crystal *(Japanese)* 77−48530
steel, austenitic stainless, high temp. alternating torsion behaviour, saturation state phenomenology 79−70111
steel, austenitic stainless, multiaxial creep equations for nonlinear and volume-nonconservative in-reactor creep 79−59164
steel, austenitic stainless, struct. and mech. props. under low temp. deform. under linear and plane stress conditions 79−1902
steel, austenitic stainless, type 304, cyclic creep during unbalanced tension-compression loading at elevated temp. 80−97545
steel, austenitic stainless, type 304, exam. of continuous cooling sensitization 79−29098
steel, austenitic stainless, type SUS 304, low cycle fatigue strength reduction factor *(Japanese)* 80−104259
steel, austenitic stainless, types 304, 316, strain growth, due to thermal stress ratcheting, exam. 78−92354
steel, austenitic stainless, viscoplatic constitutive eqns. under hot working conditions 79−57024
steel, austenitic stainless sheet, texture anisotropy influence on deformation forming limits 79−91706
steel, austenitic stainless SUS 301, stress corrosion cracking susceptibility, effect of strain-induced α'-martensite *(Japanese)* 80−104335
steel, austenitic stainless type SUS 316, low cycle fatigue tests, freq. effect on notch sensitivity at elevated temps. *(Japanese)* 80−104260
steel, bearing GCr15, stress intensity factor, S effect *(Chinese)* 77−73300
steel, C, accumulation of longitudinal strain under cyclic torsion 78−64615
steel, C, crack initiation and propagation life under repeated impact tensile loads *(Japanese)* 80−104264
steel, C, deformation strength and strain rate depend. under plain strain state *(Japanese)* 80−30028
steel, C, failure mechanisms in impact fatigue 80−40493
steel, C, fracture criterion determination, using 3-point bending 79−29216
steel, C, spheroidized, type 1090, exam. of reverse flow behaviour 78−80610
steel, C, type 45 and 1Kh2M, fatigue strength, of notched specimens with regard for cyclic plastic strains 79−43414
steel, C, type SFVV1, low cycle fatigue strength reduction factor *(Japanese)* 80−104259
steel, C-Cr (0.6, 13 wt.%), friction during working stresses and rheological charact. at high temps. *(Russian)* 77−66702
steel, C-Mn-Si, dual phase, stress-strain curves, deformation behaviour 79−52324
steel, cast, SC49, rel. between rotating and flexural bending strengths *(Japanese)* 80−81117
steel, cast automatic couplings, yield strength, crack propag. resistance and ductile-brittle transition temp. 80−104281
steel, Charpy V-notch toughness test, computer simulation 79−70138
steel, CK10, structural, temp. and freq. depend. of stress-strain behaviour under cyclic loading *(German)* 79−38888
steel, Cr, stress relaxation, superplasticity and thermal cycling *(Russian)* 80−21019
steel, Cr-Mn, strain hardening, 4.2 to 293K 80−81076
steel, Cr-Mo (2.25, 1 wt.%), strain hardening shakedown load during bending 80−20958
steel, Cr-Mo-V, biaxial cyclic deformation behaviour 80−21057
steel, Cr-Mo-V, creep deform. under const. and cyclic temp. 79−38914
steel, Cr-Mo-V, cyclic deformation under out-of-phase loads 80−40428
steel, Cr-Mo-V and stainless, biaxial cyclic deformation behaviour 80−16431
steel, Cr-Ni, strain hardening, 4.2 to 293K 80−81076
steel, Cr-Ni-Mo, dynamic and static softening behaviour at hot forming temp. *(German)* 80−25728
steel, Cr-Ni-Mo-V, plate, type HY130, exam. of elastic-plastic R curve 79−29157
steel, CrMoV, compact tension specimen, thickness effect 78−68764
steel, cyclic creep and mean stress influence on fatigue life *(Czech)* 79−43403
steel, deformation and stresses during elongation, application of Ludwig eqn. *(German)* 80−40475
steel, deformation under modified ausforming *(Japanese)* 79−11673
steel, deformed, Kh18N10T, ageing under gradually increasing load 77−90383
steel, dual-phase, notched, fatigue 79−100253
steel, ferrite-pearlite, cyclic behaviour, fatigue, chem. comp. and microstruct. effects 78−60833
steel, H_2 effect on yield 78−15474
steel, heat resistant, cyclic determ. at elev. temps. 79−66125
steel, high Si dual-phase, mech. props and microstruct. anal. 80−40444
steel, high strength, strain concentration and occurrence of fatigue cracks in welded joint *(Japanese)* 77−90452

stress/strain relations continued
steel, high-strength structural, stress-strain curves, shape effects *(German)* 80−45343
steel, induction hardened, static bending strength and correlation between static strength and endurance limit *(Japanese)* 77−70108
steel, intermediate class Kh16N6, structural aspects of work hardening 77−90369
steel, interrelation between static and dynamic strength 79−15725
steel, low alloy, cladded with monolayer austenitic stainless steel, heavy section, residual stresses *(German)* 78−35420
steel, low alloy, elastoplastic strain evaluation in crack weakened cross sections by fracture mechanics 80−45380
steel, low alloy type 10KhSND, resist. to low-cycle deformation at low temps. 79−87696
steel, low alloy-high strength, deforms. during cold crack developments in welded joints 80−81142
steel, low C, close coiled helical spring, corrosion under axial deflection and const. load 79−52428
steel, low C, cold rolled sheet, strain rate effect on yield *(Japanese)* 79−96084
steel, low C, cyclic plasticity and low cycle fatigue life 80−21058
steel, low C, cyclic plasticity and low cycle fatigue life in variable amplitude loading 80−16433
steel, low C, cyclic stress-strain response under spectrum loading *(Slovak)* 78−19886
steel, low C, dynamics of cyclic plastic deform. and fatigue life at low temps. 77−16670
steel, low C, dynamics of cyclic plastic deform. at low temps. *(Czechoslovakian)* 77−32679
steel, low C, fatigue, low cycle, cyclic stress-strain curve eval. 77−44347
steel, low C, fatigue life, variable strain ranges *(Czech)* 80−60956
steel, low C, ferrite grain size effect on cyclic stress-strain response 79−100203
steel, low C, flow stress variation after unloading, tensile load/strain diagrams *(Russian)* 78−76703
steel, low C, hardness correl. with macrostress intensity under plastic strain 79−87708
steel, low C, impact torsional test by means of dropped bar 79−100304
steel, low C, instability obs. by large strain compression 80−35253
steel, low C, low cycle fatigue props. with variable strain ranges *(Czech)* 80−45390
steel, low C, lower yield stress, grain size effects, Petch slope, temp. depend. *(Japanese)* 78−39852
steel, low C, S 35 C, annealed, crack initiation life, anal. of smooth and notched specimens *(Japanese)* 79−8347
steel, low C, type En3, high strain deform., struct. and props. 80−89301
steel, low C, weldable, precipitation hardening rel. to low cycle fatigue *(Czech)* 79−15686
steel, maraging type with 18% Ni, ageing treatment effect on fatigue crack propag. 80−16411
steel, medium C, microflow and strain hardening under cyclic loading 80−104182
steel, medium C and austenic stainless, cyclic strain induced creep, relation between modes of stress and strain superposition 78−60733
steel, medium C resulphurised, compressive strength at high strain rates, short load cells 79−29305
steel, medium strength plate, quenched and tempered, fracture toughness in ductile-brittle range 78−7036
steel, mild, plastic deform. energy const. 77−32658
steel, mild, plastic flow localisation under dynamic torsional loading, crit. variables 80−85015
steel, mild, stress/strain relation formulation for plastic deform. for strain trajectroy 78−52913
steel, Mn-C (1, 0.1 wt.%) strip, hot rolled, P effect on mech. props. 78−27532
steel, Ni-Cr-Mo, cyclic creep under increasing stress condition, constitutive eqn. 80−93593
steel, Ni-Cr-Mo, type 4340, equivalence of K_{Ic} and J_{Ic} fracture toughness meas. for range of yield stress 79−38934
steel, normalised, C-Mn-P, P effect on mech. props. 77−63745
steel, parts, stress calcs. during cooling, program system THEPLA *(German)* 80−35237
steel, pearlitic, wear behaviour rel. to basic material props. 80−108592
steel, plain C, cyclic induced creep at room temp. 80−25765
steel, plastic props., room temp. to recrystallisation temp., stress-strain relations, computer program 77−1865
steel, quasi-cleavage fracture *(Chinese)* 80−21060
steel, reinforcement, low, high temp. static strength testing 79−15902
steel, S45C, low-cycle torsional fatigue under multiple repeated loads *(Japanese)* 77−8925
steel, S45C and SS41 types, dynamic yield condition under dynamic torsion and static tension 79−34214
steel, sheet, effects of strain rate and deformation heating in tensile testing 78−85089
steel, spheroidized, medium C, strain hardening 78−52845
steel, stainless, 304, annealed and 9% prestrained, cyclic hardening and softening, room temp. 77−52483
steel, stainless, austenitic, dynamic uniaxial and biaxial stress-strain relationships 80−81122
steel, stainless, Cr-Ni, low temp. plastic deformation, in mag. field 79−83256
steel, stainless, creep test at elevated temps., based on state variable theory 79−61687
steel, stainless, effects of material properties on the dynamic response of pressure-loaded core subassembly wrappers 79−49756
steel, stainless, ferritic, 18%Cr, stress/strain curve, H_2 charging influence, room temp. *(Japanese)* 78−39884
steel, stainless, fibre reinforced Al alloy, tensile props., cryogenic cooling effect 79−61623
steel, stainless, Kh18N10T, ionised gas effects 79−70252
steel, stainless, stress/strain behaviour, exam. with high temp. short time testing facility 78−53051
steel, stainless, Ti modified 316, uniaxial tensile behaviour, Na environment effect 78−52916
steel, stainless, type 304, description of deformation induced plastic anisotropy 79−43268
steel, stainless, type 304, viscoplastic behaviour, strain rate sensitivity, creep, relaxation, tensile tests 80−66727
steel, stainless, type 304, viscoplastic model, uniaxial, based on total strain and overstress 80−64387

stress/strain relations continued
steel, stainless, type 304 welded, low temp. sensitisation, nucleation of CR carbide nuclei along grain boundaries TEM, SEM study 79−38851
steel, stainless 18KhNMA, microplastic deform. *(Russian)* 77−66681
steel, stainless 22 CND 17-13, mechanical description between 20 to 1000°C, thermoplastic calc., stress strain relations *(French)* 78−35449
steel, stainless 304, cyclic plasticity, exponential stress-strain law 77−25157
steel, stainless 304, stress corrosion cracking in high temp. water, constant strain rate meas. 78−31565
steel, stainless 304 sol. of annealed and thermally-aged, high-cycle fatigue behaviour 80−100923
steel, stainless 316, stress-strain behaviour of micron thickness foils 79−52327
steel, stainless AISI 316, biaxial cyclic deformation behaviour 80−21057
steel, stainless austenitic, low alloy 316, high temp. plasticity, B addition effects *(Russian)* 77−28852
steel, stainless type 304 L, mech. behaviour under constant stress associated with cyclic strain 80−25767
steel, stainless type 316, prediction of transient mech. response using equation of state approach 79−74207
steel, stainless/Al laminate, sandwich sheet material, plane strain compression and rolling 79−57062
steel, stainless/Al laminate, sandwich sheet materials, deform. in uniaxial tension 79−57061
steel, strengthened, high temp. deform. line charact. *(Russian)* 77−25099
steel, stress and strain intensity, determ. after plastic deform. using microhardness meas. 80−40641
steel, stress/strain diagrams of structures 79−87703
steel, structural, St37-2, crack tip displacement and flow curves *(German)* 79−47747
steel, structural, unalloyed, brittle fracture, grain size and precipitate thickness effect 78−60786
steel, SUS 304 and S15C, creep deform. under reversed cyclic stresses *(Japanese)* 80−81114
steel, type 20 and Kh18N10T, Poisson ratio, prestrain effects 79−70103
steel, type 4130, high strain rate compression, plastic flow 79−34099
steel, type SAE 1008, finite fatigue life distribs., various load-time histories 80−97589
steel, types S25C and S45C surface damage produced by pulsating impact contact load *(Japanese)* 80−104263
steel, U8A, 5KhNM and 12KhNZA, superplasticity under compression 77−86086
steel, ultrahigh strength, monotonic and cyclic stress strain curves 80−35268
steel, wave propag. effects on dynamic loading of pressure vessels 77−3090
steel, weldable, fatigue data, low and high cycle compatibility *(Czech)* 80−89343
steel 45, acoustic-emission signals, rel. to struct. 79−52297
steel compact specimens, finite element analyses of dynamic stress intensity factors, and crack arrest stress intensity factors 79−61732
steel fatigue in surface active media, adsorption facilitation mech. 80−55586
steel mild, reinforcing bars, stress strain charact. under cyclic loading 79−87688
steel plate collapse, anal. by live energy minimisation 78−52910
steel SAE 1045, thick walled cylinder, finite strain pressure-tension loading 77−32632
steel stretch-bend test strain distribution obs. 77−70243
steels, dynamic material props. for FBR safety anal., testing devices 78−60966
steels, hot plastic strain, stress- strain-time dependences *(Russian)* 80−40430
steels, structural St 37-2, cleavage fracture, report 80−25868
steels, ultrahigh C, superplastic, mech. behaviour at elevated temps 80−21028
stiff bending plates, stress-strain states, finite element effectiveness, polynomial approx. *(Russian)* 80−58921
stiffened plates, structural and by finite element and integration methods 77−3753
strain and failure relationship of stressed solids 78−9574
strain diagram plotting from data obtained during elastoplastic bending or torsion 77−81371
strain distribution near notch tip under mixed plane stress-plane strain condition *(Japanese)* 77−8891
strain energy density fracture criteria, extension to brittle and ductile fracture 78−75102
strain rate dependent materials, neck development, accuracy of long wavelength approximation 78−56719
strain rate gradient development 79−46219
strain trajectories of constant curvature for plastic deformation 80−48591
stress analysis, experimental, conf., Bradford, England (Sept. 1978) 80−17718
stress analysis of cracks, elastoplastic range 78−67144
stress wave dislocation damping, strain-amplitude depend., KGL String model 77−4101
stress-strain curve from continuous indentation test 77−90396
stressed state in reactor pressure vessels, model studies by polarised optics 78−78454
stretch components transformation using Mohr's circle 77−82393
structural deformation under dynamic loading, state variable description of material behaviour 80−85137
structures with convex strain energy density, friction problem, variational approach 79−27601
styrene butadiene rubber-glass bead composites, network density determ. from stress/strain meas. 79−34112
styrene-butadiene rubber, vulcanised $CaCO_3$ filled, stress/strain relations *(Japanese)* 80−40443
styrene-butadiene triblock copolymer films, mech. props., effect of casting solvent 79−11651
substitutional alloys, conditions for appearance of striations in stress/strain curves *(French)* 77−44319
superalloy thin walled tubes, exam. of stress/strain relations in tube eversion 79−61689
superconducting composites, stress-induced heating, finite element calc. 77−28342
superconductors, test facility for dynamic stress-strain curves meas. 77−77698
stress/strain relations continued
superconductors, type II, review of mechanical behaviour and stress effects 77−86083
superconductors under dynamic mech. stress, appl. to training effect in supercond. magnets 77−26356
superplastic flow, activation enthalpy determ. from strain rate changes in tensile tests 80−81127
superplastic flow in unsteady and steady state regions 79−42135
superplastic materials, flow and failure, review 80−50690
superplasticity, deformation mechanisms, review 80−50691
superplasticity, strain rate sensitivity of tensile flow curve *(German)* 77−63733
superplasticity rel. to strain diag. *(Russian)* 77−59854
superpotential flow problems and application to metal forming processes with friction boundary conditions 79−66119
surface shear stress, strain and displacement for screw dislocations in vertical slab 77−56594
temperature stress-state of internal combustion engines finite element study 77−80073
tensile bond strength, effect of aspect ratio, for butt joint of internal fracture 80−50823
tensile test piece, profile of contracted part after the beginning of necking *(German)* 77−86269
tension test, computer simulation, effect of testing conditions 80−7729
tension test instability *(German)* 77−52555
tension test with neck triaxiality reduction 78−7159
tension tests, analysis of misalignment 80−11864
thermo-plasticity of irradiated metals 77−4146
thermochemical equilibrium of solid under stress, nonlinear theory 78−18701
thermoplastic elastomers, crosslinked by secondary valence interactions, elasticity and processing, crosslinking behaviour 80−40320
thin shell finite element by mixed method formulation 77−9872
thin shells, heterogeneous stress/strain state, stability eqns. for small deformations *(Russian)* 80−1426
thin wafer method, analytical examination for rate independ. and rate depend. materials *(Japanese)* 79−59931
thin wall beams with deformable contour, stress/strain state 79−94500
thin-walled structures, elastoplastic analysis by finite strip method *(Japanese)* 77−42753
Thornel reinforced epoxy laminates, strength and biaxial stress-strain response, analytical expt. correlation 79−29131
three-layer cylindrical shells, thermoplastic stress state 80−96204
tip of blunt notch, plastic yielding during static and fatigue loading 79−77010
tissue properties, skin and other soft connective tissues 78−44521
torispherical vessel heads, elastic-plastic internally pressurized, stresses and buckling 77−58574
torispherical vessel heads, internally pressurised, elastic-plastic buckling 78−79241
toroidal compensator, approx. calc. method 77−14896
torsion pendulum, for continuous meas. of amplitude and damping under tensile stress 77−35099
torsional strain curves plotting 80−40638
transversely isotropic cylinder, thermal stresses for penny-shaped crack 77−89070
Tresca yield condition usage in finite element plane strain anal. 78−83263
truncated cone, semiinfinite, nonaxisymm. end loading, total stress problems, equilib. 77−65678
truncated cone, subject to axisymmetric loading, stress-strain state 78−1570
tube, viscoelastic, containing flowing fluid, bending vibrs. 79−94521
tubes, thick-walled, thermoelastoplastic creep stress anal. 80−58922
tuff, deform. charact., expt. study *(Japanese)* 78−56704
TV screen displaying instrument, exam. of design 80−21222
two joined plane strain sectors, thermal stresses 77−58559
unbounded body, weakened by circular cracks, elastic equilib. 80−53717
uniaxial tension, effect of material strain rate sensitivity and specimen heterogeneity *(Polish)* 78−84887
unidirectionally reinforced composites, large deflection, plastic constitutive relations 80−43624
unilateral contact problem, structures with nonquadratic strain energy density 77−31209
unstable fracture criteria under large plastic deformation 78−67143
upsetting tests developments for better stress/strain curve results *(German)* 80−38368
valve tissue, glutaraldehyde preserved, stress/strain and fatigue behaviour 78−40217
viscoelastic bar, transient wave propag. 80−106745
viscoelastic isotropic linear material characteristics, finite element method *(German)* 78−32681
viscoelastic linear solids, stress/strain tensor eqns. *(French)* 80−53656
viscoelastic material, linear, creep function, information theory approach to its monotonicity, concavity and symm. 77−84156
viscoelastic material, stress-strain behaviour, mathematical simulation *(German)* 80−1442
viscoelastic materials, nonlinear, creep and relax., book 77−11141
viscoelastic plastic components meas., using Moire method stress calc. from measured strain *(German)* 78−22309
viscoelastic properties dynamic evaluation for use in cardiac prosthetics 78−40405
viscoelastic rod, shock rel. to hard obstacle *(Russian)* 80−23911
viscoelasticity, nonlinear, stress relaxation, Volterra integral equation, numerical analysis 80−53646
viscoelasticity, stress/strain relationships, fluctuations 80−17802
viscoelasticity linear theory, variational and minimum principle applications *(Japanese)* 80−48599
viscoplasticity coefficient of stress concentration *(French)* 77−19541
viscous solids, stress and strain fields at crack tip *(French)* 80−14615
webs, stress state under uniform partial edge loading 79−77028
welded component fatigue life and crack propag. analysis with internal stresses 77−77576
welded dissimilar cylindrical shells under service loading, stress/strain calc. and expt. 79−83284
Westerly granite, stress-strain hysteresis loops shapes 80−26499
Westerly granite, stress-volumetric strain behaviour statistical var. 78−96196
work hardening and solid solution hardening model 79−34051
yield surface motion and loading surface 78−15449

stress/strain relations continued
Zircaloy, annealed, neutron irradiated, inhomogeneous deform. behaviour 80−85014
Zircaloy, micrograin superplasticity at 850°C 78−23758
Zircaloy, textured, interactive creep and growth, upper-bound evaluation 80−89293
Zircaloy, unirrad., stress corrosion cracking, I_2-induced, effect of test temp., alloy comp. and heat treatment 80−97632
Zircaloy cladding, effects of stress biaxiality on ballooning behaviour 79−30919
Zircaloy-2, deformation and fracture behaviour, uniaxial tension test in I_2 environment 80−13580
Zircaloy-2, martensitic transform. contrib. to strength and work hardening, and martensite flow props. 78−84842
Zircaloy-2, neutron irradiated, inhomogeneous deformation behaviour 80−50679
Zircaloy-2, polycrystn., thermal history effect on tensile props. 79−74204
Zircaloy-2, polycrystn., thermal history effect on tensile props., comment 79−74205
Zircaloy-2, pressure tubes, irrad. creep and growth, anisotropy factors 80−97536
Zircaloy-2 cladding, fracture in iodine environment 78−31581
Zircaloy-2 cladding tubes, heat treatment influence on texture and mech. anisotropy 79−91694
Zircaloy-4, H_2 effect on mech. props. *(Korean)* 79−70123
Ag, FCC, polycrystalline, deformation-strain curve description using substruct. parameters *(Russian)* 79−87690
Ag, FCC crystal, stress-strain curve, stage I to stage II transition *(Japanese)* 78−19834
Ag plastically deformed crystal, exam. of dislocation dynamics during strain rate changes 78−88506
Ag, plastically deformed crystals, exam. of dislocation dynamics during strain rate changes 78−88507
Ag-Pd, composition modulated foils, layer struct. and mech. props. 79−95300
AgCl:$Li^+(Na^+)(K^+)(Rb^+)$, impurities effect on plasticity, brittleness 78−14398
Al alloy, crack initiation at high strain rates, uniaxial and biaxial tests 80−85141
Al alloy, reverse loading stress/strain curve, w.r.t. prestrain *(Japanese)* 80−7622
Al alloy, spherical shell, three layer, stress/strain relations *(Russian)* 80−3122
Al alloy, US testing of cold worked surface, quality evaluation 78−48602
Al alloy, yield surface after proportional preloading, Tresca-type strss-strain rel. 77−32628
Al alloy, yield surfaces, effect of preloading under combined axial load and torsion 77−25091
Al alloy 1100, annealed, thick walled cylinder, finite strain pressure-tension loading 77−32632
Al alloy 2029-0, circular plates with work hardening, nonlinear behaviour, experimental deflection and strain data 79−38893
Al alloy 2618, creep and recovery under combined stress, viscous-viscoelastic model representation 79−34117
Al alloy 6061-T6, yielding of tubing under dynamic biaxial loading 80−16377
Al alloy 7050-T76, crack propagation rate and crack closure, mean stress effects 79−52336
Al alloy AMg6, multilayer shells, stress-strain state and stability at high temps. 77−54903
Al alloy D16T, acoustic-emission signals, rel. to struct. 79−52297
Al alloys, cryogenic, AMg5 and AMg6, mech. props. at −196°C 77−63748
Al alloys, deformation processes in sheet materials, application of failure maps 78−56718
Al alloys, high strength, cyclic plastic strain damage eval. and summation 79−57060
Al alloys, stress-strain behaviour at large strains 77−52442
Al alloys, stress-strain state after treatment by pressure, moire strip method appl. *(Russian)* 80−40648
Al alloys 2024-T4, 2219-T861, overaged 2219, fatigue crack propag., plastic work role 79−79070
Al, and Al alloys 6061 and 2024, burst acoustic emission during Bauschinger effect 77−48475
Al, circular tube, forming limit of free bulge-forming *(Japanese)* 80−55477
Al, commercially pure, prestrained, yield criteria and stress-strain relations anal. 79−57051
Al, commercially pure, stress-strain curves, cyclic loading initial stage *(Japanese)* 80−93617
Al, crit. resolved shear stress, orientation depend. 80−21001
Al, deformed, thermal recovery, microstruct. and stress-strain relations 80−16325
Al, FCC, polycrystalline, deformation-strain curve description using substruct. parameters *(Russian)* 79−87690
Al, isoaxial bicrystal, deformation behaviour, study by photoelastic coating and moire methods *(Japanese)* 78−11294
Al, isoaxial bicrystal, Moire investigation of mechanical behaviour 77−16647
Al notched bars, deform. behaviour and strength having biaxial state of stress at notch root *(Japanese)* 80−81116
Al, orthogonal cut surface, relations between residual stress and moire strain, exam. *(Japanese)* 78−85036
Al, plastic props., room temp. to recrystallisation temp., stress/strain relations, computer program 77−1865
Al, prestrained, isotropic hardening rule, rel. to stress/strain curve 78−23772
Al, pure, polycryst., steady-state flow, stress and temp. depend. 80−45341
Al, pure, texture influence on stress/strain curves, prestrain, solid soln. and particle hardening effect on inhomogeneous deform. *(German)* 80−30014
Al sheet alloy, type 2036-T4, in-plane deformation, correlation with Hill's theory 79−83260
Al single crystals, ⟨100⟩ oriented, deform. temp. effect on stage IV deform. *(Japanese)* 80−66587
Al single crysts., elastoplasticity, dislocation model, work hardening, tensile tests, stress/strain curves *(Japanese)* 77−52410

stress/strain relations continued
Al, superconducting, an anomalous strain-rate sensitivity of flow stress 79−43313
Al, surface strengthening of single crysts. on coating with evaporated films 77−8972
Al, tensile flow stress at room temp., grain size and strain effect 77−77528
Al, ultimate tensile strength for brief impact 80−70309
Al/Cu laminates, vapour deposited, strength enhancement 79−24576
Al-Ag (15 wt.%), precipitation hardenend cyclic stress-strain response 78−35412
Al-alloy, type PA6, under complex cyclic loading, behaviour of stress strain diagrams 80−16372
Al-Cu, flow stress, origin of high strain rate sensitivity 78−44186
Al-Cu (2.6 wt.%), sheets, effect of strain path changes on formability 79−43347
Al-Cu (4 wt.%), single crystal, anisotropy in plane strain compression 77−36599
Al-Cu (4 wt.%), with θ' precipitates, relation between elastic limit and hardness *(French)* 79−5018
Al-Cu (4 wt.%) alloy, precipitation hardened, single crystal, directional plastic behaviour, exam. 78−39788
Al-Cu full coherent precipitation hardened alloy, high temp. cyclic deform. 80−25711
Al-Cu-Mg, acoustic emission during tensile testing 80−7632
Al-Cu-Mg, cold plastic deformation, stress/strain relations 79−56991
Al-Cu-Mg/mica particulate composite mech. props. 80−100919
Al-Cu(Mg), low freq. internal friction during plastic deform. *(Chinese)* 80−103420
Al-epoxy adhesive joints, cohesive-interfacial mixed-mode fracture 79−39110
Al-Mg, acoustic emission during tensile testing 80−7632
Al-Mg, cold plastic deformation, stress/strain relations 79−56991
Al-Mg, discontinuous deform. under various conditions 77−63716
Al-Mg, dynamic uniaxial tension and compression curves 80−100884
Al-Mg, superconducting, an anomalous strain-rate sensitivity of flow stress 79−43313
Al-Mg-Si, Portevin-Le Chatelier effect, effect of precipitation hardening 77−32585
Al-Mg-Si, type 6010, microstruct. charcts. influence on formability, heat treatment 80−81090
Al-Mg-Si (0.7, 0.4 at.%), effect of precipitation hardening on strain rate behaviour and yield behaviour 79−29075
Al-Mg-Si solid solution under stress, solute atom clustering during ageing 78−31430
Al-Mg-Si-Cu, cold plastic deformation, stress/strain relations 79−56991
Al-Ni (6 wt.%), fine-grained, deform. in tension and torsion 80−85008
Al-Ni(Cd)(Fe)(Si), cold worked, struct. and props. 80−71666
Al-Zn (20 (30) (35) (40) (60) at.%), effect of UTS on cyclic creep strength *(Korean)* 80−25778
Al-Zn-Hg alloy, cathodic protection charcts., surface free energy, lattice struct. 79−29281
Al-Zn-Mg, type V-95, ultimate tensile strength for brief impact 80−70309
Al-Zn-Mg (4.5, 2.5 wt.%), fatigue crack propag. 77−86171
AlN, polycrystalline, stress-strain data up to 1.25 GPa 80−100899
Al_2O_3, polycrystalline, stress-strain data up to 1.25 GPa 80−100899
Al_2O_3/Nb, fracture mech. parameter determ. at high temps. *(German)* 79−70136
Al_2O_3-epoxy mechanical mixtures, stress-wave propag. model, dynamic response expts. 79−1477
Al_2O_3-SiO_2 (3 wt.%), J-integral meas. at high temps. *(German)* 80−93624
Al_2O_3-SiO_2 glass, annealed and tempered, fracture strength studies under dynamic conditions 79−96132
Al_2O_3-SiO_2-Fe_2O_3-CaO-MgO-TiO_2, refractory, corrosion and mech. behaviour correlations 80−40563
Au-Cd (47.5 at.%), effect of cooling rates on stress-strain behaviour 78−76721
Au-Ni, composition modulated foils, layer struct. and mech. props. 79−95300
$Au_{52.5}Ag_xCd_{47.5}$, pseudoelastic behaviour associated with thermoelastic martensitic transform. 80−16304
B fibre reinforced Al, unidirectional, K-calibration and compliance curves 78−88518
B fibres of various diameters, tensile strength, elasticity, elongation 78−3189
$BaTiO_3$, deform. and stress relax. of single crysts. 77−59542
Be, high-strength, fracture toughness determ. 77−73336
BeO, polycrystalline, stress-strain data up to 1.25 GPa 80−100899
Bi, crit. resolved shear stress of two slip systems, compression tests, 77-538K 80−59470
Bi, low temp. plasticity, temp. effect on strain hardening, slip *(Russian)* 77−31713
Bi polycrystalline, plastic deform. and stored energy of cold work 79−43348
Bi_2MoO_6, superplasticity during phase transitions 80−108498
Bi_2WO_6, superplasticity during phase transitions 80−108498
β-brass, nonisoaxial bicrystal, simultaneous hardening and softening 77−36606
C adsorbent, granules and artifacts, strength, mech. charcts. 78−23771
C fibre reinforced C, processing, room temp. mech. props., and low temp. expansion 80−25820
C fibre reinforced composite, split Hopkinson press. bar test, opt. and strain gauge methods comparison 80−85132
C fibre reinforced nylon, design parameters, fibre orientation effect 80−81141
C fibre reinforced plastic, nonlinear stress strain relations, under continuous static loading 77−59872
C fibre reinforced plastic, laminate, non Hookean behaviour in fibre direction, effect of fibre waviness on tensile props. 78−19804
C fibre reinforced polyamide thermoplastic, stiffness and strength 78−27600
C fibre reinforced polycarbonate, design parameters, fibre orientation effect 80−81141
C materials, bend strength testing, bench assembly with strain recording 79−57176
C steel, strain hardening parameters, determination from stress-strain curves 78−80562
C-C composite, structure model, Rosen model with fractional matrix 80−11719

stress/strain relations continued
Cd single crystal, low-temp. work hardening 78−3138
Cd-Ag (0.015 to 0.25 at.%), critical resolved shear stress at low temp. 77−69035
Cd-Zn single crystal, plasticity, 4 to 50K 79−43362
CdTe, crysts., mech. behaviour, yield stress function of temp., stress relaxation 79−60427
CdTe, laser window material, vap. deposition, mech. props. 77−46776
(Co,Ni)-$Cr_{23}C_6$ eutectic, microstruct. effect on fracture energy 80−7662
Co-Ni (33 wt.%), FCC deform. twinning kinetics, relationship to stress-strain behaviour 78−52887
Co-W-Cr (15,20 wt.%), surgical implant ion beam textured, stress/strain relations, fatigue characts. 78−73297
Co-WC dispersion hardened alloy, tensile deform., volume fraction of second phase effect, simulation *(Japanese)* 79−70122
Cr-Al alloy KH40NYu3, microplastic deform. *(Russian)* 77−66681
Cr-Mo-Nb, elastic-plastic mathematical model response on quasistatic loading *(Czech)* 80−29111
Cr-Ni, elastic-plastic mathematical model response on quasistatic loading *(Czech)* 80−29111
Cr-Ni-W(-Mo), heat resistant weld seam metal, tensile strength, thermophysical characts. 79−91769
CsI, exam. of kinking process, using cholesteric liquid crystals 80−7629
Cu, ⟨100⟩ oriented single crystal plastic deform. and prominent cross slip 78−19852
Cu, annealed, cyclic plasticity under cyclic nonproportional strain histories, cyclic hardening, memory erasure, strain hardening 78−88510
Cu annealed, thick walled cylinder, finite strain pressure-tension loading 77−32632
Cu, annealed O free, high cond., proportional biaxial cyclic hardening 78−84844
Cu, cyclic hardening and saturation behaviour of single crystals 78−64555
Cu, cyclic straining anal., discrete polycrystal model 77−47507
Cu, deform. of ⟨100⟩ single crystal *(Japanese)* 77−59864
Cu, dislocation mean free path at 77K under elastic deform. 78−44162
Cu, dynamic uniaxial tension and compression curves 80−100884
Cu, FCC, polycrystalline, deformation-strain curve description using substruct. parameters *(Russian)* 79−87690
Cu FCC crystal, stress-strain curve, stage I to stage II transition *(Japanese)* 78−19834
Cu, fatigue hardening and high cycle fatigue under reversed bending 79−20180
Cu, friction stress in high temp. creep 80−11723
Cu high purity, grain boundaries as dislocation sources in premacroyield strain region 79−34096
Cu, high-purity, grain size and strain rate influence on mech. behaviour, precursors existence 80−85016
Cu, hot ductility and torsional deform. *(Japanese)* 79−57069
Cu, microplastic deform. and amplitude depend. of internal friction *(Russian)* 80−45349
Cu, plastic props., room temp. to recrystallisation temp., stress/strain relations, computer program 77−1865
Cu, polycrystn., strain localisation during hot deform. 80−104195
Cu, pure, dynamic stress strain relations in combined tension and torsion, testing device 80−21197
Cu, single crysts., deformed in [001] and [111] axes, cell structs., TEM 80−70209
Cu, strain hardening parameters, 4.2 to 300K *(Russian)* 79−20063
Cu, stress strain anal. of single crystal induced by absorbed H_2 *(Japanese)* 78−11276
Cu, stress-strain behaviour over large strain range 79−15745
Cu, thick sputter deposit, microstruct., tensile props. 77−40461
Cu, transgranular cracking in 1M $NaNo_2$ solution 79−100287
Cu tubes, anisotropic, plastic deformation in hydraulic bulging 79−61688
Cu viscoplastic constitutive equations, for metal with strain rate history and temp. effects 79−61686
Cu wires, electrolytic, Young's modulus, working temp. effects 80−50667
α-Cu-Al, stress-strain behaviour, effect of grain size and composition 77−56038
Cu-Al, two-phase Cu-rich alloy, influence of microstruct. on stress-strain behaviour 80−7631
Cu-Al (10 wt.%) alloy, water-quenched, tensile fatigue strength at high temp. in vacuo *(Japanese)* 78−72837
Cu-Al (13 wt.%), polycrystn. rod specimens effect of diameter on slip mode, optical microscopy obs. 79−79051
Cu-Al (7.9 wt.%), burst acoustic emission during Bauschinger effect 77−48475
Cu-Al (9 wt.%), deformed, fatigue crack propag. 78−27621
Cu-Al (9.3 wt.%), in torsion, deformation temp. depend., superplasticity due to grain size, dislocation density *(Russian)* 79−74200
Cu-Al alloys, strain hardening parameters, conc. and temp. depend., 4.2 to 300K *(Russian)* 79−20063
Cu-$Al_2O_3(SiO_2)$ dispersion hardening single crystal, cyclic deform. *(French)* 79−1893
Cu-Al-Ni (14.0 4.2 wt.%), two stage superelasticity, successive martensite to martensite transform. 77−8826
Cu-Al-Ni (14.5, 3 wt.%), polycrystalline, pseudoelastic, cyclic stress strain response 77−86144
Cu-Al-Ni alloys, successive stress-induced martensitic transformations and associated transformation pseudoelasticity 79−43245
Cu-Al-Si-C (95, 2.8, 1.8, 0.4 wt.%) fracture characts. of superplastic single phase, exam. 78−48500
Cu-Al-Si-Co (2.8, 1.8, 0.4 wt.%), superplastic phase, exam. of mech. props. 78−52891
Cu-Cd (1.0 wt.%), yield stress and flow stress 80−97524
Cu-Cr (0.75 wt.%), deformation characts., fully reversed cyclic strain with fatigue cracks and dislocation struct. 80−81148
Cu-Ge (1 at.%), FCC crystal, stress-strain curve, stage I to stage II transition *(Japanese)* 78−19834
Cu-Ni(Pd), composition modulated foils, layer struct. and mech. props. 79−95300
Cu-SiO_2, dispersion hardened, surface plasticity effect 78−52832
Cu-Sn (4.9 wt.%), role of mech. twinning on stress/strain behaviour 80−85004
Cu-Ti(0.7 at.%), plastic deform. and precip. hardened, annealing time 78−48446
Cu-Zn, cyclic stress/strain curves in monocrystalline and polycrystalline samples, cold work and Zn addition effects 78−95786

stress/strain relations continued
β′Cu-Zn, martensite to martensite transformations 79−11615
Cu-Zn (0.25 wt.%), ductility minimum, strain rate depend. at intermediate temps. 79−79056
Cu-Zn single crystal, pseudoelastic effects 79−47739
Cu-Zn-Si, deform. close to martensitic transform. temp. 77−63714
Cu_3Au, disordered [001]-orientated single crysts., plastic deform., TEM and slip line studies 80−97541
β(CuNi)Zn alloys, effect of normal stress on {112} ⟨111⟩ slip 79−47760
Cu_2O polycrystalline and single cryst. mech. behaviour 78−95777
β-CuZn, acoustic emission rel. to stress induced martensitic transformation 80−81061
Dy, substructural changes during plastic deform., stress-strain diagrams and microhardness meas. *(Russian)* 79−52296
Er, substructural changes during plastic deform., stress-strain diagrams and microhardness meas. *(Russian)* 79−52296
Fe alloy, cast, Young's modulus and microstructure *(German)* 77−25090
Fe, Armco, microflow and strain hardening under cyclic loading 80−104182
Fe, cast, ductile, strain rate and temp., influence on strength, elongation and deformation *(Japanese)* 80−45356
Fe, cast flake and nodular, rupture strength, circumferential notch *(Japanese)* 80−93649
α-Fe, dislocation loops, equilib. shape under shear stress 79−7608
Fe, H_2 effect on yield 78−15474
Fe, high purity single crysts., thermally activated slip deformation between 4.2 and 300K 80−25801
α-Fe, high temp. deform., Cottrell-Stokes law 79−83274
Fe, model for Luders band formation and plastic instability related with strain softening due to Johnston-Gilman-Hahn theory 79−61676
Fe, plastic deform. of single crystal with shear tests in {110}⟨111⟩ and {112}⟨111⟩ slip system 77−48509
Fe, pure, cathodic charging effect on creep and tensile deformation 80−76320
Fe single crystals, size effect on slip deformation ability at very low temps. 80−21049
Fe, single crystals, work hardening and behaviour and dislocation struct. during simple shear tests 78−95762
Fe, single crysts., effect of hydrostatic pressure on plastic flow props., dislocation distribs. 79−38887
Fe sintered powder, plastic deform., constitutive eqns. 79−61667
Fe, stress strain anal. of single crystal induced by absorbed H_2 *(Japanese)* 78−11276
Fe, thermally activated slip deformation, 0.7 to 77K 79−91755
Fe-Co-V, ordered and disordered, dynamic ageing *(French)* 80−16355
Fe-Cr-Al-Ti-Y_2O_3 (20, 4.5, 0.5, 0.5) type MA956, strain rate effect on fracture behaviour at 1366K 80−16458
Fe-Mn (15(24)(30)wt.%), high hydrostatic pressure influence on stress-strain curve 80−25805
α-Fe-Mo (1.5 and 1.8 at.%), deform., testing mode effect at stages prior to steady states 77−66721
Fe-N, neutron irrad. effects on mech. props. 79−4338
Fe-N, single cryst., solid soln. softening, effect of interstitial N 80−97496
Fe-Ni (1 to 5 at.%), mech. props. below 300K *(French)* 79−8314
Fe-Ni-C austenitic single crysts., deform. props., martensitic transformation, SEM study 79−29143
Fe-Ni(Mo), solid soln., cyclic stress-strain props., depend. of fatigue crack growth rate 77−4853
Fe-Si, microflow and strain hardening under cyclic loading 80−104182
Fe-Si, microplastic deform. and amplitude depend. of internal friction *(Russian)* 80−45349
Fe-Si, polycrystalline, exam. of stress-strain state of individual grains 78−80580
$Fe_{40}Ni_{40}P_{14}B_6$, metallic glass, bending tests, evidence of ideal elastic-plastic deform. 80−97543
$Fe_{29}Ni_{49}P_{14}B_6Si_{12}$, Metglas fibre reinforced mortar, fracture props. 79−70159
Fe_3O_4, Fe_2O_3, magnetite and haematite nodules with fayalite and Ca ferrite additives, stressed state parameters *(Russian)* 80−45352
GaAs:Si, single crysts., asymmetric deform., stress-strain relations for α, β bending 79−23616
Ge, high press. appl. by spherical diamond indentor, plastic deform. obs. method 78−35619
^{4}He, HCP, free standing cryst., shear deform. 78−2333
^{4}He, solid BCC, plastic deform., stress-strain relations and US attenuation 78−38909
Hf, oxidation, microstructural study *(French)* 80−45436
Ho, substructural changes during plastic deform., stress-strain diagrams and microhardness meas. *(Russian)* 79−52296
InP single crystals, uniaxial compression deform. characts. 80−84991
K, device for press. variation of yield stress, elastic constants 78−53047
KCl, dislocation motion in micro-plastic region 78−91341
KCl, press. induced low-temp. polymorphic transition, hysteresis 78−14467
KCl single crystals, piezobirefringence and plastic deform., stress-strain curves 77−69798
KCl, stress distrib., meas. by scattered light photoelasticity *(Russian)* 80−7326
$K(D_xH_{1-x})_3(SeO_3)_2$, ferroelastic, anelastic and elastic infra-low freq. props. 80−70304
LiF single crystals, glide band sources, work hardening 80−34126
Mg, burst acoustic emission during Bauschinger effect 77−48475
Mg, plastic deform., strain rate history and temp. effects depend. 79−11684
Mg_3Cd, effect on order, of compression deformation 78−52924
MgO, compressive stress-strain behaviour at high temps. 80−25774
MgO, cryst. preliminary processing rel. to deform. curve parameters, slip line struct. 77−52421
MgO, hot-pressed, elasticity props. of polycrystals and single crystals 80−54301
MgO, single crysts., work hardening and creep 79−43262
$MgO(Al_2O_3)_n$ spinel, plastic deformation at 400°C 80−40453
$MgZn_2$, single cryst., yield strength 77−44318
Mo, dislocation structure, temp. depend., at crack tip, of fractured single cryst. 79−29210
Mo, mechanical eqn. of state *(Japanese)* 78−91375
Mo polycrystn., cyclically deformed, dislocation arrangements 80−108506

stress/strain relations continued
Mo, sintered, pure, work hardening 77−16607
Mo, strain induced damping, micro- and macro-, and dislocation structures in single crystals 78−19797
Mo-C-Zr (0.03, 0.17 wt.%), thermal treatment effect on yield drop 77−90382
Mo-Cr-V-P, load curves, structure states boundaries and strain hardening *(Russian)* 80−89241
Mo-Ti (3.5 wt.%), load curves, structure states boundaries and strain hardening *(Russian)* 80−89241
NaCl, dislocation motion in micro-plastic region 78−91341
NaCl:Sr deformation control by thermally activated processes 195 to 300K 79−24570
Na_2O-CaO-SiO_2 glass, annealed and tempered, fracture strength studies under dynamic conditions 79−96132
Nb, dislocation-free single crystal, deformed at 180K, X-ray topographic obs. 79−24587
Nb, effect of electron irradiation on low temp. deform., tensile stress-strain curves 79−55784
Nb, local heating during abrupt strain, catastrophic slip band formation 80−7652
Nb single cryst., slip localisation during discontinuous plastic flow at 4.2K *(Russian)* 77−69029
Nb, strain profile of plastic zone in dislocation-free single cryst. by X-ray topography 79−14876
Nb, stress differential in surface oxide softening of single crystals 77−86116
Nb, surface oxide softening, anisotropy 78−60716
Nb-O system, solid soln. hardening and softening 80−71665
Nb-T alloy, effect of T on low temp. yield stress of Nb, comparison with Nb-H alloy behaviour 78−39863
Nb-Ti(Zr), type II superconductor, mech. behaviour and stress effects 77−86083
Nb-Zr-C alloy, long term loading at high temps. effect on struct. and morphology of carbide phase 79−15754
Nb_3Sn, hot isostatically pressed, plastic deform. 80−108510
Nb_3Sn superconducting wires, in situ multifilamentary, mech. props. 79−47746
$NdNbO_4$, ferroelastic domain wall motion, stress-strain hysteresis curve 77−43271
Ni base alloys, heat resistant, cyclic determ. at elev. temps. 79−66125
Ni base superalloy, fatigue crack opening load variation with meas. location 80−16425
Ni, cyclic flow stress and microstructural changes during multiple step testing at elevated temperatures 79−91746
Ni, FCC, polycrystalline, deformation-strain curve description using substruct. parameters *(Russian)* 79−87690
Ni, intrinsic stacking fault energy, effect on cyclic hardening 79−11638
Ni, polycrystalline, strain hardening, dislocation link length model 80−84953
Ni single crystal, compressed, strengthening and dislocation cells *(German)* 80−66536
Ni, single crysts., strengthening, tested under compression at 293 and 77K *(German)* 80−50689
Ni, superplastic superalloy IN-738 load relaxation testing 77−40507
Ni, thick sputter deposit, microstruct., tensile props. 77−40461
Ni, work hardening, grain size effects 77−16605
Ni-Al (7.2 wt.%), fatigue crack propag., plastic work role 79−79070
Ni-Al-Cr-Co-Ti, Waspaloy, exam. of dislocation-precipitate interaction, cyclic stress-strain behaviour 78−84925
Ni-Cr, ERNiCr-3 weld metal, strain-rate effects on high temp. behaviour 79−93726
Ni-Fe metallic glass, METGLAS 2826, creep props. 79−15746
Ni-Fe(Co) alloys, fatigued, struct. and cyclic stress strain, influence of stacking fault energy and atomic size-module-interactions *(German)* 79−42082
Ni-Nb-Al-(Cr), eutectic, mech. props., high press. H_2 effects 77−63779
Ni-Ni_3Al-Ni_3Nb, directionally solidified, role of twinning in cyclic stress strain behaviour 78−80605
Ni-Pd-P amorphous alloys, tensile deform. 77−32646
Ni-Ti (49.7 at.%) alloy, deform. behaviour and shape memory effect 77−32638
Ni-Ti alloys, shape memory effect materials, criteria for efficiency assessment *(Russian)* 80−21015
Ni-W (45.5 wt.%), eutectic, mech. props., high press. H_2 effects 77−63779
Ni_3 (Al.Ti), flow stress and work hardening, exam. of temp. depend. by tensile tests 78−84839
Ni_3Al, noncoherent second phase particle effect on strain-hardening parameters *(Russian)* 79−47703
Ni_3(Al.Ti), single crysts., flow and fracture behaviour tested in tension 79−79075
Ni_3Ge single crystals, orientation and temp. depend. of flow stress 79−5008
NiTi, thermoelastic martensites, cyclic stress-strain curves obtain in tension compression 79−29166
Pb single crystal, normal-superconducting transition and plastic flow 78−3166
Pb, work hardening, and recovery rates during steady state deformation, temp. and stress effect 80−45319
Pb-2n, work hardening in mixed state *(Russian)* 79−42707
Pb-Sn, eutectic, superplastic behaviour, grain size effect 80−7635
Pb-Sn microduplex eutectic, cavitation during superplastic flow due to hard particles 77−36575
PbI_2 layered cryst. under uniaixal compression, low temp. thermal cond. *(Russian)* 80−44374
$Pb_3(PO_4)_2$, ferroelastic, deform. hysteresis loop. 77−51432
Pb(Zr,Ti)O_3:Nb ceramic, stress effects on ferroelec. hysteresis, macroscopic strain, US vel. 79−4778
Pd-Cu-Si glass, cold drawn, serrated plastic flow, optical and SEM study 79−79052
Pd-Sn-Cd alloy, non-unique stress/strain rate relations during superplastic flow 77−28855
$Pd_{82}Si_{18}$ glassy, long term creep tests, isoconfigurational viscosity rel. to annealing treatment 79−66122
$Pd_{82}Si_{18}$, stress/strain rate depend. of homogeneous flow 80−71687
polyoxymethylene, linear, plastic deform. behaviour 78−84910
$^{239}PuO_2$, stoichiometric, high-temp. deformation 80−81111
$(SN)_x$ single crystal, mech. props. 79−24580
$(SN)_x$, tensile and piezoresist. expts. 78−15447

stress/strain relations continued
Sb, compressive stress-strain curves in single crystals device *(French)* 79−47852
Sb, deformed in compression, secondary slip system *(French)* 79−66120
Sc, strength and plasticity 77−90429
Si, crack-tip dislocation pattern, X-ray topography *(French)* 80−107253
Si, dislocation dynamics during plastic deform., stress-strain characts. 79−27996
Si, high press. appl. by spherical diamond indentor, plastic deform. obs. method 78−35619
Si, mechanical strength, origin of difference in Czochralski grown and float-zone-grown cryst. 80−44212
Si, process stress analysis by IR photoelastic meas. 78−11488
Si, self-diffusion and dynamical recovery at high temps. 79−69284
Si, single crystals, dynamical recovery and self-diffusion 78−87816
Si_3N_4, stress corrosion 77−8917
Si_3N_4-Mg_2SiO_4-Si_2N_2O, compressive creep, composition effect 80−50674
SiO_2 glass, strengthened by ion exchange and quenching brittle destruction theory 80−45398
Sn-Pb eutectic, strain rate sensitivity of flow stresses, grain boundary sliding during superplastic, non-superplastic deform. 80−7645
strengthened by lattice transformations, mech. props. study *(Japanese)* 79−43332
Ta, evidence for slow strain-rate embrittlement due to O_2, SEM study 79−79109
Ta, flow stress, temp. and strain rate depend. 77−77534
Ta, slip between 0.7 and 40K 78−19808
$Tb_2(MoO_4)_3$, thermal expansivity and spontaneous strain temp. depend. 79−14943
Te, single crystals, expts. using device for pure shear deform. 77−81367
Te, strained and unstrained, SHG and propag. of CO_2 laser radiation 80−58641
Te-Ag thin film system, stress-relief appearance conditions 80−65416
Te-Bi thin film system, stress-relief appearance conditions 80−65416
Ti alloy, deform. under biaxial stress at elevated temps. 77−12675
Ti, commercial-purity, Portevin-Le Chatelier effect, mechanism 77−8886
Ti, fast neutron irrad., twinning deform. at room temp. 80−65061
Ti, grain size effect on yield stress and work hardening at 295 and 575K 78−64593
Ti, metal and alloys, compression at high strain rate, deformation anal. 80−25769
Ti, polycrystal, discontinuous electrical resistivity, low temp. active straining *(Russian)* 80−103666
Ti polycrystalline wire, electroplastic effect 79−57067
α-β Ti Widmanstatten alloy interfaces, elastic interact. stresses, effect on plastic flow onset 80−104218
α-Ti-Al, stress/strain curves 77−63738
Ti-Al-Mo-Sn alloy, elastically and plastically deformed, positron annihilation meas. of deformation 80−21038
Ti-Al-V, alloy 685, fatigue life, creep and dynamic strain ageing effect, 25 to 400°C *(French)* 80−45384
Ti-Al-V (6, 4 wt.%), superplastic, mech. behaviour and hardening characts. 79−83269
Ti-Al-V (6, 4 wt.%), targets, metallographic features after ballistic tests 79−79046
Ti-Al-V (6, 4 wt.%), void formation and growth, tensile fracture, exam. 78−80637
Ti-Al-V (6,4 wt.%), cyclic stress-strain response 77−21170
Ti-Al-V (6,4 wt.%), plastic flow instability and multiple necking during superplastic flow 77−8896
Ti-Al-V (6,4 wt.%), surface residual stresses, surface topography, fatigue behaviour 79−52366
Ti-Al-V (6,4 wt.%), surgical implant ion beam textured, stress/strain relations, fatigue characts. 78−73297
α-β Ti-Mn (8 wt.%), calc. of stress-strain curves by finite element method, comparison with expt. curve 78−84924
α-β Ti-Mn (8 wt.%), calcs. of stress-strain curve, stress and strain distribs., discussion 80−7637
α-β Ti-Mn (8 wt.%), stress-strain curve and stress and strain distrib. calcs., reply to discussion 80−7638
α, α+β, β-Ti-Mn alloys, Bauschinger effect during cyclic straining 79−43310
Ti-Ni (50.4 wt.%), thermal conversion efficiency of ideal thermoelastic marmem cycle 79−66057
Ti-Ni-Fe, plasticity, tensile stress-strain diagrams, ultimate tensile strength, elec. resist. depend. on temp. *(Russian)* 79−61652
Ti-V, cyclic stress-strain response 78−60700
β-Ti-V (40 at.%), BCC, flow stress asymmetry and cyclic stress-strain response 77−36583
Ti-Y(Er), dispersoid effect on deform. 79−24530
TiO_2, rutile, single cryst., high temp. compression in O_2 atmosphere *(French)* 79−51194
α-U, mech. props. at very high strain rates, double-notch shear test use 80−85131
α-U, polycrystalline, compressive deform. at low temps. 77−28856
α-U, strain rate effect on tensile flow and fracture 80−84992
U-Nb-Zr (7.5, 2.5 wt.%), texture development role in shape memory effect 79−87661
U_3Si, tensile ductility from 25 to 320°C 79−74225
V, different grain sizes, room temp. microstrain *(German)* 77−36614
V-H, H effect on tensile props. at moderate temps. *(Japanese)* 78−19831
V-Nb, mech. props., −196-1000°C, comp. depend. 78−39847
V-Ta, mech. props. 79−61682
V_3Si single cryst., A-15 compound supercond., plastic deform., at high temp. 79−20104
W, strain induced damping, micro- and macro-, and dislocation structures in single crystals 78−19797
W, viscoelastic wave propagation model at near-melt conditions, electron-photon impact energy deposition 79−77002
WC-Co cemented carbide, stress-strain curves using ultrahigh-pressure apparatus 79−43322
WC-Co hard alloy composite, calc. of weakest link in struct. 80−11730
WC-Co hard alloy-steel welds, effect of intermediate layer composition on structural changes and mechanical properties 78−60616
Zircaloy 2, mechanical equation of state, stress relax. meas. 78−52880
α-Zircaloy, strain ageing at 1000K 79−47725
Zn, hydrostatically compressed single crystal, work hardening studied by stress relax. method 79−20069
Zn, incompatible bicrystals, effect of grain boundaries on mech. props. *(Japanese)* 78−39798

stress/strain relations continued
Zn, oriented polycrystals, tensile behaviour under hydrostatic press. *(Japanese)* 77−52417
Zn, pure single cryst., fracture stress 80−104269
Zn single crystals, temp. and strain rate effects on strength, slip and twinning 80−16373
Zn, thermal recovery and stress-strain relations 78−11266
Zr, acoustic emission during deformation, expt. 77−73425
Zr alloys, creep and growth, irradiation induced, rate theory approach 80−89294
α-Zr, creep stress charact., 300-900K 77−66675
Zr, deformed at 77K, effect of fast-neutron irradiation on deformation twinning, TEM and optical microscopy obs. 79−37741
α-Zr, strain ageing at 1000K 79−47725
Zr-Al (8.6 wt.%), fast neutron irradiated, tensile props. and fracture toughness 80−84994
Zr-CR (1.9 wt.%), β-quenched and tempered, tensile props. rel. to tempered conditions, SEM study 79−66109
Zr-Cu (1.6 wt.%), mechanical equation of state, stress relax. meas. 78−52880
Zr-Dy dil. alloys, plastically deformed, mech. props. and microstruct. *(Russian)* 79−20112
β-Zr-Mo oxidised alloys, high temp. deformation, X-ray study 79−79045
Zr-Nb (1 wt.%), static strain ageing between 295 to 773K, TEM obs. of plastic strain 79−38855
Zr-Nb (2.5 wt.%), pressure tubes, irrad. creep and growth, anisotropy factors 80−97536
β-Zr-Nb(Cb) alloys, anneal hardening and flow softening 79−78993
Zr-Sn (1.5 wt.%), martensitic transform. contrib. to strength and work hardening, and martensite flow props. 78−84842

stresses, internal *see internal stresses*

stretch receptors *see mechanoception*

striations *see discharges (electric)*

striking *see impact (mechanical)*

strip line components
coupled Josephson junctions, microwave response *(Japanese)* 77−69454
Mach-Zehnder waveguide modulators in Ti-diffused $LiNbO_3$ 80−33203
microstrip antennas for biomedical applications of microwaves 80−3762
microstrip microwave biological exposure system 80−89924
planar dielectric waveguide, interacting discontinuities, anal. 79−27445
pulse shaping using laser-excited solid-state plasmas in Si, expt. 77−19397
SAW bandpass filter using fanned multistrip coupler 77−50837
SAW multistrip coupler, superposition model 80−74674
two-dimensional wave beam diffraction by stripline grid 80−87273
SbSI single crysts., nonlinear dielec. effects and microelectronic applics. 77−43944

strip lines
antennas, asymptotic expansions for Sommerfeld integrals 80−14272
asymmetric strip transmission line, with PbTe wall, EM wave propag. in mag. field 77−76854
dielectric small standing wave ratio and losses meas. 80−77811
diffraction on slit and on strip, scatt. pattern calc., asymptotic methods 78−86993
EM strip transmission line energy coupler, for medical diagnostic appls. 80−17045
EM wave propag. in strip transmission line in magnetic field 77−28552
enclosed dielectric microstrip, Schelkunoff analysis *(Spanish)* 80−45005
light beam streaking by electro-optically induced travelling lens 79−46045
microstrip, static field problems of dielectric objects, moment formulation 77−3512
microstrip, use in programmable delay line 79−26845
microstrip anisotropic electrostatic field problems, Green's function technique 78−70998
microstrip waveguide, theory of radiated waves using asymptotic wave diffr. theory 79−18339
mode structure influence on submillimetric-wave spectroscopy 79−30586
multimode optical waveguide propagation and interference effects *(Japanese)* 78−46764
optical, modal charact. 77−3661
optical, theory and numerical anal. 77−79956
optical stripline waveguides, dispersion charact. and radiation fields 80−64155
self-filtering S-type strip waveguides 80−33219
semiconductor, submillimetric magneto-optical props., strip line technique 80−60554
superconductive, mag. field fringing effect 78−72306
three-layer heteroepitaxial struct., strip waveguide optimum width *(Russian)* 77−7200
KD_2PO_4, ultrafast electro-optical modulator design and application 77−19432
$LiNbO_3$, diffused waveguide for acoustooptical signal processing 79−90029

stripping reactions
1p shell nuclei, DWBA applicability to stripping reactions, ladder diagram summing *(Russian)* 79−30818
A=16-40, α-spectroscopic factors between ground states, shell model prediction 79−13204
A(d,p)X, stripping at relativistic energies, Glauber theory 77−30540
absolute normalisation of (t,d) and (^{3}He,d) reactions, comparative DWBA anal. 77−14143
(d,n) on Be, C, Al, Ni, Cu, Mo, Ta and Pb, secondary neutron emission charact. 79−30843
(d,p) off-shell effects 78−62545
deuteron breakup and stripping, three-body model 79−515
deuteron scattering from N-body scatt. theory, approx. three body model 79−75934
deuteron stripping and breakup, adiabatic theory 77−18512
differential cross sections meas. by SPES I 79−75983
double stripping core independ. 2-nucleon transfer, Tang-Herndon effective interactions, (α,d), (t,p) 80−73836
eikonal approx. and distortions in heavy particle stripping mechanism *(Russian)* 78−78337
few body systems, anal. coupling constant continuation for resonance and stripping reactions *(Russian)* 80−13435
form factors anal. 78−21538
heavy ion inelastic scatt., stripping-pick-up mechanism, coupled channel theory 78−54784

stripping reactions continued
heavy ion stripping and pickup reactions on closed shell nuclei, level shifts, DWBA 80−91168
light nuclei, backward scatt. of d, ^{3}He and α-particles, heavy-particle stripping 78−13107
light nuclei, m-particle n-hole struct. from few nucleon transfer reactions, review 78−50062
light nuclei (p,π^+) reactions, π distortion effect on asymmetry 78−50176
model-independent spectroscopic information, use of spectroscopic factor and vertex constants 78−17168
multi-nucleon transfer and direct reactions, nuclear struct., review 78−50060
resonance reactions, off-shell in terms of resonant states 77−65217
single particle, two-body effective forces in light and medium nuclei 77−88049
two nucleon transfer, RPA theory, pairing vibrs., and extended basis shell model 79−481
(d,d) elastic and inelastic, diffraction scatt. theory, d dissociation and stripping reactions 79−6633
(d,p), 1.7-15 MeV, rearrangement collisions three body model, bound state approx., DWBA calcs. 79−93595
(d,p), approximate DWBA methods 77−14137
(d,p), Tabakin pot. calcs., differential cross sections, ang. distribs. 78−611
(d,p) reactions, stripping of relativistic deuterons, Glauber theory 78−94014
(d,p) reacts. at intermediate energies, triangle graph model 80−27616
(d,p) stripping reaction test from (p,π^+) 79−85436
(d,p) stripping reactions, energies below Coulomb barrier, theory 77−6394
d stripping, as two-body rearrangement collision, effect of continuum contribution 79−13262
d stripping, inclusive p spectrum, d wave function behaviour 79−17884
d stripping cross sections to a resonance, exact and DWBA anal. comparison 78−93985
(dx) breakup on nucleus, adiabatic treatment stripping and forbidden transition cross section 80−9299
(p,2p) reaction for slightly deformed nuclei 77−57657
(t,p), two-nucleon stripping reactions with Tabakin pot. 78−21570
(t,p) stripping reactions, repulsive-core effects, Tabakin potential 77−30607
t+nucleus, form factors for two-nucleon stripping process wth Skyrme potentials, DWBA 78−58287
^{27}Al(α,t), 25 MeV, DWBA anal. of triton ang. distrib. meas. 78−54776
^{27}Al(d,p)^{28}Al, 1.5 to 3.0 MeV, excitation functions 79−40932
^{27}Al(d,p)^{28}Al, 3.1 MeV, high spin states of ^{28}Al anal. 77−74856
^{36}Ar(d,p), Tabakin pot. calcs., differential cross sections, ang. distribs. 78−611
^{40}Ar(d, p)^{41}Ar, 1.354 MeV, spectroscopic factor comparison with isobaric analogue reson. 79−30787
^{10}B(p,π), microscopic model anal., stripping model test for (d,p) 79−85436
^{11}B(^{3}He,n)^{13}N, ang. distrib. at energies below Coulomb barrier 79−40938
^{9}Be(^{3}He,n)^{11}C, ang. distrib. at energies below Coulomb barrier 79−40938
^{9}Be(d,n) 83.7 MeV, 0° neutron spectra, comparison with Serber model calcs. 77−6400
^{11}Be(^{3}He,n_0)^{13}N, 5-12 MeV, excitation function and ang. distrib. 77−54231
Be(d,n), stripping-theory anal. of thick-target neutron prod. 77−6600
^{12}C(^{14}N,^{10}B)^{16}O, DWBA anal., spectroscopic factors 79−6673
^{12}C(^{6}Li,α)^{14}N, 33 MeV, multiple reaction mech., exact finite range DWBA calcs. 78−25231
^{12}C(^{6}Li,d)^{16}O, 42 MeV, α spectroscopic factors, reduced widths, stellar He burning 78−89897
^{12}C(d,p_0)^{13}C, proton polarisation in stripping reaction, obs. and DWBA calc. 79−30816
^{12}C(d,p)^{13}C, 1.5 to 3.0 MeV, excitation functions 79−40932
^{12}C(p,^{6}Li)^{7}Be, 51.9 MeV, heavy particle stripping process 78−46058
^{12}C(p,π^+)^{13}C, π distortion effect on asymmetry, polarised protons 78−50176
^{12}C(τ,d), 36 MeV, ^{12}C+p resonance line shapes 79−59076
^{40}Ca α-spectroscopic factors, direct α-stripping, zero range DWBA anal. of ^{36}Ar(^{6}Li,d) 79−45157
^{40}Ca(^{11}B,^{10}B), 51.5 MeV, n stripping, DWBA anal. with Woods-Saxon and double folding optical pots. 80−102171
^{40}Ca(t,p)^{42}Ca, form factors for two-nucleon stripping process wth Skyrme potentials, DWBA 78−58287
^{40}Ca(t,p)^{42}Ca, two-nucleon stripping process with effective interactions 78−610
Ca(d,p), A=40, 48, Tabakin pot. calcs., differential cross sections, ang. distribs. 78−611
^{40}Cd(d,p)^{41}Ca, 11 MeV, effect of Skyrme type density depend. effective pots. 78−46069
^{116}Cd(d,n)^{117m,g}In, excitation functions 78−13105
^{246}Cm(t,p)^{248}Cm, 17 MeV, shell gap obs. 77−46174
^{59}Co(α,t), 25 MeV, DWBA anal. of triton ang. distrib. meas. 78−54776
^{59}Co(d,p), ^{60}Co low lying states, DWBA anal. 78−29478
Cr (d,p), A=50, 52, 54, Tabakin pot. calcs., differential cross sections, ang. distribs. 78−611
^{52}Cr(d,p), 7-11 MeV, coupled-channel anal. 77−18579
^{52}Cr(d,p), cross section, stripping channel effect, coupled channel model, DWBA anal. 77−57676
^{52}Cr(d,p)^{53}Cr, Coulomb stripping, 2.12-2.48 MeV, DWBA anal., spectroscopic strengths 80−516
^{19}F(α,t), 25 MeV, DWBA anal. of triton ang. distrib. meas. 78−54776
^{20}F cross sections and anal. power, compound nucleus contrib. Ericson fluctuations from ^{18}O(d,p), pol. d 80−22803
Fe(^{16}O,^{12}C), A=54,56, high excitation region of ^{58,60}Ni, two- and four-nucleon transfer spectra 79−6675
^{54}Fe(^{3}He, pγ)^{56}Co, 15.15 MeV γ-ray transitions, branching ratios, level lifetimes, spin assignments 79−497
^{2}H(d,p)^{3}H, ^{2}H(d,n)^{3}H, analysing power meas. 78−25204
Hd(α,t), ^{A}Pm, A=143-153, odd-A, spectroscopic factors, shell model anal. 80−78137
(^{3}He, d) and (^{3}He, d̄), stripping reactions, zero range normalization factors 79−75956
^{204}Hg(^{3}He,n) 33.3 MeV, cross sections, DWBA anal. for data near Z=82 79−67733

stripping reactions continued
^{84}Kr(d,p), polarised and unpolarised d, ^{85}Kr level struct. and spectroscopic factors 79−471
^{86}Kr(d,p), polarised and unpolarised d, ^{87}Kr ground state spin assignment 79−471
(^{6}Li,d), ground state transitions in 1f-2p shell, 34 MeV, spectroscopic factors 79−6670
^{24}Mg(p,p′), 40 MeV, two step pickup-stripping process, negative parity states 80−32256
^{26}Mg(^{18}O,^{14}O), 87 MeV, cross section of stripping reaction, ^{30}Mg mass excess 79−3075
^{26}Mg(d,p), 3.1, 3.5 MeV ^{27}Mg energy levels, spectroscopic factors, DWBA, Hauser-Feshbach anals. 80−52581
^{98}Mo(^{3}He,d)^{99}Tc level struct., spin-parity assignments 78−8743
^{98}Mo(^{3}He,d)^{99}Tc at 18 MeV populating low-lying states 77−22894
^{14}N(d, p)^{15}N, 12 to 52 MeV, stripping reaction anal., distorted wave method 79−80948
^{14}N(d,p$_0$)^{15}N, 52 MeV, DWBA and impulse approx. anal. 77−34318
^{15}N(d,p)^{16}N off-shell effects 78−62545
^{23}Na(d,p)^{24}Na, 1.5 to 3.0 MeV, excitation functions 79−40932
Nd(^{2}He,d), ^{A}Pm, A=143-153, odd-A, spectroscopic factors, shell model anal. 80−78137
^{20}Ne(d,p), 10-12 MeV, pol. d, ^{21}Ne states cross section, anal. power, coupled channel and fluctuations anal. 80−27617
^{20}Ne(d$_{pol}$,p), 10 MeV, ^{21}Ne deduced spectroscopic factors, levels and anal. powers 80−83087
^{60}Ni(^{18}O,^{18}O′), stripping-pick-up mechanism, coupled channel theory 78−54784
^{237}Np(d,p) 12 MeV, ^{238}Np energy level scheme determ. by Nilsson model 79−26370
^{16}O(^{3}He,p), 18 MeV, ang. distribs., DWBA anal. 77−34325
^{16}O(^{6}Li,d)^{20}Ne, 43 MeV, α spectroscopic factors, reduced widths, stellar He burning 78−89897
^{16}O(d,X), X=d or N, elastic scatt. and stripping, three body calc. 80−91165
^{16}O(d,p), 12 MeV, stripping reaction differential cross section, d distortion effect *(Japanese)* 80−22796
^{16}O(p,π^+)^{17}O, polarised protons, π distortion effect on asymmetry 78−50176
^{17}O, cross sections to ground, 0.87 and 5.09 MeV states, neutron strength from ^{16}O(d,p) 80−5066
^{17}O(^{6}Li,d) 32 MeV, α-stripping, ^{21}Ne α-spectroscopic strengths and level J$^{\pi}$ assignments 79−516
^{A}Pb(^{3}He,n), A=204,206,208, 33.3 MeV, cross sections, DWBA anal. for data near Z=82 79−67733
^{204}Pb(d,p), 13.0-20.0 MeV, populating ^{205}Pb hole states below MeV 2.56 77−30478
^{204}Pb(d,p) 13.0 MeV, populating ^{205}Pb particle states 77−34216
^{207}Pb(d,p), 26.2 MeV, ^{208}Pb 7064 keV level negative parity, EM deexcitation pattern 79−36148
^{208}Pb(^{16}O,^{12}C)^{212}Po, semiclassical anal. of α-transfer, calc. of angular distrib. 79−6672
^{208}Pb(^{6}Li,d), 90 MeV, alpha-cluster transfer from alpha-decaying nuclei 80−91166
^{208}Pb(d,p), polarised d, tensor anal. powers, sub-Coulomb stripping calc. corrections 79−80918
^{208}Pb(d,p)^{209}Pb, 9.0 MeV, effects of d D state determ. 77−67752
^{208}Pb(p,π), microscopic model anal., stripping model test for (d,p) 79−85436
^{A}Pm, A=143, 145, proton states and transitions, stripping strength, shell model anal. from Nd(^{3}He,d) 80−68508
^{210}Po(d,p), 17 MeV, ^{211}Po deduced levels, J$^{\pi}$ assignments, spectroscopic factors 79−22197
Pt(^{3}He,d), A=194, 196, 198, 41.2 MeV, stripping strength, Au excitation energies, high spin states 78−78398
^{A}Pt(^{3}He,n) A=194,196, 33.3 MeV, cross sections, DWBA anal. for data near Z=82 79−67733
Pt(α,d), A=194, 196, 198, 35.1 MeV, stripping strength, Au excitation energies, high spin states 78−78398
^{32}S(d,p), DWBA anal. converging overlap integrals, stripping to decaying states 79−6530
^{45}Sc, n transfer, spectroscopic sum spin dependence for stripping and pickup 79−36219
^{45}Sc(d,p), absolute normalisations from spin depend. sum rule anal. 78−8828
S(d,p), A=32, 34, Tabakin pot. calcs., differential cross sections, ang. distribs. 78−611
^{28}Si(^{15}N,^{14}N), 44 MeV, n stripping, DWBA and coupled channel anal., two step processes 79−6552
^{28}Si(^{15}N,^{14}N), 44 MeV, modified optical pot. from backward elastic scatt. 80−32255
^{28}Si(^{3}He, ^{2}He), 52 MeV, ^{29}Si levels, J$^{\pi}$, spectroscopic factor, DWBA anal. 80−86811
^{28}Si(d, p)^{29}Si$_{g.s.}$, 12.1 MeV, vector polarization transfer coeff., deuteron D-state effect 77−14135
^{28}Si(d,p), 8.05 MeV, stripping reaction differential cross section, d distortion effect *(Japanese)* 80−22796
^{28}Si(d,p), Tabakin pot. calcs., differential cross sections, ang. distribs. 78−611
^{28}Si(d,pn), ^{29}P and ^{29}Si nucleon unbound states, spin, parity, partial width 80−102118
^{28}Si(d,pn) 10-11.8 MeV, p-n ang. correl., unbound states, DWBA anal. 77−6236
^{148}Sm(^{16}O,^{12}C), comparison of reduced widths derived from transfer reactions and α-emitters, DWBA anal. 79−6671
^{148}Sm(^{18}O,^{16}O)^{150}Sm, 2_1^+ ang. distributions, shape difference between pickup and stripping reaction 78−33209
^{120}Sn(α, p), semi-microscopic spectator model 77−26779
Sr isotopes, $1g_{9/2}$ nucleon-transfer reactions, nucleon radical distrib. 78−50068
^{88}Sr(d,p), two step processes, excitation of core coupled states, in ^{87}Sr 77−88150
^{130}Te+^{28}Si, 140 MeV, mechanism of four nucleon transfers in heavy-ion reactions 79−6674
^{232}Th(^{3}He,n), 33.3 MeV, cross sections, DWBA anal. for data near Z=82 79−67733
^{49}Ti, p transfer, spectroscopic sum spin dependence for stripping and pickup 79−36219
^{51}V(α,t), 25 MeV, DWBA anal. of triton ang. distrib. meas. 78−54776
Zn to Ni even isotope transition, α-particle spectroscopic factors, shell model calcs. 79−6385

stripping reactions continued
^{96}Zr(d,p)^{97}Zr, 5.5 MeV, effects of d D state determ. 77−67752
^{96}Zr(t,p), 20 MeV, short range correlations with Tabakin pot. 78−13115

stroboscopes
see also velocity measurement
electron microscope, stroboscopic subnanosec. illumination for thin film magnetic reversal obs. 77−18138
holographic interferometry, stroboscopic, for mech. vibrs. anal. in industrial environment 79−32422
holographic interferometry, stroboscopic, vibr. anal. with space-variant phase 77−58296
holographic interferometry, stroboscopic analysis of asymmetric membrane vibrs. 78−66786
holographic interferometry for vibrations investigation, beam modulation methods *(Polish)* 79−3649
installation for luminescence decay curve recording of crystals and glasses 77−74512
interferometer, stroboscopic, dynamic optical component evaluation, remote-site operation 79−85164
interferometry, stroboscopic, active mirror testing appl. 79−58782
LED, use as short duration stroboscope, appl. to ultrasound visualisation 77−14863
magneto-optical stroboscope for thin magnetic film pulsed magnetic reversal studies 78−4667
magneto-optical stroboscope with pulse height analyser for rapid magnetisation variations 79−67356
magnetometric stroboscopic instrument for plotting hysteresis loops, 400 Hz-50 kHz 77−71350
meter for photosensors time characts., using programmed strobing of anal. zone 78−283
multichannel nanosecond pulse generator for cyclotron stroboscopic system 79−68168
optoacoustic interactions obs. method 78−94498
particle size distribution meas., online stroboscopic microscope apparatus 80−101783
perceived motion condition for temporal facilitation, stroboscopic motion 79−53132
picosecond diagnostics of rapid processes 78−47159
pointer instrument freq. response determ. appl. *(Polish)* 78−29102
polymer film, dimensional changes meas. using stroboscopic-disk tester 79−17386
principle, design and appl. 78−55453
sampling stroboscopic convertor identification by Hammerstein model *(Russian)* 80−74495
SEM GHz stroboscopy 78−89606
strobe light with variable pulse length over 22-360 Hz frequency range 80−58716
stroboscopic TV study, interaction of two high-velocity gas jets 78−42695
US delay line trimming using stroboscopic method of signal-to-time conversion 80−19191
vibrations, strobohолographic method of investigations 77−54681
Nz pulsed laser stroboscopic fluorimeter 80−35593

strong-coupling superconductors
A15 compounds, max. T_c due to electron-photon scatt. 78−91801
A15 compounds, new aspect of superconductivity, Fermi level rel. to electron-phonon interaction 79−7927
A15 superconductors, supercond. and phonon softening in unstable systems 79−65587
A-15 compounds, coupling strength 79−19684
A-15 compounds, numerical soln. of Eliashberg, eqn. 77−59351
calorimetric properties, small changes meas. using direct difference technique 77−33988
critical temperature formula discussion *(Chinese)* 80−7017
dilute alloys, eqn. for crit. temp. 78−72300
dispersion ratio for tunnel density of states, analytic props. *(Russian)* 77−39995
electronic density of states, variation effect on transition temp. and effective mass. 80−75672
Eliashberg eqn. soln. for transition temp. *(Chinese)* 78−26985
Eliashberg eqns., numerical solns., Fermi surface calcs. 77−1514
Eliashberg equation soln., supercond. transition temp. 77−39996
Eliashberg equation solution and series expression for T_c 78−31013
Eliashberg equations at zero and crit. temps. 78−34919
EM properties, supercurrent density and penetration depth temp. depend. 77−24634
films, thick, phonon damping of virtual levels 79−4626
high T_c superconductivity, theory 78−14870
isotope effect, theory 78−91806
LF EM response function 78−10605
metal, exchange enhancement of electron-phonon coupling 78−47968
metal hydrides, anharmonicity and superconductivity 77−15988
metal-insulator-metal-superconductor junction, phonon struct., proximity effect tunnelling 79−82721
pressure coefficients of critical field, Ginzburg-Landau parameter, penetration depth 80−54833
proximity effect, McMillan tunnelling model 79−73639
quasiparticle and phonon lifetimes, theory 77−20488
spatial variance extension of strong-coupling superconductivity theory *(Chinese)* 79−11265
superconducting short bridges, critical current depend. on high. freq. field 80−44774
thermal expansion in supercond. state based on weak coupling BCS theory 78−80094
thin film, critical mag. field *(Chinese)* 80−54849
transition metal alloy, binary, conc., superconductivity and electron-phonon interactions, theory 78−14868
transition temp., Eliashberg theory 78−2614
transition temperature, local field effects, theory 78−14848
transition temperature, strong coupling theory, appl. to ^{3}He 78−47629
transition temperature eqn. 80−25032
US attenuation, finite-freq. 77−51846
Ag film-Pb sandwich, supercond., effective renormalisation interactions 79−56397
$Bi_3Sr_{1-x}Eu_x$, supercond. and mag. ordering 78−56252
CuCl, high-temp. supercond., BCS strong-coupling limit for transition temp. 80−2511
$Cu_{1.8}Mo_6S_8$, electron tunnelling spectroscopy expts. *(German)* 80−107966
Hg, finite-freq. US attenuation calc. 77−51846

strong-coupling superconductors continued
In-Mn, dil., film, ion implanted, supercond, and mag. props. 77−15987
La, DHCP and FCC phases, phonon density of states 78−67791
La_3S_4, high crit. mag. field supercond., elec. resist., sp. ht. and magnetisation 80−2532
$Mo_{1-x}Tc_x$, BCC, sp. ht. in normal and supercond. phases 79−87190
Nb, electron-coupled phonon spectrum, effects of strain 79−7943
Nb, proximity electron tunnelling spectroscopy 80−107964
Nb, strong-coupling microscopic parameters, electron tunnelling obs. 78−14888
Nb, upper crit. field, temp. depend. and anisotropy 80−80462
$Nb_{0.75}Zr_{0.25}$, effect of force constant, disorder on Eliashberg function 80−29504
Pb-In, electron tunnelling under hydrostatic press. 77−51850
Pb-Sn(Bi), dirty strong-coupling supercond., Ginzburg-Landau parameters, type II behaviour deviations 77−8249
$Pb_{0.9}Bi_{0.1}$, lifetime-broadened energy gap edge, tunnelling of junction 79−15259
$PbMo_6S_8$, electron tunnelling spectroscopy expts. *(German)* 80−107966
Pd-H, supercond. and phonon softening in unstable systems 79−65587
$TaS_2(2H)$, supercond. transition temp., upper crit. field, and interlayer coupling strength 79−56406
Tl films, supercond. amorphous, effective phonon spectrum and lattice sp. ht. 80−70895
Tl-Pb-Bi, critical field and specific heat 79−73631
YRh_4B_4, supercond., anomalous cond.-electron polaris. 80−25047

strong interactions, elementary particle *see elementary particle strong interactions*

strontium
see also nuclei with .....
abundance anomalies and p-process odd-A abundances 78−93101
adsorption by Al_2O_3, radioactive waste storage 80−99240
adsorption on anodised Al, prep. of radiation sources 79−36454
adsorption on Mo(112), interaction of adatoms 79−7754
adsorption on W and Mo (011) face, influence of substrate electronic struct. on props. 78−60032
atom, 2 keV electron excitation and ionis., ejected electron spectra 77−3466
atom, 4607.33 Å line, broadening and shift in H_2-O_2-Ar flames 77−18849
atom, 4607.33 Å resonance line, spectral width depend. on at. density in flame 77−46535
atom, 4607.3 Å resonance, collision broadened, due to laser beam interaction, anal. 78−42006
atom, 4607 Å reson. line shape, width and shift in Ar, press. depend. 79−22653
atom, 4607 Å resonance emission line, wing profile meas. 77−46534
atom, 5^1P state quenching cross sections in CO-N_2O flames 77−18836
atom, $5p^2\ ^1D_2$ level lifetime 79−63960
atom, autoionisation reson. states elec. field depend., three-photon ionisation 78−33478
atom, autoionising Rydberg states, doubly excited, by tunable dye lasers 78−33479
atom, bound even-parity J=0 and J=2 states, multiphoton ionisation spectra 77−71789
atom, bound odd-parity J=1 spectra, multiphoton excitation 79−54795
atom, diamag. quasi-Landau spectrum near ionis. threshold, two-photon ionis. spectra obs. 78−58642
atom, direct meas. of excited state lifetimes 77−65435
atom, double multi-photon ionisation *(Russian)* 77−71786
atom, efficient ionis. by reson. laser pumping 80−32685
atom, electron impact excitation, from metastable states 78−1084
atom, electron impact ionisation cross-section, calc. *(Russian)* 79−89789
atom, electron scatt., autoionis. states electron spectra *(Russian)* 79−36779
atom, excited state lifetime, delayed coincidence meas. 77−3315
atom, in $SrCO_3$, study of 4d excited states 77−26989
atom, $K\beta/K\alpha$ rel. intensity obs. 80−32665
atom, L-shell soft X-ray emission spectra, oscillator strengths 80−32651
atom, lifetime meas., stepwise excitation by pulsed dye lasers 77−83536
atom, metastable, prod. in N_2O-CO flame, u.v. spectra 77−9081
atom, multichannel quantum defect theory anal. to predict Ra states 80−52918
atom, multiphoton ionis. spectroscopy of even- and odd-parity states 78−86973
atom, multiphoton ionisation spectra of msnp$^3P^0$ states 77−83554
atom, near reson. laser beam Rayleigh scatt., collisional redistrib. and saturation 77−57938
atom, quadratic Zeeman effect, diamagnetic shift, Rydberg series, strong field mixing 78−946
atom, reson. lines, emission and absorpt. core profiles 77−50389
atom, Rydberg series, absorpt. by selectively laser-excited atoms 79−3390
atom, Rydberg states, $^1D_2 \rightarrow {}^1F_3$ microwave transition meas. using selective reson. ionisation 79−72258
atom, Sr, ejected-electron spectrum, Auger levels, autoionisation 79−22843
atom, strong correl. in 3d-Auger spectrum 78−50522
atom, Zeeman effect of J=2 states, g-factor, interacting Rydberg series 78−17609
atom X-ray spectra, mass absorpt. coeffs. in ultrasoft region, spectral depend. 77−10622
atomic and ionic spectra 79−59388
atomic quasi-Landau spectrum, semiclassical strong field mixing models 80−63847
atomic vapours, effects of magnetic fields on four-wave mixing processes 79−23024
atoms, excitation series, potential barrier effects, single configuration HFC 80−78558
atoms, fluoresc. excitation profile, laser saturation broadening in flames 80−95568
atoms, quantum defect param., ab initio calcs. 80−78525
atoms and ions in discharge, temp. and conc. determ, by spectral line shapes *(Russian)* 78−14214
basalt isotopic abundance, Earth struct. models 80−72475
basalt isotopic and element composition, Reykjanes Peninsula, Iceland 80−21725
behaviour in subsurface $CaCl_2$ brines, model, Dead Sea rift valley 80−17295

strontium continued
buffer action, in at. absorpt. spectrosc. of alkaline earths, mechanism *(Russian)* 79−29441
calc-alkaline rocks from the East Carpathians, K, Rb and Sr distrib. 78−85555
chemi-ionisation reactions of Ca, Sr, Ba, and Yb with halogens and interhalogens 77−32791
coral aragonite Sr/Ca ratio, ocean temp. determ. 80−12568
determination, by X-ray fluoresc., for radiometric age meas. 77−70356
determination in bauxite, X-ray fluoresc. method 77−36849
diffusion in Bi, mechanism 79−77819
diffusion in bitumen block coating, radioactive waste treatment *(Russian)* 80−52771
diffusion in graphite, lab. determ. 77−7900
diffusion in KCl simultaneously with Ca 78−79813
Duxbury massif (2.5 Ga), Quebec, initial $^{87}Sr/^{86}Sr$ rel. to remobilised pre 3.0 Ga sialic basement hypothesis 80−76970
Earth mantle, Nd-Sr isotope correl. and constraints on continental crust comp. and nature of lower crust 80−94498
Earth mantle materials, Nd-Sr isotopic correl. and geodynamic consequences 79−92512
electrical resistivity; 1-1000K, data tables 79−78073
electrical resistivity and thermopower, meas. at melting temp. 79−99524
enthalpy of solution, 298.15K, rel. to SrO heat of formation determ. 78−61041
film, photoemission, action of elec. field 77−48317
film, structure effects on work function, electron micrographs and photoemission meas. 79−83107
Floridan Aquifer rocks, Sr content rel. to dolomitisation 79−53346
forced-flow chromatography, detection by photometric method 80−71965
four-wave mixing production of CW VUV coherent radiation 80−58640
fuel reprocessing waste ^{137}Cs, ^{90}Sr and rare earth radioisotope separation by cation exchange 78−78486
granitoid rocks, Nd-Sr isotopic relationship and continental crust development, chemical approach to orgogenesis 80−94522
ion recombination laser 78−17923
ions, adsorbed on porous SiO_2 glass in distilled water medium, determ. 79−24814
isothermal diffusion in KCl 77−47625
isotope anomalies in Allende meteorite 78−89133
isotope comp. of Pacific Ocean Basin basalts, rel. to mantle comp. 78−65218
isotope data and crustal contamination model for calc-alkaline igneous rocks 79−79762
isotope evidence concerning petrogenesis of N.Chilean ignimbrites 79−44146
isotope evidence for petrogenesis in Mexican andesites 78−28203
isotope excretion in man, comparison of stable Sr, ^{85}Sr and ^{90}Sr 78−24153
isotopes conc in ocean floor basalts and ferromanganese deposits 78−61395
isotopic evolution in W.Greenland-Labrador craton, early Rb depletion in mantle 78−69304
isotopic studies in Indian kimberlites 79−92536
K shell photoelectric cross section, at 74.409 keV 79−72288
laser action mechanism due to 3066.2, 3011.1 nm $4d^3D_{1,2}$-$5pP^0_2$ transitions 80−9869
laser spectroscopic anal. of Rydberg series, multichannel quantum defect theory 80−18815
lattice dynamics, phenomenological model 80−44265
leaching rates from calcined natural zeolites *(Japanese)* 77−67828
leaching rates from calcined zeolites, radioactive waste processing *(Japanese)* 77−61515
liquid, density meas. at intermediate temps., method employs Archimedes' Principle 78−22784
low-level transuranic storage, radwaste Sr, Cs, Co sorption meas. on soil sediment 80−95482
metallic compressibilities, general pseudopotential approach 80−54631
nepheline syenite, dating, Rb-Sr internal isochron, ^{39}Ar-^{40}Ar plateau age methods *(French)* 78−32031
neutron activation anal., 14 MeV neutron cross sections 79−52838
photoionisation, 3d subshell absorption spectra 77−10648
PIXE anal. method 77−63973
plasma temp. diagnostics from linewidth, inductively coupled plasma 77−43083
plasmon excitation by oblique incidence of primary electron beam of medium energy 78−18987
radiative decay of autoionisation states *(Ukrainian)* 78−82682
radioactive waste, low-level, radionuclide migration in soil 79−54610
radioactive waste solidification, leaching behaviour of ^{90}Sr 78−37416
radioactive wastes, leach behaviour of hydrofracture grout 77−10478
radionuclide migration from low-level waste burial site 78−21671
recrystallisation of wires and filings by thermal processing encapsulated in metal tubulation 77−59810
separation from potash salts, ion exchange methods *(German)* 78−23940
skin transport, role of diffusion 78−20158
solution in liq. Na, elec. resistivity conc. depend. 78−84188
specific heat and thermodynamic props. 5-350K 78−47534
Sr I, II pulsed laser transitions, power characts. 79−10290
submonolayer film, on W (011) or Mo (011), disordering, LEED obs. *(Russian)* 77−89655
submonolayers adsorbed on Mo crystal, LEED and contact pot. study 80−2271
superradiant emission, visible, on three-level cascade, coupled transitions 80−58493
surface plasmons, excitation 79−28310
transport properties, elec. resist., thermoelec. power, thermal cond. deviations from Matthiessen's rule 78−39086
US attenuation due to phonon-phonon interaction and thermoelastic phenomenon 79−77686
vapour, enhanced production of coherent vacuum UV radiation by four-wave mixing 77−83923
vapour, four-wave sum freq. mixing, vacuum UV coherent radiation generation 79−10350
vapour, generation of tunable 16 μm radiation by stimulated hyper-Raman effect 78−46715
vapour, resonantly enhanced sum freq. mixing, coherence effect 77−88848
vapour pressure below 660K, heat of vaporisation 79−37825
volcanic rock isotopic composition, Grenada, Lesser Antilles 80−21724

strontium continued
volcanic rocks, Sr isotopic comp., role of ancient lithosphere in young continental volcanism 77−2133
water, natural, trace metals, energy dispersive X-ray fluoresc., at absorpt. anals., comparison 77−60175
AgBr:Sr, stress induced anomalies in internal friction, logarithmic decrement 79−66095
AgBr:Sr^{2+}, single cryst., stress-induced migration and aggregation of solute ions, internal friction 79−51200
AgCl:Sr, effect of impurity doping on Sr^{2+} diffusion 78−84002
AgCl:Sr^{2+}, plasticity, impurity hardening effect 78−47466
Al_2O_3-P_2O_5-Mg(Ca)(Sr)O glasses, Na^+, Sr^{2+} diffusion coeffs. rel. to temp. 78−30787
Ba, oxidation, SXAPS 77−73189
Ca, electrical resistivity and thermoelectric power 78−26846
Ca+Sr, laser-induced inelastic collision, fluoresc. obs. 77−54603
CaF_2:Sr^{2+}, localised vibrs. due to substitutional impurities 78−22803
^{137}Cs, in atmosphere, bioindication using needles of common pine tree 79−100550
Eu+Sr, laser induced collisional energy transfer profile, high resolution study 80−83471
Eu*+Sr+hω→Eu+Sr**, photon assisted collisional energy transfer 78−90285
He hollow-cathode discharge, Ba^+ and Sr^+ formation 78−67527
He-Sr, laser plasma, double pulse excitation, singularities *(Russian)* 77−61945
He-Sr laser, possibility of nucl. pumping, 4305 Å Sr II transition 80−58518
He-Sr pulsed laser, pumping rate and electron density meas. 80−9868
KBr:Sr, thermally stimulated luminesc., accompanying recomb. of V_F and F centres 80−55201
KBr:Sr, X-irradiated, first-stage F-centre production 77−76395
KBr:Sr^{2+}, X-irrad., hole Br_3^- centre creation and destruction 77−15411
KBr(Cl):Sr^{2+},Cu^+, thermolum. response, extension of two-step reaction model 80−89075
KCl cryst., Sr and Na impurities radial distrib., influence of form of crystn. front 80−107312
KCl:Ba(Ca)(Sr), microstruct. and hardness, impurity distrib. effects 79−24529
KCl:Ba(Sr), Z-centre, luminesc. and absorpt. spectra obs. 80−49221
KCl:CO_3^{2-}, Sr^{2+}, shift and broadening of local vibr. bands, temp. depend. 78−87755
KCl:Sr, M-centre photoluminesc. *(Russian)* 78−84649
KCl:Sr, mechanical props. as function of dopant conc., dislocations 77−69027
KCl:Sr, microcrystalline powders, role of Z-centres in stabilizing coloration 80−54227
KCl:Sr, positron annihilation and trapping in A-centres 80−84802
KCl:Sr, single crystal, thermally stimulated topochemical reactions 79−28011
KCl:Sr, structural state of impurities, hydrostatic press. effect, thermostimulated depolarisation exam. 77−39614
KCl:Sr, thermally pre-treated, glow curves 80−25470
KCl:Sr, thermally stimulated luminesc. accompanying recomb. of V_F and F centres 80−55201
KCl:Sr, thermoluminescence and colour centre thermal stability in irradiated sample 78−43941
KCl:Sr, triplet state of F_2-centres, ESR spectra 80−29616
KCl:Sr crystal, Z_4 colour centre, luminesc. study 80−64993
KCl:Sr^{2+}, conductivity, self-diffusion, lattice defect props. 77−4216
KCl:Sr^{2+}, defect parameters, self-consistent set, ionic cond. meas. 80−107487
KCl:Sr^{2+}, ionic cond., defect parameters, diffusion coeffs. 80−79978
KCl:Sr^{2+}, polarisation-plastic effect 78−2794
KCl:Sr^{2+}, Sr^{2+} precip., flotation density obs. 78−51690
KCl:Sr^{2+}, strengthening effects rel. to IV dipoles and aggregates 78−55907
KCl:Sr^{2+}, X-irrad., thermolum., impurity aggregation, trapping centre form. 78−88367
KCl:Sr^{2+}, X-irradiated, thermolum. decay, effect of impurity aggregation 77−85814
KCl:Tl^+,Sr^{2+}, electrolytic colouring, colour centre form., optical absorpt. spectra 79−15497
KCl(Br):Sr^{2+}, BeF_4^{2-}, IR absorpt. spectra, impurity cation rel. to degenerate vibr. splitting *(Russian)* 80−2807
KCl_xBr_{1-x}:Sr^{2+}, dielec. loss 77−85646
KI:Sr^{2+}, elec. field effect on mech. of recomb. 78−80397
$LaCoO_3$:Sr, anomalous $^{57}Fe^m$ charge states, Mossbauer study 80−40017
NaCl:Sr, dimer and trimer aggregate formation by NMR, ionic cond. and dielectric losses 80−15094
NaCl:Sr, high temp. phenomena Cottrell effect and thermal decomposition 79−20351
NaCl:Sr, mechanical props. as function of dopant conc., dislocations 77−69027
NaCl:Sr, positron annihilation and trapping in A-centres 80−84802
NaCl:Sr, solubility of free and assoc. Sr by elec. cond. and ionic thermocond. meas. 77−62645
NaCl:Sr deformation control by thermally activated processes 195 to 300K 79−24570
NaCl:Sr^+, ionic thermocurrent exam. 78−10833
NaCl:Sr^{2+}, strengthening effects rel. to IV dipoles and aggregates 78−55907
O_2+Be(Mg)(Ca)(Sr)(Ba), reaction kinetics in diffusion flame 77−90579
Pb-Sb-Sr alloys, corrosion props. by simplex-lattice planning method 77−56148
Rb-Sr dating of Brazilian rocks, appl. of solid-source mass spectrometer 77−70840
Sr atomic beam, time correlations between two sidebands of reson. fluoresc. triplet, multiphoton processes 80−95570
Sr I, 5s-p and 4d-p channel interactions, quantum defect model 77−30810
Sr I, oscill. strength calc. for resonance ^1S-^1P transition 78−90125
Sr I, oscillator strengths for certain transitions 79−18143
Sr I, Rydberg and autoionisation levels, laser ionisation spectroscopy 77−3331
Sr I, strong configuration interaction, multiconfiguration Hartree-Fock calcs. 77−67987
Sr I and II, excited states radiative lifetimes 79−98042
Sr II, ^2F states, fine struct. splitting 78−50494
Sr II, Hanle effect, $^2P_{3/2}$ lifetime determ. 77−18852
Sr II, resonance level lifetime meas. by pulsed laser excitation of ion beam 78−25480
Sr II, stimulated emission depend. on discharge parameters 79−13954
Sr III (IV), UV spectra, 40-100 nm, crossed electron and atomic beams *(Russian)* 78−37580
Sr^+ cyclic ion laser oscillating at 1033 and 1092 nm, single and double pulse expts. 79−22940
Sr^+, electron and ion Stark effects in plasma, widths and shifts 77−46526
Sr^+, hydration, gas phase clustering mass spectra, thermodynamics, bonding 77−16814
Sr^+, inversion and lasing on optically pumped reson. line 78−70798
Sr^{2+}, adsorption on Cu surface, ^{90}Sr tracer expt., immersion time, conc. and temp. depends. 78−87863
Sr^{2+} effect on neuromuscular junction transmitter release during repetitive stimulation 78−3469
Sr^{3+}, spectra, 250-6500 Å 78−62754
Sr-Cs mixture, laser induced collisional two-photon ionisation, fluoresc. monitoring 80−91515
Sr-He, mixture, reson. third harmonic generation 79−27328
Sr-N_2O-CO flame, candidate chem. laser reactions, intracavity dye laser absorpt. meas. 78−63108
Sr-N_2O-CO flame, Sr catalyzed, gain meas., emission band assignment 78−66815
Sr-Nd isotopic var. implications for crustal and mantle chemical evolution 79−66655
Sr-Xe, resonant third harmonic generation anal. 78−90460
Sr+Ca, laser induced collisional and radiative energy transfer 80−53108
Sr+Ca, laser-induced collisions, large cross sections meas. 79−64075
Sr+Ca, laser-induced dipole-quadrupole collision 79−98207
Sr+D(D^+), 2.7 to 31 keV, D^- equilib. charge-state fractions 78−17750
Sr+Eu absorptive collisional energy transfer, laser induced excitation spectra 80−63584
Sr+Eu*, light-induced collisional energy transfer 78−50614
Sr+F_2, crossed beam chemilum., kinetics and mechanisms 80−21264
Sr+HF, endothermic reaction, comparison of effectiveness of vibr. and translational excitation 80−93746
Sr+HF(DF), beam reaction, vibr. excitation 78−68877
Sr+HF→SrF+H, product state distrib., reagent orientation and rot. effect 79−20361
Sr+He, nonstatistical excitation of mag. substates of $^1P_1$ level 78−42194
Sr+He, Sr, $^1P_1$ level lifetime, Hanle measurement 80−23365
Sr+He(Xe), Sr reson. line width, 4607 Å, press. effects, pot. well depths 79−89643
Sr+He(2^3S_1), coherent $^2P_{3/2}$ levels excitation by Penning ionis., Hanle effect 80−5520
Sr+He($2s^3S_1$), alignment of ions in Penning collisions, polarised emission obs. 80−23533
Sr+inert gas, $^1P_1$-$^3P_1$ excitation transfer 80−102559
Sr+N_2, $A^3\Sigma_u^+$ state, vibr. excitation 80−1054
Sr+N_2O+CO reaction, intracavity dye laser spectroscopy 77−86293
Sr+S_2Cl_2→S_2*+$SrCl_2$, rearrangement reaction, crossed-beam chemiluminesc. 77−29009
Sr^++inert gas atom collision, polarisation of emitted radiation, quasimol. interf. effect *(Russian)* 77−46633
Sr_2 dimer, photoassoc., photoluminesc., collisional dissoc. 80−58303
Sr_2, low-lying states binding energy, local spin density functional formalism calcs. 79−97994
Sr_2, matrix isolated, vis. and near IR spectra 78−5214
Sr_2, Van der Waals dimer, inert gas matrix-isolated, laser excited emission spectra 78−78744
Sr_2^+, associative ionisation of laser-excited Rydberg states, mass spectrometry obs. 78−94303
SrII, near IR laser transitions in hollow cathode discharge 80−1194
Sr(^3P)+SF_6, F_5S-F bond energy bounds from chemiluminesc. obs. 79−86081
Sr^+($^2P_{3/2}$), Penning ion, polarised emission, Hanle effect obs., radiative decay rate meas. 80−5520
Sr(^1S,^3P)+ halogenated methane, laser induced fluorescence 79−66270
Sr(^1S)+Ar, Sr(^1P) collisional excitation in nonreson. laser field, four-state model 79−10191
^{82}Sr, radioactive, adsorption on alumina column for ^{82}Rb generator prod. 80−12257
^{82}Sr-^{82}Rb biomedical generator, performance obs. 79−53247
^{82}Sr-^{82}Rb generator improvement using inorganic exchangers 80−17135
^{85}Sr, blood flow and tracer uptake in normal and abnormal canine bone 80−17072
^{85}Sr, thermotransport in KCl, Soret effect meas. 77−47624
^{85}Sr, uptake in healing bone fracture rel. to blood flow 80−72187
^{85}Sr, use in revascularisation processes study, local blood flow dynamic anal. 80−81684
^{87}Sr, $^3P_2$ metastable state, hyperfine struct. at. beam mag. reson. obs. 78−17590
^{87}Sr, enrichment in Cyprus ophiolitic sulphides confirms ore form. by circulating seawater 77−81887
$^{87}Sr/^{86}Sr$, geochemistry in hydrous mantle nodules and host alkali basalts 80−56420
$^{87}Sr/^{86}Sr$, in N.Atlantic Tertiary basalts, rel. to magma source regions depletion 79−100821
$^{87}Sr/^{86}Sr$, in rocks of Cantal continental volcanic system, constraints on genesis and evolution 79−88327
$^{87}Sr/^{86}Sr$, initial ratio in Norton County enstatite achondrite 77−5508
$^{87}Sr/^{86}Sr$, initial ratios in Cretaceous kimberlites and mantle xenoliths from S.Africa 77−60372
$^{87}Sr/^{86}Sr$, initial ratios in Late Cretaceous granodiorites, Jamaica and Haiti, Greater Antilles 79−57927
$^{87}Sr/^{86}Sr$, initial ratios in Archaean rocks of English River subprvince, NW.Ontario rel. to crust form. 80−94486
$^{87}Sr/^{86}Sr$, ratios in Cretaceous mid-ocean ridge basalt (MORB) from DSDP Holes 417D and 418A 80−94520
$^{87}Sr/^{86}Sr$, ratios in oilfield brines from Kansas and Colorado 78−57225
$^{87}Sr/^{86}Sr$, ratios in Recent andesites in Ecuador and N.Chile 78−32042
$^{87}Sr/^{86}Sr$, ratios in volcanic rocks of Aleutian and Pribilof Islands, Alaska 78−57185
$^{87}Sr/^{86}Sr$ in Bay of Islands ophiolite complex, rel. to midocean ridge basalts source evolution 80−85651
$^{87}Sr/^{86}Sr$ in calc-alkaline andesites and plateau lavas from S.America 79−29726

strontium continued
$^{87}Sr/^{86}Sr$ in Kerguelen Islands igneous rocks, inferences on enriched oceanic mantle sources 80−98319
$^{87}Sr/^{86}Sr$ in mantle xenoliths, unequilibrated isotopic comp. meas. with equilibrated Nd isotopes 80−98321
$^{87}Sr/^{86}Sr$ in Murrumbidgee Batholith, isotopic equilibration 77−41026
$^{87}Sr/^{86}Sr$ in Norwegian eclogites, rel. to crustal origin 80−76978
$^{87}Sr/^{86}Sr$ in Scottish Caledonian granites, isotopic evidence for crustal provenance 80−109146
$^{87}Sr/^{86}Sr$ initial ratios and Rb-Sr ages, from Oxford Lake-Knee Lake greenstone belt, N.Manitoba 80−94485
$^{87}Sr/^{86}Sr$ ratio for fracture-filling calcite in granitic basement 77−29267
$^{87}Sr/^{86}Sr$ ratio in basalts from Sao Miguel 79−74873
$^{87}Sr/^{86}Sr$ ratio in Central North Atlantic basalts, evidence for Azores mantle plume 77−5179
$^{87}Sr/^{86}Sr$ ratio in Recent continental volcanic rocks 78−53635
$^{87}Sr/^{86}Sr$ ratio in Susquehanna River basin 77−29349
$^{87}Sr/^{86}Sr$ ratio in volcanic rocks from W.Pacific island arcs 77−33031
$^{87}Sr/^{86}Sr$ ratios in calc-alkaline volcanic rocks from Cerro Galan, NW.Argentina, evidence for crustal contamination 80−98318
$^{87}Sr/^{86}Sr$ ratios in Central American andesites, evidence for mantle petrogenesis 79−20833
$^{87}Sr/^{86}Sr$ ratios in granites from British Late Caledonian 80−36276
$^{87}Sr/^{86}Sr$ ratios in magma genesis, mineral phases and parental rocks 77−25671
$^{87}Sr/^{86}Sr$ ratios in Scottish continental volcanics, evidence for crustal contamination 79−66693
$^{87}Sr/^{86}Sr$ ratios of calc-alkaline volcanism rel. to Peru-Chile Trench granulitic basement 78−28204
$^{87}Sr/^{86}Sr$ ratios of interstitital waters from DSPD sites rel. to sediment geochem. 79−34794
$^{87}Sr/^{86}Sr$ systematics of geothermal water-rock association in Massif Central, France 77−60373
$^{87}Sr^{2+}$, aq. ions, nucl. quadrupole relax. 78−64287
$^{88}Sr/^{86}Sr$, thermal ionis. mass spectrometer obs., controllable isotope fractionation *(German)* 80−42299
^{89}Sr assay in aqueous solutions by Cerenkov radiation 79−87895
^{89}Sr behaviour in sediments in laboratory-scale aquatic ecosystem 78−3831
^{89}Sr, diffusion behaviour in SiC, 1650 to 1850°C 78−79814
^{89}Sr distribution between bound and free forms, in vitro meas. of rat soft tissue 78−28095
^{89}Sr therapy of bone metastases of prostatic gland carcinoma 80−36076
^{90}Sr, adsorption on anodised Al, oxide layer thickness, Al purity, temp. depend. studies 79−82458
^{90}Sr, balance in man, effect of P intake 78−15911
^{90}Sr bremsstrahlung radiation meas. for well logging using Ge spectrometer 80−94619
^{90}Sr, conc. variations in Baltic Sea 1973 to 1975 79−92100
^{90}Sr concentrations in pronghorn antelope bones near a nuclear fuel reprocessing plant 80−89875
^{90}Sr, content in E.Sivash waters *(Russian)* 78−77282
^{90}Sr, coyote scats, Hanford Reservation, radioactive waste distrib. 79−25120
^{90}Sr, diffusion coeffs. determ. in HTGR fuel element graphite 79−67869
^{90}Sr diffusion in feldspars, laboratory study 78−7621
^{90}Sr, effect on fetal mouse ovary rel. to time administered during pregnancy 80−51163
^{90}Sr, fast neutron influence on fission product transport in UO_2 pyrocarbon-coated HTR fuel particles 80−42777
^{90}Sr fission reactor waste management, by fusion reactor transmutation 78−70642
^{90}Sr, in atmosphere, bioindication using needles of common pine tree 79−100550
^{90}Sr in human bone, Yugoslavia 77−56490
^{90}Sr in milk and composite diet samples in India 77−86650
^{90}Sr in sample soil and water, distrib. coeff., environmental effects 77−13092
^{90}Sr in W Gulf of Mexico 77−81590
^{90}Sr leached from cemented solid, migration characts. *(Japanese)* 77−42109
^{90}Sr, radiation dose-response curves, hazard function method of resolution 79−66556
^{90}Sr, radiation-induced carcinogenesis, beagle dog obs. 79−66487
^{90}Sr, radionuclide leaching from hardened cement grout, container dimension depend. 79−13439
^{90}Sr, release from irrad. reactor fuel elements *(German)* 79−67871
^{90}Sr removal from ocean waters, adsorpt. on hydrated MnO 78−3822
^{90}Sr, time variation of low concentrations in rain water 79−43994
^{90}Sr, transmutation in high flux fission reactor, feasibility 79−85708
^{90}Sr tropospheric residence time 78−85396
$^{90}Sr/^{90}Y$ radioisotope generator, educational aid 78−78535
$Sr^* + Cl_2$, collision and reaction cross section meas. 79−59537
$Sr^* + Cl_2 \rightarrow SrCl^* + Cl$, chemiluminesc. studies 78−40030
$Sr^* + HCl$, reaction performed under high resolution, luminescence obs. 80−95662
$Sr^* + N_2O \rightarrow SrO^* + N_2$, visible chemiluminescence, absolute cross section and photon yields 78−92463
$Sr^*(^3P_1) + HCl(HF)$, laser-excited atom reaction, energy deposition 78−85134
$Sr(5p\,^1P^0) + Ca(4s^2\,^1S)$, laser-induced inelastic collisions, theory 77−14552
$Sr(5s^2\,^1S_0) + Ca^+(4s\,^2S_{1/2})$, laser induced charge transfer to excited electronic state 79−81274

strontium alloys
see also strontium compounds
Sr-Ti, phase diagrams *(Russian)* 78−80513
Al-Si-Sr phase diagram *(Russian)* 78−15363
Al-Sr-Nd phase diagram *(Russian)* 80−20893
$Bi_3Sr_{1-x}Eu_x$, supercond. and mag. ordering 78−56252
Mg-Sr, liq. alloys, thermodynamic activities determ. 80−50604
Sr containing alloy systems, prep., glass form., thermal props. 79−24461
Sr-Al-Nd phase diagrams *(Russian)* 78−27480
Sr-Al-Si system, phase diagrams construction by simplex designing method 78−6899
Sr-Nd, phase diagram, microstruct., X-ray, chemical and thermal diffusion anal. *(Russian)* 78−52761
Sr-Y, phase diag. *(Russian)* 77−59745
$Sr_2(Co_{1-x}M_x)_{17}$, M=Mn, Ti, Zr, powders, influence of substitutes on mag. props. 80−100601

strontium alloys continued
SrCu, X-ray cryst. struct. determ. 80−92478
$SrNiSn_3$, cryst. struct. rel. to $ThCr_2Si_2$ type *(German)* 78−51470
$SrPdSn_3$, prep. and crystal structure *(German)* 80−84138
$Sr_{0.67}Pt_3B_2$, cryst. struct. and supercond. props. 79−38231
Sr_2X, X=Si, Ge, Sn, Pb, occurrence, struct. 78−38663

strontium compounds
see also strontium alloys
alumoborosilicate glass, effect of vaporous and liq. Cs 77−44509
arsenates, $SrM^{IV}(AsO_4)_2$, (M^{IV}=Ge,Ti,Si,Zr,Hf), IR and Raman spectra, cryst. struct., chem. bonding 77−36225
calcium strontium propionate, compressed powder, dielectric props., particle size effects 77−59503
dicalcium lead strontium propionate, mixed cryst., phase diagram, dielec. and dilatometric anomalies 77−11689
dicalcium strontium propionate, anomalous US attenuation near ferroelec. phase transition 79−91383
dicalcium strontium propionate, cryst. symmetry in low temp. phase 79−37693
dicalcium strontium propionate, effect of particle size on dielec. behaviour 79−38429
dicalcium strontium propionate, elastic stiffness consts., determ. in US freq. region 79−37752
dicalcium strontium propionate, ferroelasticity and optical activity rel. to transition 77−76547
dicalcium strontium propionate, Raman scatt., order-disorder type transform 77−12373
dicalcium strontium propionate, temp. depend. of elastic const. c_{16} 79−28029
ferrite, hexagonal, with M, W and Y structures containing Fe^{2+} and Fe^{3+} mag. ions, saturation moment and anisotropy 80−71009
ferrite, plastic magnet appl., based on moulding ferromagnetic powder material with plastics *(Japanese)* 80−60829
formate:Mn^{2+}, cryst., e.p.r., spin Hamiltonians 77−4552
formate dihydrate:Cr^{3+}, optical absorpt. spectrum 80−50380
formate dihydrate, EPR and optical absorption spectra of VO^{2+} ion 77−40112
formate dihydrate, H bonds, deuteron mag. reson. meas. 77−85593
gaseous chemiexcited mol., modulated transmission spectra 77−86316
halides, absorpt. spectra in air-acetylene flame, using AAS with data processing 78−20102
halides, XY_4 molecules, force consts. by modified Redington and Aljibury method 80−69261
maleate tetrahydrate, cryst. struct., H-bonding scheme 80−96505
malonate, cryst. struct. 77−59003
monochalcogenides, electronic energy band struct., APW calcs. 80−65439
oxides, Sr_2MO_4, M=Mn, Cr, Tl, Ru, Hf, Mo, K_2NiF_4 structure, study by method of invariants *(French)* 80−33959
$(Pb_{0.95}Sr_{0.05})(Zr_{0.53}Ti_{0.47})O_3$+3% mol PbO, meas. and interpretation of effect *(Polish)* 79−4574
perovskite, Sr_2XReO_6, (X=Li, Mg, Ca, Mn, Fe, Co, Ni), new seignetto-magnets and ferroelectrics 78−19425
perovskite compound combination, Mossbauer spectroscopy study *(Russian)* 80−80666
perovskites, $A_2^{2+}B^{3+}U_{5/6}{}^{6+}\nu_{1/6}O_6$, struct., cation vacancies, X-ray diffr. study *(German)* 80−107147
phosphates, $SrM^{IV}(PO_4)_2$, (M^{IV}=Ge,Ti,Sn,Zr,Hf), IR and Raman spectra, cryst. struct., bonding 77−36225
propionate monohydrate, cryst. struct. 77−76385
rare earth orthocobaltites, $R_{1-x}Sr_xCoO_3$, electronic and mag. props., itinerant ferromagnetism obs. 78−10660
rare earth orthocobaltites, $R_{1-x}Sr_xCoO_3$, ferromag. reson., Lande g-factor 80−25215
rare earth strontium vanadates, $R_{1-x}Sr_xVO_{3-0.1x}$, elec. cond. and mag. susceptibility, temp. depend., 77-300K 77−47816
sodalites, aluminogermanate- and aluminate-, IR spectra rel. to T-O bond length and T-O-T ang. 79−91445
6 $(SrAl_2O_4).SrO$, cryst. struct. determ. by means of vector subsystems 79−94983
SrF_2, Eu^{2+} isomer shift, Mossbauer studies 79−56649
n-$SrTiO_3$, surface electronic struct. calc. 78−88011
strontium acetate hemihydrate:Cu^{2+}, EPR of cryst. 78−19312
strontium calcium tartrate mixed crystal, growth in silica gel 77−48325
strontium calcium tartrate tetrahydrate, crystals grown by ion diffusion through silica gels, exam. of preps. 79−52102
strontium calcium tartrate tetrahydrate, gel grown mixed single crystals, defect characterisation 80−2027
strontium uranyl tetraformate hydrate, struct. determ., orthorhombic unit cell, UR spectrum *(French)* 78−22705
synthesis, struct. and mag. props. 77−89934
$AlBr_3.SrBr_3$, CT complex, NQR 77−20747
Al_2O_3, sintering with $SrTiO_3$ admixture *(Polish)* 78−19699
Al_2O_3:$SrTiO_3$, sintering temperature effect of titanate additions 80−60808
Al_2O_3-P_2O_5-Mg(Ca)(Sr)O glasses, Na^+, Sr^{2+} diffusion coeffs. rel. to temp. 78−30787
$(Ba,Sr)Fe_{12}O_{19}$, Ferroxdure, developments and research 78−84455
$(Ba,Sr)TiO_3$, ferroelec. solid solution, dielec. nonlinearity in nonpolar phase *(Russian)* 77−32317
$(Ba,Sr)TiO_3$ ferroelectric film, phys. props. in weak elec. fields 78−35098
$(Ba,Sr)TiO_3$, ferroelec. props., press. depend., anharmonic oscillator model 80−80716
$(Ba,Sr)TiO_3$ polycrystalline solid soln., electrostriction constants, reson.-antireson. meas. *(Russian)* 78−10849
$(Ba,Sr)Nb_2O_6$ monocrystal optical homogeneity requirement for light beam control 79−82952
$Ba_{0.25}Sr_{0.75}Nb_2O_6$, inhomogeneous ferroelec., photorefractive effect 79−42935
$BaCO_3$-$SrCO_3$-$CaCO_3$, phase inhomogeneity effects on oxide cathode props. 78−52614
$BaCO_3$-$SrCO_3$-$TiO_2(ZrO_2)$, ternary systems, solid-phase synthesis 78−52733
BaO-SrO-Al_2O_3-TiO-SiO_2 glass ceramics, cryst. phases form., BaO/SrO ratio influence 80−19705
$Ba(PO_3)_2$-AlF_3-SrF_2, elec. cond., density, and IR spectra 79−95215
$Ba(PO_3)_2$-SrF_2, IR absorption spectra exam. of hydrolytic stability 80−39291

strontium compounds continued
$Ba_{0.5}Sr_{1.5}Al_4Si_{12}O_{32}.10H_2O$, brewsterite cryst. struct. refinement 77−80471
$BaSr_xCa_{1-x}Fe_4O_8$, substituted hexagonal ferrites, mag. split Mossbauer spectra obs. and X-ray struct. data 80−71250
(BaSrCa)O, cathodes, thermionic emission characts., X-ray struct. obs. 78−48270
$Ba_{0.725}Sr_{1.775}Li_xNb_{5-x}Ti_xO_{15}$, solid soln., prep., struct., dielec. props. *(French)* 77−69782
$Ba_{3-x}Sr_x(M_4Ti_4)O_{21}$, synthesis and cryst. chemistry 77−76379
$Ba_{0.25}Sr_{0.75}Nb_2O_6$, anomalous photovoltaic effect and photocond. 79−38122
$Ba_{0.25}Sr_{0.75}Nb_2O_6$, fast-response pyroelec. cryst. detector 78−49904
$Ba_{0.25}Sr_{0.75}Nb_2O_6$, ferroelec., photocond. and optical absorpt. spectra 77−8149
$Ba_{0.25}Sr_{0.75}Nb_2O_6$, ferroelec., influence of temp. on Raman scatt. spectra 77−69842
$Ba_{0.25}Sr_{0.75}Nb_2O_6$, photoresponse in transition region 77−1451
$Ba_{0.25}Sr_{0.75}Nb_2O_6$, photovoltaic current, temp. and spectral depend. 78−47828
$Ba_{0.25}Sr_{0.75}Nb_2O_6$, quadratic susceptibility dispersion meas., oscillator model including structure 78−59078
$Ba_{0.25}Sr_{0.75}Nb_2O_6$, spontaneous electroopticabsorption effect 78−19443
$Ba_{0.25}Sr_{0.75}Nb_2O_6$, thermal and spectral variations in the photovoltaic current in ferroelectrics 78−91719
$Ba_{0.39}Sr_{0.61}Nb_2O_6$, electro-optical props. 80−2728
$Ba_{0.50}Sr_{0.50}Nb_2O_6$:$La_2O_3(Tm_2O_3)(Y_2O_3)$, Raman spectra 79−78678
$Ba_{0.5}Sr_{0.5}Nb_2O_6$, electronic props. and photoresponses 80−92925
$Ba_{0.5}Sr_{0.5}Nb_2O_6$, temp. depend. of Raman spectra 78−72524
$Ba_{0.54}Sr_{0.46}Nb_2O_6$, line broadening effect in Rayleigh scatt. of Mossbauer radiation 80−50238
$Ba_{0.54}Sr_{0.46}Nb_2O_6$:Y(La)(Tm), dielectric and electrooptic props. 78−68466
$(Ba_{1-x}Sr_x)_{1-y}(Nb_2O_6)_y$:$CeO_2$ crystals, photoelectric and photorefractive props., hologram recording 80−53239
$Ba_xSr_{1-x}Nb_2O_6$ (x=0.27 to 0.54) exam. of freq. dependence of permittivity diffuse ferroelectric phase transition kinetics 80−2703
$Ba_xSr_{1-x}Nb_2O_6$, anomalous photovoltaic effect and photocond. 78−52449
$Ba_xSr_{1-x}Nb_2O_6$ crystals, optical defects and edge dislocation distributions 80−19806
$Ba_xSr_{1-x}Nb_2O_6$, ferroelec., cathodlum. spectral and temp. depend. 78−84665
$Ba_xSr_{1-x}Nb_2O_6$, ferroelectric with diffused phase transition, photoelectret states 80−20583
$Ba_xSr_{1-x}Nb_2O_6$, growth defects 78−38640
$Ba_xSr_{1-x}Nb_2O_6$, nonequilibrium processes 78−48124
$Ba_xSr_{1-x}Nb_2O_6$, photoelectretic states in real time spatial light modulators, photorefractive effect 80−80676
$Ba_xSr_{1-x}Nb_2O_6$, reduced, elec. cond., effect of oxygen vacancies 77−35939
$Ba_xSr_{1-x}Nb_2O_6$, single crystal, Mossbauer diffraction *(Russian)* 79−56644
$Ba_xSr_{1-x}Nb_2O_6$, struct. and dielec. props., isomorphic substitution effect 78−27165
$Ba_xSr_{1-x}Nb_2O_6$:Ce, pure and doped, photoelec. props. and photorefraction 80−60538
$Ba_{1-x}Sr_xNiO_{3-y}$, Sr substitution effect, powder X-ray diffr. 78−51498
(BaSr)O on Ni, cathode, oxide thickness depend. of emission 77−48299
$Ba_{1-x}Sr_xPb_{0.75}Bi_{0.25}O_3$, superconductivity, rel. to lattice const. 80−49966
$(Ba_xSr_{1-x})SO_4$:Eu mixed crystal series, X-ray diffr. study of miscibility 80−2168
(BaSr)TiO_3 film, ferroelec., dielec. props. in strong elec. fields 78−27163
$BaSrTiO_3$, model for 1/f excess noise 79−99591
$BaSrTiO_3$, semiconducting, excess noise characts. exam. 78−19110
$Ba_{0.4}Sr_{0.6}TiO_3$, ferroelec. thin film, fabrication, props. 77−28521
$Ba_{0.4}Sr_{0.6}TiO_3$ films, DC conductivity, strong microwave field effect 80−65727
$Ba_{0.60}Sr_{0.40}TiO_3$, sputtered film on Pt, pyro-effect for laser registration *(Russian)* 77−20804
$Ba_{1-x}Sr_xTiO_3$ ceramic pyroelec. responsivity, −140° to +160°C obs. 78−23405
$Ba_xSr_{1-x}TiO_3$, disordered ferroelec., dielec. const. and spontaneous polarisation meas. 78−48130
$Ba_xSr_{1-x}TiO_3$, ferroelec., with impurities, lattice dynamics 79−28061
$Ba_xSr_{1-x}TiO_3$, ferroelec. film, heteroepitaxial growth in cathode sputtering 80−93486
$Ba_xSr_{1-x}TiO_3$, thin ferroelec. layers 79−42912
$Ba_{2-x}Sr_xTiSi_2O_8$, piezoelec. crysts., SAW characts. 80−84354
(BaZnSr)TiO_3 ferroelectric film, parameters at upper end of centimetre waveband *(Russian)* 77−40185
BamSrmPb hexaferrites, prep. by cernet procedure, mag. props. 77−32174
BeO_2-Al_2O_3-SiO_2-SrF_2 system glass, role of fluoride cations during crystn. 79−65176
$(Bi_{2/3}Sr)TiO_3$, ferroelec. solid solution, dielec. nonlinearity in nonpolar phase *(Russian)* 77−32317
Bi_2O_3-SrO, solid state phase diagram, thermal and high temp. X-ray anal. *(French)* 79−65190
Bi_2O_3-SrO system, stoichiometric cpds., cryst. data *(French)* 79−99153
$Bi_{1-x}Sr_xO_{1.5-x/2}$ vacancy-type solid soln., anionic cond. *(French)* 80−49407
$(Ca,Sr)_5(PO_4)_3Cl$, partially substituted chlorapatite, cryst. struct. from X-ray data 80−96478
$CaAl_2O_4$-$SrAl_2O_4$-BaA_2O_4, binary and ternary systems, solid solubility *(Japanese)* 80−35174
CaO-SrO-Fe_2O_3 system, phase relations, Sr hexaferrite field occurrence 80−93545
$Ca_{1-y}Sr_{y/2}Ba_{y/2}Zr_{1-x}Ti_xO_3$, ceramic system, dielectric props., microwave resonator application 80−80674
$(Ca_{1-x}Sr_x)(Ca_{1/3}Nb_{2/3})O_3$ perovskites, cryst. struct. *(French)* 79−65044
$Ca_{1-x}Sr_xF_2$:Er^{3+} mixed crystal, luminesc. transition, inhomogeneous line broadening calc. 80−97332
$Ca_{1-x}Sr_xFeO_3$, Mossbauer spectra, charge disproportionation 80−15891
$Ca_{1-x}Sr_xFeO_3$, Mossbauer spectra, charge disproportionation 80−20542
$Ca_{10-x}Sr_x(PO_4)_6(OH)_2$, continuous cation migration, IR spectra study 80−93297
$(Ca_{1-x}Sr_x)RuO_3$, mag. props. 78−27027
$Ca_{1-x}Sr_xSi_2$, solid solns., α-$ThSi_2$ struct. type, comp. and press depend. 78−91322
$Cd(PO_3)_2$-$Sr(PO_3)_2$, physicochemical investigation 78−44102

strontium compounds continued
CdS-SrS, solid soln., rock salt struct., high press. phase equilibrium study 78−52777
$CdSr(PO_3)_4$, struct. from IR spectra 77−47421
$Cd_{1-x}Sr_xS$, solid soln., phase equilib. diagrams 80−108412
$CsPO_3$-$Sr(PO_3)_2$ system, physicochem. investigation 77−35666
$CsSrCl_3$, phase transitions, dilatometric and press. studies 77−15578
$CsSrCl_3$, refr. index and birefr., struct. transition effects 77−90126
$CsSrCl_3$:Mn^{2+} (Gd^{3+}), structural transitions, EPR meas. 78−34619
$Er_2Sr_3(BO_3)_4$, cryst. struct. from X-ray diffr. meas. 77−89419
Eu-Sr-S, spin glass materials, mag. field dependence of susceptibility peak 80−103840
(Eu_xSr_{1-x}) S dilute, spin-cluster freezing observation by low-freq. mag. absorpt. 79−78404
$Eu_xSr_{1-x}M_4O_{11}$, M=Nb, Ta, electrophys. and mag. props. 77−89760
$Eu_xSr_{1-x}O$, ferromag. ordering and photoluminesc. 77−66313
$Eu_{0.4}Sr_{0.6}S$, spin glass, spin dynamics, neutron scatt. study 80−65907
$Eu_{1-x}Sr_xS$, exciton refl. spectra 80−2782
$Eu_{1-x}Sr_xS$, non-metallic system, spin glass behaviour 79−24175
$Eu_xSr_{1-x}S$, blocking of pairs and spin glass freezing 79−61174
$Eu_xSr_{1-x}S$, chalcogenide-like system, crit. conc. for ferromagnet-spin glass transition 80−34662
$Eu_xSr_{1-x}S$, dil. insulator spin-glass versus blocking 80−34641
$(Eu_xSr_{1-x})S$, dilute, magnetic 'blocking' 79−78348
$Eu_xSr_{1-x}S$, dilute Heisenberg magnet, complex susceptibility of blocked spins 80−15740
$Eu_xSr_{1-x}S$, ferromag. ordering and photoluminesc. 77−66313
$Eu_xSr_{1-x}S$, ferromagnet-spin glass transition, mag. ordering, mag. susceptibility and neutron scatt. meas. 80−50135
$Eu_xSr_{1-x}S$, Heisenberg spin glass system, excitations 80−84610
$Eu_xSr_{1-x}S$, insulating spin-glass, sp. ht. near ferromag. onset 80−34667
$Eu_xSr_{1-x}S$, insulating spin glass, sp. ht. near ferromag. onset 80−97106
$Eu_xSr_{1-x}S$, mag. clusters, spinodal decomp. trend 80−65923
$Eu_xSr_{1-x}S$, mag. ordering temp. conc. depend., Eu mag. hyperfine field temp. depend. 78−14971
$Eu_xSr_{1-x}S$, mag. ordering in dil. Ising and Heisenberg systems with competing interactions 80−65914
$Eu_xSr_{1-x}S$, non-metallic spin glass system 79−61175
$Eu_xSr_{1-x}S$, onset of ferromagnetism for x near 0.5 neutron diffr. obs. 79−24181
$Eu_xSr_{1-x}S$, paramag. susceptibility, expt. and comparison with high temp. series expansion 80−60176
$Eu_xSr_{1-x}S$, spin glass, spin wave modes and low temp. sp. ht. 80−80538
$Eu_xSr_{1-x}S$, spin glass, transition temp., freq. depend. 80−97113
$Eu_xSr_{1-x}S$, spin glass to ferromag. transition, neutron scatt. and susceptibility meas. 80−60254
$Eu_xSr_{1-x}S$, spin-glass props. and mag. transition 80−97105
$(Eu_xSr_{1-x})S$, transferred hyperfine fields, NMR 80−71196
$(Eu_xSr_{1-x})S$, very dil., magnetisation dynamics 80−65915
$Eu_xSr_{1-x}SO_4$, mag. ordering temp. conc. depend., Eu mag. hyperfine field temp. depend. 78−14971
$Eu_{1-x}Sr_xSi_2$, solid solns., α-$ThSi_2$ struct. type, comp. and press depend. 78−91322
$Eu_{1-y}X_yS$ (X=Sr,Gd), spin-disorder-induced Raman scatt. from phonons, expt. investigation 80−20635
$Eu_{1-y}X_yS$ (X=Sr,Gd), spin-disorder-induced Raman scatt. from phonons, theory 80−20636
HgI_2:SrI_2, cryst. growth from soln., doping rel. to elec. cond., phase transitions 77−55880
K_2CO_3-Sr-CO_3 phase diagrams, evidence of new compound *(French)* 78−95033
KCl:RbCl, $SrCl_2$, IR window material, cryst. growth and props. 78−31333
KCl:RbCl, $SrCl_2$, laser window material, prep., grain boundary stability 77−46774
KCl:$SrCl_2$, effect of impurity on thermoelec. power 78−76098
KCl:$SrCl_2$, H_{Na} annealing, X-ray irrad., H centre capture by IV dipoles 78−10927
KCl:$SrCl_2$, Z_1-centres, dipolar relax., ITC meas. 78−75660
KCl-$SrCl_2$, photoluminescence of Z_4-centre and associated Z type colour centre *(Russian)* 79−4851
KNO_3-$Sr(NO_3)_2$ molten mixtures, electrical conductance 78−43159
K_2O-SrO-Nb_2O_5 system, selective delineation of dislocations by etching 77−72617
K_2O-SrO-SiO_2, glass, elastic constants 77−16630
K_2O-SrO-SiO_2, O_2 self diffusion exam. by proton activation anal. 79−65241
K_2O-SrO-SiO_2, solid glass, influence of composition on electrical conductivity 77−11723
$KSr(NH_2)_3$, cryst. struct. and cryst. chemistry *(German)* 79−51080
$La_{0.003}Ba_{0.66}Sr_{0.34}TiO_3$ ceramic, positive TCR near Curie temp. rel. to charge dispersion *(Russian)* 80−16511
$La_{0.5}Sr_{0.5}CoO_3$, conducting oxide powder prod. by freeze drying 79−95984
$La_{0.5}Sr_{0.5}CoO_3$, semicond. oxide O_2 electrode characts. 79−24073
$La_{1-x}Sr_xCoO_3$ ($0.5 \leq x \leq 1.0$), mag. props. 79−24154
$La_{1-x}Sr_xCoO_3$, ($0.5 \leq x \leq 0.9$), ferromag., elec. props., itinerant electron model 80−107785
$La_{1-x}Sr_xCoO_3$, specific heat meas., using laser-flash method, phase transitions obs. *(Japanese)* 80−54898
$La_{1-x}Sr_xCoO_{3-y}$, Seebeck coeff. meas., small polaron hole conduction model 80−20233
$La_{2-x}Sr_xCoO_4$, mag. behaviour obs. 80−70971
$La_{0.84}Sr_{0.16}CrO_3$, sintering 77−77440
$La_{1-x}Sr_xCrO_3$ ($0 \leq x \leq 0.4$), localised level hopping transport 80−10974
$La_{1-x}Sr_xCrO_3$, electronic struct. study by XPS 80−25518
$La_{1-x}Sr_xCrO_3$ system, phase relationships, cryst. struct. 77−69073
$La_{1-x}Sr_xCrO_3$, x=0-0.2, AC and DC cond., 77-1300K, hopping of polarons 78−2477
$La_{2-x}Sr_xNiO_4$, ($0 \leq x \leq 1$), cryst. struct. and elec. props. 78−2088
$La_xSr_{1-x}RuO_3$, metallic, mag., electronic and structural props., ^{99}Ru Mossbauer spectroscopy 77−48107
$La_{1-x}Sr_xVO_3$, Anderson transition, elec. resist. and thermopower meas. 80−100488
$La_{1-x}Sr_xVO_3$, high-temp. transport meas. 77−11917
$La_{1-x}Sr_xVO_3$, semiconductor-metal transition, Anderson localisation, Hall mobility and 1/f noise meas. 79−78142
$LiSrPO_4$, vibrational spectra and cryst. struct. 78−39536
$M_{1-x}Sr_xSi_2$ (M=Ca, Eu, Ba), solid solution with type $SrSi_2$ struct., lattice parameters at high press. 80−54203
$MgSr_xFe_{2-x}O_4$, comp. effects on ferrite characts. 78−52305

strontium compounds continued
NaF-SrF_2-CrF_3, glass transition, crystn. and melting temps., optical transmission *(French)* 80−64910
Na_2MoO_4-$SrMoO_4$, phase diagrams 77−36467
$NaNbO_3$-$SrNb_2O_6$, phase diagram, props. meas. 79−11576
Na_2O-SrO-Nb_2O_5 system, solid state equil., 800°C *(Italian)* 77−47549
$Na_2Sr_3(NH_3)_8$, cryst. struct. and cryst. chemistry *(German)* 79−51080
$NaVO_3$-BaV_2O_6-SrV_2O_6, phase diagrams, simple eutectic system 78−48379
$Nd_{1-x}Sr_xCoO_3$, Anderson transition, elec. cond. meas. 77−51786
$(Pb,Sr)_5Ge_3O_{11}$, single crysts., growth and X-ray and dielec. investigations 80−88127
$(Pb,Sr)TiO_3$, ferroelec. solid solution, dielec. nonlinearity in nonpolar phase *(Russian)* 77−32317
$(Pb,Sr)TiO_3$, ferroelec. props., press. depend., anharmonic oscillator model 80−80716
$(Pb,Sr)(Zr,Ti)O_3$, piezoceramic, effect of glass additions on props. during hot pressing 79−24475
Pb_z-$Sr_{1-z}(Zr_x$-$Ti_{1-x})O_3$:Cr_2O_3, ferroelec. ceramic, reversible characts. and dielectric losses *(Russian)* 78−84517
$PbCO_3$-$SrCO_3$ system, solid soln. form., regions of existence 79−11581
$Pb_xSr_{1-x}TiO_3$, ferroelec., with impurities, lattice dynamics 79−28061
$Pb_{0.94}Sr_{0.06}(Ti_{0.47}Zr_{0.53})O_3$-NiO, modified, dielec. and piezoelec. props. 80−11342
$Pb_{0.95}Sr_{0.05}(Ti_xZr_{1-x})O_3$, solid solns., parameters of Curie Weiss law, permittivity meas. 78−15129
$Pb_xSr_{1-x}(Zr,Ti,Nb)0_3$, hydrophone ceramic, effect of one-dimensional uniaxial stress 80−80705
$Pb_{0.95}Sr_{0.05}(Zr_x, Ti_{1-x})O_3$-$Nb_2O_5$, phase coexistence range, lattice consts. 80−92680
$(Pb_{0.97}Sr_{0.03})Zr_{0.51}Ti_{0.49}O_3$, ferroelec. phase transition under high press. 77−36188
$Pb_{0.95}Sr_{0.05}(Zr_{0.53}.Ti_{0.47})O_3$, low temp. internal friction in ferroelectric ceramic 77−21200
$Pr_{1-x}Sr_xCoO_3$, Anderson transition, elec. cond. meas. 77−51786
Pt-$SrTiO_3$ (100) interface, struct. and electronic props., AES, LEED, EELS, and UPS study 80−24986
Pt-$SrTiO_3$ (100) interface, Auger and photoemission studies, relax. and chem. shift effects 80−54749
$Rb_2O.SrO.4B_2O_3.12H_2O$, real Patterson function determ., method of rhombs, 78−5986
SRF_2:Er^{3+}, laser excitation of single ion and clustered ion sites 77−69879
SiO_2-Al_2O_3-CaO-BaO-SrO-ZnO-Na_2O-K_2O-B_2O_3, glaze effect of P_2O_5 additions 80−60824
SiO_2-CaO-ZnO-B_2O_3-Na_2O-S, SrO effect on crystallisation 80−54135
SiO_2-K_2O-Na_2O-BaO-SrO-ZnO system glass, props. optimisation 79−91611
SiO_2-TiO_2-Al_2O_3-SrO(BaO), glasses, ceramic form. rel. to Al_2O_3 content 77−25005
$(Sr,Ba)Nb_2O_6$:Ce, high sensitivity holographic storage 77−71953
Sr ferrite crystals, etch pitting, of hard magnetic ferrite crystals *(German)* 78−26568
Sr Nb_2O_6, crystallography, polymorphism and isomerism, X-ray diffr. and DTA study 80−100216
Sr-H system, equilib. H_2 press., enthalpies of soln. and formation determ. 80−107428
Sr-SiO_2 glasses, morphology effects on props. 80−49118
Sr-Te-O system, amorphous thin film, vacuum deposited, elec. cond., current cut-off *(Japanese)* 77−24625
Sr-Ti-O system, perovskite oxides, nonstoichiometry rel. to dielectric const. 77−80628
$Sr_5(PO_4)_3OH$, prep. from sulphate, X-ray diffr. and IR spectrosc. 80−29893
$(Sr/Ba)(Fe/Al/Ga)_{12}O_{19}$ solid soln. crystal for hexaferrite layer substrate *(German)* 78−23672
$SrAg_2I_4$, Raman and autocorrelation spectra, solid and soln. 79−38532
$SrAg_2I_4.8H_20$, cryst. struct. 79−23575
$Sr_2AgNb_5O_{15}$, $Sr_2AgTa_5O_{15}$, ferroelec. and ferroelastic props. *(French)* 79−24266
$SrAl(Ga)_2Si(Ge)_2O_8$, isomorphous replacements of Al by Ga and Si by Ge 77−84713
$Sr_2Al_2GeO_7$, gehlenite struct., synthesis and physicochem. props. 79−43181
$SrAl_2O_4$, cryst. struct. with 3D framework 79−86766
$SrAl_2O_4$, X-ray powder diffr. data 79−51071
$SrAl_2O_4$:Eu^{2+}, activated phosphors, luminesc. efficiency, temp. and high-press. 78−23508
$SrAl_2O_4$-$BaAl_2O_4$ system, solid solubility, α-β transition 78−63860
$Sr_4Al_4O_2[Al_{10}O_{23}]$, cryst. struct. 77−31651
$SrAl_2SiO_8$, micro-crystal, appl. of method for indexing *(German)* 78−22608
$SrAl_2Si_2O_8$, TEM obs. of feldspar aand hexacelsian polymorphs 78−83827
$SrB_{0.5}B'_{0.5}O_4$, where B=Ln, Y, Sc, Fe, In, Rh and B'=Nb, Ta, synthesis and characterisation 79−69087
$SrB_{12}H_{12}.10H_2O$, struct. dehydration, intermediate phases and thermooxidative degradation 80−33951
$SrB_{12}H_{12}.7H_2O$, cryst. growth from soln. and morphology 77−44145
SrB_2O_4:Eu^{2+}, luminesc. of high-press. phases 80−100680
$SrBPO_5$:Eu^{2+}, activated phosphors, luminesc. efficiency, temp. and high-press. 78−23508
$SrBaNaNb_5O_{12}$, X-ray powder diffraction data determ. *(Chinese)* 80−70170
$Sr_{0.61}Ba_{0.39}Nb_2D_6$, photoinduced birefr. 80−7325
$Sr_{0.25}Ba_{0.75}Nb_2O_6$ film, growth and electrophys. props. 79−42928
$Sr_{0.5}Ba_{0.5}Nb_2O_3$ piezoelectric transducer, SAW props. 80−79037
$Sr_{0.5}Ba_{0.5}Nb_2O_6$ crystals, ferroelec., dislocation free, pyroelec. props. 79−42907
$Sr_{0.5}Ba_{0.5}Nb_2O_6$, ferroelec., primary pyroelectricity 77−63371
$Sr_{0.5}Ba_{0.5}Nb_2O_6$, ferroelec., dielec. behaviour 78−80309
$Sr_{0.5}Ba_{0.5}Nb_2O_6$ film, pyroelectric effects, origin 78−88258
$Sr_{0.5}Ba_{0.5}Nb_2O_6$:Fe(Mn)(Cr)(La), ceramic, additive effects on ferroelec. and pyroelec. props. 77−16256
$Sr_{0.61}Ba_{0.39}Nb_2O_6$, electromechanical props., permittivity, elastic compliance, piezoelectric moduli 80−29691
$Sr_{0.65}Ba_{0.35}Nb_2O_6$, internal field distrib. and photorefraction 79−99843
$Sr_{0.75}Ba_{0.25}Nb_2O_6$, ceramic ageing, dielec. props. 80−88940
$Sr_{0.75}Ba_{0.25}Nb_2O_6$, electrostriction 77−48130
$Sr_{0.75}Ba_{0.25}Nb_2O_6$, ferroelectric devices for optical systems 78−90473
$Sr_{0.75}Ba_{0.25}Nb_2O_6$, large cryst. growth, control of opt. defects 78−76595

strontium compounds continued
$Sr_{0.75}Ba_{0.25}Nb_2O_6$, SBN, hologram storage, book contrib. 78−25834
$Sr_{0.75}Ba_{0.25}Nb_2O_6$ single cryst., electro-optical hysteresis curves and phase transitions *(German)* 79−28717
$Sr_{1-x}Ba_xNb_2O_6$, and Nd doped growth of low dislocation density cryst., dislocation struct. 77−40348
$Sr_{1-x}Ba_xNb_2O_6$ crysts., defect-free growth 80−108346
$Sr_{1-x}Ba_xNb_2O_6$, photorefraction in space charge field, phase transitions 80−97229
$Sr_{1-x}Ba_xNb_2O_6$, tetragonal tungsten bronze structure ferroelec. mech. for ferroelec. transition 79−38481
$Sr_xBa_{1-x}Nb_2O_6$, appl. in sub-100 ps pyroelec. detectors, 10.6 μm damage threshold meas. 80−77859
$Sr_xBa_{1-x}Nb_2O_6$, domain struct. influence on electrooptical props. 80−93283
$Sr_xBa_{1-x}Nb_2O_6$, high press. phase transitions, Raman scatt. studies 80−71402
$Sr_xBa_{1-x}Nb_2O_6$, neutron and light scatt. in phase transition region 78−64336
$Sr_{0.75}Ba_{0.25}O_6$, photorefractive effect, spectral characts. 78−43829
$Sr_{1-x}Ba_xZrO_3$, struct., X-ray powder diffr. study 80−1989
$SrBiMTeO_6$, M=Li, Na, antiferroelectric, synthesis and charact. 77−55758
Sr_2BiRuO_6, perovskites, prep., struct., emission control catalysts 77−68957
$SrBi_2Ta_2O_9$, SHG, temp. depend. ferroelec.-ferroelec. transition 78−15121
$SrBi_6Ti_3Nb_2O_{21}$, cryst. struct. 77−47428
$SrBi_8Ti_7O_{27}$, mixed-layer compound, synthesis and struct. 77−35530
SrBr, gas equilib. mass spectra, dissoc. energy meas. 77−65543
$SrBr_2$, absorpt. and refl. spectra 79−82994
$SrBr_2$, aq. solns., EXAFS meas. 80−60714
$SrBr_2$-H_2O, ^{79}Br NQR, cryst. struct. 78−27110
$SrBr_2(SrI_2)+Cl_2$, crossed beam metathesis, total cross sections 77−21354
$SrCO_3$, $NiCO_3$ impurity effect on dissoc. 78−27425
$SrCO_3$, precipitation induction errors, a method for determ. 79−5175
SrCa, matrix-isolated, laser photoluminesc., van der Waals ground state 79−41192
$Sr_{1-x}Ca_xMnO_3$, Neel points, rel. to Curie point of $LaNi_{1/2}Mn_{1/2}O_3$, superexchange interactions 77−77055
$Sr_{1-x}Ca_xO$, epitaxial layers by CVD *(Russian)* 79−56934
$(SrCaR)_2(Cr_xGa_{1-x})O_4$, R=La or Sm, mag. 2-D oxide, phys. props. 78−47974
Sr_2CaReO_6, ordered or perovskite type struct., magnetic and elec. props. 79−65053
$Sr(Ca_{1/3-x}Sr_xNb_{2/3})O_3$, perovskite, X-ray and electron diffr. study *(French)* 79−99161
$Sr_{1-x}Cd_xF_2$, lattice dynamics 78−75763
SrCl:Mn^{2+}, shape of potential well, calc. 78−87951
$SrCl_2$, absorpt. and refl. spectra 79−82994
$SrCl_2$, anion diffusion mechanism 80−2201
$SrCl_2$, anion disorder at high temps., neutron diffr. obs. 80−59614
$SrCl_2$, anion motion at high temps., quasielastic nuetron scatt. obs. 80−59715
$SrCl_2$, aq. soln., Raman spectrum, local order 78−84563
$SrCl_2$, elastic constants and acoustic wave velocity, temp. variation 78−6118
$SrCl_2$, F-centre production mechanism, radiolysis exam. 79−23602
$SrCl_2$, fast ion cond., specific heat anomaly, mol. dynamics study 80−65283
$SrCl_2$, fast ion transport 80−107558
$SrCl_2$ film, non-cryst., very-low-freq. inelastic light scatt. 80−25367
$SrCl_2$, high temp. powder neutron diffr., transition to highly conducting phase 78−47586
$SrCl_2$, in-activated, luminescence studies at 77 and 300K 80−108247
$SrCl_2$, ionic cond., activation volumes and high press. phase transitions 80−70461
$SrCl_2$, ionic cond., self-diffusion, rel. to defect motion, mol. dynamics study 80−65282
$SrCl_2$, liq., dynamic struct. factors, computer simulation 79−37611
$SrCl_2$, mass and charge transport 80−100347
$SrCl_2$, molten, struct., electrolyte 'general primitive model' prediction test 80−28902
$SrCl_2$, nearest-neighbour atom displacements derived from EXAFS spectra, temp. depend. 79−87524
$SrCl_2$, non-crystalline film, disorder-induced Raman scatt. 80−11387
$SrCl_2$, O_2^- pair centre EPR spectrum 77−24742
$SrCl_2$, orthorhombic, lattice parameters meas. 77−15382
$SrCl_2$, partial static structure factors, velocity autocorrelation functions 78−91219
$SrCl_2$, photoelectron spectra, geometry 78−29816
$SrCl_2$, point defect parameters, ionic cond. study 80−107490
$SrCl_2$, pure and doped, disorder and defect props. 80−107217
$SrCl_2$, Raman spectra, 15 to 1300K, anharmonic vibr. effects 77−43990
$SrCl_2$, self-diffusion and ionic cond. 80−107489
$SrCl_2$, single cryst., second order Raman spectrum *(French)* 78−80327
$SrCl_2$, solns. in methanol, conductance data anal., assoc. consts. 78−71875
$SrCl_2$, sp. ht. meas., Schottky-type diffuse phase transitions, defect form. energies and entropies 80−107441
$SrCl_2$, specific heat anomaly and sublattice disorder, neutron diffr. meas. 79−42238
$SrCl_2$, superionic, electrical conductivity at high temp. 78−79798
$SrCl_2$, superionic, quasielastic neutron scatt. 78−79504
$SrCl_2$, valence-electron charge density along nearest-neighbour axis 79−27944
$SrCl_2$:Cm(Bk), fluorite-struct., self-luminesc. 78−27309
$SrCl_2$:Cu^+, exciton bands, optical absorpt. and MCD spectra 80−80821
$SrCl_2$:Eu^{2+}, fluorescence lifetime and quantum efficiency for 5d→4f transitions 80−100681
$SrCl_2$:Fe^{2+}(Co^{2+}) electronic absorption spectra in far and middle infrared 78−68537
$SrCl_2$:Fe^{3+}, EPR spectra of Fe^{3+}($^6S_{5/2}$), 4-100K 78−95512
$SrCl_2$:Gd^{3+}, hyperfine interaction, X-band ENDOR 80−60457
$SrCl_2$:Gd^{3+}, Na^+, elec. field gradient at nuclei on orthorhombic sites, vs. elec. zero-field splitting 79−87070
$SrCl_2$:Gd^{3+}, small dielec. particles, cryst. field size effects 80−44913
$SrCl_2$:Gd^{3+}-m^+ complex, cryst. field parameters 78−10768
$SrCl_2$:K^+(Na^+)(Rb^+) X-irradiated, recomb. luminesc. between trapped electron and self trapped holes 77−73162

strontium compounds continued
$SrCl_2$:KCl_3, polycryst., ionic cond. 78−2292
$SrCl_2$:Mn^{2+}(Co^{2+}), cubic impurity EPR spectra, elec. field effect, mechanism 78−68361
$SrCl_2$:O_2^-, perturbed O_2^- molecule ion, EPR results 77−20682
$SrCl_2$:Pb^{2+}, intracentre luminesc. *(Russian)* 77−16395
$SrCl_2$:R, R=rare earth, dopant effect on superionic state transition 79−60547
$SrCl_2$:S, S_2^- and S_3^- mol. paramag. centres, investigation using EPR, Raman and optical spectroscopy 79−51855
$SrCl_2$-$GdCl_3$, prep. and purification 78−88420
$SrCl_2$-$PrCl_3$, prep. and purification 78−88420
SrClF, cryst., elastic consts. 80−19863
SrClF, cryst., Raman intensity anal., normal coord. anal. 78−72493
SrClF, localised vibr. of U-centres 78−75779
SrClF, long wavelength dynamics, shell model calc. 80−29134
SrClF, SrBrF, reacted flux growth, dislocation density, dielec. consts. and losses IR spectra 77−36214
$Sr(ClO_3)_2$, mol. torsional oscills., cooperative study by NQR 80−25244
$SrCl_2.2(H,D)_2O$, IR and Raman spectra, force fields 80−2753
$SrCl_2.2H_2O$, IR and Raman spectra, force fields 80−2753
$SrCl_2.6H_2O$:Gd^{3+}, evaporation technique prep. of $SrCl_2$:Gd^{3+}, H_2O content, EPR powder spectrum obs. 80−60416
$SrCoO_{2.70}$, growth and props. 78−48310
$SrCoO_3$, conducting oxide prod. by amorphous citrate process 79−95985
$SrCoO_3$:Fe^{4+}, ferromag., sign of Fe^{4+} hyperfine field, spin struct., Mossbauer study 80−39933
$SrCoO_{3-\delta}$ ($0<\delta<0.5$), ferromag., metallic elec. props. 80−70668
$SrCoO_{3-\delta}$, crystal struct. and mag. props., O vacancy effect 79−95587
$SrCoO_{3-x}$, mag. and neutron diffr. study 80−65805
$SrCoO_{3-x}$, XPS spectra, shake-up satellite of Co2p 78−52617
$Sr_2Co_2O_5$, characterisation and mag. props. *(French)* 79−90619
Sr_2CoReO_6, seignettomagnets with perovskite struct. 79−38459
$SrCrO_4$, diffuse reflectance spectra 78−88326
$Sr_{1-p}Cr_2S_{4-p}(Se_{4-p})$, modulation of intergrowth struct. 79−94967
$Sr_2Cu(OH)_6$, EPR, g-values 79−19770
SrD, UV absorpt. spectra, rot. consts. 77−14448
Sr_2EuAlO_5, X-ray cryst. struct. refinement 79−60318
$Sr_xEu_{1-x}B_6$, EPR linewidth conc. depend., $La_xEu_{1-x}B_6$ comparison, exchange interaction in EuB_6 80−20457
$Sr_{1-x}Eu_xB_2O_4$, luminesc. props. 80−34972
$Sr_{1-x}Eu_xB_4O_7$, luminesc. props. 80−34972
$Sr_{1-x}Eu_xB_6O_{10}$, luminesc. props. 80−34972
$SrEuFeO_4$, Mossbauer effect, Neel temp. and internal mag. field direction 77−12284
$SrEuFeO_4$, Neel temp. and spin reorientation, Mossbauer study 80−39934
$SrEu_2Fe_2O_7$, ferrite, Mossbauer effect study of hyperfine interactions, spin reorientation 78−19383
Sr_2EuFeO_5, X-ray cryst. struct. refinement 79−60318
Sr_2EuFeO_5-SrO-PbO, quasi-ternary system comp. diagram, rel. to Sr_2RFeO_5, Sr_2RAlO_5 cryst. growth 80−20776
$Sr_{2x}Eu_{2-2x}NbO_4$, synthesis and props. 77−52265
$Sr_{1-x}Eu_xS$, dilute spin glass, mag. props. 79−78386
SrF, $A^2\Pi$-$X^2\Sigma$ system, rot. anal. using CW tunable dye laser 79−31563
SrF, $B^2\Sigma^+$-$X^2\Sigma^+$ system, rot. anal. using a cw tunable dye laser 78−9165
SrF, excited state spectroscopic consts., dissoc., chemilum. obs. 80−21264
SrF radical, rot. spectrum of $X^2\Sigma^+$ state, MODR 78−9176
SrF, temp. depend. of chemilum. reactions, activation energies for excited state form. 78−66818
SrF:rare earth $^{3+}$, reorientation of dipoles 77−8494
SrF_2, 0.36 μ absorptance/fluence dependence obs. 79−15506
SrF_2, addition to $SrTiO_3$, effect on sintering kinetics 78−44037
SrF_2 antireflection coated, 3.8 μm CW laser damage threshold obs. 80−33053
SrF_2, band struct. determ. 77−89700
SrF_2, chem. laser window material 77−46769
SrF_2, colour centre thermal stability 78−83811
SrF_2, crack propag., cryst. props. effects 78−75720
SrF_2, dielec. const., 5.5 to 400K 80−50249
SrF_2, dielectric const. and polarisability strain derivatives 77−73125
SrF_2, dispersion calcs. of cubic nonlinear susceptibility near Raman resonance 79−94292
SrF_2, doped, far IR absorption spectra 78−76507
SrF_2, doped, Raman spectra using pulsed laser and gated detection 77−74529
SrF_2, doped with trivalent rare earths, migration entropy for bound fluorine motion 80−71303
SrF_2, electronic polarizability and dielectric const., strain derivatives 78−19406
SrF_2, F-centres, muffin-tin approx. inadequacy 78−63761
SrF_2, F-centres, single-phonon Raman scatt. meas. 77−20844
SrF_2, fluorite-struct. compound, high-temp. elasticity, US pulse meas. 77−81878
SrF_2, force consts., mean amplitudes of vibr. 78−17647
SrF_2 fusion-cast prism refractive index obs., 0.2138 to 11.475 μm 80−34882
SrF_2, high-frequency phonon lifetimes 80−70338
SrF_2, IR window coating, prep. and optical props. 77−50736
SrF_2 IR window refractive index var. with temp., −180° to +200°C obs. 79−14052
SrF_2, ionic cond., activation vols., freq. depend. cond., press. effects 80−100354
SrF_2, laser window coating material, damage at 10.6 μm 77−61991
SrF_2, laser window material, absorpt. at CO wavelengths, calorimetric meas. 78−25911
SrF_2, laser window material, surface and bulk absorpt., photoacoustic meas. 78−25912
SrF_2, linear thermal expansion coeff., capacitance method meas. 78−16772
SrF_2, long wavelength behaviour, elastic consts. 79−87441
SrF_2, mag. hyperfine const. and lattice distortion of V_k-centre 77−62864
SrF_2, melting curve, press. up to 40 kbar, rel. to high press. melting systematics 77−51475
SrF_2, mid IR laser window material, absorption props. 77−46770
SrF_2, muon Coulomb capture ratio 78−62959
SrF_2, nearest-neighbour atom displacements derived from EXAFS spectra, temp. depend. 79−87524
SrF_2, neutron irrad., role of F-centres in thermoluminesc. 79−19941

strontium compounds continued
SrF_2, optical detection of acoustic phonons at THz freqs. 80−75320
SrF_2, optical props. of cation colloidal particles 78−23503
SrF_2 piezo-optical coeffs. meas. at 0.6328, 1.15 and 3.39 μm 80−34888
SrF_2, powder, elec. cond. transition under high press. *(Russian)* 77−20370
SrF_2, press-forged laser window, polishing, cleaning and grinding 79−59849
SrF_2 purification for laser components, selective ion filter design and construction 79−14051
SrF_2, Raman spectra, 15 to 1300K, anharmonic vibr. effects 77−43990
SrF_2, refr. index, 20-85°C, temp. depend. 77−8536
SrF_2, saturated absorption of colour centres, ruby laser Q-switching appl. 78−71157
SrF_2, single cryst., linear thermal resistance temp. depend. 77−66048
SrF_2, spectral diffusion, coherent effects in ESR of Gd^{3+} 79−51852
SrF_2, strain induced splitting and oscillator strength anisotropy of IR transverse optic phonon 80−92625
SrF_2, stress-induced birefringence meas., 1-12 μm 77−24818
SrF_2, thermal props. *(German)* 80−81355
SrF_2, thermo-EMF meas., ion transfer charact. 77−7892
SrF_2, thermoluminesc. and F-centre annealing, after neutron irrad. 80−7422
SrF_2, thin film, optical props., spectral dependence, 460-1000 nm 80−76094
SrF_2, third-order elastic consts. from Lundqvist pot., many-body effects 80−39201
SrF_2, U-centre, electronic struct. and optical transition energies, SCF MS Xα calc. 79−4532
SrF_2, UPS and XPS spectra, rel. to optical props. 80−66386
SrF_2, UV visible absorpt. by laser calorimetry, wavelength modulation spectroscopy 78−66876
SrF_2, undoped, H-centre prod. by reactor neutron irrad., optical absorpt. meas. 77−59010
SrF_2, vaporisation and sublimation thermodynamics *(German)* 80−81355
SrF_2, vibr. anal., kinetic consts. method 80−18838
SrF_2, vol. depend. of refr. index 78−88275
SrF_2, width of upper valence band, tight-binding calc. 78−26814
SrF_2, XPS core-electron peaks, satellite and loss structs. 77−66571
SrF_2:Cd^{2+}, X-irrad., ESR of Cd^+ centres 77−59459
SrF_2:Ce^{3+}, cryst. field energies 80−59941
SrF_2:Ce^{3+}, dipole reorientation, Ce^{3+} conc. effect 78−10841
SrF_2:Ce^{3+}, EPR of low-symmetry sites 79−47332
SrF_2:$CeF_3(GdF_3)(TbF_3)$, absorpt. spectra of γ-irrad. cryst., 77K, 200-700 nm 78−84615
SrF_2:Cm, fluorite-struct., self-luminesc. 78−27309
SrF_2:Dy^{3+}, cluster form., IR absorption study *(French)* 80−108240
SrF_2:Dy^{3+}, nuclear spin-lattice relax. anisotropy, 78 to 300K 79−38395
SrF_2:Dy(Ho)(Pr)(Tb), V_k-centre recomb. kinetics, phosphoresc. 77−55817
SrF_2:Er, activation vol. for interstitial motion, dielec. const. meas. 80−49412
SrF_2:Er^{3+}, fluoresc. spectra of charge compensated cryst., multiphonon and energy transfer relax. 79−87496
SrF_2:Eu^{2+}, circular polarisation in luminesc. and optical orientation 78−6740
SrF_2:Eu^{2+}, ENDOR of ^{19}F ligands, under uniaxial stress 77−16207
SrF_2:Eu^{2+}, fluorescence lifetime and quantum efficiency for 5d→4f transitions 80−100681
SrF_2:Eu^{2+}, phonon spectroscopy, phonon pulse spatial, spectral and temporal evolution 78−34580
SrF_2:Eu^{2+}, spectral, spatial and temporal phonon spectroscopy, new spectrometer 78−83892
SrF_2:Eu^{2+}, superfine struct. in EPR obs. 77−1593
SrF_2:Eu^{2+}, tunable optical detection and generation of THz phonons 79−65149
SrF_2:Eu^{2+}, two-photon absorpt. spectra exam. of excited state of Eu^{2+} 77−77261
SrF_2:Gd, cryst. field parameters calc. and model of tetragonal Gd^{3+} centres 79−28328
SrF_2:Gd^{3+}, cryst. field parameters calc. 77−8048
SrF_2:Gd^{3+}, dielectric relax. and EPR line broadening 79−56608
SrF_2:Gd^{3+}, dipole relax. and equilib., ionic thermocurrent obs. 77−48121
SrF_2:Gd^{3+}, dipole strengths and conc. effects influenced by dipole-dipole interactions 79−69718
SrF_2:Gd^{3+}, high-order EPR transitions of Gd^{3+} centre 78−23335
SrF_2:Gd^{3+}, ligand ENDOR, spin Hamiltonian and hyperfine parameters 77−43903
SrF_2:Gd^{3+}, $Na^+(Kr^+)(Rb^+)(Ag^+)$, EPR of orthorhombic Gd^{3+}-univalent metal ion complexes 80−11262
SrF_2:Gd^{3+}, orientation kinetics of Gd^{3+}-F^- dipole complexes 77−51952
SrF_2:Gd^{3+}, spin-lattice relax. of Gd^{3+}, EPR line shifts meas. 78−72404
SrF_2:Gd^{3+} film, Gd^{3+} luminesc. spectrum and kinetics 78−6763
SrF_2:La, type-I dipole reorientation, activation vol. determ. from dielec. const. 80−88916
SrF_2:La^{3+}, thermal depolarisation of La^{3+}-F_i^- defect dipoles 80−75926
SrF_2:Na, γ-irrad. cryst., spontaneous and induced colour centre emission 79−7131
SrF_2:Na, tunable room temp. laser action of M-centres, luminesc. and absorpt. spectra 79−31907
SrF_2:Na^+, cryst., thermal depolarisation 79−82912
SrF_2:Nd^{3+}, linear dichroism induced by electric field orientation kinetics of Nd^{3+} centres 79−69868
SrF_2:Ni, X-irrad., optical absorpt. spectra and dichroism meas. 80−108239
SrF_2:Pb^{2+}, band struct., Jahn-Teller effect, UV luminesc. and optical absorpt. spectra 80−66243
SrF_2:Pr, Nd, Tb, Dy, Ho, Er, Tm^{3+} far IR spectra 79−33736
SrF_2:Pr^{3+}, wavelength and temp.-modulated UV absorpt. 80−2799
SrF_2:R^{3+}, far IR vibr. spectra of F^- compensation ion 78−92059
SrF_2:R^{3+}, R=rare earth ion, IR and EPR spectra meas. 77−69865
SrF_2:rare earth, dipolar complex exam. 79−38435
SrF_2:rare earth, electric dipoles, relaxation parameters and dipole-dipole interaction 79−24255
SrF_2:rare earth ion, elec. dipole-dipole interaction, ionic thermocurrent and EPR study 80−108060
SrF_2:Sm^{2+}, interconfig. luminesc., spectral and kinetic charact., appls. 77−4677
SrF_2:Sm^{2+}, interconfig. luminesc. spectra, vibronic wing 79−24358

strontium compounds continued
$SrF_2:Sm^{2+}$, pseudo-Jahn-Teller effect 79−69476
$SrF_2:Sm^{2+}$, spectra, ^5D states, Lauer-Fong formula and SCC model 79−15513
$SrF_2:Sm^{2+}$ (Tm^{2+}), vibronic spectra and dynamics of impurity-contaiing lattice 79−1787
$SrF_2:Tb_3$ and pure, UV induced processes 77−32452
$SrF_2:Tb^{3+}$, cubic Tb^{3+} centres, energy level and cryst. field parameters 77−52181
$SrF_2:Tb^{3+}$, mag., thermal and hyperfine props. 80−29368
$SrF_2:Ti^{2+}$, electronic struct. and EPR of Ti^{2+} 78−76034
$SrF_2:Tm^{2+}$, EPR, optical recording in weak mag. field 78−68376
$SrF_2:Tm^{2+}$, EPR meas. of Tm^{2+} ion pair interactions 79−95641
$SrF_2:Tm^{2+}$, modulation magnetooptic spectroscopy of cross-relaxation resonances 79−15381
$SrF_2:Tm^{2+}$ (Yb^{3+}), axial g-values of $4f^{13}$ ions with trigonal symmetry *(Korean)* 79−24135
$SrF_2:Tm^{2+}$ (Yb^{3+}), trigonal centres, point-charge approx. 78−39072
$SrF_2:Y^{3+}$, diffusion of bound and free $F_{(i)}^-$ interstitials, NMR meas. 79−78542
$SrF_2:Yb_3$ superhyperfine interaction of trigonal Yb^{3+} centres 78−27117
$SrF_2:Yb^{3+}$, trigonal centres, superhyperfine interaction, model 78−88114
SrF_2-(Y,R)F_3, R=rare earth, phase equilibria, X-ray characts. of phases 79−61570
SrF_2-BaF_2, interdiffusion 77−7912
SrF_2-CaF_2-BaF_2:Gd^{3+}, luminescence spectrum of Gd^{3+} ion and solid solution region obs. 78−84638
SrF_2-Ga_2O_3, carrier for impurity anal. of U-Pu oxides by emission spectrography 78−68944
SrF_2-LaF_3, tentative phase diagram 80−71633
SrF_2-UF_4-CeF_3 solid soln., surface degradation, complex admittance analysis 78−55980
SrF_2-ZnS, dielec. films, transparent, microscopic inhomogeneities and optical breakdown 78−10844
SrFBr, absorpt. and refl. spectra 79−82994
SrFCl, absorpt. and refl. spectra 79−82994
SrFCl, thermolum. and optical absorption spectra 80−66309
SrFCl:Eu^{2+}, fluorescence lifetime and quantum efficiency for 5d→4f transitions 80−100681
$SrF_2(Cl_2)$, Brillouin scatt. and high temp. disorder 78−80365
$SrF_2(Cl_2)$, polarised Raman scatt. in fluorite crysts., anharmonicity, high-temp. disorder 78−35132
$SrF_2(Cl_2)$, superionic conductor, theoretical investigation of Raman scatt. 78−80351
$SrF_{2-x}H_x$, synthesis and struct. determ. using neutron diffr. *(French)* 80−24425
$SrFHF_2$, ^1H and ^{19}F NMR 78−2753
$Sr(Fe_{7.2}Al_{4.8})O_{19}$, minute single crystal domain struct. 77−20646
$SrFe_8Al_4O_{19}$, thin film LPE growth and mag. props. 80−80992
$Sr(Fe_xAl_{12-x})O_{19}$, cryst. domain wall energy density determ. 77−1567
$SrFe_{12-x}Cr_xO_{19}$, effects of substitution of Fe by Cr, Mossbauer spectra 80−2674
$SrFe_{12-x}Cr_xO_{19}$, hexagonal ferrite series, Mossbauer study 80−71258
Sr_2FeEuO_5, ^{57}Fe Mossbauer study 80−39976
$SrFe_6Ga_6O_{19}$ ferrite, mag. struct., Mossbauer study 80−93087
$SrFeO_{3-x}$, NO absorpt., IR spectroscopic study 79−78675
$SrFeO_{3-x}$, neutron diffr. exam. of mag. struct. 77−20553
$SrFe_{12}O_{19}$ and $Sr_4Fe_6O_{13}$, Mossbauer spectra 80−15882
$SrFe_{12}O_{19}$, Ca^{2+} additives effect on hexaferrite lattice and mag. props. 80−60243
$SrFe_{12}O_{19}$ ceramic compact, sublattice magnetisation and textures 78−68426
$SrFe_{12}O_{19}$, exam. of factors affecting reaction kinetics, thermal analysis *(German)* 79−24471
$SrFe_{12}O_{19}$, ferrite, powder effect of SiO_2 during sintering, exam. of grain growth and phase diagram *(German)* 79−24473
$SrFe_{12}O_{19}$, formation from α-Fe_2O_3 and $SrCO_3$ 77−8786
$SrFe_{12}O_{19}$, hysteresis loops, formation processes 80−39813
$SrFe_{12}O_{19}$, M type hexaferrite, Fe ion dynamic characts. in bipyramidal position, nucl. γ reson. 79−95697
$SrFe_{12}O_{19}$, mag. props., effect of Sr dissolution by milling in water 77−25000
$SrFe_{12}O_{19}$ micropowder, high coercivity, obtained by extended wet milling, prep. and mag. props. 77−8776
$SrFe_{12}O_{19}$, microstruct. and magnetic props., electron microscope obs. 79−87290
$SrFe_{12}O_{19}$, powder, chemical plating with Co, Co-P, Ni-P and Cu 80−25593
$SrFe_{12}O_{19}$, prep. by fluidized bed technique, ceramic and magnetic props. 79−43445
$SrFe_{12}O_{19}$:Si, Sr, second phase effect on elec. and mag. props. 80−60986
$Sr_2Fe_2O_5$, brownmillerite type, NO catalytic decomp. 79−43631
$Sr_2Fe_2O_5$, order-disorder transition from brownmillerite to perovskite under heat treatment in N_2 stream 79−11612
$Sr_6Fe_{10}O_{22}$-Fe_2O_3-$ZnFe_2O_4$ system, phase relations at 1100°C 78−68676
$Sr_7Fe_{10}O_{22}$, mag. props. and spin order 78−52232
Sr_2FeReO_6, seignettomagnets with perovskite struct. 79−38459
$Sr_2Fe_xRu_{1-x}O_4$ solid soln., Mossbauer spectrosc. study 80−50235
$Sr_{0.5}FeS_2$ cathodes for nonaqueous Li batteries 80−3506
$Sr_3FeTa_2O_9$, Mossbauer and X-ray diffr. studies 80−103905
$Sr(Fe_{0.766}W_{0.234})O_3$, cryst. growth, mag. and Mossbauer studies 79−42743
$SrGa_2$, layered, dispersion of acoustic phonons, inelastic neutron scatt. 78−47484
$SrGa_{12}O_{19}$, single crystal growth, lattice const. meas. *(German)* 80−44159
$SrGa_2Si_2O_8$, ordered synthetic feldspar, cryst. struct. 78−34469
$SrGa_2Si_2O_8$-$SrGa_2Ge_2O_8$, solid solution, exam. of elastic and electrical props. 79−96057
$SrGdFeO_4$, Mossbauer effect, Neel temp. and internal mag. field direction 77−12284
$SrGdFeO_4$, Neel temp. and spin reorientation, Mossbauer study 80−39934
$Sr_2Gd_{1-x}Tb_xGaO_5$, Gd^{3+}→Tb^{3+} energy transfer, emission and excitation spectra *(French)* 80−84770
$SrGeO_3$, second modification, cryst. struct. 78−22702
Sr_2GeO_4-$Sr_3(PO_4)_2$, phase equilibria and struct. 77−85999
SrH, absorption UV spectra, (0,0)-band at 2680 Å 78−50554
SrH_2, proton chemical shift tensor, heavy ion effects 79−19791
SrH_2, XPS spectra, crystalline potentials 77−77344
$SrHAsO_4$, weilite, cryst. struct. 78−38671

strontium compounds continued
$Sr(H_2AsO_4)_2$, X-ray powder diffractometry, cryst. struct. determ. *(French)* 79−60317
α-$SrHPO_4$, triclinic, crystal structure determination *(French)* 78−91315
SrI, low-lying electronic states, vibr. anal. 80−106315
SrI, mol. dissoc. energy, high temp. mass spectra 78−58863
SrI_2 mol. struct. parameters and geom. config., gaseous electron diffr. obs. 80−37883
SrI_2, photoelectron spectra, geometry 78−29816
$Sr(IO_3)_2$, complex salts, phase transitions, cryst. struct. *(Chinese)* 80−70171
$SrIn_2Se_4$, cryst. struct. *(German)* 80−79760
$Sr_2KNb_5O_{15}$, Raman scatt. experiments in tetragonal tungsten bronze compounds 80−40113
$Sr_2KNb_{5-x}Ti_xO_{15-x}F_x$ and $Sr_{2-x}K_{1+x}Nb_5O_{15-x}F_x$, ferroelectric props., F substitution effect 77−12331
$SrLaBO_4$, crystallographic and Pb^{2+} luminesc. data 79−32971
$SrLaCoO_4$, struct. and mag. props., electronic struct. of trivalent Co *(French)* 79−86760
$SrLaFeO_4$, mag. and cryst. struct. determ. *(French)* 80−54866
$SrLaFeO_4$, Mossbauer effect, Neel temp. and internal mag. field direction 77−12284
$SrLaFeO_4$, two-dimens. mag. props. rel. to cryst. struct. 80−75776
$Sr_{1-x}La_xFeO_3$, Mossbauer spectra, charge disproportionation 80−20542
$Sr_{0.5}La_{1.5}Li_{0.5}Fe_{0.5}O_4$, high spin configuration stabilisation for Fe^{4+} *(French)* 80−88519
$SrLaMTeO_6$, M=Li, Na, antiferroelectric, synthesis and charact. 77−55758
$Sr_{0.3}La_{0.7}MnO_3$, neutron-irrad. induced phase transition 77−89952
$Sr_{1+x}La_{1-x}MnO_4$, cryst. struct. determ. *(French)* 78−6042
$SrMCrO_4$, M=La, Nd, mag. struct. determ. by neutron diffr. *(French)* 79−28507
Sr_2MNbO_6, (M=Ti, Zr, Nb), perovskite struct., synthesis, lattice constants and elec. props. 77−21369
$Sr_3M_6Si_4O_{26}$, M=Nb,Ta, IR spectra and cryst. struct. *(French)* 79−11418
$Sr_2MTa_5O_{15}$ (M=K, Rb, Tl, Cs), relative stability of struct. types, and piezoelec. props. *(French)* 80−49206
SrMg, matrix-isolated, laser photoluminesc., van der Waals ground state 79−41192
$Sr_2Mg(Co)(Zn)(Mn)(Cd)(Ca)(Sr)TeO_6$, optical SHG study of acentricity, ferroelec. of low temp. phases 80−71324
$SrMnO_{3-x}$, O-deficiency induced polymorphs and elec. cond. 80−71643
Sr_2MnReO_6, seignettomagnets with perovskite struct. 79−38459
Sr_2MnbO_6, M=Ti,Zr,Hf, semiconductors, elec. cond. 77−51748
$SrMo_4$, M=Mo,W, EPR spectrum, temp. depend. of zero field splitting 79−15346
$SrMoO_3$, perovskite-type cmpd., metallic conductivity, room temp. to 2.5K 79−65483
$SrMoO_4$, centrosymmetric cryst., linear electrogyration study 80−60540
$SrMoO_4$, Davydov splitting of vibr. levels, short range interaction 80−71418
$SrMoO_4$, external lattice vibr. modes and elastic wave vels., dispersion relations 79−33050
$SrMoO_4$, precipitation from neutral equivalent solns., cryst. numbers, final morphology and sizes 78−23597
$SrMoO_4$:Mn^{2+}, zero-field splitting of Mn^{2+} EPR 80−75531
Sr_3MoO_6, electrophys. props., effects of thermophys. props. of medium in synthesis 77−48375
$Sr(ND_2)_2$, neutron diffraction exam. 31 to 570K, temp. depend. of lattice parameters *(German)* 79−69085
$Sr(NH_3)_6$, PMR linewidth, proton tunnelling and NH_3 rot., rapid NH_3 diffusion 78−35045
$SrNO_3$, single cryst., normal Raman modes, temp. effects *(French)* 77−43998
$Sr(NO_3)_2$, Born-Mayer interaction pot. and lattice props. 79−37858
$Sr(NO_3)_2$, dynamical props., IR reflection spectra meas., 10-300K 77−1676
$Sr(NO_3)_2$, IR reflection spectra, dynamical props. and phase transition 77−16303
$Sr(NO_3)_2$, isomorphous crysts., growth defects, X-ray topography 80−70188
$Sr(NO_3)_2$, low temp. struct. changes, elec. props. 79−87377
$Sr(NO_3)_2$, press. derivatives of elastic-moduli, ultrasonic velocity meas. 78−95102
$Sr(NO_3)_2$, Raman and infrared spectra, structure of nitrate ion from space groups 78−43002
$Sr(NO_3)_2$, Raman spectra temp. depend. anomalies in symmetric stretch region 79−61361
$Sr(NO_3)_2$, X-ray Debye temp. determ. 77−59088
$Sr(NO_3)_2.4H_2O$, crystallisation kinetics 79−4264
$Sr(NO_3)_2.4H_2O$, p-p vector orient., PMR obs. 78−52361
$Sr_x(Na_{0.5}Bi_{0.5})_{1-x}$ solid solutions, piezoelec. and ferroelec. props. *(French)* 80−108158
$Sr_x(Na_{0.5}Bi_{0.5})_{1-x}TiO_3$ ferroelec. ceramic, hot pressing, numerical simulation *(French)* 80−76220
$Sr_4NaLiNb_{10}O_{30}$, electro-optic, pyroelec., dielec. and piezoelec. props. *(Chinese)* 79−69810
$Sr_4NaLiNb_{10}O_{30}$, single cryst. growth, Czochralski method *(Chinese)* 79−74078
$Sr_2NaNb_5O_{15}$, Raman scatt. experiments in tetragonal tungsten bronze compounds 80−40113
$Sr_{2.05}Na_{0.90}Nb_5O_{15}$, X-ray powder diffraction data determ. *(Chinese)* 80−70170
$Sr_{1.8}Na_{0.1}Nd_{0.1}Ta_2O_7$, solid soln., ferroelectric phase transitions, dielec. constant and thermal expansion rel. to temp. 80−88934
$SrNb_2O_6$-$NaNbO_3$-$LiNbO_3$ pseudo-ternary system, DTA, heat treatment and X-ray diffr. obs. *(Chinese)* 79−52175
$Sr_2Nb_2O_7$, crystal struct. and phase transitions, rel. to isomorphous crystals *(Japanese)* 80−49208
$Sr_2Nb_2O_7$, crystal synthesis and SHG, solid laser freq. manipulation 79−41421
$Sr_2Nb_2O_7$, electronic props. and photoresponses 80−92925
$Sr_2Nb_2O_7$, ferroelec., temp. depend. of SHG intensity 79−24267
$Sr_2Nb_2O_7$, ferroelecs., nonlinear optical props. 80−33086
$Sr_2Nb_2O_7$, ferroelectric phase transitions, dielec. constant and thermal expansion rel. to temp. 80−88934
$Sr_2Nb_2O_7$, high press. phase transitions, Raman scatt. studies 80−71402
$Sr_2Nb_2O_7$, layered ferroelectric, anomalous photovoltaic effect, photovoltaic current 80−75603

strontium compounds continued
$Sr_2Nb_2O_7$, normal-incommensurate phase transition, electron microscopy and diffraction study 80−39277
$Sr_2Nb_2O_7$, optical mode softening in incommensurate phase 80−7352
$Sr_2Nb_2O_7$, phase transition at 215°C, physical props. obs. 79−56744
$Sr_2Nb_2O_7$, sputtered films, amorphous, dielec. props. 80−54573
$Sr_2Nb_2O_7$-$Eu_2Nb_2O_7$, new system preparation 78−42994
$Sr_3NbO_{5.5}\square_{0.5}$, $Sr_2CaTaO_{5.5}\square_{0.5}$, $Sr_2CaNbO_{5.5}\square_{0.5}$, $SrZr_{0.8}Yb_{0.2}O_{2.9}\square_{0.1}$, $SrZr_{0.8}Mg_{0.2}O_{2.8}\square_{0.2}$, ionic conductivity 77−20119
$SrNdFeO_4$, Mossbauer effect, Neel temp. and internal mag. field direction 77−12284
$SrNd_2Fe_2O_7$, mag. struct., neutron diffr. determ. *(French)* 78−52224
$SrNd_2S_4$, specular IR reflectance 78−2844
$Sr(No_3)_2$, lattice parameter, 261-740K, thermal expansion and Gruneisen coeff. determ. 77−35720
SrO, at. charge densities, X-ray struct. factors 78−79566
SrO, atomic interaction effects in X-ray emission spectra *(Russian)* 79−69905
SrO, C-content determ. of single crystals grown by arc fusion 79−8456
SrO, cohesive and thermophysical props., role of three-body interactions 80−92477
SrO, crystalline pots. from XPS data 77−77344
SrO, dielec. const., temp. and press. depend. 79−65789
SrO, dielectric behaviour 79−91343
SrO, dissociation energy 77−550
SrO, EPR of molecular ions 77−90031
SrO, EPR spectra of Mn^{2+} along different mag. field orientations 79−47327
SrO, effect on crystallisation of Na_2O-CaO-Al_2O_3-SiO_2-F-B_2O_3-ZrO_2 glaze 79−60279
SrO, effect on props. of PbO containing cryst. glass 80−24637
SrO, effect on viscosity of PbO containing crystal glasses 80−19973
SrO, electronic struct., XPS meas. 77−73217
SrO, electronic struct. of F-centre 78−30887
SrO, electronic struct. of V^- and related centres 80−2355
SrO, enthalpy of solution, enthalpy of formation, 298.15K, from heat of soln. meas. 78−61041
SrO epitaxial layer, on Mo (110), secondary electron emission and struct., LEED and AES expts. 78−2958
SrO, epitaxial layers by CVD *(Russian)* 79−56934
SrO, heated on W, vaporisation behaviour, mass spectrometric thermal anal. 77−56277
SrO, hydrogenated, EPR and ENDOR meas. of γ-irradiated cryst. 77−8403
SrO, irradiated, low temp. photocond. 77−39891
SrO, logarithmic derivative reflectance spectra 80−11429
SrO, luminesc. band edge, 4-6.5 eV, optical absorpt., photoluminesc., cathodoluminescence, photocond. obs. 80−50411
SrO, mm wave spectrum, spectroscopic consts. 78−37629
SrO, modified three-body shell model, lattice dynamics 77−4165
SrO, Mollwo-Ivey relation between peak-colour absorption energy and average O ion spacing 77−90179
SrO, NaCl struct., elastic props., US meas. 78−18697
SrO, neutron- or proton-irrad., F^+ centre fluoresc. yield and lifetime, 5 to 140K 80−55181
SrO, neutron-irradiated single cryst., F^+ centres, ENDOR obs. 80−15824
SrO, phonon dispersion relations, 300K, modified three body force shell model 77−20029
SrO, proton, neutron irradiated, fluorescence from anion vacancies, F^+ centre model 78−48221
SrO, reduction by C, kinetics and mechanism *(Russian)* 80−93743
SrO, single cryst., tribolum. obs. 79−52031
SrO sintering activator, effect on α-Al_2O_3 mineralisation, alumina heat treatment 80−89186
SrO, slow-electron-stimulated desorption 79−60623
SrO surface, AES peak height calibrations 79−43072
SrO, surface states, reflectance spectra, impurity effects 77−20873
SrO, trapped hole defects, ENDOR and EPR spectra of V-centres 77−32255
SrO, XPS valence bandstruct. 80−89117
$Sr^{16}O$, ($Sr^{18}O$), $A^{\prime 1}\pi$ state, vibr. anal., isotope shifts, vibr. consts. 77−18903
SrO:Ag^{2+}, EPR spectrum, static, quasistatic and quasidynamic Jahn-Teller effect 77−85561
SrO:Co_3^{2+} noncentral and interstitial ion complexes, ESR obs. 80−71169
SrO:Co^{2+}, EPR, optical, MCD absorpt. spectra 78−43692
SrO:Cu^{2+}, ESR spectrum averaging due to motion near paramagnetic centres 77−24737
SrO:Cu^{2+}, phonon-induced tunnel hopping, ESR obs. 79−69714
SrO:D, γ-irrad., V_{OD} defects, EPR and ENDOR 78−27116
SrO:Mn^{2+}, EPR expts. 77−20691
SrO:Mn^{2+}, impurity pot. well shape calcs. 78−87950
SrO:Ni, EPR of Ni^-, two-stage increase in symmetry, reorientation of cryst. field axes 78−27085
SrO:Ni, optical absorption spectra in visible and near IR region 80−45119
SrO:Ni^+, noncentral Jahn-Teller ion, energy minimum localisation, ESR study 80−25198
SrO:Ni^+(Cu^{2+}) noncentral Jahn-Teller ion, coupled polar-tetragonal strains 80−44555
SrO:Ni^{2+}, EPR line splitting rel. to Jahn-Teller coupling and soft localised mode 80−66022
SrO:Ni^{2+}, ionic thermocurrent meas. 80−108148
SrO:Ni^{2+}, linear Stark effect for zero-phonon optical absorpt. line 80−80830
SrO:Pb^{2+}(Bi^{3+}), impurity centres vibronic spectra, lattice dynamics and electron-phonon interactions 80−7396
SrO:Pb^{2+}(Bi^{3+}). luminesc. 77−73166
SrO-Al_2O_3-B_2O_3-SiO_2, glass, corrosion by Cs vapour or liq. 77−16706
SrO-Al_2O_3-P_2O_5, struct. energetics and charging under irrad. *(Russian)* 77−84791
SrO-Al_2O_3-P_2O_5, exam. of electron beam irrad. effects on physical props. 79−4253
SrO-Al_2O_3-P_2O_5 irradiated electret glasses, relax. of external field intensity on heating 80−25282
SrO-Al_2O_3-SiO_2-TiO_2 glass-crystal material, elec. cond. 79−60876
SrO-Al_2O_3-TiO_2-SiO_2, glass formation, structure of cations *(Russian)* 80−38933
SrO-B_2O_3, ^{11}B NMR lineshape, BO_3^{-3} triangle, perfect trigonal symm. *(Korean)* 78−19367

strontium compounds continued
SrO-B_2O_3-GeO_2 system glasses, physicochem. props., alkaline earth oxides effect 79−65827
SrO-Fe_2O_3, EMF meas. with solid state cell, Mossbauer effect and magnetic props. *(Korean)* 77−28493
SrO-Fe_2O_3, splat quenching struct. and crystn. mechanism *(French)* 78−51426
SrO-Fe_2O_3 system, non-existence of single phase $SrFe_2O_4$, Mossbauer expts. 80−29178
SrO-Ga_2O_3, vitrification, spectroscopic and petrographic anal. 77−15556
SrO-Ga_2O_3-Bi_2O_3, vitrification regions 77−15557
SrO-Li_2O-Al_2O_3-SiO_2:Tb^{3+} glass, energy transfer, luminesc. efficiency under UV, neutron and charged-particle excitation 79−95822
SrO-$MMoO_4$, M=Cd,Pb, phase diag. cross sections and reactions 78−27487
SrO-OsO_2 system 79−24739
SrO-P_2O_5, glass, US velocity rel. to elastic props. 80−103425
SrO-P_2O_5 glass, diffusion of Cu^+, fluoresc. meas. 78−59980
SrO-P_2O_5 glass, ESR of VO^{2+} ions 80−100610
SrO-P_2O_5-SiO_2 glasses, photoelastic consts. and polarisability 79−65839
SrO-SiO_2 glass, effect of high-dose X-rays and reactor radiation 80−19838
SrO-SiO_2-Fe_2O_3, permanent mag. ceramics, exam. of phase diagram, using X-ray analysis, optical microscopy, electron probe anal., and thermal analysis *(German)* 79−29012
SrO-$SrCO_3$, thermal dissociation 77−86297
SrO-TeO_2 glass, struct. and props. *(Japanese)* 79−32917
SrO+ZrC, high temp. reactions 80−3320
SrO_2:Fe^{2+}(Fe^{3+}), EPR spectra, evidence for off-centre displacement of Fe^{2+} 78−72398
SrO_3, visible absorpt. and reson. Raman spectra in Ar and N_2 matrices 77−65487
SrOH, laser excited mol. fluorescence, in an air-acetylene flame 78−86908
SrO(100) surface, rumpling calc. 78−14559
4 SrO.B_2O_3.SiO_2, crystal struct., X-ray powder diffr. patterns *(Japanese)* 80−54209
SrO.HfO_2(ZrO_2), US comminution of refractory compound powders 78−23656
SrO.$R_{1-x}Sr_xVO_{3-0.1x}$, R=Nd, Eu, Gd, solid solns., elec. and mag. props. 77−89819
SrO.$3B_2O_3$.$5H_2O$, thermal dehydration 78−43132
SrO.$6Fe_2O_3$, ultrafine, microstruct. development during sintering, mag. props. 79−70022
SrO.nFe_2O_3 isotropic ferrite magnets, manuf. process and mag. props. *(Japanese)* 80−29915
$Sr(PO_3)_2$, vitreous, microhardness 80−25864
$Sr(PO_3)_2$-$AgPO_3$, phase diag., physicochem. characts. of $SrAg(PO_3)_3$ 77−52302
α-$Sr_2P_2O_7$, Raman, IR spectra, factor group anal. and band assignment 78−35126
$Sr_3(PO_4)_2$, vib. of PO_4^{3-} 77−51457
$Sr_5(PO_4)_3Cl$:CrO_4^{3-}, EPR, cryst. field parameters 79−87309
$Sr_5(PO_4)_3Cl$:CrO_4^{3-}, polarised absorpt. spectra, visible and IR, ligand field transitions 79−95812
$Sr_{10}(PO_4)_6(OH)_2$, cryst., IR spectra, band assignments 78−60442
$Sr_{10}(PO_4)_6(OH)_2$, IR spectra, stretching and librational bands of OH 78−2841
$Sr_{1-x}Pb_xTeO_3$, ferroelec. soln., prep. at room temp. *(French)* 79−43190
$Sr_xPb_{1-x}(Zr_{0.545}Ti_{0.455})O_3$, piezoelec. resonator, preparation and props. *(Rumanian)* 80−28402
$SrPrFeO_4$, Mossbauer effect, Neel temp. and internal mag. field direction 77−12284
Sr_2RAlO_5 (R=La, Pr, Nd, Sm, Eu, Ga, Tb), monocrystals growth by flux method 80−20776
$SrRFeO_4$, (R=La,Pr,Nd), Mossbauer spectra, spin reorientation 80−15880
$SrR_2Fe_2O_7$, (R=Pr,Nd,Sm,Eu,Gd or Tb), Mossbauer exam. of mag. struct. 77−40157
$SrR_2Fe_2O_7$ series, mag. struct. and spin reorientation, neutron diffr. and Mossbauer meas. 77−69503
Sr_2RFeO_5 (R=Nd, Sm, Eu, Gd), monocrystal growth by flux method 80−20776
$SrRMnO_4$, (R=La,Nd,Sm,Gd), cryst. struct. determ. *(French)* 78−6042
$Sr_2R_2O_4$ luminesc. on activation by Eu^{3+}, Nd^{3+}, Eu^{3+}-Tb^3 77−52156
SrR_2S_4, R=rare earth, ternary sulphide with Th_3P_4 struct., vib. spectra 78−2844
$Sr_4R_6(SiO_4)_6F_2$, (R=Nd, Y or Yb), synthesis and characterisation 77−24992
Sr_3ReO_6, ordered or perovskite type struct., magnetic and elec. props. 79−65053
$Sr_3Re_2O_9$, cryst. struct., mag. and semicond. props. 79−10836
Sr_xReO_3 ($0.4 \leq x \leq 0.5$), cryst. struct *(French)* 79−65041
$SrRuO_3$, mag. props., mag. torque meas. 78−23295
$SrRuO_3$ single cryst., reduced ferromag. moment obs. 77−20564
$SrRuO_3$ single cryst., magnetocryst. anisotropy and reduced ferromag. moment 77−24691
SrS, dielectric behaviour 79−91343
SrS, nearest-neighbour atom displacements derived from EXAFS spectra, temp. depend. 79−87524
SrS:Cu, phosphor, photolum. meas. 78−80393
SrS:Cu, phosphor electroluminescence characts. 79−33838
SrS:Hf, phosphor fluoresc. spectra, host lattice defect 77−12416
SrS:Hf phosphor, activation energy and freq. factor calcs. from glow curves 77−12451
SrS:Hf^{4+} phosphors, phosphorsc. decay curve 77−63450
SrS:Ho phosphor, prep. methods, X-ray diffr. appraisal 77−51350
SrS:Mn, Zr phosphor, photodielectric effect 80−107848
SrS:Nd, phosphorescence decay, trapping levels 80−104003
SrS:Pb^{2+}(Bi^{3+}), luminesc. 77−73166
SrS:Zr(Zr,Mn), yellow and red-fluoresc. mechanism 77−32419
SrS-SnS_2 system, phase diagram *(French)* 79−34013
SrS_2, prep. at high press., cryst. struct. determ. by X-ray diffr. 77−4077
$SrSO_4$, activation energies for mass transfer during crystallisation, surface active agent effects *(German)* 78−63689
$SrSO_4$, celestite, colouring mechanisms 79−82998
$SrSO_4$, celestite, crystal struct. and sulphate force consts. 78−83784
$SrSO_4$, mass transfer in precip. from mixed solvents *(German)* 78−67674
$SrSO_4$, solubility and activity coeffs. in synthetic seawater 79−91986

strontium compounds continued
$SrSO_4$, surface crystn., on $BaSO_4$, isotope exchange and electron microscopy study 80−34332
$SrS_2O_6.4H_2O$, isomorphic substitution effect on optical activity 77−32347
SrS(Se) crystalline pots. from XPS data 77−77344
$Sr_2(SbCo)O_6$, spin state of Co^{3+} ion, X-ray photoemission line broadening 79−82751
$SrSb_2O_5$, $SrSb_4O_9$, $SrSb_6O_{10}$, mixed valence cpds., prep., IR and X-ray investigation *(French)* 78−88292
$Sr_7Sb_2O_{12}$, prep. and cryst. struct. *(French)* 79−32967
$SrSi_2$, dimorphic, transform. of three-dimens. three-connected Si nets 78−42944
$SrSi_2$, high-pressure phase transform., cryst. struct. 77−35693
$SrSi_2$, phase diagram, 10 to 40 kbar, 600 to 1200°C, polymorphic transform. 80−29165
$SrSi_2$, superconducting temperature depression due to mag. field 80−54820
$Sr_3SiAl_{10}O_{20}$, Ce^{3+} activated, X-ray diffr. and luminesc. props. 80−49199
Sr_2SiO_4, gamma-irrad., ESR spectra 79−51853
$SrSmFeO_4$, Mossbauer effect, Neel temp. and internal mag. field direction 77−12284
$SrSm_2S_4$, mag. props. 78−68237
$Sr_{1-x}Sm_xS$, electron config. of Sm ions, X-ray L-absorpt. spectroscopy 80−60715
SrSn, Sr_2Sn, prep. by melting, characterisation *(French)* 77−70017
$SrSnF_4$, thermal expansion and phase transitions 79−77781
$SrSnO_3$, high-density ceramics prep. and elec. props. 80−60812
Sr_2SnS_4, $Sr_3Sn_2S_7$, prep., cryst. structs. *(French)* 79−34013
$SrSo_4$ epitaxy, on $BaSO_4$ from aqueous solns. mechanisms of growth 79−56093
$SrTa_2O_6$, structural study X-ray diffr., IR absorpt. and Raman spectra *(French)* 80−107173
$SrTa_2O_7$, ferroelectric phase transitions, dielec. constant and thermal expansion rel. to temp. 80−88934
$Sr_2Ta_2O_7$, crystal struct. and phase transitions, rel. to isomorphous crystals *(Japanese)* 80−49208
$Sr_2Ta_2O_7$, soft optic phonon responsible for structural phase transition, Raman scatt. meas. 80−96618
$Sr_2Ta_2O_7$, structural phase transition to superlattice, electron microscopy and diffraction study 80−39277
$Sr_2Ta_2O_7$:Nd,Na, SHG, effect of dopants on Curie temp. 79−24267
$Sr_2Ta_2O_7$-$Eu_2Ta_2O_7$, new system preparation 78−42994
$SrTb_2Fe_2O_7$, ferrite, Mossbauer effect study of hyperfine interactions, spin reorientation 78−19383
$SrTb_2Fe_2O_7$, Mossbauer spectra, hyperfine parameters, ordering temp. 77−90079
$SrTbO_3$, EPR study of perovskite struct. 77−69685
$SrTeO_3$, ferroelec. vacuum condensates 77−40180
$SrTeO_3$, X-ray diffractional and optical studies, ferroelectric properties 79−65805
$SrTeO_4$, powder diffr. cryst. struct. determ. 79−42020
$SrThNb_2O_8$, monoclinic-quadratic phase transform. *(French)* 77−27998
$SrTiF_6.2H_2O$, cryst. struct. refinement 79−94979
$Sr_6Ti_2Nb_4O_{20}$, new class of layer ferroelectrics. X-ray anal. and permittivity meas. 77−16266
$Sr_nTi_{n-4}Nb_4O_{3n+2}$ layer ferroelectrics, physical props. 78−10854
$SrTiO_3$ 78−6678
$SrTiO_3$, (100), LEED and UPS studies 80−100747
$SrTiO_3$ (100) surface, struct. and electronic props., AES, LEED, EELS, and UPS study 80−24986
$SrTiO_3$ (100) surface electronic structure, DV-Xα cluster method 80−39646
$SrTiO_3$ (111), O_2, H_2 and H_2O chemisorption, UPS and XPS studies, illum. effects 80−71572
$SrTiO_3$ (111), surface struct., electronic props., LEED, AES, UPS study, photoelectrochem. cell anode appl. 78−84035
$SrTiO_3$, (111) face, photoassisted reaction of adsorbed H_2O+CO_2, producing methane 78−76878
$SrTiO_3$, absolute cross sections of second order Raman scatt. 78−39548
$SrTiO_3$, absorption coeff., reflectivity, 293-853K 78−64342
$SrTiO_3$, adsorption of O_2 and H_2O, UPS, LEED and AES studies 79−4480
$SrTiO_3$, adsorption of O_2, electron energy-loss spectra obs. 80−89521
$SrTiO_3$ and $SrTiO_3$:Nb, reduced samples, optical absorpt., effect of impurity-O vacancy complex *(Korean)* 79−8163
$SrTiO_3$, anharmonic motion rel. to struct. transition 78−79718
$SrTiO_3$, anharmonic phonons and central peaks at struct. phase transitions 79−95775
$SrTiO_3$, apparatus for biaxial stress production at low temp., appl. to ferroelectric 78−45609
n-$SrTiO_3$, appl. as cathode in stable photoelectrochemical cells for splitting of water 77−44484
$SrTiO_3$ based solid solns., ferroelec., US study 79−38476
$SrTiO_3$, brilliance, sparkliness and fire of diamond simulants 78−90363
$SrTiO_3$, calc. of matrix element effects in freq. dependent dielectric function 80−70632
$SrTiO_3$, cell doubling transition Raman scatt. 79−95739
$SrTiO_3$, central peak in spectrum of ferroelec. mode fluctuations and dielec. losses, 4.2K 78−19432
$SrTiO_3$, central phonon peaks, droplet model 77−43302
$SrTiO_3$, centrosymmetric crystal, phonon polariton hyper-Raman scatt. obs. 80−76028
$SrTiO_3$ ceramic, electrocaloric effects for refrigeration at cryogenic temp. 80−77789
$SrTiO_3$, ceramic, for electrocaloric refrigeration, 4 to 15K 79−80624
$SrTiO_3$ ceramic, sp. ht and electrocaloric effects at low temps. 77−59518
$SrTiO_3$, chemisorbed phases of water, UPS meas. 78−10285
$SrTiO_3$, chemisorpt. of O_2, phase investig. by UPS 78−72684
$SrTiO_3$, cluster surface states, LCAO calc. 77−43686
$SrTiO_3$, complex refr. index meas. in far IR, by dispersive Fourier transform spectroscopy 78−92042
$SrTiO_3$, crit. behaviour under stress 77−31745
$SrTiO_3$, crit. dielec. and optical props. and storage, 4K 77−24805
$SrTiO_3$, critical elastic compliance, acoustic resonance meas. 80−65118
$SrTiO_3$, critical Rayleigh wave velocity near phase transitions 77−35803
$SrTiO_3$, crystallisation from melt, nucl. and final cryst. sizes 77−24951
$SrTiO_3$ crystals, nonlinear optical phenomena, expt. *(Japanese)* 77−38990

strontium compounds continued
$SrTiO_3$ crystals, O ion diffusion, in single and polycrystalline structures 78−22892
$SrTiO_3$, cubic, temp. depend. of X-ray reflection intensities 80−107021
$SrTiO_3$, defects grown by Verneuil method 77−51390
$SrTiO_3$, dielec. nonlinearity and parametric interactions at low temps. 79−38430
$SrTiO_3$, dielec. props. in microwave region, 4.2-78K 77−16239
$SrTiO_3$, dielectric loss at microwave frequencies *(Russian)* 78−52440
$SrTiO_3$, disorder manifestation, light scatt. spectra, high temp. 80−76017
$SrTiO_3$, doped, large gap ferroelectrics, phase transitions in mag. fields 79−33621
$SrTiO_3$, dynamic central peaks and phonon interactions near structural phase transitions 78−83903
$SrTiO_3$, EPR meas., Hamiltonians with quartic anharmonicities 78−27083
$SrTiO_3$, EPR of Fe^{3+}-V_O centre, above T_c 80−39870
$SrTiO_3$ electro-optic crystals, mechanical grinding and polishing 80−48471
n-$SrTiO_3$ electrode, flatband pot. determ. from differential stress meas. 80−75638
$SrTiO_3$, electrode, photoelectrolysis of H_2O, solar energy conversion 79−52959
$SrTiO_3$, electrode, surface photovoltage expts. 78−72227
$SrTiO_3$ electrode, surface comp. changes during photoelectrolysis, XPS obs. 79−7894
$SrTiO_3$ electrodes, photoelectrolytic, defect surface states obs. 78−14815
$SrTiO_3$, electronic density of states calc. for perovskite struct. cryst. 77−76720
$SrTiO_3$, electronic struct., XPS meas. 77−73217
$SrTiO_3$, electrooptic coeffs. 79−33673
$SrTiO_3$, energy band struct., two-photon absorption spectra study 80−15453
$SrTiO_3$, fabrication damage characterisation by internal and external meas. 80−102782
$SrTiO_3$, ferroelec., cathodlum. spectral and temp. depend. 78−84665
$SrTiO_3$ ferroelectric film, parameters at upper end of centimetre waveband *(Russian)* 77−40185
$SrTiO_3$ ferroelectric modes, Raman spectra, neutron scatt. meas. 80−80727
$SrTiO_3$, ferroelectric, first order structural phase transition, anharmonic oscillator model 80−86239
$SrTiO_3$, ferroelectric, polarisation reversal, electric field induced phase transform. 80−103925
$SrTiO_3$, field depend. sp. ht. and soft modes at low temps. 79−8105
$SrTiO_3$ film, behaviour of ferroelecs. in strong elec. microwave field 79−42884
$SrTiO_3$ film, polycrystn., dielec. props. and struct. 77−81057
$SrTiO_3$ film, polycryst. dielec. losses, influence of amplitude of measuring microwave field 79−99829
$SrTiO_3$ film, sputtered, refr. index, 0.3-1.0 μm, substrate temp. effects 77−55840
$SrTiO_3$ film, surface layer nature, AES obs., and effect on permittivity 77−24498
$SrTiO_3$, flame fusion growth of optical quality crysts. 78−11099
$SrTiO_3$, forced thermal Rayleigh scattering 78−80371
$SrTiO_3$, form. entropy and tolerance factor 80−34204
$SrTiO_3$, freq. depend. of soft mode self-energy, for IR dielec. response meas. 79−33632
$SrTiO_3$ glass ceramics, polarisation and dielec. const., 4-77K 77−32319
$SrTiO_3$, H_2 reduced, neutron scatt. study of structural phase transition, central-peak enhancement 78−30755
$SrTiO_3$, heat capacity crit. behaviour 78−10857
$SrTiO_3$, heavily reduced, soft mode behaviour 80−71409
$SrTiO_3$, hyper Raman scatt. on polaritons, polariton branches *(Russian)* 80−50334
$SrTiO_3$, hyper-Raman scatt. spectra due to lattice vibr. 80−29732
$SrTiO_3$, IR active and silent modes, hyper-Raman scatt. obs. 79−61376
$SrTiO_3$, impure, low temp. polarisation, thermoelectret state 77−12301
$SrTiO_3$, incipient ferroelectric, mode-mode coupling 78−79717
$SrTiO_3$, intrinsic quantum paraelec. below 4K, dielec. const. meas. 79−73877
$SrTiO_3$, K-edge X-ray absorpt., cond. band states 80−97382
$SrTiO_3$, low temp. phase, X-ray cryst. struct. anal. at 77K 79−37683
n-$SrTiO_3$, magnetoresist. meas., band struct. exam. 77−85242
$SrTiO_3$, mean square atomic displacement temp. depend., sublattice vibration anharmonicity 80−79890
$SrTiO_3$, model for X-ray photoelectron distrib. of d-band perovskites 79−61491
$SrTiO_3$, monodomain, O-D and O-H stretching vibrs., IR spectra 80−71449
$SrTiO_3$, Mossbauer spectroscopy, sample prep. and results 80−66078
$SrTiO_3$, neutron quasi-elastic scatt. above structured phase transition 79−27877
$SrTiO_3$ neutron scatt. data, coupling between thermal and elastic variables 77−1203
$SrTiO_3$, neutron spectroscopy of central peak energy width 77−32334
$SrTiO_3$, non-orthogonal orbitals and recursion method 78−43284
$SrTiO_3$, O K_α X-ray emission band spectra *(Russian)* 79−15563
$SrTiO_3$, optical props. above 0.14 eV 79−38546
$SrTiO_3$, optical SHG near phase transition 80−71348
$SrTiO_3$, permittivity, temp. depend., submm. spectroscopy 77−176
$SrTiO_3$, perovskite with space group I4/mcm, determ. of cryst. struct. 78−75643
$SrTiO_3$, phonon interactions and the dynamic central peak near structural phase transition 77−81114
$SrTiO_3$, photoacoustic spectra, spectrometer sample cell design investig. 77−74520
$SrTiO_3$, photoanode water photoelectrolysis at high current density 78−15679
$SrTiO_3$, photolum. and carrier drift mobility at ferroelec. transition 80−71469
$SrTiO_3$, photoluminesc., thermoluminesc. and thermally stimulated currents 78−92121
$SrTiO_3$, plasmon-phonon reson., IR reflection spectra 78−56093
$SrTiO_3$, prep. from film forming soln. 80−60811
$SrTiO_3$ prism coupler for $LiNbO_3$ integrated optics very high throughput damage resistant waveguide modulator 80−58788
$SrTiO_3$ pseudodisplacive ferroelec., temp.-dependent dielectric response obs. 77−40247

strontium compounds continued
$SrTiO_3$, pure and Nb doped, heat treated, Hall effect, electrical cond., optical absorpt., defect states 78−47812
$SrTiO_3$, Raman scatt. and ferroelec. soft modes 77−16300
$SrTiO_3$, Rayleigh scatt., crit. dynamics at struct. transition 77−12396
$SrTiO_3$, SHG and quadratic electrooptic effect 78−76429
$SrTiO_3$, second harmonic generation, bond charge theory 78−76395
$SrTiO_3$, semicond., free carrier optical absorption and scatt. *(Korean)* 78−23489
$SrTiO_3$, semicond., structural phase transitions, US velocity meas. 79−28692
$SrTiO_3$, semicond. anode in aq. electrolyte, electrolum. and electrochem. 80−76080
$SrTiO_3$ semicond. electrode, electrochem., photoelectrochem. props. 80−3352
$SrTiO_3$ semicond. electrodes, electroreduction process kinetics, cathodic dark current meas. 80−66807
$SrTiO_3$, semiconductor, soft modes, zone boundary mode 80−71357
$SrTiO_3$, single crysts., $BaTiO_3$ epitaxial growth 79−15051
$SrTiO_3$, sintering kinetics rel. to added SrF_2, ZrO_2 78−44037
$SrTiO_3$, soft phonon and central peak coexistence, theory 78−14443
$SrTiO_3$, specific heat near structural transition 77−81072
$SrTiO_3$, Sr_2TiO_4, $Sr_3Ti_2O_7$, prep. from coprecipitates of Sr and Ti 77−48374
$SrTiO_3$, stressed, trigonal-to-tetragonal transition, EPR data, realisation of 3-state Potts model 77−28525
$SrTiO_3$, struct. transition temp. from self-consistent phonon spectrum 77−89517
$SrTiO_3$, structural phase transition at 110K, theory 78−80300
$SrTiO_3$, structural phase transition, intrinsic and extrinsic central peak properties 80−34168
$SrTiO_3$ surface, oxidation and reduction by D_2O, $H_2{}^{18}O$, D_2, isotope exchange study 80−104461
$SrTiO_3$ surface, photosensitizer for water photoassisted decomp. 80−85202
$SrTiO_3$, surface defects, electronic struct., LEED, AES, UPS study 78−84273
$SrTiO_3$, surface EM wave propag., IR refl. expts. 78−39553
$SrTiO_3$, surface microrelief revealed by ion irradiation 80−54485
$SrTiO_3$, surface microrelief after ion irrad. 80−59774
$SrTiO_3$, synthesis process for solidification of ^{90}Sr *(Japanese)* 77−54319
$SrTiO_3$, tetragonal, effect of impurities on Raman spectrum 80−2770
$SrTiO_3$, thermal cond., anomalous temp. behaviour near structural phase transition *(Russian)* 80−75394
$SrTiO_3$, thermal expansion near displacive phase transition meas. 77−12345
$SrTiO_3$, thermal motion at room temp., anharmonic or disordered 79−37805
$SrTiO_3$, thermodynamic props. 77−39680
$SrTiO_3$, transition metal doped anodes for water photoelectrolysis, response to visible and UV 79−74531
$SrTiO_3$, UV refl. spectra, optical consts. 0 to 32 eV Kramer-Kronig anal., band struct. calcs. 78−43903
$SrTiO_3$ under [111] uniaxial stress, neutron scatt. 78−67798
$SrTiO_3$, undispersive nonlinear dielectric, third harmonic generation *(Russian)* 80−95955
$SrTiO_3$, uniaxial stress induced ferroelectricity *(Japanese)* 79−65814
$SrTiO_3$, vacuum condensates on US irrad. substrates, props. 77−66466
$SrTiO_3$, valence band UPS and partial p and d density of states 80−71560
$SrTiO_3$, X-ray and Mossbauer γ-ray scatt., near phase transition, energy width of central peak 78−79724
$SrTiO_3$, XPS, band struct., density of states, photoionisation cross sections, theoretical determ. 78−52629
$SrTiO_3$:^{181}Ta, quadrupole interaction, $\gamma\gamma$ cascade PAC meas. 77−81042
$SrTiO_3$:B layers, ion implanted, conductive props. Hall mobility, defect energy levels 79−82693
$SrTiO_3$:Cr^{3+} crystal, radiationless relax., photoacoustic spectra 78−27264
$SrTiO_3$:Cr^{5+}, nonlinear Jahn-Teller coupling, local dynamics, near struct. transition 80−2625
$SrTiO_3$:Cr^{5+} Jahn-Teller system, EPR, electric field effects 79−28599
$SrTiO_3$:Eu(Sm), absorption spectra, Ti^{3+} ion and Z-centre formation 77−24871
$SrTiO_3$:Fe, EPR, of Fe^{3+}-rhombic, Fe^{2+}-V_0 and Fe^{1+}-V_0 complexes 78−76302
$SrTiO_3$:Fe, photochromic Fe^{5+} in non-cubic local fields, EPR spectra of $S=^3/_2$ centre obs. 77−40127
$SrTiO_3$:Fe^{3+}, displacive struct. transition, order-disorder behaviour, phonon softening, EPR obs. 79−23695
$SrTiO_3$:Fe^{3+}, order-disorder and central peak behaviour, EPR study 80−75970
$SrTiO_3$:Fe^{4+}, opt. absorpt. 77−16349
$SrTiO_3$:H(D), controlled doping, IR spectra 79−28007
$SrTiO_3$:Mn^{n+}, reduced, EPR of Mn centres 78−35029
$SrTiO_3$:Nb, Fermi surface meas., oscillatory magnetothermal effect study 79−65357
$SrTiO_3$:Ni, photochromism, optical absorption spectra and EPR meas. 77−1708
$SrTiO_3$:V, Jahn-Teller impurity, V^{4+} EPR 80−29608
$SrTiO_3$-$Bi_2Ti_2O_7$-$CaTiO_3$ system, solid solns., elec., optical props. 79−11375
$SrTiO_3$-metal contact, surface barrier Rayleigh wave transducer 79−98578
$SrTiO_3$-Ni, electrochromism, optical and elec. meas. 79−95732
$SrTiO_3$-Si junction, photoresponse 78−72254
$SrTiO_{3-x}$, anion deficiency studies 78−22708
$SrTiO_{3-x}$, anion deficiency and anion vacancy ordering 78−51532
$SrTiO_{3-x}$, single cryst. and film, Auger spectra, surface comp. 78−27353
$SrTiO_{3-x}$-In contacts, differential capacitance, elec. field depend. permittivity effect 80−54779
Sr_2TiO_3, photoelectretic states in real time spatial light modulators, photorefractive effect 80−80676
Sr_2TiO_4-Eu_2O_3, synthesis, luminesc. of materials 79−11534
$Sr_{1-x-y}U_xCe_yF_{2+2x+y}$, solid soln., ionic cond. 79−99356
$SrUO_4$, α to β transition, anomalous behaviour 78−10182
$Sr_{0.15}VO_2$, electrical cond., thermo-EMF, and lattice consts. 80−54685
$Sr_{1.1}V_{12}O_{29.9}$, phase transitions, elec. cond., susceptibility and sp. ht. meas. 78−14776

strontium compounds continued
β-$Sr_2V_2O_7$, V-O-V bridge stretching freq. correl. with bond angle 78−74636
$Sr_3(VO_4)_2$, determination of enthalpies of formation, from heats of solution 80−2182
Sr_xVO_2, oxygen vanadium bronze, phase comp., heating in air 77−40417
$Sr_3VTa_2O_9$, prep., characterisation and mag. props. 78−26535
$SrWO_4$, Davydov splitting of vibr. levels, short range interaction 80−71418
$SrWO_4$, external lattice vibr. modes and elastic wave vels., dispersion relations 79−33050
$SrWO_4$, flux- and gel-grown, comparative microtopography 77−31852
$SrWO_4$, refr. index, single crystals having scheelite struct. 78−79082
$SrWO_4$, single cryst. growth by Czochralski method and U incorporation, effective distrib. ratios, luminesc. characts. 79−42094
$SrWO_4$, slow neutron inelastic scatt. spectra, Debye temp. calcs. *(Russian)* 80−59347
$SrWO_4$, vibr. props. and struct., effect of hydrostatic press. 77−28571
$SrWO_4$:Er^{3+}, spin-lattice and spin-spin relax. times, electron spin echo obs. 79−28609
$SrWO_4$:Mn^{2+}, zero-field splitting of Mn^{2+}, EPR 80−75531
SrW_2O_4, kinetics of crystal growth from solns. in $Na_2W_2O_4$ melts, by continuous cooling 80−11550
SrX_2, X=Cl, Br, I, valence shell electronic struct., ab initio SCF calc., photoelectron spectra 79−31383
Sr_5X_3, α, intermediate phases, cryst. struct. (X=IIb, IIIb, IVb, Vb element) 78−83793
Sr_2YRuO_6, ^{99}Ru Mossbauer spectra and other techniques 80−29659
Sr_2YRuO_6, perovskites, prep., struct., emission control catalysts 77−68957
$Sr_xZn_2Y(Y=Ba_{2-x}Fe_{12}O_{22})$, x=0, 1, 1.6, mag. moments reorientation 80−44851
$SrZrO_3$ ceramic, high-temp. corrosion resist. *(Polish)* 79−52409
$SrZrO_3$ coatings, plasma-sprayed, spectral emittance *(French)* 78−26709
$SrZrO_3$, form. entropy and tolerance factor 80−34204
$SrZrO_3$, high temp. phases, struct. determ., soft mode transitions 78−42942
$SrZrO_3$, high-density ceramics prep. and elec. props. 80−60812
$SrZrO_3$, high-temp. enthalpy and specific heat, method of mixtures 77−35712
$SrZrO_3$, $NiTO_3$, sintering additive 78−23638
$SrZrO_3$, perovskite type, X-ray K-absorpt. edge, chem. shift 79−91529
$SrZrO_3$, struct. determ. by neutron diffr. 77−15351
$SrZrO_3$:Pb^{2+}, Sb_2ZrO_4:Pb^{2+}, cryst. struct. effs. on luminesc. 77−16376
Sr_2ZrO_3, resist. to corrosion by Al_2O_3, CaO, MgO, SiO_2, K_2CO_3 and coal ash 80−16516
$Sr_3Zr_2O_7.2H_2O$, cryst. struct. and thermal stability, X-ray characterisation 78−83796
Sr0, x-irradiated, intrinsic V^- and V^0 centres, ESR exam. 77−40126
$Sr[Al_2Si_2O_8]$, hydrothermally grown, cryst. morphology study 79−46590
$Sr[Fe(CN)_5NO].2H_2O$, cryst. and mol. struct. 78−91311
$Sr[Fe(CN)_5NO].4H_2O$, cryst. and mol. struct. 77−58982
$Sr[Pt(CN)_4].5H_2O$, DC elec. cond. props. 79−51582
$Sr[Pt(CN)_4].5H_20$. energy band calcs. 77−39780
U-Sr-C FBR nuclear fuels, phase anal., 1400°C 80−66487
Y_6WO_{12}:SrO, polycryst., elec. cond., 800-7400°C 80−15517
ZnS-SrF, multilayer dielec. coatings, radiation breakdown and microinhomogeneities 80−7294
ZnS-SrF_2 dielectric film, laser irrad. and microscopic inhomogeneities 78−2157

structural transformations *see solid-state phase transformations*
structure (chemical) *see chemical structure*
structure factors (crystals) *see crystal atomic structure*
structure functions
$\lambda\phi^3$, deep inelastic struct. functions for bound states, ladder approx. 79−35952
$\phi_6{}^3$ theory, anomalous dimension, Regge cut effect on structure function 80−62847
asymptotically free colour gauge theory, electroprod. local duality and precocious scaling 77−22630
asymptotically free gauge theories, deep inelastic scatt. beyond the leading order 79−21937
asymptotically free parton model, struct. function transverse momentum behaviour, SU(3) gauge model 80−27469
bag model, spin-depend. struct. functions in deep inelastic scatt. 78−8589
baryon structure functions, dynamic relationship to baryonium trajectories 79−40763
baryonic state even wave harmonic oscillator theory, structure functions versus form factor 79−393
Bjorken scaling violation, model of quarks with size and excited states 78−74208
bounds for the ratio of anomalous dimensions, scalar gluon theories 80−57595
broken SU(6) parton model, spin depend struct. functions, deep inelastic lepton+nucleon appl. 78−428
causality, Regge behaviour, proton electroprod. struct. function, Bjorken limit of sum rule 77−67662
charmed particles, inclusive semileptonic decay, struct. functions, scaling limits 78−82165
covariant parton model, pattern of scaling violation, openings of new channels 77−41815
current-induced reactions, dual unitarisation 78−74233
deep inelastic, reconstruction from moments 78−41548
deep inelastic and semi-inclusive annihilation structure function factorisation in Bjorken limit, mass singularities 80−86713
deep inelastic electroproduction struct. funct., Abelian gauge field effects 79−71754
deep inelastic lepton-hadron scatt. in massive vector gauge models 78−74262
deep inelastic lepton-nucleon scattering, quark cascade model, struct. functions 78−25051
deep inelastic leptoproduction data, Wilson coeffs. from struct. functions 77−61292
deep inelastic scatt., corrections in asymptotically free field theories 77−38092
deep inelastic scatt., QCD predictions for singlet case 80−73707
deep inelastic scattering, contrib. of twist-four operators, struct. functions 78−78187

structure functions continued
deep inelastic scattering, struct. functions, 2nd order corrections, theoretical calcs. in QCD 79−71688
deep inelastic struct. function behaviour near physical region endpoints, QCD anal. 80−99101
deep inelastic struct. function for rest frame, quark-parton model 77−87942
deep inelastic struct. function higher order asymptotic freedom corrections for e, M, γ scatt. 79−93426
deep inelastic struct. functions, direct method for QCD predictions of scaling violations 79−80800
deep inelastic struct. functions 80−42461
deep inelastic structure function moments, QCD expt. test 80−22610
deep inelastic structure function suggested by saddle points of the anomalous dimension 79−13127
deep inelastic structure functions, moments, q^2 analyticity props. 78−78188
deep inelastic structure functions, QCD tests, Bernstein moments 80−101983
deep inelastic structure functions and the quark parton model 80−4992
deep-inelastic leptoproduction off nucleons, struct. function model in asymptotically free gauge models 79−40786
deuteron, struct. function parametrisation 77−22734
diquark contribs. to scaling violation and deep inelastic σ_L/σ_T, structure functions, QCD 80−22573
Drell-Yan conjecture in asymptotically free theories 79−17689
Drell-Yan processes, asymptotic freedom corrections, Q^2-dependence 80−62933
electron deep inelast. scatt. processes, Ward identities, struct. functions *(Chinese)* 79−93431
electron-muon symmetry of Callan-Symanzik function: two-lepton case 80−73627
electronuclear sum rules, generalised, from EM structure functions 78−89806
electroproduction, spin-dependent, sum rules, test of relativistic constituent quarks 78−25050
electroproduction, studied using light cone expansion via O_4 symm. 77−41845
electroproduction structure functions in asymptotically free theories, Regge behaviour 78−25025
factorization breaking in deep inelastic neutrino hadron production in perturbative QCD 79−80820
fermion-antifermion bound states, deep inelastic struct. functions, ladder approx. 79−35952
fibre bundles almost complex manifold approach, curvature form 78−12915
flavour nonsinglet structure function, $F_3^{\nu N}$, strong interaction field theory discrimination, QCD 79−75774
G_1, spin depend. struct. function, scaling violations 78−93880
gluon bremsstrahlung, nucleon structure functions in QCD 79−49469
gluon distrib. function, tests of QCD 78−45796
gluon operator coefficients in electroproduction 79−58926
gluons, struct. functions in QCD 79−54318
hadron collisions, lepton pair production, $q\bar{q}$ annihilation within same hadron, structure function anal. validity 80−57622
hadron inclusive electroprod. in current fragmentation region 79−30741
hadronic structure functions and form factors in low-order QCD with Migdal regularization 79−30720
hadronic structure using parton anal. of deep inelastic scattering and rel. processes 79−80803
hadronic wave functions at short distances and the operator product expansion, QCD tests 80−57564
hadrons, from parton model *(Russian)* 79−93381
hadrons, predictions of quark-parton model from dual topological unitarization 79−93361
hadrons, struct. functions in QCD 79−54318
high p_T jet pairs, parton-parton scattering and π quark struct. functions 80−47248
inclusive lepton pair prod., invariated helicity struct. funcions anal. 79−13172
intrinsic transverse parton momentum, struct. function determination 79−75722
Jost-Lehmann-Dyson representation, scale invariance breaking and spectral function 80−13316
lepton pair prod., structure function relns. at large-transverse momenta 79−17690
lepton pair prod. struct. functions, QCD improved quark-parton model 80−73671
lepton pair production, where the Drell-Yan picture breaks down 79−93372
lepton-hadron deep inelastic scatt., massive vector gauge model, struct. functions *(Russian)* 78−89720
lepton-hadron deep inelastic scattering, source theory anal., polarisation 77−34160
lepton-hadron hard reactions, scaling features, correlating quark rearrangement model 79−58939
lepton-nucleon scatt., deep inelastic nucleon constituents, parton tranverse momentum, structure function 79−2976
lepton-Reggeon inelastic scatt., definition 77−6095
light cone singularities and struct. function moment asymptotic behaviour 78−4804
longitudinal, in deep inelastic lepton-hadron scatt. 77−49979
meson structure function in covariant parton model context 80−78020
MIT bag, 1-dimens., structure function L_0 approx. correction 80−101985
MIT bag, structure functions in a translationally invariant approx. 79−36023
MIT bag model, G_2 struct. function 80−4947
moments prediction by general assumptions 80−42460
Nachtmann moments of $F_2^{\nu N}(x,Q^2)$ and energy momentum sum rule 80−57580
neutron, scaling behaviour in parton model 78−16988
neutron charge radius and deep inelastic struct. functions 78−70334
neutron EM structure functions from electron scatt. data 80−13306
neutron-proton difference in deep inelastic electron scatt. and rising $\sigma(\bar{\nu})/\sigma(\nu)$ ratio 77−49978
nucleon, Bethe-Salpeter eqn. approx. soln. in quark-gluon model 77−54080
nucleon polarisabilities α,β and deep inelastic e-N scatt. 77−49966
nucleon structure function, empirical formula, scaling violation 77−38171
structure functions continued
nucleon structure function, quark and gluon moments, gauge theory 78−50036
nucleon structure functions, overview of measurable types 80−73706
nucleon structure functions from quark distrib. functions anal. of μp and μd interactions 78−50035
parton distributions, nonsinglet, QCD parametrisation, leading and next-to-leading order corrections 80−68456
parton model, mass scale effects 78−21389
perturbative QCD in a covariant gauge, moments of struct. functions 80−32073
photon, function parametrisation 80−37267
photon structure functions, anomalous components, using Altarelli-Parisi eqns. for QCD scale breaking 79−63479
photon structure functions, QCD predictions in asymptotically free gauge theory 79−30736
photon-photon scatt. anomalous cross section in gauge theory 77−38169
pion, from nucleon low energy relation 80−52507
pion EM props., dressed quark model *(Russian)* 80−52508
point like spin-3/2 quarks, contrib. to deep inelastic struct. functions 80−47250
polarised deep inelastic electroprod., QCD higher order effects, sum rule correction 79−93428
polarised deep inelastic scatt., parton transverse momenta role, struct. function, QCD evolution 80−78034
precocious scaling in field theories 78−8525
proton, quark-parton model 79−13070
proton, scaling behaviour in parton model 78−16988
proton, struct. function parametrisation 77−22734
proton electroproduction struct. function, elastic form factor, scaling function, causal representation 79−13138
proton EM structure functions from electron scatt. data 80−13306
proton-lepton deep inelastic scattering in four-quark model *(Russian)* 77−26530
protons, flavour symmetry breaking in antiquark distribs. 79−36006
Q^2 dependence of parton transverse momenta and deep-inelastic scattering, structure functions 79−40741
Q^2 dependent parton distribution function on QCD 78−93857
QCD, 2-dimens., IR structure, EM form factors and inelastic struct. functions *(Chinese)* 79−58935
QCD, asymptotic precictions for exclusive processes, form factors, struct. functions, and low-mass jets 79−71701
QCD, charm contrib. to electroprod. struct. functions 78−58170
QCD, gauge independ. approach to hard processes, structure functions, gluons 80−86665
QCD analysis of charged-current structure functions 79−49462
QCD asymptotics and kinematic thresholds in deep inelastic scattering, structure functions 79−54315
QCD at low Q^2, structure function moments, correspondence relation 80−73673
QCD axial gauge, $O(\alpha_s)$ infra-red divergences, deep inelastic quark struct. function 80−86676
QCD calc. of structure function moments, renormalisation prescription depend. 80−4948
QCD hadronic μ pair prod., gluon gauge depend., struct. func. calc. 79−80810
QCD higher order effects of structure function moments 80−62979
QCD predictions, subtraction scheme depend., struct. function scaling 79−49450
QCD running coupling const., nonperturbative determ., N struct. functions 79−75726
QCD structure function relation between deep inelastic ν reactions and polarised electroprod. 80−37221
QCD tests and singlet struct. function moments 80−82941
quark cascade model, appl. to meson spectra in e^+e^- annihilation 78−41482
quark distributions in QCD, Q^2 dependence parametrisation 79−58938
quark gluon model of hadronic structure functions at $x\rightarrow 1$ *(Russian)* 78−54617
quark masses and structure functions 80−22585
quark parton model with large parton k_T 80−42412
quark structure functions for hadrons, Drell-Yan model anal. of $pN\rightarrow l\bar{l}X$, $\pi N\rightarrow l\bar{l}X$, $eN\rightarrow eX$ 78−21476
quark-parton distributions model, large transverse momentum hadrons, logarithmic scale breaking 78−16989
quark-parton model, strong interactions of quarks, weak interaction *(Russian)* 77−82710
quarks, struct. functions, in QCD 79−54318
renormalisation group sum rules for deep inelastic structure functions 80−22611
scaling, asymptotically-free field theory 77−18182
scaling in e-p deep inelastic scatt., possible valence gluons 77−30310
scaling props. and Gross-Neveu model anomalous dimens. 77−67660
scaling violations, parton model anal. 78−62406
shape in parton model, mass scale effects 78−25017
spin dependent photon structure functions from Drell-Yan and e^+e^- reactions 80−82973
structure function relations, lepton pair processes at large transverse momenta 78−82214
unpolarised lepton-lepton collisions, photon 3rd struct. function, QCD implications 80−73708
valence quark clusters in nucleon structure functions from neutrino scatt. 80−95252
virtual Compton amplitude, high-energy deep-inelastic scatt. 78−41550
50-250 GeV EM corrections, *(Russian)* 78−25048
d, determ. from strongly inelastic ed-scatt. in region forbidden to single nucleon scatt. *(Russian)* 77−6130
d, parton model anal. of scaling in lepton 78−8642
d, polarisation meas. in ed scatt. and d percentage D state 80−420
d, six-quark model, form factors and struct. functions 78−45871
d inelastic struct. function anal. in ed scatt. 77−26531
d magnetic structure function meas. in ed elastic scatt. at 1.0 $(GeV/c)^2$ 77−57537
e(μ)p, polarised deep inelastic scatt., scaling props. of struct. functions 78−45926
e-N deep inelastic n charge radius and quark parton model 77−71488
ed, deep inelastic scatt., nucleon struct. function moments anal., asymptotic freedom critical tests 79−54344
ed deep inelast. scatt., dispersion anal. of deuteron 77−2795
ed deep inelastic scattering, phenomenological determ. of electroprod. struct. functions 79−63478

structure functions continued
ed elastic scatt., d form factors and struct. functions, charge and struct. radius *(Russian)* 79−40841
ed scattering, neutron struct. function extraction, space-time descript. 78−62404
e^+e^- 80−63010
e^+e^- annihilation and deep inelastic scatt., VDM approach, nucleon inelastic struct. functions 77−46068
$e^+e^-\rightarrow\Delta X$, polarisation effects in nonperturbative parton model, scaling 80−105912
$e^+e^-\rightarrow\Delta(1232)X$, struct. functions and nucleon longitudinal polarisation *(Russian)* 79−22121
$e^+e^-\rightarrow\gamma$+hadrons, high energy, lepton radiation and γ struct. functions, quark parton model 80−32113
$e^+e^-\rightarrow\gamma^*\rightarrow\gamma$+hadrons, QCD predictions 80−63009
$e^+e^-\rightarrow h_1h_2X$, polarised electrons, structure functions, γ^* partial widths *(Russian)* 77−61308
$e^+e^-\rightarrow$hadron(p)+X, Callan-Symanzik eqn. for structure function moments 79−21929
$e^+e^-\rightarrow$hadrons+X, structure functions in next to leading logarithm approx., ϕ^3 field theory 80−37268
e^+e^- inclusive annihilation, many-hadron final states 78−29339
e^+e^- inclusive annihilation, leading logarithm sum for struct. functions in QCD 79−71735
$e^+e^-\rightarrow VX$, polarisation states and differential cross sections for πA_1 and $\rho^+\rho^-$ *(Russian)* 80−102059
$e^+e^-\rightarrow VX$, polarization states of produced vector meson *(Russian)* 78−25058
$e^+e^-h\rightarrow e^-X$, h=hadron, structure functions in next to leading logarithm approx., ϕ^3 field theory 80−37268
eN, deep inelastic scatt., quark model, field-theoretic, quark indistinguishability, nucleon structure function 80−62993
eN, deep inelastic scattering and asymptotic freedom, Q^2 dependence of moments 80−82978
eN deep inelastic polarised scatt., QCD corrections 80−52517
eN deep inelastic scatt., polarisation meas., struct. function anal. 79−67566
eN deep inelastic scattering, scaling prediction and prod. struct. functions 79−17738
eN$\rightarrow$eX, form factors and structure functions, review, book contrib. 80−47294
eN inelastic scatt., low energy pion electroprod. and hadron form factors, book 79−85306
ep, deep inelastic scatt., higher order asymptotic freedom corrections 80−105903
ep, deep inelastic scatt., nucleon struct. function moments anal., asymptotic freedom critical tests 79−54344
ep, deep inelastic scatt., σ_L/σ_T ratio from quark model 80−82979
ep, deep inelastic scattering on π-pole Regge *(Russian)* 78−12918
ep(d) scatt., nucleon struct. function moments, asymptotic freedom critical test 79−85300
ep deep inelastic scatt., scaling violations and QCD parametrisations, struct. functions *(Russian)* 80−37277
ep deep inelastic scattering, rest frame quark-parton model of proton, scaling 78−70374
ep$\rightarrow$e$\Lambda\bar{X}$, electroprod. of forward Λ baryon near/along virtual photon direction 79−22116
ep$\rightarrow$e'nX, π exchange, π EM struct. functions calcs. 78−70375
ep$\rightarrow$e+hadron+x, parton picture from QFT, structure function scaling behaviour 79−402
ep inclusive cross-sections meas. at 50° and 60°, 6.5-19.5 GeV 77−2843
ep inclusive scatt., QCD predictions 80−13314
ep interactions, microcausality, equal-time current commutators, sum rules *(Russian)* 77−74689
ep longitudinally polarised deep inelastic scatt., asymm., depolarisation, p struct. functions 77−6133
$e^\pm p\rightarrow e^\pm\gamma$+X, deep-inelastic bremsstrahlung, quark charges, colour gluon mass 78−74216
γ, struct. function determ. in $\gamma p\rightarrow\mu^+\mu^-X$ expts. 80−42473
γ-γ scatt., QCD higher-order asymptotic freedom, corrections, γ struct. function calc. 79−89130
Γ^0, prod. in π^-p 5 GeV/c inclusive interactions *(Russian)* 78−54652
γ+hadron$\rightarrow$lepton pair, perturbative QCD, twist-2 photon operator, parton subprocesses 80−73716
$\gamma\gamma$ collision, deep inelastic, helicity method 80−22606
K, deep inelastic structure functions in massive quark model 80−86717
K, extended vector meson dominance model 78−25046
K structure functions from inclusive prod. data, nonstrange quark distribs. 80−86715
K^-, struct. functions, predictions in quark cascade model 79−36033
K^0_L, prod. in π^-p 5 GeV/c inclusive interactions *(Russian)* 78−54652
$K^0\bar{K}^0$ pair detection, interference correlations, struct. function behaviour, statistical model *(Russian)* 79−93421
$K^-N\rightarrow\mu^+\mu^-X$, K^-/π^- structure function ratio using Drell-Yan process 80−86718
kp, large P_T pion^0 prod., meson structure functions, quark distrib. functions 80−86714
$K^+p\rightarrow pK^0X$, 32 GeV/c, total cross section and structure functions 79−40809
$K^+p\rightarrow pX$, 32 GeV/c, total cross section and structure functions 79−40809
LN scattering, structure and fragmentation function moments, meas. and QCD predictions 80−37274
MB$\rightarrow l^+l^-X$, meson quark struct. functions, and Drell-Yan process 79−63551
μ pair prod., parton model, transverse momentum distrib. determ. 77−71484
μd, deep inelastic scatt., nucleon struct. function moments anal., asymptotic freedom critical tests 79−54344
μN, deep inelastic scattering and asymptotic freedom, Q^2 dependence of moments 80−82978
μN, deep inelastic struct. function, Nachtmann moments in QCD 80−27510
μN, inclusive scatt. 96, 147, 219 GeV, nucleon struct. function determ. 80−42472
μN deep inelast. scatt., inclusive ρ^0 prod. 78−37216
μN$\rightarrow\mu\bar{X}$, colour model explanation of νW_2 rise 79−45092
μN$\rightarrow\mu$X, nucleon struct. function meas., scaling violation obs. 79−45091
μN scattering, 2.8-4.5 GeV, struct. functions and charge ratios 78−74264
μp, 219 GeV, proton struct. function determ. 78−82216
structure functions continued
μp, deep inelastic scatt., higher order asymptotic freedom corrections 80−105903
μp, deep inelastic scatt., nucleon struct. function moments anal., asymptotic freedom critical tests 79−54344
μp(d) scatt., nucleon struct. function moments, asymptotic freedom critical test 79−85300
μp inclusive scatt., QCD predictions 80−13314
N, determ. from μp and μ-nucleus deep inelast. processes 78−78185
n, parton model anal. of scaling in lepton scatt. 78−8642
n, polarisation meas. in ed scatt. and d percentage D state 80−420
N, quark distributions and quark jets from the CERN bubble chamber neutrino experiments 79−45085
n, structure function nonsinglet moments from deep inelastic lepton scatt., QCD 80−62980
N, vector and axial form factors, care model asymptotic behaviour, polarised struct. functions 77−6086
N struct. functions, scaling violation dynamical anal. 77−49976
N structure function model from hard consistent quark interactions, scaling violations 80−86719
N structure function Q^2-depend. in quark-gluon system 78−66088
ν deep inelastic scatt., four flavour quark model, struct. functions 78−45905
$\nu(\bar{\nu})$ deep inelastic scattering, scaling violations of struct. function moments and perturbative QCD 79−40736
$\nu(\bar{\nu})$N 2-200 GeV, differential cross section, struct. functions, Bjorken scaling, Callan-Gross ratio 79−392
$\nu(\bar{\nu})$N deep inelastic scatt., 45 to 205 GeV, scaling and struct. functions 78−62386
$\nu(\bar{\nu})N\rightarrow\mu^-(\mu^+)$+hadrons, renormalisable field theory, high energy behaviour 77−61279
$\nu_\mu(\bar{\nu}_\mu)$N charged current total cross sections, (V-A) interactions, nucleon struct. function scaling 78−25033
$\nu_\mu(\bar{\nu}_\mu)N\rightarrow\mu^-(\mu^+)X$, struct. functions meas., quark-parton model anal. 79−58951
νFe scattering, comparison of moments from valence struct. function with QCD predictions 79−49521
νN, charged current inclusive interactions in Fe at 30-200 GeV, struct. functions, scaling phenomena 79−75764
νN, deep inelastic scatt., structure functions, form factors, negative scaling violation 78−74241
νN, deep inelastic scattering and asymptotic freedom, Q^2 dependence of moments 80−82978
νN, $\bar{\nu}$N, y-distributions, nonscaling and longitudinal struct. function effects 78−33053
νN, scaling violation, quarks with size and excited states 78−74242
νN, structure functions of deep inelastic scatt., QCD test, high-twist contribs. 80−57579
νN scatt., QCD effects above W prod. threshold, structure functions 79−71738
νp deep inelast. scatt., and πp cross-sections 77−41843
νp interactions, microcausality, equal-time current commutators, sum rules *(Russian)* 77−74689
$\bar{\nu}p\rightarrow\mu^+$+X, 4.5 GeV^2, p struct. functions x depend., quark distrib. 80−32097
p, determ. in $^{12}C+\pi^-\rightarrow pX$, 40 GeV/c π^- momentum *(Russian)* 79−89335
p, higher order asymptotic freedom corrections from deep inelastic scatt. 80−105905
p, parton model anal. of scaling is lepton scatt. 78−8642
p, polarisation meas. in ed scatt. and d percentage D state 80−420
p, structure function nonsinglet moments from deep inelastic lepton scatt., QCD 80−62980
P, three photon structure function, quark-parton model, inelastic electron scatt. data 77−46022
p deep inelastic structure function, large-x depend. in GVMD 77−30350
p electroprod. struct. function and constituent-particle scatt. 78−45931
p struct. function determ. for μp inelastic scatt. 77−61290
p-n mass difference, anal. of expt. data, scaling violation and renormalised struct. functions 79−97628
p-nucleus collisions, $\bar{p}$ and K subthreshold prod., struct. function 78−21564
pN, $\bar{p}$N, 200 GeV/c, dimuon prod. cross section, Drell-Yan predictions, struct. functions 80−37300
$\bar{p}$p, 22.4 GeV/c, γ, K_s^0 and Λ inclusive prod., structure functions *(Russian)* 79−58985
pp, large P_T pion^0 prod., meson structure functions, quark distrib. functions 80−86714
pp$\rightarrow(\pi^\pm$ or $K^+)$+X, fast-meson production and the recombination model, proton multiquark structure functions 79−89208
pp inclusive interactions, phenomenological model of pion prod. *(Russian)* 79−30763
pp$\rightarrow$mesons, multimeson inclusive spectra and recombination model, multiquark structure functions 80−73751
$pp\rightarrow\mu^+\mu^-X$, dimuon prod. using polarised beam, Drell-Yan parton model anal. 79−58981
$pp\rightarrow\mu^+\mu^-X$, polarised p, polarisation direction, structure functions and Drell-Yan parton model test 79−63544
$pp(\bar{p})\rightarrow W^\pm(Z^0)X$, QCD perturbation theory struct. function predictions 80−42505
π, comparison between results from ep$\rightarrow$epX and Kuti-Weisskopf model *(Russian)* 80−13291
π, deep inelastic structure functions in massive quark model 80−86717
π, determ. from muon pair prod. in πN interactions 79−63553
π, determ. in two-jet calorimeter experiment at Fermilab 79−45116
π, from semi-inclusive neutrino interactions 79−80819
π, modified quark loop model, form factors, struct. functions, radiative decay 80−91088
π, structure functions from ep$\rightarrow$epX interactions *(Russian)* 79−22097
π, structure functions from inclusive prod. data, nonstrange quark distribs. 80−86715
π compositeness from wave function renormalisation constant 80−101997
π in parton model and Bethe-Salpeter wave function 77−41820
π longitudinal struct. function, exclusive and almost exclusive process asymptotic behaviour, renormalisation group 80−42464
π struct. function via deep-inelastic scatt. on virtual particles 77−18292
π structure function and scaling phenomena in Drell-Yan lepton pair prod. processes 80−405
π structure function expt. determ., quark distrib. 79−89154

structure functions continued
π structure functions, determ. sea-valence quark contribs. from $\nu\pi^{\pm}$ deep inelastic scatt. 79−26323
π^0 inclusive photoprod. and quark-parton model 78−78189
π^+, π^- behaviour in ep→e$\pi^{\pm}$+anything, various W and Q values 77−10262
π^+, struct. functions, predictions in quark cascade model 79−36033
π^+ structure from two jet events, parton scatt. anal. of π^+p and pp 79−49491
πN semi-inclusive reactions at 40 GeV/c, single particle correls., $\pi^{\pm}$ and γ struct. functions *(Russian)* 77−82792
π^-N→$\mu^+\mu^-$X, K^-/π^- structure function ratio using Drell-Yan process 80−86718
π^-N semi-inclusive reactions at 40 GeV/c, structure functions *(Russian)* 77−61332
π^+N, 200 GeV/c, dimuon prod. cross section, Drell-Yan predictions, struct. functions 80−37300
πp, cross-section asymptotic limit 77−41843
πp, direct photon prod., Compton and annihilation process contrib. 80−105925
πp, large P_T pion^0 prod., meson structure functions, quark distrib. functions 80−86714
π^-p→γX, 5 GeV/c, invariant struct. function *(Russian)* 77−74717
π^-p interactions, 5 and 40 GeV, inclusive struct. functions of γ, $\pi^{\pm}$, K^0, and Λ *(Russian)* 79−80856
π^-p→Λ+X, 4.9-40 GeV/c inclusive and semi-inclusive distribs. *(Russian)* 78−41610
π^+p→K^+X, pion struct. function from low p_T hadron prod. 79−13129
π^+p→K^+X, π struct. function from low p_T hadron prod. 79−45123
^{12}C+π^-, 40 GeV/c, secondary charged particle inclusive spectra, $\pi^{\pm}$ struct. functions *(Russian)* 78−89921
ep deep inelastic scattering, phenomenological determ. of electroprod. struct. functions 79−63478
Fe+p inclusive react., structure function of conserved hadrons, 100-1600 GeV *(Russian)* 78−41611
K, comparison between results from ep→epX and Kuti-Weisskopf model *(Russian)* 80−13291
N struct.functions, $(1-x_s)^4$ behaviour 78−74227

structure of alloys, crystal *see crystal atomic structure of alloys*

structure of elements, crystal *see crystal atomic structure of elements*

structured programming
physical appl. 77−2529

student experiments *see demonstrations*

student laboratory apparatus
accelerator physics undergraduate course, 0.5 MeV Van de Graaff 77−30
acoustic resonance, open and closed end pipes 78−81774
activated metal foil experiments, teaching expts. 79−17165
air blowers, noise emission 78−61975
air track, linear, design and construction 80−17750
air track, overcoming spark recording problem 79−35483
air track direct vel. readout, conservation of momentum demonstration 77−82346
AM radio receiver constructed from pie plates 78−81771
appearance pot. spectrometer design 80−105477
audio oscillator, modified transistor radio 78−81772
autobalancing radiometer, electrical compensation 78−86067
balloon, hot-air, lectured sized 79−75308
beam splitting device for use with smoke chamber ray optics demonstrations 80−67990
Bernoulli's principle apparatus 77−41448
biomedical equipment instruction using modularised signal processor 78−41131
biomedical instrumentation instruction, modular laboratory equipment development 78−89283
biophysics electronic apparatus, modules by Thornton 79−71206
black box electronic unknown, for undergraduate electronic laboratories, construction 77−60874
blind students, phys. apparatus 78−8189
blood pressure transducer for student use, using hybrid IC 78−8186
boxcar integrator/US recording unit using sample-and-hold circ. 80−27083
C_p/C_v resonance apparatus for physics teaching laboratory 79−84885
capillary-syringe method for prep. of air-sensitive samples for MP determ. 77−67419
centripetal force apparatus, modifications 77−71171
chart recorder, multichannel sequential switcher 78−81754
chart recorder, pen-holder design 78−16611
chart recorders, for school use 78−12503
colorimetric laboratory, calibration of set of surface colour standards 78−49625
compact solar camera, student project 80−67975
computer simulated laboratory exercises, validity of graphic approach 78−81780
cosmic ray muon lifetime, scintillation detector system 78−81752
counter-timer cct. 78−28900
counter-timer-frequency meter, evaluation 78−28901
Crookes radiometer, calibration exercise 79−62978
cryostats for laboratory course in supercond. 79−58494
crystal defects, two-dimens. model 77−78940
DC amplifiers for high impedance voltmeter, expts. 78−12505
deflecting plates, using elec. field, energy change, theory 79−71192
Dewar, for meas. of heat of vaporisation of liq. N_2 77−9840
dielectric constant meas., cell, student, research laboratory appls. 80−62433
dielectric thin films, dielectric props. meas. 79−40323
differential thermometer, for teaching appls. 79−48997
diffraction grating, electronic analog 80−46753
digital display for lecture hall use 78−86075
digital logic using integrated circuit modules 78−81755
digital mini-modules, PASCO scientific, evaluation 77−57126
directional planar plasma probe for energetic plasma electron anal. 79−9062
discrete transformations, by stored water method 79−23
drop experiment for liquid viscosity 79−40331
eddy current forces demonstration 79−62967
education, Coriolis machine, inertial motion viewed from rot. reference frame, coordinate transformation 78−69934
electrical connections, saving space and cost 77−61086
electron and ion optical bench 77−45641

student laboratory apparatus continued
electron e/m ratio measurement apparatus, power supply 77−60873
electron gun for electron motion obs. in elec. and mag. fields expt. 80−27076
electron rest-mass, Compton collisions with γ-ray spectrometer 78−16607
electronic control of solar water heating system 78−81753
electronic counter-timers, three-digit or four-digit 77−17743
electronics, modulator system for introductory physics 79−97141
electroscope, oscillating type, construction details 78−41123
electrostatic force meter, device for undergraduate laboratory 79−17164
electrostatic generator from piezoelectric gas lighter 77−37689
electrostatic motor 77−37690
electrostatic potential, laboratory and theoretical comparison 80−105461
electrostatic spray painting using Al foil and Van de Graaff generator 78−54136
entropy change experiment, Pb block lowered into liq. nitrogen 79−71194
ESR of KN_3, undergraduate expt. 80−105471
experiment design, course for high school teachers 78−36752
exploration apparatus for introductory phys. lab. 77−57121
falling objects accel. due to gravity, Doppler effect, student microwave expt. 80−105472
Faraday balance for teaching appl., strong mag. field rel. to react. rates 80−57043
field mill, electrostatic field meas. 78−16613
flame emission anal., apparatus for teaching 77−29976
fluid properties, near critical point, student apparatus 77−60881
force vectors, modified force table expt., load cells and hanging students 78−69947
Foucault pendulum, continuously operating, corridor teaching demonstration 78−54137
Foucault pendulum, improved characts. for student demonstration 78−54138
Fourier transform spectroscopy using inexpensive interferometers 78−49609
freezing by boiling, using low capacity pump without acid 78−8192
Freon 12, P-V-T relation determ. 79−62970
frequency analyzing equipment, device for scientific education in oscillatory phenomena 78−41126
galvanometer, reflecting, as harmonic oscillator with recording facilities, for teachers 78−16606
gamma-ray sources, 4.43 MeV, Am-Be or Pu-Be surrounded by hydrocarbon 78−77648
gas pressure gauge for student expt., mol. weight determ. by law of atm. 79−25795
generator-motor model for physics classes 78−65739
Hall effect, in flowing electrolyte 79−21501
harmonic force acting on free mass, simple analogue computer for soln. of motion 78−28893
high voltage pulsed system, designed for small labs. 78−86079
holograms of image plane type 78−77647
holographic animation appartus 79−97134
holographic images, 360°, a simple procedure 78−28892
holography, recording of on-axis hologram, student experiment 78−86084
holography using modified Michelson interferometer, undergraduate expt. 80−105473
hot cathode, for plasma and electron physics in underground laboratory 79−35480
hypodermic syringe, disposable, plastic, physics expts. appls. 79−5935
IC wiring tools for laboratory use 78−86073
incandescent light bulb, conversion to X-ray tube 77−33755
inertial balance, direct reading, for student demonstrations, experiment 78−86081
inertial box to illustrate the term inertial frame of reference 78−69952
infrared telescope, 6032 image conversion tube 80−42020
instrument simulator, design and use 80−4490
instrumentation in undergraduate engineering curriculum 78−8206
ion source, duofilament, for alkali metals 79−40329
IR image conversion tube, using inexpensive image conversion tube 79−71207
IR spectroscopy of solids, inert atmosphere cell 79−40338
Kelvin-Thomson atom, theory for teachers, expt. simulation 78−4439
kinetic theory simulator 79−35461
Langmuir probe, mag. field affecting characteristics 79−21502
laser, N_2 high power, inexpensive design 77−23687
laser beam alignment, reticle method 78−12495
laser communication of sound, positional modulation 78−12498
laser communication system, using US light modulator 79−40321
laser power meter, calibration, Si solar cell 80−46780
laser source, He-Ne, using cold-cathode plasma tube, optical and communication expts. appl. 78−45448
LED point light sources, appls. in undergraduate expts. 77−37686
lens-pinhole spatial filter, student laboratory apparatus appl. 79−62976
lensless real-image camera 78−8456
light polarisation by reflection, apparatus for obs. 80−62434
light velocity measurement, Foucault's method modification 79−40327
light-activated switch, photo-gate, pulse method of switching, circuit 80−42021
liquid crystal electrooptical filter, teaching expts. 77−41434
liquid crystal electrooptical switches, teaching expts. 77−41434
liquid N_2 level detector for storage Dewar 78−41125
logarithmic amplifier, schematic diagram 80−57047
magnetic liquid, surface vibr. mode obs., steady state 78−41111
magnetic materials, measurement expts., laboratory apparatus 78−81743
magnetic traces, observation technique 77−87616
magnetic wheel unipolar machine 78−12499
manometer, recording, simplified design, student laboratory apparatus appl. 79−58502
mass spectroscopy, peak height intensity normaliser, pocket device 79−35498
Maxwell vel. distrib. determ., Cenco kinetic theory appl. 77−78916
measurement errors and statistics, laboratory teaching method 79−35474
mechanical start-stop gates for air tracks 80−101698
metal-nonmetal transition, simple model 77−87615
Michelson's interferometer, instantaneous multiple use with laser light source 77−57125
microprocessor multichannel analyzer laboratory project 80−101685
Millikan experiment, analogy using quanta of mass, milli-can experiment 80−46778

student laboratory apparatus continued
molecular dipole moment, meas. using simple apparatus for undergraduates 77−57118
multi-purpose instrument for biochemical and related undergraduate studies 78−73816
multichannel analyser, built from microcomputer 79−58490
multifunctional digital instruments 78−12504
muzzle vel. expt. switches 77−87606
neutron activation analysis course experiments with 14 MeV neutron generator 77−82353
NMR detector, transistorised marginal oscillator 80−27078
NMR in undergrad. instruction, general purpose microcomputers use for hypothetical spectra synthesis 80−42009
nuclear energy level lifetime, ^{237}Np 60 keV state 79−20
numerical analysis, interactive teaching package 80−86058
optical diffraction slits, production, photographic method 79−71191
optical radiation detector laboratory, graduate-level, expts. 80−62432
optical teaching microscope for investigation of transparent biological objects 80−82622
optometry, dark adaptometer for student use and optometric practice 78−48912
oscillator, 0.25-2.5 Hz sine waves, for student lab. demonstrations 78−24624
oscillator, VLF, providing variable freq. between 0.1 and 10 Hz 79−62977
p-i-n photodiode photometer 79−32
parallax experiment 78−24615
pendulum accelerometer 79−58506
permittivity of liquid, microwave expt. 79−40320
pH meter construction 79−35510
phase and group velocity, oscilloscope expt. 78−61993
photodiode array for diffraction pattern display 78−86069
photoelectron spectrometer, design for teaching lab. 78−86078
physics laboratory experiments, graphic computer simulations 80−105470
physics teaching, recent advances, syllabus, apparatus, demonstration 77−22350
Planck's constant determ., photoelectric experiment and apparatus design 78−41109
plasma experiments on elec. cond. and similarity laws 78−24605
plasma probe for Hg discharge positive column diagnostics 79−62979
plotter for tracing oscilloscope waveshapes under 1 MHz 78−70111
polarimeter, easily constructed 79−25812
positron annihilation in solids, high temp. vacuum chamber for source protection, crystal defect obs. 79−9068
proportional temperature controller, for teaching appls. 79−48997
pulse counter, four-function pocket calculator adaption 78−12497
quantum mechanics, particle trapped in rectangular pot., simple computing system 78−28891
radioactivity detector, lengthened time const. 79−44686
Raman spectroscopy, pure rot., dry-lab expt. for H_2, CO_2 78−32634
random events, circuit for recording temporal distrib. 78−41124
recording mercury manometer, student apparatus 77−26119
refractive index, by prism method 79−21
refractive index measurement, liq., wedge-film interference method 77−22352
refractometer 78−61994
Richard's box, low-cost, superimposing mol. models on 3D electron density maps 79−35495
ripple tank, wave form. and interactions using modified elec. toothbrush 77−33756
ripple tank wave generator, using loudspeakers 77−78915
rotating chair, quantitative ang. momentum expt. 77−75789
scaling model, for biological systems 77−60875
scanning electron microscope appl., ISI Model (7) 79−89044
scatter plate prod. using laser speckle, for scatter light interference expt. 79−9063
self-contained payloads, on space transportation system 79−53951
signal generator from IC chip 79−48998
simple harmonic motion, to waves, student laboratory exercise 77−60880
sinusoidal signal source with variable phase shift 78−36782
skin effect apparatus 77−27
sky brightness and polarisation, using photomultiplier 78−81768
solar constant measurement, take-home expt. 77−49537
solar energy collector, using black liq. 79−97140
solar energy conversion 78−81763
sound-level meter, innovative high school teaching project 80−4495
spark tape anal. and mech. energy expts. 78−81758
spark timer circuit 80−67991
spectra calibration, using Edser-Butler bands 79−21504
spectrophotometer performance parameters, advanced analytical chem. expt. 79−30170
spectrophotometer/fluorimeter for university biochem. courses 77−33807
spin-orbit coupling, ball in watchglass 78−81775
steel, elastic consts., meas. app. 77−33739
stellar distances, parallax and relative magnitude, laboratory model for students 78−16610
stellar magnitude simulator, IC device 78−81742
stochastic-ergodic meas. instrument technology *(German)* 77−49705
Stokes's law experiment correction 77−33800
street lights, high press. vapour lamps, spectroscopic expts. 77−22356
sum and difference frequencies, elec. circuit demonstration 78−86088
superheated droplets, flash boiling, undergraduate student expt. 78−81748
surface tension measurement by bubble method 77−45651
table top SEM for undergraduate training 80−68002
Tel-X-Ometer apparatus for educational demonstrations 80−8763
temperature control scheme (proportional), ±0.002K for several hours 77−33806
temperature difference meas. using thermocouple, microamplifier, galvanometer, teaching appls. 78−86085
thermal conduction and diffusion, electrical circuit analogue 78−86089
thermometer using ballpoint pen case 77−49540
thermostat for optical studies of phase transformations, millidegree temp. regulation 77−33805
Thornton's electronics modules for physics courses, evaluation 77−57133
time measurement experiment in phys. education, mass and charge meas. using electronic time counter *(Japanese)* 78−41127
time-of-flight velocity measurement circuit 79−58485
timer, phototransistor adaptor for timing systems, circuit diagram 78−8
torsional pendulum, for rigidity modulus meas. 79−84894
student laboratory apparatus continued
total internal reflection, laser beam-fountain demonstration 78−81769
trajectory model device 80−46759
triggered calibrated sweep for AC oscilloscope 80−67987
ultrahigh vacuum ion pumped system, for undergraduate and postgraduate courses 79−62981
uniform acceleration, student laboratory expt. 79−40326
US pulse generation for US vel. determ. of liq. by optical diffr. 79−62963
valve oscillator, VHF, construction and transmissions line expts. 78−28894
vane radiometers, elementary model 77−64901
variable star, digitally synthesized, diagram 79−9067
water droplet interactions, expts. 78−4441
water vapour, partial press. meas., student expt. 79−44685
wattmeter, static, for use in educational establishments 78−45656
wave tank, for tsunami fluid dynamics obs. 77−13531
waveform analyser, evaluation of Pasco Model 9302 77−9842
weather forecasting games at American Universities, survey 80−98770
wind power experiment, test of kinetic theory 78−81770
wind powered boat, demonstration of conservation laws 79−19
wind tunnel, smoke tracing 78−16614
Young's modulus determination, laboratory instrument for undergraduate practical classes 77−82350
Young's modulus meas. using audio generator amplifier and speaker 80−62427
α particle scattering apparatus 77−28
^{7}Be→^{7}Li, total electron capture decay energy from inner bremsstrahlung spectrum, student experiment 78−24611
^{252}Cf fission source, undergraduate laboratory expts. 77−382
He-Ne laser tube reconditioning 77−78933
^{40}K, isotope relative abundance, radioactivity expt. for schools 79−21511
Na lamp, high-press. advantages of use in interferometry 77−9837
Na light source, use of street lamp 79−35479
NaI:Tl, fluoresc. spectra excited by γ-rays, a laboratory expt. 79−97143
^{90}Sr/^{90}Y radioisotope generator 78−78535
^{232}Th, α-decay half-life, liq. scintillator expt. for students 78−12496

studios
see also radio studios; television studios
acoustic design in recording studios 80−69601
acoustic design using scale models 79−3857
acoustic design using scale models 79−10429
acoustic treatment using modular panels, computer calcs. of reverberation time *(Spanish)* 79−32141
broadcasting and recording studios, computer-aided method for acoustical design 79−64402
film production technique and technology at Russian Mosfilm studio *(Russian)* 80−22462
hi-fi demonstration studio design *(German)* 79−94405

SU_2 theory
4-dimens. Yang-Mills theory, noninteger topological number and infiniteness of action 79−246
ν-dimensional Yang-Mills and (ν-1)-dimens. nonlinear σ-model connection, quark confinement, dual strings 80−90978
't Hooft electromagnetic tensor for Higgs fields of arbitrary isospin 80−68364
Airy function basis for ($D_{1/4}{}^{+}+D_{3/4}{}^{+}$) oscill. representation of SL(2,**R**) 80−82919
asymptotic freedom scales calc. using Monte Carlo methods 80−90988
asymptotically free SU(2)×SU(2)×SU(4) model of unified interactions 78−16968
axially symmetric multi-instanton solutions generated by conformal mappings in SU(2) Yang-Mills field 80−42337
axion mass in extended SU(2)×U(1) colour gauge theory 78−78080
B-L as fourth colour in an $SU(2)_L \times U(1)_R \times U(1)$ model 79−97589
b-quark, horizontal gauge symmetry, Cabibbo universality and fermion masses 80−22583
Backlund transformations describing SU(2) mag. monopoles 79−2915
Backlund transforms. for mag. monopoles in SU(2) gauge theory 79−2916
bases from polynomial tensors 79−40681
Bloch coherent states derivation from SU(2) van der Waerden invariant 79−3671
bound state model, confinement in two dimens. models with factorisation 79−36011
Cabibbo angle, gauge invariant rearrangement and theory, SU(2) symmetry breakdown 79−22027
Cabibbo angle calc., SU(2)×SU(2)×U(1) gauge theory 78−4776
Cabibbo angle in six quark $SU(2)_L \times SU(2)_R \times U(1)$ gauge model 79−17683
Cabibbo angle in the $SU(2)_L \times U(1)$ gauge theories 79−35991
chain, appl. to asymm. top and spectra of solids *(French)* 78−28912
charged Higgs boson in SU(2)×U(1) gauge field theory, production and decay 79−13015
charges, dual, 4-D space of constant curvature *(Chinese)* 80−68392
chiral SU(2) supergroup for Yang-Mills fields, Baker-Campbell-Hausdorff formula 79−49414
classical Euclidean Yang-Mills theory, self dual SU(2) solutions 79−2945
classical gauge field eqn., self-dual static solns. 78−45792
classical gauge field with sources 80−52416
classical particle in external Yang-Mills field and SU(2) coherent states 78−74150
classical Yang-Mills eqn., multimeron solns. 80−57477
classical Yang-Mills equations, exact solutions 79−40667
classical Yang-Mills equations, static spherically symm. solns., SU(2) gauge group 79−2914
classical Yang-Mills theory, screening solns., source within SU(2) subgroup 78−62302
Clebsch-Gordan coeffs., bilinear relns., based on anal. of Poincare, Lorentz and rotation group SO(3) 80−57509
coherent state representation, path integrals 80−62502
colour Yang-Mills theory, quark source charge screening, confinement 80−22565
constant SU(2) non-Abelian gauge pot., vacuum polarisation by fermions, integral representation 80−22543
coupling coefficients for cubic groups, 3j$\Gamma\gamma$ symbols for double octahedral SU(2) group 79−21571
covariant derivatives without gauge fields 80−73584
dimensional regulation, SU_2 gauge theory, instantons 80−18066

SU_2 theory continued
Dirac's monopole, generalisation to SU(2) gauge field theory 78−32975
dual charged solution in curved space time, Dirac quantisation, SU(2)×U(1) gauge theory 78−12827
E_7 grand unification, neutral currents problem in $SU(2)\otimes[U(1)]^3$ gauge theory *(Russian)* 80−62913
eigenstates of complex linear combinations of J_1, J_2, J_3 78−58139
eight quark model by adding horizontal SU(2) gauge to Weinberg-Salam model 79−71682
electron-muon mass ratio, $SU(2)\times U(1)\times D_4$ symmetry model 79−89090
electroweak gauge models with heavy W bosons, $SU_2\times U_1\times U_1'$ scheme *(Russian)* 80−86652
electroweak theory in SU(2|1) 79−63402
EM interactions, gauge formulation, $SU_r(2)$ internal symmetry and P- and CP-violation *(Russian)* 80−42368
Euclidean, four-dimens. SU(2) Yang-Mills theory, natural guage condition ambiguities 79−2934
Euclidean space, spherically symmetric self-dual eqns., representation theory and integration 80−77936
Euclidean SU(2) Yang-Mills theory, pseudoparticle solns. 79−35931
explosive cascade-decays of leptons. quarks, virtual photons, weak vector bosons and Higgs scalars 80−86641
fermion field with broken SU_2 symm., two-dimensional isotopic model *(Russian)* 80−73616
fermion masses and hierarchy of symmetry breaking, u and d quarks 80−86618
finite-temperature Yang-Mills gas, periodic Euclidean soln. 78−66041
flavour conservation, natural, in neutral weak currents, symm. $SU_2\times U_1\times U_1'$ model 78−12858
four-quark model, $SU_{2L}\times SU_{2R}\times U_1$ gauge group, Cabibbo angle and quark masses 78−25002
gauge field, ground state wave functionals 78−74142
gauge field, Hamiltonian formulation in interaction with external source 80−62850
gauge field, spinorial classification 79−260
gauge field, static spherosymmetric sourceless soln., selfduality and induced charge current *(Chinese)* 79−80755
gauge field classification, Lorentz invariant versus gauge invariant schemes 79−85228
gauge field configurations in curved spacetimes 80−18077
gauge field theory, nonlinear scalar field eqn., spherical symmetric exact solns. *(Chinese)* 80−62886
gauge field theory, possible construction with non-Yang-Mills field eqns. 79−93307
gauge fields, classification 78−70281
gauge fields, eigenspinor-eigenvalue eqn. 78−78076
gauge fields, interaction Hamiltonian for quark source interactions 79−67466
gauge fields, sourceless solns. of static monopole systems *(Chinese)* 78−86418
gauge fields coupled to strong gravity, Coulomb like solutions 80−82701
gauge fields in interaction with static extended quark sources 79−30709
gauge fields in Minkowski space-time reparametrisation invariant formulation 78−70257
gauge fields over 4-dimens. sphere, topological charge concentrated at a point 79−85224
gauge group, magnetic monopole as finite energy smooth soliton soln., review 78−89625
gauge hierarchy in presence of discrete symmetry, $U(1)_L\times U(1)_R$ and $SU(2)_L\times SU(2)_R\times U(1)$ 80−9094
gauge invariant S-matrix elements with Yang-Mills SU(2) instantons and antiinstanton 80−22511
gauge magnetic monopole, non-Abelian group *(Chinese)* 78−78096
gauge model, classical soln. instability 78−93806
gauge model, light neutral gauge boson, consequences for e^+e^- and $pp(\bar{p})$ reactions 78−58154
gauge symmetry, effective Hamiltonian in explicit form 78−93846
gauge symmetry, model with string type solns. 78−62317
gauge symmetry, spontaneous breakdown, grand unification of QCD and SU(2)×U(1) 79−49380
gauge theory, equivalence of massive and dimensional regularisation in the infrared 79−71612
gauge theory, exact monopole and dyon solns. for arbitrary semisimple compact group 79−71599
gauge theory, external charges, topological classification for Yang-Mills eqns. 80−90977
gauge theory, Mobius invariance and classical solutions, generalised and excited merons 79−6265
gauge theory, polarised eN scatt. anal. 78−58193
gauge theory, self-dual solns. 78−41402
gauge theory, sypersymm. breaking by pseudoparticles, supergravity implications 78−24959
gauge theory instanton solns., duality condition, Lie group interpretation, quasiparticle soln. 79−6261
gauge transformation, continuous, SU_2 as an example which cannot be continuously lifted to Lie algebra 80−52396
general Taub-NUT-De Sitter metric, self-dual Yang-Mills soln. of gravity 80−46946
geometrical unification of gauge and Higgs fields 80−99077
Gibov vacuum copies in terms of harmonic maps for SU_2 gauge theories 80−57488
global SU(2) conformally invariant theory, pseudoparticle-antipseudoparticle config. 78−24975
gravitational instanton, CP^2 props. compared with SU(2) Yang-Mills instanton 78−81909
group generators for classical Calogero system 78−62332
group potentials *(Chinese)* 78−78098
harmonic analysis as basis for quantisation 80−9116
harmonics on 3-sphere, Lie group SU(2) 78−57813
heavy atoms, P-odd effects, weak interaction eqn., SU(2) theory, four fermion theory *(Russian)* 78−93820
heavy Higgs scalars, in $SU(2)_L\times SU(2)_R\times U(1)$ gauge theory, no decoupling at low energy 79−13018
heavy lepton decay, selection rule, $SU_2\times U_1$ gauge model 79−49500
heavy quark states, weak decays and prod., jet like distrib. in SU(2)×U(1) model 79−75746
Higgs bosons in SU(2)×SU(2)×U(1) left-right gauge field, coupling strength 79−13017
Higgs induced neutral currents, natural flavour conservation and quark mixing angles 80−42392

SU_2 theory continued
Higgs-Kibble model with spontaneous symmetry breaking, covariant-formulation of Yang-Mills theories 79−54256
instantaneous Coulomb interaction in SU(2) Yang-Mills QCD 80−22574
instanton, physical interpretation of degrees of freedom 78−62312
instanton solutions, Penrose twistor transform and methods of algebraic geometry 80−73612
instanton system weakly interacting with anti-instanton system, external electric fields, structure and stability 80−77956
instantons, dynamical role in quarkless chromodynamics, bag model test 80−47246
instantons, Yang's self-duality eqns. *(Chinese)* 78−78099
integral transformation describing Clebsch-Gordan coefficients, d-function SU(2) and their symmetry *(Russian)* 79−2665
interacting instanton-antiinstanton system under external colour mag. fields in SU(2) gauge 80−101920
interaction potentials for multiquark states from instantons and other background gauge field configurations 80−101995
irreducible bases of $SU(3)\supset SO(3)$ and $SU(4)\supset SU(2)\times SU(2)$ *(Chinese)* 78−82121
Jones matrix, appl. in symmetry breaking, SU_2 theory and theory of neutrinos 79−17632
Kaluza-Klein bundle, unified theory 80−37153
Landau gauge Yang Mills theories, nonsingular spherically symmetric separable copy 79−71619
lattice gauge theories, U(N) and SU(N), non-planar diagrams in large N limit 80−47187
lattice gauge theory with fermions, renormalised phases, vacuum polarization 80−13198
lattice Yang-Mills fields, strong coupling expansion, recursive eqns. 79−245
left-right symmetric gauge models, $SU(2)_L\times SU(2)_R\times U(1)_L\times U(1)_R$, weak currents, Z^0 prod. and mass 79−253
left-right symmetric $SU(2)_L\times SU(2)_R\times U(1)$ gauge theory, atomic P violation 78−74144
left-right symmetric $SU(2)_L\times SU(2)_R\times U(1)$ theory, atomic parity, e^+e^- collisions asymm. at PETRA, PEP energies 78−12820
Lie algebra, Pauli algebra, first order power-associative deformations 79−75400
Lienard-Wiechert type of solution in SU(2) 80−4879
magnetic monopoles in broken SO_3 and SU_2 gauge theories *(Chinese)* 78−86459
many-spin system dynamics, group approach *(Russian)* 80−50221
massless QCD_2, non-Abelian travelling wave solns., SU(2) subalgebra 80−57563
matrix elements, recursive relations 79−9296
merons and other field configurations, SU(2) theory *(Chinese)* 79−63335
metastable vacuum states in SU(2) Yang-Mills theory, quantum decay process 79−250
minimal surfaces in pseudo-Euclidean space, correl. with instantons, SU(2) gauge field solns. 79−21936
monopole harmonics 79−17646
monopoles in non-Abelian gauge theory, Bogomolny eqn. for interacting monopoles 79−85225
multi-instanton solutions, conformal transformation props. of one-loop tunnelling amplitudes 78−12822
n=4 supergravity theory with local SU(2)×SU(2) invariance 78−66067
neutral current expts., left-right symmetry for $SU_L(2)\times SU_R(2)\times U(1)$ gauge group 78−21375
neutral current interactions in $SU(2)_L\times SU(2)_R\times U(1)$ gauge models, natural parity conservation, gauge bosons 79−321
neutral currents, flavour-changing, Wienberg-Salam model 80−22553
neutral currents in generalised SU(2)×U(1) gauge models 78−45832
neutral heavy lepton signatures in ν induced dilepton events, SU(2)×U(1) model 78−70353
neutral-current weak interaction without electroweak unification 80−105835
neutrino neutral current couplings in SU(2)×U(1) gauge theories, natural relations, flavour dynamics 79−89095
non-Abelian gauge theories, dual transformation, SU(2) Higgs-Kibble models 79−85234
non-Abelian symmetries, spontaneous breaking in SU(2) and SU(2)×SU(2), observable consequences 79−26252
non-self-dual static gauge fields 80−52421
nonarithmetic lattice in SU(2,1) 79−88890
nonlinear σ model, kink solns., form factor interpretation 78−24964
nonlinear SU(2)×SU(2) and SU(2)×SU(1,1) chiral theories, exact finite energy solns. 79−54253
nonlocal conserved currents for two-dimensional chiral theories 80−52413
nonstationary quantum systems, SU(2) coherent states *(Russian)* 80−90693
nucleonic form factor, pion exchange, model 80−22608
O(4) Yang-Mills, Higgs system, topologically stable solns. 80−52382
O(5) nonlinear σ-model as a SU(2) gauge theory 79−35937
parity violation in atoms, SU(2)×U(1) models, higher-order corrections 78−45807
Pati-Salam $SU(2)_L\times SU(2)_R\times SU(4)$, gauge-c 78−12851
Pauli's exclusion principle for strong interactions in hadrons, nuclei, and astrophysics 80−37206
plethysms of finite and continuous groups, generating functions 80−31548
Prasad-Sommerfield monopole, time depend. soln. of SU(2) Yang-Mills-Higgs system 79−273
pseudoparticle field, scalar propagator calc. 78−29253
pseudoparticle physics in SU(2) *(Chinese)* 79−63378
QCD, spontaneous breaking of chiral SU(2)×SU(2) symmetry 79−36013
QCD vacuum, quantum liq. model, gauge and rotational invariances of colour fields 80−13283
QCD vacuum of background SU(2) gauge field, colour mag. permeability 80−78023
quantised SU(2) gauge theory, Monte Carlo study 80−77973
quantum SU(2) gauge theory, vacuum stability, dynamical symmetry breaking 80−32000
quark flavour, crude numerical estimate in SU(2)×U(1), SU(3)×U(1), SU(2)×SU(2)×U(1) models 79−13059
quark model, zero mass, SU(2)×SU(2) symmetry improvement 78−70323

SU_2 theory continued
quark-lepton correspondence, multigeneration $SU(2)_L \times U(2)$-based model 80−22584
quarks and leptons, fermion physics in terms of $SU(2) \times SU(1)$ gauge theory 78−74197
radiative corrections to β and μ decays in $SU(2)_L \times U(1)$ models involving 2n flavors 79−40778
random walk and SU(2) Clebsch-Gordan coefficients 80−17822
reggeisation in theories with broken global symmetries, nondegeneracy of vector meson masses, non-trivial mixing 80−13236
Reggeon field theory, negative mass Reggeon multiplet 78−78110
rishon model of quarks and leptons with double SU(2) symmetry and Dirac magnetic moments 80−82943
Schwinger model on the lattice, Hamiltonian lattice perturbation exam. 78−16747
self dual Euclidean gauge fields, semisimple groups, Lie algebra, SU(2) and SU(3) fields 79−6278
self dual gauge fields, static axially symmetric solns. 79−35603
self dual SU(2) fields in multicentre spaces 80−73600
self-dual SU(2) fields in Eguchi-Hanson space 80−57483
self-dual SU(2) gauge field, Pontryagin density 78−66044
self-dual SU(2) gauge fields, Backlund transform. and Atiyah-Ward ansatze 78−21339
self-dual SU(2) gauge fields, symmetries 79−21935
sine-Gordon equation, discrete, on SU(2) lattice, group theory aspects 80−57486
six-quark theory, calc. of t-quark mass and flavour mixing angles based on $SU(2) \times SU(2)_R \times U(1)$ 79−80811
sixth quark mass in $SU(2)_L \times SU(2)_R \times U(1)$ gauge group 79−26291
Skyrme gauge model, topological solitons 80−9086
soliton, non-topological, non-Abelian internal symmetry in 3+1 dimensional space-time, quantisation, collective coord. and Lorentz covariant methods 80−47199
space-time independent potentials for SU(2), SU(1,1) and E(2) gauge theories 79−49381
spectroscopy and crystal physics, generating function techniques 80−44162
spontaneously broken gauge theory, canonical quantisation *(Chinese)* 79−49406
stability of solitons, Poincare stability, gauge theories, nonlinear Schrodinger equation 80−4881
static magnetic SU(2) Yang-Mills-Higgs system, static axial and mirror symmetric monopoles 80−90992
static SU(2) Yang Mills eqns., with external charge sources, T-invariant 79−71638
strong P and T noninvariance, natural suppression in $SU(2)_L \times SU(2)_R \times U(1)_{L+R}$ gauge model 79−9303
strongly interacting Higgs bosons, gauged nonlinear σ-model, $SU(2)_L \times U(1)$ extension 80−86656
$SU_2 \times SU_2$, field theory, chiral symmetry and pion-nucleus interactions 79−80961
$SU_2 \times SU_2$ gauge theory, appl. of pure gauge fields on coset space 79−40673
$SU_2 \times U_1 \times U'_1$ electroweak model, Weinberg-Salam intermediate bosons 80−105831
$SU_2 \times U_1$ heavy lepton model of rare μ and K decay modes 78−45898
$SU_2 \times U_1$ invariance, magnetic monopole principal bundles, physical implications 79−6296
$SU_L(2) \times SU_R(2) \times U_{L+R}(1)$ theory of neutral current effects in $pp \to \mu^+\mu^- X$, and $\bar{p}p \to \mu^+\mu^- X$ 78−17060
$SU_L(2) \otimes SU(2)_R \otimes U(1)$ and $SU(2) \otimes U_L(1) \otimes U_R(1)$ gauge theories, neutral current constraints 79−277
SU(2,1;1) nonlinear invariant σ model, superconformal group and curved fermionic twistor space 80−62831
SU(2,1), graded Lie algebra, irreducible representations 80−82913
SU(2,1) generation of electrovacs from Minkowski space 79−75427
SU(2,1) symmetry of the Einstein-Maxwell fields. II 78−93577
SU(2,2) homogeneous symplectic manifolds, conformal Lie algebra 78−45808
$SU(2\Omega) \supset Sp(2\Omega)$ chain, isoscalar factors 78−70468
SU(2|1) electroweak interactions, implications for 6 extra time dimensions 80−77998
$SU(2)_A R^4$, projective irreducible unitary representations 79−89075
$SU(2)_L \times (T_3)_R \times U_V(1)$ gauge group, grand unification, symmetry breaking and Z bosons 80−73641
$SU(2)_L \times (T_3)_R \times U_V(1)$ gauge unified model, neutral current interactions, ed and ν scatt. 80−18107
$SU(2)_L \times SU(2)_R \times U(1)_L \times U(1)_R$ gauge models, parity violation in SLAC neutral current expt. 79−9305
$SU(2)_L \times SU(2)_R \times U(1)$, CP invariance, global chiral U(1) symmetry, axion-quark coupling 79−22009
$SU(2)_L \times SU(2)_R \times U(1) \times U(1)_R$, P violation 79−6308
$SU(2)_L \times SU(2)_R \times U(1)$ based L-R symmetric gauge theory, spontaneous breakdown of parity 79−75681
$SU(2)_L \times SU(2)_R \times U(1)$ gauge group, axial-vector isosinglet neutral hadronic current coupling to ν and e 79−63371
$SU(2)_L \times SU(2)_R \times U(1)$ gauge model for weak/EM interactions, u-d quarks mass difference 78−12850
$SU(2)_L \times SU(2)_R \times U(1)$ gauge models, neutral currents, P-violation 79−54293
$SU(2)_L \times SU(2)_R \times U(1)$ gauge models, parity violating effective interaction 79−9304
$SU(2)_L \times SU(2)_R \times U(1)$ gauge symm., Higgs particles, parity conservation 78−70305
$SU(2)_L \times SU(2)_R \times U(1)$ gauge theory, left-right symm., neutral current struct. 78−41420
$SU(2)_L \times SU(2)_R \times U(1)$ gauge with permutation symmetry, quark mass and Cabibbo angles 80−47232
$SU(2)_L \times SU(2)_R \times U(1)$ Higgs scalars, vacuum expectation values, quark mass ratios 79−49404
$SU(2)_L \times SU(2)_R \times U(1)$ model, weak and EM interactions, Higgs scalars, vac. instability 79−317
$SU(2)_L \times SU(2)_R \times U(1)$ six quark model, mixing angle derivation, comments 79−75729
$SU(2)_L \times U(1)$, mass hierarchies and Cabibbo angle formula 79−63420
$SU(2)_L \times U(1)$, natural flavour conservation of Higgs couplings and Cabibbo mixing conflict 80−37200
$SU(2)_L \times U(1)$, nonlinear realisation of Weinberg-Salem model for chiral $SU(4) \times SU(4)$ meson theory *(Russian)* 79−30693
$SU(2)_L \times U(1) \times U'(1)$ left handed electro/weak model 79−54297
$SU(2)_L \times U(1) \times U(1)_R$ model, chiral symmetry and weak neutral currents 80−101980
$SU(2)_L \times U(1)$ gauge group, axial-vector isosinglet neutral hadronic current coupling to ν and e 79−63371
$SU(2)_L \times U(1)$ gauge model, mixing angles and CP violation 80−73648
$SU(2)_L \times U(1)$ gauge model with off-diagonal neutral currents, anomalous lepton events 79−2923
$SU(2)_L \times U(1)$ gauge theory, weak interactions of ultra-heavy fermions 79−75713
$SU(2)_L \times U(1)$ gauge theory of weak interactions, universal lepton mixing and mixing angles *(Russian)* 79−54298
$SU(2)_L \times U(1)$ primitive particle model 79−40708
$SU(2)_L \times U(1)$ theory, radiative corrections, simple renormalisation framework 80−101973
$SU(2)_L \times U(1)$ with four flavours, relation between Cabibbo angle and quark masses 80−105872
$SU(2)_L \otimes SU(2)_R \otimes U(1)$ calculability, fermion mass matrix and CP invariance violation 80−13252
$SU(2)_L \otimes SU(2)_R \otimes U(1)$ gauge models confronting neutral current data 79−22013
$SU(2)_L \otimes SU(2)_R \otimes U(1)$ weak model, ν mass and spontaneous P nonconservation 80−62884
$SU(2)_L \otimes U(1)$ gauge Weinberg Salam model, lepton number bound 80−82927
$SU(2)_L \otimes U(1)$ theory, CP violation and Cabibbo angle 80−52447
$SU(2)_L \times SU(2)_R \times U(1)$ gauge models, neutral current sector, natural parity conservation 79−9324
$SU(2) \times SU(2)$, dynamical rearrangement of symmetry 78−49979
$SU(2) \times SU(2) \times U(1)$ supersymmetric gauge model, atomic parity violation and neutral current predictions *(Russian)* 79−54294
$SU(2) \times SU(2)$ appl. to radiative muon capture 78−82320
$SU(2) \times SU(2)$ chiral symmetric Lagrangian description of low energy πN and NN scatt. 79−26251
$SU(2) \times SU(2)$ sigma model, $\pi^+ \to e^+ \nu_e \gamma$ decay rate. calc. 78−8659
$SU(2) \times U1$ unified theory, symmetry and renormalisation 80−22551
$SU(2) \times U(1)$, gauge invariance and fermion mass dimensions 80−62907
$SU(2) \times U(1)$, gauge theory of weak interactions 78−21328
$SU(2) \times U(1)$, $K^0 \leftrightarrows \bar{K}^0$ transition amplitude in MIT bag model 79−63450
$SU(2) \times U(1)$, leptonic colour model, expt. evidence 78−62350
$SU(2) \times U(1)$, P and T invariance violation suppression, quark mixing angles 79−54278
$SU(2) \times U(1) \times G$, hadronic neutral current in neutrino interactions and single Z-boson hypothesis 79−54295
$SU(2) \times U(1) \times G$ expanded gauge models of neutral currents, propagator momentum transfer 80−47237
$SU(2) \times U(1) \times G$ Weinberg-Salam extension, possible neutral current struct. at PETRA/PEP and LEP 79−89096
$SU(2) \times U(1) \times S_3$ model, CP violations and Kobayashi-Maskawa matrix elements 79−85243
$SU(2) \times U(1) \times SU_F(2)$ gauge model, CP violation and off-diagonal neutral currents 79−13008
$SU(2) \times U(1) \times SU_F(2)$ gauge symmetry, CP violation, neutron elec. dipole moment, muon number changing process 79−89091
$SU(2) \times U(1) \times U(1)$, V(e)V(q)+A(e)A(q) neutral currents 79−17667
$SU(2) \times U(1) \times U(1)$ gauge model, quark-lepton correspondence in neutral and charged current interactions 79−54296
$SU(2) \times U(1) \times U(1)$ gauge models, neutral current struct., parity nonconservation 79−292
$SU(2) \times U(1) \times U(1)$ gauge theory of weak and EM interactions in unified SU(6) scheme 78−41465
$SU(2) \times U(1) \times U(1)$ model, Cabibbo angle and Higgs coupling strangeness conservation 80−47233
$SU(2) \times U(1) \times U(1)$ model, neutral current, quark mass reactors, spontaneous broken Lagrangian 79−97563
$SU(2) \times U(1)$ gauge group in (V-A) model, mixing between ordinary and heavy leptons 78−41472
$SU(2) \times U(1)$ gauge model, eigenvalue condition for Weinberg mixing angle, new leptons and quarks 78−41463
$SU(2) \times U(1)$ gauge model, muon anomalous mag. moment, charged Higgs boson contrib. 80−78011
$SU(2) \times U(1)$ gauge model, polarised lepton scatt. 78−45901
$SU(2) \times U(1)$ gauge model, right-handed charm current, CP violation 78−45795
$SU(2) \times U(1)$ gauge model, symmetry breaking pattern with two Higgs doublets 79−12978
$SU(2) \times U(1)$ gauge model and parity violation in atoms 78−4775
$SU(2) \times U(1)$ gauge theories, successes and current issues 80−18064
$SU(2) \times U(1)$ gauge theories of leptons, T violation, leptonic decay and dipole moment 79−299
$SU(2) \times U(1)$ gauge theories of weak and EM interactions, neutral current contraints 78−70272
$SU(2) \times U(1)$ gauge theory, μ-e mass ratio and CP violation as quantum effect 79−30691
$SU(2) \times U(1)$ gauge theory, charged heavy lepton and neutrino 78−45794
$SU(2) \times U(1)$ gauge theory, natural suppression of CP violation 78−41421
$SU(2) \times U(1)$ model, ν interactions, trimuon prod., heavy lepton cascade decay 78−25038
$SU(2) \times U(1)$ model, quark mass matrix and discrete symmetries 78−54607
$SU(2) \times U(1)$ scheme, CP violation parametrization, quark n-doublet weak interaction *(Russian)* 80−13231
$SU(2) \times U(1)$ six quark model, uniquely determined discrete symmetry 79−93360
$SU(2) \times U(1)$ symmetry group, μe universality breaking in neutral current weak interactions *(Russian)* 79−58918
$SU(2) \times U(1)$ theories, weak isospin breaking, higher order corrections 80−95235
$SU(2) \times U(1)$ unified gauge field, Euclidean space and O_4 invariance 80−91031
$SU(2) \times U(1)$ unified gauge theory threshold effects 78−82098
$SU(2) \times U(1)$ unified model, universal Yukawa coupling 80−91032
$SU(2) \times U(1)$ vectorlike model: new leptons, quarks, and the axion question 79−40711
$SU(2) \times U(1)$ weak coupled gauge field formulation using quaternions and p, n, λ quark fields 79−63349
$SU(2) \times U(1)$ Weinberg-Salam model, possible classical solns. 80−86644

SU_2 theory continued
SU(2)×U(1) Weinberg-Salam model, weak mixing angle, grand unified gauge theories 79−89093
SU(2)⊗U(1)$_\gamma$⊗U(1)$_c$ gauge model, neutral current and ΔI=1/2 rule 79−6257
SU(2)⊗U(1)⊗U'(1), anal. in neutral current interactions, parity nonconservation in ed scatt. 79−17731
SU(2)⊗U(1)⊗U(1)' gauge theories and extensions, one-loop generated CP violation 79−89078
SU(2)⊗U(1)⊗U(1) gauge model without parity violation in heavy atoms 78−82097
SU(2)⊗U(1) gauge group theory tests from neutral current phenomena 78−24992
SU(2)⊗U(1) gauge model, strange baryon weak radiative decays and CP violation 79−6260
SU(2)⊗U(1) gauge model of EM and weak interactions, fermion mass restriction *(Russian)* 78−89650
SU(2)⊗U(1) gauge models, neutral current couplings 79−40715
SU(2)⊗U(1) gauge models of weak and electromagnetic interactions and the μe universality *(Russian)* 80−13257
SU(2)⊗U(1) model for baryon asymmetry of the universe 78−66072
SU(2)⊗U(1) standard and SU(5) grand unification models, neutral current data implications 80−78000
SU(2) and SO(2) gauge fields in 4-, 5- space-time dimens., confinement, critical dimensionality 79−89064
SU(2)/U(1) nonlinear theory, solitons with nonvanishing Hopf index 78−86410
SU(2/1) supergroup, irreducible gauge theory of a consolidated Salam-Weinberg model 79−40707
SU(5), gauge invariance and fermion mass dimensions 80−62907
SU(5), symmetry breaking patterns, Higgs fields 80−101953
SU(5)×SU(2) unification, horizontal symmetry due to quantised motion along internal axes 80−62905
SU(S) based grand unified theory, monopoles and vector bosons, symmetry breaking 80−99079
superalgebra generalisation, 3-colour extension of OSP (4,1) de Sitter and SU(2,2;1) Wess-Zumino superalgebras 79−330
supersymmetric SU(2) Yang-Mills fields, Lie groups, chiral coeffs., Baker-Campbell-Haussdorff formula 80−68355
symmetry, classical quark confining solns. incorporating colour 79−339
trimuon production by neutrinos, heavy lepton cascade mechanism using SU(2)×U(1) gauge model 78−58180
twist selection rule, mass zero representation partons 80−78027
two-dimensional SU(2) Yang-Mills theory 78−24942
U_2 (Q) invariance of principal bundles for SU_2 dual charges, and corresponding ang. operators *(Chinese)* 79−36043
U(1)×SU$_L$(2)×SU(3) theory, integer charge quarks, lepton hadronic processes *(Russian)* 80−86653
U(1)×SU(2) unified gauge field theories, field function O(4) invariance 80−37201
U(1) chiral symmetry breaking from SU(1) gauge theory 80−86617
unconfined colour quark models, weak interactions and neutral currents *(Russian)* 80−105841
unification of isospin and hypercharge, electroweak interactions of leptons 80−27439
unified model for atomic parity violation and neutral currents in gauge theories 80−4912
unifying mass scales without intermediate schiral colour symmetry, SU(2)×SU(1)×SU(3), $[SU(2n)]^4$ unified model 80−22555
unit tensor operators 80−62873
vacuum structure of SU(2) Yang Mills theories, in Coulomb gauge 78−49971
weak charge of electron, $SU_2×U_1$ theories, $\bar{\nu}_\mu$e scatt., isospin 78−16974
weak gauge boson doubling in standard SU(2)⊗U(1) model, W, Z bosons 80−62916
weak interactions, renormalisable model on gauge group SU(2)×SU(2)$_R$×U(1) 78−12855
Weinberg-Salam model, Lagrangian, invariant under SU(2/1) gauge group and rotations, in 6-D graded space 80−57537
Weinberg-Salam model, Yang-Mills theory, Higgs particle 80−4905
Weinberg-Salam SU(2)×U(1)×U'(1) extension, new neutral current structs. 79−58920
Weinberg-Salam SU(2)⊗U(1) gauge theory effective Lagrangian, neutral current results 79−35992
XY_4, tetrahedral, SU (2s+1)×ζ_r and spin statistical weights 78−50463
XY_5, trigonal bipyramidal, SU (2s+1)×ζ_r and spin statistical weights 78−50463
XY_6, octahedral, SU (2s+1)×ζ_r and spin statistical weights 78−50463
y anomaly in SU(2)×U(1) vector like model, with parity violating neutral current 79−13013
Yang's K gauge, solns. to self-dual SU(2) gauge field 79−12965
Yang's monopole, quaternionic gauge fields on S^7 80−57473
Yang Mills field, singular SU(2) symmetric potentials, bound states *(Russian)* 79−30665
Yang Mills multi-instanton paths, tunnelling pots. and WKB wave functionals 79−248
Yang Mills theory, high energy scatt. amps. 79−63346
Yang-Mills dyons, mag. charge and Pontryagin index equality in SU(2) 80−57562
Yang-Mills eqns., complex and Lienard-Wiechert solns. in Minkowksi spacetime 79−2938
Yang-Mills eqns., elliptic generalization of the one-meron configuration 80−62854
Yang-Mills eqns., local uniqueness theorem for (anti) self dual solns. 78−70263
Yang-Mills equations, classical solns. 80−4875
Yang-Mills field, 't Hooft monopole, Julia-Zee dyon, stable solns. 79−26229
Yang-Mills field, pure gauge forms 79−26228
Yang-Mills field, quantum string representation, SU_2 gauge group 80−57465
Yang-Mills field eqn. configurations in curved spacetimes 80−18076
Yang-Mills field equation instability, removal by (1+1) dimens. Higgs mechanism, SU(N) generalisation 79−58924
Yang-Mills fields, coupled to (2s+1) dimens. Higgs field, classical soln. 78−41430
Yang-Mills fields, quasi-metric with nonself-dual curvature 79−26213
Yang-Mills gauge theory, two meron configurations in transverse gauge 79−71637
Yang-Mills invariants, polynomial basis 79−17609

SU_2 theory continued
Yang-Mills lattice gauge theories, comparison with gauge groups SU(2) and Z_2 80−31966
Yang-Mills quantum field theory, meron pairs and quark confinement 78−37174
Yang-Mills static Euclidean anti-self-dual SU(2) eqns., small deformation of Prasad-Sommerfield soln. 79−71633
Yang-Mills SU(2) eqns. in compactified Minkowski space, invariance conditions 79−63342
Yang-Mills SU(2) field equations, props. of O(4)×O(2) symm. solns. 78−24931
Yang-Mills SU(2) gauge theory solns. 79−9285
Yang-Mills SU(2) theory in transverse gauge, single meron configuration 78−74145
Yang-Mills theories, classical solns., historical development and general introduction 79−93295
Yang-Mills theory, 1st and 2nd order eqn. equivalence 80−90979
Yang-Mills theory, asymptotic freedom, vacuum polarisation of unstable mode 79−9278
Yang-Mills theory, Coulomb gauge fixing 79−26235
Yang-Mills theory, deformations of instantons 78−45786
Yang-Mills theory, field-strength description of non-Abelian gauge theories 80−62856
Yang-Mills theory, finite field eqn. 80−62830
Yang-Mills theory, ground state 80−101939
Yang-Mills theory, self duality of solns. 78−37143
Yang-Mills theory, singularities and sources of static gauge fields 79−49401
Yang-Mills theory, topological and differential geometric techniques 79−71586
Yang-Mills theory, transverse pure gauge fields 79−26227
Yang-Mills theory, vacuum struct. 79−71588
Yang-Mills theory, vacuum struct. 80−57501
Yang-Mills theory in Coulomb gauge, quantisation 78−54546
Yang-Mills theory with potentials invariant under U(1) gauge subgroup 79−54255
Yang-Mills-Higgs system, classical finite energy solns. embedding in supersymmetric extension 79−2950
Yang-Mills-Higgs system, soliton solns. 79−26218
zero energy fermions in U(1) pointwise monopole field *(Chinese)* 80−42345
ed, polarised e, elastic scatt. asymmetries in SU(2)×U(1) gauge theory 79−40781
$e^+e^-\rightarrow\gamma\gamma$, weak interaction effects, QED tests, SU(2)×U(1) gauge theory 79−40767
e^+e^- high energy annihilation, possible signature of charged Higgs particles, SU(2)×U(1) model 79−35995
$e^+e^-\rightarrow\mu^+\mu^-(\tau^+\tau^-)$, cross sections, charge asymmetry, polarisation in SU(2)×SU(2)×U(1) models 79−97616
eN, deep inelastic scatt., heavy lepton mixings, Weinberg-Salam model 80−62992
en, polarised e, elastic scatt. asymmetries in SU(2)×U(1) gauge theory 79−40781
$en\rightarrow en\pi$, pol. e, P-odd asymmetry and cross sections, SU(2)xU(1), SU(3)xU(1) calcs. *(Russian)* 80−62998
e^-p, polarised e, elastic scatt. asymmetries in SU(2)×U(1) gauge theory 79−40781
$\mu\rightarrow e\gamma$, SU(2)×U(1) unified guage theory 78−8643
$\mu\rightarrow E\gamma$ predictions, $SU(2)_L×U(1)×SU(2)_R$ model for lepton decay and neutrino lifetime 78−62331
μ-e universality constraints, implications for SU(2)×U(1) gauge models of π decay 79−9368
$\mu^-\rightarrow e^-e^-e^+$, decay rate calc. SU(2)×U(1) model 78−8641
μe universality breakdown of neutral weak currents in $SU_2×U_1$ gauge *(Russian)* 79−75712
μN, deep inelastic scatt., heavy lepton mixings, Weinberg-Salam model 80−62992
NN→NN, large momentum transfer, spin effects 80−22577
$\nu_\mu e^-\rightarrow\nu_\mu e^-$, SU(2)×U(1) anal. 78−50026
$\psi'\rightarrow\psi\pi^0(\eta)$, SU_2 violation, symmetry breaking and decay amplitudes 80−52499
$\rho\rightarrow\pi\gamma$, EM decay rates, spectrum generating SU(4) approach 79−26334
u-quark masslessness, consequences for SU(2) and SU(3) 79−22022
Υ, quixotic interpretation as $Q\bar{Q}$ bound state 80−13280
Bi weak charge, SU(2)×U(1) model anal. 79−26281

SU_3 theory
(3,3*)⊕(3,3*) bilinear symmetry breaking in linear σ-model, symmetry breaking Lagrangian 79−300
27-plet hadrons, possible cause of ΔS=ΔQ violation 77−26501
27-plet mesons masses, existence of low-mass long lived exotics in quark model 78−33032
ΔS=0 weak hadron neutral current, quark parton model, νN and e^+e^- interactions 78−12859
σ model, SU(3) linear, renormalisation in one loop approx. 80−68368
σ SU(3) model, quark-loop contrib., low-energy meson dynamics 78−12869
A=12 to 24, nuclear cluster norm determ. using integral transform and SU(3) recoupling techniques 79−22214
algebra of colour 78−62354
angular momentum content of irreducible representations 78−32702
asymptotic freedom scales calc. using Monte Carlo methods 80−90988
asymptotically free parton model, struct. function transverse momentum behaviour, SU(3) gauge model 80−27469
axial vector matrix elements, chiral limit, renormalisation effects 79−17190
axial-vector-current divergences in constituent-quark basis 78−8557
b-mesons, mass splitting, SU_3 nonet of SU_6 80−47288
band structures, generalised HFB approach in SU(3) framework 80−22663
baryon decay, algebraic formulation, vector and axial vector operators, SU(3), form factors 77−71512
baryon hadronic decay, $3/2^+$ decuplet isobars in SU(3) symmetry, dynamical assumption 79−26333
baryon mass splitting by the 'strong hyperfine interaction and SU(3) breaking 78−82184
baryon octets, semileptonic decays 80−32030
baryon resonances, hadronic decay, broken SU_3 and total reduced width 78−17017
baryon SU_3 dynamical model, gravit. bound linear rotator 77−49904

SU_3 theory continued
baryon wave functions, SU_n representation transformations and phase *(Chinese)* 79−93313
baryon weak radiative decay, sum rules, sextet/octet dominance in SU(3) 78−62400
baryonium, connection between exchange-degeneracy breaking and multiquark states 79−93387
baryonium and dibaryon, quark shell model 78−41479
baryons, leptonic decays and mag. moments in nonlocal quark model *(Russian)* 80−86711
baryons, spin $1/2^+$, mag. moment sum rule, in SU_3 for u-, d- and c-quark sector 78−21428
broken SU_3 symmetry, particle correlations in multiperipheral resonance prod. model 78−45891
broken SU_3-subsymmetries of SU_4 and magnetic moments of charmed baryons 79−63382
broken SU(3) gauge model of strong and EM interactions, scatt. lengths, baryon mag. moments 78−74133
broken SU(3) hyperon anomalous magnetic moment sum rules, SU(3) Λ-Λ' mixing explanation 77−18288
broken symmetry group in central force problems 77−60960
C-G coeff., contiguous relns., derivation method 78−74171
Cabibbo angle and weak interaction invariant props. in chiral dynamics 79−71660
canonical neutral-current predictions from the weak-electromagnetic gauge group $SU(3)\times U(1)$ 80−95242
CERN bag model, effects of SU(3) breaking 77−38121
charm particles mass spectra, SU(4) and $SU(3)\times SU(3)'$ theories comparison *(Chinese)* 78−82127
charm-strange spin in SU_3 symm. for c-, s-, d-quark sector 78−37172
charmed baryon decays, EM and weak, U- and V-spin generalisations 80−47284
charmed baryon decays, weak hadronic, SU(3) dynamical scheme 80−68454
charmed baryons, dipole mag. moments, new U_3 scheme using u, d, c quarks 78−58165
charmed baryons, magnetic moments by SU_3 and SU_4 symmetry 78−82209
charmed baryons, nonleptonic decays 78−66118
charmed hadrons $\Delta C=\Delta S$ decays, sum rules, internal symm. props. 77−30376
charmed meson, non-leptonic decay in SU(3) Bose quark model 79−85278
chiral asymmetry in vectorlike weak SU(3), CP violation, one loop correction 79−287
chiral invariance for asymptotic momenta, elastic scatt. of hadrons, helicity amplitudes 78−4800
chiral $SU(3)\times SU(3)$, ρ-meson as dormant Goldstone boson 80−368
chiral $SU(3)\times SU(3)$, combined models of symmetry breaking *(Russian)* 77−6051
Chou-Yang model and s-channel helicity conservation 79−63449
classical quark matter, one dimens., Abelian approx. 78−41491
classification of states in the unitary scheme for complex nuclei and commutation properties of SU_3-irreducible ε-tensors 79−63598
classification of SU(3) mag. monopole 78−364
Clebsch-Gordan coefficients, normalisation 79−106
Clebsch-Gordan coefficients, of SU_3 group 80−36906
cluster systems, normalisation kernels, SU(3) prop., generator coordinate theory 80−73814
color embeddings, charge assignments, and proton stability in unified gauge theories 79−6309
colour gauge group, coloured monopoles 80−68360
colour gauge models, symmetry breaking and asymptotic freedom 77−13917
colour gauge theory, effective scale depend. quark masses in chiral limit 77−18222
colour geometrodynamics, eightfold way, review 80−95243
colour screening, SU(3) gauge fields 78−82102
coloured SU(3) scheme of three quarks binding in baryons, mass formulae 78−12876
congruence number, a generalization of SU(3) triality 80−95224
constituent quarks in SU(3) and SU(6), current algebra., hadron decays, review, book contrib. 80−47259
Coulomb gauge vacua of SU(3) gauge theory 80−47188
coupling S^* and ε to $\pi\pi$ and $K\bar{K}$, SU_3 couplings 80−22580
coupling strength of meson-baryon interactions in u-, d- and c-quark sector 78−25011
CP(N) ($N\geq 2$) chiral theory, 2-dimens., non-selfdual instantons 80−86585
cylindrically symmetric instantons for the gauge groups of rank 2 (SU(3), O(5) and G_2) 79−58877
decomposition theorem, appl. to CP violation through quark mass diagonalisation 80−47216
deformed even-even nuclei, application of SU(3) *(Bulgarian)* 79−9493
deformed even-even nuclei, SU_3 description of energy levels and reduced E2 transition probabilities *(Russian)* 79−13251
double folding pot. for inelastic scatt. between nuclei 80−13425
dual unitarisation, renormalisation of pomeron trajectory 77−2806
dynamical quark mass generation and the mean instanton density 79−54305
dynamical SU_3 symmetry breaking 78−21346
dynamical thresholds in dual unitarisation scheme, exotic states SU(3) struct. 77−49924
E_7 grand unification using $SU(3)\times(U(1))^3$ gauge group, neutral currents 80−27444
E based vector-like unified theory, group theoretical anal. of symm. breaking 77−87929
effective potential for non-Abelian gauge theories and spontaneous symmetry breaking 80−4863
embeddings of gauge groups in Yang-Mills theory, SU(3) case 78−93802
exotic meson mass formulae in $SU_{1,3}$ 77−65147
extension for elementary particles discovered during 1974-7 *(Czech)* 78−86103
first order SU(3) theorem for weak and EM form factors, possible expt. verification 80−415
flavour symmetry breaking and production processes in dual unitarisation, ϕ and ψ prod. 79−45080
forced harmonic oscillator, complete symmetry group 80−90705
fractional parentage coeffs., nucl. shell model, reduced SU(3), computer program 78−50097

SU_3 theory continued
G_2, weight multiplicities 78−78105
gauge field theory for weak and EM interactions with $SU(3)\times U(1)$ symmetry 78−58153
gauge fixing conditions for SU(3) gauge theory 79−97505
gauge model, Cabibbo suppression and weak universality 77−67611
gauge model of weak and EM interactions, Weinberg angle, Han-Nambu quarks 80−52452
gauge theories, statistical mechanics of field theories with broken, global, and local SU(3) gauge symmetries 79−58881
gauge theories of weak, EM and strong interactions 77−13835
gauge theories without scalars, mag. monopoles, dyons, other topologically stable solns. 77−49819
gauge theory, current synchrospherical symmetrical monopole in multisynchrospherical symmetrical case *(Chinese)* 80−22527
gauge theory, exact dyon solns. in SU_3 79−80745
gauge theory, leptonic octets and heavy lepton decays 77−34094
gauge theory, static gluon pots., appl. to fermions 79−12967
Gell-Mann's matrix algebra for SU_3 group *(Russian)* 79−9308
Gell-Mann-Okubo formula, total widths of unstable hadrons 78−45805
geometrodynamics for quarks and hadrons, currents and SU_3 theory 78−45809
group symmetries in nuclear struct., book 80−41963
hadron masses and current algebra quark masses 80−42436
hadron multiplets, realisations in SU(3) from stable particles 80−9159
hadron scattering, non-charmed, SU(1,3), dynamical group 80−62883
hadron total cross sections, semiempirical formulae, three component model with SU(3) components 78−41600
hadrons with charm, beauty and taste, SU_3 subalgebras of SU_6 80−9152
Han-Nambe and SUB quark models, modified, appl. to Weinberg-Salam unified gauge model 80−22562
hypercharge exchange reactions in quasieikonal model *(Russian)* 79−3041
hypercharge-exchange reactions, K^-p, and $\pi^+ p$, SU^3 prediction 80−13335
hyperon+nucleon interactions, one boson exchange pot. approach, multichannel Schrodinger eqn. soln. 77−57556
hyperon non-leptonic decay in (8,8) model of broken chiral symmetry 79−36072
hyperon nonleptonic decay, SU_3 symm., second class currents in effective Hamiltonian 77−41842
hyperon semileptonic decay, model with spectrum generating SU(3) symm. 77−38167
hyperon semileptonic decay, SU(3) spectrum generation, Cabibbo angle 80−9119
hyperon weak EM decays, 27th Hamiltonian component contribution 79−22101
inclusive leptoproductions, scaling violation, colour-octet model effect 79−13077
inclusive nonleptonic and semileptonic decays of charmed hadrons, sum rules determ. 77−71514
instantons, high-dimens., topological charges in SU(3) group 79−30638
instantons, topological props., non-Abelian group, SU(3) group *(Russian)* 78−45801
instantons with cylindrical symmetry, Pontryagin indices 79−286
interacting boson model, transition from SU(5) to SU(3) limits 79−13218
interaction potentials for multiquark states from instantons and other background gauge field configurations 80−101995
IR singularity quark confinement model, coloured bound state absence 79−338
irreducible bases of $SU(3)\supset SO(3)$ and $SU(4)\supset SU(2)\times SU(2)$ *(Chinese)* 78−82121
irreducible representations, commutation relations *(Chinese)* 80−52434
isospin SU(3) symmetry, spontaneous breaking of chiral symmetry in QCD 79−93352
$K^0\rightarrow\bar{K}^0$ transition in the standard $SU(3)\otimes SU(2)\otimes U(1)$ scheme *(Russian)* 80−82951
Kemmer-Duffin eqn., additional symmetry 78−89
lepton model, electron to muon mass ratio *(Russian)* 77−10187
lepton-hadron inclusive interactions, quark and target mass effects, colour SU_3 theory 77−6090
leptonic interaction gauge model in SU_3 with 30° Weinberg angle 80−4903
leptons, EM characts. and CP disturbance in $SU(3)\times U(1)$ model *(Russian)* 78−29327
leptons, SU(3) electroweak theory 80−86638
Lewis Riesenfeld oscillator, dynamical symmetry breaking 80−47210
Lie admissible pseudo-octonion algebra deformation into octonion algebra 79−17629
Lie algebra, nonlinear representations 77−13570
light quark mass and low energy η meson interactions *(Russian)* 79−67513
linear baryonic string model, dynamical SU(3) symmetry breaking 79−22036
Lorentz type internal symmetry 78−50005
low rank group enveloping algebras, reduction and generating function 80−86601
magnetic monopole solutions to SU(3) gauge model 77−6047
magntic moments and machinery of symmetry breaking 79−63477
many-spin system, group approach in dynamics *(Russian)* 80−4579
massless non-abelian gluon confinement and rising total cross sections 80−13264
meson decay, tensor, current algebra approach, symmetry-breaking Hamiltonian, chiral $SU(3)\times SU(3)$ or $SU(4)\times SU(4)$ 80−68450
meson radiative decay, consistency with vector dominance, quark models 77−79265
meson radiative decay, SU(3) octet-broken VMD anal. 77−71517
meson radiative decays 78−21419
meson spectroscopy, quark mixing and quantum chromodynamics *(Russian)* 79−54329
meson spectroscopy, review of SU_3 quark model, quark confinement and bound states 78−74228
meson theory with internal coords., Dirac eqn., Bethe Salpeter eqn., quark model 77−13937
meson wave functions, SU_n representation transformations and phase *(Chinese)* 79−93313
mesons, charmed and strange, SU(3) rules for non- and semi-leptonic weak decays 78−45916
MIT bag model, coloured quark and gluon constituents of mesons 80−4929

SU_3 theory continued
Moufang plane and octonionic quantum mechanics 78−69999
multicluster allowed states, spectroscopic amplitude of cluster transfer 77−88059
neutrino scattering scale breaking models 79−13107
Nilsson model, group theoretical treatment, deformation, pot-energy surface, oscillator shell coupling 78−33129
non-Abelian gauge theories, gauge fixing ambiguities in axial and Coulomb gauges 79−21945
noncanonical bases, of group $SU_3 \supset SO_3$ and their interconnections 80−42359
nonet struct. and quark line rule in world with more than 3 quarks 79−36022
nonleptonic hyperon decay, octet dominance in nonrelativistic quark model 79−388
nonleptonic hyperon decays 79−97624
nonlinear Dirac equation with SU(3) colour symmetry, vanishing soliton solns. 79−71693
nonlocal quark model in $SU(3)\times SU^c(3)\times U(1)$, meson decay and mass correction *(German)* 80−27456
nuclear cluster model, ang. momentum projected matrix elements 79−6445
nuclear cluster problems, SU(3) symmetry and integral kernels 80−9251
nuclear dynamics, adiabatic TDHF limit versus TDHF, in soluble model 78−50113
nuclear EM transitions, selection rules, transition probabilities *(German)* 77−2943
nuclear interacting boson model, rot. limit 78−46016
nuclear microscopic collective Hamiltonian, spin-isospin part of the matrix element 79−63609
nuclear microscopic theory, coeffs. for SU_3-irreducible decomposition of operators and props. of basic interactions 79−63608
nuclear microscopic theory, definition and eval. of collective energy 79−63607
nuclear multi-cluster problems, interaction kernels using SU(3) recoupling techniques 79−45193
nuclear physics and elementary particle physics, dynamical groups 80−42362
nuclear states, maximal restriction of basis 80−42552
octet baryons in SU_3, EM mass difference, u, d and c quark sectors 78−29334
octonion as traceless 3×3 matrices via a flexible Lie-admissible algebra 79−17630
octonionic Hilbert space description of elementary particles 79−9306
octonionic Hilbert spaces, Poincare group, SU(3) for coloured quark scheme 77−2791
octonionic quark confinement 79−17669
octonions and exceptional groups in field theory, unified interaction model *(Russian)* 79−67491
octonions in quantum mechanics 80−27479
odd-odd deformed nuclei, ground state static moments 78−66201
one-boson-exchange-potential model of baryon-baryon scatt. 80−13295
Oxford Rutherford type model, semianalytic treatment, dual unitarisation scheme, trajectory parameters 78−16996
parafermion representations of Lie-algebra chain $O_7 \supset G_2 \supset SU_3$ 78−74173
particle and field equations for gauge theory based on SO(4,1) de Sitter group 79−58868
particle under repulsive oscillator, Sl(3,R) complete symmetry group, Lie group 80−86602
path-depend. approach to coloured mag. monopoles 78−37127
Penrose theory in particle physics 78−29321
pion production by weak neutral currents, gauge theory model predictions 79−13014
Pomeron at very high energies, SU(3) anal. 77−34105
Pomeron exchange, SU(3) props., dual unitarisation scheme 77−13945
positive parity excited baryons in quark model with hyperfine interactions 78−82161
Prasad-Sommerfield soliton, excited states, SU(3) generalisation 80−4877
Prasad-Sommerfield soliton mag. monopole, excited states and SU(3) generalisation 79−40665
projective space-time, geom. of (N+1) particle system 77−74221
pseudoparticles in higher rank gauge theories 77−45960
pseudoscalar transition between spin-J and spin 5/2 baryon 78−50032
$Q^2\bar{Q}^2$ states, mass levels in (3+1) dimens. lattice gauge theory 79−58942
q meson mixing and SU(3) breaking 79−282
QCD, gauge field propagator and the number of fermion fields 80−62928
QCD, IR behaviour of higher order derivative field theories 79−30699
QCD, modified, exact global colour SU(3) symm., asymptotic freedom 78−41493
QCD, new quarks and hadrons 78−8591
QCD, six-quark model, $\Delta S=1$ weak nonleptonic decays 80−22582
QCD, strong interaction gauge theory, SU(3) colour gauge vector mesons, confinement 78−78136
QCD predictions, high p_T processes subject to sum rules, SU(3) symmetry constraints 79−354
QCD theory for the strong interaction 80−4962
QDD, quantum dath dynamics, SU(3) model for composite quarks and leptons 80−91055
quadrupole perturbation of harmonic oscill. pot. 77−60978
quark cluster, model of ordinary and exotic hadrons 79−40759
quark density model, SU(3) symmetry breaking and nonleptonic decays 79−13079
quark excitation, SU(3) model for strong interactions and ψ mesons 77−18198
quark magnetic moment, rel. to quark mass and hadron mass in SU(3) breaking 79−13050
quark mass effects as isospin and SU(3) violations in radiative decays of vector mesons 79−22091
quark mass ratio, chiral perturbation in new key 80−37208
quark masses and structure functions 80−22585
quark sea, percentage in hadron bags under constraint of quark-line rule 78−24998
quark wave eqns. 80−57571
quark-line rule for hadron nonets, review 79−26304
quark-meson σ-model, quark masses 80−47178
quark-parton model, EM mass shifts of pseudoscalar mesons 80−42459

SU_3 theory continued
quark-quark interaction, phenomenological, from s-wave baryon spectrum 80−101984
quarks with more than three colors in a class of asymptotically free gauge theories 80−394
quaternionic Hilbert space and colour confinement, admissible symmetry groups 80−27458
quaternionic Hilbert space and colour confinement 80−27457
radiative corrections to parity violation in atoms in $SU(3)\times U(1)$ gauge theory 78−62402
radiative decay of vector mesons, SU(3)-breaking models 77−18282
rare earth nuclei, validity of pseudo SU(3) model 77−34240
recoupling coeffs. 78−66050
reduced SU(3) matrix element calculation program 78−89627
Regge trajectories, dual unitarisation scheme, SU(3)-breaking and baryon exchange effects 79−26316
relativistic hadron couplings, unified framework, symms., quark models *(German)* 78−50012
right handed colour octet currents for charm and colour excitation in $\nu(\bar{\nu})$ reactions 78−93874
rotational motion, nuclear, microscopic description via SU(3) 79−36133
sd-shell nuclei, large scale shell model calcs. compared with perturbation theory in SU(3) basis 77−57613
self dual Euclidean gauge fields, semisimple groups, Lie algebra, SU(2) and SU(3) fields 79−6278
self-conjugate tensor operators, struct. props. 78−8217
self-duality eqns. for SU(3) gauge theory 77−65082
short distance analysis of weak interactions, asymptotically free theory 77−54068
simple approximations and symmetry measures for model interactions 79−17867
single particle coeff. of fractional parentage 77−79231
singular gauge instanton field, gauge zero modes, instanton determinants, and quantum-chromodynamic calculations 79−71635
SL(3,R) algebra, minimal and centred graded spin extensions 80−82910
soliton, nontopological, in three dimens. space, SU(3) gauge field 77−18168
soliton solns. of chiral $SU(3)\times SU(3)$ models 78−4761
spectrum generating $SU(3)_E$invariant form factor for pseudoscalar mesons 77−61288
spectrum-generating SU(3) and local current algebra 80−9128
spectrum-generating SU(3) and SU(4), idea and appl. 80−9118
spin-1 mixed states orbits of rotation group on density matrices 77−74612
spinning particles interacting with external fields, invariance groups of relativistic eqns., SU_3 symm. 78−49962
spontaneously broken chiral $SU(3)\otimes SU(3)$ symmetry, quark mass ratios, Goldstone pseudoscalar meson pairs 79−80770
strong coupling constants in broken SU(3) 80−27423
strong gravity contrib. to nucleonic axial-vector form factor in SU(3) 80−4902
strong interaction formalism with internal coords., partial unification of quantum theory and SU(3) classification 77−65137
strong interactions in gravitational field 80−91047
$SU_3\times U_1$ calibrating theory, weak and EM interactions appl. *(Russian)* 79−35964
$SU_3\times U(1)$ gauge models and neutral current reacts. 78−89648
SU_3 subsectors of SU_4 and mass sum rules for charmed hadrons 79−35967
$SU_L(2)\times SU_R(2)\times U(1)\times [SU(3)\times SU(3)]_c$ gauge model, chiral colour symmetry breaking 80−47234
$SU_L(3)\times SU_R(3)$, leptonic nonet anal. 77−87908
$SU_L(3)\otimes U(1)$ gauge model, exact Cabibbo universality, τ^- and X^- 80−4852
$SU(3)_{colour}\times SU(2)\times U(1)$ gauge, full operator structure of the nonleptonic $|\Delta S|=1$ weak Hamiltonian 80−99089
$SU(3)_L\times SU(3)_R$ as gauge groups of weak and associated charges, symm. breaking 78−74175
$SU(3)\times SU(3)$ chiral algebra, crossing matrix elements, Clebsch Gordan coeffs. 78−32998
$SU(3)\times SU(3)$ chiral renormalisable gauge model, nonleptonic decays 78−24938
$SU(3)\times SU(3)$ chiral symmetry breaking, BBS coupling constants, sum rules 79−35959
$SU(3)\times SU(3)$ chiral symmetry breaking, Dashen mass formula, baryon mass differences, $\eta\rightarrow 3\pi$ 79−289
$SU(3)\times SU(3)$ dynamics, broken nonlinear chiral, and $\eta\rightarrow 3\pi$ decay *(Russian)* 77−65117
$SU(3)\times U(1)$, lepton model, dynamical symm. breaking 77−5980
$SU(3)\times U(1)$, neutral currents, vectorlike model, parity violation 78−4823
$SU(3)\times U(1)\times U(1)$ model, suppression of flavour changing neutral currents 78−21350
$SU(3)\times U(1)\times U(1)$ symmetry, gauge model of weak and electromag. interactions *(Russian)* 78−45838
$SU(3)\times U(1)$ gauge group, extension of Weinberg model 77−13909
$SU(3)\times U(1)$ gauge model, polarised lepton scatt. 78−45901
$SU(3)\times U(1)$ gauge model of weak interactions, quark triplets, charmed hadron decay 77−2789
$SU(3)\times U(1)$ gauge models, exam. of weak currents and associated features 78−16975
$SU(3)\times U(1)$ gauge theory, charged intermediate boson mixing 77−87910
$SU(3)\times U(1)$ gauge theory of weak and EM interactions 78−70317
$SU(3)\times U(1)$ low-energy symmetry within the unifying $SU(4)_F\times SU(4)_C$ gauge group 79−67489
$SU(3)\times U(1)$ model, heavy lepton prod. and decay signature 78−45900
$SU(3)\times U(1)$ models, massless and supermassive quarks 79−9331
$SU(3)\times U(1)$ modified model, quark and lepton mass hierarchy 78−89653
$SU(3)\times U(1)$ theory of weak-electromagnetic interaction with charged-boson mixing 79−35988
$Su(3)\times U(1)$ unified gauge theory without μ-e universality 79−26274
$SU(3)'\times SU(3)''$ scheme of three triplet model, colour symm. ψ-mesons descript. 78−78151
$SU(3)\otimes U(1)$ gauge model of trimuon prod. in neutrino interactions 77−74671
SU(3) quark sectors, weak hadronic and radiative decays of nonstrange charmed baryons 79−22092
SU(3) subalgebras of SU(4), generalised U-spin charmed baryon magnetic moment 79−36078

SU_3 theory continued
SU(3) symmetry breaking in baryon resonance decay 78−89712
SU(4)⊗SU(3)′ model, Υ particles and SU(3)′ colour space *(Chinese)* 80−42409
SU(6) unified gauge model, based on SU(3)×U(1) and colour SU(3) subgroups 78−12847
SU(8) grand unification, natural embedding of SU(3) horizontal symmetry 80−86646
SU(N) gauge groups, N=2,3,4, meron and meronlike configurations 79−71636
subalgebras of SU(4), generalised U-spin charmed baryon magnetic moment 79−36078
subcomponent models of quarks and leptons in SU(3) subcolour, proton decay 80−78035
sum rules for matrices of generators in SO(3) basis 80−13226
supersymmetry, superfield notation for supermultiplets spontaneous breaking, Lagrangians and internal symmetry incorporation *(German)* 78−74167
symmetry breaking and partial conservation of axial vector current in constituent quark basis 77−2773
symmetry breaking and planar bootstrap eqns. 77−13939
symmetry breaking schemes for radiative decays of ρ, K^{0*}, φ vector mesons 77−6114
symmetry violation models for interactions with vector mesons, tests *(Russian)* 77−10196
tensor mesons mass, model Lagrangian, SU(3) Yang-Mills fields, tensor fields 77−13874
three-nucleon system, fractional-parentage construction of wave function 77−14041
topless model for grand unification 80−73653
two-electron atoms, channel invariants and SU(3) classification 78−41906
U(1)×SU_1(2)×SU(3) theory, integer charge quarks, lepton hadronic processes. *(Russian)* 80−86653
U(1) Goldstone boson, anal. of BRS invariance in nonAbelian gauge theories 79−80798
U gauge in Abelian and non-Abelian gauge theory, Gribov ambiguities 78−45788
unification of fundamental forces in nature, elementary particle constituents $SU(3)_c$ gauge symmetry, review 80−27448
unified gauge model with a nonlinear chiral hadron Lagrangian 80−42378
unified model of weak and electromagnetic interactions based on the gauge group SU(3)×U(1) 79−22003
unified SU(3)XU(1) gauge theory with different muon and electron neutral currents 78−58152
unified theory of gravity and strong interactions, quark confinement 77−22681
unified weak and EM interactions, semi simple SU(3l) gauge groups for hadrons 78−74195
unifying mass scales without intermediate schiral colour symmetry, SU(2)×SU(1)×SU(3), $[SU(2n)]^4$ unified model 80−22555
unitary space of particle internal states 79−30712
unitary space of particle internal states 80−18119
unitary symmetry in baryon-antibaryon systems *(Chinese)* 80−102000
up quark mass and chiral symmetry at infinite momentum 79−40685
vacuum structure of SU(3) gauge field theory in Coulomb gauge 78−62311
valance quark distribs. in π, K, D, Regge trajectories, SU(3), SU(4) breaking 79−30703
vector meson decay rates, SU(3) symmetry 78−58181
vector meson mass predictions, SU(3) formalism of S quark model 78−37177
vector meson radiative decay, off-shell factors in vector dominance model 79−22084
vector meson radiative decays, SU(3) symmetry viewpoint 80−95273
vector meson radiative decays, vector dominance model in broken SU(3) 80−73711
vector meson-nucleon interaction, SU(3) symm., coupling consts., form factors 77−13886
vector mesons, EM decay in broken SU(3) 80−82976
vectorlike SU(3)×U(1) gauge model of weak interact. $\bar{\nu}$ reactions, neutral currents 77−41805
wave equations and soln. 77−9850
weak hadronic decays of uncharmed baryons in SU(3)−dynamical considerations 79−75769
weight multiplicity for Lie groups, explicit formulae 77−26467
Weyl character formula, SU(3) representation theory, connection with SU(3) particle classification schemes 77−34101
Weyl invariants generating function *(French)* 79−93304
Wigner-Racah algebra construction, appl. to ang. momentum theory 79−58903
Yang's R gauge for self-dual SU(3) gauge fields 78−78088
Yang-Mills, unified spatial and isotopic symmetry 79−21952
Yang-Mills classical gauge theory, dyons and new topologically conserved quantity 77−6014
Yang-Mills gauge theory, classical soln. in colour meson model 78−45780
Yang-Mills theory, study of O(3) symmetric merons 79−30651
Yang-Mills-Higgs fermion-monopole system, topologically stable soln., SU(3) theory 77−13888
A_1 meson, mass formulas and selection rules in large SU(3) mixing 80−86700
α-spectroscopic factors, pseudo SU(3) approx. 78−70471
B meson, mass formulas and selection rules in large SU(3) mixing 80−86700
D-meson, gauge theoretic formulation of SU_2×U, model, mass limit 78−70316
D-meson decay, hadronic, six-quark model, quark-mass dependence, final state interactions, mixing angle effects 80−62973
D^+, D^0, weak nonleptonic decays, SU(3) symmetry and quark diagrams *(Russian)* 79−93411
D^0,D^+, SU(3) predictions for decay using new weak mixing angles 79−97619
e^-e^- annihilation, parton model, finite energy results 78−419
en→enπ, pol. e, P-odd asymmetry and cross sections, SU(2)xU(1), SU(3)xU(1) calcs. *(Russian)* 80−62998
η, vacuum symmetry, decay consts., mixing consts. in SU(3)×SU(1) QCD 80−27483
η→γγ, radiative widths, δ and S* background, SU(3) and VDM anal. 80−419

SU_3 theory continued
η→ππγ, quark loop model, SU(3) splitting of quark masses 80−62990
η→ργ(γγ), C-even meson radiative decay, SU(3), and VDM anals. *(Russian)* 80−68460
η′(957) meson, quark model description 80−62970
η′(958)→γγ, evaluation of decay rate 80−9172
η′→ργ, radiative widths, δ and S* background, SU(3) and VDM anal. 80−419
F^+, weak nonleptonic decays, SU(3) symmetry and quark diagrams *(Russian)* 79−93411
γ(10.0), two-body hadronic and radiative decays, pseudo-dimension rule, ππ and KK̄ suppression, SV_3 singlet 80−52495
γp→hX, SU(3)×SU(3) invariant interaction of quarks, large p_T, gluon bremsstrahlung 78−33072
K decay, mixing of p-wave axial vector resonances 77−30374
K→πe(μ)ν, form factors, SU(3) σ-model one loop calc., chiral symmetry breaking 80−52506
K^0_{e3} and $K^0_{\mu 3}$ decays, form factor parameters anal., SU(3) symm. violation *(Russian)* 78−450
$K^{\pm}\to\pi^0 l^+\nu_l(\bar{\nu}_l)$, decay form factors in relativistic symmetry SO(4,2)⊗SU(3)⊗SU(3) 79−36068
$K^*\to K\gamma_\beta$ quark loop model, SU(3) splitting of quark masses 80−62990
$K^{*0}\to K^0\gamma$, SU(3) and isospin symmetry breaking effects 80−95272
K̄N reaction below 1.9 GeV, dispersion theoretic discrepancy anal., SU(3), hadron coupling 78−21457
KN scatt., Z_0* resonance generalisation in SU(3) symmetry 78−37230
Kp reactions, 13 GeV/c, differential cross-sections, Regge exchange, SU_3 sum rule interpretations 77−41862
Kp/πp total cross-section ratios 77−46089
K^-p, 4.2 GeV/c, backward axial vector meson prod., isospin and SU(3) struct. 79−93458
Λ′ existence, ninth $I=0\ J^P=1/2^+$ baryon, asymptotic level realisation of SU(3), hyperon semileptonic decay anal. 77−18245
μ anomalous mag. moment in SU(3)×U(1) gauge model 79−3026
μ→e+γ decay and mixing of charged heavy leptons *(Russian)* 78−58178
$\mu^-\mu^-\mu^+$ events in ν_μ reactions, SU(3) gauge models 77−74674
μp deep inelastic scatt., charm effects, field theory anal. 78−21435
NN inelastic processes, SU(3) breaking, N(1688), Λ(1815) and Σ(1915) states 77−71526
$\bar{\nu}$N, K^0 and π^- prod. rates, SU(3) symmetry violation in quark jet 80−82966
νN inelastic scattering, possible soln. with weak neutral currents to ρ-π puzzle 79−17714
(p,pα) quasifree scattering on ^{24}Mg, ^{28}Si, ^{40}Ca, ^{58}Ni, at 157 MeV 77−6370
pp→pX, diquark fragments, large transverse momentum baryon production 80−47330
φ(3100) two-body decays and SU(3) breaking 77−18277
φ→ηγ, quark loop model, SU(3) splitting of quark masses 80−62990
φ meson, two-body hadronic decay, quark model 78−25040
φ→πγ, SU(3) algebra, appl. to ground state mesons, coupling constraints and decay rate 78−58183
πK phase shifts, perturbation expansion about SU(3)×SU(3) symm. limit 79−58975
πN σ term in hybrid chiral bag model, PCAC and SU(3)×SU(3) symmetry violation 80−78096
πp, quark-diquark elastic scatt., diquark fragments, large transverse momentum baryon production 80−47330
$\pi^+\pi^-\to K_s{}^0K_s{}^0$ scatt. cross section meas., appl. to scalar meson nonet 78−82240
ψ→η(η′)γ, SU_3 violation, symmetry breaking and decay amplitudes 80−52499
ψ→ηγ, pseudoscalar meson mixing and M1 radiative decays 77−30329
ψ meson, two-body hadronic decay, quark model 78−25040
ψ meson strong and radiative decays, SU(3)′×SU(3)″ scheme of three triplet model 77−30371
ψ/J hadronic decays, dynamics, SU(3) violation, dispersion relations, mass splitting 79−382
Q, axial vector mesons, dynamical mixing model 78−24973
Q mesons, decay amplitudes, partial widths, Lorentz and SU(3) invariant coupling constants 79−26328
Q mesons, SU(3) anal. of mass, widths 78−4802
Q_1(1280), mass formulas and selection rules in large SU(3) mixing 80−86700
Q_1(1289) decay, SU(3) octet mixing 77−18281
Q_1(1290), Q_2(1400) vector-pseudoscalar decay rates and SU(3) implications 77−61283
Q_2(1400), mass formulas and selection rules in large SU(3) mixing 80−86700
Q_2(1404) decay, SU(3) octet mixing 77−18281
Q_A-Q_B mixing angle, axial vector meson decay, A_1 and C obs., SU(3) implications 79−89148
ρ→πγ decay width, explanation using SU(3)-scalar term in the EM current operator 78−82206
t-quark, mass in SU(3) horizontal symmetry 80−37230
u-quark masslessness, consequences for SU(2) and SU(3) 79−22022
Υ(9.54) and broken SU_3 in nonstrange quark sector, vector mesons 78−58166
Y*(1385) prod., SU(3) symmetry and vector tensor universality 77−18321
Y* states from K^-p reactions, SU_3 classification 78−25077
^{11}B, SU(3) classification of 2α+t allowed states 78−50110
F^+, SU(3) predictions for decay using new weak mixing angles 79−97619
^{21}Na, parity mixing matrix element using SU_3 shell model calcs. 79−9462
^{16}O, band system composed of SU(3) components 78−50109
^{18}O, quadrupole moment of first 2^+ state, SU(3) representation 77−46113
^{28}Si(d,^{3}He)^{27}Al, multistep processes, CCBA anal., SU(3) model 77−30609
Xe-Nd region, microscopic anal. of core deform. 78−74303

SU_4 theory
$1/2^+$, baryons, vector mesonic decay, charm changing mode, SU(4) and SU(8) 80−47283
1/N dual unitarisation convergence due to SU(4) breaking, charm and strangeness implications 79−6321
$^1/_2{}^+$ charmed baryons, $C_1{}^{++}$, $C_1{}^+$, $C_1{}^0$, $X_u{}^{++}$, $X_d{}^+$, SU(4) predicted, possible observation 79−40758

SU_4 theory continued
A = 60-260 nuclei, violated Wigner SU(4) symmetry reconstruction from mass data *(Russian)* 80−37336
algebraic realisation, meson mass formula *(Russian)* 78−45895
asymptotically free SU(2)×SU(2)×SU(4) model of unified interactions 78−16968
baryon, charm changing weak decays $1/2^+ \to 3/2^+ + 0^-/\gamma$ in SU(4) and $SU(8)_w$ 79−3021
baryon nonleptonic weak decay, SU(4)-20″-dominance 78−45917
baryon weak radiative decay, SU(3), SU(4) anal. 78−33069
baryon weak radiative decay, sum rules, 20-plet dominance in SU(4) 78−62400
baryonium spectrum, SU(4) mass formulae, degenerate clustering 79−93393
baryons, ordinary and charmed, magnetic moments in broken SU(4) 80−18136
broken chiral $SU_4 \times SU_4$ symmetry at infinite momentum, have quark mass ratios 79−80768
broken isospin symmetry in chiral SU(4)⊗SU(4) and D^+-D^0 mass difference 78−89691
broken lattice gauge theory spectrum 79−49474
broken SU_3-subsymmetries of SU_4 and magnetic moments of charmed baryons 79−63382
broken symmetry, duality, baryon+baryon and baryon+antibaryon exotic mesons prod. 78−89629
broken-SU(4) model of meson decays $1^- \to 0^-\gamma$, $0^- \to 1^-\gamma$ 78−70361
canonical $SU_4 \times SU_4$ pseudoscalar meson matrix, nonlinear chiral Lagrangian 78−397
charm particles mass spectra, SU(4) and SU(3)×SU(3)′ theories comparison *(Chinese)* 78−82127
charmed baryon semi-leptonic decay and quark effective masses, SU_4 symmetry 78−58185
charmed baryons, magnetic moments by SU_3 and SU_4 symmetry 78−82209
charmed baryons, semileptonic decays, SU(4) breaking, mag. moments, suppression factors 79−387
charmed baryons, SU(4) symmetric 20-plet representation, mass, EM splitting 78−54615
charmed meson decays and right handed currents 78−8662
charmed mesons, dynamic SU(4,1) symmetry, mass spectra, anal. *(Russian)* 78−70350
chiral SU(4)×SU(4) breaking scheme, vector mesons radiative decays 79−22099
chiral SU(4)×SU(4) model, scalar meson decays 78−4801
chiral SU(4)×SU(4) symmetry, broken chiral, mass spectrum of D, F and η mesons 79−93312
chiral SU(4)×SU(4) symmetry breaking, quantitative meas. 79−93311
chiral SU(4)⊗SU(4), broken model, based on SU(4)⊃SU(2)⊗SU(2), Glashow-Weinberg model extension 78−12836
chiral SU(4)⊗SU(4) symmetry breaking parameter, meson mass 78−12838
Clebsch-Gordan coefficients for the formation of baryonium and exotic baryons 79−75739
Clebsch-Gordan coeffs., matrix, elements and symm. props. 78−45803
Clebsch-Gordan series 78−16940
current algebra including term for U(4)×U(4) to SU(4)×SU(4)×U(1) symmetry, spin zero meson spectrum 78−58176
Franzini-Radicati mass relationship in isobars, Wigner SU(4) supermultiplet 80−105958
gauge fields, pseudoparticle solns. *(Chinese)* 78−74128
gauge theories, magnetic monopoles 78−24918
gauge theory, current synchrospherical symmetrical monopole in multi-synchrospherical symmetrical case *(Chinese)* 80−22527
geometrodynamics for quarks and hadrons, currents and SU_4 theory 78−45809
hadron classification, quark model, SU(4) symmetry 78−12861
hadron decay, relativistic quark model and SU(4) 78−62366
hadrons, charmed, SU(4) mass-breaking, mass sum rules 80−62959
higher order hadronic mass formulae SU(4) framework 79−366
irreducible bases of SU(3)⊃SO(3) and SU(4)⊃SU(2)×SU(2) *(Chinese)* 78−82121
Kramers' symbolic method, extension to SU_4 80−86603
leptoquark bosons, confinement in SU_4 theory 79−45052
linear SU(4) meson σ-model, one-loop approx., spin zero mass spectrum and leptonic-decay 80−47278
low rank group enveloping algebras, reduction and generating function 80−86601
mass formula for SU_4 charmed-hadron multiplets 78−37192
mass formula in SU(4), flavour symmetry breaking 80−37250
mass formulae breaking for $^1/_2{}^+$, $^3/_2{}^+$ baryons and 1^-, 0^- mesons *(Russian)* 78−89692
mass splitting, group theory and quark model comparison 79−6290
meson decay, tensor, current algebra approach, symmetry-breaking Hamiltonian, chiral SU(3)×SU(3) or SU(4)×SU(4) 80−68450
meson decays appl. 78−12835
meson isosinglets, mixing angles, non-relativistic quark model, Schwinger-type mass relations for SU_4 and SU_5 80−18125
meson mass formula from generalisation of SU(3) Schwinger mass formulae 78−37190
meson nonet struct., mass relations, mass splittings, SU(4) framework 79−288
meson states, representation mixing, SU(4), mass formula, EM mas shifts 78−12890
meson-quark interactions, mag. moments *(Russian)* 78−45804
mesonic Bethe-Salpeter eqn. for different mass straton and antistraton, SU(4) mass relations *(Chinese)* 79−58934
monopole and dyon solns. *(Chinese)* 79−9307
nonleptonic weak Hamiltonian, current×current theory, SU(4) representations 79−17666
nonleptonic weak interaction, SU(4) symmetry struct., parity violating Hamiltonian 80−52456
nuclear struct. theory SU(4) theory role 79−3097
O(10), SU(4) colour subgroup, fractional charged gauge boson, proton half-life 80−73644
OZI relations for SU(4) coupling constants with applications to tensor mesons 79−80793
particle assignments in terms of Gelfand-Zetlin basis vectors 78−82126
Pati-Salam $SU(2)_L \times SU(2)_R \times SU(4)$, gauge-c 78−12851
pseudoscalar meson decay, symm. breaking in chiral SU(4)×SU(4) model 78−21424

SU_4 theory continued
pseudoscalar mesons, sum rule, symm. breaking of chiral SU(4)×SU(4), decay const., masses 78−33000
pseudoscalar-meson decay constants, Goldberger-Treiman relations, and chiral SU(4)×SU(4) symmetry breaking 79−293
quark line rule, generalised, SU_4 symm. scheme, reaction of hadrons containing charm quarks 78−54614
quark masses and structure functions 80−22585
quark model, non-leptonic hyperon decay anal. 78−12910
quarks, mass of u and d quarks from weak and EM interaction model 80−13254
reducible representations, projector definitions, calc. method 80−9126
semileptonic decays of charmed particles SU(4) breaking 79−63473
spectrum generating group approach, Clebsch-Gordan coeffs. 78−82126
spectrum-generating SU(3) and SU(4), idea and appl. 80−9118
spin-isospin quark model, explanation of nucleon-nucleon repulsive core 78−12984
SU_3 subsectors, U- and V-spin generalisations 80−47284
SU_3 subsectors of SU_4 and mass sum rules for charmed hadrons 79−35967
$SU_4 \otimes SU_3'$ structural model of straton with integral charges *(Chinese)* 78−12860
$SU_L(4) \times SU_R(4) \times U(1)$ model, generation of u- and d-quark masses 79−63419
$SU_L(4) \times U(1)$ as gauge symm. for quark, lepton quartets, weak and EM interactions, weak currents 78−74174
SU*(4), elementary representations and intertwining operators 79−301
$SU(2)_L \times U(1)$, nonlinear realisation of Weinberg-Salem model for chiral SU(4)×SU(4) meson theory *(Russian)* 79−30693
SU(4,1) hadron dynamical symm. anal., charmed $1/2^+$ baryon and 0^- meson mass *(Russian)* 78−74237
SU(4|N) gauge transformations, determ. of Lagrangian for supertheories 79−63118
$SU(4)_F \times SU(4)_C$ synthesis of strong, weak, and electromagnetic interactions 80−13255
$SU(4)_L \times SU(4)_R \times U(1)$ gauge, lepton weak interaction, right currents, effective Fermi interaction const. universality *(Russian)* 79−58921
$SU(4)_L SU(4)_R \times U^V(1)$ gauge group for lepton and quark weak interactions *(Russian)* 79−97566
$SU(4)_W$ symmetry, dibaryon coupling constants for γ, π and baryon interactions *(Russian)* 80−13329
$SU(4)^2$, rel. to elementary particles discovered during 1974-7 *(Czech)* 78−86103
$SU(4)^4$ unifying symmetry for light neutral Z^O boson, PETRA and PEP expts., $e^+e^- \to \mu^+\mu^-$ 78−37154
SU(4), symmetry breaking effects on strong coupling const., charmed and uncharmed B̄ BP couplings calc. 80−105802
$SU(4) \times S_3^\sigma$, straton model, meson classification *(Chinese)* 78−78145
$SU(4) \times S_3^\sigma$ scheme, straton model, Υ (9.5) props. *(Chinese)* 79−9347
SU(4)×SU(1,1) for O(4) supergravity 80−12975
SU(4)×SU(4), nonleptonic decays of charmed mesons and chiral Lagrangians *(Russian)* 79−30732
SU(4)×SU(4) breaking, association with Cabibbo angle 79−12974
SU(4)×SU(4) broken chiral symm. 78−74176
SU(4)×SU(4) broken chiral symmetry, charmed hadron masses and decay consts. 79−40686
SU(4)×SU(4) broken chiral symmetry, decay constants, smoothness, and spin-zero charm particles 79−58900
SU(4)×SU(4) chiral symmetry breaking, axial vector current divergences, kaon PCAC 79−45032
SU(4)×SU(4) current two point functions, meson decay consts. and bare quark masses from duality 78−8598
SU(4)×SU(4) symmetry breaking, Cabibbo angle, nonlinear hadronic Lagrangian, PCAC *(Russian)* 80−42360
SU(4)×U(1) gauge theory, Cabibbo mixing, new approach, CP nonconservation calc. 79−71657
SU(4)×U(1) unified gauge theory, CP nonconservation 79−71656
SU(4)×U(1) unified gauge theory, muon number conservation 79−71655
SU(4)⊃SU(2)⊗SU(2) chain, matrices of generators 78−37152
SU(4)⊗SU(3)′ model, Υ particles and SU(3)′ colour space *(Chinese)* 80−42409
SU(4) and SO(4) supergravity relations, anomalies and field transformations 79−9170
SU(6)×SU(4) tensor decomp. of effective interactions in 2s-1d shell, SU(4) irreducible tensors and norms 80−105801
sum rules for four-body semi-leptonic decays of charmed mesons 79−36067
supergravity, SU(4) invariant theory 78−41471
supersymmetry algebras with central charges, SU(4) invariance, gauge theory 78−70301
symmetry breaking, e.m. props. of D mesons calc. 78−8668
symmetry breaking and energy variation of SU(4) irreducible tensors and norms 80−105801
symmetry breaking pattern and baryon masses 78−89690
transformation matrices between canonical basis and basis of supermultiplet model in SU(4) 79−67693
$U(1) \times SU(4)_L \times SU(4)_R$ based weak-EM synthesis with manifest left-right symm. 78−8571
unified gauge model with a nonlinear chiral hadron Lagrangian 80−42378
unified theory of weak interactions of leptons and quarks, gauge model 80−22556
unifying mass scale determ. 78−45830
valance quark distribs. in π, K, D, Regge trajectories, SU(3), SU(4) breaking 79−30703
vector meson radiative decay evaluation in spectrum generating SU_4 scheme 79−54342
vector mesons, radiative decay, single parameter scheme 80−86720
vector mesons, two body photonic decays, SU(4) scheme, ideal mixing angles, amplitudes, quark sectors 78−54630
vector mesons, two-body photonic decays, 16-plet mixings in SU(4) quark symm. 78−33062
weak nonleptonic decays in SU(4) and SU(8), adjoint representation admixture 78−21426
Yang-Mills field solution 79−71584
Yang-Mills theory, SU(4) supersymmetric, charge renormalisation 78−24929
χ particles, radiative decay widths calc., broken SU(4) model 78−62395
D meson decay, SU_4 20-plet dominance model, inclusive branching ratios 80−13299

SU_4 theory continued
D^+-D^0 mass difference, form factors, SU(4) coupling, vector meson dominance model 79−391
D^*, pion and photon couplings, SU(4) violations, decay rates calc. 78−45914
$e^+e^- \rightarrow O$ particle, decay, mass, prod. from Zweig rule intermediate vector particle model *(Chinese)* 80−73697
$\eta \rightarrow 3\pi^0$, chiral SU(4)×SU(4) breaking and tadpole term 80−22532
F^+ decay, SU_4 20-plet dominance model, inclusive branching ratios 80−13299
Λ, charmed baryon mass in SU(1,4) dynamical group theory 80−62882
$NN\pi$ amplitudes, parity violating, QCD calc. in Weinberg-Salam model and SU(4) flavour symmetry breaking 79−67520
$\nu N \rightarrow \mu^-$+charmed baryon, SU(4) breaking effects, quark parton model 79−40792
$\rho \rightarrow \pi\gamma$, EM decay rates, spectrum generating SU(4) approach 79−26334
Σ_c charmed baryon mass in SU(1,4) dynamical group theory 80−62882
$\Sigma^+ \rightarrow p\gamma$, $1/2^-$ resonance poles to parity-violating amplitude, two-quark weak transitions 80−78062

SU_n theory
see also elementary particle symmetry; SU_2 theory; SU_3 theory; SU_4 theory
$1/2^+$, baryons, vector mesonic decay, charm changing mode, SU(4) and SU(8) 80−47283
1/N expansions, singular integral operator 80−57511
5-dimensional generation structure, possible signature for SU(5) semi-simple grand unification 80−82930
27-plet mesons, mass sum rules using SU_4 dynamical-group scheme 77−26505
ζ-function regularisation of fluctuations around Yang-Mills pseudoparticle 78−16919
σ model, linear in SU(n), n≥4, renormalisation in one loop approx. 79−97516
σ models, nonlinear, soft mass renormalisation of 1/N expansion 80−47164
σ SU(N) model, spontaneous symmetry breaking, renormalisation 80−42340
σ-model supersymmetric dynamics on pre-QCD level with elementary quarks and composite gluons 80−82886
$(\phi^3)_6$, asymptotic freedom, zero charge and internal symmetry *(Russian)* 77−49864
$(\bar{\psi}\psi)^2$ model, spontaneous symmetry breaking, renormalisation 80−42340
't Hooft's mag. monopole unicity 78−16908
't Hooft-Polyakov mag. monopole electric charge in CP nonconserving theories, $e\theta/2\pi$ charge dyon 79−97534
Abelian gauge theories, QED_2 generalisation, quark confinement 79−71605
Abelianizable field, duel charged soln., gauge field decomposition and reduction 79−26245
additive quark model with six flavours 80−27455
adjoint SU(N) representation, exact factorised S-matrices 79−71647
Adler chromodynamics, colour charge algebras 79−22040
arbitrary molecular point groups, fractional parentage concept 79−10225
asymptotic freedom in the infinite-momentum frame, SU(N) Yang-Mills theory renormalisation 80−22519
asymptotic reduction products of representations of covering group of SU(1,1) 78−58137
asymptotic SU_5 and a new mass constraint for the ω, φ, ψ and Υ mesons 79−36001
asymptotically free SU(5) grand unification, proton stability, renormalisation group 80−82929
atomic parity conservation, left-right symm. unified theoreies 78−70306
axial vector multiplets, mass spectrum, mixing angles, pseudoscalar mesons, decay consts. 77−13892
b-mesons, mass splitting, SU_3 nonet of SU_6 80−47288
bag model, multibaryon states, SU(6) mass formulae 78−45848
baryon, charm changing weak decays $1/2^+ \rightarrow 3/2^+ + 0^-/\gamma$ in SU(4) and $SU(8)_w$ 79−3021
baryon configuration mixing in 70 1^- multiplet of SU(6)×O(3), decoupling conditions 77−38142
baryon magnetic moments, ground-state, SU(6) symmetry 80−78064
baryon mass relations in internal SU(6) symmetry 80−82962
baryon resonance decay, l-broken $SU(6)_W$ model equivalence to relativistic harmonic oscillator quark model 78−41546
baryon resonance photocouplings, using mixed nucleon and even-wave harmonic oscillator theory of baryonic states 77−82752
baryon wave functions, SU_n representation transformations and phase *(Chinese)* 79−93313
baryon weak radiative decay, SU(3), SU(4) anal. 78−33069
baryon-lepton symmetry model, μ-number and flavour nonconserving neutral currents 78−66069
baryons, b-quark, magnetic moments, broken SU(5) symmetry 80−95257
baryons, SU(1,4) dynamical group, anal. of discrete representations, mass formulae 77−45982
baryons and baryonium, SU_6 symmetry, duality and unitarity 78−8622
bilocal gauge field theory 80−31986
boson nonets mass relations in broken SU(3) plus SU(2), mass of 9th pseudoscalar meson 77−38144
bottom hadrons, masses and allowed decays, SU(5) quark model 80−62954
bound states from instantons 78−78087
branching rule for restriction from SO(7) to G_2 78−16624
broken SU_N symm., meson mass formula 77−6043
broken SU(4), algebraic approach, D and D^* mesons 77−38097
broken SU(4), Regge trajectories with nonplanar cylinder corrections 77−45992
broken $SU(6)_w$ analysis of electroproduction 79−93436
broken SU(6) parton model, spin depend struct. functions, deep inelastic lepton+nucleon appl. 78−428
broken $SU(8)_w$ symmetry, mass formulae for 0^- and 1^- mesons 78−37191
C-G coeff., contiguous relns., derivation method 78−74171
Cabibbo angle, CP violation quark masses 78−33016
Cabibbo angle and weak interaction invariant props. in chiral dynamics 79−71660
canonical pseudoscalar-meson matrices, chiral SU(n)×SU(n) symm. of strong interactions 78−29266
charged soliton long range interactions 79−63373
charmed baryon hadronic decays, parity violation in SU(8) 79−89077

SU_n theory continued
charmed baryon mass formulae via SU(4) Regge trajectory anal. 77−79257
charmed baryon nonleptonic decays, sum rules for ΔC=ΔS=1 S-wave decays 79−58957
charmed baryons, dynamical group selection, SU(1,4) 78−37178
charmed baryons, mass spectrum from $SU_{1,3}$ dynamical group theory 80−62956
charmed baryons, nonleptonic decays 78−66118
charmed baryons, parity violating and conserving decays, $(1/2^+ \rightarrow 3/2^+ + 0^-/1^-)$ in Abe, Fujii and Sato model 79−97623
charmed hadron masses, five-quark model of ψ particles *(Russian)* 77−61263
charmed meson decay, SU(4) symm. breaking 77−26518
charmed mesons and charmoniums, masses and mixing, OZI rule breaking 78−12889
charmed-baryon nonleptonic decays, parity-violating amplitudes 78−62398
Chern classes, Pontrjagin forms and classification of gauge fields 79−67461
chiral invariance for asymptotic momenta, elastic scatt. of hadrons, helicity amplitudes 78−4800
chiral invariant SU(N) Thirring model, exact S-matrix 79−21911
chiral O(N)×O(N) and SU(N)×SU(N) 2-dimens. models, conservation laws and S-matrices 80−68389
chiral properties of fermionic determinant in two-colour QCD, symm. breaking 78−25015
chiral SU_2 symmetry, spontaneously broken, equivalence to current algebra in field theoretic model 77−82688
chiral $SU_n \times SU_n$ representation mixing, group theoretic structure 77−82687
chiral SU(2)×SU(2) theory, localised solns. 77−26451
chiral SU(3) breaking for pseudoscalar meson nonet 77−6046
chiral SU(4)×SU(4) representation mixing, algebraic struct. 77−34102
chiral SU(4)xSU(4) symm., pseudoscalar mesons as Goldstone bosons 77−30278
chiral SU(N) Thirring model, S-matrix bound state poles fixing 80−360
chiral symmetric two-dimensional σ-model with SU(N) fermions, bound states anal. 77−6028
chiral symmetry, $SU_N \times SU_N$, multiplet fermion field model 79−9299
chromodynamics, SU(n), classical noncommuting quark source charges 78−78144
classical gauge field theory eqns. with arbitrary value of topological charge 79−21954
classical limit of quantum nonspin systems 79−63134
classical SU(2) gauge theory, exact multipseudoparticle solutions 77−22649
classical SU(2) Yang-Mills field, ignorable variables extraction from Hamiltonian 80−328
classical SU(2) Yang-Mills field eqns., periodic solns. in Minkowski space-time 80−4854
classical Yang-Mills eqn., multiple meron solns. 78−32987
Clebsch-Gordan coefficients for class II representations of unitary groups 77−41506
Clebsch-Gordan coeffs. for S_n, generation programs 78−86172
Clebsch-Gordan coeffs. program for finding functions on tableaux and frames of the symmetric group S_n 78−86173
colour model of hadrons, SU(6), review 77−82702
colour-flavour symm., renormalisation effects in guage theories 78−33018
complexified SU(5) algebra, singular orbits 79−12981
confinement in colour SU(N) gauge theory 78−8592
confinement in SU(N) lattice gauge theories 80−57493
conformal transformations, unitary implementability 79−21965
conformally covariant spinor field equations 79−22004
constituent quarks in SU(3) and SU(6), current algebra., hadron decays, review, book contrib. 80−47259
coupled Einstein-Higgs field, mag. monopole and dipole soln. *(Chinese)* 78−82112
covariant n^2-plet mass formulas 79−63460
CP^{n-1} model, quantum fluctuations in the one-instanton sector 79−85209
CP^{n-1} nonlinear σ-model, lattice formulation 79−58870
current algebra including term for U(4)×U(4) to SU(4)×SU(4)×U(1) symmetry, spin zero meson spectrum 78−58176
currents in Su(5) and E_7 unified gauge theories 78−54600
cylindrically symmetric instantons for the gauge groups of rank 2 (SU(3), O(5) and G_2) 79−58877
Dashen-Frishman model free-field-like behaviour and singularity of Callan-Symanzik function 78−16928
decomposition theorem, appl. to CP violation through quark mass diagonalisation 80−47216
density matrix for arbitrary spin, equations of motion for new SU(n) parameters 80−52592
Dirac spinor, relativistic exact bound states with gauge monopole 79−268
double well oscillator, nonlinear contribs. to the partition function 79−12963
dual charges, U_1 gauge field in SU_n gauge field *(Chinese)* 78−86417
dual electromagnetism and neutral-current interactions 79−71678
dual topological unitarisation, higher rank cylinder kernel 80−27492
dynamical generation of effective degrees of freedom, flavours 79−22026
dynamical Higgs mechanism, weak ΔI=1/2 rule, sum rules, heavy quarks and leptons 80−27442
Dyon solutions, existence, rigorous results 80−73595
effective Lagrangian in spontaneously broken gauge theories 79−17653
effective potential for non-Abelian gauge theories and spontaneous symmetry breaking 80−4863
electroweak force, grand unification and superunification 79−93333
elliptic meron-antimeron soln. of Minkowski SU(2) gauge theory 80−337
EM mass splittings, Born-term contribs. 78−78181
EM properties of charmed hadrons, $SU_6 \times U_c$ calcs., mag. moments, mass differences 78−70368
Euclidean Higgs fields, topology 78−4759
Euclidean SU(2) Yang-Mills theory, degrees of freedom in pseudoparticle systems 77−45954
Euclidean Yang Mills theory, pseudoparticle parameters for arbitrary gauge groups 78−24955
Euclidean Yang-Mills theory with spherical symmetry, explicit classical solns. 79−12966

SU_n theory continued
exact SU(n) instantons with cylindrical symmetry, SO(3) symmetric 79−9290
factorised S-matrix framework, antiparticles as bound states of particles 79−49411
Fermi-Bose and internal symmetries with universal Clifford algebras 78−24970
fermion generations in grand unified theories, SU(8) model 80−78012
fermion mass, unified gauge model based on E6 80−32053
fermion-fermion high energy scatt., transverse momentum cut-off hypothesis, Yang-Mills theory 80−86575
fermions, light, mass hierarchy, grand unification, SU(N) theory 80−62911
fermions and vortex solutions in Abelian and non-Abelian gauge theories 79−12959
filling U(4) multiplets by hadrons *(Russian)* 79−22076
flavour symmetry breaking and production processes in dual unitarisation, ϕ and ψ prod. 79−45080
flavour unification in SU(11) 80−62912
fluxon solutions in non-abelian gauge models 79−9287
four flavour $SU(2)_L \times U(1)$, gauge model with unconfined colour, $\Delta I = 1/2$ rule, GIM currents 77−82708
four-element lepton models, non-diagonal neutral currents *(Chinese)* 78−78132
four-quark scheme, $\delta I = {}^1/_2$ rule, existence of $K_L{}^0$, $K_S{}^0$ 77−22688
gauge field classification, Lorentz and gauge invariants 79−30648
gauge field in stability subgroup of vacuum in nonlinear realization 78−390
gauge field theory, magnetic charges in SU_2 and U_1 theories *(Chinese)* 77−71437
gauge hierarchies beyond the tree approximation 79−67470
gauge model of weak and EM interactions with SU(3)xU(1) symm. *(Russian)* 77−6074
gauge models, symm . of Higgs pot. 78−32980
gauge SU(N) theory, baryon bound state 77−13918
gauge symmetry, spontaneous breakdown, grand unification of QCD and $SU(2) \times U(1)$ 79−49380
gauge theories without anomalies 77−2756
gauge theory, current synchrospherical symmetrical monopole in multi-synchrospherical symmetrical case *(Chinese)* 80−22527
gauge theory, suppression of flavour changing effects from neutral spinless meson exchange 79−40716
gauge theory consistency in two Euclidean spacetime dimens., SU(N) quark-gluon theory 77−74598
gauge theory with scalar fields, effective Lagrangian 80−82897
gauging SU(n/m) 79−67467
Gelfand pattern, charmed hadrons and magnetic moment 80−398
generalised Schwinger boson realisations and oscillator-like coherent states, rot. groups and asymmetric top 79−80743
generalised Schwinger representation of fermion pairs to anharmonicity 78−89807
generalized coherent states and generating invariants 80−18089
generalized dual loop expansion of $U(N_c)$ gauge theory 79−93385
generating invariants of Clebsch-Gordan coeffs. 79−302
genetic diagrams for groups of orthogonal matrices O(n) 77−29988
Gln basis labelling, Racah algebra identification with S_N 80−8835
glueball spectra, prod. and decay for QCD and SU(n) gauge theories 80−62941
grand unification with exceptional group E_6, symmetry breaking, SU(5) relations, quark masses 80−68407
grand unification with the exceptional group E_8 80−105828
grand unified model with a stable proton and no axion problem 80−95234
grand unified theory from broken SO(8) extended supergravity, SU(5) theory 80−99081
gravitational instanton, CP^2 props. compared with SU(2) Yang-Mills instanton 78−81909
gravitational instantons and universal spin structs. 78−78128
gravitons, Einstein eqn. soln., on nonsingular positive definite metric 79−49150
gross-Neveu model as $Z_3 = 0$ limit of the two-dimensional SU(N) σ model 79−35949
group representation theory, quasistandard bases of permutation group, Gelfand bases of unitary group *(Chinese)* 78−12832
group theoretical construction of two-dimensional models with infinite sets of conservation laws 80−99056
hadron bags, interactions under strict quark-line rule 78−41495
hadron electromag. and weak form factors, SU(6) scheme of relativistic quark model 78−41500
hadron interactions, inclusive processes, multiplicity and scaling, resonance production, additive quark model, SU(6) theory, review 80−63043
hadron spectroscopy, quark models and SU(5) grand unification scheme 80−4958
Heisenberg spin chain derivation from nonlinear Schrodinger eqn. 80−37184
Higgs boson mass, perturbation constraint 79−67493
Higgs bosons, masses, gauge hierarchies, SU_5 model 80−47236
Higgs fields and the determination of the Weinberg angle 79−40709
Higgs induced neutral currents, symmetries leading to flavour conservation, Cabibbo angle 79−63407
Higgs meson prod., muon-number violation 78−41422
Higgs theory, two-dimens., instanton approach 80−99053
high energy meson elastic scatt. amplitude, leading term approx. in SU(2) Yang-Mills theory 80−5017
Hilbert space $4^2(SU(2))$ as representation space for $(SU(2) \times SU(2)) s S_2$ 77−17771
hydrodynamic model, nonlinear pion+pion chiral Lagrangian, $e^+ + e^-$ and p+p collisions 78−32966
hyperon mag. moments, transition moments, SU(3) calcs. 79−13128
hyperon nonleptonic decay, sum rules for S-wave amplitudes 79−63476
identical particle indistinguishability, field quantisation Lie algebraic approach 80−77984
imbedding of groups and multiquark models 77−49903
induced representations, reproducing kernels, conformal group, ladder representations, SU(2,2) 77−13882
inequivalent embedding of SU(2), instanton interactions, gauge fields 77−10180
infrared regularizations in a model gauge theory 79−30700
inner multiplicity of unitary groups, determ. using Gelfand patterns 78−89322
instantaneous Coulomb interaction in SU(2) Yang-Mills QCD 80−396

SU_n theory continued
instanton, group theoretical aspects 79−97494
instanton distribution, external field effects in SU(2) gauge field 80−4849
instantons, geometrical description of parameter space 79−30653
instantons and quark-mass generation−the how of spontaneous chiral symmetry breaking 80−4963
instantons and the index theorem 79−21951
integer quark charge model, enhanced flavour charge 79−49457
integer-charged quarks in the SU(5) grand unified theory 80−68410
interacting boron model of collective state, O(6) limit 80−32214
interacting boson model, transition from SU(5) to SU(3) limits 79−13218
interacting boson model of nucleus in terms of Casimir operators of I(6) chains 79−45191
invariant generation, theory of representation of symmetrical group S_N 79−75700
invariant integration over SU(N) 79−243
invariant operators of unitary groups U(n) and SU(n) 78−8555
irreducible representations of compact groups, tensor product decomp. and holomorphic induction 80−47205
isoscalar axial-vector current matrix elements 78−66051
isotopic spin, possible origin from extended conformal symmetry, Yukawa interaction 79−40684
isotopic symmetry group in strong interactions, possible geom. origin 79−17628
Jaffe model, lowest states, appl. to $q^4\bar{q}$ in SU(6) 79−13060
Jones matrix, appl. in symmetry breaking, SU_2 theory and theory of neutrinos 79−17632
kerr-Schild geometry, spinors, and instantons 79−35601
l-broken U(6,6), generalised $^3P_0$ model and reln. to Melosh transform. 78−12885
lattice gauge theories, weak to strong coupling crossover 80−95212
lattice gauge theories, Z(N) system phase struct., dual variables 80−62848
lattice gauge theory, string model, hadron spectrum, Regge trajectories 77−57452
lattice SU(N) gauge theory, vacuum structure, large-scale 80−57470
lattice theory of SU(N) gauge fields, non-convergence of 1/N expansion 77−71427
left-right symm. gauge theories, CP violation, absolutely stable hadrons 78−74155
left-right symmetric SU(N) gauge models, parity violation in atoms 79−21966
left-right-symm. unified theory of quarks and leptons 78−41466
left-right-symmetric theory of weak interactions in unified gauge theory, constraints on phenomenology 78−21369
lepton structure, $SU(2) \times U(1)$ gauge theory 77−82691
Lewis Riesenfeld harmonic oscillator, unitary declension of dynamical symmetries 79−89074
Lewis-Riesenfeld time-depend. harmonic osc., dynamical symmetries 80−4588
Lie algebras associated with classical relativistic planar motion in axisymmetric EM fields 79−49064
light quarks and QCD Boson representation, dynamical symmetry breaking 80−52472
Lipkin model, quasi-spin pairing and struct. 79−485
local QFT, higher symm. interpretation, spontaneous symm. breaking, quarks and flavours 78−16942
locally flat space-time, quantised metric, spontaneous dilatation asymm. 78−16713
magnetic charge of Yang-Mills fields, in terms of Higgs fields, SO(4), SU(4) 77−45935
magnetic monopoles in broken SO_3 and SU_2 gauge theories *(Chinese)* 78−86459
many-spin system, group approach in dynamics *(Russian)* 80−4579
massless quarks in QCD, dynamical symmetry breakdown 80−52471
Maxwell's eqns. in expanding universe 78−4493
Melosh transformation, SU_2 symm. 77−87914
meron pair, introduction, motivation and formalism 80−82861
meron pairs, bare activity 80−82862
meron solutions in a non-Abelian, conformal invariant Higgs model 79−17610
meson isosinglets, mixing angles, non-relativistic quark model, Schwinger-type mass relations for SU_4 and SU_5 80−18125
meson isosinglets, mixing angles, non-relativistic quark model, SU_5 and SU_n 80−22591
meson radiative decays, higher order effects 79−13131
meson resonances, high spin, natural parity, dual reson. model with non-degenerate Regge trajectories 79−359
meson wave functions, straton model, Bethe-Salpeter eqn., SU_6 symm. *(Chinese)* 77−34125
meson wave functions, SU_n representation transformations and phase *(Chinese)* 79−93313
mesons, $SU_{1,4}$ as dynamical group, discrete representations anal., masses 77−74642
method of generating invariants 78−16945
mixing angle between ordinary and heavy leptons in a (V-A) model, constraints 78−4846
monopole bound states, SU(4) spontaneously broken 77−82679
monopole classification in SU(2) and SU(3) gauge field theory 77−38082
monopole solns. in spontaneously broken SU(n) gauge theory 78−82103
multi-instanton solution, new compact form 78−24971
multicomponent chiral and gauge models, stationary solns. 79−85213
multidimensional unified theory of gravit., EM and weak interactions 78−41462
multilevel system, group theoretical method for coherent effects calc. 80−106502
multiquark baryons and the MIT bag model in SU(6), coupling const. and decay modes 79−97600
N resonance electroproduction, helicity structure and quark motion effect 78−398
n-pseudoparticle solns., small variations 78−66042
natural flavour conservation in neutral weak interactions, SU(5) and SO(10) unified models 78−4817
net baryon number and CP nonconservation with unified fields 80−62349
neutral current couplings in neutrino-hadron interactions 78−24993
neutral current phenomena, gauge model of parity nonconservation 79−17656

SU_n theory continued
neutral currents and quark charge origin 78−21373
neutral currents in left-right symmetric unified gauge models 79−45044
neutral currents natural flavour conservation, determ. of Cabibbo angle 79−22015
neutral transitions, vector-like weak currents, parity violation *(Russian)* 78−24995
neutral weak current, structure, neutrino and antineutrino scattering experiments *(Russian)* 79−49446
neutrino number and isotropy of Universe 80−85852
Neveu-Schwarz dual model, vac. transitions *(Russian)* 78−33046
non-Abelian gauge theory of quarks and gluons in two dimens. 79−30654
non-Abelian gauge theory with many flavours, high energy processes, asymptotical behaviour *(Russian)* 80−101935
nonAbelian gauge model, Becchi-Rouet-Stora invariant, superfield struct. 78−74121
nonAbelian SU(2) gauge field, dual charge *(Chinese)* 77−34077
noncompact Lie groups and SU(1,1), continuous spectra, coherent states 78−8548
nonleptonic decays of ordinary and charmed hadrons, vector-like model 78−41545
nonlinear Lagrangians and spontaneous symm. breaking 78−70303
nonlinear SU(n) a lattice field theory, phase transition 79−252
nonrelativistic particle in spherical space, dynamical symmetries 79−26255
nonrelativistic quark model with one gluon exchange pot., baryon spectroscopy in SU(6)⊗O(3) 78−78147
nuclear cluster model using SU(3) and SU(4) coupling 77−57615
nuclear force, parity violating, unified treatment 80−47400
O(2) symmetric connections in an SU(2) Yang-Mills theory 80−4839
O(3)-symmetric merons in SU(N) gauge theory 80−82904
O(4)⊗U(1) gauge model for weak and EM interactions 79−71681
O(5)×SU(1,1) symmetric irreducible representations, orthonormal basis, interacting boson model appl. 80−78178
observable phase factors and symmetry of electric and magnetic charges 78−86428
orbital calculations, independent-particle Hamiltonian, group struct. 79−22580
order and disorder parameter inequalities 80−99051
parity violating effects in dilepton production using polarized targets 79−67613
parity violation in atoms induced by radiative corrections 78−78108
particle motion in classical gauge field, variational derivation and uniqueness of equations of motion 79−40658
Pauli-Lenz vector, extension of SO(3) to SO(4) 80−31550
periodic solutions of massive ϕ^4 and Yang-Mills theories 79−12935
pion production by weak neutral currents, gauge theory model predictions 79−13014
planar approximation for coupling N×N matrices 80−62872
planar diagrams, SU(N) asymmetric model, semiclassical approach 80−77957
Poincare supersymmetry, parafermion generalisation 79−17626
Polyakov-'t Hooft monopole and dyon, quantum theory *(Russian)* 78−392
Prasad-Sommerfield dyon (monopole) soln. of SU(2) Yang-Mills field with Higgs multiplet 80−339
pre-quarks and fractional charges 80−91048
precocious chiral grand unification based on $SU(8)_L \times SU(8)_R$ semi-simple gauge group *(Russian)* 80−42382
projective space-time, geom. of (N+1) particle system 77−74221
proton half life, Dirac approach to large number coincidences 80−27501
pseudo-oscillators, group theory 80−22226
pseudoparticle, four-dimens., quantum effects calcs., SU(2) gauge theory, chiral symm. breakdown 77−30247
pseudoparticle solns., classification in gauge theories 78−4789
QCD, 2-dimens., Bose form, SU(N) confining phase 80−52463
QCD, E_7 model, quark and lepton assignments 78−8590
QCD, gauge invariant quantum variables, $SU(N)_1 \otimes SU(N)_2 \otimes SU(N)_3$ algebra 79−30705
QCD, massless two-dimens. model, operator soln., local colour SU(n) symm. 78−41480
QCD, two dimens., renormalisation group functions 78−29242
QCD, two dimens., with SU(N) gauge symm., N→∞ limit 78−41489
QCD vacuum struct. in chiral U(N)⊗U(N) symmetry 79−93347
quadratic Hamiltonians, quadratic invariants and SU(n) symmetry group 78−36873
quantum chemistry, Clebsch-Gordan coeffs., chain $SU(2) \supset D_\infty' \supset D_4' \supset D_2'$, mol. aggregates 78−17552
quantum collective field method, planar limit appl., SU(N) theory and harmonic oscillators 80−57468
quantum flavour dynamics, quark masses and flavour mixing angles in six quark model 78−74211
quantum gravity, positive action conjecture and asymptotically Euclidean metrics 79−58611
quark and parton phys., introduction, book 79−85276
quark confinement, Dirac equation with relativistic linear potential, baryon properties, SU_6 representations 80−47261
quark confinement criteria, QED_2 model with SU(n) flavour 78−45840
quark confinement with regular cutoff via SU_n colour gauge group 77−6083
quark field, unitary invariant generalisations *(Russian)* 78−66024
quark field quantum fluctuation computation in arbitrary Yang-Mills instanton background 80−13268
quark flavour, unified theory with SU(5) subgroup 79−89102
quark mass spectrum from broken SU(6) symmetry 79−45057
quark masses and Cabibbo angles 79−9332
quark model, weak interactions, quark masses, spontaneous violation of parity 77−6054
quark model and hadron spectroscopy, review 79−80808
quark model of broken SU(8) symm., charmed meson pair prod. in e^+e^- annihilation 77−38182
quark model of nucleons, ground state wave functions, O(3)×SU(6) symmetry 78−62352
quark model of resonances, $SU_6 \times O_3$, form factors, review 77−67624
quark model relativistic generalisation minimal boosting of SU(6) scheme, meson, baryon props. 77−41814
quark model with 4 quarks pseudoscalar meson masses 77−46021
quark models, noninvariance groups, internal symms. and ghost symms. 78−25007
quark sea, SU_n flavour symm. 78−54606

SU_n theory continued
quark-diquark model with broken colour symmetry, hadron spectrum 78−12874
quark-lepton unification in SU(N>5) 80−73646
quark-quark interaction, phenomenological, from s-wave baryon spectrum 80−101984
Racah algebra of Gln, generalised back coupling rules 80−47208
recoupling coeff. and isoscalar factors, for chain of compact topological groups 78−20939
recoupling coefficients of the general linear group in bases adapted to shell theories 78−77670
recoupling coefficients of the symmetric group involving outer plethysms 78−77669
Regge behaviour of spontaneously broken non-Abelian gauge theory 78−70287
Regge spectra, symm. breaking effects, decay rates of mesons in dual resonance amplitudes 77−82715
reggeon F/D ratios in SU(4), crossing invariant soln. of baryon exchange degeneracy 77−2766
relativistic hadron couplings, unified framework, symms., quark models *(German)* 78−50012
relativistic many body theory, finite temp. and density., elementary particle symmetries 79−49403
relativistically invariant two-dimens. models, classification method *(Russian)* 78−70291
riemannian spaces with local duality and gravitational instantons 79−25938
rotation group irreducible representations, spin-1/2 representation, teaching approach 79−58488
scalar QCD in two dimens., and the parton model 78−93856
Schnurs, combinatorial hierarchy, spin dichotomy and conservation of quantum numbers 80−68383
self dual SU(N) Yang-Mills fields, nonlocal continuity eqns. 80−9096
self dual Yang Mills theory, general solns. for O(n), SU(n) and Sp(n) gauge groups 79−6281
self-dual equations for SU(n) theory, props. 79−17607
semiempirical mass formula for hadrons in quark model and QCD 78−74236
semisimple unified gauge theories 78−70282
seven lepton model, quantum flavour dynamics, mixing angle, masses, spontaneous symmetry breaking 78−89652
shell model, SU_6(s,d) boson model, collective states struct., Sm, Ba appls. 78−54672
SL(2,C) exterior forms and quantum gravity 79−35622
SL(2,C) unitary representation decomposition induced by SU(1,1) discrete series 79−21967
SL(2,R) and SL(2,Z), mass group associated with hadronic mass spectrum 79−63459
SL(n,C) actions, analytic, real, on spheres and complex projective spaces 80−68382
SO_{10} hierarchical breaking and neutrino masses 80−22550
SO(2N) grand unification in an SU(N) basis 80−62906
SO(4)×U(1) model of weak and electromagnetic interactions 79−13009
SO(4) Yang-Mills model, classical solns. with both instantons and anti-instantons 77−79211
SO(8)×SO(8) phenomenological symmetry, synthesis for leptons and hadrons 79−13035
SO(8) supergravity derivation 80−12975
soft CP-invariance violation at high temperature 79−75697
solitons, nontopological, in three dimens. space, SU(2) gauge field + spin-0 field 77−18167
space-time independent potentials for SU(2), SU(1,1) and E(2) gauge theories 79−49381
spherically symm. monopole soln. 78−8539
spherically symmetric SU(2) gauge fields and monopoles *(Chinese)* 77−74568
spinor fields in four dimensional space-time 79−6271
spontaneous breakdown of SU_N 79−9298
spontaneous symmetry breaking in chiral quantum field theory, covariant formulation 78−21347
spontaneously broken SU(2) gauge theory, nonexistence of spherically symmetric monopoles with multiple mag. charge 77−6010
standard model neutral current predictions, uniqueness 79−80789
static Euclidean SU(2) solns., global struct. 80−4862
static quark forces in classical chromodyanamics, bag models, SU(2) Yang-Mills field 79−2990
straton model, SU(5) extension, descript. of new Υ particles near 9.5 GeV *(Chinese)* 78−82168
straton model theory, extension to SU_5 *(Chinese)* 78−24996
string, relativistic, $SU_{3,1}$ in orthornormal gauge 78−437
strong interaction models, SU(n) and SU(3)×SU(3) internal symms. 77−10182
strong interactions, introductory book using potential theory 77−223
$SU_{1,3}$ calc. of exotic meson mass 77−65147
$(SU_2 \times U_1) \times S_n$ flavour dynamics, flavour number bound, n quark and n lepton generations unification 80−4907
SU_2 gauge fields, dual charge and principle bundles structure *(Chinese)* 77−71438
SU_4, spectrum generating, semileptonic decays of D-mesons 77−54098
SU_4, unified parity-conserving interactions 77−74629
$SU_4 \times SU_4$ breaking in chiral nonlinear Lagrangian, pseudoscalar meson mass 77−57513
$SU_4 \times SU_4$ chiral breaking and Cabibbo angle 77−74641
$SU_4 \times SU_4$ chiral symmetry for pseudoscalar mesons 77−67583
$SU_4 \otimes SU_3'$ structural model of straton with integral charges *(Chinese)* 78−12860
SU_5 theory, superheavy particles, decoupling at low momenta 80−52431
SU_6, dynamical symmetries, in nuclei, energy levels, transitions and collective states 78−74317
SU_6, SU_3, subalgebras and mass sum rules for hadrons with charm, beauty and taste 80−9152
$SU_6 \times Su_3^c$ scalars in E_7 irreps 78−36794
SU_7 grand unification model, two (V−A) and one (V+A) generations of quarks and leptons 80−57538
$SU_L(2) \otimes SU(2)_R \otimes U(1)$ and $SU(2) \otimes U_L(1) \otimes U_R(1)$ gauge theories, neutral current constraints 79−277
$SU_L(4) \times U(1)$ four-quark model, lepton quartets and W bosons 77−87934
SU_{m+n} containing $SU_m \otimes SU_n$, irreducible bases *(Chinese)* 78−66049
SU_{mn} containing $SU_m \times SU_n$, irreducible bases *(Chinese)* 78−66049

SU_n theory continued
$SU_n \rightarrow Sp_n$ reduction using geometrical induction procedure, SU_4 appl. 79−26256
SU_N gauge group uniqueness in grand unified model, U_1 color, proton stability 79−316
SU_n group singlet factor, recursive formula for Clebsch-Gordan coefficients *(Chinese)* 79−58902
SU_N/Z_N gauge invariant theory, phase factor operators and soliton fields 80−77947
$SU(10)_{flavour} \times SU(10)_{colour}$ unified hadron lepton theory 79−67509
SU(10) symmetry, charmed vector bosons mag. moments 78−17018
SU(12) broken symmetry in two six quark models, hadron mass relns. 77−22693
SU(1,1) Lie algebra, multiplicity free and finite multiplicity indecomposable representations 79−283
SU(1,1) non-compact group, existence of intelligent states 78−77753
SU(2,2) conformal group, unitary ray representations with positive energy 77−71450
$SU(2)_L \times SU(2)_R \times U(1)$ six quark gauge models, flavour violation 80−4951
SU(2), double groups, symmetry coupling coeffs., C_n^*, D_n^*, T^*, chem. physics 77−54499
SU(2), generalised 6-j symbols 80−31557
$SU(2) \times U(1)$ gauge model, microweak CP violation 77−71456
$SU(2) \times U(1)$ gauge model predictions for neutral current reactions 77−71424
$SU(2) \times U(1)$ gauge models, with diagonal neutral currents 77−71433
$SU(2) \times U(1)$ unified gauge theories, implications of parity violating obs. on heavy atoms 77−46006
$SU(2) \otimes U(1)$ standard and SU(5) grand unification models, neutral current data implications 80−78000
SU(2) classical gauge theory and ϕ^4 scalar field theory, relns. of solns. 77−45949
SU(2) coupling model with tachyon fields *(Korean)* 77−49844
SU(2) gauge field struct. *(Chinese)* 77−57434
SU(2) gauge fields, singular Wu-Yang soln. 77−65086
SU(2) gauge fields on Euclidean four dimens. space, self-duality condition 77−61195
SU(2) gauge group, solns. for Yang-Mills eqns. *(Russian)* 77−79226
SU(2) gauge theory, resonances, particle motion, metastable states, interaction with monopole 77−74595
SU(2) magnetic monopole solns., parameter counting in Prasad Sommerfield limit 80−352
SU(2) theory with four fermion interaction and asymptotic freedom, exact soln. 80−4858
SU(2) x U(1) gauge group, neutral current couplings 77−67567
SU(2n) principle models for integrable nonlinear systems, current constraints, conservation laws 80−86619
$SU(3)_{colour} \times SU(n)_{flavour}$, generation of diquark currents 77−65129
$SU(3) \times SU(3)$ model, meson spectrum, prod. and decay of new particles *(Chinese)* 77−49870
$SU(3) \times SU(3)$ strong interaction model, ϕ^3 field theory in 6-ε dimens. 77−82726
$SU(3) \times U(1)$ gauge models, generalised mixing and CP violation in hadron decays 78−41473
$SU(3) \times U(1)$ low-energy symmetry within the unifying $SU(4)_F \times SU(4)_C$ gauge group 79−67489
$SU(3) \otimes U(1)$ theory of weak and EM interactions 77−57481
SU(4), ψp total cross-section 77−46089
SU(4), broken, nonperturbative approach, vector mesons intermultiplet mixing 77−74653
$SU(4) \supset SU(2) \times SU(2)$, commuting missing labels operators, equivalent sets 77−60896
$SU(4) \otimes U(1)$ broken gauge theory, muon number nonconservation 77−74638
SU(4) breaking 15-plet dominance, charmed baryon spectrum 77−74663
SU(4) broken scheme for vector and pseudoscalar meson two-body decays 77−67648
SU(4) broken symm., baryon reson. 77−71455
SU(4) duality and quark parton model in deep inelastic lepton-nucleon scatt. 77−61293
SU(4) symm. model, mag. moments of 20-plet baryons, charm quantum numbers 77−61257
SU(4) theory and meson radiative decays in VMD model 77−74688
SU(5|1) superunified model in 6-dimens. 79−97557
SU(5), broken, meson mass formulae 80−47267
SU(5), Clebsch-Gordan series, quark model appl. 80−47256
SU(5), gauge invariance and fermion mass dimensions 80−62907
SU(5), Higgs scalars number and m_b/m_τ ratio 80−105826
SU(5), SU(6) vectorlike unified theories with unitary groups, Fermi oscillators, proton stability 77−67608
SU(5), unification of weak, EM and strong interactions, review 80−105814
$SU(5) \times SU(2)$ unification, horizontal symmetry due to quantised motion along internal axes 80−62905
$SU(5) \times SU(5)$ chiral symm. breaking, Cabibbo angle, meson mass spectrum 77−74614
$SU(5) \times U(1)$ unified theory, neutral current anal. 80−73647
SU(5) and SO(10) grand unification, flavour mixing and proton instability *(Russian)* 80−68413
SU(5) asymptotic symmetry, b quark flavour from Weinberg spectral function sum rules 79−67495
SU(5) combined quark-lepton decuplets, particle families *(Russian)* 80−47217
SU(5) electroweak-strong interaction model, broken colour symmetry and gluon mass 80−73650
SU(5) electroweak-strong interaction model, mass relations and mixing angles 80−73649
SU(5) grand unification, cosmological baryon asymmetry 80−86640
SU(5) grand unification, fermion mass and Higgs representations 80−27446
SU(5) grand unification, flavour number estimate 79−85264
SU(5) grand unification, heavy coloured Higgs scalars, b-quark mass 80−57543
SU(5) grand unification, nucleon lifetime, bag model calc. 80−52450
SU(5) grand unification, p lifetime and branching ratio, bag model wavefunctions 80−78004
SU(5) grand unification, spin from isospin, half integer spin charge monopoles 80−68406
SU(5) grand unification, strong CP violation, quark-lepton mass ratio 80−32057

SU_n theory continued
SU(5) grand unification, superheavy fermions and proton lifetime *(Russian)* 80−91036
SU(5) grand unification embedding in SU(N), SU(9) theory, flavour unification 80−32059
SU(5) grand unified model, inherent mixing and proton lifetime 79−49441
SU(5) grand unified theories, proton decay, flavour mixing effects 80−377
SU(5) grand unified theory, flavour number limit from fermion mass higher order corrections 80−4904
SU(5) grand unified theory, p decay modes 80−13301
SU(5) grand unified theory, proton lifetime estimate accuracy 80−101967
SU(5) grand unified theory, t-quark mass 79−97559
SU(5) interacting d-boson model, log. energy decreases 78−93955
SU(5) invariant theory, B-L nonconservation and neutron oscillation 80−78005
SU(5) mass formulae, $b\bar{b}$ states masses, mass differences and splitting 79−17691
SU(5) model, dyons and monopoles 80−82931
SU(5) model, gauge hierarchy for grand unified theory prototype 79−75711
SU(5) monopoles, magnetic symmetry and confinement 80−99078
SU(5) symmetry with beauty quark, baryon and meson mass spectra 79−45079
SU(5) theories with both proton stability and cosmological baryon-number generation 80−86642
SU(5) theory, unified theory of elementary-particle forces 80−105827
SU(5) unification, Higgs potential, coupling constants, and gauge hierarchy 80−86637
SU(5) unified gauge theory, non-Abelian electric and mag. flux 80−57545
SU(5) unified model of strong, weak and EM interactions, matter instability 79−35985
SU(5) without symmetry constraints, unified model of quarks and leptons, conservation laws 80−101968
SU(5) x SU(5) broken chiral symmetry, symmetry breaking parameters, limits 79−45026
SU(5/1) supergroup based strong-electroweak unified model with supersymmetry 80−101977
$SU(6)_w$ analysis of sums of baryonic partial widths 77−30378
$SU(6)_w$ and $\{70, 1^-\}$, $\{56, 2^+\}$ decays 77−6122
$SU(6)_W$ decay anal. of $[70, 1^-]$ and $[56, 2^+]$ multiplets 77−22733
$SU(6)_W$ models and baryon resonance decays 77−22700
$SU(6)_W$ structure of baryonic reson. photocouplings duality constraint 79−71649
$SU(6)_W$ symmetry, ang. constraints and collinearity breaking, free quark model 79−30679
SU(6), bag theory, excited states of confined quarks 77−6080
SU(6), determ. of new polarised ν sum rules 77−34144
$SU(6) \times O(3)_L$ multiplets, semilocal duality, quark-orbital Regge trajectories 80−27490
$SU(6) \times O(3)$ baryon multiplet, linear string model 78−8624
$SU(6) \times O(3)$ multiplet masses, relativistic quark model 78−8552
$SU(6) \times O(3)$ quark shell model, L=1 meson mass spectrum 78−89678
$SU(6) \times SU(3)$ as classification group for baryons, Poincare group and quarks 77−18246
$SU(6) \supset SU(3) \otimes SU(2)$ Wigner coefficients 79−97607
SU(6) based renormalisable unified gauge model with calculable masses 78−89647
SU(6) based vector-like gauge theory, unified theory with right handed currents, proton stability 77−49890
SU(6) boson model for two-nucleon transfer intensities, (t,p) appls. 78−25206
SU(6) breaking and $\Sigma^0 \rightarrow \Lambda\gamma$ lifetime 77−18284
SU(6) breaking and internal quark motion effects on baryon ground state props. 77−38128
SU(6) breaking of baryon wave functions, chromodynamic spin-spin force 79−340
SU(6) broken symmetry model, baryon mag. moment values 79−49417
SU(6) classification of states, quark model with interaction 77−74651
SU(6) configuration mixing symmetry breaking, one gluon exchange potentials 79−40739
SU(6) exotic gauge model, lepton-quark symm., CP-violation and $\mu \rightarrow e\gamma$ decay 78−12875
SU(6) grand unification model, hierarchy of symmetry breakings and neutral currents 80−52446
SU(6) grand unified theories, one loop renormalisation effects, stepwise symmetry breaking 80−32058
SU(6) model of weak interactions, neutral weak currents at high energy *(Russian)* 78−45836
SU(6) multiplet, connection with semi-local duality in quark model 79−93386
SU(6) parton model, lepton prod. with large transverse momenta in hadron-hadron collisions 78−89673
SU(6) quark model of hadron struct., field theory treatment 79−49483
SU(6) symmetry breaking in MIT bay model, neutron charge radius anal. 78−70334
SU(6) unified gauge field theory of weak, EM and strong interactions 79−17658
SU(6) unified gauge group, neutral current coupling to ν_μm and ν_e 78−54626
SU(6) unified gauge model, based on $SU(3) \times U(1)$ and colour SU(3) subgroups 78−12847
SU(7) grand unified theory with heavy colour 80−42380
SU(8), $SU_W(8)$ symmetries, mass formulae, mixing *(Russian)* 78−66097
SU(8) broken symmetry, baryon masses 79−290
SU(8) grand unification, natural embedding of SU(3) horizontal symmetry 80−86646
SU(8) mass relations among $J^P = 1/2^+$ and $3/2^+$ baryons 77−71499
SU(8) non-leptonic decay of hyperons and charmed baryons 77−49963
SU(8) quark model, charmed baryon tensorial mass operators 77−54091
SU(8) supergravity on mass shell in superspace 80−46907
SU(8) supergravity supersymmetry breaking 80−46908
SU(8) symm. mag. moments of charmed vector bosons 78−4794
SU(8) symmetry and the baryon mass spectrum 79−80814
SU(8) theory of parity violating hyperon and charmed baryon non-leptonic decay 77−26523
SU(8) unification and supergravity 80−46928

SU_n theory continued
SU(9) grand unification of flavor with three generations 80−13251
SU(N+1) σ model (or CP^N model) as nonlinear realisation of SU(N+1) symmetry 79−58871
SU(N+1) gauge theory, exact monopole solns. with spherical symmetry 79−71626
SU(n+1) invariant chiral theory, duality eqns. soln. 79−9351
SU(N>5) chiral grand unification 80−91028
SU(n), SU(2n) three quark coupling coeffs., diagrammatic group theory 79−331
SU(N)×SU(N) chiral symmetry, spontaneous breaking, instanton role 80−47219
SU(N)×SU(N) symmetry breaking with extremum constraints 80−68385
SU(N)⊃O(3), angular momenta multiplicities in system of N-dimensional harmonic oscillators 78−32702
SU(N) chiral Gross-Neveu spectrum derivation 80−47176
SU(N) colour groups, N>3, quark content 80−4938
SU(N) conformal supergravity, gauge theories for extension 78−8577
SU(N) Coulomb and Landau gauge theories vacuum struct., Gribov ambiguities, harmonic anal. 80−68363
SU(N) gauge groups, N=2,3,4, meron and meronlike configurations 79−71636
SU(n) gauge theories, directions of spontaneous symmetry breaking 80−13228
SU(n) gauge theories, spontaneous symmetry breaking pattern 80−95228
SU(N) Georgi-Glashow model, electric quark confinement in 2+1 dimens. 79−85263
SU(N) Georgi-Glashow model, electric quark confinement in 3+1 dimens. 79−97583
SU(N) grand unification with several quark-lepton generations 80−27443
SU(n) group, mixing and sequential heavy lepton weak interaction *(Russian)* 79−40720
SU(N) group, quantum fluctuations in vicinity of an instanton, quadratic Lagrangian 79−6266
SU(N) invariant non-linear σ models 79−17613
SU(N) lattice gauge model, weak coupling, monopole condensation and quark confinement 79−75683
SU(N) massive Yang-Mills field theories, struct. and renormalisability, Higgs field 79−6279
SU(N) spontaneously broken to U(1), composite magnetic monopoles 77−2765
SU(N) symmetric quantum dynamical systems, N→∞, energy spectrum for singlet and adjoint states 80−62880
SU(N) Thirring model and 1/N expansion, chiral symmetry breaking 79−12977
SU(N) unification of extra strong interactions, no-go theorem 80−32056
SU(N) Yang-Mills field eqns., constant classical solns. for N=∞ 80−73589
SU(s) grand unification, neutrino mass and oscillations, B-L nonconservation 80−52449
super Clifford algebra 79−98
superalgebra generalisation, 3-colour extension of OSP (4,1) de Sitter and SU(2,2;1) Wess-Zumino superalgebras 79−330
superalgebras, spinor representation for Lie algebra enlargement 77−34100
extended supergravity, N=2, auxiliary fields in 5, 6 space-time dimens. 79−30339
supersymmetric gauge models of weak and EM interactions 78−58106
supersymmetric models of weak and electromagnetic interactions 79−26276
supersymmetric nonlinear σ-model in 4-D, coupling to supergravity 78−49981
supersymmetric Weinberg-Salam model 79−67490
supertwistors and conformal supersymm. 78−29015
superweak gauge theory of CP-invariance violation 79−75710
symmetric versus antisymmetric mass matrices in grand unified theories 80−99082
symmetry breaking perturbation technique, tensor operators 79−12975
tensor meson radiative decay in SU(6)×O(3) broken symmetry quark model 80−73710
tensor properties of second-quantization operators and analysis of composite physical systems 79−25903
Thirring massive SU(N) model, factorisation 79−12951
Thirring model, chiral, CP^{n-1} and SU_n, exact S-matrix 80−90985
Thirring model SU(1,1) group representation theory algebraic struct. *(German)* 79−89055
Thirring model with SU_n symmetry, scale invariance 79−9288
triangular anomaly, SU(n) Lie gauge groups 78−29270
twistor theory in Weinberg-Salam and Georgi-Glashow SU(5) model 80−73651
two dimensional field theories with infinite number of conservation laws and Backlund transformations 80−9095
two-dimens. SU(N) gauge theory for mesons 77−49840
two-dimensional classical field theory, nontrivial interaction between solitons *(Russian)* 78−32698
$U(1)\times SU(4)_L\times SU(4)_R$ based weak-EM synthesis with manifest left-right symm. 78−8571
$U(1)\times U(1)(loc)\times SU_2(loc)$ invariant Weinberg Lagrangian, hypercharge group 79−71680
U(1) colour symm., Higgs coupling, proton stability 78−29290
U(N,r) σ models, generalisations of σ and Cp^N models, and instantons 79−49377
U gauge in Abelian and non-Abelian gauge theory, Gribov ambiguities 78−45788
unification mass and gauge hierachies for O(10), E_6 and $[SU(4)]^4$ models 79−80782
unification of EM, weak and strong interactions, SU(5) group and symmetry breakdown 80−73637
unified gauge field theory with torsion, symmetries 78−89386
unified gauge theories, electroweak mixing angle, sequential triplets scheme of fermions 80−86650
unified gauge theories and the baryon number of the universe 78−85842
unified SU(6) gauge theory, hierarchy of gauge symm. and CP nonconservation 78−41464
unified superconformal gauge theories for gravity+other gauge interactions 77−87928
unified theories, mass scales, alternatives to SU(5) 80−27441

SU_n theory continued
unified vectorlike gauge theory based on group SU(6) for quarks+leptons 78−4818
uniqueness of the Weinberg-Salam gauge model 79−35989
unitarity and hadron self-energy, mass shifts, and SU_6 symmetry breaking in meson spectrum 79−17687
unitary groups, functional integral representation *(Russian)* 79−9309
universal confining pot. and symmetry breaking in baryons. SU(8)⊗O(3) symmetry 79−13051
Universe baryon number asymmetry mechanism, unified calibration theory calcs. *(Russian)* 80−36756
V+A currents coupling old quarks to new quarks 77−26486
vector boson model from SL(2,C) gauge theory of gravitation and Yang-Mills theory 79−322
vector constants and their algebras for classical Hamiltonians 79−56
vector meson twenty-plet *(Russian)* 78−58220
very early Universe, phase transitions and mag. monopole prod., grand unification 80−51934
VV+AA type gauge models, effective ν interactions 78−66038
weak and EM interaction unification with strong interactions following τ and Υ, book contrib. 80−47235
weak hadronic current in models with 4 and 6 quarks *(Russian)* 77−74616
weak hypercharge embedding in strong gauge groups 79−30692
weak interaction models explaining null parity violation in Bi, tests on other weak interactions 79−2974
weak interactions of quark fields, quark masses, spontaneous parity violation 77−34115
weak interactions vectorlike model with six quarks, gauge theory, SU(2)×U(1), νN appl. 77−57480
weak nonleptonic decays in SU(4) and SU(8), adjoint representation admixture 78−21426
weak radiative decays in SU(4) and SU(8) 77−87977
weight multiplicity for Lie groups, explicit formulae 77−26467
Weinberg angle, renormalisation effects 78−62344
Weinberg-Salam model, fermion and Higgs boson mass constraints 79−49437
Weinberg-Salam model, left-right symmetric model with global symmetry 79−17657
Weyl invariants generating function *(French)* 79−93304
Wigner coefficients for SU(6)⊃SU(3)⊗SU(2) 79−45025
Wigner SU_4 symmetry mixing for nuclei in fp shell 77−6255
XY_4, tetrahedral, SU (2s+1)×ζ_T and spin statistical weights 78−50463
XY_5, trigonal bipyramidal, SU (2s+1)×ζ_T and spin statistical weights 78−50463
XY_6, octahedral, SU (2s+1)×ζ_T and spin statistical weights 78−50463
Yang's R gauge for self-dual SU(3) gauge fields 78−78088
Yang-Mills equations, SL(3,C) self dual instanton solns. 79−63369
Yang-Mills field, self-dual, parametric Backlund transformation 79−97503
Yang-Mills fields, stability and gap phenomena 80−18073
Yang-Mills instantons, space-time topology 78−8522
Yang-Mills SU(N) 2-D theory in leading 1/N expansion 78−8516
Yang-Mills theory, Regeisation of scalars and dual model struct. 78−16927
$b\bar{b}$ baryons, mag. moment sum rules, in Su(S) 80−78065
$D^+\to K^0\pi^+$, $D^0\to K^-\pi^+$, two body decays of charmed mesons, quark recombination scheme 78−37207
D^+-D^0 mass differences, chiral SU(4)×SU(4) model, broken isospin symm. 77−87917
$D_{15}\to\rho\gamma$, SU(6) selection rule violation from quark hyperfine interactions 79−6329
$D^{0*}\to D^0\gamma$, SU(4) theory, suppression factor in radiative decay amplitude 77−30372
$D\bar{D}^*$ production and decay, VDM, dual amplitude anal., e^+e^- annihilation 77−49992
$e^+e^-\to\mu^+(\tau^+)\mu^-(\tau^-)$, neutral current couplings, lepton polarisation, p violation in SU(2)×U(1) model 80−4975
eN, deep inelastic scatt., quark model, field-theoretic, quark indistinguishability, nucleon structure function 80−62993
eN scatt., polarised e, testing unified gauge theories prediction 79−17732
$e^-N\to e^-X$, parity violating asymmetry, constraint on right-handed electron weak charge 79−17734
ep deep inelastic scatt., pol. p and e, straton model, sum rule *(Chinese)* 80−42475
η decay modes of $1/2^-$ baryons, hadronic interaction symm. 77−30379
$\eta\to\pi^+\pi^-\pi^0$, on-mass-shell current algebra, SU(3)×SU(3) σ model 77−34151
$\eta'(958)\to 4\pi$, decay mode in broken $SU_6\times O(3)$ quark model 79−36071
J particle, tensor meson decays in SU_4 model *(Chinese)* 79−75767
$K\to 2\pi$, decay amplitudes in SU(2)×U(1)×U(1) model with new neutral current 80−4986
$K^\pm\to\pi^0 l^\pm\nu_l(\bar{\nu}_l)$, decay form factors in relativistic symmetry SO(4,2)⊗SU(3)⊗SU(3) 79−36068
$\bar{K}N$, below 1 GeV/c, Y* states, SU(6)⊗O(3) quark model classification 80−27523
$\bar{K}N$ system, new reson. evidence in $SU(6)_W\times O(3)$ harmonic oscill. model 79−13178
$K^-p\to M^0+\Lambda(\Sigma^0)(\Sigma^0\text{-}1385)$, 4.2 GeV/c, quark model relations 78−82233
$\mu\to e\gamma$, and other rare decays, in SU_6 superunified gauge theory 78−21408
N(1420), $SU(6)_w$ fits in baryon photo- and electroproduction 77−46057
$NN\rho$ couplings, parity-violating, QCD and MIT bag model, $1/2^-$ resonance contribs., $SU(6)_w$ symmetry 80−57540
ν neutral current data, elastic and deep inelastic, gauge model constraints 79−40718
ν-induced multilepton events, weak interaction model 78−41533
νN single- and di-muon prod., colour excitation, weak interaction model anal. 78−45906
p decay lifetime in SU(5) grand unified theory 79−71749
$\bar{p}p$, three-body annihilations, rel. to quark rearrangement model 78−21444
$\pi\to e\nu\gamma$, SU(3)×SU(3) σ-model predictions, comparison with expt. 77−10243
π field, nonlinear chiral models, many dimensional solitons 78−4792
$\pi\pi$ phase shifts, nonlinear σ model Pade calcs. 78−8695
$\psi(\psi')\to$vector meson+pion+pion, disconnected quark diagram, decay widths 77−2824
$\psi'\to\eta\psi$, $\psi'\to\pi^0\psi$, forbidden decays anal. 78−66114

SU_n theory continued
$q\bar{q}$ non Abelian gluon interactions, long distance behaviour of chromostatic potential 79−17676
ρ chiral SU(3)×SU(3) representation, spontaneous symm. breaking, VDM, PCAC 77−57512
SU(8)×SL(3,R) colour quark model, vector states in e^+e^- annihilation at 3.9-4.5 GeV 77−41850
t-quark mass in SU(2)×U(1) 79−40710
θ vector particles, calibration interaction macroscopic confinement radius *(Russian)* 80−47257
Υ (9.5), implications of Υ for ν interactions in weak gauge theories 78−70271
W, mass in SU(5) grand unified theory 80−68411
$X^0(958) \rightarrow \eta\pi\pi$, ηX^0 mixing angle, broken SU(6)×O(3) quark model 79−17721
$\xi(2800)$ as a four-quark 0^+ scalar meson, SU(5) dynamical group anal. 79−67497
Z_0 mass in SU(5) grand unified theory 80−68411
^{209}Bi, P violating eN pot., determ. of effects by optical rotation meas. 79−26277
$^{12}C(\mu^-,\nu_\mu\gamma)^{12}B$, appl. of μ^- radiative capture to nucl. spin and isospin transitions 78−86511
SU_2 exact symmetry of Dirac eqn. 77−65077
SU_4 model, wave functions, and partial decay of J particle *(Chinese)* 77−65152

subboundary structure
austenite, hot-worked, subgrain struct., X-ray diffr. and electron microscope obs. *(Russian)* 79−15698
cell wall and lattice misorientation origin during deform. 80−71712
creep deformation model incorporating recovery and thermally activated glide 79−64534
deformed crystal, theory of X-ray scatt. *(Russian)* 80−70077
diamond, synthetic disorientation of crystallite subgrains *(German)* 77−68939
fatigue crack propagation, new measurement and observation techniques 80−45463
Invar N36 melt, cast metal struct. depend. on heat treatment, subgrain struct. *(Russian)* 80−40343
muscovite, natural cryst., submicroblock struct., electron microscopy 79−14816
olivine subgrain boundaries, origin in mantle peridotites 78−85544
polycrystals, X-ray substructure anal. *(German)* 77−68895
quartz, naturally deformed, dynamic recrystn. during creep, dislocation substruct., Mg alloy comparison 80−109142
quartz, theoret. predictions and microscopic obs. methods 80−84187
secondary boundary formation during crystn. *(Russian)* 77−59767
SEM channelling contrast technique for material deform. obs. 78−23917
SEM imaging, in bulk specimens to study localised plasticity 80−66609
stainless steel, 36NKhTYu, highly deformed, discontinuous γ'-phase precipitates cell boundaries, formation during ageing 79−87641
steel, cold-rolled, recovery of lattice defects in cementite 77−90370
steel, Cr-Ni-(Mo), austenitic, strengthening by modified ausforming 78−76665
steel, high C, high alloy, $M_{23}C_6$ type carbides, effect of alloying elements on defect struct. and hardness 80−16481
steel, low C, tempered, lath martensite, Ni (5 wt.%), microstruct./yield strength relationship 77−21234
steel, Ni-Ti-Al, 36NTYu, heavily deformed, subgrain struct. due to discontinuous precipitation of γ' phase *(Russian)* 79−52218
steel, stainless, 36NkhTYu, heavily deformed, subgrain struct. due to discontinuous precipitation of γ' phase *(Russian)* 79−52218
X-ray diffraction line broadening from small subgrains containing gradients of spacing 78−67612
X-ray diffractometrical sub-structure analysis *(German)* 77−68894
X-ray misorientation contrast, lineage subgrain boundary 77−27780
Ag halide crysts., dislocations, survey of post-war research 80−62449
Ag, tensile deformed, dynamic recrystn. *(German)* 80−84959
Al alloy, D16, extruded rod, substruct. anisotropy and decomp. at subboundaries *(Russian)* 77−25095
Al, cold rolling of 1100 plates, substruct. development 80−108476
Al, deformed, thermal recovery, microstruct. and stress-strain relations 80−16325
Al, fatigue crack initiation, pre-existing subgrain effect 80−97565
Al single crystal, polygonisation at high press. kinetic regularities, dislocation struct. at 140°C 79−66070
Al, stationary creep in HVEM, cell struct. evolution 80−104242
Al, superplastic deformation depend. on subgrain struct. electron microscope study *(Russian)* 79−83257
Al-Ag, nonhomogeneity of deform. 78−84888
Al-Li, cold worked neutron irrad. alloys, He bubble behaviour, microstruct. changes 77−54359
Al-Mg (2 wt.%) subgrain formation at low stresses 78−84928
Al-Ni (6 wt.%) alloy, misorientation between subgrains, second-phase particles role, STEM microdiffr. obs. 80−104415
Al-Zn, nonhomogeneity of deform. 78−84888
Al-Zn-Mg alloy, thermomechanically treated, precip. behaviour 78−84856
Al_2O_3, cryst. subgrain misorientations, X-ray diffr. microscopy technique 77−70272
Ar, solid, diffusion processes in plastic deform. *(Russian)* 80−92591
Au-Er, dil., cold-worked, EPR expts. 80−39864
CaF_2, hot forged, laser window material, fabrication, props. 77−46773
CaF_2, laser windows, intermediate temp. forging 77−46775
CoO, single crystal and polycryst., subgrain boundary form, and creep mechanism 77−39594
Cu crystals, two-phase, recrystn. retardation, particle size, spacing effects 80−89242
Cu, electrodeposited coating, annealing effect on struct. and microhardness *(Russian)* 78−76668
Cu-Ag, solid soln., nonhomogeneity of deform. 78−84889
Cu-Ni (10 at.%), creep, substruct. and internal stresses *(Russian)* 80−97527
α-Cu-Zn, whiskers, X-ray topography, substruct. 77−11831
$CuAl_2$, single cryst., embrittlement and subboundary hardening via interstitial segregation *(Russian)* 77−12679
α-Fe, cavity formation at grain boundary-subboundary interactions 77−86040
Fe-Mo(4.1 wt.%), steady state creep at high temps. 80−89316
Fe-Ni (31 wt.%) alloy, Bridgman grown, cellular to dendritic crystn. transition, morphology and microstruct. *(Russian)* 79−14709

subboundary structure continued
Fe-P (0.14 wt.%), cavity formation at grain boundary-subboundary interactions 77−86040
Fe-Si (3 wt.%), square etch pit characts., subgrain misorientation and mag. domain patterns 77−25199
$Ga_xIn_{1-x}P$, real struct. exam. by electron microscopy and channelling 78−2143
GaP polycrystals, cathodolum. in SEM 79−1440
KCl, Czochralski-grown, dislocation subboundary characts. 78−67718
Mg alloy, dil., dynamic recrystn. during creep, dislocation substruct., quartz comparison 80−109142
MgO, subgrain boundaries form. obs. by TEM, diffusion coeff. determ. 80−79817
MgO:Ni, heavily doped, defect characterisation, rel. to use as laser material 80−65000
Mo, creep deformed single crysts., subboundary struct. obs., dislocation sets 80−103348
Mo-Re alloy wire, high-strength, rel. to fracture mechanism *(Russian)* 77−25126
Na_xWO_3 bronzes ($0.4<x<1$), domain, surface and substrate structs. 80−34281
Ni, creep, substruct. and internal stresses *(Russian)* 80−97527
Ni electrodeposit on Cu, growth and microstruct. 77−11823
Ni, growth direction orientation effect on impurity distrib. 78−47261
Ni-Cr-Al-Ti alloy, KhN78TYu, heavily deformed, subgrain struct. due to discontinuous precipitation of γ' phase *(Russian)* 79−52218
Ni_3Sn_2, single cryst. embrittlement and subboundary hardening via interstitial segregation *(Russian)* 77−12679
Se film, amorphous, block formation during crystn., electron microscope obs. 79−11030
$SrTiO_3$, defects grown by Verneuil method 77−51390
Te, screw dislocation substruct. studied by torsion expt. 79−10859
Ti, single crysts., recrystallised, X-ray topography obs. 78−10054
Y_2O_3(:Nd) single crystal growth, floating zone method with Xe arc lamp imaging furnace 80−60777
Zn cryst. subgrain misorientations, X-ray diffr. microscopy technique 77−70272
ZnTe, elec., SEM and TEM studies of impurity segregation during long annealing 80−30001
Zr alloys, creep and growth, irradiation induced, microstruct. depend. 80−93602
α-Zr monocrystal perfection using Berg method and diffractometer with omega device *(French)* 80−2035
Zr, tensile deformation behaviour, neutron irrad. effects, dislocations, twinning inhibition 77−90393

subgrain structure *see subboundary structure*

sublimation
see also heat of sublimation
adamantane, deuterated single plastic cryst., growth by slow sublimation *(French)* 79−14905
alloy, two phase microstrct. revealed by selective sublimation 79−24698
α-amino acids, mass spectrometers study of evaporation 77−86402
camphene-coated surface, convective local mass-transfer coeffs., holographic interferometry method 78−75234
ceramic powders, equipment for sublimation drying, exam. 80−25733
cometary nucleus, effect on orbital evolution of Periodic Comet Encke 80−46483
contact heat transfer between heat-liberating element and surface of subliming solid cryoagent 78−81987
cryogens, porous solids, gradientless heat transfer, metallic thermal cond. theory 79−59902
desublimation of water vapour in vacuum, heat and mass transfer and duration 77−11687
dry ice sublimation, Taylor instability 78−90689
drying in UHF EM field 78−83936
drying intensification, thermolabile porous material in contact with sorbent, in vac. 77−89641
elements, work functions and sublimation entropies 79−56283
excess component concentration, appl. to conc. determ. in nonstoichiometric appls. 78−43131
^{18}F-5-fluorouracil, synthesis and purfication by fractional sublimation 80−17134
gas flow study, temperature gradient meter for 79−86539
graphitic carbons, particle emission rel. to morphological changes during sublimation 77−47566
high-temperature chemical processes, review, book contrib. 77−40545
ice, heat and mass transfer investigation, thermal shock method 77−50864
ice, surface process affected by supplied heat 77−46889
ice nucleation on AgI, exptl. verification of ice-forming activity theory 80−101406
ice particles in solar system, sublimation rate and lifetime 77−29721
ice sublimation from frozen salt solns. 77−84918
Jupiter, atmosphere, subliming boundary layer flow, simulation 78−65545
laminar vapour-air mixture flow, around circ. cyl. with vapour desublimation, numerical anal. *(Russian)* 79−60051
lunar regolith, elements volatilisation from solid particles 77−9680
lyophilisation, effect on free radical states of animal cells 77−25391
magnetic solids, surface rate processes and vapour press. 80−34182
metals, radiation induced vaporisation, press. behaviour 80−84288
naphthalene, external mode one-density states, low freq. Raman scatt. spectra *(French)* 80−76012
naphthalene, sublimation, mass transfer at vibr. spheres 80−57220
naphthalene sublimation, radial diffusion rate, mothball lifetime, for teaching 78−54124
naphthaline, sublimation rates in axisymmetric turbulent impinging jets 77−42887
particle-vapour subliming boundary-layer flow, local nonsimilar solns. 77−80206
poly(oxycarbonylimino-1,4-phenylene), apparent sublimation: thermal decomposition+condensation repolymerisation 78−3332
porous body, sublimation, heat, mass transfer from parallel capillaries 79−37395
pumping use in ISABELLE intersecting storage ring vacuum system for 1×10^{-11} Torr operation 79−81105
rarefied gas flow in narrow slit channel with sublimation from one wall and heat inflow from other 77−15064
SEM cold stage microscopy, thin frozen hydrated specimens, temp. rise and sublimation of water 78−24198

sublimation continued
snow, rel. to grain growth 80−26553
solid solutions, freeze drying in semiconducting powder prep., solvent choice 80−11583
steam condensation heat transfer on below-freezing pt. surface 78−75042
sublimation-condensation in annular gap, heat and mass transfer 77−35141
supersonic flow over rough subliming surface, laminar boundary layer, anal. 78−51148
ternary gas mixture, natural convection, naphthalene sublimation appl. 80−6511
thermostatic control, rot. conical (spherical) jacket radiatively heated from side 77−42710
Tokamak fusion test reactor, thermal response of first wall limiters 80−79585
$Al_{10}N_8O_3$, sublimation growth, cryst. struct. determ. 80−19751
$Al_9N_7O_3$, sublimation growth, cryst. struct. determ. 80−19751
Ar, porous solid, contact heat transfer of sublimation 77−31767
Ar, sublimation temp. determination at very low pressures *(Croatian)* 79−28094
As_2S_3, thermodynamic of evaporation 77−47568
β-B, rhombohedral, sublimation, 1823 to 2253K, torsion-effusion and mass spectroscopic meas. 77−39673
Ba, adsorbed on Ir (111), thermionic emission obs. 77−85881
BiSeI, sublimation, vapour pressure 77−11686
C, low current for props. of graphite near sublimation temp. 79−50901
C particles in flame, laser heating and sublimation 78−61012
C_2 vapour, Swan bands, oscillator strength 80−63712
Cd, influence of source material and shape on sublimation props. 78−80474
CdS, anomalous behaviour of transient Langmuir dissociation 79−28092
CdS, CdSe, growth rate, sublimation rate and etching behaviour along polar axis 80−24387
CdS, surface charge and ledge dynamics, point defect annihilation during sublimation 79−90642
CdS, thermal decomp. kinetics, in vacuo, free electron density depend. 77−59111
CdS, transient phenomena in sublimation 78−30747
CdSe, influence of source material and shape on sublimation props. 78−80474
Co, sublimation rate near Curie temp. 80−49351
$CoCl_2$, vapour pressure meas. 77−89534
$CsAlSiO_4$, and $CsAlSi_5O_{12}$, cryst. evap., mass spectral investig. 80−49353
Cu-Ni (50 wt.%) alloys, estimation of sublimation energy of Cu atoms, evaporation rate and surface composition, AES meas. *(Japanese)* 80−49352
EuS, vaporisation thermodynamics, Knudsen cell mass spectra 77−47569
Ga, gaseous reduction and extraction from mica 78−92216
Ga_2Se_3, sublimation growth, closed tube, mass flow and press. meas. 77−63550
GeO formation from Ge-GeO_2 mixtures, gasification kinetics *(Russian)* 80−21273
GeP, dissociation kinetics rel. to volatile component sublattice 77−84917
GeS film, deposited on Ge (110) surface, sublimation, LEED meas., structural transitions 77−59195
GeS, growth parameter meas. during cryst. growth from vapour in closed ampules 79−19168
H_2, solid, equation of state, intramol. zero pt. energy contrib., total sublimation energy 78−71829
Hg, deposition, on W, two-dimensional condensation 80−107666
HgI_2, single crystal growth in small opened ampoules using dynamic sublimation technique 79−4904
HgS, melting point and vapour pressure 77−15549
KCl, back force effect, surface struct. 77−15571
KCl, sublimation on (100) surfaces in elec. field 79−77739
KCl surface, sublimation kinetics, elec. field influence, terrace-ledge-kink model 80−84287
K_2O, under vacuum, exam. of thermal behaviour *(French)* 79−19365
K_2SO_4, effusion studies of vaporisation/decomposition 79−95153
$LiCrO_2$, evaporation, as a corrosion product in compatability experiment of Li_2O pellets with Fe-Ni-Cr alloys, mass spectrometric study 79−73301
Li_3N, vaporisation, studied by Knudsen effusion method 80−92662
MgO-ZrO_2 ceramic sublimation at optical furnace focal spot *(Russian)* 79−95983
^{99}Mo separation from neutron irrad. UO_2 by vacuum sublimation 77−90893
^{99}Mo, sublimation separation from neutron irrad. UO_2 77−9257
N_2, porous solid, contact heat transfer in sublimation 77−31767
NaCl, back force effect, surface struct. 77−15571
NaCl:Ca, single cryst., vaporisation kinetics meas. 78−18763
Ni-Cr alloys, added metals effect on sublimation behaviour in vac. *(German)* 79−90775
Ni-Cr-Al, shape of γ′-precipitates on surface after sublimation *(German)* 77−81266
Ni-S incongruently subliming system, SEM and TEM obs. of high temp. transitions, temp.-comp. diagrams 80−104136
Ni-S system, Knudsen effusion and thermodynamics 78−79759
Ni_3Al, refractory transition metal alloying effects 78−26691
NiF_2 film preparation and characterisation 80−59815
$O_2^+AsF_6^-$, thermal decomposition, Raman spectra study, free radical mechanism 80−55652
PCl_5, sublimed phase studied by ^{31}P NMR, Raman spectra and X-ray diffr. 80−100209
$Pb_{0.93}Sn_{0.07}Se$ crysts., sublimation growth, controlled carrier concs. for IR lasers and detectors 77−52237
$Pb(Zr,Ti)O_3$, synthesis from cryochem. mixtures, chem. reacts. in sublimation drying 79−11538
PrP-I, heterogeneous equilib. 77−36777
^{103}Ru, in sublimation separation of ^{99}Mo from neutron irrad. UO_2 77−9257
SbI_3, vapour pressure 79−60496
SbSeI, sublimation, vapour pressure 77−11686
ScI_3, vaporisation thermodynamics, sublimation and formation 80−54366
$Se_{5,6}$, influence of source material and shape on sublimation props. 78−80474
Si epitaxial layers, grown by sublimation in vacuum, TEM study of surface 79−46982
SiC, cryst. growth on oriented seeds by sublimation 78−35279
sublimation continued
SiC, epitaxial growth by sublimation sandwich method, effect of impurities 80−25568
SiC epitaxial layer growth from sublimation in vac., kinetics 80−20791
Sm, vacuum sublimation method of prod. *(Russian)* 79−70012
SmF, vaporisation, Knudsen effusion method 80−6508
$SnSe_2$, temp. depend. of equilib. constants 80−88312
SrF_2, vaporisation and sublimation thermodynamics *(German)* 80−81355
SrO, heated on W, vaporisation behaviour, mass spectrometric thermal anal. 77−56277
^{132}Te, in sublimation separation of ^{99}Mo from neutron irrad. UO_2 77−9257
URu_3, sublimation thermodynamics 80−97722
WO_3 amoprhous film, sublimed under different conditions, elec. transport props. 80−7015
WSe_2, single cryst. growth by sublimation method 78−11091
$Zn_xCd_{1-x}S$, film, single-thermal-source form. 80−2492
ZnO (10$\bar{1}$0) prismatic surfaces, nonstationary sublimation *(German)* 78−60035
ZnO, ZnS, growth rate, sublimation rate and etching behaviour along polar axis 80−24387
ZnP_2, sublimation 80−34181
ZnS-Mn sublimated phosphor films, annealing effects *(Russian)* 78−43949
ZnTe growth from vapour, growth interruption 80−97416
ZrI_4, thermodynamics of vaporisation and high temp. enthalpy 78−91432
ZrO_2-HfO_2(Y_2O_3) solid soln. complex refractories *(Russian)* 78−47513

submarine cables
see also cable laying
communication lightguide cable design and manufacture 79−37027
EM field rel. to geophysical prospecting at sea *(Russian)* 78−20557
fibre optic, small, recent experiences 80−14488
glass fibre, expt. cable *(German)* 80−58711
laying using ship hull-mounted sub-bottom profiling 78−5620
low dielectric loss meas. apparatus for 0.1 to 200 MHz 80−15958
monomode optical fibre design and fabrication for submerged cable applications 80−91932
ocean thermal energy conversion, OTEC system development, Conf. Houston, TX, USA (Nov. 1978) 79−83611
Oceans 1976 conference, Washington (Sept 1976) 77−5241
offshore seismic exploration streamer cable connector design and programming 77−25803
optical fibre, jacketed, hydraulic pressure depend. of losses 78−63175
optical fibre cable unit design and test results 78−46799
PFM fibre-optic video transmission to and from undersea vehicles 80−46310
repeater housing, corrosion protection, of Be-Cu alloy 78−15583
St. Margarets Bay−La Paune, seabed measurements, sand ridges 78−15992
telecommunication, dielec. loss measurements of polyethylene at high pressure and freq. 80−27316
terminations, for sonar systems 78−45041
voltage daily variations at tidal freqs., due to induced oceanic elec. fields 77−86753
wire fracture modes and mech. props. correl. with fatigue life, large diameter cable 78−35520

submillimetre waves *see microwaves*

suboptimal control *see optimal control*

subroutines
autocorrelation coeffs. from irregularly spaced areal data, in FORTRAN 77−33191
binary mixture, internal consistency of activity coefficients program in BASIC 80−54364
biomedical surface mapping, interpolation methods, in FORTRAN 80−81750
boundary integral equation method, in FORTRAN 79−35560
combinatorial algorithm for generating positive roots of simple Lie algebras 77−2530
computer modelling of matter, conf., Anaheim, USA (March 1978) 80−51954
critical point scaling and extended scaling eqns. of state implementation, program in FORTRAN 79−46780
crystallisation in layered intrusions formation simulation, in FORTRAN 77−33069
crystallographic data Cartesian translation, in FORTRAN 77−37196
diffraction data unique reflection sets generation, in FORTRAN IV 78−18501
diversity indices computation from information theory, in FORTRAN 77−33076
eigenproblem partial soln. symmetric, truncated Lanczos method, in FORTRAN 77−5649
equations of state, search procedure, based on step-wise least-squares technique 80−19900
flow, bed topography and grain size in open-channel bends calc., in FORTRAN 77−37245
geological compositional data Q-mode factor analysis, extended CABFAC and QMODEL programs 77−9504
geological orientation data fitting to von Mises distribution, in FORTRAN 77−5201
gravity effects computation, of two-dimensional and three-dimensional bodies 78−3961
gridding of geophysical data, in FORTRAN 79−62596
IMPACT, FORTRAN program for electron-atom collision theory, soln. of coupled integro-differential eqns. 78−86948
implanted ions, energy deposition profiles from range data, in FORTRAN 77−39619
IR spectrometry, computer program LISE (Literature Search and Edit) 78−85223
light scattering, in macromolecular solutions in FORTRAN *(Rumanian)* 79−82990
linear equation solution, out-of-core assembly in FORTRAN IV subroutines 79−30213
linear prediction in least-squares scheme for max. entropy spectra, Fortran subroutines 80−98465
lithostratigraphy, parametric interpolation of digitized log segments, program in FORTRAN IV 79−62507
matrix Pade approximants, Fortran IV calc. subroutine 77−9877
molecular fluid, computer simulation of liquid-vapour surface 80−54478

subroutines continued
molecular graphs, search for self-avoiding paths, FORTRAN IV ALL-PATHS program 79−59336
molecular structures, topological code, modified Morgan algorithm 80−58122
molecular topological symmetry 79−41251
MORPHOQUANT automatic microscope image analyser, universal program system 80−56160
neutron spectra determination program, computer ES 1030, algorithm SAND-II *(Russian)* 78−48723
partial differential eqns. reduction by Galerkin, collocation, and method of lines 78−77693
petrologic modelling with extended Q-mode factor analysis, in FORTRAN 77−33070
point-density measurements using WANG 2200C minicomputer with digitiser, in BASIC 77−33072
quantum liquids and crystals, computer modelling 80−54472
radiographs processing, computer appl. 80−3259
ray-tracing for physiological optics, in FORTRAN 77−25420
rectangular and triangular diagram printer-plotting FORTRAN routines 77−5325
replicated diversity indices computation for random samples of specified size, in FORTRAN 77−37197
SNIFF self-adaptive algorithm for numerical integration 77−67261
structural stiffness matrix eqn., algorithms for direct access Gaussian soln. 78−57766
SYMAP, spatial derivatives mapping, in FORTRAN 77−40965
ternary phase diagrams, interactive computer program 80−71629
Voigt profile, fast routine in FORTRAN IV 78−7767
X-ray powder diffractometer, APD3600, file searching techniques 80−24319

subsets (mathematics) *see set theory*

substrates
see also semiconductor device manufacture
adsorbed layers, commensurate-incommensurate transitions, substrate defects effect 80−75437
adsorbed layers, two dimensional incommensurate crystal theory, thermodynamics *(Russian)* 80−49524
adsorbed monolayer, substrate-induced strain and orientational ordering 79−82460
alkali halide substrates, growth of epitaxial Au, Al, Fe 79−46979
alkali halides, gas adsorption, stress depend. of chem. pot. 78−91541
alkali halides, substrates for condensation of Au, film struct., stability and growth *(French)* 78−38989
alkali halides, surface step struct. 77−31853
alkali metal, calc. binding of deposited Au atoms 79−33208
anisotropic, SAW transverse amplitude dependence 79−7242
anthracene, for epitaxial crystn. of polyesters 79−61521
anthracene surface UV light irrad. effect on organic layer nucleation during crystallisation 80−75478
axially symmetrical, constant thickness film form. 79−27453
bending during thin film evaporation due to temp. difference between substrate faces 80−54571
biphenyl, for epitaxial crystn. of polyesters 79−61521
calibration substrate for Abeles equipment, refr. index meas. 78−77965
cemented carbide, effect on CVD of TiC 79−74096
chemostress coefficient, adatom-solid substrate interaction 78−91540
cold substrate, effect on initial resist. of In_2O_3-SnO_2 film 79−23867
conducting nonphotosensitive substrate for thin layer photoemitters 77−40325
confining substrate for micron thick liquid films, semicond. films 80−96722
crystal with island film, dislocations and stresses 79−87015
crystalline-amorphous film system, relaxation process dislocation misfit theory *(Russian)* 80−39461
cylindrical magnetron sputtering sources, substrate heating 79−24435
deformation, deposits spontaneous mactrostress calc. 80−15412
deposit-substrate systems, adhesion testing 80−50814
deposited thin film-resonating quartz crystal substrate interaction, energy transfer model 79−88914
dielectric constants, standard specimens 80−13038
dielectric crystal, dislocation detection by divergent polychromatic beam method 77−35568
dielectric multilayers, optical and geometrical thickness monitoring using monochromatic maximeter, substrate effects *(French)* 80−38140
direct ripening of crystallites on substrates 79−42417
electrochemical overgrowths, role of substrate dislocations and grain boundaries in nucleation and growth 79−51454
electrodeposit, on metallic substrate, peel test for determ. adhesion 80−50815
electron-probe microanalysis of thin coatings, charact. fluoresc. correction 80−7881
epitaxial layers, on monocryst. supports, degree of disorientation, determ. by interferometry *(Russian)* 80−24748
ferromagnetic substrates, propag. of surface magnetoelastic waves 77−55698
film edge induced stress in substrates 79−94492
film-substrate bond strength, meas. by laser spallation 80−50821
film-substrate layered systems, charcts. of phase-velocity dispersion and struct. of surface waves 80−59775
fluophlogopite, substrate for metal film epitaxial growth, orientation rels. *(Russian)* 77−31910
foreign object motion in ice, liq.-like layer model, appls. 79−46893
fused silicon, directional reactive ion etching at oblique angles 80−66428
GaAs wafer, dissolution kinetics in undersaturated isothermal solns. in Ga-Al-As systems 80−80106
gaseous impurities, distrib. in films and substrates, over broad energy ranges of implanted ions 79−69146
glass, Cr(Ti) films electron-beam deposition techniques improvement 80−7496
glass, Cr film on with ZnS or MgF_2 underlayer, thermal strength, recrystn. influence 79−87748
glass, for CC Fe_2O_3 sputtered films, optical transmission and reflection spectra depend. on substrate temp. 79−91517
glass, for Mn_3O_4 film form. from Mn^{2+} ions in water *(Japanese)* 80−45411
glass, subbing for AgBr layers, effect on photographic charcts. *(Bulgarian)* 78−78016
glass, surface temperature measurement, heated through Ga 79−97390
substrates continued
glass, thermal expansion, rel. to thermal cycling stability of Pb film tunnel junction 79−87200
glass substrate, glow discharge effect on surface props. and struct. 78−85201
glass substrate, SnO_2:Sb film, elec. props. 80−88652
graphite, growth of ^4He films, vap. press. meas. 80−70499
graphite, Si dip-coated, photovoltaic effects 80−29442
graphite for adsorbed methane submonolayer, structural transitions between epitaxially ordered phases 80−96740
heating effects during sputtering by high rate coaxial cylindrical magnetron 78−56579
heating in vacuum, heating method rel. to spectral charcts. 77−7223
holder for LPE 78−92207
holographic image and plate substrate quality relationship 80−48193
IC with Si substrate, new microanalytical method *(French)* 78−35760
III-V semiconductors for Al_2O_3 films, ion beam etching defect detection 80−89155
impurity concentration in MOS tetrodes, analytical model *(Spanish)* 79−99624
incommensurate epitaxies at finite temps., substrate pot. effect 80−88451
instantaneous bending during thin film deposition, intrinsic stresses, cantilevered plate method anal. 80−54570
insulating, thin film growth of AlSb, by metal organics CVD 80−60786
leucosapphire, crystal growth by Kyropoulous method, temp. effect on structural and optical quality 80−20784
leucosapphire, separation of Cu coating during annealing *(Russian)* 77−7997
lightweight solar array flexible substrates with anticharging layers 79−96456
low temperature, vac. deposition of thin films, cryostat *(Japanese)* 78−27403
LPE growth method to reduce thermal degradation of substrates, appl. to LED fabrication 80−104061
magnetron sputtering target/substrate configuration 78−39687
metal substrate effect on thermal positive ion emission from thick layers of KF 78−19627
metal substrates for solar selective surfaces, graphite coating props. 78−74952
metal surface, approached by substrate, surface amplitude patterns 80−75620
metal surface, electron state of atoms in ordered and amorphous adsorbed films *(Russian)* 79−51425
metal wettability, using macroscopic theory of mol. forces *(Russian)* 77−66073
metallic, enhanced vacuum deposition by pretreatment with plasmatron discharge 78−76604
metallic, temp. meas. during evap. 77−69997
metallic substrate pretreatment with plasmatron 78−11434
metals for polystyrene films, electrode effect on carrier injection, TSC, I-V charcts. 80−34463
mica, defects effect on epitaxial film struct. 78−26794
mica, surface impurity levels by static SIMS, cleaning treatment effects 77−59190
mica substrate of Au film, surface defects on heterogeneous nucleation and growth 78−47684
mica substrates, growth of Bi and Sb films, initial stages of growth and orienation, TEM study 79−28237
microwave IC substrate permittivity meas. in cylindrical cavity 78−77942
misorientation for GaAs:Si LPE layers, surface morphology, initial supercooling effects 80−34329
mullite porcelain, CVD growth of TiC whiskers, catalytic effects of various metals and refractory oxides 79−33211
muscovite, substrate for metal film epitaxial growth, orientation rels. *(Russian)* 77−31910
Mylar, growth of ^4He films, vap. press. meas. 80−70499
nanostructure fabrication, materials and techniques, substrate prep. 79−75657
naphthalene, for epitaxial crystn. of polyesters 79−61521
noble metal contact, substrate material diffusion and corrosion film formation, model 80−2312
non-metallic, temp. and pressure sensitive, micro-contacting problems with metallic layers *(German)* 80−55624
optical properties of film-substrate systems, reflectance-aided null ellipsometry 80−101827
orientation effect on amorphous Si regrowth by laser pulses 80−84409
phonon emission by metal heater film into insulating substrate, spectral distrib., model treatment 79−14896
piezoelectric film, third-order piezoelec. and dielec. consts. meas. using surface acoustic waves *(Japanese)* 80−55042
PIXE, low energy mass absorpt. coeff., meas. technique 78−7309
plasma polymerisation, mech., effect of substrate and substrate topography 78−88633
polar materials, appl. to SAW and other devices 80−66114
polyethersulphone, ion plated Cu films on, structural and resistivity study 79−42411
polyethylene, effect of glow discharge on nucleation charcts. of Au 79−77963
polyethylene terephthalate, thickness determ. of Al coating using photometry 80−62626
polyethylene/metal substrate, adhesion, role of surface topography 80−35500
polymer, amorphous Se vac. deposited, with dynamic coating device 80−100792
polymeric systems, supported on inert substrates, dynamic thermomech. study 80−55623
Pyrex, AES of Ni films, purity 77−8755
Pyrex glass, for Si evaporated semicryst. layer growth 79−82482
quartz, Cr(Ti) films, electron-beam deposition techniques improvement 80−7496
quartz, CVD of Si, using CO_2 laser for substrate heating 78−39698
quartz, fused, anthracene ultrathin film deposition 80−59812
quartz, fused, for ZnS, Na_3AlF_6 films, H_2O absorpt., IR anal. 80−75446
quasimonolithic and hybrid integrated optical circuits on Si substrates 80−64218
quench-condensed films, superconducting transition temp., elastic stress and strain effects 80−70883
recoil implantation profile for thick film 79−1454

substrates continued
refractory films, stability, high temp. and electron irrad. effects 77−39747
refractory oxides, for heteroepitaxy of Si *(French)* 77−44181
rocksalt, cleaving device for clean surface prep. 77−13738
rocksalt substrates, epitaxial growth of CuI reactively sputtered films 79−4918
rotating spherical substrate on planar wave holder, uniformity of film thickness 79−65351
rotating substrate heating by special lamp 78−59164
rough boundary substrate-thin film system, ellipsometric obs. using equiv. film theory 80−2310
rough quartz, Al thin films evaporated on rough quartz substrates surface irregularities, light scattering measurements *(Polish)* 80−88450
ruby, synthetic, CC Nb_3Pb superconducting film, prep., vac. deposition 80−89149
sapphire, Czochralski grown, etch pits and dislocations 79−37708
sapphire, polishing with colloidal SiO_2 78−39925
sapphire, solid phase Si regrowth in Si-Al-Al_2O_3 system, Hall effect 80−100413
sapphire, substrate for V, Ta, Mo, W, Nb epitaxial films, growth texture, nucleation texture *(Russian)* 80−75454
sapphire, surface quality determ. by optical reflectance method 78−43862
sapphire ($\bar{1}012$) substrate for Si epitaxial thin film growth by MBE 80−76186
sapphire film, substrate for Si, laser annealing non-thermal theory expt. test 80−89273
sapphire for $K_3Li_2Nb_5O_{15}$ film for optical waveguide, cryst. struct., dielectric props. 80−79016
sapphire ribbon crystals, EFG growth and charact., voids, grain boundaries and dislocations 80−103283
sapphire ribbon EFG prod., substrate for heteroepitaxial Si 80−108342
sapphire ribbon microvoid distribution control in edge-defined film-fed SOS growth 77−77370
sapphire substrate surface evaluation for SOS 77−76653
sapphire substrates, prep. for GaN epitaxy 78−39929
sapphire-Al interface barrier, transport and trapping obs. 77−76921
SAW device fabrication techniques, book contrib. 79−50523
SAW device substrate materials and their influence on performance, book contrib. 79−50522
selection and preparation, for heteroepitaxial Si, book contrib. 79−83128
semiconductor substrate, measurement of contact angle between water droplets and surface *(German)* 80−34276
semiconductor substrate, work function rel. to AES *(French)* 80−50479
semiconductor substrate surface, low loss electron and Auger images correl. 78−22944
solar cells, RAD process, substrate related problems 80−89635
SOS substrate quality evaluation by X-ray rocking curve technique 77−76262
spinel (100) substrate for Si epitaxial thin film growth by MBE 80−76186
sputter cleaning, substrate surface contamination from dark-space shielding 77−8968
sputtered particles-substrate, temp. overaging *(Russian)* 80−40385
sputtering, insulator film contouring over substrate topography 77−8752
stainless steel, HfN activated reactive evaporated coatings, high rate deposition, microhardness 80−25580
stearic acid, effect of glow discharge on nucleation characts. of Au 79−77963
steel, electrospark alloying to Ag, residual stresses obs. *(Russian)* 77−56145
steel, stainless, for Si evaporated semicrystalline layer growth 79−82482
steel backing plate, hot pressing with powder layer, joint form. kinetics 80−100961
steel for Cu vacuum coatings, influence of precipitation conditions on porosity *(Russian)* 80−54578
steel shot substrate, gel permeation chromatography study of degradation of polymer thin coatings 79−79134
steel substrate limiting temp. during vaporisation and condensation coating in vacuum *(Russian)* 80−100787
stepped substrate-adsorbed layer interaction, selective effect on epitaxy 78−14616
steps, fast etching phenomenon of plasma deposited Si_3N_4 films 79−34168
surface damage induced by RF-diode sputtering 77−90274
surface heterogeneity, effect on isotropic-nematic transition *(German)* 77−31759
surface relief gratings, 3200 Å period fabrication, effect on film growth 78−84089
surface temperature measurement during film deposition using thin film thermocouple 80−62668
p-terphenyl, for epitaxial crystn. of polyesters 79−61521
tetramethyltetraphenyltrisiloxane-treated substrate, effect on metal film deposition props. 79−90917
TGS substrate, ferroelec. field effect in Te films 79−42675
trace contaminants microanalysis, laser-probe pyrolysis technique 78−92553
uniformity, Kr vapour press. isotherms at 77K as standardized meas. 80−107657
uniformly thick film sputtering optimisation 79−27451
vacuum coating, surface temp. meas. 80−57297
water supercooled droplets, on ice substrate after low speed collision, freezing behaviour, cryst. struct. 80−29152
X-ray double-crystal method using nonparallel setting for lattice mismatch meas. between epitaxial layers and substrates 79−28235
Ag, electrodeposition of Au film, substrate effects on film props. 80−81329
Ag film, 1/f noise, role of substrate 79−28388
Ag, oriented crystallisation on active amorphous C centres, effect of substrate temp. on crystallisation 79−7762
Ag vacuum condensates, on Cu substrate, struct. and substruct *(Russian)* 79−73412
AgI substrates, growth of epitaxial cryst. growth, influence of saturation and elec. field 79−42408
Al (111) surface, Pb, Sn monolayer, double layer growth, struct. 80−70567
Al, adhesion of Ag films deposited from hot hollow-cathode source 77−8754
Al, for Zn film deposition, TEM and electron diffr. obs. 80−75460

substrates continued
Al sputtered coating development, porosity, durability temp. depend., electric arc metallisation regime *(Russian)* 80−39402
Al, substrate, porous anodic film form. in H_3PO_4 79−70229
Al-Zn-Mg plasma sputtered, mech. props. rel. to heat treatment *(Russian)* 80−40387
$Al_xGa_{1-x}As$, epitaxial growth, orienting substrates effects 77−43444
Al_2O_3 circuit substrate, TiO_2 dope PbO-ZnO-B_2O_3 glass corrosion protection 79−29236
Al_2O_3, Cr (Ti) films electron-beam deposition techniques improvement 80−7496
Al_2O_3 for Ni-Cr/Au films interdiffusion processes and oxidation phenomena 80−59735
Al_2O_3 for W-Al_2O_3 composite films, oxide evaporation deposited, struct., props. 80−25581
Al_2O_3, influence on adherence fracture energy of glass bonded Pt-Au thick film conductor 77−56075
Al_2O_3, laser drilling and cutting, anal. of results using computer model 79−70180
Al_2O_3, requirements and structural etching for GaN VPE *(Polish)* 77−43440
Al_2O_3 rich substrate, surface smoothness and metallization props. *(German)* 78−19906
Al_2O_3 substrates, grain growth during sintering 80−40302
Al_2O_3 substrates, tape-casted, fracture strength analysis 80−60948
Au (111), interaction layer at interface with vacuum deposited Fe film 79−99433
Au coated Si for amorphous Si, whisker growth characts. by SiH_4 thermal decomposition 80−34342
Au films on Si substrate, solid-solid reactions 78−95369
Au for evaporated Be thick films, secondary electron emission 80−104022
Au, substrate for VPE Pt, crit. thickness of pseudomorphic film growth, substrate size depend. *(Russian)* 80−29286
Au, with Ag monolayer, adsorbed pyridine giant Raman effect 80−63637
BN thick film, crystn. and semicrystn. CVD on C steel substrate 79−87586
$BaSO_4$, $SrSO_4$ surface crystn. 80−34332
Be, adhesion of Ag films deposited from hot hollow-cathode source 77−8754
Be lightweight optical substrate fabrication 79−23107
Bi, epitaxial growth of Sb 78−95246
$Bi_{12}GeO_{20}$, for interdigital transducer *(Czech)* 80−19201
C, amorphous, cluster migration in early stages of Au film growth 79−77964
CaF_2 chip, discrimination of twin orientation in Au island epitaxial films on (111) surface 79−46983
CaF_2, for Au film, interphase coincidence boundaries 79−1560
$Ca_3Ga_2Ge_3O_{12}$, substrate, electron examination of microstruct. and microsegregation 78−67919
Caf_2, Au film oriented crystn., formation of coincidence orientations on interphase boundary 79−90922
CdS, polycrystn. layers on CdS substrate, electron microscope study of surface struct. 78−22940
CdS substrates, lattice mismatch with ternary chalcopyrite films 79−87012
CdTe substrate, growth of $Hg_{1-x}Cd_xTe$ epitaxial layers 79−1829
Cr, refr. index depend. of Yb_2O_3 thin film on thickness 80−108290
Cr substrate for CdSe, thin film transistor, cryst. struct., substrate defect effects 80−70563
Cr_2O_3 substrate for CdS photoresistors, effect of heat treatment of spectral distrib. of photosensitivity 78−80017
Cu, electrodeposit on (111) Cu substrate in presence of halo-compd. of acetic acid 80−15413
Cu, electrodeposition of Au film, substrate effects on film props. 80−81329
Cu, electrospark alloying to Ag, residual stresses obs. *(Russian)* 77−56145
Cu, epitaxial electrocrystallisation, substrate imperfections effect 78−18921
Cu film, 1/f noise, role of substrate 79−28388
Cu plated substrates for Antares CO_2 laser mirrors 80−14349
Cu substrate, ion induced intermixing of Au or Ag surface film 80−15420
Cu substrate for SiO_2 film, surface EM wave absorpt. optical consts. *(Russian)* 80−108216
Cu, surface topography influence on growth struct. of sputtered Cr 80−20058
Cu-benzotriazole (benzimidazole) thin films, ellipsometric study 80−35114
CuS, covellite substrates, growth of epitaxial cryst. growth, influence of saturation and elec. field 79−42408
GaAS, semiinsulating, heat treatment effects 78−6382
GaAs, anodisation in HF O_2 plasma, oxide film form. mechanism and kinetics *(Japanese)* 80−93667
GaAs, effect on lattice consts. of MBE-grown $In_{1-x}Ga_xAs$ and $GaSb_{1-y}As_y$ 79−77942
GaAs, epitaxial growth of single crystal layers of $Cd_{1-x}Zn_xS$, close-spaced geometry 78−92198
GaAs film solar cell fabrication, substrate requirements 78−11125
GaAs, for homoepitaxy, vicinal surfaces characterisation 77−20207
GaAs, for sputtered GaSb film, growth, Hall effect, impurity levels 80−20334
n-GaAs, heat treated, origin of 1.41 eV emission band, photolum. expt. 78−72579
GaAs, O implanted, LPE growth of GaAs film 78−2592
GaAs, optical meas. of semicond. temps. *(French)* 79−35743
GaAs, out-diffusion of Cr 80−10708
GaAs, selective in situ vapour etching and growth 80−2958
GaAs, semi-insulating, thermal conversion, Hall effect and luminesc. meas. 78−6405
GaAs, semi-insulating substrate, characterisation and modification 77−81215
GaAs semi-insulating substrates, monolithic integration of optical and electronic devices, review 80−58543
GaAs semi-insulating substrates CC GaAs-$Al_xGa_{1-x}As$ transverse junction lasers with low threshold current by MBE 80−58588
GaAs semi-insulating substrates, GaAs/GaAlAs crowding effect lasers using whispering gallery mode 80−58589
GaAs, semi-insulating substrates, whispering gallery lasers 80−69405

substrates continued
GaAs, semiinsulating, epitaxy of GaAs, elec. props. rel. to growth conditions, processing 77−15977
GaAs substrate, Al MBE growth 80−24757
GaAs substrate, plasma polymerised polysiloxane film growth, dry etching process 80−25575
GaAs substrate, ZnSe film on, transition layer form. kinetics 79−87007
GaAs, substrate for epitaxial growth, backscatt. anal. of surface prep. and anodic oxidation 77−25175
GaAs substrate for p-Ge film, cond., Hall effect and transverse magnetoresist., anisotropy 79−51697
n-GaAs substrates, ion implanted, compensation 78−75680
GaAs temp. influence on Hall mobilities of GaAs and GaAs:Cr epitaxial layers 80−20335
GaAs:Cr, n-GaAs interface, elec. props. 78−6438
n-GaAs:Cr, semi-insulating, contact effects, trapping levels 78−10465
GaAs:Cr, semi-insulating, characterisation by photoelectronic data 78−68051
GaAs:Cr, site symmetry of Cr ions, ground-state splitting, ballistic phonon expts. 78−95273
n-GaAs:Zn substrate, ion implantation as predeposition process 79−19268
GaAs/SiON substrate/film system, interface formation during CVD, modelling 80−24764
GaAs-insulator film interface, evidence for growth-induced damage from photolum. expts. 78−75953
$GaAs_{2-x-z}Sb_xP_z$, LPE growth, continuous comp. grading, use as secondary substrate 77−31913
GaP, dislocation loops, effect on GaP epitaxial layer perfection 78−30843
GaP, transient-mode LPE of $Al_{1-x}Ga_xAs$ 78−72746
GaSb, LPE growth of lattice-matched AlGaAsSb 80−60794
GaSb, vapour-phase growth of epitaxial $Ga_{1-x}In_xSb$ using open-tube flow system 79−33943
GdGa garnet, Czochralski grown, substrate material dislocation propagation 78−59771
GdGa garnet single cryst. substrate surface quality *(Russian)* 77−44371
$Gd_3Ga_5O_{12}$, garnet substrate, surface polishing, damage, abrasion, brittle fracture model *(German)* 77−73357
$Gd_3Ga_5O_{12}$, garnet substrate surfaces, working damage, electron microscope investig. 77−77605
$Gd_3Ga_5O_{12}$, substrate, electron examination of microstruct. and microsegregation 78−67919
$Gd_3Ga_5O_{12}$ substrates, LPE of $Y_3Fe_5O_{12}$, substrate orientation effect 80−66438
$Gd_3Ga_5O_{12}$, orientation effect on max. vel. of domain boundaries in $(YGdYbBi)_3(FeAl)_5O_{12}$ film 79−15330
Ge (111), CdS epitaxial layers 78−18920
Ge (111)-amorphous SiO_2 or Si_3N_4 film, dislocation interactions, substrate bending and edge effects 80−39472
Ge, epitaxial growth of ZnSe 80−75469
Ge, evaporated film, lattice parameters and phase transition temp., surface influence of glass substrates 78−94996
Ge optical windows, contaminated by NH_3, CO_2, CO, HCl, methane, cryocooled, IR transmission 79−32007
Ge substrate for GaAs solar cells, thin film shallow homojunction struct., quantum efficiencies 80−35677
Ge surface, wetting by Sn, Pb rel. to cryst. orientation 78−43211
Ge/Mo substrates, device quality epitaxial growth of polycrystalline GaAs 79−69988
H, solid for liquid ^{4}He film, film transfer velocity, Van der Waals interaction *(Russian)* 80−54465
InAs, heteroepitaxial layers, $AsCl_3$ mole, fraction and substrate orientation effects on elec. parameters 80−39690
InAs, possibility of local epitaxy in depressions on unmasked substrates 79−42415
InP, (100) and {111} orientation, liquid-phase epitaxial InP film preparation *(Slovak)* 79−15037
InP (111), (110) and (001) substrates, Cd(S, Se) film growth, mismatch dislocations and lattice distortion 80−84406
InP, CC $In_{0.53}Ga_{0.47}As$, incorporation of Ga during LPE growth on (111)B and (100)InP substrates 78−91557
InP, etching and polishing in Br-methyl alcohol solution *(Slovak)* 78−56576
InP for growth of $In_{0.53}Ga_{0.47}As$, influence of orientation 79−96009
InP, HCl etching speed and polarity obs., with aid of laser beams *(Slovak)* 78−56575
InP, LPE growth of GaInAsP on (100) and (111)B oriented substrates 78−92203
InP substrates, chem. etching by H_2O_2-H_2SO_4-H_2O soln. 80−35360
InP substrates, control of thermal degradation in LPE growth with PH_2 partial pressure 79−33949
InP, surface damage induced during SiO_2 deposition by RF sputtering 79−78879
InP, thermal damage suppression by adding Ar in H_2 atmosphere 79−100275
InP, transient-mode LPE of GaAs 78−72746
InP/SiO_2 substrate/film system, interface formation during CVD, modelling 80−24764
InSb room temp. CVD of Si_3N_4 80−71597
n-InSb, surface quality improvement by low temp. CVD of SiO_2, and characterisation 80−49932
$K_2BiNb_5O_{15}$ for $K_3Li_2Nb_5O_{15}$ film for optical waveguide, cryst. struct., dielectric props. 80−79016
KBr, electron irrad., epitaxial growth and surface coverage of Te films 80−10825
KI, doped substrate for vac. deposition of Ag oriented films 80−2303
KI, F-centre effect on particularities in vac. evaporated Cr film growth 79−82496
$LiNbO_3$, for optical ICs, performance obs. *(Japanese)* 79−86265
$LiNbO_3$ substrate for InSb films, prep. and props. 80−35093
$LiNbO_3$ substrates for integrated passive optical rotation sensors using guided waves, developments 80−58781
$LiNdP_4O_{12}$ growth of $LiBi_xNd_{1-x}P_4O_{12}$ waveguide laser layer 80−23709
$LiTaO_3$ substrate, direct meas. of temp. depend. of lattice mismatches between LPE grown $Li(Nb_{1-x}Ta_x)O_3$ film 79−56087
$LiTaO_3$ substrates, LPE growth of $Li(Nb,Ta)O_3$ solid soln. thin film waveguides 79−41467
MgO, (001) film substrates for film growth studies by TEM, O_2 conditioning 79−82489
substrates continued
MgO (111) substrate, LPE growth of $NiFe_{2-x}Al_xO_4$ films 79−28238
MgO, growth of ^{4}He films, vap. press. meas. 80−70499
Mo (110) surface, molecular adsorbed CO, electronic states, photoemission spectra 80−65363
Mo alloy, interaction with Mo_5Si_3 based coating *(Russian)* 80−21167
Mo, for W-Al_2O_3 composite films, oxide evaporation deposited, struct., props. 80−25581
Mo substrate limiting temp. during vaporisation and condensation coating in vacuum *(Russian)* 80−100787
NB, contact angle with low melting metals 79−77864
NaCl (001) substrate, preferential epitaxy of evaporated films induced by electron bombard. or elec. field 80−10824
NaCl, (111) surfaces, electron bombard. effects and subsequent Ag epitaxial growth, RHEED and AES 80−15419
NaCl cleavage step decoration, nucleation and growth of metallic thin films 77−69200
NaCl cleaved surface, growth of Au island film, effect of perp. elec. field *(German)* 77−76697
NaCl, doped substrate for vac. deposition of Ag oriented films 80−2303
NaCl, elec. memory in C replicas, Au and Ag deposition expts. 77−76691
NaCl, nucleation process of Cd_3As_2 films 80−59813
NaCl, role of surface steps in nucleation of VPE Au 78−79902
NaCl, Sn film, vapour-deposited on NaCl single cryst., nucleation, growth, microstruct. 78−91561
NaCl substrates growth of Bi and Sb films, initial stages of growth and orienation, TEM study 79−28237
Ni, influence on Au electrodeposit struct., texture *(Bulgarian)* 78−79863
Ni-Ag, thin-film, elec. cond. depend. on substrate film thickness and condensation temp. 79−7911
Ni-Cr-Mo-Ti (19,11,3 wt.%) for TiC reactively sputtered coatings, adherence, XPES and wear study 80−25565
$Pb(Zr,Ti)O_3$ ceramic, substrate for In_2O_3 film, ferroelec. field effect 79−47177
Pd, for Ag epitaxial growth, influence on film growth modes *(French)* 80−84408
RbCl, Pb colloid effect on particularities in vac. evaporated Cr film growth 79−82496
Se, amorphous, vac. deposition on polymer substrates, use of temp. gradient vac. coating device 80−35099
Se film, amorphous, substrate effects on crystn. kinetics 77−1337
Si (001) substrate for Pd_2Si epitaxial islands 80−96748
Si (100), (111) substrates for rare earth metal silicide thin film formation, backscattering study 80−70542
Si (111) substrate, MBE deposition kinetics of Bi film 80−10817
Si, (111) surface substrate for $NiSi_2$ epitaxial film, interfacial order, backscatter, channelling study 80−65390
Si (111) surface substrate for Al film, struct., props. depend. on vapour flow *(Russian)* 80−75453
Si, action of plasma in capacitive electrode HF discharge *(Russian)* 78−95818
Si, amorphous film on fused silicon, transport meas., influence of interspace charge 79−15237
Si and SiO_2, for Pt-Ni vacuum condensates, X-ray anal. *(Russian)* 80−70559
Si, Au film oriented crystn., formation of coincidence orientations on interphase boundary 79−90922
Si, conditions and growth mechanism for autoepitaxial thin layers at low temp. from $SiCl_4$-H_2 system 80−20795
Si, doped oxide film formation mechanism, X-ray spectral anal. 79−87008
Si, effect of surface conditions on plasma sprayed metal coatings 80−21145
Si, effect on liq. cryst. mol. alignment 77−7663
Si, epitaxial film growth and p-n junction formation by Si beam epitaxy in high vacuum 80−16187
Si, epitaxial layer thickness meas. using phase correction function of substrate resistivity *(Rumanian)* 80−90812
Si, epitaxial stacking faults, nucleation sites 77−20201
Si, for Au film, interphase coincidence boundaries 79−1560
Si, for epitaxial crystn. of GaP films by ns laser pulses 80−107674
Si for integrated optics high quantum efficiency waveguide coupled photodetectors 80−58805
Si, for Pb, Sb, and Bi silicate films, form. kinetics and props. 80−35358
Si, for Pb thin film, residual strains 78−18915
Si, for Ta or Ta_2O_5 film, film-substrate interaction obs. 77−1324
Si for wet thermal oxide film, trap emptying kinetics 80−92983
Si, heteroepitaxy of deposited amorphous Ge layer by laser annealing 79−77952
Si, implantation effects on hardening and Si_3N_4 film stress reduction 78−71748
Si, ion implantation, channelled, through metal silicide film 80−70231
Si, local mechanical defects, annealing and effect on autoepitaxial growth *(Russian)* 80−7701
Si, nucleation controlled interaction with metal film, silicide form. 80−10711
Si, p- and n-type, establishment of inversion layer under high oxide field conditions 77−66202
Si, process-induced in-plane distortion, correl. with wafer bowing 80−54579
Si ribbons, edge-defined film-fed growth technique for solar cells 80−89138
Si, shallow contact formation substrate temp. depend., Pd-W alloys 80−96963
Si, silicide formation in Mo-W bilayer films 79−99376
Si, solar cell, from film on foreign substrate 77−77390
Si, solid state reaction with Ti film, backscatt. anal. 80−34257
Si, sputtering and sputter etching and thermal history 80−25562
Si, stress field, induced by Si_3N_4 film edge, indentation-injected dislocation half-loops obs. 78−30839
Si substrate, ion induced intermixing of Pd or Pt film 80−15420
Si, substrate for Al film, annealing effect on eutectic point *(Russian)* 80−100850
Si substrate for Au films, use of sputtering for layer removal 79−78813
Si substrate for PMMA electron sensitive layer, 400 Å linewidth electron beam lithography 80−65392
Si substrate for Pd and Pt, silicide formation by laser, electron beam annealing 80−84849

substrates continued
Si substrate for RF sputtered ferroelectric $BaTiO_3$ films, ferroelectric props. 80−80697
Si substrate for SiO_2 film, ellipsometric spectra, thickness determ. *(Chinese)* 80−86379
Si, substrate for ZnS, Na_3AlF_6 films, H_2O absorpt., IR anal. 80−75446
Si substrate package for integrated GaAs laser arrays, fabrication 79−18555
Si substrate prep. for epitaxial solar cells, low-cost, unidirectional solidification process 80−93924
Si substrate solar cells, upgraded metallurgical grade, epitaxial growth 80−93905
Si, substrate temp. influence on shallow contact formation on Si, shallow contact formation substrate temp. depend., Pt-W alloys 80−96963
Si substrate thinness, device design, solar cell processing, empirical study of interaction 80−93995
Si, substrates, semicond., stress meas. in deposited thin films, X-ray topography techniques 78−5710
Si, supercond. transition temp. of Pb ultrathin films 77−66220
Si surface, wetting by Pb, Sn, Ge in H_2+HCl 78−43210
Si surface electron beam deposited silicide formation using scanning CW laser beam 80−66862
Si, thermally oxidised, interface props., sputter deposition parameters effects *(German)* 80−40257
Si, vapour epitaxy, optimum growth conditions 78−76608
Si wafer, stress meas. in film, X-ray method 78−51860
Si wafers, process-induced in-plane distortion and wafer bowing 79−11048
Si:B^+, ion implanted, lateral spread of B^+ ions through SiO_2 mask 79−51130
Si:Fe(Al), compensated substrates for solar cells, effects of Fe and Al 80−94009
Si:P, implanted, SiO_2-film-covered, laser annealing behaviour 79−86808
Si:Sb, ion implanted doping, isotopic composition shifts on neutron activation determination 80−24487
Si:Ti substrate for epitaxial solar cells 80−61341
SiC CVD substrate, Cu mirror vapour deposition, pulsed laser damage characts. 80−48314
Si_3N_4 sample substrates, high resoln. electron beam fabrication using STEM 80−104104
SiO_2, CVD of Ta film, struct., mech. props. 77−24965
SiO_2, for interdigital transducer *(Czech)* 80−19201
SiO_2, interfacial chemistry with deposited Ba, AES obs. 80−44434
SiO_2 on Si wafer for ZnO low-loss optical waveguides 80−58793
SiO_2 solid state reaction with Ti film, backscatt. anal. 80−34257
SiO_2, substrate, glow discharge effect on surface props. and struct. 78−85201
SiO_2 substrate, obliquely evaporated for cyano-biphenyl LC, alignment 80−79677
SiO_x, growth and struct. of Au island film, effect of perp. elec. field *(German)* 77−76696
SnO_2 film, transparent cond. support for ZnS:Mn films, effect of morphology 79−56092
SnTe substrate, Ag epitaxial growth and topostactic exchanges 78−14640
$(Sr/Ba)(Fe/Al/Ga)_{12}O_{19}$ solid soln. crystal for hexaferrite layer substrate *(German)* 78−23672
$SrTiO_3$, single crysts., $BaTiO_3$ epitaxial growth 79−15051
Ti electrospark alloying to transition metals and their carbides and aluminides, residual stresses obs. *(Russian)* 77−56145
Ti for W-Al_2O_3 composite films, oxide evaporation deposited, struct., props. 80−25581
Ti-Al-V (6,4 wt.%) alloy foil, substrate temp. effect on struct. 80−7497
Ti-Al-V (6,4 wt.%) for TiC reactively sputtered coatings, adherence, XPES and wear study 80−25565
TiC, CVD coating on Co-bonded multicarbide substrate, SEM, RHEED, AES interface study 79−77927
Tl_3VS_4 single-crystal substrate SAW filter performance 77−31186
W, deposition of Au film, interface struct., FIM obs. 80−65384
W, for Cu cementation, field ion microscopy of cementation vs. substrate dissolution, pH effect 80−16206
W substrate-oxide film system with rough boundaries, ellipsometric obs. using equiv. film theory 80−2310
W-ribbon substrate, epitaxial growth of Ag, cryst. orientation *(German)* 79−65994
YAG, as substrate for $Er_3Al_{5-x}Ga_xO_{12}$ LPE film for solid laser 80−93419
YIG, magnetoelastic surface waves, magnetostatic reson. anal. 80−20441
Zn surface, Ni solar selective black coatings, electrochem. deposition 80−29885
$Zn_xCd_{1-x}S$, rough, lattice mismatch with Cu_2S and InP films 78−43263
$ZnGa_2O_4$, (111) substrate, LPE growth of $NiFe_{2-x}Al_xO_4$ films 79−28238
$ZnGa_2O_4$, flux growth, for appl. as nonmag. substrate in LPE 78−44000
ZnO, for Ni films, band bending, UPS study 80−7472
ZnS monocrystalline substrate, influence of struct. on CdS epitaxial growth and nucleation 80−88455
ZnSe, epitaxial growth, orienting semiconductive substrate effects 77−47688
Zr, contact angle with low melting metals 79−77864

sudden commencement *see magnetic storms*

sulphur
see also nuclei with .....
100 MW fluidised bed combustion district heating plant burning high S content residual oils 80−108777
^{34}S, ocean catastrophic chemical events 77−56645
abundance and distrib. in glassy rims of submarine pillow basalts 79−12111
abundance in 20 galactic planetary nebulae, spectrophotometry 78−45375
abundance in H II regions, using ionization correction scheme 78−54018
abundance in lunar rocks rel. to C content 78−4123
abundance in the ureilite meteorite Kenna 77−41365
activity in pyrrhotite at 1073K 77−72700
adlayer effect on CO and H_2 adsorption and desorption on Fe(100) 80−71573
adsorbed, role in dissolution and passivation of Ni and Ni-S alloys 79−66340
adsorbed ($\sqrt{3}\times\sqrt{3}$)R30° overlayer struct. on Ir (111) 80−15365
sulphur continued
adsorbed layer, ($\sqrt{2}\times\sqrt{2}$)R45°, and Pd(100), adsorbate induced surface reson. obs. in photoemission 80−7470
adsorbed layer interaction with substrate steps, selective effect on epitaxy 78−14616
adsorbed layer on Cu(100), electronic props., UPS, XPS and Auger spectra 77−66088
adsorbed layer on Ni, sputtering 77−36335
adsorbed layer on Ni (111) surface, bonding geometry and electronic struct. 79−77909
adsorbed on Ag (110), equilib. segregation isotherm, selvedge model 79−90883
adsorbed on AgBr dispersion in gelatin, transient absorpt. spectra, latent image form. and decay 80−66837
adsorbed on Fe, effects on surface reaction kinetics and surface self-diffusion 78−7234
adsorbed on Mo (001) surface, effect on CO adsorption 79−86981
adsorbed on Ni, photoelectron diffr. data 80−29851
adsorbed on Ni(111), surface bonding mechanism for ang. resolved photoemission 79−69360
adsorbed on Ni (001), crystallography by LEED, appl. of iso-intensity map method 79−19128
adsorbed on Ni (100), effect on photoelectron spectra *(French)* 77−36360
adsorbed on Ni (100), electron ejection by metastable He atom impact 79−8217
adsorbed on Ni (110), layer struct. from anal. of LEED pattern 79−73407
adsorbed on Ni (110) and Rh (110), surface struct. anal. using hybridisation model 80−44423
adsorbed on Ni surfaces, directional UV photoemission 78−15295
adsorbed on polycrystalline Ni surface, H_2^+ ion induced desorption 78−84069
adsorbed on Rh (110), LEED crystallographic determ. of surface struct. 80−44422
adsorbed on Ru(110), evidence for SH species, UPS and work function meas. 79−99424
adsorbed on Ru (110), UPS and work function change meas. 79−78834
adsorption, on reconstructed Ir(110)-(1×2), AES study 79−42384
adsorption and desorption kinetics of CO from clean and S covered Ru 80−6643
adsorption and desorption kinetics of H_2 from clean and S covered Ru 80−6644
adsorption effects on electrodeposition of Ag, Cu 79−20001
adsorption on Cu, influence on work function *(French)* 78−76134
adsorption on Cu (100), ang. resolved AES and LEED 78−18908
adsorption on Cu vicinal surfaces, LEED study 80−103575
adsorption on Fe(100), adsorbate coverage determ. by LEED, AES and XPS 80−103566
adsorption on Fe (110), UPS and LEED/Auger meas. 77−72773
adsorption on flyash from coal combustion, cloud nuclei form. 77−21887
adsorption on metals, thermodynamics of two-dimen. and three-dimen. sulphides 80−20036
adsorption on Ni, diffusion, multiple binding sites, photoelectron spectra, LEED struct. 77−66569
adsorption on Ni(Al)(Mg), internal and external sources of electrons 77−44097
adsorption on Ni (100), orbital identification in INS and UPS spectra 77−43427
adsorption on Ni (100) surface, ang. distrib. of S Auger emission 77−32475
adsorption on Ni (111), angle-resolved photoemission 80−40230
adsorption on Pd (110) surface, LEED study *(French)* 80−88422
adsorption on Pt (100) 78−14606
adsorption on Pt (110), LEED pattern interpretation, model 77−69184
adsorption on Ru (001), LEED, UPS, AES, and thermal desorption meas. 79−99420
aerosol particles, S assessment along urban freeway, proton induced X-ray emission anal. 77−60172
aerosols, continuous meas. and speciation by flame photometry 78−95974
aerosols, physical characts. of air pollutants 78−96284
aerosols, total conc. meas. using pulsed electrostatic precipitator and flame photometer 78−95975
aerosols from South American continent, S and trace elements concs. relationships 78−57245
aerosols in S.Hemisphere, content S and trace metals 77−49136
air pollution, balance and washout by precip. in industrial atm. *(Russian)* 79−100898
air pollution, natural and anthropogenic emissions and Central Europe, calc. from atm. meas. 77−73827
air pollution simulation over NE. United States, statistical trajectory model 77−73828
air pollution transport over N.Atlantic 78−20507
alkali, borate glass:S, blue and green coloration, absorpt. spectra 79−87470
alkali halide: S_2^-, laser-excited spectra and reorientation of S_2^- 77−28563
Allende meteorite, $^{33}S/^{32}S$ ratio anomaly 78−49402
Allende meteorite, S content, neutron capture gamma-ray spectroscopy 80−94728
alloying addition to Alnico 5 alloy, mag. props. and grindability 80−89375
amorphous, structure, random chain assembly model 78−6015
amorphous and monoclinic transform. kinetics *(German)* 79−42239
antiprotonic atoms of light nuclei and isotopes, p̄-n strong interaction effects 78−29867
Archaean volcanic rocks S content rel. to ocean floor basalts 78−88824
atmosphere, ^{38}S in SO_2 and SO_2 oxidation rate meas. 77−73814
atmosphere, Phanerozoic O budget, S isotope variations in marine sulphate evaporites 77−73810
atmosphere aerosol, level meas. using continuous flame photometric detect. system 80−81508
atmospheric aerosol characterization for particulate S, health effects 79−20984
atmospheric aerosol characts. in Florida, PIXE anal. 79−21030
atmospheric aerosol sampling and anal. system for particulate S monitoring 79−21029
atmospheric aerosols, sampling and anal. 78−96283
atmospheric meas. using compact X-ray fluoresc. analyser 78−68971

sulphur continued
atmospheric S budgets rel. to SO_2 from sour gas plants in Alberta 77−37372
atmospheric S cycle, H_2S contrib. 78−73473
atom, ^1S state photolytic prod. from OCS 79−13775
atom, ab initio effective valence shell Hamiltonian for neutral and ionic valence states 80−74117
atom, and ions, two and three-electron Auger transition, with vacancies in 2p-shell 79−63972
atom, beam-foil populations, charge state distribs., independent electron model 77−19035
atom, beam-foil study of S III-S IV, 500 to 1200 Å 78−66488
atom, chem. environent effect on Kα satellites intensity, heavy-ion collision 77−54527
atom, chemisorption on Cu, cluster theory 80−29264
atom, chemisorption on Ni, cluster theory 80−29264
atom, emission spectra in Ar plasma, lines above first ionisation limit 78−25462
atom, excited config., Hulthen and Slater type 2d functions 78−41972
atom, foil excitation, K-vacancy bearing metastable states yield, 30-50 MeV 77−54600
atom, He-like, 2^3P_1 state lifetime, X-ray emission 77−18851
atom, in CS_2 and SCO, $L_{II,III}$-absorption spectra 78−86807
atom, L X-ray emitting levels, lifetimes 78−66493
atom, lifetimes of non-penetrating states, including core polarisation effects 79−89638
atom, MINDO parameters 78−86786
atom, $O^{2+,3+,4+,5+}$ induced K-shell X-ray production cross section, 7 to 24 MeV 77−61850
atom, one-electron binding and Auger energies 80−52872
atom, photoionisation cross sections and ang. distribs., outer p subshell 80−9572
atom, photoionisation cross sections and asymmetry parameters, SCF Xα scatt. wave calcs. 80−63542
atom, pseudopotential calculations, parameter fitting scheme appls. 78−41928
atom, static multipole polarisability, frozen core approx. 79−36791
atom, UPS in VUV region 79−98153
atom, X-ray and Auger transition probabilities to 2p level 78−17640
atom nucleation particulate formation from SF_6 and SF_6-H_2 mixture photolysis 78−76836
atomic Kα X-ray satellite spectra, gas phase meas. 78−66496
automobile exhaust particulate emissions, containing H_2SO_4, X-ray fluoresc. anal. technique 77−60173
borate glass:S, (boro-ultramarine), blue chromophore identification 77−20888
brine, routine anal. by X-ray fluoresc. spectrometry applying matrix corrections 78−88690
charge-transits, flash excited, electrode-edge effects, meas. 80−2396
chemical reaction involving S, sulphide, sulphate, sulphite, application to Venus and Io 80−50837
chemisorbed c(2×2)S on Ni (100), photoemission angle-of-incidence depend. 77−32502
chemisorbed on Fe {001} surface, determ. of c(2×2) structure of S, LEED 77−85063
chemisorbed on Ni (001), dynamical calc. of angle-resolved UV photoemission 77−85890
chemisorbed on Ni (001), site determ. by angle-resolved UPS 78−71970
chemisorbed on Ni (100) and (110) surfaces, UPS 77−32500
chemisorption, on Al_2O_3-supported Ni, thermodynamic parameters meas. 80−88424
chemisorption on Ni, ang. depend. of multicentre Auger matrix element for Ni (100)-c(2×2)S 78−92151
chemisorption on Ni, orbital energy spectrum of chemisorbed electrons 78−2542
chemisorption on Ni, surface struct. from ang. resolved UPS 78−31303
chemisorption on Ni, Xα cluster model calcs. 79−65313
chemisorption on Ni(100), struct. and energy levels calc. 77−47663
chemisorption on Ni (001) and Cu(001), thermodynamics, AES study 79−82452
chemisorption on Ni (100), geometry of overlayers 78−2373
chemisorption on Ni (100), surface vibrs., electron energy loss spectra 79−33173
codeposited with O on Ag (111) surface, AES and photoelectron spectra 78−71957
composite, engineering props. 77−86093
concentration and valence state in pollution samples, X-ray fluoresc. anal. 79−48027
corrosion of C steel by wet elemental S 78−92388
defects predeposited in Si p^+-n junction diodes by low fluence ion implantation, unequal densities 80−20293
determination, combustion-gas chromatographic method, data processing 80−40762
determination, in air particulates, X-ray fluoresc. method 79−20491
determination, in fuel oil, by radioisotopic energy dispersive X-ray fluoresc. anal. 78−61122
determination, in organic compounds 79−11869
determination, in water, by neutron activation and X-ray fluoresc. analyses 78−3428
determination in submicrometric aerosols, SO_2-denuder appl. for continuous meas. 79−8699
diamond surface interaction with gases and metals 77−72758
diffusion, in α-Ti, AES meas. 78−51735
diffusion and distribution in steels St3 and 12Kh18N9 78−2306
diffusion and solubility in Ni *(Russian)* 80−70465
diffusion and solubility in solid butadiene copolymers *(Russian)* 79−33092
diffusion in γ-Fe, grain size effect 79−86930
diffusion in Ag and Cu 78−47599
diffusion in InP Schottky diode for barrier height control 77−85309
diffusion in NiO single crystal 78−95186
distribution in marine sediments 79−92523
divalent, multiple bond linking in vinyl sulphides, spectrosc. obs. *(Russian)* 78−21929
dry deposition and uptake by forest and farmland of atmospheric S 79−74939
dry deposition onto snow surface 77−37288
elasto-optic coefficient of orthorhombic crystal 79−65836
electrical conductivity, dielectric to metal transition at ultrahigh dynamic press. *(Russian)* 79−60881
electrical conductivity transition to cond. phase 79−54150
sulphur continued
electrical conductivity under shock compression *(Japanese)* 78−26923
electrode, miniature, recharging characts. in two liquid phase region 80−26127
electrode performance in Na-S battery 79−29463
electrolytes, S ion conducting *(German)* 77−90606
elemental abundances of S, K and P in aerosols from S.American rain forests 79−100910
evaporation from Fe-C(Si)(Mn)-S melts *(Russian)* 78−19716
flow on surface of Io 79−92703
fluidised-bed steam generating system to supply 100000 lb/h of saturated steam burning high S coal 80−108778
free surface and grain boundary chemistry in Fe alloys 80−75410
GaP:S, photostimulation spectra, bound electron phonon interactions *(Russian)* 77−1712
gas phase transport, definition of hydrodynamic regime acquired during crystn. 79−51029
geochemistry, influence man-made sources on S cycle of NE United States 80−26178
glass, catalytic crystallization in organic media at room temp. 77−84657
global atmospheric S cycle rel. to H_2S in marine atmosphere 79−12165
global cycle, contrib. of biologically prod. dimethyl sulphide 77−70786
global sulphur cycle study, atmospheric pollution modelling appl. 78−92902
grain boundary segregation, in α-Fe 78−72778
graphitisation, catalytic effect of S, 1400-2000°C 77−28735
high pressure phase from decomposition of S_4N_4 79−10911
high-field injection currents 78−47801
high-S coal, continuous sorbent regeneration in pressurized fluid bed combustion 80−30351
human hair surface, determination of content using minimum depth electron probe X-ray microanalysis 80−22500
implant fluence, Cr redistrib. during thermal annealing of semi-insulating GaAs 80−84199
impurity in C steel plates, effect on through-thickness props. 80−66660
impurity segregation at (111) Cu/(110)Mo and (111)Ag/(110)Mo interfaces 78−84076
insulator-conducting phase transition 77−35972
interstellar chemistry 80−101632
interstellar S, depletion on oxide grains 80−17635
Io Na cloud, forbidden S II emission rel. to Jupiter magnetosphere thermal electron density 79−40133
ion, multiplet state equilib. population in beam-foil excitation 77−19057
ion+target (Z=4-40), single and double K-shell excitation, X-ray satellites, hypersatellites 77−19058
ion+target collisions, two-electron-one-photon transitions, X-ray spectra 77−19068
ion charge distrib., 70-140 MeV, through C and Be foils 78−13364
ion implantation for InP n-type doping 78−91351
ion implantation into GaAs 78−55884
ion-foil interaction, K-shell vacancies and residual excitation 77−50519
ions, X-ray emission spectra, Kα satellite, hypersatellite yield ratios 78−86810
ions in Jupiter's S nebula, temp. anisotropy 80−17539
ions in Jupiter magnetosphere, plasma cloud injection from IO 80−90358
ions in low density plasma, dielectronic recomb., ionization equilib. and radiative energy loss, solar corona appl. 79−68903
isotope exchange between sulphate and sulphide in acid solns., expt. determ. at 300°C and 1000 bars 78−62937
isotope separation, multiphoton molecular dissociation using high-power CO_2 laser radiation 80−9657
isotope separation, SF_6 photodissoc. by IR laser pulse, selectively excited vibr. levels 78−9209
isotope studies in early Archaean sediments from W.Greenland 79−92537
isotope variations as pollution index in lakes near Sudbury, Ontario 78−57228
isotopic composition, in sulphide and sulphate minerals from DSDP Leg 37 77−91101
isotopic composition determ. using RMO-4S omegatron mass spectrometer 78−5368
isotopic composition in CS, spectroscopic meas. *(Russian)* 80−91696
isotopic composition in precipitation within Great Lakes Basin 79−16625
K-shell X-ray production, by 0.4 to 2.4 MeV ^4He and ^1H ions 79−47550
laser, atomic, pulsed microwave discharges of SF_6 and CS_2 source gases 80−48233
laser, auroral and transauroral transitions, high energy storage 77−10897
laser, photolytic, expts. for fusion research 78−63101
laser transitions, IR, in SF_6-He discharge 77−79805
laser UV transitions of ion, performance and spectroscopy 78−22111
lattice statics of α-type under hydrostatic press. 80−49175
liquid, compressibility 77−65997
liquid, conductivity meas. from melting point to 900°C 78−84209
liquid, elec. cond., 300 to 900°C 79−91050
liquid, eqn. of state determ., crit. props. and mol. comp. 80−49336
liquid, mobility variations of photoinjected charge carriers 79−91065
liquid, optical absorption spectrum, up to supercrit. conditions 78−88320
liquid, polymerisation transition, anomalous light scatt. obs. 77−19861
liquid, temp. depend. of absorption edge 77−66515
liquid droplet, optical transmission and elec. resist. changes on polymerisation 77−35460
lunar mare basalts, Fe^{2+} reduction by S loss 77−9681
lunar rock content, neutron capture gamma-ray spectroscopy 80−94728
magnetic susceptibility meas. rel. to heat treatment 78−34952
magnetoelectret, thermally stimulated discharge current 79−91341
Mars lithosphere, possible S overabundance 80−72832
measurement, model XA-300 meter for laboratory use 80−26085
mechanical strength, effect of H_2S 77−4818
metallic state, elec. resist., press. effects up to 600 kbar 78−26920
meteorites, thermal metamorphism, noble gases, C and S in Allende 79−92732
mitochondria of bovine heart, EPR investigation of two forms of Fe-S centre N-2 78−69014
mixtures containing S and surface albedo of Jupiter's satellite Io 79−40127
molecular dynamics, allotropy, solid-state phase transitions effects, Raman spectra *(French)* 77−42372
molecular laser, optically pumped, review 80−58519

sulphur continued
molecule, presence or absence in solar atm., theory 78−69765
molecule, selectively excited, coherence retention during rotationally inelastic collisions 77−46622
molecule, v.u.v. absorpt. spectrum, Rydberg transitions 77−3382
monoclinic, order-disorder transition, X-ray struct. determ. 78−30750
monoclinic allotrope, thermal behaviour 78−67813
monolayer, adsorbed on Al (111), angle resolved UPS of 2-dimens. band struct. 80−60059
muonic K-shell X-ray transitions, nuclear charge radius 78−66195
natural rubber accelerator, effect on viscosity *(German)* 78−30688
$(np)^4\ ^1S_0$-level photoionisation via autoionising levels 79−76398
ocean S budget rel. to dimethyl sulphide in seawater 78−96237
oceanic crust layer 2 S distrib., effect of low temp. seawater-basalt interaction 80−41432
odd parity levels, configuration interaction effects 79−72246
ordered overlayers on N(001) surface, elec. struct. 80−84835
Orion Nebula, Ne, S and O abundances from fine-struct. lines obs. 80−4410
orthorhombic, far IR absorpt. spectrum 77−8560
orthorhombic, photogeneration of charge carriers 80−107844
orthorhombic-monoclinic transition heat, by mass spectral determination of sublimation heat 79−73302
overlayer, on Ni (100), bonding, photoemission expts. 77−35819
particulate S in ambient aerosols, chemical state determ. by PIXE anal. 79−5225
photoelectret state in polycryst. following X-irrad. 80−60485
photoelectret state produced in polycrysts. by X-irrad. in elec. field 78−31147
photoelectric cross sections, from total absorption cross sections, 5 to 130 keV 79−26947
photographic emulsion sensitisation by S and Au 78−16869
photoinduced discharge 400 to 580 nm 77−8139
pionic atom, 2p level shifts and widths 78−46469
planetary nebulae, S abundance from IR and visible line meas. 80−82444
polymorphism and melting curve, effect of high pressure system configuration 78−43104
powdered pressings, proposed near IR reflectance standard 78−90464
probe for coal gasification systems 78−76947
production and props. in liq. Ar and N_2 by OCS photodissociation 80−43064
quench-deposited A1-type films, superconducting props. 79−15264
radiation effects, allotropic modifications and activity distrib. 80−70255
radioactivation analysis, of biological and geological materials, separation methods *(French)* 77−90700
rain and snow acidity, release by burning of fossil fuels 80−26590
in rain collected below wheat canopy, S sources 77−56698
rainwater, pH and S content in rural areas of England and Wales 79−16562
recovery during ammoniacal leaching of CuS 79−52618
replicas, of C and alloy steels, effect of methodic factors on quality 79−24691
sedimentary distrib. rel. to O_2 in Precambrian atmosphere 77−5272
segregated onto Pd surface, state, AES, EELS, UPS and XPS study 80−93452
segregation and adsorption in Fe and steel, influence on carburisation and nitrogenation 80−66701
segregation in Cr-C steel 80−66594
segregation in Ni, effect on intergranular corrosion in dil. H_2SO_4 80−30152
segregation on Fe(111) surface, LEED, AES and work-function change 80−15350
segregation to grain boundaries in Ni_3 Al and Ni_3(Al, Ti) 78−48410
shock wave method observation of transition to highly conducting state 80−4738
single crystal, photoinjection, electronic transport and Mott-Gurney transition *(Spanish)* 80−84464
soil S content and acidity in Alberta, SO_2 effect 77−73843
solar S I 1807 Å and 1900 Å lines, anal. of profiles 78−57517
solid soln. in Ni, effect on dissolution and passivation of Ni in acid medium *(French)* 78−64771
solubility, in Pd, 600-1000°C, H_2-H_2S gas phase compositon depend. *(French)* 78−87791
solubility and activity in Mn-Cu and Mn-Ni melts *(Russian)* 77−25012
solubility in Cr-rich Fe-Cr alloy *(French)* 78−30761
solubility in liquid Cu 77−21096
solubility in NiO and CoO at 1000°C 78−63858
steel, C, corrosion during cyclical exposure, to wet elemental S, and He atmosphere 78−92391
steel, C, friction faces, S, O content, secondary ion-ion emission obs. 80−55545
steel, mass spectrometric analysis of S content by remote meas. technique 78−23994
steel, stainless, crevice corrosion resistance S mechanism effect *(French)* 77−77635
steel, stainless, fracture micromechanism when kept isothermally in sulphur pulp 80−76355
steel, welded-joints, H_2 induced cracking, S content effect 80−97562
stratosphere S budget, CS_2 and COS oxidation effects 79−84423
submitochondrial particle succinic dehydrogenase, interaction of ubisemiquinone with Fe-S centre, EPR 78−69016
superconducting, transition to supercond. state at high press. *(Russian)* 79−7923
superconducting, transition to supercond. state obs. at high press. *(Russian)* 79−7922
surface, ethylene episulphide form. by laser irrad. in presence of ethylene 79−57258
surface impurity in Ta, effects on thermoelectron emission *(Russian)* 77−8712
surface segregation on Cu-Ag alloy, Auger spectral study diffusion 80−76549
TEM imaging of S atom, simulation of dark-field images of 2,3,4,5-tetraacetoxymercurithiophene 78−70229
thermochemical generation for CO chem. laser 77−68207
thermodynamic basis for generalisation of melting curves 78−2236
troposphere, global S cycle linear eight-box model 80−56506
vacancy clustering in Au 77−4100
vapour, formation of sulphide layers in S vapour on Ge surface 79−7757
vapour, reaction with monocryst. Ge, applicability of Kossel's crystal model 79−87833
sulphur continued
vapour, sulphurisation kinetics of Ti, 450-550°C, thermogravimetric determ. 77−25197
Venus, S chemistry and thermodynamics 79−44391
Venus, S chemistry of atmosphere/lithosphere system rel. to oxidation state of atmosphere and crust 80−98586
Venus atmosphere, role of gaseous S_2, S_3, S_4 and H_2S_n 80−17518
Volcan Poas, Costa Rica, subaqueous S lake 78−28206
wet fallout scale, geographical var. in S. Sweden 79−16653
X-ray fluoresc. anal., environmental samples 78−85270
X-ray L-emission spectra, in CoS, CdS, ZnS, MnS, $BaSO_4$ and K_2SO_4 *(Japanese)* 78−15254
X-ray powder diffr. pattern at −150, −75, 100°C 78−95015
XPS, in BaS and $BaSO_4$ 80−43104
zeolite-S layers, high-temp. activated dipole moments in S clusters *(Russian)* 80−20575
zone-centre lattice vibrs. of α-type, hydrostatic press. effects 80−49314
$^1S_2$, interstellar, upper limits on abundance in mol. clouds 78−28738
5^{n+}, beam-foil UV spectra, elec. dipole transition probabilities, radiative lifetimes 77−6730
Ag−S system, phase diagram, 100-600°C *(German)* 80−97471
As:S film, amorphous, chemical modification of props. 80−49250
B_2O_3-M_2O:S_2 glass, (M=Li, K, Na), absorpt. spectra of S_2 mols. 79−24337
CdTe:S, reson. interaction of local S vibr. with lattice phonons 77−11654
Ce-S-O equilibrium in molten Fe *(Chinese)* 80−104423
CeO_2:S, acceptor properties of S, free electron concentrations 80−34395
CeO_2:S, in $O_2+CO_2+SO_2$ atmosphere, elec. cond. study 80−39583
CeO_2:S, influence of S on elec. props. *(Russian)* 79−51566
Co_3O_4:S, defect struct. and elec. props., electron, hole conc. 80−44601
Cr_3O_4:S, elec. cond. and thermo-EMF 80−20231
Cu-Pb-S system, at 1473K, thermodynamic anal. 78−39746
$Cu+X^{n+}$, X=F, Al, Si, S, K X-ray production, target thickness depend. 77−75280
Fe, (100) surface, S segregation and 2D compounds precipitation *(Japanese)* 80−35188
Fe, cast, S effect on nodular graphite form. *(Japanese)* 77−56001
Fe, embrittlement, fracture mode transition as function of grain boundary sulphur 80−55520
α-Fe, S and C diffusion, AES obs. 77−51543
Fe, single cryst., segregation behaviour of S, O and P at (100) surface 80−100841
Fe-Ni-Sb-S, S/Sb surface site competition in segregation 80−40366
Fe-Si-B-S, grain-oriented, high induction, B and S addition effect on magnetic props. *(Slovak)* 79−4697
GaAs, CVD, S doping behaviour during growth, electron conc. 78−26784
GaAs:S, depth profiling using Cs^+ bombardment and negative SIMS in UH vac. 79−99232
GaAs:S, dislocation-free, TEM study of microdefects 79−82213
GaAs:S, generation of high mobility n layers, SIMS 80−103375
GaAs:S, implantation depth profiles of S^+ and S_2^+ using AES 79−55774
GaAs:S, implanted, ion channelling meas. for lattice location of impurities 79−4332
GaAs:S, ion implantation, expt. 77−11574
GaAs:S, ion implanted, evaluation by contactless mobility meas. 79−1448
GaAs:S, ion implanted, capless anneal in As controlled vapour 79−55767
GaAs:S, ion-implanted, capless anneal, effect of As partial press. 80−29038
GaAs:S, LPE, and doping characts. 79−33948
GaAs:S, MBE grown, surface exchange doping using PbS(Se) captive sources 79−10864
GaAs:S, VPE, high purity, residual donors, photocond. expts. 77−85174
GaAs:S epitaxial, VPE growth, photoluminesc. and emission spectra 80−29774
GaAs:S epitaxial layers, dopant conc. control method 77−1807
GaAs:S^+ film, ion implanted carrier characterisation by cyclotron reson. 77−20472
GaAs-S VPE layers, thickness and carrier conc. variations 79−100060
$GaAs_{1-x}P_x$:S, deep level, photoconductivity, carrier nonradiative recombination 80−20112
GaP, excited 1s-level of S-bound excitons 79−82996
n-GaP:N,O,S,C end, dielec. const. from S-C donor acceptor pair spectra 79−65788
GaP:S, defect struct. and tetrahedral precipitates, TEM study 80−107246
GaP:S, donor bound exciton excited states 80−66284
GaP:S, donor centre struct. and conduction band nonparabolicity 78−14695
GaP:S, ENDOR meas., symmetries, hyperfine parameters 78−72435
GaP:S, effects of uniaxial stress on luminesc. 79−78739
n-GaP:S, elastic moduli and mode gammas 79−73242
GaP:s, elec. props. following 1.7 MeV electron irradiation 78−80005
GaP:S, ground and excited states of bound exciton complex, stress effects 80−65463
N-GaP:S, IR absorpt. cross-section 79−38582
GaP:S, IR lattice band profile, electron spin reversion in mag. field, Nf-R curve 79−28771
GaP:S, IR photocond. response spectra 79−56257
GaP:S, nucl. relax. rel. to donor density 80−11284
GaP:S, pot.-depend. g-values and quenched diamag., props. of donor states 77−62861
GaP:S, pot.-depend. g-values and quenched diamag., pseudoacceptors D^0, X 77−62862
GaP:S, Se, Te, Si, shallow donors, excitation spectra 77−81128
GaP:S, shallow donor states, Stark effect and inversion splitting, electroabsorption spectral obs. 80−50385
GaP:S,C(Cd)(Zn), donor-acceptor pair luminesc., excitation spectroscopy 80−25440
GaP:S LEC grown crystals, HVEM investig. of defects 79−60376
p-GaP:Zn,S, spin polarisation of donors and acceptors in mag. field, optical and microwave study 80−93393
GaSb:S, cond. and Hall coeff. relax., impurity config. model 80−6786
n-GaSb:S, inhomogeneous, temp. depend. of elec. resist. 78−2482
n-GaSb:S, thermal quenching of residual cond. 78−56188
n-GaSb:S-metal surface barrier struct., elec. and photoelec. props. 78−56229

sulphur continued
Ge:S, photoionisation cross section of deep impurity centres 78−56510
Ge+S (vapour) reaction kinetics 78−35718
Ge+S(vapour) react., GeS layer form. rate rel. to S_2 vapour press. 79−43152
H production, thermochem. H_2O decomposition using S-I cycle, process eng. and bench-scale studies 80−35770
H+S^+(S^{3+}), ionization model for NGC 7027 planetary nebula 78−36671
In:S surface, impurity precipitation and resolution at melting point 78−14553
N-InAs, Moss-Burstein effect, S, Sn, Te dopants 78−64389
InAs:S, ion implanted, photocond., photo-EMF, and optical absorpt. spectra 80−70763
InAs:Te(Se)(S), intrinsic pt. struct. defects 80−33998
InAs:Zn,S, exam. of microhardness, Hall effect as function of dopant 79−95038
InAs:Zn,S, solubility and donor-acceptor interaction 80−54263
InP:S, dislocation-free, TEM study of microdefects 79−82213
InP:S, SSD growth of low dislocation density crystals 80−89135
InP:S, VPE, exam. of molar fraction controlled impurity in In-PCl_3-H_2 78−56587
InP:S^+, ion-implanted VPE layers, laser annealing, elec. and struct. anal. 79−73199
InP:Te(S), heavily doped, dislocation imaging using transmission cathodoluminesc. 80−29023
InSb:S, ion implanted, Hall effect meas. 77−20342
InSb:S, reson. states and reson. scatt. 80−49738
KBr:S, colour centres, luminesc. and photochemistry *(German)* 77−44055
KBr:S^-, Jahn-Teller model of S^- ion centre 79−82567
KCl:S, colour centres, luminesc. and photochemistry *(German)* 77−44055
KCl:S, influence of anion impurities on mech. props. of alkali halide crystals 78−87736
KCl:S^-, Jahn-Teller model of S^- ion centre 79−82567
KI:S_2, Raman spectra, orientational dynamics 78−56482
KI:S_2^-, spin-lattice relax. rate, 1.5 to 2.2K 77−20686
KI:S_2^-, Stokes' losses on cryst. vibrs. in luminesc. spectra of mol. centres *(Russian)* 77−55827
KI:S_2^- centres, luminesc., polarisation temp. depend. 78−87943
KI:S^{2-}, impurity-vacancy dipole UV absorpt. and ionic thermocurrent, F-centre form. 77−36271
KI:S_2^-, photochemical reaction, F-centre production 78−64861
KI:S^{2-}, photoinduced polarisation and depolarisation 79−33738
KI:S^{2-}, vacancy dipoles, photo-induced polarisation and depolarisation 80−2690
Mg XI-S XV ions, 2l3l-1s3l and 2l2l-1s2l radiative transitions and non-radiative decay probabilities 78−70781
MgO:S, cathodoluminesc. spectrum *(Russian)* 80−55197
Mn_3O_4:S, defect struct. and elec. props., electron, hole conc. 80−44601
Mn_3O_4:S, elec. cond. and thermo-EMF 80−20231
^{99}Mo separation using S collector in HNO_3 soln. of neutron irrad. UO_2 77−42161
Na/S batteries, load levelling and traction 80−21391
Na/S battery development program at GEC for utility lead levelling with beta alumina solid electrolyte 80−61327
Na/S cells operating with dissolved catholyte, elec. props. 80−101085
Na/S load levelling batteries, optimisation of fabrication process of beta Al_2O_3 solid electrolyte 80−72035
Na/S traction batteries, development progress and problems, review 80−61326
Na-S batteries, load levelling and motive power appls. 77−86321
Na-S cells, S electrode potential distrib. model 79−96435
NaA zeolite:S, optical spectra 78−88342
NaCl:S^{2-}, enthalpy of anion vacancy migration 80−15309
Na_2S_5-molten S interface, mass transport phenomena, rel. to Na/S battery 80−72026
Ne+S^{14+}, soft X-ray emitting slow multiply charged ion prod., recoil ion spectroscopy 77−50516
Ni, ordered overlayers of O and S, A-vector orientation depend. of angle-resolved photoemission 77−59671
Ni passivation, S influence study by Auger and electron spectroscopy 80−65347
Ni:S, impurity redistrib. under high temp. electron irrad., residual elec. resist. reduction *(Russian)* 79−82256
S adsorption in coal, content meas., using X-ray radiometric analysis 80−26077
S and S^+, one-electron capture cross sections in alkali metal vapours 79−59553
S atom, van der Waals radius, mean statistical value 77−83515
α-S, attachment energy as habit controlling factor 80−59421
S, He-like ions, X-ray emission passing through thin foils 77−3293
S I, (II), (III), reson. transitions, radiative lifetimes, astrophys. appls. 78−62767
S I, emission lines obs. in EUV spectra of late-type stars 80−82359
S I ground configuration, wavelengths of observed transitions between levels 78−50489
S II, fine-structure transitions by electron impact 78−65493
S II forbidden line emission from thermal plasma of Jupiter 78−93146
S II forbidden line emission nebula studies of Jupiter 80−67636
S II forbidden line emission round Jupiter, distrib. and intensity 80−85885
S II forbidden lines as determinant of reddening and electron density, astron. appl. 79−30114
S II Jupiter torus emission, longitudinal symmetry, visible spectra 80−82271
S II plasma in Jupiter magnetosphere, radial discontinuities obs. 80−4291
S II ring round Jupiter, var. in characts., link with Io, visible obs. 80−90360
S II-VII, spectra, 1050-5500 Å, beam-foil expt. with 100-700 keV ions 78−50495
S III, 18.71 μ forbidden line obs. in Orion Nebula 77−5557
S III, CI calcs. of oscillator strengths, L-S framework 80−14089
S III, forbidden 18.71 micron emission obs. in galactic H II regions 79−97046
S III, S IV in Io plasma torus, Voyager 1 EUV emission lines obs. 80−26792
S III 18.7 μ fine-struct. forbidden line obs. in ionised nebulae 77−37637
sulphur continued
S III 9096 Å forbidden line in Orion Nebula, Fabry-Perot obs., abundance determ. 78−96515
S III forbidden lines in Omega Nebula (W38, M17, NGC 6618), IR spectra obs. 80−90495
S IV, $3s^23p^2P$-$3s3p^2\ ^4P$ multiplet, energy levels and transitions, appl. to solar atm. 80−87028
S IV, P-, D-, S-states, oscillator strengths, transition strengths, CI calcs. 80−922
S IV IR emission line obs. of NGC 7027, planetary nebula 79−21400
S IX, excited level populations, line intensity ratios, solar corona appl. 80−32637
S IX, O I like ion, solar emission lines density depend. 79−40165
S ion+Ti, KL^n X-ray satellites, intensity distrib., photoabsorpt. effects 78−78657
S isotopic comp. in atm. precip. around Sudbury, Ontario 78−81361
S V, VI, beam foil spectra, radiative lifetimes, oscillator strengths 77−30973
S VI, spectrum, 100-8000 Å, ionis pot. 79−93946
S VII, vuv beam-foil spectrum, lifetimes 79−81174
S X, ground configs., forbidden line intensities calcs. 80−23362
S X in solar corona, density-sensitive line ratio and electron densities 79−16906
S XI, UV lines, theoretical intensity ratios 78−90108
S XI and XII solar line intensities, OSO-7 obs. of limb brightening 78−69759
S XIII, beam-foil obs. of oscillator strengths for E1 transitions 80−14112
S XIV, splitting and oscillator strengths for $2s^2S$-$2p^2P^0$ doublet 77−49348
S XV, 1s2s ^3S-1s2p ^3P transitions, Lamb shift, VUV beam foil spectra obs. 80−52919
S XV, He-like ion, oscillator strengths of transitions between low-lying S and P states 78−13470
S XV, intercomb. line obs., in laser-produced plasma 78−9106
S XVI, H-like ion, anal. of satellites to reson. lines in X-ray region 77−88421
S^-, contracted Gaussian basis sets for mol. calcs. 80−83264
S^- ion-selective electrode, sensitivity, surface heterogeneity effects 78−92526
S^-, photodetachment, fine struct. transitions, photoelectron spectra 78−55151
S^-, photodetachment cross section mag. field depend. struct., obs. 78−55148
S^-, photodetachment in mag. field 79−41143
S^+, beam-tilted C foil interactions, charge-state distrib., photon emission, 100-400 keV 79−22814
S^+ charge transfer in diffuse nebulae 80−77463
S^+, ionisation pot., periodic regularities, relativistic corrections calcs. 79−49950
S^+, mobility in He, flow-drift tube meas. 80−43831
S^+, reson. line regularities in plasma Stark widths and shifts 80−43881
S^{11+}, charge state fraction on emerging from solids, K-shell vacancies effects 78−25686
S^{12+}, S^{13+}, in-shell dipole transitions, oscill. strengths, beam-foil spectra 77−71861
S^{15+}, charge state fraction on emerging from solids, K-shell vacancies effects 78−25686
S^{2-}, parameters for analytical radial orbitals, total and binding energies 77−6668
S^{2-}, positronium formation, Doppler broadened positron annihilation line shapes 80−45164
S^{4+}, static dipole quadrupole polarisabilities and shielding factors calc. using HF scheme 80−99450
S^{4+}, travelling in solids, Kα X-ray spectra 80−100706
S^{6+}, spectra, 500-1200 Å, lifetimes 78−62756
S^{n+}, fast highly charged ions, passing through foil, multiplet states equilib. population 77−10746
S:Si, implanted, defect signature by thermally stimulated meas. 78−91643
S/N gradient in M33 galaxy, supernova remnant evidence 80−56929
S-benzene systems, liq.-liq. phase separation 80−96658
S-$CaSO_4$:Dy pellets as fast-neutron TLD 78−73251
S-He discharges, stability, emission spectra 80−107003
S-I cycle for thermochem. prep. of H_2 by H_2O dissoc. 80−16823
S+Ar, 32 MeV, $K_\alpha{}^h/K_{\alpha\alpha}$ branching ratios, S projectile charge state depend. 79−63947
S+CS_2(OCS)(CH_4), electronically excited atom, reson. fluoresc. 80−99476
S+F^-, inner-shell ionisation, X-ray cross sections 80−58369
S+He(Ar)(N_2)(H_2)(Kr)(Xe), collision-induced emission of S(^{1}S), 232 and 425K 79−81264
S+inert gas, ^{1}S-^{1}D collision-induced transitions 78−33588
S+inert gas (N_2)(H_2), rare gas sulphide S(^{1}S) emissions 78−82828
S+O_2→SO_2, chemiluminesc. matrix reaction, diffusion controlled, 8-20K 78−61013
S+OCS→S_2+CO, reaction kinetics of S($^1D_2$) reactions 79−79274
S+S→S_2, chemiluminesc. matrix reaction, diffusion controlled, 8-20K 78−61013
S+Si^{n+}(Al^{n+})(Cl^{n+})(Ar^{n+}), K-shell vacancy sharing ratio 78−42198
S+X, (X=atom with Z=11-22), K-shell ionis. cross sections 78−13596
S^-+O_3, associative detachment, rate coeffs. 78−3325
S^-+SF_6→SF_5+F+S, electron affinity of SF_5 radical 80−45495
S^++alkali metal, charge exchange, negative ion form. 79−50128
S^++Ar, double K-vacancy prod., X-ray X-ray coincidence and fluoresc. yields obs. 78−55230
S^++Kr, charge exchange cross-sections *(German)* 77−10753
S^++NO→NO^++S+1.1 eV, rate consts. kinetic energy depend., drift tube meas. 80−7778
S^++O_2→SO^++O+0.26 eV, rate consts. kinetic energy depend., drift tube meas. 80−7778
S^{15+}+Ar, K-shell vacancy sharing, interference effects 80−5606
S^{n+}+Ar, molecular K-X-ray production, projectile charge depend. 78−90188
S^{n+}+Cl(Ar), branching ratio dependence on projectile velocity and nuclear charge 79−31475
S^{n+}+inert gas, electron promotion effects for small impact parameter 79−18278
S^{n+}+inert gas atom (n=5 to 9), small impact parameter collisions, charge exchanging processes 80−14227

sulphur continued
$S^{n+}+Ne(SiH_4)(H_2S)(HCl)(Ar)$, K X-ray cross section, projectile charge depend. 77−19029
$S^{q+}+O_2(Ar)(He)$, (q=6-16), K X-ray prod., charge-state depend. 80−106391
S_2, $^1\Delta_g$ and $^1\Sigma_g^+$ states, near IR emissions 80−18852
S_2, absorpt. spectra, matrix-isolated in Ar and Kr van der Waal solids 77−52139
S_2 and S_3, absorpt. spectra in Ar matrix 79−5149
S_2, at. force consts. and internuclear distance 77−42439
S_2 B-X system, Franck-Condon factors 79−94035
S_2, $B^3\Sigma_u^-$ state lifetime, fluoresc. decay rate meas. 77−42346
S_2, chem. pumped laser emitting visible radiation, construction possibility 79−13960
S_2, dissociative chemisorpt. on Ag(111), surface layer struct. changes 79−42383
S_2, effective spin-spin parameter, ab initio calc. 78−9067
S_2, fluoresc. quenching by He, Ar, Xe, N_2, S_2, CF_4, C_2F_6, fluoresc. lifetimes 78−46386
S_2, in Ar matrix, fluoresc. and excitation spectra 78−94271
S_2 in flames, laser induced fluoresc. meas. 78−61132
S_2, ionisation pot., by photodissociative ionisation study of CS_2 79−94044
S_2 laser, optically pumped, lasing obs. 470 to 480 nm 78−63095
S_2, low lying bound molecular electronic states 79−45643
S_2, matrix isolated in solid Ar, chemilum. 79−47529
S_2, matrix-isolated, $B^3\Sigma_u^-$ predissoc., relax. processes 80−58329
S_2, microwave spectra 79-150 GHz, rot. and fine struct. parameters 79−63987
S_2 mol. $B^3\Sigma_u^-\rightarrow X^3\Sigma_g^-$ fluorescence induced by N_2 laser *(Japanese)* 80−14175
S_2, optically pumped CW dimer lasers 80−14322
S_2, optically pumped superfluorescence molecular laser 80−63990
S_2, photoionisation processes, expt. techniques, theory, review 77−14402
S_2 polymerisation, kinetics obs. by pulsed field ionis. time-of-flight mass spectrometer 77−63890
S_2, tunable visible and UV laser, $B^3\Sigma_u^-$-$X^3\Sigma_g^-$ transition 77−42522
S_2 vibrational constants, UV absorption and fluorescence spectros. of S_x vapour, x=3 to 8 80−78631
S_2^- molecular ion in alkali halide crysts., peculiarities of luminesc. spectra 77−52174
S_2+N_2 *(Russian)* 80−99711
S_3, conformation, ab initio HFS method calc. 79−36526
S_3, open and ring isomers, electronic struct., ab initio SCF calcs. 77−57862
S_3^-, stabilized on MgO surface, CNDO calcs. of g-tensors and hyperfine coupling consts. 77−83625
S_4^{2+} and S_4^{2-}, structure investigation by ab initio calcs. 80−69066
S_4^x, x=2−, 0, 2+, struct. differences explained, SCF Xα scatt. wave MO calcs. 78−74784
S_7, Raman and IR spectra, vibr. anal., force consts., thermodynamic functions 78−50545
S_8, cyclic, electron deformation density distrib., SCF-Xalpha-scatt. wave method 78−33425
S_8 rings, vibr. spectra and thermodynamic functions *(German)* 78−82742
S_8, X-ray photoelectron spectra, S2s and 2p levels binding energies 77−6844
S_8^{2+}, electronic struct. and localised MOs, bonding nature and geom. struct. 80−18798
S_8-1,2,-propylene sulphide, copolymer preparation method, anionic copolymerisation 78−64836
S_n, (n=2-12), vibr. spectra and thermodynamic functions *(German)* 78−82742
S_n, properties of small aggregates rel. to metallic character of Te_n 78−86985
S_n^{2-} (n=4-8), vibr. and rot. isomers, Raman spectra *(German)* 78−13504
$S_n+4H_2O\rightarrow 3H_2S+H_2SO_4$, chem. equilib. of aq. system, application to Venus and Io 80−50837
S_x vapour, x=3 to 8, UV absorption and fluorescence spectros., vibrational constants of S_2 80−78631
$S_2(B\,^3\Sigma_g^-, v'=10)$, radiational transitions probability calc. 77−1924
$S_2(B\,^3\Sigma_u^-)$+inert gas $(H_2)(N_2)(S_2)$, collision-induced energy transfer 79−3544
$S_2(B^3\Sigma_u^-\,v=4)$+He(Ar)(Xe), collision-induced transfer rates 79−94062
S(^{1}D, ^{3}P) isoelectronic series, Sternheimer valence shielding and anti-shielding factors 80−18807
$S(^3P)+N(^4S)$, $NS(B^2\Pi)$ form. kinetics, chemilum. obs. 79−39151
$S_{12}(S_{12}.CS_2)$, vibr. spectra and thermodynamic functions *(German)* 78−82742
SXI, solar emission lines, density dependence 80−21963
^{32}S 96 MeV heavy ion ps pulses, rebunching of MP Tandem pulses by spiral resonator 78−33357
^{32}S ions+Be(C)(Ni), radiative electron capture, X-ray ang. distrib. 77−38729
^{32}S kaonic atom, level shifts and widths, $\Lambda(1405)$ dynamics in nucleus 77−3495
^{33}S, nucl. mag. screening in SH_2, pseudopot. calcs. 79−6879
$^{33}S/^{32}S$ ratio in ocean water SO_4^{2-} 78−65340
^{34}S in natural waters, appl. to tracing of air and water pollution *(Italian)* 77−53078
^{34}S in troilite, enrichment rel. to lunar soil 80−77303
$^{34}S/^{32}S$ ratio in magmatic gases of Afar ridge volcanism 80−21732
$^{34}S/^{32}S$ ratio meas. using SO_2 and SF_6 methods, discrepancies 78−65405
$^{34}S/^{32}S$ ratios in California stratus rel. to aerosol and cloud drop origin 77−29407
^{35}S content of coolant gas in Windscale AGR, gas chromatographic and radiochemical anal. 78−73125
^{35}S diffusion in NiO crystals, simultaneous diffusion by two different modes 80−59720
S=H^+, 4 MeV beam-foil X-ray production cross-section 79−7003
$1/2S_2(g)\rightleftarrows S(1)$ equil. reaction, improved ΔG^0 values calc. 77−32822
Si:S, deep level characterisation, implantation predeposition technique 80−100444
Si:S, electron-nuclear interactions during pumping, influence of mag. field 79−95378
Si:S, existence of isotope shift for S deep level, isothermal transient capacitance meas. 78−63999
Si:S, γ-irrad. influence on elec. props. 80−6845

sulphur continued
Si:S, IR absorption and photocond., donor levels 77−55809
Si:S, i.r. photodetector, background-limited operation near 77K 77−122
Si:S, two-electron donor centre, photoionisation cross sections meas. 77−8044
Si:S diode, ionisation energies of S levels, photocapacitance meas. 77−4432
Si:S IR detectors, performance and elec. transport props. 78−45702
Si:S p^+-n junction, optical props., photocurrent meas. 77−4425
SnO_2:Sb,S CVD thin film, resist. temp. coeff. 79−38198
$SrCl_2$:S, S_2 and S_3^- mol. paramag. centres, investigation using EPR, Raman and optical spectroscopy 79−51855
TiO_2:S, acceptor properties of S, free electron concentrations 80−34395
TiO_2:S, in $O_2+CO_2+SO_2$ atmosphere, elec. cond. study 80−39583
ZnP_2:S, optical absorpt. spectra in range 0.5 to 2.2 eV 80−66250
ZnS:S, photoconductivity and negative differential photo-effect 78−39156
p-$ZnSiAs_2$:Au(Tl)(S), photoluminesc., radiative recombination 77−24883

sulphur compounds
aerosols, in atm., phys. props. 78−96285
aerosols, techniques for chem. comp. determ. 78−95976
air pollutants, conc. meas. with flame photometric apparatus 80−16883
air pollutants, conf., Dubrovnik, Yugoslavia (Sep. 1977) 78−96281
air pollutants, conf., Dubrovnik, Yugoslavia (Sept. 1977) 79−20965
air pollutants, detection using continuous flame photometric detection system 80−81508
air pollutants, large scale study in Canada 79−20979
air pollutants, long-range transport, OECD study assessment 79−20967
air pollutants, long-range transport modelling, OECD study 79−20970
air pollutants, natural and man-made emissions in Europe 79−20968
air pollutants dispersion over western Europe 79−70490
air pollutants long term deposition calc. for Europe 79−20971
air pollutants long term region patterns in Europe 79−20973
air pollutants transform. and removal, time-dependent diffusion model 79−20972
air pollution, continuous in situ meas. by flame photometry and thermal analysis 78−96296
air pollution removal mechanisms and processes *(Dutch)* 77−70824
airborne sulphates, dry deposition vel. on snow surface 77−2231
alkali halide:$SH^-(D^-)$, band centre shift 77−16346
atmosphere, information exchange concerning S compounds pollution in European Community 80−7979
atmosphere S compounds, homogeneous chemistry 78−49119
binary, with non-transition elements, at. vol. and semicond. props. 77−20089
Black Sea sediment cores, S and organic compounds geochemistry 78−49040
chalcogenide glass film, M-Sb-S-I, (M=Ge, Sn, Pb, Cd, Cu), prep. and characterisation 77−12533
CO SO_4^{2-}, atm. aerosols long-distance transport rel. to visibility, London, England 79−21015
compressed SF_6, repeated breakdown field strength in uniform field perturbed by protrusion 80−96406
concrete and mortars, containing S, durability study in temp. cycles and water resistance 78−27613
electronic struct. of some 2- and 4-valence states *(French)* 77−10591
ESCA shifts and effective charges 80−78648
ESCA using Au M_α X-rays (2123 eV) 78−72683
fluoromethane-SF_6 496-μm optically pumped laser, energy-transfer mechanisms 80−99712
Freon-12(22), gas, Rayleigh vol. scatt. coeffs., spectronephelometric meas. 78−14127
glass, flat, dependence of microbrittleness on SO_3 conc. 78−84960
graphite bisulphate, intercalation compounds, development as reagents in organic synthesis 78−27444
homogeneous oxidation in atmosphere 78−96258
metastable S species and trace metals in hot brines from French Dogger 79−62527
methane-SF_6, single-photon absorption reaction chemistry in solid state 77−73454
muonic capture rates in elements of compounds, influence of chemical bond 78−58874
one-electron binding and Auger energies 80−52872
oxide pollutants, SURE/MAP3S obs. comparison with regional model predictions 80−81501
oxides and S-bearing pollutants sensing with gas conc. cells 77−70842
pollutants wet removal from atmosphere 79−2363
polynaphthoquinone-SO_2-I_2 system for H_2O decomposition for H_2 production 80−16825
rare-earth mixed sulphides, of type $L_4Lu_{11}S_{22}$, cryst. struct. *(French)* 79−77575
reduced, emission from open oceans 79−70805
rot. spectra, 714-1667 μm, Fourier interferometric spectrometer 77−83765
salt toxic effect on activated sludge micro-organisms *(Chinese)* 79−24919
SF_6, buffered, 10.6 μm transmission props. for nanosecond pulses 80−58644
SF_6 IR mass absorption coefficients, 3 to 15 μm 79−76422
$(Sn)_x$ chain, energy band struct., Hartree-Fock and CDW solns. 79−23885
$(SN)_x$-GaAs polymer-semiconductor solar cells 79−15219
SO_2 air pollution levels modelling and forecasting, statistical approach 78−81398
SO_2 diffusion-coupled oxidation in atmosphere 78−65371
SO_2 max. surface conc. from moderate-sized power plant rel. to power plant load 79−83659
SO_2 molecules in air, remote sensing methods assessment *(Japanese)* 78−96288
SO_2 pollution levels, in Venice, meteorological factors 77−91253
steels, obs. and anal. of sulphides, using non-aqueous electrolyte-potentiostatic etching method *(Japanese)* 80−89433
sulphate, atmospheric, concs. comparison with analytical diffusion model for pollutants long distance transport 80−94125
sulphate additions and cation leaching in Douglas fir ecosystem 77−78392
sulphate aerosol, atmospheric, individual submicron particles detect. technique 78−69527
sulphate aerosol, atmospheric, meso-scale transport obs. in rurual East Midlands, England 80−94124

sulphur compounds continued
sulphate aerosol layer in stratosphere, processes, models, obs. and simulations 80−109212
sulphate aerosols, atmospheric, diurnal var. at rural sites in E.United States 80−30621
sulphate based binary solid electrolytes, props., appls. 77−84971
sulphate concentration, Southwestern Desert of US, X-ray emission anal. 80−8378
sulphate concentrations in atmosphere, correl. with total nitrate concs. 80−94123
sulphate concs. in New YOrk State, summertime trajectory analysis 79−34882
sulphate deposits, stable isotopic comp. and early Archaean origins 79−20832
sulphate particle formation by heteromol. nucleation and condensation in cavities 80−26183
sulphate reduction and marine sediment deposition rate 78−53642
sulphate residues of fresh waters, elemental, anal., spectrographic technique *(Russian)* 77−12868
sulphate solutions, electrodeposition of In, electrode reactions 78−88436
sulphate washout from stack plumes 77−37327
sulphate-water O isotope thermometry for geothermal systems 78−69383
sulphates, brine sulphate anal. by atomic absorpt. 80−89556
sulphates, residence times under non-steady-state conditions 80−77092
sulphates dissolved in hot springs and drill holes, geothermal reservoir temp. determ. using O isotopes 78−69382
sulphates in atmospheric particulates, analysis 79−83685
sulphates in Canadian air, long-range transport 79−16561
sulphates in particulate form, air quality over Los Angeles and New York 80−61483
sulphates in photochemical smog, atm. visibility reduction 77−21904
sulphide compounds of Si, Ge and Sn, struct. and chem. bonding *(French)* 78−30580
sulphide determination by gas-phase molecular absorption spectrometry 79−29430
sulphide melt, conc. EMF meas. using solid-electrolyte cell 77−40571
sulphide minerals, superstructure and modulated struct. 79−99146
sulphide minerals in CI carbonaceous chondrite meteorites, origin 79−80282
sulphide minerals in Mid-Atlantic Ridge drill core, chemistry 77−91122
sulphide ore deposits in NW.Kola Peninsula, electric near zone field development method testing *(Russian)* 80−85761
sulphides, direct leaching 77−29033
thiocyanate complexes at Ag electrode surface, Raman spectroscopic study 80−37813
thiophosgene, IR spectra, gas, liq. and matrix isolated, mol. force consts. *(German)* 79−36640
unstable molecules, forbidden transitions, laser optoacoustic spectroscopic obs. 77−61756
viscosity and diffusion coeffs. 77−89225
water-soluble, anal. of atmospheric aerosols 78−96282
$X^2\Pi_{3/2}$-state, far IR LMR spectra 79−6954
Ag-As-S system glass, struct., props. and vibr. spectra 79−65901
Al_2O_3 production, removal of S compounds in Na_2O-CaO sintering *(Chinese)* 80−55323
Ar:OCS, liq., dissoc. studies 80−78716
Ar-SF_6, thermophysical props., second virial and diffusion coeffs., thermal diffusion factors 78−42699
Ar-SF_6, volume discharge excited by electron beam, stable region *(Russian)* 78−22589
Ar+$N_2(SF_6)$, proton excited, time resolved VUV, UV and visible emission 77−14547
As-S, amorphous, glass transition and specific heat, intermolecular bond saturation 80−15011
As-S, amorphous film, photoinduced RI changes, heterodyne interferometry 77−3639
As-S, melt struct., orientation birefr., viscosity, refr. index, and density 80−84713
As-S amorphous film, photo-induced optical changes, annealing effect 78−27345
As-S chalcogenide glassy semiconductors, induced anisotropy 79−32013
As-S film, guided light reversible control by electron beam irrad. 78−1331
As-S glass media, temp. control of hologram props. 78−17883
As-S glasses, acousto-induced structural changes, optical props. 80−49122
As-S glasses, resonance Raman scatt. 80−50325
As-S semiconducting glass film holographic recording media *(Russian)* 77−10864
As-S system, glass forming ability and phase diagram 78−59760
As-S-I system glasses, IR transmission spectra, structure-chem. comp. 79−42974
As-S-Te, vitrification, density and elec. cond. measurements 79−7645
As-Sb-S-I system glasses, vitrification and volt-ampere characts. 77−31756
As-Se-S-Ge chalcogenide glass films, appls. to passive optical waveguide components 79−37048
As-Se-S-Ge chalcogenide amorphous film, computer-generated holograms using electron beam irrad. 80−95846
As_2O_3-SO_3, polarised Raman and IR spectra, force field calc. *(French)* 78−6674
As_2S_3, amorphous, elec. cond. at room temp., contact effect 77−20354
As_2S_3, thermal expansion at low temperatures 78−83982
As_2S_3-Ag light sensitive material, development of non-interchangeability under continuous laser radiation *(Russian)* 80−50870
As_xS_{1-x}, chalcogenide, covalent non crystalline topology, short range order 80−15009
As_xS_{100-x} amorphous film, photoinduced changes in optical props. 80−50445
$As_{40}S_{25}Se_{25}Si_{10}$ glass film, transient photoinduced absorpt. 77−40295
$AsS_{3.5}Te_{2.0}$ glass, gamma-irradiated, TSC meas. 77−66166
$As_{40}Se_{50-x}S_xGe_{10}$ film strip-loaded waveguide formed in graded-index $LiNbO_3$ planar waveguide 78−74965
$AsTeS_x$, chalcogenide glass, thin film crystallisation 79−7758
$As_xTe_yS_yS_{e100-3x}$ glasses, IR absorpt. spectra 77−12378
B-S compounds, relative antiwear efficiency 78−35532
Ba+SO_2→BaO+SO reaction, laser-induced fluoresc. obs., vibronic distrib. of BaO, collisional energy depend. 80−11917
Bi-S liquid soln., S activities meas. by EMF method *(Japanese)* 80−70425

sulphur compounds continued
Bi-Sb-S-I system glasses, vitrification and volt-ampere characts. 77−31756
CO-O_2-SF_6, liquid, phase matched IR third harmonic generation 78−42384
CO-SF_6, single-photon absorption reaction chemistry in solid state 77−73454
COS attack on Cu, kinetic and morphological study *(French)* 79−43488
Ca-S-O system, sulphide-sulphate equil., solid state EMF obs. 79−83492
$CdS_{1-x}Se_x$ film, resonance between Se atom dipole vibr. and interference modes, IR spectra obs. *(Russian)* 80−2888
ClO^-+NO$(NO_2)(SO_2)(CO_2)$, rate consts. at 300K 78−76829
Cu-Ni sulphidised alloys, Ru and Os behaviour during carbonylation *(Russian)* 80−40584
Cu-Sb-S-I amorphous film formation and stimulated crystallisation, electrophysial props. *(Russian)* 78−30838
Eu-As-S, glass forming region, Raman and IR obs. *(French)* 79−99080
Fe-S eutectic, Lindmann's melting law, solid-liquid core boundary, core mantle boundary 78−18743
Fe-SO_4-H_2O suspension system at 90°C, potential-pH diagram 78−61068
Ge-Bi-S system, semicond., elec. cond., glass transition temp. and optical absorption meas. 77−16329
Ge-S, amorphous, photocond., photo-induced ESR, optical edge shift 80−49809
Ge-S, glass, ESR, model of paramag. defects 79−78517
Ge-S amorphous film, defect states, ESR 80−49670
Ge-S glass, melt-quenched photoinduced ESR, annealing behaviour and glass comp. depend. 80−71156
Ge-S-Ga amorphous thin film, memory switching effects 80−88605
Ge-S-Ga(In) system glasses, photoinduced changes 80−24365
Ge-S-In, chalcogenide glass, determ. of glass phases, phys. props. meas. 79−23526
Ge-S-Sb glasses, microgravity effect on recrystn., optical and elec. props. 80−49127
Ge-S-Se, glass formation 80−103251
Ge-Si-S system, glass formation, transition temp., crystallisation and melting 80−100178
$Ge_xAs_xS_xSe_{100-3x}$ and $Ge_xTe_xS_xSe_{100-3x}$ glasses, IR absorpt. spectra 77−12378
$Ge_{33}As_{27}S_{15}Te_{25}$, chalcogenide thin films, coupled carrier theory test, high field conditions 80−100466
$Ge_{33}As_{27}S_{15}Te_{25}$ glass, switching, microstructural changes 79−65523
GeS_2, thermal expansion at low temperatures 78−83982
$Ge_{25}S_{75}$:Mn, bond struct. and character in Ge-S system, EPR obs. 80−66014
$Ge_{30}S_{70}$ glass film, Ag photodoping sensitivity 80−39121
$Ge_{40}S_{60}$, $Ge_{25}S_{75}$ glasses, Mn^{2+} EPR spectra investigation 79−11340
$Ge_{40}S_{60}$ glass, Cu doped, EPR study 79−65713
$Ge_{40}S_{60}$:Mn (Ag)(Cu), bond struct. and character in Ge-S system, EPR obs. 80−66014
$Ge_{42}S_{58}$, amorphous, bulk and film forms, elec. props. and ESR study 80−103691
Ge_xS_{1-x}, chalcogenide, covalent non crystalline topology, short range order 80−15009
H production, thermochem. H_2O decomposition using S compounds, feasibility anal. 80−35768
H, thermochemical prod. using S-Br cycle, development of lab.-scale plant 80−35774
H_2+SF_6 (tetrafluoromethane), collision-induced simultaneous transitions, IR spectra 77−50438
HI-SF_6 system, HF pulsed chemical laser 80−106514
HI-SF_6 system, HF pulsed chemical laser 80−106515
HS_2 radical, ab initio calcs. of geometry and spectra 77−34552
H_2S atmospheres, formation of contaminating layers on elec. contact materials *(German)* 80−71811
H_2S, effect on mech. strength of S, S concrete, S mortar 77−4818
H_2S, KLL Auger spectrum, obs. and ab initio SCF CI calc. 78−50654
H_2S, S K-LL Auger energies and chemical shifts 80−28069
HSO radical, ground and excited first states, ab initio SCF and CI calcs. 77−30776
H_2SO hypothetical molecule, nonempirical STO calc. of chem. bonds 80−23307
H_2SO_4 atmosphere-aerosol study of Venus cloud microstructure and optical props. 80−72808
H_2SO_4, Fe passivation, model for anodic dissolution 80−35545
H_2SO_4 gas phase meas. in stratosphere 80−36366
H_2SO_4 soln., opt. consts. in far IR 77−8574
H_2SO_4-H_2O droplets in atmosphere, equilib. size and comp., quick estimation method 79−66767
H_2SO_4-SO_2 thermochemical cycle for H_2 prod., electrochem. aspects 80−97812
H^*_2+$H_2O(SF_6)$, ionis. collisions 79−64088
I^-+SO_2, endoergic reaction, time-of-flight mass spectral obs. 77−12785
$IrSn_{1.5}(Ge)_{1.5}S_{1.5}$, new skutterudite relation compounds, prep. and charact. 78−52700
KBr:SO_4^{2-}, $Ba^{2+}(Ca^{2+})$, IR absorpt. band parameters, temp. depend. *(Russian)* 78−31226
KBr:SO_4^{2-}, IR absorpt. spectra, cation impurity influence *(Russian)* 78−10901
KCl:SO_4^{2-}, $Ba^{2+}(Ca^{2+})$, IR absorpt. band parameters, temp. depend. *(Russian)* 78−31226
KCl:SO_4^{2-}, self-diffusion, lattice defect props. 77−4216
$KClO_4$:SO_4^{2-}, AC elec. cond. and dielec. loss meas. 80−59699
K_2CrO_4:SO_4^{2-}, IR absorpt. spectra, local symmetry of impurity ions *(Russian)* 78−2893
$KHSO_4$:SO_3^-, X-irradiated, ESR saturation 78−80220
$K_xRb_{1-x}Cl$:HF_2^-,SO_4^{2-}, nonuniform broadening of IR vibr. absorpt. bands of impurities *(Russian)* 77−16357
KX:SO_4^{2-}, X=Cl,Br, impurity ion IR spectra analysis *(Russian)* 77−85762
Li/SO_2 cells, DTA, safety studies 80−81428
Li/SO_2 cells, safety studies, DTA of constituents 80−16795
Li/SO_2 cells, safety studies, kinetics of Li-organic solvent exothermic reactions 80−72030
Li/$SOCl_2$ cells, high rate discharge characts. 80−72021
Li/$SOCl_2$ hermetic primary cells, effect of type of C on performance 80−35661
Li/$SOCl_2$ primary cell, cyclic voltammetric and coulometric obs. of $SOCl_2$ reduction 80−30440

sulphur compounds continued
$Li/SOCl_2$ primary cells, $SOCl_2$ reduction mech. in supporting electrolyte 80−108792
$Li\text{-}SOCl_2$ battery for implantable cardiac pacemakers 80−30939
$Li\text{-}SOCl_2$ cells, discharge reaction mechanisms 79−100504
$Li\text{-}SOCl_2$ hermetic D cells, effect of $Li_2B_{10}Cl_{10}$ and $Li_2B_{12}Cl_{12}$ on performance 80−12000
$Li+SnCl_4(PCl_3)(SF_6)$, product mag. deflection slotted disc vel. anal. mol. beam kinetics 77−25250
Mn, corrosion, at high temp. in pure SO_4 80−50774
Mn-S-O system, sulphide-sulphate equil., solid state EMF obs. 79−83492
Mo_6S_8Sn, triple chalcogenide, NMR spectra in supercond. state *(Russian)* 80−93194
$N_2\text{-}SF_6$ laser, UV, discharge-excited, improvement in efficiency *(Japanese)* 78−33724
$N_2\text{-}SF_6$ mixture electrode surface roughness effect on breakdown voltage 77−39490
$N_2\text{-}SF_6$ pulsed discharge laser with CW X-ray preionisation 80−95910
$NH_3+NaSCN$, coolant for solar refrigeration *(French)* 79−24911
$NH_4ClO_4{:}SO_4^{2-}$, thermal depolarisation, relax. parameters 78−43779
$NO\text{-}SF_6$, single-photon absorption reaction chemistry in solid state 77−73454
$N_2O\text{-}SF_6$, single-photon absorption reaction chemistry in solid state 77−73454
$NO^+(NO)+SO_2$, cluster form., equilib. const. and rate coeffs., UV irrad. effects 77−60060
$NO(N_2O)\text{-}SF_6$, single-photon absorption reaction chemistry in solid state 77−73454
$NO(N_2O_3)\text{-}SF_6$, single-photon absorption reaction chemistry in solid state 77−73454
NSF_x, geometry and stability, LCAO-MO SCF calcs. 79−31391
$Na(3^2P)+O_2(SO_2)$, near-threshold ionis. of Na* 77−88544
Ni, corrosion rates in $SO_2\text{-}O_2\text{-}SO_3$ atmospheres under simultaneous sulfidation-oxidation 79−79162
Ni-S incongruently subliming system, SEM and TEM obs. of high temp. transitions, temp.-comp. diagrams 80−104136
$OCS\text{-}N_2\text{-}SF_6$ mixture laser, OCS photodissociation, electron dipole forbidden transition, absorpt. spectra 79−68389
P-S, amorphous, glass transition and specific heat, intermolecular bond saturation 80−15011
$\alpha\text{-}P_4S_4$, cryst. struct. 78−51486
$P_2Se_xS_y$ glass, thermophysical props., 303-413K, struct. interpretation 78−47615
P_2Se_xSy glass, vitrification temp., elec. props. and hardness meas. *(Russian)* 77−28177
$2PbO\text{-}SiO_2\text{-}xSO_3$ melts, crystn. 80−59400
$4PbO.PbSO_4$, paste mixing and curing for Pb acid batteries, effect of CO_2 79−61968
$RhGe_{1.5}S_{1.5}$, new skutterudite relation compounds, prep. and charact. 78−52700
S containing small paramag. ions on MgO g-tensors and spin densities 78−46270
S-based amorphous semicond. film, prep. by plasma decomp. of $H_2S\text{-}N_2\text{-}NH_3$, and characterisation 80−80422
S-N system, inorganic, electronic struct. obs. by photoemission XPS and UPS, CNDO calcs. 80−78653
S-Ni-Fe system containing monosulphide solid soln., elec. and struct. relations 80−90038
S-O-C, equilibrium 550 to 1100°C 79−38807
S-S bond chirality, biomolecule struct. and activity depend., review 78−27889
S-Se amorphous alloys, crystn. kinetics, elec. cond. meas. 78−34441
S-Se-Te semicond. glasses, mag. suscept. meas., refractive index 78−34952
S-Se(Te)(Tl), liq. semicond., bonding energies and entropies, mag. susceptibility meas. 80−49082
$S_2{}^{35}Cl_2$, microwave spectra and double reson., assignments, distortion consts. and struct. 79−89664
S_3^-, adsorbed on MgO, g-tensors, spin densities, CNDO calc. 78−46270
S_6, partial discharge disintegration product meas. *(Czech)* 78−67450
SB_2 photoelectron spectra, visual assessment stripping program anal. 80−28062
SBr_2, SI_2, matrix isolated, IR spectra 80−58254
SBr_2, transient species, He(I) photoelectron spectroscopy, discrete variational HFS calc. 79−31594
SC_6, electric breakdown voltage hysteresis, electrode coating effects 78−87553
SCF_2, IR, Raman and matrix isolation spectra, isotopic shifts, anharmonicity consts. *(German)* 77−83600
SCN^-, associated with metallic cations in aq. soln., press. effect, Raman spectra *(French)* 78−80333
SCN^-, electron density distrib., theoretical and expt. determ. 77−61683
SCN^-, linear mol., Compton profile bond additivity, HF calc. 79−68268
SCN^-, positronium formation, Doppler broadened annihilation line shapes 80−45164
$SCN^-+Fe(III)$, reaction kinetics, computer-controlled stopped-flow system 79−15953
$(SCN)_2$, prep., UV photoelectron spectrum and structure 80−28059
$(SCN)_2{}^-$, reson. Raman spectrum, vibr. freqs. 79−18189
$SC(NH_2)_2$, ferroelectric transitions, based on model thermodynamic pot. 78−80295
SCO, linear mol., Compton profile bond additivity, HF calc. 79−68268
SCO, S atom $L_{II,III}$-absorption spectra 78−86807
SCO^-, adsorbed on MgO, g-tensors, spin densities, CNDO calc. 78−46270
SCl_2, electronic struct., group theoretical and CNDO/2 calcs. 78−33419
SCl_2, microwave spectrum, quadratic pot. function, average struct. 77−65456
SCl_2+H, energy disposal, HCl IR chemiluminesc. obs. 78−92484
SCl_4, electronic struct., group theoretical and CNDO/2 calcs. 78−33419
S_2Cl, blue absorpt. in Ar matrix 79−5149
S_2Cl_2, electronic struct., group theoretical and CNDO/2 calcs. 78−33419
S_2Cl_2 treatment of PVC grafted butyl rubber, increase in tensile strength 79−95993
S_2Cl_2 UV photolysis in matrices, $SSCl_2$ IR spectra 78−61033
S_2Cl_2+alkali metal, matrix reaction, examination by laser excitation 79−5148
S_2Cl_2+alkali metal, matrix reaction, S_2Cl absorpt. spectrum 79−5149
S_2Cl_2+H, energy disposal, HCl IR chemiluminesc. obs. 78−92484

sulphur compounds continued
$S_2Cl_2+M\rightarrow S_2{}^*+MCl_2$, (M=Ba, Sr, Ca), crossed-beam chemiluminesc. 77−29009
S_2Cl_2+N, $NS(B^2\Pi)$ form. kinetics, chemilum. obs. 79−39151
S_4Cl_2, Raman spectra, vibrs. and rot. isomers of $S_n{}^{2-}$ (n=4-8) *(German)* 78−13504
SCl(Br), unstable radicals, matrix-isolated, IR spectra force const. *(German)* 80−43053
SF_2, ab initio LCAO MO SCF calcs., elec. struct., mol. props. 77−14344
SF_2, bond function parameter transferability 77−30770
SF_2, generalised VB calcs. of electronic struct. 77−57881
SF_2, geometry optimisation, ab initio MO calcs. 77−42232
SF_2, He I photoelectron spectra 79−10148
SF_2, microwave spectrum inertia defects, ν_1, ν_3, ν_2, equilibrium structure, vibration rotation constants, anharmonic potential functions 79−93988
SF_2, photoelectron spectra, ionisation energies, ab initio many-body Green's function calc. 79−89709
$^{32}SF_2$, $^{34}SF_2$, matrix IR spectra, vibr. and force fields, bond angle *(German)* 78−74662
SF_4, ESCA chemical shift, energy levels, SCC-MO calcs. 79−64045
SF_4, generalised VB calcs. of electronic struct. 77−57881
SF_4+ClF, thermal and photochem. reactions investig. 80−61117
$SF_4+O^+(Cl^+)$, S highly stripped core ion outer shell arrangement, Kα X-ray spectra 77−3451
SF_5, anisotropic ESR spectrum in γ-irrad. SF_6 77−21400
SF_5, IR spectrum, form. by VUV photolyses in Ar matrices 78−981
$SF_5{}^+$ ion-molecules, IR multiple-photon dissoc., lifetime meas. 80−28072
SF^+s, ion-mols. in beam, IR multiple-photon dissociation, mass spectroscopic detect. 79−89720
$SF_5{}^-+SF_3{}^+$, ion recombination, flowing afterglow, cross section meas. 77−44473
SF_6, ^{19}F NMR, chem. shielding, intermol. interactions and rovibr. motion effects 78−9171
SF_6, ^{19}F NMR vibr. anharmonicity effects 80−91580
SF_6, 10.4 μm laser pulse transmission 78−14128
SF_6 10.5 μm spectrum, high-J assignments, identification of levels pumped by CO_2 P(12) and P(22) 78−70837
SF_6, 20 kA arc, electrode vap. contamination, time depend. energy balance 78−87525
SF_6, $3\nu_2$ vibr. spectra 78−55183
SF_6, $3\nu_3$ band anal., IR spectra 78−90161
SF_6, 40 kA arc, time-resolved temp. and radius meas. using rapid-scanning polychromator 79−50907
SF_6, ab initio electronic struct., and photoelectron spectral assignment 79−54764
SF_6, absorpt. of intense laser radiation, vibr. excitation 80−9667
SF_6, absorpt. structs. in VUV region 79−3458
SF_6, absorption of intense IR radiation, statistical model 77−34626
SF_6, addition to high-press. N_2 laser, enhancement of output power 78−25859
SF_6 addition to N_2 laser discharge, negative ion prod., altered discharge parameters 80−38818
SF_6, adsorption on Cs ion source, thermionic emission 80−71557
SF_6, adsorption on Ru (001), XPS exam. 77−55866
SF_6 and atmospheric tracer gases, electron capture detection method 77−25785
SF_6 and $SF_6\text{-}N_2$ mixture, elec. breakdown and corona stabilisation obs. 78−87582
SF_6 and $SF_6{}^+$, excited states investig. 77−57882
SF_6 and SF_6-air mixture gas under impulse voltage, discharge phenomena *(Japanese)* 80−96409
SF_6, arc, temp. determ. accounting for demixing 80−70057
SF_6, arc discharge, decomposition products for SF_6 with H_2O and organic gas contaminants 79−10743
SF_6 arc field distrib. and conductance in current-zero region 78−71590
SF_6 arcs, optically thick, convection-loss dominated model 78−87519
SF_6 arcs in axial flow at const. press., steady-state charact. 78−1940
SF_6, atm. conc., rel. to tropospheric OH conc. 77−45069
SF_6, atmospheric global distrib., sources and sinks, rel. to 0_3 depletion 80−4088
SF_6, Auger emission anomalous spectra and yield, chemical species depend. 78−55152
SF_6 avalanche breakdown as stochastic process 78−67574
SF_6 axially blown arc, current-zero behaviour, theoretical model 80−38789
SF_6 based broadband gas isolator, for high power CO_2 lasers, design and evaluation 78−42339
SF_6 binary collision-induced light scatt., rot. Raman scatt. 80−78660
SF_6, binary collisions induced light scatt. 80−83428
SF_6, bond order and Raman intensity, delta function eqn. 77−61693
SF_6, breakdown at high pressure, possible cosmic ray effects 78−87577
SF_6 breakdown at moderate temps., investigation 79−27863
SF_6 breakdown charact. in non-uniform field gaps, at 0.8-2 MV range 77−15269
SF_6, breakdown charact. for 0.8 to 2.6 MV range 78−87552
SF_6 breakdown distributions, low-value fractile determ. 78−67578
SF_6 breakdown field strength, electrode surface roughness tolerance 78−67577
SF_6, breakdown performance under mixed voltages *(German)* 77−3999
SF_6, breakdown voltage at high pressure meas. *(German)* 77−55181
SF_6 breakdown voltage calc. based on elec. field strength values *(German)* 77−15264
SF_6, breakdown voltages dispersion, anal. 80−38772
SF_6, bubble formation during injection, system pressure and thermophysical effects *(German)* 79−41745
SF_6, CO_2 laser, SF_6 intracavity hysteresis, bistability, critical behaviour onset and extinction of lasing 79−98336
SF_6, CO_2 laser excited, optoacoustic meas. of energy absorpt. 77−83667
SF_6, CO_2 laser induced dissociation, energy and press. depend. 77−23523
SF_6, CW CO_2 laser spectroscopy 80−83367
SF_6, catalysis and quenching of N_2 afterglow 78−51376
SF_6 circuit breaking arc, plasma diagnostics *(Japanese)* 78−55768
SF_6 circuit-breaker, non-LTE plasma props. and at. processes, medium to high press. 80−59170
SF_6, clusters, collision induced polarisability, mol. frame distortion 80−32798
SF_6 coaxial gap breakdown probability determ., influence of meas. procedure 78−67579

sulphur compounds continued
SF_6, coexisting densities, revised and extended scaling 78−34613
SF_6, coherent emission, caused by pulsed laser in low-density gas 79−18389
SF_6, coherent resonance in pulsed fields 79−68375
SF_6, collision induced rot. Raman scatt., polarisability effects 78−86874
SF_6, collision-induced forbidden Raman transitions 77−6791
SF_6, collision-induced Rayleigh scatt. intensity calcs. 77−46569
SF_6, collisionless dissociation and isotopic enrichment, using CO_2 laser 77−18999
SF_6, collisionless dissoc. using two reson. freq. CO_2 laser fields 78−5305
SF_6, collisionless dissociation, spectral struct. of low level excitation 78−74714
SF_6, collisionless dissociation in intense IR field 79−87858
SF_6, collisionless fluoresc., 16 μm, following laser pumping, vibr. quasicontinuum 78−42111
SF_6, collisionless intramol. vibr. relax., time-resolved spectra 78−82777
SF_6, collisionless intramolecular vibr. relax. obs. 79−45706
SF_6, collisionless multiphoton laser dissoc. mechanism 77−503
SF_6, collisionless multiphoton dissoc. rate, statistical thermodynamic process 77−50482
SF_6, collisionless multiple-photon laser excitation, anharmonic splitting effect 77−61815
SF_6, collisionless multiphoton dissoc., statistical theory 78−62862
SF_6, collisionless multiple-photon excitation, mol. rot. and vibr.-rot. interaction effects 78−74720
SF_6, collisionless multiphoton dissoc., statistical thermodynamic process 78−82799
SF_6, collisionless multiphoton excitation and V-V energy transfer, coherent versus stochastic theories 78−82804
SF_6, collisionless multiphoton excitation, anharmonic oscill. model rot. effects 78−86845
SF_6, collisionless multiphoton energy deposition and dissoc. 79−61884
SF_6, collisions, laser spectroscopy investig. 80−9697
SF_6, comparison of dielectric and refractive virial coefficients and collision induced absorption bands 79−86547
SF_6, comparison of multiple-photon excitation models 78−94297
SF_6, compressed, influence of electrode macroscopic curvature upon surface roughness effects 80−40693
SF_6, compressed, ion mobility and recombination 79−60098
SF_6, compressed, low probability first breakdown voltage determ. 80−38787
SF_6, compressed, negative ion drift in applied field 78−87565
SF_6, compressed in positive rod-to-plane gaps, static breakdown anal. 80−38796
SF_6, compressed in space-charge stabilised nonuniform fields, corona threshold computation 79−19118
SF_6, conc. meas. in air over Europe 77−37351
SF_6, condensation in supersonic nozzle flow 78−34611
SF_6 condensation in supersonic nozzle expansions, trimerscritical model derivation 79−77211
SF_6 cooled gas, multiphoton dissociation with CO_2 laser, enrichment with ^{33}S 80−14245
SF_6 corona-stabilised breakdown, computations and obs. 80−64804
SF_6, critical isochore, dielectric const. critical anomaly upper bound 80−84679
SF_6, critical parameters determ. using thermodynamic and mol. similarities 77−43310
SF_6, cryst., IR and Raman spectra at 9 and 97K, cryst. struct. 79−87427
SF_6 detection in air, photoacoustic spectroscopy, resonant cell design optimisation 78−56924
SF_6, dielec. strength, electrode shape effect, overvoltage protection *(Czech)* 80−10444
SF_6, dielectric strength, breakdown tests *(Czech)* 78−30498
SF_6 dielectric strength, conductor surface irregularities influence 80−14946
SF_6, discharge, grazing, incomplete, gas temp. and electron density diagnostics 79−55600
SF_6, discharge and oscill. due to axial injection of impulsive electron beam 80−59316
SF_6, discharge development, relative motion between gas and electrode, theory 78−63616
SF_6, discharge development, high speed elec. and optical temporal resolution 78−87584
SF_6 dissoc. by multiphoton IR absorption 78−42369
SF_6 dissociation, infrared multiphoton processes, apparent step cross-sections, pulse spatial structure, irradiation techniques 80−32792
SF_6, dissociation probability for ultra-short CO_2 laser pulses 77−18998
SF_6 dissociation processes using one or two TEA CO_2 lasers 78−74713
SF_6, dissociation rate increase by red shift of nonresonant freq. under two freq. laser action *(Russian)* 77−58104
SF_6, dissolved in O_2 and Kr, cryogenic liqs., mol. motions, IR and Raman spectra 79−69823
SF_6, Doppler-limited spectroscopy, of $3\nu_3$ band 80−58244
SF_6, Doppler-limited spectroscopy of $3\nu_3$ band, rot. const. and anharmonic parameters calcs., mol. photodissoc. 80−83361
SF_6, dynamics of 10.4 μm absorption, vibr. bath model 78−17666
SF_6, effect on N_2 lasing props. 77−65591
SF_6, elec. discharges, expt. *(German)* 79−10726
SF_6 electric breakdown mechanisms, review 78−59699
SF_6, electric strength, electrode surface roughness effects, model *(German)* 78−63609
SF_6 electric strength as statistical charact. *(Russian)* 79−41787
SF_6, electrical conductivity calc., 2000 to 50000K 79−14512
SF_6, electrode surface and coating effect on DC breakdown voltages 78−87557
SF_6, electron affinity, MS Xα calc. 77−30778
SF_6, electron capture, laser radiation influence, possible laser isotope separation appl. 79−22856
SF_6, electron elastic scatt., total cross-section, multiple scatt. calcs. 79−7014
SF_6, electron elastic scatt., shape resonances 79−18289
SF_6, electron elastic scatt. resons. 80−53133
SF_6, electron impact, elastic scatt., absolute differential cross-sections meas. 79−36767
SF_6, electron impact, vibr. excitation, dissociative attachment 77−3481
SF_6, electron impact excitation, 12 eV resonance 77−88582
SF_6, electron impact excitation of inner shell, using 2.5 keV electrons 78−90303
SF_6, electron impact vibr. excitation 77−42428

sulphur compounds continued
SF_6 electron scatt., total absolute cross sections, 0.5-100 eV, incl. reson. struct. 79−45843
SF_6 electron scavenging in positron spur in nonpolar liqs. 79−100421
SF_6, electron swarm development, Boltzmann eqn. anal. 80−6205
SF_6, electronic props., (e,2e) spectrosc. obs. 80−5527
SF_6, emission spectrum of ν_3 band, 1780K, dissoc. effects 78−62795
SF_6, energy threshold effects in collisionless dissociation by IR laser radiation 77−58096
SF_6, energy-dependent absorption cross sections, use in multiphoton absorption modelling 80−32789
SF_6, equilib. composition and transport props., 300 to 15000K 77−24051
SF_6, equilib. electron-transfer reactions in gas phase involving long-lived neg. ion radicals 78−58807
SF_6, equilibrium composition calc., in 20000 to 50000K range, in dependence on pressure 79−14511
SF_6, excitation by strong IR laser field, spectral charact. 80−32713
SF_6, excited to dissoc. threshold, IR absorption 79−81245
SF_6, film, IR laser induced processes at low temp. and under ultrahigh vac. 79−69914
SF_6, first breakdown voltages 78−87554
SF_6 gas, CO_2 TEA laser-excited, slow intermol. redistrib. of vibr. energy 80−53039
SF_6 gas, compressed, initial corona voltage increase due to electrode surface roughness *(Croatian)* 80−54074
SF_6 gas, dispersion relation of spontaneous oscill., unstable regions 80−1875
SF_6, gas, electron beam irrad., delayed elec. breakdown 79−4200
SF_6 gas, excited molecule vibr. translational relaxation, nonlinear processes *(Russian)* 80−91540
SF_6, gas, heating effect on optical props., transmittance meas. 79−27737
SF_6, gas, intensity depend. transmission at 936.8 cm^{-1}, pulsed and CW laser beams 77−88867
SF_6, gas, Kerr effect, virial coeffs. 79−50843
SF_6 gas, low press., excitation of nonlinear wave by repeated pulsed electron beam 80−87878
SF_6, gas, Rayleigh vol. scatt. coeffs., spectronephelometric meas. 78−14127
SF_6, gas, sparking pots., ionisation and electron attachment coeffs. 78−42705
SF_6, gas, thermodynamical and spectral props., effect of angle-dependent part of dispersion forces 80−43138
SF_6 gas acoustic dispersion obs. by double-crystal US interferometry *(Japanese)* 79−4100
SF_6 gas blast breaker, current zero meas. 80−38795
SF_6, gas blast cct. breaking arc , energy clogging 78−87531
SF_6, gas blast circuit breaking arc, clogging transition 78−87530
SF_6, gas-liquid crit. pt. region, depolarised light scatt. 78−34612
SF_6, gaseous 1s binding energy and S $KL_2L_3(^1D_2)$ Auger energy, XPS obs. 77−3416
SF_6 gaseous saturable absorber effects on eight-beam CO_2 laser fusion system performance 80−106577
SF_6 glow discharge, non-linear effects on self-exciting wave 78−83633
SF_6, ground state, mol. consts., ν_2 Raman band calcs. *(French)* 78−9156
SF_6, ground state and vibr. heated mols., CO_2 laser pulse absorption 77−46607
SF_6 high-current arc props., influence of electrode material 78−71592
SF_6, high-current discharge plasma column, radiation charact. and struct. *(Russian)* 80−106989
SF_6, high-resolution IR Ar matrix-isolation spectra, 10K 80−32708
SF_6, high-resolution polarisation spectroscopy in 10 μm region 79−6196
SF_6, high-resolution transient double IR reson. 77−88477
SF_6, high-temp. circuit-breaking arc, axial and radial heat transport 79−19105
SF_6 high-temp. electrical breakdown parameters 78−67567
SF_6, highly excited, time-resolved IR absorpt. obs. 80−9666
SF_6, hot, vibr. anharmonicity, electron diffr. study, 298-10^3K 79−68316
SF_6, IR absorpt. of highly vibr. excited mols., double reson. meas. 78−37662
SF_6, IR absorpt. spectra of vibr. excited mols. *(Russian)* 79−36643
SF_6, IR absorption peak shift at high intensity *(Russian)* 77−42327
SF_6, IR active mols., homogeneous excitation by laser pulses 78−9202
SF_6, IR double reson. with tunable diode laser 80−14160
SF_6, IR double resonance, V-V energy transfer from ν_3 mode 77−482
SF_6, IR double resonance and energy transfer obs. 77−58105
SF_6, IR laser isotope separation 79−50150
SF_6, IR laser isotopic enrichment in low temp. matrices 78−90318
SF_6, IR laser multiphoton excitation, weak transitions in rot. band struct. 78−66614
SF_6, IR laser radiation induced dissoc., isotope separation 77−29026
SF_6, IR laser radiation multiphoton absorpt. direct meas. by pyroelec. detector 80−102545
SF_6, IR multiphoton dissoc., energy randomization 78−21982
SF_6, IR multiphoton dissociation F atoms obs. by chemi-ionis. method 78−31661
SF_6, IR multiphoton dissociation studies, inverse bottle-neck effect 80−87193
SF_6, IR multiphoton photolysis, master eqn. anal. 79−47945
SF_6, IR multiphotonic excitation, depend. on cell geometry, mol. fluoresc. and decomp. obs. 80−83430
SF_6, IR multiple-photon excited molecules, Raman spectroscopy 80−74207
SF_6, IR obs. spectra meas. using $Pb_{1-x}Sn_xTe$ diode laser *(Japanese)* 79−49306
SF_6, IR photodissoc., hydrogen halides form., IR chemiluminesc. 77−63932
SF_6, IR radiation induced mol. excitation and heating effects, time resolved 77−75142
SF_6, IR rot. spectra, orbital level splitting in octahedral symmetry, high J levels 77−69815
SF_6, IR rot. spectra orbital level splitting in octahedral symmetry, high J levels 77−69816
SF_6, IR saturation, five-level rate eqn. anal. 77−27321
SF_6, IR saturation spectrum, mag. hyperfine struct. 79−13714
SF_6, IR spectra, fine struct. of rot.-vibr. bands 80−102504
SF_6, IR spectra, ν_4 vibr. band strength 78−94240
SF_6, impulse breakdown, polarity effect, thin dielectric coating influence 80−38773
SF_6 impulse breakdown characteristics for nonuniform field gaps for switchgear design 80−84024

sulphur compounds continued
SF_6 in coaxial electrode arrangement, impulse breakdown anal. *(German)* 77−76219
SF_6, in cryogenic liqs., vibr. kinetics, IR spectrosc. obs. 79−18182
SF_6, in liq. inert gas, electron attachment, elec. field effects 77−31009
SF_6, inhibition of free radical prod. in gas-phase radiolysis of ethane 79−39178
SF_6, inhibition of homogeneous condensation by vibr. excitation, isotope separation appl. 78−37688
SF_6 insulated switching installations and devices, gas chromatography appl. *(German)* 78−88668
SF_6 insulation, predischarge-stabilised breakdown voltage *(German)* 78−63608
SF_6 insulation, under impulse voltage stress, effects of pressure and vol. on firing delay *(German)* 80−87959
SF_6 insulation breakdown characts. under operating conditions in HV apparatus 80−96414
SF_6, intense sub ns CO_2 laser pulse attenuation and reshaping 77−88870
SF_6, intramode anharmonicity const., vibr. linear absorpt. spectrum 80−18893
SF_6, ionic fragmentation after S 2p shell electron impact ionis. 78−90310
SF_6, ionisation pot., discrete variational Xα calc., Slater-type orbitals in Hartree-Fock basis 78−78837
SF_6, isotope separation, laser induced multiphoton dissoc. 77−16839
SF_6, isotope separation, selective dissociation using compressed H_2 Raman laser 77−34708
SF_6, isotope separation, TEA CO_2 laser irradiation *(Japanese)* 80−11885
SF_6, isotopic enrichment, coherent multiphoton vibr. excitation and dissociation 77−88512
SF_6, isotopically selective dissoc., intense IR laser field 77−6868
SF_6, isotopically selective photodissociation under CO_2 laser pulses, geometrical effects 77−16852
SF_6, isotopically selective collisionless laser induced dissoc. 78−1037
SF_6, KLL Auger spectrum, obs. and ab initio SCF CI calc. 78−50654
SF_6, KLL spectra of S, ab initio LCAO SCF calcs. 77−65515
SF_6, Kerr effect in gas, statistical theory 79−50842
SF_6, $L_{II,III}$-absorption spectrum, prethreshold range fine struct. 78−86847
SF_6 laser, for 16 μm range, review *(Rumanian)* 80−87408
SF_6, laser additive effects on pulsed CO TE and CS_2/O_2 chemical lasers 79−31876
SF_6, laser excitation in low temp. matrices, possible isotope selectivity 79−36788
SF_6, laser isotope separation model 77−31016
SF_6 laser isotope separation, rot. and vibr. relax. in mixture 78−25634
SF_6, laser photodissoc. energy depend. 77−10710
SF_6, laser pumped, mol. vibr. amplitude changes, gas phase electron diffr. obs. 79−76513
SF_6, laser pumping in collisional region of nozzle beam, internal excitation, time-of-flight anal. 80−95719
SF_6, laser spectroscopy using an optothermal receiver 80−37810
SF_6, laser-induced gas breakdown, wavelength depend. meas. of threshold 79−41895
SF_6, laser-induced isotope separation, threshold intensity 77−4898
SF_6, laser-irrad., high-resolution double-reson. spectroscopy, collisionless multiphoton dissoc. 80−9623
SF_6, light scatt. near crit. pt., nonzero beam diameter effect 77−85736
SF_6, liq., depolarised light scatt., dipole-induced dipole effect 77−12395
SF_6, liq., near crit. point, optical props. meas. 77−72673
SF_6, liq., positronium bubble states, temp. depend. 80−108293
SF_6, liq., transient stimulated vibr. Raman scatt. 78−71144
SF_6, long-range correlation length near liquid-vapour transition, Rayleigh scatt. 77−8593
SF_6, longitudinal mixing in pulmonary airways, impulse response 79−20568
SF_6, matrix isolated, IR photodissoc. 78−90245
SF_6, matrix isolated, IR spectrosc., temp. reversible site structural changes 80−95613
SF_6, matrix photolysis, vac. UV, using windowless discharge, IR spectra 77−71798
SF_6, microwave absorpt. 2.3 cm^{-1} region 77−46557
SF_6 mixtures, laser initiated explosions, chemilum. in near UV, visible and IR 78−48674
SF_6, model system, coherent pulse propag. effects 80−9968
SF_6, mol. beam, selective dissoc. in intense IR laser field, wavelength and energy depends. 78−73065
SF_6, mol. beam mag. resonance, rot. mag. moment spectrum 77−34661
SF_6, mol. orientation resonant optical detect. in gases, laser spectroscopy appl. 79−27742
SF_6, mol. vibr., radial distrib. function of vibr. excited mol. 79−85951
SF_6, molecular effects in F K-shell ionisation by 0.5 to 1.5 MeV protons 77−50515
SF_6, molecular vibration energy stochastization in intense IR laser field by Raman spectroscopy *(Russian)* 80−14149
SF_6, molecule, dissociation in strong IR field, appl. of CO_2 laser for isotope separation 77−83755
SF_6 molecule, matrix isolated, CO_2 laser irrad., photodissoc., IR absorpt. spectra obs. *(Russian)* 77−6877
SF_6 molecule, resonant energy absorpt. struct. in IR laser field *(Russian)* 80−5592
SF_6 molecule absorption of IR laser radiation *(Russian)* 80−986
SF_6 molecule drift mobility due to IR laser radiation *(Russian)* 80−69192
SF_6, mulitphoton absorpt., pulsed CO_2 laser radiation absorpt., press., freq., fluence depend. 80−28080
SF_6, multi-photon photo-dissociation in intense IR laser field *(Chinese)* 79−50094
SF_6 multiphoton absorpt., CO_2 laser, effect of pulse mode quality 78−66615
SF_6, multiphoton absorpt. spectrum, temp. depend. calc. 78−86927
SF_6 multiphoton absorpt. meas. by third harmonic generation 80−1036
SF_6, multiphoton absorpt., energy transfer, dissoc. probability, laser field interaction, classical trajectory approx. 80−37730
SF_6, multiphoton dissoc., producing SF_5+F, ang. and vel. distribs. 77−27130
SF_6, multiphoton dissoc., energy deposition 78−82800
SF_6, multiphoton dissoc., anharmonic force field, decoupled rigid bender model 79−41153
SF_6, multiphoton dissoc., selective mechanism, mol. beam obs. 79−41210

sulphur compounds continued
SF_6, multiphoton dissoc., unified dynamical model 80−5587
SF_6, multiphoton dissoc., collision effects 80−23467
SF_6, multiphoton dissoc., classical model 80−53076
SF_6 multiphoton dissoc. by mol. beam method, energy distribution meas. by time-of-flight spectra, dissoc. dynamics 80−78670
SF_6, multiphoton dissociation, isotope separation 78−62865
SF_6, multiphoton excitation from many rot. states by IR laser pulse 78−21986
SF_6, multiphoton excitation and dissociative ionisation, model 78−58754
SF_6, multiphoton excitation due to vibr.-rot. transitions 80−102546
SF_6, multiphoton excited, IR fluoresc. spectrum meas. 80−37828
SF_6, multiphoton IR dissoc., quantum or classical approach 78−82801
SF_6, multiphoton i.r. absorption, optoacoustic detection 77−507
SF_6, multiphoton isotope selective dissoc., pulse shape, energy, press. and geometry effects 78−25733
SF_6, multiphoton pathways, rot.-vibr. transition moments in excited states 78−25639
SF_6, multiphoton reaction, laser mode-locking effect 77−46606
SF_6, multiphoton-excited in mol. beam, photoionsation probe of vibr. energy distrib. 79−76476
SF_6, multiphoton-excited, $\nu_2+\nu_6$ absorption and emission 80−63626
SF_6, multiple IR photon absorpt., collisional effects 78−86926
SF_6, multiple photon absorption, thermal enhancement 79−68283
SF_6, multiple photon absorpt., laser pulse intensity and collisions influence 80−95699
SF_6, multiple photon dissociation threshold behaviour, chemilum. obs. 78−42145
SF_6, multiple photon excitation, collisionless 80−53079
SF_6, multiple reflection cell, laser spectroscopic meas. 78−86359
SF_6, multiple-photon absorption, experimental conditions and mol. parameters depend. 80−32790
SF_6, multiple-photon dissoc. rate determ. 77−60079
SF_6, multiple-photon excited, double reson. spectroscopy 80−53030
SF_6, multiple-photon IR laser pumping, collisional effects 80−9668
SF_6, multiple-photon two-freq. IR laser pumping, optoacoustic spectroscopy 79−36717
SF_6, multiwavelength phase conjugation using multiline CO_2 TEA laser 80−91847
SF_6, narrow reson., elastic scatt., spectroscopic studies 80−53094
SF_6, negative point-plane corona, electrical characts. 78−71567
SF_6, nonlinear absorpt. spectrum using Doppler-free polarisation spectroscopy 79−3440
SF_6, nonlinear absorpt. of CO_2 laser pulse, computer simulation 80−106575
SF_6, nonlinear optical polarisability meas. 79−54991
SF_6, nonradiative collisionless dephasing rate, two-photon coherent transient meas. 80−14176
SF_6, ν_3 band, IR spectra, in supersonic mol. beam 78−66541
SF_6, ν_3 band high-J manifolds, line freq. perturbation 79−36702
SF_6, ν_3 bands, rot. fine struct., HFS spectroscopic consts. determ., saturation spectroscopy obs. 80−53008
SF_6, ν_3 manifold, $3\nu_3$ transition, 3-quantum transition probabilities, IR spectrum 78−86866
SF_6, ν_3 mode 2nd vibr. overtone absorpt. spectrum 77−88463
SF_6, ν_3 Q-branch, CO_2 laser pumped 78−21924
SF_6, octahedral complex, ionis. energy, SCF-Xα study 78−70967
SF_6, optical Q-branch pumping in ν_3 mode 78−90232
SF_6, Orsay MP gas handling system 78−29673
SF_6, pair polarisability anisotropy, point atom polarisability approx. calcs. 80−87244
SF_6, partial discharge overvoltage dependence 77−76243
SF_6, partial photoionis. cross-sections, 20-54 eV, photoelectron spectrum 79−13769
SF_6 partial press. meas. in mixtures with N, using separation by freezing 79−71478
SF_6, partial saturation of ν_3 ladder in IR absorpt., rate process model 80−58645
SF_6, particle densities in decaying plasma 78−75442
SF_6, phase conjugation at 10.6 μm by resonantly enhanced degenerate four-wave mixing 79−64271
SF_6, photoabsorpt. cross-section, 175-770 Å 77−88462
SF_6, photoabsorption and ionic fragmentation, 5-63 eV, absolute oscill. strengths 79−72367
SF_6, photodissoc. by IR, laser pulse, selectively excited vibr. levels, S isotopes 78−9209
SF_6, photodissociation by IR laser beam *(Chinese)* 78−90236
SF_6, photoelectron ang. distrib., orbital assignments 79−819
SF_6, photoionisation spectra in XUV region 80−37837
SF_6, photon echoes, polarisation and amplitude decay meas. 77−88872
SF_6, photon-enhanced dissociative electron attachment 80−9749
SF_6, photon-enhanced dissociative electron attachment, isotope selectivity 80−18939
SF_6, physical adsorption on Ru (001), XPS expts. 77−69178
SF_6, physisorbed on Ru, XPS interpretation 77−89830
SF_6 plasma column, in Maecker type arc, diagnostics and model *(French)* 80−19652
SF_6 plasma interaction with solid polymer, emission-spectra 80−87960
SF_6 plasma thermodynamic props. at arc extinction temp. and pressures 80−79435
SF_6, plastic phase, neutron diffr. obs. and theory 79−77533
SF_6, plastic phase, orientational disorder 79−73115
SF_6, polarization-rotation and thermal-motion studies via resonant degenerate four-wave mixing 80−5779
SF_6 polyatomic molecule dissociation in IR laser field *(Chinese)* 80−106363
SF_6, population of excited vibr. level, nonequilib absorpt., 140K *(Russian)* 79−36708
SF_6, positive point-plane gap, critical press. prediction, v_c/press. characts. 78−87583
SF_6 positive-point corona phenomena, breakdown voltage/press. characts. 80−38859
SF_6, pumped by OC_6 laser, transition strengths 77−14416
SF_6, pure and H_2 mixture photolysis, S atom nucleation particulate formation 78−76836
SF_6, pure and mixtures, dielec. props., ionisation and attachment coeffs. 80−33726
SF_6 purification in const. temp. adsorption process, appl. to electrostatic accelerators 78−29672
SF_6, radiative dissoc. in laser field *(Russian)* 78−9207

sulphur compounds continued
SF_6, Raman scatt., calibration of laser light scatt. expt. in plasma devices 77−35399
SF_6 rarefied gas, coherent emission in time-separated fields 79−36954
SF_6, refl., absorpt. and transmittance depend. on irradiance at normal incidence 78−13769
SF_6, refractive index meas., intermolecular interaction effects 80−33728
SF_6, relax. mechanism, narrow reson. obs. by amplitude-modulated wave method 79−10155
SF_6, resonant single-photon dissoc. route using prelim. electron excitation 80−9662
SF_6 rod-to-plate corona discharge characteristic obs. 78−67584
SF_6, rot. spectra, asymptotic level clusters, quantum model 77−23490
SF_6, S isotope separation, multiphoton molecular dissociation using high-power CO_2 laser radiation 80−9657
SF_6 saturable absorber for CO_2 laser prepulse elimination 77−19337
SF_6, saturable absorpt. of high IR intensity CO_2 laser band 77−58391
SF_6, saturable gas absorber isolator for 9 μm band CO_2 laser amplifier 79−76709
SF_6 saturated absorption for CO_2 laser freq. stabilisation 77−75556
SF_6, saturation absorpt. characts. at 10.53 μm CO_2 P(14) line 77−38999
SF_6, saturation characts. at 10.4 μm 77−54761
SF_6, second virial coeffs. from compressibility meas., mol. pot. parameters calc. *(Spanish)* 77−47133
SF_6, selective dissoc. in two freq. i.r. laser field 77−504
SF_6, selective multiphoton dissociation by CO_2 laser irradiation 77−34707
SF_6, self-focusing and self-defocusing using IR laser 79−89978
SF_6, sign of rot. g-factor, mol. beam expt. 79−59600
SF_6, solid, NMR line shape and relax. 77−51978
SF_6, soln., cryosystem, vibr. relax. times, pulsed IR absorpt. spectral obs. 80−66188
SF_6, soln. in liquid Kr, resonant IR radiation, nonlinear absorpt., vibr. relaxation estimate 79−36642
SF_6, spark gap, KrF laser triggered, low jitter timing 80−106999
SF_6, spectral parameters, Lamb dip method investig. 78−89560
SF_6, spectroscopic consts. calc. from saturated absorption spectrum *(French)* 78−971
SF_6, spectroscopy using tunable high-press. CO_2 waveguide laser 80−43054
SF_6, spherical top mol. vibr.-rot. spectrum with tunable diode laser 78−82734
SF_6, Stokes signal amplification, effect of pump radiation incoherence 78−18015
SF_6, struct. by electron diffr. 78−29859
SF_6, supercooled, IR absorpt. spectrum 77−23574
SF_6, supersonic jet, condensation and gasdynamic cooling 80−6089
SF_6, supersonic jet expanding into vac., interaction with CO_2 laser beam 80−5584
SF_6, surface ionisation on W cathode, laser irrad. effects 80−93440
SF_6, surface tension temp. dependence from triple point to critical point *(German)* 80−100376
SF_6 thermal cond., 230-350K, up to 50 MPa 79−33123
SF_6, thermal cond. at 350 to 1300K 77−35304
SF_6, thermal conductivity at high pressures, investigation 78−67305
SF_6, thermalisation under reson. excitation by laser radiation *(Russian)* 78−26231
SF_6, threshold electron attachment cross-section 79−89708
SF_6, time-resolved IR absorpt. meas. using injection-locked single mode TEA CO_2 laser 80−9665
SF_6, total nuclear spin in rovibronic state, three calc. methods for hyperfine mag. struct 78−58658
SF_6, trace detection using phase fluctuation optical heterodyne spectroscopy 80−68266
SF_6 tracer technique for near-stack reactor effluent dispersion studies 78−11992
SF_6, transmission meas. of multiple photon absorpt. 77−83668
SF_6, tunable diode laser spectrosc. obs. 78−82061
SF_6, two IR pulse multiphoton absorpt. selective dissoc., obs. 78−82798
SF_6, two-scale factor universality near crit. point 78−55936
SF_6 type molecule, multiphoton absorption in continuum 78−90247
SF_6, unimolecular reaction model 78−7189
SF_6, universal eqns. of state and thermodynamic similarity 77−35290
SF_6, valence electron spectra, vibr. band struct. 77−23520
SF_6, valence levels, photoionisation cross-sections, MS Xα calcs. 79−54923
SF_6, very high current arcs, elec. conductance of arc gap 78−87524
SF_6, very high current gas blast arcs, local voltage and cross-sectional areas correlation 80−38779
SF_6, vibr. anharmonicity consts., ν_4 region laser absorption obs. 78−94242
SF_6, vibr. coupling in collision-induced Raman scatt. 80−83373
SF_6, vibr. Raman spectrum, Q branches shapes 78−42077
SF_6, vibr. relax., 150 to 320K, IR double reson. study *(Russian)* 78−86899
SF_6, vibr. spectra, rot. consts., IR spectra, Raman spectra obs. 80−32719
SF_6, vibr. strength, IR intensities calcs. 77−34608
SF_6, vibr.-translational relax. at high excitation rates 79−41201
SF_6, vibrational-translational relaxation, depend. on intensity of selective laser excitation *(Russian)* 78−9235
SF_6, vibrationally excited, collisionless intramolecular energy transfer 78−37663
SF_6 viscosity, investigation 78−94884
SF_6, viscosity meas., 230-800K and press. up to 5×10^8 dyn cm^2 78−95171
SF_6, viscosity meas. at low temps. 80−6193
SF_6, wall stabilised arc, current step changes, conductance transient effects 78−87547
SF_6, X-ray absorption spectra, method of coupled differential eqns. 77−88466
SF_6, X-ray absorption spectra *(Russian)* 78−50559
SF_6^-, electron impact, nearly zero energy, probability ratio meas. 79−72433
SF_6^-, matrix isolated, IR spectra, evidence for form. 77−68037
$^{32}SF_6$, anharmonic splittings, vibr. energy levels, $n\nu_3$ manifold 77−30853
$^{32}SF_6$ dissociation, infrared multiphoton processes, reaction rate, scale factors, pulse structure 80−32791
$^{32}SF_6$, multiphoton dissoc. by laser pulse, Ar, N_2 and CF_4 environments 78−73061
sulphur compounds continued
$^{32}SF_6$, point group symmetry breakdown, vibr.-rot. state, saturation spectroscopy 80−87116
$^{33}SF_6^-$, radical, prep. and EPR comparison with other hexafluoride radicals 78−68381
SF_6-air (N_2), breakdown voltage and discharge extension of long gaps 77−84550
SF_6-air mixture impulse discharge characteristics of 30 cm gaps 78−67572
SF_6-Ar, condensing flow, gasdynamic and IR meas. 80−6501
SF_6-Ar mixture, space discharge excited by electron beam *(Russian)* 78−83629
SF_6-Ar mixture, space discharge excited by electron beam *(Russian)* 78−83630
SF_6-CF_4-CH_4-CO_2, viscosity of multicomponent gas mixtures, prediction and meas. 77−31414
SF_6-ethane mixtures, viscosity, diffusion coeffs. 80−1722
SF_6-gas mixtures electric breakdown 79−37438
SF_6-H_2, high-press. radiation-chem. laser, electron beam initiation 77−75562
SF_6-H_2 electric discharge laser pumped by inductive storage unit 79−98409
SF_6-H_2 mixtures, laser irradiated, IR energy deposition and HF fluoresc. 80−23454
SF_6-H_e mixtures, collisionless multiple photon absorpt. photodissoc., HF fluoresc. 77−58099
SF_6-He extracavity saturable absorber, nsec. pulse selection in CO_2 oscillator 79−98382
SF_6-He hollow-cathode laser using F transitions 80−48289
SF_6-He(N_2)(CO_2), AC particle initiated breakdown, compressed gas mixture 78−87556
SF_6-hydrocarbon mixtures, IR laser induced ionis., mechanism 77−81415
SF_6-inert gas mixture, high power cylindrical spark discharge, dynamic and visible charact. 80−64816
SF_6-inert gas mixture, formation of inert gas fluorides in AC discharge 80−64817
SF_6-methane, mixture, CO_2 laser induced multiphoton dissociation and chemilum., laser fluence depend. 79−57233
SF_6-N_2, horizontal cylindrical power cable, convective heat transfer, simulation *(Russian)* 77−58676
SF_6-N_2 mixture, discharge inception voltages, calc. 79−68966
SF_6-N_2 mixture, electron swarm development, Boltzman eqn. anal. 80−87841
SF_6-N_2 mixture in rod-plane gaps, static field breakdown 79−68965
SF_6-N_2 mixtures, attachment coeffs. and ionic mobilities, 1.2-4 eV 80−96338
SF_6-N_2 mixtures, effective ionisation coeff. and static breakdown voltage meas. 80−19549
SF_6-N_2-Ar mixture high-current multispark discharge switching characteristic 78−67444
SF_6-N_2O solution, IR and Raman rot. correl. functions, expt. and theory 79−46541
SF_6-O_2 breathing, effect on respiratory mechanics 78−27992
SF_6-O_2-O_2, efficient CO_2 laser radiation 3rd harmonic generation, for fusion ignition 78−59087
SF_6-R-He(Ar) ternary mixtures, formation of inert gas fluorides in AC discharge 80−64817
SF_6-SO_2-fluoromethane mixture, laser irrad., IR fluoresc. meas. of equilib. and vibr. temps. 78−82766
SF_6+Al chemiluminescent reactions 77−9086
SF_6+Ar, atomic 1s states deactivation 77−50398
SF_6+Ar, differential scatt. cross-sections, intermol. pots. calcs. 79−89742
SF_6+CF_2, vibr. deactivation of CF_2 first excited single state 79−94061
SF_6+CsCl, (Cs_2Cl_2), collision induced dissoc., threshold behaviour 78−88627
SF_6+CsF, rot. inelastic collisions, mol. beam meas. 80−1049
SF_6+Cu, photon yields, chemi- and photo-luminesc. 79−5157
SF_6+D_2, optically cascaded pulsed chem. laser 77−75497
SF_6+Fe^{4+}, 20 MeV, gaseous targets, electron loss, charge state yields 79−54957
SF_6+fluoromethane, fluoromethane laser, buffer gases collisional narrowing 80−99710
SF_6+H scattering, obs. of resonance maximum 77−58126
SF_6+H_2, (oriented), total collision cross-sections, anisotropic pot. parameters calcs. 78−13568
SF_6+H_2 chemical laser, electron beam pumping 80−91784
SF_6+H_2 mixture, equilib. composition and transport props., 300 to 15000K 77−24051
SF_6+$H^+(He^+)_3$ F K-shell ionisation, AES meas. 77−10749
SF_6+H^+→SF_6^++e^-+H^+, 0.3-1.8 MeV, electron energy and ang. distrib. 78−22015
SF_6+HCl, HCl nonequilib. rot. distrib. relax., fluoresc. obs. 79−36673
SF_6+He, binary gas mixture, mutual diffusion press. depend. 77−24047
SF_6+He, differential scatt. cross-section, intermol. pot. 79−36728
SF_6+He(Ar), mol. vibrational-translational energy transfer, mass spectrometric meas. 79−36739
SF_6+K, ion-pair form. reaction, energy loss spectra 80−55630
SF_6+Li, chemiluminescence spectra, excited Li *(German)* 78−92485
SF_6+$Li^+(H^+)$, mode selective vibr. excitation 80−58351
SF_6+methane, vibr.-vibr. relax. 80−99537
SF_6+N_2, simultaneous vibr. transition, absorpt. band intensity 77−50474
SF_6+N_2O, vibr.-vibr. energy transfer, fluoresc. 80−78688
SF_6+NO+O_3, laser sensitised reaction, time-resolved NO_2* emission obs. 78−20017
SF_6+Ne, metastable state de-excitation, rate consts., radiolysis obs. 80−40709
SF_6+p-dichlorobenzene, monochlorobenzene quantum field in collision induced photodecomposition 79−79270
SF_6+Rydberg atom, reaction channels, expt. vs. theory 80−63755
SF_6+SiH_4→S_2*+SiF_4+HF+H_2, laser augmented reaction, isotopic selectivity retention during detonation 78−48673
SF_6+Si(surface), IR laser induced reaction, mol. vibr. and mol. dissoc. obs. 80−93798
SF_6+Ta→TaF_x, x=1-5, thermochem. props. of TaF_x 79−100424
SF_6+X$^-$→SF_5^-+F+X (X=O, S, F, Br, I), electron affinity of SF_5 radical 80−45495
SF_6+Xe(nf), l-changing collisions obs. 80−91633
SF_6^-+He, decomposition, SF_5^- form. 78−29833

sulphur compounds continued
$SF_6^- + SF_5^+$, ion recombination, flowing afterglow, cross section meas. 77−44473
SF_n, electron affinities from collisional ionisation with alkali atoms 78−55226
S_2F_{10}, absorpt. of intense laser radiation, vibr. excitation 80−9667
S_2F_{10}, IR laser irrad., absorpt., reaction parameters 78−94241
S_2F_{10}, multiple-photon IR laser pumping, collisional effects 80−9668
SF_6Ar, multiple photon excitation, saturation and linear absorpt., pulsed optoacoustic detect. 78−42148
SF_3BF_4:SF_3, cryst., γ-irrad., radical form., EPR 78−91955
SF_5Br, Ar matrix and solid phase Raman and IR spectra, vibr. assignments 77−6775
SF_5Br, vibr. spectrum and normal coord. anal. 77−18926
SF_5Cl AR matrix and solid phase Raman and IR spectra, vibr. assignments 77−6775
SF_5Cl, laser induced reactions, yields, product distrib. and isotropic selectivity 78−53225
SF_5Cl, multiphoton dissoc., real-time Cl atom fluoresc. detect. 78−86923
SF_5Cl, pure rot. spectra, 300 GHz, isotope effects 80−5533
SF_5NF_2, multiphoton excitation, absorption and dissoc., isotope selection 79−100408
SF_4O, vibr. spectra, struct. and thermodynamic props. 77−63416
SF_5X, (X=Cl, Br, Sf_5), VUV photolysis, SF_5 radical form. in Ar matrix, IR spectrum 78−981
SH, ($X^2\Pi_i$) radical, UPS in VUV region showing vibr. struct. 79−98153
SH, in flames, laser induced fluoresc. meas. 78−61132
SH presence in sunspot UV umbral spectrum 79−75186
SH, presence or absence in solar atm., theory 78−69765
SH, Zeeman effect, relativistic corrections 77−83646
SH^+, bond lengths derived from UPS in VUV region 79−98153
SH^+, fine struct. in $X^3\Sigma^-$ and $A^3\pi$ states, GTO and STO calcs. 77−6679
SH^+, PNO-CI and CEPA calcs. of electron correl. effects 77−34561
$SH^- + O_3$, associative detachment, rate coeffs. 78−3325
SH_2, nuclear mag. shielding of ^{33}S, pseudopot. calcs. 79−6879
SH_3^+, bond polarisability and force constants 80−69260
SH_3^+, struct., ab initio HF calcs. 79−31371
SH_n, LCAO-MO-SCF with Gaussian polarisation functions, energetic effect of p-, d-, and f-functions 78−41944
SHF, total energy, MOs nonempirical minimum STO-4LGF calcs. 78−9074
SN, struct., vibr. spectra, ab initio calcs. 78−66475
SN^+, struct., vibr. spectra, ab initio calcs. 78−66475
$(SN)_2$, theory of plasmon excitations 77−69266
$(SN)_x$, 1-D chain, ab initio treatment, HF LCAO calc. 77−1349
$(SN)_x$, acoustic phonons, inelastic neutron scatt. obs. 78−6136
$(SN)_x$, acoustic phonons 78−79698
$(SN)_x$ and S_4N_4, high press. study 78−52782
$(SN)_x$, brominated, Raman spectra meas. 78−72519
$(SN)_x$, brominated, struct. and elec. props. 80−24914
$(SN)_x$, brominated, temp. depend. of static mag. susceptibility 79−33452
$(SN)_x$, brominated, vapour species identification, mass spectrometric methods 78−44422
$(SN)_x$, brominated, X-ray absorpt. meas., 5K to room temp. 80−71516
$(SN)_x$ chain, isolated, effect of $(SCH_2)_2$ impurities, on electronic props., EHT calcs. 79−15067
$(SN)_x$ cryst., synthesis and elec. cond. *(Japanese)* 77−69308
$(SN)_x$, cryst. struct. by neutron diffr. 78−34488
$(SN)_x$ crystal, galvanomagnetic effects meas. 77−85246
$(SN)_x$, deform. and defects, lattice strain, fibrillation 80−3139
$(SN)_x$, discontinuous film, DC resist. in normal and supercond. states 79−56357
$(SN)_x$, elec. cond., galvanomag. effects 79−91091
$(SN)_x$, electrical cond. at high press., scatt., evidence for semimetallic band struct. 77−43573
$(SN)_x$, electron tunnelling, absence of supercond. energy gap 78−47769
$(SN)_x$, electronic props., ab initio LCAO HF orbital calc. 77−51635
$(SN)_x$, electronic props. and comparison with TTF-TCNQ, review 78−6306
$(SN)_x$, electronic struct., X-ray and UV photoemission obs., OPW and pseudopot. calcs. 78−6832
$(SN)_x$, electronic struct., one-electron band theory 80−65450
$(SN)_x$, electronic struct. by extended tight-binding method, comparison with S_2N_2 precursor 77−76722
$(SN)_x$, electronic struct. and opt. props. 78−6256
$(SN)_x$, energy band struct., self-consistent calc. by intersecting spheres model 79−28269
$(SN)_x$, epitaxial, optical props. and plasmon dispersion, from electron energy loss spectra 77−35882
$(SN)_x$, epitaxial crystallisation on alkali halide substrates, theory 77−24496
$(SN)_x$, epitaxial film, elec. resist., 0.03-8.9K, possible supercond. 77−15970
$(SN)_x$, fibrous struct. study by electron diffr. using TEM 79−65004
$(SN)_x$, film, brominated, XPS, electronic struct. 78−72678
$(SN)_x$ film, evaporated on low temp. substrate, elec. cond. 77−63003
$(SN)_x$ film, Hall effect, elec. cond. and magnetoresist. meas. 78−84314
$(SN)_x$ film and crystal, acoustic and optical phonons, Raman, i.r. and transmission spectra 77−4642
$(SN)_x$ films, electrical properties 78−91782
$(SN)_x$, fluctuation induced cond. and dimensionality 77−28167
$(SN)_x$, halogenated, struct. behaviour, TEM obs. 80−70126
$(SN)_x$ halogenated derivatives, cond. and magnetoresist., 4.2-300K 80−24915
$(SN)_x$, IR spectra 79−56781
$(SN)_x$, IR transmission spectrum assignment 78−15160
$(SN)_x$, intrinsic cond. anisotropy from galvanomag. effect obs. 78−6369
$(SN)_x$, kink bands, deform. and defects 79−52308
$(SN)_x$, LCAO band struct. calc. for one-dimens. chain and three-dimens. cryst. 77−76723
$(SN)_x$, lattice and electronic sp. ht. contribs. density of states 77−43344
$(SN)_x$, lattice dynamics, pseudolattices and correlation method 78−75768
$(SN)_x$, linear compressibilities, X-ray determ. 78−34565
$(SN)_x$, mag. props. in supercond. state 77−51842
$(SN)_x$, magnetization meas. in supercond. regime 79−56375
$(SN)_x$, Meissner effect, mag. susceptibility meas. 80−20351
$(SN)_x$, mol. cluster and band struct. calc. 77−8004
$(SN)_x$, negative magnetoresistance below 4.2K 79−51611

sulphur compounds continued
$(SN)_x$, neutron and heavy ion bombard., effect on elec. cond. along chain axis 78−56136
$(SN)_x$, one-dimens. supercond. mechanism *(Chinese)* 79−47189
$(SN)_x$, phonon evolution during polymerisation of SN units 78−79711
$(SN)_x$, phonon spectra, four-parameter valence force model 77−20027
$(SN)_x$, polycryst. films, single crysts., UPS, valence band struct. 77−69967
$(SN)_x$ polymer, Be_2 doped, influence of halogen on elec. and optical props. *(Japanese)* 79−51559
$(SN)_x$ polymer, elec. props. of amorphous thin film and single crystal, role of chain breaks *(Japanese)* 78−68104
$(SN)_x$ polymer, quasi-one-dimens. and metallic behaviour *(Japanese)* 77−43577
$(SN)_x$ polymer, vaporised, mass spectra 79−98249
$(SN)_x$, polymeric, electronic structure, semi-empirical pseudopotential calc. 77−72812
$(SN)_x$, polymeric, shear transformation to orthorhombic phase 77−55257
$(SN)_x$, polymerisation, EPR obs. 79−73800
$(SN)_x$, prep. and evaluation of Schottky barriers produced on III-V and II-VI cpd. semiconds. 78−6442
$(SN)_x$, preparation and properties 78−27389
$(SN)_x$, π-bonding, increased valence theory calcs. 77−46500
$(SN)_x$, quantum chem. calcs. of electronic struct. 78−6257
$(SN)_x$, quasi-one-dimens., theoretical group anal. of electron spectrum 79−82511
$(SN)_x$, reflectivity calc. taking account of fibrous struct. 79−87462
$(SN)_x$, reflectivity spectra meas. by synchrotron radn. 79−91513
$(SN)_x$, Schottky barrier to II-VI and III-V semiconds., barrier height, compared with Au 77−85312
$(SN)_x$, single cryst., elec. anisotropy, polarised refl. spectra 77−36264
$(SN)_x$ single crystal, mech. props. 79−24580
$(SN)_x$ single crystal, transverse magnetoresistance 78−72140
$(SN)_x$ single crystals, galvanomag. effects 79−19582
$(SN)_x$ single crystals, tunnelling spectroscopy investigation *(Japanese)* 80−49954
$(SN)_x$, stress-induced phase change geometry 78−23776
$(SN)_x$, struct. defects, nature and origin 77−24313
$(SN)_x$, supercond., fluctuation cond., crit. mag. fields 80−39712
$(SN)_x$, supercond., obs. of Meissner effect 78−6478
$(SN)_x$, supercond. at high press. 78−23194
$(SN)_x$, supercond. energy gap, tunnelling meas. 79−56403
$(SN)_x$, supercond. polymer, mag. props. meas. 80−107953
$(SN)_x$, supercond. props., review 78−6474
$(SN)_x$, supercond. props., press. and field depend. 78−14903
$(SN)_x$, supercond. props., press. depend., up to 9.5 kbar 78−68106
$(SN)_x$, supercond. props. rel. to fibrous morphology 80−84570
$(SN)_x$, superconducting fluctuation induced magnetoconductivity in anisotropic bulk and fibrous samples 79−95545
$(SN)_x$, superconductor, differential tunnelling resistance 79−28485
$(SN)_x$, temp. depend. of reflectance spectrum 77−85744
$(SN)_x$, temp.-depend. of elec. resist. and mag. susceptibility, density of states determ. 77−51877
$(SN)_x$, tensile and piezoresist. expts. 78−15447
$(SN)_x$, thermoelec. power, 0.1 to 4.2K, phonon drag contrib. and supercond. transition 79−56356
$(SN)_x$, thermopower from 0.15 to 4.2K 80−34427
$(SN)_x$, tight-binding SCF MO calcs., interchain interaction 78−30859
$(SN)_x$, uniaxial stress effect on room temp. elec. cond. 77−39826
$(SN)_x$, vaporisation, mass spectroscopy 77−1224
$(SN)_x$, vapour phase species, mass spectra 77−61873
$(SN)_x$, with H impurities, CPA calculations 80−44468
$(SN)_x$, X-ray and optical props. 78−39632
$(SN)_x$, XPS calc. using photoionisation cross sections 78−72697
$(SN)_x$:Br, IR spectra 79−56781
$(SN)_x$:Br, ion implantation effect on elec. props. 80−65026
$(SN)_x$:Br, X-ray absorpt. meas. of mol. struct., orientation and charge transfer 80−25486
S_2N_2, $(SN)_x$, (x=2 or 3), minimal STO-3G basis HF ab initio LCAO SCF MOC, geometry 78−903
S_2N_2, cryst. and partly polymerised films, Raman scatt., optical absorption 77−8673
S_2N_2, electronic states, ab initio, SCF, and CI calcs. 77−75053
S_2N_2, electronic struct. by extended tight-binding method, comparison with $(SN)_x$ 77−76722
S_2N_2, electronic struct. by CNDO/2 calcs. 78−62727
S_2N_2, epitaxial crystallisation on alkali halide substrates, theory 77−24496
S_2N_2, gas phase and solid state core level XPS 80−66401
S_2N_2, LCAO band struct. calc. 77−76723
S_2N_2, photoelectron spectrum, interpretation, Green's function calcs. 80−87175
S_2N_2, polymerisation, mol. struct., INDO calcs. 77−70301
S_2N_2, π-bonding, increased valence theory calcs. 77−46500
S_2N_2, semiempirical electronic struct. calcs., applicability testing, and for $(SN)_x$ 77−6681
S_2N_2, struct., vibr. spectra, ab initio calcs. 78−66475
S_2N_2, XPS, solid-state polymerisation 78−19630
S_4N_2, electronic struct. by CNDO/2 calcs. 78−62727
$S_4N_2^+$, π-bonding, increased valence theory calcs. 77−46500
S_4N_4, 6-electron 5-centre bonding units, increased valence theory calcs. 77−46500
S_4N_4, effects of pressure and temp. on phonons, Raman scattering study 80−7360
S_4N_4, electronic struct. calc. using free-electron orbitals basis set 77−79537
S_4N_4, electronic struct. and vertical electron affinities, INDO-type ASMO SCF calcs. 79−31402
S_4N_4, film, brominated, XPS, electronic struct. 78−72678
S_4N_4, pyrolysis products, mass spectrometric obs. 78−60994
S_4N_4, Raman scatt., press. and temp. depend., 0-10 kbar, 10-295K 78−15160
S_4N_4, Raman scatt. and opt. absorpt., press. and temp. depend. 77−36227
S_4N_4, solid and soln., IR and Raman spectra, vibr. assignment 78−74659
S_4N_4, solid state core level XPS 80−66401
S_4N_4, vibrational spectra, effect of temp. and press. on phonons 79−37776
$S_4N_4^-$, electronic struct. and vertical electron affinities, INDO-type ASMO SCF calcs. 79−31402

sulphur compounds continued
$(SNBr_{0.04})_x$ and $(SNBr_{0.25})_x$, solid state core level XPS 80−66401
$(SNBr_{0.43})_x$, vap., electron impact and field ionisation mass spectra 78−44422
$(SNBr_{0.4})_x$, $(SNI_{0.02})_x$, $(SN[ICl]_{0.01})_x$, influence of halogen on DC conductivity and magnetoresist. 78−91682
$(SNBr_{0.4})_x$, magnetization meas. in supercond. regime 79−56375
$(SNBr_{0.4})_x$, metallic, transport and optical props. 77−85724
$(SNBr_{0.4})_x$, structure and electronic props. 77−59349
$(SNBr_{0.4})_x$, supercond. props. rel. to $(SN)_x$ 79−65581
$(SNBr_{0.4})_x$, supercond. props., dimensionality 80−20344
$(SNBr_{0.4})_x$, supercond. polymer, mag. props. meas. 80−107953
$(SNBr_y)_x$, Raman scatt. exam. 78−39550
$S_3N_3Cl_3$, solid and soln., IR and Raman spectra, vibr. assignment 78−74659
SNF, geometry and stability, LCAO-MO SCF calcs. 79−31391
$(SNH)_x$, density of states, CPA calcs., effect of H impurities 79−42431
$S_4N_4H_4$ ($S_4N_4D_4$), vibr. spectra, force consts. *(German)* 78−13499
$S_4N_4H_4$, and -d_4, solid and soln., IR and Raman spectra, vibr. assignment 78−74659
$S_4N_4H_4$, SCF-Xα-CNDO/BW calcs., comparison 78−25435
S_7NH, solid and solns. vibr. spectra, force consts. isotope effects 77−66490
$S_{8-x}(NH)_x$, (x=1,2,3,4), and deuterates, IR and Raman spectra, isotope shifts, mol. vibr. assignment 79−10110
$(SNI_y)_x$ crystals, reson. Raman scatt. meas. 80−66203
$(SN)_n$* radicals polymerisation to $(SN)_x$ in thin films, optical spectra 80−16656
$S_4N_4.AsF_5$, molecular adduct cyclotetra(azathiene), X-ray cryst. struct. determ. 80−54180
(SN)x, halogen-doped, temp. depend. of elec. cond. 79−65563
SO, $^1\Delta$ states, corrections to effective orbital g-factor 79−7036
SO 1_0-0_1 transition in dark and molecular clouds, 30 GHz obs. 80−46639
SO, 36 GHz emission line detect. in Orion nebula, rel. to mag. fields 80−46642
SO, ($^1\Delta_g$, $^1\Sigma_g^+$) chemiluminescence sensitised by metastable $O_2(^1\Delta_g)$, energy pooling 80−26016
SO, $a^1\Delta$ state, laser mag. reson. spectrosc. 78−94265
SO, and isotopic forms, $X^3\Sigma^-$ state, CO_2 laser mag. reson. spectroscopy 80−9602
SO, deposition and transformation rates during atm. transport over Atlantic Ocean 77−66975
SO, geometry optimisation, ab initio MO calcs. 77−42232
SO, in flames, laser induced fluoresc. meas. 78−61132
SO, interstellar, millimetre wave emission obs. 78−24535
SO, interstellar abundances rel. to interstellar shocks mol. diagnostics 80−56899
SO, iow lying bound mol. electronic states, SCFCI calc. 80−23314
SO, laser excited fluoresc. 79−50077
SO, microwave absorpt. coeff. 77−64378
SO, pot. energy curves, pseudopot. multi-struct. valence bond calcs. 78−9094
SO, pot. energy curves, dissoc. energies 78−50485
SO, presence or absence in solar atm., theory 78−69765
SO, S isotope composition, vibronic spectroscopic determ. *(Russian)* 79−10124
SO, Zeeman effect, g-factors 79−3492
SO^+ ($A^2\Pi$-$X^2\Pi_r$) emission following $He^+ + SO_2$ afterglow reaction 80−95659
SO^+, form. cross section, S_2O photoionis., 650-1200 Å 77−46605
SO^+ in E-region 79−96854
$S^{16}O_2$,$S^{18}O_2$, (0,0) band rot. anal., a^3B_1 state electron spin fine struct. consts. 77−10687
SO_2, $^1B_2$ state, force field and asymm. struct. 79−22685
SO_2, 193 nm photodissoc., photofragment translational energy distrib. 79−74402
SO_2, $2^1A'$ state, electron correl. variational description, loop driven graphical unitary group approach 80−47903
SO_2, 4 μm $\nu_1+\nu_3$ band, Doppler-limited and atmospheric spectra 77−27064
SO_2 ($^3B_1$), phosphorescent lifetimes, press. saturation effect on quenching by CO_2, CO, N_2 78−1017
SO_2, absorpt. coeffs. for ν_2 and ν_3 bands 77−38668
SO_2, absorption spectrum, meas. using frequency doubled pulsed dye laser 80−87144
SO_2, absorption spectrum, meas. using frequency doubled CW dye laser 80−87145
SO_2, adsorpt. on Ti, Nb, Ta evaporated films, corrosion 78−79897
SO_2, adsorption and oxidation on atmospheric particles 78−96287
SO_2, adsorption on Fe surface, X-ray photoelectron spectra 78−27370
SO_2 adsorption on heat treated γ-Al_2O_3 79−56070
SO_2, adsorption on microporous C 78−22956
SO_2 adsorption on mixed metal films 79−87003
SO_2, aerosol-catalysed oxidation, expt. under atm. conditions 79−1941
SO_2, air pollutant, conc. in remote continental and oceanic areas 79−20983
SO_2, air pollutant dispersal, Forth Valley, Scotland 80−81497
SO_2, air pollutant levels in London, 1500-1900 period 78−44982
SO_2, air pollutant long path meas. with correl. spectrometer 78−44988
SO_2 air pollution, critical conc. determ. *(Dutch)* 78−61547
SO_2 air pollution, daily volumetric meas., PVC tubing acid release effects 77−29449
SO_2, air pollution, distrib. in Venice using air quality simulation model 79−88394
SO_2 air pollution, Helsinki study of district heating effect 79−21010
SO_2, air pollution, high vol. sampling for isotopic studies 79−70500
SO_2, air pollution, new anal. method for remote areas 79−21028
SO_2, air pollution, plume detect. 400 km from source 78−24361
SO_2, air pollution, removal from atm. by dew 78−81370
SO_2 air pollution, transport model for United States 77−37370
SO_2, air pollution, transform. and scavenging processes, plume transport model 79−20976
SO_2, air pollution deposition to pine forest, radioactive tracer method 78−20508
SO_2, air pollution emissions in Mediterranean region, remote meas. 79−20987
SO_2, air pollution emission from chem. plant, precision estimates 79−83682
SO_2, air pollution extent in India, containment and agricultural use 78−28309

sulphur compounds continued
SO_2, air pollution long-distance transport, numerical model 79−44238
SO_2, air pollution mesoscale transport over English Midlands 78−44983
SO_2, air pollution model prediction for industrial-residential area *(Chinese)* 80−3546
SO_2, air pollution reversible washout by rain, improved model 79−2364
SO_2, air pollution stochastic modelling and dosage area product forecast 79−5601
SO_2, air pollution transport over Mediterranean 78−81390
SO_2, air pollution transmission on local, regional and continental scale 79−20974
SO_2, air pollution turbulent diffusion above and within forest 77−45055
SO_2, air pollution washout coeff., data from ground level monitoring network 79−74926
SO_2, analytical pot. functions, several surface minima 78−5158
SO_2 and nitrogen oxide automatic monitors, laboratory and field calibration *(French)* 77−37455
SO_2 and SO_4^{2-} conc. relationship in urban and industrial air 79−2360
SO_2 and steady wind incidents rel. to air quality management in Pittsburgh 77−49155
SO_2 and sulphates in rain, urban and rural Norfolk, England 80−55955
SO_2, aqu., reduction of H_3AsO_4 77−4901
SO_2, atm. conc. determ. using HBr laser *(Russian)* 78−69484
SO_2, atm. pollutant, effect of sunlight UV on photochem. reactions 77−21894
SO_2, atm. trace gases and pollutants, data compilation on mag. tape 78−44995
SO_2, atmosphere conc. rel. to sulphate dry deposition on snow 77−2231
SO_2, atmospheric, dispersion correlation spectroscopy 77−73857
SO_2, atmospheric, fluoresc. monitoring using NO γ-bands 78−73121
SO_2, atmospheric, long-term monitoring method using permeation sampling, development 80−26189
SO_2, atmospheric, meso-scale transport obs. in rurual East Midlands, England 80−94124
SO_2, atmospheric, photochem. oxidation 79−70873
SO_2, atmospheric, remote sensing, $^{12}C^{18}O_2$ laser line absorption cross-sections 79−16661
SO_2, atmospheric, sampling and anal. with PbO_2 plate, Huey plate 79−62163
SO_2, atmospheric, sources in CS_2 and COS oxidation 80−4085
SO_2, atmospheric concentration determ., dye laser differential lidar system 78−32250
SO_2, atmospheric concentrations, meas. using laser absorption spectrometer 79−96497
SO_2 atmospheric pollutant dosages in urban areas 80−81499
SO_2, atmospheric pollution monitoring by lidar systems 78−53765
SO_2, atmospheric pollution detect., interferential Fourier correl. of spectrum *(French)* 79−21059
SO_2, atmospheric removal rate meas. using ^{38}S tracer *(German)* 79−53411
SO_2, atmospheric residence times under non-steady-state conditions 80−77092
SO_2, atmospheric transmittance over IR spectral bands, model 80−51535
SO_2, atmospheric transport and conversion to sulphates 79−16654
SO_2 attack of Cu, benzotriazole protective coating 78−11385
SO_2 automatic control in air by electrochem. methods 79−96491
SO_2 bond charge parameters from integrated IR absorption intensities 77−6853
SO_2, bond function parameter transferability 77−30770
SO_2, bond functions in SCF calcs. 77−14349
SO_2, catalytic surface activity, $LaNi_5$ surface segregation *(German)* 80−51008
SO_2, chemiluminescence at ($c^1\Sigma^- \rightarrow a^1\Delta$) in Ar matrix, photolysis prod. and thermoluminesc. 79−5158
SO_2, city concs., box model and acoustic sounder anal. 80−7982
SO_2 collection efficiency with 0.5 N KOH-impregnated filters 78−16168
SO_2 collection from low-vel. jets, efficiency 79−16683
SO_2, collisional quenching of $^3B_1$ state, 8-1300 torr 78−86906
SO_2, complete quartic force field calc., algorithm 80−37736
SO_2 conc., urban built-up area, Japan 79−21006
SO_2 conc. and wind in Venice, Italy, spectral anal. 77−73824
SO_2 conc. decrease near Rotterdam rel. to meteorological parameters during 1961-74 winters 77−37359
SO_2, conc. determ. for coal-burning power plant stack, Fourier spectrometry appl. 77−49196
SO_2 conc. in Milan urban atmosphere in winter *(Italian)* 78−53721
SO_2 conc. over Netherlands, source areas, dispersion model 80−61482
SO_2 concentration distributions in Paris region (1962-72) *(French)* 77−37402
SO_2 concentration in Norwegian air rel. to sulphates in precipitation 77−37385
SO_2 concentrations, maximum, and averaging time, in industrialised area of Bilbao (Spain) 80−51020
SO_2 concentrations of Venice air, time series anal. 79−57540
SO_2, continuous-running, direct-reading recorder 78−53743
SO_2 conversion in smoke plumes *(Dutch)* 77−70825
SO_2 conversion to SO_4^{2-}, meas. during manned balloon flight 79−83658
SO_2 density prediction for Tokyo, adaptive transformation network method 79−5609
SO_2, deposition and transformation rates during atm. transport over Atlantic Ocean 77−66975
SO_2 deposition velocities to snow, N.Canada 79−70478
SO_2 detect. in stratosphere, analytical technique 77−5314
SO_2, direct meas. of $^3B_1$ state lifetime in air at atm. press. 77−79653
SO_2, dispersion and wet deposition from power plant plume 80−16861
SO_2, double hole states POCI calc., Auger spectrum 78−78630
SO_2, downwind conc. from Four Corners Generating Station 80−47620
SO_2, dry and wet removal from atmosphere 79−2361
SO_2, dry deposition, field meas. with stirred chamber 79−88021
SO_2, dry deposition on forests and grasslands 79−16652
SO_2 dry deposition to land and water surfaces 77−49158
SO_2, effect on high temp. hot corrosion 78−48563
SO_2 effect on precipitation and soil S content and acidity in Alberta 77−73843
SO_2, effective spin-spin parameter and singlet-triplet transition intensities, ab initio calc. 78−9067
SO_2, electron attachment processes investig. and mobility of negative ions 80−38518
SO_2, electron impact excitation of low-lying electronic states 79−10215

sulphur compounds continued
SO_2, emission control alternatives for coal fired power stations 79−52978
SO_2 emission control and dispersion contrib. to ambient standards achievement 79−83660
SO_2 emission fluctuations during 1977 eruptions 79−39694
SO_2 emission inventory for Greater London 79−5608
SO_2 emission reduction, from steam generators burning pulverised brown coal *(German)* 78−53724
SO_2, emissivity, computer calcs. 77−84386
SO_2 evolution in soda-lime glass melting-fining, redox phenomena 80−84900
SO_2, fluoresc. and photosensitised phosphoresc. of biacetyl, quenching and triplet theory transfer 78−25608
SO_2, force field determ. from first and second order Raman spectra *(Russian)* 77−14441
SO_2, force fields using Redington method 77−18899
SO_2, form. in combustion, oxidising agent excess depend., thermodynamic anal. 78−15677
SO_2 from sour gas plants in Alberta 77−37372
SO_2, frost, IR spectra and implications for Io 80−77331
SO_2 frost or adsorbate on surface of Io, IR reflection spectrum 79−92708
SO_2, gas, photooxidation, cloud chamber obs. 79−1961
SO_2, gas complex analysis method, resonance absorption with pulsed laser light *(Japanese)* 80−36421
SO_2, gaseous 1s binding energy and S $KL_2L_3(^1D_2)$ Auger energy, XPS obs. 77−3416
SO_2, gaseous impurity, role in H_2 embrittlement of steel 77−59904
SO_2, geometry optimisation, ab initio MO calcs. 77−42232
SO_2, ground level concs. in urban areas of UK rel. to meteorology 79−12253
SO_2, ground state, ab initio and MOD POT calcs. 78−66466
SO_2, ground-level conc. calcs. near a nuclear facility 80−97823
SO_2, harmonic and anharmonic matrix elements comparison, appl. to vibrational energy transfer 80−63760
SO_2, heterogeneous conversion to SO_4^{2-}, rel. to urban air pollution 78−80789
SO_2, homogeneous oxidation mechanism in troposphere 78−96257
SO_2, homogeneous oxidation in atmosphere 78−96258
SO_2 IR absorption spectra *(Russian)* 79−25328
SO_2, IR and Raman spectra, mol. and lattice vibrs. 78−19464
SO_2, IR bands, emissivity, line shape and band model parameters 78−94246
SO_2, IR bands, line-shape parameters, 300-1200K 79−36704
SO_2, IR multiphoton excitation and inverse electronic relax., mol. vibr. and fluoresc. 80−106349
SO_2, IR obs. spectra meas. using $Pb_{1-x}Sn_xTe$ diode laser *(Japanese)* 79−49306
SO_2, IR photolysis, associated visible luminesc., 2-25 torr 79−29384
SO_2, IR spectra, Coriolis intensity perturbations 80−95617
SO_2, IR spectra, $\nu_1+\nu_2$ combination band, rot.-vibr. anal. 78−5225
SO_2, IR spectroscopy 79−98088
SO_2 identified as gas on Io 79−92704
SO_2, in air, potentiometric determ. using solid state detector 78−16151
SO_2, in Ar:OCS:O_2 matrix, $S+O_2 \rightarrow SO_2$ chemiluminescence reaction 77−48647
SO_2 in atmosphere, automatic meas., luminescence appls. *(Dutch)* 79−88041
SO_2, in atmosphere, pollution zones definition and assessment 78−81383
SO_2 in atmosphere, practical experiences with small automatic monitoring network 78−81462
SO_2 in atmosphere, remote sensing via computer assisted correl. spectrometer 78−4002
SO_2 in atmospheric samples, meas. using luminescence *(Dutch)* 80−3565
SO_2 in flames, laser induced fluoresc. meas. 78−61132
SO_2 in gas mixtures, determ. using X-ray absorpt. detector with gas chromatography 77−29069
SO_2, in O_2-variable gases, potentiometric determ. using solid state detector 78−20505
SO_2 in Orion Molecular Cloud-1 (OMC-1), rot. temp. 79−25670
SO_2, in Orion Nebula mol. cloud, distrib. obs. rel. to N_2H^+ and HCO^+ 77−26034
SO_2 in power station plumes, differential lidar meas. 79−57556
SO_2 in Sheffield industrial area, precipitation scavenging 77−29424
SO_2 in urban air of St. Louis, numerical simulation of parametric effects 79−12235
SO_2 in Venus atmosphere, distrib. and implications 79−101100
SO_2 in Venus atmosphere, IUE detect. 79−101101
SO_2, inertia defects and dipole moments by kinetic consts. method 80−928
SO_2 inhibiting effect on embrittlement, magnetisation pressure isotherms for chemisorption of SO_2 on Fe particles 78−39949
SO_2, interaction with NiO (100) surface, electron diffr. and Auger spectrosc. obs. *(French)* 80−97728
SO_2, ionis. pot., quark influence, ab initio SCF calc. 79−10058
SO_2, KLL Auger spectra of S, ab initio LCAO SCF calcs. 77−65515
SO_2, KLL Auger spectrum, obs. and ab initio SCF CI calc. 78−50654
SO_2, $L_{II,III}$ absorpt. edge, fine struct. 78−62823
SO_2, large-scale spatial and temporal distrib. of air pollutant 79−20981
SO_2, laser absorption spectra meas. air pollution detection and control 78−40672
SO_2, laser-induced phosphoresc.-excitation spectra of vibr. bands of $(^3B_1)$-$(X,^1A_1)$ transition 80−18879
SO_2, lattice dynamics, rigid mol. model 80−44266
SO_2 levels in Sarnia area, Ontario, modelling 77−37368
SO_2, liq., vibr. relax., US absorpt. and vel. meas. 80−34147
SO_2, liq. props. representation, by modified Redlich-Kwong eqn. of state 78−34590
SO_2 liquid, short range orientation effects, vibr. Raman spectra 80−2759
SO_2 liquid in sapping mechanism to explain erosional scarps on Io 79−92699
SO_2, long-path automatic monitoring using diode laser system 79−29892
SO_2, low conc. meas. using diode laser correlation spectrometer 77−91301
SO_2 low core, equilibria between air and water 78−16137
SO_2 mass spectrometric obs. in stratosphere 77−33200
SO_2, matrix elements for multiplet spin-orbit interaction 77−57905
SO_2, matrix isolated, ν_3 vibr. spectrum, diode laser spectroscopy, temp. depend. 77−50433
sulphur compounds continued
SO_2, matrix isolation spectra using tunable diode laser 78−45739
SO_2 max. conc. rel. to av. time and av. conc. in urban area 79−34454
SO_2 meas. in ambient air, Dutch-German programme 77−29443
SO_2, meas. in marine atmosphere at concs. lower than ppb 78−81340
SO_2 measurements for stability classification schemes, stack plume dispersion, Maryland 80−16862
SO_2, microwave absorpt. coeff. 77−64378
SO_2, microwave spectra, Ku-band Fourier transform spectrometer appl. 80−68265
SO_2, minor atm. components, near UV absorpt. spectra, temp. depend. *(French)* 80−36355
SO_2, mol. beam electric reson. in RF field, dipole moments of vibr. states 79−64116
SO_2, movement in atmosphere *(Dutch)* 80−97844
SO_2, nondispersive IR analyzer with compensation for optical bias 79−16103
SO_2, nonradiative transitions and intersystem crossing rates in gas phase, theory 80−23451
SO_2, ν_1-bands, absolute integrated intensity 77−6858
SO_2 on gas covered Pt surface, thermal conductivity and thermal accommodation coeff. 80−10346
SO_2 on Io, evidence from UV obs. 80−36561
SO_2 on Io, upper limit to global abundance 80−77332
SO_2 optical depth meas., mask correlation spectrophotometry, remote sensor 77−82066
SO_2, optoacoustic detect. in air-pollution control below parts per billion level 78−41355
SO_2 over E. United States, regional residence time 79−16651
SO_2, oxidation, precursor effects, rel. to air pollution 79−1960
SO_2, oxidation by O_2 and O_3 in aq. soln., kinetics, rel. to atm. rate processes 79−20905
SO_2 oxidation chemiluminesc., appl. to atm. chem. *(German)* 79−52670
SO_2 oxidation in clouds and rain, O_2, O_3 and H_2O_2 role 79−84351
SO_2 oxidation in coal-fired power plant plumes 77−87065
SO_2, oxidation in moist O_2-N_2 mixture by electron irrad., appl. to exhaust gas treatment 78−80766
SO_2, oxidation in moist atm., aerosol growth kinetics 78−96255
SO_2 oxidation in smelter plume 78−3922
SO_2 oxidation in stored rainwater samples, rel. to Mn content 79−84352
SO_2, oxidation on surface of fly ash particles under low relative humidity conditions 79−62160
SO_2 oxidation over atmospheric aerosol, absorption over V_2O_5 and C 77−70811
SO_2 oxidation rate, CO effect, smog chamber expt. 79−74925
SO_2 oxidation to SO_4 in urban atmosphere 80−81964
SO_2 oxidation to sulphates in dispersing plumes 77−70806
SO_2 oxidation to sulphate in troposphere, model predictions 80−81963
SO_2, oxidation via OH radical, rel. to atm. fate of HSO_x radicals 79−62559
SO_2 PMDR, CNDO CI calcs. 79−72342
SO_2, Penning ionisation and photoelectron spectra 77−83653
SO_2 phosphorescence, in Xe, Kr, Ar, N_2 matrices, environmental perturbation effects *(French)* 77−3407
SO_2 photo-oxidation products, smallest particle size detectable by condensation nucleus counters 78−24364
SO_2 photochem. effects on nitrate conc. in aerosols 77−49103
SO_2, photoelectron spectrum, vibr. struct., ionos. pot. 77−75217
SO_2, photomag. positronium quenching, spin conversion 77−31030
SO_2, photooxidation, aerosol evolution, rel. to air pollution 78−81392
SO_2, photooxidation, gas phase, in cloud chamber 79−47951
SO_2, photooxidation in gas phase, nucleation appls. 79−83479
SO_2 plume in atmosphere, remote sensing mask correl. spectrosc. method 80−55966
SO_2, pollutant, mesoscale air quality model appl. 78−81388
SO_2, pollutant, stationary source, quantitative meas. using Raman lidar 78−36291
SO_2, pollutant long-term mean conc. in England and Wales country areas 77−37360
SO_2 pollution electricity generation, policy options for control 80−51022
SO_2 pollution episodes in Venetian region, real-time forecasting via advection-diffusion model 80−77096
SO_2 pollution episodes in Venetian region, real-time forecasting via Kalman predictor 80−82046
SO_2, pollution high conc. duration in urban atm. 78−11982
SO_2 pollution in Montreal, Canada, anal. of meteorol. and source factors 80−104537
SO_2, pollution meas. in ambient air, International Comparison Programme 77−87066
SO_2 pollution of industrial area, occurrence affected by wind direction 80−89691
SO_2, pollution vertical distrib. in lower troposphere 79−79428
SO_2, pure gas, enthalpy, Carlson-Thodos van der Waals eqn. calcs. 80−83878
SO_2, radiation, emissivity and absorption coeff. calc. 77−55126
SO_2, radiative electron attachment spectra, vibr. stretching, electron affinity, theory 77−54617
SO_2 reaction with O_3 in water rel. to atmospheric oxidation 78−16083
SO_2, reduction by CO in presence of H_2O and O_2, catalyst effects 79−24819
SO_2 regional transport, three-dimensional grid model 77−37375
SO_2, relative Raman scatt. cross section 80−100061
SO_2 remote meas. at 4 μm with continuously tunable source 78−77365
SO_2 remote meas. by continuously tunable IR lidar 79−21025
SO_2, remote sensing of air pollution by correl. spectrometry and differential lidar 78−96298
SO_2 removal from waste gases, citrate process demonstration at 60 MW power plant 79−100553
SO_2, resonant vibrational excitation, electron impact spectrometer obs. 78−90309
SO_2, role in Io volcanism 79−92700
SO_2 rural background pollution meas. network 77−37465
SO_2, S K-LL Auger energies and chemical shifts 80−28069
SO_2, SO_4, pollutants long-range transport, airborne meas. over Denmark 78−3950
SO_2, SO_4^{2-}, air pollutants long-range transmission, simulation, dispersion model 78−57306
SO_2, SO_4^{2-}, air pollutants, budgets and turn-over times 79−20980
SO_2, SVL fluoresc. spectra, multiple vibronic origins 77−14474
SO_2, SVL fluoresc. spectra, 293 to 307 nm region 77−14475

sulphur compounds continued
SO_2, sextic centrifugal distortion consts., Watson Hamiltonian, perturbation method 77−10785
SO_2, shock heated, visible emission 80−58274
SO_2, single vibronic level fluoresc. spectra 80−91597
SO_2, solubility in molten Na_2SO_4 79−69251
SO_2, spectral determ. in atmosph. of Venus *(French)* 79−62776
SO_2, spin-forbidden singlet-triplet transition, appl. to high-resolution spectroscopic technique 77−22601
SO_2 stability in Io's atmosphere 79−92705
SO_2 surface reaction and decomposition on zeolites, resonance Raman study 80−61145
SO_2, T_2 relax. meas. using budge-type superhet. microwave spectrometer 80−91551
SO_2, T_2 relax. time meas. by microwave transient nutation 77−30862
SO_2, T_2-relax., rot. transitions, time resolved spectra, microwave pulsed spectrometer study 80−18846
SO_2 teledetection of gaseous atmos. pollutants, data acquisition and anal., pollution mapping *(French)* 80−7989
SO_2, thermal decomposition in shock waves, infrared measurements 79−47903
SO_2 to SO_4 transformation rate from atm. conc. data, aircraft meas. 77−73829
SO_2 to sulphate conversion processes in atmosphere 77−37389
SO_2, total electrostatic pot., Thomas-Fermi eqn. soln. 79−10034
SO_2 transfer resistance of European soils, laboratory meas. 77−37384
SO_2 treatment of PAN fibres 79−52403
SO_2, triplet state electronic energy delocalisation 77−3478
SO_2, two-photon spectra by three-wave mixing 78−29826
SO_2, UV absorpt. meas. using lithium formate monohydrate freq. doubling system 79−31979
SO_2, UV absorpt. spectrum, triplet states, phosphoresc. lifetime 79−50042
SO_2, UV excitation spectra, mol. fluoresc. meas., mol. predissoc. obs. 80−83389
SO_2, Venice area air pollution, real time prediction of conc. 80−55953
SO_2, vertical distrib. in atm., influence of clouds and rain, one-dimens. model 79−20982
SO_2, vibr. energy levels, semiclassical trajectory method calcs. 78−58660
SO_2, vibr. relax., phase spectrophone method obs. 80−87059
SO_2, vibr. relax. time, 300-2000K, SSH-Tanczos calc. 79−45798
SO_2, washout from atmosphere and rain composition, model 78−28253
SO_2, X→A electronic absorpt. band system, non Condon effects study 80−18837
SO_2^-, adsorbed on MgO, g-tensors, spin densities, CNDO calc. 78−46270
SO_2^-, ESR obs., on used hydrodesulphurisation catalysts 77−70342
SO_2^+, ($B^2A_1 \rightarrow X^2A_1$) fluoresc., Penning excitation, vibr. and bending freqs. 77−50507
SO_2^+, fluoresc. quantum yields and lifetimes, meas. method, ion form. 77−6815
SO_2^+, fluoresc. spectra, Penning ionis. collision with He(2^3S) 79−13758
SO_2^+ radical-ion formation 77−25285
SO_2^+, state selected vibr. levels, fragmentation, photoelectron-photon coincidence spectroscopy 79−89707
$^{34}SO_2$, $\nu_1+\nu_3$ band, high resolution IR spectrum *(French)* 77−71801
$SO_2/H_2O/X_2$ reactions (X_2=Br_2, I_2), appl. to thermochem. H prod. 80−35773
SO_2-$^{18}O_2$ mixtures, IR laser pumped, intermol. vibr. energy transfer dynamics obs. 80−87207
SO_2-alkane-H_2O gaseous mixture, photoinduced nucleation and quantum yields 79−96348
SO_2-Ar atmosphere, effect on Co at 500-900°C 78−39953
SO_2-containing ions, photodestruction 80−63722
SO_2-gas mixtures, flash photolysis, H_2SO_4 aerosol form. 79−66307
SO_2-H_2O microwave absorption, 94 GHz by mol. interaction 79−31507
SO_2-I_2 water splitting cycle, thermochem. H prod. 80−30600
SO_2-lime plaster interaction *(German)* 77−86378
SO_2-seawater, thermodynamics 77−52660
SO_2-sulphate relationships in Budapest air 77−70810
SO_2-tetrachloromethane, solns., near critical point, ultrasound absorpt. obs. 80−65160
SO_2+active N_2, excited neutral metastable SO_2 form. mass spectrometric study 80−83300
SO_2+Al, high temp. fast flow reactor obs. of kinetics 80−30226
SO_2+alkane, $^3B_1$-state lifetime saturation, chem. and phys. quenching channels 79−814
SO_2+Ar, dissoc. rate meas. behind shock wave, laser Schlieren method 80−81296
SO_2+Ar^+, emission spectra obs. 78−50622
SO_2+B, gas phase rate consts., 300K, at. absorption obs. 79−83445
SO_2+Ba→SO+BaO, reaction kinetics, BaO recoil velocity spectra 79−74361
SO_2+bromomethane, microwave spectral line width, dipole-dipole interaction calc. 78−74648
SO_2+CO_2*, near-reson. energy transfer, fluoresc. obs. 80−106348
SO_2+CO_2.CO_2^+, reaction rate coeff. and product distrib. 80−3305
SO_2+$CO(C_2H_2)$, photochem. reactions, rate consts. 78−23956
SO_2+Cl, rate const. rel. to stratosphere Cl chemistry and Venus atm. 79−84353
SO_2+fluoromethane, collisionally induced relax. processes and vibr. energy transfer 80−53107
SO_2+$H_2O(N_2)(SO_2)$, linewidths, intensities, isotope shifts, 91.5-95.5 GHz 78−42044
$3SO_2+H_2O \rightarrow 2H_2SO_4+S_n$, chem. equilib. of aq. system, application to Venus and Io 80−50837
SO_2+He, Penning ionis. due to He(2^3S), SO_2^+ fluoresc. 79−13758
SO_2+He(2^3S), Penning ionisation, mol. ion fluores., vibr. and bending freqs. 77−50507
SO_2+N_2, quenching of vibr. excited N_2, photoionis. detect. technique 78−46388
SO_2+$N_2(CO_2)(H_2O)$, collisional quenching of $^3B_1$ state, 8-1300 torr 78−86906
SO_2+NH_3, atmospheric aerosols direct form. 77−29377
SO_2+NO_2 aerosol, form. kinetics, irrad. by 488 nm light 78−40067
SO_2+NO^+, reaction rate consts. meas. 80−7782
SO_2+Ne^+, thermal energy, reaction rate coeffs. and product distrib. 79−29333
SO_2+Ne(He), Penning ionis. electron spectroscopy, energy peak shifts and shapes 77−42392
$SO_2+O_2=SO+O_2$, gas phase reaction, rate coeffs. meas. 80−97704

sulphur compounds continued
SO_2+OH, role for stratospheric HSO_3 layer, reaction rate consts. 78−32202
SO_2+OH, rot. inelastic collision, microwave spectra 79−45806
$SO_2+O(^3P)$, vibr. excited, collision induced intramol. deactivation 78−25670
SO_2+olefin+thiirane+O_3 excited neutral metastable SO_2 form. mass spectrometric study 80−83300
SO_2+SO_2, potential well depth estimation method 79−86034
SO_2+SO_2(Ar)(He), vibr. relax., shock tube study 80−48062
SO_2+Sc(Y), nascent product state distribs., laser fluoresc. detect. 78−7187
SO_2+Tb^{3+}(Dy^{3+}), in H_2SO_4 soln., electrochemiluminesc. emitters quenching by electrolysis products 79−1794
SO_2+W, reaction kinetics, 1600-2100K 79−20266
SO_3, dissoc. pathways and mol. vibr., compliance consts. and min. energy coords. 78−35661
SO_3, electron impact mass spectrometry, proton affinity, ion-mol. reactions 78−3415
SO_3 emissions remote meas. from Asama Volcano, Japan *(Japanese)* 79−70772
SO_3 evolution from anhydrous α-$CoSO_4$, gas equilib. and kinetic approach *(German)* 78−23943
SO_3, gaseous, IR absorpt. coeffs., partial press. variations 78−56922
SO_3, photoelectron spectrum assignment, ionisation pot. and electron affinity, Green's function method 77−54576
SO_3, reversible dissociation, thermal energy storage appl. 79−48186
SO_3, rotational Raman spectrum, rot. consts. and bond lengths 79−18195
SO_3^- containing alkali borate and silicate glasses, γ-irrad., paramag. SO_3^- radicals 79−42838
SO_3^{2-}, SO_4^{2-}, O K-emission spectra, electron struct. 80−87099
$SO_3+Ar \rightarrow SO_2+O+Ar$, rate const. of spin forbidden dissoc. in shock wave 79−57214
$SO_3+H_2O \rightarrow H_2SO_4$, gas phase kinetics, CNDO/2 calc. of H_2SO_4 and $SO_3.H_2O$ struct. 78−76840
SO_3+NH_3, donor-acceptor adduct form., ab initio calcs. 78−82612
SO_4 aerosol, geographical extent in Midwestern and Southern USA 77−49145
SO_4, and isotopic forms, struct., normal coord. anal. 78−965
SO_4, atmospheric distribution, moving high pressure system, E.United States 79−83664
SO_4 dispersion, wind, temp. and conc. fields 78−3929
SO_4, distortion from T_d symm. 78−63706
SO_4^{2-} aerosol form., CO effect, smog chamber expt. 79−74925
SO_4^{2-} aerosol form. and growth in stratosphere 79−5604
SO_4^{2-} aerosol layer, form. and evolution model for stratosphere and troposphere 80−21801
SO_4^{2-} aerosol layer in stratosphere, formation and evolution model 80−17327
SO_4^{2-}, aerosol particles size depend. on relative humidity 79−20906
SO_4^{2-} aerosols, ambient, laser-Raman monitoring 78−69532
SO_4^{2-}, aerosols, in atm., large-scale spatial and temporal distrib. 79−20981
SO_4^{2-}, air pollutant, conc. in remote continental and oceanic areas 79−20983
SO_4^{2-}, air pollutant, spatial and temporal distrib. in United States 79−20985
SO_4^{2-}, air pollution, natural sources in tropical humid area *(French)* 78−81371
SO_4^{2-}, air pollution, Regional Experiment (SURE) in NE.United States 79−20977
SO_4^{2-}, air pollution, sources and sinks, stochastic model 79−100930
SO_4^{2-}, air pollution determ. in Netherlands, 1971-76 period 79−21031
SO_4^{2-}, air pollution transport over Mediterranean 78−81390
SO_4^{2-}, airborne particles, size meas. and chem. comp. by diffusion sampling 78−45007
SO_4^{2-}, atm. aerosol hazes and long-range pollution transport, satellite detect. 79−20975
SO_4^{2-}, atm. prod. rel. to cloud water acidity 79−5546
SO_4^{2-}, conc. in atm. precip. 79−100915
SO_4^{2-}, conc. in rainwater, obs. by European Atmospheric Chemistry Network 79−2365
SO_4^{2-} containing aerosols, dynamics, review 78−96286
SO_4^{2-}, contrib. to acidity of rain 79−2327
SO_4^{2-}, detect. in subway air 78−36273
SO_4^{2-}, dry and wet removal from atmosphere 79−2361
SO_4^{2-}, effect on Ti crystallisation *(Chinese)* 79−51440
SO_4^{2-}, in ambient aerosols, assay via ion chromatography anal. 78−68974
SO_4^{2-}, in atm. aerosol particles, sampling and anal. techniques 78−28304
SO_4^{2-} in E United States precip., concs. behaviour 78−92962
SO_4^{2-}, in Greenland snow and ice, natural and anthropogenic origins 79−70815
SO_4^{2-}, in natural water, determ. by at. absorpt. spectroscopy 77−40595
SO_4^{2-}, in stratosphere, concs. at high altitudes 78−20468
SO_4^{2-}, individual submicron size particles detect. method 78−95973
SO_4^{2-}, ionisation energies, SCF-Xα transition state calcs. 80−74115
SO_4^{2-}, level in reacting atmospheric aerosol, calcs. 80−26056
SO_4^{2-}, maritime atm. aerosols, sources over N.Atlantic Ocean 79−20904
SO_4^{2-}, meas. in particulate matter from coal and oil combustion 79−74569
SO_4^{2-}, ν_1 Raman linewidth, in acidic aq. soln. 77−65481
SO_4^{2-}, pollution vertical distrib. in lower troposphere 79−79428
SO_4^{2-} production in rain and raindrops in polluted atm. 79−88388
SO_4^{2-}, quantitative determ. in aerosol particles 79−20474
SO_4^{2-}, sampling and anal. of atm. aerosols 78−96283
SO_4^{2-}, spatio-temporal distrib. in Antarctic snow 79−20870
SO_4^{2-} species, identification in air pollution by Raman spectroscopy 79−5625
SO_4^{2-}, tropospheric aerosols chem. props. 78−96254
SO_4^{2-} vibr. spectra, press.-scanned Fermi reson. spectroscopy appl. 79−73937
SO_4/Cl ratio in Ionian Sea coastal waters *(Italian)* 79−5499
SO_5^{2-}+Tb^{3+}(Dy^{3+}), in H_2SO_4 soln., electrochemiluminesc. emitters quenching by electrolysis products 79−1794
SO_x removal from atmosphere, by absorption reaction, using MARTZ-CLEAN reagents based on $NaClO_3$ and K_2CO_3 *(Japanese)* 80−61147

sulphur compounds continued
S_2O, 3400 Å bands, rot. anal., upper state struct. 78−13506
S_2O, forbidden transitions, laser optoacoustic spectroscopic obs. 77−61756
S_2O, force field determ., Redington's method applicability 79−81168
S_2O, isotopes, force consts., mean amplitudes of vibr. 78−970
S_2O, photoionis. mass spectrum, heat of form., dissoc. energy 77−46605
S_2O, UV excitation spectra, mol. fluoresc. meas. 80−83389
S_2O^+, form. cross section, S_2O photoionis., 650-1200 Å 77−46605
$SO_2(^3B_1)$, isolated mol., phosphoresc. decay efficiency 77−75194
$SOCl_2$, immersion medium for Nd:glass disc laser 78−1262
$SOCl_2$, microwave discharge, chemiluminescence of $SO(^1\Delta_g, ^1\Sigma_g^+)$ 80−26016
$SOCl_2$+H, energy disposal, HCl IR chemiluminesc. obs. 78−92484
SO_2Cl^- and $(SO_2)_2Cl^-$, heats of formation, determ. by mass spectroscopic technique 80−76540
SO_2Cl_2, photoabsorption and photodissociation, 190-300 nm 79−50038
SO_2Cl_2+H, energy disposal, HCl IR chemiluminesc. obs. 78−92484
SO_2ClF, reduction by anhydrous HI 79−5150
SO_2F_2, bond function parameter transferability 77−30770
SO_3F, dye laser excitation of vibr. levels of upper electronic state, mol. fluoresc. meas. 80−83402
SO_3F, laser fluoresc. spectrum 80−28047
$S_2O_6F_2$, heating and laser excitation fluorosulphate radical prod. and spectrum 78−35647
SOH, ground and first excited states, geometry, ab initio SCF calcs. 78−50657
SOH radical, ab initio SCF and CI calcs., electronic states and transitions 77−46488
$S_2O_8^{2-}$-I^- aqueous redox mixtures, γ-radiolysis 79−16017
$S^{16}O_2(S^{18}O_2)$, $^1B_2('A')$ state, force field for large amplitude motions 80−43023
$SO_3(SO_3^+)$, Jahn-Teller interaction, Franck-Condon factors and vibronic energy level calc. 78−50536
$SO(^1\Sigma^+ \rightarrow ^3\Sigma^-)$, in O-COS-$O_2(^1\Delta_g)/O_2$ system, chemiluminescence 80−66806
SO_2XY, (X,Y=Cl,F), positive and negative ion chemistry 78−85140
$SO_2.BF_3$, ^{10}B enrichment by low-temp. exchange *(Japanese)* 78−55251
$SO_3.H_2O$ and H_2SO_4, CNDO/2 calc. of thermal stability 78−76840
$SPBr_3$, mol. struct., electron diffr. and spectroscopic vibr. amplitude 80−58387
SPF_3, electronic struct. of valence shell, UV photoelectron spectroscopy 78−82781
SPF_3, IR spectra, matrix isolated, force const. calc. 78−62802
SPF_3, isotopic forms, microwave spectra, centrifugal distortion consts., vibr. and rot. states, IR matrix spectra 77−10665
SPF_3 vibr. spectrum, assignment using matrix isolation and isotope substitution *(German)* 78−13498
$SSBr_2$, IR matrix isolation spectra in Ar matrix at 9K 79−93995
$SSCl_2$, IR spectra, prod. in S_2Cl_2 photolysis 78−61033
SSF_2, FSSF, and ^{34}S isotropic forms, matrix IR and Raman spectra *(German)* 79−89674
SSO^-, adsorbed on MgO, g-tensors, spin densities, CNDO calc. 78−46270
SSe_{20}, crystalline phase growth in amorphous solid and liquid samples 78−43107
$SSe_{22.5}$, amorphous, photo-effect on crystn. kinetics, elec. cond. obs. 79−77522
$SSe_{22.5}$, amorphous-cryst. transition, light effect, rel. to polymer crystallisation 79−99076
SSe_{40}, amorphous alloy, crystn., elec. cond. meas. 78−34440
SSe_9, stable thermoelectret, effects of anisotropic external perturbation *(Russian)* 77−63361
SSe_x (x=10, 15, 40), amorphous crystal transition, appl. of Kolmogorov-Avrami equation 78−67649
S_xSe_y, s=6-3, y=2-5, thermal behaviour 78−67813
$S(SiD_3)_2$, gaseous, liquid, solid phases, Raman spectra, IR spectra gas and solid phases, molecular vibr. exam. 78−25547
$S(SiH_3)_2$, gaseous, liquid, solid phases, Raman spectra, IR spectra gas and solid phases, molecular vibr. exam. 78−25547
S0 in Orion Molecular Cloud, line profile rel. to rotational explanation of high-vel. mol. emission 80−36688
$^{32}SF_5{}^{35}Cl$, microwave rot. spectra, mol. parameters *(French)* 77−456
$^{32}SF_6$, multiphoton dissoc., temp. depend. 79−89722
^{35}S compounds, beta decay, transition probabilities, ab initio calcs. 77−61387
Se-S, glassy alloy, order-disorder transition kinetics 78−67650
Sf_6, absorpt. of pulsed CO_2-laser radiation at 140K 79−22707
Sf_6, high resolution X-ray emission, valence electron struct. and chemical bonding, LCAO comparison 79−31545
Sf_6, IR-IR double reson. following IR laser excitation, ν_3 mode 79−54872
Sf_6, integrated IR band intensities and transition moments 80−95611
Sf_6, simultaneous multiline saturation at 10.6 μm 77−88868
Sf_6, third harmonic generation at 10.6μ 77−14775
Sf_5Cl, mol. image reconstruction by electron holography 79−68367
SiO_2-Al_2O_3-Fe_2O_3-CaO-MgO-Na_2O-B_2O_3-SO_3, exam. of white flaky inclusions, causes and formation time 79−29237
SiO_2-Na_2O-CaO-MgO-Fe_2O_3-Al_2O_3-SO_3-Sn thermally polished, exam. of strength of surfaces 80−25887
$(Sn)_x$, superconducting polymer, elec. cond., heat capacity and optical props. 80−7028
Xe+$NH_3(H_2S)(SO_2)$(HCl), ionis. cross sections calc. 77−68103

sum rules
0^--mesons in broken SU(4), improved mass formula 77−30352
$3/2^+$ charmed baryons, mass splitting by weight diagrams, parallelogram law sum rules 77−49915
27-plet mesons, mass sum rules using SU_4 dynamical-group scheme 77−26505
η' meson as pseudoscalar gluon, current sum rule saturation in QCD *(Russian)* 79−71718
A=2, 4, 16, photonuclear sum rule enhancement factor, Hartree Fock, Bethe-Goldstone eqns. 79−3137
additive quark model with six flavours 80−27455
Adler's, deep inelast. νp scatt. and πp cross sections 77−41843
Adler's sum rules in source theory 77−38099
Adler sum rule subtractions and charge symmetry violation 77−18202
Adler-Weisberger sum rule and the σ-commutator for the kaon-proton system 80−101956
Adler-Weisberger sum rule and the σ-commutator for the kaon-neutron system 80−101957
atoms, bound system, generalised virial theorem and dipole sum rules 78−21088
axial vector multiplets, mass spectrum, mixing angles, pseudoscalar mesons, decay consts. 77−13892
b-mesons, mass splitting, SU_3 nonet of SU_6 80−47288
bag model, spin-depend. struct. functions in deep inelastic scatt. 78−8589
baryon mag. moment sum rules in SU_4 charm symmetry scheme 77−30380
baryon magnetic moments, implications for quark model 80−13290
baryon resonance decay, π emission, quark model, widths, amplitudes, sum rules 77−57534
baryon weak radiative decay sum rules, octet/sextet and 20-plet dominance 78−62400
baryons, spin $1/2^+$, mag. moment sum rule, in SU_3 for u-, d- and c-quark sector 78−21428
beautyonium bound states, Υ, Υ′, Υ″, dispersion sum rules *(Russian)* 80−13235
Bessel functions, squares of positive zeros, nonlinear eqns. and sum rules 78−49639
Bethe-Levinger, meson exchange current theories 79−71798
Bloom-Gilman duality and pion form factor 79−9352
bootstrap, planar pole, and existence of good finite mass sum rules 78−16948
broken SU(3) hyperon anomalous magnetic moment sum rules, SU(3) Λ-Λ′ mixing explanation 77−18288
bromomethane($-d_1,d_2,d_3$), F and G sum rules as vibr. intensity data error indicators 79−3494
causality, Regge behaviour, proton electroprod. struct. function, Bjorken limit of sum rule 77−67662
charm baryons, mass splitting and weight diagrams 79−26314
charm particle photoproduction total cross sections, quantum chromodynamics *(Russian)* 78−45880
charm particles, sum rules for four-body semi-leptonic decays 79−36067
charm scheme of subhadronic constituents, weak decay processes 78−25012
charmed baryon nonleptonic decays, sum rules for ΔC=ΔS=1 S-wave decays 79−58957
charmed baryons, mass splitting sum rules 79−89083
charmed hadron masses, from effective quark masses, sum rules 80−4965
charmed hadrons, SU(4) mass-breaking, mass sum rules 80−62959
charmed hadrons ΔC=ΔS decays, sum rules, internal symm. props. 77−30376
charmed particles, hadronic props., superconvergence sum rules 80−78043
charmonium, C-even, decay sum rules in QCD 77−54081
charmonium, masses of 2P and higher levels, sum rules 78−4805
charmonium and charmed mesons on QCD, sum rules 77−30327
class of sum rules for system of identical particles 80−91019
closure approximation, appl. to perturbation theory, muon capture and pion electroproduction 78−16680
coefficients of fractional parentage for 3- and 4-body nuclear systems, sum rules 77−50067
collective states and crossing symmetry 79−93497
Compton profiles, directional, sum rule based on kinetic energy integral 80−2889
conserved axial second class current, sum rule, commutation relations and axial formfactor 80−18090
conserved axial second class current, sum rule, dispersion calc. 80−77986
Cottingham formula, nuclear Coulomb energy differences 78−37256
counting rules and determination of quark masses in chiral $SU_4 \otimes SU_4$ 79−63437
critical correlation function and exponent η: a sum rule 79−63387
crossing sum rules for partial-wave amplitudes 78−21355
cubic inverse energy-weighted and adiabatic inertial parameters in HF calcs. 77−79316
current algebra and electromagnetic hadron interactions, review, book contrib. 80−47240
current correlation function finite temp. spectral function sum rules 77−67591
de Gennes' model sum rules, decoupling procedure in Green's function method *(Russian)* 78−56434
deep inelastic scatt., mass corrections, asymptotically free theories 77−61297
deep inelastic sum rules in source theory 77−61190
deformed nuclei, surface thickness effects and multipole excitation splitting, sum rule approach 79−453
dimuon prod., sum rules and moments, valence quark transverse moments 78−54660
dipole, estimate of $\chi_J \rightarrow \gamma\psi$ widths 77−13958
dipole sum rule schematical eval., collective isovector quadrupole strength 80−47428
dipole sum rules for products of 3-j symbols 78−65803
dispersion sum rules and exotic baryon resonances, reggeon scatt., E_{55} resonance *(Russian)* 80−101955
dispersion sum rules for Reggeon-particle scatt. 78−54583
doubly closed shell nuclei, isovector giant monopole resonances, sum rule approach 80−78244
Drell-Hearn-Gerasimov sum rule determ. in low energy Compton effect anal. 78−21433
Drell-Yan process higher order corrections, QCD and parton model sum rules 80−95251
duality, phenomenological, strong interactions description using finite energy sum rules 77−82716
duality and four reggeon amplitudes 77−233
duality sum rule, inclusive e^+e^- annihilation semi-local duality 77−49985
dynamical Higgs mechanism, weak ΔI=1/2 rule, sum rules, heavy quarks and leptons 80−27442
effective NN interaction and exchange current vel. depend., dipole sum rule enhancement 80−63100
eikonal approx., electron-oriented nucleus scatt., polarisation of e , nuclei and emitted γ rays 78−37331
electro- and photonuclear EM sum rules 80−22810
electron-nucleus nonintegrated sum rules and projection operator method 77−2967

sum rules continued
electronuclear energy weighted sum rules and excited state quadrupole moments 79−36150
electronuclear sum rules, generalised, from EM structure functions 78−89806
electronuclear sum rules, linear energy weighted, nuclear struct. determ. method 79−75897
electroproduction, polarised, flavour singlet coefficient functions, QCD corrections, sum rules 80−47301
electroproduction, spin-dependent, sum rules, test of relativistic constituent quarks 78−25050
electroproduction above pion threshold, EM interactions and mag. sum rules 80−42639
EM multipole transitions, nuclear force contrib., model independ. of energy weighted sum rules 78−66241
energy momentum sum rule beyond the leading order in QCD 80−78024
energy weighted electronuclear sum rules, centre-of-mass corrections 80−5091
energy weighted sum rules for spin-dependent excitations of nuclei 80−86833
ethylene, transition moment closure tests of basis sets 79−6968
even nuclei, 2^+ excited states quadrupole moments, energy weighted sum rule appl. 80−9229
even-even nuclei, static quadrupole moments of arbitrary excited states, sum rule approach 80−91135
exotic baryon resonance with isospins $\geq 5/2$, existence, sum rule in Reggeon field theory *(Russian)* 78−93824
few-nucleon systems, energy-weighted longit. sum rule for electron-nucleus scatt. and nuclear forces 78−58238
field and algebra struct. on null planes 77−18154
field theory, renormalisation of single particle states 78−24926
fine structure of inclusive spectra, sum rules and Feynman-Yang scaling generalisation *(Chinese)* 79−49557
finite energy, for pion and photon couplings for D*-D system, D* width 77−67649
finite energy sum rule for nucleon polarizabilities difference *(Russian)* 79−58905
finite energy sum rules, high-energy Regge expansion 77−45988
finite-mass, for reggeon-reggeon scatt. 77−41828
Freidrichs model, Lyapunov function evaluation 78−73876
Gelfand pattern, charmed hadrons and magnetic moment 80−398
gluonium, scalar, J/ψ radiative decay as gluon source, QCD sum rules 80−47296
hadron interactions, effective radius quantum number depend., quark sum rules *(Russian)* 80−102062
hadron spectrum, planar amplitudes without Regge cuts 80−27464
hadronic deep inelastic production, sum rules in quark parton model 77−87981
hadronic structure using parton anal. of deep inelastic scattering and rel. processes 79−80803
hadronic targets, spin-$^1/_2$, Compton scatt., optimal sum-rule inequalities 80−105815
hadrons, multipole polarisabilities from Compton scatt. amplitudes 80−13311
hadrons with charm, beauty and taste, SU_3 subalgebras of SU_6 80−9152
Hartree-Fock anal. of nucl. many-body problem 77−18457
heavy-quark channels and threshold prediction, pomeron hypothesis, sum rules relating NN, πN, KN cross sections 78−89755
Heisenberg ferromagnet system, temp. Green's function sum rules *(Chinese)* 80−31678
high-mass diffraction in the supercritical region 79−22081
hypernuclei, Friedel sum rule, hadron phys. meaning, nuclear matter density, binding energy 78−82305
hypernuclei, produced by strangeness exchange reactions, sum rule cross section calcs. 78−17130
hyperon nonleptonic decay, sum rules for S-wave amplitudes 79−63476
hyperon nonleptonic decays in SU(3) 79−97624
hyperon radiative weak decays sum rules, branching fractions and asymmetry parameters 80−410
I=1 bosonic reggeon-particle scatt., dispersion sum rules *(Russian)* 80−32089
I=1 reggeon-baryon scatt., superconvergent dispersion sum rules and vertices struct. *(Russian)* 80−27494
inclusive hadron production in high energy particle+nucleus collisions, sum rules, scaling law 77−57673
inclusive nonleptonic and semileptonic decays of charmed hadrons, sum rules determ. 77−71514
inclusive reactions, induced by EM or hadronic weak currents, single obs. π sum rules, PCAC 77−34161
ionisation potentials, sum rule, Manne Åberg theorem connection, many body Green's function formalism 80−27930
Ising model with transverse field, method of two-time Green's functions 80−2543
isoscalar giatn resonances, sum-rule approacH 77−82898
isoscalar meson-nucleon couplings, finite energy sum rules, duality determ. 77−13940
isotopic molecules, new sum rule connecting vibr. freq. parameters 79−36615
jet cross sections and quark current-photon pointlike coupling, sum rules 80−32104
large-amplitude collective nuclear motion in fission and heavy ion reactions 80−22675
Lepton pair production cross section using Drell Yan formula, sum rules, moments 78−54611
lepton-hadron deep inelastic scatt. 77−79233
lepton-proton deep inelastic scatt., energy momentum sum rule approx. using QCD model 79−63439
light nuclei, total photonuclear cross sections 79−71841
mass-sum rule, Veneziano-type amplitudes π and K mesons 78−74180
Melosh transformation and light cone current algebra 77−41791
meson radiative transition, symm. and duality constraints 78−78178
meson spectrum in simple planar bootstrap model 78−8618
mesonic effects in photonuclear sum rules, book contrib. 80−476
minimally coupled N-particle scatt. integral eqns. 77−88090
multipole moments, form factors, energy weighted sum rules, cnetre-of-mass bounds 80−27590
Nachtmann moments of $F_2^{\nu N}(x,Q^2)$ and energy momentum sum rule 80−57580
nonlinear molecule rotation-vibration motion, sum rules calculations 79−98062
sum rules continued
nucl. sum rules, electron scatt., giant reson. 77−14114
nuclear binding energy, relativistic sum rule 77−14023
nuclear collective excitations 79−59002
nuclear dipole polarisability sum rule, HF calc.,, ^{16}O, ^{40}Ca appl. 78−21504
nuclear direct reaction orbital rearrangement and energy sum rule, ^{40}Ca anal. 77−79353
nuclear elastic form factors, properties from energy weighted sum rules 78−37319
nuclear electro-excitation, energy-weighted isoscalar sum rules 80−63174
nuclear EM sum rules for (γ,γ), (e,e), transitions and giant resonances 80−5090
nuclear field theory, phonon renormalisation, eigeneqns. and sum rules *(Chinese)* 80−102127
nuclear giant multipole resonances, energies, transition densities, sum rules from RPA eqns. 77−61365
nuclear hydrodynamic models, current density sum rule 77−79314
nuclear magnetic multipole transitions, energy weighted sum rule 79−9505
nuclear matter, correlated, electric dipole sum rule 80−83056
nuclear matter, Landau parameters sum rules, tensor force effects 79−80892
nuclear radiative muon capture rates, maximum photon energy, sum rule correction calc. 79−6517
nuclear spin depend. excitations 79−59018
nuclear sum rule anal. of one-neutron transfer data, shell model validity 77−67730
nucleon polarisabilities and dispersion relation sum rules 77−49966
null plane current anticommutators, sum rules and appls. 80−52436
octet baryons in SU_3, EM mass difference, u, d and c quark sectors 78−29334
one-dimensional oscillator, matrix elements, upper and lower bounds using quantum mech. sum rules 79−35578
partial wave amplitudes asymptotic behaviour, Regge models and dispersion relations 77−10204
partially conserved axial vector currents, corrections, light-plane commutators, sum rules, meson decay 79−304
parton model, corrections in asymptotically free field theories 77−38092
parton transverse momentum dependence on longitudinal momentum 78−25016
photoabsorption, σ_{-2} sum rule, gauge invariance and locality 77−34286
photonuclear reactions 77−79362
photonuclear sum rule, spin current contribs., strong violations 80−18291
photonuclear sum rules from continuum calcs., dependence on residual interactions 80−22807
photoproduction polarisability sum rules in QED 79−2960
pion-charmed baryon scatt. and coupling strengths, superconvergence sum rules 80−52532
pion-nucleus scatt. amplitude determ. using derivative sum rules and dispersion relations 77−10373
polarised deep inelastic electroprod., QCD higher order effects, sum rule correction 79−93428
polarizabilities of proton and pion, sum rule relation *(Russian)* 79−93420
polyatomic molecules, intensity distribution in vibronic bands, Dushinsky effect 79−93983
polyelectron atom He-Xe, strength sum evaluation method 77−75229
polynomials, zeros, sum rules 80−57521
polynomials, zeros, sum rules 80−62888
progenitor sum rules, π-nucleon coupled fields, ρ-mesonic effects 78−17111
progenitor sum rules, nuclear theory appl., meson+nucleon interaction, inelastic form factors 78−54690
pseudoscalar mesons, sum rule, symm. breaking of chiral SU(4)×SU(4), decay const., masses 78−33000
QCD, charm photoprod., ψ, D, F etc. prod., sum rules, cross sections 78−58169
QCD, resonance props. from sum rules 79−26301
QCD, spectral function sum rules in charged current sector 79−80796
QCD, sum rules for light quarks *(Russian)* 78−45812
QCD and resonance physics, appl. of sum rules to ρ-ω mixing 79−22060
QCD and resonance physics, appl. of sum rules to reson. props. of mesons 79−22059
QCD and resonance physics, general technique for deriving sum rules 79−22058
QCD predictions, high p_T processes subject to sum rules, SU(3) symmetry constraints 79−354
QCD spectral function sum rules, EM current flavour components 80−99084
quantum two-component plasma third sum rule and local mean-field theory 78−5982
quark model with 4 quarks pseudoscalar meson masses 77−46021
quark recombination model, meson and baryon prod. sum rules 80−4922
quark-parton, for various Reggeons 77−6095
quark-parton model, strong interactions of quarks, weak interaction *(Russian)* 77−82710
quarkonia, spectra, decays, levels, jets, sum rules 80−18112
quarkonium, quantum mechanical applications, masses and leptonic widths of ψ and Υ 80−27484
quarkonium radiative transition amplitudes, QCD dispersion sum rules 80−52511
quarkonium systems, sum rules 80−68423
Racah algebra of Gln, generalised back coupling rules 80−47208
radiative decay widths of charmonium states, superconvergent sum rules 78−21422
Reggeon amplitudes satisfying good finite mass sum rules 78−16953
Reggeon vertices and finite mass sum rule, bootstrap eqn., dual resonance model 80−13292
relativistic quark model, spectral function sum rules 79−63428
S- and P-wave hyperon decay amplitudes, $\Delta I=^1/_2$ rule deviations, weak current-current interactions 80−9166
scattering problem, universal sum rules 78−4806
scattering theory and polynomials orthogonal on the unit circle 79−30294
self-consistent mean-field theory, progenitor sum rules, giant dipole reson. 77−67729
semiclassical sum rules for bound state energy relations 78−70308
semileptonic decay of charmed particles, formalism using helicity amplitudes 78−4852

sum rules continued
sine-Gordon field, spectral sum rules 77−6000
single quark transition model, sum rules among charmed hadron decay amplitudes 78−12907
spectral function sum rule and onium 79−26329
spectral function sum rules for quark and baryon fields, using lightlike charges 78−93822
spherical nuclei with pairing, M1-reson. calc. 79−6390
spin/isospin saturated system, two-body distribution function, direct and exchange sum rules 80−27212
strengh distributions and statistical spectroscopy, general theory 77−79322
strength distributions and statistical spectroscopy, shell model comparisons 77−79323
structure functions, deep inelastic renormalisation group sum rules 80−22611
SU_3 subsectors of SU_4 and mass sum rules for charmed hadrons 79−35967
SU(3)×SU(3) chiral symmetry breaking, BBS coupling constants, sum rules 79−35959
SU(3) in SO(3) basis, sum rules for matrices of generators 80−13226
SU(4)×SU(4) broken chiral symm. 78−74176
SU(4)×SU(4) current two point functions, meson decay consts. and bare quark masses from duality 78−8598
SU(4) broken symm., duality, baryon+baryon and baryon+antibaryon exotic mesons prod. 78−89629
SU(4) spectral function, pseudoscalar mass spectrum, η' assignment 77−38143
SU(5) asymptotic symmetry, b quark flavour from Weinberg spectral function sum rules 79−67495
Υ' (10040) as an I=1 vector meson resonance 80−47241
time dependent HF polarisability and RPA sum rules, collective model restoring force 79−6461
time dependent HF polarisability and RPA sum rules, isovector giant resonances 79−6462
TRK sum rule, exchange contrib. 79−45035
two-particle scattering systems, general, sum rules 80−8862
unitary sum rules and collision time in large resonance level overlaps *(Russian)* 78−70309
vector meson-nucleon scatt., sum rules 78−45810
vector mesons, leptonic decays, six-quark sequental model 80−52490
virtual Compton amplitude, high-energy deep-inelastic scatt. 78−41550
weak hadronic $\Delta S=0$ baryon-π amplitudes, Melosh transformation 78−12857
weak nonleptonic decays in SU(4) and SU(8), adjoint representation admixture 78−21426
Weinberg sum rules, derivation of meson spectrum, duality unification with chiral symm. 78−29272
x^4 potential, associated ground state wavefunction, sum rules 79−45036
A_1, spectral function sum rules and A_1-W coupling const. 80−27429
$A_2 \rightarrow \pi\gamma$, suppression factors for VMD couplings calc., duality constraints anal. 77−13960
$\chi_J \rightarrow \gamma\psi$, charmonium states radiative and hadronic widths, gluon spin 80−4998
d inelastic screening, form factor at $t \neq 0$ 80−91070
D^+-D^0 mass difference, broken isospin symmetry in chiral SU(4)⊗SU(4) 78−89691
(e,e'p) quasi-free scatt., spectral function, sum rule discrepancy, shell model deviation 80−42641
e+nucleus scatt., multipolar sum rules *(Russian)* 78−21548
ed scatt., energy weighted sum rules, almost realistic NN pot. anal. *(Russian)* 80−13465
$e^+e^- \rightarrow$hadrons, finite energy sum rules in QCD 79−40754
e^+e^-, jet cross sections and quark current-photon pointlike coupling, sum rules 80−32104
e^+e^- annihilation, hadron jets transverse momentum and ang. distribs. from QCD 79−40793
e^+e^- annihilation, sum rules for Υ-family formation, QCD anal. *(Russian)* 79−54347
e^+e^- calorimetric experiments, $\gamma\gamma$ processes, tests of QCD 80−22628
$e^+e^- \rightarrow \gamma$+hadrons, quark-parton model predictions, sum rules, charge asymm. 77−10219
$e^+e^- \rightarrow$hadrons, below 2 GeV, comparison of QCD sum rules with expt. 79−49458
$e^+e^- \rightarrow$hadrons, finite energy sum rules, cross section, QCD calcs. 78−62413
$e^+e^- \rightarrow$hadrons, QCD perturbation theory sum rule, ρ, ω and ϕ mesons 79−85268
eN deep inelastic polarised scatt., QCD corrections 80−52517
ep deep inelastic asymmetry meas., Bjorken sum rule, p spin struct. models 78−70376
ep deep inelastic scatt., pol. p and e, straton model, sum rule *(Chinese)* 80−42475
ep interactions, microcausality, equal-time current commutators, sum rules *(Russian)* 77−74689
$ep \rightarrow \pi^0 X$, duality and finite energy sum rules 80−42477
$e^+p \rightarrow e^\pm\gamma + X$, deep-inelastic bremsstrahlung, quark charges, colour gluon mass 78−74216
η_c mass determ. from QCD sum rules 78−74223
η_c mass from dispersion sum rules in QCD, identification with X(2.83) *(Russian)* 78−89681
η', QCD sum rules for mass, possible pseudoscalar gluonium, instanton effects 80−388
$\eta''(2.8)$ radiative decay, charmed quark content of ω and ϕ mesons 77−71511
GpN and πK scattering, chiral dynamics and asymptotical restrictions, sum rules *(Russian)* 78−17047
γ^*N scattering amplitude, nonreson. part, dispersion sum rule with derivative *(Russian)* 78−66121
$\gamma\gamma$, jet cross sections and quark current-photon pointlike coupling, sum rules 80−32104
$\gamma\gamma$ elastic scatt., meson couplings to two photons 77−6128
$\gamma\gamma \rightarrow$hadrons, sum rules and non-Regge terms 78−25093
γp elastic scatt., <400 MeV, dispersion relation anal. 77−82744
$\gamma p \rightarrow p$+vector meson, total cross section *(Russian)* 78−8674
$\gamma p \rightarrow \pi^0 X$, duality and finite energy sum rules 80−42477
$\gamma p \rightarrow W^+ n$, current algebra and sum rules high energy W^+ prod. 80−102039
$\gamma\pi$, hadron photoprod. and saturation of sum rules *(Russian)* 79−49529
$J/\psi \rightarrow \eta(\eta')\gamma$ decay rate, QCD sum rules 80−52497

sum rules continued
(K^-,π^-) reactions, 900 MeV/c, sum rule for hypernuclear formation, distorted wave impulse approx. 78−70572
$K^*(982) \rightarrow K\pi\pi$, finite energy sum rules and finite dispersion relns. 77−22731
KN finite energy sum rules, Regge pole models, exchange amplitudes 78−470
KN scatt. length for S-wave I=0, dispersion reln. sum rules 78−37231
Kp reactions, 13 GeV/c, differential cross-sections, Regge exchange, SU_3 sum rule interpretations 77−41862
$K^-p \rightarrow K^0\Delta^0$, 13 GeV.$c^{-1}$, sum rule in kaon-nucleon cross section meas. 78−82236
$K^-p \rightarrow \bar{K}^0 n$, 13 GeV.$c^{-1}$, sum rule in kaon-nucleon cross section meas. 78−82236
Λ recoilless prod. on nuclei by (K^-,π^-) reaction 77−3053
μp high energy data, QCD energy momentum sum rule, gluon fraction of proton 77−49971
$\mu p \rightarrow \mu n W^+$, current algebra and sum rules high energy W^+ prod. 80−102039
NNπ amplitudes, weak, sum rules and theoretical description of nonleptonic hyperon decays 79−17663
$\nu(\bar{\nu})N \rightarrow N'\gamma e(\bar{e})$, current algebras and high energy γ-prod., sum rules 80−102039
$\nu e(\bar{\nu}e)$ forward elastic scatt. amplitudes, new sum rules 79−54332
νN cross-sections, polarised deep inelastic sum rules 77−13952
$\nu N(\bar{\nu}N)$ forward elastic scatt. amplitudes, new sum rules 79−54332
νp interactions, microcausality, equal-time current commutators, sum rules *(Russian)* 77−74689
νp polarised cross sections, new polarised ν sum rules 77−34144
$\omega \rightarrow \pi\gamma$, suppression factors for VMD couplings calc., duality constraint anal. 77−13960
pd→Xd, diffractive interaction, test of finite mass sum rule 77−22819
$p\bar{p} \rightarrow \gamma\gamma$ annihilation, influence on sum rule proton polarisability 80−18143
pp→Xp diffractive interaction, test of finite mass sum rule 77−22819
$\phi \rightarrow \pi\gamma$, suppression factors for VMD couplings calc., duality constraints anal. 77−13960
π electroprod., light cone dispersion sum rules, axial vector currents 78−41556
π inclusive prod., sum rules, π bremsstrahlung 78−45811
π radiative decay amplitude, low-energy expansion, currents, sum rules 80−52509
$\pi^0,\pi^\pm$ EM polarisabilities, sum rules, coloured quark field theory 80−57561
$\pi N \rightarrow \pi\Delta$, finite energy sum rules and duality 77−22763
$\pi N \rightarrow \pi N$, finite-energy sum rules, three component duality 80−82996
πN scattering off-mass shell model, calc. of finite-energy sum rules 79−63517
πN total cross section sum rule, reln. of sea quark distrib. and pomeron 79−63441
πp forward symmetric amplitude, asymptotic parametrisation by continuous-moment sum rules 77−18341
$\pi^-p \rightarrow \eta n$, tensor-exchange amplitude and polarisation determ. 78−45962
$\pi\pi$ resonances, anal. of asymptotical sum rules *(Russian)* 79−54359
$\pi\pi$ scatt. sum rules on crossing-symmetry basis 77−57467
$\pi\pi$ t-channel isospin-1 scatt amplitude, crossing constraints 77−67592
$\pi\rho$ scatt. amplitude asymptotic limit, sum rules, predicted resonance with A_1 meson quantum numbers *(Russian)* 78−78214
$\pi\Sigma$ scattering amplitude, sum rules for $\pi\Sigma$ reson. parameters *(Russian)* 79−22137
$\psi \rightarrow 3\gamma$, dispersion sum rule charmonium theory, decay probability lower bound *(Russian)* 78−89716
$\psi \rightarrow 3\gamma$, dispersion theory of charmonium, self consistency test, decay probability *(Russian)* 78−89717
ψ leptonic decays, spectral-function sum rules 78−4857
Q mesons, sum rule for decay widths 78−449
^{9}Be(γ,π), photoabsorption and sum rules, structure, RMS radius, polarisability and exchange parameters 80−22686
^{13}C, charge transition density, sum rules, oscillation form factors *(Russian)* 79−22186
^{12}C($\pi\ \gamma\gamma$), branching ratio, ang. correlation 79−85526
Ca isotopes, $f_{7/2}$ neutron occupancies 78−78240
^{56}Fe(e,α), E2 isoscalar resonance sum rule, DWBA anal. 80−68621
^{2}H, photonuclear sum rules and interaction effects, integrated cross-section determ. from double commutator 78−21542
^{2}H(e,e), EM interactions and mag. sum rules 80−42639
^{2}H(e,e), energy weighted sum rules, almost realistic NN pot. anal. *(Russian)* 80−13465
^{2}H(e,n)p EM sum rules, exchange currents and isobar configurations 79−93526
^{2}H(γ,n), forward angle cross section and sum rule from Siegert's theorem 79−80925
^{2}H(n,n)^{2}H, sum rules linking doublet and quartet phase-shifts with ^{3}H binding *(Russian)* 77−74831
^{3}H, enhancement factor calc. in photonuclear electric dipole sum rule 78−37288
^{3}H, muon capture 78−37314
^{3}H photoeffect, electric dipole sum rules 79−36231
^{3}H photoeffect, hyperspherical harmonics and elec. dipole sum rules 77−57650
$^\Lambda$H, A=2, 3, EM sum rules, total absorption cross sections 79−71818
^{2}He(e,e) energy weighted sum rules *(Russian)* 80−86900
^{3}He, enhancement factor calc. in photonuclear electric dipole sum rule 78−37288
^{3}He, muon capture 78−37314
^{3}He, photonucl. sum rules 79−6427
^{4}He harmonic oscillator sum rules for photonuclear reactions, shell model, perturbative corrections 78−41692
^{4}He photodisintegration, total, dipole, and quadrupole cross sections, sum rules *(Russian)* 80−83094
^{4}He, superfluid, singular f-sum rule, applicability to inelastic neutron scatt. 80−6577
^{4}He, TRK dipole sum rule reevaluation including isobar effects 78−66221
^{4}He(π,π), derivative sum rule and scatt. parametrisation 79−76037
$^\Lambda$He, A=3, 4, EM sum rules, total absorption cross sections 79−71818
$^\Lambda$Li(γ,π), A=6, 7 80−22686
^{16}O, longit. isoscalar electroexcitation, sum rules and mean excitation energy 78−521
$^{16}O+\mu$, total muon capture rate, Skyrme forces, closure approx., sum rule technique 78−54742

sum rules continued
^{18}O 1.98 MeV 2^+ state static quadrupole moment, from nuclear sum rules 80−13374
^{208}Pb, longit. isoscalar electroexcitation, sum rules and mean excitation energy 78−521
^{208}Pb(p,p′), sum rule anal. of inclusive cross section 78−33183
Pb(p,t), A=204,6,8, E=35 MeV, spectra and ang. distribs. meas. DWBA anal., sum rules 78−13101
^{45}Sc, neutron stripping and pick-up, reanalysed data, sum rule anal. and spectroscopic factors 78−8828
Sr isotopes, $1g_{9/2}$ nucleon-transfer reactions, sum rules 78−50068

summing circuits
see also adders
inductive transducer summing circuit errors 77−18046

Sun
see also solar .....
see also cosmic ray solar modulation
absolute solar motion, rel. to discrete redshift 78−49530
acoustical oscillations, period comp. 77−29756
Alfven wave flux, rel. to solar wind accel. 80−85923
angular semidiameter, new meas. from limb darkening function obs. at 5012 Å 80−67677
angular vel. distrib. 77−56904
apex, rel. to protocometary cloud 77−25984
apparent diameter fluctuations due to Earth's atmosphere turbulence 77−74026
apparent instantaneous diam., atmospheric limits on astrometric precision 77−74021
apparent solar diameter long period oscills., obs. 78−89138
apparent yearly precession, rel. to photospheric vel. research 78−20809
astrophysics, extension to stellar and galactic astrophysics 77−9736
atmospheric effects on setting and rising 77−91271
azimuth meas. for spacecraft location determ. on planetary surface 78−49287
basic solar motion components, calcs. *(Italian)* 79−12414
as binary star, possible existence of companion 78−12198
brightness distrib. at 8.6 mm, interferometer obs. 80−56800
centre-to-limb solar observation of Ca II K-line component *(French)* 80−82331
chromosphere-corona transition zone of solar active regions, non-thermal velocities *(French)* 80−77371
colour rel. to Hyades metal content and distance 80−101569
compact companion, mass, vel. and luminosity 79−2490
companion star, reality questioned 78−57475
companion star influencing comet orbits 80−31260
constant mass solar model, differentially rotating gaseous polytropes configurations 80−82338
convection zone, ensemble-averaged eqns. for granulation, supergranulation and giant granules 80−67698
convection zone, scales of motion 79−25589
coronal temp. and holes and solar activity quiescent periods 79−2538
diameter, comparison of transit obs. and photoelectric driftscans 78−4169
diameter, secular decrease, Tobias Mayer obs. refute hypothesis 80−90389
diameter pulsations, phase coherence 79−92747
diameter vars. correl. with atm. electron and gamma-ray fluxes short-period vars. 79−21115
differential rotation/global convection system, modulation by nonlinear dynamo rel. to solar cycle 78−40889
diffusion time scales and accretion, convection zone mass 77−33454
distance from galactic centre, determ. from radial vels. of O and B stars 80−101584
education, solar physics, simple approx. model 78−36756
Einstein effect (gravitational deflection of light), obs. at solar eclipse (1981 July 31) *(Russian)* 80−51651
ellipsoid of inertia, model rel. to perihelia of inner planets orbits 80−67531
equator orientation errors not cause of sunspot drift oscillation 80−41786
equatorial acceleration, effects of outward transport of ang. momentum by gas convection 77−53531
equinox, position and motion during 250 yrs. 77−73935
filigree model and faculae 79−71013
five-minute oscillations, horizontal energy flows struct. 80−62103
formation rel. to origin of planets, monograph 78−32625
free oscills., theoretical spectrum 79−5805
galactic spiral density wave interaction with Sun and galactocentric radial motion 79−8998
gaseous sphere contraction vel., virial-based soln. 79−48665
global oscillations, long-period, observational evidence 79−2539
global oscillations, obs. as oscills. in apparent limb darkening function 79−35226
global oscillations energy transport, upper bound from photosphere radiative equilib. 78−32430
global oscillations of solar brightness 77−25988
global solar velocity oscillation, supergranulation origin 77−13305
gravitational contraction of protosun and Laplacian gas ring shedding 79−62765
gravitational deflection of light, effect of meas. on Gorky latit. *(Russian)* 78−40462
gravitational deflection of microwaves, improved upper limits on polarisation depend. 77−2596
gravitational potential harmonics, effects on Earth rot. axis precession angle 78−48953
gravitational red shift, Fe I line meas. 80−90391
heliographic coordinates, rel. to use of solar graticules 78−16299
heliosphere H atoms, ionis. by light and solar wind in near Sun region 80−105145
inhomogeneous models, neutrino flux survey 78−4166
interstellar dense clouds encounters 77−87497
Jacobi's virial eqn. soln. for celestial bodies 79−8832
JOSO workshop on solar optical obs., proceeding (Firenze, Italy, 7-10 Nov. 1978) 79−75178
large scale oscillation rel. to fluctuations at centimetric and millimetric wavelengths, model 77−22175
magnetic field measurement by Mt. Wilson magnetograph, effects of ang. resolution 77−22082
magnetic field structure, Pioneer 11 confirmation 77−82162
magnetic fields and convections, basic props. of mag. flux tubes 77−13297
magnetic star 77−53566
mass loss from primitive Sun, rel. to origin of lost cloud 78−57502
mass loss rel. to meteoroid swarm evolution 80−8592
Mercury transit, 1973 November 10, photographic obs. at Pulkovo *(Russian)* 78−28562
MHD surface waves on cylindrical fluxtubes rel. to Sun 79−75098
models, H-R diagram fits rel. to He content and convective mixing length 80−26835
motion relative to neighbouring galaxies *(Russian)* 78−24553
motion with respect to external galaxies 77−91619
NASA solar terrestrial programme, planning 79−5731
network model 79−48747
non-radial oscills. with initial chemical discontinuity 80−82341
nonradial p mode eigenfrequencies depend. on solar envelope struct. 78−16364
nonradial p-mode oscillations 78−32428
nonresonant second-order interaction of waves, generation of deeply penetrating gravity-like oscill. 78−28508
oblateness rel. to facular excess brightness, wavelength depend. 78−7955
observational ephemeris, 1977, September to October *(French)* 77−87241
observational sites testing with balloon borne radiosondes, turbulence and seeing meas. 77−29645
origin and history to earliest geological times, rel. to origin of life 78−69923
oscillation frequencies, line broadening due to convective fluctuations 80−31293
oscillation periods, correl. with cosmic ray short-term fluctuations periods 80−67483
oscillations, Fe I 5124 Å Doppler shift obs. 78−53905
oscillations, influence of Sun outer layers on detect. 79−5800
oscillations, obs. results and theories 78−12182
oscillations, period obs. rel. to internal struct. 80−105226
oscillations, representation of observable signals in Chebyshev polynomials 79−89857
oscillations, review 78−69777
oscillations in solar diameter, obs. and techniques *(Danish)* 77−22153
oscillations with 160 min. period, magnetograph obs. 79−40156
oscillations with 160 minute period, evidence 80−82324
p-mode eigenfrequencies, radial rotational vel. gradient effect 79−30027
p-mode oscillations, tracer of radial differential rot. 79−35221
photosphere oscillations, PEPSIOS spectrometer obs. 78−93203
photosphere structure and dynamics, rel. to Sun as variable star *(French)* 79−2540
photospheric image quality, influence of atmospheric thermal disturbances *(French)* 77−53532
photospheric oscillations, search for long period modes 77−41370
physics, future progress prediction *(Italian)* 78−81606
plasma diagnostics of solar interior, use of MHD pulses 80−109405
polar regions, study by out-of-ecliptic space probes 77−87228
position, ephemerides calc. formulae *(German)* 80−77367
position computation procedure 79−5734
position obs. with CERGA astrolabe *(French)* 77−45380
position sensors using fibre optic selector 77−49262
positions, low-precision formulae 80−61990
positions in 1976, CERGA astrolabe obs. *(French)* 78−69760
primitive accretion disk physics 78−81566
proper motion, apex rel. to cometary orbits perihelion distrib. asymmetry 78−96429
pulsation, rotation and sunspot cycle, relationship of periods 77−53519
pulsation with 2^h40^m period, possible magnetospheric origin 78−7961
pulsations at periods from 7 to 70 minutes, observational search 78−93180
quadrupole moment influence on perihelion shift of Mercury, modified theory of gravitation *(German)* 79−88844
quiet spatial structure during 1977 October eclipse, VLA 6 cm obs. 80−72895
radial oscillations, first twenty modes of 1968 non-standard solar model 77−41371
radial velocity, meas. using HF absorpt. cell 80−12681
radio antenna using gravitational lens, interstellar communication 80−62040
radio obs. of quiet Sun using student-designed radiotelescope, multidisciplinary exercise 80−17759
radio radius at centimetre wavelengths, and brightness distrib. across disc 80−21968
radio signal retardation by solar gravity, Viking expt. results 80−36933
radiowave deflection by Sun, General Relativity test 77−70994
radius and temperature, vars. due to mag. buoyancy 79−92749
radius at 35 GHz, obs. 77−22174
radius oscillations, effects of seiches in supergranules 77−13310
review of present knowledge 78−40895
ring of rocky material, hypothesis 80−21961
Saturn's rings, thickness caused by satellite and solar perturbs. and planetary precession 80−36569
secular accel. rel. to Earth-Moon tidal friction, Earth moment of inertia change 80−81803
semidiameter meas., light deflection effects *(German)* 80−46531
solar and solar-terrestrial physics, illustrated glossary 78−57537
solar constant, Smithsonian Astrophysical Observatory program, (1902 to 1962) 80−36606
solar flare build-up, study workshop, Cape Cod, Mass., USA (1975 September 8 to 11) 77−17473
solar motion, rel. to centroid of Local Group 78−12376
solar motion, vel. and apex determ. from open clusters proper motions 80−46418
solar motion and galactic rotation consts., from stellar proper motions 78−32440
solar motion corrections to general catalogue for southern stars, proper motions in α *(Russian)* 79−92685
solar motion vector, correl. with nodes and perihelia distrib. of nearly parabolic cometary orbits 80−67661
space motion, rel. to kinematics of Galaxy and Andromeda nebula (M31) 77−91518
speckle image reconstruction of solar features 77−33354
spectral analogues, photoelectric scanner obs. of solar-type stars 78−40938

Sun continued
spectrometric research, automation system for on-line signal processing *(Russian)* 80−12659
stability against nonradial thermal modes 80−82322
standard model and stellar evolution calc. programme 80−67703
stellar convection, hydrodynamics rel. to solar obs. 78−89182
structure from global studies of 5-min. oscills. 80−26838
Sun and heliosphere, conference, London, England (1979 April 3 to 4) 80−82574
sunrise, sunset and eqn. of time 77−33326
surface oscillations, geophysical effects 79−8777
surface oscillations and pulsations, rotation speeds 80−67676
T Tauri stage of evolution 77−5467
T Tauri phase, appl. to carbonaceous chondrite fission Kr and Xe origin 79−35199
temperature minimum in far IR, var. with solar cycle 80−94769
thirteen-colour photometry, derived 77−22230
three-body problem, restricted, families of three-dimens, double-symm. periodic orbits, Sun-Jupiter case 80−26722
tidal action on accreting protoplanets, rel. to planets rot. origin 79−8859
torsional oscillator with 11 year period 80−105217
transit of Mercury, 1973, November 10, photographic obs. *(German)* 77−22127
turbulent medium with density gradient, MHD effects, appl. solar convection *(Russian)* 78−47055
Tycho Brahe's solar observations 79−88785
UV Doppler camera for transition zone studies 79−25485
velocity field meas. using Fabry-Perot spectrometer 80−90333
X-ray photographs, anal. and interpretation 78−4179
zodiacal constellations and solar movement *(French)* 77−70981

sunlight
see also atmospheric optics; sky brightness
1950-2150 Å solar radiation, ground level meas. using NH_3 actinometry 79−2345
absence, nighttime darkness duration, depend. on latit. 77−25632
absorption by CuO, Al oxide, Pt black surfaces, comparison with Planckian black body *(German)* 77−35026
absorption by water vapour, thermotidal exciting function 78−28310
absorption in Venus atmosphere 80−46434
absorption of shortwave radiation by plant cover, calc. procedures 78−16219
aerosol, solar radiation absorpt., visual photometric meas. technique 80−85750
aerosol extinction at 500 nm in urban and rural air at Milwaukee, USA 79−100946
airport control tower cab, optical design 80−58661
anisotropic diffuse insolation, calc. of instantaneous flux on tilted surfaces 80−101412
Arctic regions, sunlight rel. to layering of summertime stratus cloud 77−5290
atmopsheric scattering of solar radiation refl. from ocean surface *(Russian)* 77−29435
atmosphere, aerosol extinction coeff. from outgoing solar radiation meas. in O_2 0.76 μm band *(Russian)* 79−8690
atmosphere, internal gravity waves generation by movement of terminator 77−91348
atmosphere, photon fluxes calc. including mol. scatt. and refl. 79−53512
atmosphere, sunlight scattering, Rayleigh and Mie theory 80−56605
atmosphere attenuation, effect of O_3 and H_2O vapour content and atmos. turbidity 80−93855
atmosphere attenuation in visible and near IR, experimental profiles up to 30 km *(Russian)* 78−61558
atmosphere disturbance production by terminator, allowance for terminator boundary slope 77−91208
atmosphere emergent radiation, computation method for region ranging from UV to IR 77−87069
atmosphere extinction, meas. in mountainous regions 80−90202
atmosphere scattering, Monte Carlo simulation of twilight obs. *(Russian)* 77−33186
atmosphere temp. drop due to airborne volcanic dust 80−85726
atmosphere transmission, 1923 to 1957, from Smithsonian Astrophysical Observatory pyrheliometric meas. 80−17374
atmospheric propagation, rel. to solar power systems 77−73798
atmospheric transmission measurement and prediction, 4.0 to 5.3 μm, CO_2, N_2 continuum absorpt. contribs. 79−92589
atmospheric transparency from ground actinometric meas. 79−39859
atmospheric turbidity at Athens Observatory, solar radiation meas. 78−7768
biological influences and appls. of optical radiation *(Japanese)* 78−44556
blinds with internal diaphragms, light-blocking effectiveness 79−50405
brass photocorrosion in $CuCl_2$ and $FeCl_3$ aq. solns. 79−57145
bright sunshine, differences between morning and afternoon, in New Zealand, statistical anal. 77−29401
British spring weather, survey (1950 to 1979) 80−98427
building interior lighting, sun tracking concentrators 77−62043
Campbell-Stokes recorder rel. to Dirmhirn global radiation recorder *(German)* 78−44953
Campbell-Stokes sunshine recorder traces, turbidity determ. 78−88912
chromaticity locus of daylight *(Japanese)* 77−78355
circular polarization of sunlight reflected from planetary atmospheres 78−28558
circumsolar radiation, single and multiple scatt. contribs. 79−25325
clear sky conditions, solar radiation and illumination simultaneous meas. 80−81985
clear sky normal incidence solar insolation measured with RG2 filter, charact. 78−69426
climate sensitivity to incident radiation vars. 80−56595
climatology of global solar radiation in California and an interpolation technique based on orthogonal functions 80−67402
cloud diffuse reflectance, semiempirical model 79−80014
clouds, solar radiation refl., transmission and absorpt. props. parameterisation 80−56601
coastal zone, indicators of long-term var. of hydrometeorologic elements *(Russian)* 78−77258
concentrated, pulsed, heliotherapy unit, integral concentrator, irradiation technique improvement, medical physics 79−83885
cumulus clouds, downward scatt. solar radiation 78−3876
cumulus clouds, scattered and total solar radiation fluxes *(Russian)* 77−41169

sunlight continued
Czechoslovak radiation climate evaluation, w.r.t. solar power utilisation *(Czech)* 78−88874
daily irradiation, ARIMA modelling with constant and seasonal parameters 80−55821
daily solar total irrad. fluctuations, temporal statistical anal. *(French)* 80−61292
daily sunshine durations and temps., spatial variability over uniform terrain 78−3887
data, stochastic modelling and forecasting 78−36243
data collection system using microprocessors 78−69542
daylight, spectral distrib., 280-2800 nm, Australia 78−69452
daylight from north sky at Nagaoka, Japan, principal component anal., spectral distribs. *(Japanese)* 77−64433
diffuse irradiance measurement using shadowband, corrections 80−101410
diffuse reflection by Earth, radiation press. perturbations of near-Earth satellite 78−24444
diffuse solar radiation below overcast sky, ang. distrib. 80−85719
diffuse solar radiation field in cloud layer *(Russian)* 79−29851
direct beam solar irradiance and illuminance computation 80−90174
direct irradiance at the ground, parametric modelling 80−101411
direct solar energy, Markov chain simulation with one minute binning *(French)* 80−61293
direct solar irradiance, indirect meas. 80−45644
Earth satellite orbits, effects of resons. with respect to solar radiation press. perturbations 80−90326
Earth surface radiation balance, influence of irrigation 79−29863
Earth surface UV radiation regime, effects of stratosphere pollution 78−16153
Earth zonal radiation balance, perturbation by stratospheric aerosol layer 80−56602
evolution implications for Earth's early atmosphere 78−36285
fluctuations observed at Earth surface rel. to stratosphere aerosol content fluctuations 80−82035
flux var. rel. to O_2 density in thermosphere 80−72659
forward scattering from water surface 78−44872
global solar radiation at Lyon and at Macon, France, for (1978) *(French)* 80−55812
global solar radiation est. and prediction by stepwise multiple regression anal. for Greece (1961 to 1975) 80−61880
Global Solar Radiation Index, vars. at Kew 77−17217
global spectral distrib. determ. using rapid spectral radiometer for solar cell appls. 80−61369
global surface irradiance, effect of aerosol props. and surface reflectivity 80−76611
Great Britain, global solar radiation distrib. on horizontal surface, monthly maps 79−79959
halo phenomena due to reflection by ice crystals *(Norwegian)* 79−84475
incident solar radiation at Earth surface, estimation from geostationary satellite data 80−82006
insolation, long-term variations 79−88469
insolation, SOLMET data, 1953 to 1975, anal. rel. to solar availability for winter space heating 80−81421
insolation and climatology relations, solar energy availability estimation 78−81344
insolation meas., Si-cell based sunstation system 79−5582
insolation measurements at Las Vegas, in United States 78−69427
insolation modelling, review of solar radiation resource assessments 80−35640
insolation prediction at Fort Hood, Texas, rel. to climatological variables 78−24333
insolation stability characterisation by stochastic time series 79−57396
intensity, data rehabilitation, SOLMET-2 procedures criticised 80−4071
intensity obs., global insolation on horizontal and tilted surfaces 78−81275
Io Na cloud, solar radiation press. as cause of east-west asymmetries 80−36560
irradiance meas. from NIMBUS 6 satellite 77−25766
irradiance meas. using optical fibres and Si detectors 79−100960
irradiance on horizontal surface, estimation of totals from UK average meteorological data 80−81422
irradiance outside atmosphere, Bouguer method for ozonometer determ. *(Russian)* 80−61918
Israel, estimation of solar radiation and ambient temps. 80−76607
Italy, solar radiation distrib. *(Italian)* 77−81987
Japanese sunshine project *(Japanese)* 77−87034
Jupiter atmosphere, UV radiation rel. to hydrocarbon photochemistry and Lyman alpha albedo 80−105194
Jupiter reflected sunlight, absorpt. bands rel. to atmospheric comp. and cloud struct. deduced from absorpt. bands in refl. sunlight 80−56758
light sources for simulating sunlight 80−87454
luminous efficacy of daylight at Tokyo *(Japanese)* 80−72631
lunar surface, intense local photoelectric charging in sunset terminator region 77−45330
lunar terminator, localised photoelectric supercharging with progression of sunset 77−45331
Lyman-α, mesospheric extinction meas. during Winter Anomaly Campaign (1975-76) 78−45001
Lynman α radiation, atmospheric absorpt. rel. to O_2 densities 77−87010
Mars dusty atmosphere, solar heating rates 78−85878
Mars thermosphere, depend. of struct. on solar activity 77−64686
measurement, using automatic solar-radiation meter 80−89592
mesoscale mapping of available solar energy at the Earth's surface by use of satellites 80−72613
metameric white samples for testing relative UV content of light sources and daylight 79−58767
meteorological aspects of solar and wind power 78−36250
monitoring system, biological response study appl. 77−52839
monthly average diffuse radiation, cloudiness index and sunshine duration correlating methods 80−98384
monthly mean global solar radiation maps for Japan 80−109185
monthly mean solar radiation calc. using daily time intervals 80−17353
monthly sunshine percentage rel. to 700 mb height field 78−3867
multilayer antisolar glazing heat throughput calc. 78−94415
near IR direct and scattered fluxes *(Russian)* 78−81299
Neptune, sunlight absorpt. rel. to thermal evolution, comparison with Uranus 78−85903
obscuration by cometary dust, rel. to ice ages and ecological catastrophes 78−53714

sunlight continued
ocean, diurnal var. of underwater irradiances on horizontal surfaces 80−72549
ocean, solar radiation effect on temp. meas. with Aanderaa thermistor chains *(French)* 79−62611
ocean surface with waves, radiance distrib. over surface, glitter and sky contrib. 77−21902
p-n junction solar cell response to concentrated sunlight and partial illum. 79−61996
photochemical smog enhancement by N,N′-diethylhydroxylamine in polluted ambient air 77−91262
photon scattering in turbid atmosphere, path length distrib. 77−45147
polarising radiometer meas., skylight at South Pole station, Antarctica 78−57320
pollution affecting solar radiation incident on St. Louis, USA 80−109247
radiation flux density, solar and terrestrial radiation dependent on the amount and type of cloud 80−67403
radiation incident on slopes of different orientations meas. using pyranometer 77−53164
radiation intercepted by a tilted surface, estimation of daily, clear sky, spatial distrib. 80−81423
radiation loading on fixed, tracking surfaces, solar energy availability investig. 80−40838
radiation pressure, appl. to satellites inertially fixed pitch stabilisation 80−101523
radiation statistics, linear spatial interpolation 80−93859
radiative transfer, cloud shape and mutual shading effects 80−101430
radiative transfer through turbid atmosphere, single-scatt. solution 79−16663
radiative transfer under cumulus cloud conditions, Monte Carlo method *(Russian)* 80−21793
radiative transfer under fractional cloud cover, two-stream approx. 80−51534
radiometer, portable, with Cu_2S-CdS photo-cell, solar radiation meas. appl. 78−53763
reflected from polygonal heliostat, analytic evaluation 79−29452
reflected sunlight from Venus, polarisation, planetary atm. struct. and comp. determ. 80−36533
reflected sunlight polarisation, meas. from high-altitude balloon 78−61561
reflection by clouds, fast azimuthally dependent model 80−51532
reflection by ocean-atmosphere system, spectral struct. of refl. radiation field *(Russian)* 77−33086
reflection from Earth, brightness field, atm. transmission function calc. *(Russian)* 80−4105
rocket, monoaxial controlled solar pointer for atmospheric occultation meas. *(Japanese)* 78−32312
scattered light intensity and polarisation degree in model atm., mol. anisotropy effect 80−77104
scattering by clouds, dimensions and orientation effects 77−33188
scattering by noctilucent cloud particles 78−11945
scattering from gradient particulate atm., background noise in optical communication 79−62576
scattering from hexagonal ice crystals 79−94150
sea, wind-ruffled, sunlight glitter pattern, time-averaged intensity calcs., oil pollution detect. appl. 79−53349
sea surface, Sun glitter pattern appl. to surface slope distrib. function determ. *(Russian)* 80−94611
sea surface, wind-ruffled, isophotes of sunlight glitter 77−45001
seawater, chlorinated, sunlight-induced bromate form. 77−49088
seawater penetration of solar radiation in Indian Ocean, calc. 79−2278
seawater sunlight polarisation, reflection, and biological effects 77−56648
Seoul, Korea, useful radiation intensity for NH_3-H_2O solar absorption refrigeration system *(Korean)* 78−51052
sky brightness indicatrix rel. to single scatt. optical depth, new formula *(Russian)* 78−11999
solar battery performance and thermal characteristics *(German)* 79−96443
solar central receiver system, flux density integral for reflected sunlight, numerical anal. 80−93863
solar collectors orientation, optimisation 77−81965
solar constant, accurate determs. by avity pyrheliometers 79−2341
solar constant, Smithsonian Astrophysical Observatory program, (1902 to 1962) 80−36606
solar constant vars., sunspots influence rel. to weather 77−91238
solar energy: four sites demonstrate potential 79−61946
solar energy utilisation, global and sky radiation estimates for Austria 80−93861
solar energy utilisation, prediction of hourly diffuse solar radiation from measured hourly global radiation on a horizontal surface 80−93864
solar images quality, influence of atmospheric thermal disturbances *(French)* 77−53532
solar irradiance, model for determining the spectral quality of daylight on a horizontal surface at any geographical location 80−93856
solar radiation, monthly mean calcs. on vertical and inclined surfaces 80−45746
solar radiation characts. and intensity calc. 80−45649
solar radiation data, statistical correl. between daily and monthly averages 80−8409
solar radiation data base using bright sunshine data approach 77−25763
solar radiation levels on tilted surfaces, computer model validification 80−35641
solar-radiation regime, energy structure distribution laws analytic representation 80−98378
spectral actinometric observations, appl. to atmospheric aerosol turbidity characts. determ. 78−92986
spectral attenuation at Mauna Loa by aerosols 80−41494
spectral composition in 4000-7000 Å range at Moscow 78−16133
spectral distrib. data, $300<\lambda<1500$ nm range 77−25764
spectral distribution monitoring, broadband filter radiometry error anal. 77−53163
spectroradiometry of daylight at sea level in Durban. 79−100955
stratosphere, NO_2 light extinction rel. to Cretaceous-Tertiary extinctions 78−32215
stratosphere UV heating, rel. to zonal winds var. correl. with 27-day solar rot. 78−88878
sunset IR spectra and stratospheric NO and NO_2 mixing ratio profiles determ. 80−94563
sunshine duration rel. to mean daily solar radiation in Iraq 78−81337
sunlight continued
sunshine possibility, sky cover predictions 79−16565
Tanggula region, global and net radiation *(Chinese)* 79−92568
total hourly horizontal data, pyranometer data acquisition system, USA 77−25765
total luminous energy transfer, scatt. medium effect 77−65577
total solar radiation, cooling tower plume effects, obs. 79−12177
total solar radiation at Earth's surface using satellite measurements 80−4147
transfer in clouds, finite geometry effect 79−58085
transmission through uniform waterdrop atmosphere, computer calculation 78−36244
troposphere and low stratosphere, scattered solar radiation field meas. *(Russian)* 79−16667
turbid atmosphere, transparency characts. calc. 78−81407
twilight, Raman scattering spectrum 79−92596
underwater chlorophyll *a* fluorescence sensing, sunlight penetration depth estimation 79−79874
underwater irradiance, meas. in Central Atlantic Ocean *(Russian)* 78−77257
underwater sunlight fluctuations in sea spatial and temporal correlation 80−94533
United States, recent increase in sunshine duration rel. to cloudiness 79−20930
United States, solar climates 80−76612
upper atmosphere extinction, theory 77−78546
Uranus, sunlight absorpt. rel to thermal evolution, comparison with Neptune 78−85903
UV, intensity of direct and scattered radiation at large air masses *(Russian)* 77−49166
UV irradiation solar flux meas. between 120 and 400 nm, current position and future needs 78−57536
UV meas. and physics 80−41784
UV radiation changes at Earth surface, effects of possible O_3 changes 80−94577
UV radiation in stratosphere, rel. to solar cycle signal in tropospheric winds 80−72604
UV radiation photometric obs. with Sun near horizon *(Russian)* 79−8691
UV spectral distribution under clear day conditions 77−41171
UV spectrum 140 to 350 nm, NASA meas. using SURF storage ring calibrations 80−94721
variation of spectral distribution obs., at various geographical locations (1968 to 1974) 77−37313
Venus atmosphere, results of solar flux radiometer expt. aboard Pioneer Venus multiprobe mission 79−48718
Venus atmosphere, scattered solar radiation fluxes spectral and altitude distrib. 80−62059
Venus thermosphere, depend. of struct. on solar activity 77−64686
water penetration imagery, surface/depth data separation by multispectral scanning 78−69539
water suspensions, radiative property measurements 80−9811
winter sunshine totals for English city centres 79−84457
zenith photoelectric measurements during annular solar eclipse (1976, April 29) 78−3900
C I photoionisation by sunlight, C II line excitation 80−58223
Cu photocorrosion in $CuCl_2$ and $FeCl_3$ aq. solns. 79−57145
H Lyman-α radiation, mesospheric meas. rel. to O_2 density, press. and temp. profiles 78−44947
Si solar concentrator cell, effects of nonuniform illumination and temp. profiles under concentrated sunlight 80−93941

sunshine *see sunlight*

sunspots
see also solar activity
11-year cycle and weather, timed by internal solar chronometer 79−16921
11-year solar cycle, double maximum features 77−49363
17th century, 1625 to 1626 and 1642 to 1644, anomalous solar rot. from sunspot drawings 78−36550
17th century solar activity from auroral and sunspot obs. *(French)* 77−29747
20 year variations in number rel. to Earth diurnal rot. vel. and geomag. vars. 78−32005
30-day periodicity in sunspot activity and rainfall 79−84765
80 year sunspot period, maximum in 1944-53 period 77−17468
80-90 year cycle in solar activity 77−53536
1611 to 1613, Thomas Harriot's sunspot obs. rel. to solar rot. 79−75182
1970 June flare activity rel. to sunspots movement 78−89141
1972 August, struct. and dynamic props. of large sunspot group 78−49409
1972-1975 period, unusual flare and sunspots phenomena 79−16914
active regions gross energy balance 78−28633
active regions heliographic oscills. in longitude, sunspot zone modulation *(French)* 77−64714
activity Cycle 21 prediction with early 1980 max. 78−69778
activity cycles continuity *(Chinese)* 78−85925
activity in 1943-1977 period, Catania obs. 79−25584
activity periods, correlation analysis *(Chinese)* 77−67082
Alfven wave propagation in density gradient 77−33437
Alfven waves in corona above sunspots 77−78732
alkaline earth oxides, possibility of occurrence in sunspots 78−85933
annual mean no. rel. to Bombay geomagnetic and climatic (1848-1967) data 80−81811
annual mean numbers, max. entropy spectral anal., confidence limits 80−22284
annual sunspot numbers, vars. rel. to Earth day length, seismic activity and geomag. moment 77−90981
area on solar disc, effect on solar constant 80−77376
axisymmetric convection in prescence of mag. field, solar granulation and sunspots appl. 80−12724
bipolar groups, asymmetry 79−21264
bipolar groups, circularly polarised radioemission obs. at 1.35 cm *(Russian)* 78−57532
bipolar magnetic group rel. to angular vel. distrib. and magnetic rope twisting 77−56904
broad-band circular polarisation, origin 78−45301
butterfly diagram, 1959-1974, rel. to general mag. fields and convection zone struct. 77−22166
chromosphere, fine structs. extension into corona, Hα obs. *(French)* 78−28607

sunspots continued
chromosphere, radial vel. and brightness oscills. regimes *(Russian)* 80−51727
chromosphere above sunspot umbrae, Ca II H, K and IR lines interpretation 78−53501
chromosphere above sunspot umbrae, obs. of emission cores in Ca II H- and K-lines 78−53900
chromosphere above umbrae, temperature and electron density 78−53908
chromosphere-corona transition zone over sunspot, dynamics, OSO-8 obs. 77−9728
circular polarisation of type III solar radio bursts in 24 to 220 MHz range *(Russian)* 78−16384
climate-sunspot relations, statistical evidence from long-term temp. records 78−69439
climatic changes, rel. to sunspots occurrence 79−58309
convective propulsion of magnetic flux tubes 80−4313
cool corona pressure and energy balance over sunspots 77−13291
cooling by Alfven waves refl., theory 79−5799
cooling mechanism, overstability and Alfven wave prod. 77−78733
coronal magnetic field, struct. rel. to local sources of solar radio emission S-component 80−46528
cosmic ray intensity daily variation, rel. to sunspot numbers and solar flux 79−35082
cosmic rays 11 year modulation cycle rel. to sunspots and solar general mag. field 79−21114
cycle 21, use of dynamo theory to predict sunspot number 78−81597
Cycle 21 prediction, comparison with previous cycles *(Chinese)* 80−8608
Cycle 21 prediction, Sargent's anal. 79−2537
cycle before Maunder minimum, evidence for 11-year periodicity 78−61825
cycle influence on geomag. field 77−78090
cycle irregularity, historical evidence 79−58307
cycle morphology, theory *(Chinese)* 80−12722
cycle period-amplitude relation, hysteresis of nonlinear mag. oscill. and 55-year cyclic modulation 79−35214
cycles during 1540-1700 period, from solar and auroral obs. 79−21267
daily cosmic ray flows during solar cycle in solar equator vicinity 78−69622
darkness difference between sunspots, mag. and vel. field effects 78−28629
decay mechanism, turbulent processes in strong mag. field *(Russian)* 78−93193
differential rotation meas., 1978, from recurrent and non-recurrent sunspots 79−84780
distribution between N and S solar hemispheres, var. with solar cycle 77−56881
drift in latitude and longitude, one-year oscill. explanation 78−73693
drift oscillation not explained by solar equator orientation errors 80−41786
early records in 'The Book of Changes' *(Chinese)* 80−77366
effects on satellite performance 80−56812
eleven-year cycle, correl. with ionosphere equatorial spread-F occurrence in American zone 80−109298
emission line spectrum of sunspot in UV, obs. 77−13296
equator-crossing spot, development and motion 80−90394
EUV emission from B-like ions, density sensitivity 79−16910
EUV spectrum, H_2 emission lines obs. 79−16908
Evershed flow in chromosphere-photosphere transition region 78−65593
excited states of magnetic configurations 77−29762
F_2-layer over Gauhati, penetration freq. study, India 77−5394
faculae and sunspots, mag. field effects on solar luminosity 80−46515
faculae rel. to sunspot cycle 80−90390
fine struct., image motion due to atmospheric heat turbulence 80−77108
flare-sunspot associations rel. to Hα-flare visual features 80−41803
formation, assoc. vel. field 77−2396
formation mechanism 77−45395
formative stage, mag. knots mutual attraction 78−53898
global rotation rate determ. using 1967-74 sunspot data 80−90387
granule diameters near penumbra 80−8607
group, local radiosource fine structure *(Russian)* 79−21260
group development, pattern recognition methods appl. *(Russian)* 77−64722
group development rel. to local source radioemission fluctuations *(Russian)* 79−30035
group rotation rates 80−41797
group velocities, statistical distrib., depend. on solar activity cycle phase 80−72918
groups, kinematic parameters rel. to convective zone cophasal regions 78−96469
groups fragmentation vars., rel. to size and 11-year cycle 78−73691
groups number frequency distribution, var. during eleven-year cycle, group size depend. 77−78739
heat flow in convective downdraught 80−4314
heat flux in subphotospheric layers, rel. to umbral granulation 78−73692
historical background to sunspot research, rel. to sunspot physics and sunspot cycle *(Norwegian)* 79−75312
influence on weather, possible mechanism 77−91238
intensity meas., correction for stray light during 1973 June 30 eclipse 78−28596
IR opacity due to molecular vibration rotation bands 80−41798
IR umbral intensity rel. to phase in solar cycle 78−69773
isolated magnetic configurations rel. to Hα-flares and microwave bursts 78−16387
large group sequences 77−53560
large sunspot groups occurrence frequency in cycles 14 to 19 77−17467
largest area per solar cycle, statistics 80−41796
largest number per solar cycle, statistics 77−22159
latitudinal drift of groups, 22-year or 11-year cycle 77−17503
latitudinal drift on solar surface 77−53554
latitudinal zonality, movement of material and activity cycle 77−17535
lifetimes and numbers of groups, predictions from statistical anal. 80−82327
light bridges fine structure 79−66984
line shifts and asymmetries in sunspot penumbrae 80−51715
linearly polarised light intensity distribs., influence of magneto-optical effects 80−21965
long term vars. in solar wind and sunspots, implications of auroral changes during 18th and 19th centuries 80−98498
magnetic and vel. field evolution of sunspot group 78−89143
sunspots continued
magnetic buoyancy in rotating gas, effect of fine electrical and thermal conductivities 78−57436
magnetic configurations, rel. to Hα flares and microwave bursts 77−53527
magnetic field and vel. quasiperiodical oscills. *(Russian)* 78−12186
magnetic field for August 1972 flare-active region 80−46521
magnetic field gradients determ. from Zeeman line rot. and profiles *(Chinese)* 80−85920
magnetic field motion rel. to proton flares 77−17488
magnetic field oscillations, rel. to chromospheric flares occurrence 77−67084
magnetic fields, flux changes rel. to chromospheric network evolution *(Russian)* 78−57531
magnetic fields, meas. from saturated and blended lines via Fourier transform techniques 77−22165
magnetic fields, model rel. to active corona field three-dimensional struct. 77−67085
magnetic fields, rel. to photospherical granule dimension *(French)* 78−89145
magnetic fields and motions, granulation and sunspots *(Russian)* 78−16376
magnetic fields and proper motions, 1968 October 20-27 complex group obs. *(Russian)* 78−65583
magnetic fields and proper motions *(Russian)* 77−64731
magnetic fields higher rot. rate at photosphere, Doppler meas. 80−46516
magnetic fields of active regions and spots, contrib. to solar mean field compared to background field *(Russian)* 78−57530
magnetic fields spiral config. 77−82192
magnetic flow tubes physics, mutual hydrodynamic forces between neighbouring tubes 79−101127
magnetic flux elements, stability in horizontally stratified compressible plasma 78−28610
magnetic flux of colinear bipolar spot pairs 79−75185
magnetic flux tube physics, connective overstability in mag. field in downdraft 80−21960
magnetic flux tubes, aerodynamic lift on thin cylinder in convective flows 79−101126
magnetic flux tubes, physics, rel. to general nature of sunspots 79−75168
magnetic flux tubes, physics, rel. to sunspots, aerodynamic, drag 79−71012
magnetic flux tubes physics, aerodynamic lift 79−101125
magnetic flux tubes physics, umbral dots and longitudinal overstability 80−26825
magnetic structures, correl. with radio noise storms 78−4185
mass flow in complex sunspot 80−51732
Maunder minimum, 1645-1715 period 77−71103
Maunder Minimum, catalogues of auroral obs. 80−51722
Maunder minimum, rel. to 11-year, 80-90 year and 600 year cycles 78−77549
Maunder Minimum, rel. to Andrew Marvell's poetry 80−12877
Maunder minimum, solar surface rotation rate 77−2377
Maunder Minimum, sunspot numbers not correlated with temps. during Little Ice Age 80−82050
Maunder minimum nature, explanation of differential rot. effect on convection struct. 80−101573
Maunder minimum rel. to auroral freq. in 17th and 18th centuries 79−66856
McMath 14275, sunspots correl. with 6 cm emission maxima from 6″ resolution obs. 80−62096
McMath region 13043, opposite polarity sunspots collision rel. to centimetre-wave sources rapid var. 80−67688
meridional motions, rel. to mag. fields and convection 77−53493
MHD oscills. ensemble, interaction with quasiuniform mag. field, sunspots 77−76041
MHD wave damping, theory 77−5514
moats, lifetimes from magnetograph obs. 80−21966
molecular line haze opacity in sunspots 79−75188
monthly mean number, correl. with geomag. H-component regular daily var. at Alibag 79−8593
morphological analysis of 1972 October large group *(Chinese)* 78−28603
morphological features of large solar active region, 1978 April to May *(Chinese)* 80−8613
north-south distribution of flares, sunspot mag. classes and sunspot areas, 1955-74 period 77−71088
number, correl. with freq. of coronal transients 77−22181
number and solar activity forecasting 77−29757
numbers, quasi-biennial variation correl. with quasi-biennial geomag. var. 78−32006
numbers, rel. to equatorial solar rot. and terrestrial climatic changes 78−7960
numbers, rel. to solar far IR brightness temp. minima 80−62035
numbers during solar cycle, relation to Pc 5 micropulsations features 78−36406
numbers in current millennium, rel. to ^{14}C prod. in atm. 80−85730
ohmic dissipation in sunspot decay 77−13312
origin, strong downdraught development, hydrodynamic anal. 80−72908
penumbrae, fine struct. of mag. field and brightness 77−22179
penumbral bright grains, characts. of displacement 77−22177
penumbral edge continuum bright point, characts. 80−98638
penumbral spiral morphology correl. with energetic flares *(Chinese)* 77−22155
penumbral vortical pattern anal., 1972 August *(Chinese)* 77−22157
penumbral waves, fluid layer stability in horizontal magnetic field 79−25573
period stability investigation by periodic anal. of aurora and earthquake records in ancient China *(Chinese)* 79−21253
photography, of solar faculae and sunspots with balloon-borne 10 cm telescope *(Japanese)* 79−80292
photoheliographic results, (1968 to 1971) 79−2487
photosphere, granular vels. around sunspots 77−29776
photosphere darkening, rel. to heat flow near obstacles in solar convection zone 78−28609
photospheric gas motions in single sunspot *(Russian)* 78−65582
pigeon homing performance, correlation with magnetic storm due to sunspots 79−2087
plage fragments, characts. assoc. with photosphere network props. 80−98634
planetary influence refuted *(French)* 78−69770

sunspots continued
pores in sunspot groups, proper motion meas. 80−12733
potential magnetic fields, comparison of meas. and calc. 78−77532
power spectrum anal. of time series 79−16705
preiodicity rel. to solar rot. 79−35223
pretelescopic records from Orient, catalogue, 28 BC-AD 1604, activity excursions 79−66975
quasi-biennial variation, correl. with neutrino flux 79−44440
radiative transfer, through model sunspot 80−21964
radio bursts, peak flux spectra, statistical anal. 80−98641
radio communications, sunspot cycle 21 79−58308
radio emission, 6 cm obs. with 6 arc seconds resolution 77−33444
radio emission, obs. by RATAN 600 telescope 77−78760
radio emission obs. at 1.9, 2.5 and 3.5 cm wavelength, assoc. with 1974 July sunspots *(Russian)* 78−65585
radio radiation, spectral polarisation obs. of local sources during March (1970) 77−53535
rare earth oxides, possibility of occurrence in sunspots 78−85933
relative numbers, long-term vars. rel. to solar cosmic-ray prod. rate 79−92735
relative numbers variations within 10-100 years range, rel. to Earth rot. rate and K_p-index 77−90980
rotation during 19th and 20th cycles 77−53552
rotational motion of gases *(Russian)* 77−64716
running penumbral waves origin 78−93188
Schluter Temesvary sunspot, vertically orientated mag. flux tubes, exact static equilib. 80−98637
SHF emission at 6 cm wavelength, model 80−51712
solar atmosphere struct. above sunspots, two-component model 79−96989
solar constant, effects of sunspots and faculae 78−4163
solar cycle 21, predicted maximum annual sunspot number 78−73696
Solar Cycle 21, radio communication effect 79−75181
solar cycle 21, sunspot number prediction from polar coronal holes and geomag. activity 80−21979
solar cycle and solar luminosity 79−75176
solar cycles 19 and 20, morphology of sun form. 77−78763
spectrum, Doppler shifts rel. to solar rot. determ. 79−92745
spiral sunspots, flares and prominences photographic obs., 1972 October *(Chinese)* 78−69761
stability, of axisymmetric mag. flux tube 77−64734
steady force-free dynamos, theory 78−20777
stochastic cycles, normalisation according to period, algorithm *(Russian)* 79−75117
structure from Solar Stratospheric Observatory obs. 79−25574
temperature distribution, anisotropic heat transfer *(German)* 77−45386
terrestrial weather data, sunspots and geomag. activity, cross-spectral anal. 77−78313
thermal models 79−84773
thermal structure, rel. to mag. fields conc. 77−64735
thermal structure, theory 77−5517
tidal theory of solar activity 79−30034
transition region, emission meas. in far UV 77−78750
turning points and aurorae since (AD 1510) 80−21980
twisted magnetic fields 80−41799
umbrae, internal structure 80−82328
umbrae, IR Ca II lines 80−85918
umbrae, mag. field gradient from echelle spectrograms 77−33456
umbrae, material motions obs. 77−45374
umbral area/penumbral area ratio, vars. correl. with Earth climate 80−31272
umbral boundaries, convection and sunspot depths 77−29761
umbral bright points, morphology and intensity *(French)* 78−89146
umbral brightening assoc. with two-ribbon flare 80−41804
umbral dots, dynamic and struct. behaviour for photometry obs. 80−109409
umbral dots, improved obs. 80−26831
umbral dots rel. to intense mag. fields in weak background field 77−29783
umbral fine struct. and granulation, statistical anal. 77−74032
umbral flares 79−25579
umbral flashes and overstable magnetoacoustic modes 80−12734
umbral spectrum, synthesis with mag. fields 77−17459
umbral spectrum, TiO rot. lines, temp. determ. 78−96451
umbral spectrum in 6812-6898 Å range 79−101136
umbras, outward wave propag. and motions in mag. tubes 79−16927
UV spectra, preliminary results from OSO-8 LPSP instrument 78−49317
variability index, solar cycle parameter *(Polish)* 79−58311
Wilson effect *(Chinese)* 80−12721
Wolf number, reliability in estimating long term periodicities 77−49355
Wolf number data, new ARMA models 79−12442
Wolf numbers, rhythmic struct. amplitude-phase disturbances anal. 79−62806
Wolf numbers secular course, prediction formula 77−45393
Wolf relative number, rel. to originating groups and average lifetime 80−67684
Wolf sunspot numbers, freq. anal. and forecasting 80−56797
Wolf-Zurich number conversion, reduction factors *(German)* 80−98631
X-ray bright points anticorrel. with sunspot number, 1970-78 period 79−53789
X-ray bright points correl. with sunspot intensity, cycle var. 80−41783
yearly sunspot numbers, Box-Jenkins modelling appl. 77−87633
Zeeman line profile, mag. field determ. 80−82221
Zurich annual sunspot number link with temp. and precipitation for USA 80−17328
Zurich sunspot number, monthly averages vars. correl. with total atmospheric O_3 79−16571
Zurich sunspot numbers, 1972 to 1977, rel. to solar wind proton temp. heliocentric gradient 79−40052
AlF lines, intensities prediction 78−20803
CO emission lines in UV spectra of sunspots and flare 79−53795
CO fluorescence in sunspot EUV spectrum, obs. 78−93184
Ca II, H and K lines shapes and centre to limb. var. in sunspot umbrae 77−22178
FeH bands identification in spectra 78−7952
FeH, column densities rel. to Wing-Ford band identification 78−24507
H_2, detect. in sunspots EUV spectra 78−12184
H_2 emission in UV spectra of sunspots and flare 79−53794
H_2 emission lines, reson. fluoresc. with Lyman α 79−8821
He I 10830 Å triplet in umbral spectrum *(Russian)* 80−36604

sunspots continued
Mg I resonance line core obs., possible rapid vars. 79−40163
MgO red and near UV bands calc. rel. to umbral spectrum 80−12736
NO spectrum, gamma system equivalent widths calcs. 79−12457
NO vibration-rotation bands, equivalent widths 77−2395
O_2 Schumann-Runge band system in umbral UV spectrum 80−12735
SH presence in sunspot UV umbral spectrum 79−75186
SiO (A-X) system in sunspot UV umbral spectrum 79−75187
SiO isotopic lines, for $^{28}Si/^{29}Si/^{30}Si$ isotopic abundance ratio determ. 79−30044
SiO vibration rotation bands in sunspots, equiv. widths at 8 μ 78−40903
TiH in sunspot spectra, possibility 79−48789
TiO equivalent width meas., theoretical interpretation, line form. process 80−72902
TiO, rot. temp., rel. to photospheric and sunspot models 78−69766

superaerodynamics *see rarefied fluid dynamics*

superalloys
aluminide, corrosion resistant coatings, high temp. 79−57138
anomalous response to notch under superplastic conditions 78−52930
Astroloy, grain coarsening by critical strain annealing 79−47711
earth reentry exposure, simulated, effect on mech. props., oxidation of Haynes 188 and Hastelloy X 79−5086
Hastealloy X, relations between weld heat affected zone cracking and microstruct., Gleeble test *(Japanese)* 78−52858
Hastelloy, C-276, H transport rel. to ageing treatment 80−75384
Hastelloy, C-276, H-induced crack growth 80−71747
Hastelloy X, mech. props. effect of solidification substruct. 77−25040
Hastelloy-X, low cycle fatigue crack propagation at 25°C and 760°C 80−104270
Hastelloy-X, Ni-Cr-Fe-Mo, cyclic oxidation resist. improvement by high temp. etching treatment 80−97627
hot consolidation of rapidly solidified powders, review 79−33965
IN-100, fatigue crack growth retardation at elevated temp. 80−3158
Incaloy IN 738, dispersion hardened 78−11156
Incoloy 800, nuclear grade boiling tubing superalloy, Co and C content anal. 80−78397
Inconel 600, nuclear grade boiling tubing superalloy, Co and C content anal. 80−78397
Inconel 617, creep, morphological changes of carbides, affect on creep props. 80−108509
Inconel 706 and 718, relations between weld heat affected zone cracking and microstruct., Gleeble test *(Japanese)* 78−52858
Inconel 718, environment effect on high temp. fatigue crack growth 80−30090
Inconel 718, grain growth during sintering 80−97449
Inconel 718, superalloy, wear of superhard tool during cutting, SEM and metallographic obs. 78−64720
Inconel X-750, deform. and fracture characts., 24-816°C 80−108551
laser-assisted hot spot machining, advantages and potential 79−70199
microcrystalline, rapidly quenched particulates, appl. 80−84887
Nimonic, IN100, γ' precipitates, casting conditions effect on morphology 80−7548
Nimonic 115, superalloy, critical strain model for creep fracture 77−32648
Nimonic 80 A, TEM obs. of cellular transformation products 80−3045
Nimonic 80A, struct., fracture characts. 80−3071
Nimonic 80A superalloy, contrast from cavities in HVEM 80−79780
phase extraction, chemical and X-ray diffr. anal. 78−72951
phases *(Chinese)* 78−95728
powder metallurgy techniques applied to superalloys 78−3073
Rene 41, Ni-Cr-Co-Mo-Ti-Al-Fe (18.96, 11.09, 9.65, 3.06, 1.59, 0.89 wt.%) formation of Cr_2O_3 monocrystals on heat treatment 79−52455
Rene 80, dislocation behaviour during plastic deform. *(Japanese)* 80−108504
Rene 95, as hot isostatically pressed (HIP) and HIP+forged, low cycle fatigue 80−25854
satellite, hardness and erosion resistance to aqueous SiO_2 slurry 79−43441
skin technology, industrial appl. of space processing 79−28991
steel, ultrahigh C, superplastic struct. development by heat treatment 80−11703
thermodynamic study of corrosion 79−57161
thin walled tubes, exam. of stress/strain relations in tube eversion 79−61689
Ticonal, effect of rare earth metals on mag. props., struct., and phase transformations 79−99732
Udimet 520, γ' distribution in slip plane, dislocation loop form. during creep *(Japanese)* 79−42075
Udimet 520, γ' phase composition variation with ageing 77−8866
Udimet 520, Nicralloy-coated, microstruct. degradation, influence of corrosioin protective coating 80−40611
Udimet 520, precipitation hardening *(Japanese)* 79−43259
Al alloys, tensile deform. behaviour *(Japanese)* 78−27558
Al bronze, low cycle fatigue 78−27632
Al-Cu-Zr, superplastic alloy Supral, solidification and recrystallisation 80−7550
Al-Zn eutectoid, fracture, electron microscope obs. 78−31533
Al-Zn-Mg superplastic alloy, cavity growth under creep conditions 80−60940
Co base, cast, high temperature fatigue behaviour 80−40485
Co base, rupture life, prior temperature cycling effect 78−60840
Co, superalloy, attritious wear in grinding 77−32696
Co-base superalloy, machine thixocast, mech. prop. deficiencies 79−74244
Co-based, low temp. hot corrosion, Na_2SO_4-induced, mechanism, burner rig tests 80−40610
Co-Cr-Ni superalloy Mar-M509 standard and Mo modified, phase anal. 77−63675
Co-Cr-Ni-Ta-Al-Y (25, 10, 5, 3, 0.5 wt%), exam. of hot corrosion 79−20251
Co-Ni-Cr superalloys, γ'-precipitation-strengthened, yielding 77−8894
Co-Ni-Cr-Al-Ta, S-57 alloy hot corrosion, cyclic oxidation, depth of attack determinations 80−11837
Co-Ni-Cr-W-Fe, HA-188 alloy, hot corrosion, cyclic oxidation, depth of attack determinations 80−11837
Cu alloy, activation energy of plastic flow 78−64584
Cu-Al-Si-C (95, 2.8, 1.8, 0.4 wt.%) fracture characts. of superplastic single phase, exam. 78−48500
Cu-Al-Si-Co (2.8, 1.8, 0.4 wt.%), exam. of mech. props. 78−52891

superalloys continued
Fe alloys, Al-based coatings for high temp. appl., process development and props. 80−40614
Fe base superalloy, PHACOMP appl. to σ-phase estimation of various heats *(Chinese)* 79−100109
Fe base superalloy, type A-286, elevated temp. fracture toughness testing of thin section irrad. materials 80−61063
Fe-Cr-Ni-Ti-Al, Ti, Ni, Al, H_2 variations effect on mech. props. 78−3188
Fe-Ni-Al-Co-Cu-Ti YuNDK type, S effect on mech. props. 80−60927
Fe-Ni-Co-Cu-Ti YuNDKT alloys, impaired mag. props. with C and S additions 80−60368
Fe-Ni-Cr (35, 15 wt.%) superalloy, stress rupture and tensile props., C and B additions effect *(Chinese)* 80−104244
Fe-Ni-Cr-Al-Ti-W-Mo (35, 15, 2.4, 2.3, 2.2 wt.%) wrought superalloy, freckles *(Chinese)* 80−104137
Fe-Ni-Cr-Mo superalloy, mech. props., η-phase form. effect *(Chinese)* 80−20925
Fe-Ni-Cr-Si, superalloy, Cr and Si effect on mech. props. and microstruct. *(Chinese)* 79−100207
Fe-Ni-Cr-Ti-Al, Ti and Al effect on microstruct. and mech. props. *(Chinese)* 79−74130
Fe-Ni-Cr-Ti-Mn-Mo, (25.8, 14.04, 2.17, 1.27, 1.30 wt.%), superalloy A-286, precipitation hardening, exam. of fracture toughness and mech. props. 78−92355
Fe-Ni-Cr-base superalloys, characterization for PNP components 80−5242
Mg-Mn-Ce alloy, MA8, dislocations at grain boundaries and grain-boundary glide 78−64605
Mo, high temperature properties 78−44173
Ni alloy, IN-100, aluminised, microstruct. degradation, influence of corrosioin protective coating 80−40611
Ni alloys, Si-based coatings for high temp. appl., process development and props. 80−40614
Ni base, dispersion strengthened, creep stress component rationalization *(Korean)* 79−66115
Ni base, internal stresses due to dislocation walls around second phase particles 79−99210
Ni base, rupture life, prior temperature cycling effect 78−60840
Ni base, SIGMA-SAFE, phase diagram approach to sigma phase problem 78−64547
Ni base IN 100, corrosion resistant intermetallic coating, microstruct. effect on mech. props. 78−85058
Ni base Rheocast high performance superalloy, solid-liquid phase charact. 77−28803
Ni base superalloy, directionally solidified, struct. and props. *(Chinese)* 80−20918
Ni base superalloy, fatigue crack opening load variation with meas. location 80−16425
Ni base superalloy, γ′ precipitate size determ. technique 79−34221
Ni base superalloy, γ′-precipitation influence on recrystallisation 80−29955
Ni base superalloy, instrumental anal., use of HF induction melting and centrifugal casting *(Japanese)* 77−56280
Ni base superalloy, single crystal, apparent and effective creep parameters, incubation period 77−63715
Ni base superalloy IN-738, γ′ precipitate coarsening during ageing and creep 79−52271
Ni base superalloy Nimonic 80A, microstruct. anal. by high-resolution electron microscopy 80−76459
Ni base superalloys, rapid solidification, use in gas turbine engines 80−84888
Ni base superalloys, recrystallisation 77−16616
Ni based Rene 80 superalloy, initial stages of pack aluminisation 80−76188
Ni based superalloys, aluminide and MCrAlY (M=Ni, Co, Fe) coating characterization by phase diagrams 79−8276
Ni based superalloys, sigma phase prediction techniques 80→7567
Ni, cast, microstruct. and microanalysis 78−35393
Ni powder, thinning technique for microstruct. obs. using analytical electron microscopy 78−48587
Ni, sintered carbonyl type and with dispersed ZrO_2 inclusions, struct. effect on high-temp. ductility 77−63757
Ni superalloy, STEM microanal. of precipitates and their nuclei 80−81067
Ni, superplastic superalloy IN-738 load relaxation testing 77−40507
Ni-(Co)-Cr, aluminide coating, microstruct. and chem. 80−76189
Ni-Al, (2 and 6 wt.%), oxidation, α-Al_2O_3 growth, microstruct., precip. 80−108626
Ni-Al-Cr superalloy IN-100, crack retardation at elev. temp., hold time effect of single overload 79−79068
Ni-Al-Ti cast superalloy, eutectic transform. on ageing *(Chinese)* 79−100110
Ni-Al-Ti-Cr superalloys, estimation of conjugate γ and γ′ compositions 79−8282
Ni-base, powder metallurgical, creep-rupture at intermediate temps. 80−97568
Ni-base, STEM microanalysis of precipitates 80−104492
Ni-base coated with Ni-Co-Cr-Al-Y, fatigue cracking in coating 78−11438
Ni-base superalloy, ⟨111⟩ monocrystals under compression, inhomogeneous deformation 77−63736
Ni-base superalloy, conventional and powder metallurgical, σ-phase precipitation 80−11646
Ni-base superalloy, effects of grain boundary carbides on creep and back stress 80−3130
Ni-base superalloy, microscopic inhomogeneity of plastic strain influence on fatigue cracks *(German)* 80−40470
Ni-base superalloy, phase extraction *(German, English)* 77−52599
Ni-base superalloy IN713LC, hot corrosion, thermal cycling effects 77−70204
Ni-base superalloys, emission spectral anal. with fixed time integration technique *(Japanese)* 80−71974
Ni-base superalloys, stacking fault energy rel. to mech. props. *(French)* 79−43339
Ni-base superalloys, technique for replication of γ′ 80−79648
Ni-base type IN 718, acoustic emission interpretation of ductile fracture processes 80−35300
Ni-base wrought superalloy, creep and stress rupture behaviour in air and vacuum 80−60918

superalloys continued
Ni-based, hot workability, effect of S, Ca, Mg, Y and Zr minor elements 80−66552
Ni-based, low temp. hot corrosion, Na_2SO_4-induced, mechanism, burner rig tests 80−40610
Ni-based superalloys, TEM obs. of cellular transformation products 80−3045
Ni-Co-Cr superalloy, powder produced, necklace struct. development 80−40395
Ni-Co-Cr-Al-Ti-Mo superalloy IN738, casking porosity removal using hydrostatic press. sintering 80−55322
Ni-Co-Cr-Mo-Al, Astroloy, extruded powder metallurgy superalloy, recrystallisation study 79−4976
Ni-Cr superalloy, interactions between creep and low cycle fatigue *(Chinese)* 80−66572
Ni-Cr-Al-ThO_2, hot corrosion, cyclic oxidation depth of attack determinations 80−11837
Ni-Cr-Al-Y_2O_3 superalloy, recrystn. and texture development 80−16328
Ni-Cr-Co base superalloy APK1, hot isostatically pressed, heat treatment, fracture props. 77−73251
Ni-Cr-Co superalloy, σ-phase effect on mech. props. *(Chinese)* 79−74229
Ni-Cr-Co superalloy IN-792, crack growth resistance, metallurgical effects 77−36655
Ni-Cr-Co-Al super alloy, IN-738, creep failure criteria 80−65150
Ni-Cr-Co-Mo-Al, IN-67 alloy, hot corrosion, cyclic oxidation, depth of attack determinations 80−11837
Ni-Cr-Co-Mo-Ti-Al, powders, HCl surface treatment to prevent TiC precipitation, fracture props. 79−8397
Ni-Cr-Co-Ti, superalloy sintering thermochemical surface treatment 80−25617
Ni-Cr-NbC (18, 10 wt.%) eutectic composite, unidirectional solidification, thermal cycling, temp. range effect on microstructural degradation 80−89272
Ni-Cr-Ti rapidly solidified superalloys, surface segregation 80−76263
Ni-Cr-Ti-Co-W-Al-Mo alloys AF-115 and AF2 1DA, superalloy powder compacts, fatigue origins 78−48521
Ni-Cr-W-Mo-Al-Ti (15,6,3,2,2, wt.%), wrought, Si effect on transition brittleness *(Chinese)* 80−55491
Ni-Cr-base superalloys, characterization for PNP components 80−5242
Ni-Fe-Ce superalloy, vacuum melted, Ce effects on microstruct. 77−36552
Ni-Fe-Cr (18, 18 wt.%) superalloy, mech. props., 4-295K 77−44327
Ni-Fe-Cr base superalloy, addition effect on mech. props. *(Chinese)* 80−20998
Ni-Fe-Cr superalloy 718, heat treatment effect on room temp. and elevated temp. fracture toughness response 80−100922
Ni-Nb-Al-Cr, directionally solidified, exam. of growth and morphology 79−11601
Ni-Nb-Cr-Al, directionally solidified eutectic superalloy, high temp. oxidation resistant coatings 78−39937
Ni-Ti-Al superalloy, pendant drop melt extracted, struct. and props. 80−76242
Ni-W-B, M_5B_3 type boride 78−44131
β-NiAl, oxidation, α-Al_2O_3 growth and microstruct. 80−108627
Ni_3(Al.Ti), single crysts., flow and fracture behaviour tested in tension 79−79075
NiTa C-13, advanced fibre reinforced eutectic superalloy, creep and rupture 77−63744
NiTaC eutectic superalloy, casting, furnace atm. effects 80−84880
NiTaC eutectics, high cycle fatigue at room temp. 80−16459
Pb-Sn, eutectic, roll load and torque necessary for rolling *(French)* 78−95761
Pb-Sn (62 wt.%), activation energy for superplasticity 77−86112
Pb-Sn (62 wt.%), eutectic, exceptional ductility 78−27579
Pb-Sn eutectic, anelasticity effect on stress relaxation 78−31443
Pb-Sn superplastic alloy, cutting, stress distrib. *(German)* 79−24682
SiC-Ni based superalloy reaction, at elevated temps. 80−3287
SiO_2-base cores, for superalloys, high temp. characterisation 80−10640
Ti-70A superalloy, fusion reactor blanket structures, radiation resistance 80−63379
Ti-Mn, microduplex grain struct. stabilisation 78−44058
Zn-Al, high strength superplastic alloy, exam. of precise forging method 79−4929
Zn-Al (20 wt.%) superplastic alloys, Zn diffusion, strain influence *(Russian)* 79−37870
Zn-Al (22 at.%), heat treatment and straining effect on fracture and corrosion 79−87672
Zn-Al (22 wt.%), activation energy for superplasticity 77−86112
Zn-Al (22 wt.%), eutectoid alloy, ductility and fracture 78−60819
Zn-Al (22 wt.%), superplastic eutectoid cavitation evidence 77−63741
Zn-Al (22 wt.%) eutectoid, superplastic, factors affecting ductility 77−86097
Zn-Al (22 wt.%) eutectoid, grain size effect on plastic deform. at room temp. *(Japanese)* 78−31462
Zn-Al (22 wt.%) superplastic alloy, cavitation and neck form. 80−30022
Zn-Al (40 wt.%), superplastic deform., dislocation effects 77−48515
Zn-Al alloys, comp. effects on intergranular slip during superplastic deform. *(Russian)* 77−32633
Zn-Al eutectoid, superplasticity, study by electron microscopy 77−48479
Zn-Al eutectoid superplastic alloy, fatigue, microstruct. obs. and frequency effect 77−36659
Zn-Al superalloy, transform. kinetics 79−100114
Zn-Al-Cu (18, 5 wt.%) alloy, superplasticity *(Russian)* 77−59856
Zn-Al-Cu-Mg (22, 0.5, 0.01 wt.%), superplastic alloy, strengthening mechanism *(Japanese)* 77−55975

superconducting cables
applied superconductivity, conf., Pittsburgh, USA (Sept. 1978) 79−33374
composite wire critical current density rel. to tensile stress at 4.2K, obs. 79−33439
conference, Stanford, Calif., USA (Aug 1976) 77−28272
cryogenic current safety lead for magnet quench 77−83232
cryogenic systems, circulating cooling time for laminar and turbulent flow coolant 77−5849
fusion reactor, induction heating coils, 50 kA prototype superconducting cable, critical current 80−106196
heavy-current cabled and soldered multifilament superconductor AC losses 79−32808
insulation, elec. discharges in He at low temps. studied 77−27757

superconducting cables continued
magnetisation anisotropy meas. in hysteresis loss using Hall sensors 80−17966
multifilamentary and cabled superconductors, cryogenic stability anal. 79−59260
polycarbonate, plastic insulation for cryogenic power cable, exam. of dielectric, tensile props. 80−25823
polyester (Mylar), plastic insulation for cryogenic power cable, exam. of dielectric, tensile props. 80−25823
polyethylene, low temp. dielec. loss due to antioxidants 79−99822
polyethylene, plastic insulation for cryogenic power cable, exam. of dielectric, tensile props. 80−25823
polyethylenes, dielec. losses, for use in AC superconducting power transmission lines 80−25302
polypropylene, plastic insulation for cryogenic power cable, exam. of dielectric, tensile props. 80−25823
polypropylene-polyurethane laminates, meas. of dielectric losses at cryogenic temps. 80−25301
polysulphone, plastic insulation for cryogenic power cable, exam. of dielectric, tensile props. 80−25823
power line conductor, thermal stability 78−52163
PTFE, spacer material, dielec. loss meas. using supercond. reson. cavity 77−8501
rows of wires, in transverse mag. field, AC losses *(Japanese)* 80−60143
telecommunication, cryogenic envelope, determination of struct. and thermal insulation performance 79−58731
Tokamak power reactor supercond. poloidal magnet system design, experimental 79−31207
transient losses in cables for PF and TF coils 78−62635
He cooling systems, large, review of hydrodynamics and heat transfer 79−204
He refrigerators for transmission lines, optimisation w.r.t cost and reliability 78−24802
He requirements for superconducting power network 79−50897
He, supercritical, dielec. breakdown 79−65796
He unit requirements, for superconductive energy appl. in USA 78−89999
Nb sputtered film interface with stainless steel, for supercond. AC cables 79−74089
Nb-Ti, multifilamentary, Mirror Fusion Test Facility, superconductor core manufacturing and quality 80−93521
Nb-Ti multifilamentary cable magnet, quench development 77−26351
Nb_3Al multifilamentary cable fabrication and props. 79−33438
Nb_3Sn monofilamentary wires, supercond. crit. current density, bending effects 80−50018
Nb_3Sn, multifilament, production and props. *(German)* 80−3081
Nb_3Sn multifilamentary conductor production and testing 79−32809
Nb_3Sn multilayered supercond. power line conductors, elec. props. and growth morphology 77−28325

superconducting critical field
A15 multifilamentary high-field superconductors, status of development 79−61004
A15 superconductors, effects of material parameters on H_{c2} 79−61005
A-15 compounds, superconducting props. and structural transition *(Russian)* 77−12052
alloy, theory of upper crit. field 77−63038
amorphous superconductor, high-κ, upper and lower crit. fields 79−4629
anisotropic lower critical field, orientation depend. 80−20361
anisotropic superconductors, upper critical field theory 80−75692
antiferromagnet, uniaxial, critical magnetic field, influence of superconductivity 79−87219
antiferromagnetic superconductors, new pairing state, pair destruction, theory 80−54847
boson method, impurity and temp. effects 78−91826
Chevrel phase materials, indirect meas. of Fermi surface parameters 79−60686
clean cubic type II superconductor, anisotropy of generalised Ginzburg-Landau parameters 79−4630
conduction electron spins, surface relax. 79−60995
rel. to continuous field generation, future prospects, using supercond. coils 79−71493
critical temp. and critical mag. field of superconductor *(German)* 78−84343
definitions of terms for supercond. phenomenology, meas. practices 78−52117
dislocation structures, supercond. states 79−69627
dislocation systems, superconducting states, impurity effects *(Russian)* 80−11131
experimental data, anal. for type A and type B superconductors *(Chinese)* 80−60151
filament formation near edge dislocation *(Russian)* 79−4635
filamentary superconductor, Ginzburg-Landau theory of upper crit. field 79−78276
filamentary superconductor, upper and lower crit. fields 80−25053
film, crit. mag. field calc. using Ginzburg-Landau eqns. *(French)* 79−60999
film, superconducting props. 79−38215
fluxoid quantum number at H_{c3} 79−78275
granular superconductors, percolation theory, crit. props. 80−84575
graphite-K intercalation compounds, Fermi surface, transport and supercond. props. 79−65367
hard superconductor, flux trapping, penetration depth determ. 80−100572
hard superconductor flux jumps under time depend. external conditions 80−7038
high performance wire development 77−20487
impurities with Kondo effect, Green's function calcs. 77−89894
impurity mode effects on crit. characts. of superconductors, zero temp. crit. field *(Russian)* 79−19692
inhomogeneous superconductor, crit. fields 78−84367
intermetallic phases, technical superconductor applications *(German)* 78−27005
Josephson coupled layered supercond., upper critical field *(Russian)* 80−100551
Josephson self-resonant modes analysis, using mechanical analogue model *(Chinese)* 80−34563
Kondo effect in supercond., transition temp. and upper crit. field 77−55634
Kondo effect in type II superconductors, upper critical field and Ginzburg-Landau parameter 78−14874
Kondo superconductor, self-consistent theory of pairbreaking 78−26989
large-scale applications of supercond. materials, review 79−69640
layered compounds, upper crit. fields and reduced dimensionality 80−70910
layered superconductors, effect of random distortions on crit. field 80−54851
local state form. along dislocation, crit. field and current for destruction *(Russian)* 78−14905
magnetic impurities, crystalline-field-split in supercond., free energy and thermodynamical crit. field 77−32127
magnetic impurity low temp. behaviour, transition temp., specific heat, free energy 80−88691
materials and methods development trends *(Czech)* 78−23213
metallic glasses, mats. props. review 77−4043
microbridges, neg. resist. and hot electrons, model 78−60254
molybdenum chalcogenides, multicomponent, physical props. 80−84577
molybdenum chalcogenides, supercond., prop. preparation and struct. *(French)* 79−73619
molybdenum ternary chalcogenides, structures and properties survey *(Czech)* 80−70870
neutron irradiation effects 78−52121
non-pure superconductor, type I-type II transition and lower crit. field 78−2615
paramagnetic limit, Fermi surface dielectric gap *(Russian)* 80−2533
paramagnetic limit in superconductors with dielectric gap in Fermi surface *(Russian)* 78−95402
paramagnetic susceptibility for H_2, supercond. crysts. without symm. centres 77−15994
periodic structures, crit. fields *(Russian)* 80−88700
polysulphur nitride, temp. depend. and anisotropy of H_{c2} 80−25054
power apparatus appls. for superconductivity, research study *(Japanese)* 78−19192
properties of selected superconductive materials 79−56366
quantum polarisation effect in critical freq. EM field 80−75677
quasi-one-dimensional superconductor, critical mag. field, transition temp. *(Russian)* 80−93058
quasi-zero-dimensional superconductor, theory of upper critical field 80−107968
rare earth compounds, $R_xMo_6S_8$, high crit. field Chevrel phase 79−61003
rare earth compounds, ternary, superconductivity and ferromagnetism 79−69617
rare earth compounds, ternary, theory of superconductivity 79−73628
rare earth rhodium boride system, ternary, supercond., phase diagrams at upper crit. fields 80−2531
rare earth superconductors, upper crit. fields in the dirty limit, depend. on intra- and interaction exchange interactions 79−56461
rare earth ternary compounds, supercond. and antiferromag. coexistence 80−25030
rare-earth, mag. supercond., appl. of boson theory to mixed state 80−7050
relationship with energy gap 79−65621
standard measurement techniques for determ. of supercond. props. 79−69622
strong coupling superconductor thin film, critical mag. field *(Chinese)* 80−54849
superconductivity and magnetism *(Hungarian)* 79−47226
superconductor, magnetic, shape effects 80−103773
superheating field for finite κ calc. 77−12060
surface relaxation time of conduction electron spins 78−91814
synthesis from thermalised sputtering and changes in Tc and depend. of H_{c2} on temp. 79−56350
technical superconductor radiation damage obs. 79−33422
ternary superconductor, mag. interactions 79−73613
thin cylinder in transverse mag. field, metastable supercond., Ginzburg-Landau eqns. 79−60961
transition metal chalcogenides, quasi-one-dimens., elec. mag., and supercond. props., review *(Russian)* 80−93022
transport current effects on superconducting thin-walled cylinder in mag. field *(Russian)* 80−100573
type I superconducting film, cylindrical domain struct. in mag. field 80−15666
type I superconductor, crit. field for nucleation of n-domains 77−1515
type I-type II transition and lower crit. field 78−2615
type II supercond. cylinder, magnetisation change induced by current near upper crit. field 80−70890
type II superconducting film, crit. region near H_{c2} rational approx. 79−91198
type II superconductor, bounded, intermediate state struct. form. near crit. field, role of surface 80−80465
type II superconductor, fluctuations in crit. region near upper crit. field 80−25048
type II superconductor, neutron irradiation effects *(Rumanian)* 78−52144
type II superconductors, anisotropic, demagnetisation effects on lower critical field 80−97043
type II superconductors, high field expts. on press. effects up to 15 kbar 79−61006
type II superconductors, order parameter change near H_{c2}, influence of transport current 80−75690
type II superconductors, thermodynamics near $H_{c2}(T)$ and scaling law 79−60968
type-II superconductor, magnetisation, rel. to anisotropy of upper crit. field 80−54832
type-II superconductors, anisotropic, lower crit. field 80−60153
upper critical field at low temps. 77−66230
weakly coupled supercond.-insulator multilayer stack, calc. 78−52161
Al film, granular, crit. field anisotropy and fluctuation cond. 78−26994
Al film, supercond. crit. field, spin-polarized tunnelling meas., test of high-field supercond. theory 79−87220
Al film in microwave radiation field, resistive state transition *(Russian)* 80−93038
Al particles, Zeeman crit. field, NMR spin echo meas. 79−56453
Al/Ge multilayered superconducting films, crit. fields and crit. temps. 79−7945
Al-formvar superconductive junction, Ginzburg's generalised jellium model 80−15663
Am, superconducting critical field, sp. ht. 80−11136
As, A1-type superconductor, critical mag. field 79−69638
AuGa, and $AuGa_2$, supercond. transition temp. and crit. field 79−38232

superconducting critical field continued
$AuGa_2$, press. depend., theor. *(Russian)* 77−51843
$(Au_{1-x}Pd_x)Ga_2$, supercond. transition temp. and crit. field 79−38232
$BaPb_{1-x}Bi_xO_3$, supercond. T_c and crit. fields, comp. depend. 79−73623
$BaPb_{1-x}Bi_xO_3$, superconducting props., Hall coeff. and elec. resist. meas. 80−84531
Be-Zr alloy, glassy, quenched from melt, supercond. props. 78−26983
Bi, A1-type superconductor, critical mag. field 79−69638
Bi, amorphous, superconductivity and the very strong electron-phonon interaction *(Japanese)* 79−95552
Bi, ultrathin film, crit. mag. fields *(Russian)* 78−23214
Bi, whiskers, hardness, elec. props. *(Russian)* 78−51874
Bi-Fb amorphous alloys, superconductivity and the very strong electron-phonon interaction *(Japanese)* 79−95552
C_8K, intercalation compound, superconductivity 78−91827
C_8K, intercalation cpd. with graphite, supercond. props. 80−44755
Cs_xWO_3, normal phase and supercond. props 80−25035
Cu-Nb_3Sn multifilamentary tapes, in situ formed, crit. current density anisotropy 80−84576
Cu-Nb_3Sn superconducting composite, crit. props., AC hysteretic losses 80−50014
Cu-V_3Ga, supercond. in situ composites, stress effects on crit. props. 80−65757
Cu_xLa_{1-x}, splat-cooled, phase diagram and supercond. props. 80−70881
$Cu_2Mo_6S_8$, normal state and superconducting property measurements 78−91660
$Cu_xMo_6S_8$, Chevrel phase supercond. prep. and supercond. props. 79−28434
$Cu_xMo_6S_8$, evaporated films, superconducting upper crit. fields, crit. currents 79−42714
$Cu_xMo_6S_8$, sintered and sputtered, supercond. upper crit. field 78−23215
$Cu_xMo_6S_8$, supercond., two-phase, upper crit. field meas. 80−29509
$DyMo_6S_8$, supercond. and antiferromag. coexistence, neutron study 78−95401
$Dy_{1.2}Mo_6S_8$, mag. ordering in supercond. state, resist. and AC susceptibility meas. 78−19194
$(Er_{0.6}Ho_{0.4})Rh_4B_4$, reentrant supercond., magnetisation meas. near lower crit. temp. 80−25043
$Er_{1.2}Mo_6S_8$, mag. ordering in supercond. state, resist. and AC susceptibility meas. 78−19194
$ErRh_4B_4$, supercond. and mag. props. 79−4631
$ErRh_4B_4$, supercond. transition temp., upper critical field, local spin fluctuations 79−38250
$ErRh_4B_4$, superconducting thin films, critical mag. field 80−75693
$ErRh_{11}Sn_{3.6}$, synthesis, supercond. and mag. props. 80−100547
$Er_xY_{1-x}Rh_4B_4$, mag. and supercond. transitions 80−70874
Ga film, crit. transverse mag. fields and transition temp. *(Russian)* 80−7048
Ga, films, distorted, crit. mag. fields *(Russian)* 78−39273
B-Ga, metastable, elec. props. in normal and supercond. states *(Russian)* 80−65520
$Gd_xEr_{1-x}Rh_4B_4$, effects of Gd ion on supercond. transition temp., mag. transition temp. and upper crit. field 79−56392
Ge, A1-type superconducting thin film, critical mag. field 78−31023
GeTe film, semicond., supercond. energy gap and crit. field, tunnelling meas. 77−24644
$HbSe_2$:Mn layered superconductor, crit. temp. and fields 77−51836
Hf-V foil, rapidly quenched and heat treated, supercond. props. 80−54852
Hg filament, crit. mag. field and supercond. transition temp. 77−16013
$Ho_{1.2}Mo_6S_8$, supercond. transition temp., upper critical field, local spin fluctuations 79−38250
I, metallic A1-type modification, normal conductivity and superconductivity 80−20348
In, crit. RF mag. field, rel. to superheating 78−2632
In, divided superconducting thin film, superheating and supercooling field resistive meas. *(French)* 80−44751
In film, He ion implantation effects on parallel crit. field, vortex state *(Russian)* 77−69459
In, stress depend. of supercond. parameters 77−12045
In-Bi, crit. RF mag. field, rel. to superheating 78−2632
In-Bi, single spheres, supercond. props. 79−73617
In-Bi (2 at.%), supercond. film, thermal cond. in perpendicular mag. field 77−8229
In-Bi(Tl)(Pb), small κ supercond., phase transitions higher than second order 80−88668
In-Mn, dil., supercond. film, H_{c2} meas., mag. impurity effects, pair breaking theory 79−42708
In-Pb (7 at.%) alloy cylinder, magnetisation change induced by current near upper crit. field 80−70890
α-In-Sn, stress depend. of supercond. parameters 77−12045
$In_{\sim 3}Mo_{15}Se_{19}$, high field supercond., crit. temp. and crit. field 79−47211
In_3Sn, anisotropy of upper crit. field 80−20360
In_3Sn, tetragonal supercond., lower and upper crit. field, anisotropy and temp. depend. 80−97042
La film, tunnelling investig., multiple band effects 77−8244
La, heat capacity and supercond. props. 80−65247
La-Al(Ge)(Au), amorphous, alloying effect on supercond. props. 79−60951
$La_{1-c}Ce_cAl_2$, Kondo superconductor, self-consistent theory of pairbreaking 78−26989
$La_{1-x}Ga_x$ foils, amorphous, splat cooled, calorimetric and resistive meas. 79−33417
$La_{1-x}Gd_xMo_6Se_8$, supercond. transition temp., upper critical field, local spin fluctuations 79−38250
$La_{1-x}Gd_xRu_2$, mag. ordered superconductor, re-entrant superconductivity 78−88059
$(La_{.993}Lu_{.007})_{1-x}Gd_xRu_2$, exchange enhanced supercond., compensation effect on H_{c2} 77−4474
(LaPr)Sn_3, supercond., free energy and thermodynamical crit. field 77−32127
La_3S_4, high crit. mag. field supercond., elec. resist., sp. ht. and magnetisation 80−2532
$La_{0.80}Th_{0.20}Ce$, re-entrant supercond. matrix-impurity system additive pair breaking 77−69460
$LiTi_2O_4$, prep., characterisation and supercond. props. 77−40010
$Li_{2.6}Ti_xO_4$, upper critical field, paramag. limiting effects 77−8251
Lu_2C_3, superconductivity 79−73621
Mo ternary chalcogenide, MMo_6X_8 (M=metal, X=chalcogen) Chevrel phase, supercond. and normal state props. 78−56267
superconducting critical field continued
Mo-C film layer structure obs. of supercond. transition temp. and crit. mag. field oscills. 77−69438
Mo-chalcogenides, crit. mag. fields *(Russian)* 78−34936
Mo-Re, σ phase alloy, critical mag. field, elec. resistance 80−54850
Mo_6NaS_8, specific heat and supercond. critical field *(Russian)* 77−77004
$(Mo_{0.6}Ru_{0.4})_{0.8}G_{0.2}$-Fe (G=P,B), amorphous supercond., upper crit. field as function of temp. 79−73646
$(Mo_{1-x}Ru_x)_{80}P_{20}$, amorphous alloys, superconductivity, mag. susceptibility and electronic props., liq. quenching 78−88057
$(Mo_{1-x}Ru_x)_{80}P_{20}$, amorphous, liq. quenched, mag. susceptibility, supercond. and electronic props. 79−56376
MoS_2 intercalation compounds, reaction with alkali and alkali earth metals, band struct., superconductivity 78−26541
Mo_6Se_8, Chevrel phase, anisotropy of H_{c2} 79−56460
Mo_6Se_8, heat capacity and mag. props., 2-30K 79−42692
$Mo_{70}Si_{20}B_{10}$, amorphous alloys obtained by liq. quenching, superconductivity 80−75670
Nb, and Nb-V alloy, effect of purity and alloying with Ta, Cr, Mo or Re 77−85375
Nb, anisotropy of crit. field, magnetisation meas. 79−78260
Nb, critical current density, deviation from critical state model 80−84578
Nb, critical field, muon spin relaxation *(German)* 80−50015
Nb, cylindrical and ellipsoidal, rotational magnetisation and torque meas. in mag. field 78−43515
Nb, deviation function 79−7947
Nb film, crit. temp., crit. field, and surface resist. 77−55635
Nb, film, critical mag. fields and currents, temp. depend. *(Russian)* 80−103798
Nb film, struct. and electrophys. props. at 4.2K 80−80436
Nb, flux pinning by voids during neutron irrad. 77−40008
Nb, hypersonic attenuation near critical field H_{c1} 77−77005
Nb, lower critical field anisotropy 78−76201
Nb, peak effect due to vortex pinning in subsurface layer *(Russian)* 80−93060
Nb, supercond. surface resistance derivative meas. for annealed and unannealed crysts., crit. mag. fields 79−33395
Nb, superconducting, deformed, oscillation in current-voltage characts. near H_{c2} 79−28491
Nb, US attenuation, hysteresis near and below H_{c1} 80−75676
Nb, upper crit. field, temp. depend. and anisotropy 80−80462
Nb:N, H_{c2} anisotropy, impurity and temp. dependence 78−43533
Nb-Ga (16 to 28 at.%), transition temp., upper critical field and magnetisation curves 77−80866
Nb-Ge-Fe, effect of Fe on supercond. and mag. props. 79−56351
Nb-Ir, A 15- and σ-phases, supercond. 79−73645
Nb-Pt alloy, superconducting parameters of A15- and σ-phases 78−39242
Nb-Rh, σ-phase alloy, superconductivity and resistance behaviour 80−70882
Nb-Si(−V)(Zr)(Mo)(Ta)(W)(C)(B)(Ge), ductile amorphous, superconductivity 80−60131
Nb-Sn, diffusion couple, phase equilibria, effect on T_c and H_{c2} 79−56462
Nb-Ti, multifilament superconductor, metallurgical design 79−33434
Nb-Ti, optimised pinning struct., crit. data 1.8-4.2K 77−89913
Nb-Ti, pinning curves, high field J_c and scaling behaviour 80−93064
Nb-Ti, superconductivity after heavy ion irradiation at low temps. and high fluence 77−69437
Nb-Ti alloy, supercond. and mag. props., anisotropy *(Russian)* 77−59361
Nb-Ti-Ta, pinning curves, high field J_c and scaling behaviour 80−93064
Nb-Ti-Zr ternary system, high-field supercond. 80−97045
Nb_3/Sn-Cu composites, in situ processed, supercond. props. 80−75698
Nb_3(Al, Ge) tape, effect of thermal treatment on supercond. props. 79−61016
Nb_2Al, $NbAl_3$, supercond. and mag. props. 77−47922
Nb_3Al tape, effect of thermal treatment on supercond. props. 79−61016
Nb_3Al-Ni(Cr)(Fe) mag. impurities effect on supercond. props. 77−1524
$Nb_3Al_{0.83}Ge_{0.21}$, A-15 phase, sp. ht. meas., Debye temp., energy gap and crit. field 79−19689
Nb_3As, electronic and supercond. props. 77−16011
$Nb_{\sim 3}Au$, upper crit. field 79−82729
NbB_2, superconductivity below 1K 80−20342
NbC_x, reactor irrad. effects on elec. resist. and supercond. props. *(Russian)* 78−47895
NbCN, preparation methods and supercond. properties *(French)* 79−73618
Nb_3Ga, critical data, under hydrostatic pressure to 15 kbar 79−47217
$Nb_{78}Ga_{22-x}Mn_x$, supercond. props., influence of Mn mag. impurities 80−54825
$Nb_{80}Ga_{20-x}Mn_x$, supercond. props., influence of Mn mag. impurities 80−54825
Nb_3(Ge, X), X=Si, Ga, CVD tapes, supercond. props. at high mag. fields 79−38279
$Nb_{1-x}Ge_x$, supercond., mag. field props. 80−54822
Nb_3Ge, α-particle irrad., relationship between density of states and supercond. transition temp. 79−42684
Nb_3Ge CVD tapes, supercond. props. at high mag. fields 79−38279
Nb_3Ge, CVD-prepared, high field props. and scaling 79−56455
Nb_3Ge, density of states from critical field meas. 79−42690
Nb_3Ge, effect of ^{16}O and ^{32}S ion irrad. and thermal recovery on T_c, residual resist. and slope of crit. field 79−56348
Nb_3Ge film, prep. by coevaporation, supercond. props. 78−91830
Nb_3Ge film, sputtered and evaporated, transition temp., critical field and current anisotropy 77−28328
Nb_3Ge sputtered film, struct. and superconducting props. 77−28337
Nb_3Ge tape, prep. by continuous CVD process 78−11121
Nb_3Ge-based superconducting alloys, upper critical field temp. depend. *(Russian)* 78−10622
$Nb_2Ge_{1-x}Ga_x(Sn_x)$ CVD films, supercond. props., 4.2 to 19K 79−42713
$Nb_{78}Gn_{22-x}Fe_x$, $Nb_{80}Ga_{20-x}Fe_x$, A15 phase supercond. 79−87181
$(Nb_{0.99}Mo_{0.01})_{1-x}Ge_x$, supercond. transition temp. and crit. field 79−38220
NbN, critical data, under hydrostatic pressure to 15 kbar 79−47217
NbN diffusion wires, crit. currents and supercond. crit. field under high press. 79−38287
NbN film, supercond., upper crit. field 78−64172

superconducting critical field continued
NbN, supercond. RF reactively sputtered films, deposition parameter effects on props. 80−80972
NbS, supercond. props. at press. up to 20 kbar 79−24111
NbS_2 (2H), anisotropy of upper critical field 78−76200
Nb_3S_4, anisotropic superconductor, critical field and specific heat meas. 80−44779
$NbSe_2$ (2H), layered, anisotropy and electron-phonon coupling effects on sp. ht. 77−51844
$NbSe_2$ (2H), pure and Fe doped, layer supercond., anisotropy and temp. depend. of H_{c2} 77−51857
$NbSe_2$ (2H), supercond., thermodynamic props., exhibiting anisotropy and strong-coupling effect 77−12062
2H-$NbSe_2$, layer struct. supercond., H_{c2} temp. and ang. depend. 77−8248
$NbSe_2$-Fe, dil. alloy, magnetotransport and superconductivity 77−55516
$NbSe_2$(2H), specific heat and critical field, anisotropy and strong coupling effects 77−36021
Nb_3Si, electronic and supercond. props. 77−16011
Nb_3Si, supercond. props., effect of neutron irrad. 79−38211
Nb_5Si_3, supercond. props. and cryst. struct. 79−78245
Nb_3Sn, α-particle irrad., relationship between density of states and supercond. transition temp. 79−42684
Nb_3Sn bronze process, flux pinning scaling law depend. on strain 80−75696
Nb_3Sn, bronze processed, effect of third element additions 77−28333
Nb_3Sn composite processes with Cu-Sn-Zn matrix, superconducting props. 78−84370
Nb_3Sn, critical data, under hydrostatic pressure to 15 kbar 79−47217
Nb_3Sn, current carrying capacity increase by Hf addition 80−7056
Nb_3Sn, density of states from critical field meas. 79−42690
Nb_3Sn, effect of diffusion couple Sn content on superconductivity 79−61009
Nb_3Sn, electron beam deposited, microstruct., rel. to supercond. props. 79−37935
Nb_3Sn, fast neutron irradiation, effect on critical current density 78−19197
Nb_3Sn film on insulating substrate, crit. mag. fields *(Russian)* 79−11277
Nb_3Sn in bronze, supercond. props. thermally induced matrix stresses 77−32134
Nb_3Sn, low field microwave props., H_{c1} 77−28317
Nb_3Sn monofilament wires, supercond. props., effect of Be alloying additions to bronze matrix 79−87222
Nb_3Sn, multifilament superconductor, metallurgical design 79−33434
Nb_3Sn multifilamentary composites, crit. currents, flux pinning, and crit. field 79−78280
Nb_3Sn, multifilamentary high-field superconductor, status of development 79−61004
Nb_3Sn, neutron irrad. effect on upper crit. field and crit. current 77−72954
Nb_3Sn, supercond., crit. fields Pauli paramag. limiting and material parameters 79−78277
Nb_3Sn, supercond., fast particle irradiation effects, using anti-site defect model, electronic state influences 79−56346
Nb_3Sn, supercond. props., effect of neutron irrad. 80−80463
Nb_3Sn, supercond. props. and struct., neutron irrad. dose depend. 77−15985
Nb_3Sn, supercond. tape, crit. current, effect of Sn-Nb phase, annealing 79−24119
Nb_3Sn superconducting multifilamentary composites, strain depend. of crit. current and crit. field 79−33432
Nb_3Sn, superconducting props., effect of radiation induced atomic disorder 78−52133
Nb_3Sn superconductors, bronze-processed, effect of Ta additions 78−95404
Nb_3Sn, ternary additions effect on upper crit. field at 4.2K 77−28316
Nb_3Sn, thick walled tube, calc. of transverse dipole mag. field distributions *(French)* 79−47209
Nb_3Sn-Al_2O_3 composite, electron beam deposited, microstruct., rel. to supercond. props. 79−37935
Nb_3Sn-Fe(Co)(Mn), mag. impurities effect on supercond. props. 77−1524
Nb_3(SnGa), wire, neutron effect on T_c, I_c and flux pinning 79−38216
$Nb_3(Sn_{1-x}Ga_x)$, bronze processed wires, critical current densities in fields up to 23.5 T 78−47922
Nb_3(SnIn) tapes, diffusion processed, high field props. 79−38266
Nb_3(SnIn) wires, prep. by ductile fabrication process and props. 79−38265
$Nb_{30}Ta_{70}$, microwave props. of 8.6 GHz supercond. cavity 77−28297
$Nb_{0.95}Ta_{0.05}Se_3$, resist 0.5K to room temp., supercond. transition temp. and crit. field 79−82704
$Nb_{1-x}Ta_xSn_2$, supercond. transition temp. and upper crit. field 80−39723
$(Nb_{0.99}Ti_{0.01})_{1-x}Ge_x$, supercond. transition temp. and crit. field 79−38220
$(Nb_{0.99}Ti_{0.01})_{1-x}Ge_x$, supercond., mag. field props. 80−54822
$(Nb_{0.99}Zr_{0.01})_{1-x}Ge_x$, supercond. transition temp. and crit. field 79−38220
$(Nb_{0.99}Zr_{0.01})_{1-x}Ge_x$, supercond., mag. field props. 80−54822
$NdRh_4B_4$, possible obs. of coexistence of supercond. and long-range mag. order 79−82730
Ni-Nb(-Cu)-C, NbC dispersed supercond. tapes, fabrication and charcts. 78−19773
Pa, superconducting transition temp. and upper critical mag. field 80−44756
Pb, crit. mag. field, functional derivatives 78−91798
Pb, crit. RF mag. field, rel. to superheating 78−2632
Pb film, hypersonic attenuation investig. of crit. field, intermediate state 77−8246
Pb, superconducting phase condensation in bulk sample *(German)* 79−56447
Pb-Bi alloy, crit. mag. fields, influence of parameters 80−75691
Pb-Bi-Tl alloy, crit. mag. fields, influence of parameters 80−75691
Pb-In, superconductive to normal transition due to external mag. fields, dynamic behaviour 80−39722
Pb-In (1 to 20 at.%), upper critical field anisotropy 77−36033
Pb-In alloys, strong coupling effects in temp. depend. of flux-flow resist. near H_{c2} 77−36036
Pb-Mn, dil., supercond. film, H_{c2} meas., mag. impurity effects, pair breaking theory 79−42708

superconducting critical field continued
Pb-Sb, dynamic destruction of supercond. 80−2529
Pb-Sn(Bi), dirty strong-coupling supercond., Ginzburg-Landau parameters, type II behaviour deviations 77−8249
Pb-Tl alloy, crit. mag. fields, influence of parameters 80−75691
Pb-Tl alloys, pinning parameters 78−52173
$PbMO_6S_8$, supercond., upper crit. field meas. up to 600 kG 80−93057
$PbMo_{5.1}S_6$, supercond. wire prep. by powder technique 78−52705
$PbMo_6S_8$, high crit. field Chevrel phase 79−61003
$PbMo_6S_8$, normal state and superconducting property measurements 78−91660
$PbMo_6S_8$, supercond. wires prod. and characteris. 77−69462
$PbMo_6S_8$ wire, powder processed, crit. current density and field 80−80466
$Pb_xMo_6S_8$, Chevrel phase supercond. prep. and supercond. props. 79−28434
$PbMo_6Se_8(S_8)$, anisotropy of H_{c2} 78−39274
PdH_x, upper crit. field determ. 78−47919
PdH_x, $x\simeq1$, type I supercond. props. 79−56448
Rb_xWO_3, anisotropy in H_{c2} 80−6879
$(SN)_x$, supercond., fluctuation cond., crit. mag. fields 80−39712
$(SN)_x$, supercond. props., review 78−6474
$(SN)_x$, supercond. props., press. and field depend. 78−14903
$(SN)_x$, supercond. props., press. depend., up to 9.5 kbar 78−68106
$(SN)_x$, supercond. props. rel. to fibrous morphology 80−84570
$(SNBr_{0.4})_x$, supercond. props. rel. to $(SN)_x$ 79−65581
$(SNBr_{0.4})_x$, supercond. props., dimensionality 80−20344
Sb, A1-type superconductor, critical mag. field 79−69638
Sc_4C_3, superconducting phase synthesis at high press. and temp., critical field *(Russian)* 80−65732
ScS, supercond. props. at press. up to 20 kbar 79−24111
Si, A1-type superconducting film, critical mag. field 78−31023
$SmRh_4B_4$, coexistence of supercond. and antiferromag. order 80−11140
Sn, A1-type superconducting thin film, critical mag. field 78−31023
Sn, crit. RF mag. field, rel. to superheating 78−2632
Sn film, crit. mag. fields, temp. depend., penetration depth thickness depend. 80−70908
Sn, stress depend. of supercond. parameters 77−12045
Sn, supercond. fine particles, sp. ht., fluctuations under mag. field, crit. field and transition temp. 77−80873
Sn, surface, superconductivity suppression by microwave radiation *(Russian)* 79−24098
Sn-Bi(Sb), small κ supercond., phase transitions higher than second order 80−88668
Sn-In, crit. RF mag. field, rel. to superheating 78−2632
$Sn_{1.2(1-x)}Eu_xMo_{6.35}S_8$, supercond. transition temp., upper critical field, local spin fluctuations 79−38250
$Sn_xMo_6S_8$ and $(Sn\text{-}Al)_xMo_6S_8$, Chevrel phase supercond. prep. and supercond. props. 79−28434
$SnMo_6Se_8$, anisotropy of H_{c2} 78−39274
$SnMo_6Se_8$, high crit. field Chevrel phase 79−61003
Ta, critical field, muon spin relaxation *(German)* 80−50015
Ta:N, H_{c2}-anisotropy obs. 78−80105
Ta:N, superconductive to normal transition anisotropy 80−25031
Ta-N, supercond. props. 77−20507
Ta-Rh, σ-phase alloy, superconductivity and resistance behaviour 80−70882
TaN, mag. field direction determining whether type I or II 79−15266
TaS_2 (aniline)$_{3/4}$, low-field magnetisation meas. on small cryst. in supercond. phase 79−87188
TaS_2 intercalated with methylamine, supercond. layer cpd., crit. field enhancement and reduced dimensionality 80−60152
TaS_2-Fe, dil. alloy, magnetotransport and superconductivity 77−55516
TaS_2(2H), supercond. transition temp., upper crit. field, and interlayer coupling strength 79−56406
$TaSe_2$-Fe, dil. alloy, magnetotransport and superconductivity 77−55516
$TaSe_3$, superconducting crit. field rel. to anisotropic cryst. struct. 78−80104
TaS_2(pyridine)$_{1/2}$ intercalation complex, supercond. transition temp., upper crit. field, and interlayer coupling strength 79−56406
TaS_2(pyridine)$_{1/2}$, upper and lower critical fields, supercond. props. from Ginzburg-Landau theory 79−56456
$Tb_{1.2}Mo_6S_8$, mag. ordering in supercond. state, resist. and AC susceptibility meas. 78−19194
Tc-C film layer structure, obs. of supercond transition temp. and crit. mag. field oscills. 77−69438
Tc-Fe, dil., effect of Fe impurities on superconductivity 79−61007
Tc-Fe dilute alloys, supercond. and mag. props. 80−29494
Ti-Nb superconducting alloys and cmpds. with A15 struct., H_2 effect on supercond. props 79−28438
Ti-Nb-Si, amorphous alloy, supercond. props. and crystn. behaviour, TEM and DTA study *(Japanese)* 80−84536
Ti-Nb-Zr-Ta, superconducting props. comp. depend., stress effects and precipitation behaviour, X-ray scatt. 80−93059
TiN, high dispersed superconductivity 78−43505
TiN, low-energy ion-stimulated deposited, supercond. props. 80−88664
TiN, superconductivity 78−2605
Tl-Pb-Bi, critical field and specific heat 79−73631
$Tl_2Mo_6Se_6$, one dimensional supercond. crystal struct., resist. and upper crit. field 80−50016
V, amorphous film, supercond. props., gaseous impurities effect *(Russian)* 78−72301
V, and V-Nb alloy, effect of purity and alloying with Ta, Cr, Mo or Re 77−85375
V, anisotropy of genera-ised Ginzburg-Landau parameters 79−4630
V columnar films, crit. field anisotropy, depend. on prep. conditions *(Russian)* 80−93056
V film, crit. temp., crit. field, resist. and struct. *(Russian)* 77−4475
V film, inhomogeneous, crit. field anisotropy 79−56459
V, lower critical field anisotropy 78−76201
V, thermal conductivity in ultrapure normal, mixed and supercond. states *(Russian)* 79−4617
V-Al/Cu-Ge composite superconductors, transition temp. and upper crit. field, heat treatment effects 79−38268
V-Al/Cu-Ge composite tape, transition temp., upper crit. field 78−68126
V-C film layer structure, obs. of supercond. transition temp. and crit. mag. field oscills. 77−69438
V-Hf-Nb(Zr), multifilamentary, superconducting props. improvement 79−38267
V-Ti superconducting film, electron spin effects 79−28488
V_3Ga, crit. temp. and field, prep. from V-Al and Cu-Ga 78−43506

superconducting critical field continued
V_3Ga, high current density multifilament wire, neutron effects on equilibrium and transport props. 78−52126
V_3Ga, multifilamentary high-field superconductor, status of development 79−61004
V_3Ga multifilamentary wires, effect of low temp. neutron irrad. 77−32132
V_3Ga, neutron irrad. effect on upper crit. field and crit. current 77−72954
V_3Ga, supercond., μ^+ probe study *(Russian)* 79−7946
V_3Ga-Cu composites, supercond. props. 79−95557
V_2Hf base Laves phase compound tapes, supercond. props., prep. 77−40011
V_2Hf-base C15 compounds, development as high field supercond. 79−61015
$V_{1-x}Pt_x$, A-15 struct., Knight shift in normal state, upper crit. field curves *(French)* 78−43519
V_3Si, H_{c2} anisotropy in high field, grain boundary flux pinning 78−43532
V_3Si, mixed state, ultrasonic anomaly 77−55644
V_3Si, mixed state A15 struct., Gibbs free energy and lower crit. field temp. depend. 77−55643
V_3Si, neutron irrad., grain boundary pinning, field-depend. change of crit. current density 80−65759
V_3Si, neutron irrad., sound velocity, magnetic susceptibility and upper critical field 78−88074
V_3Si, supercond., crit. fields Pauli paramag. limiting and material parameters 79−78277
V_3Si, supercond. props., effect of neutron irrad. 80−80463
V_3Si, thermodynamic study, intrinsic type II superconductivity 79−47193
V_3Si-Fe, mag. impurities effect on supercond. props. 77−1524
$W_{70}Si_{20}B_{10}$, amorphous alloys obtained by liq. quenching, superconductivity 80−75670
$Y_{1-x}Gd_xRh_4B_4$, mag. supercond., anomalous temp. depend. of upper crit. fields 80−29510
Y_2O_3, synthesis at high-press and temp., supercond. 80−2513
$Y_{0.7}Th_{0.3}C_{1.55}$, superconducting crit. mag. field curve, initial slope 77−28318
$YbMo_6S_8$, supercond., low temp. thermal and mag. props. 78−14904
Zr-Rh alloys, amorphous, thermal relax. effects on electronic and supercond. props. 79−65575
Zr-V foil, rapidly quenched and heat treated, supercond. props. 80−54852
ZrC_x, x=0.99 to 0.13, elec. cond., supercond. state 78−43504
$(Zr_{1-x}Er_x)_3Rh$, amorphous, influence of mag. ordering on supercond. props. 80−29511

superconducting critical temperature *see superconducting transition temperature*

superconducting devices
see also cryotrons
accelerator structs. for medium energy protons 77−83151
accelerometer, using Nb-on-sapphire RF resonator 79−49210
accelerometers, gravitational wave detection, and general gravit. expts. 78−45555
applied solid state physics, book 80−94936
applied superconductivity, conf., Pittsburgh, USA (Sept. 1978) 79−33374
bimetallic ring, thermoelec. effect 79−4616
bolometer, effect of LF noise on threshold sensitivity 79−89005
bolometer, free floating, sensitive heat pulse detection 77−79149
bolometer, high-speed, based on Ag-Sn double films 80−57368
capacitive transducer with superconducting resonator for mechanical vibration meas. 78−21127
cavity, Nb reentrant, for heavy ion LINAC 77−26896
cavity multipactoring suppression in accelerator appls. 77−83121
chopper amplifier, improved sensitivity 77−26306
chopper amplifier for resistance meas., sensitivity and noise calc. 79−12817
Cocatron, servo valve for liq. He II level control, superfluidity and supercond. applic. 78−18855
coil energy storage power supply 79−34442
coil simulation, AC loss meas. 80−37050
coils, for Tokamak, active energy transfer rate control using inductor-convertor bridges 78−13338
composite superconducting transition edge bolometer 77−71371
cooling, microminiature cryogenic refrigerators design and construction 79−26059
cooling by supercritical He refrigerator, recovery time after thermal upset 77−17992
cryocooler for supercond. instruments, requirements 78−93710
cryocoolers for superconductive electronics 79−26058
cryocurrent comparators, ring cavity elements, field attenuation 77−144
cryogenic engineering, conf., Grenoble, France (May 1976) 77−17988
current carrying elements, size effect 79−61019
current comparator, appl. to meas. of Kapitza conductance of Evanohm 77−41645
cyclotron, magnetic field calcs. for proposed supercond. machine at Milan 77−83200
cyclotron in Milan, beam extraction studies 77−83361
cyclotron in Milan, injection studies 77−83195
Earth conductivity determ. using single superconducting coil 77−41184
electron accelerators, elimination of electron multipacting in supercond. structs. 78−9004
fabrication technology for superconducting ICs 79−28493
field emitter, max. current density, rel. to cathode geometry and kinetic props. 78−72704
field-emission cathode peak current, size effect 80−29863
field-frequency lock, for a superconducting spectrometer 78−86312
flux pump power supply, using inductive current transfer 78−12704
fluxmeter, quantum, with 15 to 20 kHz passband 80−57345
fusion reactor, T-10M Tokamak, normal and supercond. inductive energy storage and switching 78−55018
fusion reactor supercond. switches of high specific breaking power 78−55020
gamma camera, for clinical utilisation 79−63330
gravimeter, general struct., detection system and precision *(Chinese)* 79−34995
gyroscope, high accuracy all angle readout using quantised flux 77−26223

superconducting devices continued
gyroscope, shielded, mag. torque, for tests of gravit. theories 77−13678
gyroscope, to test Einstein's general theory of relativity 80−8897
gyroscope, trapped-flux spin-down torques 78−57941
heat switches, effect of surface prep. 79−60966
heavy ion post accelerator test section, operation experiences 77−83149
heavy ion superconducting booster, split ring resonator 77−83126
heavy-ion booster, Stony Brook project 77−83125
heavy-ion superconducting cyclotron at Chalk River, status 77−83192
ion source, high-perveance electron beam superconducting ion source 77−23333
ISABELLE, two superconducting storage rings 79−36440
laser frequency measurement using supercond. point contacts 80−90824
lens, for imaging organic materials in electron microscope 80−73553
levitation expt., search for quarks in matter 78−488
linac, Argonne superconducting heavy ion accelerator 77−38459
linac, superconducting heavy-ion, hybrid solenoid as focusing element 77−38460
linac recyclotron at Stanford, initial performance 77−83145
linac with MUSL-2, a second microtron 77−83198
linacs, heavy-ion superconducting 77−83141
linear accelerator, closely-coupled cavity chain, unit cell reson. freq. meas. method 77−83179
linear accelerator, comparison of short muffin tin structs. *(French)* 78−33330
linear accelerator, electron acceleration characts. 77−83178
linear accelerator, superconducting slow-wave structures 77−38458
linear accelerators, ion acceleration at 4.4K by superconducting resonators 77−34483
liquid He level indicator *(Japanese)* 78−12705
magnetic flux-free environment creation, cryogenic appl. 80−101797
magnetic gradiometer, LF noise spectra 77−33203
magnetic gradiometer for meas. of mag. gradients from ocean waves 79−29867
magnetic shield, superconducting shell, closed axisymmetric, for weak mag. fields 77−74470
magnetic shielding by superconducting shell, theory 79−68351
magnetic susceptometer, high sensitivity, based on SQUID magnetometer 78−49872
magnetometer, modification of sample holders 77−26367
magnetometer, oscillating sample, for water solns. vol. suscept. meas. 77−49753
materials for supercond. electronics 79−28470
memory device utilizing storage of Abrikosov vortices at array of pinning sites 79−28487
metrology appl. *(Japanese)* 78−37030
microwave noncontacting accelerometer for gravitational wave antenna 77−30076
microwave resonators used for high sensitivity dielectric loss meas. 77−10043
mm wave superconducting devices, present status 79−26119
multicontact thin-film switch, prod. 78−4661
NMR spectrometer, efficient decoupler coil design to reduce heating in conductive samples 80−31828
noise, conference, Bad Nauheim, West Germany (Mar. 1978) 79−24031
point contact microwave detector/receiver 77−79153
positive-sensitive detector of ionizing particles 80−63460
power network, He requirements 79−50897
powered superconductor MM range receiver for radio astronomy 80−21919
QED circuits at ultralow temp. 80−13247
quantum magnetometer with Hanle effect, three layer superconducting shield 77−53962
reference temperature, 0.015 to 0.21K, based on superconducting phase transitions 80−17948
refrigeration requirements for future superconductive energy related applications 79−58711
refrigerator, closed-cycle, for supercond. electronic systems, design 78−93711
refrigerator requirements, conf., Boulder, CO, USA (1977) 78−93696
relativity gyroscope expt., high accuracy test facility 77−30077
resonator, bar-loaded, electron accelerator appl. 79−36434
resonator, FM, analysis and appls. 77−26893
resonator, high-Q, for solid dielec. loss meas. 78−93733
resonator, Q-factor depend. on mag. flux line motion 77−32110
resonators, coaxial type, mech. vibration meas. appl. 77−74383
resonators, development and production for Argonne heavy ion linac 79−36435
resonators, high stability oscillators, appl. to fundamental physics, metrology 79−26034
resonators, RF contact 77−26923
review of superconducting device symposium of 1967 held at Charlottesville 79−28448
RF particle separator, negative 16 to 37 GeV beam, results 78−89589
RF particle separator CERN 79−81113
RF particle separator for CERN 77−26948
RF superconducting resonators for booster linac 79−54623
rotary switch, multicontact, cryoelectronic appls. 78−89497
solenoid, current regulated sweep unit 78−4659
solenoid with flowthrough opt. cryostat, for magnetoopt. investigations 80−105651
solid dielectric props. meas. with superconducting resonators 78−21180
solid-state oscillator with superconducting sapphire resonator, freq. stabilisation 79−12823
spectrometer for p polarisation meas. in high energy elastic scatt. 77−30439
spheres and current carrying coils, integral representation of inductance 80−80469
split ring resonator as accel. struct. for ^{16}O and ^{32}S beams 77−6577
split-loop resonator as heavy ion accelerating element 77−26894
split-ring resonator as heavy-ion accelerating struct. 77−26895
SQUID magnetometer for ocean bottom magnetic field meas. 77−87102
submillimetric composite bolometers with metal film absorbers 77−37997
SUPER-SOLO solenoid, switch and cryostat 79−54222
superconducting heavy-ion resonator, microprocessor based feedback system 77−88292
superconductive electronics, conf., Charlottesville, USA (Mar. 1978) 79−28447
superheated granules as X-ray and gamma-ray imaging detectors, astronomical appl. 79−25504

superconducting devices continued
superheated superconducting detectors, magnetic field dependence 80−27893
superheated superconducting suspension as transition radiation detector, electron meas. 77−6628
switch for large heat flow below 50 mK 78−54376
temperature fixed point device, prep. and calibration 80−82770
temperature fixed point device for temps. above 0.5K 79−63221
temperature fixed point device to provide reference temps. below 0.5K 79−63220
thermometer, low temp. stabilisation appls. *(German)* 78−86250
thermometer, sensitivity, temp. and field depend. 80−4708
thin film probe, for detection of second-sound shock waves in superfluid He 79−73355
transformer-rectifier flux pump power supplies performance anal. 78−12703
X-band Pb cavity expt., closed-cycle mech./adsorption refrigeration appl. 78−93708
Al heat switch and plated press-contacts 78−54377
He liquid, transient heat transfer, static coolant 78−75049
He refrigerators and liquefiers for large superconducting systems, optimization 79−63233
Nb, microwave cavity of muffin-tin type, for accelerator use 77−26905
Nb, RF superconductivity, appl. to particle acceleration, overview 79−31244
Nb, supercond. film, switching, storage and erasure effects 77−8253
Nb superconducting C-band cavities for linear accelerator appl. 79−36432
Nb superconducting cavities, AES depth profile meas. on oxide layer 77−8984
Nb TM_{010} superconducting RF cavities for high energy storage rings, 700 MHz meas. 79−68059
Nb-sapphire RF superconducting resonator, fabrication and props. 79−51704
Nb-Sn sintered material tubes for magnetic shielding 79−67446
Nb_3Sn cavities with high microwave qualities 77−26890
Nb_3Sn disc loaded waveguide, for linear accelerator appl., fabrication and props. 77−26892
Nb_3Sn flux exclusion tube for mag. field shielding in particle spectrometers 79−13578
Nb_3Sn, superconducting accelerating struct., high field exam. 79−36439
Nb_3Sn superconducting microwave resonator for measuring dielectric loss in polymeric solids 79−67316
$Nb_{30}Ta_{70}$, microwave props. of 8.6 GHz supercond. cavity 77−28297
NbTi monofilamentary wire in current sharing state, supercond. temp. sensor use 80−57288
Pb resonators, polishing procedure for high surface electric fields 77−83197
Pb shell, mag. vacuum prod. by supercond. transition 78−8427
$PbMo_6S_8$, supercond. wires prod. and characteris. 77−69462
Sn-Pb supercond. loop, laser irrad. effects 79−56419

superconducting energy gap
A15 compounds, microscopic model of supercond. and martensitic transform. 77−8226
A15 compounds, supercond. crit. temp. for model density of state using Eliashberg gap eqns. 80−93034
A15 compounds, supercond. rel. to struct. transform. 78−14873
A15 compounds, T_c reduction due to defects, gap anisotropy mechanism 77−43773
A15 superconductors, radiation induced Tc, gap anisotropy effects 78−52125
A-15 compound, defect influence on T_c 80−20345
A-15 compounds, coupling strength 79−19684
amorphous superconductor, ratio of energy to transition temp. 78−10619
anisotropic superconductors, nonmag. impurities effect on supercond. transition temp. 80−93035
anisotropy, Eliashberg eqns., review *(Spanish)* 80−84544
anisotropy, normal layer proximity effect 80−84558
anisotropy of energy gap, quasi-particle approach 79−61225
barium stearate single-layer Langmuir films, elastic and inelastic tunnelling 80−80403
charge imbalance relaxation freq. depend. near T_c 80−93030
collective oscillations and electric field penetration, review 80−88678
Cooper coupling, increase due to strong longitudinal sound 80−49990
Cooper pairs formation, and nature of supercond. currents 80−65736
determination by point contact tunnelling 78−19185
energy dependent electronic density of states, gap and crit. temp. 80−84538
Fermi surface-phonon isoenergetic surface intersection topology changes, prediction *(Russian)* 78−64164
Fermi systems, review of methods in quantum field theory 78−8338
ferromagnetic superconductor, paramagnetic fluctuations, influence on superconductivity 80−70900
film, gap enhancement due to quasiparticle tunnel injection 78−56262
film, illuminated, heating model and spectral characts. of phonon emission 79−28442
film stripline, association with freq. range limitation of pulse propag. 78−43524
impurity mode effects on crit. characts. of superconductors, zero temp. energy gap *(Russian)* 79−19692
inelastic electron tunnelling spectroscopy, advantages of supercond. electrodes 79−4625
insulator to superconductor in DC electric field 78−6481
junction, nonequilibrium phenomena *(Russian)* 78−34934
kinetic eqns., nature and decay rate of new mode 80−49978
kinetic eqns. for electron excitations and phonons 80−7032
magnetic impurities, EM penetration depth 77−66225
magnetic properties of superconductors, effect of insulating pairing of electrons 80−15651
metallic thin film, superconducting state realisation 80−49977
multivalley semiconductors, supercond., crit. temp. effects 79−1638
Nb_3Ge, supercond., single phase, sp. ht. meas., 4-29K 78−72307
nonequilibrium states, narrow nonequilibrium sources *(Russian)* 80−88687
nonequilibrium superconducting states with two coexisting energy gaps 79−51724
nonequilibrium superconductor, high-freq. AC process dynamics 80−88674
nonequilibrium superconductor, optical pumping, transition point *(Russian)* 77−12064

superconducting energy gap continued
nonequilibrium superconductor, order parameter dependence on optical pumping intensity 78−91816
nonequilibrium superconductor with tunnel injection quasiparticles, phase transitions 79−69636
nonequilibrium superconductors, transients, phonon distrib., supercond. gap, Boltzmann-BCS formulation 78−52149
nonlinear acoustic attenuation effects, energy gap widening *(Russian)* 77−43780
nonsymmetric tunnel junctions, I-V characts., inhomogeneities and meas. current effects *(Russian)* 79−87196
nonthermal quasiparticle distribs., energy gap instability 78−39256
order parameter oscill. in nonequilib. state due to quasiparticle injection 79−42697
paramagnetic limit, Fermi surface dielectric gap *(Russian)* 80−2533
phonon mechanism for sound-affected energy gap *(Russian)* 77−43781
phonon Raman scattering in superconductors 80−100657
photon-assisted tunnelling obs. of supercond. gap variations *(Russian)* 77−43786
proximity systems with magnetic impurities, DC Josephson effect 80−100554
proximity-effect sandwiches, theory 79−1646
quasi-two-dimensional dirty superconductor, nonstationary Josephson effect *(Russian)* 80−100556
relationship with critical field 79−65621
relaxation and collective motion two-fluid theory 79−73625
semimetallic system, critical temp. depend. on band gap for dielectric-supercond. transition *(Russian)* 79−65578
stability of superconducting states out of thermal equilib. 80−2526
superconducting film, gap enhancement due to microwave irradiation 78−14892
superconducting proximity effect, transition metal impurities in normal metal 77−59356
superconductivity proximity effect, McMillan tunnelling model 79−73639
superconductor-semicond. device research, future prospects 79−28467
TCNQ salts, electron tunnelling 78−47769
transition metal chalcogenides, quasi-one-dimens., elec. mag., and supercond. props., review *(Russian)* 80−93022
tunnel junction, nonequilibrium phonon effect on supercond. states with 2 coexisting energy gaps 80−84561
tunnel junction, selfblocking of tunnel current, current-voltage characteristics *(Russian)* 78−95397
tunnelling, sum rules *(Russian)* 79−87195
two-band model tunnelling density of states 77−51854
type I and II superconductors, energy gap and penetration depth *(Chinese)* 79−51718
virtual bound state alloys with resonant impurity scatt. centres theory 79−99654
weak links, order parameter and quasiparticle dynamic props. 80−100555
Al, energy gap enhancment by tunnelling extraction 80−34564
Al film, deviations of equilib. order parameter from mean field theory 77−69453
Al film, quasiparticle branch mixing rates 79−78269
Al film in tunnel junction, new supercond. state obs. at high quasiparticle injection 77−72949
Al film strips, radiation stimulated supercond. 77−28298
Al, microwave enhanced energy gap, tunnelling meas. 77−51853
Al, narrow superconducting bridges, microwave radiation stimulated T_c enhancement 80−84537
Al, phonon absorption and pairbreaking at 35 GHz 77−32120
Al, supercond. film, quasiparticle injection, tunnel junction characts. 78−76193
Al, superconducting band gap anisotropy and Fermi surface anisotropy *(Spanish)* 80−84544
Al, superconducting order parameter relax. time, temp. depend. 77−77011
$Al-Al_2O_3-Ir$, tunnel junction, supercond. props. of Ir film 79−56444
Al-formvar superconductive junction, Ginzburg's generalised jellium model 80−15663
Al-Mn(Cr)(V), dil., supercond., nucl. spin relax. and quasiparticle excitations 80−88680
Al-monolayer-Pb, supercond. junction, electron tunnelling meas. 79−28482
$Cu_{1.8}Mo_6S_8$, electron tunnelling spectroscopy expts. *(German)* 80−107966
$Cu_{1.8}Mo_6S_8$, supercond. energy gap and phonon-induced structs. in tunnelling density of states 79−51728
Fe-In, superconducting Kondo alloys and alloys with strong electron-magnetic impurity interaction, EM absorpt. of light 80−39711
Ga-Ag tunnel junction, evidence for existence of anisotropy of supercond. energy gap 80−20357
GaAs-Pb junctions, electron tunnelling under high press., transition temp., energy gap, phonon energies 79−15257
GeTe, film, semicond., supercond. energy gap and crit. field, tunelling meas. 77−24644
Hg films, superconducting, far-IR and electrodynamic props. meas. 80−103957
Hg, law of corresponding states, Eliashberg eqn. *(Russian)* 79−87183
In, energy gap and phonon frequencies under press., tunnelling meas. 77−32112
In-Mn, dilute alloy, local excited states, electron tunnelling observation 80−34565
Ir, thin film, supercond. energy gap, temp. depend. 79−56444
La film, tunnelling investig., multiple band effects 77−8244
Mo-Re alloys, supercond. energy gap and transition temp., tunnelling meas. 79−56405
Mo-Si(Ge)(Al), amorphous supercond. alloy, produced by coevaporation, struct. and supercond. 79−91179
Mo_xRe_{1-x}, (x=0.4 and 0.6), search for strong coupling superconductivity 79−28441
$(Mo_{0.5}Ru_{0.5})_{80}P_{20}$, amorphous normal and mixed supercond. state, ^{31}P NMR 79−87193
$Mo_{0.18}Tc_{0.82}$, search for strong coupling superconductivity 79−28441
$Mo_{0.4}Tc_{0.6}$, A15 and BCC, sp. ht., 4-20K 78−68111
$Mo_{1-x}Tc_x$, BCC, sp. ht. in normal and supercond. phases 79−87190
Nb, effect of changes in $\alpha^2(\Omega)F(\Omega)$ on the zero-temp. energy gap 80−97025
Nb, Eliashberg eqns. soln. 77−43776
Nb, energy gap determ. by pt. contact tunnelling 78−19185

superconducting energy gap continued
Nb film, supercond. relax. phenomena at microwave freqs. *(Russian)* 79−47187
Nb microbridges, heating and flux flow, I-V curves and microwave mixing 79−28474
Nb, single cryst., superconductive tunnelling meas. 79−47203
Nb, superconducting, thermodynamic props. 80−107955
Nb, superconducting parameters, tunnelling meas. 79−91192
Nb-Ge(Si), amorphous supercond. alloy, produced by coevaporation, struct. and supercond. 79−91179
Nb-I-Pb junctions, fine struct. of current-voltage curves, energy gaps, barrier layer *(Russian)* 79−19693
Nb-NbO_x-Pb tunnel junction, temp. depend. of effective Nb energy gap 80−80454
Nb-Zr, effect of band structure on elastic constants and superconductivity 79−8313
$Nb_3Al_{0.83}Ge_{0.21}$, A-15 phase, sp. ht. meas., Debye temp., energy gap and crit. field 79−19689
Nb_3Ge film, in supercond. proximity sandwich, energy gap struct., appl. to electron-phonon spectra 79−56401
Nb_3Ge, ordered and disordered A15 phases, energy gaps, tunnelling 77−8235
Nb_3Ge, superconducting thin films, energy gaps from tunnelling meas. 80−25050
Nb_3S_4, anisotropic superconductor, critical field and specific heat meas. 80−44779
$NbSe_2$, 2H phase, layered type II supercond., NMR meas. 77−36024
$NbSe_2$ (2H), layered, anisotropy and electron-phonon coupling effects on sp. ht. 77−51844
$NbSe_2$ (2H), Raman scatt. from supercond. gap excitations 80−93340
$NbSe_2$ (2H), Raman scatt. by supercond. gap excitations, coupling to CDWs 80−103956
Nb_3Sn, cavities, quasiparticles in energy gap corresponding to weak spots 79−56386
Nb_3Sn, effect of changes in $\alpha^2(\Omega)F(\Omega)$ on the zero-temp. energy gap 80−97025
Nb_3Sn, gap anisotropy, electron irrad. effect on transition temp. 78−10599
Nb_3Sn, supercond., thin film, US attenuation of SAWs 80−49988
Nb_3Sn, superconducting thin films, energy gaps from tunnelling meas. 80−25050
$Nb_{0.75}Zr_{0.25}$, supercond. energy gap, proximity tunnelling method determ. 79−56404
Pb, effect of changes in $\alpha^2(\Omega)F(\Omega)$ on the zero-temp. energy gap 80−97025
Pb film, quantized resistances, RF fields effects 78−10604
Pb, law of corresponding states, Eliashberg eqn. *(Russian)* 79−87183
Pb superconducting film, nonequilib. gap instability and phase transition under intense tunnel injection 79−28476
Pb-Cd thin films, electron tunnelling study of supercond. proximity effect 80−2525
Pb-Cu(Ag) double layers, intermetallic boundary effects, tunnelling 80−88692
Pb-I-NiCr-Cu double tunnel junction struct., supercond. energy gap suppression and instability 79−56417
Pb-In, electron tunnelling under hydrostatic press. 77−51850
Pb-In alloys, supercond. energy gap determ. by pt. contact tunnelling 78−19185
$Pb_{0.9}Bi_{0.1}$, quasiparticle recombination time, tunnelling of junction 79−15259
$Pb_{55}Bi_{45}$ film, amorphous, supercond. energy gap and transition temp. 78−14866
PbIn oxidised electrodes, symm. and asymmetric supercond. tunnel junctions, subharmonic gap struct. study 79−60981
PbIn-oxide-Pb tunnel junction, subharmonic gap struct., line shape and rel. magnitude 77−80882
PbIn-oxide-Pb(PbTl) tunnel junction, subharmonic group struct., multiparticle tunnelling theory 79−56438
Pb_xIn_{1-x}-Pb_yTl_{1-y} asymmetric supercond. tunnel junctions, subharmonic gap struct. 79−15260
$PbMo_6S_8$, electron tunnelling spectroscopy expts. *(German)* 80−107966
$PbMo_6S_8$:Gd^{3+}, powder EPR spectra, cryst. field, supercond. energy gap 80−34769
$Pb_{1.125}Mo_6Se_{7.5}$, Chevrel phase supercond., NMR study 80−49989
$(SN)_x$, electron tunnelling, absence of supercond. energy gap 78−47769
$(SN)_x$, supercond. energy gap, tunnelling meas. 79−56403
$(SN)_x$, superconductor, differential tunnelling resistance 79−28485
Sn, bulk supercond., method of determ. of energy gap 77−85384
Sn film, energy gap reduction by quasiparticle injection 77−47941
Sn film, energy gap suppression and instability under strong quasiparticle injection 80−7042
Sn, superconductor, bulk non-equilib. quasiparticles probed by ballistic phonons 79−56391
Sn-insulator-Sn, supercond. tunnel junction, phonon emission caused by subharmonic energy gap 79−56437
Sn-KCl granular superconductors, far IR absorpt. 80−84548
Sn-SnO_2-Sn, supercond. tunnel junctions, energy gap suppression by quasiparticle self-injection 78−80102
$SnMo_6S_8$:Gd^{3+}, powder EPR spectra, cryst. field, supercond. energy gap 80−34769
Ta, effect of changes in $\alpha^2(\Omega)F(\Omega)$ on the zero-temp. energy gap 80−97025
V, mixed state, US attenuation purity depend., crit. temp. and energy gap 77−47935
V, thermal conductivity in ultrapure normal, mixed and supercond. states *(Russian)* 79−4617
V, thin film, determ. of energy gap, tunnel effect method 79−42704
V/Al-Al_xO_y-Pb tunnel junction, superconducting transition, critical currents, Josephson effect *(Russian)* 80−29507
V-C sandwiches, energy gap fluctuations *(Russian)* 78−34930
V_3Si, A15 compound, microscopic model of supercond. and martensitic transform. 77−8226
V_3Si, single crystals, supercond. tunnel characts. 80−7044
V_3Si, superconducting thin films, energy gaps from tunnelling meas. 80−25050
V_3Si thin film far IR laser thermal spectroscopy 80−60144
V_3Si, thin films in supercond. and normal states, far IR laser spectroscopy 79−61453
V_3Si tunnel junctions, energy gap investigation 80−84569
$W_{0.65}Re_{0.35}$, search for strong coupling superconductivity 79−28441
$Y_{0.7}Th_{0.3}C_{1.58}$, specific heat 78−91813

superconducting energy gap continued
Zn, cyclotron mass and superconducting energy gap calc. as a function of Fermi surface position 79−69625
Zn film, supercond., SAW US attenuation 79−73633
Zn, superconducting, ultrasonic attenuation 78−88071

superconducting junction devices
AC Josephson like effect with linear periodic current phase relation 77−32124
acoustic transducers for 50-1000 GHz range 77−50851
automatic thermal cycling apparatus, for superconductive thin film devices 78−37014
bidimensional junction lattices, proximity effects *(French)* 80−49998
bolometers for submillimetre waves 78−37063
bridge, inhomogeneous, in UHF field, superconducting transition *(Russian)* 79−19690
bridge, phase slip dynamics and excess current *(Russian)* 80−103786
bridges, collective modes in arrays 79−56435
bridges, switching process depend. on control impulse ascent time *(German)* 78−2627
capacitively shunted microbridge, I-V characts., subgap struct. 77−15998
cavity-coupled Josephson device, parametric dependences, I-V characts. 80−20356
coherent microbridges coupled by external shunts, props. 79−28460
coherent tunable Josephson radiation generation, 2-18 GHz, with narrowed linewidth 78−88078
compact preset SQUID for total field measurement 80−22392
conference, Stanford, Calif., USA (Aug 1976) 77−28272
Cooper-pair tunnel triode, anharmonic wave coherent radiation *(Chinese)* 79−65604
coupled Josephson weak links, phase locking 78−72309
critical current, effect of UHF field *(Russian)* 78−72313
cryogenic current comparators, double constant current source, appl. 79−21775
cryogenic current standard based on AC Josephson effect 77−82557
cryogenic free-precession ^{3}He magnetometer using a SQUID 79−6153
cryogenic refrigerator, low power closed-cycle 78−77921
current-switched Josephson gate 79−82713
Dayem bridges, two interacting, coherent behaviour 78−14891
DC SQUID, ultra-low-noise tunnel junction, design, fabrication and noise props. 80−29506
DC voltage monitor for standard cell using AC Josephson effect 77−82552
digital Josephson technology−present and future 79−28472
dirty S-N-S sandwiches, Usadel equations, and props. boundary conditions 79−60990
dirty superconductor limit, microjunction phonon spectroscopy *(Russian)* 79−11272
dirty superconductor-normal metal interface, boundary conditions, pot. barriers effects 80−34554
double Dayem bridge structures, Josephson-like behaviour 77−8238
double Josephson junction interferometer, dynamics 78−68118
doubly-connected loops containing two Josephson junctions, flux penetration 77−85391
dynamic props. of supercond.-normal-supercond. junction *(Russian)* 80−103785
edge-grown low-capacitance supercond. tunnel junctions props. 80−54837
electron-tunnelling junction fabrication technique 79−38261
fabrication techniques *(Japanese)* 77−4470
fabrication technology for superconducting ICs 79−28493
far IR Josephson junction voltage-tunable differential heterodyne spectroscopy 79−30578
fast response time meas. system under fast EM radiation 79−35782
femtovoltmeter and voltage tunable heterodyne receiver based on DC resistive SQUID 79−63276
film bridge, supercond. stimulated by UHF radiation, crit. currents 77−16008
film bridges, supercond. stimulation by microwaves, length depend. *(Russian)* 79−33408
film bridges, supercond. stimulation by microwaves, threshold *(Russian)* 79−33409
film structure with degenerate semiconductor bridge, Josephson effect 80−20359
FIR detectors, Josephson-junction direct devices and transition edge bolometers, review 80−77865
fluxons on a Josephson line with loss and bias 80−103794
Ge-Sn barrier Josephson tunnel junctions 78−68114
gradiometer, balancing, system of adjustable superconducting plates, biomag. signal meas. 79−25162
gradiometers, for measuring magnetic effects of geophysical origin 80−101463
granular films as weak link in Josephson devices 80−88685
granular microbridges, fluctuations and crit. current determ. 80−84562
granular supercond. contact, Josephson-coupled, behaviour in microwave field *(Russian)* 78−52158
granular superconductor, quantum interference, coherence and percolation *(French)* 79−56434
gravitation antenna, quantum interferometer as recording element *(Russian)* 78−45557
gravity gradiometer 79−29868
gyroscope, development of London moment readout 79−26090
high-frequency, high-voltage effects on useful limit 77−1521
high-resolution cryogenic resist. bridge using SQUID null det., construction and performance 79−2792
highly stable, resettable const. current supply, SQUID appl. 79−67289
hypersonic generation and detection using Josephson junction *(Polish)* 77−14870
hysteretic RF SQUID as reactance and possibility of phase sensitive detection on RF SQUID 78−54410
impurities in normal metal layer of supercond.-normal metal-supercond. junction, pair penetration depth determ. 80−29508
inhomogeneous distributed Josephson struct., mag. flux dynamics 78−34932
inhomogeneous junction in UHF field, stimulation of supercond. *(Russian)* 79−78272
interferometer design, current stabilisation appl. 77−53945
interferometers, threshold curve anal. 80−49999
interferometric meas. technique for inductance and penetration depth 78−72306
inverse AC Josephson effect voltage standard 78−16808

superconducting junction devices continued
Josephson, interaction between two junctions separated by small superconducting granule 79−33399
Josephson, junction, near-ideal, fabrication and behaviour, expt. 77−20502
Josephson, phase-depend. cond. and nonequilib. props. probed by flux entry into weakly closed loops 77−66228
Josephson array, relation between critical current and order parameter 79−87197
Josephson contact, mixed state, parametric reson. 77−8245
Josephson contact, vortex pinning and energy *(Russian)* 78−68117
Josephson contact microwave detector sensitivity and cutoff frequency rel. to capacitance 78−49902
Josephson contacts with semicond. layer, critical current *(Russian)* 79−99661
Josephson coupled layered supercond., upper critical field *(Russian)* 80−100551
Josephson critical current in supercond.-insulator-supercond. contacts near T_c *(German)* 78−84361
Josephson current, paramag. impurities effect *(Russian)* 80−70903
Josephson devices, voltage standard *(Japanese)* 77−51851
Josephson effect, current-versus voltage source model 78−6484
Josephson effect, physical principles and appls. *(Croatian)* 79−11271
Josephson effect, through locally lowered tunneling barriers 80−100558
Josephson effect applications 77−20503
Josephson effect heterodyne receiver 78−12754
Josephson effect higher harmonics, flux tunnelling, thermodynamic free energy 80−60147
Josephson effect in supercond. bridges, microscopic theory *(Russian)* 78−56258
Josephson effect voltage standard, at zero current bias 80−57245
Josephson element principles, applications to precision meas. of electric potential and magnetic flux at high freq. *(Norwegian)* 80−80447
Josephson elements, elec. controlled *(Russian)* 79−91189
Josephson FET, hybrid, feasibility 80−80451
Josephson harmonic mixer, freq. meas. of methyl alcohol laser at 4.25 THz 80−95078
Josephson interferometer, static characts. 78−76192
Josephson interferometer flux detrapping by ground plane thickness modulation 80−2523
Josephson interferometer resonance amplitude theory, SFQ memory cells 80−27317
Josephson interferometers, large arrays, device parameter meas. 80−75682
Josephson junction, appl. to frequency modulation 79−82724
Josephson junction, barrier inhomogeneities, effect on junction behaviour *(German)* 78−91818
Josephson junction, broadband tunable microwave generation 77−72944
Josephson junction, coherent radiation induced bistability 80−80453
Josephson junction, discriminating props., use in microwave spectral anal. 77−49748
Josephson junction, externally pumped, singly and doubly degenerate microwave parametric amplifiers 79−26122
Josephson junction, finite length, steady oscillatory states 80−44773
Josephson junction, finite size, current distribution *(Russian)* 78−80103
Josephson junction, flux flow characteristics 78−84351
Josephson junction, frequency-agile, biasing for precise freq., analogue computer study 79−28455
Josephson junction, in inhomogeneous field *(Russian)* 78−84350
Josephson junction, long, boundary between static and dynamic states *(Russian)* 77−40002
Josephson junction, long, oscills., exact solns. of sine-Gordon eqn. 78−68115
Josephson junction, mag. flux annihilation 80−11139
Josephson junction, millimetre-wave, far-infrared and infrared detectors *(Japanese)* 78−32872
Josephson junction, nonlinear behaviour, qualitative theory 78−52159
Josephson junction, oxide formation process, ellipsomesric meas. *(Japanese)* 80−11561
Josephson junction, quantum interference, determ. of characteristics *(Russian)* 78−88081
Josephson junction, radiation power spectrum 78−43522
Josephson junction, semiconductor-barrier, cavity resonances 78−84352
Josephson junction, sputtering system for fabrication *(Japanese)* 80−55293
Josephson junction, voltage standard, commercial prototype 79−26068
Josephson junction, with linear periodic current-phase relations, phase locking and microwave impedance 80−93043
Josephson junction composed of N series loops, kinetic momentum quantum effect 79−87199
Josephson junction detector of microwave and far IR radiation, response 77−61119
Josephson junction dynamics, sine Gordon eqn. solns. 79−28481
Josephson junction interferometer, loop inductance 80−97034
Josephson junction noise thermometer, comparison with nuclear orientation thermometer, 0.011-0.05K 79−63218
Josephson junction noise thermometers 79−21752
Josephson junction parametric inductance fluctuations, upconvertor 80−25052
Josephson junction resistively shunted, AC, DC components of source current *(Chinese)* 79−11270
Josephson junction threshold viewed as crit. point 78−56264
Josephson junction with matched RF source, analogue simulation 80−75683
Josephson junctions, applications in plasma physics 80−103194
Josephson junctions, as nonlinear elements *(Japanese)* 77−1519
Josephson junctions, coupled, I-V charact., model calc. 80−84559
Josephson junctions, half-harmonic parametric oscills. 80−50001
Josephson junctions, long, current thresholds, resonant fluxon propagation, loss, bias, and open-circuit boundary conditions 80−50003
Josephson junctions, mixing in the FIR 79−26121
Josephson junctions, natural fluctuations in tunnel current *(Russian)* 77−47937
Josephson junctions, nonlinear effects in RF field *(Russian)* 79−65603
Josephson junctions, series-connected, noise characts. 77−66229
Josephson junctions, system of two junctions, radiation interaction *(Russian)* 79−82715
Josephson junctions, types, props., and limitations 79−28456
Josephson junctions fabrication, tunnelling through edge-grown barriers 80−100567

superconducting junction devices continued
Josephson junctions in self-pumping mode of operation, anomalies of freq. conversion 80−54839
Josephson junctions mounted in a waveguide, wide-band detect. characts. 80−4767
Josephson junctions with Sn-Ge barriers, adjustable tunnelling transmission 79−65613
Josephson logic and memory devices for process computer, refrigeration requirements 79−58726
Josephson logic circuits, nonlinear current injection switching 79−11269
Josephson long junction, switching behaviour 77−77007
Josephson microbridge, I-V charact. microwave irradiation depend. 80−25051
Josephson microbridge, thin-film, millimeter-wave conversion 79−73644
Josephson microbridge, variable thickness, DC and UHF props. *(Russian)* 78−10620
Josephson microbridges, submicron, fabrication using optical projection lithography and liftoff techniques 79−28458
Josephson microwave source, short term emission fluctuations 79−15263
Josephson mixer receiver, at millimetre and long submillimetre wavelengths 77−34027
Josephson mixers, mm wave, using Nb point contacts 79−26123
Josephson mixers for heterodyne reception at submillimetre wavelengths present expt. status, future developments 79−26120
Josephson multiple junction generated higher voltage standard 79−26069
Josephson nondestructive readout RAM cells, design criteria 80−50000
Josephson optical modulator with weak-link diffraction grating 79−98486
Josephson oscillators, synchronisation props., single point junctions and chains 79−19703
Josephson pair-quasiparticle interference, in meas. of flux entry into supercond. interferometer 78−14895
Josephson parametric amplifiers, gain-dependent noise temp. 80−84552
Josephson point contact, in wide-band radiometer for short-wave millimetric radioastronomical obs. 79−96916
Josephson point contact, Riedel anomaly and nonlinear effects 78−60253
Josephson point contact detector, high-sensitivity, for 1.5 t 2 mm band, radioastronomical obs. appl. 78−4106
Josephson point contact junctions and microbridges, HF props. 79−28461
Josephson point contacts with low capacitance *(Russian)* 79−4624
Josephson point junction, nonlinear effects 77−40003
Josephson point junction chain, solitary wave solns. 79−87212
Josephson point-contact resonance responses 79−99658
Josephson receivers, mm- and submm-wave, close-cycle cooling 78−93709
Josephson resistive junction, I-V characteristics 78−91820
Josephson self-oscillator mixer, submillimetre and far IR detector 77−34026
Josephson symmetric two-junction interferometers, self-induced reson., theory 80−107962
Josephson transmission line, appl. of perturbation anal. of fluxon dynamics 79−11280
Josephson transmission line oscillators, soliton solns. 79−87211
Josephson tunnel junction, flicker (1/f) noise 77−1520
Josephson tunnel junction, long, microwave induced resistive state 78−47914
Josephson tunnel junction, nonresonant vortex motion 80−97037
Josephson tunnel junction, parametric amplification at 35 GHz 79−95547
Josephson tunnel junction, Q-factor and reson. amplitude, calc. 78−10617
Josephson tunnel junction, quasi-particle heterodyne mixing 79−56395
Josephson tunnel junction, two gap state induced by singular IV characts. 79−1645
Josephson tunnel junction, vortex width broadening 79−82718
Josephson tunnel junction array parameter amplifier 79−65611
Josephson tunnel junction in arbitrary cct., response 78−39265
Josephson tunnel junction parameters, microwave freq., temp. depend. 80−34561
Josephson tunnel junction parameters near transition temp. 79−65610
Josephson tunnel junctions, current density distrib. Fiske mode field depend. 79−78264
Josephson tunnel junctions, current steps in current-voltage characts. 79−65612
Josephson tunnel junctions, fabrication and four terminal resistance study *(Chinese)* 78−68116
Josephson tunnel junctions, high frequency losses 78−88083
Josephson tunnel junctions, large, current-voltage characts. 78−6483
Josephson tunnel junctions, light-sensitive, self-reson. modes 77−63033
Josephson tunnel junctions, resistively shunted 78−47916
Josephson tunnel junctions, semiconductor barrier props. *(German)* 78−84360
Josephson tunnel junctions containing vortices, excess DC current, mag. field depend. 79−38259
Josephson tunnel junctions of nonuniform width, max DC Josephson current vs. external mag. field charact. calc. 80−65747
Josephson tunnelling current, theory of cos ϕ term. 78−14890
Josephson tunnelling in supercond.-insulator-supercond. contacts *(German)* 78−84359
Josephson tunnelling junctions, self resonant modes with zero external magnetic field, theory 79−24105
Josephson tunnelling junctions, supercond. fluctuations, below trasntiion temp. 78−84354
Josephson video-detector, optimisation for mm wavelengths 80−4768
Josephson voltage standard system, influence of voltage divider 78−74027
Josephson voltage standards, recent advances 77−18023
Josephson weak link, model *(Russian)* 78−88080
Josephson weak-link, simplification of resistively shunted junction model 77−72946
Josephson-effect absolute noise thermometer, resolution of unmodelled errors 78−62196
Josephson-effect differential heterodyne receiver, freq. conversion at 0.4 mm wavelength 79−26125
Josephson-effect voltage-standard instrument, features 78−93729
Josephson-junction arrays, radiation props. *(German)* 78−88077
Josephson-junction capacitor, QED theory 80−93049
Josephson-junction ccts., dynamics 79−73635
LF spectral analyser with HF SQUID, threshold sensitivity 78−41328
light induced weak link 78−34926

superconducting junction devices continued
light-sensitive Josephson junctions, post developments, future appl. 79−28462
long superconducting bridges with variable thickness, Josephson effects 78−14897
low temperature transport physics, appl. of SQUIDs 79−26067
magnetic auditory evoked response using SQUID 78−80889
magnetic field gradiometer 78−77947
magnetic transition-metal impurities effect on tunnel characts. *(Russian)* 78−34927
magnetometer, RF SQUID, construction, geomag. microfluctuation meas. appl. *(Japanese)* 79−5641
magnetometer, use in strain transducer 77−37877
magnetometers, RF-driven SQUID, rock magnetism and palaeomag. appls. 77−45201
magnetometers for very weak fields 79−30510
magnetopneumographic meas. with SQUID fluxgate magnetometers 80−104711
MB DC-SQUID, crit. current mag. modulation, logic device appl. 78−84371
metal point contacts, double-phonon backflow-process 79−56441
metal-insulator-metal-superconductor junction, phonon struct., proximity effect tunnelling 79−82721
microbbridges and point contacts, nonstationary Josephson effect 79−38256
microbridge, high-resistance, with Bi crosspiece 80−93050
microbridge, I-V characts. and excess current 79−73641
microbridge, Josephson radn., subharmonic energy gap struct. 79−91186
microbridge, thin film, nonreson. detection of Josephson radiation 78−43523
microbridge Josephson junction, current-phase relation, size dependence 80−44767
microbridge Josephson junction, fabrication using electron beam lithography 79−28457
microbridge properties in pure limit *(Russian)* 77−89903
microbridge SUPARAMPs, phase instability noise in Josephson junctions 79−26124
microbridge with normal bank, I-V characts. 79−87204
microbridges, basic props. and appls. 77−26400
microbridges, effective capacitance, normal-current injection in supernormal junctions 78−47911
microbridges, enhancement of crit. current by microwave radiation 77−28298
microbridges, neg. resist. and hot electrons, model 78−60254
microbridges, non-equilib. effects, superconductivity stimulation by RF radiation and DC current *(Russian)* 80−39714
microbridges, response times and low-voltage behaviour 79−65602
microbridges, short, dynamic props. 79−47202
microbridges, triggering of phase slip by impact of low-energy atoms 80−93045
microbridges, with paramag. impurities, Josephson steady-state effect *(Russian)* 80−93042
microbridges and arrays, I-V characts. temp. depend., Josephson radiation 79−28459
microbridges and filaments, high-freq. AC process dynamics 80−88674
microbridges and tunnel junctions, half-harmonic generation at RF induced steps 79−56439
microbridges in resonant cavity, enhanced Josephson radiation and linewidth-narrowing 79−56433
microjunction, supercond.-normal metal-supercond., microwave enhanced crit. current 79−82720
microscopic theory of Josephson effect on supercond. bridges *(Chinese)* 78−14887
microwave SQUID using pump signal at 9 GHz 79−35798
MIM diode, US effect on tunnel current for normal and supercond. metals 77−16006
miniature preset multihole SQUID, sensitivity 77−37952
neuromagnetic fields sources location, using SQUID system, comparison with electrical method 80−101190
non-equilibrium superconductivity characterisation, via Josephson effect 80−100557
nonequilibrium phenomena *(Russian)* 78−34934
nonequilibrium superconductors, mag. field depend. of relax. times 79−28477
nonstationary Josephson effect in short supercond. junctions *(Russian)* 79−78273
nonsymmetric tunnel junctions, I-V characts., inhomogeneities and meas. current effects *(Russian)* 79−87196
normal metal-constriction-superconductor microbridge, I-V characts. and excess current 79−73641
normal metal-superconductor structure, laser irrad. theory of current voltage characts. *(Russian)* 77−80877
optical waveguide controlled Josephson junction 78−66955
optically induced non-equilibrium and heating effects in superconductors *(Russian)* 78−95398
oscillator, current-drive, quantum modelling 80−75687
oxide-barrier-tunnel junctions, low-noise 115 GHz mixing 79−51722
parametric convertor type pulse amplifiers, AC Josephson effect appls. 78−19184
parametrically coupled Josephson bridges, resistive state, promixity effect *(Russian)* 80−100550
partially phase-correlated junction states 79−65606
pendulum type mechanical analogue of Josephson junction *(Japanese)* 77−72948
phase slip centers, interactions obs. using coupled microbridges 77−47940
phonon generation and detection expts. with supercond. tunnelling junctions, sources of losses 78−18718
photon detection in nonlinear tunneling devices, theory 79−6177
point contact, excess current *(Russian)* 79−19702
point contact, in wide-band radiometer for short millimetre range 79−62750
point contact, LF fluctuations, cond. and voltage *(Russian)* 77−20500
point contacts, DC Josephson effect investig. *(German)* 80−39713
point contacts, phase-depend. cond. at microwave freq. 77−16001
point contacts, sub mm band mixer 77−49774
point contacts, three-dimens. assembly, crit. currents and penetration depth 80−84560
point contacts excess current temp. and press. depend. *(Russian)* 79−69635
point junction under high voltage, nonstationary Josephson effect *(Russian)* 79−60987
point-contact Josephson junctions, capsule type, MM-wave video detection 80−13141
proximity effect bridge, thermal effects 77−63030
proximity effect tunnel junctions with amorphous Nb-Si(Al) barriers 79−65614
proximity effect weak links, control of characts. 79−65615
proximity effect weak links, steady-state and RF props. 80−84563
proximity sandwiches, mag.-supercond.-mag., phase diagram 78−95399
quantised resistances in supercond.-normal-supercond. film struct. 79−56426
quantum magnetometer cct. and characteristics 79−40594
quantum magnetometer with two-contact sensor, asymptotic characteristics 79−6155
quasiparticle mixers, supercond.-insulator-supercond., conversion gain prediction 80−70901
quasiparticle nonlinear relax. to nonequilib. state *(Russian)* 80−7040
quasiparticle scattering and current-volt. characts. of supercond.-normal-supercond. film struct. 78−10615
quasiparticle superconductor-insulator-superconductor tunnel junctions as microwave detectors 80−65744
refrigerator, closed-cycle, 4.5K, for supercond. susceptometer 78−93707
resistance from superconductor in supercond.-normal metal interface 78−43525
resistive SQUID appl. to heat capacity meas. 79−63213
resistive SQUID thermometer, theory 79−21753
RF biased SQUID, meas. of absolute intensity of weak mag. field 80−82794
RF instrumentation based on superconducting quantum interference 78−57995
RF SQUID, hysteretic, input noise 80−70905
RF SQUID, hysteretic behaviour, spiral model *(German)* 78−49868
RF SQUID, narrow-band ultra-low current meas. 79−63274
RF SQUID, quantum interference in supercond. ring closed by weak link 80−97035
RF SQUID, use in magnetocardiography *(Dutch)* 79−79670
RF SQUID magnetometer, effect of noise on performance 79−54159
RF SQUID magnetometer, synchronous demodulation, amplitude- and phase-sensitive detection 80−105679
RF SQUID structures, topology and theory 80−97036
RF SQUID system, microwave biased, appl. to magnetic aftereffect 79−26089
RF SQUIDs, extension to noise theory rel. to gravit. radiation detectors 77−87685
RF-biased SQUID, with half-wavelength transmission line 80−22342
RF-SQUID magnetometer, biased by harmonic magnetic flux meas. stability 79−93175
S-C-S(N) pure short microjunctions, nonstationary Josephson effect theory *(Russian)* 80−50010
self-oscillating Josephson mixer as submillimetric and far IR detector 77−38004
short bridges, critical current depend. on high. freq. field 80−44774
shunted Josephson junction model, autonomous case 78−34929
shunted Josephson junction model, nonautonomous case 78−39267
shunted superconducting bridges, transition from relaxational to Josephson oscillations 78−72312
SINIS junction proximity system, crit. Josephson current calcs. *(German)* 78−88079
solid-state device conference, Tokyo, Japan (Sept. 1976) 77−76901
space applications of LF supercond. sensors inc. SQUID devices 80−56691
spectroscopy of high-frequency phonons, transport phenomena, review 80−49325
SQUID, A/D conversion, conditions for countable pulse train 79−91191
SQUID, AC, low inductance, low crit. current, analysis 77−10071
SQUID, appl. to cardiac recording, phase and amplitude relationships of elec. and mag. events 80−104695
SQUID, appl. to human brain mag. response monitoring 77−29231
SQUID, appl. to magnetic ion concentration, in maser crystals 78−82007
SQUID, commercial superconducting systems 79−28452
SQUID, DC, noise limitations 79−21784
SQUID, DC, present and future status 79−28450
SQUID, DC, voltmeter and magnetometer circuits optimisation 80−13056
SQUID, DC-thin film, magnetocardiogram meas. first order gradiometer 80−89877
SQUID, fabrication and LF and HF appls. 77−22583
SQUID, for Earth's mag. field meas. using magnetotelluric sounding technique 78−96322
SQUID, for magnetic field and spatial gradient meas., design and advantages 77−26369
SQUID, future of superconducting instruments in metrology 79−26020
SQUID, granular supercond. characterisation 79−28489
SQUID, gravitational wave detector, resonant transducer matching between cryogenic antenna and low-noise amplifier 80−46949
SQUID, high temperature, props. and production method 79−28451
SQUID, laser irrad. effects 79−56419
SQUID, low-inductance, with two microwave junctions 77−82579
SQUID, medical application *(Japanese)* 80−12290
SQUID, Nb_3Sn film for operation above 14.5K 77−66226
SQUID, operating principles *(Hungarian)* 80−75686
SQUID, oxidised Nb granules as three-dimens. Josephson junction array 79−67362
SQUID, recent developments and appl. of Josephson effect *(Japanese)* 78−91819
SQUID, review of development and future 79−33398
SQUID, RF, LF noise expt. exam. 80−98947
SQUID, RF, nonhysteretic, weak link parameters effect on resonant circuit 79−28454
SQUID, RF, review of state of the science 79−28449
SQUID, RF biased, theory of nonhysteretic regime 77−24643
SQUID, RF sensor, automatic monitoring circuitry 77−18044
SQUID, RF-biased, mag. flux meas. on superfluid ^3He 77−31827
SQUID, ring interferometer in mag. field *(Russian)* 79−93179
SQUID, sensing element for gravitational antenna *(Russian)* 77−45773
SQUID, single contact RF bias, low freq. external interference 79−67361
SQUID, thermally generated mag. flux in supercond. loops 79−56452

superconducting junction devices continued
SQUID, thermodynamic equilibrium fluctuations generation by Josephson junction, Werthamer theory 80−100564
SQUID, thin film, for mag. field meas. 77−74463
SQUID, thin film type, mag. field sensitivity, galvanic coupling to supercond. antennae *(German)* 79−85154
SQUID, UHF, tapped tank circuit, anal. and operation 78−41334
SQUID, use in NMR spectrometer 80−37064
SQUID, V-V_xO_y-Pb tunnel junctions, IV characts. 79−19704
SQUID, with RF bias, fluctuation characts. 79−9229
SQUID, with two Josephson junctions, limiting magnetic field sensitivity *(Russian)* 77−77010
SQUID, with V-VO_x-Pb Josephson tunnel junctions, quantum interference, critical currents 78−91821
SQUID 3-axis magnetometer, for magnetotelluric meas. with remote reference 79−29866
SQUID (DC) as mag. flux detector 77−26358
SQUID adjustment using cryostat *(Polish)* 80−31768
SQUID appl. to nuclear gyros and magnetometers, high stability and sensitivity 80−98949
SQUID appl. to somatically evoked field meas., transient responses to elec. stimulation of median nerve 80−104706
SQUID application to measurements in fundamental physics 79−26087
SQUID applications in biophysics 79−29640
SQUID applications to weak magnetic field measurement 80−86267
SQUID appls. portable refrigerator 80−27313
SQUID arrays, for mag. field meas., geophysical, biomedical appls. 78−32830
SQUID based detection systems, mag. field meas., comparison between two methods 80−104712
SQUID biomedical appl., iron overloaded liver non-invasive diagnosis 80−101244
SQUID coupled to piezoelectric transducer, detection of gravitational waves 78−21218
SQUID detection, low temp., NMR imaging improvement towards mol. kinetic meas. 80−104723
SQUID detection of EPR at mK temps. 79−63290
SQUID detection of high sensitivity mag. reson. 79−75560
SQUID detection of NMR, appl. to liq. ^{3}He 79−67368
SQUID detector appl. in biomagnetism, techniques 78−96061
SQUID differential magnetometers, design criteria 79−26088
SQUID fabrication and applic. to magnetometer *(Japanese)* 77−65048
SQUID for AC current meas. down to 10^{-14} A 78−49859
SQUID gradiometer, DC, thin-film, design optimisation 80−98951
SQUID gradiometer, second-derivative, magnetocardiogram meas. 80−104696
SQUID gradiometer, thin film DC device 77−30187
SQUID gradiometric magnetometers, balancing system 79−63285
SQUID in mag. field, stationary and transport currents *(Russian)* 80−50009
SQUID instrumentation for biomagnetic meas. in unshielded and noisy environments 80−104710
SQUID instruments and shielding for low level mag. meas. 77−40840
SQUID magnetometer, 430 MHz, AC-biased, quantum limited 80−101809
SQUID magnetometer, AC-biased, noise, slew rate and stability 80−98948
SQUID magnetometer, archaeomagnetic intensity meas. 78−352
SQUID magnetometer, broadband and higher-power, for small signal A-D convertor 78−62211
SQUID magnetometer, enhanced sensitivity using resonant input circuit 79−35799
SQUID magnetometer, optomagnetic meas. appl. 80−98950
SQUID magnetometer, use in determ. of diamag. props. of metalloproteins 79−53036
SQUID magnetometer, with independent pumping 80−105685
SQUID magnetometer appl. to nucl. mag. thermometry 77−26292
SQUID magnetometer for dilute magnetic alloy studies, calibration 79−67358
SQUID magnetometer for meas. of macroscopic quadrupole field for antiferromagnetic order determ. 79−24140
SQUID magnetometer for meas. of magnetocardiogram and cardiac output 80−104709
SQUID magnetometer for vector magnetocardiogram meas. 77−29213
SQUID magnetometer in conjunction with superconducting magnets as susceptometers 79−26086
SQUID magnetometer with selective pickup loop to biomagnetic meas. 79−63286
SQUID magnetometer with temp. control, spontaneous magnetisation and mag. susceptibility meas. 80−68221
SQUID magnetometers, AC-biased, classical to macroscopic quantum transition 80−98953
SQUID magnetometers, AC-biased, macroscopically quantised, higher harmonics in Josephson effect 80−98952
SQUID magnetometers, geophysical dewar systems design 80−101462
SQUID magnetometers, magnetoretinographic meas. of retina injuries in eye 80−104702
SQUID magnetometers, signal detection of 1/f noise 79−26091
SQUID magnetometry, low-level, of human heart in small ferromag. enclosure 78−92726
SQUID NMR techniques, appl. to liquid ^{3}He 79−26093
SQUID picovoltmeter operating in mag. fields up to 3.2 T 79−58698
SQUID resistance bridge, ultra high resolution 79−63275
SQUID ring, fluxoid transition mechanisms, quantum vs. thermally excited 80−100565
SQUID sensor, offset temp. coeff. 77−26359
SQUID signal in the hysteresis mode, triangular to square wave signal transition 77−74469
SQUID signal strength versus frequency 79−28453
SQUID system, double hole biased at 30 MHz, characts. *(Japanese)* 77−5858
SQUID system for low drift high sensitivity magnetisation meas. 80−86347
SQUID systems, low noise circuitry 78−4672
SQUID technique for magnetoencephalogram power spectrum estimation of human brain 80−104704
SQUID used in superconducting shield for mangetoencephalography 80−104708
SQUID using low crit. current Al-Al_2O_3 film 77−40013
SQUID using Nb thin film microbridge *(Japanese)* 80−31816
SQUID with tunnel junction, reson. effect, step voltage meas. 79−7940

superconducting junction devices continued
SQUID-based NMR spectrometers, sensitivity limits 80−98961
SQUIDs, multiple mag. flux entry, cosϕ conductance exam. 79−4623
SQUUD system for low-drift magnetisation meas. 77−82574
standard cell calibration against Josephson voltage reference 77−5874
strip line coupled Josephson junctions, microwave response *(Japanese)* 77−69454
submillimetric Josephson mixer receivers, potentials and limitations 77−38003
super-Schottky diode, space appl., microwave and IR detectors 80−85836
superconducting-normal metal-superconducting junction, crit. currents, mag. field depend. 80−50008
superconducting-normal-metal infinite geometry, extrapolation length near T_c 79−82723
superconductor-constriction-superconductor, microbridge, I-V characts. and excess current 79−73641
superconductor-degenerate semiconductor-superconductor structures, critical Josephson current calc. 78−52162
superconductor-insulator-superconductor tunnel junctions, responsivity to microwave radiation 80−100553
superconductor-metal point junction as microwave radiation detectors 78−16847
superconductor-metal-insulator-metal-superconductor system, Josephson current, weak supercond. *(Russian)* 80−54842
superconductor-normal metal interface, boundary conditions and critical currents *(Russian)* 80−15665
superconductor-semiconductor contact amplification props. 79−7941
symmetric double weak link device, hysteresis behaviour in mag. field 78−39268
thin film technology, appls. in energy, optics, and electronics, review 80−78932
thin-film bridges, microwave-induced effects on crit. currents 79−87202
thin-film DC SQUID gradiometer 79−9228
transistor, superconducting 79−28466
transistor, three-film three-terminal device, theory and construction 78−47908
tunnel junction, nonequil. excitation distrib. and phonon generation *(Russian)* 78−23204
tunnel junction, normal conductance change, origin 80−65753
tunnel junction, selfblocking of tunnel current, current-voltage characteristics *(Russian)* 78−95397
tunnel junction, supercond.-insulator-supercond., optically irrad., quasiparticle energy distrib. function 80−2527
tunnel junction fabrication, two-level e-beam resist process with 1000 Å resolution 80−49996
tunnel junction instabilities, depend. on mag. field and barrier thickness 79−56436
tunnel junction mixers, quantum limited detection 80−18015
tunnel junctions, quantum noise effects in 0-1 mV bias range 80−80449
tunnel junctions as low noise 10 GHz mixers 79−82714
tunnel-junction refrigerator 80−57311
tunnelling devices as mm wave photon detectors 79−30554
tunnelling junction, thermal cond. meas. 77−36029
tunnelling junctions, quasi-particle recomb. and 2Δ-phonon-trapping 77−8236
two- and three-dimensional superconducting constrictions, static props. 79−28479
two-junction Josephson interferometer, reson. phenomena, anal. 78−47910
UHF radiometer with superconducting detector 79−71526
UHF SQUID magnetometer using coded (4.2K) GaAs FET preamplifier, biased at 430 MHz 80−52282
UHF SQUID magnetometer using varactor-tuned 4.2K GaAs FET amplifier 80−31814
variable thickness bridges, submicron dimensions, nonequilibrium phenomena in weak link region 79−56421
voltage cell using Josephson junction, computer simulation 79−93089
voltage locking and other interactions in coupled superconducting weak links 80−39719
voltage measurements within equilibrium region near phase slip centres 78−26997
voltage reference system Josephson junction *(French)* 77−67470
voltage standard, cryogenic voltage comparator 77−18030
voltage standard, for standard cell calibration 77−18029
voltage transfer standard based on AC Josephson effect, standard cell calibration appl. 77−82553
weak link, props. 79−38262
weak link, RF impedance 78−14889
weak link, RF-induced pot., quasiparticle effects 77−16002
weak link, short, space, time variations of order parameter, supercurrent, normal current 78−91823
weak link, short, with distinct chem. potentials at boundary 80−2528
weak link, solns. of nonlinear eqn. of resistively shunted model of Josephson junctions 78−2628
weak link fabrication, electron beam lithography, ion implantation 78−47913
weak links, applicability of Josephson effect theory in tunnel junctions 79−56431
weak links, gapless, coupled dynamics of order parameter and quasiparticle distrib. 79−56422
weak links, interaction in stationary states 78−31020
weak links, Josephson junction model, current steps *(Chinese)* 79−91187
weak links, low-voltage dynamical props., Ginzburg-Landau model 79−60982
weak links, model for non-equilibrium behaviour at low voltages 79−56424
weak links, nonequilib. effects, Ginzburg-Landau model *(Chinese)* 78−95396
weak links, order parameter and quasiparticle dynamic props. 80−100555
weak links, quasiparticle-injected, simple-heating-induced Josephson effects 80−70904
weak links, review of physical processes 79−60983
weak links, SNS and SS_1S types, current-phase relation 79−60991
weak links, symmetric, crit. current densities and current phase relations 79−87207
weak links, thermal switching times 78−76191
weak links and films, scatt. model for Josephson behaviour 78−56261
weak links for freq. multiplication 79−11273

superconducting junction devices continued
weak-link, non-ohmic transverse potential 78−76196
weak-link, one-dimensional, time depend. supercond., relax. oscills. of order parameter 79−28475
weak-link junction, evaporated, voltage-switching effect 77−28305
Ag-Sn, supercond. proximity-effect bridge, thermal effects 79−78265
Ag-Sn proximity effect bridges, long, voltage anomaly 79−51725
Ag-Sn proximity-effect bridges, T* anomaly under phonon injection 80−34566
Ag-Sn proximity-effect bridges, phonon-injection-induced first-order transition obs. 80−39718
Al bridges, nonequilibrium phenomena under microwave radiation 79−56420
Al granular bridges, with different thicknesses and widths, crit. current, temp. depend. 80−88688
Al microbridges, non-equilibrium phenomena 79−56410
Al, narrow superconducting bridges, microwave radiation stimulated T_c enhancement 80−84537
Al shielded room for biomag. meas. 80−104846
Al tunnel junction, quasiparticle recomb. times and electronic density of states at Fermi level 79−56414
Al weak link, props. 77−28302
Al/AlO_x/La-rare earth metal tunnel junctions, cond. meas., cryst. field effects 80−88694
Al/formvar/Al(Sn) structures, low frequency phonon spectroscopy by tunnel effect 78−23206
Al-Al_2O_3-Ir, tunnel junction, supercond. props. of Ir film 79−56444
Al-Al_2O_3-Nb, quantitative proximity tunnelling spectroscopy 79−91193
Al-Al-PbBi double tunnel junction structs., quasiparticle relax. times, energy and temp. depend. 79−56412
Al-AlO_x-Pb junctions, organic ring cpd. doped, asymmetries in elastic and inelastic tunelling 79−95549
Al-C-Al sandwich, microwave irradiated, superconductivity at room temp. *(Russian)* 80−11138
Al-In_xO_y-Pb tunnelling junctions, fabrication 77−36027
Al-Pb proximity sandwiches, Josephson and quasi-particle tunnelling expts. 79−65616
Al-Pb:Bi, tunnel-junction relax. oscillator, appl. to thermometry 79−85138
Al-PbBi tunnel junction as phonon spectrometer 78−47477
Au/In proximity effect bridges, finite size array 79−78270
Au/In proximity effect bridges, square arrays, transition temps. 80−84557
Au/Pb/In-oxide-PbBi tunnel junctions, supercurrent interference patterns and excess currents 80−100563
Bi, amorphous, microbridge prep. and transition from superconducting to normal state 78−34933
$Bi_{1-x}Pr_x$-Al oxide-Al tunnel junction, cryst. field struct. obs. in conductance 78−84358
In microbridges, non-equilibrium phenomena 79−56410
In superconducting microbridge, voltage locking and other interactions 80−39720
In, superconducting-normal interface, boundary resist. 80−50006
In-CdS-In, tunnel junction light-induced DC Josephson current 79−47204
In-CdS-In Josephson junction, exhibiting nonuniform max. current distrib. self-resonant modes 78−56263
In-In_2O_3-Pb, Josephson tunnel junction fabrication for MM-wave detector 80−100427
In-In_xO_y-Pb tunnel-junction barriers, evidence for chemical annealing effects 79−42701
Ir Dayem-type microbridges, supercond. props. of Ir films 79−56444
Mo weak leak, ion-implanted, Josephson to depairing behaviour transition 77−1522
Nb bridges, variable thickness, microwave mixing 77−85390
Nb, film microbridge, fabrication and I-V charcts. 79−87198
Nb, ion-implanted bridge with thick Pb banks, fabrication and characterisation of film parameters 80−100569
Nb Josephson junctions, excess current anal. 79−28465
Nb Josephson junctions, submicron, fabrication by evaporation 79−28920
Nb Josephson point-contact far IR detector props. 79−30543
Nb microbridges, heating and flux flow, I-V curves and microwave mixing 79−28474
Nb microbridges, vertical type, fabrication and DC charcts. 80−103788
Nb, nanobridges Josephson effect, quasiparticle diffusion time, inelastic scatt. time 80−34556
Nb on thin Si membranes, super-Schottky and Josephson-effect devices 79−28469
Nb point contact, 9 GHz complex impedance 77−28303
Nb, point contact Josephson junctions, thermally recyclable, as low-noise mixers 78−62224
Nb point contacts, AC Josephson effect meas. at 604 GHz 77−80876
Nb point contacts, Josephson effects in far IR, high freq. behaviour 79−1643
Nb SQUID, low-noise DC type, with 1 μm tunnel junctions 80−80450
Nb SQUID point-contact operation in very low-power cryocooler 78−93699
Nb selective plasma etching 78−39940
Nb, superconducting bridges by electron beam lithography and ion implantation Josephson effect 80−20355
Nb superconducting point contacts, DC and HF behaviour 78−31021
Nb superconducting point contact, high freq. props. in far IR 80−54840
Nb superconducting point contact, singularities of I-V curve and voltage fluctuations 80−93044
Nb thin film microbridge, video detection of far IR radiation *(Japanese)* 80−97038
Nb thin film microbridges, fabrication and charcts. 79−19705
Nb thin-film Josephson tunnel junctions, fabrication and props., in situ ellipsometric meas. 80−65749
Nb, thin-film SQUID working at 4.2K, fabrication and characterisation 80−100570
Nb tunnel junction, temp. dependent props., 2-9L 77−24642
Nb, variable thickness bridges on GaAs substrates, props. 79−28464
Nb, variable thickness bridges, mm wave response 79−28463
Nb weak link SQUID 79−38258
Nb/Ta thin film proximity effect bridge 79−82712
Nb-I-Pb junction, double-peak structure *(Russian)* 79−82716
Nb-I-Pb junctions, fine struct. of current-voltage curves *(Russian)* 79−19693

superconducting junction devices continued
Nb-Nb Josephson junctions, submicron, thermally recyclable, fabrication and charcts. 80−100566
Nb-Nb point contact junction, supercond. weak couplings, high-freq. props. 78−68122
Nb-Nb superconducting point junctions, I-V charcts. *(Russian)* 79−51727
Nb-Nb_2O_5-Pb Josephson junction formed on Nb film edge 80−107960
Nb-Nb_2O_5-Pb(In) Josephson junctions, props. of Nb_2O_5 thermally grown tunnel barriers 80−100568
Nb-Nb_xO_y-Pb, tunnelling junction, current-voltage charcts., knee struct. 79−38261
Nb-Nb_xO_y-Pb, two-dimens. Josephson junction, supercurrent vs. mag. field charcts. 80−34562
Nb-Nb_xO_y-Pb Josephson tunnel junction form. and ageing, adsorbed gas effect *(Russian)* 78−14899
Nb-Nb_xO_y-Pb(In) Josephson junctions, preparation and props. *(Russian)* 79−91188
Nb-Nb_xOy-Cu/Pb supercond. proximity junction, max. DC Josephson current, thickness depend. 79−82719
Nb-NbO_x-Pb, miniature tunnel junction, gap voltage determ. 79−7939
Nb-NbO_x-Pb Josephson junction, self-reson. modes 78−64169
Nb-NbO_x-Pb Josephson junctions with high current densities, critical current 80−100552
Nb-NbO_x-Pb Josephson tunnel junctions, fabrication using FR glow discharge oxidation 80−34559
Nb-NbO_x-Pb tunnel junctions, oxide tunnelling barriers, ESCA characterisation 80−65745
Nb-NbO_x-Pb tunnel junction, temp. depend. of effective Nb energy gap 80−80454
Nb-NbO_x-PbIn Josephson junctions, penetration depth of supercond. films 79−42691
Nb-NbO_x-PbIn window type junctions, critical Josephson current depend. on magnetic field 79−65607
Nb-NbO_x-Sn long Josephson junctions, flux-flow voltage, dynamic vortex motion 79−4620
Nb-Nb(Nb_3Sn) supercond. point contacts, crit. currents, effect of laser radiation *(Russian)* 79−28484
Nb-oxide-Pb, for frequency-voltage convertors, design 77−82555
Nb-oxide-Pb Josephson junctions, anomalous microwave-induced voltages 78−39266
Nb-oxide-Pb Josephson tunnel junction, capacitance and ellipsometrically determined oxide thickness 77−4469
Nb-Pb, long, magnetic field behaviour of zero field steps 80−100561
Nb-PbSn, Josephson tunnel junction, 3rd yr undergrad. expt. 78−54126
Nb-Si amorphosamorphous thin film tunnel junctions 79−28473
Nb-Te-Pb Josephson junctions, prep. and props. 80−65754
NbC weak link SQUID 79−38258
Nb_3Ga Josephson junctions, excess current anal. 79−28465
Nb_3Ge, bridge contact, Josephson effect 80−70906
NbN granular microbridges, Josephson effects 80−84556
NbN thin film SQUID biased at 20 MHz and 9.2 GHz 78−72311
NbN weak links, granular, Josephson behaviour 80−75681
NbN-NbN point-contact Josephson junction, fabrication and charcts. 78−19189
NbN-V_3Ga point-contact Josephson junction, fabrication and charcts. 78−19189
NbO_x-Pb Josephson junction, with high tunnel current density, fabrication and appl. to high speed switching 77−24645
$NbSe_2$ microbridges, current-voltage curves, hysteresis of crit. current *(Russian)* 77−69452
Nb_3Sn film contacts, quantum interference at H_2 temp. *(Russian)* 77−12041
Nb_3Sn, nonstationary Josephson effect, 13-18.3K, 9-10 GHz, 20 MW *(Russian)* 78−2631
Nb_3Sn superconducting bridge junction, crit. current temp. depend. *(Russian)* 78−34938
Nb_3Sn, thin film weak-links SQUIDs, localised region radiation damage, fabrication and properties 78−47912
Nb_3Sn-Nb_3Sn supercond. point contacts, crit. currents, effect of laser radiation *(Russian)* 79−28484
Nb_3Sn-Pb tunnel junction, Josephson props. 79−7937
NbV-VO_x-Pb Josephson tunnel junction, VO_x effect on props. 79−87203
Pb alloy Josephson tunnelling gate, thermal cycling 78−19188
Pb, detection of high energy phonons from Sn junction generators 77−4161
Pb, distribution function branch imbalance, relaxation 79−33401
Pb film tunnel junction, thermal cycling stability enhancement using substrate with large thermal expansion 79−87200
Pb microbridges, supercond. breakdown under electron beam irrad. 79−56418
Pb microbridges, two-dimens. imaging of resist. voltage changes caused by electron irrad. 80−15659
Pb, narrow film strip, weak link induced by optical guided waves 78−14886
Pb, small Josephson junction, temp. and mag. field variations in resist., cos ϕ conductance and effective capacitance 78−84357
Pb, supercond., strips, resistive transition in surface sheath state 79−56443
Pb superconducting contact to p-InAs, charcts. 79−38254
Pb superconducting variable thickness microbridge, microwave response 79−82717
Pb, tunnel junction, basis Josephson parameters, depend. on temp. below T_c 79−56442
Pb tunnel junction, quasiparticle recomb. times and electronic density of states at Fermi level 79−56414
Pb tunnel junctions, nonequilibrium occupation of quasiparticle states 79−56416
Pb/Bi-I-Al tunnel injected nonequilibrium supercond. struct., diffusive quasiparticle instability, multiple gap states 80−50005
Pb-alloy Josephson tunnel junctions, effect of process variables on elec. props., cryogenic memory appls. 80−65748
Pb-Cd-Pb junctions, pair pot., mag. field depend., crit. currents meas. 80−84555
Pb-$Cu_{91}Ni_9$-Pb superconducting junction, crit. currents 79−69633
Pb-$Cu_{99.8}Mn_{0.2}$-Pb superconducting junction, crit. currents 79−69633
Pb-I-NiCr-Cu double tunnel junction struct., supercond. energy gap suppression and instability 79−56417
Pb-In, series-connected Josephson tunnel junctions, fabrication procedure diagnostics 78−47909
Pb-In_xO_y-Pb tunnelling junctions, fabrication 77−36027

superconducting junction devices continued
Pb-In-Au, series-connected Josephson tunnel junctions, fabrication procedure diagnostics 78−47909
Pb-In-Au Josephson tunnel junctions, strain relax. effects 79−65617
Pb-In(-Au) base electrode film Josephson junctions, tunnel barrier oxide struct. 80−65750
Pb-Nb-Pb bridged, variable thickness, ion implant, coherent vortex motion props. obs. 80−100562
Pb-Pb_xO_y-Pb Josephson junction, long-term stability at liq. N_2 temp., voltage standard 77−72945
Pb-Pb_xO_y-Pb thin film Josephson junctions, prep. *(Slovak)* 79−42699
Pb-PbO-Pb, Josephson tunnel junction fabrication for Mm-wave detector 80−100427
Pb-Sn eutectic, directionally solidified, periodic array of supercond.-normal contacts, supercurrent and dynamic resist. 78−34928
Pb-Sn Josephson junctions, small area high current density normal resistance, RC times 80−34555
Pb-Sn lamellar eutectic alloy, supercond. normal-supercond. junction arrays 77−24641
Pb-Te-Pb Josephson junction, cavity resonances 78−84352
Pb-Te-Te oxide-Pb Josephson junctions, prep. and props. 80−65754
$Pb_{0.98}Bi_{0.02}$-Cd, superconductor-normal-metal boundary resist., mag. field depend. 80−44772
$Pb_{0.99}Bi_{0.01}$, superconducting-normal interface, boundary resist. 80−50006
PbIn-oxide-Pb junction, two-particle tunnelling and microwave effects 78−43527
PbIn-oxide-Pb(PbTl) thin film tunnel junction, subharmonic group struct., multiparticle tunnelling theory 79−56438
Pb_xIn_{1-x}-Pb_yTl_{1-y} asymmetric supercond. tunnel junctions, subharmonic gap struct. 79−15260
Pd-CdS-In, tunnel junction, light induced DC Josephson current 79−47204
Si strongly-doped monocrystal Josephson junctions 79−56400
Sn, and $Sn_{0.99}In_{0.01}$, superconducting-normal interface, boundary resist. 80−50006
Sn double tunnel junction, film energy gap suppression and instability under strong quasiparticle injection 80−7042
Sn, double tunnel junction 79−33401
Sn film, vac. deposition rate effect on supercond. Josephson tunnel junctions 80−2954
Sn film bridge, obs. of operating conditions and shunting effects in small size supercond. 77−16005
Sn microbridges, non-equilibrium phenomena 79−56410
Sn microbridges, nonequilibrium enhanced supercurrents 78−43526
Sn, nuclear spin-lattice relax. time meas. using SQUID magnetometer, appl. to thermometry 79−63212
Sn superconducting thin-film bridge, IV curves oscill. instability and quasi-particle recomb. *(Russian)* 80−44769
Sn, superconducting variable thickness microbridge, microwave response 79−82717
Sn thin-film superconducting bridge microwave impedance anomalies 79−7942
Sn tunnel junction, quasiparticle recomb. times and electronic density of states at Fermi level 79−56414
Sn, variable thickness bridges on GaAs substrates, props. 79−28464
Sn-In, distribution function branch imbalance, relaxation 79−33401
Sn-insulator-Sn, supercond. tunnel junction, phonon emission caused by subharmonic energy gap 79−56437
Sn-O-Sn Josephson tunnel junction, parametric amplification on RF-induced steps 79−78266
Sn-oxide-Sn Josephson tunnel junctions meas. temp. depend. of cos 0 conductance 78−10611
Sn-SnO_2-Sn, supercond. tunnel junctions, energy gap suppression by quasiparticle self-injection 78−80102
Sn-SnO_x-SN tunnel contacts, spatially inhomogeneous state under strong injection conditions 80−80457
Sn-SnO_x-Sn long Josephson junctions, flux-flow voltage, dynamic vortex motion 79−4620
Sn-SnO_x-Sn tunnelling junctions, fabrication by modified RF plasma oxidation method 80−103787
Sn-SnO-Sn Josephson junction current-voltage characts., resonance detection cct. 78−54406
Ta point contact, 9 GHz complex impedance 77−28303
Ta-Ta_xO_y-Pb, tunnelling junction, current-voltage characts., knee struct. 79−38261
V/Al-Al_xO_y-Pb tunnel junction, superconducting transition, critical currents, Josephson effect *(Russian)* 80−29507
V-CdS-In Josephson junctions preparation and behaviour obs. 80−100559
V-CdS-In Josephson structures, light-sensitive 79−99660
V-V_xO_y-Pb tunnel junctions, Josephson characteristics *(Russian)* 77−47938
VNb-NbO_x-Pb Josephson tunnel junction, compared with VNb-VO_x-Pb 79−87203
V_3Si bridge contacts, nonstationary props. 80−103793
V_3Si superconducting bridge junctions, vortex model appl. *(Russian)* 79−60986
V_3Si-SiO_x-Mo_3Re_2, supercond. tunnel junctions 80−107961

superconducting lenses *see magnetic lenses*

superconducting machines
50 MVA, thermal design of cryogenic rotor 79−58710
500 kVA alternator, liquid-He cooled, design and tests 77−26309
AC generator, heat losses in rotating liquid transfer union, simulation 77−84116
alternators, with rotating field windings, research using rotating He rig 79−58719
applied superconductivity, conf., Pittsburgh, USA (Sept. 1978) 79−33374
cryogenerator magnet field transient change calc. *(French)* 77−26303
fusion reactor, inductive and rotating machinery energy storage and transfer 79−85782
fusion reactor, Tokamak, commercial, plasma driving system requirements 78−54954
generator, 2 GW, cryogenic aspects *(French)* 77−26304
heat transfer in rotating windings, free convection in cryo-fluid He-I modelling 78−26745
heat transfer to liq. He in centrifugal acceleration fields, free convection and boiling regimes 77−89604

superconducting machines continued
homopolar machine, 10 MJ, fast-discharging, for fusion reactor 78−54950
homopolar machine, 10 MJ, superconducting magnet design 78−54927
magnetic energy storage system, switching technology in theta-pinch fusion reactor 77−23285
multifilamentary composite superconductor power losses 79−30507
optimisation, of the refrigerators and liquefiers 80−8994
refrigeration requirements for future superconductive energy related applications 79−58711
rotary machines as I/O system for superconducting magnetic energy storage system *(Japanese)* 80−85306
rotor refrigerant circuit operating as zero mechanical work thermal pump, liquid He rotating cryostat 79−58717
temperature telemetry via optical channel *(Russian)* 78−57966
turbogenerators, heat transfer in rotating excitation winding using He in rotating thermosiphon loops 79−58718
unit helium requirements for superconductive energy applications in the USA 78−89999
He cooling systems, large, review of hydrodynamics and heat transfer 79−204
He requirements for superconducting power network 79−50897

superconducting magnets
see also superconducting machines
2.6 T supercond. magnet design and manufacture for polarised target 79−31293
3 GeV proton synchrotron magnet design and meas. 79−31303
220 MeV/c superconducting π spectrometer for tissue irradiation 79−34667
AC loss measurement, analogue digital double integration joulemeter 80−57325
accelerator magnets, relationship between supercond. and high energy phys. 79−33441
ANDROMEDA, supercond. magnet system for particle detection in medium energy physics 79−13582
aperture limitation due to coil block errors 77−386
applications in next decade 77−10069
applied superconductivity, conf., Pittsburgh, USA (Sept. 1978) 79−33374
Argonne National Laboratory Experimental Power Reactor, superconducting magnet system 78−50372
Argonne/GA TNS Tokamak reactor supercond. ohmic heating coil design 79−31197
barrier resistance meas. in multifilamentary composite superconductor 79−30506
beam line magnets, fast energy dump 79−68091
beamline dipole magnets, design and testing 77−26354
bending, for energy saver doubler project, testing and field meas. 77−26899
bending magnets, 10.8, design and construction 78−82559
bending magnets CESAR for CERN SPS machine 79−31251
Bitter magnet development, stabilisation and calibration 79−30501
Bitter solenoid efficiency factor, allowance for cooling holes 79−30502
BNL AGS, high field superconducting beam transport 79−76203
built-up superconductors, current transfer 78−62633
central field, influence of magnetization in multifilamentary composites 79−65599
CERN ISR, 120 GeV superconducting conversion study 78−58509
CERN ISR, supercond. quadrupole magnets, wire dimension meas. and short circuit detection 79−31255
CERN ISR, superconducting high luminosity insertion 79−72049
CERN superconducting proton storage rings, 400 GeV, feasibility study for e-p, p-p and p-$\bar{p}$ facilities 78−58510
circulating cooling system, based on commercial 6.3 helium liquefier 78−57961
circulating cooling system, exptl., with rotary pump 77−82528
circulation cooling system based on He liquefaction apparatus 78−57992
coaxial transfer lines for gas and liq. He 79−58758
coil, appl. to mag. field modulation 77−18056
coil, buckling, vibr., lateral constraint and damping effects 78−63344
coil, losses in multifilamentary composite 78−62637
coils with ferromagnetic frames, direct meas. of dynamic mag. induction coeffs. *(French)* 77−61096
cold neutron beam polarising supercond. hexapole magnet 79−31300
commercial circular dichroism instruments, magnetic shielding problems 77−87807
commercial superconductors, test facility for dynamic stress effects 77−77698
composite, eddy current losses 78−62636
composite media, effect of axial conduction and metal-helium heat transfer on local stability 78−91832
composite superconductor, losses under hi-high rate pulsed transverse field 79−33385
composite superconductor, normal zone evolution, dynamic simulation rel. to magnet design 77−89914
composite superconductor continuous resistive transition self-field instability depend. 78−50369
composite superconductor stability in typical coil configs. 77−26350
composite superconductors, stability anal. by thermal analyser digital computer program 78−54995
composite superconductors, stress-induced heating, finite element calc., appl. to magnets 77−28342
composite superconductors for fusion magnets, current distrib. and losses 77−28331
conductor configurations for large magnets 77−26360
conductor materials, review *(Japanese)* 80−25042
conference, Stanford, Calif., USA (Aug 1976) 77−28272
conference on cryogenic engineering, London, England, (July 1978) 79−54137
continuous field generation, future prospects 79−71493
cooling channels, nucleate boiling crisis of He I 79−32196
cooling system, optimal cryogenic gas flow 79−93149
cooling system design, for fusion reactor appl. 77−23289
cooling system using liquid He 78−54998
cooling using superfluid He, cryostabilisation 78−54996
cryogenic current safety lead for magnet quench 77−83232
cryogenic systems, circulating cooling time for laminar and turbulent flow coolant 77−5849
cryogenic technology and superconductivity in controlled thermonuclear reaction programs 79−54600

superconducting magnets continued
cryostat for supercond. magnet, low He evaporation rate *(Japanese)* 79−44910
CTR blanket design *(Japanese)* 78−46164
CTR blanket design and associated problems *(Japanese)* 77−50286
cyclotron, heavy ion, proposed for Chalk River, mag. field related mech. tolerances 78−58511
cyclotron magnet 1:6 model construction and operating experience 79−31261
cyclotron neutron source for radiotherapy 79−20655
D-shaped toroidal field coil, design 79−9225
DC, use in generator system for pulsed power 77−34426
DC electromagnetic pump using supercond. magnet, performance charcts. 77−82994
DC superconducting magnets, pot. damage due to HF EM wave propag. 78−50371
DEALS, demountable superconducting magnet system, for fusion reactors 80−52777
demountable TF magnet system, appl. to Tokamak 78−54925
design for 10 MJ homopolar machine 78−54927
development at Intermagnetics General Corp. 79−58699
dipole, cooled by forced circulation of two-phase He 80−9009
dipole, ESCAR, experimental study of gas-cooled Cu leads 79−67995
dipole magnet, quench levels induced by proton beam spray meas. 77−26906
dipole magnet models of combined type 79−31301
dipole magnet system for MHD facility, with integrated control system 79−52948
dipole magnets for CERN beam line 79−31294
dipole magnets for Fermilab synchrotron, magnetisation effects 77−83229
dipole magnets for high energy accelerators, stress and strain distribs. 79−31250
dipole models for accelerator-storage ring complex 79−31259
dipole quenching by proton beam induced heating 79−30504
dipole ultra stable window frame magnet 77−83235
dipole window-frame type high precision magnets at BNL 77−83228
dipoles, 2.5 T window-frame type, for small synchrotrons 79−54224
dipoles SPD-3 and SPD-3′, testing 77−26904
doubler tevatron microprocessor quench protection system 79−72088
drift chamber performance in supercond. mag. field, electron drift angle meas. 78−37485
electron lenses, direct meas. of dynamic mag. induction coeffs. *(French)* 77−61096
electron microscopy, superconducting lenses applic. 77−71408
electron storage ring VEPP-3, proposal to install supercond. wiggler magnet, synchrotron radiation prod. 78−62671
ELMO Bumpy Torus Reactor toroidal magnet system design 79−31196
emergency cold valve, operating in He II 80−22367
energy doubler central liquefier 77−82530
energy doubler magnets, AC loss meas. 79−31277
energy doubler magnets, production characts. 79−31276
energy doubler quenches, pressure development 79−76200
energy loss, measuring device 79−71489
energy loss meas. device for superconducting magnets excited by AC 79−2796
energy storage, 10000 MWh, underground rippled He dewar system 79−58705
energy storage appl., 1970-9 development at Wisconsin University, Madison (USA) 80−26176
energy storage application for particle accelerators and power networks 78−25360
energy storage coil, 0.54 MJ 78−54924
energy storage coils, conductor design 78−62639
energy storage magnet, single layer, design and cost-related parameters 80−108815
energy transfer applications, Nb alloys, construct., stabilisation methods, mech. and elec. props. *(Dutch)* 78−49871
epoxy fracture after low-temp. irradiation 79−34147
epoxy impregnated superconducting composites, mech. props., strain effect at 4K 80−25822
epoxy resin, for supercond. magnet, deform. rate depend. of mech. props. at cryogenic temps. 80−55456
epoxy resin, low temp. irradiation effects on mechanical props., use in superconducting magnets 78−60737
epoxy resin based composites, superconducting magnet insulators, gamma-ray radiation effects 80−24495
epoxy resin composite, powder-filled, of adjustable thermal contraction, mech. props. 79−61691
ESCAR, tests of superconducting bending magnets 79−76202
ESCAR bending magnets, design, construction and operation 79−36444
ESCAR magnet cooling system 79−30485
ESCAR superconducting fully cryogenic accelerator 77−83236
failure experience rel. to fusion power reactors 77−26870
Fermilab, appl. of NMR cct. to superconducting mag. field meas. using signal ave. 77−83231
fermilab doubler magnet design and fabrication techniques 79−36443
Fermilab energy doubler, dipole magnet technology 77−26901
Fermilab energy doubler, mag. field meas. 79−31258
Fermilab energy doubler construction progress 79−36441
Fermilab energy doubler magnets, support design and cryostat system 79−31257
Fermilab energy doubler/saver mag., radiation damage limitations 77−83238
Fermilab energy doubler/saver project, ring of superconducting mags., status report 77−83212
Fermilab main accelerator quadrupole transistorised regulators 77−83243
Fermilab switchyard, superconducting dipole 79−76204
field orientation rel. to magnetisation of supercond. wires 78−52151
five coil partial torus, buckling and vibrs. 77−79128
force cooled superconductor cryostability expt. 78−50378
force-cooled conductors design 78−54999
force-cooled superconductor design for large fusion magnets 79−31216
forced flow cooling, numerical anal. of heat-induced transients in He 80−82773
frictional heating of metal-insulator pairs at cryogenic temps., rel. to supercond. magnet technology 80−66671
fusion, toroidal field superconducting coil cryogenic stability and field anal., design parameter 80−106200
fusion energy research *(Japanese)* 79−18039

superconducting magnets continued
fusion magnet development 77−26869
fusion magnetic systems, struct. anal. methods and standards 80−86972
fusion magnets, radiation effects 78−50294
fusion reactor, CC NbTi, pool cooling superconducting test coil, Japanese design 80−99340
fusion reactor, cluster test facility, design 80−90835
fusion reactor, ELMO Bumpy Torus Proof-of-Principle, proposed mag. system 80−99296
fusion reactor, field-reversed mirror 80−42857
fusion reactor, finite element anal. of structural response of superconducting magnet 77−3166
fusion reactor, HFCTR, demonstration reactor conceptual design, high force density magnets and modularisation 80−95439
fusion reactor, high current density superconducting coils, cryostability 80−106201
fusion reactor, JXFR, superconducting mag. system conceptual design 80−99295
fusion reactor, Large Coil Program, coil winding development support 80−106190
fusion reactor, Large Coil Program, General Dynamics Convair/IGC manufacturing engineering 80−106169
fusion reactor, Large Coil Program, Nb_3Sn forced flow superconducting test coil, Westinghouse design 80−99337
fusion reactor, Large Coil Program, NbTi superconducting test coil, General Electric design and manufacture program 80−102319
fusion reactor, Large Coil Program, Westinghouse superconducting mag. elec. design 80−91250
fusion reactor, Large Coil Task, CC NbTi forced flow superconducting test coil, Swiss design 80−99341
fusion reactor, Large Coil Test Facility test stand design description 80−102320
fusion reactor, large superconducting toroidal field coil program, progress report 80−99335
fusion reactor, maximum toroidal mag. field value by core constraint 80−102349
fusion reactor, MFTF, mag. cryostability 80−106198
fusion reactor, MFTF, superconducting mag. quench vent rate 80−106197
fusion reactor, mirror machine, supercond. mags. 80−42862
fusion reactor, multiple mirror, coil design and economic optimisation 80−99284
fusion reactor, multipole fusion confinement with 2 MA levitated superconducting coil 80−106191
fusion reactor, press. induced flow cooling, highly stable superconducting mag. systems 80−106192
fusion reactor, Princeton large torus 3-coil test 78−54945
fusion reactor, reversed-field-pinch, superconducting windings 80−27804
fusion reactor, SLPX TF coil, stress anal. using COSMIC-NASTRAN 80−106168
fusion reactor, STARFIRE project, superconducting poloidal coils design study 80−106185
fusion reactor, STARFIRE project, toroidal field coil system preliminary assessment 80−106186
fusion reactor, superconducting toroidal system, force anal. for all fault conditions 80−91258
fusion reactor, Tandem Mirror Reactor, end plug mag. system design 80−102347
fusion reactor, Tokamak constant tension D-shaped coils, lateral support struct. 78−55013
fusion reactor, torsatron, superconducting mag. engineering design 80−99297
fusion reactor and plasma physics magnets, USA development 79−31193
fusion reactor and plasma physics magnets, W.European development 79−31194
fusion reactor Large Coil Program, NbTi, superconducting test coil, General Dynamics Convair Division, Intermagnetics General Corp. design 80−99338
fusion reactor Large Coil Segment test, struct. anal., mag. force loadings 78−50373
fusion reactor large magnet systems safety 78−770
fusion reactor large system, structure, insulators, conductors 80−32471
fusion reactor magnetic coil, Large Coil Program, test heater conceptual designs 80−91251
fusion reactor magnets, safety and structural aspects 77−26874
fusion reactor solenoid, orthotropic, finite element stress anal. 78−55010
fusion reactor superconducting magnet joints, resistance welding 80−91259
fusion reactor superconducting magnet magentoelastic energy calcs., finite element anal. 78−55002
fusion reactor superconducting magnets, structural design 80−86974
fusion reactor superconductor strain and mag. system design parameters, closed-form anal. 78−50377
fusion reactor systems for Tokamak design 77−71691
fusion reactor TESPE coil, finite element method calc., winding package modelling 78−50376
fusion reactor toroidal field coil thermal design and anal. 78−50368
fusion reactor toroidal field magnet system utilizing normal metal trimming coils 78−54931
fusion reactors, differences between mirror and toroidal fusion systems, superconducting magnets 80−32429
fusion reactors, Large Coil Program, low temp. stability, joints, design method 80−106195
fusion reactors, Large Coil Program, pool boiling mag. quench press. calc. 80−106199
fusion reactors, Large Coil Program, superconducting mag. coil struct. design status 80−106189
fusion reactors, large Coil Program, Westinghouse coil cooldown and warmup 80−106193
fusion reactors, Large Coil Program, Westinghouse coil stability testing, pulsed induction heating 80−106194
fusion reactors, Large Coil Task, NbTi, forced flow superconducting test coil, EURATOM design 80−99339
fusion reactors, Large Coil Test Facility, liq. He cooling system 80−102321
fusion reactors, MFTF superconducting mag. design and construction 80−101008
fusion reactors, supercond. toroidal field magnets, large coil program 79−36400
fusion reactors, Tokamak and tandem mirror reactors, neutral beam injection and superconducting magnets 80−63391

superconducting magnets continued
fusion reactors, Torsatron T-1, demountable resistive joint for high current superconductors 80−106202
fusion research, supercond. mirror magnets 79−36401
fusion tokamak, development of superconducting magnet *(Japanese)* 79−73026
fusion-fission breeder reactor, supercond. poloidal field coil design 78−70640
gas-cooled current leads 80−37056
General Atomic PGFR concept, 10 tesla toroidal field magnet system 79−49835
glass fibre reinforced epoxy, struts for superconductive storage magnets, mech. props. 80−25824
glass fibre reinforced polyester, struts for superconductive storage magnets, mech. props. 80−25824
glass-epoxy laminate, superconducting magnet insulators, gamma-ray radiation effects 80−24495
gyromonotron design, 240 GHz, using supercond. magnet system 80−58498
heavy ion accelerator magnet configuration and construction technology 79−31264
heavy ion storage supercond. coil radial sector guiding field calc. 79−31262
heavy-current cabled and soldered multifilament superconductor AC losses 79−32808
heavy-ion cyclotron at Chalk River, extraction system, design 77−83266
helium refrigeration system and cryogenic system for superconducting Switchyard magnets at Fermilab 79−67990
Helmholtz coils, optimisation, critical current rel. to mag. induction 79−67353
HEUB dipoles, operating experience 77−83234
high current density magnet, thermal stability 80−37057
high current materials for Tokamak toroidal field coils 77−31530
high energy accelerators, superconducting dipole magnets with high field uniformity, development and investigation *(Russian)* 80−5416
high energy beam line dipole-magnetostatics, design 77−83363
high energy physics applications, review 77−26949
high energy physics program at BNL, equipment, experiments, future research 77−18716
high field facilities at Francis Bitter National Magnet Lab. 79−71497
high field magnet laboratory of Grenoble, facilities and utilisation 79−71495
high field superconductors, large internally cooled, development, production and testing 79−54144
high field test facility, and initial performance 79−30447
high homogeneous field, for polarised proton target 77−26911
high magnetic field facility at Univ. of Wurzburg 79−71492
high magnetic field installation at Univ. of Nijmegen 79−71496
high-energy physics appl. 80−68990
hollow conductors, cooled by supercritical He 78−54997
hollow conductors for force-cooled superconducting magnets, fabrication and properties *(Japanese)* 80−90868
HV insulation problems 79−30512
hybrid magnets for high mag. field generation, polyhelix coils, optimization calcs. 80−240
hyperon bubble chamber 11.7 T solenoid 78−50435
Hyperon-1 supercond. magnet for high-energy physics expts. 79−31302
hysteresis losses in multifilamentary coil 77−26363
induction coil system, superconducting for a doublet Tokamak reactor 77−30657
instability sources and possible explanations of training problem 77−22584
integrated composite conductor for fusion program 78−62631
intersecting storage accelerator supercond. magnet construction and performance 79−31263
intersecting storage ring supercond. solenoid installation and performance 79−31270
ion source, electron beam type, using supercond. solenoid, low-vel. heavy ions prod. 80−58017
irradiation effects at low temp. on materials and components for supercond. mag. for high energy phys. appl. 77−69012
ISABELLE dipole magnets, forced flow cooling 77−26907
ISABELLE dipole magnets, magnetization effects on field shape 79−31253
ISABELLE half-cell prototype, magnet power supply system 77−83244
ISABELLE insertion quadrupoles 79−76197
ISABELLE magnet support and adjustment system 79−76198
ISABELLE quadrupoles 77−83227
ISABELLE ring magnets, operating characts. 77−26900
ISABELLE storage rings magnet cryostats, mech. design 77−83218
JET Tokamak inner poloidal field coil design 79−31209
JET Tokamak toroidal field coil design 79−31205
JET Tokamak toroidal field coil manufacture 79−31206
Kapton (polyimide), insulators for superconducting magnets, effect of low temp. irradiation 80−25817
large, electron/positron intersecting storage ring appl. 77−46435
Large Coil Program, cryostabilised conductor cooling system 78−50393
Large Coil Program, General Dynamics Convair conceptual design test coil 78−50389
Large Coil Program, General Electric test coil conceptual design 78−50390
Large Coil Program, He liquefier-refrigerator and distrib. system 78−50398
Large Coil Program, Nb_3Sn forced flow superconductor design considerations 78−50394
Large Coil Program, pulse coil concepts 78−50397
Large Coil Program, research and development activity 80−99336
Large Coil Program, struct. response of toroidal field coils, finite element anal. 78−50396
Large Coil Program, superconducting toroidal field coils for Tokamaks 78−50388
Large Coil Program, support struct. conceptual design 78−50395
Large Coil Program, Westinghouse Electric conceptual design for test coil 78−50392
large diameter solenoids, mag. spectrometers for colliding beam accelerators 77−26919
large-scale applications of supercond. materials, review 79−69640
leads, detachable, up to 100 A for mag. field of 5.0 T 79−75557
lens system for 500 kV electron microscope 80−68321
loss measurement in coils, electronic meas. apparatus 77−26361

superconducting magnets continued
low current DC beam line magnets, supercond. coil manufacturing method 77−82575
low current superconducting coil for beam transport dipole magnet 79−31256
low permeability meas. at cryogenic temperatures 79−30514
magnetic energy storage system with superconducting rotary machines as I/O system *(Japanese)* 80−85306
magnetic field inhomogenity measurement method, Hall probe appln. *(Czech)* 80−13107
magnetic field prod. and meas. 78−8425
magnetic flux compression, compression generator, PULSAR, design optimisation 80−68957
magnetooptical cryostat with superconducting solenoid at 83 kOe 79−71461
magnetothermal conductivity measurement for selected metals, 4 to 20K 79−67317
mechanical and thermal stresses in superconducting accelerator and beam-line mags. 77−83362
MHD circular saddle coil magnet, structural analysis 77−27739
MHD generation developments *(Czech)* 79−87996
MHD generator magnet systems 78−55759
MHD power generator system appl., design and trade-off analyses 79−52950
MHD superconducting magnet system (U-25, Argonne) 77−27740
MHD superconducting magnets 77−27741
Milan superconducting 1:6 model magnet, mag. field meas. 79−54669
mirror fusion experiment magnet system 77−27743
mirror fusion test facility, beams and supercond. magnets 79−49849
mirror fusion test facility, supercond. coils for plasma confinement field 79−36402
mirror fusion test facility, supercond. magnet prod. system 79−36408
mirror fusion test facility 80−43962
Mirror Fusion Test Facility supercond. coil development 79−31202
mirror fussion test facility, supercond. Yin-Yang coil fabrication 79−36403
model magnet for superconducting cyclotron at Milan 77−83194
monolithic conductor manufacture 78−62642
multifilament superconductors, effect of local heat dissipation on stability 80−60156
multifilamentary composite superconductor power losses 79−30507
multifilamentary composite superconductor transport current distrib. 79−30505
multifilamentary superconductors with alternating twist, losses in transverse pulsed fields 79−30508
multiple superconducting energy doubler accelerator magnets, series operation 77−83214
Mylar (polyester), insulators for superconducting magnets, effect of low temp. irradiation 80−25817
neutron irradiation effects on organic insulators at 5K for superconducting magnets 80−107336
NMR applications, for studies in biochemistry 79−74811
NMR measuring head for expts. in supercond. mag., characts., appls. *(German)* 77−41661
NMR spectrometer, widebore supercond. magnet systems, sideways-spinning 20 mm tube probe 79−30518
Nomex (nylon paper), insulators for superconducting magnets, effect of low temp. irradiation 80−25817
NUWMAK fusion reactor, toroidal field magnet system 79−36406
Oak Ridge National Laboratory superconducting coil fabrication development 78−50370
ohmic heating coil, fast ramp superconductor 78−62638
ohmic heating pulsed superconducting coil 78−62640
ohmic heating solenoid, appl. to Tokamak TNS 78−54928
ohmic testing coil for fusion reactor 78−62634
ORPUS-3, pulsed superconducting solenoid for poloidal field coils 78−62641
particle accelerator, ESCAR, magnet design 77−26902
particle accelerators at Karlsruhe, quadrupole magnet design and construction 77−26889
particle beam bending magnets, large aperture design for Brookhaven AGS 77−26910
particle separator, large scale He II cryostat design 77−30742
plasma and fusion appls. 77−19759
plasma confinement in fusion reactors appl. 79−23441
plasma physics and fusion reactor research in USSR, appls. *(Slovak)* 78−87474
plasma physics research appl., USSR 79−31192
polarised proton target, for pion photoproduction 79−22508
poloidal coil air-core system for experimental power reactor 77−26873
poloidal field coil design and development of JT-60 Tokamak 79−31204
poloidal field coils in Tokamak fusion reactor, interaction and protection 77−42189
polycarbonate, insulators for superconducting magnets, effect of low temp. irradiation 80−25817
polymer films, superconducting magnet insulators, gamma-ray radiation effects 80−24495
polypropylene, insulators for superconducting magnets, effect of low temp. irradiation 80−25817
portable 16.5 T system for shared use 77−148
portable self-contained refrigerants transfer system, for use with supercond. magnet dewars 80−8993
precooling using Cryomech GB02 cryocooler and gas-filled thermal switches 80−52245
protection device, with superconducting switch 80−9007
proton beam exposure in synchrotron, quench thresholds 79−31254
Proton-Electron Tandem Ring Accelerator 'transparent' solenoid superconductor 79−31274
prototype supercond. quadrupole magnet for CERN intersecting storage rings 79−31265
pulse loss and voltage meas., elec. method 77−37949
pulsed, hysteretic and mechanical loss calcs. 79−80649
pulsed, stability studies, fusion reactor appls. *(Japanese)* 80−106158
pulsed and DC types, high energy physics appl. *(German)* 78−21834
pulsed solenoid ORPUS-1, poloidal field coil performance 77−26352
pulsed superconducting coil, 1.5 MJ, and cryostat, performance tests 79−49259
pump for liquid He, design and construction 77−45849
quadrupole collector with large solid angle for heavy-ion expts. at high-energy 77−34506
quadrupole magnet construction for CERN ISR 77−10507

superconducting magnets continued
quadrupole magnet design for ion beam fusion linac 79−36433
quadrupole magnets for CERN intersecting storage rings, testing using flexible cryogenic system 79−58706
quadrupoles, magnetic field calc. by harmonic current layer method *(Croatian)* 77−28341
quadrupoles used in CERN hyperon-beam, cryogenic design and performance 79−54220
quench protection system for ISABELLE 77−83233
quenching of technical superconductors by ht. and mag. field pulses 78−43537
'R and A' magnet for ANL polarised proton target 77−38525
racetrack, press.-impregnated, training behaviour 77−22585
radiation damage to materials for fusion reactors *(Japanese)* 78−54873
recovery of supercond. systems, laboratory obs. and computer calc. 79−30494
research in Europe and appl. trends *(German)* 77−55649
RF particle separator, 300 W 1.8K refrigerator for 77−18770
RST, RF driven steady state toroidal expt., design 80−91276
Saclay high-energy physics supercond. magnet programme 79−31352
saddle-shaped, MHD generator appl., construction 78−22579
safety of superconducting fusion magnets: twelve problem areas 80−102348
segment test facility, 7.5 Tesla 78−54929
separation of mag. minerals using supercond. mags. *(Czech)* 78−88923
solenoid, 60Hz AC loss meas. 77−26362
solenoid, Al stabilised supercond., design and construction, for CERN intersecting storage rings 77−46428
solenoid, Basque project 77−23325
solenoid, biaxial sample rot. use *(Czech)* 80−37010
solenoid, control of field-changing tasks by microcomputer 79−216
solenoid, effect of constructional features on magnetic parameters 79−21786
solenoid, hysteresis losses 78−84345
solenoid, in persistent mode, magnetothermodynamic meas. error anal. 79−17454
solenoid, large high current density, for use in high energy physics expts. 77−23326
solenoid, large high-current density, for Time Projection Chamber expt. 79−54219
solenoid, mag. field stability in persistent mode *(Czech)* 78−29131
solenoid, mag. parameters, NMR study of effect of constructional features 79−71488
solenoid, magnetisation, field dependent, automatic M-H curve recorder in high magnetic fields *(Japanese)* 79−71500
solenoid, optimisation of aperture solenoid with rectangular windings 80−4747
solenoid, supercond., mag. flux conc. using Tb cryst. 78−49869
solenoid, superconducting, homogeneous, for superconductor props. meas. by NMR *(Czech)* 78−29130
solenoid, use of cylindrical drift chamber 79−3311
solenoid, with magnetometer for magnetocrystalline anisotropy meas. from 4 to 300K 77−2673
solenoid, with variable current density, optimisation 79−17450
solenoid design optimisation 77−147
solenoid field magnet for large polarised target, 2.6 T field 79−54221
solenoid for intense meson beam channel *(Czech)* 77−38527
solenoid for time projection chamber at PEP 79−31320
solenoids, detachable leads, for use in liquid He dewars 79−63240
solenoids, square-ended design for optimum performance 78−82009
solenoids and resonators for H^- collective accelerator, Q-values and field profiles 78−46188
solenoids and resonators for H^+ collective accelerator 78−46187
solenoids fields meas., automatic, using NMR 80−57344
solenoids using Nb-Ti alloy wire 79−93174
solid state physics, high mag. fields, generation and application 80−27321
space applications 80−37058
space applications 80−41694
spacers, epoxy resin, powder filled, exam. of mech. props., thermal contraction 80−25821
spin-tipping solenoids for polarized beam synchrotron, magnet and cryostat design 79−31252
split-coil magnets for generating high homogeneous mag. fields 77−57366
split-pair systems for polarised proton target 77−14291
stabilisation of large magnets, expt. models 77−26349
stability, against localised disturbances of limited magnitude 78−39264
stability, critical current margin design criterion 80−31807
stability, vapour form. and heat transfer in liq. He cooling channels under transient and steady state conditions 79−32197
stability problems in accelerators under high energy particle interactions *(Russian)* 80−68972
static and dynamic characteristics, appl. of experiment planning 79−67352
storage ring, torroidal, for neutrons 78−21795
storage ring facility, POPAE, 6 T dipole magnet design 77−26898
storage ring magnet for ISABELLE ISR, update 79−36442
storage rings, ISABELLE, superconducting dipole prototypes, operational parameters 77−83215
stress-induced heating of multifilamentary composite conductor, influence on mag. performance 77−26357
strong and ultrastrong pulsed mag. field generation 79−71494
structural alloys for superconducting magnets in fusion energy systems, props. at 4K 80−86976
SUPER-SOLO solenoid, switch and cryostat 79−54222
superfluid He bath to improve performance 77−30188
synchrotron, power supply and quench protection scheme 79−36445
synchrotron dipole magnets coil motion 77−83237
synchrotron dipoles, eight tesla range 79−76201
systems 80−9008
T-10 M tokamak toroidal field coil shape struct. anal. 78−50374
T-7 Tokamak superconducting magnet test program, some results 79−37528
tape-wound cylindrical, trapped fields 77−26355
TESPE toroidal coil for Tokomak fusion plasma containment 79−54223
testing instrumentation and methods 77−26882
tevatron, Fermilab proton accelerator with supercond. mag. ring 78−835
TF superconducting magnet, demountable, for catalysed D-D and D-^{3}He fusion reactors 77−88280
superconducting magnets continued
THOR Tokamak toroidal field system design and manufacture 79−32807
Tokamak, Oak Ridge Experimental Power Reactor toroidal coil system 77−26872
Tokamak, TNS, equilib. field coils and free boundary equilib. considerations 78−58420
Tokamak design, TORUS II SUPRA 79−37527
Tokamak EF coil energy transfer supercond. solenoids and phase-shifting bridge 79−31213
Tokamak energy storage superconducting solenoids 78−66369
tokamak fusion reactor, generic PSAR for TF coil system 78−58407
Tokamak fusion reactor, material and design options for superconducting TF magnets 79−85801
Tokamak fusion reactor, structural anal. 77−3162
Tokamak fusion reactor, supercond. ohmic-heating coils, simulation expts. 79−36404
Tokamak fusion reactor prefabricated toroidal supercond. field magnet system 79−31211
Tokamak fusion reactor supercond. toroidal coil bending moment computation 79−41867
Tokamak fusion reactors, superconducting heating coils and toroidal field coils design 77−6559
Tokamak fusion reactors, superconductor design considerations for poloidal field coils 79−63236
Tokamak ohmic heating coil design and testing 79−32806
Tokamak plant, superconducting toroidal field magnet model 78−17425
Tokamak power reactor supercond. coil design, experimental 79−31198
Tokamak power reactor supercond. poloidal magnet system design, experimental 79−31207
Tokamak power reactor toroidal field coil design and manufacture 79−31201
Tokamak reactor, compact high-density, system of field coils 77−34464
Tokamak reactor, magnet coil radius optimisation 77−42191
tokamak reactor superconducting toroidal field magnet computational model, technical and economic 78−50375
Tokamak reactors, supercond. toroidal magnets, mag. and thermal loading 79−36407
Tokamak reactors, supercond. toroidal magnets, max. mag. fields, mech. stress calcs. 79−36405
Tokamak requirements for supercond. materials and devices w.r.t. thermonucl. fusion *(French)* 78−13322
Tokamak superconducting long-pulse expt., SLPX, design features 79−50898
Tokamak superconducting toroidal field coil concept 79−31200
Tokamak TF coil system, protective control features 78−62625
Tokamak toroidal field coil shielding calc. 79−31212
Tokamak toroidal field coils, pulsed field losses, expt. simulation 77−26871
Tokamak toroidal field coils, reduction of bending moments 80−47697
Tokamak toroidal field coils, superconducting 78−62632
Tokamak toroidal field magnet 77−31496
Tokamak toroidal magnet supercond. cluster test design 79−31199
Tokamak toroidal magnet system development, cluster test facility 79−30495
Tokamak-7, circulating superconducting magnet system, design and operational tests 79−89498
Tokamak-7, mag. system sections, test results 77−27742
Tokamak-type experimental power reactor, interaction and protection of supercond. and pulsed coils 77−23262
Tokamak-UWMAK systems, magnet design of toroidal field coils 77−6558
toroidal, for FINTOR 1 fusion reactor 77−27694
toroidal field coil, 10 Tesla 77−27692
toroidal field coil design and development for JT-60 Tokamak 79−31203
toroidal field coil design for fusion-driven actinide burner 77−27693
toroidal field coils, bending-free, for Tokamak reactor 78−55012
toroidal field magnets conceptual design for expt. fusion reactor 78−50391
toroidal field superconductors for fusion devices, development and testing 79−59263
toroidal fusion magnet systems, radiation damage effect on max. attainable magnetic field 78−50295
toroidal magnet coil design and testing 79−31195
toroidal magnet design for Tokamak fusion reactor 79−76135
toroidal system for demonstration fusion reactor FINTOR-D, preliminary design 79−67953
toroidal-field coils, flow characts. of forced-flow Nb_3Sn conductors 79−58741
training and degradation phenomena *(Slovak)* 79−6152
training behaviour, effect of adhesion between turns 78−89507
training phenomenon, influence of mech. props. 77−26356
transformer-rectifier flux pump using inductive current transfer and thermally controlled Nb_3Sn cryotrons 80−4727
transient heat transfer, temp. meas. with μs response time 78−71270
transient losses in cables for PF and TF coils 78−62635
transversely isotropic solenoid, electromech. stress anal. 77−79127
ultracold neutron storage ring supercond. magnet design 79−31266
ultrathin-coil supercond. solenoids for high-energy accelerators and storage rings 79−31260
UWMAK II, conceptual demountable TG magnet design 78−17426
warm Fe dipoles, stress anal. 79−68041
wiggler magnet, 5T design for dedicated synchrotron radiation source at Daresbury 78−62672
windings, transient heat transfer to liq. He from bare Cu surfaces 78−83219
Ying-Yang magnet system for mirror fusion test facility 78−54922
ZGS beam transport for transverse and longitudinally polarised protons 78−55074
ZGS high-energy beam line 77−26903
Al, use in design of composite superconductors in elasto-plastic region 77−28851
Al-NbTi solenoid magnet for high energy particle detector, conductor and cryostat design 79−31319
Cu, electrical conductivity, effect of cyclic strains and work hardening at 4.2K 78−91655
Cu, stabiliser, 400 GeV proton irrad., resist. meas. 77−37948
H_2 atoms trapping and thermal detection using superconducting magnet of low temp. 80−73396
He cooling systems, large, review of hydrodynamics and heat transfer 79−204

superconducting magnets continued
He cryostat with refrigerator for supercond. magnet 79−58733
He distrib. system for Large Coil Test Facility 78−55001
He, liq., dewar, temp. profile 77−41621
He, liq., narrow channel flow and heat transfer charact., void fraction in steady and transient states 78−55000
He transfer lines for cooldown or warmup 79−63234
He unit requirements, for superconductive energy appl. in USA 78−89999
Nb-Ti, multifilamentary, Mirror Fusion Test Facility, superconductor core manufacturing and quality 80−93521
Nb-Ti, superconductor optimisation for 12 Tesla toroidal field coils 80−91272
Nb-Ti 10 kA conductor development for Tokamak toroidal coil 79−31217
Nb-Ti alloy, supercond. Helmholtz coils, optimisation 79−2795
Nb-Ti coils, for thermonuclear fusion *(French)* 80−95399
Nb-Ti in Cu matrix composite superconductor, cyclic stress effects on transport props. 77−28336
Nb-Ti multifilamentary cable magnet, quench development 77−26351
Nb-Ti superconducting magnet system, for short sample test on Tokamak superconductor 80−9010
Nb-Ti-Ta, superconductor optimisation for 12 Tesla toroidal field coils 80−91272
Nb_3Ge film, CVD fabrication of supercond. tape for high-field magnets 78−95698
Nb_3Ge, long tapes, CVD prepared, high current densities, use in producing 20 T magnet 79−33436
Nb_3Sn filamentary composite conductor design 79−30515
Nb_3Sn filamentary hexapole magnet construction and testing 79−30503
Nb_3Sn in Cu matrix composite superconductor, cyclic stress effects on transport props. 77−28336
Nb_3Sn, low temp. neutron irrad. expts., E_n=14 MeV 79−33424
Nb_3Sn magnets for Tokamak reactor 78−54983
Nb_3Sn multifilament conductor critical current rel. to mech. strain 79−31215
Nb_3Sn multifilament superconductors, designed for high B appl., losses 79−33414
Nb_3Sn multifilamentary conductor, for fusion research magnets, manufacture and props. 77−28760
Nb_3Sn multifilamentary conductor for fusion research 79−35797
Nb_3Sn multifilamentary conductor production and testing 79−32809
Nb_3Sn multifilamentary conductors for large-scale magnets, crit. currents, stability, and stress effects 79−38291
Nb_3Sn, multifilamentary coils for Lawrence Livermore Laboratory superconducting High Field Test Facility 80−90834
Nb_3Sn multifilamentary dipole magnet, construction and performance 77−28758
Nb_3Sn multifilamentary dipole magnets, supercond. props., 4.2 to 15K 79−31275
Nb_3Sn multifilamentary hollow superconductor and magnet, fabrication and crit. currents 79−38289
Nb_3Sn multifilamentary supercond., Cu-stabilised, recent developments 77−28759
Nb_3Sn, neutron irrad. effect on supercond. fusion magnet props. 78−52128
Nb_3Sn, supercond. props. and appls., state-of-the-art 79−33413
Nb_3Sn-V_3Ga concentric solenoid magnet system, 17.5 T operation 77−26353
NbTi, 7 T multipurpose split-coil system for Mossbauer spectroscopy and susceptibility measurements, 2 to 300K 79−58746
NbTi cabled and soldered superconds. with low losses, for fusion research magnets, development 79−35796
NbTi, dynamic stress effects, supercond. magnet training problems 78−49870
NbTi, neutron irrad. effect on supercond. fusion magnet props. 78−52128
NbTi solenoid, operating at 9 T in He gas 77−74461
NbTi split coil superconducting magnet system, for Mossbauer spectroscopy and susceptibility meas. 79−71486
NbTi superconducting magnet, 0.8 m free bore toroidal magnet module 78−54923
Si(Li) electron spectrometer with superconducting transporting magnets 80−27376
Tb single crystal flux concentrator for supercond. solenoids 78−57991
V_3Ga composite prep. and testing for high-field supercond. magnet 79−30513
V_3Ga, development by diffusion processes and use in 17.5 T supercond. magnet 79−61015
V_3Ga superconducting tape, stress effect on critical current *(Japanese)* 80−50020

superconducting materials
see also composite superconductors; dirty superconductors; strong-coupling superconductors; superconducting semiconductors; superconducting thin films; type I superconductors; type II superconductors
A15 cpds., high-press. synthesis 77−70022
AC conductor, cooled by cryogenic liq., heat transfer models 80−5926
alkali metals, heavy, supercond. and high temp. resist. at high press. 77−47917
alkaline earth metals, lack of supercond. in Mg and Ba above 0.3K 77−12053
alloys containing paramag. impurities, Raman scattering of light 79−73634
aniline black, superconductivity at room temp. 78−80089
anisotropic superconductor, finite freq. US attenuation 79−1640
anisotropic superconductor, functional derivative of critical temp. with electron phonon spectral density 80−49971
borides, conference, Varna, Bulgaria (Oct. 1978) 80−12842
built-up superconductors, current transfer 78−62633
charge inbalance generation by temperature gradient 79−95541
commercial superconductors, test facility for dynamic stress effects 77−77698
conference, Stanford, Calif., USA (Aug 1976) 77−28272
conference on cryogenic engineering, London, England, (July 1978) 79−54137
cryogenic engineering, conf., Grenoble, France (May 1976) 77−17988
dislocation motion 77−47929
dislocation motion 77−47930
dislocation-point defect interaction, rel. to internal friction *(Russian)* 77−36018

superconducting materials continued
DNA, superconductivity, dynamical model 79−62172
Electrochemical Society Meeting, Boston, USA, (May, 1979) 79−91959
epoxy impregnated superconducting composites, mech. props., strain effect at 4K 80−25822
fatigue testing, in normal and superconducting states 78−19959
friction between like metals, 4.2-80K, superconductivity effects 78−48543
high field, large internally cooled, development, production and testing 79−54144
high performance wire development 77−20487
Hubbard model, transforms 77−72972
internal friction near critical temperature at acoustic frequencies 80−100305
Israel Physical Society 1980 annual meeting, Rehovot, Israel (April 1980) 80−94909
layered structures, book contrib. 77−39994
layered superconductors, Josephson coupling effects, review 80−84554
magnet conductors, review *(Japanese)* 80−25042
magnetic superconductors, mag. scatt. of neutrons 80−103819
magnetic superconductors, spin fluctuation and US attenuation 80−80445
magnetothermal conductivity measurement for selected metals, 4 to 20K 79−67317
metal, flow stress relation with thermal conductivity discontinuity at supercond. transition 78−60246
metals with $Z \lesssim 49$, electron-phonon interaction, mass-enhancement factor and supercond. transition temp. 77−66221
metastable compound synthesis with high supercond. transition temp. 80−93024
metrological problems 79−73650
MHD conversion appl. *(Japanese)* 78−47925
noise, conference, Bad Nauheim, West Germany (Mar. 1978) 79−24031
nonlinear acoustic attenuation effects, energy gap widening *(Russian)* 77−43780
physical properties of superconductors, elec. engineering appl. *(German)* 77−55648
polysulphur nitride, temp. depend. and anisotropy of H_{c2} 80−25054
properties, review and table 77−4460
radiation induced damage, review 78−51580
rare earth metals, lack of supercond. in Ce, Pr, Nd and Yb above 0.3K 77−12053
rare earth-Sn-X, X=Rh, Ir, Ru, Co, cryst. growth and cryst.-chem. invest, supercond./mag. ternary cpds. 80−100777
research and elec. engineering appl., European trends *(German)* 77−55649
review of search for new materials 77−59350
ribbon-form material, rapid quenching from melt *(Japanese)* 78−92210
semiinfinite sheet, current coil interaction, electrodynamic suspension system *(Russian)* 80−83539
small metal particles ground state energy and orbital mag. susceptibility 80−49983
soldering superconducting wire to cryogenic leads, simple repeatable method 80−4728
standard measurement techniques for determination of props. 79−69622
superheated supercond. colloid neutron detector, detection and background rejection tests 78−78580
tabular data, stabilisation and manufacture *(French)* 79−7931
technical superconductor radiation damage obs. 79−33422
ternary compounds, supercond., p-state pairing and magnetism 80−54819
$(TMTSF)_2PF_6$, one dimens. conductor, superconds., resist. meas. and mag. field effects *(French)* 80−44753
transition metal, normal state, resistivity, anomalous temp. coeff. at high temp. 78−2458
TTF-TCNQ, effect of benzene ring substitution on supercond. and metallic props. 80−20193
wire, coil simulation, class and instability meas. 79−71487
Al, superconducting, an anomalous strain-rate sensitivity of flow stress 79−43313
Al-Al_2O_3 granular film, crit. current density, normal state resist. depend. 77−40013
Al-Mg, superconducting, an anomalous strain-rate sensitivity of flow stress 79−43313
AlH_x, electronic struct. and electron-phonon interaction, hydrogenation effect, rel. to supercond. 80−107694
Am, discovery of superconductivity up to 0.79K 79−11262
CuCl, disordered, diamag. transition 80−34636
CuCl, interface superconductivity? 80−39696
CuCl, interface supercond., piezoelec. hypothesis 80−60128
CuCl, possibility of excitonic dielectric-supercond. phase transition 77−43797
CuCl, possibility of high temp. superconductivity 79−51711
$ErMo_6S_8(Se_8)$, ternary superconductor, paramagnetic relax. effects 78−68112
$ErRh_4B_4$, ternary superconductor, paramagnetic relax. effects 78−68112
$Eu_xSn_{1-x}Mo_6Sn_8$ (Se_8), ternary superconductor, paramagnetic relax. effects 78−68112
Ga-$GaCl_2$, finely disperse system, supercond. props. 77−85376
Hg filament, ultrathin, influence of fluctuations on supercond. transition 77−8234
Hg, supercond. crit. temp., functional derivative with electronic density of states, Eliashberg eqns. 79−56368
In-InCl, finely disperse system, supercond. props. 77−85376
Lu, T_c meas. up to 200 kbar 77−47916
$Mo_3M_3S_4(Se_4)$, M=transition metal, prep. from $Mo_3S_4(Se_4)$ by topotactic reaction 77−90598
Nb-Ge system, reaction diffusion, electron probe anal. 79−28152
Nb_3Sn high field superconductors, filamentary, manuf. and appl. limits *(German)* 77−55647
Nb_3Sn, irradiated, critical current density 79−38293
NbTi superconductors, R&D in Czechoslovakia *(Croatian)* 77−28339
Pb film, quasiparticle and phonon lifetimes, tunnel junction meas. 77−20498
Pb-$PbCl_2(I_2)$, finely disperse system, supercond. props. 77−85376
$PbMo_6S_8$, supercond. wires prod. and characteris. 77−69462
Pd, search for supercond. at very low temps. 78−91799
Pt, search for supercond. at very low temps. 78−91799
Rb, search for supercond. at high press., elec. resist. meas. 79−56359
Rh, search for supercond. at very low temps. 78−91799
$(SN)_x$, electronic struct. and opt. props. 78−6256

superconducting materials continued
$(SN)_x$, supercond. polymer, mag. props. meas. 80−107953
$(SN)_x$, supercond. props., review 78−6474
$(SN)_x$, thermopower from 0.15 to 4.2K 80−34427
Sn film bridge, obs. of operating conditions and shunting effects in small size supercond. 77−16005
Sn, superconducting fine particles, specific heat exam., fluctuations in zero mag. field 77−28295
$(SnBr_{0.4})_x$ 80−107953
Tl, supercond. crit. temp., functional derivative with electronic density of states, Eliashberg eqns. 79−56368
V film, crit. temp., crit. field, resist. and struct. *(Russian)* 77−4475
V, ultrafine particles, sp. ht., 1.3-10K, supercond. transition 77−12061
$YbMo_6S_8$, ternary superconductor, paramagnetic relax. effects 78−68112

superconducting quantum interference devices *see superconducting junction devices*

superconducting semiconductor materials *see superconducting semiconductors*

superconducting semiconductors
amorphous semiconductor superconductivity feasibility model *(Russian)* 78−80092
high-temperature electron-hole supercond. 80−2512
laser induced supercond. props. 77−72960
many-valley degenerate semiconds., supercond. transition temp. *(Russian)* 78−56254
metal-insulator transition, electron pairing, effect on optical props. of supercond. 80−60139
multivalley semiconductors, supercond., crit. temp. effects 79−1638
semiconductor-insulator-semiconductor film system, response to EM field 77−32125
transition in DC elec. field 78−6481
$BaPb_{1-x}Bi_xO_3$, semiconductor-metal transition and supercond., IR absorpt. and struct. meas. 77−28278
CdS-In, photosensitive granular superconductor 79−78246
$Co_2Mo_6S_6O_2$, O-containing Chevrel phases, synthesis and props. 80−108368
CuCl, amorphous/cryst. interface, supercond. mechanism 80−44783
CuCl, high-temp. supercond., BCS strong-coupling limit for transition temp. 80−2511
$Cu_2Mo_6S_6O_2$, O-containing Chevrel phases, synthesis and props. 80−108368
GaP, metallic modification, supercond. transition temp. at high temp. *(Russian)* 77−80867
GaSe, press. induced metallic and supercond. state 80−75666
Ge, amorphous, possible ABB-type excitonic superconductor *(Chinese)* 80−7029
Ge, amorphous/cryst. interface, supercond. mechanism 80−44783
Ge, supecond, friction layer formed during friction between Ge and Pb *(Russian)* 78−52143
Ge, supercond. at high press., crit. temp. 80−60130
GeTe, film, semicond., supercond. energy gap and crit. field, tunelling meas. 77−24644
GeTe, supercond., metal-insulator transition, electron pairing, effect on optical props. 80−60139
InAs, supercond. of surface *(Japanese)* 78−14864
InSb, rapidly condensed film, metastable supercond. *(Russian)* 77−72937
InSb, superconducting phases at high press. 78−88063
$Ni_2Mo_6S_6O_2$, O-containing Chevrel phases, synthesis and props. 80−108368
$PbMo_6S_6O_2$, O-containing Chevrel phases, synthesis and props. 80−108368
Si, amorphous, possible ABB-type excitonic superconductor *(Chinese)* 80−7029
Si, amorphous/cryst. interface, supercond. mechanism 80−44783
Si strongly-doped monocrystal Josephson junctions 79−56400
SnTe, supercond., metal-insulator transition, electron pairing, effect on optical props. 80−60139

superconducting thin films
A15 materials, α-particle induced defects and stoichiometry 77−32101
A15 struct., supercond. enhancement, review 78−64161
acoustic coupling and effective quasiparticle lifetime 77−20499
acoustic matching to substrates 80−15652
automatic thermal cycling apparatus, for superconductive thin film devices 78−37014
bridge, Josephson effect and collective oscillations *(Russian)* 78−31022
bridge, supercond. stimulated by UHF radiation, crit. currents 77−16008
bridges, switching process depend. on control impulse ascent time *(German)* 78−2627
conductivity meas. using ultra-high vacuum compatible probe 78−49867
contacts, critical currents, density, penetration depth 80−25059
cooper pairs, photon scatt. on plasmons, Landau-Ginzburg theory 80−65738
Coulomb superconductor with inverse quasiparticle distrib., behaviour in mag. field 77−20490
critical dimensions, Ginzburg Landau theory *(Russian)* 77−15990
critical electric fields and currents in two dimensional systems *(Russian)* 80−107972
critical temperature increase due to size effect 78−88062
current carrying, nonequilib. hysteresis 79−15256
current-field relation, nonlocal, differential operator method 79−69637
cylindrical superconducting film, resistive part of current voltage charcts. *(Russian)* 77−77000
dirty proximity-effect sandwich system, theoretical investigation of transition temp. 79−73638
electric field under tunnel injection conditions 80−103792
electron beam codeposition, synthesis and props. 78−72296
electron-hole superconductivity influence of struct. defects 77−20489
EM field absorption *(Russian)* 78−34924
energy transport without loss *(German)* 79−60955
far IR absorption, in films with spatially varying order parameter 77−28284
Faraday effect obs. in polarising microscope 80−70892
ferromagnetic, long reentrant, self-heating-induced phenomena 80−50013
film, superconducting props. 79−38215
flux lattice melting, phase diagram 80−84571
flux pinning in films with periodic thickness modulation 80−88702
gap enhancement due to microwave irradiation 78−14892
gap enhancement due to quasiparticle tunnel injection 78−56262

superconducting thin films continued
gapless superconductor, destruction of supercond. by alternating elec. field 77−1518
geometrical reson. effect, electron tunnelling density of states meas., review *(French)* 78−2626
granular films, percolation threshold and crit. current, theory 80−88706
granular metal film, supercond. quenching when charging energy exceeds Josephson coupling energy 77−47943
granular microcylinder, flux quantisation phenomena above T_c *(Russian)* 80−70899
hotspot minimum current in long, thin-films superconductors 80−15656
illuminated, heating model and spectral charcts. of phonon emission 79−28442
inhomogeneous, pair-breaking current, Ginzburg-Landau theory 80−97029
inhomogeneous crit. dynamics 77−8230
inhomogeneous film, cond. near superconducting transition temp. 80−93031
inhomogeneous superconductor, excess elec. cond. calc. 77−55637
inversion temperature in pinning of vortices by periodic struct. 78−56274
Josephson behaviour in films and weak links, scatt. model 78−56261
long, second crit. current, microwave power depend. 77−43794
long thin-film, paradox in crossover of mech. causing hysteresis 80−107971
long-range order, off-diagonal, observability of decay 77−59352
magnetic flux quanta, obs. using decoration and electron vortex microscopy 77−47945
melting of two-dimensional vortex lattices 80−2539
memory device utilizing storage of Abrikosov vortices at array of pinning sites 79−28487
metal film, effect of chemisorption on supercond. 80−39703
metal-nonmetal film system, quantum oscills. in supercond. transition temp. *(Russian)* 77−32107
metallic, superconducting state realisation 80−49977
metastable alloys, review of current work 80−81002
metastable systems, high transition temps., survey *(Russian)* 78−19172
microbridge with normal bank, I-V charcts. 79−87204
microwave irradiation stimulated superconductivity, Josephson effect 79−47201
multilayered supercond. films, critical currents as functions of mag. field and temp. *(French)* 77−72955
multisource deposition rate control using mass spectrometer as sensing element 78−72730
nearly two-dimensional superconductor, crit. exponent 78−14884
non-equilibrium superconductors, formation of inhomogeneity 78−52150
nonequilibrium, inhomogeneous state onset 78−14875
nonequilibrium distribution functions of quasiparticle and phonons calc. 77−89904
nonequilibrium energy spectra of emitted phonons 77−27957
nonequilibrium excitation of quasiparticles and phonons 77−43783
nonequilibrium induction of superconductivity by tunnelling injection 79−91194
nonequilibrium states, kinetic eqn. approach 77−47925
nonequilibrium superconductivity 78−52146
normal metal-superconductor double-layer, photon struct. induced into normal side by proximity effects 79−99659
optically excited, spatial instability driven by quasiparticle diffusion 77−80870
optically induced non-equilibrium and heating effects in superconductors *(Russian)* 78−95398
optically irradiated, phonon spectrum and phonon temp. definition 80−93037
order parameter, dynamic behaviour in EM field *(Russian)* 79−91184
ordering parameter and current density, depend. on paramag. impurity conc. and electron pair rel. *(Russian)* 78−6489
paramagnetic impurities, depend. of crit. conc. on mag. field 78−14863
parametric amplification region calc. 77−80860
Pauli paramagnetism and Fermi surface topology changes under press., rel. to supercond. phase transition 78−2612
periodic pinning structures, supercond. vortices 79−38269
photoexcited, phonon spectrum 80−11132
pin distribution effect on DC voltage-current charcts. 79−99666
pin-free, vortex chain size effect and negative resist. 77−80888
probe, fast response, for detection of second-sound shock waves in superfluid He 79−63237
properties, review and table 77−4460
proximity effect weak links, steady-state and RF props. 80−84563
quantised resistances in supercond.-normal-supercond. film struct. 79−56426
quasiparticle charge imbalance induced by supercurrent with thermal gradient 80−34546
quasiparticle energy distrib. function in optically irrad. films 80−2527
quasiparticle scattering and current-volt. charcts. of supercond.-normal-supercond. film struct. 78−10615
quench-condensed films, superconducting transition temp., elastic stress and strain effects 80−70883
rare earth lead molybdenum sulphides, $R_xPb_{1\pm x}Mo_{6+y}S_8$, R=La, Nd, Pr, Gd, sputtered, supercond. props. 80−50019
resistive domains in long supercond. of small cross section, close to crit. temp. 78−26995
resistive state, linear depend. on applied microwave power of second crit. current 77−32121
resistive transition 80−7049
resistivity, vortex-antivortex depairing 79−69639
resistivity evidence in Monte Carlo studies 80−80434
RF complex impedance meas. 80−84573
second critical current in long film in perpen dicular mag. field 77−63045
self-heating effects in long thin film over wide temp. range 79−51717
split planar thin-film superconductor, anomalous crit. currents 79−51731
SQUID, granular supercond. characterisation 79−28489
SQUID, mag. field sensitivity, galvanic coupling to supercond. antennae *(German)* 79−85154
standard cell voltage monitor using AC Josephson effect 77−82552
stripline, propag. const., attenuation and phase vel. expressions, pulse propag. 78−43524
strong coupling superconductor thin film, critical mag. field *(Chinese)* 80−54849
supercond. cylinder, order parameter enhancement by microwave irrad. 80−70896

superconducting thin films continued
superconducting fluctuation influence on magnetoresistance *(Russian)* 80−54815
superconductor-semiconductor contact amplification props. 79−7941
surface impedance, effects of quasiparticle redistrib. 80−44764
surface polariton modes at interfaces, theoretical anal. 77−24639
surface relaxation time of conduction electron spins 78−91814
thermal induced potential, quasiparticle thermal transport coeffs. 77−85385
thickness determination, using backscattered electrons as tool 79−21704
tilted vortices, mixed state features in surface layers *(Russian)* 80−29512
topological excitations in two-dimensional superconductors 79−56458
transition metal glasses and amorphous films, supercond. and electronic props. 79−73612
transition metal-Ge, RF cosputtered system, supercond. props. 77−51835
tunnel injection into superconductors, theory *(Russian)* 79−47198
tunnelling in films containing single flux vortices 77−59360
tunnelling with spin polarised electrons 79−4627
two-layer model for ultrathin films 78−14849
type I superconducting film, cylindrical domain struct. in mag. field 80−15666
type I-superconductors, cylindric superconducting domain lattices in mag. field, lattice stability determ. *(Russian)* 80−44775
type II superconducting film, crit. region near H_{c2} rational approx. 79−91198
type-I, current induced resistive state, noise in flux tube nucleation 79−24109
ultra-thin films, transition temp., interface and fluctuation phenomena 80−84527
virtual levels, phonon damping 79−4626
voltage measurements within equilibrium region near phase slip centres 78−26997
voltage transfer standard based on AC Josephson effect, standard cell calibration appl. 77−82553
vortex-antivortex pair dissoc. in 2-dimens. superconds. 79−56457
vortices, local mag. flux density and elec. current density 80−84572
vortices, phase transitons, review 80−88698
vortices, static and dynamic interaction with periodic pinning potential 78−52170
weakly damped collective oscillations, EM excitation, surface impedance *(Russian)* 80−65739
Ag-Mn, supercond. proximity effect and pair breaking, normal state mag. interactions 77−63035
Ag-Sn proximity effect bridges, long, voltage anomaly 79−51725
Al, 2 GHz SAW attenuation meas. of mean free path 77−39999
Al, anomalous resistive state due to light pulse 78−52157
Al, cylindrical, granular, crit. currents and electron mean free paths 80−7057
Al, cylindrical, order-parameter variations meas. 80−103797
Al, deviations of equilib. order parameter from mean field theory 77−69453
Al, dielectric coating effect on superconductivity 80−7026
Al, edge pinning in perpendicular mag. fields 79−4633
Al film, crit. temp. enhancement *(Russian)* 80−93021
Al film, implanted at low temp. by H or D, critical temp. enhancement *(French)* 77−8237
Al film, metastable current states, mean free path variation *(Russian)* 80−2538
Al film, permanent resistive states created by light pulses 79−56450
Al film in microwave radiation field, resistive state transition *(Russian)* 80−93038
Al, film in presence of Formvar, excess elec. cond. above T_c 78−60250
Al film in tunnel junction, new supercond. state obs. at high quasiparticle injection 77−72949
Al film with magnetically weakened section, Josephson effect obs. 77−28302
Al films, Al^{2+} irrad., increase of resist. and supercond. transition temp. 80−7027
Al films, microwave induced supercond. above crit. temp. 79−56364
Al, fine particles, supercond. transition temp. meas. 77−12044
Al, getter sputtered at low temp. 78−35305
Al, granular, crit. field anisotropy and fluctuation cond. 78−26994
Al, granular, hopping cond., supercond., magnetoresist., Zeeman splitting 78−60243
Al, granular, transition to localisation, elec. resist. 80−70877
Al, granular film, heat capacity, 0-4.5K, crit. coupling between grains 78−84348
Al granular film, vortex chain size effect and negative resist. 77−80888
Al granular films, inhomogeneous supercond. transitions, microwave meas. 80−103789
Al granular films, self-ion implantation, supercond. transition temp. enhancement 80−103774
Al granular films, vortex noise at supercond. transition 80−84530
Al granular films as weak link in Josephson devices 80−88685
Al granular superconducting bolometer as mol. beam detector 80−73524
Al, intrinsic and expt. quasiparticle recomb. times 77−15999
Al, metastable current states 79−15265
Al, microwave enhanced energy gap, tunnelling meas. 77−51853
Al, nonlinear conductivity of thin films in mixed state *(Russian)* 80−80464
Al, perforated, crit. currents associated with interaction of commensurate flux-line sublattices 78−34937
Al, perforated with triangular lattice of 1 μm holes, critical currents 77−28332
Al, precursor diamagnetism, magnetisation meas. 77−32115
Al, quasiparticle branch mixing rates 79−78269
Al, resistive states, voltage switching effect in tunnelling systems *(Russian)* 79−7938
Al, self-heating effects in long thin film over wide temp. range 79−51717
Al strips, freq. depend. of microwave-enhanced supercond., and local injection of electrons 78−6492
Al strips, on Si substrates, microwave-enhanced crit. currents, phonon effects 79−56451
Al strips, supercond., order-parameter relaxation meas. 79−47207
Al, supercond., meas. of effective quasiparticle recombination times, density of electronic states at Fermi level 79−38264
Al, supercond. film, resistance, effective medium approach 78−60249
Al superconducting film, granular, O content and oxide barrier thickness, transition temp. meas. 79−15250
superconducting thin films continued
Al, superconducting film, microwave enhanced critical current, charact. time const. meas. 79−24102
Al superconducting strips, with local injection of electrons, microwave-enhanced crit. currents 77−63044
Al, superconducting thin film, evidence for Kosterlitz-Thouless transition 80−39721
Al, supercooling mag. field and thermal fluctuations 78−34925
Al, thick film, supercond., tunnelling characts., geometrical reson. in Al-Pb struct. 79−38260
Al, transition edge bolometer 77−71371
Al, transition to zero vorticity, long-range topological order 80−93039
Al tunnel junctions, superconductivity enhancement by microwaves 80−107956
Al, tunnelling with spin polarised electrons 79−4627
Al:O, perforated film, RF resist. in mag. field, pinning force const. 79−56471
Al:O, RF complex impedance meas., dynamic pinning 80−84573
Al:WO_3 films, resistive state, effect of UHF rad. on dynamic cond. *(Russian)* 78−52154
Al/Ge multilayered superconducting films, crit. fields and crit. temps. 79−7945
Al-Al_2O_3, supercond. granular film, mag. penetration depth, depend. on normal state resist. and temp. 79−56378
Al-Al_2O_3 granular film, crit. current density, normal state resist. depend. 77−40013
Al-C(Si)(Ge), ion-implanted, enhancement of supercond. transition temp. 77−32103
Al-Cu, dil. alloy, quench condensed thin films, supercond. and struct. from electron diffr. patterns 78−47901
Al-Cu, superconducting amorphous films of high stability 80−70889
Al-Formvar-Sn coupled films, Ginzburg's excitonic supercond. model 80−97039
Al-Ge, double supercond. transition in resistance-temperature and current-voltage characts., percolation theory 79−56365
Al-Ge thin film alloy, critical currents near metal-insulator transition 79−65626
Al-Si(Ge) film, ion-implanted, percolation and superconductivity 78−26982
Al-V-Ti junction, spin-dependent electron tunnelling 79−19700
As, A1-type superconductor, critical mag. field 79−69638
As, film A1-type supercond. vapour-quenched transition temp., A7-type phase transition 78−52145
$AuGa_2$, magnetic susceptibility and Knight shift press. depend. 77−43777
Ba, A1-type quench-condensed, prep. and crit. temp. 77−69443
$BaPb_{1-x}Bi_xO_3$, RF sputtered, T_c as function of comp. and annealing conditions 79−24100
$BaPb_{1-x}Bi_xO_3$, superconducting thin films, RF sputtering prep. 80−76181
Bi, A1-type superconductor, critical mag. field 79−69638
Bi, amorphous, microbridge prep. and transition from superconducting to normal state 78−34933
Bi, amorphous, supercond. fluctuation effects in resist. transition 78−10609
Bi, amorphous film, temp. dependence of SAW attenuation 80−75679
Bi, amorphous films, supercond. fluctuation effects in perpendicular mag. fields 79−60980
Bi, film A1-type supercond. vapour-quenched transition temp., A7-type phase transition 78−52145
Bi, superconducting amorphous film, Kosterlitz-Thouless transition 80−88699
Bi, superconducting ultrathin film, metastable, supercond. props. *(Russian)* 79−7917
Bi superconduting film, critical temp., thermal equilibrium *(Russian)* 80−80438
Bi, ultrathin film, crit. mag. fields *(Russian)* 78−23214
Bi-Sb film, tunnel conductivity, proximity effect *(Russian)* 79−51726
Bi-Tl film, superconductivity and phonon spectrum *(Russian)* 79−91190
Cd-Mn, dil., lattice state effects on pair breaking 77−8219
Ce, A1-type quench-condensed, prep. and crit. temp. 77−69443
Cs, A1-type quench-condensed, prep. and crit. temp. 77−69443
$Cu_{2.5}Mo_6S_8$, evaporated two-phase, crit. current and scaling laws 78−91831
$Cu_xMo_6S_8$, Chevrel phase supercond. prep. and supercond. props. 79−28434
$Cu_xMo_6S_8$, Chevrel-phase sputtered film, supercond. critical currents 77−80892
$Cu_xMo_6S_8$, evap. film prep., supercond. props., lattice parameters 78−23195
$Cu_xMo_6S_8$, evaporated films, superconducting upper crit. fields, crit. currents 79−42714
$Cu_xMo_6S_8$, inhomogeneous superconductor, scaling laws for pinning forces 79−47214
$Cu_xMo_6S_8$, sputtered, supercond. crit. currents and scaling laws 78−47923
$Cu_xMo_6S_8$, superconducting reactively evaporated film, crit. currents 79−28492
$Cu_xMo_6S_8$, thin films, low temp. normal state, resist., temp. depend. 78−91783
$ErRh_4B_4$, film, sputter deposition and low temp. props. 80−2948
$ErRh_4B_4$, superconducting and mag. transitions, alpha particle irradiation damage effects 79−60954
$ErRh_4B_4$, superconducting thin films, critical mag. field 80−75693
Ga, amorphous thin films, supercond. surface resist. 77−72961
Ga film, crit. transverse mag. fields and transition temp. *(Russian)* 80−7048
Ga, films, distorted, crit. mag. fields *(Russian)* 78−39273
B-Ga, metastable, elec. props. in normal and supercond. states *(Russian)* 80−65520
Ga, supercond. thin film, tunnelling meas. in high mag. field 78−68120
Ga, T_c and residual resist., variation with coating thickness 78−47900
Ge, A1-type superconducting thin film, critical mag. field 78−31023
$Ge_{0.6}Cu_{0.2}Au_{0.2}$ film, superconducting transition temp., resistivity meas. 77−43774
GeTe, semicond., supercond. energy gap and crit. field, tunnelling meas. 77−24644
$HfGe_2$ film, supercond. obs. 77−72939
Hg films, superconducting, far-IR and electrodynamic props. meas. 80−103957

superconducting thin films continued
Hg-Xe film, random mixtures, superconducting transition temp. and metal-nonmetal transition 80−29498
Hg-Xe vapour deposited films, cond. transitions, effect of disorder on supercond. 80−88659
In, amorphization by ion implantation 78−52135
In, current-induced resistive state, fluctuations in flux nucleation process 79−38252
In, discontinuous film, DC resist. in normal and supercond. states 79−56357
In, divided superconducting thin film, superheating and supercooling field resistive meas. *(French)* 80−44751
In film, crit. current hysteresis prod. by electron overheating 79−56449
In, film, embedded with He particles, superconductor ion implantation study of inhomogeneities 78−52181
In, film, flux nucleation meas. in current induced resistive state 78−27002
In film, Josephson arrays, proximity effect junctions 80−84553
In film, metastable current states, mean free path variation *(Russian)* 80−2538
In film with dirty type II supercond. props., flux flow resistivity 77−51859
In films, crit. temp. enhancement *(Russian)* 80−93021
In films, supercond., sp. ht. discontinuity and transition temp. meas. 79−60969
In, He ion implantation effects on parallel crit. field, vortex state *(Russian)* 77−69459
In, metastable states supercond. parameters 78−47903
In, resistive transitions scaling behaviour 79−15248
In superconducting films, metastable states, supercooling fields 80−97031
In ultrathin films on TbTe and Te, prep. and characterisation 77−7995
In-Bi (2 at.%), thermal cond. in perpendicular mag. field 77−8229
In-Cr, electronic thermal cond., 1.5 to 3K 77−47934
In-Cr(Mn) films, supercond., sp. ht. discontinuity and transition temp. meas. 79−60969
In-Fe, Raman scatt. of light 79−73634
In-In_2O_3-Pb, Josephson tunnel junction fabrication for MM-wave detector 80−100427
In-Mn, dil., ion implanted, supercond. and mag. props. 77−15987
In-Mn, dil., supercond. film, H_{c2} meas., mag. impurity effects, pair breaking theory 79−42708
In-Pb-In thin film bridge, instability current enhancement in perpendicular mag. field 77−85396
In-Sn film, supercond. transition temp. and crit. currents *(Russian)* 77−55632
In_2Bi-In, thin lamellar eutectic strips, unidirectionally solidified, morphologic and crystallographic study *(French)* 77−55264
InSb, rapidly condensed film, metastable supercond. *(Russian)* 77−72937
In−Gd film, dil., fluctuation induced cond. above supercond. transition temp. 79−47196
Ir, superconducting film, props. 79−56444
La, A1-type quench-condensed, prep. and crit. temp. 77−69443
La, tunnelling investig., multiple band effects 77−8244
$La_{100-x}Au_x$, amorphous film, stability, supercond. temp. and residual resistivity 79−4636
$La_{1x}Au_x$, splat cooled amorphous alloy, sp. ht. 78−19182
$LaGe_2$ film, supercond. obs. 77−72939
$LaMo_6S_8$ thin films, crit. currents and pinning forces 80−34575
Mo superconducting film, amorphous and crystalline, transition temp. exam. by UPS 79−28433
Mo, T_c and residual resist., variation with coating thickness 78−47900
Mo:N, high T_c amorphous phase stabilisation by interstitial nitrogen 78−23622
Mo:N, implantation effect on supercond. and struct. transform. 77−4462
Mo-Ge(Bi) amorphous films, supercond. transition temp. and residual elec. resist. *(Russian)* 79−19680
Mo-Re, electron beam deposited, supercond. transition temp. conc. depend. 77−28279
Mo-Si(Ge)(Al), amorphous supercond. alloy, produced by coevaporation, struct. and supercond. 79−91179
Mo-Sn-Se system, supercond. crit. temp. and cryst. struct. *(Russian)* 80−107947
Mo_3Ge, RF sputtered, crit. temp. 78−14853
Mo_3Sn, thin films with A-15 struct., prep. 78−80478
Nb based A-15 type, universal defect behaviour, transition temp. rel. to lattice parameter 77−69440
Nb, critical mag. fields and currents, temp. depend. *(Russian)* 80−103798
Nb, deposited in quasi-closed vol., supercond. props. 79−91180
Nb, devitrified glass or ruby substrate, elec. props. 77−55635
Nb, electron beam evaporated film, struct., supercond., purity *(German)* 77−52253
Nb, far IR reflection and transmission spectra, room temp. 77−55792
Nb film, bias sputtering prep. 79−1826
Nb film, critical currents due to microwave field 80−25058
Nb, film, epitaxy, struct. and supercond. props., on (001) surface of fluorophlogopite *(Russian)* 80−80101
Nb, film microbridge, fabrication and I-V characts. 79−87198
Nb film sputtered onto Cu substrate, microstruct. and supercond. props. 77−85370
Nb films, ion beam sputtered, supercond., laser annealing effects 80−97024
Nb films, penetration depth measured with Nb-NbO_x-PbIn Josephson junctions 79−42691
Nb films, supercond. props. and electronic density of states *(Russian)* 79−28439
Nb granular films, ratio of supercond. transition temps. 80−84529
Nb granular films as weak link in Josephson devices 80−88685
Nb, granulated film, critical current temp. depend. *(Russian)* 80−103803
Nb heteroepitaxial layers on sapphire, residual mechanical stress and strain influence on superconductivity 80−15644
Nb, ion-implanted bridge with thick Pb banks, fabrication and characterisation of film parameters 80−100569
Nb layer, ion bombarded, supercond. props. and struct. 80−88671
Nb, magnetron-sputtered, intrinsic stresses and supercond. props. 80−24772
Nb, nanobridges Josephson effect, quasiparticle diffusion time, inelastic scatt. time 80−34556

superconducting thin films continued
Nb on thin Si membranes, super-Schottky and Josephson-effect devices 79−28469
Nb, props. control, bias sputtering model 78−72720
Nb, sputter deposited film, O contamination, Auger anal. 78−52669
Nb, struct. and electrophys. props. at 4.2K 80−80436
Nb, supercond. relax. phenomena at microwave freqs. *(Russian)* 79−47187
Nb superconducting amorphous film, conductivity and transition temp., ion bombardment effects *(Russian)* 80−49969
Nb, superconducting bridges by electron beam lithography and ion implantation Josephson effect 80−20355
Nb, superconducting film, thickness depend. of electrophys. parameter *(Russian)* 78−10590
Nb superconducting film prod. by electron beam sputtering *(Russian)* 78−15308
Nb superconducting films, crit. depairing currents, temp. and mag. field depend. 80−7058
Nb superconducting weak link, props. 79−38262
Nb, surface impedance 79−24110
Nb, switching, storage and erasure effects 77−8253
Nb, thin-film SQUID working at 4.2K, fabrication and characterisation 80−100570
Nb, transition temp. and crit. current, Gd ion implantation effects 77−39986
Nb, transition temp. and transition width, impurity effects *(Russian)* 77−66222
Nb, vacuum deposited, deposition parameter effects on crit. temp. 80−2514
Nb/Cu, layered ultrathin coherent structs., supercond. props. 80−84525
Nb-Al proximity sandwiches, supercond. transition temp. and tunnelling meas. 80−7045
Nb-Al-(Ge) film, depend. of supercond. props. on sputter deposition conditions and heat treatment 77−36399
Nb-Au film, in versatile multicontact switch 78−4661
Nb-Ge, A15 struct. superconductor, high field transport props. TEM study 80−34574
Nb-Ge, CVD and sputter deposited, critical current density and stability 77−28327
Nb-Ge, coevaporated, supercond. critical temp. and struct. 77−28275
Nb-Ge, compounds with A15 structure, films, TEM study *(French)* 80−80135
Nb-Ge, supercond. film, prep. and props. *(Russian)* 77−66218
Nb-Ge, TEM expts., correl. of struct. and elec. props. 78−14628
Nb-Ge, two-phase tetragonal Nb_5Ge_3 phase identification by electron diffr. 77−89665
Nb-Ge film, sputtered, high press. induced shifts in supercond. transition temp. 77−85374
Nb-Ge supercond. thin film characterisation by ion scatt., ion-induced X-rays, and ion resonance 77−40617
Nb-Ge superconducting film, prod. by electron beam sputtering *(Russian)* 78−15308
Nb-Ge vapour deposited films with T_c of ~20K, preps. *(Japanese)* 77−12048
Nb-Ge-Si, A15 struct. superconductor, high field transport props. TEM study 80−34574
Nb-Ge-Si, CVD, struct., comp., stability and homogeneity 80−15421
Nb-Ge-Si, compounds with A15 structure, films, TEM study *(French)* 80−80135
Nb-Ge-Sn A15 cpds., CVD, superconductivity 79−38222
Nb-Ge(Si), amorphous supercond. alloy, produced by coevaporation, struct. and supercond. 79−91179
Nb-N, superconducting layers, sputtering in high vacuum apparatus *(German)* 80−89147
Nb-N system, ion-implanted, supercond. crit. temp., effect of implantation conditions 78−19176
Nb-Nb_2O_5-Pb Josephson junction formed on Nb film edge 80−107960
Nb-NbO_x-Pb tunnel junctions at 4.2K, conductance of oxide barrier 80−7046
Nb-NbO_x-Sn long Josephson junctions, flux-flow voltage, dynamic vortex motion 79−4620
Nb-sapphire RF superconducting resonator, fabrication and props. 79−51704
Nb-Si, compounds with A15 structure, films, TEM study *(French)* 80−80135
Nb-Si compounds, CVD, struct. and supercond. props. 79−24447
Nb-Si film, superconductivity close to A15 stoichiometric phase 79−95540
Nb-Ti, film, composition determ. by ^3He elastic scatt. 78−76974
Nb-Ti films, ion beam sputtered, study by ^4He backscattering and nucl. reaction microanal. 79−42400
Nb-Zr sputtered films on Ta, struct. and supercond. props. *(Japanese)* 78−52138
Nb_3Al, complex refractive index meas. 80−93264
Nb_3Al film, electron-beam coevaporated, prep. and characts. 80−76187
$Nb_3Al_{1-x}Ge_x$, RF sputtering synthesis, supercond. transition temp. variation 77−81216
$Nb_3(AlSi)$, ternary supercond. alloy films, T_c, props. *(Russian)* 78−88055
$Nb_3(AlSi)$, thermomodulation spectra, 1.1-2.8 eV 78−48250
NbCN, high field critical current densities and resistive transition 79−61018
NbCN, preparation methods and supercond. properties *(French)* 79−73618
NbCn, high field critical current densities and resistive transition 79−73648
Nb_3Ga, critical data, under hydrostatic pressure to 15 kbar 79−47217
Nb_3Ga, RF sputtered, supercond. and struct. props. 77−28274
$Nb_3(Ge,Si)$ A15 film, supercond. and structural props. 79−87177
$Nb_3(Ge, X)$, X=Si, Ga, CVD tapes, supercond. props. at high mag. fields 79−38279
$NbGe_2$, sputtered, supercond. transition temp. meas. 80−7019
Nb_3Ge, amorphous film, supercond., flux flow resist., vortex pair dissoc. 80−88701
Nb_3Ge amorphous films, X-ray diffr. analysis of microstruct. 78−72035
Nb_3Ge, amorphous nongranular thin superconducting film, thermodynamic and resistive transitions 80−34571
Nb_3Ge, α-particle induced defects and stoichiometry 77−32101
Nb_3Ge, α-particle irrad., supercond. transition width 78−23193
Nb_3Ge, CVD deposited, second phase (tetragonal Nb_5Ge_3) rel. to critical current 77−32131

superconducting thin films continued
Nb_3Ge, CVD on inside of Cu tube, AC losses 77−28312
Nb_3Ge CVD tapes, supercond. props. at high mag. fields 79−38279
Nb_3Ge coevaporated film, high supercond. transition temp., nucleation and growth 80−76185
Nb_3Ge, critical current density and flux pinning 77−20510
Nb_3Ge, critical temp., resistivity, structure depend. on comp. 78−6470
Nb_3Ge, DC sputtered films, annealing and mech. deform. effects on struct. and supercond. props. 79−38217
Nb_3Ge, electron beam co-deposited, prep. and supercond. crit. temp. 78−15310
Nb_3Ge, electron beam codeposition in O_2, Cl_2, or air, phase diagram 77−28728
Nb_3Ge, energy gap from tunnelling meas. 80−25050
Nb_3Ge, epitaxial growth of polycryst. films with high supercond. transition temp. 77−63015
Nb_3Ge, far IR reflection and transmission spectra, room temp. 77−55792
Nb_3Ge film, CVD fabrication of supercond. tape for high-field magnets 78−95698
Nb_3Ge film, EXAFS meas. 78−2935
Nb_3Ge film, in supercond. proximity sandwich, energy gap struct., appl. to electron-phonon spectra 79−56401
Nb_3Ge film, low temp. sputter deposition 78−48315
Nb_3Ge film, prepared by cosputtering, supercond. props. 79−4634
Nb_3Ge film, supercond., epitaxial growth on Nb_3Ir and Nb_3Rh substrates 78−80473
Nb_3Ge film, superconducting, A-15 type, getter-sputtering with controlled additions of O 78−88427
Nb_3Ge film, superconductivity, relevance of mag. interactions, EPR study 80−100545
Nb_3Ge films, correl. between crit. current density and microstruct. 79−38277
Nb_3Ge films, form. of A15 phases by DC sputtering 79−38740
Nb_3Ge films, magnetron sputtered preps. and microstruct. 79−38276
Nb_3Ge films, prep. by DC sputtering and solid state diffusion, supercond. props. and struct. 79−38212
Nb_3Ge, growth by co-evaporation in O_2, critical temp. enhancement 77−28273
Nb_3Ge, high T_c film with impurity expanded lattice, form. and stabilisation 79−56099
Nb_3Ge, high T_c films, electron tunnelling and AES anal. 79−28471
Nb_3Ge, high T_c supercond., anal. of X-ray traces 79−56098
Nb_3Ge, high-temp. supercond. phase stabilisation w.r.t. prep. conditions *(Russian)* 80−70871
Nb_3Ge, Nb_5Ge_3 and NbO content, X-ray diffr. obs. 80−2515
Nb_3Ge, nucleation of high-T_c phase in presence of impurities 78−88054
Nb_3Ge, ordered and disordered A15 phases, energy gaps, tunnelling 77−8235
Nb_3Ge, prep. by chem. transport reaction, critical props. 79−47635
Nb_3Ge, projected critical current, comparison with $PbMo_6S_8$ 79−69642
Nb_3Ge, RF and DC sputtered films comparison, O content effect 78−72022
Nb_3Ge, RF sputtered film, high superconducting transition temp. 77−59346
Nb_3Ge, scaling laws for pinning forces 79−47214
Nb_3Ge, sputter-deposited, superconducting T_c and phase relationship 79−56344
Nb_3Ge, sputtered, chemical composition versus lattice parameter a_0 and supercond. transition temp. relations 77−43771
Nb_3Ge, sputtered, ion scatt., AES, depth profiling 77−11806
Nb_3Ge, sputtered and evaporated, transition temp., critical field and current anisotropy 77−28328
Nb_3Ge sputtered and evaporated, struct.-depend. anisotropy of supercond. crit. currents 79−38292
Nb_3Ge sputtered film, struct. and superconducting props. 77−28337
Nb_3Ge sputtered films, Ge surface segregation exam. by AES 79−56084
Nb_3Ge, sputtered on Cu, film-substrate interface obs. by electron microscopy 80−65398
Nb_3Ge, supercond., intercorrelations between composition, lattice parameter a_0 and T_c 77−8217
Nb_3Ge, supercond. film, amorphous content, X-ray diffr. study, rel. to transition temp. 80−75668
Nb_3Ge, supercond. film, CVD, crit. temp., crit. current density 78−76204
Nb_3Ge supercond. film, of high transition temp., US attenuation 80−49991
Nb_3Ge supercond. thin films, He- and Ar-irradiated, X-ray diffr. studies 80−29503
Nb_3Ge superconducting film preparation and props. 79−11515
Nb_3Ge superconducting films, role of O_2 in form. of struct. *(Russian)* 79−60950
Nb_3Ge superconducting film, crit. temp. correl. with resist. relations and film struct. *(Russian)* 80−15646
Nb_3Ge superconducting films, high critical temp., optimum sputtering conditions 80−15647
Nb_3Ge superconducting films, quantitative Auger anal. 80−55740
Nb_3Ge, TEM obs. of microstruct., foil prep. method 77−55642
Nb_3Ge tape, prep. by continuous CVD process 78−11121
Nb_3Ge tape conductors, strain depend. of crit. current density 79−38278
Nb_3Ge, tunnelling obs., X-ray and electron diffr. obs. 77−32123
Nb_3Ge:H film, sensitivity of supercond. transition temp. to H content 78−47894
$Nb_3Ge_{1-x}Ga_x$ CVD films, supercond. transition temp. depend. on lattice parameter 79−38219
$Nb_2Ge_{1-x}Ga_x(Sn_x)$ CVD films, supercond. props., 4.2 to 19K 79−42713
$Nb_3Ge(Sn)$, defect prod. under ^4He irrad., T_c var. 77−8220
$Nb_3Ge(Sn)$, electron irradiation at cryogenic temps., effect on T_c and transport props. 78−52122
Nb_3In, thin films with A-15 struct., prep. 78−80478
NbN, 2-dimens. supercond. phase transition, universal current scaling in crit. region 79−28429
NbN, critical data, under hydrostatic pressure to 15 kbar 79−47217
NbN film, supercond., upper crit. field 78−64172
NbN film, ultrathin granular, zero dimensionality and Josephson coupling 78−10612
NbN granular films, crit. current behaviour 80−15672
NbN granular films, supercond., crit. props. 80−88661
NbN granular films as weak link in Josephson devices 80−88685
NbN, granular thin film, phase transition between incoherent and coherent supercond. states 79−56394

superconducting thin films continued
NbN, granulated film, critical current temp. depend. *(Russian)* 80−103803
NbN, supercond. props., SQUID behaviour 78−72311
NbN superconducting reactively sputtered film, Auger anal. 78−72297
Nb_2N, supercond. props. and structural phase transform. induced by C^+ and N^+ implantation 80−107942
Nb_3Pb superconducting film, prep., vac. deposition 80−89149
$NbS_{1.6}Se_{0.4}$, layered supercond., fluctuation induced diamag. and dimensionality 77−77006
$NbSe_2$, layered supercond., fluctuation induced diamag. and dimensionality 77−77006
$NbSi_2$, sputtered, supercond. transition temp. meas. 80−7019
Nb_3Si epitaxial layers, ion implantation synthesis, supercond. transition temp. optimization 79−38218
Nb_3Si film, supercond., obtained by vaporisation in vacuum, props. 78−14865
Nb_3Si films, form. of A15 phases by DC sputtering 79−38740
Nb_3Si, high T_c supercond., anal. of X-ray traces 79−56098
Nb_3Si, supercond., A15 film, electron beam evaporation 80−29284
Nb_3Sn, AC losses, low field behaviour, morphology depend. 77−24655
Nb_3Sn, atomic displacements induced by radiation damage, X-ray study 80−2085
Nb_3Sn, α-particle induced defects and stoichiometry 77−32101
Nb_3Sn, critical data, under hydrostatic pressure to 15 kbar 79−47217
Nb_3Sn, delayed flux entry and surface barriers, tunnelling obs. 77−59355
Nb_3Sn, electron beam deposited, microstruct., rel. to supercond. props. 79−37935
Nb_3Sn, electron beam evaporation, growth morphology 77−44167
Nb_3Sn, energy gap from tunnelling meas. 80−25050
Nb_3Sn film, electron beam codeposited, growth morphology and tensile props. 78−10301
Nb_3Sn film, high T_c, high-rate magnetron sputtering, supercond. transition temp. meas. 77−43770
Nb_3Sn film contacts, quantum interference at H_2 temp. *(Russian)* 77−12041
Nb_3Sn film formation, solubility, precipitating processes *(Russian)* 80−92792
Nb_3Sn film on insulating substrate, crit. mag. fields *(Russian)* 79−11277
Nb_3Sn films, deposition by quasi-closed vol. method, supercond. crit. temp. 80−15645
Nb_3Sn, gap anisotropy, electron irrad. effect on transition temp. 78−10599
Nb_3Sn, growth by high-rate magnetron sputtering, transition temp. and crit. currents 77−28718
Nb_3Sn, high critical temperature and high sensitivity ratio on quartz 77−24502
Nb_3Sn, high-rate sputter-deposited, effect of oxygen on microstruct. 80−20343
Nb_3Sn multilayered supercond. power line conductors, elec. props. and growth morphology 77−28325
Nb_3Sn, O^{4+} bombarded, Mossbauer studies 80−2672
Nb_3Sn, on $LiNbO_3$ substrate, US attenuation of SAW in applied mag. field 80−75678
Nb_3Sn patterned film, appl. to refractory lift-off process using Nb-Cu bilayers 79−47626
Nb_3Sn SQUIDs for operation above 14.5K 77−66226
Nb_3Sn, supercond., thin film, US attenuation of SAWs 80−49988
Nb_3Sn, TEM microanalysis 80−104491
Nb_3Sn tape, diffusion process and chemical vapour deposition *(Croatian)* 77−28340
Nb_3Sn thin film bridges, AC Josephson effect 79−42702
Nb_3Sn, thin film weak-links SQUIDs, localised region radiation damage, fabrication and properties 78−47912
Nb_3Sn, vap. deposited supercond. film, effect of N_2 and tape heating 78−34939
Nb_3Sn, vapour deposited, supercond., surface resist. and penetration depth 79−33392
Nb_3Sn-Al_2O_3 composite, electron beam deposited, microstruct., rel. to supercond. props. 79−37935
Nb_3Sn-Cu superconducting composite, electron beam co-evaporated, TEM study 79−28247
Nb_3Sn_4 film, critical currents due to microwave field 80−25058
$Nb_3Sn(Ga)(Al)$, formation of supercond. phase by heat pulse action on quasiamorphous film 77−63017
$Nb_3Sn(Ge)$, resistivity and T_c measurement after low temp. neutron irradiation 78−52123
P quench-deposited A1-type films, superconducting props. 79−15264
Pb, amorphous, nucleated with Mo, supercond. and normal elec. cond. 77−24633
Pb anomalous temp. depend. of quasiparticle injection-induced voltage onset 78−56256
Pb, conducting coating effect on supercond. transition temp. and normal-state cond. 77−16007
Pb, current-induced flux motion, studied at 100 ns time resolution 79−47208
Pb, film, first order transition due to quasiparticle injection 78−23208
Pb film, monocryst., heteroepitaxial growth, struct. defects, and elec. props. *(Russian)* 80−84403
Pb film, near supercond. transition temp., Hall effect 79−42698
Pb, film, spatially inhomogeneous state appearance under laser pumping conditions 80−93053
Pb film, ultrathin quench-condensed, two-dimensional elec. cond., onset of supercond. 78−39233
Pb film tunnel junction, thermal cycling stability enhancement using substrate with large thermal expansion 79−87200
Pb, flux dynamics during current-induced breakdown magneto-optical flux detection 77−24646
Pb, flux nucleation in current-induced resistive state 78−23210
Pb granular film, Josephson coupled, resistive transition 80−88683
Pb, granular film, superconducting, Josephson-coupled, role of clusters in localisation 80−39716
Pb, hypersonic attenuation investig. of crit. field, intermediate state 77−8246
Pb, interaction between crystal lattice and vortices 77−28307
Pb, intermediate state, shadow electron microscopy 79−11276
Pb, intrinsic and expt. quasiparticle recomb. times 77−15999
Pb, narrow film strip, weak link induced by optical guided waves 78−14886

superconducting thin films continued
Pb on Cu and Ag substrates, tunnel conductivity, proximity effect *(Russian)* 79−51726
Pb, polycryst. or amorphous, thermal cond., 0.5-11K 78−39260
Pb, quantized resistances, RF fields effects 78−10604
Pb, quasiparticle and phonon lifetimes, tunnel junction meas. 77−20498
Pb, supercond., meas. of effective quasiparticle recombination times, density of electronic states at Fermi level 79−38264
Pb superconducting amorphous film, conductivity and transition temp., ion bombardment effects *(Russian)* 80−49969
Pb superconducting contact to p-InAs, characts. 79−38254
Pb superconducting film, nonequilib. gap instability and phase transition under intense tunnel injection 79−28476
Pb, superconducting film, radiation induced critical temp. 79−87179
Pb, superconducting thin film resonator, high-freq. characts. in mag. field *(Russian)* 78−31014
Pb, T_c and residual resist., variation with coating thickness 78−47900
Pb thin strips, supercond., optical wave illum., critical current behaviour 80−50012
Pb ultrathin films deposited on Si, transition temp. 77−66220
Pb ultrathin films on PbTe and Te, prep. and characterisation 77−7995
Pb:Au(In)(Bi), type II film, penetration depth meas. 77−28285
Pb/Bi-I-Al tunnel injected nonequilibrium supercond. struct., diffusive quasiparticle instability, multiple gap states 80−50005
Pb-Al_2O_3-Al tunnel junction, Pb supercond. film behaviour in mag. field 78−14894
Pb-Au (2.5 wt.%) film, In diffusion, alloy form. 78−22899
Pb-Bi film, amorphous and polycrystalline, specific heat meas. 77−80715
Pb-Cd, supercond. proximity effect, electron tunnelling study 78−10616
Pb-Cu contacts, proximity effect *(Russian)* 80−34558
Pb-Fe, supercond. films, modification of props. by Fe grains *(French)* 79−60957
Pb-Ga(Ge)(Si)(Mo)(Bi) amorphous films, supercond. transition temp. and residual elec. resist. *(Russian)* 79−19680
Pb-Ge thin film alloy, critical currents near metal-insulator transition 79−65626
Pb-In, supercond. surface sheath, dynamic pinning model of elec. dissipation 77−28320
Pb-In film, RF sputter anodisation, Josephson junction form., ellipsometry anal. 79−29258
Pb-In film, superconducting tunnel junction, pulsed quasiparticle injection 80−84565
Pb-In multilayered film, critical currents 79−61017
Pb-In-Au, penetration depth 78−72306
Pb-In-Au alloy, Josephson junction electrode materials, strain relax. 79−38255
Pb-M, M=Bi, La, Sm, vacuum deposited supercond. films, T_c chem. comp. depend. *(Russian)* 78−19174
Pb-Mn, dil., supercond. film, H_{c2} meas., mag. impurity effects, pair breaking theory 79−42708
Pb-PbO-Pb, Josephson tunnel junction fabrication for Mm-wave detector 80−100427
PbCu film, amorphous supercond., phonon heat transport, thermal cond. meas. 78−19181
$Pb_{0.9}Cu_{0.1}$, polycryst. or amorphous, thermal cond., 0.5-11K 78−39260
PbIn films, penetration depth measured with Nb-NbO_x-PbIn Josephson junctions 79−42691
$PbMo_6S_8$, inhomogeneous superconductor, scaling laws for pinning forces 79−47214
$PbMo_6S_8$, projected critical current, comparison with Nb_3Ge 79−69642
$PbMo_6S_8$, thin films, low temp. normal state, resist., temp. depend. 78−91783
$Pb_xMo_6S_8$, Chevrel phase supercond. prep. and supercond. props. 79−28434
Pd, confined geometry, p-wave supercond. or itinerant ferromag. 80−11129
Pd, irradiated film, supercond. 79−78249
$PdAl_xH_y$ films, ion implantation prop., supercond. crit. temp. 79−87182
PdH_x film, elec. resist. meas. 78−31011
$PdH_x(D_x)$ films, electron-phonon coupling, elec. cond. obs. 80−50011
$PdIn_xH_y$ films, ion implantation prop., supercond. crit. temp. 79−87182
Re, plasma deposited, from $Re_2(CO)_{10}$ vapour decomp. 80−20799
Re, T_c and residual resist., variation with coating thickness 78−47900
Re_3Ge_3, RF sputtered, crit. temp. 78−14853
S quench-deposited A1-type films, superconducting props. 79−15264
$(SN)_x$, discontinuous film, DC resist. in normal and supercond. states 79−56357
Sb, A1-type superconductor, critical mag. field 79−69638
Sb film A1-type supercond. vapour-quenched transition temp., A7-type phase transition 78−52145
Sb-Te, A1-type, superconductivity 80−29496
Se, A1 type, supercond. destruction by mag. field 78−91825
Se, A1 type metallic phase, optical consts. and refl. 77−32455
Si, A1-type superconducting film, critical mag. field 78−31023
Si-Au films, quenched condensed, elec. resist. and supercond. 80−54669
Sn, A1-type superconducting thin film, critical mag. field 78−31023
Sn bridge, obs. of operating conditions and shunting effects in small size supercond. 77−16005
Sn, crit. mag. fields, temp. depend., penetration depth thickness depend. 80−70908
Sn, critical heat flux in He-II 79−23795
Sn, cross-like film structures, microwave irrad. stimulated superconductivity and Josephson effect 79−60988
Sn, cylindrical and plane films, crit. current transverse distrib. 77−43795
Sn, electron mean free path depend. of crit. currents and pair-breaking limit 77−20504
Sn, energy gap reduction by quasiparticle injection 77−47941
Sn, energy gap suppression and instability under strong quasiparticle injection 80−7042
Sn, excess conductivity above supercond. transition temp. 77−32100
Sn film, crit. current hysteresis prod. by electron overheating 79−56449
Sn film, crit. temp. enhancement *(Russian)* 80−93021
Sn film, effect of rate of deposition on supercond. props. and struct. 80−2954
Sn film, HF pair-breaking current *(Russian)* 77−32130
Sn film, limitation in microwave stimulation of supercond., crit. current meas. *(Russian)* 80−88695
Sn film, metastable current states, mean free path variation *(Russian)* 80−2538
Sn film, metastable supercond. alloys, produced by low temp. ion implantation 80−88670
Sn film, substrate dependent excess electrical conductivity above superconducting transition temp. 78−84324
Sn, film, superconducting, current-voltage characts. in microwave field 79−69631
Sn, film, superconducting fluctuations, transition temp. *(Russian)* 80−65740
Sn, film, superconducting transition curve stepped struct. due to microwave radiation *(Russian)* 78−2610
Sn, film at supercond. transition temp. thermal noise fluctuations 78−47907
Sn films covered by Ge, effect on excess elec. cond. 80−65741
Sn, intrinsic and expt. quasiparticle recomb. times 77−15999
Sn, long, order parameter relax. during flow of crit. current 77−59364
Sn, long film, crit. currents in microwave EM fields 80−70898
Sn microstrip, optically illuminated, resistive transition and supercond. props. 80−54821
Sn, nonlinear conductivity of thin films in mixed state *(Russian)* 80−80464
Sn, paraconductivity 80−54845
Sn, phonon-injection-induced destruction of supercond. 80−6956
Sn ribbon, penetration depth of nonequilibrium elec. field, temp. depend. *(Russian)* 78−23202
Sn, spatially inhomogeneous state under tunnel injection conditions 80−80457
Sn, supercond., quasiparticle recomb. time and normal electronic density of states at Fermi surface from tunnel junction expts. 79−24108
Sn, supercond. film, resistance, effective medium approach 78−60249
Sn, superconducting current carrying film, resistive region boundary movement, ambient media depend. 80−44763
Sn, superconducting film, radiation induced critical temp. 79−87179
Sn superconducting thin-film bridge, IV curves oscill. instability and quasi-particle recomb. *(Russian)* 80−44769
Sn, surface, superconductivity suppression by microwave radiation *(Russian)* 79−24098
Sn, thermal processes in current-loaded *(Russian)* 77−55639
Sn, thin film, supercond., acoustic wave absorpt., quasiparticle distrib. 78−10603
Sn, thin layers, EM field penetration, depend. on temp. in mixed and intermediate states 79−65598
Sn thin strips, nonequilibrium resistive state, penetration depth meas. 79−56377
Sn thin-film superconducting bridge microwave impedance anomalies 79−7942
Sn-Cu film, metastable supercond. alloys produced by low temp. ion implantation 80−88670
Sn-In, nonlinear conductivity of thin films in mixed state *(Russian)* 80−80464
Sn-In multilayered film, critical currents 79−61017
Sn-Sb, A1-type, superconductivity 80−29496
Sn-SnO_x-Sn long Josephson junctions, flux-flow voltage, dynamic vortex motion 79−4620
$Sn_xMo_6S_8$ and $(Sn\text{-}Al)_xMo_6S_8$, Chevrel phase supercond. prep. and supercond. props. 79−28434
Ta film sputtered onto Cu substrate, microstruct. and supercond. props. 77−85370
$TaGe_2$, sputtered, supercond. transition temp. meas. 80−7019
TaN, prep., comp. anal., and supercond. T_c 79−15605
$TaSi_2$, sputtered, supercond. transition temp. meas. 80−7019
$TaS_2(pyridine)_{1/2}$ intercalated layered supercond., fluctuation induced diamag. and dimensionality 77−77006
Tc, electrodeposited, supercond. transition, AC susceptibility meas. 79−95539
Tc film, supercond. transition, complex susceptibility 80−29495
Te, A1 type, supercond. destruction by mag. field 78−91825
Te-Au, ion irrad. induced supercond. 80−34544
Te-Au film, metastable supercond. alloys, produced by low temp. ion implantation 80−88670
Te-I, A1-type, superconductivity 80−29496
TiN films, reactively RF sputtered, struct. and elec. props., substrate bias effects 80−96763
TiN, low-energy ion-stimulated deposited, supercond. props. 80−88664
TiN, VPE, and superconductivity *(German)* 77−24964
Tl films, supercond. amorphous, effective phonon spectrum and lattice sp. ht. 80−70895
$U_xPb_{1+x}Mo_{6+y}S_8$, sputtered supercond. props. 80−50019
V, amorphous film, supercond. props., gaseous impurities effect *(Russian)* 78−72301
V columnar films, crit. field anisotropy, depend. on prep. conditions *(Russian)* 80−93056
V, crit. temp., crit. field, resist. and struct. *(Russian)* 77−4475
V, determ. of energy gap, tunnel effect method 79−42704
V, evap. layer, ion bombardment effect on superconducting transition temp. 78−52136
V film, resist. supercond. transition 80−25033
V film, scaling behaviour of resistive supercond. transitions 79−56363
V, inhomogeneous, crit. field anisotropy 79−56459
V, resistive transitions *(Russian)* 79−95546
V, resistive transitions scaling behaviour 79−15248
V, superconducting tunnelling, meas. of annealing characteristics 79−7944
V, superconducting vacuum-deposited film, electrophys. props. *(Russian)* 77−59345
V-Al junction, spin-dependent electron tunnelling 79−19700
V-M, M=Ti, Nb, Sm, vacuum deposited supercond. films, T_c chem. comp. depend. *(Russian)* 78−19174
V-Si-C alloy, struct., crit. temp., resist. 78−72299
V-Ti superconducting film, electron spin effects 79−28488
V-Ti(Cr) amorphous films, supercond. transition temp. 79−60953
V_3Al, formation of supercond. phase by heat pulse action on quasiamorphous film 77−63017
V_3Ge, α-particle induced defects and stoichiometry 77−32101
$V_3Ge(Si)$, defect prod. under ^4He irrad., T_c var. 77−8220
V_3Si alloy, struct., crit. temp., resist. 78−72299
V_3Si, α-particle induced defects and stoichiometry 77−32101
V_3Si, complex refr. index and reflectivity of thin film, microscopic characts. and superconductivity 78−31267
V_3Si, energy gap from tunnelling meas. 80−25050
V_3Si, far IR reflection and transmission spectra, room temp. 77−55792
V_3Si film, optical props. *(Russian)* 80−93418

superconducting thin films continued
V_3Si film, sputtered, high press. induced shifts in supercond. transition temp. 77−85374
V_3Si film, superconducting props. 79−38215
V_3Si, formation of supercond. phase by heat pulse action on quasiamorphous film 77−63017
V_3Si, ion irradiated, influence on struct., resist., and supercond. transition temp. 80−54823
V_3Si superconductor film, Fourier and laser spectroscopy comparison in far IR-sub. mm. range 79−93237
V_3Si thin film far IR laser thermal spectroscopy 80−60144
V_3Si thin films, Holstein processes and electron-phonon spectral function, far IR meas., 19K 79−87445
V_3Si, thin films in supercond. and normal states, far IR laser spectroscopy 79−61453
V_3Si-SiO_x-Mo_3Re_2, supercond. tunnel junctions 80−107961
YGe_2 film, supercond. obs. 77−72939
$Y_xPb_{1\pm x}Mo_{6+y}S_8$, sputtered supercond. props. 80−50019
Zn film for energy selective phonon detection 80−92621
Zn, SAW US attenuation 79−73633
ZrGe, film, supercond. obs. 77−72939
$ZrGe_2$, RF sputtered, crit. temp. 78−14853

superconducting transition temperature
A15 binary alloys, supercond. transition temp., computer assisted estimate 79−38240
A15 compound, superconducting transition depend. on non-hydrostatic stress 80−107948
A15 compound trends, self consistent band calcs. 78−79925
A15 compounds, density of states broadening and its effect on T_c 79−65577
A15 compounds, disordered, reordering kinetics, recovery of supercond. transition temp. 80−96678
A15 compounds, high press.-high temp. treatment, phase props. 77−28746
A15 compounds, high supercond., T_c, attributed to linear chains or cubic symmetry 79−38221
A15 compounds, martensitic and supercond. transition models, anisotropy of vortices and US anomaly, review *(Japanese)* 78−23216
A15 compounds, max. T_c due to electron-photon scatt. 78−91801
A15 compounds, microscopic model of supercond. and martensitic transform. 77−8226
A15 compounds, mode softening and high supercond. crit. temp. 78−14851
A15 compounds, new aspect of superconductivity, Fermi level rel. to electron-phonon interaction 79−7927
A15 compounds, supercond. crit. temp. for model density of state using Eliashberg gap eqns. 80−93034
A15 compounds, T_c reduction due to defects, gap anisotropy mechanism 77−43773
A15 compounds, T_c related to residual resist. 79−15134
A15 films, electron beam codeposition, synthesis and props. 78−72296
A15 supercond. with defects 78−76183
A15 superconductors, radiation induced Tc, gap anisotropy effects 78−52125
A15 superconductors, supercond. and phonon softening in unstable systems 79−65587
A15 type compounds, A_3B type, supercond. transition temp.-solid solution range correlation 77−85373
A15 type compounds, supercond. T_c in terms of Debye temp. and effective and reduced ionisation pots. 79−28435
A15-phase superconductors, metallurgical possibilities of raising transition temp. *(German)* 77−69441
A15-type compounds, review of superconducting props. and structure 80−70909
A-15, A_3B type, cryst. chemical laws 78−34914
A-15 compound, defect influence on T_c 80−20345
A-15 compounds, disordered, resist. and supercond. transition temp. 80−107944
A-15 compounds, disordered, T_c depression, appl. to Nb_3Ge 80−7020
A-15 compounds, effect on critical temp. for supercond. of disorder, induced by α-particles 78−47897
A-15 compounds, radiation damaged, supercond. crit. temp. 78−76185
A-15 compounds, radiation induced damage, TEM and heat capacity meas. 79−56349
A-15 compounds, superconducting props. and structural transition *(Russian)* 77−12052
A-15 compounds, superconductivity 79−60947
A-15 diffusion layers, influence of additions of growth and supercond. props. *(German)* 80−11130
A-15 materials, effect of neutron irradiation 78−6472
A-15 structure alloys, influence of composition on supercond. transition temp. 77−20486
A-15 superconductors, transition temp., d band relative displacement *(Chinese)* 80−103770
A-15 superconductors with defects, transition temp. 78−14857
A-15 type compounds, relation between martensitic and supercond. phase transition 80−29497
alkali metal ternary chalcogenides, $M_{0.33}TaS_2$ and $M_{0.5}NbS_2$, supercond. props., alkali cation and topotactic solvation influences 79−87180
alkali metal tungsten bronzes, enhanced supercond. T_c, possible explanation 78−14850
alkali metal tungsten bronzes, superconductivity at press. up to 20 kbar 79−38226
alkali metals, heavy, supercond. and high temp. resist. at high press. 77−47917
alkali tungsten bronzes, dynamic fluctuations between local struct. states in supercond. TI phase 78−26981
alkali tungsten bronzes, struct. and supercond. 79−82703
alloy, effect of transition metal impurities, role of s-d Coulomb interaction 78−88061
alloy, theory of upper crit. field 77−63038
alloys, binary, supercond. transition temp. lowering by nonmagnetic impurities 80−100546
alloys, Kondo effect, specific heat jump at transition temp. 78−6479
alloys, nondiagonal disorder effects, appl. to V-Ta 79−73622
alloys and intermetallic cpds., metallurgical factors influencing T_c 79−38225
aluminides of non-magnetic transition metals, atomic volumes deviation from additivity 79−82178
amorphous alloys, liq.-quenched 79−38234

superconducting transition temperature continued
amorphous superconductor, Eliashberg function, tunnelling and crit. temp. anal. 80−80455
amorphous superconductor, ratio of energy to transition temp. 78−10619
Anderson impurity ordering, critical temp., Gor'kov eqn. calcs. *(Russian)* 80−65731
anisotropic superconductor, functional derivative of critical temp. with electron phonon spectral density 80−49971
anisotropic superconductors, nonmag. impurities effect on supercond. transition temp. 80−93035
anisotropic superconductors, upper critical field theory 80−75692
antiferromagnet to superconductor transition, model 79−82706
approximate T_c formula, Eliashberg eqn. *(Chinese)* 80−107941
BCS-superconductor with mag. impurities, transition temp. in spin fluctuation limit 77−32104
binary system, T_c-X state diagrams 78−31010
biological membranes as excitonic superconductors *(Russian)* 78−23190
bridge, inhomogeneous, in UHF field, superconducting transition *(Russian)* 79−19690
calculation, for very large electron-phonon coupling 79−73620
charge imbalance relaxation freq. depend. near T_c 80−93030
close packed compounds, superconducting T_c, heterogeneous hybridisation *(Chinese)* 80−107940
composite superconductor, granulated, superconducting transition, influence of particle size 79−69619
compound superconductors, radiation effects on critical currents 78−52175
contactless measurement method, high press. 78−23191
correlation with Hall coefficient sign 79−78247
critical dynamics far from equilibrium 80−27258
critical temp. and critical mag. field of superconductor *(German)* 78−84343
critical temp. correlation with electronic and phonon props. 79−69620
critical temperature depend. on radiation defects, electron density of states calcs. 80−44758
critical temperature mag. field depend., strong diamagnetism *(Russian)* 80−7022
cryostat for contact pot. difference changes meas. between metal and supercond. at transition temp. 77−22573
cryst. struct., supercond. T_c comp. depend. 78−51494
cybernetic prediction of supercond. cpds. 80−39697
definitions of terms for supercond. phenomenology, meas. practices 78−52117
determination, influence of effective phonon spectra 79−78252
dilute alloys, eqn. for crit. temp. 78−72300
dipstick cryostat, with temp. controller for high thermal stability 80−37044
dirty layer superconductors, fluctuation sound attenuation, depend. on critical temp. *(Russian)* 80−34553
dirty proximity-effect sandwich system, theoretical investigation of transition temp. 79−73638
dirty superconductors, time-depend. Ginzburg-Landau eqns. near supercond. transition temp. 80−70886
dislocation mobility, change at supercond. transition 77−15993
dislocation systems, superconducting states, impurity effects *(Russian)* 80−11131
dynamic instabilities in high T_c materials 78−10607
electric field penetration and collective oscillations, review 80−88678
electronic density of states, variation effect on transition temp. and effective mass 80−75672
electronic density of states depend. 78−76186
electronic structure of solids, appl. of fast self-consistent cluster calc. for large systems, transition temp. calc. 79−82513
Eliashberg eqn. soln. *(Chinese)* 78−26985
Eliashberg equation, solution at $T=T_c$ 78−34918
Eliashberg equation soln. for weak and strong electron-phonon coupling 77−39996
Eliashberg equation solution and series expression for T_c 78−31013
Eliashberg equations at zero and crit. temps. 78−34919
Eliashberg theory, strong-coupling superconductors 78−2614
energy dependent electronic density of states, gap and crit. temp. 80−84538
enhancement, role of locally nonequilib. energy distrib. of electronic excitations *(Russian)* 77−80863
excitonic insulator transition under press., calc. 79−4611
f-band metals, mode softening and lattice instability under press. 77−51833
fast neutron irradiation effects, comparison for C-15 Laves phase, A-15 and Chevrel phases 77−55633
ferromagnetic superconductor, new phase, crit. temp. and wave number determ. 79−82705
ferromagnetic superconductor, paramagnetic fluctuations, influence on superconductivity 80−70900
ferromagnets and spin glasses, supercond. and mag. order 80−93029
filament formation near edge dislocation *(Russian)* 79−4635
film, depend. of crit. conc. of paramag. impurities on mag. field 78−14863
film, enhancement 78−64161
film, Pauli paramagnetism and Fermi surface topology changes under press. 78−2612
film, sputtered, high press. induced shifts in supercond. transition temp. 77−85374
film, superconducting props. 79−38215
film, T_c increase due to size effect 78−88062
film, ultrathin, two-layer model 78−14849
film systems, metastable, high transition temps., survey *(Russian)* 78−19172
finite geometry, microscopic investigation of proximity effect 79−33402
functional derivative with electronic density of states, Eliashberg eqns. 79−56368
gap equation calc., theory of high T_c superconductors 79−65582
Ginzburg-Landau parameter crit. value 78−10597
Ginzburg-Landau theory, time depend., dissipative current carrying states in supercond. filaments 78−47906
granular, percolation model, specific heat, elec. resistance 80−93025
granular composite superconductors, Ginzburg-Landau theory, props. 80−88673
granular metal-semiconductor system, exciton enhancement of supercond. transition temp. 79−7921
granular superconductors, coherence transition, structural disorder effects 80−88657

superconducting transition temperature continued
granular superconductors, effect of charging energy on transition temp. 79−91181
granulated superconductors, phase transitions, Josephson energy *(Russian)* 80−84540
graphite, phonon thermal conductivity, rel. to elec. cond., possible supercond. 80−49434
graphite intercalation compound, $C_{8.8}K$, mag. susceptibility fluctuations near supercond. transition temp. 79−78259
graphite-K intercalation compound, effect of H addition on superconducting transition temp. 80−70872
heterogeneous superconductor, crit. temp. determ. *(Russian)* 77−76992
high Debye temperature material, theoretical upper limit of crit. temp. 80−60129
high performance wire development 77−20487
high T_c superconductivity, theory 78−14870
high transition temperature mechanisms *(German)* 78−68105
high-Tc superconductors role of quasilocal excitations 80−2508
high-temperature electron-hole supercond. 80−2512
high-temperature superconductivity non-specialist review 77−12070
increased, by adsorption of light metal atoms *(Russian)* 78−84337
inhomogeneous film, cond. near superconducting transition temp. 80−93031
intermetallic compounds, press. depend. of martensitic and supercond. transition temp. 79−19681
internal friction near crit. temp. at acoustic freqs. 80−100305
interstitial compounds, electronic structure and useful phys. props. 77−89683
ion-ion interaction in metals and intermetallic compounds, connection with supercond. transition temp. 78−47896
irradiated ordered materials, temp. variation of phase transition *(Russian)* 78−76181
isotope effect, theoretical anal. 78−91806
itinerant magnets and superconductors, structural instabilities, phase diagrams 78−14922
Josephson coupled layered supercond., upper critical field *(Russian)* 80 100551
Josephson FET, hybrid, feasibility 80−80451
Josephson tunnel junction parameters, microwave freq., temp. depend. 80−34561
Kondo alloys and supercond. proximity effect 78−19190
Kondo effect in supercond., transition temp. and upper crit. field 77−55634
Kondo superconductor, self-consistent theory of pairbreaking 78−26989
laser light scatt. spectroscopy, phase transitions 78−10156
lattice instabilities in non-A15 superconductors, struct. instability temp., 78−10591
lattice instability, high superconducting transition temp. 80−88663
layered compounds CDW instability rel. to supercond. T_c 78−14856
linear chain system, exciton model of supercond. 78−6476
local field effects, theory 78−14848
localised states, T_c enhancement, band struct., electron-phonon interaction 78−47902
lossless and dissipative current carrying states of quasi-one dimens. superconductor 77−32109
low-lying vibrational modes and theory of local and transport props. at transitions 78−14425
magnet training and degradation phenomena *(Slovak)* 79−6152
magnetic field, weak, meas. of absolute intensity, use of RF biased SQUID 80−82794
magnetic impurities in supercond. *(Hungarian)* 77−28277
magnetic impurity effect, case of high Kondo temp., Anderson model 77−63023
magnetic impurity low temp. behaviour, transition temp., specific heat, free energy 80−88691
magnetic properties of superconductors, effect of insulating pairing of electrons 80−15651
magnetically impure superconductors, finite relax. time at zero field transition point, exptl. obs. 78−23219
many-valley degenerate semiconds., supercond. transition temp. *(Russian)* 78−56254
materials for supercond. electronics 79−28470
melting of two-dimensional vortex lattices 80−2539
metal, flow stress relation with thermal conductivity discontinuity at supercond. transition 78−60246
metal, high resistivity, supercond. transition temp., influence of electron mean free path 79−82702
metal, supercond. as probe of mag. state of local moments 77−20491
metal, superconducting transition, effect of change of electrostatic interaction of defects 78−10610
metal and alloy softening at transition *(German)* 77−89898
metal film, effect of chemisorption on supercond. 80−39703
metal film, energy transport without loss *(German)* 79−60955
metal superconductivity, generalized jellium model, effect of ion core repulsion *(Russian)* 79−11260
metal-NH_3 mixture, attractive electron-electron interaction from molecular tunnelling mode, possible supercond. transition predicted 79−37793
metal-nonmetal film system, quantum oscills. in supercond. transition temp. *(Russian)* 77−32107
metal-semiconductor disordered interface, supercond. transition temp. enhancement by bipolaron interface centres 80−84528
metal-semiconductor interface, disordered, supercond. 80−20347
metallic elements and A-15 compounds *(Chinese)* 78−52116
metallic fine particles, anharmonic lattice vibr. theory, Einstein model appl. 78−18714
metallic glasses, electronic structure rel. to elec. cond., supercond. and mag. props. 80−65429
metallic glasses, mats. props. review 77−4043
metallic glasses, structure and properties, review 78−47245
metallic thin film, superconducting state realisation 80−49977
metallic ultrathin filaments, dielectric and superconducting fluctuations, Peierls transition *(Russian)* 80−65742
metals, simple, binding energy, compressibility, interionic pot. and transition temp. using pseudopot. method 79−46598
metals, simple, model pot. calc. 79−99650
metals, triplet supercond. transition in strong mag. field 80−25040
metals with $Z \leq 49$, using self-consistent potentials 77−66221
metastable compound synthesis with high supercond. transition temp. 80−93024
micropower-induced enhancement *(Russian)* 80−93023
superconducting transition temperature continued
microscopic theory of supercond., nonequilibrium and high T_c supercond. 79−65591
mode propagation in superconductors near T_c 79−19682
molybdenum chalcogenides, multicomponent, physical props. 80−84577
molybdenum chalcogenides, supercond., prop. preparation and struct. *(French)* 79−73619
molybdenum ternary chalcogenides, structures and properties survey *(Czech)* 80−70870
Mossbauer isomer shift at phase transitions, book contrib. 79−87352
multiband system, electron pairing, radiation effect 80−88679
multivalley semiconductors, supercond., crit. temp. effects 79−1638
neutron irrad., elec. resist., temp. depend. 79−91024
neutron irrad. effects on transition temp. *(Japanese)* 79−82707
neutron irradiation effects 78−52121
NMR and US absorpt. of superconductor with struct. transform. *(Russian)* 79−95544
noble metal alloys, superconductivity, correlations and predictions 78−23192
non-transition elements and alloys, supercond. transition temp., Hall const. correl. 79−47186
nonequilibrium superconductors, phase transitions, theory allowing for phonon reabsorption 78−68107
nuclear magnetic relaxation rate, in superconducting state *(Rumanian)* 78−60247
nuclear spin relaxation rate fluctuation growth, mag. field effect 78−10606
one-dimensional systems, impurity effects on ordered phases 80−24905
order parameter, rel. to macrowave function, near T_c 79−47191
order parameter spatial variations near Anderson impurity with high Kondo temp. 79−38245
paramagnetic limit, Fermi surface dielectric gap *(Russian)* 80−2533
periodic lattice, theory of coexistence of supercond. and magnetism, supercond. transition temp. 80−34543
perturbative corrections, direct and indirect ladder diagrams 80−49979
phonon spectrum, generalised moments, in Allen-Dynes formula for crit. temp. *(French)* 80−39702
phonon spectrum effect on critical temp. at type 5/2 phase transition 79−28437
phonon spectrum influence on T_c of superconductors *(Chinese)* 79−51707
polysulphur nitride, low temp. thermal cond. 80−24689
polysulphur nitride, temp. depend. and anisotropy of H_{c2} 80−25054
porous glass:In, effect of press. on transition temp. 80−97027
pressure dependence effect of $2^1/_2$-order transitions and Kohn discontinuities *(Russian)* 77−47914
properties of selected superconductive materials 79−56366
pseudopotential, Bragg planes, effect on superconducting pairing and crit. temp. 80−15648
quasi one-dimensional metal, crit. temp. for phase transition *(Russian)* 79−78253
quasi-one dimensional metals, transition temp., tunnelling amp. depend. 79−42683
quasi-one-dimensional conductor, Peierls instability and superconductivity, possibility of coexistence 78−31028
quasi-one-dimensional conductors, impurity effect on phase transitions 78−6297
quasi-one-dimensional superconductor, critical mag. field, transition temp. *(Russian)* 80−93058
quasi-two-dimensional superconductivity in quantising mag. field *(Russian)* 77−40001
quench-condensed films, superconducting transition temp., elastic stress and strain effects 80−70883
rare earth alloys with Cu_3Au lattice, cryst. chemistry and supercond. crit. temp. 79−86744
rare earth compounds, phenomenological study of supercond. 78−43512
rare earth compounds, $R(Rh_{0.85}Ru_{0.15})_4B_4$, mag. ordering and supercond. 78−14861
rare earth compounds, RMo_6X_8, X=S,Se, coexistence of supercond. and antiferromag. order 79−65579
rare earth compounds, RRh_4B_4, coexistence of supercond. and ferromag. order 79−65579
rare earth compounds, ternary, superconductivity and ferromagnetism 79−69617
rare earth cpds., $RMo_6S_8(Se_8)$ and RRh_4B_4, coexistence of supercond. and mag. ordering *(Russian)* 80−84542
rare earth cpds., RRh_4B_4 and RMo_6X_8 (X=S, Se), mag. order and supercond., neutron scatt. studies 80−44807
rare earth iridium borides, RIr_4B_4, supercond., magnetism and metastability 80−29501
rare earth iron silicides, $R_2Fe_3Si_5$, superconductivity 80−49968
rare earth lead molybdenum sulphides, $R_xPb_{1\pm x}Mo_{6+y}S_8$, R=La, Nd, Pr, Gd, sputtered, supercond. props. 80−50019
rare earth metal compounds, high temp. paramagnetic-supercond. phase transitions, mag. cell symm. *(Russian)* 79−78255
rare earth metal compounds, phase stratification in superconductors *(Russian)* 79−42685
rare earth molybdenum chalcogenides, Chevrel phase correlation between struct. and supercond. transition temp. 80−7023
rare earth molybdenum sulphides, $R_{1.2}Mo_6S_8$, low temp. magnetisation meas., and supercond. props. 79−8018
rare earth rhodium borides, RRh_4B_4, NMR and sp. ht. in supercond. and mag. ordered phases 80−7037
rare earth system, superconductivity, review 79−69621
rare earth ternary borides, RRh_4B_4, ferromag. Curie Temp., high supercond. transition temp. 77−89893
rare earth ternary borides, RRh_4B_4, supercond., re-entrant magnetism, energy band calcs. 78−52140
rare earth ternary compounds, coexistence of superconductivity and long-range magnetic order 79−11264
renormalisation group recursion relations involving dynamics, in mag. field 80−60137
resistive state, phase-slip centres, current-voltage characts. *(Russian)* 80−80437
review and table of props. 77−4460
review of calc. techniques, BCS theory and phonon spectra *(Spanish)* 80−84535
review of superconducting critical temps. theory *(Chinese)* 79−38241
rigorous formula *(Chinese)* 78−26986
second order phase transitions, superspace group description *(Chinese)* 80−8942

superconducting transition temperature continued
semimetal, mixed superconducting-excitonic insulator phase, diamagnetism, virtual intraband transitions 80−2520
semimetallic system, critical temp. depend. on band gap for dielectric-supercond. transition *(Russian)* 79−65578
series expression, convergence region *(Chinese)* 78−52115
series expression convergence 78−80090
series formula of supercond. critical temp. applications *(Chinese)* 80−54816
slightly dirty superconductors, EPR relaxation time, thermal behaviour 79−47195
solders, transition temp. determ. 77−28281
solid solution disordered alloy, conc. depend. of superconducting transition temp. *(Russian)* 79−28427
standard measurement techniques for determ. of supercond. props. 79−69622
standards for practical superconductors, development 79−33442
strong coupling supercond., transition temp. eqn. 80−25032
strong coupling superconductors, critical temperature formula discussion *(Chinese)* 80−7017
strong-coupling superconductors, press. coeffs. of critical field, Ginzburg-Landau parameter, penetration depth 80−54833
student experiment 77−24632
superconducting thin hollow cylinder, mag. field penetration, Ginzburg-Landau calcs. *(Russian)* 80−75674
superconducting-normal-metal infinite geometry, extrapolation length near T_c 79−82723
superconductivity and magnetism *(Hungarian)* 79−47226
superconductivity proximity effect, McMillan tunnelling model 79−73639
superconductivity-ferromagnetism coexistence, transition temp., magnon freq., indirect exchange 80−44757
superconductivity-ferromagnetism coexistence in two-band model *(Russian)* 80−84539
synthesis from thermalised sputtering and changes in Tc and depend. of H_{c2} on temp. 79−56350
technical superconductor radiation damage obs. 79−33422
temperature fixed point device, prep. and calibration 80−82770
temperature fixed point device for temps. above 0.5K 79−63221
temperature fixed point device to provide reference temps. below 0.5K 79−63220
ternary compounds, supercond., p-state pairing and magnetism 80−54819
ternary superconductor, mag. interactions 79−73613
Th, calc. using cluster approach 79−7928
theory, series formula *(Chinese)* 79−91177
theory, soln. of series expression for T_c and its radius of convergence 79−78251
thermometer referenced by superconducting to normal transition point *(Japanese)* 80−77785
tilted vortices, mixed state features in surface layers *(Russian)* 80−29512
$(TMTSF)_2PF_6$, one dimens. conductor, superconds., resist. meas. and mag. field effects *(French)* 80−44753
$(TMTSF)_2PF_6$, organic one-dimensional superconductor, transition temp. 80−44754
transition element cpds. and their dil. alloys, supercond. crit. temp., s-d Coulomb interaction 78−31012
transition metal alloy, binary, conc., superconductivity and electron-phonon interactions, theory 78−14868
transition metal alloys, amorphous, reduced supercond. transition temps. 77−39991
transition metal alloys, deformation and solute-induced microstructural effects on superconductivity 79−7925
transition metal binary alloy, amorphous and crystalline, superconducting transition temp. correlation with solute conc. 78−52139
transition metal carbides, influence of implanted ions on supercond. transition temp. 77−28276
transition metal chalcogenides, quasi-one-dimens., elec. mag., and supercond. props., review *(Russian)* 80−93022
transition metal compounds, electronically driven lattice instabilities, role of p-d hybridisation 79−7669
transition metal compounds, reduced ionisation potentials as parameters in superconducting transition temp. calcs. 80−75671
transition metal dihydrides, band struct. and electronic props., electron-phonon coupling 79−47011
transition metal glasses and amorphous films, supercond. and electronic props. 79−73612
transition metal hydrides, electron-phonon interaction const. calc. 79−65160
transition metal hydrides, isotope effects on supercond. props. 79−65580
transition metal sulphides, selenides and phosphides, NaCl struct., supercond. props. 79−4613
transition metal superconductors, specific heat anharmonic components, phonon freq. temp. shift *(Russian)* 79−91183
transition metal-Ge, RF cosputtered system, supercond. props. 77−51835
transition metal-metalloid glasses, struct., elec., supercond., and mech. props. 80−6365
transition metals, amorphous, superconducting transition temp. *(Chinese)* 80−54817
transition metals, and their carbides high temp. superconductivity and phonon softening 78−14848
transition metals, BCC, supercond transition temp. and press effects 77−4461
transition metals, Cauchy discrepancy with supercond. transition temp. 80−84533
transition metals, influence of implanted ions on supercond. transition temp. 77−28276
transition metals, resistivity and superconductivity 79−51550
transition metals, supercond., effect of s-, d-electron hybridisation *(Russian)* 78−39243
transition metals, supercond. transition temp., ab initio calc. 80−25036
transition metals and alloys, BCC, T_c related to residual resist. 79−15134
transition metals silicides, atomic volume deviations and supercond. T_c 80−75203
transport current effects on superconducting thin-walled cylinder in mag. field *(Russian)* 80−100573
tungsten bronzes, hexagonal, supercond. and special phonons, neutron scatt. obs. 80−15643
tunnelling experiments, supercond. crit. temp. calc. 78−60241

superconducting transition temperature continued
two-band superconductor with nonmagnetic impurities, transition temp. 78−2607
two-band systems, BCS pairing and Peierls distortion compatibility 78−88068
two-dimensional fluctuation-induced cond. above crit. temp. 78−10608
two-dimensional superconductor, resistivity evidence in Monte Carlo studies 80−80434
two-fluid model, electron distrib., energy spectra *(Russian)* 79−15252
type I and II superconductors, influence of effective phonon spectrum on T_c *(Chinese)* 79−51705
type I and II superconductors, T_c and penetration depth *(Chinese)* 79−51706
type I superconductor, mag. dipole effect on order parameter *(French)* 77−89899
type I superconductors, approximate T_c formula, Eliashberg eqn. calcs. *(Chinese)* 80−88662
type II materials, radiation-induced changes in crit. props., radiation defects *(Russian)* 80−25027
type II superconductor, A15 struct., electronic density of states and T_c changes with atomic ordering 78−91800
type II superconductor, dielastic, interaction of flux line lattice with internal stresses of cryst. imperfections 78−14906
type II superconductor, neutron irradiation effects *(Rumanian)* 78−52144
type II superconductors, high field expts. on press. effects up to 15 kbar 79−61006
ultra-thin films, transition temp., interface and fluctuation phenomena 80−84527
volume dependence, dielectric screening functions effect, appl. to Pb and Al 77−4471
α-AG-Ge(Al), T_c depend. on electron per atom ratio, lattice deform. 77−8222
Ag-In (Sn) multilayers, vapour quenched, supercond. transition temp. 80−20346
Ag-Nb-Ga, phase relations, A15 phase diffusion layer formation 78−52764
$Ag_xMo_3S_4$, chevrel phase, charge transfer and valence electron conc. 78−6029
$Ag_{1-x}Sn_{1+x}Se_{2-y}$, supercond. and normal state props. 77−36008
Al bridges, nonequilibrium phenomena under microwave radiation 79−56420
Al, defect structure depend. on Ga and Ca implanted ions 80−59494
Al, electron-phonon interaction press. depend., rel. to supercond. transition temp. 79−95106
Al, energy gap enhancment by tunnelling extraction 80−34564
Al film, crit. temp. enhancement *(Russian)* 80−93021
Al film, deviations of equilib. order parameter from mean field theory 77−69453
Al film, fine particles, supercond. transition temp. meas. 77−12044
Al film, getter sputtered at low temp. 78−35305
Al, film, granular, transition to localisation, elec. resist. 80−70877
Al film, implanted at low temp. by H or D, critical temp. enhancement *(French)* 77−8237
Al film, quasiparticle branch mixing rates 79−78269
Al, film, superconducting transition temp. and lattice dynamics 80−93028
Al film strips, radiation stimulated supercond. 77−28298
Al films, Al^{2+} irrad., increase of resist. and supercond. transition temp. 80−7027
Al films, microwave induced supercond. above crit. temp. 79−56364
Al granular films, inhomogeneous supercond. transitions, microwave meas. 80−103789
Al granular films, self-ion implantation, supercond. transition temp. enhancement 80−103774
Al granular films, vortex noise at supercond. transition 80−84530
Al, narrow superconducting bridges, microwave radiation stimulated T_c enhancement 80−84537
Al, nonlinear sound wave interactions, sound attenuation in weak superconducting state *(Russian)* 80−75310
Al strips, microwave-enhanced supercond. meas. 80−2509
Al, supercond., appl. of non-local extension to Gaspari-Gyorffy theory 78−80093
Al superconducting film, granular, O content and oxide barrier thickness, transition temp. meas. 79−15250
Al, superconducting order parameter relax. time, temp. depend. 77−77011
Al, superconducting transition temp., electron-phonon mass enhancement, pseudopot. calcs. 78−2604
Al, superconducting transition, effect on jump-like deform. *(Russian)* 80−34538
Al thin films, dielectric coating effect on superconductivity 80−7026
Al/Ge multilayered superconducting films, crit. fields and crit. temps. 79−7945
Al-3d transition metal, dil., transport props., sp. ht. and supercond. ant. temp. calcs. 77−1393
Al-C(Si)(Ge) film, ion-implanted, enhancement of supercond. transition temp. 77−32103
Al-Ce, very dil., low temp. sp. ht. 79−51745
Al-Cu, dil. alloy, quench condensed thin films, supercond. and struct. from electron diffr. patterns 78−47901
Al-Cu, superconducting amorphous films of high stability 80−70889
Al-formvar-Sn junction, supercond. order parameter fluctuations below T_c 77−66227
Al-Ge, film, double supercond. transition in resistance-temperature and current-voltage characts., percolation theory 79−56365
Al-Si(Ge) film, ion-implanted, percolation and superconductivity 78−26982
$Al_{10}V$, supercond. transition temp. determ., localised phonon modes 77−63016
Am, discovery of superconductivity up to 0.79K 79−11262
As, electrical resistivity meas., 50 mK-7K 79−60839
As, film A1-type supercond. vapour-quenched transition temp., A7-type phase transition 78−52145
As_2Te_3, amorphous, press.-induced semicond.-metal and supercond. transitions 77−43671
Au, pure, supercond. transition temperature estimated 78−43358
Au/In proximity effect bridges, square arrays, transition temps. 80−84557
Au-Al-In solid soln., elastic strain energy depend. of supercond. T_c 79−38229

superconducting transition temperature continued
Au-Ga, resist. and supercond. meas., electron-phonon interaction and Coulomb pseudopot. determ. 78−43358
Au-Ga-In solid soln., elastic strain energy depend. of supercond. T_c 79−38229
α-Au-Ge(Zn), T_c depend. on electron per atom ratio, lattice deform. 77−8222
AuGa, and $AuGa_2$, supercond. transition temp. and crit. field 79−38232
$AuGa_2$, press. depend., theor. *(Russian)* 77−51843
$AuGa_2$ type supercond., mag. impurity and press. effect on crit. temp. *(Russian)* 78−23189
$(Au_{1-x}Pd_x)Ga_2$, supercond. transition temp. and crit. field 79−38232
Ba, BCC, superconductivity under press. 78−14858
Ba film, A1-type quench-condensed, prep. and crit. temp. 77−69443
Ba, superconductivity, pressure dependence, ion core 78−91805
$BaGe_2$, superconducting temperature depression due to mag. field 80−54820
$BaPb_{1-x}B_xO_3$, critical temp. depend. on band gap for dielectric-supercond. transition *(Russian)* 79−65578
$BaPb_{1-x}Bi_xO_3$ film, RF sputtered, T_c as function of comp. and annealing conditions 79−24100
$BaPb_{1-x}Bi_xO_3$, semiconductor-metal transition and supercond., IR absorpt. and struct. meas. 77−28278
$BaPb_{1-x}Bi_xO_3$, supercond. T_c and crit. fields, comp. depend. 79−73623
$BaPb_{1-x}Bi_xO_3$, superconducting thin films, RF sputtering prep. 80−76181
$BaPb_{1-x}Bi_xO_3$, superconducting props., Hall coeff. and elec. resist. meas. 80−84531
$Ba_{0.67}Pt_3B_2$, cryst. struct. and supercond. props. 79−38231
$Ba_{1-x}Sr_xPb_{0.75}Bi_{0.25}O_3$, superconductivity, rel. to lattice const. 80−49966
Be alloys, enhancement of supercond. transition temp. 80−60129
Be film, vapour quneched, mech. stresses and elec. cond., supercond. transition temp. 79−73414
Be-Nb-Zr alloys, glassy and partially crystalline 78−60239
Be-Zr alloy, glassy, quenched from melt, supercond. props. 78−26983
Bi, amorphous, microbridge prep. and transition from superconducting to normal state 78−34933
Bi, amorphous film, supercond. fluctuation effects in resist. transition 78−10609
Bi, band structure model 80−25034
Bi, film A1-type supercond. vapour-quenched transition temp., A7-type phase transition 78−52145
Bi, lightly doped, superconductivity, resist. obs. 78−64160
Bi, superconducting amorphous film, Kosterlitz-Thouless transition 80−88699
Bi, superconducting modification obtained by impact compression *(Russian)* 80−93020
Bi, superconducting ultrathin film, metastable, supercond. props. *(Russian)* 79−7917
Bi superconduting film, critical temp., thermal equilibrium *(Russian)* 80−80438
Bi-Pb alloy, effects of press. up to 30 kbar *(Russian)* 77−20484
$Bi_{1-x}Sb_x$, press. depend., 30-80 kbar 77−8223
$Bi_3Sr_{1-x}Eu_x$, supercond. and mag. ordering 78−56252
C films with high conductivity, prep. and props. 80−80983
C_8K, intercalation compound, superconductivity 78−91827
C_8K, intercalation cpd. with graphite, supercond. props. 80−44755
$Ca_{0.67}Pt_3B_2$, cryst. struct. and supercond. props. 79−38231
Cd, electronic properties depend. on $2^1/_2$-th order phase transition under high press. *(Russian)* 80−11128
Cd whisker, stress depend. 77−39989
Cd-Cr, dil., estimates of s-d interaction from supercond. transition temp. and mag. susceptibility 78−43561
Cd-Cr(Mn)(Ni), dil., mag. and supercond. props. 79−38237
Cd-Mn, dil., lattice state effects on pair breaking 77−8219
Cd-Sn alloy, superconductivity and microstructure 80−107949
CdS-In, photosensitive granular superconductor 79−78246
Ce film, A1-type quench-condensed, prep. and crit. temp. 77−69443
Ce, high press. superconductivity, phonon softening 78−14852
$CeCu_2Si_2$, strong Pauli paramagnetism, superconductivity obs. 80−29499
$Ce_{1-x}Gd_xRu_2$, superconductivity and ferromagnetism coexistence, 60 mK-4.2K, spin echo NMR 78−84349
$Ce_{0.73}Ho_{0.27}Ru_2$:Co, spontaneous mag. order below superconducting transition temp., Mossbauer study 80−39701
$CeRu_2$, change of valence of Ce ions, induced by H absorption, supercond. disappearance 79−47185
$CeRu_2$, H absorption induced Ce valence change, mag. and supercond. props. 80−50042
$Co_2Mo_6S_6O_2$, O-containing Chevrel phases, synthesis and props. 80−108368
Cr film, vacuum-evaporated, with A-15 struct., absence of superconductivity 77−62768
Cs film, A1-type quench-condensed, prep. and crit. temp. 77−69443
Cs, supercond., elec. resist. and phase transforms. under high press. *(German)* 80−107763
Cs_xWO_3, normal phase and supercond. props 80−25035
Cu alloy-Nb composite wires, resist.-temp. meas., percolation theory 79−28490
Cu-Ga porous solid formed by shock compression 80−29905
Cu-Nb, supercond. wire, directional solidification of melts, supercond. ionisation temp. *(Russian)* 78−76596
Cu-Nb (0,4 at.%), splat quenched, aged, superconductivity *(Japanese)* 77−63018
Cu-Nb_3Sn, in situ formed multifilamentary composite, supercond. and mech. props. 78−39279
Cu-Nb-Sn dil. alloys containing Nb_3Sn precipitates, superconductivity 78−43507
Cu-Nb-Sn system, phase equilibria and supercond. props. *(Russian)* 80−50589
α-Cu-Si(Ge), T_c depend. on electron per atom ratio, lattice deform. 77−8222
Cu-V-Ga dil. alloys with V_3Ga particles, supercond. props. and microstruct. 78−39278
Cu-V-Si, supercond. props. 80−107945
Cu-V-Si, two-step supercond. transition 80−34539
CuCl, high-temp. supercond., BCS strong-coupling limit for transition temp. 80−2511
CuCl, pressure depend. of structural, chemical, elec. and mag. props. 80−96596
Cu_xLa_{1-x}, splat-cooled, phase diagram and supercond. props. 80−70881
superconducting transition temperature continued
$Cu_2Mo_6S_8$, normal state and superconducting property measurements 78−91660
$Cu_2Mo_6S_8$, phonon density of states, mode softening correl. with supercond. transition temp. 79−51714
$Cu_xMo_3S_4$, chevrel phase, charge transfer and valence electron conc. 78−6029
$Cu_xMo_3S_4$, superconductivity, lattice transforms., electronic instabilities 77−39990
$Cu_xMo_3S_4$, superconductivity and cryst. struct. 79−78250
$Cu_xMo_6S_8$, $1.5 \leq x \leq 3.55$, low temp. phase diagram, 1.2-320K 77−85371
$Cu_xMo_6S_8$, Chevrel phase supercond. prep. and supercond. props. 79−28434
$Cu_xMo_6S_8$, evap. film prep., supercond. props., lattice parameters 78−23195
$Cu_xMo_6S_8$, prep. by topotactic electrode reactions, struct., supercond. 79−99158
$Cu_xMo_6S_6I_2$, x=0 to 1.2, superconducting Chevrel-phase system, synthesis and transition temps. 79−69618
$Cu_2Mo_6S_6O_2$, O-containing Chevrel phases, synthesis and props. 80−108368
$Cu_xMo_6S_8(Se_8)$, prep., metallurgical and supercond. props. 77−32102
$Cu_{0.7}Mo_3Se_4$, Chevrel-phase, low temp. struct. instability rel. to supercond. 77−47919
$CuRhS_4(Se_4)$, press. depend. of supercond. transition temp. meas. 77−12050
Cu(Sn)/Nb(Al), composite superconductor fabrication and charact. 77−81242
$Cu_{40}Zr_{60}$, amorphous alloys, supercond. transition temp., press. depend. 80−84524
$Dy_xCe_{1-x}Ru_2$, supercond., mag. props. 79−11267
$Er_{1-x}Gd_xRh_4B_4$, supercond. and mag. transitions at press. up to 19 kbar 79−38236
$Er_{1-x}Ho_xRh_4B_4$, ferromagnet, sp. ht anomaly at lower superconducting transition temp. 79−47194
$Er_{1-x}Ho_xRh_4B_4$, mag. and supercond. transitions, cryst. field effects 80−107950
$Er_{1-x}Ho_xRh_4B_4$, re-entrant supercond. and mag. ordering 78−60240
$(Er_{1-x}Ho_x)Rh_4B_4$, superconductive and mag. interactions, hydrostatic press. effect 80−49973
$Er_xMo_6Se_8$, long-range antiferromag. order and supercond. coexistence 78−10715
$ErRh_4B_4$, ferromag. superconductor, vortex phase 80−80441
$ErRh_4B_4$, film, sputter deposition and low temp. props. 80−2948
$ErRh_4B_4$, supercond., thermal cond. between 0.05 and 4K 79−60967
$ErRh_4B_4$, supercond. transition temp., upper critical field, local spin fluctuations 79−38250
$ErRh_4B_4$, superconductivity destruction at onset of long-range mag. order 77−76994
$ErRh_4B_4$, superconducting and mag. transitions, alpha particle irradiation damage effects 79−60954
$ErRh_4B_4$, superconducting thin films, critical mag. field 80−75693
$Er_{1-x}Tm_xRh_4B_4$, mag. and supercond. transitions, cryst. field effects 80−107950
$Er_xY_{1-x}Rh_4B_4$, mag. and supercond. transitions 80−70874
$Er_xY_{1-x}Rh_4B_4$, supercond. phase transitions, recentering temp. to normal ferromag. state 80−7024
$EuIr_2$, superconductivity 79−78248
ε-Fe, low temp. supercond., transition temp. estimated 80−34540
$FeMo_6S_8$, mixed Chevrel phases, crystallography 80−39038
$FeZnMo_6S_8$, mixed Chevrel phases, crystallography 80−39038
Ga film, crit. transverse mag. fields and transition temp. *(Russian)* 80−7048
Ga film, T_c and residual resist., variation with coating thickness 78−47900
Ga II, superconducting high pressure phase, sp. ht. 80−70894
B-Ga, metastable, elec. props. in normal and supercond. states *(Russian)* 80−65520
Ga, nonlinear sound wave interactions, sound attenuation in weak superconducting state *(Russian)* 80−75310
Ga, superconducting modifications in bulk samples *(Russian)* 79−65574
Ga ultrathin metallic filaments, appearance of dielec. instability, coexistence with supercond. 80−103784
Ga-Cu, fast quenching of A15-phases *(German)* 77−36014
Ga-$GaCl_2$, finely disperse system, supercond. props. 77−85376
Ga-insulator compound, obtained by impact compression method, superconducting properties *(Russian)* 79−7919
GaAs-Pb junctions, electron tunnelling under high press., transition temp., energy gap, phonon energies 79−15257
GaP, metallic modification, supercond. transition temp. at high temp. *(Russian)* 77−80867
GaSe, press. induced metallic and supercond. state 80−75666
$Gd_xEr_{1-x}Rh_4B_4$, effects of Gd ion on supercond. transition temp., mag. transition temp. and upper crit. field 79−56392
$Gd_xEr_{1-x}Rh_4B_4$, mag. and supercond. transitions 78−68127
$Gd_xEr_{1-x}Rh_4B_4$, mag. ordering near supercond. region 79−73696
$Gd_xY_{1-x}Rh_4B_4$, mag. and supercond. transitions 78−68127
Ge, supecond, friction layer formed during friction between Ge and Pb *(Russian)* 78−52143
Ge, supercond. at high press., crit. temp. 80−60130
$Ge_{0.6}Cu_{0.2}Au_{0.2}$ film, superconducting transition temp., resistivity meas. 77−43774
H_2, metallic, electron-phonon interaction and superconductivity, APW calcs. 78−14854
H_2, metallic, phonons, supercond. transition, nonlinear self consistent screening approach 79−95537
$HbSe_2$:Mn layered superconductor, crit. temp. and fields 77−51836
Hf-V, superconductivity and metallurgy of C15 materials 79−4610
$HfC_xN_yO_z$, valence band XPS, correl. to supercond. 79−65980
$HfGe_2$ film, supercond. obs. 77−72939
$Hf_{0.65}Nb_{0.35}$, superconducting alloy, transition temp. and flux line pinning 77−43772
HfV_2, C-15 struct., phase transitions, elec. cond., crystal lattice parameters *(Russian)* 80−54826
HfV_2, C15 Laves phase, supercond. and stoichiometry 78−39245
HfV_2H_x and HfV_2D_x, composition depend. of supercond. crit. temp. 77−20482
$HfV_2H_x(D_x)$, superconducting transition temp. var., isotope effect 77−12047
$Hf_{0.5}Zr_{0.5}V_2H_x(D_x)$, enhanced supercond. transition temp. on H(D) additions 78−80083

superconducting transition temperature continued
Hg filament, crit. mag. field and supercond. transition temp. 77−16013
Hg, supercond. transition temp. from Eliashberg eqns. 79−51709
Hg ultrathin metallic filaments, appearance of dielec. instability, coexistence with supercond. 80−103784
Hg-Xe film, random mixtures, superconducting transition temp. and metal-nonmetal transition 80−29498
Hg-Xe vapour deposited films, cond. transitions, effect of disorder on supercond. 80−88659
$Ho(Ir_xRh_{1-x})_4B_4$ pseudoternary system, supercond. and mag. ordering 80−70876
$Ho_{1.2}Mo_6S_8$, re-entrant ferromag. supercond., heat capacity and AC mag. susceptibility 79−60948
$Ho_{1.2}Mo_6S_8$, supercond. transition temp., upper critical field, local spin fluctuations 79−38250
I, metallic A1-type modification, normal conductivity and superconductivity 80−20348
In alloys, superconducting transitions temp. rel. to electronic struct. 77−80865
In, amorphization by ion implantation 78−52135
In, discontinuous film, DC resist. in normal and supercond. states 79−56357
In, fibres, supercond. transition at 6K *(Russian)* 77−80868
In film, resistive transitions scaling behaviour 79−15248
In films, crit. temp. enhancement *(Russian)* 80−93021
In films, supercond., sp. ht. discontinuity and transition temp. meas. 79−60969
In, Lifshits transition, electron-phonon interaction 80−29502
In, shell model for clad particles *(Chinese)* 79−69623
In, stress depend. of supercond. parameters 77−12045
In, supercond. transition temp. from Eliashberg eqns. 79−51709
In, superconducting transition temp., electron-phonon mass enhancement, pseudopot. calcs. 78−2604
In, superconductivity destruction singularities, intermediate state, hysteresis *(Russian)* 80−80460
In ultrathin films on TbTe and Te, prep. and characterisation 77−7995
In ultrathin metallic filaments, appearance of dielec. instability, coexistence with supercond. 80−103784
In whisker, stress depend. 77−39988
In whiskers from Sn-In alloys, current carrying, superconductivity breakdown 80−60133
In-Bi, single spheres, supercond. props. 79−73617
In-Bi (2-33.3 at.%), phase diagram DTA, X-ray diffr. and supercond. T_c meas. 79−38795
In-Bi(Tl)(Pb), small κ supercond., phase transitions higher than second order 80−88668
In-Cd-Sn, supercond. transition temp. depend. on electron conc., and electron mean free path 79−56345
In-Cr(Mn) films, supercond., sp. ht. discontinuity and transition temp. meas. 79−60969
In-InCl, finely disperse system, supercond. props. 77−85376
In-Mg, ordered equiatomic, lattice specific heat meas., Debye temp., superconducting transition 80−54396
In-Mn, dil., film, ion implanted, supercond, and mag. props. 77−15987
In-Mn, discontinuity in sp. ht. at supercond. transition 79−60971
In-Sb, cryst. struct. after appl. of high press., supercond. transition temp. 80−70169
α-In-Sn, stress depend. of supercond. parameters 77−12045
In-Sn alloy, Lifshits transition, electron-phonon interaction 80−29502
In-Sn alloy, phonon spectra and superconductivity, single-particle electron-tunnelling expts. 77−40005
In-Sn film, supercond. transition temp. and crit. currents *(Russian)* 77−55632
In-Sn(Pb)(Tl) alloy whisker, stress depend. 77−39988
In-Tl alloy, superconducting transition temp., phonon mode softening 79−1637
In-Tl alloys, supercond. transition in martensitic two phase region 77−72936
In_2Bi, press.-induced supercond. phase transform. 79−24099
$In_xMo_3S_4$, chevrel phase, charge transfer and valence electron conc. 78−6029
$In_{\sim 3}Mo_{15}Se_{19}$, high field supercond., crit. temp. and crit. field 79−47211
InSb, superconducting phases at high press. 78−88063
In_3Sn, superconductivity, and phase diagram of In-Sb system 79−38794
$In_{0.69}Tl_{0.31}$, supercond. transition temp., specific heat, pseudopotential form factor 80−97026
Ir borides, MIr_3B_2 (M=La, Th, U), supercond. and mag. props. 80−97028
Ir-Y eutectic alloy, supercond. transition enhancement due to lattice softening 80−103775
$(La,Ce)Ru_2$, supercond. transition temp., its press. depend., and structural phase transform. 78−6473
(La, Ce)Sn_3, dil. alloys, supercond. and normal state props. 78−76184
(La,Na)Sn alloys, supercond. transition temp. 79−78254
(La, Nd)Sn_3, superconducting props. 79−60958
(La,Y)Ce, dil., Kondo supercond., transition temp., susceptibility and resist. 80−65733
La, DHCP and FCC phases, phonon density of states 78−67791
La film, A1-type quench-condensed, prep. and crit. temp. 77−69443
La film, tunnelling investig., multiple band effects 77−8244
La, low temp. P-T diagram 77−47550
La particles, supercond. props. *(Russian)* 80−7018
La, press. depend., mode softening 78−14847
La, superconducting, electron-phonon coupling, hydrostatic press. depend. 78−80087
La-Ag alloys, amorphous, elec. resist. and supercond. 80−70885
La-Al(Ge)(Au), amorphous, alloying effect on supercond. props. 79−60951
La-Au, splat-quenched, Mossbauer effect and elec. resist., amorphous struct. 80−84676
La-Ce, Kondo system, intermediate temp. supercond. under hydrostatic press. 79−24097
La-Eu, dil., DHCP, impurity effects on T_c, electron pair breaking 77−36013
La-Eu(Gd), EPR investig. of local moment, correl. with supercond. props. 77−63282
La-Gd, dil., DHCP, impurity effects on T_c, electron pair breaking 77−36013
La-Gd(Tb,Dy,Ho,Er,Tm) alloys, FCC, supercond. transition temp. 79−4614
La-In alloys, cohesive and superconducting props. from electronic struct. calcs. 79−99113
La-pnictides, supercond. props. 77−85366
La-Sm-Sn, dil. alloy, Kondo effect obs., supercond. transition temp. meas. 77−51837
LaAg, under hydrostatic press., supercond. and phase transform, elec. resist., 1-300K, 78−10595
$LaAl_2:Gd^{3+}(Eu^{2+})$, cryst. field parameters, relax. rates 78−84482
La_4As_3, superconductivity 77−20481
$La_{100-x}Au_x$, amorphous film, stability, supercond. temp. and residual resistivity 79−4636
$La_{78}Au_{22}$, amorphous supercond., T_c and fluctuation cond. under high press. 79−7935
La_4Bi_3, La_4Bi_2Pb and La_4BiPb_2, superconductivity 77−20481
La_2C_3, solid solution, lattice const. and superconducting transition temp. *(Russian)* 80−92496
$La_{1-n}Ce_n$, supercond. mag. alloy, effect of interconfigurational fluctuations 78−19175
$La_{1-c}Ce_cAl_2$, Kondo superconductor, self-consistent theory of pairbreaking 78−26989
$(La_{1-n}Ce_n)_3Al$, mag. impurity effects in normal and supercond. state, NMR 78−2622
$La(Ce)Sn_{3-x}Pb_x$ system, mag. impurities in supercond., supercond. transition temp. and sp. ht. 78−39244
$La_{1-x}Ga_x$ foils, amorphous, splat cooled, calorimetric and resistive meas. 79−33417
$(La_{1-n}Gd_n)_3Al$, mag. impurity effects in normal and supercond. state, NMR 78−2622
$La_{80-x}Gd_xAu_{20}$, amorphous, supercond. and spin-glass regime, magnetisation and resist. meas. 77−36011
$La_{1-x}Gd_xMo_6Se_8$, supercond. transition temp., upper critical field, local spin fluctuations 79−38250
$La_{1-x}Gd_xRu_2$, mag. ordered superconductor, re-entrant superconductivity 78−88059
$LaGe_2$ film, supercond. obs. 77−72939
La_3In, alloying effects 79−38227
$(LaNd)Sn_3$, containing Nd impurities, supercond. and normal state props. 80−49967
$La_{80-x}Pr_xAu_{20}$, amorphous, mag. and supercond. props. 80−75713
$LaRu_2$, H absorption induced Ce valence change, mag. and supercond. props. 80−50042
$LaRu_2$, supercond. disappearance on H absorption 79−47185
La_4Sb_3 and $La_4(Sb_{0.5}Bi_{0.5})_3$, superconductivity 77−20481
$LaSn_3$, dilute alloy containing light rare earth impurities, press. depend. of supercond. transition temp. 79−47184
La_3Sn, cubic phase, high press. and high temp. synthesis, and characterisation 78−19687
$La_{1-y}Tb_yAg$, crystal field effects, normal and superconducting states 78−2621
$(La_{1-x}Th_x)_{1-n}Ce_n$, supercond. mag. alloy, effect of interconfigurational fluctuations 78−19175
$(La_{0.80}Y_{0.20})Ce$, three superconducting crit. point behaviour 78−10625
$La_{1-y}Y_y(Ce)$ system, mag. impurities in supercond., supercond. transition temp. and sp. ht. 78−39244
$LaYSb_3$, superconductivity 77−20481
$LiTi_2O_4$, prep., characterisation and supercond. props. 77−40010
$LiTi_2O_4$, press. depend. of supercond. transition temp. meas. 77−12050
$LiTi_2O_4$, single-phase, prep., crystal struct. and superconducting transition characts. 80−50583
Lu, T_c meas. up to 200 kbar 77−47916
Lu_2C_3, superconductivity 79−73621
MRh_4B_4 (M=trivalent transition metal, usually rare earth) supercond. and ferromagnetism, role of Sc 78−95438
Mg, superconducting transition temp., electron-phonon mass enhancement, pseudopot. calcs. 78−2604
Mo and Nb-Mo alloys, superconductivity and phonon softening, between electron bands and phonons 78−14859
Mo chalcogenide superconductors with $T_c>10K$ 79−33381
Mo, electron-phonon coupling and supercond. transition temp. 79−56360
Mo film, T_c and residual resist., variation with coating thickness 78−47900
Mo selenides, ternary, Chevrel phase supercond., compressibility and vol. depend. of Tc 78−31008
Mo single crystal 78−52136
Mo sulphides, ternary, Chevrel phase supercond., compressibility and vol. depend. of Tc 78−31008
Mo superconducting film, amorphous and crystalline, transition temp. exam. by UPS 79−28433
Mo ternary chalcogenide, MMo_6X_8 (M=metal, X=chalcogen) Chevrel phase, supercond. and normal state props. 78−56267
Mo ternary chalcogenides, supercond. props. 79−38230
Mo ternary cpds., $R_ySn_xMo_6S_8$ (R=La, Ce, Pr, Eu, Gd, Ho, Lu, Y, In, U), supercond. props. 80−97023
Mo:N film, high T_c amorphous phase stabilisation by interstitial nitrogen 78−23622
Mo:N film, implantation effect on supercond. and struct. transform. 77−4462
Mo-Be solid solutions, superconducting transition, temp. changing peculiarity due to press. *(Russian)* 80−70878
Mo-C film layer structure obs. of supercond. transition temp. and crit. mag. field oscills. 77−69438
Mo-chalcogenides, crit. mag. fields *(Russian)* 78−34936
Mo-Ge(Bi) amorphous films, supercond. transition temp. and residual elec. resist. *(Russian)* 79−19680
Mo-Re, σ phase alloy, critical mag. field, elec. resistance 80−54850
Mo-Re alloys, supercond. energy gap and transition temp., tunnelling meas. 79−56405
Mo-Re film, electron beam deposited, supercond. transition temp. conc. depend. 77−28279
Mo-Ru(-Si), amorphous superconductors, prep. by electron beam evaporation and liq. quenching, crit. temp. 80−103776
Mo-Si(Ge)(Al), amorphous supercond. alloy, produced by coevaporation, struct. and supercond. 79−91179
Mo-Sn-Se system, supercond. crit. temp. and cryst. struct. *(Russian)* 80−107947
Mo-Tc system, supercond. behaviour, quick-quench production technique 78−56251
MoB_2, hexagonal, form. by plasma heating and props. 79−28996
Mo_3Ge, RF sputtered 78−14853

superconducting transition temperature continued
Mo_3Ge, superconductivity, T_c related to disorder and density of states 79−15249
Mo_3Os, effect of high energy neutron irradiation on supercond. transition temp. 77−36012
Mo_3PbS_8 embedded in resin, composite supercond., high transition temp. 80−88660
$(Mo_{0.6}Ru_{0.4})_{82}B_{18}$, supercond. metallic glass, neutron irrad. effects 80−29060
$(Mo_{0.6}Ru_{0.4})_{0.8}G_{0.2}$-Fe (G=P,B), amorphous supercond., upper crit. field as function of temp. 79−73646
$(Mo_{1-x}Ru_x)_{80}P_{20}$, amorphous alloys, superconductivity, mag. susceptibility and electronic props., liq. quenching 78−88057
$(Mo_{1-x}Ru_x)_{80}P_{20}$, amorphous, liq. quenched, mag. susceptibility, supercond. and electronic props. 79−56376
$(Mo_{0.6}Ru_{0.4})_{80}Si_{10}B_{10}$, amorphous supercond. matrix, flux pinning by MoRu precips. 80−65756
Mo_5RuTe_8, synthesis, struct., and elec. props. 80−92877
MoS_2 intercalation compounds, reaction with alkali and alkali earth metals, band struct., superconductivity 78−26541
Mo_6S_8, relationship between electronic struct. and supercond. transition temp. 77−85368
$Mo_6S_6Br_2$, supercond., crit. temp. meas. 77−85367
$Mo_6S_6I_2$, supercond., crit. temp. meas. 77−85367
Mo_6Se_8, Chevrel phase, isotope effect on supercond. T_c 78−52141
Mo_6Se_8, Chevrel phase, isotope effect on supercond. transition temp., phonon modes 79−51713
Mo_6Se_8, isotope effect, theory 78−91806
Mo_6Se_8, isotope effect on transition temp. 79−73615
Mo_6Se_8, relationship between electronic struct. and supercond. transition temp. 77−85368
$Mo_6Se_{8-x}Br_x$, supercond. obs. crit. temp. determ. 77−85367
$Mo_6Se_{8-x}I_x$, supercond. obs. crit. temp. determ. 77−85367
$Mo_{70}Si_{20}B_{10}$, amorphous alloys obtained by liq. quenching, superconductivity 80−75670
$Mo_5SnGa_xS_6$ heat capacity from 2 to 25K 78−43518
$Mo_6Te_{8-x}I_x$, supercond obs., crit. temp. determ. 77−85367
$Mo_{1-x}V_x$, supercond., NMR and mag. susceptibility meas. 79−56388
Mo_6X_8 (X=S, Se), phonon density of states, mode softening correl. with supercond. transition temp. 79−51714
NaCl, high press. metallic modification, superconduction obs. *(Russian)* 79−65576
Na_xWO_3, anomalous supercond. transition temp., electron pairing by acoustic plasmon exchange 79−56358
Na_xWO_3, dynamic fluctuations between local struct. states in supercond. TI phase 78−26981
Na_xWO_3 enhanced T_c, interband coupling 78−91804
Na_xWO_3, semiempirical model for lattice instabilities in nonstoichiometric materials 78−14442
$(Nb,Ti)N_x$, metastable supercond. phase, effects of rapid quenching on transition temp. 78−2611
Nb and alloys, dynamic destruction of supercond. 77−69461
Nb and Nb-Mo alloys, superconductivity and phonon softening, between electron bands and phonons 78−14859
Nb, and Nb-V alloy, effect of purity and alloying with Ta, Cr, Mo or Re 77−85375
Nb based A-15 type superconductors, universal defect behaviour, transition temp. rel. to lattice parameter 77−69440
Nb, effect of O ion irradiation on supercond. 78−52131
Nb, electron-phonon interaction electronic contrib. 77−15524
Nb film, crit. temp., crit. field, and surface resist. 77−55635
Nb film, deposited in quasi-closed vol., supercond. props. 79−91180
Nb, film, epitaxy, struct. and supercond. props., on (001) surface of fluorophlogopite *(Russian)* 80−80101
Nb film, Gd ion implantation effects 77−39986
Nb film, magnetron-sputtered, intrinsic stresses and supercond. props. 80−24772
Nb film, struct. and electrophys. props. at 4.2K 80−80436
Nb film, superconducting tunnelling, meas. of annealing characteristics 79−7944
Nb film, transition temp. and transition width, impurity effects *(Russian)* 77−66222
Nb film, vac. deposited, deposition parameter effects on crit. temp. 80−2514
Nb film sputtered onto Cu substrate, microstruct. and supercond. props. 77−85370
Nb films, ion beam sputtered, supercond., laser annealing effects 80−97024
Nb films, penetration depth measured with Nb-NbO_x-PbIn Josephson junctions 79−42691
Nb, flux pinning by voids during neutron irrad. 77−40008
Nb granular films, ratio of supercond. transition temps. 80−84529
Nb heteroepitaxial layers on sapphire, residual mechanical stress and strain influence on superconductivity 80−15644
Nb layer, ion bombarded, supercond. props. and struct. 80−88671
Nb, O enrichment of surface layers, penetration depth and resist. meas. 78−19180
Nb, optical props. and electron-phonon interactions 80−2510
Nb, plastic deform. effect on positron annihilation and supercond. transition *(Russian)* 77−39993
Nb, plastic deformation effects on superconducting specific heat transition 80−20352
Nb, spin fluctuations effect on T_c, from sp. ht. and mag. suscept. 80−7030
Nb sputtered film, tunnelling characts. 79−4621
Nb, supercond., influence of plastic deform. 77−85378
Nb, supercond. crit. temp. enhancement by radiation damage 78−2609
Nb, supercond. transition temp. from Eliashberg eqns. 79−51709
Nb superconducting amorphous film, conductivity and transition temp., ion bombardment effects *(Russian)* 80−49969
Nb, superconducting bridges by electron beam lithography and ion implantation Josephson effect 80−20355
Nb superconducting film prod. by electron beam sputtering *(Russian)* 78−15308
Nb, superconducting transition temp., correl. with resist. anomalies and defect struct. 77−47920
Nb, superconductive transition point as reference temp. 80−107943
Nb, T_c control by N ion implantation 78−2606
Nb/Cu, layered ultrathin coherent structs., supercond. props. 80−84525
Nb/Cu-Sn-Mg, superconductor, effect of Mg addition to Cu-Sn matrix 80−25028

superconducting transition temperature continued
Nb/In composite superconductor, transport props. 80−88658
Nb-Al, A15 and σ-phases, supercond. and normal state electronic props. 77−43765
Nb-Al alloy, A-15 struct., influence of composition on transition temp. 77−20486
Nb-Al alloy, σ-and A15-phases, Knight shift and supercond. 77−15984
Nb-Al proximity sandwiches, supercond. transition temp. and tunnelling meas. 80−7045
Nb-Al-Si, supercond. transition temp., Si conc. depend. 78−84339
Nb-Al-(Ge) film, depend. of supercond. props. on sputter deposition conditions and heat treatment 77−36399
Nb-Al(Ga)(Ge), fast quenching of A15-phases *(German)* 77−36014
Nb-epoxy, interface, Kapitza resist. in supercond. and normal states 77−66085
Nb-Ga (16 to 28 at.%), transition temp., upper critical field and magnetisation curves 77−80866
Nb-Ga alloy, A15 type, melt produces specimens, supecond., homogeneity, transition temp. *(German)* 78−2608
Nb-Ga-Cu, fast quenching of A15-phases *(German)* 77−36014
Nb-Ga-Cu, phase diagram, metallographic and X-ray study, annealed and as-cast supercond. crit. temp. *(Russian)* 78−56617
Nb-Ga-Fe ternary system, phase equilib. at 1000°C, supercond. transition temp. 80−35158
Nb-Ga-Ir system, phase equilib. at 1000°C and supercond., Nb-rich portion 77−36480
Nb-Ga-Sc, superconducting transition temp., X-ray, microscopic and microprobe anal. *(Ukrainian)* 80−75667
Nb-Ga-Y, X-ray and microprobe anal., isothermal section and supercond. transition temp. *(Ukrainian)* 79−38793
Nb-Ge, A15 struct. superconductor, high field transport props. TEM study 80−34574
Nb-Ge, amorphous supercond. alloy, resistivity, transition temp. 80−60126
Nb-Ge, supercond. A-15 phase, supercond. transition temp. after ion implantation 80−49972
Nb-Ge, supercond. film, prep. and props. *(Russian)* 77−66218
Nb-Ge, supersuperconducting transition temp., correl. with resist. anomalies and defect struct. 77−47920
Nb-Ge, transition metal atom stabilised superconductivity 79−7924
Nb-Ge film, coevaporated, supercond. critical temp. and struct. 77−28275
Nb-Ge film, supercond., TEM expts., correl. of struct. and elec. props. 78−14628
Nb-Ge film, supercond. transition temp., rel. to prep. conditions 77−36009
Nb-Ge superconducting film, prod. by electron beam sputtering *(Russian)* 78−15308
Nb-Ge vapour deposited films with T_c of ~20K, preps. *(Japanese)* 77−12048
Nb-Ge-Cu, phase equilib. and supercond. props. *(Russian)* 80−40332
Nb-Ge-Fe, effect of Fe on supercond. and mag. props. 79−56351
Nb-Ge-Ni, phase composition and superconducting props., influence of Ni *(Russian)* 80−20898
Nb-Ge-Si, A15 struct. superconductor, high field transport props. TEM study 80−34574
Nb-Ge-Si, Si effect on raising superconducting transition temp. in pelicular specimens *(Russian)* 78−23188
Nb-Ge-Si, supercond. state transition temp., influence of Si on alloy constitution *(Russian)* 79−78244
Nb-Ge-Sn A15 cpds., CVD, superconductivity 79−38222
Nb-Ge-Sn(Pt)(Ir), A15 cpds. prod. by liq. quenching, phase stability and supercond. props. 79−95538
Nb-Ge(Si), amorphous supercond. alloy, produced by coevaporation, struct. and supercond. 79−91179
Nb-Ge(Si) and Nb-Ge-Si, A15 cpds., CVD prep. and supercond. crit. temp. 79−60949
Nb-I-Pb junction, double-peak structure *(Russian)* 79−82716
Nb-I-Pb junctions, fine struct. of current-voltage curves, crit. temp. reduction *(Russian)* 79−19693
Nb-Ir, A 15- and σ-phases, supercond. 79−73645
Nb-Ir-O, phase struct., supercond. H-phase 78−39246
Nb-Mo system, electron-phonon coupling const. and supercond. transition temp., average T-matrix approx. 80−39707
Nb-N, superconducting layers, sputtering in high vacuum apparatus *(German)* 80−89147
Nb-N system, ion-implanted, effect of implantation conditions 78−19176
Nb-Nb_3Al, fabrication by quench-age method 77−40403
Nb-$Nb_3(Al,Ge)$ multifilamentary supercond., fabrication and props. 77−20480
Nb-Pt, A15 phase, comp. and order effects on supercond. props. 77−85372
Nb-Pt alloy, superconducting parameters of A15- and σ-phases 78−39242
Nb-Pt-O system, phase equilibria, diagram, unit cell parameters, supercond. 80−55352
Nb-Rh, σ-phase alloy, superconductivity and resistance behaviour 80−70882
Nb-Si compounds, CVD, struct. and supercond. props. 79−24447
Nb-Si film, superconductivity close to A15 stoichiometric phase 79−95540
Nb-Si-Sn(Pt)(Ir), A15 cpds. prod. by liq. quenching, phase stability and supercond. props. 79−95538
Nb-Si(−V)(Zr)(Mo)(Ta)(W)(C)(B)(Ge), ductile amorphous, superconductivity 80−60131
Nb-Sn, depend. of supercond. transition temp. on composition *(Russian)* 78−19173
Nb-Sn, diffusion couple, phase equilibria, effect on T_c and H_{c2} 79−56462
Nb-Sn filamentary composite, as function of reaction conditions 77−28330
Nb-Ti, multifilament superconductor, metallurgical design 79−33434
Nb-Ti, radiation effects on critical currents 78−52175
Nb-Ti, superconductivity after heavy ion irradiation at low temps. and high fluence 77−69437
Nb-Ti, thermal conductivity in low temp. range 78−39259
Nb-V(Ta) alloys, electron-phonon interaction and supercond. transition temp. *(Russian)* 79−28426
Nb-Zr sputtered films on Ta, struct. and supercond. props. *(Japanese)* 78−52138
$Nb_3(Al,Ge)$ and $Nb_3(Al,Si)$, liq. quenched, supercond. props. 80−84580

superconducting transition temperature continued
$Nb_3(Al, Ge)$ tape, effect of thermal treatment on supercond. props. 79−61016
Nb_2Al, $NbAl_3$, supercond. and mag. props. 77−47922
Nb_3Al, and $Nb_3Al_{0.76}Ge_{0.24}$, supercond. props. of cold worked core wires an basis of A15 phases 77−85369
Nb_3Al base ternary solid solns., T_c meas., dopant depend. 77−1510
Nb_3Al based ternary solid solns., supercond. transition temp., paramag. susceptibility and lattice parameters meas. *(Russian)* 77−43766
Nb_3Al core wires and pressed powder compacts, supercond. transition 80−34541
Nb_3Al film, electron-beam coevaporated, prep. and characts. 80−76187
Nb_3Al, liq.-quenched, crit. current density and T_c 77−72957
Nb_3Al, mechanical and supercond. props. 79−38214
Nb_3Al multifilamentary composite, metallurgy, fabrication and supercond. props. 77−28764
Nb_3Al multifilamentary cable fabrication and props. 79−33438
Nb_3Al, neutron irrad. effects on transition temp. *(Japanese)* 79−82707
Nb_3Al, nuclear magnetic relaxation, near T_c *(Russian)* 79−42852
Nb_3Al, supercond. props. and lattice parameter, comp. and neutron irrad. effects 80−70880
Nb_3Al, superconductivity, crit. temp., paramag. susceptibility comp. depend. *(Russian)* 77−66219
Nb_3Al tape, effect of thermal treatment on supercond. props. 79−61016
Nb_3Al-Nb_3Ge-Nb_3Ga system, supercond. crit. temps. 77−8218
Nb_3Al-Ni(Cr)(Fe) mag. impurities effect on supercond. props. 77−1524
$Nb_3Al(Ga)$, NQR freq. temp. depend., supercond. transition temp. 80−93207
$Nb_3Al_{0.8}Ge_{0.2}$, supercond., sp. ht. meas. 77−28296
$Nb_3(AlSi)$, ternary supercond. alloy films, T_c, props. *(Russian)* 78−88055
$Nb_3Al(Sn)$, electron-phonon coupling and supercond. crit. temp. 79−33379
Nb_3As, electronic and supercond. props. 77−16011
Nb_3As, structural and supercond. props. press. effects 80−39700
Nb_3Au, BCC, density of states, comparison with A-15 78−80095
NbB_2, superconductivity below 1K 80−20342
NbC, C implanted, channelling crit. angle and min. yields 78−47458
NbC, diffuse, production and superconductive props. *(Bulgarian)* 80−80467
NbC, electronic struct. of vacancies, effect on supercond. transition temp. 80−29347
NbC, supercond. critical temp., neutron irrad. effect 80−80433
NbC, supercond. transition temp. and lattice dynamics 79−56361
NbC, superconductor, appl. of non-local extension to Gaspari-Gyorffy theory 78−80093
NbC, ultrafine powders and sintered compacts, prep. and supercond. props. 77−40015
$NbC_{0.89}$, implantation or diffusion of C rel. to supercond. transition temp. 77−69442
NbC_x, light element implantation effect on T_c 80−107951
NbC_x, reactor irrad. effects on elec. resist. and supercond. props. *(Russian)* 78−47895
NbC(N), critical temp. enhancement, surface effect on phonon spectrum and electronic state density *(Chinese)* 80−2507
NbCN, preparation methods and supercond. properties *(French)* 79−73618
Nb(CN), supercond. critical temp., neutron irrad. effect 80−80433
NbC_xN_{1-x}, obs. of phonon anomalies, sp. ht. meas. and supercond. transition temp., 1.5-90K 77−39985
NbC_xN_{1-x}, s.p. ht., 4.2-100K, phonon anomaly rel. to supercond. transition 78−14880
$Nb_{0.75}Ga_{0.25}$, A 15 phase high transition temp., sp. ht. determ. 80−60140
Nb_3Ga, comp. and LRO effects 77−39992
Nb_3Ga film, RF sputtered, supercond. and struct. props. 77−28274
Nb_3Ga, heat treatment and stoichiometry effects 77−43769
Nb_3Ga, transition temp. increase by rapid hardening with annealing 80−76275
Nb_3Ga-Nb_3Pt alloy, comp. depend. *(Russian)* 77−59347
$Nb_{78}Ga_{22-x}Mn_x$, supercond. props., influence of Mn mag. impurities 80−54825
$Nb_{80}Ga_{20-x}Mn_x$, supercond. props., influence of Mn mag. impurities 80−54825
$Nb_3(Ge,Si)$ A15 film, supercond. and structural props. 79−87177
$NbGe_2$ single crysts., elec. resist. and superconductivity 79−38233
$NbGe_2$, superconducting transition temp. meas. of sputtered films and bulk 80−7019
$Nb_{1-x}Ge_x$, supercond., mag. field props. 80−54822
Nb_3Ge, A15 superconductor, rel. between transition temp. and density of states 79−15247
Nb_3Ge, amorphous and crystalline A-15 phases 78−83896
Nb_3Ge, amorphous nongranular thin superconducting film, thermodynamic and resistive transitions 80−34571
Nb_3Ge, and $Nb_{0.82}$, structural and supercond. props. press. effects 80−39700
Nb_3Ge, α-particle irrad., supercond. transition width 78−23193
Nb_3Ge, α-particle irrad., relationship between density of states and supercond. transition temp. 79−42684
Nb_3Ge, CVD, impurity doping effect on supercond. crit. props. 78−52174
Nb_3Ge composite filament, continuous, high-strength, prep. and supercond. props. 77−28765
Nb_3Ge continuous supercond. tape, prep. by CVD 77−80893
Nb_3Ge, DC sputtered films, annealing and mech. deform. effects on struct. and supercond. props. 79−38217
Nb_3Ge, effect of ^{16}O and ^{32}S ion irrad. and thermal recovery on T_c, residual resist. and slope of crit. field 79−56348
Nb_3Ge, epitaxial growth of polycryst. films with high supercond. transition temp. 77−63015
Nb_3Ge film, α-particle induced defects and stoichiometry, effect on T_c 77−32101
Nb_3Ge film, electron beam deposited, comp. depend. 78−6470
Nb_3Ge film, electron beam co-deposited, prep. and supercond. crit. temp. 78−15310
Nb_3Ge film, growth by co-evaporation in O_2, critical temp. enhancement 77−28273
Nb_3Ge film, high-temp. supercond. phase stabilisation w.r.t. prep. conditions *(Russian)* 80−70871
Nb_3Ge film, low temp. sputter deposition 78−48315
superconducting transition temperature continued
Nb_3Ge film, nucleation of high-T_c phase in presence of impurities 78−88054
Nb_3Ge film, prepared by cosputtering, supercond. props. 79−4634
Nb_3Ge film, sputtered, chemical composition versus lattice parameter a_o and supercond. transition temp. relations 77−43771
Nb_3Ge film, sputtered and evaporated, transition temp., critical field and current anisotropy 77−28328
Nb_3Ge film, supercond., intercorrelations between composition, lattice parameter a_0 and T_c 77−8217
Nb_3Ge film, supercond., epitaxial growth on Nb_3Ir and Nb_3Rh substrates 78−80473
Nb_3Ge film, superconducting, A-15 type, getter-sputtering with controlled additions of O 78−88427
Nb_3Ge films, magnetron sputtered preps. and microstruct. 79−38276
Nb_3Ge films, prep. by DC sputtering and solid state diffusion, supercond. props. and struct. 79−38212
Nb_3Ge films, tunnelling obs., X-ray and electron diffr. obs. 77−32123
Nb_3Ge, high crit. temp., prep. *(Japanese)* 79−78914
Nb_3Ge, high pressure and temp. treatment effect on supercond. props. *(Russian)* 77−1512
Nb_3Ge, low fluence alpha irradiation, behaviour of supercond. transition temp. 78−43510
Nb_3Ge, low temperature electron, neutron irrad. effects on critical temp. *(French)* 80−75669
Nb_3Ge, neutron irradiated, A15 compound, recovery of T_c by annealing 78−52132
Nb_3Ge, projected critical current, comparison with $PbMo_6S_8$ 79−69642
Nb_3Ge, RF and DC sputtered films comparison, O content effect 78−72022
Nb_3Ge, RF sputtered film, high superconducting transition temp. 77−59346
Nb_3Ge, sputter-deposited, superconducting T_c and phase relationship 79−56344
Nb_3Ge, sputtered film, nonstoichiometry effect 77−11806
Nb_3Ge sputtered film, struct. and superconducting props. 77−28337
Nb_3Ge, supercond. film, amorphous content, X-ray diffr. study, rel. to transition temp. 80−75668
Nb_3Ge, supercond. film, CVD, crit. temp., crit. current density 78−76204
Nb_3Ge supercond. film, of high transition temp., US attenuation 80−49991
Nb_3Ge, supercond. film, prep. by chem. transport reaction, critical props. 79−47635
Nb_3Ge supercond. thin films, He- and Ar-irradiated, X-ray diffr. studies 80−29503
Nb_3Ge, superconducting A-15 type compounds, transition temp., radii ratio and structure *(Chinese)* 80−44752
Nb_3Ge superconducting film preparation and props. 79−11515
Nb_3Ge superconducting films, role of O_2 in form. of struct. *(Russian)* 79−60950
Nb_3Ge superconducting film, Nb_5Ge_3 and NbO content, X-ray diffr. obs. 80−2515
Nb_3Ge superconducting film, crit. temp. correl. with resist. relations and film struct. *(Russian)* 80−15646
Nb_3Ge superconducting films, high critical temp., optimum sputtering conditions 80−15647
Nb_3Ge, superconducting transition temp. 78−47898
Nb_3Ge tape, prep. by continuous CVD process 78−11121
Nb_3Ge tape, prepared continuously by CVD, props. 78−60257
Nb_3Ge:H film, sensitivity of supercond. transition temp. to H content 78−47894
Nb_5Ge_3, 0.30K T_c meas. with 0.14K transition width 78−6468
$Nb_3Ge_xAl_{1-x}$, ternary supercond. alloys, comp. variations 80−97022
$Nb_3Ge_{1-x}Ga_x$ CVD films, supercond. transition temp. depend. on lattice parameter 79−38219
$Nb_3Ge(Sn)$, electron irradiation at cryogenic temps., effect on T_c and transport props. 78−52122
$Nb_3Ge(Sn)$ film, ^4He irrad. induced defect prod., T_c var. 77−8220
$Nb_3Ge(Sn)$, optical props. and electron-phonon interactions 80−2510
$Nb_3Ge(Sn)$, resistivity and T_c measurement after low temp. neutron irradiation 78−52123
$Nb_{78}Ga_{22-x}Fe_x$, $Nb_{80}Ga_{20-x}Fe_x$, A15 phase supercond. 79−87181
NbH_x, supercond. T_c and low temp. resistivity, morphology 77−72940
$NbMo_2Be$, predicted A15 struct. and T_c=30K 78−76182
$(Nb_{0.99}Mo_{0.01})_{1-x}Ge_x$, supercond. transition temp. and crit. field 79−38220
$(Nb_{1-y}Mo_y)_3Ge$ system, composite transition metal atom supercond. 77−39984
$Nb_{1-x}Mo_xSe_2$, supercond. transition temp. and mag. susceptibility 77−12043
NbN, 2-dimens. supercond. phase transition, universal current scaling in crit. region 79−28429
NbN, diffuse, production and superconductive props. *(Bulgarian)* 80−80467
NbN embedded in resin, composite supercond., high transition temp. 80−88660
NbN granular films, supercond., crit. props. 80−88661
NbN, γ- and δ-forms, cryst. growth and supercond. transition temp. 80−107946
NbN, Raman spectra and superconductivity of various phases 78−68506
NbN single crystal preparation, transition temperature determination 80−60776
NbN, supercond. props., SQUID behaviour 78−72311
NbN, supercond. RF reactively sputtered films, deposition parameter effects on props. 80−80972
NbN, supercond. transition temp. and lattice dynamics 79−56361
NbN, ultrafine powders and sintered compacts, prep. and supercond. props. 77−40015
Nb_2N, supercond. props. and structural phase transform. induced by C^+ and N^+ implantation 80−107942
$NbN_{0.7}C_{0.3}$, cryst. growth and supercond. transition temp. 80−107946
$Nb_3Nb_{1-x}Si_x(Ge_x)$, impurity stabilised A15 supercond., transition temp., lattice consts., specific heat 80−93026
Nb_3Pt, neutron irrad. effects on supercond. props. 79−38224
Nb_3S_4, supercond., prep. and transition temp. 78−84341
$NbS(Se)_2$, polymorphism at high press. and temps., T_c and band struct. 78−26528
$Nb_3S_{1.7}Se_{2.3}$, supercond., prep. and transition temp. 78−84341
$NbSe_2$ nonstoichiometry, electrical props. *(Japanese)* 78−10593

superconducting transition temperature continued
$NbSe_2$:Mn, Kondo effect, mag. ordering and superconductivity 77−62915
$NbSe_2$:Mn, supercond., anomalous flux flow and matching 77−12069
$NbSe_2$-Fe, dil. alloy, magnetotransport and superconductivity 77−55516
$NbSe_3$, Fermi surface, press. effects, supercond. transition at 3.5K 80−20068
$NbSe_3$, superconducting transitions and diamagnetism 80−84526
$NbSe_3$, superconductivity under press. 77−76995
$NbSe_3$:Zr, dopant effect on supercond. transition temp. rel. to CDW 80−39699
$NbSe_x$, x=1.48-2.0, nonstoichiometric, elec. props., supercond. transition temps. 79−73624
Nb_3Se_4, supercond., prep. and transition temp. 78−84341
$NbSe_2$(2H), CDW onset temp. and supercond. crit. temp., press. effects up to 20 kbar 77−39987
$NbSi_2$, superconducting transition temp. meas. of sputtered films and bulk 80−7019
Nb_3Si, A-15 type, growth by levitation melting, transition temp. meas. *(Chinese)* 79−24424
Nb_3Si, electronic and supercond. props. 77−16011
Nb_3Si epitaxial layers, ion implantation synthesis, supercond. transition temp. optimization 79−38218
Nb_3Si film, quasiamorphous, supercond. phase formation by heat pulse 77−63017
Nb_3Si film, supercond., obtained by vaporisation in vacuum, props. 78−14865
Nb_3Si, high press. phase, prod. by recrystn. of metastable sputter deposits, struct. and supercond. props. 78−60571
Nb_3Si, high T_c, supercond. props. from extrapolation of sp. ht. meas. on A-15 Nb-Si 80−25045
Nb_3Si, hypothetical, electronic struct., lattice parameters and possible supercond. transition temp. 79−23891
Nb_3Si, metastable A-15 struct. synthesis by ion implantation, supercond. transition temp. 80−55319
Nb_3Si, structural and supercond. props. press. effects 80−39700
Nb_3Si, substituted, splat cooling influence on supercond. T_c and stoichometry 80−80439
Nb_3Si, supercond. phase, formation by explosive compression 79−82701
Nb_3Si, supercond. props., effect of neutron irrad. 79−38211
Nb_3Si, superconducting, high transition temp., sputtering 78−15309
Nb_3Si, superconducting A-15 type compounds, transition temp., radii ratio and structure *(Chinese)* 80−44752
Nb_3Si type alloy with A15 struct., depend. on stoichiometry *(German)* 77−69444
Nb_5Si_3, supercond. props. and cryst. struct. 79−78245
$Nb_{1-x}Sn_x$, sp. ht., supercond. T_c and martensitic transform. *(French)* 78−43508
Nb_3Sn, A-15 struct. Nb based superconductors, irrad. type influence on radiation defects 80−15093
Nb_3Sn, alloying agent influence on struct. and supercond. props. *(Russian)* 80−39698
Nb_3Sn, anisotropic thermal parameters of Nb, rel. to transition temp. 79−99282
Nb_3Sn, α-particle irrad., relationship between density of states and supercond. transition temp. 79−42684
Nb_3Sn bronze process, flux pinning scaling law depend. on strain 80−75696
Nb_3Sn, cavities, quasiparticles in energy gap corresponding to weak spots 79−56386
Nb_3Sn, coherence parameter, nonlinear high temp. supercond. elements with A-15 lattice *(Russian)* 80−60127
Nb_3Sn composite processes with Cu-Sn-Zn matrix, superconducting props. 78−84370
Nb_3Sn, crit. temp. and transition width, 25 MeV O ion irrad. effects 77−69439
Nb_3Sn, Cu admixture in Sn bath effect on critical current and stability temp. 80−7059
Nb_3Sn, deform. effects on supercond. transition temp. 77−12051
Nb_3Sn, degradation mechanism of superconducting transition temp. under high energy neutron irradiation 78−52124
Nb_3Sn diffusion layer material, characterisation 79−38213
Nb_3Sn, effect of diffusion couple Sn content on superconductivity 79−61009
Nb_3Sn, effect of O ion irradiation on supercond. 78−52131
Nb_3Sn, effect on critical temp. for supercond. of disorder, induced by α-particles 78−47897
Nb_3Sn, electron beam deposited, microstruct., rel. to supercond. props. 79−37935
Nb_3Sn, fast neutron irradiation, effect on critical current density 78−19197
Nb_3Sn filamentary wires, fabricated by infiltration method, supercond. props. 77−28761
Nb_3Sn, filaments in Cu matrix, thermal strain effects on superconducting critical temp. 80−93032
Nb_3Sn film, α-particle induced defects and stoichiometry, effect on T_c 77−32101
Nb_3Sn film, growth by high-rate magnetron sputtering, transition temp. and crit. currents 77−28718
Nb_3Sn film, high T_c, high-rate magnetron sputtering, supercond. transition temp. meas. 77−43770
Nb_3Sn films, deposition by quasi-closed vol. method, supercond. crit. temp. 80−15645
Nb_3Sn, gap anisotropy, electron irrad. effect on transition temp. 78−10599
Nb_3Sn, high-rate sputter-deposited, effect of oxygen on microstruct. 80−20343
Nb_3Sn, high-temp. supercond., tunnelling spectra, electron pairing anal. 79−87205
Nb_3Sn, highly disordered, elec. resist. and supercond. T_c 78−52142
Nb_3Sn in bronze, supercond. props. thermally induced matrix stresses 77−32134
Nb_3Sn, low fluence alpha irradiation, behaviour of supercond. transition temp. 78−43510
Nb_3Sn, low temp. irrad. with 20 MeV S ions, effect on supercond. props. 79−38223
Nb_3Sn, martensitic transform. coupling with supercond. transition 78−44126
Nb_3Sn monofilament wires, supercond. props., effect of Be alloying additions to bronze matrix 79−87222
Nb_3Sn multifilament conductors, strain effect on crit. props. 78−80108
superconducting transition temperature continued
Nb_3Sn, multifilament superconductor, metallurgical design 79−33434
Nb_3Sn multifilamentary composite superconductor, reaction treatment, crit. current, transition temp. and bend props. 79−33430
Nb_3Sn multifilamentary composite superconductor, effect of heat treatment on supercond. props. 79−33376
Nb_3Sn, multifilamentary supercond., stress effects 77−32133
Nb_3Sn multifilamentary superconductor, crit. current up to 18 T and supercond. transition temp. 77−47950
Nb_3Sn multifilamentary superconductor, stress induced normal⇄supercond. transition 79−33377
Nb_3Sn, neutron irrad., elec. resist., temp. depend. 79−91024
Nb_3Sn, neutron irrad. effects on transition temp. *(Japanese)* 79−82707
Nb_3Sn, neutron irradiation at 8K, supercond. crit. current and crit. temp. meas. 77−28334
Nb_3Sn, O^{4+} bombarded, Mossbauer studies, supercond. transition determ. 80−2672
Nb_3Sn, phonon softening and T_c, strong electron-phonon coupling 78−31009
Nb_3Sn, produced by Sn implantation, supercond. and Mossbauer effect 79−4612
Nb_3Sn, radiation damage effect on superconducting props. 78−52127
Nb_3Sn, supercond., fast particle irradiation effects, using anti-site defect model, electronic state influences 79−56346
Nb_3Sn, supercond., thin film, US attenuation of SAWs 80−49988
Nb_3Sn, supercond. props., effect of neutron irrad. 80−80463
Nb_3Sn, supercond. props. and struct., neutron irrad. dose depend. 77−15985
Nb_3Sn, supercond. props. of cold worked core wires an basis of A15 phases 77−85369
Nb_3Sn, superconducting, formed from Cu-Sn alloy, props. 79−42709
Nb_3Sn superconducting multifilamentary wire, stress effects 79−33431
Nb_3Sn, superconducting props., effect of radiation induced atomic disorder 78−52133
Nb_3Sn, superconducting transition temp., crit. parameters 77−28280
Nb_3Sn superconductors, bronze-processed, effect of Ta additions 78−95404
Nb_3Sn tapes, transition temp. meas. using Si linear thermometer 77−57330
Nb_3Sn, vap. deposited supercond. film, effect of N_2 and tape heating 78−34939
Nb_3Sn-Al_2O_3 composite, electron beam deposited, microstruct., rel. to supercond. props. 79−37935
Nb_3Sn-Cu superconducting composite, electron beam co-evaporated, TEM study 79−28247
Nb_3Sn-Fe(Co)(Mn), mag. impurities effect on supercond. props. 77−1524
Nb_3Sn(Al), neutron irradiated, A15 compound, recovery of T_c by annealing 78−52132
Nb_3Sn(Al)(Ga)(Ge)(Si), supercond. transition temp., rel. to A15 phase stability 78−52137
Nb_3(SnGa), wire, neutron effect on T_c, I_c and flux pinning 79−38216
Nb_3Sn(Ga)(Al) film, quasiamorphous, supercond. phase formation by heat pulse 77−63017
$Nb_{0.95}Ta_{0.05}Se_3$, resist 0.5K to room temp., supercond. transition temp. and crit. field 79−82704
$Nb_{1-x}Ta_xSn_2$, supercond. transition temp. and upper crit. field 80−39723
Nb_3Te_4, supercond., prep. and transition temp. 78−84341
NbTi, supercond. critical temp., appl. of cryogenic calorimetry 79−40577
NbTi superconducting state, stability under localised heat pulses 79−73611
NbTi/In composite superconductor, transport props. 80−88658
NbTi-Cu, composite superconductor, acoustic emission 80−84546
$(Nb_{0.99}Ti_{0.01})_{1-x}Ge_x$, high T_c, resist. meas. 80−88531
$(Nb_{0.99}Ti_{0.01})_{1-x}Ge_x$, supercond. transition temp. and crit. field 79−38220
$(Nb_{0.99}Ti_{0.01})_{1-x}Ge_x$, supercond., mag. field props. 80−54822
$Nb_{1-y}Ti_ySe_2$, supercond. transition temp. and mag. susceptibility 77−12043
$Nb_{1-x}W_xSe_2$ x=0 to 0.15, elec. resist., mag. suscept., heat capacity, structural, supercond. transition *(Russian)* 78−31006
Nb_3X, X=Ge, Gu, Al, Sn, Pt, composition effects on T_c 77−76993
$Nb_{1-x}Zr_x$, supercond., McMillan-Rowell tunnelling spectroscopy 79−60985
$(Nb_{1-x}Zr_x)_3$ Sn, bronze-processed tape, AC losses between 5 and 16K 79−82727
$Nb_{20}Zr_{80}$, supercond. and normal, sp. ht. meas., 2-20K 80−70893
$(Nb_{0.99}Zr_{0.01})_{1-x}Ge_x$, supercond. transition temp. and crit. field 79−38220
$(Nb_{0.99}Zr_{0.01})_{1-x}Ge_x$, supercond., mag. field props. 80−54822
$nbSe_2$ (2H) single crystal, elec. resistivity, effect of hydrogen intercalation *(Russian)* 78−84338
Ni-Nb(-Cu)-C, NbC dispersed supercond. tapes, fabrication and characts. 78−19773
NiH_x, electronic band struct. and interatomic bond 78−43295
$Ni_2Mo_6S_6O_2$, O-containing Chevrel phases, synthesis and props. 80 108368
Os borides, MOs_3B_2 (M=Lu, U), supercond. and mag. props. 80−97028
Pa, superconducting transition temp. and upper critical mag. field 80−44756
Pb, band structure, and electron-phonon interaction, supercond. transition temp. determ. 79−19512
Pb, effect of O ion irradiation on supercond. 78−52131
Pb, effect of supercond. transition on phonon energies and lifetimes 79−28432
Pb film, amorphous, nucleated with Mo, supercond. and normal elec. cond. 77−24633
Pb film, conducting coating effect on supercond. transition temp. and normal-state cond. 77−16007
Pb film, T_c and residual resist., variation with coating thickness 78−47900
Pb, high press. superconducting transitions determ. via X-ray diffr. 77−11442
Pb layer in Al-SiO_2-Si-Pb MIS system, supercond. transition effect on photocurrent 78−72271
Pb, phonon softening, neutron scatt. at high press. 78−80091
Pb, plastic deform. rate rel. to supercond. transition, temp. depend. *(Russian)* 78−31015
Pb, shell model for clad particles *(Chinese)* 79−69623

superconducting transition temperature continued
Pb single crystal, normal-superconducting transition and plastic flow 78−3166
Pb, strength loss in supercond. state, size factor effect *(Russian)* 80−88677
Pb, supercond. transition temp. from Eliashberg eqns. 79−51709
Pb, supercond. transition temp., theoretical calc. 79−73614
Pb, superconducting, press. depend. of supercond. transition temp. 78−84340
Pb superconducting amorphous film, conductivity and transition temp., ion bombardment effects *(Russian)* 80−49969
Pb, superconducting film, radiation induced critical temp. 79−87179
Pb, superconducting transition temperature, resistive transition meas. 77−80861
Pb, superconducting transition temp., electron-phonon mass enhancement, pseudopot. calcs. 78−2604
Pb, superconducting transition curves, meas. during plastic deform. 79−60956
Pb, transverse acoustic phonons, freq. and damping, supercond. transition temp. effects 79−42687
Pb ultrathin films deposited on Si 77−66220
Pb ultrathin films on PbTe and Te, prep. and characterisation 77−7995
Pb:Ni, paramag. impurity effect on work hardening at superconducting transition *(Russian)* 77−47915
Pb-Bi, splat quenched, solubility limit, vacancy conc. and supercond. transition temp. 77−12046
Pb-Bi alloy, T_c evaluation, from ab initio band struct. calcs. on Pb 80−75502
Pb-Cd, supercond. proximity effect, electron tunnelling study 78−10616
Pb-Cd thin films, electron tunnelling study of supercond. proximity effect 80−2525
Pb-Fe, supercond. films, modification of props. by Fe grains *(French)* 79−60957
Pb-formvar-Al tunnel junction, excitonic superconductivity, BCS theory, generalised jellium model 80−75684
Pb-Ga(Ge)(Si)(Mo)(Bi) amorphous films, supercond. transition temp. and residual elec. resist. *(Russian)* 79−19680
Pb-In, electron tunnelling under hydrostatic press. 77−51850
Pb-In, viscous drag on mobile dislocations, plastic deformation, critical temp. magnetic data 78−43514
Pb-M, M=Bi, La, Sm, vacuum deposited supercond. films, T_c chem. comp. depend. *(Russian)* 78−19174
Pb-$PbCl_2(I_2)$, finely disperse system, supercond. props. 77−85376
Pb-Sb, crystal struct., supercond. after subjection to high press. 78−88064
Pb-Sn, lamellar eutectic alloy, proximity effect, entropies, free energies and transition temps. 77−51849
Pb-Sn system, soft solder, elec. and thermal cond. at low temps., superconducting transition temp. 80−20150
Pb-Sn(Bi) alloys, dil., impurity effects on softening at T_c *(Russian)* 78−23220
Pb-Sn(Bi)(Ni), strength loss in supercond. transition, nonmag. and paramag. impurities influence *(Russian)* 80−70875
$Pb_{55}Bi_{45}$ film, amorphous, supercond. energy gap and transition temp. 78−14866
PbIn films, penetration depth measured with Nb-NbO_x-PbIn Josephson junctions 79−42691
$PbMo_{5.1}S_6$, high supercond. T_c, soft mode behaviour 78−14855
$PbMo_{5.1}S_6$, supercond. wire prep. by powder technique 78−52705
$PbMo_6S_6$, cold-worked core-wires, supercond. transition temp. and lattice instability 78−6469
$PbMo_6S_8$ and ternary sulphides, lattice parameter rel. to supercond. T_c 78−52119
$PbMo_6S_8$, influence of Fe on superconduction transition temp., and mag. props. *(Russian)* 79−42686
$PbMo_6S_8$, normal state and superconducting property measurements 78−91660
$PbMo_6S_8$, prod. by solid state reaction, supercond. crit. temp. *(Japanese)* 79−42682
$PbMo_6S_8$, projected critical current, comparison with Nb_3Ge 79−69642
$PbMo_6S_8$, relationship between electronic struct. and supercond. transition temp. 77−85368
$PbMo_6S_8$, supercond. wires prod. and characteris. 77−69462
$Pb_xMo_6S_8$, Chevrel phase supercond. prep. and supercond. props. 79−28434
$Pb_xMo_6S_{8-y}$, phase relns., stoichiometry, T_c 78−15378
$PbMo_6S_6O_2$, O-containing Chevrel phases, synthesis and props. 80−108368
$Pb_xMo_6S_8(Se_8)$, prep., metallurgical and supercond. props. 77−32102
$PbMo_6S_8(Se_8)(Te_8)$, Chevrel phase correlation between struct. and supercond. transition temp. 80−7023
$PbMo_6Se_8$, relationship between electronic struct. and supercond. transition temp. 77−85368
$PbMo_6X_8$ (X=S, Se), phonon density of states, mode softening correl. with supercond. transition temp. 79−51714
Pd, disordered film, supercond., occurrence and crit. temp. after He^+ irrad. 79−11261
Pd, elec. resist. and supercond. transition temp., electron-phonon contrib. 78−80085
Pd, electron-phonon coupling and supercond. transition temp. 79−56360
Pd, irradiated film, supercond. 79−78249
Pd, triplet pairing, spin fluctuation and phonon contribution 79−7929
Pd-Ag-D system, instability and superconductivity 78−39248
Pd-Cu(Ag)(Au) alloys-H solid solutions, superconducting transition temp. behaviour *(Russian)* 80−70879
Pd-H, supercond. and phonon softening in unstable systems 79−65587
Pd-H alloys, press. depend., Gruneisen parameters and electron-phonon enhancement 77−63026
Pd-H like compounds, T_c increase by optical phonons 77−1509
Pd-H system, anharmonicity effects on superconducting transition temp. 79−33380
Pd-H system, instability and superconductivity 78−39248
Pd-H(D), band struct. and supercond. props., APW calc. 79−56354
Pd-H(D), conc. depend. and inverse isotope effects 77−80864
Pd-H(D), isotope effect, theory 78−91806
Pd-H(D), isotope effects in supercond. properties 78−6471
Pd-H(D), superconductivity and electron-phonon interaction 80−49975
Pd-H(D) system, superconductivity and phonon softening 79−73626
Pd-Ni-H, hydride formation in high press. range 80−65235
Pd-Ni-H alloys, hydrogenation under high press., superconducting crit. temp. 78−88058
superconducting transition temperature continued
Pd-Ni-H alloys hydrogenised under high press. 77−51834
Pd-Rh-H and Pd-Ag-H, band struct. and supercond. props., APW calc. 79−56354
Pd-Si-H(D) alloys, superconductivity in solid solution and amorphous phase regions, isotope effect 79−56347
$Pd_{1-x}Ag_xH_c$, superconducting transition temp. conc. var. 77−8221
$Pd_{1-y}Ag_yH_x$, electronic struct. and supercond., APW calc. 79−95318
$Pd_{1-y}Ag_yH_x$, superconducting transition temp., APW band struct. calcs. 78−95393
$Pd_{0.91}Ag_{0.045}Rh_{0.045}H_x$, supercond. transition temp. rel. to optical phonon spectrum 79−56355
$PdAl_x$ hydrides, supercond. transition temp. 79−47188
$PdAl_xH_y$ films, ion implantation prop., supercond. crit. temp. 79−87182
PdB_xH_c, superconducting transition temp. conc. var. 77−8221
$Pd_{1-x}Cu_xH_c$, superconducting transition temp. conc. var. 77−8221
PdD, electron-phonon mass enhancement factor and supercond. crit. temp. 79−87184
PdD, isotope effect on transition temp. 79−73615
PdH, electron-phonon mass enhancement factor and supercond. crit. temp. 79−87184
PdH, isotope effect in supercond. *(Russian)* 77−89892
PdH, supercond., book contrib. 80−25037
PdH, superconducting transition critical temperature, BCS theory, phonon spectra *(Spanish)* 80−84535
$PdH_{0.97}$:Fe(Cr), supercond. transition temp. depression, coexistent mag. behaviour 80−49976
PdH_x film, elec. resist. meas. 78−31011
PdH_x, supercond. below 1.5K *(Russian)* 79−91178
PdH_x, superconducting transition temp., inverse isotope effect, Einstein model 80−65734
PdH(D), isotopic vol. effect 77−1511
PdH(D), stoichiometric, ^1H and ^2D NMR, rel. to supercond. T_c 78−72430
PdH(D), superconducting, electronic spin density, isotope effects 78−39262
$PdH_x(D_x)$, 0.2K to 4K 79−99651
$PdH_x(D_x)$, band struct., supercond. props., APW calcs. and neutron scatt. 78−43511
$PdH_x(D_x)$ films, electron-phonon coupling, elec. cond. obs. 80−50011
$PdH_x(D_x)$, isotope effect *(Russian)* 80−88665
$PdIn_xH_y$ films, ion implantation prop., supercond. crit. temp. 79−87182
$Pd_{1-y}Rh_yH_x$, electronic struct. and supercond., APW calc. 79−95318
$(Pd_{95}Rh_5)_1H_x$, elec. resistivity studies 80−59957
$Pd_{30}Zr_{70}$, amorphous alloys, supercond. transition temp., press. depend. 80−84524
radiation induced enhancement of superconductivity 78−39249
Rb_xWO_3, anisotropy in H_{c2} 80−6879
Rb_xWO_3, anomalous supercond. transition temp., electron pairing by acoustic plasmon exchange 79−56358
Rb_xWO_3, phase transitions, supercond. transition temp. and elec. props. 79−28431
Re film, T_c and residual resist., variation with coating thickness 78−47900
Re, plastic deform. rel. to low temp. sp. ht., supercond. *(Russian)* 78−31005
Re-based HCP-BCC binary systems, electronic struct. and supercond. *(Russian)* 79−33375
Re_5Ge_3, RF sputtered 78−14853
Rh borides, RRh_3B_2 (R=rare earth), supercond. and mag. props. 80−97028
Ru borides, RRu_3B_2 (R=rare earth, Y, Th, or U), supercond. and mag. props. 80−97028
Ru-Fe, dil., localised spin fluctuation system, supercond. transition temp., conc. depend. 78−56253
S, transition to supercond. state obs. at high press. *(Russian)* 79−7922
S, transition to supercond. state at high press. *(Russian)* 79−7923
$(SN)_x$, brominated, struct. and elec. props. 80−24914
$(SN)_x$, discontinuous film, DC resist. in normal and supercond. states 79−56357
$(SN)_x$, electronic struct. and opt. props. 78−6256
$(SN)_x$, one-dimens. supercond. mechanism *(Chinese)* 79−47189
$(SN)_x$, supercond. at high press. 78−23194
$(SN)_x$, supercond. props., review 78−6474
$(SN)_x$, supercond. props., press. and field depend. 78−14903
$(SN)_x$, supercond. props., press. depend., up to 9.5 kbar 78−68106
$(SN)_x$, thermoelec. power, 0.1 to 4.2K, phonon drag contrib. and supercond. transition 79−56356
$(SN)_x$, thermopower from 0.15 to 4.2K 80−34427
$(SNBr_{0.4})_x$, effect of bromination 77−59349
$(SNBr_{0.4})_x$, supercond. props. rel. to $(SN)_x$ 79−65581
$(SNBr_{0.4})_x$, supercond. props., dimensionality 80−20344
Sb film A1-type supercond. vapour-quenched transition temp., A7-type phase transition 78−52145
Sb-Te, A1-type, superconductivity 80−29496
$(Sc,M)Rh_4B_4$, M=Ca, Th or rare earth, supercond. and ferromagnetism 78−95438
Sc, superconducting high-pressure phase 79−33378
Sc_4C_3, superconducting phase synthesis at high press. and temp., critical field *(Russian)* 80−65732
Se, A1 type, supercond. destruction by mag. field 78−91825
Si, metallic, superconducting transition temp., press. effects, elec. cond. 80−103777
Si-Au films, quenched condensed, elec. resist. and supercond. 80−54669
Sn, chem. potential change on becoming superconducting 77−28301
Sn, effect of O ion irradiation on supercond. 78−52131
Sn film, crit. temp. enhancement *(Russian)* 80−93021
Sn film, metastable supercond. alloys, produced by low temp. ion implantation 80−88670
Sn, film, superconducting fluctuations, transition temp. *(Russian)* 80−65740
Sn, film, superconducting transition curve stepped struct. due to microwave radiation *(Russian)* 78−2610
Sn, film at supercond. transition temp. thermal noise fluctuations 78−47907
Sn, shell model for clad particles *(Chinese)* 79−69623
Sn, stress depend. of supercond. parameters 77−12045
Sn, supercond. fine particles, sp. ht., fluctuations under mag. field, crit. field and transition temp. 77−80873
Sn, supercond. whiskers, current induced phase transition 78−10600
Sn, superconducting film, radiation induced critical temp. 79−87179

superconducting transition temperature continued
Sn superconducting films, Ge-covered, effect on excess elec. cond. 80−65741
Sn, superconducting fine particles, specific heat exam., fluctuations in zero mag. field 77−28295
Sn, superconductor, paramagnetic effect fine struct. apparent mag. permeability *(Russian)* 79−95550
Sn ternary intermetallic systems, new supercond./mag. cpds., X-ray powder diffr. data 80−100215
Sn, thin layers, EM field penetration, depend. on temp. in mixed and intermediate states 79−65598
Sn ultrathin metallic filaments, appearance of dielec. instability, coexistence with supercond. 80−103784
Sn whisker, stress depend. 77−39988
Sn, whiskers, current-carrying, mutual influence of votlage steps in V-I characts. 78−10601
Sn-Au, amorphous film, elec. resist., temp. depend., supercond. transition temp. 79−91159
Sn-Bi, crystal struct. and superconductivity after appl. of high press. and quenching 80−10531
Sn-Bi(Sb), small κ supercond., phase transitions higher than second order 80−88668
Sn-Cu film, metastable supercond. alloys produced by low temp. ion implantation 80−88670
Sn-In(Cd)(Sb)(Bi) alloy whisker, stress depend. 77−39988
Sn-Sb, A1-type, superconductivity 80−29496
$(Sn)_x$, superconducting polymer, elec. cond., heat capacity and optical props. 80−7028
$Sn_{1.2(1-x)}Eu_xMo_{6.35}S_8$, supercond. transition temp., upper critical field, local spin fluctuations 79−38250
$SnMo_5S_6$, high supercond. T_c, soft mode behaviour 78−14855
$SnMo_6S_8$, cryst. struct., superconducting characts. changes 79−86773
$SnMo_6S_8$, mixed Chevrel phases, crystallography 80−39038
$SnMo_6S_8$, phonon density of states, mode softening correl. with supercond. transition temp. 79−51714
$Sn_xMo_3S_4$, chevrel phase, charge transfer and valence electron conc. 78−6029
$Sn_xMo_5S_6$, supercond. props., effect of W and Re alloying additions, Mossbauer and X-ray diffr. meas. *(Russian)* 79−15245
$Sn_xMo_6S_8$ and $(Sn\text{-}Al)_xMo_6S_8$, Chevrel phase supercond. prep. and supercond. props. 79−28434
$Sn_xMo_6S_8$, struct. anal. supercond. props. 80−97023
$Sn_xMo_6S_8(Se_8)$, prep., metallurgical and supercond. props. 77−32102
$SnMo_6S_8(Se_8)(Te_8)$, Chevrel phase correlation between struct. and supercond. transition temp. 80−7023
$Sr_{0.67}Pt_3B_2$, cryst. struct. and supercond. props. 79−38231
$SrSi_2$, superconducting temperature depression due to mag. field 80−54820
TTF-TCNQ, one-dimens. supercond. mechanism *(Chinese)* 79−47189
Ta film, supercond. transition temp. rel. to struct. and deposition parameters 77−85377
Ta film sputtered onto Cu substrate, microstruct. and supercond. props. 77−85370
Ta, flow stress at superconducting transition, temp. and strain rate depend. 78−2617
Ta, internal friction at T_c *(Russian)* 77−36026
Ta, plastic deform. effect on positron annihilation and supercond. transition *(Russian)* 77−39993
Ta, superconductive transition point as reference temp. 80−107943
Ta wire, emission current effect on superconductor critical parameters 79−91185
Ta:N, superconductive to normal transition anisotropy 80−25031
Ta-Nb-V, solid solutions, superconductivity and charge transfer 79−7926
Ta-Nb-V BCC solid solutions, supercond. and normal state, sp. ht. meas. 78−84347
Ta-Rh, σ-phase alloy, superconductivity and resistance behaviour 80−70882
TaC_xN_y, supercond. and normal props. under hydrostatic press. 77−12049
$TaGe_2$, superconducting transition temp. meas. of sputtered films and bulk 80−7019
Ta_3Ge, superconducting transition temp. 78−47898
TaN film, prep., comp. anal., and supercond. T_c 79−15605
TaS_2 ($4H_b$), press. effects on CDW transitions 77−51680
TaS_2, alkali metal and alkali metal hydroxide intercalates, lattice parameters, supercond. transition temps. 80−25029
TaS_2 intercalates with alkali metals, prep., X-ray anal. and supercond. transition temp. 78−31007
TaS_2 intercalation complexes, superconductivity 78−91803
TaS_2-copper tetra-4-dimethylaminophthalocyanine, dye intercalated layered cpd., struct. and superconductivity 78−84342
TaS_2-Fe, dil. alloy, magnetotransport and superconductivity 77−55516
$TaS_{2-x}Se_x$ layer compound, Hall coeff., 4-200K, rel. to supercond. transition temp. 78−95305
TaS_2(2H), supercond. transition temp., upper crit. field, and interlayer coupling strength 79−56406
TaS_2($4H_b$), electrical cond. and CDW transitions under press., rel. to supercond. 77−43574
$TaSe_2$-Fe, dil. alloy, magnetotransport and superconductivity 77−55516
$TaSe_3$, effect of press. on supercond. transition temp. 79−91182
$TaSe_3$, one-dimens. monoclinic, supercond. below 2.1K, mag. field effect *(Japanese)* 77−43767
$TaSe_3$, superconducting transition *(Japanese)* 78−30880
$TaSe_3$, superconducting transitions and diamagnetism 80−84526
$TaSi_2$, superconducting transition temp. meas. of sputtered films and bulk 80−7019
Ta_5Si_3, elec. resist. and mag. permeability meas., 2.1K *(Russian)* 77−20485
TaS_2(pyridine)$_{1/2}$ intercalation complex, supercond. transition temp., upper crit. field, and interlayer coupling strength 79−56406
TbAl-NdAl, existence of high-temperature superconducting phase *(Russian)* 79−42685
Tc film, electrodeposited, supercond. transition, AC susceptibility meas. 79−95539
Tc film, supercond. transition, complex susceptibility 80−29495
Tc, superconducting transition temperature, resistive transition meas. 77−80861
Tc, superconductivity and Fermi surface calcs. 80−70873
Tc-C film layer structure, obs. of supercond. transition temp. and crit. mag. field oscills. 77−69438
Tc-Fe, dil., effect of Fe impurities on superconductivity 79−61007
superconducting transition temperature continued
Tc-Fe dilute alloys, supercond. and mag. props. 80−29494
^{99m}Tc, supercond. effect on decay rate, lattice consts., transition temp. 78−41671
Te, A1 type, supercond. destruction by mag. field 78−91825
Te, high-press. metallic, supercond. transition temp. press. depend. 80−80435
Te-Au film, metastable supercond. alloys, produced by low temp. ion implantation 80−88670
Te-Au film, supercond. by ion irrad. 80−34544
Te-I, A1-type, superconductivity 80−29496
Th-Cr, supercond., press. meas. to 20 kbar 80−88667
Th-H system, supercond., book contrib. 80−25037
Th-La(Y)(Ce)(Zr)(Bi)-H, hydride form. and supercond. 77−36007
Th-Zr, supercond. transition temp. depend. on constitution 78−88056
Th-Zr alloys, BCC phase, supercond. props. 79−87178
Th_4H_{15}, superconductivity and electron-phonon interaction 80−49975
Th_4H_{15}, ThH_2, phonon densities of states rel. to supercond. props. 77−27960
$Th_4H_{15}(D_{15})$, massive, prep. and characts., supercond. props. 77−43768
$Th_4H_{15}(D_{15})$ normal and supercond., low-temp. sp. ht., Debye temp. and supercond. props. 77−4466
Ti-based HCP-BCC binary systems, electronic struct. and supercond. *(Russian)* 79−33375
Ti-Mo (3 to 35 wt.%), high pressure influence on transition temp. to supercond. 80−107952
Ti-Mo (5 at.%) based alloy, supercond. transition temp. enhancement by varying struct. state 77−20483
Ti-Nb superconducting alloys and cmpds. with A15 struct., H_2 effect on supercond. props 79−28438
Ti-Nb-Si, amorphous alloy, supercond. props. and crystn. behaviour, TEM and DTA study *(Japanese)* 80−84536
Ti-Nb-Zr-Fe, supercond. and paramag. props., effect of Fe additions *(Russian)* 80−65730
Ti-U(Cr)(Mo)(W), dilute, superconducting transition temp. and mag. suscept. 78−47899
Ti-V (19 at.%), aged ω-phase precipitation, incomplete proximity effect 78−60252
Ti-V(Nb)(Ta), influence of different factors on supercond. transition width *(Russian)* 79−1636
$Ti_{1-x}Co_x$, electronic struct. and anomalies of elec. and mag. props. 80−6710
$Ti_{1-x}Fe_x$ alloys, $(0<x\leq 0.2)$, nonmetallic resistivity and simultaneous superconductivity *(Russian)* 77−36005
TiN, high dispersed superconductivity 78−43505
TiN, low-energy ion-stimulated deposited, supercond. props. 80−88664
TiN, Raman scatt. supercond. transition temp., phonon density of states, Debye temp. 78−52499
TiN single crysts., supercond. T_c at high press. 79−38228
TiN, supercond. critical temp., neutron irrad. effect 80−80433
TiN, superconductivity 78−2605
TiN, VPE, and superconductivity *(German)* 77−24964
$Ti_{1-x}Ni_x$, electronic struct. and anomalies of elec. and mag. props. 80−6710
Tl films, supercond. amorphous, effective phonon spectrum and lattice sp. ht. 80−70895
Tl-Pb-Bi, critical field and specific heat and crit. temp. 79−73631
$Tl_{0.33}WO_3$ bronze, elec. resist. meas., anisotropy, supercond. 80−75569
U, phonon-softening 78−10592
α-U-Mo, dil., electronic properties depend. on $2^1/_2$-th order phase transition under high press. *(Russian)* 80−11128
$U_6Fe_{0.98}$ supercond. transition temp. reduction by neutron irradiation 77−63020
$U_xPb_{1+x}Mo_{6+y}S_8$, sputtered supercond. props. 80−50019
$(V,Fe)_3M$, M=Si, Ge, Ga, solid soln. form. and supercond. T_c *(Russian)* 78−80512
$(V,Nb)_3Ga$, $(V,Nb)_3Ge$ and $(V,Nb)_3Si$ solid solns., conc. depend. 77−36006
$(V,Nb)_3Si$ type alloy with A15 struct., depend. on stoichiometry *(German)* 77−69444
V, amorphous film, supercond. props., gaseous impurities effect *(Russian)* 78−72301
V, and V-Nb alloy, effect of purity and alloying with Ta, Cr, Mo or Re 77−85375
V, effect of O ion irradiation on supercond. 78−52131
V, evap. layer, ion bombardment effect on superconducting transition temp. 78−52136
V, Fermi surface area, effective heat, optical masses, surface anisotropy critical temp. depend. *(Russian)* 79−90943
V film, crit. temp., crit. field, resist. and struct. *(Russian)* 77−4475
V film, resist. supercond. transition 80−25033
V film, resistive transitions scaling behaviour 79−15248
V film, scaling behaviour of resistive supercond. transitions 79−56363
V, mixed state, US attenuation purity depend., crit. temp. and energy gap 77−47935
V, plastic deform. effect on positron annihilation and supercond. transition *(Russian)* 77−39993
V, spin fluctuations effect on T_c, from sp. ht. and mag. suscept. 80−7030
V, supercond., influence of plastic deform. 77−85378
V/Al-Al_2O_3-Pb tunnel junction, superconducting transition, critical currents, Josephson effect *(Russian)* 80−29507
V-Al/Cu-Ge composite superconductors, transition temp. and upper crit. field, heat treatment effects 79−38268
V-Al/Cu-Ge composite tape, transition temp., upper crit. field 78−68126
V-C film layer structure, obs. of supercond. transition temp. and crit. mag. field oscills. 77−69438
V-Ga(Ge)(Si), fast quenching of A15-phases *(German)* 77−36014
V-Hf-Nb(Zr), multifilamentary, superconducting props. improvement 79−38267
V-M, M=Ti, Nb, Sm, vacuum deposited supercond. films, T_c chem. comp. depend. *(Russian)* 78−19174
V-Nb-Ta, elec. resist. and electron-phonon interaction parameters, comp. depend. 78−14862
V-Re system, discovery of supercond. A-15 phase 78−88060
V-Si-C alloy film, crit. temp. and elec. resistivity, correl. with C content 78−72299
V-Ta alloys, electron-phonon interaction and supercond. transition temp. *(Russian)* 79−28426
V-Ti(Cr) amorphous films, supercond. transition temp. 79−60953

superconducting transition temperature continued
V-Zr-Nb alloy, rel. between density of states and martensitic and superconducting phase transition temps. 78−10594
V_3Al film, quasiamorphous, supercond. phase formation by heat pulse 77−63017
VC, metastable supercond. phase, effects of rapid quenching on transition temp. 78−2611
$(V_{1-x}Cr_x)_3Si$, elastic moduli, 4.2 to 290K, softening near supercond. transition *(Russian)* 80−92582
$V_{3-x}Cr_xSi$, x=0 to 3, struct., supercond. and mag. props. 80−1962
$V_3(Fe,Ge)$, struct. and supercond. transition temp. *(Russian)* 79−7920
V_3Ga, A15 cpd., hydrogenation effects on supercond. transition temp., lattice parameters 80−103772
V_3Ga, as-cast and annealed *(Russian)* 78−56618
V_3Ga, cast, effect of hydrostatic extrusion on supercond. props. *(Russian)* 77−21215
V_3Ga, comp. and LRO effects 77−39992
V_3Ga composite prep. and testing for high-field supercond. magnet 79−30513
V_3Ga, crit. temp. and field, prep. from V-Al and Cu-Ga 78−43506
V_3Ga, high current density multifilament wire, neutron effects on equilibrium and transport props. 78−52126
V_3Ga, long-range order parameter variations determ. and correls. with supercond. T_c 77−11504
V_3Ga, neutron irrad. effects on transition temp. *(Japanese)* 79−82707
V_3Ga, nuclear magnetic relaxation, near T_c *(Russian)* 79−42852
V_3Ga, single crystal prep. by iodine transport, supercond. T_c meas. 78−48294
V_3Ga, structure effects on supercond. props. and electron spectrum *(Russian)* 77−80862
V_3Ga, supercond., neutron-induced disorder revealed by isochronal annealing 77−72938
V_3Ga, supercond. A15 phase, prep. by controlled precip. 80−81000
V_3Ga, superconducting transition temp. and electron density of states 77−32105
V_3Ga, superconducting transition temp., metallurgical processing, struct. 77−63019
V_3Ga-V_3Pt alloy, comp. depend. *(Russian)* 77−59347
$V_3Ga(Si)$, high T_c supercond., electron-phonon coupling, effect of electronic density of states sharp struct. 78−14877
V_3Ge, A-15 cpds., nucl. mag. relax. in normal and supercond. state 80−49993
V_3Ge, A15 cpd., hydrogenation effects on supercond. transition temp., lattice parameters 80−103772
V_3Ge, anisotropic thermal vibrations, lattice const. X-ray study 80−34164
V_3Ge, bronze-processed, stress-induced enhancement of supercond. T_c 78−64159
V_3Ge film, α-particle induced defects and stoichiometry, effect on T_c 77−32101
V_3Ge, forbidden Bragg refls., rel. to supercond. transition temp. 79−15251
V_3Ge, formation by composition diffusion process, and crit. temp. determ. 77−85959
V_3Ge, superconducting, high transition temp., sputtering 78−15309
V_3Ge, superconducting A-15 type compounds, transition temp., radii ratio and structure *(Chinese)* 80−44752
V_3Ge, superconducting transition temp. and electron density of states 77−32105
$V_3Ge_xOs_{1-x}$, low temp. props. 79−99652
$V_3Ge(Si)$, electron-phonon coupling and supercond. crit. temp. 79−33379
$V_3Ge(Si)$ film, ^4He irrad. induced defect prod., T_c var. 77−8220
$V_3Ge(Si)$, supersuperconducting transition temp., correl. with resist. anomalies and defect struct. 77−47920
V_2Hf base Laves phase compound tapes, supercond. props., prep. 77−40011
$V_2Hf_{1-x}Zr_x$, normal and supercond. state, transition temps., mag. susceptibility and specific heat determ. *(Russian)* 80−60132
V_3In, hypothetical, electronic struct., lattice parameters and possible supercond. transition temp. 79−23891
$V_{75-x}M_xGa_{25}$, M=Ti, Cr, Mn, Fe, Co, Ni, supercond. transition temp. and electron-phonon coupling parameter 79−60952
VN, electronic struct. of vacancies, effect on supercond. transition temp. 80−29347
$VN_{0.74}$ and $VN_{0.89}$, low-temp. specific heat and superconducting critical temp. meas., density of states 80−54835
V_3P, superconducting transition temp. 78−47898
$V_{1-x}Pt_x(Ga_x)(Si_x)$, A-15 cpds., nucl. mag. relax. in normal and supercond. state 80−49993
V_3Si, A15 compound, microscopic model of supercond. and martensitic transform. 77−8226
V_3Si, A15 cpd., hydrogenation effects on supercond. transition temp., lattice parameters 80−103772
V_3Si based ternary solid soln., supercond. T_c and paramag. susceptibility *(Russian)* 77−59348
V_3Si, channelling, at displacements and electron phonon/defect interactions 77−84815
V_3Si, chemical composition effect on phase transition and transition temp. 78−14860
V_3Si, electron spectrum characts., mag. susceptibility depend. on resistivity ratio 79−95320
V_3Si, electronic struct., electron-phonon interaction and high temp. superconductivity, APW calc. 78−14871
V_3Si embedded in resin, composite supercond., high transition temp. 80−88660
V_3Si film, α-particle induced defects and stoichiometry, effect on T_c 77−32101
V_3Si film, optical props. *(Russian)* 80−93418
V_3Si film, quasiamorphous, supercond. phase formation by heat pulse 77−63017
V_3Si film, sputtered, high press. induced shifts in supercond. transition temp. 77−85374
V_3Si film, superconducting props. 79−38215
V_3Si, Hall effect, 77K to superconducting transition temp. 78−43359
V_3Si, ion irradiated, influence on struct., resist., and supercond. transition temp. 80−54823
V_3Si, low fluence neutron irradiation, behaviour of supercond. transition temp. 78−43509
V_3Si, low temp. irrad. with 20 MeV S ions, effect on supercond. props. 79−38223
superconducting transition temperature continued
V_3Si, martensitic transform. coupling with supercond. transition 78−44126
V_3Si, neutron irrad., sound velocity, magnetic susceptibility and upper critical field 78−88074
V_3Si, neutron irradiated, A15 compound, recovery of T_c by annealing 78−52132
V_3Si, neutron irradiated single crystal, superconducting transition temp. widths, resistivity and heat capacity meas. 78−91802
V_3Si, neutron-irrad., ht. capacity and resistivity 78−88075
V_3Si, nontransforming, press.-induced phase transformation 78−80084
V_3Si, nuclear magnetic relaxation, near T_c *(Russian)* 79−42852
V_3Si, optical props. and electron-phonon interactions 80−2510
V_3Si, plastic deform. effect on supercond. props. 80−29500
V_3Si, single cryst., double supercond. transitions 79−28430
V_3Si, single cryst. growth by electron beam melting 78−64467
V_3Si, supercond. and struct. transitions *(Russian)* 78−52118
V_3Si, supercond. props., effect of neutron irrad. 80−80463
V_3Si, supercond. structure and properties *(German)* 80−93631
V_3Si, supercond. transition temp. and phase transform. at press. up to 45 kbar 79−56352
V_3Si, superconducting transition temp. press. depend., for shear-stress induced tetragonal phase 77−36010
V_3Si, transforming and nontransforming, high press. effects 78−80086
V_3Si, US anomaly when cooled below martensitic and supercond. transition temps. 80−20354
V_3Si-Fe, mag. impurities effect on supercond. props. 77−1524
$V_3(Si_{1-x}C_x)$, bulk, effect of C on supercond. transition temps. and microstructure 80−54824
$V_3Si(Ga)$, coherence parameter, nonlinear high temp. supercond. elements with A-15 lattice *(Russian)* 80−60127
$V_3Si_{1-x}Ge_x$, elastic props., 77 to 290K, rel. to supercond. transition temp. *(Russian)* 80−66560
$V_3Si_xOs_{1-x}$, supercond. transition temp. and paramag. susceptibility 79−28436
V_3Sn, A-15 cpd., normal-state elec. resist. 80−75542
V_3Sn, ultrafast quenched and subsequently tempered, supercond. T_c 78−64162
V_3Ti, metastable supercond. phase, effects of rapid quenching on transition temp. 78−2611
$(V_{1-x}Ti_x)Ge$, pseudobinary A15 compound, supercond. transition temp. 80−49970
$W_{70}Si_{20}B_{10}$, amorphous alloys obtained by liq. quenching, superconductivity 80−75670
Xe, metallic state transition under high press., supercond. *(Russian)* 79−60713
$(Y,La)B_6$, superconducting transition temps., impurity effects 80−20341
YGe_2 film, supercond. obs. 77−72939
$Y_xLu_{1-x}Ir_4B_4$, supercond., magnetism and metastability 80−29501
Y_2O_3, synthesis at high-press and temp., supercond. 80−2513
$Y_xPb_{1\pm x}Mo_{6+y}S_8$, sputtered supercond. props. 80−50019
YRh_4B_4, supercond., anomalous cond.-electron polaris. 80−25047
$Y(Rh_{0.85}Ru_{0.15})_4B_4$, mag. ordering and supercond. 78−14861
YS, supercond. transition temp. and lattice dynamics 79−56361
YS, superconductor, resonances in generalised susceptibility and phonon anomalies 79−60443
$YbFe_xMo_6S_8$, singularities in mag. and supercond. props. 79−51710
$YbMo_6S_8$, supercond., low temp. thermal and mag. props. 78−14904
Zn film, supercond., SAW US attenuation 79−73633
Zn film for energy selective phonon detection 80−92621
Zn, superconducting transition temp., electron-phonon mass enhancement, pseudopot. calcs. 78−2604
Zn whisker, stress depend. 77−39989
Zn-Mn, dil., Kondo effect and impurity interactions in resist., transition to supercond., 0.05-14K 78−14721
$ZnMo_6S_8$, mixed Chevrel phases, crystallography 80−39038
$ZnMo_5S_6(Se_6)$, Chevrel-phase, low temp. struct. instability rel. to supercond. 77−47919
Zr, H(D) implanted, superconductivity enhancement obs. 80−70884
Zr-Pd, metallic glasses, electronic props. and supercond. 79−73486
Zr-Rh alloys, amorphous, thermal relax. effects on electronic and supercond. props. 79−65575
Zr-Rh-H(D), superconducting transition temp., effect of H(D) conc. 80−84532
Zr-V, superconductivity and metallurgy of C15 materials 79−4610
Zr_xBe_{1-x} noncrystalline alloy, phonon-electron scatt., superconducting temp. 80−54330
ZrC, supercond. transition temp. and lattice dynamics 79−56361
ZrC_x, x=0.99 to 0.13, elec. cond., supercond. state 78−43504
$Zr_{70}Co_{30}$, metallic glass, low temp. resist., supercond. T_c 79−38235
$Zr_3Co_{1-x}M_x$, M=Cu, Ni, Fe, Mn, Ag, and Ru, phase stability and supercond. T_c 78−80519
$Zr_{65}Cu_{35}$, metallic glass, low temp. resist., supercond. T_c 79−38235
ZrGe, film, supercond. obs. 77−72939
$ZrGe_2$, RF sputtered 78−14853
$Zr_3Ge(P)(Sb)(Si)$, superconducting transition temp. 78−47898
$Zr_xHf_{1-x}V_2$, polycrystalline superconductor, resist. and mag. susceptibility, transition temp., temp. depend. 80−25113
ZrN, plasma-formed, ESCA and supercond. transition temp. 78−19697
$Zr_{70}Ni_{30}$, metallic glass, low temp. resist., supercond. T_c 79−38235
$Zr_{1-x}S$, correl. with short- and long-range ordering of vacancies 77−19945
$Zr(V,Al)_2$, struct., supercond. props., elec. resist. and mag. susceptibility, 4.2 to 300K *(Russian)* 79−15246
ZrV_2, C-15 struct., phase transitions, elec. cond., crystal lattice parameters *(Russian)* 80−54826
ZrV_2, supercond. rel. to struct. instability *(Russian)* 78−23196

superconductive tunnelling
see also Josephson effect; proximity effect; superconducting junction devices; tunnelling spectra; tunnelling spectroscopy
A15 films, electron beam codeposition, synthesis and props. 78−72296
A15 type compound, props. and one-dimensionality 80−2530
A15-type compounds, review of superconducting props. and structure 80−70909
acoustic coupling and effective quasiparticle lifetime 77−20499
amorphous superconductor, Eliashberg function, tunnelling and crit. temp. anal. 80−80455
amorphous superconductor, ratio of energy to transition temp. 78−10619
branch-imbalance relaxation times 80−20358
Chevrel-phase superconductors, lattice dynamical calcs. 79−33056

superconductive tunnelling continued
coherent longitudinal phonon injection effect in nonequilib. superconds. 79−47205
conduction electron spins, surface relax. 79−60995
critical temperature calc. using tunnel expts. results 78−60241
current characteristics of supercond. tunnel junctions 80−60150
Current-monitored superconducting bridge junctions *(Russian)* 78−23205
dielectric crystals, doped, phonon spectroscopy using supercond. tunnel junctions 79−90738
dirty type I superconductors,, Al-Formvar-Sn junctions, mode propagation, well below Al transition temp. 80−15662
dynamical problems, approx. Hamiltonian, variational method *(Chinese)* 80−44768
elastic tunnelling spectroscopy of single-particle excitations 78−56260
electron tunnelling spectroscopy, review of principles and techniques, superconductivity 78−90253
electron-phonon interaction function determ. using dispersion relation 78−34931
energy gap anisotropy, normal layer proximity effect 80−84558
energy gap determ. by pt. contact tunnelling 78−19185
ferromagnet-Al_2O_3-Al, electron spin-polarisation, band model 77−72947
film, electric field under tunnel injection conditions 80−103792
film, gap enhancement due to quasiparticle tunnel injection 78−56262
film, geometrical reson. effect, electron tunnelling density of states meas., review *(French)* 78−2626
film, nonequilibrium, energy spectra of emitted phonons 77−27957
film, thick, phonon damping of virtual levels 79−4626
film, ultrathin, two-layer model 78−14849
films, containing single flux vortices, tunnelling 77−59360
films, thin normal metal, tunnel electron injection *(Russian)* 79−19696
Formvar, phonon spectrum from Al-Formvar-Pb junction electron tunnelling 77−59080
function, quasi-particle injection and disappearance of supercond. 77−20497
Ginzburg-Landau equations, electron-hole pairing, quantum coherent phenomena *(Russian)* 77−80869
granular metal, supercond. transition, increased resistance rel. to quasiparticle tunnelling 80−88689
helical order of spins in supercond. 80−70888
high temperature superconductors, tunnelling spectra, electron pairing anal., appl. to Nb_3Sn 79−87205
inelastic electron tunnelling spectroscopy, advantages of supercond. electrodes 79−4625
Josephson junctions fabrication, tunnelling through edge-grown barriers 80−100567
junction, characterisation of electron tunnelling conductance curves, use of barrier parameters 78−84356
junction, electron tunnelling, effect of dissolved O^{2-} 78−80100
junction, extension of Feuchtwang method, Green's function theory 78−68121
junction, involving high temp. A15 lattice-type superconds., nonlinear phenomena 78−14898
junction, nonequil. excitation distrib. and phonon generation *(Russian)* 78−23204
junction, nonequilibrium phonon effect on supercond. states with 2 coexisting energy gaps 80−84561
junction, phonon spectroscopy of paramagnetic crystals 80−84634
junction, quasi-particle recomb. and 2Δ-phonon-trapping 77−8236
junction, selfblocking of tunnel current, current-voltage characteristics *(Russian)* 78−95397
junction, two-band model 80−2524
junction resistance effect on microwave-Josephson tunnel coupling *(Chinese)* 78−80099
junctions of superconds. with paramag. impurities *(Russian)* 77−80878
layered metal structure, acoustic size effect, sound attenuation anisotropy *(Russian)* 79−46752
magnetic transition-metal impurities effect on tunnel charact. *(Russian)* 78−34927
metal, ferromag., electron spin polarised tunnelling from superconductors 79−78263
metal, reliability of tunnel density of states 79−28483
metal-insulator-superconductor junction, electron interactions with phonons and mag. impurities 77−16004
metal-oxide interface, surface states, enhanced tunnel conductivity 80−80456
metal-semiconductor disordered interface, supercond. transition temp. enhancement by bipolaron interface centres 80−84528
metal-semiconductor interface, disordered, supercond. 80−20347
microbridge properties in pure limit *(Russian)* 77−89903
microbridges, neg. resist. and hot electrons, model 78−60254
microwave-induced effects 79−87202
microwave-induced step height, mag. field effect *(Chinese)* 78−6482
MIM diode, US effect on tunnel current for normal and supercond. metals 77−16006
N-S boundary resistivity, tunnelling contact resistance *(Russian)* 80−93048
nonequilibrium distribution functions of quasiparticles and phonons calc., possible existence of negative resist. 77−89904
nonequilibrium double junction, tunnelling charact. 78−14893
nonequilibrium double tunnel junction, anal. 79−19698
nonequilibrium induction of superconductivity by tunnelling injection 79−91194
nonequilibrium state, studied by large quasiparticle injection from external current source 78−10614
nonequilibrium states, narrow nonequilibrium sources *(Russian)* 80−88687
nonequilibrium states, tunnel injection into superconductors, theory *(Russian)* 79−47198
nonequilibrium states of film, supercond.-insulator-supercond. tunnelling charact. 77−47925
nonequilibrium states of normal metal films in regime of electron tunnel injection *(Russian)* 79−19695
nonequilibrium supercond. states under tunnelling injection 79−56415
nonequilibrium superconducting states with two coexisting energy gaps 79−51724
nonequilibrium superconductor, normal component drag by condensate, tunnelling *(Russian)* 80−93051
nonequilibrium superconductor with optical and tunnel quasiparticle pumping, threshold instability and inhomogeneous states *(Russian)* 79−87209

superconductive tunnelling continued
nonequilibrium superconductor with tunnel injection quasiparticles, phase transitions 79−69636
nonequilibrium superconductors, obtained by tunnel injection, quasiparticle distrib. function 79−56413
nonequilibrium superconductors, transients, phonon distrib., supercond. gap, Boltzmann-BCS formulation 78−52149
nonthermal quasiparticle distribs., I(U) characts. 79−65609
normal conductance change, origin 80−65753
normal electron tunnel elements, interaction with 0.6-40 μm EM radn., radn. detection appl. *(German)* 79−24103
normal metal-superconductor structure, laser irrad. theory of current voltage characts. *(Russian)* 77−80877
order parameter fluctuations, pair tunnelling, review 79−1642
order parameter reson. fluctuations rel. to tunnel current *(Russian)* 78−31019
order parameter singularities, tunnelling currents, Fermi surface calcs. *(Russian)* 80−80458
phonon generation and detection by tunnelling *(Japanese)* 77−28306
photon-assisted tunnelling obs. of supercond. gap variations *(Russian)* 77−43786
proximity effect for superconductors containing transition metal impurities, tunnelling conductance calc. 78−52160
quantum noise effects in tunnel junctions in 0-1 mV bias range 80−80449
quasi one-dimensional metal, crit. temp. for phase transition *(Russian)* 79−78253
quasi-one-dimensional metals, supercond. transition temp., tunnelling amp. depend. 79−42683
quasiparticle and phonon lifetimes, theory 77−20488
quasiparticle charge imbalance induced by supercurrent with thermal gradient 80−34546
quasiparticle mixers, supercond.-insulator-supercond., conversion gain prediction 80−70901
quasiparticle superconductor-insulator-superconductor tunnel junctions as microwave detectors 80−65744
quasiparticle tunnelling, enhancement in superconductivity 78−76197
refrigerator, cooling power and efficiency, tunnelling calc. 80−57311
resistance from superconductor in supercond.-normal metal interface 78−43525
resistive states at superconducting junctions *(Russian)* 79−19706
ring with low capacitance Josephson point contact junction, flux transition mechanisms 80−44770
ring with weak links, critical voltage for flux tunnelling 80−75685
spin polarised electrons 79−4627
SQUID ring, fluxoid transition mechanisms, quantum vs. thermally excited 80−100565
stability of superconducting states out of thermal equilib. 80−2526
superconducting bridge, quantized vortex formation *(Russian)* 78−43521
superconducting-normal interface, boundary resist. 80−50006
superconductivity proximity effect, McMillan tunnelling model 79−73639
superconductor-insulator-superconductor tunnel junctions, responsivity to microwave radiation 80−100553
superconductor-semicond. device research, future prospects 79−28467
surface relaxation time of conduction electron spins 78−91814
teaching, cryostats for laboratory course in supercond. 79−58494
thermal conductivity of tunnelling junctions meas. 77−36029
thermoelectric quasiparticle transport, tunneling potentials 79−47200
transistor, superconducting 79−28466
transition metal, tunnel junctions, phonon struct., junction quality 79−11274
transition metal glasses and amorphous films, supercond. and electronic props. 79−73612
tunnelling density of states, ultrasound attentuation, in superconductors with overlapping bands 79−7934
two-band model tunnelling density of states 77−51854
Ag film-Pb sandwich, supercond., effective renormalisation interactions 79−56397
Ag-Mn, spin-flip scatt. time, superconductive tunnelling 79−8003
Al film, deviations of equilib. order parameter from mean field theory 77−69453
Al film, implanted at low temp. by H or D, critical temp. enhancement *(French)* 77−8237
Al film, quasiparticle branch mixing rates 79−78269
Al film, supercond., meas. of effective quasiparticle recombination times, density of electronic states at Fermi level 79−38264
Al film, supercond. crit. field, spin-polarized tunnelling meas., test of high-field supercond. theory 79−87220
Al film in tunnel junction, new supercond. state obs. at high quasiparticle injection 77−72949
Al film with Er impurity, spin-flip scatt. and supercond. order parameter dynamics 79−78267
Al, microwave enhanced energy gap, tunnelling meas. 77−51853
Al, supercond., crystalline and granular, tunnelling meas. 78−84355
Al, supercond. film, intrinsic and expt. quasiparticle recomb. times 77−15999
Al, supercond. film, quasiparticle injection, tunnel junction characts. 78−76193
Al, superconducting, quasiparticle charge distrib. due to tunnel injection 80−44771
Al, superconducting film, resistive states, voltage switching effect in tunnelling systems *(Russian)* 79−7938
Al tunnel junction, quasiparticle recomb. times and electronic density of states at Fermi level 79−56414
Al, tunnelling characts., phonon struct. enhancement by high energy spectral weight 79−60984
Al/AlO_x/La-rare earth metal tunnel junctions, cond. meas., cryst. field effects 80−88694
Al/formvar/Al(Sn) structures, low frequency phonon spectroscopy by tunnel effect 78−23206
Al-Al oxide-$Bi_{1-x}Pr_x$ tunnel junction, cryst. field struct. obs. in conductance 78−84358
Al-Al_2O_2-ferromagnet struct., electron tunnelling into ferromagnetic metals 80−60104
Al-Al_2O_3-Pb junction, Pb supercond. film behaviour in mag. field 78−14894
Al-Al_2O_3-ferromagnetic alloy junction, spin polarised tunnelling results for Ni alloys 78−39372

superconductive tunnelling continued
Al-Al-PbBi double tunnel junction structs., quasiparticle relax. times, energy and temp. depend. 79−56412
Al-AlO_x-Pb junctions, organic ring cpd. doped, asymmetries in elastic and inelastic tunelling 79−95549
Al-AlO_x-PbBi tunnel junction, quasiparticle energy distrib. in nonequilib. supercond. 77−80881
Al-Er, dil., order parameter dynamics and collective modes, pair tunnelling meas. 79−56409
Al-formvar superconductive junction, Ginzburg's generalised jellium model 80−15663
Al-Formvar-Sn coupled films, Ginzburg's excitonic supercond. model 80−97039
Al-insulator-Pb, clean and doped tunnel junctions, barrier profiles 79−56445
Al-monolayer-Pb, supercond. junction, electron tunnelling meas. 79−28482
Al-Ox-Ag-Cu-Pb and Al-Ox-Cu-Ag-Pb trilayer junctions, tunnelling characts. 79−87208
Al-Pb junction, intensity and line-shape measurements in inelastic electron tunneling spectroscopy 79−24104
Al-Pb:Bi, tunnel-junction relax. oscillator, appl. to thermometry 79−85138
Al-PbBi superconducting tunnel junctions, optically illuminated, quasiparticle energy distribution 80−75688
Al-V-Ti junction, spin-dependent electron tunnelling 79−19700
Al_2O_3, doped, phonon spectroscopy in supercond. tunnel junctions 79−90738
Al_2O_3, inelastic electron tunnelling spectroscopy of adsorbates, MgO comparison 80−88686
$Al_2O_3:Fe^{2+}$, phonon spectroscopy using superconducting tunnel junctions 78−91389
Bi-Tl film, superconductivity and phonon spectrum *(Russian)* 79−91190
Co-Al_2O_3-Al, electron spin-polarisation, band model 77−72947
$Cu_{1.8}Mo_6S_8$, electron tunnelling spectroscopy expts. *(German)* 80−107966
$Cu_{1.8}Mo_6S_8$, supercond. energy gap and phonon-induced structs. in tunnelling density of states 79−51728
Fe-Al_2O_3-Al, electron spin-polarisation, band model 77−72947
Ga-Ag tunnel junction, evidence for existence of anisotropy of supercond. energy gap 80−20357
GaAs-Pb junctions, electron tunnelling under high press., transition temp., energy gap, phonon energies 79−15257
GeTe, film, semicond., supercond. energy gap and crit. field, tunelling meas. 77−24644
^{4}He cryostat design, superconductive tunnelling study *(Spanish)* 80−73347
In, energy gap and phonon frequencies under press., tunnelling meas. 77−32112
In-Mn, dilute alloy, local excited states, electron tunnelling observation 80−34565
In-Sn alloy, phonon spectra and superconductivity, single-particle electron-tunnelling expts. 77−40005
InAs-oxide-$Pb_{50}Bi_{20}$ junction, hot electron temp. in InAs meas. by tunnelling 77−4352
La film, tunnelling investig., multiple band effects 77−8244
La-Pr, superconductive tunnelling, cryst. field effects 78−88085
$LaAl_2$, doped with Tb, Nd, or Pr, crystal field effects, tunnelling within mK range 80−70907
$(La_{1-x}Ce_x)Al_2$, Kondo supercond., tunnelling density of states 78−14900
$(La_{1-x}Ce_x)Al_2$, Kondo supercond., tunnel junction fabrication with wax barriers, tunnelling meas. 78−19191
$LaPb_3$, doped with Tb, Nd, or Pr, crystal field effects, tunnelling within mK range 80−70907
$LaSn_3$, doped with Tb, Nd, or Pr, crystal field effects, tunnelling within mK range 80−70907
MgO, inelastic electron tunnelling spectroscopy of adsorbates, Al_2O_3 comparison 80−88686
Mo-Re alloys, supercond. energy gap and transition temp., tunnelling meas. 79−56405
Mo-Si(Ge)(Al), amorphous supercond. alloy, produced by coevaporation, struct. and supercond. 79−91179
Nb, at thermally oxidised junctions, supercond. parameters determ. 79−19699
Nb, electron-coupled phonon spectrum, effects of strain 79−7943
Nb, energy gap determ. by pt. contact tunnelling 78−19185
Nb film, meas. of annealing characteistics 79−7944
Nb, plastically deformed, changing lattice dynamics 78−67793
Nb, single cryst. 79−47203
Nb sputtered film, tunnelling charact. 79−4621
Nb, strong-coupling microscopic parameters, electron tunnelling obs. 78−14888
Nb, superconducting, state of art of tunnelling 79−69634
Nb, superconducting parameters, tunnelling meas. 79−91192
Nb tunnel junction, temp. dependent props., 2-9L 77−24642
Nb:N,H(D), thermal cond., 0.07 to 1.5K, influence of N interstitials 79−65601
Nb-Ge(Si), amorphous supercond. alloy, produced by coevaporation, struct. and supercond. 79−91179
Nb-I-Pb, junctions, fine struct. of current-voltage curves, tunnel currents *(Russian)* 79−19693
Nb-NbO_x-Al/Pb supercond. proximity function, production by RF sputtering and photolytographic techniques 77−43787
Nb-NbO_x-Pb tunnel junctions at 4.2K, conductance of oxide barrier 80−7046
Nb-NbO_x-PbIn tunnel junctions with ultra-thin Nb electrodes 79−56398
Nb_3Ge, high T_c films, electron tunnelling and AES anal. 79−28471
Nb_3Ge, ordered and disordered A15 phases, energy gaps, tunnelling 77−8235
Nb_3Ge superconducting film 77−32123
Nb_3Ge, superconducting thin films, energy gaps from tunnelling meas. 80−25050
Nb_3Sn, delayed flux entry and surface barriers, tunnelling obs. 77−59355
Nb_3Sn, high-temp. supercond., tunnelling spectra, electron pairing anal. 79−87205
Nb_3Sn, superconducting thin films, energy gaps from tunnelling meas. 80−25050
Nb_3Sn tunnel junctions, tunnelling density of states and electron-phonon spectral function 79−65618

superconductive tunnelling continued
$Nb_{1-x}Zr_x$, supercond., McMillan-Rowell tunnelling spectroscopy 79−60985
$Nb_{20}Zr_{80}$, supercond., US attenuation 80−44766
Ni and Ni alloys, tunnel currents, spin polarisation, simple band theory interpretation 79−78451
Ni-Fe(Cr) alloy film, electron spin polarisation, meas. using supercond. tunnel junction 77−69637
Ni(alloy)-Al_2O_3-Al, electron spin-polarisation, band model 77−72947
Pb, distribution function branch imbalance, relaxation 79−33401
Pb, Fermi electron vel. change under press., Tomasch tunnelling *(Russian)* 77−72950
Pb, film, first order transition due to quasiparticle injection 78−23208
Pb film, quasiparticle and phonon lifetimes, tunnel junction meas. 77−20498
Pb film, supercond., meas. of effective quasiparticle recombination times, density of electronic states at Fermi level 79−38264
Pb, laser irradiated tunnel junction, nonequilibrium quasi-particle distrib. function, thermal regime *(Russian)* 79−42700
Pb, supercond., quasiparticle and phonon propagation 79−42689
Pb, supercond. film, intrinsic and expt. quasiparticle recomb. times 77−15999
Pb superconducting film, nonequilib. gap instability and phase transition under intense tunnel injection 79−28476
Pb superconducting junction, neutron irradiated, tunnel spectroscopy 78−10618
Pb tunnel barrier, oxidation in humidity-controlled O_2 regulated atm. 78−19187
Pb tunnel junction, quasiparticle recomb. times and electronic density of states at Fermi level 79−56414
Pb tunnel junctions, nonequilibrium occupation of quasiparticle states 79−56416
Pb/Bi-I-Al tunnel injected nonequilibrium supercond. struct., diffusive quasiparticle instability, multiple gap states 80−50005
Pb-Bi, supercond. tunnelling, effect of phase composition and press. 79−15261
Pb-Cd thin films, electron tunnelling study of supercond. proximity effect 80−2525
Pb-Cd-Pb, supercond.−normal-metal−supercond. junction, crit. currents 80−107965
Pb-Cu(Ag) double layers, intermetallic boundary effects, tunnelling 80−88692
Pb-Fe multilayers, zero pair pot. verification by supercond. tunnelling 80−54841
Pb-formvar-Al tunnel junction, excitonic superconductivity, BCS theory, generalised jellium model 80−75684
Pb-I-NiCr-Cu double tunnel junction struct., supercond. energy gap suppression and instability 79−56417
Pb-In, electron tunnelling under hydrostatic press. 77−51850
Pb-In alloys, supercond. energy gap determ. by pt. contact tunnelling 78−19185
Pb-In film, superconducting tunnel junction, pulsed quasiparticle injection 80−84565
Pb-PbO-Pb junction with nonequilib. quasi-particle population, tunnel effect under laser irrad. *(Russian)* 77−43788
Pb-Si superconducting solutions, effect of hydrostatic compression on tunnelling *(Russian)* 80−65746
Pb-Si:Sb Schottky tunnel junction, variable range hopping assisted tunnelling 80−39670
Pb-SiO_2-$Pb_{0.8}Sn_{0.2}Te$, prop. of insulating film for tunnelling study on zero bias anomaly 79−15608
Pb-Tl-Bi-In, localised phonons studies by supercond. tunnelling 79−87210
Pb-Tl-In, localised phonons studies by supercond. tunnelling 79−87210
$Pb_{0.9}Bi_{0.1}$-insulator-$Pb_{0.9}Bi_{0.1}$ junction, I-V charact. for quasiparticle recombination 79−15259
PbIn oxidised electrodes, symm. and asymmetric supercond. tunnel junctions, subharmonic gap struct. study 79−60981
PbIn-oxide-Pb tunnel junction, subharmonic gap struct., line shape and rel. magnitude 77−80882
PbIn-oxide-Pb(PbTl) thin film tunnel junction, subharmonic group struct., multiparticle tunnelling theory 79−56438
Pb_xIn_{1-x}-Pb_yTl_{1-y} asymmetric supercond. tunnel junctions, subharmonic gap struct. 79−15260
$PbMo_6S_8$, electron tunnelling spectroscopy expts. *(German)* 80−107966
PbTe-based structures, zero anomaly of tunnel cond. 79−24107
Pd-H(D) system, normal state phonon resist. and supercond. tunnelling density of states 79−56402
PdD_x, optical phonon spectra, supercond. tunnelling meas. 79−19701
PdH_x, optical phonon spectra by supercond. tunnelling meas. 79−19701
$PdH_x(D_x)$ films, electron-phonon coupling, elec. cond. obs. 80−50011
PdZr, amorphous, supercond., US props. 80−44765
SN, quasiparticle recomb. time and normal electronic density of states at Fermi surface from tunnel junction expts. 79−24108
$(SN)_x$, differential tunnelling resistance 79−28485
$(SN)_x$, supercond. energy gap, tunnelling meas. 79−56403
Si oxidised amorphous layers, supercond. tunnel junction barriers 80−93040
SiO thin films at 60 mK, high-freq. phonon propagation 79−19347
Sn, double tunnel junction 79−33401
Sn film, energy gap reduction by quasiparticle injection 77−47941
Sn film, thermal processes in current-loaded bridges *(Russian)* 77−55639
Sn, supercond. film, charge imbalance generation by supercurrent 79−95548
Sn, supercond. film, intrinsic and expt. quasiparticle recomb. times 77−15999
Sn, supercond. tunnel junction, quasiparticle excitation by α-particles 80−103791
Sn, superconducting film, energy gap suppression and instability under strong quasiparticle injection 80−7042
Sn tunnel junction, quasiparticle recomb. times and electronic density of states at Fermi level 79−56414
Sn-In, distribution function branch imbalance, relaxation 79−33401
Sn-SnO_2-Sn, supercond. tunnel junctions, energy gap suppression by quasiparticle self-injection 78−80102
Sn-SnO_x-SN tunnel contacts, spatially inhomogeneous state under strong injection conditions 80−80457
Sn-SnO-Pb, supercond. tunnel struct., nonequilib. state, influence of illumination 79−15262

superconductive tunnelling continued
Sn-SnO-Sn Josephson tunnel junction, temp. depend. of cosφ conductance, plasma reson. expt. 79−33405
Sn-SnO-Sn junction with nonequilib. quasi-particle population, tunnel effect under laser irrad. *(Russian)* 77−43788
Tl films, supercond. amorphous, effective phonon spectrum and lattice sp. ht. 80−70895
V, thin film, determ. of energy gap, tunnel effect method 79−42704
V-Al junction, spin-dependent electron tunnelling 79−19700
V-C sandwiches, energy gap fluctuations *(Russian)* 78−34930
V-Ti superconducting film, electron spin effects 79−28488
V_3Si, single crystals, supercond. tunnel characts. 80−7044
V_3Si, superconducting thin films, energy gaps from tunnelling meas. 80−25050
V_3Si tunnel junctions, energy gap investigation 80−84569

superconductivity
see also BCS theory; coherence length; composite superconductors; Cooper pairs; critical currents; dirty superconductors; fluctuations in superconductors; Ginzburg-Landau theory; Meissner effect; penetration depth (superconductivity); strong-coupling superconductors; superconducting critical field; superconducting devices; superconducting energy gap; superconducting materials; superconducting transition temperature; superconductive tunnelling; type I superconductors; type II superconductors
A-15 type compounds, props. and one-dimensionality, book 80−3
absorbed film, disordering due to supercond. transition in metal substrate 80−50022
AC losses from combined action of transport current and applied field 79−33383
AC superconductor, uniform, behaviour of normal zones 80−11127
acoustic wave propag. in solid superconductors 78−95395
acoustoelectric effect, difference compared to thermoelec. effect 79−38246
amorphous, s-p superconductor, Eliashberg function, phonon spectrum 78−88066
amorphous metals, superconducting properties rel. to ordering 80−65735
amorphous superconductivity *(Chinese)* 80−44759
ampere determination from levitation of supercond. mass 77−30178
anharmonism, effect on supercond. *(Russian)* 78−39255
anisotropic supercond., boson method derivation *(German)* 77−85379
application to high energy physics 79−33441
applied, conference, Stanford, Calif., USA (Aug. 1976) 77−28272
Bardeen, John, contrib. to solid state physics 80−57057
basic principles, appls. *(German)* 77−89896
bimetallic ring, thermoelectric effect 79−65597
biological effects of microwaves, non-thermal 77−2022
biological materials, remanent magnetization as evidence for room temp. superconduction 80−35926
Boltzmann kinetic equation, scatt. by paramag. impurities *(Russian)* 77−36015
boson method, extension to systems containing randomly distrib. non-magnetic impurities 78−39253
branch-imbalance relaxation times 80−20358
bulk superconductor, nonequilibrium and superlattice effects, US attenuation meas. 79−56390
charged gapless superconductor, order parameter modes, dynamical pair-field susceptibility 78−2613
classification of superconductors, new scheme based of series expression for T_c 79−78252
clean superconductor, effect of impurity scatt. on thermally induced charge imbalance 80−60135
coexistence with magnetism, appl. of multicritical point anal. 79−77717
coherent longitudinal phonon injection effect in nonequilib. superconds. 79−47205
coherent-state formalism in supercond. and Josephson-junction calcs. 79−51723
collective excitations, appl. of generalized self-consistent field method 78−10598
collective modes and nonequilibrium effects in current-carrying supercond. 79−69626
complex molecules, π-electron pair correl. of supercond. type, appl. to optical and mag. props. 79−54778
composite materials, phys. props. review 77−4720
constricted superconductors, non-equilibrium effects 79−65590
contactless method for supercond. detect. in inhomogeneous media *(Russian)* 77−8254
cosmological superfluid vacuum state, time-varying constant and nonsingular models 77−13512
Coulomb superconductor with inverse quasiparticle distrib., behaviour in mag. field 77−20490
critical dimensions, Ginzburg-Landau theory *(Russian)* 77−15990
critical parameters during field emission of electrons 80−88682
critical phenomena, simulation, using Wien bridge oscillator, threshold instabilities 77−1211
critical slowing down, dynamic-exponents, Ginzburg-Landau theory 80−103783
critical state in combined superconductors, stability 77−15997
cryoelectrics, computerised measurement instrumentation 80−98920
cryogenics, a critical review 78−89485
cryogenics critical review 78−37022
cryogenics of Sulzer, Switzerland 80−82769
cryostat using supercrit. He coolant, for meas. on superconductors 77−30155
cubic to tetragonal structural transition, effect of supercond., due to two-fold degenerate electronic band 79−4615
current carrying elements, size effect 79−61019
current variation with gravitational field variation, general relativistic phenomenological theory 80−54827
cylinder, magnetic behaviour 79−65584
cylinder of rectangular cross section, 2-D current and field distrib. 78−72303
definition of terms for fundamental states, flux phenomena, meas. practices 78−34916
demonstration based on In-Pb covered manganin wire 79−35751
destruction by optical pumping, theory 78−47905
dielectric-superconductor boundary, Kapitza discontinuity *(Russian)* 79−51732
dislocation electrostatic interaction *(Russian)* 78−23198
dislocation mobility in superconductors, cond. electron effects 79−7932

superconductivity continued
dislocation systems, superconducting states, impurity effects *(Russian)* 80−11131
dissipative structures in quasi-one-dimensional superconductors, soliton solns. 79−87186
edge dislocation screening in metals and superconductors, metal softening *(Russian)* 80−64997
education, gauge symmetry breaking, geometrical approach, superconductivity and spontaneous symmetry breaking 80−57028
effective potentials, Ginzburg-Landau model 78−52287
elastic constants, single crystals, rel. to vibr. behavior, supercond. 78−10114
electric charge density oscillation, superconductor with magnetic impurities *(Russian)* 78−56255
electric confinement and magnetic superconductors, appl. of QCD 78−58157
electric field penetration into supercond. 78−76188
electrical field penetration into supercond. 77−69446
electrically conducting body, forces in mag. field using hydrodynamic analogy 80−34551
electrodynamic suspension system, current coil interaction with semiinfinite superconducting sheet *(Russian)* 80−83539
electrodynamics and quantum field theory 80−60134
electrodynamics of superconductors as a consequence of local gauge invariance *(German)* 80−103778
electron density of states for material with transition metal impurities 77−63024
electron gas, one-dimens., interacting, ground-state energy in mean field approx. and instabilities 80−88493
electron gas, screening props., CDW and singlet supercond. response functions 77−47745
electron gas propagation, normal phase, in long superconductors of small cross-section 79−78274
electron microscopy applications 77−38059
electron-hole pairing system, interband transitions and current state possibility *(Russian)* 77−36017
electron-hole superconductor, linear response to EM field 77−32125
electron-ion system, multiplicity and pseudomultiplicity 77−1389
electron-phonon interaction, matrix element calculation, phase transition 78−79703
electron-phonon system, parallel spin electron-electron interaction 80−10622
electron-phonon thermal cond. *(Russian)* 78−26993
elementary particle unified supercond. model of weak, EM and strong interactions 77−49888
Eliasberg's equations, solvability *(Russian)* 78−39250
Eliashberg equation, solution at $T=T_c$ 78−34918
Eliashberg equations, soln. by means of N-point Pade approximants 78−6475
Eliashberg formulation, electron-phonon density rel. to phonon inverse lifetime, review 80−84543
Eliashberg gap equation, approx. BCS-like soln. 77−1513
EM properties, general lecture 78−26901
EM wave nonlinear absorpt. near one-photon threshold 80−60142
energy technology relationship 78−88053
exchange enhancement of electron-phonon coupling 79−7930
exciton and polariton mechanisms of superconductivity 79−60959
excitonic, applic. of biological membranes *(Russian)* 78−23190
excitonic, possibility 79−38243
exotic spinors in supercond., charge depend. of quantised flux and Josephson current 79−33400
Fermi liquids at surfaces quasiclassical boundary conditions 80−4641
Fermi-liquid, electromagnetic response, formal solutions 80−100548
fermion systems, eqns. of motion for field operators and energy spectrum for isotropic systems 78−36926
ferromagnet, magnetic ordering, spin wave dispersion *(Russian)* 80−54818
ferromagnet, many-domain, indirect interaction of electrons via spin waves 77−85382
ferromagnetic superconductor, mag. domain struct., sample thickness effects 80−39704
ferromagnetic superconductor, uniaxial, domain struct. parameters 80−39705
ferromagnetic superconductor, with domain struct. mag. induction vector 79−65585
ferromagnetic superconductor mean-field theory 79−65586
ferromagnetic superconductors, phase transitions, renormalisation group treatment 80−29505
ferromagnetic transition, EM effects 79−51708
ferromagnetism coexistence, intersection lines 77−47924
filament and cluster crystals, liqs. in ultrathin channels, rel. to supercond. materials development 79−19162
filamentary superconductor, upper and lower crit. fields 80−25053
filaments, phase-slip state theory 79−56371
fine particles, nucl. spin relax. *(Russian)* 77−80875
flux flow curves as function of temp. 78−84344
forced flow cooled superconductor, normal zone propagation velocity 79−82732
Frohlich model, macroscopic phonon wave function 77−51839
gapless superconductor, pairing, Hartree-Bogolubov method 77−55636
gapless superconductor film, destruction of supercond. by alternating elec. field 77−1518
gapless superconductors, antilinear operators, pairing for broken time reversal symmetry systems 79−51716
gapless superconductors, elec. field behaviour 78−72305
gas liquefaction and liquefying cycles, thermodymamics *(Croatian)* 77−28294
Gaspari-Gyorffy theory, non-local extension 78−80093
gauge invariant model, local, collective excitations 77−87902
gauge theory solitons, quantisation, Feynman rules, Nielsen Olesen vortex 77−2734
Ginzburg-Landau equations, time-depend., soln. for external time variable mag. field *(German)* 78−10596
Ginzburg-Landau theory of two antagonistic order parameters, magnetism and superconductivity 79−38242
Ginzburg-Landau theory origin, development and applications, importance w.r.t. other theories *(Slovak)* 77−63022
Gorkov theory, higher order decoupling, moment conserving procedure 77−66223
granular, percolation model, specific heat, elec. resistance 80−93025
granular materials, size effects in cond. and supercond. 80−77581

superconductivity continued
granular superconductors, simple model for resistive-nonresistive transition 78−72298
ground state of quasi-orbital electrons 78−39252
hadron superconducting quark model quantum corrections 77−6082
hard superconductor flux jumps under time depend. external conditions 80−7038
helical order of spins, coexistence with magnetic order 79−65588
helical ordering of spins in supercond. 80−88669
HF cut offs of Coulomb interaction, real freq. Coulomb pseudopotential derivation 80−49980
high magnetic field behaviour of solids and plasmas, conference, Cambridge, MA, USA (Sept. 1978) 79−60667
high pressure effects, review 77−43278
high temperature, characteristics of superconductors, causes *(Hungarian)* 77−72935
high temperature, mech. coherence effects, repulsive interactions 79−69624
high temperature, possible mechanism based on metallic excitonium formation 79−38244
high temperature, superconductivity mechanism, metallic excitonium form. *(Russian)* 78−39254
high temperature supercond., contactless expt. methods 78−23221
high temperature superconductors, microscopic theory 79−87187
high vacuum evaporation system with low-temperature substrate for superconducting meas. 78−84716
high-temperature superconductivity non-specialist review 77−12070
history and fundamental concepts *(French)* 79−7931
inhibited, weak itinerant magnetism 79−51715
inhomogeneous, conf., Berkeley Springs, WV, USA, 1979 80−82562
inhomogeneous, Ginzburg-Landau theory 80−88672
instable systems, supercond. and phonon softening 79−65587
interband transitions and currents in systems with electron-hole pairing 78−72302
interface of two media, quasiparticle interaction 79−65532
introduction to phenomenon, applications 79−47182
ion-ion interaction in metals and intermetallic compounds, connection with supercond. transition temp. 78−47896
kinetic eqns., nature and decay rate of new mode 80−49978
Kondo superconductor, transport props. 79−65600
Lagrangian formulation 77−89897
lattice distortion and supercond., three-dimens. models anal. 77−8225
lattice dynamics of disordered or unstable lattices 78−75790
lattice model, correl. between quark confinement and mag. flux tubes in superconductor 78−78057
law of corresponding states for ideal and nonideal superconductors, Eliashberg eqn. *(Russian)* 79−87183
layer crystals, superconductivity using BCS model 79−15254
layered compound, supercond. and charge-density waves 80−34542
layered crystals, excitonic pair formation *(Russian)* 77−36016
layered structures, book contrib. 77−39994
layered system, coexistence of superconductivity and ferromagnetism *(Russian)* 79−7918
lens, electron microscope appl. 80−86530
linear chain crysts. containing impurities, Peierls instability and supercond. *(Chinese)* 79−51486
linear chain system, exciton model of supercond. 78−6476
long thin superconductor, resistive domain of small cross section in microwave EM field 79−28446
longitudinal acoustic wave absorpt., nonlinear effects, hysteresis *(Russian)* 79−19691
longitudinal sound attenuation in supercond. with mag. impurities *(Russian)* 79−11268
low lying lattice vibrational modes, conf., San Juan, Puerto Rico, (Dec 75) 78−10131
low temperature physics, conf., Grenoble, France, (Aug. 78) 79−51462
low-dimensional crystals, excitonic superfluidity 78−6359
low-dimensional materials, cond. temp. depend., metal-insulator transition, supercond. and semicond. behaviour 79−95391
lysozyme, search for superconducting regions 80−101149
macrometals as possible excitonic superconductors 79−42688
magnetic fields, calculation method from boundary conditions *(Ukrainian)* 80−34545
magnetic flux quantum, in supercond. ring, theory, teaching approach 79−84902
magnetic impurities, coexistence of superconductivity and ferromag., BCS and Zener models 80−88676
magnetic impurities in supercond. *(Hungarian)* 77−28277
magnetic impurity effects, Anderson model 78−52148
magnetic impurity interactions, theory 77−39997
magnetic instability of superconducting wire in the changing magnetic field 80−34569
magnetic order coexistence 78−19177
magnetic ordering in superconductors, SCF model *(Russian)* 79−15253
magnetic ordering in superconductors, susceptibility calcs. 79−99656
magnetic superconductor, Fermi surface nesting effect on mag. instability 80−54831
magnetic superconductor, spin-spiral ordering 80−2517
magnetic superconductor, thermodynamics of magnetism and supercond., mol. field theory 80−34668
magnetic-surface states 79−33389
magnetism and magnetic materials, conference, Cleveland, USA (Nov. 1978) 79−73651
metal, criterion for supercond. rel. to compressibility *(Russian)* 78−23200
metal, hot electron distrib. at low temp. *(Russian)* 77−12056
metal, superconducting and normal, attenuation, EM generation and detection of US shear waves 78−39261
metal, superconducting and normal, non-linear acoustic props. of cond. electrons 79−60975
metal, superconductivity and ferromagnetism 79−73616
metal-H systems at high H press., physicochemical props., book contrib. 80−24535
metals, frictionless heat motion at low temps. 79−69495
metals, normal to superconducting transition, thermo-inertial mechanism of plasticity enhancements *(Russian)* 79−47183
metals, superconductivity studied by electron-phonon and Coulombian e-e coupling strength and quasi particle mass 80−88666
metrology appl. *(Japanese)* 78−37030
microscopic mechanism for the macroscopic asymmetry of superconductivity 79−19687
superconductivity continued
microscopic theory, introductory remarks recent developments *(Chinese)* 79−47192
multi-valley semimetals with Coulomb interaction between electrons *(Russian)* 78−64165
mutual compatibility with ferroelectricity 78−15104
N-particle Schrodinger eqn., macroscopic behaviour, superconductor and fermion systems 78−60242
narrow channels, voltage jumps in current-voltage characts. *(Russian)* 78−23197
neutron stars, superconducting props. of π condensates 78−32993
NMR and US absorpt. of superconductor with struct. transform. *(Russian)* 79−95544
NMR theory in supercoductors with paramag. impurities in singlet state 79−28445
non-adiabatic systems, quasi-orbital conduction electrons 79−33382
non-equilibrium superconductivity 80−44762
nonequilibrium, phase transitions induced by quasiparticle injection 78−91808
nonequilibrium distribs. in superconductors, review *(Russian)* 79−19688
nonequilibrium distribution, electron-electron collisions effect *(Russian)* 80−7033
nonequilibrium distribution functions of quasiparticles and phonons calc. 77−89904
nonequilibrium phenomena in superconductors, review 80−49982
nonequilibrium states of thin films, kinetic eqn. approach 77−47925
nonequilibrium superconductor, effect of pair breaking on branch relax. 79−78257
nonequilibrium superconductor, with wideband source of quasiparticles, kinetic theory 80−80442
nonequilibrium superconductors, T^* model of quasiparticle and phonon distribs. 80−25039
nonequilibrium superconductors, BCS-Boltzmann and Ginzburg-Landau descriptions 79−65589
nonequilibrium superconductors, crit. intensity of optical pumping, temp. depend. *(Russian)* 79−7933
nonequilibrium superconductors, microscopic and Boltzmann eqn. approach 80−15649
nonequilibrium superconductors, phase transitions, theory allowing for phonon reabsorption 78−68107
nonequilibrium superconductors, pot. difference meas., mag. field dependence of branch imbalance relax. time 79−65592
nonequilibrium superconductors, transients, phonon distrib., supercond. gap, Boltzmann-BCS formulation 78−52149
nonequilibrium superconductors hypersound enhancement *(Russian)* 80−34552
nonlinear transient phenomena in supercond., Ginzburg-Landau eqn. generalisation 77−32110
normal domain formation by acoustic methods 78−60248
normal metal-superconductor boundary excess resist. temp. depend., quasiparticle Andreev reflection *(Russian)* 79−73640
normal zone propagation, of superconductor carrying time-dependent current 78−84346
nucleic acids, discontinuous mag. field effects, room temp. superconductivity 79−62195
numerical investigation of basic eqn. 77−85381
one-dimensional Peierls-Frolich state, impurity pinning of charge density wave 78−6298
one-dimensional system, supercond. order and CDW coexistence, Peierls instability *(Russian)* 77−69445
one-dimensional Tomonaga model with impurities, localisation versus delocalisation 78−6311
order-disorder transitions, static precursor nuclei, anomalies in high temp. superconductors, ferroelectrics, organic conductors 78−10165
ordered continuously degenerate systems, props. 79−93040
phase slip centre, charge imbalance waves and nonequilib. dynamics 80−54830
phase-slip centres interaction in supercond. filaments, step structs. 79−56367
phenomenological generalised theory, superdiamagnet theory *(Russian)* 80−7031
phenomenological parameters, thermodynamic and quantum mech. derivation 77−12054
phenomenological unifying approach to London and Ginzburg-Landau theories 80−103779
physical acoustics and exploration of superconducting state, 1st, 2nd, 3rd, 4th and 5th sound, review 80−96090
physical properties of superconductors, elec. engineering appl. *(German)* 77−55648
physics of transitions, introduction 78−26660
pion condensates, supercond. props., σ model anal. with nucleons 79−59029
plasmon mechanism for supercond. in two-, three-dimens. electron systems 78−88065
plastic deformation of superconductors, Cooper pair scatt. model 80−39709
plasticity at very low temperature, dislocation motion, rel. to supercond. and tunnelling *(Czech)* 77−32630
plate, hysteresis losses 78−84345
polyvalent metals, Brillouin zone boundary influence on Coloumb interactions 80−24827
practical applications of superconductivity 80−49965
precision electrical meas. using superconductivity *(German)* 77−79124
problems of very low temperatures *(German)* 77−55650
propagating normal zone (quench), induction, by local energy release 79−38210
quantum defects, electron defect interactions *(Russian)* 80−15650
quantum field theory of solids, book 77−31922
quantum polarisation effect in critical freq. EM field 80−75677
quantum polarisation effect of uniform superconductor in EM field having crit. frequency 78−34923
quark matter, asymptotically high density 78−12863
quasi-one-dimensional conductor, Peierls instability and superconductivity, possibility of coexistence 78−31028
quasi-one-dimensional conductor, supercond. transition, impurity effect 77−15986
quasi-one-dimensional conductors, order in coupled metallic chains problem 78−6358
quasi-one-dimensional electron gas with strong on site interactions 77−4306

superconductivity continued
quasi-one-dimensional electron systems, effect of interchain electron transfer on phase transition 78−51911
quasi-one-dimensional electron systems, instabilities, mean field approx. 78−23036
quasi-one-dimensional electron-phonon system, electron jump effect on phase tansition *(Russian)* 80−92673
quasi-one-dimensional metal systems with random impurities, cond. at T=0 78−6360
quasi-one-dimensional systems, three-dimens. ordering in system of weakly coupled chains 78−6295
quasi-orbital conduction electron model 78−34917
quasi-two-dimensional superconductivity in quantising mag. field *(Russian)* 77−40001
quasiparticle charge imbalance relax. in superconductors 79−60960
quasiparticles, nonequilib. distrib. function 78−91810
quenching of technical superconductors by ht. and mag. field pulses 78−43537
radiation stimulated, current density Eliashberg, theory 77−89895
radiation-stimulated superconductivity, stability, theory 77−47923
radiometric effect and thermal cond. size effect 78−60245
Raman sound scattering in normal metals and superconductors *(Russian)* 78−23199
rare-earth, mag. supercond., appl. of boson theory to mixed state 80−7050
Rayleigh sound absorpt. in normal and supercond. metals *(Russian)* 78−43233
reentry of superconductivity, rel. to ferromagnetism 78−39247
refrigeration technology for superconductors 77−82529
relativistic Bogoljubov equations, derivation from nonlinear bispinor Lagrange density 79−73627
relaxation and collective motion, two-fluid model 79−56369
relaxation and collective motion two-fluid theory 79−73625
relaxation processes, nonequilib. electrons and phonons 78−91807
renormalisability of superconductivity models, nonlinear spinor models, fermions, collective bosonic states 77−18179
renormalisation group recursion relations involving dynamics, in mag. field 80−60137
residual RF surface resist., acoustic generation effects, nonlocal theory 77−89901
resistive phase-slip states in superconducting channels 80−103780
resistive state, occurrence of topologic singularity *(Russian)* 79−19686
resistive states and elec. oscills. in supercond. channels, quantum kinetic theory 77−32108
response functions of superconductors and ^{3}He(B), autocorrelation functions of density and transversal current, acoustic and quasihomogeneous 80−49449
response functions of superconductors and ^{3}He(B), density and current correlation functions 80−49448
review and table of props. 77−4460
review of superconductivity and magnetism *(Hungarian)* 79−47226
RF expectations and limitations 79−1648
rotating multiply-connected superconductors, induced mag. field 77−85383
rotation induced electromotive forces in normal and superconducting metals 79−24120
S-wave and P-wave superconductors, absence of proximity effect 80−93033
SAW absorption in bulk superconductor in presence of supercurrent 79−28443
SEM, low temp., appl. to superconductors 80−80443
semimetal, intrinsic, dielec. and supercond. phase transitions 77−66111
semimetals, laminar, superconducting props., Coulomb electron interaction considerations 79−87185
shell model for clad particles of supercond. *(Chinese)* 79−69623
single-photon absorption in superconductor near threshold *(Russian)* 78−91815
slab in AC mag. field, I-V characts. *(Japanese)* 78−19183
sliding Frohlich waves, lack of superconducting behaviour 78−10378
small superconductor, phase transitions in mag. field, book 80−3
small superconductor in magnetic field, first and second order phase transitions 80−2519
solid-state theory, introduction, book 79−33215
space applications 80−41694
spatial structure in nonequilib. supercond., pumping under microwave irrad. *(Russian)* 77−43784
sphere rot. in mag. field, induced EM field *(German)* 80−54828
spin glasses, superconductivity, total compensation of paramag. effect 80−7021
spin glasses, superconductivity 79−28428
spin susceptibility of conductivity electrons, spatial dispersion *(Russian)* 79−51719
stability, in forced flow He cooling system, numerical anal. of heat-induced transients 80−82773
structural instabilities in superconds. 79−38294
superconducting loop, bimetallic, acoustically generated mag. flux 77−16010
superconductivity, general relativistic phenomenological theory 80−2518
superconductivity and elementary particles theory, review 80−4911
superconductivity-ferromagnetism coexistence in two-band model *(Russian)* 80−84539
supercurrent-thermal gradient interaction, branch imbalance generation 79−99657
superfluidity and superconducting phenomena demonstrated with He cryostat *(Polish)* 80−86059
superstructures, condensate band spectrum and current carrying states anal. *(Russian)* 80−39706
surface, ponderomotive phenomena theory, magnetic forces *(Russian)* 77−12058
surface current and magnetic field, boson transformation method 78−91809
surface EM waves in superconductors 78−88072
surface phenomena and topological singularities, Josephson phenomena, EM surface waves, transient phenomena 79−99653
surface polariton modes at interfaces, theoretical anal. 77−24639
surface sheath, Brownian motion 79−19708
surface thermoelectric effects *(Russian)* 78−34921
Swiss Physical Society, autumn sessions 78−72053
symposium contrib., Florida, USA (March 1979) 80−51946
teaching, cryostats for laboratory course in supercond. 79−58494
technological survey *(German)* 79−65573

superconductivity continued
terminology for practical superconductors 80−7034
theory based on revised classification of states of matter rel. to charge transmission props. 79−19683
theory developments from 1950s to 1980s, w.r.t. elementary particles theories *(Czech)* 80−80440
thermal conductivity at Lifshitz electronic transition point *(Russian)* 80−11135
thermal conductivity meas. from 4.2-300K 79−60970
thermoelectric and acoustoelectric effects, influence of mutual drag of excitations and phonons 80−44761
thermoelectric branch imbalance currents 79−56370
thermoelectric effect in nonequilib. superconductor 79−65594
thermoelectric effect in supercond. with low conc. of mag. impurities 77−69448
thermoelectric effects 79−65593
thermoelectric effects in superconductors, general and theoretical anal., review 80−11133
thermoelectricity, toroidal sample config. 79−65595
thermonuclear reaction programs, controlled, cryogenic technology and superconductivity .79−54600
thermopower, possible existence in supercond. state 78−23201
transition element compounds, supercond. props., lattice symm. and instability 77−8224
transition meas., contactless, circuitry 79−17442
transition metal, one-electron theory, atomic sphere approx. to KKR and LMTO methods 78−91584
transition metal nitrides and carbides, surface energy for brittle fracture from phonon freqs., rel. to soft-mode induced supercond. 79−86837
transition metals, 4d electron-phonon matrix element, supercond., and ion-core enhancement 77−62811
transition metals, conf., Toronto, Canada (Aug. 1977) 78−91577
TTF-TCNQ complex *(Japanese)* 77−1412
two order parameter system, one subsystem supercond., in const. ordering field 78−34915
two-band superconductor, effect of nonmag. impurit. on nucl. spin-lattice relax. *(Russian)* 77−51845
two-band system, coexistence of dielec. and supercond. ordering 80−10853
two-fluid model, electron distrib., energy spectra *(Russian)* 79−15252
ultralow temperature physics, future prospects 79−65268
US attenuation and Fermi surface topology *(Russian)* 78−23203
US study of cond. 79−60976
vortices interaction energy 79−78256
weak and EM field model, self-interacting lepton field Lagrangian, lepton antilepton composite particles 77−41800
weak coupling superconductors, single particle excitation decay theory 78−52147
weak superconductor with current in external mag. field, free energy 80−25046
weak-coupling supercond., quasiparticle, charge and energy conservation 79−19685
weak-coupling superconductor, effect of electron-phonon renormalisation on thermodynamics 79−99655
weakly illuminated superconductor, nonequilib. props., theory 77−66224
yrast bands of negative parity, gapless superconductivity, exactly solvable R(8) model 77−14015
Au-Pd-Au sandwich, obs. of strongly enhanced mag. susceptibility, possiblity of p-wave supercond. 80−93076
Bi-Sn, superconductive microsegregations, 3.7K resist. drop 79−69646
Cr_3Si phase structure, rel. between phase diagrams and superconductivity 80−88330
CuCl, behaviour under press., possibility of superconductivity 79−38239
CuCl, optical absorpt. meas., evidence against intrinsic electron-hole supercond. 80−108172
CuCl, possibility of high temp. superconductivity 79−38238
CuCl, possibility of high temp. superconductivity 79−51711
H metal, superconductivity and crystal struct. *(Hungarian)* 78−38659
H_2, solid *(Hungarian)* 77−72935
He technique appl. in Czechoslovakia *(Croatian)* 77−28282
^{4}He, Bose condensate density temp. depend., rel. to supercond. *(Russian)* 79−33140
Nb spheres, mag. levitation, obs. of fractional charge on matter 77−49709
Nb/H, heat capacity and supercond. between 1.5 and 16K 80−2521
Pb-Sb, dynamic destruction of supercond. 80−2529
Pd, disordered film, supercond., occurrence and crit. temp. after He^+ irrad. 79−11261
Pd-H, optical phonons in supercond. 77−63021
Pd_cAg_{1-c}, possibility of superconductivity 80−10862
PdH_x, local, soft modes, superconductivity thermal neutron inelastic scatt. *(Chinese)* 80−70331
$(SN)_x$, epitaxial film, elec. resist., 0.03-8.9K, possible supercond. 77−15970
$(SN)_x$, fluctuation induced cond. and dimensionality 77−28167
$Ti_{1-x}Fe_x$ alloys, $(0<x\leq0.2)$, nonmetallic resistivity and simultaneous superconductivity *(Russian)* 77−36005
V/H, heat capacity and supercond. between 1.5 and 16K 80−2521
Y_2O_3, synthesis at high-press and temp., supercond. 80−2513
$ZrZn_2$, phonon contrib. to Stoner enhancement factor, ferromag. and possible superconductivity 80−25070

superconductors *see superconducting materials; superconductivity*

supercooling
acenaphthene-α-nitronaphthalene, binary mol. system, phase diagram 77−39664
amorphous state, Gaussian core model 79−73101
austenitic steel, 17G1S struct. and austenite transformation kinetics variation on deform. *(Russian)* 79−70060
austenitic steel, pearlitic transformation incubation effect, Mossbauer spectra *(Russian)* 79−70061
benzyl benzoate, supercooled, depolarised lines in quasielastic light scatt. 80−45095
boiling, nucleate, subcooled, latent heat transport contrib. 78−75046
boiling, subcooled, nucleate, mechanistic model 78−90697
boiling mechanism during burnout phenomena in subcooled two-phase water flows 78−94529
bubbles, active nucleation site spatial distrib., bubble flow density 78−71267
channel, rectangular, forced flow boiling and burnout 78−94530

supercooling continued
cholesteric liquid crystal, phase transitions and critical phenomena *(Russian)* 79−4407
cholesteryl esters, kinetics of cholesteric/blue phase transform. 79−95140
classical liquid, metastable supercooled state, props. 78−55796
classical nucleus in liq.-liq. miscibility gap, undercooling in binary system 77−28002
crystal growth, from melt, effect of supercooling and atomic kinetics on crystn. front and growing cryst. radius 79−94937
crystal growth by travelling solvent method, heat flow, diffusion and convection 77−39549
crystallisation from melt, nucleation on supercooling, inter-nuclear separation distrib. function *(German)* 77−19885
crystallisation in supercooling condition, a false high-press. effect under nonequilib. conditions 79−77728
crystallisation of supercooled liquid in sound field, steady-state dynamics 80−15223
4-cyano-4′-n-pentylbiphenyl, refr. index meas. and isotropic-nematic phase transition study, surface plasmon technique 80−84282
cyclic carbonates, supercooled liqs., dielec., acoustic, NMR, viscoelastic relax. props. 77−1609
1,1′-diacetylferrocene, MBBA soln. nematic glass-supercooled nematic transition, Mossbauer temp. obs. 79−95687
dibenzyl-tolane, single cryst. growth from melt, influence of supercooling and impurity conc. on growth rate of faces 79−14714
dilute binary alloy, unidirectional growth, morphological stability of planar interface 80−84920
electron-hole droplet, supercooling in adiabatic spraying *(Russian)* 78−43306
electropatented wire, austenitizing, supercooling and heating temp. effects 78−23737
eutectic colony growth, supercooling dynamics, stability in presence of external perturbations *(Russian)* 80−16291
flow instabilities in sustained and transient boiling, inlet subcooling effect 78−94809
garnet LPE layers, growth rate depend. on supercooling, induced striation expt. 79−24453
gas, in supersonic nozzle, nonequilibrium heterogeneous-homogeneous condensation *(Russian)* 77−51096
gas, IR spectroscopy 77−23574
gases, high velocity flows, nonequilib. homogeneous condensation, determ. of maximal supercooling 80−6086
glass transition, soft-sphere model, mol. dynamics study 80−49343
glass-forming liquids, relax. times, temp. depend. 78−83924
glycerol, supercooled, Mossbauer effect and model of mol. motion 78−64301
glycerol, supercooled liq., dynamical struct. factor, Mossbauer spectroscopy 78−27126
glycerol, supercooled liq., mol. motion, Mossbauer effect, Rayleigh scatt. obs. 77−73099
glycerol(-d_3), single cryst., glassy, and supercooled, polarised Raman spectra, anharmonic multiphonon interactions 79−91419
hard-sphere liquid, glass transition, computer mol. dynamics simulation 77−11674
heat transfer during subcooled forced convection boiling at subatmospheric press. 78−94525
heat transfer mechanism with boiling in narrow spaces, interferometry obs. 78−94527
HOAOB, isotropic-nematic transition, supercooling and nucleation, interface dendrites 78−42896
ice, nucleation threshold on Cu_2S, Ag_2S, Mo_2S and CdS photosensitive surfaces 77−55343
inorganic hydrate, solidification, heat transfer processes *(Japanese)* 80−6372
Josephson element principles, applications to precision meas. of electric potential and magnetic flux at high freq. *(Norwegian)* 80−80447
Lennard-Jones liquid, mol. dynamics studies of glass form. 80−38896
leucosapphire, supercooling and crystn. temp. determ. 79−51237
liquid, dielectrophoretic heat transfer 78−94874
liquid, long wavelength density fluctuations 79−90515
liquid, thermal conductivity and viscosity, mode-mode coupling 80−88370
liquid metallic thin film, supercooling, electron diffraction study *(French)* 79−7676
lunar igneous rocks, review of analogue information on supercooling 77−60652
2-6-lutidine-water, anomalous supercooling near critical point 80−70384
melting, cylindrical, subcooling effect 79−32214
metals, supercooling on homogeneous crystn. *(Russian)* 80−19914
microminiature cryogenic refrigerators, design, construction 79−26059
nucleation, liquid superheat and vapour subcooling, corresponding states correlation 79−32218
PAA, isotropic-nematic transition, supercooling and nucleation, interface dendrites 78−42896
polyethylene terephthalate, glass conversion zone determ. from DTA *(German)* 77−20059
polymer, crystn. at low supercooling 79−10823
polymers, crystallisation phenomena 79−82162
rime growth, splintering mechanism 79−39788
salol, liq., supercooled, relax. kinetics, optical Kerr effect obs. 77−84613
salol, liq. and supercooled, VH light scatt. spectra *(French)* 77−1755
skin freezing temperature, human finger 77−21486
smectic-B liquid crystal, supercooled monotropic, Mossbauer studies of ^{57}Fe bearing solute 77−81041
soft core system, crystallisation, mol. dynamics method 78−18565
solute redistribution during crystallisation, interface field effects 80−84119
steam, method for calculating expansion 77−27573
steam, thermodynamic props., virial eqn. of state 80−14872
steam bubble, nonspherical, collapse in suddenly pressurised water *(French)* 78−33997
steel, alloyed with Cr, Mo, Co, Mn, martensitic point position depend. on cooling rate *(Russian)* 79−70063
steel, austenitic, high speed, supercooled, austenite decomposition kinetics 78−92233
steel, austenitic stainless, fracture toughness and transition temp., T_{50}, effect of cooling rate and supercooling temp. 78−84987
steel, austenitic supercooled, transformation kinetics into spheroidised pearlite *(Russian)* 78−95742
supercooling continued
steel, Mn-Ni-Cr-C, supercooled austenite, influence of constant mag. field on diffusional decomp. *(Russian)* 79−4964
steel, pearlitic and bainitic transformations in austenite, processes during incubation period 80−40348
steel, SiO_x inclusion formation on introduction of solid SiO into molten steel *(Russian)* 78−80530
steel, structural, supercooled austenite, structural characts. of decomposition 80−60870
succinonitrile, low entropy of fusion plastic crystal, dendritic growth, expt. test of theory 77−35842
superconductor, paramagnetically limited, supercooling curve meas. 78−14885
supercooled, struct. refinement mech. *(Russian)* 80−20975
trimethylphosphate, plastic and hard crysts., liq., nucl. spin-lattice relax. mol. motion 78−48065
tristearin irreversible liq.-liq. phase transition, ^{13}C NMR meas. 78−26681
tube, vert., uniformly heated, forced convection boiling, crit. heat flux 79−27498
tube, vert., uniformly-heated, crit. heat flux prediction, generalised graphical method 79−46313
water, anomalous compressibility to 1-9 kbar, correl. with supercoding 79−65134
water, appl. of polychromatic correlated site percolation 80−22296
water, convection effect on dendritic ice growth 77−7999
water, heterogeneous crystallisation, role of adsorption 79−95125
water, I^- charge transfer to solvent spectra, water struct., solvated electron 77−50447
water, LF sound velocity and related thermodynamic props. 79−73255
water, metastable liquid, US vel. under atmospheric press. 79−10897
water, probability of ice nuclei form. 78−3909
water, saturated (subcooled), crit. discharge through differently shaped channels 78−55681
water, self diffusion, high-press., low-temp. spin-echo NMR obs. 77−8446
water, sound vel. dispersion, struct. relax. effect, Brillouin scatt. obs. 80−107375
water, structure and motion at high pressure 78−87606
water, subcooled, choked expansion and the isentropic homogeneous equilib. model for 2-phase flow 78−91034
water, supercooled, dispersed within emulsions, freezing, differential scanning calorimetry meas. 77−15552
water, supercooled, US vel. and attenuation *(French)* 79−90730
water, supercooled liq., high freq. sound vel. and absorpt., thermodynamic singularity, 228K 77−76489
water, supercooled to −33°C, sound vel. determ. by acoustic levitation method 80−88269
water(-d), high-press. supercooled, density max. 77−1162
water supercooled, hypersonic sound vel., thermodynamic interpretation 78−59860
water-ice transition, production of stimulated coherent radiation 78−83920
wedge, forced-convection film boiling, boundary layer flow 79−46366
wet-steam flow, critical pressure ratio 77−84300
Ag, dendrite growth from supercooled melt 77−51628
Al alloys, liquid, kinematic viscosity temp. depend., porosity, H solubility, supercooling *(Russian)* 80−54425
Al kinematic viscosity temp. depend. porosity, H solubility, supercooling *(Russian)* 80−54425
Al, liquid, kinematic viscosity temp. depend., porosity, H solubility, supercooling *(Russian)* 80−54425
Al-Cr(Mn), struct. form. and phase transform. kinetics *(Russian)* 78−15359
(Al-Zn):Cd eutectic system, cellular growth, unidirectional solidification investig. *(Korean)* 77−28805
AuIn-Pb pseudobinary system, DTA 78−23667
Bi film, supercooling, exam. by electron diffr. and electron microscopy *(French)* 78−14636
Bi thin film, structural evolution 8 to 573K, supercooling effects *(French)* 79−90921
$6Bi_2O_3.SiO_2$, stable γ-phase cryst. form. from supercooled melt, metastable δ-phase precip., surface contamination role 79−91635
CO_2, supercooled, IR absorpt. spectrum 77−23574
$Ca(NO_3)_2$-H_2O solns., ice I homogeneous nucleation temp., slow vitrification mechanism 78−26666
$Ca(No_3)_2$-H_2O system, induction period supercooling depend. meas. 80−19918
Co-C alloys, graphite nucleation on surface *(Russian)* 80−40360
Cu, dendrite growth from supercooled melt 77−51628
Cu-Ni(Su), supercooled melt, dendrite growth morphology *(Japanese)* 78−11216
D_2, supercooled, possible phase change to superfluid state 77−62707
D_2O, appl. of polychromatic correlated site percolation 80−22296
Dy_2O_3, soln. in $K_2O.2(3)MoO_3$, rel. supersaturation and supercooling 80−40245
Fe, supercooling by method of microvolumes *(Russian)* 77−21092
Fe-Ge (10 to 50 at.%), phase diagram rel. to heat treatment, supercooling diagram *(German)* 78−92240
Fe-Mg, cast ferrite-based, graphite nucleation on surface *(Russian)* 80−40360
Fe-Ni, martensite burst transformation, supercooling 78−84806
Fe^{3+}-Fe^{3+} distances, in aq. NO_3^- and ClO_4^- solns., from small-ang. X-ray diffr. maxima 78−42880
α-Fe_2O_3 crystal flux growth, solubility and relative supersaturation in Fe_2O_3-PbO-V_2O_5 fluxed melt system 80−64934
Ga, liq. supercooled, double hard sphere model 77−43128
Ga, liquid., supercooled, dynamics 79−27902
Ga metastable states, supercooling and polymorphism *(French)* 78−14325
Ga single crystals, rate equations for dislocation-free and dislocation-assisted growth 79−4262
Ga, with 100 ppm Ag single cryst. growth by pulling, thermal parameters governing purity *(French)* 78−2046
GaAs, multiple layer LPE growth by controlled supercooling of Ga soln. 77−77429
Ge, single cryst. growth, supercooling needed for Czochralski and Stepanov methods 78−3015
Ge single crystals, constitutional supercooling growth conditions, structural and chem. inhomogeneities 80−93473

supercooling continued
H_2O, supercooled, longit. proton relax. times, press. and temp. depend. 77−85598
^4He, superfluid, heat transport, Kapitza resistance of Al 79−23794
Hg, liquid structure, X-ray diffr. obs., 173-473K 80−14997
In film, metastable states supercond. parameters 78−47903
In, ideal superheating and supercooling limits 77−4465
In superconducting films, metastable states, supercooling fields 80−97031
In-Bi, dil., supercond., ideal superheating and supercooling limits 77−4465
In-In-P-GaP, liquidus surface obs. 78−22829
$In_{0.53}Ga_{0.47}As$, growth on (100)-oriented InP, from supercooled solution 79−70001
InGaAsP-InP layers, grown by LPE techniques, lattice const., bandgap, thickness and surface morphology meas. 80−59818
InP layers, grown by LPE from supercooled solns., thickness meas. 78−10307
InSb, morphological instability under constitutional supercooling during cryst. growth from melt and stabilising thermal gradient 79−4910
KNO_3-$Cd(NO_3)_2$ molten mixtures, elec. cond. 79−90813
$LiNbO_3$, Czochralski grown single crysts., cellular interface and struct. due to constitutional supercooling *(Chinese)* 79−51026
$Na_2S_2O_3.5H_2O$, glass transition, anal. of large stable supercooling 77−51477
$Na_2S_2O_3.5H_2O$, glass transition, theory 77−84890
$Na_2S_2O_3.5H_2O$, solidification, heat transfer processes *(Japanese)* 80−6372
$NdAl_3[BO_3]_4$, single phase crystallisation region from solvent melt 80−38977
Ni alloy powder, crystallised by supercooling methods, struct. props. *(Russian)* 80−54483
Ni, solidified from supercooled condition, Si conc. influence on struct. *(Russian)* 77−16567
Ni, supercooled, struct. refinement mech. *(Russian)* 80−20975
Ni-C alloys, graphite nucleation on surface *(Russian)* 80−40360
$PO(SCN)_3$:Nd^{3+} solns., spectroluminesc. props. 77−16362
Pb, supercooled liquid thin films, liq. struct. factor determ. by STEM 80−10487
SF_6, supercooled, IR absorpt. spectrum 77−23574
Si ribbon parallel twinned structure development by shaped crystallisation 78−64465
Si:Pt, implanted and laser annealed, segregation and increased dopant solubility 80−65016
SiO_2, high press. supercooled liq., density max. 77−1162
$(Sm,Y)_3(Fe,Ga)_5O_{12}$, epitaxial mag. layer, LPE, growth rotation rate, effect on props. 78−56053
Sn, $\beta \rightarrow \alpha$ polymorphic transformation, mechanism of growth of cubic modification nuclei *(Russian)* 77−44239
Sn melt, highly supercooled, dendrite growth *(Russian)* 77−81253
Sn-Bi (Pb) alloys, supercooled, dendritic growth rates *(Russian)* 78−80533
steel, high C, graphite nucleation on surface *(Russian)* 80−40360
Tl, α and β-phase stability range and supercooling, electron diffr. obs. *(French)* 77−84924
UF_6, supercooled, IR absorpt. spectrum 77−23574
WF_6, supercooled, IR absorpt. spectrum 77−23574
$(Y,Sm,Lu,Ca)_3(Ga,Ge,Fe)_5O_{12}$, film growth and mag. props. for bubble-memory appl. 79−87297
$Y_3Ga_xFe_{5-x}O_{12}$, film growth conditions rel. to memory element props. 77−66399
ZnAl (18.75 wt.%), supercooling phase β break up kinetics *(Polish)* 80−25654
ZrO_2-SiO_2, liquid immiscibility, microstruct. of plasma dissociated $ZrSiO_4$ 80−107429

superexchange interactions
alkylammonium copper chlorides, high-temp. susceptibility obs., 80-300K, ferromag. interactions 77−66274
amorphous ferromagnet, effective-field distrib. and resistivity minima 79−73501
antiferromagnet, charge transfer light absorpt. 78−34975
calcium copper acetate hexahydrate, $CaCu(CH_3COO)_4.6H_2O$ and $CaCu(CD_3COO)_4.6H_2O$ 78−2680
channel model in exchange theory 78−14950
copper acetates, antiferromag. exchange coupling, superexchange mech. 78−39310
copper dichloride dipyridine, ground state wave function and superexchange interaction 79−42752
crystal with many-electron paramag. ions and strong cryst. field, perturbation theory 77−59402
1,4- dibromonaphthalene, highly disordered quasi-one-dimens., excitation transport 80−34961
ferrimagnet, indirect hyperfine and superexchange interactions 77−69537
ferromagnetism, basic models, classification of theories *(Rumanian)* 78−91840
garnets, superexchange operator and cryst. field interactions 80−59931
guanidine aluminium sulphate hexahydrate type ferroelectrics, ESR of Fe^{3+} exchange pairs 77−90022
Heusler alloy, Mn-containing theory of spin waves 79−78354
insulating solids, long-range ferromag., antiferromag. superexchange, limit function 80−54883
insulator, interaction between mag. ionis., case of degenerate orbitals 79−11309
insulators, refined LCAO scheme 78−91861
ion orbitals, frozen, ang. depend. of superexchange 77−32185
iron tetraphenylporphyrin chloride, electron spin pairs, low and ultralow temps. 77−77092
magnetic insulator, supertransferred hyperfine interaction 77−85403
magnetic insulators, potential exchange theory 78−19242
magnetic semiconductors, long-range exchange interactions 77−69531
models, prospects for ab initio calcs. 77−69281
naphthalene, long range exciton percolation, superexchange, energy denominator 77−28609
naphthalene $^1B_{2u}$ resonance pairs, energy denominator depend. of excitons absorpt. 77−39783
one-particle states 79−91011
orthochromites, superexchange, ang. depend. for frozen ion orbitals, mol. orbital model 77−32185
perovskites, ordered, mag. props. *(French)* 78−95434

superexchange interactions continued
rare earth orthoferrites and orthochromites, exchange interactions 78−60279
ruby, energy transfer between different emitters and spatial diffusion 80−103978
transition metal compound, effective spin-orbital Hamiltonian 80−70998
transition metal compound, multielectron theory 80−70997
transition metal ions, exchange-coupled in ionic crystals, optical spectra *(Rumanian)* 79−87474
transition metal oxides (fluorides), potential exchange theory in mag. insulators 78−19242
tri-p-tolylamine and its paramag. radical cation, disordered mol. solid, direct obs. of superexchange 80−39848
xanthine oxidase (dehydrogenase), EPR, mag. spin-spin dipolar interaction 80−53026
BaF_2:Tm^{2+}, EPR meas. of Tm^{2+} ion pair interactions 79−95641
$BaLaMRuO_6$, (M=Mg, Fe, Co, Ni, Zn), cubic ordered perovskites, Mossbauer and mag. susceptibility meas. 80−75889
$BaZn_2Fe_{16-x}Al_xO_{27}$, saturation magnetisation, anisotropy field and Mossbauer meas. 77−69508
CaF_2:Tm^{2+}, EPR meas. of Tm^{2+} ion pair interactions 79−95641
$CaIr_xRe_{1-x}O_3$, (0<x<1), sintered, exam. of mag. and electrical props. 78−80135
$CaIr_xTi_{1-x}O_3$, semiconductor, struct., mag. and elec. props. 79−91046
$CoCl_2.6H_2O$, antiferromag., spin flop and paramag. resons. at very low temp. 77−66426
$CoFe_2O_4$, superexchange interactions, three-sublattice anal. 79−61095
$Co_{2-y}Zn_yTiO_4$, cation distrib. and mag. props. 78−14939
$Co_{2-y}Zn_yTiO_4$, spinel series, exchange integrals, mag. struct. and coercive force, magnetisation meas. 77−69507
Cr complex, dimer di-μ-diphenylphosphinatoacetylacetonatochromium(III), EPR of exchange coupled Cr^{3+} pairs 78−88172
CrTe, effect of high pressures on magnetic properties 78−52238
$CsCuCl_4.2H_2O$, hyperfine and super-exchange interactions 80−103654
$Cs_2CuCl_4.2H_2O$, ferromag., hyperfine and exchange interactions, NMR study 80−50208
$Cs_2Cu(SO_4)_2.6H_2O$, long exchange paths between mag. ion pairs, singlet-triplet separation determ. 77−69283
$CsMnCl_3.2H_2O$:Cu(Co), quasi one-dimens. antiferromag., mag. impurity effect on Neel temp. and spin-flop field 79−61099
$CsMnF_4$, planar ferromag., cryst. and mag. struct., Jahn-Teller effect 80−75715
$Cu_yCr_2Se_{4-z}Br_x$, paramagnetic-ferromagnetic phase transition temp. depend. on element conc. 79−69672
$CuFe_2O_4$, superexchange interactions, three-sublattice anal. 79−61095
Cu_5FeS_4, mag. ordering and vacancy clustering, mag. susceptibility and Mossbauer spectra meas. 77−85625
$Cu(NO_3)_2.2^1/_2H_2O$, singlet ground-state system, mag. props., short-range ordered state 78−23289
EuO:Gd, mag. props. and instability phenomena 79−1666
Eu_2O_2S, cooperative optical absorption obs. in luminesc. excitation spectra 78−27308
EuO(S)(Se)(Te), superexchange interaction parameters, many-electron model calc. 79−7988
Fe complex, bis(N,N-dialkyldithiocarbamato) iron III halides, short range antiferromag. coupling, Mossbauer spectra 77−90076
Fe complex (2, 9-dimethylphenanthroline) sulphate, mag. props., Mossbauer spectra 80−66081
Fe-Al, spin glass transition, Monte Carlo study 80−39801
Fe-Al (0.27 to 0.50 at.%), spin glass behaviour, microscopic model, Ising lattice, exchange and superexchange 80−39800
$Fe_xCu_{1-x}Cr_2Se_4$, crystallographic and image props. 80−39049
Fe_3O_4, superexchange interactions, three-sublattice anal. 79−61095
$Fe_{1+x}Sb$, Mossbauer meas. of lattice and interstitial Fe atom mag. ordering 79−99807
GdN, mag. interaction and carrier conc. 80−71005
$GdN_{1-x}O_x$, magnetic interaction and carrier conc. 80−71005
GdP-GdS systems, mag. exchange interactions, free carrier conc. 78−60278
$GdVO_4$:Ho^{3+}, optically excited doublet splitting in magnetically ordered state 78−19238
$(HF)_2$, H-bonding and indirect exchange ('superexchange') in 79−93912
$(H_2O)_2$, H-bonding and indirect exchange ('superexchange') in 79−93912
$H_2O.HF$, H-bonding and indirect exchange ('superexchange') in 79−93912
$KCrF_3$, mag. struct. and cooperative ordering or orbitals 79−99687
$K_2CuCl_4.2H_2O$, and isomorphous cpds., mag. interactions of H and D nuclei, NMR obs. 79−87251
$K_2CuCl_4.2H_2O$, ferromag., hyperfine and exchange interactions, NMR study 80−50208
$K_2CuCl_4.2H_2O$, hyperfine and super-exchange interactions 80−103654
$KCuF_3$, mag. struct. and cooperative ordering or orbitals 79−99687
K_2IrCl_6, thermal expansion meas. near antiferromag. transition 77−20610
$KMnF_3$, exchange interaction of excited $Mn^{2+}(^4A_1)$ ions, Anderson model 80−25124
K_2NiF_4, 2D antiferromag., volume depend. of superexchange, US velocity meas. of T_N 78−19237
$LaNi_{1/2}Mn_{1/2}O_3$ and $Sr_{1-x}Ca_xMnO_3$, Curie and Neel points rel., common exchange integrals 77−77055
$La_{1-x}Sr_xCoO_3$ ($0.5 \leq x \leq 1.0$), Co^{3+}-O-Co^{3+}, Co^{3+}-O-Co^{4+}, Co^{4+}-O-Co^{4+} interactions 79−24154
$Li_{0.5}Fe_{2.5}O_4$, superexchange interactions, three-sublattice anal. 79−61095
$Li_{0.5}Ga_xFe_{2.5-x}O_4$, superexchange interaction parameters, Mossbauer spectra obs. 77−51899
$MnAs_{0.97}P_{0.03}$, orthorhombic, mag. anisotropy 77−43832
$MnAs_{1-x}P_x$, double exchange ferromag. coupling, magnetisation meas. 80−75751
$Mn(CN)_3.(H_2O)_{0.57}$, mag. interactions, theory 80−97085
$Mn_{1-y}Cr_yAs$, double exchange ferromag. coupling, magnetisation meas. 80−75751
MnF_2, molten, superexchange, EPR linewidth 79−19774
$MnFe_2O_3$, superexchange interactions, three-sublattice anal. 79−61095
MnO, paramag., μ^- spin rotation at O site 77−20785
$(NH_4)_2CuBr_4.2H_2O$, ferromag., hyperfine and exchange interactions, NMR study 80−50208
$(NH_4)_2CuBr_4.2H_2O$, hyperfine and super-exchange interactions 80−103654
$(NH_4)_2CuCl_4.2H_2O$, ferromag., hyperfine and exchange interactions, NMR study 80−50208

superexchange interactions continued
$(NH_4)_2CuCl_4.2H_2O$, hyperfine and super-exchange interactions 80−103654
$NiFe_2O_4$, superexchange interactions, three-sublattice anal. 79−61095
$Rb_2CuBr_4.2H_2O$, ferromag., hyperfine and exchange interactions, NMR study 80−50208
$(Rb)_2CuBr_4.2H_2O$, hyperfine and super-exchange interactions 80−103654
$Rb_2CuCl_4.2H_2O$, ferromag., hyperfine and exchange interactions, NMR study 80−50208
$Rb_2CuCl_4.2H_2O$, hyperfine and super-exchange interactions 80−103654
Si_3N_4:Fe, α- and β-phases, Mossbauer and Raman obs. of state of Fe 79−33572
SrF_2:Tm^{2+}, EPR meas. of Tm^{2+} ion pair interactions 79−95641
$SrFe_{12}O_{19}$, mag. props., effect of Sr dissolution by milling in water 77−25000
UIG, Ga-substituted, computer simulation of temp. and field depend. of sublattice magnetisation and spin-flip transition 79−11300
$YCrO_3$, exchange interactions 78−60279
$YFeO_3$, exchange interactions 78−60279
YIG, Al substituted, transferred hyperfine fields, Mossbauer effect meas. 79−1726
YIG, magneto-optical coeffs. induced by elec. and mag. dipole transitons 77−52060
YIG, superexchange and applied field depend. of Faraday rot. induced by elec. dipole transitions 77−36206
$Zn_cM_{1-c}Fe_2O_4$, M=Ni^{2+}, Co^{2+}, Fe^{2+}, $Zn_cMFe_{2-c}O_{4-c}Fe$, M=Ni^{2+}, Co^{2+}, calc. of saturation magnetisation by cluster components 77−43817

superfluid helium-3
5-d spin theory 80−49450
β-phase, negative ions mobility 79−86956
A_1 phase, broken relative symmetry and dynamics 80−24705
A_1 phase, mag., macroscopic dynamics 77−7929
A_1 phase, topology of singularities 78−51772
A_1-phase, domain wall exam. 79−42332
A⇄B transition in mag. field near polycritical point 77−11760
A and B phases, mobility of positive and negative ions 77−80672
A and B phases, US props. 79−65278
A and B phases, vortex solns. *(Russian)* 77−11762
A phase, effect of mag. dipole interaction on collective modes 77−89610
A phase, helical textures and NMR frequencies 79−95235
A phase, homogeneous case orbital dynamics 80−75399
A phase, intrinsic angular momentum value in BCS theory 79−51340
A phase, NMR on textural defects 78−38895
A phase, obs. of magnetisation reversals during relax. meas. 78−79842
A phase, phenomenological model of collapsed superflow and orbital relax. 79−51348
A phase, planar textures 78−79837
A phase, possible existence of monopole-antimonopole pairs 79−51341
A phase, slowly rotating, textures 79−95236
A phase, stability of superflow 78−14532
A phase, textures bearing surface singularities solns. 78−79841
A phase, theory of orbital dynamics, hydrodynamic eqns. 80−54461
A phase, theory of sound propag. 78−38896
A to B phase nucleation 80−100371
A- and A_1-phases, spin dynamics 79−51350
A- and B- phases, book 80−2227
A- and B-phases, disortion in elec. and mag. fields, NMR shifts 77−35780
A- and B-phases, linear and point singularities *(Russian)* 77−20151
A-phase, absence of orientational elec. field effect 79−19417
A-phase, analogy between disclination rank and vortex line invariant, in Cosserat continuum *(French)* 78−1977
A-phase, and its magnetic properties 79−42333
A-phase, angular momentum and singularities 77−66056
A-phase, anisotropic, orbital hydrodynamics, large angles of rotation of orbital momentum 77−80669
A-phase, anisotropy and flow 79−73367
A-phase, anisotropy of electric suscept. 77−80670
A-phase, arbitrary textures, hydrodynamics 77−31833
A-phase, attenuation of zero sound 77−24461
A-phase, boojums, analogy with cholesteric liq. crystals 78−56014
A-phase, collective modes of gap parameter for axial state 77−7937
A-phase, composite magnetic solitons 77−31832
A-phase, composite solitons, mag. reson. 78−51779
A-phase, composite solitons and mag. reson. 77−80674
A-phase, composite solitons in presence of superflow 80−2233
A-phase, Cooper pairs vs. Bose condensed mols., ground-state current 80−49451
A-phase, coreless vortices, in presence of heat flow 79−14980
A-phase, coupled spin orbit relaxation theory 78−6192
A-phase, direct obs. of orbital dissipation and superflow collapse 79−51347
A-phase, dissipation of flow, NMR study 80−92745
A-phase, dynamic spin behaviour in presence of textures 79−1536
A-phase, effect of order-parameter collective modes on NMR and US attenuation 79−51344
A-phase, entropy production and non-linear hydrodynamic eqns. 77−80668
A-phase, equilibrium textures, hydrodynamic and mag. effects in cylindrical pore 77−72734
A-phase, evidence for metastable mode, pulsed NMR meas. 77−85013
A-phase, existence of helical texture around superflow 79−60586
A-phase, ferromag. props. 78−14529
A-phase, ferromagnetic orbital magnetisation 78−38902
A-phase, field-induced $\hat{l}$ textures and mag. resonance 79−46864
A-phase, field-induced surface texture, in presence of superflow 79−46869
A-phase, first order current induced textural transition 79−95237
A-phase, gauge wheel, rot. symmetry and phase of order parameter 79−82409
A-phase, generation of textural defects 79−60588
A-phase, Hamiltonian equations of hydrodynamics 77−69138
A-phase, have persistent currents been obs.? 80−10731
A-phase, helical texture in presence of superflow and mag. field 79−7726
A-phase, helical texture stability, hydrodynamic free energy 79−95238
A-phase, helical textures, hydrodynamic stability study 79−55990
A-phase, helical textures, NMR response 80−70496

superfluid helium-3 continued
A-phase, helical textures and anisotropic heat flow 79−23800
A-phase, hydrodynamic eqns. *(Russian)* 77−4237
A-phase, hydrodynamics equations in presence of vortices *(Russian)* 79−33141
A-phase, hydrodynamics in Lagrange formalism *(Russian)* 77−55413
A-phase, in rotating bucket 78−2328
A-phase, instability of persistent currents and heat flow 80−15327
A-phase, internal struct. of de Gennes disgyration 79−60584
A-phase, intrinsic angular momentum, and its hydrodynamics with unclamped normal fluid 78−22922
A-phase, intrinsic angular momentum 78−56013
A-phase, ion mobility tensor, ion-quasiparticle scatt. 80−59753
A-phase, $\hat{l}//V_s$ texture, helical instability, mag. field effect 79−11000
A-phase, Lagrange and Hamilton hydrodynamic eqns. *(Russian)* 78−10248
A-phase, line singularities energies 79−86954
A-phase, linear singularities and structures 77−51564
A-phase, linear texture, and mag. reson. 79−4451
A-phase, longit. and transverse NMR modes, satellite resons. 77−7936
A-phase, longitudinal mag. relax. 80−59751
A-phase, mag. field effect on texture 79−65276
A-phase, mag. resons. associated with linear textures 79−60585
A-phase, magnetic texture relax., NMR meas. 79−60581
A-phase, mass current, intrinsic orbital angular momentum 80−84338
A-phase, microscopic theory for orbital hydrodynamics 80−70494
A-phase, new phase-transfer decay mechanism for persistent currents 80−6586
A-phase, NMR in presence of disgyration 79−19418
A-phase, omegism, order parameter structure 77−66062
A-phase, orbital angular momentum at finite temps., local plane-wave approx. 80−65330
A-phase, orbital angular momentum density at finite temps. 80−59752
A-phase, orbital dynamics 80−2232
A-phase, orbital dynamics in presence of heat flow and mag. field 79−51337
A-phase, orbital dynamics in spin fluctuation feedback approx., out-of-phase mode 80−54457
A-phase, orbital dynamics near transition temp. 79−37893
A-phase, orbital motion in presence of heat current 79−51349
A-phase, orbital motions 79−19416
A-phase, orbital relaxation viscosity coeff. 77−66066
A-phase, orbital solitary wave solution 77−31824
A-phase, order parameter collective modes, effect on NMR and US attenuation 79−46866
A-phase, order parameter singularities, confined to small cylinders, NMR 79−55994
A-phase, phase diagram for helical texture 80−24704
A-phase, phase slippage without vortex cores 77−31831
A-phase, planar $\hat{l}$ textures and mag. reson. 77−80673
A-phase, planar-twist soliton near A-A_1 transition, NMR props. 79−33145
A-phase, props. near transition to A_1-phase *(Russian)* 79−7728
A-phase, rotating, vortex lattice detectability 80−29240
A-phase, screening effect and nucleation of coreless vortices, in stationary and rotation containers 79−69311
A-phase, slab, nonplanar textures, Ginzburg-Landau theory 78−51777
A-phase, slab in mag. field, deformed textures, Ginzburg-Landau eqns. 77−39718
A-phase, slowly rotating, textures and free energy 79−60587
A-phase, small cylinders, evidence for textural transition for NMR expts. 78−56015
A-phase, soliton lattice for NMR behaviour 80−2234
A-phase, soliton study 80−88386
A-phase, solitons in the vicinity of the transition to A_1-phase *(Russian)* 78−87840
A-phase, spin disgyrations 77−89611
A-phase, spin relax. and zero sound attenuation at low temp. 80−107595
A-phase, stability of aligned state in superflow 78−56007
A-phase, stability of superflow 79−14979
A-phase, strong-coupling orbital 79−51346
A-phase, superflow, topological aspects 79−60580
A-phase, superflow collapse, orbital dissipation 78−91501
A-phase, superflow in torus 79−23797
A-phase, surface spin waves 79−86955
A-phase, textural critical vel. in limit of large mag. fields 79−99383
A-phase, textural singularities 77−59168
A-phase, texture and supercurrents 79−65279
A-phase, textures, hydrodynamic and mag. effects in slab 77−1273
A-phase, textures in narrow cylinders 80−24703
A-phase, topological anal. of cores of singularities 79−4450
A-phase, topological struct., nucleation and screening effect of coreless vortices 79−1537
A-phase, transverse magnetisation relaxation and superfluid spin flows *(Russian)* 80−34265
A-phase, transverse response for parallel plate geometry, coupled fluid and orbital motion 77−31828
A-phase, uniform magnetisation precession instability in mag. field *(Russian)* 79−95232
A-phase, unusual NMR effects 77−66059
A-phase, viscosity tensor, generalised paramagnon model 80−39379
A-phase, vortex ring without singular cores 78−67880
A-phase current-driven textural transition 79−55993
A-phase in a half-space, exact soln. for fountain-like texture 78−43199
A-phase rotating, textures 79−11002
A-phase slab, mag.-field-induced cellular superflow, periodic texture 80−24706
A-phase soliton lattice, flow induced 79−82407
A-phase texture elec. orientation 80−6585
A-phase vortex ring without singular cores 79−11001
A-phase weak ferromagnetism and peculiarities of superfluid transition *(Russian)* 78−67885
acoustic shear impedance meas. 77−11759
Anderson-Brinkman-Morel phase, orbital dynamics 77−24462
anisotropic A-phase, nonlinear sound interactions *(Russian)* 77−11761
anisotropic superfluid, ang. momentum of BCS ground state 79−90840
anisotropic superfluid, orbital angular momentum 77−89612
anisotropic superfluid phases, book contrib. 79−99387
anomalous magnetic relaxation *(Russian)* 79−23801
antiferromagnet, itinerant electron, dynamic magnetisation as internal Josephson effect 78−47931

superfluid helium-3 continued
B phase, mag. collective excitations 77−69136
B phase, motion of negative ions 77−11757
B phase, soliton-like spin waves 80−44385
B phase, spin waves creation 79−82411
B phase, surface textures and NMR 79−37895
B phase, textural singularities, NMR analysis 77−89608
B-phase, acoustic shear impedance 79−51343
B-phase, anisotropic gap distortion due to superflow and depairing crit. current 80−88383
B-phase, appl. of two-fluid hydrodynamic equations 79−46865
B-phase, Balian-Werthamer system, stability and inequalities for autocorrelation functions 80−96714
B-phase, bound spin wave states associated with n-solitons 78−67884
B-phase, collective excitations, kinetic eqn. approach 79−60579
B-phase, collective excitations exam. by kinetic equation method 78−18860
B-phase, collective excitations in presence of superflow 80−92744
B-phase, crit. current obs. 80−15328
B-phase, domain struct., derived from Ginzburg-Landau eqns. 78−63896
B-phase, dynamic magnetism relaxation, wall-pinned mode 78−43201
B-phase, dynamic NMR and static suscept. using RF-SQUID 77−51565
B-phase, existence of states with J=1 and 2 *(Russian)* 77−35779
B-phase, first-sound attenuation and viscosity 80−75401
B-phase, gap distortion, depairing critical currents, all temperatures 80−92743
B-phase, gap parameters and collective modes in strong mag. field 80−15325
B-phase, HF sound propag. meas. 80−88391
B-phase, low freq. zero sound attenuation, satellite peak struct. press. depend. 78−75901
B-phase, low temp. spin relax. 80−15323
B-phase, low-temp. spin relax. 79−55989
B-phase, macroscopic pairty nonconservation due to neutral currents 77−80671
B-phase, microscopic evaluation of transport parameters 79−51354
B-phase, n solitons in crossed mag. field and superflow 80−44386
B-phase, nonlinear hydrodynamics 80−59750
B-phase, nonlinear NMR, instability analogous to ferromag. reson. predicted 78−43202
B-phase, orientational electric field effect 79−46868
B-phase, phase transition to inhomogeneous state induced by elec. field *(Russian)* 77−51566
B-phase, press. depend. of superfluid density 79−51358
B-phase, pulsed NMR expts., spin waves *(Russian)* 79−7727
B-phase, shear viscosity, s-p-d wave approximation 80−96715
B-phase, shear viscosity calc. 77−51562
B-phase, sound dispersion and neutral superfluids with BCS pairing at T=0 79−51345
B-phase, spin collective excitations 79−46861
B-phase, spin relax. far below T_c 79−51353
B-phase, spin susceptibility in acoustic limit *(Russian)* 77−4236
B-phase, spin wave breathers, double sine-Gordon equations 80−15329
B-phase, standing spin wave mode obs. 77−24463
B-phase, static spin susceptibility 78−30807
B-phase, susceptibility in acoustic limit at nonzero temp. 78−84020
B-phase, textural spin waves 77−66058
B-phase, textures and NMR theory 77−39717
B-phase, textures effect on sp. ht. 78−75900
B-phase, transport coeffs. 79−51342
B-phase, transport processes at low temp. 77−55412
B-phase, transverse zero sound 77−31829
B-phase, viscosity, T-matrix calcs. *(Russian)* 78−63895
B-phase, viscosity meas. to 1 mK 79−51360
B-phase, viscosity near superfluid transition 78−38903
B-phase, zero sound attenuation peak obs. 80−88390
B-phase at equilib., formalism 80−88384
B-phase dynamics, broken spin-orbit symmetry 78−71898
B-phase ferromagneticlike reson. behaviour obs. in NMR 78−10245
B-phase spin oscills. in prescence of dipole forces 80−6583
Barnett effect 80−88388
Bogoliubov transform for spatially varying gap, gradient free energy 78−38901
Bose spectra stability, phonon branches, dispersion coeff. *(Russian)* 80−49452
Bose spectrum nonphonon branches *(Russian)* 80−92750
bound states of one-particle excitations near vessel walls 77−31826
boundary effects, transition temp. between ABM- and BW-states 77−31834
chiral fields, in Ginzburg-Landau region 79−55991
collective oscillation hybridisation near A. phase transition *(Russian)* 80−80020
collisionless collective modes 77−66067
conference, Brighton, England (Aug. 1976) 77−66055
cooling to 1 mK by nuclear demagnetisation of $PrNi_5$ 77−65037
correlated pairing theory 78−10247
creation of mag. solitons 77−15653
critical fluctuations, Anderson-Morel phase stabilisation *(Russian)* 79−73368
density and viscosity measurement 77−66061
density of superfluid, fourth sound Helmholtz resonator study 79−51359
density tensor meas. for A and B phases 77−15652
depairing critical currents 78−56009
dewar for IRAS telescope 79−54143
dissipative current structure, hydrodynamic calcs. *(Russian)* 80−100372
distortions around small object 77−85012
domain wall energy and spatial conformation in parallel plate geometry 80−96716
dynamic orbital effects, US propag. and viscosity, book contrib. 80−2235
electron bubble mobility 77−43402
exact Green function eqns., extraordinary phases 77−47642
experimental properties rel. to BCS theory 78−59998
Fermi liquids at surfaces quasiclassical boundary conditions 80−4641
Fermi superfluid hydrodynamics, time-depend. BCS formalism, compared with He II, finite nuclear systems 78−22920
Fermi systems, review of methods in quantum field theory 78−8338
fifth sound propag. 80−6580
film on metal surface, superfluidity mechanism *(Russian)* 78−30809
flow properties, comparison with ^{4}He 78−59997
flowing, NMR 79−4448

superfluid helium-3 continued
fluid-superfluid transition phase diagram, thermodynamic stability, fluctuations *(Russian)* 80−80023
fountain press., sp. ht. and thermal cond. meas. 77−35782
free energy, strong coupling corrections, spin-fluctuation theory 78−38899
frequency sums for free energy 79−33148
frictionless flow behaviour and mag. effects 77−43403
gauge group and p-wave phases 79−23798
gauge groups and phases 79−55992
Ginsburg-Landau region, phase equilib. in Lie group method 79−23799
Ginzburg-Landau free energy 77−28063
heat capacity, spin susceptibility, NMR and viscosity *(Danish)* 78−22921
heat capacity anomalous near transition, 0.8-20 mK 80−15326
heat capacity from CMN-^{3}He capacity meas. *(French)* 79−1097
heat transfer with solids below 100 mK 80−24701
helical textures stability with superflow in A-phase 79−46871
hydrodynamic action functional, phase transitions *(Russian)* 78−14534
hydrodynamic modes interaction, sound propag. and spin waves *(Russian)* 79−37897
hydrodynamic parameters and correlation functions 79−82406
hydrodynamic stability of ^{3}He-A uniform superflow, truncated variational approx. 78−67881
hydrodynamics and inhomogeneous states, review 80−49453
hydrodynamics and macroscopic dynamics in high mag. field 77−72733
incipient superfluidity, above superfluid transition temp. 78−79846
inert p-wave phases in strong coupling theory 77−31825
interface with Ag, thermal boundary resist. from 0.4 to 10 mK 79−56000
interface with nonmagnetic solid, Kapitza resist., quantum perturbation treatment 80−88385
ion mobilities in normal and superfluid phases 79−65280
ion motion and mobility, A and B phases 78−18861
ion motion using unified description of drag force 77−66054
Jastrow wavefunctions containing attractive correlations 78−56001
kinetic properties, model for calc. of helium-helium excitations cross-section *(Russian)* 78−56006
liquid-vapour porous-plug separators for cryogenic space system 79−54142
localised spin wave states in mag. field gradient 77−51563
longitudinal magnetic relaxation 78−79840
longitudinal magnetisation, relax. meas. 79−51355
low temperature physics, conf., Grenoble, France, (Aug. 78) 79−51462
low temperature props., review 79−37896
magnetic and electric-orientational effects, influence of internal fields 78−51775
magnetic field-dependent phase diagram below polycrit. point 77−66053
magnetic Kapitza conductance between paramag. substances 77−4235
magnetic relaxation, tip-angle-depend. 78−43203
magnetic relaxation and high amplitude spin waves *(Russian)* 80−92749
magnetic relaxation in hydrodynamic region *(Russian)* 79−95239
magnetic relaxation near crit. temp. 78−18862
magnetic resonance, electron cloud distortion, viscosity and density meas. 79−65277
magnetic solitons and monopoles 77−66065
magnetisation, nonlinear motion, parallel ringing 80−107597
magnetisation, p-wave spin triplet pairing Hamiltonian, 5-D spin 80−75400
magnetisation 77−31827
magnetoelectric textures in ^{3}He-A slabs, capacitive meas. 78−22924
mobility of negative ions, theory 80−107598
multipole pair vibrations, BCS soln. 78−47627
negative ion motion in normal and superfluid phases 78−38900
negative ions motion, model for A, B phases 78−2326
new phases *(Chinese)* 79−99385
NMR, I-texture effects on satellite frequencies 79−60583
NMR, low temp. orbital dynamics 77−66057
NMR, pulsed, nucl. susceptibility, spin-lattice relax., freq. shifts, A and B phases 78−47628
NMR and ion mobility experiments 78−91505
NMR in restricted geometries 77−7933
nonequilibrium processes, transport and relaxation 77−66068
orbital dynamics, homogeneous systems 79−33144
orbital dynamics in two-fluid model 78−30806
orbital dynamics of ABM state, microscopic approach near absolute zero 77−39716
order parameter, sp. ht., mag. props., sound propag., hydrodynamic props., book contrib. 79−99388
order parameter relaxation and hydrodynamics near A-transition 77−66064
ordered nonsingular systems, topology appls. 78−10166
orientational dynamics, two-fluid model 77−69135
oscillation viscometer results for A- and B-phase resonances, and normal phase viscosity 79−51351
oscillatory flow, temp. depend. of crit. vel. 80−10732
p-wave superfluidity in long narrow pores 79−28168
pair breaking by electron bubbles 79−51352
particle like solitons, A- and B-phases *(Russian)* 77−80675
phase transitions not controlled by stable fixed points 77−47640
physical properties of superfluid ^{3}He *(Danish)* 78−2325
planar textures, Ginzburg-Landau eqn. solns. 80−10729
point and line singularities 78−47625
Poisson brackets, nonlinear hydrodynamics eqns. in condensed matter physics 80−54296
positive ion mobility in normal and superfluid phases 79−4449
positive ion mobility meas. 79−55995
properties, general review *(French)* 79−33149
properties and phase diagram *(Polish)* 79−37894
properties and phenomena of condensed ^{3}He 77−35783
quasiparticle interactions, superfluid transition temps. 79−95233
quasiparticle interactions, transport coeffs. and superfluid free energy 79−95234
quasiparticle interactions and superfluid transition temps. 79−51356
quasiparticle transport equation, shear viscosity 78−14531
refrigerator with double nuclear stage for research on superfluid ^{3}He 79−58704
response functions of superconductors and ^{3}He(B), autocorrelation functions of density and transversal current, acoustic and quasihomogeneous 80−49449

superfluid helium-3 continued
response functions of superconductors and ^{3}He(B), density and current correlation functions 80−49448
response theory calcs., corrections to mag. susceptibility, binding energies, density 78−67883
review of phases, theoretical and expt. work 77−76639
rotating, equilibrium order parameters, chemical potentials 80−96713
rotating, stationary vortex arrays, obs. with TV/photographic method 79−77851
rotating A-phase, periodic structure of peculiar vortices *(Russian)* 77−35784
second viscosity and attenuation of fourth and second sound near transition temp. 77−31830
second-sound shock wave detection using fast-response superconducting thin-film probe 79−63237
singularities, investigation by homotopic topology methods *(Russian)* 77−69140
size effect influence on fluid density and transition temp., fourth sound meas. 80−80022
soliton exam. 79−33146
soliton solns. for spin orbital freedom wave eqns. *(Japanese)* 78−38904
soliton-antisoliton pair interaction in double sine-Gordon eqn., numerical simulation 80−46821
sound propagation and kinetic coeff., book contrib. 80−2237
specific heat, in weak-coupling-plus model 79−46867
specific heat discontinuities, rel. to Ginzburg-Landau parameters 80−54459
specific heat jump at superfluid transition and effective mass, press. depend. 80−65331
spin and orbital dynamics, book contrib. 80−2236
spin dynamics equations soln., strong mag. field 78−56010
spin dynamics theory, spin-orbit interactions, spin waves *(Russian)* 80−54462
spin flow density fluctuations, superfluidity *(Russian)* 80−65328
spin fluctuation peak, low-energy, theoretical anal. of neutron obs. 80−6584
spin relax., transport, spin fluctuation dominance model 77−66052
spin relaxation effects in nonlinear parallel ringing of magnetisation 78−6193
spin susceptibilities, flow depend. 78−14528
spin triplet pairing, Hartree-Bogoliubov theory 79−55988
spin wave interactions 79−86957
SQUID NMR techniques, appl. to liquid ^{3}He 79−26093
stability conditions, small-gap spin excitations 78−87839
static magnetisation 78−56008
strong coupling effects 78−47626
strong-coupling effects 77−11758
superflow, gap functions, critical currents, susceptibilities 80−103531
superfluid A-phase, composite soliton in narrow circ. cylinder, satellite freq., thermal fluctuations 80−34266
surface, topological singularities *(Russian)* 78−79847
surface energy and textural boundary conditions between A and B phases 80−54458
surface energy assoc. with interface between A- and B-phases, NMR obs. 77−47641
surface magnetism 79−51361
susceptibility measurement, by double bundle nuclear demagnetisation refrigerator 78−93692
texture topology in planar phase 79−69310
textures 79−82410
textures in narrow cylinders 78−95200
textures near $A \rightarrow A_1$ transition, NMR and current effects 78−59994
theory, introduction 78−59996
thermal boundary resistance between ^{3}He and CMN, preliminary meas. 77−66060
thermal contact with Pd sinter down to 0.4 mK, anomalous Kapitza boundary conductance 79−69312
thermometry of superfluid transitions 77−65038
topological classification of line singularities in cylindrical pore 79−4447
topological theory of defects in ordered media 79−93072
topology of non-singular textures using relative homotopy groups 78−84021
transition temperature, strong coupling theory 78−47629
transition temperature and pressure obs. with La-CMN thermometer 79−7731
transport and relax. processes close to transition temp. 77−55411
transport and relaxation properties, kinetic eqn. and Bogoliubov quasiparticle relax. rate 78−79838
transport and relaxation properties, viscosity, thermal, cond. and normal fluid density relax. 78−79839
transport parameters, Kubo formulae and BCS-Green's functions 80−88382
two-dimensional, phase transitions 79−33143
vacuum manifolds, gauge groups and topological invariants 79−237
viscosity and superfluid density meas. of A and B-phases 77−66063
viscosity of normal and superfluid phases 79−51357
vortex solns. for A and B phases *(Russian)* 77−11762
vortex-free slippage of phase, I vector oscill. in A phase *(Russian)* 78−63897
zero gravity behaviour 79−55987
zero sound and spin waves coupling near T_c 79−69309
zero-sound attenuation from order-parameter fluctuations in liquid ^{3}He 78−79845
B-phase, n-solitons, and NMR freq. calcs. 78−34670
He II-^{3}He dilute mixture, ^{3}He phase transition 77−80677
^{3}He, solid, possible explanation for recently obs. phase transition in high mag. fields 80−20006
^{3}He-^{4}He mixture superfluid thin film, third sound vel. calc. 80−107602
^{3}He-HeII solutions, van der Waals molecular dimers $(^3He)_2$, bound states *(Russian)* 80−49454
^{3}He-superfluid ^{4}He solutions, mag. phases of superfluid ^{3}He 80−59755
^{4}He-^{3}He, dilute soln., low temp., ^{4}He effective interaction 80−10734

superfluid helium-4
^{3}He bound states on ion bubbles in liq. ^{4}He 78−2329
^{3}He-^{4}He superfluid injection dilution refrigerator, process anal. 79−97394
λ point, US absorption, dynamic scaling 80−44380
acoustic vibration field density of states in piecewise const. parameter media 80−6483
adsorbed film, density profile, effect of substrate on superfluidity suppression 78−10252
adsorbed film on Vycor glass, superfluid transition 77−72737
anharmonic effects in US propagation near λ transition 80−96707
atomic order, gauge theory 77−76636
attenuation of fourth sound 79−51332
axial heat transport through annular duct with rotating inner cylinder 79−60575
behaviour near λ point 77−59166
boiling, heat transfer crises 79−94466
Boltzmann transport equation, search for exponentially damped surface solns. 78−67878
Bose gas, temp. depend. of quasiparticle sound velocity 77−69128
bound 2-roton state by neutron scatt. meas. *(Russian)* 79−86951
bound excitations 78−59993
bound roton-ion states, energy spectrum *(Russian)* 79−4445
bound states of rotons to impurities 78−55999
boundary with quantitative meas. of phonon energy transmission coeff. 77−66084
breakdown of superfluidity, excitation emission from negative ions with extreme supercritical vels. 80−65323
bubblon generation on charged surface, and instability generation *(Russian)* 78−18858
bubblons, speed camera obs. 79−65272
cable-in-conduit conductor, heating-induced flows 80−38229
capillary flow props., instabilities and vortex motion 77−55408
capillary geometry, effect of boundary conditions 79−69307
capillary isothermal flow, persistent current obs. 79−55955
charge trapped vertex ring, teaching 77−45650
charged surface stability breakdown, He ion geyser ejection *(Russian)* 80−15320
circulation, in ^{3}He-^{4}He dilution refrigerator 80−57304
Cocatron, servo valve for liq. He II level control, superfluidity and supercond. applic. 78−18855
combined axial mass and heat transport 78−63894
condensate fraction, neutron diffr. exam. 77−72728
condensate fractions and pair correlations 80−39375
confined film near T_λ, sp. ht. scaling 78−38894
continuum mechanics theory 77−69133
continuum theory, classical theory of irreversible processes 80−29236
coolant, superfluid plug control device 80−82774
cooled colour centre laser cavity 80−48282
counterflowing, superfluid transition temp., second sound vel. 77−89606
critical angular velocities for two-dimensional superfluidity 79−99379
critical dynamics at lambda pt., eqn. of motion approach 79−86943
critical fluctuations near lambda point, energy-density correl. function 79−12753
critical phenomena and superfluid transition 78−59989
critical superflow through Grafoil, two-dimens. random bond model 80−15319
critical thermal cond. near λ-point, light scatt. spectrum 80−24697
critical velocity, flow through cylindrical channel 77−69127
current flow effects *(Dutch)* 79−1534
cyclotron reson. freq. increase, electric field on surface dimple electrons 78−47624
density depression by velocity 78−51760
density fluctuation spectrum at finite temps. 79−82403
density in submicrometer diameter channels, Helmholtz resonator meas. 79−77852
density regions, λ transition and roton physical picture 79−82402
dewar for IRAS telescope 79−54143
didactic demonstrations of superfluidity and superconductivity phenomena *(Polish)* 80−86059
dielelctric const. meas. in liq. and solid 77−20143
droplets, heavy nucleus analogue 78−59992
dynamic scaling and US attenuation near superfluid transition point 78−84016
dynamic scaling near lambda point, two-loop calcs. 79−14977
dynamic scaling near lambda point 80−15321
dynamic scaling near T_λ 80−34264
dynamic struct. factor, temp. depend. 78−95197
dynamic structure, neutron diffr. determ. 77−11749
dynamic structure factor near λ temp. 77−66049
dynamical behaviour close to λ-line light scatt. review 79−7717
Ekman time for relax. of rotating He II following spin-up of container 78−75897
electron crystal, appearance of crystallised layer in superfluid He *(French)* 79−73364
electron escape from image-potential-induced surface states 80−49440
elementary excitation, structure factor and phase velocity 80−80012
elementary excitation line shapes, energies and linewidths, neutron scatt. obs. 79−60572
elementary excitation spectra 79−60568
elementary excitation spectrum, zero temp., anomalous dispersion, microscopic calc. 79−55976
elementary excitations, μeV resolution study by neutron spin echo 80−65327
elementary excitations, Brillouin-Wigner perturbation theory with correlated basis functions 78−2319
elementary excitations below 1K, exptl. evidence for interactions, entropy meas. 77−85006
energy spectrum, concave nature at very low wave numbers 79−4438
entropy meas. under press. between 0.7 and 1.35K 78−56004
entropy under press. *(French)* 77−72726
equilibrium superradiance in Bose gase 78−55994
evaporation by rotons and phonons, heat-pulse technique 79−33135
evaporation through narrow channels 79−60578
excitation energy spectrum, roton contrib. 80−24699
excitation spectrum, Bogoliubov theory 79−7722
excitation spectrum, RPA calc. involving simple pseudopot. 80−92738
excitation spectrum of system of interacting bosons 78−71897
fifth sound, vel. meas. 80−39377
fifth sound 79−60569
fifth sound in planar film 79−60570
fifth sound mode 80−75398
film, adsorbed on Al_2O_3 powder, surface tension sound 80−24691
film, adsorbed on Vycor substrate, superfluid mass and transition temp. 79−51385
film, Bose-Einstein condensation, thermodynamic functions 79−82399

superfluid helium-4 continued
film, Brownian motion, boundary layers and quantised vortex prod. 80−6579
film, complete decay of persistent currents, pulsed third sound TOF expts. 79−51378
film, compressible and layered, third sound 80−65325
film, crit. surface density 78−63891
film, dissipation below 1K 79−51376
film, dissipation by pinned vortex lines 77−80662
film, dynamics 80−59748
film, dynamics of vortex pairs using Fokker-Planck equation 79−69313
film, energy dissipation rate meas. 77−80663
film, finite size effects, effect of boundary conditions, below 0.5K 78−47616
film, heat cond. by ripplons 79−51375
film, influence of substrates on superfluid density at T=0 77−69144
film, jump in superfluid density 80−44387
film, long wavelength excitations, ripplon dispersion 79−73356
film, modified eqn. of state, mech. reson. meas. 80−24692
film, neutron scatt., surface effects 78−10251
film, nonequilibrium statistical mechanics 79−33137
film, on oscillating planar substrate, energy dissipation 78−47620
film, rate of energy dissipation 79−51377
film, rotating, melting of two-dimensional vortex lattices 80−2539
film, saturated, oscills. induced by persistent circulation 77−47637
film, saturated superfluid, on rough surfaces, persistent currents in presence of third-sound reson. 77−20156
film, solitons at low temps., Korteweg-de Vries eqn. 80−96717
film, specific heat near Tλ 77−80664
film, strong decay of persistent currents, thickness depend. 79−33133
film, superflow decay, vortex pinning effects 80−84332
film, superflow onset, 2-dimens. XY model 78−47623
film, superfluid density and dissipation in transition region 79−51384
film, superfluid healing length and density, ring diagram approx. 80−54452
film, surface electrons, quantum oscill. effects *(Russian)* 79−11105
film, third sound, two-dimens. hydrodynamics and elementary excitations 79−7721
film, third sound attenuation, 0.1-200 Hz 77−20159
film, third sound propag. and attenuation *(Russian)* 80−92733
film, two-reservoir, oscillations below 1K, damping 78−14535
film, universal jump in superfluid density 78−18856
film, unsaturated, direct obs. of third-sound mass displacement waves 78−30804
film, vortex pair prod., boundary layer problem 79−99378
film adsorbed on Grafoil, onset and third sound vel. meas. 80−44388
film and bulk, superflow in very long glass-capillaries 79−65273
film boiling anal. 80−10716
film growth on graphite, MgO, and Mylar substrates, vap. press. meas. 80−70499
film in zero gravity 80−54464
film on oscillating substrate, superfluid transition 78−67877
film thinning during crit. and subcrit. flow 80−20002
film thinning during persistent flow 79−73360
films, geometry induced third sound splitting 80−96712
films, vortices and superfluid decay 80−96710
first and second sound attenuation near lambda point 79−95227
first sound, order parameter fluctuation critical attenuation near critical temp. 80−2229
flow, exchange of heat with sintered Cu 77−82526
flow, slow thermal wave *(Russian)* 78−56005
flow, thermally-driven, in two coupled capillaries 79−86950
flow hydrodynamics, normal density component velocity depend. *(Russian)* 80−65326
flow of unstable isotope ^{6}He in ^{4}He, possible detection temp. 79−19411
flow through 2 μm-diameter orifices, obs. of quantised vorticity 79−19412
flow through porous plugs, space cooling system appl., plug characts. 78−49842
flow through porous Vycor glass under small press. gradient 80−49442
flows, healing and relax., first, second and fourth sound 78−47617
flows, healing and relaxation comparison with Khalatnikov-Lebedev theory 80−107587
fluctuating force in turbulent He II thermal counterflow 79−42330
fluctuations in turbulent counterflow, vortex line density fluctuation power spectra 80−84335
fountain effect 78−22917
fountain pump 78−59987
fourth sound attenuation 80−100370
fourth sound phenomenon under adiabatic and isothermal conditions 80−100369
fourth sound propag. and flow props. in very long capillaries 80−44384
fourth sound vel. and attenuation 79−86942
fourth sound vel. under press. 78−2322
fourth-sound-like propagation in grafoil-filled resonators 80−34263
free convection at supercritical pressures 78−26745
free convection film boiling from flat surfaces immersed in saturated He II, size and orientation effects 79−60577
free surface, book contrib. 80−2231
free surface, crit. behaviour near λ point 80−2228
freely suspended, rot. vel. nonregular variation *(Russian)* 80−88376
fundamentals and origins of superfluidity, crit. vel. problem, book contrib. *(French)* 77−85009
gauge wheel of superfluid ^{4}He, two fluid model 80−44379
Gorter-Mellink convection in He II, axial heat slow eqn. and dimens. anal. 80−64545
ground state energy and struct. 77−66051
hard-sphere model, crit. anal. 78−51769
healing and relaxation in flows, Landau's eqns. generalisation 77−55404
heat exchange with solid effect of surface roughness on dynamical props. 78−75923
heat transfer at wall, healing and relax. 78−75899
heat transport, steady state, at atm. press., practical data 79−60565
heat transport in long tube 79−60576
heat transport in restricted geometries, 0.8-2K 80−29237
HF crit. attenuation, 0.55-1.7 GHz 79−55958
HF sound scatt. near λ-transition *(Russian)* 77−59165
hydrodynamic eqns. accounting for ponderomotive forces, superfluid flow appl. *(Russian)* 79−19409
hydrodynamic equations, canonical *(Russian)* 78−79835
hydrodynamic stability of vortex ring in counterflow 79−86944
superfluid helium-4 continued
hydrodynamical modes when the vapour volume is small 80−88379
hydrodynamics, canonical eqns. 78−91497
hydrodynamics, Zilsel's variational principle derived from Lin's principle 80−24695
hydrodynamics equations in presence of vortices *(Russian)* 79−33141
hydrodynamics of three particle condensate model 78−22919
hydrodynamics quantisation for superfluid helium *(German)* 80−39371
interaction with ultra-cold and cold neutrons 77−83434
interface conditions between liq. and vapour 80−10723
interface with clean Ag, Kapitza cond. and enhanced power anomaly, 1-2K 80−88378
interface with clean Cu, static and transient anomalous Kapitza conductance 79−19444
interface with normal ^{4}He, temp. jumps across phase boundary 79−51334
interface with sapphire, ballistic-phonon-pulse transmission at 0.25K 79−95229
ion motion along vortex lines, in RF elec. field 79−51323
ion radius anomaly near lambda transition 77−76634
isochores between 25 bar and melting curve 78−14523
isotopic purification 77−35769
isotopically pure, roton-driven mech. for nucleation of negatively charged vortex rings 80−59746
isotopically pure, vortex nucleation 80−44378
Kapitza conductance, depend. on dislocation density near Cu interface 79−33170
Kapitza conductance, direct electronic contrib. 78−95221
Kapitza conductance of Ag, proof of surface superfluidity in enhanced power anomaly 80−15359
Kapitza resistance, axiomatic acoustic mismatch theory, with loss 79−33132
Kapitza resistance meas. using second sound *(Russian)* 80−88375
Kapitza thermal resistance and tunnelling states of atoms, theory 77−85046
lambda point, light scatt. props., static and dynamic scaling phenomena 80−92739
lambda transition, dynamic scaling correction 79−73357
lambda transition, microscopic theory, thermodynamic potential 79−73365
lambda transition during heat flow at supercritical press. 78−91499
laminar flow through capillary tubes 79−55949
Landau critical vel., negative ion expts. 77−55405
Landau critical velocity meas., excitations 80−103528
laser light scatt., multiplicative and additive stochastic processes 78−84596
level detector for pumped bath 78−49843
light scattering, near T_λ 80−29238
light scattering, spontaneous, by superfluid liquid surface, spectral features *(Russian)* 77−62696
light scattering 78−59991
liquid-vapour porous-plug separators for cryogenic space system 79−54142
local boiling, rel. to electron-hole drops in Ge in superfluid He *(Russian)* 79−42462
low and ultralow temp. cryogenic coolers for space missions 80−77790
low temperature physics, conf., Grenoble, France, (Aug. 78) 79−51462
many boson systems, representation of coherent states 79−30363
momentum distribution at 1.1 and 4.2K from neutron scatt. meas. 77−80665
monolayer film, third sound modes, superfluid solitons 79−10998
motion and thermodynamics, high density of vortex lines 78−54290
multi-electron bubbles *(Russian)* 78−30805
multiphonon boundary in excitation spectrum *(Russian)* 79−51324
multiple phonon spectrum boundary and props. *(Russian)* 78−63893
mutual friction force temp. depend. near λ-point *(Russian)* 77−35778
negative ion motion at supercritical drift velocities at low temps. 77−80667
negative ion velocity-field characts., effect of one-roton emission process 78−47622
negative ion vortex nucleation rate for ions whose drift vels. are limited by roton emission 79−55969
negative ions, dynamical interactions with superfluid ^{4}He 79−55954
negatively charged vortex rings, nucleation near solidification press. 78−55997
neutron inelastic scatt. studies of elementary excitations 79−65275
neutron scattering, book contrib. 80−2230
neutron scattering, role of two roton bound state 79−4446
neutron scattering, role of two-roton bound state 78−55993
neutron scattering 78−59990
neutron scattering and thermodynamic quantities, need for more precise data 78−22916
neutron scattering measurements, roton-roton interactions 79−46860
neutron spin-echo study of excitations 80−80014
neutron storage 79−86948
nonlinear combination interactions between first and second sounds *(Russian)* 77−69125
nonlinear conversion of second sound to first sound within a waveguide 79−55974
nonrotating vortex states 78−55996
nonstationary rotation regime, rel. to superfluidity of pulsars 80−98683
normal density viscosity, meas. at different freq. *(Russian)* 79−33130
normal fluid heat-exchange drag 80−49441
ODLRO and superfluidity in He-II 79−55986
one phonon excitation spectrum and interaction pot. 80−54455
optically observed second sound resonance 78−71894
order parameter relax. near T_λ, HF first sound meas. 79−55960
ordered media containing defects, gauge-like variables 79−88889
phonon dispersion, neutron scatt. study 79−51336
phonon dispersion curve from entropy meas. down to 0.75K 77−7922
phonon dispersion in He II 80−10722
phonon energy spectrum emitted into ^{4}He from thin-film heater 77−76633
phonon heat transport and Knudsen's minimum below 0.6K 79−33136
phonon relaxation theory in He II 77−85005
phonon temp. depend. above and below T_λ, neutron scatt. meas. 79−55973
phonon-roton excitation 80−107586
physical acoustics 77−51561
Poisson brackets, nonlinear hydrodynamics eqns. in condensed matter physics 80−54296

superfluid helium-4 continued
potential dependence of pairing solution 79−55977
pressure release sound modes 79−51331
pressure release superleak sound modes 80−54453
pressure-modulated flow in narrow channels, nonlinear friction force effect on vel. *(Russian)* 78−22914
pressure-volume and acoustic virial coeffs., temp. depend., quantum range 80−47056
pressurised, cooling of composite superconductor, triple-phase phenomena 80−20364
pressurised, vortex nucleation by neg. ions, thermal roton influence 80−10721
pressurized, attenuation and dispersion of first sound near superfluid transition 78−14524
pulsed perturbation relaxation, intense short heat pulse passage, compression wave propagation *(Russian)* 79−82400
purification technique from ^{3}He, for neutron source bottle 78−17823
quantised vortex rings, trajectories near orifice 78−55995
quantum hydrodynamics and two-fluid dynamics 77−69130
quantum lattice gas as microscopic model 78−59986
quasiparticle sound velocity, temp. depend., imperfect Bose gas picture 78−51761
Raman experiments, interpretation 79−73362
resonance mode conversion and other second order effects 77−51559
resonant nonlinear mode conversion 78−79831
ripplon canonical conjugate momenta 79−55951
ripplon damping at low temp., calc. 79−7720
ripplons, microscopic theory 78−14525
rotating, continuous model of vortex oscills. 80−70490
rotating, effect of hysteresis, second sound attenuation meas. *(French)* 79−55965
rotating, equilibrium order parameters, chemical potentials 80−96713
rotating, obs. of quantisation of circulation 80−59747
rotating, Poisson brackets and continual dynamics of vortical lattice *(Russian)* 79−73359
rotating, pressurised, relaxation phenomena, transition to ^{4}He II 79−99381
rotating, quantum steps in circulation around fine wire 79−55967
rotating, second sound vel., mutual friction 78−51766
rotating, Tkachenko waves 80−39376
rotating, vortex critical creation vels., equilib. vortex density *(Russian)* 79−19408
rotating, vortex free energy 79−51329
rotating, vortex position photography technique 80−96708
rotating Couette flow, hydrodynamic instabilities, attenuation of second sound resonances 79−55964
rotating cylinder, vortex patterns and energies 80−6578
rotating dynamics, rel. to pulsar astrophysics problems accessible in laboratory 78−49469
rotating freely, spontaneous accel. as manifestation of new type of quantum phase transition 79−55971
rotating He II, vortex-disc interaction 78−10237
rotating high speed frame, normal-superfluid λ transition 78−38892
rotating superfluid, vortex oscills., continuum model 78−34669
rotating system, equilibrium Onsager-Feynman vortex lattice *(Russian)* 80−29234
rotating under high press. collectivisation ang. speed shift of vortex oscills. 79−51326
rotating with vortices, defect hydrodynamics *(Russian)* 80−49445
roton lifetime, inelastic neutron scatt. meas. *(Russian)* 79−7723
roton lifetime effects on thermodynamic props. 79−55957
roton second sound dispersion 77−31819
roton-roton interaction for large and zero momentum 80−84336
roton-roton interactions, in elastic neutron scatt. spectra 78−95194
roton-roton interactions and thermodynamic props. 79−60571
rotons, temp. depend. of spatial correls. 78−71896
rotons and solidons 79−95228
sapphire superfluid ^{4}He interface, 0.25K, ballistic phonon pulse transmission 79−19415
sapphire-^{4}He interface, transmission of ballistic longitudinal and transverse phonon pulses at 0.25K 79−51416
second shock waves, detection by superconducting thin film probe 79−73355
second sound, boundary conditions 79−46857
second sound, self-focusing *(Russian)* 79−10996
second sound damping, crit. dynamics below T_λ 80−10727
second sound damping near superfluid transition, rel. to renormalisation gp. predictions 80−10725
second sound discharge and compression shock wave propagation *(Russian)* 80−103529
second sound shock waves, pulse characts. and temp. depends. 78−67876
second sounds, nonlinear profile, heat pulse method 78−75896
second-sound shock wave detection using fast-response superconducting thin-film probe 79−63237
self-consistent description of an interacting Bose gas at T=0K 80−80015
self-diffusion of turbulence through porous media 79−55961
short range order parameter 78−83712
single atom neutron scatt. and two roton connected state branches *(Russian)* 80−44381
singular behaviour of mass conductivity in superleak at superfluid transition 77−28059
singular f-sum rule, applicability to inelastic neutron scatt. 80−6577
slowly rotating, spontaneous acceleration, phase transition in system of macroscopic quantum vortices 79−33131
solid-superfluid interface, roughening transition 80−103536
solid-superfluid interface, struct., surface tension 80−88380
sound absorption, theory *(Russian)* 77−89607
sound conversion phenomena at free surface, acoustic coeffs. 80−96709
sound propagation, asymmetry phenomenon *(Russian)* 78−22913
sound propagation in liq.-vap. quasistatic equilib., crit. props. of sp.ht. 79−33134
sound transformation at free surface 80−54451
sound velocity, temp. depend. 79−33139
spatial distribution of order parameter, spectral approach of inverse problem *(Russian)* 77−80659
spatial order, temp. depend. 80−39374
specific heat, 65-850 mK, and phonon dispersion 79−4442
specific heat near lambda point, under press., exptl. tests of scaling laws and universality 78−84017
specific heat of confined sample, near superfluid transition 79−46859

superfluid helium-4 continued
spherically confined superfluid, quantised vortices *(Russian)* 80−70487
static heating length calc. 79−60567
static struct. factor and pair correls., neutron diffr. study, 1.00 to 4.27K 80−80010
stationary flow, 1.5K 79−73358
stationary flow, combined meas. 80−49446
statistical thermodynamics of cubic system below 0.5K 79−86939
steady-state heat transport at 1 bar 79−60574
stress tensor form 77−51558
structure factor, dynamical, two component character, superfluid and normal fluid 80−70488
structure factor anal. 78−34667
structure factor and sound vel., first and second sound 78−34668
subcooled, Kapitze resistance of Al 79−23794
sum rules at finite temps. 79−65270
superflow, healing and relax. in He II flows 79−14976
superflow dissipation near lambda point 79−55947
superflow into a solid superleak 80−39372
superfluid flow induced by crossed electric and magnetic fields *(Russian)* 78−84019
superheating and bubble formation 78−56000
surface, electron lifetime 79−77849
surface, hydrodynamic modes for ripple waves 78−43195
surface, ripplons, adsorbed ^{3}He and heat conduction meas. 80−49459
surface deformation and surface motion due to standing second sound waves 79−55984
surface electron mobility, 0.02 to 1K 79−55985
surface electron system with Coulomb interactions *(Japanese)* 78−51771
surface electrons, HF cond. 78−10238
surface excitations, effect on damping in two-dimens. electron gas *(Russian)* 79−10995
surface profiles, evidence of large superfluid vortex 78−18857
surface tension and contact angle, against solid ^{4}He 79−42339
surface tension and surface entropy 78−10235
surface wave, small amplitude long wave propag., linearised theory 78−56002
temperature fluctuations 79−19414
temperature gradients near heated surface 79−73363
theory of liquid ^{4}He 79−73361
theory of superfluidity 80−39378
thermal counterflow, vortex line drift velocity effects on temp. diff. data anal. 78−51765
thermal counterflow at large heat currents, geometry effects 78−51763
thermal counterflow in rot. flow, vortices and turbulence 79−86946
thermal expansion coeff. and phase transition 79−51333
thermal hydrodynamic fluctuations at interface *(Russian)* 78−23477
thermal quenching behaviour for formvar-coated composite superconductor 79−61633
thermally induced flow oscillations 79−82404
thermo-osmotic convection at incipient lambda transition, above crit. press. 78−95199
thermodynamic properties, interacting boson systems 78−2320
thermodynamic props., appl. of theory of temp. depend. energy levels 77−59163
thermodynamic versus neutron meas. at low temp. 79−51327
thermodynamics 77−69131
thermorotation effects 78−79832
thermorotation effects 79−55966
thin film, superfluidity 80−107594
thin rotating annulus 77−55407
third sound measurement as capillary condensation probe in porous material 80−20005
third sound pulses in doubly connected systems 79−55956
three-dimensional solitons *(Russian)* 78−63892
three-particle structure function, convolution approx. for ground state 78−26746
time-dependent Gross-Pitaevskii equation at T≠0 77−51560
transient heat transport 80−10715
turbulence, electron photography *(French)* 80−54456
turbulence, homogeneous, self-preserving structures 79−55962
turbulence, penetration through porous filters 79−46855
turbulence, steady homogeneous counterflow 78−87836
turbulence, vel. and temp. depend. from thermal resist. meas. 80−20003
turbulence and fully turbulent state 79−65274
turbulence during rotation, critical lengths 80−49443
turbulence in He-II counterflow jet 77−72732
turbulent counterflow, steady-state vortex-line density 78−95198
turbulent counterflow, vortex line density by second sound burst technique 79−55963
two dimensional system, phase transitions review 80−52149
two-dimensional, critical temp. gap and phase condensation 78−95201
two-dimensional, microscopic theory, excitation spectrum and thermodynamics props. 80−24709
two-dimensional and three-dimensional fluids, energy spectrum and phase vel. 80−70489
two-dimensional superfluid, dissipation near crit. point 78−47619
universality under press. near superfluid transition, critical exponents and scaling corrections 77−47638
unsaturated films, decay of persistent currents obs. 80−75397
US attenuation and dynamical scaling near T_λ 77−24460
US attenuation near λ line under high press. 79−55972
US finite amplitude wave propag. 80−80024
US generated quantised vorticity 78−38893
vacancy wave and tunnelling effect 78−47618
velocity dependence of superfluid-density near λ-point 79−37890
velocity fluctuation spectrum 80−34262
Venturi level differences 80−24698
viscosity, ion mobility and λ-transition 77−72731
viscosity and thermal conductivity *(Russian)* 80−10720
viscosity behaviour near superfluid transition 77−89605
viscosity near superfluid transition under press. 79−19413
viscosity near superfluid transition under press. 79−55959
viscosity properties depend. on oscill. freq. 80−6576
vortex form., crit. vel. depend. on oscill. period *(Russian)* 80−92732
Vortex formation near protuberances on a solid surface and the structure of the Ginzburg-Pitaevski equations 79−86947
vortex generation in modulated superfluid, flow through pinhole 77−72730

superfluid helium-4 continued
vortex lattice form. relax. times in two-valued vessel subjected to ang. accelerations *(Russian)* 80−92731
vortex line generation, threshold first sound amplitudes 79−55970
vortex lines, stability and interaction 78−47621
vortex motion in uniformly or nonuniformly rotating He II, eqns. *(Russian)* 78−87838
vortex nucleation inhibition by strong electric fields 80−92735
vortex photography progress report 79−55968
vortex pinning, surface roughening effects 80−88381
vortex quantisation and Higgs mechanism 78−2321
vortex rings, neutron elastic scatt. cross section calc. 79−4443
vortex-induced torque on porous disc, quantum calc. 78−51762
vortex-line density fluctuations 77−80666
vortices, quantized, and dielec. const. splashes in crossed fields *(Russian)* 79−19410
vortices pinning in nucleopores, effect on second sound resonators 80−49439
vorticity, nondissipative two-fluid eqns. 79−7724
vorticity fluctuations in turbulent counterflow 79−33138
vorticity threshold and vortex-core parameter near T_λ, second sound probe meas. 77−85007
wave process propag. in flow, new related phenomenon 79−51330
wave processes, in parallel channels, with different degrees of damping *(Russian)* 78−91496
zero point motion 77−76635
He, density correlation function and dynamic transient exponents at and above T_λ 79−51325
He II rotating, geostrophic and Tkachenko wave threshold intensity, Raman scattering *(Russian)* 78−43192
He II-^{3}He dilute mixtures, scatt. function S_{33} (q,ω) 79−56010
^{3}He-^{4}He, dil. soln., ^{3}He excitation spectrum at zero temp. 79−60592
^{3}He-^{4}He, dil. solns., sp. ht. and ^{3}He quasiparticle excitation spectrum 78−71901
^{3}He-^{4}He, superfluid, spin waves *(Russian)* 79−95240
^{3}He-^{4}He, superfluid soln., dil., low temp. props., book contrib. 80−15330
^{3}He-^{4}He, superfluid solution, second sound velocities *(Russian)* 79−33150
^{3}He-^{4}He, superfluid solutions, second sound attenuation and dissipation processes, 1.3-2.0K *(Russian)* 79−42335
^{3}He-^{4}He mixture, conc. susceptibility near superfluid transition 78−18865
^{3}He-^{4}He mixture near tricritical point, thermal diffusion ratio and thermal conc. gradients 77−76640
^{3}He-^{4}He mixture superfluid thin film, third sound vel. calc. 80−107602
^{3}He-^{4}He mixtures, coherence length effects on nucleation of superfluid transition 77−66069
^{3}He-^{4}He mixtures, superfluid transition temp., Green's function calc. method 77−72735
^{3}He-^{4}He superfluid mixture, second sound velocity, influence of spin 77−80676
^{3}He-He II degenerate soln., kinetic coefficients, thermodynamic props., hydrodynamic, acoustic and spin wave propag. *(Russian)* 78−18867
^{3}He-He II solns., magnetokinetic effects 79−19419
^{3}He-HeII solutions, van der Waals molecular dimers $(^3He)_2$, bound states *(Russian)* 80−49454
^{4}He atoms, scattering from superfluid ^{4}He surface, quantum interference 79−99382
^{4}He film, adsorbed, few atomic layers, excitations, two-dimensional roton. 80−39381
^{4}He, in fine regular pores, superfluid density and superfluid onset temp. 79−51335
^{4}He, liq., phase transitions, positive and negative ion mobilities meas. 78−87833
^{4}He, solid, nucleation in Vycor under press., superfluid oscills. near melting press. 79−51388
^{4}He, superfluid vortex lattice collective oscills. *(Russian)* 78−51759
^{4}He-^{3}He, dil. soln., ^{3}He quasiparticle excitation spectrum and second sound vel. meas. 80−24708
^{4}He-^{3}He, dilute soln., low temp., ^{4}He effective interaction 80−10734
^{4}He-^{3}He solution, Tomonaga model, 3-D analogue *(Russian)* 78−71900
interface with Cu, exponentially damped surface solutions generated by heat flow 79−55980
Si-^{4}He boundary, phonon energy transmission coeff., quantitative meas. 77−66084

superfluidity
see also quantum fluids; superfluid helium-3; superfluid helium-4; vortices
λ-transition, time development of coherent and superfluid props. 79−4439
acoustic turbulence, first and second sound kinetic eqn. soln. *(Russian)* 78−43193
antiferromagnet, existence of states with superfluid flow, Ginzburg-Landau theory *(Russian)* 78−72085
Bose condensate of electron-hole pairs *(Russian)* 77−31957
Bose liquid, hydrodynamics allowing for dissipative processes 79−23796
Bose liquid mixtures at finite temp. 79−19411
Bose superfluid, pot. depend. of pairing soln. 79−55977
Bose system, degenerated, superfluid ground state theory 77−20141
Bose-condensated electron-hole fluid, phase fixation, excitonic and spin superfluidity 78−30872
Bose-condensed quantum crystal, superfluidity 78−75905
Bose-Einstein condensation, suppression in restricted geometries, coherent states 79−46854
Bose-gas model, dil. hard sphere, calc. of low density atomic H gas props. 80−87194
boson condensate, dynamic eqn. functional formulation, many body theory 80−84334
boson gas, ideal and weakly interacting, phase transition kinetics 77−35775
boson system, interacting, ground state 79−58630
boson system, LF asymptotics of self energy parts at T=O *(Russian)* 79−95230
boson system, superfluid flow rel. to local gauge invariance 80−54450
Cl ^{3}He, A-phase, entropy production and non-linear hydrodynamic eqns. 77−80668
Cocatron, servo valve for liq. He II level control, superfluidity and supercond. applic. 78−18855
conditions for existence, phase fluctuation spectrum, Thomas-Kuhn sum rule 77−39709

superfluidity continued
critical angular velocities for two-dimensional superfluidity 79−99379
in crystals, two possible types 79−4454
degenerate Bose systems, condensate theory versus pairing theory 79−67224
degenerate fermi gas, hydrodynamic eqns. allowing for finite coherence length *(Russian)* 80−12989
dense matter, transport props., neutron stars appl. 79−67236
Dirac's monopole analogy 80−6575
excitons, Bose condensation, DLRO and ODLRO 77−43515
excitons, Bose condensed long range order, superfluidity 77−43514
Fermi gas, hydrodynamic action and Bose spectrum 78−139
Fermi liquid, small-gap excitations at zero temp. and in acoustic limit 79−7725
Fermi liquids, stability conditions, small-gap spin excitations 78−87839
Fermi superfluid hydrodynamics, time-depend. BCS formalism, compared with He II, finite nuclear systems 78−22920
Fermi superfluids, microscopic theory 79−65281
Fermi system, Bose spectrum, hydrodynamic action functional *(Russian)* 78−14534
Fermi systems, appl. to low density hard sphere systems 79−51339
Fermi systems, binary expansion in microscopic theory 79−51338
fermion systems, eqns. of motion for field operators and energy spectrum for isotropic systems 78−36926
fermion systems, superfluid, microscopic derivation of hydrodynamic equations, appl. to ^{3}He-B 79−46865
flow birefringence, depend. on normal-superfluid component relative motion *(Russian)* 80−45032
Frenkel exciton spectrum under the condition of Bose condensation 79−56133
Frenkel excitons, superfluidity for DLRO or ODLRO 77−43516
Galilean presymmetry and quantisation of circulation 77−35772
Green function for Bose liq. near lambda point 77−87689
Gross Pitaevskii eqn., generalised solns. 80−49437
hadron superfluidity in neutron stars, determ. from pulsars and compact X-ray sources 80−77442
hadronic matter, anisotropic superfluidity, analytic formulation 80−105869
hadronic matter, Pomeron and critical temp. 80−22566
helicity modulus at low temperatures 78−70052
helicity modulus for ideal Bose fluid 77−71267
hydrodynamical action functional in Bose and Fermi systems *(Russian)* 77−47639
hydrodynamics of superfluid systems with an account for ponderomotive forces *(Russian)* 79−19409
hydrodynamics quantisation for superfluid helium *(German)* 80−39371
isotopic invariance and pairing energies 80−22687
Josephson's relation and ε expansion for helicity modulus, renormalisation group approach 78−10239
liquid in crossed elec. and mag. fields *(Russian)* 79−55946
low-dimensional crystals, excitonic superfluidity 78−6359
macroscopic quantum phenomena in superfluid He and supercond., appl. *(Chinese)* 79−38263
macroscopic systems, linear response theory, Thomas-Kuhn sum rule 77−28060
magnetic superleaks, tests on natural magnetites 77−43399
metallic crystals, low-dimensional, excitonic 'superfluidity' 77−20248
model Hamiltonian for one- and two-dimensional superfluids 80−44377
molecular crystals with several sublattices, exciton-phonon interaction and Bose-Einstein condensation of Frenkel excitons 80−107713
neutral superfluids with BCS pairing at T=0, sound dispersion 79−51345
neutron $^3P_2$ superfluidity under π^0 condensation in neutron star matter 80−47417
neutron fluid, stationary flow in $^3P_2$ paired state *(Russian)* 80−103527
neutron star matter, superfluid phase transition 79−59025
neutron stars, rotating, form of quantum vortex filaments 80−67770
neutron stars, superfluidity 80−77441
neutron stars superfluid interiors, relax. processes between superfluid and crust 78−65645
nuclear physics, high spin rotation, collective aspects of heavy ion collisions 80−78309
nuclear structure at high angular momenta, review *(German)* 79−40832
nucleon superfluidity in neutron stars, influence on cooling 79−101170
ordered continuously degenerate systems, props. 79−93040
periodic solid, perfect one-component, microscopic and hydrodynamic theory 77−43405
physical acoustics and exploration of superfluid state, 1st, 2nd, 3rd, 4th and 5th sound, review 80−96090
physics of transitions, introduction 78−26660
Poisson's formulas for wave propagation 78−38891
polaritonic Bose condensation, effects of superfluidity 78−18976
problems of very low temperatures *(German)* 77−55650
pulsar crust superfluid, pinning and threading of quantized vortices 77−45475
pulsar-type superfluid system, rotating, dynamics of Onsager-Feynman vortices *(Russian)* 77−82270
pulsars, rotational behaviour rel. to superfluidity 80−98683
pulsars, superfluid liquid rotation, theory, relativistic effects in vortices *(Russian)* 78−61876
quantised vortices nucleation in small channels 79−37891
review 79−42328
review of investigations near absolute zero early investigation to present day discoveries 78−69958
rotating superfluid, vortex oscills., continuum model 78−34669
rotating superfluid dynamics, rel. to pulsar astrophysics problems accessible in laboratory 78−49469
rotational speedups accompanying angular deceleration 80−10738
sound field due to moving source in superfluid 79−90054
strong coupling theory of superfluid transition temp., appl. to ^{3}He 78−47629
superfluid as a source of all interactions 79−21620
turbulence, 2-D, hydrodynamic and plasma applications, dynamical eqns., diffusion, MHD, superfluidity, review 80−69769
turbulence, penetration through porous filters 79−46855
two dimensional system, ordering 80−107407
two-dimensional superfluid, dissipation near crit. point 78−47619
two-dimensional systems, superfluid density, XY model 79−95242
ultralow temperature physics, future prospects 79−65268
viscous Bose liq., hydrodynamics and transport coeffs. 77−69134

superfluidity continued
Vortex formation near protuberances on a solid surface and the structure of the Ginzburg-Pitaevski equations 79−86947
wave propagation, variational and reciprocity principles 77−72727
wave propagation in superfluid, scatt. problem 79−55948
D_2, supercooled, possible phase change to superfluid state 77−62707
H, Bose condensed spin-aligned, elementary excitations 77−72729
H, system of H atoms with polarised spin 78−30812
He, density correlation function calc. near T_λ in symmetric planar-spin model 77−4232
He, fifth sound propag. 80−6580
He film, multilayer adsorbed, in restricted geometries, book contrib. 79−99391
He, film, superfluid props. 80−34270
He film, superfluidity and the two dimensional XY model 79−28498
He film, very thick, electrohydrodynamic instability 79−51382
He film near λ point, phase transition 77−66070
He films, crit. attenuation of sound at 9 GHz 77−4241
He films, effect of substrate on suppression of superfluidity 79−69314
He, flowing superfluid, hydrodynamics of vortex generation 77−1272
He II, motion in rapidly rotating bucket 77−31817
He II, superfluid behaviour near λ point 77−59166
He, phase transition, fluctuational character *(Russian)* 77−47633
He, solid and liquid, book 79−99377
He, transformation of first sound into second sound *(Russian)* 77−11755
He, universal relations among crit. amplitude, calc. up to order ε^2 for systems with continuous symm. 77−17936
^{3}He and ^{4}He monolayer systems, book contrib. 79−99390
^{3}He, Bose spectra stability, phonon branches, dispersion coeff. *(Russian)* 80−49452
^{3}He, dissipative current structure, hydrodynamic calcs. *(Russian)* 80−100372
^{3}He, liquid, superfluid transition temp. calcs. 80−103530
^{3}He, superflow, gap functions, critical currents, susceptibilities 80−103531
^{3}He-^{4}He, at λ transition, universality 78−51782
^{3}He-^{4}He, liquid, nucleation of superfluid phase transitions at container walls 79−56014
^{3}He-^{4}He, mixture film, superfluidity precipitous onset 79−23802
^{3}He-^{4}He II, pulsed NMR investig. of ^{3}He flow vel. 77−59171
^{3}He-^{4}He liquid mixture, nucleation of superfluidity and phase separation 78−43204
^{3}He-^{4}He mixture, dilute, diffusion const. and thermal cond. along λ line 77−47644
^{3}He-^{4}He mixture, dilute, thermal cond. conc. depend. on λ line 77−51567
^{3}He-^{4}He mixture, film, superfluidity and phase separation 79−77857
^{3}He-^{4}He mixture, HF crit. sound attenuation near T_λ 79−95241
^{3}He-^{4}He mixture, liquid, differential osmotic press. meas. of conc. suscept. near lambda curve and tricritical point 79−73371
^{3}He-^{4}He mixture, superfluid phase transition, universality and scaling laws 77−11763
^{3}He-^{4}He mixture, superfluid fraction, density near λ point oscillating disc method 77−43404
^{3}He-^{4}He mixture, thermal transport properties near and below superfluid transition 79−60590
^{3}He-^{4}He mixture, transport props. near superfluid transition and tricritical point 80−29242
^{3}He-^{4}He mixture, tricritical crossover exponent 77−4239
^{3}He-^{4}He mixture, US propagation near tricritical point 77−59169
^{3}He-^{4}He mixture films, tricritical behaviour in vicinity of walls 79−51387
^{3}He-^{4}He mixtures, ^{3}He superfluidity 79−19420
^{3}He-^{4}He mixtures, concentration susceptibility near superfluid transition 79−56006
^{3}He-^{4}He mixtures, homogeneous phase separation obs. 80−107599
^{3}He-^{4}He mixtures, normal density at elevated press. *(Russian)* 79−90841
^{3}He-^{4}He mixtures, phase diagram and conc. susceptibility near tricritical pt. 79−56005
^{3}He-^{4}He mixtures, sound propagation near superlfuid transition 78−79848
^{3}He-^{4}He mixtures, superfluid transition onset props. 77−35786
^{3}He-^{4}He solution film, thermodynamic theory 77−4238
^{3}He-^{4}He solutions, ^{3}He supercritical states contrib. to thermodynamics *(Russian)* 79−65282
^{3}He-^{4}He solutions, roton spectrum, calc. *(Russian)* 77−4240
^{3}He-^{4}He superfluid mixture, early stages of spinodal decomposition, calc. 80−20004
^{3}He-^{4}He superfluid solution in superleak waveguide, acoustic-modes *(Russian)* 79−90842
^{3}He-He II dilute solution, fourth sound velocity 80−70498
^{4}He, Bose-Einstein condensation, interacting boson theory without anomalous propagators 77−33942
^{4}He solid, search for superfluidity 78−10254
^{4}He-^{3}He, fifth sound 79−60569
Pd, triplet pairing, spin fluctuation contrib. 78−10711

supergiant stars
16 M⊙ supergiant with 1 M⊙ neutron star companion, double core evolution 78−53980
A, F, G-type supergiants kinematics, appl. to galactic spiral structure parameters derviation 80−17665
A 0538−66, recurrent transient LMC X-ray source, precise position, supergiant star counterpart 79−62933
A-type bright supergiants in LMC, spectra, line intensities 77−22215
A-type supergiant stars, reson. line profiles from IUE and Copernicus spectra 80−90424
α and β Aquari, G-type supergiants, evidence for hybrid atmospheres and winds from UV spectra 80−72948
α Aquarii, chromospheric event detect. from UV spectrum obs. 80−31299
α Aquarii, supergiant, Ca II H and K line variation 77−22227
η Aquilae, Cepheid variable, absolute energy distrib. in radiation spectrum *(Russian)* 80−72974
atmospheres, light scattering, in circumstellar dust shell, stellar interferometry 79−80309
ε Aurigae, dual aspect of wavelength depend. fluctuations 80−62190
ζ Aurigae, eclipse data rel. to radius change of K-type supergiant component 79−84820
supergiant stars continued
ε Aurigae, eclipsing binary, astrometric study from Sproul 61-cm refractor plates 78−89219
ε Aurigae, eclipsing binary, distance from astrometric obs. 79−53859
ζ Aurigae, eclipsing binary, UV obs. of supergiant atmos. 80−94836
ε Aurigae, fine analysis of atmosphere of primary F-type supergiant 78−85976
B2 to G0 type, small amplitude light vars. 78−32469
B 1 Ia-0 supergiants, mass loss meas. 79−16948
B supergiants, kinematical parameters from UBV photometry 77−26011
B-type, intrinsic colour indices 79−84794
B-type, radial vel. vars. 79−21285
B-type supergiant assoc. IR source GL 2636, IR and visible obs. 80−105302
Balloon-borne UV Stellar Spectrograph, first obs. results 79−70955
BD −14° 5037, B-type, radial vel. vars. 79−21285
blue supergiant+neutron star, evolution 80−98689
bright IR star monitoring at 2.7 μm 78−16433
bright stars in SMC, structure and kinematics study 79−101192
α Camelopardalis, O-type, spectroscopic study, model atm. anal. 78−28681
XX Camelopardalis, R Coronae Borealis star, photometry in optical and IR ranges 80−101601
α Camelopardalis (O9.5 Ia), stellar wind terminal vel. short time changes from UV spectrum 80−36625
α Camelopardalis (O9.5 Ia), variable Hα P Cygni profile 80−41818
UW Canis Majoris, absolute dimensions and evolution 79−12496
VY Canis Majoris, apparent orbit, rotating holey dust cloud hypothesis 79−40191
VY Canis Majoris, diameter upper limits 79−16974
VY Canis Majoris, irregular variable supergiant, OH maser source, UHF spectra obs. 80−90550
UW Canis Majoris, O7f supergiant, mass loss rate meas. 80−67736
VY Canis Majoris, OH and H_2O microwave maser emission obs. 78−53949
VY Canis Majoris, OH/IR star, 1612 MHz OH maser multibaseline VLBI obs. 80−12766
VY Canis Majoris, supergiant OH maser source, optical radial vel. 77−49378
α Canis Minoris (Polaris), interferometry, first fringe meas. 80−82215
AG Carinae, P Cygni supergiant, spectrum of ring nebula 77−67100
α Carinae (Canopus), generalised Compton effect in spectrum 78−53938
Cassiopeia A supernova, progenitor, consistent evolutionary picture involving supergiant mass loss 78−36623
ρ Cassiopeiae, absolute energy distrib. in 3400-7100 Å range 78−49440
SU Cassiopeiae, Cepheid variable, spectrophotometric determ. of effective temp. 80−90435
κ Cassiopeiae, effective temp. radius, mass loss and luminosity 80−51748
AZ Cassiopeiae, interacting eclipsing binary, mass loss of cool supergiant component 78−32522
κ Cassiopeiae, OBC star, spectrophotometry, 3300-7100 Å region 79−67009
UV Cassiopeiae, R Coronae Borealis star, photometry in optical and IR ranges 80−101601
6 Cassiopeiae, spectroscopic obs., equivalent widths, microturbulence and radial vel. 80−22006
PZ Cassiopeiae, supergiant OH maser source, optical radial vel. 77−49378
V509 Cassiopeiae (HR 8752), no emission at Hβ (1979 July 31) 79−92782
V509 Cassiopeiae (HR 8752), spectrum variable supergiant, Hα emission obs. 79−88672
V509 Cassioperae (HR 8752), light vars. during period of spectrum vars. 79−101161
UW Centauri, visual magnitude estimates, UBV photometry 78−40962
V810 Centauri (HD 101947), yellow variable supergiant near Cepheid instability strip, VBLUW photometry 80−98672
9 Cephei, B2-type supergiant, circumstellar CO lines discovery 79−84793
VV Cephei, eclipsing binary, distance from astrometric obs. 79−53859
VV Cephei, eclipsing binary, UV spectrum 80−82415
δ Cephei, Hα radial vel. behaviour 80−51788
μ Cephei, late-type supergiant, possible H_2O thermal emission identification 78−81628
μ Cephei, M supergiant, circumstellar shell and mass loss rate 77−45415
19 Cephei, O-type, spectroscopic study, model atm. anal. 78−28681
μ Cephei, polarization across TiO bands 79−97005
VV Cephei, spectroscopic obs. during 1976/77 eclipse ingress phase 78−45359
μ Cephei, supergiant, relationship to young open cluster Trumpler 37 77−22284
VV Cephei, UBV obs. 80−17611
VV Cephei, UBV photometry during ingress phase of 1976-78 eclipse 78−20862
VV Cephei, UV spectrum obs. during chromospheric eclipse phase 80−109498
9 Cephei (B2 Ib), circumstellar CO obs. 80−94795
VV Cephei system, distant, in Puppis, spectral classification, UBV photometry and polarimetry 80−51810
Cepheid variables determ. of colour term in period-luminosity colour relation 80−94812
circumstellar dust shell effect on photospheric line profiles 79−30058
circumstellar ring systems, SiO and H_2O maser line evidence 78−89195
classical Cepheids, mass-luminosity relationship 79−35278
cool stars, effective temps; ang. dias. and reddening determ. from 1 to 5 μm flux curves 79−44458
cool stars, near IR excesses 78−16406
cool stars, supersonic stellar winds and rapid mass loss 79−21268
R Coronae Borealis, UBVRIHKLMN photometry, interpretation 80−67756
R Coronae Borealis stars rel. to Type I supernovae, appl. to Crab Nebula 79−5845
31 and 32 Cygni, ζ Aurigae stars, UV spectroscopic obs. 80−109499
α Cygni, anomalous spectral line contours of Fe II multiplet *(Russian)* 78−93243
P Cygni, Copernicus UV obs. 79−30066
V367 Cygni, eclipsing binary, spectroscopic study 78−53984
P Cygni, effective temp. radius, mass loss and luminosity 80−51748
P Cygni, electron scattering in expanding atmosphere 79−21311
P Cygni, extreme B-type supergiant, UV spectroscopy 80−22004

supergiant stars continued
P Cygni, H Balmer line profiles, accel.-decel. envelope, mass loss 79−40205
P Cygni, H Paschen α obs. 80−62156
P Cygni, high resolution UV spectrum obs. 80−26873
NML Cygni, IR speckle interferometry 80−31216
α Cygni, mass loss from mid UV spectrum obs. 78−93217
α Cygni, Na I interstellar lines hyperfine struct. 78−24542
V729 Cygni, O-type evolved contact system, masses 78−93309
32 Cygni, opacity wavelength depend. in atm. of K-type supergiant component 78−73741
α Cygni, radial vel. and line profile vars. in supergiant 80−22010
γ Cygni, radio emission upper limits rel. to nature of Cygnus X radio source 78−28809
32 Cygni, supergiant eclipsing binary, λ6575 and λ4870 light curves anals. 79−88700
α Cygni (Deneb), Ca II K line high-resolution obs. 78−16408
α Cygni (Deneb), Ca II K-line core asymmetry 80−85981
α Cygni (Deneb), Copernicus obs. of UV spectrum 78−45330
P Cygni in far UV *(Russian)* 79−8919
Cygnus OB2 No.12, high resolution 2μ spectroscopy rel. to interstellar and stellar features 78−57613
Cygnus OB2 number 12, spectral classification and membership of association 80−51760
Cygnus X-1 (HDE 226868), optical photometry, (1972-1976) 78−32609
degenerate neutron cores, equilib. models struct. 77−33472
S Doradus, LMC Hubble-Sandage variable, IUE and ground based spectroscopic obs. 80−101595
S Doradus (HD 35343), luminous LMC supergiant, long time baseline VBLUW photometry 80−36630
30 Doradus region, in LMC, interstellar extinction and stellar population 78−96517
early-type mass-losing supergiants, two-core model and evolutionary status *(Russian)* 80−109425
early-type supergiants, Balmer discontinuity from uvby photometry 77−53591
early-type supergiants, in Bochum 15 stellar aggregate, photoelectric and spectroscopic obs. 77−87490
early-type supergiants, spectrum variability, UV obs. *(Italian)* 78−32458
extended atmospheres, sphericity effects in red giants, model study 80−22012
extragalactic distance indicators 78−93396
extreme galactic B and A supergiants, light vars. 77−56927
F and G-type supergiants, search for light vars. 79−88657
F- and G-type, enhanced He abundance effects on visible spectra 80−12759
F- and G-type, luminosity calibration using O I 7774 Å line equivalent width 78−53942
F-type stars, southern, visible spectra obs. 80−98660
F-type supergiants in Magellanic Clouds, Ca abundances 80−98655
G and K Ib supergiants, C, N and O abundances 78−24509
G and K supergiants, observational evidence for mass loss 77−56928
G- and K-type, Li abundances 78−28676
G- and K-type giants and supergiants, correl. between motions and CN anomalies 77−17566
G- and K-type Ib supergiants, metal abundances 77−33482
galactic G-type supergiants, UBV photometry 80−41824
galactic supergiants, five-channel photometric obs. 78−16398
HD 101947, yellow supergiant star, Cepheid with 125 day period 79−88671
HD 105056, ON supergiant, radial vel. study 80−90427
HD 152236, B-type, radial vel. vars. 79−21285
HD 152667=OAO 1653−40, physical parameters 79−17021
HD 152667 (V861 Scorpii), eclipsing binary X-ray source, possible black hole 79−53858
HD 152667 (V861 Scorpii), phys. props. and orbital parameters, supergiant star with black hole companion model 79−71067
HD 153919, Of supergiant, X-ray binary 3U 1700−37 optical counterpart, light curve anal. 78−32470
HD 153919 (=4U 1700−37), supergiant-neutron star, optical variability 80−82419
HD 154368, interstellar species, excitation temps. and column densities in direction of supergiant 79−8981
HD 159378 (Tr 27-102), yellow variable supergiant near Cepheid instability strip, VBLUW photometry 80−98672
HD 166734, Of binary system, evolutionary state, visible obs. 80−82414
HD 168607 (B9 Ia^+), S Doradus type star candidate, spectral line profiles *(Russian)* 80−90456
HD 169454, B-type, radial vel. vars. 79−21285
HD 183143 and wavelength depend. of interstellar circular polarization 79−92819
HD 18391, characts. of HIA 0255+574 nearby radiosource 78−81701
HD 188209, O-type, spectrophotometry, 3300-7100 Å region 79−67009
HD 190603, effective temp. radius, mass loss and luminosity 80−51748
HD 33579, 35343, HDE 286757, 269006, most luminous LMC supergiants, long time baseline VBLUW photometry 80−22007
HD 33579, HD 35343 (S Doradus), HDE 268757, HDE 269006, most luminous LMC supergiants, long time baseline VBLUW photometry 80−36630
HD 34664 (S 22) in LMC, peculiar emission lines, mass loss and wind 80−77416
HD 698, massive spectroscopic binary, spectral obs., evolutionary state, mass loss 78−57590
HD 74180, F2 Ia^+ supergiant, common distance with open clusters Pismis 6 and 8 and (Wat 6) 79−88712
HD 77581 (3U 0900-40), X-ray binary, spectroscopic orbit and masses of components 78−16461
HD 77581 (=Vela X-1), supergiant+neutron star, X-ray, UV and visible obs. 80−94892
HD 91619, 96919, B-supergiants, peculiar H_α profile variations 77−17577
HD 93129A, O3 supergiant, rel. to Carina nebula 77−87520
HDE 226868 (Cygnus X-1), Hα emission in (1977) 80−51919
HDE 269700, B-type, radial vel. vars. 79−21285
heavily reddened young open cluster Trumpler 27, spectra and photometry 77−78836
α Herculis, 1.25-3.25 μ airborne photometric obs. 78−40934
AC Herculis, curve-of-growth analysis of RV Tauri variable 80−22026
α^1 Herculis, He I 10830 Å emission obs., high-temp. chromosphere 79−48792
supergiant stars continued
α Herculis, M supergiant, circumstellar shell and mass loss rate 77−45415
α Herculis, M-type supergiant, Mg II h and k emission obs. 78−53945
AC Herculis, RV Tauri star, UBV obs. 80−56857
α Herculis A, M-type supergiant, Li abundance in atmosphere *(Russian)* 80−72950
high luminosity stars in Galaxy and Magellanic Clouds, UBV intrinsic colours 80−26855
HR 8752, binary emission feature variability, visible obs. 80−109463
HR 8752, spectrum var. of G-type supergiant 79−62828
HR 8752, spectrum var. of superluminous supergiant, near IR obs. 78−81630
HR 8752, superluminous star, hot companion discovery by IUE 79−16947
HR 8752 (HD 217476), superluminous superiant, line spectrum changes rel. to expanding shell 79−80308
HR 8752 (V509 Cassiopeiae), emission-line spectrum rapid changes 80−36645
I-15, distant B-type object in Norma 80−62129
instability effects, brightness limits and coronae 80−109432
intrinsic and interstellar polarization components separation 79−30079
intrinsic colours rel. to interstellar reddening material distrib. 79−8908
IR spectral observations, of late-type supergiants *(Japanese)* 79−80307
IRC+10420, high-resolution OH maser obs. at 1612 MHz 79−44471
IRC+10420, new OH maser feature spatial struct. 79−48946
IRC+10420, stellar OH maser VLBI obs. rel. to mag. field 79−25742
K-type, macroturbulence rel. to luminosity 79−96997
late-type, 1.25-3.25 μ airborne photometric obs. 78−40934
late-type, in Magellanic Clouds, IR photometry 79−35254
late-type, sphericity effects in extended atms., models 78−81617
late-type southern stars, chem. comp., solar neighbourhood metallicity distrib. 80−12758
late-type stars, anal. of balloon-borne near IR multicolour photometry 80−98654
late-type stars, near IR multicolour photometry from BAT *(Japanese)* 80−31298
late-type supergiant stars, S I emission in EUV 80−82359
late-type supergiants, atmospheric struct. from freq. depend. diam. 77−56924
late-type supergiants, luminosity effects in spectra 77−60753
late-type supergiants, near IR photometry with balloon-borne telescope 78−73713
late-type supergiants, near IR photometry with balloon-borne telescope 80−4357
late-type supergiants, radio emission search 77−87392
ρ Leonis, effective temp. radius, mass loss and luminosity 80−51748
η Leonis, mass loss from mid UV spectrum obs. 78−93217
ρ Leonis, non-anomalous diffuse interstellar absorpt. features 78−16418
LMC, blue to red supergiant star ratio across face, rel. to star form. 80−26984
in LMC, long-term light vars. 78−45326
in LMC, luminosity and extinction values, UV obs. 80−77477
in LMC, photoelectric UBV photometry *(German)* 80−21932
in LMC, photometric luminosity calibration, visible obs. 80−94797
in LMC, spectra, diffuse interstellar 4430 Å feature 80−73033
in LMC, spectral types and magnitudes, catalogue of 1882 objects 78−32361
LMC members, IUE obs. and 2200 Å feature detection 79−16959
LMC members, IUE obs. of UV spectra and flux distribs. 80−101593
LMC OB and supergiant stars, deep objective prism survey catalogue 79−40090
LMC supergiant stars, comments on catalogue of Stock et al. *(French)* 78−53941
LMC supergiants, BVI photometry 77−33490
LMC supergiants, distrib. rel. to spiral struct. 77−29924
LS I+61°303, variable binary radio star (B1 Ib), X-ray emission detect. 80−105400
LS I +61°303, radio variable Be star, UV spectrum, stellar models 80−26879
LSI+61°303, supergiant Be star, radio emission and radial vel. periodic vars. 80−62149
LSS 1916, 3371, new VV Cephei stars, spectra and colours 79−35299
luminous blue variable stars in M31 and M33, IR detect. 78−49437
luminous stars in NGC 6822 and IC 1613, visible spectra and photometry 80−82345
luminous variable stars in M31 and M33, spectra and photometry 78−28686
δ^2 Lyrae, M-type supergiant, Li abundance in atmosphere *(Russian)* 80−72950
in M31, photometric and spectroscopic studies in Baade's Field IV 80−36622
in M33, supergiants distrib. rel. to spiral struct. and star form. 79−21437
M6 field, supergiant IR photometry and interstellar matter towards galactic centre 78−16405
M-type, circumstellar envelopes, observational study 78−53939
M-type, circumstellar gas and dust shells, optical and IR obs. 79−21281
M-type, classification from spectral scans 80−62127
M-type, highly reddened IRC objects, IR photometry and near IR spectra 79−84796
M-type, in central region of 30 Doradus, IR survey 78−32544
M-type, in LMC, MK spectral types, luminosities 79−62820
M-type, in solar neighbourhood, absolute magnitudes 78−81631
M-type, IR spectral bands in 1-5 μ region prospects 78−69801
M-type, SiO maser sources, 43 GHz obs. 79−16942
M-type, spectral type and luminosity classification from near IR spectrograms 79−16952
M-type in SMC rel. to low metallicities 79−96995
M-type maser stars, radial vel. determ. 80−77410
M-type southern objects, search for OH 1612 MHz emission 78−69792
M-type supergiants, photoelectric two-dimensional spectral classification 78−53936
M-type supergiants in reddened Ara cluster, IR photometry rel. to thermospheres 77−41395
M-type with OH, H_2O or SiO maser emission, catalogue 79−70965
in Magellanic Clouds, supergiants birthrate and mass function 80−67699
mass loss and convective overshooting influence on evolution 79−84789
mass loss rates 77−91534
massive luminous stars, stellar winds effect on evolution 79−12467

supergiant stars continued
massive single stars, main sequence evolution with and without stellar wind 79−16936
massive stars, bulk yields of nucleosynthesis 78−36552
massive stars, evolution in Galaxy and LMC 79−101191
massive stars presupernova evolution 79−16930
Milky Way, supergiants and O-type stars props. and catalogue 79−40183
in NGC 2439 association, photometry and spectra 78−16470
in NGC 5102, lenticular galaxy, dust and young supergiant stars obs. 79−44609
in NGC 654, young open cluster B to F-type supergiants identification from UBV photometric study 80−109502
nonvariable supergiants, classical Cepheids and bright giants, spectrophotometric comparison 80−56837
O and B0 supergiants in Magellanic Clouds, spectral classification 77−78777
O- and B-type stars, ionization conditions in expanding envelopes 78−28671
OB supergiant X-ray binaries, line distortion effects 78−7995
OB supergiants, mass loss and massive binary evolution 77−57020
OB supergiants, minimum flux corona theory 80−26844
OB supergiants, X-ray flux and ionization in wind, corona effects 79−48783
OB supergiants in X-ray binary systems, possible mass transfer mechanism 77−9809
OB-type stars, search for H Paschen α 80−62156
OB-type supergiants, effective temps., ang. diameters, distances and linear radii 80−17584
OBA supergiants and Of stars, IR photometry and mass loss rates 77−45414
OH maser emission from late-type stars, UHF obs. 80−56826
OH/IR sources, microwave spectra, galactic distrib., radial velocity 78−16432
open cluster NGC 3105, photoelectric UBV obs. 77−64811
α Orionis, 1.25-3.25 μ airborne photometric obs. 78−40934
α Orionis, 14.9 GHz obs. 79−75210
α Orionis, ang. diameter, speckle interferometry *(Russian)* 78−40922
α Orionis, angular diameter meas. with large altazimuth telescope *(Ukrainian)* 79−96925
κ Orionis, B0.5 Ia star, Hα profile variable 79−101146
β Orionis, B8 Ia star, UV spectrum 77−22221
α Orionis, circumstellar shell heterodyne interferometry 78−8000
α Orionis, CO and SiO millimetre line emission search rel. to circumstellar shell props. 78−49423
α Orionis, CO circumstellar absorpt. obs. in 4.6 micron spectrum 80−26858
α Orionis, detect. of surrounding refl. nebulae from polarisation obs. 77−13340
α Orionis, emission lines in UV spectra 79−71028
κ Orionis, interstellar B II 1362 Å detect. 80−51841
ε Orionis, interstellar K-line, photographic obs. 79−16956
ζ Orionis, interstellar MgI line structure, balloon UV obs. 79−35251
α Orionis, IR speckle images, two-dimens. obs. *(French)* 80−46553
α Orionis, M supergiant, circumstellar shell and mass loss rate 77−45415
β Orionis, mass loss and shell, IUE and balloon UV obs. 80−51765
β Orionis, mass loss from mid UV spectrum obs. 78−93217
ζ Orionis, O-type supergiant, wind and corona struct. from Hα line profile anal. 78−40947
ε Orionis, Orion OB1 association star, interstellar lines obs. by Copernicus 80−22050
α Orionis, polarized light scattered by dust shell 79−12473
α Orionis, reconstructed images using stellar speckle interferometry 77−22222
ζ Orionis, Reticon obs. of Hα P Cygni profile 80−82365
α Orionis, variable, mass loss, visible spectra obs. 80−67755
α Orionis, vel. fields in shell from Fe II emission line obs. 79−101144
β Orionis, visible spectrum 79−44479
α Orionis (Betelgeuse), circumstellar gas shell spatial extent 78−28673
α Orionis (Betelgeuse), K I 7699 Å emission from circumstellar shell 77−22210
α Orionis (Betelgeuse), optically thin dust shells 80−22011
α Orionis (Betelgeuse), radio emission 79−48788
α Orionis (Betelgeuse), UV flux meas. 77−22231
ζ Persei, interstellar C_2 rot. fine-struct. lines obs. 80−67811
S Persei, supergiant 22 GHz H_2O maser emission temporal var. 78−49461
S Persei, supergiant OH maser source, optical radial vel. 77−49378
S Persei, supergiant OH star, conditions for circumstellar OH emission 77−22218
photometric histories of three highly reddened blue supergiants 79−5916
photometry, intrinsic lines in (B-V), (V-I_{KC}) diagram 78−73704
photospheres, large turbulent elements 79−75206
Population I stars, kinematical trend of vel. residuals 79−48863
pulsation mass calcs. 80−46556
ζ Puppis, of supergiant, mass flow var., visible and UV obs. 80−90431
ζ Puppis, visible and UV spectroscopy of stellar wind var. 79−16949
R Puppis (HD 62058), G-type supergiant, UBV photometry and variability confirmation 80−41824
R148, B5 supergiant in LMC, possible identification with (LMC X-1) 79−5923
radial vel. meas., expanding dust cloud effects on maser source 79−5816
radial velocities of supergiants in SMC 78−93237
red giants and supergiants, mass loss 77−9743
red supergiants, detect. of surrounding refl. nebulae from polarization obs. 77−13340
red supergiants, envelope dynamical instability and lower mass limit for C detonation supernovae 77−17553
red supergiants, model atm. based on band-model opacity 77−56934
reddened OB supergiant, as optical counterpart of (3U 1538-52) 78−12412
reddened objects in IRC catalogue 79−62841
Roberts 22, bipolar nebula assoc. with A2 Ie star, radio, IR and visual obs. 80−94859
FG Sagittae, anomalous planetary nebula, spectrophotometry and UBV photometry (1968 to 1977) 79−88687
FG Sagittae, photometric radius and pulsation mass 78−36576
FG Sagittae, planetary nebula central star, radial vel. meas. rel. to binary star model 80−98664
μ Sagittarii, binary star, obs. of eclipse of unseen companion 80−4401
supergiant stars continued
V3955 Sagittarii, field RV Tauri/SRd variable 79−88665
RY Sagittarii, spectra near min. light 80−36642
VX Sagittarii, supergiant OH maser source, optical radial vel. 77−49378
VX Sagittarii, VLBI obs. of SiO maser 79−92779
V861 Scorpii=OAO 1653−40, physical parameters 79−17021
α Scorpii, 1.25-3.25 μ airborne photometric obs. 78−40934
α Scorpii, balloon-borne near IR multicolour photometry 80−4356
α Scorpii, circumstellar absorption lines in UV spectrum 80−51804
α Scorpii, circumstellar shell heterodyne interferometry 78−8000
α Scorpii, emission lines in UV spectra 79−71028
ζ^1 Scorpii, extreme B1 supergiant, IUE obs. of line spectrum and continuum energy distrib. 80−17583
ζ^1 Scorpii, extreme B1 supergiant, UV reson. lines obs. 80−4349
ζ^1 Scorpii, extreme B-type supergiant, UV spectroscopy 80−22004
α Scorpii, location of α^2 Scorpii along line of sight 78−73739
α Scorpii, M supergiant, circumstellar shell and mass loss rate 77−45415
AH Scorpii, supergiant OH star, conditions for circumstellar OH emission 77−22218
α Scorpii (Antares), spectrum of nebula 78−41014
ζ^1 Scorpii (HD 152236), UV spectroscopic and photometric vars. 80−101594
V861 Scorpii (HD 152667), X-ray binary, behaviour of Hα 79−101171
α Scorpii A mass loss of M-type supergiant 79−8916
RY Scuti, silicate grains IR emission from early-type supergiant binary system 80−41827
semi-period of variation for B2 to G0 supergiants 78−61854
semi-period-luminosity-colour relation for late B- to G-type supergiants 78−61853
SMC, atlas of variable stars, clusters, emission regions and supergiant stars, book 79−44619
SMC, MK classifications 77−87390
in SMC, radial stars, radial vel. determ. by spectrographic and photometric data study 79−101147
SMC, structure from supergiant distrib. 77−45549
SMC, supergiant spectrometry and photometry, catalogue 78−16411
in SMC, UBV photoelectric photometry *(German)* 78−77594
solar neighbourhood initial mass function determ. from upper H-R diagram study 80−36626
spectral classification of 26 supergiants in SMC 77−29936
spectral types of red supergiants in Magellanic Cloud clusters 79−40190
spectral types of stars with unusual photometric indices 79−71033
spectroscopic binaries, Ca II H and K line emissions in late-type giants and supergiants 77−91566
sporadic mass ejection in red supergiants 79−40186
SU Tauri, R Coronae Borealis star, photometry in optical and IR ranges 80−101601
SU Tauri, R Coronae Borealis variable, brightening after long minimum, 1980 August to September 80−109438
SU Tauri, visible and IR photometry and polarimetry *(Russian)* 78−61860
RV Tauri and yellow semiregular variables, photometric investigations 80−26865
BL Telescopii, eclipsing binary, unusual variability of bright supergiant companion 77−64797
BL Telescopii A, yellow variable supergiant near Cepheid instability strip, VBLUW photometry 80−98672
Tr 27-102 (HD 159378), GOIa supergiant, possible long-period Cepheid 78−45336
4U 1538−52, binary X-ray pulsar, early B-type supergiant as counterpart 78−93472
4U 1538-52 optical counterpart, spectroscopy and system parameters 79−5924
4U 1907+09, optical identification and OB supergiant binary hypothesis 80−82542
α Ursae Minoris, astrometric obs. (1953-61) for Pulkovo large transit instrument orientation parameters determ. *(Russian)* 79−96910
variable star discovery in M33, light curve, magnitude 78−73717
λ Velorum, K-type supergiant, UV spectrum rel. to chromosphere and wind struct. 80−72948
γ_2 Velorum, Wolf-Rayet binary, orbital element determ. from spectral obs. 80−85950
very luminous supergiants assoc. with groups of luminous OB stars 77−17555
S Vulpeculae, 67 day Cepheid, case for membership in (Vulpecula OB2) 80−41831
winds from O and B supergiants in Magellanic Clouds 80−51863
WRA 977, B-type supergiant, spectroscopic obs., X-ray source identification 79−101148
WRA 977 (4U 1223−62, GX 301−2), binary star orbit determ. from X-ray obs. 80−90570
Wray 977, optical counterpart to X-ray binary pulsar, 4U 1223−62, optical spectra 80−72984
Wray 977 (4U 1223−62), B-type supergiant, spectral classification 79−80305
yellow semiregular and RV Tauri variables, photometric investigations 80−26865
yellow stars in LMC direction, UBV photometry and LMC members number 78−93417
in young galaxies, role in contribution to X-ray background 80−82550
C IV resonance lines in B- and early A-type objects 80−46550
C shell burning to Fe core collapse, evolution of 15 M$\odot$ star 80−72937
$^{12}C/^{13}C$ ratio in giant and supergiant atms. 77−13337
H_2O masers, detect. of new sources 78−32466
He shell flashes in red supergiants, convective penetrations and observable effects 80−51755
N deficient supergiants in loose assoc., LTE and non LTE abundance anals. 79−44478
O-rich late-type stars, 16 to 39 micron spectroscopy 80−22002
OH large-scale sky survey at 1612 MHz 78−32358
SiO 86.2 GHz maser sources, polarisation props. 80−4449

supergravity
(3/2,1) superfield of O(2) supergravity 80−52105
11 dimensional theories 78−70038
11-dimensional supergravity, dimensional reduction, masses from extra dimensions 79−71332
σ model, supersymmetric nonlocal conservation laws 80−46938
advances and significance of quantum theory of gravity 79−93028
algebraic approach in superspace 79−17314

supergravity continued
algebraic approach to supergravity in superspace 80−46915
algebraic simplifications in supergravity theories 77−87681
anomalies, topological invariants and Gauss-Bonnet theorem 79−85046
anomalies in supergravity 79−2700
anti De Sitter space, supersymmetry nonlinear realisation 77−87915
antigravity as extension of supergravity 80−46911
antigravity from supergravity with N=2-8 ferrionic generators 80−27198
antisymmetric tensor fields coupled to gravity, renormalisability 80−90765
antisymmetric tensor gauge fields, local supersymmetry without gravity 80−46910
asymptotically flat instantons 80−46932
auxiliary field structure in chirally extended supergravity 78−78126
auxiliary fields 78−49743
auxiliary fields and tensor calculus for N=2 extended supergravity 80−46920
auxiliary fields and ultraviolet divergences 78−78127
auxiliary fields of supergravity 79−17315
axial and conformal anomalies for arbitrary spin 78−70040
axial and trace anomalies for spin 3/2 79−2690
axial anomaly for spin 3/2 fields 78−8580
axial currents, supercurrents and anomalies in supersymmetric QED 80−46933
axial gauge invariant supergravity 77−41790
axial superfield and the supergravity group *(Russian)* 79−17319
B quark, member of colour sextet 79−71712
background field gauge in supergravity 80−46912
background metric in supergravity theories 78−70043
Bargmann-Wigner and Weyl spin-3/2 fields, spinors, chiral operator 80−31981
Bianchi identities, complete soln. in superspace with supergravity constraints 79−58610
Bianchi identities and supercovariant derivative 80−17852
Bose analogs to supergravity, construction problems 80−46926
broken supersymmetry and supergravity 77−61212
BRS gauge and ghost field supersymmetry in gravity and supergravity 77−38116
calibration invariance 78−4548
calibration invariant local divergences, general structure *(Russian)* 79−63119
canonical formulation 78−29016
canonical quantization of massless and massive spin 3/2 field in general covariant gauges 79−71334
Cartan's geometrical structure 78−49745
chirality, self-duality, and supergravity counterterms, quantum corrections 79−75429
classical field theories, non-signification of super gravitation 80−27193
classical solutions 78−122
classical supersymmetric particles 80−86560
complex and quaternionic supergeometry 80−46941
complex spinors and unified theories 80−46943
component formalism follows from the superspace formulation 79−12688
conference, supergravity, Argonne, Il, USA (Oct. 1977) 78−77788
conference, supergravity, Stony Brook, USA (Sept. 1979) 80−46738
conformal gravity as a gauge theory 79−49144
conformal supergravity, constraints and invariance 80−46917
conformal supergravity, curvature constraints for dependent gauge fields 79−67209
conformal supergravity, linear and scalar N=2 multiplets with central charges 80−105562
conformal supergravity, ordinary space and superspace connections 80−98844
conformal supergravity, props. 78−78085
conformal supergravity on basis of SO(4,2) gauge *(Chinese)* 79−93021
consistent supergravity with complex spin-3/2 gauge fields 77−5731
constrained local superfields, and super Higgs mechanism 79−71342
constraints for supergravity 80−46918
covariance group structure, graded conformal, affine groups 80−22264
covariant canonical formulation, subsidiary conditions and physical S-matrix unitarity 80−12974
covariant canonical quantization of massless spin 3/2 field in general covariant gauge 79−40440
covariant quantization 78−41470
curvature in terms of torsion and convariant derivatives, Bianchi identities 80−62561
differential forms on supermanifolds *(Russian)* 80−4889
differential geometry methods in gauge and gravitational theories 80−90768
dimensional regularization and supersymmetry at the two-loop level 80−17854
Einstein's theories extended, book 80−22164
Einstein supergravity, symmetry, spin connection simplifications 80−22258
Einstein supergravity supergroup, simplest example *(Russian)* 80−36929
Einstein theory, energy positivity 78−32741
electroweak force, grand unification and superunification 79−93333
eleven-dimensional supergravity on the mass shell in superspace 80−68116
energy density commutator for massless spin 3/2 field in a covariant gauge 79−71335
exact plane-wave solutions of supergravity field eqns. 79−2707
extended, algebraic props. 77−49875
extended, gauge internal symmetry 77−38115
extended, geometrical interpretation 77−49660
extended, higher order invariants 79−35614
extended geometric supergravity on group manifolds with spontaneous fibration 80−31649
extended spontaneously broken supergravity models, properties 80−46924
extended supergravity, auxiliary fields 80−46919
extended supergravity, dimensional reduction simplifications 80−52110
extended supergravity, irreducible representations of extended supersymmetry algebras on superfields 80−98843
extended supergravity, N=3,4, meson type classical solns. 80−90755
extended supergravity as geometry of superspace 78−65856
extended supergravity in De Sitter space, algebraic props. 77−79021
extended supersymmetry invariants by dimensional reduction 80−47213
fermionic Goldstone-Higgs effect 78−29291
fermions and bosons in a unified framework 79−21630
fiber bundle model of the gravitational field 80−46923
fibre bundles and supersymmetries, super-Poincare group 80−105559
first nontrivial exact solution of supergravity 79−30337
flat superspace with supertorsion 79−2705
G-index theorem for natural operators on ALE gravitational instanton spaces 80−46940
gauge group and geometry of supergravity 80−8888
gauge invariance and spinor calculus, de Sitter, gravitation theory 80−12978
gauge quantization for spin-3/2 fields 77−2735
gauge supersymmetry and supergravity 77−2593
gauge theories, Quantum inequivalence of different field representations, supergravity appl. 80−95214
gauge theory of gravity and supergravity on a group manifold 79−21635
gauge theory of supersymmetry 78−8576
gauge theory of the conformal and superconformal group 77−74300
gauged N>4 supergravity, vanishing one loop β-function, infinite renormalisation 80−86186
geometrical description, fibre bundle analogy 80−98841
geometrical formulation of supergravity theories on orthosymplectic supergroup manifolds 80−95019
geometrical formulation on supergroup manifold 80−46916
geometrization in superspace and local supersymmetry 80−8890
ghost counting in supergravity 78−93589
ghost-free axial gauge in supergravity 80−57162
global theory of supermanifolds 80−82911
globally supersymmetric multiplets without local extensions 80−17856
grand unified theory from broken SO(8) extended supergravity, SU(5) theory 80−99081
gravitational axial superfield and the formalism of differential geometry *(Russian)* 80−57164
gravitational field equations of fourth order 79−12674
gravitational index theorems and super theorems 79−75432
gravitational spin-3/2 axial anomaly 78−93588
gravitino, axial current anomaly, Faddeev-Popov ghosts 80−68120
gravity and supergravity as gauge theories on a group manifold 78−41469
group structure 79−21619
hadron fundamental supergeometrodynamic theory 79−40725
Hamiltonian formalism, quantization and S-matrix 78−16972
Hamiltonian formulation 78−24722
Higgs effect, gravitino masses and couplings 80−62562
Higgs mechanism in (1+1) supergravity 78−74199
higher spin gauge fields, beyond 3/2, systematics 80−46937
hypergravity, consistency problems, massless spin 5/2 field coupling 79−93023
hypergravity, consistency requirements 80−46936
linarized and conformal structure 78−45546
linearisation of supergravity 79−12679
linearised supergravity, supersymmetric quantisation, ghost fields and superpropagation 79−93022
local complex supersymmetry in two dimensions 77−45985
local extended supersymmetry and supergravity 77−17894
local supersymmetry for spinning particles 77−2768
local supersymmetry in (2+1) dimensions 78−49980
local supersymmetry in superspace 79−12979
local supersymmetry transformations, fermion solutions in presence of instantons 78−74177
local symmetry of superspace-time of supergravity 79−12689
locally supersymmetric Maxwell-Einstein theory 77−2582
massive, self-interacting scalar multiplet coupled to supergravity 77−74633
massive scaler multiplet coupling 78−82137
massive spinning particle in Minkowski space equivalence to massless particle in de Sitter space 80−119
massive supergravity from non-linear realization of orthosymplectic gauge symmetry 78−33019
massive supergravity from spontaneously breaking orthosymplectic gauge symmetry 78−77787
massive vector multiplet coupled to supergravity 80−17855
massive vector multiplets, lagrangian construction 80−31645
massive vectormultiplets in supergravity 80−46927
massless Rarita-Schwinger field, covariant canonical quantisation 79−97280
massless spin-2 plus spin-3/2 particle interaction theory 79−63113
matter coupling and BRS transformations 78−93837
matter couplings 77−17895
minimal auziliary fields 78−49742
modified Feynman rules 79−132
N=2 extended, auxiliary fields in 5 and 6 space-time dimens. 79−30339
N=2 extended supergravity, superfields, auxiliary fields and tensor calculus 80−57157
N=2 extended supergravity, superspace constraints, algebraic derivation 80−57159
N=2 extended supersymmetry, multiplgt of currents 79−40438
N=2 Poincare supergravity multiplets, transformation rules 80−73248
N=2 theory with a gauged central charge 78−62349
N=4 theory with local SU(2)*SU(2) invariance 78−66067
N=8, on-shell theory in superspace 80−27199
N=8 spontaneously broken supergravity, mass matrix, gauge couplings 79−97281
N=8 supergravity theory, the Lagrangian 79−17311
no-hair conjecture example, Schwarzschild background, static helicity 3/2 perturbatiqn 80−31647
non-distinguishable field and space variables in QFT, supergravity appl. 80−98845
non-integral gauge theories 79−12675
non-linear realisations in two dimens., supergravity coupling 77−79024
non-metrical supergravity for a spin-two nonet 79−71333
nonlinear de Sitter symmetry and restricted space-time regions 79−85043
nonlinear gauge fields, structure of gravity and supergravity theories 78−77791
nonlinear realization of graded conformal group 80−105561
nonlinearly realised supersymmetric theory, canonical quantisation 79−97283
O(2) extended, exact plane wave solns. 79−25955
O(2) supergravity, coupling with several vector multiplets 78−33020
O(4) to O(8) extended supergravity, finiteness calcs. 79−97282

supergravity continued
O(N), quartic ghost interactions, auxiliary fields 79−85044
O(N) model, dynamical mass generation in $S^1 \times R^3$ 80−99046
off-shell N=8 supersymmetry with central charges for maximally extended supergravity 80−95230
on-shell 11-dimens. supergravity in superspace, eqns. of motion 80−57160
one-loop divergences in the quantum theory of supergravity 77−13674
one-loop finiteness of quantum gravity of mass shell 78−62142
one-loop renormalisability of pure supergravity and of Maxwell-Einstein theory in extended supergravity 77−5730
open problems with spins >2 80−46934
OSp(1,4) renormalisable theory with higher derivatives 80−36930
OSp(1,4) supergroup, Wess-Zumino model classical solns. 80−36928
OSp(4,1) invariant fermionic σ model, graded orthosymplectic geometry 79−54277
Poincare and conformal models with closed algebras 78−74198
Poincare supergravity as broken superconformal gravity 78−62348
post-Einstein unified theory, book contrib. 80−22260
prepotentials in a superspace formulation 79−12683
properties of supergravity theory 77−81
pseydoinvariant gauge Lagrangians' gravity and supergravity 79−12680
quantum corrections to the quadratic mass formula of broken supersymmetry 80−46942
Rarita Schwinger eqn. solns. in Kerr Newman space 80−116
Rarita-Schwinger Majorana field, exact soln. and eqns. of motion 80−90756
recent developments 79−30336
renormalizability properties 77−34087
review of present status of supersymmetry and supergravity 79−63112
S-matrix and supergravity 77−46010
S-matrix for the theories that admit closure 78−81911
S-matrix in supergravity 79−135
scalar multiplet coupled to supergravity, modified interaction 77−67366
scalar multiplet coupled to supergravity 77−46012
Schwinger source formalism for Fermi-Bose transform. 79−63114
self-duality and helicity in supergravity 80−46929
self-duality in superspace, functional anal. 80−46902
six dimensional, superspace torsion and curvature constraints 80−52104
SO(2) extended supergravity, algebra closure, minimal set of auxiliary fields 79−80490
SO(2) linearised supergravity, multiplets 79−80488
SO(3) and SO(3) supergravity fineteness, nonremornalisability of scalar multiplet coupling 78−4821
SO(3)-invariant extended supergravity 77−22475
SO(8) extended supergravity 78−16970
SO(8) extended supergravity 80−4914
SO(8) supergravity derivation 80−12975
space-time properties of supergravity 80−8887
spacetime foam 79−9172
spin, supersymmetry, and square roots of constraints 79−12676
spin 2 matter-gravity coupling problems 80−46939
spin 3/2 field and Cartan's geometry 78−16712
spin 5/2 theories, supergravity extensions beyond SO(8) 80−46935
spin-3/2 theory of gravitation 79−49148
spin-5/2 supergravity 79−21624
spinning particle in metric-torsion field, eqn. of motion 80−62543
spinning string, complete action 77−13943
spinning strings, the scalar multiplet, and supergravity in (2+2)-dimensional superspace 80−90757
spinor dual model and supergravity 77−13675
spontaneous breaking of supersymmetry through dimensional reduction 79−40441
spontaneous symmetry breaking, Higgs effect in supergravity without cosmological constant 79−17310
spontaneously broken N=8 supergravity 79−67212
square root of general relativity 77−82437
square roots of constraints and supergravity 77−49663
status as unified gauge theory 80−46925
strong spin-two interaction and general relativity 79−45046
structure of supergravity 79−2971
SU(2,2/1) superconformal group, Yang-Mills-like Lagrangian 80−62560
SU(4|N) gauge transformations, determ. of Lagrangian for super-theories 79−63118
SU(4) and SO(4) supergravity, anomalies, field transformations 79−9170
SU(8) supergravity on mass shell in superspace 80−46907
SU(8) supergravity supersymmetry breaking 80−46908
SU(8) unification and supergravity 80−46928
super-Higgs effect in a class of scalar models and model of super QED 78−29268
super-self-duality *(Russian)* 79−44831
superalgebra stability in supergravity models *(Russian)* 80−52109
superconformal gravity advantages over normal supergravity 80−8889
superconformal group nonlinear realisation and conformal supergravity 79−12695
superconformal invariance of superspace with nonminimal auxiliary fields 79−17317
superconformal supergravity and internal symmetry 77−54056
superconformal symmetry breakdown as guide to supergravity constraints 80−46930
superconnections in extended supergravity 80−36927
supercurrent anomaly 78−29267
supercurrent generated vector superfield 77−71453
superfield analysis using supertorsion and supermanifold 79−85038
superfield covariant derivatives for O(1) and O(2) supersymmetry 80−46914
superfield critique, supergravity theories 79−54028
superfield Feynman graphs, loop calculations 80−46906
superfield formulation 79−17312
superfield Lagrangian 78−41468
superfield supergravity 79−17309
superfield supergravity with symmetry 80−8891
supergraph formalism UV finiteness in gauge supersymmetry 80−46913
supergraphs, perturbation theory description from globally-supersymmetric gauge breaking 79−67203
supergravity has positive energy 77−74299
superspace action for simple supergravity 80−27197
superspace and component formulations, tensor calculus transcriptions 79−63116
superspace Bianchi identities and 6-dimens. spacetime 79−67204
supergravity continued
superspace constraint algebraic origins 80−98842
superspace equations redundancy elimination 79−12678
superspace formalism, construction of supervielbeins and superconnections off-shell 80−105558
superspace formulation 77−30084
superspace formulation 79−2972
superspace formulation consistency checks 78−37170
superspace formulation for supergravity, book contrib. 80−22261
superspace formulations 80−46931
superspace geometry 78−49744
superspace geometry and N=1 non-minimal supergravity 80−57155
superspace geometry in supergravity, Riemannian theory reduction, Yang-Mills connections 80−57156
superspace geometry of supergravity 80−46909
superspace tensor calculus formulations, relations to supergravity 80−46922
superspaces WITH Bose and Fermi coordinates, geometry, supergravity appl. 77−26143
supersymmetric black holes 78−93300
supersymmetric dimensional regularization via dimensional reduction 79−67202
supersymmetric gravitation, two-loop divergences 77−49659
supersymmetric non-linear alpha-model in four dimensions 78−49981
supersymmetry, physico-geometrical comments, unified field theories and supergravity, gauge transformations 80−364
supersymmetry and supergravity, review *(Czech)* 80−86183
supersymmetry constraints, algebraic understanding 80−46921
supersymmetry geometry, graded manifold theory 79−58896
supersymmetry transformations of noninteracting massless particles 80−95015
superunified field theories, geometrical transformation laws 79−63117
superunified theories based on geometry of local (super-) gauge invariance 78−24723
surface deformations, their square root and the signature of spacetime 80−8874
surface integrals as asymmetry generators 77−74634
symmetry breaking by instantons 79−21625
sypersymmetry, supergravity theories and the dual spinor model 77−49923
sypersymmetry breaking by pseudoparticles 78−24959
tachyon solns. in classical relativity 80−36917
tachyons, absence in supergravity and classical Einstein gravity 79−67208
tensor calculus for supergravity 78−70037
three-loop counterterms 78−65854
trivial solution identification, gauge transformation to Einstein vacuum soln. 80−68115
twisted supermultiplets, topological effects 80−98839
two-loop renormalizability 77−17897
U(N) invariance in extended supergravity 77−61003
ultracold neutrons, supergravitation and gravitino 3/2 investig. 79−85047
unification of laws of physics *(Polish)* 80−36926
unification of the laws of physics 78−50001
unified approach to matter coupling in Qeyl and Einstein supergravity 78−54275
unified field theories with U(N) internal symmetries 78−8577
unified geometric theory of gravity and supergravity 77−41521
unitarity, ward identities, and quantisation rules 78−54279
unitarity in general covariant gauge 79−75428
unitary field theories 79−35613
vacuum symmetries quantum effects 79−17634
vector and scalar multipletz and gauge invariance 79−12684
vector multiplet coupled to supergravity 78−86214
vector multiplets, massless limit 80−73250
weak field approximation *(Russian)* 80−27201
Wess-Zumino constraints, superconformal transformations and six-dimensional spacetime 80−27196
Wess-Zumino supergravity formalism, constraints soln. 79−2970
WU(4) invariant theory 78−41471
Yang-Mills theory and supergravity, unification 77−46011
zero Riemann curvature flat space topology and gravitino eqn. of motion 80−86187
SO_2 model of extended supergravity, minimal set of auxiliary fields 79−58608

superheating *see heat transfer*

superheavy nuclei
see also nuclei with mass number 220 or higher
^{258}104 compound nucleus, prod. method optimisation 78−46103
^{260}104, detection methods, comparison of reactions ^{246}Cm+^{18}O, ^{248}Cm+^{16}O, ^{249}Bk+^{15}N 77−23106
^{260}104, synthesis by ^{249}Bk(^{15}N,4n) 79−30850
^{260}106 compound nucleus, prod. method optimisation 78−46103
^{262}[105] spontaneous fission, fragment mass distrib., total kinetic energy release 78−17256
^{263}106, identification from alpha-decay chain ^{263}106→ ^{259}Rf→ ^{255}No→ ^{251}Fm 77−26637
^{294}110, naturally occurring superheavy element search, alpha emission half-life 80−63139
^{298}114, high spin pot. energy surfaces, fission barrier, α-, γ-decay half lives, yrast spectrum 80−73764
^{298}114, self consistent K-matrix model calc. 77−6257
A=114, theoretical chem., heat of form. 77−32824
A=114-116 superheavy elements produced in ^{48}Ca ion reactions on Am, Pu, Cm 78−29493
A=354, Z=126, spontaneous fission, α-decay, β-decay half-lives calc. 77−6469
A>92 superheavy elements, nonexistence in nature *(German)* 77−41031
A-116, theoretical chem., heat of form. 77−32824
in Allende meteorite, search for fission tracks 78−32415
alpha half-lives, alpha particle struct. effects 78−17158
atomic collision systems, intermediate and superheavy nuclei, UNILAC expts. 80−63751
atomic X-ray spectra 77−38631
background re-evaluation in superheavy element data from monazite 77−33077
bound states of superheavy nuclei from weak unsaturated two nucleon forces *(Russian)* 80−462

superheavy nuclei continued
carbonaceous chondrites, superheavy element fission hypothesis for Xe origin 77−78726
Cheleken Peninsular geothermal waters, USSR, search for superheavy nuclei 79−96781
collective motion, stability and prod. in heavy ion collisions 80−18169
collision system, radiative processes, search for positron emission 80−63752
compound nucleus reaction, superheavy element prod. method optimisation 78−46103
compound reaction prod. calcs., barriers, shapes 77−46184
critical nucl. charge, electron shells, positron creation in collisions 79−9603
decay in bubble chambers *(Russian)* 79−93568
delayed fission produced in synthesis induced by heavy-ion beams and neutron currents *(Russian)* 79−89341
Earth samples, meteorites and cosmic rays, superheavy element search *(Russian)* 79−84277
element 114, search in galena using EM isotope separator and fission track detectors 77−27203
elements, detection by fission activity detect. *(Russian)* 79−13358
elements search in terrestrial substances *(Chinese)* 79−84281
fermion charge accumulation in nucl. matter rel. to existence and props. *(Russian)* 77−57597
fission of $^{300}120$, effect of nuclear force finite range on fission and heavy-ion reactions 78−13180
giant haloes and search for superheavy elements in Yugoslav biotites 78−16008
giant haloes assoc. with monazite, prod. by ^{244}Pu fission alpha particles 77−29300
group separation procedure for superheavy elements using diethyldithiophosphoric acid 77−26953
growth points in nuclear physics, book 80−94928
Hartree-Fock calcs. for magic numbers Z=126 and 138 77−88062
heavy ion collisions, superheavy atoms, electronic binding energy, wave functions 78−46252
heavy ion collisions up to 10 MeV/nucleon on UNILAC, review of SHE searches 78−50194
heavy ion experiments at UNILAC *(German)* 78−66435
HF calcs. using Skyrme and finite range forces 77−46101
ion-atom collisions, quasiats., K-vacancy form., positron emission 80−63753
K X-ray fluoresc. anal. 77−81449
K- and L-shell ionis. cross section estimates, comparison with actinide fission prod. X-rays in micas 77−50581
lifetime, theoretical prediction of nonoccurrence in nature 78−662
magic numbers, energy density method 77−14059
meteorite Kr and Xe isotopes, study of spontaneous fission products 80−63215
meteorites of iron type, superheavy element fission tracks 80−26821
monazite, from South Indian beach sand, superheavy element search, K X-ray fluoresc. anal. 80−61801
monazite, giant halo inclusions, evidence against superheavy elements 78−40554
monazite, superheavy elements search in bulk samples by ^{32}S ion backscattering 77−21773
monazite from South India beach sands, superheavy elements search using X-ray fluorescence 78−16017
monazite inclusions, PIXE search for superheavy elements 77−49066
monazite inclusions possessing pleochroic halos, PIXE anal. 78−69350
monazite ore search, neutron fission of mass separated samples 77−13078
monazites examination in search for superheavy elements 80−36297
monozite search via ^{7}Li elastic scatt., upper limits 77−86896
Moon, superheavy elements as heat source for primaeval melting 78−24478
naturally occurring, rel. to radioactivity distribs. and isotopic abundances 78−20407
nonexistance in UNILAC expts. *(German)* 80−42731
nuclear skin thickness variations 77−14025
nucleosynthesis, current astrophysical theory review 77−29644
pionic condensation, superdense nuclei *(Russian)* 77−46129
primary cosmic ray nuclei, obs. with solid-state track detectors and X-ray films *(Japanese)* 78−61688
primordial, X-ray anal. of monazite inclusions in mica 77−25685
primordial superheavy elements, proton-induced X-ray emission from monazite inclusions in mica 77−9429
production and natural searches, review 80−37411
production cross section limits from ^{238}U(^{63,65}Cu,x) at 9.6 MeV/nucleon 77−34343
production in ^{48}Ca ion+^{248}Cm, spontaneous fission, radiochem. separation 78−74390
production via collective mass transfer in ^{238}U+^{238}U 77−337
production via r-process 77−56825
quasi-atom concept and expts. 77−14177
quasi-molecules, positron creation from K-shell vacancy 77−58220
quasimolecules, superheavy, inner shell electronic states calc. 79−89817
r-process nucleosynthesis, beta-delayed fission 77−23012
review of recent searches for superheavy elements in nature 79−79845
search and synthesis, review 78−50117
search for, using solid state nuclear track detectors 80−91200
search for high energy α-particles 79−59040
search in Allende meteorite and cordierite giant halos 80−21752
search in giant-halo inclusions using synchrotron radiation 77−22925
searches for, review, book contrib. 78−85121
searches in nature and accelerators, review 77−57616
selections from 1977 Comments on Modern Physics, book 79−30181
self-consistent energy density mass formula extrapolation 78−93932
shell struct. in 250≤A≤500 mass region 77−22833
spin-orbit pot. effect on single particle levels 79−59000
spin-orbit symmetry potential, stability of superheavy elements 78−50104
spontaneous fission, natural 78−13172
spontaneous fission half lives, odd A nuclei, Z≥96 78−86556
spontaneous fission props. for 98≤Z≤106 and 150≤N≤164, shell model 78−82401
spontaneously fissioning new nuclide in Allende meteorite, chemical conc. *(Russian)* 77−87353
spontaneously fissioning new nuclide in meteorites, chemical conc. *(Russian)* 77−87352
stability, proton orbital 1/2$^-$[521] obs. in ^{251}Es and ^{247}Bk 77−67698
stability and fission barriers, crit. ang. momentum depend. 80−32262
stability and nuclear props., review of research 79−89218
supercritical nuclei, Z>137, WKB method appl. *(Russian)* 79−49587
superdense nuclei stability region, pion condensation *(Russian)* 77−46128
superheavy elements, search for fission decay in Madagascar monazite 77−17105
superheavy elements, search in nature based on spontaneous fission meas. 77−29518
superheavy elements in monazite crystals, proton induced X-ray spectra 77−17106
synthesis, using ^{48}Ca ion beam, fragmentation theory 77−74881
synthesis and properties, ^{48}Ca induced reactions 77−54242
synthesis in fusion reactions, failure 79−45317
ternary fission, three-centre shell model 79−36226
transuranium elements, z>100, stability *(Czech)* 77−50040
volatile element synthesis and identification 78−46239
volatile superheavy elements, synthesis and identification in heavy-ion reactions 79−45288
Z=100 to 173, Dirac-Fock-Slater calcs. of energy eigenvalues and total eigenvalues 77−71739
Z=104, tetravalent hydride, Dirac-Fock one-centre calcs. 77−88380
Z=106, atomic and chemical props. by gas chromatography and aqueous chemistry, book contrib. 78−85121
Z=106, hexavalent hydride, Dirac-Fock one-centre calcs. 79−6837
Z=110, Dirac-Slater SCF relativistic mol. calcs. 78−41970
Z=114, Dirac-Fock one-centre calcs., tetravlent hydride prediction 77−34551
Z=114, existence in S.American hypogene lead ores, exptl. evidence *(German)* 79−55019
Z=114, tetravalent hydride, relativistically parameterized extended Huckel theory 79−49924
Z=114-126, nuclear stability reexamination using deformed Woods-Saxon pot. lifetimes level density 79−3094
Z=116, possible detection expt. in marine creatures 77−3503
Z=118, 172, 226, symm. and stability of 2(2l+1) electron configurations of elements 80−1100
Z=119 to 137, anomalous solns. for Dirac electron in Coulomb field 77−14331
Z=126, even-A, ternary fission rates calc. 77−54264
Z=126, search in X-ray spectra in monazite from Malaysia 77−86895
Z=126, source and concentration anal. 77−19111
Z=132 quasi-atom I-Au system, X-ray spectra 77−14177
Z>103, method for rapid separation and identification 77−26952
Z≃126, form. during decompression of cold neutron star matter 77−33544
α-decay, absolute probability, four projectors theory, plateau model 77−14074
α-decay lifetimes 79−36203
α-particle stability of superheavy nuclei in Z=126 region 77−300
^{258}104 prod. from cool compound nucleus formation with oriented heavy ions 80−99179
^{260}106 prod. from cool compound nucleus formation with oriented heavy ions 80−99179
^{262}105, shell model anal. of spontaneous fission props. 78−82401
^{241}Am-Be thermal neutron flux standard density variation obs. 77−83409
Bi_2S_3, superheavy element search using neutron multiplicity counter 80−4011
^{252}Cf fission, search for abnormal energy release reln. to superdense nuclei *(Russian)* 79−89340
^{252}Cf source in tissue-equivalent phantom, neutron absorbed dose obs. 80−12278
^{248}Cm+^{48}Ca, 267 MeV, search for superheavy elements 77−74871
^{248}Cm+^{48}Ca, search for volatile superheavy elements 78−94027
^{256}Es 7.6 hr β-decaying high-spin isomer, discovery following ^{254}Es(t,p) 77−22964
Fe meteorites, superheavy elements possible existence 79−48742
Fm isotopes, A=254 and 259, low-energy spontaneous fission systematics 77−23125
^{257}Fm, shell model anal. of spontaneous fission props. 78−82401
^{257}Fm(t,p), 16 MeV, ^{259}Fm detection from spontaneous fission activity 77−26795
^{257}Fm(t,p), prod. of ^{259}Fm, half-life and fission mass distrib. meas. 77−26776
^{259}Fm 1.5 sec activity obs. in ^{257}Fm(t,p) at 16 MeV 77−26795
^{259}Fm prod. in ^{257}Fm(t,p) half-life and fission mass distrib. meas. 77−26776
Ha, (element 105), atomic and chemical props. by gas chromatography and aqueous chemistry, book contrib. 78−85121
Pb targets, possibilities for producing super-heavy elements Z>102, new projectiles *(Russian)* 78−86548
Pb targets for superheavy element synthesis 77−82960
^{208}Pb+^{86}Kr, 469 MeV, search for superheavy nuclei, Z>106, lifetimes >2 ps 78−46102
^{208}Pb(^{136}Xe,X)Y, 470 MeV, search for delayed fission products from superheavy nuclei 78−70562
^{241}Pu in ^{241}Am, determ. by γ spectrometry 79−52808
Rf, (element 104), atomic and chemical props. by gas chromatography and aqueous chemistry, book contrib. 78−85121
U+^{136}Xe, search for superheavy elements 79−6692
^{235}U fission fragment thermonuclear superheavy nuclei synthesis, prod. cross sections 80−95331
^{238}U+^{238}U, 7.5 MeV/u, theoretical estimates for transuranium element prod. in heavy ion collisions 79−54454
$^{260}X_{105}$, prod., L X-ray spectra, decay 78−8780
$^{294}X_{116}$, prod. at barrier energies in ^{48}Ca (^{248}Cm, 2n) 79−13368
^{276}X synthesis search in ^{237}Pa(^{48}Ca, 3n) *(Russian)* 79−40954
^{111}^{279}X synthesis search in ^{233}U(^{48}Ca,Zn) *(Russian)* 79−40954
^{112}^{228}X, primordial and other nuclei, shell model calc. 78−8752
^{126}^{298}Z, triple clustering at fission barrier, Hartree-Fock calc. 77−10454

superheterodyne receivers
astronomical mm wave spectrometers, intensity calibration 77−33353
biotelemetry and radiotracking receiver 77−48892
CMOS ICM 7555 capacitance meter cct., using radio receiver indicator 80−62692
femtovoltmeter and voltage tunable heterodyne receiver based on DC resistive SQUID 79−63276

superheterodyne receivers continued
frequency analyzing equipment, device for scientific education in oscillatory phenomena 78−41126
HF, receiver design principles 78−45714
microwave, low-noise 115 GHz receiver on Columbia GISS 4 ft radiotelescope 79−53718
optical, beam splitter transmissivity 79−18528
optical, CO_2 waveguide laser for space link transceiver 77−19322
optical, in turbulent atm., signal current probability distrib., theory 78−78916
optical, in turbulent atm., signal current probability distrib., expt. 78−78917
optical heterodyne receiver output signal dependence on angle of incidence 79−45910
quasi-optical radiometer receiver design 78−8447
quasioptical superheterodyne radiometer for upper atmosphere 77−41241
Schottky diode concepts, heterodyne radiometry 78−45713
submillimetric heterodyne receiver with laser local oscillator 77−38042
submillimetric Josephson mixer receivers, potentials and limitations 77−38003
submillimetric radiation, heterodyne vs. direct detection receivers 77−38006
swept-frequency heterodyne receiver with CRT display for spectral analysis *(Spanish)* 77−37875

superionic conducting materials
see also ionic conduction in solids; mixed conductivity
AC properties of ionic conductors 78−47578
activation volume for fast ionic cond. in solid and molten salts 80−59711
β''-Al_2O_3, Mg- and Li-stabilized, high electron microscopy images of defects 79−73135
β-Al_2O_3-Ag_2O, antiferroelectric transformation, Potts' model universality class 80−50277
β-Al_2O_3-Cu_2O, phys. and chem. props., use in determ. of thermodynamics of Cu-Sn alloys 80−107502
β- and β''-Al_2O_3-Na_2O, fast ion conductors, TEM obs. 79−86920
β-Al_2O_3-Na_2O, geometrical aspects of breakdown, TEM study 79−79096
β-Al_2O_3-Na_2O, Monte Carlo calc. of Na diffusion 77−89579
alkali glasses, rapidly quenched, alkali ion cond. 80−107559
alkaline earth fluoride based solid electrolytes, in galvanic cells 80−3501
β''-alumina, K^+ ion nonuniformity, in contact with $NaNO_3$ and Na_xS_y melts 78−10215
ambient temperature solid state battery developments, review 80−61328
anomalous frequency-dependent conductivity in disordered one-dimensional systems 79−46834
applications, accumulator with high energy density *(French)* 80−26131
B_2O_3-Li_2O-LiCl, ionic conductor, IR refl. Raman study 80−66173
battery appls. and developments, conf., Brussels, Belgium (Jan. 1979) 80−72032
book 80−22156
borate glass, Li^+-rich, high elec. cond. 78−84000
Brillouin scatt. from thermal fluctuation 77−20866
Brownian motion in polarisable lattice, appl. to superionic cond. 77−76603
collective excitations, dynamics, in one dimensional superionic conductors 79−14958
collective motion, AC conductivity calc. 79−99368
concentration gradients of cations in centrifugal field 79−28142
conductivity measurement, four-probe AC bridge technique 80−57340
confined-gas model for ion flow 80−65276
continuous stochastic models, book contrib. 80−24663
cooperative phenomena within generalized lattice gas models 79−46827
correlation effects, thermoelectric power, model calcs. 77−39688
correlation functions theory 78−79674
correlations among mobile ions role, microscopic model 80−107534
current-pot. curves discontinuities in solid electrolyte systems 80−24660
density fluctuations, long-wavelength 78−79808
dielectric response 80−10899
diffusion and conductivity, effects of disorder and mobile particle interactions 80−107536
diffusion in periodic potentials, dynamic correlation functions 77−59138
diffusion of labelled particles on one-dimens. chains, density fluctuations 79−4426
domain formation, thermodynamic theory 77−84963
domain states in solid electrolytes with structural disorder 79−42307
dynamic behaviour, theory *(German)* 78−79796
dynamic properties 78−79673
dynamics, review *(Japanese)* 78−30791
electrode preparation techniques, in solid electrolytes *(Japanese)* 80−24658
electronic conductivity 77−76882
for energy storage and conversion systems, characterisation 77−76596
enhanced diffusion mechanisms, review 78−67847
EXAFS investigation of struct. and ion motion, excluded vol. model 80−108302
EXAFS studies of struct. and cond. process, book contrib. 80−25485
excluded volume model, constraints of immobile ion lattice 80−107543
fabrication and properties of solid electrolytes 80−70463
fast ion transport in solids, conf., Lake Geneva, USA (May 1979) 80−57006
fast ion transport in solids, conf., Lake Geneva, USA (May 1979) 80−105427
fast ionic conductors, review, device appls. 78−51724
fast ionic transport in solid electrolytes and mixed conductors, material stability and chem. diffusion 80−65292
film, size-selective photochromism 79−99668
film electrolyte systems, materials charact. and appls., review 77−77781
fluoride solid electrolytes 80−70464
fluorite ceramics, doped, short range order anal. by electron diffr. 78−83672
fluorite crystals, disorder at high temp., Brillouin scatt. 78−2866
fluorite structure, activation vol. 80−107557
fluorite structure, Brillouin scattering and lattice defect energetics 78−80369
fluorite structures, superionic props., IR spectra 80−107483
fluorite type crystal, effects of anharmonicity and disorder on Raman scatt. at high temp. 78−80349
fluorites, disordered anions exam. 79−42299
fluorites, structure and transport 80−84318
frequency dependent cond., correl. effect, Scher-Lax model 80−34238

superionic conducting materials continued
frequency dependent conductivity 77−84973
glass, ionic conductivity, weak electrolyte theory 80−84322
glass and ceramic developments for electrical industry appls. 79−78925
glasses as solid electrolytes 80−84321
hard sphere fluid model 80−44363
Haven ratio, temp. depend., correl. effects role 80−107504
high temperature meas., solid electrolytic cell, meas. at 700K and higher 80−31760
hollandites, cryst. growth and structural props. 80−89129
hopping among inequivalent octahedral sites in body-centred tetragonal lattice 79−1520
hopping conduction, one-dimensional, and diffusion, theory 78−6355
hopping conductivity, freq. depend., model calcs. 80−107507
hopping conductivity in quasi-one-dimensional lattice gas with three-dimensional ordering 78−91473
hopping conductivity of interacting particles 78−10214
hopping model 79−37869
hydrodynamic theory for collective excitations, appl. to α-AgI 79−1524
hydrodynamic theory for collective excitations 80−107530
impedance and modulus spectroscopy 77−12309
independent particle model 80−6551
interacting Brownian particles and correlations 80−29202
interacting Brownian particles in periodic medium model 80−59712
introduction to fast ion conductors 80−6549
ionic crystals, defects, computer modelling, review 80−107205
ionic crystals, transport phenomena, appl. to solid state devices 78−55976
ionic plasma oscills. 80−29212
ionic thermoelectric power, lattice gas model 78−26717
lattice dynamics, conf., Paris, France (Sept. 1977) 78−59869
lattice dynamics of disordered or unstable lattices 78−75790
lattice gas, phys. correl. factor in Nernst-Einstein relation 80−105591
lattice gas model, critical cond., rel. to cond. in superionic conductors 78−93614
lattice gas models, book contrib. 80−24661
lattice potential effects on ion flow in superionic conductor 80−65274
layer and tunnel compounds, fast ion transport and electrochem. storage 80−61324
light scatt. and IR absorpt. book contrib. 80−25382
linear chain, two-sublattice, hopping particle occupancy correlation function normal modes 80−49402
magnetic resonance, book contrib. 80−25240
materials showing fast ion cond., review 77−7891
melting, appl. of microscopic theory 78−79748
metal-solid electrolyte interface, DC and current-voltage charact. 77−28251
metal-solid electrolyte interface, low-amplitude AC passage 77−32080
N-methylhexamethylenetetramine bromide-CuBr, solid electrolyte galvanic cell applic. 77−77775
microscopic model, physical principles and applications *(German)* 78−67861
microscopic models for ionic cond. 80−70454
microscopic theory 78−79809
microwave conductivity of solid electrolytes 79−55929
microwave conductivity theory, hopping model 80−59710
mixed conductivity, superionic-electronic, electrodes, partial cond. meas. technique 80−44360
mobility paths for MI_4^{-3} clusters, ab initio electronic struct. calc. 80−70458
Na-S batteries, solid electrolyte β-Al_2O_3 formation from m-Al_2O_3 by new method 80−89606
NASICON solid electrolyte, processing and phys. props. 80−60820
NMR investigations in solid electrolytes, review 80−60432
nonlinear collective excitations 78−55979
nuclear magnetic relaxation by paramag. impurities 79−42866
one-dimens. disordered solid, anomalous specific heat, rel. to superionic conductors 79−23746
one-dimensional, soliton Brownian motion and impurity effects 79−77814
one-dimensional, thermal cond., ion-ion interaction contrib. 78−55977
one-dimensional ionic conductors, cooperative diffusion and soliton Brownian motion 78−95177
one-dimensional models 77−35741
oxide glasses, fast ion transport 80−107470
oxides, review 80−49414
oxides, standard free energy of formation, by EMF method with solid oxide electrolyte at low temps. *(Japanese)* 80−88338
paramagnetic impurity contribution is NMR relaxation in one-dimension 80−20477
phase transition to high ionic cond. state for solid electrolyte *(Russian)* 79−51304
phase transitions, book contrib. 80−24662
phase transitions, free energy and eqn. of state 78−75826
phase transitions and dynamics 78−59924
phase transitions in unsymmetric disordering systems, thermodynamics *(Russian)* 77−61045
phase transitions induced by elec. field 78−63856
polyamine iodide-AgI solid electrolytes, elec. cond. and cryst. struct. 80−107537
polyamine iodide/AgI solid electrolytes, conc. depend. of elec. cond. 80−24647
polyether-alkali metal salt adducts, cond. investigation rel. to use as solid electrolytes 80−59708
prefactor anomalies, absolute rate theory breakdown 78−47559
prefactor anomalies, absolute rate theory breakdown 78−47560
prefactor anomalies, effect of low dimensionality 78−48061
preparation for lab. teaching program, electrochemistry in solid state 78−93498
pyridine-Ag_5I_6, dynamical aspects 78−79695
pyridinium cuprous bromide, solid electrolyte, crystal growth from melt 78−64462
pyridinium pentasilver hexaiodide, solid electrolyte, contrib. of non-Brownian motion to transport props. 80−70453
pyridinium pentasilver hexaiodide, sp. ht. and cond., gradual solid electrolyte transition 77−76604
pyridinium pentosilver hexaiodide, freq. depend. ionic conductivity 78−2291
pyridinium silver iodide, fast ion conductor, phase transitions, thermoelec. power meas. 80−107540

superionic conducting materials continued
quasi-elastic scattering of light, neutrons and electrons, Debye-Huckel eqn. *(Chinese)* 78−68521
quasi-lattice gas model 80−44364
Raman scattering from mobile ions, theory 78−80352
Raman spectra, interpretation using liquid like model 78−2855
review, props. of solid electrolytes *(Czech)* 77−59142
review, superionic conductors, some experimental facts and fallacies 79−23774
review *(German)* 78−79795
review 79−55923
scattering of light and neutrons in diffusion model 78−26719
self-discharge currents in systems with solid electrolytes, shelf-life of cell 79−100502
silver iodide-N,N,N,N′,N′,N′-hexamethyl-1,3-propylenediomine diiodide, solid electrolyte, cryst. struct. determ. 77−7705
sine-Gordon model, overdamped, Brownian diffusion 80−27223
soft-core model for ionic crystals, normal ionic salts and superionic conductors 80−49411
solid electrolyte, diffusion and ionic cond., correl. factor meas. problems 80−59709
solid electrolyte dielectric permeability, phase transition to superionic state *(Russian)* 80−49403
solid electrolyte galvanic cell for gas sensing, response speed 77−60149
solid electrolyte gas sensor developments 80−61217
solid electrolyte interface, small signal AC response 78−6444
solid electrolyte materials chemistry problems 80−96680
solid electrolyte with structural disorder, current flow mechanism 80−19982
solid electrolyte-metal interface adsorption layer capacitance calc. *(Russian)* 80−59697
solid electrolytes, phase transitions and thermodynamic states 77−84975
solid electrolytes, two-state model, cationic disorder theory 79−73337
solid electrolytes containing both mobile and immobile alkali ions 80−96690
solid solution electrodes, characterisation and performance, secondary battery appl. 80−72033
solid state chemistry of batteries, electrodes, and electrolytes, conference, Miami Beach, Florida, USA (Sept. 1978) 79−100393
solids, high energy density batteries appls. 79−70445
space charge phenomena and cond. 78−71877
statics and local dynamics of solid electrolytes near phase transition 80−107542
statistical mechanics of superionic conductors 79−42294
structural transition theory 79−23731
structure and dynamical props., X-ray and neutron scatt. studies, book contrib. 80−24433
sublattice disorder, phenomenological models 77−35663
sublattice disorder and dynamics, exptl. techniques, review 78−91476
sublattice melting, rel. to melting transitions in binary salts 77−43364
sulphate based binary solid electrolytes, props., appls. 77−84971
summer school, Aleria, Corsica, France (Sept. 1977) 80−6339
superionic conductors, transitions, structures, dynamics and spectra, review 79−60549
superionic solid film, surface diffusion coeff. 80−92709
survey and appls. *(Dutch)* 77−7894
ternary fluorides, high anionic cond. of new solid electrolytes 80−107546
tetraethylammonium iodide-Ag_nI_{n+1}, ionic conductors, electrochem., props. 77−31808
tetramethylammonium silver iodide superionic film, electrocodeposition, electrochem. cells 80−107478
theoretical models, review 80−107465
theory of superionic conduction, including struct. principles 80−6550
thermodynamic peculiarities of solid electrolytes 79−33114
thermoelectric power 79−46835
thermoelectric power calc., nature of hopping process 78−51727
transition temperature to high cond. state as function of press. 80−44365
transport properties, review 77−62671
two component particle transport 77−84964
unipolar conduction model for solid electrolytes 79−28144
Ag orthophosphates and sulphates, anhydrous, struct. relationships w.r.t. fast ion cond. 80−107188
Ag^+ superionic conductors, US attenuation due to hopping of Ag^+ ions 78−22890
$Ag/RbAg_4I_5/I_2$ solid state battery, low temp. degradation 80−61331
Ag-β-Al_2O_3, test for solid electrolyte by EMF meas on Ag/Au couples *(German)* 80−104307
Ag-Ge-S glasses, X-ray determ. of struct. *(Japanese)* 80−10501
Ag-Zn, molten, EMF meas. of activities using ZrO_2 solid electrolytes *(Japanese)* 80−88339
AgBr, far IR spectra, cond., cation local motion 79−1754
AgBr, phonons at elevated temp. 78−79810
AgBr(Cl), ionic transport, defect form. and migration energies, quasiharmonic model 80−107538
$AgCrS_2(Se_2)$, superionic and electronic cond. meas. 77−89577
$Ag_{0.85}Cu_{0.15}Br$, far IR spectra, cond., cation local motion 79−1754
$Ag_{1-x}Cu_xI$-QI, Q=NH_4, $(CH_3)_4N$, $C_5H_5NCH_3$, elec. cond., −20 to 130°C 77−55387
AgCuSe, mixed conduction 79−78140
Ag_2HgI_4, order-disorder transform. at 51°C, sound vels. and dielec. losses 78−10129
Ag_2HgI_4, polycryst., Raman spectra, press. depend. 77−73137
Ag_2HgI_4, superionic cond., cation disordering 77−84692
α-AgI, activation vol. for ionic cond. 80−59711
AgI, α and melt phases, light scatt. from correl. ion fluctuations 79−95771
AgI based, superionic conductors, geometric struct. principles 77−89574
α-AgI, cation distrib. and anharmonic thermal vib. 77−66005
α-AgI, collective motion in superionic conductors, AC conductivity calc. 79−99368
α-AgI, cond. mechanisms in superionic phases, neutron diffr. obs. 80−59714
AgI, conductivity, hopping system, master equation 80−39348
α-AgI, current-current correlations 78−51732
AgI, density of states, IR cond., and Raman scatt., lattice dynamics calc. 78−30709
AgI, density of valence states, photoelectron spectra meas. 80−25523
α-AgI, diffusion dynamics, quasielastic neut. scatt. expt. 80−107484
α-AgI, diffusive motion of Ag^+ ions, quasielastic neutron scatt. 77−11726

superionic conducting materials continued
α-AgI, dynamic cage effect 80−107541
AgI, dynamical aspects 78−79695
AgI, EXAFS investigation of struct. and ion motion 80−108302
α-AgI electrolyte, degree of disorder of anion lattice 78−59975
α-AgI, fast ion conductor, phase transitions, thermoelec. power meas. 80−107540
AgI group superionic conductor, phase transition detection by thermoelectric power method 80−92669
α-AgI, I_2 diffusion obs. using ^{131}I radiotracers 78−18830
β-AgI, ion dynamics and transition to superionic state, nucl. spin-lattice relax. meas. 78−43179
α-AgI, ionic cond. in 8-40 GHz range 80−44358
α-AgI, ionic motion, low freq. Raman scatt. 78−80354
α-AgI, ionic motions nature, mol. dynamics calcs. 80−107533
AgI, lattice dynamics of binary superionic conductors 80−107393
AgI, lattice potential effects on superionic cond. 80−65274
β-AgI, low temp. electronic hopping 78−39111
α-AgI, molecular dynamics exam. of Ag diffusion 78−55981
AgI, molten, freq. depend. ionic cond. 77−7882
α-AgI, neutron scatt. expts., Ag^+ ion motion 80−6552
AgI, phase transition, statics and local dynamics, mean field and Mori theory 80−39347
β-AgI, phonon-induced X-ray scatt. from lattice dynamical model 79−37790
AgI, position and dynamics of Ag ions using EXAFS, jump-diffusion cond. model 77−59643
α-AgI, Raman scattering evidence for sublattice melting 78−80350
α-AgI, Raman spectra, freq. depend. cond. exam. 78−10883
α-AgI, Raman spectra, interpretation using liquid like model 78−2855
AgI, Raman study 78−80353
AgI, single cryst. neutron diffr. meas., Ag distrib. determ. 78−10025
α-AgI, single particle and collective aspects of Ag^+ ion motion 80−6553
αAgI, solid electrolyte, contrib. of non-Brownian motion to transport props. 80−70453
AgI solid electrolyte α-phase stabilisation 80−29209
AgI solid electrolyte plastic deformation and thixotropy obs. 78−79660
α-AgI, state of order, config. model 80−6390
α-AgI, struct. and dynamics, two-dimens. mol. dynamics model 80−49413
α-AgI, structural and dynamical behaviour 80−107544
AgI, structural model 78−79797
α-AgI, structure, X-ray scatt. anal. 80−28983
α-AgI, superionic, anal. of Ag K-EXAFS data 80−97377
α-AgI, superionic, continuous order-disorder transition, Raman spectroscopic evidence 80−45070
α-AgI, superionic compound struct., cation distrib., powder neutron diffr. 77−72595
α-AgI, superionic cond., correlations in motion of particles, mol. dynamics calcs. 77−66043
AgI, superionic cond., cryst. struct., neutron diffr. study 79−42041
α-AgI, superionic cond., freq. depend. cond. 77−84973
α-AgI, superionic cond., sublattice melting, Raman spectra, rel. to AgBr(Cl) melts 78−10882
α-AgI, superionic cond., statistical thermodynamic description *(French)* 80−65281
α-AgI, superionic conductor, appl. of Brownian motion in polarisable lattice 77−76603
α-AgI, superionic conductor, microscopic model *(German)* 78−67861
AgI, superionic conductor, lattice dynamics 79−95111
α-AgI, superionic conductor, microwave absorption spectrum 80−11515
α-AgI, superionic conductor, soft-core model, Monte Carlo study 80−54430
α-AgI, superionic phase, struct., X-ray scatt. anal. 80−28983
α-AgI, superionic. liquid-like Raman scatt. 79−95769
α-AgI type compounds, struct. and phase transition *(Japanese)* 79−65250
AgI type solid electrolytes, sp. ht. anomaly, theory *(Russian)* 78−10198
AgI type solid electrolytes, expt. props. 78−63877
AgI/Ag oxysalt system, vitreous solid electrolytes, conductance mechanism 80−107560
AgI-Ag oxosalt systems, solid electrolytes with glass-like struct., thermodynamic and electrochem. props. 79−10978
AgI-Ag oxysalt high cond. glasses, struct. obs. 79−32908
AgI-$Ag_2Cr_2O_7$ system, solid electrolyte stability 77−15619
AgI-$Ag_2Mo_2O_7$ system, solid electrolyte stability 77−15619
AgI-$Ag_2Mo_2O_7(Ag_2Mo_4O_{13})$, solid, intermediate compounds with fast ion transport 77−43371
AgI-Ag_2MoO_4 pseudobinary system, superionic cond. glasses, comp. depend. of ionic cond. 80−75380
AgI-Ag_2O-MoO_3, superionic conducting glass, IR spectra and struct. 79−10804
AgI-Ag_2O-MoO_3 glass glass superionic cond., struct. and transport props. 80−88602
AgI-Ag_2O-P_2O_5 system, glass form. and superionic cond. characts. 78−26722
AgI-Ag_2O-$P_2O_5(MoO_3)$ glassy electrolyte galvanic cells 80−104513
4AgI-Ag_2XO_4, (X=Cr, Mo, W), ionic cond., complex admittance 77−84969
AgI-Ag_3AsO_4 system, solid electrolyte stability 77−15619
AgI-based solid electrolyte cell discharge mechanism 80−35663
AgI-type solid electrolytes, introductory survey 80−6549
Ag_4I_5, ionic cond., effect of press. 78−51733
$(AgI)_x(Ag_2O\ B_2O_3)_{1-x}$, amorphous superionic compound, ^{11}B lineshape and relaxation 80−108107
$(AgI)_x(Ag_2O.B_2O_3)_{1-x}$ glass, ionic cond. and disorder modes 80−39344
$Ag_7I_4AsO_4$ vitreous electrolyte, ionic cond. 79−77807
$Ag_{44}I_{53}(C_{11}H_{30}N_3)_3$, cryst. struct. determ. 78−26553
$Ag_7I_4PD_4$, superionic solid film, surface diffusion coeff. 80−92709
$Ag_7I_4PO_4$ film formation from electrolysis of HI-H_3PO_4 soln., electrocodepositional method 80−55315
$Ag_7I_4PO_4$, solid electrolyte, ionic cond. meas., 4-79°C 80−54433
$Ag_{26}I_{18}W_4O_{16}$, cryst. struct. and ionic conductivity 77−80647
$Ag_{26}I_{18}W_4O_{16}$, order-disorder type ferroelectric transitions, ionic conductivity meas. 80−66122
$Ag_{26}I_{18}W_4O_{16}$, solid electrolyte, anisotropic elec. cond., low temp. phase transitions 80−65289
$Ag_{26}I_{18}W_4O_{16}$, struct. phase transition, dielectric, cond. and Raman obs. 79−19368
Ag_2MI_4 (M=Cd, Zn), fast ionic cond. and order-disorder transition 79−99363

superionic conducting materials continued
$AgNbO_3$.4AgI room temp. solid electrolyte and galvanic cell performance 78−79803
Ag_2O-MgO-Al_2O_3, ionic cond. 80−107480
$AgPO_3$-AgX, X=I,Br,Cl, ionic conductivity *(French)* 78−79805
$Ag_xRb(PO_4)_2$, struct., density and elec. cond. 80−33952
β-Ag_2S, cond. mechanisms in superionic phases, neutron diffr. obs. 80−59714
α-Ag_2S, cryst. struct., X-ray scatt. determ. 79−46613
β-Ag_2S, fast-ion conductor, Ag ion density, neutron diffr. study 80−34234
Ag_2S, liquid, ionic and electronic cond., thermoelec. power 80−39329
α-Ag_2S, struct., X-ray scatt. intensity anal. 78−38672
Ag_2S-As_2S_3-AgI glasses, temp. and comp. depend. of ionic cond. *(French)* 80−34229
$Ag_2S+Ln_2S_3$, powdered mixtures, reaction rate, production of ionic semiconductors 80−93741
Ag_3SBr, superionic conductor, phase transition, struct. 80−107144
βAg_3SI, anharmonic thermal vibr. of cations 80−65214
Ag_3SI, dynamical aspects 78−79695
Ag_3SI, struct. and phase transition *(Japanese)* 79−65250
Ag_3SI, superionic conductor, ordered phase struct. 78−83792
Ag_3SI, superionic cond., phase transition and cryst. structs., sp. ht., neutron and X-ray diffr. obs. 80−10662
Ag_2S(Se), ionic-electronic mixed conductor, solid state controlled growth using cryst. rotation 78−31338
α-Ag_2S(Se), single cryst. growth through capillary tube 80−108331
Ag_2Se, liquid, ionic and electronic cond., thermoelec. power 80−39329
α-Ag_2Se, superionic cond., X-ray diffr. study 77−84719
$Ag(T_1)/AgI/Ag(T_2)$ cell, thermo-EMF of highly conducting solid electrolytes 80−24659
Ag_2Te, liquid, ionic and electronic cond., thermoelec. power 80−39329
$Ag_2Tl_6I_{10}$, one-dimensional ionic conduction 79−7707
β-$AgVO_3$.4AgI room temp. solid electrolyte and galvanic cell performance 78−79803
Al solid electrolytic capacitors, pit etching method for improving freq. and temp. characts. 80−100944
β-$Al_{11-y}Mg_yO_{16}$, X-ray diffuse scatt. obs. of struct. 80−107186
β-AlO_3-$(Na,Li)_2O$, NMR, Raman and IR spectra, and X-ray diffr., heat treatment induced changes 80−107508
β-Al_2O_2-Na_2O, between metal electrodes, cell complex admittance diagrams, grain boundary effect *(French)* 80−45653
β-Al_2O_3, additive modified charact. by NMR 78−10785
Al_2O_3, β- and β″-phases, defect struct. obs. by high resolution TEM, battery ageing relevance 80−107501
β-Al_2O_3 compounds, stoichiometry, phase transition and conductivity 79−23773
β-Al_2O_3, defect props. and ionic transport 80−107486
β-Al_2O_3 electrolyte, polycryst., impedance of electrochem. cells, cond. relax. 79−100401
β-Al_2O_3, field assisted bonding to metals 80−45474
β-Al_2O_3, ionic superconductors *(French)* 80−39346
β″-Al_2O_3, Li_2O-stabilised, deterioration under electrolytic conditions 80−40592
β″-Al_2O_3, Mg- and Li-stabilised, high-resoln. electron microscopy images 80−107277
β-Al_2O_3, Na, K and Ag substitued, lattice vibrs., ion transport spectra 77−20121
β-Al_2O_3, new fabrication methods 79−78916
B-Al_2O_3 solid electrolyte, optimisation of fabrication process, for Na/S load leveling batteries 80−72035
β-Al_2O_3 solid electrolyte based Na/S traction batteries, development progress and problems, review 80−61326
β-Al_2O_3, solid electrolyte for Na/S battery, GEC development program 80−61327
β-Al_2O_3 solid electrolytes, elec. cond. and activation energy *(Chinese)* 80−79987
β-β″-Al_2O_3, solid electrolytes, resist. obs. 200-1000°C 80−107500
β-Al_2O_3, stoichiometric, Raman and IR spectra, Frenkel defects, order-disorder transition and cation cond. 80−55086
β-Al_2O_3 structures, superionic props., IR spectra 80−107483
β-Al_2O_3-$(Na,K)_2O$, equil. distrib. of ionic species 80−107511
β-Al_2O_3-$(Na,K)_2O$, model calcs. of cond. anomalies, pot. energies of cation arrangements 80−107510
β-Al_2O_3-$(Na,Li)_2O$, β-Al_2O_3-$(K,Li)_2O$ and β-Al_2O_3-$(K,Sn)_2O$, ionic cond. and Raman spectra 80−107509
β-Al_2O_3-$(Na,Li)_2O$, first-order quadrupole NMR obs. of cation distrib. and ion motion 80−108113
β-Al_2O_3-$(Na,Li)_2O$, ionic motion obs. using NMR and internal friction 80−108099
β-Al_2O_3-$(Na,Li)_2O$ solid electrolyte, Li motion and activation obs. using ^{7}Li NMR 80−108100
β-Al_2O_3-Ag_2O, Haven ratio, temp. depend., Ag diffusivity and ionic cond. 80−107503
β-Al_2O_3-Ag_2O, stoichiometric A phase, X-ray diffuse scatt. obs., sublattice phase transition 80−64944
β-11Al_2O_3-Ag_2O, sublattice phase transition, stoichiometric 79−42241
β-Al_2O_3-Ag_2O, superionic conductor, microwave absorption spectrum 80−11515
β-Al_2O_3-Ag_2O, thermal cond. below 300K 77−24454
β-Al_2O_3-$Ag_2O(D_2O)(NH_4^+)$ 80−107512
β″-Al_2O_3-$Ag_2O(H_3O)(K_2O)(Li_2O)(NH_4^+)(Na_2O)$, ionic cond. at room temp. 80−107513
β-Al_2O_3-$Ag_2O(K_2O)(Li_2O)(Na_2O)$, low-energy excitation spectra, localised modes 80−59606
β″-Al_2O_3-$Ag_2O(K_2O)(Li_2O)(Na_2O)(Rb_2O)$, single cryst. Raman scatt., cond. mechanism and cryst. struct. 80−66209
β-Al_2O_3-D_2O, anhydrous, prep. and struct. of $DAl_{11}O_{17}$ 80−107187
Al_2O_3-H_3O^+, β and β″ phases, protonic, conductance and spectroscopy 80−70450
β-Al_2O_3-H_3O^+, ESR of paramag. defects in cond. planes 80−29617
β-Al_2O_3-H_3O^+, high press. thermal stability 79−23678
β-Al_2O_3-H_3O^+ protonic cond., struct. investig. 79−19213
β″-Al_2O_3-$H_3O^+(Na_2O)$, struct. basis for superionic cond. 80−107498
β-Al_2O_3-$H^+(H_2O)_n$, IR and Raman spectra, OH stretching freqs., struct. and cond. 78−27210
β″- Al_2O_3-$H^+(H_2O)_n$, IR study 80−16037
β-Al_2O_3-K_2O, ESR of paramag. defects in cond. planes 80−29617
β-Al_2O_3-K_2O, thermal cond. below 300K 77−24454
β-Al_2O_3-Li_2O, thermal cond. below 300K 77−24454
β-Al_2O_3-Li_2O-Na_2O, solid electrolytes, elec. props., stability 77−84978

superionic conducting materials continued
β-Al_2O_3-Li_2O-Na_2O, spin-lattice relaxation and Li motion 80−70451
β-Al_2O_3-M_2O, M=Ag, K, Rb, Na, Eu, X-ray diffuse scatt. 78−71725
B-Al_2O_3-M_2O, M=Na, Ag, Rb, K, far IR absorption and ionic cond. 78−72512
β-Al_2O_3-M_2O, M=monovalent metal, superionic cond., phonon spectra and sp. ht. calc. 77−24368
β-Al_2O_3-M_2O (M=Li,Na,K,Ag), sp. ht., 0.1-1 K, evidence for localised low-energy excitations 78−34632
Al_2O_3-MgO-H_2O fast proton conductor 78−91480
β-Al_2O_3-NH_4^+, high press. thermal stability 79−23678
β-Al_2O_3-NH_4^+, NH_4^+ jump diffusion and rotational tunnelling, proton NMR, spin isomerism theory 79−99778
β-Al_2O_3-NH_4^+, PMR relax. time obs. of ionic motion 80−71213
β-Al_2O_3-NH_4^+, protonic cond., struct. investig. 79−19213
β-Al_2O_3-NH_4^+, single cryst. characts. and AC cond. obs. 80−107514
β-Al_2O_3-NH_4^+ and β″-Al_2O_3-NH_4^+-H_3O, single cryst. PMR and proton motion 80−108101
β-Al_2O_3-NH_4^+ proton dynamics neutron scatt. study 80−59408
β- Al_2O_3-Na_2-CaO, microstruct. and ionic resistivity 80−44357
β-Al_2O_3-Na_2O, ^{23}Na NMR spectrum, correl. effects 78−76324
β″-Al_2O_3-Na_2O, ^{23}Na NMR obs. of ionic diffusion, 180 to 800K, attempt freq. 80−108097
β-Al_2O_3-Na_2O, ^{23}Na NQR and two-dimens. diffusion, model analysis 80−108111
β-Al_2O_3-Na_2O, ^{27}Al NMR obs., Na motion and cond. characts. 80−108096
β-Al_2O_3-Na_2O, AC impedance, microstruct. and strength 80−100349
β-Al_2O_3-Na_2O, AC ionic cond., dielec. and NMR relax. 80−59713
β″-Al_2O_3-Na_2O, absorbed water effect on NMR lineshape and spin-lattice relax. time 80−108098
β-Al_2O_3-Na_2O, anomalous Na behaviour obs. using pulsed and CW NMR 80−108095
Al_2O_3-Na_2O, β and β″ phases, stability, cond., paramag. impurity effects obs. 77−84976
Al_2O_3-Na_2O, β and β″ phases, formation by solid state reaction between $NaAlO_2$ and γ-Al_2O_3 80−29912
Al_2O_3-Na_2O, β′ and β″ phases, engineering props. data compilation, rel. to energy storage 80−49415
β-Al_2O_3-Na_2O, calculation of simultaneous ionic cond. and tracer diffusion 78−43178
β-Al_2O_3-Na_2O, ceramic and powder specimens, various Na_2O content, NMR study 79−61240
β-Al_2O_3-Na_2O, colour centers, AES, electron energy loss, and optical spectroscopy obs. 78−35176
β-Al_2O_3-Na_2O, colour centre ESR by localised tunnelling states 80−108073
β″-Al_2O_3-Na_2O, computer simulation of ionic conductivity 77−89580
β-Al_2O_3-Na_2O, cond. plane struct. and energetics 80−92715
β-Al_2O_3-Na_2O, conductivity dispersion in single crystal 77−28037
β-Al_2O_3-Na_2O, development for Na/S battery 80−71615
β-Al_2O_3-Na_2O, EPR and optical absorpt. studies of X-ray produced defects 78−95517
β-Al_2O_3-Na_2O, ESR of paramag. defects in cond. planes 80−29617
β-Al_2O_3-Na_2O, electrolytes, electric modulus spectroscopy 77−84974
β-Al_2O_3-Na_2O, fracture stress, effect of microstruct. defects 77−44338
β-Al_2O_3-Na_2O, H_2O effect on Na^+ diffusivity 77−31806
β-Al_2O_3-Na_2O, ionic cond. temp. depend., comparison with NASICON 80−107520
β-Al_2O_3-Na_2O, layered material, contact free conductivity 80−2195
β″-Al_2O_3-Na_2O, Li_2O stabilised, electrolyte polarisation anal. by complex admittance method 80−2689
β-Al_2O_3-Na_2O, low-temp. ^{23}Na satellite spectra, Na ion motion 80−108112
β-Al_2O_3-Na_2O, microwave absorpt., low-temp. dielectric props. anomalies, ion tunnelling states 78−92013
β-Al_2O_3-Na_2O, motion of charge carrying ions, mol. dynamics simulation 80−107506
β″-Al_2O_3-Na_2O, NMR of ^{23}Na, elec. quad. interaction, 185 to 419K, ion motion obs. 80−108110
β-Al_2O_3-Na_2O, non-stoichiometric, amorphous, US attenuation and velocity 80−39228
β″-Al_2O_3-Na_2O, nonstoichiometric, correl. effects in diffusion, Haven ratio, point defect interactions 80−107505
β-Al_2O_3-Na_2O, nucl. double reson. interferometry, satellite spectrum 78−31123
β-Al_2O_3-Na_2O, planar [00.l] disorder, TEM obs. 77−31680
β″-Al_2O_3-Na_2O, polycryst. Na^+ ion diffusion rel. to cond. 77−72715
β-Al_2O_3-Na_2O, potential energy distrib. and ionic motion 80−70455
β-Al_2O_3-Na_2O, preferable orientation for Na^+ cond. 80−35144
β-Al_2O_3-Na_2O, protonic, conductance and spectroscopy 80−70450
β″-Al_2O_3-Na_2O, rapid ion conductor, Na penetration 80−24653
β-Al_2O_3-Na_2O, single cryst. and polycryst., elec. props. 77−72714
β-Al_2O_3-Na_2O, single crystal ionic conductor, migration losses 77−80643
β-Al_2O_3-Na_2O, single cryst., non-Debye capacitance 80−107497
β″-Al_2O_3-Na_2O, solid electrolyte, behaviour at high current density, sodium heat engine mode 80−61330
β-Al_2O_3-Na_2O, superionic anisotropic ceramic, prod. by microwave sintering *(French)* 78−52742
β-Al_2O_3-Na_2O, superionic conductor, microwave absorption spectrum 80−11515
β-Al_2O_3-Na_2O, synthesis, ceramic form., sintering, cond. 79−11537
β-Al_2O_3-Na_2O, synthesis by chem. methods 77−24993
β-Al_2O_3-Na_2O, thermal cond. below 300K 77−24454
β-Al_2O_3-Na_2O, thermal desorption of ions 77−7973
β-Al_2O_3-Na_2O, Young's modulus and internal friction obs. 77−35624
β-Al_2O_3-Na_2O 79−19396
β-Al_2O_3-Na_2O ^{23}Na asymmetry parameter, temp. variations 80−6540
β-Al_2O_3-Na_2O doped with transition metal ions, complex plane anal. of impedance and admittance 80−70452
β-Al_2O_3-Na_2O electrolyte development for Na-S battery 79−29461
Al_2O_3-Na_2O solid electrolytes phase composition 77−36468
β″-Al_2O_3-Na_2O solid electrolyte, tube fabrication from cast ceramic tape 80−60819
β″-Al_2O_3-Na_2O solid electrolyte, processing and phys. props. 80−60820
β″-Al_2O_3-Na_2O solid electrolyte, strength degradation under electrolytic conditions 80−61329
β″-Al_2O_3-Na_2O solid electrolyte, heat treatment effects on ionic cond. and microstruct. 80−65293
β-Al_2O_3-Na_2O:Mg, with and without Co co-doping, ionic cond. and cryst. struct. 78−26723

superionic conducting materials continued
β-Al_2O_3-Na_2O:Mn^{2+}, EPR of Mn^{2+} 78−6569
β-″-Al_2O_3-Na_2O:Na^+,Ca^{2+}, charge compensation mechanism, Na^+ and Ca^{2+} ion movement 78−22891
β-Al_2O_3-Na_2O_3:Ag^{2+}, EPR measurements 78−95515
β-Al_2O_3-Na_2O-Li_2O, ^{7}Li NMR 79−15361
β″- Al_2O_3-Na_2O-Li_2O (8.85, 0.75 wt.%) pressing powders, prep. by spray drying 80−40294
β-Al_2O_3-Na_2O-SiO_2, solid electrolytes, exam. of microstruct. ionic resistivity 78−80566
β-Al_2O_3-Na_2O(Ag_2O), Raman scatt., 12-400K, 2nd order phase transition 77−81091
β-Al_2O_3-Na_2O(Li_2O)(K_2O)(Ag_2O)(H_3O), with mobile ion species, dielec. relax. 79−91351
β″-Al_2O_3-NaO-LiO_2, stabilised, effect of phase composition, grain size, on Na ion cond. 78−47582
β-Al_2O_3-OH_3^+, proton dynamics neutron scatt. study 80−59408
β-Al_2O_3-X_2O, (X=Na,K,Rb,Ag,Tl), infrared and Raman spectra 79−1761
β-$Al_2O_3Na_2O$, H-exchanged, effect of moisture, on H_2 activity changes and thermal stability 78−47580
β-Al_2O_3.(K_xNa_{1-x})$_2O$, anomalous behaviour in ionic cond. obs. 78−87818
β-Al_2O_3.$(NH_4)_2O$, neutron scatt. study of NH_4^+ motion 78−30785
β-Al_2O_3.Na_2O cryst. or sintered disc, Au electrode interface impedance rel. to roughness 77−4437
β-Al_2O_3.Na_2O, single cryst. and polycryst., anisotropic cond., low temp. modulus spectra 77−4217
ArO_2-ScO_3 solid electrolytes, thermoEMF 78−95184
Au/solid electrolyte/Au primary cells, charge storage with various electrolytes 80−89605
Au-Zn, molten, EMF meas. of activities using ZrO_2 solid electrolytes *(Japanese)* 80−88339
AuI, elec. cond. 79−42302
B_2O_3-Li_2O-LiCl glass system, exam. of ionic conductivity of Li *(French)* 78−51730
B_2O_3-Li_2O-LiCl glass system, new solid electrolytes, conductivities and activation energies 79−28137
B_2O_3-Li_2O-LiCl glasses, solid electrolyte, NMR meas. 80−29208
$BaCl_2(F_2)$, sp. ht. meas., Schottky-type diffuse phase transitions, defect form. energies and entropies 80−107441
BaF_2 solid electrolyte, n-type electronic cond., 700-900°C 80−29448
BaF_2, theoretical investigation of Raman scatt. 78−80351
BaF_2:R, R=rare earth, dopant effect on superionic state transition 79−60547
δ-Bi_2O_3, thermoelectric power, heat of transport of O^{2-} ions 80−92713
Bi_2O_3-M_2O_5(M_2O_3) (where M=V,Nb,Ta,Y,Gd) ion cond. and oxide ion vacancy 79−28139
Bi_2O_3-$M2O_5$, sintered, (M=V, Nb, Ta), high oxide ion cond. 78−14503
β-AgI, ionic cond. and dielec. meas., Frenkel defect formation energy 78−87814
$(C_5H_5NH)Ag_3I_6$, solid electrolyte, low-temp. phase transitions 77−72686
CaF_2, anion motion at high temps., quasielastic nuetron scatt. obs. 80−59715
CaF_2, computer simulation 78−43173
CaF_2 electrolyte for thermodynamic study of alkaline earth oxide compounds 78−53241
CaF_2, fast ion transport, computer simulation 80−107485
CaF_2, mol. dynamics studies of superionic conductors 80−107547
CaF_2 solid electrolyte, meas. of O chem. pot. 80−3359
CaF_2 solid electrolyte use in galvanic cells for thermodynamic obs. on refractory double oxides *(French)* 80−85190
CaF_2, theoretical investigation of Raman scatt. 78−80351
$Ca^{2+}F_2^-$, particle motions, ionic conduction, self-diffusion 77−15620
CaF_2:R, R=rare earth, dopant effect on superionic state transition 79−60547
$CaF_{2-x}H_x$, ionic cond. determ. from admittance and dielec. loss meas. *(French)* 80−107479
CaS-Y_2S_3 (1 wt.%), solid electrolyte, elec. cond. under low partial pressures of S *(Japanese)* 80−49409
$Ca_{1-x}Y_xF_{2+x}$, fast ionic conduction of F^- ions 79−99360
$Ca_{1-x}Y_xF_{2+x}$, solid anionic conducting electrolytes, struct., elec. props. 77−84977
CeF_3, ^{19}F spin-lattice relax. and mag. couplings 79−65753
CeF_3, doped with aliovalent cation dopants, ionic cond. 77−20115
CeO_2, ionic conduction, doping effects and defect interactions 80−19978
CeO_2:Y, slow transient phenomenon 80−107550
CeO_2-Y_2O_3 film, surface characterisation, XPS, ESCA, and AES expts. 78−72028
Cu free electrolytic films, tensile creep for various film thicknesses calcs. *(Russian)* 80−11697
Cu halides, lattice dynamics of binary superionic conductors 80−107393
Cu^+ ion conductor, $Py_2Cu_5Br_7$, cryst. struct. 78−51527
Cu-CuI-graphite secondary cell, transient ionic current obs. 80−108790
Cu-CuI-graphite secondary cell, steady state hole current obs. 80−108791
CuBr, cond. mechanisms and struct. at high temps. 77−84711
β-CuBr, far IR spectra, cond., cation local motion 79−1754
CuBr, superionic behaviour at high temp., EXAFS study 80−107496
CuBr, superionic cond., cryst. struct., neutron diffr. study 79−42041
CuBr(Cl)(I), LF light scatt. spectra in superionic cond. phases, ion motion obs. 80−108217
7CuBr.$C_6H_{12}N_4CH_3Br$, solid electrolyte galvanic cell appl. 77−77775
CuCl, superionic behaviour at high temp., EXAFS study 80−107496
CuCl-RbCl, room temp. high cond. 77−72712
Cu_2HgI_4, fast ionic cond. and order-disorder transition 79−99363
Cu_2HgI_4, polycryst., Raman spectra, press. depend. 77−73137
Cu_2HgI_4, superionic cond., cation disordering 77−84692
CuI and CuI:CdI_2, ionic cond., vacancy and interstitial mobilities, phase transitions 77−20116
CuI, α and melt phases, light scatt. from correl. ion fluctuations 79−95771
CuI, cond. mechanisms and struct. at high temps. 77−84711
CuI, EXAFS investigation of struct. and ion-motion 80−108302
CuI, ionic motions nature, mol. dynamics calcs., sp. ht. anomaly due to order-disorder transform. 80−107533
CuI, lattice dynamic meas. and calcs. 79−99880
CuI, NMR relax. evidence for sublattice melting 77−15623
CuI, Raman study 78−80353
CuI solid electrolyte α-phase stabilisation 80−29209
CuI, superionic cond., cryst. struct., neutron diffr. study 79−42041

superionic conducting materials continued
CuI, superionic cond., EXAFS study 80−50462
CuI, superionic cond., Raman spectra in all 3 phases 78−19486
CuI, superionic conductor, lattice dynamics 79−95111
$CuIn_{11}S_{17}$, defect spinel, cryst. growth, search for new superionic cond. cpds. 78−31307
$CuInSnS_4$, spinel, cryst. growth, search for new superionic cond. cpds. 78−31307
$Cu_xMo_6S_{8-y}$, mixed conductor, partial Cu ion cond. and chem. diffusion 80−84323
$Cu_xMo_6S_{8-y}$, mixed conductor, equilib. partial thermodynamic props. 80−85270
Cu_6PS_5Br, cryst. struct. of new superionic conductor 78−26514
Cu_6PS_5Br, cryst. struct. at 293 and 473K, thermal parameters, neutron diffr. obs. 80−59450
$Cu_2S+Ln_2S_3$, powdered mixtures, reaction rate, production of ionic semiconductors 80−93741
$Cu_{2-\delta}S$, $Cu_{2-\delta}Se$ and $Cu_{2-\delta}(S,Se)$, ionic and electronic cond., thermopower and Hall coeff. 77−20117
$Cu_2S(Se)$, ionic-electronic mixed conductor, solid state controlled growth using cryst. rotation 78−31338
$Cu_{2-x}Se$, X=0-0.23, cond. transition to superionic state, crit. conc. 79−55924
CuTeBr, ionic cond., phase transition obs. by millimetre wave spectroscopy 78−22855
CuTeBr, superionic conductor, microwave absorption spectrum 80−11515
CuTeX (X=Cl, Br, I), solid ionic cond., props. 79−14963
Cu_3VS_4, out of equil. mixed cond., electronic cond. decrease in ionic soln. 80−107874
Cu_3VS_4, out of equil. mixed cond., off-centre positions and order-disorder transition, ultrafast nucl. relax. obs. 80−108103
Cu_3VS_4, out of equil. mixed cond., chem. origin of mobile ions, spin-lattice relax. and NQR obs. 80−108104
$DAl_{11}O_{17}$, anhydrous, cryst. struct. from powder neutron diffr. 80−1983
β- and β″-Ga_2O_2-Na_2O, fast ion conductor, Na^+ self diffusion and Na-K exchange 79−28133
Ga_2O_3-Na_2O, β- and β″-phases 77−40234
Ga_2O_3-Na_2O, β- and β″-phases, ionic cond., room temp. to 350°C 77−43368
Ga_2O_3-Na_2O, β- and β″-phases, IR spectra 78−39552
β″-Ga_2O_3-Na_2O, single cryst. growth by Na_2O evaporation from molten Na_2O-Ga_2O_3 77−44141
β″-Ga_2O_3-Na_2O-K_2O mixed crystals, cond. anomaly 79−46838
$HUO_2AsO_4.4H_2O$ and $HUO_2PO_4.4H_2O$ layered cpds., struct. investigs. below antiferroelec. transition temps., H bond ordered structs. 80−107416
$HUO_2AsO_4.4H_2O$ and $HUO_2PO_4.4H_2O$ layered cpds., single and polycryst., proton cond. behaviour w.r.t. antiferroelec. transition temps. 80−107481
$H_{5n-2}UO_2(IO_6)_n.4H_2O$, n=0.5 to 2.0, high proton cond. 80−107562
$H(UO_2P(As)O_4)4H_2O$, H motion, PMR obs. 78−80239
$HUO_2PO_4.4H_2O$, rapid H^+ cond. 77−76602
$HUO_2PO_4.4H_2O$, H^+ ion cond., struct. mechanism, X-ray diffr. obs. 78−34651
$HUO_2PO_4.4H_2O$, H^+ ion solid electrolyte, cryst. struct. 79−14759
$HUO_2PO_4.4H_2O$, film fabrication and appl. as solid electrolyte in electrochromic displays 80−70462
$HUO_2PO_4.4H_2O$ solid proton conductor, appl. as electrochromic cell 80−89497
$HuO_2P(As)O_4.4H_2O$, water deficiency, enthalpy of dehydration, thermogravimetric anal. 80−65251
In_4CdI_6, fast ionic cond. and order-disorder transition 79−99363
$In_2ZnBr_4(I_4)$, fast ionic cond. 79−99363
In_2ZnI_4 and In_4CdI_6 solid electrolytes, ion transport mechanism and polarisability role, comparison with Cu^+ and Ag^+ cond. 80−107531
K-Hollandite, one-dimens. ionic conductor, modulation and incommensurability 80−19980
KAg_4I_5, pressure effect on phase transitions 80−70405
KAg_4I_5, solid electrolyte, Raman spectra 79−73934
KAg_4I_5, superionic film, elec. ionic cond. and electron spectra 80−6543
KAg_4I_5, superionic phase transition, dynamical and crit. pt. props. 80−107535
KAg_4I_5, superionic solid films, preparation and elec. cond. 79−82380
$KBiF_4$, fast ionic conduction of F^- ions 79−99360
$KBiF_4$, new solid electrolytes, conductivities and activation energies 79−28137
$K_{1+x}Fe_{11}O_{17}$, ionic cond. and chemical diffusion 77−47618
$KInO_2$-MO_2, M=Zr, Hf, Sn, Pb, lamellar struct., cond. meas. *(French)* 77−1257
$K_x(L_{x/2}Sn_{1-x/2})O_2$ (L=Mg, Ca, Zn; x<1), new family of cationic conductors *(French)* 79−60546
$K_{1.54}Mg_{0.77}Ti_{7.23}O_{16}$, hollandite, cationic short range order, ion-ion interaction 77−11729
$K_{1.54}Mg_{0.77}Ti_{7.23}O_{16}$, one-dimens. superionic cond., ionic order, defect cond. 78−87815
$K_{1.54}Mg_{0.77}Ti_{7.23}O_{16}$, hollandite, one-dimens. superionic cond., transport model 80−107529
$K_{1.6}Mg_{0.8}Ti_{7.2}O_{16}$, solid electrolyte, dielec. response, 5.2-77K 79−56709
$K_2Mg_xTi_{8-x}O_{16}$, stochastic Langevin dynamics study of correlated ionic motion in 1-D solid electrolytes 80−65279
$(K_xNa_{1-x})_2$ 0.58 Ga_2O_3, anomalous behaviour in ionic cond. obs. 78−87818
$KNbO_3$ glass, quenched, ionic cond., appl. as solid electrolyte 79−1522
β-K_2O-Al O_3, cation distrib. 77−80487
K_2O-Ga_2O_3-Al_2O_3, solid solns., K ionic cond. 77−35747
K_2O-MgO-Al_2O_3, ionic cond. 80−107480
$K_2O_{5-x}Ga_2O_3.xFe_2O_3$, K ion cond. 78−83998
K_2OsCl_6, impurity H^+ ion motion, ^{35}Cl NQR obs., 77 and 298K 80−60451
K_2OsCl_6, single cryst. with H^+ interstitials, protonic cond. from dielec. meas. 80−107515
K_2SO_4, anhydrous, struct. relationships w.r.t. fast ion cond. 80−107188
$KScO_2$-MO_2, M=Zr, Hf, Sn, Pb, lamellar struct., cond. meas. *(French)* 77−1257
$KTaO_3$ glass, quenched, ionic cond., appl. as solid electrolyte 79−1522
$LaAlO_3$ perovskite electrolytes for high-temp. fuel cells 79−29467
La_2O_3, fast ionic O_2 diffusion, neutron scatt. evidence 79−99357
Li battery solid electrolyte evaluation 79−29465
Li ionic conductors, review 77−84979

superionic conducting materials continued
Li salt based solid electrolyte, synthesis and characterisation, secondary cell appl. *(French)* 80−72034
Li solid electrolyte materials, review of crystal and electrochem. props. 80−107524
Li solid electrolytes, review 77−84980
Li-ion conductors in solid electrolytes 80−71610
LiAl/FeS, battery system research developments at ANL 80−61323
$LiAlCl_4$, fast ionic conductor, thermodynamic and phase props. 80−89211
$LiAlCl_4$, solid and molten electrolyte, thermodynamic stability 80−107447
α-$LiAlO_2$, NMR study of Li^+ motion 79−42863
Li_5AlO_4, α and β phases, NMR study of Li^+ motion 79−42863
Li_5AlO_4, ionic cond., effects of Li_2SO_4 addition, moisture, and LiOH 79−99362
Li_5AlO_4, Li_5FeO_4 and Li_5GaO_4, additives and moisture effect on ionic cond. 80−107523
Li_5AlO_4, NMR relaxation by paramag. impurities 79−42866
Li_5AlO_4 pure and doped ionic conductivity increase obs. 78−14506
$LiAlSiO_4$, β-eucryptite one-dimens. fast ion cond., temp. depend. of cryst. struct. 80−107191
$LiAlSiO_4$, crystalline, glass and glass-ceramic form, effect of composition changes, substitutions and press. on ionic cond. 78−43172
β-$LiAlSiO_4$, NMR relax., Li^+ motion, order-disorder transition 77−12220
β-$LiAlSiO_4$, superionic cond., ionic cond. and NMR line narrowing 79−42306
$LiAlSiO_4$:Cu, β-eucryptite solid electrolyte, Cu^{2+} EPR obs. of ion exchange props. 80−108056
$LiAlSi0_4$, β-eucryptite, superionic conductor, order-disorder transition, microwave impedance obs. 79−14966
$Li_{4+x}B_7O_{12+x/2}Cl$, solid electrolyte, NMR meas. 80−29208
$Li_4B_7O_{12}Cl$, new solid electrolytes, conductivities and activation energies 79−28137
$Li_4B_7O_{12}Cl(Br)$, Li^+ mobility, isotropic cond. *(French)* 77−1258
$LiCl$-Li_2O-B_2O_3 system of vitreous electrolytes *(French)* 78−27767
LiF-$Al(PO_3)_3$ glass, phase decomp., X-ray diffr. and IR spectra study 80−30003
$LiFe_5O_8$, elec. props. 77−80641
$LiGaO_2$, single crystal ionic conductor, migration losses 77−80643
Li_4GeO_4-Zn_4GeO_4, solid electrolyte system, phase diagram 80−66489
LiI complexes, ionic cond., electrochem. props. 77−60072
LiI dispersed in large surface area Al_2O_3, solid state storage batteries appls. 79−43754
LiI:α-Al_2O_3, model for fast ionic cond. 79−77811
LiI-WO_3 solid-state electrochromic cell, fabrication and charact. *(Japanese)* 80−84717
$Li_6In_2O_6$, ion mobility, NMR meas. *(French)* 79−65240
$Li_6In_2O_6$, pseudo-two-dimens. electrolytic solid, Li ion mobility, NMR study *(French)* 80−34235
$LiMSO_4$, M=Li, Na, K, Li_2SO_4-$ZnSO_4$, ht. capacity and ht. of transform. 78−26690
$Li_{16-2x}Mg_x(GeO_4)_4$, $0<x<4$, synthesis, resistivity and structure 78−18831
$Li_{16-2x}Mg_x(SiO_4)_4$, $0<x<4$, synthesis, resistivity and structure 78−18831
LiN_3, low temp. method for single cryst. growth 79−74077
Li_3N, cryst. growth and struct., phys. props., book contrib. 79−42308
Li_3N, defect props. and ionic transport 80−107486
Li_3N, defect struct., quartet state paramag. centres, EPR meas. 79−42837
Li_3N, diffusion processes and struct. NMR study 80−108090
Li_3N, electron density study using Compton scattering 80−79750
Li_3N, far IR absorption, temp. and isotope effects 79−51969
Li_3N, IR and Raman spectra and lattice dynamics 78−48177
Li_3N, interstitial sites and anharmonic thermal vibrs. in cryst. struct., ionic cond. mechanism 80−107190
Li_3N, ionic conductivity obs. 78−14507
Li_3N, ionic hopping model, NMR relax. data anal. 80−92714
Li_3N, ionic transport mechanism and defect props. 80−107528
Li_3N layer structure with fast ion cond., ^6Li NMR obs. of diffusion 80−108102
Li_3N, NMR exam. of ion diffusion 79−19397
Li_3N, photoluminesc. props. 80−50414
Li_3N, single cryst., ionic conductivity 77−72711
Li_3N single crystal and sinters, Li ion conduction 80−70449
Li_3N, sinter prep. and Li ionic cond. props. 79−99361
Li_3N, superionic conductor, local ionic motion, anisotropic dielec. behaviour 78−87817
Li_3N thin film, vacuum evaporation on WO_3, retarded deposition 80−108351
Li_3N:H, ionic cond. 79−42305
Li_3N-LiBr(Cl)(I) quasibinary cuts, fast ionic cond. props., 25 to 400°C 80−107527
$LiNbO_3$ glass, quenched, ionic cond., appl. as solid electrolyte 79−1522
Li_7NbO_6, ion mobility, NMR meas. *(French)* 79−65240
Li_7NbO_6, pseudo-two-dimens. electrolytic solid, Li ion mobility, NMR study *(French)* 80−34235
$Li_x(NbO)_4Nb_{30}O_{90}$, struct. and ionic cond. 79−65246
Li_3Ni, densified polycrystalline, use in solid state batteries 79−86921
Li_2O-B_2O_3 glasses, fast ion transport 80−107470
Li_2O-Li_2SO_4-B_2O_3 vitreous electrolytes, ionic cond. and Raman spectra *(French)* 80−24656
Li_2O-LiCl-B_2O_3 system, fast Li^+ ion vitreous superconductors, EPR study *(French)* 80−11269
Li_2O-LiF-B_2O_3 glasses, fast Li^+ conduction 80−79984
Li_2O-LiF-B_2O_3-Li_2SO_4 glasses, DC cond. and secondary struct. relax. 80−107469
Li_2O-LiX-B_2O_3 glass, X=halogen, high anionic cond. of new solid electrolytes 80−107546
Li_2O-TiO_2, pseudobinary phase rotations, DTA and X-ray anal. 80−108411
Li_2S-P_2S_5-LiI, ionic cond. meas. from room temp. to glass transition temp. *(French)* 80−88355
Li_2SO_4 based solid electrolytes, FCC phase transport mechanism studies and uses 80−107525
Li_2SO_4, fast ion conductors, X-ray diffr., neutron diffr., and Brillouin scatt. study 80−107170
Li_2SO_4, high temp. fast ion cond. phases, neutron diffr. obs. of struct. 80−107512
superionic conducting materials continued
Li_2SO_4 solid electrolyte plastic deformation and thixotropy obs. 78−79660
$LiSiO_4$, pure and doped ionic conductivity increase obs. 78−14506
Li_4SiO_4-Li_3PO_4, ionic cond. enhancement by Li_3PO_4 addition 77−7893
Li_4SiO_4-Li_3PO_4 solid solns., Li ion cond., struct. and comp. effects 77−89575
Li_8SnO_6, ion mobility, NMR meas. *(French)* 79−65240
Li_8SnO_6, pseudo-two-dimens. electrolytic solid, Li ion mobility, NMR study *(French)* 80−34235
$LiTaO_3$ glass, quenched, ionic cond., appl. as solid electrolyte 79−1522
$Li_2Ti_3O_7$, channel-structured superionic conductor, anisotropic conductivity 80−6546
$Li_2Ti_3O_7$, Li^+ ion conductor, X-ray cryst. struct. determ. 79−46604
$Li_2Ti_3O_7$, NMR data for new ionic hopping rate prefactor expression 78−47559
$Li_2Ti_3O_7$, NMR data for new ionic hopping rate prefactor expression 78−47560
$Li_2Ti_3O_7$, superionic cond., ionic cond. and NMR line narrowing 79−42306
$Li_x(WO)_4W_{30}O_{90}$, struct. and ionic cond. 79−65246
$Li_{14}Zn(GeO_4)_4$, crystal struct. and ionic conductivity 78−51728
$Li_{14}Zn(GeO_4)_4$, LISICON, AC meas. of ionic cond., 298 to 573K 80−107526
$Li_{16-2x}Zn_x(GeO_4)_4$, $0<x<4$, synthesis, resistivity and structure 78−18831
$Li_{16-2x}Zn_x(SiO_4)_4$, $0<x<4$, synthesis, resistivity and structure 78−18831
$NH_4Ag_4I_5$, pressure effect on phase transitions 80−70405
$NH_4Ag_4I_5$, Raman spectra, internal vibrs. of NH_4^+ ions 78−72497
$NH_4Ag_4I_5$, solid electrolyte, Raman spectra 79−73934
$NH_4Ag_4I_5$, superionic solid film, prep. and elec. cond. 80−54431
$NH_4Ag_4I_5$, superionic solid film, surface diffusion coeff. 80−92709
$NH_4Ag_4I_5$, superionic phase transition, dynamical and crit. pt. props. 80−107535
$NH_4Ag_4I_5$, thin film solid state battery 78−76876
$NH_4Cu_4Cl_3(I_{2-x}Cl_x)$, highly conducting solid electrolyte 80−65280
Na, orthophosphates and sulphates, anhydrous, struct. relationships w.r.t. fast ion cond. 80−107188
6NaCl.$CdCl_2$, 60 wt.% powders, Suzuki phases prep. and stability 80−35123
$Na_{0.70}Ga_{4.72}Ti_{0.29}O_8$, one-dimens. Na^+ ion cond., cryst. struct. and cond. meas. 80−107521
$Na_{5-x}Li_xErSi_4O_{12}$, solid electrolytes for Na/TiS_2 cells, synthesis, charact. and utilisation 80−107518
β-Na_2O-Al_2O_3, single cryst. Czochralski growth 77−77367
β-Na_2O-CaO-Al_2O_3, impurity conc. at grain boundaries, AES obs. 77−35570
Na_2O-Ga_2O_3 system, new superionic conductor *(French)* 78−14504
Na_2O-Ga_2O_3 system β and β'' phases, fast ion cond., prep. and phase comp. 80−59716
Na_2O-Li_2O-Al_2O_3, local electrode current density and flow decoration 80−100935
Na_2O-MgO-Al_2O_3, ionic cond. 80−107480
β''-$Na_2O.Ga_2O_3$, reaction with water, particle size effect 77−21379
$Na_2O.Li_2O.Al_2O_3$, comp. and props. for use in Na-S battery 79−87745
Na_3PO_4, high temp. fast ion cond. phases, neutron diffr. obs. of struct. 80−107512
Na_3PO_4, pure and doped ionic cond., doping effect 78−51725
$Na_5RSi_4O_{12}$ (R=Sm to Lu, Y, Sc), solid electrolytes, struct. charact. 80−1997
$Na_5RSi_4O_{12}$, superionic conductors, Na conductivity paths 78−91482
$Na_3Sc_2P_3O_{12}$, fast-ion conductor, struct. phase transition 80−88362
$Na_3Sc_2P_3O_{12}$, synthesis, cryst. struct. and ionic cond. 80−107519
$Na_{4-x}(Si_{1-x}P_x)O_4$, $(O\leq x\leq 0.25)$, exam. of Na ion conductivity by impedance meas. *(French)* 78−51731
$Na_{0.9}Ti_{1.1}Fe_{0.9}O_4$, short period β-alumina type cpds., cryst. struct. and superionic cond. 80−107499
$Na_3Zr_2PSi_2O_{12}$, NASICON, ^{23}Na NMR obs. of ionic diffusion, 180 to 800K 80−108097
$Na_4Zr_2Si_3O_{12}$, struct. analysis at 300 and 600°C, rel. to ionic cond. 80−107189
$Na_{1-x}Zr_2Si_xP_{3-x}O_{12}$, press. and comp. effect on fast Na^+ ion transport 80−107516
$Na_3Zr_2Si_2PO_{12}$, NASICON, phase transition, X-ray diffr., ionic cond. and sp. ht. meas. 80−19979
$Na_3Zr_2Si_2PO_{12}$, NASICON, ionic cond. temp. depend., comparison with β-Al_2O_3-Na_2O 80−107520
β''-$Na_2O.6Al_2O_3$, polycrystalline Na^+ ion drift and diffusion anomalies in elec. field 77−43372
NdF_3, ^{19}F spin-lattice relax. and mag. couplings 79−65753
Pb/PbF_2/BiF_3/Bi thin solid film reversible galvanic cell 79−52928
$Pb_{1-x}Al_xF_{2+x}$, ionic cond. of quenched and annealed specimens, interstitial cond. mechanism 80−2199
$Pb_{1-x}Bi_xF_{2+x}$, new solid electrolytes, conductivities and activation energies 79−28137
$Pb_{1-x}Bi_xF_{2+x}$, solid anionic conducting electrolytes, struct., elec. props. 77−84977
$Pb_{1-x}Bi_xF_{2+x}$, solid soln., struct. and ionic cond. correl., neutron diffr. study *(French)* 80−84324
PbF_2, anion disorder at high temps., neutron diffr. obs. 80−59614
β-PbF_2, anion mobility from noise meas. 79−46836
β-PbF_2, complex impedance exam. 78−47579
PbF_2, cubic, dielec. const., ionic cond., soft modes 78−14427
PbF_2, cubic and orthorhombic, press. and temp. depends. of ionic cond. 79−95207
PbF_2, fast ion conductor, phonon freq. distrib., temp. variation 80−84264
PbF_2, inelastic neutron scatt. study of phonon dispersion relation 78−30712
PbF_2, lattice dynamics 78−79697
PbF_2, phonon temp. depend., neutron scatt. study 79−60450
β-PbF_2, solid electrolyte, mobile species mobility and conc., temp. depend. 77−20113
PbF_2, sp. ht. meas., Schottky-type diffuse phase transitions, defect form. energies and entropies 80−107441
PbF_2, superionic, electrical conductivity at high temp. 78−79798
PbF_2, superionic, F^- motion and F sublattice melting, NMR obs. 77−43374
PbF_2, theoretical investigation of Raman scatt. 78−80351
PbF_2:Fe^{3+}, F^- motion, ESR study 80−66023

superionic conducting materials continued
PbF_2:Mn_3, NMR relaxation by paramag. impurities 79−42866
PbF_2:Mn^{2+}, cryst. field fluctuation dynamics, EPR 78−23328
PbF_2:Mn^{2+}, NMR linewidth with mag. tagging for superionic cond. parameters determ. 77−81021
PbF_2-AlF_3, ionic cond., characts., effect of trivalent cations 77−89576
$Pb_{1-x}M_xF_{2+x}$ (M=Bi,Th), fast ionic conduction of F^- ions 79−99360
Pb_2MnF_6, antiferromag. and superionic conductor, EPR and NMR meas. 79−99366
$PbSnF_4$, α- and β-, new solid electrolytes, conductivities and activation energies 79−28137
$PbSnF_4$, fast ionic conduction of F^- ions 79−99360
$PbSnF_4$, fast ionic cond. of F^- ions, NMR study *(French)* 80−39345
$PbSnF_4$, high anionic cond. of new solid electrolytes 80−107546
$Pb_xSn_{1-x}F_2$ solid soln., struct. evolutions *(French)* 80−96488
$Pb_{1-x}Th_xF_{2+2x}$, new solid electrolytes, conductivities and activation energies 79−28137
PrF_3, ^{19}F spin-lattice relax. and mag. couplings 79−65753
$RbAg_{4-x}Cu_xI_5$, solid electrolyte, elec. cond. 77−15624
$RbAg_4I_5$, Ag^+ ion pot. energy calcs. 79−10828
$RbAg_4I_5$, contact in solid state cells, electrochem. study 80−76527
$RbAg_4I_5$, critical dynamics, role of acoustic phonons, and Z-branch 77−84887
$RbAg_4I_5$, cryst. growth from soln. 79−33916
$RbAg_4I_5$, depolarisation of light by crit. fluctuations 79−61333
α-$RbAg_4I_5$, dynamic cage effect 80−107541
$RbAg_4I_5$, EXAFS, RDF studies 79−87526
$RbAg_4I_5$ film, thermopower meas. temp. depend., correl. effects role 80−107539
$RbAg_4I_5$, I_2 diffusion obs. using ^{131}I radiotracers 78−18830
$RbAg_4I_5$, ionic cond., effect of press. 78−51733
$RbAg_4I_5$, ionic cond. near order-disorder transition 77−11728
$RbAg_4I_5$, low temp. phases, α→β→γ transitions 77−15586
$RbAg_4I_5$, nonequilibrium thermodynamic description, variation of ionic cond. with temp. 79−61391
$RbAg_4I_5$, phase transition, statics and local dynamics, mean field and Mori theory 80−39347
$RbAg_4I_5$, single cryst., dielectric relax. *(German)* 79−4764
$RbAg_4I_5$, single particle excitations, inelastic neutron scatt. obs. 80−59599
$RbAg_4I_5$, solid electrolyte, polarised Raman scatt. meas. 77−12376
$RbAg_4I_5$, solid electrolyte, cond., phase transitions 77−84972
$RbAg_4I_5$, solid electrolyte, electronic cond. meas. 78−2483
$RbAg_4I_5$, solid electrolytes, co-ionic cond. 78−26721
$RbAg_4I_5$, solid electrolyte, neutron scattering study 78−79696
$RbAg_4I_5$, solid electrolyte, thermodynamics and electrochem. behaviour of I_2 electrode 79−70348
$RbAg_4I_5$, solid electrolyte, Raman spectra 79−73934
$RbAg_4I_5$ solid electrolyte, interface with metal, photocurrent obs. on illumination 80−34513
$RbAg_4I_5$, solid electrolyte, contrib. of non-Brownian motion to transport props. 80−70453
$RbAg_4I_5$, solid electrolyte development, Ag^+ cond. 80−107532
$RbAg_4I_5$, static and dynamic NMR effects at 208K and 122K phase transitions 80−108105
$RbAg_4I_5$, struct. transition at 209K, Ising like behaviour 78−14460
$RbAg_4I_5$, superionic conductor, absence of Hall effect for Ag ions 77−31805
$RbAg_4I_5$, superionic conductor, evidence for first-order phase transition 78−83949
$RbAg_4I_5$, superionic conductor, phase transition detection by thermoelectric power method 80−92669
$RbAg_4I_5$ superionic films, elec. cond. and optical absorpt. studies 79−99355
$RbAg_4I_5$, superionic phase transition, dynamical and crit. pt. props. 80−107535
$RbAg_4I_5$, US absorpt., ionic cond., relaxing sp. ht. 78−14505
$RbAg_4I_5$, US attenuation near 208K phase transition 79−33085
$RbAg_4I_5$:AgI,Rb_2AgI_3, polycryst., ionic cond., impurity conc. effects 78−51734
$RbAg_4I_5$-metal interface, photocurrents, photoelectrochem. effects 78−34897
$RbBiF_4$, fast ionic conduction of F^- ions 79−99360
RbCl-CuCl, AC cond. and phase relations meas. 77−72713
$RbCu_4Cl_3I_2$, development of Cu^+ ion cond. 80−107532
α-$RbCu_4Cl_3I_2$, solid electrolyte, cryst. struct. and anal. 79−82382
$Rb_4Cu_{16}I_7Cl_{13}$ in CuCl-CuI-RbCl system, high Cu ion cond. solid electrolyte, elec. props. and powder X-ray diffr. anal. 80−15295
$Sb_2O_5.nH_2O$, crystalline, ^1H NMR study of proton transport 80−60446
SmF_3, ^{19}F spin-lattice relax. and mag. couplings 79−65753
$SrCl_2$, anion disorder at high temps., neutron diffr. obs. 80−59614
$SrCl_2$, anion motion at high temps., quasielastic nuetron scatt. obs. 80−59715
$SrCl_2$, fast ion cond., specific heat anomaly, mol. dynamics study 80−65283
$SrCl_2$, high temp. powder neutron diffr., transition to highly conducting phase 78−47586
$SrCl_2$, ionic cond., self-diffusion, rel. to defect motion, mol. dynamics study 80−65282
$SrCl_2$, sp. ht. meas., Schottky-type diffuse phase transitions, defect form. energies and entropies 80−107441
$SrCl_2$, superionic, electrical conductivity at high temp. 78−79798
$SrCl_2$, superionic, quasielastic neutron scatt. 78−79504
$SrCl_2$:R, R=rare earth, dopant effect on superionic state transition 79−60547
$SrF_2(Cl_2)$, theoretical investigation of Raman scatt. 78−80351
ThO_2, ionic conduction, doping effects and defect interactions 80−19978
ThO_2:Ce^{3+}(Ce^{4+}), mixed ionic and electronic transport 80−107875
ThO_2:Y_2O_3, electrochem. cell, complex impedance, temp. and freq. depends. 77−1458
$TlBiF_4$, fast ionic conduction of F^- ions 79−99360
α-$TlBiF_4$, new solid electrolytes, conductivities and activation energies 79−28137
Tl_4CdI_6, fast ionic cond. 79−99363
β-Tl_2O-Al_2O_3, cation distrib. 77−80487
$Tl_2ZnBr_4(I_4)$, fast ionic cond. and order-disorder transition 79−99363
$Tl_2ZnBr_4(I_4)$, solid electrolytes, ion transport mechanism and polarisability role, comparison with Cu^+ and Ag^+ cond. 80−107531
ZrF_4 based glass, elec. and dielec. props. in freq. and temp. ranges 5-500 kHz and 130-280°C *(French)* 79−23772

superionic conducting materials continued
ZrF_4-BaF_2-$ThF_4(LaF_3)(NdF_3)(PrF_3)$, F^- ion cond. glasses, cond. process 80−107477
$Zr(HPO_4)_2.H_2O$, Na^+ transport, gas-solid and solid-solid reaction kinetics 80−61086
ZrO_2 based solid electrolyte, use for study of O_2 solubility and diffusivity in liq. metals 80−59669
ZrO_2, CaO stabilised, exam. of O_2 permeability and p-type electronic cond. 79−10980
ZrO_2, cell electrolysis of H_2O at 800° to 1000°C *(French)* 80−26024
ZrO_2, doped, ionic cond., theoretical model 80−107552
ZrO_2 solid electrolyte, electrochem. reduced, electrocatalytic decomp. of NO 80−61113
ZrO_2:Cu, point defects, electrochem. characterisation 80−35599
ZrO_2:Y_2O_3, solid electrolytes, charge carrier conc. and diffusion 77−11930
ZrO_2/Pt solid electrolyte/porous electrode system, interface polarisation effects 80−61114
ZrO_2-CaO, microstruct., ordering, elec. props. 77−15374
ZrO_2-CaO (12-19 mole%), AC elec. behaviour, 300-900°C, grain size, electrode material, and sintering effects 78−34649
ZrO_2-CaO RF sputtered film, solid electrolyte, comp., struct. and AC cond. 77−39741
ZrO_2-CaO(Y_2O_3), fluorite related ordered compounds, prep. struct. 77−68958
ZrO_2-Y_2O_3, Faradaic reaction kinetics, impedance dispersion anal., electrode/electrolyte interface process 79−11798
ZrO_2-Y_2O_3, solid electrolyte, cond. maximum 78−47577
ZrO_2-Y_2O_3, solid solns., density meas. rel. to O vacancy model 78−2113
ZrO_2-Y_2O_3 film, surface characterisation, XPS, ESCA, and AES expts. 78−72028
ZrO_2-Y_2O_3 superionic cond. cell, complex impedance 80−10702
ZrO_2-Y_2O_3/Pt interface, electrode kinetics, complex impedance dispersion anal. 79−96325

superlattices
adsorbed layers, general principles of construction of structural models 80−84351
alloy, stabilisation of long-period superlattices 79−95348
alloy, theory of ordering, crystal lattice parameters rel. to composition and order *(Russian)* 79−77543
alloys, substitutional disorder description within supercell model 78−26479
antiferromagnet, Ising model, crit. props., calc. 80−65946
bonding, superlattices and diffr. 79−19535
γ-brass, inversion antiphase domain boundaries, superlattice diffr. spots 78−6071
γ- brass type alloys, superstructures and defect obs. 80−107284
Bravais-lattice operator in one band of solid 80−10519
bulk superconductor, nonequilibrium and superlattice effects, US attenuation meas. 79−56390
chloranil, neutron superlattice reflection, soft phonon and central peak scatt., phase transition 78−18732
copper formate tetrahydrate, short-range order, diffuse neutron scatt. 78−15124
cubic lattices, ordered dispersal of point defects, appl. to fluorite related structs. 77−47447
defect superlattices, hardening influence, computer simulation *(Russian)* 79−83206
derivative lattices, determ. of relationships 80−107012
p-dibromo-tetrafluorobenzene mol. cryst., in commensurate phase, quasielastic neutron scatt. 80−107386
electron gas statistical and thermodynamic props. *(Russian)* 79−87051
electronic band struct. in mag. fields 79−65355
FCC lattices, ordered superstruct., phase diagrams, cluster variation calc. 80−39256
ferroelectric substances, electron microscopy investigations, review *(Japanese)* 80−71366
graphite intercalation compound $C_{24}K$, order-disorder transition, X-ray study 80−33922
graphite intercalation compounds, low energy optical transitions, refl. spectra and X-ray diffr. 80−25371
graphite-AsF_5 intercalation compounds, de Haas-van Alphen effect, charge transfer rate 80−54595
group VIII and nearly related elements, cmpd. and superlattice form. 79−94955
heterojunction superlattice, energy spectrum 78−6259
heterojunction superlattices, Green's function of electron in periodic field 80−49857
HF characteristics at low temps., multiphoton absorpt., tunnelling *(Russian)* 78−68073
hypersound amplification by a quantizing electric field 80−6915
III-V compounds and alloys, MBE process and problem areas, review 80−10815
III-V semiconductor *(Slovak)* 80−88620
image potential enhancement by static elec. field 80−92846
inhomogeneous semiconductor structures, instability of plasma oscills. 79−11167
jamesonite, cryst. struct., superlattice variations, order-disorder struct. 79−86770
lattice image calculations for imperfect crysts., superlattice approach 80−107030
layer structures, intercalation with N_2H_4, charge density waves or artefacts 80−100221
magnetic semiconductor, conduction electron spectrum, influence of nonlinear spin waves 79−28270
MBE production of superlattices and barrier structures *(Chinese)* 79−46986
metal, one- and two-dimens., periodic lattice distortion and CDWs 79−60678
modulated structures, conference, Kailua Kona, Hawaii, USA (March 1979) 79−94928
modulated structures, review 79−94929
MOSFET structure, artificial superlattice near carriers 78−64130
multilayer stacks, very thin nonideal, wavelength variation of transmissivity, refl. 80−100701
narrow band gap semiconductor, high elec. field conduction in space and time superlattices 80−49756
nonlinear plasma oscillations in high freq. elec. field 79−19612
nonstoichiometric compounds, intermediate phase 79−65013

superlattices continued
4-n-octyloxybenzoyloxy-4'-cyanostilbene, re-entrant polymorphism, nematic-smectic A-nematic-smectic A, X-ray study 80−34172
one-dimensional, band structure instability under strong population inversion 77−43470
one-dimensional periodic medium, nonlinear optical props. 77−50728
one-dimensional superlattices, electronic density of states 80−75488
ordered superlattices, X-ray studies, rel. to microstructure 79−94844
pair correlation splitting in phases with long range order 79−15109
partial Patterson function, use for superlattice reflection phase determ. 80−79627
perturbed crystals in Kg representation, orthonormal localised states 78−6327
piezoelectric semiconductor layers, periodic pot. 78−19142
plasma oscillations 77−72878
plasma oscillations under strong high freq. elec. field 80−10904
plasmons, two-dimens., due to piezoelec. effect 80−92845
polymeric series of coverings, symmetry, comparison with layers of real structs., Belov subclass development 80−84129
rare earth oxide film, short-range order to long-range order transition 78−10288
semiconductor, cond.-valence band interactions, subband struct. 77−72815
semiconductor, electron temperature superlattice, nonlinear theory *(Russian)* 79−78112
semiconductor, electronic props. 79−95490
semiconductor, electroplasmon parametric resonance 80−34475
semiconductor, EM field nonlinear penetration, self-induced transparency 78−25930
semiconductor, odd photomagnetoresistance effect 79−95425
semiconductor, optical props. with electron temp. superlattice *(Russian)* 80−34879
semiconductor, plasma oscills. in strong elec. field 80−44637
semiconductor, size quantised, superlattice state 78−39142
semiconductor, soliton propagation 78−72162
semiconductor, superlattice doping, electronic states, elec. props. 79−95480
semiconductor, temperature superlattice with hot electrons 80−20202
semiconductor, with hot electrons, temp. superlattice, transport props. effects *(Russian)* 78−34839
semiconductor, with superlattice, heating photocond. 79−19622
semiconductor, with superlattice, magneto-oscillatory effects 77−85132
semiconductor, with superlattice, plasma resonant interaction with Stark oscills. 80−107842
semiconductor multilayer heterojunction struct., impurity and phonon scatt. 80−2456
semiconductor superlattice, geometrical and physical props. of constant-energy surface 77−69213
semiconductor superlattice, phonon spectrum, effect of strong elec. field, parametric reson. 80−44273
semiconductor superlattice, transverse electron effective mass 80−100429
semiconductor superlattice microwave/infrared detectors 80−13138
semiconductor superlattices, optical and transport props., review *(Slovak)* 80−20288
semiconductor surface excitonic wave-phonon coupling 77−15775
semiconductor thin films, fabrication for device appls. 80−100418
semiconductor with sumperlattice, optoelectric effect, theory 80−70768
semiconductor with superlattice, Coulomb screening 78−14684
semiconductor with superlattice, EM wave absorpt. by free carriers, high freq. quantum transport eqn. 78−60148
semiconductor with superlattice, EM wave propag., mag. field effect 80−70745
semiconductor with superlattice, Hall effect 80−39612
semiconductor with superlattice, high freq. cond. 79−69542
semiconductor with superlattice, impurity photocond., electron spectrum reconstruction 80−24966
semiconductor with superlattice, nonlinear EM wave amplification 77−88835
semiconductor with superlattice, nonlinear interaction of two waves 78−10494
semiconductor with superlattice, nonlinear plasma oscills. 78−26897
semiconductor with superlattice, optical absorpt. by impurities 79−69867
semiconductor with superlattice, optical phonon excitation by light absorpt., impurity photoionisation 80−44275
semiconductor with superlattice, phonon spectrum, electron-phonon interaction effects 77−47528
semiconductor with superlattice, two-photon absorpt. 77−16331
semiconductor-dielec., high freq. electromagnetic, response 78−19073
semiconductors, absolute negative resist. *(Russian)* 78−34838
semiconductors, cond. in strong elec. fields 77−55539
semiconductors, EM wave absorption in quantising electric field 80−108182
semiconductors, EM wave interaction in weakly nonlinear medium with superlattice 80−93257
semiconductors, narrow band gap, superlattices, acoustic wave absorpt. and amplification 80−29445
semiconductors, third harmonic generation *(Russian)* 77−27315
semiconductors with negative differential conductance, surface EM wave excitation, helicon and Alfven waves 79−69543
semiconductors with superlattices, Stark-cyclotron resonance, Larmour freq. *(Russian)* 80−60421
semiconductors with superstructure, weakly bound states of elementary excitations 79−60733
single crystal surface, electrochemistry, surface struct., superlattice struct. 80−76519
solid surface, physics, review *(Japanese)* 78−79870
spinodal decomposition of vacancies, void lattice formation 79−10845
sputtered film, ion-bombardment-enhanced diffusion during growth 78−87882
stearic acid-based, layer periodic structure, prep. and optical props. 77−69199
superconducting superstructures, condensate band spectrum and current carrying states anal. *(Russian)* 80−39706
TCNQ salt, $(TMA^+)_3(I_3^-)(TCNQ^-)_2(TCNQ^0)$, struct., phys. props. and lattice distortion evidence 78−6305
ternary alloys, AB-AC quasi-binary sections of order-disorder phase diagram 78−88463
tetramethylammonium tetrachlorozincate, low temp. phases, superstruct., X-ray study 80−39065
transition metal dichalcogenides, periodic lattice distortions, charge density waves 79−82536

superlattices continued
transition metal layered compound, excitonic wave-phonon coupling 77−15775
$TTF_{0.97}Se_{0.03}$-TCNQ, Peierls-superlattices and soft phonon anomalies, X-ray scatt. meas. 78−75795
TTF-SCN, quasi one-dimens. conductor, CDW phase transform., X-ray scatt. study 80−24594
TTF-TCNQ, Peierls-superlattices and soft phonon anomalies, X-ray scatt. meas. 78−75795
TTF-TCNQ, periodic lattice distortions, charge density waves 79−82536
TTF-TCNQ, phonon anomalies and superstructures, Peierls transition, X-ray diffuse scatt. obs. 77−27962
TTF-TCNQ, theory of structural phase transitions 78−38831
two dimensional superlattice of misfit dislocations, possibility of X-ray and electron diffr. struct. determ. 80−54560
two-dimensional system, electronic props., conf. Berchtesgaden, Germany (Sept., 1977) 78−60177
Ag_xTiS_2, intercalation cpd., Raman scatt. and electron diffr. meas. 79−24321
AgZn-AgMg quasibinary alloy, phase relation and superlattice form. 78−3097
AlAs-GaAs (001) interface and superlattice, electronic props., band struct. 79−95485
AlAs-GaAs (100) superlattices, band struct. 78−30868
$Al_4(Ni, Co)_3$ ternary phase in Al-Ni-Co system, cryst. struct., vacancy controlled phase *(Chinese)* 80−70164
β''-Al_2O_3-$H_3O^+(Na_2O)$, struct. basis for superionic cond. 80−107498
β-Al_2O_3-M_2O,`M=Ag, K, Rb, Na, Eu, X-ray diffuse scatt. 78−71725
Au-Cu-Ag dental alloy, age-hardened, struct. and morphology 78−92272
Au-Cu-Ag-Pd (35.4, 17.8, 9.7 at.%), dental alloy, age-hardenable, TEM obs. 77−21156
Au_3Cd, sputtered epitaxial films, order-disorder reaction obs. 78−84092
Au_5Mn_2, monoclinic, ordering, high resolution electron microscopy 79−43290
Au_4V, effect of structural changes on phys. props. 78−31400
Ba_2XRuO_6(X=La,Eu), ^{99}Ru Mossbauer spectra and other techniques 80−29659
Ca Mg $(CO_3)_2$ (dolomite), modulated struct. 79−100832
CaF_2, anion-void superlattices *(Danish)* 79−14796
CaF_2, fluorite, electron irrad., {100} faceted anion voids 79−51153
Ca_2XRuO_6 (X=Y,La,Eu), ^{99}Ru Mossbauer spectra and other techniques 80−29659
CdTe/HgTe superlattice, new IR material 79−72634
CdTe-HgTe ideal superlattice, electronic props. calc. 80−49885
CdTe-HgTe superlattice on CdTE layers, evanescent states, tight binding calcs. 80−70611
CdTe-PbTe(InSb) superlattices, laser deposition of multilayer heteroepitaxial structs. 80−44450
Co-V alloy system, Co rich, low temp. phase, electron microscopy 77−84766
Co_xZrS_2, ($0<x\leq0.50$), intercalation compounds, ordered phases obs. 80−33962
$Co_{0.83}[Pt(C_2O_4)_2].6H_2O$, quasi-one-dimens. conductor, Peierls distortion and superlattice, X-ray study 80−29397
$Cs(B_xW_{3-x})O_9$ (B=Na, Ca, Co, Ni, Cd, Ga, Bi, Nb, Ta) cryst. struct., temp. dielec. anomalies 80−1998
CsCl-type lattice, (111) superlattice screw dislocation motion, computer simulation 80−79793
$Cs_{1.75}[Pt(CN)_4].xH_2O$, one-dimensional, X-ray diffuse scatt. meas. 77−19937
Cu, He gas-bubble superlattice form. 80−2086
α-Cu-Al, short range ordered, struct. and new superlattice phase 78−52756
Cu-Al alloy, ordered, superlattice fringe images, computer simulation 80−103296
Cu-Au off-stoichiometric alloys, long period superlattice 79−55699
Cu-Au system, two-phase mixtures, long-period superlattices 80−84140
Cu-Ni-Al (5, 2.5 at.%), precip. hardening *(Japanese)* 80−71663
Cu-Ni-Sn (10, 6 wt.%), spinodal decomposition, X-ray and electron diffr. study 80−81063
Cu-Pd, mag. susceptibility and electronic struct. of ordering *(Russian)* 80−11161
Cu-Sn alloy system, long period superlattice obs. and impurity effects 80−103297
Cu-Zn-Al Marmem alloy, β_1 phase superstruct. obs., rel. to transform. mode 78−39776
CuAu, mag. susceptibility and electronic struct. of ordering *(Russian)* 80−11161
Cu_3Au, alloys, superlattice-fringe imaging theory, images formed from two beams 80−79649
Cu_3Au, electrical resistivity and LRO, energy gap formation in Fermi surface 80−88533
Cu_3Au, mag. susceptibility and electronic struct. of ordering *(Russian)* 80−11161
Cu_3Au, neutron irrad., displacement cascades, direct obs. method 80−107335
Cu_3Au-$Cu_3Pd(Pt)$, quasibinary system, order-disorder transform., superlattice form. 80−2159
Cu_3Au-Ni, antiphase domains morphology 80−108460
$CuCrS_2$, domain struct. and superstructure, TEM obs. 80−79779
Cu_5FeS_4, bornite, superstructuring, vacancy clustering, high-resolution electron microscopy 78−42981
Cu_xMS_2, ($0<x\leq0.50$) (M=Zr, Hf), intercalation compounds, ordered phases obs. 80−33962
r-CuMn, annealing ordered phase study by neutron diffr. 80−89265
Cu_2NiZn, characterisation of superlattice dislocations by TEM 79−55748
Cu_2NiZn, separation of partials of superlattice dislocations, anisotropic elasticity theory, ordering 79−65082
Cu_2NiZn, superlattice dislocations 78−83816
Cu_3Pt, antiphase domains morphology 80−108460
Cu_9S_5, digenite, superstructuring, vacancy clustering, high-resolution electron microscopy 78−42981
EuTe, exchange and superlattice band splittings, magneto-optical meas. in high mag. fields 79−61342
Fe-Al alloy, antiphase boundary energies 77−36460
Fe-Al alloy, ordered, superlattice fringe images, computer simulation 80−103296
Fe-Al alloys, pairwise interaction energy 77−36461
Fe-Co alloy, V addition effect on atomic order parameters, dislocation struct., mechanical props. 79−91762

superlattices continued
Fe-N (10 at.%), structural transforms., expt. investig. *(Russian)* 77−12613
Fe-Ni, ordered phase, Llo superstruct., Mossbauer spectrum, Debye-Scherrer pattern from LL-chondrite 80−50241
Fe-Ni (31 at.%), austenitic, ageing, absence of at. order 77−11502
FeAl, order parameter, atomic scattering factor, thickness fringes in electron micrographs 79−10832
Fe_3Al, alloys, superlattice-fringe imaging theory, images formed from two beams 80−79649
Fe_3Al, electrical resistivity and LRO, energy gap formation in Fermi surface 80−88533
γ-Fe_2O_3, small particles, vacancy sintering 77−65975
Fe_xZrS_2, ($0<x\leq0.50$), intercalation compounds, ordered phases obs. 80−33962
$Ga_{1-x}Al_xAs$, Shubnikov-de Haas oscillation, in semiconductor superlattice 77−62947
$Ga_{1-x}Al_xAs$ superlattices, multilayers, periodic and near-periodic, small-angle interferences of reflected X-rays 79−94846
GaAs, intrinsic surface gratings, low-angle X-ray diffr. obs. 77−85035
GaAs, periodic doping structure, nipi superlattices, HBE growth and charcts. 79−95484
GaAs, Shubnikov-de Haas oscillations in semiconductor superlattice 77−62947
GaAs-$Al_xGa_{1-x}As$, heterojunction and superlattice, magnetophonon reson., polaron mass 80−44715
GaAs-$Al_xGa_{1-x}As$ modulation-doped heterojunction superlattices, electron mobilities 79−7877
GaAs-$Al_xGa_{1-x}As$ superlattice, mag. field induced dimensionality change 78−64381
GaAs-$Al_xGa_{1-x}As$ superlattice, electronic props. 80−11080
GaAs-AlAs, one-dimensional superlattice, X-ray diffr. 77−27860
GaAs-AlAs alternating monolayers, zone folding effects on phonons 78−72510
GaAs-AlAs superlattice, folded acoustic phonons obs., Raman scatt. 80−88996
GaAs-AlGaAs heterojunction superlattices, electron mobilities 80−29473
GaAs-AlGaAs heterojunction superlattices, obs. of intersubband excitations in multilayer two dimensional electron gas 80−29753
GaAs-AlGaAs heterojunction superlattices, inelastic light scatt. by two-dimens. electron gas 80−93360
GaAs-AlGaAs superlattice, selective transmission of HF phonons 80−34154
GaAs-$Ga_{1-x}Al_xA$ heterostruct. superlattice, props. in high mag. fields 79−73570
GaAs-$Ga_{1-x}Al_xAl$ superlattice, reson. Raman scatt., 2-D quantum states 77−8577
GaAs-$Ga_{1-x}Al_xAs$, superlattice umklapp processes in resonant Raman scattering 78−64362
GaAs-$Ga_{1-x}Al_xAs$, semiconductor superlattices by MBE 79−95939
n-GaAs-$Ga_{1-x}Al_xAs$, superlattice, subband struct. and optical spectra, self-consistent calc. 80−15443
n-GaAs-$Ga_{1-x}Al_xAs$, heavily doped superlattice, electronic props., perpendicular low temp. mobility 80−65660
GaAs-$Ga_{1-x}Al_xAs$ heterostructures, quantum size effect in superlattices, electronic props. 80−29471
GaAs-$Ga_{1-x}Al_xAs$ superlattices, resonance enhanced Umklapp Raman process 78−39547
GaAs-$Ga_{1-x}Al_xAs$ superlattice, sub-band dimensionality 78−63981
GaAs-$Ga_{1-x}Al_xAs$ superlattice, Raman scatt., polar phonon anisotropy 80−45052
GaAs-$Ga_xAl_{1-x}As$ superlattice, photoconductor with high sensitivity and reduced dark current appl. 79−7881
GaAs-GaAlAs, subband related anisotropy in negative magnetoresistivity 80−11082
GaAs-GaAlAs superlattices, metalorganic VPE growth, in sites ellipsometry monitoring 80−70547
$(GaAs)_n(AlAs)_m$ multilayers, MBE, interdiffusion, X-ray diffr. study 80−70474
$GaP_{0.1}As_{0.9}$, gas-transport condensate with superlattice, structural and chemical inhomogeneity 77−85088
GaP_xAs_{1-x} ($0\leq x\leq0.32$) epitaxial film, one-dimens. superlattice, X-ray spectrometer scanning, struct. variations 78−47681
GaP_xAs_{1-x}-GaAs one dimens. superlattice, possibility of X-ray and electron diffr. struct. determ. 80−54560
Ge, (111) surface, clean, double diffr. spots in RHEED patterns 79−90855
Ge-$Ga_{1-x}Al_xAs$, MBE of ultra thin film superlattices on GaAs substrates, TEM study 79−37932
Ge-GaAs superlattice and interface, electronic struct. 78−52065
Ge(111) surface, Sn monolayer, induced 7×7 superlattice struct., RHEED obs. 78−91521
^4He, on graphite, ground-state energy, variational calc. 80−24710
InAs/GaSb (001) superlattices, electronic struct., two dimensional effects 80−11064
InAs-GaSb, semiconductor-semimetal transition obs. 80−44710
InAs-GaSb (001) superlattice, electronic struct., tight binding calc. 78−95350
InAs-GaSb (001) superlattices, two-dimens. effects and effective masses 80−49883
InAs-GaSb (100) superlattice, electronic struct., self-consistent pseudopot. method 80−49884
InAs-GaSb heterostruct. superlattice, props. in high mag. fields 79−73570
InAs-GaSb superlattice energy struct. and semiconductor-semimetal transition 79−23893
InAs-GaSb superlattice, cyclotron resonance, energy level quantisation 79−73430
InAs-GaSb superlattice, electronic struct., self-consistent pseudopot. calc. 80−29470
InAs-GaSb superlattices, crystallography, Rutherford backscatt. and channelling obs. 80−49533
InAs-GaSb superlattices, semicond.-semimental transition obs. 80−49882
InAs-GaSb superlattices, mag. field induced semimetal-semicond. transition 80−65656
$In_{1-x}Ga_xAs$-$GaSb_{1-y}As_y$ superlattice, optical absorption 79−19887
$In_{1-x}Ga_xAs$-$GaSb_{1-y}As_y$, semiconductor superlattices by MBE 79−95939
$In_{1-x}Ga_xAs$-$GaSb_{1-y}As_y$, electronic subband struct. 77−72815
$In_{1-x}Ga_xAs$-$GaSb_{1-y}As_y$, new heterostruct. characts. 78−72247
$In_{1-x}Ga_xAs$-$GaSb_{1-y}As_y$ superlattice, with nonlinear energy-wave and energy-momentum relationships 79−7871
superlattices continued
InSb/GaSb superlattice thin films, sputtered, ion-bombardment-enhanced diffusion during growth 78−87882
InSb-CdTe(PbTe) superlattices, laser deposition of multilayer heteroepitaxial structs. 80−44450
InSb-GaSb, compositionally modulated sputtered superlattice, growth and interlayer diffusion 79−56930
InSb-GaSb superlattice, interlayer diffusion 77−85086
K, vacancy superlattice 77−7713
$K(B_xW_{3-x})O_9$ (B=Na, Ca, Co, Ni, Cd, Ga, Bi, Nb, Ta) cryst. struct., temp. dielec. anomalies 80−1998
KC_{24}, press. induced staging transition 80−79938
KCN, cryst., struct., phase transition, 6-300K, neutron diffr. obs. 77−76347
K_xVF_3 (x=0.45 to 0.56), non-stoichiometric, struct. depend. on composition 79−99152
$K_{1.75}[Pt(CN_4)].xH_2O$, one-dimensional, X-ray diffuse scatt. meas. 77−19937
Kr, monolayer on graphite, commensurate-incommensurate transition, X-ray scatt. 79−73382
LaF_3 single cryst., electron diffr., superlattice struct. 78−42993
β-$LiAlSiO_4$, eucryptite, one-dimensional ionic conductor, neutron scatt. study 80−49361
$Li_{0.5}Fe_{2.5}O_4$, ht. treatment conditions effect on superlattice formation 77−84922
Li_xTiS_2, intercalation cpd., Li ordering, electrochem. obs. 78−59795
$Li_{0.44}Zn_{0.09}Fe_{2.47}O_4$, ordering, elect. of V_2O_5 additions 77−35532
$Mn_{0.25}NbS_2$, mag. anomaly rel. to struct. disordering 78−43557
$MoSe_2$ and other layer structs. containing hohlstellen, electron diffr. 77−80397
$MoSe_2$, TEM exam. 77−35548
$(NH_4)_2BeF_4$, paraelec. and ferroelec. phases, X-ray diffuse scatt. and superlattice struct. *(Japanese)* 77−43189
Na, vacancy superlattice 77−7713
Na-zeolite, matrix, Te cluster superlattices, N and S type volt-ampere characts., elec. cond. *(Russian)* 80−70665
NaCN, cryst., struct., phase transition, 6-300K, neutron diffr. obs. 77−76347
$Na_xTi_4O_8$ bronze, hydrothermal prep., Na ion arrangement 80−75209
NaX-Se semiconductor superlattice absorpt. edge, light scatt. *(Russian)* 80−71438
Nb/Cu layered ultrathin coherent struct. 80−80122
Nb-Zr, acoustic phonon anomalies and superstructure, neutron inelastic scatt. meas. 80−19892
Nb_3Ge superconducting film, tunnelling obs., electron and X-ray diffr. obs. 77−32123
NbS_2-$(pyridine)_{1/2}$ intercalation complex, superlattice struct., NMR meas. 80−70180
$NbSe_2$ (2H), charge density wave transitions, neutron diffr. exam. 77−89515
$NbSe_3$ and related cpds. bands, bonds and charge density waves 79−95327
$NbSe_3$, CDW form., direct electron diffr. 78−30877
$NbSe_3$, quasi one-dimens. conductor, CDW phase transform., X-ray scatt. study 80−24594
$NbSe_3$, satellite electron diffr. below 59K, Fermi surface features 78−84136
$NbSe_2$(2H) microscopic theory of charge density wave instability 78−79732
Ni, He gas-bubble superlattice form. 80−2086
Ni-Cr film, long range order 79−60657
Ni-Cr-type alloys, theory of ordering, superstruct. form. *(Russian)* 77−81256
$Ni_{1-x}Al$ solid solution, vacancy ordering exam. by electron diffr. after annealing 78−3123
Ni_3Al based alloys, mean square atomic displacements 79−28053
Ni_3Al, Mossbauer spectra, exam. of struct., superlattice population anal. 78−88240
Ni_2Cr ordered alloy, mech. twinning *(French)* 77−72624
Ni_3Fe, superlattice dislocations, compression induced mag. anisotropy 77−85442
Ni_3Fe, superlattice dislocations, compression induced mag. anisotropy 77−85443
Ni_3Ga, with $L1_2$ struct., dissociated struct. of superlattice dislocations 79−37706
$Ni_{3\pm x}Te$, two-layer system, diffr. features 79−82187
Ni_xZrS_2, ($0<x\leq0.50$), intercalation compounds, ordered phases obs. 80−33962
PbI_2 intercalated with organic mols., superlattice and quantum dimens. effect *(Russian)* 79−46628
$Pb_xNb_yO_6$ pyrochlore phases, three odd superstructures *(French)* 77−68946
PbTe-CdTe(InSb) superlattices, laser deposition of multilayer heteroepitaxial structs. 80−44450
γIPdD, refl. struct. determ. by neutron diffr. 79−7593
$PdD_{0.73}$, (1, 1/2, 0)-superlattice reflection splitting near 50K, neutron diffr. studies 80−70168
β-PdD_x, (1, 1/2, 0) superlattice reflection, neutron diffr. exam. 79−65038
Pd_3Fe, X-ray and electron microscope obs. of antiphase domains and superdislocations *(Russian)* 77−86017
Pt (111) and (100) superlattices formed by dissociative adsorption of HI, LEED, AES, and thermal desorption studies 80−55715
Pt complex, $(C(NH_2)_3)_2Pt(CN)_4Br_{0.23}.H_2O$, pseudo-one-dimens. cpd., solitary wave excitations, and cryst. struct. 78−6307
Pt complex, $[C(NH_2)_3]_2[Pt(CV)_4]Br_{0.23}.H_2O$, one-dimensional, X-ray diffuse scatt. meas. 77−19937
Pt complex, KCP, periodic lattice distortions, charge density waves 79−82536
$Rb(B_xW_{3-x})O_9$ (B=Na, Ca, Co, Ni, Cd, Ga, Bi, Nb, Ta) cryst. struct., temp. dielec. anomalies 80−1998
$RbCaF_3$, structural phase transition, superlattice points, neutron diffr. obs. 80−19944
$RbH_3(SeO_3)_2$, order parameter 77−66460
Rb_xVF_3, non-stoichiometric, struct. depend. on composition 79−99152
$Rb_{1.75}[Pt(CN)_4].xH_2O$, one-dimensional, X-ray diffuse scatt. meas. 77−19937
$(SN)_x$, halogenated, struct. behaviour, TEM obs. 80−70126
Sb_2Tl_7, single-cryst. struct., X-ray diffr. determ. 77−65963
Si, (001), clean, double diffr. spots in RHEED patterns 79−90855
Si (111) 7×7 surface structure investigation, RHEED 80−96723

superlattices continued
Si (111) surface structure induced by Ag evaporation, RHEED meas. 78−22942
Si, high index surface, natural orientational superlattice in 2D electron gas 79−99598
Si, influence of one-dimensional superlattice on two-dimensional electron gas 77−43683
Si, periodic stepped structure, on vicinal planes, LEED obs. 80−24725
Si, superlattice and 2-D electron gas 78−64080
Si, two-dimensional electrons in superlattice, HF cond. 78−64055
Si-SiO_x interface, evidence for superlattices, magnetocond. expts. 77−89868
SiC (1 OH), phonon spectrum, dispersion curves energy discontinuity and vibr. modes, IR spectra obs. 80−44274
SiC (6H), semicond. with one-dimens. electron superlattice, interband optical absorpt. 79−15483
SiC crystal, energy band struct. and optical spectra 78−18962
SiGe, ultra high vacuum epitaxy on Si substrates *(German)* 77−47702
Si(110), clean surface structural transitions, LEED obs. 78−6203
Si(111) reconstructed 7×7 surface superlattices, microdomain model 80−107625
$Sr_2Ta_2O_7$, structural phase transition to superlattice, electron microscopy and diffraction study 80−39277
$SrTiO_{3-x}$, anion deficiency and anion vacancy ordering 78−51532
$SrTiO_{3-x}$, superlattices in anion-deficient compound 78−22708
Sr_2YRuO_6, ^{99}Ru Mossbauer spectra and other techniques 80−29659
T 79−8885
Ta_2H, ordered, distortion-induced superstruct. modulation, from X-ray scatt. 80−49186
TaS_2, 1T polytype, intercalated with Li(Na)(K)(Eu), CDW's and superlattice patterns 77−47746
TaS_2, polytypes, charge density waves and superlattice effects, intercalation with hydrazine 78−39043
TaS_3, Peierls superstruct., low temp. X-ray diffr. obs. 78−59793
$TaSe_2$ (2H), CDW and accompanying periodic structural distortions 78−72094
$TaSe_2$ (2H), charge density wave transitions, neutron diffr. exam. 77−89515
$TaSe_2$ (2H), optical absorpt., band struct., plasmons, and CDW 80−45104
2H-$TaSe_2$, commensurate superlattice vibr., Raman spectra 77−16299
$Ta_{1-x}Zr_xSe_2$ (1T), CDW stacking order, interlayer interactions and impurity effects 77−7699
$Ti_{1-x}Hf_xSe_2$ mixed cryst., elec. resist. and phase transition temp. 80−24928
$TiO_{1.95}iFe$, quenched near melting point, transverse composition waves 79−99220
$TiSe_2$ (1T), electronic and vibronic struct. 80−44500
$TiSe_2$ (1T), phonons and CDWs, inelastic neutron scatt. meas. 79−28059
$TiSe_2$, mechanism for 200K transition, sp. ht. meas. 78−22853
$TiSe_2$, semimetal, electronic props., superlattice form. 77−15532
$TiSe_2$, structural distortion, band Jahn-Teller type mechanism 77−62875
$TiSe_2$, superlattice formation, Raman and far IR spectra 78−35135
$Ti_{1+x}Se_2$, superlattice form., phase transform., electron and X-ray diffr. meas. 77−15383
$Ti_{1+x}Se_2$, superlattice form. and phase transition, IR reflectivity meas. 79−24322
$Ti_{1-x}V_xSe_2$ ($0 \leq x \leq 0.1$), elec. resist. and Hall effect 80−2386
Ti_xVF_3, non-stoichiometric, struct. depend. on composition 79−99152
UO_2, antiferromag. new type mag. domains *(Russian)* 77−59430
V_2D, BCC α-phase, metal atom-induced diffuse X-ray scatt. from short range order 79−60358
V_2D, ordered, distortion-induced superstruct. modulation, from X-ray scatt. 80−49186
VO_x, struct., model based on O vacancy superlattice 77−84707
Zr_3Al, deformed and irrad., lattice defects obs., superlattice dislocations and defect clusters 80−107261

supernova remnants
1181 optical remnant assoc. with 3C 58 discovered 78−65678
acceleration of high-vel. clouds 78−20877
adiabatic phase, thermal X-ray spectra 80−82475
blast model, parameters from X-ray data and SNRs of known age *(Chinese)* 80−77471
blast wave instabilities, adiabatic and isothermal models 80−67814
blast waves, propag. rel. to interstellar medium mechanical heating 80−36682
blast waves, propagation rel. to hot interstellar medium filling factor 80−17634
blast-wave, two-fluid model 79−80345
Brahe's SN 1572, location from original obs. rel. to remnant 78−12256
3C 391, obs. at 1.4 and 10.7 GHz 80−4417
3C 58, comparison of optical and radio emission of plerion 80−73023
3C 58, soft X-ray flux upper limits 80−56915
3C 58, spectra of faint knots 78−93375
3C 58 (SN 1181), plerionic supernova remnant, supernova absolute magnitude and type classification 80−56862
candidates, spectroscopic survey in 6000-6800 Å region 77−60815
η Carinae, evidence for circumstellar disc and asymmetric explosion *(Italian)* 79−53893
Cassiopeia, A, weak X-ray source, ANS meas. 80−46701
Cassiopeia A, 38 MHz flux density meas. 78−12344
Cassiopeia A, 90 GHz map of young SNR 79−2561
Cassiopeia A, 927 MHz emission secular decrease 79−75255
Cassiopeia A, ^{14}N radioemission at 26 MHz 80−41886
Cassiopeia A, absolute radio spectrum 78−8090
Cassiopeia A, anal. of motion of details in thin shell model *(Russian)* 80−56920
Cassiopeia A, CO emission obs. 78−8071
Cassiopeia A, continuous particle injection model for radio flux var. 77−13426
Cassiopeia A, evidence for illumination by binary neutron star 77−33615
Cassiopeia A, explanation of secular flattening of radio spectrum 80−101637
Cassiopeia A, flux density meas. and confirmation of 38 MHz anomaly 77−45531
Cassiopeia A, foreground interstellar HCN absorpt. obs. 80−101624
Cassiopeia A, HF obs. using interference-excising correlator 79−75110
supernova remnants continued
Cassiopeia A, high-resolution X-ray obs., struct., expansion phase, mass 80−26960
Cassiopeia A, identification as black hole 79−75244
Cassiopeia A, image tube spectrograms 78−16485
Cassiopeia A, intensity and polarisation at 9 mm wavelength 80−36732
Cassiopeia A, interpretation of spectra, massive presupernova star hypothesis 78−36652
Cassiopeia A, numerical model 80−12790
Cassiopeia A, progenitor, consistent evolutionary picture involving supergiant mass loss 78−36623
Cassiopeia A, proper motion obs., expansion centre determ. 77−22289
Cassiopeia A, proper motions and temporal flux changes of compact features 77−60818
Cassiopeia A, radio emission evolution, freq. dependence *(Russian)* 78−4387
Cassiopeia A, radio emission evolution 79−67074
Cassiopeia A, radio spectrum evolution 79−30104
Cassiopeia A, radio spectrum rel. to cosmic ray electrons spectrum and diffusion 79−53677
Cassiopeia A, relativistic electrons streaming at speeds above Alfven vel. 79−40068
Cassiopeia A, search for X-ray line emission 78−57607
Cassiopeia A, secular decrease in 927 MHz flux, radio flux density obs. 80−67840
Cassiopeia A, secular decrease in radio emission flux density at 437 and 510 MHz *(Russian)* 80−8702
Cassiopeia A, spectral intensity variations *(Russian)* 77−91661
Cassiopeia A, statistical particle accel. models 78−57606
Cassiopeia A, X-ray spectrum, line emission obs. 80−26961
Cassiopeia A, X-ray struct. 77−41401
Cassiopeia A, young SNR, radio emission evolution according to observational data 79−75256
Cassiopeia A direction, OH and formaldehyde absorpt. obs. 78−45381
Cassiopeia A historical records 80−77430
Cassiopeia A supernova remnant, abundance inhomogeneities 80−12797
Cassiopeiae A, historical records rel. to 3 Cassiopeiae 80−72792
Cassiopeiae A, mag. field origin 80−85989
catalogue of optical candidates in nearby galaxies 80−62037
chemical and isotope fractionation by grain size separates 80−67831
CL 4, H I absorption from compact radiosource 79−48944
compact remnants, positional coincidences with COS-B γ-ray sources 78−45435
compact sources in directions of SNRs, 2.8 and 3.7 cm obs. *(Italian)* 79−53925
conference, Erice, Italy (May 1978) *(Italian)* 79−53836
conference, Sydney, Australia, (April 1978) 79−75230
Copernicus UV interstellar lines obs. in direction of HD 50896 77−26036
coronal line emission obs. and shock-heated plasma temp. determ. 78−65676
coronal lines, RGO spectrograms *(Italian)* 79−53892
cosmic ray acceleration 80−82192
cosmic ray electrons, source spectrum rel. to diffusion model of propag. 79−53677
cosmic ray production, particles escape and adiabatic energy losses 79−16771
cosmic ray transport coeffs. 79−101033
cosmic rays, trapping by hydromag. waves in high β plasmas 80−17482
cosmic rays accel. in shock fronts rel. to synchrotron emission 78−32302
cosmic rays in dense shell 77−33599
Crab, age and distance determ., student exercise 78−12520
Crab, emission region size, electron transport and mag. field models 77−17650
Crab, emission-line spectra of condensations 79−35327
Crab, evidence for detect. of 1-10 MeV emission in 1971 August 77−45605
Crab, extended soft X-ray emission obs. 77−13438
Crab, high energy X-ray spectrum, OSO-8 obs. 78−12315
Crab, interplanetary scintillations of PSR 0531+21 at 74 MHz 78−36625
Crab, interstellar medium characts., soft X-ray and radio obs. reconciliation 78−12328
Crab, magneto-parametric instabilities, two-fluid model of interaction with pulsar EM waves 80−85851
Crab, near IR photometry and spectral index 80−8675
Crab, photoelectric spectrophotometry of filaments, abundances 78−41006
Crab, relativistic particles injection 78−36678
Crab, search for 1-20 MeV gamma rays, balloon-borne obs. 80−67912
Crab, search for 400 keV γ-ray line 78−12345
Crab, spectrograms of filaments, faint forbidden lines 78−45388
Crab, X-ray polarization, precision meas. without pulsar contamination 78−41086
Crab Nebula, 2695 MHz high-resolution maps *(Italian)* 79−53891
Crab Nebula, 2.7 GHz study with 3.7×10 arcsec ang. resolution 79−40248
Crab Nebula, anomalously low expansion vel. 77−53676
Crab Nebula, compact source flux density meas. by interferometer 80−62252
Crab Nebula, continuous particle injection model for radio flux var. 77−13426
Crab Nebula, disrupted the star in close binary containing neutron star, model 79−25696
Crab Nebula, emission line spectrum 80−22068
Crab Nebula, far IR emission, upper limit 79−58406
Crab Nebula, final SAS-2 gamma-ray results 77−33688
Crab Nebula, flux density at 1.8 mm *(Russian)* 78−32558
Crab Nebula, general props. of recent SNR 78−61912
Crab Nebula, imaging by balloon-borne X-ray telescope *(Japanese)* 79−80220
Crab Nebula, interstellar O edge in X-ray spectrum 79−67079
Crab Nebula, low-energy gamma-ray obs. 77−29894
Crab Nebula, lunar occultation obs. at 114 and 26.3 MHz, small-scale struct. 80−46627
Crab Nebula, lunar occultation obs. at decametre wavelengths 80−62248
Crab nebula, magnetoparametric instabilities theory 79−8829
Crab Nebula, millimetre and submillimetre meas. 79−75267
Crab Nebula, model 80−62230
Crab Nebula, obs. by gamma-ray telescope with modulating anticollimator *(Russian)* 79−16832

supernova remnants continued
Crab Nebula, parametric instabilities of commensurable and incommensurable nonlinear plasma waves 79−66915
Crab Nebula, parametric plasma instabilities 78−45220
Crab Nebula, physical theory rel. to optical and X-ray surface brightness 80−51834
Crab Nebula, polarimetry with OSO-8 X-ray polarimeter 78−12426
Crab nebula, polarised radioemission occultation by solar corona during weak solar activity *(Russian)* 78−77527
Crab Nebula, possible line feature at 73 keV, intensity and width 79−92829
Crab Nebula, prod. by explosion of R Coronae Borealis type star 79−5845
Crab Nebula, radiation origin through pulsar magnetosphere cyclotron instability *(Russian)* 80−8645
Crab Nebula, radio emission from compact source, HF meas. with URAN-1 interferometer 80−31343
Crab Nebula, remarkable spectra in outskirts of supernova remnant 78−36662
Crab Nebula, remnant, nature of EM field and radiating particles *(Russian)* 78−12351
Crab Nebula, search for coherent ELF radiation at pulsar freq., upper limit 79−16728
Crab Nebula, search for thermal X-ray line emission 78−8095
Crab Nebula, shock waves by hydrodynamics effects on filaments spectra 78−85997
Crab Nebula, short-wave millimetric obs. with wide-band radiometer 79−96916
Crab Nebula, small-scale polarisation obs. 79−25656
Crab Nebula, SN 1054 as probable Type II supernova 77−87522
Crab Nebula, struct. at 327 MHz from occultation obs. 78−12339
Crab Nebula, wisps, possible cosmic laser 77−87505
Crab Nebula, wisps struct. 79−25682
Crab Nebula, X-ray line emission, balloon-borne obs. 80−41884
Crab Nebula contrib. to dispersion measure of NP0532 pulsar 77−74122
Crab Nebula occultation by Moon, 1974, Sept., 180 and 1646 MHz obs. 77−26043
Crab Nebula plasma model and NP 0532 X-ray and gamma-ray radiation 80−41885
Crab Nebula radio struct. 79−75257
Crab Nebula search for gamma ray lines 78−8013
Crab Nebula wisps, reanal. of coherent radiation 79−35345
Crab Nebula-type objects 77−87524
Crab-like remnants, radio props. of plerions *(Italian)* 79−53888
Crab-type objects, plethoric SNRs 79−35338
Crab-type supernova remnants (plerions), probably short-lived objects 79−12504
CTA1, continuum obs. at 2695 MHz 79−62890
CTB 1, kinematics and evolution 80−67823
CTB 1, UHF emission and radio shell 80−77461
CTB 80, as possible remnant, optical emission and historical evidence 80−51853
CTB 80, peculiar supernova remnant, central radio source optical and H I obs. 80−56896
γ Cygni, ang. diameter from 1.4 GHz aperture synthesis obs. 78−4328
γ Cygni nebula, SNR gas collision with dense cloud 79−97055
in Cygnus, high vel. gas obs. *(Russian)* 79−21403
Cygnus Loop, abundances and filament shock vel., UV obs. 80−94848
Cygnus Loop, ANS X-ray obs. 80−82455
Cygnus Loop, CO emission obs. 78−8071
Cygnus Loop, far UV emission line spectrum, C depletion in interstellar medium 79−21398
Cygnus Loop, fast shock wave detection, optical spectra 80−82467
Cygnus Loop, high-rel. gas Hα emission origin 80−41873
Cygnus Loop, imaging X-ray obs., temp. struct. 80−41876
Cygnus Loop, ionization struct. 77−87525
Cygnus Loop, radial distrib. of Fe X and XIV forbidden line emission 80−51828
Cygnus loop, radial vels. 77−17666
Cygnus Loop, radio source Cl 4 optical identification and position 79−21453
Cygnus Loop, search for O VII X-ray line emission 78−93379
Cygnus Loop, soft X-ray image *(Italian)* 79−53895
Cygnus Loop, soft X-ray spectra emission line features obs. 80−94849
Cygnus Loop, supernova high vel. gas obs. and filaments spectra *(Russian)* 78−41028
Cygnus Loop, UHF emission and filamentary structure 80−77461
Cygnus Loop, UV spectra interpretation using radiating shock wave models 80−90498
Cygnus Loop, UV spectral obs. of bright filament 78−45387
Cygnus Loop, Voyager 2 UV spectrometer obs. 79−92816
Cygnus Loop, X-ray image 79−25663
Cygnus Loop, X-ray spectra var. with position 80−82472
Cygnus Loop, X-ray spectrum two component appearance interpretation 80−82475
Cygnus Loop forbidden Fe XIV emission radial distrib. 78−32545
Cygnus Loop H I distrib. rel. to high-vel. gas 79−71083
Cygnus region, new optical remnant discovery 78−4330
Cygnus X region, supernova remnant component of γ Cygni radio source 78−28809
Cygnus X-1, possible remnant of SN 1408, from Chinese historical records *(Chinese)* 79−80343
Cygnus X-ray superbubble, multiple supernovae 80−90575
in dense molecular clouds, struct. and IR emission 80−82450
density and energy 78−20868
discovery in southern sky 77−45518
30 Doradus nebula, supernova remnants contrib. to struct. 80−62226
early evolution in homogeneous medium, electron thermal cond. effects 77−78843
electron acceleration mechanism 80−85988
electron-ion equilib. and ionization nonequilib., X-ray evidence 80−41879
energetic particle trapping by Alfven wave instabilities 80−31205
estimates of physical parameters 77−13431
evolution, numerical model *(Italian)* 78−93383
evolution, Tycho SNR and CTB1 examples 77−87523
evolution of line intensity ratios in Galaxy and LMC 77−17656
expanding gas shells in Canis Major R1 and OB1 associations 78−93336
expanding shell assoc. with loop structures in Orion and Eridanus 79−53866
expansion characteristics in mol. cloud 80−94846
supernova remnants continued
extended 0.1-2.0 keV soft X-ray emitting regions 78−16581
filamentary structure, prod. by stellar wind from presupernova 80−62249
filamentary vels. in southern objects *(Italian)* 79−53889
G120.1+1.4, Tycho's SNR, rot. measure and turbulent struct. 79−88718
G126.2+1.6 near 4U 0115+63 X-ray transient 80−8668
G127.1+0.5, central source, optical obs. 79−17067
G127.1+0.5, centred on very compact radiosource 78−16555
G127.1+0.5, VLBI obs. of assoc. compact radiosource 78−86029
G127.3+0.7, possible supernova remnant in open cluster, 1.4 GHz obs. 77−64826
G127+0.5, continuum obs. at 2695 MHz 78−61903
G206.9+2.3 (=PKS 0646+06), optical identification 78−36660
G206.9+2.3 (PKS 0646+06), optical supernova remnant discovery 78−96518
G286.8−0.5, nonthermal radiosource in front of Carina Nebula, SNR 79−35355
G287.8−0.5, possible assoc. with X-ray source 77−2492
G287.8−0.5, possible supernova remnant in Carina *(Italian)* 79−53924
G287.8−0.5, X-ray emission obs. 77−2488
G290.1−0.8, optical emission detect. 79−30103
G290.1−0.8, optical SNR photographed 79−40249
G291.0−0.1, location in Tr 18 open cluster 78−20875
G292.0+1.8, abundance anomalies, radial vels., possible Crab-like SNR 80−46628
G292.0+1.8, optical identification and spectrum 79−84839
G292.0+1.8, unusual SNR, synthesis map at 1415 MHz 77−49454
G292.0+1.8, young supernova remnant, high vel. material obs. 80−22064
G296.1−0.7, radio object in Crux, assoc. optical nebulosity 78−16499
G321.9−0.3, possible assoc. with runaway star (Circinus X-1) 80−67910
G321.9-0.3 rel. to Cirinus X-1, simultaneous radio and optical obs. 79−17137
G326.3−1.8, G348.5+0.1, G348.7+0.3, unusual supernova remnants, radio obs. 79−84841
G326.3−1.8, peculiar supernova remnant, optical identification 79−25675
G339.2−0.4, radio recombination line obs. refutes SNR nature 80−46650
G339.2−0.4, supernova remnant or planetary nebula, radio and optical obs. 80−22104
G46.8−0.3, galactic supernova remnant, kinematic distance estimate 79−84833
G55.7+3.4, shell source, high resolution obs. at 610 and 1415 MHz 78−8140
G65.2+5.7, 1420 MHz continuum obs. *(Italian)* 79−53886
G65.2+5.7, 1420 MHz continuum obs. of new SNR 79−44587
G65.2+5.7, soft X-ray spectrum and structure 79−71093
G74.9+1.2, continuum obs. at 2695 MHz 80−67830
G74.9+1.2, distance estimate from H I absorpt. line meas. 78−28765
G74.9+1.2, distance of supernova remnant and nearby point source 77−64864
G74.9+1.2, VLBI obs. of assoc. compact radiosource 78−86029
G78.1+1.8, compact radio source discovery from interstellar scintillation obs. 79−101213
G78.2+2.1 in Cygnus X region, H I 21 cm line emission maps 80−56917
G 21.5−0.9, resembling Crab Nebula, obs. 77−5553
G 261.9+5.5, H I 21 cm obs., H I clouds 80−62229
G 74.9+1.2, total intensity and polarization struct. 79−8980
G 84.2−0.8, high resolution 1415 and 2695 MHz obs. 80−98702
G 84.2−0.8, new supernova remnant in Cygnus 77−29906
galactic, spectra, comp. and kinematics of ejected material from supernovae *(Italian)* 79−53844
galactic 79−48894
galactic centre region, compact radio continuum sources obs. 79−21430
galactic coronae, production by supernovae rel. to intracluster medium origin and quasar absorpt. lines 80−31355
galactic distribution, search for optical remnants *(Italian)* 79−53882
galactic loops *(Hungarian)* 79−40263
galactic nucleus radio source, supernova remnant hypothesis 77−5572
galactic radio loop II, contrib. to diffuse soft X-ray brightness distrib. 79−53942
galactic radio supernova remnants, systematic search for optical nebulosity 79−29998
galactic supernova remnants, 5 GHz obs. 77−29907
galactic supernova remnants, new catalogue corrected for distance from galactic plane 79−75120
galactic supernova remnants, new optical obs. 80−17636
galactic supernova remnants, search for stellar remnants 80−26890
galactic type I remnants, appl. ot supernova models with slow energy pumping 78−73726
galatic supernova remnants, radio evolution and population characts. 79−75254
gamma-ray sources 79−92887
gas dynamics of supernovae and their remnants 77−17605
general processes and theory 77−57001
Gum nebula, Balmer alpha photographic obs. and interpretations 78−24545
Gum Nebula, cometary globule obs. 77−2464
Gum nebula, distance from photometry of stars in reflection nebulae 78−32449
Gum Nebula, evidence for star form. triggered by nebula expansion 77−29821
Gum Nebula, temp. and density vars. *(French)* 80−26951
H1207−52, soft X-ray emission detect. from southern SNR 78−77620
H1616−51, soft X-ray emission detect. from southern SNR 78−77620
H2027+19, Delphinus soft X-ray source, model, X-ray obs. 80−90576
H 1538−32, new extended soft X-ray source detect., possible old supernova remnant 80−51912
HB3, X-ray emission obs. 78−81679
HB 3, kinematics and evolution 80−67823
HB 3, soft X-ray obs. 80−56915
HB 9, soft X-ray emission obs. 80−36697
He 2-111, planetary nebulae, giant halo with very high vels. discovery 79−25691
high energy neutrinos of extraterrestrial origin, possible detection with DUMAND 79−80179

supernova remnants continued
high-velocity H I clouds, map and local supernovae shell model 80−26923
historical supernovae and possible remnants *(Italian)* 79−53837
hot interstellar gas, contrib. to galactic corona 79−25709
hydrodynamical evolution, analytical methods 79−5885
IC 443, assoc. with low latit. negative vel. H I clouds in galactic anticentre 77−45506
IC 443, CO emission obs. 78−8071
IC 443, detect. of gas at 10^6K 79−53875
IC 443, fast filaments and high vel. gas, Hα obs. 79−30106
IC 443, H_2 detection at 2.1 μm 80−17630
IC 443, Hα inteferometric obs. of fast filaments and high vel. gas 79−75258
IC 443, H I cloud and jet obs. 77−33592
IC 443, H I distrib. rel. to high-vel. gas 79−71083
IC 443, high-rel. gas Hα emission origin 80−41873
IC 443, shock enhancement of HCO^+ 80−82464
IC 443, shocked clouds of subthermally excited OH in SNR 79−35349
IC 443, shocked CO discovery 80−8669
IC 443, supernova remnant, CO emission from dense cloud 77−29897
IC 443, X-ray images 79−48889
IC 443, X-ray spectrum and structure 77−49453
identification in nearby galaxies *(Italian)* 79−53884
interacting supernova remnants, struct. and evolution 80−4423
interacting supernova remnants, tunnels in sky 80−4409
interaction, simulation rel. to interstellar hot tunnels 77−17645
interstellar medium heating, rel. to delayed star form. in galaxies 80−105349
isothermal blast wave model 77−9778
isothermal self-similar blast wave theory 77−82295
isotopically anomalous material, injection into early solar nebula 79−101094
Kepler's, struct. at 327 MHz from occultation obs. 78−12339
Kepler's SN 1604 remnant, spectrum 80−85982
Kepler's SNR, distance from interstellar absorption determ. 80−46651
Kepler's SNR, weak soft X-ray emission detec. 79−58403
Kepler's supernova remnant, X-ray obs. from Einstein Observatory 80−82465
kinematics and evolutionary sequence in cloudy interstellar medium, interferometry obs. 80−67823
in LMC, obs. in O III and S II forbidden lines 77−91607
inLMC, SHF obs. 80−67864
LMC, SNRs identification from Einstein Obs. X-ray meas. 80−26980
LMC N 49, X-ray source 0525.9-66.1, gamma-ray burst obs. *(Russian)* 80−36739
LMC supernova remnants N49 and N63A absolute photometry 77−74116
LMC X−1, luminous extended X-ray source as supernova remnant 78−16570
location with respect to galactic plane 77−74127
Loop I, X-ray features, SNR model 80−22066
low surface brightness remnants, optical and radio obs. 79−88717
Lupus Loop, soft X-ray emission detect. 79−53876
Lupus Loop, X-ray spatial extent and spectrum 80−82457
Lupus region, soft X-ray structure 79−71085
in M33, emission regions catalogue 80−46416
in M33, N/S abundance gradient, SNR evidence 80−56929
in M33, radio and optical obs. *(Italian)* 79−53890
in M33, spectra, element abundances 79−35354
in M33, supernova remnants catalogue 80−41734
in M33, supernova remnants optical identification 79−62894
in M33 detected by strong S II forbidden line emission 78−36665
M87, model for optical knots in jet 79−30127
Magellanic Cloud supernova remnants, high-resolution mapping in coronal [Fe XIV] emission 79−97051
Magellanic Cloud supernova remnants, optical emission from shocks 79−92831
in Magellanic Clouds, direct photography 77−91612
in Magellanic Clouds, optical obs. review 79−75259
Magellanic Clouds, SNR populations *(Italian)* 79−53887
in Magellanic Clouds, spectroscopic study 77−91613
magnetic field distribs., Faraday rot. and depolarisation 77−13428
MHD wave fronts, filamentary struct. form. 78−81668
MHD wave fronts and old SNR simulation *(Italian)* 79−53885
Milky Way near l=333°, 8.87 GHz obs. 80−22102
model for clusters of discrete gamma-ray sources 78−49558
Monoceros Loop, high vel. gas, Na I lines obs. 78−12348
Monoceros Loop, narrow band photography, shock wave model 78−32547
Monoceros Loop, photographic obs. of diffuse and filamentary nebulosity 78−32548
Monoceros ring, rel. to supernova-induced star form. in Monoceros OB2 assoc. 80−31334
MSH 11−54, rel. to new H1122−59 X-ray source in Centaurus 78−28859
MSH 11-54, X-ray obs. 80−82463
MSH 14−63, probable remnant of A.D. 185 supernova, X-ray emission obs. 78−45427
MSH 14-63, soft X-ray emission obs. 77−37636
MSH 15-56=GX 326.3−1.8, soft X-ray emission detect. 79−44639
N132 D in LMC, rapidly moving material, visible and UV obs. 80−82449
N132D, supernova remnant in LMC similar to Cassiopeia A, photographic and spectroscopic study 78−93345
N49, in LMC, possible assoc. with gamma ray burst (1979, March 5) 79−58441
N49, LMC supernova remnant, as source of fast intense unusual gamma-ray transient 80−73073
N49, LMC supernova remnant, as source of gamma-ray transient event of 1979 March 5 80−73074
N49, SNR in LMC, Pioneer Venus Orbiter obs. of 1979 March 5 gamma-ray transient 80−77518
N49 and N63 in LMC, UV spectra interpretation using radiating shock wave models 80−90498
N49 SNR in LMC, X-ray obs. of gamma-burst field 80−27019
N49 supernovae remnant as source of March 1979 γ-ray burst 80−105270
N51D, giant filamentary shell in LMC, nature and dynamics 80−105343
N63A, lower limit to mass of original supernova 80−62165
supernova remnants continued
N 132D in LMC bar, possible correl. with X-ray source 80−82491
in NGC 4449, extraordinary extragalactic supernova remnant spectrophotometry 80−56895
NGC 604, giant H II region in M33, SNRs rel. to content of high mass stars 80−31340
in NGC 6946, search for radio emission from four young SNRs 80−77473
NGC 7822 (W 1), 2.8 and 6 cm wavelength obs. 78−4383
nonthermal radio emission spectra 77−57101
North Polar Spur, old reheated SNR 78−16580
North Polar Spur, reheated supernova remnant model appl. to X-ray obs. 80−105370
North Polar Spur, soft X-ray spectra emission line features obs. 80−94849
North Polar Spur, X-ray features 77−45554
North Polar Spur *(Russian)* 78−41072
OA 184, interferometric obs. in Hα line, expansion vel. *(Russian)* 79−88728
OA 184, kinematics and evolution 80−67823
old supernova remnants in solar neighbourhood, evidence from interstellar He I obs. 80−62234
V843 Ophiuchi (Kepler supernova 1604) remnant, soft X-ray emission detect. 79−40244
ζ Ophiuchi interstellar cloud, CO obs., density and identification as supernova remnant 78−36656
optical counterparts of gamma-ray sources 79−35429
optical emission from shock waves 77−64816
optical filaments form. problem, observational approach 78−45384
optical supernova remnant candidates in M33 central region, discoveries 79−21402
Origem Loop, 0.610 GHz obs. rel. to proposed Milky Way companion galaxy 77−29941
Origem Loop, assoc. with low-latit. negative vel. H I clouds in galactic anticentre 77−45506
Orion OB1 association direction, supernova remnants rel. to Copernicus obs. of interstellar matter 80−22050
particle acceleration in collisionless shocks, regulated injection and high efficiency 79−44311
periodicity investigation at 21 cm 80−82529
physical parameters, estimates 77−13431
physical processes in interstellar medium studied in SNRs 79−67071
PKS 1209−52, soft X-ray emission detect., evolutionary phase 79−62892
primaeval galaxies, model emission spectra 80−46655
PSR 0950+08, ghost SNR, 327 MHz obs. 79−12506
pulsar-driven isothermal blast-wave models 77−78847
pulsar/supernova remnant associations, possible origin in close binary systems 78−85965
Puppis A, Fe X and XIV forbidden line emission 79−44580
Puppis A, Fe XIV coronal line and filamentary emission 79−84843
Puppis A, O VIII 18.97 Å resonance line emission detect. 77−45535
Puppis A, optical and radio comparison 78−28760
Puppis A, optical spectral obs. of filaments *(Italian)* 79−53883
Puppis A, X-ray and Fe XIV 5303 Å emission 80−26962
Puppis A, X-ray images 79−48889
Puppis A, X-ray spectrum and struct. 78−20876
Puppis A, X-ray spectrum two component appearance interpretation 80−82475
Puppis A, X-ray struct. from Copernicus data 79−8982
Puppis A X-ray spectra var. with position 80−82472
radial distrib. within parent galaxies, exponential law 77−45473
radial distribution within parent galaxies, exponential law 77−45473
radial instability of adiabatic self-similar blast waves 78−8089
radiative shocks and UV precursors, theoretical models 79−25660
radio dynamical evolution of young remnants 78−93365
radio emission from possible SNR in NGC 4449 irregular galaxy 79−17056
radio emission shells asymm., large-scale gradients in surrounding medium 78−69861
radio evolution, generalized theoretical approach 80−85990
radio maps, explosion processes 77−37642
radio remnants, X-ray obs. by ANS 79−92833
radio remnants resembling Crab Nebula, props. 79−53881
radio struct. obs. 77−13435
radio supernova remnants, source counts rel. to galactic supernova outbursts frequency 80−62168
radioactivity and elec. charge of interstellar grains 77−87499
radiosource in irregular galaxy NGC 4449, possible SNR with broad optical emission lines 79−17057
RCW 103, soft X-ray emission detect., evolutionary phase 79−62892
relativistic and nonrelativistic gas flows, low press. limit 77−9655
S147, assoc. CO absorpt. detect. 80−67836
S147, kinematics 79−44585
self-similar flow behind blast wave 77−53415
self-similar spherical expansion, Rayleigh-Taylor instability 79−8823
shell nebulae in Magellanic Clouds, survey in S II, N II and O III forbidden lines and Hα 79−67085
shock wave intermediate zone radiative cooling, effect on optical emission spectra 80−109517
shock waves, post-collisional propag. and amplification *(Russian)* 79−44360
Simeiz 147, filamentary nebula, optical obs. 77−13445
Simeiz 147, Hα emission of optical filaments, shock wave vel. 78−8103
SN 1006, soft X-ray emission detect. 79−53876
SN 1006, X-ray emission models 77−17646
SN 1006, X-ray spectrum 80−82457
SN 1006 optical remnant, peculiar spectrum obs. 79−21371
SN 1006 remnant, Ariel V X-ray obs. 79−40250
SN 1006 remnant, optical emission from shock wave 79−5890
SN 1572 (Tycho's supernova), small dia. radio source discovery near centre of remnant 80−98680
SN 1604 (Kepler's supernova), optical remnant expansion time scale, brightness, reddening 78−28747
SN 393, no optical nebulosity near nonthermal radiosource posns. 79−58366
soft X-ray emission from SNR in Cygnus 78−54013
soft X-ray sources in Cygnus region 78−4397
southern supernova remnants, high resolution radio obs. 80−51849
spectral index distrib. of radio shells 80−77462
spherical clouds in hot gas, radiation effects on evaporation 77−78842

supernova remnants continued
in spiral galaxies, characts. rel. to disc radio continuum flux 77−13460
SS 433, associated filamentary optical nebulosity detect. 79−88723
near SS 433, faint, highly-contorted nebular filament discovery 80−94855
stellar remnants, identified with new class of radio star 79−17117
surface brightness-diam. correl. 77−29899
synchrotron radio surface brightness rel. to SNR radius 79−58409
Taurus A, intensity and polarisation at 9 mm wavelength 80−36732
Taurus A, secular decrease in 927 MHz flux, radio flux density obs. 80−67840
Taurus A (Crab Nebula), 927 MHz emission secular decrease 79−75255
thermal X-rays theoretical spectra of young remnants 78−73751
Tycho, filaments spectrum 78−73747
Tycho, search for fossil Stromgren sphere 78−36661
Tycho's, mag. field amplification in collisionless shock waves 77−49459
Tycho's SNR, HEAO 1 obs. and structure study 80−51842
Tycho's SNR (3C 10), 10.7 GHz obs. 79−75264
Tycho's SNR (3C 10), distance, Westerbork H I obs. 80−101633
Tycho's supernova, optical remnant expansion obs. 79−8962
Tycho's supernova (SN 1572), unsuccessful search for optical stellar remnant 80−101603
Tycho's supernova remnant, optical emission from shock wave 79−5890
Tycho's supernova remnant, radio flux density meas. separated by 15-year interval 80−26955
Tycho SNR, weak X-ray source, ANS meas. 80−46701
Tycho SNR spectrum, model of optical emission from fast shock wave 80−46631
Tycho supernova remnant, radio struct. 80−56919
Tycho supernova remnant, Type I SNR, elemental abundances from X-ray spectrum 80−46635
Tycho supernova remnant, X-ray line emission obs. 80−46636
type rel. to supernovae type, mag. field effects 80−77474
ultrahigh energy neutrino emission from cosmic ray sources 78−65723
Vela, assoc. UV absorpt. lines 77−33604
Vela, filamentary struct. rel. to change in pulsar rot. measure 77−29867
Vela, interaction with cloudy interstellar medium 77−2463
Vela, IUE UV spectrum 80−101635
Vela, obs. of extended X-ray source centred on Vela pulsar 78−41095
Vela SNR, X- and gamma-ray emission *(Russian)* 80−94861
Vela supernova remnant, rot. measure and turbulent struct. 80−51836
Vela supernova remnant, X-ray maps 80−51838
Vela X, X-ray spectrum two component appearance interpretation 80−82475
Vela X supernova remnant, radio polarisation maps 80−56909
velocity distrib. of interstellar gas, UV absorption line obs. 78−89235
VRO 42.05.01, Hα emission of optical filaments, shock wave vel. 78−8103
VRO 42.05.01, Hα inteferometric obs. of fast filaments and high vel. gas 79−75258
VRO 42.05.01, high vel. gas expansion *(Russian)* 79−17069
W1 (S171), optical supernova remnant radial vel. field 80−62250
W28, RATAN-600 2-13 cm wavelength obs. of W28 A $_2$ H II region *(Russian)* 80−17642
W44, ANS obs. of X-ray emission 78−54010
W44, associated molecular cloud obs. 78−8079
W44, CO obs. 77−64836
W44, expansion into surrounding interstellar medium, dense cloud encounter 77−22298
W44, IR obs. of nearby star formation regions 79−58399
W44, relation to W48 and mol. cloud 78−28762
W49B, distance from CH radio emission obs. 77−87511
W50, assoc. with Stephenson-Sanduleak 433 emission-line star/X-ray source/radiosource 79−8930
W50, associated filamentary optical nebulosity detect. 79−88723
W50, continuum obs. at 2695 MHz 80−67830
W50, extended struct. correl. with SS 443 radio jet 80−31381
W50, interstellar medium interaction with SS 433 relativistic jets visible obs. 80−101629
W50, N II emission enhancement and distance rel. to assoc. with (SS 433) 79−92783
W50, optical filaments spectra rel. to SS 433 mass loss rates and lifetime 80−12804
W50, optical spectrum of faint filamentary nebula 80−90557
W50, probable supernova remnant, relation to (SS 433) 80−72987
W50, spectrum of optical nebulosity 80−51851
W50 (SS 433), optical remnant discovery 80−56916
W50 containing SS 433, object with unique spectrum 80−82381
W51, first optical detection, rel. to galactic spiral struct. 78−61900
W51, high vel. H_2O maser features obs. 77−9779
W51 H_2O source obs. with Crimea-Haystack interferometer *(Russian)* 78−69865
X-ray emission from optically thin plasmas, abundance effects on continuum spectrum 78−53814
X-ray emission rel. to evolutionary phases 77−87521
X-ray emissions, obs. 79−58404
X-ray obs. and quark stars in young SNRs, neutrino cooling 80−56858
X-ray obs. and supernova process studies *(Italian)* 79−53894
young remnants, search for radio emission at 3.7 and 11 cm 78−40972
young supernova remnants, radio emission evolution according to observational data 79−75256
young supernovae remnants, X-ray props. rel. to neutron stars cooling 80−77443
CO emission obs. 78−8071
Fe X and XIV forbidden line emission from Puppis A and other objects 79−44580
H I+molecular/H II shells from 1 to 2000 pc dia., wind-driven or supernova remnants 79−25678
Hα emission of optical filaments, shock waves interaction with interstellar medium 78−8103
Hα/N II forbidden line ratio, evidence for grain destruction 77−45520
O, N and S abundances, optical emission from shock waves 77−49447
Si XIII and Si XIV line emission, search with ANS crystal spectrometer 79−17131

supernovae
see also supernova remnants
16 M⊙ supergiant with 1 M⊙ neutron star companion, double core evolution and envelope ejection 78−53980
185, positional coincidence with planetary nebula with high-vel. giant halo (He 2-111) 79−25691
1006, historical records rel. to position, brightness and visibility duration 77−82267
1006, optical remnant identification and Lupus Loop form. 79−29998
1969l in NGC 1058, obs. and theoretical light curves comparisons 77−13370
1972e in NGC 5253, Type I, spectrum after 365 and 435 days 78−4255
1973f in NGC 4944, photometric obs. 79−21318
1973r in NGC 3627, obs. of type II supernova 77−49407
1974g, type I, in NGC 4414, post-maximum spectral obs. 77−78806
in 10-16-117, discovery, magnitude 78−69817
acceleration processes in young supernova remnants 77−33613
analytic models of supernovae and black holes, Einstein eqn. solns. 78−4258
anisotropic explosion of rotating, self-gravitating uniform spheroids, appl. to supernovae 79−8822
in anon. galaxy, discovery obs. 78−20846
in anon. galaxy in Grus, discovery, position 78−93289
in anonymous faint spiral galaxy, discovery obs. 78−8031
in anonymous galaxies, three new discoveries 80−46589
in anonymous galaxy, discovery report 79−2549
in , anonymous galaxy in Camelopardalis, discovery, photographic magnitude 79−5849
in anonymous galaxy in Canes Venatici discovery obs. 80−67759
in anonymous galaxy in Centaurus, discovery, posn. and magnitude 80−85961
in anonymous galaxy in Centaurus, magnitude (1980 June 30) 80−85962
in anonymous galaxy in Cygnus, photometric and spectrophotometric obs. 79−5847
in anonymous galaxy in Cygnus, UBV photometry and spectrum 79−5846
in anonymous galaxy in Grus, discovery and magnitudes (1980 May 23 to July 12) 80−94820
in anonymous galaxy near k Centauri, discovery and magnitudes 80−85962
in Aquila, 4 BC, identification with Christmas Star and binary pulsar 78−81781
asymmetric explosions and binary pulsar origin 78−69816
axion production, astrophys. implications of new light Higgs boson 79−22007
beta transition rates in hot dense stellar matter 78−73699
binary star orbital elements and run-away vels. caused by symmetric explosion 77−91570
in binary systems, implications for evolutionary status of stars with M≳50 M⊙ *(Russian)* 80−109425
in binary systems, rel. to HD 108 possible collapsed companion 77−13369
binary X-ray sources, relation of type I supernovae 77−57021
blast wave, Lagrangian coordinate transforms. in self-similar-model 77−57072
blast waves and the interstellar medium *(Italian)* 79−53845
Brahe's SN 1572, location from original obs. rel. to remnant 78−12256
BV magnitudes, spectroscopic obs., brightness, distance 79−16999
Canis Major R1, supernova-induced star formation region 77−87494
Canis Major R1 association, supernova induced star formation 78−8063
η Carinae, possible future supernova 77−87520
Cassiopeia A supernova, low luminosity rel. to identification as black hole 79−75244
Cassiopeia A supernova, O burning rel. to remnant abundance inhomogeneities 80−12797
Cassiopeia A supernova, probable Flamsteed observation 80−62436
Cassiopeiae A rel. to 3 Cassiopeiae 80−72792
celestial chaos related to Earth's climatic and biological catastrophes 79−53509
Cepheus OB3 association, supernova-induced star form. 78−12306
characteristics and evolution, from radio, X-ray, and γ-ray obs. 77−37611
collapse, high temp. matter comp. and adiabatic index 79−44354
collapse and transport supernovae with neutrino degeneracy 78−40977
collapse of massive star cores, supernova explosion from shock heating 80−56863
collapsing core, shock struct. and neutrino radiation, rel. to supernova explosions 78−49427
collapsing cores and supernovae 79−62815
in Coma cluster of galaxies, light curves anal. 78−32497
conference, Erice, Italy (May 1978) *(Italian)* 79−53836
conference, Grenoble, France (Sept. 1976) 77−87456
convection, lepton-driven, in collapsing cores, theory 79−84811
core collapse, effects of neutrino ang. momentum losses 77−56916
core collapse, neutral currents and neutrino Comptonisation in high-temp. nuclear matter 80−21905
core collapse, neutrino prod. and inelastic scatt. by nuclei at extreme temps. 80−36488
core collapse, shape instability pressure stabilisation 80−8537
core collapse, theory 80−77389
core collapse, Thomas-Fermi model of warm nuclei 80−51648
core collapse outcome, effects of core eqn. of state 80−85928
core gravitational collapse, shockwave prod., neutrino transport effects 80−94818
cosmic ray accel. from dense shell around supernova *(Russian)* 77−87454
cosmic ray electrons, discrete galactic sources 79−35078
cosmic ray prod., intensity var. at Earth from cosmogenic isotope obs. 80−101503
cosmic ray production, spatial inhomogeneities in low-energy cosmic ray diffusion model 77−5402
cosmic ray production, time delay between nucleosynthesis and accel. to relativistic energies 78−28455
cosmic ray sources *(Italian)* 79−53846
cosmic rays accelerated in shock, early radiation spectrum, cooling and escape, radiation spectrum, cooling and escape 79−48626
cosmic rays injection into dense supernova shells by pulsars 78−65638
cosmological deceleration parameter determ. from supernovae obs. 77−49509
Crab, 0.511 MeV gamma-rays meas. with balloon-borne Ge(Li) spectrometer 77−53373
Crab, balloon obs. of lunar occultation, of hard X-ray source *(Japanese)* 77−82319

supernovae continued
Crab, ionisation and thermal equilib. of filaments 77−74117
Crab, mapping and total flux determ. at 1 mm wavelength 77−49460
Crab, obs. of linear polarisation at 7.2 cm during occultation by solar corona 77−60837
Crab, optical linear polarization obs. from Durham 77−74126
Crab, possible γ-ray line detect. 77−49458
Crab, thin scatt. diffusion of radiating electrons rel. to observed size 77−87502
Crab Nebula, 1054 supernova mass from search for extinction in and near nebula 77−67118
Crab Nebula, explosion date from pulsar proper motion 77−82269
Crab Nebula, optical spectrum rel. to baryon star magnetosphere *(Russian)* 77−91555
Crab supernova explosion of 1054, sighting in Near East 78−62028
Cretaceous-Tertiary extinctions, effects of supernovae and stratospheric aeronomy 78−32215
Cygnus Loop, radio struct. at 25 MHz 78−54027
in Cygnus X-ray superbubble, power source 80−90575
degenerate C/O cores, detonation formation 77−45398
diffuse interstellar lines 79−21401
disrupted the star in close binary containing neutron star, model for Crab Nebula 79−25696
distance determ. by Baade's generalised method, appl. to H_0 and q_0 80−73082
distant (z=0.5) supernova light curve, photometric obs. 80−94821
dynamical r-process, nuclei far from β-stability 77−26004
Earth showered by lunar γ-ray ablation debris 80−56731
education, explosion in binary system, classical mechanics appl. 80−62428
ejecta, chemical condensation sequences 79−58365
ejecta, dust grains sudden nucleation and growth 80−26941
ejecta condensation, presolar grains and meteorites isotopic anomalies 78−20845
electron capture in nuclear statistical equilibrium 79−92663
emission lines, broadening and displacement during nonlinear transfer in turbulent plasma *(Russian)* 77−91418
energetic electrons production rel. to X-ray and γ-ray background radiation origin 77−33703
energy loss rate due to electron capture in highly evolved stars 77−64752
envelope acceleration by pulsar radiation 79−62859
equations of state in pre-supernova collapse, nuclear partition functions at high temperature 79−101059
in ESO 153-G27, discovery and magnitudes (1979 August 19 to October 15) 80−26892
expanding envelopes, Lyman α quanta scattering *(Russian)* 80−67556
expanding shell, site for r-nuclei prod. 80−72932
exploding inner shells, nucleosynthesis evidence 79−62860
explosion, massive star core hydrodynamics 79−16995
explosion mechanisms 77−87465
explosion models, new solns. 80−12751
explosions, effect on stellar evolution 80−31315
explosions, off-center, rel. to high vel. pulsars form. 80−46587
explosions, pseudoscalar bosons rule *(French)* 79−44361
explosions, Rayleigh-Taylor instability 78−36551
explosions and low-energy neutrino elastic scattering 78−89056
explosions in clusters of galaxies, microwave pulsed emission upper limit 78−69890
explosive core overturn, rel. to mass ejection 80−72988
explosive nucleosynthesis, massive star evolution preceding and during supernova, element abundances *(German)* 79−44469
explosive nucleosynthesis 80−72766
explosive r process cooling process 78−69791
external galaxy investigations of nature of supernovae 77−49408
extragalactic, X-ray bursts search using HEAO-1 satellite 80−46585
extragalactic supernovae, types I and II, radial distribs. in spiral and elliptical galaxies 80−62163
extragalactic supernovae spectra, comp. and kinematics of ejected material *(Italian)* 79−53844
in faint ScI galaxy, discovery and position 77−22257
final evolution of stars *(Italian)* 79−53805
flares, CC ^{14}C concentration in Earth's atmosphere, corrections with astrophysical and geophysical phenomena 78−61477
galactic events, colour curves and visual light curves 79−58368
galactic supernova outbursts, frequency estimate 80−62168
galactic supernovae, occurrence freq. and long-lived remnants prod. 77−64784
galactic supernovae, seismic detection of gravit. radiation *(Russian)* 77−13371
galactic winds, supernovae-driven, rel. to Hubble sequence 79−8989
in galaxies, rel. to galactic coronae and intracluster medium origin 80−31355
galaxies spiral structure, influence of supernovae and stochastic star form. 78−93395
gamma-ray emission, continuum intensity and spectrum 80−101602
gas dynamics of supernovae and their remnants 77−17605
gas ejection from dwarf spheroidal galaxies driven by supernovae 80−22088
general processes, remnants and theory 77−57001
grain condensation in expanding envelope, as source of presolar grains in meteorites 78−24520
grains ejected from supernovae rel. to solar system isotopic abundance anomalies 77−87285
gravitational collapse, weak interactions and supernova outbursts 77−87464
gravitational radiation, generation by escaping neutrinos 78−93092
gravitational radiation from supernova neutrino bursts 78−81642
gravitational waves emission, theory and astronomical appls. 79−92664
gravitationally collapsing stars, criteria for mass ejection 77−33534
guest star of AD 1408, Japanese record 80−90641
heavy and neutron-rich elements synthesis by rapid neutron capture process 78−77488
heavy element, origin in star development supernovae and galactic matter *(German)* 79−44468
heavy element nucleosynthesis, current astrophysical theory review 77−29644
heavy elements expulsion, accretion by Sun, rel. to terrestrial ice ages *(Polish)* 79−58310
Hercules X-1 (HZ Herculis) binary system, pre-supernova parameters 80−62318
supernovae continued
historical records, book 79−17002
historical records 77−2448
historical records of Cassiopeia A 80−77430
historical supernovae and possible remnants *(Italian)* 79−53837
hot CNO nucleosynthesis, $^{18}O/^{17}O$ abundance ratio 77−78767
Hubble constant determ. from Type I supernovae enveloped model 77−87459
Hubble diagram for type I and II objects 78−53967
hydrodynamical acceleration of particles in supernovae and extragalactic radio sources 80−31313
IC 443, remnant, negative vel. H I condensations obs. 78−54016
in IC 5201, discovery report 79−44514
interacting neutron fluid at high temp., eqn. of state, supernovae hydrodynamics 79−2718
interacting neutron matter model at postsupernova temps. 77−45399
intergalactic supernovae, limit on frequency in Coma cluster of galaxies 77−17604
interstellar hot gas, nature, origin and evolution 78−16506
interstellar medium, mechanical heating rate by supernova blast waves 80−36682
interstellar medium heating, rel. to delayed star form. in galaxies 80−105349
interstellar three component model regulated by supernova explosions in inhomogeneous substrate 78−16486
ionisation events in stratosphere, effects on NO_2, O_3 and climate, rel. to life extinction 78−96273
ionisation of interstellar H_2 clouds 78−69856
IR excesses, role of Fe II dielectronic recomb. 78−32478
Kepler's star of 1604, translation of original description 77−33536
light curves, pulsar theory, dynamical effect and thermalisation of strong waves 78−8028
light curves, radiation dynamics and envelope ejection theory 77−64783
light curves and spectra obs. at Asiago Astrophys. Observatory 77−87457
light curves rel. to existence of central pulsar 78−4256
in M100 (NGC 4321), discovery of possible type II object before max. 79−48835
in M33, freq. from supernova remnants catalogue 80−41734
magnetorotational explosion, one-dimensional cylindrical model 80−101605
mass ejection and core hydrodynamics *(Italian)* 79−53842
mass of supernova that produced N63A, lower limit 80−62165
massive close binaries, post-supernova stage, tidal instability 77−57024
massive close binary stars, effects of supernova explosion on evolution 78−49479
massive close binary systems, late evolutionary stages 77−57023
massive star, Mg, Al isotope yields from C and Ne zones 80−90406
massive stars presupernova evolution 79−16930
master list of non-stellar objects 77−78668
maximum of outburst as opportunity for mutual CETI search strategy 80−56723
in MCG 10-16-117, classification and spectrum 78−69818
in MCG −3-34-61, discovery of 17 mag. object 80−72989
in MCG −3-34-61, Type I spectrum revealed (1980 June) 80−82401
in MCG -4-32-23, precise position, photographic magnitude 78−57568
in MCG-4-32-23, discovery 78−53968
in MCG-5-9-22, discovery 78−81643
in MCG-5-9-22, spectrum and absolute magnitude 78−81644
mechanism for young galaxy contribution to X-ray background 80−82550
MHD model, numerical anal. 80−46588
MHD processes near compact superdense objects rel. to supernova explosions 79−40206
model, heavy element origin 77−56825
model, neutrino degeneracy effects 77−2447
models with gradual energy release, shell struct. and light curve 77−78807
molecular clouds, critical mass rel. to supernova phase 77−78770
in molecular clouds, spectra and luminosity, evolution 80−82399
Monoceros OB2 association, evidence for supernova-induced star form. 80−31334
near-Earth supernova, effect on Cretaceous-Tertiary environment 78−32499
near-Earth supernova and extinctions at end of Cretaceous, astronomical evidence 78−32500
nearby, impact on climate and biology on Earth 78−28297
nearby supernova, effects on terrestrial atmosphere 80−94584
neutrino emission, review and possible obs. 78−77486
neutrino energy equilibration, models 80−105265
neutrino interactions with envelope, rel. to prod. of bypassed elements 77−45408
neutrino mediated shocks 80−94818
neutrino processes, reaction rates 78−45215
neutrino radiation, rel. to damping of collapsing core nonradial pulsations 77−56999
neutrino radiation for hot neutron star form., rel. to envelope outburst problem 78−45350
neutrino radiative lifetimes, limits from supernovae 79−16785
neutrino transport, direct simulation and aspects of equilibration 78−89050
neutrino transport, time-dependent, out of dense stellar cores, theory 80−94783
neutrino transport, weak neutral currents; supernova model 78−62391
neutrino transport in collapsing core, Fermi statistics 77−26019
neutrino transport in collapsing stellar core model 78−8029
neutrino transport in supernova models, multigroup diffusion scheme 79−25590
neutrino-induced nucleosynthesis, appl. to D and p-process nuclei 77−87582
neutrinos, high energy, emission from point sources and detect. techniques 79−2484
neutron gas interactions at high density and temp., supernova models appl. 77−33330
neutron star binaries formation rel. to gravit. radiation 79−35291
neutron stars formation, neutrinos and gravit. waves emission 78−12266
neutron stars formation rate in Galaxy, upper limit rel. to gaseous remnants form. 78−49471
neutron-proton electron mixture with zero charge density, eqn. of state, rel. to supernova explosions 77−53416
in NGC3733, spectrophotometry (1980 March 22) 80−62164

supernovae continued
in NGC 1199, mag. 17 object, 1979 Sept. obs. 80−41846
in NGC 1325, Type II, UBV photometric obs. 78−16444
in NGC 1411, discovery of SN in elliptical galaxy 77−67104
in NGC 1411, spectral obs. and precise position 77−82266
in NGC 3226, discovery, magnitude 77−33537
in NGC 3733, discovery of mag. 15 object (1980 March 17) 80−51793
in NGC 3780, probable supernova 79−5848
in NGC 3780, spectrophotometry of type II object 79−17000
in NGC 3913, B magnitude and spectrophotometry 79−44513
in NGC 3913, discovery report 79−44512
in NGC 3913, type I characts. and likely max. magnitude 79−48834
in NGC 4275, possible visual obs. 77−29865
in NGC 4278, possible supernova 77−53616
in NGC 4321, IUE UV and visible obs. (1979 April) 79−53834
in NGC 4321, JHKL mags., 1980 Jan obs. 80−41847
in NGC 4321, spectrograms (1979 April) 79−48836
in NGC 4321, spectrophotometry, type II characts. 79−67044
in NGC 4321, spectrum, lightcurve and magnitudes of type II object 79−71061
in NGC 4321, type II characts. and 1979 April UBV and visual obs. 79−58364
in NGC 4321, UBV photometry, light curve and type 79−67045
in NGC 4321, UBV photometry 79−53835
in NGC 4321, UBVR photometry 80−77428
in NGC 4321, UBVRI photometry and visual mag. estimates 79−80330
in NGC 4321, UV and visible obs. (1979 April-May) 79−58363
in NGC 4321, visual magnitude estimates, 1979 May-Jun. 79−75229
in NGC 4321 (M100), interstellar Na I and Ca II absorption in spectrum 80−51847
in NGC 4340, discovery obs. 77−22256
in NGC 4402, Type I, UBV photometric obs. 78−16444
in NGC 4647, classification and time since maximum 79−25620
in NGC 4647, discovery, magnitude 79−25619
in NGC 488, NGC 977, photometry 79−62857
in NGC 4902, discovery and magnitude (1979 August) 79−88693
in NGC 5253, high supernova rate, previous high luminosity explanation 80−77489
NGC 5367, young star cluster star form. initiation by supernova 77−82294
in NGC 5406, 1977, March 28 photovisual magnitude 77−57002
in NGC 5406, discovery of 14th magnitude object 77−33535
in NGC 5854, discovery of mag. 15 Type I object (1980 March 20) 80−51793
in NGC 7723, Type I, UBV photometric obs. 78−16444
NGC 7822 (W1), remnant, optical studies of kinematics and struct. 78−54028
in NGC 977, discovery obs. 77−17606
nucelosynthesis, rel. to Ap and Am stars comp. anomalies origin 79−35277
nucleosynthesis, by n-process of neutron capture 77−2336
nucleosynthesis, mechanisms for explosion and element synthesis *(French)* 80−72933
nucleosynthesis mechanisms 77−87463
nucleosynthesis rel. to Martian atmosphere, implications of Viking data 77−87307
nucleosynthetic yields of metals and stellar birthrate 80−51741
in OB associations, interaction with interstellar medium to form H I supershells 80−82468
V843 Ophiuchi (Kepler supernova 1604) remnant, soft X-ray emission detect. 79−40244
outburst, role of neutral currents of weak interactions *(Czech)* 77−45472
outburst light, expanding gas shell external excitation 78−40976
p-process isotopes nucleosynthetic origin in supernova explosions 78−57541
parent galaxy redshifts 79−44612
peculiar H II regions with nonthermal radioemission, supernova shell interaction *(Russian)* 77−91610
photometric classification *(Russian)* 78−12255
photon helicity detection for matter/antimatter star discrimination 78−12092
piston problem, one-dimensional, in non-ideal gas, time-dependent soln. 80−82185
in planetary systems 80−56860
pre-supernova behaviour of 15 M⊙ star 79−35282
pre-telescopic obs., uses in modern astronomy 79−96930
precursor stars, mass loss by stellar winds *(Italian)* 79−53841
presolar meteoritic sulphides, supernovae origin 77−29866
presupernova models and supernovae 80−56864
presupernova stellar wind, as possible cause of supernova remnant filamentary struct. 80−62249
progenitors, masses 77−87461
progenitors evolution 77−87462
protosolar OB association supernovae, rel. to Allende isotopic anomalies and cosmochronology 80−4462
PSR 1952+29 and 1929+10, evidence of binary system disrupted by supernova explosion 79−35285
quasar luminosity model, galactic nucleus evolution with stellar coalescence and supernovae 77−87568
quasars, multiple supernova model rel. to colour variability 79−9021
r-process nucleosynthesis, required conditions 79−44459
r-process nucleosynthesis, supernovae mass range 79−5844
r-process seed nuclei prod. at low densities and temps. 77−64742
radial distrib. in galaxies, correction for galactic diameters 77−2465
radio emission from immediate postoutburst, origin and evolution 78−40973
radio pulses, searches and possible sensitivity improvements 78−40975
radio pulses from distant supernovae, sensitive RF search 79−25626
Rayleigh-Taylor convective overturn in stellar collapse, supernova explosion mechanism 80−41815
Rayleigh-Taylor convective overturn of core, rel. to supernova explosion 80−77429
Rayleigh-Taylor driven explosion, 2-D numerical study 80−94819
relativistic astrophysics, pulsars, supernovae, and X-ray sources *(German)* 79−101060
relativistic blast waves that accelerate 80−67534
relativistic electrons accel. in explosion 78−28710
relativistic many-body theory, quantum chromodynamics and neutron stars/supernova 79−40752
supernovae continued
relativistic particles generation during outburst, kinetics *(Russian)* 79−21319
relativistic particles total energy upper limit in early stages of explosions, rel. to galactic nuclei and quasars 79−71059
remnants evolution, hydrodynamic code for interacting remnants 80−4423
review, of history and theory *(Norwegian)* 79−80329
review of properties 77−87455
runaway stars, as witnesses to supernova explosions 78−32448
runaway stars and supernovae *(Italian)* 79−53812
in Sc-type galaxies, max. likelihood estimate of occurrence rate 78−45402
Sedov-Taylor blast wave solns. stability 79−35104
selection effect for supernovae in external galaxies 79−80328
self-similar oscillations of gas, theory *(Russian)* 79−17001
Seyfert nuclei as successive supernovae 77−91652
shell expansion, cooling wave props. 77−9760
shell explosions, mechanism by neutron lepton radiative decay *(Russian)* 79−8934
shell shock waves, cosmic ray acceleration, energy loss effects *(Russian)* 80−17449
shock steepening and prompt thermal emission 79−16998
shock wave acceleration of energetic charged particles 80−31189
shock wave acceleration of Galaxy cosmic rays 80−82154
shock waves, cosmic ray particles accel. 78−49241
shock waves in interstellar medium, cosmic ray acceleration 80−31179
shock waves structure 77−17603
slowly rotating stars, gravit. collapse, supernova explosion, neutron star or pulsar remnant 78−96472
SN 1006 optical remnant, peculiar spectrum obs. 79−21371
SN 1054, possible European record 80−62437
SN 1181 (3C 58), absolute magnitude and type classification 80−56862
SN 1181 (3C 58), discovery of optical counterpart 78−32546
SN 1572 (Tycho's supernova), small dia. radio source discovery and precise position 80−98680
SN 1970g, in M101, spectra of type II supernova 78−8030
SN 1970j, 1971l and 1971u, spectra and type identifications 77−22255
SN 1972e in NGC 5253, spectrum 80−41844
SN 1979c in M100, coordinated obs. (1979 April-June) 80−101604
SN 1979c in M100 (NGC 4321), gamma-ray emission, continuum intensity and spectrum 80−101602
SN 1979C in M100 (NGC 4321), precise position 80−85962
SN 1979c in M100 (NGC 4321), spectrophotometry 80−62166
SN 1979c in NGC 4321 (M100), detect. at 60 nm wavelength 80−82402
SN 393, no optical nebulosity near nonthermal radiosource posns. 79−58366
soft X-ray flux prediction method 79−71060
solar system encounter with nearby supernova, rel. to Earth ice ages and viological catastrophes 77−29662
solar system formation, role of supernova, isotopes found in primitive meteorites 79−44380
solar system formation, supernova trigger, evidence from meteorites isotopic anomalies 78−77499
solar system formation, supernova trigger for collapse of interstellar cloud 77−37512
solar system formation 80−82232
solar system origin, relation to supernova explosions 80−17509
spatial distrib. and birth-rate 79−25624
spectra of type I supernovae, effects of line overlapping in conservative scatt. case *(Russian)* 80−105266
spectrum before max. luminosity in Type I objects 80−41845
standard candle for cosmology 79−101167
star formation trigger 80−26891
statistical properties *(Italian)* 79−53838
statistics, rate calc. for Galaxy and external galaxies 77−87460
stellar, A>20 nuclei in advanced stellar evolution and supernovae 80−41817
stellar collapse, adiabatic hydrodynamics and shock wave propag. 80−56861
stellar collapse, effects of nuclear forces, partition function and dissoc. 79−48833
stellar collapses, rate in Galaxy 77−71122
stellar evolution, final phases rel. to supernova phenomenon *(Italian)* 79−88646
stellar gravitational collapse, hydrodynamics 78−45318
stellar remnants, spectroscopic search 80−26890
synchrotron radiation from MHD shock wave front of magnetic field discontinuity, astrophysical appls. 77−25939
thermodynamics of nucleon, lepton, photon mixture, quantum mechanical calcs. 80−77273
thermonuclear astrophysics, element abundances rel. to nucleosynthesis *(Italian)* 79−53715
thermonuclear combustion of C, neutrino mechanism, form. of neutrino stars and supernova outbursts *(Russian)* 77−87379
Thomson scattering in envelopes and emission line profiles *(Russian)* 78−16445
Tien-Kuan guest star of 1054, Crab supernova, historical records *(Chinese)* 78−65743
trigger for solar system formation, Allende meteorite evidence 80−12683
Tycho's supernova, distance and luminosity from fast shock wave model for remnant 80−46631
Tycho's supernova, optical remnant expansion obs. 79−8962
Tycho's supernova (SN 1572), unsuccessful search for optical stellar remnant 80−101603
Tycho supernova, Type I supernova, nucleosynthesis rel. to remnant elemental abundancies 80−46635
Type I, early part of light curve, modelling, H abundance effects 77−87458
type I, element stratification in ejected envelopes 79−16997
Type I, envelope model, Hubble constant determ. 77−53617
type I, in ESO 290-G50, spectral obs. 78−96496
Type I, light curve postmax. stages, model *(Russian)* 78−36624
type I, list of 44 objects, luminosity peak on secondary distance indicator *(French)* 78−4257
Type I, luminosity *(Italian)* 79−53843
Type I, luminosity calcs. 80−82400
type I, photographic and spectroscopic obs. 77−57000
Type I, photometric class depend. on parent galaxy type *(Russian)* 78−32498

supernovae continued
Type I, photometric props. *(Italian)* 79−53839
Type I, progenitor stars, moderate He stars *(Italian)* 79−53806
Type I, theory, light curve anal., evolutionary sequence 79−62858
Type I, use as cosmological clocks 77−2446
type I and II, neutrino mechanism of thermonuclear explosion of degenerate C-O cores 80−62162
Type I envelope, cooling mechanisms *(Russian)* 77−74076
Type I outbursts 79−58367
Type I supernovae, appl. to Hubble const. determ. 79−40304
Type I supernovae, interpretation of spectra 78−49467
Type I supernovae, models 78−65636
Type I supernovae, origin from short-lived stars 79−88692
Type I supernovae, radioactive excitation source model for late time spectra 80−105264
Type I supernovae and supernova remnants, H abundances 78−53969
Type I supernovae in galactic halo, contrib. to galactic corona 79−25709
type I supernovae light curves, colour curves and expansion vel. rel. to brightness decline rate 78−96495
Type I supernovae rel. to R Coronae Borealis stars, appl. to Crab Nebula 79−5845
type II, comparison of theoretical and obs. light curves *(Russian)* 77−57003
type II, nonequilib. processes in evolution 80−46586
Type II, O I absorpt. lines obs. in spectra *(Russian)* 77−45474
Type II, photometric classification and observed charact. 79−25621
Type II, X-ray bursts 78−93287
Type II and peculiar supernovae, photometric props. *(Italian)* 79−53840
Type II events, spectral analysis from 8 to 15 months after explosion 78−40974
Type II events as extragalactic distance indicators, UBV data and light curve models 79−62856
type II objects, photometric props. 79−44511
type II supernovae, light curves analytic solns. 80−77427
type rel. to supernova remnants type, mag. field effects 80−77474
Type V, in galaxy MCG 43223, spectrum obs. 78−93288
ultrahigh energy neutrino emission from cosmic ray sources 78−65723
Virgo cluster supernovae, gravit. waves detectability by reson. antennas 80−8545
in Virgo galaxy cluster, discovery 80−90460
visual hunting by amateur astronomers, prospects 77−91556
VV 5-42-11(=Zw 171-20), probable supernova in interacting galaxy 77−53615
W41, supernova remnant, OH radio lines absorpt. obs. 78−54068
warm neutron degenerate matter, eqn. of state 79−84810
weak interaction rates for sd-shell nuclei 80−82336
weak neutral current, effects in stellar collapse, review, book contrib. 78−85964
wind driven circumstellar shells, struct. and evolution 78−16400
Wolf-Rayet stars as supernova progenitors *(Italian)* 79−53830
X-rays and gamma-rays recorded in Antarctic ice core 80−31314
in Zw 310-31 = VV 11-10-52 faint galaxy NE of nucleus 78−4259
$\nu(\bar{\nu})$ emission from supernovae, form. and cooling of neutron stars 78−8038
^{26}Al, prod. from stellar evolutionary sequence 79−5809
^{26}Al production from explosion near solar system rel. to lunar interior melting 78−40849
^{26}Al production in explosive C burning 78−20814
^{26}Al, synthesis in explosive H burning 80−85929
C degenerate core thermonuclear reaction propag., neutrino mech. *(Russian)* 79−5812
C detonation models, lower mass limit 79−17053
C detonation supernovae, effects of URCA process in convective degenerate cores 77−22203
C detonation supernovae, evolved C cores energy generation and dissipation 80−82339
C detonation supernovae, lower mass limit rel. to dynamical instability in supergiants envelopes 77−17553
C ignition in stellar C-O core, reaction rate enhancement due to strong screening 80−36613
C layer, ^{11}B neutrino-induced prod. 80−82337
C-burning flash in degenerate C-O stellar core supernova outburst 77−78774
Fe group elements production, relative abundances from e-process nucleosynthesis *(Russian)* 80−62167
Fe-O stars collapse, physical and mathematical formulation and computational method 77−87369
Fe-O stars with masses of 2M⊙ and 10 M⊙, gravit. collapse 78−20815
H II regions, origin from supernovae explosions 80−67877
He burning shells, explosive neutron processing rel. to metoeritic abundance anomalies 79−58302
He-driven r-process, rel. to solar system isotopic anomalies 78−57567
in IC 5201, UBV photoelectric meas. 79−17000
K, Ar, nucleosynthesis rel. to interstellar isotopic anomalies 78−28761
^{25}Mg(p,γ) reaction, relative yields of ^{26}Al^{g} and ^{26}Al^{m} 79−101058
^{26}Mg(p,γ)^{27}Al, isotopic anomaly, stellar reaction rate, astrophysical aspects 80−99132
Ne-E, anomalous meteoritic Ne component, thermonuclear origin, supernova models 78−45292
^{22}Ne and ^{26}Al nucleosynthesis in novae and supernovae outbursts 80−62143
O VI gas in solar corona, origin in supernova explosion 78−57528

superparamagnetism
see also magnetic properties of fine particles
basalts, mag. grains nature and implications for palaeomag. 79−84243
catalyst, mag. characterisation, review 78−64881
classical theory of superparamag. relaxation 77−8411
coercive force as function of temp. 79−87292
crystals with dislocations, phase transitions of the second kind, dislocation superparamagnetism *(Russian)* 80−1957
cubic anisotropy, asymptotic superparamag. time consts., negative anisotropy const. 78−10679
cubic anisotropy, asymptotic superparamag. time consts., positive anisotropy 78−10678
dipole interaction and mag. props. *(Russian)* 78−60316
FCC particles, relaxation times in external mag. fields 78−95482
Fe particles in glass-like C matrix, identification and props. 80−11229
fine particle system, coercivity and remanence, particle size distrib. effect 77−73053

superparamagnetism continued
frustrationless models, rel. to spin glasses 80−29561
GaAs:Fe, superparamagnetism, spontaneous magnetization 79−11285
glass, magnetic susceptibility measurement, torsional reson. technique 80−82796
interacting single-domain grains, thermoremanence and ideal magnetization calc. 79−25232
inverted state, relax. to equilib. state *(Russian)* 77−80968
iron(II)-A-zeolites, reduction, mag. and Mossbauer study 80−71115
magnesioferrite precipitated particles in MgO, resonance anisotropy field 77−69541
magnetic moment time development and discrete orientation model of particles 80−60378
magnetisation curling in superparamagnetic spheres 77−8363
magnetisation vector diffusion coeff., anisotropy energy, vol. distrib. of particles by Mossbauer effect 78−48099
magnetisation vector movement in superparamag. particles case, relax. freqs. *(Russian)* 79−95610
magnetisation vector of superparamag. particles 79−56494
magnetodipole broadening of reson. line *(Russian)* 79−38385
Metglas 2826-A, anomalous magnetisation, critical effects, superparamagnetism 77−8328
Mossbauer effect study of superparamagnetism, relax. of magnetisation vector 78−19402
Mossbauer relaxation spectra of superparamag. particles 77−66448
particles, Mossbauer spectra, magnetisation vector precession 80−15872
particles, mutual attraction 80−29581
red ochre, chem. anal. by Mossbauer spectroscopy, and superparamagnetism 78−20397
relaxation times, high order, superparamagnets with cubic anisotropy 77−69632
resonance anisotropy field of superparamag. particles 77−69541
spin glass materials, mag. field dependence of susceptibility peak 80−103840
spin glasses, theory, review 78−2696
spinels, domain wall formation inhibition, effect on bulk mag. props. 80−11220
spontaneous coherent state, phase transitions 78−47991
steel, stainless, sp. ht. 4 to 30K 79−61115
time constants of superparamag. particles 77−69631
ultrafine particles, VEROS prep. method and superparamag. props. *(Japanese)* 77−85954
$(Al_2O_3)_{0.2}(Ho_2O_3)_{0.2}(SiO_2)_{0.6}$, amorphous low temp., AC susceptibility, freq. depend. of spin freezing temp. 79−82808
Au-Fe, mictomagnet, freq. depend. of susceptibility max. 78−95445
$BaFe_4Ti_2O_{11}$, R-type hexaferrite, spin struct. and mag. props. 78−52216
$Bi_7Ti_{2.5}Sn_{0.5}Fe_3O_{21}$, layered ferroelec. antiferromag., superparamagnetism, Mossbauer spectra obs. 77−51999
$CaO-Al_2O_3-Fe_2O_3$, and resonance spectroscopy study *(Russian)* 77−55733
Co, anisotropy field, resonance meas. 78−64227
β-Co superparamag. FCC particles, hyperfine interaction, relax. Mossbauer spectra 79−78573
Co, ultrafine particles prepared by vacuum evap. on running oil substrate, mag. behaviour 79−28565
Co-Al alloys, deformed, superparamag. inclusions *(Russian)* 77−85416
Co-Ga, binary alloy, small-angle neutron scatt. from superparamag. behaviour 78−19217
Co-Ga-Mn, small-angle mag. neutron scatt., states of mag. order study rel. to Mn and Fe substitution 79−11292
$CoFe_2O_4$ ultrafine particles, prep. and mag. props. 80−71116
CoGa, onset of ferromag., diffuse mag. neutron scatt. meas. 77−63113
$Co_{0.54}Ga_{0.46}$, frequency depend. magnetisation, superparamagnetic behaviour 80−84624
$Co_{54}Ga_{46}$, superparamag. response to low DC fields 80−44860
$Co_2Ga_{2-x}Cu_x$, mag. and struct. phases from magnetisation, neutron, X-ray diffr. techniques 78−52253
$Co_2Ga_{1.95}Fe_{0.05}$, mag. behaviour, Mossbauer effect and DC magnetisation meas. 80−50244
$Co_2Ga_{2-x}Ni_x$, mag. and struct. phases from magnetisation, neutron, X-ray diffr. techniques 78−52253
$Co(N_2H_5)_2(SO_4)_2$:Co, Mossbauer effect and paramag. relax., superparamag. behaviour of correl. spin domains 77−69756
$CoO-Al_2O_3-SiO_2$, spin glasses, low-field susceptibility, freq. depend. 78−47981
$CoO-Al_2O_3-SiO_2$, spin glass, magnetic aftereffects 79−61176
$CoO-Al_2O_3-SiO_2$ glass, mag. ordering, Mossbauer exam. 77−24764
Cr-Fe, antiferromagnetic phase, superparamagnetic behaviour of Fe nearest neighbour atoms 79−15299
Cr-Fe, superparamagnetism and mag. order charact. near critical conc., neutron scatt. study 79−11293
Cu-Co, superparamagnetic, mag. aftereffects, dynamic neutron depolarisation study 80−50147
Cu-Co superparamagnetic particles, macrospin glass form. *(Russian)* 80−25165
Cu-Fe, dilute, low temp. heat capacity in mag. field, superparamagnetism 80−39804
Cu-Mn-Al, Heusler alloys, ferromag. inclusions, mag. props. and struct. study *(Russian)* 80−80570
Cu-Ni-Fe alloys superparamag. early stages of decomp. *(Russian)* 78−6890
Cu-Ni-Fe solid solution, after precip., susceptibility of interacting superparamag. grains 79−99733
$CuRb_2Br_1.2H_2O$, three-dimens. ferromag., crit. susceptibility exponents in Curie temp. region using relax. techniques 77−66304
$(Eu_xSr_{1-x})S$, dilute, magnetic 'blocking' 79−78348
$Eu_xSr_{1-x}S$, insulating spin glass, mag. props. 80−2589
$Eu_xSr_{1-x}S$, spin-glass props. and mag. transition 80−97105
Fe clusters, supported, Mossbauer spectra 80−7220
Fe colloidal dispersion, mag. props., struct. and oxidation 80−34699
Fe film, on Cu and Ag substrates, mag. props., Mossbauer spectra meas. 80−11233
Fe, finely dispersed, superparamagnetism, Mossbauer meas. 78−68303
Fe particles in Hg, ferromag. liquid, mag. props., ageing effects 77−12154
Fe ultrafine particles prepared by vacuum evaporation, mag. props. 78−35007
Fe, ultrafine particles prepared by vacuum evap. on running oil substrate, mag. behaviour 79−28565
Fe-Al, ferromag.-mictomag. transition, intermediate superparamag. 77−12140

superparamagnetism continued
Fe-Al_2O_3 granular film, interface props., Mossbauer spectroscopy 80−34336
Fe-Al_2O_3 granular films, superparamagnetism and relax. effects 80−71118
Fe-Cr-Ni, mag. state at low temps. *(Russian)* 78−56298
Fe-Gd film, amorphous, O_2 contamination effects on mag. props. 78−64231
Fe-SiO_2, granular compund, superpara- to ferromag. transition temp. meas. 77−69633
Fe-SiO_2 granular film, interface props., Mossbauer spectroscopy 80−34336
Fe-$SiO_2(Al_2O_3)(ZrO_2)$ granular films, superparamag., Mossbauer effect 80−7131
Fe-Ti, magnetism and H_2 storage 80−70941
Fe-ZrO_2 granular film, interface props., Mossbauer spectroscopy 80−34336
$Fe_{1-x}Al_xOOH$, Mossbauer study, determ. of Al content and mag. props. 80−39938
$FeGa_2O_4$, magnetic props. by Mossbauer effect, neutron diffr. and magnetisation meas. 77−43918
$FeMO_2S_4$, Mossbauer investigation, Neel point, superparamag. effects 80−97170
$Fe_{2(1-y)}Mg_{(1+y)}Ti_yO_4$, Mossbauer spectra anal., model 80−20560
$Fe(N_2H_5)_2(SO_4)_2$:Co, Mossbauer effect and paramag. relax., superparamag. behaviour of correl. spin domains 77−69756
$Fe_{1.6}Ni_{78.4}B_{10}P_{10}$ metallic glass, superparamag. behaviour, chem. inhomogeneities role 80−84625
$(Fe_{0.04}Ni_{0.96})_{80}P_{10}B_{10}$, amorphous magnetisation, field and temp. depend. 80−39755
$(Fe_xNi_{100-x})_{80}P_{10}B_{10}$, amorphous, elec. resist., 2 to 300K, composition depend. 80−44562
γ-Fe_2O_3 acicular particles, coercivity, magnetic recording tape appls. 78−14983
Fe_2O_3 amorphous layer on graphite, Mossbauer spectra, superparamag. props. 80−60474
α-Fe_2O_3, analysis of car exhaust by Mossbauer spectroscopy 78−92963
α-Fe_2O_3, inclusions in α-Al_2O_3, superparamag. props. 78−48405
γ-Fe_2O_3, small particle composite, preparation methods, superparamagnetism, optical transparency 78−60315
γ-Fe_2O_3 small particles, hyperfine field below superparamag. blocking temp., Mossbauer obs. 78−19392
Fe_2O_3 ultrafine particles in PTFE matrix, EPR and Mossbauer study 80−100625
α-Fe_2O_3-Cr_2O_3 solid solution, Mossbauer effect studies 80−71249
Fe_3O_4 ferrofluid suspension, mag. props., stability 79−87293
Fe_3O_4, ultrafine particles in ferrofluid, superparamag. and ferromag. reson. 78−15026
β-FeOOH, colloidal suspension, ionic spin relax. theory for Mossbauer spectra 78−19384
FeS_2, oxidation, Mossbauer spectroscopic and magnetokinetic studies, 400-500°C 80−44880
FeS_2, pyrite, magnetokinetics of oxidation, appl. to mag. separation from coal 77−12161
FeTi, hydrogenation, effect of surface segregation on mag. props. 78−84819
$Fe_{1-x}Ti_{1+x}$, Mossbauer study, superparamag. clusters 77−85633
$Fe_{3-x}Ti_xO_4$, spin glass behaviour, susceptibility and hysteresis meas. 80−65917
$GdCu_{1-x}Zn_x$, mag. struct. determ. 79−87238
Hg, liquid, ferromag., containing Fe particles, time depend. magnetisation 80−44877
$(Ho_2O_3)_{0.194}(Al_2O_3)_{0.227}(SiO_2)_{0.579}$, amorphous, low temp. spin glass behaviour 80−60297
(La, Gd)Al_2 spin glass, suscept. and sp. ht., mag. field depend. 79−61173
$LaNi_5$, magnetism and H_2 storage 80−70941
Li-Mg alloy, BCC, paramag. enhancement *(Russian)* 77−51878
$MgFe_2O_4$, small mag. particles, anisotropy field, resonance meas. 78−64227
$Mg_{0.5}Fe_{2.5}O_4$, ferrimag. epilayer, superparamag. interface, mag. props., FMR 78−95492
$(Mg_xFe_{1-x})_2SiO_4$, olivine, Fe-rich superparamagnetic clusters, Mossbauer study 79−82831
Mg_2Ni, magnetism and H_2 storage 80−70941
MnBi, mictomag. alloys, elastic props. *(Russian)* 80−7141
MnO-Al_2O_3-SiO_2, amorphous spin glass, AC susceptibility 80−80520
MnO-Al_2O_3-SiO_2, spin glasses, low-field susceptibility, freq. depend. 78−47981
MnO-Al_2O_3-SiO_2 glass, spin freezing, muon spin depolarisation 78−39491
MnO-Al_2O_3-SiO_2 glass, spin freezing, muon spin depolarisation, superparamag. domain model 78−68272
$Na_2O.2Al_2O_3.5SiO_2:Fe^{3+}$, Mossbauer effect and magnetometric exam. 78−6613
$Na_2O.2B_2O_3$-Fe_2O_3 glass, Fe_2O_3 crystallite formation, Mossbauer obs. 78−68429
Ni dispersions, semi-amorphous, on Al_2O_3-graphite, mag. characterisation 80−44876
Ni film, adsorbed $H_2(CO)$, ferromag. reson. exam. 78−15028
Ni microcrystals, H_2 chemisorption effect on superparamagnetic relax. time, Mossbauer meas. 79−61284
Ni, ultrafine particles prepared by vacuum evap. on running oil substrate, mag. behaviour 79−28565
Ni-Cr, low temp. sp. ht. near ferro-paramag. transition 77−63218
Ni-Cu, nearly ferromag., heat capacity meas. in mag. field 0.3 to 4K, superparamag. clusters 77−69579
Ni-P electrodeposit, magnetisation coercivity and magnetostriction 78−68338
Ni-V, low temp. sp. ht. near ferro-paramag. transition 77−63218
$NiFe_2O_4$ precipitation from silicate glass, Mossbauer study 80−54998
NiO catalyst, superparamagnetic, elec. props. 79−65506
$Ni_{0.25}Zn_{0.75}Fe_2O_4$, Mossbauer study, spin fluctuations 80−60471
Pt-Fe alloys, supported, mag. prop. meas. in H_2 and O_2, 77 to 700K 79−91257
Pt_3Fe, collision cascades, neutron induced superparamagnetism *(Russian)* 78−2166
$RbFeCl_3.2H_2O$, 2D Ising system, crit. fluctuations, Mossbauer spectra study 80−44842
Sm, polycrystalline with ferromag. impurities, mag. props., 1.5-300K 77−69547

superparamagnetism continued
$SmCo_5$, amorphous, supermag.-ferromag. transition and directional crystallisation 80−65891
$(Ti_{1-x}V_x)_2O_3$ spin glass, mag. props., metallic antiferromagnetism 79−82791
$V_{1-x}Fe_x$, low temp. sp. ht. and mag. props. 80−2548
$V_{1-x}Fe_xH_n$, low temp. sp. ht. and mag. props. 80−2548
$Y_{1-x}Fe_x$, amorphous, spin resonance exam. 79−51860
$ZnFe_2O_4$, neutron damage effects, superparamag. state replacement cascades 77−16051
$Zn_{0.8}Mn_{0.2}Fe_2O_4$, spin interaction, neutron diffr. and Mossbauer effect meas. 77−4501

superplasticity
activation enthalpy determ. from strain rate changes in tensile tests 80−81127
alloy, anomalous response to notch under superplastic conditions 78−52930
alloy, flow and failure, review 80−50690
alloys, cavity growth 80−93627
alloys, grain size effect on maximum strain rate sensitivity 79−100227
α/β brass, cavitation during superplastic deform. 79−5011
α/β brass, grain boundary sliding and intergranular cavitation during superplastic deformation 79−5009
brass, recrystallization during induction heating 80−97511
brass, superplastic deform. rate rel. to flow stress, determ. methods 78−60709
brass α/β, two-phase superplastic alloy, hydrodynamical behaviour, constitutive law 80−40452
cast Fe, white, superplasticity parameters 77−56042
cavitation of superplastic materials, validity of diffusion creep mechanism 77−44296
cavity growth anal. during superplasticity 80−60923
creep, grain-boundary sliding controlled, grain rolling, superplasticity 77−90399
deformation mechanisms, review 80−50691
Duralumin 2017, superplasticity *(Korean)* 79−38902
Earth mantle, structural superplastic creep and linear viscosity 77−5155
feldspars, superplastic flow and cryst. chemistry changes 79−79831
finely crystalline materials rel. to displacement along grain boundary *(Russian)* 80−15184
flow in unsteady and steady state regions 79−42135
grain boundaries during superplastic deform., dislocation density and diffusion parameters 79−65099
grain boundary sliding and its accommodation during creep and superplasticity 77−40436
heat-resistant alloys, installation for mech. tests under superplasticity conditions 80−55603
internal friction in superplastic alloys 77−16635
mechanism rel. to hyperfine grain struct. 78−84930
metal, dislocation kinetics of superplasticity and creep 77−76404
metal, high plasticity, fracture nature *(Russian)* 77−25149
metals, mechanical props., testing and modelling 80−25811
microcrystalline alloys, metastable, rapidly quenched particulates, props. appl. and production 80−84887
microstructure resulting from alloying and heat treatment, effect on creep, fatigue, fracture strength 78−11246
porous materials, sintering kinetics, superplasticity of polycryst. materials 79−100072
porous structure, shrinkage kinetics, boundary slip and superplasticity 77−36611
powder metallurgy superalloy, wrought, phase relations and microstruct., C and Hf conc. effect 77−44218
refractory multiphase systems, infusible, some novel effects, rel. to practical appls. 80−55460
region I characteristics 80−107357
rheological and metallurgical discussion of superplastic behaviour 78−30200
slip band theory, model for creep based on dislocation climb at grain boundaries 79−37756
steel, 0Kh12G14N4Yu2, struct. after deformation under conditions of superplasticity 80−21031
steel, austenitic stainless, ferritic, prep. with fine grains by cold rolling and recrystallisation, superplasticity *(French)* 78−35406
steel, C, deformation peculiarities at high temp. under superplasticity with cyclic thermal load *(Russian)* 78−95776
steel, carbon content influence on superplastic charcts. *(Russian)* 77−21218
steel, cavitation during superplastic flow, affecting factors 78−60728
steel, Cr, stress relaxation, superplasticity and thermal cycling *(Russian)* 80−21019
steel, eutectoid, superplasticity parameters 77−56042
steel, eutectoid and hypoeutectoid stress relaxation during rapid heating transform. *(Japanese)* 78−11258
steel, eutectoid and hypoeutectoid viscoelasticity under transformational superplasticity *(Japanese)* 77−52416
steel, high C, Cr addition effect on superplasticity 79−15729
steel, Kh20N80, during creep resist. testing *(Russian)* 77−44294
steel, low C, high temp. plastic flow under thermal cycling in superplasticity interval 77−70130
steel, martensitic, Cr-Ni, grain refining and phase transforms. effect on plasticity *(Russian)* 78−39837
steel, stainless, 0Kh12G14N4Yu2, effect of plastic deform. on biphase struct. 78−44176
steel, stainless, ferrite to austenite decomposition 80−3073
steel, U8A, 5KhNM and 12KhNZA, superplasticity under compression 77−86086
steel USA, spheroidised pearlitic, superplasticity *(Russian)* 78−19826
steels, ultrahigh C, superplastic, mech. behaviour at elevated temps 80−21028
strain diagram relationship *(Russian)* 77−59854
strain rate sensitivity of tensile flow curve *(German)* 77−63733
structural, theory 80−16386
structural theory 77−63735
superalloy, hot consolidation of rapidly solidified powders, review 79−33965
superplastic deformation, grain rearrangements 78−83828
theories 79−19309
two-phase materials, role of interphase-boundary dislocations, ledges and diffusion 78−11295
two-phase structures, high-temp. deform. 78−68738

superplasticity continued
Zircaloy, micrograin superplasticity at 850°C 78−23758
Zircaloy-4, exam. of plastic props. at elevated temps. in air 77−4811
Zircaloy-4, strain rate sensitivity parameter measurement, from expt. load vs. time curves, superplastic range 79−8406
Al alloy V96Ts, superplasticity 79−52326
Al, high purity, cyclic torsional deform., factors influencing ductility 77−56031
Al, impurity influence on superplasticity, elongation decrease at rupture *(Russian)* 79−91735
Al, single and polycrystals in torsion, superplasticity *(Russian)* 78−3180
Al, single crystal 79−1901
Al, superplastic deformation depend. on subgrain struct. electron microscope study *(Russian)* 79−83257
Al-Ca-Zn (5,5 wt.%) superplastic sheet alloy, mechanical properties, superplastic forming behaviour 80−60920
Al-Cu, single and two phase, superplastic behaviour 80−11709
Al-Cu (33 wt.%) eutectic, superplasticity, in-situ obs. by TEM 77−28876
Al-Cu-Zr, particle stabilized structures, hot deform. 79−47733
Al-Cu-Zr, superplastic alloy Supral, solidification and recrystallisation 80−7550
Al-Cu-Zr (6, 0.3 wt.%), superplastic, texture studies 79−83210
Al-Cu-Zr (6, 0.3 wt.%), superplastic, mech. anisotropy and deformation mechanisms 79−83254
Al-Cu-Zr (6, 0.4 wt.%), superplastic flow activation energy 80−11701
Al-Cu-Zr (6, 0.4 wt.%), superplastic deformation charact. 80−16387
Al-$CuAl_2$ eutectic, superplastic behaviour during compressive deform. 77−52429
Al-Ge, structural changes during superplastic deformation, grain boundary porosity *(Russian)* 79−83258
Al-Ge (0 to 8 wt.%), superplastic props. *(Russian)* 80−45345
Al-Ge (4 wt.%), superplasticity exam. *(Russian)* 78−39836
Al-Mg, fracture during superplastic flow 78−60729
Al-Mg, grade 5083, superplastic, interaction effects during growth of drilled holes 79−38923
Al-Mg alloy, superplastic behaviour, effects of bidirectional twisting 77−70129
Al-Mg alloy AMg6, US vibr. during superplastic deform. effect on struct. 79−38911
Al-Mn-Zr (0.9, 0.4%), strain induced continuous recrystn., rel. to superplastic behaviour 78−84915
Al-Si eutectic alloys, superplasticity 80−11710
Al-Zn, tension deformed superplastic specimens, instantaneous strain rate variation *(Russian)* 79−79033
Al-Zn (22 wt.%), superplastic strain rate sensitivity, rel. to ductility 78−31478
Al-Zn alloys, recrystallisation and superplasticity, HVEM straining 80−39207
Al-Zn eutectoid, superplasticity, test machine rigidity effect 79−70250
Al-Zn-Mg, cavitation during superplastic deform. *(Japanese)* 78−15464
Al-Zn-Mg (9, 1 wt.%), superplastic flow, relative motion of grains 77−52426
Al-Zn-Mg superplastic alloy, cavity growth under creep conditions 80−60940
AlGe (4 wt.%), struct. peculiarities of superplastic behaviour due to porosity 79−34111
Be, brittleness problems, elevated plasticity and superplasticity, temp. depend. *(Russian)* 79−15758
Be-Ni(Y), plastic deform., flow stresses, fracture *(Russian)* 80−108496
Bi-Pb-Sn, eutectic alloys, struct. instability and absence of superplasticity *(Russian)* 77−8882
Bi_2MoO_6, transform. superplasticity 80−108498
Bi_2WO_6, transformational superplasticity 80−108498
C steel, superplasticity due to successive deformations *(Russian)* 80−55464
Cd-Sn, eutectic alloys, struct. instability and absence of superplasticity *(Russian)* 77−8882
Cu alloy, superplastic, microscopic examination of internal void formation 80−16383
Cu alloys, cavitation during superplastic flow, affecting factors 78−60728
Cu foil, role of grain-boundary porosity in superplasticity *(Russian)* 78−56690
Cu-Al (9.3 wt.%), in torsion, deformation temp. depend., superplasticity due to grain size, dislocation density *(Russian)* 79−74200
Cu-Ni-Zn, microduplex, superplastic deform., cavitation and fracture 78−64640
Fe, Armco and carbonyl, kinetic singularities of plastic deform. during $\gamma \rightarrow \alpha$ transform. *(Russian)* 78−92262
Fe, commercially pure, viscoelasticity under transformational superplasticity *(Japanese)* 77−52416
Fe laminates, superplastic bonding 80−25981
Fe-Mn-C, struct. superplasticity 80−76317
Fe-Ni-Cr-Ti based alloy, 36 NKhTYu, high temp. deform. charact. *(Russian)* 77−63719
Mg-alloy, superplastic deformation mechanism, deformation model 78−31477
Mg-Mn-Ce, structural changes and deformation during superplastic flow 78−15472
Mg-Mn-Ce (1.5, 0.3 wt%), superplasticity role of diffusional creep *(Russian)* 80−97528
Mg-Mn-Ce (1.5%, 0.3%) alloy, dislocation slip during superplastic deform. *(Russian)* 77−21214
Mg-Mn-Ce alloy, superplastic deform., role of grain boundaries 78−19843
Ni alloy ZhS6KP, heat-resist., superplastic deformation, effect on struct. 79−96090
Ni-Al_2O_3 alloy, electron beam evaporated, struct. and mech. props. 78−11114
Ni-Co-Cr-Ta-Al-W-Mo-Ti, cast, phase volume fraction determ. using manual point count practice 78−53052
Pb and Pb-Tl (2.5 wt.%), grain boundary sliding, grain size and stress effects 78−27571
Pb, film, hillock formation by grain boundary sliding 80−107673
Pb-In (40 wt.%), solid soln., single phase, superplastic behaviour 80−21048
Pb-Sn, eutectic, electron emission avalanche obs., during isothermal superplastic deform., *(Russian)* 77−48324
Pb-Sn, eutectic, superplastic behaviour, grain size effect 80−7635

superplasticity continued
Pb-Sn, eutectic alloys, struct. instability and absence of superplasticity *(Russian)* 77−8882
Pb-Sn (62 wt.%), activation energy for superplasticity 77−86112
Pb-Sn (62 wt.%), intercrystalline and interface boundary sliding, tensile tests, SEM obs. 79−38886
Pb-Sn eutectic, appl. of SEM specimen holder for cold tensile deform. expts. *(French)* 77−36704
Pb-Sn eutectic, cavitation during superplastic flow, affecting factors 78−60728
Pb-Sn eutectic, strain rate sensitivity index, expt. comparison of different methods 80−3144
Pb-Sn eutectic alloy, superplastic deform. of circular sheets *(French)* 77−28871
Pb-Sn eutectic alloy, superplastic deform. at relatively high strain rates 79−57042
Pb-Sn microduplex eutectic, cavitation during superplastic flow due to hard particles 77−36575
Pb-Tl, sliding and its accommodation during creep and superplasticity 77−40436
Pd-Sn-Cd alloy, non-unique stress/strain rate relations during superplastic flow 77−28855
Sn-Bi, eutectic, superplastic anisotropy *(German)* 80−25808
Sn-Pb eutectic, strain rate sensitivity of flow stresses, grain boundary sliding during superplastic, non-superplastic deform. 80−7645
Sn-Pb-(Bi)(Ag)(Sb) (Cu), microduplex eutectic, cavitation during superplastic flow 78−48457
Sn-Zn (9.8 wt.%), eutectic superplasticity 77−36582
SnPb 38, superplasticity, effect of ageing *(Czechoslovakian)* 77−32644
Ti alloy OT4, high plasticity effect 80−35272
α and $\alpha+\beta$Ti alloy of different stability, exponential law use for anal. of strain hardening process 79−15697
Ti alloy TA6V, superplastic behaviour of welded specimens 77−86100
Ti alloy VT6s, superplastic state eqn. for sheet in biaxial tension 79−66131
Ti-Al-V (6, 4 wt.%), superplastic, mech. behaviour and hardening charcts. 79−83269
Ti-Al-V (6,4 wt %), superplasticity, effect of temp. 80−7639
Ti-Al-V (6,4 wt.%), effects of grain size on superplasticity, deformation mechanisms, microstructural characteristics 79−52323
Ti-Al-V (6,4 wt.%), plastic flow instability and multiple necking during superplastic flow 77−8896
Ti-Al-V (6,4 wt.%) superplastic deform. 78−31471
Ti-Al-V (6,4 wt.%) superplastic alloy, maximum attainable ductility 80−60919
Ti6A14V, superplastic deform. of circular sheets *(French)* 77−28871
U-Mo (1.5 wt.%), superplastic behaviour 450 to 720°C *(French)* 79−74203
UO_2, superplastic creep 79−15730
Zn-22 wt.% Al superplastic eutectoid alloy tensile deformation obs. *(Japanese)* 79−90714
Zn-Al, dislocation slip peculiarities during superplastic deform. 79−20102
Zn-Al (0.4 wt.%), intergranular slip during in situ superplastic deform. 80−96538
Zn-Al (1.1 wt.%) superplastic alloy, grain size determ. *(Czech)* 80−81118
Zn-Al (20 wt.%) superplastic alloys, Zn diffusion, strain influence *(Russian)* 79−37870
Zn-Al (22 at.%) eutectic, superplastic, microscopic examination of internal void formation 80−16383
Zn-Al (22 wt.%), activation energy for superplasticity 77−86112
Zn-Al (22 wt.%), eutectoid alloy, ductility and fracture 78−60819
Zn-Al (22 wt.%), eutectoid, low stress and superplastic creep behaviour 80−81120
Zn-Al (22 wt.%), meas. of plasticity parameters under superplastic flow 78−60710
Zn-Al (22 wt.%), superplastic eutectoid cavitation evidence 77−63741
Zn-Al (22 wt.%), superplastic deform. mechanism, electron microscope obs. 78−3167
Zn-Al (22 wt.%), superplastic deform. rate rel. to flow stress, determ. methods 78−60709
Zn-Al (22 wt.%), superplastic, of very high purity, cavitation 79−24586
Zn-Al (22 wt.%), superplastic eutectoid, concurrent grain growth and deformation mechanism 79−74222
Zn-Al (22 wt.%), texture effect on superplasticity 79−20103
Zn-Al (22 wt.%) eutectoid, superplastic, factors affecting ductility 77−86097
Zn-Al (22 wt.%) superplastic alloy, grain growth texture 80−81075
Zn-Al (40 wt.%), superplastic deform., dislocation effects 77−48515
Zn-Al alloys, comp. effects on intergranular slip during superplastic deform. *(Russian)* 77−32633
Zn-Al alloys, dislocations obs. in superplastic deformation 78−51549
Zn-Al eutectoid, superplasticity, study by electron microscopy 77−48479
Zn-Al eutectoid superplastic alloy, fatigue, microstruct. obs. and frequency effect 77−36659
Zn-Al superplastic eutectoid alloy, low strain rate behaviour 80−40458
Zn-Al-Cu (18, 4 wt.%), plastic deform. at room temp., superplastic props., tensile strength *(Czech)* 80−45360
Zn-Al-Cu (18, 5 wt.%) alloy, superplasticity *(Russian)* 77−59856
Zn-Al-Cu-Mg (22, 0.5, 0.01 wt.%), superplastic alloy, strengthening mechanism *(Japanese)* 77−55975
Zn-Al(22 wt.%), alloy sheet, superplastic, cold-rolling effects on mech. props. and microstructure *(Japanese)* 80−71671
Zr-Nb (2.5 wt.%), superplasticity 77−12669
Zr-Nb (2.5 wt.%), superplastic and strain rate depend. plastic flow, 873 to 1373K 80−30052
Zr-Nb microduplex alloys, struct. and props. 78−3170

superradiance
see also acoustic superradiance
alkali metal, Rydberg states and microwaves, spectroscopy, masers and superradiance study 80−53248
amplified spontaneous emission in spherical and disk-shaped laser media 80−1177
amplifier, degenerate, swept-gain, steady-state pulse behaviour 78−87033
atom, superfluorescence initiation 79−781
atom-coupled-to-field system, coherent radiation, phenomenological theory 77−14683
atomic oscillatory superfluorescence, statistical props. 80−47938

superradiance continued
atomic state, superradiant, excitation by pulse of quantum field 80−87359
atomic system, superrad. phase transition nonoccurrence 79−41360
atomic system, superradiant Raman scatt. of light *(Russian)* 79−36964
atoms, spontaneous and stimulated emission 77−79788
backward Raman amplifier for excimer laser pulse compression, parasitic superfluoresc. suppression 80−69453
bidirectional laser amplifiers, amplified spontaneous emission intensity fluctuations 80−37988
coherence properties, initiating noise source obs., intrinsic delay time quantum fluctuations 80−58492
collective effects in weakly ampiifying media *(Russian)* 77−83841
collective processes in slightly inverted and absorbing media 80−87367
computerised analysis, collaboration collection report 80−73106
cooperative cascade emission, linear stochastic theory 80−74326
cooperative cascade emission theory, nonlinear evolution 80−74327
cooperative emission by polyatomic system, homogeneous and inhomogeneous broadening *(Russian)* 77−46713
cooperative spontaneous emission theory 79−27223
counterrunning light waves interaction in mirrorless device 79−98333
crystals with paraelectric impurities, superradiative transitions, acoustic and EM excitation 78−66872
Dicke Hamiltonian, spin-spin interaction on super-radiant phase transition 78−16762
Dicke model, generalised, canonical transform theory 77−19216
Dicke model, nonlinear extensions, second order phase transitions 77−34855
Dicke model Hamiltonian, coherence props. of radiation field 78−58959
Dicke model of phase transitions, rel. to optical bistability 79−81402
Dicke models, generalized, superradiant phase transition 77−65585
Dicke state N two level atom assembly, radiation emission theory 80−69350
Dicke superradiance angular depend., rel. to angular correlation between far IR and pump radiation 79−41370
Dicke-maser model dynamics, phase transition to the spontaneous coherent state 78−66792
diffusion eqns. invariant solns. 77−75458
distributed feedback due to meeting of oppositely propag. noise waves, beats *(Russian)* 77−71965
Doppler beat observation 78−66794
dye, tunable superradiant emission, planar cell 77−7116
dye amplifier, amplified spontaneous emission and spatial depend. of gain 78−42332
dye DFB laser, N_2 laser pumped, external mirror effect on characts. 78−42352
dye energy transfer laser, intermol. interactions and spectral shifts 78−74902
dye laser, superluminesc. pulse waveform *(Russian)* 78−22120
dye laser, superluminescent source of optical noise for nonlinear optics *(Russian)* 78−79033
dye laser, superradiant, coherence and beam geometry 78−37876
dye laser amplifiers, exam. of photonic efficiency *(French)* 78−59004
dye solution, amplified spontaneous emission, effect of O_2 80−95885
dye solution amplifying dynamic holograms, wavefront reversal 80−48331
dye solutions, amplified spontaneous emission with picosecond light pulses 78−82965
dye solutions, light-induced grating form. by two independ. laser beams, DFB effect 79−94230
dye superradiance and damping characteristics obs. 77−83869
dye vapour pumped by N_2 laser, fluorescence and amplified spontaneous emission characts. 79−3694
dynamical behaviour in model mag. insulator 80−87358
education, spontaneous emission and superradiance, coherence effects, semiclassical 77−82347
exciton, superradiance and free induction decay, theory 79−37992
exciton echo intensity, closely spaced energy levels effect 77−20244
extended optically thick medium, superradiance theory 77−23637
extended system, semiclassical model *(Russian)* 79−36864
fluctuating field source superfluorescence, quantum mech. derivation of Maxwell-Bloch eqns. 79−55096
fluoromethane, single-mode optical pumping, superradiant far IR emission 78−42329
free electron laser, coherent transients, laser lethargy and coherence brightening 79−94204
gain measurement in optically pumped materials, diffr. effect 77−19225
gas superluminescence in high-current discharge, polarisation due to Zeeman splitting 80−100060
harmonic oscillators system, superradiant decay 78−42314
independent-atom picture for superradiant system 77−58303
indrr gas halogen exciplex, spontaneous and superfluoresc. emission, pumping of I laser 77−34883
Josephson oscillators, quantum stochastic process in thermodynamic limit 77−37814
Kerr black hole, massive fermion superradiance 79−25948
laser amplifier, amplified spontaneous emission and gain saturation nonlinearity 77−31087
level degeneracy, theory 77−75461
level degeneracy effects, $j=1/2$ to $j'=1/2$ dipole transition 79−22924
limiting characts. 79−36863
many-level molecules, unitary dynamical symmetry for superadiance, classical limit 78−9355
many-level system, spontaneous coherent responses, from states involving super-radiative phase transitions *(Russian)* 78−71069
master equation, exact soln., for arbitrary initial excitation 77−83839
master equation, exact solution for complete initial excitation 77−68200
metal atom lasers, finely dispersed metal particle active medium 80−91777
metal surface, reson. interaction with neutral mol. 77−80702
methyl fluoride, Dicke superradiance obs. in far IR emission 77−38841
microwave superradiance and maser action, in alkali Rydberg atom system 79−86153
molecular system, superradiant Raman scatt. of light *(Russian)* 79−36964
molecular system interacting with radiation field, equilib. mean values 79−27224
multi-level system, swept excitation model 78−9354
multilevel system, group theoretical method for coherent effects calc. 80−106502
superradiance continued
multiplication of spontaneously emitted photons by means of quantum mech. amplifier *(Russian)* 77−75463
N two-level atoms, interaction with radiation field in restricted rotating wave approx. 80−5713
N-atom system, superradiance and energy transfer 77−3558
N-two level atoms, interaction with radiation field in restricted rotating wave approx., numerical anal. 80−5714
non-centresymmetric media, phase transitions into spontaneous coherent state *(Russian)* 80−69353
nonlinear swept gain amplifiers, energy and power fluctuations 79−55095
octupole and hexadecapole dynamics in solid state physics, algebraic struct. 77−88682
organic molecules in solution, selective two-stage excitation, ultrashort-pulse oscillator 79−64283
oscillatory, quantum fluctuations effect 77−14682
oscillatory superfluorescence, Markovian master eqn. model 79−27222
oscillatory superfluorescence, quantum statistics 79−917
parametric amplification based on four-wave parametric processes in two-photon reson. 79−94296
parasitic superfluorescence suppression in backward Raman amplifiers 80−38073
phase transition problem, applicability of Wang-Hion method 80−31695
phase transitions, superradiant, gauge invariance theory 78−66795
photonic efficiency of dye laser amplifiers *(French)* 78−59004
plasma, nonideal, in electric field 80−38568
plasma flow, spontaneous superradiance of at. and mol. ions 77−3470
polyatomic molecules excited by CO_2 laser pulses, stimulated emission *(Russian)* 79−94214
polymethine dye unstable photoisomers, superluminesc. and stimulated emission 79−31896
POPOP dye vapour lasers, optical and electron beam pumping, review 80−48237
POPOP vapour, electron beam excited superradiance 78−66820
POPOP vapour, picosecond generation of radiation 80−48238
pulse intensity fluctuations, quantal macrovariables calcs. 77−3559
pulsed amplified spontaneous emission source, statistics and spatial distrib. meas. 78−22102
pump depletion effect, superradiance in Raman light scatt. 80−9957
quantum beats, superfluoresc. chirping role, Lamb shift sign change 79−31474
quantum theory, for N-two-level atom system 77−75459
relaxation from complete inversion, fluctuations, scaling theory 77−38840
resonance fluorescence of thin crystal films, superradiance 78−68573
resonant scattering of intense beam of radiation by assembly of atoms in small vol. 77−34853
RF, optical pulse generated under photon-echo conditions 80−95858
rhodamine 6G, emission kinetics in ps. range 78−13699
rhodamine 6G, superluminesc. band structureless spectra 79−7124
rhodamine 6G solns., picosec. kinetics of emission 79−76685
rhodamine dye solns., amplified spontaneous emission 79−45941
rhodamine dyes, amplified spontaneous emission, picosecond pulse generation 79−3691
ruby laser, generation, amplification of high power picosecond pulses depend. on superluminescence 80−53305
ruby NMR laser, dynamic props. from point of view of synergetics 80−43341
ruby NMR laser, spontaneous nucl. spin system self organisation 79−916
scaling, nonequilibrium systems near instability point, anomalous fluctuation theorems in extensive region 77−2612
scaling theory and exact soln., fluctuations and relax. near instability point 78−37864
Schwinger source theory 80−48195
semiconductor, superradiant phase transition 77−44047
semiconductor laser diode, modulated optical output, relax. oscills., superradiation effects 77−7150
semimetal, superradiant phase transition 77−44047
slightly detuned sources, quantum theory 80−14307
solid state, review 79−51988
spatial structure formation 79−64215
spatial variation with time, numerical anal. *(Russian)* 80−78821
spatially extended medium, oscillating superfluoresc., leading pulse shape and delay 80−23648
spectroscopy, superradiance triggering 80−52324
spin systems in phase transition to superradiant state, dynamics and thermodynamics 79−22925
subharmonic, two-level atom system 79−18385
superfluorescence, delay-time statistics and inhomogeneous line broadening 80−99684
superfluorescence, macroscopic quantum fluctuations 79−76651
superfluorescence, oscill., appl. of soln. of sine-Gordon eqn. with boundary conditions 79−27221
superfluorescence, phase-wave fluctuations 80−23652
superfluorescence, tipping angle and quantum fluctuations, pumping process effects 80−5718
superfluorescence beats, theory incl. quantum fluctuations and finite sample size 80−102686
superfluorescent pulse fluctuation 80−58490
superfluorescent systems, fluctuations, semiclassical theory 77−58301
superluminescence, spatial coherence 80−99683
superluminescence polarisation obs. of high-current pulsed discharge in gas with anisotropic gain 79−14515
superluminescent laser theory for dye soln. *(Russian)* 79−951
supernonradiative phase transition, appl. to paramag. impurities in strong mag. field 79−14898
swept-grain amplification, semiclassical theory 79−31846
thin-film distributed optically excited laser, signal suppression by superluminescence radiation *(Russian)* 78−87091
thin-film waveguide laser amplifier with lossy cladding 80−64074
three-level atoms, streak camera obs. of superradiance development 79−18384
three-level molecular system, cooperative evolution, transient effects of dephasing and relax. 80−28184
three-level molecules, cooperative behaviour, transient effects of coherent optical pumping 79−13938
three-level system, cooperative cascade emission 78−78659
three-level systems, superradiance and subradiance 80−83570

superradiance continued
transition point from conserving to non-conserving regimes, emission rates and critical times 77−23638
transverse effects in superfluorescence 80−37979
two level atoms, quantum stochastic process in thermodynamic limit 77−37814
two-(three-)level systems, steady and transient behaviour 78−1200
two-level atom system, superfluorescence and amplified spontaneous emission 79−85933
two-level atomic system, superfluoresc. fluctuations 80−23651
two-level atoms, Dicke superradiance and superluminosity, fine struct. and time evolution 77−65438
two-level atoms, effect of high-power coherent radiation on spontaneous emission 79−55094
two-level atoms, inhomogeneously broadened, superfluoresc. and amplified spontaneous emission 80−106499
two-level atoms, spontaneous polarisation capacity, Dicke model *(Russian)* 79−10277
two-level atoms system, quantum theory, incl. propag. effects 80−58491
two-level degenerate system, superradiance 78−46553
two-level ensemble interacting through EM field, phase transition, collective polarisation 77−19218
two-level molecular ensemble, cooperative decay 77−88681
two-level molecule interacting with light, Dicke model asymptotic behaviour 79−3508
two-level molecules, gauge-invariant system, superradiant state, phase transition 80−69352
two-level system in radiation field, dynamics, temp. depend. props. 78−66793
Volterra cycles and cooperative fluoresc. crit. point 79−3667
Wannier excitons, radiative decay in thin crystal fields 80−92823
wave front inversion in superluminescence *(Russian)* 79−3669
waveguide laser, stimulated emission spectrum, leaky modes *(Russian)* 80−87400
X-ray superradiance, criteria 77−88680
γ-rays from pair recombination in travelling wave struct., stimulated emission 78−37863
Al^{3+} ion, plasma in fast evolution, time-resolved soft X-ray absorpt. transitions 77−18827
$Al_xGa_{1-x}As$ DH laser material, Ar laser induced catastrophic damage 79−86178
$Al_xGa_{(1-x)}As$-$Al_yGa_{(1-y)}As$ DH optically pumped laser, room temp. single pass gain 77−75511
ArCl superfluorescent laser, discharge-pumped, laser action at 175 nm 77−38859
ArF superradiance laser excited by electric discharge 77−19236
CdS active surface, exciton stimulated emission and superradiance refl. spectra, props. 80−25411
CdS crystals, one-photon pumping, active layer structure, light amplification 80−78858
CdS, gain spectroscopy and plasma recomb. 78−88327
CdS, induced absorption and gain from high density excitons 78−68533
CdS laser radiation under excitation by pulsed bremsstrahlung X-rays 79−91467
CdS, superluminescence due to pulsed X-rays, 170 and 295K 78−42338
Cs atom, F-levels lifetime meas. using partially superradiant population 80−9575
Cs, superfluorescence, comparison with theory, quantum beat spectroscopy appls. 78−86837
Cs, superfluorescence of vapour, effective initial tipping angle 79−22923
Cs, superradiance triggering spectroscopy 80−52324
Cu I lines, superradiance obs. in pulse vaporisation of pulverised Cu_2O, CuO 79−45934
Cu, superradiance at 511, 578 nm during two discharge current pulse vaporis. *(Russian)* 78−29942
Cu vapour pulsed laser, spectral comp. of superradiance, stimulated and spontaneous radiation 80−102713
Cu-Ne mixture, 3-20 kHz pulse discharge obs. 78−71092
D_2O, far IR superradiant laser, 114, 66 μm emission, time-resolved pulse and wavelength meas. 77−88715
D_2O laser, optically pumped, superradiant line obs., 235, 280, 97 and 98 μm 78−1215
D_2O laser, zigzag-pumped, oscillator and superradiance characteristics 79−31873
D_2O, laser oscillator-amplifier system, superradiant background radiation 77−54724
D_2O oscillator, zigzag pumped, superradiant 66 μ emission 78−33743
D_2O, single-mode optical pumping, superradiant far IR emission 78−42329
D_2O superradiant laser, Raman shifts of 99 μm output, Fabry-Perot freq. meas. 79−55120
D_2S, CO_2 laser pumped, high power far IR superfluorescent emission 79−27243
Eu, visible Dicke superradiant transitions *(French)* 79−45690
Eu, visible Dicke-superradiant transitions 79−45692
Eu, visible superfluorescence cooperative reson. Stokes radiation 80−5500
$Fe(CO)_5$ photodissociation laser 78−74886
FeF_2:Mn, mag. polariton, impurity mode enhancement and superradiance effects 79−28622
GaAs injection laser, intensified luminesc. *(Russian)* 78−90416
GaAs, junction laser, spectral hole burning 79−50291
HDS, CO_2 laser pumped, high power far IR superfluorescent emission 79−27243
He-Ne laser, field distrib. and spatial coherence of superluminescence at 3.39 μ transition *(Russian)* 78−13682
He^{2+} + Li collisions, soft X-ray emission obs. 80−83591
^4He atomic Bose system, equilibrium superradiance 78−55994
Hg photodissociation laser, optically pumped 77−68206
I_2, B-X system superfluoresc. emission obs., 1.1 to 1.3 μm 79−81412
InGaAsP-InP DH lasers, spatial hole burning, spontaneous emission saturation, direct obs. 80−95892
KCl:Li^+, coherent excitation by EM and acoustic waves, induction and echo signal study 78−67773
KCl:OH^- type paraelec. systems, phonon superradiant phase transition *(Russian)* 79−69206
KH_2PO_4, ultrashort light pulse parametric transform. under optimum interaction conditions 80−99791
KrF superradiance laser excited by electric discharge 77−19236
$La_2Mg_3(NO_3)_{12}.24H_2O:Nd^{3+}$, proton raser, self-radiating nuclear spin system *(German)* 80−53298
superradiance continued
LiF single crystals, visible superradiance of excited F_2-centres 79−33733
N_2 laser, compact high-power TEA, superradiant laser pulses 78−90427
N_2 laser, single freq. emission, superradiance line splitting 77−75495
N_2 laser, superrad., inexpensive construction *(Korean)* 78−22147
N_2 superfluorescent UV laser, demonstration 80−105475
N_2 superradiant UV laser, method for brightness increase 79−36917
N_2^+ discharge laser, superluminosity, spatial-spectral struct. 79−55116
N_2^+ high-pressure laser, superradiance spatial structure 79−64215
NH_3, efficient energy extraction by superradiant emission 80−53271
$^{14}NH_3$, high power vibr.-rot. emission, optically pumped off reson. 77−7068
Na, laser excited fluoresc., saturation power, calc. and obs. 77−42276
Na vapour, superradiance, quantum beat spectra 80−106311
Nd:YAG giant pulse lasers, energy charact., superradiance effects 80−64031
Ne, pulsed amplified spontaneous emission source, statistics and spatial distrib. meas. 78−22102
Ne, pulsed amplified spontaneous emission intensity, spatial and frequency distribs. 79−50270
Ne superradiation propagation through reson.-absorbing positive column plasma, pulse shape change 79−4117
Ne superradiation pulse variation interacting with Ne reson.-absorpt. plasma 78−71489
$Pr_xLa_{1-x}P_5O_{14}$, laser emissions, fluoresc. 79−72572
PrP_5O_{14}, laser emissions, fluoresc. 79−72572
$Pr_xY_{1-x}P_5O_{14}$, laser emissions, fluoresc. 79−72572
Rb, Doppler-free superradiance, polarisation charact. 79−782
Rb, radiative lifetimes up to n=12 excited states, pulsed dye laser and superradiance excitation 80−83322
Rb, superrad. between degenerate levels, polaris. charact., coupled transitions 80−58493
Rb, superradiant cascading effects, Rydberg levels 79−31491
Rb vapour, modulation of intensity from transition to low levels 79−45691
Rb_2, vapour, laser radiation absorpt. superradiance 78−46553
S_2, optically pumped superfluorescence molecular laser 80−63990
Sr, visible emission on three-level cascade, coupled transitions 80−58493
Tl, green line superradiance, selective optical excitation and inversions via excimer channel using Tl-Hg and Tl-Cd-Ar systems 79−50281
Xe 3.51 μm laser amplifiers, spectral narrowing and saturation induced rebroadening optical heterodyne obs. 80−63976
Xe-He, 3.51 μm laser amplifiers, spectral narrowing and saturation induced rebroadening optical heterodyne obs. 80−63976
Xe-He source, intensity fluctuations of amplified spontaneous emission at 3.51 μm 80−32957
XeF superradiance laser excited by electric discharge 77−19236
XeF, superradiant laser, gain saturation effects 78−66808
ZnO, optical gain and induced absorption from excitonic mols. 78−84609
ZnO, optical gain spectra, direct recording using laser modulation 78−66834

supersaturation control *see chemical variables control*

supersaturation measurement *see chemical variables measurement*

supersonic flow
see also shock waves
acoustic wave nonlinear distortion in propagation through supersonic flow 78−22367
aerodynamic heating of bodies with deep cavity 79−86454
aerodynamic shape optimisation for bodies in supersonic flow 80−38438
aerodynamics, SOUSSA computer code 78−71352
aeroelasticity of unsteady aerodynamics, force calc. methods *(French)* 78−75095
aft bodies, two-dimensional, min. pressure drag in supersonic flow 77−27555
aft-body drag reduction, combined boat-tailing and base blowing at M=3 77−23988
air flow through high press. gas valves into atm., noise and flow pattern obs. 80−59067
air in supersonic nozzle, shock activation with overexpansion, jet form. 78−18330
air scoops at supersonic and hypersonic vels., throttling, separation and central body cooling 80−14739
airfoil, leading-edge separation bubbles, shear layer and transitional reattaching flow 77−27580
airfoil design by numerical optimisation 79−98750
airfoil in supersonic and hypersonic flow, wedge problem 79−41705
amplification coefficient, effect of mixing conditions in a laval nozzle 80−6085
analogue modelling, supersonic flow around a wing 80−28530
annular jets for supersonic and sonic flow 80−100019
asymmetric nozzle, off-design regimes with supersonic inlet vel. 77−24009
asymptotic, supersonic, 2-dimens. turbulent wakes, fully developed mean flow criteria 80−14706
atmospheric O_3 depletion, supersonic gas sampling error 77−33193
atomic O_2 supersonic nozzle beam source development 80−58016
attached supersonic turbulent boundary-layer/flap interaction pressures, correlation technique 80−48683
axisymmetric accretion in astronomy, energy considerations 77−33335
axisymmetric bodies, aerodynamic coeffs. in supersonic flow *(Russian)* 78−34153
axisymmetric flow past body of revolution *(Russian)* 78−34154
axisymmetric flow past pointed body of revolution *(Russian)* 77−55034
axisymmetric nonstationary flow around an obstacle in a cylindrical tube 79−77169
axisymmetric steady flow, slightly conducting gas in mag. field 77−15128
axisymmetric supersonic turbulent base pressures 78−94764
base flow at supersonic vel., rockets and re-entry vehicles appl. 78−67243
base influence on supersonic flow around a cone, power-law injection 80−100010
base pressure correlation technique, turbulent supersonic flow, conical bodies 77−89146
beam skimmers, transition regime behaviour 77−3491
blast wave computations using the flux-corrected transport algorithm 79−77184
blunt axisymmetric bodies, supersonic flow modelling, drag and entropy layer 80−48740

supersonic flow continued
blunt biconic at incidence, laminar viscous shock layer, supersonic/hypersonic flow 78−30313
blunt bodies with combined cross sections, num. comput. 77−58728
blunt body, boundary and wake, supersonic viscous gas flow, numerical soln. 80−38441
blunt body, unsteady supersonic flow, grid characteristic method 80−38442
blunt body flow of viscous perfect gas and nonequilib. gas mixture 80−28578
blunt body in supersonic flow, Navier-Stokes eqns. numerical computation 80−10263
blunt body injection into supersonic flow, expt. study 79−90277
blunt cone hypersonic and supersonic flow, near wake Reynolds number effects, interferometric obs. 80−43733
blunt cone with following body, base press. meas. 78−51187
blunt wedge at angle of attack, ideal gas flow 79−86460
bodies with arbitrary cross section, aerodynamic coeffs. 79−68741
body of revolution, slender, nonlinear normal forces, Reynolds no. influence *(German)* 78−51191
body of rotation in supersonic turbulent flow, base press. 79−86455
body oscillating in supersonic stream, entropy and total energy 79−86456
boundary layer, blown off, reattachment by injection cut off 77−3844
boundary layer, external acoustic perturbations *(Russian)* 78−34152
boundary layer, free interaction with supersonic flow, dispersion eqn. solutions 80−69867
boundary layer, prediction by hybrid marching integration procedure 77−65761
boundary layer, Reynolds number effects on turbulence field 80−19434
boundary layer, two-dimens., viscous-inviscid flow matching, numerical method *(French)* 78−79334
boundary layer flow about cones, method of integral relations 79−10589
boundary layer in external acoustic field 79−68740
boundary layer on cone, transition 78−38368
boundary layer on cone at Mach 5, transition 78−38369
boundary layer on plate with leading edge blunting, stability 79−64688
boundary layer response to oblique slot blowing 77−11220
boundary layer visualisation in shock tube, book contrib. 80−1715
boundary layers, supersonic, interacting with cooling wall jets, turbulent and optical characteristics 80−106792
bow wave distance for infinitely long plate in ultrasonic flow *(German)* 79−81920
Burgers' turbulence, similarity law and renormalisation 78−46994
cascade, linearised theory *(French)* 78−94766
cascade deviation, prediction and measurement 80−24049
cascade with strong in-passage shocks, unsteady flow 78−14041
cascades, aerodynamic anal., response predictions 78−34160
cascades, aerodynamic anal., unsteady press. field 78−34159
cascades, supersonic and transonic compressor, unstarted choked regime calc. *(Chinese)* 80−43730
cavitation zone, acoustics and hydrodynamics in supersonic regime 77−27567
channel contour construction, transforming supersonic flow cross-section 79−37349
channel flow, influence of rarefaction and compression waves on base pressure *(Russian)* 79−27656
characteristics method for calculating irrotational supersonic space flows *(Russian)* 79−18908
chemical laser flowfield, laser induced I_2 fluorescence meas. 80−38008
chemical laser nozzle, TRW CL XV, fluid mechanical and optical analysis, LAMP and BLAZER code calcs. 79−98350
chemical lasers, supersonic mixing flow field 77−42528
chemically reacting gas mixture, thermal crisis suppression by laser radiation 80−75000
chemically reactive MHD flow near slender wing with supersonic leading edge *(Italian)* 79−14495
circuit breaking arcs, current zero arc model based on forced convection 80−33831
circular cane, vibr. relaxing gas, numerical anal. 78−46993
circular cone, surface blowing, fluid injection and suction 77−27554
collisional relax. of vibr. excited mol., reson. enhanced 79−64081
combined bodies, supersonic inviscid flow, shock interactions *(Chinese)* 80−6084
compound lifting surfaces at high supersonic flight speeds 77−19622
compressed boundary layer on two-dimens. plate, unstable localised disturbance characts. 77−55031
compressible and incompressible flows, recent theoretical and expt. developments, book 80−1620
compressible boundary layer flows, curvature near separation 78−55661
compressible flow fields, two-dimensional, computation by modified local stability scheme 78−1681
compressible flow problems, modified FLIC method, finite element anal. 80−74911
compressible supersonic turbulent boundary layers, compressible press. gradient effects 79−60001
cone, slender, at high incidence 78−90932
cone with arbitrary surface deviations in supersonic gas flow, aerodynamic characts. 77−19620
cones, axisymmetric impingement of supersonic air jets, shock pattern 80−48741
cones at incidence, supersonic viscous flow 80−38439
cones at large incidence, floating shock fitting method 78−71367
cones with near-critical and supercritical vertex angles 79−81918
confluence of three shock waves in three-dimens. flow 78−59422
conical crossflow sonic line, flow patterns and bubble props. 80−69862
conical flow, without axial symmetry, numerical method 77−89147
conical nozzle, flowfield induced by secondary gas injection 77−62290
conical supersonic flow around yawed circular cones in the transonic region *(German)* 79−77175
continuum source particle beam properties, comput. modelling 80−26062
contrary wall jet, interaction with supersonic flow on plate with turbulent boundary layer *(Russian)* 78−22398
control jets, gasdynamic features, 3-D subsonic and supersonic flows 80−6112
convergent supersonic jet, wave struct. in interaction with infinite 2-dimens. obstruction 77−55064
corner, three-dimens., Navier-Stokes eqn. soln., numerical code 78−30314
corner flow, boundary region 79−32559
corner flow, viscous-inviscid interaction of laminar boundary 79−32563
supersonic flow continued
corner flow, vortical and entropic distortions 79−32532
corner flow with compression and expansion numerical and exptl. results 78−18313
corner interaction of boundary layer and shock wave, flow separation 80−96287
CW supersonic chemical laser, porous nozzle, chemically reacting boundary layer 80−100022
cylindrical channel, sudden expansion of supersonic jet 80−48800
cylindrical shell in supersonic flow, response to shock load 77−42771
data reduction technique for flow angle and mass flow rate meas. in unknown flowfield 79−77306
DC arc in supersonic nozzle flow, appl. to gas blast circuit breaker 79−23469
degeneration of supersonic flow due to interaction of centered compression and rarefaction waves 80−69864
delta wings in supersonic flow, crossflow shocks 80−48749
density distribution for free supersonic jet emerging against pressure difference *(German)* 80−1666
diffuser with surface cooling, flow and heat transfer meas. in pseudo-shock region 77−42868
dispersed supersonic two-phase flow, shock characts., droplet size depend. at nozzle 80−106815
disturbances generated by supersonic flow over deep cavity, laser appl. 79−98748
drag, supersonic wave, of planar singularity distribs. 78−83430
droplet-vapour flow, normal shock waves 79−32651
duct, supersonic flow downstream oscillations from abrupt cross section increase, nozzles 80−74976
duct flow, base press. oscills. 79−46386
duct flow, quasi-one-dimensional fluid, boundary conditions on time depend. computations 77−84324
ducted and exhaust plume flow fields, computer anal. 79−7397
electric discharges, transversally combined, low temp. *(Russian)* 78−22590
electrogasdynamic supersonic flow over wedge in presence of charged massive particles 80−33685
elliptic cones with large semiaxis ratio, num. soln. method 77−58729
excess noise from supersonic underexpanded jets in flight 80−69815
expansion corner effect on shock-wave and boundary layer interactions 80−14737
exponential atmosphere, supersonic flow round large body 79−90278
external supersonic flow, turbulent boundary layer interaction on concave corner and spherical intake 77−55032
finite difference method, supersonic three-dimens. flow 78−51190
finite difference method calcs. *(French)* 78−34157
finite element formulation for subsonic and transonic flow 80−28526
finite length plate in supersonic low density flow, surface pressures and corrections 80−14741
flame, atm. press., supersonic sampling, boundary layer cooling 77−60143
flame, premixed, propag. in supersonic airstream 77−84339
flat faced cylinders, second order shock capturing finite difference method *(Japanese)* 79−4038
flat insulated plate, supersonic laminar boundary layer stability 79−98749
flat plate trailing edge in rarefied supersonic airflow, boundary layer 80−24046
flattened bodies and sharp tip wings 79−46341
flight, longitudinal stability conditions *(German)* 77−31330
floating heat layer interaction with solid wall, computation, book contrib. 80−1642
flow field meas. by laser shearing interferometer *(Chinese)* 79−32715
flow past cone with large wall injection velocity, model 79−32561
fluid channels indirect design using global variational method with trial functions 77−27595
flutter in elastic rotating bodies 77−39257
freon gas flow around blunt object, bow shock instability 80−10266
gas, shock wave under continuous energy supply 80−103042
gas centrifuge, pressure recovery of supersonic flow in diffuser 78−29104
gas diffusion in supersonic jet 79−32604
gas ejector, with slotted nozzle, effect of viscosity on limiting performance 77−27572
gas flow behind supersonic spheres *(Russian)* 79−14423
gas flows, selfgravitating, thermodynamic processes and radiation, numerical method, shock fronts 80−14848
gas flows in gravitational field *(Russian)* 78−67212
gas jet, interaction with plane barrier *(Russian)* 77−27571
gas jet, nonstationary, wave structure and density distrib. 77−62286
gas jet blowing into supersonic flow without 3-dimens. boundary layer separation, nozzle shape 80−100009
gas mixture, binary, spherical expansion into flooded space, components separation 79−81948
gas mixtures with vibr. relax., nozzle flow 79−64727
gas particle flows over wedge *(German)* 80−43731
gas plane flows in presence of weak supply of energy *(Russian)* 79−32498
gas stream, supersonic, stationary, conical flow about plane wedge and circular cone 80−74912
gas-film cooling efficiency in supersonic axisymmetric nozzles 79−98715
gas-jet visualisation by laser induced I_2 molecular fluorescence 77−80257
gas-particle mixtures, supersonic flow past wedge, shock wave *(Japanese)* 77−47070
gasdynamic laser, two-phase mol. vibr. relax. in gas-aerosol system 79−45807
gases, high velocity flows, nonequilib. homogeneous condensation, determ. of maximal supercooling 80−6086
Gaussian beam self-focusing in supersonic gas flow, thermal self-action effect 79−76768
general point performance equation, calc. of pitch and climb angles *(German)* 79−77176
generation for circular cascade of aerofoils, design of annular nozzle *(French)* 77−7433
halogens, supersonic atomic and mol. nozzle beam source 77−31028
heat and mass transfer and friction under complex thermogasdynamic conditions 79−1209
heat pipe, supersonic flow and shock waves 79−32568
heat source moving through fluid, sound radiation 78−1688
heat transfer, highly cooled turbulent boundary layers 78−9652

supersonic flow continued
heat transfer meas. using local heat flux sensor, appl. to heat transfer in supersonic flow 79−82015
heat transfer on flat porous wall with alternating injection and suction zones 79−98719
heat transfer to axisymmetric bodies, freestream turbulence effects 77−75916
heavy species velocity, in low density supersonic free jet 79−94754
heavy-particle impurity suspension effect on viscous shock layer gas flow 80−28554
high angle of attack aerodynamics (conf. Sandefjord, Norway (Oct. 1978)) 79−77159
high Reynolds number supersonic flow, compression corner flowfields, turbulent boundary layer separation 80−14735
high-temperature supersonic jet, noise spectrum 79−94691
hot wire anemometry, rarefied gas flow vel. meas. 80−100040
hot-wire anemometer freq. response, comments on determination and optimization 80−87832
hot-wire anemometers, freq. response of constant temp. anemometers 80−59149
hot-wire fluctuation data anal. with end-loss correction 78−55703
hyperbolic wave eqn., unsteady supersonic aerodynamic theory 77−42862
ideal gas flow, choked and supercritical, through orifices and convergent conical nozzles, numerical soln. 80−38474
ideal gas flow around blunt wedge, sonic line shape 80−64577
inert gas supersonic jets as vacuum UV source 77−75639
inert impurity, optical method for measuring intensity of fluctuations of conc. of inert impurity 77−80234
inlet, flowfield computation using bicharacteristics method with shock wave fitting 80−38443
instability zones due to acoustic pulse striking a vortex sheet on a supersonic stream 79−64689
interacting boundary layers in high Reynolds number laminar separated flow 77−42865
inverted population gas flow round blunt bodies, amplification factor 78−5828
inviscid conical corner flowfields, complex shock interactions 80−48739
inviscid conical flowfield structure about external axial corners 79−94646
inviscid hyperbolic flow, computational algorithms tests 80−27140
inviscid supersonic flow, over external axial corner, shock wave and vortical singularities 77−42866
ion beam, intense, adiabatic wall focusing for thermonuclear microexplosion ignition 77−61611
ionised gas, nonequilibrium, supersonic, corner expansion flow, physical aspects 80−1639
ionising shock waves in EM field in supersonic flow *(Russian)* 77−89155
isotope separation, by probe in supersonic flow, Monte Carlo simulation 79−94098
jet, acoustic perturbations *(Russian)* 77−58751
jet, acoustic reflections effect on discrete component of noise spectrum 79−68775
jet, axisymmetric, counterflow problem, num. soln. procedure 77−58757
jet, flow characts. of large scale wave-like struct. 77−89178
jet, flowing onto infinite perpendicular barrier, limiting expansion ratio 78−59439
jet, imperfectly expanded, model describing sound generation 79−4053
jet, impinging on barrier, sound field 78−9495
jet, Mach wave emission 78−26172
jet, nonsteady interaction with barrier, math. model of oscillatory cycle 80−19462
jet, shock layer ahead of barrier 79−64723
jet, stream model 77−89180
jet, supersonic, cold, coaxial, acoustic, flow characts. 80−1656
jet, supersonic, noise, Reynolds number depend. 78−14053
jet, supersonic gas, penetration into the ground *(Russian)* 80−28544
jet, thermogasdynamic interaction with inclined permeable baffle 79−98773
jet, turbulent wave, laser velocimeter meas. 78−26173
jet, two-dimens., impingement on flat plate, shock-interference heating 79−94688
jet, two-dimensional, impingement on normal ground surface 77−24003
jet, underexpanded, discharging into opposing supersonic stream, wave structure anal. 80−19461
jet, underexpanded, press. pulsations on flat plate 78−94778
jet compressor, constant-area-mixing type, design theory 79−86482
jet flame stabilisation in subsonic and supersonic flows 78−34206
jet flow from nozzle, coords. of acoustic cross-section 78−5778
jet flow over obstacle, discrete tones generation 78−1708
jet from nozzle with inclined rim 79−64724
jet inflow into cavity, press. fluctuations and heating 79−64726
jet injection, separation zone, boundary layer thickness and transverse curvature effects 80−48745
jet noise, amplification by higher-mode acoustic tone 78−9664
jet noise spectrum, discrete component 78−9493
jet noise suppression by coaxial cold/heated jet flows 78−63468
jet structure produced by slit orifices *(German)* 79−77210
jet-barrier interaction, shock layer flow near axis 79−90282
jets, acoustic radiation using double-pulse holographic interferometry 80−14678
jets, axisymmetric subsonic and supersonic, in parallel stream, turbulence meas. 77−31349
jets, colliding supersonic coaxial underexpanded, investigation of flow 78−67237
jets, two-phase supersonic flow around a sphere 80−6114
Kelvin-Helmholtz instability in supersonic and super-Alvenic fluids 80−87816
laminar boundary layer on conical body with gas injection *(Japanese)* 78−59417
laminar boundary layer reattachment, num. soln. 80−53809
laminar boundary layer separations, quasi-3-dimens. 78−46995
laminar boundary layer with conjugated heat transfer 79−64687
laminar boundary layers, compressible problem in three dimens. 77−31277
laminar boundary layers, strong slot injection, flow separation 80−48738
laminar boundary-layer reattachment in supersonic flow 79−46342
laminar boundary-layer separation by slot injection 79−98747
laminar flow over backward facing step, numerical soln. at high Reynolds number 77−47040
laminar separation, second order asymptotic soln. 80−83828

supersonic flow continued
laminar separation of supersonic stream, Reynolds no. effect 80−19432
laminar viscous, numerical anal., separation 80−24062
laser, chemical, pressure recovery, 1D flow model, comparison with DF laser results 77−71979
laser, recombination dynamic H plasma, freely expanding, from supersonic nozzle 77−19240
laser velocimetry and visualisation, two-phase supersonic streams, gas-dust 79−68830
Laval nozzle, supercritical steam supersonic discharge 80−48765
Laval nozzles, subsonic, transonic, supersonic flow characts. calc. *(Chinese)* 79−32623
Laval plane nozzles, approx. for special flows *(Russian)* 78−87374
leading shock wave front in front of blunt object with recess instability *(Russian)* 77−75940
leeside flowfields of planar delta wings, Reynolds number 79−60003
linear supersonic flow round a yawed elliptic cone *(German)* 77−65762
linearised, improved higher-order panel method 80−6082
linearised boundary layer equations with self-induced pressure, anal. for $M_\infty=1$ case 79−86458
liquid containing gas bubbles, struct. of supersonic waves and cavitation development 80−33643
liquid film stability adjacent to supersonic boundary layer 77−930
liquid jets, high speed, mechs. of emergence and flight 77−80193
liquid layer adjacent to gas stream, surface waves, subsonic and supersonic disturbances 79−23336
local supersonic zone near wing profile of infinite span flow calcs. 79−32565
Lorentz-like coordinate transform. in supersonic regime 79−37348
low density supersonic gas flow, temp. meas. probe 80−74913
low Reynolds number supersonic air jets, noise generation by instabilities 80−23831
low supersonic flow over hemisphere-cylinder at incidence up to 19° 78−59419
low supersonic lifting surface, finite element anal. and collocation method 78−1687
Ludwieg tube with downstream valve, starting process 79−72965
Mach 6 hydrodynamic flow past permeable wedge, holographic interferometry meas. *(Russian)* 78−14108
Mach wave radiation of hot supersonic jets 80−69894
Mach waves, kinematics inside and outside supersonic jets, book contrib. 80−1640
magnetoaerodynamic forces on oscill. circular cylindrical shell, simple harmonic motion 79−1257
mass transfer in near wake 78−9650
Maxwell gas, shock struct., numerical integration of Burnett eqns. 79−94677
MHD convertor, acceleration nozzle, with supersonic flow deformation 78−26181
MHD generator, combustion-driven, boundary-layer profile meas. 77−24194
MHD generator, supersonic, working body thermodynamic props., chem. kinetics effect 78−91163
MHD generator, with inclined input stream, supersonic flow *(Russian)* 78−94837
MHD streams, interaction of bounded subsonic and unbounded supersonic MHD streams 79−37419
MHD-generator channel, with slanted entrance stream 79−77429
microwave discharge, supersonic flow in waveguide, electron densities, possible laser 80−38842
Mira variable stars, supersonic mass ejection 77−53605
mixed 2-D flows of supersaturated and two-phase medium with nonequilib. phase transitions 79−77224
molecular beam nozzle, use of pulsed valve 80−100045
molecular beams, intensity dependence on stagnation temp. 77−68629
molecular beams, rotor accelerated 78−66686
multiphase mixture, two-dimens. nozzle and jet supersonic flows 80−48780
Navier-Stokes equations, parabolic, implicit finite-difference method using fractional steps technique 80−69866
near-sonic region, steady inviscid flow field calc. *(German)* 80−1643
near-wake for slender cone, Mach number depend. of laminar transition 77−62277
near-wake phenomena, with and without external compression, axial and radial air injection effects 80−10273
non-stationary slightly supersonic flow past instantaneously generated bodies *(German)* 77−65757
nonequilibrium gas relaxation in supersonic nozzle, analysis method 80−74941
nonequilibrium two-phase flow in Laval nozzles 79−68820
nonstationary boundary layer with self-induced pressure, flow near vibrating wall 79−86459
nonstationary separation of laminar boundary layer, numerical method *(Russian)* 79−14425
nonstationary two-stage axisymmetric escape of gas into a submerged space, numerical modeling 79−77200
nonuniform supersonic flow past the circular cone 79−55400
not-so-slender wing theory 77−58717
nozzle, chem. nonequilib. flow, specific momentum losses 78−59505
nozzle, influence of transonic flow throat region for maximum thrust 79−41729
nozzle, nonequilibrium heterogeneous-homogeneous condensation of gas *(Russian)* 77−51096
nozzle, pulsed jet wave struct. in nonstationary flow stage 80−59094
nozzle, subsonic and supersonic, turbulent boundary layer heat transfer 79−1229
nozzle flow, start-up shock wave struct. 79−7398
nozzle flowfields, fully viscous and Navier-Stokes solns., comparison, book contrib. 80−1641
nozzle flows of condensible vapour, near-equil. heterogeneous nucleation and similarity rules 77−58759
nozzle flows with boundary layer, CO_2-N_2-He, gain coefficients 80−14312
nozzle in different jet regimes, internal and external flows, separation and wakes 80−100023
nozzles, flat and axisymmetric, supersonic flow calc. method for arbitrary inlet gas props. 77−68657
nozzles, supersonic, thermal protection by gas curtain, vel. gradient 78−51215
nozzles, supersonic axisymmetric, film cooling efficiency 80−48710

supersonic flow continued
nucleation homogeneous, gasdynamics of supersonic flow with condensation 77−62292
numerical simulation of supersonic cone flow at high angle of attack, laminar and turbulent flow 79−77178
open tubes, resonant oscillations of gas 77−68628
oscillating airfoil surfaces in supersonic flowfield, time-variant aerodynamics 79−77167
oscillations, self-induced, in boundary layer flow 78−67215
panel structural optimisation under supersonic flutter conditions *(Italian)* 79−41600
parallel elastically-coupled flat plates, supersonic flutter analysis 77−75838
parawings, conical, with small camber, trailing edge slope and membrane weight effect *(German)* 77−31331
particles in supersonic flow, vel. lag expts. 79−7402
permanent one-dimens. flow, small unsteady perturbations *(French)* 77−51024
perturbations, high and low freq., growth calc. for perfect inviscid gas *(Russian)* 78−46992
planar sonic nozzle, three dimens. wave struct. of nonstationary gas outflow 77−55068
plane flow, past a curved wedge, quasi-linear hyperbolic systems *(French)* 80−10261
plasma, ablation at steel plate, electron heat transfer mech. 78−71496
plasma, low-density, electrostatic field struct. in wake of sphere 77−60509
plasma, steel target impact effect, boundary layer role 79−32780
plasma, supersonic-subsonic flow transition, shock formation, enhancement by microwaves 77−65845
plasma jet, supersonic damaging of metals, mech. momentum hole 80−2065
plasma jet from magnetoplasmadynamic source, gasdynamic struct. of initial section 77−35332
plasma stream, dense, shock braking processes, radiation-gasdynamic obs. 80−19635
plate with periodic suction and injections in supersonic region, boundary layers *(German)* 80−59069
plate with vertical cylindrical projection, aerodynamic coeffs., approx. method 80−48746
point-to-plane gap corona and breakdown in supersonic airstream 78−67573
potential flow, panel flutter, finite element calc. 78−26152
Prandtl supersonic jet problem, linear aerodynamic theory formulae, validity, book contrib. 80−6090
pressure discontinuity system with 1 or 2 triplets, supersonic object, air equilib. physicochem. transforms. 79−90350
pseudo-transonic eqn. with diffusion term 78−38365
pulsed gasdynamic device with ring type supersonic nozzle 77−75998
pulsed supersonic He jet, space time charact. 77−51093
quasihomogeneous flow, turbulence in presence of density and vel. fluctuations 80−1638
radial gas expansion from rapidly started source 79−46340
radiating gases, sonic wave propagation 77−47114
radiative gas dynamics, spectral models, applicability 78−14100
radiative transfer in supersonic flows, probabilistic approach 79−53712
rapid surface vaporisation with back pressure, Knudsen layer, flow Mach number 79−77168
rarefied plasma flow around body, electrostatic field struct. in wake 77−91402
rarefied supersonic CO_2 flow, fluctuations in intensity of radiation excited by electron beam in jet core 77−55104
reacting gas, steady axisymmetric supersonic free jet, approx. analytical soln. 77−55099
reattaching laminar and turbulent separated flow, three-dimens. heat and mass transfer 77−65759
recombination, in steady supersonic flow, in devices for laser isotope separation 79−31717
resonance tube, oscillation excitation from supersonic jet *(Japanese)* 80−24116
review of laser anemometry applications in France and Germany 77−35272
rocket engines, meas. turbulence parameters in exhaust plume, laser crossed beam correl. method 79−86541
rocket exhaust anemometry, Doppler difference and two focus methods, correlator and photon counting 79−60084
rotating propulsive nozzle flowfields for nonequilibrium chemically reacting supersonic flow 80−48764
rough subliming surface, laminar boundary layer, anal. 78−51148
ruled bodies, linear theory 79−77170
segmented-conic body, flow structure close to lateral surface and formation of breakaway zones 77−58727
self-similar explosion waves of variable energy at the front 80−103040
separated, self-excitation of acoustic oscillations 77−7411
separated rarefied gas flow at low Reynolds no., heat transfer 79−98713
separated supersonic boundary layer, moderate injection with reattachment, shear layer 79−32562
separated turbulent boundary layer, laser velocimetry meas. 77−35274
separation, incipient, viscous interaction, laminar and turbulent boundary layers, similitude props. 77−72325
separation flow, 2- and 3-dimens., turbulent boundary layer and shock wave 80−100017
sharp cone, symmetry plane viscous layer 77−58639
shell, cylindrical in supersonic flow, vibration, finite element anal. 80−5973
shell deformation by supersonic gas flow, drag 80−96279
shock and combustion waves around supersonic cone 78−26154
shock propagation along 90 degree bends, curvature effects on stability 78−18314
shock separated turbulent boundary layer at compression corner, mean flow meas. 77−42867
shock stand-off distance for sphere, formula 77−55030
shock wave−turbulent boundary layer interactions, Reynolds no. effect 78−1689
shock wave analysis flow through body wall 80−38447
shock wave ignition of metal powders, pre-ignition processes 77−40546
shock wave interaction in turbulent boundary layer 79−41711
shock wave profile about hemispherical nose 77−89149
shock-wave boundary-layer interaction, appl. laser anemometer 77−35275
supersonic flow continued
shock-wave-turbulent boundary layer interaction, appl. photon correlation anemometry 77−35277
skin friction in supersonic laminar and turbulent flows 79−98751
slender cone at high angle of attack, supersonic flow field meas. 79−77177
solar wind flow past planets, axisymm. implicit blunt body computation technique 78−96370
solids of revolution, small perturbation theory 79−68742
sonic boom propag. in thermosphere 80−33305
sonic boundary layer counterjet interaction with supersonic flow 79−64728
sonic injection, auxiliary blowing effect on conc. profiles downstream *(French)* 77−65778
sonic-boom press. signature distortion by high-speed jets 78−79156
sound waves, resonance interaction with plane parallel flow 77−814
sphere, flow pattern visualisation by broad light source holographic interferometry 80−19008
sphere drag at Mach numbers from 0.3 to 2.0 at Reynolds numbers approaching 10^7 79−81919
spherically blunted cone with massive surface blowing, laminar and turbulent flows, shocks 80−38445
spiked bodies in supersonic flow, nonstationary separation 80−38460
spontaneously condensing and wet steam discontinuous flows in steam turbines, numerical investigation *(Russian)* 80−87800
stationary supersonic flow of compressible fluid, distrib. eqns. *(French)* 77−62278
steady flow about blunt bodies, finite difference methods 80−96280
steady two- and three-dimensional, shock discontinuities detection method 77−58736
steam, wet, supersonic flow, total- and static-press. probe characts. 77−84353
steam condenser, supersonic nozzle discharge, heat transfer and gasdynamics 78−55671
steel, stainless, cylinder, in thermal aerodynamic tube, nonsteady heat transfer method 79−37147
stepped rod in wind tunnel, flow separation downstream 77−58718
stream flow past thin sharp bodies with intensive blow *(Russian)* 77−31329
supersonic boundary layer, separated bubble induced by wall depression 78−9651
supersonic combustion past a conical body with normal surface blowing 79−41770
supersonic to subsonic transition with local supersonic regions, book contrib. 80−1627
supersonic wings with subsonic leading edges, minimum drag *(German)* 77−15058
supersonic/hypersonic flow past an oscillating flat plate at high angles of attack 79−14424
s-tetrazine, cooled supersonic jet, Van der Waals complex, isotope effects, fluoresc. obs. 78−55194
thermal boundary layer, effect of wall hollow-induced separated bubble *(French)* 78−5784
thermally nonequilibrated flow through supersonic nozzle, cooling, population inversion *(Russian)* 77−7412
thin airfoil in stratified atmosphere, supersonic-transonic flow 78−5764
thin body, subsonic and supersonic flow of chemically reacting inviscid gas 79−98820
thin flat plate parallel to supersonic stream, laminar near wake, centreline velocity 79−55392
thin turbulent layer, hot-wire anemometry, error reduction 78−34235
three dimensional separated turbulent flows at supersonic speeds 80−19435
three dimensional stationary supersonic flow fluid, progonka process calcs. 79−7383
three-dimensional, calc. by method of characts., approx. eqns. 77−19619
throttling in round duct, separated flow changes 78−63446
trailing edge flow, numerical soln. of 2D laminar and turbulent flows 79−77172
transverse gas stream, penetration and mixing of secondary liq. injection 77−24018
triple deck problem for supersonic and subsonic flow, numerical technique for separation 80−14757
turbine, steam, high-capacity, converging cascade flow calc. 78−87360
turbulence, near wake flow 78−22368
turbulence in supersonic boundary layer, laser Doppler velocimeter meas. 77−35273
turbulence meas., using hot-film and modified hot-wire sensors 79−90356
turbulence model development expts. with numerical simulations 77 27551
turbulence separation, subsonic and supersonic, ultra-short duration visualisation *(French)* 78−75128
turbulent, vel. meas. and shock fronts, appl. Doppler velocimeter with Fabry-Perot interferometer 77−39377
turbulent axisymmetric near wake behind bluff-base bodies 78−1665
turbulent boundary layer, interacting, over wavy wall 79−55366
turbulent boundary layer, on nonadiabatic surface, solution to equations 77−89148
turbulent boundary layer, supersonic, wall temp. effect 78−94765
turbulent boundary layer of equilib. dissoc. and ionised gas 77−47039
turbulent boundary layer separation and reattachment on flat plate with ramp 77−23990
turbulent boundary layer-transonic shock wave interaction, integral computation method 79−1213
turbulent boundary layer/shock-wave interaction sweep effect on separation conditions 77−62280
turbulent boundary layers, flare-induced separation 77−3843
turbulent boundary layers, separation ahead of protuberances 78−14040
turbulent boundary-shock wave interaction, aerodynamic heating 78−26155
turbulent compression corner flow, numerical simulation 77−62276
turbulent flow, turbulence production 78−94767
turbulent free jets, subsonic and supersonic, laser velocimeter meas. 79−77307
turbulent mixing with transverse jet 79−32603
turbulent near-wake behind step with supersonic jet 79−14448
turbulent shear layer, instability waves, radiation of sound 80−79341
turbulent shear stresses in compressible boundary layers 80−14736
turbulent skin friction at subsonic and supersonic speeds, wake component influence 80−19340

supersonic flow continued
turbulent surface flow around yawed cone 79−4037
turbulent wake, external compression effects 79−32560
two-dimens. time-marching supersonic flow calcs. 77−51081
two-dimensional supersonic flows of mixture, vapour and drops in nozzle and submerged jet, determ. 79−23357
two-dimensional supersonic viscous in reactions near walls, prediction method 77−58726
two-dimensional transverse sonic jet interaction with supersonic stream, application factor 80−24047
two-parameter skin friction formula for adiabatic compressible flow, shocked relaxing boundary layer 78−51188
two-phase flow, energy dividing props. in discharge from supersonic jet *(Russian)* 77−39332
two-phase flow, nonequilib. condensation, boundary condition numerical anal. 80−64565
two-phase flow, nonequilib. subsonic/supersonic, acoustic vel. obs. 78−42642
two-phase flow, phase separation 79−23358
two-phase flow, vertical density surges, rel. to sound vel. *(German)* 78−42641
two-phase flow in Laval nozzle, direct problem, numerical soln. 78−63475
two-phase fluid, 2-D supersonic flow, condensation effects calcs. *(French)* 77−84272
underexpanded gas jet issuance into supersonic flow 80−38468
underexpanded jet, first roll geometrical struct., cone angle and degree of contraction effects 77−11229
unsteady aerodynamic modelling for arbitrary motions 80−19433
unsteady flow of supersonic gas stream past a slender profile, asymptotic expansion of nonlinear effects 80−69863
unsteady inviscid flow 78−71350
unsteady lifting surface theory in subsonic and supersonic flow, integral transform method 80−19437
unsteady supersonic flow around wings with detached shock wave, numerical soln. 79−94647
unsteady two-dimensional subsonic, transonic and supersonic flow calcs. by method of characts. 77−55021
unsteady-state flow around bodies of variable form 80−6087
upstream adiabatic zone, subsonic, supersonic downstream boundary layer heat transfer effects 78−83379
upstream perturbation propagation, supersonic flow, self-induced press. boundary layer on moving surface 80−74914
upwind second-order difference schemes for transonic flow with embedded supersonic and shock regions 77−23975
in vacuum, meas. by electron diffr. instrument 78−75235
vibrational relax. in supersonic flow, meas. using high temp. spectropyrometric unit 78−9275
viscous, past corner, energy eqn., asymptotic solns., heat transfer 79−32564
viscous compressible flow at high Reynolds number, global approach and coupling approach 80−48742
viscous flows, interactive numerical calc. procedure 77−31326
viscous gas flow, subsonic and supersonic, simplified Navier-Stokes eqns. 80−31520
viscous laminar jet flow in slipstream calculation *(Russian)* 79−77209
viscous supersonic flow over external axial corners, shock and bubble generation computation 80−14734
vortex flow, with adiabatic index $\gamma=2$ 77−901
wake, laminar, of thin flat plate set parallel to stream, centre line vel. variation 78−14042
wake, supersonic, of transverse circ. cylinder, laminar to turbulent transition, external noise effect 78−38367
wake of axisymmetric body, ideal gas, numerical anal. 78−59420
wake struct. in supersonic gas flow around sphere 79−77119
water film flow behaviour and effect on cocurrent air flow, press. distrib. along rigid wavy structures 77−55029
water flow with air contents, partially- and super-cavitating hydrofoils in cascade, analysis method *(Japanese)* 80−14763
wave drag, nonplanar singularity distribs., Hayes' algorithm extension 77−84271
wave equation generalised axial radiation soln., flow patterns, wakes in supersonic field *(German)* 78−14043
wave system of flow past slender body 77−31327
wave system of flow past slender body 78−34155
wavy wall, boundary layer effects *(German)* 77−84274
wedge, intense supersonic gas blowing through wall, dividing static press. determ. 77−84273
wedge flow, anisotropic radiatively coupled, Milne-Eddington approx. 77−31398
wind tunnel, Mach 5, development 78−38437
wind tunnel, wall cavity, effect on starting characts. 77−58827
wind tunnel calibration by shock standoff distance computation up to Mach 1.2, schlieren method 77−27557
wind tunnel test program for determining effect of spin on boundary-layer transition at Mach numbers 5 and 8 on 9-deg. cone configurations 80−14864
wind tunnels, pressure fluctuations, freestream 78−14102
wing, supersonic gas flow, numerical method and routine 80−38440
wings, delta, lift with leading-edge vortices, at low speeds 79−14422
wings, sharp-edged 79−10587
wings with attached shock wave on leading edge, num. soln. 77−51080
Ar arcs in supersonic flow, numerical analysis 80−38776
Ar, cluster formation and homogeneous nucleation, comparison of expt. and theory, for supersonic nozzle flow 80−79925
Ar jet, supersonic, electron beam-excited, continuous VUV emission spectrum origins 79−6964
Ar, low-density expansion, non-Maxwellian vel. distrib. function 79−98762
Ar, nonequilibrium condensation and surface tension in supersonic jet flow *(Russian)* 80−65210
Ar nucleation, Ar in He carrier gas, supersonic nozzle flow 78−94871
Ar plasma, supersonic nonequilib. corner expansion flow, electron and particle temp. 77−89235
Ar, reflected shock wave, press. anal. at Mach numbers of 10 to 35 77−15060
Ar supersonic jet, spark line emission, 300-1000 Å 77−19793
Ar, supersonic pulsed flow from conical nozzle 80−103056
Ar-He rarefied mixture in supersonic nozzle and jet, longit. translational nonequilib. 79−27678

supersonic flow continued
Br_2, dissociating flow in supersonic nozzles, atomic recomb. and vibr. relax. effects 78−42677
Br_2 recombination in supersonic expansion in nozzle *(Russian)* 78−1757
CO, vibr. population distrib. in supersonic expansion 78−71364
CO-N_2-Ar mixture, supersonic expansion, CO vibr. level populations, gasdynamic laser appl. *(French)* 77−23659
CO_2 gasdynamic laser, gain supersonic flow heating effect, condition optimisation 78−82947
CO_2 lasers, high flow rate, gain and discharge characteristics 77−38855
CO_2, supersonic jet, $(CO_2)_n^-$ cluster formation and electron attachment 78−5385
CO_2-N_2, gasdynamic laser, gain-optimisation, theory 79−76664
CO_2-N_2, gasdynamic laser, theoretical gain-optimisation, parametric study 79−76665
CO_2-N_2-H_2O gas mixture, oscillatory nonequilib. in planar supersonic nozzle flow 78−1758
CO_2-N_2-He mixture in gas-dynamic system with independent thermal excitation, population inversion in two-step mixing 79−89888
Cl, shock heated, radiative recombination under nonequilib. expansion in supersonic nozzle *(Ukrainian)* 79−37421
D+O_3+CO_2 mixture supersonic jet, gain meas. for CO_2 laser 79−89902
D_2-HCl electric discharge gasdynamic laser, turbulent mixing characts. 78−9366
H supersonic flames, chemical kinetics and unmixedness effects on burning 80−64649
H_2, supersonic combustion in vitiated airstream, using transverse injection 78−14095
H_2O low density flow temp. and density meas. by submillimetre spectroscopy 80−43816
He plasma expansion, supersonic, population inversion 79−27755
He-CO_2-Cs mixture in rapidly circulating laser, interaction rate of Cs and CO_2, gasdynamic parameters 79−86173
He-N_2-CO_2 mixture in supersonic nozzle, shock activation with overexpansion, jet form. 78−18330
N_2 in supersonic nozzle, shock activation with overexpansion, jet form. 78−18330
N_2 jet, freely expanding, quantum effects in rot. relax. 80−58355
N_2 molecular beam generation, parameters rel. to stream perturbation before skimmer 79−86468
N_2 plasma, spatial distrib. in transverse-discharge supersonic stream, continuum theory and probe meas. 80−48866
NH_3, condensation by homogeneous nucleation in supersonic nozzles 77−11230
Na vapour heat pipe performance rel. to nozzle discharge theory 78−75033
Na vapour jet target, gating and pumping action 80−10281
SF_6, condensation in supersonic nozzle flow 78−34611
SF_6 condensation in supersonic nozzle expansions, trimerscritical model derivation 79−77211
SF_6, inhibition of homogeneous condensation by vibr. excitation, isotope separation appl. 78−37688
SF_6, supersonic jet, condensation and gasdynamic cooling 80−6089
SF_6, supersonic jet expanding into vac., interaction with CO_2 laser beam 80−5584
XeF, supersonic expansion jet, $B \leftarrow X$ system rot. and vibr. anal., isotope intervals, fluoresc. spectra 80−14174

supersonics *see supersonic flow*

supersymmetry
see also supergravity
σ model, nonlocal charges from zero curvature 80−31995
σ model, supersymmetric nonlocal conservation laws 80−46938
σ-model, nonlinear, superconformal invariance in 4-dimens. space-time 80−37154
σ-model, nonlinear, sypersymmetric, Ricci-flat Kahler manifolds and supersymmetry 80−90994
σ-model, U(N,r), supersymmetric, and O(2) extended supersymmetry 80−82878
σ-model supersymmetric dynamics on pre-QCD level with elementary quarks and composite gluons 80−82886
σ-model supersymmetric extensions, dynamical conservation laws, symmetric space valued fields 80−95227
σ-models, nonlinear, supersymmetric, nonlocal conserved currents and instanton-like solutions 80−86544
σ-models, nonlinear, with N=Z extended supersymmetry in 4-dimens. 80−47174
σ-models, supersymmetric, Kahler geometry and renormalisation 80−105789
A(0,1) Lie superalgebra, Fock-type representation 80−37181
A(0,n) Lie superalgebra, Fock space representation 80−86606
Abelian gauge theory supersymmetric aspects, Becchi-Rouet-Stora supertransformation, QED reformulation 77−34103
Abelian Higgs Kibble model, generalised Slavnov invariance, supersymm. struct. 78−78070
action principle for Neveu Schwarz Remond string and other systems using supernumerary variables 77−46030
algebra including topological charges for supersymmetric theories with solitons 78−89630
algebraic approach to supergravity in superspace 80−46915
algebras, unusual, appls. in particle physics 80−27419
antisymmetric tensor gauge fields, local supersymmetry without gravity 80−46910
auxiliary fields and tensor calculus for N=2 extended supergravity 80−46920
axial and conformal anomalies for arbitrary spin in gravity and supergravity 78−70040
axial anomaly for Majorana spin 3/2 loop with external gravitons in supergravity 78−8580
axial currents, supercurrents and anomalies in supersymmetric QED 80−46933
Bianchi identities for supersymmetric gauge theories 78−62299
black holes in supergravity, spin 3/2 perturbation of Schwarzschild black hole 78−93300
Bose analogs to supergravity, construction problems 80−46926
breaking of symm., massless spinors anal. 77−22658
broken supersymm. and supergravity 77−61212
broken supersymmetry, existence of massless colour octet quarks and unstable hadrons 78−89631
broken supersymmetry mass formula, quantum corrections 80−27424

supersymmetry continued
broken supersymmetry theories, parity conservation 77−41785
BRS supersymmetry, non-trivial realisation 80−82882
Casimir invariants and characteristic identities for generators of graded Lie algebras 80−13227
chiral field, supersymmetric, 1/N perturbation theory and quantum conservation laws 80−68373
chiral gauge spinor superfield as scalar multiplet 79−85241
chiral models, instanton type solns. *(Russian)* 79−58901
chiral SU(2) supergroup for Yang-Mills fields, Baker-Campbell-Hausdorff formula 79−49414
chirally extended supergravity, Maxwell-Einstein supergravity, auxiliary field struct. 78−78126
classical chiral models in two-dimens. time-space, supersymmetrical generalisation *(Russian)* 79−12980
classical field theories, non-signification of super gravitation 80−27193
classical particle spin dynamics and supersymmetry 77−82690
classical particles with spin, supersymmetry model *(Russian)* 80−101946
classical solns. in two-dimens. field theories 78−16943
classical supersymmetric particles 80−86560
complex and quaternionic supergeometry 80−46941
complex spinors and unified theories 80−46943
conference, supergravity, Stony Brook, USA (Sept. 1979) 80−46738
conformal and superconformal gravity and non-linear representations 79−17308
conformal invariant supersymmetric theory, CPT transformation 77−13884
conformal spinor current anomalies 78−8520
conformal spinor current anomaly from symmetry arguments 78−4803
conformal superalgebra, new representations 77−61199
conformal supergravity, props., gauge theory 78−78085
conformal supergravity, superconformal group, nonlinear representation 79−12695
conformal transformations in superspace 78−70295
constrained local superfields, and super Higgs mechanism 79−71342
constraints for supergravity 80−46918
coupling of O(2) supergravity with vector multiplets, Yang Mills field appl. 78−33020
covariance group structure, graded conformal, affine groups 80−22264
CP^{N-1} model, (2+1) dimens. supersymmetric, supersymmetry algebra and central charge 80−86568
CP^{n-1} model with quarks, confinement and chiral symmetry breaking 79−54302
CP^{n-1} supersymmetric model, central charge, superalgebra and Dirac brackets 80−99044
differential forms on supermanifolds *(Russian)* 80−4889
differential geometry methods in gauge and gravitational theories 80−90768
dimensional regularisation, supersymmetric form inconsistency 80−91013
dimensional regularization and supersymmetry at the two-loop level 80−17854
Dirac particle, supersymmetry and position operators 79−6305
Dirac particle propagator, supersymmetric methods 80−342
Dirac particles in external fields 80−82918
dual model superconformal group, isomorphic function, Fock space representations 78−74230
dual spinor model, low energy region, supersymm. Yang-Mills theory, supergravity theory 77−49923
Duffin-Kemmer-Petiau formulation of Bose field for supersymmetric model 78−93814
dynamical Bose-Fermi supersymmetries in complex nuclei 80−57703
dynamical growth of supersymmetry 80−105809
Einstein equations, supersymmetry, and flat limits of curved superspace 79−25932
elastic scattering amplitude asymptotics in a supersymmetric theory *(Russian)* 79−75748
elementary particle theory, mathematical method, conf., Liblice, Czechoslovakia (June 1978) 79−21891
expanded, spontaneous violation, Goldstone fields *(Russian)* 80−47218
explicit symmetry breaking in fermion-conserving model 77−54055
extended N=4 supersymmetric gauge theories, off-mass-shell formulation 80−77959
extended supergravity, dimensional reduction simplifications 80−52110
extended supergravity, eqns. of motion in terms of geometrical quantities in superspace 78−65856
extended supergravity, gauge internal symmetry 77−38115
extended supergravity, irreducible representations of extended supersymmetry algebras on superfields 80−98843
extended supergravity, three loop counterterms, nonrenormalisability 78−65854
extended supersymmetric theories, spontaneous generation of massive multiplets and central charges 79−35958
extended supersymmetry, derivation of unextended superfields 79−89076
extended supersymmetry invariants by dimensional reduction 80−47213
extended supersymmetry involving minimal interaction 77−26468
extended sypersymmetric Yang-Mills theories, superfield formulation, auxiliary component fields 80−90995
exterior calculus and two-dimensional supersymmetric models, super sine-Gordon model 80−47214
Fermi-Bose and internal symmetries with universal Clifford algebras 78−24970
fermion-fermion scattering in supersymm. field theory, high energy behaviour 77−13887
fermionic Goldstone-Higgs effect in (2+1) dimens. supergravity 78−29291
field theory, fermion (meson)-meson scatt., high energy behaviour 79−295
finite affine extensions of supersymm., graded Poincare Lie algebra 78−70300
flat superspace with supertorsion, supergravity, quantisation, renormalisable theory 79−2705
$g\phi^3$ model, supersymmetric, massive and massless, renormalised supercurrent and anomalies 79−6267
Galilean supersymmetry 79−17625
gauge models of weak and EM interactions 78−58106
gauge supersymmetry, spontaneous breaking, supergravity gauge invariance 79−9277
gauge supersymmetry, spontaneously broken, quantum loops UV finiteness 79−21919
gauge supersymmetry, supergraph anal. 80−27422
supersymmetry continued
gauge supersymmetry and supergravity 77−2593
gauge sypersymmetry eqns., spherically symm. soln. 78−4532
gauge theories, facts and prospects, conf., Schladming, Austria (Feb.-Mar. 1978) 79−26203
gauge theories, invariant regularisation 79−71646
gauge theories, supersymmetric and nonsupersymmetric regularisation by dimensional reduction 80−77951
gauge theories with extended supersymm., superfields formulation 78−41410
gauge theory, developments *(Chinese)* 80−77978
gauge theory, supersymmetric, charge renormalisation vanishing 78−24930
gauge theory of gravity and supergravity on a group manifold 79−21635
gauging Lie superalgebras 80−73618
general relationship between linear and nonlinear realisations of supersymmetry 79−9297
general relativity, superspace, local supersymmetry, superfibre bundle theory 78−77782
general relativity and spin via square root procedure, supersymmetry 77−82437
generalised superalgebras, Lie structs., Z_N+Z_N grading 78−78106
generalized Lie algebras 79−58898
geodesic in gauge supersymm. 78−12634
geometric aspects of supergauge theory 78−8506
geometric model 78−54579
geometry of superspace with Fermi and Bose coords. 77−26143
ghost field supersymmetry and BRS gauge in gravity and supergravity 77−38116
global, explicit model exhibiting a generalisation, Poincare algebra extension 79−35961
global theory of supermanifolds 80−82911
globally supersymmetric multiplets without local extensions 80−17856
goldstino couplings and neutral currents, mass relation for lepton and quark superpartners 79−75717
Goldstone neutrinos avoidance mechanism, spontaneously broken supersymm. theories limits 77−30279
graded Lie algebra of generators of symmetries, supersymmetry in de Sitter space 79−93305
graded manifold theory, supersymmetry geometry 79−58896
graded spin extension of the algebra of vol. preserving deformation 78−65855
grand unified field theories, mass relations and renormalisation effects 79−49436
Grassmann character, explicit solns. 80−91015
Grassmann spaces, model for supersymmetric quark-twistor string 79−22018
gravitational field equations of fourth order and supersymmetry 79−12674
gravity and supergravity unified geometric theory 77−41521
Higgs effect, supergravity and supersymm. massless QED 78−29268
Higgs mechanism and non-linear realisation for extended supersymmetry 78−16941
Higgs mechanism in (1+1) supergravity 78−74199
Higgs-Kibble mechanism, superfield theoretical treatment 78−89616
higher spin gauge fields, beyond 3/2, systematics 80−46937
Hilbert superspaces and Grassmann numbers, Fermi oscillator system appl. 80−95223
hypergravity, consistency requirements 80−46936
induced spontaneous sypersymmetry breaking in first order 77−211
instantons, local supersymmetry transf. and fermion solns. 78−74177
invariant supersymmetry space integrals using nonmetric formalism 78−4796
inverse scatt.-like problem for supersymmetric models, eqn. of motion linear problem 78−93818
irreducible representations direct product reduction, rest frame *(Russian)* 77−61216
Ising field theory, 'doubled' model, and supersymmetric sine-Gordon kink struct. 79−71614
Killing vectors in gauge supersymmetry 79−131
Lagrangian field theory and supersymmetry 77−6041
Lie superalgebras, Casimir invariants, calcs. 79−12976
Lie-Backlund supergroup, supersymmetry transformations *(Russian)* 79−80771
light hypernuclei quasifree formation and supersymmetry 77−14057
linearised supergravity, supersymmetric quantisation, ghost fields and superpropagation 79−93022
local, geometric interpretation 77−38096
local cohomology and superselection struct. 77−10192
local complex supersymmetry in two dimens., O(2) string model 77−45985
local extended and supergravity 77−17894
local quantized superfield, local commutativity from spin and statistics 77−57435
local supersymmetry in (2+1) dimens., spinning membrane 78−58138
locally supersymmetric extension of QED 77−18212
locally supersymmetric theories with model-independent transformation laws 78−93819
many-instanton problem, Euclidean supersymmetry 77−74615
many-particle Regge poles in supersymmetric theory *(Russian)* 77−46034
mass and number limits of neutral weakly interacting particles, cosmological approach 77−71000
mass formula in broken supersymmetry 79−97535
mass generation in a normal product formulation 78−25027
massive gluinos 79−2987
massive QED, renormalisation in Veltman gauge, supersymmetric transformation 77−46000
massive scalar multiplet coupling to supergravity, generalisation 78−82137
massive spinning particle in Minkowski space equivalence to massless particle in de Sitter space 80−119
massive supergravity, from spontaneous breaking orthosymplectic gauge symmetry 78−77787
massive supergravity nonlinear realisation of orthosymplectic gauge symm., coupling to spin 1/2 spin 1 multiplet 78−33019
massive supersymmetric pairs, neutrino as massless stable bound state 79−85242
massive U(1) Thirring model, S-matrix and dynamical supersymm. 77−67586
massive vectormultiplets in supergravity 80−46927

supersymmetry continued
massless field supermultiplets with arbitrary spin, gauge transformations and Lagrangians 79−85240
massless gauge theories, supersymmetric extension, supercurrent construction principle 79−40664
massless supersymmetric Wess-Zumino model and SU(2) gauge supermultiplet, classical solns. 78−8549
massless Wess-Zumino model in 4-dimens., asymptotic estimates 80−82877
matter couplings in supergravity theory 77−17895
mixing of weak and gravit. interactions, massive gravitino 78−8578
modified supersymmetries 79−45024
N=2 extended supergravity, superspace constraints, algebraic derivation 80−57159
N=2 extended supersymmetry, Noether current multiplets, extended supergravity 79−40438
N=2 supergravity with gauged central charge 78−62349
n=4 supergravity theory with local SU(2)×SU(2) invariance 78−66067
N=4 supersymmetric Yang-mills theory, 3-loop β function zero value 80−105783
N=8 spontaneously broken supergravity, mass matrix, gauge couplings 79−97281
N=8 supergravity theory, lagrangian 79−17311
Neveu Schwarz Ramond model, complete action for spinning string, field eqns., constraints 77−13943
new hadronic states, production, decay and detection 78−70302
Noether's theorem in superspace 80−73621
non-metrical supergravity for a spin-two nonet 79−71333
non-perturbative quantum field theory, lattice renormalisation construction 80−9098
non-relativistic model, spontaneous supersymmetry breaking and superconductivity 80−32031
non-Riemannian generalised super-gauge formalism, corresponding invariant physical theory 78−82122
nonAbelian gauge theory, supercurrent anomaly 78−24958
nonlinear σ model, 2-D, topology and higher symmetries 79−26241
nonlinear σ model, nonlocal charges and currents 80−27410
nonlinear σ model in two dimens., supersymm. form 78−24957
nonlinear gauge fields and the structure of gravity and supergravity theories 78−77791
nonlinear model supersymmetric extension, Kahler manifolds, Grassmann manifolds and CP^{n-1} models 80−9113
nonlinear realisation in anti de Sitter space 77−87915
nonlinear superfields and quark confinement *(Chinese)* 80−42346
nonlinearly realised supersymmetric theory, canonical quantisation 79−97283
nonlinearly realised theory, quantisation 77−65088
nonlocal currents for supersymmetric nonlinear models 80−52414
nonrelativistic supersymmetry, relevance to many-body problems 80−22537
O(4) to O(8) extended supergravity, finiteness calcs. 79−97282
off-shell N=8 supersymmetry with central charges for maximally extended supergravity 80−95230
OSp(1,4), superfield formulation in anti-de Sitter space 80−57508
OSp(1,4) supergroup, Wess-Zumino model classical solns. 80−36928
OSp(4,1) invariant fermionic σ model, graded orthosymplectic geometry 79−54277
partial wave analysis for supersymm. scatt. amplitudes 77−49872
perturbation theory supergraphs 80−13229
photino and goldstino, scatt. cross sections on matter 79−97558
physico-geometrical comments, unified field theories and supergravity, gauge transformations 80−364
physico-geometrical considerations of supersymm. concept, superfield theory 78−74172
physico-geometrical remarks on unified gauge field and supersymm. concepts 78−37167
Poincare invariance without Poincare group 79−12992
Poincare supergravity as broken superconformal gravity 78−62348
Poincare supersymmetry, parafermion generalisation 79−17626
and pseudoclassical dynamics for particle with arbitrary spin 77−57464
pseudoclassical relativistic electron and supersymmetries 77−13845
QCD, hadronic and supersymm. string states 79−75724
QED, absence of radiative corrections to axial current anomaly 80−13242
QED, supercurrent gauge invariance, α-independ. 80−95233
QED, supersymmetric, renormalised supercurrents and scale anomaly 80−105818
QFT, supersymm., space time symm., internal symm. groups, relativistic invariance *(Russian)* 77−49871
quantum corrections to the quadratic mass formula of broken supersymmetry 80−46942
quantum gauge supersymmetry, props. of globally supersymmetric Green's functions 79−63352
quantum gravity and path integrals, supersymmetric theory, virtual Planck-mass black holes 79−2706
quantum mass corrections to supersymmetric soliton theories in two dimensions 79−54254
quantum parafield theory and supergroup transformations 80−9124
radiative mass generation in perturbation theory and the renormalization group 80−86611
real simple Lie superalgebras, finite-dimens., classification 80−57516
relativistic harmonic oscillator, model 77−38086
relativistic string quantized in four-dimensional space, supersymmetrical Lagrangian in QCD principles *(Russian)* 80−13276
renormalisation theory, perturbative, general features, quantum action principles, pure Yang-Mills theory 80−105794
representations determ. for more than 1+1 dimens. 78−54580
restored symmetries, quark system, Pomeron as Josephson current 77−61211
review of present status of supersymmetry and supergravity 79−63112
review of principles and historical development 77−18197
reviews, algebraic props., applic. to particle physics 77−87918
Riemannian space-time, differential forms 77−82441
S-matrix amplitude props. in supersymm. theories 77−67582
S-matrix of supersymmetric nonlinear σ model determ. 78−66052
scalar and spinor free fields, supersymmetry charges 77−6049
scalar supersymmetric theories, characterisation by Bose field transformation 80−32033
scalar supersymmetric theory, α-representations 79−30680
scale invariance in superspace 79−17313
Schwinger source formalism for Fermi-Bose transform. 79−63114

supersymmetry continued
self-duality, helicity, and supersymmetry: the scattering of light by light 79−93327
self-duality and helicity in supergravity 80−46929
sine-Gordon eqn., inverse scatt. in higher dimensions 80−47165
sine-Gordon eqn., polongation struct. and inverse scatt. formalism 80−47173
sine-Gordon equation, supersymmetric, prolongation struct. inverse scatt. formalism 80−99032
Sine-Gordon model, infinite set of local quantum conservation laws 80−47207
sine-Gordon model, supersymmetric, exact soliton like solns. 79−30643
sine-Gordon model, supersymmetric solitons and monopoles 80−31991
sine-Gordon model and two-dimens. bag 78−21382
sine-Gordon supersymmetric model, higher local quantum conserved currents 80−52435
sine-Gordon supersymmetric model, quantisation of conservation laws and superrenormalisation 79−89058
sine-Gordon supersymmetric theory, infinite set of bosonic conserved currents 78−62313
SL(3,R) algebra, minimal and centred graded spin extensions 80−82910
SO_2 extended supergravity, geometrical interpretation 77−49660
SO(8) extended supergravity 78−16970
SO(8) extended supergravity 80−4914
SO(8) supergravity derivation 80−12975
soft spin 3/2 massless fermions, gravity, supersymm. 77−49869
soliton quantum mechanical mass in supersymmetric theories 80−22536
space-time lattice supersymm. formulation 77−82689
spin, supersymmetry, and square roots of constraints 79−12676
spin 1/2 classical particle, supersymmetric actions 79−2952
spin 3/2 field and Cartan's geometry 78−16712
spin 5/2 theories, supergravity extensions beyond SO(8) 80−46935
spin representation of orthogonal group, superfield interpretation 77−49874
spin system, critical, in random mag. field, supersymmetry, neg. dimensions 79−97533
spin systems, supersymmetric, extensions 78−21344
spin-1 fields, supersymmetric non-polynomial vector multiplets and causal propagation 80−91012
spinning membrane, locally supersymmetric, reparametrisation invariant action 77−79230
spinning particle, local supersymmetry 77−2768
spinning string, local supersymmetry and reparametrisation invariant 77−18244
spinor charges, internal and space-time symmetry fusion 77−22660
spinor field geometrodynamical superspace, quasi-catastrophe theory 78−41137
spinor operators of Weiss-Zumino type and their irreducible components 79−71602
spinor representation for Lie algebra enlargement 77−34100
spinor Yang-Mills superfield 78−12825
spinorial charges and twistors 77−13885
spl(2,1), basic superalgebra representations 80−82908
spl(2,1) superalgebra, irreducible representations, tensor product 80−82909
spontaneous breakdown inducing IR anomaly 77−38095
spontaneous breakdown of chiral symmetry in supersymmetric nonlinear σ model 78−54549
spontaneous breakdown of fermion number conservation and supersymm. 77−30248
spontaneous breaking in non-Abelian gauge theories 77−49878
spontaneous breaking of supersymm., unified gauge models appl. 77−71452
spontaneous breaking through dimensionsal reduction 79−40441
spontaneous symm. breaking in Wess-Zumino supersymm. model 78−74170
spontaneous symmetry breaking and Goldstone fermions 77−22659
spontaneously broken local gauge supersymm. struct., real gravit. interactions 77−49843
spontaneously broken supersymmetic model at high temperature, Green's function props. 79−26257
spontaneously broken supersymmetry in QFT 78−54582
spontaneously broken theories of weak, EM and strong interactions 77−79244
stability and supersymmetry, general formalism, explicit two-loop appls. 77−79228
stability and supersymmetry, models with local gauge symmetry, renormalisation group anal. 78−70296
strong gravity, supersymmetric theory for f- and g-gravitons and massive gravitinos 78−62141
SU(2,1;1) nonlinear invariant σ model, superconformal group and curved fermionic twistor space 80−62831
SU(2)×SU(2)×U(1) supersymmetric gauge model, atomic parity violation and neutral current predictions *(Russian)* 79−54294
SU(2)×U(1) gauge model, low-energy theorems for Goldstone neutrino 77−2769
SU(2) gauge theory, sypersymm. breaking by pseudoparticles, supergravity implications 78−24959
SU(2) supergroups, Yang-Mills, Lie groups, chiral coeffs., Baker-Campbell-Haussdorff formula 80−68355
SU(2) Yang-Mills-Higgs system, classical finite energy solns. embedding in supersymmetric extension 79−2950
SU(4|N) gauge transformations, determ. of Lagrangian for supertheories 79−63118
SU(5/1) supergroup based strong-electroweak unified model with supersymmetry 80−101977
SU(8) supergravity supersymmetry breaking 80−46908
SU(N) conformal supergravity, gauge theories for extension 78−8577
super $(\phi^3)_2$ model, large order perturbation theory 80−82876
super Clifford algebra 79−98
super sine-Gordon eqn., supergroup geometrical interpretation, supersymmetric extension 80−57475
super Weyl transformations in two dimensions 79−25953
super Yang-Mills theory, anomalies and supersymmetric regularisation by dimensional reduction 80−82916
(super-ϕ^3)$_4$, Euclidean model, normalisation of Schwinger functions 79−89060
(super-ϕ^3)$_4$, regularisation of Euclidean model, supersymmetry Ward identity derivation 79−89059
super-gauge symmetry in general relativity, Einstein's A transformation *(German)* 78−86199

supersymmetry continued
superalgebra generalisation, 3-colour extension of OSP (4,1) de Sitter and SU(2,2;1) Wess-Zumino superalgebras 79−330
superalgebra in (0,1) integration of supersymmetrical Liouville eqn. *(Russian)* 80−101947
superalgebra with spinor-vector generator, Goldstone spin 3/2 particle, Higgs effect 77−49876
superconformal algebra, two-point and three-point Green's functions of scalar superfield 77−30280
superconformal group in flat superspace 77−2763
superconformal invariance of superspace with nonminimal auxiliary fields 79−17317
superconformal supergravity and internal symm., proliferation of gauge fields 77−54056
superconformal symmetry breakdown as guide to supergravity constraints 80−46930
superconformal transformations group 79−2953
superconformal unified field theory 78−12848
supercurrent, existence and deduction from an arbitrary superfield Lagrangian *(Russian)* 78−89633
superdiagram technique for gauge theories, renormalisation 77−30267
superfield covariant derivatives for O(1) and O(2) supersymmetry 80−46914
superfield eqns. of motion 78−8503
superfield Feynman graphs, loop calculations 80−46906
superfield formulation of supergravity 79−17312
superfield notation for supermultiplets spontaneous breaking, Lagrangians and internal symmetry incorporation *(German)* 78−74167
superfield representations of supersymmetry algebras with central charges, SU(4) invariance 78−70301
superfield supergravity formalism of Wess Zumino, constraints 79−2970
superfield supergravity with symmetry 80−8891
superfields and supersymmetric linear multiplet *(Chinese)* 80−101950
superfields in higher-dimensional spacetime 79−17316
superfields with arbitrary spin, spectral representation of two-point function 77−6050
supergauge invariant Yang-Mills eqns., exact solns. 79−67471
supergeometry mathematics 78−73891
supergrand exceptional unification and quark-lepton constituents 80−91030
supergrand unification in E_8, quark-lepton assignments, symmetry breaking scheme 80−68408
supergraph formalism UV finiteness in gauge supersymmetry 80−46913
supergravity, 2-loop divergence, with external gravitons on-shell cancellation 77−49659
supergravity, auxiliary fields, matter coupling, BRS transformations 78−93837
supergravity, auxiliary fields 79−17315
supergravity, auxiliary fields and UV divergences, supersymmetric Yang-Mills-Einstein system 78−78127
supergravity, auxiliary fields for closed algebra using S-matrix 78−81911
supergravity, canonical formulation 78−29016
supergravity, Cartan's geom. struct. 78−49745
supergravity, classical solns. 78−122
supergravity, constraint-free superfield formalism 79−17309
supergravity, coupling to scalar multiplet 77−67366
supergravity, covariant quantisation 78−41470
supergravity, extended, U(N) invariance 77−61003
supergravity, extended, with gauge internal symmetry in de Sitter space 77−79021
supergravity, extended, with SO(4) symmetry 77−64991
supergravity, extended theories, algebraic props. 77−49875
supergravity, fibre bundles and supersymmetries, super-Poincare group 80−105559
supergravity, geometrization in superspace and local supersymmetry 80−8890
supergravity, global supersymmetry transformations of noninteracting massless particles 80−95015
supergravity, Hamiltonian formalism, quantisation and S-matrix 78−16972
supergravity, Hamiltonian formulation 78−24722
supergravity, local supersymmetry in (2+1) dimens., differential forms. 78−49980
supergravity, locally invariant supersymmetric gauge field theory 78−49742
supergravity, minimal set of auxiliary fields, gauge algebra closure 78−49743
extended supergravity, N=2, auxiliary fields in 5, 6 space-time dimens. 79−30339
supergravity, O(2) extended, exact plane wave solns. 79−25955
supergravity, one-loop renormalisability 77−5730
supergravity, Poincare and conformal, multiplication rule and supersymmetric densities for multiplets 78−70037
supergravity, Poincare and conformal models with closed algebra 78−74198
supergravity, renormalisability props., superinvariant local counterterms 77−34087
supergravity, SO(3) and SO(4), finiteness and renormalisability of scalar multiplet coupling 78−4821
supergravity, SO(3)-invariant extended 77−22475
supergravity, space-time spin struct., and Hamiltonian constraint square roots 77−49663
supergravity, SU(4) invariant theory 78−41471
supergravity, super Higgs effect, gravitino masses and couplings 80−62562
supergravity, supercurrent anomaly 78−29267
supergravity, superfield Lagrangian 78−41468
supergravity, superspace and component formulations, tensor calculus transcriptions 79−63116
supergravity, superspace constraint algebraic origins 80−98842
supergravity, superspace formulation, consistency checks 78−37170
supergravity, supersymmetric dimensional regularization via dimensional reduction 79−67202
supergravity, supersymmetric generalisation of differential geometry tensors 78−45546
supergravity, surface integrals as symmetry generators 77−74634
supergravity, two-loop renormalisability 77−17897
supergravity, unified theory of basic forces 78−50001
supergravity, unitarity, Ward identities, and new quantisation rules 78−54279

supersymmetry continued
supergravity, Weyl and Einstein, unified approach to matter coupling 78−54275
supergravity and cosmological const. 77−74171
supergravity and gravity as gauge theories on group manifold 78−41469
supergravity and S-matrix 77−46010
supergravity and supersymmetry, review *(Czech)* 80−86183
supergravity and Yang-Mills theory unification 77−46011
supergravity as gauge theory of supersymmetry 78−8576
supergravity constraints, algebraic understanding 80−46921
supergravity coupled to massive self-interacting scalar multplet, spontaneous symmetry breaking 77−74633
supergravity coupled to scalar multiplet 77−46012
supergravity coupling to nonlinear realisations of supersymmetry in two-dimens. 77−79024
supergravity in 11 dimens., action and transform. laws 78−70038
supergravity in superspace, algebraic approach 79−17314
supergravity review, phenomenological appls., and lower spin fields unification 78−77788
supergravity structure, gauge actions, multiplets 79−2971
supergravity superfield analysis using supertorsion and supermanifold 79−85038
supergravity supergraphs, perturbation theory description from globally-supersymmetric gauge breaking 79−67203
supergravity theories, algebraic simplifications 77−87681
supergravity theories, background metric, conformal anomalies calc. 78−70043
supergravity with axial-gauge invariance 77−41790
supergravity with complex spin-3/2 gauge fields, invariant under local complex supersymm. 77−5731
supergravity with general scalar interactions, super Higgs effect, gravitinos, spontaneously broken supersymmetry 79−6037
supergravity without cosmological constant, spontaneous symmetry breaking and Higgs effect 79−17310
supergroup transformation, paraGrassmann algebra of relativistic fields 79−45029
supermanifolds, Lie superalgebras and superspace 80−9125
superspace, auxiliary mass BPHZ renormalisation procedure 78−16902
superspace, effective potential calc. 78−16944
superspace, explicit form for chiral multiplet tensor calculus 79−9302
superspace, generally covariant theories of gauge fields 78−54568
superspace, new class of superalgebras and local gauge groups 78−29230
superspace affine theory, simple Lagrangian 80−105813
superspace as a fibre space 79−17637
superspace as family of concrete spinor structures 80−95225
superspace formulation for supergravity, book contrib. 80−22261
superspace formulation of supergravity using vierbeins 79−2972
superspace gauge theories, superspace Maxwell and Yang-Mills actions 80−86582
superspace geometry and N=1 non-minimal supergravity 80−57155
superspace geometry of supergravity 80−46909
superspace tensor calculus formulations, relations to supergravity 80−46922
supersymmetric gauge theories and their possible applications to the weak and electromagnetic interactions 79−49419
supersymmetric Liouville and sine-Gordon eqns., method of inverse scatt. and Backlund transforms. 79−2951
supersymmetric models of weak and electromagnetic interactions 79−26276
supersymmetric nonlinear σ-model in 4-D, coupling to supergravity 78−49981
supersymmetric point particles and monopoles with no strings 80−52432
supersymmetric solitons in four space-time dimens., the mag. monopole 79−21896
supersymmetrical field theories, mathematical base *(Russian)* 79−67478
supersymmetrical string model, physical states *(Russian)* 79−67523
supertranslated soliton solution, two dimens. supersymm. quantum theory construct. using Dirac's method 78−45783
supertwistors and conformal supersymm. 78−29015
superunified field theories, geometrical transformation laws 79−63117
superunified theories, geometry of gauge invariance 78−24723
tachyons, absence in supergravity and classical Einstein gravity 79−67208
tensor calculus for vector multiplet coupled to supergravity 78−86214
Thirring model, supersymmetric generalisation 79−40682
three-loop charge renormalization effects due to quartic scalar self-interactions 80−57489
topological charges for N=4 supersymmetric gauge theories and monopoles of spin 1 79−63364
trace and axial vector anomalies, for spin 3/2 Majorana field, derivation using zeta function regularisation procedure 79−2700
transformation laws for chiral multiplet 77−71454
two-dimensional supersymmetric models, group theoretical construction 80−99069
unification of EM, weak and strong interactions, extension to gravity 80−73637
unification of fermions and bosons, interacting model 79−21629
unification of fermions and bosons, math. structures and phys. questions 79−21630
unification of fermions and bosons, physical foundations of local (algebraic) approach 79−21628
unification of fundamental forces in nature, elementary particle constituents $SU(3)_c$ gauge symmetry, review 80−27448
unified field theory applications 80−91040
unified gauge field underlying supersymmetry space, physico-geometrical remarks 79−13007
unified gauge theories and Higgs bosons 77−45948
unified superconformal gauge theories for gravity+other gauge interactions 77−87928
unified theory of gauge fields and supersymmetry 78−58150
universal supersymmetry and its need for grand unification theories 80−13230
vacuum symmetries of gauge supersymmetry, quantum effects 79−17634
vector superfield as Abelian gauge field, Lagrangian density 77−18170
vector superfield generated by supercurrent, supergravity formulation 77−71453
vector-like model of lepton interaction 78−412
Volkov-Akulov model, constrained linear realisation 78−78107
weak and EM interactions, supersymmetry and gauge theories 79−26208
Weinberg-Salam model, Lagrangian, invariant under SU(2/1) gauge group and rotations, in 6-D graded space 80−57537

supersymmetry continued
Weinberg-Salam model 79−67490
Weinberg-Salam model of lepton interactions, supersymm. extension, low energy studies 77−49887
Wess-Zumino model, massive, dimensional regularisation, supersymmetry 80−27398
Wess-Zumino model as linear σ-model of spontaneously broken conformal and OSp(1,4) supersymmetries *(Russian)* 79−93315
Wightman distributions, globally conformal invariant quantum field theory, conformal superworld 77−49824
Yang Mills string theories 77−79216
Yang-Mills field theory, point splitting regularisation, superformal anomaly 80−91014
Yang-Mills fields, Ward identity, one-loop level, renormalisation 80−73597
Yang-Mills supersymmetric gauge theory, cancellation of supercurrent anomaly 78−8518
Yang-Mills supersymmetric theory, mag. monopoles and dyons, quantum corrections 78−62334
Yang-Mills theories 77−45944
Yang-Mills theory, allowed supersymmetric vacuums 78−4783
Yang-Mills theory, point-splitting derivation of anomalous divergence for the spinor current 78−74148
Yang-Mills theory, SU(4) supersymmetric, charge renormalisation 78−24929
Yang-Mills theory and instantons 78−32986
Yang-Mills theory in superspace 79−12979
Yang-Mills theory in Wess-Zumino gauge, supersymmetric regulators and supercurrent anomalies 80−86614
zero-mass representations of Poincare supersymmetries with arbitrary spinor generators 80−99065
e^+e^- annihilation, spin-0 electron or muon pair prod., cross section supersymmetry predictions 80−32092
$pN \rightarrow R\bar{R}+X$, R-hadron prod. bounds from calorimetry expts. 79−13167
$\bar{p}p$, heavy lepton prod. and decay, supersymmetrical model of weak and EM interactions *(Russian)* 80−86748
$\psi \rightarrow$gravitino+antiphotino, gravitino mass lower limit, light gravitino weak interactions 79−75698
t-quark mass in super unified O(10) model 79−49439
supervisors (programs) *see supervisory and executive programs*
supervisory and executive programs
see also multiprogramming; online operation
PDP 11 and MBD branch driver for data acquisition 79−89567
proton storage ring, NAP-M, supervising system 77−65365
supply systems (electric) *see power systems*
supports
see also poles and towers
cable-stayed cantilever beam dynamics 78−46889
cooling towers with column supports, free vibration analysis 78−83292
EHV transmission line, vibration dampers, Indian standards 77−5660
fusion reactor, compact toroidal ignition experiment, support struct. anal. by numerical code 80−106167
fusion reactor, RST, support struct. 80−102342
fusion reactor, TFTR toroidal field coil support restraint struct. 80−95428
fusion reactor, toroidal field coil in-plane bending stress, struct. support design 80−106164
fusion reactors, TFTR neutral beam support system 80−102376
machine vibrations anal. and obs. block deformability influence *(Italian)* 78−51108
PWR core support barrel motion monitoring by ex-core detectors 79−13446
rigid body systematic deflection by suspension vibration in mag. field *(Russian)* 79−9223
skirt-supported pressure vessel free vibrations, finite element analysis 79−68632
Tokamak fusion reactor prefabricated toroidal supercond. field magnet system 79−31211
two-way continuous rectangular plate free vibration theory 79−68631
ultraprecision spindle unit construction on aerostatic supports 78−77880
Si-loaded support, effect on transverse modes in gap-coupled surface-wave devices 79−46138
suppression wavemeters *see wavemeters*
suppressors (surge) *see surge protection*
surface acoustic wave devices
see also acoustic microwave devices; acoustic parametric amplifiers; acoustic parametric devices; acoustic parametric oscillators
1.2 GHz temperature stable SAW oscillator 78−59226
2.148 GHz SAW oscillator using AlN/Al_2O_3 delay line 80−74680
2-D separated media semiconductor convolver for acoustic Fourier transforms of optical images 80−74308
31st Annual Frequency Control Symposium, Atlantic City (1977) 78−57905
58 MHz TV intermediate-frequency filter, using ZnO sputtered film 77−80022
300 MHz oscillators using SAW resonators and delay lines 78−59255
300 MHz resonator oscillator close-in phase noise rel. to vibration 79−55289
400 MHz SAW timing filter for optical fibre transmission 79−50415
acoustic focusing device with IDT on thin piezoelectric plate 80−1398
acousto-optic Bragg deflector, wideband, guided wave, technology and applic. 77−58471
acousto-optic lens, Fourier and Mellin transform props. 78−78926
acousto-optic memory correlator, long duration, using acousto-photorefractive effect 78−79124
acousto-optic memory correlator using acousto-photorefractive effect 78−71248
acousto-optic modulators for integrated optics 79−90032
acousto-optic real time two crystal correlator 78−42497
acousto-optic real-time radar and sonar signal processing 79−72515
acousto-optic signal processors 80−102640
acousto-optic signal processors using multichannel SAW correlation and convolution 80−74611
acousto-optic time integrating correlator 80−64295
acousto-optic tunable TE-TM mode convertor on diffused waveguide 80−53477
acousto-optical devices critical assessment and development trends *(Czech)* 80−23777
acousto-optical devices for real- and near-real-time signal processing 80−10024
surface acoustic wave devices continued
acousto-optical light diffraction grating, gas laser tuning *(Russian)* 78−33759
acousto-optical modulator and correlator, for optical link 78−38040
acousto-optical planar deflector, with colinear propagation of optical and surface acoustic waves *(Russian)* 77−62053
acousto-optical total internal reflection modulator 77−19435
acoustoelectric, wideband signal processing 77−27442
acoustoelectric memory correlators, fabrication, experimentation and anal. 79−32179
acoustoelectric SAW image scanner applications 79−45912
acoustoelectronic devices based on interaction of SAW with electrons in semiconds. 77−80025
acoustooptic Bragg deflector, wide-band guided wave, using tilted-finger chirp transducer 80−14440
acoustooptic TE⇌TM mode convertor utilizing doubly confined optical and acoustic waveguide struct. 78−83087
acoustooptical film deflector, efficiency for Gaussian beam 78−13791
actively controlled SAW power divider 78−18120
admittance sheet deposited on piezoelectric substrate 77−80689
amplifiers, monolithic, of continuous operation 77−80023
amplifiers, study of saturation power 77−39133
amplitude response, optical meas. method 79−94435
analogue CCD and SAW filters 77−39172
analogue signal processing appl. 77−27437
analogue signal processing C-CD and SAW devices appl. 77−27439
analogue signal processing technology, transversal filters and resonators 80−87656
anisotropic crystal surface $\Delta V/V$ waveguide SAW propagation and mode excitation 77−31161
asymmetric three-transducer configuration analysis 77−39165
automatic response measurements for large time-bandwidth SAW devices 80−74677
band-pass filter, with three-transducer configuration 80−74610
band-pass filter synthesis, acoustic surface waves, transfer characts. *(Russian)* 77−58510
bandpass filter using fanned multipstrip coupler 77−50837
bandpass filter with −50 dB sidelobes using unweighted interdigital transducers 78−71244
bandpass filters, approx. parameter anal. *(Russian)* 80−23858
bandpass filters, characteristics 77−68332
bandpass filters, technique, construction, appl. *(German)* 79−50544
bandpass filters, TV receiver appls. 78−51008
bandpass filters, two-port model 77−62117
bandpass filters, withdrawal weighted CAD 78−66991
bandpass filters exhibiting arbitrary phase and amplitude response charcts., design 77−80021
bandpass filters with quarter wave reflections, design 80−19183
bandpass transversal filtering technology 77−27440
Bleustein-Gulyaev waveguides with gratings, anal. Bleustein-Gulyaev waveguides with gratings, anal. 80−1391
book 79−50518
Bragg deflection of guided optical wave by surface acoustic waves in $LiNbO_3$ Ti-diffused waveguides 79−14118
broad-band filters, tap weight enhancement 78−22239
broadband chirp transducers for integrated optics spectrum analyzers 80−74514
Broadband modified chirp transducers for integrated optics spectrum analyser 80−58802
broadband probe, materials testing appls. 78−23904
broadband SAW delay lines using weakly piezoelectric substrates 78−22230
buffer memory, SAW/CCD device 79−46137
bulk waves anal. 79−7259
Butterworth contiguous filters, design, fabrication and testing, 248.8 to 401.2 MHz 79−68493
C-CD/SAW devices for signal and image processing, conf., Ottawa, Canada, 1977, Oct. 79−32159
capacitive tap weighted SAW transducers 77−80041
cascaded gratings, transmission response 77−23835
cascaded SAW gratings as passband filters 77−68333
ceramic SAW filter development and applications 79−23156
characteristics measurement in frequency domain, methods 77−75755
chirp filter FFT processor 78−87209
chirp filters, spectrum analyser appl. *(Japanese)* 80−79065
chirp filters based Fourier transformation processors 79−7270
combined bandpass and rejection filters, design and eval. *(Russian)* 80−83718
compensated filter used in wide spread MSK waveform generator 80−74670
conference, ferroelectric materials and their applications, Kyoto, Japan, Nov. 17-19, 1977 79−19846
conference, New Orleans, LA, USA 80−73101
controllable electroacoustic phase shifter 79−81640
conversion to bulk plate modes in shallow gratings 80−1385
convolution in hybrid piezodielectric-semiconductor system 79−7268
convolver, degenerate elastic, nonliner interactions 80−64254
convolver, in monolithic MIS struct., charact. 77−80027
convolver, semicond. surface state meas. appl. 79−42617
convolver, wideband, utilising Sezawa waves in metal-ZnO-SiO_2-Si config. 78−66988
convolver comprising monolithic ZnO on Si 77−7261
convolver for surface-states concentration profile and capture cross section determ. 80−80341
convolver in monolithic MIS struct., basic charcts. 77−23791
convolver used to study photoconductivity of semiconductors 79−42587
convolvers, enhancement of convolution voltage due to transverse drift of carriers 80−1381
correlators for US flaw detection 77−19470
coupled SAW grating resonator filter synthesis 77−23821
crystal parabolic frequency/temp. characteristic compensation 79−55294
deeply-etched resonators, long-term aging improvement 79−55290
degenerate elastic convolver, theory 80−74628
delay line, beam tracking, multiply reflected Gaussian beams in circular cross section 79−18343
delay line, tunable, using layered piezoelectric-liquid-piezoelectric structure 79−94431
delay line, variable, using magnetostrictive metallic glass film overlays 78−63240
delay line acousto-optic signal processing devices 79−94328
delay line and resonator oscillators for phase locking 78−59254

surface acoustic wave devices continued
delay line complex transfer coeff. calc., Shockley-Ramo induced current theorem 79−7264
delay line filters, wideband, low insertion loss, VHF band 80−28398
delay line filters for GHz SAW oscillators, fabrication and performance 79−14185
delay line signal processors using acousto-optic interactions, real time system 80−28384
delay line used for obs. of elec. props. of CdS-$NiCl_2$ interface 79−56302
delay line with ZnO film, elastic-surface-wave temp. coeffs. 77−88987
delay lines, appls. of amorphous magnetic-layers 80−28389
delay lines, combined triple-transit and bulkwave suppression 80−53565
delay lines, temp. dependence of surface wave diffraction on α-quartz 77−15674
delay lines, towards an idean photon correlator 80−68252
delay lines, triplet-transit suppression technique 79−64453
delay lines, true quadrature taps 78−87222
design and appls., review 77−50853
dielectric/piezoelectric layered waveguide, surface acoustic wave amplification *(Russian)* 78−23138
diffused p-n diode memory correlator 77−23831
digital filter design using optimum pulse response techniques 77−46872
digital FM compression system *(Russian)* 78−55541
and digital techniques, interfacing and comparison 77−27438
diode array SAW correlator model and expt. 78−9508
disc delay line beamguide 'optical' transfer function 77−31183
dispersive delay line for real-time spectral anal. of D_2O far IR laser pulses 79−45983
dispersive delay lines, new cut of quartz for temperature stability 80−19185
doubly-rotated-cut, numerical anal. 80−74616
driven equilibrium Fourier transform sensor operating at 100 MHz 80−74612
dual-gate depletion-mode FET/piezoelectric film transducer 79−50563
echo-tomographic imaging with SAW processing, ultrafast 80−74639
edge bonded transducer design and application 79−55304
edge reflection SAW absorber, FM discriminator appls. 78−1517
edge-bonded surface-acoustic-wave transducer array 80−1395
elastic surface waves propag., charact. for SAW filters, book contrib. 80−1378
electrode-withdrawal weighted filters, method for reducing sidelobes 80−5875
electrode-withdrawal weighted SAW filters, suboptimization 79−27471
electronically variable delay using a SAW tapped delay line and digital shift register 78−63241
electronically-addressed bulk acoustic wave Fourier transform device 80−74637
electrostatic voltage sensor *(Japanese)* 80−105632
EM periodic SAW transducers 78−13880
EM transducer model and flexible design for NDT 77−23844
EM transducer range resolution improved by pulse compression 77−19509
equivalent circuit model for SAW transducers 77−46870
externally coupled resonator-filter (ECRF), loss minimizing 79−41542
fabrication techniques, book contrib. 79−50523
fast SAW-based discrete Fourier transformers 79−18613
film thickness monitor, quartz crystal, based on SAW oscillator 78−3036
filter, band-pass, design and expt. results *(Czech)* 80−19201
filter, band-pass, transversal, principle, design and performance 78−38147
filter, L-band low loss SAW filters 80−74673
filter, TV receiver appl. *(Japanese)* 78−71247
filter appls. in consumer electronics, review 80−74675
filter design, low-sidelobe cascaded 80−74679
filter design and implementation, book contrib. 80−1394
filter design applied to group-delay equaliser in TV rebroadcast transmitters 80−74676
filter design for nonlinear phase response, building-block method 77−27433
filter design for TV, CATV and radar appls. 80−53579
filter design using linear programming technique *(Japanese)* 77−23839
filter design using linear programming technique 79−32154
filter design using optimisation technique 80−74671
filter design with arbitrary phase and amplitude characteristics 77−23826
filter design with diffraction compensation 80−74672
filter developments, for high frequencies 78−51010
filter technological advances 78−46862
filter triple transit suppression by mech. and regeneration reflection cancellation 77−23829
filter using waveguide between input and output transducers, freq. response 77−39162
filter with low insertion loss using group-type unidirectional interdigital transducer *(Japanese)* 78−33980
filter with narrow pass band, transmission systems appl. *(Japanese)* 78−90602
filters, compensation technique using multistrip couplers 77−75750
filters, design, construction, appl., book 80−1393
filters, fine frequency adjustment by modifying propagating direction 78−18125
filters, fundamentals of design, interdigital transducer circuit model, book contrib. 79−50520
filters, introduction 79−55282
filters, low insertion loss, using multiphased unidirectional transducers 80−28397
filters, low insertion loss *(Japanese)* 79−72772
filters, manufacturing inaccuracies influence on transmission charact. 79−10434
filters, method for accurately adjusting the centre freq. 79−32155
filters, narrow band transversal types and interdigital transducers, review 80−28395
filters, narrow pass-band, for transmission system appls. 79−50517
filters, operator, transfer function *(French)* 77−54846
filters, props. and appls. *(Japanese)* 79−18644
filters, resonator, scattering analysis and design 79−68492
filters, SAW propag. and amplification, appls. in TV systems *(Italian)* 79−81642
filters, signal sorting, identification in communications receivers, military appl. 79−18615
surface acoustic wave devices continued
filters, synthesis, limitations of phys. model in terms of number of fingers and material consts. 80−28399
filters, use in communications equipment 78−38152
filters with asymmetric amplitude-freq. response, synthesis *(Russian)* 79−68521
filters with weighting of electrode overlap without beam integration *(German)* 78−51011
finite SAW transducer, surface charge density and elec. field distrib., moment method 80−23857
flat conductor, EM SAW transducers, fields 77−23842
frequency control 32nd Annual Symposium, Atlantic City (1978) 79−54100
frequency filters, mathematical design model *(French)* 77−68331
frequency synthesizers for fast frequency hopping 77−39176
frequency to voltage convertor using SAW linear FM chirp filter 80−19182
GaAs holographic grating transduction from bulk to surface acoustic waves 77−31199
gap-coupled Schottky diode array/$LiNbO_3$ imager for scanning of optical images 80−74632
gap-coupled surface-wave devices, transverse modes 79−46138
generation of SAW in crysts. with high dielec. const. 78−83203
grating acoustic scanner for material defects 79−47878
grating cascades, bulk scatt. loss 77−46869
grating resonators, mode pattern verification 78−1532
grating resonators, modes 78−42498
grating resonators, reflection-dependent coupling 77−23822
grating-array reflectors and transducers 80−58884
grating-resonator filter, behaviour of unidirectional transducers 80−5877
gratings, theoretical anal. of stored energy 80−74622
grooved reflective array SAW compressor and resonator performance 77−23820
grooved reflector array, groove depth var. effect on performance 78−75017
grooved reflector arrays, reflection and bulk wave loss charact. 78−9510
grooved SAW reflective grating, field theory 77−31162
guide step analysis 78−1487
guided acousto-optical beam deflector 77−19433
guided-wave acousto-optic interaction on Si substrate 79−37050
Gulyaev-Bleustein and Rayleigh wave reflection, rel. to signal processing appl. 77−80028
HF acousto-optic mode conversion and deflection 77−54776
high speed signal processing, optical and acoustic integration 78−51012
high volume markets trends and charact., review 77−50815
holographic image scanning by SAW on monolithic MIS structure 77−23771
horizontal-shear surface wave grating resonators 78−59249
horn design for focused SAW radiation into waveguide 78−1542
hydrophones for use in sonobuoy system 79−94437
IDT, Al evaporation conditions 80−92007
IDT, bulk wave radiation suppression, theoretical investigation of crystalline orientation 80−58886
IDT, electrode charge distrib. as element factor, anal. 80−1396
IDT, input admittance calc. using moment-method technique 79−94439
IDT filter with three inclined tapered transducers 79−81637
implantable SAW pressure transducer/transmitter 79−29575
impulse response modelling of SAW transducers 79−81665
in-line chirp filter applications 78−59207
in-line reflective array compressor 80−74626
information processing using surface acoustooptic interaction, side entry config. 78−42461
information storage and correlation in semiconductor diode arrays 78−9505
integrated optic Bragg spectrum analyser design 80−33237
integrated optic spectrum analyser, design of Bragg cells 80−74515
integrated optic spectrum analyser design and fabrication 79−72720
integrated optical RF spectral analyser acousto-optical readout scheme 79−50446
integrated optical spectral analyser design and fabrication 79−50445
integrated optics spectrum analyser, development progress 80−58803
integrating correlators; four-wave interactions 79−98547
interacting SAW transducer equivalent circuits 77−27456
interdigital SAW transducers, freq. charact. improvement *(Japanese)* 79−23164
interdigital transducer, book contrib. 80−1400
interdigital transducer, electromechanical coupling coeff. 79−23163
interdigital transducer, excitation of surface and shear acoustic waves on nonpiezoelec. materials 78−66997
interdigital transducer and 1.1 GHz SAW oscillator, photolithographic contact printing *(Japanese)* 78−33981
interdigital transducer design, redefined element factor 79−7266
interdigital transducer design and component specification tradeoffs 77−27455
interdigital transducer finger pattern, modification of aperture 78−13883
interdigital transducer for Lamb wave devices for AM, influence of electrical termination 79−41549
interdigital transducer in layered anisotropic semiconducting struct., elec. input admittance matching 78−22238
interdigital transducer transfer function rel, to fabrication tolerances 77−27452
interdigital transducer transverse electrostatic end effects 77−27453
interdigital transducer using basal plane of semi-infinite, hexagonal piezoelect. cryst. 78−22244
interdigital transducers, equiv. cct. parameters from surface waves dispersion relations 77−39187
interdigital transducers, equivalent network model 79−46145
interdigital transducers, excitation profiles 79−41544
interdigital transducers, finger withdrawal admittance eval. by normal mode anal. 78−33978
interdigital transducers, generation and detection of surface and bulk acoustic waves 77−39186
interdigital transducers, scatt. parameters 77−39188
interdigital transducers and delay lines, fabricated using simple mask printers 78−59229
interdigital transducers for one-port SAW resonators, narrow band filters appl. *(Japanese)* 79−27478
interdigital transductors in 3-layer CdS-SiO_2-Si structure *(Dutch)* 78−22242
inverse filter for NDT 77−28970

surface acoustic wave devices continued
ion beam etching, for SAW refl. struct. fabrication, role of redeposition 77−56123
IR scanning by SAW modulation 79−80687
isotropic elastic waveguides, numerical anal. by mode-matching method 78−9465
isotropic elastic waveguides, rectangular rods, mode-natching method 78−9466
Israel Physical Society 1980 annual meeting, Rehovot, Israel (April 1980) 80−94909
Lamb wave transducer with three operation modes, communication system appls. 80−43583
Lamb-wave device with three operation modes 79−14183
large time-bandwidth acousto-optic signal processors 79−46118
large-scale lossy groove array finite difference analysis 77−27420
laser beam/acoustic surface wave interaction in metal-diffused optical waveguides, TE-TM mode conversion 78−42411
laser pulse detector, using SAW generation 77−57392
layered piezoelectric-semiconductor surface state acoustic memory 78−90615
lensless acouto-optical convolver using polarisation discrimination detect. 78−79170
low-distortion FM demodulator using SAW delay device 78−51014
magnetoelastic Rayleigh wave convolver internal efficiency calc. 77−23817
manufacturing methods and technology progress report 77−39173
matched filter device development using monolithic integration of SAW and semiconductor ccts. 79−32164
material design parameters for optimum performance, SAW propag. theory 79−32161
materials development 78−6636
memory, monolithic, with long storage time 77−80026
memory, using semicond. laser 77−80024
memory correlator using GaAs Schottky diodes 78−66989
memory correlator using nonlinear interactions *(French)* 80−33294
memory correlators, charge storage 79−64455
memory correlators, p^+n SAW, modified theory 80−43563
memory-correlator for Fourier transform optical imaging 78−83090
metal powder on piezoelec. substrate, dynamic SAW reflecting struct. 80−74565
metal-dielectric contact, surface barrier Rayleigh wave transducer 79−98578
metal-ZnO-SiO_2-Si structure for SAW appl., fabrication related deterioration 78−14829
metal-ZnO-SiO_2-Si structures, charge injection 80−49919
metallic gratings, equivalent circuit of step discontinuity, rel. to SAW devices 80−33389
metallisation, use of Cu-doped Al 80−23856
microwave SAW components fabrication process 79−32162
MIS SAW convolver, minority carrier response 77−80847
MIS structure, parametric amplification and generation of SAW 79−10438
modulator for ruby laser, by US surface waves on resonator mirror 77−50699
monolithic SAW amplifier and periodic grating oscillator 79−50447
monolithic storage correlator, appl. to adaptive filter 78−87208
multichannel commutation of analogue signals using SAW transducers governed by MOS ICs 78−33963
multichannel signal processing using acoustooptic techniques 80−19160
multimode SAW resonators, optimum design 77−23823
multistrip coupler, superposition model 80−74674
multistrip coupler for coupling of surface skimming bulk waves 80−74630
multistrip coupler mode analysis 77−27419
multitrack nonperiodic multistrip couplers, cct. model 78−75026
narrow pass band filter, frequency stability study *(Japanese)* 78−90603
narrowband matched SAW filters realisation *(Russian)* 80−23850
one-port SAW resonators, config. and cct. anal. 78−63258
one-port SAW resonators using long IDTs and their application to narrow band filters 79−76934
optical film waveguide, SAW signal convolution 77−27428
optical image acoustic scanning 79−36845
optical image processing, two-dimensional high-speed acoustic Fourier transform 79−36844
optical image processing appls. 78−71051
optical image scanner, using transverse acoustoelec. effect in photocond. CdS 77−11001
optical image scanning, by electronic control of CdS SAW delay lines, 78−26006
optical probing, diagnostic and device appl. 77−59198
optical processing systems, seminar, Huntsville, USA (May 1979) 80−46732
optical spectra meas. using SAW spectrum analyser 79−21819
optical tunable switched directional couplers of two thin film waveguides using SAW 78−75003
optoacoustic deflector planar, expt. 78−74995
optoacoustic device, planar, SAW loss meas. using light beam diffraction 78−74996
oscillator, temperature independent *(Japanese)* 79−81613
oscillator frequency stability developments 78−59253
oscillator quartz cuts for improved temp. stability 79−55292
oscillator with two acoustic paths 77−23846
oscillators, development 77−34987
oscillators, influence of acceleration *(French)* 79−32176
oscillators, role in biotelemetry 77−90926
oscillators, status and designs review 78−55542
overlay ridge waveguide SAW mode analysis 79−46100
overlay waveguides, analytical method for characts. determ. 79−94383
p-n diode storage correlator, charging process 78−9500
parallel-channel SAW filter bank transfer function synthesis 77−23828
periodic dot arrays, selective reflection of SAW 80−74624
periodic grating oscillator performance 77−39190
periodic interdigital transducer for SAW 79−7269
periodic interdigital transducers with arbitrary voltages, generalized model 79−68534
phase shifter with 3 interdigital transducers 80−79062
phase velocity and frequency/temp. characteristic analyses 77−85044
photoacoustic surface wave generation system using CW laser, NDT appl. 80−87683
photoresists, standing waves and other interference elimination 80−69614

surface acoustic wave devices continued
physical props. and communication signals processing applications and devices 80−38162
picture colour component detection in SAW scanning 78−59149
piezoceramic SAW propagation loss reduction by hot pressing 78−2356
piezoelectric film, third-order piezoelec. and dielec. consts. meas. using surface acoustic waves *(Japanese)* 80−55042
piezoelectric film filter, ferrite propagation, under external magnetic field 78−22229
piezoelectric semiconductor SAW convolver, effect of transverse drift of carriers on operation, theory and expt. 80−14529
piezoelectric semiconductor SAW convolver, efficiency 78−18124
piezoelectric transducers, characterization of RF sputtered ZnO and ZnS films by X-ray diffraction anal. 80−80138
planar electrodes, distributed capacitance, optic and SAW device appls. 77−27387
plasma etched SAW resonator ageing effects 77−39148
polar materials, appl. to SAW and other devices 80−66114
polyvinylidene fluoride transducers, evaluation of performance 80−74617
precision TV demodulator using high-performance SAW transversal filters 79−49258
pressure sensing SAW resonator 77−23850
prism couplers for Rayleigh and Lamb waves, anal. 80−69619
production and test programme progress report 78−59206
production methods, electron beam erosion, photographic process *(Russian)* 78−18134
programmable transversal filtering using baseband compatible SAW processors 79−98548
propagation losses due to surface roughness 78−38926
propagation velocity meas. on $LiNbO_3$ 80−92003
pulse compression filter using reflective dot array 77−75749
pulse compression techniques *(German)* 79−81639
quartz, delay line second harmonic generation in SAW *(French)* 80−34285
quartz, film acoustic surface waveguides, electrically controllable polarisation conversion and its appl. 79−76924
quartz, ion-etching of grooves for SAW devices 78−95822
quartz, resonator transverse modes, SEM obs., phase effects 79−68452
quartz piezoelectric crystal, electron-acoustic signal processing *(Russian)* 77−62111
quartz powder on piezoelec. substrate, dynamic SAW reflecting struct. 80−74565
quartz SAW oscillator higher-order temp. coefficients 79−55291
quartz SAW resonator deep etching 78−59248
quartz SAW resonator design with Al metallisation 77−39147
quartz SAW resonator tuning by shorted reflector opening 78−59246
quartz with metallic overlay films for temp. compensation, SAW device appls. 80−79043
radar pulse Doppler processing with low-loss SAW delay line 77−31184
Rayleigh wave line with continuously variable optically controlled delay 77−68360
recirculation loops, for signal processing 78−22228
reflection gratings, theoretical investigations of energy storage effects and 2nd harmonic responses 80−74621
reflective arrays, coupled mode vector anal. and flowchart 79−7241
reflective dot array SAW filter 77−23825
reflective dot arrays, wave reflection 79−90052
reflective-array-compression filters, nonsynchronous scatt. loss 78−71246
reflector, determination of centre freq. and intrinsic refl. coeff. 80−74620
reflector, metallic strip grating expts. 78−13875
reflector grating, shallow grooved, SAW reflection and bulk-wave loss characts. 77−39129
reflector performance rel. to fabrication tolerances 77−27452
reflector-array-compressor devices, effects of temperature-dependent anisotropy and use of Y-cut quartz 80−74625
resonator, 310 MHz, with Q at material limit, design and fabrication 78−5608
resonator, as stress sensor, freq./stress sensitivity 77−2645
resonator, distributed-feedback, design, computer model and construction *(Flemish)* 80−5899
resonator, quartz, two-port design 77−23819
resonator, two-port, terminal characteristics, S-matrix approach 77−23848
resonator, VHF and UHF, Q-factors, reflective array design, calc. method *(Dutch)* 77−34988
resonator bandpass filter design for various coupling mechanisms 78−33967
resonator cavities with unidirectional transducers 77−23849
resonator coupling and multimode filter design 77−23824
resonator filter for radio receiver 79−7271
resonator filters, direct transmission, suppression by inverse phase interdigital transducer *(Chinese)* 78−79181
resonator filters, improved temp. stability using multiple coupling paths 80−19175
resonator filters 79−55283
resonator filters using tapered gratings 78−87224
resonator filters with enhanced out-of-band rejection 80−19179
resonator optical waveguide model 77−39146
resonator Q rel. to fabrication tolerances 77−27452
resonator reflector and transducer characteristic effects 77−39168
resonator substrates, SAW attenuation due to platelet defects 79−95253
resonator transverse modes, effects of anisotropy 78−5609
resonators, characts. from Fabry-Perot cavity anal. 77−39131
resonators, fundamental mode oscillators, narrowband filter at 1.43 GHz 80−87687
resonators, radiation losses formed by interdigital type reflectors 80−69603
resonators, study of Q and modes using metal waffle-iron and strip arrays 78−51030
resonators, transverse mode anal. 80−96169
resonators and long IDTs, coupled-mode analysis *(Japanese)* 79−27477
resonators and resonator filters, design and performance 79−32178
resonators composed of long interdigital transducers, anal. rel. to electrode loading effect 78−9517
resonators on quartz, loss reduction and cavity maximizing 79−41543
resonators using withdrawal weighted reflectors 80−19180
response to high-speed thermal radiation 79−41545
RF spectral analyser, integrated optics structure employing acousto-optic effect 77−27389
ring filter geometry 77−39175

surface acoustic wave devices continued
rotation sensor using EM-SAW transduction 77−31194
SAW, frequency band broadening of phase shifters 78−55532
SAW resonators, using long IDTs, coupled mode anal. 79−76933
SAW space-charge coupled signal processor with storage 78−9507
SAw/CCD accumulating correlator for analogue signal processing 79−72757
SAW/CCD high-speed analogue programmable tapped delay line 77−39167
SAW/CCD programmable matched filter 80−5896
Schottky diode/$LiNbO_3$ acoustoelectric integrating correlator 77−88990
second harmonic SAW generation in devices involving semiconductor coupling 79−46148
segmented bidirectional amplifier SAW oscillator 78−1528
SEM diagnosis, voltage contrast obs. 80−69618
semiconductor light-sensitive diode acoustic airgap convolver, theory 79−49288
semiconductor surface space charge layer study using SAW convolver 77−46871
semiconductor-airgap-piezoelectric convolver, theory 77−7260
semiconductor-compatible SAW devices 77−80044
semiconductor-on-piezoelectric SAW convolver saturation phenomena 78−2358
semiconductor-piezoelectric gap coupled convolver, simplified operation theory 77−39163
shallow bulk acoustic wave devices, recent developmental advances 80−74629
shallow bulk acoustic wave excitation by interdigital transducers 78−59251
shallow bulk acoustic wave generation by interdigital transducers 79−51411
side-entry surface acousto-optic interaction signal processor 80−48174
signal processing, comparison of optical and SAW techniques 80−48173
signal processing appls., comparison with digital devices 79−32145
signal processing appls., review, book contrib. 79−50519
signal processing appls., review 80−38204
signal processing devices, fundamental aspects, book contrib. 79−50521
signal processing equipment, component review *(French)* 78−51013
signal processing research programme of United States Air Force 80−48171
signal processing technology assessment seminar, Aviemore (1976) 77−39166
signal processing using HF strain transducer 77−88991
signal processor theory and production method *(German)* 80−58867
single-channel reduced-bandwidth processor for US imaging 80−74636
slanted device technology for radar system appl. 80−19181
sonar beamforming by CCD scan conversion for SAW chirp-Z transform 80−43552
spaced interdigital transducers, SAW probing 77−80045
spectrum analyser, digital signals processing 78−26007
spectrum analysers in photon-counting mode, statistical props. 80−105712
spiral SH_0 waveguide, Al film evaporated on $Pb(Zr,Ti)O_3$ disc, characts. 77−72123
split strip periodic metal gratings on piezoelec. surface, wave propag. 77−39130
ST-quartz SAW resonators and coupled resonator filters 77−39174
status report of SAW and magnetostatic wave devices, transversal filters appl. 80−28394
storage convolution, correlation, signal processing appl. *(French)* 79−32146
storage convolver use in signal correlation 77−23832
storage correlator, input correlation 77−84085
storage correlator equivalent circuit models 78−9506
strain gauge 77−79091
strain transducer, diffused MOS device for SAW signal detection 77−5825
strip-coupled varactor SAW convolvers, parametric cct. anal. 78−71245
submicron SAW interdigital transducer fabrication by contact printing 79−46147
substrate materials and their influence on performance, book contrib. 79−50522
surface acoustic waveguides, microwave network anal., rectangular ridge guides 77−23790
surface charge on unapodized periodic IDI 80−91947
surface elastic wave devices, RF leakage *(Slovak)* 78−55522
surface skimming bulk wave bandpass filters using Y-rotated quartz 80−74583
surface skimming shear-wave guidance by corrugated surface 80−74582
surface wave and bulk wave observation using frequency-shift holography 79−81600
surface wave interaction CCD prototype 77−23818
surface-skimming bulk wave controlled quartz crystal oscillator 78−59250
survey of component technologies in subsystem signal processing 79−32160
switchable SAW filter banks at UHF 79−41533
Swzawa wave broadband thin-film interdigital transducers 80−74681
tapered highly reflective surface-wave grating, refl. spectrum, distortion 78−13867
tapped delay line suppressing reflection from interdigital transducers *(Japanese)* 78−63247
temperature behaviour, piezoelectric coupling in quartz, $LiNbO_3$, $LiTaO_3$, Tl_3VS_4, acoustic surface wave propag. *(French)* 78−35093
temperature compensation techniques 80−74614
temperature effects of devices integrated on Si 80−79066
temperature stable oscillators employing parallel-connected SAW resonators 80−74615
test head, for generation and reception of US surface waves in high temp. mild steel 78−95901
thermal shearing effects on the temperature stability 80−69613
thermal stress effects of acoustic surface waves in layered media *(Japanese)* 79−98573
thin film acousto-optic devices, theory and experimental results 77−58472
thin film devices and filters *(Japanese)* 77−73116
thin film interdigital transducers for SAW devices at GHz freqs. form. by electron beam lithography 80−4702
three-phase interdigital transducer for acoustic imaging in fluids 79−72774

surface acoustic wave devices continued
tilted-finger chirp transducer for design of wideband guided-wave acousto-optic Bragg deflector 80−74510
transducer, 2-phase interdigital, with unidirectional props. 79−1044
transducer, micro-fabrication technique for Al electrode 77−80042
transducer, mixed matrix representation of interdigital transducers 80−19184
transducer, new model 78−59232
transducer, tunable, appl. of nonlinear interaction of SAW with Josephson junction 77−85392
transducer, very narrow aperture acoustic diffr. effects 78−22240
transducer analysis by equivalent parameter representations 78−1541
transducer array for surface defect imaging in metals 80−74660
transducer with capacitive electrode weighting, band-pass filters 80−48544
transducers, apodized, radiation conductance 80−96174
transducers, asymmetrically truncated with finite impulse response 78−87225
transducers, bulk-wave, field distributions for surface-skimming 79−64472
transducers, charge distribution for non-periodic transducers using cct. model 80−74691
transducers, parameter calc. with power scattering coeffs. *(Russian)* 80−64317
transducers, surface to bulk wave conversion at local surface defects 78−38165
transducers, withdrawal weighting combined with series sections weighting 79−81666
transducers based on layered systems, calc. of electromech. coupling coeff. squared 80−87690
transducers on nonzero conductive Si substrate, calcs. of fractional velocity 78−1533
transducers on Si substrates with polyvinylidene fluoride films 80−74618
transmitting hydrophone development and performance 79−53586
transversal equaliser using SAW tapped delay line and PIN diode control ccts., characts. 79−68532
transversal filters, interdigital transducer models for accurate design implementation 80−28396
transversal filters, synthesis using interdigital transducer models 80−5897
tunable magnetoelastic surface wave oscillators, freq. control 79−32177
tunable resonator oscillator, appls. of amorphous magnetic-layers 80−28389
tunable variable bandwidth/frequency SAW resonator 78−59247
TV IF filter, temp. stable ZnO/Pyrex glass substrate 80−43566
TV receiver ghost image cancelling circuit and SAW image sensor appls. *(Japanese)* 77−27429
two dimensional image scanning of movies using surface acousto-optic interaction 79−94352
two dimensionally periodic transducer *(Japanese)* 78−33984
two step electron beam lithography process for submicron SAW device fabrication development 79−55281
two-phase PSK modulator employing SAW delay line, fundamental performance 80−33398
two-port quartz SAW resonator construction and performance 77−39145
two-port resonator using long interdigital transducers *(Japanese)* 78−33982
U-path HF periodic grating oscillator 77−23847
UHF filters using unidirectional interdigital transducers 79−32170
UHF oscillator for radio receiver 79−7272
ultrasonic symposium, Phoenix, AZ, USA (Oct. 1977) 79−46096
ultrasonics symposium, Annapolis (1976) 77−19469
ultrasonics symposium, Cherry Hill (1978) 79−50472
underwater sound sensor using SAW resonator-controlled oscillators 80−74631
unidirectional SAW transducers with ZnO film on glass substrate 77−68355
unidirectional transducer with 3 electrode groups for Lamb wave devices 78−51034
unidirectional transducers, 3-phase equivalent cct. model 80−74627
US beam scanning by SAW transducer arrays 79−55266
US delay lines, transverse surface waves propag. on cylindrical surfaces of anisotropic solid 78−10270
US filtering and correlation 78−60969
US military investment and usage 77−39189
US surface wave velocimeter, phase sensitive 80−102947
variable frequency SAW resonator on ferroelectric-ferroelastics 78−33977
voltage-controlled SAW resonator oscillators 77−27450
waveguide, nonlinear interaction of elastic waves with reson. *(Russian)* 78−6206
waveguides, microwave network anal., flat overlay guides 77−27411
waveguides, types and props., book contrib. 79−50488
wedge transducers, efficient broadband design using coupled-mode theory 78−63253
weighted SAW transducers, electrostatic neighbour and end effects 77−31200
withdrawal weighted SAW filter design from electric field interactions in finite arrays 77−23827
ZnO, film, reactively RF sputtered, anal. of texture 78−67921
ZnO/Si acoustoelectric devices 80−80332
Al-ZnO-SiO_2-Si monolithic MIS struct., charge-transfer device using SAW 79−11229
AlN, piezoelectric film, low temp. growth by RF reactive planar magnetron sputtering method 80−76175
$AlPO_4$, berlinite, material for SAW devices 79−56735
$AlPO_4$, berlinite, temperature-compensated cuts for SAW devices 78−60018
$AlPO_4$ high piezoelectric coupling temp. compensated cuts for SAW devices 78−13869
As_2S_3, film waveguide, acoustooptic deflection and modulation of light by stationary phase grating struct. 80−5841
$Ba_2Si_2TiO_8$ fresnoite, characts. for SAW devices 79−82430
$BaTiO_3$-metal contact, surface barrier Rayleigh wave transducer 79−98578
$Bi_{12}SiO_{20}$, pulling large crystals 79−11507
CdS bulk wave-$LiNbO_3$ SAW piezoelectric coupling 77−23845
CdS crystal with thin photoproduced semiconducting layer, tests of convolver on transverse surface waves 77−42646
CdS film, double-layered polycrystalline on $LiNbO_3$ substrate, fabrication and props., rel. to SAW appl. 78−64480

surface acoustic wave devices continued
CdS film SAW two-dimensional image processor 77−39164
CdS SAW convolver, effect of transverse drift of carriers on operation 80−14529
CdS SAW monolithic convolver with high resistivity surface layer, non-linear cond. 79−98554
CdS thin-film Lamb wave delay line characteristics and strain effects 77−31185
CdS/$LiNbO_3$ system SAW convolution signal photoenhancement obs. 77−27431
CdS-$LiNbO_3$ monolithic two-dimensional Fourier transformer 79−72516
CdS-$LiNbO_3$ separated medium convolver, illumination effects 77−72766
Ge slow surface states, optical image storage for $LiNbO_3$ SAW readout 77−23773
InAs/$LiNbO_3$ structure, SAW generated transverse acoustoelectric voltage, image scanning and signal processing appl. 80−49826
InSb thin films for acoustoelectronics 80−103765
InSb/$LiNbO_3$ acoustoelectric convolver, gap-coupled, for IR imaging device 78−94492
InSb-$LiNbO_3$ SAW convolver, efficient struct. realisation, Hall mobility meas. 80−83705
β-$LiAlSiO_4$, eucryptite, temperature-compensated cuts for SAW devices 78−60018
$LiNbO_3$ 400 MHz saw filters 79−23158
$LiNbO_3$ acoustic conversion, piezoelect. surface wave behaviour at discontinuities 77−31198
Y-Z $LiNbO_3$, acoustic effects of filamentary defects 80−75314
$LiNbO_3$, acousto-optic interaction with surface waves, for image scanning 77−3673
$LiNbO_3$ acousto-optic convolver with large time-bandwidth product 77−27432
$LiNbO_3$ acousto-optical SAW interaction multicolour image scanner 77−58483
$LiNbO_3$ acousto-optic memory correlator 77−88992
$LiNbO_3$, acoustophotorefractive effect, appl. at acousto-optic memory correlator 78−15145
$LiNbO_3$ acoustophotorefractive memory correlator enhancement 79−55080
$LiNbO_3$ device, obs. of bulk waves and surface waves through side planes of several cuts 78−71238
$LiNbO_3$, diffusion of Ti, surface acoustic waveguide formation 77−79998
$LiNbO_3$ $\Delta V/V$ waveguide SAW propagation obs. and modal analysis 78−38128
Y-Z $LiNbO_3$, filamentary defects visualisation at wafer inspection stage 80−75315
$LiNbO_3$, ion implanted, acoustic model of SAW delay lines *(French)* 78−55540
$LiNbO_3$ low-loss high-coupling volume mode 79−51409
$LiNbO_3$, obs. of bulk waves by freq. shifted holography 77−19505
Y-Z $LiNbO_3$, radiation patterns of bulk acoustic modes from finite interdigital transducer 80−43491
$LiNbO_3$ SAW devices, SAW and bulk wave propag., freq. shift holography *(Japanese)* 79−59895
$LiNbO_3$ SAW filter bulk wave suppression by triangular metal film overlay 77−23830
$LiNbO_3$ SAW plate convolvers at 1 GHz 80−1382
$LiNbO_3$ SAW resonator design with Al metallisation 77−39147
$LiNbO_3$ SAW-CdS bulk wave piezoelectric coupling 77−23845
$LiNbO_3$, tapped SAW delay line, coupling with CdS bulk wave 77−1289
$LiNbO_3$, temp. coeff. of freq. determ. 80−75316
$LiNbO_3$ UHF SAW filters using group-type unidirectional interdigital transducers 78−59252
$LiNbO_3$, use as surface acoustic wave devices 78−91525
$LiNbO_3$ waveguide, thin-film optical filtering using acoustooptic interaction 79−81572
$LiNbO_3$ wedge, apodized ID transducer, radiation conductance 78−38164
$LiNbO_3$ X-cut plate shear transducer, direction of displacement 78−51031
$LiNbO_3$, Y-cut, SAW right angle reflection coeff. from metal strip array meas. 77−23814
$LiNbO_3$, Y-cut, SAW $\Delta V/V$ waveguides in arbitrary propag. directions 79−81602
$LiNbO_3$:He^+, ion implanted SAW guides, air-gap Si convolver data 78−42500
$LiNbO_3$:Na^+ (Co^{2+}, Zr^{4+}) film, improvement in temp. stability and SAW device appl. 80−75939
$LiNbO_3$:Ti thin film acousto-optic deflector 77−75698
$LiNbO_3$-CdSe structure, electroacoustic effects and signal convolution 80−10098
$LiNbO_3$-gap coupled Schottky diode memory correlator, grating coupled optical imaging 80−64143
$LiNbO_3$-InSb layer structures, fabrication and use in SAW amplification 79−41540
$LiNbO_3$-liquid-CdS-liquid-$LiNbO_3$ structure, acoustic wave propag. and amplification 77−42654
$LiNbO_3$-pn-diode airgap convolver struct. optical scanner using single SAW pulse 80−64144
$LiNbO_3$-Si, acoustoelec. SAW phase shifter 78−13866
$LiNbO_3$-Si acoustically-matched surface elastic wave transducer 78−90623
$LiNbO_3$-SiO_x-InSb-SiO_x monolithic acoustoelectronic amplifier with pulsed power supply 79−56269
$LiTaO_3$ crystals for commercial SAW TV IF filters, fabrication 80−80961
$LiTaO_3$ SAW delay line with −70 dB spurious responses 77−31182
$LiTaO_3$, single cryst. prep. for surface acoustic wave device appls. *(Japanese)* 80−60772
$LiTaO_3$, single crysts., Czochralski growth for SAW device appl. 79−33922
$LiTaO_3$-SiO_2, temp. compensated SAW device fabrication 79−76923
$MgAl_2O_4$ spinel material for SAW devices 79−56735
Ni film, evaporated, for use as variable delay SAW device, magnetostrictive effects 80−71144
PVF_2 thin film SAW tranducers for 8 MHz delay line 80−58876
$Pb(Cu_{1/4}Nb_{3/4})O_3$-$Pb(Li_{1/4}Nb_{3/4})O_3$-$PbTiO_3$-$PbZrO_3$, piezoelec. ceramic materials for SAW devices 79−11390

surface acoustic wave devices continued
$Pb(Cu_{1/4}Nb_{3/4})O_3$-$Pb(Li_{1/4}Nb_{3/4})O_3$-$PbTiO_3$-$PbZrO_3$, optimisation of composition for SAW devices 79−33609
$Pb_2KNb_5O_{15}$ material for SAW devices 79−56735
$PbTiO_3$-$PbZrO_3$-$In(Li_{1/5}W_{2/5})O_3$, piezoelec. ceramic characteris. for surface wave filters 78−95215
Si array/$LiNbO_3$ gap-coupled imaging devices 79−46057
Si charge transfer by SAW in ZnO 77−27415
Si guided-wave acousto-optical devices 80−102864
Si SAW delay line design, inclusion of cond., equivalent cct. 77−88989
Si-SiO_2 structure, appl. to integrated oscillators 78−83186
$SrTiO_3$-metal contact, surface barrier Rayleigh wave transducer 79−98578
Tl_3TaSe_4, new SAW zero temp. cuts 78−2351
Tl_3VS_4, SAW zero freq.-temp.-coeff. configs. 77−43418
Tl_3VS_4 single-crystal substrate SAW filter performance 77−31186
YIG magnetoelastic transducers, approximate theory 79−68533
YIG nonreciprocal thin film acoustic device, design, appl. of cct. theory of elastic waveguides 77−85042
ZnO, CVD of epitaxial films on sapphire, SAW interdigital transducer fabrication 80−66430
ZnO, film, SAW resonators 78−83199
ZnO film on Si convolver, with surface-controlling junctions 77−88988
ZnO interdigital transducer, efficient bulk-wave excitation in layered media 77−69156
ZnO monolithic SAW device, separation of storage effects 79−18611
ZnO piezoelec. film, fabrication and appl. *(Japanese)* 78−23616
ZnO Sezawa mode pn-diode array memory correlator 79−78178
ZnO thin film SAW device manufacture, sputtering system and film characterisation 78−95692
ZnO thin film SAW filters 79−23157
ZnO thin films, surface acoustic-optic interaction, diffr. 77−3685
ZnO thin-film, for HF range *(Japanese)* 80−53598
ZnO/quartz for device materials, expt. study of props. 80−80050
ZnO/SOS monolithic SAW amplifier 78−6205
ZnO/Si structs., anal. of charge injection 80−80049
ZnO-on-Si SAW convolver development 77−27430
ZnO-Si p-n diode monolithic storage correlator 78−18119
ZnO-Si structure, MIS and SAW propag. characts. 78−30988
ZnO-SiO_2-Si monolithic convolver, long time storage of surface-acoustic-wave signals 77−1287
ZnO-SiO_2-Si SAW device, interface transduction 80−102949

surface acoustic waves
see also acoustic waves; Rayleigh waves; surface acoustic wave devices; surface phenomena
acoustic waveguides, damping of normal and surface waves, depend. of vel. on losses 79−14135
acousto-optic interaction on nonpiezoelectric substrates 79−46090
acousto-optic interaction with guided optical waves, in integrated optical systems 78−42465
acoustoelectric surface waves at interface between media, electrostriction-induced 77−16255
acoustooptic guided wave Bragg diffr., phased SAW array in $LiNbO_3$ 77−58439
amplitude limitation observable in freq. shift holography 78−71058
amplitude measurement, optical probe 79−28185
anisotropic elastic waveguide normal-mode anal., appl. to Rayleigh-Love wave mode converter 79−23113
anisotropic graded index waveguide, acoustooptic interaction efficiency freq. depend. 80−23776
anomalous sound absorpt. for fluid-fluid interface 80−74562
atmospheric sound propagation, surface waves over layer with large refr. index 77−50805
attenuation due to thin film finite conductivity and air loading 77−31154
attenuation of waves propag. along boundary with periodic inhomogeneities 80−102905
backscattered echoes rel. to circumferential waves impinging on submerged Al cylinders 79−86276
backward waves and acoustic scanning, nonlinear interaction of vol. and surface waves 80−79040
bandpass filter design, use of charge distribution model 80−74678
Bleustein-Gulyaev wave amplification in tetragonal and hexagonal crystals 77−7959
Bleustein-Gulyaev wave propag. characts. at surface imperfections 78−43226
Bleustein-Gulyaev wave transmission characts. at corner 77−59197
Bleustein-Gulyaev waves, penetration depth in CdS photoconductor 79−28186
Bleustein-Gulyaev waves, propag. and amplification in materials with strain depend. dielec. const. 79−41469
bone, US surface wave propag. 78−44578
bone, US surface waves for studying props. of human tibia 77−25619
bone, US vel. rel. to mech. props. 77−32937
book 79−50518
Brillouin scattering by Stoneley waves, elasto-optic and surface ripple mechanisms 80−71435
Brillouin scattering from surface waves, appl. of surface Green's function mapping method 80−40125
Brillouin surface ripple scattering by solids, for acoustoelec. amplified bulk acoustic waves 78−39559
broadband generation on GaAs by conversion from acoustoelectrically amplified bulk waves 77−54852
bulk particle motion fields induced in optically transparent plate, differential optical measurements 80−53576
case hardening depth meas. using ultrasonic goniometer, corner reflection method, book contrib. 79−100325
ceramic surface flaw detection by SAW scatt. 79−47866
ceramics, surface cracks, acoustic surface wave meas. 80−61055
ceramics containing volatiles mechanisms for attenuation 80−74560
circlar tube, relationship between plate and surface modes 77−80002
circumferential waves, cylindrical shell supported by a continuum, dispersion relations 78−90564
coherent optics methods appl. to acoustic field investigations 80−106691
coherent scatt. into bulk waves by grooves 77−3691
colinear interaction between acoustic and optical waves in planar waveguide, radiation into substrate 80−53452
collimated laser beam interactions with SAW-induced bulk particle motion 79−76742
composite thin-plates, equivalent microwave network analysis 79−3820

surface acoustic waves continued
conversion electron Mossbauer spectroscopy, dynamic theory, possibility of investigating Rayleigh surface waves 77−51997
corrugated surface, horizontal shear surface wave propagation 77−7957
coupling of elastic surface waves in piezoelectric crystals 77−85045
critical surface wave velocity near phase transitions 77−35803
cubic crystal, (001) plane, surface modes, computer program 78−2352
cubic crystal/cubic crystal interface, transverse surface acoustoelec. wave propag., due to electrostriction 77−66082
cubic crystals, elastic surface wave propagation 78−2357
cylindrical crystal surfaces, influence of piezoelectric effect of transverse SAW 78−94479
delaminations in thin sheets, elongated, interaction with Lamb waves, book contrib. 79−98574
delay calc. under uniform finite strain 77−39138
delay line fabrication by direct optical projection 79−81667
dielectrics, influence of field strength on phase vel. and localisation depth 78−95218
differential optical interferometry 77−72120
diffraction and guidance, theory 78−13828
diffraction in quartz 80−38160
dislocation motion, acoustic emission, surface and bulk waves 78−87856
dispersion equations, anal. of roots in problem of elastic surface waves in anisotropic media 79−14997
dispersion relations for Rayleigh waves in cubic crysts. 80−102906
dynamical properties of solid surfaces, analytic approach 78−71929
eccentric spheres, interior and exterior boundary-value wave problems 77−75384
edge waves in isotropic solids 77−31860
elastic body, attenuation of surface Rayleigh acoustic waves travelling along periodically surface 80−80047
elastic half-space containing cylindrical inclusion, dynamic surface stresses 78−90748
elastic medium, surface waves in presence of inviscid flow field 77−49603
electric field, effect of external flow of charged particles 79−82432
electroelastic surface wave excitation, detect. and scattt., integral eqn. approach 77−812
electron beam induced excitation of surface acoustic and electrostatic waves 77−24473
electronic absorption, temp. depend. 77−55585
electrostatic probe for absolute measurement of SAW amplitude 79−50543
EM transducer harmonic operation 79−46152
EM transducer with periodic permanent magnets, horizontally polarised shear elastic wave excitation 79−76932
end-fire piezoelectric transducers, wideband excitation of surface elastic waves in microwave range 80−10105
fast surface wave near first critical angle, prediction, detection and charact. 79−23117
ferrite propagation, under external magnetic field 78−22229
ferrite/semiconductor composite struct., SH type wave propag. 78−23319
ferroelectric, SAW propagation along domain boundaries, low temp. sp. ht. contrib. 77−77158
ferroelectric crystal with piezoeffect, Rayleigh wave propag. near Curie temp. 77−89630
ferroelectrics, $BaTiO_3$ type, surface acoustic waves on domain boundaries 79−90860
ferromagnetic conductor magnetoelastic surface wave attenuation 77−20667
ferromagnetic metallic glasses, Brillouin scattering 78−92085
ferromagnetic-semiconductor structure, thermal fluctuations during amplification of magnetoacoustic surface waves 78−88158
field pattern visualisation in multistrip structures 78−9511
film coated materials, Rayleigh wave dispersion, approx. solution 77−39731
Franz-type wave, rel. and attenuation, generation on outside of solid cylinders in water *(French)* 80−28370
frequency translated holography, S/N, smallest detectable vibr. 77−7022
gap waves between two piezoelectric half spaces 78−50970
garnet epitaxial film, elastic surface wave propag., magnetoelastic effect 77−20669
generation, linear and nonlinear growth 79−56057
generation anal., synchronous, new theory 79−81593
generation and detection by interdigital transducers 77−39186
generation at 20 MHz, from pulsed thermoelectric expansion of constrained surface 77−35007
generation by means of CW laser, NDT appl. 80−87683
generation by nonlinear mixing of bulk waves 79−50490
GHz quartz transversal filters, fabrication limits and characteristics 80−43562
glass 7059, film acousto-optical props. for integrated optical Bragg cell 79−55251
glass film, Brillouin scatt. from surface phonons, SAW vel. and attenuation 78−95587
grating coupling between SAWs and plate modes 80−102895
grating waveguide modes 78−59172
guided elastic waves, generalised transmission-line equations appl. 77−62728
guided optical beam scatt. by surface acoustic waves 79−98508
guided waves propag. along edge of semiinfinite slit 78−1457
Gulyaev-Bleustein wave excitation, wave field structure 79−19442
harmonic generation, detection of mol. films 77−80688
harmonic generation, overlap-integral anal. 79−55259
harmonic generation at unbonded interfaces and fatigue cracks 78−90562
heterodyne optical probing of partial standing waves 78−13870
hexagonal crystals, semiinfinite, surface waves characts. 79−60614
HF, phase/amplitude meas. using phase sensitive laser probe 79−14171
HF elastic surface wave propagation on cylindrical obects 77−24472
holographic visualisation, improved S/N ratio *(French)* 78−75023
hybrid signal processor using SAW/CCD technologies 79−32163
ice detection using surface acoustic waves 78−18129
interaction with discontinuities, computer model 79−68461
interdigital transducer on piezoelectric half space, spectrum of emanating acoustic waves 80−79044
interfacial stress effects on Stoneley wave propag. 77−46833
interferometer for monitoring Rayleigh waves 78−74052
Josephson junction, nonlinear interaction with SAWs 77−85392
Lamb wave diffraction by finite crack in elastic layer 80−64244

surface acoustic waves continued
Lamb wave equivalent US mode propagation in thin-walled tubing 79−68459
Lamb wave excitation in yz-cut plates *(Russian)* 78−55483
laminated composite, horizontal shear surface waves 77−80687
laser light diffraction at solid-liquid interface 78−38127
layered media, SAW propag. characts., thermal strain effects 79−19440
layered systems, direction control of acoustic wave propagation 80−103557
layered systems, film-substrate characts. of phase-velocity dispersion and struct. of waves 80−59775
leaky Rayleigh waves, restrictions on the existence 79−82429
light beam propag. parallel to surface, diffr. by acoustic wave 78−66752
light scattering from Rayleigh waves 78−50993
light scattering on internal refl. 78−64345
$LiNbO_3$, finite difference anal. 80−75423
liquid-metal interface, surface wave generation by US wave *(French)* 78−18885
liquid-solid interface, superimposed grating, backward displacement of waves 77−1288
liquid-solid interface, US wave interaction at Rayleigh angle 77−39132
longitudinal US wave propag. near surface of a solid 78−95217
Love wave interaction in thin film with periodic surface corrugation 79−14130
Love waves on layer-coated cylinder 78−2354
Love waves propag. along cylindrical surface, excitation 80−102907
low-dimensional crystals, SAW propagating along free boundary 79−73388
magnetoacoustic surface wave excitation by meander lines 78−19298
magnetoelastic Rayleigh waves on bulk YIG, convolution 79−64404
magnetoelastic wave velocity on magnetised ferrite substrate, nonreciprocity 80−80587
magnetostrictive SAW generation efficiency meas. of residual stress 77−28972
matched filter, realisation, electronically tunable *(Russian)* 79−98538
metal, light scatt. from surface acoustic phonons 78−76484
metal, mode conversion, by EM generation of US 80−84357
metal, resonance absorption of Rayleigh sound by surface electrons 78−71924
metal, SAW absorption with and without external mag. field *(Russian)* 77−31936
metal, surface acoustoelectric H-waves, theory 77−69159
metal, US surface wave vel. meas. on plane and cylindrical samples, optical methods 77−46875
metal-electrolyte interface, ultrasound generation, prelim. meas. 78−91526
metallic thin film surface wave attenuation due to electron-phonon interaction 79−55848
metallic thin films, attenuation and phase vel. of SAW interacting with charge carriers 79−46136
metals, effect of magnetic field on propag. 78−18095
metals, SAW attenuation coeffs. and wave speeds 79−46903
metals, strain, US characts., meas. apparatus 78−60898
microscopic derivation of theory of extended objects in crysts. 79−37704
microsphere removal by SAW displacement field 79−45884
MIS structure, SAW charge transfer theory 79−56327
monolithic layered piezoelectric-semicond. structures, acoustoelectric coupling 77−32050
multimode cylindrical surface wave excitation, multiple impedance boundary condition simulation 78−26000
noncollinear interaction with RF elec. field 79−69566
noncollinear three-phonon interaction in an isotropic plate 78−66970
nonlinear acoustics 8th symposium, conf., Paris, France, July 1978 80−33277
nonlinear acoustoelectro-luminescence excited by SAW 80−45143
nonlinear elastic interactions between acoustic bulk and surface waves 77−50797
nonlinear interaction with bulk waves in piezoelectric crystals, signal transformations *(Russian)* 77−3703
nonlinear propag. characts. of finite amplitude SAWs excited by monochromatic line source 80−96091
nuclear reactor pressure vessels, US pulses propag. by means of acoustic emission *(German)* 80−3274
observation in SAW devices using frequency-shift holography 79−81600
optical heterodyne method for SAW study using laser beams *(Russian)* 80−64271
optical image storage and scanning with oppositely-directed surface waves 79−55238
optical probing, diagnostic and device appl. 77−59198
optical probing of HF guided wave surface displacements with arbitrary profile 80−69612
optical waveguide, Bragg electrostriction, power balance approach 77−75660
optical waveguide, electrostrictive mixing, acoustic surface wave generation, theory 77−19424
optical waveguide, interaction between optical and acoustic surface waves, expt. 77−19428
optical waveguide, light diffraction by oppositely propagating SAWs 79−41453
optical waveguides, SAW electrostrictive mixing analysis 77−27390
parallel optical flat SAW meas. by reflective interferometry 79−76931
parametric mixing, approx. theory 79−86279
parametric mixing and harmonic generation anal. 79−50489
particle motion fields anal. 80−79042
passage through gap between piezoelectric coated with insulating films 79−28187
periodic coupling of piezoelec. and magnetoelastic surface waves 78−10269
periodic electrode system in piezodielectric, acoustic waves oblique incidence 79−7267
periodic structures, noniterative technique using Languerre functions and Fourier series 79−81596
in periodically corrugated piezoelectric medium, Bleustein-Gulyaev surface waves behaviour 80−87616
phase velocities on solid-liquid boundary 78−83151
phosphor, EL-590 M type, electroluminesc. excitation by SAW, nonlinear effects 80−16104
photochromic film waveguide, acousto-optical props., integrated optics appl. 80−33207
photoelastic film, fluctuations of acoustic waves and light scattering *(Russian)* 77−28543

surface acoustic waves continued
photographs on TV images of travelling waves using strobed electron beam 80−102894
photoinduced surface storage of SAW patterns in $LiNbO_3$ 80−74309
physical props. and communication signals processing applications and devices 80−38162
piezoceramic material, SAW, nonsynchronous interaction *(Russian)* 78−26002
piezocrystal, interaction of two-dimens. plasmons with surface piezoacoustic waves, appl. to MOS structs. 79−28683
piezoelectric, coupled surface, electroacoustic waves 78−2355
piezoelectric, elastic wave leakage across gap 78−6204
piezoelectric, perturbation anal. of attenuation and dispersion 78−47653
piezoelectric, velocity rel. to uniaxial biasing stresses 77−27416
piezoelectric boundary waves propagating along SiO_2 and $LiTaO_3$ interface, characts. 79−14149
piezoelectric coated with semicond. film, Bleustein-Gulyaev wave amplification 79−61309
piezoelectric crystal, Gulyaev-Blustein wave excitation by developing defects *(Russian)* 78−56030
piezoelectric crystal, line acoustical waves anal. 78−34692
piezoelectric crystal, plasmon transformation into SAW 80−59903
piezoelectric crystal, surface wave anal. using orthogonal functions 78−51810
piezoelectric crystal surface, periodic film form. due to SAW 78−72038
piezoelectric crystals, shear surface waves, generalised 80−92770
piezoelectric crystals, surface modes, acoustic wave propagation 80−20026
piezoelectric crystals, surface wave solns. nonexistence example 80−6611
piezoelectric crystals, theory in symm. form. 78−10848
piezoelectric crystals, variation of phase vel. and wave struct. of finite amplitude SAW 78−95219
piezoelectric film, third-order piezoelec. and dielec. consts. meas. using surface acoustic waves *(Japanese)* 80−55042
piezoelectric insulator, nonlinear interaction of SAW with electron beam 80−70517
piezoelectric media, two separated, coupling of propagating SAW 78−38929
piezoelectric medium, semibounded, body waves and quasi-body surface waves 80−107367
piezoelectric plate, elastic surface wave propag., elec. screening effect *(Russian)* 79−14999
piezoelectric semiconductor, surface electroacoustic wave, excitation by drifting cond. electrons 77−66083
piezoelectric semiconductor film, surface mode phonon amplification theory 78−34691
piezoelectric semiconductor film, surface phonon amplification 77−31864
piezoelectric semiconductor plates, natural oscills. modulated by charged particle beam, energy losses *(Russian)* 80−2259
piezoelectric semiconductors, acoustoelectric surface phonon-conduction electron interaction 79−42360
piezoelectric semiconductors, surface phonon acoustoelectric interaction, elastic anisotropy effects 80−6610
piezoelectric semiconductors, synchronisation 77−11964
piezoelectric shear wave, two-dimens. electron plasma interaction *(Russian)* 79−19842
piezoelectric solid, semi-infinite, SAW generation 78−51809
piezoelectric substrate coated with admittance films, attenuation and vel. of surface waves 79−98540
piezoelectric substrate small attenuations and vel. variations 79−86281
piezoelectric surface excitation by far IR laser beam 79−46906
piezoelectric surface waves on cubic cryst., slowness surface Gaussian curvature 79−77887
piezoelectric-semiconductor struct., nonlinear acoustoelectric effects for large amplitude SAW 80−92942
piezosemiconductor film, surface-mode acoustic wave amplification 79−46907
plasma ion-acoustic waves excitation by piezoelectric surface acoustic wave 80−10381
plasmon-acoustic wave interactions due to deformation potential *(Russian)* 80−15356
powders, SAW interactions, for various directions of propagation 80−49486
power densities determination, simple approximation method 77−79987
propagation, temp. behaviour, piezoelectric coupling in quartz, $LiNbO_3$, $LiTaO_3$, Tl_3VS_4 *(French)* 78−35093
propagation along periodic struct. on piezoelec. medium anal. soln. of inhomogeneous infinite simultaneous eqns. 78−30109
propagation along X-axis on Y-cut plate of Se 80−75313
propagation in homogeneous piezoelectric halfspace 79−3970
propagation in split strip periodic metal gratings on piezoelec. surface 77−39130
propagation patterns in $LiNbO_3$ SAW devices, generated by interdigital transducers *(Japanese)* 79−59895
propagation patterns obs. by freq. translated holography method *(Japanese)* 78−22222
propagation study based on coherent light diffraction *(Russian)* 79−14172
properties and types, book contrib. 79−50487
quartz, doubly-rotated cuts 80−74584
quartz, effects of the ion implantation on SAW propag. 80−75421
quartz, fused, light scatt. by SAW on refl. and transmission 79−24288
quartz, fused, photoelastic light scatt. from surface Rayleigh waves 80−97235
quartz, He^+ ion implanted, SAW velocity, influence of annealing 79−14996
quartz, ion-implanted, SAW velocity 0.9 to 6K 78−84040
quartz, isotropic fused, SAW generation by nonlinear mixing of bulk waves 79−50490
quartz, piezoelectric layer, non-crystalline characteristics after ion implantation *(French)* 77−73117
quartz, piezoelectric surface wave velocity, flexural biasing state influence 79−56730
quartz, propag. meas. by acoustoelectric methods 80−84359
quartz, resonator transverse modes, SEM obs., phase effects 79−68452
quartz, SAW cut with orthogonal temp. compensated propag. directions 80−10770
quartz, SAW delay, zero temp. coeff. 79−86972
α-quartz, temp. dependence of surface wave diffraction 77−15674
α-quartz SAW temp. depend. 78−51813
quartz SAW velocity/temperature dependence calc. 79−56062
surface acoustic waves continued
quartz substrate, SAW attenuation due to platelet defects 79−95253
quartz substrate, surface and bulk acoustic waves excited by interdigital transducers, optical diffr. study *(Chinese)* 78−50965
α-quartz surface skimming bulk wave theory 79−56064
quartz wedge, reflection, transmission and conversion of normally incident SAW 80−2257
quartz with zero temp. coeff. of delay, SAW propag. characts. 80−75420
quasibulk surface waves, existence criterion 78−67898
quasivolume surface elastic waves, in low-symmetry crysts. 77−28070
Rayleigh wave, propag., isotropic elastic material with homog. strain 78−94460
Rayleigh wave excitation and detection using piezoelectric polymer sheet transducers *(French)* 79−14182
Rayleigh wave interaction with periodic surface corrugation 79−50484
Rayleigh wave nonlinear interaction in $LiNbO_3$-CdS system, expt. investigation 80−102946
Rayleigh wave propagating along rough surface, dispersion and damping 80−102892
Rayleigh wave propagation in strongly magnetostrictive materials 77−40111
Rayleigh wave reflection from periodic corrugations of surface in oblique incidence 80−58850
Rayleigh wave scatt. by normal discontinuities, influence of elastic props. 77−46835
Rayleigh wave scatt. by post spacers 79−27456
Rayleigh waves, attenuation of elastic waves by surface inhomogeneities 79−23822
Rayleigh waves on smooth surfaces of arbitrary shape 80−64272
rectangular ridge, edge localised vibr. modes 77−89629
reflection and bulk-wave conversion at single shallow groove 77−51586
reflection by strips, grooves and arrays of strips and grooves 78−63214
reflection from finite system of periodic perturbations 80−10059
reflection from local surface inhomogeneities at oblique incidence 78−18094
reflection from thin-strip overlays, first-order coeff. 80−1376
resonant transmission across piezoelectric gap 78−87855
review, major types 79−95254
Rochelle salt, dehydration kinetics in ferroelec. and paraelec. phases, surface acoustic waves influence 80−97204
rock, appl. of direction-sensitive displacement analysis by multiple freq. holographic interferometry 78−54338
rotated Y-cut quartz surface skimming bulk wave analysis 79−56065
rough surface sound reflection, surface wave effects *(Russian)* 80−1377
roughness effects on dynamical props. 78−75923
scanning of optical images using acoustoelectric memory correlator struct. 80−74632
scattering, surface wave formation and resonance relation *(French)* 80−8809
scattering by edges of thin surface layers at oblique incidence 78−18085
scattering by interdigital transducer, model and appl. to SAW track changer 79−59899
scattering by surface breaking cracks 79−56058
scattering from elastic cylinders, Regge poles 78−50967
scattering from elliptical cracks for failure prediction 80−55608
scattering from surface cracks, angular and frequency dependence obs. 79−57197
scattering in piezoelectric material, by metallic electrodes anal. 78−83157
second harmonic generation in finite amplitude SAW, anisotropic media *(French)* 80−34285
semiconductor, opaque, light scatt. from surface acoustic phonons 78−76484
semiconductor surface characterisation using SAW 80−11069
semiconductor surface eval. using SAW convolver 80−97677
semiconductor with negative differential conductivity, amplification of SAW by transverse current 79−7741
semiconductor-metal contact, depletion depth, acoustic determ. 79−99621
semiconductor-piezoelectric structure, SAW attenuation and transverse acoustoelec. field 78−10516
semiconductor-piezoelectric structure, vol. acoustic wave excitation in nonlinear interaction with surface waves 80−69582
shear acoustic surface waves on a cylindrical surface of a solid coated with a layer of a different material 79−32117
shear SAW at periodically nonuniform boundary between two solids 79−32112
shear SAW in high permittivity three-layer system *(Russian)* 80−80048
shear volume waves conversion to surface acoustic waves at solid surface *(Russian)* 79−69332
shear waves in periodic structures, electronic damping and amplification shear waves in periodic structures, electronic damping and amplification 80−19124
shear waves in periodic structures on solids 79−90055
signal processing appls., review, book contrib. 79−50519
slow, shear surface acoustic waves in a slow-wave structure on a solid surface 79−18567
slow shift SAW in attenuating piezo-electric and piezosemicond. surface structs. 78−79872
slow waves on hard substances, theory 77−39122
solid insulator interface, parametric interaction with EM waves in microwave field, 80−92771
solid-liquid interface, surface wave reflection from periodic irregularities 79−18562
solids, transverse SAW in microwave field 80−92945
special total reflection on anisotropic crystals 79−56054
spherical wave reflection from reactive impedance boundary, Cagniard's method modification 77−11064
steel, dispersion in cold-worked layer of used railroad rail 79−1014
steel, mild, rolled, critical angle US reflectometry of stressed bar, book contrib. 79−100324
steel high-temperature ultrasonic testing *(Italian)* 79−96242
Stoneley wave amplification at interface between piezoelectric semicond. and dielectric crystal 79−19441
Stoneley wave amplification between two piezoelecs. separated by thin semicond. film 79−14998
Stoneley wave meas. using differential interferometric optical scanning system 78−75919
Stoneley wave study of adhesively bonded interface 80−49530

surface acoustic waves continued
Stoneley waves at interface between two hexagonal crystals *(French)* 77−31859
strength of nonlinear interaction between collinear surface acoustic waves 80−33295
stroboscopic visualisation, surface wave travelling on a glossy plane *(French)* 78−79175
strongly anisotropic crystals, slow surface waves 79−69333
strongly inhomogeneous SAW in solids 79−64374
structure, properties and appls. of SAW, overview *(Italian)* 80−69574
superconductor, bulk, absorption of SAW in presence of supercurrent 79−28443
surface cracks, SAW excitation, length and depth resonances 79−8403
surface cracks, small, size estimation using SAW 78−76793
surface skimming bulk wave propag. in Y-rotated quartz 80−74583
surface skimming bulk waves, coupling with multistrip coupler 80−74630
surface skimming bulk waves, excitation and detection on rotated Y-cut quartz 80−43492
surface skimming shear-wave guidance by corrugated surface 80−74582
surface-skimming bulk wave excitation, analysis using Green's function formulation 80−53519
temperature compensated materials with high piezoelectric coupling 77−40184
TGS, electromech. coupling of surface acoustic waves near ferroelec. transition 78−19415
TGS, SAW phase velocity in b-plane 77−85043
thermal stress effects of acoustic surface waves in layered media *(Japanese)* 79−98573
thermopiezoelectric material, monoclinic symmetry, surface wave propag. 80−44403
thin film elastic constants and SAW velocity and attenuation meas. 79−56101
transition metal dichalcogenides, layered, surface Brillouin scatt. obs., surface ripple and elasto-optic mechanisms 80−16048
transition radiation of Gulyaev-Bleustein SAW in piezocrystals 78−43231
transverse amplitude dependence on anisotropic substrates 79−7242
transverse modes in SAW resonators 80−96169
transverse surface waves, on cylindrical surfaces of anisotropic solid 78−10270
two-layer systems with an air gap, interaction with electrons 77−39901
ultrasonic wave transmission through rough surface *(Russian)* 80−100387
US, nonlinear interaction in 2-6 MHz range *(French)* 80−33296
US leaky wave attenuation by near-surface defects 77−32757
US surface wave velocity measurement using reflections from laser scribed grooves 78−90614
US wave diffraction, expt. and anal. 80−5898
variational limits on piezoelectric problem parameters 79−81594
velocity, attenuation and reflection meas., interf. acoustical method 79−18638
velocity dispersion induced by laser radiation absorpt. 77−51585
velocity meas. by phase-sensitive laser probe 79−46911
velocity measurement, high accuracy method 80−38189
velocity measurement, pulse technique 78−5618
velocity variation measurement, recirculating pulse generator 78−5619
viscoelastic media, surface wave propagation 78−42555
viscous heat conducting fluid, acoustic boundary layer 80−107377
visualisation, by acousto-optical holography *(German)* 80−70515
X-ray topographical representation 79−47870
Al alloys, fatigue, microcrack development, acoustic SHG study 80−35440
Al, Brillouin spectra, light scatt. cross section for surface ripples 80−71434
Al film on α-quartz, SAW velocity/temp. dependence 77−31861
Al superconducting film, 2 GHz SAW attenuation meas. of mean free path 77−39999
Al, surface wave scatt. from elliptical cracks for failure prediction 80−55608
AlN, epitaxial film growth by MBE, physical and optical props. 80−2293
AlN, piezoelectric film, low temp. growth by RF reactive planar magnetron sputtering method 80−76175
Al_2O_3 film on stainless steel in water, Gaussian ultrasonic beam refl. 78−67896
$\alpha AlPO_4$ as SAW substrate material, piezoelec. props. 80−80710
$AlPO_4$, berlinite, piezoelectric coupling for SAW applications 79−56055
α-$AlPO_4$, berlinite, SAW props. 78−79871
α-$AlPO_4$, berlinite, SAW velocity and piezoelec. coupling obs. 79−56056
α-$AlPO_4$, berlinite, surface skimming bulk wave theory 79−56064
α-$AlPO_4$, berlinite, temperature-compensated surface and pseudo-surface acoustic wave props. 77−51584
α-$AlPO_4$, berlinite, X-axis boule cut SAW props. 79−56061
$AlPO_4$, SAW velocity calc. 78−13869
Au film on ⟨100⟩ Si, measurement of SAW dispersion using acoustic microscopy 80−53575
Au film on α-quartz, SAW velocity/temp. dependence 77−31861
Au film on Si, SAW dispersion and film thickness meas. 80−10769
$Ba_2Si_2TiO_8$, elastic consts., thermal expansion and piezoelec. props. 77−85651
$Ba_2Si_2TiO_8$, fresnoite, SAW props., expt. and calc. 78−43229
$Ba_2Si_2TiO_8$, fresnoite single cryst. SAW characts. 79−37913
$Ba_{2-x}Sr_xTiSi_2O_8$, piezoelec. crysts., SAW characts. 80−84354
$BaTiO_3$, Rayleigh wave generation by surface piezoelectricity 78−71925
Bi, amorphous film, temp. dependence of SAW attenuation 80−75679
$Bi_{12}GeO_{20}$, finite amplitude SAW distorted rippling profiles, optical probing obs. 80−34287
$Bi_{12}GeO_{20}$-CdS, air gap coupled system, SAW energy transfer 77−11774
$Bi_{12}SiO_{20}$ crystal, piezoelec. and saw props. 80−75949
$Bi_{12}SiO_{20}$ surface and pseudosurface wave props. 79−46908
$Ca_{12}Al_{14}O_{33}$, piezoelectric material, cryst. growth and characterisation 79−99825
CdS, acoustic-wave-induced increase in cond. 77−59307
CdS, acoustoelec. interaction, influence of surface pot. 77−1455
CdS, bulk acoustic phonons, light scatt. from phonon-induced surface ripples 78−75924
CdS crystal, SAW amplification, bulk and acoustic noise 80−39637
CdS crystal with thin photoproduced semiconducting layer, tests of convolver on transverse surface waves 77−42646

surface acoustic waves continued
CdS cylindrical crystal, transverse SAW obs. 78−84042
CdS, epitaxial film, conductivity control by S vacancy form., light modulation appls. 77−4455
CdS film, strain-induced modulation of photoconductivity 79−24009
CdS heteroepitaxial films on ZnS, surface-wave acoustoelectric domain excitation and probing 79−46904
CdS, light scatt. by Bleustein-Gulyaev waves on refl. and transmission 79−24288
CdS, parametric interaction of acoustic surface waves *(French)* 77−62083
CdS, photocond. meas. using surface wave acoustoelec. current 77−8131
CdS, photoconducting, surface acoustic noise amplification by carrier drift 78−72208
CdS, photoconductive, transverse electric current effect on SAW propagation 79−47127
CdS, SAW absorpt., effect of transverse electron drift 77−76879
CdS, SAW meas. of surface elec. props. 77−20387
CdS, SAW superheterodyne amplification 77−55589
CdS, semicond., coexistence of surface and bulk acoustic waves in acoustoelec. domains 80−44404
CdS, semicond. piezoelec. crysts., US Rayleigh waves rel. to acoustoelectric characts. 77−1456
CdS, sputtered film, Rayleigh wave propag. *(French)* 77−62727
CdS, surface acoustoelec. current due to Rayleigh wave, ambient medium effects and surface state changes 77−69383
CdS, surface elastic wave propag. in piezoelec. plate, elec. screening effect *(Russian)* 79−14999
CdS surface spectroscopy using acoustic surface waves, spectral response 77−69402
CdS, surface state meas. by SAW convolver 79−42617
CdS, transverse acoustoelec. effect rel. to SAW intensity 78−26917
CdS-$LiNbO_3$ structure, acoustoelectric interaction of surface waves with inhomogeneously distributed free carriers 77−43668
$ErFeO_3$, SAW meas. of magnetoelastic effects 80−75839
$Fe_{80}B_{20}$, ferromagnetic metallic glasses, Brillouin scattering 78−92085
$Fe_{40}Ni_{40}P_{14}B_6$, ferromagnetic metallic glasses, Brillouin scattering 78−92085
GaAs, Brillouin spectra, light scatt. cross section for surface ripples 80−71434
GaAs, bulk acoustic phonons, light scatt. from phonon-induced surface ripples 78−75924
n-GaAs epitaxial film, surface mode phonon amplification, numerical analysis 78−34691
GaAs, laser irradiated, origin of periodic surface struct. 78−91513
GaAs, SAW meas. of surface elec. props. 77−20387
GaAs, surface characterisation using SAW 80−11069
GaAs:Cr (Cr-Te), and undoped, transverse-acoustoelec.-voltage spectroscopy 79−99586
GaP, powder, electroluminesc. excitation by SAW, nonlinear effects 80−16104
GaP, surface characterisation using SAW 80−11069
GaYIG, magnetoelastic surface wave attenuation 77−20667
Gal, Brillouin spectra, light scatt. cross section for surface ripples 80−71434
$Ho_{0.58}Tb_{0.20}Dy_{0.22}Fe_2$, magnetoelastic surface wave propagation, mag. field depend. 77−85535
$Ho_{0.58}Tb_{0.2}Dy_{0.22}Fe_2$ magnetoelastic surface wave dispersion obs. 79−47321
InAs/$LiNbO_3$ structure, SAW generated transverse acoustoelectric voltage, image scanning and signal processing appl. 80−49826
KCl, surface radiative absorption meas., acoustic technique 77−3596
$KTaO_3$, Rayleigh wave generation by surface piezoelectricity 78−71925
$KTaO_3$-metal contact, surface barrier Rayleigh wave transducer 79−98578
$LiIO_3$ crystal elastic, piezoelec., dielectric and acoustic props. 79−46740
$LiIO_3$, piezoelec. coated with semicond. film, Bleustein-Gulyaev wave amplification 79−61309
$LiIO_3$ single crystal, surface acoustic wave parameter meas., coherent optics method 80−106691
$LiIO_3$, transverse gap elastic waves, expt. 80−59576
$LiIO_3$, US wave tunnelling across piezoelectric gap 78−87857
$LiIO_3$, Z-cut, temp. coeff. of delay for SAWs 77−76654
$Li_{1-x}Na_xNbO_3$, LPE, growth and temp. coeff. of SAW velocity 78−43227
$LiNbO_3$, acoustooptic interaction, unguided light deflection via SAW 77−8543
$LiNbO_3$, aluminum-coated YZ, measurements of SAW attenuation 80−74619
$LiNbO_3$, and $LiTaO_3$, finite amplitude SAW distorted rippling profiles, optical probing obs. 80−34287
$LiNbO_3$ crystals, velocity and propag. loss meas. of surface shear waves 80−74581
$LiNbO_3$ delay line, bulk wave generation due to nonlinear interaction of SAW 79−42359
$LiNbO_3$, diffr. effects from very narrow surface wave transducers 78−22240
$LiNbO_3$, diffusion waveguide, acousto-optic mode conversion at surface wave freqs. *(Russian)* 78−1348
$LiNbO_3$, effects of the ion implantation on SAW propag. 80−75421
$LiNbO_3$, electroacoustic echo excitation with aid of surface waves 77−14834
$LiNbO_3$, excitation and propagation patterns, frequency translated holographic obs. 77−80690
$LiNbO_3$, film lightguide, pulse signal convolution in acoustooptic interaction *(Russian)* 78−1345
$LiNbO_3$ interfaces, SAW reflection, light scatt. meas. 80−34286
$LiNbO_3$ laser beam/SAW mode conversion 79−46056
$LiNbO_3$, leaky SAW and guided light Bragg interaction, theoretical anal. 78−72484
$LiNbO_3$, line acoustical waves anal. 78−34692
$LiNbO_3$ optical waveguide, Bragg interaction of leaky and Rayleigh waves 77−23783
$LiNbO_3$, optical waveguide, anisotropic planar, acoustooptic interaction 77−68273
$LiNbO_3$, optical waveguide, diffr. of modes by standing elastic surface waves *(Russian)* 78−1343
$LiNbO_3$, parametric mixing of SAW in 20 to 100 MHz range 79−86279
$LiNbO_3$, partial waves of SAW, direct meas. by light scatt. 78−66994

surface acoustic waves continued
$LiNbO_3$, phase and amplitude relations between fundamental and second harmonic SAW 77−69157
$LiNbO_3$, piezoelec., SAW interaction with secondary electrons 80−80708
$LiNbO_3$, piezoelec. layer, non-cryst. characts. after ion implantation *(French)* 77−73117
$LiNbO_3$, piezoelectric surface wave velocity, flexural biasing state influence 79−56730
$LiNbO_3$, propagation losses due to surface roughness 78−38926
$LiNbO_3$ pure and Fe doped, IR induced acousto-photorefractive memory effect 80−80746
$LiNbO_3$, SAW, suppression of harmonic generation by ZnO thin-film loading 80−84355
$LiNbO_3$, SAW convergence props. 80−24726
$LiNbO_3$, SAW propagation and scatt., finite difference anal. 80−20595
$LiNbO_3$, SAW reflection from conducting strips 80−5853
$LiNbO_3$, surface elastic wave propag. in piezoelec. plate, elec. screening effect *(Russian)* 79−14999
$LiNbO_3$, wedge fabrication for line acoustic wave propag., using cleavage method 78−30818
$LiNbO_3$, Y-Z, Rayleight-wave reflection from groove 79−51408
$LiNbO_3$, Y-Z, SAW scatt. from groove 78−60019
$LiNbO_3$, Y-Z cut, surface to bulk mode wave conversion, at interfaces ang. spectrum meas. 78−47652
$LiNbO_3$, y-z, x-z and $41^1/_2$-x cuts, SAW SHG, laser probing 77−31153
$LiNbO_3$, y-z crystal, line shape of light scattered by SAW upon total internal refl. 79−24287
$LiNbO_3$, y-z cut, light scatt. from SAW 78−6652
$LiNbO_3$:Na structure field stability limits, LPE film growth, SAW velocity 80−80102
$LiNbO_3$:Na^+(Co^{2+},Zr^{4+}) films, LPE growth from Li_2O-V_2O_5 flux, X-ray and acoustic characterisation 80−15383
$LiNbO_3$:phosphor, piezoelec., interaction with SAW, excitation of electrolum. 79−60615
$LiNbO_3$-CdS, layered structure, acoustoelectric surface current kinetics 78−43232
$LiNbO_3$-CdS, layered struct., transverse acoustoelectric effect 79−69567
$LiNbO_3$-CdSe, piezoelec.-semicond. layer struct., acoustic-wave-induced increase in cond. 77−59307
$LiNbO_3$-CdSe layer structure, SAW absorpt., elec. field effects 80−65355
$LiNbO_3$-InSb struct., electroacoustic interaction temp. depend. 79−69336
$LiNbO_3$-liquid-CdS-liquid-$LiNbO_3$ structure, acoustic wave propag. and amplification 77−42654
$LiNbO_3$-p-Si, frequency doubling of the two-pulse and three-pulse echoes in surface acoustic waves 79−69335
$LiNbO_3$-Si(CdTe) structure, acoustoelectronic interaction between SAW and transverse drift current 77−69424
$LiTaO_3$, propagation with arbitrary cut *(Japanese)* 80−92769
$LiTaO_3$, rotated Y-cut, SH and Rayleigh surface waves 79−46910
$LiTaO_3$ rotated Y-cuts for SAW launching 79−56060
$LiTaO_3$ SAW substrate minimal diffraction cuts 78−33934
$LiTaO_3$ surface skimming bulk wave theory 79−56064
$LinBO_2$, adjacent to thermally oxidised Si, SAW attenuation obs. of semicond. surface props. 79−87131
Mo film, constrained, 20 MHz thermoelastic wave generation 79−47880
$NH_4H_2PO_4$, Z-cut, SAW velocity, electromechanical coupling coeff. 80−84358
(Na,Li)NbO_3 ceramic, optimum prep. conditions and characterisation 78−3079
Nb_3Sn, on $LiNbO_3$ substrate, US attenuation of SAW in applied mag. field 80−75678
Nb_3Sn, softening of surface phonons in (100) plane 80−107627
Nb_3Sn, supercond., thin film, US attenuation of SAWs 80−49988
Ni, Brillouin spectra, light scatt. cross section for surface ripples 80−71434
Ni crystals in strong mag. field, EM excitation and vel. dispersion of sound *(Russian)* 80−39837
Ni film, 618 MHz SAW attenuation rel. to mag. field 77−40110
Ni film, mag. field depend. surface acoustic wave attenuation meas. 77−20674
Ni, film, mag. susceptibility correlation with SAW attenuation 79−47310
Ni film, RF sputtered on $LiNbO_3$, SAW delay variation obs. 79−56102
Ni-7070 pyrex glass boundary, 9 MHz Stoneley wave generation 79−82433
Ni-$LiNbO_3$, layered structure, mag. control of surface elastic waves 77−20666
Pb/Cu(Ag) proximity effect semiconductor, US surface wave attenuation 79−60994
$Pb_2KNb_2O_5$, SAW props., rel. to device appl. 78−71923
$Pb_2KNb_5O_{15}$ piezoelectric coupling for SAW applications 79−56055
$Pb_2KNb_5O_{15}$, strong electromechanical coupling of SAW 78−63919
$PbMoO_4$, SAW props. 78−63920
$PbTiO_3$ ceramics, temp.-compensated, for SAW appl. 80−15355
Se, SAW vel. and electromech. coupling factor 80−75422
n-Si ion implanted surface potential barriers, $LiNbO_3$ SAW obs. 77−28234
Si, ion-implanted, impurity activation monitoring by SAW techniques 80−65020
Si, SAW meas. of surface elec. props. 77−20387
Si, surface characterisation using SAW 80−11069
Si wafer, surface exam. of ion-implantation using SAW convolver 77−72897
Si wafers eval. using SAW 80−76470
Si:H, amorphous, Brillouin scattering from acoustic bulk and surface waves 80−11425
n-Si-SiO_2-ZnO-Al, SAW convolver in monolithic MIS struct. 77−23791
SiC, power, electroluminesc. excitation by SAW, nonlinear effects 80−16104
Si_3N_4 film acousto-optical props. for integrated optical Bragg cell 79−55251
Si_3N_4, hot pressed, surface wave scatt. from elliptical cracks for failure prediction 80−55608
SiO_2, and $SiO_{0.7}$, amorphous sputtered thin film, US anomalies, 0.5-300K 80−34145
SiO_2, finite amplitude SAW distorted rippling profiles, optical probing obs. 80−34287
SiO_2, phase an amplitude relations between fundamental and second harmonic SAW 77−69157
surface acoustic waves continued
SiO_x, thin film on YZ-$LiNbO_3$, SAW props. 80−84356
SiO_x-GaAs, vacuum evaporated system, acoustoelec. signal, interface props. 80−75646
Sn, u.s. surface generation, below 20K 78−2353
$Sr_{0.5}Ba_{0.5}Nb_2O_3$ piezoelectric transducer, SAW props. 80−79037
Ta_2O_5 film acousto-optical props. for integrated optical Bragg cell 79−55251
Tl_3TaSe_4, for SAW devices, temp. compensated cuts with zero power flow 77−12313
Tl_3TaSe_4, new SAW zero temp. cuts 78−2351
Tl_3TaSe_4 SAW coupling and temperature coefficients 79−51410
Tl_3VS_4, for SAW devices, temp. compensated cuts with zero power flow 77−12313
Tl_3VS_4, growth of inclusion free crystals, for surface wave and bulk wave acoustic devices 80−25549
Tl_3VS_4 SAW coupling and temperature coefficients 79−51410
W, SAW excitation using wedge-shaped transducers 79−69334
YIG, dilute, magnetoacoustic surface wave excitation by RF field on Bloch walls 80−25178
YIG, nonreciprocal attenuation of elastic surface waves 77−55696
YIG substrates, magnetoelastic surface waves, magnetostatic reson. anal. 80−20441
YIG:Gd, Ga, optical probing of magnetoelastic Rayleigh waves 79−78495
Zn film, supercond., SAW US attenuation 79−73633
ZnO film, longit. elastic wave attenuation, 9.4 GHz 78−18888
ZnO film acousto-optical props. for integrated optical Bragg cell 79−55251
ZnO films, RF sputtered single-cryst., on sapphire, struct. and SAW props. 80−80105
ZnO monocrystal and RF sputtered heteroepitaxial film, SAW attenuation comparison 79−56063
ZnO piezoelectric films formed by RF reactive ion-plating 79−83140
ZnO piezoelectric films, RF planar-magnetron sputtered, characterisation 80−96751
ZnO, RF sputtered epitaxial film, appl. to integrated optics 77−14821
ZnO triode sputtered film elastic props. rel. to structure and composition 79−46988
ZnO/quartz for SAW device materials, expt. study of props. 80−80050
ZnO/substrate higher order mode SAW propagation obs. 79−46909
ZnO-SiO_2-Si layered structure, SAW props., anal. 77−62729
ZnS, surface acoustic wave modes 78−2352

surface activity *see surface energy*

surface-atomic beam collisions *see atom-surface impact*

surface chemistry
see also chemisorption; corrosion; oxidation
ablating layer, rate of physical and chemical transformation *(Ukrainian)* 80−50887
ablating plane (axisymmetric) body, turbulent boundary layer with neg. press. gradient 78−79389
acetylene, adsorbed on Ni(111), benzene form., vibr. spectra 78−95952
acetylene, chemisorbed on Pt (111), self-consistent EHT studies 79−61896
acetylene, chemisorption on Pt(111), reaction at room temp., form. of vinyl-like species 79−46939
active ion bombardment induced chemical reactions at surfaces detected by SIMS 79−16034
adatom laser stimulated migration and multiphoton excitation, relax. and reaction enhancement 79−39200
adhesion, surface chemistry studies, anal. appls. 80−88440
adsorbed atoms thermal desorption, one dimens. microscopic model, weak binding case 80−96729
adsorbed species, surface reactions, dipole interactions effects 80−61143
aerodynamic levitation flow reactor and applics. 77−29046
AES of surfaces 78−85277
AES with secondary emission imaging 78−11475
alien layer build-up on contact materials *(German)* 80−7852
alkali halide, screw dislocations in puncture rosettes, motion-starting-stresses, surface-active media effects *(Russian)* 78−10051
alkali silicate glasses in aqueous solutions, leaching kinetics rel. to surface pot. 80−11803
alloy, high-temp., scale behaviour in carbonaceous gas atmos. 77−36693
alloy surface chemistry, sample morphology effects 78−7233
aluminisation in Al packs, for protective coating form., kinetic diffusion theory 77−32727
analysis by ion scattering and secondary ion mass spectrometry 77−40621
analysis instruments for vacuum electronics *(Czech)* 77−18145
anthracene, in atmosphere, photooxidation on particulate matter 80−61487
antiscale forming effectiveness of seeding crystals in thermal power plant 80−89527
aqueous magnetic fluid prep. by peptisation with anionic surfactant 78−44408
atom-surface reaction, EPR anal. via ultrahigh vacuum/flow system 78−7232
Auger electron spectroscopy, quantitative analysis 77−85852
bentonite, selectivity of ion-exchange reactions 79−34360
biopolymer synthesis on solid supports 79−29397
boiler inlet temps. and corrosion product deposits, water chemistry effects 80−89528
book 77−25310
boride coatings, reaction with Mo substrate 77−32716
boriding, with a thermally unstable gas (B_2H_6) 80−30159
brass, sphere, dissolution in H_2SO_4 in elec. field *(Russian)* 77−4867
1-butene, adsorbed on δ-Al_2O_3, isomerisation, IR study 80−76554
1-butene adsorption on delta alumina, microgravimetric-IR study 80−75432
carbonaceous chondrite meteorites, surface catalysis rel. to organic matter origin in early solar system 78−20767
catalysis and surface science, review 80−40740
catalyst, granular bed, static, flow transfer processes 80−45554
catalyst surface mag. field effect on mol. dissoc. rate 80−16721
catalytic heterogeneous, bimolecular surface reactions, defect renormalised propagator stochastic theory 78−95955
catalytic reactions at high press. 79−47972
cell for surface studies using IR transmission spectroscopy 78−41361
cells, electrochemical, photovoltaic phenomena and mechanisms 78−8198
ceramics, local in depth anal. by neutral beam SIMS 80−89565

surface chemistry continued
chalcopyrite, aq. oxidation in hydrochloric acid 79−61764
chalcopyrites, acidic fermic sulphate leaching, reaction mechanism 79−83511
charcoal, wood, prep., chem. activation 79−28973
chemical states at surfaces exposed to high-temp. vapours 78−11559
chemisorption kinetics, power adsorption isotherm, entropy correction 80−40734
chemisorptive luminescence systems for surface reaction obs. 78−7236
chymotrypsin hydrolysis of N-succinyl-L-phenylalanine-p-nitroanilide, enzymatic reactions 78−95992
colloid stabilisation by polymers, excluded volume effects 77−60129
colloidal systems, surface forces, direct meas., elastic deform. effect 80−93805
condensed adsorption layers, effect on electrode reaction rates 80−93769
conference, Budapest, Hungary (Sept. 1975) 78−11567
conference on surface science, Cambridge, England (March 1979) 80−36773
contaminants analysis by plasma chromatography-mass spectroscopy 78−3433
cortisol, gas phase fragmentation, high voltage scanning field desorption obs. 78−3320
crystal growth and deposition, gaseous phase, chem. transport reaction 80−44161
crystal plasticity, surface effects, review 77−47505
α-cyanoacrylate adhesive in first monolayer on bulk Al surface, IR spectra, H-bond form., stretching vibr. 80−87119
cyclobutene, strong collision and thermal decomp. on surface, variable encounter method calcs. 80−50885
cyclopropane, surface isomerisation to propylene, role of vibr. energy 79−74376
cylinder array, convective mass transfer with surface reaction 78−79369
defects role, review 78−14551
desorption rates, neutral and ionic, meas. via surface ionisation detector with field reversal 77−2710
diffusion-controlled reactions on a two-dimensional lattice 80−71940
diphenanthra[4,5,6-abcd, 4,5,6-jklm]perylene, high photoresponse, O_2, N_2 and SF_6 effects 77−32036
1,1-diphenylethylene, adsorbed on porous Vycor glass, reson. Raman spectrum, surface species identification 78−42066
dynamics, laser probe investigs. 79−43580
electrochemical electron transfer at electrodes in soln., review, in book, for teaching 78−8203
electrochemical surface processes, kinetics simulation 79−16004
electrochemical surface reacts. driven by linear pot. sweep, kinetics 77−25275
electrochemistry, steady-state conversion rate rel. to surface reaction process, catastrophe theory 80−108717
electrode processes possessing charge transfer mechanism, overvoltage theory, in book, for teachers 78−8204
electrode surface, covalently bound molecules, redox reactions, steric effects 78−73077
electrode systems, nonequilib. polaris. states props. overvoltage theory, in book, for teachers 78−8205
elementary reactions on single crystal surfaces, kinetics 80−108729
ellipsometry of electrochem. surface layers 78−56874
enzyme-substrate interactions, educational model 77−26110
ESCA, quantitative surface anal., limitations, depth profiling, catalyst surface anal. 78−53298
ESCA, X-ray type, C 1s contaminant buildup on conductors and insulators 78−95981
ethanol+Al_2O_3, surface reaction, 295-575K, surface specieis study 79−100435
ethylene, adsorption on W (100) and decomposition to acetylene, AES obs. 79−66353
ethylene, chemisorption on Pt(111), reaction at room temp., form. of vinyl-like species 79−46939
ethylene chemisorbed on W, reaction with atomic H 77−36789
EXAFS obs. 80−108735
fatigue crack growth, surface reaction and transport controlled, model 80−75299
ferric ion behaviour during chemical cleaning 79−43625
flammability resistance by radiation processing 78−95942
float glass, attack by water, behaviour of Al traces *(French)* 80−89378
in flocculation 77−60134
flow on flat plate with chem. surface reaction, mass transfer *(German)* 79−72961
fluid-solid reactions, law of additive reaction times 79−83452
formaldehyde, adsorbed on W(100) single cryst., XPS obs. of decomp. 77−4927
formaldehyde, oxidation on Cu (110), temp. programmed desorption obs. 79−87878
formic acid, on Ni surface, decomp., dipole interactions effects 80−61143
formic acid on Ni (100)-p(2×2)C, decomp. 79−91995
fusing xerographic toner images against bare metal surfaces, release mechanisms 79−17527
fusing xerographic toner images against bare metal surfaces, release agent chemistry 79−17528
gas mixture, multicomponent, transport equations near catalytic surfaces 80−43821
gas-solid interface, electronic struct. HFR calc. 80−54745
gas-solid reaction, transient anal., sigmoidal conversion-time behaviour 77−66768
gas-solid reaction with changing particle size, unsteady state heat transfer 78−92503
gas-solid reactions, book 77−63958
gas-surface reactions, semiempirical generalised LEPS pot. 78−68923
E-glass fibre, silane coupling agent deposited on surface, hydrolysis and drying effect on siloxane bonds 80−85072
glaze/glass-ceramic, interface reactions, electron microprobe anal. 80−84398
glow curves and desorption spectra anal. method 80−80053
graphite, acidic surface oxides, struct. investigation using diazomethane 79−52404
graphite, burning permeable surface, accel. flow, turbulent heat/mass transfer 78−38417
graphite, conditioning of surface by atomic H 80−93665
graphite, reaction with H_2, mol. beam-surface expt., quasi-equilib. treatment 77−86376
graphite+Be→Be_2C layer, limiting stage investig. 77−36786

surface chemistry continued
graphite fluoride, chemical reactivity, rel. to lubrication appl. 79−66349
graphite monolayer on Ni (110) surface, oxidation mechanism 80−101037
haematite particles, crud deposition on heat transfer surface, surface chemistry 80−35376
halide dioxide radical form., H_2O_2 decomposition of halide-coated surface, EPR obs. 80−7851
halides, adsorpt. of water, mol. studies of ice-forming capabilities 77−31872
heavy metal ion removal in clay suspensions 77−86955
heterogeneous atom recombination on surface sites, kinetics of Langmuir-Rideal mechanism 79−87876
heterogeneous catalysis, conference, Varna, Bulgaria (Oct. 1979) 80−82578
heterogeneous catalysis reaction mechs., electron pair behaviour and surface orbitals 80−55705
heterogeneous chem. reactions under action of turbulent jet, modelling 78−64885
heterogeneous chemical kinetics by modulated mol. beam mass spectrometry 77−25305
heterogeneous surface with mass transfer, boundary layer transport 79−70371
heterogeneously catalysed reactions, kinetic instabilities, oscill. instabilities 79−24717
heterogeneously catalysed reactions, kinetic instabilities rate multiplicity 79−20341
1-hexene-water(-D_2O), field-induced surface reactions, field ionis. mass spectra obs. 78−95949
high temperature metallic species, absorpt. and fluoresc., high temp. fast flow reactor technique 80−42231
hydrazine, decomp. on Ir(111) surface, N_2 emission, ang. depend. 80−97731
hydrocarbon formation on interstellar graphite grain surfaces 80−82458
hydrocarbons, formation on metal surfaces in fusion reactors 80−21322
hydrocarbons, reactions, rate consts., temp. depend., photolysis, high temp. fast flow reactor technique 80−42231
hyrocarbons, on activated C, rel. between adsorption and polarizabilities 80−76558
ice nucleation threshold on Cu_2S, Ag_2S, MoS_2 and CdS photosensitive surfaces 77−55343
ilmenite, roasted ore, Fe chlorination kinetics in fluidized bed reactor 79−47979
immobilised enzyme systems, industrial appls. 79−29399
inelastic electron tunnelling spectroscopy, surface chem. and heterogeneous catalysis appls. 78−92512
inorganic compounds, field ionisation mass spectrometry, review 78−35764
integrated surface physics and chemistry laboratory planning for automation 79−67269
interface, stability problem, diffusion, reaction and convection 80−33567
interface composition determ. methods 79−70396
interfacial organic chem. processes 80−26050
interstellar dust, surface chemistry in mixed oxide grains model 80−26934
interstellar grains, H_2 form. on surfaces 79−21367
interstellar grains surface activity, adsorbed mol. ions rel. to diffuse spectral bands 77−26040
interstellar oxide grains, mol. prod. 79−25690
ion beam analysis and ion implantation in single UV vacuum sample chamber 77−4970
ion beam effects, ESCA obs. 78−52612
ion implantation, chemical and electrochem. aspects, review 80−100271
ion-metal surface soft landing, chem. surface modification 77−24916
ionic solid volatilisation, surface charge effects 78−14457
IR photoacoustic spectroscopy of solids and surface species 80−90909
isolated discharge electroerosion craters, interelectrode surfactant effect *(Russian)* 79−83462
isotope separation, by semipermeable membrane, secondary-stage processes, photoexcitation effects *(Russian)* 77−6962
laser induced reactions 77−25308
laser stimulation of surface reactions by excitation of adsorbed molecules 77−56242
liquid alkali metal-solid metal interfaces, chemistry and physics 77−51576
liquid crystal, colloid and surface chemical aspects 78−9950
liquid phases interface, hydrochemical stability 78−22933
liquid-liquid interfaces in isolation and in interaction, review 77−47651
magnetite electrochemical polarisation in surfactant solns. *(Russian)* 79−83465
marine sediment particles, surface organic layer containing U and Th, thickness meas. 78−40592
mass spectrometry, molecular beam, appl. to coupled diffusion and chem. reaction 77−73497
mass transport and surface reactions, in Leveque's approx. 78−76907
materials chemical resistance medical laboratory techniques 79−88926
membrane system, closed, vesicular, mechano-chemistry 77−60189
merocyanine dye monolayer on p-chloranil cryst. in sandwich cell, electrochromic detection of internal charges 78−11549
metal, atomic transport and surface reaction mechanisms using stable isotope tracers 79−52448
metal, H_2-diffusion-rate-limited hydriding and dehydriding kinetics 80−35764
metal, oxidisable, DC reactive sputtering, glow discharge mass spectrometry and X-ray diffr. 79−38701
metal hydride, oxide, nitride prod. in electron diffr. camera 77−65937
metal melt, treatment by high-temp. gas stream, math. model, applic. to nitriding *(Russian)* 78−53016
metal oxides, nonstoichiometric, work function and near-surface chem. diffusion 80−80034
metal powder mixture with decomposing oxide, growth kinetics of surface film during annealing 79−96216
metal surface oxidation study, vacuum microbalance investigation 80−76552
metal surface treatment by ionic bombardment new technique *(French)* 77−77643
metal surfaces, characterisation by SIMS and XPS 79−16054
metal-gas interactions, kinetics and mechanisms, book contrib. 78−11558
metal-gas reactions, surface chemiluminesc. study 80−55708
metal-gas systems, surface reaction rate meas., resist. relax. method 79−66355

surface chemistry continued
metallic surface, catalysed thermal desorption and dissoc. processes, microscopic theory 80−75439
metals and alloys, sulphidation, high-temp., thermobalance for studying kinetics 78−23876
metals and alloys, sulphidation mechanism, review *(Polish)* 80−45413
metals in gaseous oxidative medium, reaction diffusion theory 79−20463
methane, chemisorption on Rh, vibr. excitation and surface reactivity 79−73393
methane prod. on electrodes of electrical arcs in ultra high vacuum 77−60065
methanol, chemisorption on Ni(111), methoxy species, electron energy-loss spectra 79−29391
methanol adsorption onto oxidised surface, oxidation by methanol *(Russian)* 79−51435
mineral surface interactions with organic solutes, groundwater vel. determ. 80−98492
minerals, surface reactions rel. to dissolution rate control under Earth surface conditions 79−20817
mischmetal-$Ni_{5-x}Al_x$ ternary alloys, Al addition effects on structural and H_2 absorpt. props. 79−52761
modulated mol. beam mass spectrometry, reaction prod. vector, surface reaction 77−63952
modulated molecular beam mass spectrometry, anal., appl. to nonlinear systems 78−56944
molecular beam reactive scatt. 77−24469
molecular metal clusters rel. to chemisorpt. and catalysis 77−76668
molecule-metal interaction and surface reactions, theoretical description 80−39652
molten metals, reaction rates, interface phenomena *(French)* 79−43632
Mossbauer spectroscopy applics. 77−12749
multivalent binding to substrate, linear differential equations in chemical equilibrium calculations 80−30279
neutron bottles, surface physics and chem. rel. to storage time anomaly 79−85575
neutron scattering techniques in applied research, medium-flux research reactors 79−13514
nitriding process, monitoring systems 79−52556
non-crystalline solid, surface and thin film chem. anal. techniques *(French)* 77−73495
oblating heat shield, Jupiter probe, C vaporisation into nonequilib. stagnation point boundary layer 79−1264
optical surface figuring by laser controlled chem. reactions 78−63209
organic compounds, field ionisation mass spectrometry, review 78−35763
organometallic decomposition by reaction with photoelectron, appl. to metal film deposition 80−71599
orientationally selective reaction, diffusion controlled effective reaction rate 79−16040
oscillating surface, thermal accommodation coeffs., translational and internal energy 77−86354
oscillations in surface reactions 79−47982
oxide surfaces, electron donor sites and acid-base props., adsorbed radical ESR 77−21417
particulate solid, reactions, viscous flow and Knudsen diffusion 77−4937
passivated and unpassivated surfaces, heat treatment effects 79−73383
phosphate glass, thermal expansion and chem. durability 77−80636
phospholipid vesicle walls, photosensitised electron transport 78−80787
photochemistry and photodesorption, isotope separation aspects 78−64863
pinacyanol sensitizer adsorbed on CdS, spectral sensitization at low surface density 79−47973
pitch weathering processes, IR multiple internal refl. obs. 79−74461
plasma etching, electron or ion bombardment, Ar^+ enhancement 79−82073
plasma magnetic confinement system, surface problems caused by dissolved H_2 80−57946
plastic foils for neutron dosimeters, electrochem. etching prep. techniques 79−76298
PMMA electron resists, molecular weight depend. of developed contours 79−87859
polyethylene, surface fluorination effects, internal refl. spectroscopy obs. 78−86340
polymer, degration, reaction product volatility effect on thermogravimetric anal. 80−104316
polymer carbons, water vapour adsorption, porosity, and surface chem. 79−52753
polymer film, formation, time-lapse IR spectroscopic obs. 79−74458
polymer surface, struct., bonding and reactivity, ESCA meas. 79−52073
polymer surface oxidation, LCAO-SCF calc. of core binding energies of O-containing organic mols. 79−76344
polymers, high-temp. pyrolysis, heat transfer processes at gas/solid surface *(Russian)* 80−61152
polypropylene, surface fluorination effects, internal refl. spectroscopy obs. 78−86340
polyvinylidene fluoride, chem. etching of fission tracks, growth of fine holes, TEM, SEM study 79−76297
porous oxide pellet, spherical, reduction by gas flow *(French)* 79−27713
porphyrin metallation, in monolayer films and assemblies 79−11817
Portland cement, hydration mechanism 78−35349
propane, radiative thermal cracking on porous glass *(Russian)* 79−39205
propiolic acid, adsorbed in thin film tunnel junctions, hydrogenation and deuteration, IETS obs. 80−45547
protein-substrate binding, linear differential equations in chemical equilibrium calculations 80−30279
pulmonary surfactant film, surface dilatational viscosity obs. 79−62278
pulsed differential reactors for kinetic study of the H_2S-alkaline minerals reaction in coal 79−20465
PVC, Cu evaporated film, electron-induced metallochromic reaction for metal image formation 80−86476
PVC, rigid plate, simultaneous diffusion and dechlorination in H_2SO_4 *(Japanese)* 77−52521
PVC surfaces, natural and stabilised, composition, ageing, oxidation and weathering, ESCA obs. *(French)* 80−61139
pyrocarbon, methane formation during p and d irrads. and thermal release of K 77−36788
quantitative analysis using ion-induced secondary ion and photon emission 77−86423
quartz, mechanically activated, reactivity *(German)* 79−29395
γ-quartz, reaction, with NaCl-kCl melt, exam. of struct., IR absorption spectra 80−55706

surface chemistry continued
quartz, theory of etching in HF 78−27666
quinoline, photooxidation on rutile, ESR and effects of surface states 79−66352
reactions, kinetics and dynamics, conf., La Jolla, CA, USA (Aug 1979) 80−105415
reactions in plasma generated near ferroelectric surface, obs. 78−68931
reactive polymers, for enzyme immobilised enzymes 79−29398
reactive solid exposed to step in surface temp., ignition 79−83458
reactivity of surfaces, exptl. techniques and appls., review *(French)* 79−92000
reactivity with Y_2O_3, exam. by thermal anal. 78−85154
refractory metals, gasification by atomic F, high temp. kinetics 78−53019
refractory solid/liquid reaction zones, electron probe micro analysis applic. *(French)* 77−32848
reinforced organic composite, graphite, or C-C, ablation, mathematical modelling 79−41564
reversible alloys, hydrogenation for H_2 storage *(French)* 79−74549
RF plasma utilisation in sputtering and surface reactions 78−84714
rheological props., terminology and symbols 80−26065
Rochelle salt, dehydration kinetics in ferroelec. and paraelec. phases, surface acoustic waves influence 80−97204
sapphire substrate for Nb and V highly-oriented films, surface chem. treatment 77−66097
segregation, effect on metallurgical props., SIMS, XPS and AES *(French)* 80−80045
semiconductor, direct conversion of chem. to elec. energy 80−66984
semiconductor, prereduced surfaces, room temp. activity for oxygen isotopic exchange 79−91998
semiconductor, tetrahedrally coordinated, review of surface struct., chem. and spectroscopy 80−59764
semiconductor crystal surface, nonequilib. electron effects due to chem. excitation 78−72238
semiconductor crystal surface, nonequilib. electron effects due to chem. excitation 78−72239
semiconductor metal interface, Schottky barrier, chemical reaction and charge redistrib. 78−95365
semiconductor surface physicochemical processes, ellipsometric installation 77−18071
semitransparent rotating disc electrode, photochem. and electrochem. surface reactions 78−40056
Si, complexing mechanism, effect of ion etch rate 79−70197
silica gel, IR spectra of dry transparent plates, surface struct. study 79−87884
silicate glass, hydration in steam atmosphere 80−85211
silicate glass surface, $Ca_3(PO_4)_2$ film form., bonding to bone 80−85212
silicide formation in thin layers of W or Mb *(German)* 80−7859
SIMS, appl. to surface reactions *(French)* 80−45603
single crystal surface, electrochemistry, surface struct., superlattice struct. 80−76519
solar energy utilisation, photoelectrochemical systems *(German)* 80−45713
solid surface, mol. dynamic processes interaction with laser radiation 80−71943
solid surface and thin film analysis by SIMS and AES 78−80825
solid surface fluorescence analysis, calibration curves 78−31719
solid surface monolayers, anal. by mass and energy spectrometry methods 77−56248
solid surfaces, surface processes, and solid/gas interactions 80−73125
solid-fluid reactions, law of additive reaction times 79−83453
solid-gas and solid-liquid interfaces, struct. rel. to reactivity 77−72775
solid-gas heterogeneous reaction, general kinetic eqn. *(French)* 78−92444
solid-gas reactions, existence of instabilities 80−7861
solid-gas surface reaction, nonequilibrium thermodynamic anal. 79−79285
solid-solid interface chemistry, characterisation, theory 80−75448
sols, primary and secondary coagulation and heterocoagulation, role of surface chemistry 80−45551
Spheron 6, surface group obs. using gaseous reagents, surface acidity evolution during heat treatments *(French)* 77−66767
spin combustion, mathematical model 79−29364
stable surface chemical reactions, interfacial hydrodynamic instability 80−66874
static AES technique, appls. 78−84685
steel, AISI 4340, subcrit. crack growth, fracture mech. and surface chemistry obs. 79−8392
steel, C, H attack kinetics and service behaviour 78−39951
steel, carbide layer form. in fused borax bath containing metals and metal chlorides or oxide powders *(Japanese)* 77−48684
steel, cold-rolled, good and bad paintability, AES, SEM and X-ray diffr. characterisation of surfaces 79−42344
steel, cold-rolled sheet, surface chemistry 80−61146
steel, complex carbide V-Nb-C layer form. in fused borax bath *(Japanese)* 77−56150
steel, ferrite-austenite transition, diffusion const. of C and carburisation rate consts., thermopower meas. 80−89216
steel, high-C, ShKh15, interaction with controlled atmospheres during annealing 77−44269
steel, hydrogen absorption, anilines surfactants effectiveness, HCl conc. effect 80−108638
steel, industrial, surface chem. characterisation by SIMS, glow discharge spectrometry and other techniques 80−66907
steel, mild, electrodes, in H_2SO_4, H evolution reaction kinetics 80−97630
steel, molten, deoxidised, reaction with oxidising gas bubbles 78−88438
steel, molten deoxidised, reaction with oxidising gas bubbles 78−84739
steel, plasma thermochemical treatment 79−94823
steel, sheet, type 08Kp, blackness degree rel. to heat treatment in controlled atms. 79−57165
steel, sphere, dissolution in H_2SO_4 in elec. field *(Russian)* 77−4867
steel, stainless, Cr-Ni-Mo, surface, scraping, mech. (electrolytic) polishing, ion etching, effects on ESCA 78−53037
steel, stainless, reduction of oxide layer by H atoms 80−40738
steel, stainless, stabilised with Cr-Ni-Nb, reaction with Te vapour 77−8986
steel, stainless, stress corrosion cracking in high temp. water, surface prep. effect 79−5088
steel, stainless, surface chem. rel. to metallurgical props., SIMS, XPS and AES *(French)* 80−80045

surface chemistry continued
steel, stainless, wear in dibenzyl disulphide-containing oil, X-ray photoelectron spectroscopy of surface chemistry 78−64736
steel, stainless Kh18N10T, surface treatment by plastic deform. effect on gas evolution and H_2 permeability *(Russian)* 79−15853
steel, superheated-steam oxidation, exam. of catalyst influence 78−85030
steel, type AISI 316, thermal passivation in controlled vacuum 80−76276
STEM use for two-dimensional molecular assemblies construction 78−24201
strontium alumoborosilicate glass, effect of vaporous and liq. Cs 77−44509
surfactant inhibition of electrochem. reaction rate, random error effect on characteristic parameters 80−40705
synchrotron radiation and sputter Auger techniques 78−61130
temperature programmed desorption with reaction 80−6621
tetrabenzo-[a,cd,j,lm]perylene thin films, high photoresponse, O_2, N_2 and SF_6 effects 77−32036
theory, aims and recent accomplishments 80−75413
thermal desorption mass spectroscopy, computer control, data acquisition, appls. 80−61181
thermal instability of vibr.-excited mol. gas, appl. to surface ignition *(Russian)* 78−56895
thermokinetics of H_2 generation from transition metal-H compounds 79−74421
thermosphere satellites, gas-surface reactions impact on N mass spectrometric meas. 79−66849
Tokamak discharge chamber, AES anal. *(Russian)* 79−4163
transition metal carbides, nitridation in NH_3 stream *(German)* 78−68928
transition metal sulphides, ion bombardment damage, XPS obs. 80−97404
transition metal surface reactions with N, 10^{-3} to 10^{-10} mbar, 77 to 370K, reactions 78−64889
transition metal surface reactions with O, 10^{-3} to 10^{-10} mbar, 77 to 370K, reactions 78−64889
transition metals, nitridation in NH_3 stream *(German)* 78−68928
transition metals, on Si, silicide form. at interface, interface marker technique obs. 80−59734
transition metals, reaction with gases, exam. of mech. and kinetics *(Russian)* 79−57289
transport and reaction, stochastic calcs. 80−108736
triboelectric charging process 79−78157
triboelectric charging technique for surface contamination analysis 80−11966
tunnelling spectroscopy, appls., review 78−92588
two-dimensional colloidal state concept and role in activity of solids 80−55704
water reaction with pyrolytic graphite surface 78−15707
wood, vapour phase reaction of 2,4-tolylenediisocyanate *(Japanese)* 77−77603
X-ray photoelectron spectrochem. quantitative analysis *(French)* 77−36836
zeolite-water desorption, complex reaction interphase boundary kinetics 79−57203
Zircaloy-4, heat treatment in SiO_2 capsules, vapour transport of Zr and Si 80−55437
γ-Al_2O_3, physisorption and reaction of $Mo(CO)_6$, IR spectra obs. 80−80064
Ag (110), adsorption, O_2-induced, and reaction of H_2, water, CO, and CO_2 80−55714
Ag (110), ethylene-O_2 interaction, LEED and AES obs. 80−89520
Ag (111), chemisorbed Rb struct., and NO reactivity on Rb-dosed Ag 79−28207
Ag, adsorption and surface reaction of formic acid 80−40741
Ag formation on Ag-halide surface, flash photolysis expts. on Ag halide photochromic glasses 79−94310
AgBr, (100) and (111) face, influence on aggregation of sensitising dyes 79−39202
Ag(I) reduction by tartrate in HN_3 solns. *(Russian)* 79−47976
AgI/RbI quasibinary system, solid state reactions and transport props. 80−96700
Ag(111) surface, dissociative chemisorpt. of S_2, surface layer struct. changes 79−42383
Al etching surfactant evaluation 77−77646
Al film+vitreous silica substrate, reaction 77−86380
Al, reaction with H_2, influence of surface reactions on rate *(Russian)* 80−66863
Al surface, oxidation, synchrotron radiation photoelectron obs. 78−52634
Al surface hydrous, oxide film formation 78−15602
Al-C-silaceous sand mixture in N_2 atmos., weight loss during heating, compaction *(Japanese)* 80−35151
Al-Cu, type 2219-T851, fracture mechanics and surface chemistry of fatigue crack growth 80−81168
Al-Mg (7 wt.%), bare surface reaction rates in aq. solns. 80−101022
Al-SiO_2, film system, kinetics of interaction 77−44459
Al-SiO_2, reactions and wetting behaviour 77−15664
Al-SiO_2, surface reactions and interdiffusion, photoemission study 80−49532
Al+H_3PO_4, porous anodic films nucleation and growth 78−44273
Al+NO_3^-, reactions between metal and aq. nitrate solns., XPS 77−12825
Al_xCy, on diamond 77−72758
$Al_2Ge_2O_7$ reduction by C, gaseous and metallic Ge yields *(Russian)* 80−40737
Al_2O_3, mass spectroscopic investig. of chem. reactions between adsorbed species 77−40600
γ-Al_2O_3, OH layer, IR spectra, outgassing temp. effects 80−66175
η-Al_2O_3 outgassed at 400, 650°C, heat of adsorpt. of pyridines from soln., surface acidity 80−61154
Al_2O_3, pure and SiO_2 coated, surface props., catalytic activity 79−79287
η-Al_2O_3, surface, laser Raman fluoresc. background, OH^- excitation 78−10875
Al_2O_3, surface microstructural changes due to reduction by C *(Russian)* 80−100378
Al_2O_3/CuO, thin film interaction, $CuAl_2O_4$ form. *(Russian)* 78−52697
Al_2O_3+W interaction, 2200 to 3200°C *(Russian)* 79−39194
Al-AlOOH, disapore, superstructure form. on dehydration, electron microscopy obs. 80−3327
Al(100) oxidised surface structure anal., extented appearance potential fine struct. study. 80−75411

surface chemistry continued
As_2S_3 films, kinetics of light-enhanced vaporisation rel. to photocond. 77−84919
Au films on Si substrate, solid-solid reactions 78−95369
Au surface, clean, hydrophilic nature 80−80029
Au/Ti thin films, effect of Cl_2 on elec. resistance, Ti atom migration and preferred orientation 80−34530
Au-Pb-In solder joints, layer growth, ageing 77−32764
B_4C, reaction kinetics with liq. Al, Si, Ni and Fe 80−84344
B_4C-Ti(V)(Cr), contact reaction with liq. Ni 80−55707
B_2O_3 containing glasses, wetting and reactions on Pt, effect of C and water 77−7951
BP+$N_2(NH_3)$ 79−43627
Ba films, chemisorptive luminescence systems for surface reaction obs. 78−7236
Ba getter film, initial reaction probability with O_2, water, CO and CO_2, AES obs. 80−61153
BaF_2, formation and growth of oxidation centres result of O^{2-} diffusion 80−7706
Bi, molybdates on SiO_2, EPR *(French)* 78−64271
C black, acidic surface oxides, struct. investigation using diazomethane 79−52404
C black, surface S-containing group complexing 78−68920
C blacks, surface polarity, surface activity, slurry pH, oxidation effects 78−68915
C fibres, PAN-based, surface charcts., investig. by flow microcalorimetry 78−48694
C film, oxidation, IR spectroscopic study 79−96162
C particles growth, during hydrocarbon pyrolysis 79−91919
C polymer chars, associated O_2 and H_2 78−11551
C, surface groups, acidimetry, formation of derivatives 78−68918
C, surface groups, spectroscopy 78−68919
C target, O^+ low energy ions, interaction obs. 79−34352
CF_x, exam. of graphite fluorination kinetics, meas. of activation energy, reaction rate 79−96284
CO, adsorbed on Pd (111) surface, catalytic oxidation, mol. beam investig. 78−88656
CO, catalytic oxidation on Pt, CO_2 product vel. and ang. distribs. 78−20065
CO, catalytic oxidation on ferrites, IR spectrosc. investig. 80−89524
CO, chemisorbed on metals, electronic struct., vibr. spectra, and chem. 79−42390
CO, chemisorpt., surface struct. chemistry and electron impact props. on Rh(110) 78−6225
CO, hydrogenation on Fe foil, AES and XPS study 80−7858
CO, influence on N absorpt. in plasma melting of steel *(Russian)* 79−39193
CO, on CoO, catalytic oxidation 80−71945
CO oscillatory oxidation over Pt, theory 80−85215
CO oscillatory oxidation over Pt, theory 80−85216
CO oxidation on Pt, AC pulsing technique 79−100439
CO photodesorption from metal, forming CO_2 79−52777
CO, reactions with NO over Rh flash desorption spectra, titration, reaction kinetic calcs. 78−61045
CO, titration of pre-adsorbed O on Ir (111), XPS investigation 79−91994
CO+N_2O catalytic reaction on Sc_2O_3 and MgO, kinetic obs. 79−29389
CO+O, adsorbed on Ir (111), Langmuir-Hinshelwood reaction mechanism 79−29408
CO+O on Rh surface, Langmuir-Henshelwood reaction 79−47965
CO+O_2, chemisorbed on Ru(001), electron energy loss spectra 79−46924
CO+O_2 on Ag (111) ordered and damaged surfaces 78−14583
Ca-Mg-Ni-B, hydriding behaviour 80−71942
$Ca_3Al_2O_6$, retardation of hydration by sulphates 77−56249
CaO+CO_2→$CaCO_3$, reaction kinetics, effect of temp. and CO_2 press. 80−45552
Ca_2O:Bi, positive ion nonequilibrium emission in heterogeneous chemical reaction, mass spectra 80−55277
$CaSO_4.{}^1/_2H_2O$, (α and β-phase), surface chem. and porosity 78−85200
CdO_2, catalyst on isopropanol, surface active sites during dehydrogenation 79−43621
CdS-metal interface, chemical reactions and local charge redistrib. 79−19661
CdSe-metal interface, chemical reactions and local charge redistrib. 79−19661
Cl_2, interaction with H_2SO_4 and water, surface reactions at low temps. 79−79288
Co (0001), adsorption and reactivity of NO, LEED, AES, and thermal desorption study 80−80090
Co, adsorption-desorption kinetics of CO, surface carbide form. effects 80−103574
Co-Al_2O_3 catalysts, reducing and sulphiding treatments, XPS obs. 78−85196
Co-Ni, selective catalytic surface behaviour, tight-binding approx. calcs. 78−76924
Co_2-rare earths, H_2 reaction, thermal anal. 79−100434
$CoFe_2O_4$, thermally induced surface chemistry and struct., XPS 78−22939
CoO+H_2S, sulphurisation of (100) face, low-press. *(French)* 79−52754
Co_3O_4 MOS device, detection of CO 78−76908
Co_3O_4-H_2, interaction with surface, quantum chemical study 80−45549
Cr, CVD on Ni, reaction mechanism, growth rate and struct. obs. 80−39476
Cr, oxidation, Cr-O bonding, characterisation by high resolution AES *(French)* 79−100468
Cr particle nitrogenation, metallographic obs. *(Bulgarian)* 78−15712
Cr surface reactive, field ion microscope and atom probe obs. 79−29410
Cr-Ni steel, austenitic, effect of Si on carburising mechanism at 930°C 77−56155
Cr_2O_3 dissociation in presence of C in Ar, CO and vac. atm., Cr_3C_2 form. *(Russian)* 80−35570
Cr_2O_3-H_2, interaction with surface, quantum chemical study 80−45549
Cu (100), adsorbed formate and acetate species, EELS study 80−76120
Cu (100), chemisorption and decomp. of formic acid, EELS study 80−16729
Cu (100) reaction with ethanol and methanol, EELS study 80−16728
Cu (100) surface, interaction with O_2, AES, EELS, LEED and work function studies 80−24731
Cu (111), hydroxylation and dehydroxylation, XPS obs. 80−7850
Cu (111), partially Cs covered, oxidation effect on UPS 79−78826

surface chemistry continued
Cu, adsorption and surface reaction of formic acid 80−40741
Cu surface, interacting mechanisms with organic sulphides rel. to friction and lubrication behaviour 80−45546
Cu, surface film of 2-mercaptobenzothiazole and 2-mercaptobenzimidazole, XPS and X-ray induced Auger spectra obs. 80−40600
Cu-Ag, surface segregation of S, Auger spectral study diffusion 80−76549
Cu-Fe (0.2 at.%), surface oxidation, Mossbauer obs. 80−55564
$Cu+NO_2$, relative humidity depend. 79−5176
$CuFe_2O_4$, thermally induced surface chemistry and struct., XPS 78−22939
Cu(110), adsorption of O_2 and its reaction with CO 80−15373
D exchange reaction between H_2 and water a hydrophobic catalyst supporting Pt 80−30208
D_2+H_2O, isotope exchange on Pt over hydrophobic support 79−11823
D_2+H_2O, isotope exchange on Pt, CO poisoning effects 79−11824
Er, film, reaction with H_2O vapour, spectroscopic and X-ray diffr. obs. 77−40575
Er powder, hydride form. under water vap. 79−91997
ErD_2, thin film, reaction with H_2O vapour, spectroscopic and X-ray diffr. obs. 77−40575
ErT_2, film, surface oxide form. and interfacial metal loss, AAS, XES 78−31733
$EsCl_2(Br_2)(I_2)$, prep., characterisation and decay of Es(II) 80−16727
EuTe, high-temperature evaporation and reactivity 80−103469
$F+SiO_2$, heterogeneous reaction, discharge-flow tube meas. 80−21274
Fe (110) surface, adsorption and decomposition of NH_3, identification of surface species using SIMS 79−90862
Fe, adsorbed S effects on surface reaction kinetics and surface self-diffusion 78−7234
Fe, adsorption, segregation and reactions of non-metal atoms, LEED and AES obs. 80−59783
Fe, adsorption and surface reaction of formic acid 80−40741
Fe, carburization, methane gas→C(dissolved)+$2H_2$ (gas), kinetics 80−55712
Fe dissolution kinetics, and passivation depend. on temp. and ionic strength 80−97626
Fe, evaporated, adsorbed acetylacetone, XPS study 80−76133
Fe, free surface and grain boundary O_2 and S chemistry 80−75410
γ-Fe, kinetics of carburisation in CO-He and CO-H_2 atmospheres at 920°C *(German)* 78−85024
Fe liquid, C saturated, decarburization by CO_2, effect of S 79−11726
Fe, oxidation at 300°C 79−61792
Fe, pure circular disc electrodes in (Na, H)ClO_4 solns., complex formation meas. 80−55569
Fe surface, form. and decomp. of nitrides 79−24831
Fe surface, interacting mechanisms with organic sulphides rel. to friction and lubrication behaviour 80−45546
Fe surface, nitride layer formation, activated surface, passivation 80−16577
Fe:C, decarburisation by H_2, conversion electron Mossbauer obs. 78−85198
Fe-Al (up to 7.2%), oxidation process 78−85022
Fe-Cr, surface and bulk alloys, oxidation at 300°C 79−61792
Fe-Ni, carburization, methane gas→C(dissolved)+$2H_2$ (gas), kinetics 80−55712
Fe-Ni alloy, fluorination kinetics and fluoride film form., chem. nature obs. 80−101035
Fe-Si layer, growth kinetics and morphology 78−95700
Fe-Zn system, Zn vapour interaction with solid Fe, Zn chem. potential effect on interaction layers 78−11416
$Fe+H_2O$, clean surface oxidation and passivation by vapour, XPS, FeOOH formation 77−81424
Fe_2-rare earths, H_2 reaction, thermal anal. 79−100434
FeO surface, water-gas shift reaction kinetics 80−11949
α-Fe_2O_3, reduction to active magnetite and direct air oxidation to α-Fe_3O_4 *(German)* 78−7060
Fe_2O_3:Mn, surface props. 79−65302
Fe_2O_3-H_2, interaction with surface, quantum chemical study 80−45549
Fe_3O_4-$FeAl_2O_4$-$FeTiO_3$ titaniferous magnetite, chlorination, 1273 to 2273K 80−55752
α- FeOOH, goethite, surface OH groups, D_2O isotopic exchange, IR investig. 80−2254
α-FeOOh, goethite, superstructure form. on dehydration, electron microscopy obs. 80−3327
FeS_2, oxidation, Mossbauer spectroscopic and magnetokinetic studies, 400-500°C 80−44880
FeTi, surface segregation, catalytic effect on hydrogenation 80−45814
GaAs (110) surface oxidation process, XPS study 79−15585
GaAs, CO(O_2) interactions, surface electronic struct. (surface chem.) using synchrotron radiation 78−53254
GaAs film, RF sputtered, ESCA, surface chemistry suitability for photovolt. appl. 80−7476
GaAs, impurity distribs. by chemical methods 77−43237
GaAs, nitridation, following oxidation, surface and contact props. of GaN produced 77−20436
GaAs, surface chemistry and electronic struct., adsorption of O_2, photoemission meas. 77−20985
GaAs-Al interfaces, chemically induced charge redistrib. 79−33342
GaAs-Al(Ga)(Ge), surface reactions and interdiffusion, photoemission study 80−49532
GaN on Si, form. with GaCl-NH_3-H_2(He), ESCA and RHEED meas. 79−90909
GaP (110) surface oxidation process, XPS study 79−15585
GaP:Cs-O simultaneous adsorption, oxidation interface chemical struct. 80−103584
GaSb, surface chemistry and electronic struct., adsorption of O_2, photoemission meas. 77−20985
Gd film, hydride form. under water vap. 79−91997
Ge, chemomagnetic effect, elec. cond. change due to surface recomb. of H atoms 77−8086
Ge, formation of sulphide layers in S vapour 79−7757
Ge, monocryst., reaction with S vapour, applicability of Kossel's crystal model 79−87833
$Ge+Br_2$, heterogeneous photochem. reaction kinetics, laser radiation intensity effect 79−66326
$Ge+Br_2$, rate-limiting step, ellipsometric and photochem. meas. 80−16730

surface chemistry continued
$Ge+GeBr_4$, single crystal+vapour system, reaction kinetics and laws of soln., heat of adsorption 79−39196
GeS layers form. on Ge surface, S_2 vapour press. rel. to growth rate 79−43152
H+C, surface chemical reaction of thermal at. H 78−20071
H_2, ortho⇌para conversion, on CoO, MnO mag. surfaces 79−47969
H_2+D_2, exchange reaction, steady-state, surface reaction effects *(French)* 78−85148
H_2+D_2, exchange reaction, gas phase, heterogeneous initiation *(French)* 78−85149
H_2+D_2 exchange reaction, on Pt(111) or (332) surface, mol. beam obs. 79−66269
H_2+D_2→2HD on stepped Pt surface, selective adsorption effect 78−20066
H_2+Fe(001), gas-surface reactions, semiempirical generalised LEPS pot. 78−68923
H_2+N_2O, HO radical form. on Pt surface, laser-induced fluoresc. obs. 80−108738
H_2+O_2, adsorbed on Pt (111), reaction kinetics 77−55461
H_2+O_2, adsorbed on Pt particles supported on SiO_2 gel, low press. reaction 77−52668
H_2+O_2, chemisorbed on Pt, Pt-Au and Ni (100) surfaces, UPS investig. 77−51600
H_2+O_2, on Pd (111), mol. beam relax. and isotopic exchange meas. 80−35575
H_2+O_2 on polycryst. Ni surface, SIMS and thermal desorption meas. 80−40742
HD, dissociative adsorption on Re surface 79−86987
HI-H_2-I_2, H_2 separation in thermogravitational column 80−45561
H_2O+CO_2, photoassisted reaction on $SrTiO_3$ (111) face, methane form. 78−76878
H_2SO_4 bulk surfaces, reactions with atmospheric species rel. to aerosols role as tropospheric sinks 80−72612
Hf, decomp. of hydrocarbons, O or N surface segregation effects 80−55654
$HgCl_2$, reaction on metallic Cu, reaction velocities, effect of neutral salt addition 78−64887
I_2 surface chemi-ionisation by Rb_2 beam 78−7231
InAs, thermal oxidation, growth rate and chem. comp., temp. depend. 80−108619
n-InP, epitaxial layer, (100) surface chemistry, ESCA study 80−103552
InP, surface chemistry and electronic struct., adsorption of O_2, photoemission meas. 77−20985
InSb (110) surface oxidation process, XPS study 79−15585
Ir, (100) and (111) surfaces, chemisorptive bonding and reaction of NO, UPS obs. 77−72786
Ir (110), adsorption of CO and reaction with O_2, transient study 80−30284
Ir, (111) surface, flash desorption spectra of NO, recombined mol. identification 79−86996
Ir, adsorption of H_2 and O_2, surface reaction, thermal desorption and FEM obs. 79−52774
Ir film, CO oxidation, IR absorpt. spectroscopy 80−71398
Ir(100), chemisorpt. and reaction of acetylene, ethylene and benzene, geometric and electronic effects 77−21421
K, Na, superthermal neutral beams impact on W surface, stimulated chemical reaction 77−9123
K_2O glasses, partially leached, dehydrated surface reaction with water 80−3406
LaB_6 cathodes, residual gas poisoning in vac. system, thermionic emission decay 78−27364
$LaNi_5$, H storage using metal hydrides, self restoring of active surface 80−45815
$LaNi_5$, self restoring of active surface, photoemission, mag. susceptibility study 78−48280
$LaNi_5+3H_2$⇄$LaNi_5H_6$ reaction, absorpt. capacity and reaction kinetics 79−43626
$LaNi_{5-x}Al_x$, ternary alloys, Al addition effects on structural and H_2 absorpt. props. 79−52761
Li, adsorption of methyl groups, complex form., STO calcs. 77−9124
Li, surface characterization of film growth 80−81240
LiH, effect of surface hydrolysis to LiOH on IR absorption, X-ray luminesc. and EPR spectra 80−60660
LiH+Te exothermic solid-state reaction, ion backscatt. obs. 78−20064
LiO_2, reactions with Mo in fusion blanket feasibility tests 80−26055
Li_7Pb_2, fusion reactor breeding material, reaction with H_2O 80−13830
Mg films, chemisorptive luminescence systems for surface reaction obs. 78−7236
Mg nitridation in HF discharge, temp. effect 80−3399
Mg, surface nitridation in N_2 DC glow discharge, 0.3-5 torr, mechanism 78−3370
Mg/Mg_2Cu eutectic, hydriding and dehydriding kinetics obs. by press. sweep method 80−35765
Mg-noble metal alloy, sintered, supercorroding for heat and H_2 gas generation, seawater reaction 78−15607
MgO, catalytic behaviour, rel. to XPS obs. 79−24820
MgO, dissolution mechanism in acids 80−39296
MgO, irrad., effects, O_3^- ion form. 79−100431
MgO, surface, laser Raman fluoresc. background, OH^- excitation 78−10875
MgO, vaporization in O_2-H_2O atmos. *(Japanese)* 79−74279
MnO, reduction by C, surface reactions, CO regeneration *(Russian)* 80−66772
MnO-H_2, interaction with surface, quantum chemical study 80−45549
Mn_3O_4 film, form. on glass surface from Mn^{2+} ions in water *(Japanese)* 80−45411
Mo (111) planes, adsorption of NH_3, preferential nitriding, FEM study 80−66877
Mo film, carbonisation and oxidation, electron diffr. exam. *(Russian)* 77−44399
Mo, interaction with gases, H_2, N_2, O_2, CO, water vapour and hydrocarbons *(German)* 79−74296
Mo, sulphidation, cryst. of MoS_2 77−52539
Mo-Al_2O_3, catalysts, reducing and sulphiding treatments, XPS obs. 78−85196
Mo-Si diffusion couples, $MoSi_2$ or Mo_3Si/Mo_5Si_3 form. 79−77836
$Mo+H_2S$→MoS_2 78−3078
MoF_6 reduction by H, chemical kinetics eqn., adsorbed component interactions *(Russian)* 80−35569
MoO_3-TiO_2, reduction, Mo^{5+} and O_2^- form. 77−90590

surface chemistry continued
MoS_2 on Mo, sulphate coating growth kinetics and mechanism 77−86220
Mo(100), chemisorpt. of O_2, low-energy SIMS, ion yields depend. on surface chem. and primary ion energy 78−73105
N_2 fixation using fusion energy heat source 80−32510
N_2^+ + first row transition metal surface reactions 79−96363
N_2^+ + Group IV elements and oxides, XPS and UPS prod. determ. 78−73084
NH_3, decomposition by Re filament at low press. above 500K 79−61906
NH_3, decomposition kinetics on single cryst. planes of Pt 77−1948
NH_3 on Pt surface, heterogeneous reaction of decomp., stimulation by CO_2 laser 78−61052
N_2H_4, dissociative adsorption on Fe(111) 79−46956
NO, adsorbed on Cu, species identification, struct., dissoc. chemisorption, desorption, UV photoelectron spectroscopy 78−52635
NO, adsorbed on Ru (001), inelastic electron scatt. dissoc. energies adsorbed state depend. 78−95956
NO+CO, on polycrystalline Pt at low press., reaction kinetics study *(German)* 79−15988
NO+CO, on polycrystalline Pt surface at low press., reaction kinetics study *(German)* 79−15989
NO_2 on Cu, ultrahigh vacuum ESR studies 80−97729
N_2O, chemisorbed on Cu (111), decomposition probability 79−65317
$NO_2(N_2O_4)$ surface decomposition, resonance and spontaneous Raman spectra 80−61144
NaCl-kCl melt, reaction with LiO_2-$2SiO_2$ X-ray, IR exam. 80−55706
Na_2O glasses, partially leached, dehydrated surface reaction with water 80−3406
Na_2O-Al_2O_3-SiO_2 glass, leaching in HCl solns., Na conc. distrib. in surface layers 80−21141
Nb electrode, surface changes induced by strong cathodic polarisation 79−100388
Nb film, ion bombardment with N_2^+, Ar^+, struct. changes, chemical compound formation *(Russian)* 78−95084
Nb, interaction with gases, H_2, N_2, O_2, CO, water vapour and hydrocarbons *(German)* 79−74296
Nb-H system, enthalpy and entropy changes for non-stoichiometric hydride formation 79−52741
Nb+O_2, high temp. interaction kinetics and mechanism 79−100432
NbC_x+Be→Be_2C layer, limiting stage investig. 77−36786
Ni (100), chemisorption and decomp. of formic acid -d_1 79−34361
Ni (100), interaction of adsorbed H_2, CO, and methanol, temp. programmed desorption study 80−66876
Ni (100), kinetics of C deposition from adsorbed CO 80−76553
Ni (111), dehydrogenated adsorption of ethylene, thermal desorption and AES study 80−29274
Ni, B-containing diffusion layer formation *(Russian)* 77−48570
Ni, B-containing multicomponent diffusion layer formation *(Russian)* 77−44400
Ni, corrosion, high temp., SO_4 induced, studied at 900°C in O_2+4.2% SO_2 80−97639
Ni, evaporated, adsorbed acetylacetone, XPS study 80−76133
Ni film, vacuum-deposited, ethylene adsorption and reactivity with adsorbed H, surface pot. meas. 79−86995
Ni films, adsorption and decomp. of ethylene, coverage depend. meas. 80−96743
Ni, pack aluminisation process kinetics 77−32718
Ni, passive film, XPS study 79−100469
Ni, reaction with CO_2 interfacial kinetics, $^{14}CO_2$-CO exchange reaction, S effect 79−47978
Ni, role of adsorbed S in dissolution and passivation 79−66340
Ni, sulphidation in H_2S-H_2 mixtures, 450-600°C 78−3257
Ni, sulphidation kinetics, in H_2S-H_2 550 to 600°C 78−64780
Ni surface, stepped, acetylene dehydrogenation 79−52752
Ni/Al_2O_3 catalysts, coprecipitated methanation type, metal-support interaction, XPS obs. 80−80936
Ni-Cr alloy, phosphidation in P vapour, 700°C, phosphide layer struct. and kinetics 80−25906
Ni-Fe, (100) surface, O interaction, Fe segregation, LEED and XPS studies 79−82437
Ni-P, electroless deposition on Al, X-ray and SEM obs. 79−90907
Ni-S, role of adsorbed S in dissolution and passivation 79−66340
Ni-Si-B powder, oxidation at 850°C, SEM, ESCA, and elec. cond. meas. 80−7717
Ni^{2+} + MoO_3 catalyst on Al_2O_3, Raman spectrum 80−108742
Ni_2-rare earths, H_2 reaction, thermal anal. 79−100434
Ni_3C films, on graphite, thermal decomp., AES lineshape study 79−79293
$Ni(CO)_4$, form. on single Ni cryst., reaction kinetics and induced surface facetting 80−71948
$Ni(CO)_4$, form. reaction rate, substrate mag. phase depend. 80−108737
$Ni_{1-x}Cu_x$+CO, $Ni(CO)_4$ form. activation energy, mag. phase depend. 80−3409
$NiFe_2O_4$, thermally induced surface chemistry and struct., XPS 78−22939
NiO (100) surface, sulphurisation by H_2S, AES, LEED, RHEED structural study *(French)* 78−64888
NiO, (100) surface interaction with SO_2, electron diffr. and Auger spectrosc. obs. *(French)* 80−97728
NiO, doped and undoped, elec. props. and surface charact. 80−65571
NiO, nonstoichiometric, near-surface and bulk chem. diffusion 80−80035
NiO-Al_2O_3 reaction at film-substrate interface, Rutherford backscatt. obs. 80−59733
NiO-H_2, interaction with surface, quantum chemical study 80−45549
$Ni_{1-x}S$, oxidation, TG/DTA/MS obs. 78−31745
Ni_xS_y, interaction with Pd *(Russian)* 79−52758
Ni(001), reaction of CO and H_2, extended muffin-tin orbital theory 80−76557
Ni(100) oxidised surface structure anal., extented appearance potential fine struct. study. 80−75411
Ni(111), coadsorption of CO and H_2, surface carbide influence, vibr. electron energy loss obs. 79−52772
O_2 adsorbed on Cu (110) surface reaction with CO, ellipsometry, AES, LEED study 80−6635
O_2, chemisorbed on Cu (111), decomposition probability 79−65317
Pb (100) and (110) surfaces, oxidation and sulphidation, LEED and XPS obs. 78−20070
Pb electrode, in situ surface phase study by laser Raman spectroscopy 80−103542
Pb, sphere, dissolution in H_2SO_4 in elec. field *(Russian)* 77−4867

surface chemistry continued
PbSe surface, clean and O_2-exposed, XPS (UPS) obs., electronic struct. 78−52637
$Pb_{1-x}Sn_xTe$ anodic oxide film form. conditions, IR absorpt. spectra 80−11494
$Pb_{1-x}Sn_xTe$ IR detector, ESCA, surface chem. and leakage current correl. 77−20402
Pd (111), scattering, adsorption, and absorpt. of H_2 and D_2, mol. beam study 80−29277
Pd, chemisorption and decomp. reactions of O containing organic mols., UPS 77−63953
Pd film, vacuum-deposited, ethylene adsorption and reactivity with adsorbed H, surface pot. meas. 79−86995
Pd surface chemical reactions using MOS structure 77−73470
Pd-H system, enthalpy and entropy changes for non-stoichiometric hydride formation 79−52741
Pd+MgO, reaction and bonding, below MP of starting materials, obs. in TEM 77−21419
Pd+SiO_2, reaction and bonding, below MP of starting materials, obs. in TEM 77−21419
Pt (110), acetylene adsorption, desorption and surface dissoc. 77−62749
Pt (111), surface reaction with acetylene ethylene, and H_2, EELS 78−71947
Pt, adsorption and decomp. of ethylene, 90 to 500K 79−46933
Pt, adsorption of O_2 on (110) surface, Ar^+ bombardment effects on reactivity 80−89099
Pt, adsorption of water, H_2 and reaction between H_2 and adsorbed O 80−49514
Pt, $CO(O_2)$ interactions, surface electronic struct. (surface chem.) using synchrotron radiation 78−53254
Pt catalyst surface morphology, faceting induced by NH_3 and propane oxidation 77−52669
Pt film, vacuum-deposited, ethylene adsorption and reactivity with adsorbed H, surface pot. meas. 79−86995
Pt on C, crystallite behaviour on sintering 78−7235
Pt oxidation, XPS spectra study 80−3254
Pt, polycryst. wire, multilayer surface oxidation 78−88579
Pt, surface area loss, on graphite support, in H_3PO_4 78−73076
Pt target, O^+ low energy ions, interaction obs. 79−34352
Pt-Rh alloys, surface behaviour on heating in air, XPS and SIMS *(French)* 77−40327
PtAl, form. in hollow cathode discharge, emission spectrum obs. 78−27819
PtD, form. in hollow cathode discharge, emission spectrum obs. 78−27819
PtH, form. in hollow cathode discharge, emission spectrum obs. 78−27819
Pt(IV), reduction to Pt(II), X-ray irrad., Ar ion bombardment, XPS obs. 80−35573
PtO, form. in hollow cathode discharge, emission spectrum obs. 78−27819
Pu, oxidation, binding energies, Auger and X-ray photoelectron spectra study 80−76550
Pu-Ga (1 wt.%), alloy powder, hydriding kinetics 80−76503
Re, adsorption, oxidation, and hydrogenation of CO, XPS, UPS, and thermal desorption study 80−71571
Re, O_2 and CO isotope exchange reactions 77−70338
Re surface, interaction with N_2^+ beam, reaction dynamics studied by XPS and thermal desorpt. spectrometry 80−93797
Re-O-Cl system, gas-transition metal interaction, kinetic model *(French)* 80−108740
Rh/Al_2O_3 catalysts, surface interaction between NO and CO, IR study 79−70369
Ru ($10\bar{1}0$) surface, oxide form., thermal desorption and ESCA obs. 79−82442
Ru (101), chemisorption of O_2, CO+O_2 interaction 77−73471
Ru (110), kinetics of C deposition from adsorbed CO 80−76553
Ru (110), methanol reaction, thermal desorpt. meas. 78−31685
Ru electrodes, adsorption and surface reactions, cyclic voltammetry and X-ray emission spectrometry 78−61018
Ru electrodes, reversibility and growth behaviour of surface oxide films 79−20263
RuO_2, catalyst on isopropanol surface active sites during dehydrogenation 79−43621
Ru(110), adsorption of H_2S, H_2, and S, evidence for SH species 79−99424
S interstellar molecule formation, ion reactions at grain surfaces 80−101632
S surface, ethylene episulphide form. by laser irrad. in presence of ethylene 79−57258
S^- ion-selective electrode, sensitivity, surface heterogeneity effects 78−92526
SF_6+Si(surface), IR laser induced reaction, mol. vibr. and mol. dissoc. obs. 80−93798
SO_2, heterogeneous conversion to SO_4^{2-}, rel. to urban air pollution 78−80789
SO_2 surface reaction and decomposition on zeolites, resonance Raman study 80−61145
ScD_2, surface, interactions with reactive gases 78−23964
Si (111), surface reaction with acetylene and NH_3, 1225 to 1380°C 79−100441
Si, amorphous, hydrogenation using DC and HF plasma treatment 80−59497
Si and its cpds., chemical aspects of fluorocarbon plasma etching 79−83350
Si, CF_3^+ ion bombardment, XPS and Auger study 79−70367
Si, CVD, gas phase diffusion and surface reactions 79−15614
Si, chemisorption of XeF_2 and SiF_4, XPS and Auger spectra, surface chemistry 80−81358
Si deposition by SiH_4 pyrolysis at low temps. and atm. press. 79−91595
Si, dry etching induced surface contamination, SIMS, AES, and XPS obs. 80−11810
Si, early oxidation stages, AES study *(French)* 79−8379
Si, laser induced formation of metal silicides 79−70366
Si, laser induced reactions with metal films, silicide formation 79−70365
Si, multigrained, grain boundary elec. and compositional props., surface anal. 80−76575
Si n-p planar diode, Al layer covered, laser beam produced alloy areas, characterisation 79−69594
Si, nitridation, effects of Fe and Al additions 77−16708
Si, powder, effect of Fe and $FeSi_2$ on nitriding 79−33985

surface chemistry continued
Si powder, nitriding *(German)* 79−74414
Si, reactivity with organic nitrogen compound, rel. to polishing *(Russian)* 79−70192
Si, solubility and transport behaviour of water, dissolution 80−93801
Si surface electron beam deposited silicide formation using scanning CW laser beam 80−66862
Si, thermal oxidation in O_2-trichloroethylene mixture, 900, 1000 and 1100°C 80−3221
Si-containing films, formed by reaction of Si with organic compounds of N, struct. investigation 79−87009
Si-metal thin film reactions, laser annealing 79−70364
Si-SiO_2 system, structural defect formation rel. to thermal oxidation kinetics *(Russian)* 78−43478
$Si+2XeF_2 \rightarrow SiF_4+2Xe$, surface reaction, IR chemiluminesc. 79−83504
Si+H, solid surface and low-press. plasma, reactivity 79−47968
Si+metal oxides, spray coated, IR investig. 79−39197
$Si+NH_3$, surface nitride form., XPS excited by Zr Mζ radiation 80−40236
$Si+XeF_2(F_2)(Cl_2)$ plasma etching, electron or ion bombardment, Ar^+ enhancement 79−82073
SiC-fission product isothermal rections in HGTR TRISO UC_2 and UC_xO_y 80−42744
SiC-fission product reaction kinetics in HTGR TRISO UC_2 and UC_xO_y fuel in thermal gradient 80−47570
Si_3N_4, nitriding *(German)* 79−74414
Si_3N_4, reaction-bonded, internal oxidation processes role in high-temp. mech. props. 79−38915
$Si_3N_4+XeF_2(Cl_2)(F_2)$, plasma etching, electron or ion bombardment, Ar^+ enhancement 79−82073
SiO_2, adsorption of H_2O, surface treatment and methylation effects 78−84058
SiO_2, dry etching induced surface contamination, SIMS, AES, and XPS obs. 80−11810
SiO_2, HF vapour phase etching, prod. viability for semicond. manufacturing and reaction model 80−81219
SiO_2, on Si, reduction by heating in Ga mol. beam at 800°C 80−50730
SiO_2, surface, NH_2 photodissoc., rate, mechanism *(Russian)* 78−53233
SiO_2, surface reactivity modification by Ar/O_2 plasma treatment 78−64890
SiO_2 surface reactivity with water and acid mols. *(French)* 79−79284
SiO_2, vaporisation in steam atmosphere 80−44306
SiO_2, vitreous, H impregnated, γ radiation effects, hydride, hydroxyl formation 79−87874
SiO_2, vitreous, hydroxyl free, reaction with H, diffusion, absorpt. spectra 80−85210
SiO_2/InP interface formation, thermodynamic considerations 80−100529
SiO_2+H_2 reactions, rate controlling processes for H_2 transport in vitreous silica 78−26733
Si_2Te_3 surface reaction, AES exam. 78−63931
Si(111) and (100), reaction of ethylene at high temp., crit. conditions for SiC growth 79−47981
$SmCo_5$ hydriding kinetics, inverse over pressure effect 80−55944
$SmCo_5$ thin film, hydride form., kinetics, mag. monitoring 80−35571
SnO_2, reduction by C 79−61901
SnTe substrate, Ag epitaxial growth and topostactic exchanges 78−14640
$SrSO_4$, activation energies for mass transfer during crystallisation, surface active agent effects *(German)* 78−63689
$SrTiO_3$ surface, oxidation and reduction by D_2O, $H_2{}^{18}O$, D_2, isotope exchange study 80−104461
$SrTiO_3$ surface, photosensitizer for water photoassisted decomp. 80−85202
Ta auto-cathodes, effect of O_2 on emission and surface diffusion *(Russian)* 79−77892
Ta, decomp. of hydrocarbons, O or N surface segregation effects 80−55654
Ta film, ion bombardment with $N_2{}^+$, Ar^+, struct. changes, chemical compound formation *(Russian)* 78−95084
Ta foil, reaction with acetylene, effect on mech. props. 79−91590
Ta, interaction with gases, H_2, N_2, O_2, CO, water vapour and hydrocarbons *(German)* 79−74296
Ta, nitridation by ionised glow-discharge to form FCC Ta_xN_y 77−52266
Ta, simultaneous interactions with Cl_2 and O_2 under low press. and high temp. 80−71938
$Ta+F_2$, reaction, 690-930K modulated mol. beam mass spectrometry expts. 77−70341
TaS_2-2H electrodes, topotactic reduction nechanism, neutron diffr. obs. and intercalation cpd. form. 80−108748
Ti alloys, surface layers examination using vacuum UV spectrograph *(French)* 80−71987
Ti film, ion bombardment with $N_2{}^+$, Ar^+, struct. changes, chemical compound formation *(Russian)* 78−95084
Ti film, ion stimulated N_2 sorption, TiN_x form., sorption ratio, capture coeff. anal. 80−39411
Ti, nitriding, ESCA study *(Japanese)* 80−11833
Ti, sulphurisation kinetics, 450-550°C, thermogravimetric determ. 77−25197
Ti, surface layer, study using vac. UV spectrograph *(French)* 80−71987
Ti:N surface, ion nitriding by a DC glow discharge method, surface anal. 78−80672
Ti-Ni alloy, effect on $[Cu(NH_3)_4.(H_2O)]^{2+}$ solns. on drilling *(Russian)* 78−53017
Ti-O alloys+Li melt, ternary solid soln. formation *(Russian)* 78−11396
Ti(C,N), hydrolysis 78−15713
$TiN_{0.91}$ plates, oxidation kinetics *(French)* 78−85199
Ti_2NiO_x (x=0 to 0.5), hydrogen characts., thermogravimetry/DTA meas. 79−52760
TiO_2 electrode, chem. modification for dye sensitisation, rel. to H_2O oxidation 79−91964
TiO_2 electrode, silanisation effects on semicond. props. 79−96364
TiO_2, in desert sand, photoreduction of N_2 to NH_3 79−83483
TiO_2, photodesorption of H_2O, pulsed-laser-dynamic-mass-spectrometer study 80−35568
TiO_2-Ni (100) interface, electronic props., struct., comp., chemical bonding 80−84499
$TiO_2.nH_2O$, U extraction from seawater by adsorption-exchange concentration 78−36198
$Ti_xV_{1-x}H_2$ system, reaction and press.-composition isotherms meas. 80−108391
surface chemistry continued
$Ti_{1-x}Zr_xMn_2$, hydride formation, hydriding characts. of reversible uptake 78−44402
U extraction from seawater, tests of adsorbents 78−36198
U powder, hydriding kinetics, 13.3 and 26.6 kPa, 50-250°C 80−16725
U+F surface reactions, UF_6^- form. 77−73465
$U+H_2$, surface reaction, temp. depend. 79−91996
UF_6 on C-coated Pt(Pt-W), mol. negative surface ionisation 78−56913
UO_2-UC_2-C microspheres, carbothermic prep., rate-controlling preps. 80−45257
V surface, chemisorption of Br_2, struct., Na adsorption effects 80−101039
V surface interaction with O_2, H_2, H_2+O_2 and H_2O, SIMS, EID 77−62753
V_2O_3-H_2, interaction with surface, quantum chemical study 80−45549
V_2O_5, interaction with adsorbed propene, IR emission spectra obs. 79−90881
W (100), electron and photon-stimulated desorption of CO 79−99414
W, Br_2+O_2 reaction, rate of reaction meas., gas flow experiment 78−92510
W, carburisation by methane, initial kinetics 79−47824
W, carburization, catalytic Co effect 80−3255
W, catalytic decomp. of NH_3 single pulses, mol. beam relax. spectrometry 80−21321
W, desorption of D_2, meas. of fast desorption kinetics by laser heating technique 79−23837
W film, carbonisation and oxidation, electron diffr. exam. *(Russian)* 77−44399
W, interaction with gases, H_2, N_2, O_2, CO, water vapour and hydrocarbons *(German)* 79−74296
W, powder, sulphiding with H_2S 79−5071
W, reaction with CO_2 and D_2O at high temps. and low press. 77−86379
W ribbon, with adsorbed CO, CO_2, or methane electron beam induced C deposition, AES obs. 77−89651
W surface wetting by liquid Cu depend. on preliminary surface treatment *(Russian)* 80−35388
W-O-Br system, appl. of mass transfer model of halogen doped incandescent lamps 77−32832
$W+SO_2$, reaction kinetics, 1600-2100K 79−20266
W_2C, single cryst., decarburization, field emission microscopy and TEM 79−70368
WO_3 electrode, surface growth of ternary compds., in electrolyte containing redox couples 78−61016
W_xO_y, carburisation/reduction with CO, morphological study 79−47977
W(100), chemical effects in electron loss spectrum 77−4705
W(100), chemisorpt. of O_2, low-energy SIMS, ion yields depend. on surface chem. and primary ion energy 78−73105
W(110) vicinals, adsorption of N_2, step sites as dissoc. centres 80−6642
XeF_2+Si, surface reaction, IR chemiluminesc. 79−43633
$YNi_{5-x}Al_x$ ternary alloys, Al addition effects on structural and H_2 absorpt. props. 79−52761
Y_2O_3, U, C interactions, thermal anal. 78−85154
YbTe, high-temperature evaporation and reactivity 80−103469
Zn (0001), interaction with Te, UPS investigation 79−91563
Zn, phosphidation in P vapour, kinetics and associated diffusion coeffs. 80−3405
Zn surface oxidation, 78-493K, kinetics 78−64886
Zn, surface oxidation, Auger spectrosc. obs. 80−97388
Zn+P reaction mechanism and kinetics, effect of Ag and Mn impurities 77−21416
ZnO $10\bar{1}0$ surface, reaction of O_2, AES, LEED, EPR, desorpt., surface cond. and work function expts. 78−95950
ZnO $(000\bar{1})$ and $(10\bar{1}0)$ surfaces, clean and contaminated, reactivity to Cl_2 79−61904
ZnO electrode, reson. Raman spectra of adsorbed rose bengal 78−76446
ZnO electrode, role of triplet states in xanthene dye sensitisation 78−76869
ZnO, photodesorption of CO_2, pulsed-laser-dynamic-mass-spectrometer study 80−35568
ZnS 80−35096
Zr:N surface, ion nitriding by a DC glow discharge method, surface anal. 78−80672
$Zr(BH_4)_4$ catalytic reactions on Al_2O_3, inelastic electron tunnelling spectra 80−75425
Zr(C,N), hydrolysis 78−15713
ZrC formation on graphite via activated cementation *(French)* 77−52552
$ZrC_x+Be \rightarrow Be_2C$ layer, limiting stage investig. 77−36786
ZrN-Al_2O_3, sintering reaction thermodynamics 80−2989
ZrN-Mo, cermet, sintering reaction thermodynamics 80−2989

surface composition *see surface structure*

surface conductivity
see also surface scattering
anisotropic metals in perpendicular mag. field, surface impedance behaviour *(Russian)* 78−39145
anthracene, surface states and persistent internal polarisation via photocurrent transients 77−89825
antiferromagnetic superconductor, surface impedance 79−82709
cathode, oxide coated, emission local nonuniformities 77−20978
cathode, oxide type, conductivity model 79−15159
chemisorption kinetics, determ. from substrate current fluctuations 80−84383
conducting ferromagnets, surface impedance resonance depend. *(Russian)* 79−91089
dielectric, irrad. by electron beams, effect of bulk and surface cond. on pot. 80−2446
electron gas, semi-infinite, nonlocal cond. tensor calc., effective optical surface region 80−20283
electron gas, two dimensional, elec. cond., mean free path *(Russian)* 80−44702
electron mobility of two-dimens. electron-impurity system, theory 78−43457
flat capillary, ion transport numbers, surface conductance 80−11071
glass, surface conductivity at solid/liq. interface 79−78152
glass surface resistance changes during dew form. initial stages 77−11777
hexafluoropropylene-tetrafluoroethylene copolymer, surface component of vac. absorpt. and resorpt. currents, source of dielec. loss 80−70792
III-V compounds, electron transport in quantised inversion and accumulation layers 79−60935

surface conductivity continued
insulator-semicond. interface, impurity-band hopping conduction in surface layers 80−75649
ionic crystal, effect of surface cond. on crystal bulk anal. 78−6177
Kapton, optical, elec. props., struct., ion textured surface 78−72904
maximum metallic resistance, in two dimensions as 30000 ohms 78−95335
metal, conduction electrons, surface scatt. under spin resonance conditions *(Russian)* 79−82857
metal, Doppler-shifted cyclotron reson., excitation of dopplerons and Gantmakher-Kaner waves *(Russian)* 77−32261
metal, electric surface impedance 78−88017
metal, in mag. field normal to surface, reson. singularities of surface impedance 78−10495
metal, semi-infinite, transverse dielec. response, surface effects 77−47878
metal, surface impedance near anomalous skin-effect limit, electron-electron N processes 80−100497
metal, surface scattering of conduction electrons and kinetic phenomena *(Russian)* 79−56210
metal, temp. depend. of low freq. surface impedance 78−56207
metal film, cond. electron focusing by inhomogeneous mag. field *(Russian)* 80−70850
metal film, surface impedance oscillation effects due to one sided RF excitation *(Russian)* 80−11106
metal surface problems in microwave region, theory and meas. *(Chinese)* 80−44704
metal-insulator-semiconductor structure, DC cond. and Shubnikov-de Haas effect 80−11012
metals, cyclotron resonance in weak mag. fields surface impedance, current density asymptotic *(Russian)* 80−2641
metals, surface impedance, extreme anomalous limit, diffuse refl. from boundary 80−29460
metals, surface impedance in mag. field, theory *(Russian)* 78−6427
MIS capacitor, current transient response, effect of insulator surface conduction 78−34910
MIS structure, charge-transfer, surface mobility and Hall mobility determ. 78−23175
MIS structures, surface recombination and photoeffect, statistics *(Russian)* 78−39221
MOS system photocapacitance, influence of surface charge fluctuations *(Russian)* 78−43480
MOS system surface charge inhomogeneity modelling and analysis *(Russian)* 78−43479
nonequilibrium conducting media, boundary conditions *(Russian)* 79−91127
organic semiconducting polymer, Z synthesis from Cu^{2+} chelate of PVA and iodine, optimum prep. conditions 79−91612
organic solid surface-conductivity vacuum meter *(German)* 77−57340
paper sheets, charge decay and resistance parameters correlation determ. 80−70795
Permalloy, thin film, oscillatory metallic field effect and surface magnetoelasticity 79−56282
polar semiconductor, surface inversion layers, energy loss of warm and hot carriers 77−11981
polyacrylonitrile, pyrolyzed, surface layer, anal. of elec. cond. mechanism by impedance diagram *(Japanese)* 78−23148
polyethylene terephthalate, lateral motion of charge 78−43458
polymer coated glass, current leakage path form. by water diffusion 78−10535
polymers, oriented, conduction anisotropy meas. *(Japanese)* 80−54707
polymers, surface component of vacuum absorpt. and resorpt. currents, surface charge accumulation 80−60063
polymers, surface component of vacuum absorpt. and resorpt. currents, origin and magnitude 80−70791
polystyrene particles, monodisperse, dil. and conc. aqueous dispersions, elec. cond., surface cond. and double-layer polarisation 80−89533
porcelain, charge carrier prod. by degradation in SF_6 80−7707
quartz, adsorbed gas effects 77−85297
quasi-two-dimensional semiconductor, warm carrier relax. via acoustic phonons 77−43694
semiconducting surface inversion layer, cyclotron reson. of interacting electrons 78−34885
semiconductor, ambipolar hot-carrier size effect kinetics 80−107799
semiconductor, bounded, transport effects when a current passes along an energy inhomogeneity 79−7845
semiconductor, H recomb., nonequilib. charge carrier generation *(Russian)* 79−91126
semiconductor, magnetodiode and magnetoconcentration effects, influence of field effect 80−107903
semiconductor, photodesorption, role of C 77−36787
semiconductor, polydispersed, surface elec. cond. of particles influence on dielec. characts. *(Russian)* 77−16270
semiconductor, relax. time energy depend. and surface galvanomagnetic props. 78−43459
semiconductor, surface helicon waves in Faraday geometry, existence 80−44703
semiconductor, surface space charge layer spectroscopy 77−20386
semiconductor, two-layer nondegenerate, dimens. depend. of elec. cond. *(Russian)* 77−51804
semiconductor (semimetal) film, calc. 78−91751
semiconductor contact potential difference and surface cond., combined meas. method 77−18042
semiconductor crystal surface, nonequilib. electron effects due to chem. excitation 78−72239
semiconductor surface eval. using SAW convolver 80−97677
semiconductor surfaces, surface photovoltage spectroscopy 77−69391
semiconductor with surface doping, surface parameters determ. 77−15933
semiconductors, antiferromagnetic resonance rel. to surface impedance, magnetoelastic contrib. 80−50200
semiconductors, carrier mobility-meas. technique on inverted surfaces near cond. threshold, appl. to Si 79−69602
semiconductors, surface magnetoplasma wave spectrum in HF mag. field 80−24995
sheet glass, chemical resistance to water testing by surface cond. meas. *(Polish)* 79−70271
silicide fabrication, surface resist. meas. for control 77−89854
solar cell, diffusion equation, surface boundary condition 80−66975
solid dielectrics, surface resistivity meas. and calc. 79−1617
solid disperse systems, electro-osmotic mass transfer, surface cond. influence *(Russian)* 80−76546

surface conductivity continued
superconductor film, weakly damped collective oscillations, EM excitation, surface impedance *(Russian)* 80−65739
superconductors, surface resistance, theory 77−51841
surface charge state change during thermodesorpt. 77−80825
surface resistivity, effect of hydrofluoric acid treatment 78−10537
Teflon, optical, elec. props., struct., ion textured surface 78−72904
thin epitaxial layer surface As concentration meas. 79−95037
thin metal conductors, surface impedance oscills. in RF range *(Russian)* 79−91090
transparent conducting film surface resistance obs. 77−77313
trapping phenomena rel. to surface states 77−39916
two-dimensional electron-impurity system in strong mag. field, electron spectrum and cond. *(Russian)* 78−88016
ultra-thin dielectric layer on semicond. substrate, surface charge density determ. *(Polish)* 79−51675
vacuum deposited resistive foils, manufacture and props. of multicomponent alloys *(Polish)* 80−35131
Ag film, chemisorption effects on optical reflectance and elec. resistance 79−33361
AgBr, epitaxial layer, ionic field effect 78−10588
AgBr, film and microcrystal, interstitials and surface conductance 79−23776
AgBr, thin epitaxial layer, surface ionic cond., lattice disorder, space charge region 77−11730
Al, nonlinear skin effect at 4.2K, surface resist. determ. *(Russian)* 79−87122
Al, superconducting and normal state, anisotropic impurity scatt. and EM surface resist. 78−30970
Al thin films, HF induction plasma treatment, effect on phys. props. *(Russian)* 80−24961
Al-SiO_2-Si capacitor C-V characteristic determ. of surface minority carrier lifetime *(Polish)* 77−89855
Al_2O_3 ceramic, surface elec. resist. in Cs vapour 77−51802
Al_2O_3, D plasma interaction, surface structure, chemistry and resistivity changes 78−53010
Al_2O_3 films for Si devices, surface and bulk elec. conduction obs. 77−43761
γ-Al_2O_3 interface with electrolyte solns, adsorption of ions, surface conductance, ion mobility and surface pot. 80−75622
As-Se, glassy, surface phenomena, gas adsorption effects on elec. props. 79−42621
As_2Se_3, glassy, with adsorbed $H_2O(NH_3)(NO_2)(O_2)(CO_2)(CO)$, surface cond., photocond. 78−80038
Au, evaporated, 890 GHz surface resistivity meas. by pyroelectric detector 77−39915
Au film, surface resistivity at 337 μm 77−39913
BN glass transfer process 80−107459
Bi, transverse magnetoresistance, field depend., static skin effect 79−11149
Cd, cyclotron resonance of holes, nonlinear surface resist. effects *(Russian)* 77−8010
Cd, surface impedance, Gantmakher-Kaner oscills. *(French)* 77−66195
Cd, surface impedance, in mag. field *(Russian)* 78−19079
Cd, surface impedance in mag. field, influence of nature of electron reflection 77−51803
Cd, surface resist. in mag. field, doppleron and Gantmakher-Kaner oscills. *(Russian)* 77−32261
$Cd_xHg_{1-x}Te$ single crystal, photoconductivity spectral distrib. rel. to surface condition 79−78136
CdS, SAW meas. of surface elec. props. 77−20387
CdS:Cu(Cl) thin films, surface and bulk photoconc. 80−88653
CdS_xTe_{1-x}, surface layer conductivity type inversion by ruby laser radiation *(Russian)* 77−15948
Cu, resonant cavities, RF loss reduction at 35 GHz by cryogenic cooling 78−93761
Cu surface, fine interaction of conduction electrons 80−34500
n-GaAs, low temp. field generation of carriers, liberation from surface states 80−92959
n-GaAs, nature of low temp. field generation of carriers, liberation from surface states 80−92960
GaAs, photoelectric memory effect, effect of metallic island struct. on surface 77−55570
GaAs, photomag. effect anomalies and state of surface layer 80−100482
GaAs, SAW meas. of surface elec. props. 77−20387
GaAs, semi-insulating, effects of heat treatment characterised by SIMS 78−6091
GaAs, surface, distrib. of surface states 80−44692
GaAs, surface photogalvanic effect, polarisation depend. photocurrents *(Russian)* 80−80322
GaAs, surface recombination rate reduction by Ru chemisorption 80−49866
GaAs:Cr, semi-insulating, I-V characts. and surface currents 79−56234
GaAs:Cr (Cr-Te), and undoped, transverse-acoustoelec.-voltage spectroscopy 79−99586
GaAs:Se, and undoped sample, annealed, surface cond. change, n-p double layer 78−64095
GaAs-oxide interface, field effect 79−87160
GaP:Mg, ion implanted, elec. profiles 79−77628
p-GaSe, resistivity, anisotropy 77 to 750K 79−4559
Ge (111), adsorption of K and Cs, effect on surface elec. props. 79−90880
Ge, ambipolar hot-carrier size effect kinetics 80−107799
Ge bicrystal cleavage plane, Shubnikov-de Haas oscills. *(Russian)* 78−64094
n-Ge, cathodically treated, surface mobility of electrons 77−51801
Ge, chemomagnetic effect, elec. cond. change due to surface recomb. of H atoms 77−8086
Ge, cleaved in liquid He, surface elec. cond. *(Russian)* 80−15588
Ge, conductivity of cleaved surface *(Russian)* 79−51654
Ge during X-irradiation, oxide hydration degree determ. 77−24605
Ge, field effect characts. rel. to surface inhomogeneity 78−26933
Ge, H atom recombination at surface, elec. cond. and chemomag. effect *(Russian)* 79−91125
Ge heteroepitaxial film, ethanol pulsed adsorption effect on elec. cond. 80−93014
Ge, high purity, surface inversion layer electron and hole mobilities 77−76937
Ge, illumination influence on surface cond. irreversible elec. cond. increase *(Russian)* 80−92963

surface conductivity continued
Ge, near intrinsic, negative differential cond., ambipolar size effect due to hot carriers 78−72185
Ge, relax. time energy depend. and surface galvanomag. props. 78−43459
Ge slab, intrinsic, longit. cond., influence of surrounding gas *(French)* 78−10448
n-Ge surface, chemical channel of recombination 80−39656
Ge, surface, Hall effect study, channel cond. *(Russian)* 80−92909
n-Ge, surface electron mobility, Hall effect and cond. meas. 79−56281
Ge surface Hall effect and cond., electron, hole conc. and mobility *(Russian)* 80−44619
Ge surface microwave cond. observations *(Russian)* 80−2447
Ge, surface mobility of irrad. sample, interpretation using two-layer model *(Russian)* 77−51804
Ge:Na (111) surface, O_2 adsorpt., work function, surface cond. changes meas. 78−79875
n-Ge:Ni, quasi-surface conduction effects on photocond. spectrum and IR quenching 77−1452
Ge-Ge (Sn) friction pairs, elec. cond. of Ge tribolayers at He temp. 79−87140
He, liq., surface electron mobility due to electron-ripplon interaction *(Russian)* 77−35770
He, liq. surface, electron liq., high freq. cond. electron correlation effects 80−107589
He, liquid, surface electron high freq. cond., electron system heating, I-V characts. *(Russian)* 80−29244
^{4}He, liq., HF cond. of electrons trapped at surface 78−10238
^{4}He liquid, hot electron theory 78−22915
^{4}He, liquid, surface warm electrons, non-Ohmic transport, scatt. mechanisms 77−20142
In, film, vac. deposited, influence of ion bombardment during condensation 79−82483
p-InAs, surface conductance of Ar-ion-bombard. samples 79−60910
InP film, electron-beam annealed, surface conduction 80−84500
InSb (110), cleaved, gap states, field effect meas. 80−84501
InSb (110), ion bombard. effect on surface struct. and electronic props. 80−6923
InSb (110) surface, LEED and surface conductivity during gas adsorption 77−62760
InSb (110) surface, struct. and electronic props., RHEED and field effect meas. 80−11068
n-InSb, compensated cryst., influence of surface cond. on Hall coeff. and elec. resist. 79−69579
InSb, Ettingshausen effect, influence of surfaces, narrow-gap semicond. characterisation 77−24571
n-InSb film, galvanomagnetic meas. of surface layer carrier conc. and mobility 77−55628
p-InSb inversion layer, magnetotransport 78−64138
InSb, MISS struct., surface electron and hole mobility and conc. *(Russian)* 80−44701
InSb, magnetically frozen-out, evidence of surface cond. from etching expts. 79−47152
InSb, magneto-surface transport props. 77−43693
n-InSb, surface recomb. velocity, temp. and α-bombardment dose effects 77−8173
InSb(111) surface, oxidation props., LEED and surface cond. meas. 78−15559
K, calc. of change in surface impedance, due to cyclotron wave excitation 78−6429
KCl crystal, use of photoelectrons to investigate surface charges 80−2444
MgO single cryst., γ-irrad. in presence of O_2, H_2 and H_2O adsorbates, thermostimulated surface cond. 80−34499
Mo, RF surface impedance, new type of oscills. 79−15070
Mo, surface thermoelectrotransport of atoms 80−2448
Na_2O-CaO-Bi_2O_3-SiO_2, electro-conducting glass-ceramic production by ion-exchange and reduction treatment 79−1616
Nb, O enrichment of surface layers, supercond. penetration depth and resist. meas. 78−19180
Nb, superconducting thin film, devitrified glass or ruby substrate, elec. props. 77−55635
Nb_3Sn, low field microwave props., H_{c1} 77−28317
Ni plate, thin, helicon-Doppleron effect on spin wave prop. 77−66394
Ni-Co, ferromagnetic resonance, surface anisotropy 78−95526
NiO:C, surface charge, O(1s), C(1s) and Ni(2p) XPS 80−45196
NiO:Li^+(Na^+), finely divided catalyst, low-temp. doping 79−51128
Pb, superconducting RF surface resist., 136 to 472 MHz and 1.5 to 4.2K 77−63029
Pb-Bi, supercond. alloys, microwave surface resist., mag. field depend. *(French)* 77−24647
PbS_xS_{1-x} epitaxial film, Hall mobility meas., surface charge transport 77−20473
$Pb_{1-x}Sn_xSe$ epitaxial film, Hall mobility meas., surface charge transport 77−20473
$Pb_{0.82}Sn_{0.18}Te$ epitaxial films, surface transport of carriers at 77K 79−28419
$Pb_{1-x}Sn_xTe$ IR detector, ESCA, surface chem. and leakage current correl. 77−20402
Sb, effect of surface layer current, on transport coeffs., and meas. of Kapitza resist. 77−69348
Sb, magnetoresist., superficial cond. effects 77−28235
Si (100) inversion layer, hot electron drift velocity, Monte Carlo calcs. inc. 3 subbands 78−91752
Si (111), adsorpt. of Cs, LEED, work function and thermal desorpt. 78−14590
Si, adsorbed Pd impurity, effect on surface electronic props. *(Russian)* 79−91124
Si covered by ultra thin oxide layer, surface cond. mechanism 79−38149
Si, electron irradiated, high resist. surface layer, Schottky barrier meas. 78−64093
Si, field effect characts. rel. to surface inhomogeneity 78−26933
Si, high-resistivity layer form. during electron irrad. 80−80352
n-Si, IR spectra of surface photocond. and photo-EMF 77−76868
Si, inversion layer, dynamic conductivity of electrons, temp. depend. 78−19115
Si inversion layer, elec. cond., freq. depend. 78−72270
p-Si, inversion layer, screening effect and quantum transport in strong mag. fields 78−19155
p-Si inversion layers, hot carrier effects in high mag. field, 1.25-20K 78−34908
Si inversion layers, magnetocond. in ground Landau level, defect diffusion in Wigner cryst. 77−39914
Si MIS capacitors, C-V curves, outer oxide surface conditions effects 80−97000
Si MOS structure, low leakage, determ. of surface- and bulk-generation currents 79−24055
p-Si, Na impurity diffusion, ion irrad., defect form. effects *(Russian)* 77−43386
Si, quasi-two dimensional space charge layers, transport phenomena 79−95508
Si, SAW meas. of surface elec. props. 77−20387
Si, spin-depend. carrier recomb. at surface, photocond. expt. 78−19096
Si surface, MOS struct. band structure, minigaps, magnetoresistance, cond., space charge layers 80−92980
n-Si, surface conductivity anisotropy in accumulation layers 78−10536
n- Si, surface electron states, props. determ. at 77K 77−55598
Si, two-dimensional inversion layer on surface, minigap and conductivities 80−20267
Si:B, use of BN source to achieve high surface concentration of B *(Russian)* 80−107639
p-Si:P, annealing behaviour, recovery, surface carrier density and Hall mobility meas. 77−32012
Si-B, exam. of two stage diffusion of B, under a gas phase oxide film 79−95044
Si-on-sapphire MOS devices, effects of planar defects near Si-SiO_2 interface on elec. props. 79−11231
Si-SiO_2 microsensor, surface conductivity effect of aliphatic alcohol molecule adsorption *(Russian)* 78−34887
Si_3N_4 films for Si devices, surface and bulk elec. conduction obs. 77−43761
SiO_2 grown on polycryst. Si, surface asperity mechanism of cond., SEM obs. 78−19153
SiO_2-Li_2O-Al_2O_3-K_2O:Ag_2O(-CeO_4) (-Sb_2O_3), surface resist. meas. 80−44700
Si_2Te_3, passivated single cryst., elec. conductivity 78−95299
Sn, film, vac. deposited, influence of ion bombardment during condensation 79−82483
SnO_2, CVD semicond. film, surface and bulk cond., process parameters effect 77−1502
$SrTiO_3$:B layers, ion implanted, conductive props. Hall mobility, defect energy levels 79−82693
Te film, atm. comp. influence on elec. surface props. 78−26980
Te film, field effect meas. 77−43757
Te, galvanomagnetic props., surface layer effects reduced by etching 77−51769
TiN-Nb(Ta)N, microcomposite film prod. for radio resistors 78−3052
TiO_2, chemical implantation of 10-keV H^+ and D^+, resist. and optical absorpt. expts. 77−59031
V, film, vac. deposited, influence of ion bombardment during condensation 79−82483
W, chemisorbed H, surface cond. and intrinsic surface states, surface refl. spectra 80−15378
W plate, impedance oscillations in mag. field 78−39140
W, RF surface impedance, new type of oscills. 79−15070
W, RF surface impedance at different sample surface states 79−60911
W, single cryst. plates, magnetoresistance, temp. depend. *(Russian)* 79−7820
W, surface impedance and HF cond. in strong mag. field, thin single cryst. plates *(Russian)* 77−89831
W, surface thermoelectrotransport of atoms 80−2448
W thin plate, oscillations of surface impedance in circularly polarised RF fields *(Russian)* 78−39144
W-O system, surface elect. cond. of oxides in equilib. with gas phase 79−61791
ZnO 10$\bar{1}$0 surface, reaction of O_2, AES, LEED, EPR, desorpt., surface cond. and work function expts. 78−95950
ZnO accumulation layers, Hall mobility and work function, correl. 78−60185
ZnO crystals, adsorbed dye laser, charge transfer, field effect and spectrally sensitised photocond. meas. 80−49815
ZnO film, prep. by reactive ionized cluster beam deposition, and characterisation 80−10829
ZnO, nonpolar surface, interaction with CO and CO_2, changes in elec. cond. and surface pot. 79−65321
ZnO, photodesorption of CO_2, rel. to surface cond. and AES, band-bending model 77−47671
ZnO, polar (000$\bar{1}$) surface, annealing and Ar^+ bombard. effects on conductivity, LEED obs. 79−51653
ZnO, polar faces, space charge layers, anomalous electron mobility 77−62981
ZnO polar surfaces, H and O_2 exposed, ion irrad., and heat treated, cond., EELS study 80−71525
ZnO, powder, effects of O_2 chemisorption and CO_2 photodesorption 77−11980
ZnO, prismatic surface, O_2 interaction obs. 77−31899
ZnO, surface charge transfer in presence of photosensitising dyes 78−68049
ZnO surface extreme accumulation layers due to He^+ ions 77−72909
ZnO, surface phenomena, interpretation by compensation model 78−95323
ZnSe, minority carriers diffusion length by surface photovoltage method 80−60003

surface contours
see also surface structure; surface topography measurement
abraded surfaces, topography rel. to contact area and abrasion mechanism 80−58986
astronomical optical surface shaping automation methods 79−84675
atom-surface impact, roughness effect on capture of gas atoms 80−60726
B_2O_3-SiO_2 glass, surface flattening kinetics by sinusoidal profile decay method *(Japanese)* 80−34284
carbon tetrachloride drops falling through H_2O, surfactants rel. to deform., oscill. *(French)* 80−66880
channels for steam generation, roughness rel. to heat exchange intensification 79−55371
coating, thin film surface irregularities rel. to optical props. *(Russian)* 77−11047
complex profiled surface alloying, automatic electrode feeding *(Russian)* 78−19936

surface contours continued
component tolerance control, two-dimensional shadow image mapping filters *(Russian)* 79−94155
computer-controlled machine tool for diamond-turned surface accuracy improvement 80−1367
configuration control by conc. loads applic., mirrors case 79−94317
configuration control of nonuniformly heated shells, actuators effectiveness 79−94318
contouring method by parallel light Moire holography 78−33702
contrast of time-averaged speckle patterns produced by small vibrations of diffuse objects 79−94169
cytomorphological contour classification for mass cancer screening 79−79682
deformation of surface irregularities under static loads 80−58985
diamond turning precision machine tool system 80−69568
discrete actuator deformable mirror 80−33133
ferromagnetic fluid, in appl. mag. field equilib. surface patterns 77−84332
glass, polished, 1.064 μm laser damage threshold rel. to pulse duration and surface roughness 80−33055
heat transfer of rough cylinder in transverse water flow *(Russian)* 79−10449
holographic contour fringe computer-aided analysis 77−49766
holographic contour fringe generation by dual-index immersion 77−49765
Inconel 625, plasma nitriding, surface topography obs. by SEM 80−45442
liquid, transient behaviour due to pulsed US transducers 80−95073
machine tool computerised control for diamond-turned surface finish 79−98517
metals, abrasive finishing with refractory carbide micropowders 80−11842
mica, metamorphic white, surface microtopography 80−54493
MIM tunnel junction, anomalous surface enhanced mol. Raman scatt. 79−72324
Moire contouring of large objects by scanning technique 78−32791
Moire contouring system, lateral grating movement *(Japanese)* 77−87817
moire patterns, contour fringes of optical surface 77−14659
Moire topographic method, anal., concave convex region discrimination 78−65901
NC diamond turning system evolution 80−1369
nitrided steel surface wear-related topography 78−60847
nucleate boiling, surface topography 78−90653
ophthalmic lens surface working machinery 80−28363
optical surface microtopography, generated by diamond turning machine 80−33263
paper, surface characterisation and printability criteria, stochastic approach 78−18878
particles in porous polycrystalline solids, mechanism hindering boundary sliding 79−95962
patient contour drawing using US compound B-scanner 79−83865
plane surface deviations, meas. system *(German)* 77−30127
plastically deformed crystal, acoustic emission, bubble formation mechanism in liq. He *(Russian)* 78−85066
plotting, moire technique 80−42002
polymer, friction coefficient calc. for contact surfaces with nonspherical asperities 79−20200
polyvinyl furfural, CdO, MoS_2 and graphite filled, contact area, filler effect 79−57040
profiles reference line selection and fitting, based on random process analysis 78−45594
quartz, cultured, hydrothermal growth, prism face develop. rel. to microcryst. form. 77−72572
rainbow holographic contour generation 80−63948
reflecting surface roughness evaluation, statistical approach 78−90367
rough surfaces computer simulation of contact 79−19470
SEM method and apparatus for quantitative anal. of microrelief 79−7530
semiconductor structure, electrodeless meas. of resist. and spherical curvature 79−49252
semiconductor wire, quantised monochromatic wave absorpt., indirect transitions due to surface roughnesses *(Russian)* 79−91397
solid body-microparticle impact, cratering, viscous effects 79−66255
stepped surfaces, surface geometry, RHEED study 79−77881
terrestrial hills, wind, flow profile, numerical soln. 77−33173
topography, rel. to adhesion props. 79−96280
triangular microprofile containing surfaces, oblique incidence sputtering, topographic changes 80−66372
two-wavelength contour holography, fringe form. 77−19194
wetting film, thickness on rough substrates 79−56044
zero order diffraction microimage reproduction from surface relief gratings 79−17518
Ag film vacuum deposition and ion plating, effects on surface topography 79−82427
Al-Cu, high strength, type 2024-T3, crack growth, fatigue induced surface deform., holographic detect. 80−85120
Al-Cu-Si, effect of sample conditions on sputtering and intensities, emission spectrochem. anal. using glow discharge *(Japanese)* 80−21349
As_2S_3 chalcogenide film surface relief hologram selective etching *(Russian)* 79−94181
As_2Se_3 chalcogenide film surface relief hologram selective etching *(Russian)* 79−94181
As_3Se_2 chalcogenide film surface relief hologram selective etching *(Russian)* 79−94181
CU, effect on polyethylene adhesion 79−74340
$Cd_xHg_{1-x}Te$, crystallisation from solution in Hg 77−19883
Cr, CVD protective coating on steel, struct. and carbide form. 77−40387
Cu, electroplated surface roughness and brightness rel. to periodic reverse current 79−96201
Cu-Be, dynode surface, SEM and Auger microanalysis 80−100384
Fe-Cu-Ni-Cr_3C_2-C based sintered friction material, wear, surface geometry and struct. effects 80−25875
GaAs, VPE, surface defects rel. to technological parameters 78−44015
$Gd_3Ga_5O_{12}$, garnet substrate, surface polishing, damage, abrasion, brittle fracture model *(German)* 77−73357
$Gd_3Ga_5O_{12}$, garnet substrate surfaces, working damage, electron microscope investig. 77−77605
GeS, film on Ge, evaporation, thermogravimetric, electron microscopy investigs. 77−15715
surface contours continued
$Hg_{1-x}Cd_xTe$, surface topographic stoichiometry variations, electrolyte electrorefl. obs. 78−27249
MgO, smoke particles, size distrib. 80−104471
NaCl single crystal, surface relief obs. using PbS epitaxial replicas 77−51577
NaCl, single crystal, surface markings, left by unsteady cleavage crack propag. 79−46746
$NaClO_3$, dislocations rel. to growth mechanism from aq. soln., X-ray topography 80−59464
Na_2O-CaO-SiO_2 glass, surface viscous flattening kinetics, sinusoidal profile decay method 79−79139
Ni coatings, detonation powder spray deposition 80−61028
Ni, Czochralski growth conditions rel. to cryst. imperfections, mag. domain walls 77−68937
Pb surface erosion by supersonic plasma stream, mech. momentum role 80−2065
PbO-SiO_2, surface flattening kinetics by sinusoidal profile decay method *(Japanese)* 80−34284
Si, substrates, semicond., stress meas. in deposited thin films, X-ray topography techniques 78−5710
Te-Ag thin film system, stress-relief appearance conditions 80−65416
Te-Bi thin film system, stress-relief appearance conditions 80−65416
W, ion sputtering yield reduction by special surface microtopography 77−36330

surface diffusion
see also sorption
adatom and cluster motion, simulated using mol. dynamics 79−99411
adatom laser stimulated migration and multiphoton excitation, relax. and reaction enhancement 79−39200
adatom mobility on metal surface, density functional approximation calc. 80−103577
adhesion energy of two crystals, effect of surface diffusion 78−2380
adsorbable gases, surface diffusion through porous media 77−80694
adsorbate diffusion on single cryst. surface 78−38969
adsorbate diffusion on single crystal surfaces, influence of lateral interactions 78−38953
adsorbed atom migration, dynamical theory 77−1293
adsorbed atoms, diffusion and density fluctuations on solid surfaces 80−39452
adsorbed gases on solid surfaces, mobile and localized adsorption, theory 80−65379
adsorbed layer, dynamics near surface 79−95271
adsorbed species 80−80070
adsorption, surface band theory and surface transport props. 77−43680
alkali halide (100) surface, adsorbed monomers and dimers, pot. surfaces, diffusion dissoc. 77−66769
alkali halide cryst., surface impurity distribution, Fick's 2nd law calc. 77−47673
alkali silicate glasses in aqueous solutions, leaching kinetics rel. to surface pot. 80−11803
alloy, single phase, annealing of diffusion layer 78−14518
amorphous surface, energy profile and binding energy, computer simulation 80−100381
anodic oxidation, mobility of foreign atoms 77−90494
anthracene, radical cation, EPR, acidic surface anisotropic rot. diffusion 78−27095
atom, chemisorbed on solid, diffusional motion, microscopic anal. 79−4467
atom on solid surface, diffusion equation 78−79890
atomic diffusion mechanisms *(Hungarian)* 78−38868
atoms on metal surfaces diffusion parameters, binding energy and dipole moment 79−51422
Au film, diffusion of Ag along grain boundaries, scanning Auger microscopy obs. 78−22897
benzene on graphitized C black, adsorbed layer mobility 78−6216
binary alloy, kinetics of nuclei coalescence by reactive diffusion *(Russian)* 79−42398
binary alloys, diffusion-controlled growth of solid soln. scales 77−70232
binary alloys, kinetic nucleation model 77−85118
Brownian diffusion model 78−6214
Brownian particle motion in periodic field of force, diffusion coeff. in large friction limit 78−38869
Burton-Cabrera-Frank surface diffusion model, 80−59415
butadiene iron tricarbonyl, adsorbed on graphite, diffusion and melting, Mossbauer meas. 79−61270
cavity growth controlled by surface diffusion, numerical study 79−90668
chemically active surface, boundary conditions for aerodynamic eqns. and diffusion *(Russian)* 77−55105
chemisorbed atom, coherent and diffusional motion 77−1292
CIDEP, two-dimens., surface diffusion and spin polarisation, asymptotic Green's function method appl. 80−91584
CIDN(E)P, in two-dimensional fluid, and Heisenberg spin exchange 80−14157
cluster motion, stochastic model 78−14550
coefficient, expt. determ. method 77−1298
coefficient, from sorption kinetics, time-lag theory 78−38937
crystal surface, (1n0), stepped relief machine model 80−34283
crystalline surface, diffusion of atomic clusters, stochastic model 77−28077
crystallite migration on surface, Monte Carlo calc. 78−26783
cutting tools, diffusive wear, mag. field effect 80−60985
cyclohexane on graphitized C black, adsorbed layer mobility 78−6216
depth profiling of H, He isotopes, proton elastic scatt. technique 77−24327
desorption, non-isothermal, approx. kinetic relation describing diffusion *(French)* 79−90864
diffusion at low temperature, anal. of surface accumulation method for film systems 79−77838
diffusion bonding, in Ar atmosphere, aspects *(Japanese)* 78−11491
diffusion-controlled reactions on a two-dimensional lattice 80−71940
diffusive cavitation of grain interfaces, non-equilib. models 79−46668
disordered surfaces, atomic migration, theory 80−54516
electrochemical electrode processes, kinetics from transitional sections of polarisation curves 77−25283
electron irradiation effects on surface prop. of solids 80−70261
electron microscope contamination by surface diffusion of adsorbed hydrocarbon mols., theory 80−99013
energy transfer effects 79−82420
epitaxial island mobility, one-dimens. model sinusoidal pot. 80−44457

surface diffusion continued
exciton diffusion and annihilation, inhomogeneous surface layer effect *(Russian)* 79−60730
field emission microscopy appls. 79−65982
film, effect of surface condition at low temps. 78−91469
film, multiple grain boundaries and surface diffusion 77−4276
film, polycryst., nodule mechanism of diffusion-induced disintegration *(Russian)* 78−51829
film deposition, adatom diffusion and capture by clusters, random-walk problem 78−2385
film growth, initial stages, ion bombardment effects 78−14639
film growth by ionised-cluster beam deposition, adatom migration effect 77−32527
film growth kinetics under high adatom conc., surface diffusion parameters 77−28088
flavanthrene molecules, stationary stochastic adparticle flip-flop as a precursor to surface diffusion 80−15371
foreign atom, coverage on surface as function of adsorption, sputtering and diffusion rates 79−69354
free molecular gas flow in capillary, effect of absorption time differences 77−89164
gas desorption from solid, two diffusion mechanisms 80−92784
gas diffusion through surfactant films, interfacial resistance 80−39385
glass, conc. distrib. in surface layer after contact with $AgNO_3$ melt, $AgNO_3/NaNO_3$ mixture 80−44372
grain boundary groove evolution in presence of evaporation 78−14364
grain boundary groove profile, effects of surface free energy anisotropy 79−7734
grain boundary grooving under action of surface diffusion and evaporation or corrosion 80−39397
grain boundary grooving under influence of evaporation or corrosion 79−28179
graphite, adsorption and migration of O_2, CNDO/2 calcs. 79−28205
graphite, Ag particle motion on heating in gaseous environments 78−34695
graphite, interaction with Cs, study of surface diffusion, computer simulation 78−30837
graphite, mobility of 2-dimens. hypercrit. fluid methane, neutron scatt. obs. 77−20193
graphite, of benzene molecules on basal planes, neutron scatt. study 79−42385
hexamethylene tetramine, cryst. growth kinetics from soln., role of solvent-solute interactions 77−24282
hydrocarbon molecules, strongly adsorbed, contamination rate reduction 79−1550
hydrodynamic interfacial instability, mechanical, chem. and elec. constraints, review 80−34278
ice, I_h, water monomer on basal plane, static interaction model 78−18891
ice surface viscosity, activation energy, vacancy migration 80−107458
impurity distribution, calc. for cryst. solid with inhomogeneous layers *(Russian)* 78−14500
interface, stability problem, diffusion, reaction and convection 80−33567
interface of two phases or liquids, selective processes induced by resonance laser radiation 78−64867
interfacial instability, mass transfer, Marangoni effect and interfacial longit. waves 79−46890
ion, near metal surface, friction parameter and Brownian motion 80−15584
ion beam texturing of surfaces 79−77876
ionic crystal, gas-solid interaction potential, adsorption sites and surface migration 80−24738
ionic crystal, phys. adsorption of nonpolar gases, localised and mobile phases, hopping adsorbates 80−24739
island films, diffusive mass transfer, review 80−20054
islands, rotation and translation on substrate 80−10811
lattice defects and diffusion processes in solids, book 80−107207
LED, DH, output power and response time, thickness depend. 79−95479
Lennard-Jones two-dimensional system, mol. dynamics method 79−90873
liquid films, dynamic behaviour, surface mobility effects 80−88409
mass spectrometry, molecular beam, appl. to coupled diffusion and chem. reaction 77−73497
metal, direct obs. of individual atoms, FIM 77−62724
metal, FIM direct obs. of surface diffusion and atomic interactions 78−34716
metal, surface self-diffusion near ambient temp. by surface pot. meas. *(French)* 79−51397
metal, with low and adsorption activity, diffusion coeff. of H, steady-state flow method 80−10795
metal oxides, nonstoichiometric, work function and near-surface chem. diffusion 80−80034
metal surface, electron correl. in chemisorbed H atom, friction coeff. 78−60026
metal surface, electron density depend. on modulation, adsorption, diffusion 80−54526
metal surface, kinetics of adsorpt., desorpt. and migration, review 79−46921
metal surface, near point-defect, annealing, diffusion theory and Monte Carlo anal. 78−47646
metal surface electrochemical smoothing, roughness, diffusional preelectrode layer *(Russian)* 80−76401
metal surfaces self-diffusion of single atoms and diffusion of adatoms, activation energies calc. 80−24732
metal tip profile change meas. for evaporation rate determ. 77−24403
metallic thin film, vacuum deposition, early stage obs. using microbalance technique and electron microscopy *(Japanese)* 80−54554
metallic thin films, surface and grain boundary diffusion, charact. temp/melting point ratio 79−90919
metals, carburising, surface-gaseous medium interaction laws 80−76411
metals, individual atomic events on surfaces, quantitative examination 80−75409
methane, adsorbed monolayer on graphite, two-dimens. diffusion by mol. dynamics method 79−90873
methane, adsorbed on graphite, NMR pulsed field gradient method, diffusion coeff. meas. 80−15362
MHD generator, cathode spot erosion, thermal conduction-diffusion 78−5955
molecular sieves, 5A, modelling, appl. to Ar diffusion coeff. determ. *(French)* 80−54508
molecule desorption and surface diffusion from critical deposition rate 80−92786
Monte Carlo simulation diffusion and evaporation on (100) surface of FCC crystal 78−30836
morphological changes occurring by surface diffusion on body with anisotropic surface energy, elec. stress effects 78−6202
multistate diffusion in perfect and defective systems, stochastic theory 79−93067
neopentane, adsorbed on graphite (TiO_2), NMR pulsed field gradient method, diffusion coeff. meas. 80−15362
nonpolar molecules, adsorbed on metal surface, depolarisation interaction 78−51820
oxides at high temperatures obs., crystalline and non-crystalline, use of sinusoidal profile decay method *(Japanese)* 80−54479
particle drag retardation of surface smoothing and sintering 77−12561
perylene, anthracene, radical cation, EPR, acidic surface anisotropic rot. diffusion 78−27095
phthalic anhydride+8-hydroxyquinoline, solid-state reaction kinetics 77−36746
planar surface discontinuity, annealing by surface diffusion 79−23812
polystyrene latex, grain boundary struct. obs. and boundary diffusion 78−51552
polyurethane foams, elastic, stability against organic solvents *(German)* 80−85074
pore velocity, due to surface diffusion under temp. gradient, finite thermal conductivity correction 80−15428
potential depth resolution of ion analyser, model development *(French)* 77−85867
powders, surface area measurement using Knudsen diffusional flow of gas 79−40536
quartz, surface quality determ. using Ag diffusion and neutron-activation method 79−51401
reactive gas flow through porous barrier, exit flux, composition depend. 77−31383
refractory metal, surface geometry and emission parameters, changes during directional mass transport 78−2344
self-diffusion consts. of surface adatoms from growth or evaporation spiral evolution kinetics, appl. to NaCl and KCl 79−65301
SEM with ultrahigh vacuum system for surface physics expts. 78−38925
sintering, diffusion controlled sphere-sphere, simulation 80−20814
sintering, surface redistribution by grain boundary diffusion 80−84871
sintering map effects 79−74117
solid, diffusional mass transfer exam. by light diffusion method *(Russian)* 77−7953
solid surface, mol. dynamic processes interaction with laser radiation 80−71943
solid surfaces, surface processes, and solid/gas interactions 80−73125
solid-liq. metal diffusion layer, phase growth kinetics *(Russian)* 79−37882
sorbent solid, moisture diffusion, diffusion cell and pore diffusion 78−10210
sorption process, diffusion coefficient estimation 77−80696
spherical powder sintering by surface diffusion, computer simulation 78−48344
sputter induced surface morphology, analytical modelling 77−16445
sputter profiling, depth resolution, surface transport effects, calc. 80−97393
sputtered alloys and compounds, surface layer composition changes 77−73200
stearic acid monolayers on HCl subsoln., surface diffusion by ^{14}C-tracer 78−34679
steel, C, siliciding in US field 79−39043
steel, chemicothermal treatment quality control by fractographic method 79−39080
steel, Cr, carburising kinetics, in endothermal atm. 80−76410
steel, Cr, carburising with high-activity carburiser 80−76412
steel, endurance, effect of surface diffusion alloying 77−81344
steel, high-C, carburising kinetics, in endothermal atm. 80−76410
steel, ionic nitriding, procedure and equipment, nitrided layer hardness obs. 80−45414
steel, sintered, diffusion treatment with B, Si, Cr and C, corrosion and wear improvement 77−77642
steel carburisation process, diffusion modelling 80−108632
steel cladding, 8 distrib. after Na exposure and high-temp. 77−57719
steel temper embrittlement control progress 78−72797
STEM, at. resolution, adsorpt. and diffusion of heavy atoms on light element substrates 77−24484
STEM use for direct obs. of atomic diffusion on thin film substrates 77−89644
substrate, VPE growth of Si *(French)* 77−59236
superionic solid film, surface diffusion coeff. 80−92709
supersaturated soln., shape stability of growing cylindrical particle due to diffusion and interface kinetics 80−79720
surface analysis, influence of surface diffusion, model calc. 79−15016
tetracene, radical cation, EPR, acidic surface anisotropic rot. diffusion 78−27095
tetramethyltin, adsorbed on graphite, nature of 2 D diffusion, Mossbauer meas. 80−84372
thin film growth, surface self-diffusion coeff., adhesion energy of evap. material 78−84080
thin film growth due to crystallite surface migration, review 80−10810
three-phase system, diffusion laws 80−107310
transition metal alloys, surface segregation 79−34044
transition metals, adatom surface diffusion charact., pair potential calcs. 80−39446
two-dimensional substrate lattice, migrating adatom capture by point capture centres 78−43236
W (110), chemisorption of N, surface diffusion, scanning Auger spectroscopy exam. 77−55452
water adsorbed on protein molecules, investigation using spin-echo NMR method and pulsed magnetic-field gradient programme 79−21794
Ag (110), adsorption of S, equilib. segregation isotherm, selvedge model 79−90883
Ag, adsorbed O_2 layer, EPR of O_2^-, rate of angular reorientation 78−72413
Ag film, void growth, TEM obs. 80−59833
Ag films, hillock form. hole growth and agglomeration 80−44455
Ag surface, diffusion of labelled adsorbed Cl^-, I^- ions 80−39413
Ag, surface self diffusion coefficient, O_2 pot. effect *(Japanese)* 78−60014

surface diffusion continued
Ag, surface self-diffusion coeff., O_2 potential effect 80−15354
Ag, thin film, hillock growth due to thermal stress relax. of diffusion creep and surface diffusion 79−65345
Ag, vacuum deposition, on evaporated AgBr layers, growth mechanism 80−35095
Ag-Au, nucleation and growth on substrates, surface diffusion activation energy 79−77956
Ag-Au, surface layer, effect of Ar^+ bombardment, AES and SIMS 80−25504
$Ag_7I_4PD_4$, superionic solid film, surface diffusion coeff. 80−92709
Al film, nucleation and growth on C layers, adsorption energy and surface diffusion 79−99451
Al, oxide films, metal and O_2 transport, AES and inert marker, techniques 80−97641
Al-Zn, plastic deform. effect on struct. transform. at elev. temp. *(Czech)* 79−79044
Al_2O_3, activated, moisture diffusion 78−10219
Al_2O_3, initial sintering, method for obtaining surface diffusion coeffs., appl. to shrinkage data 78−95713
Al_2O_3 surface diffusion coefficient obtained by free sintering 77−72765
Au deposited on alkali metal substrates, calc. binding energy of Au atoms to substrates 79−33208
Au film, adatom surface diffusion at low temps., elec. resist. study *(French)* 80−65376
Au foil, radiation damage, in situ study by HV electron microscopy 78−6101
Au sol, grain boundary struct. obs. and boundary diffusion 78−51552
Au-Ag, deposition on alkali halide, kinetic nucleation model 77−85118
Au-Ag film system grain-boundary diffusion at low temp., meas. by surface accumulation method 79−77839
Bi film, adatom surface diffusion at low temps., elec. resist. study *(French)* 80−65376
Bi film, deposition props. on specially prepared substrate, desorption energy and surface diffusion 79−90917
C, activated, adsorption in countercurrent flow 80−70524
C, adsorption of Ag and U, scanning-transmission electron microscope obs. 77−51597
C, dissolution into Ni through (110) surface, 615-660K, AES, LEED 78−63932
Cd film, deposition props. on specially prepared substrate, desorption energy and surface diffusion 79−90917
Co-C alloys, graphite nucleation on surface *(Russian)* 80−40360
Cu (100), self-diffusion near ambient temp. by surface pot. meas. *(French)* 79−51397
Cu and Cu alloys, diffusion in systems involving group VA elements, review 77−39697
Cu electrocrystallisation from $CuSO_4$ solns., current density under stationary surface diffusion *(Russian)* 79−8237
Cu electrocrystallisation from $CuSO_4$ solns., expt. and slow surface diffusion theory *(Russian)* 79−11505
Cu, evaporated film, roughening and flattening by surface diffusion, influence on surface struct. 79−69381
Cu film, polycryst., nodule mechanism of diffusion-induced disintegration *(Russian)* 78−51829
Cu, friction surface structural investigation, O_2 surface diffusion *(Russian)* 80−96726
Cu, initial sintering, method for obtaining surface diffusion coeffs., appl. to shrinkage data 78−95713
Cu, sintering, contact resist. determ. of neck growth rate and mass transport mechanism 77−55899
Cu-Ni, clean surface, surface segregation and growth process of altered layer *(Japanese)* 80−24720
Cu-Ni, surface layer, effect of Ar^+ bombardment, AES and SIMS 80−25504
Fe, adsorbed S effects on surface reaction kinetics and surface self-diffusion 78−7234
Fe, Armco, carburising kinetics, in endothermal atm. 80−76410
α-Fe, O_2 potential effect on surface self-diffusion coeff. 80−15353
Fe particles, motion on graphite surface 79−90850
Fe, polycrystalline, H_2 adsorpt. and embrittlement, work function changes 80−96741
Fe:Ti, C induced amorphous surface layers 80−107287
Fe-Mg, cast, ferrite-based, graphite nucleation on surface *(Russian)* 80−40360
Fe-Ni alloy, fluorination kinetics and fluoride film form., chem. nature obs. 80−101035
Fe_3O_4, low temp. sintering 78−92221
GaAs (111), Ga-As-H-Cl CVD system, adsorption of Cl, GaCl, As, As_4, Ga, AsGaCl, 973 to 1223K, equilib. adsorption layers 79−23858
GaAs, rel. to VPE in CVD systems, anisotropic phenomena 80−54563
Gd on W in field ion microscope *(Russian)* 77−47662
$Gd_3Ga_5O_{12}$, interface processes with $(YSm)_3(FeGa)_5O_{12}$ film, LPE, horizontal dipping obs. 80−49552
Ge (111), desorption kinetics of two-dimens. condensed phases of Ag 79−90882
H_2O, adsorbed, surface-induced NMR line splittings and augmented relax. rates 78−64288
H_2O, adsorbed molecule in pores of zeolites, intermed. state of enhanced mobility 78−60027
^3He adsorbed on Grafoil, nuclear spin relax. and atomic motion 79−51369
Hg on metal surfaces, flow kinetics in temp. grad. *(Russian)* 78−6198
Ir, field evaporation end form at 4.2K 77−1790
Kr in charcoal bed, breakthrough characts., effect of carrier gases, temp. and intraparticle diffusivity *(Japanese)* 79−73392
LaB_6, field emission and FIM expts. 77−90255
Mg film, deposition props. on specially prepared substrate, desorption energy and surface diffusion 79−90917
Mo (011) face, submonolayer Ba film, surface diffusion, manifestation of phase states *(Russian)* 78−91539
Mo (011) face, surface diffusion and interaction between adsorbed Ba atoms *(Russian)* 80−6658
Mo, surface thermoelectrotransport of atoms 80−2448
NH_3, adsorbed on graphite, NMR pulsed field gradient method, diffusion coeff. meas. 80−15362
$NH_4Ag_4I_5$, superionic solid film, surface diffusion coeff. 80−92709
NaCl, evaporating surface, step motion obs. and simulation 78−26766
NaCl, of CO_2, gas-solid interaction potential, adsorption sites and surface migration 80−24738
surface diffusion continued
NaCl, of methane, adsorpt. pot., localised and mobile phases, hopping adsorbates 80−24739
NaCl, single cryst. in vac., influence of dislocations on evaporation 79−10935
NaCl:Ca, surface segregation and diffusion 77−43416
Na_2O-(CaO)-SiO_2, diffusion controlled attack by aq. solns. 80−81218
Na_2O-CaO-SiO_2 glass, surface viscous flattening kinetics, sinusoidal profile decay method 79−79139
$Na_2O.2SiO_2$ glass, diffusion of Ag into surface layer from $AgNO_3$ melt 80−44371
Nb, H absorption rate, metallic film effect 80−49525
Nb, magnetic surface barrier breakdown by O diffusion, permeability meas. 79−56601
Nb superconducting, O_2 diffusion profiles in surface layer 79−24101
Nb, surface, coverage of O atom as function of adsorption, sputtering and diffusion rates 79−69354
Nb_3Sn, supercond. diffusion layer, Zr content and Nb cold working effects 77−16015
Ni (001), adsorpt. of S, multiple binding sites and diffusion, photoelectron spectra and LEED struct. 77−66569
Ni (100), interaction with methane, diffusion of deposited C, AES-LEED study 79−99418
Ni (110), anisotropy of surface self diffusion 77−43367
Ni (110), surface self-diffusion, sinusoidal profile decay technique 79−99404
Ni, absorbed on W(111), surface site geometry, diffusion charact. 78−75944
Ni, oxide films, metal and O_2 transport, AES and inert marker, techniques 80−97641
Ni, polycryst., bulk-to-surface precip. and surface diffusion of C, AES data interpretation 78−34713
Ni, self-diffusion of singel atom, in (331) plane, field-ion microscopy 78−67895
Ni surface, single-atom self-diffusion FIM study 80−103548
Ni, surface diffusion effect on sintering 79−74117
Ni, surface self-diffusion in presence of adsorbed halogens *(French)* 80−24723
Ni:C, bulk-to-surface precip. and surface diffusion, AES meas. 77−11784
Ni-C alloys, graphite nucleation on surface *(Russian)* 80−40360
Ni-Pd (1 at.%), surface comp. and surface segregation, AES obs. 79−51404
β-NiAl, oxide films, metal and O_2 transport, AES and inert marker, techniques 80−97641
NiO, grain boundary thermal grooving, mass transport, self-diffusion coeffs. 80−44217
NiO, nonstoichiometric, near-surface and bulk chem. diffusion 80−80035
NiO-Al_2O_3 system, concurrent meas. of vol., grain boundary and surface diffusion coeff. 77−55399
Ni(110), surface self diffusion, temp. depend. directional anisotropy 78−87851
Pb (111) surface, vacuum deposition of Cu, Ag, substrate diffusion effects, RHEED, LEED, AES 80−65410
Pb film, deposition props. on specially prepared substrate, desorption energy and surface diffusion 79−90917
PbS, hot-pressed compact, elec. behaviour, adsorbed atmos. gas effects 77−66601
PbSe surface, clean and O_2-exposed, XPS (UPS) obs., electronic struct. 78−52637
PbTe (111) epitaxial films, localised electron irrad. effects on elec. props. and O_2 sorption 80−49472
Pt (110), two-dimens. diffusion of Pt adatom 79−28183
Pt, diffusion energies for Pt, Ir, Au adatoms, Lennard-Jones pair pot. calcs. 79−77923
Pt, of Ba, vaporisation expts. on Pt-Ba cathodes 78−10272
Pt, of single atoms of Pt, Ir and Au, FIM expts. and Morse potential calcs. 78−34717
Pt-Rh alloys, surface comp. determ. by ion scatt. spectroscopy 80−6602
Pt(111) surface, of C, AES 78−71954
Re, oxide formation and surface rearrangement, field ion microscope obs. 77−28936
Rn, diffusion coefficient and exhalation rate from building materials, meas. technique 80−4694
Si (111), adsorption of Cl, H, Si, SiCl, $SiCl_2$, equilib. adsorption layers 79−23858
Si (111), of Al, surface diffusion 79−28184
Si (111) surface, atomically clean, diffusion of adsorbed Au 78−72037
Si, CVD from SiH_4-HCl-H_2 system, rate-determining reactions and surface species 80−84405
Si, epitaxial layer, growth mechanism from ion-molecular beams 80−2299
Si, surface self-diffusion, investigation by slow electron diffr. method *(Russian)* 78−51808
Si:Ag (Zn,Fe), diffusion mechanism of fast impurities, distrib. in surface layers 77−11735
Si:As, segregation and desorption kinetics for evaporation of As 79−99410
Si:B, inhomogeneous surface layer, diffusion and implanted, X-ray rocking curves 80−6603
Si:B, P, long range enhancement of B diffusivity by P diffusion 80−103386
Si:B, use of BN source to achieve high surface concentration of B *(Russian)* 80−107639
SiO_2 film on Si substrate, Na transport caused by ion and atom impact 80−6682
steel, high C, graphite nucleation on surface *(Russian)* 80−40360
Ta auto-cathodes, effect of O_2 on emission and surface diffusion *(Russian)* 79−77892
Ta, diffusion and surface distrib. of N, probed by (p,γ) resonance broadening method 78−38918
Ta, electron-stimulated desorption of O_2 bound state obs., 300K 77−85082
Ta, H absorption rate, metallic film effect 80−49525
Ti fibres, high-temp. nitriding kinetics *(Russian)* 80−21166
Ti, friction surface structural investigation, O_2 surface diffusion *(Russian)* 80−96726
TiO_2, rutile, mass transport mech. determ. by sinusoidal profile decay method 78−6178
UO_2-zircaloy-4, reaction kinetics at high temps., O_2 diffusion 80−16667

surface diffusion continued
V, oxidised in air during laser irradiation, switching effect *(Russian)* 80−24977
V surface interaction with O_2, H_2, H_2+O_2 and H_2O, SIMS, EID 77−62753
W (100), coadsorption of Zr and O_2 at high temp. 80−6653
W (110), mobility of adsorbed O, 300 to 800K, field emission current meas. 79−33187
W (110), O_2 diffusion, coverage-distance plots, diffusion coeff. 77−62755
W (110), surface mark migration, anisotropy of thermal mass transport 77−51583
W (110) mobility and two-dimens. compressibility of adsorbed Xe, field emission current fluctuation method 80−80089
W (110) plane, tunnelling of H in surface diffusion 80−75416
W (110) surface, of O_2, contact pot. difference meas. 77−39921
W (111), (211), and (311), adsorption of W single atoms, surface site geometry determ. by FIM 80−39447
W (111) surface, surface site geometry and diffusion characts. of Ni atoms 78−71953
W (310), field emission current instability induced by migrating atoms 78−35254
W {123} plane, clean and H saturated, surface diffusion of single W atoms 80−80081
W adatoms, on Ir(110), surface diffusion by atomic exchange mech. 80−49508
W, adsorpt. surface migration and thermal desorpt. of LaB_6, field emission microscopy 79−56075
W, adsorption of Ga, In and Sn, field emission, FIM 77−16470
W, anisotropy of surface self-diffusion 78−34689
W, diatomic cluster migration on W {100} plane, elementary displacement steps 80−88436
W emitter tip, surface shape changes, field ion microscopy meas. 78−26754
W field emitter, surface migration and overgrowth of LaB_6 77−85902
W, field evaporation end form at 4.2K 77−1790
W, LEED and electron microscopic investigs., review *(Hungarian)* 77−47654
W, of Pd, anisotropy effects due to substrate struct. 79−99422
W, periodic struct. development, under conditions of thermal mass transfer *(Russian)* 77−59187
W points, micro-size, change in shape and electron field emission 79−74067
W, self-diffusion, effect of Ni adsorption layer, FEM characts. *(French)* 77−1296
W, surface, self-diffusion coeff., determ. from van der Mast's expt. data between 3000-3600K 79−11011
W, surface diffusion 79−56048
W, surface diffusion of adsorbed Pd and Au layers, spreading behaviour 79−99421
W, surface diffusion of adsorbed O, secondary electron emission study 80−76117
W, surface energy anisotropy and faceting behaviour in vac. and in H_2 77−7961
W surface self-diffusion, ion impact induced, FIM study 80−103549
W, surface self-diffusion by ion impact, protrusion formation 78−75938
W, surface thermoelectrotransport of atoms 80−2448
W, with adsorbed Pd, field emission obs. of adsorpt., diffusion and self-diffusion 78−38945
W, with H adatoms, PMR meas. of adsorption state, surface migration 78−10275
W-Re, surface diffusion 79−56048
W-Re (3%) alloy, W adatom-substitutional Re atom interaction, FIM obs. 77−89626
W-SiO_2, adsorbed O_2^-, EPR 78−84046
W(110), adsorption and diffusion of CO 79−46955
W(211), Re adsorbed atoms and dimers, surface diffusion 77−20183
$(YSm)_3(FeGa)_5O_{12}$ film, LPE on $Gd_3Ga_5O_{12}$, interface processes, horizontal dipping obs. 80−49552
Zn film, deposition props. on specially prepared substrate, desorption energy and surface diffusion 79−90917
Zr, adsorbed on W(Ta)(Re), low-temp. mobility, surface struct. 77−20197
Zr, adsorption and absorpt. of CO, NO, N_2, O_2, and D_2, dissoc. and diffusion 80−80085
Zr fibres, high-temp. nitriding kinetics *(Russian)* 80−21166

surface discharges
see also corona
air-dielectric surface discharge, flash-energy spectra anal. 77−4009
air/glass interface, ns. grazing discharge, X-ray emission 80−33846
cathode surface heating by high pressure glow discharge, catastrophic bridging 78−87574
ceramic substrate, spark, channel spreading and substrate vaporisation 77−89336
charge density distribution along positive streamer on dielectric surface 78−87536
chemical reactions in plasma generated near ferroelectric surface, obs. 78−68931
corona discharges from ice points on metal electrodes 78−67587
creep discharge, probability of discharge phenomena, theory and obs. 80−38838
creep discharge at dielectric surface, statistical anal., independ. discharges model 78−1938
creep discharge plasma channel props., dielectric surface effects 80−15973
creep discharge self-sustaining at dielectric surface, Paschen's law 80−38837
creep discharge surface injected carrier half-life meas. 80−15972
current flow in corona discharges with arbitrary outer-conductor geometries 77−62418
DC partial discharge, repetition rate, cavity surface cond. depend. 77−11421
dielectric conduction and breakdown, conf., Gainesville, FL, USA (Oct.-Nov. 1979) 80−82564
dielectric in vacuum, surface breakdown, dielectric strength calc., quantitative model 80−34855
dielectric materials spacecraft, surface discharge arc propag. and damage 80−71314
dielectric solid surface breakdown in vac., desorption mechanism 78−67464
surface discharges continued
dielectric stimulated arcs in lighting-arrestor connectors, substantial lowering of breakdown voltage 79−99013
dielectric surface, gas discharge, flash amplitudes meas. 77−80384
dielectric surface, photoinduced surface discharge 80−88929
dielectric surface creep discharge flash intensity and time distrib. obs. 78−67562
dielectric surface creep discharge photon intensity rel. to charge transport 78−67561
dielectric surface grazing discharge, elec. field config. 80−44069
dielectric surface with accumulated air positive ions, vacuum breakdown obs. 78−75464
electrolyte surface discharge development and influence on model reactions *(Russian)* 79−96320
electrophotographic two-component developer discharge and contact interaction *(German)* 78−62258
electrostatically rechargeable liquids, max. discharge energy estimate *(German)* 80−38737
epoxy mica generator insulation, dielectric stress conc. influence on voltage endurance 78−15094
fast insulator surface flashover, investigation using electro-optical elec. field meas. 80−64820
fast insulator surface flashover in vacuum, mechanism, electro-optical investig. 80−103206
flashover of insulator surface in vacuum mag. inhibition 77−11411
fracture, ionisation wave generation, microbreakdown mechanism 79−33032
gliding linear discharge over dielectric surface, obs. 80−38826
high-pressure atomic and molecular impurities, preionisation by UV irrad. of surface discharge 80−38847
hydrocarbon liquids, electrostatically charged, incendivity of sparks from surface 80−6303
insulating solid, elec. strength and degradation 78−83631
insulation as affected by immobile high-current discharge and arc resist. 79−37563
insulator flashover in HV vacuum transmission line, mag. effects 77−24236
insulator surface flashover in vacuum, electro-optical meas. 80−38823
Kapton H, discharge area scaling and surface/subsurface damage due to electron beam irrad. 80−34853
mechanism and charge quantities due to steep front impulse voltages, expt. *(Japanese)* 77−7608
metal, current pulse effects on structure at crack tip *(Russian)* 77−44332
metal cathode, electrically stressed surface elec. phenomena, electrolum. and breakdown with medium gap spacings 80−20710
metal surface, electrical pulsed discharge action under air environment *(Russian)* 77−43091
metal surface with incident microwave radiation, secondary emission discharge 77−1026
metal target, gas breakdown near surface, pulsed CO_2 laser focusing effect 79−52051
multichannel surface spark gaps 79−18436
Mylar, discharge area scaling and surface/subsurface damage due to electron beam irrad. 80−34853
organic insulating material, arc tracking, comparative tracking index 77−90528
organic insulator, wetting and discharge inception in atmosphere of fog *(Japanese)* 79−4201
partial discharge at dielectric surface, charge transported rel. to no. of photons emitted 77−80383
plasma, UV pulse form. by EM shock wave front 77−58917
plasma source, ion form. and secondary electrons *(Russian)* 78−71503
plasma switches, high press. surface discharge, review 80−103208
PMMA, immersion in high press. gaseous media, breakdown characts. for direct voltages with ripple 80−45009
polycarbonate plate, impulse surface flashover in vacuum, effect of normal elec. stress 79−4199
polyethylene surface field strength under DC stress 80−15967
polymer, dielectric film on cond., sliding spark development in air 79−86634
pulsed surface flashover mechanism involving electron-stimulated desorption 80−70055
Rochelle salt ferroelectric surface creep discharge plasma channel and domain interactions 80−15996
sliding discharge, guided, explosive emission phenomena 80−19649
smouldering discharge at O_3 liq. surface in N_2, thin solid pellicle formation of N_2O_5 80−38827
solid dielectric, surface discharge initiated breakdown, in high pressure gaseous mixtures 78−48117
spark discharges, high current, light emission props. and appls., book contrib. 79−77449
statistical model of creep discharges in air dielec. surface 79−99012
streak photography of solid insulator surface flashover in vacuum 78−59700
Teflon FEP, discharge area scaling and surface/subsurface damage due to electron beam irrad. 80−34853
Townsend discharge spark voltages, cathode surface state effects *(Korean)* 80−19643
tracking phenomena in solid dielectric materials under moist conditions, expt. 77−43934
UV light source, surface spark discharge type, for H_2/F_2 laser initiation 80−78923
UV spectral efficiencies of surface-spark discharges, appl. to I laser 77−75496
$Ba_2NaNb_5O_{15}$, ferroelec. phase, thermally stimulated light flashes, surface elec. props. effects 79−73885
CO_2 laser, vac. UV preionisation source spectral characts. 79−31938
CO_2 TEA laser, laser output depend. on initial photoelectron density 80−43320
Cu cathodes, broad area type, electrolum. regions, current-voltage characts. 80−84019
H_2, superluminescence in surface discharge *(Russian)* 78−37676
$LiNbO_3$, spontaneous elec. breakdown 77−66458
$LiTaO_3$, spontaneous elec. breakdown 77−66458
N_2, liq., dielectric breakdown, using discharge figures 80−11338
NaCl, mechanoluminesc. peaks, microbreakdown mechanism, generation of ionisation waves 79−33032
S, single crystal, photoinduced discharge 400 to 580 nm 77−8139
SF_6 breakdown field strength, electrode surface roughness tolerance 78−67577

surface discharges continued
SnO_2 coated glass, surface elec. breakdown 80−25303
TiO_2-polycarbonate laminate, impulse surface flashover in vacuum, effect of normal elec. stress 79−4199
ZnS, single crysts. excited by laser beam and elec. field, streamer luminesc. and photolum. obs. 80−34986

surface electron states
see also interface electron states; surface scattering
1/f noise, theoretical analysis *(Polish)* 78−91737
ab initio SCF LCAO calc., impurity clustering, surface states three-dimens. cryst. 78−56201
absorbed atoms, effect on surface electronic props. 79−60905
adatom, electronic states, correlation effects, self-consistent T-matrix calc. 80−44691
adatom density of states, impurity atom effects 80−92958
adatom effects, quantum mech. approach 77−85294
adatom monolayer, on model transition metal surface, densities of states, chemisorption effects 78−26769
adatom on transition metal surface, vibr. model using pair interactions 80−15357
adatom pair interaction asymptotics, degenerate electron gas permittivity 80−29281
adatom valence-level position variation on metal surface 80−88611
adatoms, correlation effects, s-d hybridization in substrate 80−107886
adatoms, electron state at high coverages 79−28400
adatoms, electronic state, depend. on conc. 78−72001
adsorbate, photoelectron core level spectra calc. 77−85896
adsorbate and clean surfaces, electronic props. *(French)* 80−80344
adsorbate bond geometry, determ. using photoemission 78−71951
adsorbate induced electronic states, rel. to photoemission, book contrib. 78−95326
adsorbate induced photoemission, book contrib. 78−95668
adsorbate on single crystal, anal. of electronic state by angle-resolved photoelectron spectroscopy 80−11541
adsorbates, angle-resolved photoemission, book contrib. 78−95669
adsorbates, core level spectra, exactly soluble limits of model 78−80459
adsorbates, photoexcitation theory rel. to angle-resolved UPS and surface EXAFS 80−39426
adsorbates, surface plasmon effects on satellites in XPS 79−61493
adsorbates, XPS, plasmon effects on core level spectra 78−60547
adsorbates deep level spectroscopy, many body effects 80−39441
adsorbed atom interaction, LEED exam. 78−95237
adsorbed atom on solid surface, photoemission from valence band, surface plasmon emission, model Hamiltonian calcs. 80−50525
adsorbed atoms, electronic struct. and UPS, appl. to O on Ni 78−15281
adsorbed atoms, soluble relax. model for core level spectroscopy 79−8226
adsorbed atoms and molecules, core level spectroscopy, surface relax. energies, theory 77−89830
adsorbed atoms and molecules XPS, many-body effects 80−55266
adsorbed atoms interactions, plasmon mediation in presence of metallic surface 78−71991
adsorbed atoms on metal surface, XPS satellite spectra 77−20993
adsorbed atoms surface band splitting, theory, with appl. to He/graphite 80−60058
adsorbed diatomic on electrode, reson. Raman scatt. 79−51421
adsorbed layer, electron density oscills, around adatom 79−87138
adsorbed layer, electronic transforms, near boundary separating mag. and nonmag. states 80−92961
adsorbed layer, nonuniform charge distribution, phase transitions, Hartree-Fock calcs. 80−54525
adsorbed layer, struct. and electron alterations, electron-phonon interaction effects *(Russian)* 78−87880
adsorbed molecules, surface plasmon enhanced light absorption 80−40176
adsorbed species, plasmon versus shake-up satellites in XPS 78−48286
adsorption, surface band theory and surface transport props. 77−43680
adsorption of atoms on metals, Green's function formalism for studying electronic struct., local density of states calc. 80−107884
AES, obtaining density of states information from self-deconvolution of Auger band-type spectra 78−92150
Al (001) surface, nearly-free-electron metal, origin of surface reson. states 78−95322
alkali adsorbates and surface states in (111) covalent faces 79−42601
alkali halide, band struct. of selectively adsorbed atoms 79−28399
alkali halide film, low energy electron scatt. 78−26928
alkali metal chemisorbed layers, changes in work function due to charge transfer 78−18900
alkali metal submonolayer on metal substrate, geom. struct. rel. to electronic props. 77−85080
alkali metals, adsorbed on metal substrates, electronic struct. 79−87139
alkaline earth metals 79−28310
alkaline earth oxides photoluminescent spectra of surface states 79−47505
alloy, cleaved, electronic theory, off-diagonal disorder 79−4596
alloy, disordered, bulk and surface density of states, effect of surface segregation 77−15729
alloy surfaces, sputtering process and sputtered ion emission models 80−35044
alloy thin film, thickness depend. of CPA electronic densities of states 80−65644
alloys, A_3B type, surface effects on order-disorder phase transition 77−76556
amorphous and ordered films, adsorbed on metal surface, electron state of adsorbed atoms *(Russian)* 79−51425
amorphous film, surface phonon assisted tunnelling at low temp. 77−4421
analysis of surfaces, atomic beam scatt., SIMS, and vibr. spectra, book contrib. 79−42357
angle resolved secondary emission and electron energy loss study of electronic struct. 79−61477
angle-resolved photoemission, review 80−45214
anisotropic continuum, with anisotropic surface layer, coeff. of attenuated total reflection 80−60535
anisotropic crystal films, surface polaritons 78−26822
anthracene, intermol. relax. energies, UPS 78−31304
anthracene, polarised refl., surface excitons, Davydov splitting 77−16327
anthracene, polarised reflection spectra, surface and vol. exciton coupling, vibronic states 78−72543
anthracene, single crystal, contact charging and photoemission 79−47586

surface electron states continued
anthracene, surface polaritons, attenuated total refl. 77−63423
anthracene, surface states and persistent internal polarisation via photocurrent transients 77−89825
anthracene, thin surface layer, delayed fluoresc. obs., surface trap influence 77−77291
anthracene, total reflection spectra, site shift surface exciton dispersion 77−77233
anthracene films, optical props., comparison between free and optical contact mounting 80−89079
anthracene surface, Ar impact, Penning ionisation electron spectra and photoelectron spectra 80−66352
antiferromagnet, FCC lattice of second kind, surface magnons and mag. structs. 78−23261
atom near metallic surface, resonant state, Schrodinger eqn. soln., jellium model 78−80033
atom-surface scattering, selective adsorption phenomena, elastic theory 79−100012
atomic and electronic struct. 80−54746
atomic chemisorption on simple metals, chem. trends, core-hole relax. 78−14586
atomic cluster on metallic surface, density functional calculations 80−44699
atomic electronic levels, near crystal surface, pot. drop effects 78−19123
attenuated total reflection spectra of surface excitons polaritons 77−24867
Auger electron APS, extended fine struct. analysis 79−28863
band models, appl. of Green's function matching procedure 77−59320
biexciton in polar semicond., binding energy calc. 80−96796
bimetallic junctions, interface plasmon modes, theoretical anal. 80−54767
bound electron gas, static semiclassical response 78−56089
bounded chain of potential centres, electron states 79−7874
cadmium arachidate monolayer, Ag(Au) substrate, reson. surface plasmon reflection 78−56536
cadmium arachidate monolayer, surface plasmon spectra, refractive index dispersion 78−64424
Casimir effect in dielectrics using source theory, surface tension and latent heat 79−8109
catalysis, heterogeneous, role of surface science expts. 78−15710
cathode material choice methodology to obtain low work function 80−100500
CdS, transverse acoustoelec. voltage inversion 77−47885
CdS thin films, slow electron mean free path 79−99998
p-CdTe, surface photovoltage spectroscopy in IR and visible range 80−39632
CDW of two-dimensional electrons, in strong mag. fields 78−43316
characterisation, state-of-the art and need for standards 78−38916
characterisation by X-ray techniques 77−55868
charcoal, adsorbed H_2 monolayers, H_2 dynamics 79−66341
charge disturbances, surface-induced, in filled bands 78−10532
charge exchange scatt. 78−43974
charged particle interaction with surface modes 80−20275
charged particles surface excitation system, ground-state energy 80−15462
charged surface layers, collective excitations *(Chinese)* 79−51646
charged two-dimensional isotropic Fermi liq., static and dynamical props. 79−19532
chemisorbed atoms, spatial variation of extraorbital screening charge 79−60886
chemisorbed systems, model, exact and approx. results for electron densities of states 79−42605
chemisorbed systems, review of electronic struct. calcs. 77−28226
chemisorption, electronic and ionic motion, exact unidimensional model 80−15369
chemisorption, image charge effects, surface plasmons 80−84381
chemisorption, image charge effects on adsorbate valence spectra, perturbational study 80−84380
chemisorption, spin-fluctuation description 77−76666
chemisorption of single atom on transition metal surface, relax. shifts and singular broadening in spectra 77−59203
chemisorption on model insulator 77−85072
chemisorption on Ni (001), electronic struct., KKR model calcs. 78−56200
chemisorption on transition metals, semiempirical model calcs., extended basis set 77−72793
chemisorption systems, IR spectral linewidth and sticking coeffs., nonadiabatic effects 80−39423
classical two-dimensional electron system, correlations and plasma oscills. 79−69446
clean metal surface physics, review 77−15659
clean surfaces, electron states, photoemission data anal., book contrib. 78−95325
cleaved crystal, surface electronic Green's functions in terms of the bulk Green's function via random-walk theory 79−60898
cluster Bethe-lattice method appl. 80−49852
collective modes, ground state energy of semi-infinite electron gas, rel. to surface props. 77−66134
complex tight binding systems, surface density of states determ. 80−20272
conference, Eindhoven, Netherlands (June 1976) 77−62708
conference, New York, USA (Oct. 79) 80−73093
conference on solid-vacuum interface, Amsterdam, Netherlands (June 78) 79−42342
conference on surface physics, Tagow, Poland (June 1976) 78−26747
conference on surface science, York, England (March 1977) 78−14540
contact potential meas., surface pot. jump effect of spots, coatings and cryst. faces 77−51805
cooperative emission of excited mol. monolayer into surface plasmons of metallic substrate 80−20666
copper phthalocyanine film, electron acceptor surface states due to O_2 adsorption 80−88586
covalent and ionic solids, determ. of electronic struct. 78−2409
covalent surface, pot. and charge distribs. and dangling-bond state 78−2537
crystal lattice electron energy spectrum depend. on external electric field *(Russian)* 80−34498
crystal slab, 3-D, surface states, relativistic Green matrix method, muffin-tin potential 80−80345
crystal surface form., remarks on boundary conditions and resolvent method 79−42599

surface electron states continued
crystal surface states, calc. by relativistic Green matrix method 79−47139
CTIP, exciton surface polaritons at room temp. 79−47476
cubic ferromagnet, magnetic crystal, semi-infinite, impurity states, Green's function method *(Russian)* 79−51647
4-cyano-4′-n-pentylbiphenyl, refr. index meas. and isotropic-nematic phase transition study, surface plasmon technique 80−84282
γ-cyclopropyl-bis (1,3,3-trimethylindolenine-2-yl)pentamethinium fluoroborate, exciton surface polaritons, reflecting faces obs. 80−65645
cyclotron resonance, two dimensional electrons interacting with surface and volume phonon 78−80221
cyclotron resonances, Coulomb interaction effects in 2-dimens. 78−60073
d-band width, surface at. relax. effects 78−34878
deep levels, effect of vibration of adsorbed molecules on electron capture 80−29458
degenerate electron liquid, skipping orbit cyclotron resonance, surface state transitions 80−103889
degenerate semiconductor, with surface depletion layer, surface polaritons, hydrodynamical model 80−6752
density of states in tight-binding formalism 78−10530
density-density correlation function, exchange corrections 78−14786
desorption, multiphonon processes, quantum-statistical theory 80−107641
desorption, time dependent escape rate from potential well 78−79888
diamond, (100) surface states, SCF extended tight-binding method 77−47881
diamond, (111) surface states and relax., modelling and using mol. SCF calcs. 78−39186
diamond, surface electronic struct., self consistent pseudopotential calc. 78−47842
diamond-type crystals, LCAO band structure, overlap and distant neighbour effects 80−49585
diatomic linear chain, semi-infinite s-p hybrid, surface states 77−4419
dielectric, energy struct. determ. by electron absorpt. spectra 78−11040
dielectric films, transition layer vibrs., resonance region auxiliary surface polaritons *(Russian)* 80−2347
dielectric interface, surface polariton effects in spontaneous emission 77−20391
dielectric parabolic wedge, electrostatic edge modes 77−28231
dielectric response in local representation, microscopic theory 77−85289
dielectric sum rule for electron response function 78−39184
dielectric surfaces, phenomenological model for optical props. 80−20605
dielectric surfaces, rough, interaction of EM waves 77−43688
dielectric wedge, electrostatic edge modes 77−28230
dielectric-vacuum interface, spatial dispersion in optical props. 77−4613
diodes, thin film glass based structures, surface electron states effect on switching *(Russian)* 80−107887
disorder at surfaces and interfaces, effect on electronic props. 78−26932
disordered solids, surface states 80−103736
dye crystal, CTIP, exciton surface polaritons detect. by ATR spectra at 295K 79−4818
dye in contact with Ag film, enhanced total refl. with surface plasmons 79−59694
dyes, photographic emulsion spectral sensitisation, latent image form., subcond. band events 78−32905
electric field sustained in δ-well crystal, energies greater than work func. 78−10528
electron binding energies reference level problem in photoelectron spectra of solids and adsorbates 78−63936
electron density, bulk and surface atoms, from ab initio model calcs. 79−4590
electron eigenstates, near surface of solids, mathematical theory 78−76125
electron emission spectroscopy probe 77−51798
electron energy loss spectroscopy, book contrib. 77−63509
electron gas, Bloch, surface mag. props. in opposing elec. and mag. fields at 0K 78−63992
electron gas, correlation energy, appl. of coupled cluster approx. 78−72102
electron gas, degenerate, in metal or semicond. slabs, surface plasmon damping 80−88501
electron gas, multipole surface plasmons, bulk-selvedge coupling theory 79−28394
electron gas, neutrally charged with surface, props. 79−38144
electron gas, spin polarised, model for conduction electrons of simple metal in mag. field and ferromag. Gd 77−8034
electron gas with surface, Green function theory, exchange and correlation effects 77−8164
electron liquid, cyclotron reson. at skipping orbits *(Russian)* 78−72240
electron liquids, two-dimens., short-range order onset, thermodynamic props. 78−43454
electron spectroscopic analysis of surfaces *(French)* 80−16153
electron spectroscopy, (e,2e) reactions, theory 78−39640
electron spectroscopy and surface chemical bonding, book contrib. 80−24992
electron spectroscopy of surfaces, review 78−92169
electron-hole droplet reson. radiation, radiative decay of surface plasmons *(Russian)* 77−62841
electron-hole liquid, two-dimensional, ground-state energy 77−28233
electron-hole plasma, LF degenerate surface modes 77−28137
electron-plasmon and electron-phonon interactions in bulk and near surface, Kikuchi patterns 78−26759
electronic structure and UV photoemission 77−62975
electronic surface resonances and crystal surface structure 78−71648
electronic surface resonances of crystals for Al(001), W(001), Ni(001) and oxygenated Ni(001) 79−95464
elements, sputtering process and sputtered ion emission models 80−35044
ellipsometry of clean surfaces, submonolayer and monolayer films, review 80−103546
EM surface wave exam. by appl. of optical technique 77−76893
energy conversion radiation enhancement using surface polaritons 80−7941
energy spectrum in periodic magnetic field, band struct., surface states anal. *(Russian)* 80−39645
epitaxial islands, equilibrium struct., one-dimens. model 79−15035
ESCA, surface anal. and electronic structure *(French)* 80−7891
exchange-correlation energy functional, gradient approx. 79−90983
exciton energies and radii 80−92829
exciton luminescence spectra, surface polaritons and Brewster waves *(Russian)* 79−43033
surface electron states continued
exciton-polariton *(Japanese)* 77−39910
excitons in mixed molecular crystals, theory 79−47135
excitons near hard walls, Green's theorem calc. 79−78014
experimental studies *(Chinese)* 79−99602
far IR surface polariton obs. by attenuated total reflection 77−39790
fast-moving charge near surface, self-energy 79−47138
Fermi systems, spectral function calculation, time depend. approach 79−43096
ferroelectric semiconductor, band bending in surface layer 80−60061
ferroelectric semiconductor, spontaneous polarisation field screening by free charge carriers *(Russian)* 80−50274
ferromagnetic metal, spin-polarised field emission, many-body and spin-dependent surface pot. effects 79−74065
ferromagnetic semiconductor, surface localised low energy electron-magnon states *(Russian)* 80−88734
field emission spectroscopy, extended range 78−39669
field ion emission, surface plasmon excitation and Jason effect, comment 77−28699
field ion emission, surface plasmon interpretation, comment 77−28700
film, band structure, appl. of extended rigorous cellular method 78−52055
film, electron states in longitudinal mag. field 78−91784
film, electronic props. in longit. mag. field 79−73603
film, HF formalism for calc. of total energies and charge densities 80−49850
film, surface density of states calc. within tight-binding scheme 77−55594
films, linearized APW method for electronic band struct., appl. to Fe, Co, Ni, Cu and Al 79−69393
films, thin, quantised, electronic energy spectrum *(Russian)* 80−44688
FIM role of surface states, one-dimens. model 78−26399
finite crystals, surface deformations 78−76127
foil, surface guided modes, excitation by electrons 77−59310
force constant changes near surface 77−85047
friction coeff. of atom near metal surface 77−59312
gas-solid interface, electronic struct. HFR calc. 80−54745
graphite, adsorbed He, band struct. and thermodynamic props. 80−80349
graphite, chemisorbtion of CO, CNDO calc. using cluster model 80−54522
graphite, chemisorpt. of N periodic overlayers, CO-NDO calcs. 79−7745
graphite, H chemisorption, cryst. orbital NDO calcs. 77−7965
graphite, He scattering, bound state reson. and inelastic effects 79−28876
graphite, interaction and band struct. effects for He derived from scatt. data 78−92162
graphite (0001), scattering and selective adsorption of H_2 (D_2) 80−71553
graphite (0001) surface, He atom scatt., bound state reson., interaction pot., band struct. effects 80−29840
graphite adsorbed H_2 monolayers, H_2 dynamics 79−66341
graphite film, relativistic excitations by inelastic electron scatt. 77−1463
Green's function and generalised phase shift for surface and interface problems, Green's function and generalised phase shift 79−60895
Green's function for surface physics, partial differential eigenvalue eqn. 80−6929
Green's function formalism for N-interfaces 78−39179
Green function method for electronic struct. and vibr. modes calc. at surfaces 78−88012
H_2, electron surface barriers for dense phases 78−91754
halides, electron spectroscopy of crystals, book 80−36786
Heisenberg ferromagnet, mag. excitation near surface of high Miller indices 77−51871
heterogeneous catalysis reaction mechs., electron pair behaviour and surface orbitals 80−55705
hexamethylcyclotrisilazane film, glow-discharge-polymerized, in MIM and MIS structs., elec. cond. mechanism 79−42680
HV electrode, Fe microsphere impact, charge reversal, oxidation effect 77−12042
hypersound resonant excitation by 2-dimens. plasmons *(Russian)* 79−78032
III-V compounds, (110) surface, energy distrib. of dangling-orbital surface states 80−80347
III-V compounds, electron transport in quantised inversion and accumulation layers 79−60935
III-V semiconductor, cubic, high symmetry surface, dispersion law calc. for Tamm states 80−15587
III-V semiconductor, theory for surface (110), relax. effects 80−6938
III-V semiconductor based layered multielectronic systems, electronic process investig. survey *(Russian)* 80−107891
III-V semiconductor surfaces and interfaces, Green's function technique, tight binding approx. 80−49855
image force for parallel incident particles, surface plasmon dispersion and single-particle effects 79−42602
image force on moving charge 77−39982
impurities, near-surface, adiabatic potential, symmetry props., group theory methods 80−70786
impurities, surface bound states, quantum and classical liquids 78−18859
impurity effect, transfer matrix approach 78−95321
infinite crystal, surface states determ. by complex extension of tight binding 78−80032
inhomogeneous electron systems, exchange and correlation effects calc. 80−20104
inhomogeneous media, surface plasmon dispersion, reply to comment 79−42609
inhomogeneous media, surface plasmon dispersion 77−24602
inhomogeneous media, surface plasmon dispersion 77−28229
inhomogeneous media, surface plasmon dispersion relation 79−42608
n-InSb, surface recomb. vel., repeated cyclic surface treatment effects 77−32065
integral characteristics of the electron structure of crystalline surfaces 78−64078
inversion layer, threshold conduction 78−43450
inversion layer localisation and two-dimensional white noise problem 78−84271
inversion layers, far IR emission, Hamiltonian for one-dimensional Coulomb field 77−43764
ion, near metal surface, friction parameter and Brownian motion 80−15584

surface electron states continued
ion bombardment-induced photon emission, spectral features, mechanisms band struct. depend., review 77−44072
ion-induced kinetic electron ejection, pot. emission, semiconductors and insulators, review 77−44109
ionic crystal, surface parameter calc. by pseudopotential method *(Russian)* 78−76130
ionic crystal-degenerate semiconductor interface, localised plasmon-optical phonon coupled modes 78−38930
ionic crystals, surface electron states in continuous spectrum 78−26931
ionic crystals, surface F centres, electronic struct., numerical soln. of one electron Schrodinger eqn. 78−64091
ionic crystals, surface polaron 78−60020
ionic crystals, weakly bound surface polaron 79−69576
ionically bonded surfaces, stability in ionising environments, core hole Auger decay mechanism 80−29457
itinerant-electron ferromagnetic film on nonmagnetic metallic substrate, mag. props. 80−20371
jellium, chemisorption, effective-medium theory of chem. binding 80−65367
jellium, chemisorption of H, simple model 77−69171
jellium, chemisorption of Li(H), simple model 79−60625
jellium metal, bounded, linear response function in RPA 79−69444
jellium metal, surfaces props., statistical calc. 80−24987
jellium metal surface, work function calc. 79−65536
jellium metal surface densities, electronic density, variational calc. 79−15205
jellium metallic surface, corrections to local density approx., gradient expansion vs. wave-vector analysis 77−51796
jellium metallic surface, exchange-correlation energy, wave-vector analysis 77−47877
jellium model with finite discontinuity in potential, response function 77−1466
jellium surface props., statistical calc. 79−60897
jellium-vacuum interface, charge distrib., nuclear density profile 78−30962
Kane semiconductors, parametric excitation of surface waves 79−38014
Kronig-Penney cryst., semiinfinite, generalised existence conditions 77−51794
laminated systems, two dimensional and surface plasmon mixing *(Russian)* 80−15466
laser irradiation effects 80−84812
lattice and symmetrical description of surface bands 80−70785
layer metal particles, surface plasma oscillations 77−76765
layer metal particles, surface plasmons 77−1465
layered structure, surface polaritons, dispersion relations, recursive soln. 77−69390
LEED Kikuchi pattern, contrast change due to plasmon excitation 78−34686
light emission from inelastic tunnelling spectroscopy, surface plasmon modes 79−3598
light metal, surface effects on X-ray level widths 79−47147
liquid, surface CARS 80−1280
liquid surface electron layer, parametric excitation of collective modes 77−15928
local densities of states near a crystal surface with disordered overlayer 79−15201
local orbitals, optimisation for electronic struct. calc. 77−47711
localised, surface structure and energy spectra 79−60885
lossy media, nonlinear excitation of surface polaritons 79−90974
magnetoplasmon type polaritons, LF, existence criterion in Faraday config. 80−96961
many-valley cubic semiconductor, light absorpt. by free carriers at surface 78−48200
matching Green function method, surface electronic struct. calc. 78−88013
mechanical metal-semiconductor contacts, I-V characts., press. effects 78−2564
mechanical surface excitons, interaction with radiation, refl. and transmission spectra 79−15098
metal, 'surf-riding' electrons on wake potential of ion beams 77−80747
metal, adsorption of He, HF calc. of repulsive pot. contrib. 77−43434
metal, BCC, chemisorption of monolayer of atoms, charge in density of states determ. 77−47682
metal, charge screening and Friedel oscillations of electron density *(Russian)* 78−79951
metal, chemisorption, effect of gradient correction to exchange and correlation energies 77−11978
metal, chemisorption, intra-adsorbate Coulomb correl., surface structure 77−15685
metal, chemisorption, theoretical models, chemical and solid state approaches 78−18911
metal, conduction electron distribution function and corrections to surface impedance for normal skin effect *(Russian)* 78−76100
metal, density functional theory, review 80−44698
metal, effect on ground state of approaching H atom 77−35979
metal, electrochemical exam. of multiple states of chemisorbed atoms 77−44512
metal, electrodynamics, optical refl. coeffs. and surface plasmon dispersion law 80−75619
metal, electron gas, local density functional for kinetic energy near defect, metal surface 80−20105
metal, electron scatt., effect of surface on lattice defects, surface Landau level reson. 79−65534
metal, electron-surface-plasmon scatt. using parabolic nontouching trajectory 77−28228
metal, electronic surface reson. band struct. and lineshapes 79−82655
metal, energetics of chemisorption, book contrib. 80−24740
metal, exchange-correlation hole 78−80037
metal, excitation by fast electrons of surface plasmons on spherical voids 77−11975
metal, FCC, (100) surface, chemisorption-induced interaction between electronic levels of two-level adsorbate 80−39644
metal, gradient approx, anal. appl. 80−96810
metal, H chemisorption, surface sp-conduction electrons, spin-density functional formalism 79−33321
metal, HCP, LCAO description of (0001) surface electron states, appl. to Sc 78−72232
metal, image-potential-induced states, plasmon model 79−78147
metal, inhomogeneous strain effects on surface props., rel. to fracture model development 77−72907
surface electron states continued
metal, interacting metal half spaces, effect of retarded-surface-plasmon dispersion and Van der Waals interaction 79−69452
metal, interaction with neutron mol. 77−80701
metal, IR absorption, contribution of conduction electron scattering 79−42971
metal, jellium model, H chemisorption, linear response theory 78−91543
metal, jellium model, H chemisorption, relax. energies in UPS 78−91544
metal, jellium model, nonlocal density based self consistent surface calcs. 77−72898
metal, light reflection, adatom characts. depend. 78−10918
metal, periods IV, V, and VI, work function depend. on plasmon energy 78−18986
metal, physisorbed inert atoms, polarisation due to short range interaction with substrate 80−39428
metal, plasmon mechanism for energy loss, dissoc. and orientation of fast ions excited by grazing collisions 80−11523
metal, plasmon model for image-potential-induced surface state, appl. to positron surface states 79−19559
metal, refraction effects in angle resolved photoemission from surface states 79−38720
metal, reson. interaction with neutral mol. 77−80702
metal, resonance absorption of Rayleigh sound by surface electrons 78−71924
metal, review of chemisorption 79−42377
metal, semi-infinite, nonlinear interaction of oppositely travelling surface plasmons 79−28393
metal, semi-infinite, transverse dielec. response, surface effects 77−47878
metal, simple, self-consistent, calc. of surface energy including ion pot. perturbation effect 77−8166
metal, sticking probability, correl. with adsorbate-induced electron struct. 80−39425
metal, struct. induced surface plasmon polariton modes using ATR, theory 79−60890
metal, surface charges waves *(Russian)* 78−64077
metal, surface dipole barrier, calc. 80−96958
metal, surface electrons, reson. and cyclotron waves *(Russian)* 77−73081
metal, surface energies and work function, simple analytic model 80−49862
metal, surface energy 78−91528
metal, surface energy calc. in model of discrete positive charge *(Russian)* 78−38911
metal, surface energy of electron gas, virial theorem 77−69398
metal, surface excitations in contiguous plasma 80−38667
metal, surface photoeffect, energy and angular energy distribs. 77−63535
metal, surface plasmons *(Russian)* 79−33327
metal, surface plasmons in thin film, circular cylinder and spherical void, RPA calcs. 77−80823
metal, surface region, absorption of EM radiation 78−43456
metal, surface roughness effect on light absorptivity 78−80314
metal, surface-plasmon dispersion relation from reflectivity of parallel-polarised light 79−78030
metal, surface-resonance fine struct. in LEED intensity profiles 77−39518
metal, ultrafine particles, positron annihilation exam. 78−56542
metal, virial theorem for jellium model 79−60892
metal, with substitutional disorder, density of states, Green's function theory 78−23145
metal, work function changes due to absorpt. 77−7972
metal cavity, lifetime of trapped excited atom, broadening mech. for optical absorption line 79−38578
metal circular cylinders, inhomogeneous, non-radiative surface plasmon-polariton modes 80−29455
metal crystal with and without surfaces, asymptotic displaced charge round impurities 79−95364
metal electrodes, plasma-type electroreflection, mechanisms 77−1659
metal film, carrier relax. time, optical determ. by surface plasmon excitation 77−1499
metal film, surface impedance oscillation effects due to one sided RF excitation *(Russian)* 80−11106
metal film, surface plasmons, rel. to structure-related optical characts., visible and UV 77−55841
metal films, one-dimens., electronic states 80−54758
metal oxide, molecular adsorption, UPS studies, review 80−84374
metal oxide surface, adsorption of electron acceptors, strength and distrib. of electron donor sites 78−84055
metal oxides, d-band, surface enhanced covalency and effect on surface states 77−35975
metal particles, spherical, surface plasmon dispersion relation, hydrodynamical model 78−84277
metal shallow grating diffr. efficiency, Rayleigh type and surface plasmon reson. type anomalies 79−55050
metal spheres, optical surface plasmon modes, theory 78−2539
metal spheres, small, plasmon freqs., calc. by hydrodynamic theory 78−43319
metal substrate, H chemisorption, model, including image charge effects 79−73405
metal surface, adsorbed atoms, oscillatory indirect interaction, non-asymptotic behaviour in tight-binding models 78−72000
metal surface, adsorbed layer, structural and electronic reconstruction 78−84280
metal surface, approached by substrate, surface amplitude patterns 80−75620
metal surface, band effects and dipole interaction between two adatoms 79−33323
metal surface, electron correl. in chemisorbed H atom, friction coeff. 78−60026
metal surface, electron-phonon coupling in image-potential bound states 80−54752
metal surface, electron-plasmon interaction 80−39649
metal surface, excited molecules located above surface, theory of damping 79−15203
metal surface, fast ion scatt. by plasmons, theory 80−45190
metal surface, force on moving charge, spatial dispersion effects 80−65646
metal surface, Friedel oscillations around adatom 78−30967
metal surface, indirect long-range oscillatory interaction between adsorbed atoms 78−71997

surface electron states continued
metal surface, integro-differeneial eqn. for electron density and formula for surface tension of jellium 80−44689
metal surface, interaction between adatom and substitutional impurity atom 79−56076
metal surface, light refl. from dye molecule monolayer 78−48246
metal surface, linearised secondary electron cascades, surface and subsurface sources 78−11036
metal surface, linearised secondary electron cascades 78−11035
metal surface, mol. chemisorption, self-consistent calc. 79−95260
metal surface, narrow band, self consistent model calc. of electronic states 78−95333
metal surface, neutral molecule, resonance interaction 78−84279
metal surface, normal mode anal. of image pot. 79−33325
metal surface, optical SHG effects of electron band struct. 77−740
metal surface, positron-electron correlations, RPA calc. 80−40181
metal surface, retarded Van der Waals' force 79−38146
metal surface, self consistent electronic struct. effect on atomic positions, computer simulation 78−30969
metal surface, semiclassical infinite barrier model 78−64079
metal surface, sticking rate, transmission problem, model Hamiltonian 80−107640
metal surface, tight-binding, dissociative chemisorption of molecule 78−2368
metal surface, van der Waals, interaction with mol., effect of spatial dispersion 78−10534
metal surface, vector potential calc., semi-infinite electron gas approximation 77−32063
metal surface, with adsorbed at., XPS intrinsic plasmon satellites, dispersion and lifetime effects 79−56151
metal surface bonding, book contrib. 80−24990
metal surface electronic barrier, elec. field effect in presence of adsorbate, Thomas-Fermi model 80−49864
metal surface electronic density of states, random distribution of impurity atoms 78−6424
metal surface electronic struct., linear response theory, appl. to Na 78−56197
metal surface energies, variational calc. 77−24603
metal surface energy, gradient corrections in interpolation formulae, surface plasmons 80−2441
metal surface exposed to external radiation, solns. of Maxwell's eqns. 78−52054
metal surface interaction with external mol. complex 79−47140
metal surface or metal-metal interface, plasmon dispersion 78−52053
metal surface plasmons, direct energy transfer from excited dye mol. 79−91119
metal surface props., Rayleigh-Ritz variational calcs. 79−69570
metal surface props. in square barrier and linear one electron potential model 79−19645
metal surface region, electrostatic energy and screened charge interaction for different Fermi surface shape 80−70631
metal surface with substitutional disorder, electronic struct. 78−23144
metal surfaces, chemisorption, historical review 79−46920
metal surfaces, dipole barrier and work func. calc. 79−15208
metal surfaces, electronic spectrum of ordered monolayers 77−85293
metal surfaces, exchange and correlation energy, wave vector anal. 80−20273
metal-adsorbate system, appl. of cluster model theory, book contrib. 80−24991
metal-air interface, far IR propag. distances of surface EM waves 79−42616
metal-dielectric interface, p-polarised light total absorpt. by surface plasma waves 78−88373
metal-insulator-semiconductor struct., magnetooptic interband absorption by semicond. surface layer 80−93288
metal-insulator-semiconductor structure, DC cond. and Shubnikov-de Haas effect 80−11012
metal-semiconductor contact, frequency relationships of photocurrent and photo-EMF *(Russian)* 80−107908
metal-semiconductor contact, surface doping effect *(Russian)* 77−47896
metallic atom chemisorption, work function variations 79−46936
metallic film, electron density and potential, variational calc. 79−78218
metallic films, adsorption studies using modulated surface plasmon reson. 79−82439
metallic interfaces, conf., Ghent, Belgium (Sept. 1978) 80−41946
metallic rough surface, reflection loss for s and p polarised waves near surface plasmon freq. *(French)* 80−97225
metallic sphere, very small, surface plasmon dispersion, RPA 77−47886
metallic surface, collective effects in physical adsorption of inert gas atoms 79−19456
metallic surface, dispersion of surface plasmons 80−2440
metallic surface, effect on cooperative Lamb shift 77−3317
metallic surface, electrodynamics, microscopic effects *(Russian)* 80−6936
metallic surface, self-consistent electron theory, review 80−88616
metallic surface, surface traps and vacancy trapping, slow positron obs. 79−87522
metallic surface energy, exchange and correl. contrib., wave-vector decomp. 80−75615
metallic surface state, influence of refr. of p-polarised light on photoemission 80−20772
metallic surface states, effect of refraction of p-polarised light on photoemission 78−72686
metallic surfaces, interaction between two pieces of jellium 77−32061
metallic thin films, density response function and dynamic struct. factor, nonlocal effects 79−69447
metallic thin films, optical props., effect of quench condensation 79−78773
metallic thin films, surface plasmon light scatt. 79−87517
metallic thin films *(French)* 80−60692
metallic thin layered structures, coupled surface plasmons 79−56873
metals, adhesion theory for two surfaces 80−20270
metals, chemisorption of gases, book 79−69370
metals, density of states and spin susceptibility, normal and giant surface effects 78−10322
metals, ground state, variational self-consistent method 78−56204
metals, liq., charge density fluctuations in surface layer *(Russian)* 80−15580
metals, photoelectron spectroscopy of surface states 79−56909
metals, s-p bonded, review of electronic struct. calcs. 77−28226
metals, surface effects in hydrodynamic model review 79−78148

surface electron states continued
metals, surface electron density crimping, Ashcroft potential, density functional calcs. *(Russian)* 79−82653
metals, surface relax. time of conduction electron spins 78−91814
metals separated by dielectric, electronic component of metal-metal interaction force, calc. 78−52056
Mg, K X-ray emission spectra, double plasmon high energy satellite 80−11510
MIM structure, surface plasma oscillations, refl. coeff. and energy density repartition for p-polarised waves *(French)* 79−69606
MIM tunnel junction, surface plasmon excitation 78−10578
MIM tunnel junction, surface plasmon excitation by electron tunnelling 78−91779
MIOS memory structs., degradation, fast surface state density 79−38179
MIS dielectrics, charge centre removal, low press. RF annealing technique 78−56230
MIS solar cell, effects of pinholes, oxide traps and surface states 78−80055
MIS solar cell open-circuit photovoltage rel. to oxide thickness 79−61985
MIS structure, calc. of surface states in band gap by Green's function method 80−15611
MIS structure, capacitance-voltage charact., built-in charge fluctuation effects, negative surface state density 80−6992
MIS structure, determ. of deep level parameters in surface layer of semiconductor 80−15612
MIS structure, fast surface states density, photoelectric methods of determ. 80−70835
MIS structure, high- and low-freq. steady state capacitance 80−54796
MIS structure, in presence of radiation, dielec. deposition temp. effect 77−89872
MIS structure, photovoltaic efficiency, effect of insulating film and interface states *(French)* 77−1488
MIS structure, SAW charge transfer theory 79−56327
MIS structure, semicond. surface states, capacitance, admittance, freq. depend. 80−49940
MIS structure, thermal generation of carriers through surface centres 79−69603
MIS tunnelling Schottky barrier, surface state effect on electrical characts. 78−47877
MISIM struct. inversion layer, symmetrical, carrier conc. calc. 80−75651
mixed crystal, semi-infinite, local electronic states, CPA extension 79−65401
MNOS p-channel transistor, memory charact., H_2 anneal effects 80−80388
MNOS structures, high temp. H anneal, effects of fast surface states 79−38178
MNOS structures with tunnelling-thickness SiO_2 films, charge trapping obs. 78−95379
model calculation using Koster-Slater type surface potential 79−7872
molecular crystal, surface exciton energy calc. 77−20400
molecular crystal, surface exciton levels, radiation corrections 80−34962
molecular crystal, surface excitons theory 77−15927
molecular crystal/electrolyte interface, illuminated, space charge behaviour 78−84290
molecular crystals, semi-infinite, with surface point defect, exciton states 80−20271
molecular solid, surface props., review 78−34886
molecule-metal interaction and surface reactions, theoretical description 80−39652
MOS capacitor, surface state distrib. determ. from transient capacitance plots 79−42658
MOS inverted-channel carrier scatt., effect of oxidation in Cl media 78−76156
MOS layer structure, UV illumination effect on elec. props. 79−82676
MOS p-channel transistors, boundary surface band bending 78−34903
MOS pulsed capacitor, minority carrier lifetime meas. influence of Si-wafer surface state density 80−60098
MOS structure, charge motion, surface state effects 78−2573
MOS structure, effect on surface and bulk generation currents 78−47883
MOS structure, surface state spectrum meas. by pulsed C-V method 80−88641
MOS structure, use of mini-computer for rapid evaluation of C-V-plots *(Russian)* 79−28413
MOS structures, inversion layer near electrode edge, pot. and charge density distribution 80−88642
MOS structures, surface piezoacoustic waves, interaction with two-dimens. plasmons 79−28683
MOS structures with external p-n junction, linear gate volt., impulse-current behaviour *(German)* 79−56319
MOS surface states, DLTS spectra synthesis and anal. 80−11090
MOS transistor, Au-doped, Au surface-state energy levels 80−11092
m.o.s.f.e.t., inversion layers, localised state wave functions 77−4417
MOSFET and gated diode, surface states, density and capture cross section determ. *(German)* 78−23173
Mossbauer spectroscopy and surface phenomena study 80−39916
MOST channels, quasi-Fermi level gradient distrib., Hall voltage 80−29481
MOST structures with process-induced defects, elec. props. 80−54788
muffin tin orbital method for surface and films 78−95331
multi-scattering method for cryst. surface band struct. calc. 80−2439
multipole surface plasmons, attenuated total refl. spectra 79−78149
n-type semiconductor anode, illum., charge transfer modes, digital simulation 80−2464
narrow band gap semiconductors, conference, Warsaw, Poland (Sept. 1977) 79−82582
narrow band gap semiconductors, conference, Warsaw, Poland (Sept. 1977) 80−49703
narrow gap semiconductor, surface states in energy gap 77−69401
neutral particles interaction pot. with surfaces *(Russian)* 80−6937
nickel phthalocyanine film, electron acceptor surface states due to O_2 adsorption 80−88586
p-nitroaniline, adsorbed layer, core ionisation, negative shake-up energy 79−56913
noble metal, electronic structure and d-holes of films and surfaces 78−39180
noble metal film, modulated surface-plasmon reson. in situ meas., O_2 adsorpt. 77−77311

surface electron states continued
noble metals, surface electronic structure, calc. method 77−89828
non-local density based self-consistent surface calculations, Thomas-Fermi soln. 77−28227
non-specular conducting surfaces, classical electrodynamics 77−85280
non-specular dielectric surfaces, classical electrodynamics 77−85279
one dimensional crystal with square well pot. 79−82652
one dimensional model, existence conditions for surface states 77−89826
one-dimensional crystal, semiclassical WKB approx. calcs. 78−52046
one-dimensional crystal in external field, with internal Kronig-Penney type pot. 77−72896
one-dimensional crystals, matching conditions, Bloch functions, logarithmic derivatives 80−15475
one-dimensional deformed semi-infinite cryst., surface states 79−65529
one-dimensional inversion (enrichment) layers in MOS structure semicond. surface, production method 79−42663
one-dimensional model crysts., surface density of states, rel. to adsorbed molecule 80−107889
one-dimensional semi-infinite crystal with arbitrary potential at boundary, surface states 77−43681
one-dimensional semiinfinite systems, surface state energies 80−88607
one-dimensional theory, Green's function soln. *(Russian)* 77−59311
ordered adlayers, density of surface states, Green's function calc. method 77−85291
ordered adlayers, electronic struct. 79−38142
ordered overlayers, on FCC metal surface, electronic struct. calcs. 79−60906
organic crystals, exciton surface polaritons 79−4519
organic monolayer/metallic substrate, exciton-surface plasmon interaction 79−69569
oscillating dipole-metal surface interaction, jellium model and random phase approx. 80−92955
oxidised surfaces, sputtering process and sputtered ion emission models 80−35044
p-n heterojunction differential admittance theory in the presence of surface electron states 80−96981
perovskites, d-band, concepts of surface states and chemisorption, book contrib. 80−107651
perovskites, d-band, surface electronic props., π-bands exam. 79−38145
perturbed crystals in Kg representation, orthonormal localised states 78−6327
phonon-polaritons, semi-infinite crysts., review 77−89827
photoelectric work function, depend. on light freq. *(Russian)* 77−32066
photoelectron excitation process theory, book contrib. 78−95664
photoelectron spectroscopy, solid-state, with synchroton radiation, review 80−71570
photoelectron spectroscopy, theories for expt. data anal. 77−63541
photoelectron spectroscopy of clean and adsorbate covered surfaces *(French)* 80−50519
photoelectron spectroscopy of localised levels near surfaces, scatt. effects and relax. shifts 78−15291
photoemission, angle-resolved, from localised orbitals at solid surfaces, theory 78−15292
photoemission, many-body effects, book contrib. 78−95667
photoemission and surface electronic properties, book 78−95662
photoemission and surface electronic props., book contrib. 78−95663
photoemission spectroscopy, angle-resolved, final-state symm. and polarisation effects 77−40332
photovoltage transients, surface state parameters determ. 77−72905
piezoelectric crystal, optical SHG with surface plasmons 78−18008
piezoelectric crystal, surface polaron states, polaron-phonon interactions 80−70790
piezoelectric semiconductors, acoustoelectric surface phonon-conduction electron interaction 79−42360
piezoelectric semiconductors, surface phonon acoustoelectric interaction, elastic anisotropy effects 80−6610
plasmarons, effect of finite thickness of accumulation layer, theory 80−103636
plasmon, eigenmodes, Fredholm integral eqns. *(French)* 78−56195
plasmon, EM surface wave, energy flow and group vel., hydrodynamic approx. calcs. 78−84272
plasmon, momentum or energy fixed dispersion relations 78−14687
plasmon dispersion and damping, effect of surface irregularities 77−24604
plasmon dispersion relation at short wavelengths 80−96962
plasmon dispersion relation in presence of spatial dispersion 79−42612
plasmon effects in electron spectroscopies and chemisorption 79−33190
plasmon light emission induced by fast electrons on modulated surface 78−80424
plasmon obs. using X-ray emission 78−92146
plasmon oscill. eigenmodes and Van der Waals energy, chain of aligned spheres *(French)* 77−80821
plasmon oscills., eigenmodes, geometrical shapes 77−80822
plasmon resonances in 2-D system, dispersion relation 78−63997
plasmon-acoustic wave interactions due to deformation potential *(Russian)* 80−15356
plasmon-phonon modes in quantizing mag. field, nonlocal shift 77−72908
plasmons, around cavity surface, in semiinfinite metal *(French)* 78−56196
plasmons, counterpropagating, for coherent SHG 80−33081
plasmons, Nonlinear mixing of oppositely travelling surface plasmons 79−95460
plasmons, surface, theory of non phase-matched SHG 78−72101
plasmons at inhomogeneous liq. metal/dielec. interface, second dispersion branch 77−32059
plasmons on rough surface, dispersion relation splitting 79−60739
plasmons on rough surfaces, dispersion relation changes 77−69394
polar liquids, surface dipolar plasmons, nonradiative, dispersion relations 78−6308
polar semiconductor, surface inversion layers, energy loss of warm and hot carriers 77−11981
polar semiconductor surface, energy levels and geometry, theory 80−49481
polarisation wave instability in quasitwo-dimens. system 78−68065
polariton effects in spontaneous emission, effects of spatial dispersion 78−34879
polariton frequency shift, cryst. surface and dielec. function depend. 80−44522
polariton generation through grating couplers 77−85153
polariton interaction with periodic surface struct. 77−47879
surface electron states continued
polariton motion in thin surface layer, nonstationary phenomenological theory *(German)* 80−88608
polariton scattering by order parameter fluctuations near phase transition 77−35981
polariton use in optical storage 80−48414
polaritons, bulk and surface, nonlinear spectroscopy 77−50730
polaritons, effect of surface roughness 79−73451
polaritons, hybrid bulk-surface type 80−49626
polaritons, hybrid bulk-surface type 80−49627
polaritons, linear photon and two photon absorpt. 80−49863
polaritons, molecular thin plate, with near-surface polariton transition layer, reflection and transmission spectra *(Russian)* 78−14677
polaritons, nonlinear optical spectroscopy, stationary and nonstationary, theory *(German)* 80−6922
polaritons, Raman scatt., active spectroscopy theory 77−59576
polaritons, spectrum, coupling to excited fluorescent molecule near surface 77−69395
polaritons, theory and spectroscopy uses 80−92835
polaritons due to spatial dispersion 79−69438
polaritons in anisotropic crysts. 78−87919
polaritons in semi-infinite crystals, review 78−72087
polaritons in spatially dispersive medium, surface effects 78−56081
polarons, electrons in surface phonon field 80−107885
polarons and excitons, surface self-trapped states *(Japanese)* 80−2445
poly-2,4-hexadiyne-1,6-diol bis (p-toluene sulfonate), exciton surface polaritons, reflecting faces obs. 80−65645
poly-2,4-hexadiyne-1,6-diol bis (p-toluene sulphonate), cryst., exciton surface polaritons, reflectivity of (100) face, 295K 78−80372
polyethylene, surface charge release, crossover phenomenon, thermally stimulated discharge current study 80−50255
polyethylene terephthalate, mechanism of photocarrier generation 77−89798
polymer, contact electrification, extrinsic surface state contrib. 77−11984
polymer, surface props., review 78−34886
polymer films, photoelectric emission and contact charging, surface states 79−33885
polymer surface modification by RF plasma, difference ESCA spectra 77−63529
polymeric materials, high-energy electron emission, in breaking adhesive contact 79−65981
polymers, vacuum-UV irrad. photoelec. emission and contact charging 79−52075
polymers powders, corona-charging props. 80−6946
polystyrene coated Ag holographic grating, Raman spectra enhancement by plasmon surface polaritons 80−80885
positron binding energies at surfaces, thermal activation meas. 79−95371
positron surface states, emission of positrons, positronium 80−54655
in potential jump model *(Russian)* 77−85278
powder semiconductors, HF conductivity depend. on surface energy band bending *(Russian)* 77−15890
pseudopotential surface and interface calculations 80−49853
pseudopotentials, reliability criteria 80−49563
PTS, exciton surface polaritons at room temp. 79−47476
pyridine, adsorbed on Ag, giant Raman scatt. 79−95768
quantum chemical calc. methods 80−49849
quantum insulator, plasma oscillation spectrum charges, continuum approx. free electron surface state binding energy 79−69575
quantum resonance impedance oscillations *(Russian)* 78−91781
quartz glass surface, in vacuum, mechanism of appearance of elec. charges 79−69743
α-quartz surface, XPS study 80−93451
quasi-two-dimensional electrons, electrodynamics 77−89829
quasi-two-dimensional system in perpendicular elec. field, hydrogenic model 80−29454
quasiparticles, density of states, in anisotropic flat slab, in effective mass tensor approx. 79−28266
Raman scattering, surface enhanced, surface plasmon model 80−108211
Raman scattering by surface polaritons and compensation effect 78−10374
random alloy, optical absorption and photoemission spectra 80−45216
rare earth alloys, surface effects on valence 78−91746
rare earth atoms at surface, photoionisation of 4f electrons 78−11077
rare earth compounds, XPS, intermediate valence states 79−33887
rare earth element submonolayer films, electronic phase transitions, heat of absorption 80−24736
rare-earth metals, surface valence state from surface tension props. 79−95462
refractory materials, emission and adsorption props., rel. to electronic struct., review 77−76899
resonance band structure, lateral surface struct., determ. method 78−68067
resonant elastic scatt. of electrons for surface struct. meas. 77−63505
rhodamine B surface state hole traps, surface photovoltage meas. 80−39654
rough surface, dispersion relation for surface plasmons, quantum mechanical approach 78−72099
rough surface, surface plasmon radiation, roughness assisted, ang. distrib. 78−52521
rough surface light scatt., vector theory, surface plasmon effects 79−59638
Rydberg states, existence and detection via LEED 78−56198
Schottky barrier, mag. surface levels in presence of depletion-type band bending 80−20285
Schrodinger equation for surface pot. barrier including spin-orbit interaction, anal. and numericai soln. 79−58492
secondary ion and photon emission under medium-energy ion bombard., influence of surface plasma 79−33881
semi-infinite array of identical potentials, surface effects and electronic density of states 78−54110
semi-infinite crystal with surface impurity, electronic states 79−24046
semi-infinite solid, elementary excitations in surface region 79−60618
semiconducting surface inversion layer, cyclotron reson. of interacting electrons 78−34885
semiconducting surface inversion layers, exchange and correl. 80−75618
semiconductor, 2-dimens. plasma formed by quantising surface channel *(Russian)* 77−15936
semiconductor, amorphous, tetrahedrally bonded, electronic density of states, surface bond effects 77−8002
semiconductor, appl. of surface photovoltage spectroscopy 77−69391

surface electron states continued
semiconductor, core-level photoyield exam. of empty surface states 77−55593
semiconductor, covalent, non-orthogonal tight-binding approach 80−2442
semiconductor, cpd., conf., Princeton, USA, (Feb, 1977) 77−85300
semiconductor, deep level profile anal. by double deep level transient spectroscopy 77−20378
semiconductor, effect of surface space charge region 78−43939
semiconductor, effect on chemisorption of H_2 78−51823
semiconductor, electron emission from surface subband, reduced work function 80−60757
semiconductor, electron states at planar and stepped surfaces 78−10531
semiconductor, electronic struct. of point defects, surfaces and interfaces, Green's function scatt. theoretic method 79−33258
semiconductor, electronic struct. rel. to sorption 78−14784
semiconductor, generalised tridiagonal Hamiltonian resolvent matrix, exact soln. 80−29307
semiconductor, interface form., initial steps, surface states and thermodynamics 80−49503
semiconductor, localised states near displacive transition 80−70644
semiconductor, magnetoplasmon-polariton surface modes, Voigt geometry 78−43451
semiconductor, meas. of surface and interface states *(Japanese)* 80−20269
semiconductor, MM wave guiding and control by surface plasmons 80−103713
semiconductor, narrow gap, boundary conditions, energy spectrum, and optical transitions 79−42614
semiconductor, nonpolar, empty surface states and surface order effects on sorption 77−85281
semiconductor, optical orientation of electrons, surface quality effects 79−11466
semiconductor, optoelectric effect and oscillations near surface 77−8172
semiconductor, p-type, field emission theory, surface states and recomb. processes 77−85901
semiconductor, photocond., influence of surface space-charge layer 80−15563
semiconductor, photoemission meas. of surface and bulk states 80−25527
semiconductor, possible role in FIM, Kronig-Penney model 77−47883
semiconductor, prereduced surfaces, room temp. activity for oxygen isotopic exchange 79−91998
semiconductor, quasi-two-dimensional, crit. conc. of hot carriers 77−35977
semiconductor, quasi-two-dimensional, electron scatt. by polar optical phonons 78−72237
semiconductor, size effect, influence of space-charge regions on boundary conditions 77−89790
semiconductor, struct. induced surface plasmon polariton modes using ATR, theory 79−60890
semiconductor, surface electronic props., optical spectroscopic techniques, review 80−11070
semiconductor, surface energy level determ., thermally stimulated contact pot. difference method 79−99601
semiconductor, surface final-state effects on core electron transition energies 78−91745
semiconductor, surface properties, investigation by laser and photovoltages *(Russian)* 78−23130
semiconductor, surface reconstruction, dynamical theory 80−10773
semiconductor, surface reconstruction, theory 77−85282
semiconductor, surface space charge layer spectroscopy 77−20386
semiconductor, surface state excitons 77−51799
semiconductor, surface-state props., using field effect anal. 79−24053
semiconductor, surface-states concentration profile and capture cross section determ. using SAW convolver 80−80341
semiconductor, tetrahedrally coordinated, review of surface struct., chem. and spectroscopy 80−59764
semiconductor, unipolar, n-type, field-effect mobility, energy spectrum of surface states 80−39657
semiconductor, unipolar high-resistivity, directionality of longitudinal photocurrent 79−11177
semiconductor, with defects adsorbed mols. and metal overlayers, electronic structure 79−95466
semiconductor crystal surface, nonequilib. electron effects due to chem. excitation 78−72238
semiconductor crystal surface, nonequilib. electron effects due to chem. excitation 78−72239
semiconductor cyclotron resonance 78−6575
semiconductor doped surfaces, inversion layers, quantum model 78−30961
semiconductor electrode, charge injection, space charge region, simulation 77−15949
semiconductor electrode, surface state charge transfer in photoelectrolysis of water 79−28405
semiconductor film with surface states, light absorption under superhigh vac. *(Russian)* 78−72618
semiconductor in quantizing mag. field, plasma surface states of electrons 79−11195
semiconductor interface and overlayer electronic struct., review 80−49841
semiconductor interfaces, conf., San Diego, Calif., USA (Feb. 1976) 77−20377
semiconductor layer structure, laser-induced photolum. and collective effects *(Russian)* 79−95830
semiconductor of simple geometries, field penetration and band bending in high elec. fields 79−87106
semiconductor plasma, magnetically active, longit. propag. of surface waves 77−15934
semiconductor plasma, surface helicons, theory 80−60019
semiconductor plasma, surface waves 79−1612
semiconductor plasma, surface-helical instability *(Russian)* 77−15885
semiconductor space charge layers, subband struct., perturbation theory 80−84497
semiconductor stepped surface, electron states 78−95327
semiconductor surface, atomic and electronic struct. 78−72223
semiconductor surface, chemisorption of mol. complexes, bond orbital model *(German)* 80−59807
semiconductor surface, electron beam prod. of plasma oscillation instabilities *(Ukrainian)* 79−33318
semiconductor surface, electron-electron interaction and electronic props. of space charge layers 78−60210
surface electron states continued
semiconductor surface, field ionisation and field evaporation mechanisms 79−15594
semiconductor surface, heterogeneous, slow relaxation kinetics 77−85288
semiconductor surface, instrument for angle-resolved UV photoemission spectroscopy *(Japanese)* 80−93455
semiconductor surface, macroscopic recomb. centres 80−6933
semiconductor surface, resonance inelastic light scattering by carriers 80−20655
semiconductor surface and adsorbate states, charge injection into space charge layers 80−100496
semiconductor surface characterisation using SAW 80−11069
semiconductor surface electronic structure determ. by low energy electron loss spectroscopy *(Japanese)* 78−88007
semiconductor surface eval. using SAW convolver 80−97677
semiconductor surface plasma, van der Waals interaction with neutral atom, mag. field effects 77−59316
semiconductor surface plasmon dispersion, appl. to InSb 77−1464
semiconductor surface properties, methods of influencing 77−15965
semiconductor surface spectroscopy, exciton effects, theory 80−49856
semiconductor surface steps, Bethe-Peierls approx. 77−39911
semiconductor surface with incomplete impurity ionisation, quantum model 78−34877
semiconductor surfaces, optical props., book contrib. 80−80737
semiconductor surfaces and interfaces, calcs. 79−1613
semiconductor surfaces and interfaces, electronic struct. calc., scattering theoretic approach 80−6940
semiconductor tunnelling, bound levels and band struct., rel. to inelastic electron tunnelling spectroscopy 79−4597
semiconductor with surface doping, surface parameters determ. 77−15933
semiconductor-dielecltric interace, surface polaritons of LO-phonon-plasmon coupled modes 79−7792
semiconductor-electrolyte interface, charge transfer via surface states, water photoelectrolysis anal. 80−75636
semiconductor-insulator boundaries, capture coeff. of neutral surface traps, influence of image forces 79−51683
semiconductor-liquid junctions, differential capacitance measurement by desk calculator controlled system 79−78170
semiconductor-vacuum interface, electronic struct. self-consistent pseudopot. method 77−20428
semiconductor-vacuum interface, phase rule 78−52049
semiconductor/adsorbate system, local density of states calcs. *(German)* 80−60062
semiconductors, amorphous, doped, electronic props. 80−80283
semiconductors, calc. based on chemical pseudopotential 77−69393
semiconductors, covalent, tight binding analysis of step-depend. density of ⟨111⟩ surface states 77−59321
semiconductors, density waves in one, two and three dimensions 79−95353
semiconductors, electroreflectance, crystal termination effects, field reversal 77−69802
semiconductors, empirical tight-binding method, critique 80−49854
semiconductors, interband transitions, electron-hole effects 77−66192
semiconductors, photoelectron spectra, book contrib. 80−16155
semiconductors, review of electronic struct. calcs. 77−28226
semiconductors, surface and interface electronic struct., book contrib. 79−42619
semiconductors, surface potentials using electron energy anal., SEM study 80−15582
semiinfinite crystal with surface substitutional disorder, electronic struct. 77−72903
shielding of electric fields by surface electron states in an ionic lattice 78−52059
Shockley states in a semi-infinite Kronig-Penney model 79−73562
Si (111), surface relax., EHT and cluster calcs. *(Chinese)* 80−59762
n-Si-electrolyte junction, Schottky barrier height and reverse current 80−6979
simple cubic crystal, localised states, next-nearest neighbour approx. calcs. 79−7870
simple metals, atomic chemisorption, atom-jellium model, state density calc. 78−84066
simple metals, density functional theory of chemisorption, book contrib. 80−107647
sintering, Samsonov electronic theory 77−90288
sinusoidal surface grating, surface plasmons effect on diffr. orders 77−42618
solar selective absorbers and diffr. gratings, surface plasmons 79−14103
solid, semi-infinite, electronic instability of surface 77−43682
solid plasma slabs, hybrid bulk-surface polaritons 79−60904
solid surface, physics, review *(Japanese)* 78−79870
solid surface studies, recent progress *(Japanese)* 80−15347
solid surfaces, non-ideal, optical props., phenomenological models 80−88950
solid surfaces props. characterisation, structural, chemical and electronic, use of LEED methods *(Italian)* 80−49467
solid-electron interaction, nature and consequences 78−72230
solid-gas and solid-liquid interfaces, struct. rel. to reactivity 77−72775
space charge layers, HF magnetoconductivity 78−60231
specific heat of two dimens. electron gas, exchange interaction contrib., calc. 80−44331
spectral densities, transfer matrix approach 77−35976
spectroscopy using synchrotron radiation 77−20882
spherical particle, max. charge imparted by pulse-charging 80−6945
spherical particle with extremely high resistivity, corona charging 80−6944
spherical wave method for surface electronic wave functions in semi-infinite muffin-tin lattice 79−42603
sputtering characteristics, surface-barrier shape effects 80−93447
n-$SrTiO_3$, surface electronic struct. calc. 78−88011
$SrTiO_3$ (100) surface electronic structure, DV-Xα cluster method 80−39646
stilbene:rhodamine-6Zh, luminesc. of adsorbed mols., excitonic energy transfer to surface 78−31255
submonolayer films on metallic surface, struct. and props. review 78−38972
substrate-split localised adsorbate levels, spin polarisation effects in photoemission 79−19971
superconductors, surface relax. time of conduction electron spins 78−91814
superlattice, image pot. enhancement by static elec. field 80−92846

surface electron states continued
surface, narrow-band, self consistent model calcs. of electronic states 77−85295
surface channel, CCD, surface state parameters, transfer loss meas. 79−56279
surface channel tunnel junctions, subband spectroscopy 78−64104
surface charge state change during thermodesorpt. 77−80825
surface chemical bond, book 80−22147
surface phase shift rule, and density of states 78−2538
surface plasmon dispersion relation in presence of surface roughness 80−65650
surface polaritons allowing for spatial dispersion *(Russian)* 78−14675
surface properties of materials, Conf., Missouri, USA (August 1977) 78−87867
surface roughness effect on image potential electron energy loss, plasmon electron scatt. 80−54748
surface wave dispersion relation for non-local media 79−28398
surface-atom polarisability derivation from field-ion energy deficits 80−76155
surface-exciton polaritons, dispersion theory 78−72089
synchrotron radiation techniques 80−80945
TCNQ, exciton surface polaritons at room temp. 79−47476
TCNQ, single crystal, exciton surface polaritons, attenuated total reflection spectra 79−91460
Teflon FEP, annealed electret, charge stability 80−6943
Teflon FEP-A, corona and electron beam charged, TSC peak identification and surface-voltage stability 79−78614
tetracene surface states, electric field effects, exciton-charge carrier interactions *(Russian)* 80−24989
theoretical models of the electronic structure at surface irregularities 78−80031
theory, aims and recent accomplishments 80−75413
theory of solid surfaces, book 80−36787
thermoelectrets, surface charge density maximum during forming 77−36169
thin crystals, surface state calc. 78−14778
thin film, 11-layered, CPA calc. of local density of electronic states 80−65643
thin film heterostructure, energy spectrum study 80−70787
thin surface layer, interactions between nondegenerate electrons, effect on cyclotron resonance, mag. cond. *(Russian)* 80−15802
thin surface layers, thickness and optical consts. using surface plasmon excitation 79−47533
thin-film geometry, harmonic generation of surface-plasmon nature, off-synchronous treatment 79−18475
three-dimensional crystal, Hartree-Fock theory of surface states 80−44468
tight binding metal, vibr. freq. of atom normal to surface, Einstein model 79−51412
tight binding method, first principles 80−49564
tight-binding Green's functions for surfaces, thin films, and solid interfaces using random-walk theory 80−54753
transition and noble metals, d-band metals, chemisorption, book contrib. 80−107649
transition metal, adsorption of CO, electronic struct., localised orbital pseudopot. method 80−39653
transition metal, adsorption of rare-earth atoms, effects of changes in valence state 79−69367
transition metal, chemisorption of H, effect of surface spin fluctuations 80−75613
transition metal, chemisorption of ordered atomic layers, HF Green's function formalism and phase shift technique 80−24733
transition metal, chemisorption of ordered overlayers with C(2×2) and (2×1) structs. 79−46925
transition metal, electronic perturbations 78−95334
transition metal, electronic structure and d-holes of films and surfaces 78−39180
transition metal, magnetic moment near surface, one-electron band model 79−82747
transition metal, photoemission theory 78−95679
transition metal, projected surface energy bands, Shockley surface states 78−68061
transition metal, Shockley surface states, projected surface energy bands 78−88009
transition metal, spin fluctuations 78−95451
transition metal, surface density of states, continued fraction method 77−20388
transition metal, surface electronic structure calculations 78−95329
transition metal, tight-binding theory of interactions between transition metal adatoms 77−1304
transition metal (001) surface, model, chemisorption, coverage depend. of adsorption behaviour 78−71976
transition metal complex, surfaces, and supported catalysts, analogies among active sites 78−56917
transition metal cpds., rock salt struct., surface energy bands, Shockley surface states, bonding 80−92956
transition metal surface, chemisorbed H_2, Hartree-Fock-Slater model cluster calc. 78−26929
transition metal surface, electron states at steps, cluster-Bethe lattice approx. 78−52045
transition metal surface (adsorbate), intermediate UPS/XPS synchrotron radiation study 78−52633
transition metal surface clusters, Hartree-Fock-Slater model calcs. 77−72899
transition metal surface electronic states, self-consistent model calcs. 79−42618
transition metal surface electronic struct., influence of size and roughness 78−14785
transition metal surfaces, independent electron theory of atomic interactions 79−60903
transition metals, chemisorption of light gas atoms, on (100) surface, model calcs. 77−11797
transition metals, chemisorption on, theoretical model, formalism 80−6651
transition metals, conf., Toronto, Canada (Aug. 1977) 78−91577
transition metals, core levels between surface and bulk atoms, variation of binding energy shifts 80−88615
transition metals, d-electron surface density of states 77−85296
transition metals, field emission and field ionisation, role in heterogeneous activation of gas molecules 78−35271
transition metals, review of electronic struct. calcs. 77−28226
surface electron states continued
transition metals, self-consistency role in evaluation, tight-binding calcs. 77−39908
transition metals, stepped surface, electron states 78−95327
transition metals, surface electronic structure, calc. method 77−89828
transition metals, surface states, qualitative theory, Shockley model 80−6924
transition models, and free-electron like metals, alkali metal adsorpt., valence electronic struct., wave-function matching calcs. 78−72235
trapping of positive energy electrons on infinite sheet 78−14779
trapping phenomena rel. to surface states 77−39916
triboelectricity, charging between metal and insulator 79−78157
TTF-TCNQ, XPS, surface electronic struct. 78−52627
tube, ambient axial electric field, temp. depend. surface shielding effect 77−58221
tunnel junction, small-particle type, light emission, local plasmon modes 79−19676
two atom surface coupling, double reson. at plasmon freq., collective effects 80−34934
two dimens. Brillouin zone and Wigner-Seitz cell integrations, special point formulae generation 80−70783
two dimensional electron gas, correlations 78−63996
two dimensional electron spectrum spin splitting, specified by surface potential *(Russian)* 80−15583
two-band crystal, surface reconstruction, Green's function formalism 78−14543
two-band crystal, surface reconstruction, model for CsCl struct. 78−14544
two-dimensional, Hartree-Fock soln. of CDW in mag. field 79−28302
two-dimensional classical plasma, on dielectric film, collective excitations *(Russian)* 78−34788
two-dimensional electron gas in mag. field polarisability 80−107888
two-dimensional electron impurity system, quantum theory of cyclotron reson. lineshape 78−64083
two-dimensional electron system in strong mag. field, Anderson localisation 77−15929
two-dimensional electron system in strong mag. field, crystallisation 78−30966
two-dimensional electron-impurity system in strong mag. field, electron spectrum and cond. *(Russian)* 78−88016
two-dimensional quantum plasma in mag. field, exchange energy 77−72904
two-dimensional surface layer, ground state energy and effective mass of polaron 79−23910
two-dimensional system, electronic props., conf. Berchtesgaden, Germany (Sept., 1977) 78−60177
two-dimensional Wigner glass in strong mag. field, numerical study 78−63993
ultrathin doping levels as model for 2-dimens. systems 78−60182
uniaxial crystal foil, electron energy loss probability at oblique incidence 80−25506
UPS, angle-resolved, initial state symmetries from polarisation effects 80−40227
valence band spectroscopy in ultrasoft X-ray region 77−55852
virtual, simple modelistic treatment 80−103739
virtual surface states, Green function theory 80−80342
voids and particles, Van der Waals energy between them, from asymptotic to close contact 80−80351
VUV isochromat spectrometer for surface anal. 79−54197
Vycor glass, positronium-surface interaction in pores 78−27347
Wannier-Stark ladders of finite crystal, level shifts 78−30895
water, surface dipolar plasmons, nonradiative, dispersion relations 78−6308
wide-gap semiconductors, thermionic emission current, surface states effects 79−15581
Wigner crystal on liq. He surface, cond. *(Russian)* 80−6594
Wigner crystallisation of two dimensional electron gas in strong mag. field 78−60005
XPS, solid-state and adsorbate shifts, equivalent cores calc. 79−28888
XPS and AES techniques for surface characterisation 77−32495
zincblende (110), surface relaxation 79−38143
zincblende compounds, (111) and $(\bar{1}\bar{1}\bar{1})$ faces, surface electron states 78−80035
zincblende compounds, (111) face, dangling bond surface state 78−84278
zincblende compounds, electronic struct. and atomic config. at cleavage surface 77−62974
(e,2e) reaction, possibility for solids, expt. conditions 77−90225
Ag (001) surface, photoemission, electron escape effect 79−1814
Ag (100), (110), (111), high resolution photoelectron energy distrib. curves 77−28693
Ag (100) and (111) surfaces, positronium form. due to slow positron trapping 80−107748
Ag (110), electroreflectance, surface state contrib. 80−80755
Ag (111), adsorbed layers of $O_2(N_2)(S)$, electronic props., XPS and UPS 78−10279
Ag (111) surface, obs. of surface plasmon splitting by electroreflectance spectroscopy 79−61338
Ag, angular resolved photoemission from low index faces 78−48282
Ag, CESR, influence of freq. and surface effects 79−51856
Ag clean (111) surface, absence of filled surface states in s-p gap, LCAO calc. 78−2543
Ag, electrode pot. effects on surface plasmon excitation 78−15149
Ag, electroreflectance spectroscopy, longitudinal surface plasmons 80−40137
Ag film, angular depend. UPS, surface electronic struct. 79−83095
Ag film, bounded by dielectric slabs, attenuated total refl. angular spectra 78−92135
Ag film, dye monolayer effect on surface plasmons, ATR obs. 79−87001
Ag film, energy transfer from excited dye mol. to surface plasmons 79−91119
Ag, film, lifetimes of surface plasmons 79−47143
Ag film, surface plasmon wave excitation of dye mol. fluoresc. emission 79−89703
Ag film coated with dye monolayer, anomalous dispersion of surface plasma oscills. 79−8203
Ag films, underlayer effect on surface roughness, surface plasmon excitation meas. 79−51456
Ag foil, surface-plasmon resonance, roughness-induced wavelength corrections 80−108288

surface electron states continued
Ag foils, surface plasma-wave reflectance and roughness-induced scatt. 80−66228
Ag grating, surface plasmons rel. to diffr. order intensity profile, higher harmonics influence 78−25981
Ag halide, photographic image form., defect and impurity states, LCAO calc. 78−16876
Ag, intrinsic surface states, UV photoemission meas. 77−20983
Ag, nature of 3.8 eV plasmon in XPS 79−78838
Ag, positronium formation at (100) surface 79−82654
Ag rough film, multiple light scatt. of surface plasmons 77−48262
Ag rough surface, transition radiation for 77 keV electrons, surface plasmon light emission 78−60530
Ag, single cryst. electrodes, electroreflectance obs. in aqueous solns. 80−25342
Ag surface, (111) and (100), crystallographic anisotropy in surface plasmon decay to photoelectrons 79−24052
Ag surface, clean and oxidised, $M_{4,5}VV$ Auger spectra, anal. based on self-convolution of measured UPS 77−77332
Ag surface, periodically modulated, radiative decay of surface plasmons excited by fast electrons 77−24599
Ag surface, time-resolved mol. electronic energy transfer interaction with pyrazine 80−92957
Ag, surface Landau level resonances, effect of k_H-broadening 79−65533
Ag surface layers, reflectivity, contrib. of longit. polarisation waves 79−83046
Ag, surface plasma oscills., sinusoidal surface 77−73179
Ag, surface plasma waves, dispersion curves, attenuated total reflection spectra 78−88015
Ag, surface plasma waves 79−47151
Ag, surface plasmon dispersion relation in presence of surface roughness 80−65650
Ag, surface plasmon light emission induced by fast electrons on modulated surface 78−80424
Ag, surface plasmon reson. interaction with dye monolayers 78−84674
Ag, surface polariton absorption and emission spectra, edge effects 78−10375
Ag, surface-plasmon modulated reson. for adsorption studies 79−83045
Ag surfaces, Cs and Cs-O covered, surface plasma waves, ATR study 80−39451
Ag, thin layer on Al surface, surface plasmon ATR spectroscopy 79−78770
Ag thin layered structures, coupled surface plasmons 79−56873
Ag-Cu, surface segregation, electronic theory, density of states, cluster-Bethe-lattice approx. 80−49369
Ag-In_2S_3-Si layered struct., Hall effect, I-V characts., surface states *(Russian)* 80−97001
AgBr film, surface space charge region 77−1508
AgBr, localisation of polarons on (100) surface, rel. to photographic sensitivity *(Russian)* 77−35983
AgCl, luminescence, theory and measurement 79−19934
AgI film, light-induced changes, ellipsometric meas. 78−56537
Al (001), 100-2000 eV electron backscatt., surface and bulk plasmon losses 77−32480
Al (001), enhanced photoexcitation 80−80937
Al (001), scatt. matrix method for surface states 79−60894
Al (100), inelastic LEED at beam emergence condition 78−83690
Al (100), photoemission, ang. terms in optical pot. 80−55269
Al (111), angle-resolved UPS obs. of 2-dimens. band structs. of S, Se and Te 80−60059
Al (111), bonding of O, electronic struct. calcs., rel. to UPS data 80−59801
Al (111), LEED Kikuchi pattern, contrast change due to plasmon excitation 78−34686
Al (111), ordered O overlayer, angle-resolved photoemission, band struct. 80−40229
Al, adsorption of O_2, intrinsic and extrinsic plasmon coupling, XPS of adsorbed atoms core states 78−10278
Al, adsorption of O_2, relation between energy-band and cluster model 78−52048
Al, adsorption of small molecules, photoelectron spectra, surface plasmon spectroscopy 79−47148
Al, ang. depend. of plasmon loss features in XPS 78−43987
Al, anisotropic Fermi vel., surface Landau level reson. 78−10333
Al, bulk and surface plasmon loss intensities in XPS, Auger and electron energy loss spectra 79−38012
Al, characteristic energy losses on C contaminated surfaces, secondary electron spectra, AES, and EELS 79−99997
Al, chemisorption of O, unoccupied extrinsic surface resonances and site struct. determ. by soft X-ray absorpt. 79−73403
Al, mean free path of electrons needed to form surface plasmons 77−51800
Al, photoemission from (100), (110), and (111) cryst. faces, surface states 79−4893
Al, plasmon sideband exam. by synchrotron radiation tuning of electron escape depths, UPS 77−47755
Al, SCF Xα scattered wave calc. for clusters up to 43 atoms 78−10323
Al, single cryst., surface reson. and oxidation 78−72225
Al surface, light diffr., photon excitation of compound plasmon resonances 79−28307
Al, surface, single cryst. unoccupied surface resonances, surface soft-X-ray absorption spectroscopy 79−28862
Al, surface broadening of 2p core level photoemission spectra 80−25524
Al, surface photoelec. effect, surface photoemission spectroscopy on jellium 79−4900
Al, surface plasmon dispersion, high-energy electron loss spectroscopy obs. 77−20390
Al, surface plasmon dispersion curves, splitting by Ag surface layers 78−60178
Al, valence band Auger spectra, surface effect 80−80915
Al, with plastic surface coating, g-factor and spin relax. time of cond. electrons 77−32258
Al-Al_2O_3-Ag tunnel junction, 4-pyridine carboxaldehyde-doped, surface enhanced Raman spectra, surface plasmons 79−98111
Al-Al_2O_3-SnTe, junction, tunnelling, Fermi level depend. on carrier conc., influence of surface states 80−25016
Al-In_2S_3-Si layered struct., Hall effect, I-V characts., surface states *(Russian)* 80−97001
Al-Si_3N_4-Si struct., surface energy bands under step function illumination 80−49840
Al-SiO_x-Si MIS solar cells, short-wavelength response 79−57428

surface electron states continued
Al_2O_3, adsorpt. of TCNQ anion radical salts, EPR and electronic spectra 77−72776
Al_2O_3 amorphous layers in MIS structures, prep. and physical props. *(Slovak)* 78−64122
Al_2O_3 monolayer, core excitons and inner well resonances in surface soft X-ray absorpt. spectra 80−40187
Al_2O_3, valence band density of states from self-deconvolution of $L_{23}VV$ Auger spectrum 79−47561
Al_2O_3:Eu, surface luminesc. centres excitation characts. 78−52560
Al_2O_3:Si thermoluminescent phosphor, annealing characts. and nature of traps 77−85817
β-Al_2O_3-Na_2O, adsorption of Na, surface electronic struct. calcs. 80−75431
AlSb (110), wave functions and surface struct. 78−91519
Al(100), angular resolved photoemission from intrinsic surface states 78−39665
Ar, solid, n=1 surface excitons and LO-TO splittings of bulk excitons 79−73445
Ar, solid, surface excitons 77−76892
As_2Se_3 amorphous thin films, illumination-induced change in contact pot. 80−20251
Au (100), characterisation of reordered and normal surfaces by LEED, AES and EELS 78−34687
Au (100), normal and reconstructed, electronic struct. changes, ang. resolved photoemission obs. 80−25520
Au (110), electroreflectance, surface state contrib. 80−80755
Au, AES and characteristic energy loss spectra, expt. and interpretation 78−27354
Au alloys, surface electron states, photoelectron spectra meas., rel. to Au 78−14781
Au clusters on alkali halide surface, size depend. of valence bands, XPS study 80−65647
Au, core level binding energy and density of states from first atomic layer, XPS meas. 79−87563
Au, electrode pot. effects on surface plasmon excitation 78−15149
Au electrodes, adsorpt. of Br^-, specular reflect. investig. 78−61047
Au, electron tunnelling from particle, plasmons and polarised light emission 79−51685
Au film, angular depend. UPS, surface electronic struct. 79−83095
Au film on Ag, optical constants, 4000-6000 Å, using surface plasmon optical excitation 77−69925
Au, intrinsic surface states, UV photoemission meas. 77−20983
Au, L_β emission band, surface plasmons in X-ray emission bands 78−92146
Au, monolayer, on W(001), elec. struct. 78−72236
Au, photoelectron spectra, occupied surface-state bands in sp gap 79−43094
Au, photoelectron spectra, bulk and surface, rel. to band struct. 80−20770
Au, photoemission study of bulk and surface electronic struct. 79−4894
Au, single cryst. electrodes, electroreflectance obs. in aqueous solns. 80−25342
Au, surface atoms, XPES, core level binding energy, density of states 79−8224
Au, surface dipole moment calc. 80−60060
Au, surface electron states, photoelectron spectra meas., rel. to Au alloys 78−14781
Au surface electronic structure, XPS study 80−55259
Au, surface plasma waves, dispersion curves, attenuated total reflection spectra 78−88015
Au, surface plasma waves 79−47151
Au, surface state on (111), $E(k_\parallel)$ relation, ang. resolved photoemission 78−76582
Au, surface valence state from surface tension props. 79−95462
Au, surface-plasmon modulated reson. for adsorption studies 79−83045
Au, with cadmium arachidate monolayer, surface plasma reson. 77−90210
Au, Xe physisorption, electronically excited atoms coupling to cond. states 77−89642
Au-Ag(Cu), surface segregation, electronic theory, density of states, cluster-Bethe-lattice approx. 80−49369
Au-oxide-n-GaAs structs., reverse-bias depend. photocurrent, photoionisation of surface states 80−20323
Au(111) and polycrystalline surfaces, O_2 adsorption, LEED, AES and energy loss spectra 80−34310
Ba, ang. depend. of characteristic energy loss, surface plasmon excitation 78−2962
BaO epitaxial films, cathode poisoning due to O_2, CO_2, and S, surface anal. 79−42600
BaO, monolayer on W (110), film struct. and electron state 80−100498
BaO, surface states, reflectance spectra, impurity effects 77−20873
$BaTiO_3$ (001), LEED and UPS studies 80−100747
$BaTiO_3$, cluster surface states, LCAO calc. 77−43686
$BaTiO_3$, controlled surface layers 78−48120
$BaTiO_3$, defect chemistry and elec. cond. improved positive temp. coeff. model 77−39859
$BaTiO_3$, exam. of PTC effect as function of Ti excess *(German)* 79−23960
$BaTiO_3$, photoelectron and optical spectra derived from self-consistent charge MO and band calcs. 80−96785
$BaTiO_3$, surface layer exam. 78−43805
$BaTiO_3$, XPS and UPS from surface defects 80−76136
Be, electronic surface states, (001) surface, Brillouin zone 79−24047
BeO, film, TSEE, low energy electron impact excitation 77−12505
Bi, and Bi_2O_3, AES and characteristic energy loss spectra, expt. and interpretation 78−27354
Bi film, charge carrier scatt. *(Russian)* 78−80079
Bi film, quantum size effect and band struct. Bi-dielec.-metal system obs. 80−54811
Bi film, transparency meas. in mag. field, electronic isoenergetic surface cross section *(Russian)* 79−47532
Bi, oscillations with short periods of collector voltage for transverse focusing of electrons *(Russian)* 77−47837
Bi, oxidation, UPS, valence band, cond. band and 5d core states 77−20995
Bi, skipping electrons cyclotron resonance, electron-electron interaction parameter determ. 80−34351
Bi thin film, structure and electronic props. 80−70562
BiI_3, layered compound, exciton spectra, surface and stacking fault effects 80−40134

surface electron states continued
$Bi_{1-x}Sb_x$ alloy films, quantum resistance oscills. at low temps., surface band distortion *(Russian)* 80−11110
$Bi_2Te_{3-x}Se_x$ films, surface band struct. and scatt. mechanism 80−34535
C allotropes, diamond, graphite, gas-solid interface, electronic struct. HFR calc. 80−54745
C:Ni, X-ray photoemission studies 80−76138
CO, chemisorbed on metals, electronic struct., vibr. spectra, and chem. 79−42390
CaO, chemisorption of O_2, adsorboluminescence from surface F-centres 80−20723
Cd, electronic surface states, (001) surface, Brillouin zone 79−24047
n-$Cd_xHg_{1-x}Te$, recombination due to surface excitation, photoconductivity, impurity states *(Russian)* 80−60042
CdS cleaved in ultrahigh vac., elec. surface props. determ. 77−15926
CdS, exciton luminescence, surface recombination, space-charge-layer effects 78−80410
CdS, exciton obs. in thin surface layers, refl. spectrum *(Russian)* 78−2877
CdS, exciton spectra anomalies, surface state effects 78−18974
CdS film, cryst. and electronic surface struct., stimulated recrystn. effects 79−78151
CdS film, surface energy levels, thermally stimulated contact pot. difference method 79−99601
CdS film, surface states, surface photovoltage spectroscopy meas. 77−1504
CdS, influence of surface states on absorption edge 77−16344
CdS MIS devices surface states 78−72267
CdS, photorefl. in exciton region, surface layer influence 78−76489
CdS, polycrystalline evaporated layers, donor and trap densities 80−20213
CdS, SAW meas. of surface elec. props. 77−20387
CdS, spatial dispersion and surface layer effects on the phase of reflected light *(Russian)* 78−35182
CdS, surface acoustoelec. current due to Rayleigh wave, ambient medium effects and surface state changes 77−69383
CdS, surface electronic struct., slow electron reflection, total current spectroscopy *(Russian)* 80−54759
CdS, surface energy levels, O(C) adsorpt., AES study *(Japanese)* 78−88008
CdS, surface energy struct. changes during ion cleaning and thermal annealing 80−92962
CdS, surface photovoltage in exciton absorpt. range 78−19119
CdS, surface photovoltage, characterisation 80−60033
CdS, surface props., photoreflectance spectra in the exciton region 78−95324
CdS surface spectroscopy using acoustic surface waves, spectral response 77−69402
CdS, surface state meas. by SAW convolver 79−42617
CdSe ($11\bar{2}0$), surface electronic struct. and chem. struct. 78−14788
CdSe, rel. to photovoltage transients 77−89802
CdTe, bulk and surface states anal. using synchrotron radiation 77−66574
CdTe, clean and oxidised surfaces, O_2 sticking coeff., ionicity effects, XPS expts. 77−85887
CdTe, clean and oxidised surfaces, surface states, low-energy EELS study 80−11522
CdTe, nonpolar surface, tight-binding calc. 77−20383
CdTe, surface photovoltage 78−2540
Cf, surface valence state from surface tension props. 79−95462
Co (0001) surface state, photoemission and synchrotron radiation obs., symmetry determ. 80−20771
Co-Si, surface physicochemical state, Auger electron spectroscopy study 80−100715
CoO and Co_3O_4, XPS interpretation, valence band structure 77−12497
Cr, (100) surface, clean $(\sqrt{2}\times\sqrt{2})R45°$ struct. 80−2255
Cr, antiferromagnetic, surface Raman scatt., calc. 80−45069
Cr, charact. electron energy loss mechanism 79−91547
Cr, surface atom electron binding energy depend. on composition, Auger spectra, APS spectra 80−39655
Cr, surface electronic struct., tight-binding approx. calcs. 78−64090
Cr-GaAs, Schottky-barrier diode, surface electron states 79−73578
Cr-SiO_2-n-Si tunnel diodes elec. characts. meas. and modelling 77−39955
CrTe, film, attenuated total refl., magneto-optical effects 77−52196
Cs-O film, metallic, on Ag substrate, photoemission, surface plasmon excitation 77−16461
CsBr, (110) surface, electronic struct. of valence bands calc. *(Russian)* 80−75621
CsCl, (110) surface, electronic struct. of valence bands calc. *(Russian)* 80−75621
CsI, (110) surface, electronic struct. of valence bands calc. *(Russian)* 80−75621
Cs(100), calc. by mixed-representation method 77−20399
Cu, (001), electronic struct. of steps 78−34884
Cu (001), electronic surface barrier resons., LEED study 80−39651
Cu (001), M-point surface state, high-resolution angle resolved photoemission study 80−108322
Cu (001), O_2 chemisorption, Cu3d-O2p interaction study by angular-resolved photoemission using synchrotron radiation 80−84836
Cu (001) and (110) electronic wave functions by spherical wave method 79−42604
Cu (001) monolayer, electronic struct., self-consistent LCAO calc. 79−4606
Cu (001) monolayer, level ordering of states 78−91748
Cu (001) monolayers, electronic struct. 78−72233
Cu (001) surface, tight-binding calcs., self consistency effects 77−39909
Cu (100), adsorbed layers of N, O and S, electronic props., UPS, XPS and Auger spectra 77−66088
Cu (100), electronic struct., self-consistent local-orbital calc. 80−80348
Cu (100), interaction of CO and CO_2, molecular orbital calc. 77−31898
Cu (100), surface state-surface resonance density 79−28392
Cu (100), three-layer film, work function and density of states, self-consistent calc. 77−35978
Cu (100), XPS of chemisorbed CO 79−15589
Cu, (100) and (111), surface states, d-band, angle-resolved photoemission spectra obs. 80−20768
Cu, (100) and (111) faces, response function with d orbital effects on electronic screening 77−62977
Cu (100) film, chemisorbed N_2, electronic struct. 77−59315
Cu (100) monolayer, self consistent electronic struct. 80−6926

surface electron states continued
Cu (100) surface, angle-resolved PES study 80−55273
Cu, (100) surface, d-like surface state band, angle-resolved photoemission obs. 79−78840
Cu (110), adsorption of pyridine, angle-resolved photoemission, selection rules 80−40231
Cu (110), electroreflectance, surface state contrib. 80−80755
Cu (110) film, energy bands, tight binding calc. 77−15761
Cu, (110) surface, photoemission obs. of new surface state band 79−91121
Cu, (111), (100), (110), energy band parameters, EHT calc. 78−34883
Cu (111), Cs adsorption system, electronic surface band energy 80−2443
Cu (111) face, surface states and surface pot. 77−4418
Cu (111) face, surface state band, photoemission cross section 77−90252
Cu (111) film, energy bands, tight binding calc. 77−15760
Cu (111) surface, partially Cs covered, oxidation effect on UPS 79−78826
Cu (111) surface, positronium form. due to slow positron trapping 80−107748
Cu (111) surface, self-consistent electronic struct. calcs. on bulk and thin films 79−1614
Cu (111) surface band energy shift upon adsorption of Cs and O, angle-resolved UPS study 80−40228
Cu, (111) terrace of stepped (211) face, photoemission meas. 78−84697
Cu (111)/Cs, adsorption-induced changes of photoemission spectra and surface electronic struct. 80−55260
Cu, angle-resolved photoemission, prediction of spectra peak intensities 78−72695
Cu, bulk and (001) film, extended tight-binding calcs. 80−70592
Cu, CESR, influence of freq. and surface effects 79−51856
Cu, chemisorption of H, density of states and chemisorption energy calc. 80−34315
Cu, chemisorption of N atoms, electronic struct. of Cu_5N cluster, Xα scattered-wave calcs. 79−60902
Cu, d-band narrowing, obs. using angle-resolved XPS 80−11062
Cu, electron emission, ang. distrib., final state effects 77−66580
Cu, electronic structure and d-holes of films and surfaces 78−39180
Cu, energy band dispersions and lifetimes using angle-resolved photoemission 79−77998
Cu film, angular depend. UPS, surface electronic struct. 79−83095
Cu film, surface electronic struct., determ. by ab initio calc. 77−43679
Cu, film growth on graphite and amorphous C, electronic struct. by photoemission and Auger obs. 79−77947
Cu, intrinsic surface states, UV photoemission meas. 77−20983
Cu metal cluster, adsorption of CO, mol. orbital calc. 78−18895
Cu, N covered, self-consistent electronic struct. calc. 78−2544
Cu, on polystyrene, unusual core level spectra, XPS obs. 79−24415
Cu, ordered monolayer on Zn (0001), electronic struct., photoelectron spectra 78−39660
Cu, photoemission spectra, interpretation in terms of surface density of states 79−52081
Cu, single cryst. electrodes, electroreflectance obs. in aqueous solns. 80−25342
Cu surface, (001), O_2 adsorption effect on surface barrier, LEED study 80−84378
Cu surface, (110), adsorbed pyridine, photoemission selection rules 80−100751
Cu surface, Ar^+ ion bombardment, O_2 enhancement of sputtered ion yields 79−38705
Cu, surface d-band narrowing, angle resolved XPS 78−19635
Cu, surface energy band calc., significance for photoemission 78−95330
Cu, surface plasma waves 79−47151
Cu, surface polariton absorption and emission spectra, edge effects 78−10375
Cu, surface spin-flip probability from TESR 78−91953
Cu, surface states, (100) and (111), polarisation depend. photoemission 80−100495
Cu, surface-plasmon modulated reson. for adsorption studies 79−83045
Cu, surfaces and twin faults, electronic states calc. by surface Green's functions 80−39647
Cu-Ni, optical absorption and photoemission spectra 80−45216
Cu-Ni, UPS, surface and bulk density of states, comp. depend. 77−44125
CuBr, surface exciton polariton, ATR meas. 77−77236
CuCl (100), obs. of p- and d-like surface states, angle resolved UPS study 80−104045
CuCl, surface exciton polariton, ATR meas. 77−77236
CuNi alloys, electronic theory of surface segregation 79−23819
Cu_2O, electric field screening by surface electron states 78−52058
Cu(100), N chemisorption, bonding, MO theory 77−76659
Cu(100), photoemission via Bloch states and evanescent band gap states, polarised synchrotron irradiation 79−61492
Cu(111), (100), temp. depend. of bulk and surface energy bands using angle-resolved photoemission 79−69572
Cu(111), adsorption of Cs, struct. and electronic props. 78−23147
Cu(111), bulk s orbital bands, sensitivity to oxidation, photoelectron spectra 79−47597
Cu(111) frequency depend. photoelectric surface state cross section periodic oscills., PES study 80−50522
Cu(111) surface, UPS at const. wavevector component 80−16151
Cu(111) surface 77−62979
D_2, electron surface barriers for dense phases 78−91754
Dy, electron energy loss spectra 77−85860
EuTe, antiferromag. FCC lattice of second kind, surface magnons and mag. structs. 78−23261
Fe (001) surface, spectral density of transfer matrix formalism 78−39185
Fe, (111), (100) and (110) surfaces, UPS obs. 79−38712
Fe, ferromag. film, surface states, surface magnetisation and electron spin polarisation 80−65648
Fe, ferromagnetic, chemisorption of H, spin-spin interactions, UPS spectra calc. 80−6630
Fe, field-emitted electron spin polarisation by tunnelling through surface pot. 80−29861
Fe film, transverse Kerr magneto-optical effect enhancement by surface magnetoplasma waves 77−52056
Fe, Shockley surface states, three faces of BCC cryst. 78−76126
Fe, surface atom electron binding energy depend. on composition, Auger spectra, APS spectra 80−39655
Fe-Cr, surface atom electron binding energy depend. on composition, Auger spectra, APS spectra 80−39655

surface electron states continued
Fe-Ni, electronic struct. calc., effects of chemisorption; contact pot. and surface magnetisation 80−103734
$Fe_{1-x}O$, surface struct., XPS study 80−20759
n-Fe_2O_3 electrodes, characterisation and behaviour in acetonitrile solns. 80−25004
γ-Fe_2O_3, sat. moment *(French)* 77−85431
Fe_2O_3, semicond. anode in aq. electrolyte, electrolum. and electrochem. 80−76080
GaAS (110), wave functions and surface struct. 78−91519
GaAS, O_2 chemisorption on (110) surface, bonding sites 78−38938
GaAlAs, surface vacancies, bound state energy levels calc. 80−80340
GaAs (100), angle-resolved photoemission spectra 80−50516
GaAs (100), electronic struct., scattering-theory formulation 79−42607
GaAs (100) surface, pot., wave functions, spectrum and charge density calc. 77−20382
GaAs, (100) surfaces, reconstructed, ang. resolved photoemission from surface states, adsorption and annealing effects 80−16143
GaAs (110), adsorption of In, N, P, and As, UPS and EELS study, tight-binding calcs. 80−49496
GaAs (110), adsorption of O_2, H_2, H_2O and H_2S, surface photovolt. spectroscopy 80−49499
GaAs (110), chemisorbed O_2, extrinsic surface states 78−91535
GaAs (110), chemisorption of Cl, photoemission spectra and tight-binding calcs. 80−6629
GaAs (110), chemisorption of Al, electronic struct., tight binding calc. 80−49842
GaAs (110), chemisorption site geometry and interface electronic struct. of Al and Ga, photoelectron spectra 80−49843
GaAs (110), chemisorption of O and Al, ab initio theory 80−75612
GaAs (110), clean, cleaved, surface states, work function meas. 80−49847
GaAs (110), double-dangling-bond defects and band bending 79−69411
GaAs (110), electron states from transfer matrix method 78−56203
GaAs (110), electronic states and initial steps in oxidation 78−91534
GaAs (110), low O_2 exposure effects on electronic surface props. 79−47146
GaAs (110), optical technique, detection of external reflectivity change on oxidation 80−6939
GaAs (110), pseudocharge density calcs. 78−84275
GaAs (110), reconstruction and oxidation initial stages, ab initio calc. 80−49473
GaAs (110), self-consistent pseudopotential calcs., electronic struct. and atomic co-ords. 80−49848
GaAs (110), steps 80−49846
GaAs (110), surface core-level binding-energy shifts 80−103737
GaAs (110), surface electronic struct., ang. resolved photoemission expts. and tight binding calcs. 78−91743
GaAs (110), surface electronic struct. calcs. 80−80343
GaAs (110), surface states and matrix elements in angle-resolved photoemission 78−91741
GaAs (110), surface states symmetry determ. using polarisation-depend. ang. resolved photoemission 78−91742
GaAs (110), unrelaxed, surface states in bond orbital model 78−91749
GaAs (110), valence band Auger spectra 78−35230
GaAs (110), valence band Auger spectra, from Ga and As CCV transitions 78−92149
GaAs (110) relaxed surface, electronic states 79−51649
GaAs (110) surface, chemisorption of O_2, electronic struct. theory, oxidation, electron spectra interpretation 79−42376
GaAs, (110) surface, electronic struct. of clean and O_2 covered surface 77−43685
GaAs (110) surface, electronic states near band gap 77−85290
GaAs (110) surface, electronic struct., pseudopot. calc., surface relax. model 80−29456
GaAs (110) surface, exposed to O and O_2 photoemission spectra meas., Space Shuttle expt. 78−35246
GaAs (110) surface, oxidation model 77−32703
GaAs (110) surface, relax. effects 77−24601
GaAs (110) surface, surface states, angle-resolved photoemission meas. 77−20984
GaAs (110) surface states, surface relax. models, tight-binding calcs. 79−4594
GaAs (110)-Al(Ga)(In), Schottky barrier form., defect mechanism 80−49902
GaAs ($\bar{1}\bar{1}\bar{1}$), MBE prep., angular resolved UPS of surface states 79−47598
n-GaAs, absorption tails in surface depletion layer and bulk 78−64379
GaAs, adsorbed O, (110), surface electronic struct., synchrotron irradiated photoemission 78−43453
GaAs, adsorbed O_2^- EPR spectrum, HFS 77−40118
GaAs, adsorption of Sb_2, surface state exam. by energy loss spectra 77−15935
GaAs base laminated epitaxial struct., surface plasmon phonon polaritons *(Russian)* 80−59905
GaAs, CO(O_2) interactions, surface electronic struct. (surface chem.) using synchrotron radiation 78−53254
GaAs, chemisorption and oxidation states of (110) surfaces 79−24049
GaAs, chemisorption of Li, charge injection into space charge layers 80−100496
GaAs, clean and oxidised surfaces, O_2 sticking coeff., ionicity effects, XPS expts. 77−85887
GaAs, contact pot. difference meas. 77−20403
GaAs, deep trap study by free exciton refl. spectra 79−60761
GaAs, electrodes in acetonitrile soln., mediation of electron transfer 79−70341
GaAs, electronic structure of (111) and ($\bar{1}\bar{1}\bar{1}$) surfaces 79−87137
GaAs, electronic surface props., interaction with Au and O adsorbate layers 77−20385
GaAs, electronic surface structure Cs(Rb)(Na) adsorpt. processes, AES, LEED, EELS, study 78−68068
GaAs, epitaxial, impurity gradients caused by surface states and substrate doping 77−84784
GaAs epitaxial film, surface trap exam. by surface doping and field effect 77−76896
GaAs epitaxial layers, electronic surface props., photoluminesc. exam. 77−20901
n-GaAs, far IR propag. of surface EM waves 79−42615
p-GaAs, field emission, role of surface electron states 78−2993
GaAs, field penetration in FIM, band bending 79−87567
GaAs in acetonitrile solns., photoelectrochem. behaviour 79−4600

surface electron states continued
GaAs, in MIS system, nature of surface carrier depletion layers 77−1469
n-GaAs, low temp. field generation of carriers, liberation from surface states 80−92959
GaAs, MBE (001) layers, work function meas. 80−49870
n-GaAs MIS structs., native oxide, effect on interface props. and removal by sputter etching 79−11228
n-GaAs, MIS structures, C-U curves, surface state densities 77−85335
p-GaAs MOS capacitors, anodized, C-V characts., surface pot. 79−11227
GaAs MOS structure, props. of surface carriers 77−20453
GaAs MOS system, surface and interface exam. by derivative surface spectroscopy 79−82674
n-GaAs, nature of low temp. field generation of carriers, liberation from surface states 80−92960
GaAs, O_2 sorption and excitonic effects, photoemission expts. 77−85055
GaAs, photocathodes, photoelectron emission, energy levels, influence of dimens. quantisation *(Russian)* 78−64447
n-GaAs, photoemission and work function of (111A) and (111B) surfaces, energy states 77−20980
GaAs, photoemission modulation by IR illumination, surface band bending height interpret. 80−108318
GaAs, positron annihilation in disturbed surface layers 78−6809
n-GaAs, real epitaxial surface, photoelec. spectroscopy, mechanisms 78−34858
GaAs, rel. to photovoltage transients 77−89802
GaAs, SAW meas. of surface elec. props. 77−20387
GaAs Schottky-contact, influence of surface states and hole traps *(Bulgarian)* 80−25006
GaAs, semi-insulating, surface layer thermal conversion mechanism, Hall effect meas. 80−49772
GaAs, struct., elec. props., effects of illumination, O_2 absorpt., electron bombard. *(French)* 78−34690
GaAs, surface, (110), ang.-resolved photoelectron spectra 78−43984
GaAs surface, cluster model approach for electronic struct. 78−56205
GaAs, surface, distrib. of surface states 80−44692
GaAs, surface, electron struct. and Fermi level pinning by O_2 and metals 80−11066
GaAs, surface, vacancies, bound state energy level calcs., tight binding approx. 80−44694
GaAs, surface (111), ($\bar{1}\bar{1}\bar{1}$), (110), XPS, photo-Auger ionisation cross section, electron mean free paths 78−56558
GaAs, surface characterisation using SAW 80−11069
GaAs, surface chemistry and electronic struct., adsorption of O_2, photoemission meas. 77−20985
GaAs, surface electron states, (110), photoemission 80−25529
GaAs, surface exciton energy 80−92829
GaAs, surface photovoltage spectroscopy appl. 77−69391
GaAs, surface photovoltage due to photo-thermo-ionization of surface states 78−14787
GaAs, surface recomb. vel., psec. optical techniques 80−70784
GaAs, surface states, band struct. by discontinuous potential method 80−20276
n-GaAs, surface states, photoemission yield obs. 77−16459
GaAs surface states obs. by XPS 80−50515
GaAs, surface states XPS 80−25528
GaAs surfaces, electronic struct., tight-binding calc. 80−54755
GaAs surfaces (110) and (111)As, UPS and LEED 78−91514
GaAs, UPS, 5-450 eV, surface states, oxidation behaviour 77−66579
GaAs, UV photoemission, polarisation-depend., angle-resolved spectroscopy 77−66573
n-GaAs, valence band studies of clean and O_2 exposed surfaces 78−43298
GaAs:Ar^+-metal, semi-insulating layer capacitor, surface-state charge density estimation 79−56316
p-GaAs:Cd, (110) cleaved surface, defect-induced surface states 80−6925
GaAs:Cr, surface and bulk recombination parameter determ. from photoluminesc. spectra 77−55820
GaAs:Cr semi-insulating substrate, photoluminescence obs. of surface degradation during LPE growth 78−6865
GaAs:Cr wafers, semi-insulating, surface degradation by heat treatment at 900°C 77−80820
GaAs:Sb (100) surface, Sb-induced surface states 78−10529
GaAs:Se, ion implanted, surface state study from photoreflectance 79−91465
GaAs-Al_2O_3 MOS struct. model for surface states associated with As atom dangling bonds 79−60927
GaAs-AlGaAs heterojunction superlattices, obs. of intersubband excitations in multilayer two dimensional electron gas 80−29753
n-GaAs-oxide, plasma-grown, surface states, modified DLTS meas. 80−11094
GaAs-Pt-air system, far IR propag. distances of surface EM waves 79−42616
GaAsP, negative-electron-affinity, photoemission transmission coeff. 78−56560
GaAs(110), high resolution photoemission yield, surface states 77−69392
GaAs(110), photoemission spectroscopy and tight binding calcs. 77−85888
GaAs(110), surface and interface states, effects of atomic and electronic rearrangements 77−85284
GaAs($\bar{1}\bar{1}\bar{1}$)As surface, 3 states, comp., struct., surface states and O_2 sticking coeffs. 77−66080
GaP (III) B surface, negative-electron-affinity, photoemission transmission coeff., comparison with GaAsP 78−56560
GaP (110), electronic surface states, initial steps of O_2 chemisorption 80−49844
GaP (110), surface bands in relaxed cleavage surface, tight binding model 78−91744
GaP (110), wave functions and surface struct., EPR expts. 78−91519
GaP, cleaved (110) surface, electron surface props. 80−11067
GaP, contact pot. difference meas. 77−20403
GaP, Cs(Cs-O) activated, with negative electron affinity, near UV photoemission and secondary emission 78−11074
n-GaP electrode, photoanodic dissolution rate, effect on surface electronic band energies 80−103748
p-GaP electrodes with metal adatoms, surface states form. due to impregnated H 80−54778
GaP, electron-hole drops, self-consistent surface calculation 80−65464

surface electron states continued
GaP, photovoltage transients, intensity and chopping freq. depend. 77−47859
GaP, polaritons, freq. depend. of associated functions 79−78020
GaP, Raman scatt. from surface polaritons, selection rules 77−52083
GaP, surface characterisation using SAW 80−11069
GaP, surface polariton linear photon and two photon absorpt. 80−49863
GaP, surface polaritons, light scattering studies, effect of surface roughness 80−6753
GaP:Te(S), IR lattice band profile, electron spin reversion in mag. field, Nf-R curve 79−28771
GaP(As)(Sb), contact potential difference and photoemission expts. 77−47884
GaP(As)(Sb), contact pot. difference, photoemission, and low energy loss spectra expts. 77−85285
GaP(Sb)(As), (110) surface, trned in energy distribs. of Ga dangling orbital surface states 79−28397
GaSb (100) surface, Sb-induced surface states 78−10529
GaSb (110), chemisorption of Cl, photoemission spectra and tight-binding calcs. 80−6629
GaSb (110), oxidation, initial stages, photoemission study 80−16529
GaSb (110), surface core-level binding-energy shifts 80−103737
GaSb, chemisorption and oxidation states of (110) surfaces 79−24049
GaSb, photoemission investig. of surface states, effects of O_2 and alkali metals 77−48312
GaSb, real surface elec. props., light effects *(French)* 77−72906
GaSb, surface, electron struct. and Fermi level pinning by O_2 and metals 80−11066
GaSb, surface chemistry and electronic struct., adsorption of O_2, photoemission meas. 77−20985
GaSb, UPS, 5-450 eV, surface states, oxidation behaviour 77−66579
GaSb-InAs system, (110) surface and interface electronic struct. 80−100494
$GaSb_{1-y}As_y$ alloy, (100) surface electronic properties obs., using electron energy loss spectra 79−15202
Gd, electron energy loss spectra 77−85860
Ge (100), density of states, simple modelistic treatment of virtual surface states 80−103739
Ge (100), electronic struct., scattering-theory formulation 79−42607
Ge (111), adsorption of K and Cs, effect on surface elec. props. 79−90880
Ge (111), adsorption of polar molecules, surface recomb. centre neutralization 79−38147
Ge (111), electron struct., photoelec. props. 80−100493
Ge (111), spectroscopy of electron subbands 80−71422
Ge, (111) surface, clean and O_2 adsorbed photoemission yield spectroscopy of electronic surface states 79−91122
Ge (111) surface, clean and CO-covered, UPS and ion-neutralisation spectroscopy 80−10785
Ge (111) surface, n-channel inversion layer, subband energies 80−11063
n-Ge accumulation layers, effect of low-energy Ar^+ ion bombardment on electron scatt. 77−66205
Ge, adsorbed metal atoms effect on surface electron props. 77−55597
Ge, adsorption of water, neutralization of surface recomb. and fast capture centre 79−33184
Ge bicrystal cleavage plane, Shubnikov-de Haas oscills. *(Russian)* 78−64094
Ge, chemisorption of Cl_2, photoemission polarisation effects with synchrotron radiation 78−14580
Ge, clean surface, geometrical struct. rel. to electronic props. 77−62719
Ge during X-irradiation, oxide hydration degree determ. 77−24605
Ge, electronic inversion channel anomalous Hall factors *(Russian)* 79−95467
Ge, electroreflectance, effect of surface and nonuniform fields 78−68511
Ge heteroepitaxial film, ethanol pulsed adsorption effect on elec. cond. 80−93014
Ge, LCAO band structure, overlap and distant neighbour effects 80−49585
Ge, photoemission spectroscopy of surface states and oxidation 77−55863
Ge read out, by SAW, optical image memory in slow surface states 77−79942
Ge, relaxed (111) surface, self consistent pseudopot. calc. 77−47880
Ge, review of optical methods of detection 77−66191
Ge single cryst., atomic H interaction, highly efficient electron accommodation *(Russian)* 79−78818
Ge slab, intrinsic, longit. cond., influence of surrounding gas *(French)* 78−10448
Ge, slow states conc. determ. by field effect meas. 77−28232
Ge, slow surface, states, optical excitation investigation 78−76129
Ge slow surface states, optical image storage for $LiNbO_3$ SAW readout 77−23773
Ge surface, adatom indirect interaction 80−44696
n-Ge surface, chemical channel of recombination 80−39656
Ge surface, Cl chemisorption, cluster calc. by iterative EHT 77−32062
Ge, surface, cluster model approach for electronic struct. 78−56205
Ge surface, field penetration and band bending in high elec. fields 79−42613
Ge, surface, high freq. cond. and cyclotron reson. 80−11273
Ge surface, X-irradiated, slow relaxation of surface states 77−62980
Ge, surface electronic props. meas. by SEM, sand-blasting effect 77−62976
Ge, surface electronic struct., self consistent pseudopotential calc. 78−47842
Ge, surface photovoltage spectroscopy appl. 77−69391
Ge surface states, recomb. centres, regularities, electrolyte contact effects *(Russian)* 80−65652
Ge, surface states, recombination centre formation *(Russian)* 80−29459
Ge surface states, Tamm-like and field sustained, model studies, localisation props. 78−64092
Ge surfaces, electronic struct., tight-binding calc. 80−54755
Ge, ultra high vac. cleaved, photolum., role of intrinsic surface states 78−52571
Ge, work function, meas. by thermionic emission 78−19628
Ge:Au, Sb 79−69577
n-Ge:Ni, negative differential conductance of surface channels 79−11134
Ge:Pd and pure, photoelectric props., surface states *(Russian)* 80−60043
Ge:Sb, effect of degree of doping on surface state charact. 79−69577
Ge:Sb(Au) cleaved surface, influence of impurities on local surface states 79−78150

surface electron states continued
Ge-GaAs, p-n heterojunctions, surface electron states 79−73578
Ge-GaAs interface, surface and interface states of (111) surfaces 79−15206
GeS (001), density of empty states, core-level EELS and photoemission spectra meas. 79−78145
GeS (001) surface, electronic struct., Auger and electron energy loss spectra meas. 77−59314
GeSe (001), density of empty states, core-level EELS and photoemission spectra meas. 79−78145
Ge(100) surface electronic state localisation, layer density of states calcs. 80−6931
Ge(111), atomic geometry effects, photoemission and electron energy loss spectra 77−85283
Ge(111), chemisorption of Cl, threefold co-ordinated site chemisorption, cluster model calc., extended Huckel theory 78−39178
Ge(111), dangling-bond surface states 78−43452
Ge(111), high resolution photoemission yield, surface states 77−69392
Ge(111)2×1, oxide layer, surface states detect optical reflectivity obs. 80−50368
Ge(111)2×1, surface electron states detected by external reflectivity 78−80036
H, adsorbed on jellium surfaces, charge density oscills. and adatom-adatom interaction 79−42389
H, chemisorbed atom, surface charge fluctuations effect on spectral density 80−65368
H-like atom near metal surface, quasi-stationary spectrum 79−18132
H_2, electron localisation at surface *(Russian)* 79−60893
H_2, liq., localisation of electrons on surface *(Russian)* 79−33322
He, adsorbed on graphite, band struct. effects in heat capacity 80−59788
He atom-surface scattering pot., surface electron density depend. 80−104027
He, liq., electron gas struct. formed in image-pot. induced surface states 79−65400
He, liq., electrons localised at surface, cyclotron freq. shift *(Russian)* 80−6582
He, liq., escape rate of two-dimensional electrons, around 1K 79−46856
He, liq., image-pot.-induced surface states, in strong elec. and mag. fields 78−946
He, liq., local disorder, for IR transmittance meas. 80−75395
He, liq., surface, escape rate of two-dimensional electrons 79−28165
He, liq., surface, two-dimensional electron gas, cyclotron reson. 79−60566
He, liq., surface electron system, liq. to cryst. phase transition *(Russian)* 80−6593
He, liq., surface electrons over macroscopic periodic struct. *(Russian)* 79−10997
He, liq., two-dimens. electron gas, CDW 80−65476
He, liq., two-dimensional electron system *(Japanese)* 78−51771
He liq. surface, cyclotron reson. of two-dimens. electrons *(Russian)* 80−88374
He, liq. surface, electron solid, phonon-ripplon coupling 79−42337
He, liquid, charged surface, current instability theory *(Russian)* 80−29243
He, liquid, cyclotron reson. with surface electrons *(Russian)* 77−59319
He, liquid, cyclotron reson. freq. increase, electric field on surface dimple electrons 78−47624
He, liquid, nonlinear cyclotron resonance of localised surface electrons *(Russian)* 77−59318
He, liquid, short-wave surface excitation study using electron gas nonlinear I-V charact. *(Russian)* 80−10717
He liquid, surface electron states, two-dimens. cryst. form. 78−60006
He, liquid, surface electron high freq. cond., electron system heating, I-V charact. *(Russian)* 80−29244
He, liquid, surface state electron lifetime, rel. with chemical potential of electron liquid 79−78028
He, liquid, velocity autocorrel. time in surface electron liq. from spectral line broadening 77−20146
He liquid surface, collective excitation spectrum of electron Wigner cryst. *(Russian)* 77−47647
He, liquid surface, electron sheet liq. to cryst. transition 79−42341
He liquid surface, localised electron states 78−60007
He liquid surface, parametric excitation of electrons in mag. field 79−51389
He, parametric excitation of electrons *(Russian)* 79−37892
He, superfluid film, surface electrons, quantum oscill. effects *(Russian)* 79−11105
He surface, collective excitations and electrodynamic behavior in three layer structure 78−60079
^{3}He, liq., electron escape from image-potential-induced surface states 80−49440
^{3}He, liq., localised electron states, cyclotron reson. above surface *(Russian)* 80−6587
^{3}He, liq. and dense vapour, electron surface barrier, density depend. determ. 77−1270
^{3}He, liquid, electrostatic image force depend. on spatial dispersion, energy spectrum *(Russian)* 80−107593
^{3}He, liquid cyclotron resonance of localised electrons above surface *(Russian)* 78−14533
^{3}He-^{4}He, liquid solution, bound impurity pair effect on surface tension *(Russian)* 80−65332
^{4}He, liq., broadening of inter-subband transitions in image-pot.-induced surface states 78−43194
^{4}He, liq., dimple lattice of electrons on surface, struct. 79−99380
^{4}He, liq., electron escape from image-potential-induced surface states 80−49440
^{4}He, liq., localised electron states, cyclotron reson. above surface *(Russian)* 80−6587
^{4}He, liq. and dense vapour, electron surface barrier, density depend. determ. 77−1270
^{4}He, liquid, electrostatic image force depend. on spatial dispersion, energy spectrum *(Russian)* 80−107593
^{4}He, liquid, surface electron interaction with EM radiation *(Russian)* 80−54449
^{4}He liquid surface, hot carrier mobility 78−59988
^{4}He liquid surface, theory of hot electrons 78−22915
^{4}He, superfluid, surface, electron lifetime 79−77849
^{4}He, superfluid, surface, hydrodynamic modes for ripple waves 78−43195
^{4}He surface, hot electrons theory 79−42329

surface electron states continued
Hg electrode, electroreflection spectra calc., electromodulation mechanisms 77−1658
Hg, liquid, surface plasmon dispersion 77−62978
$Hg_{0.8}Cd_{0.2}Te$-ZnS MIS struct., nonparabolic bond semicond., surface state studies, capacitance measurements 79−78190
$Hg_{1-x}Cd_xTe$, far IR cyclotron resonance in inversion layer 77−69396
$Hg_{1-x}Cd_xTe$ films, Tamm surface states, Kane model 79−28395
$Hg_{1-x}Cd_xTe$, n-surface inversion layers study 80−25017
$Hg_{1-x}Cd_xTe$, Tamm surface states 77−55595
Ho, electron energy loss spectra 77−85860
II-VI semiconductor-electrolyte boundaries, electrolyte boundaries, photo e.m.f. meas., semicond. energy bands 77−1481
In, surface plasmon dispersion, high-energy electron loss spectroscopy obs. 77−20390
InAs, contact pot. difference meas. 77−20403
InAs, contact potential difference and photoemission expts. 77−47884
InAs, supercond. of surface *(Japanese)* 78−14864
InAs, surface potential and surface states rel. to n-, p-, compensated n-type behaviour 77−15932
InAs, surface space charge investig., reson. enhanced Raman scatt. 77−20849
InAs, two dimensional accumulation layer, Anderson localisation 80−107871
InAs:Sb (100) surface, Sb-induced surface states 78−10529
$In_{1-x}Ga_xAs$ alloy, (100) surface electronic properties obs., using electron energy loss spectra 79−15202
InN, thin film, characterisation using XPS electron energy loss spectra 79−87561
In_2O_3, thin film, characterisation using XPS electron energy loss spectra 79−87561
In_2O_3-SnO_2-InP solar cell junctions, efficiency, InP surface props. 80−85288
InO_xN_y, thin film, characterisation using XPS electron energy loss spectra 79−87561
InP (110), oxidation, initial stages, photoemission study 80−16529
n-InP, (110) surfaces, photolum. intensities in vac. and gas ambients 79−61412
InP, and $In_xGa_{1-x}As_yP_{1-y}$ binary and quaternary cpds., surface and dielec.-semicond. interface props. 80−93001
InP, chemisorption and oxidation states of (110) surfaces 79−24049
InP, cleaved surface, angle resolved photoelectron spectroscopy 80−55258
InP cleaved surfaces, and interfaces with metal electrodes 78−10554
InP, deep trap study by free exciton refl. spectra 79−60761
InP in acetonitrile solns., photoelectrochem. behaviour 79−4600
InP, rel. to photovoltage transients 77−89802
InP, surface, electron struct. and Fermi level pinning by O_2 and metals 80−11066
InP, surface chemistry and electronic struct., adsorption of O_2, photoemission meas. 77−20985
InP, surface recomb. vel., psec. optical techniques 80−70784
InP, surface space charge layers and Schottky barrier form., Raman scatt. study 80−50319
InP, surface vacancies, bound state energy levels calc. 80−80340
InP-electrolyte struct., field effect of photoluminesc. 79−99928
InP-Langmuir film MIS structures, surface state distrib. obs. 77−89859
n-InP-metal surface barrier struct., props. 79−11223
InP(As), contact pot. difference, photoemission, and low energy loss spectra expts. 77−85285
InSb (110), chemisorption of Cl, photoemission spectra and tight-binding calcs. 80−6629
InSb (110), clean, O_2 adsorption, AES, LEED, RHEED and field effect meas. 80−49501
InSb (110), cleaved, gap states, field effect meas. 80−84501
InSb (110), ion bombard. effect on surface struct. and electronic props. 80−6923
InSb, (110) surface, core level photoionisation spin-orbit branching ratio, initial and final state effects 79−83094
InSb (110) surface, struct. and electronic props., RHEED and field effect meas. 80−11068
n-InSb, damped surface magnetoplasmons, theory 79−7873
InSb, electronic surface struct., Cs(Rb)(Na) absorpt., AES, LEED, EELS study 78−68068
InSb inversion layer, electromagnetic mode 78−60080
InSb inversion layer, spectroscopy of electron subband levels 78−10569
InSb inversion layer, spectroscopy of electron subband levels 78−64364
n-InSb, n-type, photoconductivity with different surface treatment 78−2517
n-InSb, recomb. of hot electrons, photoelectromag. and dynamic photocond. meas. 79−38081
InSb surface, IR spectroscopy of subband levels 80−20277
InSb, surface, reson. excitation of electron subbands 80−49865
n-InSb, surface accumulation layer, sub mm electron cyclotron reson. 78−6576
n-InSb, surface magnetoplasmons 79−19646
InSb, surface magnetoplasma waves, reson. spectrum and dispersion characts. 79−38148
InSb surface magnetoplasma wave struct. 80−6934
n-InSb, surface recomb. velocity, temp. and α-bombardment dose effects 77−8173
InSb(111) surface, oxidation props., LEED and surface cond. meas. 78−15559
Ir (001), surface electronic props. 78−95332
Ir (100)-1×1 surface struct. and reconstruction kinetics, LEED, UPS and work function meas. 79−90851
Ir (111) surface, step effects on total energy distrib. 79−100026
Ir, (111) surface states, surface Umklapp effects, photoelectron spectra 80−93457
Ir, chemisorbed CO and O on (100) and (110) faces, electron field emission 78−84704
Ir clean (001) surface, electronic props. 77−72901
Ir, clean and adsorbate covered surfaces, field emission energy distrib. spectra 80−25535
K (001) surface, electronic struct. by density matrix method 79−60900
K film, adsorbed on Ni (100), plasmon losses in electron energy loss spectra 79−61480
K film, splitting of surface plasmon emission spectra 79−99954
K, surface electron states and optical props. in IR spectral range *(French)* 80−54757

surface electron states continued
KBr, electronic states at (100) surface, accounting for spin-orbit interaction *(Russian)* 78−91750
KCl, and KCl-AgCl, surface positron and positronium states, positron annihilation expts. *(Russian)* 78−39623
KCl crystal, use of photoelectrons to investigate surface charges 80−2444
KCl, detection by photocharging spectroscopy 77−66193
KCl, electronic states at (100) surface, accounting for spin-orbit interaction *(Russian)* 78−91750
KI, electronic states at (100) surface, accounting for spin-orbit interaction *(Russian)* 78−91750
KI microcrystals, UV spectra by diffuse reflectance technique, surface electronic transitions obs. 80−75614
$K_{1.62}Pt(C_2O_4)_2.2H_2O$, plasma resonance absorpt. from small particles 77−24841
Kr, solid, n=1 surface excitons and LO-TO splittings of bulk excitons 79−73445
Kr, solid, surface excitons 77−76892
LaB_6 (001), surface state exam. by angular resolved UPS 78−19114
LaB_6 (001) surface, struct., initial oxidation, XPS, UPS, LEED, AES, work function meas. 79−99403
LaB_6 (100) surface, O_2 adsorption, UPS and LEED study 80−49519
LaB_6, Shockley surface states, angle-resolved photoemission 79−56278
LaB_6 surfaces, (100), (110) and (111), electron states, UPS study 80−100752
LaB_6(001) surface, struct. and initial oxidation, UPS, XPS and work functions meas. 77−86195
Li, valence band Auger spectra, surface effect 80−80915
LiF (001), H and D beam scatt., specular bound state reson. struct. 79−52069
LiF, selective adsorption of He, band struct. effects 79−73402
α-$LiIO_3$, attenuated total reflection spectra of anisotropic surface polaritons 78−87919
$LiIO_3$, surface polariton spread length by modified DCIR method *(Russian)* 79−73566
$LiNbO_3$ surfaces, ion and electron bombard., photoelectron spectroscopy and electronic props. 80−71559
$LiNbO_3$, XPS and UPS from surface defects 80−76136
$LiNbO_3$:Fe, intrinsic field effect, photoelectric emission study 79−69961
Li(100), calc. by mixed-representation method 77−20399
Mg, ang. depend. of characteristic energy loss, surface plasmon excitation 78−2962
Mg, deposits of different roughness, refl. drops and surface plasmons 77−20392
Mg, electronic surface states, (001) surface, Brillouin zone 79−24047
Mg, surface structure autocorrelation functions and Fourier transforms for rough deposits 79−69450
MgO, (001) surface, charge deform. and geometric relax., shell model 79−95255
MgO, chemisorption of O_2, adsorboluminescence from surface F-centres 80−20723
MgO, chemisorption on (100) surface, surface electronic struct. 79−11016
MgO, intrinsic surface states at (100) and (110) surfaces 78−91740
MgO, ionic cryst., surface electronic struct., discrete variational Xα cluster method 79−4591
MgO surface, $H_2+D_2 \rightleftharpoons 2HD$ catalysis, SCF UHF calc. 77−9120
Mo (001), self consistent electronic struct., pseudopotential calcs. 79−42606
Mo (001) surface, electronic susceptibility and surface phase transition 79−33169
Mo, (001) surface, electronic origin of reconstruction 80−11065
Mo (001) surface, surface CDW phase transitions 78−43455
Mo (001) surface, surface states and photoemission 79−60887
Mo (001) surface with saturated H adsorption, band structure self-consistent calc. 80−15585
Mo (011) face, adsorption of Sr and La, influence of substrate electronic struct. on props. 78−60032
Mo (100), adsorption of CO_2 and trimethylamine, adsorbed O effect, LEED and AES obs. 80−39443
Mo (100), effect of metallic adsorbates on surface reson. 79−65983
Mo (100), surface resonances, photoemission and field emission meas. 79−4593
Mo (100) and (110) surface, directional UPS obs. 77−8722
Mo, (100) and (110) surface density of states 78−52047
Mo (100) clean surface electron struct., positron annihilation study 80−24988
Mo (100) face, surface reson. 78−72226
Mo (100) plane, surface reson., field emission energy distrib., LCAO calc. 77−32507
Mo (100) surface, clean and O_2 covered electron energy loss spectra meas. 77−16440
Mo, AES and characteristic energy loss spectra, expt. and interpretation 78−27354
Mo, adsorption of CO, O_2, metastable He de-excitation spectroscopy and UPS study 80−34314
Mo, adsorption of O_2, low energy SIMS and electron induced desorpt. exam. 77−76667
Mo, charact. electron energy loss mechanism 79−91547
Mo, electron-surface plasmon scattering using a parabolic non-touching trajectory 78−95328
Mo, electron-surface-plasmon scatt. using parabolic nontouching trajectory 77−28228
Mo polycrystalline surface, CO chemisorption, substrate mediated C-O interaction, photoelectron spectra 79−34353
Mo, RF surface impedance, new type of oscills. 79−15070
Mo, slow electron inelastic scatt., vol. and surface plasmon excitation 77−52207
Mo, surface bands of (001) surface 77−72902
Mo, surface relaxation and electronic structure of (100) surface 79−73561
Mo, surface resonances on (100) plane, angle-integrated photoemission spectra 77−85894
Mo, UPS, angle-resolved, surface resonances on (100) face 78−2987
MoS_2, surface electronic struct., slow electron reflection, total current spectroscopy *(Russian)* 80−54759
Mo(001), H chemisorbed, self-consistent electron struct. 80−44693
Mo(001) surface, atomic displacements and electronic struct. 78−30963
Mo(001) surface, electronic struct., self-consistent pseudopot. calcs. 78−76128

surface electron states continued
Mo(001), surface electron struct., matching Green function method calcs. 78−88014
Mo(110) and (100) surface, surface reson. states and adsorption of 4d atoms 78−71982
Mo(110), surface densities of states for normal photoemission 78−35251
N_2 film, on metal or sapphire substrates, luminescence and nonradiative energy transfer to surfaces 80−97350
Na (001) surface electronic struct., linear response theory 78−56197
Na (110), surface states in nearly-free-electron approx. *(French)* 79−33326
Na, adsorbed on Al, adatom valence-level position variation 80−88611
Na, adsorbed on Ni, substrate, hybridisation between s and p resons., jellium model 80−6932
Na, CESR, influence of freq. and surface effects 79−51856
Na film, adsorbed on Ni (100), plasmon losses in electron energy loss spectra 79−61480
Na film, slow electron bombarded, light radiation 80−40168
Na, IR and optical props., surface-plasmon-mediated absorpt. mechanism 80−93308
Na surfaces, (100) and (111), electron energy states *(French)* 80−34496
NaCl crystals, electronic and hole centres and surface, quantum-chemical calcs. 80−65489
NaCl, detection by photocharging spectroscopy 77−66193
NaCl, energy struct. determ. by electron absorpt. spectra 78−11040
NaCl, quantum-chem. calcs. of electronic and hole centres and surface 80−20118
NaF (001), H and D beam scatt., specular bound state reson. struct. 79−52069
Na(100), calc. by mixed-representation method 77−20399
Nb (001), pseudopotential calc. 77−8167
Nb (001) ideal surface, self-consistent pseudopot. calcs. 77−76894
Nb surface, clean and oxidised, electronic struct., UPS meas. 78−95682
NbC, rock salt struct., surface energy bands, Shockley surface states, bonding 80−92956
Nd film, on W(100), struct., electronic and dynamic props. *(Russian)* 77−76702
Nd, threshold pot. spectra, $N_{4,5}$ absorpt. widths 79−69578
Ne, dense, electron injection, comparison with H_2 and He 79−73567
Ne, electron localisation at surface *(Russian)* 79−60893
Ne, solid, bulk and surface excitons, transmission and refl. spectra obs. 79−95340
Ne, solid, n=1 surface excitons and LO-TO splittings of bulk excitons 79−73445
Ni (001), adsorbed c(2×2) Na overlayer, core level excitation effects, synchrotron radiation UPS study 80−40234
Ni (001), chemisorpt. of O_2, MS$X\alpha$ total energy calcs. with non-muffin-tin corrections 77−72795
Ni (001), chemisorption of O and S, dynamical calc. of angle-resolved UV photoemission 77−85890
Ni (001), O_2 overlayer struct. and theory of electron struct. 79−65319
Ni (001) and (001)c(2×2)S adsorbed, electronic surface resonances by LEED 79−24051
Ni (001) film, self consistent calc. of surface phenomena 79−73560
Ni (001) surface, c(2×2) Se overlayer, angular resolved UPS 78−76584
Ni (001) surface, chemisorbed O_2, electronic struct. and overlayer struct. theory 79−28391
Ni, (001) surface, chemisorption bonding c(2×2)O, self-consistent electronic struct. 79−78146
Ni (001) surface, electronic struct. of ordered S overlayers 80−84835
Ni, (001) surface, local density of states, asphericity of pot. and charge transfer, ab initio self-consistent calcs. 79−15064
Ni (001) surface, O monolayer, angle-resolved UV photoemission calc. 77−24927
Ni, (001) surface, spin polarised photoemission theory, surface states and dead layer existence 79−15584
Ni (100), bonding of O 78−79889
Ni (100), chemisorption of first row atoms, molecular cluster theory 77−1309
Ni (100), chemisorption of O, S and Se, struct. and energy levels calc. 77−47663
Ni (100), chemisorption of CO, Hartree-Fock-Slater mol. cluster calcs. 79−51650
Ni (100), electron field emission, positive spin polarisation and band model of magnetism 77−52226
Ni (100), electronic struct. of c(2×2) and p(2×2) O overlayers 79−47144
Ni (100), initial oxidation, electron energy loss spectra, LEED, AES, and work function meas. 79−61795
Ni (100), surface electronic struct., self-consistent local orbital calc. 80−65649
Ni (100) and (111) surface, chemisorption of CO, tight-binding theory 77−20395
Ni (100) surface, bonded Se, electronic orbitals 78−72224
Ni (100) surface, clean and gas-covered, electron energy loss spectra 79−47570
Ni (100) surface, spectroscopy by He metastable beam 77−36334
Ni (110) surface, electron spin polarisation, effect of H_2 adsorption, electron capture spectroscopy 78−14933
Ni (111), adsorption of chalcogens, angle-resolved photoemission 80−40230
Ni (111), chemisorbed CO, orientation of CO from angle resolved photoemission 77−8721
Ni (111), chemisorption and reaction of NH_3, LEED, desorption and photoemission expts. 80−59799
Ni (111), chemisorption of H, electronic struct. of H using angle-resolved photoemission 79−69573
Ni (111), isothermal desorption of CO, UPS study, time-resolved approach 80−39440
Ni (111) and (110), laser-induced charge transfer to adsorbed CO, photoemission expts. 80−59798
Ni (111) surface, clean and with CO absorbed layer, angle-resolved photoemission meas. 77−16463
Ni, (111) surface, Λ_1-symmetry surface state, angle resolved photoelectron spectra 78−80034
Ni, (111) surface, pyrazine physisorbed, UV spectroscopic ellipsometry obs. 79−86997
Ni (111) surface, with O_2, Se, S and Te adsorbed layers, bonding geometry and electronic struct. 79−77909

surface electron states continued
Ni, adsorbed CO, core level spectrum, satellite struct., ab initio HF-LCAO calc. 80−40233
Ni, adsorbed O, electronic struct. and UPS 78−15281
Ni, adsorption of N_2, photoemission and electronic struct., cluster calcs. 80−97403
Ni, CO adsorbed on (001), orbital energy spectrum 78−2369
Ni, chemisorption of H, embedded cluster model 80−39427
Ni, chemisorption of H, model, comparison with UPS data 79−46932
Ni, chemisorption of H_2, interaction between adsorbates, model Hamiltonian calc. 79−46964
Ni, chemisorption of H_2, molecular complex model, electronic struct. calc. 77−1314
Ni, chemisorption of O(S)(Se)(Te), orbital energy spectrum of chemisorbed electrons 78−2542
Ni clusters local densities of states 80−88466
Ni, d-band narrowing, obs. using angle-resolved XPS 80−11062
Ni, ferromag. film, surface states, surface magnetisation and electron spin polarisation 80−65648
Ni, ferromagnetic, chemisorption of H, spin-spin interactions, UPS spectra calc. 80−6630
Ni, ferromagnetic, photoemission spectra and band struct., spin polarisation of bulk photoemission 79−78843
Ni, field-emitted electron spin polarisation by tunnelling through surface pot. 80−29861
Ni film, ferromagnetic (100) and (110), energy bands 79−1630
Ni film, surface properties and photoelectron spin polarisation 78−14782
Ni film, transverse Kerr magnet-optical effect enhancement by surface magnetoplasma waves 77−52056
Ni, film growth on graphite and amorphous C, electronic struct. by photoemission and Auger obs. 79−77947
Ni films, electronic struct. calc., effects of chemisorption; contact pot. and surface magnetisation 80−103734
Ni foil, hydrogenated, surface states of chemisorbed H_2 and elec. cond. 77−69399
Ni, hydrocarbon chemisorption, C 2s levels, initial state shift 78−34703
Ni, hydrogenated foil, surface states and thermo EMF 78−91674
Ni, magnetic surface anisotropy of transition metals, model calc. 80−34625
Ni metal cluster, adsorption of CO, mol. orbital calc. 78−18895
Ni, polarisation-dependent angle-resolved photoemission for band structure studies 78−95678
Ni, rel. to absorption spectrum anomalies, 2-3 eV, optical anisotropy *(French)* 78−43893
Ni, rigid exchange splitting model 77−11977
Ni, spin polarisation of field emitted electrons 77−32508
Ni surface, adsorption, chemisorption of at., mol. H_2, semi-empirical CNDO MO calcs. *(German)* 79−95465
Ni surface, spin distribution of electrons, electron capture spectroscopy 78−14932
Ni, surface density of states in simple model 77−47874
Ni, surface vibrs., chemisorbed O influence 80−84361
$Ni_{1-x}Cu_x$ (x=0.03, 0.16, 0.24), photoemission study, surface, bulk electronic struct. 78−48281
$Ni_{23}Cu_{77}$ random substitutional alloy, (001) surface, angle resolved photoemission 77−85895
NiFe, magnetic surface anisotropy of transition metals, model calc. 80−34625
NiNO, ground and core hole states, config. depend. HF LCAO SCF calc., relax. and binding energy 80−29453
NiO (001). diffr. of monoenergetic He atoms, energy levels from bound-state reson. 79−61487
NiO (100) surface, electronic states, electronic energy loss spectroscopy 78−6426
NiO, H chemisorption, perfect surfaces, cation vacancies, self-consistent HF-VB calcs. 79−69351
Ni(001) surface, O chemisorption induced states, angle-resolved photoemission from adsorbates 78−23585
Ni(001), surface electron struct., matching Green function method calcs. 78−88014
Ni(001) surface states, surface magnetisation, electron spin polarisation 80−88612
Ni(100) magnetic surface states, photoelectron spectra, surface Brillouin zones 80−6928
Ni(110), mag. exchange splitting of electronic surface states 80−88610
O, on Al (100), overlayer electronic struct. 77−85058
O_2 chemisorbed on TiO_2 and $SrTiO_3$, phase investig. by UPS 78−72684
O_2 covered metals, secondary ion yield, quantitative determ. *(German)* 79−48003
O_2 monolayers, on graphite, mag. α-phase and α-β-phase transition 80−70530
Pb films, conduction electron surface scatt. phase shift, tunnelling meas. 79−51648
Pb, surface density of electronic states 77−20397
PbI_2, layered compound, exciton spectra, surface and stacking fault effects 80−40134
PbO powder layers, adsorbed rhodamine B dye, charge storage and photocond. 78−64056
PbS (100) surface, electronic struct., O_2 adsorption effects, UPS study 80−54756
PbS film surface with oxysulphate layer, photoelec. memory effect 77−55584
PbS oxide, optical excitation meas. of trap charging surface film *(Russian)* 78−76180
PbS(Se)(Te), chemisorption of O_2, room temp., UPS and XPS obs. 78−91529
PbSe surface, clean and O_2-exposed, XPS (UPS) obs., electronic struct. 78−52637
p-$Pb_{0.82}Sn_{0.18}Te$, mag. susceptibility, inversion layers effect *(Russian)* 77−72996
$Pb_{1-x}Sn_xTe$:Cd, photoelec. props., surface recomb. effect 80−44659
n-PbTe, accumulation layer, quantised surface states 80−20279
PbTe, magnetoreflectance of surface space charge layers 78−52475
Pd (100), adsorption of Xe and CO, lateral interactions, effect on work function, UPS, and IR spectra 79−77904
Pd (100), chemisorption of CO, adsorbate band formation, UPS expts. compared with calcs. 79−77916
Pd (100), with CO adlayer, band formation, calcs. and photoemission expts. 79−95463
Pd, (100) surface, benzene chemisorbed, angle-resolved photoemission symm. anal., polarisation depend. and lateral interactions 79−91568

surface electron states continued
Pd (111), electronic states calc. and adsorbate-induced photoemission struct. interpretation 78−60179
Pd (111), interaction with O_2, EELS, AES and LEED obs. 79−86985
Pd (111) clean surface, electronic struct. using LCAO band model 79−65531
Pd (111) surface, adsorbed O_2, UPS and thermal desorpt. characts. 80−54754
Pd, chemisorption of H, embedded cluster model 80−39427
Pd, chemisorption of H, model, comparison with UPS data 79−46932
Pd film, work function changes due to adsorbed H_2, surface and interface dipoles 80−96972
Pd, film growth on graphite and amorphous C, electronic struct. by photoemission and Auger obs. 79−77947
Pd overlayers, on Nb, form. of Pd (111) surface states and reson. d-levels, photoemission obs. 80−50523
Pd particle array, on amorphous SiO_2 substrate, model catalyst, electron microscopy and UPS expts. 79−4899
Pd, single cryst., ang. resolved photoemission at 21.2 and 16.8 eV 77−63543
Pd surface, segregated S state, AES, EELS, UPS and XPS study 80−93452
Pd-Si (111) interface, microscopic Pd_2Si form., UPS obs. 80−24743
Pd(111) chemisorption of H, photoemission spectra, SCF electrical struct. 79−33320
Pt 6(111)×(100), clean and O_2-covered, UPS studies 80−76151
Pt (001), surface electronic props. 78−95332
Pt (100), chemisorption of O_2 and H_2, comparison of (1×1) and (5×20) configs. 77−51599
Pt (100), cyanogen adsorbed layers, electron energy loss spectrum 78−14592
Pt (111), adsorption of CO, XPS, UPS, thermal desorption, and work function meas. 79−77905
Pt (111), chemisorbed CO, orientation of CO from angle resolved photoemission 77−8721
Pt, absorption of CO on (111) surface, photoemission, 40-150 eV 77−16465
Pt, $CO(O_2)$ interactions, surface electronic struct. (surface chem.) using synchrotron radiation 78−53254
Pt, chemisorption of H, embedded cluster model 80−39427
Pt, chemisorption of H, model, comparison with UPS data 79−46932
Pt clean (001) surface, electronic props. 77−72901
Pt cluster, conduction electron density oscills., NMR spin-echo meas., indirect exchange interaction 80−44954
Pt complex, coordinatively unsaturated, electronic struct. and catalytic activity 78−72228
Pt, electrochemical adsorpt. of H_2, adsorpt. states, tensiodynamic meas. 77−20196
Pt electrodes, chemisorbed H, anion effects on multiple states, reflection spectra obs. 79−43634
Pt surface, stepped or flat, H_2 chemisorption, calcs. 79−28208
Pt, surface dipole moment calc. 80−60060
Pt, surface struct. and electronic props., CO_2, O_2, H_2 chemisorption 77−1300
Pt, UV photoemission, from (111) and [6(111)×(100)] surfaces 79−91566
Pt(III), electronic struct. of adsorbed Na 78−19117
Pt(111) surface, identification of adsorbed OH species 80−49509
Rb film, adsorbed on Ni (100), plasmon losses in electron energy loss spectra 79−61480
Re (0001), chemisorption of CO, role of d-orbitals, angular resolved UPS and thermal desorption meas. 80−40232
Re, chemisorption of alkali metal ats., bond, adatom valence energy level broadening *(French)* 79−33176
Rh (111) surface, UPS meas. of chemisorbed and condensed CO using synchrotron radiation 79−33902
Ru (001), dissociation of adsorbed H_2S, chemisorption and electronic struct. of S layer 79−79292
Ru (001), electron stimulated desorption of CO, correl. with other meas. 78−47658
Ru (110), adsorption of H_2S, H_2, and S, UPS and work function change meas. 79−78834
Ru, physisorbed SF_6, XPS interpretation 77−89830
Sb, Sb_2O_3 and Sb_2S_3, AES and characteristic energy loss spectra, expt. and interpretation 78−27354
SbI_3, layered compound, exciton spectra, surface and stacking fault effects 80−40134
SbSI, ferroelectric semiconductor, polarisation switching processes, effect of surface electron states 77−90115
SbSI, surface layer exam. 78−48119
Sc (0001), H adsorption, geometric vs. electronic factor in surface electronic structure 80−70788
Sc (0001), surface states 79−91120
Se, amorphous, density of surface states 77−76897
Se diode surface states determ. by conductance and capacitance 77−85318
Si, (001) (2×1) reconstructed surface, dimer model self consistent calcs. 80−88613
Si, (001) and (111), geometrical and electronic struct., review 80−80039
Si (100), atomic and electronic structs., energy minimisation calcr. 80−49480
Si (100), chemisorption of H, new type of chemisorptive bond, theory 78−26930
Si (100), chemisorption of H, pairing model calcs., compared with expt. 78−34719
Si (100), dimer reconstruction, photoemission obs. 80−80939
Si, (100), effective mass and collision time 78−64081
Si (100), electronic struct., scattering-theory formulation 79−42607
Si (100), intrinsic surface states, photoemission study 80−50514
Si (100), surface space charge layer, inter-subband optical transitions 77−15931
Si (100) inversion layer, hot electron drift velocity, Monte Carlo calcs. inc. 3 subbands 78−91752
n-Si (100) inversion layer mobility depend. on intersubband scatt. at low temps. 79−95506
Si (100) surface, cyclotron reson. of electrons in surface space charge layers 77−8169
Si (100) surface, intersubband optical absorption in space-charge layers 77−35984
Si (100) surface, pairing model, electronic pot., charge density, Fermi energy and surface density of states 77−47875
surface electron states continued
Si (100) surface, reconstructed, atomic and electronic struct. 79−73381
Si (100) surface, surface cyclotron resonance, freq. depend. 77−8170
Si (100)-SiO_2 inversion layers, exchange and correl. contribs. to subband energies 79−42654
Si (110), chemisorption of Cl, LCAO calcs., Auger line shapes, localized density of states 78−56202
Si (111), 2×1 reconstructed, self-consistent anal. 78−91518
Si (111), (100) and (110) ideal surfaces, valence-band Auger lineshape theory 77−48286
Si (111), (e,2e) reactions, theory 78−39640
Si (111), adsorption of Cl, electronic energy states, cluster-type calcs. 79−47149
Si (111), chemisorbed O_2 electronic struct. tight-binding calc., XPS and UPS meas. 80−49845
Si (111), chemisorption of H_2(Cl), conduction-band surface resonance 78−52051
Si (111), chemisorption of H, localised model, ab initio HF-LCAO calc. 80−6930
Si (111), dynamic effective charge and surface reconstruction, soft-mode theory 79−4460
Si (111), electronic states and initial steps in oxidation 78−91534
Si (111), intermediate oxidation state, core photoelectron absorpt. vs. chemical shifts 80−81220
Si, (111), struct. depend. oxidation, high resolution photoemission yield spectroscopy 77−1305
Si (111), surface relax., mol. SCF calcs. 78−91522
Si (111), surface states and surface struct., angle-resolved PES 79−28390
Si (111), with chemisorbed Cl and F, electronic energy struct. calcs. 79−78144
Si (111) 1×1, chemisorption of Cl in surface vacancies 79−77910
Si (111) 7×7 clean surface and O chemisorbed stage valence band density of states from $L_{23}VV$ Auger spectra 80−100717
Si, (111) 7×7 surface, adsorption of Al, electron energy loss spectroscopy and LEED 77−43432
Si (111) 7×7 surface, giant core-exciton effects, electron energy loss spectra and XPS 77−24600
Si (111) 7×7 surface, Schottky barrier formation, photoemission, exam. of filled surface states and band bending 77−28250
Si (111) 7×7 surface, secondary electron emission from surface state resonances 79−69930
Si (111) 7×7 surface electronic struct., angle-resolved UPS study 80−50513
Si (111) 7×7 surface states, low-energy electron loss spectroscopy 79−60891
Si (111) (7×7) surface structs., LEED anal. and energy minimisation calcs. 80−49478
Si (111) covalent surface, pot. and charge distribs. and dangling-bond state 78−2537
Si (111) face, surface states and photoemission 77−72900
Si, (111) surface, Ag interaction, AES 78−14589
Si (111) surface, chemisorbed Al, local density of states 79−47142
Si (111) surface, clean, ESCA obs., Ni(Au) surface impurities 78−52640
Si (111) surface, clean and O_2-chemisorbed, electron states by AES 80−54747
Si, (111) surface, electron inversion layers, obs. of sixfold valley degeneracy 79−38176
Si, (111) surface, electronic density of states changes during O adsorption, AES obs. 79−65528
Si (111) surface, H chemisorbed, electronic struct. 78−39182
Si, (111) surface, low press. baked, dominant interactions and average distances between paramag. centres 80−15783
Si (111) surface, relax. of surface atoms, Si_4H_9 clusters 77−8171
Si (111) surface, relax. of surface atoms, Si_4H_9 clusters 77−35980
Si (111) surface, surface energy bands and atomic position of chemisorbed Cl 78−56041
Si (111) surface, with Al overlayers, electronic states 80−11061
Si (111) surface with Al overlayers, electronic struct., self-consistent pseudopotential method 79−4595
Si (111) surfaces, cleaved, electronic structure following Al adsorption 80−75610
Si (111)-1×1, electronic struct. of surface, model pseudopot. calc. 80−65651
Si (111)7×7, dangling-bond surface states and O_2 adsorption, reflectometric study 79−99600
Si (111)7×7 surface electronic struct., angle-resolved UPS study 80−40226
Si, ⟨111⟩ surface, 2×1 reconstruction mechanism 77−66079
Si, adsorbed metal atoms effect on surface electron states 77−55597
Si, adsorbed Pd impurity, effect on surface electronic props. *(Russian)* 79−91124
Si, amorphous, clean and O_2 adsorbed, light sensitive electron laser meas. 79−24396
Si amorphous film, optical props., electronic states 80−25475
Si, bonding states of adsorbed O_2, photoemission obs. 78−92170
Si, bulk and surface equlib. props., self-consistent pseudopotential calcs. 79−60750
Si, chemisorption of Cl_2, photoemission polarisation effects with synchrotron radiation 78−14580
Si chemisorption of Ga on (111) surface, Ga-induced surface states 79−19644
Si, chemisorption of H on (111) 77−62743
Si, clean and gas (O_2 and H_2O) covered surface, appl. of UPS ultrahigh vacuum apparatus *(Japanese)* 80−37125
Si, clean cleaved, surface photovoltage, effects of atomic steps 78−19120
Si, clean surface, geometrical struct. rel. to electronic props. 77−62719
Si, dangling bonds, EPR, localised states and unpaired electrons on microcrack surfaces 78−52351
Si, deformed surface, defect struct. rel. to elec. props. 78−72231
Si, field emission, role of surface electron states 78−2993
Si, field penetration in FIM, band bending 79−87567
Si, high index surface, natural orientational superlattice in 2D electron gas 79−99598
n-Si, IR spectra of surface photocond. and photo-EMF 77−76868
Si inversion layer, elec. break-through, exactly solvable model 78−56234
Si inversion layer, Γ and X electric breakthrough interference effect 79−47137
Si inversion layer, high freq. cond., Drude relax., 2D plasmons and minigaps in surface lattice 78−60230

surface electron states continued
Si inversion layer, IR spectrum, 10^5G effect on linewidth 78−946
Si inversion layer, influence of natural superlattice on 2-dimens. electron gas spectrum *(Russian)* 78−68064
Si, inversion layer, interacting electron system, cyclotron reson. 78−87902
Si, inversion layer, polaron model for localisation 80−20280
Si inversion layer, valley splitting, effects of misorientation 79−73564
Si, inversion layer, voltage tunable far IR emission 80−25018
Si inversion layer surface cyclotron resonance, temp. and stress effects 78−60229
n-Si inversion layers, broken symmetry states 79−15229
Si inversion layers, CDW mag. fields and stability 78−10533
Si inversion layers, cyclotron and subband emission 78−64128
n-Si inversion layers, electronic g-factor, spin-split Landau levels 80−80346
Si inversion layers, random pair attractive interaction model of carrier correl., compared with expt. 78−60212
n-Si inversion layers, stress and temp. depend. of subband struct., plasmon-pole approx. 79−95461
n-Si, inverted MOSFET surfaces, quantum oscills., valley splitting, lineshape in state density effects 79−56318
n-Si, inverted MOSFET surface, evidence for Lande factor g=2, finite valley splitting 80−6989
n-Si ion implanted surface potential barriers, $LiNbO_3$ SAW obs. 77−28234
Si, local density of states method and bond orbital model calc. 77−8165
Si MNOS structures with tunnelling-thickness SiO_2 films, surface channel hole mobility obs. 78−95380
Si MOS capacitors, pulse response anal., lateral depletion region around gate area 79−38187
Si MOS diode charact. obs., electron irradiation damage effects *(Japanese)* 79−42646
p-Si MOSFET, intersubband reson. photoresponse, mechanism 79−82677
Si MOSFET, n-type inverted, surface, mag. field depend. of valley splitting 79−19650
Si MOSFET, spin orbit interaction and many body effects in surface states 78−64132
Si MOSFET, surface quantum states, two-dimensionality of many-body effects 80−103740
Si, morphology and electronic struct. 79−78194
Si, n-channel (100) inversion layers, valley splittings due to elec. break through 79−4592
Si, n-type inverted MOSFET (100) surfaces, quantitative determ. of valley splitting 79−51678
Si, O_2 adsorption, UPS, new adsorption state 78−34702
Si, oxidised in trichloroethylene-O_2, Cl incorporation and elec. props. 79−91827
Si, photoemission spectroscopy of surface states and oxidation 77−55863
Si phototransistors, slow contamination and fast surface state effects, SEM study 80−107896
Si, plasmon sideband exam. by synchrotron radiation tuning of electron escape depths, UPS 77−47755
Si, polarisation dependent electrorefl. spectra, surface phenomena 78−68479
Si, quasi two-dimensional, crit. conc. of hot carriers 77−35977
Si, reconstructed surface (111)2×1, polarization depend. of optical absorpt. spectrum 79−28396
Si, review of optical methods of detection 77−66191
Si, SAW meas. of surface elec. props. 77−20387
Si, step depend. surface states, self-consistent pseudopot. calcs. 77−20384
Si, superlattice and 2-D electron gas 78−64080
Si surface, (111), energy states, computer renormalisation-group calc. 80−75617
Si surface, (111), metastable 2×1 reconstructed, dangling bond mediated attractive electron-electron model 78−91520
Si, surface, (111) 2×1, cleaved, O_2 adsorption, low-energy electron loss spectra 79−15840
Si surface, (111)7×7, electronic struct. calc. 80−24993
Si surface, adatom indirect interaction 80−44696
Si surface, Ar^+ ion bombardment, O_2 enhancement of sputtered ion yields 79−38705
Si surface, Cl chemisorption, cluster calc. by iterative EHT 77−32062
Si, surface, cluster model approach for electronic struct. 78−56205
Si surface, electron states, surface photovoltage spectroscopy study, doping effects 80−49860
Si surface, field penetration and band bending in high elec. fields 79−42613
Si surface, ideal and 2xl chain-reconstructed, electronic struct. determ. 78−52050
Si surface, MOS struct. band structure, minigaps, magnetoresistance, cond., space charge layers 80−92980
Si surface, metal doped, recomb. of nonequilib. carriers at high excitation rates 79−7835
Si, surface, stressed, n-inversion layers, Hartree calc. 78−68066
Si surface, valence band Auger line shape, corrected numerical results 78−52602
Si surface (100), vicinal plane surface band struct. electron inversion layers, minigaps 78−68062
Si, surface characterisation using SAW 80−11069
Si, surface charging during illumination, effect of various surface treatments 79−51651
n- Si, surface electron states, props. determ. at 77K 77−55598
Si, surface electron states using discontinuous potential model 79−69574
n-Si, surface photocond. and photo-emf spectra 79−73544
Si, surface photovoltage spectroscopy appl. 77−69391
Si, surface potential, influence of metal impurities, surface photo-EMF obs. 78−19122
Si, surface props. using SAW attenuation in adjacent $LiNbO_3$ 79−87131
n-Si, surface quantum oscills. in inversion layers under uniaxial press. 78−88041
Si, surface space charge layer, electron subbands, mag. field effect 77−20393
Si surface space charge layers, cyclotron reson. of holes 77−76932
Si, surface space charge layer, anisotropic and tilted valley systems, absorption 77−85726
n- Si, surface space-charge layer, intersubband-cyclotron combined reson. 78−68063

surface electron states continued
Si, surface state distrib. after treatment with HF and H_2O using photovoltage pulses 79−60888
Si, surface with incomplete impurity ionisation, quantum model 78−34877
Si surfaces, electronic struct., tight-binding calc. 80−54755
Si, transition layer form., band struct., electroreflectance 77−16333
Si, under stress, density functional calc. of subband struct. 80−20321
Si:Ag, surface layer, ellipsometry 78−19121
n-Si:Ar(P), single cryst., positron annihilation parameters, energy-band struct. on surface in free-electron approx. 79−15555
Si:As, amorphous, field effect and thermoelectric power 79−33289
Si:Au, nonequilib. population of electron states and photomemory of surface pot. 78−56206
Si:Au surface, electronic props. 77−66194
Si:Au(Hg), photomag. effect 77−4401
Si:B, RF glow discharge sputtering damage centres, barrier formation 79−33329
p-Si:B-SiO_2 interface in MOS structures, carrier mobility and impurity distrib. 78−34902
Si:H, amorphous, surface activated, photoemission spectra, minority carrier diffusion length 80−40235
Si:H, amorphous, surface states distribution using MOS tunnel junctions 80−103735
Si:H,P, amorphous, in MOS tunnel junction, electron tunnelling charact. 79−73592
n-Si:Pd, surface, photocond. and photo-emf spectra 79−73544
Si:Zn (Mn) (In), surface characterised by negative electrochemical pot., electronic props. 80−44695
Si-Ge alloys, temp. depend. of ESR line intensity of surface centres 77−32246
Si-SiO_2, flat-band voltage due to fixed surface charge density, modified expression 79−56317
n-Si-SiO_2, MOS structures, radiation states 80−103758
Si-SiO_2 interface, effect of high-temp., post-oxidation annealing on elec. props. 79−82673
n-Si-SiO_2 interface, hot carrier surface thermo EMF depend. on surface band bending 80−44734
Si-SiO_2 interface traps energy distribution meas., in MOS devices, under non-steady-state *(Korean)* 78−64119
Si-SiO_2 MOS interface, surface-state density and minority carrier generation rate, meas. by DLTS, hot hole effect 80−100527
SiC with dielectric coating, surface polaritons, waveguide modes 80−80195
SiO_2 (100), electronic struct., scattering-theory formulation 79−42607
SiO_2, electron irrad. effects, EELS study 80−24985
SiO_2, HCl-grown oxides, characterisation of surface states using MOS transient currents 80−65696
SiO_2 monolayer, core excitons and inner well resonances in surface soft X-ray absorpt. spectra 80−40187
SiO_2, surface defect studies, AES, theoretical model, and expt. 79−7738
SiO_2, surfaces, electronic struct. calc., scattering theoretic approach 80−6940
SiO_2, valence band density of states from self-deconvolution of $L_{23}VV$ Auger spectrum 79−47561
Si(100) 1×1 surface, interacting with H monolayer, electronic props., self-consistent calc. 77−43690
Si(100) inversion and accumulation layers, effective mass and collision time of electrons, oscillatory magnetoconductance 78−34909
Si(100) surface, temp. depend. of electron intersubband reson. 78−14783
Si(111), atomic geometry effects, photoemission and electron energy loss spectra 77−85283
Si(111), chemisorption of H, formation of monohydride and trihydride phases 79−15004
Si(111), conduction-band surface resonance 78−52051
Si(111), dangling-bond surface states 78−43452
Si(111), high resolution photoemission yield, surface states 77−69392
Si(111) ideal and relaxed surface, electronic struct. 79−60901
Si(111) surface, interpretation of intrinsic surface states 78−6423
Si(111), surface density of states from soft X-ray absorpt. spectra 80−40187
Si(111), water vap. and O_2 interactions, EELS 78−14571
Si(111)-(7×7), and impurity stabilised Si(111)-(1×1) surface, photoemission studies 80−104041
Si(111)2×1, oxide layer, surface states detec., optical reflectivity obs. 80−50368
Si(111)2×1, surface electron states detected by external reflectivity 78−80036
Sm, divalent surface states, photoemission meas. 78−47841
Sm metal, XPS evidence for weak surface divalent component 77−39808
Sm surface, valence change 79−56280
Sm surface electronic structure, XPS study 80−55259
Sm, surface mixed valence, XPS study 80−60753
Sm, surface valence state from surface tension props. 79−95462
Sm, XPS, 50-250 eV, 4d→4f transition and surface mixed valence 79−15588
Sm, XPS, electronic struct. determ. for surface 80−20765
SmB_6, surface mixed valence, XPS study 80−60753
SmS, mixed valence states at surface 77−20398
Sn, positron annihilation in fine particles, surface trapped states 80−84800
SnO_2-Si, solar cell, max. theoretical efficiency 79−83598
SrO, surface states, reflectance spectra, impurity effects 77−20873
$SrTiO_3$, (100), LEED and UPS studies 80−100747
$SrTiO_3$ (100) surface, struct. and electronic props., AES, LEED, EELS, and UPS study 80−24986
$SrTiO_3$ (111), surface struct., electronic props., LEED, AES, UPS study, photoelectrochem. cell anode appl. 78−84035
$SrTiO_3$, cluster surface states, LCAO calc. 77−43686
$SrTiO_3$, electrode, surface photovoltage expts. 78−72227
$SrTiO_3$ photoelectrolytic electrodes, defect surface states obs. 78−14815
$SrTiO_3$, semicond. anode in aq. electrolyte, electrolum. and electrochem. 80−76080
$SrTiO_3$ semicond. electrode, electrochem., photoelectrochem. props. 80−3352
$SrTiO_3$, surface defects, electronic struct., LEED, AES, UPS study 78−84273
$SrTiO_3$:B layers, ion implanted, conductive props. Hall mobility, defect energy levels 79−82693
Tb, electron energy loss spectra 77−85860
Te accumulation layer, surface states calc. 77−43692

surface electron states continued
Te cyclotron resonance, transport and surface phenomena 77−40132
Te films, elec. props., 77 to 450K, thermal width of band gap 79−51698
Te, inversion layer, calc. from Shubnikov de Haas meas. and triangular surface pot. well 79−15207
Te inversion layers, surface quantum oscillations 77−89777
Te inversion layers, surface quantum transport 78−64088
Te inversion layers in mag. fields 80−44690
p-Te, photocond. and lifetime, surface trapping, spectral distrib. 78−34840
Te:Sb, surface carrier effects on Hall mobility at low temp. 77−80794
Ti (0001), H adsorption, geometric vs. electronic factor in surface electronic structure 80−70788
Ti (0001), surface states 79−91120
Ti (0001), valence band struct. and chemisorption, XPS and UPS study 80−35062
Ti (0001), with adsorbed N (1×1) layer, underlayer geometry, electronic struct. calcs. and UPS meas. 80−54751
Ti (0001) film, electronic struct., Fermi level, surface states, GO calcs. 80−6927
Ti (0001) film, with adsorbed H (1×1) monolayer, electronic struct., surface geometry 80−54750
Ti (10$\bar{1}$1) surface, HCP→BCC transition He II UPS study 79−42345
Ti, band struct. effect on photon emission from sputtered Ti atoms 80−58208
Ti, polycryst., absorpt. of O at room temp., XPS and UPS 77−89645
TiC, Shockley surface states and bonding 78−91739
TiH_x and $TiD_{0.9}$, surface characts., AES, EELS, SIMS, and XPS study 80−65343
TiO, (001) surface, spectral density of states 78−39187
TiO, TiO_2 band struct. effect on photon emission from sputtered Ti atoms 80−58208
TiO_2, (110) and (100) surfaces, LEED and electron spectra 77−72757
TiO_2 (rutile), (001) and (110) faces, UPS and LEED obs. 80−45206
TiO_2 (rutile), (001) and (110) surfaces, surface and bulk density of states calcs. 80−49858
TiO_2, cluster surface states, LCAO calc., electron energy loss peak interpretation 77−43686
TiO_2, clusters, surface electron struct. and defect states, DV-Xα calc. 80−20268
TiO_2 electrode, silanisation effects on semicond. props. 79−96364
TiO_2 electrodes, in aq. electrolytes, surface states, photocurrent obs. 80−49895
TiO_2, OH^- adsorption on defect site, electronic struct. 79−47150
TiO_2, rel. to elec. props. of Ti-TiO_2-Au diode 80−15617
TiO_2, semicond. anode in aq. electrolyte, electrolum. and electrochem. 80−76080
TiO_2, sputtering defects, associated surface electron states, UPS, XPS and AES obs. 80−60755
TiO_2, surface electronic struct. by discrete variational Xα cluster calc. 78−43449
TiO_2 treated with quinoline, photooxidation and effect of surface states, ESR obs. 79−66352
TiO_2, UV photon induced secondary electron emission 79−52079
n-TiO_2-electrolyte interface, charge-transfer-controlled photocurrent 80−50992
n-TiO_2-electrolyte interface, charge transfer via surface states, water photoelectrolysis anal. 80−75636
V, and its cpds. with light elements, surface state, XPS investigation 78−11070
V, magnetic moment near surface, one-electron band model 79−82747
V, single cryst., surface investigation by positron annihilation 79−15552
VO, (001) surface, spectral density of states 78−39187
VO, surface states in unreconstructed (001) surface 77−32060
W, (001), (011) and (111), projected surface energy bands 78−88009
W (001), adsorbed H_2, LCAO calc. of band struct. 77−8168
W (001), chemisorption of H, HF Green's function formalism and phase shift technique 80−24733
W (001), electronic surface reson. band struct. and lineshapes, LEED meas. 79−82655
W (001), surface bands dispersion 77−15930
W (001), surface phase transition, electronic contribs., surface susceptibility, ab initio self-consistent thin-film energy band calc. 80−29255
W (001), surface reson. bands, dispersion relations 77−51797
W (001), surface resonance bands 78−47843
W (001), surface resonance band fine struct. in LEED 78−47844
W (001) clean surface, spectral density of states 78−39181
W, (001) surface, electronic origin of reconstruction 80−11065
W (001) surface, surface CDW phase transitions 78−43455
W (011) face, adsorption of Sr and La, influence of substrate electronic struct. on props. 78−60032
W (100), adsorption of O_2, surface struct. and thermally stimulated reaction 77−55451
W (100), surface resonances, photoemission and field emission meas. 79−4593
W (100) and (110) surface, chemical effects in N_7 VV Auger spectra 77−32474
W (100) effect of metallic adsorbates on surface reson. 79−65983
W (100) face, surface reson. 78−72226
W (100) surface, adsorbed Au, Cu layers, electron field emission revealing unmasked surface reson. 79−15595
W (100) surface, energy loss mechanisms in low energy electron scatt. 77−85859
W (110), chemisorption of CO, LEED, XPS and Auger meas. 77−89647
W (110) surface, adsorption of H, band struct. and adsorbate geometry, surface-reflectance-spectroscopy 80−44416
W (110) surface states, characterisation and transferability obs. 79−33319
W, adsorbate covered, field emission energy distrib., overlayer geometry effects 77−8730
W, charact. energy loss mechanism 79−91547
W, chemisorbed H, surface cond. and intrinsic surface states, surface refl. spectra 80−15378
W faces, simultaneous adsorption of Ba and Cu atoms, work function changes 80−65378
W, field electron energy distrib., surface density of states 77−16471
W films, (010), energy band calc. including spin-orbit interactions 80−20274
W, LEED and electron microscopic investigs., review *(Hungarian)* 77−47654
surface electron states continued
W, polarisation-dependent angle-resolved photoemission for band structure studies 78−95678
W, RF surface impedance, new type of oscills. 79−15070
W, RF surface impedance at different sample surface states 79−60911
W, secondary electron emission rel. to LEED 78−84689
W, semi-infinite cryst., secondary electron emission, obs. of electronic struct. 79−33871
W, slow electron inelastic scatt., vol. and surface plasmon excitation 77−52207
W surface, (110), chemisorpt. effects on dielec. function, refl. spectra 80−75616
W surface, (110), X-ray photo emission spectra, bulk atom 4f splitting 79−100020
W, surface dipole moment calc. 80−60060
W, surface electronic structure and spectral densities 77−80824
W, surface relaxation and electronic structure of (100) surface 79−73561
W, surface state transferability, UPS meas. for (011) states 80−39650
W tip, photon assisted field ionisation 78−3000
W, UPS, angle-resolved, surface resonances on (100) face 78−2987
(W-Au)-SiO_2-Si:B MOS transistor, ion implantation effect on threshold voltage 78−34903
WO_3, semicond. anode in aq. electrolyte, electrolum. and electrochem. 80−76080
WO_3 semiconducting electrode, influence of surface states, impedance meas. *(French)* 77−1468
W(001), electron loss spectrum, momentum transfer effects 77−85858
W(001), electronic surface reson. and thermally induced struct. transition 80−88614
W(001), surface density of states for directional photoemission spectroscopy 77−20396
W(001), surface state resonance exam. above vacuum level 78−30965
W(001), surface states and surface resonances, self-consistent electronic struct. 80−96960
W(100) surface, angle-resolved photoemission from surface states, refraction effects 78−48279
W(111), surface densities of states for normal photoemission 78−35251
W(21$\bar{1}$), adsorption of Be, work function changes and scatt. electron energy losses 79−46947
Xe, physisorbed on Pd (100), angular-resolved photoemission 79−43102
Xe, solid, n=1 surface excitons and LO-TO splittings of bulk excitons 79−73445
Xe, solid, surface excitons 77−76892
Y_2O_3:Eu, surface luminesc. centres excitation characts. 78−52560
$YbAu_2$, surface electronic structure, XPS study 80−55259
Zn (0001), adsorption of Te, UPS investigation 79−91563
Zn, electronic surface states, (001) surface, Brillouin zone 79−24047
Zn, oxidation, MVV Auger spectra, line shape, relax. energies 77−73195
Zn/Cu film system, UPS during atomic diffusion 79−43097
$Zn_xCd_{1-x}S$:Cu crystallophosphors, spectra of IR electrophotographic sensitivity *(Russian)* 80−50423
ZnO 10$\bar{1}$0 surface, reaction of O_2, AES, LEED, EPR, desorpt., surface cond. and work function expts. 78−95950
ZnO (0001), (000$\bar{1}$) and (10$\bar{1}$0), UPS rel. to elec. struct. 78−15288
ZnO (0001) surface, hardness, electrolyte pH and bias voltage effect 78−47654
ZnO (000$\bar{1}$) surface, surface and bulk excitations, reflection electron energy loss spectroscopy 77−20389
ZnO (10$\bar{1}$0) surface bias voltage effect on hardness, charge exchange near dislocations 78−52078
ZnO, adsorption of H, space charge accumulation layers effect on secondary ion yields, H conc. meas. 79−83087
ZnO, bulk and surface plasmons, single and multiple excitation 77−12474
ZnO ceramic varistors, trapping by localized states, effect on dielec. and elec. props. *(Russian)* 79−28671
ZnO, chemomechanical effects 79−82431
ZnO electrode, role of triplet states in xanthene dye sensitisation 78−76869
ZnO, electronic surface and bulk transitions exam. by electron energy loss spectra 78−30964
ZnO epitaxial film, nonuniform cond. due to H chemisorption *(Russian)* 80−65723
ZnO, field emission energy distrib., surface state emission obs. 78−35258
ZnO, photodesorption of CO_2, rel. to surface cond. and AES, band-bending model 77−47671
ZnO, polar surface, clean (O_2-H-exposed), reflection energy loss spectra, 2-30 eV 78−64434
ZnO, polar surfaces (0001), (000$\bar{1}$) specificity, field emission, H adsorption 77−21009
ZnO powder, CO_2 desorption during electron irrad. and interaction with atomic H 77−89638
ZnO, strong accumulation layers, negative magnetoresistance 78−6428
ZnO substrate, for Ni films, band bending, UPS study 80−7472
ZnO, surface charge transfer in presence of photosensitising dyes 78−68049
ZnO, surface exciton dispersion relations, additional boundary conditions 77−43687
ZnO, surface exciton polariton, nonlinear optical excitation 77−59259
ZnO, surface exciton polaritons, ATR obs., book contrib. 79−42620
ZnO, surface exciton polaritons, nonlinear optical excitation and dispersion relation 79−82657
ZnO, surface photovoltage spectroscopy appl. 77−69391
ZnO, work function, band bending, and electron affinity 79−47145
ZnS bulk and surface states anal. using synchrotron radiation 77−66574
ZnS, nonpolar surface, tight-binding calc. 77−20383
ZnS:Ag, electroluminesc., surface barriers *(Russian)* 78−2919
ZnS:Cu, polycryst. phosphor, excitation storage, recombination barrier participation 78−27316
ZnS(Se)(Te), clean and oxidised surfaces, O_2 sticking coeff., ionicity effects, XPS expts. 77−85887
ZnSe (100), electronic struct., scattering-theory formulation 79−42607
ZnSe (100) surfaces, surface states meas. by LEED, AES and EELS *(Japanese)* 79−99599
ZnSe (110), LEED intensity anal. and electron spectroscopy 77−43678
ZnSe (110) surfaces, obs., by low-energy-electron loss spectroscopy *(Japanese)* 79−83071
ZnSe (111), low-energy electron loss spectra, bulk and surface transitions 78−11042

surface electron states continued
ZnSe, bulk and surface states anal. using synchrotron radiation 77−66574
ZnSe, electroluminescent MIS diodes, surface state density determ. 77−35993
ZnSe film, surface polaritons, thermostimulated emission *(Russian)* 78−10904
ZnSe film, thermostimulated polariton emission 78−2436
ZnSe, nonpolar surface, tight-binding calc. 77−20383
ZnSe surface states, electron interaction characterisation, by low energy electron transmission photovoltaic modulation 79−60896
ZnSe(Te), clean and oxidised surfaces, surface states, low-energy EELS study 80−11522
ZnSe(100) surface, anomalous oxidation props. 78−15558
ZnTe (110) and (111) surfaces, electron energy loss spectra, bulk and surface losses 79−43080
ZnTe (110) and (111) surfaces, O_2 adsorption, electron energy loss and Auger spectra 79−47568
ZnTe based metal-semicond. struct., spectral photosensitivity obs. 79−95492
ZnTe, bulk and surface states anal. using synchrotron radiation 77−66574
ZnTe clean and adsorbed O_2 (110) surfaces, UV photoemission spectra *(Japanese)* 80−93456
ZnTe, free exciton refl., surface layer effects 78−76493
ZnTe, luminescence spectra struct. surface and volume polaritons *(Russian)* 80−16089
ZnTe, nonpolar surface, tight-binding calc. 77−20383
ZrO_2 film, CVD from organometallic cpds. and characterisation 78−23626

surface energy
see also surface electron states; surface energy measurement
acetone-chloroform solution, Monte Carlo calcs. for interface struct. with directed intermol. forces *(Russian)* 78−1975
adhesion, interfacial energy-contact angle relation 79−91904
adhesion of solids, review of physical mechanisms *(French)* 78−6231
adhesive wear and friction, state of the art 77−8955
adsorption, intermolecular surface forces in plane densely packed hexagonal model 80−59785
adsorption system surface properties variational calcs., binding energy, Lang model 80−29279
aliphatic acids, thermodynamics of adsorption at air/aqueous soln. interface 80−10752
aliphatic alcohol, thermodynamics of adsorption at air/aqueous soln. interface 80−10752
alkali halides, surface energies, surface tensions and surface struct. 79−60610
n-alkanes, anisotropic London dispersion forces, surface effects 80−74214
alloy, FCC, Monte Carlo simulation of surface segregation 78−31413
anthracene, intermol. relax. energies, UPS 78−31304
antiphase boundary motion, microscopic diffusional theory, appl. to domain boundary coarsening 79−61563
artificial blood substitutes, surface energetics anal. 80−41321
p-azoxyanisole, depend. of phase transition temp. on thickness 78−26669
binary alloy, concept of partial elastic energy in anal. of surface segregation *(French)* 79−77884
binary alloy, morphological stability, discrete lattice theory, appl. to interfacial zones 78−3133
binary alloys, surface conc. profile and surface energy 80−84350
biphasic alloy, surface composition, cherry model 79−90849
borate glass, crit. stress intensity factor and fracture surface energy *(French)* 77−76487
brittle material, surface energy determ. from AE, automatic system 79−91899
brittle materials, effective surface energy of rupture determ. 80−21074
p-n-butyl-p′-heptanoyloxyazoxybenzene oriented on NaCl MgF_2 coated NaCl, surface phenomena and IR spectra 80−79678
β-casein, molecular structure of adsorbed film 79−79462
charged particles surface excitation system, ground-state energy 80−15462
coherent interphase boundary energy anisotropy between cubic-type crystals 80−54252
colloid, spherical particle, diffuse double layer, modified nonlinearised Poisson-Boltzmann equation 79−79305
contact adhesion between solids in vacuum, deform. and interfacial energy 78−22306
copolymer mesophases, scaling laws 79−94872
covalent or ionic-covalent crysts., dislocation-free contact 80−80096
crack resistance, characteristics correlation of material α_p and γ 80−21075
crack tip lattice trapping, relation between macroscopic and microscopic thermodynamic surface energies 80−59572
cracks, discrete dislocation analysis 80−84236
crystal, energy of step on rough face 77−43421
crystal growth from solution, mechanism role of solvent-solute interactions, surface entropy factor 77−24281
crystal surface-electron-hole drop interactions, interaction energy 80−29335
crystal-solution interfacial tension, from crystn. meas. 79−69045
crystallite growth on curved metal surface, fragmentation *(Russian)* 78−22676
cubic metals, theoretical eqn. 78−43234
cyclotrimethylene trinitramine, high explosive, fracture surface energy determ. 77−44337
cyclotrimethylene trinitramine, high explosive, surface energy from contact angle meas. 79−51393
cylindrical particle at fluid interface, equilib. position, force and free-energy anal. 77−55428
dialkyl phthalates, plasticizers, surface tension, contact angle, surface energy, entropy determ. *(Japanese)* 77−31843
diamond, synthesis from graphite, nucleation rate 79−16032
diamond (111) surfaces, relax. and reconstruction using C_4H_9 clusters, MINDO/3 calc. 79−42356
diamond solid-fluid interface roughening transition, Monte Carlo simulation 79−99088
4.4-dihexylazoxybenzene, nematic liq. cryst., alignment on surfactant treated obliquely evaporated surfaces 80−49092
dilute alloy, surface segregation, bond and strain energy effects, atomic calc. 79−69256

surface energy continued
dipolar crystal, surface local field effect, dipole moment, self consistent electric field calcs. 80−49178
drops, rotating, captive between co-rotating parallel faces, shapes and stability, capillarity eqns. 80−64592
drops, surface energies, contact angle wetting *(German)* 77−62710
elastic solids, contact deforms., role of mol. forces 79−23824
elastic solids, contact deforms., role of mol. forces 79−23823
electrocapillary theory, Lippmann relation, surface thermodynamics 78−61048
electron response function, dielectric sum rule 78−39184
electron-hole liquids, relation between bulk compressibility and surface energy 80−65465
eutectic alloys, surface energy considerations 78−44152
fatty alcohol solid monolayers in H_2O, interface struct., model 80−54505
FCC crystal, surface energy and chem. pot., microscopic capillarity approx. 80−5654
fermion system, exchange contrib. to surface energy infinite barrier model 79−85067
ferroelectric thin film, anisotropy properties, thermodynamic anal. *(Russian)* 79−28686
ferroelectric thin films, phase transitions, second order, thermodynamics *(Russian)* 78−52458
ferroelectrics, surface sound waves on domain boundaries, low temp. sp. ht. 78−71937
ferromagnetic-paramagnetic transition, surface energy effect *(Russian)* 79−87260
filled polymer solution, structural strength 79−64973
fluoro epoxy resins, surface props., appls., wear resistance and friction 78−64713
fracture stress obtained from the elastic crack tip enclave model 80−71730
free energy, anisotropic, method for absolute meas. 77−85062
gas-liquid interface of rising bubbles, adsorption rate determ. *(Japanese)* 80−6595
gas-liquid surface of mol. fluids, mol. dynamics computer simulations 80−39387
gas-liquid surface of penetrable sphere model, surface energy and tension 77−4249
gas-liquid surface of penetrable sphere model 79−73380
glassy organic polymers, total fracture surface energy, theory 79−43406
grain boundaries decohesion energy, solute adsorption influence 80−65009
grain boundary groove profile, effects of surface free energy anisotropy 79−7734
graphite, determ. using high temp. vacuum metallography *(Russian)* 77−15677
graphite fibre, surface anal. by XPS and polar/dispersive free energy anal. 80−65340
graphite fibre, Type-A, surface comp. and energetics 77−70024
graphite fibres, HM, surface comp. and energetics 80−54480
haemoglobin equilibria in soln., surface free energy model 80−81535
4-heptyl-4′-cyanobiphenyl, nematic liq. cryst., alignment on surfactant treated obliquely evaporated surfaces 80−49092
interface forces and interactions, roughness and ductility depend. 77−24476
interfaces of two bulk phases, non-equilibrium thermodynamics including EM effects 80−13021
interfaces separating compressible bulk phases, stability 80−107610
interfacial energy, surface energy, surface tension and lattice friction relation 79−69341
interfacial tension var. with supersaturation, one-layer adsorpt. model 80−103563
intermediate state, superconducting-spot and normal-spot models 79−11275
ionic crystal, surface stability 80−20016
ionic crystal, surface vibrational properties, review 78−71928
ionic crystals, statistical theory calcs. of surface energy and surface tension 80−17894
ionic crystals, vibrational surface modes, vibrational contributions to surface thermodynamic functions 77−47659
Ising antiferromagnet, square lattice, interface free energy and transition temp. 77−73041
Ising model, boundary free energy, natural iteration and cluster variation methods, critical points 77−17913
Ising systems, frustrated, interface entropy, phase transitions 79−19711
isotropic solid soln. cryst. surfaces, surface stress and chem. equilib. 80−107628
jellium metal, surface props. in linear pot. approx. 77−43689
jellium metal, surfaces props., statistical calc. 80−24987
jellium metallic surface, exchange-correlation energy, wave-vector analysis 77−47877
jellium-metal surface energies in infinite and step-pot. approx. 77−47876
leucosapphire crystals, block boundary energies 78−55877
Lippmann eqn., statistical mech. deriv., dielec. const. 77−20404
liquid, simple, nonadditivity contrib. 78−18874
liquid crystal, isotropic phase, surface induced ordering, birefringence obs. 80−14998
liquid crystal films, disjoining pressures isotherms *(French)* 79−99401
liquid crystal surface, statistical thermodynamics, local order parameter 80−88023
liquid crystals, surface alignment using polynuclear metal complexes 80−1924
liquid drop on solid substrate, deviations from Young's equation 77−66075
liquid in equilibrium with vapour, surface tension rel. to cohesive energy density 78−34680
liquid layer, insulating, cellular deformation mechanism, charge flux *(French)* 80−70507
liquid metal, surface entropy using hard-sphere model 79−37906
liquid phase sintered systems, particle coalescence probability estimation 80−104086
liquid surface, atomic processes, book contrib. 79−60605
liquid-vapour interface, surface tension and energy 77−76647
lysozyme, molecular structure of adsorbed film 79−79462
macroscopic metal catalysts, morphology and etching processes, review 80−7856
magnetisation theory, of slab of finite thickness, role of positive surface energy 80−15724

surface energy continued
MBBA, nematic liq. cryst., surface alignment using lecithin monolayers, contact angle meas. 79−4247
melt surface boundary, mass transfer, influence on crystal habit during growth 79−14712
membrane system, closed, vesicular, mechano-chemistry 77−60189
metal, adsorption of metal atoms, enthalpy calc. 80−100406
metal, classical cleavage energy, layer summation method 77−85287
metal, crystal melt interfacial free energy calc. from exptl. radial distrib. function data 79−10926
metal, cubic, relation between surface energy and Debye temp. 78−10271
metal, exchange and correl. contrib., wave-vector decomp. 80−75615
metal, FCC, anisotropy of surface free energy, computer simulation *(Russian)* 78−87858
metal, gradient corrections in interpolation formulae, surface plasmons 80−2441
metal, inhomogeneous strain effects on surface props., rel. to fracture model development 77−72907
metal, interacting metal half spaces, effect of retarded-surface-plasmon dispersion and Van der Waals interaction 79−69452
metal, one component substances, surface energy, temp. depend. 77−72753
metal, semi-empirical theory 77−76895
metal, simple, self-consistent, calc. of surface energy including ion pot. perturbation effect 77−8166
metal, solid 79−23825
metal, solid-solid and solid-liquid interfacial energy 79−42396
metal, surface energies and work function, simple analytic model 80−49862
metal, surface energy calc., exchange contrib., convergence of gradient expansion 77−43684
metal, surface energy calc. in model of discrete positive charge *(Russian)* 78−38911
metal, surface energy meas. by zero creep method at extremely low O_2 partial press. *(Czech)* 78−63926
metal, surface energy of electron gas, virial theorem 77−69398
metal, surface free energy of solid, at MP, estimated from liq. surface tension data 77−31866
metal, surface relaxation, lattice statics calc. 78−63925
metal, vacancies and change of surface free energy at melting point 79−42219
metal 78−91528
metal surface, gradient correction to electron exchange-correl. energy 77−43691
metal surface, ground state, variational self-consistent-method 78−56204
metal surface, influence of submonolayer films on props., calc. *(Russian)* 80−2273
metal surface energies, variational calc. 77−24603
metal surface free energy for BCC, FCC and HCP structs. etch pit depend. 80−29258
metal surface interaction with external mol. complex 79−47140
metal surface props., Rayleigh-Ritz variational calcs. 79−69570
metal surface-void van der waals interaction energy 78−10036
metal surfaces, adhesion theory, electron distribution tail effective length *(Russian)* 79−99430
metal-liquid, effect of lubricants, plasticity during cold working stresses *(Russian)* 77−55419
metallic film, electron density and potential, variational calc. 79−78218
metallic surface, self-consistent electron theory, review 80−88616
metals, adhesion theory for two surfaces 80−20270
metals, atomic binding energy and surface energy rel. to prediction of physical props. 80−59434
metals, free-electron like, interface energy 77−62984
metals, surface atom polarisation energy, effect of depolarisation 79−60620
metals, surface effects in hydrodynamic model review 79−78148
metals and alloys, diffusion layers, effect of chemicothermal treatment on struct., surface energy, and bulk props. 79−96207
mica, surface free energy dispersive component, adhesion to water and n-alkanes 77−55435
mica, surface free energy nondispersive component, adhesion to polar liq. 77−55436
microdrop, energy and mol. structure, mol. dynamics method 79−11004
microemulsions, lattice gas model, surfactant effects 78−23974
microindentation method, for surface energy evaluation 80−16473
molten metal, relation between surface energy melting temp. and Fermi wavelength 77−51571
molten salt, model for two-particle distrib. functions 79−33158
monocarbide, cubic, calc. of surface energy, rupture energy, and theoretical strength 77−11775
morphological changes occurring by surface diffusion on body with anisotropic surface energy, elec. stress effects 78−6202
naphthalene, cryst. plasticizing by surface active organic media, creep rate meas. 79−55813
naphthalene, surface dynamics, calc. 80−92772
naphthalene single crysts., surface active substances effect on plastic flow 80−44248
nematic liq. cysts. surface alignment, temp. depend. of pretilt angles 79−55656
nematic liquid cryst., surface alignment on TGS surface controlled by domain struct. 79−99068
nematic liquid cryst., surface alignment using lecithin monolayers, contact angle meas. 79−4247
nematic liquid crystals, surface alignment, easy axis determ. and temp. depend. of field energy 79−90541
nematic liquid crystals, surface and anchoring energies, van der Waals contrib. 80−92455
nematic liquid crystals, surface and interfacial free energy, Van der Waals dispersion force contrib. 79−99399
nematic liquid crysts., molecular alignment using alkoxysilanes, rel. to surface energy 80−100164
nitrides, surface energy for brittle fracture from phonon frequencies 78−67790
nonionic surfactants, stabilisation of bubble nuclei in agarose gels 80−76562
nuclear ceramics, grain boundary energy to surface energy ratio, as determ. from pore geometry 80−34291
nucleation processes, and surface energy values for substance of different crystn. struct. 80−49144
oil, spreading on water, rel. to surface contamination 79−43795
surface energy continued
optical glass strength limit rel. to Knoop microhardness 79−72641
optical material radiation strength, dissipative characteristic 79−27344
organ eutectics, roughness parameter and surface energy rel. to surface nucleation 79−19163
oscillatory forces between two solid surfaces arising from struct. in intervening liquid, meas. 80−70521
pentaerythritol tetranitrate, high explosive, fracture surface energy determ. 77−44337
pentaerythritol tetranitrate, high explosive, surface energy from contact angle meas. 79−51393
pentylcyanobiphenyl, isotropic phase, surface induced ordering, birefringence obs. 80−14998
pentylcyanobiphenyl, liquid crystal, isotropic phase, surface induced ordering, birefringence obs. 80−14998
percolation clusters in nucleation theory 79−52785
phyllosilicates, dioctahedral and trioctahedral, calc. of electrostatic energy relations 80−19743
plasmon contrib. to surface correlation energy 77−69397
plasmon oscill. eigenmodes and Van der Waals energy, chain of aligned spheres *(French)* 77−80821
PMMA, surface energy anal., comparison of one- and two-liq.-contact-angle methods 77−59181
polar liquids, electrostatic contrib. 80−20014
poly(dihydroxypropyl methocrylate), surface charact., by contact angle methods 80−61140
poly(hydroxyethyl methacrylate), surface charact., by contact angle methods 80−61140
poly-1,1-dihydropentadecafluorooctyl methacrylate barrier films, props. 79−51197
polyethylene, oxidised, energy of adhesion with polar and nonpolar liquids 77−55427
trans-1,4-polyisoprene, kinetics of thin film growth from melt 80−10505
polymer, deform. polarisation effect on interaction with liquid environment, fracture *(Russian)* 77−25166
polymer, electric charge, effect on interaction with liq. medium 79−56036
polymer, surface free energy determination *(Polish)* 80−84362
polymer-water interfaces, contact angle 80−20010
polymeric material, amorphous, surface free energy estimation 77−55438
polypropylene oxide, isotactic, crystallisation, heterogeneous nucleation, interfacial energy effects 79−69023
polysilicane gel on glass plate, elastic deformation in adhesion of solids 78−60010
polystyrene, crosslined, swollen, surface energy, contact angles 79−73379
polystyrene interfacial colloidal crysts., microscopic obs. 80−97737
powder science, laboratory techniques for handling powders 80−45475
PTFR, surface energy anal., comparison of one- and two-liq., contact-angle methods 77−59181
pure liquids, predictions of total surface energy 80−29250
PVC, surface energy anal., comparison of one- and two-liq.-contact-angle methods 77−59181
rare earth hexaborides, obtained by melting, micromech. props., rel. to bonding 80−21082
Rebinder effect in breakdown of dielectrics 77−44328
rods, with anisotropic surface free energy, stability 80−20013
roughness effects on dynamical props. 78−75923
rubber, peeling initiation and propag. 78−76824
salt, molten, surface tension calcs., Fowler model modification 78−67888
serum albumin, bovine, molecular structure of adsorbed film 79−79462
silicate glasses, surface energy calc. from wettability data 77−35804
smei-infinite solid, edge dislocation behaviour with surface energy effects 79−55743
solid, new measurement method 78−44187
solid, surface energy density by wedging method 77−75858
solid, universal model 80−39409
solid or liquid, surface free energy theory, thermodynamics, mol. forces and struct. 77−55437
solid surfaces and interfaces, elastic energy of point defects and inclusions 80−73272
solid surfaces in contact, adhesive force 79−15026
solid surfaces props. characterisation, structural, chemical and electronic, use of LEED methods *(Italian)* 80−49467
solid-gas interfaces, topographic and thermodynamic aspects 78−68927
solids, surface energy and theory of friction 77−51609
spherical particle at fluid interface, equilib. position, force and free-energy anal. 77−55429
stearic acid, microscopic obs. of cleaved surface 79−95248
steel, austenitic, high content of low melting additives, high temp. neutron irradiation embrittlement *(Russian)* 79−73218
steel, C, martensites, fractography, facets classification *(Slovak)* 79−20173
steel, stainless, creep ductility, intergranular particle size and spacing effect 80−40461
steels, strength reduction by adsorpt., stress corrosion *(Russian)* 79−29265
step excess energy 78−47254
stilbene, depend. of phase transition temp. on thickness 78−26669
succinonitrile, grain boundary groove shapes, at a solid/liquid interface 79−65101
succinonitrile, grain boundary groove shapes, at solid/liquid interface appl. to Arbel-Cahn theory 79−69114
supersaturated soln., shape stability of growing cylindrical particle due to diffusion and interface kinetics 80−79720
surfactant, insoluble, adsorpt. on monolayer-covered surface, Gibbs eqn. calcs. 80−59781
surfactant micelles, hydration 80−89518
surfactant solutions, aggregation, micelle and microemulsion form. 80−89547
surfactant solutions, review of concepts 80−89542
TGS, pure and deuterated, domain wall thickness and surface energy 79−87408
theory and appls., symposium, New York, USA (Apr. 1976) 77−55422
thermodynamics equilib. forms of crystals 80−107629
transition metal, group VIa, layered dichalcogenides, hole reactions, electrochem. solar energy conversion appl. 79−7893
transition metal alloy, surface segregation, electronic theory 77−43414
transition metal carbides and nitrides, surface energy for brittle fracture from phonon freqs. 79−86837
type superconductor with field-dependent surface barrier, AC losses 79−87216

surface energy continued
water, electrostatic contrib. 80−20014
water droplet interactions, expts. for educational use 78−4441
wetting, mechanism, mol. dynamics 78−51789
zinc oxalate, crystallisation kinetics, specific surface energy at cryst.-soln. interface 78−26471
Ag, dendrite growth from supercooled melt, interfacial free energy 77−51628
Ag epitaxial films, grain boundary struct. evolution during recrystn., interface energy effect *(Russian)* 80−15387
Ag-Sn system intermetallic formation rate, H_2 adsorption effect 79−90819
AgBr melts, surface energy and surface tension coeffs., effect on photographic emulsion microcryst. growth rate *(Russian)* 80−47132
AgCl melts, surface energy and surface tension coeffs., effect on photographic emulsion microcryst. growth rate *(Russian)* 80−47132
Al, adhesion props. 80−10774
Al epitaxial films, grain boundary struct. evolution during recrystn., interface energy effect *(Russian)* 80−15387
Al, Kapitza resistance, heat transport through subcooled He II 79−23794
Al, liq., thermodynamic props., pseudopot. calc. *(Russian)* 79−46549
Al, neutron irradiated, void surface props. determ., anisotropic small-angle neutron scatt. 78−10095
Al powder, liq.-solid phase transforms. *(French)* 80−45294
Al-In (40, 70 wt.%), liq. phase immiscible system, solidification in microgravity 78−84770
Al-Mg, alloy, surface activity of Mg, XPS and AES meas. 79−86975
Al-Zn-Hg alloy, cathodic protection characts., surface free energy, lattice struct. 79−29281
Al_2O_3 surface energy measurement by const. temp. method data for liquid Cu-Sn and Au-Ag 78−6208
Al_2O_3, surface energy meas. by temp. variant method for liquid metals 78−6209
AlSb (110), surface struct., EPR meas. and elastic energy minimisation calcs. 79−51405
Ar, liq., surface thickness, near triple point, using surface tension data 79−99400
Ar monolayers, on graphite, condensation and compression, high resolution LEED obs. 79−77906
Ar, surface energy and surface tension near triple pt. 78−43218
Au epitaxial films, grain boundary struct. evolution during recrystn., interface energy effect *(Russian)* 80−15387
Au fine particles, adhesion, role of twinning and surface energy, TEM obs. 78−72009
Au, vacancy size effect, surface energy in small particles and bulk specimens 80−75223
Au-Cu, surface conc. profile and surface energy 80−84350
α-B, rhombohedral, surface energy calc. 77−85048
$BaTiO_3$ polymorph, hexagonal, low temp. and surface CO_3 adsorption and desorption 80−80713
C fibre, friction, expt. and adhesion theory 77−1877
C fibres, PAN-based, surface characts., investig. by flow microcalorimetry 78−48694
$Ca_{10}(PO_4)_6(OH)_2$ dissolution kinetics, nucleation-controlled 80−59659
$Ca_{10}(PO_4)_6(OH)_2$, hydroxyapatite, aq. solution system, interfacial props. and equilibria 79−77751
$CdB^4C^5_2$, chalcopyrite struct., surface energy and compressibility, rel. to glass form. 79−51417
Ce_2O_3, hydrated, sorption props. rel. to dehydration conditions 79−66345
$CeO_2La_2O_3$, ceramic, thermal stability, sintering, deform., effect of La_2O_3 79−11532
Co-Fe epitaxial films, singularities of $\gamma \rightarrow \alpha$ transform., X-ray diffr. obs. *(Russian)* 79−52198
Co_5Ge_3, solid and liquid, physicochemical props. and structure 80−39548
Cu (111) surface, self-consistent electronic struct. calcs. on bulk and thin films 79−1614
Cu, dendrite growth from supercooled melt, interfacial free energy 77−51628
Cu, liq., surface tension rel. to temp., surface enthalpy, entropy 78−38912
Cu, metallic adhesion, use of fracture mechanics and contact resistance meas. 77−70271
Cu-Au system, two-phase mixtures, long-period superlattices 80−84140
Cu-Fe, growth kinetics and interfacial energy of coherent γ-Fe particles *(Japanese)* 78−19765
Cu-Ni, liq., surface conc. profile and surface energy 80−84350
Cu-Sn system intermetallic formation rate, H_2 adsorption effect 79−90819
Fe, cast, influence of interfacial energy on shape of graphite 80−16360
α-Fe, FIM specimens annealed at $0.5T_m$, surface energy anisotropy 77−20181
Fe, metallic adhesion, use of fracture mechanics and contact resistance meas. 77−70271
Fe-Al, antiphase boundary motion, microscopic diffusional theory, appl. to domain boundary coarsening 79−61563
Fe-As, liquid alloy, density and surface free energy *(Russian)* 78−11204
Fe-B, metallic glasses and vapour deposited films, amorphous to cryst. transition 80−88048
Fe-Si-B, surface tension, density, and oxidation kinetics 80−20028
GaAs (110), surface struct., EPR meas. and elastic energy minimisation calcs. 79−51405
GaP (110), surface struct., EPR meas. and elastic energy minimisation calcs. 79−51405
Gd, ferromag., spin polarised electron gas model 77−8034
Ge, electron hole drop, surface energy calcs. 77−47741
Ge, nonuniform electron-hole liq., props. in high density limit 77−43505
Ge, surface energy effect on electon-hole drop luminesc. 77−48239
H_2O, surface tension and energy, Fowler model 80−10754
He crystals, meas. of surface tension and contact energy, standing waves *(French)* 80−92753
^{3}He, liq., surface energy calc. 77−85011
^{3}He, superfluid, surface energy assoc. with interface between A- and B-phases, NMR obs. 77−47641
^{3}He, superfluid, surface energy and textural boundary conditions between A and B phases 80−54458
In, vacancy size effect, surface energy in small particles and bulk specimens 80−75223
K (001) surface, electronic struct. by density matrix method 79−60900
KCl, (100) face, mol. dynamics computer simulation of surface props. 78−18880
KH_2PO_4, kinetics of crystn. from soln., activities, interfacial energy and solubility 77−76340
K_2SO_4, kinetics of crystn. from soln., activities, interfacial energy and solubility 77−76340
$LaNi_5$ surface segregation, influence of O_2, H_2, H_2O, SO_2 *(German)* 80−51008
Li/H_2O_2 surface energy for 10 atom Li model using ab initio SCF calc. 79−69359
LiH, crystalline, surface struct., quantum mechanical ab initio calc. 77−1281
Mg-Sn melt, density and free surface energy *(Russian)* 77−66074
$MgAl_2O_4$ spinel, surface energy calc. contribs. from Coulomb and Born-Mayer interactions 78−18890
MgO, cryst. surface strain and polarisation fields, breathing shell model calcs. 78−22946
MnO_2 porous powders, Al_2O_3 and SiO_2 coated, changes in surface free energy for N adsorption 80−84363
MoS_2, specific surface energy determ. 77−28073
NaCl, dislocation movement, effects of adsorpt. of octadecylamine *(Russian)* 77−51372
Na_2O-B_2O_3-SiO_2, mechanical strength and swelling in liq. 80−85024
Na_2O-CaO-SiO_2 glass, surface viscous flattening kinetics, sinusoidal profile decay method 79−79139
Nb-Fe(Co)(Ni)(Os), alloying element influence on strength, ductility, surface and grain boundary energies *(Russian)* 79−74234
Ni-Au alloys, surface segreg., surface energy and solute strain energy effects 77−72760
Ni-Ge alloys, liq., temp. depend., 1000-1700°C *(Russian)* 77−15662
Ni-Sn system intermetallic formation rate, H_2 adsorption effect 79−90819
Ni_5Ge_3, solid and liquid, physicochemical props. and structure 80−39548
Pb, superconducting film, intermediate state, shadow electron microscopy 79−11276
Pb-In films, atom redistrib., ion-ion emission obs. *(Russian)* 78−18926
Pt-W interface, contaminated, contact adhesion, deform. and interfacial energy 78−22306
Si (100), atomic and electronic structs., energy minimisation calcr. 80−49480
Si (111) (7×7) surface structs., LEED anal. and energy minimisation calcs. 80−49478
Si (111) surface reconstruction, milk-stool model, quantum chem. ab initio calc. 80−49477
Si (111) surfaces, relax. and reconstruction using Si_4H_9 clusters, MINDO/3 calc. 79−42356
Si, bulk and surface equlib. props., self-consistent pseudopotential calcs. 79−60750
Si, electron-hole drop luminescence, hysteresis effect and surface energy 78−2907
Si, reconstructed surface physics, review 80−10766
Si, structurally related bulk and surface props., self-consistent pseudopot. method 80−54632
SiC, $\beta \rightarrow \alpha$ transformation, microstructural aspects 79−8295
SiC, $\beta \rightarrow \alpha$ transformation, interfacial energetics 79−8296
Si_3N_4, hot pressed, fracture phenomenology, fracture surface energy, crack propagation 79−57090
SiO_x thin films, deposition and characterisation study 80−80133
Ti, surface and grain boundary free energy, zero-creep determ. 79−4313
Ti-Al-V (6,4 wt.%), surface and grain boundary free energy, zero-creep determ. 79−4313
Ti-Ni alloy, effect on $[Cu(NH_3)_4.(H_2O)]^{2+}$ solns. on drilling *(Russian)* 78−53017
UO_2 and UO_2-Ni, surface, grain boundary and interfacial energies 78−21649
UO_2, nonstoichiometric, surface and interfacial props. 77−69161
UO_2, surface energy, determ. by Hertzian indentation 80−93641
UO_2, surface energy *(German)* 79−7742
UO_2, surface props. of low index faces, calc. 80−6604
UO_2-(Ni), surface, grain boundary and interfacial energies 78−71905
UO_2-Gd_2O_3, interfacial energy meas. 77−59763
UO_2-stainless steel, interfacial props. 79−65223
W, (100) oriented cryst., plastic relax. effect on semi-brittle fracture 77−69036
W, adsorption of Ga, In and Sn, field emission, FIM 77−16470
W, secondary electron emission rel. to LEED 78−84689
W, surface energies and vacancy-surface interactions calc. 79−19448
W, surface energy anisotropy and faceting behaviour in vac. and in H_2 77−7961
Zn, pure single cryst., fracture stress 80−104269
$ZnB^4C^5_2$, chalcopyrite struct., surface energy and compressibility, rel. to glass form. 79−51417
ZrO_2, crystallisation from $Zr(OH)_4$, influence of water vapour *(Japanese)* 79−78865
ZrO_2, wet vibro-grinding with surfactants, superhigh density sintering suitability 79−33989

surface energy measurement
adhesive energy measurement techniques 80−50803
analyser, combining secondary ion mass spectrometry and ion scattering spectrometry 79−5189
film balance of wide range (80 dynes/cm) and high sensitivity (10^{-3} dyne/cm) 80−98910
Hertzian cracking, anti-plane elastic solid model, surface energy meas. *(Spanish)* 77−31260
organic polymers, comparison of one- and two-liq.-contact-angle methods 77−59181
polymers, specific fracture surface energy, meas., review *(French)* 80−104275
vacuum ultramicrobalance, for surface studies 79−71465

surface hardening
alloy, surface layer alloying effect on electroerosion working *(Russian)* 78−64760
automatic induction hardening equipment 78−92284
boride coatings, reaction with Mo substrate 77−32716
boriding of high purity Fe with cryst. B powder 80−84951
boronising, powder, physicochem. characts. 80−61024
brass, repeated friction contact, form. of thick hardened surface layer 79−39056

surface hardening continued
brass, surface hardening by electrohydraulic forming *(Japanese)* 80−16571
case carburising, in commercial elec. furnaces 80−27310
case hardened components, exam. of fracture surface by TEM. *(Japanese)* 78−52949
case hardening depth meas. using ultrasonic goniometer, corner reflection method, book contrib. 79−100325
cemented carbides, indentation fracture, surface fracture toughness nature 78−60849
consolidating soil indentation effect of Poisson ratio 78−83340
controlled nucleation thermochemical deposition, improvements over chemical vapour deposition 78−92387
electron beam surface hardening 79−61773
electrospark alloying with TiC-Ni-Mo alloys 77−59998
electrospark coating improvement by laser action *(Russian)* 79−15850
fatigue crack growth, effect of notches and surface hardening 77−86165
Fe, cast, compact graphite inclusions, surface hardening by continuous action laser emission *(Russian)* 78−15567
Fe, strengthening in H_2S04, H_2 hardening rel. to struct., anodic behaviour *(Russian)* 79−15855
ferromagnetic material, induction heating for case hardening 78−15570
finishes for wear reduction, data sheet 79−91814
glass, polished surfaces, environment sensitive, ellipsometric obs. 77−48559
glass fibre reinforced epoxy laminate, metallization by Cu and chem. treatment by H_2CrO_4 *(German)* 80−93670
hardened metal, sintered, CVD of C rel. to atmosphere *(German)* 79−95966
HF cyclically operated generator appls., charact. *(German)* 80−81070
Inconel 625, nitriding in N_2-H_2 glow discharge 80−16590
induction hardening universal feeders 79−83243
laser beam appl., CW, CO_2, 5 kW 79−15879
laser surface transformation hardening, heat flow model for cylinder 80−93700
measurement and control problems *(German)* 77−44267
metal, cavitation erosion resist., increase by case hardening, possible mechanism 80−11845
metal, erosive wear by impinging SiC particles, surface hardness and material props. effect 77−66705
metal, hardening and softening during absorption fatigue in surface active medium, governing laws 77−86230
metal surface hardening by plasma nitriding 79−8400
metal systems, mech. prop. improvement by pulsed laser generated shock wave 77−48443
metal-ceramic containing diamond, impact hardening 79−15828
metals, carburising, surface-gaseous medium interaction laws 80−76411
metals, laser heat treatment, wear resist., corrosion protection, hardening, review 78−72939
metals, thermochemical treatment *(German)* 78−15598
nitriding process, monitoring systems 79−52556
plastic deformation hardening; exam. of selecting condition for component hardening 78−88479
polyethylene prostheses, radiation crosslinking improvement of shock- and abrasion-resistance 77−60307
refractory metal, disturbed layer depth on abrasive lapping with TiC, NbC, WC micropowders 77−44391
steel, 12KhN3A, case-hardened, friction austenite, electron diffr. obs. *(Russian)* 77−21286
steel, 45, case hardening quality control by ferromagnetic coercive force transducer probes 78−53151
steel, AISI 1045, laser transform. hardening, fatigue and wear rates 79−70198
steel, Al-Cr-Mo, nitride hardened roller, surface fatigue failure under pure rolling and sliding rolling contacts 79−79183
steel, Al-Cr-Mo, nitride hardened rollers, surface fatigue resistance under pure rolling and sliding-rolling contacts 79−79184
steel, alloy, corrosion-impact-cyclic strength of boring bars, effective hardening treatment 78−53034
steel, alloy, Cr, austenitic boundary layers, form. by short laser pulse reaction 78−88555
steel, alloy, quenched, high strength, shot blast hardening effect on repeated impact bending 79−1914
steel, alloy and C, ion nitrided and ion-softnitrided, comparison of compound layers *(Japanese)* 79−8386
steel, austenitic, carbonitriding, high-temp., saturation kinetics *(Russian)* 79−52450
steel, austenitic, mechanism 78−85048
steel, austenitic stainless, Cr-Ni (18,8 wt.%), X-ray meas. of residual stress in ground surface layer *(Japanese)* 77−48491
steel, austenitic stainless, nitrided, type 03kh17N8G5MFAB, alloying charact. and phase comp. 80−30166
steel, austenitic stainless, surface hardening by electrohydraulic forming *(Japanese)* 80−16571
steel, bonded, nitrided, corrosion behaviour in aqueous media 78−95837
steel, by focused laser beam *(Russian)* 78−27670
steel, by heating in electrolytic plasma *(Russian)* 78−11390
steel, C, induction hardened, surface durability, optimum case depth 80−30137
steel, C, rolling contact fatigue, tufftriding effect on 0.2% C cylindrical specimen 80−100954
steel, C, spinning machine ring, increasing wear resist. by boriding 80−21115
steel, C, structural transform. and surface hardening by laser treatment 77−70233
steel, C, wear charact. of worn surface layer under lubrication *(Japanese)* 78−35526
steel, C and alloy, nitriding, effect on struct. and internal stresses 80−30162
steel, C and alloy, wear resistance, change through hardened layer 79−96153
steel, C and alloys, ion-softnitriding effects on metallurgical props. of nitrided layer *(Japanese)* 79−5079
steel, C type 45 hardened layer structure and props. with intensive spray cooling and hardening 79−38859
steel, C-Cr (1.0, 1.5 wt.%), 52100 bearing steel, control of surface residual stress by heat treatment 80−97501
steel, carbonitrided, case struct. investigation by warm electrolytic etching 80−35414
steel, carbonitrided 25KhGT, 25 KhGM, exam. of hardenability and phase composition 78−44272
surface hardening continued
steel, case hardened, MnCr, shot peening effect on bending fatigue strength *(German)* 78−56777
steel, case hardened gas carbonitrided, holographic interferometry study of plastic flow *(German)* 77−77723
steel, case hardening and carbonitriding treatment, comparative effects on operation props. *(French)* 77−59991
steel, case-hardened cast, contact endurance rel. to austenizing *(Russian)* 78−56805
steel, casecarburized and hardened, relationship between fatigue strength and case hardness distrib. *(Japanese)* 79−61782
steel, chemicothermal treatment quality control by fractographic method 79−39080
steel, composition effect on carburizing 80−35432
steel, Cr, carburising with high-activity carburiser 80−76412
steel, Cr plated, high strength, with and without surface strengthening prior to plating 79−39051
steel, Cr plated, laser treatment 80−21191
steel, Cr-Ni, case hardened rollers, surface fatigue failure under pure rolling and sliding rolling contacts 79−52472
steel, cylindrical parts, case hardening 77−90507
steel, die types 4Kh5MFS and 5Kh2MNF, nitriding in vibrofluidised bed 80−35410
steel, diffusion coatings, carbide and boride, props. *(Russian)* 79−52443
steel, electrospark alloying with TiC-Ni-Mo alloys 77−59998
steel, En8, surface hardening by 2 kW CW CO_2 laser 79−83396
steel, fatigue strength, low-cycle, under severe loading, friction-strengthening treatment effect *(Russian)* 79−52435
steel, fatigue strength of 30 KhGSNA, 12 KhN3A, effect of friction in abrasive medium after hardening 78−35507
steel, fatigue strength on combined surface strain-hardening and tempering *(Russian)* 77−59900
steel, ferritic, by gas nitriding, process improvements 80−97499
steel, gas carbonitriding, N, saturation 79−57152
steel, gas nitrosulphurized, in temp. range 813-903K, wear props., surface and cross-sectional hardness, X-ray diffr. and SEM study *(Japanese)* 79−29224
steel, high strength, surface work hardening effect on life 77−70234
steel, hot forging die type, fractography *(Japanese)* 80−108547
steel, ion-carbo-nitriding in CO-N_2-H_2 gas mixtures, expt. *(Japanese)* 80−71670
steel, ionic nitriding, procedure and equipment, nitrided layer hardness obs. 80−45414
steel, low C, electroboronising by superimposed cyclic current, Na_2CO_3, B_4C, NaCl, NaOH activator studies 80−85081
steel, low C, gas nitrocarburized, cyclic stressing 79−57098
steel, low C, Si effect on gas nitriding, surface hardness *(Japanese)* 77−48582
steel, low-C, fatigue strength, low-cycle, effect of shock wave press. 79−29205
steel, medium C, type 35 laser treatment effect on struct. and mech. props. 79−39041
steel, mild, fatigue strength, effect of grinding surface *(Japanese)* 77−48533
steel, mild, surface hardness improvement by dynamic recoil implantation 80−61008
steel, mild, with different grain sizes, surface strengthening by high frequency loading *(Czechoslovakian)* 77−28934
steel, Mn-Cr, tempered, case hardened, shot peening effect on bending fatigue strength *(German)* 79−24645
steel, moving target in N_2-Ar-He, action of laser beam at high pressures, surface hardening *(Russian)* 78−94925
steel, Ni (21 wt.%), ageing, nitrided case struct. investigation 80−35416
steel, Ni-Cr, case-hardened, surface durability in rolling contact fatigue testing 77−63684
steel, Ni-G rollers, case hardened, surface durability in pure rolling and sliding-rolling contacts 79−61739
steel, nitrided EN41B, effect of residual stresses on fatigue failure 78−64698
steel, nitriding, diffusion layer hardening calc. 79−52456
steel, nitriding, mag. field effect 79−57153
steel, rapid, surface modification by ZrB_2 treatment 79−66203
steel, rolls for cold-rolling mills, surface hardening, contact fatigue strength 79−24664
steel, sintered, diffusion treatment with B, Si, Cr and C, corrosion and wear improvement 77−77642
steel, sintered, mech. props., effect of small cold reduction 79−39048
steel, stainless, 95Kh18, vacuum quenching 78−85047
steel, stainless, liquid boronizing, wear resistant coating *(Korean)* 79−43475
steel, stainless, nitrided, type 316, microhardness and N_2 conc. profile 79−96226
steel, stainless, nitriding in glow discharge in crossed electric and magnetic fields 80−16578
steel, stainless martensitic, nitriding in metastable condition 80−30167
steel, surface hardened, luminescent-discharge optical emission spectrometry appl. to surface anal. *(French)* 79−79164
steel, surface hardening by US treatment *(Russian)* 77−73364
steel, surface hardening during electrospark alloying with transition metals IV-VI *(Russian)* 78−95849
steel, surface structural changes on exposure to plasma, etch resistance *(Russian)* 79−83234
steel, tool, type KhBG, carburising and quenching, effect on fracture toughness 80−29997
steel, tool type M2, surface hardening and microstruct. refinement by laser melting, electron beam melting, heat treatment *(Korean)* 79−70093
steel, tufftrided, hardened, fatigue life, effect of programmed load history *(Japanese)* 79−20160
steel, type 12Kh2N4A, belt grinding, struct. transformations 80−30169
steel, types S25C and S45C surface damage produced by pulsating impact contact load *(Japanese)* 80−104263
steel, using CO_2 laser beam 77−90490
steel, using linear-contour laser beam *(Russian)* 77−12731
steel, WC reinforced surface layer, serviceability improvement by Ni, Cu-Ni, V alloying additions 77−21290
steel, wear resist., effect of rolling friction strengthening, oil abrasive environment *(Russian)* 79−15799
steel 40Kh, surface working effects on crack resist. *(Russian)* 78−56734

surface hardening continued
steel 45, hardened layers, struct. and composition, after electrospark doping *(Russian)* 77−70213
steel carbonitriding high-speed struct. and props. 79−57155
steel components, residual stress distrib. on surface cold working *(Russian)* 77−59975
steel nitriding, distortion prediction, appl. 79−24663
steel rollers, case-hardened, nitrided, surface failure, durability 78−84959
steel ShKh15, high C, wear tests in fuel oil, O_2 conc. effect in oil *(Russian)* 77−16694
steel surface HF inductive pulse hardening *(German)* 78−27687
steels, 110G13 and 40Kh10G10, hardening and structural transformations during friction *(Russian)* 77−52527
steels, alloy, surface plastic deform., effect of heating conditions, types 45, 40 Kh 78−53033
steels, N-implanted, surface hardness and abrasive wear resist. 80−50746
structural material hardening by laser irradation *(Russian)* 79−15851
US energy use in surface improvement, of mech. and corrosion props. *(Rumanian)* 79−15821
US peening *(German)* 78−85020
vacuum furnace fusion requirements for self-fluxing overlays 79−83367
Al alloy 2024-T3, work hardening in surface layers and bulk during fatigue 78−48428
Al FCC single crystal, crystal rotation accompanying scratch deform. *(Japanese)* 79−15733
Al, high temperature hard anodizing 79−96230
Al, surface fatigued single crystal, inhomogeneous positron trapping 77−90216
Al, surface strengthening of single crysts. on coating with evaporated films 77−8972
Al/Sn, composite, kinetics of adsorption softening of solid interface *(Russian)* 79−61619
Al-Ti alloy spark alloying, cathode weight change and hardened layer obs. *(Russian)* 80−61005
α-Al_2O_3, annealing, stable hardened subsurface layer form. 77−56128
Al_2O_3, chemically-strengthened polycryst. mat., flexural strength at high temps. 77−21302
Be, surface hardening by B ion implantation 80−16604
C fibre coated with Si or ZrC, mech. props. 77−70197
Cu, FCC single crystal, crystal rotation accompanying scratch deform. *(Japanese)* 79−15733
Cu, polycryst., surface layer hardening by multiple impact 80−108469
Cu-Ni, erosive wear by impinging SiC particles, surface hardness and material props. effect 77−66705
Cu-SiO_2, dispersion hardened, surface plasticity effect 78−52832
Fe and alloys, refining effect of diffusion impregnation with added Fe powder to impregnant mixture 77−28044
Fe and Fe_3Si, hardening and softening during adsorption fatigue in surface active medium, governing laws 77−86230
Fe, cast, grey, fracture kinetics, surface hardening effect 80−76354
Fe, cast, grey, surface hardening by continuous laser emission *(Russian)* 77−70212
Fe, cast, nitrided, wear resistance *(Korean)* 80−21178
Fe, cast, steel cam-roller pair, wear resistance strengthening treatment *(Russian)* 78−31542
Fe, cast, using CO_2 laser beam 77−90490
Fe, cast, wear resist., effect of rolling friction strengthening, oil abrasive environment *(Russian)* 79−15799
Fe, contact interaction with graphite at high press. and temp. *(Russian)* 79−11722
α-Fe, exam. of structural defects due to shock waves, and induced hardness 78−48427
Fe, Fe-C, diffusion coating by Cr and Pb melt bath, kinetics *(Korean)* 78−60873
Fe, ion-carbo-nitriding in CO-N_2-H_2 gas mixtures, expt. *(Japanese)* 80−71670
Fe, nitriding, thermodynamic considerations *(German)* 78−60874
Fe, sintered, austenitic nitriding and bainitic hardening 80−85084
Fe, wear of surface due to friction, surface hardening 78−44227
Fe-Al(Cr)(V)(Ti), hardness after nitriding, metallographic, electron microscopic and microprobe anal. 78−51608
Fe-based materials, wear resistance, surface hardening processes, review 78−72894
Fe-C-Mo-Nb-Al-Ti-B (0.015, 5.75, .7, 1.6, 2.5, 0.1 wt.%), TZM sheet, wear resistance, effect of surface hardening 77−59985
Fe-M, (M=Cr,W,Mo,V,Ti), morphology and growth kinetics of δ-pearlite formed by carburisation 80−108485
Fe-Mo alloys, carburised, austenite-carbide colonies struct. *(Russian)* 79−52449
α-Fe-Ti, ion implanted, microstruct., ion beam anal. and TEM study 80−107294
Mo, chromizing, formation of ordered solid soln. *(Russian)* 78−11402
Mo, strengthening by vacuum-deposited W film *(Russian)* 77−66714
Mo, surface oxide softening in single crystals 78−95860
Mo, wear resistance, effect of surface hardening 77−59985
Nb alloy, VN2AE, influence of nitriding on heat resist. and brittleness *(Russian)* 79−8380
Nb, single crystal, surface oxide softening, TEM obs. 77−40462
Nb, stress differential in surface oxide softening of single crystals 77−86116
Ni, B-containing diffusion layer formation *(Russian)* 77−48570
Ni, B-containing multicomponent diffusion layer formation *(Russian)* 77−44400
Ni-Cr-B-Si, hard faced with WC, exam. of abrasion and wear props. 79−34202
Si, doped and intrinsic, chemomech. effect 78−64751
SiO_2, vitreous, strengthening by coating application 77−32636
SiO_2-Na_2O-CaO-MgO-Al_2O_3, toughening by electrochemical treatment in Sn melt 80−11800
steel, Ni-Cr, rolling contact fatigue failure 80−16608
Ti alloy VT9, fatigue strength estimation after US hardening 77−12746
Ti, nitriding kinetics in RF discharge, surface hardening 77−36684
Ti-Al-V (6, 4 wt.%), friction characts. improvement by O_2 dissolution and controlled surface hardening *(French)* 80−45401
Ti-Al-V alloy, friction coeff. reduction on injection with TiC particles 80−85086
(W, Mo)C, hard-facing applications, effect of Mo on struct and hardness of WC 80−108474
W, carburization, catalytic Co effect 80−3255
surface hardening continued
W, surface oxide softening in single crystals 78−95860
WC-Co, TiC coated, TiC stoichiometry effects on mech. props. 77−66715

surface-ion beam collisions *see ion-surface impact*

surface ionisation
absolute ionisation coefficients, meas. via ionisation detector with field reversal 77−2710
adatom, valence shell energy level shift *(French)* 78−67900
adsorbed atom, on metal containing dislocations, calc. 78−47670
amine, chemisorbed on metal or oxidised metal, mass spectra expts. 78−2360
cluster ions, field desorption, ion form. mechanism 79−15006
dielectric surface with accumulated air positive ions, vacuum breakdown obs. 78−75464
dilute low-temperature plasma, ionisation in presence of solid phase and alkali metal component 77−42989
dynamic characts. of neutral particle desorption by surface ionisation voltage method 80−44426
EPMA correction procedure, Monte Carlo derivation 78−20119
halogens, surface ionisation, on LaB_6, using ion source 78−60538
ice, sputtering by MeV light ions, erosion rate 78−48268
ion source, for mass separator operating on heavy-ion beam 78−5083
ion source using surface ionisation process 80−68999
ion trap sensitivity for spectroscopic applications, $^{137}Ba^+$ ground state hyperfine splitting 80−22447
ionisation density, spatial distrib. calc. in a material due to electron beam irradiation 80−55234
isobar nuclei, separation of alkali and alkaline earth elements using surface ion source 80−37688
physicochemical surface processes investigated by alpha-particle effect on electron work function 78−2547
polyatomic ions, thermal desorption lifetime and kinetic characts. determ. 79−11018
radiation damage, defects and surfaces in bulk metallic, covalent and ionic systems, review 80−34049
sputtering products, elemental anal. *(French)* 80−50905
Teflon films, hole transit, trap modulated mobility and dispersive hopping discussion 79−69616
transient ion desorption, work function, evap. rate, ion heat of adsorption 77−20198
zinc blende structured semiconductor surface analysis by X-ray photoelectron spectroscopy *(Japanese)* 78−88672
Al, elemental anal. of sputtering products *(French)* 80−50905
Al plasma anodisation current efficiency *(Japanese)* 79−24655
Cu, elemental anal. of sputtering products *(French)* 80−50905
Cu-Al, elemental anal. of sputtering products *(French)* 80−50905
Dy, surface ionisation on W (110) 79−87142
Gd, surface ionisation on W (110) 79−87142
H_2^+, negative surface ionisation on ThO_2, plasma diagnostics appl. 80−6280
In, surface ionisation meas. after ion sputtering *(French)* 80−27374
Ir (111), phase state of adsorbed Ba (C-Ba), thermionic emission 77−85881
K, on W, stimulated ionisation by Na, Cs beams, energy depend. 78−31292
LaB_6, negative surface ionisation 77−77335
LaB_6, negative surface ionisation, intense halogen ion source 79−93850
LaB_6, polycrystalline, negative surface ionisation of I atoms, negative ion desorption heat 79−78848
Li plasma, electrode pot. layer characts., surface ionisation and Schottky effects 77−15260
Mo, coadsorption of O_2 and Cs, electron emission props., thermal stability 80−66878
Na, on Re with adsorbed O_2, mol. beam surface ionisation detection 77−90232
Pd surface, adsorbed CO, Penning ionisation by metastable He beam, theory 80−60735
Pt surface, mean residence time and ionisation efficiency meas. of K 77−85874
Re, by laser-excited Li beam, quantum yield 79−87540
Re surface, long range and temp.-depend. interaction with alkali metal atom, theory 80−59802
SF_6, negative ion form. on W cathode, laser irrad. effects 80−93440
Si (111)-Cl(7×7), angle resolved secondary emission and electron energy loss study of electronic struct. 79−61477
Si, negative electron affinity surface activation, laser beam scanning obs. 79−4890
Ta, by laser-excited Li beam, quantum yield 79−87540
Ta, negative surface ionisation 77−77335
TaC, negative surface ionisation 77−77335
Tb, surface ionisation on W (110) 79−87142
ThO_2, negative surface ionisation 77−77335
UF_6 on C-coated Pt(Pt-W), mol. negative surface ionisation 78−56913
W, desorption of Cs, dynamic characts. of neutral particle desorption by surface ionisation voltage method 80−44426
W, hot emitter, surface struct. change during baking above 2000K 79−65971
W, K atom beam impact, mean residence time of K^+ and ionisation efficiency 77−73208
W surface, Cs ions evap. isotherms from single cryst. faces 79−24829
ZrC, negative surface ionisation 77−77335

surface-molecular beam collisions *see molecule-surface impact*

surface phenomena
see also surface.....
see also atom-surface impact; capillarity; crazing; crystal surface and interface vibrations; emissivity; field evaporation; interface phenomena; ion-surface impact; magnetic surface phenomena; molecule-surface impact; sorption; surface acoustic waves
ablation of melting solid surfaces, in impingement region of H_2O jet 80−14766
adhesion, surface and interfacial aspects, review 80−108690
adsorbed monolayer parameter determ. by full current spectroscopy method *(Russian)* 80−70539
adsorption isotherm and solute activities from spreading pressure-surface charge data 78−14576
air-water interface, modified technique for dynamic surface press. and relax. meas. 78−6201
aliphatic surface monolayer, on water, phase transition model 79−56041

surface phenomena continued
anthraquinone, UV light effect on nucleation during crystallisation on anthracene surface 80−75478
anthrone, UV light effect on nucleation during crystallisation on anthracene surface 80−75478
atomic and surface physics, conf., Salzburg, Austria (Feb. 1980) 80−57010
atomically clean surface environment, confirmation using field electron emission 80−52250
binary metal alloys, surface segregation correlation with bulk diffusion 80−54388
brass, surface reddening during strip reduction process 79−43490
caffeine in aq. electrolyte, adsorpt. isotherm and solute activities from spreading pressure-surface charge data 78−14576
catalysis research, heterogeneous IR spectroscopy appl., literature review *(German)* 78−53256
chemical physics of solids and their surfaces, book 80−82587
composite materials, surface, flame propagation velocity rel. to thermal props. *(Russian)* 80−7797
conference, Budapest, Hungary (Sept. 1975) 78−11567
conference, Cambridge, England (March 1979) 80−36773
conference, Eindhoven, Netherlands (June 1976) 77−62708
conference, general congress, Societe Francaise de Physique, Toulouse, France (June 1979) 80−77536
conference, Gothenburg, Sweden, June 1979 80−51950
conference, San Juan, Puerto Rico (June 1976) 77−25318
conference, trends in physics, York, England (Sep. 1978) 80−31416
conference on solid-vacuum interface, Amsterdam, Netherlands (June 78) 79−42342
conference on surface physics, Tagow, Poland (June 1976) 78−26747
conference on surface science, York, England (March 1977) 78−14540
contamination, anal. using mass spectrometer system with laser heating 79−87903
conversion electron Mossbauer spectroscopy, dynamic theory appl. to surface phenomena 77−51997
cratering explosion, pulsed hydrodynamic model 78−51180
crystal surface elastic props., surface tension tensor, volume stress *(Russian)* 80−100389
crystal surface morphology development during sputter erosion 80−88414
crystal surface problems, expansion technique, appl. to ferromag. spin waves 77−4244
diatomic molecules, laser-induced predissoc., surface mag. field effect 80−106365
dielectric three-ply system with space heterogeneity, surface EM waves *(Russian)* 78−55288
diffusion bonding, in Ar atmosphere, aspects *(Japanese)* 78−11491
diffusion-reaction produced layer growth rate, heat release effects *(Russian)* 77−55397
Earth surface, mechanical interaction with fluid-filled crustal fracture 79−79779
effusion and related surface processes, review 77−51151
elastic crystal, equilib. shape due to surface stress 77−35030
elastic interface wave guided by thin film between two solids 80−100385
elastic skin, periodic surface ripples 77−31845
elastic wave propagation, free surface of cryst., spatial dispersion 80−54310
electrolyte soln. surface interaction, grand canonical ensemble method appl. 80−54092
ellipsometry work at Gakashuin University from 1955, review 80−9019
epoxide resin with maleic anhydride hardened, edge effect of time, surrounding medium effect 77−86211
equilibrium characteristics in the condensed state with the nearest-neighbours interaction *(Russian)* 79−12726
ferroelectric films, surface effects on phase transitions, local spontaneous polarisation 80−2708
float glass, commercially produced, thermally toughened and untoughened, surface damage resistances on air and tin side 79−61612
fluid surface correlations, density profiles 78−6196
fluid surface density variation, Bose hard-sphere fluid model 77−20163
fluorescence, meas. by SPEKOL spectrocolorimeter 79−80664
Fourier emission IR microspectrophotometer for surface anal., lubrication problem appls. 80−13162
free surface, wrinkling 78−5676
gas adsorption, surface areas calc. using programmable calculator 78−15706
glass, thermally tempered sheet and plate, surface stress meas. using optical waveguide effect 80−25967
glass liquid-liquid immiscible regions, surface effects on energetics 80−33903
Hellmann-Feynman theorem, appl. in surface physics 79−95262
hot wall with impinging liq. droplet, transient temp. profile 78−75050
integrated surface physics and chemistry laboratory planning for automation 79−67269
interatomic forces, theories 80−107632
layer surfaces, reflectivity at 3.39 μm, meas. method, relevance to pipelines 80−52340
lecithin surface films, equilib. and metastable states rel. to use as biological model 77−60188
liquid, Laplace molecular pressure and internal pressure, rel. to capillary theory formulas 77−25303
liquid crystal, smectic-A surface skin, on liq., periodic ripple form. 77−47352
liquid crystal phase transformations, size and surface effects 77−15555
liquid crystals, alignment by amphiphilic monolayers 79−37614
liquid droplet, surface thickness and surface oscillations, quantum and classical calcs. 78−91511
liquid film, surface deformation under charge *(French)* 77−31848
liquid film, surface deformation under charge flux *(French)* 77−31847
liquid surface deform. due to laser radiation thermal action, lens effect 80−33048
liquid surface relief prod. by US field, holographic interferometry meas. 78−1519
liquid-liquid system interfacial instability and longitudinal waves 80−33566
liquid-solid interaction forces, meas. by detachment of liq. from solid substrate 80−10740
meas. of lubricated sliding surfaces *(German)* 80−14643
melt surface velocity, expt. meas. and prediction in 30000 lb inductively stirred melt 78−11139
melting, mol. dynamics method 78−75807

surface phenomena continued
metal, pack rolling, bonding, deform. struct., small reduction before seizing 77−90503
metal, surface strain meas. by intensity of reflected light flux 77−17972
metal interaction with gases and C, conf., Stuttgart, Germany (Sept 1977) *(Russian)* 79−57134
metal sheets, frictional surface damage during press forming 78−76768
metal surface, flash mechanism caused by monochromatic laser radiation 79−95878
metal surface, mol. vibr. energy transfer, classical EM theory 80−96806
metal surface chemisorption theory, electron localisation, surface interactions 80−84376
metal surface heated, charge separation from electrolyte drops 80−88617
metal surface laser beam irrad., effective absorpt. coeff., temp. field determ. *(Russian)* 80−76108
metal surface molecule enhanced Raman scatt., rough surface spheroidal model 80−84744
metal surface struct. and initial stages of reactivity, review 78−68837
metals, cyclotron resonance depend. on surface, anomalous skin effect *(Russian)* 80−75860
metals, surface positronium formation, stopping distance, positron-phonon interactions 80−96582
meteors surface layer, thermal fracture and detached particles mean dia. 80−62081
mica surfaces, van der Waals interactions 78−30973
molecular clusters adsorbed on conductor surfaces *(Russian)* 80−80078
molecular ion formation on molecular cryst. surface UV laser irrad. *(Russian)* 80−71521
molecular processes on surfaces 80−34339
molten salt, model for two-particle distrib. functions 79−33158
Monte Carlo methods in statistical physics, book 79−80528
Monte Carlo studies, surface physics appl., book contrib. 79−82426
Mossbauer effect appl., conference, Kyoto, Japan (Aug.-Sept. 78) 80−7199
near surface region of solid, H_2 effect on deform. and fracture, Rebinder-Westwood effect 79−39001
nematic mesophase, surface disclination lines rel. to surface-induced homogeneously tilted alignment 77−58950
n-nitroaniline, UV light effect on nucleation during crystallisation on anthracene surface 80−75478
ocean, heat exchange in small-scale sea-air interaction 78−3810
optical heterodyne interferometer, appl. to surface inspection 77−90529
percolation problem and surface effects in semi-infinite medium repulsive wall case 80−62588
percolation processes, scaling theory and real space renormalisation group 80−86223
phase boundaries and multiphase systems, conf., Tokyo, Japan (Sept. 1977) 79−29415
phase boundary, Fresnel refl. coeffs., optical thickness *(German)* 77−69794
photoelectron spectrometer for surface studies, gas press. up to 1 Torr 80−4822
piezoelectric powder, polarisation echo and surface props. theory *(Russian)* 77−48122
PMMA moist surface mech. strength reduced by electric charge *(Russian)* 80−60486
polyethylene, anisotropic surface stress 78−14562
polyethylene, effect of ketones, temp. depend., environmental stress relax. study 80−45336
polymer films adhesion, to metals and non-metals, principles and meas. methods *(Czech)* 78−80709
polymer solution, surface fluorescence, determ. using SPEKOL spectrocolorimeter 79−79301
polymer surface, flame propagation velocity rel. to thermal props. *(Russian)* 80−7797
polyvinyl furfural, CdO, MoS_2 and graphite filled, contact area, filler effect 79−57040
potentiostatic tests, use of free-corrosion potential time transients to distinguish between pitting and crevice corrosion 79−39058
powders and porous materials, specific surface, determ. using Hg porosimetry 80−29896
Raman scattering by forced surface oscills. in liquid drop 80−92763
reactivity of surfaces, exptl. techniques and appls., review *(French)* 79−92000
refractory, castable, stability in steam-N_2 and steam-CO atmos. at 199°C 78−20063
review of surface science 79−19427
SEM, insulating surfaces, charge neutralisation by gas ionisation 79−6235
semiconductor, struct. and props., review *(Japanese)* 80−49483
semiconductor physics, conf., Edinburgh, Scotland (Sept. 1978) 79−95303
semiconductors, conference, Pacific Grove, USA (Jan.-Feb. 1979) 80−46725
semiconductors, interface and surface physics, review 80−49872
skinned sintering kinetics, cryst. surface calcs. *(Russian)* 80−40276
slab, surface displacements for high speed rubs 80−83767
solid, surface stress effects on plane wave propag. 77−3761
solid films and surfaces, conference, Tokyo, Japan (Jul. 78) 80−10739
solid state physics, contrib. of Conyers Herring in 1930s 80−57056
solid surface and thin film anal. methods, review 79−34410
solid surface response to high-power incident flux, with temperature dependent absorptivity 78−51038
spectroscopic analysis and electronic struct., book 79−42428
spherical particle, surface enhanced Raman scatt. by molecules 80−95629
steel, austenitic, thermonuclear reactor walls, ferromagnetic layer form. magneto-optical testing method 80−35465
steel, C, H attack kinetics and service behaviour 78−39951
steel, carbide layer form. in fused borax bath with electrolytically dissolved Vn, Nb, Cr and Ta *(Japanese)* 77−52671
steel, Cr-Mo (2.25, 1.0 wt.%), C transfer between structural steels and Na in LMFBR 79−97805
steel, H_2 absorption, effect of organic inhibitors *(Russian)* 78−35570
steel, oxidation-reduction processes on surface during heating in vacuum *(Russian)* 78−11403
steel, stainless, gas liberation, 20°C, surface oxide effects *(Russian)* 80−3286
steel, stainless, surface roughness influence on equilib. of liq. spreading 80−39389

surface phenomena continued
steel, strengthened by surface plastic deform., tempering effect on physicomech. props. *(Russian)* 78−35409
steel against Al_2O_3, elastohydrodynamic contact, lubricated by naphthenic hydrocarbon, IR meas. of surface temp 79−15807
step trains, modes of vibr., rhythmical bunching, expt. obs. to show periodicity in step patterns 79−41996
superconductor, inhomogeneous, surface barrier influence on vortex pinning 77−55645
supersaturated vapour, critical clusters, theory and Monte Carlo simulation, review 80−82734
surface and colloid science, conf., Stockholm, Sweden (Aug. 1979) 80−86035
surface layers of NbC and VC formed by immersion in hot bath containing Fe-V or Fe-Nb and carbonate *(Japanese)* 77−52672
surface magnetisation profile singularities near critical point 80−103843
surface physics research development, review *(Chinese)* 79−37898
surface science, American vacuum society symposium, Chicago, (Sep. 1976) 77−39722
surface science, rel. to energy development and technology 78−88553
surface stress in solids 78−63290
survey of recent research 80−39384
suspended particles in estuarine and coastal waters, surface films form. rel. to elec. charge 80−36331
temperature meas. in continuous rating using separately applied detectors *(French)* 77−27466
thermal contacts fluxes modelling, electrolytic *(Italian)* 77−24504
thermal coupling of 2.8-μm laser radiation to metal targets 80−76107
thermally induced structural changes, specimen surface influence 80−103559
thermodynamics, equilib. and nonequilib. processes, review 77−44505
thermodynamics, fundamental eqns. 80−107630
thermoplastic films, quasistatic theory of frost deform. 79−56052
thermoplastic recording material, latent image and surface deformation *(German)* 80−42284
Tomkeieff eqn. applicability to truncated multiphase systems 77−44437
transition metal alloys, surface segregation 79−34044
TTF-TCNQ powder, phase transition at 49K 77−89539
ultrasonic wave transmission through rough surface *(Russian)* 80−100387
uracil in aq. electrolyte, adsorpt. isotherm and solute activities from spreading pressure-surface charge data 78−14576
vacuum science and technology, undergraduate and post-experience courses 79−62954
vacuum techniques applied to surface and thin film phenomena 78−86280
vaporisation, partial wave propag., influence of rapid particle fluxes *(Russian)* 79−38696
water surface EM wave excitation 79−13893
waves, derivation from general grain boundary theory 79−1442
Weissenberg effect, review of expts. 79−60025
Al melt-NaF filter material interaction mechanism *(Russian)* 80−108743
Al, surface roughness influence on equilib. of liq. spreading 80−39389
Al-Li-Mg-Be alloys, phase composition of surface films, oxidation protection mechanism *(Russian)* 80−65417
BN in contact with W, barrier layers for good high-temp. stability 79−70194
C blacks, surface polarity, surface activity, slurry pH, oxidation effects 78−68915
C steel joints, with interference, increasing supporting capacity, by electrophysical methods, exam. 78−85055
Cr-Ni compressor disk, surface plastic deform., optimal method 80−60924
Cr_2O_3 polycrystalline powder, crystallite sizes and surface areas 77−66086
Cs-Rb(K)(Na), solute atom-grain boundary interaction energy, electron-statistical calcs. *(Russian)* 79−73175
Cu, creep rate, effect of surface anodic dissolution in acetate buffer soln. 78−3249
Fe-N system, spattering phenomenon during arc melting 79−39053
Fe-Zn system, Zn vapour interaction with solid Fe, Zn chem. potential effect on interaction layers 78−11416
(FeNi)PB amorphous wires, surface oxidation and annealing influence on induced anisotropy 80−100957
Ga, amorphous thin films, supercond. surface resist. 77−72961
Ga ionisation mechanism on W field emitter 80−76156
GaAs-$Al_{0.2}Ga_{0.8}As$ periodic layered media, optical surface waves 78−43946
Ge, heterodiffusion due to H atom surface recombination stimulation, Cu, Zn, In coated *(Russian)* 80−59726
He, liq., 2D electron plasma, RF absorpt., parallel pumping *(Russian)* 78−22911
He, liq., charged surface stability *(Russian)* 77−35791
He, liq. surface, electron solid, phonon-ripplon coupling 79−42337
He, liq. surface, electron sheet liq. to cryst. transition 79−42341
He, liquid, charged surface vibrations in metal approx. *(Russian)* 80−10718
He liquid, plane surface layer, density profiles and pair correlation asymptotics *(Russian)* 80−88371
He, liquid, surface liquid-crystal transition in two dimensional electronic system 80−88303
^{3}He, liquid, electrostatic image force depend. on spatial dispersion, energy spectrum *(Russian)* 80−107593
^{4}He, liquid, electrostatic image force depend. on spatial dispersion, energy spectrum *(Russian)* 80−107593
^{4}He liquid, localised ion states, effective mass, binding energy, surface displacement 80−84333
^{4}He superfluid, charged surface stability breakdown, He ion geyser ejection *(Russian)* 80−15320
^{4}He superfluid film, neutron scatt., surface effects 78−10251
K-Rb(Cs)(Na), solute atom-grain boundary interaction energy, electron-statistical calcs. *(Russian)* 79−73175
$LiNbO_3$:Fe, photoinduced refractive index discontinuities at surface 80−75999
$LiNbO_3$:Ti optical waveguide, surface wave mode conversion, static strain-optic effect 80−87561
MgO, dense layer form. in pitch bearing magnesite brick, kinetics and mechanism 79−11717
MgO short time chemomechanical effects, dislocation generation and motion, drilling simulation 79−87749

surface phenomena continued
MnF_2, ATR spectra and surface EM wave dispersion anisotropic case 77−77215
Mo ion incorporation into TiO_2 matrix, ESR, UV, and ESCA spectral anal. 79−43670
Mo-Zr, nitride form. in N_2 atmos. *(Russian)* 78−19938
Na-K(Rb)(Cs), solute atom-grain boundary interaction energy, electron-statistical calcs. *(Russian)* 79−73175
$NaNO_2$, compressed powder, dielec. props., surface layer effects 78−76413
$NaNO_2$ powder, surface layer effects on dielec. props. 77−1631
Na_2O-Al_2O_3 (CaO)-SiO_2 glass, surface charge in aqueous electrolyte soln. 79−29245
PbO_2(Pb) electrode, anodic impedance during suspension-electrolysis leaching of β-ZnS in 1N H_2SO_4 soln. *(Japanese)* 79−43594
Pt (111) surface, backscattering, channelling spectra, H adsorption, surface relaxation 80−71552
Rb-K(Cs)(Na), solute atom-grain boundary interaction energy, electron-statistical calcs. *(Russian)* 79−73175
Si, temp. rise induced by laser beam, nonlinear heat cond. 79−11487
SiC, dielectric coating effect on surface polaritons, optical consts. *(Russian)* 80−88489
Si_3N_4-CeO_2, surface stress development during oxidation 80−50736
Si_3N_4-MgO, reaction with Fe to produce surface pitting 78−76778
SiO_2 film on Cu substrate, surface EM wave absorpt., optical consts. *(Russian)* 80−108216
SiO_2, fused, surface charge in aqueous electrolyte soln. 79−29245
SiO_2-Al_2O_3-Fe_2O_3-CaO-MgO-Na_2O-B_2O_3-SO_3, exam. of white flaky inclusions, causes and formation time 79−29237
Sn, extremely fine crysts., surface melting 77−62622
Ti-Al-Mo-Zr, compressor disk, surface plastic deform., optimal method 80−60924
$VH_{0.55}$, ultra-high vacuum cleavage, H_2 desorption 80−54514
W, (110) surface, conduction electron interaction with diffracting electrons *(Russian)* 80−79643
W, contact with BN, barrier layers for good high-temp. stability 79−70194
W-Zr field emitter, time-of-flight atom-probe study 80−80949
Zn, strengthening by electroplastic strain, surfactant effect *(Russian)* 80−20953

surface phonons *see crystal surface and interface vibrations*

surface potential
adatom on transition metal surface, vibr. model using pair interactions 80−15357
adsorbed monolayer, substrate-induced strain and orientational ordering 79−82460
alkali halide crystals, ultrahigh vacuum equipment for surface charge and pot. meas. 78−12708
alkali silicate glasses in aqueous solutions, leaching kinetics rel. to surface pot. 80−11803
alkaline earth phosphate (MO-Al_2O_3-P_2O_5) irradiated electret glasses, relax. of external field intensity on heating 80−25282
alklylammonium ions, adsorpt. potential determ., at soln.-solid interface 79−56068
atom chemical potential rel. to diffusional motion and distortion of macroscopic inclusions *(Russian)* 77−66676
atom-surface bound states, surface averaged pot. energy function 77−11789
axisymmetric field problem soln. by Gaussian surface charge simulation 80−95758
band-discontinuity surface, temp. of electron gas induced by passage of electron currents 78−14793
barrier, Schrodinger eqn., anal. and numerical soln. incl. spin-orbit interaction 79−58492
biological particle surface, elec. double layer phenomena *(Rumanian)* 80−94144
biomembranes, potential, rel. to surface pot., ionic permeab. 80−35853
biporous media, influence of double layer on dynamics of ion adsorption 79−11827
C-CD, signal charge and surface pot., steady-state distrib. calc. 80−100525
capillary surface, zeta potential determ. method using oscillating laminar flow streaming pot. meas. 78−76873
β-casein, adsorpt. isotherm, at air-water and air-oil interfaces 79−79461
chalcogenide glasses, localised states calc. rel. to contact capacitance and field effect 79−11090
charge density and polarisation from sessile drop contact angle meas. 77−85365
colloid, spherical particle, diffuse double layer, modified nonlinearised Poisson-Boltzmann equation 79−79305
colloid particle separation by potential barrier chromatography 77−73474
colloidal particles, interaction force, calc. of electronic component 79−11829
conducting body of revolution covered with thin layer of dielectric, axisymmetrical excitation 79−81327
corona charged polyethylene thermally stimulated current and surface potential decay obs. 80−15945
covalent surface, pot. and charge distribs. and dangling-bond state 78−2537
crystal surface discrete dipole layer effect on surface barrier shape 79−95468
Cu, adsorption of CO, on (110), LEED, surface pot., IR spectra 77−66092
degenerate semiconductor, surface photo-EMF 79−69580
desorption, fission fragment induced mol. ions desorption, electrochemical surface pot. effect *(German)* 78−6228
desorption, multiphonon processes, quantum-statistical theory 80−107641
dielectric, electron penetration, 20-50 keV, sandwich method meas. 80−6436
dielectric, irrad. by electron beams, effect of bulk and surface cond. on pot. 80−2446
dielectric, mean potential and electric field determ. 79−24262
dielectric surface, conductor-like behaviour 79−101046
dipole layers, forces between plates 80−70793
discrete stochastic electric double layer, electrostatic props. 79−96318
distribution meas. by vibrating electrode 79−67340
electrochemical machining, approx. method for solving problems 78−44241
electrolyte, free surface struct., single ion hydration energies 78−26752

surface potential continued
electrolyte double layer potential change meas., transistor method 77−85298
electron gun, surface change method, computer anal. of characteristics 80−101891
electron scattering on micron-size pinholes, surface pot. mapping 79−81351
electrophotographic films, instrument for meas. potential microprofile 77−45913
electrophotographic films, surface charge meter using electrostatic induction *(Japanese)* 80−77886
equipotential and mag. intensity contour line visualisation by SEM 79−6149
exciton wave phase, effect of surface potential *(Russian)* 77−89708
exoelectrons, energy and angular distribution 77−85904
ferroelectric domains, quantitative electron mirror microscopy 78−15132
ferroelectric materials, repolarisation in SEM 79−15424
ferromagnetic metal, spin-polarised field emission, many-body and spin-dependent surface pot. effects 79−74065
flat capillary, ion transport numbers, surface conductance 80−11071
galvanomagnetic-recombination field effect, theoretical model 78−43420
glass, particle size influence on force moving particle in inhomogeneous elec. field, influence of field frequency 79−11795
glass reactions with aq. solns., influence of surface pot. on kinetics 80−108612
glass/Cu-polymer compound powders, prep. and corona charging props. *(Japanese)* 78−19679
graphite (0001) surface, He atom scatt., bound state reson., interaction pot., band struct. effects 80−29840
guanidinium aluminium sulphate hexahydrate, surface obs., SEM and AES expts. 80−71362
guarded electrode design which has small gap between electrode and guard ring 80−68215
heterocoagulation, interaction energy of two unequal spheres 79−29411
heterogeneous system, thermodynamic theory of nucleation on charged particles 79−39216
highly dispersed substances, electrosurface props. meas. 78−53249
hydrocarbon liquids, electrostatically charged, incendivity of sparks from surface 80−6303
hydrodynamic interfacial instability, mechanical, chem. and elec. constraints, review 80−34278
ice, surface pot. obs., rel. to thunderstorm charge separation 80−51495
III-V semiconductor based layered multielectronic systems, electronic process investig. survey *(Russian)* 80−107891
image charge pot. at interface of two semi-infinite media, Thomas-Fermi soln. 79−87155
insulating film, detection of self-drifting of ionic charges by surface potential decay method 78−72295
insulators, XPS, binding energy, surface pot. and work function calcs. 80−89113
interfaces, with two types of ionising group, electrokinetic and surface pots. 78−76136
ion adsorption dynamics, in long bed when double layer taken into account 79−69349
ion beam, scatt. by solid surface, skipping motion due to surface pot. 80−45191
ionic crystals, mirror chips, in contact with liq. phase, ellipsometric investigation 80−11516
ionic solid, induced dipole contribs. 77−47882
jellium surface, interaction of H_2 80−29259
LiF, mirror chips, wetting contact angle 80−10746
lipid bilayer membrane interaction forces in zone of contact 78−53345
liquid metal, surface ion density, nonmonotone, perturbative discrete ion introduction into jellium 78−72222
liquid-air interface, dipole layer, electrolyte effect 78−51796
localised state, surface potential model *(Russian)* 77−85278
lysozyme, adsorpt. isotherm, at air-water and air-oil interfaces 79−79461
measurement in high vac., vibrating capacitor method modification 77−71343
measurement of local variations on solid surface, device with high spatial resolution 77−39921
mechanical surface excitons, interaction with radiation, refl. and transmission spectra 79−15098
metal, classical cleavage energy, layer summation method 77−85287
metal, surface charge density prod. in satic electrification 78−14797
metal, surface pot. drop and contact pot. difference in terms of orbital electronegativity 78−2546
metal and semiconductor surfaces, electrostatic interaction of charges 80−24996
metal film, size effect in Landau diamagnetism, surface pot. effect *(Russian)* 80−93012
metal oxides, nonstoichiometric, work function, high temp. meas. using dynamic condenser 78−64097
metal oxides and binary metal oxides, spinel struct., isoelectric point meas. 80−88609
metal surface, step potential model, static semiclassical response of bounded electron gas 78−72221
metal surface barrier, transmission and reflection of low-energy electrons 78−18507
metallic films, interacting, surface pot. 78−30968
metallic surface, anisotropic contrib. to optical pot., in electron spectroscopy, theory 80−44086
metallic surfaces, interaction between two pieces of jellium 77−32061
metals, liq., charge density fluctuations in surface layer *(Russian)* 80−15580
microporous solid, electrical double layer on surface 80−11955
MIS structure, interface states, thermally stimulated surface pot. 78−68091
MIS structure, MM wave modification by surface carrier scatt., surface pot. depend. 80−44736
MIS structures, surface potential distributions *(Russian)* 78−80065
monolayers, elastic and viscoelastic, dynamic surface potentials 80−3603
MOS capacitor, interface state parameter determ. by DLTS 80−65642
MOS capacitor photovoltage characterisation 78−10573
MOS devices, inversion layer, pot. and carrier distrib., quantum mechanical determ. 80−29483
MOS structure, surface potential and interface disorder *(French)* 77−15966
MOS structure, use of mini-computer for rapid evaluation of C-V-plots *(Russian)* 79−28413
MOS structure semicond. surface potential, quasistatic meas. 79−56323

surface potential continued
MOS structures, inversion layer near electrode edge, pot. and charge density distribution 80−88642
MOS structures with superthin gate dielectric, hole mobility in inversion layers 80−29482
naphthalene, deep exponential distrib. of traps, long-time decay of surface pot. 79−47041
naphthalene, surface pot. decay, trap modulated mobility 78−72164
one dimensional crystal with square well pot. 79−82652
one-dimensional crystal, surface pot. influence on electron refl. intensities 77−63506
one-dimensional theory of surface states, Green's function soln. *(Russian)* 77−59311
organic adsorbed layers, Si-SiO_2 interface as electrode for electrical and ellipsometric meas. 80−15366
pattern measurement by potential probes, crevice depth determination in metallic testpieces appl. *(German)* 78−35597
pentadecanoic acid, monolayer on water, surface pot. meas. in coexistence region 77−28236
phosphate glass, electron irrad., elec. flield, distrib. above surface *(Russian)* 77−43763
photocathodes, alkali metal multilayers, high field enhancement of photoemission 78−19639
photoconductor-air gap-semiconductor system, calc. of surface charges under voltage in darkness 80−6905
photostimulated field emission, triangular barrier pot. model 80−100759
phthalocyanine film, surface photovoltage, central ligand effect 79−78231
PLZT electrooptic ceramic, electron beam surface charging, rel. to optical modulation 80−6952
polar liquid, electric double layer at surface 78−53212
poly(alkyl methacrylate)s, corona charged, decay of surface charge and TSC *(Japanese)* 80−54712
poly-(bisphenol) carbonate, photocond., of double layer polymer systems doped with charge transfer complexes 79−87124
poly-N-vinylcarbazole, electrophotographic film, dark discharge 78−34864
polyethylene, corona charged, direct drift mobility meas. 78−10837
polyethylene, high density corona charged, TSC, oxidation effect 78−26882
polyethylene, surface charge release, crossover phenomenon, thermally stimulated discharge current study 80−50255
polyethylene film, corona charged, surface potential decay 78−14795
polyethylene film, effect of corona generated excited molecules on surface pot. decay 80−6941
polyethylene film, elec. charge decay characts. 77−28238
polyethylene film, high density, corona charged, thermally stimulated surface pot. 80−11327
polyethylene film, surface pot. decay, drift mobility determ. 77−11979
polyethylene films, corona charged, charge trapping 80−88571
polyethylene films, high density, corona-charged, surface pot. decay 79−24254
polyethylene films, surface pot. decay, appl. of Scher-Montroll method 79−7851
polyethylene terephthalate, TSC due to mobile ions and ionic conduction *(Japanese)* 80−54432
polyethylene terephthalate film, corona charged, surface voltage decay mechanism, TSC meas. 80−11326
polymer, surface electric charge, effect on interaction with liq. medium 79−56036
polymer electret, absorpt. and relax. of charge 80−6942
polymer electret, charge dissipation, transport mechanisms 80−7268
polymeric double layer system, high field cond., xerographic characts. 79−95448
polypyrimidines, with azomethine in main chain, decaying process of surface potential *(Japanese)* 79−24095
polyvinylcarbazole, photocond., of double layer polymer systems doped with charge transfer complexes 79−87124
polyvinylidene fluoride, corona-charged, surface effects 80−66102
polyvinylidene fluoride film, uniaxially stretched and corona poled, piezoelec. meas. 80−25311
probe for 77K operation and with nanosecond response 78−12726
quartz resonator surface patterns obs., using SEM 80−71323
rare earth-transition metal amorphous thin films, mag. potential distribution and wall velocity meas. 80−34725
rhodamine B adsorbed on NaCl, photoelectric meas. and contact charging 79−19643
satellite geomagnetic substorm charging simulation 79−96886
scanning mirror electron microscopy, quantitative evaluation of elec. microfields 78−74110
Schottky barrier, excitonic refl. of light 80−10885
SEM meas., electron energy analysis 80−68307
semiconductor, excitonic surface potential 78−76000
semiconductor, potential barrier height, temp. depend. *(Russian)* 78−68070
semiconductor field-effect anal. for surface-state props. 79−24053
semiconductor surface potential distrib. meas. using mirror electron microscope 79−35784
semiconductor with surface doping, surface parameters determ. 77−15933
semiconductors, cause of appearance of potential contrast, in SEM 79−27883
semiconductors, surface potentials using electron energy anal., SEM study 80−15582
serum albumin, bovine, adsorpt. isotherm, at air-water and air-oil interfaces 79−79461
shielding of electric fields by surface electron states in an ionic lattice 78−52059
Shockley states in a semi-infinite Kronig-Penney model 79−73562
Shuttle Orbiter, skin electrical charging during electron gun operator 77−22042
solid surface in localised physi-sorption, gas desorption times, local or nonlocal surface pot. calcs. 80−54499
sols, primary and secondary coagulation and heterocoagulation, role of surface chemistry 80−45551
spectral sensitisation, physical basis for models 77−5941
sputtering characteristics, surface barrier curvature influence 80−60739
steel, deformed and welded mild, potential distrib. meas. technique, appl. to corrosion study, apparatus *(Japanese)* 78−53049
stratified spheroidal volume conductors excited by electric dipole source 80−32867

surface potential continued
Teflon FEP-A, corona and electron beam charged, TSC peak identification and surface-voltage stability 79−78614
transition metal, surface density of states, pot. shift for ferromag. and paramag. states 77−20388
TSEE, role of surface pot. 77−8732
two dimensional electron spectrum spin splitting, specified by surface potential *(Russian)* 80−15583
two-domain analysis of field producing bodies using fictitious poles 78−33649
type II superconductors, flux flow state, static electric potential structure 78−43535
ultra-thin dielectric layer on semicond. substrate, surface charge density determ. *(Polish)* 79−51675
virtual surface states, Green function theory 80−80342
water, free surface struct., single ion hydration energies 78−26752
water interface, mol. orientation and surface pot. at 4°C 80−15339
work function and surface pot. meas. from secondary electron emission energy in SEM 80−66343
Ag (111), clean or Na-covered, adsorpt.-desorpt. props. of Br_2 78−38944
Ag, vac. deposited films, surface pot. and work function rel. to thickness 79−42672
AgBr and AgBr:$PbBr_2$, emulsion grains, dielec. loss, ionic cond. and surface space charge 77−28038
AgBr emulsion grains, edge length dependence of ionic conductivity, space charge characteristics 80−88360
AgBr:Pb^{2+}, cubic microcryst., ion influence on ionic cond. and space charge charact. 79−55928
AgCl(Br), point defect form. energies, atomistic calc. and surface pot. meas. 80−107221
Al alloys, contamination, automated nondestructive inspection 80−16629
Al plasma anodisation forming voltage limitation mechanism *(Japanese)* 80−16579
Al-Si_3N_4-SiO_2-Ge structure, small signal HF photo EMF meas. 78−52097
Al-SiO_2-Si structure, small signal HF photo EMF meas. 78−52097
γ-Al_2O_3 interface with electrolyte solns, adsorption of ions, surface conductance, ion mobility and surface pot. 80−75622
As_2S_3, crystalline and amorphous, surface charging effects on valence band spectra in XPS 77−8725
As_2Se_3, amorphous, dark discharge, relaxation current meas. *(German)* 80−49760
As_2Se_3 layers for electrophotographic use *(German)* 80−42283
Au, adsorption of Xe and CO on (100) 77−15691
Au, vac. deposited films, surface pot. and work function rel. to thickness 79−42672
BaO, cond. band edge, electron affinity, LEER 77−24606
$BaSO_4$, TSEE and surface charging, simultaneous meas. 80−29864
Bi, spheres, mean inner pot., elec. biprism and interf. electron microscopy 80−49063
Bi, surface potential under high mag. fields 78−26887
$Bi_{1-x}Sb_x$, thin film, elec. props., composition variations *(Russian)* 79−7841
C, black, surface acidity effects on work function 78−2548
CO on Rh(110) 78−6225
CaF_2, mirror chips, wetting contact angle 80−10746
$Ca_{10}(PO_4)_6(OH)_2$, hydroxyapatite, aq. solution system, interfacial props. and equilibria 79−77751
CdS, acoustoelec. interaction 77−1455
CdS, O and CO adsorption effects on surface pot. *(Russian)* 77−47686
CdS, photoanode, flat band pot., depend. on surface ion effects 79−62013
CdS, photopotential changes due to Ar ion bombardment 77−8174
CdS powder layers, surface pot. dark decay, moisture sorption and heat treatment effects 80−18038
CdS, SAW meas. of surface elec. props. 77−20387
CdS, surface charge and ledge dynamics, point defect annihilation during sublimation 79−90642
CdS, surface photovoltage, characterisation 80−60033
CdS, thermal desorption of O_2, photopot. and surface pot. changes 77−11795
Co film, evaporated, adsorption of H_2, surface pot. meas. 77−31890
Cr-covered objects, dispersion forces at 132-670 nm distances 79−42681
Cr_2O_3-Al_2O_3, solid soln., effect of Cr on point of zero charge 78−61021
Cs^+, adsorpt. potential determ., at soln.-solid interface 79−56068
Cs/W, work function measurement in SEM 80−80918
Cu (001), surface potential energy barrier model, LEED, intensity profiles 78−64089
Cu (001), surface relax. and thermal expansion calcs., simple surface Madelung force 79−23820
Cu (100), self-diffusion near ambient temp. from surface pot. meas. *(French)* 79−51397
Cu (111), chemisorption of CO, IR spectra, LEED, and surface pot. meas. 80−39438
Cu (111) face, surface states and surface pot. 77−4418
Cu (111) surface, self-consistent electronic struct. calcs. on bulk and thin films 79−1614
Cu/Zn galvanic couple, potential distrib. meas. technique, appl. to corrosion study, apparatus *(Japanese)* 78−53049
Cu_2O, electric field screening by surface electron states 78−52058
α-Fe, (001), surface relax. and thermal expansion calcs., simple surface Madelung force 79−23820
Fe, field-emitted electron spin polarisation by tunnelling through surface pot. 80−29861
FeO_x, work function, high temp. meas. using dynamic condenser 78−64097
Fe_2O_3-Al_2O_3, solid solns., effect on Fe on point of zero charge 78−61021
p-GaAs MOS capacitors, anodized, C-V charact., surface pot. 79−11227
GaAs, oxide film influence on adsorption and electrophys. props. 79−42369
GaAs, SAW meas. of surface elec. props. 77−20387
GaAs, surface passivation using composite Al_2O_3 and native oxide, MIS charact. 80−93004
p-GaAs/rare earth metal contacts, surface pot. barrier 80−60086
GaAs-Ge interface, abrupt, electronic struct., self-consistent calc. 77−24611
GaAs-insulator interface, elec. props. 78−95370
GaAs-Ta_2O_5, surface pot. variation, capacitance-voltage meas. 79−61769
surface potential continued
Ge (111), adsorption of polar molecules, surface recomb. centre neutralization 79−38147
Ge, adsorbed metal atoms effect on surface electron props. 77−55597
Ge, adsorption of N_2 and CO, adsorption potentials and trapped electrons role 79−90872
Ge, field effect charact. rel. to surface inhomogeneity 78−26933
Ge, galvanomagnetic-recombination field effect, theoretical model 78−43420
Ge surface, field penetration and band bending in high elec. fields 79−42613
^{4}He-^{3}He mixture, surface pot., heats of vaporisation, ^{3}He bound state 77−1274
HgI_2:CdS binder layer photoreceptor, surface charge charact. thickness depend. 80−57409
HgI_2-CdS binder layers, surface charge charact. for electrophotography 77−10123
HgI_2-CdS photoconducting binder layers, surface charge decay charact. 77−43642
In-Ga, eutectic alloy, zero point determ. from uncharged surface pot. 77−90611
InAs, surface potential and surface states rel. to n-, p-, compensated n-type behaviour 77−15932
InP, surface passivation using composite Al_2O_3 and native oxide, MIS charact. 80−93004
InSb, degenerate semicond., surface photo-EMF depend. on bulk consts. 79−69580
InSb, magneto-surface transport props. 77−43693
n-InSb, photoconductive lifetime, surface pot. effects 80−11029
Ir, adsorption of H_2, influence of surface steps and clusters, field emission investig. 77−28698
LiF, powder, irradiated with ^{60}Co γ-rays 77−12504
LiF, selective adsorption of He, band struct. effects 79−73402
Mg vermiculite, adsorbed water mol. orientation, elec. pot. calc. 78−26763
Mo (001) surface, surface states and photoemission 79−60887
NaCl (001) surface, relax. and rumpling effects on point ion potential 77−72770
NaCl, cleavage of single crystals, investigation of fast electrical processes 79−24045
NaF, ^{4}He scattering, selective adsorption effects on diffr. beam intensity 77−12480
Nb, adsorption of O_2, continuous meas. of surface pot. variations using mirror electron microscope 77−47680
Ni (001), surface potential energy barrier model, LEED, intensity profiles 78−64089
Ni (110), chemisorption of N_2, mol. and dissociative mechanisms 80−39431
Ni, field-emitted electron spin polarisation by tunnelling through surface pot. 80−29861
Ni film, vacuum deposited, ethylene adsorption and reactivity with adsorbed H, surface pot. meas. 79−86995
Ni films, electronic struct. calc., effects of chemisorption; contact pot. and surface magnetisation 80−103734
Ni, spin polarisation in LEED 77−43696
Ni-Fe, electronic struct. calc., effects of chemisorption; contact pot. and surface magnetisation 80−103734
NiO (001), gas-surface pot., derivation from diffr. of monoenergetic He atoms 79−61487
n-PbTe, accumulation layer, quantised surface states 80−20279
PbTe substrate for MIS capacitor, C-V and G-V charact. 78−26962
Pd film, adsorption of H_2 or$_2$, reciprocal titration of gases, film surface area determ. 77−1318
Pd film, vacuum deposited, ethylene adsorption and reactivity with adsorbed H, surface pot. meas. 79−86995
Pt, electron wave interference in adsorbed CO film 79−33332
Pt film, vacuum deposited, ethylene adsorption and reactivity with adsorbed H, surface pot. meas. 79−86995
Pt with adsorbed H, field emission study 77−24477
Pt-Cr(Si) interface, low-temp. diffusion, ambient effects 80−100355
Re, effect of O_2 adsorption on surface pot. 79−65323
Se photoreceptors, phthalocyanine sensitized, elec. cond., charge decay charact. 80−15630
Si (100), chemisorption of H, pairing model calcs., compared with expt. 78−34719
Si (100) surface, pairing model, electronic pot., charge density, Fermi energy and surface density of states 77−47875
Si (111), chemisorption of H_2(Cl), conduction-band surface resonance 78−52051
Si (111) covalent surface, pot. and charge distribs. and dangling-bond state 78−2537
Si, adsorbed metal atoms effect on surface electron states 77−55597
Si, field effect charact. rel. to surface inhomogeneity 78−26933
Si, influence of metal impurities, surface photo-EMF obs. 78−19122
Si MOS diode charact. obs., electron irradiation damage effects *(Japanese)* 79−42646
n-Si, passive, complete activation initiation by local photoactivation 79−100403
Si, SAW meas. of surface elec. props. 77−20387
Si solar cells, effect on surface recombination 80−12017
Si surface, field penetration and band bending in high elec. fields 79−42613
Si, surface electron states using discontinuous potential model 79−69574
Si, surface potential spread rel. to chemical treatment *(Russian)* 78−11363
Si:Au, nonequilib. population of electron states and photomemory of surface pot. 78−56206
Si:P solar cell, minority carrier lifetime degradation during ion implanted processing, surface photovoltage 79−39305
Si:Zn (Mn) (In), surface characterised by negative electrochemical pot., electronic props. 80−44695
p-Si/rare earth metal contacts, surface pot. barrier 80−60086
Si-on-sapphire MOS devices, effects of planar defects near Si-SiO_2 interface on elec. props. 79−11231
Si-SiO_2, Fowler-Nordheim tunnel injection into SiO_2, Si surface pot. effect 79−91151
Si-SiO_2, interface, distinction between donor and acceptor character of surface states 78−39216
Si-SiO_2 interface, thermally grown, inhomogeneities of surface potential 80−34524

surface potential continued
$Si-SiO_2$ interface, thermally grown, surface pot. inhomogeneities after stress ageing 80−92993
$Si-SiO_2$ structure, oxide charge evaluation, appl. of Kelvin method 78−19157
SiO_2 surface, adsorpt. pot. and electrophysical props. *(Russian)* 79−91123
SiO_2, surface charge, effect of doping with P+B, differing vacuum deposition conditions *(French)* 77−85286
SiO_2, surface pot. during ion implantation 80−19826
SiO_2-InP MOS struct., capacitance-voltage and surface photovoltage meas. 79−60931
SiO_2-Si in MIS, interface states, thermally stimulated charge decay 77−12009
Si(111), conduction-band surface resonance 78−52051
Te film, annealing effect on elec. cond. and Hall effect 77−8213
Te, inversion layer, surface quantum levels, calc. from Shubnikov de Haas meas. and triangular surface pot. well 79−15207
TiO_2 electrodes, chemically modified, nature of surface states 80−107905
V (100), sorption investig. using total current spectroscopy of slow electrons 77−8694
W, field electron energy distrib., surface density of states 77−16471
W, surface pot. barrier effect on photofield emission 78−60551
W, work function measurement in SEM 80−80918
W(110) surface, Ba monolayer, struct. transformation stages 77−47681
YAG, interrelationship between mech. props. and elec. relief on surface layer 79−23821
ZnCdS:(Cu+Ag) binder layer for electrophotography 80−4797
ZnCdS:Cu, high field photoconduction in binder layer 79−47121
$Zn_{0.35}Cd_{0.65}S$ binder layers, doped and undoped, xerographic characts. 79−56288
ZnO (10$\bar{1}$0) surface bias voltage effect on hardness, charge exchange near dislocations 78−52078
ZnO, adsorbing p- and n-type dyes, surfaces pot., UV light illum. effect 80−75624
ZnO ceramic varistors, trapping by localized states, effect on dielec. and elec. props. *(Russian)* 79−28671
ZnO, chemomechanical effects 79−82431
ZnO, nonpolar surface, interaction with CO and CO_2, changes in elec. cond. and surface pot. 79−65321
ZnO powder layers, dyed, dependence on adsorbed dye amount *(Japanese)* 79−24003

surface scattering
used for carrier scattering by surfaces
see also surface conductivity
defects at surfaces and interfaces, electronic struct. 80−84498
disorder metal systems, conduction electron surface scatt. *(Russian)* 80−24917
ferrometnatic metal slab, transmission of 24 GHz radiation, effect of diffuse surface scatt. of carriers, calc. 80−34780
film, Cottey conduction model extension 78−84183
foils, surface scatt. data table 79−60907
III-V compounds, electron transport in quantised inversion and accumulation layers 79−60935
junction current, luminesc. near dislocation, surface, integral representations, appl. to LED's 78−68079
metal, conduction electrons, under spin resonance conditions *(Russian)* 79−82857
metal, conduction electrons spin magnetisation kinetics, role of surface scatt. *(Russian)* 77−80989
metal, cyclotron resonance with almost specular boundary *(Russian)* 78−10778
metal, EM sound generation in cyclotron reson. regime *(Russian)* 77−69381
metal, surface scattering of conduction electrons and kinetic phenomena *(Russian)* 79−56210
metal, US generation by EM radiation, surface scatt. effects 80−24973
metal cylindrical wire, elec. resist., scatt. processes, Monte Carlo calc. 80−75560
metal film, boundary scatt. indicatrix of cond. electrons, expt. data *(Russian)* 77−39969
metal film, elec. cond., size effect 78−76162
metal film, surface impedance oscills. in perpendicular mag. field *(Russian)* 78−76165
metal surface, disordered, multiple scatt. of cond. electrons 80−10959
metallic film, conduction electron surface scatt. process, magnetoacoustic oscillations *(Russian)* 80−15575
metallic film, oscill. kinetic effects, boundary electron scatt. *(Russian)* 78−52104
metallic film, strain gauge factor anal. 78−6458
metallic films, size effects, resistivity derivation 78−76163
metallic films, ultrasound attenuation, size magnetoacoustic effect *(Russian)* 80−107869
metallic thin films, free-electron, optical props., theory including electron surface scatt. 80−29817
metallic thin films, grain boundary and surface scatt., statistical model 80−103762
metallic thin films, unlike surface properties, transport coeffs., diffuse surface scatt. 80−20331
metals, complex, RF size effect, mean free path depend. of reson. strength 79−56202
metals, surface impedance, extreme anomalous limit, diffuse refl. from boundary 80−29460
MIS structure, MM wave modification by surface carrier scatt., surface pot. depend. 80−44736
multilayer thin film struct. thermoelec. props. 80−92964
semiconductor (semimetal) film, surface resistivity calc. 78−91751
semiconductor film, quantised, indirect interband absorption rel. to surface irregularity 78−39618
semiconductor surfaces, relaxation time spectrum of slow traps *(Russian)* 77−15937
semimetal, compensated, hydrodynamic cond., surface scatt. and phonon drag *(Russian)* 77−8088
SOS MOS devices, elec. characts., cryst. defects and residual stress effects 78−34906
surface CCDs, electron mobility surface diffuse scatt. model 78−47879
Ag, transverse electron focusing and specular refl. from cryst. faces 80−6823

surface scattering continued
Al foil, electrical conduction, electron mean free path, surface scatt. 80−88535
Ar jet, supersonic, electron beam-excited, continuous VUV emission spectrum origins 79−6964
Au, films, optical props. meas. rel. to electron surface scatt. theory 80−29818
Au, polycryst. film, RF bias-diode and triode sputtered, resist. and microstruct. 78−80072
Au, pure, small resistivities, size correction 77−43742
Bi bounded semimetals, phonon two-stage drag of electrons, thermoelectric power, scatt. mechanism 80−92919
Bi, cylindrical thin crystal, size effect oscills. in longit. magnetoresist. *(Russian)* 77−69357
Bi, epitaxial film, magnetoresist., carrier scatt. at grain boundary planes and surfaces 77−32095
Bi, film, size effect of carrier heating, surface scatt. *(Russian)* 80−100474
Bi, thin film, 1/f noise, boundary scatt. effect 80−49836
Bi wire, field effect and magnetoresist., surface scatt. 77−43570
$Bi_2Te_{3-x}Se_x$ films, surface band struct. and scatt. mechanism 80−34535
$Cd_xHg_{1-x}Te$, vac. evap. film struct. rel. to carrier scatt. 77−85116
Cu, mirror refl. of cond. electrons from cryst. surface *(Russian)* 77−35985
GaAs, surface recombination velocity, diffr. from picosecond transient free carrier gratings 79−47109
n-GaAs-$Ga_{1-x}Al_xAs$, heavily doped superlattice, electronic props., perpendicular low temp. mobility 80−65660
Ge, electronic inversion channel anomalous Hall factors *(Russian)* 79−95467
InP, surface recombination velocity, diffr. from picosecond transient free carrier gratings 79−47109
K, electron scatt. effect, excitation of cyclotron waves, calc. 78−6429
Mo, elec. resist., quadratic contrib., 2 to 40K *(Russian)* 80−92874
Mo, film, specularity coefficient of conduction electrons, angular dependence *(Russian)* 79−87167
Mo film, sputtered, elec. resist., annealing and struct. effects 80−60109
Pb films, conduction electron surface scatt. phase shift, tunnelling meas. 79−51648
Re, elec. resist., quadratic contrib., 2 to 40K *(Russian)* 80−92874
Ru, elec. resist., quadratic contrib., 2 to 40K *(Russian)* 80−92874
Si (100) inversion layer, hot electron drift velocity, Monte Carlo calcs. inc. 3 subbands 78−91752
n-Si (100) inversion layer mobility depend. on intersubband scatt. at low temps. 79−95506
p-Si, inversion layer, screening effect and quantum transport in strong mag. fields 78−19155
Si inversion layers, mobility temp. depend., Coulomb and surface roughness scatt. 80−80390
$Si-SiO_2$ boundary, surface charge transport in valence band of Si 80−70789
Sn, aggregate film, resist., temp. depend. 78−39230
W, atomically clean surface, static skin effect and transverse electron focusing *(Russian)* 79−91036
W, elec. resist., quadratic contrib., 2 to 40K *(Russian)* 80−92874
W, film, specularity coefficient of conduction electrons, angular dependence *(Russian)* 79−87167
W, mirror refl. of cond. electrons from cryst. surface *(Russian)* 77−35985
W, RF size effect, surface electron scatt. influence *(Russian)* 80−2414
W, surface, atomically conduction electron reflection, skin effect, transverse electron focusing, simultaneous meas. 78−76131
W, surface reflection of conduction electrons *(Russian)* 78−43373
ZnO, strong accumulation layers, negative magnetoresistance 78−6428

surface structure
see also interface structure; surface texture
$A_{1-x}B_xC$, rapid localised non-destructive optical charact. of ternary layer *(French)* 77−62725
ABS polymers, deposited in internal magnet magnetron sputtering system, adhesion of Cu films 79−83121
absorbed film, disordering due to supercond. transition in metal substrate 80−50022
adsorbates, thermal desorption and conversion kinetics, AES study 78−71959
adsorbed layer, superelastic electron scattering *(French)* 78−56039
adsorbed layers, general principles of construction of structural models 80−84351
adsorbed layers, photoelectron diffr. aximuthal patterns, struct. sensitivity 80−107644
adsorbed monolayer, substrate-induced strain and orientational ordering 79−82460
adsorbed monolayers, intrinsic defects, deep potential relief surface *(Russian)* 79−99415
adsorbed surface structure and dynamics, neutron scatt. studies, review 79−60639
AES, anal. techniques 79−43691
AES, by computer *(French)* 80−7890
AES, low beam current density, surface anal. 78−15748
AES, qualitative and quantitative surface analysis appls., review 77−90704
AES, quantitative, applic. to impurity segregation and depth profiling 78−19611
AES, quantitative, formalism for surface conc. calcs. 78−19612
AES, quantitative analysis *(Polish)* 78−76967
AES, surface composition, quantitative anal., review 79−24854
AES, surface topography development during depth profiling, sputter-etching effects 79−46900
AES and ESCA combined with SEM *(French)* 80−47154
AES depth profiling with N_2^+ ion sputtering 77−16889
alkali chlorides, thin film, crystal-vacuum (100) surfaces, mol. dynamics computer simulation 80−34288
alkali halide, brittle fracture of single crysts. and active struct. of cleavage surfaces 79−28039
alkali halide, morphology of growth and evaporation surface 78−79544
alkali halide adsorbate motions and reactions at surface defects, mol. beams 77−59205
alkali halide surfaces, adsorbate binding energies and struct. at surface defects 77−59206
alkali halide surfaces, step struct. 78−79865
alkali halide surfaces, step struct. 78−79866

surface structure continued
alkali halides, surface energies, surface tensions and surface struct. 79−60610
alkali halides, surface step struct. 77−31853
alkali halides, thin films, crystal-vacuum (110) interfaces, mol. dynamics computer simulation 80−34289
alkali halides with NaCl struct., differential ionic relax., shell model, (100) 77−69151
alkaline silicate glass, surface layers, plasticity and microcrack formation, electron microscopy *(German)* 80−40469
alloy, BCC, order-disorder transform. in surface layers, theory *(Russian)* 78−19739
alloy, binary, calibration line introduction for comp. determ. by AES 79−56892
alloy, binary, surface dehomogenisation during evaporation and ion sputtering 77−73207
alloy, binary, surface segregation prediction using bulk alloy variables 79−65300
alloy, effects on bulk props. 78−85049
alloy, segreg., surface miscibility gaps, reg. soln. theory 78−18882
alloy, surface composition changes on ion bombardment 80−2913
alloy, surface segregation, appl. of quantification of atom-probe FIM data 78−62263
alloy, surface segregation, existence of surface miscibility gaps within regular soln. theory 78−71909
alloy, surface segregation prediction from bulk melting curve shape 77−12597
alloy sputtering 80−50503
alloy surface, anal. by secondary ion-ion emission 77−56200
alloy surface, enhanced diffusion effect on preferred sputtering 78−43973
alloy surface, free energy of segregation 80−29256
alloy surface, theory of segregation 79−77886
alloys, A_3B type, surface effects on order-disorder phase transition 77−76556
alloys, binary, surface composition, regular soln. theory 78−10265
alloys, binary, surface segregation kinetics 80−80044
alloys, machining damage, depth of surface layers determ. 80−85094
alloys, surface composition after fabrication by SIMS 80−65351
amino acid monolayers and ordered films on Cu, surface struct. LEED 78−38968
amorphous surface, energy profile and binding energy, computer simulation 80−100381
amorphous surface, RHEED patterns, refr. correction 78−71646
analysis, electron probe methods, AES, electron stimulated desorpt. 77−44098
analysis, He^{2+} induced X-ray emission technique 79−43548
analysis, trajectory focusing in surface scatt. of channelled ions 78−68594
analysis, using SIMS, Mossbauer spectra and spectrometry 79−16050
analysis and characterisation, conf., Les Arcs, France (Jan. 1978) *(French)* 79−8466
analysis by combined Auger, X-ray and SEM studies 80−81413
analysis by ion sputtering and thermal ionis. *(French)* 77−63510
analysis by photon-induced field ionisation mass spectroscopy 80−40780
analysis of surfaces, atomic beam scatt., SIMS, and vibr. spectra, book contrib. 79−42357
analysis techniques, AES, ESCA, and photoelectron spectroscopy 79−95252
analysis techniques and appls., symposium, Dayton, USA (Jun. 1979) 80−62363
analysis using alpha-induced X-ray emission 78−20132
analytical techniques, quantification, review 80−65342
anodic oxide superficial layer, X-ray emission spectrometry and ion backscattering *(French)* 80−49482
anodised films on metals, ellipsometer obs. interpretation using film form. models 80−101828
apparatus for low-energy alkali ions scatt. from solid surface 77−40318
atom diffraction by cryst. surfaces, reson. effects 77−35447
atom-surface classical scattering, cutoffs and shadows 78−80448
atomic and electronic struct. 80−54746
atomic and molecular processes, review 77−24469
atomic beam diffraction from solid surfaces, struct. studies 80−65349
atomic relaxation effect on d-band width 78−34878
atomically clean surfaces, instruments for anal. and imaging 80−105749
atoms as structural components in metallurgy *(Dutch)* 80−96465
Auger electron appearance potential spectroscopy, core level spectroscopy *(Japanese)* 80−50473
Auger electron spectroscopy, review 79−92043
Auger electron spectroscopy microanalysis, in SEM 80−101058
Auger spectrometry, analytic approach 80−50474
ball bearings, surface comp., AES and ion sputter profiling 77−40465
bent single crystal, equilib. face, surface relief form. during annealing 78−47651
benzene, epitaxial film, on metal (111) substrates, surface struct., LEED obs. 79−86969
benzene film, on metal substrate, surface struct. using LEED 79−77879
bimetallic cluster, segregation and short range order props. at boundaries 79−29071
binary, segregating alloy, theory of surface effects 79−19435
binary alloy, surface composition determ., review 79−90849
binary alloys, homogeneous, surface anal. using quantitative AES 79−24395
binary alloys, surface conc. profile and surface energy 80−84350
binary liquid solutions, surface cluster functions 78−67631
binary ordering alloy, theory of surface effects 79−19434
biological implant, ion beam sputter of surface morphology SEM exam. 77−44836
bisphenol A-phthallic anhydride epoxy resin, diglycidyl ether, Rayleigh scatt., Brillouin and IR spectra 80−66211
blistering by ion bombardment, SEM and TEM obs., review 77−43261
and bonding, review 77−4252
bonding and crystallography of surfaces, book contrib. 80−24724
borided surface layers, Mossbauer and metallographic anal. 80−50769
borosilicate glass, surface struct. rel. to HF etching and stressed state 79−100276
brass, surface microstruct. changes on immersion in $CuSO_4+H_2SO_4+HI$ soln. 78−19945
brittle materials, water drop impacted, damage thresholds 80−81149
butadienepstyrene, surface phenomena in struct. rearrangement after deform. *(German)* 78−19913

surface structure continued
carbon tetrachloride, surface study, ellipticity coeff., ellipsometric method 80−84343
carburised and carbonitrided surface layer structure and phase composition 78−95830
β-casein, molecular structure of adsorbed film 79−79462
cast Fe, grey and ductile, subsurface defects, SEM and EDAX study 80−44400
catalysis, heterogeneous, role of surface science expts. 78−15710
catalysis and surface science, review 80−40740
catalysts, surface investig. methods 78−14546
cathode arc spot crater form. model 77−62414
cavitation erosion, observation of eroded surface by SEM 78−15536
cellulose hydrated film, orientational heterogeneity, IR spectra and dichroism obs. *(Russian)* 78−38990
channelling studies of surfaces and defects 79−4358
characterisation, literature review 1970-76 77−77816
characterisation, physical methods, review *(French)* 80−7889
characterisation, state-of-the art and need for standards 78−38916
characterisation using ion, electron and X-ray beams, combined, studies of surfaces and thin films 77−86412
chemical analysis, comparative survey of methods, book contrib. 79−66393
chemisorbed layers, surface defects and thermodynamics 80−80068
chemisorption on defective surface, theory 78−2362
chemisorption on metal, intra-adsorbate Coulomb correl. and surface struct. roles 78−71979
chemisorption on metal, intra-adsorbate Coulomb correl. and surface struct. roles 78−71980
clean metal surface physics, review 77−15659
coating characterisation 77−31919
coating chemical characterisation by surface and near-surface sensitive techniques 79−15053
coeff. and surface conc. 80−39122
coherence length and transfer width in LEED and mol. beam diffr. 79−42347
collision spectroscopy of backscatt. medium energy ions, quantitative surface anal. 77−8704
composites, surface charact., combined ion scattering spectrocopy, SIMS, SEM, energy dispersive X-ray techniques 79−43702
composition anal. by Penning ionisation electron spectroscopy, metastable He impact, electron energy distrib. 79−52060
composition analysis, by ion beams *(French)* 79−8467
composition changes in sputtering 78−2343
composition depth profiles, ion sputtering effects 80−35616
compositional and structural analysis of single cryst. surfaces using low energy ion scatt., review 79−87547
compound, surface composition changes on ion bombardment 80−2913
computer controlled ESCA for nondestructive surface characterization utilizing a TV-type position sensitive detector 78−76969
conducting and semiconducting materials, surface study using Johansson three-electrode objective *(French)* 80−47152
conference, Eindhoven, Netherlands (June 1976) 77−62708
conference, Gothenburg, Sweden, June 1979 80−51950
conference, New York, USA (Oct. 79) 80−73093
conference on ion beam anal., Washington, USA (June-July 1977) 79−5194
conference on neutron inelastic scattering, Vienna, Austria (Oct. 77) 79−41912
conference on solid-vacuum interface, Amsterdam, Netherlands (June 78) 79−42342
conference on surface science, York, England (March 1977) 78−14540
copper phthalocyanine, cryst. growth from vapour, hollow cryst. form, mechanism *(German)* 77−55252
corundum, optical, polished, surface layer obs. by IR reflection spectra *(Russian)* 78−19458
corundum, shaped crystal, grown from melt, struct. perfection 78−3021
corundum, subjected to thermal shock, study of substruct. and surface morpholoy 79−43292
Cosserat's medium, linear and surface defects, stresses 78−83813
crystal plasticity, surface effects, review 77−47505
crystal surface, (1n0), stepped relief machine model 80−34283
crystal surface morphology development during sputter erosion 80−88414
crystal surface steps, statistical props. 78−47648
crystalline solids, electronic industry, chem. anal. instrumental methods progress 80−66903
cubic crystals, microfacet rotation for high Miller-index surfaces with terrace, step, and kink structs. 80−54495
cyano-biphenyl LC alignment on obliquely evaporated SiO_2 films 80−79677
cyclohexane, monolayers and thin crystals grown on Pt (111), LEED obs. 77−59230
cyclohexane, thin crysts. and monolayers on Ag(111) surface, LEED 79−11014
decoration, localization of crystallites along steps 79−14992
defect surface structures, LEED studies, review 77−80685
defects, review 78−14551
deformation due to non-homogeneous distrib. of solute atoms in cryst. 79−33164
depth profiling by ion microprobe with high mass resolution 79−46894
determination, by ion beam sputtering, spectrochem. anal. 77−48701
diamond, and interaction with gases and metals 77−72758
diamond, cryst. surface layers treatment and study by HF ion-plasma etching *(Russian)* 80−16517
diamond, form. by shock compression of graphite, cryst., surface struct. 78−44060
diamond, identification by electron refl. *(German)* 80−54080
diamond, inelastic scatt. differential cross-sections 77−76652
diamond, metastable overgrowths in dissoln. medium in Ni presence at atm. pressure, SEM surface study 79−51030
diamond, sub-surface contamination by hot-atom recoil in neutron activation anal. 77−60144
diamond, synthetic, topographic structures and origin *(German)* 77−85036
diamond, total secondary electron emission spectrum 77−72759
diamond (111) surfaces, relax. and reconstruction using C_4H_9 clusters, MINDO/3 calc. 79−42356
diamond subsurface damage exam. using cathodoluminescent mode of SEM 77−80398
diamond surface, polished, RHEED pattern 80−65345

surface structure continued
diatomic surfaces, LEED/MEED intensity calcs. 80−44083
dielectric solid, absorpt. of laser radiation by defects in surface layer *(Russian)* 80−25497
differential geometry, distortion, torsion, Burgers circuit 80−64996
diffusional mass transfer exam. by light diffusion method *(Russian)* 77−7953
dilute alloy, surface segregation, bond and strain energy effects, atomic calc. 79−69256
dipropylammonium manganese chloride, layer perovskite, step bunching obs. by compound holographic microscopy 78−63682
dislocation wall form. in contact with surface active melt, stacking fault energy *(Russian)* 77−72626
dislocations, universal concept, rel. to disclinations and grain boundaries 80−100231
effects due to probing electrons and sputtering 77−90706
elastic and inelastic slow electron scatt. in solids 79−90857
elastic crystal, relationship between dislocations and surfaces 80−24446
electrohydraulically formed tube properties *(Japanese)* 78−87848
electrolyte, free surface struct., single ion hydration energies 78−26752
electron capture spectroscopy, technique for surface science and ferromagnetism 80−92766
electron microprobe analysis *(French)* 79−48034
electron microscopy, sample preparation effects on decoration patterns 79−86658
electron re-emission Mossbauer spectroscopy, appl. to surface films 77−1622
electron spectrometer for surface analysis, design, book contrib 77−61169
electron spectroscopic quantitative surface analysis 78−92552
electron spectroscopy, for bulk and surface microscopy and microanal. 80−52367
electron spectroscopy, introductory survey, book contrib. 77−63502
electron spectroscopy, quantitative, electron inelastic mean free path 79−92041
electron spectroscopy for surface analysis, book 77−63545
electron spin polarisation, appl. to surface study *(Japanese)* 79−37911
electron-excited core level spectroscopies for surface analysis, book contrib. 77−63503
electronic material and device characterisation using surface-sensitive analytical techniques 80−65341
electronic surface resonances and crystal surface structure 78−71648
electrostatic interactions and the structure of water, conf. Brussels, Belgium (1972) 78−26413
ellipsometric measurement of surface anisotropy 78−56452
ellipsometry, metallic films and surfaces, nonlocal effects, theory 80−104006
ellipsometry, principles and appls. 78−16834
ellipsometry applied to surface films and film growth 78−39619
ellipsometry of clean surfaces, submonolayer and monolayer films, review 80−103546
energy spectra of scattered ions, new method of surface struct. determ. 78−87854
epidermal imprinting by celloidine 79−25170
equilibrium surface topography, developed by sputtering, stability 79−14988
equilibrium surfaces, adsorption energy 77−31896
ESCA, surface anal. and electronic structure *(French)* 80−7891
ESCA of surface structure at high press., technique 78−73103
EXAFS, application to surface struct. and adsorbate config. 77−51602
EXAFS from X-ray refl. meas 80−71512
EXAFS-Auger process for surface struct. anal. 77−51580
exoelectron emission for tribomechanical surface treatment *(German)* 77−4870
extended appearance pot. fine struct. surface anal. 80−11512
extended X-ray absorpt. fine struct.-Auger process for surface struct. anal. 77−11768
faceted microcrystal, surface tension meas. by lattice parameter changes 77−47660
faceted surfaces, investigation by slow electron diffraction 80−100377
fatigue crack closure, computer model, based on surface roughness and residual strain 77−73347
ferrites, Mn-Zn, machining effect obs., on magnetisation curves *(Japanese)* 77−21295
ferrogarnet crystal, surface layer damage thickness meas. 79−5106
ferromagnetic article, surface monitoring by defect field harmonics 79−39093
ferromagnetic thin films, influence fo surface-rearrangement on soft modes 79−69702
fibre optic elements, damaged layer struct. after diamond grinding and polishing 79−7220
field emission, surface studies 79−67444
field emission micro SEM, for UHV surface anal. 80−86519
field emitting micro-points, location, nanosecond UHV discharges 78−332
field ion microscopy, developments 79−67445
film analysis using computer-controlled Auger spectrometer, digital methods 77−56268
film profiling using proton excited X-rays 79−4490
film surface analysis techniques survey, for development and production *(Hungarian)* 80−54537
films, (111) oriented, and surface layers, unified weak field magnetoresistance 79−95514
flaw detection using optical filters 78−53163
Fourier transform IR spectroscopy, surface analysis appl. 78−76943
friction surfaces microstructure, during tribotechnical processes *(German)* 78−15540
fusion reactor first wall, surface impurities and cleaning techniques in ORMAK 77−34435
fusion reactor materials, surface anal. in Princeton Large Torus 77−57743
GaAs, Schottky barrier, effect of oxide composition on elec. behaviour, AES meas. 79−87141
garnet epitaxial layer, decomposition caused by annealing 78−18918
gas-liquid surface of penetrable sphere model 79−73380
Gaussian TEM_{00} mode laser beam scatt. from surface defect, normlaization 80−48313
glass:Nd, surface struct., laser beam effects, IR spectra appl. 79−95250
glass, adsorption of Au, AES study, electron bombardment effects 80−65380
surface structure continued
glass, chem. tempered, surface stress meas. using opt. waveguide effect *(Japanese)* 80−45473
glass, co-acting (synergistic) flaws and strength 77−20168
glass, float, low-Fe, weathered, surface, characterisation 80−93666
glass, glass surface, inhomogeneities and defects, detection using microbubbles, implantation technique *(German)* 78−47647
glass, physical chemistry exam. 78−2018
glass, polished surfaces, environment sensitive, ellipsometric obs. 77−48559
glass, structure and processes *(German)* 80−38928
glass, surface comp. profiles by Auger spectroscopy and ion etching 77−90223
glass, surface damage by abrasive contact, effect on strength 80−85066
glass, surface flaws, decoration technique 78−14547
glass, surface struct. and reactivity influence of separation *(German)* 78−30817
glass fibre, surface struct. effect in solubility in water *(Japanese)* 80−34198
glass substrate, glow discharge effect on surface props. and struct. 78−85201
glass surface, sputtering with inert gas ions 78−64438
glass surface anal. by AES 78−60013
glass tip, surface and crystallographic struct. using field-ion and electron microscopy 80−10767
glow discharge and ion-microprobe sputtering, SEM and ion-microprobe mass anal. 78−43977
grain boundary grooving under action of surface diffusion and evaporation or corrosion 80−39397
grain boundary grooving under influence of evaporation or corrosion 79−28179
graphite, Auger electron appearance potential spectroscopy *(Japanese)* 80−50473
graphite, bending strength, surface roughness effect at high temp. *(Japanese)* 79−70131
graphite, energetic deuteron irradiated surface struct. quantitative meas. 78−95210
graphite, Fe-catalysed gasification, electron, microscopy 80−104358
graphite, N adsorption, surface homogeneity changes on gasification 79−51396
graphite, phase contrast electron microscopy of holes and steps 77−38063
graphite, pyrolytic, ion bombarded, surface deformation *(Japanese)* 78−18879
graphite, pyrolytic crystals, surface topography, bombarded with Ar^+, N^+, He^+ ions 78−6820
graphite, rel. to low energy sputtering, theory 79−28880
graphite, surface alteration by interaction with Ar^+ and Xe^+ beams 78−91347
graphite, surface behaviour under various vacuum conditions, Au decoration obs. 78−75915
graphite, surface erosion by ion bombardment crystal anisotropy effect 78−23845
graphite, surface morphology changes after irrad. with energetic He ions 78−21767
graphite fibre, surface anal. by XPS and polar/dispersive free energy anal. 80−65340
graphite fibre, Type-A, surface comp. and energetics 77−70024
graphite fibres, HM, surface comp. and energetics 80−54480
graphite monofluoride, surface alteration by interaction with Ar^+ and Xe^+ beams 78−91347
graphite surface, adsorbed Cs, dissolution, lamellar cpd. form. *(French)* 80−100399
graphite thin film, high resolution phase contrast electron microscopy 80−103224
gratings, 3200 Å period fabrication, effect on film growth 78−84089
growth and composition on NaCl substrate 77−89677
guanidinium aluminium sulphate hexahydrate, surface obs., SEM and AES expts. 80−71362
Hastelloy B-2, corroded surface, electron bombardment effect during Auger electron anal. 80−61014
Hastelloy C-276, cold worked, annealed, surface segregation, Auger spectroscopy study 79−83204
heterogeneous catalysis, conference, Varna, Bulgaria (Oct. 1979) 80−82578
heterogeneous surface, adsorpt. energy distrib., surface topography effects 77−89649
hexagonal symmetry surfaces, anal. of two-dimens. superstructs. obs. by LEED and RHEED 79−23817
hexamethylcyclotrisilazane film, plasma-polymerised, TEM study 80−44456
hexamethylene tetramine crystals, growth from aqueous and ethanolic solns., (110) surface struct. 77−76338
high energy molecular beam apparatus for solid and surface anal. 77−21443
high resolution Rutherford backscatt. techniques, appl. to near surface anal. 79−5207
hydrogel coatings, and impregnations in silastic, dacron and polyethylene 79−20719
hydroxide surface, XPS exam. of chemical changes induced by Ar^+ ion bombardment 79−14993
ice, epitaxial film, on metal (111) substrates, surface struct., LEED obs. 79−86969
ice, film, on metal substrate, surface struct. using LEED 79−77879
ice, intrinsic surface order near melting point 79−14986
ice, monolayer ledges on basal surfaces 77−35809
ice, surface transition layer, ellipsometric study 80−103545
ice surface, liquidlike layer, thermal expansion meas. 79−19381
ice surface, near 0°C, 100 keV proton channelling meas. 78−14549
ice surface layer, viscosity, from thermal contraction meas., 0 to −50°C 80−49469
III-V compounds, surface comp., low-energy ion scatt. spectrometry 80−100382
III-V semiconductor, surface microhardness depend. on surface treatment method 78−15560
III-V semiconductors, surface and interface anal., secondary ion mass spectrometry technique 80−59763
imaging atom probe for surface studies 78−14555
imaging atom probe mass spectroscopy 79−23818
impurity, Auger spectral analysis 77−15671
Inconel 600, XPS exam. of initial growth of oxide films 79−20240

surface structure continued
inelastic particle reflection by Rayleigh waves 79−74022
inert gas absorbate-substrate system, surface phonons, superstructures 77−15676
influence on image speckle pattern contrast 80−17985
n-InSb, surface recomb. vel., repeated cyclic surface treatment effects 77−32065
interface roughness, calc. *(Russian)* 80−103587
interior planes acoustic microscopy 80−5886
interstellar oxide grains, surface defects rel. to mol. prod. 79−25690
ion beam analysis *(Japanese)* 80−20021
ion beam material characterisation, conf., Aleria, Corsica (Sept. 1976) 79−96403
ion beam surface crystallography, channelling and blocking effects, double alignment backscattering 80−65350
ion beam texturing of surfaces 79−77876
ion bombarded faceted cone symm. rel. to ejection patterns 78−64439
ion bombarded surfaces, energy analysed SIMS with Auger and XPS meas. 79−4457
ion bombardment, electron microscopical anal. of surface effects and volume defects, review *(Rumanian)* 80−29093
ion bombardment crystal surface, equilib. at. struct. 79−56051
ion bombardment of three-dimens. surface 80−104029
ion channelling, appl. to surface studies 79−95064
ion etched surface microstructures 79−83362
ion induced Auger spectroscopy for surface anal. 80−55756
ion induced optical emission for surface and depth profile analysis 79−4333
ion irradiated solids, energy spectra of Auger electrons, possible surface diagnostic method 79−69946
ion microprobe analysis, elemental imaging errors, polarity role 78−20103
ion optics for surface anal. 79−46902
ion plating process features and surface film props. 79−83361
ion scattering, atomic chain model, surface semi-channelling *(Japanese)* 80−50501
ion scattering, medium and high energy, two-atom model for surface blocking calc. 79−4886
ion scattering analysis double scattering effect 79−47584
ion scattering methods for determ., review 78−71907
ion scattering spectrometry, high-resolution energy analyser 77−36333
ion scattering spectrometry and secondary ion mass spectrometry for surface anal. 80−103541
ion-bombardment Auger spectroscopy for studying surfaces of solids 79−20497
ion-nitrided steel surface structure and hardness, heat treatment effects *(Japanese)* 79−87718
ion-plated metal film structure on plastic substrate 79−82501
ion-surface impact, surface atomic struct., effect on recoil atom energy distrib. 80−35050
ion-surface scattering, review of elastic ion-surface interaction 79−47583
ionic compounds, monovalent, solid soln., surface comp. calc. using monolayer model 80−6607
ionic crystal, FCC, point defects at surfaces 77−47443
ionic crystal, surface stability 80−20016
ionic crystal surfaces, defect struct. 79−19439
ionic crystals, layer spacing relax. at surfaces 80−6609
ionic crystals, surface rumpling at finite temps, Verwey model 79−51402
ionic solid, elec. potential in surface region, induced dipole contribs. 77−47882
ionically bonded surfaces, stability in ionising environments, core hole Auger decay mechanism 80−29457
ISS/SIMS, developments 78−76971
joint strength, effect of change in surface morphology of adherend 77−36672
Kapton, optical, elec. props., struct., ion textured surface 78−72904
Kikuchi pattern intensity, angular and temp. depend. 78−2349
kinetic stability of plane-faced crystal growth forms 78−47259
laser fusion targets, vapour deposited coatings, surface finish obs. 78−60863
laser-annealed surfaces, characterisation by ellipsometry 80−103544
lateral structure, surface reson. band struct. determ. method 78−68067
latex films, surface struct., vulcanisation, radiothermoluminesc. obs., 100-230K 78−75575
LEED, data averaging, objective approach 77−15668
LEED, defects in surface structure 80−44402
LEED, diffuse, of ordered cryst. surface, correl. between statistics and multiple diffr. 79−4461
LEED, dynamic installation 80−44399
LEED, Fourier transform deconvolution procedure, multiple scatt. effects 79−32862
LEED, photographic-vidicon camera method for intensity meas. 79−37596
LEED, reliability factor 77−35802
LEED, review 78−83691
LEED, review 79−10764
LEED, single-reflection layer scatt. theory 80−49059
LEED, surface characterization, tutorial 79−68986
LEED, surface defect struct. determ., book contrib. 77−62726
LEED, theoretical advances 78−83688
LEED, ZA 78−42870
LEED anal., book contrib. 79−42358
LEED analysis method, comparision of rel. intensities of diffraction beams 80−54082
LEED applications, review *(Russian)* 79−14994
LEED beam intensity measurement by photographic method, use of Vidicon camera 77−7638
LEED crystallography, review of struct. anal. 79−14656
LEED crystallography of clean surfaces and chemisorbed species 77−24470
LEED determ., multiple scatt. theory based FORTRAN computer programs, book 79−86971
LEED determination of surface structure of solids and adsorbates 78−94953
LEED for surface crystallography 77−80686
LEED from disordered overlayer, model calc. 78−84074
LEED intensities anal., transform deconvolution method 77−62717
LEED intensity curves, spin-depend. features, model calcs. on W (001) 78−34685
LEED intensity meas., reliability determ. 80−92424
LEED methods in surface crystallography 79−42349
surface structure continued
LEED one-electron potential 77−31567
LEED patterns, intensity dynamics 78−10267
LEED reliability determ. 80−49474
LEED rotation diagrams appl. 78−38917
LEED spectra measurements *(Japanese)* 79−37595
LEED surface crystallography, past and present 78−14253
LEED technique, accuracy-limiting factors 80−75127
liquid film, mol. dynamics simulation 77−15666
liquid of charged particles in equilib. with vapour, surface dipole layer and surface tension 80−70505
liquid surface, atomic processes, book contrib. 79−60605
low energy ion backscattering, struct. anal. 78−15271
low energy ion scattering analysis of surface and thin film composition *(French)* 77−59663
low energy ion scattering for composition and struct. anal. of outer surface 79−4458
low energy ion scattering spectroscopy, UHV apparatus *(Japanese)* 80−20746
low-energy ion scattering, appl. to surface anal. 79−95890
LPE ripple wavelength, morphological stability theory 78−34725
lysozyme, molecular structure of adsorbed film 79−79462
machined surface layer structure determ. using Barkhousen noise probe *(German)* 79−24710
macroscopic metal catalysts, morphology and etching processes, review 80−7856
mass spectrometry, sputtered neutral, for surface analysis and depth profiling 77−77833
MBBA, isotropic, surface-induced ordering 80−108176
measurement, by electron resonant elastic scatt. dispersion 77−63505
melt fragmentation, initiation in fuel-coolant interactions, mixing of drops of hot liquid fuel with volatile coolant 80−13537
meson transfer reactions in solids, surface struct. effects 80−104015
metal, chemisorption, intra-adsorbate Coulomb correl., surface structure 77−15685
metal, compositional variation and impurities using ion beam and nucl. techniques 79−52448
metal, direct obs. of individual atoms, FIM 77−62724
metal, electrodynamics, optical refl. coeffs. and surface plasmon dispersion law 80−75619
metal, ion beam induced desorption of overlayers 80−59786
metal, IR spectroscopy methods of investigation *(Japanese)* 78−19470
metal, oxidation, Auger electron, X-ray fluoresc. spectroscopy appls. 77−44412
metal, radiation blistering developments, review 80−44239
metal, sliding wear, surface topography and integrity effects 78−3235
metal, small angle neutron scattering by surface imperfection 77−51578
metal, surface O_2 content anal. by reson. α-scatt. from ^{16}O 78−64778
metal, surface relax. from LEED, Fourier transform-convolution method 79−4459
metal and oxide surfaces, and interfaces, slow exchange processes study using SIMS 80−55653
metal BCC crystals, surface indentation pyramids, kinetics of shape changes 77−43417
metal film, evaporated, surface area rel. to temp., gas adsorpt., nature of substrate 78−79909
metal film, surface effect on laser-induced damage 77−16436
metal film, vacuum deposited, grain struct., influence of impurities and alloying elements *(Russian)* 78−56048
metal films, on alkali halide substrates, nucleation and growth, surface study techniques, review 80−10809
metal monolayers, on metal cryst. surfaces, surface struct., review 80−80067
metal oxide, molecular adsorption, UPS studies, review 80−84374
metal oxide powder, quantitative surface meas., XPS method and appl. 78−40104
metal surface, adsorbed layer, structural and electronic reconstruction 78−84280
metal surface, anal. by secondary ion-ion emission 77−56200
metal surface, near point-defect, annealing, diffusion theory and Monte Carlo anal. 78−47646
metal surface, order-disorder phase transforms., CDW and mass density waves 80−39281
metal surface, self consistent electronic struct. effect on atomic positions, computer simulation 78−30969
metal surface, soot covered, refl. of slow electrons 77−36327
metal surfaces, dipole barrier and work func. calc. 79−15208
metal with terraced surface, work function calc. 80−6950
metallic film, appl. to adsorption and catalysis 78−75943
metallic surface, electrodynamics, microscopic effects *(Russian)* 80−6936
metallic surface, mirror electron microscopy for total electron refl. coeff. determ. 78−5994
metallic thin film, structure-related optical characteristics in visible and UV 78−35217
metallic thin films, surface and grain boundary diffusion, charact. temp/melting point ratio 79−90919
metallic thin films *(French)* 80−60692
metals, abrasive finishing with refractory carbide micropowders 80−11842
metals, adhesion, fundamental nature 79−52616
metals, individual atomic events on surfaces, quantitative examination 80−75409
metals, review 79−37912
metals, slow positron studies 80−55223
metals, surface charact., combined ion scattering spectrocopy, SIMS, SEM, energy dispersive X-ray techniques 79−43702
metals, surface layers, cross-sectional struct., appl. of cryogenic fracturing technique 77−30219
metals and alloys, diffusion layers, effect of chemicothermal treatment on struct., surface energy, and bulk props. 79−96207
metals and alloys, refractory, surface investigation by FIM and atom probe *(German)* 79−55623
metals electrochemical polishing, AC current influence obs. *(Russian)* 79−1922
mica, defects effect on epitaxial film struct. 78−26794
mica, impurity levels by static SIMS, cleaning treatment effects 77−59190
mica, metamorphic white, surface microtopography 80−54493
mica substrate of Au film, surface defects on heterogeneous nucleation and growth 78−47684

surface structure continued
mica surface, static SIMS anal. 78−38922
micro Auger analysis, using field emission source 80−104020
microanalysis, electron spectroscopy apparatus *(French)* 80−47151
microanalysis, using heavy ion 400 kV accelerator of Thomson-CSF Central Research Lab. *(French)* 78−41880
microfractography *(Japanese)* 80−71841
microstructure determ. and microanalysis by ultrahigh vacuum field emission gun SEM 80−96423
microsurfaces, obs. using thermal desorption spectroscopy combined with TEM and transmission electron diffr. 79−90888
modular surface analysis system, combined ESCA, UPS, AES and SIMS 78−73107
molecular beam scattering, coherence length and transfer width 79−83090
molecular beam scattering, coherence length and transfer width 79−83091
molecular beam study of single crysts. and catalysts 79−47971
molecular solid, surface props., review 78−34886
molten salt, Fowler model, electroneutrality correction 79−28174
monatomic lattice, modified lattice-statics approach to surface calc. 77−62718
monolayers on crystal substrate, orientational ordering of incommensurate structure, static distortion waves 77−59235
Monte Carlo simulation of crystal surface structures, appl. of statistical tests, cryst. growth 77−4060
mullite-corundum ceramics, electron microscopy of damaged surface 80−88413
multicomponent surface phase, comp. determ. from gas adsorption data 80−88417
multiple ion scattering, review 77−63517
naphthalene, (001) and (100) surface struct. models 79−86966
naphthalene, epitaxial film, on metal (111) substrates, surface struct., LEED obs. 79−86969
naphthalene, films, on metal substrate, surface struct. using LEED 79−77879
near-surface microanalysis of solids using ion beam techniques 79−24868
nematic liquid crystal, surface structural crit. point 78−91247
neutron scattering from adsorbed mols., surfaces and intercalates, review, book contrib. 80−84394
nitriding in glow discharges, influence on phase comp. and plasticity of diffusion layer *(Russian)* 80−76400
NODUS, ion scatt. spectrometer for surface composition anal. 78−76968
nuclear fuel and materials, nondestructive surface exam. 80−21246
nuclear techniques for bulk, surface anal. 78−85238
nylon 66 films, superstructural ordering 80−15344
one- and two-dimensional periodic superstructures, possibility of formation 79−11044
optical examination and monitoring of surfaces, review 79−67375
optical fibre, fracture surface anal. 80−58754
optical surface layer, reflection related to density profile Fourier transform *(Russian)* 78−31269
organic surface contaminants, anal. by plasma chromatography-mass spectroscopy, and Raman microprobe technique 80−108773
oxide film characterisation, using low energy electron induced X-ray spectroscopy *(French)* 78−41386
oxide layers on Ni-Cr and Fe-Ni-Cr alloys, compar. study of comp. and struct. by secondary ion emission and electron microprobe *(French)* 77−56286
oxide surface, XPS exam. of chemical changes induced by Ar^+ ion bombardment 79−14993
oxidised Iconel surface, quantitative anal. by XPS and rastered ion bombardment 77−40604
n-paraffins, monolayers and thin crystals grown on Pt (111), LEED obs. 77−59230
PDX Tokamak, surface analysis station 80−79586
penetrant inspection, high temp. 77−12756
perfect crystal, disturbed surface layer, X-ray diffr. 77−85038
phosphor bronzes, surface Cs^+ impact, 5.5 keV negative secondary ion emission obs., rel. to Cu *(French)* 77−66562
phosphosilicate glass, AES quantitative anal., electron irrad. induced surface comp. changes 77−48709
photoacoustic reflection-absorpt. spectroscopy for IR anal. of surface species 80−105723
photoelectron spectroscopy, solid-state, with synchroton radiation, review 80−71570
photoelectron spectroscopy of clean and adsorbate covered surfaces *(French)* 80−50519
photoemission electron microscopy in high vacuum region, image brightness and contrast 78−55791
photographic emulsion layers, surface microstructure *(Russian)* 79−58819
photomacrography and photomicrography, oblique transmitted light techniques 78−306
phthalocyanine monolayers and vapour-grown films, surface struct., LEED 77−35830
planar structures, hexagonal and cubic models, surface forces 80−20022
planar surface discontinuity, annealing by surface diffusion 79−23812
PLT Tokamak vacuum vessel, residual gas and surface comp. changes with H_2 discharge cleaning 79−80631
PMMA, crack growth rate effect, fracture surface structure 80−16466
PMMA, fracture surface parabola markings, temp. 78−52969
PMMA, optical strength rel. to surface defectiveness 77−28665
PMMA, solvent cast, surface characts., chromatographic study 80−20020
PMMA, struct. of boundary layers on solid substrate determ. by total internal reflection *(Russian)* 79−32922
PMMA, uniaxial tension, fractographic anal. of crack growth kinetics 80−40519
point defect interaction energy, influence of solid surfaces 77−62520
point defect-edge dislocation interaction near solid surface 80−79834
point defect-inclusion interaction energy near solid surface *(Germany)* 78−38750
point defects, elastic interactions in semi-infinite medium 80−39146
point defects, inclusion and segregation zone, elastic energies *(German)* 78−95049
polar semiconductor surface, energy levels and geometry, theory 80−49481
pollutant particles, characterised by AES and XPS 79−43694
surface structure continued
poly-γ-benzyl-L-glutamate, monolayers, struct. studies, IR, ATR, and TEM obs. 80−44396
polyacrylic acid film, structurisation and mech. props., EM obs. *(Russian)* 80−59406
polyamide-6, surface defects and mech. strength, oriented polymer *(Russian)* 78−51451
polyethylene, linear, single cryst., surface melting, X-ray diffr. 77−31755
polyethylene films, hard elastic, deform. mechanism 77−32652
polyethylene terephthalate fabric, surface struct., props. rel. to plasma surface treatment 78−95831
polymer, supramol. struct. characterisation, use of C X-radiation 80−79705
polymer, surface props., review 78−34886
polymer model adhesives, peeling, morphology and rheology obs. 78−92439
polymer surface, struct., bonding and reactivity, ESCA meas. 79−52073
polymer surface modification by RF plasma, difference ESCA spectra 77−63529
polymers, crystalline formations study, light refl. from untreated surface 77−28945
polymers, ESCA investigation of struct., reactivity and bonding, O_2 (inert gas) surface modification 78−3438
polymers, mol. config. packing statistics near surface 77−35491
polymers, surface charact., combined ion scattering spectrocopy, SIMS, SEM, energy dispersive X-ray techniques 79−43702
polymethyl methacrylate, direct obs. of zero field surface 80−16133
polystyrene substrate, Cu vapour deposition, surface complex, XPS obs. 78−72026
polystyrene-polymethylmethacrylate system, phase relationships and fracture surface morphology 79−61571
porous solids, pore struct. anal. using adsorpt. data, appl. to active C 77−32763
positron annihilation in crystal materials, determ. of vacancy conc. *(French)* 79−69901
positron apparatus 80−86500
probing and imaging techniques 80−54487
Pt-Au, chemisorption of H_2 and CO, effect of surface segregation 77−51601
pure elements, photoelectron line intensity meas. 78−56563
PVC surfaces, natural and stabilised, composition, ageing, oxidation and weathering, ESCA obs. *(French)* 80−61139
pyrocarbon coatings, refl. anisotropy and struct. determ. by perpendicular incidence microellipsometer 80−101824
pyrographite, surface struct., amorphisation, secondary electron spectra and AES 79−43077
quantitative surface anal., comparison of XPS results with model 78−40091
quartz, cultured, hydrothermal growth, prism face develop. rel. to microcryst. form. 77−72572
quartz, dissolution of grown synthetic quartz inside the autoclaves 78−63911
quartz, hydrothermally grown single crystals, real struct. investig. of rhombohedral faces *(German)* 78−2348
quartz, laser-induced spherical defects 77−44093
quartz, microtopographical obs. of 2nd order prism faces, hydrothermally-grown crysts. 80−54481
quartz, single crysts., Ar and O_2 interaction at high temp., surface struct. changes *(German)* 80−96725
quartz, surface damage by X-rays, γ-rays, neutrons, SEM study 80−79837
quartz, surface quality determ. using Ag diffusion and neutron-activation method 79−51401
quartz, surface structural modification by high temp. gases, computer simulation of RHEED patterns *(German)* 79−95251
quartz, synthetic, Z-surfaces, SEM examination *(French)* 80−24719
quartz, theory of etching in HF 78−27666
quartz, twinned crystals, after Japan Law, investigation of regrowth 80−54162
quartz fused, refractive index distrib. normal to polished surface, ellipsometric meas. 79−86965
quartz natural microcrystals, elementary growth layers on faces 78−14634
α-quartz surface, XPS study 80−93451
random distributed steps at interfaces and surfaces, quantitative LEED evaluation 78−63912
rare earth garnets, preparation, substrate and epitaxial layer surface quality control, X-ray topography *(German)* 77−55432
Rayleigh wave dispersion, subsurface struct., estimation, dense data 77−39730
Rayleigh wave dispersion, surface layer struct. estimation, anal. theory for sparse data case 78−38928
Rayleigh wave dispersion, surface layer struct. estimation, sparse data case 79−14995
reconstructed surfaces 78−95214
reconstruction, physical realisation of two-dimensional Ising and X-Y models 80−15351
reconstruction as source of growth steps 77−55251
refinements in reliability factors for surface crystallography 77−59193
refractory metal, disturbed layer depth on abrasive lapping with TiC, NbC, WC micropowders 77−44391
refractory metal, surface geometry and emission parameters, changes during directional mass transport 78−2344
replica, surface profile, reference line analysis 77−15672
resistive layer microstructure on superconducting Al surface *(Russian)* 80−34567
resistivity relaxation measuring system, for surface reaction meas. 80−55718
resonant defect enhancement of laser elec. field 77−63499
review of physics of solid surface *(Japanese)* 78−79870
RHEED, appls. of new techniques 77−62452
RHEED, theory for general surfaces 79−42353
RHEED developments *(Japanese)* 78−22607
RHEED scattering intensities 79−42354
RHEED-AES combined system, simultaneous struct. and comp. information 78−47216
roughening transition of crystal surface, exactly solvable model 77−47368
ruby, optical strength rel. to surface defectiveness 77−28665
Rutherford backscattering *(French)* 78−43976
Rutherford backscattering and LEED 79−82419

surface structure continued
Rutherford backscattering spectrometry, signal overlap subtraction, surface struct. studies 80−50486
saddle-field ion sources, props. and appl. 79−76239
sapphire, absorbing microdefects effect on anisotropy of optical strength 78−2952
sapphire, cryst. surface layers treatment and study by HF ion-plasma etching *(Russian)* 80−16517
sapphire substrates, prep. for GaN epitaxy 78−39929
scanning electron microscope with field emission gun for solid surface studies *(Czech)* 79−6240
scanning electron stimulated desorption, appl. to surface anal. 78−34700
secondary electron yield, determ. of surface spacings 80−66341
secondary ion emission, intensity changes correction via new total ion monitoring method 78−12796
section topograph technique, high resolution, applicable to synchrotron radiation sources 80−57449
segregation, effect on metallurgical props., SIMS, XPS and AES *(French)* 80−80045
segregation, quantitative theory 78−71910
SEM appl., field emission, electron channelling and microdiffraction from surfaces 80−59355
SEM with ultrahigh vacuum system for surface physics expts. 78−38925
semi-infinite isotropic elastic medium, reson. scatt. of Rayleigh waves by mass defect 80−20025
semiconductor, cpd., conf., Princeton, USA, (Feb, 1977) 77−85300
semiconductor, cubic tetrahedral and layered structs., review 77−85032
semiconductor, nonpolar, empty surface states and surface order effects on sorption 77−85281
semiconductor, reconstruction-induced subsurface strain, theory 78−91516
semiconductor, review 79−37912
semiconductor, struct. and props., review *(Japanese)* 80−49483
semiconductor, superstructure, excitonic wave-phonon coupling 77−15775
semiconductor, surface reconstruction, theory 77−85282
semiconductor, tetrahedrally coordinated, review of surface struct., chem. and spectroscopy 80−59764
semiconductor microcharacterisation, using electron microscopy, review 80−101911
semiconductor supersaturated solid solns., decomp., surface impurity content 78−51681
semiconductor surface, atomic and electronic struct. 78−72223
semiconductor surface, atomic geometry, ELEED meas. 79−51399
semiconductor surface, depth profiling, optoacoustic technique 80−65337
semiconductor surfaces, LEED reliability 79−37910
semiconductors, covalent and ionic, surface (110) atomic struct. bulk elastic consts. and phonon freqs. 79−69331
semiconductors, subsurface strain, reconstruction induced, theory, appl. to Si (100) 78−63914
semiconductors, surface analysis by ion beam backscattering *(Chinese)* 79−82425
serum albumin, bovine, molecular structure of adsorbed film 79−79462
Si (111), surface relax., EHT and cluster calcs. *(Chinese)* 80−59762
silica gel, IR spectra of dry transparent plates, surface struct. study 79−87884
silica gel, skeletal struct. modification with alcohols and water vap., thermal analysis obs. 78−88659
silicate gardens, growth morphology, mechanisms 80−100765
silicate glasses, polishing, surface characts. using grazing X-ray reflection *(French)* 80−65353
silicates, core-level XPS peak intensity ratio ang. variations rel. to surface anal. and chemisorption 80−40225
SIMS, appl. to surface anal., review 80−40204
SIMS, solid surface investig. applications *(Rumanian)* 80−49510
SIMS, surface anal., advantages and disadvantages rel. to ion scattering spectrometry 79−12883
SIMS, tridimensional characterisation of solid surfaces 78−73110
SIMS, using DC accelerator 79−92042
SIMS attachment, extending SEM capabilities for chem. charact. of semiconductors and metals 79−17555
SIMS data quantification 78−76942
SIMS/SEM, surface anal. appls. 79−26187
single crystal surface, electrochemistry, surface struct., superlattice struct. 80−76519
soda-lime glass, depth profiles of Na and Ca by SIMS and AES 78−51805
solid state physics, conf. Munster, Germany (March 1979) 80−41941
solid surface, microgravimetric-IR study 80−76577
solid surface, physicochemical props. investigation by SIMS *(Czech)* 80−90927
solid surface anal. by secondary ion mass spectrometry *(Rumanian)* 77−47655
solid surface analysis, ion beam sputtering 77−12477
solid surface and thin film analysis by SIMS and AES 78−80825
solid surface characterisation techniques, review 78−22945
solid surface studies, recent progress *(Japanese)* 80−15347
solid surfaces, ion and neutral scatt., backscatt. energy spectra anal. by TOF technique 79−5236
solid surfaces, problems *(Japanese)* 78−43222
solid surfaces, surface heterogeneity in physical adsorption 79−23829
solid surfaces, surface processes, and solid/gas interactions 80−73125
solid surfaces props. characterisation, structural, chemical and electronic, use of LEED methods *(Italian)* 80−49467
solid-electron interactions conf., Southampton, England (Apr. 1976) 77−44570
solid-gas and solid-liquid interfaces, struct. rel. to reactivity 77−72775
solid-gas interfaces, topographic and thermodynamic aspects 78−68927
spectroscopy, total current, study of surface regions and bulk physics 80−31952
spin polarised electron source for LEED 78−83693
sputter induced surface composition changes, in alloys 80−49470
sputter induced surface morphology, analytical modelling 77−16445
sputter profiling, depth resolution, surface transport effects, calc. 80−97393
sputtered alloys and compounds, surface layer composition changes 77−73200
sputtering, angular distrib. and yield from faceted surfaces 79−15575
sputtering, non-elemental solid surface, surface composition, yields, desorption effects, review 77−44111

surface structure continued
sputtering by slow energy ions, theory taking surface microstruct. into account 79−28880
sputtering of single cryst., differential yield, surface struct., review 77−44112
stainless steel:C, surface, obs. at very low accel. voltage (200 V-1 kV) by SEM 80−10764
stainless steel, coated with C, surface damage by D^+ and He^+ ions irrad. 80−23146
stainless steel, in $MgCl_2$ solutions, Cl distrib. in oxide films, SIMS *(French)* 80−108765
stainless steel, machine faceted, low-energy ion erosion studies 80−80923
stainless steel, surface layer anal. after exposure to N_2O_4 *(Russian)* 77−40478
stearic acid, evaporating cryst. surfaces in vacuum 79−77740
stearic acid, microscopic obs. of cleaved surface 79−95248
steel, 0.45% C, annealed, roller, macroscopic and microscopic changes in surface layer due to rolling contact 77−77518
steel, Al killed BOP, degreased and annealed, surface exam. *(German)* 77−52686
steel, austenite, blistering after 40 keV He ion bombard. 80−39175
steel, austenitic, Cr-Ni, ion-implanted N, chem. state study by AES and XPS 80−79825
steel, austenitic, friction in vacuum of type U8 steel under microshock loading *(Russian)* 80−108583
steel, austenitic 30KhGSA, white phases structure after heat treatment 80−76281
steel, austenitic stainless type AISI 304, surface comp. after different surface treatments 80−3253
steel, austenitic stainless type AISI 316, L sheet and LN plate surface comp. after different surface treatments 80−3253
steel, bearing, type AISI 52100, tricresyl phosphate treated, Auger anal. 79−52413
steel, C, machined, microdefects on surface 80−16607
steel, C, pore formation in surface layers, during As diffusion redistrib. 80−49421
steel, C and Cr, surface damage during friction, struct. effect 80−35339
steel, cold-rolled, good and bad paintability, AES, SEM and X-ray diffr. characterisation of surfaces 79−42344
steel, cold-rolled sheet, surface chemistry 80−61146
steel, contact fatigue life of S-P type extreme pressure additive lubricated surfaces 79−47780
steel, Cr, cold roll, frictional heating surface damage 80−76289
steel, Cr, exam. of surface layer after electrochemical treatment, effect on mech. props. *(Russian)* 80−7727
steel, Cr (25 wt.%) polarised light, recrystallisation annealing 77−28947
steel, ferritic stainless, effect of Cl ions on passive layers 80−59766
steel, high-C, boriding, boride case struct. 79−24665
steel, industrial, surface chem. characterisation by SIMS, glow discharge spectrometry and other techniques 80−66907
steel, low C, high strength impact deposited white-layer on X65 78−48566
steel, low C structural, fracture toughness and X-ray diffr. obs. of surface *(Japanese)* 80−66634
steel, medium C, Ni-Cr-Mo, overheated, fractographic study *(Chinese)* 80−66616
steel, mild, AISI 1009 and 1018, corrosion incipient processes in hypersaline geothermal brine at 90°C 80−50753
steel, mild, surface analysis rel. to annealing *(French)* 77−32857
steel, mild and type EN31, eval. of cold rolling oils and boundary lubrication characts. by SEM 80−85068
steel, Mo^+ ion bombardment, phase composition and struct. change of surface layers *(Russian)* 80−24506
steel, Ni-Cr, case hardened rollers, macroscopic and microscopic changes in surface layer due to rolling contact 77−77518
steel, Ni-P plated, electroless, fatigue strength and plated layer microstruct. *(Japanese)* 80−93645
steel, nitrided, chem. state anal. by conversion electron Mossbauer spectrometry 80−7718
steel, rapid, ZrB_2 surface treatment, phase comp. and struct. of layers 79−66203
steel, segregation and adsorption of S, influence on carburisation and nitrogenation 80−66701
steel, stainless, 0Kh16N15M3B *(Russian)* 80−39170
steel, stainless, 305, surface composition changes with plasma discharges 77−34434
steel, stainless, 316, surface analysis by SIMS, SEM AND ESCA 79−52825
steel, stainless, 410 type, surface segregation using atom-probe FIM 79−77883
steel, stainless, austenitic, oxidation mechanism, oxide thickness, comp. and growth, nuclear technique study 80−61022
steel, stainless, depth profiling of passive film by quantitative AES 78−19611
steel, stainless, ground surface ion bombardment, in DC glow discharge 78−95098
steel, stainless, surface treatment, X-ray photoelectron spectrosc. study 80−50764
steel, stainless, Type 304, surface analysis by SXAPS *(Japanese)* 77−70231
steel, stainless, type 316, neutron irrad. damage simulation using HVEM, surface effect on void swelling 78−29572
steel, stainless, type 316, surface comp. rel. to crevice corrosion initiation 80−93680
steel, stainless, type 430, Ni^+-implanted, struct., comp. and electrochem. anal. of surface alloy 80−16603
steel, stainless, type EP838 ion irradiated, surface structure changes during post-irradiation heating *(Russian)* 80−75272
steel, stainless 304, Auger electron appearance potential spectroscopy *(Japanese)* 80−50473
steel, stainless type 304 attack morphology of stress corrosion cracking, TEM study *(French)* 79−83368
steel, surface structural changes on exposure to plasma, etch resistance *(Russian)* 79−83234
steel, trace element UV emission, spectrochem. anal. *(French)* 80−71997
steel, type 1Kh17N2, alloying element redistrib. during friction *(Russian)* 77−81326
steel, type 1Kh17N2, white zone formation and props. during friction in vac. *(Russian)* 80−40542

surface structure continued
steel, type 40 Kh, electron emission depend. on surface mechanical treatment *(Russian)* 80−100945
steel, types 60G, ShKh15, structural changes near holes and inclusions due to pulsed currents *(Russian)* 80−108459
steel, W-Mo, types R6M5 and R6M5K5, decarburising layer evaluation 80−21164
steel, wear testing in oils containing organosulphur cpds., XPS obs. of surface comp. rel. to wear 77−36668
steel, white layers forming at high rates of friction, struct. props. *(Russian)* 79−15800
steel, Zn coated, cold rolling influence on struct. and deform. of diffusional layer *(Russian)* 80−55465
steel 1095, quenched, Mossbauer study of surface martensite 77−32578
steel 1Kh18N9T, physico-mech. props. after boring in metallic melts *(Russian)* 78−56736
steel C60, machined, surface morphology, struct., SEM, topographic investigs. *(German)* 77−73372
steel low C, surface segregation of Mn during annealing 77−36555
steel sheets, surface composition, degreasing and batch annealing effects 80−66700
steel sheets, surface layer composition charact. by glow discharge spectrometry *(French)* 79−87923
steels, stainless, passive state, electron spectroscopy anal. 80−59765
steels ShKh15 and 12KhN3A, white phases structure after heat treatment 80−76281
STEM, single atom microscopy, instrumental aspects 80−86522
step densities, two-dimens. random probability model 80−80036
step structure, decoration technique 80−103554
step thickness determination, on crystal surfaces, use of defocus contrast of TEM 79−7531
step thickness measurement, TEM 80−103555
step-step interaction on clean surfaces, morphological changes 78−14552
stepped surface exam., LEED vs. RHEED 77−72762
stepped surfaces, surface geometry, RHEED study 79−77881
steps, thermodynamic props., solid on solid model 77−7683
strengthening by electrospark alloying *(Russian)* 79−96198
structure sensitive factors in molecular cluster formation by ion bombardment of single crystal surfaces 79−19964
submonolayer films on metallic surface, struct. and props. review 78−38972
subsurface structure detection by scanning photoacoustic microscopy 80−6323
sunlight absorber, struct. and thermal efficiency 77−125
superstructures rel. to surface phonons 77−62731
surface (100), atomic struct., angle-resolved XPS, LEED and ISS investigation 80−10765
surface analysis techniques 79−70411
surface chemical bond, book 80−22147
surface dislocation model, Z-phase interface boundary problem 80−39085
surface layer, segregation of ferromag. Ni, magnetooptic investigation 80−2256
surface layer structure, rel. to neutron refl. on boundary *(Russian)* 78−1976
surface properties of materials, Conf., Missouri, USA (August 1977) 78−87867
surface state resonance effect, obs. by convergent beam RHEED 80−107622
surface-dynamics of growing crystals 80−44160
synchrotron radiation and sputter Auger techniques 78−61130
synchrotron radiation techniques 80−80945
sytrene-tetrahydrofuran block copolymer, H_2O contact angle and surface struct. *(Japanese)* 78−79861
Teflon, optical, elec. props., struct., ion textured surface 78−72904
Teflon, surface alteration by interaction with Ar^+ and Xe^+ beams 78−91347
TEM obs. *(Spanish)* 77−47308
tetrabrommethane, surface melting, transition from atomically smooth to rough struct. 77−76648
TGS, cleavage surface, electron microscopy using shadow decoration technique 77−7955
TGS, ferroelec. cleavage surface microscopic struct. by electron microscopy 79−51403
theory, aims and recent accomplishments 80−75413
thin film, and surface anal., modern methods 80−54486
thin film, electron-induced X-ray spectrometry anal. *(French)* 79−43067
thin film surface anal. and depth profiling by spark-source mass spectrography, discharge model 80−40781
thin films, segregation effects at surfaces and interfaces 80−39475
thin films, surface anal., survey of ESCA, AES, SIMS, and ISS *(Hungarian)* 80−70544
thin films and interfaces, analytical techniques, review 80−80120
threshold-potential spectrometer appl., based on Auger electron spectrometer 80−52365
tinplate surfaces, Auger depth profiling and anal. 80−59768
tools for surface anal., review 80−103540
topography, high-resolution polymer replication 78−10264
topography, numerical interpretation 79−51406
topography, rel. to adhesion props. 79−96280
total current spectroscopy, review 80−45185
trace analysis *(Japanese)* 78−40102
transition metal alloy, surface segregation, electronic theory 77−43414
transition metal compound surfaces, review 80−84349
transition metal dilute alloys, component segregation to interfaces 79−51398
transition metal oxide and hydroxide surfaces, chem. changes induced by Ar^+ bombardment, XPS obs. 79−83084
transparent dielectric, enhanced localised intensities in surface scratches rel. to laser damage 79−22999
transparent materials, defective surface layer formation during abrasion, laser-induced breakdown *(Russian)* 78−53007
two-band crystal, surface reconstruction, Green's function formalism 78−14543
two-band crystal, surface reconstruction, model for CsCl struct. 78−14544
Udimet 700, superalloy, melted by laser beam, microstructure and topography exam. 79−69919
ultra-high vacuum systems for surface anal. 79−67323
ultrahigh depth resolution surface analysis, appls. 78−71917
surface structure continued
ultrasonic wave transmission through rough surface *(Russian)* 80−100387
UPS determination of surface structure, angle-resolved method 79−91567
USb_2, single crystal growth, structural perfection 80−15024
vacancies in close packed crystal surfaces 79−77871
vacuum deposited film, orientation axis tilt rel. to vapour angle of incidence 80−88456
vicinal surface, system of regularly spaced steps, LEED *(French)* 80−49060
W, field emission tip, microscopic protuberance formation, min. elec. field and temp. 78−6835
water, free surface struct., single ion hydration energies 78−26752
wedge disclinations near surface of semi-infinite cryst. *(Russian)* 80−49224
X-ray fluorescence, Ar ion induced, for surface anal., preliminary obs. 79−5228
X-ray photoelectron spectra, surface chemical analysis through even derivatives 79−100463
X-ray spectroscopy, methods, results of studies of atomic states and elemental composition 77−29063
X-ray standing wave field excitation, meas. apparatus, appls. 77−15285
X-ray total external refl., differential eqn. calcs. 78−71625
XPS and AES techniques for surface characterisation 77−32495
Zircaloy-2, neutron irradiated, inhomogeneous deformation behaviour 80−50679
AG {110}, re-exam. by LEED 77−85029
Ag (110), ethylene-O_2 interaction, LEED and AES obs. 80−89520
Ag (110), struct. and effect of surface roughness on LEED intensities 77−24471
Ag (110), surface relax., LEED results anal. by convolution-transform method 77−89624
Ag (110), surface struct., LEED determ., const. momentum transfer averaging 79−42350
Ag (111), chemisorbed Rb struct., and NO reactivity on Rb-dosed Ag 79−28207
Ag (111), epitaxially grown on mica, surface defect struct., LEED study 80−80038
Ag (111) surface, Ar ion bombardment, effect on struct. and reactivity, ellipsometry and LEED meas. 77−59192
Ag, (111) surface electron microscopy 80−103556
Ag electrode, metal ion adsorption kinetics, surface struct. 78−79873
Ag electroplated lead frames, surface struct. rel. to bonding behaviour, IC prod. *(German)* 79−11010
Ag evaporated film, adsorbed CO, enhanced Raman scatt. mechanism in ultrahigh vacuum 80−107645
Ag, film, sputtering mechanism, SEM 80−29839
Ag film, substrate surface structure effects on absorptance 78−19585
Ag, multiply twinned particles, internal and surface struct. by electron microscopy 80−84189
Ag, single crystal, electrochem. grooving, gross linear defect obs. 78−67894
Ag, surface roughness induced electronic Raman scatt. 80−50347
Ag thin film, X-ray fluoresc. spectroscopy of surface using RHEED-solid state detector method 80−108760
Ag, vacuum deposited film, surface struct., HEED meas. 78−6234
Ag:Al_2O_3:Al tunnel-junction struct., surface polariton mean free path, roughness 80−93008
Ag-Au, calibration line introduction for comp. determ. by AES 79−56892
Ag-Au, composition changes under ion bombardment, scanning Auger microprobe obs. 79−83076
Ag-Au, corrosion in HNO_3 80−85091
Ag-Au, sputtering, ion yield depend. on alloy comp. 77−20976
Ag-Au, surface layer, effect of Ar^+ bombardment, AES and SIMS 80−25504
Ag-Au, surface segregation, ion scatt. spectroscopy meas. 79−82423
Ag-Au alloy, Auger exam. of preferred sputtering 77−44106
Ag-Au alloy, determ. of surface versus bulk composition, low energy ion scatt. spectroscopy 77−1284
Ag-Au alloy, ion irrad., surface segregation and selective sputtering, AES expts. 79−7740
Ag-Au alloy, surface after sputtering, AES obs. 77−55858
Ag-Au alloy, surface enrichment, AES meas. 77−1283
Ag-Au system, surface segregation 79−69330
Ag-Cd (45 at.%), morphology and struct. of bainite plates in β' phase 79−52213
Ag-Cu (6.6% at.wt.), melted by laser beam, microstructure and topography exam. 79−69919
Ag-Cu alloy, surface comp. after sputtering, AES obs. 77−55858
Ag-Cu surface alloyed films, laser melt quenched, microstruct. 80−76423
Ag-Ge, liquid, surface tension exam., sessile drop method *(French)* 77−20162
Ag-Ni solid solution, reversible surface segregation, radioactive tracer, LEED, and AES expts. *(French)* 77−69155
Ag-Pd, surface comp. changes under ion bombardment, AES study 80−55250
Ag-Pd alloy, surface comp., AES expts., correl. with O_2 heat of chemisorpt. data 78−34684
Ag-Pd alloys, inert gas ion bombardment, dynamic surface composition changes, AES obs. 80−60745
Ag-Pd system, surface segregation 79−69330
AgBr layer, sensitised, topography of developed centres 80−73491
AgBr:Pb, impurity segregation to surface, ion scattering spectroscopy obs. 77−19979
AgBr(Cl), vapour-deposited epitaxial film 80−59814
Ag_2S-K_2SO_4 mixtures, surface comp., AES and XPS obs. 80−81386
Ag−(100)InP, metal-semicond.cathode contact, metallurgical, physical, chemical processes 80−107911
Ag(111) surface, adsorbed I_2, adsorbate-substrate bond length, X-ray anal. 78−84679
Al, (001) and (110) surfaces, LEED intensities 77−47656
Al (110), surface relax., LEED results anal. by convolution-transform method 77−89624
Al, (110) and (100) surfaces, MEED intensity calc. using chain method 77−20169
Al (111), ordered O overlayer associated with chemisorption state 78−47665

surface structure continued
Al, (111) surface, adsorbed O, surface struct., LEED and SEXAFS data 80−92782
Al alloy, 2024-T3, adherend surface, chem. comp., effects of chem. and thermal treatments 78−39939
Al and Al alloys, Auger spectroscopy produced in glow discharge *(Russian)* 78−14545
Al, and Al-Cu(Pb) dil. alloys, pulsed ruby laser irrad., noncryst. phase form 80−35012
Al, annealed and powder sintered (SAP 895), sputtering under D^+ and $^4He^+$ bombardment, microstruct. effects study 80−84821
Al, chemisorption of O, unoccupied extrinsic surface resonances and site struct. determ. by soft X-ray absorpt. 79−73403
Al, contamination by exposure to DC-704 silicone liq., IR refl. spectra anal. 77−59630
Al, extrusion, pick-up form. on surface 78−39882
Al, film on Si(111) substrate, struct., props. depend. on vapour flow, ionisation *(Russian)* 80−75453
Al, foil, influence of O_2-pressure on oxidation rate, TEM study 80−104355
Al foil electrolytic perforation, surface film phase composition obs. *(Russian)* 80−61004
Al, industrial, depth profiling by ion microprobe with high mass resolution 79−46894
Al lithographic sheet, AC etching 80−35547
Al, low vacuum condensates, struct., IR refl. obs. *(Russian)* 78−30850
Al sheet surfaces, chem. characterisation by SIMS, glow discharge spectrometry and other techniques 80−66907
Al, sputtered by He^+, photon emission, dose depend. 77−8695
Al sputtered coating development, porosity, durability temp. depend., electric arc metallisation regime *(Russian)* 80−39402
Al surface, (111), interlayer spacing, LEED data anal. 80−54484
Al, surface, pure, oxidised element determ. by SIMS 78−85247
Al, surface relaxation using surface EXAFS 79−23816
Al thin film evaporated on quartz substrate, surface irregularities 79−90920
Al-Ag (7.27 wt.%), peculiarities exhibited during fatigue loading *(Chinese)* 80−71723
Al-Ag alloy, thin foil, X-ray microanalysis, surface film effect 78−44428
Al-Cu, surface enrichment of Cu due to Xe sputtering, AES and He ion backscatt. meas. 77−4250
Al-Cu (4 wt.%), non IPS geometric surface relief effects associated with diffusional phase transform. 77−32575
Al-Cu-Mn-Mg-Fe-Si-Zn alloy D16, surface layers chem. composition rel. to fatigue resist., corrosion-fatigue resist. 79−29275
Al-GaAs interface, thermal ageing of Al film, optical microscopy and SEM obs. 77−20203
Al-Mg, foil, oxidation in O_2 atm., TEM study 80−104356
Al-Mg (2.5wt.%) sheet, surface oxide state and weldability 80−59769
Al-Mg-Li alloy, 01420, surface layer props. *(Russian)* 78−80674
Al-Sb, laser induced surface alloy formation and Sb diffusion 80−54439
Al-Xe film, ion implanted radiation enchanced Xe outdiffusion, Rutherford backscatt. 77−76609
Al-Zn-Mg type 7017 and 7018 alloy plate, fractographic study of stress-corrosion crack propag. 79−57158
AlGaAs-GaAs heteroepitaxial wafers, Mg doping, surface morphology and photoluminesc. props. laser applics. 77−3591
$Al_xGa_{1-x}As$, MBE grown film, in situ surface characterisation by RHEED, SIMS and AES 77−43410
$Al_xGa_{1-x}Sb$, surface flatness depend. on LPE condition 79−15042
Al_2O_3, adsorbed ethanol, acetic acid and acetaldehyde, inelastic electron tunnelling spectra, surface vibr. struct. determ. 80−35572
Al_2O_3 adsorpt. of isobutyl alcohol, gravimetry, IR investigs. 79−1546
Al_2O_3 anodic layer formation in H_3PO_4 solns., surface charact. 78−15603
Al_2O_3, anodic oxide film, behaviour of emulsion particles during electrodeposition 80−104357
Al_2O_3, bending strength, surface roughness effect at high temp. *(Japanese)* 79−70131
Al_2O_3, D plasma interaction, surface structure, chemistry and resistivity changes 78−53010
Al_2O_3, dense, steam-enhanced Ca segregation, AES and SEM obs. 79−83352
Al_2O_3, films, form., cross-sections, struct. obs. 78−67917
Al_2O_3 hard anodic coatings, effects of cellular structures 78−11448
γ-Al_2O_3, hydrate covering, surface struct., IR spectra meas. 77−89622
α-Al_2O_3, ion bombard., vol. expansion, annealing compaction, surface props. 78−67748
Al_2O_3, layer, obtained by reactive evap., surface struct. and morphology *(Polish)* 79−28242
γ-lAl_2O_3, OH layer, IR spectra, outgassing temp. effects 80−66175
Al_2O_3, quantitative surface anal., comparison of XPS results with model 78−40091
Al_2O_3 rich substrate, surface smoothness and metallization props. *(German)* 78−19906
Al_2O_3 rod, damaged, mech. strength, surface defects effect, appl. as insulators *(German)* 80−76330
Al_2O_3, surface microstructural changes due to reduction by C *(Russian)* 80−100378
Al_2O_3-Cu composite, vapour deposition, microstruct., texture and surface topography 77−70001
Al_2O_3-SiO_2 glass ceramic, surface streaks and blisters, UV fluoresc. study 80−84347
$Al_2(SO_4)_3$-K_2SO_4.$2PH_2O$, rel. between etch pits or growth hillocks and dislocations on (111) faces 79−77602
AlSb (110), surface struct., EPR meas. and elastic energy minimisation calcs. 79−51405
AlSb (110), wave functions and surface struct. 78−91519
Al(100) oxidised surface structure anal., extented appearance potential fine struct. study. 80−75411
Al(111), oxide layer amorphous to cryst. surface transition, slow positron obs. 80−75417
Ar, liquid, surface study, ellipticity coeff., ellipsometric method 80−84343
As, (111) surface, freshly cleaved, vaporisation, surface morphology changes obs. 77−80612
$As_{15}S_{40}Ag_{45}$ glass, photosurface deposition of metallic Ag discs 77−76650
Au (100), characterisation of reordered and normal surfaces by LEED, AES and EELS 78−34687
Au (100), disordered, diffuse LEED intensities obs. 79−4462
surface structure continued
Au (100) surface, reconstruction, superstruct., model 80−103551
Au (101), disordered surface, diffuse LEED intensities, statistical disorder theory 79−4463
Au (110), (1×2) and (1×3) superstructures, LEED study 80−20024
Au (110), electron spin polarisation in LEED 78−83692
Au (110), reconstructed surface, LEED anal. 79−77878
Au (111), anomalous surface superstruct., UHV electron microscope obs. 80−10760
Au (111), relativistic effects on LEED intensities 79−7737
Au (111) film, sputtered, surface struct., HV electron microscopy and theoretical model 78−22981
Au, (111) surface electron microscopy 80−103556
Au, adsorbed layer comp. anal., by ion-forwarded electron spectra 77−31850
Au, chemisorption of I, AES and LEED study 80−100405
Au coins, surface anal. by X-ray fluoresc., SEM and scanning Auger spectroscopy 80−89552
Au electrode, metal ion adsorption kinetics, surface struct. 78−79873
Au, electrodeposit, struct., texture, influence of As on brightness *(Bulgarian)* 78−79862
Au, electrodeposit, struct., texture, influence of substrate *(Bulgarian)* 78−79863
Au evaporated film, adsorbed CO, enhanced Raman scatt. mechanism in ultrahigh vacuum 80−107645
Au film, (001), vapour-deposited, surface struct. and lattice const., TEM obs. 77−1326
Au film, (001) surface atomic steps obs. using TEM 77−20173
Au film, ion bombarded, surface craters induced by displacement cascades 80−107344
Au film, on Ni, AES anal., influence of ion bombardment on depth resolution 77−20210
Au film, on Si (100) substrate, growth and struct., LEED and AES obs. 79−51457
Au film, surface step structure imaging by dark field electron microscopy 80−15346
Au film (001), high resolution TEM 80−100383
Au film (001) surface, computer modelling of high resolution TEM images 80−6330
Au films, (111), sputtering in high voltage electron microscope 80−35027
Au films on Cu, oxidation exam. by ion scatt. spectra 79−79153
Au islands in polymer surface, laterally inhomogeneous sample, ang. and spatial depend. intensity for ESCA spectroscopy 79−74468
Au, lattice images, obs. with a field emission electron microscope 79−14659
Au, multiply twinned particles, internal and surface struct. by electron microscopy 80−84189
Au, spherical crystal, drop grown from melt, RHEED obs., superstructs. 78−43225
Au, stepped surface, edge atom dipole moments 78−14791
Au surface, clean, hydrophilic nature 80−80029
Au, surface dipole moment calc. 80−60060
Au, vacuum deposited film, surface struct., HEED meas. 78−6234
Au-Ag, surface segregation 79−77873
Au-Cr alloys, Cr conc., quantitative Auger electron analysis 77−85852
Au-Cu, surface conc. profile and surface energy 80−84350
Au-Cu alloy, surface comp. as function of temp., AES expts. 78−95212
Au-Cu-O surface, quantitative Auger analysis using relative sensitivity factors 78−7295
Au-Cy alloy, surface comp. after sputtering, AES obs. 77−55858
Au-Ni, surface segregation, strain effects 80−80042
Au-Ni-O surface, quantitative Auger analysis using relative sensitivity factors 78−7295
Au-Ni(Pd)(Pt), surface composition determ. 79−69328
Au-Pd, surface comp. changes under ion bombardment, AES study 80−55250
Au-Pd alloy, surface comp., polishing, cleaning and Ar sputtering effects 77−72763
Au-Sn alloys, surface comp. by Auger spectroscopy, sputter cleaning 77−59648
Au(111)/Ag(111) thin film system, diffusion processes, diffused Ag composition profile 79−90832
B, CVD, morphologies, influencing factors, temp. range 1390-1640K 80−89154
B fibre, prep. by closed CVD system, mech. props. and surface defects 79−52311
B fibres, quality evaluation from morphological and fractographic characteristics *(Russian)* 79−70150
B fibres, surface morphologies rel. to mech. props. 80−11749
BN, cubic, growth pressure-temp. region in system BN-Mg 79−66053
BP coatings, on Mo by CVD and their composition and microhardness 79−28942
Ba, adsorbed layers on W, Auger and work function meas., impregnated W cathode model 79−43073
Ba-O system, adsorbed layers on W, Auger and work function meas., impregnated W cathode model 79−43073
BaB_6 powder, surface struct. effects on thermionic emission characts. and vapour pressure *(Japanese)* 80−50506
BaO, AES peak height calibrations 79−43072
BaO epitaxial films, cathode poisoning due to O_2, CO_2, and S, surface anal. 79−42600
$BaT:O_3$, surface microrelief revealed by ion irradiation 80−54485
$BaTiO_3$ (001), LEED and UPS studies 80−100747
$BaTiO_3$, ferroelec. to paraelec. transform., influence of domain boundaries on interface struct. 79−95718
$BaTiO_3$, ferroelectric-paraelectric transform., basic struct. and charact. 79−95717
$BaTiO_3$, pure and doped crysts., surface and domain struct., AES and SEM expts. 80−71363
$BaTiO_3$, surface microrelief after ion irrad. 80−59774
$BaTiO_3$, surface study using AES and ion scatt. spectroscopy 80−65339
$BaTiO_{3-x}$, ferroelec., Auger spectroscopy of surface layers 79−42343
$BaTiO_{3-x}$, single cryst. and film, Auger spectra, surface comp. 78−27353
$BaWO_4$, flux- and gel-grown, comparative microtopography 77−31852
Be (0001) surface, work function and purity, AES, LEED and photoelectron spectra meas. 78−68606
Be, blistering model, correlation between blister diameter and skin thickness 78−95067

surface structure continued
Be, irradiated with He^+ at 20 keV, surface damage and gas trapping profile meas. *(French)* 80−84218
Be, slowly oxidised, secondary electron yield changes, and AES characterisation 80−71524
Be, surface morphology, effect on low energy H ion erosion yield 79−42121
Be-Cu, calibration line introduction for comp. determ. by AES 79−56892
Be-Cu dynode, depth profiling anal. of surface layer 80−2253
Bi, intervalley scattering processes, surface struct., transverse electron focusing study *(Russian)* 80−84352
Bi, single crystal from Bridgman's method, triangular facet formation 80−28933
Bi surface, detection of high mass cluster ions by SIMS and XPS surface monitoring 77−16442
Bi thin film, structural evolution 8 to 573K, supercooling effects *(French)* 79−90921
C, (001)-(2×1) surface, reconstruction-induced mean-square displacements 80−15343
C, activated, of I_2, pore struct. 77−31870
C fibre, metal-coated with Cu, Co or Ni, coating struct., SEM study 80−97605
C fibre layers on arc anodes props. and cooling behaviour 79−52245
C fibres, PAN-based, surface charact., active surface area, microporosity 78−35536
C fibres, PAN-based type I, II and III, TEM study of structural heterogeneity 79−77465
C fibres with large breaking strain, prep., mech. props., struct., appl. 78−44077
C films, surface struct., graphitisation, secondary electron spectra and AES 79−43077
C, glassy, surface erosion by ion bombardment crystal anisotropy effect 78−23845
C materials, optical microscopy, reflection, interference colours, terminology 78−42871
C materials, thermodynamic props. rel. to struct. 77−80597
C, on Fe(100), adsorbate coverage determ. by LEED, AES and XPS 80−103566
C, reconstruction-induced subsurface strain, theory 78−91516
C, secondary electron spectroscopy 77−85854
C steel, fatigue, residual stresses, surface cracks *(Japanese)* 77−25121
C vacuum deposited coatings for prosthetic devices 77−40374
CO adsorbed layers, on W (210), surface struct., LEED obs. 79−82449
CU(311), LEED meas. 77−89623
$Ca_3Al_2Si_3O_{12}$-$Mg_3Al_2Si_3O_{12}$, synthetic garnet, soln. grown, surface features 78−2346
$CaC_2O_4.2xH_2O$ ($0<x<5$ zeolite water fraction), weddellite, growth morphology, PBC analysis 80−24388
CaF_2, Au decoration and C replica techniques 77−1286
CaF_2, fluorite crystals, surface struct., growth mechanism 79−99096
CaF_2, polished crysts., rocking curve meas. *(German)* 78−2347
CaO (100), surface struct., LEED study 80−39396
CaO, (100) surface struct. using LEED meas. and rumpled ionic models 80−20019
CaO, AES peak height calibrations 79−43072
CaO, produced from $CaCO_3$ powder decomp. in vac. and in CO_2 80−45255
CaO-Al_2O_3-SiO_2 glass-$MoSi_2$ filler, vitreous composite prod. 77−90313
Ca_3SiO_3, hydrated, composition and morphology 78−26755
Ca_3SiO_5, fracture surfaces, quantitative anal. using energy dispersive X-ray spectrometry *(French)* 80−89571
Cd (0001), oxidation, LEED and AES obs. 79−87756
Cd deposited layers on Ti (0001), LEED and AES determ. of struct. 77−72804
Cd deposited layers on Ti (0001), LEED and AES determ. of structure 77−76688
ω-Cd-Hg alloy, melt-growth, morphology of single crysts. 78−64464
$Cd_xHg_{1-x}Te$, correlation between structural and chemical inhomogeneity *(Russian)* 80−49484
$Cd_xHg_{1-x}Te$, surface microhardness depend. on surface treatment method 78−15560
CdS, clean surface, AES and LEED exam. 80−10762
CdS film, cryst. and electronic surface struct., stimulated recrystn. effects 79−78151
CdS film, surface stoichiometry rel. to CdS-Cu_2S cell performance 78−2956
CdS, film, surface struct. and elec. props. 80−34531
CdS, film for solar cells, struct. and elec. props., thickness depend. 78−72289
CdS, polycrystn. layers on CdS substrate, electron microscope study of surface struct. 78−22940
CdS, single cryst., polar (0001) and (000$\bar{1}$) surfaces, comparison of AES signals 80−16130
CdS(Se), uncoated and liq. layer coated, vaporisation mechanism, surface morphology 77−35683
CdS(Se)(Te), evap. onto electron bombarded NaCl substrates, epitaxial growth and characts. 79−28948
CdSe film, laser annealing effects on surface struct. and elec. characts. 79−73605
CdSe:Cu, doping profile rel. to photoelec. props. in alloyed surface layers *(Russian)* 77−85268
CdSe:Cu surface layer of CdSe, microstruct., photoelec. props. 78−43221
$CdSe_xTe_{1-x}$ film, polycrystalline, deposition and physical props. 77−4741
CdTe epitaxial films, surface morphology, layer and spiral growth 80−10823
CdTe surface, sputter cleaning and dry oxidation, XPS and LEED study 80−108618
CdTe, surface layers formed by etchants, XPS meas. 78−44240
CdTe surfaces, SIMS, Rutherford scatt. and ellipsometry 79−56046
Ce oxidised surface, comparative sputtered neutral mass spectrometry and SIMS studies 79−90856
CeB_6, thermionic emission rel. to surface state 78−39654
CeO_2-Y_2O_3 film, surface characterisation, XPS, ESCA, and AES expts. 78−72028
CeTe, surface characterisation by high resolution Rutherford backscatt. 80−25511
Cl adsorbed layer on Ag(111), props., struct., AES study 78−72024
Co (0001) surface, LEED and AES meas. 77−31857
surface structure continued
Co (0001) surface, LEED meas. 77−59188
Co (100), clean and C-covered, LEED-Auger expts. 78−38921
Co (10$\bar{1}$2), struct. and CO chemisorption obs. 79−4474
Co {001} surface, LEED struct. anal. 78−47645
Co, corrosion in Ar-SO_2 atmospheres, scale struct. obs. *(Japanese)* 80−55568
Co, martensitically transforming, state of surface 78−43223
Co, surface structure in HCP and FCC bulk phases 78−51807
Co-C, dil., C segregation to single cryst. surfaces 80−39301
Co-Ni, surface chemical comp. changes due to ionic bombardment *(Russian)* 77−1776
Co-Si, surface physicochemical state, Auger electron spectroscopy study 80−100715
$CoCr_2S_4$, CVD grown, surface microstruct. 79−4905
$CoFe_2O_4$, thermally induced surface chemistry and struct., XPS 78−22939
$Co_{1-x}Fe_{2+x}O_4$, prep. by wet and ceramic methods, struct., mag. and surface props. 78−52307
$Co_{1-y}Fe_{2+y}O_4$, equilib. surface comp., cation comp. with stoichiometric oxygen content 78−79867
$Co_{1-y}Fe_{2+y}O_4$ ferrite, $-0.1\leq y\leq 0.1$, surface composition, AES 78−14557
$Co_{1-y}Fe_{2+y}O_4$, role of vacant and chemisorbed O and charge transfer effect 78−79868
CoO (100), LEED anal. 80−15352
CoO (100), surface struct., LEED study 80−39396
CoO (111), surface relax., ionic model 80−6608
CoO, surface layer spacing relax., electrostatic argument 79−46901
Co(10$\bar{1}$2), surface struct. of non-unique planes, LEED obs. 79−99402
Cr, (100) surface, clean ($\sqrt{2}\times\sqrt{2}$)R45° struct. 80−2255
Cr, cryst. surface layers treatment and study by HF ion-plasma etching *(Russian)* 80−16517
Cr-Au, matrix sensitive and insensitive factors evaluation using quantitative AES 79−24395
Cr-Ni, blistering after 40 keV He ion bombard. 80−39175
CrO_2, epitaxial growth on rutile, possible appl. as bit oriented mag. material 77−16127
Cr_2O_3/Cr solar-absorber surfaces, chemical and struct. anal. 79−95283
Cr_2O_3/γ-Fe_2O_3/Pt electrode, two layer oxide surface film anal. by modulation spectroscopy *(Japanese)* 80−11491
Cr_2O_3-Cr film, electrodeposited, optical degradation rel. to surface morphology, SEM and AES obs. 79−79401
Cr_3O_4 anode, wear-resistant, use in applied electrochem. 80−40701
Cr_2S_3, single crystal, exam. of unit cell structures by interference contrast microscopy 78−67670
CsI:Na, crystal, kinetics of decay of surface solid soln. 79−23810
CsI(Na) scintillating crystals in cosmic X-ray detectors, growth of deactivated layers 77−10554
$CsSn_2I_5$, surface props., Auger study, elec. cond. meas., photochem. study 80−66339
Cu (001), adsorbed O c(2×2), surface geometry determ. by deep-core-level XPS 80−40224
Cu (001), chemisorbed O, Ar^+ bombardment, angle resolved SIMS, surface struct. 79−77913
Cu (001), surface barrier struct., LEED study 80−65354
Cu (001), surface relax. and thermal expansion calcs. 79−23820
Cu (100), chemisorption and decomp. of formic acid, EELS study 80−16729
Cu (100), N adsorption, LEED, data averaging, objective approach 77−15668
Cu (100), self-diffusion near ambient temp. from surface pot. meas. *(French)* 79−51397
Cu, (100) single crystal surface oxidation 80−11846
Cu, (100) surface, Auger emission ang. depend., overlayer effects 78−39637
Cu (100) surface crystallography, LEED I-V profile anal. 80−75415
Cu (110), LEED anal. 78−71914
Cu, (110) surface, contraction determ. by LEED intensity anal. 79−73385
Cu, (110) surface struct., ion focusing effect *(Russian)* 78−26757
Cu, (111), low-energy positron diffr. 80−70511
Cu (111), vicinal stepped surface obs., LEED vs. RHEED 77−72762
Cu, (111) and (100) surfaces, Sn segregation 78−14554
Cu (111) surface, structural determ. using reliability factor proposed for LEED 78−43224
Cu, (111) surface atomic steps obs. using TEM 77−20173
Cu, (111) surface electron microscopy 80−103556
Cu (111)/Cs, adsorption-induced changes of photoemission spectra and surface electronic struct. 80−55260
Cu (410) surface, edge atom depression, ion scatt. spectroscopy study 80−54492
Cu, adsorbed mol. monolayers, UV-visible spectra 78−72619
Cu, cathode, ns voltage pulse breakdown of emitting sites, field emission microscopy obs. *(German)* 77−63547
Cu, cementation, on Fe, deposit struct., reaction rates, SEM 80−104421
Cu, electrochem. nucleation and growth on Te and Al, TEM 80−104451
Cu electrodeposition potential and electrolyte composition effects on surface morphology *(Russian)* 78−48337
Cu, electron emission depend. on surface mechanical treatment *(Russian)* 80−100945
Cu, electroreflectance, influence of surface microtopography 79−15437
Cu, evaporated film, surface struct. 79−69381
Cu evaporated layer on Ge, RHEED Kikuchi bands, anomalous contrast 78−87597
Cu, film, sputtering mechanism, SEM 80−29839
Cu films on Ru (0001), growth, struct. and electronic props. 79−77958
Cu, friction surface structural investigation, O_2 surface diffusion *(Russian)* 80−96726
Cu, He ion irrad., 1 to 25 keV, range profiles, reemission, blistering 78−38758
Cu, ion bombarded, cone struct. initiation 79−51171
Cu, ion irrad., topographical features relative stability 80−2092
Cu, irradiated with 20 keV He^+, surface damage and gas trapping profile meas. *(French)* 80−84219
Cu, point emitter, surface microrelief under explosive electron emission 78−2973
Cu, pyramidal structure stability on ion bombarded surface 79−51170
Cu, pyramidal structures, development on ion bombarded surfaces 80−84177
Cu, rel. to low energy sputtering, theory 79−28880

surface structure continued
Cu selective surfaces on Al-Cu alloy, chemical brightening and etching 79−62037
Cu single crystal spheres, dissolution, formation of etch pits, surface structure study using SEM 79−23735
Cu, sputtering, surface topography, appl. of thermodynamics of capillarity 80−20749
Cu stepped and disordered surfaces, adsorbed Xe, two-dimens. phase transformations 80−103580
Cu surface, (001), adsorbed c(2×2)CO layer, struct. 80−88428
Cu, surface (100), adsorption of O_2, LEED study 80−100408
Cu, surface contaminant anal. by ion-electron spectroscopy 80−54490
Cu, surface topographical features formed by ion bombard., crystallographic depend. 80−70266
Cu surfaces, O_2 adsorbed, exam. of structure by LEED, O_2 pressure-temp. diagram *(Japanese)* 78−79884
Cu, thin film, oxidation, RMEED/SEM studies 80−100968
Cu, vacuum deposited film, surface struct., HEED meas. 78−6234
Cu vicinal surfaces, LEED study, S, O and Pb adsorption effects 80−103575
Cu whiskers, Bragg case diffr. curves by X-ray triple cryst. diffr. method, surface quality 79−51461
Cu, with Al_2O_3 inclusions, breakdown and emission props., effect of inclusions 79−87389
Cu:Au:C, surface, obs. at very low accel. voltage (200 V-1 kV) by SEM 80−10764
Cu-Ag, surface segregation of S, Auger spectral study diffusion 80−76549
Cu-Al, surface segregation during adsorption and low pressure oxidation *(French)* 78−75932
Cu-Al spherical crysts. grown from drop of melt, topography 80−84353
Cu-Au, corrosion in HNO_3 80−85091
Cu-Au, surface anal. by LEED and AES 77−69153
Cu-Au(Pd), surface structures, LEED obs. 80−10761
Cu-Be, dynamic segregation, ESCA obs. 77−8718
Cu-Be, dynode surface, SEM and Auger microanalysis 80−100384
Cu-Co-Si (0.36, 0.11 wt.%), surface layer struct. on annealing, SIMS and AES exam. 80−88415
Cu-Fe, explosive plasma sputtered coatings, struct. and props. *(Russian)* 80−100783
Cu-Ga, ion bomard. effect on surface comp., reflectometry AES 77−81190
Cu-Ga alloys, effect of ion bombardment on surface composition using differential reflectometry and AES 77−59189
Cu-M alloys (M=Zn,Al,Sn,Mn,Pb), diffusive redistrib. during friction *(Russian)* 78−52999
Cu-Mn (3, 5, 10 at.%) alloys, surface segregation of Mn and oxide film form., AES study *(French)* 79−66065
Cu-Mn-S, Mn surface segregation and Mn/S cosegregation 80−40367
Cu-Ni, clean surface, surface segregation and growth process of altered layer *(Japanese)* 80−24720
Cu-Ni, evaporation limited segregation 80−70513
Cu-Ni, liq., surface conc. profile and surface energy 80−84350
Cu-Ni, oscills. in composition depth profile, UPS meas. 78−71919
Cu-Ni, preferential sputtering Auger electron spectra obs. 79−33880
Cu-Ni, quantitative AES anal. of M_1 VV transition, computer simulation 79−91542
Cu-Ni, sputter-induced subsurface segregation, Auger electrons obs. 80−10757
Cu-Ni, surface composition cluster size distrib., Monte Carlo method calc. 78−63915
Cu-Ni, surface layer, effect of Ar^+ bombardment, AES and SIMS 80−25504
Cu-Ni, surface segregation, comparison of low-energy ion-scatt. results with theory 78−38923
Cu-Ni (50 wt.%), preferential sputtering, thickness and in-depth comp. profile of altered layer, AES 78−39649
Cu-Ni (50 wt.%) alloys, estimation of sublimation energy of Cu atoms, evaporation rate and surface composition, AES meas. *(Japanese)* 80−49352
Cu-Ni alloy, oxidised with NO, surface comp., AES obs. 77−20176
Cu-Ni alloy, sputtered altered layers, in-depth profile, model 78−19613
Cu-Ni alloys, surface comp. calc. by regular soln. theory, surface relax. effects 79−42355
Cu-Ni alloys, surface comp. and catalysis, AES and thermal desorption meas. 79−46898
Cu-Ni alloys, surface segregation and in-depth profile, AES 77−31856
Cu-Ni:polyethylene, surface, obs. at very low accel. voltage (200 V-1 kV) by SEM 80−10764
Cu-Ni-Sn (9, 2 wt.%), surface comp., Auger electron spectroscopy study, manufacture and storage influence 80−65348
Cu-Ni-Zn (18, 27 wt.%), surface comp., Auger electron spectroscopy study, manufacture and storage influence 80−65348
Cu-Ni-Zn alloy, surface comp., outdoor exposure influence 80−59770
Cu-Pd, surface comp. changes under ion bombardment, AES study 80−55250
Cu-Pd, surface struct. from LEED and AES meas. 79−77882
Cu-Pd alloy, (100) and (110) surfaces, LEED patterns 77−85031
Cu-Pt, surface segregation, comparison of low-energy ion-scatt. results with theory 78−38923
Cu-Sn, ε and η phases, surface struct. changes due to sputtering 77−73206
Cu-Sn, Sn surface segregation in monolayer regime, model of kinetics and equilib., AES data explained 79−7739
Cu-Sn alloy, surface comp., outdoor exposure influence 80−59770
Cu-Sn-P (5, 1-5 wt.%), effect of P on friction and wear characts. 80−16494
Cu-Zn alloy, surface layer composition determ. by XPS 79−43682
Cu-Zn alloys, surface comp., outdoor exposure influence 80−59770
Cu-Zn-Al wire, made from pendant drop melt extraction technique from bulk material, X-ray diffr. and thermal anal. 79−43227
$CuAl_2O_4$, pure and NiO promoted catalysts, surface oxidation state and comp., XPS study 80−76134
$CuFe_2O_4$, thermally induced surface chemistry and struct., XPS 78−22939
$CuFeS_2$, superficial degradation in air and water, XPS obs. *(French)* 80−89110
$CuGaSe_2$ thin film, surface morphology study using RHEED 79−65564
$Cu_xMg_{1-x}Al_2O_4$, spinel solid solns., solid-state and surface props. 77−66415
CuNi alloys, electronic theory of surface segregation 79−23819

surface structure continued
CuO selective surfaces on Al-Cu alloy, chemical brightening and etching 79−62037
Cu_2O-Au(Mg)(Mn)(Yb) Schottky barrier solar cells, surface anal. using AES 79−43759
Cu_2O(111) growth modes, on (111)Cu surfaces, UHV-RHEED and TEM study 79−19481
Cu_2S-CdS thin film solar cells, Cu_2S layer separation, struct. 79−95282
Cu(100), adsorption and incorporation of O_2 78−56042
Cu(100), adsorption of CO, LEED study of c(2×2) struct. 79−86983
Cu(100), N chemisorption, bonding, MO theory 77−76659
Cu(311) surface, struct. determ. by multiple scatt. calcs. of LEED intensities 78−56028
EuO (100), surface struct., LEED study 80−39396
$Eu_{0.14}Si_{0.31}O_{0.55}$, insulating amorphous mag., optical, mag., and magneto-optical props. 79−61344
EuTe, high-temperature evaporation and reactivity 80−103469
f.c.c. crystals, layer by layer LEED and 2-dimens. space group symmetry 77−1280
α-Fe, (001), surface relax. and thermal expansion calcs. 79−23820
Fe (001) surface, clean, LEED anal. 77−43411
Fe (100), adsorption of Br_2, AES, LEED, work function, and thermal desorption study 80−15375
Fe (100), adsorption of carbon tetrachloride, AES, LEED, work function, and thermal desorption study 80−15376
Fe (100), adsorption of Cl_2, AES, LEED, work function, and thermal desorption meas. 79−82465
Fe (100), adsorption of I_2, AES, LEED, thermal desorption, and work function study 80−15374
Fe (100), equilib. surface segregation of dissolved C, N and S 77−62723
Fe, (100) surface, S segregation and 2D compounds precipitation *(Japanese)* 80−35188
Fe {110}, atomic struct., LEED anal. 80−88410
α-Fe, BCC, LEED intensity spectra of (100), (110) and (111) surfaces *(German)* 77−31854
Fe, cast, structural changes, due to pulsed action of high temps. and pressures *(Russian)* 80−7554
Fe, cast, wear mechanism of friction couples 79−83329
Fe, casting, fatigue strength, section size and surface struct. effect *(Japanese)* 79−20170
Fe, free surface and grain boundary O_2 and S chemistry 80−75410
Fe, nitrided, X-ray and Mossbauer study of surface 78−48568
Fe, oxidation, FIM obs. 80−89388
Fe, reaction with methane at 750 C micro Auger anal. 80−104020
Fe, segregation and adsorption of S, influence on carburisation and nitrogenation 80−66701
Fe, sintered, austenitic nitriding and bainitic hardening 80−85084
Fe struct. effect on CO hydrogenation 78−73034
Fe surface, adsorbed O_2 effect on chem. reaction kinetics 80−55572
Fe, surface, contamination in vac. depth selective conversion electron Mossbauer spectroscopy 80−2671
Fe, surface segregation of Sn, AES obs. 77−20172
Fe zone refined crystals, cryst. orientation and distrib. of stray grains 80−70509
Fe-Al (1 to 4 wt.%), effect of nitriding on surface structure and props., and on diffusion layer *(Russian)* 79−34197
Fe-CR alloys, ion-etched, surface comp., effect of adsorbed CO, AES obs. 79−46896
Fe-Co, surface comp. and surface segregation 80−34280
Fe-Cr, Auger electron and appearance pot. spectroscopic study of surfaces 80−11520
Fe-Cr, mechanically polished, XPS determ. of comp. of surface and surface oxide 78−7074
Fe-Cr, nondestructive in-depth surface anal. by XPS with different excitation X-ray energies 79−20328
Fe-Cr, surface covered with anodic oxide film, in-depth composition profiles 80−10763
Fe-Cr, surface segregation of impurities (C,N and S) *(French)* 77−56192
Fe-Cr (25wt.%) alloy, surface comp. rel. to passivation phenomena *(French)* 79−43479
Fe-Cr alloy, (100) and (110) surfaces, lateral lattice spacings, simultaneous LEED and AES 77−20174
Fe-Cr-Al, electrical heating material, SEM obs. and surface analysis of oxide films formed at high temps. 77−16738
Fe-Cr-Al(-Y), isothermal oxidation behaviour at 1200°C, SEM 80−50755
Fe-Cr-Al(-Y), thermal cycling influence on oxidation behaviour at 1200°C, SEM 80−50756
Fe-Cr-Mn alloys, Mn content effect on Cr distrib. in suboxide layers *(Russian)* 77−12732
Fe-Cr-Mo, sputtering effect on surface comp., AES obs. 80−6601
Fe-Cr-Ni, foil, in situ oxidation in HVEM 80−104354
Fe-Cr-Ti (18, 0.1-0.9 wt.%), high temp. oxidation *(Japanese)* 80−71806
α-Fe-Fe_3C alloys, ground surface layer exam. of props. 78−84840
Fe-Mn, high-temp. sulphidation, scale struct., corrosion kinetics 80−50777
Fe-Ni, surface comp. obs. by AES 78−10266
α-Fe-Ni (3-12 wt.%), structure and $\gamma \rightarrow \alpha$ polymorphic transform. kinetics 80−71645
Fe-Ni (50 wt.%), surface comp. and oxide film thickness after various surface treatments, AES study 80−66693
Fe-Ni-Mn (20, 5 wt.%), surface martensite, crystallography and morphology 80−40354
Fe-Ni-Sb-S, S/Sb surface site competition in segregation 80−40366
Fe-Si, dislocation wall form. in contact with surface active melt, stacking fault energy *(Russian)* 77−72626
Fe-Si, grain oriented sheet, AC hysteresis, surface struct. and elastic stress effects 80−88791
Fe-Si (1%), LEED-Auger exam. of $(1\bar{1}0)$ surfaces 78−71915
Fe-Si (2-8 wt.%), single crysts., growth striations, X-ray studies 80−79774
Fe-Si-Al, surface oxide layer struct., AES study 80−89396
Fe-Si-B, surface tension, density, and oxidation kinetics 80−20028
Fe-Ti (0.15 wt.%), Ti distrib., segregation, FIM anal. 80−84200
Fe-Zr, dilute solid solution, surface segregation, AES exam. 77−43413
$FeCr_2S_4$, ferrimag. semicond., elementary step growth on surface of vapour grown cryst. 77−76649
$FeCr_2S_4$, pure and doped, CVD grown, surface struct., elec. props. and band struct. 79−4905

surface structure continued
$FeCr_2S_4$, vapour grown, growth mechanism of multisteps on surface 78−75605
$Fe_{72}Ni_8P_{13}C_7$, glass, erosion craters produced by spark machining, scanning microscopy obs. 78−44268
$Fe_{1-x}O$, surface struct., XPS study 80−20759
α-Fe_2O_3, haematite, etch figure shapes on most stable faces *(French)* 77−16707
Fe_2O_3 sputtered films, optical transmission and reflection spectra depend. on substrate temp. 79−91517
α-Fe_2O_3, surface struct., adsorptive interactions rel. to rusting process, IR spectra 79−34363
Fe_2O_3:Mn, surface props. 79−65302
α- FeOOH, goethite, surface OH groups, D_2O isotopic exchange, IR investig. 80−2254
α-FeOOH, surface struct., adsorptive interactions rel. to rusting process, IR spectra 79−34363
$FeO.Fe_2O_3.MgO.P_2O_5$ glass, conversion electron Mossbauer anal. of surfac struct. and chem. state 77−63333
FeS_2, pyrite, single cryst. growth by chem. vapour transport, surface struct. and morphology 79−23550
FeS_2, superficial degradation in air and water, XPS obs. *(French)* 80−89110
FeTi, hydrogen energy storage, surface segregation *(German)* 79−77872
FeTi, surface and mag. props., heat treatment and hydrogenation effects 80−75447
Ga, (3×3) superstructure on W(011) and Mo(011), FIM obs. 79−99425
GaAS (110), wave functions and surface struct. 78−91519
$Ga_{1-x}AlAs$ (110) oxide-free Schottky barriers, surface comp. and charcacts., AES obs. 79−82661
$Ga_{1-x}Al_xAs$ layer, surface conc. x determ. by rapid localised non-destructive optical method *(French)* 77−62725
$Ga_xAl_{1-x}As$, Schottky barrier, effect of oxide composition on elec. behaviour, AES meas. 79−87141
GaAs, (001) vicinal stepped surface obs., LEED vs. RHEED 77−72762
GaAs, (100), comp. and struct. of differently prepared surfaces, LEED and AES 78−91524
GaAs, (100) surface, etch pit density meas. using automatic struct. analyser EPIQUANT *(German)* 77−72619
GaAs (100) surface struct. determ. by LEED, UPS, and EPR 80−49475
GaAs, (100) surfaces, reconstructed, ang. resolved photoemission from surface states, adsorption and annealing effects 80−16143
GaAs, (100) surfaces, struct. and stoichiometry during molecular beam epitaxy, RHEED anal. 79−4921
GaAs (110), atomic struct. of clean and As covered surfaces, LEED study 80−49476
GaAs (110), chemisorption of O and Al, ab initio theory 80−75612
GaAs (110), comparison of LEED intensities for chemically polished and cleaved surfaces 78−18884
GaAs, (110), correl. of short-range order and sputter dose, using vidicon-based LEED system 79−83082
GaAs (110), LEED intensities, dynamical calc. 79−77462
GaAs (110), order-disorder interaction with O_2, LEED anal. 80−75445
GaAs (110), reconstruction and oxidation initial stages, ab initio calc. 80−49473
GaAs (110), self-consistent pseudopotential calcs., electronic struct. and atomic co-ords. 80−49848
GaAs (110), subsurface atomic displacements, evidence from LEED/CMTA analysis 78−38920
GaAs (110), subsurface atomic displacements, LEDD exam. 78−71912
GaAs (110), surface and near-surface atomic struct., LEED 78−91515
GaAs (110), surface electronic struct. calcs. 80−80343
GaAs (110), surface struct., EPR meas. and elastic energy minimisation calcs. 79−51405
GaAs (110), surface struct., LEED and AES study, comparison of MBE and ion bombard. surface prep. 80−54496
GaAs (110) clean surface, internal pot., interplanar spacing, LEED 77−89627
GaAs (110) surface, atomic geometry from elastic LEED intensities 77−20170
GaAs, (110) surface, bond angle and lengths of rearranged As and Ga atoms 78−71918
GaAs (110) surface, O_2 interaction, order-disorder effects, LEED, UPS anal. 80−6634
GaAs, (110) surface structure, rotational relaxation, cluster model *(Chinese)* 80−107621
GaAs ($\bar{1}\bar{1}\bar{1}$), MBE prep., angular resolved UPS of surface states 79−47598
GaAs (111) and ($\bar{1}\bar{1}\bar{1}$) surfaces, XPS study 79−83102
GaAs, chemisorption of Cs, isobars, LEED and loss spectroscopy meas. 77−4262
GaAs, diffusion of Sn effect of ambient As vapour press. on surface stability 80−2208
GaAs, epitaxial layer, surface morphology 79−90852
GaAs epitaxial layers, substrate prep. effect on surface morphology 78−26780
GaAs epitaxial layers, non-doped, from Ga-$AsCl_3$-H_2 system, TEM and RHEED study of micromorphology and defects 79−65340
GaAs epitaxial layers on polycryst. GaAs substrates, LPE growth charcacts. 80−75471
GaAs epitaxial multilayer photocathode structures, TEM obs. of dislocations generated 80−100241
GaAs, epitaxially grown (001), (111) and ($\bar{1}\bar{1}\bar{1}$) surfaces, LEED, AES, photoemission 78−38924
GaAs, GaP, field ion microscopy 78−19644
GaAs, homoepitaxy and epitaxy, surface anal. during growth, using RHEED and Auger spectroscopy 80−66433
GaAs, intrinsic surface gratings, low-angle X-ray diffr. obs. 77−85035
GaAs, ion bombardment, composition changes, AES 78−72662
GaAs, ion implanted, encapsulation surface effects 77−1883
GaAs, ion-implanted, laser pulse annealing of amorphous surface layer, TEM 80−55436
GaAs, laser irradiated, origin of periodic surface struct. 78−91513
GaAs, layer structures revealed by decoration method and electron microscopy 77−27902
GaAs layers, from gas phase, impurity influence on growth micromechanism 80−45237
GaAs, MBE, growth temp. depend. and charcacts. 79−28946
GaAs, MBE (001) layers, work function meas. 80−49870
surface structure continued
GaAs, MBE grown film, in situ surface characterisation by RHEED, SIMS and AES 77−43410
GaAs, multilayer liquid phase epitaxy, transition to faceting 80−96750
GaAs on GaAs and Ge, epitaxy, mechanism, effect of substrate surface struct. 77−51614
GaAs, photo-field cathode, ageing and surface state effects *(Russian)* 77−28703
GaAs, positron annihilation in disturbed surface layers 78−6809
GaAs, struct., elec. props., effects of illumination, O_2 absorpt., electron bombard. *(French)* 78−34690
GaAs, substrate for epitaxial growth, backscatt. anal. of surface prep. and anodic oxidation 77−25175
GaAs, substrate for homoepitaxy, vicinal surfaces characterisation 77−20207
GaAs surface, energy-minimisation approach to atomic geometry 78−95213
GaAs, surface characterisation by high resolution Rutherford backscatt. 80−25511
GaAs, surface chem. changes on annealing, optical and electron microscopy study 79−73383
GaAs, surface cryst. regularity by X-ray photoelectron diffr. 80−89112
GaAs surface impurities, struct. and comp. of compounds using IR spectroscopy 78−63918
GaAs surface morphology during etching with H_2O vapour 80−39094
GaAs, surface structure and orbital symmetries of (110) surface state 78−72229
GaAs, surface studies during MBE growth 79−90899
GaAs surfaces (110) and (111)As, UPS and LEED 78−91514
GaAs, VPE, fast growth at low temp. and high partial pressure 79−51446
n-GaAs, wafer surface contamination study by ASLEEP 79−19256
GaAs:Au, back surface gettering 80−10758
GaAs:Cr, gettering by back surface mech. damage 80−10759
GaAs:Cr, semi-insulating, Cr redistrib. during thermal annealing as function of encapsulant and implant fluence 80−84199
GaAs:Cr semi-insulating wafer, heat treatment technique for no thermal conversion 80−100857
GaAs:Cu, supersaturated solid solns., decomp., surface impurity content 78−51681
p-GaAs:Ge, (111) surface, LPE grown, cryst. struct., phys. and chem. props. by Auger obs. 79−73386
GaAs:Ge(Sn), LPE layer growth, impurity effect on terrace form. 79−95288
GaAs:Se^+, TEM structural study, surface and interior damage 80−34025
GaAs:Si LPE layers, surface morphology, substrate misorientation, initial supercooling effects 80−34329
GaAs:Si(Cr), LPE, spiral growth patterns, dopants role 77−72800
GaAs:Sn, surface segregation of Sn during MBE, SIMS and AES 78−72031
GaAs:Te, implanted and laser annealed, surface crystallinity, refl. and channelling meas. 79−95036
GaAs:Te, ion implanted, surface crystallinity and stoichiometry of laser annealed samples 79−73198
GaAs:Zn, surface conc. control 79−55758
GaAs-AlGaAs LPE layers, baking effect on surface morphology 78−14625
GaAs(-GaP) single cryst., defect distrib. near abraded surface 80−92533
$GaAs_{1-x}Sb_x$, MBE grown, surface struct. exam. by MEED 78−87847
GaAs(110), kinematical LEED calcs. 77−85034
GaAs(110), surface and interface states, effects of atomic and electronic rearrangements 77−85284
GaAs($\bar{1}\bar{1}\bar{1}$)As surface, 3 states, comp., struct., surface states and O_2 sticking coeffs. 77−66080
GaN, epitaxial growth on sapphire substrate, surface feature exam. 79−4919
GaN:Zn epilayers, growth parameters effect on props., device struct. 78−26975
GaP (100), prep. of negative electron affinity surface by Cs adsorption 80−10768
GaP (110), surface struct., EPR meas. and elastic energy minimisation calcs. 79−51405
GaP (110), wave functions and surface struct., EPR expts. 78−91519
GaP, heteroepitaxial deposition on GaAs, Sn solvent inclusion, surface morphology *(German)* 79−28968
GaP single cryst., defect distrib. near abraded surface 80−92533
GaP, surface layers produced by chemical treatment, comp. and struct. 79−96173
GaP_xAs_{1-x}, surface defects and comp. inhomogeneity during gas-phase heteroepitaxy 77−85090
GaSe, photoemission anisotropy, possible surface struct. determ. 78−11076
Gd, AES, by computer *(French)* 80−7890
Gd oxidised surface, comparative sputtered neutral mass spectrometry and SIMS studies 79−90856
Gd-Co amorphous films, resputtering processes 78−64242
GdGa garnet single cryst. substrate surface quality *(Russian)* 77−44371
$Gd_3Ga_5O_{12}$, garnet substrate, surface polishing, damage, abrasion, brittle fracture model *(German)* 77−73357
$Gd_3Ga_5O_{12}$, garnet substrate surfaces, working damage, electron microscope investig. 77−77605
$Gd_2(MoO_4)_3$, surface study using AES and ion scatt. spectroscopy 80−65339
Ge, (001)-(2×1) surface, reconstruction-induced mean-square displacements 80−15343
Ge (100), dimer reconstruction, photoemission obs. 80−80939
Ge (100), surface structure and chemical state 77−15670
Ge (111) Cd adsorption, struct. and surface coverage, RHEED-mol. beam obs. 77−4265
Ge, (111) cleavage face, struct. changes, LEED and Auger spectroscopy study 79−95249
Ge (111) surface, annealed, atomic structure 78−75916
Ge, (111) surface, clean, double diffr. spots in RHEED patterns 79−90855
Ge (111) surface, clean and CO-covered, UPS and ion-neutralisation spectroscopy 80−10785
Ge, amorphous, ideal surface, definition and charcacts. 80−107623
Ge, black, solar selective absorber characterisation 80−80112
Ge, clean surface, geometrical struct. rel. to electronic props. 77−62719

surface structure continued
Ge, contamination by exposure to DC-704 silicone liq., IR refl. spectra anal. 77−59630
Ge, cryst. surface layers treatment and study by HF ion-plasma etching *(Russian)* 80−16517
Ge, electron irrad., defect growth, struct. rel. to temp. 77−11591
Ge, epitaxial growth from monogermane at 685°C 78−51833
Ge film black, solar selective absorber surface 79−29484
Ge, liquid, surface tension exam., sessile drop method *(French)* 77−20162
Ge, order-order type phase transition at surface *(Russian)* 77−39728
Ge, photo-field cathode, ageing and surface state effects *(Russian)* 77−28703
Ge, reconstructed (001)2 x 1, LEED intensity calcs., dimer model variations 79−77875
Ge, reconstruction-induced subsurface strain, theory 78−91516
Ge surface, (111), ion-bombarded and annealed, spectroscopic ellipsometry study 80−103543
Ge, surface structure, LEED and spot photometric meas. 79−23811
Ge, vicinal surface, LEED obs. 78−14561
Ge:Li, supersaturated solid solns., decomp., surface impurity content 78−51681
GeS, (001) surface struct., LEED expt. 78−84034
GeS, film on Ge, evaporation, thermogravimetric, electron microscopy investigs. 77−15715
Ge(100) surface, Ar ion bombarded, determ. of atomic steps, LEED 78−63913
Ge(111) surface, diffuse scatt. at high temp., RHEED study 80−80043
Ge(111), surface electronic struct., atomic geometry effects, photoemission and electron energy loss spectra 77−85283
^{4}He, liquid 78−87837
HgCdTe, crystal and photodiode, imperfections and surface conditions using electron induced current technique 79−67385
$Hg_{0.8}Cd_{0.2}Te$ surface, sputter cleaning and dry oxidation, XPS and LEED study 80−108618
$Hg_{1-x}Cd_xTe$, surface topographic stoichiometry variations, electrolyte electrorefl. obs. 78−27249
Hg_2Cl_2, surface composition, electron impact, mass spectrometry, AES and LEED meas. 79−60607
HgTe surface, sputter cleaning and dry oxidation, XPS and LEED study 80−108618
In film, RF plasma oxidised, surface analysis using ESCA 80−50742
In film, submonolayer superstructures on Si (111) isothermal desorption, RHEED meas. 79−86992
In, impurity precipitation and resolution at melting point 78−14553
In, quantitative surface anal., comparison of XPS results with model 78−40091
In-Au double layer, ultrathin, quantum size effect *(French)* 77−20466
In-Sn liquid alloy, 2-butanol vapour adsorption, effect on surface tension and surface comp. 79−14981
InAs, possibility of local epitaxy in depressions on unmasked substrates 79−42415
$In_{0.53}Ga_{0.47}As$, phase diagram at 650°C and LPE growth of lattice-matched layer 79−96009
InGaAsP, LPE grown, impurity effect on surface morphology 80−29291
InGaAsP-InP layers, grown by LPE techniques, lattice const., bandgap, thickness and surface morphology meas. 80−59818
InGaSb, LPE growth characteristics, substrate surface contamination dependence 80−39470
InP (100) surfaces, chem. treatment effects on comp. and nature 79−47794
InP (110) surfaces, cleaved and polished-sputtered-annealed, LEED and AES study 80−103550
n-InP, epitaxial layer, (100) surface chemistry, ESCA study 80−103552
InP film, electron-beam annealed, surface conduction 80−84500
n-InP, heat treatment in controlled P vapour 80−88137
InP, LPE grown, impurity effect on surface morphology 80−29291
InP, LPE grown, surface morphology 77−62771
InP, surface damage induced during SiO_2 deposition by RF sputtering 79−78879
InP surface decomposition prevention in LPE growth 80−96749
n-InP wafer, defect studies by ASLEEP, SEM and scanning AES 79−19256
InP:S^+(Se^+), ion-implanted VPE layers, laser annealing, elec. and struct. anal. 79−73199
InSb (110), clean, O_2 adsorption, AES, LEED, RHEED and field effect meas. 80−49501
InSb (110), ion bombard. effect on surface struct. and electronic props. 80−6923
InSb (110), surface struct. by elastic LEED, comparison with GaAs(110) and ZnTe(110) 80−80040
InSb (110) surface, LEED intensity dynamical anal. 80−88412
InSb (110) surface, struct. and electronic props., RHEED and field effect meas. 80−11068
InSb (110) surface struct. determ. by LEED, UPS, and EPR 80−49475
InSb, (111) surface, anal. by low energy ion scattering spectroscopy, LEED and AES *(Japanese)* 80−20746
InSb, Cu-coated, surface contamination, ion microprobe mass analyser obs. 77−52729
InSb, ion implanted, efficient void form., TEM obs. 80−44237
InSb, LPE growth characteristics, substrate surface contamination dependence 80−39470
InSb, single crystal, chem. and ion etching, surface changes *(French)* 80−108614
InSb, surface analysis, X-ray photoelectron spectra, surface oxidation-etchant correlation 78−56029
InSb(111) surface, oxidation props., LEED and surface cond. meas. 78−15559
InSe, photoemission anisotropy, possible surface struct. determ. 78−11076
$In_{2-x}Sn_xO_{3-y}$-ZnS:Mn thin film structure, surface morphology and electro-optical props. *(Russian)* 80−49554
Ir (100), adsorption of Xe, local surface struct., UPS study 80−39429
Ir (100), superstructure from LEED meas. 79−73259
Ir (100) surface, reconstruction, superstruct., model 80−103551
Ir (100)-1×1 surface struct. and reconstruction kinetics, LEED, UPS and work function meas. 79−90851
Ir (110), O adsorbed, surface struct. anal. using hybridisation model 80−44423
Ir (110), unreconstructed and constructed surface, LEED obs. 79−77880

surface structure continued
Ir (110) 1×2 reconstructed surface, struct. study by LEED, reliability factor anal. 80−39399
Ir (110)-(1×2) reconstructed surface, LEED expts., test of struct. models 79−56050
Ir (111), ($\sqrt{3}\times\sqrt{3}$)30° S overlayer struct., LEED obs. 80−15365
Ir (111), oxidation, combined LEED/UPS obs. 78−19955
Ir (111) surface, structural anal. of (2×2) O overlayer, LEED study 80−2264
Ir, adsorption of H_2, influence of surface steps and clusters, field emission investig. 77−28698
Ir, chemisorption, clean normal and reconstructed (100) surfaces, multiplets role 77−15694
Ir surface, (110), unreconstructed, determ. of atomic arrangement by LEED 79−14990
Ir, surfaces (111), (100)-(5×1) and metastable (100)-(1×1) struct. depend. 4f-core-level binding energies for surface atoms 80−44406
Ir, with adsorbed Xe, 5p photoemission, local surface struct. influence 80−2920
Ir(110), adsorption of O, structure of c(2×2)O overlayer 79−19463
Ir(111), LEED 77−85040
K, on Fe(100), adsorbate coverage determ. by LEED, AES and XPS 80−103566
KBr in contact with KCl, mutual diffusion, development of relief on contact surfaces 78−22964
KBr, single cryst., lattice structure distortion on freshly formed surface, electrification 77−51582
KCl crystal, surface elementary steps interaction with Au particles 80−39400
KCl, monatomic surface step effect on Au nuclei 77−15719
KCl, sublimation on (100) surfaces in elec. field 79−77739
KCl, sublimation struct., back force effect 77−15571
KCl surface, sublimation kinetics, elec. field influence, terrace-ledge-kink model 80−84287
KCl:Sr, single crystal, thermally stimulated topochemical reactions 79−28011
KH_2PO_3, mechanically treated single crystal, depth and struct. of disturbed layer *(Russian)* 78−23839
KH_2PO_4, prism faces microtopographical study 79−42346
KH_2PO_4, real structure influence on optical strength 79−7187
K_2SO_3-Ag_2SO_4 mixtures, surface comp., AES and XPS obs. 80−81386
Kr, mono- and bilayers on graphite, two-dimens. struct., neutron diffr. study 79−42393
Kr, monolayer on graphite, commensurate-incommensurate transition, X-ray scatt. 79−73382
LaB_6 (001) surface, struct., initial oxidation, XPS, UPS, LEED, AES, work function meas. 79−99403
LaB_6, (001) surface struct., XPS, LEED meas. 78−63909
LaB_6 (100), (110), and (111), surface structs. and work functions 80−70512
LaB_6 (210) surface, work function, struct. and chemisorpt. stability, XPS, UPS and LEED 80−65344
LaB_6 and $La_{0.58}Sm_{0.42}B_6$, FIM study 80−71578
LaB_6, clean and oxidised (100) surface, LEED, AES, work function, evaporation meas. 78−71989
LaB_6, field emission and FIM expts. 77−90255
LaB_6 single crystal cathode, thermionic emission, surface struct. 80−97395
LaB_6, surface (100), atomic struct., angle-resolved XPS, LEED and ISS investigation 80−10765
LaB_6 surface stoichiometry, thermionic emission B conc. effects 79−87556
LaB_6, thermionic emission rel. to surface state 78−39654
LaB_6:C, AES, LEED and energy-loss spectra study of C layer on (100) surface 77−62715
LaB_x x=4.24 to 29.2, thermoelectric electron emission, work function, 1400-2100K 78−60539
$LaNi_5$ surface segregation, influence of O_2, H_2, H_2O, SO_2 *(German)* 80−51008
Li electrode, in lithium perchlorate-propylene carbonate solution, surface anal. *(French)* 80−50859
LiF (001), He elastic scatt., hard corrugated surface model, GR Method 77−85863
LiF, (100) face, surface layer and dislocation etch pits 77−19962
LiF, single crystal, neutron and gamma irradiation, SEM and Bragg profile anal. 80−15158
LiH, crystalline, surface struct., quantum mechanical ab initio calc. 77−1281
α-$LiIO_3$, surface defect layer struct. due to mechanical working *(Russian)* 80−100238
Li_3N:H, ionic cond., nuclear reaction anal. 80−34454
$LiTaO_3$ monocrystal lapping and precision machining characteristics *(Japanese)* 79−80593
Lu, crystal surface study from refl. electron energy loss spectra obs. 80−20742
Mg rough deposits, surface struct. autocorrelation function, electron microphotographs 78−26756
Mg, surface structure autocorrelation functions and Fourier transforms for rough deposits 79−69450
Mg-Mg_2Ni eutectic alloy and Mg_2Ni, catalytic effect in hydrogenation, surface analysis 80−30283
MgO (001), LEED Kikuchi pattern, surface state reson. 78−83689
MgO (001) cleavage face, LEED Kikuchi pattern, surface reconstruction 78−84038
MgO (100), chain method of LEED/MEED intensity anal. 80−20018
MgO (100), surface struct., LEED study 80−39396
MgO (100) surface differential ionic relax., shell model 78−63917
MgO, atomic C anal. by $^{12}C(d,p)^{13}C$ method 80−108766
MgO, cryst. surface strain and polarisation fields, breathing shell model calcs. 78−22946
MgO, dissolution, surface roughening effects and mechanism distinction 79−47975
MgO, etching in acids, surface micromorphology 77−15419
MgO, intrinsic defects at (001) and (011) surfaces 77−47443
MgO, reconstruction of the (001) surface 78−75922
MgO, segregation of aliovalent solutes adjacent {100} surfaces 79−78979
MgO single crystals, surface atomic steps obs. by electron microscopy, dark- and bright-field techniques 80−84040
MgO surface, characteristics of electron-beam-cleaved surfaces by in situ Au decoration 77−51579

surface structure continued
MgO surface, electron beam cleaved, characterisation by Au decoration 77−47657
MgO, surface layer spacing relax., electrostatic argument 79−46901
MgO-ZnO, solid soln., surface comp., Auger and XPS investig. 78−51806
Mg_2SiO_4 crystals, morphology and dislocation etch pits, (010) surface 80−24457
Mn-substituted garnet film, growth characts. and mag. props. 80−39826
Mn-Zn ferrite, single crystal, surface damaged layer study *(Japanese)* 77−86260
Mn-Zn ferrite single crystals, mech. polishing effect on mag. props. *(Japanese)* 80−16569
$MnAu_4$, domain struct. exam. by powder method *(German)* 78−91883
MnO (100), surface struct., LEED study 80−39396
MnZn ferrites, form. of comp. heterogeneity during high-temp. sintering 80−60818
Mo (001), surface struct. determ. using LEED 79−42351
Mo (001) surface, electronic susceptibility and surface phase transition 79−33169
Mo, (001) surface, electronic origin of reconstruction 80−11065
Mo (001) surface struct., LEED anal. 80−34282
Mo (100), chemisorption of H, phase changes, LEED obs. 79−77911
Mo (100) surface, phase transition exam. of LEED 77−55433
Mo (112) surface adsorption of Li film, LEED and contact pot. method 80−10794
Mo, blister erosion reduction by multi-groove surface microstruct. 78−95211
Mo cathode, H_2 glow discharge, FCC surface layer form., electron diffr. obs. 77−55311
Mo cathode, ns voltage pulse breakdown of emitting sites, field emission microscopy obs. *(German)* 77−63547
Mo, energetic deuteron irradiated surface struct. quantitative meas. 78−95210
Mo foil electrolytic perforation, surface film phase composition obs. *(Russian)* 80−61004
Mo, glow-discharge surface treatment, struct. defect prod. 77−63832
Mo, He ion irradiated, TEM 77−19994
Mo, point emitter, surface microrelief under explosive electron emission 78−2973
Mo, polycrystn., 2 keV Ne^+ ion bombard., dose and microstruct. effects on surface topography and sputtering yield 79−65124
Mo, sintered, thermally induced surface composition variations 79−5078
Mo surface, adsorbed Ga and Sn, struct., FIM obs. 80−103576
Mo, surface impurities, depend. on prep. method, ion scatt. spectroscopy 80−40200
Mo, surface machined, struct., electron diffr., TEM *(German)* 77−73371
Mo, surface relaxation and electronic structure of (100) surface 79−73561
Mo, surface sensitive structure in angular resolved photoemission *(French)* 77−40326
Mo, surface structure changes due to ionic bombardment, LEED and AES obs. *(Russian)* 77−1775
Mo Tokamak limiter, surface observation, infrared techniques 80−38693
Mo:C (110) surface, segregation, precip. and desorpt. of C, AES and LEED study *(French)* 80−103480
Mo-base alloy, TZM, blistering under He ion bombard. 80−92567
Mo-Fe metalloceramic alloy, brittle fracture investigation, segregation, morphology, struct. *(Russian)* 80−55503
Mo-Mn metalloceramic alloy, brittle fracture investigation, segregation, morphology, struct. *(Russian)* 80−55503
Mo-Re-C (0.3, 0.2 at.%) time-of-flight atom-probe expts. 80−55741
Mo-TiC(ZrC)(HfC), thermionic emission, surface structural characts. after prolonged use, work function variation 80−20758
Mo-W, calibration line introduction for comp. determ. by AES 79−56892
MoO_3, ESCA of surface composition changes under ion bombardment 77−20974
MoS_2 (2H), surface struct. determ. by dynamical LEED 77−43415
MoS_2 (2H), surface struct. and interplanar separation by LEED 77−59191
MoS_2, clean surface, AES and LEED exam. 80−10762
Mo(001), clean and H chemisorbed, atomic displacements, LEED obs. 80−70514
Mo(001) surface, atomic displacements and electronic struct. 78−30963
n-Si, ion implantation causing surface defects, electroreflectance 79−19274
N_2 adsorbed layers, on W (210), surface struct., LEED obs. 79−82449
N_2 overlayer on graphite, orientational ordering, neutron scatt. meas. 80−10783
NH_3, epitaxial film, on metal (111) substrates, surface struct., LEED obs. 79−86969
NH_3, film, on metal substrate, surface struct. using LEED 79−77879
$NH_4H_2PO_4$, {100} faces cryst. growth kinetics, low supersaturations range, dislocations 79−56047
$NH_4H_2PO_4$, surface effects on strength of whiskers and microcrysts. *(Russian)* 78−51864
NH_4HSO_4, ferroelectric powder dielectric behaviour particle size depend. 80−55046
NO, first monolayer on MgBr cleavage face, triple point 78−6227
Na (110), Na_2O (111) surface comp., LEED obs. 77−72761
Na c(2×2) overlayer on Ni (001), surface struct. effects via photoexcited core electron diffr. 79−74063
Na halides, surface rumpling at finite temps, Verwey model 79−51402
NaA-zeolites, XPS, analytical and struct. information 77−90239
NaCl, (100), (110) and (111) surfaces annealed in vac. 400-800°C, evap. struct. 77−15572
NaCl (100) surface perturbations during LEED investig. *(French)* 77−28069
NaCl, bent single crystal, equilib. face, surface relief form. during annealing 78−47651
NaCl, cleavage faces, evaporation pattern determ. by decoration method in electron microscopy *(German)* 80−107626
NaCl, cleavage of single crystals, investigation of fast electrical processes 79−24045
NaCl cleavage step decoration, nucleation and growth of metallic thin films 77−69200
NaCl cleaved surface structure, electron microscope 79−7735
NaCl crystal, annealed near thermodynamic equilib. of cryst. and vapour, {110} surface struct. and coarsening 77−28067
surface structure continued
NaCl crystal surface struct., effect of ionic bombardment *(German)* 80−24507
NaCl, energy spectra of sputtered Na atoms from 20 keV rare gas ion bombard. 79−52068
NaCl, etched cleavages, moisture effect on spiral and terraces steps 77−4251
NaCl, evaporating cryst. surfaces, successive monatomic step trains with different density 80−29254
NaCl, evaporating surface, step motion obs. and simulation 78−26766
NaCl, filamentary crystal, vacancy-enriched surface layers 78−51536
NaCl, intrinsic defects at (001) and (011) surfaces 77−47443
NaCl, liq. surface, Fowler model, electroneutrality correction 79−28174
NaCl, rocksalt (h10) faces, terrace like step trains, evaporation, TEM obs. 77−35801
NaCl, single cryst., lattice structure distortion on freshly formed surface, electrification 77−51582
NaCl, single crystal, surface markings, left by unsteady cleavage crack propag. 79−46746
NaCl stepped and disordered surfaces, adsorbed Xe, two-dimens. phase transformations 80−103580
NaCl, sublimation struct., back force effect 77−15571
NaCl substrate, role of surface steps in nucleation of VPE Au 78−79902
NaCl surface conditions of step decoration 80−15349
NaCl type structure, chain method of LEED/MEED intensity anal. 80−20018
NaCl, with dispersed Au particles, age hardening of surface, double decoration obs. 79−11634
$NaF:Ca^{2+}(K^+)(Li^+)$, substitutional impurities, defect props. of (001) and (011) surfaces 77−47443
Na_2O-CaO-SiO_2 glasses, fluorinating agents effect on comp. and surface struct. 80−35364
Na_2O-Al_2O_3-SiO_2 glass, leaching in HCl solns., Na conc. distrib. in surface layers 80−21141
Na_2O-Al_2O_3-SiO_2 glass, interaction with aq. salt solns., alkali ions distrib. in surface layers 80−21142
Na_2O-CaO-SiO_2 glass, Na surface conc. determ., by $^{23}Na(p,\alpha)^{20}Ne$ reaction 77−20171
Na_2O-CaO-SiO_2 glass, surface viscous flattening kinetics, sinusoidal profile decay method 79−79139
Na_2O-K_2O-Al_2O_3-SiO_2, structure of modified surface layer, internal friction method 80−103258
Na_2O-NaF-CaO_xZnO_{1-x}-Al_2O_3-SiO_2, opal glasses, strength, surface composition 80−30066
Na_2O-SiO_2 glass, internal and surface struct. by X-ray scatt. 80−84074
Na_2O-SiO_2 glass surface anal., effect of electron bombardment during AES on composition 79−83065
Na_2O-ZrO_2-SiO_2 glass, treated with 2 N solns. of $NaCO_3$ and NaOH, surface layer comp. 80−35366
Na_xWO_3 bronzes ($0.4<x<1$), domain, surface and substrate structs. 80−34281
Na_xWO_3, domain struct., optical microscope obs. 79−19436
Na_xWO_3, x=0.6 and 0.8, surface characts. 80−39392
Nb (110) and (750), interaction with O_2, LEED, AES, SIMS, and EELS obs. 80−44408
Nb electrode, surface changes induced by strong cathodic polarisation 79−100388
Nb film sputtered onto Cu substrate, microstruct. and supercond. props. 77−85370
Nb, surface damage caused by He^+ ion bombard. 80−39177
Nb, surface topography formation due to elec. transfer processes *(Russian)* 80−54482
Nb-Mo(Ti)(Zr), nitriding, diffusive saturation, lattice spacing and activation coeffs. *(Russian)* 80−21168
Nb-Zr (1.5 wt.%) alloy, field ion microscopy investigation, surface struct. 80−45220
$Nb_3Al_{0.2}Si_{0.8}$, A-15 alloy synthesis by ion implantation 78−80489
NbO, single cryst. growth by chem. transport reactions 77−12508
Nb_2O_5, and Nb oxidized foil, Nb enrichment on surface due to electron irradiation induced dissociation 79−28015
Nb_2O_5-ZrO_2 sputtered thin layer structure and optical props. 79−28851
$NbSe_2$ (2H), surface struct. determ. by dynamical LEED 77−43415
$NbSe_2$ (2H), surface struct. and interplanar separation by LEED 77−59191
Nb_3Sn, flux density gradient determ. by Faraday effect 80−107969
Ni (001), adsorbed CO c(2×2), surface geometry determ. by deep-core-level XPS 80−40224
Ni (001), adsorption of N_2, c(2×2) struct. form 80−80083
Ni (001), azimuthal anisotropies of ejected dimer ions, SIMS expt., struct. effects 80−60730
Ni (001), structural parameters and interplanar spacing by LEED averaging 77−11771
Ni (001), surface barrier struct., LEED anal. 80−20023
Ni (001) surface, adsorbed N_2, p(2×2) struct., LEED and AES study 80−54515
Ni (001) surface, chemisorbed O_2, electronic struct. and overlayer struct. theory 79−28391
Ni (001)/CO(O) system, adsorbate geometries determ. from final state scattering in X-ray photoemission 80−54488
Ni (100), adsorbed chalcogen, structure, force consts., binding energies and photoemission, importance of final state multiplet splitting 78−71966
Ni (100), adsorption of C, substrate reconstruction, LEED constant momentum transfer averaging study 80−39445
Ni (100), adsorption of water $(O_2)(H_2)(CO)$, combined XPS/LEED/SIMS exam. 79−83075
Ni (100), clean surface and with chemisorbed O, rapid LEED intensity meas. 80−44420
Ni (100), O and S chemisorption, surface vibrs., electron energy loss spectra 79−33173
Ni (100) and (110) surface at open circuit in H_3PO_4, changes in surface struct. after anodic etching 79−61777
Ni (100) face, O-Ni system vibrs. rel. to struct. during oxidation 77−66089
Ni (100) surface, coadsorption of Sn on Pb, P or O contaminated surface, AES study 80−88437
Ni (100) surface, oxidation study using low energy ion scatt. technique 79−49338
Ni (100)-c(2×2)-O system, adsorbed monolayer, RHEED study 79−77912

surface structure continued
Ni (100)-c(2×2)CO, LEED meas. 80−6647
Ni (110), adsorbed H, adatom configuration, He diffr. study 80−103569
Ni (110), adsorption of H, substrate reconstruction, LEED constant momentum transfer averaging study 80−39445
Ni (110), anisotropy of surface self diffusion 77−43367
Ni (110), clean and H saturated, structural investig. by He diffraction 79−86984
Ni (110), clean and S covered, atomic struct., medium energy ion scatt. 79−61483
Ni (110), S and O adsorbed, surface struct. anal. using hybridisation model 80−44423
Ni (110), struct. anal. during O_2 adsorption, low energy ion scatt. meas. 79−82424
Ni (110), surface damage induced by bombard. with 3-30 keV noble gas ions 80−60728
Ni (110), surface relax., LEED results anal. by convolution-transform method 77−89624
Ni (110), surface relax., O_2 coverage effects, medium energy ion scatt. obs. 79−28181
Ni, (110), surface relaxation and composition, medium energy ion scatt. spectra 78−63916
Ni, (110) and (111) surfaces, oxidation exam. at room temp. by combined SIMS-AES/LEED method 79−20241
Ni, (110) surface, S adsorbed layer struct. from anal. of LEED pattern 79−73407
Ni (111), adsorption of acetylene and ethylene, surface structs., LEED and AES obs. 79−60636
Ni (111), Mossbauer effect emission spectroscopy and AES 79−91329
Ni (111) surface, C interaction, monolayer form. and struct. stability 80−10756
Ni, (111) surface, S free and covered, D_2 desorption, ang. depend. of flux, mean energy and speed ratio 79−86993
Ni, (111) surface, scatt. of mol. and atomic H ions 79−69943
Ni {100}, adsorption of O, low energy ion scatt. study 80−39420
Ni {100} and Ni {100} with O overlayer, crystallographic effects in low energy ion scatt., local ion-atom neutralisation 80−84377
Ni, adsorbed S and Se, photoelectron diffr. data 80−29851
Ni alloy, ZhS6K, diffusion layer form. on Nb addition, struct., comp. *(Russian)* 78−56814
Ni alloy powder, crystallised by supercooling methods, struct. props. *(Russian)* 80−54483
Ni alloys, dilute, near surface composition, effect of irradiation and sputtering 79−33168
Ni alloys, heat resistant EI437B and EI929, surface condition, air stream effect 80−76409
Ni, blistering model, correlation between blister diameter and skin thickness 78−95067
Ni, cavitation-erosive wear in surface-active media, dislocation struct. and fracture study by FMR *(Russian)* 79−52384
Ni epitaxial monocrystal structure rel. to externally applied stress 77−76708
Ni foil electrolytic perforation, surface film phase composition obs. *(Russian)* 80−61004
Ni foils, 20 keV $^4He^+$ irrad., depth distrib. of bubbles 79−69166
Ni, lattice images, obs. with a field emission electron microscope 79−14659
Ni, Medicus matrix cathode, surface characts. 80−66378
Ni passivation, S influence study by Auger and electron spectroscopy 80−65347
Ni plated Fe single crystal, deformed at 77K, surface obs. 78−19916
Ni, segregation of C to (100) surface, isosteres 77−1282
Ni sheet, adsorbed ^3H, ethylene-^{14}C determ., autoradiography method 77−63989
Ni single crystal, surface hyperchannelling, scatt. of low energy Ar ions, computer simulation 80−34110
Ni stepped surface, morphology exam. by LEED and ARS 78−71913
Ni surface, (001), adsorbed c(2×2)CO layer, struct. 80−88428
Ni surface, oxidation, structural changes, low energy ion scatt. study 80−35423
Ni surface damage due to two component He^+ and D^+ ion beam 79−49880
Ni, surface self-diffusion in presence of adsorbed halogens *(French)* 80−24723
Ni target, surface layer anal. medium energy ion backscatt. expts., solid state detector 79−4456
Ni, with Te overlayer, surface sensitivity of MeV He ion scatt. 79−56904
Ni/Cr multilayers, AES depth profiling by sputtering with N_2^+ ions 79−95881
Ni-Al, (2 and 6 wt.%), oxidation, α-Al_2O_3 growth, microstruct., precip. 80−108626
Ni-Au, dil., orientation depend. of surface segregation, AES and SEM obs. 78−71908
Ni-Au alloys, surface segreg., surface energy and solute strain energy effects 77−72760
Ni-Co, ferromagnetic resonance, surface anisotropy 78−95526
Ni-Co-W, electrodeposition, surface morphology and cryst. struct. 80−71602
Ni-Cr-Al, oxidation, NaCl vapour effects on microstruct. 78−44274
Ni-Cr-Ti rapidly solidified superalloys, surface segregation 80−76263
Ni-Cu, sputtering rate, radiation-induced segregation and preferential sputtering effects, kinetic model 80−40199
Ni-Cu, surface composition, AES 78−14558
Ni-Cu, surface segregation using atom-probe FIM 79−77883
Ni-Cu, surface segregation, computerised atom-probe FIM study 80−75412
Ni-Cu alloy, surface comp. and catalysis 80−54489
Ni-Cu(5%), absolute composition depth profile, surface segregation, field-ion microscope obs. 79−33166
Ni-Fe-Pd thin films, mag., surface and corrosion props. 80−34707
Ni-Mo, sputtering rate, radiation-induced segregation and preferential sputtering effects, kinetic model 80−40199
Ni-P amorphous alloy prep. by ion implantation 78−22748
Ni-Pd (1 at.%), surface comp. and surface segregation, AES obs. 79−51404
Ni-Pd surfaces, electrochem. passive film form. and comp. determ. by SEM, SIMS, XPS 80−39401
Ni-Th (1 at.%), surface comp., temp. and O_2 exposure effects, AES study 80−80914

surface structure continued
Ni-Ti (1.6, 7.64 wt.%), monophase high temp. scaling, metallography study 80−21159
Ni-V, dil., oxidation behaviour at 1200°C 77−77636
β-NiAl, oxidation, α-Al_2O_3 growth and microstruct. 80−108627
$Ni(CO)_4$, form. on single Ni cryst., reaction kinetics and induced surface facetting 80−71948
$NiFe_2O_4$, thermally induced surface chemistry and struct., XPS 78−22939
βNiH, decomposing, α-phase precipitate detection by Bitter powder pattern 79−28104
NiO (001) surface, chemisorption of H, surface and second-layer defect effects 80−65369
NiO (100), surface struct., LEED study 80−39396
NiO (100) surface, dynamical LEED calc. 77−62721
NiO (100) surface, LEED expt. and calc. down to 60 eV 80−92767
NiO (100) surface, sulphurisation by H_2S, AES, LEED, RHEED structural study *(French)* 78−64888
NiO, surface layer spacing relax., electrostatic argument 79−46901
NiO/SiO_2, catalyst, XPS for surface struct. and composition 79−43093
$NiO-Al_2O_3/SiO_2$ catalyst, XPS for surface struct. and composition 79−43093
NiO-MgO solid solns., surface comp. study by XPS 80−104035
$Ni_{0.96}Sb_{0.04}$, surface segregation, XPS and AES obs. 80−76135
$NiSi_2$ epitaxial film on (111) Si substrate, interfacial order, backscatter, channelling study 80−65390
Ni(001) surface N adsorption due to ion beam irrad., surface struct. LEED study *(Chinese)* 80−84364
Ni(100), adsorption of CO, LEED study of c(2×2) struct. 79−86983
Ni(100) oxidised surface structure anal., extented appearance potential fine struct. study. 80−75411
Ni{001}c(2×2)-CO struct., LEED study 79−86982
O, on Fe(100), adsorbate coverage determ. by LEED, AES and XPS 80−103566
PLZT, refr. index, 405-764 nm, surface layer 78−35110
Pb, deposition on Au, quantitative Auger electron spectroscopy, substrate and instrumental effects 80−71523
Pb electrode, in situ surface phase study by laser Raman spectroscopy 80−103542
Pb, film, sputtering mechanism, SEM 80−29839
Pb film, vacuum deposited, reflectance spectra, structural rearrangement effects 77−24905
Pb, quantitative surface anal., comparison of XPS results with model 78−40091
Pb thin films, thermal strain, multiple cycling to 4.2K effects 79−90918
$PbCO_3$, cryst. growth, Liesegang ring form., pH effect 80−49140
PbInAu film, RF plasma oxidised, surface analysis using ESCA 80−50742
$PbMoO_4$, hollock growht origin in gel growth 80−49139
PbS, clean surface, AES and LEED exam. 80−10762
PbS, superficial degradation in air and water, XPS obs. *(French)* 80−89110
PbS, surface defect annealing *(Russian)* 77−47658
PbSe films, current carrier conc. and type control, elec. cond., synthesis process *(Russian)* 80−100412
$Pb_{1-x}Sn_xSe$ epitaxial layers obtained by LPE, growth conditions correl. with morphology 80−104079
$Pb_{1-x}Sn_xTe$ layers, LPE growth on metal-etched substates 80−55313
PbTe (111) epitaxial films, localised electron irrad. effects on elec. props. and O_2 sorption 80−49472
PbTe(Se) vacuum deposited thin films, struct. and growth 79−19482
Pd (100), adsorption struct. of CO, LEED and high-resolution EELS study 80−20037
Pd (110) surface, adsorption of S, characterised by LEED *(French)* 80−88422
Pd, (111) surface electron microscopy 80−103556
Pd coated Si wafers, interference effects on irrad. with laser beam 80−66333
Pd crystallite morphology, surface struct., electron microscopy obs. 80−29257
Pd, film, on ZnO, struct., elec. props., AES, UPS study 78−76168
Pd-Ag, ion bombarded, surface segregation, XPES obs. 79−77885
Pd-Ag, surface segregation, Auger studies 78−87849
Pd-Ag (Cu) alloys, epitaxial growth and surface characterisation 78−14638
Pd-Ba (1.5 wt.%), thermionic emitter, Auger spectrum fine struct. 78−2954
Pd-C, dil., C segregation to single cryst. surfaces 80−39301
Pd-Ni, Auger sensitivity factors 78−43964
Pd-Ni alloys, surface comp. and catalysis, AES and thermal desorption meas. 79−46898
Pd-Pt, with adsorbed Xe, 5p photoemission, local surface struct. influence 80−2920
$Pd_{781}Cu_{55}Si_{164}$ glass, erosion craters produced by spark machining, scanning microscopy obs. 78−44268
Pd_2Si, on Si substrate, thermally induced Si accumulation, AES study 80−24718
Pd(001), adsorpt. of CO, LEED, electron energy loss spectra study, surface struct. effect on weak chemisorpt. bonding 78−71987
Pt (100), adsorbed Cs layer, surface struct., LEED anal. 77−89654
Pt (100), chemisorption of O_2 and H_2, comparison of (1×1) and (5×20) configs. 77−51599
Pt (100), superstructure from LEED meas. 79−73259
Pt (100) (5×20) and (1×1) surfaces, stability and reactivity, adsorption of H 80−75434
Pt (100) surface, LEED intensity spectra, double diffr. model 77−31858
Pt (100) surface, reconstruction, superstruct., model 80−103551
Pt (110), surface structs. during S adsorption, LEED pattern interpretation model 77−69184
Pt (110) reconstructed surface, LEED-AES study, O_2 treatment effect 80−39398
Pt (111), at. steps role in H interaction 77−15690
Pt (111), relax. effects, and thermal vibrs., medium energy ion scatt. 79−28182
Pt (111) and (100), surface struct. anal. by MeV ion backscatt. and channelling 78−71916
Pt (111) and (100) superlattices formed by dissociative adsorption of HI, LEED, AES, and thermal desorption studies 80−55715
Pt (111) surface, 400 eV H^+ ion scatt. obs. of surface relax. 78−43972
Pt (111) surface, relax., dynamical LEED calcs. 77−59196

surface structure continued
Pt (111) surface, surface struct. and bonding of (2×2) acetylene overlayers, LEED analysis 77−85067
Pt (997), terrace bending obs. from He beam scatt. 80−40202
Pt (997) surface, partial facetting, He beam scatt. and LEED study 80−103547
Pt, adsorption and decomp. of ethylene, 90 to 500K 79−46933
Pt, adsorption of CO, O_2, NH_3, surface composition, AES and temp. programmed desorption meas. 80−34313
Pt, adsorption of H, electrode surface exam. by LEED and AES 77−47665
Pt, adsorption of O_2, surface struct. depend., LEED, AES, and electron energy loss spectra 79−46934
Pt, adsorption of O_2 on (110) surface, Ar^+ bombardment effects on reactivity 80−89099
Pt catalyst surface morphology, faceting induced by NH_3 and propane oxidation 77−52669
Pt crucibles, surface changes rel. to Fe anal. 80−61192
Pt crystallite morphology, surface struct., electron microscopy obs. 80−29257
Pt, effects on rates of O_2 adsorpt. and CO oxidation 78−43251
Pt electrode, compact layer struct., absorpt. EHT calcs. 77−16828
Pt, secondary electron spectroscopy 77−85854
Pt, stability and struct. of high Miller index forces in vacuum and with adsorbed C and O 77−76651
Pt, stepped surface, edge atom dipole moments 78−14791
Pt surface, atomic interplanar spacing determ. from insulation of channelling expts. 77−80563
Pt surface, chemisorbed CO, IR refl.-absorpt. spectra, absorbate island struct. 80−84385
Pt, surface dipole moment calc. 80−60060
Pt, surface struct. and electronic props., CO_2, O_2, H_2 chemisorption 77−1300
Pt-Au, surface segregation using atom-probe FIM 79−77883
Pt-Au, surface segregation, comp. depth profiles meas. using atom-probe field ion microscope 80−100380
Pt-Ba alloy, elemental comp. and chem. state of surface during thermal activation, AES obs. 78−2345
Pt-C, dil., C segregation to single cryst. surfaces 80−39301
Pt-Cr(Fe)(Ni) dilute alloys, surface segreation, equilib. surface composition, AES meas. 77−85039
Pt-Cu, surface composition, XPS *(Portuguese)* 80−24722
Pt-Cu, surface segregation, ion scatt. spectroscopy meas. 79−82423
Pt-Ir alloys, surface composition 79−19433
Pt-Ir solid solutions, investigation of field-ion micropattern contrast, selective evaporation and ionisation models 79−69962
Pt-Pd alloy, surface composition determ. by AES 78−79869
Pt-Pd(Au) alloys, surface comp. and catalysis, AES and thermal desorption meas. 79−46898
Pt-Rh, surface composition using ion scatt. spectroscopy 79−82422
Pt-Rh alloys, surface behaviour on heating in air, XPS and SIMS *(French)* 77−40327
Pt-Rh alloys, surface comp. determ. by ion scatt. spectroscopy 80−6602
PtSi, 10-160 keV Ar ion sputtering, Rutherford backscatt. obs. 79−15574
PtSi, impurity effects 80−80037
Pt(111), LEED, quantitative anal. 80−44085
Pt(111) surface relaxation, temp. depend., He scatt. 79−19447
Re (10$\bar{1}$0), LEED anal. 80−75414
Re, electrodeposited from fused salts, (10$\bar{1}$1) texture *(Russian)* 80−92791
Re, O_2 adsorption, effect of struct. defects, steps and kinks 80−29269
Re, oxide formation and surface rearrangement, field ion microscope obs. 77−28936
Re, steps, effect on adsorption of CO *(French)* 78−43250
Rh (100) surface, structural determ. using reliability factor proposed for LEED 78−43224
Rh, (100) surface struct. determ. by LEED 77−69152
Rh (110), S adsorbed, surface struct. anal. using hybridisation model 80−44423
Rh (110), S-adsorbed, LEED crystallographic determ. of struct. 80−44422
Rh (110) surface structure, LEED exam. 78−87853
Rh (111), adsorption of O_2, AES, LEED, and thermal desorption mass spectra meas. 79−77900
Rh, (111) surface struct. study by LEED 79−14987
Rh, film, annealing effect on struct., TEM, electron diffr. study 78−76682
Rh, struct. effect on CO hydrogenation 78−73034
Rh supported surface, CO chemisorption, activated surface processes, IR spectra 80−16724
Rh(100), adsorption of H_2S, (2×2) surface struct., LEED anal. 79−99426
Rh(111), surface geometry, vibrational props., Debye temp., LEED study 78−87852
Ru (~001) stepped surface, O_2 chemisorption, LEED and AES obs. 80−11947
Ru surface, clean, oxidation, FIM study 79−47796
Ru surface, clean, oxidation, atom probe anal. of oxide films 79−47797
Ru, with adsorbed Xe, 5p photoemission, local surface struct. influence 80−2920
RuO_2-TiO_2 anode, wear-resistant, use in applied electrochem. 80−40701
S, on Fe(100), adsorbate coverage determ. by LEED, AES and XPS 80−103566
Sb, cleavage faces, evaporation pattern determ. by decoration method in electron microscopy *(German)* 80−107626
Sb_2Te_3, cleavage faces, evaporation pattern determ. by decoration method in electron microscopy *(German)* 80−107626
Sc, crystal surface, N and O adsorption, refl. electron energy loss spectra obs. 80−20742
Sc surface, single cryst., segregation of impurities 79−65299
Se surface, (10$\bar{1}$0) and (12$\bar{1}$0), LEED study *(French)* 79−14991
Se-Ge, amorphous thin film, photocontraction rel. to surface struct. 80−49551
Si, 5 MeV α-particle irrad., X-ray exam. of surface layer struct. changes 78−6114
Si, (001), clean, double diffr. spots in RHEED patterns 79−90855
Si (001), high energy ion scatt. study 80−59772
Si (001), RHEED, expt. compared with calcs. 78−91523
Si, (001) and (111), geometrical and electronic struct., review 80−80039
surface structure continued
Si, (001)-(2×1) surface, reconstruction-induced mean-square displacements 80−15343
Si (100), atomic and electronic structs., energy minimisation calcr. 80−49480
Si (100), H adsorption, MeV ion scatt. study 80−80071
Si (100), intensity-energy spectra 77−47653
Si (100), intrinsic surface states, photoemission study 80−50514
Si (100), struct., LEED study, atomic arrangement model 78−71922
Si (100), vicinal, LEED obs. of stepped surface 80−59773
Si (100) (2×1) clean surface, struct. using averaged LEED 77−59194
Si (100) reconstructed surface struct. study using thermal energy He diffr. 80−60731
Si, (100) surface, Auger emission ang. depend., overlayer effects 78−39637
Si (100) surface, diffr. of He atoms obs. 78−52609
Si (100) surface, LEED meas. 78−60016
Si (100) surface, models of (2×1) surface struct., quasidynamical calc. of LEED intensities 78−71921
Si (100) surface, reconstructed, atomic and electronic struct. 79−73381
Si (110) surface peak anal. by 100-350 keV protons 80−55247
Si (111), 2×1 reconstructed, self-consistent anal. 78−91518
Si (111), cleaved, geometrical struct., LEED expts. 78−91517
Si (111), dynamic effective charge and surface reconstruction, soft-mode theory 79−4460
Si (111), impurity stabilised by Te deposition, atomic arrangement, LEED exam. 77−11770
Si (111), ion bombard., struct. changes, AES obs. 80−79842
Si (111), low-pressure-baked, EPR study 79−82860
Si (111), MEED, secondary electron emission under surface state reson. 78−84688
Si (111), nitridation, AES and LEED results 80−80041
Si (111), surface relax., mol. SCF calcs. 78−91522
Si (111), surface reproducibility and impurity segregation ion neutralisation spectra and UPS obs. 78−34688
Si (111), surface states and surface struct., angle-resolved PES 79−28390
Si (111), surface structure, high temp. RHEED obs. using metal-backed fluoresc. screen 80−75126
Si, (111) 2×1 surface, LEED theory and expt. 79−46895
Si (111) 7×7, He at. beam diffr. obs. 79−33165
Si (111) 7×7, structure model from anal. of RHEED patterns 80−49471
Si, (111) 7×7 surface, adsorption of Al, electron energy loss spectroscopy and LEED 77−43432
Si (111) 7×7 surface structure investigation, RHEED 80−96723
Si (111) (7×7) surface structs., LEED anal. and energy minimisation calcs. 80−49478
Si (111) clean surface, internal pot., interplanar spacing, LEED 77−89627
Si, (111) surface, annealing of scratches 79−60609
Si (111) surface, clean, ESCA obs., Ni(Au) surface impurities 78−52640
Si (111) surface, clean, new diffr. phenomena in RHEED 78−63910
Si (111) surface, O_2 adsorption, atomic steps and residual gas effects 80−54517
Si (111) surface reconstruction, milk-stool model, quantum chem. ab initio calc. 80−49477
Si (111) surface structs., induced by Ag evaporation, RHEED obs. 79−23814
Si (111) surface structure induced by Ag evaporation, RHEED meas. 78−22942
Si, (111) surface structure phase transform, screw dislocations RHEED study 80−88153
Si (111) surfaces, 2×1 to 7×7 struct. transition during annealing, LEED obs. 79−42352
Si (111) surfaces, cleaved, electronic structure following Al adsorption 80−75610
Si (111) surfaces, geometric struct., LEED obs. 80−49479
Si (111) surfaces, relax. and reconstruction using Si_4H_9 clusters, MINDO/3 calc. 79−42356
Si (111)($\sqrt{31}\times\sqrt{31}$)R ±9°-In struct., RHEED obs. 79−60612
Si, ⟨111⟩ surface, 2×1 reconstruction mechanism 77−66079
Si, amorphous, ideal surface, definition and characts. 80−107623
a-Si, Ar^+ bombardment induced ripple topography 77−77336
Si, CVD, surface anal. during growth using RHEED and Auger spectroscopy 80−66433
Si, chemically etched, model of structural transforms. during thermal oxidation 78−79557
Si, chemisorption of H_2, magnetic-sector atom-probe field ion microscopy exam. of hydride form. 77−80699
Si, clean and gas (O_2 and H_2O) covered, appl. of UPS ultrahigh vacuum apparatus *(Japanese)* 80−37125
Si, clean cleaved, surface photovoltage, effects of atomic steps 78−19120
Si, clean surface, geometrical struct. rel. to electronic props. 77−62719
Si, coincidence site superpositions 77−69154
Si, crucible grown, virgin and implanted, laser irradiation effects on surface structure 80−92768
Si, cryst. surface layers treatment and study by HF ion-plasma etching *(Russian)* 80−16517
Si, dangling bonds, EPR, localised states and unpaired electrons on microcrack surfaces 78−52351
Si, decontamination of Au impurities by etching 80−55559
Si defects in surface due to oxidation, exam. using double crystal back reflection topography *(German)* 79−51098
Si, diffusion of Ga in closed capsule, surface damage elimination 78−87691
Si, doped with metal impurities contact angle, water adhesion energy *(Russian)* 77−89620
Si, epitaxial (111) surface, etching observation of stacking faults, dislocations, S-pits, etch pits *(Chinese)* 80−70197
Si, epitaxial layer grown by saturated Sn melt undercooling, morphology 78−22969
Si epitaxial layers, grown by sublimation in vacuum, TEM study of surface 79−46982
Si, filamentary crystals, branching and bending obs. 77−7954
Si, forbidden 200 diffr. spots 78−47214
Si, heavy ion induced disorder in surface and at shallow depths 80−59535
Si high-dose implantation, surface cryst. and buried amorphous layers 77−7743

surface structure continued
Si, intensity dynamics of slow-electron diffr. patterns 78−10267
Si, ion bombard. effect on surface struct., RHEED and Au decoration 80−2096
Si, ion implanted, electron beam annealing, surface struct. study using SEM 80−70235
Si, ion-implanted, period surface struct. in laser annealing, new expt. evidence 80−29836
Si, laser annealed layers, Raman spectroscopy characterisation 79−73189
Si, laser induced surface deforms. 79−82262
Si, laser irrad., anisotropic melting and epitaxial regrowth, surface struct. 79−33163
Si, laser pulse train shaping for polycrystal recovery in self-ion implanted samples 79−47555
Si, lattice strains induced by localized oxidation, high temp. real-time X-ray topographic studies 80−108489
Si, local mechanical defects, annealing and effect on autoepitaxial growth *(Russian)* 80−7701
Si, MBE growth and surface struct. 80−10816
Si, melting and resolidification, laser-induced, surface morphology 79−87529
Si, morphology and electronic struct. 79−78194
Si on sapphire, gettering effect by O implantation, Hall and Rutherford backscattering meas. 79−65103
Si, order-order type phase transition at surface *(Russian)* 77−39728
Si, oxidised surface, irregular growths of $B(OH)_3$ 78−39926
Si, Pb implantation, channelling and RHEED anals. 78−30657
Si, periodic stepped structure, on vicinal planes, LEED obs. 80−24725
Si, photo-field cathode, ageing and surface state effects *(Russian)* 77−28703
Si phototransistors, slow contamination and fast surface state effects, SEM study 80−107896
Si plasma etching as diagnostic technique 77−44385
Si, pure and with adsorbed Al(Au), thermal expansion and at. vibr. singularities 77−89635
Si, purity for semicond. appls., neutron activation anal. 80−71979
Si RF sputter-etched surface, cryst. damage, spectroscopic ellipsometry obs. 80−103538
Si, reconstructed (001)2 x 1, LEED intensity calcs., dimer model variations 79−77875
Si, reconstructed surface physics, review 80−10766
Si, reconstruction-induced subsurface strain, theory 78−91516
Si ribbons grown by capillary action shaping technique, surface quality and impurity distrib. 80−108343
Si, self-implanted, ⟨100⟩ and ⟨111⟩, crystallised layers by laser annealing, struct. 78−47644
Si, short range order in surface layers, electroreflection exam. 78−6703
Si, slip dislocation nucleation during laser annealing 80−84179
Si sputter-machined surface, Ar^+ ion, lattice disordering obs. *(Japanese)* 80−3228
Si, structurally related bulk and surface props., self-consistent pseudopot. method 80−54632
Si surface, (111), metastable 2×1 reconstructed, dangling bond mediated attractive electron-electron model 78−91520
Si, surface, (111) 2×1, cleaved, O_2 adsorption, low-energy electron loss spectra 79−15840
Si surface, (111)7×7, electronic struct. calc. 80−24993
Si, surface, energy-minimisation approach to atomic geometry 78−95213
Si, surface, etched and heat-treated, optically stimulated ESR investigation 80−11245
Si, surface, pure, oxidised element determ. by SIMS 78−85247
Si, surface, sputter etched, damage, contamination, ion backscatt. obs. 79−33167
Si, surface, stacking fault generation due to mech. damage, preoxidation annealing influence 80−54261
Si, surface layer, thin, density meas. by total external X-ray reflection 78−14635
Si, surface layer defects, influence of multiple oxidation *(Russian)* 78−47650
Si surface layers, impurities, elec. and photoelec. props. 80−2298
Si, surface quality estimation after polishing, Kikuchi reflection obs. *(German)* 77−86208
Si, surface relief after Ar^+ bombardment at low-energy *(Russian)* 79−15028
Si, surface self-diffusion, investigation by slow electron diffr. method *(Russian)* 78−51808
Si, surface structure, LEED and spot photometric meas. 79−23811
Si, surface structure changes by laser pulses 78−14548
Si, surface structures after pulsed laser annealing, LEED obs. 80−54494
Si, surface topography changes due to pulsed laser annealing 80−84348
Si, surface-damaged, X-ray triple-crystal diffractometer appl. to dynamical and kinematical diffr. from perfect and damaged crysts. 78−55784
Si surfaces, amorphous, hydrogenated, and monocryst., AES and LEED, comparative study *(French)* 80−44398
Si, thermal oxidation, high resolution Rutherford backscatt., implanted ions analysis 79−87911
Si, vicinal surface struct., LEED exam. 79−60611
Si wafer, HCl etching, smooth or pitted surface struct., gas phase comp. effect 78−11360
Si wafer, high resolution SIMS 78−56929
Si wafer, surface characterization by ellipsometry 79−90853
Si wafer, thin surface layers, amorphous to cryst. transform., obs. technique 80−107288
Si, wafers, HCl etched, surface morphology, etch pit origin 79−96166
Si wafers, saw damage reduction in lubricant environment 80−108585
Si:Ag, surface layer, ellipsometry 78−19121
Si:As, ion implanted layers in device structures, boundary effects in laser annealing 79−73188
Si:As, ion-implanted, channelling anal. of CW Ar laser annealing 79−73186
Si:As(B), ion implanted, pulsed laser annealing appl. to device fabrication 79−73180
Si:As(Sb), ion-implanted, CO_2 laser annealing 79−73183
Si:B, inhomogeneous surface layer, diffusion and implanted, X-ray rocking curves 80−6603
Si:B, polycryst., effect of laser annealing on struct. and elec. props. 79−11243
Si:B(P)(As)(Sb)(Cu)(Fe), ion implanted, doping profile, pulsed laser annealing effects 80−88197

surface structure continued
Si:O, CVD layer, RHEED study of surface crystallinity, annealing effect on structure 79−69371
Si:P, ion implanted, subsurface damage, TEM and channelled Rutherford backscatt. study 80−107337
Si:Sb, laser doping, evaporation loss and diffusion of Sb, under pulsed laser irrad. 80−59508
Si/surface porous oxide film, impurity distrib. during P diffusion 77−39944
Si-Al-Al_2O_3 system, solid phase Si regrowth on sapphire 80−100413
Si-containing films, formed by reaction of Si with organic compounds of N, struct. investigation 79−87009
SiC, 10 keV H^+ irrad., C deposition, surface swelling, surface morphology changes 77−35608
SiC, cryst. surface layers treatment and study by HF ion-plasma etching *(Russian)* 80−16517
SiC, energetic deuteron irradiated surface struct. quantitative meas. 78−95210
SiC, radiation defect annealing, recovery of LEED maxima 80−65075
SiC, strength-grain size relation, surface finish effects 77−81333
SiC, subjected to thermal shock, study of substruct. and surface morpholoy 79−43292
SiC, surface defect annealing, following Ar ion and electron irrad. 80−7603
α-SiC(6H), radiation defect distrib. anisotropy near $(000\bar{1})$ surface, LEED study 80−96577
$SiCl_4$-$GeCl_4$-BCl_4 particulate layers consolidation, in fabrication of optical fibre preforms 80−60787
Si_3N_4 ceramic, surface and subsurface struct. by photoacoustic spectroscopy 78−68481
Si_3N_4 films on Si wafers, O determ. by ^3He activation anal. 80−71981
Si_3N_4, pyrolytic, amorphous and crystalline, chemical vapour deposited fracture surfaces rel. to struct. features 79−5038
SiO, obliquely coated on In_2O_3 coated substrate, TEM exam. of surface topology 77−39726
SiO_2, amorphous, induced crystallisation exam. 78−6016
SiO_2, amorphous, struct. model, surface struct. *(German)* 79−90859
SiO_2, amorphous forms, surface struct. ESCA, X-ray line shift meas. *(Russian)* 77−66775
SiO_2, disperse, EPR, O_2 vacancy relax. rel. to substrate struct., gas adsorpt. *(German)* 79−95645
SiO_2 film, on Si, structure determ. by electron diffr. anal. 79−15050
SiO_2, fused, surface crystn. by Li^+ ion implantation and annealing 80−89383
SiO_2 gel, internal and surface struct. by X-ray scatt. 80−84074
SiO_2 glasses surface textures and defects, exam. using liq. crysts. 80−6364
SiO_2, stoichiometric condensate form. during electron beam evaporation of quartz, electrophysical props. 77−16496
SiO_2, substrate, glow discharge effect on surface props. and struct. 78−85201
SiO_2 surface, Ar plasma-treated, O_2 adsorption reactivity, EPR obs. 79−51418
SiO_2, surface characterisation by free radical spin labels 77−90701
SiO_2, surface defect studies, AES, theoretical model, and expt. 79−7738
SiO_2:Na^+, heat treated, heat of immersion in H_2O, organic compds. 80−3396
SiO_2-based glass, with thin metal films, exam. using emission electron microscope 77−1285
SiO_2-Na_2O-CaO-MgO glasses, surface and near surface struct. 78−87850
SiO_2-Na_2O-CaO-MgO float glass, surface SnO_2 distrib., ellipsometry and XPS study 80−84346
Si_2Te_3, surface exam. by Auger spectroscopy 77−69150
Si(001)2×1 surface, struct. determ. by LEED 79−19438
Si(100), (1×1)H struct., averaged LEED 77−62720
Si(100) (1×1)H surface structure, LEED meas. 78−14602
Si(110), clean surface structural transitions, LEED obs. 78−6203
Si(111) 7×7, LEED, theory and expt. 77−35033
Si(111) 7×7 surface struct., LEED seventh order diffr. beams interpretation 77−62716
Si(111) 7×7 surface struct., LEED intensity calc. 78−34683
Si(111), adsorption Ag, cohesive energy and 2-dimens. phase diagram, AES exam. 78−43246
Si(111) reconstructed 7×7 surface superlattices, microdomain model 80−107625
Si(111) surface, Auger spectra intensity var. due to diffr. 77−85849
Si(111), surface electronic struct., atomic geometry effects, photoemission and electron energy loss spectra 77−85283
Si(111)-(7×7), and impurity stabilised Si(111)-(1×1) surface, photoemission studies 80−104041
Si(111)-$\sqrt{3}\times\sqrt{3}$-Ag structure, atomic arrangement, low energy ion scatt. spectroscopy 80−96724
Si(111)(7×7) surface models, LEED anal. 80−75418
Si{001}2×1 reconstructed surface, atomic struct., LEED intensity analysis 77−28068
SmB_6 (001) surface, azimuthal anisotropy in low-energy ion scatt. 79−28875
SmB_6, FIM study 80−71578
Sm_2O_3, surface step thickness measurement 80−103555
SmS (001) surface, mixed valency and phase transitions 80−39658
SmS, mechanical polishing, stabilisation mechanism for metallic phase on surface 78−60015
Sn diffusion in Cu, via surface segregation 77−7905
Sn film, vacuum deposited, reflectance spectra, structural rearrangement effects 77−24905
Sn plate surface, ion-bombardment conditions effect on chem. profile 80−54287
Sn-Au double layer, ultrathin, quantum size effect *(French)* 77−20466
Sn-Ni equiatomic electrodeposited alloy, surface comp. 78−47649
Sn-Ni metastable alloy, surface film comp., time depend., XPS 78−60870
Sn-Pb surfaces ageing, detrimental effect in PC fabrication 80−108625
SnO_2 CVD coating on glass, elec. resist. rel. to cryst. microstruct. 80−84520
SnO_2:Sb film on glass substrates, elec. props. 80−88652
SnO_2-ZnS:Mn thin film structure, surface morphology and electro-optical props. *(Russian)* 80−49554
SnTe, film, heat treatment in air, effect on struct., props. 79−11037
SrO, AES peak height calibrations 79−43072
$SrTiO_3$, (100), LEED and UPS studies 80−100747

surface structure continued
$SrTiO_3$ (100) surface, struct. and electronic props., AES, LEED, EELS, and UPS study 80−24986
$SrTiO_3$ (111), surface struct., electronic props., LEED, AES, UPS study, photoelectrochem. cell anode appl. 78−84035
$SrTiO_3$ electrode, surface comp. changes during photoelectrolysis, XPS obs. 79−7894
$SrTiO_3$, fabrication damage characterisation by internal and external meas. 80−102782
$SrTiO_3$, surface defects, electronic struct., LEED, AES, UPS study 78−84273
$SrTiO_3$, surface microrelief revealed by ion irradiation 80−54485
$SrTiO_3$, surface microrelief after ion irrad. 80−59774
$SrTiO_{3-x}$, single cryst. and film, Auger spectra, surface comp. 78−27353
$SrWO_4$, flux- and gel-grown, comparative microtopography 77−31852
Ta film sputtered onto Cu substrate, microstruct. and supercond. props. 77−85370
Ta, thermoelectron emission, S impurity atom effects, electron spectra *(Russian)* 77−8712
TaC surface, effect of C oxidation on work function, 1250-2000K, AES 79−24054
Ta_2O_5, hydrated, heat treatment effect on physicochem. props. 80−20966
Ta_2O_5, ion-bombarded cryst., structural and compositional changes 79−46724
Ta_2O_5, oxidised Ta foil, electron bombardment effects on surface composition, Auger spectroscopy, electron desorption measurements 79−77874
Ta_2O_5, XPS, low energy ion backscatt. spectra 78−72660
TaS_2 (2H), surface struct. and interplanar separation by LEED 77−59191
Te film, surface morphology depend. on vacuum deposition angle 80−103553
Te, vacuum deposited film, effects of electron irradiation on surface coverage *(Japanese)* 79−82477
Te(10$\bar{1}$0), LEED intensities anal. 80−88411
Te(1$\bar{2}$10) face, epitaxial growth of Se, LEED and AES meas. 77−1328
Th (111), struct., Debye temp., and oxidation, LEED and AES obs. 77−89625
Th, $He^+(Ne^+)(Ar^+)$ impact, appl. of double pass cylindrical mirror analyser 78−72658
Th, ion irrad., surface C and O, AES obs. 78−71775
(Ti,V)C, activated reactive evaporation deposited films, annealing study, microstructure 80−24762
Ti, 300 keV He^+ irrad., exfoliation, flaking, blistering, in-situ SEM obs. 77−35598
Ti (0001), with adsorbed N (1×1) layer, underlayer geometry, electronic struct. calcs. and UPS meas. 80−54751
Ti (0001) film, with adsorbed H (1×1) monolayer, electronic struct., surface geometry 80−54750
Ti (0001) surface, oxidation, LEED and AES meas. 77−31851
Ti (10$\bar{1}$1) surface, HCP→BCC transition He II UPS study 79−42345
Ti alloys, electrochemical working, film form. and surface roughness *(Russian)* 80−76397
Ti alloys, grinding, effect on surface struct. 80−25878
Ti alloys, surface layers examination using vacuum UV spectrograph *(French)* 80−71987
Ti, Auger electron appearance potential spectroscopy *(Japanese)* 80−50473
Ti, chemisorption of N_2 on {0001}, at. underlayer form. 77−15693
Ti diffusion coated cast Fe, wear resistance 79−52459
Ti foil electrolytic perforation, surface film phase composition obs. *(Russian)* 80−61004
Ti, friction surface structural investigation, O_2 surface diffusion *(Russian)* 80−96726
Ti, HCP to BCC type struct. transition at surface, FEM obs. *(Japanese)* 78−22938
Ti, serrated {10$\bar{1}$2} twin interfaces 80−84182
Ti, surface impurity segregation, quantitative AES 78−19611
Ti, surface layer, study using vac. UV spectrograph *(French)* 80−71987
Ti, using digital scanning Auger electron microscope 78−12797
Ti-Al, elec. spark Al doping of VT-18, surface struct. and props. *(Russian)* 80−76398
Ti-Al-Cr-Mo alloy VT3-1, reactions with some refractory compounds 80−16585
Ti-Al-Sn-Cu-Zn, (5, 2.5, 3, 1.5 wt.%), embrittlement after high temperature long-time exposure *(Chinese)* 78−95792
Ti-N_2, condensate formed by plasma flow precipitation in vacuum, cryst. and surface props. *(Russian)* 80−100788
TiC, activated reactive evaporation deposited films, annealing study, microstructure 80−24762
TiC coatings, on cemented carbides, struct. and hardness 80−59771
TiC-Ni-Mo sintered hard alloy TN-20, fracture surfaces 80−7684
TiD_2, clean and contaminated films, fabrication and AES 78−52600
TiH_x and $TiD_{0.9}$, surface characts., AES, EELS, SIMS, and XPS study 80−65343
TiO_2, (110) and (100) surfaces, LEED and electron spectra 77−72757
TiO_2 (rutile), (001) and (110) faces, UPS and LEED obs. 80−45206
TiO_2, rutile, superficial constitutive water, NMR study 80−88881
TiO_2:H photoanodes, diffusion and surface chemistry 80−35546
TiO_2-Nb_2O_5 sputtered thin layer structure and optical props. 79−28851
TiO_2-RuO_2 anode, wear resistant, use in applied electrochem. 80−40701
TiO_2-ZrO_2 sputtered thin layer structure and optical props. 79−28851
TiS_2, LEED, single-reflection layer scatt. theory 80−49059
TlI-TlBr mixture, KRS-5, contamination by exposure to DC-704 silicone liq., IR refl. spectra anal. 77−59630
TlTe, melt, elec. cond., surface tension, microhardness, influence of impurities 80−88551
$(U, Pu)O_{2\pm x}$, gradient of U, Pu and O at surface 77−18665
U, $He^+(Ne^+)(Ar^+)$ impact, appl. of double pass cylindrical mirror analyser 78−72658
$UAl_2(Co_2)$, surface comp. and electronic struct., photoemission study 80−66382
UIr_3, (100) surface reconstruction, LEED, AES, electron energy loss spectra study 78−75918
UO_2, (110), (100), and (111) surfaces, struct. study using He^+ ion scatt. spectroscopy 80−40206
UO_2 (111), $He^+(Ne^+)(Ar^+)$ impact, appl. of double pass cylindrical mirror analyser 78−72658
UO_2, (111) and (553) surface struct., He^+ ion scatt. spectra 78−75917
UO_2 (~100), vicinal surfaces, LEED and AES expts. 79−4464
surface structure continued
UO_2 pellet surfaces, β-$UO_{2.33}$ formation in air at 229 to 275°C, X-ray diffr. study 80−35362
UO_2, surface props. of low index faces, calc. 80−6604
(V,Ti)C+Ni cermet, binder grain size 80−44401
V, and its cpds. with light elements, surface state, XPS investigation 78−11070
V, clean surface, nearest neighbour spacings from extended appearance pot. fine struct. 79−69329
V, H_2 permeability, surface impurity layer effect 77−24440
V, irradiation with 2 MeV He ions, low cycle at elev. temp. 78−95086
V surface, chemisorption of Br_2, struct., Na adsorption effects 80−101039
V-Pd, dil. alloys, surface segreg. 78−18883
V_2O_5, (001) surface modification, during catalytic oxidation of propene *(French)* 80−45557
V_2O_5 and lower oxides, electronic, optical, structural and surface props., review 80−88120
W (001), anal. of surface barrier struct. using LEED data 78−84037
W (001), displacive transition, H adsorpt. effects, theoretical model 80−65352
W (001), LEED spectra, expt. rel. to theory 78−84039
W (001), spin-depend. features in LEED intensity curves, model calcs. 78−34685
W (001), surface phase transition, electronic contribs., surface susceptibility, ab initio self-consistent thin-film energy band calc. 80−29255
W (001), surface relax., LEED rotation diagrams 79−28180
W (001), surface relax. determ. using LEED rot. diagrams 78−38917
W (001), surface structure, LEED anal. 78−38919
W (001), with adsorbed Cs, photoemission anisotropy, possible surface struct. determ. 78−11076
W (001) (1×1) surface contraction using LEED intensity anal 80−6606
W (001) clean surface displacive phase, long-range inhibition by N 80−2266
W (001) face, surface contraction, LEED exam. 77−43412
W, (001) surface, electronic origin of reconstruction 80−11065
W, (001) surface, reconstruction and reordering by H adsorption, MeV ion scatt. studies 79−82443
W (001) surface, spin polarisation in LEED, theoretical predictions 77−31855
W (001) surface structure by MeV ion backscattering, channelling 80−6605
W (001) surface with adsorbed S, struct. and effect on CO adsorption 79−86981
W (100), adsorbed H-induced lattice reconstruction, surface vibr. obs. 79−19445
W (100), adsorbed O, electron stimulated desorption ion energy distrib. and surface struct. 78−75940
W (100), adsorption of Cl_2, LEED and AES study 79−90878
W (100), chemisorption of H, phase changes, LEED obs. 79−77911
W (100), LEED intensities, temp. depend., surface struct. phases and surface Debye temp. 80−39395
W (100), O covered, ion scatt. spectroscopy 77−73205
W (100), reconstruction in presence of O half monolayer, struct. props. 80−44421
W (100), surface reconstruction kinetics in presence of O half-monolayer 80−65375
W (100) single crystal, surface studies by MeV He scatt. 79−4455
W (100) stepped surface, adsorbed O, electron stimulated desorption ion ang. distribs. 80−20035
W (100) surface, phase transition exam. by LEED 77−55433
W, (100) surface, scatt. of mol. and atomic H ions 79−69943
W (110), chemisorption of O, displacement reconstruction model 79−46949
W (110), D^+ depth distrib., effect of surface impurities, channelling model 79−1451
W (110), WO_2 and O_2 adsorption by LEED and AES 80−34317
W (110) surface, adsorbed Pd, growth, struct., stability, desorption 80−59794
W, (110) surface, low energy ion scatt. features, inelastic loss and surface crystallography 80−66371
W (110) surface defect. exam., LEED obs. 79−82421
W (110)-O chemisorbed layer, island size determ., response function and substrate struct., LEED meas. 79−42414
W (111), (211), and (311), adsorption of W single atoms, surface site geometry determ. by FIM 80−39447
W (111) surface, surface site geometry and diffusion characts. of Ni atoms 78−71953
W {001} (1×1)→($\sqrt{2}\times\sqrt{2}$)R45° surface struct. transition, LEED, AES, and work function meas. 79−42348
W {001}($\sqrt{2}\times\sqrt{2}$)R45°, low temp. surface struct., space group determ. by LEED 77−85037
W, adsorption of Ga, In and Sn, field emission, FIM 77−16470
W clean {001}-(1×1) surface, struct. determ., dynamical and exptl. LEED results 78−14560
W, coadsorption of La and B, field emission meas. 78−47662
W crystal-atom and W(001) surface, low-energy positron diffraction, theoretical study 80−84034
W, deformed, surface layer struct. effect on polygonisation and recryst., X-ray diffr. anal. and metallographic exam. *(Russian)* 80−84948
W, dendritic surfaces, antireflection coated, reflectance geometrical study 79−91511
W dispenser cathodes, Ba-activated, surface characts., ion scatt. spectrometry and SIMS study 80−66377
W emitter tip, surface shape changes, field ion microscopy meas. 78−26754
W, FIM study of lattice damage caused by low-energy He ion bombardment 78−95090
W faces, simultaneous adsorption of Ba and Cu atoms, work function changes 80−65378
W, fine tip microcrystal, microscopic protuberance form., crit. remoulding obs. 78−27380
W, fine tip microcrystal, thermal smoothing after critical remoulding 78−27381
W, fine tip microcrystal, vertex remoulding, effects on field emission 78−27379
W, hot emitter, surface struct. change during baking above 2000K 79−65971
W, LEED, low index surfaces, spin polarisation, intensity profiles 77−62722

surface structure continued
W, LEED and electron microscopic investigs., review *(Hungarian)* 77−47654
W monocrystals in alkaline electrolyte, surface orientation, effect on anode current *(Russian)* 80−75360
W, periodic struct. development, under conditions of thermal mass transfer *(Russian)* 77−59187
W points, micro-size, change in shape and electron field emission 79−74067
W, regularly stepped single crystal surfaces, work function determ. by thermionic emission 77−59665
W, stepped surface, edge atom dipole moments 78−14791
W surface, adsorbed W, Ga, Sn, struct., FIM obs. 80−103576
W surface, atom zigzag chains obs. by field ion microscopy 78−84036
W, surface, isothermal ramped field-desorption of benzene 79−90870
W, surface cleanness control using secondary electron spectroscopy *(Russian)* 79−90858
W, surface diffusion of Pd, anisotropy effects due to substrate struct. 79−99422
W, surface dipole moment calc. 80−60060
W surface layer struct. during milling, plastic deform., failure *(Russian)* 80−40586
W, surface relaxation and electronic structure of (100) surface 79−73561
W, surface structure and topological modification during depth profiling, FIM obs. 79−78816
W, surface structure changes due to ionic bombardment, LEED and AES obs. *(Russian)* 77−1775
W, thermal field cathode emitters, end form changes, electron microscope obs. 77−4718
W-Al_2O_3 cermet films, oxide evaporation deposited on Mo, Ti, Al_2O_3 substrates, struct., props. 80−25581
W-Mo, refractory, surface investigation by FIM and atom probe *(German)* 79−55623
W-Tic(ZrC)(HfC), thermionic emission, surface structural charact. after prolonged use, work function variation 80−20758
WC, explosive plasma sputtered coatings, struct. and props. *(Russian)* 80−100783
WC-Co cemented carbide, bending strength, surface roughness effects *(German)* 77−8947
WC-Co DC and RF sputtered coatings, bias effect, struct., X-ray-Auger study 80−70565
WC_x, (3×5) struct. on W (110) surface, at. beam diffr. and scatt., surface characteris. 79−78819
WO_3, oxidised W foil, electron bombardment effects on surface composition, Auger spectroscopy, electron desorption measurements 79−77874
WO_3, powder, electron bombardment effects on surface composition, Auger spectroscopy, electron desorption measurements 79−77874
W(001), electronic surface reson. and thermally induced struct. transition 80−88614
W(100), atomic struct. using FIM 79−73384
W(100), clean thermally induced c(2×2) surface struct. 77−62714
W(100), I adsorption at room temp., LEED and AES study 80−84389
W(100) surface, instability, distortion and dynamics 80−84360
W(110) vicinals, adsorption of N_2, step sites as dissoc. centres 80−6642
W{001} (1×1) surface structure, pseudo-relativistic LEED calcs. and R-factor anal 80−70510
W{001} surface, clean, reconstructed, field-ion microsc. obs., 15-400K 80−15348
W{100}, adsorption of N_2, surface disorder effects on work function change 77−20192
Y-Y_2O_3-Au junction, defect struct. and local conduction 78−26970
$Y_3Al_5O_{12}$, laser cryst., struct. inhomogeneity obs. by vac. decoration 77−35701
$Y_3Al_5O_{12}$, layer structuresrevealed by decoration method and electron microscopy 77−27902
YIG, magnetocrystalline surface anisotropy energy, one-ion mechanism 79−78362
YbTe, high-temperature evaporation and reactivity 80−103469
ZNSe, surface, energy-minimisation approach to atomic geometry 78−95213
Zircaloy-4, heat treated in SiO_2 capsules, Zr and Si vapour transport surface struct. anal. of deposits 80−55437
Zn, electron emission depend. on surface mechanical treatment *(Russian)* 80−100945
Zn, film, sputtering mechanism, SEM 80−29839
Zn film growth, HEED and projection microscope obs., surface orientation depend. on deposition parameters 77−32523
ZnO (000$\bar{1}$), adsorption of alkali metal, anomalous behaviour of Na 78−79883
ZnO (0001) and (000$\bar{1}$) polar surfaces, 6-fold LEED patterns 78−71920
ZnO (10$\bar{1}$0), LEED anal. of atomic geometry 77−69149
ZnO (10$\bar{1}$0), surface struct. from LEED anal., matrix inversion method 79−46897
ZnO (10$\bar{1}$0) and (11$\bar{2}$0) surface, atomic geometry from elastic LEED intensities 77−20170
ZnO (10$\bar{1}$0) prismatic surfaces, nonstationary sublimation *(German)* 78−60035
ZnO, film for solar cell appl. structural, optical and elec. props. 80−2294
ZnO, hexagonal spot pattern production with light source and electron beam 77−69148
ZnO, prismatic surface, O_2 interaction, effect of surface defects 77−31899
ZnO, thin Zn or O rich layers, thermolysis, photolysis, SEM, XPS 77−11821
ZnS, (110) cleavage stratigraphic etch patterns, displacements 77−7680
ZnS, clean surface, AES and LEED exam. 80−10762
ZnS, electrolum. phosphors, surface phenomena occurring during ageing *(Russian)* 79−33842
ZnS, film, laser evaporation synthesis, surface struct. 79−28954
ZnS ion beam etching, topographic changes, amorphisation, luminescence study 80−76078
ZnS, superficial degradation in air and water, XPS obs. *(French)* 80−89110
ZnS, uncoated and liq. layer coated, vaporisation mechanism, surface morphology 77−35683
ZnS, vaporisation, negative whisker form. by solid-liq.-vapour mechanism 77−35684
ZnS:Mn, phosphor, surface changes following interaction with H *(Russian)* 78−72602

surface structure continued
ZnS:Mn films, surface struct., microrelief rel. to morphology of SnO_2 transparent cond. support 79−56092
ZnS:Mn on SnO_2/glass transparent conductive base, surface morphology effects on electroluminesc. *(Russian)* 78−48238
ZnS:Mn-H atom systems, surface physiochem. changes, radical recombination luminesc. investig. 79−56863
ZnSe (100) surfaces, surface states meas. by LEED, AES and EELS *(Japanese)* 79−99599
ZnSe (110), LEED intensity anal. and electron spectroscopy 77−43678
ZnSe, crystallographic polarity and etching behaviour 77−85030
ZnSe, evap. onto electron bombarded NaCl substrates, epitaxial growth and characts. 79−28948
ZnSe(110), kinematical LEED calcs. 77−85034
ZnTe (110) surface, elastic LEED anal. 79−86967
ZnTe (110) surface struct. determ. by LEED, UPS, and EPR 80−49475
Zr, (0001) surface struct., HCP phase, LEED study 80−20017
Zr, FIM, specimen prep. and results 77−11449
Zr, serrated {10$\bar{1}$2} twin interfaces 80−84182
Zr-CR (1.9 wt.%), β-quenched and tempered, tensile props. rel. to tempered conditions, SEM study 79−66109
Zr-N_2, condensate formed by plasma flow precipitation in vacuum, cryst. and surface props. *(Russian)* 80−100788
Zr-Ni, surface layer, segregation of ferromag. Ni, magnetooptic investigation 80−2256
Zr-Ni-H, surface segregation of Ni, influence on catalytic activity 80−30275
ZrC-Re, spectral emissivity, 1400 to 2500K, surface relief and composition 77−24420
ZrNi, surface segregation of Ni, influence on catalytic activity 80−30275
ZrO_2, near-surface phase transforms., effect of grinding and polishing 78−15557
ZrO_2-CaO, stabilised microspheres, structure, mechanical props. *(Russian)* 80−100379
ZrO_2-Y_2O_3, stabilised microspheres, structure, mechanical props. *(Russian)* 80−100379
ZrO_2-Y_2O_3 film, surface characterisation, XPS, ESCA, and AES expts. 78−72028

surface tension
acrylic coating, surface tension effects 80−53487
adsorbed film on crystal, spreading press., direct meas. 77−15692
adsorbed layer, spreading press. 78−38971
adsorption, intermolecular surface forces in plane densely packed hexagonal model 80−59785
adsorption on solid surface, surface stress and tension at gas-solid interface 79−60627
aerosol, two-layer spherical liquid particle with solid core, thermophoresis 79−39211
air entrainment at solid/liquid/gas interface 77−1276
alcohols, normal, semiempirical theory of surface tensions 79−51391
aliphatic acids, thermodynamics of adsorption at air/aqueous soln. interface 80−10752
aliphatic alcohol, thermodynamics of adsorption at air/aqueous soln. interface 80−10752
alkali halides, molten, rigid sphere model 77−7946
alkali halides, surface energies, surface tensions and surface struct. 79−60610
alkanediol-eicosane, interface tension, sessile bubble method *(Japanese)* 78−79857
alkanediols, surface tension, sessile bubble method *(Japanese)* 78−79857
n-alkanes, anisotropic London dispersion forces, surface effects 80−74214
alkanes, normal, semiempirical theory of surface tensions 79−51391
alloy, binary, with strong chem. interactions, model using surrounded atom concept 77−15665
alveolar surface tension in excised lungs 79−92257
aqueous heterogeneous systems, thermal anomalies 77−32829
artificial blood substitutes, surface energetics anal. 80−41321
azo dye sulphonates and analogs., aqueous solns., surface tensions 78−47641
bacterial adhesion, influence of substratum critical surface tension 79−79493
binary liquid alloys, surface tension, compressibility and surface segregation 78−67889
binary liquid mixture, horizontal layer, surface tension driven instability in presence of Soret effect 80−10227
binary liquid mixture, surface tension, free energy density expansion 78−91509
binary metallic system, rel. to conc. profiles across solid-liq. interface 80−55382
binary mixture of non-electrolytic liquids, surface tension *(French)* 77−15660
binary mixtures, excess surface tension calc. and theories of solns. 78−91508
black lipid film stability, interfacial props. effects 78−15798
black lipid membranes and bilayer vesicles in solution, thermodynamic stable states anal. 80−45856
body loading with cracks, energy conditions for brittle failure *(Russian)* 80−96234
bromides, and mixtures, molten, elec. cond., density, viscosity, surface tension, review 77−80638
bronchial collapsibility of excised dog lungs, effect of lung surface tension 80−67118
bubble cavitation problem, numerical soln. 78−79347
bubble columns, axial dispersion coeffs. rel. to fluid props. 77−3861
bubble growth dynamics, isothermal, gas bubble in liq. 79−14459
bubble motion in vertical temp. gradient, buoyancy and Marangoni forces 79−46372
bubble nonhemispherical, attached to solid wall, collapse motion, numerical variation soln. 77−51103
n-butane, and +octafluorocyclobutane mixtures, surface tension meas. 79−19371
di-butylphthalate, critical nuclei, meas. of number of mols. and surface tension from rate of nucleation 79−65293
calculation for incompressible nonviscous liquid of finite depth *(Russian)* 77−68604
capillarity, van der Waals' thermodynamic theory under hypothesis of continuous variation of density 79−56043

surface tension continued
capillary condensation, Kelvin eqn. direct exptl. verification 79−33159
capillary phenomena in cylindrical pores, appl. to pore size anal. 80−15340
Casimir effect in dielectrics using source theory, surface tension and latent heat 79−8109
cavitation, surface tension effects 79−64719
cavitation flows, combined influence of surface tension and gravity *(Russian)* 78−75178
CBOOA, smectic A, nematic and isotropic phases 77−39539
cellular motion in liquid heated below rel. to surface deformation and active agents *(Russian)* 77−54973
charged fluids, theory of density profiles and surface tension 80−44689
charged particles, two-component liquid, in equilib. with vapour, surface dipole layer and surface tension 80−70505
chlorophyll black lipid membranes in dil. electrolyte solns., bifacial tension meas. 79−16162
classical Lennard Jones 6-12 fluid, surface characts., density functional theory 77−24255
clean metal surface physics, review 77−15659
cloud droplet condensation growth in turbulent medium, hygroscopicity and surface tension effects *(Russian)* 77−33142
coating of flat sheet during withdrawal from wetting liq., meniscus shape, flow model 77−29044
colloidal systems, surface forces, direct meas., elastic deform. effect 80−93805
computation in molecular dynamics experiments 78−30815
conducting liq. layer, surface tension effects, MHD convection stability and thermocapillarity *(Russian)* 78−47054
conference, Budapest, Hungary (Sept. 1975) 78−11567
contact of spherical particle with a droplet, approx. eqn. 79−60604
convection, Benard-Rayleigh, finite amplitude, nonlinear stability anal. 79−46311
convection, surface-tension induced, at reduced gravity 78−83374
convection driven by non-uniform surface tension 80−10116
copolymers, triblock, lamellar domain dimensions, prediction 77−39547
cryolite melts saturated with alumina, interfacial tension between Al and melt 78−38913
crystal growth, diffusive, numerical soln. accounting for growth rate and surface tension anisotropy 80−33912
crystal surface elastic props., surface tension tensor, volume stress *(Russian)* 80−100389
cyanobiphenyl, meas. near nematic-isotropic transition temp. 78−43219
cylindrical slab of fluid, in weightlessness condition, surface-tension driven convection *(Russian)* 78−90872
cytoplasm spherical drop with effective surface tension influenced by oscillating enzymatic reactions 80−108862
deformable solid surfaces, thermodynamics 78−34694
demonstration, teaching aids, convention of secondary school physics teachers *(Hungarian)* 80−67957
dendrites, growth theory, surface tension effects 79−11051
density functional theory for simple liquids, appl. to liq. metals 80−103537
density-gradient term in free energy near crit. temp. 77−89617
dialkyl phthalates, plasticizers, surface tension, contact angle, surface energy, entropy determ. *(Japanese)* 77−31843
dielectric fluid-fluid interface, stability in elec. and gravit. *(Russian)* 77−27617
dielectric liquids, HF electric field influence on surface tension *(Russian)* 80−49463
diethylene, critical nuclei, meas. of number of mols. and surface tension from rate of nucleation 79−65293
dimethyltetraphenylmethylphenylsiloxanes, density, viscosity, surface tension and crit. temps. 79−86830
diphenyl methane, critical nuclei, meas. of number of mols. and surface tension from rate of nucleation 79−65293
diphilic polyelectrolytes, aqueous solns., Wilhelm method 80−10745
dispersed two-phase single-component system, modification of charact. functions by interphase boundary and surface tension 77−90647
drop, incompressible fluid, equilib. and stability analysis 80−59092
drop deformation and orientation in shear and extensional flow fields, dynamic interfacial props. 80−107611
drop dynamics in shear fields, role of dynamic interfacial effects 80−107612
droplet, viscous, deform. due to deposition of surfactant 78−18876
droplets, surface tension, size effect, self-consistent calcs. 77−51569
drops, diffusophoresis in viscous media 78−35731
drops, interfacial tension inferred from quadrupole resonance props. 80−33275
drops, liquid, rotating, held together by surface tension, equilibrium shapes and stability 80−79367
Dynamic fluid interface displacement and prediction of air entrainment 78−2337
dynamic liquid surface tension determ. from drop oscillation frequency and capillary jet instability 78−56026
dynamic surface tension excess at compressed interface, bulk-to-surface diffusion interchange 79−56042
eddy diffusivity, near open channel free surface, heat transfer expt. 78−5798
education, Brownian motion, melting, surface tension and rubber networks, thermodynamic anal. 80−73132
education, bubble cohesion in foam, binding energy calc. 78−61978
education, soap film on wire frame in zero gravity, variation problem branching 79−9057
elastically deformable bodies, wetting, influence of vol. deform. of solid 79−11008
electrocapillary emulsification 78−48697
electrohydrostatic theory 78−43213
1.1-electrolyte solutions, conc. aq., by means of Wilhelmy and laser light scatt. 77−72745
electron-hole drops, stability of spherical form *(Russian)* 79−42464
electron-hole liquid, in semiconductors, equilib. props., review *(Russian)* 78−34773
electrostatic drop formation, effects of conductive liquid props. 78−1122
emulsion, inverse-type, coalescence of drops in uniform elec. field 78−53265
ethyl n-dodecoate, photocapillary effect, temp. depend. *(Russian)* 78−34682
ethylene glycol, critical nuclei, meas. of number of mols. and surface tension from rate of nucleation 79−65293
surface tension continued
ethylene oxide-propylene oxide copolymers, composition sessile bubble method *(Japanese)* 79−69323
ethylene-propylene copolymer, surface tension, composition and temp. depend. *(Japanese)* 78−79860
faceted microcrystal, surface tension meas. by lattice parameter changes 77−47660
fatty alcohol, oil-water interface adsorption, high-press. effect on phase transition 79−99395
ferromagnetic system, invariant equilibrium states and surface tension 79−40491
filament and cluster crystals, liqs. in ultrathin channels, rel. to supercond. materials development 79−19162
film, thermodynamic theory of clustering and percolation transitions 77−47697
film flow, meniscus shape theory, Navier Stokes eqn. 78−38270
film on liquid surface, persistence in presence of disturbance 77−31839
flow, separating, fluid-surface interface, static contact line, slip at wall and shape of free surface 80−53737
flow instability, of liq. film down heated incline, surface tension driven 79−27620
flow of liq. film down vertical or inclined surface, surface tension effects 80−106778
fluid, multiphase system, vapour bubble collapse, charact. functions 78−18156
fluid dynamics, free boundary flow, surface tension effects, finite element fluid flow simulators 80−82647
fluid dynamics expts. and problems *(French)* 78−9645
fluid interface, perturbations surface tension and gravity effects *(Russian)* 78−10256
fluid interfaces, isothermal and deformable, mass transfer and surface tension, review 80−33564
fluid interfacial stress and struct., gradient theories 79−19428
fluid/fluid interfaces, capillary phenomena, review 80−70506
Fowkes' hypothesis, statistical mechanics basis 80−2249
free energy theory, using Lennard-Jones 6-12 pot. 80−10751
gas bubble, growth or dissolution, general soln., analyticity 80−10747
gas bubble adhesion to heat transfer surfaces 79−89375
gas-liquid surface, penetrable sphere model 78−10261
gas-liquid surface of mol. fluids, mol. dynamics computer simulations 80−39387
gas-liquid surface of penetrable sphere model, surface energy and tension 77−4249
gas-liquid surface of penetrable sphere model 79−73380
gas-liquid system, digital simulation 78−2341
general physics and heat, book 79−25814
Gibbs states, non-translation invariant with coexisting phases, analyticity 80−8923
glass, Twyman effect in plane-parallel plates, effective surface tension *(Russian)* 77−31867
glass fibres, evaluation of surface tension 78−47657
glycerin nonadecane, critical nuclei, meas. of number of mols. and surface tension from rate of nucleation 79−65293
glycol-alkane systems, interfacial tensions, regular soln. theory and Antonow's rule 79−14983
graphite, surface, wettability, surface tension, contact angles of liqs. 79−37901
gravity waves, non-uniform free surface, superficial viscosity and tension *(French)* 80−48728
group structure for general lattice systems and surface tension 80−4675
hard sphere fluid, near wall 79−73081
hard sphere system, surface tension, compressibility, bulk modulus press. coeffs. and Rao's acoustical parameter 80−80027
hard-sphere fluid, interacting with wall, virial coeffs. 79−23808
hard-sphere fluid, near a wall, surface tension, approx. method calcs. 78−59724
heavy fluid, surface tension forces effect on unilateral overflow characts. *(Russian)* 77−55416
heterogeneous system, thermodynamic theory of nucleation on charged particles 79−39216
n-hexadecane-acetone, noncritical interface near crit. end point, surface tension meas. 79−69322
history Berthelot's first publication, 1850, subjection of liqs. to tension 78−32639
horizontal crystal ribbon growth, meniscus stability 80−103281
hydraulic characts. of liqs. flowing through porous metal fibre mats., permeability laws 78−67848
hydrocarbon mixtures, estimation of surface and interfacial tension 78−67887
hydrodynamic stability of liquid films and jets, effect of soluble surface-active substances 80−6027
ice-water interface, surface tension meas. by grain boundary groove method 77−24481
immiscible liquids, binary system, wetting hypothesis, validity, Antonow's rule appl. *(French)* 80−49462
inhomogeneous charged fluids, density functional theory, rel. to molten salts surfaces 80−79660
insoluble monolayer, ionised, of surfactant, thermodynamic eqn. of state 79−8450
interface, noncritical, near a crit. end pt., struct. and tension 77−84885
interface, stability problem, diffusion, reaction and convection 80−33567
interface between liquid and vapour, surface of tension location 79−37909
interface instability in presence of chemical potential gradients *(French)* 80−75338
interfaces, pure, thermodynamics and dynamics rel. to Spacelab 79−28910
interfacial energy, surface energy, surface tension and lattice friction relation 79−69341
interfacial instability, mass transfer, Marangoni effect and interfacial longit. waves 79−46890
interfacial order parameter profile near critical point, renormalisation group approach 78−6200
interfacial phenomena interpretation using schematic density profiles 78−60012
interfacial statics differential eqn., micromech. derivation 79−46882
interfacial tension minima, dynamic, equilibration of surface-active solute between two liquid phases 80−80026
internal cohesion of liquids, Reynolds' work 79−58511
invariant Gibbs states, cluster props., surface tension 79−49172

surface tension continued
iodides and mixtures, molten, elec. cond., density, viscosity, surface tension 77−80638
ionic crystals, statistical theory calcs. of surface energy and surface tension 80−17894
Ising ferromagnet, surface tension using real-space renormalisation group methods 79−73760
Ising ferromagnet, two-dimens., surface tension of diagonal interface 77−59369
Ising model, using real-space renormalisation group methods 78−47985
isobutyric acid-H_2O, liquid-vapour surface tension near liquid-liquid consolute point 80−107613
isotropic solid soln. cryst. surfaces, surface stress and chem. equilib. 80−107628
jet flow, viscous, with surface tension, finite element soln. 78−79349
jets, Newtonian, axisymmetric, die-swell, Galerkin finite element method 80−83830
Kelvin equation, effect of surface tension on vapour pressure, derivation 80−2248
kinetic theory 78−56022
laminar film condensation, on vertical plate, surface tension effects 78−95148
lattice systems, phase transition and surface tension 80−77713
lattice systems, surface tension and phase transition 80−27226
Lennard-Jones 12-6 fluid, liq.-vap. interface, density and surface tension 79−90772
light modulator, using oil film deform. by surface tension var. 80−5831
light scattering by surface tension waves 79−58469
lipid bilayer membrane interaction forces in zone of contact 78−53345
lipid bilayer thermal excitations detect. by light beating spectroscopy 77−48762
lipid monolayer phase transitions, model 78−2338
Lippmann eqn., statistical mech. deriv., dielec. const. 77−20404
liquid, cohesive energy density, surface and interfacial tension and heat of mixing 77−55431
liquid, in vessel, vibr. amplitude determ., structural damping and surface tension applied to stress anal. 80−19417
liquid, statistical mechanical theory 79−82414
liquid binary metallic systems, rule for surface enrichment 80−75406
liquid crystal, colloid and surface chemical aspects 78−9950
liquid crystal, nematic-vapour and nematic-isotropic interfaces, mol. theory 77−15307
liquid crystal surface, statistical thermodynamics, local order parameter 80−88023
liquid drop in immiscible liquid, evaporation, surface tension effects 77−47648
liquid drop on solid substrate, deviations from Young's equation 77−66075
liquid film, free, stabilised with ionic surfactants, EHD 78−87403
liquid film, mol. dynamics simulation 77−15666
liquid film flow down inclined plane, deflection toward underside 79−18867
liquid in equilib. with vapour, lattice model 77−43409
liquid in equilib. with vapour, rel. to cohesive energy density 78−34680
liquid ionic salts, melting transition statistical model, dielectric const., surface tension 80−70378
liquid jet hydrodynamic development, surface active materials effect 79−46883
liquid metal, appl. to calc. of surface free energy of solid at MP 77−31866
liquid metal, pure, surface tension and electron density 78−51803
liquid metal, temp. depend. 77−4248
liquid metal spreading on solid substrate 77−51575
liquid metals, radial distrib. function and thermodynamic characts., interparticle interaction pot. *(Russian)* 80−49086
liquid metals, surface properties, hard-sphere and square-well models 80−19684
liquid metals, surface tension and critical props. 79−28176
liquid microclusters, thermodynamics, size effects, theory 78−22935
liquid mixtures, static surface tensions, monolayer model 77−4245
liquid mixtures, theory 80−88404
liquid penetrant testing, continuum fluid mechanics aspects 80−43818
liquid spreading on liquid surface, hydrodynamics 78−30814
liquid spreading on solid surface, physical regularities *(Russian)* 77−62712
liquid spreading on solid surfaces, static and dynamic contact lines, book contrib., review 80−20015
liquid zone stability, static or rot. 77−59182
liquid-liquid interfaces in isolation, and in interaction, review 77−47651
liquid-vapour interface, gravity effects, van der Waals theory 77−72744
liquid-vapour interface, struct. at 110K, Monte Carlo method, for Ar-like fluid 80−54477
liquid-vapour interface, sum rules, surface tension appl. 78−63900
liquid-vapour interface, surface tension and energy 77−76647
liquid-vapour interface, surface tension-compressibility relation 80−44397
liquid-vapour interface nature, non uniform classical fluids statistical mechanics 79−77468
liquid-vapour system in gravit. field, interface correlations 77−1275
liquids, mol. theory, teaching 77−57123
liquids, potential and flux conserving static equilibria in elec. or mag. fields, determ. 80−88399
liquids, simple, surface tension and density profile from expression for excess free energy 77−80681
longitudinal instabilities in exit flow from a slit, surface tension origin 79−98684
LPE 78−88432
lubrication, hydrodynamic, free boundary problem including surface tension 80−19542
lung structure and elasticity, 3-dimens. modelling 77−36992
magnetic colloid, theory of large agglomerates 79−79310
material transport rate and stress distribution during grain boundary diffusion driven by surface tension 79−61525
MBBA, anisotropic interactions with surface-treated substrates, wall effects on Freedericksz transition 79−99070
mean spherical model approx. 78−75514
measurement of low interfacial tensions from light scatt. intensity by liq. interfaces *(French)* 80−20007
membrane, rel. to 2-D phase transformation 77−1980
membrane system, closed, vesicular, mechano-chemistry 77−60189
surface tension continued
meniscus, equilib. and stability props., exact determ. of surface tension 78−10263
meniscus joining vertical rod to liquid bath, stability 77−4247
meniscus profiles between concentric cylinders, expt. and computation 77−20164
meniscus shape in rot. vertical tube 78−51797
metal, high temp. creep, remarks rel. to zero creep method 77−12671
metal, liquid, critical temp. and temp. coeff. *(German)* 77−35800
metallic particle, surface tension depend. on size, vaporisation time *(Russian)* 80−34290
metallic surface rippling induced by surface tension during laser melting 78−11405
metals, atomic binding energy and surface energy rel. to prediction of physical props. 80−59434
metals, liq., compressibilities, surface tension at melting temp. 78−91370
metals, liq., temp. depend. *(Russian)* 80−15336
metals, theory of adhesion *(Russian)* 77−44455
methane, liq., surface tension and density profile from expression for excess free energy 77−80681
methylphenylsiloxanes, density, viscosity, surface tension and crit. temps. 79−86830
micelle formation of cationic surfactants, influence of perfluorinated counter-ions *(German)* 79−74423
microcluster formation, free energy, curvature-depend. surface tension effect 80−100056
microdrop, pressure tensor and surface tension, mol. dynamics method 79−11005
microemulsions, thermodynamic stability, theory 78−85203
microemulsions, thermodynamic stability 78−95962
mixed halide melts, elec. cond., surface tension, density and viscosity, tables 79−60531
mixture, binary, nucleate boiling heat transfer, conc. depend. 78−87249
molecular fluid, computer simulation of liquid-vapour surface 80−54478
molten salt, model for two-particle distrib. functions 79−33158
molten salt mixtures, surface tensions 80−29246
monolayer, interfacial, thermodynamic treatment, excess quantities, adsorbed and spread layers 80−40732
monolayer, mobile or registered, surface tension and spreading press. 78−38960
monolayers at fluid-fluid interfaces, hydrodynamic stability, ion interactions 80−6598
monolayers at fluid-fluid interfaces, hydrodynamic stability, dipole interactions 80−6599
monolayers on liquid-liquid interfaces, interfacial tension *(French)* 79−73376
multicomponent systems, approx. theory of interfacial tensions, appl. to binary liquid-vapour tensions 79−51390
nematic liquid crystal, surface tension, mol. theory 77−1075
nematic liquid crystal, surface tension, pre- and post-transitional effects 79−77511
nematic liquid crystals, Marangoni effect 78−6009
nematic liquid crysts., molecular alignment using alkoxysilanes, rel. to surface energy 80−100164
nematics, Benard-Marangoni instability *(French)* 78−75538
Newton black film, line tension, determ. by cnt. bubble method 80−88406
Newton black films, line tension determ. by diminishing bubble method 80−88407
nitroethane-3-methylpentane, liquid-vapour surface tension near liquid-liquid consolute point 80−107613
non-Newtonian fluid, rot. liq. film, free surface instability 79−37294
nonpolar liquids, surface tension, geometric model 79−86963
nonuniform simple hard-sphere fluid, interface props., statistical mech., perturbation theory 77−84607
nonviscous liquids, free surface flow, gravity waves with surface tension depend. on impurities *(French)* 79−90267
ocean, surface tension effect on waves development from periodic disturbances in non-uniform fluid *(Russian)* 78−77253
octafluorocyclobutane, and +n-butane mixtures, surface tension meas. 79−19371
oil droplets, motion and optical props. by interf. method 78−67893
oil-water interface, electroadsorption and electrocapillarity 80−44393
optical fibre coating with conical shape applicator 80−58820
optical fibre ends when fusion spliced *(Japanese)* 80−28317
optical glass, melting, fining, surface tension, diffusion, nucleation in microgravity 80−81016
optical materials, Twyman effect theory based on Van der Waals interactions *(Russian)* 79−77890
organic liquids, branched-chain, surface tension temp. coeff. *(Japanese)* 78−75913
organic liquids, butyl alcohol, benzol and diesel fuel, AC field influence calc. comparison with exptl. data *(Russian)* 77−55417
oscillating jet method, surface elasticity effect 80−10743
oscillations of doubly connected free liq. surface 77−80682
oscillatory flow in U-tube manometers, effect of drag reducing polymer additives 80−64584
overstability in horizontal layer of binary liq. mixture with Soret effect 80−106782
oxides, liq., calc. *(Russian)* 80−15335
particle size, surface tension, stabilizer conc. effects meas. *(German)* 79−24834
particle size effect on acoustic phonon spectrum, rel. to Debye temp. 77−72666
pendant drops, surface area meas. 78−30813
pendent drops, equilibrium and stability 79−23805
pendular ring condensation on spherical adsorbent, surface tension curvature depend. 79−46926
pentanol activity in bulk phases, distribution and surface activity *(French)* 80−24712
petrol surface tension and flow, high-voltage effects *(Russian)* 79−83464
phase interfaces, balance eqns. and struct. models 78−59453
phospholipid vesicles, hydrostatic press. 80−56000
photographic emulsions, high shear rate viscosity and dynamic surface tension 79−19495
photon correlation spectroscopy, liquid surfaces, effect of instrumental broadening 77−87852
planar structures, hexagonal and cubic models, surface forces 80−20022
plane pendent drops, instability 80−29247

surface tension continued
PMMA, monolayers collapse mechanism, surface press. and ellipsometric obs. 78−43214
PMMA, surface energy anal., comparison of one- and two-liq.-contact-angle methods 77−59181
polar liquid, calc. 77−31841
polar liquid, surface tension, effect of elec. field 78−51791
poly(alkylene glycol), surface tension, sessile bubble method *(Japanese)* 78−79857
poly(alkylene glycol)-eicosane, interface tension, sessile bubble method *(Japanese)* 78−79857
poly(ethylene terephthalate), surface props. rel. to UV irrad. *(Japanese)* 78−79859
polyalkylene isophthalates, by sessile bubble method *(Japanese)* 80−75405
polybutadiene, adsorption behaviour, surface tension exam. *(Japanese)* 78−31690
polyethylene films, adhesive props. improvement by corona discharge appl. *(French)* 78−92438
polyethylene films, preliminary treatment before corona discharge printing, technical parameter effects *(German)* 79−15838
polyethylene-co-vinyl alcohol-g-ethylene oxide aq. soln., surface tension *(Japanese)* 80−24716
polymer, adhesion phenomena and influence of various factors, work of adhesion *(Polish)* 80−3292
polymer, breakup of anisometric drops on mixing 77−40578
polymer melts, immiscible, surface and interfacial tension, thermodynamic theory *(German)* 78−26753
polymer melts, theory 79−65296
polymer mixtures, molten, interface props. near consolute point 78−87792
polymeric composite, interphase, physico-chemical problems 80−16262
polymers, amorphous high, surface tension temp. depend., appl. of significant liquid struct. theory 80−44394
polyvinyl alkylates, surface tension *(Japanese)* 79−95247
porous materials, sintering, behaviour of pore filled with const. amount of gas 80−66450
positive surface tension gradients, Rayleigh-Benard convection *(French)* 80−75404
profile area as useful pendent drop parameter 79−23806
protein crystal dehydration, conformational changes with hydrostatic compression *(Russian)* 77−43339
protein-lipid interaction, appl. of surface tension meas. 79−24940
PTFR, surface energy anal., comparison of one- and two-liq., contact-angle methods 77−59181
pulmonary surfactant film, surface dilatational viscosity obs. 79−62278
pulsed laser-induced shattering of water drops 80−50471
pure liquid, theory 79−65296
pure liquids, temp. depend. correl. 78−91512
PVC, surface energy anal., comparison of one- and two-liq.-contact-angle methods 77−59181
PVC pastes, rheological, surface props. rel. to density of prep. foams *(Polish)* 78−85212
quartz, vitreous and cryst., plates, Twyman effect and effective surface tension *(Russian)* 77−31867
rare-earth metals, surface valence state from surface tension props. 79−95462
Rayleigh waves, surface tension dispersion effects 80−14513
Rayleigh-Taylor instability, method of generalised coords. 78−65771
review of theory 79−77866
rigid sphere model and evaluation of surface tension of liquids 79−56040
rimming flow, numerical simulation of free-surface flow with surface tension 78−22353
rotating fluid dynamics, review *(French)* 78−30300
rotating thin-ring electrode, bubble nucleation 78−48664
salt, molten, surface tension calcs., Fowler model modification 78−67888
sea, surface tension variability with mean wind speed 78−7656
semiconductor, phase diagrams for electron-hole droplet condensation 79−38001
semiconductor-liquid metal structure, electrocapillarity effect 79−73588
silicone oil drop spreading on horizontal surfaces 80−2250
silicone oil thin films, convective heat transfer, surface tension effect 78−94681
simple fluid, one-component, liquid-vapour phase coexistance, surface tension determ. from many body pot. 80−49465
simple fluids, surface tension formulae 79−73378
small particles, cause of reduction in lattice spacing *(Russian)* 80−38967
solid, eqn. of state anal. 80−6618
solid or liquid, surface free energy theory, thermodynamics, mol. forces and struct. 77−55437
solid-liquid interface, study of interfacial tension, elec. field depend. 78−87845
solid-liquid metallic binary alloy, interfacial tension, chem. adsorption and temp. depend. 80−59777
solid/melt interfacial tension and contact angles of small particles, determ. from crit. vel. of engulfing 80−79915
solidifying melt, particle engulfment, thermodynamic aspects 77−4184
solitons in condensed matter physics, theory 80−50122
soluble inorganic salts, crystal-solution interfacial tension, from crystn. meas. 79−69045
solution, different-sized mols., orientation effects, surface region, lattice model 79−1540
specific acoustic impedance in organic liquids, interdependence on surface tension *(Polish)* 80−39223
sphere in continuum model, surface tension rel. to internal press. 78−2336
statistical mechanics of short chain mols. at interface 77−43426
statistical theory 79−51392
steel, interfacial tension in phase boundary with MnO-TiO_2-SiO_2(Al_2O_3) *(Czech)* 78−63907
steel, molten interfacial tension in phase boundary molten CaO-SiO_2-Al_2O_3-CaF_w2 slag *(Czech)* 78−63908
steel, Si-Mn, melt, surface tension *(Russian)* 78−43212
steel-(MnO-SiO_2-ZrO_2) slag system, molten, interface, wetting angles, surface tension *(Czech)* 79−19432
steep water waves, surface tension effects 80−38424
styrene-acrylic terpolymer surface tension rel. to temp., compatibility of external plasticiser 79−15834
submerged moving bodies, free surface and surface tension effects 80−1522
surface oscillations, viscosity and surface tension relax. effects 77−62266
surface tension driven convection, solidification effects 80−43703
temperature, rel. to surface tension *(Chinese)* 78−18873
tetra-n-pentylammonium salts, molten, thermodynamic props., cation struct. 79−55639
tetrabutylammonium iodide, alcoholic soln., repulsion phenomena in thin layers 80−107619
tetrahydrofran-propylene oxide copolymer, surface tension, composition and temp. depend. *(Japanese)* 78−79860
thermo-optical convertor with liq. modulating medium 80−91927
thermodynamic viscous interface theory and associated stability problems 79−95246
Thermodynamics of adsorption and Gibbsian distance parameters in two and three-phase systems 78−10282
thermoplastic recording media, electrocapillary effect, tangential extension influence on 'frost' deform. *(Russian)* 77−68249
thin liquid films in emulsions, tension and contact angles 80−92761
transient axisymmetric wave motions due to sources in presence of surface tension 77−72312
triethylene glycol, critical nuclei, meas. of number of mols. and surface tension from rate of nucleation 79−65293
triple point surface tension and bulk modulus, theoretical relationship 78−47638
two-phase fluid equilibrium, thermodynamic functions and surface tension 78−2262
vaporisation entropy/surface tension relation near melting point *(Japanese)* 79−99397
vapour-liquid interface, surface thickness determ. assuming linear density profile 79−69324
vinylacetate-H_2O suspensions, particle size, surface tension, stabilizer conc. effects meas. *(German)* 79−24834
viscida, buckling and stretching, surface tension effects 79−10512
viscoelastic non-Newtonian liquids, resist. to tensile stress 80−1505
viscometer, capillary, Ubbelohde-type, surface tension effects for spherical fluid reservoir case *(German)* 79−86534
viscosimeter, capillary, Ubbelohde-type and types with different reservoir bulbous form, surface tension effects calc. *(German)* 79−86535
viscous or perfect incompressible fluids, gravity waves with surface tension and capillarity strain *(French)* 77−65749
vortex sheet discretised evolution with buoyancy and surface tension effects 77−27579
vortex sheet evolution, buoyancy and surface tension effects 78−9643
water, autoadsorption and surface entropy in 20-50° temp. range 77−28065
water, cavitation expts. in steel Berthelot tube 80−87788
water, coalescence times of H_2S and CO_2 bubbles 77−42899
water, distilled, AC field influence calc. comparison with exptl. data *(Russian)* 77−55417
water, normal and heavy, surface tension from Skeleton table *(German)* 80−75407
water, press. effects on surface tension, adsorpt. of hydrocarbon gases and CO_2, 0-50°C 78−56024
water, surface tension, temp. coeffs. meas. 78−43216
water, Thakur-Hickman meas. 77−85019
water jet, penetration through water surface, high-speed photography 78−42693
water waves, steep, surface tension effects 79−55398
water-nitrobenzene interface, mechanoelectrical energy conversion using interfacial tension changes 79−14982
water-toluene-sodium dodecyl sulphate-butanol 1 mixture, interface light scatt., interface tension meas. 80−76039
water/air surface tension, effect of air diffusion and interface struct. 77−4246
waterbed, teaching apparatus 79−13
wetproofed electrode, pore filling degree with electrolyte and liq. reactant 80−40702
wetting tension depend. on meniscus curvature, adjacent liquid film disjoining press. isotherm 80−2247
Ag-Au, liquid, surface tension *(Japanese)* 79−19431
Ag-Cu, liquid, surface tension 78−43217
Ag-Ge, liquid, surface tension exam., sessile drop method *(French)* 77−20162
AgBr melts, surface energy and surface tension coeffs., effect on photographic emulsion microcryst. growth rate *(Russian)* 80−47132
AgCl melts, surface energy and surface tension coeffs., effect on photographic emulsion microcryst. growth rate *(Russian)* 80−47132
AgCl-KCl, solns., activity coeffs., surface tensions, 860 to 1000K 78−76897
AgCl-NaCl molten solns., activities and surface tension 80−10748
Al, liq., thermodynamic props., pseudopot. calc. *(Russian)* 79−46549
Al-Cu, liq. alloys, surface tension meas. *(French)* 78−18875
Al-halide systems, liquid-liquid interfacial tension meas. 80−10750
Al-Pb(Bi)(Sn) liquid alloy, surface tension and surface adsorpt. determ. *(French)* 79−69325
Al-Pb(Sn), liquid, surface tension, size effect *(French)* 80−15341
Al-Si alloys, surface tension *(Czech)* 79−77865
Al_2O_3-Cr_2O_3 melt, exam. of surface tension and density 79−1541
Al_2O_3-SiO_2 melt, exam. of surface tension and density 79−1541
Ar, liq., surface properties of classical Lennard-Jones liquid *(Russian)* 79−77869
Ar, liq., surface tension and density profile from expression for excess free energy 77−80681
Ar, liq., surface thickness, near triple point, using surface tension data 79−99400
Ar, liquid-vapour interface, surface of tension near triple point, theory 80−100375
Ar, liquid-vapour interfacial width near central pt. 78−22931
Ar, nonequilibrium condensation and surface tension in supersonic jet flow *(Russian)* 80−65210
Ar phase stability boundary, nucleus surface tension rel. to surface radius of curvature 79−60603
Ar, surface energy and surface tension near triple pt. 78−43218
Ar, triple point, surface tension effect on transition zone 77−35798
Au, surface valence state from surface tension props. 79−95462
Ba, liquid thermophysical properties, up to 1800K 78−30767
Bi, liq., in fused alkali chloride binary mixtures, electrocapillary phenomena 77−40553
Bi, liq., in fused KCl-KBr mixtures, electrocapillary phenomena 77−40554
Bi, molten, density, surface tension, temp. depend. 77−69147

surface tension continued
Bi-Pb-Hg, liquid, surface tension and density *(Russian)* 77−55418
Bi_2O_3-Mo(W)O_3 melts, electrophys. props. 77−89817
Bi_2O_3-Si(Ge)O_2 melts, phys. props. 77−89566
C, vitrified, surface, wettability, surface tension, contact angles of liqs. 79−37901
CaF_2, melts, elec. cond., surface tension, viscosity, density *(Russian)* 80−92758
CaF_2-MgO-SiO_2, melts, elec. cond., surface tension, viscosity, density *(Russian)* 80−92758
CaF_2-MgO(SiO_2), melts, elec. cond., surface tension, viscosity, density *(Russian)* 80−92758
$Ca(No_3)_2$-H_2O system, induction period supercooling depend. meas. 80−19918
CaO-SiO_2-Al_2O_3-Na_2O-CaF_2 melts, surface tension and limit wetting angle in contact with C and CrNi steels *(Czech)* 79−37908
Cd-$CdCl_2(Br_2)(I_2)$ molten solution 77−85024
$CdTl_2Se_4$:Au(Ag)(Cu), doping effect on surface tension of melt and cryst. microhardness 80−49464
Ce, surface and volume props., flow props., surface layer thickness *(Russian)* 80−59760
Cf, surface valence state from surface tension props. 79−95462
Cl_2, liquid-vapour surface, computer simulation 80−54478
Co melt, calc. using model potential obtained from X-ray expts. *(Russian)* 77−31580
Cr-Ge liquid and amorphous alloys, struct. props., cond., viscosity, surface tension *(Russian)* 80−54119
CsCl-UCl_3 melts, density, surface tension and viscosity 78−67764
CsI-KI, binary molten mixture, surface tension meas. 79−65294
Cu, liq., surface tension rel. to temp., surface enthalpy, entropy 78−38912
Cu, liquid, dissolved O below 0.02 wt.% effect on surface tension 80−107618
Cu, liquid, surface tension meas. with levitated metal droplets, influence of oscill. amplitude 78−51798
Cu, liquid droplets, surface tension meas., 1000 to 1330°C 77−62711
Cu, molten, O_2 absorption, surface tension driven flow effect 78−6199
Cu, surface tension at intermediate and high temps., influence of additional elements 78−15476
Cu, surface tension cct. cavities under Cu^+ ion irradiation, O_2 and He effects *(French)* 77−35611
Cu-Fe(Co)(Ni), liquid, surface tension *(Japanese)* 79−19431
Cu-Pb, liquid, surface tension, size effect *(French)* 80−15341
F, liquid, hard sphere model with attractive interactions 80−96434
Fe, high C, interfacial tension in phase boundary with MnO-TiO_2-SiO_2(Al_2O_3) *(Czech)* 78−63907
Fe, liquid, surface tension meas. with levitated metal droplets, influence of oscill. amplitude 78−51798
Fe melt, calc. using model potential obtained from X-ray expts. *(Russian)* 77−31580
Fe ore concentrate, sinter quality improvement *(Chinese)* 80−104089
Fe-Ag-Cu melts, phase interface props., Cu influence *(Russian)* 79−51261
Fe-As melts, influence of Sn, Si, Mn and Cr additions on surface tension and density *(Russian)* 80−15337
Fe-As melts, surface tension, density, adsorption *(Russian)* 80−92757
Fe-C (graphite), adhesion and wettability of graphite *(Russian)* 80−20008
Fe-Si, liq. alloys, surface tension, sessile drop method meas. *(French)* 78−84029
Ga, liq., low-temp. H_2 plasma influence, elec. double layer form. 79−33160
Ge, determ. of crystal-liquid interfacial tension 78−75809
Ge, electron-hole droplet condensation model, phase diagram and surface tension 80−6734
Ge, electron-hole droplet shape under uniaxial stress 77−43518
Ge, liquid, surface tension exam., sessile drop method *(French)* 77−20162
Ge, solid-liquid interfacial tension determ., glassy sphere nucleation by rapid cooling 77−51570
p-H_2, liq.-vap. phase equilib., surface tension *(Russian)* 79−65178
$HN(SO_2Cl)_2$, physical props. meas. 79−51293
H_2O, surface tension and energy, Fowler model 80−10754
He crystals, meas. of surface tension and contact energy, standing waves *(French)* 80−92753
He, liq., dynamic struct. factor function, surface contrib. 77−47634
He, liq. and vapour phases, thermodynamic and thermophysical props. calc. using HEPROP computer program 80−6529
He, liquid, free surface, book contrib. 80−2231
^{4}He, superfluid against solid ^{4}He, surface tension and contact angle 79−42339
^{3}He, liq., surface tension, density profile, variational calcs. 78−67882
^{3}He liq. and ^{3}He-^{4}He dil. soln., quasiparticle theory of surface tension for normal systems 79−56012
^{3}He, liquid, ground state surface tension 77−7935
^{3}He, liquid, surface fluctuation influence on free energy, surface tension *(Russian)* 80−92746
^{3}He, liquid, surface tension and density profile at 0K 79−55997
^{3}He, significant structure theory, thermodynamic props. 78−51774
^{3}He-^{4}He, liquid solution, bound impurity pair effect on surface tension *(Russian)* 80−65332
^{3}He-^{4}He mixture, near absolute zero, holographic interferometry exam. of phase changes 78−38905
^{3}He-^{4}He mixtures, free surface, book contrib. 80−2231
^{3}He-^{4}He mixtures, interfacial tension near tricritical point 77−69141
^{3}He-^{4}He phase separated mixtures under press., interfacial tension, 0.3-0.7K 79−51367
^{3}He-^{4}He solutions, interfacial tension near tricrit. point 78−2330
^{4}He, droplets, surface energy, tension, thickness 78−84015
^{4}He, HCP crystal, roughening transition 80−88397
^{4}He, liq., free surface, crit. behaviour near λ point 80−2228
^{4}He, liquid, surface structure 78−87837
^{4}He, solid-superfluid interface, struct., surface tension 80−88380
^{4}He, superfluid, surface tension and surface entropy 78−10235
^{4}He superfluid film, adsorbed on Al_2O_3 powder, surface tension sound 80−24691
Hg, in Rankine-type capillary viscometer *(Japanese)* 80−14859
Hg/electrolyte interface, adsorpt. of ethylammonium bromide, from H_2O, D_2O solns., solvent props. 79−83459
In, liq., low-temp. H_2 plasma influence, elec. double layer form. 79−33160

surface tension continued
In-Sn liquid alloy, 2-butanol vapour adsorption, effect on surface tension and surface comp. 79−14981
InP, molten stoichiometric, surface tension 78−39684
KCl, aqueous film on Hg, secondary electrocapillary effects, interfacial tension and entropy 77−55420
KCl, molten, vapour-liq. interface, mol. dynamics model 80−54362
La, surface and volume props., flow props., surface layer thickness *(Russian)* 80−59760
La_2O_5-$Na_2Si_2O_5$ molten glasses, surface tension and density, 900-1500°C 80−15334
LiH, liq., density and surface tension, 982-1280K 80−59548
LiH, liq., surface tension investigation, 964-1300K 80−70503
$MgCl_2$-NaCl(RbCl) binary melts, surface tensions *(Japanese)* 78−10260
Mg_2SiO_4, floating zone method growth, interface shapes 80−60775
Mo, doped, surface tension driven flow in electron beam floating zone expts. 80−19731
N_2, liq., surface tension and density profile from expression for excess free energy 77−80681
N_2, liquid-vapour surface, computer simulation 80−54478
N_2O_4-HNO_3-H_2O dissociating system, surface tension at liquid-vapour boundary *(Russian)* 78−47643
$Na_xH_2P_xO_{3x+1}$, conversion products in presence of orthophosphate effect on melt props. 77−25355
NaI-KI(RbI) binary molten mixture, surface tension meas. 79−65294
$NaNO_3$ floating zone melting, surface tension driven flow 78−48313
Nd, surface and volume props., flow props., surface layer thickness *(Russian)* 80−59760
$Nd_3Ga_5O_{12}$, floating zone method growth, interface shapes 80−60775
Ni epitaxial electrodeposition, surface-stress phenomena at start 80−35542
Ni melt, calc. using model potential obtained from X-ray expts. *(Russian)* 77−31580
Ni-O, liquid alloys, surface tension and wettability of Al_2O_3 *(Japanese)* 79−99398
Pb, molten, density, surface tension, temp. depend. 77−69147
Pb, surface tension liquidus temp. to 550°C *(Korean)* 79−90848
Pb-Bi molten alloys, density, surface tension, temp. depend. 77−69147
Pb-Sn(-Sb), surface tension liquidus temp. to 550°C *(Korean)* 79−90848
PbO/PbF_2/B_2O_3 solvent system, density, surface tension and expansivity data, effect of B_2O_3 conc. 79−19985
PbSe-flux, interfacial tension at boundary of fused systems 77−35797
PbTe-flux, interfacial tension at boundary of fused systems 77−35797
Pd-C (graphite), adhesion and wettability of graphite *(Russian)* 80−20008
Pr, surface and volume props., flow props., surface layer thickness *(Russian)* 80−59760
Pt-C (graphite), adhesion and wettability of graphite *(Russian)* 80−20008
Pt-Pd (Co)(Su)(Al)(Si) melts, surface tension and density *(Russian)* 80−39388
Pu, liq., hard-sphere model, phys. prop. meas. interpret., adjacent solid phase implications 77−19866
RbCl-UCl_3 melts, density, surface tension and viscosity 78−67764
Rh-C (graphite), adhesion and wettability of graphite *(Russian)* 80−20008
Rh-Cu(Si), melts, surface props. *(Russian)* 78−26750
Se, liq., surface tension isotherms, struct. changes 79−37904
Se_xTe_{1-x} melt, densities and surface tensions 79−86831
Si, electron-hole droplet condensation, phase diagram and surface tension 79−19521
Si, electron-hole droplet condensation model, phase diagram and surface tension 80−6734
Si film, critical surface tension, aligning props. of nematic MBBA mols. 79−90846
p-Si, photosensitivity of elastic moduli and surface tension 78−83864
Si-B system, liq., surface tension, density, and oxidation kinetics, 1410-1700°C 80−20011
SiC, wetting by Cu-Ti and Cu-Sn-Ti melts 78−68664
$SiCl_4$ physical and thermodynamic properties, rel. to Si technology 79−65218
SiO_2, critical surface tension anisotropy, liq. cryst. alignment 79−86676
SiO_2-Al_2O_3-CaO-MgO, liq. silicic and slag, struct, density, surface tension *(Polish)* 78−83711
Sm, surface valence state from surface tension props. 79−95462
Sn, surface tension liquidus temp. to 550°C *(Korean)* 79−90848
Te, liq., surface tension isotherms, struct. changes 79−37904
Te, liquid, meas. of viscosity, density and surface tension *(French)* 78−91371
Tl-Te system melts, conc. depend. 79−37904
$TlNO_3$-$LiNO_3$(KNO_3) mixtures, molten, surface tension, regular solution theory 78−71903
TlTe, melt, elec. cond., surface tension, microhardness, influence of impurities 80−88551
Tl_2Te, melt, resistivity, surface tension, microhardness, influence of impurities 80−88552
Tl_2Te_3 melt, impurities effect on surface tension polytherm and adsorption obs. 77−7947
U, liq., hard-sphere model, phys. prop. meas. interpret., adjacent solid phase implications 77−19866
UCl_4 molten mixtures with alkali metal chlorides, physicochemical props. 78−38915
UO_2, liquid, surface tension 79−7733
UO_2, surface props. of low index faces, calc. 80−6604
W, molten drop break up in gas flow, surface drag, capillary excitation *(Russian)* 80−100024
YAG solutions, in PbO/PbF_2/B_2O_3 solvent systems, density, surface tension and expansivity data, effect of B_2O_3 conc. 79−19985
$YFeO_3$, floating zone method growth, interface shapes 80−60775
YIG, floating zone method growth, interface shapes 80−60775
Zn, liq., temp. depend. *(Russian)* 80−15336
Zn, molten, surface tension, positive temp. coeff. 77−72751
Zn, Zn-Sn and Zn-Sn-Pb, intergranular and solid-liquid interfacial tensions 77−36452
Zn-Bi liquid alloy, surface tension and surface adsorpt. determ. *(French)* 79−69325
Zn-Pb(Bi), liquid, surface tension, size effect *(French)* 80−15341

surface tension measurement
absolute method, max. force exerted by meniscus formed by cone on free liq. surface 80−39390
automatic sample movement unit, operation at specified constant speed 77−51572
contact angle, for sessile drop on horizontal surface, projected image magnification 77−55421
contact plate method *(German)* 77−62713
cryostat for surface tension meas. at low temp. 79−17426
drop volume principle, new apparatus construction 77−59179
drop weight volume method 77−1277
drops, surface and interfacial tension determ. by drop shape meas. 77−59176
dynamic surface tension, meas. by excited capillary jet axisymmetric disturbance growth rate 78−95205
dynamic surface tension of solns., bubbles, maximal pressure, dead time of formation 80−10744
using filter paper Wilhelmy plates with insoluble monolayers 78−357
floating foil method 80−325
grain boundary groove method, for ice-water interface 77−24481
holographic interferometry of surface deformations of transparent fluids 79−7094
inks, dynamic surface tension, determ. from capillary instability of jets 78−84031
insulating liquids, capacitive sensing of capillary rise 78−41399
interfacial tension, electrochem. data numerical differentiation by Fourier transformation 78−41139
interfacial tension meas. using rods 77−31842
interfacial tension meas. with spinning drop in gyrostatic equilibrium 78−51799
Langmuir film balance meas. system 80−62659
lattice parameter change method, theory for faceted microcryst. 77−47660
Lippmann electrometer, for interfacial tension meas., capillary wear effects 78−26751
liquid, by method of highest press. in gas bubble, meas. device 77−43407
liquid dynamic surface tension meas. instrument 80−42313
liquid gas interfaces, contactless method 79−1277
liquid interfacial tension meas. from scatt. light intensity 80−20012
liquid metals, apparatus for 80−59759
liquid-liquid interfacial tension meas., appl. to molten Al-halide systems 80−10750
menisci around plates and pins dipped in liq., Wilhelmy plate and solderability meas. 77−59185
molten salts, ring method technique 78−54521
multicell spinning drop interfacial tensiometer 78−45770
oil droplet, shape when suspended in aq. soln. with density gradient, meas. of low interfacial tension 79−77863
organic polymers, comparison of one- and two-liq.-contact-angle methods 77−59181
oxide melts, specific weight, electrical conductivity, viscosity and surface tension meas. methods survey *(Slovak)* 80−47079
pendent-drop method, surface interfacial tension meas. 79−46891
ring tensiometry, effect of contact angle 78−60011
Sentis' method, extn. to surface tension of liqs. 79−46888
solid-liquid interphase surface tension, thermal meas. procedure *(French)* 77−66072
sphere tensiometry: wall effects and correction factors 78−63899
spin drop surface tensiometer, alternative soln. 78−47642
spreading pressure of adsorbed film, direct reading strain gauge 77−15692
striascopic imaging of profiles with laser light 79−2845
student experiment, bubble method 77−45651
temperature dependence from triple point to critical point *(German)* 80−100376
wall effect in surface tension determ. using Wilhelmy plate 80−2246
water on semiconductor substrate surfaces, measurement of contact angle *(German)* 80−34276
Al, liquid, pure, surface tension meas. *(German)* 77−35799
Cu, liquid, pure, surface tension meas. *(German)* 77−35799
H_2O, adsorption of proteins, meas. at interfaces by drop volume technique 78−60009
He, and other liquified gases, proposed quick method 78−43208
Sn, liquid, pure, surface tension meas. *(German)* 77−35799

surface texture
adsorbed molecules, Raman and fluoresc. enhancement by surface roughness 80−102511
adsorption, capillary condensation on rough surfaces 79−1544
autocorrelation, surface texture assessment 80−47013
benzene submonolayer on silica gel, PMR and DMR dynamics and surface heterogeneity 79−69735
binary liquid mixtures adsorption onto solid surface, effect of surface heterogeneity 80−44411
biological implant, ion beam sputter of surface morphology SEM exam. 77−44836
boiling heat exchange, of light hydrocarbons and N_2, surface roughness depend. *(Russian)* 79−68562
boiling liquid thin film rupture, heat-transfer surface state effect 78−55552
cartilage, articular, meas. of surface microgeometry 80−3880
catalyst, diffusion in pores, gas chromatography obs. 79−70372
ceramic/metal layer adhesion mechanism for metallization of electronic ceramics, elec. props. *(German)* 80−76381
cholesteric helix surface, elec. field-induced high-order ref. 78−35115
cholesterylpelargonate, cholesteric-smectic A transition, metal-supercond. analogue 79−23712
colour reproduction of surface texture, visual qualities 78−16881
computer-aided three-dimensional anal. of surface roughness *(Polish)* 77−67411
contact resistance, metal-metal effect of surface roughness and surface films 78−10540
corundum, derived from dehydration of diaspore (α-AlOOH), periodic regular texture 79−99328
corundum ceramic, roughness depend. on initial grain size of alumina *(Polish)* 78−30816
crystal, energy of step on rough face 77−43421
digital capacitance-based meas. instrument 78−4593
divalent metal oxides, (100) surfaces, rumpling calcs. 78−14559
dynamical properties, effects of surface roughness 78−75923

surface texture continued
elastic body, attenuation of surface Rayleigh acoustic waves travelling along periodically surface 80−80047
electrode, equipot., electrophoretic force 78−61024
electrode surface and coating effect on DC breakdown voltages in SF_6 78−87557
electrode surface roughness, effect on electric breakdown in air 80−84018
electron reflection from metal surfaces, surface roughness, IR absorpt. 80−71526
electrospark coating formation factors *(Russian)* 78−19908
ellipsometry for surface roughness meas. 80−52294
exciton luminescence spectra, surface polaritons and Brewster waves *(Russian)* 79−43033
Fabry-Perot electro-optic type wide-band modulator sensitivity, surface error influence 79−50392
film, method of obs. of contact area and mech. breakdown 79−37939
fine particle profile, ruggedness and texture specification by fractal dimension 79−40535
finely grooved solid surface, apparent contact angle of liquids, SEM study 77−51573
flat plate streaming potential investigations: hydroynamics and electrokinetic equivalency 80−106777
fluoro epoxy resins, surface props., appls., wear resistance and friction 78−64713
fluoropolymers, ion-beam textured, adhesive bonding 79−87752
Fourier method of shape and surface texture and of planar sections of particles 77−77690
glass, ground, surface height and correlation length from reflection scatt. of laser light *(French)* 80−54491
glass, obs. by laser damage in Au coating 77−1279
glass, sheet, striation form. mechanism, luminous point method meas. 79−61751
glass ceramic, bonding thermosprayed Si 78−23848
glass ceramic, surface prep. for Si thermosprayed coating 78−11367
glass surface roughness effect on 1064 nm 150 ps laser pulse damage 79−14013
glazed ceramic insulators, surface quality monitoring 79−61813
gloss appearance by means of moire patterns *(German)* 80−52300
graphite, N adsorption, surface homogeneity changes on gasification 79−51396
graphites, ARV, VPP, MPG-6, contact thermal resistance, surface finish and compression depends. 78−79829
grinding, role of elastic and plastic behaviours *(Japanese)* 80−100868
heterogeneous surface, topography effects on adsorpt. energy, asymptotically correct condensation approx. 79−7753
high press. gas discharge prebreakdown processes, electrode surface inhomogeneity effects 79−14628
image speckle pattern rel. to object surface profile, simulation 77−19175
interface forces and interactions, roughness and ductility depend. 77−24476
ion bombardment effects *(Rumanian)* 77−28673
laser damage thresholds for mirror and window materials, 10.6 m 77−50708
laser fusion targets, vapour deposited coatings, surface finish obs. 78−60863
laser speckle and surface roughness 80−102622
layer-by-layer crystal growth, step motion kinetics 77−4063
liquid crystal, texture, light scatt. determ. in dynamic scatt. regime 79−27913
liquid crystals, nematic and cholesteric, surface and bulk configurations, topology 80−59381
LMFBR, Na test of bellows expansion joints, metallographic study *(Japanese)* 79−67850
lunar samples, surface texture from polarimetric and photometric obs. 77−60673
luster quality, meas. method, texture and microreflection characteristics *(Japanese)* 80−35466
magnox fuel cladding, surface struct. data acquisition and processing system 80−898
mathematical models 79−82428
measurement, evaluation of fibre optic proximity transducer 80−36985
measurement by differential light scattering 80−36991
measurement developments, future implications 80−36984
metal, bumpy, Raman scatt. by adsorbed molecules 79−15448
metal, ion beam texturing 77−44402
metal, optical functions, effect of surface roughness 78−56447
metal, surface roughness effect on light absorptivity 78−80314
metal, thin sheet, tensile instability and limit strains, growth of surface roughness 77−86084
metal film, structure-related optical characts. in visible and UV 77−55841
metal film and foil, surface IR wave propag. distance, imperfection and oxidation effects 77−28641
metal mirrors, diamond turned, surface, optical and laser damage charcts. 77−50705
metal ribbons, amorphous Newtonian-quenched, formed by melt spinning and melt extraction, dimens. variations 79−56943
metal sheets sliding on dies under plane strain drawing, sliding surface damage obs. *(Japanese)* 77−44369
metal surface, rough, hemispherical emittance 80−70434
metal surface finish meas., backscattered electron intensity *(Japanese)* 79−4465
metal surface micro-inhomogeneity effect on optical breakdown of gas 80−48922
metal surface roughness meas. using laser speckle 78−8383
metal surfaces, abrasion mechanism rel. to groove sizes, shapes 79−20216
metals, elastic constants and moduli of axial textures 80−75286
metals, ion-beam textured, adhesive bonding 79−87752
metals, submicroscopic surface relief after finishing 79−29276
metals, surface plasmons on rough surfaces, dispersion relation changes 77−69394
metals, surface sliding damage, no lubrication, materials depend. *(Japanese)* 78−56780
meteorites regmaglyptic relief index, meas. 80−56782
Michelson interferometer, double-passed, influence of surface roughness on photometric setting-accuracy 78−12746
microspreading on rough surfaces by SEM 77−72746
molecules adsorbed on rough surfaces, Rayleigh, Mie and Raman scatt. 80−83378

surface texture continued
multiple layer adsorption, on foreign substrate, surface roughness and surface free energy variation 77−24497
NDT, surface detects appearance, effects of roughness and method of surface preparation of rods 77−63860
nematic liquid crystals, texture, light scatt. determ. in dynamic scatt. regime 79−27913
nematic-cholesteric mixture, surface boundary conditions influence on transition *(Russian)* 79−23705
nitrided steel surface wear-related topography 78−60847
non-IPS geometric surface relief effects rel. to diffusional phase transform. 77−15667
nuclear tracks, etched, statistical distrib. of quadratic holes on planar surface, computer simulation 80−37705
optical examination and monitoring of surfaces, review 79−67375
optical glass, surface layer structure after grinding and polishing, Kr sorption meas. 77−31122
optical glass diamond grinding kinetics 80−64224
optical pattern recognition by diffraction pattern sampling 80−99643
optical properties, effect of surface texturing 78−56443
optical properties of rough surfaces, discontinuous films, heterogeneous materials, review 80−103935
optical properties of rough surfaces, general theory and small roughness limit 77−75423
optical surface meas. using FECO scanning interferometer 77−7219
optical surface roughness dependence of laser induced damage threshold 79−81469
optical surfacing, struct. of fine ground surface 77−27393
organic eutectics, roughness parameter and surface energy rel. to surface nucleation 79−19163
orientation distribution function, calc. of odd part 80−20954
orthodontic adhesive joints, adherend topography effects 77−52916
oxide films, As doped, thermal stress effects on roughening 79−23813
paper, surface characterisation and printability criteria, stochastic approach 78−18878
particles, textured and structured, fractal dimension characterisation, dilation logic appl. 79−58673
phonon transport in bounded systems, influence of size effect and surface roughness 79−46849
pole figure anal. by computer 77−71303
poly(ethylene terephthalate), surface props. rel. to UV irrad. *(Japanese)* 78−79859
polycarbonate film, by aq. acetone solns., roughness form. mechanism *(Russian)* 78−48554
polycrystalline surface texture analysis, modern methods, review 78−75914
polyethylene, surface fluorination effects, internal refl. spectroscopy obs. 78−86340
polyethylene film, oriented, soln. growth 80−45244
polymer surface contacting blood, roughness effect on thrombus form. 79−48369
polymer surfaces, abrasion mechanism rel. to groove sizes, shapes 79−20216
polymers, corrugated surface, Rayleigh wave excitation, modified wedge method 79−37261
polypropylene, surface fluorination effects, internal refl. spectroscopy obs. 78−86340
polypropylene fibre, with helical internal texture, SEM obs. of surface morphology 80−39394
powder, ultra fine, surface roughness effect on formation by rotating friction mill *(Japanese)* 78−95709
quartz, amorphous layer on mech. treated single crysts. electron microscope and RHEED obs. 80−24721
quartz, IR reflection spectra of rough surfaces *(Russian)* 77−48175
quartz, obs. by laser damage in Au coating 77−1279
quartz fused, refractive index distrib. normal to polished surface, ellipsometric meas. 79−86965
quartz grains, from sub-glacial and assoc. environments, characterisation using SEM 79−25238
quartz grains in Einbeck, W.Germany, loess profile, weathering rel. to stratigraphy *(German)* 79−20823
quartz grains of podzols, surface texture, SEM study 78−36151
quartz ground surface, structure features of dull layer 77−54763
Raman scattering, surface enhanced, surface roughness effect 80−83377
random generation of rough surfaces, numerical procedure 78−62060
randomly stepped surface, He backscattering 78−11055
Reynolds roughness effects in hydrodynamic lubrication 79−1919
riffle formation model 78−63482
rock joint surface roughness, statistical representation 79−48464
rough curved surfaces, theoretic considerations on surface roughness meas. *(Czech)* 80−193
rough surface, random, reflectance derived with Fresnel approx. 80−87309
rough surface contact, review of expt. work 80−76377
rough surface description, Rayleigh wave dispersion 77−39727
rough surface heat transfer in turbulent boundary layer, mixing length hypothesis 78−83378
rough surface turbulent flow heat and mass transfer, Reynolds analogy deviations 78−83380
rough surfaces, anisotropic, light scatt. 79−60606
rough surfaces, topographic characts. by virtue of profile 79−56049
roughened surfaces in gas cooled fast breeder reactor heat exchanges, improved transfer 77−18650
roughness improvement using US energy *(Rumanian)* 79−15821
roughness persistence between surfaces in static contact 77−11632
rubber, friction against paper and polymer film surfaces, microroughness effect 80−71763
rubber, surface texture effect on hysteretic friction 79−61741
scattering object, coherently illuminated, speckle pattern statistics in diffr. field 80−63924
semiconductor characterisation and analytical techniques *(Japanese)* 77−84735
semiconductor substrate surface, low loss electron and Auger images correl. 78−22944
SF_6 compressed, breakdown threshold, effects 78−75449
silica optical fibres, surface flaws obs., fracture strength 77−14793
silicate glasses, polishing, surface characts. using grazing X-ray reflection *(French)* 80−65353
sinters, texture anal., appl. to Ca ferrites in sinters of rich Fe ores 80−18009
smoothing, particle drag retardation 77−12561

surface texture continued
smoothness measurement, currently employed instruments 77−67409
snad grain surface texture rel. to wind vel. conditions 80−41443
solar cells *(Chinese)* 79−57435
speckle, white light, contrast at defocused image plane 80−23621
speckle patterns, partially developed correlated, statistical props. 79−3629
steel, austenitic stainless, 316, surgical implant ion beam textured, stress/strain relations, fatigue characts. 78−73297
steel, maraging, 18 wt.% Ni, solution heated and aged, surrface damage during machining, unlubricated 78−15599
steel, stainless, brightness, vacuum heating effect *(Japanese)* 79−61752
steel, stainless, emittance, oxidation and surface roughness effects 80−96673
steel, stainless, emittance meas. rel. to surface roughness parameters 80−100342
steel, stainless, ground surface ion bombardment, in DC glow discharge 78−95098
steel, stainless, type 304, laser surface melted, topographical characts. 79−70200
steel, stainless, type 304, surface condition effects on IR absorptivity 79−56754
steel 1018, laser surface melted, topographical characts. 79−70200
steel C60, machined, surface morphology, struct., SEM, topographic investigs. *(German)* 77−73372
steel medium C, type 45, electroerosion, white-layer structures detection method 79−52485
stylus instrument developments 80−36983
substrate topography, insulating film contouring 77−8752
surface plasmon dispersion relation in presence of surface roughness 80−65650
thermal conductivity, surface roughness effects, low temp., including defect and boundary scatt. of phonons 77−28057
thin-wall cylinder cold rolling method 80−66535
topography, correlation with profile statistical parameters 80−88418
topography as nonstationary random process 78−24739
transition metal surface electronic struct., influence of size and roughness 78−14785
US ellipsometer design and performance 79−57196
vortex tube efficiency, hot end inner rifling influence 79−94462
Walsh function assessment method 80−36995
waveguide scattering problem, comparison of two perturbation theories 80−83662
waviness, roughness and shape deviations standardisation 77−5805
wetting, effects of solid surface roughness, expt. study 80−34275
wetting, surface roughness effects 77−59178
X-ray imaging system, surface roughness and scatt. effects 80−77921
X-ray study of rough surfaces, effect of 1° glancing angle on penetration depth 79−35665
Zircaloy cladding, stress corrosion cracking, inner surface texture effect 80−66695
ZnO, film, reactively RF sputtered, anal. of texture 78−67921
Ag (110), struct. and effect of surface roughness on LEED intensities 77−24471
Ag electronde, enhanced Raman effect from adsorbed cyanide 80−50348
Ag film, friction and fear in ultrahigh vacuum, effects of speed, film thickness and substrate surface roughness 79−20202
Ag film, polycrystalline with artificial surface roughness, electrical resistivity temp. coeff. *(Russian)* 79−82688
Ag film, surface roughness determ. from light scatt. meas. 78−5541
Ag film, surface roughness, light scatt. meas. 80−107624
Ag films, underlayer effect on surface roughness, surface plasmon excitation meas. 79−51456
Ag foil, surface-plasmon resonance, roughness-induced wavelength corrections 80−108288
Ag foils, surface plasma-wave reflectance and roughness-induced scatt. 80−66228
Ag sinusoidally modulated, light emission of nonradiative surface plasmons 77−1467
Ag surface, adsorbed pyridine, enhanced Raman scatt., ultrahigh vac. study, surface roughness depend. 80−88993
Ag surface, electrochemically roughened, nature and role in promoting anomalous Raman scatt. intensity 78−84587
Ag, surface plasmon dispersion relation in presence of surface roughness 80−65650
Ag, surface-plasmon modulated reson. for adsorption studies 79−83045
Ag wire, ultrapure, cryst. forms of hillocks and voids formed by electromigration 77−31811
Ag-MgF_2 layered system, optical excitation of surface plasma waves 78−6803
Ag-Pd and Ag-Ag contact resistance, effect of surface roughness and surface films 78−10540
Al alloy, 2024 T-351, laser surface melted, topographical characts. 79−70200
Al, deformed surface layer, block misorientation 79−99405
Al film, vacuum deposited, 7 to 65 μ thick, morphology and purity determ. 77−76699
Al laser target, multiple-pulse thermal coupling at 3.8 μm wavelength 80−96371
Al, MEED, multilayer scatt. effects 78−83682
Al, sputtering by 15 keV Ar^+ ions, microroughness 79−91556
Al, surface deformation and wear track obs. using analytical electron microscope 80−108687
Al, surface roughness effects on the energy dispersion of backscattered protons 79−24403
Al, surface roughness meas. using Rutherford backscattering of protons 79−51400
Al-Al_6Fe, fibre reinforced eutectic, deformation behaviour by rolling, TEM and SEM study 79−29129
Al_2O_3, Ni dispersed epitaxial layer, textural effects on catalyst, ferromag. reson. 78−23963
Al_2O_3, surface smoothness and densification, effects of SiO_2 additive 78−27462
Al_2O_3-MgO-Cr_2O_3, effect of Cr_2O_3 on surface grain growth 79−23815
Al_2O_3-SiO_2 glasses, thermally toughened, residual compressive stresses evaluation 78−31523
β-$Al_2O_3.Na_2O$ cryst. or sintered disc, Au electrode interface impedance rel. to roughness 77−4437
As_2Se_3, glassy, with adsorbed $H_2O(NH_3)(NO_2)(O_2)(CO_2)(CO)$, surface cond., photocond. 78−80038

surface texture continued
Au, electrodeposit, struct., texture, influence of As on brightness *(Bulgarian)* 78−79862
Au, electrodeposit, struct., texture, influence of substrate *(Bulgarian)* 78−79863
Au film, ellipsometric obs. of optical props., rel. to surface roughness 79−78776
Au film, surface roughness effects on the energy dispersion of backscattered protons 79−24403
Au, surface-plasmon modulated reson. for adsorption studies 79−83045
Au wire, ultrapure, cryst. forms of hillocks and voids formed by electromigration 77−31811
Au-Co electrodeposits, heating effect on microstruct. and surface topography 77−43456
$BaTiO_3$ surface voids, Auger spectrochem. anal., organic contamination 79−24467
Be, RF sputtered film, props. rel. to deposition conditions 77−39965
Be, thick film, amorphous, RF magnetron sputtering 80−80971
Bi film, ellipsometric obs. of optical props., rel. to surface roughness 79−78776
Bi film, X-ray diffr. anal., {001} textured growth 78−72016
Bi thin film, structural evolution 8 to 573K, supercooling effects *(French)* 79−90921
C fibres, oxidation, surface props. *(French)* 78−44238
C fibres, oxidation by NO_2, struct., props. modification 78−44237
C fibres, PAN-based, surface charact., investig. by flow microcalorimetry 78−48694
C materials, optical microscopy, reflection, interference colours, terminology 78−42871
Cd films, nucleation and growth, props. 80−29878
$CdCO_3$, topotactic decomp., X-ray diffr. obs. 77−44478
CdS, single cryst., surface treatment effects on photoluminesc., struct. and optical props. *(Russian)* 78−15224
CdS thin film solar cell fabrication, HCl etching 80−81474
Co-W-Cr (15,20 wt.%), surgical implant ion beam textured, stress/strain relations, fatigue charact. 78−73297
Cr, oxidation kinetics, 300 to 600°C, struct. and morphology of oxide film 77−59982
Cr-Cr_2O_3, black chrome films, surface microstruct. rel. to optical props. in solar absorbers 79−52036
Cr-Cr_2O_3, chrome black, electroplated selective surface, thermal emittance, solar absorpt., refl., and roughness 79−79406
Cr_2O_3 films, black, microstruct. depend. of optical props., SEM, XPS, and sputter depth-profiling 79−43049
Cr_2O_3-Cr black, selective coating, optical and topographical props. 80−26165
Cu, cementation, on Fe, deposit struct., reaction rates, SEM 80−104421
Cu coating, bias sputter parameters effect, hollow cathode 77−40369
Cu, electroplated coating, levelling kinetics, interferometric investigation *(Bulgarian)* 78−79864
Cu, erosive wear mechanisms, combined TEM and SEM obs. 80−108601
Cu, evaporated film, grain boundary grooving and hillock form. 79−69381
Cu film, diffuse optical scattering from variable roughness surfaces 80−100704
Cu, horizontal plate, pool-boiling heat transfer, nucleation centre size, surface roughness 78−90652
Cu, polycrystalline, intracrystalline slip bands in high temp. creep, comparison with brass single crystal *(Czech)* 79−77604
Cu, sputtered surfaces, stability of cones and pyramids 79−78812
Cu substrate, surface topography influence on growth struct. of sputtered Cr 80−20058
Cu surface, boiling props. of H_2O rel. to organics 78−90654
Cu, surface morphology influence on sputtered yield angular distribution 80−65338
Cu, surface roughness effect on H_2 dissociation, classical trajectory calcs. 78−76925
Cu, surface-plasmon modulated reson. for adsorption studies 79−83045
Cu-Al_2O_3 dispersed composite, electron beam deposition, struct. characterisation 77−44197
Cu_2S-CdS thin film solar cells, Cu_2S layer separation, struct. 79−95282
Fe alloy, surface layers examination, X-ray method 78−35606
Fe, cast, grey, chromisation, influence on surface roughness *(German)* 79−11729
Fe-Si (3.25 wt.%), single crystals and polycrystals, cutting surface texture 79−20291
δ-Fe-Zn layer formed on hot dip galvanising, texture 77−9001
Fe_5Ge_3, crysts., roughness of (212) face vs. solution conc. 79−61515
α- Fe_2O_3, hematite, derived from dehydration of geothite (α-FeOOH), periodic regular texture 79−99328
Fe_2O_3:Mn, surface props. 79−65302
δ-FeO(OH) crystallites, TEM imaging investigation 80−39096
GaAs, VPE, fast growth at low temp. and high partial pressure 79−51446
GaAs:Cu, sensitivity of impurity photocond., ordered surface irregularities 79−24018
GaAs/In-Ge-Ag, semiconductor surface condition, effect on ohmic contact barrier height 77−4435
GaAs(Sb), electrochemical sectioning and surface finishing 80−108611
GaN epitaxial layers for LED, X-ray diffr. topography and cryst. characterisation 79−65336
GaN, formed from initial oxidation and nitridation of GaAs, surface and contact props. 77−20436
GaP, surface polaritons, light scattering studies, effect of surface roughness 80−6753
Ge, rough surface, polarisation angles, ellipsometric meas. 78−56449
He scattering by surfaces, diffr. intensities, topographic curves 78−15274
^{3}He, superfluid B phase, surface textures and NMR 79−37895
^{3}He-A, superfluid, instability of persistent currents and heat flow 80−15327
^{4}He, film, saturated superfluid, on rough surfaces, persistent currents in presence of third-sound reson. 77−20156
^{4}He, superfluid, vortex pinning, surface roughening effects 80−88381
In film, friction and fear in ultrahigh vacuum, effects of speed, film thickness and substrate surface roughness 79−20202
InP, MBE growth, expt. *(Japanese)* 77−4743
InP:Sn film, mol. beam epitaxial growth 77−16505
InP/$In_xGa_{1-x}As_yP_{1-y}$ interfaces, sputter-profiled, depth resolution degradation by cone form. 80−80094
surface texture continued
$KBrO_3$, polarised IR reflection spectra, surface damage effects 79−19872
KCl diamond turned window surfaces, 10.6 μm pulsed laser damage 77−50704
KCl, etching, double poison role 80−54240
KCl surface texture and optical props. after forging between polished dies 80−33102
KH_2PO_4, cryst. laser irrad. damage threshold, surface finish and defects effects *(German)* 78−59058
LiF ground surface, structure features of dull layer 77−54763
LiF TLD, plastic deform. effects on thermolum. sensitivity, rel. to handling technique 77−16988
Mg, surface structure autocorrelation functions and Fourier transforms for rough deposits 79−69450
Mo alloys (MChVP and TsM10VD), erosion, effect of ion bombardment dose and previous surface treatment 80−89419
Mo electrolytic dissolution at high anodic potentials, surface quality *(Russian)* 79−39025
Mo, film on sapphire substrate, orientational growth, epitaxial textures, nucleation textures *(Russian)* 80−75454
Mo sheet, 45° brittleness due to partial recrystallisation, 45° crack formation and propagation *(Russian)* 79−100238
Mo, surface machined, struct., electron diffr., TEM *(German)* 77−73371
Mo_2 single crysts., surface orientation effect as high temp. creep and fracture type 80−16403
MoS_2 film, sputtered, solid lubricant, morphological growth 77−35825
MoS_2, unsupported hydrosulphurization catalyst promoted by group VIII metals, catalytic, structural and textural props. 79−79289
NaCl crystal, annealed near thermodynamic equilib. of cryst. and vapour, {110} surface struct. and coarsening 77−28067
NaCl, deformed surface layer, block misorientation 79−99405
$Na^{14}NO_3$, $Na^{15}NO_3$, polarised IR reflection spectra, surface damage effects 79−19872
Nb, film on sapphire substrate, orientational growth, epitaxial textures, nucleation textures *(Russian)* 80−75454
Nb, supercond., surface effect on crit. current density 79−61014
NbC, and NbC-ZrC solid soln., prep. by impregnation, strength, surface submicrocracks 77−16661
Nb_3Ge, high T_c supercond., anal. of X-ray traces 79−56098
Nb_3Si, high T_c supercond., anal. of X-ray traces 79−56098
Ni, (111) surface, S free and covered, D_2 desorption, ang. depend. of flux, mean energy and speed ratio 79−86993
Ni, erosive wear mechanisms, combined TEM and SEM obs. 80−108601
Ni, smooth electrode, potentiodynamic investig. 77−21395
Ni, substrate surface effects on C deposition 77−28721
Ni-Al, Raney nickel catalyst, surface texture studied by N_2 adsorption and ESCA *(French)* 79−69348
Ni-Cr multilayer structs., sputter profiling, depth resolution and surface roughness effects, AES obs. 77−76694
Pb film, friction and fear in ultrahigh vacuum, effects of speed, film thickness and substrate surface roughness 79−20202
PbO, polycrystalline layers, influence of prep. conditions on phase comp., texture and struct. 79−4495
Pt, adsorption of H_2, electrolyte environment and crystallite size effects 78−27774
Pt coated razor blades, surface roughness effects on the energy dispersion of backscattered protons 79−24403
Pt-Ir solid solutions, investigation of field-ion micropattern contrast, selective evaporation and ionisation models 79−69962
Re, adsorpt. of CO on basal (0001) and stepped $|14(0001)\times(10\bar{1}1)|$ planes 78−14594
SF_6, compressed, influence of electrode macroscopic curvature upon surface roughness effects 80−40693
SF_6/N_2 pressurized mixtures, electric breakdown, surface roughness effects 80−14877
Sb, film, microrelief, electron microscope obs., grain size and condensation rate 77−55469
Sb film, X-ray diffr. anal., {001} textured growth 78−72016
Se, thin film selective absorber coatings, prod. using an oblique vacuum deposition technique 80−81488
Si (111) surface, heating effects on ellipsometric parameters 77−72764
Si, CVD amorphous films, effect of surface charact. on visible and UV optical props. 80−60698
Si epitaxial layers, grown by sublimation in vacuum, TEM study of surface 79−46982
Si film, polycryst., grain struct. and surface roughness, TEM study 80−70556
Si films, CVD, amorphous and polycryst., microscopic surface roughness, effective-medium models, ellipsometric expts. 80−24756
Si, optical reflectance rel. to surface damage 79−14985
Si, polycryst., oxidation, morphological aspects 80−76388
Si, porous layer, struct. and heat-treatment effect 79−1557
Si, rough surface, polarisation angles, ellipsometric meas. 78−56449
Si solar cells, proton irradiated, processing influence on elec. performance 80−94001
Si substrates, reactive ion etching 79−83351
Si, surface, pulsed electron beam processing, doping, annealing 80−75254
Si, surface, selectively roughened, polarimetry of specular and non-multiple scatt. EM radiation 79−13904
Si, surface relief after Ar^+ bombardment at low-energy *(Russian)* 79−15028
Si, thermal oxidation, mechanism of appearance of surface roughness and surface defects 77−7956
Si wafer, chemically etched, surface roughness by gas adsorption techniques 80−15398
Si, X-ray diffr., meas. of dynamical and kinematical components with triple cryst. diffractometer 79−50948
Si:P, polycrystalline laser recrystallised film on Si substrate, cryst. struct., thermal oxidation 80−65391
Si:Sb vacuum deposited coating, p-n junction, pulsed electron beam annealing doping, diffusion 80−75480
SiC, reaction-bonded, impact erosion by ang. Al_2O_3 particles 80−89362
Si_3N_4 film, amorphous, optical props., band gap and surface roughness 77−32396
Si_3N_4 film deposited from SiH_2Cl_2 and NH_3, characterisation 79−11521
SiO_2 film, on Si wafer, surface roughness by gas adsorption techniques 80−15398
SiO_2, fused, laser damage threshold rel. to surface roughness 77−40306

surface texture continued
SiO_2, fused, laser damage threshold rel. to subsurface struct. 77−40307
SiO_2, fused, surface damage threshold rel. to prep. and OH^- conc. 77−62026
SiO_2, fused, surface roughness rel. to prep. and treatment history 79−14058
SiO_2, Ni dispersed epitaxial layer, textural effects on catalyst, ferromag. reson. 78−23963
SiO_2, surface roughness effect on 1064 nm 150 ps laser pulse damage 79−14013
SiO_2, thin films on rough polycryst. Si surfaces, oxide thickness and refractive index meas. 80−93422
SiO_2-TiO_2 antireflection coatings, 1064 nm 150 ps laser pulse damage rel. to barrier layering and smoothness 79−14018
Sn, sputtered film, exam. of frictional props. 79−15814
surface roughness, liq. superheat and heterogeneous nucleation 79−37146
Ta, film on sapphire substrate, orientational growth, epitaxial textures, nucleation textures *(Russian)* 80−75454
Te textured thin films, prep., high solar absorptivity by multiples refl. 80−11568
Te, thin film selective absorber coatings, prod. using an oblique vacuum deposition technique 80−81488
Ti, coatings, electrolytically deposited, texture, anti-corrosional props. *(Russian)* 80−66532
Ti, emittance, during nonstationary high temp. heating by Ar flow *(Russian)* 80−84308
Ti metal-metal interface, adhesion energy, surface treatment and ion implantation effects 80−107660
Ti-Al-Mo-Zr, compressor disk, surface plastic deform., optimal method 80−60924
Ti-Al-V (6,4 wt.%), laser surface melted, topographical characts. 79−70200
Ti-Al-V (6,4 wt.%), surgical implant ion beam textured, stress/strain relations, fatigue characts. 78−73297
V, film on sapphire substrate, orientational growth, epitaxial textures, nucleation textures *(Russian)* 80−75454
V, radiance temperature at melting point, surface roughness depend. 80−59683
V, rolling textures, microstructure, micro orientation *(Russian)* 79−91663
V superconducting heat switches, effect of surface prep. 79−60966
W, film on sapphire substrate, orientational growth, epitaxial textures, nucleation textures *(Russian)* 80−75454
WS_2 unsupported hydrosulphurization catalyst promoted by group VIII metals, catalytic, structural and textural props. 79−79289
Y-Er, surface, high-freq. elec. cond. dispersion function, effects of polishing and annealing 78−19506
ZrC, and ZrC-NbC solid soln., prep. by impregnation, strength, surface submicrocracks 77−16661

surface topography measurement
abrasive surface profile meas. system, computer controlled 77−52603
adhesive bondline interrogation using Stoneley wave methods 80−49530
aerospace components, holographic interferometry 77−7039
anisotropy, surface, review of characterisation processes 79−12770
aspheric profile gauging using bootstrap data interpretation technique 79−59786
aspheric surface contour meas. machine and computer system 80−14494
aspherical surface profile testing by goniometer 79−76895
aspherical surface testing by holographic interferometry 79−85116
automatic pattern processor for simple and complex interference patterns 80−13129
cartilage, articular, meas. of surface microgeometry 80−3880
ceramic surface metrology using peak counting, quality control 80−95065
circular surface trueness testing by laser speckle photography 79−86266
complex surface shape inspection, coherent optical method evaluation 79−81578
component profile inspection equipment 80−105608
conference New Delhi, India (1977) 78−4590
contactless laser interferometer sweep gauge for diamond-turned surfaces 80−73441
contour holography of moving object, using injection locked flash pumped dye laser 78−50737
contour line of object, real time moire topography equipment controlled by microcomputer 78−89441
contour slope meas. of an object, coherent optical method 78−32862
corneal topography using moire contour fringes 80−26316
cracking metal surface deformation obs. by interference microscopy *(German)* 77−56210
cylindrical surface linearity testing device 77−30129
cylindrical surfaces, artificial holograms by photographic method 79−7095
dark-field surface inspection using total internal reflection 80−74519
deflection contour generation by white light projection speckle method 80−98881
defocused speckle photography, tilt topology technique 77−26419
defocused speckle photography, topological information extraction technique 77−41676
depth contours determ., double photography in coherent light *(French)* 77−87733
depth measurement of bright flat holes by means of projected fringe pattern methods 79−75583
depth profile generation using moire fringes 79−75488
developments, future implications 80−36984
diamond turned surface production, interferometric test repeatability 80−74538
dichromatic speckle pattern, for surface roughness meas. 78−89428
differential light scattering method 80−36991
diffraction grating, sinusoidal groove depth determ. using laser 77−83949
diffuse reflectance rel. to partial coherence and IR laser photogoniometric meas. 80−14283
diffuse surfaces, automated contouring, phase-locked moire fringe analysis 79−26023
diffusing object surface state study by double speckle photography 79−85120
diffusing surface determ. by speckle photography 79−85117
diffusing surface optical autocorrelation 80−99646
digital capacitance-based meas. instrument 78−4593

surface topography measurement continued
dispersive device linear in wave-numbers, space-time optics appls. 77−72071
displacement meas., coherent optical correlation technique 79−75499
dynamic representation by TV moire topography *(German)* 78−89430
EHD contacts, asperity interactions 79−20215
elastohydrodynamic film thickness, meas. of artificially produced dents and grooves 80−36975
electrode surface finish, backscattered electron intensity meas. *(Japanese)* 77−66081
electronic speckle pattern interferometry of surface shapes 78−94380
ellipsometry for surface roughness meas. 80−52294
endoscopic contour technique for meas. dimensions of object detail *(German)* 80−31839
engineering struct. surface deform. meas. by laser speckle photography 79−40534
epoxy resin DGEBA, cured with TETA, crack propag. and fractography, Talysurf meas. 79−70154
eye optic disc topography, by laser contour angiography, error model 77−60236
feeler instrument meas. errors, effects of probing system dynamics 78−73965
fibre optic proximity transducer evaluation 80−36985
film, optical consts., thickness and surface roughness determ., technique and appl. to AlN *(German)* 77−41670
films deposited on semicond. substrates, X-ray topographic meas. method 78−5710
flatness deviation meas. instrum. with aerostatic basis 79−6083
flatness meas., moire angular readout device 79−93209
flatness meas. by roundness gauge with reference rotation 77−30128
flatness of test glass, reading errors of interf. fringes 79−32097
flexed plate, slope and curvature contours meas. using interferometer 77−87810
fluctuations obs. by laser damage in Au coating 77−1279
Fourier method of shape and surface texture and of planar sections of particles 77−77690
fracture surface SEM analysis, microtopography 80−68312
friction surfaces, wear meas. using profilograph, mould producing material quality factors 78−7116
fringes, running, profile measurement using projection 78−93647
glass film, RF sputtered, roughness parameters 77−69202
height difference detection by digitised moire pattern processing 80−52156
height meas. of surface features by SEM 77−60019
height probability density function on ground glass surface from far-field coherent light scatt. 79−93099
height standard deviation on ground glass surface using interference microscopy 79−93098
high sensitivity interferometric measurement study *(Japanese)* 78−37048
holographic contour fringe computer-aided analysis 77−49766
holographic contour fringe generation by dual-index immersion 77−49765
holographic contour mapping application *(Japanese)* 77−88674
holographic contouring, of surface topography and contact rigidity study of rough surfaces 80−64494
holographic contouring by displacing object and illum. beam 78−74864
holographic double-exposure and fringe projection techniques comparison *(Polish)* 78−32788
holographic interferogram quantitative evaluation procedures *(German)* 80−87344
holographic interferometry of plastic parts 77−7037
holographic-moire technique, extension to 3D, to separate patterns corresponding to components of displacement 79−35661
human platelets, air-dried, topography and thickness measured by correlative TEM and SEM 79−84041
image moire method for determination of partial slopes in fixed plates 80−14645
image processing of additive-obtained moire patterns *(German)* 80−47017
image speckle contrast for meas. of object surface roughness 78−1168
incoherent optical correlator using projected fringes patterns, for object shape and contour control 79−97357
induction profilometer for surface irregularity recording 77−74358
interference surface testing with quarter-wavelength sensitivity 78−32870
interferograms, two wave, sensitivity improvement process *(French)* 80−98968
interferometer design, construction and interferogram processing, optical testing appl. 80−79020
interferometric examination of lenses, mirrors and optical systems, 3D display 80−69497
interferometric flatness testing by self-levelling reference plane 78−63207
interferometric surface mapping with variable sensitivity, IC manufacturing appl. 78−45592
interferometry at 10.6 μm 80−86385
ion etching, SEM dynamic study 80−50734
large curved surface coordinate determ. apparatus 78−77863
large monocrystal X-ray reflection/scanning and transmission topographic methods 80−96415
laser beam meas. of surface profile and angular deflection 79−85125
laser dot matrix space-coded surface topographical mapping 80−98885
laser heterodyne apparatus for roughness measurement of polished surfaces 79−21696
laser interferometric profilographs for surface irregularities meas. 77−74363
laser profilograph, description 77−74356
laser reflectance patterns for machined surface finish meas. 79−85126
laser scanning analyser, roughness meas. 80−36992
laser scanning beam for surface profile meas. and ang. deflection monitoring, noncontact method 79−9203
laser section method for surface roughness estimation *(German)* 79−49198
laser speckle granularity growth, appl. to surface inspection 78−12750
laser speckle interferometry, anal. of double aperture speckle and shearing camera techniques 79−6169
laser speckles, bibliography (1976 to 1978) 80−82593
lasers in metrology and testing, review 77−5817
layer thickness measurement by kinetic method 77−24503
light interferometry, correlation functions determ. 78−5428
light rangefinder and profilometer, high-resolution gas laser 80−102754

surface topography measurement continued
linearity of large surfaces determ. using universal optical string 77−26269
liquid, transient behaviour due to pulsed US transducers 80−95073
lunar surface bistatic radar surveillance with FM signal 79−5758
machine part, rotating, surface finish, laser method for determ. 80−89454
machined part flatness and parallelism meas., contactless interferometric method 78−21208
machined surface time series modelling 80−36998
magnetic tape roughness measurement using stereoscopic SEM 79−67254
MC planar, design based on TMS 9980 *(Italian)* 79−21697
mean lines of surface profiles from different electrical filters 78−16773
metal, impact abrasive wear, anal. 79−43443
metal film, on pyrex, surface roughness meas. by ellipsometry and TEM 77−20205
metal mirrors, diamond turned, evaporated and sputtered, surface and optical studies 78−79098
metal surface, diamond turned, finish meas. by differential light scatt. 78−5544
metal surface finish meas., using backscattered electron intensity *(Japanese)* 79−4465
metal surface roughness meas. using laser speckle 78−8383
metal surfaces, laser technique *(German)* 80−52155
metal surfaces, shape and deformations, holographic contour immersion method *(Polish)* 80−62630
metallic mirror surface topography determ. by Nomarski reflection microscopy, theory 79−54185
metalworking rectilinearity and planarity deviations meas. 79−97348
methods survey *(German)* 78−4591
microcomputer application to surface roughness meas. 80−47014
microgeometry meas. by stylus instrument 79−80575
microinterferometer, apochromat objective, with increased resolution, surface roughness testing 79−71519
microlocal analysis using laser mass spectrometer *(Russian)* 77−12862
microroughness estimation for solid surfaces, light scatt. method 77−74355
microscope, phase-locked interf., for surface roughness, curvature meas. 78−49894
microscope, phase-locked interferometric, design and construction 78−45687
microscope, portable, design and performance 77−67495
microwave scatterometer, backscatter optimisation using complex charact. polarisation concept 79−100966
mirror, plane lattice point light source appl. *(Japanese)* 78−9463
mirror optical scatter meas. specification proposal 80−48390
mirror surface curvature and local distortion meas. by holographic interferometry 79−76796
moire, computer generated, for profile testing 80−105689
Moire contour lining, reference plane orientation by optoelectronic methods 77−2636
Moire contouring of large objects by scanning technique 78−32791
Moire contouring system, lateral grating movement *(Japanese)* 77−87817
Moire contouring using virtual moving gratings simulated on computer 78−73968
moire contourography, computer-aided replication of human anatomy 80−67189
moire fringe biostereometry using parallel light beam 79−100701
moire fringe electronic processing, comparison of moire topography and photogrammetry 79−40601
moire fringes, geometric effects *(German)* 79−2746
Moire holography contouring method 78−1183
Moire method applied to high speed deform. meas. 78−36970
Moire patient imaging system, evaluation of 79−39464
moire patterns, contour fringes of optical surface 77−14659
Moire photography, appl. to human face mapping 80−85462
Moire projection topography accuracy and sensitivity 78−45677
moire surface contouring by addition method 79−30420
Moire technique, null-test using synthetic deformed gratings 77−34021
Moire topographic method, anal., concave convex region discrimination 78−65901
moire topography, historical review 80−9024
moire topography, meas. accuracy evaluation 79−40528
Moire topography, projection-type, theory 78−16776
moire topography, real-time and time-resolved, in microseconds region 80−52154
Moire topography, theoretical aspects and practical appls. 79−39463
moire topography, theory and applicable limit for divergent light rays 78−86237
moire topography using grating hologram, appl. to human body 77−5893
monochromatic, point source X-ray emission, use in topographic mapping *(Russian)* 79−30416
multilayer dielectric mirror, light scattering due to surface roughness 80−58460
Nomarski polarisation interferometry, for slope determ. of microscopic surface features 78−16840
non-optical surfaces, by oblique fringe projection from diffr. gratings 78−89437
noncontact optical gauging by remote image tracking in production environment 80−8961
noncontact optical profilometer, fast, precise, automated measurement 79−54095
noncontact optoelectronic position transducers 79−50406
nonplanarity of surface plates, errors in measurement by optical planarity meter 80−17919
nosetip ablation holography in 10 MW plasma arc facility 78−20621
oblique incidence interferometer for surface testing 77−26389
online topographical analysis in SEM 80−68310
opaque polished surface roughness determ., diffuse reflection method 79−49274
opaque surface, roughness determ., photometric method 80−95072
optical component, surface evaluation techniques 79−46094
optical element flatness, interferometric examination techniques 80−69498
optical Fourier spectrum analysis, metal surface roughness measurements 79−49195
optical Nomarski microscopy, differential interf. contrast, for topography quantitative determ. 80−73318
surface topography measurement continued
optical noncontacting transducer, for machined surface profile meas. 79−58765
optical parabolic reflectors, medium size, surface shape quantitative evaluation 79−72654
optical planimeter IS41M for flatness checks on large workpieces 79−97350
optical profile transducer for machined surfaces testing 79−85124
optical profilometer, fast versatile, for surface roughness of workpieces meas. 80−37069
optical shop computer-controlled interferometry, in-process production tool 80−74531
optical surface, scratch classifier for inspection of scratch severity 77−75722
optical surface mapping with quarter wavelength fringes 78−46846
optical surface meas. using FECO scanning interferometer 77−7219
optical surface profile testing with set of spherometers, math. analysis 78−13823
optical surface quality standards based on total integrated scatt. 80−48391
orientation determ. from multiple images, photometric method 80−52163
parameters calc. *(German)* 78−4592
particles, textured and structured, fractal dimension characterisation, dilation logic appl. 79−58673
patient's surface contour measuring device 80−104717
periodic surface characterisation by US diffraction spectroscopy 78−60974
phase locked interferometers, phase difference, surface topography measurements, transparent phase object applications 79−58775
phase-lock interference microscopy, real-time, design, appls. 79−17480
photo-optic measuring systems using bifurcated fibre-optic probe 79−81569
photokeratography using moire techniques 77−21590
photometry appl. 78−4682
pipes, soldered, device for automatic scrapping 79−29308
planarity determ., by interference pattern assessment, using laser source 80−31711
plane surface deviations, meas. system *(German)* 77−30127
planimeter, used with trinocular microscope and TV receiver for TV photomicrography 79−71523
ploughed soil, microwave backscatter determ. *(French)* 80−82072
polished surfaces, smoothness parameter meas. using spectral analysis optical system 80−86261
polychromatic speckle patterns, use for surface roughness meas. 80−31708
power spectrum measurement by optical Fourier transformation 80−36989
profile computerised meas., digital voltmeter output recording on punched tape 80−22327
profile digitised diffractographic data processing 77−58276
profile digitization for stylus instruments 80−36993
profile from horizontal light source reflection, calc. from observed image 80−101777
profile from horizontal light source reflection, image calc. 80−101776
profiles reference line selection and fitting, based on random process analysis 78−45594
profilograph needle radius of curvature, effect on roughness parameter of finely machined surfaces 77−53859
profilometer, EBR-II subassembly, at HFEF 77−54299
profilometers 252 and 283, with direct indication 80−22329
pyroceramic plate surface quality obs. after mechanical polishing 79−72732
radio reflector surface of radiotelescope antennae, surface contour control 79−80221
radiotelescopes, reflector surface errors, rapid meas. method 77−41301
random water waves, optical meas. technique 77−29503
reflecting surface shape determ. of fast-scanning Fabry-Perot interferometer 79−12842
relocation profilometer stage, three dimensional 77−77725
remote profilemeter, converted streak camera 77−79058
replica materials, film type, surface reproduction characteristics 80−36988
replica materials and techniques, comparative study 80−36987
reversible fringe counter in laser interferometry 77−87816
rock joints roughness determination, new laboratory method 78−96315
rotating surface roughness meas. apparatus 78−4588
rough curved surfaces, theoretic considerations on surface roughness meas. *(Czech)* 80−193
rough surfaces, characterisation by meas. of single roughness constant 80−86264
roughness, by amplitude density distribution and autocorrelation function of surface profile *(Hungarian)* 78−12668
roughness, influence of stylus tip geometry on meas. *(German)* 80−68182
roughness, standards and methods *(German)* 79−17398
roughness and surface slope measurement, comparison of Talysurf and optical methods 80−36990
roughness evaluation from interference extremum amplitudes 79−78766
roughness filtering using digital filters 80−36994
roughness meas., alternatives to stylus techniques 79−75496
roughness meas. by reflected-light microscope *(German)* 80−31861
roughness measurement, electrical stylus tip instrums. 80−90818
roughness measurement methods using SEM techniques, research and development *(German)* 80−105612
roughness measurement using improved pneumatic Wheatstone bridge 80−62629
roughness meter using backscattered electron intensity *(Japanese)* 79−93131
roughness of small-diameter channels, non-destructive inspection by replicas 77−30136
roughness of technical surfaces, statistical charact. of profile angles *(German)* 77−17944
roughness parameter determ., profilometer attachment 78−36967
roughness parameters, error due to feeler probes 78−169
roughness profile description, separation of random and periodic components 80−36997
roughness values comparison, measured by M- and E-systems 77−5807
Rutherford backscattering meas. of surface roughness, appl. to Al 79−51400
Rutherford proton backscatt. 80−47015
SAW X-ray topographical representation 79−47870

surface topography measurement continued
scanning gauge for surface form meas., spherical and aspherical 79−32100
scanning moire topography, automatic 3-D shape meas. 77−79139
schlieren instrument large-aperture adapter for optical surface quality evaluation 79−14122
sea wave profile meas. by radar altimeter, computer simulation 77−5367
SEASAT-A satellite ocean surface truth expts. 77−5419
SEM, automatic topographical surface reconstruction 80−62803
SEM, photomicrograph anal. with symmetric pair scintillation detector 79−6232
SEM, stereoscopic observation and three-dimens. meas. instrument 78−21287
SEM, three-dimensional stereo data acquisition, presentation and treatment 78−21297
SEM analysis of object microrelief, metallurgy appls. 80−73319
SEM computer-aided topographical analysis 80−70094
SEM in analysis of material surface texture 80−73548
SEM method and apparatus for quantitative anal. of microrelief 79−7530
SEM topographical measurements at grazing incidence, alignment problem 80−99014
semiconductor characterisation and analytical techniques *(Japanese)* 77−84735
semiconductor manufacturing, interferometric method for surface deform. meas. 78−32793
semiconductor structure, electrodeless meas. of resist. and spherical curvature 79−49252
shadow-moire fringes, interpretation, grating rot., translation effects, surface topography appls. 79−20304
shadow-Moire method with continuously variable sensitivity 77−74361
signal processing and analysing device, Herbert-Sigma *(French)* 80−57254
silicone rubbers, dimensional stability, interferometric gauge meas. system 79−21807
single crystal, surface relief obs. using epitaxial replicas 77−51577
site tolerance, and surface roughness, standard rel. 80−62634
smoothness, currently employed instruments 77−67409
solid corrugated surface, by reflection of EM wave, anal. 79−13875
solid surface characterisation techniques, review 78−22945
Soviet instruments and meas. systems exhibition 80−52161
speckle, polychromatic, for surface roughness properties meas. 78−21210
speckle applications *(French)* 77−67494
speckle contrast, roughness props. meas. 77−18082
speckle correlation of diffuse surface image *(French)* 77−61115
speckle interferometry, book contrib. 79−75584
speckle interferometry, decorrel. effects, contouring and surface roughness meas. 77−45886
speckle pattern correlation, real time roughness meas. 77−18081
speckle pattern interferometry, holographic illum. elements, object geometries comparison, speckle pattern interferometry, holographic illum. elements 78−66785
speckle pattern structural difference for surface roughness meas. 77−79056
speckle patterns, non-gaussian statistics, surface roughness meas. 78−66762
speckle patterns appl. to surface inspection 77−26385
speckle topography, appl. to surface relief obs. of diffuse reflection object 79−54096
speckle wavelength decorrelation for surface roughness meas. 79−30418
sphere, laser interferometric system for positioning of sphere and meas. roundness 79−97416
spherical surface error absolute definition technique, use in interferogram analysis 79−86268
standardisation development, waviness, roughness and shape deviations 77−5805
standardised hand-held instrument, with in-built data processor *(German)* 80−57255
standards development in Soviet Union, All-Union test scheme 80−22328
steel, hot rolled strip and plate shape meas. device 80−35498
steel, square parts, surface inspection, defect depth meas., eddy current method 79−29307
steel, stainless, surface, roughness factor measurement, energetic D^+, He^+, Ar^+ irradiation 80−39172
steel, stainless, surface morphology of H ion eroded samples 79−86968
step height measurement in μm range by two-ray interferometry with adjustable light wavelength *(German)* 77−82489
step-height measurement uncertainties, stylus type instrument calibration against interferometer appl. 78−77862
structure influence on image speckle pattern contrast 80−17985
stylus instrument developments 80−36983
stylus radius rel. to surface roughness meas., digital simulation 77−67413
stylus tip instrums., standards and calibration *(German)* 80−101782
supersmooth surfaces, meas. using electron mirror interference microscope 79−93260
surface finish automatic inspection by laser scanning *(German)* 78−170
surface mapping, absolute optical path meas. by interferometry 79−6093
surface potential pattern measurement by potential probes, crevice depth determination in metallic testpieces *(German)* 78−35597
surface profile waviness and roughness separation technique, Fourier anal. *(German)* 77−74352
telescope PPS 12, meas. of surfaces up to 30 m in extent 78−94423
TEM technique for observing atomic surface steps 77−20173
terrain analysis FORTRAN program 77−9509
texture, autocorrelation function appls. 80−47013
thin wire defect parameters meas. using capacitance method 80−35489
three dimensional uneven object protrusion using Moire fringes *(Japanese)* 77−87730
three-dimensional inspection using computerised electro-optical instrument 79−86272
three-dimensional topographic mensuration, laser electro-optic system 80−99784
tissue characterisation by US backscattering 79−70595
tools for surface anal., review 80−103540
toolsetters, optimal adjustment parameters, one-way adjustment 79−97349
tooth surface moire topography *(German)* 78−80992
transducers appl., mechanical and optical *(French)* 79−170
surface topography measurement continued
transparency, large area, distortion measurements using shearing interferometer with scanned photodiode array and microcomputer 79−80675
tunable moire grating for optical mapping 80−5832
two wavelength holographic interferometer, metrological charact. 77−26393
two-frequency microwave holographic imaging with axial resolution 78−1184
two-wavelength contouring with automated thermoplastic holographic camera 80−74318
universal instrument, modular with indicator and strip recorder *(German)* 80−57283
US backscatter at normal incidence for randomly rough surface characteristics meas. *(French)* 80−52165
US pulse echo techniques for flaw detection in metal components *(French)* 80−55613
very-small-angle light scatt. apparatus design and performance 77−10082
wavefront correlation effect on topogram sensitivity 80−69345
wear measurement by thin layer activation 78−60932
X-ray anal., conf., Denver, USA (Aug. 1976) 77−70382
X-ray diffraction characterisation, highly collimated beam, appl. to Si 78−9912
X-ray diffraction topography *(Chinese)* 80−1883
X-ray image processing, quantitative, with SEM, surface meas. appls. *(French)* 78−41379
X-ray mirror profile meas. machine 80−69496
X-ray scattering and differential interference contrast microscopy 79−30410
X-ray study of rough surfaces, effect of 1° glancing angle on penetration depth 79−35665
Zygo interferometer system 80−73437
Ag film, surface roughness determ. from light scatt. meas. 78−5541
AgCuAg sandwich target, proton induced K-shell X-ray yield ratios 77−48724
Al alloys, contamination, automated nondestructive inspection 80−16629
Al surface damage, meas. and detect. after static contact loading 80−64495
Al thin films evaporated on rough quartz substrates *(Polish)* 80−88450
Al-Cu, high strength, type 2024-T3, crack growth, fatigue induced surface deform., holographic detect. 80−85120
Be substrate for lightweight mirror, surface quality and thermal props. 80−23762
C surface, pyrolytic, roughness factor measurement, energetic D^+, He^+, Ar^+ irradiation 80−39172
$CaHPO_4$, powder and granules with starch mucilage binder, surface topography variation under compression 80−80998
Co, effect on surface roughness on backscattering spectra 80−47016
Fe ore, adsorption methods for determ. of specific surface 78−21096
Mo laser mirror, optical and metallurgical characterisation 80−33129
Si, surface roughness evaluation by UV refl. 80−39393
SiC coatings for first-wall candidate materials by RF sputtering 80−25563
SiC surface, roughness factor measurement, energetic D^+, He^+, Ar^+ irradiation 80−39172
SiO film, obliquely evaporated, topography rel. to liquid crystal orientation 77−69190
SiO_2, film on Si, electron beam damage, obs. using scanning AES 80−2070
Ti-Al-V (6,4 wt.%), surface residual stresses, surface topography, fatigue behaviour 79−52366

surface treatment
see also etching; polishing; surface hardening
ABS mouldings, selective Cu plated in areas, effect on mech. props. 79−34182
acoustic cleaning, electrolytic method for quality control 79−34233
alkali-borosilicate glasses, antireflection film production by heat and chem. treatment 80−66677
alloy, effects on bulk props. 78−85049
alloy, laser surface melting 77−90492
alloy surface composition modification by high-power CW lasers 80−93699
alloys, improvement of props. by ion implantation 80−16601
alloys, nitriding methods and programmed control system 78−95857
aluminas, surface modified, DTA and TGA exam., gas chromatographic eval. 77−36785
American Vacuum Society National Symposium, Boston, USA (Nov 1977) 78−72718
antiscale forming effectiveness of seeding crystals in thermal power plant 80−89527
austenitic solid solution, chem. evaluation of B and its correlations with hardenability and hardness *(German)* 79−39230
austenitic stainless steel thermal treatment for spectrally selective surface fabrication 80−35752
ball bearings, surface comp., AES and ion sputter profiling 77−40465
bone-cement interface bond enhancement technique 78−31980
boride coatings, high temp. resist. and struct. 79−39008
boride coatings on C and alloy steel, spectroscopic thickness determ. 80−85099
boriding, with a thermally unstable gas (B_2H_6) 80−30159
borosilicate glass, cleaning for biological appl. 77−29234
borosilicate glass, porous, surface area change with acid treatment, adsorption of N_2 and H_2O *(Japanese)* 78−44244
bronze-steel, phase composition and struct. of diffusional interlayer in fusion zone, X-ray analysis 78−56821
BWR, Dresden 1 plant, prototype operation for decontamination of primary system 79−54538
BWR decontamination, research and development program 79−54539
carborundum, oxidation protection via phosphate impregnation 77−44374
carburising, process parameters and gas conditions 79−96208
carburising and nitriding, conf., Cincinnati, USA (Nov. 1975) 79−24656
carburizing, determining the limits of regulating carbon potential 78−85052
carburizing, high-rate, direct-current glow discharge furnace 79−83370
carburizing in glow discharge methane plasma 79−11724
chalcopyrites, acidic fermic sulphate leaching, reaction mechanism 79−83511
chemicothermal treatment, mathematical modelling 80−100955
clean surface preparation *(Japanese)* 78−80664

surface treatment continued
cleaning, DIP device for small parts 79−39037
cleaning, metal and glass, liquid spraying technique, appl. to laser surfaces 78−72921
cleaning *(Japanese)* 80−16527
cleaning for thin film technology 79−15843
cleaning techniques review, for atomically clean surfaces preparation 80−11804
coating technology, conference, London (1978) 79−83358
complex profiled surface alloying, automatic electrode feeding *(Russian)* 78−19936
container processing for parenteral products 77−28923
controlled environment exposure of atomically clean surfaces 78−19954
corrosion resistance of L68, LMsh68, MNZH 5-1 to scale-removing solns. *(Russian)* 77−59971
corundum single crystal, premetallizing with Mo-Mn-SiO_2 79−47792
crystal, in-situ cleaning by ion sputtering in EM 80−101895
crystal units, vacuum system for cleaning and cold welding *(Polish)* 80−31776
DC glow discharge techniques for surface treatment and coating 78−11374
decontamination tests, practice-related procedures *(German)* 77−28916
decoration, film growth, initial stages, ion bombardment effects 78−14639
diamond smoothing techniques 78−50957
dielectric surface, charge accumulation, losses, electron-beam treatment *(Russian)* 80−75931
diffusion welding, surface treatment by glow discharge effect 78−7089
E-glass fabric, acid-treated, elec. resistivity studies 79−70178
electroboronizing, Al effects on hardness and wear resistance *(Korean)* 77−73356
electrochemical treatment cathode with honeycomb arrangement of drain apertures *(Russian)* 79−96164
electrolytic coating, ionic evaporation, paints, organic coatings *(French)* 80−30127
electron microscope components, RF sputtering apparatus for cleaning 77−54022
electroplating, acid-Cu electrolytes, effect of periodic reverse current process on deposit props. 79−33951
electrospark alloying, residual stresses obs. *(Russian)* 77−56145
epoxy laminate, surface prep. to promote electroless Cu bonding 77−21300
erosion by ion bombardment *(Russian)* 78−23567
ferric ion behaviour during chemical cleaning 79−43625
ferrite, surface metallisation via elec. discharges 77−77626
ferrite reduction using plasma methods *(Russian)* 80−7700
ferrous material fractured surface exam., oxide scale removal 78−95886
fibre reinforced composite, discontinuous, effect on mechanical strength analysis and obs. *(Japanese)* 77−77596
fibre reinforced plastic laminates, US evaluation of hygrothermal effects 80−7730
fibre reinforced polyurethane foam, with chopped fibres, morphology and fracture 77−36447
film cleaning by ultrasonic liquid cavitation and acceptable solvents 80−62769
fluoropolymer adhesive joints, fracture and surface anal. by SEM and ESCA 77−55434
fracture preservation and cleaning, for fractography 80−71866
fretting corrosion control using coatings and surface treatments 80−35368
fused silicon substrate, directional reactive ion etching at oblique angles 80−66428
gas nitriding, automatic control of NH_3 dissociation 77−70223
gas washing of fracture surface by explosive detonation products 77−77611
glass, clean, bibliography 77−28922
glass, glass-ceramic surfaces, glow-discharge surface-treated, adhesion of vacuum deposited oxide *(Russian)* 77−44372
glass, removal of stearic acid monolayers with organic solvents 77−28924
glass, surface modification by chemical and electrochemical methods *(Polish)* 77−86213
glass, surface props. and contact angle after treatment with glow discharge and heating 80−21139
glass, surface treatment, improvement in mech. and optical props. recent progress *(Japanese)* 79−79141
glass, surface treatment effect, on chemical polishing time of crystal products 78−92436
glass ceramic, bonding thermosprayed Si 78−23848
glass ceramic, surface prep. for Si thermosprayed coating 78−11367
E-glass fibre, silane coupling agent deposited on surface, hydrolysis and drying effect on siloxane bonds 80−85072
glass fibre reinforced polyester resin, interfacial bond strength, effect of surface treatment 77−21303
glass surface, difluorodichloromethane thermochem. treatment, mech. props. 80−40565
glass surfaces, cracked layer thickness determ., chemical method 80−64226
glass workpiece, US drilling, structural alterations 78−48555
glass-ceramic, chemical plating with Ni and Cu 77−44379
glasses, alkali-silicate, chem. stability, cations coordination, leaching vacancy mechanism 80−35526
glasses, alkali-silicate, chem. stability depend. on cation O_2 structs. 80−35527
glasses, partially leached rods, contact-damage resist. 80−50707
glazing machine, which improves quality of glazing, exam. of design 80−11801
glow discharge, struct. changes in vacuum deposited metal coatings *(Russian)* 79−15852
glow discharge cleaning effectiveness rel. to base material atomisation rate *(Russian)* 80−20797
graphite, bending strength, surface roughness effect at high temp. *(Japanese)* 79−70131
graphite, conditioning of surface by atomic H 80−93665
graphite, surface cleaning, air cleavage and UHV cleavage, obs. using Au decoration 78−80665
graphite, ZrC formation via activated cementation *(French)* 77−52552
graphite fibre, Type-A, surface comp. and energetics 77−70024
graphite fibres, HM, surface comp. and energetics 80−54480
ground surface profile, crest and trough height distrib., Monte Carlo simulation *(Japanese)* 79−34180
surface treatment continued
ground surface profile power spectrum, Monte Carlo simulations *(Japanese)* 79−34179
Hastelloy-X, carbonization and carburisation in high press. He environment *(Japanese)* 79−26516
heat exchanger, total efficiency, uniform fouling deposit effects 79−1091
high pressure boiler in-service scavenging by intermittent dosing with chelating agent 80−89485
hydrogel pilocarpine release rate control by plasma polymerisation 77−60284
III-V semiconductor, surface microhardness depend. on surface treatment method 78−15560
Incoloy 800 and 802, influence of carburisation on mech. props. 79−20254
Inconel 600, thermal outgassing after various surface preparations 79−67952
Inconel 600 and 601, influence of carburisation on mech. props. 79−20254
Inconel 625, organic contamination removal by plasma cleaning and etching 80−97645
Inconel 625, plasma nitriding, hardness meas., Rutherford backscatt. surface anal. 80−45442
Inconel 625, surface treatment of plane and hollow components in glow discharges 79−1923
Inconel X-750 foil, surface pretreatment for improved coating adherence 79−15877
industrial, review *(French)* 80−16528
n-InSb, surface recomb. vel., repeated cyclic surface treatment effects 77−32065
instrumentation engineering, laser beam appls. in drilling, welding, cutting, definite abrasion and surface treatment *(German)* 80−108608
integral glass covering of spacecraft solar cells by electrostatic bonding 80−93676
ion beam sputtering, appl. to surface machining 80−30129
ion bombardment, thermal release of ionically pumped inert gases 77−67450
ion bombardment by low-energy ions of plasma accelerators 80−97608
ion deposition techniques, AES exam. of surface cleaning methods 79−15878
ion implantation, surface treatment process in production engineering 80−34028
ion plated filament, improved strength *(Japanese)* 77−90282
ion sputter gun, in-situ cleaning of crystal surfaces in EM 80−101895
ionic cleaning, plasma accelerator with closed drift of electrons for ion beam formation *(Russian)* 79−38993
ionic deposition and electron bombardment industrial equipment, pollution control *(French)* 80−7699
ionic nitriding thermochemical process, equipment, process details and advantages and prospects *(French)* 80−108641
joint strength, effect of change in surface morphology of adherend 77−36672
laser applications in materials processing, seminar, San Diego, CA, USA (Aug. 79) 80−90609
laser beam materials processing, thermophys. and hydrodynamic effects 78−19957
laser material processing, overview 78−56826
laser material processing, welding, cutting, drilling and surface hardening 78−80663
laser material processing, workpiece focal point window tolerances 80−5776
laser treatment of material influence of oxidising atmosphere *(Russian)* 78−23840
laser-surface purification of ferrous metals 78−92392
lens surface geometry model, high-speed generating, smoothing and polishing 78−50889
liquid crystal surface alignment treatment giving controlled low angle tilt 77−19871
liquid filtration US enhancement 78−59526
localised surface modification, CW CO_2 laser appl. 79−15879
low-pressure applications 79−94824
material processing by high power lasers, comparison of available systems 78−30003
metal, cleaning and surface preparation 79−15876
metal, electroerosion and electrochemical treatments compared *(Russian)* 79−15846
metal, fusion and evacuation after elec. contact treatment *(Russian)* 77−73365
metal, heating by laser emission, spatial nonlinear problems *(Russian)* 80−7440
metal, ion implantation, corrosion mechanism 77−8982
metal, nitridation and oxidation, comparison of behaviour at high temp. 79−74288
metal, resistance to plastic deform. under HF vibrs. rel. to surface treatment *(Russian)* 77−52400
metal, RF reactive plasma cleaning 77−44409
metal, surface contamination detection by nondestructive test, surface potential difference meas. method 79−83424
metal, surface properties improvements, using vacuum thermal process techniques 79−100283
metal, thermomechanical treatment by ionic bombardment *(French)* 78−11418
metal cleaning, by electron cyclotron resonance plasma *(Japanese)* 80−16572
metal hydride, oxide, nitride prod. in electron diffr. camera 77−65937
metal melt, treatment by high-temp. gas stream, math. model, applic. to nitriding *(Russian)* 78−53016
metal mirrors, for high-power appls., multithreshold damage analysis 77−88884
metal oxide metaphosphate glasses, vibr. study of metal cation reduction at surface 78−56797
metal oxide reduction using plasma methods *(Russian)* 80−7700
metal powder, atomised, refining by ultrasound 77−44187
metal surface, 10 eV ion impact, chem. modification, ESCA obs. 77−24916
metal surface, electrical pulsed discharge action under air environment *(Russian)* 77−43091
metal surface, heat treatment, using W-inert gas arc 79−96209
metal surface, metastable alloy formation by ion implantation 80−15130
metal surface, plasma cleaning and etching, removal of C 80−97645
metal surface cleaning, by electron cyclotron resonance plasma of H 79−47821

surface treatment continued
metal surface cleanness control by photoemission recording *(Russian)* 80−49839
metal surfaces, radioactive contamination 80−68771
metal working, surface hardening and alloying using high power CW CO_2 lasers 78−79026
metal working by CW CO_2 lasers 77−90493
metal working with high power lasers 78−80682
metallic glass, surface oxide film removal suing US oscill. energy *(Russian)* 78−72935
metallic materials, thermochem. treatment *(German)* 78−15598
metallic substrate pretreatment with plasmatron 78−11434
metallic surface, heat treating and melting with scanning laser or electron beam 78−11406
metallic surface alloying methods *(Russian)* 78−19931
metallic surface rippling induced by surface tension during laser melting 78−11405
metals, abrasive finishing with refractory carbide micropowders, surface struct. 80−11842
metals, carburising in fluidised bed of C-graphite materials 79−20276
metals, chemical conversion coatings for wear resist., review 78−72893
metals, electrochemical surface treatment method for reducing H_2 absorption *(Russian)* 79−15858
metals, evaluation by microdensitometry *(Czech)* 79−30524
metals, ion surface treatment 78−11415
metals, ionic bombardment, new technique *(French)* 77−77643
metals, submicroscopic surface relief after finishing 79−29276
metals and alloys, chemicothermal treatment, process kinetics 80−35415
metals and alloys, diffusion layers, effect of chemicothermal treatment on struct., surface energy, and bulk props. 79−96207
metals and alloys, finishing, use of ion implantation techniques, effect on wear and corrosion props. 79−34204
metals and alloys, laser erosion, influence of metallic target temp. *(Russian)* 79−39028
mica, surface impurity levels by static SIMS, cleaning treatment effects 77−59190
microalloy layer formation by ion implantation 80−16600
MIS inversion channel hole mobility rel. to field treatment in active media 78−91774
moderator surface preparation for increased slow positron yield 80−61011
negative photoresist, RF O_2 plasma stripping, visible spectra 77−40591
negative photoresists, RF O_2 plasma stripping, optical detect. systems 77−40585
neutron activation analysis installation with automatic surface contamination removal 78−88671
nitrided layer, fracture toughness determ. from hardness impressions *(German, English)* 80−97575
nitriding in glow discharges, influence on phase comp. and plasticity of diffusion layer *(Russian)* 80−76400
nonferrous metals, C, O, AND N content., microanal., surface treatment effects 78−11596
nuclear power plant Dresden Unit 1, chemical cleaning 79−54591
Nylon 6, unidirectionally reinforced, mech. props. and fracture 77−21252
optical coating removal by Al_2O_3 powder and NH_4HF_2 soln. 80−74521
optical fibre, furnace drawn, tensile strength 80−58751
optical fibres, low-loss step-index, fabrication using modified rod-in-tube method 79−50467
optical glass surfacing, using loose abrasives, impregnated diamonds and electro-plated diamonds 78−50956
optical materials, deleterious effects of US cleaning 77−42631
optical surface, cleaning techniques 79−46093
optical surface programmed aspherisation accuracy rel. to tool size 79−72727
oxidising metal heating by periodically pulsed CO_2 laser 80−7445
palliative treatments for fretting fatigue, review 80−21126
PAN fibres, SO_2 treatment 79−52403
PET fibres, adhesivity improvement by plasma surface treatment 79−15823
plasma industrial utilisation, synthesis, powder, metallurgical and surface treatments, review *(French)* 80−96398
plasma processing apparatus, RF discharge plasma conditions 77−72521
plasma surface heater, magnetically scanned, appls. 79−94826
plasma torch anode design improvement to increase deposition efficiency 79−87750
plasma torch with magnetically traversed arc for surface heat treatment 79−32832
plastic deformation treatment, tool design for 78−13824
plastic laminate removal from metal using laser beam 78−7061
plastic sample containers, for trace element samples, selection, cleaning methods 78−35745
PLT Tokamak vacuum vessel, residual gas and surface comp. changes with H_2 discharge cleaning 79−80631
poly(ethylene terephthalate), surface props. rel. to UV irrad. *(Japanese)* 78−79859
polycarbonate film, by aq. acetone solns., roughness form. mechanism *(Russian)* 78−48554
polyester fibres, plasma surface treatment, ESR detect. of free radicals 79−15824
polyethylene, melting against Al, XPS obs. 77−32700
polyethylene, pretreated surface, nitrobenzene contact angle, H_2O environment *(Japanese)* 78−79858
polyethylene, surface activation by corona treatment *(Japanese)* 77−77604
polyethylene films, adhesive props. improvement by corona discharge appl. *(French)* 78−92438
polyethylene films, plasma surface treatment, ESR detect. of free radicals 79−15824
polyethylene films, preliminary treatment before corona discharge printing, technical parameter effects *(German)* 79−15838
polyethylene low density flame treatment of surface, XPES study 79−66179
polyethylene terephthalate fabric, surface struct., props. rel. to plasma surface treatment 78−95831
polyethylene terephthalate film, surface modification by corona discharge, adsorption and wettability 77−86212
polyethyleneterephthallate, sorption of low MW solvents on struct. and mech. props. *(Russian)* 78−11358
polymer, plasma treatment in O, ESCA and XPS obs. 78−72910
surface treatment continued
polymer coated graphite fibre-epoxy resin composites, prep., adhesion 79−15644
polymer film, plasma etching and cleaning 80−1855
polymer film coating, electropolymerisation in aq. medium book contrib. 80−50778
polymer lattices, purification 78−7243
polymer modification by plasma treatment 77−70198
polymer surface modification by RF plasma, difference ESCA spectra 77−63529
polymeric thin coating, mechanochem. degradation, substrate effects 79−79134
polymers, plasma surface treatment and plasma induced grafting 79−15825
polyolefin film, corona discharge treatment 77−56129
polypropylene, effect of corona treatment on dielectric props. for capacitor appl. 79−33607
polypropylene films, plasma surface treatment, ESR detect. of free radicals 79−15824
polystyrene, form. of Cu-O-polymer complex 78−92372
polystyrene lattice cleaning, dialysis, steam stripping and ion exchange effectiveness 80−3414
pore struct., effect of washing with aq. solns. containing Mg^{2+}, Ca^{2+} ions 79−52786
porous materials, effects of different methods of prep. on reproducing surface 80−60995
powder coatings, in metal finishing, review 80−104330
powder metal sprayed coatings, bond strength, influence of surface preparation 78−11150
powder purification by US cleaning and pickling, effectiveness of working liq. comp. 77−63587
prefired substrate, acid treatment, improvement in as-fired surface finish 79−24636
PVC+Br_2(I_2), reaction in surface-modified film subject to thermal-radiative and photochem. action *(Russian)* 77−21385
PWR steam generator chemical cleaning 79−93819
pyroceramic plate scribing by pulsed CO_2 laser 79−52410
quartz, grinding and surface treatment by ball mill in cetyl alcohol *(Japanese)* 80−25890
quartz, mechanically activated, reactivity *(German)* 79−29395
quartz, surface structural modification by high temp. gases, computer simulation of RHEED patterns *(German)* 79−95251
quartz oscillator plate, surface treatment by 100 keV B ion implantation *(Japanese)* 78−59826
quartz plates, surface irregularities due to mechanical treatment *(Polish)* 80−89380
quartz wafer cleaning, surface contaminant estimation methods *(Polish)* 80−89381
radioactive effluent monitoring problems, loss and error reduction procedures 78−89987
recoil implantation, film thickness optimisation 77−35578
refractory metals, nitriding reactions and processing conditions, thermodynamic approach *(Russian)* 80−21169
residual stress measurement, bending deflection and stress source methods *(French)* 79−34265
residual stresses determ., ground and lapped metal surfaces 79−34211
resin-coated optical fibre, tensile strength tests *(German)* 78−33871
rocksalt, cleaving device for clean surface prep. 77−13738
sapphire substrate for Nb and V highly-oriented films, surface chem. treatment 77−66097
semiconductor processing, residual film monitoring by ellipsometry 80−13124
semiconductors, plasmatron appl. *(Russian)* 79−77428
shearing process, basal section profile effect 79−47754
shot-blasting, development and appl. *(French)* 79−96170
silica gels, surface treatment, adsorption properties *(Japanese)* 78−95855
silica oxidation furnace, cleaning procedures to minimise Na contamination 77−59955
silicate photochromic glass, CeO_2 activated, surface treatment effect on absorpt. 78−71168
silicone membrane progesterone release rate control by plasma polymerisation 77−60285
single crystal surfaces, grinding and electropolishing using simple goniometer 78−4604
sintered mats., complex diffusion alloying 78−68650
smectic liquid crystal structural order effects of surface treatment, sample thickness, and cooling rate 78−63667
Spectrofloat glass, theoretical anal. of optical transmission and refl. props. 77−90120
sputter cleaning, substrate surface contamination from dark-space shielding 77−8968
sputter cleaning, technological appl., review 77−44107
stainless steel, colouring processes 77−8981
stainless steel, laser surface melting for corrosion protection 80−93698
steel, alloy, 08kp, denitriding annealing, affect on mech. props. 79−52461
steel, alloy, carburisation, internal oxidation of excess carbides *(Russian)* 80−25903
steel, alloy, carburised, kinetic parameter determ. *(Rumanian)* 79−29259
steel, alloy, diffusion modelling of carburization 79−24657
steel, alloy, quenched carbonitrided, multicycle fatigue failure 80−104283
steel, alloy, structure and properties after nitriding in molten salts, steel 08kp with Al diffusion coating 80−35418
steel, alloy, surface quality improvement, thermomech. treatment 80−61020
steel, alloy, thermodynamic aspects of gas-metal heat treating reactions 79−24547
steel, alloy, type 25Gs, increasing fatigue resistance by surface plastic deformation 78−88530
steel, alloy, types CT40, CT40X, CT45, texture form. 80−25721
steel, alloy cast, optimal alloying, carburising effect 80−50771
steel, alloy U8, wear resistant diffusion coatings of B-Cr(Si) 78−56823
steel, ATSI 9310, fretting, selected fretting resistant surface treatments 79−29223
steel, austenitic, containing Ti, nitriding and nitride composition 79−20278
steel, austenitic, Mn-Al-V-F2, EM charact. after nitriding, aging, austenitizing, NDT of nitrided layer depth 79−11750

surface treatment continued
steel, austenitic 18KhGT, carburising in vac., rate, austenite grain size, C distrib. 79−20277
steel, austenitic stainless, 12Kh18N10T, nitriding accel. 79−96204
steel, austenitic stainless carburisation, X-ray microanalysis *(French)* 80−11981
steel, austenitic stainless type AISI 304, surface comp. after different surface treatments 80−3253
steel, austenitic stainless type AISI 316, L sheet and LN plate surface comp. after different surface treatments 80−3253
steel, bearing, type AISI 52100, tricresyl phosphate treated, Auger anal. 79−52413
steel, boride coatings, form. mechanism and struct. during crystn. of castings 80−35412
steel, boride coatings from induction heating microstruct. and props. 80−30165
steel, borided, 45, 20Kh, 30KhGSNA and Kh12F1, relative wear resistance 77−73351
steel, boriding, electrolytic, effect of iron oxides 79−39042
steel, boriding by ion bombardment with B_2H_6 *(French)* 78−60876
steel, boriding with B_4C based paste 80−16583
steel, C, 45, surface wearing ability, surface finishing method and running-in effects 80−11794
steel, C, carbide deposition on surface, exam. *(Russian)* 79−34200
steel, C, carbide formation during chromising, exam. in terms of ternary phase diagrams 78−56818
steel, C, Cr-Mo and Cr-Mo-Al, NH_3 gas addition to N_2-H_2(-C_3H_8) gas mixture and its effect on nitrided layer *(Japanese)* 80−35403
steel, C, fatigue, residual stress and crack growth expts., notch and surface treatment effects 79−8356
steel, C, ion nitriding, wear resistance *(Japanese)* 77−63828
steel, C, siliciding in US field 79−39043
steel, C, sintered, diffusional boronizing, exam. of process 79−96219
steel, carburisation by polymer paste, exam. of saturation 80−16582
steel, carburised, fracture resistance 79−24612
steel, carburised, microstruct. and fracture 79−24658
steel, carburised, transform. of residual austenite, mag. field effects *(Russian)* 80−29952
steel, carburising, carbide-austenite layers, form. and development 80−35413
steel, carburized and quenched, residual stresses *(Japanese)* 80−89262
steel, carburizing, vacuum, case depth 80−100956
steel, case carburised, residual stress effect in mech. performance 79−24659
steel, chemicothermal treatment, diffusional basis 80−104343
steel, chromisation, influence on surface roughness *(German)* 79−11729
steel, cleaning corroded surfaces for electron microscope exam. by cathodic polarisation 79−70242
steel, combined saturation with C, N and O by chemicothermal, surface treatments, oxidation carburisation 78−95856
steel, constructional, nitriding process in glow discharge *(Russian)* 80−55560
steel, Cr, carburising kinetics, in endothermal atm. 80−76410
steel, Cr, thermodynamic anal. of facing process using other metals 78−60878
steel, Cr plated, high strength, with and without surface strengthening prior to plating 79−39051
steel, Cr-Ni-Mn, type 4340, decarburisation by gaseous atomic hydrogen 80−30160
steel, Cr-V, hardened sping, surface finish effect on fatigue strength *(Japanese)* 79−61708
steel, cylindrical parts, centreless smoothing 77−90507
steel, decarburised layer effects on fracture toughness of 60S2 77−59930
steel, electric, EO-100 and E-11, surface cleansing with ML-51 combined with monoethanolamine, corrosive action study 79−39052
steel, endurance, effect of surface diffusion alloying 77−81344
steel, Fe-Cr-Al, sulphidation behaviour, 750°C, preoxidation effect *(French)* 78−15566
steel, friction and wear during hot forging 80−89358
steel, galvanised, identification of grains with (0001) orientation, chem. test 79−47853
steel, galvanised strip, passivation treatment 80−61146
steel, glass-enamel coating prod. by induction fusion method, heating rate effect 80−11825
steel, hardness, effect of laser irrad. in inert gas atm. *(Russian)* 79−38935
steel, high Mn mandrels, wear resist., surface layer chem. comp. influence *(Russian)* 79−52444
steel, high speed tool, laser surface melting 79−24654
steel, high-C, boriding, boride case struct. 79−24665
steel, high-C, carburising kinetics, in endothermal atm. 80−76410
steel, high-speed, atomised powders and sintered blanks, particle size effects 77−44188
steel, high-strength maraging, N18K9M5T, nitriding effect on fracture resist. 80−21092
steel, hypereutectoid, form. of surface graphitisation centres *(Russian)* 79−11720
steel, impact strength, effect of surface decarburization and carburization of faces and core struct. 78−23811
steel, internal oxidation during carburizing and heat treating 79−24660
steel, ion nitriding, case depth vs process time 78−72922
steel, ion-softnitriding of type S15C with N_2-H_2-CH_4 mixture, mech. props. of surface *(Japanese)* 79−61780
steel, laser-irradiation surface treatment *(Russian)* 77−59978
steel, low and medium C, surface alloyed with nitride forming elements, nitriding *(Russian)* 78−31569
steel, low C, current density and voltage effect on cpd. layer growth by ion-softnitriding *(Japanese)* 80−35402
steel, low C, kinetic aspects of diffusion zone and compound layer formed during ion-softnitriding *(Japanese)* 79−15866
steel, low C, surface shot blasting, prep. for plasma deposition 80−16586
steel, low-alloy, oxidation resist., N effect 80−66706
steel, low-C, corrosion inhibitors, effect on corrosion fatigue *(Russian)* 77−59977
steel, maraging, Ni-Co-Mo (18, 8, 5 wt.%), fatigue strength charact. *(German)* 77−21241
steel, martensitic, low C, nitriding, exam. of case props. 78−85045
steel, mech. strength, effect of H_2 sorption and Al and N_2 surface treatment *(Russian)* 78−31570
steel, medium C, surface burnishing effect on low cycle corrosion fatigue *(Russian)* 77−16730

surface treatment continued
steel, mild, adhesion of Al plasma sprayed coating, substrate pretreatment effect 79−83391
steel, mild, adsorbed H distrib. rel. to electrochemical treatment in pure alkali 80−16589
steel, mild, descaling by HCl *(French)* 80−108642
steel, mild, nitrided, oxidation resist. 78−95846
steel, mild, surface analysis rel. to annealing *(French)* 77−32857
steel, Mn, solutioning of castings in salt baths 78−23871
steel, Mn-Cr, blank hardened, shot peening effect on bending fatigue strength *(German)* 78−35402
steel, Mn-Cr, normalised, shot peening effect on bending fatigue strength *(German)* 78−35401
steel, MnCr (16, 5 wt.%), bending fatigue behaviour improvement by surface treatment *(German)* 78−84957
steel, N_2 implantation, nitride form., wear rate reduction 78−27149
steel, Ni-Cr-Mo, surface burnishing effect on low cycle corrosion fatigue *(Russian)* 77−16730
steel, nitrided, chem. state anal. by conversion electron Mossbauer spectrometry 80−7718
steel, nitrided layer depth, electroinduction meas. method 80−104379
steel, nitriding in molten nitrates 80−35417
steel, nitriding processes, controlled 79−100294
steel, nonpropagating fatigue cracks, in steel component strenthened by surface plastic deformation, anal. 78−88529
steel, plasma thermochemical treatment 79−94823
steel, powder forged, fatigue, surface treatment effect 80−85048
steel, SC49, tufftrided, surface treatment effect on cast, SC49, rel. between rotating and flexural bending strengths *(Japanese)* 80−81117
steel, segregation and adsorption of S, influence on carburisation and nitrogenation 80−66701
steel, sintered, boronizing 79−96210
steel, sintered, diffusion chromising 77−66607
steel, stainless, 304, shot peened, stress corrosion cracking, const. strain rate investig., cold work, sensitisation effect 79−20259
steel, stainless, 304 and 316, lowering of degassing level *(French)* 79−57159
steel, stainless, 95Kh18, vacuum quenching 78−85047
steel, stainless, carbonisation and carburisation in high press. He environment *(Japanese)* 79−26516
steel, stainless, Cr-Ni-Mo, surface, scraping, mech. (electrolytic) polishing, ion etching, effects on ESCA 78−53037
steel, stainless, electron-bombardment surface prep. for Princeton Large Torus 77−59957
steel, stainless, gas liberation in vac., effect of different methods of surface treatment *(Russian)* 80−45429
steel, stainless, highly protective film development by surface treatment 80−66699
steel, stainless, Kh18N10T surface treatment by plastic deform. effect on gas evolution and H_2 permeability *(Russian)* 79−15853
steel, stainless, nitriding charact. at low atmos. press. of NH_3, thermodynamic *(Russian)* 78−15573
steel, stainless, sensitised surface normalisation by laser melting 78−60869
steel, stainless, surface morphology of H ion eroded samples 79−86968
steel, stainless, surface preparation for adhesive bonding, surface characteris. techniques 77−56132
steel, stainless, surface treatment, X-ray photoelectron spectrosc. study 80−50764
steel, stainless, surface treatment of plane and hollow components in glow discharges 79−1923
steel, stainless, type 304, physicomechanical and wear props., influence of ion implantation and overlay coatings 80−40603
steel, stainless, type 304, surface treatment effect on protium uptake, AES anal. 77−59984
steel, stainless, type 316, surface comp. rel. to crevice corrosion initiation 80−93680
steel, stainless, type AISI 316, carburisation of crevices by impure liquid Na 78−80680
steel, stainless, vacuum components, pre-vacuum surface finish influence on electron stimulated desorption in ultrahigh vacuum 80−57320
steel, stainless 304, metallurgical factors on the corrosion and mass transfer in liq. Na *(Japanese)* 80−71804
steel, stainless type 304, surface cleanup and sputtered ion production, AES and SIMS obs. 79−66209
steel, surface cleaning in glow discharge, ion bombardment effect *(Russian)* 78−95848
steel, surface deposit of ZrC, exam. of composition *(Russian)* 79−34201
steel, surface saturation with Sb and As under glass fusion treatment *(Russian)* 78−35585
steel, surface treatment process in nontoxic salt bath 79−83398
steel, surface treatment protective coatings for scuffing and adhesive wear resistance 77−86217
steel, surface wearing ability, finished surface direction effect on wearing ability 80−11793
steel, type 40 Kh, electron emission depend. on surface mechanical treatment *(Russian)* 80−100945
steel, type 55SM5FA, formation of hardened layer during burnishing 78−85046
steel, types 45, 50, U8, U10, diffusion chromizing, 79−43357
steel, US cleaning incorporation in continuous annealing plants 77−1884
steel, US critical angle reflectivity, near-surface metallic prop. gradient effect 80−70516
steel, W-Mo-Cr-V tool, laser surface melted, struct., heat treatment effect 80−76424
steel, wear charact. of burnished machined surfaces 80−108595
steel, wear resistance of broaching bits in relation to boriding and heat treatment 78−85051
steel, wear resistance of low temp. nitriding treatment 80−89357
steel, white layers effects on stress-corrosion resistance rel. to C content *(Russian)* 78−11393
steel, work-hardenable, N26T low magnetic phase, fatigue strength effect of surface treatment 77−48546
steel 10, carburizing in fluidized bed 78−19951
steel 1Kh17N2Sh, fatigue failure, surface finishing influence 80−60972
steel 40Kh, surface working effects on crack resist. *(Russian)* 78−56734
steel antioxidation protective glass enamel cladding exam. of development 78−85031

surface treatment continued
steel C60, machined, surface morphology, struct., SEM, topographic investigs. *(German)* 77−73372
steel C, fatigued, strengthening by surface plastic deformation 78−88505
steel carburisation process, diffusion modelling 80−108632
steel casting surface alloying feasibility trials 79−83395
steel cold plastically deformed, exam. of structure of diffusion layers after borating *(Russian)* 79−34054
steel fatigue in surface active media, adsorption facilitation mech. 80−55586
steel hardfaced, effects of quenching on structure and wear resist. 77−21175
steel nitridation process, ionic, in glow discharge *(Russian)* 77−11412
steel plates, plastic coated, RF welded, quality and strength *(German)* 79−34185
steel powder, high speed, S and O reduction in a H_2 gas stream 80−61015
steel sheets, surface composition, degreasing and batch annealing effects 80−66700
steel ShKh15, fatigue strength and residual stress distrib., machining method effects 78−31528
steel stainless, solar energy collector optical props. rel. to heat treatment 78−94455
steel surfaces, machined, X-ray diffr. residual stress meas. methods, comparison 77−56212
steel surfacing, with up to 0.8% C, self-shielding flux-cored wire development 79−8402
steels, mechanism of H_2 entry during acid cleaning 79−39023
strengthening by electrospark alloying *(Russian)* 79−96198
superalloy, aluminide coating, improvement by sputtering *(French)* 79−29278
superalloy, laser melted, epitaxial resolidification 77−90491
surface resistivity, effect of hydrofluoric acid treatment 78−10537
surface structure, distribution of defects, LEED 80−44402
surfaces, machined, X-ray diffr. residual stress meas. methods, comparison 77−56212
TEM contamination exam. and specimen cleaning methods 79−54232
thermocyclic stress effects in corrosive-media, electrochem. polarization applic. *(Russian)* 78−11356
thermoplastic layers, isothermal smoothing of surface deformation *(Russian)* 80−76394
tinplate, passivation treatment 80−61146
transition metal, penetration of interstitial elements during surface treatment 77−12737
ultrasonic cleaning using Freon 113, ethylene tetrachloride, methylene chloride anisotropic mixtures *(Polish)* 79−15839
US cleaners and disintegrators, review, latest instruments 79−37101
US energy use in surface improvement, of mech. and corrosion props. *(Rumanian)* 79−15821
UV/O_3 cleaning procedure and results 77−25168
vacuum deposition equipment cleaning, practical procedures 80−57318
vacuum equipment cleaning procedures 79−71467
vacuum metallisation chamber condensate removal system 79−58752
vacuum outgassing material selection and treatment 78−81994
wear resistance, surface treatments, selection procedure, review 78−72892
wood, vapour phase reaction of 2,4-tolylenediisocyanate *(Japanese)* 77−77603
Zircon, fine ground, mechanised method of cleaning with acid 79−83357
Ag films deposited from hot hollow-cathode source, adhesion, ion precleaning 77−8754
Al alloy, cast, forging and heat treatment effects on diamond planishing treatment 79−43237
Al, alloy, laser surface melting 78−48557
Al alloy, surface preparation for adhesive bonding, surface characteris. techniques 77−56132
Al alloys, chemical cleaning, Pourbaix diagrams appl. 79−83380
Al alloys, fatigue of fillet welds, peening effect 79−91853
Al alloys, laser surface melted, porosity form. 78−44279
Al alloys, surface shot blasting, prep. for plasma deposition 80−16586
Al, effect on interface reactions with polyurethane adhesive 77−81384
Al, laser strengthening, struct., hardness and dislocation density *(Russian)* 80−76399
Al, physicomechanical and wear props., influence of ion implantation and overlay coatings 80−40603
Al, porous anodic film, ion beam thinned, electron microscopy 78−92390
Al pretreatment and anodisation, before Cu plating *(German)* 80−45243
Al surface, plasma cleaning and etching, removal of C 80−97645
Al, TEM/XPS study of Cr^{6+}/Cr^{3+} colloidal SiO_2 surface films 80−85090
Al, thermal desorption of oxide film, influence of grain boundaries and recrystn. 80−61023
Al, US cleansing process 78−11417
Al-Cu-Mg, tpye RR55, high strength, creep behaviour, effect rel. to anodic coatings, SEM study 80−97542
Al-Cu-Mg-Mn alloys, shot peened, positron annihilation meas. 77−63833
Al-Li, diffusion coeff. determ. during hydriding *(German)* 79−29288
Al-Mg (2.5wt.%) sheet, surface oxide state and weldability 80−59769
Al-Mg alloy, nitridation process study 80−61013
Al-Mg-Li alloy, 01420, surface layer props. *(Russian)* 78−80674
Al-Zn-Mf-Cu-Cr alloys, shot peened, positron annihilation meas. 77−63833
Al_2O_3, bending strength, surface roughness effect at high temp. *(Japanese)* 79−70131
Al_2O_3, cutting tools, effect of acid etching on cutting performance 79−96169
Al_2O_3 sintered surfaces, premetallizing with Mo-Mn-SiO_2 79−47792
Au-CdS, Schottky junction, surface defects, photovoltaic, piezoelectric and V-I characteristics *(French)* 80−49898
Au-Pd alloy, surface comp., polishing, cleaning and Ar sputtering effects 77−72763
Au-Sn alloys, surface comp. by Auger spectroscopy, sputter cleaning 77−59648
$BaFe_{12}O_{19}$ powder, chemical plating with Co, Co-P, Ni-P and Cu 80−25593
Be, zincating, deposition conditions, film characts. 77−40397
Be-Cu surface preparation for Au electrodeposition 78−7100
C fibre reinforced polymer, strength props., fibre surface treatment effects 78−27636
C fibres, oxidation by NO_2, struct., props. modification 78−44237

surface treatment continued
C fibres, PAN-based, surface characts., active surface area, microporosity 78−35536
C fibres, PAN-based, surface characts., investig. by flow microcalorimetry 78−48694
C fibres, surface treatment with tetra-(octadecyl) titanate, X-ray and electron microscope study *(Japanese)* 79−74280
C fibres and C fibre reinforced epoxy phenol, oxidation, effect on props. 80−40574
CaF_2, press-forged laser window, polishing, cleaning and grinding 79−59849
$Ca_{10}(PO_4)_6X_2$ (where X is F, Cl, OH or Co), influence of mech. treatment on struct. and reactivity *(German)* 79−43272
$Cd_xHg_{1-x}Te$, surface microhardness depend. on surface treatment method 78−15560
CdS, Au deposition, Schottky diodes and MIS devices, surface treatment effects, SEM obs. 80−54794
CdS, cathodolum. in red and exciton regions, surface treatment influence 77−77303
CdS, polycrystn. layers on CdS substrate, electron microscope study of surface struct. 78−22940
CdS, surface photovoltage in exciton absorpt. range 78−19119
$CdSe_xTe_{1-x}$ crystal, acoustoelec. oscillations affected by surface treatment *(Russian)* 78−10517
CdTe surface, sputter cleaning and dry oxidation, XPS and LEED study 80−108618
Cr powder, thermogravimetric exam. of nitridation rate *(Japanese)* 79−20292
Cr-Ni compressor disk, surface plastic deform., optimal method 80−60924
Cr-Ni steel, austenitic, effect of Si on carburising mechanism at 930°C 77−56155
Cr-Ni steel, carburised, effect of atm. during heating to quenching temp. on austenite decomp. 77−56157
Cu (111), chemisorpt. of CO on differently prepared surfaces 78−6223
Cu, acoustic emission under action of single elec. pulse discharge *(Russian)* 77−59071
Cu adhesion to Au, surface treatments and surface impurities 77−15701
Cu, CESR, influence of freq. and surface effects 79−51856
Cu cathodes, erosion, vacuum to atmospheric press. arcs 78−79482
Cu electrocrystallisation from $CuSO_4$ solns., exptl. methods *(Russian)* 79−8235
Cu, electron emission depend. on surface mechanical treatment *(Russian)* 80−100945
Cu mirror, microstruct. effect on Ag overlayer deposition, 10.6 μm reflectivity 77−42543
Cu pickling in HCl waste free system 80−71795
Cu, surface, electron stimulated desorption, glow discharge treatment 79−65964
Cu surface, plasma cleaning and etching, removal of C 80−97645
Cu surface shot blasting, prep. for plasma deposition 80−16586
Cu-Al, sulphurisation solid state phenomena 78−64781
Cu-Be(2 wt.%), tarnish surface films, formed in ammoniacal Cu(II) solns. 80−97624
Cu-Ni sulphidised alloys, Ru and Os behaviour during carbonylation *(Russian)* 80−40584
FE-Zn, prep. and phase diagrams *(French)* 80−76231
Fe and Fe-C, (0.8 wt.%), sintered, hot forging ahd chemicothermal treatment, effect on wear resistance 80−25606
Fe, Armco, borided surface layers, Mossbauer and metallographic anal. 80−50769
Fe, Armco, carburising kinetics, in endothermal atm. 80−76410
Fe, Armco, nitriding charact. at low atmos. press. of NH_3, thermodynamic *(Russian)* 78−15573
Fe, Armco, siliciding with Si-SiO_2 mixture, exam. of corrosion resistance 80−16584
Fe, atomically clean, N_2 treatment, corrosion inhibition 78−19954
Fe, boriding by ion bombardment with B_2H_6 *(French)* 78−60876
Fe, carbonyl powder, kinetics of phosphatizing reaction 79−96218
Fe, carburisation rel. to interstitial penetration 77−12737
Fe, carburization, methane gas→C(dissolved)+$2H_2$ (gas), kinetics 80−55712
Fe, cast, atomised powders, particle size effect on purification in US pickling 79−28985
Fe, cast, diffusion saturation and form. of FeB and Fe_2B coatings 78−53032
Fe, cast, grey, carbide-free Cr diffusion coating 79−96205
Fe, cast, heated in CO atm., obs. cracks around graphite flakes *(Japanese)* 78−84974
Fe, cast, high strength, wear resist., electrocontact surface facing influence *(Russian)* 79−52385
Fe, cast powder, exam. of reaction between C and O, before and after annealing in converted gas 79−33973
Fe chromised layers, fatigue fracture kinetics study by reverse bend tests *(Russian)* 78−31511
Fe, decarburisation of white and malleable in H_2 atmosphere *(Russian)* 77−70210
Fe, H_2 permeation, rel. to embrittlement, organic inhibitors, surface treatment 80−108635
Fe, hot galvanising with liquid Zn, Fe-Zn compound form. *(French)* 79−20275
γ-Fe, kinetics of carburisation in CO-He and CO-H_2 atmospheres at 920°C *(German)* 78−85024
Fe liquid, C saturated, decarburization by CO_2, effect of S 79−11726
α-Fe, nitrided, aging at room temp. 80−71679
Fe, powdered compacts and Armco, electrolytic boriding 79−39044
Fe, pure, nitrided layers obtained by ion bombardment, microstruct. exam. *(French)* 78−15581
Fe, refining by electric fields in vacuum, surface active impurity elimination *(Russian)* 80−55563
Fe, segregation and adsorption of S, influence on carburisation and nitrogenation 80−66701
Fe, sintered, austenitic nitriding and bainitic hardening 80−85084
Fe, solid, liquid, reaction with solid Fe, interdiffusion exam. *(Japanese)* 78−39944
Fe surface, laser doping with V *(Russian)* 78−95065
Fe surface, nitride layer formation, activated surface, passivation 80−16577
Fe, surface treatment process in nontoxic salt bath 79−83398
Fe, triboelectric charging, effects of fluorinated compounds 78−60188

surface treatment continued
Fe-Al (1 to 4 wt.%), effect of nitriding on surface structure and props., and on diffusion layer *(Russian)* 79−34197
Fe-Al(V)(Ti), nitrided, struct. and props. 78−19950
Fe-based powder PZh2K, porous struct., effect of diffusion chromising with sintering 79−66219
Fe-Cr, high-temp. oxidation, borate inhibitors 80−66705
Fe-Cr, thermodynamics of chlorination *(Russian)* 79−52168
Fe-Cr-C, steel carbide formation during chromising, exam. in terms of ternary phase diagrams 78−56818
Fe-Mo(V), nitrided by const. activity ageing, X-ray studies 77−32720
Fe-Ni, carburization, methane gas→C(dissolved)+$2H_2$ (gas), kinetics 80−55712
Fe-Ni (50 wt.%), surface comp. and oxide film thickness after various surface treatments, AES study 80−66693
Fe-Ni alloy, surface decarburisation rate in dry H_2, soft mag. material manufacture 78−60882
Fe-Si (3 wt.%), grain oriented, mag. props., effect of decarburizing *(Chinese)* 80−103821
Fe-Si(Cr)(Ni)(Mn)(C), alloy layers formed by reaction with molten Al, X-ray, EPMA anal., hardness meas. *(Japanese)* 78−72926
Fe-V (1 wt.%), nitrided and annealed, struct. 77−8998
Fe-V (1.06, 5.23, and 15.55 wt.%), nitriding 78−3253
δ-Fe-Zn layer formed on hot dip galvanising, texture 77−9001
FeS_2, acid bacterial leaching, lixiviant alteration by fungal absorpt. of Fe 80−108617
GaAs (001) surface, thermal treatment before MBE growth, RHEED-AES meas. 79−61754
GaAs, clean or contaminated (001) surface, Au film growth 78−26785
GaAs, etchant, universal, multipurpose 78−53008
GaAs, impurity distribs. by chemical methods 77−43237
GaAs, positron annihilation rel. to surface treatment *(Russian)* 77−44081
n-GaAs, real epitaxial surface, photoelec. spectroscopy, mechanisms 78−34858
n-GaAs Schottky barrier junction, SEM meas. of hole diffusion length, surface effects 79−87110
GaAs:Cr erosion by laser beams *(Russian)* 78−2950
GaAs:Cr wafers, semi-insulating, surface degradation by heat treatment at 900°C 77−80820
GaP, surface cleaning by oxidation and heating, characterisation for electron emitter appl. 78−35548
$Gd_3Ga_5O_{12}$, chemical-mechanical polishing characteristics, magnetic bubble device appl. *(Japanese)* 79−5067
$Gd_2(MoO_4)_3$, ferroelectric domain decoration 78−10862
n-Ge, cathodically treated, surface mobility of electrons 77−51801
Ge, magnetic field influence on 1/f noise, surface origin evidence 79−99592
Ge, surface electronic props. meas. by SEM, sand-blasting effect 77−62976
$Hg_{0.8}Cd_{0.2}Te$ surface, sputter cleaning and dry oxidation, XPS and LEED study 80−108618
HgTe surface, sputter cleaning and dry oxidation, XPS and LEED study 80−108618
InAs anodic oxide films prep. and props. 80−55553
InP (100) surfaces, chem. treatment effects on comp. and nature 79−47794
InP (110) surfaces, cleaved and polished-sputtered-annealed, LEED and AES study 80−103550
InP substrate, thermal damage suppression by adding Ar in H_2 atmosphere 79−100275
InP surface preparation for Schottky barrier and ohmic contact formation 80−39671
InSb, oxidised surface, photocond. meas. *(Russian)* 77−43664
InSb, surface analysis, X-ray photoelectron spectra, surface oxidation-etchant correlation 78−56029
KCl, cryst., plasma prod. by laser impact, effect on surface 78−1866
$KCoF_3$, strain sensitive props., Mossbauer spectra obs. 77−20765
$KFeF_3$, strain sensitive props., Mossbauer spectra obs. 77−20765
KH_2PO_4, cryst. laser irrad. damage threshold, surface finish and defects effects *(German)* 78−59058
Li, surface characterization of film growth 80−81240
LiF, thermocyclic stress effects in corrosive-media, electrochem. polarization applic. *(Russian)* 78−11356
$LiTaO_3$, refr. index distrib. after surface lapping, theory 78−72479
Mg nitridation in HF discharge, temp. effect 80−3399
Mg-Ce, diffusion coeff. determ. during hydriding *(German)* 79−29288
MgO, (001) film substrates for film growth studies by TEM, O_2 conditioning 79−82489
MgO, spherical particle impact damage, effect of crystallographic orientation 79−79135
$MgO-Al_2O_3-SiO_2$ based cordierite glass-ceramic, strength and thermal shock, surface treatment effect 80−25884
$MgSiO_2$, kinetics of dislocation etching 80−6409
Mo electrolytic dissolution at high anodic potentials, surface quality *(Russian)* 79−39025
Mo, glow-discharge surface treatment, struct. defect prod. 77−63832
Mo, ionic siliciding, diffusion layer prod. 78−23855
Mo, nitriding kinetics 80−35415
Mo, rolled sheet, boriding, Cu effect 80−21165
Mo, siliconised thermal stress and thermal expansion 77−21324
Mo single crystal, endotaxy during carburisation 77−70228
Mo, sintered, thermally induced surface composition variations 79−5078
Mo, sulphidation, cryst. of MoS_2 77−52539
Mo, surface machined, struct., electron diffr., TEM *(German)* 77−73371
Mo-N, nonporous metal production accompanying arc plasma nitriding *(Russian)* 80−7712
Mo-Ti (up to 5.48 wt.%), internal nitriding, hardness, nitride type, precipitation *(Japanese)* 79−79157
Mo-Ti-La-C, influence of high pressure on mech. preps. after nitriding *(Russian)* 79−57137
Mo-W (50 wt.%), emissivity, 1200-3000K, effects of annealing and surface treatment 78−43154
NaCl, cryst., plasma prod. by laser impact, effect on surface 78−1866
NaCl crystal rough surface smoothing, during evaporation or condensation 80−103470
$NaNbTiO_5$, high temp. chlorination kinetics 79−61765
$Na_2O-Al_2O_3-SiO_2$ glass, leaching in HCl solns., Na conc. distrib. in surface layers 80−21141
surface treatment continued
$Na_2O-Al_2O_3-SiO_2$ glass, interaction with aq. salt solns., alkali ions distrib. in surface layers 80−21142
Na_2O-CaO glass, wettability, effect of cleaning procedures 80−65336
$Na_2O-CaO-Bi_2O_3-SiO_2$, electro-conducting glass-ceramic production by ion-exchange and reduction treatment 79−1616
$Na_2O-CaO-SiO_2$ glass, surface viscous flattening kinetics, sinusoidal profile decay method 79−79139
Nb nitriding, high-temp., kinetics and mechanism *(Russian)* 79−74300
Nb, nitriding kinetics 80−35415
Nb, surface carburisation with propane 79−8382
Nb-Mo(Ti)(Zr), nitriding, diffusive saturation, lattice spacing and activation coeffs. *(Russian)* 80−21168
Ni, B-containing diffusion layer formation *(Russian)* 77−48570
Ni, B-containing multicomponent diffusion layer formation *(Russian)* 77−44400
Ni, kinetics, Ni_2Al_3 layers growth by cementation *(French)* 80−35127
Ni, sulphidation kinetics, in H_2S-H_2 550 to 600°C 78−64780
Ni, surface decarburisation rate in dry H_2, soft mag. material manufacture 78−60882
Ni-Cr alloy, heat-resistant, conc. of hardening γ′-phase, effect on electrochem. shaping *(Russian)* 77−8979
Ni-Cr alloy, phosphidation in P vapour, 700°C, phosphide layer struct. and kinetics 80−25906
Ni-Cr type alloys, Co surface pretreatment to attain pore-free aluminised coatings 80−40612
Ni-Cr-Co-Mo-Ti-Al, powders, HCl surface treatment to prevent TiC precipitation, fracture props. 79−8397
Ni-Cr-Co-Ti, superalloy sintering thermochemical surface treatment 80−25617
Ni-In, protective coating on Kovar, vacuum seal for borosilicate glass appl. *(Italian)* 80−40621
NiAl, kinetics, Ni_2Al_3 layers growth by cementation *(French)* 80−35127
$Pb_{1-x}Sn_xTe$:Cd, photoelec. props., surface recomb. effect 80−44659
$PbTiO_3$, spontaneous polaris. shielding destruction by polishing and scribing 79−15427
$Pb(Zr,Ti)O_3$ polycrystalline ceramic, fracture and strength, surface treatment effects 80−11704
Re, interaction with F_2 and fluorides at low temp. and high press. 78−39700
Rn barrier, interior of building structs. foundations built on U mill tailings material 79−2138
SI, nitridation, fluoride accelerated 80−7705
Si (111), nitridation, AES and LEED results 80−80041
Si (111) surface, heating effects on ellipsometric parameters 77−72764
Si, direct thermal reaction with N_2, very thin Si_3N_4 film growth 78−52665
Si, form. of carbonaceous layer during high dose ion implantation, removal by cleaning, annealing and oxidation 79−70374
Si, gettering effects *(Japanese)* 79−83356
Si, lifetime control through impact sound stressing 77−85238
Si, nitridation, effect of Fe and H 79−57129
Si, nitridation, effects of Fe and Al additions 77−16708
Si, nitridation, H_2 effects 79−57128
Si, nitridation by ion beam method 77−16705
Si, nitridation to form α- or β-Si_3N_4 80−50609
Si, nitriding kinetics and mechanisms 79−70190
Si photodiode, refl. and external quantum efficiency change after surface cleaning 79−93212
Si, positron annihilation rel. to surface treatment *(Russian)* 77−44081
Si, powder, effect of Fe and $FeSi_2$ on nitriding 79−33985
Si powder, nitriding *(German)* 79−74414
Si, prior to thermal oxidation, rel. to chem. struct. of interface 78−27654
Si processing technology, appls. of scanning CW lasers and electron beams 80−100932
Si, residual stress and defects induced by scribing 80−60990
Si semiconductor plates, control of quality of surface treatment, using Al spraying technique 80−60989
Si, sputter cleaning using Ar^+ ions, temp. depend. of residual damage, 25 to 800°C 77−48558
Si substrate, Si_3N_4 growth using anhydrous NH_3 79−43141
Si, surface, controlled stripping, automated system 78−31557
Si, surface, pulsed electron beam processing, doping, annealing 80−75254
Si, surface charging during illumination, effect of various surface treatments 79−51651
Si, surface cleaning by pulsed laser irrad. 80−45173
p-Si, surface elec. behaviour after chem. treatment 80−20185
Si, surface potential spread rel. to chemical treatment *(Russian)* 78−11363
Si, surface state distrib. after treatment with HF and H_2O using photovoltage pulses 79−60888
Si, transition layer form., band struct., electroreflectance 77−16333
Si wafer, thermal characts. of $H_2SO_4-H_2O_2$ cleaning soln. 80−3225
Si, X-irrad., photocond. spectrum 77−15903
Si:B high-temp. diffusion, glass layer formation obs. 78−7069
$Si-SiO_2$-Mg-Cu powder compact, nitridation to form Si_2ON_2 whiskers *(Japanese)* 80−93674
α-SiC, lattice absorpt. bands in IR spectra, surface treatment effects 77−52071
SiF_4, thermocyclic stress effects in corrosive-media, electrochem. polarization applic. *(Russian)* 78−11356
Si_3N_4, factors affecting α, β phase formation, during nitridation of Si powders 78−52738
Si_3N_4 films, prep. by thermal nitridation of Si in NH_3, comp. and oxidation resist. 80−3215
SiO_2, adsorption of H_2O, surface treatment and methylation effects 78−84058
SiO_2, fused, surface crystn. by Li^+ ion implantation and annealing 80−89383
SiO_2, fused, surface damage threshold rel. to prep. and OH^- conc. 77−62026
SiO_2, fused, surface roughness rel. to prep. and treatment history 79−14058
SiO_2, on Si, reduction by heating in Ga mol. beam at 800°C 80−50730
SiO_2 surface, Ar plasma-treated, O_2 adsorption reactivity, EPR obs. 79−51418
SiO_2, surface reactivity modification by Ar/O_2 plasma treatment 78−64890

surface treatment continued
SiO_2-Al_2O_3-CaO-MgO-NaO-K_2O-B_2O_3-ZrO_2, glaze, exam. of zircon crystallisation 79−19155
SiO_2-Al_2O_3-CaO-MgO-Na_2O, ion exchange and electrodiffusion of Li ions in surface layer 79−20227
SiO_2-B_2O_3-Na_2O-K_2O system glass, phase separated, loss of oxides during acid leaching, atomic absorpt. anal. 79−11716
SiO_2-B_2O_3-Na_2O-K_2O glass, strengthening by partial leaching 80−60993
SiO_2-Na_2O, alkali, grain-cleaning procedures effect on crushed glass chem. durability tests 80−66678
Sn fine powders, electrodeposition, effect of cathodic current density on structure 80−16238
Sn plate, passivation by cathodic dichromate treatment 77−56139
SrF_2, press-forged laser window, polishing, cleaning and grinding 79−59849
$SrFe_{12}O_{19}$, powder, chemical plating with Co, Co-P, Ni-P and Cu 80−25593
steel, Cr plated, factors influencing durability 80−108643
steel, Si killed, effect of Al addition to Zn on phase composition and morphology of products of Fe-Zn reaction *(Polish)* 78−85021
Ta, interaction with F_2 and fluorides at low temp. and high press. 78−39700
Ta, nitridation by ionised glow-discharge to form FCC Ta_xN_y 77−52266
Ti alloy, hydrogenation during electrochemical treatment *(Russian)* 79−39024
Ti alloy VT3-1, fatigue failure, surface finishing influence 80−60972
Ti alloys, pseudo-α, salt-corrosion effects on long-term strength, vacuum annealing and stress concentrators effects *(Russian)* 78−11392
Ti fibres, high-temp. nitriding kinetics *(Russian)* 80−21166
Ti, ion nitriding by a DC glow discharge method, surface anal. 78−80672
Ti metal-metal interface, adhesion energy, surface treatment and ion implantation effects 80−107660
Ti, nitriding, ESCA study *(Japanese)* 80−11833
Ti, nitriding, high temp., heat release kinetics *(Russian)* 77−66751
Ti, permeation of H plasma reduced by layer of interstitially built ϵ-Ti_2N 80−16566
Ti, physicomechanical and wear props., influence of ion implantation and overlay coatings 80−40603
Ti powder, exam. of mechanicochemical comminution, in the presence of epoxy resin or polysulphide rubber 80−16236
Ti, surface layer alloying element distrib. *(Russian)* 78−19934
Ti, wear and corrosion resistance, effect of surface alloying with Nb and Si *(Russian)* 77−25191
Ti-Al-Cr-Mo-Zr hard alloy VK15, shot blasting in strength improvement 77−81272
Ti-Al-Mo-Zr, compressor disk, surface plastic deform., optimal method 80−60924
Ti-Al-V (6,4 wt.%), phase transformation after hydrogenation 80−7560
Ti-Al-V-(Sn), surface finishing effect on internal stresses, X-ray study *(German)* 79−34210
Ti-Mo, boronizing, reaction kinetics 79−61797
Ti-Zr-Nb-Si, Nb and Si surface alloying effects on wear and corrosion resistance *(Russian)* 77−25191
TiO_2, adsorpt. of O_2, vacuum heat cleaned, O_2^- radical form., EPR 77−35806
TiO_2, metal-TiO_2-Si structure, I-V characteristics, deposition, post-deposition oxidation effects 78−80063
$TlCl_3$.$(TlCl)_3$, labelled, exchange of Tl ats. rel. to γ-irrad., heat treatment, grinding 78−92470
W, acoustic emission under action of single elec. pulse discharge *(Russian)* 77−59071
W, carburisation by methane, initial kinetics 79−47824
W, carburizing rate, Co effects *(Japanese)* 79−52453
W high-current multicavity thermionic cathode, erosion mechanisms, sputtering 79−55570
W, interaction with F_2 and fluorides at low temp. and high press. 78−39700
W, ion sputtering yield reduction by special surface microtopography 77−36330
W, porous, chromising 80−100959
W, powder, sulphiding with H_2S 79−5071
W, rolled sheet, boriding, Cu effect 80−21165
W surface layer struct. during milling, plastic deform., failure *(Russian)* 80−40586
W:ThO_2, uncarburized filament activation by sputtering 78−52608
W-Co, carburizing rate, Co effects *(Japanese)* 79−52453
W-Co mixed powder, carburizing *(Japanese)* 79−52454
W-Cu pseudoalloy, porous, chromising 80−100959
WC powder, chemical plating with Co and Co-P 80−25593
YAG brittleness anisotropy, microcrack formation due to surface treatment 80−40526
Zn and Zn coated surfaces, cathodic pretreatment 78−19929
Zn, electron emission depend. on surface mechanical treatment *(Russian)* 80−100945
Zn, phosphate coating, effect of grain size on film formation kinetics 79−34203
Zr fibres, high-temp. nitriding kinetics *(Russian)* 80−21166
Zr, ion nitriding by a DC glow discharge method, surface anal. 78−80672
Zr, ion-implanted polycryst., thermal oxidation 80−71786
Zr, nitriding in RF discharge 77−86222
Zr-Nb (1 at.%), high-temp. nitriding, chemical and metallographic anal., disintegration test 79−24668

surface vibrations *see crystal surface and interface vibrations*

surface waves (fluid)
see also liquid waves; oceanography
air flow above water waves, numerical model 77−81912
air-water film flow, transport phenomena, wary interface motion 77−35213
air-water interface, adequacy of theories of capillary wave damping 77−72750
air-water interface, surface waves damping rel. to adsorpt. and spreading films detect. 79−5690
airflow above waves, numerical simulation *(Russian)* 80−4076
asymptotic motion on flowing liquid, stationary solns. *(Russian)* 79−90269
axisymmetric waves on the surface of viscous fluids 80−96266
baroclinic oceans, semi-implicit numerical model 77−29316

surface waves continued
beach slope sand granulometric composition variations during wave cycle *(Russian)* 78−15991
boundary layer growth on vertical plate due to waves 79−72884
bubbles, oscillating, pulsation amplitude threshold for surface waves 79−18900
capillarity-gravity waves, third-order reson. interactions 78−34148
capillary fluids rot. in cylindrical vessel, free oscill. *(Russian)* 77−27542
capillary wave theory and mean field theory of interfaces 78−18309
capillary waves, large amplitude, on fluids sheets 77−7406
capillary waves, progressive, periodic, finite-amplitude 80−79339
capillary-gravity waves, 2-dimens. wave packet 77−35154
capillary-gravity waves, exact eqn. numerical soln., closed bubbles 80−14715
Cauchy problem for nonstationary surface waves of perfect fluid *(French)* 79−27653
Cauchy problem for nonstationary surface waves of perfect liquid *(French)* 79−27652
Cauchy-Poisson problem on sphere *(Russian)* 77−35156
caustic region, nonlinear theory for shallow water waves 77−11211
charged liquid, parametric surface wave excitation by AC elec. field 79−23375
circular solitary wave on shallow water 79−55397
cnoidal wave, existence downstream after flow under sluice gate 79−86403
cnoidal waves, higher order solns. *(Japanese)* 78−42625
conducting fluid, run-off is elec. field, undamped waves 79−90271
continental shelf wave side band instability and long wave resonance 78−16030
creeping waves, on shallow water, numerical investigation 78−90928
crossed wave pattern, wind interaction rel. to Langmuir circulations 79−23330
data analyser system for buoys 77−5362
diffraction and refraction computation, using finite and infinite elements, structures loading at sea calc. 77−81910
diffraction by object, integral formulation of Helmholtz eqn. 80−81919
direction-sensing water wave probe design 77−58819
drag sphere velocity probe, miniature, development and testing 78−55705
eddy diffusivity, near open channel free surface, heat transfer expt. 78−5798
EDH, surface waves, nonlinear stability 79−50810
EHD surface wave propagation, nonlinear effects 78−67278
electrolyte nonlinear wave processes, in dispersive media, MHD stimulation 77−7473
elevation produced by oscillatory press. distrib. in uniform translation on surface 77−47027
energy flux for trains of inhomogeneous plane waves 80−46817
excitation near cut off freq. 77−68607
film, liq., falling, 3-dimens. wave characts., laser beam refraction obs. 79−27654
film, liq., flowing down inclined plane with heat transfer, interfacial shear, stability 79−37290
film, vertical wall, large amplitude waves 78−14030
film, wavy, instantaneous vel. profile meas. 78−79299
film on liquid surface, persistence in presence of disturbance 77−31839
finite depth water with immersed vertical boundaries, surface waves 79−77151
finite-amplitude deep-water waves on currents 79−92958
flat finite wave tank radiometric measurements, 3-dimensional vector modelling and restoration 77−17238
floating finite-width plate in a periodic pressure system 80−6070
free and forced edge waves, finite amplitude effects 78−79330
free surface, simple fluid between torsionally, oscill. cylinders 77−57202
free surface flows under gravity, exact selfsimilar solns. 80−48725
free surface vibrations caused by internal waves, experimental investigation *(Russian)* 79−16478
Freon-113, pure and mixed with methanol, EHD coupled minimum film boiling, surface wave model 78−87240
frustrated total reflection, demonstration apparatus 77−67158
gas-liquid film interface stability behind slipping shock wave front *(Russian)* 78−55630
gas-streamlined liquid film, quasiharmonic motion development in vertical flow 77−55014
Gaussian random wavetrain, randomness effects on stability 78−90923
generated by forced heaving half-immersed sphere(s), HF limiting virtual-mass coeffs. 77−51072
generation of stationary flow *(Russian)* 79−39731
gravitational-capillary, asymmetric, plane forced, wave shape on liquid surface of const. depth *(Russian)* 79−86448
gravity surface wave diffraction by cylinders *(Russian)* 77−68605
gravity surface waves, hydrodyanmic diffraction at vertical obstacles *(Russian)* 77−55012
gravity surface waves, tsunami wavelength, wave equation soln. 78−90927
gravity wave diffraction, in shallow water, optimal control problem *(Russian)* 80−74896
gravity wave diffraction at underwater axisymmetric obstacle, polynomial approx. *(Russian)* 79−77143
gravity wave diffraction by arbitrary obstacles *(Ukrainian)* 80−48722
gravity wave diffraction over underwater channel of varying depth *(Russian)* 80−79333
gravity wave horizontal asymmetry *(Russian)* 80−74897
gravity wave reflection in variable depth water 77−15051
gravity wave-current interaction, energy propag. stopping 77−47029
gravity waves, air-water interface effects 79−57947
gravity waves, growth and equilib. in wind-wave tank 78−1679
gravity waves, interaction with arbitrarily disposed submerged inhomogeneities *(Russian)* 80−79334
gravity waves, long period, on beach, generalised KdV-eqn., soln. 78−92844
gravity waves, non-uniform free surface, superficial viscosity and tension *(French)* 80−48728
gravity waves, surface, multi-dimensional packets 78−42624
gravity waves, triple roots and curved caustics 78−40584
gravity waves, uniformly analytic initial domains 79−72901
gravity waves, vertical asymmetry over a limited depth *(Russian)* 80−79337
gravity waves diffraction, ray methods 78−40574
gravity waves incident on submerged horizontal plate 78−5758

surface waves continued
gravity waves on rot. fluid, numerical method 77−51071
gravity-capillary surface waves, nonlinear interactions 78−18310
Hamilton's principle for surface waves 78−5759
Hamiltons principle 78−5760
harbours, reson. in closed L-shaped channel 77−78190
heated pounds, turbulent boundary layer of stratified airflow, surface waves 80−92133
heavy liquid layer, discontinuous solutions 77−67286
height meas., new acoustical methods 79−1276
HF surface wave generation by partially immersed heaving cylinders 77−42853
hydraulic surge phenomena *(Norwegian)* 80−27141
hydrodynamic effects of a travelling wave *(Russian)* 80−38423
ideal fluid with free surface, laminar flow instability, reson. surface wave buildup 78−34106
incipient wave propagation on shallow water *(Russian)* 80−74895
induced atmospheric pressure field above spectrum of surface gravity waves 80−92168
infinite depth fluid, steady free surface gravity-capillary waves, integro-differential formulation 80−6072
infinite depth water with immersed vertical boundaries, surface waves 79−77150
infinite elements in fluid-struct. interactions 77−35132
inhomogeneous liquid-vapour interface, surface waves origin 78−75158
interaction between short surface waves and long internal waves 80−48723
interfacial gravity waves, form. by submerged vorticity regions and fluid inhomogeneities 79−64682
interfacial instability, mass transfer, Marangoni effect and interfacial longit. waves 79−46890
interfacial waves launched by an explosive line-source in a submerged elastic half-space 78−75088
inviscid flow over elastic medium, surface waves generation 77−49603
irrotational free-surface flow, time-dependent, formation of sharp corners 80−83808
irrotational free-surface flow, time-dependent 80−83807
irrotational waves and convergence of Levi-Civita's series 77−58711
Kelvin instability development in unstationary flow 77−7405
kinematic characteristics of travelling waves 78−67205
Korteweg-de Vries equation and nonlinear waves 79−92956
Lake Suwa, wind driven currents, obs., numerical calcs. *(Japanese)* 77−37254
laminar film, mass transfer with dissolution 78−26098
Langmuir circulations, wave-current interaction theories 80−100004
large amplitude progressive interfacial waves, Boussinesq waves 79−86447
light scattering by surface tension waves 79−58469
linear waves, asymptotic behaviour and wave patterns construction *(Czech)* 80−69
linearised interface-wave problems for superposed inviscid liquids 80−87782
liquid, damping effect of monolayers on surface wave motion 78−67206
liquid, three-dimensional gravitationally-elastic, gravitationally-capillary surface waves *(Russian)* 79−32537
liquid boiling wave processes at heat releasing surfaces 79−90773
liquid dispersion, suspended impurities effects on wave excitation in sound field 80−81372
liquid drop in EM field, Raman line splitting 77−69826
liquid film, falling, laminar, transport augmentation by surface waves 78−71343
liquid film, surface wave propag. under charge flow *(French)* 77−31849
liquid film flow, drop form., size spectrum 78−34187
liquid interface, mol. light scatt., heat fluctuations *(Russian)* 78−23477
liquid layer adjacent to gas stream, surface waves, subsonic and supersonic disturbances 79−23336
liquid of finite depth (nonviscous incompressible), calc. of surface wave propagation *(Russian)* 77−68604
liquid surface electron layer, parametric excitation of collective modes 77−15928
liquid surface wave due to shock wave interaction, viscosity effect 77−11202
liquid wave-fronts in free-flow transients, position fixing method based on Ti memory property *(Italian)* 80−43723
liquid-gas interface, surface wave generation and detection method 79−1277
liquid-liquid system interfacial instability and longitudinal waves 80−33566
liquid-solid interface, waves generated at interface with viscoelastic solid 79−68729
liquid-vapour flow, wave pattern and liq. film burnout 78−90985
liquid-vapour interface, kinetic eqn. at mean field level 79−37905
long and short surface waves interaction 77−41049
long-period wave problems, finite element method 79−4026
lubrication, cavity-fluid interface, wavy interface anal. 77−55059
magnetic fluid, surface wave excitation, by travelling mag. field *(Russian)* 77−47099
magnetic liquid, surface vibration mode obs., steady-state, for teaching lab. 78−41111
magnetic liquid thin layer with two free boundaries, instability conditions, surface wave dispersion eqn. *(Russian)* 78−1752
magnetised liquids, separated by thin elastic film, surface stability 79−94727
meas. using resistance wave gauge, accuracy and calibration 80−24110
MHD anisotropic surface wave system, common wave phenomena appl. 77−24029
MHD dispersive surface wave generation 77−47111
MHD gravity waves, dispersion on running stream of inviscid elec. cond. liq. 78−59502
MHD waves in arc discharge, low freq. spectrum, instabilities *(Russian)* 77−68762
mineral oil, finite amplitude equilib. waves on surface of nonvertical falling film 77−19614
minimum wind stress for wave inception 78−57285
momentum flux in monochromatic waves of large amplitude *(Russian)* 77−31317
natural oscillation solns., variational method *(Russian)* 77−80176
Nekrasov's integral equation, soln., wave of greatest height, Stokes's conjecture 78−94754
non-Newtonian fluid, rot. liq. film, free surface instability 79−37294
non-Newtonian incompressible liquid film, surface waves 80−43748
surface waves continued
nonisothermal liquid film, nonlinear dispersive surface waves 80−33617
nonlinear baroclinic waves, exptl. study of instability and mode selection in large basis 80−85669
nonlinear stern wave production in pot. flow past flat bottomed body 80−38425
nonlinear surface waves with gravity or surface tension restoring forces 78−22357
nonlinear waves and solitons, stability in three dimens. 79−97211
nonlinear waves in closed basin, random behaviour 80−26557
nonlinear wind-wave system, model and expt. 79−34846
ocean, calcs, of main waves generated by tropical hurricane *(Russian)* 78−16021
ocean, interfering waves rel. to lower thermosphere heating by acoustic waves dissipation 77−53266
ocean, long waves effects on wind boundary layer and ripple slope statistics 77−45005
ocean, meas. using pulse compression radar scatterometer system, expt. 77−29483
ocean, rough surface rel. to underwater light field fluctuations, numerical modelling *(Russian)* 77−33090
ocean, surface waves breaking rel. to turbulence generation *(Russian)* 78−16022
ocean, surface/internal waves energy transfer model 77−923
ocean, wave height and wave celerity obs. in surf zone 77−45012
ocean, wave-induced atmospheric mag. field, attenuation 77−13058
ocean, waves orbital vels. rel. to vel. fluctuations scaling in mixed layer 77−45009
ocean, waves rel. to rhomboidal lattice struct. on sandy beaches 77−37178
ocean capillary waves, laser probe for 2D wave slope spectra meas. 77−60472
ocean long-period waves on beach 77−21780
ocean rough surface, effects on sound attenuation in shallow water 77−62091
ocean surf, atmospheric elec. space charge generation 78−36235
ocean wave height barometric sensor 77−78487
ocean wave slope meter, fast response instrument, wind-wave moments meas. 78−45012
ocean waves, analogue model for induced geomag. vars. 77−49003
ocean waves, statistical distrib. of periods and heights 77−45006
ocean waves, synthetic aperture radar imaging, focusing effects 78−40555
ocean waves on erodable base, bottom vel. and scouring 78−49029
oil thickness variation on wavy water 80−6134
oil-water interface, US emulsification drop form. by capillary wave instability 79−32643
opto-acoustic antenna, floating, acoustic field statistical characts., surface waviness depend. *(Russian)* 78−1536
oscillations, viscosity and surface tension relax. effects 77−62266
parametric excitation, by sound waves *(Russian)* 77−46841
parametric excitation of waves, heating effect 78−67209
parametric wave excitation at liq. surface *(Russian)* 77−58709
periodic long wave deformation, over gently sloping bottom 78−90921
periodically rough water surface, thermal radiation critical phenomena *(Russian)* 78−81188
plasma, ion-acoustic LF surface waves, parametric instability *(Russian)* 77−68766
propagation theories for water waves, variational principles 80−24043
protein solution, propagation of surface shear waves 79−77146
pseudoplastic liquid film, wave motion 79−32583
pulsed plasma generation by surface wave 78−75385
radar backscatter from water waves, induced current effects on microwave backscatter, expt. 77−25688
radiation and scatt., by cylinders, for short waves 79−27657
random signal analysis, for level and velocity meas. in rivers and open channels 77−45205
random water waves, optical meas. technique 77−29503
random wave fluid, wave groups presence modelling 79−2245
ray theory of ship waves, rel. to streamlined ships 79−59994
rectilinear surface waves incident on submerged circ. sill 78−1677
reflection, at permeable quaywall with reservoir, of obliquely incident waves *(Japanese)* 79−32546
reflection, from tangential discontinuity of velocity *(Russian)* 79−4024
remote level and velocity measurement by random signal anal. from surface waves 79−72976
resonant nonlinear interaction of waves in stratified fluid 78−83418
ring vortex instability, wave formation dependence on vorticity distrib. 78−34146
ripple, annular, two phase flow, statistical characteristics 78−9672
ripple growth to swell, ang. momentum conservation explanation 80−56478
ripple tank wave generator, using loudspeakers, student demonstration 77−78915
roll waves, small amplitude, behaviour in turbulent liquid films *(German)* 78−94756
rotating circular cylinder, radially progressive surface waves 80−14722
rotating cylindrical layer of fluid *(Russian)* 77−925
rotating fluid, finite depth, Green's function anal. 79−37324
rotating fluid, waves due to sources and internal boundaries 79−37323
rotational surface waves, comparative theorem 79−50745
run off models, two dimens., kinematic wave approx. 79−4099
scattering, by submerged sphere 78−34145
scattering by compact obstacles 78−90925
sea irregular surface, amplitude and phase var. of refl. narrow sound bundle 77−46825
sea state and wind sensing by HF skywave radar 78−24396
sea wave profile meas. by radar altimeter, computer simulation 77−5367
sea wave space and time structure measurement from Doppler frequency shift 77−29482
shallow water, open channel wave propag. numerical method anal. 79−10582
shallow water basin, wind-driven current, eddy viscosity, bottom friction 78−65319
shallow water in polygonal bottomed tank, wave motion, initial condition influence 79−50746
shallow water wave equation model, finite element tidal computations 79−84282
shallow water waves, improved finite difference scheme 79−4028
shear layers, nonlinear evolution of waves 80−83809
shear waves on liq. surface, theory 79−64679

surface waves continued
shoaling of finite-amplitude surface waves on water of slowly-varying depth 80−69853
shoaling waves, breaking invariants 78−85577
short crested waves, boundary layer vels. and mass transport 80−92169
short gravity waves, phase speeds of upwind and downwind travelling waves 80−98332
short surface scattering by cylinder 77−89132
short-crested waves, third order approx. calcs. 79−50741
slender floating body, wave radiation, charact. wavelength 79−2640
small amplitude surface waves due to an oscillatory pressure 79−32539
small amplitude water waves, uniqueness in region of varying depth 80−1613
solar atmosphere, five-minute oscills. in temp. min. as surface waves 79−62808
solar photosphere, props. of surface (capillary) waves *(Russian)* 80−12726
solitary wave interactions, finite difference soln. of Boussinesq eqn. *(Russian)* 79−77141
solitary waves, review, book contrib. 80−94962
solitons, horseshoe-shaped, on flowing viscous film of fluid 79−18906
spectral energy transfer from surface waves to internal waves, oceanic main thermocline 79−70812
spin and angular momentum in gravity waves 80−53798
standing surface waves, double boundary layers 77−25694
standing waves, finite amplitude, on finite-depth perfect liq. surface *(Russian)* 78−75155
standing waves of finite amplitude on surface of ideal liquid of finite depth 79−81906
stationary temperature boundary layers generation by surface waves *(Russian)* 80−1611
stationary waves at the surface of a magnetizable liquid in a stream impinging on a point barrier 80−83805
steep progressive gravity wave, rounded crest, transcendental eqn. 77−56643
steep surface wave deformation, growth of normal mode instabilities 79−1206
steep wind waves, amplitude modulation 80−103036
steepness over a limited depth *(Russian)* 80−79336
Stokes waves, higher order solns. *(Japanese)* 78−42625
submerged obstacle, finite-difference method 79−4027
surface waves and internal waves interaction 79−10576
symmetric finite-amplitude rotational waves, streamfunction soln. 77−41044
tabular iceberg, off Newfoundland Grand Banks, wave erosion 77−56646
thermally induced surface fluctuations on simple fluids 80−88403
thermoconvective waves in horizontal bounded layer of incompressible fluid 77−89134
thin fluid layers under centrifugal forces, wave flows, obs. 79−23335
thin liquid sheet, instability and its break-up 77−11205
thinning liquid film, surface wave development 80−19416
topographically trapped waves, review, book contrib. 80−96273
transient flow problems, Lagrangian soln. using triangular mesh 79−64678
transient waves generated by a moving oscillatory pressure on a sloping beach 80−56476
trapped waves around circular island, amplitude relation 79−7380
travelling gravity-capillary waves on liq. film surface falling past permeable bed 78−87351
tsunamis, simple demonstration apparatus 77−13531
turbulent boundary layer, wave generation on elastic surfaces, expt. study 80−74843
two-dimensional boundary-value problems of small amplitude waves in finite water depth, num. analysis method 77−9444
two-layer 'shallow water' model 80−59061
two-layer fluid, waves caused by periodic press. near thin wall *(Russian)* 77−27541
two-layer shallow water flow, internal and surface waves, numerical anal. 80−19472
two-phase flow, hydrodynamics and heat exchange in film flow 78−91000
two-phase liquid film flow, hydrodynamic and heat transfer in downward annular motion 77−89190
underwater ridge, wave guide properties for surface waves 80−96268
unidirectional sinusoidal, channel propagation, Korteweg-de Vries equation application 79−50742
uniform depth ocean, energy transmission by surface waves through an opening 80−61811
unsteady, numerical method for initial stages of wave breaking 77−68613
unsteady flow damping by compliant boundaries 77−31274
unsteady wave development, surface tension effect *(Russian)* 79−100856
Venice lagoon inlets, maximum waves forecasts computation *(Italian)* 77−37205
vertical body of revolution beneath surface, focus on body 78−38347
viscoelastic polymers, surface wave calcs. 79−32593
viscous fluid film, approx. eqns. for long nonlinear waves 78−38346
viscous fluid layer, solitary waves *(Russian)* 77−51070
viscous fluid of variable depth 77−11210
viscous incompressible liquid, wave generation by radially symm. press. on free surface 78−26133
water, irrotational waves, existence theory 78−38348
water, long-wave propag., modelling criteria, appl. to tsunamis 78−26132
water, nonlinear propagation, effect of random inhomogeneities 77−11204
water, oscillatory boundary layer beneath waves, meas. using laser Doppler anemometry 79−27719
water, oscillotory waves, Korteweg-de-Vries and Schrodinger eqns. solns. and expt. 78−26131
water, surface gravity water propag., wave action and set-down on shear current 78−90920
water, surface waves due to moving press. strip 79−59996
water, wave generation, Rayleigh method 79−68730
water flume, orbital vel. meas. by two-component laser Doppler anemometer 77−3898
water of finite depth, soliton solns. of Davey-Stewartson eqn. for long waves 78−38351
surface waves continued
water of variable depth, conf., Canberra, Australia (July 1976) 78−40572
water surface, free, roughness determ., from air flow struct. anal. 78−63441
water surface, optical pulse refl., probability charcts. *(Russian)* 78−22081
water surface roughness rel. to air flow *(Russian)* 77−70669
water wave, steady, numerical soln. using Riemann Hilbert method 80−33618
water wave damping, effect of large grooves 77−11209
water wave generation by wind, airflow separation 77−70734
water wave probe, parallel wire type 79−18979
water wave propag. over circular shoal, parabolic eqn. method 80−14717
water wave propagation over underwater source 78−83416
water wave reflexion by permeable barrier 80−14716
water waves, in nonhomogeneous incompressible fluid, nonlinear differential eqns. 78−55657
water waves modulation near kh=1.363, Stokes wave stability 77−84265
wave amplitude measurement, surface standing, using capacitance meas. circuit 79−50833
wave and force measurement system 79−41780
wave generator model, traction force determ., Navier-Stokes liquid motion description 79−77152
wave height spectrum of two-component composite waves in surf-zone *(Japanese)* 80−100006
wave resistance due to vessel near solid walls *(Russian)* 77−55013
wave spectrum changes due to shoaling and breaking, −3 power law *(Japanese)* 80−100007
wave-slope spectra in capillary-gravity range, increasing wind, laser beam meas. 77−3836
wavelets, initial generation by coupled shear flow instability wind wave evolution 79−94635
wavy water surface thermal radioemission obs. at 3.5 and 14.5 MHz *(Russian)* 78−61425
wind driven capillary waves meas. in wave tank, rel. to ocean 79−64673
wind generated wave damping in medium with natural turbulence *(Russian)* 77−41058
wind wave generation, Phillips-Miles theory 78−79328
wind waves, directional slope and curvature distribs. 77−31316
wind waves, long-term parameter distrib. function 78−81202
wind waves on water, duration-limited, 1-dimens. spectra of growth 78−46990
wind waves problems, similarity theory appl. *(Polish)* 77−21795
wind-driven water waves, numerical model calcs. 77−922
wind-generated, interaction with sub-surface water jet *(Russian)* 79−4025
wind-generated in deep water, Rayleigh method *(Russian)* 78−36178
wind-generated water waves, spatial correls. rel. to freq. independent phase vels. 80−98333
wind-generated waves obs. on variable current 77−41053
wind-induced waves, exptl. investig. of freq. spectrum components dispersion ratio *(Russian)* 79−10581
wind-wave generation of surface gravity wave 78−49033
wind-wave interaction, two-layer flow, numerical simulation 78−92823
wind-wave tank, microscopic and macroscopic surface structs. growth and decay rates 80−48726
He, liq., surface, macroscopic electron lattice formation 79−77861
^{4}He, superfluid, second sound, boundary conditions, standing surface waves obs. 79−46857
^{4}He superfluid, surface wave, small amplitude long wave propag., linearised theory 78−56002
^{4}He, superfluid surface, spectral features of spontaneous light scatt. *(Russian)* 77−62696
Hg, shallow surface-wave simulator for jet noise sources 77−80146

surge absorbers *see surge protection*

surge protection
see also divertors; surges
doubler tevatron microprocessor quench protection system 79−72088
Fermilab magnet protection using ZNR surge suppressors 79−68043
GaAs laser diode power supply control cct. *(German)* 80−78852
image intensifier protection against damage from high intensity flashes 79−37046
neutral beam injector, high voltage series protection by cross field interrupter 80−13884
power supply, three-phase system, computer aided cct. design 78−54959
superconducting beam line magnets, fast energy dump 79−68091
Si:Al lamellar devices, surge protector, solar cell, HV diode and negative resistor appls. 78−10068

surge suppressors *see surge protection*

surgery
abdominal surgery, role of rapid-sequence image intensifier fluorography 79−92340
acrylic surgical bone cement fracture behaviour 80−56277
anaesthesia administration, computer-aided, use of dynamic programming model 77−5107
anaesthesia stage indicator, signal divider 80−3858
aneasthesia delivery system, closed loop design 78−40402
angiographic universal setups for general hospital with vascular surgery facility 79−92336
aortic and mitral regurgitation patient surgery and vectorcardiogram changes 79−44050
aorto-coronary saphenous bypass surgery, ^{201}Tl myocardial perfusion scintigrams 79−25068
aortocoronary sapheneous bypass surgery, evaluation by ^{201}Tl myocardial perfusion scintigrams 80−12235
aspiration automatic control device for cardiac surgery *(French)* 78−61282
atrial septal defect repair, sinus node dysfunction and atrioventricular conduction disturbances 77−81647
autotransfusion, variable speed pump head control 77−52918
autotransfusion, variable-speed pump head control 78−57121
blood cell damage in extracorporeal circulation, haemorheological effects of mech. factors 79−62280
bone, orthogonal machining, forces and energies 79−29559
bone marrow, autologous transplantation, treatment for X-ray, neutron, exposure, monkeys 79−29572
bone tissue preservation, effect of treatment on chemilum., rel. to bone fragment transplantation 77−86709

surgery continued
cancer management, status of low linear energy transfer radiation 79−20621
cardiac, deep body temperature monitoring, thermistors, digital display, continuous recording 77−29223
cardiac patient postoperative management, computerised intensive care 77−40918
cardiac surgery, data acquisition and processing during operation by multiplexer *(German)* 78−92743
cardiac surgical patient postoperative computerised meas., analysis, and treatment 78−36044
cardiology, development progress 78−3646
cardiovascular surgery, endothelial lesions associated with vascular clamping 79−53278
cell microsurgery using UV laser beam *(German)* 77−60235
cerebral blood flow automated analyser for ^{133}Xe studies 77−86597
choke-earthed surgical diathermy circuit analysis 79−20705
choledochoscope, rigid optical-fibre, KhVS-1, bile duct inspection appl. 77−37071
claw hand optimal surgical correction, finger biomechanical model 79−92268
cold finger, for cryosurgery, heat transfer charcts. *(Russian)* 77−22556
combination surgery cell with laminar air flow *(German)* 79−16335
corneal mechanised trepan control 79−29659
coronary artery bypass fluid mechanics, for introductory physics course 77−78911
coronary artery bypass graft patient recovery trajectory classification algorithm 80−94411
coronary bypass surgery, left ventricular function and myocardial metabolism evaluation by atrial pacing 77−81646
coronary-artery bypass surgery, correls. with myocardial scintigraphy using ^{99M}Tc pyrophosphate 79−39475
crest factor definition for surgical equipment 80−56273
cryocatheter tourniquet, appl. 78−7521
cryogenic instruments for local tissue destruction, choice of instrument working temps. for cryogenic instruments 78−36036
cryogenic instruments for treatment of head and neck tumours 77−78029
cryogenic technique in treatment of neoplasms of oral cavity and pharynx 77−78030
cryogenic techniques, clinical appl. 80−12295
cryoirrigator, stomatological 77−21654
cryoprobe, for medical surgery 80−56274
cryosprayer improvements 77−78033
cryosurgery, freezing patterns of normal and diseased tissues 78−44685
cryosurgery, math. and biophys. foundation 77−40920
cryosurgery, self-contained apparatus 80−56271
cryosurgery instruments, effects of heat transfer material on working parameters 78−36037
cryosurgical apparatus coolant supply system 77−81637
cryosurgical applicator, temp. distrib. reproducibility 79−39589
cryosurgical applicator for dermatology 77−78034
cryosurgical heat tube instrument design 77−78031
cryosurgical instrument for proctological and gynaecological operations for malignant tumours 79−70699
cryosurgical instruments, open and closed circuit supplies compared 79−39592
cryosurgical instruments for otorhinolaryngology 77−78032
cryosurgical probe, heat transfer coeff. within cavity formed by tip 80−36188
cryosurgical probe, Stefan-like problem in biological tissue analysis 77−17005
cryotumourectomy control with LF impedance meter 77−25591
cryoultrasonic surgical instrument 77−78027
dental electrosurgery, evaluation of patient elec. load by analogue cct. 77−40912
dental pain reliever with increased stabilisation of working current 77−48922
diathermy indifferent electrodes, performance electrodes. 80−72367
diathermy units, selection guidelines 77−73613
ECG monitor, non-fade, battery-powered, features 78−7528
EEG automatic pattern recognition, patients under general anaesthesia during operations 80−17154
EEG preamplifier for monitoring 77−40916
electrosurgery, tissue coagulation, effects of HF current parameters 80−3746
electrosurgery system using HF surgery unit Radiotom 704 78−73292
electrosurgical dispersive electrode site temp. and current density distrib. model 79−92424
electrosurgical dispersive electrodes, dry metal-foil, thermal props., skin temp. rises 80−98171
electrosurgical dispersive electrodes, thermal performance evaluation method 79−74735
electrosurgical hazard monitor 79−83882
electrosurgical instrumentation review 78−44680
electrosurgical load-independ. const. current generator 78−44684
electrosurgical passive grounded electrode/patient equivalent circuit analysis 77−78025
electrosurgical return electrode capable of steam sterilisation and reuse 77−40911
electrosurgical safety precautions 79−92317
endometrial cryosurgery of perfused human uterus, investigation of temp. field produced 80−55995
engineering in medicine and biology, conf. Atlanta, USA (Oct. 1978) 79−39332
eye, detached retinal tears computer localisation for scleral buckling procedure 78−7529
eye lens replacement, accurate meas. of eye length using US echo-oculometer 77−37030
eye operations, photographic documentation using model 310 surgical microscope 80−56161
femoro-popliteal by-pass graft, flow in idealised models 79−39429
femur fractures, reduction apparatus 79−16343
ferrofluid seal, for blood flow statis during surgery, hydrostatic loading 77−13031
fibre optics in medicine, diagnostic and therapeutic appls. 79−39466
fish surgery, low-cost audible heart rate monitor 77−70575
glaucoma surgery, Nd:glass laser with freq. doubling capability 78−40403

surgery continued
gross surgical specimen photography, centimetre rule/elevator rod technique 78−61287
gynaecological cryogenic treatment apparatus 79−57807
gynaecological endoscopic photography, increased mobility using articulated lens 77−48928
gynecological cryosurgical apparatus using N_2O as coolant 78−7525
heart surgery, interference suppression for EEG recording 79−100784
HF current surgery, instruments and problems *(Hungarian)* 80−98172
hydrocephalus surgical treatment, valve system design *(Japanese)* 78−31963
hypothermia in heart surgery; intercellular oedema due to reduced membrane efficiency 77−29225
implants, corrosion fatigue behaviour of Ti-Al-V 79−39027
intraoperative angiography in cardiac, thoracic and vascular surgery 77−90880
intraoperative coronary arteriography for graft patency prediction 79−92343
intraoperative use of X-ray TV chain with video recorder 79−92334
intraoperative X-ray diagnosis, exposure reduction by magnetic disc store 79−92345
ischaemic heart disease studied by cardiac pacing 77−81628
kidney transplantation, effect on evoked pots. and EEG freq. 78−61160
laparoscopic sterilisation techniques, preclinical and clinical testing 77−48929
laparoscopic surgery, bipolar sterilising forceps and uterine manipulator 77−48926
laparoscopic tubal sterilisation instrumentation 77−48927
laser action, possible head surgery appl. of Ar laser 79−8529
laser application, state of the art 77−40729
laser application in clinical rhinology, Ar^+ laser instrument *(German)* 78−69177
laser applications, advantages 79−34704
laser applications, in USSR 77−73555
laser applications in clinical medicine *(Japanese)* 80−12211
laser applications in medical research, biophysical aspects 80−51201
laser applications in medicine *(German)* 77−9235
laser applications in otology, review 78−48860
laser applications in surgery, using CO_2 laser 77−9297
laser beam applications in medicine and surgery, review *(French)* 79−34626
laser beam operation in surgery and treatment, safety 78−35903
laser biomedical research in USSR 78−48858
laser effects on blood vessels 79−66505
laser endoscope treatment of urinary tract strictures *(German)* 78−35914
laser in clinical otorhinolaryngology appl. of Ar^+ laser 77−90870
laser iridectomy, energy required, hazards and techniques 78−11713
laser medicine development trends 80−51198
laser medicine in Japan, current status *(German)* 80−98059
laser microsurgery, CO_2 laser use and laryngology applics. 78−35905
laser neurosurgery, CO_2 laser uses *(German)* 78−35912
laser osteotomy, new results *(German)* 78−24114
laser possibilities, limits and prospects *(Italian)* 80−56156
laser scalpel and micromanipulator for neurosurgery, CO_2 laser system *(German)* 80−3753
laser surgery, acute and long term laser beam effects on fibroblasts and smooth muscle cells in culture 78−40268
laser surgery, Ar ion laser treatment of haemangiomas, teleangectasia, radiodermatitis and tattoos 78−35906
laser surgery, flexible fibre-optic beam-guiding system, oto-rhino-laryngology appls. *(German)* 79−83886
laser surgery, healing of tissue wounds following CO_2 laser action *(German)* 78−35913
laser trabeculotomy in glaucoma treatment 78−53470
lasers, effect on lining tissue and applics. 77−90871
lasers in medicine, appls. and equipment development 78−48862
ligament and tendon replacement, polylactic acid polymer-filamentous carbon tissue scaffold 79−92434
microneurology, appl. of colour TV as surgery teaching aid 78−40396
microprocessor-based patient monitoring system 78−44681
microwave radiation, rapid protein coagulation appl. 79−5336
mitral valve replacement, prediction of postoperative systolic left ventricular wall stress 78−40427
monitoring, 4-channel telemetry system 78−31961
monitoring, developing crisis 78−40401
monitoring, inexpensive general purpose computer 78−36045
muscle relaxation in surgical patient indicated by frontalis muscle spontaneous elec. activity 78−44686
myocardial activity determ. at surgery using shrinking stress meas. 78−31966
myocardial perfusion index calculator for prediction of subendocardial ischaemia in cardiac surgery 77−40915
myringoplasty, comparison of implant materials after tympanic membrane perforation in rat 79−39597
nasopharyngeal anaesthetic apparatus adaptor 77−81639
neurosurgery, laser appls., review 80−26317
neurosurgical cryoprobe, self-contained, with replaceable flask, features 78−7526
neurosurgical intraoperative X-ray equipment use 79−92344
oesophageal multiprobe for temp., ECG and heart and lung sound meas. 78−77146
open-heart surgery, brachial artery blood flow measurement, noninvasive ultrasonic Doppler technique 77−86570
operating room airborne contamination protection using electrostatic particle repulsion system 78−28125
operating table with interchangeable top 78−36042
operating theatre patient monitoring problems and trends 79−92422
operating theatre safety fundamentals *(Japanese)* 79−2149
operating theatre X-ray installation planning 79−92339
ophthalmology, extraocular muscle system mechs. model 78−40155
orthopaedic surgery, role on intraoperative X-ray diagnostics 79−92341
orthopedic surgery, prevention of deep wound infection 79−16265
pacemaker electrode insertion via cephalic vein, thrombosis obs. 77−81714
pacemaker implantation, therapy/measuring combined unit *(German)* 78−7519
pacemaker implantation surgery, intracardiac ECG derivation during electrocoagulation 78−40397
paediatric intertrochanteric osteotomy fixation of modified Kuntscher's nail *(Croatian)* 78−44675

surgery continued
partial hepatecomy using high power CW and Q-switching ND:YAG laser *(German)* 77−44734
photocoagulating scalpel for laser surgery 78−48866
plasma scalpel, cuts and cauterises, animal studies 77−52912
plastic surgery, biomechanical aspects 80−56103
prosthetic limb joints, use of Al_2O_3 ceramics *(German)* 77−25593
quality health care and cost containment, conf., Washington, USA (Mar.-Apr. 1978) 79−39333
radioactive glove box accident, surgical treatment of wound contaminated by ^{239}Pu and Am *(French)* 78−53521
rehabilitation engineering *(Japanese)* 80−12304
renal and ureteral calculi, surgical treatment under fluoroscopic control 79−92342
rewarming after surgery, hyperthermia study in dogs 78−80834
scoliosis correction using Dwyer cable, noninvasive telemetric determ. of anterior spinal fusion 77−44851
Sharplan 791 CO_2 laser for clinical surgery 78−35904
skin, human, reconstructive surgery, in-plane compressive strain limits prediction 80−41069
spinal deformities correction, force meas. 80−76861
stereotaxic surgery, computer system for anatomical and functional mapping of thalamus 77−37097
stomach tissue, canine, temp. increase comparison for Ar and Nd:YAG laser irrad. 79−92290
supraorbital Doppler evaluation of blood flow in vascular surgery 79−88144
supraventricular tachycardia, diagnosis and management, instrumentation and therapeutic techniques, review 79−39598
surgical implant materials, corrosion fatigue props. 79−39604
surgical implant materials, corrosion props. 79−39605
tissue suturing apparatus, multiple staple, with needle-shaped matrices 79−57808
tissue temperature simulation in cryosurgery 80−85355
transposition of great arteries in infants, cardiovascular simulation 77−44713
transurethral surgery HF power generation requirement *(German)* 79−16338
US, refinements in methods and apparatus 80−21508
US applications and new developments, review 78−11712
US concentrator, equivalent cct. anal. 78−50997
US equipment, selection of material for concentrator-instrument section 80−21242
US in medicine and biology, review 77−66830
vascular occlusion treatment by cryothrombectomy and cryovenectomy 77−78026
ventilation feedback control in small infants after open-heart surgery 79−70710
ventilatory monitoring in operating room, current techniques and future requirements 78−20307
ventricular arrhythmia on-line study, computer system 78−81060
ventricular septal defect plastic repairing instrument 78−7522
vitreous surgery via pars plana, instrument design 78−81056
wound preoperative force meas., transducer device 78−36041
wrist kinematic and kinetic analysis rel. to surgical reconstructive procedures 80−16999
O_2 consumption continuous measurement, under N_2O anaesthesia 77−81640
Ti for implantation, biological props. 78−3678

surges
see also overvoltage; transients
air insulation gaps, critical impulse voltage stress determ., test 77−4018
explosion of double wire, optical flashes, photographic appl. 80−1865
oil electric strength for switching surges and long flash-over distances, expt. *(Czech)* 78−56427
pump pipeline, pressure surges calc., method of characteristics appl. *(Spanish)* 79−23364
spark gaps, electrode shape effect on SF_6 dielectric strength, overvoltage protection *(Czech)* 80−10444
spark gaps, HV switching surges, influencing factors *(German)* 80−87958
spark gaps, long air, disruptive voltage calc. with positive switch voltages *(German)* 80−87964
switching, long distance discharge probability calc. *(French)* 77−39493
switching, long spark modelling, voltage and flashover distance conversion factors *(Czech)* 77−15254
switching, long spark modelling *(Czech)* 77−1028

surgical operations *see surgery*

surveying
aerial photographic equipment developments, aerial survey camera and navigation telescope 77−66997
aerial photography, high altitude, aspects and results 78−36309
aerial survey image interactive hybrid optical/video processing system 77−53254
aerial triangulation, bridging with independent horizontal control 79−25184
aerotriangulation by Skylab Earth terrain camera photography 77−33209
Alps, precision levelling and recent vertical movements *(German)* 77−2139
altitude observations, Fourier transform. *(German)* 78−61312
American Society of Photogrammetry, use of International System of Units 79−21692
angular goedetic cross bearings, accuracy *(Russian)* 79−92476
Asama Volcano, Japan, geodimeter survey during 1977, ground deform. *(Japanese)* 79−70732
Asama Volcano, Japan, joint geophys. and geochem. obs. in 1977 *(Japanese)* 79−70771
Asama Volcano, Japan, precise levelling surveys *(Japanese)* 79−70731
astronomical azimuths of terrestrial objects, as indicators of continental blocks rot. 78−53613
atmosphere refraction correction to levelling *(Russian)* 80−77127
Autocollimation Outfit for JENA surveying instruments 77−82030
automatic drafting system, appl. to problems of geodesy *(German)* 78−15952
automtic optical plumbline requirements and design *(German)* 77−70877
Baikal rift zone, recent crustal movements, precise levelling data 78−36139

surveying continued
Bavarian land survey, development of present 1:500000 outline map *(German)* 77−2081
Bavarian surveying administration, centralised and decentralised data processing *(German)* 77−2288
block aerotriangulation adjustment data for analytical rectification using artificial points 79−2177
Bohemian Massif and W.Carpathian border, recent crustal movements 79−79791
Briones Hills, California, geodolite meas. near earthquake 78−92803
cadastral maps and new technical developments *(German)* 77−70589
California State geodimeter data, possible bias, comment 77−17018
China, Zhang Sui and first astronomical geodetic survey *(Chinese)* 77−64911
collocation, with help of Gaussian algorithm *(German)* 79−79730
contemporary crustal movements in Canada 80−8273
criterion matrices, appl. to design of homogeneous isotropic geodetic networks *(German)* 79−100983
crustal movements, conf., Palo Alto, California, USA (July 1977) 79−79785
crustal movements monitoring by geodetic meas., statistical anal. 79−79726
data acquisition and processing, microprocessor-based system features 79−29913
densification of ground control networks, computer program package *(German)* 80−94452
Diablo Plateau, W.Texas, contemporary uplift from levelling meas. 79−20798
Digital Terrain Model, use of electronically controlled drawing machines *(German)* 78−20348
distance measurement, electro-optical nonperiodic errors rel. to use of plane mirrors *(German)* 77−9324
distance measurement, micrometer errors and short period errors of graduated circles *(German)* 78−45038
distance measurement, multi-wavelength instrument 77−29484
Earth's surface, air survey methods *(Dutch)* 78−3972
Earth exploration from satellite Soyuz 22, Raduga expt. *(German)* 77−56765
Earth resource surveying and interpretation 78−24391
electronic distance meas. technology 77−67410
electronic tachymetry, ten years of Zeiss equipment *(German)* 79−34999
electrooptical distance meas. instruments, Zeiss ELDI 2 type, error anal. *(German)* 79−21081
extended-range three-wavelength distance measuring instrument design 79−80053
extreme value problem, tunnel building appl. *(German)* 77−52967
fault creep records and long-baseline strain data, Hollister, California 79−79776
fault displacement in Peking district *(Chinese)* 79−62462
fluid tube tiltmeters, thermally induced errors 78−36303
forest fire survey application of microwave radiometry 77−87127
Gauss-Helmert model, singular covariances, least-squares adjustments *(German)* 80−56340
geodesy, an ordering factor in society *(German)* 77−60344
geodetic data systematic inversion, central California 79−84076
geodetic free nets, modification of Helmert-Wolf's soln. *(German)* 80−94453
geodetic level testing, vertical and horizontal settings 77−29489
geodetic reference systems for crustal motion studies 79−79720
geological joints, mapping via photogrammetry and EDP appl. 80−56470
German Bight, trilateration distance meas. *(German)* 80−8248
German Standards Institute, 50 years of standardisation in surveying *(German)* 78−45591
graduated circles, short-period, error determ. *(German)* 78−88791
gravimetric networks, adjustment *(German)* 79−44084
gravity base at Newcastle upon Tyne University, England 79−29693
gravity vector and geodetic position survey, inertial navigation system appl. 79−29914
ground cracking, instrumentation and field monitoring 79−79729
height vars., basic determ. problems *(German)* 79−34725
horizontal crustal deformation from historic geodetic measurements in southern California 79−84197
hybrid distance-direction networks, Helmert-type variance-covariance-component estimator appl. 80−101318
image analysis system for Earth resources surveys 79−5644
inertial meas. systems, basic eqns. and error models *(German)* 80−56655
inertial navigation system for automatic position, azimuth and gravity disturbance meas. 77−5353
inertial rotation sensors for surveying and geophysical meas. 80−12571
inertial systems, geodetic appls. *(German)* 80−56656
instrument manufacture 77−82027
interactive computer graphical systems appl. *(German)* 79−21023
interactive lake survey programme for water resource surveillance 78−81257
interferometric methods for distance meas., recent crustal movements appl. 79−80057
interpolation, via groups of triangulation data points of different statistical characts. *(German)* 77−9321
interpolation by linear least squares, numerical aspects *(German)* 77−9322
interpolation method using multiquadratic eqns. *(German)* 78−15951
IR distance meas. instrument 77−49201
Izu Peninsula, Japan, geodimeter surveys, horizontal strain meas. *(Japanese)* 78−96163
Japan, crust horizontal deform., first-order triangulation meas. 79−79727
Juan de Fuca plate aseismic subduction, geodetic evidence 79−84209
LAGEOS high-mobility ranging station, geodesy appl. 79−79723
level testing, autocollimation equipment 79−67369
levelling, influence of temp. in Telyvel electronic system *(German)* 78−45037
levelling, systematic errors of compensator levels, new instrumental developments *(German)* 77−2289
levelling data, automatic evaluation prospects *(German)* 78−32258
levelling networks, Helmert-type variance-covariance-component estimator appl. 80−101318
literature survey for the year 1976, appendices *(German)* 77−90993
Lompoc, California earthquake, 1927 November 4, source mechanism from geodetic data 79−84126

surveying continued
magnetic surveying using horizontal gradient vectors 78−28334
marine geophysical surveying, new techniques appl. 79−53560
marine survey vessels, multiple use 79−53561
Mekometer measurements in Imperial Valley, California 79−79728
Mini Range III positioning system, meas. range improvements, technical details and charact. *(Italian)* 80−56611
motorized precision levelling with NI 002 Automatic Level 77−86743
Mount Etna, large ground deform. from precise levelling obs. 77−37172
mountain peaks uplift determ. by three dimens. triangulation *(German)* 77−52966
objectives of surveying, meas. techniques and data processing methods *(German)* 80−101317
offshore surveys, accurate positioning at distances to 400 km 80−12328
orthomapping review 78−88777
orthophotography, history, advantages and uses 77−66995
perimeter survey by photogrammetric methods 79−25185
Phlegrean Fields, Naples, geodetic and geophys. meas., elevation changes 79−29734
photogrammetric meas. for field mapping *(German)* 78−92776
photogrammetric network densification by aerotriangulation *(German)* 77−60496
photogrammetry, orientation, triangulation and digitisation, numerical methods 78−36312
photogrammetry, SEM appls., simplfied numerical transform. for distortion correction *(German)* 79−17572
photogrammetry, use in network densification and land register surveying *(German)* 79−92633
photogrammetry using digitally controlled differential rectifiers *(German)* 77−60495
Point Mugu earthquake, California, 1973 Feb. 21, epicentral region elevation changes 77−56587
polar motion analysis by radio interferometric surveying, POLARIS project 79−79721
precise direction measurement by laser, techniques and instruments *(Czech)* 79−30414
precise levelling error propag. rel. to recent crustal movements 77−44884
precision circular scale manufacture by contact photographic printing 79−75638
precision levelling with two-fluid tiltmeter 77−21919
radio interferometric differential baseline meas. comparison with conventional geodesy 79−79722
reduced three rosettes measuring method for ang. deviations determ. *(German)* 77−60497
refraction-free direction meas., coincidence method *(German)* 78−87124
refraction-free directions, coincidence procedure 78−87125
relevelling data, secular gravity var. effects, orthometric corrections *(German)* 80−56341
remote sensing surveys in geologic exploration 77−56631
Rhenish Massif, recent vertical crustal movements determ. 79−79789
N.Upper Rhine Graben, negative height change causes *(German)* 79−34727
Upper Rhine Graben, repeated levellings, errors *(German)* 79−34726
Upper Rhine Graben and Rhine Shield, levelling data, multivariate analysis *(German)* 79−34728
Rhinegraben, geodetic high-precision meas. in active tectonic area 79−79788
Salton Trough, California, deform. meas., 1973-77 period 79−84079
Satellite Emission Radio Interferometric Earth surveying (SERIES), GPS geodetic system 79−100804
satellite systems, American developments *(Norwegian)* 79−62723
satellite universal telemetering system for magnetospheric and ionospheric research *(German)* 77−73924
scale and orientation in combined Doppler and triangulation nets 80−101311
seismic surveys, residual static and crossdip corrections simultaneous estimation 79−92500
semi-automatic precision surveying system for PEP accelerator 77−83246
short range distance measurement by EM phase comparison technique 77−87090
singular compensation problems, hypothesis tests *(German)* 78−44758
slip monitoring along major faults in southern California 79−48388
STEREOMETROGRAPH model G with fast motor drive 77−66996
stress field anal. of northern Hsiaokiang fault, Yunnan *(Chinese)* 79−62464
Switzerland geomagnetic survey instrumentation and results *(French)* 78−15966
tacheometer, electrooptical, EOT 2000, design parameters, performance figures 78−77858
Theo 002 Universal Theodolite for geodetic astronomy 77−82028
THEO 020 A universal theodolite for surveying 77−82029
theodolite, reduction of influence of vertical axis error on horizontal angle meas. *(German)* 79−44278
theodolite, THEO 020 A, field test 78−77859
theodolite, THEO 080 A, with attachable circular compass 80−56634
theodolite, type 2T, highly unified instrum. 80−13120
theodolite microprocessor selection, development, and programming 78−24218
theodolite standardised series, specification 78−73543
theodolites, electrooptical and microprocessor-based *(Czech)* 78−77860
theodolites, use of polyhedral prisms in testing 79−67370
three dimensional test net, investigations in Stuttgart area *(German)* 79−79731
triangulation, microwave distance meas. in German net *(German)* 78−88792
triangulation network adjustment to new European system *(German)* 77−70590
trigonometric networks calculation, development and form. *(German)* 78−15947
trilateration network, adjustments to account for meteorological conditions 80−77131
underwater surveys by submersibles, acoustic navigation system 79−5683
United States, western region, strain accumulation rates, 1970-78 period 80−21607
United States east coast, recent vertical crustal movements 78−32052
USA Geological Survey low-level radioactive waste burial site selection 78−94116
vertical crustal movements, solvability and multiquadric anal. appl. 79−79787
surveying continued
vertical crustal movements in Atlantic coastal plain, USA 79−79790
Very Long Baseline Interferometry (VLBI), foundations and geodetic appl. *(German)* 78−45036
VLBI Earth surveying, miniature radio interferometer terminals 79−100805
water levels, obs. via electrooptical distance meas. *(German)* 78−69280
Zeiss Eldi 2 electro-optical rangefinder, accuracy and range *(German)* 77−68274
U, National Uranium Resource Evaluation (NURE) aerial radiometric survey data interpretation via principal components anal. 80−101438
susceptance, electric *see electric admittance*
susceptance, electric, measurement *see electric admittance measurement*
susceptibility, dielectric *see optical susceptibility*
susceptibility, magnetic *see magnetic susceptibility*
susceptibility, optical *see optical susceptibility*
suspensions
absorbing particles, simultaneous meas. of dichroism and birefringence in elec. field., photocurrent signal obs. 80−82801
adsorbed polymer layer, on particles in suspension, thickness meas. by mag. birefringence 80−42191
aerocolloidal suspension of solid particles, shock wave entering aerocolloid domain 78−51227
Aerosil in cetane, suspension, thermal cond. rel. to elec. field, struct. form. 77−9138
aggregable particles, conc. suspension, viscosity calc. 79−7362
air, particulate matter, suspended, X-ray fluoresc. anal., semicond. detector X-ray spectrometer construction, calibration 77−56321
aircraft vibration isolation for high-performance cameras 77−74543
algae aqueous suspension, fragile nonspherical solid particle hydraulic transport investigation 77−73618
algal suspension, light scatt. expts. and theory, ang. depend. 79−16166
alkali n.-alkanoates, long-chain, ethanolic solns., solubility temp. depend. 78−15724
alumina powder, particle size analysis, using centrifugal sedimentation *(German)* 78−57890
Amazon River, fine sediment non-uniform vertical distrib. 79−84313
1,8-anilinonaphthalene sulphonate in bacterial suspension, fluoresc. spectra 79−88052
anisotropic micropolar fluid theory 80−31515
anisotropic suspension of aligned ellipsoids, heat conduction 77−7286
aqueous suspensions, three flux method for predicting radiative transfer 80−6052
aqueous suspensions of spherical colloid particles, phase transitions 77−4938
asbestos fibre suspension, heat transfer and friction coeffs. for tubular flow 78−22405
bacteria, E.coli strains in aq. suspension, polarisability anisotropy and aminoglycoside antibiotic effects 80−85441
bacterial suspension, physico-chem. changes on cooling, cell elec. cond. anal. 77−86458
Baltic Sea, estuary region, suspension distrib. under river drifts influence *(Russian)* 80−98345
Baltic Sea sedimentation, role of river suspensions *(Russian)* 78−7616
benzene, liq., laser pulsation kinetics, optical damage effects 80−58614
biological cell suspension, electrophoretic analysis, Doppler spectra line shape smoothing 79−84053
biological material dilute suspensions, meas. via differential US velocimeter 77−78065
blood, red cells, rheological props. meas. by Couette viscometer 80−97992
blood, US propag., effects of red cell shape and orientation 78−24104
blood cell aggregation, conductometric meas. 77−25614
blood droplet deformation in Courette flow suspension, expt. *(German)* 79−16227
blood suspension aggregation in Couette flow *(French)* 80−97991
blood type suspensions in circular tube, blood flow model 79−29543
Brookfield viscometer adaption for use with slurries and suspensions 77−4884
Brownian movement of suspended particle with nonlinear friction 80−146
Brownian particles, diffusion of interacting spherical particles suspended in fluid 78−54304
Brownian rotational-translational particles, at finite conc., dynamics and hydrodynamics 79−7401
butadiene-styrene latexes, ageing *(Polish)* 79−70098
calorimeter problem, nonadiabatic, transfer processes in suspensions of solids 79−23353
β-carotene, solubilised in lecithin liposomes, linear dichroism, absorption statistics 78−1014
Casson fluid flow between approaching discs, plug flow region 78−67230
cell separation, local conc. gradient determ. by conductivity meas. *(German)* 79−5411
cell suspension six-channel aggregometer 78−81001
cement, settling and flow props., effect of cellulose ethers and lignosulphonates 77−11242
centrifugal sedimentation of large particles 78−59462
ceramic, rheological properties, effect of grainy filler ceramic suspensions 80−43685
ceramic body growth, diffusion theory *(Czech)* 79−69269
ceramic suspension, automated meas. of viscosity 79−37258
ceramic suspension, ferromagnetic filtration apparatus improvement 78−11561
ceramic suspension, ferromagnetic treatment, optimum system construction with FOL instruments 78−4666
ceramic suspensions, sputter drying *(Russian)* 80−55324
cermet electrodeposition, effect of electrolyte in charge carried by suspended ceramic particle 78−68665
chalk, grain size determ., sample preparation methods 79−24694
channel flow, two dimensional model of steady laminar flow 80−106834
charged particles, laminar tube flow, entrance deposition 80−59100
charged particles in ionic solutions, elec. cond. 80−7866
charged rigid sphere suspension, rheology, suspension mechs. 78−40086
chloroplast suspension, photoinduced changes in oxidation-reduction pot. rel. to photosystem II activity 77−25399
chloroplasts, in suspension, near IR radiation dispersion *(Russian)* 78−24045
clay aqueous suspension turbulent flow, average velocity profile and functional loss in pipe 80−48778
clay plate suspensions, ordering, statistical mech., theory 78−23968

suspensions continued
clay suspensions, with negative thixotropy, hysteresis loops, deflocculant addition effect 79−52789
clay-water suspension turbulent flow in tube, velocity profile and frictional losses *(Russian)* 77−31364
cluster settling, appl. of distrib. of kth nearest neighbours 80−40758
coagulated colloidal suspensions, couette flow, viscosity effect 79−90317
coagulated suspensions, flow equation 78−63487
coagulating droplets, statistical distrib. 79−74425
coal-organic solvent mixture, fast-dump reactor apparatus for short reaction times 77−44575
colloid suspensions in a polymer solution *(French)* 79−87879
colloidal, radiometric method for particulate processes characterisation, theory 80−45578
colloidal, radiometric method for particulate processes characterisation, expt. 80−45579
colloids, hydrophobic, coagulation mechanism 78−40085
complete suspension of particles in stirred tanks 78−27824
concentrated, rheological relations, self consistent field theory *(German)* 77−14972
concentrates, physical stability criteria, review 80−45562
conducting fluid with spherical particle suspension oscillating flow in mag. field 80−79408
continuous models of suspensions, nonequilib. thermodynamic approach 80−28479
continuum two-phase theory, volume averaged balance eqns. *(German)* 80−92212
convective heat transfer in coaxial horizontal channel, influence of electroviscous effects 79−77100
creeping flow, hindered settling, particle shape effect 80−14797
degree of agglomeration assessment 77−70343
deposition, onto rot. disc, convective diffusion, external force field 78−40081
deposition in channel entrance, combined influence of diffusion, electricity and gravity 80−1674
deposition in channel entrance 77−89194
deposition in entrance of diffuser, electrostatic and gravitational effects, laminar flow, numerical investigation 80−14785
deposition in entrance of parallel-plate channel, gravity effect 80−83834
diamond, aq. suspension, particle size distrib. function electrooptical diffusion method for determ. 80−8956
diamond vibrating suspension, defective surface layer formation on transparent materials *(Russian)* 78−53007
dielectric properties in plane channel, flow with perpendicular elec. field *(Russian)* 77−62305
dielectric separation of solid particles 80−16213
dielectric suspension, convective heat transfer, rheodynamics, in horizontal coaxial cylindrical channel 78−59494
dielectric theory, interfacial polarisation, anal. of biological cell suspensions 80−45563
diffuser entrance region, suspension laminar flow and particle deposition 80−53845
dilute, effective thermal cond., flow effects 77−1952
dilute, of spherical particles in non-Newtonian liq., rheological behaviour 80−24058
dilute, single component multiphase mechanics 77−55079
dilute colloidal suspension, Krishnan effect, theory 77−34824
dilute suspension, boundary layer in presence of electric field *(Russian)* 78−63503
dilute suspension, low Reynolds number flow in slowly varying tubes 79−46389
dilute suspension of ellipsoidal particles flowing in channel, elec. field effects *(Russian)* 77−68696
dilute suspension of spheres in power model fluid, apparent stress deform. behaviour 78−42578
dipalmitoyl lecithin vesicles in dil. suspension, light scatt. obs., of phase transitions 77−16915
dipalmitoylphosphatidylcholine, changes in vol. mag. susceptibility at the phase transition 80−76770
disc-shaped particles in liquid, appl. to US holograms recording 77−14857
disperser for powder, suspension and emulsion production 78−23636
dissociative and associative substances, appl. of Gibbs-Thomson eqns. 77−4944
divinyl benzene suspension, dielectrophoresis 80−3362
droplet-laden gas, attenuation of high-intensity sound 77−62082
dumbbell shaped particles in power-law liq., struct.-phenomenological theory 78−1730
dust-laden gas flow, heat transfer 78−14067
dust-liquid channel flow, with varying inlet temp., transient forced convection soln. 78−87375
dusty gas flow in horiz. and vertical tubes, heat transfer 78−22409
dusty viscous conducting liquid, unsteady flow in annulus in mag. field 78−38412
dusty viscous fluid, unsteady flow through uniform pipe 78−59450
effective thermal conductivity calc. *(Russian)* 78−76935
effective transport processes, for interactive particles calc. method 79−50836
effective viscosity, statistical theory 79−90290
elastic sphere suspension, steady flow in tube 78−67251
electric polarisability, anisotropy, length depend. of ionic contrib. 80−85224
electric polarisability, stability 80−85222
electrical meas. of suspended particles, blood counting appl. *(Japanese)* 77−44869
electrically cond. suspensions moving in mag. field, continuity eqns. *(Russian)* 77−55098
electro-optical phenomena, induced dichroism rel. to elec. field calc. 78−50699
electrophoretic mobility, mass transport method 78−35696
electrophoretic mobility of particles suspended in low-cond. liqs., field depend. 78−56919
electrophotographic liquid developer, permittivity and conductivity meas. *(German)* 78−62257
electrorheological, spontaneous rotation of dielectric rotor 77−15130
electrorheological suspension, effect of contamination *(Russian)* 77−44519
electrorheological suspension flow, vibr. effect *(Russian)* 80−53877
electrorheological suspensions, struct. form in electric fields *(Russian)* 77−86390
electrorheological suspensions, struct. form. in electric fields *(Russian)* 77−86391
ellipsoid freely suspended, rotation about a slow viscous flow's vorticity axis 78−38386
elliptical particle suspensions covered with shell, dielec. behaviour, rel. to biological cells 80−51057
enamel slips, control of rheological props. 79−29136
estuarine environment, natural suspended matter flocculation and electro-kinetic pot. *(French)* 80−61817
extensional viscosity of a dilute suspension of spherical particles at intermediate microscale Reynolds numbers 80−106835
fast moving, particle size and vel. meas. 77−42935
ferrite F-600, suspension in caster oil, residual magnetisation *(Russian)* 79−1689
ferrocene derivatives in smectic B phase liquid cryst. BBOA, ^{57}Fe Mossbauer study 78−27136
ferrofluid, mag. birefringence pulsed field meas. 79−82943
ferrofluid, suspension, magnetodiffusion, interferometric obs. *(Russian)* 77−4946
ferrofluid motion, rot. mag. field effects 77−950
ferromagnetic, birefringence in mag. field *(Russian)* 77−43979
ferromagnetic suspension, bulk viscosity calc. *(Russian)* 77−81429
ferromagnetic suspension, heat transfer for shear flow conditions 79−46394
ferromagnetic suspension, mag. field effect on heat transfer, thermal cond. 78−59500
ferromagnetic suspension, magnetorheological characts. meas., errors 80−33550
ferromagnetic suspension, residual magnetisation 80−84623
ferromagnetic suspension serving as a liquid magnet 80−84622
ferromagnetic suspensions, convective heat transfer and thermophysical props., mag. field effects 79−77264
ferrosuspension, magnetorheologic characts. *(Russian)* 77−65786
ferrosuspension, MHD flow, heat transfer *(Russian)* 78−26203
ferrosuspension, motion in rot. homogeneous mag. field *(Russian)* 77−27604
ferrosuspension, motion induced by travelling mag. field *(Russian)* 77−27606
ferrosuspensions, internal rotations and the other transport phenomena 80−28573
ferrosuspensions, mag. field effects on mech. props. 78−87321
fibre suspension, conc. rheology of tube flow, uniform fibre length distrib. 77−58628
fibre suspension, concentrated, rheology of tube flow 77−58627
fibre suspension, dil., mechanistic aspects of drag reduction in turbulent pipe flow 80−6102
fibre suspension, rheology, rel. to turbulent drag reduction 78−22315
fibre suspension flow in pipes, transition regime analysis, drag reduction 77−89186
fibre suspension in water, turbulent jet, analogous behaviour to polymer solns. 78−1732
fibre suspensions, fibre degradation effects 79−72918
filtering of liquid suspension by deposited layers in filter device *(Russian)* 77−53872
filtering of suspension with a compressible residue, intensification by pulsation *(Russian)* 79−90324
filtration, 2-component, conc. wave bifurcation *(Russian)* 78−22420
filtration in porous membranes, pore and particle size distribs. correl. *(Japanese)* 80−3418
flocculation, polymer aided, shear effect 79−52779
flocculent, sedimentation, review 80−35577
flotation of fine particles, effects of size and charge 77−16865
flotation of fine particles by group of bubbles, kinetics 78−53261
flow, memory impairment, Brownian rotation of spheroids 80−79386
flow, time-depend, dilute arbitrary-shape particles, Brownian rot. effect 78−26188
flow, two-phase, in entrance region of circular pipe, effect of conc. of suspended particles 80−19481
flow in cylindrical pipe, using ultrasonic debitmetry Doppler spectra *(French)* 80−96303
flow in pipe, velocity field asymmetry *(Russian)* 77−68671
flow in tube, energy balance and concentration distribution rel. to diameter *(Russian)* 77−35203
flow in tube, solid particle concentration rel. to vertical diameter *(Russian)* 77−31365
flow of dense suspensions, review 78−67255
flow of gas with dispersed solid particle impurity in viscous shock layer 80−28554
flow of suspension-carrying bottom layer *(Russian)* 77−55070
flow rate meas. ultrasound propagation and scatt. approach 80−43806
flow through ultrafine capillaries 78−94822
fluid dynamical aspects of operating conditions of suspension stirrers *(German)* 80−26058
fluidised beds, dehydration of solutions and suspensions, rel. to granulation 80−81373
gas, finitely conducting, effect of suspended particles on hydromagnetic thermal convection instability 79−53709
gas, turbulent annular flow, gas vel. profile 77−35215
gas and solid particles, energy balance 77−77812
gas bubble suspensions, incompressible nonNewtonian and Newtonian fluids, dilatational props. 78−30343
gas suspension, closed dynamic eqn. system using kinetic theory 80−6190
gas suspension flow in long horizontal pipe, heat exchange investig. 80−19388
gas suspension vertical flow, wall-particle interaction 78−59461
gas-conveyed solid suspension flow, press. losses 77−80197
gas-hard particle mixtures, nonstationary waves, shock wave interactions *(Russian)* 77−27587
gas-liquid ascending flow, monodispersed, funciton stress on wall, bubble size effect 80−59098
gas-particle flow, physico-computational model 79−32650
gas-particle flows in shock waves, radiant interchange among suspended particles *(Japanese)* 77−15063
gas-particle mixtures, supersonic flow past wedge, shock wave *(Japanese)* 77−47070
gas-solid, free turbulence influence on heat transfer 77−42898
gas-solid, turbulent heat transfer during motion in tubes *(Russian)* 77−24020
gas-solid suspension, heat transfer rel. to turbulence 79−72928

suspensions continued
gas-solid suspension flow, laser anemometry meas. 77−35268
gas-solid suspension flow in tube, press. drop, entry length 78−42647
gas-solid suspension flow through packed beds, convective heat transfer 79−4075
gas-solid suspensions flowing in steel and insulating coated pipes, electrification 77−77811
gas-solid turbulent suspension flow, frictional pressure drop Prandtl's mixing length anal. 79−14458
geophite, suspension, electrooptical diffusion method for determ. particle distrib. function 80−8956
giant lecithin vesicles, alignment and opening by elec. field 80−3708
glass, complex raw material, hydrothermal prep. 80−104106
glass bead-air suspension, local particle conc. in turbulent duct flow 77−11239
glass beads in polystyrene soln., suspension, time depend. viscoelastic behaviour 80−99982
graphite, in liq. dicyclopentadiene, CO_2 laser pulse induced chem. reactions 80−66821
graphite, suspensions, particle shape influence on light absorpt. in mag. field 80−60549
graphite particles, diamag. levitation, Brownian-motion press. gauge appl. 78−24807
graphite suspension in He, high-temp. power plant coolant, efficiency enhancement *(Russian)* 79−68549
NE Gulf of Alaska, processes affecting suspended matter distrib. and transport 80−12398
haemoglobin in solution, conc. depend. of diffusion coeff. 79−29546
hard-sphere suspension, viscosity, direct inter-macromolecular interactions effects 79−95199
heat and mass transfer in a suspension of matter in gas with capillary-porous particles 79−87885
heat conduction, averaged-equation approach 77−1949
heat transfer in channel flow, particle-wall interactions 78−5787
heat transfer to suspension with solid separation at wall 78−9685
heavily filled, viscosity relations 80−48776
heavy metal ion removal in clay suspensions 77−86955
horizontal gas-suspension stream, local heat exchange 77−47071
hydrodynamic screening and viscous drag at finite conc. 78−35725
hydromagnetic, physical property variations *(Russian)* 78−47022
hydrosol particles in suspension, dispersivity effect on light scatt. *(Russian)* 78−68932
impulsive motion, effect of antisymmetric stresses and particle rotation, two-phase continuum theory 80−106833
inclinable pipe, suspension in turbulent flow, Markovian model, eddies 80−48790
inertial coupling in dynamic eqns. of components 78−63483
instability conducting anisotropic suspension, macroscopic transport coefficients *(French)* 78−35729
interpenetrating EM structured continua, thermodynamic and mech. props. calcs. *(Russian)* 77−47580
kaolin, aq. suspension, flocculated and dispersed, rheological behaviour in pipe flow 79−37361
kaolin suspensions, aq., flocculated and dispersed, rheological behaviour in pipe flow 80−64510
kaolinite, aq. suspension, mag. and optical props., Fe_2O_3 impure particles 78−76933
lakes, suspended solids, anal. using Landsat multispectral data 79−16523
laminar flow with diffusive gravit. deposition at entrance of converging and diverging channels 80−14825
laminar Poiseuille flow, particle lateral migration, tubular pinch effect 79−98783
laminar tube flow, gravitational deposition of growing aerosol particles 80−59099
laser diagnostic irradiation of fluid-suspended cell flow 77−21594
laser pulsation kinetics, optical damage effects in liqs. 80−58614
laser-Doppler technique, local size and vel. probability distrib., two-phase suspension flow 78−59517
latex, colloidal cryst., optical props. near MP 78−11562
latex, monodisperse, order-disorder phase transitions, short-range order 77−29056
latex, monodisperse, phase transition pressure determ. from sedimentation equil., Alder transition model 77−70344
latex, monodisperse, reflectivity obs. of phase separation into ordered and disordered phases 77−70345
latex, monodisperse particle size determ., spectroscopic method 77−29055
latex, purification 78−27828
latex particles, size determ. by combined filtration and turbidimetry method 79−79313
latex solids, agglomerating and dewatering 80−104470
latex sphere aggregates, dynamic shape factors determ. by sedimentation vel. meas. in capacitor 80−26063
latex sphere suspensions, ordering, statistical mech., theory 78−23968
latex suspension liquid film flow, local thickness meas. 79−4070
light absorption in non-homogeneous objects, sieve effect 79−22896
light scattering, form-anisotropy, Rayleigh-Gans-Debye type approx. validity 79−1770
light scattering, turbidity 78−44407
lipid lamellar liquid crystalline systems, orientation studies of probe molecules by linear dichroism 77−90718
lipid vesicle suspensions, particle size distrib. determ. by photon correl. spectroscopy 77−86711
liquid dispersion, suspended impurities effects on wave excitation in sound field 80−81372
liquid suspensions, membrane filter mounts and quick-change device 77−53873
low-frequency dielectric dispersion, of ideally polarisable spherical particles 79−61912
macromolecules, interacting, spherical, light scatt., conc. fluctuations, transport eqn. 79−1775
magnesite-phosphate mortar, rheological props. 77−23927
magnetic, influence of dispersion factor *(Russian)* 79−52788
magnetic suspensions, magnetic and rheological props. *(Russian)* 79−55350
magnetisable suspensions, hydrodynamic in travelling mag. field 80−48807
magneto-rheological suspensions, mag. field effects on elec. cond. 80−11960
magnetorheological systems, heat transfer 79−81988
marine mineral suspensates and geochemical exploration 78−88936
suspensions continued
memory impairment in flow, expt. 79−41736
memory impairment in flow, theory 79−41735
metal powder suspension in air, spontaneous ignition temperature *(Russian)* 78−47027
methacrylic acid-methyl methacrylate statistical copolymer suspension polymerisation, stabilisation effects, viscosity 78−85157
MHD laminar flow, suspended particle motion stability *(Russian)* 78−5808
microconvective heat, mass transfer processes 79−86435
microfluids, theory of chemically reacting mixtures 80−14777
microhydrodynamics, characteristic effects, developments 77−68681
micropolar fluid, pulsatile flow 77−7359
microspecimen suspensions, simple magnetic holders for critical point drying 77−52946
mineral particles settling in liq., X-ray photography 79−20469
mixed colloidal suspensions, selective coagulation 79−74426
monodisperse, rigid bodies, time dependent relaxation behaviour 79−47411
monodisperse latex, simulation study of eqn. of state of simple liquid 77−63964
motile solid particles in fluid, two dimens., convection numerical study 77−56399
motion of particles suspended in stationary turbulent medium at large Reynolds number 80−83836
movement in porous solid interior *(French)* 80−43770
mud suspension, batch sedimentation in inclined tube 79−64743
multigranular, aqueous, sedimentation in oblique plate separator under laminar flow conditions *(German)* 77−44513
multiple light scattering, Brownian polymer particles in water 78−78912
nascent, microcryst. growth, optical absorpt. investig., photographic appls. 77−12835
natural water bodies, universal multispectral algorithms for suspended sediment remote sensing 79−53558
Navier-Stokes flow with suspended particles, mathematical modelling, numerical simulation 77−72348
Newtonian fluid containing rigid particles, peristaltic pumping at low Reynolds number 79−10604
non-Newtonian fluid, steady flow, numerical modelling 78−51205
non-Newtonian fluids, particle movement, appl. to dyeing and haematology *(German)* 78−87369
non-Newtonian liquid filtration eqn. 78−55690
nonstationary axial-symmetric suspension flow in viscous liquid 77−39326
nonstationary flow, rheological behaviour 80−6130
nonstationary motion in grav. field, volume conc. effect *(Russian)* 80−75002
nonstationary suspension flow in viscous liquid 77−39325
nonuniform suspended load, non-equilibrium transportation *(Chinese)* 80−8339
nonviscometric flow, drop suspension model, deformation and vorticity 79−60022
ocean, fine suspended particles, removal mechanisms and residence times 78−32106
ocean, remote acoustic monitoring of natural suspensates and slope/shelf water intrusions 79−2241
ocean acid waste dump, particulate Fe mapping 80−56497
oceans, Atlantic and Pacific, suspended particles rel. to chem. processes 78−36201
Onsager transition in hard plate fluid 77−48696
organic pollutants in water, influence of detergent traces on hydrosolubility and maintenence in suspension *(French)* 80−7961
oriented non-spherical particles, polarisation characts. 79−81362
oscillatory parallel flow in channel 77−68677
parallel flows with boundary layer characts. 77−15093
particle, solid spherical hydrodynamic interaction with rising bubble 78−51221
particle coagulation using US 79−32152
particle counting and vol. determ. in suspensions, optical-electronic device 78−57894
particle distribution in Poiseuille flow of suspension in micropolar fluid model 80−10314
particle interactions in fluid suspension, averaged-equation approach 78−23972
particle mobility, meas. via alternating field microelectrophoresis apparatus 77−29237
particle mobility in liqs., meas. by optical and elec. transients 79−77303
particle motion in turbulent flow in open channel 78−51225
particle motions in a viscous fluid, review, book contrib. 80−96289
particle size and concentration, determ. by light backscatter technique 78−85214
particle size and number concentration, meas. method 80−9082
particle size distrib., on-line measurement techniques, instruments *(German)* 78−60895
particle size meter using laser light scatt. spectroscopy 80−77754
particle swarm moving in viscous fluid 78−26186
particle transverse motion in turbulent boundary layer 78−79358
particles in dilute suspension in general flow, mass flow and density meas. 80−101784
particles in laminar tube flow, thermophoretic deposition 79−46371
particles suspended in turbulent fluid, dispersion 78−14073
particles suspension in turbulence, small sphere motion in rot. vel. field 77−58771
particulate emission monitor calibration in gas-solid suspension 77−37454
particulate matter suspended in water, vol. scatt. function at near-forward angles 78−55299
particulate sedimentation, mixture theory formulation 77−21423
particulate suspensions, weak wave propagation 77−80207
paste-like composite with polymer binding, rheological props., wall effect 77−47072
n-pentane, liquid, containing suspended particles, superheating expt. 78−90642
pentane/chloroform mixture, liquid, containing suspended particles, superheating expt. 78−90642
percolation, sol-gel transitions, stirred percolation, and laminar flows of passive suspensions *(French)* 80−77724
phase interfaces, balance eqns. and struct. models 78−59453
pigment dispersion rheology, kinetic model, expt. results 79−7361
plastic disperse systems, generalised flow theory with account of wall effect 78−87320

suspensions continued
platelet adhesion to solid surfaces, effects of plasma proteins and substrate wettability 78−35814
Poiseuille flow stability for slender fibres 78−71388
Poiseuille to plug flow transition in tubes 79−90316
polar fluid microstructure, relative force 77−72343
Polirit, optical polisher powder, particle size distrib., dispersion analysis 77−9141
Polirit suspension, factors reducing polishing ability 80−74543
Polirit suspension for optical component polishing, chem. antifoaming agents 80−74542
poly (N,N-dipropylacrylamide), 'feathered' polymer resin, prep. from suspension 80−35533
polydisperse, two-parameter size distribs. eval. using photon correl. data 79−92011
polydisperse discs, particle size distrib., transient elec. birefr. data, two-parameter distrib. functions 78−40083
polydisperse ellipsoids, particle size distrib., transient elec. birefr. data, two-parameter distrib. functions 78−40084
polydisperse gaseous suspension, heat transfer between subsonic nozzle walls, rel. to particle motion parameters 77−24019
polydisperse materials gravitational classification in horizontal flow *(Ukrainian)* 77−68668
polydisperse rod suspension, elec. birefringence relax. 78−23430
polyethyl acrylate modified mortars, inner struct. and flexural props., suspension and emulsion studies *(Japanese)* 77−86092
polyethylene crystals in suspension, heat of fusion 79−87870
polyethylene oxide, elec. polarisation in suspension, Kerr effect 77−63359
polyethylene single crystal in suspension, Fourier transform IR study 78−10877
polyethylene single-crystal suspensions, small-angle X-ray scatt. lamellar thickness determ. 79−10784
polymer, random coil, nonzero thickness, suspension, shear viscosity conc. depend. 79−10238
polymer crystal in suspension, light scatt. in streaming system, dimens. characterization 79−69852
polymer melt containing suspension, cell model theory of shear viscosity 80−103048
polymer melt suspension, plastic-viscoelastic constitutive eqn. 79−60014
polymer melts, particle filled, viscosity 78−87319
polymer solution, free precipitation of spherical particles in centrifugal force field 77−11247
polymer solutions, concentrated, transport properties, hydrodynamic mean field theory of voscisity of sphere suspension 79−4422
polymeric systems, rheology, review 78−87317
Polyox dilute soln., elongational flow obs. 79−60029
polystyrene, suspension of monodisperse spherical colloidal particles, layered sedimentation 79−39217
polystyrene charged particles in water, quasielastic light scatt. 79−24835
polystyrene latex particle size by electron microscopy and light scattering 79−66365
polystyrene latex particles, particle sizing by forward lobe scatt. intensity ratio 78−71031
polystyrene latex particles in CTAB (Na_2SO_4), gas bubble surface charge meas. 78−21100
polystyrene particle colloidal suspension in KCl(LiCl) aq. solns., dielectric loss 78−35728
polystyrene solutions, ordered and disordered, particle dynamics determ. from time depend. multiple light scatt. 78−33672
polystyrene sphere crystals, in aqueous suspensions, solid-like phase transiton 80−50893
polystyrene spheres, crystallised suspension, gravitational compression 78−23975
polystyrene spheres suspended in air jets, effect of particle proximity on drag force 80−96306
polystyrene spheres suspended in isodecane, field depend. of electrophoretic mobility 78−56919
polystyrene suspension, laminar flow, augmentation of heat and mass transfer, correl. of data 80−53840
polystyrene-polyethylene oxide copolymer, elec. polarisation in suspension, Kerr effect 77−63359
polyvinyl alcohol, hydrocarbon suspension, temp. depend. of electroviscous effect and dielectric parameters 79−79299
polyvinyl dispersion, ageing *(Polish)* 79−70098
porous particle suspension, linear shear flow 77−15094
porous particles suspension, effective viscosity, flow 79−18929
powders, emission spectrometric anal., suspension sampling method 77−86393
power reflection spectroscopy, analytical techniques 80−62714
power-law liquid, dil. suspensions of dipole dumbbells, rheological eqns. of state and shear flow in elec. field 79−86473
prolate spheroids in shear flow, bulk heat flux 79−46370
pulverised fuel gas flow distrib. in manifolds of uniformly variable section *(Russian)* 80−33666
purple membrane fragment suspensions, elec. dichroism obs., trimer model interpret. 80−89728
PVC, mechanochemical degradation in primary struct., mech. vibration effects, IR spectra *(German)* 78−19769
PVC, suspensions, melts, rheological props. rel. to struct. 79−3983
PVC composite, MBS type multifunctional impact modifier effect on mech. and rheological props. *(Polish)* 78−52751
PVC dispersion, rheology, particle size effects 79−92007
PVC plastisol, steady shear rheological behaviour 79−37274
PVC suspension rheological props. *(German)* 79−94579
quartz glass-water, electrolytes effect on viscosity, pH and zeta pot. props. 79−34365
quartz sand, high-conc. suspension, prod. principles 80−66463
radiational flame propagation over gas suspension of solid combustible particles 80−53880
random behaviour simulation, interval of quiescence method 78−31708
Rayleigh-Taylor instability, two superposed cond. fluids, with suspended particles 78−87399
real-time US spectroscopy in suspensions, pulse transmission system 77−19495
red blood cell suspensions, steady state O_2 diffusion 77−40644
red cells in dilute suspensions, turbulent flow and effect on O_2 uptake kinetics 77−60223
resin particles, dispersed, precipitation on cellulose fibre in elec. field 78−53262
rheological behaviour, dense suspensions 79−32431
suspensions continued
rheological props., steady flow 79−18930
rheological thixotropy analogue simulation study with plane-cone Ferranti-Shirley viscometer *(French)* 77−65725
rheology of suspension of deformable particles, elastohydrodynamic theory 77−35104
rheometer for the investigation of disperse systems 79−82012
rigid ellipsoidal particles in external field, dil. suspension, rheological eqns. *(Ukrainian)* 80−48661
rigid ellipsoids, rheological props. *(Russian)* 78−75187
rigid sphere suspensions, micropolar fluid model, viscous Couette flow 77−84302
rigid spherical particle suspension, two-phase theory, volume averaging and governing eqn. *(German)* 80−87801
rivers, suspended sediments vertical distrib. in translational flow 78−3841
rod photoreceptor disc membrane, cooperative conform. change induced by bleaching 77−81499
rod-like molecular particles, anisotropy of interfacial elec. polarisability, length depend. 79−38520
rods suspended in silicone oil, interactions between rods in shear flow 77−55075
Saguenay Fjord, suspended particulate matter geochemistry 78−92852
sand grains, mobile, in ocean, underwater detect. 78−96192
sea suspended material and chlorophyll conc., estimation from outgoing radiation spectrum meas. from helicopter 80−36333
sea water, dielectric permeability calc. *(Russian)* 78−77261
seawater, ^{210}Pb particulate and soluble activities in deep oceans 77−5223
seawater, particulate trace metals concs. in Laccadive Sea 80−104997
seawater, surface charge of suspended particles in estuarine and coastal waters 80−36331
seawater from Pacific, size distrib. of suspended particles in surface water 80−4047
seawater-clay suspension, turbulent boundary layer 79−20858
second-order fluid, migration of spheres in two-dimens. unidirectional shear flow 77−940
sediment analysis using vibration-frequency method 79−49202
sediment hindered settling, two-phase flow anal. 77−89193
sedimentation, settling instability, horizontally homogeneous suspension 78−42652
sedimentation, theory and expt. comparison 77−40577
sedimentation, three-parameter Markov model 78−34183
sedimentation Markov model for very slow settling of dilute suspension 78−22406
sedimentation of monodisperse suspension of solid particles in viscous fluid, Markov model 80−28551
sedimentation of suspension of spherical particles *(Russian)* 78−67254
sedimentation phenomena of fine particles investigated by vibrational force field and interferometry 79−60086
sedimenting suspension, conc. distrib. determ. by radioactive solids 79−32634
sediments, agglomerated, in N.Chesapeake Bay estuary, microstruct. 79−53336
sepiolite, clay mineral, anisotropy of interfacial elec. polarisability, length depend. 79−38520
sepiolite, electric polarisability, anisotropy, length depend. of ionic contrib. 80−85224
settling, accelerated by addition of buoyant particles 79−96369
settling, modelling of suspended solids 77−84298
settling velocity 79−46360
shear flow, particle orientation distrib. 79−96372
shear flow, particles self-diffusion 77−24015
shear viscosity of settling suspensions meas. 79−82011
sheared, effective thermal conductivity 77−7436
sheared, macroscopic transport props. 77−32840
silt suspension turbulent boundary layer, steady state model 78−28242
simple shear flow of dilute fluid suspension, orthokinetic collisions of hard spheres 77−35199
simulated microbes, suspension, size determ., teaching expts. 79−71178
slender particles oriented in extensional non-Newtonian flow, stress field 77−19632
slurries, solids content determ. by X-ray scatt. 80−3467
small particles suspended in turbulent fluid, convection, mass transfer 80−87793
sodium bentonite, Wyoming suspension, comparison of optico-optical scattering and birefringence 80−85226
solar absorbing working fluid properties obs., molten salt heat transfer fluid with solar-absorbing oxide particles 78−87112
solid dielectric particle dilute suspension in flat duct, electric field effect 80−53868
solid particle suspension, wave propagation *(French)* 79−46361
solid particle suspension in compressible fluid, wave propag. 80−69858
solid particles in turbulent stream, gravitational transport theory *(Russian)* 78−75188
solid particles lateral migration in laminar flow near plane 77−35207
solid particles suspension in agitated tank 79−7400
solid solitary grains in water stream, saltation and suspension trajectories 77−44517
solid-liquid mixtures, rheological characts., shear stress/strain rate relationships 80−10287
solids in water, measurement standard, macerated glass fibre filter paper, water analysis appl. 79−8454
solloidal solution droplets, solid, particle form., heat and mass transfer 78−95967
sphere suspended in fluid, vel. in sound wave 77−23800
spheres, hydrodynamic interactions, Navier-Stokes eqn. calc. *(Russian)* 79−32652
spheres, porous, in a linear flow field, motion and rupture 79−64755
spheres, uniform suspension, effective shear viscosity theory 78−11565
spheres in non-Newtonian fluid, viscosity 78−90807
spheres in viscoelastic media, alignment and aggregation effects, photographic obs. 77−80129
spherical agglomeration in conical drum 78−14064
spherical drops, mean drag and ave. velocity *(Russian)* 78−67259
spherical particle suspension, Brownian motion effect on bulk stress 78−7246
spherical particles in cylindrical pores, constrained Brownian movement 77−32841
spheroids, in streaming suspension, dynamics, dielectric consts. 78−76374

suspensions continued
stability, net repulsive van der Waals forces between different particles, macromolecular, or biological cells in liqs., appls. 80−34274
stability against coagulation 77−32843
starch, hydrocarbon suspension, temp. depend. of electroviscous effect and dielectric parameters 79−79299
statistical theory, review, book contrib. 80−96288
stirred, suspended particles absorpt. of solute molecules 78−30342
Stokes problem for a suspension of spheres at finite concentrations 78−55967
Stokes problem for suspension of spheres, effective medium theory 79−81836
stress near rigid boundaries 77−80200
styrene-H_2O suspensions, particle size, surface tension, stabilizer conc. effects meas. *(German)* 79−24834
surface chemistry effects in particle deposition 77−60134
suspended sediment transport theory, elliptic boundary value problem 79−14466
suspensions, crystallisation, aggregate stability and effect on purity of product 80−100769
suspensions, rheology, colloidal forces role, review 80−103063
Syton determination of size distribution of submicron particles in colloidal suspension, FODA 78−61057
technology for coatings production purposes 77−73476
thermal EM radn. 2-dimens. multiple scatt. 77−39209
thermomagnetophoresis of particles in magnetic suspensions 80−35581
thick clay suspensions, electroenforced sedimentation in consolidation region 80−26057
tobacco mosaic virus suspensions, ordering, statistical mech., theory 78−23968
transport properties, role of inertia 77−32839
transversal undostatic forces prod. by border effects 77−72316
turbulence, suspended particle motion 78−22408
turbulent, combined radiative and convective heat transfer 78−9724
turbulent, heat transfer and struct. 78−9683
turbulent and pseudo-turbulent transport 78−14068
turbulent characts. of open channel flows *(Japanese)* 77−68676
turbulent energy balance in pressure pipe flow for suspension bearing flow 80−48777
turbulent flow, diffusion model description, appls. *(German)* 78−59446
turbulent flow of particle-fluid mixture, energy balance 77−47076
turbulent pipe flow, vertical cond. distrib. 78−1714
turbulent suspension flow, gravitational theory, discrete model 80−48779
turbulent two-phase isobaric jet, anal. *(Russian)* 77−27586
two-dimensional fluid motions induced by motile particles, convection field and geotactic components 77−55080
two-phase flow, constitutive eqns. for lift force and Brownian motion 77−937
two-phase flow of particles during crystallisation in gaseous stream, modelling by aerothermochemistry of suspension eqns: *(French)* 80−53844
two-phase unpolymerised system, particle size, surface tension, stabilizer conc. effects meas. *(German)* 79−24834
US attenuation 79−41475
US propagation, effects of particle shape and orientation 78−59171
velocity-turbidity system, amplitude-frequency characteristic *(Russian)* 78−75195
vinyl chloride suspension polymerisation monitoring by US attenuation and velocity 79−70328
vinylacetate-H_2O suspensions, particle size, surface tension, stabilizer conc. effects meas. *(German)* 79−24834
viscoelastic fluid, motion of rigid particles 80−103044
viscoelastic fluid, suspension of two identical spheres, interaction anal., general homogeneous flow 78−63455
viscoelastic properties 79−92006
viscosity, modified cell model approach 80−74944
viscosity of suspension of nonharmonic dumbell mols. 78−2282
viscous sound attenuation 80−74577
water, adsorbed on cellulose, NMR relaxation times 79−78552
water, air and oil, dynamic behaviour under periodic perturbations *(Russian)* 77−19631
water suspended solid analysis by single-particle scatt. 79−79435
water suspensions, radiative property measurements 80−9811
water suspensions of latex spheres, laser heterodyne apparatus for small angle scatt. meas. 80−1261
water-in-oil cream, viscoelastic props. 77−58629
wave motions in thin film of suspension flowing down an inclined plane *(Ukrainian)* 79−77220
yeast cells in suspension, vacuole detect. by transmittance radiometry 80−26418
AgBr, adsorption of cyanine, pH depend. 78−62254
Al suspension in Ar stream, Nd laser radiation interaction, spark form., breakdown intensity *(Russian)* 77−35435
Al_2O_3 suspended particles, behaviour on solidification of Al-Cu (33%) under reduced gravity *(German)* 80−60853
β-Al_2O_3, suspension, mobility and zeta potential meas. in various solvents 77−36761
Al_2O_3 suspensions, grinding method influence on rheology and suitability for high-density sintering 79−29001
As_2S_3 suspension dispersed in gelatin, photoinduced dichroism 79−98453
$BaSO_2$, suspension, light scatt., optical anisotropy determ. by polarisation ratio 79−1772
C black conc. suspensions in low mol. wt. vehicles, rheology anal. 80−19312
C black particles, simultaneous meas. of dichroism and birefringence in elec. field., photocurrent signal obs. 80−82801
$CaCO_3$ polydisperse particles, in $Ca(HCO_3)_2$ soln., growth, soln. in mag. field 78−53260
CdS, monodisperse particles form. from soln., light scatt. theory use in size estimation 80−76560
Co particles, ferromagnetic colloids in toluene, small-angle X-ray scatt., interparticle correlations 79−11831
Cr_3C_2-Ni alloys, electrophoretic deposition from conc. suspensions for P/M prep. of hard alloys 77−63575
Cr_2O_3-ZrO_2 granules, from spray drying of suspensions 80−104100
Cu, dielec. const. determ. 77−40579
Fe plating cathode current distrib. influences *(Russian)* 79−96197
Fe-SO_4-H_2O suspension system at 90°C, potential-pH diagram 78−61068
FeO, deposition on Zircaloy heated surface from boiling water 78−58353

suspensions continued
Fe_2O_3, flocculated suspension in ethylene glycol, intrinsic viscosity rel. to shear rate 80−1502
Fe_2O_4, suspension in oil, motion in rotating mag. field *(German)* 77−75983
Fe_3O_4, magnetite, analysis using magnetovibr. analyser 78−4668
Fe_3O_4, suspensions, ferrofluid motion, rot. mag. field effects 77−950
$Fe(OH)_3$-$Fe(OH)_2$ suspension system, potential-pH diagram 80−55728
KCl, colloidal suspension, radiowave dielec. dispersion 80−11311
LiCl, colloidal suspension, radiowave dielec. dispersion 80−11311
MgO, liq., imaginary part of complex refr. index, suspension meas. *(Russian)* 79−33659
MnO, hydrated, adsorpt. of Cs and Sr radioisotopes 78−3822
Ni, dielec. const. determ. 77−40579
PbI_2 suspension, chem. sensitization 80−73492
PbS, colloidal, light scatt. and electron microscopy 78−3379
Pt complex, $[Pt(dapn)_2][Pt(dapn)_2Br_2](ClO_4)_4$, (dapn=1,2-diaminopropane), optical absorpt. spectra of small particles 79−56812
$^{239}PuO_2$, fragmentation of respirable particles in water by alpha decay 77−56487
$^{239}PuO_2$, in vivo solubility in rat lung 78−28093
Si_3N_4, aqueous suspension rheological and processing props. 77−23928
SiO_2 gel, hydrocarbon suspension, temp. depend. of electroviscous effect and dielectric parameters 79−79299
TiO_2, aq. suspension, flocculation effect on dilatant flow 79−61916
TiO_2, in glycerine, Bingham plastic flow through annuli 80−64521
TiO_2 particles in suspension, light scatt. phenomena and abs. *(German)* 77−10835
TiO_2, suspended in highly insulated liq., photoelectrophoretic phenomenon, direct imaging system 77−54005
TiO_2 suspension, adsorption-desorption of IO_3^- 80−93804
V_2O_5-water, EPR of VO_{aq}^{2+} formed by solar light photoreduction, electrolysis appl. 78−11540
ZnO/Al_2O_3, microstratified mixing of suspensions, viscosity dependence 79−70023
$ZrSiO_4$-Al_2O_3 (SiO_2) suspensions for slip casting, prep. and props. 80−104103

swelling
absorbed molecules from medium, Raman spectrosc. technique 79−42364
AGR fuel cladding, development of high strength, ductile stainless steel alloys 80−45367
alloys, irradiated, effect of defect trapping and solute segregation, on defect recombination rates and void swelling 78−47369
biophenol-A-polycarbonate, liquid induced crystallisation 80−30125
bounded media, dislocation loop growth and void swelling by charge particle damage 78−6110
carbide fuel pins, mixed, radial distrib. of Xe bonded fission gas, electron probe anal. 79−36318
carbides, brittle materials, swelling, blistering, p, d, and He ion irrads. porosity effects 77−35603
ceramic fuel, irradiation device for creep and swelling study 77−42063
ceramics, technique for studying internal and external gas pressure within pores 80−11606
concrete, creep during drying and wetting 79−52319
concrete and mortars, containing S, durability study in temp. cycles and water resistance 78−27613
correl. between void swelling and thermodynamic stability 80−641
creep, swelling and growth, radiation induced, bias factors estimated from self-consistent model 80−88249
crosslinked collagen membranes, transport props., physical props. effects 78−77028
N,N-diethylacrylamide, cross-linked copolymer, improved mech. props. 80−61091
diffusion with discontinuous swelling, type II diffusion as particular soln. of conventional eqn. 78−91471
dislocation bias and point defect relaxation volumes 79−99248
dislocation loop growth during intrinsic point defect-impurity atom mobile complex formation *(Russian)* 79−90653
EBR-II, duct dilation expts. 79−93702
EBR-II, multiaxial in-reactor creep in presence of significant void swelling 79−55818
EBR-II reactor components, creep and swelling 79−54499
elastomers, filler type, effect on concentration rel. to equilib. swelling in solvents 79−64979
elastomers with inert fillers, swollen state, network density determ. from stress/strain meas. 79−34112
epoxy/graphite composite and cured epoxy resin, thermal expansion and swelling 80−92450
ethylene copolymers, partially cryst. pseudoeutectoid, swelling, thermodynamics 80−39311
extended plane fluid sheet, swelling finite element anal. 79−37277
extrudate swell, inelastic theory 80−43684
extrudate swell, thermally induced, Galerkin method 80−79312
fast reactor materials, fast neutron damage 78−10093
fast reactor peripheral fuel element shells, radiational swelling circumferential nonuniformity 79−19289
fast reactor subassemblies, irrad. swelling induced bow 79−93724
FBR fuel cladding alloys, phase instabilities and swelling behaviour 79−54500
FBR structural materials, design appl. of irrad. creep and swelling data 79−59167
fibrin, modification by synthetic polymers 80−61090
fission, gas swelling, physical processes and mechanisms 79−97808
fission fuel grain boundary loss terms, use in fission gas release and swelling models 80−63257
fission reactor core system, bowed, NUBOW-3D program for static anal. including irrad. creep and swelling 80−5215
fission reactor fed, effect of solid fission products and dislocations on swelling and fission gas release during fast overpower transient 78−8917
fuel element modelling, interpreting and predicting irradiation creep 77−42058
fuel pins, fast breeder, fuel-cladding mech. interaction, obs. and anal. 80−86959
fusion materials, heavy ion irradiation, swelling theory 80−34090
fusion reactor first wall material, mobile He inclusion in void swelling rate theory model 80−34069
fusion reactor materials, fracture resistance 78−82515

swelling continued
fusion reactor materials, ion bombarded, swelling induced stresses, crystalline orientation effects 80−34093
fusion reactor materials, irradiation creep by the climb-controlled glide mechanism in Tokamaks 80−102304
fusion reactor materials, material requirements exam., review 78−50257
fusion reactor materials science 79−97899
fusion reactor metals, irradiated, defect cluster nucleation, He injection effect 80−34091
GCFR cermet cylindrical core swelling *(Russian)* 79−13425
gel, heterogeneous two-phase, permeability 80−76563
gel swelling kinetics theory, polyacrylamide gel obs. 79−39214
gelatin hardened layer structuralisation, kinetic anal. using swelling 78−62255
gelatin layers in photog. developers, effect of diffusion on swelling *(Russian)* 79−97461
gels, swelling kinetics device 80−21210
glass, swelling, blistering, 140 keV p, d and He ion irrads., porosity effects 77−35603
glass fibre reinforced epoxy composite, unidirectional, hygroelasticity, angular depend. 80−50663
glass fibre reinforced plastic, residual strength, hygrothermal history effect 77−77513
glassy polymer, solvent osmotic stresses, prediction of Case II transport kinetics 80−26049
glassy polymer multi-phase Stefan problem describing swelling and dissolution 78−2263
graphite, fusion reactor first wall appl., radiation damage 79−86822
holograms, 3-dimens., emulsion thickness change effects 78−78968
2-hydroxyethyl methacrylate-methacrylonitrile or acrylonitrile copolymer network, mech. response 79−57031
Inconel 600, Neutron irradiation using HFIR for evaluation as fusion reactor material 78−13324
irradiated materials, cascade damage and self-ion injection effects on swelling 78−34549
irradiation creep, temp. depend. 77−43252
irradiation effects, low dose, void incubation, rate theory approach 79−77635
irradiation effects, void nucleation, swelling, creep, rate eqns. 80−49274
irradiation-induced swelling, and creep, effects of pt. defect trapping and solute segregation 79−79040
LMFBR advanced MX-type fuels, fission gas swelling, temp. depend. 80−57842
LMFBR advanced MX-type fuels, low-temp. microscopic swelling, phenomenological model 80−57851
LMFBR advanced MX-type fuels, swelling mechanism anal. 80−57850
LMFBR core design, irradiation creep data 77−46211
LMFBR core materials, effect of swelling and creep on performance 78−13261
LMFBR fuel disruption following LOF accident, in-pile expt. using high-speed cinematography 80−78366
LMFBR highly-rated MX-type fuels, fission gas release and microscopic swelling 80−57848
LMFBR performance, effects of irradiation creep and swelling 78−78482
LMFBR reactor materials, simulation of void swelling and radiation-induced creep 78−8907
metal, heavy irradiation damage at high temps., void swelling problems *(Japanese)* 77−59049
metal, irrad., peak void swelling temp. 77−72608
metal, irradiation creep and swelling, cascade damage effect 77−19991
metal, radiation blistering developments, review 80−44239
metal, void growth in irrad. sample, fully dynamic rate theory 79−73212
metal swelling, max. point on temp. scale rel. to point defect generation *(Russian)* 78−38751
metals, influence of a surface coating, on void formation 78−47416
metals, irradiation induced swelling, bias factor 80−2062
metals, radiation creep speed and swelling, self diffusion mechanisms *(Russian)* 80−92595
metals, radiation-induced creep and swelling, radiation dose depend. *(Russian)* 80−29050
metals, swelling during pulsed irrad., model, void growth exam. 78−47436
metals, vacancy porosity kinetics at high irradiation doses of fast neturons 79−28018
metals, void swelling, depth dependent, by self-ion irradiation, generalized model 79−14856
metals and alloys, irradiated, solute segregation and precipitation effects on void swelling 78−67741
metals and alloys, radiation damage prediction and measurement 78−75693
metals irradiated general rate theory model of void swelling 79−23655
methacrylic acid-N,N'-ethylenedimethacrylamide crosslinked copolymer soln., 3-dimens. struct. peculiarities *(Russian)* 79−55678
α,ω-methoxy-poly(ethylene oxide) effect of swelling on longitudinal acoustic mode 80−29739
mineral, swelling examination method 77−53232
multicomponent inhomogeneous system, diffusion with moving boundaries and swelling at const. volume 80−44353
MX type reactor fuels, microscopic swelling meas., effects of grain boundary migration 78−66348
MX-type fuel and fuel pin swelling, 1973-76, fabrication and characterisation 79−41001
neutron and heavy ion damage correlation, predicted temp. shift on swelling with radiation dose rate change 79−7630
neutron irradiation, discrete ordinate codes, discrete cross section expansion 79−69162
Nimonic PE-16, electron irrad. in HVEM, void growth, vacuum environment influence 80−107323
nuclear fuel, gas release and swelling, operational model, grain boundary gas 80−95346
nuclear fuels, fission gas precipitation into intra- and intergranular porosity, theory 80−57849
nuclear fuels, role of fission gas swelling and release in reactor accidents 80−57854
nuclear oxide fuel element in fast overpower transient, effect of solid fission products and dislocations 80−623
nuclear reactor fuel and fission gas response to simulated thermal transients 78−74453
nuclear reactor materials, depend. of evolving cavity distrib. functions on cavity growth kinetics 79−3206
swelling continued
nuclear reactor materials, radiation damage, fast breeder and fusion reactors *(Japanese)* 79−81011
nylon, stress cracking induced by $ZnCl_2$ solns. 78−27594
nylon 6, swelling by absorbed water, mol. orientation effect 78−11285
Nylon 6 film, prior high-press. treatment effects, weight swelling, density, IR crystallinity, X-ray and viscosity obs. 80−81025
optical materials and components, space charged particle environment effect 80−69472
oxide nuclear fuel, fission gas release and swelling, simple operational model 80−92565
oxides, brittle materials, swelling, blistering, p, d and He ion irrads. porosity effects 77−35603
PCP, oriented swollen soln., IR dichroism, short-range orient. order *(Russian)* 79−51941
PET, effect of liquid aliphatic compounds on mech. props. 80−55488
PMMA, diffusion-controlled penetration by monohydric normal alcohols 78−76918
PMMA, in distilled water, influence of liquid environmental media on mech. behaviour 78−52902
PMMA, reactor irrad., growth of macroscopic radiolytic gas bubbles, diffusion model 80−65058
PMMA, sheets, in methanol, case II swelling and transport kinetics 78−76922
point defect production in irradiation, swelling, cascade diffusion theory 80−34044
point defect sink strength in irradiated materials 77−51368
point defect trapping, effect on irradiation induced creep and swelling 78−71756
polethylene-polypropylene blend, extruded, thermal swelling and mech. characterisation 80−81110
poly(butadiene-co-styrene), rubber, radiation cured, dynamic phys. props. 77−69003
polyacrylamide, mech. degradation, polymerisation effect *(Japanese)* 78−11194
1,2-polybutadiene, crosslinked in states of strain, entanglement networks, swelling anisotropy obs. 80−79666
polybutadiene networks, cis-trans, thermoelastic obs. 79−74220
polycarbonate, amorphous morphology, from NMR obs. of swelling penetrant mol. motion 79−27929
polycarbonate fibre, highly-oriented, drawing behaviour and mech. props. 78−76708
polycarbonate film, by aq. acetone solns., roughness form. mechanism *(Russian)* 78−48554
polydimethylsiloxane, end-linked chains, elastomeric properties, dilution effects 79−90570
polydimethylsiloxane, end-linked model network, elastic modulus and equilib. deg. of swelling 77−35616
polydimethylsiloxane chains, end-linked, swollen model networks, stress/strain isotherms and elastic modulus 80−79668
polydimethylsiloxane end-linked chains, nonGaussian effects 80−65127
polyester resin, unsaturated, $CaCO_3$ system, $CaCO_3$ addition effect on degradation in boiling water *(Japanese)* 78−11281
polyester resin, unsaturated $CaCO_3$ system, $CaCO_3$ addition effect on water absorption in boiling water *(Japanese)* 78−11282
polyester resin mortar, degradation in boiling water *(Japanese)* 78−11280
polyester resin-filler system, resistance to degradation in boiling water *(Japanese)* 78−11283
polyethyl acrylate modified mortars, inner struct. and flexural props., suspension and emulsion studies *(Japanese)* 77−86092
polyethylene, environmental stress cracking, theory 79−34176
polyethylene, in toluene, pressure crystallised, swelling behaviour, rel. to densities 80−2167
polyethylene, low density, with a single texture, oriented crystallisation of biphenyl 78−9966
polyethylene, low-temp. relax., effects of chem.- and electron irrad.-crosslinking 79−4990
polyethylene crystals, soln. formed, low mol. weight, swelling 79−94920
polyethylene in organic fluids 79−60255
polyhydroxyethyl methacrylate swollen network filled with polyhydroxyethyl methacrylate, viscoelastic and ultimate behaviour in rubbery region 79−83247
polymer, glassy, sheets and spheres, gel diffusion with discontinuous swelling 80−44354
polymer, isotropically swollen networks, vol. depend. of elastic eqn. of state 78−67832
polymer, non-ion-exchange type, electrolyte solubility *(Russian)* 80−54391
polymer chain, scaling props., excluded vol. expansion, Monte Carlo study 80−96435
polymer film, swollen, diffusion-relax. cojpling, two-stage sorption correl. 79−94864
polymer gels, thermodynamic props., review *(German)* 78−20073
polymer membrane, penetrant sorption kinetics, transverse differential swelling stresses 78−76923
polymer network, small ang. neutron scatt. 79−90569
polymer networks, deformation free energy, vol. depend. 80−40454
polymers, glassy, sorption of solvents, sample-dimension effects 79−52766
polymers, struct. determ. from elastoosmometric parameters 80−64923
polymethacrylic acid, swollen networks, viscoelastic photoelastic behaviour 80−59366
polyoxymethylene-copolyamide blend melt, viscoelastic peculiarities *(Russian)* 78−38263
trans-1,5-polypentenamer, stress-opt. behaviour 77−90128
polysiloxane dizwitterionomers, sorption of H_2O, mechanism 80−49506
polystyrene, crosslined, swollen, surface energy, contact angles 79−73379
polystyrene, swollen network in benzene, pendent chains, influence on thermodynamic and viscoelastic props. 80−28481
polystyrene latex particles, swollen, aggregation studied by photon correlation spectrosc. 80−66886
polystyrene model-networks, structure 77−89385
polystyrene networks swollen in cyclohexane, swelling equil. and light scatt. at theta conditions 80−107036
polystyrene-polyolefin blends, mech. and swelling properties on heating 79−57053
polythene-polystyrene blends, differential scanning calorimetry and swelling characterisation 79−57053
polyurethanes, vapour press. of solvent above swollen crosslinked networks rel. to rubber elasticity theory 80−45536

swelling continued
polyvinyl alcohol, absorption of H_2O mols. from liq., Raman spectrosc. technique 79−42364
polyvinyl alcohol, atactic, thermoelasticity of networks swollen in water, polymer-diluent interactions 80−29102
polyvinyl alcohol networks, swelling equil. with dil. salt solns., thermoelastic behaviour, hydroxyl group interact. 80−79667
polyvinyl alcohol swollen in aqueous glycol, network thermoelasticity, interactions 80−104201
polyvinylidene fluoride, γ-ray irradiation effect on mech. props., in presence of triallyl trimellitate *(Japanese)* 77−86091
PTFE grafted membranes, struct.-properties relationships *(French)* 80−61136
pulsed radiation effect on void growth and swelling 80−34043
PVA, H_2O-swollen sorption of $TiCl_4$ from benzene solns. *(Polish)* 79−4471
PVA, swollen crystallinity determ. by laser Raman spectroscopy 80−38953
PVC, suspensions, melts, rheological props. rel. to struct. 79−3983
radiation creep and void swelling, bias factors in reaction-rate-theory anal. 79−46700
reactor core bowing history computer program 79−9688
reactor materials, radiation-induced embrittlement and swelling due to void form, ASTM research 78−13231
reactor materials, void swelling simulation, review 78−8906
refractories, swelling on proton, deuteron and He ion bombardment 78−67750
refractory fusion reactor materials, neutron irrad., microstruct., voids, nucleation TEM study 80−29065
rubber, natural, crosslinked by dicumyl peroxide, modulus, swelling relations 80−59551
rubber elasticity, molecular aspects book contrib. 78−84886
rubber network, stress-optical coeff. and amorphous order 77−77169
rubbers, swollen, low-freq. dynamics, optical and mech. props. 80−43626
SAP 895 (Al-Al_2O_3) alloy containing ^4He and ^3H, tensile props. 80−34129
self-ion bombardment induced swelling, effect of implanted interstitials 78−10099
silicate glasses, swelling on proton, deuteron and He ion bombardment 78−67750
sink strengths for thin film surfaces and grain boundaries 80−88207
stainless steel in FBRs, correl. between void swelling and thermodynamic stability 80−641
stainless steels, type 304, fast-neutron swelling behaviour 79−67864
steel, AISI 316, fast reactor irradiated, solution treated, struct. 77−69008
steel, austenitic, annealed, Ni ion bombardment, swelling temp. depend. effect of He implantation 80−29080
steel, austenitic, cold worked, derivation of simple void-swelling equation 79−7631
steel, austenitic, gas implantation effects, fusion reactor first wall damage simulation 80−29079
steel, austenitic, Ni-Cr, neutron-irradiated solute segregation and void swelling 79−60407
steel, austenitic 316, displacement energy determ., HVEM obs. and electron bombardment 78−6100
steel, austenitic stainless, creep, rel. to radiation swelling and stacking fault energy *(Russian)* 78−27562
steel, austenitic stainless, fast neutron irrad., effect on mech. props. 78−92309
steel, austenitic stainless, HVEM irrad., point defect trapping influence on void swelling 79−23652
steel, austenitic stainless, irradiation induced creep, AISI 316, 20% cold worked effect of temp. change 78−72816
steel, austenitic stainless, neutron dose rate depend. of swelling in fission reactors 80−104233
steel, austenitic stainless, type 316, irradiated with 46.5 MeV Ni^{6+} ions, soluble C effect on void swelling and low dose dislocation structs. 80−49280
steel, austenitic stainless, type FV 548, 20% cold worked irradiated with 22 MeV C^{2+} ions or 46 MeV Ni^{6+} ions, study of void swelling 79−37744
steel, austenitic type 316, continuous gas generation effects in neutron and simulation environments 80−34068
steel, austenitic-ferritic stainless, radiation swelling in fission reactors 80−65063
steel, cold worked FV548, electron irradiated, void swelling after 10 ppm He preinjection 77−19989
steel, ferritic, FV607, void swelling, theory 78−71763
steel, ferritic, FV607, void swelling in 1 MeV electron irradiation 78−71762
steel, ferritic, void swelling during irradiation, suppression mechanisms 80−6441
steel, ferritic alloy and martensitic stainless, void swelling response after fast reactor irradiation 80−6437
steel, low C, cold swaged, exam. of H_2 attack mechanisms 78−76791
steel, neutron irradiation induced swelling, empirical relationship with dose and temp. 77−50247
steel, stabilised, pressurised capsules in-pile creep meas. 77−42077
steel, stainless, 304, void form., effect of sequential and simultaneous He implantation 78−71719
steel, stainless, 304L, irrad. induced creep and swelling 79−93723
steel, stainless, α-irradiated, He cavitation, rel. to TiC precipitation 80−45399
steel, stainless, cladding, irradiation enhanced creep 77−42074
steel, stainless, cladding dimensional changes in FBR $(U,Pu)O_2$ fuel pins due to swelling and inelastic strain 80−104296
steel, stainless, depth distrib. of swelling, TEM exam. 80−15165
steel, stainless, dilation and bowing in EBR II ducts and cladding 80−625
steel, stainless, dose rate and cascade collapse effects on swelling 79−23656
steel, stainless, EBR-II fuel pin cladding, obs. of in-reactor creep and swelling 80−13600
steel, stainless, EBR-II reflector assembly irrad. induced bowing, implications for core restraint design 80−104234
steel, stainless, fast neutron irradiated, solution annealed tubing, residual stress behaviour 80−65054
steel, stainless, FBR cladding stress distrib., effect of irradiation-induced swelling 80−19850
steel, stainless, He effects on microstruct. in ion-irrad. 80−29078
swelling continued
steel, stainless, in-pile irrad. effect simulation by Ni ion bombardment, dislocation density, swelling 77−347
steel, stainless, ion bombardment, primary recoil energy spectra characts. 78−10103
steel, stainless, irradiated, vacancy loop effect on swelling 79−14852
steel, stainless, irradiation creep and swelling, microstructural modelling 77−52407
steel, stainless, neutron irrad., solution-annealed and cold-worked, swelling 78−13229
steel, stainless, neutron irradiated, stress effects on microstruct. 77−47490
steel, stainless, phase instability effect on cladding deform. profile of LMFBR fuel elements 77−74921
steel, stainless, solution treated, irradiated to low doses with 22 MeV C^{2+} and 46.5 MeV Ni^{6+} ions, interstitial loops 79−14855
steel, stainless, solution treated FV 548, irradiated with 22 MeV C^{2+} and 46.5 MeV Ni^{6+} ions void swelling 78−22771
steel, stainless, swelling, effect of free surface 78−10097
steel, stainless, type 304, void swelling, 200 keV C^+ bombardment, dose and temp. depend. 77−55309
steel, stainless, type 304L, neutron irradiated, rapid swelling behaviour with $\gamma \rightarrow \alpha$ transformation, TEM study 79−42112
steel, stainless, type 316, electron irradiated, void swelling 78−55891
steel, stainless, type 316, influence of preirrad. thermal-mechanical treatment on phase stability and swelling 79−55792
steel, stainless, type 316, neutron irrad. damage simulation using HVEM, surface effect on void swelling 78−29572
steel, stainless, type 316, neutron irrad. induced, neutron flux and irrad. temp. dependence 78−79636
steel, stainless, type 316, stress-free swelling at high neutron fluence, rel. to LMFBR core environment 78−13239
steel, stainless, type 316, struct. life anal. for fusion reactor first-wall appl. 78−13326
steel, stainless, used as reactor cladding material, void swelling obs. by HV electron microscope *(Japanese)* 79−42108
steel, stainless 316, 20% cold worked, swelling increase due to inreactor temp. reduction 78−34547
steel, stainless 316, carbide precipitation rel. to in-reactor deform. 79−8302
steel, stainless 316, irradiated void swelling incubation period, stress effects 78−6105
steel, stainless 316, irradiation induced swelling, stress effects 78−34545
steel, stainless 316, soln. annealed, cavity alignment and precipitation during dual ion bombardment 80−70273
steel, stainless AISI 316, neutron irradiated, rel. between irradiation induced swelling and shear modulus 80−15157
steel, stainless AISI 316, Si and Ti effect in phase stability and swelling behaviour 79−78972
steel, stainless austenitic, neutron irrad., swelling due to gamma prime and $M_{23}(C_1Si)_6$ form. 78−51590
steel, stainless type 304, ion bombarded, He effects 80−29076
steel, stainless type 316, irrad. induced nuclear cladding swelling, empirical development of design equation 80−59527
steel, stainless type 316, temp. effects on swelling 80−32347
steel, type 316 stainless, Neutron irradiation using HFIR for evaluation as fusion reactor material 78−13324
steel, type FV548, 1 MeV electron irradiated, influence of pre-injected He on void nucleation and growth 80−34054
steel, type X16H15M3B, radiation swelling, predictions for conditions in fast reactors *(Russian)* 79−67870
steel, voids and swelling following $^{56}Fe^{3+}$ bombardment, fast neutron effects simulation 77−30651
steel austenitic stainless, Cr-Ni 316 type, electron irradiated, void swelling 79−42104
styrene butadiene rubber-glass bead composites, network density determ. from stress/strain meas. 79−34112
styrene-acrylonitrile copolymer swelling, glass transition and crazing, polar group incorporation 78−85017
styrene-divinylbenzene copolymers, porosity variation and swelling 80−97493
styrene-divinylbenzene grafted copolymer, structure investigation by IR spectroscopy *(Russian)* 77−62487
transient fuel fission gas behaviour, NEFIG model calcs., bubbles and swelling 80−618
viscoelastic thin shell, swelling under const. loading 78−63326
void growth, rel. to intrinsic point defect properties 78−47315
void swelling, bulk recombination role 78−83847
void swelling, effect of recombination of sink strengths in rate theory 79−14851
void swelling, nucleation theory 80−65038
void swelling, rate theory, effect of recombination on sink strengths 78−87712
void swelling, rel. to in-pile precipitation 78−70595
void swelling, role of bulk point-defect recombination 79−42105
void swelling, transition from gas bubbles 78−14383
void swelling and irradiation induced creep 77−44297
void swelling depth distribution produced by 5 MeV Ni ions 77−7771
void swelling in metals and alloys under irradiation, theory 78−75692
void swelling rate, vacancy dislocation loop effect 80−2084
void swelling simulation, effect of self ion injection 78−22772
void swelling simulation, theoretical evaluation of dual beam irradiation expts. 78−79646
void volume, swelling, errors in determ. by TEM 80−84208
void-swelling, response to temp. changes 79−65116
Zircaloy-2, annealed, neutron irradiation growth 79−42109
Zircaloy-2, irradiation growth, shape and volume changes 80−92562
Al, Al ion irradiated, void swelling and annealing of voids, electron microscopy study 80−88216
Al alloys, neutron irradiation effects, on microstruct., mech. props. and swelling 79−65121
Al, creep, rel. to radiation swelling and stacking fault energy *(Russian)* 78−27562
Al film, deform. under He ion bombardment 80−65073
Al, surface exfoliation and blistering induced by He ion bombard. in energy range 10-80 keV 80−39173
Al-Cu (4 wt.%), effect of semicoherent precipitation on void swelling, when neutron irradiated 79−42115
Al-Mg, Si alloy, void form. under different precip. conditions, after Al ion irrad. 80−59529
B_4C, effect of fast neutron irradiation on struct. 78−26597

swelling continued
B_4C, used as control rods in FBR, irradiation effects 78−67742
Be, neutron irradiated, annealed, tensile props. and swelling, effect of He bubbles 78−22765
Be, neutron irradiated, gas porosity, Brownian motion 79−73222
C, swelling, blistering, 140 keV p, d and the ion irrads., porosity effects 77−35603
Cu, blistering by He atoms, (10-20 keV), exam. of skin structure, thickness, He distribution and swelling 79−60412
Cu, He ion irrad., 1 to 25 keV, range profiles, reemission, blistering 78−38758
Cu, surface tension at intermediate and high temps., influence of additional elements 78−15476
Cu-Fe (1.5 wt.%), precipitation-effect on void formation during electron irradiation 80−84211
Fe alloys, swelling, correlation with number of bonding d electrons 77−47491
α-Fe, irradiation induced void swelling, Cr additions effect 80−55408
Fe, metallised pellet, factors influencing crushing strength after H_2 reduction 79−11531
α-Fe, void swelling during irradiation, suppression mechanisms 80−6441
α-Fe, void swelling response after fast reactor irradiation 80−6437
Fe-Cr, irradiation induced void swelling, Cr additions effect 80−55408
Fe-Cr-Ni, austenitic, self-diffusion and swelling under irradiation 80−39343
Fe-Cr-Ni, neutron irradiated, rel. between irradiation induced swelling and shear modulus 80−15157
Fe-Cr-Ni, solid soln. strengthened and precipitation hardened, in-reactor creep 79−43327
Fe-Cr-Ni alloy, dual-ion-irradiated, swelling anal. 78−86600
Fe-Cr-Ti-Mo-TiO_2 (13, 3.5, 1.5, 2 wt.%) dispersion hardened, void swelling 80−65046
Fe-Ni alloy, disordered, short-range order study by time-depend. PAC method 78−6618
Fe-Ni-Cr, pulsed HVEM irrad., effect on microstruct. evolution 80−34053
Fe-Ni-Cr (20, 15 wt.%), single and dual ion irrad., microstruct. studies 80−29077
$Fe_{40}Ni_{40}P_{14}B_6$, irradiation swelling 78−30682
interstitial cluster nucleation, effect of trapping at onset of irradiation 79−78974
$KMg_2LiSi_4O_{10}F_2$-$NaMg_2LiSi_4O_{10}F_2$, solid soln., solid solubility and swelling characts. 80−59660
Mg alloys, neutron irradiation effects, on microstruct., mech. props. and swelling 79−65121
Mo, ion bombardment by Ni^{2+}, TEM study of damage depth distrib. 78−10101
Mo, microstruct., swelling induced by ion bombard., He injection effects 80−29083
Mo, neutron irradiated, void swelling and shrinkage, TEM study 80−34079
Mo, neutron-irradiated, high-temp., positron annihilation characts. meas. 77−89480
Mo-Ti-Zr (0.5, 0.1 wt.%), neutron irradiated, void swelling and shrinkage, TEM study 80−34079
Mo-Zr, heavy ion irradiated, void swelling, phase instability 80−29084
Mo-Zr-B, porosity and mech. props. after neutron bombard., 780-1080°C *(Russian)* 80−24502
NaCl, single cryst. expt. on distension of gas-filled cavity 80−49286
Na_2O-B_2O_3-SiO_2, mechanical strength and swelling in liq. 80−85024
Nb, blistering by He atoms, (10-20 keV), exam. of skin structure, thickness, He distribution and swelling 79−60412
Nb, He blistering, large swelling meas., gas press. model 80−88218
Nb, swelling correlation with local gas concentration following He irrad. 80−70271
Ni alloys, swelling, correlation with number of bonding d electrons 77−47491
Ni, cavity evolution in 500 keV $^4He^+$ irrad. 80−29082
Ni, creep, rel. to radiation swelling and stacking fault energy *(Russian)* 78−27562
Ni, creep, volumetric, irradiation induced, stress effect on swelling 77−43253
Ni, form. of vacancy micropores during bombardment by 300 keV Ni ions 78−2172
Ni, ion irrad. with 20 and 500 keV $^4He^+$, depth distrib. of cavities and dislocation damage 80−107346
Ni, irradiated with Cu and Ni ions, depth depend. damage profile 79−14857
Ni neutron and heavy ion damage correlation, dose rate and He injection effects 79−7629
Ni, oxidation, role of grain growth 77−81337
Ni, self-ion irradiated, He effect on void form. 78−6112
Ni, void swelling caused by neutron and self-ion bombardment, 573 to 873K 78−14387
Ni, void swelling rates in self-ion irrad. sample 80−29081
Ni, voids and swelling following $^{56}Fe^{3+}$ bombardment, fast neutron effects simulation 77−30651
Ni-Al, neutron irradiated, rel. between irradiation induced swelling and shear modulus 80−15157
Ni-Al(Cr)(Ti), ion irradiation induced void swelling and defect microstructs., TEM obs. 79−51164
SiC, 10 keV H^+ irrad., C deposition, surface swelling, surface morphology changes 77−35608
SiC, fusion reactor first wall appl., radiation damage 79−86822
Si_3N_4, swelling, blistering, 140 keV p, d and He ion irrads., porosity effects 77−35603
Ta, neutron irradiated, microstruct. and swelling 77−69006
Th alloys, irradiation effects 78−86606
Ti, trapping coeff. of energetic H at high doses 77−31699
Ti-Al-V, (6,4 wt.%), single and dual ion irrad., microstruct. studies 80−29077
Ti-Al-V (6,4 wt.%), ion irradiated, microstruct. study using TEM 80−96572
Ti-Fe-C-N, ion irradiated, microstruct. study using TEM 80−96572
TiB_2, swelling, blistering, 140 keV p, d and He ion irrads., porosity effects 77−35603
(U, Pu) C, nuclear fuel, irradiation induced creep meas. 80−93605
$(U,Pu)C_{1-x}N_x$ LMFBR MX-type fuels, fission gas release and microscopic swelling 80−73921
$(U,Pu)O_2$, in pile creep 77−42060
swelling continued
$(U,Pu)O_2$, reactor fuels, fission gas swelling, temp. and burnup depend. 80−63252
U core fuel elements, of A-1 reactor, volume growth *(Czech)* 80−27745
U-alloys, thermal creep and swelling, characterisation 79−74226
U-Cr-Al (0.2, 0.1 at.%) fuel elements with high swelling resistance for KS-I5O reactor 78−78471
U-Si-Al fuel rods, Zr-Nb cladding, irradiation behaviour with peripheral voidage 78−54835
UC, effect of porosity on fission-gas-induced swelling 78−8959
UC, MX-type LMFBR fuels, TEM exam. of microscopic swelling 78−70596
U_2C_3+UC, MX-type LMFBR fuels, TEM exam. of microscopic swelling 78−70596
UN, fission enhanced creep and swelling, in-pile meas. 77−42061
UO_2 and $(U, Pu)O_2$ fuel, gaseous and solid fission product behaviour, swelling 77−34396
UO_2, commercial fuel pin, irradiation induced volume changes, comparison with model 78−78465
UO_2, high density, fuel kernel, burn-up swelling *(German)* 77−46283
UO_2, irradiated, spacing of intergranular fission gas bubbles 78−66340
UO_2, irradiated sample, 1000 to 2100K, swelling and fission gas obs. 78−78462
UO_2, matrix swelling rate 78−8900
UO_2, microstruct. depend. model for fission product gas release and swelling 80−42757
UO_2, reactor fuels, fission gas swelling, temp. and burnup depend. 80−63252
UO_2, relative growth rates of fission-gas bubbles on grain faces 79−6739
UO_2, swelling and gas release at low and intermediate temps. 77−50241
UO_2:Cr_2O_3, fission gas release and swelling 80−47567
$U_{0.8}Pu_{0.2}C_xN_{1-x}(0\leq X\leq 1)$, MX-type LMFBR fuels, TEM exam. of microscopic swelling 78−70596
V, He preinjected, void swelling on neutron irradiation 77−7765
V, neutron irradiated, void swelling, O_2 effect 78−6106
V:N, ion bombard., void form. 80−34097
V-Cr (wt.%), 3.5 MeV $^{51}V^+$ irrad. induced void swelling and solute segregation 79−7637
V-Ni, ion bombard., void form. 80−34097
V-O (1 to 4 at.%), solid soln., void swelling, V ion beam irradiation, 550 to 905°C 78−63795
V-O alloy, temp., dose and conc. depend. of void form. following V^+ ion beam irradiation 78−10105
Zr alloys, creep and growth, irradiation induced, rate theory approach 80−89294
Zr, void swelling during electron irrad., HVEM study 80−92559
Zr-Al (8.6 wt.%), effect of fast neutron irradiation on irradiation growth of Zr_3Al 78−55896
Zr-Al (8.6 wt.%), neutron irradiation effect on tensile props., swelling 77−7768
Zr-B (1.3 wt.%), investigation of swelling due to neutron irrad. *(Russian)* 79−60404
Zr_3Al, Ar^+ ion and electron irradiation, irradiation swelling, lattice parameter changes 79−65123
$ZrH_{1.9}$, neutron irrad. induced defects, nature and thermal stability 77−50246

swept-frequency oscillators
optical fibre transfer function meas., swept-frequency technique 78−1375
wideband freq.-swept marginal oscillator detector for ion cyclotron reson. spectrometer 80−9069

swept-frequency reflectometry
liquid and solid complex permittivity meas., rectangular waveguide method 80−15941

switchboxes *see switchgear*

switched filters
precision TV demodulator using high-performance SAW transversal filters 79−49258
Cs beam frequency standard design for satellites 78−57911

switches
see also relays; semiconductor switches; time switches
600 MW pulsed energy convertors for toroidal field coil, design philosophy 78−58496
acoustic, for noise level control, monostable multivibrator appl. *(German)* 77−65649
active Y-junction switching devices in Ti diffused $LiNbO_3$ optical waveguides 79−23091
balanced-bridge switch modified config. with two straight waveguides 79−98506
bistable switch, based on waveguide coupler, exam. 78−38086
cold-cathode controlled gas discharge switch 78−86300
contact thermometer, bimetallic, basic parameters *(Czech)* 78−12692
crossed field tube for high power on-off switching 77−24222
digital beam switch for agile beam laser radar 80−58620
duplexing switch with high isolation, for pulsed NMR spectrometer 80−86363
dye CW laser, electrooptically tuned, optical switching and bistability 79−59708
electro-optic multimode waveguide modulator or switch 80−23783
electro-optical active components for guided light 78−42470
electro-optical channel waveguide switch for computer communication bus 80−9987
electro-optical devices for multimode optical switching 79−76882
electro-optical directional coupler switch, used as amplitude modulator, exam. 78−42467
electro-optical waveguide 3×3 switch, tuning and control theory 79−41458
electron beam switch, microwave energy compression 80−96396
Fabry-Perot optical switch driven by fast $Pb(Zr,Ti)O_3$ transducer 79−86251
fibre, single-mode, optimised design 80−106607
fibre-optic, crossbar 80−74497
fibre-optic, single-throw, single-pole 79−37001
fibre-optic repeater bypass DPDT switch 79−98484
fibre-optic switch with electrostatic deflection cantilever 80−53427
four-channel, IC, for oscilloscope appl. *(German)* 77−65030
fusion reactor, High Voltage Switch Tube, for Neutral Beam Power System 80−99291
fusion reactor, T-10M Tokamak, normal and supercond. inductive energy storage and switching 78−55018

switches continued
fusion reactor supercond. switches of high specific breaking power 78−55020
high current diffuse vac. arc, stable mode with ring array rod electrodes 78−9894
high current switch, fast closing, for fusion reactor field coils 78−74484
high current switch, fast closing, fusion reactor fast discharge expt. 78−74483
high voltage opening switch using spoiled electrostatic confinement 80−103205
high-voltage water switches, streamer model 80−107002
HV switch tube development, for Tokamak fusion test reactor 78−66385
ignitrons, high current, for plasma physics expt. equipment *(German)* 78−75435
integrated astable optical multivibrator using Mach-Zehnder interferometric optical switches 80−87560
integrated optical device used as switch, amplifier, limiter and memory logic element 79−32090
integrated optical switch, optically controlled two channel, based on directional coupler 78−83116
integrated optical switch, polarization-independent, for use with single-mode optical fibres 79−37059
integrated optics switch, total internal refl., theoretical evaluation 79−18551
integrated waveguide-hologram memory design approach 80−32940
IR to visible AC Kerr efficient switches using liquid O_2 and liquid CS_2 80−19078
Kalousek electromechanical switch, for potentiostatic conditions 80−85236
laser triggered Krytron-Blumlein electro-optic switch 78−9450
laser triggered solid dielectric switches with low jitter and inductance 80−54066
laser triggered switching of solid insulated spark gap 80−54065
laser triggering through fiber optics of a low jitter spark gap 80−107000
light-activated switch, photo-gate, pulse method of switching, circuit 80−42021
liquid crystal electro-optic switch, four-port, for unpolarized fibre light 80−58715
low-loss SPDT fibre-optic switch 79−41445
Mach-Zehnder interferometer, switch, integrated optical format 78−38084
Mach-Zehnder interferometric switch for integrated optical multivibrators 80−53479
Mach-Zehnder interferometric waveguide modulator, polarization-independent operation 79−18552
mechanical multimode one-to-many fibre-optic switch 79−76814
microoptical switch, Mach Zehnder interferometer, for use with optical fibre transmission lines, exam. 78−38085
miniature triggered spark switch, high repetition rate 80−103203
modulator switch, balanced bridge, using Ti-diffused $LiNbO_3$ strip waveguides 78−63201
multicontact thin-film superconducting switch, prod. 78−4661
multimode 3×2 fibre optical matrix switch 80−58764
multiposition optical-fibre switch 79−41438
neutral beam power supply, series switch/regulator system, 40 kV, 80 A, 10 ms, for fusion reactor 78−66366
nonlinear Fabry Perot devices, integrated optic format 78−38087
nuclear fusion expt., switch for mag. cct. supply *(German)* 78−37441
opening switch, chemically enhanced, for generating high-voltage pulses 77−49744
optical, bistable, multimode integrated 78−79145
optical Bragg switch, thin film 78−38088
optical bypass switch for fibre-optic data bus systems 80−99826
optical channel waveguide double-pole double-throw switch/coupler, using total internal refl. 78−71233
optical fibre switch, four-way, mechanically operated 80−53464
optical fibre switch driven by $Pb(Zr,Ti)O_3$ bimorph 79−18502
optical fibre switch with high reproducibility for communication systems 79−64329
optical fibre switches for fault terminal isolation 78−46833
optical matrix switch, low-loss 4×4, for fibre-optic communication 79−76823
optical moving fibre, switch, using V-grooved connecting device 79−18509
optical switch array, mirror-type, integrated on $LiNbO_3$ substrate 79−27436
optical switch constructed of graded-index rod lenses, for multimode fibre systems 79−27439
optical switches for integrated optics and fibre optics appls. 79−37057
optical switching device using leaky surface wave, controlled by electro-optic effect 79−23090
optically activated switch/modulator using photoconductor and two channel waveguides 78−1437
plasma confinement, Eta Beta machine, spark gap switches charact. *(Italian)* 79−55533
plasma switches, high press. surface discharge, review 80−103208
plasma valve design with liq. metal cathodes, high-power conversion/switching appls. 78−9865
plasma-filled fast-opening switch for use with relativistic electron beam diode 77−47275
plasma-jet-triggered, 10 to 100 kV operation 79−55574
polarisation-conversion wavelength-selective fibre switches 80−58736
polarisation-independent optical switch using weighted directional coupler 80−58798
pressurized spark gap switch with high repetition rates in multimegawatt average power range 77−23275
railgap multichannel high-energy switch 78−55770
rib waveguide switches with MOS electrooptic control, monolithic integrated optics in GaAs-$Al_xGa_{1-x}As$ 78−87168
spark gap, for main capacitor banks switching in ZT-40 fusion reactor, development 78−55036
spark switches, high repetition rate, with Al and brass electrodes, surface ageing 80−106997
spring, complex arch type, movable, snap-through action characts., appl. to microswitches 78−63339
spring, complex arch type, movable, snap-through action characts., microswitch appls. 78−63340
superconducting Al heat switch and plated press-contacts 78−54377
superconducting heat switches, effect of surface prep. 79−60966
superconducting multicontact rotary switch, cryoelectronic appls. 78−89497
switches continued
superconducting switch for large heat flow below 50 mK 78−54376
tetrodes, high-power, fusion research appl. 79−54592
thermal, gas-filled, for use in precooling system for superconducting magnet 80−52245
thyratron-spark gap hybrid for high voltages and currents 80−54067
triggered spark gap switch system, long life, high repetition rate 80−106998
triggered vacuum gap, plasma buildup and breakdown delay 79−73048
two-stage opening switch technique, for high inductive voltage generation 78−55034
water-cooled equipment, emergency switch design 78−81962
Cs-Ba triode arc switch, high-current, low-voltage, pulsed control 78−71551
Hg wetted reed, heat treatment variations effects on Fe-Ni alloys surface conditions and on switch behaviour 80−66547
$LiNbO_3$ fast-response broad-band electrooptic elements for laser beam control systems 79−89944
Nb, supercond. film, switching, storage and erasure effects 77−8253
SbSI single crysts., nonlinear dielec. effects and microelectronic applics. 77−43944

switchgear
see also circuit breakers; switches
fast crowbar switching system for Texas turbulent heating fusion expt. 77−23260
high current switching, Al foil explosion caused by electric discharge, cylindrical foil, obs. 79−55597
LV switchgear contacts, AgMgO properties *(Slovak)* 78−56603
quasistatic magnetic field generation using prototype switching system 80−42244
triggered vacuum gap, anode spot formation, characts. 77−39485
vacuum interrupter, for for high voltage DC current, for fusion reactors 78−74489
SF_6, breakdown characts. for 0.8 to 2.6 MV range 78−87552
SF_6, breakdown performance under mixed voltages *(German)* 77−3999
SF_6 insulated switching installations and devices, gas chromatography appl. *(German)* 78−88668
SF_6-insulated substations, insulation design and co-ordination 80−100102

switchgear testing
ASDEX circuit breaker system, design, calcs. and tests 78−55032
CRO technological improvements and applications *(French)* 77−61091
fusion reactors, interrupter and hybrid-switch testing 80−99289
HV four-electrode field emission pre-ionised triggered spark-gap switches, 10 to 30 kV, parallel operation 80−70075
HVDC interrupter test facility, dual 30 kA systems 78−55035
liquid metal plasma valve circuit breaker, 15 kA-30 kV, fusion reactor application 78−74488
SF_6-insulated metal-clad, arcing, decomposition products and pressure rise 80−100101

switching
see also electrical conductivity transitions; ferroelectric switching; magnetic switching; switches
automated multichannel meas. systems, microcircuit program device for analog signal switching 79−26042
biplanar image converter, photocathode switching 80−19105
bistable nonlinear Fabry-Perot resonator switching speed and energy calc. 80−64095
chemical laser flameout using fluidic switching 78−29943
Fabry-Perot resonator, bistable, use as optical switch, limiter or memory element 77−39024
fast-action, of signals on SAWs governed by MOS ICs 78−33963
fuel cell electrodes, galvanostatic switching curve shapes 80−66965
high currents, Al foil explosion caused by electric discharge, cylindrical foil, obs. 79−55597
high-current vacuum arc in a magnetic field 78−71572
initiation, Anderson model 78−10524
Josephson long junction, switching behaviour 77−77007
laser diodes in optical transmitters, switching dynamics and noise *(German)* 79−89919
laser emission spectrum switching by external optical signal 80−9892
laser logic elements, transients during switching *(Russian)* 80−23697
LV switching-off process, phenomena *(Slovak)* 78−55761
metal-insulator-Si(n)-Si(p^+) device, switching voltage criteria 80−15610
MHD devices, plasma ionization instability, dynamic suppression, switching modelling 80−59308
MHD generator, arc switching near electrodes, elec. current oscills. 79−55569
nematic liquid crystal adjustable access couplers for fibre-optic switching 80−33217
neutral beam, pulsed, arc (arc filament) power supplies, for fusion reactor 78−70637
optical, gyrotropic waveguide switching elements at optical wavelengths 79−37049
optical communication, conference, Amsterdam, Netherlands (Sep. 1979) 80−46733
photothermoplastic recording with rapid switching 80−32941
PMMA film in small area lateral MIMS device, cond., switching 80−97003
semiconductor, IR switching, ultrafast optically controlled 80−58626
solenoid, supercond., mag. field stability in persistent mode *(Czech)* 78−29131
stepped switched optical directional couplers with unequal section lengths 80−33235
surge, long spark modelling *(Czech)* 77−1028
surges, long spark modelling, voltage and flashover distance conversion factors *(Czech)* 77−15254
triggered vac. gap, $Pb(Zr,Ti)O_3$, dielec., low-voltage firing characts. 77−80381
wall reattachment device, loading effects on switching *(Japanese)* 79−10548
GaAs, picosecond optoelectronic switching 77−23742
MIS structure, electronic processes *(Russian)* 79−56312
SF_6-N_2-Ar mixture high-current multispark discharge switching characteristic 78−67444
Si:Au p^+-i-n^+ diode, double injection switching, effect of trapped space charge 77−1473
Si-SiO_2 MIS systems, dynamic props. of switching, appl. to charge transfer devices 80−92997
Te-Au thin film interface, evolution, switching effects *(French)* 80−6660

switching circuits
see also choppers (circuits); emitter-coupled logic; switching networks; trigger circuits
control circuits using diode switches with switching of nsec pulses 78−8415
CTR neutral beam source, SCR series switch and impulse crowbar 78−66395
ECG amplifier with automatic lead switching 78−28106
electrometric circuit switching by magnetically controlled contact 77−79108
FET Q-switch circuit for pulsed NMR 77−49760
light-activated switch, photo-gate, pulse method of switching, circuit 80−42021
linear transmission gate for nuclear electronics 80−23267
programmable quadrupole mass spectrometer *(Japanese)* 77−86415
respiratory flowmeter switching device incorporating delay for synchronisation with mass spectrometer 80−17160
six-channel MOSFET commutator, monopolar mass spectrometer appls. *(Russian)* 78−74099
spark source, adjustable-waveform, thyratron-diode switch element, appl. emission spectrometry 77−63998
static interruptor cct., triac, thermostatic and lighting control appl. *(Italian)* 78−73984
temperature regulator for inductive loads using IC zero voltage switch U 106 BS with triac *(German)* 80−77779
transmitter-receiver matching network for US pulse-echo system 77−78012
US, two-board design, alarm and data transmission systems appl. 78−46870
switching equipment, telephone *see telephone switching equipment*
switching networks
matrix switching network for fibre-optic communication 80−58735
optical, terminated crossbar matrix 77−19386
optical matrix switch, low-loss 4×4, for fibre-optic communication 79−76823
switching systems
see also electronic switching systems
electrical contacts in switching equipment, welding resistance meas. 77−57353
fusion reactor, MFTF, sustaining neutral beam power supply, shunt preconditioner, IBM-ASTAP anal. 80−102332
fusion reactor, ZT-40, switching components development 78−55036
integrated optical switching system with input modulator 80−99884
optical fibre communication systems, low loss 4×4 switching network 80−58718
optical fibre single mode switching terminal 78−59159
optical waveguide switch, 3×3, for optical switching system 78−55470
superconducting magnetic energy storage system, switching technology in theta-pinch fusion reactor 77−23285
two-stage opening switch technique, for high inductive voltage generation 78−55034
X-ray diagnostic sets with automatic exposure relays, switching delays 77−48903
switching transitions *see electrical conductivity transitions*
symbol manipulation
atom, first-order wave functions, computer calcs. using Green's functions 78−41934
automatic dimensional analysis using symbolic maths. 77−57173
crystallographic computing correlation with artificial intelligence research 77−17960
finite element stiffness matrix, symbolic generation 79−32244
formula manipulation with FORMAC73 language 77−41522
gravitational fields, Bel-Petrov classification 78−93566
LISP appls. *(Polish)* 78−61749
non-numerical matrix products using FORMAC 78−50540
problem soln. by symbolic computer processing of formulae 80−17803
space time curvature tensor, Newman Penrose formalism, CAMAL program calcs. 78−24701
structural mechanics, computerised symbolic manipulation 79−32327
symbols *see nomenclature and symbols*
synchrocyclotrons
beam intensity monitoring, Ni, Cu foils 77−38578
CERN 600 MeV, ISOLDE-2 on-line isotope separator 77−23330
CERN 600 MeV synchrocyclotron, status report 79−54647
CERN accelerators, radiation protection *(Dutch)* 77−46434
CERN reconstructed 600 MeV performance and prospects 77−83288
conference on cyclotrons and their appl., Bloomington, USA (Sept. 1978) 79−54626
construction principles, advantages and appls. *(German)* 78−5078
conversion projects, discussion of projects at CERN, Nevis, Orsay, Uppsala, and JINR at Dubna 79−54645
general orbit theory for accelerated particles in cyclotrons, appl. to synchrocyclotrons and omegatrons 80−74052
Harvard Univ. 160 MeV proton beam, clinical experience and implication for designers 79−54693
induced activity of building and structural mats. in 680 MeV accelerator hall 77−50319
injector, functional generator of controlling voltage of energy modulator 80−68975
JINR synchrophasotron, neutron prod. by deuteron stripping 78−33340
McGill synchrocyclotron engineering improvements 79−54652
neutron beams of the Leningrad Institute of Nuclear Physics synchrocyclotron 80−87003
neutron TOF spectrom. of 1 GeV proton synchrocyclotron 77−26927
Nevis facility, status and exptl. program 77−14279
Nevis machine operation status 77−83289
Nevis proton synchrocyclotron extraction system, design, operation 77−83265
Nevis pulse synchrocyclotron ion source using single cold cathode 79−54679
Orsay 200 MeV proton synchrocyclotron, beam optics and beam monitoring in beam lines 79−54636
Orsay 200 MeV synchrocyclotron, machine parameters, beam handling and extraction, current status 79−54635
proton spectra, high energy, emerging from 680 MeV synchrocyclotron shielding 78−17530
secondary particle beams, average momentum and comp. meas. 77−65382
π meson channel, layout and characts., Leningrad Inst. of Nuclear Phys. 77−23323
synchronisation
30th Annual Frequency Control Symposium, Atlantic City (1976) 77−37852
31st Annual Frequency Control Symposium, Atlantic City (1977) 78−57905
airborne clock synchronisation by minimum variance methods 77−37853
artificial hand, myoelectrically operated with dynamic control, practical trial *(German)* 79−12029
atomic clocks, SIRIO satellite signals experiment *(Italian)* 79−2751
atomic clocks, VLBI obs. 78−29092
biotelemetry system, with time division of channels 80−94386
cine film with EMG data by LED display device, rats appl. 77−81754
cinefilm with magnetic tapes carrying sound track, digital technique *(German)* 79−35866
cinema film projection, sound track synchronisation, new system *(German)* 79−67402
cinematography, EBU/IRT time codes with modified setting instrument *(German)* 80−18029
circuit for gas laser and camera synchronisation 80−73489
clock synchronisation, India-W.Germany, relativistic corrections 80−95077
clock synchronisation circuit, digital clocks, using transmitted time code 79−67257
clock synchronisation in rotating frame of Earth, time discontinuity obs. 77−60333
clock synchronisation in uniformly rotating frame, one way speed of light 79−49034
clock synchronisation rules and transitivity 77−29982
clocks, Symphonie satellite appl. 80−68184
clocks for VLBI, influence of relativity theory *(Russian)* 77−5664
diagnostic and treament techniques 80−61727
Digitron fast multichannel time recorder 77−67949
domestic time synchronisation method using TV broadcasting satellite *(Japanese)* 77−17956
dropping Hg electrode, synchronisation in natural drop expts., high speed device 80−37049
dye laser, tunable, improved freq. doubling for 217-360 nm 78−33781
dye laser synchronisation, CW laser injection, spectral purity *(French)* 78−63118
educational aids, synchronising visual to audio material 77−57135
error monitoring, correction cct. for electronic clocks 78−73970
fast solid-state camera for high-speed event diagnostics 80−78985
global coordinate time scale, practical implications of relativity 80−47030
high precision time comparison, via satellite, synchronisation discrepancy obs. 77−17953
high-speed motion picture photography and oscillography 80−8969
injection diode modulated laser pulse generator and digital control cct. *(Russian)* 80−14372
intercontinental clock synchronisation, ramp method 80−47034
intercontinental time comparison by spread-spectrum random-access geostationary satellite system 77−5815
intermittent sinusoidal voltage phase difference meas. device 78−77941
international time synchronisation, precision tracking package TEMPUS, NAVSTAR satellite network appl. 80−22332
Josephson junctions, system of two junctions, radiation interaction *(Russian)* 79−82715
Josephson oscillators, synchronisation props., single point junctions and chains 79−19703
laser, solid-state, ring, synchronisation regimes of opposite waves and beats *(Russian)* 79−3717
laser by small external signal, capture dynamics 78−46559
laser pulse timing by combined passive and active mode-locking, anal. 78−55391
lasers, injection, for optical pulses meas. 80−23711
LASSO experiment on Spiro-2 spacecraft laser synchronisation from stationary orbit 80−82211
lip synchronised recording technique for speech translation in cinefilms *(Russian)* 80−105737
luminous flux meas., automatic null method *(French)* 80−27331
magnetic bubble propagation, recurrence and synchronism *(Japanese)* 79−56579
magnetic recording, one-channel, direct and reversible synchronisation unit 78−3620
maser, circulating resonance monotron by electron beam modulation *(Russian)* 77−38842
masers, MCR monotron synchronization by external harmonic signal applied to resonator 80−43312
METEOSAT synchronisation and image channel system *(Italian)* 77−82110
multichannel GaAs laser array output synchronisation 78−42417
optical discharge image, as registered with streak camera, with electrical parameters 80−31919
optical multichannel analyser, full synchronisation for picosecond spectroscopy 77−38022
oscillators, two-mode self-excited, synchronisation and stochastisation by external field 79−80524
PCM encoding and decoding for optical memories 80−102658
pulse synchronisation technique, dispersion meas. in single-mode optical fibres 80−48410
Q-switched laser pumping lamp trigger circuit 79−68403
quantum frequency store and Cs atomic transition frequency comparison system 77−79064
recorder, six colour, six channel, synchronised by a microprocessor *(French)* 78−77885
relativistic synchronization procedures, geophysical tests in rotating frame 78−24662
remote atomic clocks synchronisation using injection laser diodes 77−82493
remote site timescale intercomparison technology 77−37855
respiratory flowmeter switching device incorporating delay for synchronisation with mass spectrometer 80−17160
ring lasers, solid-state, synchronisation modes of colliding waves and beats 79−72602
satellite time transfer technology, review 80−47029
single mode fibre 1.1-1.3 μm dispersion meas. by pulse synchronisation 80−64192
sinoatrial bradycardia treatment by transvenous atrial synchronised pacing 77−81683
sound triggered electronic photo flash unit, using variable time delay 80−57407

synchronisation continued
stochastic self-oscillations and turbulence, review 80−4537
Symphonie geostationary satellite, time transfer link for atomic clock synchronisation 80−47038
synchroniser cct. for image, sound in amateur cine films *(Russian)* 79−6210
thalamocortical interaction model for petit mal seizure pathogenesis 79−83759
thermal TV camera, noise, synchronisation, spatial resolution and lifetime characts. 79−35833
time, by VLBI technique *(Japanese)* 80−26755
time and frequency, conf., Helsinki, Finland (Aug. 1978) 80−46728
time comparison *(German)* 80−37000
time comparison of JJY signal reception via the E-region 78−65910
time measurement, freq. method, fundamental problems *(French)* 77−53865
time synchronisation using ATA standard time broadcast 80−47024
time-freq. secondary standard comparison based on LF/VLF radio link 77−87737
timekeeping clock synchronisation and comparison problems and equipment 77−71302
TIROS-N weather satellite, detection circuits and sync pulses for picture facsimile machine 79−53577
tissue mutual impedivity spectrometry 80−17046
US pulsed Doppler blood flow and dimension meas. in conscious dogs 79−62318
voluntary selfpaced movement, event-related desynchronisation evaluation 79−96531
walking, synchronisation of optical press. distrib. and 3-dimens. force meas. under sole human foot *(German)* 78−35975
weather satellite, detection of 300 Hz pulses 78−36420
Cs clock, laser synchronisation between observatories of Paris and San Fernando *(French)* 78−89461
H-maser clocks, synchronization using very-long-baseline interferometry 79−88920
$NaNH_4SeO_4.2H_2O$ ferroelectric crystal optical SHG and pulse modulation *(Russian)* 77−14771
Nd:YAG laser, kinematic mode synchronisation *(Russian)* 77−34892
Nd^{3+}:YAG laser with nonstationary resonator, axial mode synchronisation *(Russian)* 77−75582

synchronism *see synchronisation*

synchronous generators
see also alternators
JET, large flywheel-generator-diode convertor, modelling and simulation 80−13894

synchronous machines
see also synchronous generators
rotary machines as I/O system for superconducting magnetic energy storage system, appl. *(Japanese)* 80−85306
slot-less, armature and excitation field, analytical calc. method using polar coordinates *(German)* 80−32870
slot-less, winding reactances and inductances determ. under stationary conditions *(German)* 80−32871

synchros
selsyn rotor angle-to-digital code convertor, design *(Russian)* 78−65915

synchroscopes *see cathode-ray oscilloscopes*

synchrotron radiation
absolute photon flux and ang. distrib. of the VUV Tokyo synchrotron radiation 78−66731
accelerated electron cluster in synchrotron, rot. disc, method investig. of synchrotron radiation 79−3264
accelerated particle resonances, perturbation treatment in classical dynamics 79−22506
accelerator source, book contrib. 80−5421
ACO storage ring, design of undulator, use as free electron laser 80−91334
Adone e^+e^- ring, beam-beam effects 80−37649
Adone wiggler magnet, status report 79−68081
Aladdin storage ring, status of the Synchrotron Radiation Center of the University of Wisconsin, Madison 80−91326
angle resolved photoelectron spectrometer for atoms and molecules 80−90932
angular and spectral distrib., modified Bessel functions of fractional order 80−91738
angular distribution, electron beam phase vol. effect 79−76563
angular-spectral distribution and polarization of synchrotron radiation from a 'short' magnet 79−94137
application, review 78−74825
application to EXAFS and angle resolved photoemission spectros. *(Korean)* 80−74453
applications, characteristics and sources 78−74960
applications, comparison of characteristics of X-ray and γ-ray sources 80−14030
applications, purpose, design of SR facilities 78−78543
applications, review 78−9010
applications, review 79−44997
applications, review 79−67448
applications, to study of matter 77−74566
applications to struct. of matter determ. 78−32963
UX Arietis, binary star, synchrotron radio emission obs. 77−64793
UX Arietis, RS Canum Venaticorum binary, two-freq. radio polarimetry 79−21335
astronomical, X-ray sources, emission mechanisms, detection techniques 77−22061
astronomical polarised compact radio sources, physical conditions 78−4384
astrophysical plasma synchrotron reactor as RF source *(Russian)* 78−4098
atomic non-Rydberg spectroscopy, review 78−90127
atomic photoionisation studies in extreme UV and X-ray regions 80−43017
atomic physics with synchrotron radiation 80−63583
atomic spectroscopy using synchrotron radiation, book contrib. 80−4779
Auger and line optical data acquisition, synchrotron radiation source 78−63019
BESSY, a 800 MeV storage ring dedicated to synchrotron radiation, review 79−68021
BESSY storage ring, 800 MeV dedicated light sources, choice of principal parameters and light source 80−91333
synchrotron radiation continued
BESSY SX/700: a monochromator system covering the spectral range 3 eV $\lesssim \hbar\omega \lesssim$ 700 eV 80−90952
betatron electron beam, struct. determ. via synchrotron radiation 77−65368
betatron oscillation linear coupling depend. 80−91345
betatron vibration role in synchrotron radiation formula *(Russian)* 78−50684
biological structural determinations using synchrotron X-rays 80−46112
black holes, accreting, synchrotron gamma ray emission spectrum 78−32504
BNL National Synchrotron Light Source, 100 to 700 MeV booster synchrotron 79−67973
BNL National Synchrotron Light Source, 2.5 GeV X-ray ring, design status 79−68023
BNL National Synchrotron Light Source, 700 MeV VUV storage ring 79−68031
book 77−75402
boundary effects and circular polarisation of synchrotron sources 79−48668
brightness of synchrotron radiation from electron storage rings 80−91330
3C 111, 3C 236, radio galaxies, 150 GHz obs. 80−41908
3C 273 microwave emission, self-Compton process rel. to X-rays and γ-radiation 80−22106
caesium hydrogen tartrate, Cs L_{III}-edge anomalous X-ray scatt., meas. by synchrotron radiation 79−24389
Cassiopeia A, supernova remnant, continuous particle injection model for radio flux var. 77−13426
Cassiopeia A, supernova remnant, explanation of secular flattening of radio spectrum 80−101637
CESR, synchrotron radiation exit ports, thermal design 79−68035
channelled electrons in crystals quasi-synchrotron radiation characts. 80−92572
channelling, spontaneous radiation, coherent bremsstrahlung and synchrotron radiation 80−6446
charge moving in helical path, ultrarelativistic case *(Russian)* 78−74826
charged particle acceleration, three-photon vacuum radiation *(Russian)* 78−5406
charged particle crossing boundary between dielectric media, synchrotron radiation *(Russian)* 77−61903
charged particle in plasma with random inhomogeneities synchrotron-transient radiation spectrum 78−45213
Cherenkov radiation, angular distrib. 78−62998
CHESS−the Cornell high energy synchrotron source 80−91328
CHESS synchrotron radiation facility, high energy tunable X-ray source 80−68984
CHESS synchrotron source, photon position sensitive monitors 80−91336
circular electron accelerator, with strong mag. field, errors introduced by oscillations 79−6779
coherent, from relativistic electron bunch, influence of beam longit. distrib. *(Russian)* 77−31053
collection mirrors, soft X-ray throughput 78−62275
Coma cluster of galaxies, synchrotron emission rel. to X-ray flux spatial distrib. 77−33686
compact radio sources, energetics 78−57671
compact variable radiosources, small-pitch-angle synchrotron radiation model 79−53919
Compton scattering in sources with synchrotron reabsorption, rel. to quasars 80−72761
Compton scattering spectroscopy appl. 78−23547
conference, storage ring beam-beam interactions and nonlinear dynamics, Upton, NY, USA (March 1979) 80−36758
conference, trends in physics, York, England (Sep. 1978) 80−31416
conference, user group's activities and progress, Stoughton, USA (Oct. 1978) 79−94138
conference on particle accelerator engineering and technology, San Francisco, USA (Mar. 79) 79−67979
conference on synchrotron radiation instrumentation, Orsay, France (Sept. 1977) 78−62999
contact projection of micro-objects by X-ray synchrotron radiation 79−26193
cosmic radiation, sources, discovery, spectra, review 77−5585
cosmic ray electrons, detect. by synchrotron radiation in geomag. and interstellar mag. fields 78−57412
cosmic spherically-symmetric nonthermal sources, Compton and synchrotron processes 79−88583
Crab and Vela pulsars, pulsed emission prod. by synchrotron mechanism 79−35283
Crab Nebula, continuous particle injection model for radio flux var. 77−13426
Crab Nebula, relativistic particles injection rel. to synchrotron spectrum 78−36678
Crab Nebula, synchrotron radiation and shock waves hydrodynamics rel. to filaments spectra 78−85997
Crab Nebula, thin scatt. diffusion of radiating electrons rel. to observed size 77−87502
Crab Nebula, wisps struct. rel. to nonlinear plasma effects 79−25682
Crab Nebula, X-ray polarisation meas. rel. to synchrotron emission model 78−12426
crystal monochromatized beams, investigation using X-ray monochromators with order sorting and polarizing props. 80−31963
crystallite dimensions determ. using synchrotron radiation X-ray diffr. photographs 80−24313
crystallography appl., energy-dispersive powder diffr. 77−24245
Cygnus A, radio galaxy, 150 GHz obs. 80−41908
cylindrical mirror analyser, design and use with synchrotron radiation, autoionisation obs. 80−18049
Daresbury 2 GeV storage ring with 600 MeV booster synchrotron, review 79−68022
Daresbury 2 GeV synchrotron radiation source, X-rays and VUV, progress report 78−62666
Daresbury SRS, VUV and soft X-ray monochromators 80−90942
data acquisition system for EXAFS and photo-electron spectroscopy expts. 78−62676
depolarisation, in orbital plane in presence of vertical betatron oscillations *(Russian)* 78−33656
developments in photon beam technology 78−78051

synchrotron radiation continued
diamond, synchrotron electron beam damage, study by optical, cathodoluminesc. and X-ray topography 80−39155
diffraction gratings, efficiency synchrotron radiation monochromisation 78−63189
diffractometer, high-resolution energy-dispersive, using synchrotron radiation 79−14640
directed beam, possibility of obtaining from relativistic charge *(Russian)* 78−1139
DORIS, luminosity limitations 80−37648
DORIS double storage ring, synchrotron radiation source in X-ray and UV regions 78−62668
EAS radio emission spectra, Cherenkov and synchrotron radiation mechanisms 77−64566
electron and particle discrimination, transition and synchrotron radiation 77−10568
electron beam spectrum monitor using synchrotron light 79−72146
electron bunch coherent radiation, electron distrib. effects 78−66734
electron bunch source, X-ray monochromatisation, phase space analysis 78−62276
electron cyclotron plasma radiation, in L-2 stellarator *(Russian)* 79−4178
electron moving in field of two plane waves and mag. field, theory of emitted radiation *(Russian)* 77−79733
electron produced synchrotron radiation spectrum, high energy struct. from $^{12}C(\gamma,\gamma)$ scatt. 78−13062
electron ring optical diagnostics using synchrotron radiation and light scattering meas. 80−5405
electron storage ring, Be windows for synchrotron radiation beam lines 79−68026
electron storage ring, focusing condition 77−42584
electron storage ring, horizontal wiggler, modelling of effect on beam parameters 79−68029
electron storage ring, vacuum control system for synchrotron radiation beam lines 79−68027
electron storage ring, vacuum system for synchrotron radiation source 79−63830
electron storage ring, vacuum ultraviolet and soft X-ray radiation sources appl. *(Japanese)* 78−25941
electron storage ring coherent microwave emission fine struct. 78−78875
electron storage ring SOR-RING as synchrotron radiation source 77−6584
electron storage ring VEPP-3, proposal to install supercond. wiggler magnet, synchrotron radiation prod. 78−62671
electron storage rings, SPEAR and PEP, estimate of spin polarisation 79−72093
electron storage rings, VEPP-2M, -3 and -4 as synchrotron radiation sources, beam characts. 78−62667
electron synchrotron orbit radiation characts. in visible spectrum, rel. to use as radiometric standard 78−9008
electron synchrotron-Cherenkov detectors 80−884
electrons acceleration by weak MHD turbulence, energy spectrum, radiosources appl. 79−88582
enhancement by storage ring beam modulation 78−82550
ethene, optical synchrotron-Cherenkov radiation threshold effects 80−28154
excitation spectroscopy, time-resolved photoluminescence emission and lifetime meas., synchrotron radiation use 78−66687
excitation standard, for light pulse shape calibration of H_2 flash lamp 79−72642
extragalactic compact X-ray sources, observational consequences of synchrotron self-Compton models 77−29961
extragalactic IR sources, synchrotron radiation model 80−31387
extragalactic radiosources, synchrotron radiation, contour maps and energy source *(French)* 79−75291
far UV spectroscopy using synchrotron radiation 77−67513
filtering methods, for Mossbauer source production 78−25374
fluorescence lifetime meas., single photon counting or phase shift techniques 79−13841
fluorescence lifetime measurement with subpicosec. resolution, use of synchrotron radiation 79−72447
flux measurement from SURF II storage ring using Si radiometer 80−90895
focusing on single point without time distortion, electron storage ring radiation 77−10991
galactic cosmic rays, contrib. to diffuse X-ray flux in 2 to 7 keV range 80−98745
galactic electron spectrum below 1000 MeV 79−5718
galactic halo radio emission, synchrotron radiation model 78−96544
galactic non-thermal radio radiation from polar regions, spectra 80−22082
galactic nonthermal radio spectrum, rel. to cosmic ray electrons spectrum and gamma-rays prod. 80−62257
galactic radio continuum, interpretation using new model of spiral struct. 77−13465
galactic radio spectrum, influence of primordial black holes 80−62179
galactic synchrotron radiation, distrib. from cosmic ray electrons propag. diffusion model 79−53679
galactic synchrotron radiation, rel. to cosmic ray electrons source spectrum and diffusion 79−53677
galactic synchrotron radio emission, rel. to Galaxy cosmic rays and mag. field distrib. 80−4207
galaxies, nearby, nonthermal radio continuum emission obs. *(German)* 80−109544
Galaxy, synchrotron radiation in inhomogeneous mag. field 77−67127
Galaxy, synchrotron radiation rel. to mag. field configurations 78−20884
gas-phase time-of-flight photoelectron spectrometer using synchrotron radiation 80−4818
generation, properties and appls. *(Czech)* 80−37945
generation and applications 80−32896
geological samples, chem. microanal., by X-ray microscopy near absorption edge with synchrotron radiation 78−20527
grazing incidence for UV monochromators using toroidal holographic gratings 80−90946
grazing incidence monochromator, ultra high vac., SSRL, design considerations and operating experience 78−62269
grazing incidence monochromator FLIPPER, ultra high vac., for synchrotron radiation 78−62237
grazing incidence monochromators, optimisation for synchrotron radiation 80−90943

synchrotron radiation continued
grazing incidence monochromators with holographic toroidal gratings, 10 to 150 eV 80−90947
growth of synchrotron radiation research, comments and reflections 78−63001
gyrosynchrotron emissivity peak freq. of weakly relativistic electrons in isotropic plasma 77−64633
halomethanes, synchrotron radiation photoabsorption cross sections, Rydberg states 80−28033
heavy-ion accelerator, dimensions of electron ring meas. by synchrotron radiation 80−42877
high flux grazing incidence monochromator based on holographic grating for synchrotron radiation 78−62271
high vacuum two crystal monochromator for soft X-ray synchrotron radiation 78−62272
historical aspects and appl. of synchrotron radiation 79−41310
holographic grating monochromator for 5 to 1000 eV synchrotron radiation 78−18049
holographic transmission diffraction gratings for soft X-rays 80−90965
holographic transmission gratings appl. to UV and X-ray synchrotron radiation monochromators 78−63186
holography, X-ray synchrotron radiation, coherence props. and power 77−75442
HR 1099, binary star, synchrotron radio emission obs. 77−64793
HR 1099, RS Canum Venaticorum binary, nonthermal flare emission during February 1978 outburst 79−21332
HR 1099, RS Canum Venaticorum binary, rapidly variable polarisation obs. at radio freqs. 79−21336
HR 1099, RS Canum Venaticorum binary, strong radio flaring discovery 79−21330
HR 1099, RS Canum Venaticorum binary, two-freq. radio polarimetry 79−21335
HR 1099, RS Canum Venaticorum type binary, radio emission detect. 77−9772
inelastic scatt. of X-rays and synchrotron radiation in crystals, review 78−39625
inner level spectroscopy with synchrotron radiation, theoretical aspects, book contrib. 80−4778
instrumentation, conf. Gaithersburg, MD, USA, June 1979 80−90607
instrumentation utilising surface photoelect. effect 80−92927
interacting beam models, summary 80−37644
inverse synchrotron radiation, energy exchange between focused laser beam and free relativistic electron 80−74286
IR, photometric anal. of radiation from Orsay storage ring 77−34922
ISABELLE, beam-beam interaction, transfer map approach 80−37651
isomeric nuclear state excitation by synchrotron radiation, Mossbauer effect 79−42508
ISR, beam-beam investigations, review 80−37645
Jupiter, bounce averaged synchrotron loss in dipole field 77−87316
Jupiter, decametric radiation source, synchrotron process 77−71056
KEK photon factory storage ring lattice, design principle 79−68033
RT Lacertae, RS Canum Venaticorum binary, gyrosynchrotron radio emission obs. 79−58379
BL Lacertae, visible and IR polarisation rel. to synchrotron emission 77−9803
laser-to-microwave frequency division using synchrotron radiation 79−76562
light velocity meas., Marinov's expt. 78−32673
low angular scatter in biopolymer solns., use of proportional chambers 78−65155
luminescence spectroscopy, VUV time and energy resolved, system using synchrotron radiation excitation 78−65982
LURE grazing incidence spectromonochromator, soft X-ray synchrotron radiation, 2 years operating experience 78−62270
LURE Rowland circle grazing incidence monochromator, performance 110 to 280 eV 80−90945
M87, nature of jet and synchrotron radiation source 78−54055
M87 jet, synchrotron optical and radio emission origin *(Russian)* 80−8694
macromolecular structural studies, with synchrotron radiation, X-ray television area detectors 79−55610
magnetic field inhomogeneity effect 77−79736
magnetic system appl. 77−24730
Markarian 421, optical and radio obs., identification with 2A 1102+384 X-ray source 79−5899
MAXIMOC grazing incidence monochromator for XUV investigations with synchrotron radiation 78−62238
Maxwellian synchrotron sources, spectral characts., model for 3C 273 radio and X-ray spectra 79−35107
MHD shock wave front of magnetic field discontinuity, astrophysical appls. 77−25939
mirror system, wideband, for electron ring diagnostics using synchrotron radiation 78−78518
mirrors, vac. UV and soft X-ray, for synchrotron radiation 78−83071
mirrors, vacuum UV and soft X-ray, for synchrotron radiation 79−3762
modulation spectroscopy, in vacuum UV, with synchrotron radiation, review 78−4710
molecular dynamics and photochem., synchrotron radiation obs. appls. 80−66830
molecular photoselected excited states, dynamics, advances using synchrotron radiation 80−37836
molecular spectroscopy appls. 80−53166
molecular spectroscopy using synchrotron radiation, book contrib. 80−4780
monazite, giant halo inclusions, evidence against superheavy elements using synchrotron radiation excitation 78−40554
monochromator system for synchrotron radiation 78−62278
monochromator using wavelength dispersion 78−296
monochromator with three-wave Bragg diffr. 80−87993
monochromators, conical diffraction mounting 80−91910
monochromators, curved, X-ray diffr. characts. for synchrotron rad. 79−9268
monolithic monochromators for synchrotron radiation, 1 to 4 Å, order sorting, focusing and polarising 80−90955
Moscow State University, synchrotron radiation research review 78−66730
multiphoton radiation, relativistic electron near nucleus in mag. field, soft photon approx. *(Russian)* 77−46676
multipole expansion 79−50199
N-100 storage ring, vacuum ultraviolet-radiation extraction channels 78−5071

synchrotron radiation continued
narrow band visible radiation from high-energy proton beams 77−58241
National Synchrotron Light Source basic design and project status 80−91329
National Synchrotron light source magnetic component system 79−68038
normal incidence monochromator, 2m high throughput, for SURF II storage ring 80−90951
normal incidence monochromator for synchrotron radiation, charact. modification using holographic concave gratings 78−62236
normal incidence monochromators for synchrotron radiation sources, experimental uses 78−62235
NP 0532, Crab pulsar, model, X-ray, optical and radio emission 78−4265
NP 0532, Crab pulsar, radiation, role of magnetosphere cyclotron instability *(Russian)* 80−8645
nuclear physics appls., review 80−106216
OJ 287, BL Lacertae object, purely synchrotron interpretation for synchronous optical-radio outbursts 80−8679
optical synchrotron radiation interference effects 80−63906
optical synchrotron-Cherenkov radiation threshold effects 80−28154
orbital radiation in storage ring, spectral chart *(Japanese)* 78−55290
Orsay, e^+e^- interactions, beam-beam effect observations, review 80−37650
Orsay's ACO storage ring LURE 77−10505
PAMPUS storage ring synchrotron radiation, physical applications *(Dutch)* 77−61639
particles accelerated by Alfven waves, distrib. function self-similar solns. 79−32757
PEP storage ring vac. system, synchrotron-radiation-induced heating effects 79−81107
PETRA, luminosity limitations 80−37648
PETULA device, electron beam interaction, UHF radiation *(Russian)* 78−38532
photodiode detector calibration using synchrotron radiation 80−90810
photoelectron spectroscopy, appl. to GaAs and Pt surfaces 78−53254
photoelectron spectroscopy, solid-state, with synchrotron radiation, review 80−71570
photoelectron spectroscopy, synchrotron radiation appls., book contrib. 80−14035
photoemission from noble metal surface (adsorbates), intermediate UPS/XPS synchrotron radiation study 78−52633
photoemission spectroscopy, angle-integrated, experimental geometry for studying polarisation effects 79−67395
photoemission using synchrotron radiation source, book contrib. 78−95677
photon factory project *(Japanese)* 77−83343
picosecond phase shift measurements at 358 MHz using synchrotron radiation 79−44949
PKS 0548−322, BL Lacertae object, synchrotron self-Compton model for X-ray spectrum 80−17654
PKS 0735+178, flat spectrum radio source struct. 78−16549
plasma, dense, synchrotron-like X-radiation produced by intense laser beam heating 78−67322
plasma, magnetised, synchrotron radiation from relativistic electron circ. orbits 79−55474
plasma turbulent reactor, relativistic electrons spectrum, synchrotron radio emission 79−40071
plasmas, laser produced, as X-ray source for synchrotron radiation research 80−320
polarisation and spectral-ang. charact. in a medium *(Russian)* 77−14647
polarised radiation transfer in inhomogeneous self-absorbed synchrotron sources 77−78623
polarising effect of monochromators on synchrotron VUV and X-radiation, polarisation meas. 78−66732
polyisobutylene fibres, stretched, crystn. kinetic study using synchrotron radiation 80−33909
power luminance spectral density unit, USSR state standard, 0.05 to 0.25 micron wavelength range 79−2819
principles, prod., and research appls. *(French)* 77−68159
properties and introduction to synchrotron radiation, book contrib 80−5669
props. and appls., review 79−36830
proteins, small angle X-ray scattering using sychrotron radiation, mol. wts. determ. 78−66700
proton beam at mag. field edge, obs. of visible synchrotron radiation 79−86119
proton beam in storage ring or synchrotron, monitoring by narrow band synchrotron radiation 77−83293
pulsars, incoherent synchrotron radiation model 78−40979
QSOs, synchrotron radiation rel. to optical polarisation alignment with radio struct. 79−25751
quantum beats from nuclei excited by synchrotron pulses 78−88239
quantum corrections, radiated power of spin $^1/_2$ particle 79−21995
quantum corrections, second order effects 78−1136
quantum corrections 80−37193
quantum corrections to power spectrum 78−21362
quasars and active galactic nuclei, magnetic flare model, magnetised accretion disc around massive black hole 80−22113
quasars and BL Lacertae objects, optical polarisation model 77−2479
quasi monochromatic, from undulators, spectra for strong and weak fields 78−63000
quasi-thermal electrons gyrosynchrotron emission, appl. to solar flares 80−36602
radiationless transitions, synchrotron radiation obs. 80−63706
radio galaxies, radiation transfer, dynamics, stability and evolution of synchrotron plasmon, book 78−24564
radio sources, compact, extragalactic, interpretation of spectra 80−62299
radio sources, form. of universal and diffusion regions of relativistic electrons non-linear spectra 80−109555
radio sources, relativistic corrections in expanding synchrotron sources theory 80−12821
radio sources variable at low freqs., evidence for relativistic expansion and electron synchrotron radiation 79−9018
radiometric transfer standards calibration in UV and VUV 79−12847
radiometry, synchrotron radiation as an absolute standard source 80−90879
radiosources, compact extragalactic, super-luminal expansion 77−53695
radiosources, extended, particle accel. and radiative losses effects on source dynamics 80−46687
synchrotron radiation continued
radiosources, extragalactic, decimetric variability *(Russian)* 79−21454
radiosources, nonuniform, with internal absorpt., radio spectra 77−5580
radiosources, nonuniform struct. effects on physical parameters 78−8138
radiosources, self-absorbed synchrotron, polarized radiation transfer 77−53413
radiosources, superlight flux vars. in relativistically expanding sources, models 78−4377
radiosources nonlinear spectra, rel. to relativistic electrons accel. in plasma turbulent reactors 79−8824
radiowave generation by gyrosynchrotron and Langmuir-wave processes, solar and stellar appl. 79−21172
rare earth germantes, flux-grown, X-ray topography 80−64939
relativistic, electrons in soft photon spectrum, external field effects *(Russian)* 77−14648
relativistic charged particle, effect of multiple scattering on synchrotron radiation *(Russian)* 80−13245
relativistic charged particle in arbitrary EM field, radiation, accel. 78−42269
relativistic electrons, emission harmonics, inhomogeneous line broadening 78−25782
relativistic electrons, synchrotron radiation oscillatory behaviour 79−26271
relativistically expanding spherical radiosources, flux vars. 79−17112
resonance scatt. by nuclei, time delay 79−15386
resonant filtering, pure nucl. refls. and X-ray interferometry, impedance matched grazing incidence films 80−37141
review, origin, charact. and appls. 77−58243
review of appl. in biology, solid state and atomic physics *(Danish)* 79−81345
review of props., facilities, and source parameters and optimisation 79−68018
review of synchrotron radiation research, book contrib. 79−22161
review of synchrotron radiation research 79−22505
Sagittarius A region, 8.2 mm obs. 78−28794
Schwarzschild black hole in ext. mag. field, radiation emitted by relativistic particles 78−96501
section topograph technique, high resolution, applicable to synchrotron radiation sources 80−57449
selective X-ray absorption microanal. using synchrotron radiation, transition metals in Mn nodules 78−68957
short-wave synchrotron radiation prevention by rotatable mirrors 78−62274
single-particle dynamics, electron motion 78−78892
small angle scattering camera for synchrotron radiation X-rays, description and results 78−66020
soft X-ray microscopy and lithography using synchrotron radiation 78−66018
soft X-ray microscopy/lithography branch line at SSRL 80−91344
soft X-ray small angle scattering, appl. to polystyrene latexes 78−51395
soft X-ray synchrotron radiation focusing using toroidal mirror 78−45760
solar moving type IV bursts, gyro-synchrotron modulation obs. 80−26833
solar moving type IV radio burst, three freq. obs. and modified synchrotron model 78−69776
solar moving type IV radio bursts, obs. and interpretation 79−40174
solid state physics applications 77−51283
solid state spectroscopy using synchrotron radiation, book contrib. 80−7375
source for electronic states and struct. anal. *(Chinese)* 80−44075
sources, properties, and research appl., review 77−75403
sources, props. and charact. 80−62729
sources and utilisation, review 78−41390
SPEAR, beam-beam functional dependencies of machine parameters 80−37647
SPEAR, synchrotron radiation beam ports, installation and thermal design 79−68034
SPEAR, synchrotron radiation source 77−83186
SPEAR storage ring, as synchrotron radiation source for X-ray spectroscopic studies 77−41745
SPEAR storage ring, initial operation of mag. wiggler 79−68025
SPEAR storage ring and synchrotron radiation research 79−41052
spectra, radio and electron, effect of interstellar mag. field inhomogeneities 80−85849
spectra investigation, difluoroethylene 79−59514
spectral chart of radiation from circular accelerator 78−46498
spectral radiance calibration of light sources in vac. UV using synchrotron radiation 78−65954
spectral tip calc. refinement, transition rates for mag. bremsstrahlung, computing techniques 79−49430
spectrometer for 100 to 130 nm 80−90953
spectrometer for ultra soft X-ray emission from synchrotron radiation excitation 78−62273
spectroscopic applications, properties, characteristics as radiation source *(Norwegian)* 80−63420
spectroscopic applications, review 77−58239
spectroscopic instruments applic. in synchrotron emission channels *(Russian)* 77−82623
spectroscopic source, appl. to elec. struct. determ. of solids 77−20882
spectroscopy, review *(German)* 79−40624
spectroscopy, use of synchrotron radiation *(Japanese)* 79−63311
spectroscopy appls. in VUV and X-ray regions, lecture 78−24870
spectroscopy instrumentation and appls., book contrib. 80−4782
spectroscopy of fast fluoresc., nanosec. range 80−62736
spin-flip and normal synchrotron radiation from rot. charge in mag. plasma 80−28153
Stanford Synchrotron Radiation Laboratory, operation and development, review 79−68020
Stanford Synchrotron Radiation Laboratory, status report 80−91327
statistical state of radiation field anal. 78−66736
storage ring, use in obtaining high resolution molecular X-ray absorption spectra 77−27199
storage ring design considerations for parasitic use of synchrotron radiation in the infrared 80−91340
storage ring synchrotron radiation far IR source 79−30577
storage rings, beam-beam interaction, radical diffusion simulation 80−37653
storage rings, expt. enclosures and beam line safety components 80−91341
storage rings, free electron laser amplifier operation 79−68399

synchrotron radiation continued
storage rings, interaction effects of EM fields on particle beams 80−37643
straight groove toroidal grating monochromators, 10 to 500 Å, design optimisation for synchrotron radiation 80−90944
superconducting wiggler magnet, 5T design for dedicated synchrotron radiation source at Daresbury 78−62672
superlight source *(Russian)* 77−6983
supernova explosions, relativistic electrons accel. 78−28710
SURF II, 250 MeV storage ring for UV synchrotron radiation, progress report 79−68032
SURF II storage ring, status report 80−91325
surface analysis by synchrotron radiation and sputter Auger techniques 78−61130
surface atomic and electronic struct. studied with synchrotron radiation 80−80945
surface EXAFS study of adsorbate Auger electron intensity on single cryst. surfaces 78−66562
Synchrotron Radiation Source booster magnet power supply 79−31272
Synchrotron Radiation Source booster synchrotron combined-function magnets 79−31269
Synchrotron Radiation Source storage ring multipole magnet prototype 79−31268
synchrotron-Cherenkov radiation, expt. aspects 77−19146
Tantalus I electron storage ring radiation, synchrotron and laboratory discharge light sources comparison 79−10371
techniques and appls., book 80−5668
time resolved spectrofluorometry, appl. of synchrotron radiation 78−65978
time resolved spectroscopy at storage rings 80−31902
time resolved X-ray scattering, synchrotron radiation camera and data acquisition system 80−99023
Tokamak synchrotron emission and runaway electron distrib., time evolution 77−39447
Ton 1542, Seyfert galaxy nucleus, optical polarisation and synchrotron radiation *(French)* 77−26053
transfer standard radiometric sources and detectors, calibration using synchrotron radiation 78−65967
transition rates in intense-field regime 80−77991
two-photon, for ultrarelativistic electron, Dirac eqn. anal. *(Russian)* 77−2719
UHV beam line at SSRL for spectral range 4-4000 eV, monochromatised radiation 78−62673
ultra-high-vacuum double crystal monochromator beam line for studies in the spectral range 500-4000 eV 80−90957
ultrahigh-energy electrons traversing cosmic blackbody photon gas, synchrotron losses 79−5742
undulator emission from 'Pakhra' synchrotron *(Russian)* 78−5409
undulator for the 700 MeV VUV-Ring of the National Synchrotron Light Source 80−91337
undulators and 'free-electron lasers', review 80−9794
Uranus, 34.3 MHz synchrotron flux upper limit 77−60724
UV, photodiode calibration appl. 78−77959
UV and X-ray spectroscopy, synchrotron radiation as intensity reference 79−75619
UV beamlines for National Synchrotron Light Source 80−91342
UV laser possible pumping by synchrotron radiation, NaCl:I(Br) luminesc. 78−66835
UV source, 50 MeV electron synchrotron with cyclotron preaccel. 77−61641
UV spectral emission scales establishment appl. 78−78001
vacuum UV circular dicroism spectroscopy using synchrotron radiation 80−91575
vacuum UV energy brightness spectral standard source, 0.05-0.25 μm range 77−79909
vacuum UV radiation scales, plasma blackbody lines and synchrotron radiation 78−1309
vacuum UV radiation scales 77−30124
vapour absorption cells and beam generating ovens for synchrotron radiation spectroscopy 78−66688
VEGA device, electron beam interaction, UHF radiation *(Russian)* 78−38532
Vela pulsar (PSR 0833−45), synchrotron radiation model for optical and gamma-ray emission 80−94824
VEPP-2M storage ring, synchrotron radiation use to test VUV detectors absolute efficiency 80−82824
VUV 4 m normal incidence monochromator 80−90950
VUV beam line instrumentation for National Synchrotron Light Source storage ring 80−91343
VUV monochromators, 10 to 300 Å for synchrotron radiation, evaluation 80−90907
VUV monochromators with toroidal holographic gratings, Strehl criterion 80−90949
wavelength dispersion system normal incidence monochromator 78−296
white beam, X-ray energy dispersive diffractometry using synchrotron radiation, special features 78−66019
white dwarf stars, magnetic, polarised synchrotron radiation emission 77−2428
wiggler, helical, radiation source, orbits and fields 77−79203
wiggler, helical wiggler and free electron laser *(Japanese)* 80−37658
wiggler magnets, standard, effects on synchrotron radiation spectrum and storage ring operation 78−62670
wiggler magnets, use as synchrotron radiation source at SPEAR storage ring 80−91332
wiggler with short period helical path as radiation source 77−79202
Wisconsin Synchrotron Radiation Center, UHV Seya-Namioka and adjustable slit 'Grasshopper' monochromators 78−62234
X- and γ-ray production by template modulated coherent light, energy spectra, freq., polarisation 77−13833
X-ray, high power, pumping of possible VUV laser crystals media 79−41387
X-ray, use in determ. photoelectron spectra of Pb, In, Sb and Pb compounds 77−44118
X-ray camera, double focusing, use with synchrotron radiation 80−313
X-ray camera, small-angle, using synchrotron radiation for structural studies 77−43108
X-ray crystallography applications, absorpt. factors of DNA 78−76988
X-ray crystallography source, appl. to mag. domains in Fe-Si 78−67620
X-ray crystallography source, white beam topography 78−67621
X-ray crystallography technique, phase determ. 78−67618

synchrotron radiation continued
X-ray crystallography white radiation methods using synchrotron sources 80−44076
X-ray energy-dispersive diffractometry using synchrotron radiation 78−18487
X-ray focusing mirror 80−90961
X-ray interferometry, appl. of synchrotron radiation 80−90954
X-ray laser holography, pumping by synchrotron radiation from storage rings 78−55322
X-ray lasers pumped with synchroton radiation and low-energy photons 79−41371
X-ray lithography application 77−22628
X-ray lithography using synchrotron radiation, resist sensitivity 80−62820
X-ray microscopy, high resolution, for chem. microanal. 80−81416
X-ray monochromatisation by crystal diffraction, synchrotron radiation 78−62277
X-ray monochromator development for synchrotron radiation facilities 80−91351
x-ray monochromator geometry for focusing synchrotron radiation above 10 keV 80−90958
X-ray monochromator system 78−62279
X-ray monochromators, channel-cut, identification of spurious reflections 80−90959
X-ray optics and monochromators for synchrotron radiation 77−54027
X-ray photoabsorption of solids by specular reflection 79−15561
X-ray small angle scattering, and diffr. exp. in biology and physics employing synchrotron radiation and energy dispersive techniques 79−12051
X-ray source for struct. determ. of biopolymers 78−47210
X-ray synchrotron source, design status 79−68024
X-ray topography, appl. of synchrotron radiation from electron storage rings 80−64830
X-ray topography, developments, review 80−64836
X-ray topography, using synchrotron radiation, microscopic struct. investig. 77−76424
X-ray topography, white beam settings 78−67619
X-ray transmission diffraction gratings for synchrotron rad. sources, modelling 80−90964
X-rays, from electron storage rings, meas. of detector losses 78−86752
XUV mirror reflectivities from 50-150 eV 80−90966
XUV monochromator design for use with synchrotron radiation sources 80−90940
e^+e^- storage rings, beam-beam effects expts. at SPEAR 80−37646
Al clean films, O_2 interaction study using synchrotron-radiation-induced-photoemission 80−55709
Al, single crysts., misfit recrystn. dislocations formation study during recrystn. by X-ray synchrotron topography 79−38849
Al surface, oxidation, synchrotron radiation photoelectron obs. 78−52634
Al-Cu, type 1100, synchrotron radiation microradiography 80−85121
Al-Cu-Mn, type 2219, synchrotron radiation microradiography 80−85121
Ar,K inner-shell level energies, absorpt. spectroscopy with synchrotron radiation 80−99583
Ar, spin-polarised photoelectrons by circularly polarised synchrotron radiation 80−91516
Be, neutron focus in synchrotron radiation *(Russian)* 78−33344
CO, partial photoionisation cross-section determ. using synchrotron radiation 77−75243
CO_2, partial photoionisation cross-sections, branching ratios, synchrotron radiation meas. 78−42141
CO_2, spin polarised photoelectrons, synchrotron excited 80−43101
Cr I, inner shell absorpt. spectrum, 3d wavefunction collapse 77−23455
Cs, polarised photoelectrons produced by circ. polarised synchrotron radiation 80−18830
^{57}Fe, 14 keV, nuclear resonance excitation by synchrotron radiation 78−78363
^{57}Fe Mossbauer level excitation using synchrotron radiation 80−7204
$^{57}Fe^m$, Mossbauer level excitation using specific characts. of synchrotron radiation 78−66447
Ge, hot microdeformation and simultaneous X-ray topography apparatus *(French)* 80−38871
H_2, synchrotron radiation scattering cross sections 78−55213
He, synchrotron radiation scattering cross sections 78−55213
Ir (100), chemisorptive bonding of CO, photoemission investig. using synchrotron radiation 77−12498
K_2 excitation, prod. and decay of 0_u^+ and 1_u states 80−43109
Kr, $^3P_1$ state, reson. fluoresc., Zeeman beats, time-resolved VUV spectra using synchrotron radiation 78−33454
Kr, K inner-shell level energies, absorpt. spectroscopy with synchrotron radiation 80−99583
Kr, spin-polarised photoelectrons by circularly polarised synchrotron radiation 80−91516
LiF, anisotropic Compton scattering using synchrotron radiation 80−60703
Mg clean films, O_2 interaction study using synchrotron-radiation-induced-photoemission 80−55709
N_2, partial photoionisation cross-section determ. using synchrotron radiation 77−75243
N_2O, non-Franck-Condon transitions in resonant autoionization 79−50092
N_2O, spin polarised photoelectrons, synchrotron excited 80−43101
$OH(A^2\Sigma^+ \rightarrow X^2\Pi_i)$ yields from H_2O photodissoc. 80−71927
SF_6, photoionisation spectra in XUV region 80−37837
Si radiometer for storage ring synchrotron radiation 80−86411
Xe, $^3P_1$ state, reson. fluoresc., Zeeman beats, time-resolved VUV spectra using synchrotron radiation 78−33454
Xe, 5s electron photoionisation cross section with synchrotron radiation 78−5180
Xe, L_1,L_2,L_3 inner-shell level energies, absorpt. spectroscopy with synchrotron radiation 80−99583
Xe_2, time and energy resolved fluorescence, radiative lifetime, collisional mixing, pulsed synchrotron radiation obs. 79−98136
Xe_2^*, synchrotron radiation excited, time resolved spectroscopy 80−69092

synchrotrons
see also cosmotrons
3 GeV proton synchrotron magnet design and meas. 79−31303
28 GeV proton synchrotron and intersectig storage rings, interconnected vacuum system 78−86706

synchrotrons continued
400 GeV proton synchrotron, CERN, preliminaries to commencement of operation 77−83185
500 MeV synchrotron ring magnet power supply 79−18068
600 MeV booster synchrotron for Daresbury 2 GeV storage ring 79−68022
800 MeV proton synchrotron for pulsed spallation neutron source 77−67930
accelerated electron cluster in synchrotron, rot. disc, method investig. of synchrotron radiation 79−3264
accelerated particle resonances, perturbation treatment in classical dynamics 79−22506
accelerating resonator of ion synchrotron, tuned power amplifier 79−68063
AES sources for use at low energy 80−77913
AGS, efficient slow extraction, nonlinear growth of betatron oscillations, magnetic septum 80−47793
AGS, max. orbit distortion distrib. for randomly distributed magnet misalignments 78−82549
AGS, microprocessor based beam loss monitor system 79−72070
AGS slow extracted beam, size meas. 80−37672
alternating gradient, ψ(J) particle, discovery, props., experimental apparatus develop. *(Czech)* 78−78232
ANL ZGSynchrotron, 1 to 12 GeV beam transport for polarised protons 79−72056
ANL ZGSynchrotron, high energy polarised deuteron beams 79−72054
Argonne intense pulsed neutron source, commissioning 79−67997
Argonne ZGS, polarised proton target, using high homogeneous field supercond. magnet 77−26911
bakable Al vacuum chamber and bellows with flange and seal for ultrahigh vacuum 79−30486
beam depolarisation in magnetic field 78−33336
beam detector assembly for the Fermilab Energy Doubler 79−72156
beam energy distribution control technique for proton synchrotron 79−72128
beam lifetime in KEK PS main ring 77−83278
beam production with high line-density by azimuthal combination of bunches 79−72114
beam RF phase lock loops, effect of large delays 79−68046
BEAMSCOPE, device for meas. of emittances and betatron amplitude distribs. 79−72145
Bevalac, partially stripped heavy ion accel. 77−83187
bevatron, intercomparison of high-energy accelerator field dosimetry 78−25331
BNL AGS, high field superconducting beam transport 79−76203
BNL AGS, polarised proton acceleration 79−72055
BNL AGS slow extraction improvements 79−72045
BNL AGSynchrotron, 1.5 GeV/c multiturn shaving extraction and its transport line 79−72062
Bonn, polarised electron accel., and possible depolarisation 79−63826
Bonn 2.5 GeV synchrotron, acceleration of polarised electrons, and subsequent depolarisation 79−68002
book, synchrotron radiation 77−75402
booster synchrotron, 100 to 700 MeV, for BNL National Synchrotron Light Source 79−67973
Brookhaven AGS, longitudinal coupling impedance meas. 79−72104
Brookhaven AGS, polarisation studies, past, present and future 77−30737
Brookhaven AGS superconducting bending magnets, large aperture design 77−26910
bunch lengthening and microwave instability 77−83370
bunches with local elliptic energy distribs. 79−76565
CAMAC based high-resolution repetitive waveform generator 79−76214
CERN, Intel 8080 microprocessor development system 77−83314
CERN, international scientific cooperation *(Dutch)* 77−45669
CERN's 28 GeV proton accelerator, RF power supply system, control equipment 77−79488
CERN's 400 GeV super proton synchrotron, design and construction 79−68064
CERN 400 GeV proton synchrotron control consoles 77−38518
CERN 400 GeV SPS, ISR merging for 60 GeV collider 78−58513
CERN 400 GeV Super Proton Synchrotron, multipurpose He refrigerator/liquefier 79−58737
CERN 400 GeV super proton synchrotron, review *(Dutch)* 77−46432
CERN 400 GeV superproton synchrotron, facility description 78−37471
CERN 50 MeV linac for proton synchrotron, operation and modification 77−38442
CERN accelerators, radiation protection *(Dutch)* 77−46434
CERN experiments in 1979 80−408
CERN proton synchrotron, automatic procedures 79−72074
CERN proton synchrotron, electron ring addition, proposal for weak interaction study 78−55062
CERN proton synchrotron, improvement project for computer assisted controls 79−72209
CERN proton synchrotron, stand alone control system for continuous transfer ejection to SPS 78−82552
CERN proton synchrotron booster, improved recombination of 20 PSB bunches and merging to 5 dense bunches 79−76192
CERN Proton Synchrotron focus control, pole face winding design and field correction 79−31299
CERN PS, collective phenomena at very high intensity 79−76193
CERN PS, computer controlled beam local radial perturbation and rotation 79−72072
CERN PS, SPS, beam production with high line-density by azimuthal combination of bunches 79−72114
CERN PS beam, online evaluation of mean radial position 78−82548
CERN PS booster, microprocessors in control and beam obs. 77−88302
CERN PS booster, reliability and maintenance anal. 77−83281
CERN PS booster, simultaneous dynamic stopband compensation and correction lens location 79−76191
CERN SPS, 148 MW pulsed power supply, mains voltage stabilization and filtering 79−76207
CERN SPS, 200 MHz accelerating systems and 800 MHz Landau damping cavity 79−72063
CERN SPS, acceleration and storage of dense single bunch 79−72094
CERN SPS, collective transverse beam instabilities damper description 79−72143
CERN SPS, control systems operating experience, suggested principles for future accelerators 79−72211
CERN SPS, external proton beams and splitter system 77−83386
CERN SPS, fast resonant extraction 79−72137
synchrotrons continued
CERN SPS, high freq. longitudinal and transverse pick-ups 79−72152
CERN SPS, NODAL control system 79−9987
CERN SPS, proton beam at mag. field edge, obs. of visible synchrotron radiation 79−86119
CERN SPS, review of performance and operation reliability 79−72048
CERN SPS, supercond. bending magnets CESAR 79−31251
CERN SPS, target stations and beam dumps 77−83385
CERN SPS, zer flux DC current transformer 77−88306
CERN SPS system, travelling wave drift tube structure 77−38517
CERN Super Proton Synchrotron, beam observation via optical transmission system 80−38119
CERN super proton synchrotron, experimental programme *(Dutch)* 77−46431
CERN super proton synchrotron, experiments with light particles *(Dutch)* 77−46433
CERN super proton synchrotron, review 78−78529
CERN Super Proton Synchrotron beam-splitting steel septum magnets 79−31295
CERN Super Proton Synchrotron extraction channel septum magnets 79−31296
CERN supersynchrotron, radiation protection *(German)* 77−14270
CESR control system, interface hardware 79−72069
chromaticity correction in KEK main ring 80−74049
closed orbit distortions, stability of large synchrotron 79−76186
colliding beam facilities, overview 80−37642
combined monochromator instrument, synchrotron electron current determ. and light source calibration 78−65954
CPS at CERN, pulse to pulse modulation, extraction modes, beam intensity 77−83277
CPS continuous transfer, modulated fast bump 77−83240
cryogenic current safety lead for magnet quench 77−83232
depolarising resonance crossing, Froissart and Stora procedure 77−38510
dipole magnets in eight tesla range 79−76201
doubler tevatron microprocessor quench protection system 79−72088
Dubna heavy ion synchrophasotron facility 79−72125
electron, circularly polarised photon beam prod. by imperfection resonance methods 77−38512
electron, cryostat with large cooling power, for polarised target 77−34496
electron, review of photonuclear research at Lund and future accelerator plans 77−82907
electron, synchrotron, beam lifetime increase using pulsed mag. field 79−3265
electron, synchrotron orbit radiation characts. in visible spectrum, rel. to use as radiometric standard 78−9008
electron beam intensity, synchrotron with cyclotron preaccel. 77−61642
electron beam spot, photographic obs., rel. to amplitude of betatron oscillation 78−55059
electron beam spot, photographic obs. 77−71709
electron bunch lengthening in storage rings due to fast longitudinal instability 77−83340
electron distributed computing system for data acquisition and control 77−38513
electron produced synchrotron radiation spectrum, high energy struct. from $^{12}C(\gamma,\gamma)$ scatt. 78−13062
electron relativistic beam in synchrotron, ang. spread of vel. using undulator radiation electron 80−14021
electron synchrotron storage ring RF power supply *(German)* 78−17453
electron-photon cascades separation by scintillation counter system 78−78563
energy doubler quenches, pressure development 79−76200
ESCAR, tests of superconducting bending magnets 79−76202
ESCAR superconducting fully cryogenic accelerator 77−83236
fast cycling, separated function magnet systems, power supply tracking problem *(Chinese)* 79−49882
feedback-stabilised proton synchrotron, beam interaction 78−78527
Fermi National Accelerator Laboratory, description 77−57782
Fermilab, appl. of NMR cct. to superconducting mag. field meas. using signal ave. 77−83231
Fermilab, cryostat mass production 79−68045
Fermilab, dynamic loss properties of Ni-Zn accelerator RF system ferrite 79−68053
Fermilab, high energy electron cooling 79−72090
Fermilab, magnetisation effects in superconducting dipole magnets 77−83229
Fermilab 1000 GeV switchyard, microprocessor control of He refrigerator system 79−68006
Fermilab 500 GeV accelerator, operating experience 77−83280
Fermilab 500 GeV main accelerator RF cavity 128 MHz mode damper 77−83299
Fermilab booster, antiproton deceleration 79−72102
Fermilab Booster, design of additional extraction/injection area 79−72047
Fermilab booster, low level RF system 79−76205
Fermilab booster, transverse instabilities suppression, fast feedback system 77−83298
Fermilab booster accelerator, mag. system modification, increased energy 77−83222
Fermilab booster beam, longitudinal dipole oscills., effects, damping 77−83259
Fermilab booster beam damper, logic and control module 77−83313
Fermilab booster beam damping system, high-speed RF data transmitter 77−88296
Fermilab booster bunches, linac bunch struct. during adiabatic capture and accel. 77−83261
Fermilab booster low level RF system, high speed voltage controlled oscillator 79−68049
Fermilab booster main ring beam transfer phase lock cct. 79−72073
Fermilab Booster Ring, 30 to 53 MHz super cavities for 10-GeV acceleration 79−68058
Fermilab Booster synchrotron, broadrange beam signal limiter 79−72082
Fermilab booster synchrotron, transverse instability damping electronics 77−83318
Fermilab capacitor tree 77−83242
Fermilab control system, computerized network of distributed processors 77−83302
Fermilab electron cooling, electron beam diagnostics 79−72147
Fermilab electron cooling expt., design and construction of electron beam 79−72138
Fermilab electron cooling expt., proton beam diagnostics 79−68005

synchrotrons continued
Fermilab energy doubler, dipole magnet technology 77−26901
Fermilab energy doubler correction magnets, construction 79−68042
Fermilab energy doubler/saver mag., radiation damage limitations 77−83238
Fermilab energy doubler/saver project, ring of superconducting mags., status report 77−83212
Fermilab facilities, future projects, perspective 79−85841
Fermilab magnet protection using ZNR surge suppressors 79−68043
Fermilab main accelerator quadrupole transistorised regulators 77−83243
Fermilab main ring, azimuthal beam redistribution 79−72103
Fermilab main ring magnet supplies, bipolar operation 79−76206
Fermilab main ring magnets, operational reliability 79−72044
Fermilab main ring power supply, minicomputers control system 77−83303
Fermilab master slave servo-manipulator, control system 77−83309
Fermilab neutrino focusing horn, 10 msec. 150 kA pulsed power supply 79−68092
Fermilab phase controlled pulsed power supplies, charact. of inversion operation 77−83223
Fermilab switchyard, superconducting dipole 79−76204
Fermilab synchrotron, attainment of 500 GeV proton beam 77−83275
Fermilab Tevatron He liquefier power supply 79−68044
free electron devices for light prod., history, book contrib. 79−27147
heavy ion accel. for inertial fusion 77−83189
heavy ion facility for radiation therapy 77−86588
heavy ion variable charge synchrotron theory 79−72124
heavy-ion accelerators, book contrib., review 78−90003
HEUB superconducting dipoles, operating experience 77−83234
high energy accelerator system for intense heavy ion beam, inertial fusion igniter 79−72040
high energy heavy ion acceleration, prospects 79−68010
high energy physics program at BNL, equipment, experiments, future research 77−18716
injection method at zero gradient synchrotron 77−83133
injection methods in Fermilab booster synchrotron 77−83132
INS electron 1.3 GeV synchrotron, polarised electron acceleration 80−37660
intense pulsed neutron source, vacuum system 79−63261
Intense Pulsed Neutron Source (IPNS-1) accelerator 500 MeV fast kickers 79−72131
Intense Pulsed Neutron Source (IPNS-1) accelerator RF system 79−67998
ion, ferrite accelerating resonator with tunable freq. from 2.5 to 30.8 MHz 79−97914
ionisation monitor, bakeable weldable vacuum gauge 79−40589
jumping an intrinsic depolarization resonance in synchrotrons, Froissart-Stora formula 79−72058
KEK, 750 keV beam line construction 77−38438
KEK, beam diagnostics with wall current monitor 79−72080
KEK, beam position monitor system, design, operation 77−83306
KEK, closed orbit control system for main ring 79−68008
KEK, harmonic current AC filters 78−33333
KEK, low energy kaon beam line charact. 79−72053
KEK, minicomputer assisted function generator for the dynamic control of chromaticity correction sextupoles 79−68009
KEK 12 GeV proton synchrotron, computer control system of main ring magnet power supply 79−72071
KEK 12 GeV proton synchrotron, voltage flicker suppression 77−83230
KEK 12 GeV synchrotron, and current status of accelerator facilities in Japan 79−72041
KEK 500 MeV fast cycling booster synchrotron 77−83282
KEK beam line magnets control by CAMAC serial highway 79−68007
KEK booster, beam loss in initial acceleration 79−76182
KEK booster, longitudinal beam behaviour 79−76184
KEK booster, transverse coherent instability anal. 79−76183
KEK booster to main ring beam transfer system, construction operation 77−83264
KEK main ring, dipole magnets field meas., B-clock system 77−83308
KEK main ring, prototype multipole magnets, design, field uniformity 77−83220
KEK main ring, RF acceleration 79−68048
KEK proton synchrotron, control computer system 77−88301
KEK proton synchrotron, initial operation, 12 GeV energy, peak intensity 77−83272
KEK proton synchrotron, power supply 77−83245
KEK proton synchrotron, status of beam lines 77−10499
KEK proton synchrotron, synchronous beam transfer from booster to main ring 77−83263
KEK proton synchrotron vacuum system design and construct. 77−83225
KEK proton synchrotrons, coupling resonance $2\nu_H$-$2\nu_V$ 79−76185
KEK synchrotron, proton attenuation lengths in paraffin, concrete and iron around targets 80−102412
KEK-PS, duoplasmatron ion source 77−83390
KEK-PS main ring, slow beam extraction schemes 79−72046
large multiwire proportional chambers for experiment NA3 at the CERN SPS 80−102388
LEP, 15 GeV injector alternatives, storage ring and synchrotron 79−72052
LEP 100 GeV e^+e^- storage ring, synchrotron injector design 77−67913
magnetic spectrometer, SPES II, use with multiwire props. counters of three-body nuclear reaction study *(French)* 79−708
magnetic spectrometer SPES I, for use with Saturne synchrotron *(French)* 79−709
magnetic undulator in electron synchrotron motion and radiation of relativistic electrons *(Russian)* 78−62997
magnets for spallation neutron source 79−68039
medical ion accelerator, cyclotron and synchrotron design studies 79−54661
miniature pulse deflector construction 78−82545
MWPC instrumentation for CERN SPS secondary beams 78−46206
National Synchrotron light source magnetic component system 79−68038
neutrino, beam channel charact., Protvino Inst. 78−37474
neutrino beam focusing system, Protvino Inst. 78−37477
NUMATRON project, high energy heavy ion facility, design, performance 78−62665
Numatron project, high-energy heavy-ion accelerator *(Japanese)* 79−26791
synchrotrons continued
NUMATRON project at INS, Tokyo Univ., heavy ion source 79−68016
optical reflector for energy extraction 80−78467
Pakhra synchrotron, split microtron injector, design and charact. 77−83136
particle physics overview, role of CERN and FERMILAB *(Dutch)* 77−45928
passive filter for annular electromagnet 78−5074
PETRA, damping of coherent transverse bunch oscills. 79−72142
photodisintegration and π photoprod. coincidence expts. at Bonn 500 MeV synchrotron 80−22815
photon dose rate from induced activity in the beam stop of a 400 GeV proton accelerator 78−94144
polarised beam acceleration possibilities with Brookhaven AGS 79−63844
polarised ions, acceleration by synchrotons, review 79−63840
polarised particle, production and accel., status report, Saturne 79−63847
polarised proton acceleration in CERN synchrotron 77−38509
polarised protons, acceleration by 12 GeV synchrotron at KEK, possibilities 79−63846
proton, 12 GeV, beam size meas. by fast rotary scraper 79−72078
proton, beam position monitor for ΔR feedback on RF system 79−72079
proton, CERN, online function generation optimisation 78−834
proton, ESCAR bending magnets, design, construction and operation 79−36444
proton, high energy electron beam prod. *(Russian)* 79−41058
proton, KEK preinjection accelerating column 77−38436
proton, magnetisation of ferrites in tunable accelerating resonators 80−68983
proton, radioactivity of subsurface water in ground shield 77−67907
proton, Rutherford, pulsed neutron facility 78−29208
proton, with short accel. time, accelerating resonators 77−46429
proton, Zero Gradient Synchrotron, H^- injection 77−83369
proton beam, 70 GeV, channel, shaping system, for Protvino Inst. neutrino expts. 78−37476
proton beam 70 GeV, for Protvino Inst. neutrino expts., charact. 78−37475
proton beam in storage ring or synchrotron, monitoring by narrow band synchrotron radiation 77−83293
proton KEK 12 GeV, beam profile meas. 77−83404
proton KEK synchrotron, simple Q-measurement 77−83316
proton recapture and moderation on magnetic field decay in proton synchrotron 79−68062
proton synchrotron, intense beam, bunched optimum critical energy transition 77−83346
proton synchrotron, multiturn injection efficiency increase 77−83129
proton synchrotron, oscillations, effects of induced voltage and forces of space charge on motion *(Bulgarian)* 80−47792
proton synchrotron accelerator theory 77−67925
proton synchrotron booster, CERN, longit. active damping system 77−83371
proton synchrotron booster model for multiturn injection 77−83130
proton synchrotron booster RF accelerating system, dynamic closed loop control 77−83379
proton synchrotron for intense pulsed neutron source facility 77−83191
proton synchrotron slow extraction beam parameter monitoring and control system in CAMAC standard online with ES 1010 computer 78−29674
proton synchrotrons, future expts. 78−78528
proton synchrotrons, intensity and energy spread at injection 77−83131
proton synchrotrons, non-linearities 78−78897
Proton-Electron Tandem Ring Accelerator magnet field meas. 79−31271
protons in synchrotron, beam parameter diagnostics via IR undulator emission *(Russian)* 78−836
PS booster at CERN, longit. active damping system electronics, tracking band pass filters 77−83297
pulsed septum magnet for extraction from Fermilab booster synchrotron 77−83219
pulsed spallation source for neutron scattering research 77−83351
radial damping by octupole for zero gradient synchrotron beam 77−83383
rapid cycling synchrotron magnet with separate AC and DC circuits 79−68101
relativistic electrons, emission harmonics, inhomogeneous line broadening 78−25782
review of synchrotron radiation research 79−22505
RF accel. in KEK booster synchrotrons 77−83279
Saclay Saturn synchrotron, facilities and expts. 77−61636
Saturn 2, 100 MeV-3 GeV proton accelerator *(French)* 80−32547
SATURNE, MIMAS-low energy accumulator injector, project description 79−71985
SATURNE, status report on upgrading and future programmers 79−68001
Saturne 2, strong focusing and polarised beam acceleration in strongly modulated structures 79−72057
Saturne experimental facilities, energies and types of particle *(French)* 80−78465
Saturne I, five years of expts. with high-energy projectiles *(French)* 79−3262
Saturne II, beam liner computerised control system, organisation, function, hardware 77−83400
Saturne II, CRYEBIS, a multi-purpose EBIS 79−72166
Saturne II, new nucleation up to 2 GeV performance, research programs *(French)* 79−695
Saturne II, secondary emission detector system for beam profile monitoring 77−83402
Saturne II at Saclay, RF system 77−83301
SATURNE II proton synchrotron, magnet design and meas. 77−83241
Saturne II proton synchrotron, polarised ion source 77−34491
secondary emission chamber, stability tests in high flux photon beams 79−72077
secondary emission chamber at Brookhaven AGS 79−72187
Serpukhov, two stage synchrotron and IHEP storage complex, status report *(Russian)* 79−63829
Serpukhov proton synchrotron ion-getter pumps, operation evaluation 77−83347
Serpukhov proton synchrotron shield, mixed radiation dose equivalent outside 80−32530
SIRIUS, experimental study of the spectral, angular and polarization properties of undulator radiation 80−91338

synchrotrons continued
Sirius, shaping of highly stable flat top in excitation current pulse of electromagnet 78−5075
spin flip by adiabatic passage of depolarisation resonances 80−5415
SPS, CERN, damping of longit. instabilities 77−83372
SPS, CERN, extraction modes anal. 77−83255
SPS, FODO separated function lattice, design 77−83262
SPS, real-time control system, operating system principles 80−875
SPS, second order effects in sextupole-corrected SPS lattice 79−76196
SPS beam instrumentation, closed orbit correction 77−83305
SPS computer control system, operational experience 77−83292
SPS magnet system, nonlinear fields and their compensation 77−83268
super-proton-synchrotron at CERN, microtechniques *(Swedish)* 77−65370
superconducting, power supply and quench protection scheme 79−36445
superconducting dipole magnets coil motion 77−83237
superconducting dipoles, 2.5 T window-frame type, for small synchrotrons 79−54224
superconducting magnets in synchrotron, quench thresholds after proton beam exposure 79−31254
superconducting quadrupole magnets for hyperon expt. at CERN 77−26889
superconducting warm Fe dipoles, stress anal. 79−68041
synchrophasotron, 10 GHz, origin and development *(Russian)* 77−67921
synchrophasotron, acceleration of laser-injector-generated C nuclei 78−29675
synchrophasotron, Dubna, drift chamber system, charact., on line operation 77−6627
synchrophasotron, overload protection circuit for pulsed current using ICs 79−3263
synchrophasotron, system for coupling freq. of accelerating voltage with mag. field 80−23193
synchrotron, 50 MeV, with cyclotron preaccel., VUV source 77−61641
Synchrotron Radiation Source booster synchrotron combined-function magnets 79−31269
tevatron, Fermilab proton accelerator with supercond. mag. ring 78−835
therapeutic proton and heavy ion source capabilities 79−20629
Tomsk synchrotron, system of tagged photons 78−833
TRIUMF data interface 77−88304
TRIUMF facilities and kaon factory designs 79−85837
vacuum feedthrough, bakeable, with 22 pins, for monitor system of proton synchrotron 78−21798
vacuum technology, medium, high and ultrahigh, conf., Oxford, England (Apr. 1978) 79−63242
weakly focusing, polarised electron accel. *(Russian)* 77−75012
wiggler, helical wiggler and free electron laser *(Japanese)* 80−37658
zero gradient, betatron tune profile using main magnet pole face windings 77−83317
zero gradient synchroton proton recoil polarimeter 77−38511
zero gradient synchrotron, resonance extraction slow spill control system 77−83256
zero gradient synchrotron, synchronisation with booster injector 77−83253
ZGS, 30″ bubble chamber 80−91304
ZGS, 30 μA beam toroid for 750 keV polarised proton beam monitoring 79−68072
ZGS, acceleration of polarised protons 77−34488
ZGS, computerised meas. of injection betatron tunes 77−83312
ZGS, conception to turn-on 80−91298
ZGS, construction history 80−91299
ZGS, design engineer's view 80−91315
ZGS, early adventures 80−91301
ZGS, Effective Mass Spectrometer 80−91310
ZGS, experimental area operations 80−91316
ZGS, external proton beams 80−91307
ZGS, highlights and speculations 80−91324
ZGS, history, conference, Argonne, IL, USA (Sept. 1979) 80−90600
ZGS, history as seen from Washington 80−91323
ZGS, low level beam diagnostics for polarised proton operation 77−83311
ZGS, mini-computer based digital RF control system 77−83310
ZGS, non high energy physics programs 80−91320
ZGS, operations 80−91319
ZGS, polarised beam history 80−91311
ZGS, polarised beam program 80−91312
ZGS, polarised beam results, review 80−99361
ZGS, polarised targets 80−91309
ZGS, role in high energy physics 80−91306
ZGS, scientific program start-up 80−91302
ZGS, strong interaction counter expts. 80−91305
ZGS, superconducting magnet bubble chambers, history 80−91368
ZGS, technical history 80−91313
ZGS, the peak years 80−91303
ZGS, titanium vacuum chamber installation 80−91317
ZGS, universities role in the seventies 80−91322
ZGS, visual reminiscences 80−91321
ZGS 500 MeV booster synchrotron, data acquisition and control, sequential logic and minicomputer 77−83304
ZGS as seen from the midnight shift 80−91314
ZGS at Argonne, depolarising resonances effects on circulating polarised proton beam 77−83274
ZGS beam transport for transverse and longitudinally polarised protons 78−55074
ZGS booster, intensity and position meas. systems 77−83307
ZGS history, the early stages 80−91297
ZGS history, universities' role 80−91300
ZGS polarised proton beam splitting 78−13366
ZGS polarized beam facility, supercond. solenoids, magnet and cryostat design 79−31252
ZGS streamer chamber and kaon physics 80−91308
ZGS superconducting high-energy beam line 77−26903
ZGS technician's view of high energy physics 80−91318
d acceleration in CERN PS and ISR 77−83283
Al vacuum chamber and bellows, proton synchrotron appl. 79−68056
H^- polarised ion source, pulse operated, Lamb shift type, for acceleration of polarised protons *(Japanese)* 77−67929
Na vapour charge exchange cell 77−38542
$SmCo_5$ permanent magnets for accelerators 79−31273

synoptic climatology *see climatology*
synthetic rubber *see rubber*
system documentation *see program and system documentation*
system failure and recovery
see also operating systems (computers)
mass storage directory entry repair for lost data retrieval 78−77954
optical long focal length aerial reconnaissance system response to thermal shock 80−78939
system recovery *see system failure and recovery*
system theory
see also artificial intelligence; identification; information theory; modelling; pattern recognition; simulation
2-D polynomial matrices, factorisation and coprimeness 77−64915
biological systems and systems theory *(Japanese)* 78−24018
biology and medicine, systems theory, importance and motivations *(Spanish)* 80−104549
cerebral energy metabolism and memory 79−74629
classical philosophies of science, general systems theories challenge 78−86107
diffraction in dispersive media, system theoretical approach 79−98272
dissipative open system, dynamical transitions 79−64629
energy system synthesis, solar energy system 80−76614
environmental systems planning, design and control, conf. Kyoto, Japan, (Aug. 1977) 79−52962
Fabry-Perot interferometer response to AM light beams 78−16836
functional electrical stimulation orthoses, gait parameter variability *(French)* 77−9302
hydrological cycle in Lake Biwa basin, study *(Japanese)* 77−81951
incoherent electro-optical meas. systems with arbitrary stops and misfocusing *(German)* 78−1366
instability of evolving systems, elastic stability theory and catastrophe theory approaches 78−44442
learning in networks with minimal disruption 79−74628
linear systems with periodic coeffs., stability determ., numerical method 77−2535
magnetic hysteresis, probabilistic mathematical models *(Polish)* 77−80960
materials science, concept of system 80−101003
measurement dynamics rel. to system and information theory 78−8377
measurement techniques, error anal. using information, signal and system theory *(German)* 80−68164
metrology appls., survey 79−85111
multiexponential fluorescence decay, systems theory approach to anal. 79−59495
non-conservative systems, dynamics 77−2538
optical bilinear transformations, general props. 79−98305
radiography, systems approach to scale of equipment 78−57064
stratosphere, O_3 reduction due to pollution, system-theoretic model 77−73848
subharmonic and superharmonic synchronisation in weakly nonlinear systems 77−2534
transistor current gain characteristic as model for living structure 79−74590
visibility reduction by aerosols, visual acuity theory appl. 78−11997
volume-conductor fields of isolated axon, linear filtering problem 78−3463
walking-stick maps, syncope, rel. to chaos 77−63894
systems analysis
see also program and system documentation
accelerator and storage ring systems for inertial fusion 77−83474
algebraic model for CW thermal-blooming effects 79−94303
automated counting system, design philosophy 79−88923
biochemical systems anal., mol. biology, book 77−21468
biomedical instrumentation requirement 77−48894
conversion from two to three functional modes of logical address space 78−36981
Earth obs. systems, planning, design and control 79−58220
education, systems approach 79−35450
fission-fusion systems, laser-driven, nuclear and thermohydrodynamic calcs. 80−47696
LWR emergency core cooling component experience data, defect anal. programme 79−18010
neurotransmitter dynamic balance, systems and control theoretic anal. 78−44495
nuclear engineering, probabilistic systems reliability analysis for students 77−37698
nuclear power reactors in elec. utility system, short range system analysis method 77−50252
optical fibre communication systems, digital 77−65631
performance optimisation 79−89579
search for extraterrestrial intelligence 80−4274
storage reservoir analysis, mass-curve techniques, systems and perspective 80−8457
underwater camera data correl. and interpretation, systems approach 79−5688
water resources management, systems anal. and modelling techniques appl. 79−5518
wear, systems anal. and description *(German)* 80−103417
West German solar energy utilisation programme technologies 79−57366
systems design *see systems analysis*
systems engineering
see also systems analysis
air pollution control, prediction of pollutant concentration 79−52992
biomedical system development 77−5094
electro-optics, systems aspects, seminar, Huntsville, AL, USA (May 1979) 80−94921
heat transfer, artificially intelligent problem solver, system design outline 80−99916
high-performance quartz crystal oscillators, systems approach 79−54109
holographic one-tube goggle 80−78988
IEEE International EMC Symposium, Atlanta (1978) 78−82876
IR detector system limitations 78−77988
magnetron sputtering equipment and application status 79−83124
measurement engineering development trends *(German)* 80−86243
nuclear reactor safety analysis, BWR 77−38359
optical design, fabrication and operation 80−95986
optical storage medium specification and performance trends, review 80−43415
optical system tolerancing plan activities and documents 80−48382

systems engineering continued
optical-fibre communications 77−7016
pacemaker automated test system developments 80−30944
photovoltaic-solar thermal system role of high performance solar cells 79−61978
power satellite solar array blanket interface problems 79−96466
RF automatic test equipment, synthesised signal generator design 77−53875
solar power satellite design and system engineering issues 79−96465
transmission system design, influence of optical component baseband frequency response 78−1415
vacuum system engineering, integrated approach 79−67320
vacuum systems, integrated approach 78−70134

systems programming *see systems analysis*

systems software
see also operating systems (computers); program processors; utility programs
cephalometric tracing processing system, software development *(Japanese)* 80−94409

Szilard-Chalmers reactions *see radiochemistry*

T invariance
θ-vacua energy depend., P and T conservation in the presence of instantons 78−89628
atom+diatom, rot. inelastic scatt., mag. transitions, time reversal symm. 80−48066
axion properties, strong T and P conservation enforcement 79−67481
bound states from instantons 78−78087
broken symmetries at high temperature 80−42357
chiral symmetry spontaneous breaking, using vacuum stability condition 79−35986
colour gauge theory of strong interactions, P and T invariance 78−37153
cosmic matter-antimatter asymmetry and gravitational force 80−90586
Dirac equation, two-component first-order equations for the quantum-relativistic electron 79−17649
dynamically broken-gauge theories, P and T violation in QCD 80−9093
Einstein paradox and intrinsic time symmetry 79−71287
electromagnetic simulation of T-invariance in β-decay 79−30807
EM systems, parity and time inversion symmetries 77−45721
EM systems, parity and time inversion symmetries 79−67169
experimental progress, few-body aspects 77−22665
extended relativity, T-violation and new particle 80−37182
false effects in decay triple correlation, time-parity violation search *(Russian)* 78−78180
ferroelectrics, P- and T-nonconserving interactions, macroscopic effects 78−84532
fundamental physics with reactor neutrons and neutrinos [conf. ILL, Grenoble, France (Oct. 1977)] 79−59112
gauge theories, manifest L-R symmetry, strong P and T noninvariances and neutron electron dipole moment 79−63372
Glauber model and time reversal invariance 80−91020
hadronic interaction, time reversal invariance present evidence 79−63386
lepton-hadron scatt., polarised beam and target, review and survey of expts. and theoretical implications 79−67560
magnetic monopoles, PT-invariant theory of massive dually charged particles, Dirac-like eqn. 80−52429
massive particles with any spin. consistent eqns., Klein-Gordon divisor, review 80−73577
mechanical systems, follower load type, time invariant functionals 80−77609
(non)conservation of isospin, parity, charge conjugation, and time reversal invariance in intermediate energy phys. 79−80772
nonequilibrium stationary states, light scatt., broken time reversal symm. 79−28776
nucleon decay, T violation possibility and consequences in superunified theories 80−82917
P and T violating electromagnetic interaction of the quark in the instanton field 80−52430
Planck's constant, time invariance 78−93556
Poincare group, irreducible representations of groups containing subgroup of finite index 80−68384
PT asymmetry and four-fold EM degeneracy lifting, appl. to ring laser mode splitting 80−23606
quantum field theory, relativistic, discrete symmetries 80−68387
quantum gravity and time reversibility 80−82704
quantum mechanical eqn. of Kadanoff and Baym, time reversal noninvariance 79−17332
Racah time reversal and K_2^0 decay problems 80−78056
relativistic classical nonlinear field theory, PCT violation 77−65081
relativistic QFT, spontaneous symmetry violations 80−52411
rotationally inelastic scattering, mag. transitions, time reversal symm. 80−53105
S-matrix theory of overlapping resonances, constraints imposed by analyticity and unitarity 77−22656
static SU(2) Yang Mills eqns., with external charge sources, T-invariant 79−71638
strong hadron interactions, possible test in NN polarised scatt. 77−30402
strong P and T noninvariance, natural suppression in $SU(2)_L \times SU(2)_R \times U(1)_{L+R}$ gauge model 79−9303
strong P and T noninvariances in a superweak theory 78−82123
SU(2)×U(1), P and T invariance violation suppression, quark mixing angles 79−54278
SU(2)×U(1) gauge theories of leptons, T violation, leptonic decay and dipole moment 79−299
SU(3)×U(1) gauge models, exam. of weak currents and associated features 78−16975
superheavy boson decay, neutrino number and isotropy of Universe in grand unified theories 80−85852
tests in strong, EM and weak interactions 77−57532
time asymmetries and classical and quantum physics 80−22216
time reversal logic 79−30677
TP inversion in quantum gravity 79−58613
violation testin ^{184}W 922 keV γ-ray transition 77−71581
Wigner's random matrix model, time reversal violation 77−30542
β-decay, time reversal invariance and second class weak currents, review 78−37309
$D \rightarrow K^* \mu \nu$, in e^+e^- annihilation, T-odd asymmetry in CP violation model *(Russian)* 80−105885
$e^+e^- \rightarrow FF$, with polarised particles, weak asymmetries, unified gauge theory anal. 78−8636

T invariance continued
eN elastic scatt., polarisation effects, C- and T-invariance perturbation *(Russian)* 77−10256
K^0 decay, T-violation without assumed CPT 79−26249
K_1^0-K_2^0 system, T violation K^0 decay, book contrib. 78−78173
$K_2^0 \rightarrow k\pi$, k=2 or 3, Racah time reversal, a C,P,T scheme 80−78056
$K_L^0 \rightarrow \pi^- \mu^+ \nu_\mu$, transverse polarisation of μ, violation of time-reversal invariance 80−68448
Λ, polarised, β decay, ang. correl. parameters meas. 78−25044
μ decay correlations and lifetime meas. 80−77996
NN interaction, time reversal noninvariant NN potential in two nucleon system 79−54352
NN scatt. formalism 78−21463
$\nu(\bar{\nu})$p elastic scatt., final state polarisations, test for T-invariance and 2nd class currents 79−63466
ν oscillation, CP or T violation effects 78−21349
ν+hadron inclusive interaction, single-lepton and dilepton prod., test of T invariance 77−34146
$\nu_l \mathcal{L} \rightarrow \mathcal{L} \nu_l$ processes, possible T-violation, phenomenological model of neutral currents 77−30359
$\nu n \rightarrow \mu$ p, bounds on outgoing baryon transverse polarisation, T-odd effects 77−87966
$\bar{\nu} p \rightarrow \mu^+ n$ or $\mu^+ \Lambda$ or $\mu^+ \Sigma^0$, bounds on outgoing baryon transverse polarisation, T-odd effects 77−87966
$\nu p^+ \rightarrow \mu^- \Delta^{++} (\nu \Delta^+)$, Δ polarisation, test of T-invariance of weak and charge currents, comment 79−67531
$\bar{\nu} p^+ \rightarrow \mu^+ \Delta^0$, Δ polarisation, test of T-invariance of weak and charge currents, comment 79−67531
pp elastic scatt., 6 GeV/c, polarisation anal. 78−41568
π, photoproduction in E<450 MeV region, dispersion relations, CT invariance, review, book contrib. 80−47311
ψ' decay, Higgs bosons, five-quark model, P and T nonconservation 77−74686
$\Sigma^+ \rightarrow \Lambda e \nu$, transverse polarisation anal. 78−45919
$\tau \rightarrow K^* \pi \nu$, in e^+e^- annihilation, T-odd asymmetry in CP violation model *(Russian)* 80−105885
$\tau \rightarrow \nu_\tau n\pi$, T-violation effects, neutrino mass *(Russian)* 80−95294
^{110m}Ag, oriented, T-reversal test and struct. study 78−86505
^{56}Co beta decay, limit on time-reversal violation from β-γ correl. meas. 77−34261
^{57}Fe, γ-ray emission, test of time reversal invariance 78−29421
^3He(p(polarised),p)^3He, nuclear force and T-violation effects 78−4797
^{191}Ir 129 keV transition, atomic screening, time reversal violation 80−106011
$^{19}Ne \rightarrow {}^{19}F + e^+ + \nu$, test of time reversal symmetry 77−30521
^{49}Ti, polarised, T violation test, γ-ray directional correlation 78−62330
TlF, P- and T-violating interactions in hyperfine struct., mol. beam reson. expt. 80−53019

Ta *see tantalum*

table lookup
see also data handling
attenuator monitoring, computational tables and computers for efficiency improvement 77−79073
formant frequency and bandwidth conversion to reflection coefficients 80−91975
holographic numerical optical processor configurations 80−48194
magnetic field reduction to pole, fast Fourier series algorithm 77−5333
nuclear reactor multivariable parameter meas. and display microprocessor solution 79−72221
signal processing of ECG waveforms, automatic, using syntactic methods 79−62386
truth-table look-up optical processing utilizing binary and residue arithmetic 80−69334

table-top computers *see minicomputers*

tables (data) *see collections of physical data*

tables (decision) *see decision tables*

tachometers
see also angular velocity measurement
biological precision rate calibrator 79−20731
cardiac tachometer, instantaneous, with extendable range 79−20700
cardiotach, heart-rate monitoring cct., construction 80−30920
DC, AC and pulse generator, features 79−63198
digital, error analysis 80−90832
digital, for heart rate measurement 80−17162
digital, for meas. steady-state shaft speed 79−6101
digital tachometer using LEDs *(Spanish)* 79−54112
Doppler effect based, microwaves non-conventional appl. survey *(Italian)* 80−13093
flowmeter for exact meas. and reproduction of high gas flow rates 79−77309
gyro, parameter meas., mechanical spring simulation under work conditions 79−67263
gyrotachometer, error autocompensation at angle vibr. of base *(Russian)* 78−16782
hot wire tachometric probes, calibration instrument features *(Italian)* 79−72966
induction tachometer for measuring speed of rotating rolling mill rollers 79−80584
light activated, non-contact, with 0 to 20000 and 10000 to 30000 RPM ranges 79−80602
optical, with contamination prevention 80−73344
optoelectronic revolution counter for X-ray tube anodes *(German)* 78−12678
speed meas. devices survey, industrial appl. *(French)* 79−93105

tachyons
active Lorentz transformations, consequence of lack of invariance 79−84951
active Lorentz transformations, consequence of lack of invariance, reply 79−84952
Backlund transformations in nonlinear systems, tachyon solitons and their interactions 78−54181
Bethe-Salpeter eqn., Lagrangian bound state formalism, dynamical vacuum instability 78−74146
bi-metric gravitation theories, kinematical consequences of causal tachyons 78−21038
black hole EM energy extraction through charged tachyons 79−17013
black holes, test particle motion in crossing Schwarzschild surface, book contrib. 79−44816
bradyon interactions, superluminal and subluminal EM fields 80−12902

tachyons continued
bradyons and tachyons, unified approach by conformal transformations 77−67282
bradyons and tachyons, unified description using dynamical SO(4,2) symmetry, book contrib. 79−44834
causal and noncausal wave propag. 77−49593
causality, problems in theory of tachyons 78−28945
causality for tachyons in macrophysics, extended relativity 77−22411
causality in macrophysics, paradoxes, extended relativity theory 77−22406
causality laws, violation with tachyon discovery, book contrib. 79−44720
causality problems in special relativity, tachyons in an expanding universe 79−67155
causality recovery in macroscopic processes 77−2542
causality recovery in special relativity for tachyons 78−73843
causality violation 77−22412
causality violation by controlled creation and absorption of tachyons 77−45693
causality violation by controlled creation and absorption of tachyons, answer 77−45694
causality violation in controlled creation and absorpt. of tachyons 77−22413
charged, detect., theory, rel. to general relativity 78−41614
charged extended tachyon EM radiation, collision with neutral particles 80−4522
charged tachyon in dispersive medium, EM radiation *(Russian)* 78−74187
charged tachyon in dispersive medium, radiation energy *(Russian)* 78−74186
charged tachyons, Cherenkov radiation in vac. 77−57210
Cherenkov radiation, thought expts. at superluminal relative velocities 77−57186
classical field theory 77−64949
classical special relativity mechanics, classical particles with unusual props. 80−77615
classical theory of Recami and Mignani, rigorous approach, formal proof 77−26171
complex physical quantities and space-like states, book contrib. 79−44723
conformal relativity, unified description of bradyons and tachyons based on dynamical SO(4,2) 77−67352
cosmic ray extension air showers, $\geq 10^{14}$ eV, 290 μs preceding period 77−78588
cosmic ray tachyon monopole search 79−16770
cosmological evolution, role and nature of tachyons *(Russian)* 79−17150
covariant quantum equations in curved spacetime, Lorentz covariance and tachyons, book contrib. 79−44725
detection, using Cherenkov and ToF detectors, book contrib. 79−45125
detection by black holes 79−17012
dual string theory, lattice approach, tachyon problem exhibited 78−4840
EAS, search for tachyons 79−16780
electromagnetic and hadronic props., book contrib. 79−44721
elementary particle strong interactions, tachyons and virtual fields 79−12970
EM analogue, production by reflected ultrashort laser pulse *(Russian)* 77−46680
emission and absorpt. in six dimensional relativity 80−31502
emission from white holes 77−33718
existence of quarks, monopoles, tachyons, etc., review of expts. 78−12872
extended relativity, absorpt. of tachyons 78−32672
extended relativity, macroscopic tachyons absorpt., paradoxes 77−57188
faster than light phenomena in special and general relativity, book contrib. 79−44817
faster than light processes, causality 77−54061
field model, Lee-like *(Korean)* 78−50058
field theories with tachyons, conventional treatment book contrib. 79−58888
fluid droplet model in framework of two centres particles 80−105868
four-velocities in quantum theory, K-space 78−49720
free falling body in field of black hole, superluminal speeds 77−78816
general relativistic eqn. solns. 80−36917
gravitational field eqns. 77−57242
gravitational field of charged tachyon 78−54282
hadronic resonance props., consideration as compound of bradyons and tachyons 78−58163
hadrons, tachyon and bradyon compound system model based on conformal relativity 79−93343
hadrons as compounds of bradyons and tachyons, ground state and decay anal. 78−58156
information flow, causality and classical theory of tachyons 79−9429
information flow, causality and the classical theory of tachyons 78−82261
interaction with gravity, rel. to cosmology and black holes 79−25839
joint distributions and tachyons 79−58541
Kerr source, energy extraction by tachyon injection 79−48844
kinematics and dynamics of faster than light motions *(Russian)* 79−71247
kinematics for scatt. of spacelike momentum 78−12559
Klein Gordon equation, propag. of solns. with arbitrary complex mass 79−21924
Klein-Gordon eqn., one-dimens., nonrelativistic reduction and interpretation 77−74262
light radiation from tachyons, direction of emission 77−33862
light-like motions of particles in gravitational fields 78−4480
Lorentz group, relativistic semigroup and tachyons *(Russian)* 77−82386
Lorentz transformation, comment on Gonzalez-Gascon effect 77−33863
Lorentz transformation, reply to comment 78−49656
Lorenz invariance of tachyon theories 78−54581
magnetic monopoles, tachyon monopoles, existence in 6 dimens. space, superluminal transforms. in Dirac theory 78−54183
magnetic monopoles and tachyons in the de Sitter universe, book contrib. 79−44726
magnetoelectric dipole gas as explanation of biocosmic phenomena, summary of phenomena 80−8241
magnetoelectric dipole gas as explanation of biocosmic phenomena, theoretical concepts 80−8242
magnetoelectric dipole gas as explanation of biocosmic phenomena, theory development 80−8243
tachyons continued
magnetoelectric monopoles, polymerised, delocalised clouds as possible cause of auras 80−41362
massless 't Hooft model, tachyonic modes, vanishing of scalar density 80−77949
massless chromodynamics, vacuum rearrangement 78−70327
meta universe, tachyon energy and momentum, contribution to gravitational field 77−45760
Minkowski space, complex, superluminal boost in x-direction, Lorentz transformation, tachyonic connections 80−105497
monopoles, tachyons and related topics, book 79−44718
monopoles and massive photons 78−20986
multiply-connected space-time, black holes and tachyons 79−30315
non-Abelian gauge theory of quarks and gluons in two dimens. 79−30654
nonequatorial tachyon trajectories in Kerr spacetime, and second law of black hole phys. 79−71244
observations in nucl. emulsions possibly overlooked 80−12963
photon-tachyon interactions and the isotropic photon flux 80−446
production branching ratio in e^+e^- annihilation, search using Michelson expt. 77−54127
propagator of spinless tachyons determ. 77−74263
pseudospherically symmetric tachyon perfect fluids 79−35599
quantum field theoretical study of tachyons, book contrib. 79−58887
quantum field theory description 80−18069
quasi catastrophe theory, appl. to classical tachyon theory, imaginary units 77−22414
quasi-catastrophe theory, tachyon existence, imaginaries, and causality, book contrib. 79−44815
quaternion quantum mechanics as the description of tachyons and quarks 79−30273
quaternionic formulation superluminal transformation, in complex space-time 79−53973
quaternions and subluminal and superluminal Lorentz transformations, book contrib. 79−44724
reference frames and the velocity of light, book contrib. 79−58542
relativistic quantum theory, space-time states, book contrib. 79−58886
relativistic semigroup, Lorentz group and tachyons *(Russian)* 77−82801
relativity, special, 6-D, centre-of-mass frames of pairs of particles, bradyons, luxons, tachyons 80−77614
relativity, superluminal frames and tachyons 79−58543
rest frames for tachyons and photons 77−60928
scalar waves in Schwarzschild space-time 78−45558
Schwarzschild black hole, tachyons from free falling body 77−53625
Schwarzschild metric and tachyon production inside horizon 78−36635
search for preferred frame of reference, book contrib. 79−44722
second law of black hole physics and tachyons 79−49117
six dimensional space time formalism of electromagnetism, mag. monopole behaviour of electrically charged tachyons 78−54182
space-like geodesics in fields of charged mass point and uncharged static cylinder 77−53805
spacelike geodesics in the Nordstrom geometry 79−88852
special relativity, causality recovered 77−82387
special relativity, tachyons and causal paradoxes, reinterpretation principle 79−84949
spin 1/2 tachyons, nonexistence of conserved probability, Dirac eqn. general soln. 77−67554
spin-1/2, quantum mechanics 77−5693
spin-s tachyons and tachyon wave propag., book contrib. 79−58890
spinning tachyons as particle constituents, free spinning point particle theory 78−41155
strong interaction field theory, role of tachyons and virtual fields, book contrib. 79−58889
strong interaction field theory, tachyon role 79−9353
SU(2) coupling model with tachyon fields *(Korean)* 77−49844
supergravity, tachyon absence in supergravity and classical Einstein gravity 79−67208
superluminal and subluminal causal transformations through transformations of metrics 78−28943
superluminal frames and tachyons, introductory review, generalised Lorentz transform. derivation 78−69983
superluminal frames and tachyons, introductory view, book contrib. 79−44719
superluminal Lorentz transformations, imaginary quantities problem in extended relativity 80−52020
superluminal Lorentz transformations, imaginary units, motion of tachyon 80−86082
superluminal particles and rods, visual appearance 78−89334
superluminal particles motion in gravit. field of nonrot. black hole *(Russian)* 78−93103
synchronization in special relativity and related theories 79−71243
tachyon dust universe 78−24583
tachyon wave propag. and spin-s tachyons, book contrib. 79−58891
tachyon-reggeon scatt., string interaction, physical picture 77−18241
tachyonic matter, based on discrete unitary representations of Poincare group for spacelike momenta 79−44822
tachyons without paradoxes 77−60931
time symmetric tachyon universe, momentum flux, press. 78−86153
toxic air ion effects due to tachyon magnetoelectric dipoles and beta rays 80−35999
two body correlations through tachyon exchange 80−42367
two-body interactions, tachyon exchange 80−82960
unified approach to bradyons and tachyons by conformal transformations 77−60934
vacuum instability, tachyon existence 77−9884
Yang-Mills coloured theory, string like phase 78−32990
Yang-Mills theory, tachyon bound state and vac. instability 78−29244

tackiness *see adhesion*

TADMR *see microwave-optical double resonance*

tandem accelerators *see particle accelerators*

tantalum
see also nuclei with .....
absorption kinetics of H_2, 77-700K, effect of O_2 sorption layers 79−95169
absorption rate of H, metallic film effect 80−49525
adatom, on W (110), dipole moment, field emission meas. 77−47674
adsorbed layers of H_2, energy loss spectra *(French)* 79−83069
adsorption, of LaB_6, work function 80−20039
adsorption of CO, AES obs. 77−35818

tantalum continued
adsorption of $CO(CO_2)$, FEM and flash filament method exam. 78−43245
adsorption of Cs, direct meas. of adsorpt. isobars 78−43235
adsorption of K, work function depend. on surface coverage 77−11788
adsorption of O_2, FEM obs. of work function changes 78−26771
adsorption of Zr, low-temp. mobility, surface struct. 77−20197
adsorption on Au on (100) surface, model 77−1321
adsorption on W (100), effect on surface reson. 79−65983
AES at very low energies, caesiation 77−69946
anodic barrier film characts., ISS/SIMS 78−53021
anodic film, electrochem. reactions by tunnel current 77−81340
anodic oxidation, open-cct. transient method for overpotential anal. 78−27776
anodic oxide coating effects on mechanical behaviour 77−32659
anodic oxide films, space charge, TSC obs. 77−32326
anodic oxide layers, depth profiling by sputtered neutral mass spectroscopy 77−77833
anodisation constants, for oxide thickness prediction 77−48574
anodised layer, structure and stoichiometry, thickness effects 77−77634
atom, 5d level open shell interactions, 304 Å photoelectron spectrum 80−87087
atom, α-particle impact K-shell ionisation, 40 to 110 MeV 78−17752
atom, γ-ray absorption cross-sections, 10-160 MeV 78−90136
atom, elastic scatt. of 145 keV gamma rays 79−13680
atom, even config., parametric calcs. 78−82631
atom, Kα line widths, precise meas. 78−62761
atom, K X-ray energy, excitation mode depend. 78−17597
atom, K X-ray energy, excitation mode depend. 78−17598
atom, K-shell electrons, Compton scatt. of 1.12 MeV gamma-rays 77−68016
atom, K-shell X-ray energy, excitation mode depend. 77−18824
atom, K-shell X-ray energy, excitation mode depend. 79−26926
atom, KLL Auger emission, de-excitation of double L vacancy states 77−18886
atom, L-shell internal excitation accompanying L-capture 80−95726
atom, L-subshell ionisation cross-section ratio by ion beam impact, projectile charge and vel. depend. 77−6920
atom, L-subshell ionisation with high vel. positive ions 79−50122
atom, magnetic hyperfine struct. 78−934
atom, nuclear K-X-ray satellites, Z=50-83, by α-bombard., 17.5-22.5 MeV 80−42984
atom, partial level density, statistical props. of atomic energy levels 78−70732
atom, photoelectric cross section, derived from total absorpt. cross sections 77−10646
atom, photoelectric cross sections for 323 keV gamma rays 77−88432
atom, Rayleigh scattering at 59.34 keV through 60° to 150° 77−83547
atom, total to K-shell photoelectric cross section ratios, 145 to 662 keV γ-rays 77−54545
atom, X-ray fluoresc. yields in KLL Auger emission 77−54525
atom total to L-shell photoelec. cross section ratio 77−30836
auto-cathodes, effect of O_2 on emission and surface diffusion *(Russian)* 79−77892
autocathode, influence of electric field and heating on work 80−7478
bamboo struct., wire, high-temp. rheology 77−1851
BCC, band struct., generalised APW method using variational expression 80−6695
BCC, neutron-irradiated, Frenkel defect spontaneous recomb. volumes 79−60355
BCC, stress-induced interaction and ordering 79−42057
BCC crystal, elastic constants, thermal expansion and bulk modulus 80−6452
BCC lattice, strain ordering in interstitial solutions 80−107420
bombarded by Cs^+, transient emission of continuous photon spectrum by cathodic sputtering products 79−74046
bremsstrahlung emission meas., using vac. UV isochromat spectrometer 77−74521
capacitor, stress wave emission anal. in resistance welding 79−11739
chemical vapour deposited, kinetics and microstruct., pressure and temp. depend. 80−11569
coating of mild steel at atm. press. using CVD method 80−55591
coating of mild steel by CVD 78−15594
corrosion by molten alkali metal hydroxides and liquid Li 77−44414
corrosion resistance in 1M $LiAsF_6$/THF, suitability for organic electrolyte Li secondary batteries 79−100387
corrosion resistant pure metal, passivity and pitting in chloride solutions 78−44258
deformed at 4.2K, electrical resistivity recovery spectrum, stage III 77−8895
density, rel. to elastic const. calc. from US meas. 77−86079
density of unoccupied electronic states, UV isochromat spectra and SXAPS 79−77977
desorption kinetics of halogens, pulsed ion beam method 80−34300
desorption of O_2 in vacuum, thermodynamic props. calcs. *(Russian)* 80−54501
determination, in Mg alloy, emission spectrographic DC arc-powder technique 78−48713
determination in ore, spectrochem. method 79−16075
diffusion and surface distrib. of N, probed by (p,γ) resonance broadening method 78−38918
diffusion anomalies, vacancy model *(French)* 77−43366
diffusion in V, 1100 to 1800°C 77−24443
diffusion of H_2, in single crystal, Debye-Waller factor, neutron spectroscopy 79−37881
diffusion of H_2, isotope effects, crystal field stabilisation 80−59728
diffusion of H_2 *(Japanese)* 78−10221
diffusion of H, book contrib. 79−82390
diffusion of H, expt. compared with theory for light interstitial diffusion *(Russian)* 77−15632
diffusion of H, neutron radiography meas. 77−39696
diffusion of H and D at high conc. 78−26731
diffusion of H and D in Ta, low temp., from quenching and annealing study 80−6555
diffusion of H and trapping 80−70447
diffusion of interstitial O_2, sink/barrier phenomena 79−60553
diffusion of O, new EMF method 77−84994
diffusion of O and N, statistical calcs. on Arrhenius lines 80−59722
diffusion of U at high temp., determ. by neutron fission tracks meas. 77−89587
tantalum continued
edge dislocations, study by transmission channelling of MeV ions, expt. setup 80−29098
elastic constants, temp. depend., H_2 effect 77−32610
elastic moduli, effect of H and UHV annealing 77−90389
elastic properties, at high temp. 80−30007
electrical and thermal resistance at low temp. *(Russian)* 78−68007
electrical resistance temp. depend. in solid and liq. states, 2200-4200K 78−10415
electrical resistivity, 4.5-300K, singularities found *(Russian)* 78−26842
electrical resistivity due to interstitial H (D) 80−96848
electrnic sp. ht. and heat conduction, temp. depend. 78−71865
electrode, anodised, meas. of electrochem. reactions, appl. to tissue stimulation 78−95931
electrolytic polishing, use of pure FSO_4H 78−85094
electromigration of H, temp. depend. *(Russian)* 77−84986
electromigration of H, temp. depend. of mobility, 20-250°C *(Russian)* 78−47587
electron irradiated, energy and orientation depend. of at. displacement 79−99244
electron irradiation, bremsstrahlung yield and absorbed energy distrib. 79−99245
electron-phonon interaction, calc. using APW band struct. calcs. and measured phonon spectra 78−14869
electron-phonon interaction, relativistic, APW calc. 80−92837
electron-stimulated desorption of O_2, bound state obs., 300K 77−85082
electronic density of states, optical mass and DC elec. resist., Slater-Koster interpolation 77−15731
electronic properties and reflectivity, iterative empirical pseudopot. calc. 77−76745
electronic structure, APW calcs., self-consistency and exchange effects 77−66109
electronic structure, thermoreflectance studies 80−76047
electrotransport in Th, 1370-1665°C 78−59979
electrotransport of H(D) at high H concs. 80−34246
embrittlement, by O_2 study using tensile strengths, SEM fractrography 79−79109
emission current effect on superconductor critical parameters 79−91185
emittance at 400 to 850K and normal spectral reflectance at room temp. 77−20813
enthalpy, 2400 to 3270K *(Russian)* 77−66031
epitaxial layers, influence of formation conditions on struct. *(Russian)* 80−20045
evaporated film, adsorpt. of CS_2 and H_2S, 195 to 473K 79−33197
field evaporation patterns, multilayer 77−59675
film, β-phase, Ta^{n+} transport number during anodic oxidation 79−39036
film, amorphous, UHV deposited, elec. and struct. props. obs. 78−6233
film, anodisation voltage relationship to oxide thickness *(German)* 78−11443
film, BCC, optical props. 79−78781
film, bias ion beam sputter deposited, elec. props. and structures 79−82692
film, CVD on silica, struct. and mech. props. 77−24965
film, deposited by cylindrical magnetron sputtering, internal stresses, optical reflectance and elec. resist. 77−43449
film, deposition by ion beam sputtering 77−73228
film, deposition parameters, struct., and elec. props. 77−81222
film, determ. of thickness and O, N content 78−80824
film, electron beam evaporator for in situ deposition studies in UHV electron microscope 80−40264
film, evaporated, adsorpt. of SO_2, corrosion 78−79897
film, evaporated, interaction with BCl_3, HCl, adsorpt. 78−75945
film, evaporated, supercond. transition temp. rel. to struct. and deposition parameters 77−85377
film, H^+ and D^+ sputtering in energy range 0.6 to 15 keV 79−78808
film, ion bombardment with N_2^+, Ar^+, struct. changes, chemical compound formation *(Russian)* 78−95084
film, nucleation of α or β phase, impurity effects 77−24493
film, on Si, obs. of film-substrate interaction 77−1324
film, oxidation in ambient conditions resist. and ellipsomatic meas. 79−34209
film, photoemiss. from conduction band and core levels 77−16464
film, planar-magnetron-sputtered, phys. and elec. props. 80−6673
film, planar-magnetron-sputtered, props. 79−82474
film, reactively sputtered, N content determ. from Fourier anal. of X-ray diffr. profile 77−76693
film, RF sputtered, thermoelec. power, Hall coeff. and struct. props. 77−43743
film, sputtered, physical props. 79−77938
film, superimposed on Nb film, cation-transport processes during anodic oxidation, Rutherford backscatt. and nucl. microanal. 79−20264
film, vacuum-deposited, gas adsorpt. effects on photoelec. props. 78−15298
film deposition by sputtering, influence of Ar plasma 77−69988
film on Corning glass, N and O content nondestructive determ. *(German)* 78−43272
film on GaAs, form. of Ta_2O_5 after oxidation 79−61769
film on sapphire substrate, orientational growth, epitaxial textures, nucleation textures *(Russian)* 80−75454
film sputtered onto Cu substrate, microstruct. and supercond. props. 77−85370
films, vac. evaporated, optical cond. 80−76100
flow stress, temp. and strain rate depend. 77−77534
flow stress at superconducting transition, temp. and strain rate depend. 78−2617
flow stress temp. depend., effect of interstitial atom clustering and embrittlement *(Russian)* 78−34538
foil, crack growth resistance, straining stage of SEM 77−25124
foil, defective anodic oxide films, elec. characts. 77−12039
foil, electron beam deposited, periodic chemical var. effect on mech. props. 79−91590
foil, electron energy loss spectra 80−7452
foils, coated with thin H-permeable Pd film, AES and SIMS 79−52467
gamma-ray attenuation meas. using Ge(Li) detector 78−17539
gamma-ray elastic scatt. cross section at 279 keV 79−26421
gasification by atomic F, high temp. kinetics 78−53019
heat capacity, 10^8-10^9 K s^{-1} pulsed heating, (2-4)×10^3K 78−14473
high temp. radiative props., expt. determ., spectral emissivities 80−74718
hollow arc cathode, emission current density 78−76574
hydrogen embrittlement, effect on ductility *(Japanese)* 80−66636

tantalum continued
implantation of Si, Al, Hf, Ta into InP and GaAs, form. of protective oxide 78−79622
implanted Ne, depth profiling using $^{20}Ne(p,\gamma)$ 79−7621
interaction with gases, H_2, N_2, O_2, CO, water vapour and hydrocarbons *(German)* 79−74296
interatomic pair potential, phonon spectra 80−33927
intermediate state, muon spin rotation 79−56446
internal equilibrium, cryst. dynamics, lattice dynamical theory of BCC metals 78−79688
internal friction and elastic constants, reson. vibrs. of metal spheres 78−15443
internal friction measurements, of O_2 and N_2 diffusion 78−75888
internal friction peaks, induced by work hardening, low temp. relax. spectra *(French)* 77−1844
interstitial ordering, O effect, $Ta_{64}C$ artifact 79−99185
ion, electron cyclotron resonance source *(French)* 78−29680
ion bombardment, energy distrib. of positive secondary ions and sputtered atoms 77−32485
ion implantation effect on corrosion behaviour of pure Fe 78−31559
ion induced continuum emission 80−89025
ion irradiated, ordered void arrays 78−34553
ion plated with Pd and Ni, prep., H_2 absorption and desorption rate *(Japanese)* 80−108358
ion prod. in hollow cathode source 78−74525
kinetics and thermodynamics of reaction with N_2 *(German)* 79−74415
Knight shift and hyperfine fields, core polarisation contrib., nucl. acoustic reson. determ. 79−51868
Knight shifts obs. with 6.2 keV ^{181}Ta Mossbauer resonance 79−11369
L-subshell ionisation cross section, branching ratios, fluoresc. yield, Coster-Kronig factors 80−43166
lattice atom displacements near end of implanted μ^+ tracks 78−55890
lattice distortion and migration energy of H impurities 78−30796
lattice dynamics, local frequency spectrum, mean thermal displacement of H 80−59604
lattice dynamics, seven parameter model 79−90739
lattice parameter, X-ray meas. 77−89406
lattice vibrations, Debye temp., freq. wave vector dispersion relations 78−63818
light ion ranges meas. by (p,γ) reson. broadening, 20-100 keV 77−69023
liquid, thermophysical measurements, up to 7500K 78−43136
LMFBR control material, integral capture cross section meas. in CFRMF 77−26760
luminescence characteristics of pure surfaces acted on by flux of field emission electrons 80−100695
magnetic hyperfine field meas. in Cr, spin density waves detected 78−60364
melt, thermal expn., 1146-2288K 78−43148
metallisation of Si-SiO_2 interface, induced stress meas., X-ray transmission topography 79−24434
microvoid form., gaseous impurity atom effects, positron annihilation study 80−49275
microyielding in single crystal, high amplitude damping 77−52396
microyielding in single crystals, microflow parameters 77−52395
molten, static struct. factor 77−19865
Mossbauer spectra, 2nd-order Doppler shift, 1-100K 79−91317
Mossbauer states at 6.2 keV, freq. modulation 80−7212
Mossbauer transition of ^{181}Ta at 6.2 keV and high temps. 77−12269
muon$^+$ spin resonance, diffusion, temp. depend. 78−39490
muon diffusion, μ^+SR meas. 78−39487
muon location and diffusion, μSR 79−56693
muon quadrupolar interaction expansion of crystal lattice *(Russian)* 79−15388
muon trapping, Knight shift, rel. to H interstitials 80−50247
near-threshold displacements in single crysts., electron-irrad. induced defects, resistivity meas. 79−60356
negative surface ionisation 77−77335
neutron irradiated, microstruct. and swelling 77−69006
neutron yield calcs., electron beam incidence 78−95622
nitridation by ionised glow-discharge to form FCC Ta_xN_y 77−52266
NMR-γ double resonance, Mossbauer absorpt. spectra *(Russian)* 80−34824
NMR-Mossbauer double reson. 80−40019
optical properties and electronic props. 79−42439
optical spectroscopy, for investigation of electronic struct. 78−91611
oxidation comparison with O_2 adsorption, SIMS 78−15273
oxidation in O_2-N_2 and O_2-inert gas mixtures 78−3255
oxide layers, combined SIMS, AES and XPS investigation 79−33199
phonon density of state determ. from thermodynamic crystal functions *(Russian)* 79−82291
phonon frequencies calc. 79−19329
photo field emission spectroscopy of band structure by He-Ne laser irrad. 80−55276
photodesorption of CO forming CO_2 79−52777
photoelectric cross section, total to K-shell ratios 78−5188
photoelectric cross sections, from total absorption cross sections, 5 to 130 keV 79−26947
photoelectric cross sections of low energy photons 78−46309
photoelectric cross-section at K-edge measurements 78−2983
photoemission, two-photon, induced by picosecond laser pulses 77−77347
photofield emission spectroscopy of band struct. 78−35261
photoneutron yields released by incident electrons, improved calc. 80−27630
pionic atom, quadrupole hyperfine interactions, nucl. moment 78−37772
plasma production, relativistic electron beam impacting foil 79−77403
plastic deformation effect on positron annihilation and supercond. transition *(Russian)* 77−39993
polycrystalline, dislocation relaxation under high pressure 79−77605
polycrystalline, trace diffusion of nuclear reaction products, lanthanides 78−22896
positive muon diffusion in single cryst. 78−80267
positron annihilation and vacancy formation 80−16119
positron trapping and annihilation at vacancies 80−29823
powder, cathodic electrodeposit, effect of electrolyte composition and process parameters, on particle size distribution 80−16233
powder, extraction of N_2 by vacuum hot extraction method, effect of graphite *(Japanese)* 78−84729
powder, particle shape effect on parameter of vol.-porous anodes of electrolytic capacitors 79−61539
powdered, N_2 determ. by vacuum hot extraction with graphite addition *(Japanese)* 77−48683

tantalum continued
proton implanted, anelasticity, internal friction meas. 79−24560
purification from Nb during precipitation from gaseous phase, during H_2 reduction of $NbCl_5$ and $TaCl_5$ *(Russian)* 78−44017
quantitative anal., for D, by ion microanalysis 78−56945
radiance temperature at melting point 77−15603
radioisotopic X-ray fluorescence determ. in industrial samples 77−52702
range and range straggling of heavy radioactive ions 78−22776
range of $^{27}Al^+$ ions, meas. by (p,γ) reson. broadening 79−46729
rare metal ores, quantitative relns. between Ta, U, Th and Zr 77−56629
reactive sputtering yield 77−66566
resistivity variations caused by H and D interstitials, isotope effects 77−89750
resonance absorpt. at L edges and white line 79−61469
rolled single crystal, recovery and recrystallization 80−3093
secondary electron emission coeffs. for multiply charged ion bombard. 78−11051
secondary ion emission, normalised energy spectra from Hg^+ impact 80−45193
SEM exam., ultra-high vacuum, secondary electron emission dependence on electron beam dose, surface interactions from AES and ELS 80−61209
shear elastic constant, anomalous temp. behaviour, US study 80−79855
sintering with transition metal additions 78−15335
slip, between 0.7 and 40K 78−19808
solubility of H_2 at high temp. 77−84934
spectrometer graphite furnace, Ta foil lining, at. spectrosc. 78−74078
spray coating form. in pure Ar atm. 77−32709
sputtered film., internal stresses, effect of substrate orientation and rotation 79−77968
sputtered film, stabilisation of β-modification by Ta-Si interlayer, SIMS depth profiling 80−54568
sputtered films, difference between α-phase layers and β-phase layers 79−52116
sputtered layer, thermal oxidation, reaction kinetics 78−39959
sputtering, low energy, H, D and He ions 80−100734
static and dynamic props. of O and H impurities, Mossbauer meas. 80−7246
stopping power for 0.3-1.5 MeV protons 79−55801
stopping power for 28 MeV α-particles, re-evaluation 78−79651
stopping powers for 28.8 MeV α-particles 77−80556
stopping powers for 8.78 MeV α-particles 77−80557
substrate, TiB_2 coating prep. by CVD and interaction with substrate 79−24680
superconducting, muon spin relaxation *(German)* 80−50015
superconducting crit. temp., functional derivative with electronic density of states, Eliashberg eqns. 79−56368
superconducting intermediate state, mag. props. and N-S surface energy 78−2633
superconducting point contact, 9 GHz complex impedance 77−28303
superconducting transition temperature, ab initio calc. 80−25036
superconductive transition point as reference temp. 80−107943
superconductor, effect of changes in $\alpha^2(\Omega)F(\Omega)$ on the zero-temp. energy gap 80−97025
superconductor, internal friction at T_c *(Russian)* 77−36026
surface, adsorbed C^+ layer removal, by 20-30 keV Ar^+ bombardment, in plasma 77−76103
surface, decomp. of hydrocarbons, O or N surface segregation effects 80−55654
surface, H_2 adsorption, mass spectra and field-emission obs. 77−76673
surface, interaction with F_2 and fluorides at low temp. and high press. 78−39700
surface, Lyman-α emission from proton bombard. 79−91503
surface, nonstationary heating and oxidation in low temp. plasma flow, heat and charge transfer obs. *(Russian)* 80−104341
surface, secondary ion emission mechanism, under Hg^+ ion bombardment 79−100013
surface, simultaneous interactions with Cl_2 and O_2 under low press. and high temp. 80−71938
surface (110), electron-stimulated desorpt. of O 78−2363
surface (111), 100 eV electron bombardment adsorbed mol. luminesc., coherent bremsstrahlung *(Russian)* 78−31290
surface (111), electroluminescence in 200 to 630 nm range 80−103997
surface (112), oxidised, emission and work function, K adsorption effects 78−11060
surface energy distrib. of secondary electrons during relax. of metastable inert gas atoms *(Russian)* 77−85861
surface ionisation by laser-excited Li beam, quantum yield 79−87540
surface layers, Mossbauer conversion electron studies 78−15068
target impurity effect on laser produced expansion, ion spectrography 80−43945
thermal cond. and emissivity meas. using imaging furnace 80−103667
thermal conductivity, 0.3-20K, temp. and impurities effects 78−14883
thermal conductivity, 4.5 to 200K *(Russian)* 80−103665
thermally oxidised, ^{16}O conc. profiles anal., using (d,p) and (d,α) reactions 79−5215
thermo EMF, effect of H diffusion 79−23950
thermoelectron emission, S impurity atom effects, electron spectra *(Russian)* 77−8712
thermophysical meas. above 2500K, apparatus 77−45845
thermophysical props. and neutron absorpt. 80−103488
thin film, elec. cond., strain gauge factor, ion bombardment effects 80−80417
thin film deposition by high current ion beam sputtering, struct. and elec. props. 80−59837
thin film standard target for Rutherford backscattering microanalysis 79−2882
transport of H, study by neutron radiography, review of results 78−59961
treatment, of graphite atomiser tubes, for high temp. AAS 78−73093
unipolar arc damage in hot, dense D plasma 79−3235
vacancy annealing stage after heavy ion implantation, Mossbauer meas. 78−39463
vacancy formation and migration energies, positron annihilation meas. 77−84739
vacuum technology appl., melt processing and appl. *(Hungarian)* 80−55318
valve metal thin films, deposited on dielectric supports, exam. of anodisation kinetics *(Russian)* 80−7702
vaporisation, influence of inert gases on losses *(Russian)* 79−55878
wetting by Cu-Ag-P alloy 79−82417

tantalum continued
wire, H-absorption kinetics between 500 and 700K 80−49528
wire, strain ageing by return of elastic limit method *(French)* 78−68713
wires, supercond. destruction by current, long N-S interfaces 79−56480
zone refining effect on recryst. grain orient. in rolled and annealed cryst. 77−36532
μ^{181}Ta atom, X-ray transitions, radial charge parameters, quadrupole moment 77−34226
Ag/$RbAg_4I_5$/Ta, solid electrolyte timing cell and coulometer 80−68216
Al/Ta double layer on Si, anal. by low energy ion scatt. *(French)* 77−59663
Al-Ta-poly-Si interdiffusion, Ta barrier effect, Auger anal. 78−71888
Al_2O_3-Ta system, phase comp. of solid products formed in vacuum heating *(Russian)* 77−44185
$CaHfO_3$:Ta, electric field gradient temp. depend., TDPAC 77−20768
Dy:^{181}Ta, ferro- and antiferromag. phases, temp. depend. of mag. hyperfine field, TDPAC obs. 77−36165
GaP:Ta, donor centre struct. and conduction band nonparabolicity 78−14695
H uptake rates, enhancement by thin surface overlayers of Pd or Pt 79−82345
β-Hf, electrotransport and diffusion of Ta impurities *(German)* 78−87826
HfC:Ta, perturbed ang. correlation spectra, elec. quadrupole interaction 80−15916
$HfCo_2$:Ta, perturbed ang. correlation spectra, elec. quadrupole interaction 80−15916
$HfFe_2$:Ta, perturbed ang. correlation spectra, elec. quadrupole interaction 80−15916
liquid, polyvalent, electrical resistivity by harmonic model potential 80−54668
Nb, stress induced interaction of point defect pairs, in BCC solutions 78−79608
Nb/Ta thin film proximity effect bridge 79−82712
Nb-Ta bimetallic loop, supercond., thermoelec. flux effects due to penetration depth changes 77−24636
$NbSe_3$:Ta, elec. cond., anomalous, and microwave absorpt. 79−42527
Ni:Ta, ion-implanted, laser irrad. effect 80−108306
Pt:^{181}Ta, lattice defect induced elec. field gradient, PAC meas. 79−42878
Se:Ta, electrophysical meas. rel. to control of conductivity type 77−24323
Ta, deformed at 77K, dislocation substruct. 77−32647
Ta I and Ta II, oscill. strength determ. in 40 MHz inductively coupled plasma 79−48031
Ta IV, 2900 to 200 Å spectrum anal. 78−58615
Ta, K-shell photoionisation, cross section meas. K X-ray-photoelectron coincidence method 79−72285
Ta, phonon dispersion curves compared with Ta-H and Ta-D 77−76504
Ta, photo field emission characteristics, band struct. influence 78−27373
Ta, resistivity due to H incorporation 80−70666
Ta XLVI X-ray spectra from laser produced plasmas 80−42981
Ta XLVI(XLVII), $3d^k$-$3d^{k-1}$npnf transitions in laser plasma 78−9108
Ta:H, recovery after cold working at 4.2K, resist. meas. 79−4977
Ta:N, H_{c2}-anisotropy obs. 78−80105
Ta:N, non-pure supercond., Ginzburg-Landau parameter 77−76997
Ta:N, superconductive to normal transition anisotropy 80−25031
Ta:N film, triode sputtered, struct.-related cond. props. 79−78225
Ta:Xe, BCC, heavy ion implanted, vacancy recovery, Mossbauer spectroscopy 79−82896
Ta-Al_2O_3, vaporis. at elevated temp., mass spectrometric obs. 79−29388
Ta-Al_2O_3 heterophase film, elec. props. rel. to Al_2O_3 content 77−15969
Ta-D, dil. soln., high temp. thermodynamics 78−43128
Ta-Ga phase relationships, X-ray anal. of struct. 77−36453
Ta-H, BCC, tetrahedral interstitial site H band modes, neutron scatt. obs. 79−55852
Ta-H, dil. soln., high temp. thermodynamics 78−43128
Ta-H, incoherent spinodals, meas. by Gorsky effect 78−19712
Ta-H, interstitial position of H from entropy of soln. 77−65989
Ta-H, N interstitial trapping of H, hydride precip., resist. meas. 77−20293
Ta-H, spinodals and diffusion coefficients of H, sample shape depend. 78−19713
Ta-H system, with mobile H impurities, anomalous nuclear acoustic reson. line shape 77−20730
Ta-H(D), lattice expansion due to interstitially dissolved impurity, isotope effect 77−39600
Ta-Nb superimposed metallic layers, ionic movements during anodization, Rutherford backscatt. and nuclear microanal. 80−71913
Ta-Nb-Ta sheet, interface topology, exam. method 77−72797
Ta-O, dil. soln., high temp. thermodynamics 78−43128
Ta-O, relaxation anal. after ageing under stress *(French)* 80−16365
Ta-O, steady state O_2 solubility *(German)* 80−44322
Ta-Si, interface modification by ion implantation 80−70475
Ta-Ta_2O_5-Ag junctions, polarity-depend. tunnelling cond. 80−70846
Ta-Ta_2O_5-InP thin refractory MIS struct. deposition 80−75647
Ta-Ta_2O_5-ZnS:RF_3-Au struct., R=rare earth, electrolum. and cathodolum. meas. *(French)* 77−16398
Ta-Ta_2O_5-ZnS:TbF_3-Au thin films, MIS struct., DC electrolum. obs., Poole-Frenkel effect 78−88038
Ta-Ta_xO_y-Pb, tunnelling junction, current-voltage characts., knee struct. 79−38261
Ta+F_2, reaction, 690-930K modulated mol. beam mass spectrometry expts. 77−70341
Ta+F_2 reaction, modulated molecular beam mass spectrometry 78−15678
Ta+H^+, K-shell ionisation, 7-15 MeV, relativistic effects 78−82830
Ta+Kr^{n+}, K-L level matching, X-ray obs. 79−63948
Ta+SF_6→TaF_x, x=1-5, thermochemical props. of TaF_x 79−100424
Ta^{n+}+H, single electron capture cross-section 79−59560
Ta_6 clusters, electronic struct., scattered wave-Xα calc. 79−11053
$TaD_{0.06}$, D diffusion, 6.2 keV Mossbauer reson. of ^{181}Ta 78−39472
$TaD_{0.10}$, lattice location of D, ion channelling obs. 78−67708
$Ta^{n+}H_2$, single electron capture cross-section 79−59560
TaH_x, proton Knight shift and mag. suscept., high resolution meas. 77−55716
Ta_2O_5/Ta, heat-treated anodic film, exoelectron emission and radiation dosimetry *(Japanese)* 79−83110
^{178}Ta, chemical separation from parent ^{178}W, applications to nuclear medicine 79−16301

tantalum continued
^{178}Ta, energy spectra and spectral resolution in Xe-filled multiwire chamber 79−49901
^{178}Ta radiopharmaceuticals for lung and liver imaging, rat expts. 80−51254
^{178}Ta, scintigraphic imaging with the Anger scintillation camera 80−12231
^{178}Ta, short lived nuclide for nuclear medicine, production of the parent ^{178}W 79−16300
^{181}Ta impurities in Hf_xZr_{1-x}, electric quadrupole interactions, TDPAC meas. 78−76364
^{181}Ta in Te, quadrupole interaction, TDPAC meas. 80−20521
^{181}Ta, isomer shifts of 6.2 keV γ-rays, book contrib. 79−87358
^{181}Ta, L X-ray spectrum, L_1 subshell yield 79−49608
^{181}Ta nuclear acoustic reson. line shapes, quadrupole exchange contrib. 79−61242
^{181}Ta, pionic 4f→3d transition, pionic 3d state strong interaction level shift and width 79−98251
^{182}Ta Mossbauer sources *(French)* 80−74064
TiO_2:Ta, slightly doped, elec. cond. and defect struct., charge compensation, point defect model 80−75568
TiO_2:Ta, Ti^{3+}-Ti^{3+} exchange interaction *(French)* 77−89945
$TiSe_2$:Ta, transport props. and phase transition 78−72149
Zn:^{181}Ta, quadrupole interaction, TDPAC meas. 78−52392
ZrB_2-Ta composite, vacuum hot-press sintering and microstruct. *(Japanese)* 78−23649
ZrO_2-Ta and ZrO_2-Y_2O_3-Ta aligned eutectic composites, solidification and fracture behaviour 77−48387

tantalum alloys
see also tantalum compounds
BCC ternary, solid soln. hardening model, compared with expt. results 77−44262
magnetic susceptibility and Knight shift meas., d-metal alloys 80−66055
thermal conductivity at slow temps., temp. depend. *(Russian)* 79−91019
thermotransport of O 79−95216
Ti-Ta system, high-temp. oxidation *(Russian)* 79−74301
WC-TiC-TaC-Co, CVD and activated reactive evaporation of TiC, AES obs. of substrate-layer interactions 79−24679
Ag-Ta film, optical absorption spectra meas. 77−85823
CC TaC based hard metal, non-stoichiometric sintering, mech. props. 80−25616
(Co,Cr,Ni)-TaC, eutectic alloy, directionally solidified, struct. defects, autoradiographic investig. *(Russian)* 77−25038
Co-Al(Cr)-Ta, eutectic alloys, charact. by melting, oxidation resistance and composition 78−52768
Co-Cr-Ni-Ta-Al-Y (25, 10, 5, 3, 0.5 wt%), exam. of hot corrosion 79−20251
Co-Cr-Ni-TaC, directionally solidified eutectic, mech. props. and sruct., thermal cycling effects *(Russian)* 78−92282
Co-Cr-Ni-W-Ta-C, alloy Mar M-509, TEM exam. of thermal fatigue crack propag. in cast alloy 78−76740
Co-Cr-Ni-W-TaC (15.7, 9.5, 3, 12.77 wt.%) alloy Co50B3W, temperature cycling effect on rupture strength 78−39898
Co-Cr-NiTaC eutectic, directionally solidified, microstructural stability 79−38815
Co-Cr-Nr-TaC eutectic alloys, fatigue, microstructure effects 78−23803
Co-Cr-Ta, high temperature wear resistant coatings, CrO_2 hardened 79−24677
Co-Ni-Cr-Ta-C (10, 10, 14, 1 wt.%), aligned eutectic, directionally solidified, fatigue crack propag. 78−27624
Co-Ta, dendritic segregation 80−76260
Co(Cr,Ni)-TaC fibrous eutectic, deformed, thermal stability of microstruct. *(Russian)* 79−1895
Co_2Ta, mag. susceptibility, 77-500K *(Russian)* 77−80911
Cr-La-V-Nb-Ta, La, V, Nb Ta effect on hardness and strength *(Russian)* 79−34050
Cr-M, optimum alloying with rare earth metals, Ti, Zr, Hf, Nb, Ta 78−68651
Cr-Ta, Invar alloys, thermal expansion, plasticity *(Russian)* 79−55907
Cr-Ta, mixed SDW and Zeeman hyperfine interactions, TDPAC calc. 79−99797
Cu-Ta, metastable alloy layer formed by Ta^+ ion implantation 78−71709
Cu-Ta metastable alloy form. by ion implantation, combined TEM and ion channelling obs. 78−34530
Dy-Ta, dil., elec. field gradient at ^{181}Ta, temp. depend., TDPAC meas. 79−95689
Er-Ta, dil., elec. field gradient at ^{181}Ta, temp. depend., TDPAC meas. 79−95689
Er-Ta, dil., mag. hyperfine field determ., TOPAC meas. 79−91330
Fe-Co-Mo-Ta semihard mag. alloy, mag. props., thermal expansion, elec. resistivity and hardness *(Japanese)* 80−88789
Fe-Co-Ta for semipermanent magnets *(French)* 79−47675
Fe-Cr-Al-TaC (13.5, 3.7, 9 wt.%) eutectic alloy, directionally solidified, thermal cycling effects on microstruct. 77−32686
Fe-Cr-Ta, eutectic alloy, exam. of eutectic temp., composition, and oxidation resistance 78−52767
Fe-Mo-Ta, ternary Laves phase strengthening 80−108466
Fe-Ni-Ta (-Co), alloys, Co effect on martensite ageing at 300-600°C *(Russian)* 80−20972
Fe-Ta, nuclear mag. moment of ^{182}Ta NMR-ON study 80−78139
Fe-Ta alloy, mech. drawn and aged, exam. of electrical resistivity, hardness, microstruct., and mag. props. *(Japanese)* 78−48545
Fe-Ta-Co, Recalloys, semihard mag. alloys, mag. and elec. props., hardness, thermal expansion *(Japanese)* 79−5066
Ga-Ta, liquid binary alloys, magnetic susceptibility *(Russian)* 77−24671
Gd-Ta, dil., elec. field gradient at ^{181}Ta, temp. depend., TDPAC meas. 79−95689
Gd-Ta, dil., mag. hyperfine field and elec. field gradient at ^{181}Ta impurities, TDPAC meas. 79−47361
Hf-Ta, dil., hydrostatic and uniaxial compression, elec. field gradient at Ta, time differential PAC meas. 77−69739
Hf-Ta, prep. by carbide-oxide reaction 77−12554
Ho-Ta, dil., elec. field gradient at ^{181}Ta, temp. depend., TDPAC meas. 79−95689
Ho-Ta, dil., mag. hyperfine field determ., TOPAC meas. 79−91330
^{181}Ho-^{181}Ta, dil., elec. field gradient at impurity, anomalous temp. depend., host 4f levels, γ-γ correls. 78−95272
Mn-Ni-Ta, non-ferromagnetic Elivar type 77−48473

tantalum alloys continued
$(Nb,Ta)_3Sn$, supercond., bronze-processed, effect of Ta additions 78−95404
Nb-Ta, and Nb-B-Ta, supercond. crit. temp. and crit. field, Ta alloying effect 77−85375
Nb-Ta, resistivity due to H incorporation 80−70666
Nb-Ta, supercond., transport current distrib., neutron small angle scatt. study 79−42711
Nb-Ta, supercond. theory of upper crit. field, shift of Fermi level 77−63038
Nb-Ta, terminal solubility of H and characts. of solid solns. 79−86894
Nb-Ta (13 wt.%) alloy, flux line bending by transport currents, neutron diffr. 77−8247
Nb-Ta (20.at.%), optical props., 0.1-25 eV, band models 78−10892
Nb-Ta (54 at.%) cylinder, superconducting mag. and resistive behaviour 77−8252
Nb-Ta alloys, electron-phonon interaction and supercond. transition temp. *(Russian)* 79−28426
Nb-Ta alloys, H diffusion at 296K 80−84329
Nb-Ta system, short-range order exam. by diffuse X-ray scatt. *(Russian)* 77−31644
Nb-Ta type II supercond., defect-free, AC permeab. 77−8250
Nb-Ta-O solid soln., thermodynamic props. 78−31386
Nb-Ta-Si, ductile amorphous, superconductivity 80−60131
Nb-Ti-Ta, pinning curves, high field J_c and scaling behaviour 80−93064
Nb-Ti-Ta, superconductor optimisation for 12 Tesla toroidal field coils 80−91272
Nb-Ti-Ta alloys, metallurgical anal. and crit. current densities 79−38286
Nb-W-Zr-Ta, long-term strength props., vac. level effect 80−55484
Nb-W-Zr-Ta (90, 4.5, 3.5, 2 wt.%) creep and creep limit in super vac. at 1100°C, heat treatment effect 80−81133
$Nb_{30}Ta_{70}$, microwave props. of 8.6 GHz supercond. cavity 77−28297
$Nb_{53}Ta_{47}$, effects of hydrostatic pressure on changes in elastic consts. caused by addition of H 80−75287
$Nb_{53}Ta_{47}$, pure and hydrogenated crysts., effect of pressure on elastic consts. 80−7614
$Nb_{73}Ta_{27}$, supercond., flux density distrib. meas. 77−32129
$Nb_{73}Ta_{27}$, supercond., flux pinning by precipitates 77−47948
$Nb_{80}Ta_{20}$, supercond., phonon cond. below 1k 78−14881
Ni base alloy IN792, carbide morphology 77−36508
Ni-Al-Ta, heat resist., solidification range 80−35177
Ni-Al-Ta, solvus surface determ. using precipitation method 79−15674
Ni-Al-Ta (7.5, 2.0 wt.%), dendritic monocrystal, microsegregation and nonhomogenisation 79−37940
Ni-Al-Ta dendritic monocrysts., directionally solidified, coarsening kinetics 80−108425
Ni-based TaC eutectic, directionally solidified, elastic moduli 80−84984
Ni-based-Ta(Cn,N) hard metals, isostatic hot pressing influence on mechanical properties 78−92219
Ni-Co-Cr-Mb-W-Ta, Cr, Mb, W, Ta effects on σ phase occurrence 77−36507
Ni-Co-Cr-Ta-Al-W-Mo-Ti, cast, phase volume fraction determ. using manual point count practice 78−53052
Ni-Cr-Al-TaC, eutectic composite, microstructure, fatigue props. 80−85038
Ni-Cr-Co-Al-Ti-W-Ta-Mo, IN 738 LC, loading frequency and environmental effects on high temp. fatigue crack growth 78−64675
Ni-Cr-Co-Al-W-Mo-Ti-Ta, heat resist. and struct., Ta effect 80−76312
Ni-Cr-Ta alloy, precipitation hardening, 650 to 800°C 77−59798
Ni-Cr-Ta system, phase equilib. of Ni rich region at 1523 and 1273K 80−93541
Ni-Cr-Ta-Ti-Si, EP557 precipitation hardening alloy, mech. props., heat treatment effect 80−60877
Ni-Cr-TaC eutectic-like composite, obs. of interfacial diffusion by high resolution TEM 79−4432
Ni-Fe-Cr-Nb-Ta-Mo alloy, fatigue crack growth, stress ratio and hold-time effects 80−40531
Ni-Fe-Ta-W, high magnetic permeability alloys, Hardperm 77−48012
Ni-Ta, dil., crit. behaviour, ^{181}Ta PAC expt. 78−43723
Ni-Ta, dil., crit. behaviour of local magnetization, PAC and magnetisation meas. 78−48098
Ni-Ta, dil., mag. props. at elevated temps. 77−63089
Ni-Ta (70, 30 wt.%) metallic glass, struct. and crystn. *(Russian)* 80−70136
Ni-Ta ion implanted surface alloys, solid solubility and radiation-induced disorder, backscatt. obs. 79−46692
Ni-Ta system, phase diagram diffusion relation *(Russian)* 77−52287
Ni-Ta-Al system, phase equilibria and diagram, electron probe, X-ray diffr. anal. 80−29927
Ni-Ta-Al-Fe, Al and Fe effect on precipitation kinetics 79−20054
Ni-Ta-C, composites of γ+TaC 77−85965
Ni-Ta(7 at.%), short-range order, pseudopot. calc. and diffuse X-ray scatt. *(Russian)* 77−28008
$Ni_3(Mo,Ta)$, quenched alloys, DO_{22} type ordered phase form. 78−95768
NiTa C-13, advanced fibre reinforced eutectic superalloy, creep and rupture 77−63744
NiTa, exam. of oxidation 79−96221
NiTaC eutectic superalloy, casting, furnace atm. effects 80−84880
NiTaC eutectics, high cycle fatigue at room temp. 80−16459
NiTaC-13, directionally solidified eutectic alloy, chem. compatibility with ceramic materials 79−87623
$Ni_3Ti_{0.5}Ta_{0.5}$, conservative domain struct., TEM study 80−79776
Re-Ta-Mo, phase diag. *(Russian)* 77−59747
$Sm_2(Co, Cu, Te, Fe, Ta)_{17}$, permanent magnet, improved props. 77−89978
$TABe_{12}$, by diffusion saturation in vacuum, resistance to heat 78−44259
Ta-8W-2Hf wt.% (t-111) alloy, dissolution kinetics of small amounts oxygen, internal oxide disp. reactions, annealing 77−16612
Ta-Al-C, phase diagram and lattice constants, X-ray diffr. method 80−89207
Ta-Ar amorphous metal films, struct. and elec. characterisation 79−87017
Ta-Co amorphous metal films, struct. and elec. characterisation 79−87017
Ta-Cr (15 wt.%), solid soln., discontinuous precipitation *(German)* 80−45314
Ta-Cr-Si-Al, heat resistive films, prepared by sputtering, lifetime meas. 80−80132
Ta-D, dil. soln., high temp. thermodynamics 78−43128
tantalum alloys continued
Ta-D, stability curve for phase separation of D, neutron small-angle scatt. study 79−15672
Ta-D system, phase equilibria study *(Japanese)* 79−78936
Ta-Fe, X-ray emission spectra study of electron struct. of Laves phases *(Russian)* 78−23555
Ta-Ga, crystal struct. at high press., polymorphism 80−88112
Ta-H, BCC, quasimolecular Jahn-Teller reson. states 80−44550
Ta-H, BCC, tetrahedral interstitial site H band modes, neutron scatt. obs. 79−55852
Ta-H, degree of positron localisation on components 77−85833
Ta-H, dil. soln., high temp. thermodynamics 78−43128
Ta-H, elastic constants, temp. depend, H_2 effect 77−32610
Ta-H, electron work function, 300 to 600 degrees C, contact potential difference meas. 80−29462
Ta-H, fracture modes *(Japanese)* 80−66636
Ta-H, incoherent spinodals, meas. by Gorsky effect 78−19712
Ta-H, interstitial position of H from entropy of soln. 77−65989
Ta-H, N interstitial trapping of H, hydride precip., resist. meas. 77−20293
Ta-H, physical properties, plastic deformation, H ordering *(Ukrainian)* 80−71689
Ta-H, prod. using Pd layer coating technique 79−47816
Ta-H, spinodals and diffusion coefficients of H, sample shape depend. 78−19713
Ta-H, thermokinetics of H_2 generation from transition metal-H compounds 79−74421
Ta-H alloy, high conc., Huang diffuse X-ray scatt. from lattice strains 78−38746
Ta-H system, acoustic emission induced by hydride formation 80−76257
Ta-H system, phase diagram and transforms., struct. obs. of various phases 80−104125
Ta-H system, phase equilibria studies *(Japanese)* 79−78935
Ta-H system, positron localisation *(Russian)* 77−66555
Ta-H(D), lattice expansion due to interstitially dissolved impurity, isotope effect 77−39600
Ta-H(D), phonon freqs. and dispersion curves 77−76504
Ta-H(D) system, single cryst. prep. and characterisation 79−95910
Ta-Ir (1 wt.%), positron annihilation, photon ang. distrib. meas. effect of deformation, annealing temp. *(Russian)* 78−35220
Ta-Ir(Rh) system glasses, form., crystn. and microhardness, resist. obs. 80−89178
Ta-N, amorphous metal films, struct. and elec. characterisation 79−87017
Ta-N, domain configurations of new phase *(French)* 78−56648
Ta-N (0.6 to 6.5 at.%), supersaturated solid soln., precipitation 79−96028
Ta-N (4 at.%), TEM obs. of ordering 79−96021
Ta-N(O)(C) system, specimen prep. for metallography *(German, English)* 80−89439
Ta-N(O)(O-N), electrolytic polishing, use of pure FSO_4H 78−85094
Ta-Nb-V, solid solutions, superconductivity and charge transfer 79−7926
Ta-Nb-V BCC solid solutions, supercond. and normal state, sp. ht. meas. 78−84347
Ta-Nb(Re)(W) (50,20,0 at.%), with N_2, spectral emissivity, N_2 absorption rate, N_2 solubility, thermodynamic data *(German)* 77−25026
Ta-Nb(W)(Re), kinetics and thermodynamics of reaction with N_2 *(German)* 79−74415
Ta-Ni amorphous metal films, struct. and elec. characterisation 79−87017
Ta-Ni film, amorphous, UHV deposited, elec. and struct. props. obs. 78−6233
Ta-O, BCC, Snoek type reordering during strain ageing *(French)* 79−8312
Ta-O, dil. soln., high temp. thermodynamics 78−43128
Ta-O solid soln., interstitial ordering and precipitation at 100 to 270°C, exam. 78−52813
Ta-Pd system, phase diagram exam. of composition by X-ray diffr., electron microprobe anal., and metallography 78−76632
Ta-Pt, electrospark alloying for obtaining stable effective electrodes for electrochemical processing *(Russian)* 79−39157
Ta-Pu, metastable, high rate sputter deposition, annealing behaviour of deposits 77−21025
Ta-Re-Y-La alloy, Y, La determ., spectrochem. method 79−16076
Ta-Re-(N), deformed at 77K, dislocation substruct. 77−32647
Ta-Rh, σ-phase alloy, superconductivity and resistance behaviour 80−70882
Ta-Si-Cu, struct. and supercond., Cu influence 80−50592
Ta-T(D), diffusion and resistivity at low temps. 78−14511
Ta-V system, short-range order exam. by diffuse X-ray scatt. *(Russian)* 77−31644
Ta-W, electronic density of states, temp. depend. of elec. resist. and mag. susceptibility 77−11891
Ta-W, thermoelec. power, 4.2 to 300K 80−70684
Ta-W BCC, press. derivatives of elastic moduli, Fermi surface topological changes, band struct. 79−61639
Ta-W optical props., temp. depend., 4.2-1100K 78−2874
Ta-W TV-10 alloy, thermal expn., 1146-2288K 78−43148
Ta-W-Hf, embrittlement, effect of composition 77−21247
Ta-W-Hf, small-angle electron scattering in TEM from lattice strains accompanying precipitation 79−14658
Ta-W-Hf (8,2 wt.%), T-111, O_2 absorption, effect on lattice parameter and specimen dilation 78−83958
Ta-W(Re)(Ir) film, amorphous, temp. stability 78−63948
TaAl, α phases, lattice parameter and order 77−76359
TaB_2-Cr-Si-Al, heat resistive films prepared by sputtering, lifetime meas. 80−80132
Ta(C,N)-Ni-HfC(HfN)(Mo_2C)(VC), sintering, prod. of hard metals 78−11155
Ta(C,N)-Ni-VC, sintering behaviour, VC effect 80−93520
TaC-Co-C directional eutectic, high-strength, interphase boundaries *(Russian)* 79−38812
TaC-Ni-Cr directional eutectic, high-strength, interphase boundaries *(Russian)* 79−38812
TaC-NiC, powder for plasma arc spray coating appl. 78−15591
TaC-Ni(-W) alloys, oxidation resistance 77−60000
$TaD_{0.06}$, D diffusion, 6.2 keV Mossbauer reson. of ^{181}Ta 78−39472
$TaD_{0.10}$, lattice location of D, ion channelling obs. 78−67708
$TaGe_2$, superconducting transition temp. meas. of sputtered films and bulk 80−7019

tantalum alloys continued
$TaH_{0.257}$, influence of H on bulk band struct., optical absorptivity spectra obs. 77−89692
α-TaH_x, electronic struct., thermoreflectance studies 80−76047
TaH_x, proton Knight shift and mag. suscept., high resolution meas. 77−55716
β-Ta_2H, ordered alloy, electron microscope study of lattice distortions 77−11507
Ta_2H, single cryst., X-ray diffr. study on H ordering 79−14736
$Ta_{70}Nb_{30}$, Abrikosov vortex formation kinetics *(Russian)* 80−93055
TaS_2-Fe, dil. alloy, magnetotransport and superconductivity 77−55516
$TaSe_2$-Fe, dil. alloy, magnetotransport and superconductivity 77−55516
$TaSe_3$, electronic props. variation with struct. 79−42438
$TaSe_3$, one-dimens. monoclinic, supercond. below 2.1K, mag. field effect *(Japanese)* 77−43767
$TaSi_2$, superconducting transition temp. meas. of sputtered films and bulk 80−7019
Ta_3Si, superconducting, shock synthesis *(Russian)* 77−85957
Ta_5Si_3, supercond. transition temp. meas. *(Russian)* 77−20485
Tb-Ta, dil. elec. quadrupole interaction, temp. and press. depend., TDPAC meas. 80−60469
Ti-Al-Nb-Ta-Mo (6, 2, 1, 0.8 wt.%), elevated temp. flow strength, creep resist., diffusion welding characts. 80−30033
Ti-Nb alloys, Fe, Mo, V, Ta alloying additions on microstruct. after combined treatment *(Russian)* 77−59826
Ti-Nb-Ta-Ge (40,20,0.8 wt.%) foil, dispersion hardening, TEM and electron diffr. obs. *(Russian)* 79−1873
Ti-Nb-Zr-Ta, superconducting props. comp. depend., stress effects and precipitation behaviour, X-ray scatt. 80−93059
Ti-Ta, influence of different factors on supercond. transition width *(Russian)* 79−1636
Ti-Ta (4.37 wt%), oxidation kinetics, 1258-1473K, and at pressure of 0.013, 0.133 and 1.0 bar 80−89411
Ti-Ta-Co system, phase stability, X-ray anal. 79−61580
Ti-ZrO_2(HfO_2), eutectic system metallographic investigation *(Russian)* 77−66629
V-Nb-Ta, supercond., elec. resist. and electron-phonon interaction parameters 78−14862
V-Ta, and V-Nb-Ta, supercond. crit. temp. and crit. field, Ta alloying effects 77−85375
V-Ta, mech. props. 79−61682
V-Ta, superconducting transition temp., nondiagonal disorder effects 79−73622
V-Ta, X-ray emission spectra *(Russian)* 77−55851
V-Ta (5 wt.%), strain hardening, screw dislocations and microtwinning *(Russian)* 80−29971
V-Ta alloys, electron-phonon interaction and supercond. transition temp. *(Russian)* 79−28426
$V_2Hf_{1-x}Ta_x$, C15 supercond., electronic and lattice props. 78−68110
V_3Si-Ta solid soln., supercond. T_c and paramag. susceptibility *(Russian)* 77−59348
V_3Ta, NMR meas., mag. susceptibility, Knight shift and elec. field gradient determ. *(Russian)* 78−23359
W-C-Ta, vacuum melted, phase composition, struct. and props. 78−31403
WC-Co-Ta, cemented carbide, deformation, high temp., stress relaxation, and strain rate depend. 78−39854
WC-Co-Ta-Ti-Nb, cemented carbide, deformation, high temp., stress relaxation, and strain rate depend. 78−39854
WC-Co-TaC-TiC-NbC cemented carbide, microstructure, high temp. deformation, uniaxial plastic compression 80−40451
WC-TaC-Co, cemented carbide, strength improvement by hot isostatic pressing 78−84969
WC-TiC-TaC, powder for plasma arc spray coating appl. 78−15591
WC-TiC-TaC-Co cemented carbides, transverse-rupture strength at 600 to 1000°C obs. *(Japanese)* 79−43374
WC-TiC(TaC, NiC)-Co, hard, homogeneity and wear resistance estimation, by magnetic method 77−90558
ω-Zr-Ta, electric field gradients at substitutional Ta atoms, TDPAC high-pressure study 78−52384
Zr-Ta (5 wt.%), β-precipitation in martensitic struct., tempering temp. effect 79−34045
Zr-Ta (5 wt.%), martensitic transform. by rapid cooling, non-equilib. precipitation 79−34075
Zr-Ta (5 wt.%) martensite, β_1 precipitation, thermodynamics 79−74164

tantalum compounds
see also tantalum alloys
anodic barrier film characts., ISS/SIMS 78−53021
anodised layer, structure and stoichiometry, thickness effects 77−77634
borides, chemical vapour deposition *(French)* 77−36406
carbides, changes in phase structure during prolonged heating in vacuum 78−44095
chalcogenides, layered, soln. mechanism of metals 79−42249
CVD on quartz substrate from gas mixture of $TaCl_5$-BCl_3-H_2-Ar 80−29880
dichalcogenide, domain-like incommensurate CDW states and first order incommensurate-commensurate transition 78−26824
$(H_3O)_{5-x}Ta_{11+x/5}O_{30}$, synthesis, non-stoichiometry, density and ionic cond. meas. *(French)* 78−52741
minerals, cryst. struct., X-ray powder diffr. study 80−107169
oxide, anodic film on Ta, electrochem. reactions by tunnel current 77−81340
oxide film, anodic, photodepolarisation *(Russian)* 77−32316
rare earth oxide (R_2O_3)-Ta_2O_5 glassy systems, rapid quenching by laser beam, exam. of composition and crystallization 78−52856
refractory carbides, borides and nitrides, wetting by and interactions with liq. metals 80−54473
sital, structural glass component, strength in complex stress state 79−91763
sitall cylindrical shell reinforced with internal stiffening ribs, stress-strain state under external press. 80−71684
Sitalls, soln. rate in alkali soln. 80−16531
TaS_2, amine intercalation, water effects, X-ray diffr. meas. 80−44178
1T-TaS_2, nearly commensurate phase, harmonics effect on phase transitions 78−14462
tungsten bronze, tetragonal, type structure cpds, transition sequences *(French)* 77−89538
Al-anodised Ta_2O_3/native oxide-n-GaAs MOS structure evaluation 80−84514
Al-Ta_2O_5-Al, healing of defects in dielec. film by anodisation 80−65406

tantalum compounds continued
BaO-Al_2O_3-SiO_2-Ta_2O_5-Mo glass ceramic metal composites, cermet prep. 80−11618
$Ba_4TaRu_3O_{12}$, $(Ru_3O_{12})^{13-}$ cluster obs. in presence of orbital degeneracy and spin-orbit coupling *(French)* 80−70655
$Ba_3(Ta_4Ti_4)O_{21}$, effects of Sb substit., synthesis and cryst. chemistry 77−76379
Bi_2O_3-Ta_2O_5, sintered, high oxide ion cond. meas. 78−14503
$Ca_3(MTa_2)O_9$, M=Ca, Cd, Mn, Fe, Zn, Co, Mg, Ni, monoclinic perovskite-type struct. 77−84725
$CeTaO_{4+x}$, oxidation-reduction reactions, phase equilibrium, thermogravimetry and magnetic susceptibility meas. 78−39930
Cr-Ti/MgO-TaC dispersion-strengthened, high temp. wear and oxidation resist. 80−25877
Cr-Ti/TaC dispersion-strengthened, high temp. wear and oxidation resist. 80−25877
$Cr_{8-x}Ta_{3+x}Si_8$, cryst. struct. *(French)* 78−38675
D_xTaS_2, struct., form. by cathodic reduction, neutron diffr. obs. 79−73150
Er_2O_3-Ta, oxide grain growth at interface 77−81245
$3Er_2O_3$-Ta_2O_5 refractories, prep. and anal. 77−48384
Eu_2O_3-Gd_2O_3-Ta_2O_5 system at 25, 50 and 75 mole.% Ta_2O_5, cross section investig. 77−12607
Eu_2O_3-R_2O_3-Ta_2O_5, R=La, Gd, Y, quasibinary cross sections 77−90333
Eu_2O_3-Sc_2O_3-Ta_2O_5 system, orthotantalate section, X-ray diffr. and luminesc. obs., conc. depend. 80−54205
Eu_2O_3-Ta_2O_5, microcracking, elastic props., internal friction 78−92326
Eu_2O_3-Y_2O_3-Ta_2O_5, struct., phase form., luminesc. and X-ray diffr., obs. *(Russian)* 78−6765
1T-$Fe_{0.1}Ta_{0.9}S_2$, mag. modulation of lattice electric field gradient 77−85628
Fe_xTaS_2, metallic, mag. susceptibility at low temp. 80−70972
$Fe_xTa_{1-x}S_2$ (1T), low-spin high-spin equilib., susceptibility and Mossbauer expts. 77−48109
1T-$Fe_xTa_{1-x}S_2$, Anderson localisation, elec. resist. and magnetoresist. meas. 80−44596
$Fe_xTa_xV_{2-2x}O_4$ complex solid solns., synthesis and phase diagram, semicond.-metal transition temp. 79−43214
H_xTaS_2, nonstoichiometric, incoherent neutron spectra, X-ray diffr. 78−42998
$HTaWO_6$, and $HTaWO_6.H_2O$ defect pyrochlores, NMR study of proton motion 79−82889
HfC-TaC alloys, microhardness rel. to valence electron conc. 77−86130
$Hf_xTa_{1-x}C$, thermal cond. and diffusivity, 1000-2200°C, elec. cond. 78−91491
$Hf_xTa_{1-x}C_y$ solid solns., mag. susceptibility, 20-1300K *(Russian)* 78−39287
$In_3Ta_2O_7$, new phase of mixed oxide 78−59787
$K_{6-2x}Ba_xTa_6Si_4O_{26}$, IR spectra, appl. to nonstoichiometry in cpds. with $(M_6X_4O_{26})$ layers (M=Nb,Ta; X=Si,Ge) *(French)* 79−11418
K_2O-Ta_2O_5 mixed oxides, cryst. struct., electron microscopy study 78−91309
K_2O-Ta_2O_5 mixed oxides, cryst. struct., electron microscopy study 78−91310
$K_{10}(Ta_8O_{21})_2.Ta_6X_4O_{26}$, X=Si, Ge, cryst. struct. *(French)* 77−76378
$KTa_{1-x}Nb_xO_3$, holographic storage using photorefractive effect, dielectric const. 80−78800
$KTa_{1-x}Nb_xO_3$, quantum ferroelec., elastic compliance, impurity effects 79−99835
$KTaO_3$, complex electronic dielectric const. from tight binding energy bands 78−60054
$K_2Ta_2O_3F_6$, Marignac's salt, X-ray diffr. study of cryst. struct. 77−89417
$K_{1+x}Ta_{1+x}W_{1-x}O_6$ pyrochlore system, comp. depend. of ionic cond. 80−107517
La_2O_3-GeO_2-$Ta_2O_3(HfO_2)(ZrO_2)$, vitrification, crystn. 77−15559
$LiBa_3Ta_3Ti_5O_{21}$, insertion of Li, X-ray and neutron diffr. study *(French)* 78−91324
$Li_{1-x}Hf_{2-x}Ta_x(PO_4)_3$, new solid ionic conductors 77−35953
Li_2O-Ta_2O_5 system phase diagram 79−47668
$LiTaO_3$, for substrate used in fabrication of SAW Butterworth contiguous filters 79−68493
Li_xTaS_2, chem. diffusivity of Li at 30°C 80−59737
$Li_{1-x}Zr_{2-x}Ta_x(PO_4)_3$, new solid ionic conductors 77−35953
$MgTaCuO_4$, cryst. struct., synthesis 78−83790
$Na_{5-x}Ta_{11+x/5}O_{30}$, synthesis, non-stoichiometry, density and ionic cond. meas. *(French)* 78−52741
Na_xTaS_2, Na chem. pot. and free energy of intercalation, electrochemical meas. 79−100396
$Na_{1+x}Ta_{1+x}W_{1-x}C_6$ pyrochlore system, comp. depend. of ionic cond. 80−107517
$Na_xTa_yW_{1-y}O_3$, substitution of W with Ta, Anderson type transition *(French)* 79−60879
(Nb,Ta)As, X-ray cryst. struct. determ. 79−69078
$(Nb,Ta)_8N_9$, cryst. struct. determ. *(German)* 80−107145
Nb-Ta-N sputtered films and their anodic oxides, elec. props. of resist. and dielec. films 80−11126
$(Nb_{1-x}Ta_x)_2C$, modulated structs., periodic antiphase domains 79−94969
$Nb_{0.95}Ta_{0.05}Se_3$, resist 0.5K to room temp., supercond. transition temp. and crit. field 79−82704
$Nb_{1-x}Ta_xSe_3$, thermoelectric power meas., 10-300K 80−20177
$Nb_{1-x}Ta_xSn_2$, supercond. transition temp. and upper crit. field 80−39723
Ni-TaC, eutectic alloy, fibre reinforced, directionally solidified, anisotropic yielding behaviour 79−11675
$Pb_2Ta_{2-x}M_{2x}O_{7-x}$, (M=Ti, Sn Zr), oxygen deficient, form., IR spectra, dielec. const. *(Japanese)* 77−48171
PuC-TaC, solubility study 78−83956
Rb_2-Ta_2O_5, phase equilib. relns. and crystal chemistry, structs. useful as ionic conductors 79−20033
$Rb_{5-x}Ga_{11+x/5}O_{30}$, synthesis, non-stoichiometry, density and ionic cond. meas. *(French)* 78−52741
Rb_2O-Ta_2O_5 mixed oxides, cryst. struct., electron microscopy study 78−91309
Rb_2O-Ta_2O_5 mixed oxides, cryst. struct., electron microscopy study 78−91310
$Rb_{10}Ta_{29.20}O_{78}$, layered cryst. struct. 80−107166
SiO_2-CaO-Na_2O-Ta_2O_5 system, water, alkali, acid resist., chem. durability 79−34162
SiO_2-Ta_2O_5 film, refr.-index-adjustable, for integrated optical ccts., prep. and props. 78−63203

tantalum compounds continued
SiO_2-Ta_2O_5 film channel optical waveguide, fabrication using CO_2 laser 79−27386
$SnTaS_2$ intercalate, cryst. struct. determ. 78−26534
$(Ta,Ti)B_2$ on graphite, CVD coatings, hardness meas., SEM study 80−24760
Ta complex, prep. by halide reaction with tetramethylurea and tetramethylthiourea, and characterisation 79−15972
Ta complex, $TaCl_5$ complex with O- and S-containing ligands, prep., and characterisation 79−14729
Ta-Al-N thin film resistors with improved elec. props. 80−100544
Ta-C-B system, mech. and physical props. 77−59731
Ta-D system, thermodynamic stability of Ta_2D, rel. to long-range order parameters *(Japanese)* 78−15376
Ta-H, degree of positron localisation on components 77−85833
Ta-H, electron work function, 300 to 600 degrees C, contact potential difference meas. 80−29462
Ta-H, phase diagram revision 77−63641
Ta-H(D), anelasticity due to long-range diffusion 80−60904
Ta-H(D), H ordering, review 80−60850
Ta-H(D) system, single cryst. prep. and characterisation 79−95910
Ta-N, supercond. props. 77−20507
Ta-O supersaturated solid solution, precipitation processes, hardness change meas. 80−25712
Ta-O(N), dislocation pinning, impurity interactions, strengthening *(Russian)* 80−92532
Ta-Ta_2O_5-Ag junctions, polarity-depend. tunnelling cond. 80−70846
Ta-Ta_2O_5-InP thin refractory MIS struct. deposition 80−75647
Ta-Ta_2O_5-ZnS:RF_3-Au struct., R=rare earth, electrolum. and cathodolum. meas. *(French)* 77−16398
Ta-Ta_2O_5-ZnS:TbF_3-Au thin films, MIS struct., DC electrolum. obs., Poole-Frenkel effect 78−88038
Ta-Ta_xO_y-Pb, tunnelling junction, current-voltage characts., knee struct. 79−38261
Ta-Ti-N, reactive sputtered film, elec. props. 78−84336
Ta-Ti-O, reactive sputtered film, elec. props. 78−84336
Ta_3As, arsenic decomp. pressures and enthalpy of form. 77−70329
Ta_3As, X-ray cryst. struct. determ. 79−69078
TaB_2, single cryst. growth, floating zone and Al soln. methods 79−86729
TaB_2, vapour transport in temp. gradient in presence of iodine 79−19997
TaB_2-Cr-Si-Al, heat resistive films prepared by sputtering, lifetime meas. 80−80132
TaB_2-ZnS:Ag(Ag,Ni)-glass binder, thermally stable, comp. 77−63617
$TaB_{2.11}$, heat capacity thermodynamic properties from 5 to 350K 78−91446
$TaBr_5$, gaseous, electron diffr. obs. of vibr. assignment, mol. struct. and barrier to pseudorot. 79−81293
TaC, abrasive action, X-ray investig. 77−52497
TaC, adsorption of Cs(K), adsorpt. energy, thermionic emission 77−7978
TaC and Ta_2C, self-propag. high-temp. synthesis 80−60815
TaC, bond energy and ionization efficiencies from SIMS 79−24400
TaC CVD coating, on W-ThO_2 and SiC filaments, effect on high temp. mech. props. 78−15347
TaC coated emitters, thermionic emission props. *(Japanese)* 77−40322
TaC, diffusion of W, correl. with self-diffusion 77−24437
TaC, etchant for revealing microstructure 80−85097
TaC, generalised susceptibilities and electronically driven phonon anomalies 79−42208
TaC, high temp. supercond., role of electronic struct. on obs. phonon anomalies 77−24363
TaC, micropowder, abrasive props. 77−63821
TaC, negative surface ionisation 77−77335
TaC, phonon anomaly rel. to Fermi surface 77−11853
TaC, phonon dispersion, deformation dipole model 79−99281
TaC, pressing regime influence on high-temp. creep *(Russian)* 80−100852
TaC, quasi-self-consistent energy band structures using relativistic KKR calcs. chemical bonding 79−51484
TaC, reactions with Ti-Al-Cr-Mo alloy VT3-1 80−16585
TaC, single crystal growth by plasma heating 78−60569
TaC, solid-phase reacts., effect of nonstoichiometry, thermodynamic evaluation 78−60632
TaC, sputtering, low energy, H, D and He ions 80−100734
TaC surface, effect of C oxidation on work function, 1250-2000K, AES 79−24054
TaC, thermal and electrical conductivity, 1500-3000K 78−43385
TaC, true heat capacity meas. by pulse method 80−19953
TaC, ultrafine grain, high pressure hot pressing 79−70024
TaC, ultrafine powder prep. in HF plasma 77−12562
TaC, X-ray emission band exam. and electronic struct. 77−8689
TaC-C fibre composite, neutral beam target appls. 78−66399
TaC-Ni base eutectic, oxidation protection 77−40475
TaC-TaB_2, exam. of high temp. friction and wear, and deformation behaviour 79−34152
TaC-TaB_2, phase diag., solubilities, reactions 77−63643
TaC-VC, phase diag. calc. 77−90329
TaC_x, complex phases with NaCl struct., microhardness rel. to electronic structure 77−90438
TaC_x, solubility of H, X-ray diffr. exam. 80−44318
TaC_x, static distortions and Debye temp. determ., neutron diffr. exam. *(Russian)* 77−80482
Ta_2C_x, solubility of H, X-ray diffr. exam. 80−44318
TaC_xN_y, supercond. and normal props. under hydrostatic press. 77−12049
$Ta_2C_xO_y$, solubility of H, X-ray diffr. exam. 80−44318
$TaCl_5$, mol. struct., vibr. assignments, barries to pseudorotation 78−29858
$TaCl_5$, photoelectron spectra 79−821
$TaCl_5OPCl_3$, vibr. amplitude and normal coord. anal. *(German)* 78−66536
$TaCl_5.CD_3CN$, Raman spectra and Teller-Redlich product rule 79−69817
$TaCl_5.CH_3CN$, Raman spectra and Teller-Redlich product rule 79−69817
$Ta_2Co_4O_9$, flux growth and chem. characts. 78−23595
TaD, structs. phase diagrams, morphologies, prep. methods, book contrib. 80−25675
Ta_2D, atomic displacements determ. by deuteron magnetic resonance *(Japanese)* 78−15035
tantalum compounds continued
Ta_2D, neutron diffr. meas. of disorder-order phase transitions 80−29947
Ta_2D_{1+x}, atomic displacement of Ta determined by deuteron magnetic resonance 79−37701
Ta_2D_{1+x}, phase relations in terms of long-range order 79−38808
TaF_x complex, with 4-(2 pyridylazo)-resorcinol, stability investig. by spectrophotometry 77−36782
TaF_x, x=1-5, reaction of SF_6 admitted to Ta effusion cell, thermochem. props. 79−100424
Ta_3Ge, superconducting transition temp. 78−47898
TaH, structs. phase diagrams, morphologies, prep. methods, book contrib. 80−25675
$TaH_{0.13}$, diffusion of H, neutron scatt. study 79−60550
$TaH_{0.75}$, calorimetric study of phase transform. 77−48426
TaH_x, diffusion of H atoms, quasielastic neutron scatt. obs., book contrib. 79−82383
TaH_x, H diffusion and electronic struct., pulsed NMR obs. 80−54967
TaH_x, phase diagram, mag. susceptibility 78−84778
TaH_x, positron localisation *(Russian)* 77−66555
Ta_2H, ordered, distortion-induced superstruct. modulation, from X-ray scatt. 80−49186
Ta_2H, single cryst., X-ray diffr. study on H ordering 79−14736
$TaH_x(D_x)$, acoustic and optic phonons, neutron diffr. obs., book contrib. 79−82296
$TaH_x(D_x)$, cryst. struct., phase diagrams, order-disorder transition 78−55836
$Ta_{0.97}Hf_{0.03}S_2$ (1T), charge density waves, ESCA, XPS investigs. 77−12490
$(TaI_5)_2$, X-ray cryst. struct. determ. *(German)* 80−19754
ε-TaN, cryst. struct. determ. by neutron diffr. exam. 78−26522
TaN, cubic phase formation from hexagonal by plasma jet heating 78−84726
TaN diffusion barrier in Si device metallisation 80−65304
TaN, electronic struct., relativistic energy band struct. calc. 80−34354
TaN, energy band struct. calc., symmetrised APW method 80−96784
TaN film, growth by CVD, microhardness and corrosion resist. 77−36404
TaN film, prep., comp. anal., and supercond. T_c 79−15605
TaN film, press. depend. of elec. props. appl. to press. meas. 79−78241
TaN film, simple vacuum gauge, 10^{-5} to 10^{-3} Pa press. range 78−70148
TaN, matrix isolated, electronic and vibr. absorpt. spectra 79−64014
TaN, sputtered thin films, cross-sectional composition by SIMS, elec. resist. calcs. 79−77953
TaN, superconductivity, mag. field direction determining whether type I or II 79−15266
TaN, thin film, characteristics of Pirani type vacuum gauge *(Japanese)* 80−13086
TaN, thin film, in Pirani type vacuum gauge *(Japanese)* 80−52257
TaN, X-ray emission band exam. and electronic struct. 77−8689
TaN_x film, triode sputtered, struct. and elec. props. 79−78242
TaN_x, films, thermal oxidation and resist. 80−60125
TaN_x metastable FCC, band struct. calc. 79−33231
Ta_2N film, high temp. nitriding kinetics depend. on press. *(Russian)* 80−50838
Ta_2N, films, thermal oxidation and resist. 80−60125
β-Ta_2N, growth by annealing Ta in N_2, cryst. struct. 77−35533
Ta_2N, sputtered layer, thermal oxidation, reaction kinetics 78−39959
Ta_2N, thin film deposition by closed anode bias sputtering *(Japanese)* 80−93484
β-Ta_2N-ε-TaN, prep. by exothermic reaction and by zone melting, cryst. struct. 77−35533
Ta_3N_5, polycryst. film, cryst. struct., electron diffr. *(French)* 77−76677
Ta_xN_y, FCC, formation in ionised glow-discharge 77−52266
TaO, displacement function calc. 80−34047
TaO, energetic heavy ion irrad., elastically deposited energy, numerical calc. 77−59057
TaO_4^{4-}, normal vibr. freqs., force consts. calc. *(Russian)* 77−6759
TaO_5 film, used in making lenses and waveguides in collimator 79−68446
TaO_6^{7-}, octahedral cluster, ionisation energies and atomic populations, XPS and SCFMS Xα calc. 79−93923
TaO_n, combined SIMS, AES and XPS investigation 79−33199
TaO_x film, optical const. var. with struct., ellipsometric meas. 77−63478
Ta_2O_3, cathodic luminesc. of oxide covering on Ta electrode in electrolyte soln. 77−69915
Ta_2O_3, form. on GaAs after oxidation of Ta 79−61769
$2Ta_2O_3$ thin film, FCC cell struct. investigation 80−92796
Ta_2O_5, $^4He^+$ ion scatt. spectrometry below 1.0 keV 79−83088
Ta_2O_5, amorphous, range of ^{27}Al meas. by (p,γ) reson. broadening 77−69023
Ta_2O_5, amorphous and cryst., elec. cond. mechanism, admittance meas. 80−70705
Ta_2O_5, anodic, on sputtered Ta_2N, dielec. props., 20-10^5 Hz, 150-500K 79−87386
Ta_2O_5, anodic, sputtered, equilib. surface comp., mass and energy depend. 79−19472
Ta_2O_5 anodic film, scintillation 79−91500
Ta_2O_5, anodic film, thermally stimulated exo-electron emission 80−11546
Ta_2O_5, anodic film on Al, strain to failure, failure characts. 77−12734
Ta_2O_5 anodic film with Au counterelectrodes, conduction process 78−84312
Ta_2O_5 anodic films, reanodisation effect on exoelectron emission 79−43110
Ta_2O_5, anodic oxide film, adhesion, ductility and fracture, spectrophotometric thickness meas. and SEM obs. 79−99460
Ta_2O_5 anodic oxide film, model for ionic cond. 80−2197
Ta_2O_5, anodised film, nonuniformities, optical props., spectrophotometric obs. 78−2933
Ta_2O_5 antireflection coatings for Au-GaAs solar cells parameters determ. 77−763
Ta_2O_5, chemical effect, influence on stopping power 80−47830
Ta_2O_5, defective anodic film on Ta, elec. characts. 77−12039
Ta_2O_5 doped systems, struct. and ordering, high resolution TEM obs. 78−35378
Ta_2O_5, elec. breakdown during anodic growth 80−55033
Ta_2O_5, elec. props. as dielec. in Ta solid dielectric capacitor *(Spanish)* 78−19405
Ta_2O_5, ε-modification, cryst. struct. and microstruct. 79−51083
Ta_2O_5 film, atomic composition depth distrib. by energetic ion anal. 80−35617

tantalum compounds continued
Ta_2O_5, film, dielec. props. meas., two layer Maxwell-Wagner model 78−76373
Ta_2O_5 film, electrical breakdown by impact ionisation, models compared with expt. 79−91373
Ta_2O_5 film, for MIS device, CVD and characterisation 77−4742
Ta_2O_5 film, on Si, antirefl. coating for solar cell, film-substrate interaction obs. 77−1324
Ta_2O_5 film, reactively sputtered on SI, dielectric and optical props. obs *(Bulgarian)* 80−89144
Ta_2O_5 film, refractive index 80−84792
Ta_2O_5, film, sputtering conditions rel. to electronic cond. 77−40365
Ta_2O_5 film, temp. and time charact. of breakdown *(Russian)* 77−55751
Ta_2O_5 film acousto-optical props. for integrated optical Bragg cell 79−55251
Ta_2O_5 film capacitative humidity sensor Panahume *(Japanese)* 80−105658
Ta_2O_5, film form. by reactive HF sputtering with voltage bias 78−3045
Ta_2O_5, film on Al, Cu, Au, Ag electrode, electric strength of MIS system 80−96999
Ta_2O_5 film with protective coating, optical waveguide prod. 79−72682
Ta_2O_5 films, Poole-Frenkel effect and cond., effect of heat treatment in oxygen and in vacuum 80−39693
Ta_2O_5, hydrated, heat treatment effect on physicochem. props. 80−20966
Ta_2O_5 inversion layers for Si solar cells 80−94075
Ta_2O_5, ion-bombarded cryst., structural and compositional changes 79−46724
Ta_2O_5 optical waveguides, colinear interaction between acoustic and optical waves in planar waveguide, radiation into substrate 80−53452
Ta_2O_5, oxidised Ta foil, electron bombardment effects on surface composition, Auger spectroscopy, electron desorption measurements 79−77874
Ta_2O_5, plane optical waveguide, fabrication by reactive sputtering 78−71221
Ta_2O_5, preferential sputtering by Ar^+ ions, XPS obs. 79−83083
Ta_2O_5, RF-sputtered thin-film optical waveguide, effect of deposition parameters on optical loss 79−76881
Ta_2O_5, reactive DC sputtering deposited films with magnetron-plasmatron, mechanical elec., optical props. 80−25566
Ta_2O_5, sputter deposition onto GaAs, and MIS struct. charact. 77−89864
Ta_2O_5, sputter depth profiling with low press. HF plasma 79−95041
Ta_2O_5 sputtered film for integrated optics, refr. index meas. *(Italian)* 79−32088
Ta_2O_5, sputtering by Ar^+ below 1 keV 78−88397
Ta_2O_5, thermoluminesc., in H_2O vap. atm., temp. depend., time decay *(Russian)* 77−44074
Ta_2O_5 thin film protection of unstable OF-type glass components 79−14079
Ta_2O_5, with hexagonal lattice in thin layers, atomic struct., electron diffr. 80−84160
Ta_2O_5, XPS, low energy ion backscatt. spectra 78−72660
Ta_2O_5/Ta, heat-treated anodic film, exoelectron emission and radiation dosimetry *(Japanese)* 79−83110
Ta_2O_5-GaAs interface, fabricated by interactive oxidation, props. 80−49935
Ta_2O_5-H_2O_n, influence of preparation on pore structure and ion exchange props. 79−1970
Ta_2O_5-semicond. oxide interface, electron injection and reactions 77−76936
Ta_2O_5-SiO_2, plane optical waveguide, fabrication by reactive sputtering 78−71221
Ta_2O_5-TiO_2, anodic film, Rutherford backscatt., capacitance 77−16734
Ta_xO_y deficient $Ta_{10}O_{18}$ struct., monoclinic, cryst. struct. by electron diffr. 77−39570
$Ta_2O_5N_x$, sputtered birefr. film, deposition conditions effect on refr. index 77−39118
$Ta(OR)_2Cl_3.L$, halo-alkoxide complex, prep. and props. 78−18605
TaS, (1T), effect of CDW on optical spectra 79−95738
TaS_2, 1T, anomalous magnetoresist., CDW state 78−72173
TaS_2, 1T, quasi-octahedral layer compound, band struct. and Fermi surfaces 77−76747
TaS_2, 1T and 1H polytypes, fast neutron irrad., defect prod., effects on resist. and charge density waves 80−65060
TaS_2, 1T polytype, charge density waves effects on phonon modes, Raman spectra meas. 77−36245
TaS_2, 1T polytype, intercalated with Li(Na)(K)(Eu), CDW's and superlattice patterns 77−47746
TaS_2, $1T_2$ phase, Kohn anomaly, neutron scatt. meas. 77−69056
TaS_2, $1T_2$ polytype, incommensurate periodic lattice distortions, real space TEM 77−47432
TaS_2, $1T_\beta$ to $1T_\alpha$ phase transform., cinematographical obs. 77−84925
TaS_2, 1T-, 2H-, 6R- thin cryst. polymorphs, anomalous resistivity, 0-350K 77−11909
TaS_2, 2H polytype, effect of incipient CDW on second-order Raman spectra 78−80357
TaS_2, 2H polytype, Li intercolation kinetics PAC hyperfine spectrosc. 79−87337
TaS_2 (1T), angular resolved photoemission at low energy and high atomic number 77−36373
TaS_2 (1T), CDW and accompanying periodic structural distortions 78−72094
TaS_2 (1T), CDW-transition temp., press. depend. 77−51730
TaS_2 (1T), charge density waves, ESCA, XPS investigs. 77−12490
TaS_2 (1T), commensurate and incommensurate CDW state, far IR reflection spectra 79−95755
TaS_2 (1T), domain-like incommensurate CDW states and first order incommensurate-commensurate transition 78−26824
TaS_2 (1T), generalised electronic suscept. and CDW 77−43471
TaS_2 (1T), Hall effect 79−38103
TaS_2 (1T), low temp. elec. props. 77−85205
TaS_2 (1T), nonlinear cond. in two-dimens. CDW system 80−10997
TaS_2 (1T) and (2H), bonding and charge density wave phase transitions 80−44282
TaS_2 (1T) electron irradiated, lattice contraction 80−59520
TaS_2 (2H), intercalation with deuteropyridine, neutron diffr. meas. 79−90612
TaS_2 (2H), quantum oscillations and Fermi surface 79−37960
TaS_2 (2H), Raman scatt. 77−1679
TaS_2 (2H), sp. ht. and resist. near CDW phase transitions 78−34786

tantalum compounds continued
TaS_2 (2H), surface struct. and interplanar separation by LEED 77−59191
TaS_2 (2H) intercalated with pyridine, ionic bonding model 79−65052
TaS_2 (2H) single crystal, specific heat meas. in mag. field, 0.3 to 3K, AC calorimetry technique 78−43516
TaS_2 (2H)+NH_3(N_2H_4)(pyridine)(O_2) gases, reacts., intercalation X-ray diffr. investig. 77−12828
TaS_2 ($4H_b$), Fermi surface calcs. 77−51640
TaS_2 ($4H_b$), press. effects on CDW transitions 77−51680
TaS_2 (4Hb) layer cpd., oscillatory magnetotransport obs. 77−85241
TaS_2 (aniline)$_{3/4}$, low-field magnetisation meas. on small cryst. in supercond. phase 79−87188
TaS_2, alkali metal and alkali metal hydroxide intercalates, lattice parameters, supercond. transition temps. 80−25029
1T-TaS_2, and 1T-$TaS_{2-x}Se_x$, Anderson localisation, elec. resist. and magnetoresist. meas. 80−44596
4Hb-TaS_2, band structure calculations, charge transfer and charge density waves 78−79926
TaS_2, charge density waves, mol. beam diffr. obs. 79−73453
TaS_2, decomp. press. and enthalpy of decomposition 79−66042
TaS_2, enthalpy and specific heat, temp. depend. 80−54406
TaS_2 intercalate with tetraalkylammonium hydroxide, prep. and struct. 80−79752
TaS_2 intercalated with NH_3, charge transfer, PAC meas. 78−76366
TaS_2 intercalated with methylamine, supercond. layer cpd., crit. field enhancement and reduced dimensionality 80−60152
TaS_2, intercalated with organic cpds., upper crit. fields and reduced dimensionality 80−70910
TaS_2 intercalates with alkali metals, prep., X-ray anal. and supercond. transition temp. 78−31007
TaS_2, intercalation compounds, octahedral, microstructural study 77−84729
TaS_2 intercalation complexes, superconductivity 78−91803
TaS_2 intercalation complexes with 3d transition metals, mag. and metallic transport props. 80−44814
TaS_2, intercalation cpd. with pyridine, nucl. spin-lattice relax. meas. 80−54962
TaS_2, kinetic study of NH_3/ND_3 exchange by neutron diffr. 79−29350
1T-TaS_2, layered cpd., anisotropic X-ray absorption 78−39629
TaS_2, layered dichalcogenide, US vel. rel. to CDW 77−76490
TaS_2 mixed coordination polytypes, optical props. 0.5-6.0 eV range 79−15476
1T-TaS_2, nearly commensurate phase stabilisation 77−15588
TaS_2, nucl. spin-lattice relax. meas. 80−54962
TaS_2, Peierls transit transition 77−66119
TaS_2, phase transformations and domain structures *(French)* 78−27509
TaS_2, polytypes, charge density waves and superlattice effects, intercalation with hydrazine 78−39043
TaS_2 polytypes, in situ intercalation in TEM, using N_2H_4 gas 79−8254
1T-TaS_2, pure and cation-doped, charge carrier localisation 80−44597
TaS_2, supercond., upper crit. field 77−15994
TaS_2, TDPAC meas., CDW, structural and charge transfer effects 78−39468
TaS_2, texture and lubricating props. 77−44368
TaS_2, thermal expansion, lattice parameter meas. 78−18804
TaS_2:Fe, local moment form., mag. susceptibility meas. 79−82756
TaS_2:NH_3, mol. motion, neutron quasielastic scatt. obs. 79−90827
TaS_2/pyridine intercalated, struct. and bonding 78−91323
TaS_2-2H electrodes, topotactic reduction nechanism, neutron diffr. obs. and intercalation cpd. form. 80−108748
TaS_2-copper tetra-4-dimethylaminophthalocyanine, dye intercalated layered cpd., struct. and superconductivity 78−84342
TaS_2-NH_3 intercalation complex, press. induced diffusion effects, NMR study 79−19797
TaS_3 and TaS_2, modulated struct. phenomena, survey 79−95033
TaS_3, CDW state, Raman spectroscopy obs. 78−60439
TaS_3, electron diffr. evidence for one-dimens. Peierls distortion 78−10024
TaS_3, monoclinic form, cryst. struct. determ., Peierls type transition obs. *(French)* 80−88109
TaS_3, one-dimensional compound, phase anal., X-ray and elec. meas. 79−51086
TaS_3, Peierls superstruct., low temp. X-ray diffr. obs. 78−59793
TaS_3, Peierls transition *(Japanese)* 78−30880
TaS_3, press. depend. of metal-semicond. transition 79−47016
TaS_3, Raman spectra, CDW induced metal-semicond. transition 80−11404
TaS_3, transport props. 80−20175
$TaSCl_3$, prep. and characterisation 77−59705
Ta_6SH_x, H locations and motions, PMR linewidth meas. 77−77115
$TaS_2(ND_3)$, intercalation system, wideline NMR, temp. effects 77−16184
$TaS_2(NH_3)$ and $TaS_2(NH_3)_{1/3}(H_2O)_{2/3}$, incoherent inelastic neutron spectra 80−84163
$TaS_2(NH_3)$, intercalation complex, wideline NMR obs., translational and reorientational effects 77−1602
$TaS_2(NH_3)_x$, NMR spectral densities and two-dimens. diffusion 80−50215
$TaS_{1.6}Se_{0.4}$, pure and intercalated with organic cpds., upper crit. fields and reduced dimensionality 80−70910
$TaS_{2-x}Se_x$ (1T), transport props. 80−103710
1T-$TaS_{2-x}Se_x$, electronic cond. process, resist. meas., 1.3-240K 80−44595
$TaS_{2-x}Se_x$ layer compound, Hall coeff., 4-200K 78−95305
$TaS_2(Se_2)$, 1T phase, CDWs, electronically driven phonon anomalies and phase transforms. 78−63834
$TaS_2(Se_2)$, 2H and 4Hb polytypes, layered cpd., thermal props. at CDW transitions 77−47750
1T$TaS_2(Se_2)$, Hall effect meas., 1.4-360K 80−44616
$TaS_2(Se_2)$, intercalated with ethylenediamine, Raman spectra 78−48182
$TaS_3(Se_3)$, phase transitions and elec. props. 80−20178
TaS_xSe_{2-x}, growth by I_2 vap. transport, cryst. struct. 77−73223
TaS_2(1T), anomalously large negative magnetoresist. at ultra low temps. 79−60852
TaS_2(1T) pure and doped, electrical, structural and mag. props. 79−78141
TaS_2(1T) pure and doped, Mott and Anderson localisation, commensurate phase transition 80−39641
TaS_2(1T), surface CDW, obs. by atomic beam diffr. 80−39195

tantalum compounds continued
TaS_3(1T), inequivalent lattice sites in charge density distorted phases 80−15835
TaS_2(1T)(2H), nucl. quadrupole interactions, high press. effects 78−35072
TaS_2(2H), Li intercalation, electrochemical studies 80−39048
TaS_2(2H), supercond. transition temp., upper crit. field, and interlayer coupling strength 79−56406
TaS_2($4H_b$), electrical cond. and CDW transitions under press., rel. to supercond. 77−43574
TaS_2:Sn, intercalated, Mossbauer effect, hyperfine interaction, lattice dynamics 77−8473
TaS_2.$(pyridine)_{1/2}$, intercalation complex, vib. spectra 77−59076
$TaSe_2$, 1T, quasi-octahedral layer compound, band struct. and Fermi surface 77−76747
$TaSe_2$, 1T and 2H superstruct., cryst. struct. using X-ray diffr. 80−39044
2H-$TaSe_2$, 2D displacive modulation, struct. using superspace-group concept 80−79726
$TaSe_2$, 2H, CDW, action on Fermi surface 77−76736
$TaSe_2$ 2H, CDW effect on thermoreflectance spectra 77−52120
$TaSe_2$, 2H phase, CDW band struct. and IR and visible thermoreflectance meas. 77−28556
$TaSe_2$, 2H polytype, effect of incipient CDW on second-order Raman spectra 78−80357
$TaSe_2$, 4Hb polytype, CWD induced atomic shifts 80−39045
$TaSe_2$ (1T and 2H), charge density waves, ESCA, XPS investigs. 77−12490
$TaSe_2$ (1T), CDW obs. by Mossbauer reson. of ^{57}Fe impurity 77−73104
$TaSe_2$ (1T), commensurate and incommensurate CDW state, far IR reflection spectra 79−95755
$TaSe_2$ (1T), generalised electronic suscept. and CDW 77−43471
$TaSe_2$ (2H), anisotropy in mag. susceptibility 78−43558
$TaSe_2$ (2H), CDW amplitudes determ. by ^{77}Se NMR 77−77116
$TaSe_2$ (2H), CDW and accompanying periodic structural distortions 78−72094
$TaSe_2$ (2H), CDW and discommensurations, ^{77}Se NMR study 80−88883
$TaSe_2$ (2H), charge density wave transitions, neutron diffr. exam. 77−89515
$TaSe_2$ (2H), domain-like incommensurate CDW and first order commensurate-incommensurate transitions 78−56084
$TaSe_2$ (2H), effect of CDW fluctuations on Raman active optic phonon freq. 78−87750
$TaSe_2$ (2H), effect of CDW on optical spectra 79−95738
$TaSe_2$ (2H), Fermi surface, de Haas van Alphen meas. 77−20229
$TaSe_2$ (2H), first-order phase transition, thermal expansion meas. 79−51256
$TaSe_2$ (2H), incommensurate and commensurate struct., Raman scatt. 79−95739
$TaSe_2$ (2H), magnetoresistance in commensurate CDW state, Fermi surface topology 77−43576
$TaSe_2$ (2H), optical absorpt., band struct., plasmons, and CDW 80−45104
$TaSe_2$ (2H), Raman scatt. from CDW 80−93340
$TaSe_2$ (2H), softening of CDW excitation, at superstructure transition 78−79728
$TaSe_2$ (2H), sp. ht. and resist. near CDW phase transitions 78−34786
$TaSe_2$ (2H), thermal and elastic props., X-ray diffr. exam. 79−37754
$TaSe_2$ (2H) and (1T), Raman spectroscopy of CDW state 78−35141
$TaSe_2$, (2H) CDW, reentrant lock in transition at high press. 80−88320
$TaSe_2$ (2H) microscopic model of CDWs 77−89719
$TaSe_2$ (4Hb), atomic displacements in CDW induced superstructure 80−10536
1T-$TaSe_2$, CDW obs. by ^{181}Ta Mossbauer effect 78−39469
2H-$TaSe_2$, commensurate superlattice vibr., Raman spectra 77−16299
$TaSe_2$, evaporation, mass spectroscopic anal. 77−76530
$TaSe_2$, $TaSe_3$, comparison of elec. cond. 78−14715
$TaSe_2$:Fe, competition between charge and spin density waves, Landau-Ginzburg theory 79−95352
$TaSe_2$:Fe, local moment form., mag. susceptibility meas. 79−82756
$TaSe_2$/(2H) layer cpd., oscillatory magnetotransport obs. 77−85241
$TaSe_3$, chain-like compound, low temp. phase transition 78−80088
$TaSe_3$, effect of press. on supercond. transition temp. 79−91182
$TaSe_3$, oscillatory magnetotransport, Fermi surface anisotropy, Hall effect, g-factor, Dingle temp. 78−51975
$TaSe_3$, phonon study of chemical bonding 80−20645
$TaSe_3$, superconducting crit. field rel. to anisotropic cryst. struct. 78−80104
$TaSe_3$, superconducting transition *(Japanese)* 78−30880
$TaSe_3$, superconducting transitions and diamagnetism 80−84526
$TaSe_3$, transport props. 80−20175
$TaSe_2$(S_2), layer type dichalcogenides, reflectivity, 6 to 40 eV, electronic deep level excitation 77−55801
$TaSe_2$(2H), CDW layered cpd., phase diagrams 79−69243
$TaSe_2$(2H), CDW phase transition, effect of electron-phonon scattering 78−95265
$TaSe_2$(2H), layer cpd. commensurate-incommensurate transition 79−69244
$TaSe_2$(2H), plasmon behaviour at charge density wave onset 80−10900
$TaSe_2$(2H), Raman scatt., charge density wave mode softening at superstruct. transition 77−8584
$TaSe_2$(2H), Raman spectra of soft modes at CDW transition 77−16301
$TaSe_2$(6R), stacking layer study, appl. of convergent beam electron diffr. 80−39116
$TaSi_2$ film, elastic stiffness and thermal expansion coeffs. 80−107451
$TaSi_2$ films, on polycrystalline Si, oxidation characts. 80−97602
$TaSi_2$ refractory formation by As^+ ion beam bombardment 80−107286
$TaSi_2$, self-propag. high-temp. synthesis 80−2988
$TaSi_2$-$CrSi_2$, phase equilib., struct. and props. 80−50608
Ta_5Si_3 and $TaSi_2$ form. in thin cosputtered (Ta+Si) films on polycryst. Si and SiO_2 80−70546
TaS_2(pyridine)$_{1/2}$ intercalated layered supercond., fluctuation induced diamag. and dimensionality 77−77006
TaS_2(pyridine)$_{1/2}$ intercalation complex, supercond. transition temp., upper crit. field, and interlayer coupling strength 79−56406
TaS_2(pyridine)$_{1/2}$, pyridine orientation, X-ray diffr. meas. 79−55679
TaS_2(pyridine)$_{1/2}$, superconducting intercalation complex, proton spin lattice relaxation time 78−80096
TaS_2(pyridine)$_{1/2}$, upper and lower critical fields, supercond. props. from Ginzburg-Landau theory 79−56456

tantalum compounds continued
$Ta_{1-x}Ti_xS_2$ (1T), magnetoresistance in the Anderson localized states near the metal-nonmetal transition 80−88479
$Ta_{1-x}Ti_xS_2$ (1T), magnetoresist. near metal-nonmetal transition at ultra low temps. 80−88600
$Ta_yTi_{1-y}S_2$, Li intercalation, electrochemical studies 80−39048
$Ta_xTi_{1-x}Se_2$, cryst. struct. and elec. props. 79−47133
$Ta_{16}W_{18}O_{94}$, characterisation of thermally contracting tungstates 78−63869
Ta_2WO_8, characterisation of thermally contracting tungstates 78−63869
Ta_2WO_8, neutron powder diffr. study of cryst. struct., profile anal. 79−55706
$Ta_{22}W_4O_{67}$, characterisation of thermally contracting tungstates 78−63869
$Ta_{1-x}Zr_xSe_2$ (1T), CDW stacking order, interlayer interactions and impurity effects 77−7699
^{181}Ta, isomer shifts of 6.2 keV γ-rays, book contrib. 79−87358
TiC-TaC, prod. and props. 77−28772
TiC-WC-TaC carbide mixture in plasma reactor *(German)* 77−1819
TiN-Nb(Ta)N, microcomposite film prod. for radio resistors 78−3052
TiO_2:Ta_2O_5, conduct. rel. to defect structure, obs. 77−76392
TiO_2:Ta_2O_5(Nb_2O_5), rutile, defect struct. and elec. cond. at 1273K 80−44604
TiO_2-Ta_2O_5 system, surface microphases investigation by X-ray electron spectral anal. 79−51269
$TiSe_2$ (1T), lattice dynamics and phase transitions 78−79727
$Ti_{1-x}Ta_xO_2$, solid soln. formed in TiO_2-Ta_2O_5-Ta at 1100°C *(French)* 78−35375
TlH, ab initio SCF calcs. using relativistic effective core pot. 80−95524
$Tl_{5-x}Ta_{11+x/5}O_{30}$, synthesis, non-stoichiometry, density and ionic cond. meas. *(French)* 78−52741
Tl_3TaSe_4, for SAW devices, temp. compensated cuts with zero power flow 77−12313
Tl_3TaSe_4, new SAW zero temp. cuts 78−2351
$Tl_{1+x}Ta_{1+x}W_{1-x}O_6$ pyrochlore system, comp. depend. of ionic cond. 80−107517
$Tl_{1+x}Ta_{1+x}W_{1-x}O_6.nH_2O$, pyrochlore type, stoichiometry and ionic cond. 80−24648
UF_6-TaF_5, dil sol., liq.-vap. equilib. 77−62632
$Zn_2Ta_2O_6$, metastable orthorhombic variety, crystallographic characts. *(French)* 79−82185
ZrC-TaC solid solns., high-temp. creep 79−11661
ZrO_2-$YO_{1.5}$-$TaO_{2.5}$, cubic fluorite phase, elec. cond. 80−107551
6.14ZrO_2.Ta_2O_5, elec. cond. meas. 80−100463

tantalum electrolytic capacitors *see electrolytic capacitors*

tantalum rectifiers *see electrolytic rectifiers*

tape recorders
see also magnetic heads; magnetic recording
4-channel cassette recorder for 24-hour epileptic patient EEG monitoring 78−3639
ambulatory ECG monitoring problems 78−11763
bat detection instruments 80−69609
biomedical ECG recording, correction of timing errors due to tape speed variation 80−72354
biomedical recording system, TDM multiplexing system for multichannel signal averaging of visually evoked responses 80−36165
Braille display cassette tape recording for text reproduction *(Spanish)* 79−39612
cassette, amplitude variations measuring set *(German)* 79−32156
cassette data recorder *(Spanish)* 79−30441
and chart recorder timing waveform generator 79−17415
cortical evoked response audiometry, portable programmable tape recorder 77−60279
data output device using narrow tape recorder for radio receivers 79−29993
data recording and reproduction using magnetic tape 79−88934
dual capstan drive tape recorder *(German)* 80−95092
ECG cassette recording and automatic processing microprocessor system 78−36021
ECG continuous monitoring on commercial pilots appl. 77−86659
EEG analogue multiplexer for FM tape recording 79−34691
EEG cassette recording system, portable four-channel 77−56498
EEG digital recording system for epileptic event observation 78−3641
EEG recording system, portable pulse-interval modulation telemetry/multiplexing system, home use 80−67261
elements with large time constants *(Russian)* 78−187
equipment and services, 1979 video yearbook 79−14197
FM electronics system for biomedical data recording 79−44010
holography, sequential information retrieval 77−7024
instrumental, applications vs. recording mode 78−62188
instrumentation recorders, for data acquisition 78−49817
kit of instruments for statistical research 78−87215
low intensity data recording, estimation of reliable spectral information 79−21724
low-frequency FM tape recording of nerve action potentials 79−57832
magnetic head alloy Fe Al-Pr, resist. depend. on rolling process, thermal treatment *(Polish)* 80−39555
meteorology radar signal recording on video machine, coherent Doppler radar 80−46275
microprocessor-controlled tape drive 79−93123
minicomputer-controlled high-speed transient recording system *(Russian)* 77−9992
NMR spectra recording processing and accumulation, using mag. tape system *(Russian)* 79−26097
PCM, wideband, Space Shuttle Orbiter appl. 77−64614
physiological 4-channel recording 78−24154
physiological signals, analogue tape recorder, low cost using hi-fi cassette player 80−41282
portable, FM- and direct-recording types comparison 79−1028
punched-tape recording system, radioastronomy appl. *(Russian)* 78−65501
read head for magnetic tape recorders using magneto-resistance principle 80−87688
seismometer stationed on ocean bed, self-contained unit with mag. recorder *(Russian)* 80−36410
shipboard meteorological data system 80−46299
single-track multiplex FM conversion unit 77−45828
slide sync tape recorder, sensory modality matching tests 80−41334
smoking pattern recorder, portable 80−94385
spectrophotometer kinetic curve recording unit 78−86352

tape recorders continued
stereo, sound track production for home cinefilm 78−16883
stereo cassette, digital system for recording analogue voltages 77−61061
thermoplastic photoconductor tape performance for optical recording 80−43305
three-channel modulation scheme for biological signals 78−61272
thresholds of pain and hearing, cassette recorder noise and music levels *(German)* 80−81616
time reference singal for tape recording, IRIG and NASA code formats 80−57262
tutored videotape instruction advantages for science and engineering courses 78−8194
video, high-resolution for medical X-ray work 78−24120
wideband video facility, stress-wave emission signals recording appl. 77−37873
wind energy survey anemometer and recording instrumentation 77−33222

taste *see chemioception*

Taylor instability *see flow instability*

t.d.m. *see time division multiplexing*

teaching
see also demonstrations; education; student laboratory apparatus; training
Abraham-Minkowski controversy, EM momentum in static fields 80−101678
AC power line, reasons for grounding (earthing) 80−77594
academic motivation, objective measurement 79−17154
accelerated reference frames, theory 80−41991
acceleration, by 'racetrack' game 78−62022
acceleration and velocity teaching, racetrack game 80−31458
accelerator physics undergraduate course, 0.5 MeV Van de Graaff 77−30
acoustic absorption, classroom experiment 80−42016
acoustical propag. in ocean, appl. of parabolic approx. 79−25794
acoustics of percussion instruments 77−9838
additivity, rapidity, relativity, teaching 80−41984
advanced energy systems, future needs and developments 78−8197
advanced undergraduate physics laboratory, industrial research roleplaying 78−36755
Aharonov-Bohm effect, first-order perturbation theory 79−21497
Aharonov-Bohm scatt. by thin impenetrable solenoid 79−9058
aids and materials 80−94942
airphoto interpretation, teaching using computer 79−48999
Airy functions, stress problem solns., teaching appl. 78−86063
algorithms, fast least squares, on-line data fitting 77−33787
alkali metals, cohesive energy 80−90630
alkenes, π bond dissoc. energies, derivation from isomerisation kinetics 79−58498
American Association of Physics Teachers, 1979 winter meeting 80−42042
analogue computers, teaching appls. with biological examples 79−84890
analytical chemistry, problems 78−81736
analytical chemistry, role of audio-visual learning aids laboratory 80−94944
angular momentum conservation, rel. to springboard divers, gymnasts and trampolinists 79−84884
angular velocity vector, attached to moving reference frame, time variation 80−41986
antiferromagnetic and ferromagnetic parallel susceptibilities, graphical illustration 78−41118
applied mathematics, math. modelling techniques 79−35492
approximation methods for 80−105474
Arrhenius activation energy, derivation using collision theory 78−93495
astrology in undergraduate astronomy courses 78−61991
astronomy, infrared, 3K cosmic background radiation, star form., nuclei of active galaxies 80−67958
astronomy, orbital elements, nonlinear least squares minimisation 77−33761
astronomy, position finding, spherical projections, teaching appl. 77−41437
astronomy, radius vector determ. from two position obs. 77−33760
astronomy, the dark night sky, 'Olbers' paradox', history and resolution 77−33758
astronomy, use of computers in schools 80−73126
astronomy, use of line-of-sight transparency 79−35508
asymptotic freedom 80−17761
atmospheric oscillations and Ruchhardt's experiment, theory, for teachers 79−71198
atomic electronic 4s, 3d energy levels, textbook diagram, teaching 78−73801
atomic energy levels for p-block ats., electron repulsion integrals 78−93494
atomic orbital contour calcs., teaching approach 78−93500
atomic orbitals, hydrogen-like, shape, teaching appl. 78−93496
atomic radiative decay, electrical analogues for two- and three-level systems 77−33793
atomic spectra, Rydberg-Schuster law 78−16591
atomic spectral line breadth, conversion from freq. to wavelength widths 78−32632
atomic structure, var. calcs. 77−61679
audio-visual systems, Hungarian developments, BEAG activities 78−46860
Aufbau principle, subshell filling order, method for determining 77−26111
automated simulation of direct school/society interaction 79−35487
automobile whip antenna, first overtone vibrational mode obs. 80−17747
automobiles, air and rolling resistance effects 77−11
ball and spring, elliptical motion 80−82613
ballistics, collision of aimed and initially stationary balls 79−21506
ballistics, snowballs and ICBM's 79−58465
ballistics of shot put, maximum range 78−61985
ballistics pendulum 77−78914
Balmer wavelength calc. with hand calculator, student project 78−12512
bar magnets, torque theory 77−13527
barometric distribution, elementary kinetic derivation 77−62323
batteries, combinatorial rules 79−62962
Bernoulli's theorem, misinterpretation 77−87614
Bernoulli force, coffee cup demonstration 79−35482
bi-lingual audio-visual aids for technical education in developing Arab countries 80−94943

teaching continued
bicycle dynamics, nongyroscopic aspects, lab. demonstration 78−36769
bicycle stability, teaching approach using unsuccessful nongyroscopic theory 80−42001
binary elastic collision in rel. space, isosceles trapezoid representation 78−61981
binary heterogeneous vapour-liquid equilibrium, student experiment demonstrating miscibility effects 77−82352
bioinstrumentation teaching laboratory, efficient use of animal expts. 77−37700
biological membranes, single-file diffusion 78−54127
biomembranes, teaching demonstration using molecular membrane model 77−57117
black hole geometry, photon orbit charts 77−33783
black holes, nature of interior universe theory 77−67107
black holes, particle emission and critical mass, Kessler model 79−71190
black holes, particle emission model 78−62018
blackbody spectrum, interpretation of quantum theory 78−54130
blind students, musical acoustics course 80−77584
Bode's law and the 'missing moons' of Saturn 79−58480
bond free energies, table for chem. student use 80−22171
book, secondary school general physics course 78−57725
Born's discovery of the quantum-mechanical matrix calculus 80−82615
Bose's second paper, conflict with Einstein, history of science 77−33813
bouncing ball experiment, theory of time of flight, for teachers 79−71196
bound diatomic molecules, covalent bonding concept in undergrad. chem. courses 80−22177
bowling ball path, rot. coord. system 77−33788
brachistochrones, tautochrones, evolutes, and tesselations 79−25798
braking distance versus mass for automobiles 77−45644
Brecht's Galileo, changing perceptions of Galileo Galilei as scientific exemplar 80−51996
Brewster angle in semi-infinite dielectric moving perpendicularly to interface 80−57034
Bronx High School of Science, physics teaching 80−77562
Brownian motion, account of discovery 78−86090
Brownian motion, correl. in Langevin theory 79−97133
Brownian motion, melting, surface tension and rubber networks, thermodynamic anal. 80−73132
Brownian motion, two-dimens., simulation on micro-computer *(Japanese)* 80−31461
Brownian motion with viscous drag, Monte Carlo simulation 78−61984
bubble chamber, electromagnetic shower photographs 78−65737
bubble cohesion in foam, binding energy calc. 78−61978
bubbles with interconnection, equilib. states 79−15
CAI, audible, use of audio or video recordings 80−42008
calculus teaching, discrete approach using computer 79−80398
camera flare rel. to internal finish, student examination project 79−25782
cancer, cervical, treatment by cathetron 78−49617
canonical transformation to the free particle 77−49521
capacitor, mag. field between discharging plates, Ampere's law 79−21490
capacitor complete discharge time, thermal noise 80−17727
car tyre, friction and traction 78−81751
cardiovascular system simulation by elec. compartmental model 79−5388
cart wheels on inclined plane, theory and expt. 78−61977
cascade decay processes, probability theory calc. 79−44670
catastrophe theory, appl. to ferromag. mol. field 79−35467
catastrophe theory, soap film simulation 79−62974
celestial mechanics, diurnal motion of Sun seen from Mercury, computer aided soln. 78−61969
celestial mechanics, elementary derivation of perturbation eqns. 77−6
celestial navigation, with stereographic projection 77−60866
cells, electrochemical, photovoltaic phenomena and mechanisms 78−8198
centrifugal buoyancy forces, particle in rotating fluid 78−12487
centrifugal buoyancy forces from energy considerations 80−82609
CGS to SI conversion for electromagnetism 78−16592
charged particle, motion in mag. monopole field, classical theory 79−97139
charged particle motion in dipolar axially symmetric field 77−68155
chemical, osmotic and electrochemical equilibrium, principle of virtual work 77−33767
chemical analysis, quantitative, grading methods 79−48993
chemical bond orders, lengths, MO calc. methods, correl. with experimental values, teaching appl. 77−29974
chemical equilibria, double scales as visual representations 79−84908
chemical equilibrium, entropy differences and statistical effects, symmetry corrections and entropy of mixing 79−21480
chemical equilibrium, entropy gradient, heuristic approach 79−48991
chemical equilibrium teaching, computer method using minimisation of free energy 79−30168
chemical kinetics computer simulation 77−13555
chemical reaction, complex, kinetics, Markov chain appl. 80−27085
chemical reaction kinetics, teaching, Monte Carlo method, computer program 77−24
chemical reaction kinetics 78−69928
chemical reaction rate eqn. integration, interactive computer program system 80−31469
chemical spectroscopy, computer-assisted learning methods 79−84906
chemical thermodynamics, applicability of $dE=TdS-PdV$ 77−87609
chemistry, electron pair mechanism, non-specialist teaching appl. 78−89279
chemistry, first order kinetic data anal., optimisation method 78−12500
chemistry, M-C-O deformation modes, no. and symmetry determ., group theoretical method 78−11
chemistry, method of successive approx., teaching 78−89281
chemistry curriculum, ion-ion, ion-dipole, dipole-dipole interactions 78−10
chemistry teaching, courses, laboratories, for nonscientists, bibliography, 1968-1977 79−84881
chimney breaking while falling 77−33768
chiral molecules, detection, identification by Cahn-Ingold-Prelog rules, computer program 79−58499
circuit theory, DC, teaching approach using rectangle dissection 80−46757
circular motion with friction, numerical and analytical solns. 80−57029
class notetaker, rotating assignment of student 78−81734
classical and quantum uncertainties, particle in box, harmonic oscill. and atom 79−25789

teaching continued
classical field theory, classical deflection in a central field 80−41993
classical inverse scattering in one dimension 80−82595
classical Kepler problem in momentum space 78−36764
classical machanics, freely moving balls on rotating discs, stable circular orbits 80−27074
classical mechanics, anharmonic oscillator, Hamilton's principle appl. 79−84896
classical mechanics, complementary Lagrange formalism 78−36745
classical mechanics, fundamental laws and concepts *(Hungarian)* 77−37691
classical mechanics, Hamilton's principle, variational formulation approx. solns., simple pendulum 77−33774
classical mechanics and Neother's theorem 77−45635
classical mechanics gauge invariance, derivation of Maxwell's eqns. 80−73131
classical mechanics operator formulation, wave packets in config. space 80−73137
classical mechanics perturbation expansion method, calcs. 77−33741
clavier, tuning, freq. matching using pocket calculator 78−81728
climate, astronomical theory, teaching approach 79−84891
clinical experiences, computer simulated patients 79−17162
clock escapement mechanisms, mathematical theory 78−41108
clocks, mains and battery operated, energy efficiency 78−81773
closed universe, S^3 topology, rel. to Dante's Divine Comedy 80−41980
coal-fired power station pollution, physics 79−44659
cognitive preferences, comparative studies of Israeli chem. students 79−48985
coherent optics, T_2 as collision time, dephasing time, or reciprocal linewidth 80−27075
college astronomy and physics texts, readability 80−77583
collision theory, hockey ball goal scoring approach 77−41435
collisions, linear, elastic, dynamic solns. 80−17769
colour, primaries as used in physics and art 79−35464
colour centres, absorption wavelength, finite-pot. well models 78−12463
colour reproduction of surface texture, visual qualities 78−16881
compact storage for iterative soln. of large sparse linear systems of eqns. 78−57713
comparative evaluation of instructional systems, survival principle 79−92906
composite potential well, energy level determ. using Green's function factorisation theorem 79−97148
compound and intermediate nuclear struct. wave packet scatt. time evolution, simple model 79−9054
Compton shift, energy-momentum relation for electron 79−40322
computer assisted learning in nuclear engineering 77−13557
computer graphics and electromagnetic fields 77−33781
computer programs for high-school expts. 78−86094
computer used to improve unit teaching 77−53721
computer-aided instruction, appl. to ecological population dynamics 79−30166
computer-aided ship structural design for diploma and undergraduate courses 79−35494
computer-assisted learning in the University of Surrey Chemistry Department 79−30167
computer-assisted-learning agency, staffing needs and position in vertical organisational struct. of educational institution 80−42007
computers in educational technology 78−49615
condensation of lattice gas, one-dimens. 79−18
conditionally divergent series, rearrangement, induced charge on parallel plates 77−87599
conservation effects on resource usage, integral expressions 78−69941
conservative motion in phase space *(Spanish)* 78−36785
continuity equation, 1-dimens., for unsteady flow 80−82598
contour plotting, moire technique 80−42002
coordinate transformation of Laplace operator in 2-D 78−61999
coordinate-free rotation operator, for rotations in Euclidian space 79−97145
Coriolis effects in fixed frame, physical meaning 77−75788
Coriolis machine, inertial motion viewed from rot. reference frame, coordinate transformation 78−69934
Coriolis phenomenon in nuclei and planets, rot. alignment 80−90636
correspondence principle, rel. to potential step scattering, theory 80−46761
cosmologies with varying gravity, theories and effects 77−60858
cosmology, generalised Doppler formula for nonstatic universe 77−78900
Coulomb's law in moving medium, Maxwell's eqns. and Dirac function 78−61987
Coulomb phase shift, of quantum theory, and classical time delay 79−97135
Coulomb problem, symmetry and invariance, canonical transformations 80−41989
coupled harmonic oscillators, natural freqs. from anal. geometry 79−25806
cranking model, perturbation theory and Dalgarno Lewis method 77−45640
creativity model, alternating intuitive and rational critical phases *(French)* 77−9159
crisis question technique 78−81738
critical damping of simple-harmonic motion 79−17
Crookes radiometer, physics anal. 79−35504
crystal, one-dimens. with Morse pot., stability 78−54134
crystal optics, group vel. and energy density, monochromatic wave dispersion depend., for teaching 78−25792
crystal vibrations, matrix paradox 78−49611
curl operator when A.curl A≠0 78−62020
curve fitting, interactive computer program, for science students 77−60913
dark night sky paradox, expansion and hierarchical struct. of the universe 78−86055
data analysis, exponential growth factors by Mangelsdorf's method 79−71195
data manipulation and handling problems of analogue signals, digital filtering use 80−4489
David Ausubel learning theory as reference system for content organisation in physics 80−22172
de Broglie wave relativistic Doppler shift 78−49613
deep one-dimens. periodic pot., zero energy gaps, Kronig-Penney model 80−62426
degree-day measurements 80−77574
delocalisation, organic chemistry courses 78−4426
teaching continued
density matrix, asymptotic high temperature expansion 78−54115
detonation, theory, one-dimensional compressible flow 80−41985
developing countries, electromagnetism and telecommunication, course content 78−3
diamagnetic susceptibility calculation using Pascal's consts., BASIC program 80−37717
diatomic molecule, quantum mech. model 78−86050
diatomic molecules vibr. consts. determ., IR spectroscopic, quantum chem. teaching project 79−84914
dielectric cylinder, scattered light polarisation characts. 77−75409
differential operators, direct derivation in curvilinear coords. 78−12478
diffraction in time and the time-energy uncertainty relation 77−13518
diffraction of plane δ-function pulse at a half plane, boundary pulse effects 78−12460
diffraction pattern classroom anal., image-space method 80−51983
diffraction pattern of selected area, indexing, graphical technique 78−54132
diffusion, random walk approx., theory of generating function and method of steepest descent 78−36744
diffusion equation, derivation from Fokker Planck equation using perturbation methods 78−54117
dimensional analysis, modification and generalisation in physics teaching 80−105481
dimensional analysis in electricity and mechanics 79−97165
dipole relaxation in electric field 80−90625
Dirac γ matrices 77−45637
Dirac delta function, appl. elec. current and mag. multipole distribs. 80−17740
Dirac delta function, appls. to elec. charge and multipole distribs. 77−75356
Dirac equation for the H atom 80−46760
Dirac monopole, calc. of strength 77−33764
Dirac theory, Hermitian interaction terms 77−33752
discrete transformations, by stored water method 79−23
dispersion eqn., long wavelength approx., appl. EM wave in plasma 80−17735
displacement currents and magnetic fields in empty space, theory 77−22347
distance-teaching projects, cost effectiveness evaluation 79−40312
Doppler effect, relativistic dynamics 79−97164
Doppler effect formula, acoustic, derivation on intuitive basis 78−24621
Doppler effect in special relativity for teaching 78−24609
Doppler redshifts in oblique approach of source and observer 79−58475
Doppler shift formula for radar echo without transformation eqns. 77−82344
Doppler-shifted photons, origin of increased energy explained by mechanics of source 78−28897
double group theory, half-shell and two-level system, optical polarisation 78−49594
double group theory, half-shell and two-level systems, rot. and half integral spin states 78−45447
dry friction problems, graphical soln. for teaching 78−12511
dynamic load line construction 80−67963
dynamics, brachistochrone, arbitrary initial vel. object 79−21500
dynamics, infinitesimal rotations, invalidities in usage 80−57036
dynamics, laws of, teaching in Soviet schools *(Hungarian)* 78−9
dynamics of variable mass system, flexible inextensible rope 78−86071
E-layer height, calc. errors 77−22346
Earth's interior and const. gravity models 77−45645
Earth's size measurement, from sunset obs. 79−35459
Earth gravity values at poles, rel. to equator, density effects 80−46758
Eastern mystical philosophy, quantum mechanics and the bootstrap-quark controversy 79−84883
eddy currents, levitation, metal detectors and induction heating 78−61967
eigenfunctions and eigenenergies, N-space dimensions calcs., for H and relativistic π-mesic atom 80−41988
eigenvector of general rot., geometrical construction 80−57025
Einstein, light quanta, radiation, relativity in 1905 77−31
Einstein's 1907 essay-translation 77−87619
Einstein's 1925 unified field theory, equivalence with relativistic theory of the nonsymmetric field 79−58484
Einstein's General Theory of Relativity and press reaction 80−57075
Einstein's principle of equivalence, sources of confusion 77−45646
Einstein's relativity paper (1905) and the electromagnetic world picture 78−16616
Einstein and ΔtΔE 80−51986
Einstein and general relativity, historical perspectives 79−40316
elastic collisions, theory 77−67264
elastic collisions of theee spheres in a line, eigenvalue and difference eqns. solns. 77−33786
elastic scattering, large-ang., approx. classical theory 79−25801
elastic three-body linear collision, inverse scatt. problem 79−35468
elasticity, its development during the 17th and 18th centuries 79−17167
electric car, physical principles 77−41440
electric discharge, multipacting breakdown mechanism in HF discharge, for teachers 79−97144
electric energy density in dissipative medium by cct. analogue 78−36759
electric field strength, dissipative media, equivalent cct. 79−40319
electric motor, made from ball bearing 79−21488
electric resistance, temp. depend., qualitative anal. by audible demonstration 80−46775
electrical circuit geometrical representation 78−12513
electrical circuits, current in external circuit, induced by charged particle motion in device 79−21503
electrical conductivity, Kubo-Greenwood formula 78−62017
electro-and magnetostatics, point-multipole expansion 78−61992
electrochemical electron transfer at electrodes in soln., review, in book, for teaching 78−8203
electrochemical oscillations, of voltage and current, spontaneous, maths. anal. of mechanisms, in book, for teaching 78−8201
electrochemical species-selective sensor, use of semi-permeable membranes, in book, for teachers 78−8200
electrochemistry, solid state 78−93498
electrochemistry, special topics, undergraduate level teaching, book 78−8196
electrode processes possessing charge transfer mechanism, overvoltage theory, in book, for teachers 78−8204
electrode systems, nonequilib. polaris. states props. overvoltage theory, in book, for teachers 78−8205

teaching continued
electrodynamics, cause and effect relationship 78−54108
electrodynamics, charge hyperbolic motion and radiation 78−49587
electrodynamics, extended charges, motion, radiation reaction effects 77−33748
electrodynamics, Lienard-Wiechert field expression, circulating charge in static mag. field 78−69933
electrolyte solutions, ion motion due to elec. field, units, nomenclature, teaching appl. 77−14
electromagnetic radiation fields: a simple approach via field lines 80−51991
electromagnetic theory, Hertz vector potentials, instructional appls. 78−12490
electromagnetism, Maxwell's theory, Faraday induction term and Galilei invariance 80−41995
electromagnetism, to undergraduates, showing practical appls. 78−20922
electromagnetism, vector fields, Debye pot. representation 78−73797
electromotive force: Volta's forgotten concept 80−73143
electron in strong mag. field, degenerate perturbation theory 77−33801
electron microscopy, autotutorial methods utilizing sound-on-slide presentations 80−73534
electron optics, charged particle trajectory calc. in electrostatic field 80−90635
electron optics, spherical aberration 78−54135
electron properties, meas. of single isolated electron 78−81776
electron relax. time in metals, waiting time paradox 78−36771
electron spin, nonrelativistic quantum mechanics derivation from Schrodinger eqn. 78−69942
electron trajectories, in homogeneous elec. fields, relativistic and classical 77−41436
electron wave packet in uniform electric field wave mechs. 78−61983
electron-dipole system, semiclassical quantisation 79−25799
electron-photon scattering, symmetrical formulation in relativistic quantum mech. 77−67599
electronics, systems approach 77−45625
electronics, undergraduate laboratory course 80−105478
electronics design course curriculum study, overview 80−27063
electronics study group, integrated circuit appls. *(German)* 80−67970
electronics technology development, teaching 80−31470
electrooptics for electrical engineers, undergraduate curriculum 79−11
electrostatic fields, points of equilib. 80−31453
electrostatic paradox and resolution, teaching approach 77−75357
electrostatic problems with simple dielectric boundary, solution method 78−12458
electrostatics, point charge between grounded planes, conditionally convergent series 79−71201
electrostatics, relax. calcs. 79−58489
elemental evolution and isotopic composition, teaching 78−41128
elementary particle interactions, cross-sections, Lorentz contraction 77−33743
elementary particle phenomena, rel. to undergraduate physics 78−54118
elementary particle spectrum, series classification 77−74652
elementary particle weak interactions, resource letter, WI-1 78−16601
elementary particles, quarks and the concept of particle, Richtmyer memorial lecture 78−62286
elementary particles since J/ψ, review 80−57018
elliptical orbits and inverse square law of gravity 80−46755
elliptically polarised light, polar intensity profile calcs. 77−13526
EM field, static, angular momentum 80−46771
EM field multipole expansions, spin-weighted spherical harmonics 77−33766
EM field problem with a non-linear condition 79−18326
EM field theory, moment methods, for undergraduates 78−28886
EM fields, multipole expansions, using Debye potentials 78−41116
EM induction history 79−44682
EM plane wave accel. of free electron 77−78917
EM theory, undergraduates 77−71167
EM theory of prism couplers, tutorial approach *(French)* 77−37694
EM vector pot., physical interpretation 80−46772
EM vector pot. and its physical reality 78−61974
EM vector potential, interpretation 79−25809
EM wave interaction with matter, gauge invariant formulation 78−62006
EMF, pot. difference, voltage 79−58478
EMF, potential difference and voltage, definitions 78−12469
emission from blackbody, thermodynamic laws 80−105451
energy conservation and human body weight, diet, exercise and differential eqn. 77−87598
energy conversion processes, performance standards, Atwood machine as example 78−62008
energy efficiency, problems and solns. 78−81762
energy projects, undergraduate physics 77−13530
engineering design, creativity testing 80−27062
engineering design curricula, computer appls. 80−27065
engineering education, modern methods and instructional media roles 80−27064
engineering education, perspective and some current problems 79−10
engineering-science summer programme 79−2588
entropy, crystal model *(Hungarian)* 77−64906
entropy, definitions by Boltzmann and Clausius, reversible processes 77−10
entropy, molecular model *(Hungarian)* 77−64903
entropy, perfect gas model *(Hungarian)* 77−64904
entropy, rubber model *(Hungarian)* 77−64905
entropy and rubbery elasticity, teacher resource paper 80−17777
entropy increase principle for collection of thermally interacting systems 77−33785
entropy maximisation, chemically organising effects 77−26107
entropy maximisation controversy 79−58477
equipartition theorem generalisation 78−49603
equivalence principle, monkey and hunter demonstration 80−67984
equivalence principle, or formal mathematical statement, for teachers 79−71200
equivalent electrons, J allowed values in jj coupling 80−90624
error estimation, use of quartiles 77−60868
errors, approximate treatment 77−12
Euler's theorem on rigid-body motion, matrix theoretic proof 79−62964
Eulerian and Lagrangian coordinate systems 79−21491
European computer network, engineering design computer packages, teaching 80−31465
exclusion principle, undergraduate teaching approach 78−81746

teaching continued
exponential function, appl. to problems of steady inflation 77−13576
exponential function, growth and compound interest 77−5637
exponential growth factors, determ. by Mangelsdorf's method 80−67980
exponential law, concepts prior to 1900 78−86052
extended Galilean transformation 79−25788
exterior algebra and exterior differential forms for electromagnetic problems 80−57037
factoring 111...11, applications, teaching approach for pre-calculus students 78−57714
Faraday's law problem, including nonlinear term, rel. to perturbation theory 79−35470
fast Fourier transforms for spectral analysis 78−81750
feedback, sequential test methods and quality criteria *(German)* 80−67968
Fermat principle, tutorial for physics teachers *(Hungarian)* 78−36775
ferromagnetism, Bethe-Peierls-Weiss model, phase transition calc. 79−2585
Feynman path integral and gauge invariance 80−82601
Fibonacci numbers, recurrence relation soln., combinatorics function anal. 80−51988
field effect transistors, computer simulation, student lab expt. 79−44673
finite antenna, EM radiation calcs. 77−68149
finite rigid-body rotations, kinematics 78−12482
finite rotations and angular velocity 80−46766
Fizeau effect, theory, expt., and Zeeman meas., for teaching 78−24597
flow, Stokes law, Reynolds no., appl. to erythrocyte sedimentation rate 78−49610
fluorescence quenching rate constant, undergraduate expt. using Spectronic 20 77−57119
fluorescent intensity analysis, absorption and self-absorption quenching effects 77−37693
Fokker-Planck equation, simplified derivation for teaching 79−71188
forced harmonic oscillator, Hamiltonian for time-depend. damping 79−21495
forced harmonic oscillator, quantum mech., interaction 77−60951
forensic science, for criminal justice students 79−48986
Foucault pendulums, long and short, precessional periods 78−73794
Fourier, series convergence rate, graphical illustration 79−80399
Fourier series, recursive evaluation 79−35477
Fourier transform imaging, systems theory appl. *(German)* 78−74851
fracture, (materials science), description of Open University course 'Materials under Stress' 78−57720
fracture, teaching in universities 78−77645
Franklin, Benjamin, exptl. philosopher, theory of electricity, for teaching 78−24630
Fraunhofer diffraction, transcendental eqns., numerical soln. method 77−33750
Fraunhofer diffraction and polarisation 79−44666
Fraunhofer diffraction patterns, from apertures illuminated with nonparallel light 80−67983
fraunhofer diffraction patterns from apertures illuminated with nonparallel light 79−35465
free-electron gas, n-dimens., specific heat and density of states 78−12466
Fresnel's eqn. for light reflection and refraction 80−101688
Fresnel diffr. of slow neutrons, by pointed and square straight-edges 77−33794
Fresnel integrals, computer evaluation 77−33795
Friedmann cosmology luminosity distance eqn. 78−6
Friedmann models, views of the evolving Universe 78−24598
Friedmann universe, closed, black-body spectrum evolution 78−24599
frontier molecular orbital theory, appl. to Hammett correls. 78−93499
frozen-in field condition, Lie derivative calcs. 79−2586
fuel saving by thermostat setback 78−24626
Fues potential, vibr.-rot. spectra, Schrodinger eqn. soln., pot. energy curves *(Spanish)* 78−36784
Galileo's two bodies falling through air, numerical anal. 80−17755
Galileo and Aristotle re-assessed 77−49541
Galileo and Tower of Pisa expt., discussion 78−49582
gas, forbidden volume, van der Waal's gas equation 77−60864
gas, relativistic energy and momentum transformation 78−24618
gas atom scattering, from solid surfaces, undergraduate course 77−60863
gas transport processes, alternative approach to kinetic theory 78−28890
gauge invariance, analogy with relativity, particle internal symmetry 78−49595
gauge symmetry breaking, geometrical approach, superconductivity and spontaneous symmetry breaking 80−57028
general relativity, metrics for moving reference frame, teaching approach 77−67337
general relativity, two-, three-dimens. space times 78−5
general relativity, uniformly accelerated reference frame 78−36747
generalized bound-state perturbation theory 80−17748
geometrical analogy for the formal definition of entropy 80−51990
geometrical optics, advanced, for engineers, matrix algebra methods 80−62415
geometrical optics, handling of spherical mirrors and lenses *(Hungarian)* 78−12449
geometrical optics, lens Fourier transform properties 80−57024
geometrical optics, programmable pocket calculator appls. 79−58468
geometrical optics, thin lenses formulae 79−35509
geometrical optics 78−77638
geophysics, applied MSc programme in Nigeria 80−105463
geothermal energy, energy source possibility 79−35507
geothermal energy resources, in Great Britain 79−17166
Gibbs mixing entropy paradox, quantum gases 78−49588
glass tube cutter, hot wire technique 78−20925
glider on inclined linear air track, viscous damping and restitation coeffs. 80−46768
granular materials, size effects in cond. and supercond. 80−77581
gravitation, inverse square law from Kepler's 1st two laws, Cartesian coords. 77−33802
gravitation, Newton's law, deductive and inductive nature 78−24617
gravitational accel., g radial variation, comments 77−82343
gravitational and magnetic crossed fields, accel. of metal 77−33775
gravitational fields, brachistochrones and isochrones 77−87596
gravitational fields whose brachistochrones and isochrones are identical curves 79−25807
gravitational mass change in two point charges system 79−35460
gravity acceleration as a function of mass 78−81766

teaching continued
Green's functions in space and time 79−58474
group representation theory, intuitive approach 77−87592
group theory, from common objects to mols. 78−32631
group theory in chemistry, pedagogical approach to direct product represent. 80−17771
group theory of covariant harmonic oscillators, interacting quarks 78−61970
Gurney's ballistics calc. 80−67946
gyroscope, reaction to impulsive torque, description for teaching 78−24604
gyroscope motion, elementary discussion 78−16605
haemodynamics, coronary artery bypass surgery 77−78911
Hall effect, positive voltage interpretation by electron motion 78−69945
Hall effect discovery 80−27099
Hamilton's principle for canonical equations of motion 80−105464
Hamilton-Jacobi equation solns. in Coulomb pot. and quasiclassical approx. 80−46765
handing chain natural freqs. 77−78913
harmonic oscillator, damped, canonical approach, for teaching 80−17757
harmonic oscillator wavefunctions, asymptotic behaviour 80−67979
harmonic plane waves, particle displacement 80−73138
harmonic waves, introduced through Fourier synthesis 80−27080
hearing mechanism, phys., review 77−90808
heat conduction, generalised eqn., parabolic or hyperbolic soln. 78−36746
heat diffusion in solid sphere, Fourier theory 80−31456
heat engine using clear night sky as heat sink 80−27082
heat engines and external work, thermodynamics, conceptual expt. 78−49586
heat of adsorption, determined by gas-solid chromatography 79−35497
Heisenberg microscope, crit. ang. aperture 80−41981
Hermitian, antiHermitian and unitary operators, basic props. for quantum mechs. appl. 78−54113
high energy process, with strong absorption, elementary quantum mech. 78−86053
history and physics, educational course 77−41429
history of mathematics, causal and formal logic unification 78−77639
HMO calculations, minicourse in HMO theory using small computers 78−25444
holography, intensity ratio setting method 80−77588
holography, recording of on-axis hologram, student experiment 78−86084
homogeneous ellipsoidal inclusions, general theorems, Poisson theorem, dielectric polarisation, conduction and elasticity 78−61979
Hooke's law, potential energy curve 80−67961
Hooke's law oscillator, ideal, anharmonic vibrs. 78−36743
human body, live, thermodynamics of cooling for treatment purposes 80−73128
hydrogenlike atoms, spin-orbit terms derivation 80−73148
hyperbolic mirrors, holography and Fermat's principle, geometrical anal. 77−45647
ideal Fermi gas, ultradegenerate, ground state press. 79−58471
illustrated technical talks, planning and preparation guidelines 77−9832
image formation in lenses and mirrors, graphical representation for teaching 77−49539
improper integrals, programmable pocket calculator calcs. 80−101696
increasing weight of falling bodies, Aristotle's conclusion 80−46770
induced angular momentum, classical and quantum calcs. 78−86060
industrial internship programme in nuclear engineering education 78−4432
inertia, concept development from Aristotle to Newton 78−81786
inertia, mechanical mutual inertia in spring coupled system, mutual inductance analogue 78−49590
infi-nitelinear array of atoms, props., Morse pairwise pot. calcs. 77−76331
infinite-well potential, soln. using SO(2), for teachers 77−33791
information theory density matrix for a simple quantum system 79−58470
instantaneous axis of rotation, theory and demonstration apparatus 79−84903
instructional evaluation by students, appl. in teaching diagnosis, improvement 79−35448
instrumental functions, asymmetric, generalised Lloyd's graphical deconvolution methods 79−84905
instruments in advanced physics, a final year undergraduate course 79−21486
integrated optics laboratory for teaching and research in optical waveguides 77−39034
interactive computer assistance with calculations arising in undergraduate laboratory experiments 79−35493
interference colours produced by white light refl., teaching paper from films 80−8754
interference fringes, formation and optimisation 78−36766
interference fringes of Fresnel double mirror, localised and unlocalised, theory extended to wedge 80−67960
internal cohesion of liquids, Reynolds' work 79−58511
internal forces cancellation 80−27079
international organisations for physics teaching 80−77561
inverse-square orbits; A geometric approach 79−44662
ionospheric radio wave propag. model 79−97159
irreversible processes, linear coeff. calc., kinetic and Onsager reciprocity theorems, gas flow appl. 79−9053
isotachophoresis process 79−25784
isotropy of light velocity convention 80−101689
iterative soln. for square-well pot. eigenvalues, pocket calculator 77−33778
J^2 eigenvalues 80−17742
jacobians and curvilinear metrics 79−62961
jerk: the time rate of change of acceleration 79−5928
Joule's constant determination, large scale 19th century expt. method 80−77572
K-harmonics in one dimension 79−2584
Keller plan course improvement 77−49518
Kelvin-Thomson atom, the one- to six-electron atoms 77−88367
Kepler's third law, mean radius calcs. 78−24612
Kepler's third law, synodic period statement 77−87601
Kepler ellipse, some props. 79−97151
Kepler ellipse, symmetry prop. of vel. 80−101694
Kepler initial value problem, geometry, two-circle calcs. 79−71182
Kepler orbit, from initial conditions via Lenz vector 78−16602

teaching continued
Kepler problem, formal equivalence with Maxwell fish-eye theory 78−81733
kinematics, vector calc., kinematic strategy of self-preservation for the jogger 79−97157
kinetic theory, mean time between collisions paradox 77−33771
kinetic theory of matter 78−81767
Kirchoff's laws of spectral analysis, computer laboratory exercises 78−73790
knots, topology friction and strength 77−33769
knuckleballs, aerodynamics and spin 77−22344
Kronig-Penney electron 79−22
Kronig-Penney model, energy band structure, nearly-free and tightly-bound electron approxs. 78−73792
laboratory practice, the principle investigator concept, comment 77−33777
Lagrangians and Hamiltonians, constructed from eqn. of motion 78−62016
Landau damping, linearised eqns. of motion 78−57723
Landau levels, analytic function theory, energy eigenvalues and eigenfunctions determ. 77−69259
landuse anal. using BASIC interactive image processing 77−74176
Laplace transforms, real variable inversion 79−21496
laser beam diffraction, teaching approach 79−71177
laser driven fusion 80−42012
laser light, monochromaticity, theory 79−84886
laser oscillator bandwidth, role of spontaneous emission 78−41114
lateral-angular magnification relationship for simple magnifier 80−57031
lattice, one-dimensional, finite length effects, Debye-Waller factor and specific heat 77−33798
lattice vibrations, in 1-dimens. defect system 80−31454
least squares fit, uncertainty calc. 78−86068
Leidenfrost effect, demonstrations 78−81744
lens aperture, rel. to depth of focus, appl. to reading with relaxed eye 78−12489
lens maker's equation 79−44683
lens object-image relations 78−36780
liberal arts physics, history and philosophy, relevance 77−22348
lifelong learning adapted to adults, principles and practice, University of Mid-America 79−12
light, correlation velocity, in dispersive media 77−68165
light, intrinsic angular momentum 79−58483
light deflection by Sun, principle of equivalence calcs. 78−81729
light momentum density in refracting medium, electrostriction, Peierls method 77−33772
light polarisation on reflection 78−24616
light power, relativistic transformations 79−84887
light propag. in birefringent cryst., projection dyadic treatment 77−33789
light propagation tutorial *(Hungarian)* 78−36774
light reflection and refraction, analogue model 80−67948
light trapping in fluid media, teaching, approach 79−71179
light velocity meas., nuclear timing technique 80−90637
linear chain Ising model, energy states 77−33779
linear chain molecules, cooperative ligand binding, teaching approach 77−87610
linear differential eqns. with polynomial coeffs., appl. Schrodinger eqns. 77−49522
linear lattice of atoms, Lennard-Jones pot. basis 78−61997
linear least squares parameters, stat. significance, student guide 80−17770
linear programming, introduction and appl. to simple cct. 80−73136
linear regression, least-squares eqns. derivation, appl. to g determ. 78−45450
linear systems, response to square wave force, transients, teaching appl. 80−31467
Lippman-Schwinger equation, soln. for n delta-shell pots. 78−41112
liquid, possible excitations, ball bearing model 77−45642
liquid crystals, crystal display, cyclobiphenyl compounds 80−67962
localised interference fringes 80−101680
logarithms! and estimation 78−36748
logical abilities and success in physics courses, correl. 80−17731
longitudinal standing wave in gas, press. var. 78−12514
Lorentz groups, homogeneous and inhomogeneous, teaching method to illustrate difference 80−17766
Lorentz theory for classical radiation reaction of accel. charged particle, dumbell model 78−49592
Lorentz transformation, accel. 80−90639
Lorentz transformation, derivation in acoustic and ballistic situations 78−24623
Lorentz transformation, kinematic consistency 77−33754
Lorentz transformation, kinematic consistency 78−24608
Lorentz transformation, self-inverse form 77−82345
Lorentz transformation, self-inverse form 79−25808
Lorentz transformation, vector formulation, as student introduction to special relativity *(Italian)* 78−12447
Lorentz transformation and causality condition 78−7
Lorentz transformation without rot., matrix representation, for undergrads. 80−17760
Lorentz transformations, nonlinear vector product, appls. 79−44668
Lorentz-Dirac eqn. for classical charged particle, mass renormalisation 78−62007
lunar centre of mass displacement from geometric centre, comment 78−69937
lunar halos, geometrical optics of formation 77−45634
Mach's principle, Einstein's equation and classical physics anal. 77−49524
Mach's principle, equivalence principle violation 78−61998
macromolecular solns., educational courses, integration with phys. chem. 78−77642
magnetic, interior force field 78−54123
magnetic charge quasiclassical quantisation 77−87595
magnetic domains, dynamic behaviour, struct., rel. to ferromag., teaching appls. 78−86080
magnetic Faraday's law analogue, appl. to slow charge convection 78−49607
magnetic field, inside long rod of magnetised material, calcs. 78−73795
magnetic flux quantum, in supercond. ring, theory, teaching approach 79−84902
magnetic monopole mobility spectrometer 78−62000
magnetic multipole expansion 80−105456

teaching continued
magnetic objects, current loops, thermodynamics 80−90633
magnetism w.r.t chemistry, guide to units 80−12871
magnetostatic monopoles in Cartesian coordinates 79−5932
magnetostatic multipole expansion, using scalar pot. 78−61995
magnetostatics, magnetic multipole expansion using scalar potential 79−58493
malpractice suits problem in instructional technology 79−92907
manpower studies relating to college physics teaching in the midwest 78−62039
Markov processes, approaches to linear birth-and-death and similar processes 79−80400
martial arts, deform. of solid objects, energy considerations 77−33745
Mathematical Association of America, activities relevant for physicists 78−41107
mathematical modelling, introductory course for undergraduates 78−57717
mathematics, insight and intuition, appl. to geometrical problem 79−80397
mathematics, new naturalistic style 77−60867
mathematics, remedial work for university students in engineering courses 80−86054
mathematics and statistics, development for appl. to all sciences, secondary level 78−57716
mathematics courses, effect of class evaluation method on learning 78−57719
mathematics learning, effect of specially constructed advance and post-organisers 79−35452
mathematics module, description and evaluation 80−86056
mathematics teaching by computer, long-division practice program in BASIC 80−98775
mathematics teaching by computer-assisted learning 79−80401
matrix differential equation, rotations as solns. 78−62021
matrix optics, principal plane concept generalisation 80−73140
Maxwell's eqns., Lorentz and conformal covariance, normal transformation rules 78−49589
Maxwell's equations, derivation 79−21487
Maxwell's equations, derivation from local gauge invariance 78−54109
Maxwell's equations, inside and outside of source, vector spherical harmonics 78−81747
Maxwell's equations as one quaternion eqn., appl. to wave propag. 78−54133
Maxwell's gas velocity law functional eqn. derivation 77−13
Maxwell equations, equivalence with inhomogeneous wave eqns. 79−97138
Maxwell fish-eye pot. and Coulomb pot. from mechanics 78−49585
Maxwell stress tensor derivation, electrostrictive effects in cryst. 77−33792
measurement errors, random, simulation (Monte Carlo) method, teaching appl. 78−86062
measurement errors and statistics, laboratory teaching method 79−35474
measurement theory, for student physics labs., university level 78−24601
measurements, quantum and classical correlations 78−73866
mechanical laws, optoelectronic apparatus for classroom demonstrations 80−46773
mechanical resonance, $J_0(x)$ obs. on reson. rot. vertical chain 80−42006
mechanics, determ. of vels. on inclined plane 77−5661
mechanics, non-isochronous small oscills. 78−36749
mechanics, safety in falling elevator 77−41441
mechanics, teaching approach starting with dynamics *(Hungarian)* 79−17157
mechanics of catching a stray goose 79−44665
mechanics teaching in Britain to undergrad. students, eval. of standard 77−53722
mechanics teaching in Italy 79−17160
media effectiveness comparison, video tape, audio tape and printed transcript 79−80403
medical diagnostics, computerised axial tomography 78−49619
medical diagnostics, US imaging techniques and appls. 78−49620
medical diagnostics, xeroradiography 78−45449
medical electronics for meas. of temp., press. and flow 78−49621
medical measurements, in intensive care 78−49622
medicine, nuclear diagnostics 78−49618
megalithic astronomy 77−33759
Mercury, perihelion precession, nonrelativistic contrib. 79−71184
mesh analysis using graph theory, generalised procedure 80−101681
metallic glasses, phase transition and mech., elec. and mag. props. 78−36765
metrological research on prospective measuring techniques, conf. Wroclaw, Poland, Sept. 1978 *(Hungarian)* 80−86247
micelles, distrib. of solubilised mols. 79−58497
microcomputers in education, hardware, software and personnel problems 80−98771
microcomputers in schools, software and equipment choice 80−98772
microelectronics revolution, appl. in telecommunications, medicine, education 80−31446
microscopy, course at North Carolina State University 80−95135
Millikan experiment, analogy using quanta of mass, milli-can experiment 80−46778
mirage, ray theory anal. 77−87605
mirages, form., wave eqn. calcs. 77−33749
mirages, stratified medium light ray trajectories 78−69940
mirrors, semireflecting lossless, transmitted and reflected optical fields phase shift 80−46769
MIS diode, abrupt depletion layer approximation 79−58473
models and their use in chemistry teaching 78−86064
models as a pedagogical tool 78−86065
models in science, philosophical discussion 78−86108
molar volumes microscopic insight from macroscopic data, teaching appl. 78−69930
mole, amount of substance 77−87723
mole, importance in school chem. courses 77−87589
mole, introduction in teaching of ideal and real gases 77−87611
molecular beam effusive flow, vector flux density distrib. calc. for any aperture 80−22165
molecular dissociation model, dynamics and time averaged behaviour 78−61968
molecular electronic structure theory, computer program for graduate instruction 77−78937
molecular geometry predictions using simple MO theory 78−93497
molecular model of t-RNA, appl. as teaching aid 77−78936
teaching continued
molecular models based on Petri dishes stereochem. appls. 78−73817
molecular orbitals, homonuclear diatoms, σ_p and π level permutation 79−40336
molecular orbitals, localised and delocalised for polyatomic mols., undergraduate course 78−32630
molecular orbitals calcs., back-of-the-envelope type 78−16593
molecular vibration, biharmonic oscillator, coincident energy levels 79−40324
molecule, diatomic, hyperfine struct. transitions, quantum theory 80−17762
moment of inertia in quantum mechanics, Harris cranking model 79−35475
moments of inertia and Mohr's circle 77−45643
momentum autocorrelation functions from classical Green's functions. [Teaching] 78−61976
momentum distributions, in at., nucl. and proton struct. 78−24596
momentum flow as force, alternative conceptualisation for teaching mechanics 80−67993
momentum operator in nonCartesian coords. 78−24620
momentum operators for curvilinear coordinate systems 80−17743
monopoles, elec. and mag., without strings, heuristic pot. theory 79−5931
moon centre-of-mass offset 77−2353
Morse oscillator, classical motion, calcs. 78−73796
Moseley's expts.: Kα line freqs., rel. to at. number, reinterpretation 80−82616
mothball lifetime, naphthalene sublimation, radial diffusion rate 78−54124
motional EMF, rel. to animal navigation 77−60879
moving vertical line, apparent appearance for v>c, v=c and v>c 78−69935
M.Sc. theses, for pedagogical direction of studies *(Polish)* 78−73808
multi-purpose instrument for biochemical and related undergraduate studies 78−73816
multiple scattering theory, target nucleus wave function antisymmetry 77−49523
multiple-choice questions, item bank 77−60869
multipole radiation theory, in senior undergraduate physics course 78−54120
musical acoustics, room reverberation time meas. 80−42000
musical acoustics for the musician 79−71205
musical complex tones, interval-based representations 80−101684
musical string vibrations 77−49536
N-body disintegration theory, Maxwellian distrib., nuclear appls. 80−57033
n-body potential energy functions 79−40318
N-rays, 1903-1906, expt. investigation of spurious radiation 77−33814
nculear collective model, two-dimens., for even-even nuclei 77−61358
negative absolute temperature and Carnot cycle 78−61996
negative energies 77−13553
nerves, electrochem. theory, steady and transient pots., in book, for teaching 78−8202
Newton's 2nd law, spatial translation symmetry 78−54129
Newton's laws, in rotating Cartesian frames 77−33751
Newton's second law of motion and translational symm. of space 77−8
Newton-Raphson method cf. method of Scoring 79−17201
Newtonian mechanics, estimates of human body mechanical performance 78−40211
Newtonian motion analysis on micro-computer *(Japanese)* 80−31462
newtons laws of motion: some interpretations of the formalism 80−51984
noise formulae, elec. derivation, using Campbell's theorem 78−24602
nonequilibrium phase transitions, stability and dissipation 80−105479
nonequilibrium thermodynamics, available energy theory 79−44669
nonideality effects in kinetic theory, student experiment with surprise value 77−82351
nonrelativistic quantum mechanics and anomalous part of g-factor 77−74238
nonscience majors, innovative course based on mass-radius diagram of states of matter 78−62002
nonspreading wave packets, physical interpretation of Berry Balazs wave function 80−57040
nonspreading wave packets 79−44672
normal coordinates, rel. to natural coords., theory 77−22343
normal ordering, identities 78−86059
nuclear angiocardiogram anal. program for radiology trainees 80−8143
nuclear chain reaction demonstration model 80−46774
nuclear engineering, teaching laboratory for expansion of student knowledge horizons 78−4445
nuclear engineering, teaching project management as part of international technology transfer 78−4428
nuclear engineering laboratory, computer modules for calculation of prompt-neutron generation time 78−4447
nuclear engineering teaching laboratory, development at Ecole Polytechnique 78−4444
nuclear fuel management analysis core, computer code for teaching assistance 78−4449
nuclear instrumentation, computer-based data acquisition system for multi-station teaching laboratory 78−4446
nuclear laboratory course at Purdue University 78−4443
nuclear power plant health risks 79−35506
nuclear reactor analysis 80−36806
nuclear reactor development, secrecy and simultaneous discovery, 1938-45 78−12523
nuclear reactor dynamics, theory and computer simulation 77−45636
nuclear reactor safety, MIT nucl. engineering dept. courses, USA 78−58378
nuclear reactor thermal hydraulics, computer graphics 80−36824
nuclear scattering simulation in one-dimens. 77−33780
nuclear structure, one-dimensional many-boson systems 80−27071
nucleon-nucleon hard-core systems, bound states and scatt. 78−41115
numerical analysis, interactive teaching package 80−86058
numerical electronic technique, in physics education 80−46777
off-axis Helmholtz field 79−2587
oil paintings, neutron activation anal. 78−81761
Olbers' paradox, comment 78−86070
one-dimens. many body model with two- and three-body forces, exact Hartree soln. 79−9065
one-dimensional crystal, Debye, Einstein and exact heat capacities, theory 77−68376

teaching continued
one-dimensional oscillator systems, density of states-frequency theorem 80−82602
one-dimensional particle-in-the-box problem, perturbation theory illustration using champagne bottle situation 80−36816
Open University, adoption of unorthodox TV practices 79−40332
operational amplifier behaviour, review 80−67959
operator props. through three-dimens. rot. 80−105469
ophthalmological instruments and eye models in teaching, training and education 80−51993
optical design education program, desktop computer appl. 79−84922
optical waveguide and quantum mechanical tunnelling, some additional references 77−33776
optics, analogy between nonrelativistic particles and optical rays 77−14657
optics, faculty of Inst. of Optics, profile 80−62422
optics, graduate training at Optical Sciences Centre, programmes 80−62418
optics, the principal plane, its pedagogic role 79−97150
orbital angular momentum and parity 80−77564
orbital angular momentum eigenvalues, integralness calcs. 80−67977
orbital motion on an interactive-graphics terminal, teaching appl. 80−73152
order of magnitude estimation 77−13560
organic chemistry, textbook, undergraduate level 78−57711
organic chemistry courses, unified approach to teaching of struct. and bonding 80−17732
organic chemistry for master's degree, Keller method 79−58461
organic conductors and semiconductors, electronic struct. 79−35496
orthogonal curvilinear coord. representation of quantum mechanical operators, exterior differential form 79−9049
oscillation theory, use of mathematical models 78−86087
oscillations, free damped, differential eqn. soln., teaching appl. 79−62950
oscillations by matrix theory 78−61986
osmotic pressure, teaching, solvent tension, dilution explanations 78−73803
Pade approximants via continued fraction approach 78−61972
paradoxes in teaching 80−105453
partial derivatives, teaching, appls. to environmental problems 77−13523
particle accerator theory, rel. to fundamental consts. 77−22345
particle collisions, conservation of energy and conservation of vector momentum 80−101693
particle detectors, multiwire proportional chamber and drift chamber 77−18745
particle heavy spring system, oscills., Stieltjes integral calcs. 79−71180
particle in a one-dimensional box, momentum correl. function calcs. 77−33740
particle in box, position versus momentum representation 77−33762
particle in potential well, adiabatic invariants for varying mass 77−33797
particle motion in central force, without orbit precession 78−86057
particle scattering from target, spin-spin interaction calcs. 78−81730
particles, angular momentum in centre-of-mass frame 80−90631
partons, ancient Greek theory 77−64910
partons, similar concepts in ancient Greek, Hindu and Chinese philosophy 78−54143
Pauli's σ matrices, intuitive understanding 79−97153
Pauli principle in Euclidean geometry 80−17768
pencil point breaking, stress anal., size and shape of points 79−84901
pendulum, simple, large-amplitude, Fourier anal. 80−17767
pendulum, string-coupled, normal mode anal. 79−21494
pendulum motion, computer simulation, undergraduate teaching aid *(German)* 77−67166
pendulum with oscill. support, square wave model 78−49597
pendulums, massive cord, oscill. freq. calcs. 78−54121
pendulums, spherical compound, natural freqs. 77−67265
pendulums in orbiting spaceship, equilibrium and stability 79−44667
percolation clusters, teaching film 79−58509
percussion instrument acoustics, multidimens. vibrs. 77−57128
performance assessment, sequential test method in physics *(German)* 80−67969
Periodic Table, subclassification of lanthanides and actinides 77−26109
permittivity of liquid, microwave expt. 79−40320
permutation operator, explicit representation 79−35469
perspective distortion in photography, eye as simple lens 80−17734
perturbation theory, continuum contribution to bound states 77−33803
perturbation theory, normalisation of states 77−33770
perturbation theory, stationary state function ambiguity, resolution, for teaching 78−24603
PET 2001, multidisciplinary summer course for schoolchildren 80−98774
ph-sics for engineers and scientists, book 78−57710
phase change derivation, phys. chem. textbook assumption removal 80−17772
phase changes, soap film simulation 79−62974
phase transitions, mean field theory, Ginzburg criterion and marginal dimensionality 77−69067
phonons, atoms and waves 77−62591
photoacoustic effect and wave physics 80−42003
photoelectric effect and Planck's constant 79−28
photon emission from mol. and electronic transitions, quantum dynamics, semiclassical description 80−105466
photon interference, quantum field theoretic description using QED methods 78−12464
photons, quantum mech. theory 77−13519
photosynthesis, carbon fixation cycle, model, teaching appl. 78−73806
physical chemistry teaching, macromol. principles 78−77643
physicists' thinking skills, in laboratory 80−31443
physics, 'talk and chalk' method 79−44660
physics, A-level, computer managed independent learning 79−62948
physics, changes in methods, emphasis and subject matter 80−77587
physics, dialectical approach *(German)* 80−68006
physics, performance assessment and control *(German)* 80−73127
physics, performance assessment rel. to syllabus *(German)* 80−67967
physics, power station game 79−62949
physics, practical exercises *(German)* 80−68007
physics, school-university interface 77−87590
physics, scope, tasks and needs of didactics *(Polish)* 79−88781
physics, sequential examination processes appl. *(German)* 80−4487
physics, Spanish course based on Keller plan 79−58495
physics, teacher training at Bremen University *(German)* 77−22349
teaching continued
physics, undergraduate students teaching eighth grade classes 78−12446
physics, use of models, pedagogical approach rel. to history of science 80−77567
physics 13: teaching modern physics through science fiction 80−90626
physics computer assisted learning using microcomputers 79−62972
physics computer-aided teaching, hinted finding scheme, simulation appls. *(French)* 80−98777
physics homework solutions, recording methods 80−77573
physics in Europe, bibliography 79−40341
physics students, mathematics ability 80−77591
physics teachers, discussion skills, evaluation 77−33721
physics teaching, effects on intellectual development of students 77−33722
physics teaching aids, convention of secondary school physics teachers *(Hungarian)* 80−67957
physics teaching and personality development assessment *(German)* 80−67966
physics teaching and Piaget, understanding students 80−31473
physics teaching for related sciences and professions 77−22339
physics teaching methods, of Joseph Henry, biographical review 79−44692
physics teaching using SWTP 6800 system in BASIC 80−98776
Piagetian approach to physics teaching 80−41978
Piagetian-type testing, engineering and liberal arts majors at Cornell, performance 80−67955
piano tuning, using dual trace oscilloscope 79−71199
planar electrostatics 80−90623
plane wave solns., rel. to const.-identity 3-dimens. wave 80−17749
plasma, computer simulation, statistical mechs. 78−62014
plasma, Landau damping, application of Laplace transform inversion 79−21496
plasma physics, low-cost advanced undergraduate lab. expt. 78−12456
plasma waves, delay line simulation, wave propag. in dispersive and attenuating media 80−82606
point charge in three-dielectric medium with planar interfaces, method of images 79−9055
point charge near cond. plane, force acting 78−49605
point charge system, pot. energy of equilib. config. 77−87602
point groups, continuous, characters and representations 80−36809
point groups, continuous, reduction of representations 80−36808
point groups, continuous, reduction of representations 80−36810
Poisson brackets, canonical invariance 79−25810
Poisson distribution, expectation value and variance 78−69943
polar gas, polarisation by external and internal elec. fields 78−12459
polar intensity profile of elliptically polarised light, comment 77−87600
polarising microscopy, college course 77−22360
porphyrins, isomers, enumeration by combinatorics, Polya's theorem 78−93501
positron annihilation gamma ray energy broadening demonstration 78−73814
positronium, QED predictions rel. to expts. 77−58213
potential scatt., classical and quantum transport theories 78−16603
Poynting vector introduction at elem. stage of physics courses 80−12865
practical work, relevance to comprehension of physics 80−27068
Prestel viewdata system, introduction 80−42013
primary cell systems without liq. junction, use of central connectors 78−8199
principles of equivalence 78−12455
probability and statistics, rel. to tennis 80−41997
probability games, modelling stellar evolution and fusion 80−77590
probability in submicroscopic processes, dice games illustrating reactor neutron flux and radioactivity 78−12515
problem-solving in physics, teaching and understanding 80−8752
projectile fragmentation and momentum 77−45654
projectile motion, air resistance, speed depend. 77−75932
projectile motion, symmetry and geometrical arguments 79−35463
projectile motion, teaching to sixth-form level 77−60862
projectile range, generalised launching point soln. 79−62965
projectile range formula for above ground level launch 78−8190
proportional navigation 80−82611
pseudopotentials, for excited states of H atoms 79−84893
pseudostationary wave, anal. 80−82605
pseudowork-energy principle nonrigid or rot. bodies 78−49602
psychology, theories and research of Jean Piaget 79−49000
push-me-pull-you capacitor, student discussion topic 79−97160
QED, radiation-matter interaction Hamiltonians 78−54114
QED charge-electric dipole interaction in 1 dimens. 80−42005
quantal problems, soluble, using solns. of Schrodinger eqn. 77−67307
quantisation and independent coordinates 79−16
quantization of inequivalent classical Hamiltonians 79−35466
quantum chemistry course problems using model pseudopots. 79−30165
quantum clocks, time meas. 80−90632
quantum electrodynamics, gauge invariance, diagrammatic proof 78−74183
quantum measurements, interactive computer program, for teaching 78−41113
quantum mechanics, 1-dimens. singular pots. 77−13522
quantum mechanics, canonical transformations, development from Hamilton's principle 79−71185
quantum mechanics, computer graphic presentation for non-physical science students 77−49526
quantum mechanics, domain and range of operator 79−97149
quantum mechanics, Feynman path integrals, classical limit 78−12476
quantum mechanics, group representation theory, intuitive approach 79−25804
quantum mechanics, interpretation, spin and uncertainty 79−58481
quantum mechanics, Kac ring model, illustrative calcs. using projection tech. 77−78918
quantum mechanics, mechanical model 78−49591
quantum mechanics, non-Hermitean Hamiltonians, dissipative forces 77−33763
quantum mechanics, perturbation formulas for energy, derivation 78−86051
quantum mechanics, Schrodinger eqn., bound state solutions, var. calcs. 77−33747
quantum mechanics, self-adjointness and spontaneously broken symmetry 77−87593
quantum mechanics, spherically symmetric pots., ladder operators, energy levels and degeneracy 78−62013
quantum mechanics, vector operators and spherical harmonics 79−44674

teaching continued
quantum mechanics, Wigner distrib. for ang. coords. 79−35472
quantum mechanics, zero probability problems 77−41499
quantum mechanics *(Hungarian)* 78−36753
quantum mechanics and perturbation theory, perturbed harmonic oscillator *(Spanish)* 78−36786
quantum mechanics in secondary schools, review of Dutch program *(Hungarian)* 79−44657
quantum particle in square well, bound state energy 79−35478
quantum pendulums, classical, semiclassical and quantum aspects 80−101679
quantum state determination, one dimensional particle, quantum 79−35473
quantum statistical mechanics, Dirichlet's integral formula and phase vol. 80−17744
quantum theory, accelerating transformation operator appls. 77−74239
quantum theory, completeness in quantum mechanics 78−89278
quantum theory, its cognitive repression in contemporary physics 79−97169
quantum theory, Lagrangian and dissipation 79−84892
quantum theory, operator functionals and path integrals 77−33736
quantum theory, plane rotator, degenerate perturbation theory, Zeeman and Stark effects 79−9059
quantum theory, transmission past rectangular barriers or wells, $|\Psi|^2$ and flux anal. 79−71183
quantum transition concept in undergrad. courses, explanation of photon creation and absorpt. 80−36807
quantum transitions without quantum jumps, theory 77−67306
quantum virial theorem, derivation 79−71193
quark confinement, limiting spectra from confining potentials 79−84895
quasar redshifts, teaching consideration 80−90621
quasi-ideal pendulum, small amplitude oscills. 79−84897
radar echo Doppler shift formula by wave superposition 79−97147
radiation exposure in daily life, review 77−49535
radiation health physics, graduate educational program to prepare science majors for career 78−4427
radiation safety in laboratories 80−73154
radioactivated metal foil experiments 79−17165
radioactive dating and population growth by dice game 80−57030
radioactivity, binomial distrib. and Poisson statistics 77−49525
radioactivity, probabilistic description based on good-as-new postulate 79−35471
radiotelescope design, multidisciplinary exercise, Jupiter bursts and quiet Sun obs. 80−17759
radiotherapy by external ionising radiation beams 78−49616
raindrop growth physics 79−35502
rare earth garnet thin films, macroscopic magn. props., magneto-optical expts. 80−46764
Rayleigh hysteresis loops, visualisation, geometrical method 77−77072
reaction kinetics, interactive simulator, teaching appls. 79−48992
reaction kinetics, nonisothermal, studied by thermal anal. and DTA 79−40335
reactor kinetics, computer assisted learning package 77−33809
reading through pinholes 80−17765
reasoning development, influence of studying physics 77−29971
recursive method for partition function calc., average energy calc., APL program 79−9050
reduced gas pressure in centrifugal field 79−58491
reflection and elastic scatt., Compton scatt. and special relativity 80−46756
refraction, apparent level of beer in glass, optical illusion 77−68166
refractive index of floor, Brewster's angle method 79−71202
regression line analysis 80−73144
relative motion, problem of boat crossing flowing rivers 77−60883
relative velocities, running in the wind 78−86072
relative velocity, problem involving a jogger (runner) and wind direction 79−84904
relative velocity problems concerned with boating 78−12510
relativistic cube, two-dimens. appearance to stationary observer 79−97142
relativistic harmonic oscillators and hadronic struct., 1st year graduate quantum mechs. 78−61971
relativistic line of charge over ideal conductor, net force 78−36762
relativistic massive particles, gravitational deflection, general relativistic anal. 80−46767
relativistic motion in a plane 80−101686
relativistic negative acceleration components 78−86058
relativistic paradox 77−49530
relativistic quantum mechanics, free localised Dirac particle, Zitterbewegung 80−17739
relativistic rot. disc circumference 77−87603
relativistic statics, covariant formulation 78−49593
relativistic torque, comment on 'right-angle lever paradox' 78−36750
relativistic transformations, Newtonian force and EM field 78−49601
relativistic two-body electrodynamics 78−54112
relativistic vector formulation, of electric and mag. fields *(Italian)* 78−12448
relativity, accel. and weight of extended bodies 77−33746
relativity, appearance of objects moving at relativistic speeds, computer programs 78−12484
relativity, Bohr-Einstein weighing of energy debate, time and gravity 79−97152
relativity, Einstein's 1907 essay, discussion 78−12454
relativity, Einstein's 1907 paper, retranslation 77−71173
relativity, Einstein's first paper, retranslation, comments 77−33811
relativity, energy flow velocity, rel. to energy momentum tensor 79−21498
relativity, physicists' reactions and popular attitudes, historical account 80−77602
renormalisation group theory, second order phase transitions, undergraduate statistical physics 78−62012
renormalisation rule for WKB-type wave functions 78−69944
resistance variation with temperature 80−77575
resonance Raman spectroscopy 78−4425
restricted three-body problem, L_4 and L_5 points, stability at pot. maxima 79−7
Riemann curvature tensor and closed geodesic paths, for teachers 78−24600
rigid rotator, account suitable for basic quantum mechanics course 77−33773
road vehicle stopping distance, weight transfer effect 79−25800

teaching continued
rotating water sprinkler anal. 79−9064
rotation about arbitrary axis, matrix formalism 77−60922
rotation group irreducible representations, spin-1/2 representation, teaching approach 79−58488
rotation operators, time-depend. aspects 80−90634
rotational gradient operator, Eulerian angles for rigid body orientation 77−67266
rotational partition function, for rigid asymmetric mol. rot. 79−84899
rotations, Lorentz transformations, and arbitrary axes 79−97155
rotations, nonlinear vector products calc. methods. 77−71201
rubber, balloon, internal press. eqn. 79−14
Rutherford's scattering formula via the Runge-Lenz vector 80−73141
Rutherford scatt., electron deflection, inverse 1st, 2nd and 3rd power field, program 77−87594
Rydberg constant, using a hand-calculator 78−81765
S-matrix theory, quark as redundant concept, order concept, review 79−25786
Saha equation, elementary derivation, rel. to mol. dissoc. 80−82599
satellite motion in vicinity of triangular libration points 78−12488
satellites, orbital speed, in Kepler ellipse, theory 77−70984
scalar diffraction theory, near-field, Fourier transform appls. 80−31455
scattering, particle in central field, deflection function 79−24
scattering cross-sections, two-asymptote approx. 77−7
scattering from inverse square law potential, algebraic eqn. 78−81749
SCF calculations on LiH for undergraduates 80−82597
school teachers' subjective response to aircraft noise 79−70496
schools specialised in physics and mathematics *(Hungarian)* 80−67956
Schrodinger's cat paradox, separation of macroscopic and microscopic domains 77−33742
Schrodinger eqn. for free particle, wave packet spreading in coord. representation 80−17736
Schrodinger eqn. solns. using approximate nucleon-nucleon and Λ-nucleon pots. 80−62429
Schrodinger equation, numerical integration, using WKB approx., eigenvalue estimates 78−12486
Schrodinger equation, trigonometric soln. of polar function, for H atom 77−67308
Schrodinger equation and the accel.-gravity equivalence principle, for teaching 78−24614
Schrodinger wave functions at pot. discontinuities, continuity conditions 80−27077
Schwarzschild field geodesic, Newtonian limit 78−86056
science, use of models 80−77566
science and technology, philosophy of new methods, special reference to biomedical engineering 78−28883
science and the humanities, The Two Cultures gap, teaching 80−41979
scientific creativity, Newton and Beethoven contrasted, Kepler's laws from conservation principles 78−49583
scientific discovery, roles of dreams and inspiration 79−49007
scoring systems allowing for partial knowlege 79−48994
screened Coulomb potentials, energies calcs. 80−31452
second law of thermodynamics, molecular model *(Hungarian)* 77−64903
second law of thermodynamics, perfect gas model *(Hungarian)* 77−64904
second quantisation, in weak external EM field, as one-particle problem 78−12462
seismic refraction technique for geophys. surveying 79−97161
SEM, methods for short courses 80−73533
SEM, slide/tape modules 80−68005
SEM, video tape appls. 80−68004
SEM teaching philosophy and methodology 80−67964
semi-infinite array of identical potentials, surface effects and electronic density of states 78−54110
semiclassical scattering theory, spurious excitation 80−73142
sensitometric sources, photometric and radiometric calibration, tutorial 77−34044
series, infinite, evaluation using physical analogues 79−25803
SI metric units, in college phys. texts 80−101697
SI units, classification 78−36962
SI units, conventions and practices, physics teacher's viewpoint 80−36968
SI units, group props., dimensionality 80−17746
SI units, group props. 80−17745
SI units, rationalisation and need for approximation to SI 80−36969
simple DC circuits, student concepts 80−77569
simple harmonic motion, noncalculus derivation for introductory physics 77−17742
simple harmonic motion, to waves, student laboratory exercise 77−60880
simple pendulum, flexible cord mass effects, eqn. of motion perturbation expansion 77−82341
simplified relativistic force transformation equation 79−25791
simulation games, critical analysis 78−49579
single slit diffraction, theory testing expt. 80−77568
site symmetry approach to hybridized orbitals 77−13552
snow and avalanche phenomena 80−57044
soap film in a wedge, expts. for teachers 79−17169
soap film on wire frame in zero gravity, variation problem branching 79−9057
soap films as analogue for minimum path and minimum area problems 77−17740
soft spring, dynamic behaviour, mathematical anal. 78−12491
solar eclipse demonstration *(Hungarian)* 78−36773
solar energy concepts, in chem. teaching 78−73805
solar energy conversion 78−81763
solar energy conversion technology 78−86092
solar physics, simple approx. model 78−36756
solid angle, relativistic transformation 80−101683
solid state diffusion, atomistic model, pedagogical use of Monte Carlo method 79−25797
solid state physics, review of experimentation, undergraduate level *(Spanish)* 80−82624
solid state physics based on quantum theory shaping ideas *(Hungarian)* 77−87608
solid structure, coordinated polyhedra approach 77−78934
solid-state diffusion in elec. field, Monte Carlo demonstration 80−27072
solitary wave solns. of classical nonlinear field eqns. 80−17756
soliton solns. to nonlinear wave eqns. 80−17737
solution of $dy/dx=(a_1x+b_1y+c_1)/(a_2x+b_2y+c_2)$ 78−77641
sound, sixth form physics course 79−62973

teaching continued
sound reproduction systems, high fidelity, components and characts. 80−77582
sound vel. meas., Raman-Nath theory, mol. struct., liq. mixture, temp. depend. 77−33796
space colonisation 79−44663
spatial Bose-Einstein condensation, teaching examples 79−71176
special relativity, addition of parallel velocities, theory 77−67274
special relativity, developments and changes 80−8758
special relativity, Einstein simultaneity, meas. methods 79−8
special relativity, event method 80−31450
special relativity, length paradox in three dimens. 78−62015
special relativity, mass velocity dependence without momentum principle 78−24613
special relativity, rel. to classical electromagnetism 78−54116
special relativity, rigidily connected accelerated clocks, teaching approach 79−58487
special relativity, secondary-school course not relying on historical approach 78−86096
special relativity, teaching module 79−21483
special relativity 77−33810
special relativity and Michelson-Morley experiment, history of physics, role in education 80−8759
specific heat curves, exact, Einstein and Debye for one-dimens. crystal 78−86076
spectral density, time-depend. perturbation theory calcs. 77−13525
spectroscopy quantum chem. teaching, fluctuating elec. dipoles, light absorpt. 78−73802
spectroscopy with supersonic jets 80−41996
speed, Galilean and Einsteinian concepts, vel., rapidity and celerity 80−73130
speed and displacement relations for tire skids, program for PET 80−57038
spin resonance phenomena, classical calcs. 77−69665
spin-1 matrices, props. 79−67128
spin-1 matrices, props. 80−101695
spin-1 problems, soln. using spin-1/2 methods 78−73793
spinning top, on surface with friction, behaviour 79−58467
spiral spring, (nonhelical) simple harmonic motion, Bessel functions, closed form solns. 80−57026
spontaneous reasoning in elementary dynamics 80−4482
spring-mass system, equivalence of horizontal and vertical systems 77−9841
springs, static and dynamic effects, influence of mass 80−41990
sprung pendulum, anal. of nonlinear coupling 80−51987
square-well potential, integral eqns. and scatt. solns. 80−31451
starfield, appearance from relativistic spaceship, nonexistence of 'starbow' 79−62955
stationary waves 80−67999
statistical concepts in physics 79−35501
statistical distributions, quantum and classical, derived 77−5
statistical mechanics, equilibrium distribution functions, thermodynamic derivation 79−71175
statistical mechanics, information-theoretic, system in contact with heat reservoir 78−36770
statistical mechanics, partition functions, series expansion problems 77−33753
statistical methods for non-Gaussian distribs. 77−33782
statistical thermodynamics, partitions 79−58496
statistical thermodynamics, teaching demonstration for 3rd form of secondary school *(Hungarian)* 77−49528
statistics, choice of mean 78−16604
statistics course, teaching approach for non-specialists 78−57715
steady-state response of difference eqns., digital computation schemes 78−57718
stellar aberration and the Kepler problem hodograph 78−24622
stochastic model, radioactive decay, difference-differential eqns. 80−51992
stratospheric photochemistry, computer simulation 79−21481
structured tutorials to develop students' creative thinking, problem-solving and formulation 79−35451
student experiment, evolution of theoretical models *(Polish)* 80−36819
Sturm-Liouville problem, eigenfunctions normalization 77−78910
suggestopaedia, training technique 79−17153
superconductors, search for new materials 77−59350
superfluid He, charged trapped vortex ring 77−45650
supernovae in binary systems: an application of classical mechanics 80−62428
superposition of acoustic or EM waves, false paradox 80−41999
supply and demand phenomena, math. anal. 80−77589
surface potential barrier, Schrodinger eqn., anal. and numerical soln. incl. spin-orbit interaction 79−58492
surface tension in liquids, mol. theory 77−57123
swing motion, example of parametric amplification 77−4
symmetry and conservation in nature 79−26
synchrotron radiation, origin, characts. and appls., review 77−58243
Synge's triads of null rays 80−73146
telecommunication, at university, of Rio de Janeiro, course structure 78−2
temperature concept without zeroth law 78−24607
tennis racket physics, teaching approach 79−71173
terminal velocity, analogue technique 79−97163
terminology, gravis as synonym for the phrase, force of gravity 78−69936
thermal conduction and diffusion, electrical circuit analogue 78−86089
thermodynamic energy distribution *(Hungarian)* 77−64907
thermodynamic equilibrium, teaching approach 79−27
thermodynamic equilibrium 80−46751
thermodynamic work and harmonic oscill. 78−49598
thermodynamics, 1st law, axiomatic vs. conventional formulation 78−24619
thermodynamics, air conditioners, second law efficiency, energy efficiency ratio and performance coeff. 78−36742
thermodynamics, analogy with mechanics, symplectic struct. 79−71174
thermodynamics, Caratheodory's integrating factor choice 78−41110
thermodynamics, classroom example, free energy change during liq. vaporisation 80−42010
thermodynamics, misconceptions in school 77−60865
thermodynamics, pressure-volume work exercises illustrating the first and second laws 80−22173
teaching continued
thermodynamics, quasi-Carnot cycles, negative Kelvin temps., theory 78−54111
thermodynamics, zilch cycle and 1st law 77−82342
thermodynamics for calculating chem. equilibria, review for teachers 77−26108
thermodynamics violation of second law, linear decompressive expansion followed by adiabatic compression, cyclic 80−42019
Thomas precession, geometrical kinematical origin 79−6
three-electron bonds, stability and dissoc. energies 77−78935
tidal power, alternative energy sources 78−86091
time dependent Hamiltonian, scale gauge transforms., adiabatic approx. principle, suitability for teaching 78−45506
time dilation and twin paradox, intuitive understanding 78−86093
time evolution operator, derivation and appl. 79−58476
time evolution operator in quantum mechanics 80−82610
tippe top, spinning motion 77−33735
Titius-Bode law, Piagetian learning cycle for astronomy study unit 80−51985
topological solitons in physics 79−25793
torque and Newton's third law 78−12517
training model 79−35447
training with computers 77−33734
transient beats, determ. using operational amplifier cct. 79−54
transport processes in gases, relax. approx. to Boltzmann eqn. approach 78−73804
trapped species in host lattice 78−16594
tropical year, its astronomical meaning 79−97136
TRS-80, teaching at Keene High School 80−98773
tsunami-generating earthquakes, ionosphere detect. method 79−44681
TV appl. in colleges, closed-circuit system preparation and installation *(German)* 78−12521
TV instruction by satellite, India, reception systems, overall appraisal 78−8185
TV picture 'ghosts', used to locate offending building 78−81764
twin paradox, round trip, gravitational field eqns. and geodesic eqns. of motion 79−58463
twin paradox in special relativity 80−105465
two-body problem, orbits from Lenz vector 78−36763
two-capacitor problem, using circuit self-inductance 79−62960
two-electron atom, 1snl excited levels, ionisation energy calc., perturbation, Schrodinger eqn. methods 80−17728
uncertainty principle, paradoxes 78−89280
uncertainty relation, mathematical proof 79−84888
uncertainty relation between angular momentum and angle variable 80−27073
underdeveloped countries, electromagnetism, telecommunications, factors against learning 78−4
undergraduate, field problem computation by numerical methods 77−10803
undergraduate engineering education, physics requirements 79−44656
unimolecular gas reactions, Lindemann theory 78−27753
university engineering course, first semester subjects and projects *(French)* 80−27066
University of London Institute of Education, Science Department, teacher training, curriculum devel. 80−27061
university physics teaching and research, vocational aspects 79−62951
US velocity, of liq., determ. using optical diffr. by short acoustic pulses 79−62963
v=gt expression, origins of derivation 80−77593
valency concept development, reln. to chemical bonds, teaching approach *(Hungarian)* 79−756
van der Waal's crystal, P-V-T diagram, Helmholtz free energy, mean field model 77−33784
variational technique,73 variational technique, for two-electron atom 79−21505
vector calculus and algebra, geometrical meaning of curl operation 77−45639
vectors in physics teaching *(German)* 80−82623
velocity of string pulse, derivation without calculus 78−24610
verbal computation problem-solving, hierarchical struct. of learner abilities rel. to material strength 79−35453
vibrating string anal. 77−9
vibrating strings, intrinsic nonlinear effects 80−82607
video monitor, large screen, for computer output display 80−77597
virial theorem and scale transformations 80−17763
virtual image in hyperbolic mirror, for holography 79−35476
virtual levels, in three-level atoms, definition 79−44671
viscosity, variation with temp. 77−89222
von Neumann's theorem on composite systems, group theoretical interpretation 79−71189
vorticity vector, rot. theory 80−82604
water sprinkler, rotating, range calcs. 77−13528
waterbed physics, theory 79−13
wave and particle descriptions of light, equivalence, rel. to radar freq. shift 80−101692
wave functions, rotation in phase space, Fourier transform method 77−33744
wave functions of 1/2-integral spin particles, 720° rot. effect, teaching models 79−62958
wave mechanics, invention, Schrodinger-Einstein correspondence 79−84898
wave mechanics, origin, pedagogical approach *(Portuguese)* 80−22166
wave mechanics, three dimens. wave packet tumbling motion 77−82340
wave packets, propag. and spreading theory 77−13521
wave packets, time dependent elastic scatt. in one dimens. 78−12461
wave propagation, step in amplitude of d.c. pulse of wave packet 79−97137
wave propagation in continuous and discrete systems, eqns., props. 79−5
wave scattering, fluctuating inhomogeneous media, model 79−21492
wave-packet, position probability, classical and quantum spreading, for teaching 78−24606
waveguide, quantisation of radiant energy 78−36757
waveguide theory, translational invariance and normal modes 79−25
wind energy as alternative energy source, energy science course material 78−61973
wind powered boat, demonstration of conservation laws 79−19
windmills, max. power extraction, theory 79−58482
work, teaching of mechanics 79−21493
zeroth law and transitivity, empirical temp. 77−33790
^{11}B, NMR, for senior level inorganic courses 78−4424

teaching continued
^{252}Cf fission source, undergraduate laboratory expts. 77−382
Co_3O_4, crystal field calcs. for normal spinel struct. 77−13554
H atom, variations, quantum theory calcs., generator coord. calcs. 80−41987
H, atomic struct., relativistic Dirac eqn. 78−62019
H, neutron scattering, 0.1 to 14 MeV, slowing down times and distances calcs. 77−65409
H, one-dimens., $\Psi(x)=\Psi(-x)$ even states 80−90638
H, photon emission, Bohr theory covariant eqns. 80−105482
H, Schrodinger eqn. in two-dimens. 80−31457
H, Stark effect, theory, teaching appls. 79−5933
H_2, electron correl. as rot. polarisation, Heitler-London-Rosen calc. 80−4492
H_2^+ bonding and virial theorem 78−49599
He, ^1S ground state, variational perturbation calc., teaching 78−41129
He atom, one-dimensional, bound states 79−40317
He, Schrodinger eqn. solns., existence criterion 78−41117
He-Ne laser wavelength drift 80−67978
^{3}He and ^{4}He superimposed spectra, isotope shift, mass and vol. effect, Fe arc spectrum calibration 80−46763
LiH, lattice energy calc. 78−16595
Na Rydberg states, anomalous fine struct., perturbation model 80−57035
S-S bond chirality, biomolecule struct. and activity depend., review 78−27889
U isotope separation appl. to nucl. fuel cycle, teaching module 80−36805

teaching approaches to particular topics *see teaching*

teaching demonstrations *see demonstrations*

teaching machines *see computer-aided instruction*

technetium
see also nuclei with .....
atom, Lα X-ray spectra, $_{40}$Zr to $_{48}$Cd, linewidths 79−41131
band structure calc., effect of correlation 79−60699
bleomycin-^{99m}Tc thyroid scans, evaluation of cold areas 80−56183
EHDP labelled with ^{99m}Tc, uptake quantification in sacroiliac scintigraphy, comparative study 80−94326
Fermi surface, constant-energy-search KKR band theory calc. 77−89689
film, electrodeposited, supercond. transition, AC susceptibility meas. 79−95539
film, supercond. transition, complex susceptibility 80−29495
hardness, temp. depend. *(Russian)* 79−74202
HCP, elec. field gradient 78−14698
heparin labelled with ^{99M}Tc for imaging of acute myocardial infarcts, dog expts. 80−81733
HIDA labelled with ^{99m}Tc, synthesis of 5 new isomers and comparison with ^{99m}Tc-(2,6-dimethyl)HIDA 80−72323
internal conversion, scattered-wave cluster technique 80−107696
long-term environmental behaviour, chemical approaches 79−93765
MDP labelled with ^{99m}Tc, lymphography appl. *(Japanese)* 80−94352
MDP labelled with ^{99m}Tc, quantitative assessment of bone scans in diffuse alterations 80−72287
paramagnetic form factor, polarised neutron diffr. study 80−39745
pertechnetate [^{99m}Tc], evaluation of renal grafts 80−46017
plastic strain, temp. depend. *(Russian)* 79−74202
radiochemical characts. and role in nuclear fuel reprocessing, review *(Czech)* 78−82496
radioisotope adsorption by minerals 80−83203
recovery and use of noble metals from radioactive waste 80−99242
red blood cells, in vivo labelling with ^{99m}Tc with stannous pyridoxylideneaminates 80−46049
red blood cells labelled with ^{99m}Tc, evaluation of gastrointestinal hleeding 80−51219
red giant stars, Tc I absorpt. lines obs. 78−28689
reduction and sorption in granitic bedrock, biological hazard estimation 79−79415
selective on-line gas phase separation from fission products 79−97907
separation from fission products, fast chem. methods 77−16856
stannous pyrophosphate labelled with ^{99m}Tc, mouse myocardial uptake obs. 80−46019
stellar spectral analysis and Tc in late-type stars 80−8623
superconducting transition temperature, resistive transition meas. 77−80861
superconductivity and Fermi surface calcs. 80−70873
in T Cephei, Me variable star, Tc I lines obs. 78−32483
^{99M}Tc, muco-ciliary transport monitoring method, bronchiectatic patient appl. 80−30840
^{99m}Tc labelled aerosol particles rel. to ^{81m}Kr ventilation imaging for lung function assess. 79−100716
^{99m}TC, intrahepatic lithiasis detection, sequential scintiphotography 80−72309
Tc I, HFS from spectra, mag.-dipole and electric-quadrupole hyperfine consts. 77−68002
Tc:^{57}Fe, dilute, quadrupole splitting and isomer shift, Mossbauer spectrum 78−48096
Tc-C film layer structure, obs. of supercond. transition temp. and crit. mag. field oscills. 77−69438
^{99}Tc accumulation by plants 77−56489
^{99}Tc accumulation by tumbleweed and cheatgrass grown on arid soils 78−80974
^{99}Tc in reactor waste, sorption by minerals 79−49721
^{99}Tc lifetime in generator-produced ^{99m}Tc, calc. 79−88188
^{99}Tc migration potential in radioactive waste 80−3537
^{99}Tc separation regeneration of breeder reactor fuel *(Czech)* 78−82496
^{99}Tc sorption on USA subsoils from differing weathering intensity areas 78−16014
^{99}Tc^m, β-decay rate for estimation of ultra-high pressure 78−77927
^{99}Tc^m, simulated standard by ^{141}Ce 78−61261
^{99}Tc^m generator of higher activity 80−17136
^{99}Tc^m hepatobiliary imaging, jaundiced adults, infants 79−5339
^{99}Tc^m hepatobiliary imaging in non-jaundiced patients 79−5338
^{94m}Tc, cardiac blood pool visualisation, labeled red blood cells and serum albumin 79−29601
^{99m}Tc, assay of radioactive impurity in pertechnetate eluted from ^{99}Mo−^{99m}Tc generator *(Japanese)* 80−81735
^{99m}Tc, atmospheric release, dose evaluation 79−25119
^{99m}Tc, automatic dispensing system, radiation exposure evaluation 79−96663
^{99m}Tc, beta-decay and dose calcs. 80−91154

technetium continued
^{99m}Tc, bilateral renal scintigraphy, quantitative anal. 79−34662
^{99M}Tc, blood flow and tracer uptake in normal and abnormal canine bone 80−17072
^{99m}Tc, blood plasma, vol. meas. in man using labeled serum albumin 79−29602
^{99M}Tc, bone marrow scanning in pediatric oncology 80−17067
^{99m}Tc bone scintigraphy, use in uremic pulmonary calcification detect. 80−3788
^{99m}Tc, brain imaging, artifact in supine posterior projection 79−34661
^{99m}Tc brain scintigraphy, early and delayed image evaluation 80−3790
^{99m}Tc, cardiomyopathy scintigraphic diagnosis, method sensitivity 80−17061
^{99m}Tc, clinical comparison of ^{99m}Tc HEDP and ^{99m}Tc MDP for bone metastases detect. 79−83904
^{99m}Tc, comparison of colloids for lymphoscintigraphy 79−29580
^{99m}Tc contamination of laboratory personnel, its degree and routes 80−98147
^{99M}Tc DTPA, radiolabelled liposomes as metabolic and scanning tracers in mice 80−17073
^{99m}Tc, determination in bleomycin-^{99m}Tc preparations, thin layer and paper chromatography *(Russian)* 77−77855
^{99m}Tc, dynamic renal transplant imaging, transplant perfusion index 79−34653
^{99m}Tc, energy spectra and spectral resolution in Xe-filled multiwire chamber 79−49901
^{99m}Tc, gamma camera array of ^{99}Mo impurities 80−36100
^{99m}Tc, generation from ^{99}Mo, influence of radiation dose on elution yield 79−29624
^{99m}Tc generators, operational assessment by performance indices 80−94332
^{99m}Tc, heart, anal. of high speed multicrystal gamma camera recording 79−25077
^{99m}Tc, hepatobiliary agent, liver pharmacokinetic and imaging studies 79−29597
^{99m}Tc, hepatobiliary dynamic flow study 79−53217
^{99m}Tc, hepatobiliary study of liver-transplant patients 80−3793
^{99m}Tc imaging of acute myocardial infarction in dogs, emission-computed tomography appl. 79−79638
^{99m}Tc, improved labelling of proteins by stannous tartrate reduction of pertechnetate 80−72324
^{99m}Tc, kidney function studies following radiation therapy of spleen 79−20615
^{99m}Tc labelled 2,3-dimercaptopropansulphonate, prep. and distrib. in the rat 80−51244
^{99M}Tc labelled (Sn)DTPA, comparison of 4 commercial preps. in glomerular filtration rate meas. 80−81704
^{99m}Tc labelled (p-butyl) iminodiacetic acid, clinical evaluation in hepatobiliary imaging *(Japanese)* 80−67236
^{99m}Tc labelled bovine thrombin and streptokinase-activated human plasmin, in vitro assessment 80−41238
^{99m}Tc labelled DTPA and MDP, compensative value on brain lesion *(Japanese)* 80−67235
^{99m}Tc labelled erythrocytes, rat, factors affecting splenic deposition of heat damaged cells 79−29596
^{99m}Tc labelled fibrinogen, usefulness of phlebography for pulmonary embolism patients 80−36093
^{99m}Tc labelled human serum albumin kits, evaluation for cardiac blood pool imaging 80−17130
^{99m}Tc labelled liposomes, lymph node imaging agent 79−96649
^{99m}Tc labelled possible cholescintigraphic agent, formed from 3-hydroxy-4-formylpyridine, glutamic acid 79−79653
^{99m}Tc labelled pyrophosphate, changes in bone imaging after X-irrad. 80−72239
^{99m}Tc labelled pyrrolidino-methyl tetracycline, prep. and control 79−29623
^{99m}Tc labelled radiopharmaceuticals, internal dosimetry in clinical nuclear medicine 79−12007
^{99m}Tc labelled radiopharmaceuticals, comparison of 2 types for lymphoscintigraphy 80−41185
^{99m}Tc labelled red blood cells, ultrafiltration labelling technique 80−51243
^{99m}Tc labelling of red blood cells 80−41236
^{99m}Tc, left ventricular function evaluation by myocardial scintigraphy and radionuclide angiocardiography *(Japanese)* 80−81724
^{99m}Tc, liver scanning agents, comparison of ^{113m}In-phytate, ^{99m}Tc-phytate and ^{113m}In-colloid 79−96650
^{99m}Tc lung imaging kit, radiochem. impurities 77−56469
^{99M}Tc macroaggregates, pulmonary regional perfusion assess., compared to ^{81M}Kr continuous intravenous infusion 79−39477
^{99m}Tc manipulated in syringes, radiation exposure obs. 80−67252
^{99m}Tc, medical abnormality detection, influence of size and radiopharmaceutical concentration ratio 79−16272
^{99m}Tc methylene diphosphonate, immediate renal imaging and renography, clinical evaluation 80−98126
^{99M}Tc, myocardial scintigrams, specificity of pyrophosphate in prior infarction cases 79−39476
^{99M}Tc, myocardial scintigraphy, correls. with coronary-artery bypass surgery 79−39475
^{99m}Tc myocardial scintigraphy, use of blood-pool imaging 80−12228
^{99m}Tc, pancreas scanning, extension of the subtraction technique 79−66506
^{99m}Tc, point source depth, meas. from γ-ray spectra 79−39492
^{99m}Tc, production from ^{99}Mo 78−37353
^{99M}Tc, pyrophosphate and hydroxymethylene diphosphonate carriers, comparison in acute myocardial infarction 80−94342
^{99m}Tc pyrophosphate scintigrams, diagnosis and localisation of myocardial infarction 79−5350
^{99m}Tc, quantitative lymphoscintigraphy, mammary metastases detect. 79−16266
^{99m}Tc radiolabelling of mouse spleen leucocytes 79−100739
^{99m}Tc radiopharmaceutical kits, rapid colour spot test for stannous Sn levels 77−86630
^{99m}Tc radiopharmaceuticals, As for P substitution, bone-seeking agent analogues 80−51250
^{99m}Tc radiopharmaceuticals evaluation, miniaturised chromatography systems 79−96391
^{99m}Tc, rel. to ^{125}I in thyroid imaging 80−36077
^{99m}Tc, S colloid, liver perfusion in vivo meas. in normal and partially hepatectomized rat 79−79636

technetium continued
^{99m}Tc scintiangiograms, importance in optimum radiation schedule in treatment of superior vena caval obstruction 80−72334
^{99M}Tc, sequential myocardial scintigraphy, following myocardial infarction 79−39474
^{99m}Tc, simultaneous emission and fluorescent scanning of thyroid 79−16275
^{99m}Tc, supercond. effect on decay rate, lattice consts., transition temp. 78−41671
^{99m}Tc tracers, femoral head activity in Perthes' disease 79−29606
^{99m}Tc, tumour tracer accumulation, autoradiographic study, experimental infectious lesions 79−5348
^{99M}Tc, venography, features of inferior vena cava obstruction 79−34655
^{99m}Tc, venography, large vol. injection without tourniquet, lower extremities 79−34654
^{99m}Tc/^{67}Ga, computerised double-tracer subtraction scanning for inflammatory diseases 79−70612
^{99m}Tc-DTPA, limitations of single sample tracer method for determ. glomerular filtration rate 79−16271
^{99m}Tc-E-HIDA, characts. in hepatobiliary scintigraphy *(Japanese)* 80−81729
^{99m}Tc-Ti-DTPA, prep., control and biological distrib. 80−51246
^{99m}Tc-1-hydroxy-ethylidene-1,1-disodium phosphonate labelling using Sn(II) reductant 79−88190
^{99m}Tc-bleomycin selective labelling for tumour imaging 79−53228
^{99m}Tc-diethylentriaminepentaacetic acid freeze-dried kit prep. 79−88189
^{99m}Tc-dimercaptosuccinic acid, renal differential function in dogs 79−79639
^{99m}Tc-diphosphonate, scintigraphic assessment in human bone tumours 79−20613
^{99m}Tc-hepatobiliary agents, absorbed dose estimation 80−72330
^{99m}Tc-labelled erythrocytes, spleen scanning in humans 80−67230
^{99m}Tc-labelled radiopharmaceuticals, brain uptake by passive membrane transport 80−51053
^{99m}Tc-labelled red blood cells, kit preparations 79−11999
^{99m}Tc-microspheres, bladder wall dose after administration 80−109030

technetium alloys
see also technetium compounds
Mo-Tc system, supercond. behaviour, quick-quench production technique 78−56251
$Mo_{0.18}Tc_{0.82}$, search for strong coupling superconductivity 79−28441
$Mo_{0.4}Tc_{0.6}$, A15 and BCC, sp. ht., 4-20K 78−68111
$Mo_{1-x}Tc_x$, BCC, sp. ht. in normal and supercond. phases 79−87190
Nb-Mo-Tc alloys, supercond., point-group symmetry 78−64163
Tc-Fe, dil., effect of Fe impurities on superconductivity 79−61007
Tc-Fe, dil., local magnetisation, Mossbauer meas. 80−66091
Tc-Fe alloy, Mossbauer spectra, hyperfine field 80−20526
Tc-Fe dilute alloys, supercond. and mag. props. 80−29494

technetium compounds
see also technetium alloys
hexahalides, X_n-SW-calc. of chemically induced decay const. variation of ^{99m}Tc in TcO_4^- and hexahalides 79−54769
reduction and sorption in granitic bedrock, biological hazard estimation 79−79415
$^{99}Tc^m$, chemically induced decay constant variation 78−93968
Pu-Tc-C systems, phase relationships 77−21127
TcB_2, electron struct., Fermi energy and surface, bonding 80−20076
TcB_2, possibility of semicond. props., rel. to atomic volume 77−69317
$^{99m}TcBr_6^{2-}$, preparation problems, decay const. 80−106020
$Tc(CO)_5Cl(Br)(I)$, thermodynamic props. tabulation 79−24808
$^{99m}TcCl_6^{2-}$, preparation problems, decay const. 80−106020
$TcCl_8^{3-}$, metal-cluster, EHT calcs. of electronic struct., metal-metal bonding *(Russian)* 77−61687
$Tc_2Cl_8^{3-}$ ion, visible spectra, electronic struct. 78−5240
TcF_6, heat capacity, entropy Gibbs energy, 2.23-350K 78−38852
$^{99m}TcI_6^{2-}$, preparation problems, decay const. 80−106020
TcO_4^-, X_{α}-SW-calc. of chemically induced decay const. variation of ^{99m}Tc in TcO_4^- and hexahalides 79−54769
$^{99m}TcO_4^-$, diffusible aerosol inhalation for imaging pulmonary ischaemic lesions 77−37047
TcO_3Cl, near UV absorpt. spectra, dynamical Jahn-Teller effect 78−86881
TcP_2O_7, $Tc_4(P_2O_7)_3$, prep. and comparative biological props. 79−12000
^{99m}Tc radiopharmaceuticals, rapid miniaturised chromatographic quality control procedures 78−28070
^{99m}Tc radiopharmaceuticals, radiation decomposition 79−83907
^{99m}Tc-EDTA complex production method and renal retention obs. 80−12254
^{99m}Tc-pertechnetate labelling of human plasma proteins, rapid chemical method 79−29618
^{99m}Tc-radiopharmaceuticals, ligand determ., electrophoretic method 80−40699
$^{99m}TcO_4^-$, thyroid scintigraphy, clinical comparative study with ^{123}I-Na *(Japanese)* 80−81728
^{99m}TcS colloid lymphoscintigraphy 80−36114
U-Tc-C systems, phase relationships 77−21127

technical information centres *see information services*

technical presentation
electron diffraction gas-phase, guide for publication of expt. data 77−1048
lectures, presentation technique 77−53719
scientific paper writing, component parts 77−53718
technical meetings, visual and oral presentations, preparatory tech. for technicians 78−8215

technicians *see personnel*

technological forecasting
see also research and development management
adaptive optics technology, historical review and prospects 79−59793
adaptive optics technology status and prospects 80−33132
AGR development and exploitation prospects 80−23109
all solar power supply for France, technological forecasting *(French)* 79−100497
Australian wind-powered generator potential and requirements 79−29444
cancer treatment by microwave hyperthermia *(French)* 80−3764
chemical analysis, instrumentation, discussion of future under microcomputer advances 79−83536
cinematographic equipment development, 35 mm cameras appl. *(Russian)* 80−284

technological forecasting continued
coal utilisation review and forecast (1950-2000) *(French, English)* 80−21363
cooperation among developing countries, evaluating potential of technology transfer 80−82628
data logging status and prospects 79−93114
ECG data processing development, status, and trends 79−39558
electret US transducer performances and prospects 78−59244
electronics appl., conf., Portland, Ore., USA, May, 1977 77−81598
energy, forecasting of future requirements 79−57348
energy forecasting models and their validity 80−89582
energy modelling and forecasting at US ERDA 78−49629
energy production and consumption, developments up to year 2000 *(French)* 79−92048
energy projections for USSR and Eastern Europe 80−26100
energy resources, projections to 2050 *(Dutch)* 80−61221
energy supply, (late 1970's till 2000) *(German)* 79−96411
European thermonuclear fusion programme, role of technology 80−86982
fast particle therapy status and prospects in Europe 79−20641
fibre optic communication systems, development during next decade 80−1329
fission material reprocessing plant, United Reprocessors in Europe *(Dutch)* 77−14254
French natural gas industry developments and prospects *(French, English)* 80−21364
French plan VII, energy forecasting 78−49628
fuel cell development status and prospects *(French)* 79−79389
fusion, ETF, engineering challenges 80−95422
fusion, international fusion technology program 80−95423
fusion, US magnetic fusion program, survey 80−91249
fusion inertial confinement, advanced engineering requirements 80−95421
fusion power status and prospects 77−67878
high energy physics detectors−limits to growth 79−89537
high energy physics expts., computer technology effects 79−89536
holographic storage principles and application prospects 79−89860
India, need for and consequences of technological assessment 80−68017
India, present and future 79−67140
integrated optics long-term role in optical and electronic systems 80−33232
integrated optics planar technology electro-optic devices *(Czech)* 77−46820
interferometric optical testing status and prospects 80−74529
material sciences development, Spacelab era influence (1981) 79−19981
medical electronics, worlwide inequalities and development prospects *(French)* 79−70660
nuclear fuel reprocessing plant, optimal installation program 77−46370
nuclear physics, impact of changing computer technology 79−89538
nuclear physics, impact of changing computer technology 79−89539
nuclear power development in US, Pu recycle's influence 79−36394
oil and gas, geophysical exploration forecasting up to year 2000 *(Russian)* 77−87122
optical ceramic, gas-moulded, characteristics and application prospects 79−81495
optical fibre communications, appls., techniques and predictions 80−87472
optical fibre communications history and prospects 80−9994
optical fibre transmission, American view *(German)* 78−33845
optical fibres, future developments, impact on 'next generation' of electronic equipment, data ring concept 80−102808
optical hybrid image processing trends and prospects 80−32927
optical instrument manufacturing, cyclical growth characteristics and prediction 79−76862
radioactive waste storage and disposal, US policy 79−49792
solar cells, power supply appls., technology and research 79−92076
solar cells combined with heat pumps, domestic space heating appl. *(Swedish)* 80−7919
solar panel in-orbit performance, of orbiting solar observatory (OSO-8) 79−48652
solar thermal power plants, dispersed, performance and economic risk evaluation, by computer Monte Carlo simulation 79−52902
sonar, fifth generation digital distributed signal processing 77−88995
Southern African solar energy resources and requirements 79−57383
space research programmes *(Japanese)* 78−24418
space technology, forecast 79−66905
substitute fuel prospects *(French)* 79−92055
technical projects realisation, appl. to O'Neill space colonies 77−87230
thermonuclear power plants, problems and perspectives *(Polish)* 78−54876
uK energy modelling 80−72003
USA Federal solar energy programme achievements and prospects 79−57370
wavelength division multiplexing technology status and prospects 80−64203
worldwide energy prospects, synthesis of studies published in 1976 and 1977 *(French)* 79−29443
Si ribbon growth, technology assessment 1978-1986, computer anal. using PECAN 79−8244
U, demand and reprocessing requirements estimate, 1976 to 2000 77−14232
U supply for fission reactors, world's resources survey 77−10468

tectonics
absolute plate motions and intraplate stress rel. to mantle rheology 77−33046
abyssal fractures rel. to tectonics *(Russian)* 78−3731
accretion at trenches, model, rel. to subduction complexes tectonic evolution 79−20797
active continental margins, earthquake foci three-dimensional projection 80−72453
active margins 78−57191
Adak Canyon region, central Aleutians, seismicity and tectonics 80−61772
Adelaide Geosyncline, Australia, Late Precambrian palaeomagnetism rel. to sigmoidal structural trends 80−101325
advective folding deformations, modelling and natural analogues 77−81858
N.Aegean region, evidence of crustal shortening 77−53028
Aegean region, geodynamics 78−69307
Aegean Sea and surrounding regions, active tectonics 78−96181

tectonics continued
Afar, accreting plate boundary, seismic and volcanic evidence 80−21700
Afar depression, Ethiopia, an Atlantic type continental margin in the making 77−21692
Afar depression, palaeomagnetism of axial zone lavas rel. to tectonics 77−37126
Afar region, geological evolution and geophysics 79−5468
Afar region rifting, geodetic evidence and elastic-brittle model 80−21697
Afar triangle, geodetic evidence for rifting, model for vertical displacements 80−98295
Afar triangle, seafloor spreading obs. during November 1978 fissure eruption 79−57912
Afghan Pamir, geology and tectonics of Himalayas 80−72513
E.Afghanistan, shallow earthquakes and tectonic activity 80−72444
W.Africa, Archaean supracrustal relics zonation rel. to tectonic settings 78−44815
Africa, evidence for late Tertiary uplift 78−77207
SW.Africa, geodynamic model for evolution of continental margin 77−21740
S.Africa, kimberlites, palaeomagnetic obs. and tectonic implications 80−109093
W.Africa, kimberlites and plate tectonics 78−11868
NW Africa, Late Palaeozoic-Early Mesozoic palaeogeography 77−70659
W.Africa, late Precambrian plate tectonics 79−44166
S.Africa, principal horizontal stresses 77−91093
southern Africa, seismicity and incipient rifting 77−81813
Africa and Antarctica, present relative motion 77−29272
W.Africa and Gulf of Guinea since Jurassic, membrane tectonics, comments and reply 79−44161
W.Africa continental margin, subsidence and uplift, DSDP Leg 41 geological results 77−21754
southern Africa continental margins, continental breakup and deep crustal struct. 77−21742
W.African and Gulf of Guinea tectonic activity since Jurassic, membrane tectonic theory 78−65248
African Archaean mobile belts and granite-greenstone terrain 77−33074
African plate, deformed by post-Jurassic drift 80−17245
African plate, evidence for western sector N-S shift from mag. anomaly study 77−53035
African plate, tectonics rel. to mantle convection pattern and stress system 77−81859
E.African Rift, cross-cut by volcanic chain in N.Tanzania, gravity survey 80−98301
E.African rift system, tectonic history, theory and laboratory expts. 80−21669
African/Adriatic promontory, rel. to Alpine orogeny and Carpatho-Balkan region plate movements 77−9394
aftershocks of Canal de las Ballenas, Gulf of California, earthquake, rel. to plate tectonics 78−20363
Agulhas Basin of S.Atlantic, seafloor spreading history, geomag. study 80−21696
Al Jubail, Saudi Arabia, evidence for recent coastal uplift 79−79799
Alabama Piedmont, structural development 78−65290
Alaska, 1964 earthquake faulting mechanism regional var. from static displacement data anal. 80−30998
S.Alaska, tectonic development rel. to Denali fault system 78−81137
Alaska, tectonic implications of palaeomag. data 77−32998
central Alaska plate tectonics, implications of Bouguer anomaly map 80−51380
Alberta, Canada, crustal stress evidenced by bore hole asymm. 80−21671
Albian open seaway between northern and southern proto-Atlantic 78−40538
Alcaparrosa Formation, Argentina, palaeomagnetism and K-Ar age rel. to Gondwana plate tectonics 78−96135
Aleutian and Alaskan volcanoes as tectonic stress orientation indicators 77−91087
Aleutian and Pribilof Islands, volcanic rocks Pb and Sr isotopes rel. to lithosphere subduction 78−57185
Aleutian arc, tectonic blocks, episodic subduction, strain diffusion and magma generation 77−33037
Aleutian subduction zone seismicity, volcano-trench separation, rel. to great thrust-type earthquakes 80−21655
central Aleutians, double Benioff zone and lithosphere unbending 78−32047
Alpine fault, New Zealand, frictional metamorphism, Ar depletion and tectonic stress 80−41440
Alpine geology, resoln. of fundamental questions *(French)* 78−24281
Alpine metamorphism, thermal budget 78−61373
Neo-Alpine orogenesis, thin-skinned plate tectonics 79−84207
alpine peridotite near Pinchi Lake, BC, tectonic fabric 77−44987
Alpine region, tectonic stress directions, correl. with joint orientations 80−105052
Alps, continental convergence 77−78149
Alps, foreland folding model 78−81141
S.Alps, Late Mesozoic pelagic limestone, megatectonic obs. from palaeomagnetism obs. 80−109095
S.Alps, Permian volcanics palaeomag. props. rel. to S.Alpine block plate tectonics 80−89948
Alps, precision levelling and recent vertical movements *(German)* 77−2139
Alps, shearing subductions mechanisms *(French)* 78−20376
Alps, tectonic progradation rel. to plate tectonic evolution 80−56452
Alps in Valais-Valle d'Aosta area, formation *(French)* 79−2206
E Alps tectonics and N.Italy earthquake, 1976 May 6, fault-plane soln. 77−64228
N.America, effect of craton on distrib. of seismicity and intraplate stresses 80−98248
S.America, equatorial transcurrent faulting and oceanic fracture zones 78−65245
N.America, Lower Palaeozoic tectonics rel. to New Brunswick rock units palaeomagnetism 79−100809
N.America, palaeopoles and palaeolatits, displaced terrains 80−12367
N America, possible Proterozoic plate boundary 77−91079
N.America, unconventional Proterozoic palaeomag. polar wander path rel. to tectonic events 79−66619
Middle America Trench, S.Mexico, progressive accretion 80−26487
N.America west coast, upper Mesozoic subduction complexes distrib. and character 78−81136
N.American Cordillera near Fortieth Parallel, tectonics and chronology 78−81138
tectonics continued
N.American intra-plate crustal deformation, implications of VLBI meas. 80−51379
Central American isthmus, emergence rel. to Gulf Stream Late Cenozoic vel. fluctuations 80−12432
N.Anatolian fault zone, Plio-Pleistocene reversal of displacement 80−94512
ancient big river systems significance and origin 78−77281
Ancona area, Italy, seismotectonics 78−65246
Ancona region, Italy, seismo-tectonic considerations *(Italian)* 78−40492
Andaman Sea crust, seismotectonics and tectonic history 80−8283
Andaman-Nicobar region, neo-tectonics and time-space seismicity 79−12082
Andean andesites, petrogenetic composition variations 80−8313
Andean subduction zone, intermediate aseismicity and recent andesitic volcanism 77−49055
Andean Wadati-Benioff zone morphology, andesitic volcanism, Nazca plate tectonic features 78−32039
central Andes, plate tectonics rel. to Plio-Quaternary tectono-magmatic zonation 77−29273
andesitic island arcs of SW.Pacific, peralkaline rhyolites origin rel. to tectonics 78−32043
anisotropic Earth model, appl. of tensor spherical harmonics to Navier eqn. of dynamic elasticity 80−98296
Antarctic Peninsula, subduction rel. to transverse geochemical vars. and calc-alkaline magmas genesis 80−56466
Antarctic plate boundary near Bouvet triple junction, tectonic structure 78−53639
Antarctica, palaeomag. results and test for oroclinal bending 78−73311
Anti-Atlas, Morocco, Pan-African province geodynamic interpretation from geology and geochronology *(French)* 80−76952
apatite fission track ages, from Himachal Himalaya, India, tectonic interpretation 78−57182
N.Apennine chain, heat flow meas. of folded continental arc 77−86841
Apennines, anticlockwise rot. rel. to Tuscan anatectic magmatism eastward migration 79−16428
NW.Apennines, seismicity and relation with surface structs. 79−34749
Appalachian fold belt, palaeomagnetism of Middle Ordovician volcanic rocks from Quebec 78−15965
Appalachian foreland fold and thrust belt, New York State, deform. nature 80−3973
Appalachian Orogen in Canada 80−8304
Appalachian orogen western margin, basement slice at Saint-Malachie, Quebec 79−20824
Appalachian salients and recesses, Lake Precambrian continental breakup and Iapetus Ocean opening 77−17057
N.Appalachian-Caledonides and Acadian Orogeny, palaeomagnetic results 77−9390
Appalachians, recent thrusting 79−79836
Appalachians, structural trends NE of Newfoundland and Trans-Atlantic correlation 80−85656
Appalachians, tectonics in St. Dominique region, Quebec *(French)* 77−78144
S.Appalachians, tectonics of W.Piedmont and Blue Ridge 78−61383
apparent polar movements, 1850 to 1600 Myr, palaeomagnetic meas. of SW Greenland metamorphic rocks 77−13059
N Appennines, collisional orogen model 79−92515
Apuane Alps structural evolution, continental margin deform. in N.Appenines, Italy 79−25245
aquifer water extraction leading to land deformation 80−105003
Arabian Shield, ophiolite belts and island arc collisions 78−20421
arc-arc junction, continental plate stress state, model 80−46163
arc-trench gap accretion, rel. to episodic plutonism in magmatic arcs 80−76956
Archaean greenstone belt, Island Lake, Manitoba, diapiric structs. and regional compression 79−57922
Archaean greenstone belt, Yellowknife, Canada, structs. induced by granite diapirs, rel. to tectonics 77−81892
Archaean greenstone belts, tectonic hypothesis rel. to Agnew belt, Australia 80−94507
Archaean Superior Province, tectonic model, thermal conditions 80−31018
Archaean tectonics constraint from geothermal gradients and plate prod. rate 79−34770
Archaean tectonism, numerical models of vertical tectonism in greenstone belts 80−81861
Arctic Basin, detailed aeromag. survey, rel. to tectonic evolution 79−70746
Arctic basin, seismic and gravity profiles 77−33030
Arctic Basin, tectonic evolution, Jurassic to present 79−48446
Arctic geophysical review, summary 79−48456
Arctic Ocean, Alpha Ridge is not spreading centre 79−48455
Arctic Ocean, formation and plate-tectonic processes *(Russian)* 77−29278
Arctic Ocean, mag. anomalies rel. to sea-floor spreading 79−48398
Arctic Ocean Basin, form. by circum-Arctic plate accretion and Pacific plate fragments isolation 80−98294
Arctic Ocean Basin, plate tectonic evolution 80−76953
Arctic regions, seismicity, 1908 to 1975, rel. to tectonics 79−48423
Arctic seafloor, rotation of N. Alaska 79−88328
Arizona, palaeomag. poles, polarity zonation and polar wandering from Cambrian and Devonian strata 78−28156
N.Armenia, motion on plate from Jurassic rock palaeomagnetic obs. 80−104870
Armenia, tectonic fault zones, geophysical investigations *(Russian)* 77−9386
Armorican Massif, France, Late Devonian to Early Carboniferous palaeomag. poles rel. to tectonics 79−84100
Asal-Ghoubbet rift zone, Afar, 1978-9 geodetic survey after seismo-volcanic activity 80−46164
aseismic ductile shear zones, dynamic model 79−79763
central Asia, active faulting and Cenozoic tectonics of Tien Shan, Mongolia and Baykal 80−8278
Asia, central and south-central, large-scale Cenozoic tectonics as prods. of continental collision 80−17246
S.E. Asia, crustal tectonic stress field details *(Chinese)* 80−56414
Asia, evidence for large Cainozoic crustal shortening from palaeomag. data 78−57189
E. and SE.Asia, evolution of marginal basins and adjacent shelves 78−32055

tectonics continued
central Asia, seismic moments of major earthquakes and average slip rate 77−86796
Asia, slip-line field theory and large-scale continental tectonics 77−5173
Middle Asia seismoactive regions, geomag. investigations rel. to crustal blocks compression and tension 80−26464
asteroidal terrestrial cratering, plate tectonics and evolution of life 78−96421
asthenosphere, frictionally heated shear flows stability 79−44164
asthenosphere, thermal stability or instability of shear flow 78−20370
asthenosphere thermal instability beneath moving plate 80−31007
asthenospheric counterflow, kinematic model 79−25220
asymmetric folding and monoclinal kinking of compressible elastic multilayers 77−17093
S.Atlantic, evolutionary history from deep sea drilling results 77−21756
N.E.Atlantic, rifting and subsidence on continental margins 77−73713
N. Atlantic, sea floor spreading and early opening, mag. and gravity data 78−65247
Atlantic continental margins, obs. and ideas rel. to plate tectonics 77−21691
N.Atlantic crustal structure, deep drilling results 80−26478
Atlantic equatorial fracture zone trends, plate kinematic implications 78−85527
N.Atlantic Mesoic crust reconstruction 80−51365
Atlantic mid-oceanic ridge, axial temp. profile and crustal struct. 80−26476
S Atlantic Ocean, age of opening from palaeomag. of Cretaceous Pirgua Subgroup (Argentina) 77−90998
Atlantic Ocean, graben development assoc. with initial rifting 77−21721
Atlantic Ocean, history of growth and topography of ocean bottom 80−3993
N.Atlantic Ocean, opening rel. to Messejana Dolerite fault-dike system (Iberia) age 79−2198
NE Atlantic Ocean, spreading history rel. to continental margin bathymetry, around British Isles 80−12372
N Atlantic Ocean, surrounding continents reassembly 77−53036
Atlantic Ocean floor vertical tectonic movements during Mesozoic-Cenozoic period 79−2210
N.Atlantic Ocean formation, rel. to E.Greenland dyke swarm offshore continuation 78−73352
N.Atlantic Ocean opening, basalt magma sources 79−100821
Atlantic Ocean opening, palaeomag. study 80−51320
S.Atlantic Ocean opening, prior and post continental movements from palaeomag. data 77−21744
Atlantic Ocean palaeobathymetry from Jurassic to present 78−20387
S.Atlantic oceanic crust in Mesozoic and subsequent evolution, mag. and gravity data 80−21699
N.Atlantic opening from palaeomagnetism of Notre Dame Bay lamprophyre dikes 80−26440
S.Atlantic opening time from palaeomagnetism of Mesozoic igneous rocks from N.Brazil 79−44089
Mid Atlantic plate boundary between Iceland and Azores, seismicity and earthquakes 79−88266
N.Atlantic region Upper Triassic tectronics, implications of salt deposits on Newfoundland Grand Banks 80−94516
Mid Atlantic Ridge crest, geological and geophys. investigations 80−8284
Mid-Atlantic Ridge. Eocene limestones and tectonics 79−12106
Atlantic rifting initiation, paleomag. evidence 80−51350
Atlantic S.E. of Azores, crustal struct. rel. to mag. anomalies and bathymetry 80−51384
Atlantic seafloor spreading, Kane fracture zone 80−21668
N Atlantic subduction directions and evolution of Caledonides 77−2135
Atlantic type continental margins, conference, Sao Paulo, Brazil, (13-18 Oct. 1975) 77−21690
Atlantic type continental margins, struct. from geophysical meas. 77−21702
Atlantic-type continental margins, distinction of two basic struct. types 77−21741
Atlantic-type continental margins, form. and geodynamic development 77−21737
Atlantic-type continental margins, sedimentary histories rel. to rifting styles 77−21738
Atlantic-type continental shelves, major synchronous events 77−21720
Atotsugawa Fault, Japan, seismicity and focal mechanism of local earthquakes *(Japanese)* 80−94482
W.Australia, Cundeelee area, regional geology and tectonic processes 79−2194
Australia, isostasy and evolution of compensation mechanism 78−65252
Australia, plate collision, seismic shear waves excitation and propag. 80−104887
Australia, tectonic, igneous and metallogenic provinces rel. to mantle convection and subcrustal stresses 80−72484
Australia continental slope and shelf, sedimentary basins evolution from Mesozoic times 78−96175
N.Australia Precambrian shields and platforms, struct. and tectonic style 80−3982
Australia-Antarctica, revised computer fits 77−53032
Australian Mesozoic revised palaeomag. data rel. to Gondwanaland breakup 77−52984
Australian region, contrasts between oceanic and continental Oligocene unconformities 78−73370
Austria, palaeomag. data from Northern Calcareous Alps, tectonic implications 79−53307
Avalon zone, Atlantic Canada, extent determ. from mag., seismic and gravity data 80−12384
Azores, earthquake (1980 January 1), aftershock sequence and present day tectonics 80−104911
Azores, K-Ar age of oldest volcanics, volcanic history 80−46158
b-values and seismic source models, tectonic stress vars. along active crustal fault zones 79−84150
back-arc basins, asymmetric spreading 80−85636
back-arc opening and subduction mode 79−70778
Badra area of Iraq, gravity investigation rel. to fault region 79−34729
central Baffin Bay, sea-floor spreading 80−51373
Baffin Bay continential margin and Lancaster Sound, seismic refr. meas., continental/oceanic crust boundary determ. 78−20368
Baie d'Audierne (Brittany) basic-ultrabasic complex, age and tectonic implications 78−11852
Baikal rift, deep struct. and formation mechanism from geophysical exploration *(Russian)* 80−12364

tectonics continued
Baikal rift zone, fault evolution 78−36132
Baikal rift zone, recent crustal movements, precise levelling data 78−36139
Baikal rift zone, seismotectonics 78−36134
Balcones Faults, effect on groundwater movement in S. central Texas 78−53672
Balei gold region (E.Transbaikalia), structural features and tectonics 80−98300
Baltic Shield, Proterozoic tectonics from palaeomag. study of Swedish rapakivi suite 80−56346
Banda Arc, continent-island arc collision 79−84211
Banda Sea (E.Indonesia), subducted lithosphere geometry from seismicity and fault plane solns. 78−81131
banded deformation structures description and origin, regional strain, local perturbs. 78−7629
basic concepts of plate tectonics, plate motion, earthquakes, geology 78−61386
basic intrusions emplacement mechanism 78−61374
Basin and Range province, tectonic extension thermal effects rel. to heat flow 79−70763
Bathurst and McDonald faults, N.W.T., aeromagnetic anomalies 77−5168
Bay of Biscay, rifting, crustal attenuation and subsidence 79−2209
bedded formations tectonics, struct.-forming props. from modelling data *(Russian)* 79−8627
bedding tilt and rotation correction in palaeomagnetic studies 80−109097
Belchertown pluton, W. central Massachusetts, palaeomag. evidence for tectonic rot. 77−44919
Bellingshausen Sea earthquake, Feb. 1977, ocean ridge generated compression mechanism 80−46142
bending of subducting plate in central Aleutians, ocean bottom seismograph meas. 80−89978
Benin Gulf, Africa, tectonics of Niger delta sediments 77−21693
Benue Trough, Nigeria, early Cretaceous basalt volcanism and initial continental rifting 78−61417
Benue Trough, Nigeria, gravity field rel. to tectonic evolution 80−21701
Benue Trough, tectonic evolution and implications for W.Africa Upper Cretaceous palaeogeography 79−2230
Bergell region, uplift history of Alps, apatite fission track age 80−21727
Bering Island, tectonic struct. of mountainous region 80−90045
Bering Sea, crustal heat flow and tectonic explanation 80−109123
Bering Sea and NW.Pacific Ocean, S_n waves propag. rel. to trapped old lithospheric unit 80−51346
Betic Zone, S.Spain, geotectonic evolution of westernmost Alpine belt 79−48443
Black Sea, mantle material intrusion age rel. to mag. anomalies nature *(Russian)* 78−85473
block faulting mechanism, geological and expt. studies 79−66692
block folding, mechanical model 77−81841
block tectonics analysis in Mongolia, appl. of two-dimensional autocorrelation anal. 80−56469
Blue Mountains, Oregon, Jurassic plutons tectonic rot., palaeomagnetic obs. 80−109099
Blue Ridge and Piedmont provinces, recent vertical crustal movements from levelling surveys 79−79794
blueschists at Shangla Pass, N.Pakistan, early Tertiary, evidence for subduction 79−2229
Bohemian Massif, heat flow pattern, rel. to tectonic struct. 77−64241
Bohemian Massif and W.Carpathian border, recent crustal movements 79−79791
Bohemian Massif and W.Carpathians, geothermal models 77−81848
Botswana, dyke swarm interpretation as failed Gondwana spreading axis 78−57180
Brawley, California, surface faulting assoc. with 1975 January earthquake swarm 77−9349
Brawley earthquake swarm, California, 1975 January, tectonic implications 77−9348
Brazil, coastline Quaternary formations, littoral zone evolution 77−21755
NE.Brazil, Post-Palaeozoic volcanism and tectonic significance 77−21735
S.Brazil, structural mapping, mineral deposits rel. to tectonics 77−81855
Brazil, Uruguay and Argentina continental margin geology and tectonics, rel. to S.Atlantic opening 77−21704
SE.Brazil and SW.Africa, geotectonic features correl. 77−21703
N.Brazil continental margin, evolution, sediment distrib. and hydrocarbon potential 77−21697
E.Brazil continental margin, salt deposits distrib. rel. to plate tectonics 77−21698
S Brazil intracratonic and marginal basins tectonic evolution 77−21743
Brazilian Continental Margin, Panafrican thrusting and melting 77−21769
S.Brazilian continental margin, structural study rel. to plate tectonics 77−21694
Brazilian marginal basins, evolutionary stages 77−21699
British Columbia, geotectonics of Cretaceous and Eocene plutons, palaeomag. fold test 77−91090
British Columbia, mag. anomalies and magnetizations, rel. to subduction 78−11796
British Columbia, north-central, northward displacement during late Cretaceous/early Tertiary 80−76955
S.British Columbia, tectonics rel. to Mesozoic-early Cainozoic activity 77−81852
brittle fault zones, grain size as shear strain indicator 77−17062
Bulgaria, plate tectonic theory of geological evolution 77−78148
SE.Bulgaria, Upper Cretaceous resedimentation phenomena rel. to tectonics 78−36160
Burma and S China, seismicity and tectonics 80−89983
Butte mining district, Montana, palaeomagnetism, rock magnetism and aspects of structural deform. 80−101326
Cabo-Ortegal mafic/ultramafic massif, emplaced nappe, gravity data 80−21689
Caledonian fold belt of N.Britain, tectonics rel. to Lithospheric Seismic Profile in Britain (LISPB) 78−73329
Caledonian orogeny, subduction tectonics rel. to Norwegian eclogites crustal origin 80−76978
Caledonian orogeny, tectonic implications of palaeomagnetic meas. 79−88244
California, crust tectonic tilt rate, lake level obs. 80−90065

tectonics continued
S.California, crustal deformation model 80−51377
California, earthquake swarms and local crustal spreading along major strike-slip faults 79−66645
S.California, N.Peninsular Ranges province early 20th century upwarping 79−79796
central California, preliminary stress meas. by hydrofracture 77−91097
central California, source parameters of earthquakes, (1972, February 24 and September 4) 77−2112
S.California, strain accumulation and stresses across thrust faults 77−53033
S.California, strain and uniaxial N-S regional contraction 79−74883
S California, tectonic process numerical simulation 78−11860
S.California downwarping, tectonomagnetic anomaly and seismicity 80−21626
S.California uplift area, Recent vertical movements four-dimensional modelling 79−80055
S. California uplift rel. to dilatancy hypothesis 77−49056
Cambrian Arden Pluton tectonic history, palaeomagnetic study 80−61752
Cambrian greenstone belts, Australia, marginal sea crust slices in Lachlan Fold Belt 79−29765
Cambrian slate belt of N Wales, mag. susceptibility anisotropy and correl. with strain 79−79832
E.Canada, passive margin, earthquake focal mechanisms and postglacial faulting 79−96741
W.Canada, seismicity, 1899-1975 period 79−5452
W.Canada, tectonic rotation of Queen Charlotte islands 77−73701
Canada, vertical crustal movements, map 80−109130
E.Canada tectonically active region, magnetotelluric fields time depend. 80−26451
Canadian continental margins, evolution and geophys. features 80−8274
Canadian Cordillera, geodynamic evolution 80−8276
Canadian Cordillera, Mesozoic-Tertiary basin models, geological constraints 78−28232
Canadian Pacific margin, subduction zone 78−40530
Canadian prairies, tectonics 78−85526
NW Canadian Shield, geochronology of Bear-Slave provinces granite rel. to crustal breakup 77−91080
Canary Island palaeomagnetism, and continental margin evolution 80−56363
Canary Islands, tectonic significance of joints 79−8625
Cape Breton Is., Canada, post-Mississippian thrust faulting 78−61360
N.Caribbean, crustal plate subduction history 80−41429
Caribbean Basin, transitional intercontinental sutural geostructure model 80−31015
Caribbean plate evolution and buoyant ocean floor 78−96183
Caribbean plate seismic wave attenuation near Lesser Antilles Island arc 77−40990
E.Caribbean Sea floor, heat flow meas. rel. to subduction processes 79−39683
Caribbean seismotectonics, implications from Caracas, Venezuela 1967 earthquake 79−20761
Caribbean-North American plate boundary, Quaternary faulting in Central America 79−79804
Caroline Plate, petrochem. of troughs and crustal accretion 80−12385
Caroline plate existence, from marine geophys. and seismological data 79−29731
Carpathian Mountains, disjunctive dislocations revealed by interpretation of space television photographs *(Russian)* 80−104958
Carpathian region, expected earthquakes, max. magnitude, seismo-tectonic anal. 77−53002
Carpathian system, geophysical data and Earth structure *(Hungarian)* 77−86829
E.Carpathians, plate tectonics rel. to rare earth elements in volcanic rocks 77−5151
Carpathians, recent vertical crustal movements, geoid residual local undulation *(Russian)* 78−15987
Carpathians internal region, in depth dynamics and tectonic movements *(Russian)* 79−48444
Caucasus, Alpine history, example of active continental margin evolution 77−78147
S.E.Caucasus, young tectonic disturbances and seismicity 79−44165
Cayman Trough, mag. anomalies inversion and sea floor spreading 79−34789
Cayman Trough, rock and palaeomagnetic evidence for spreading centre 79−84215
Cenozoic explosive volcanism recorded in deep sea cores, tectonic effects, climatic implications 77−49052
Cenozoic volcanic rocks, SE.California, regional stratigraphy, K-Ar ages and tectonics 79−70798
Central Alps, structual zones and continental collision 78−81124
Central Alps, Switzerland, heat flow, heat prod. and vertical crustal movements 77−81847
central anomaly magnetization high and sea floor spreading, comments 77−5133
Cerro Galan Caldera, NW.Argentina, volcanic history rel. to plate tectonics setting 78−85523
Chad basin, Africa, active intra-continental sedimentary basin 77−21726
Chagos-Laccadive Ridge, earthquake swarm and tectonic implications 79−16395
Chagos-Laccadive Ridge (Indian Ocean), geophysical study rel. to plate tectonics 77−44952
Charleston-Summerville area of South Carolina, Geological and geophysical studies of seismicity 78−11837
Charlie Fracture Zone, relationship to continental crust NE of Newfoundland 77−25664
chelogenic cycles in continental crust evolution *(Chinese)* 80−89984
Chile, Camaraca Formation of Middle Jurassic, palaeomag. and plate rotation 80−85586
Chile, Quaternary tectonics 78−44980
China, active faulting and tectonics 77−86848
NE China, physical interpretation of Hiacheng earthquake prediction 77−49028
China, seismicity and Quaternary faulting 77−40995
China, seismicity and seismotectonics charact. *(Chinese)* 79−16406
China, tectonic deform. charact. from seismological data *(Chinese)* 80−76951
SW.China, tectonic evolution 78−32054
China, tectonic stress field rel. to plate movement 79−62478
S.W. China, tectonic stress field rel. to recent tectonic activity *(Chinese)* 77−91089
China, tectonics rel. to Mongolian earthquakes of (1905, July 9 and 23) 77−37142
China, tectonics structure *(Chinese)* 77−73702
S China and Burma, seismicity and tectonics 80−89983
S.China Sea, 1965 October 7, intraplate thrust earthquake 80−26461
Chuko fault, Taiwan, underlying Tsengwen reservoir, seismicity 80−81930
E.Churchill Province, Andean-type tectonism 80−36222
circum Pacific mountain belts from continental collisons, lost Pacifica continent hypothesis 78−11863
Coast Plutonic Complex of S.British Columbia, Canada, tectonics and geothermal resources 79−70429
coastlines, tectonic settings rel. to barrier islands global distrib. 79−2214
Cocos Plate, lower oceanic crust fine struct. 79−88337
Coldbrook Group in Caledonia Highlands of S New Brunswick, stratigraphy, palaeogeography and tectonic setting 77−91128
Colombia deep earthquake, 1970, July 31, spatio-temporal history rel. to fault process 77−86813
Colorado, tectonomag. study using field difference method 80−21850
S.W.Columbia, active plate boundary dynamics, deep seismic sounding study 77−13074
conference on passive margins, Jun. 1978, Nova Scotia, Canada 80−36774
conference on plateau uplifts, Flagstaff, Arizona (August 1978) 80−57004
Connemara Antiform, tectonic evolution from palaeomag. data 78−36093
contemporary crustal movements in Canada 80−8273
continental blocks rotational motions, evidence from terrestrial objects astronomical azimuths 78−53613
continental coalescence of Guyana Shield and W.African Craton 80−26613
continental convergence zones, temp. modelling 77−81850
continental crust evolution by tectonic processes 77−64255
continental crust shortening, by reactivated basement reverse faulting 80−36284
continental drift, high-latit. continents as cause of glaciation 79−20961
continental drift, hydrodynamic mechanism 79−44386
continental drift, influence on true polar wandering 79−44079
continental drift, rel. to Earth albedo contrast and glaciation 79−74950
continental drift and large-scale polar wandering 79−79719
continental drift debate, historical review 77−29277
continental drift from time and latitude obs. 77−13072
continental drift mechanisms, review 78−92813
continental drift motion of latit. observatories, rel. to rotation pole secular trend 77−86734
continental drift of islands, effect on Earth rotation period 80−94445
continental drift ref. to astronomical time determs. 79−40063
continental drift theory, scientific growth 79−62992
continental evolution, basement and sedimentary recycling 80−56430
continental growth and emergence timing 78−11867
continental lithosphere thermal evolution 78−65234
continental lithospheric boundary layer, liability to sink into less dense asthenosphere 80−56447
continental margins, stress state 78−3742
continental margins, tectonic fabric rel. to oceanic fracture zones, appl. to Equatorial Atlantic 77−21695
continental margins, tectonics rel. to big river sands 79−25274
continental margins, vertical evolution 77−21739
continental movements and rotation determ. using astronomical methods *(French)* 78−40529
continental plates pre-Tertiary velocities from palaeomag. data 80−21848
continental platform subsidence mechanisms and eustatic sea level changes 77−21718
continental rift fault patterns, analytical model 79−79805
continental shear zones, geological aspects of deform. 78−3768
continental splitting mechanism, rel. to plateau uplift stress distribs. 79−34777
continental tectonics and seismicity, review 79−44160
continental tectosphere comp. and development 78−81133
continents, deep structure 79−66665
continents, secular changes in marine inundation of USSR and N.America during Phanerozoic 78−3735
convection currents in mantle 77−29265
convection rates of viscous fluid, upper mantle and continental drift appl. *(Russian)* 80−1581
convective heat transfer model for lithospheric thinning and crustal uplift 79−84199
convective instability of upper mantle models 79−88323
convergent plate margins, volcanic activity rel. to great earthquakes 78−7588
Coral Sea basin tectonic evolution from marine mag. anomaly data 80−21698
Cordillera evolution 79−62475
W.Cordillera of N.America, plate linkage mechanism rel. to oroclinal deform. 77−66901
Cordilleran Benioff zones 78−11866
Cornwallis Fold Belt, Canada, history and mechanism of basement uplift 77−91091
Cornwallis Pb-Zn District, Canada, Mississippi Valley-type deposits controlled by stratigraphy and tectonics 77−91130
Cornwallis Pb-Zn district, deposits controlled by stratigraphy and tectonics, discussion 78−73366
Coronation Geosyncline, palaeomag. poles rel. to arrangement of continents in middle Proterozoic 79−84101
Corsica, rotation rel. to palaeomag. data, comment 77−64251
Corsica (France), Quaternary tectonic movements 78−57234
Corsica-Sardinia microplate evolution from magnetisations of Tertiary volcanics 80−56343
Corsican granite, deformation effects on ^{39}Ar-^{40}Ar systematics 79−53347
Coso Range, California, tectonics and stress field 80−90003
Costa Rican orogen, tectonics of outer arcs 80−8311
creep in geodynamic processes 78−3744
Crimea, crustal tectonic stresses rel. to weak earthquake foci *(Russian)* 78−11862
Crimea, seismic processes rel. to tectonics *(Russian)* 78−3721

tectonics continued
Crimea, tectonodynamic regionalisation rel. to Earth crustal struct. *(Russian)* 79−8616
crust and mantle struct. explainable by plate tectonic processes 80−81855
crust gravity gliding tectonics, orogenic wave simulation, model 80−94506
crustal deformation, line length changes resolution by EM distance meas. ratio method 80−4143
crustal deformation, migration 79−79800
crustal deformation, transition between regimes dominated by intercrystalline diffusion and creep 77−53047
crustal deformation, viscoelastic, by finite quasi-static sources 79−39686
crustal deformation analysis, models for estimation of parameters *(German)* 80−101319
crustal deformation by dilatancy model, earthquake precursors 80−51347
crustal deformation due to volcanic eruptions, piezomag. field assoc. with Mogi model 80−67334
crustal doming and rifting mechanism, Upper Rhinegraben rift development appl. 78−61387
crustal movement data from strain meas. in Honshu, Japan 80−8277
crustal movements, conf., Palo Alto, California, USA (July 1977) 79−79785
crustal movements, precision meas. of gravity differences 79−92467
crustal movements, recent, estimation, geodetic obs. goodness concept restatement 79−57840
crustal movements observation for earthquake prediction *(Japanese)* 78−28180
crustal rifting and subduction causes, appl. to Atlantic margin of Brazil 78−3743
crustal rifting and volcanism relative timing and tectonic implications 78−81129
crustal stress state, statistical anal. 80−81852
crustal stresses determ. from seismic b-value scanning, appl. to earthquakes development modelling *(Chinese)* 79−12072
crustal structure formation using plate tectonics and rotation hypothesis *(Russian)* 78−15986
crustal structures formation, mechanical modelling rel. to interpretation of regional gravity anomalies *(Russian)* 78−49154
crustal subduction, P.J. Holmquist theories 78−20379
crustal vertical movements, rel. to surface relief in Bulgaria, statistical investig. 78−81126
Cuban Shelf, quantitative anal. of vertical tectonic movements 79−53333
Cuvier Basin, off W.Australia, crust form. by rifting, seismic study 80−12368
cycle recurrence, correl. with Mohorovicic relict discontinuities *(Russian)* 77−44947
Dalradian slide, NW Ireland, strain history from deformed pebbles 80−4013
Damara-Ribeira orogen, continental collision interpretation 80−21703
Danakil Depression and Dead Sea Rift, comparative study of sedimentary fills 78−69347
Davie fracture zone and movement of Madagascar 78−65249
Dead Sea Rift and adjoining areas, gravity and density distrib. rel. to tectonics 79−57893
Dead Sea Rift and N.Israel, mag. and gravity obs. and interpretation 80−98233
Dedham granodiorite, E.Massachusetts, Rb-Sr age and relation to Avalonian orogenic belt 77−81835
Deep Sea Drilling Project of Scripps Institution of Oceanography, results 78−69464
deep seismic zone, Tohoku, Japan, freq.-magnitude obs. rel. to geochem. changes 80−72447
Delhi region, seismotectonics, earthquake data, strain distribs. 77−17044
Dellwood knolls, role in triple junction tectonics off northern Vancouver Island 80−90067
Denali fault system, Alaska and Canada, displacement history 78−88805
descending lithosphere, effects of accretion on geometry 77−29275
descending lithosphere thermal regime, effect of varying angle and rate of subduction 78−77206
descending plate lithospheric split, obs. from N Apennines 80−85639
descending slab stress state, anal. of seismic source parameters 80−104946
Devonian Catskill red beds, evidence for tectonic motion 79−2183
Deweras Group sedimentary environment, Rhodesia, palaeorift system 78−53650
Dezadeash flysch sedimentology rel. to strike-slip faulting along Denali Fault 77−17098
Diablo Plateau, W.Texas, contemporary uplift from levelling meas. 79−20798
Diablo Plateau region, W.Texas, new evidence for tectonic uplift 80−72481
diapir formation, finite element model of density instability 80−51366
Dinarides, tectonic framework and evolution 78−32053
Dinarides, Yugoslavia, middle Triassic volcanism rel. to peri-Mediterranean tectonics 78−77238
dipping plate in Aegean Arc causing P-wave travel time residuals 77−33011
discrete islands formation in linear island chains due to discrete mantle plumes 78−44796
displacement calc. from finite strain, compatibility eqns. 77−73703
Djibouti Republic, magnetic anomaly map and tectonic interpretation 80−61753
dolines, terrestrial and lunar, form. *(French)* 77−86826
dolomite, stacking faults obs. 78−3761
double seismic zone in downgoing slabs and mesosphere viscosity 80−26472
downgoing slab, olivine to spinel transition kinetics and deep focus earthquakes 77−5190
driving mechanism for plate tectonics 77−44961
W dronning Maud Land, Antarctica, Precambrian folding and metamorphism 77−86894
DSDP abyssal igneous cores, remanent mag. inclinations, postemplacement tectonic effects 78−28161
ductile deformation zones, mechanical processes involved in crystalline basement rocks deform. 79−53344
Duncansby volcanic neck, NE.Scotland, palaeomag., K/Ar ages, tectonic implications 78−61369
dunite complex, S.Shetland Islands, deform., serpentinisation and emplacement rel. to fracture zone tectonics 78−44814

tectonics continued
dyke injection direction determination, new criterion based on wall minerals ang. relations 79−79843
dynamic processes, extraterrestrial causes, rel. to extinction of life 78−92820
Early Cretaceous remanent spreading centre in central Pacific Basin 80−21706
Earth crust, struct. and evolution 79−96749
Earth crust in situ stress field, determ. via hydrofracturing, fracture mechanics approach 78−81435
Earth crust stress changes, in situ monitoring 79−29884
Earth sciences frontiers, orthodoxy and creativity, symposium, Hobart, Tasmania (1977 February 7 to 10) 80−62380
Earth upper mantle, nonlinear stress propag. 79−16422
earthquake aftershock sequence, frictional fault model 80−30992
earthquake cycle, asthenosphere readjustment effects on free surface deform. 78−85490
earthquake cycle in underthrust zones, model 80−26457
earthquake fault mapping in Japan *(Japanese)* 80−51348
earthquake fault model (stochastic) 80−109114
earthquake faults, premonitory slip rel. to foreshocks characts. and earthquake prediction 80−3944
earthquake focal mechanism consistency, new parameter describing seismic activity *(Chinese)* 79−12074
earthquake focal mechanisms in Hollister area, S.Coast Ranges, California 79−79752
earthquake foci motion, typification technique, seismotectonic problems soln. 78−61350
earthquake fracture energy for shallow events as tectonic indicator 78−20358
earthquake mechanisms, Izu Peninsula, Japan 80−12345
earthquake precursory rock cracking, size estimation of preparation zone 80−76930
earthquake prediction based on tectonics *(Chinese)* 78−61335
earthquake prediction based on tilt anomaly 80−104917
earthquake prediction rel. to plate tectonics *(German)* 80−98267
earthquake recurrence intervals 79−92490
earthquake seismic moments beneath island arcs, phase changes and subduction vels. 77−33007
earthquake swarms, model involving dike clusters 77−44934
earthquake-source parameters, relation to magnitude 78−96154
earthquakes, centrifuge modelling 78−81429
earthquakes, fault plane soln. from relative amplitudes of P and pP 77−73669
earthquakes, similarity laws rel. to fault rupture 77−81808
earthquakes and tectonic patterns, central Mississippi valley 78−85504
earthquakes at plate boundaries, magnitude-freq. relation 80−56390
earthquakes connected with human engineering activity, tectonic and tectonophysical conditions for occurrence 77−81802
earthquakes focal regions, tectonics rel. to P-wave amplitudes regional anomalies 79−79751
earthquakes in and near Japan, energy release statistics (1915 to 1978) 80−94471
earthquakes in Jan Mayen, Iceland and Svalbard, focal mechanism solns. reanal. 79−44140
earthquakes maximum magnitude prediction, geotectonic method and appl. to N.Italy area 78−40493
East Africa, isostatic compensation 79−8623
East Pacific Rise, 9° to 12°S, anal. of fast-spreading ridge crest 77−33039
East Pacific Rise at 21°N, hydrothermal activity and crestal struct. 78−28216
East Pacific Rise at 31°S, local axial migration and spreading rate variations 77−29274
Easter volcanic chain, S.E.Pacific, mantle hot line 77−70628
Eastern Rift, Africa, volcano spacings and lithospheric attenuation 77−5167
Echzell/Wetterau, earthquake, 1975 November 4, seismotectonics 78−40512
N Egypt, shear zones from gravity data 78−28208
El Golfo earthquake, Mexico, 1966 August 7, source mechanism 79−66627
El Pilar fault zone, NE.Venezuela, brief review 79−79775
elastic dykes, pre-cleavage, at New Paltz, New York, redistrib. by folding 79−100837
elastic plate, earthquake stress drops and plate driving stresses 77−91100
NE Ellesmere Island, NWT, Canada, post-glacial uplift dating 78−77233
Ellsworth Mtns. crustal fragment, Antarctica, age and tectonic posn. 77−29262
Elsonian magmatism in Labrador, age, characts. and tectonic setting 78−73365
energy and mineral resources rel. to plate tectonic research 78−7606
energy coupling between tectonic processes and earthquakes 78−73321
energy release in great earthquakes 77−86798
Eolian Islands, S. Thyrrenian Sea, basement structural trends from aeromagnetic and gravimetric data 78−40519
SW.Ethiopia, dating of volcanic and rifting history 80−51369
Ethiopian rift geodimeter survey 77−70633
Ethiopian rift valley, present day strain rates 78−32051
Eurasian and North American plates, relative rot. pole determ. 80−85637
central Europe, active or residual tectonics stresses 77−91094
Europe, heat flow, temp. distrib. and geothermal models, tectonic implications 77−81849
Europe, tectonic and geophysical implications of preliminary heat flow map 79−70765
Central Europe, tectonic units rel. to mantle heat flow and geotherms 79−70767
European territory, tectono-magmatic processes rel. to heat flow 79−96751
W.Eurpoe and E.Canadian continental shelves, basement fractures, trans-Atlantic correls. 78−73327
evolution of surface features of Earth, endogenic and exogenic forces 80−3972
expansion of Earth or new global tectonics, comparison *(Russian)* 78−28211
Explorer ridge, off W.Canada, marine geophys. survey 79−25224
extension behind island arcs and motions rel. to hot spots 79−20796

tectonics continued
Fairweather fault Late Quaternary offsets and crustal plate interactions in S.Alaska 78−88804
Falkland escarpment and Agulhas fracture zone, boundary between oceanic and continental basement 77−21700
Falkland-Agulhas Fracture Zone, ridge-crest offset history 80−26490
Farallon Escarpment vicinity, seismicity and tectonics 78−32018
Farallon plate beneath Western USA, seismol. study 80−85621
Farallon plate fragmentation by pivoting subduction 78−77208
fault blocks and plate tectonics, theory 80−46166
fault creep events, empirical law 78−3745
fault creep records and long-baseline strain data, Hollister, California 79−79776
fault gouge, structural changes during stable sliding and stick-slip 78−32079
fault gouge composition effect on frictional sliding stability 78−3759
fault gouge deformation, simulation expts. on sandstone 80−81880
fault growth dynamics, physical basis for aftershock sequences 77−21688
fault mechanics and earthquake prediction, conf., Stanford, California, USA (Dec. 1977) 79−84143
fault motion, energy balance 77−56593
fault motion, source parameters rel. to tectonics field 78−88801
fault motion in presence of friction and inhomogeneous initial stress, rupture propag. 77−86835
fault motion meas. by satellite laser ranging, San Andreas appl. 79−79786
fault rupture propagation, theory 80−104910
fault slip stabilisation by coupled deformation-pore fluid diffusion 80−56378
fault strain field, included rectangular fault in semi-infinite media 80−98261
fault stress directions, for given fault population, theory 80−8455
fault termination deformation, a clay expt. 80−21734
fault termination deformation, normal fault in shade 80−90048
fault unstable slippage, facing media of different elastic consts. 80−72506
faulting, interpretation of seismic glut moments of total degree two or less 77−91038
faulting in southcentral Arizona, caused by groundwater extraction 79−57979
faulting inception in rock mass with weakened zone 77−33064
faulting of geological structures, cryst. defect theory approach 80−21731
faults, discontinuous structural surfaces, regression program in FORTRAN 79−84495
faults, local gravit. field effects on cloudiness distrib. 78−32136
faults, size and distrib. rel. to earthquake elastic energy release and heat prod. 79−44106
feldspars, superplastic flow and cryst. chemistry changes 79−79831
Fennoscandian land uplift gravity lines 79−92474
Finland, meas. at Fennoscandian land uplift gravity lines 79−92472
fluid-filled fracture, mechanical interaction with Earth surface 79−79779
fold shape analysis, expansion of dip isogons use and preliminary investigations implications 79−39986
folding, finite element models 79−20788
folding, three-dimens. strains in hinge zones 77−81863
folding in simple shear, expt. anal. 78−32077
folding of sedimentary rocks, Malaguide Complex, Spain 80−8312
folding of single viscous layer, exact infinitesimal-amplitude soln. 77−73729
folds and gravity tectonics in ice and rocks 77−70658
folds slope angle effect on rocks primary magnetisation direction 77−53041
forearc basins development, implications of large thrust earthquakes and tsunamis 79−57905
fracture system, statistical anal. *(Chinese)* 80−41417
France, heat flow rel. to deep struct. and mantle convection 80−98291
Franciscan formation, California, pedestrians guide to rock exposures 80−81849
Franciscan melanges, comparison with olistostromes of Taiwan and Italy 78−81159
French Alps, relations between tectonic stresses and mag. props. of Guil valley Permian volcanics *(French)* 77−25679
French Western Alps, internal mineralogy, petrology rel. to Alpine metamorphism and tectonics 78−36157
Friuli aftershocks during 1977 80−85597
Friuli area, NE Italy, seismicity, rel. to 1976 May 6 earthquake 77−73690
Friuli earthquake, 1976 May 6, focal mechanism 80−85603
Friuli earthquake, Italy, 1976 May 6, past and future seismicity, plate tectonic model 79−79753
Fruili area, seismic activity rel. to neotectonic movements 78−24229
Fuji river, active faults anal. by track etch method *(Japanese)* 80−109127
Galapagos hotspot, spreading centre jumps and subaxial asthenosphere flow 77−33042
Galapagos Inner Rift, 86°10′W, struct. and tectonics 79−79808
Galapagos Islands, t, spreading centre jumps 80−104877
Galapagos Rift at 86°W, regional morphological and struct. anal. 80−26491
Galapagos Rift at 86°W, rift valley sheet flows, collapse pits and lava lakes 80−21708
Galapagos Rift at 86°W, sealed topography and magmatic episodes 80−21681
Galapagos Rift at 86°W, volcanism struct. and evolution of rift valley 80−21707
Garm geodynamic polygon, surface deformation 79−79792
Garm region, crustal fracturing rel. to weak earthquakes space-time sequence 80−21653
Gazli earthquake, 1976 May 17, search for tectonomagnetic effect 79−57859
geodesy applied to crustal movement measurement, instrumentation trends and prospect 79−29738
geodesy contributions to geodynamics *(German)* 78−81101
geodetic data systematic inversion, central California 79−84076
geodynamic interpretation of pot. field anomalies, physically based source models *(German)* 79−34782
geodynamic monitoring and earthquake research, radiointerferometry appl. 80−31151
geodynamics, of oceans and continents, rel. to seismic anisotropy 77−49011
tectonics continued
geodynamics and palaeomagnetism 79−79737
geologic evolution of terrestrial planets 77−53442
geological faults, fracture, creep and strain 78−69345
geological folding process, laboratory expt. and theory 80−21733
geological history computation from field survey and map data in FORTRAN 77−9522
geological sciences, evolution rel. to plate tectonics 78−7605
Georgia Inner Piedmont, hornblende and biotite $^{40}Ar/^{39}Ar$ ages, rel. to tectonothermal history 78−48990
geosyncline processes, energy aspects *(Russian)* 78−96182
German Democratic Republic, geomag. secular var. anomalies rel. to vertical and horizontal crustal movements 80−26449
Gettysburg Bank, N.Atlantic Ocean, K-Ar data rel. to plate boundary transform motion 79−88322
glacial isostatic adjustment and sea level, global finite element model 79−20800
global, framework for seismic microzonation 79−88270
global asymmetry rel. to other planets *(Russian)* 78−73346
global geodynamics, Canadian contribs., 1971-79 period. 80−8262
global gravity anomalies and two-scale mantle convection 77−17067
global heat flow map and flow pattern, plate tectonics interpretation 78−7603
global isostatic overcompensation 79−62474
global plate reorganization during early Cenozoic 79−34788
global plate tectonics, rel. to pole secular motion 78−65172
global tectonics, Palaeozoic and Precambrian, rel. to polar paths and palaeomag. cycles 79−66618
Gondwana configuration in Early Palaeozoic, palaeomag. study of Argentina 80−89938
Gondwana Palaeozoic apparent polar wander path 78−36094
Gondwanaland, breakup rel. to evolution of Indian Ocean 80−41428
Gondwanaland, east-west fit from palaeomagnetic data 80−61792
Gondwanaland, India and Madagascar fit based on matching Precambrian lineaments 79−62477
SE.Gondwanaland, plate tectonics Campbell plateau and Lord Howe Rise 80−17244
Gondwanaland break up, revised model *(German)* 78−44797
Gondwanaland break-up rel. to flood basalt volcanism and subduction 78−65251
Gondwanaland fit, plate tectonics of India and SE Asia 80−8282
NW Gondwanaland Proterozoic tectonics, new evidence from E Newfoundland 79−57908
Gondwanaland reconstruction, Antarctic Napier complex rel. to S. India 80−76946
Gondwanaland reconstruction 77−66903
Gondwanaland reconstruction for Indian Ocean 77−70632
Gondwanaland reconstruction from lower Palaeozoic sequence of N. Victoria Land, Antarctica 77−17069
Gondwanan glaciation, cyclothems, continental positioning, and climate change 79−62526
Gorda Ridge spreading centre, active faulting meas. by sonobuoy array 78−85494
Gore Range (Summit County, Colorado), Quaternary geology, and reported surface faulting 79−2238
graben-type sedimentary basins form. by continental crust extension 77−25665
grabens of Canyonlands National Park, Utah, geometry, mechanics, kinematics 80−21728
Grampian orogeny in Scotland: arc-continent collision and polarity reversal 79−39696
granite magmatism initiation and thermal diversity 78−65240
gravimetric geoid over Alps, and tectonic interpretation *(French)* 79−66600
gravity anomalies and tectonics, review 80−98593
great earthquake occurrence, chaos theory of fault block behaviour 80−72448
W.Great Kabylia (Algeria), granite, deform. by ductile shear *(French)* 79−39716
Great Slave Lake, Canada, early history and tectonics of East Arm graben 78−49017
Greater India rel. to palaeomagnetic data from Hindukush, Pakistan 79−44087
Greece, lithospheric model for earthquake interp. 78−3726
E Greenland, continental rifting rel. to struct. of coastal dyke swarm and assoc. plutonic intrusions 80−56467
E.Greenland, Jurassic basin evolution 78−73344
E Greenland, southern Caledonian fold belt polyorogenic nature from isotopic age study 80−76938
S.E.Greenland continental margin, struct. and tectonics 77−33014
E.Greenland continental margin, Tertiary basalts ages rel. to plate separation 77−5153
greenstone belts, ancient marginal basins or ensialic rift zones 78−61418
greenstone belts, Archaean, thermal modelling and tectonic environment 79−70762
greenstone belts from Superior Province in Manitoba, tectonic evolution 79−62497
Gregory Rift Valley, Kenya, magnetotelluric and magnetovariational study rel. to tectonics 77−91000
Grenville Belt, Rb-Sr and palaeomag. evidence from Sweden rel. to magnetisation age and tectonics 77−81839
Grenville Province, palaeomag. and tectonics 78−88794
Grenville Province, tectonics from palaeopoles $^{40}Ar/^{39}Ar$ dating 79−20778
Guacanayabo Bay, Cuba, tectonic processes rel. to Holocene sedimentation 78−3752
Guatemala earthquake, 1976 February 4, tectonic aspects 77−2137
Guatemala earthquake (1976, February 4), seismological aspects 78−85493
Guaymas Basin spreading axis, high-temp. hydrothermal deposit 80−101355
Gulf of Aden, mag. survey, seafloor spreading phases determ. 78−32049
Gulf of Aden and Afar, mag. anomaly map and plate tectonics 80−56364
Gulf of Aqaba, sinistral movement rel. to Red Sea opening 80−76954
Gulf of Elat (Aqaba), continental breakup evidence 80−72485
W.Gulf of Mexico, sedimentary section rel. to Jurassic plate boundary 77−21749
Gulf of Mexico-Caribbean area, Permian-Triassic continental reconstruction 80−56431
Gulf of Oman, fold development 78−15984

tectonics continued
Gulf of Oman, sediment deform. and plate tectonics 77−5176
W.Gulf of Oman, tectonics 80−8279
Gulf of Valencia, W.Mediterranean, aeromagnetic survey *(French)* 77−29243
Hackett River greenstone belt, Slave Province, NWT, regional deforms. and granitoid plutons emplacement 79−100834
Hadrynian Polar Track discovery rel. to Grenville problem 77−48991
Harp Lake Complex, Labrador, palaeomagnetism and Precambrian polar wandering path 77−90997
Haute-Pointe massif, France, new tectonic interpretation *(French)* 77−49054
Hawaii earthquake, Nov. 1975, low dip angle faulting mechanism 80−56406
Hawaiian Island chain, volcanism linear migration from Kauai shield-building volcanism age 80−36281
Hawaiian Islands, isostasy and lithosphere flexure 80−26485
Hawaiian volcanoes, rift zones as expressions of plume generated radial stress fields 80−90051
heat flow and tidal drag as driving forces of plate tectonics 78−32050
heat flow from tectonic units, Romania *(Rumanian)* 80−8268
Hellenic Arc, dynamic model deduced from geophysical data 77−21734
Hellenic Arc, recent Quaternary tectonics from geological obs. on land 79−79797
Hellenic arc and trench system, key to E.Mediterranean area neotectonic evolution 80−56451
Hellenic Arc tectonic evolution since late Miocene 78−96185
Hellenic trench system, subduction to transform motion, Seabeam survey 80−8285
S Hemisphere, plate to tectonics rel. to circum-Antarctic Ocean and Antarctic glaciation 78−16063
Hercynian Front in Ireland, probably local feature 78−32035
Hercynian Ocean northern margin, sedimentary facies and basin subsidence 77−21725
Hess Rise, W.Pacific, plate tectonic history 80−90026
N. Hida region, Japan, seismicity and focal mechanism of local earthquakes *(Japanese)* 80−94482
W.Himalaya, Central Crystallines, geology and tectonics 80−72516
Himalaya, intracontinental subduction initiation mechanics 79−16431
Himalaya, its rise and plate tectonics 79−53334
Himalaya, two intracrustal boundary thrusts 80−104948
Himalaya, uplift and cooling rates from geochronological data 80−85627
Himalaya and Tibet Plateau region, tectonic history 80−72486
Himalaya geological structure study using satellite imagery *(German)* 77−66907
Himalayan geothermal belt *(Chinese)* 79−79759
Himalayan mountain front NW termination, active tectonics from microearthquakes 78−40505
Himalayan Suture Zone, Landsat picture obs. 80−76948
Himalayas, seismicity, earthquake mechanisms and tectonics 78−40514
Himalayas, seismotectonics, continental plate convergence 78−7593
Himalayas region, conf., Mar. 1978, Katmandu, Nepal 80−72523
Hindu Kush, tectonic lineaments from ERTS imageries 78−3739
Hindu Kush region, microearthquake seismicity and fault plane solns. 80−72446
Hindukush, Baluchistan arc, seismotectonics and struct. (1890-1970) 80−104922
Hinterland Belt, Canadian Cordillera, deformation episodes 78−88825
Hispaniola, Cretaceous and Tertiary rocks palaeomagnetism rel. to Caribbean plate tectonics 79−44103
Hokkaido and Tohoku, Japan, intraplate seismicity and large quakes 80−51337
Honshu, Japan, deep seismic zone and plate tectonics 80−8269
horizontal stresses from satellite pictures *(Russian)* 79−20791
Horse Canyon earthquake, California, stress-release process 80−56387
hotspot islands, Rodriguez, Darwin and Amsterdam Islands 79−20793
Hungarian depression, horizontal compression and extension rel. to gravity nontidal vars. *(Russian)* 79−8621
hydro-isostatic flexure rel. to Holocene sea level changes 79−84295
Iapetus Ocean, evidence for Cambrian opening 80−98299
Iapetus Ocean suture location in Newfoundland 77−66915
Iberian margin ocean-continent boundary struct., discovery of serpentinite diapir W. of Galicia Bank 80−94489
ice ages and continental drift, theory 79−44209
Iceland, continuum model of crustal generation, kinematic aspects 80−90059
Iceland, crustal stress, hydrofracture meas. rel. to tectonics 77−91098
Iceland, evidence for asthenosphere diapiric updoming from 1977 Seismic Project 79−57889
N Iceland, gravity and height vars. during present rifting episode 80−90060
E.Iceland, lava $^{40}Ar/^{39}Ar$ age for ocean ridge spreading rate 80−36273
N.Iceland, major rifting episode with intense earthquakes, ground deform. and magmatism 77−37175
N.Iceland, microearthquakes rel. to geomorphology and tectonics 77−81801
N.Iceland, plate boundary rifting, 1975-78 period 79−84210
Iceland, rift jumping rel. to oceanic plagiogranites melting and rhyolites generation 77−86885
Iceland, tectonic spreading, problems and mechanism 78−36137
N Iceland, vertical crustal movements from height meas., (1965 to 1977) 80−89931
N.Iceland fissures, relative movements and tile changes 80−90062
Iceland Plateau, tectonic synthesis from sea floor morphology and mag. anomalies N of Iceland 80−89953
Iceland position and plate tectonics 77−33041
NE Iceland rift zone, geodetic meas. and horizontal crustal movements 80−89930
Iceland-Faeroe Ridge, subsidence history rel. to Lower Tertiary laterite and Thulean land bridge 78−85514
Icelandic crust, lateral magma flow during rifting episodes 78−73339
Icelandic plate boundary rift and earthquake activity *(German)* 79−5467
Icelandic volcanism, rift zones as expressions of plume generated radial stress fields 80−90051
Ile de Groix blueschists, progressive shear rel. to subduction or obduction 78−53652
inclined seismic zones rel. to age-length depend. of subducting margin 78−57175
N.E. India, and N. Burma, seismicity, gravity and tectonics 77−25654
India, Bouguer gravity anomaly map and tectonics 80−61791
tectonics continued
India, Holocene deform. and crustal movements in type areas 79−79793
India, northward motion since Late Cretaceous, palaeolatitudes 78−28209
India, peninsular, fan faults rel. to origin of Himalayas 80−85630
NE.India, seismicity and focal mechanisms rel. to faults and tectonics 78−24221
India, seismotectonics 78−44782
India-Asia collision from Indian apparent polar wandering path 80−26452
Indian intra-cratonic sedimentary basins, deep struct. features and evolution 77−21728
Indian Ocean, model of evolution rel. to breakup of Gondwanaland 80−41428
Indian Ocean, seafloor spreading history 80−61790
Indian Ocean and surrounding areas, contemporaneous tectonic events 77−64256
Indian subcontinent, two-stage collision model 79−88241
Indian subcontinent collision with Eurasia 77−78146
Indian/Pacific plate boundary, microearthquake study of New Zealand 80−109131
Indo-Australian plate, evidence for internal deform. 80−109134
Innuitian Province, Arctic Canada, tectonic history 80−8275
inter-arc basins, kinematic model 78−81127
intra-plate deformation, faults activated by 1978 Thessaloniki earthquakes 79−39697
intra-plate volcanism during Cainozoic, rel. to mantle convection 80−98293
intracratonic basin, formation model involving deep metamorphism 80−85618
intraplate events, Tangshan earthquake analysis 79−92495
intraplate seismicity, zones of weakness, alkaline magmatism and tectonism 79−74882
intraplate seismicity on bathymetric features, 1968 Emperor Trough earthquake 80−30997
intraplate volcanism, geological and geophysical parameters 78−65243
intraplate volcanism, magma flow through lithospheric fractures, tensional tectonics 78−65242
Iran, seismotectonic implications of relocated aftershock sequences 79−44119
Iran, seismotectonic provinces, discussion 79−92499
Iran, seismotectonic provinces 77−9357
Iran, tectonics rel. to earthquakes instrumental and relocated epicentres 79−88258
Iranian Makran, Recent faulting episode 78−32038
Iranian Plateau, quantitative seismotectonic study 79−88279
Iraq, seismicity and seismotectonics, 1900-72 period 77−73665
E. and SE.Ireland, geochemistry and tectonics of Upper Ordovician volcanics 79−44144
S.Irish Caledonides, plate tectonics and evolution 77−5174
island arc development, obs. expts. and speculations 80−98298
island arc merging and Superior province of N.W.Ontario development 77−17066
island arcs, curvature rel. to convergence vel. and subduction angle 78−81128
island arcs, tectonic flow 79−25223
island-arc volcanism, magma formation and ascension due to sinking of tectonic plates 79−100823
isostacy and long term flexural rigidity of crust 80−46161
isostasy at midocean ridge crests 80−31022
isostasy investigation, correl. coeffs. between elevations and Bouguer anomalies 77−86850
isostatic and dynamic processes rel. to viscosity 77−21745
isostatic compensation and viscosity differences between crust and asthenosphere 80−104947
isostatic compensation on continental scale, local and regional mechanisms 78−11859
isostatic tilting, post-glacial, induction of regional trend to river meander migration 80−101391
central Israel, evidence for pre-Late Jurassic east-west fossil continental margin 79−34766
Israel, Mesozoic palaeomag. results and inferences for microplate struct. in Lebanon 80−61760
Italy, fault-plane solns. and stress regime 78−69299
S.Italy, geotectonic features rel. to seismic risk map 79−44113
Italy, heat flow meas. rel. to tectonic features 79−70769
Italy, rotation rel. to volcanic rocks palaeomag. 79−66613
Italy, rotation rel. to volcanic rocks palaeomag. 79−66614
NE.Italy, surface geology rel. to seismically active tectonic structures 78−24286
Iwate-Oki (Japan), earthquake, 1968, June 12, focal mechanism and tectonics 77−78123
Izu Block, Japan, accommodation of colliding plates 80−41424
Izu Peninsula, Japan, active faults in Amagisan area *(Japanese)* 78−96164
Izu Peninsula, Japan, geoelectric survey near anomalous upheaval zone *(Japanese)* 80−46122
Izu Penisula, active faults anal. by track etch method *(Japanese)* 80−109127
Izu-Oshima-kinkai earthquake, Jan. 1978, fault mechanism 80−41390
Izu-Oshima-kinkai earthquake, Japan, Jan. 1978, associated surface faulting 80−41408
Izu-Tokai District, Japan, tectonic activity rel. to earthquake prediction *(Japanese)* 78−96145
Jamaica, blueschists, coaxial pure shear rel. to deform. assoc. with subduction 79−2236
Jamaica, Late Cretaceous and Miocene igneous rocks, palaeomag. rel. to tectonics 78−20352
James Bay gravity survey rel. to Kapuskasing Gneiss Belt, Ontario 78−48959
Jan Mayen fracture zone, Norwegian Sea, seismicity map 77−78127
Jan Mayen Ridge, Cepan 1 1975 survey 78−96184
Japan, continental drift and Permian greenstone palaeomag. 80−21629
SW.Japan, earthquake activity rel. to plate tectonics 80−21663
Japan, geomagnetic secular change anomalies rel. to tectonic activities 77−2091
SW.Japan, major earthquake focal mechanisms rel. to tectonics 78−11827
Japan, subduction tectonics rel. to geology 78−20377
Japan geosyncline outer margin, structural characts. and tectonisms around microcontinent 78−81139

tectonics continued
SW.Japan island arc, uppermost mantle differential stress lateral var. 80−98275
Japan Trench, form. and evidence for eastward extension of Honshu *(German)* 79−84200
Japan trench, microearthquake activity off Sanriku rel. to tectonics 77−81803
Japanese and Izu-Bonin Islands junction, gravity meas. rel. to plate tectonics 77−78085
Jotunheimen Caledonian structure, geological evidence 79−25222
Juan de Fuca and Explorer Ridges, recent plate interactions, model 77−66900
Juan de Fuca plate aseismic subduction, geodetic evidence 79−84209
Juan de Fuca plate movements 79−44162
Juan de Fuca Ridge crest, E.Pacific, tectonic topography compensation 80−56448
Jura fold limb rotation, geometrical adjustments 77−21747
Jura mountains, stratigraphy and tectonics, rot. tectonics on laramide fault pattern *(French)* 79−34785
Jurassic sea-floor spreading in E.Equatorial Atlantic 77−64253
Kalapana, 1975 November 29, intra-plate earthquake rel. to geothermal processes 79−39664
Kambalda dome, W.Australia, tectonics rel. to sulphide fabrics in Ni sulphide ores 78−77229
Kamchutka, volcanic zone, tilt meas. 80−3984
Kane fracture zone in western Central Atlantic Ocean 77−5170
S.Kanto and Tokai districts, Japan, crustal plate dynamics *(Japanese)* 80−51382
Karakorum, tectonic lineaments from ERTS imageries 78−3739
Kenya rift valley, geophysics 77−86825
Khurgu earthquake, Iran, 1977 March 21, field report, seismotectonics 79−12083
kinematics from Euler vectors 78−53637
King's Trough, NE.Atlantic Ocean, struct. from bathymetric, seismic and gravity data 78−49005
King Island, Australia, fission track ages rel. to continental rifting 78−53628
Klamath Mountains, Oregon, Jurassic island arc sequence identification in Rogue and Galice formations 79−100836
Krafla Caldera, NE Iceland, gravity and elevation changes caused by magma movement 80−90052
Krafla fissure swarm, Iceland, surface deform. in rifting events 80−90061
Krafla volcano area, N. Iceland, horizontal magma flow rel. to subsidence events, (1975 to 1979) 80−90053
Kurile trench-Hokkaido rise system, flexure profile by plate model 80−72482
Kurile-northern Honshu arcs junction, mantle earthquakes mechanism rel. to slab tectonics 77−81805
coastal Labrador, granite intrusions, Rb-Sr ages and tectonics 77−81836
Labrador Sea and North Atlantic evolution 78−28210
Labrador Trough, Canada, early recumbent folds in northeastern part 78−65300
Lachlan Fold Belt in New South Wales, description, tectonic history 78−96211
Lageos for crustal movement meas. 78−65441
Lake Baikal rift system 77−37163
Lake Biwa, Japan, secular gravity change meas. rel. to vertical crustal movement 78−40463
Lake Eyre North, S.Australia, bottom profile and tectonic grooves 78−69376
Lake Van, E.Turkey, volcanism evolution and plate interaction 77−29270
Lake Van tectonic activity and sedimentation study *(German)* 78−3843
Laksefjord, Finnmark, fold rotation during overthrust processes 78−88812
land subsidence in England and Wales, implications of Flandrian sea level changes in Thames Estuary 78−24304
Laramide folding and faulting in SE.Arizona, basement cored uplift model 80−8272
Laramide orogeny, seismic profiles in Wyoming, USA 80−85626
Laramide Wind River uplift, Wyoming, USA, gravity and seismic refl. data 80−21679
Late Cretaceous fore-arc basin, California, petrologic evolution rel. to arc development 79−2232
Late Palaeozoic slate belt, structural succession and tectonic significance 78−81140
late Precambrian mafic dykes, Montana, geochemistry and Rb-Sr geochronology rel. to Belt tectonics 78−77196
Late Quaternary uplift in New Hebrides, U series ages 78−3741
Laurentia, Precambrian plate tectonics from Gardar lavas (S.Greenland) palaeomag. meas. 77−40973
Laxfordian deformation in Carloway area, Isle of Lewis, Scotland 78−7638
Leon line, N.Spain, wrench deformation, facies differentiation 78−88831
Lewisian foreland, NW.Scotland, central zone palaeomag. rel. to tectonics 80−26443
linear and planar structure, rot. and strain in three-dimens. progressive deform. 77−78171
liquid-filled vertical crack propagating due to hydrostatic press. 80−72505
lithosphere, elastic-perfectly plastic bending under generalised loading, appl. to Kuril Trench 78−73341
lithosphere, isostatic disturbances rel. to elastic stresses 77−81842
lithosphere bending at trench, elastic-perfectly plastic anal. 78−81135
lithosphere creep deformation model, deformation due to geologic load 80−104939
lithosphere flow and rupture, analogy with creep rupture in cold ice sheet 79−2306
lithosphere individual plates, absolute motion estimate from ridge and trench boundaries location 78−85529
lithosphere plates, accretion and subduction effects on shallow global mantle flow 79−44163
lithosphere slab, penetration into lower mantle beneath Sea of Okhotsk 77−73700
lithosphere-mantle decoupling, role of shear heating 79−20790
lithospheric downgoing slabs, temps. rel. to seismic zone lengths 79−25212
lithospheric necking and slowly accreting plate boundaries 79−2208
lithospheric plates driving force, induced suction phenomenon 78−40534
lithospheric plates movement, influence on mantle convection 79−74880

tectonics continued
lithospheric plates underthrusting zone, oceanic sediments subduction mechanism 77−53030
lithospheric strain model using generalised Norton-Hoff law *(French)* 78−88809
lithospheric thinning, hot spots and island subsidence 78−53631
S.Long Island, New York, Holocene submergence history 79−74881
longitudinal folds, high-amplitude, form. and stress state 77−9382
Lord Howe Rise and SE.Australian margin, rift valley breaching 78−96179
Los Angeles basin (California) SW block, thermal subsidence and petroleum generation 80−3967
lower mantle convection, inferred from low Q zone 80−76944
Loyality Islands uplift rates, $^{230}Th/^{234}U$ dating of raised coral terraces 78−73347
magma series erupted in different marine tectonic settings, trace element anal. 80−21667
magmagenesis 79−12103
magmatic diapir folds tectonic evolution, influence of temp. and heat exchange with crustal rocks *(Russian)* 80−104957
magnetic variation due to stress change, theory of electrokinetic-mag. anomalies 80−21627
major continental blocks, drift since Devonian 78−11864
Makran coast, Iran and Pakistan, seismic harzards, regional tectonics and geology 79−88295
Malaguide complex, structural facing and Palaeozoic rocks 77−49046
mantle, geodynamic consequences of Nd-Sr isotopic correl. 79−92512
mantle, implications of Spanish deep-focus earthquake (1954 March 29) 77−9375
mantle, kinematic models of large-scale flow 79−70777
mantle, parametrised convection model rel. to Earth thermal history 79−16429
mantle, seismic vel. variations, origins 80−81854
upper mantle, tectonics rel. to magmas and volatile components 80−41418
mantle, thermal convection, time dependent simulation 80−101352
mantle, thermoconvective waves, propag. without attenuation 80−90064
mantle, two-dimensional flow beneath rigid accreting lithosphere 79−12102
mantle, two-scale convection rel. to global gravity anomalies 78−85528
mantle, upper, thermal and mechanical struct., continental and oceanic models 77−37169
mantle convection, depth extent from seismic energy release of deep and intermediate earthquakes 80−41404
mantle convection, finite deformation during fluid flow 79−92519
mantle convection, internal radiogenic heating rel. to oceanic bathymetry flattening 80−85642
mantle convection, numerical anal. 80−51371
mantle convection, plate movements as obs. evidence 79−84692
mantle convection, rel. to inertia and gravity asymmetry 80−98269
mantle convection, scale rel. to plate motion 77−44963
mantle convection, simple plate models 79−25221
mantle convection, two-scale flow model rel. to plate tectonics 78−73348
mantle convection driven by radioactive energy, model for decaying source 80−72461
mantle convection model, plate tectonics mechanism 77−81860
mantle convection models, laboratory expt. 77−9396
mantle convection pattern and subcrustal stress field under Asia, rel. to seismicity 78−57190
mantle convection rolls, stability anal. 80−76957
mantle convection shaping by tidal bulge, rel. to global tectonics 78−32048
mantle convection with moving surface plates, model 80−85634
mantle convective instability, thermomechanical model 80−90063
mantle creep (steady state), anal. of olivine eqns. of state 80−104924
mantle creep rate, influence of natural radioactivity 79−92520
mantle evolution beneath mid-ocean ridges 77−44962
mantle flow, one-dimensional modelling 79−39698
mantle flow pressure rel. to subduction angle, non-Newtonian corner flows theory 79−39695
mantle plumacy problems, graphic solns. 77−91081
mantle plume, fluid-dynamic model of ascending flow 80−12370
mantle viscous flow under moving lithospheric plates and under subduction zones 77−56613
marginal basins, diffuse magnetic anomalies and their tectonic and petrologic significance 78−32064
Mariana Trough, back arc spreading characts. 78−53640
marine geology and geophysics, 1967-77 review 77−64260
marine geomagnetism, plate tectonics, plate boundaries and mag. field reversals *(French)* 79−66621
Markansu Valley earthquake, Tadjikstan, USSR, 1974 August 11, seismotectonics 80−21659
Massachusetts, regional tectonics rel. to metamorphism temp. and press. 77−2148
Massif central, France, upper mantle struct. and dynamics from basalt xenoliths obs. *(French)* 79−48424
Massif Central, upper mantle regional struct. and geodynamics 78−81120
Maubisse Formation, East Timor, palaeomag., tectonic implications 78−3716
mechanical models for absolute plate motions in Early Tertiary 77−33036
E.Mediterranean, deep struct. and tectonics 78−69309
W.Mediterranean, gravity and bathymetry rel. to tectonics 77−32973
E.Mediterranean, struct. and tectonic setting of Levant continental margin 78−69310
Mediterranean Alpine Belt, geodynamics of eastern region 77−13071
E.Mediterranean and Levant fracture zone, tectonics of continental collision 78−69319
Mediterranean and marginal seas origin 78−69322
Mediterranean arc evolution at continental stage *(Italian)* 79−66670
Mediterranean area, surface wave and seismotectonic studies 77−37151
E.Mediterranean gravity anomalies, volcanic activity rel. to tectonic development 78−69318
Mediterranean interarc basins, comparison of Tyrrhenian and Pannonian basins 77−13075
Mediterranean region, Holocene eustatic changes and coastal tectonics, crustal consumption 78−81201
Mediterranean region, struct. and tectonics, conf., Haifa, Israel (Aug.-Sep. 1976) 78−69306
E Mediterranean regional vertical tectonics from gravity obs. 77−5172

tectonics continued
Mediterranean Ridge, young submerged chain assoc. with Hellenic arc, struct. and tectonics 77−53014
Mediterranean Sea, plate movements rel. to Messinian salinity crisis 77−91151
E.Mediterranean Sea, tectonic elements and crustal struct. 78−44801
melt production in mantle, by viscous dissipation 80−72463
Mentese region, SW Turkey, LANDSAT imagery appls. 78−77236
Mesozoic volcano-tectonic rift zone and back-arc basin development, South America 79−29762
Mesozoic-Cainozoic sedimentary basins development in W. North America 77−5169
Messina, Italy, earthquake, 1908 December 28, seismotectonic study 79−84177
Messina Layered Intrusion, Limpopo Mobile Belt, S.Africa, tectonic setting, geology and age 80−76969
metamorphic sodic amphibole from Newfoundland Appalachians, tectonic implications 77−29298
meteorite craters, geophysical and geomechanical aspects 80−17265
trans-Mexican volcanic belt, seismic refl. and geomag., leg 17 of project CICAR *(Spanish)* 80−36280
Mexico, apparent polar wander path, tectonic implications 79−25191
E.Mexico tectonic significance of alkaline volcanism 77−78143
Michigan Basin, crustal stress meas. 79−39681
Michigan Basin, Keweenawan turbidites as foundered basin sequence developed during protoceanic rift system evolution 79−39712
Michigan Basin, thermal and mechanical evolution, lithosphere elastic flexure 77−21719
Mid Atlantic Ridge, long-range sonar study and tectonic implications 77−33049
Mid Atlantic Ridge and Kurchatov Fracture Zone, sonar obs. 78−28214
Mid Atlantic Ridge crest at 26°N, magnetic anomaly patterns, spreading rate 77−32991
mid ocean ridge median valleys, faulting 77−44964
Mid-Atlantic Ridge, median valley tectonic model from gravity obs. 80−90071
Mid-Atlantic Ridge, oblique intersection with Charlie-Gibbs transform fault 79−84212
Mid-Atlantic Ridge at 37°N, geophysical anomalies rel. to spreading rate vars. 77−91070
Mid-Atlantic Ridge crest at 37°N, crustal struct. 77−9378
Mid-Atlantic Ridge fracture zone, deep crustal architecture and identification as transform fault *(Russian)* 79−96747
Mid-Cayman Rise spreading centre, tectonic setting rel. to basalt glasses geochemical var. and petrogenesis 80−101364
mid-ocean ridge spreading rate, petrological evidence 80−109135
mid-ocean ridges, spreading rate rel. to oblique spreading, model 79−34786
mid-oceanic ridge axes, topography and tectonics from fluid dynamic models 80−41433
mid-plate hot-spot swells, thermal origin 79−8619
Middle America arc, focal mechanism solns. and tectonics 78−77191
Middle Ordovician formations, E.Tennessee, tectonic significance of distal turbidites 78−65296
Middle-America Trench, visual obs. of sea-floor subduction line 77−66902
Midland Craton of England and Wales, Precambrian polar wander path from palaeomag. study 79−66617
Midland Valley evolution in Scotland rel. to clasts in Ordovician conglomerates 79−92540
midocean ridge, existence of mantle double partial melt zone 80−104940
migmatite rise, numerical expts. based on continuum dynamics 80−51381
migmatite tectonics, Hidaka metamorphic belt, Japan 80−8310
Mindanao earthquake, 1976 August 16, preliminary seismological assessment 79−66635
mineral exploration and plate tectonics 78−7607
minimum-dissipation theorem, usage in temp. depend. viscosity problems 80−12369
Minnesota, crustal struct. and seismicity, rel. to historic earthquakes 78−11840
Mississippi embayment, remote sensing appls. to tectonics and seismicity 77−81856
Moine thrust zone, differential stress determ. from deformation-induced microstructs. 80−85652
Moine Thrust Zone, Eriboll, Scotland, palaeostress estimates 79−79835
molasse and nonmarine-paralic sedimentary basins 79−57902
Mole (Haute-Savoie, France), geological profile of south flank rel. to struct. and tectonics *(French)* 78−69348
Molucca Sea collision zone, Indonesia 78−61384
Mongolo-Okhotsk mobile belt, rift formation and tectonic history 80−90066
Morro Rock-Islay Hill igneous complex, palaeomag., rel. to crustal block rot. in California 79−84106
Mount Carmel, struct. and extension into E.Mediterranean, marine geophys. survey 77−33026
mountain peaks uplift determ. by three dimens. triangulation *(German)* 77−52966
mountain territories, formal morphostructural zoning 77−73876
mountains origin, implications of Sun and Moon accels., appl. to gravit. const. var. 79−8592
moving continents and oceans, book 79−12104
Mull lava succession palaeomag. study rel. to Eurasian Plate motion 77−48995
Munich-Milan Alpine section, active faulting and tectonics, LANDSAT imagery 77−53037
Muskoka region, Canada, tectonic interpretation of rock joint orientations 77−70653
mylonites flow strength, role of grainsize reduction and grain boundary sliding 80−21721
mylonites formation, mechanical processes involved in crystalline basement rocks deform. 79−53344
mylonites from Grenville Front Tectonic Zone, Ontario, distortional strain estimation 78−7628
Nain anorthosite (Labrador), palaeomagnetic results and tectonic implications 78−77178
nanogravity survey in Canada rel. to tectonic movement detect. due to groundwater movements 77−33038
Narmada-Son lineament, extension towards Murray Ridge 78−15985
Nazca group volcanic rocks, Peru, volcanic history 80−12357
Nazca plate, finite element modelling of stresses 79−20802

tectonics continued
Nazca plate off S. Peru, crustal model from ocean bottom seismometer obs. 78−32032
Nazca plate subduction beneath Peru, earthquake spatial distrib. 79−66671
Nelson River gravity anomaly, SE.Saskatchewan, seismic survey 78−28153
Nemaha Uplift in Oklahoma, Kansas and Nebraska, geological survey of seismicity and tectonic rels. 78−7589
Nepal, basic intrusions of volcanic origin 80−72477
W.Nepal, gravel deposits indicating tectonic uplift 80−72487
Nepal Himalaya, body waves from earthquakes, focal mechanism and tectonics 80−72455
Nepal Himalaya, struct. geology of Kusma-Sirkang section 80−72478
SW New Brunswick and SE Maine, stratigraphy and tectonic setting of Palaeozoic sedimentary rocks 78−57199
New Guinea-Solomon Islands region, seismicity maps 78−7592
New Hebrides, Quaternary volcanism geochemistry and origin rel. to tectonics 78−20375
New Hebrides Island Arc, anomalous propag. through shearing contact zone 80−3948
New Hebrides island arc, earthquakes precise relocation rel. to seismotectonics 79−16404
New Hebrides island arc, geodynamic model rel. to upper mantle struct. in convex side 79−74861
New Hebrides island arc, tectonic troughs form. mechanisms 78−73349
New York state, microzonation and neo-tectonics 79−88275
New Zealand, plate tectonics developments 79−84208
New Zealand, present tectonics and Late Cenozoic evolution 78−20378
New Zealand plate boundary distortion *(German)* 78−20382
W.Newfoundland, $^{40}Ar/^{39}Ar$ ages and ophiolite obduction 77−33034
E. Newfoundland, aborted Proterozoic rifting 78−57200
Newfoundland, Early Palaeozoic plate tectonic model 80−94509
central Newfoundland, folded thrust faults 77−33068
Newfoundland, Late Wisconsinian glacitectonic struct. and post glacial permafrost 78−61440
SW Newfoundland, ophiolites rel. to tectonic models 77−17103
W.Newfoundland, palaeomag. evidence against rotation hypothesis 77−37129
SW Newfoundland, Proterozoic-Palaeozoic thermal history from Grenville basement rocks $^{40}Ar/^{39}Ar$ ages 79−20771
Newfoundland Basin, Mesozoic evolution 78−32045
Newfoundland Ridge, seismic structure, nature of crust, oceanic origin 79−25211
Nias Island, Indonesia, Neogene trench-slope deposits palaeobathymetry and tectonic uplift 80−104950
Nias Island, Indonesia, structural geology implications for subduction zone tectonics 80−109120
Nigerian and Sergipe-Alagoas sedimentary basins, Cretaceous transgressions 77−21701
Ninetyeast Ridge area, seismicity and tectonics, Indian plate internal deform. 78−73343
Nizky Jesenik Mts., Czechoslovakia, mag. anisotropy meas. rel. to rock cleavage origin 77−9410
Nootka Fault Zone, new plate boundary off W.Canada 79−92518
E.North America, tectonic implications of earthquakes surface wave focal mechanisms 80−3942
North America Early Carboniferous palaeomag. field rel. to N. Appalachians tectonics 80−8249
North American Atlantic continental margin, rapid Cretaceous subsidence and sedimentation 77−21722
North American Atlantic continental margin, sedimentary basins 77−25666
W.North American plate, intraplate tectonics 77−41017
North Island, New Zealand, axial tectonic belt 79−2173
North Sea, Buchan and Witchground Grabens, seismology study 80−51364
North Sea basin, subsidence in post-mid-Cretaceous 80−109133
N.Norway, continental margin crustal struct. and tectonic history 80−51360
W Norway, Devonian basins subsidence and sedimentation 77−21727
Norwegian Caledonides Trondheim Nappe melange and tectonic model 80−3985
Norwegian gneiss eclogites, giving evidence for Precambrian continent-continent collision 77−49057
Norwegian-Greenland sea, thermal evolution in sea floor spreading model 80−56427
ocean floor spreading, driving mechanism 79−100824
ocean floor spreading, mid-ocean ridges *(Russian)* 79−88333
ocean palaeocirculation, influence of plate tectonics 77−45017
ocean ridge activity, Phanerozoic history and climatic instabilities 77−66981
ocean spreading centre processes, qualitative models including hydrothermal penetration 77−33045
oceanic aseismic ridges, isostasy anal. and tectonics implications 80−3971
oceanic aseismic ridges, subsidence 77−37162
oceanic basins, volcanic evolution of marginal and interarc basins 80−8271
oceanic circulation with partial shallow return flow rel. to oceanic plates 78−40520
oceanic crust, serpentinite protrusions tectonics 77−5149
oceanic crust, structure, composition and origin 77−29268
oceanic crust, tectonics rel. to time scales and dynamic models of deep-sea sedimentation 78−15988
oceanic fracture zones, vertical tectonism 78−53638
oceanic fracture zones of equatorial Atlantic (7 to 10°N), lithosphere struct. *(Russian)* 80−104932
oceanic isostatic thermally-expanded ridge crests, gravity signatures 79−66604
oceanic lithosphere age-dependent subduction beneath western South America 79−2211
oceanic lithosphere flexure and uplifted atolls, comment 80−26486
oceanic lithosphere isostasy, anal. for Hawaiian-Emperor seamount chain 79−39688
oceanic lithosphere mechanical behaviour, implications of two earthquakes seaward of Tonga Trench 79−16405
oceanic lithosphere thermal structure rel. to ridge-crest and transform earthquakes source parameters 79−88265
oceanic mantle beneath S.Rio Grande Rift, tectonic history 79−29724

tectonics continued
oceanic plate motions driven by lithospheric thickening and subducted slabs 79−8622
oceanic ridge system, thermal struct. rel. to global sea-level changes 79−29743
oceanic spreading ridges, upper mantle partial melting 78−65237
oceanic trench outer rise, dynamic support 78−81116
oceanic trench outer rise width, model of crust thickness as function of age 80−56426
Oita, Japan, tectonic topography rel. to 1975 April 21 earthquake *(Japanese)* 77−2109
Okhotsk and Japan Seas abyssal depressions, struct. and origin 77−37168
Oklo natural fission reactors geological environment, tectonic anal., petrography, geochemistry *(French)* 80−21742
Oklo natural reacors, fluid phases contemporaneous with sandstone diagenesis, and tectonic movements *(French)* 80−21746
Oklo natural reactors, mining, geology and tectonics *(French)* 80−21743
Ondrejov laser satellite-tracking station, regional tectonics and seismicity 78−36418
NW.Ontario, granitoid complexes and Archaean tectonics 80−31019
Ontong Java and Manihiki Pacific oceanic plateaus, seismic struct. 80−21680
Onverwacht Group, Transvaal, sedimentology rel. to early Earth tectonics 78−44812
ophiolite emplacement on continental margins, similarity to thrust faulting 77−2136
ophiolite genesis, tectonic regimes 79−57898
ophiolite nappes emplacement, Mesozoic-Cenozoic examples 77−41012
ophiolites, Chilean, hydrothermal metamorphism vars., ocean floor metamorphism implications 79−88354
ophiolitic metabasalts in Mediterranean area, clinopyroxene comp. rel. to plate tectonics 79−57925
ophiolitic rocks tectonic emplacement in Precambrian Mona Complex, Anglesey 79−8631
Ordovician volcanic rocks, N.Maine, magmatic affinity and tectonic significance 77−44984
orogenesis, chemical approach to Nd-Sr isotopic relationship in granitoid rocks and continental crust development 80−94522
orogenic volcanism caused by thermal runaways? 80−90057
orogeny, caused by tidal deformation of crust 80−85625
Oroville, California, surface faulting assoc. with 1975 August 1 earthquake 77−9345
Otago schist megaculmination, origins and tectonic significance in New Zealand Rangitata Orogen 78−81142
overthrusting, model of const. thickness overthrust on visco-plastic sole 80−51378
Owen Basin, Arabian SE margin, and Owen Fracture Zone evolution 79−84217
SW.Pacific, Eocene subduction zone, disruptive ophiolitic belt evidence 80−104949
W Pacific, evolutionary history 77−44965
S.W.Pacific, gravity anomalies and main tectonic units 77−17078
W. central Pacific, Mesozoic evolution 77−44953
N.E.Pacific and Alaska, plate tectonics and palaeomagnetism 77−91092
SW.Pacific basin, reverberant subbottom layers distrib. rel. to plate northward drift 80−8290
Pacific lithosphere, flexure seaward of Bonin and Mariana trenches 79−57903
Pacific lithospheric plate, elastic thickness from geoid heights along Hawaiian-Emperor seamount chain 80−3899
Pacific Margin, Vancouver Island and adjacent regions, tectonic-stratigraphic evolution 78−20399
W.Pacific marginal basins, sea floor spreading evidence 77−37177
NW.Pacific Ocean and Bering Sea, S_n waves propag. rel. to trapped old lithospheric unit 80−51346
Pacific Ocean basin, volcanic history since Jurassic, crustal loading study 80−46165
Pacific plate, central stress fields delineated by linear volcanic chains 77−17068
Pacific plate, evidence for roll cell mantle convection 78−73345
Pacific plate, mantle convection and stress field from geopot. harmonics 77−9393
Pacific plate, Neogene motion relative to mantle and Earth spin axis 79−44167
Pacific plate motions rel. to N Pacific basalts mag. props. 78−40543
Pacific plate subduction *(Japanese)* 80−94514
Pacific plate subduction beneath Japan Islands, 3-D seismic struct. 80−51376
N.Pacific plate tectonics under Alaska, implications of earthquakes focal mechanisms 79−79806
circum-Pacific region, timing of geological events 77−64233
E.Pacific Rise, equatorial, regional shape and tectonics 78−44800
E.Pacific Rise, sea-floor spreading rel. to young cratered volcanoes pair history 80−12374
E.Pacific Rise, struct. of crust, volcanism periodicity and magma flow 80−17243
E.Pacific Rise−Galapagos rise system, topography rel. to sea-floor spreading 78−73331
E.Pacific Rise evolution between 3-13°S since Middle Miocene 78−88813
E.Pacific Rise near 3°25′S, structural geomorphology of fast-spreading rise crest 78−44799
E.Pacific Rise spreading centre, geophysical expts. and hot springs 80−101360
Pacific subduction zones, great earthquakes recurrence 77−17045
Pacific-N.American plate interaction and Californian Neogene volcanism 80−21702
Pacific-Nazca plate boundary, fast slipping transform fault zone near-bottom reconnaissance 79−25226
Pakistan and N.W. India, seismicity patterns assoc. with continental collision 77−25655
palaeo-oceans and continental drift *(Russian)* 77−25672
palaeomagnetism and plate tectonics, book 80−36789
palaeostrain analysis, distortion and dilatation 77−78167
Palaeozoic base maps, palaeogeography and plate tectonics 80−41441
Palaeozoic igneous rocks, Welsh Borderlands, palaeomag. survey rel. tectonic rot. of Britain 78−48961
palaeozoic sequences palaeobathymetric anal., rel. to basin tectonics 78−69341

tectonics continued
Palmahim structure in SE Mediterranean off Israel, continuous tectonic activity since Upper Miocene 79−34790
Pamir, tectonic lineaments from ERTS imageries 78−3739
Pamir-Himalayan deep fault zone description 79−39676
Pamir-Hindu Kush, upper mantle high-Q zone from earthquakes spectral content 77−86795
Pamir-Hindu Kush region, seismicity and fault plane solns. 80−72445
Pan-African mobile belts, no evidence of 500 Myr detrital zircons or high mountains 79−84213
Panamint Valley fault zone, W.Basin and Range province, California, Holocene offset and seismicity 79−79802
Pangaea, reconstruction for Permian period using mag. field configuration calcs. 77−56577
Pangaea and movement of crustal fragments on shrinking Earth 78−57187
Papua New Guinea, delayed partial melting of subduction-modified mantle 78−57183
Papua New Guinea, Late Cainozoic geotectonics and volcanism 80−51372
Papua New Guinea-Solomon Islands region, 1964-1973 earthquakes, seismotectonics 80−8270
Papuan Ultramafic Belt, mode of emplacement 79−84214
paraffin model experiment 77−13073
paratectonic porphyroblasts, inclusion trails spiral direction reversal 79−39717
Parece Vela Basin, E.Philippine Sea, evolution and chronology 80−41431
passive continental margin, evolution in light of drilling results 80−76942
passive continental margin, thermal evolution in sea floor spreading model 80−56427
passive continental margins, isostatic gravity anomaly rel. to ocean-continent boundary evolution 77−81777
Pau D'Albo struct., Sao Paulo, Brazil, form. mechanism 79−48441
Pearson Formation (Great Slave Supergroup, NWT), palaeomagnetism and Coronation loop 78−77179
Peking region, convection-generated stress concentration and Tangshan earthquake seismogenic models 79−92507
Pelusiam Line, major transcontinental shear 77−53034
Permo-Triassic and Jurassic ^{40}Ar-^{39}Ar ages from Greek igneous rocks rel. to rifting 79−74872
Permo-Triassic Tethys, mid-Mesozoic closure 79−70780
central Peru, Eocene uplift and unroofing of coastal batholith near Lima 79−2199
Peru-Chile Trench, faulting rates and angles 78−36138
Peruvian continental margin, Andean geosynclinal pair 77−21724
Phanerozoic palaeomagnetic restructurings, chronological distribution curves 79−53302
Phanerozoic plate tectonics 78−92812
Phanerozoic sedimentary basins, Australia, tectonic implications 78−96174
Phanerozoic tectonics and volcanism rel. to pulsation and expansion of Earth *(Russian)* 79−2202
Philipine Sea Plate, activity of northern boundary *(Japanese)* 80−51382
W.Philippine Basin, DSDP sediments palaeomagnetism, mag. anomalies phase shifting and Basin rots. 77−86764
Philippine Islands, tectonic struct. revealed by seismicity and volcanicity 80−94511
Philippine Sea origin and development, ^{40}Ar-^{39}Ar ages from DSDP Leg 31 77−64254
Philippine Sea plate instantaneous rotation vector rel. to Eurasian plate 78−7608
Philippine Sea-Eurasian plate boundary, crustal deformation in S.Kanto, Japan 78−40533
Philippines, subduction zone south of Mindanao, evidence from 1976 August 16 earthquake 79−44117
Phlegraean fields, Italy, intercrustal hydrodynamic correlation with geodynamics 77−2138
Pinchi Fault Zone, central British Columbia, geology and evolution 77−91129
Pine Mountain block thrust sheet, USA, energetics of driving force 80−21730
plate bending at trenches, mechanical models constraints from earthquakes 80−41426
plate boundaries, seismic activity dynamic interaction along rising and sinking edges 77−73706
plate boundary seismic pot., major boundaries 80−85606
plate deformation, dislocation differential geom. in 2D space 78−22719
plate deformation rel. to nonNewtonian antiplane mantle flow 77−73704
plate driving forces 77−64249
plate effects in N.Pacific subduction zones 77−37176
plate fracture rel. to asthenosphere flow stress 78−53606
plate motion and mantle return flow response 80−46152
plate motion and thermal instability in asthenosphere 77−17073
plate motion rel. to large energy release from earthquakes 78−28186
plate motions, present day, Relative Motion 2 model 79−20792
plate motions, rel. to asthenosphere flow model 78−96180
plate motions, rel. to geoid and single-cell mantle convection 77−60362
plate reconstruction method, Pacific-Nazca plate evolution appl. 78−81130
plate relative motion problem, linear formulation 80−72480
plate resting on deformed incompressible elastic halfspace, axisymm. flexure 77−46913
plate tectonic controls on diagenesis 80−12387
plate tectonics, appl. of geodetic research to geodynamic problems *(German)* 80−101317
plate tectonics, convection models having multiplicity of large horizontal scales 79−16430
plate tectonics, driving force models for plate stress, review 80−56450
plate tectonics, Earth crust evolution rel. to prebiotic chemical evolution 78−40666
plate tectonics, rel. to impact origin of ocean basins 77−91085
plate tectonics, review 77−44959
plate tectonics, role of C in Earth upper mantle 80−81845
plate tectonics, roles of boundary friction, basal shear stress and deep mantle convection 78−57188
plate tectonics, theoretical problems, conf., Aug. 1978, Caracas, Venezuela 80−51400
plate tectonics and lithosphere petrology, comparison with Venus tectonics and comp. 80−72805

tectonics continued
plate tectonics conf., Grenoble, France, 1975, Sept. 77−44958
plate thickness rel. to continental lithosphere thickening model 78−77200
plate triple junction, of type TTT(b), stability condition *(Japanese)* 80−94513
plate vel. rel. to oceanic transform earthquakes 78−53620
plateau uplift mechanisms 79−92517
plates relative motions, rel. to marginal basins form. 80−41427
Pleistocene drift, ice-marginal sedimentary, glacitectonic and morphologic features, Newfoundland example 78−57233
polar wander excitation, effects of ridges and trenches 79−16367
post glacial uplift mechanism, phase boundary reaction to medium press. changes 80−90058
post-metamorphic uplift and erosion, depth meas. from metamorphic bathozones and bathograds 78−81113
postglacial uplift of crust, mechanism 80−104943
postseismic surface stress, viscoelastic model 80−98278
postseismic viscoelastic surface deform. and stress, theory 80−94496
pre-Tertiary system, Shimokita Peninsula, NE Japan, geological structure 77−5163
Precambrian, time divisions in South America, chronotectonic boundaries 79−48442
Precambrian basement, W.Canada, U and Th conc., petrologic and tectonic controls 80−17257
Precambrian dykes, preferred orientation of intrusion 78−88829
Precambrian geodynamics, palaeomagnetic data for Africa, Australia and N.America 77−66889
Precambrian geologic history 77−2131
Precambrian mobile belts of Africa, crustal evolution towards plate tectonics 77−66906
Precambrian polar wandering rel. to plate tectonics 80−31024
Precambrian thermal regimes 78−65235
premonitory crustal deformations, strains and seismotectonic features (b-values) preceding Koyna earthquakes 79−79755
pretlercynian continental configuration, palaeomag. data from NW.France 80−72414
Prince Edward fracture zone and Mozambique basin evolution, S.W.Indian Ocean 77−17077
proterozoic intraplate deformation, comparison with SE Asian neotectonics 78−65250
Proterozoic rocks of Sweden indicating ancient subduction zone 80−46162
pseudofaults and plate tectonics, propagating rift model 78−32046
Puerto Rico Trench origin and gravity anomalies 78−11861
punctuated evolution of tectonic style 79−16432
N Pyrenean metamorphism, age and tectonic implications 79−34819
Pyrenees, central southern region, gravity gliding and compressive nappes 78−69342
Pyreness, subduction and collision model 77−81854
quadrupole junctions, stability 79−29737
quartz-rich rocks folding, implications of c-axis fabrics of experimentally folded ice 79−57983
quartzites, intracrystalline deform. comparison in natural and exptl. deform. 79−79830
Quebec, LG-3 dam fault average net slip, dome and basin structs. *(French)* 77−73732
Quipungo mobile belt, Western Angola, geological evolution *(Portuguese)* 79−70796
recent crustal movements as determined by geodetic meas. 77−44960
Red Sea, crustal age and extent 77−29284
Red Sea, tectonics rel. to heat flow map 77−91083
Red Sea opening with two poles of rotation, comments 77−5171
Red Sea spreading centre, implications of thiocyanate in deep sea brine 79−57975
Red Sea-Gulf of Aden area, plate tectonic anal. 78−69320
Reggio Calabria earthquake, 1975 Jan. 16, seismological results and geostructural appl. 77−49007
regional strain analysis, geometric interpretation 77−73705
Reykjanes Peninsula, Iceland, 1972 September earthquake swarm and tectonic significance 77−33009
Reykjanes Ridge, fracture zones obs. south of 60°N rel. to evolution between 40 and 12 Myr BP 80−90069
Reykjanes Ridge, SE.flank, lithosphere evolution, seismic surface wave study 80−90022
Reykjanes Ridge, stress directions rel. to ridge crest morphology near 62°N 80−90070
Reykjanes Ridge crest, rifted and nonrifted regions transition 79−88338
Rhenish Massif, recent vertical crustal movements determ. 79−79789
Rhinegraben, geodetic high-precision meas. in active tectonic area 79−79788
Rhinegraben rift system, Holocene movements and stress state 79−79801
Ridge Basin, S.California, earthquake focal mechanisms and hypocentres, tectonics 80−21695
ridge migration and asymmetric sea floor spreading 78−11858
rift geometry near former India-Australia-Antarctica junction 78−96166
rift valley formation over oceanic ridge, upwelling flow model of topographic profile *(Chinese)* 80−8280
rift-transform struct. of seafloor ridge system, thermal convection and tidal bulge formation 77−64252
rifted arch basins and post-breakup rim basins on passive continental margins 77−81861
rifted continental margins, thermal history and subsidence, Nova Scotian and Labrador Shelves 80−12353
rifted ocean ridges, evolution 79−34787
rifts at high angles to orogenic belts, origin, Upper Rhine Graben example 78−48989
riftward younging of volcanic units in Ethiopian rift valley 79−84204
Rivera-Tamayo oceanic fractures, ocean bed renewal, photographic/seismographic obs. *(French)* 79−74887
rock deformation, crack-seal mechanism causing extension veins 80−61798
rock deformation, elliptical particles non-coaxial deform. 79−79829
rock folding under confining pressure, anal. of faulted drape-folds 78−7626
rock mechanics constraints on lithosphere stress and temp., consuming plate 80−31021
rock sheet, Dent-Blanche, stressing subductions and Eocene flexure *(French)* 78−24282
tectonics continued
rock strain, estimation from deformed ellipsoidal objects, algebraic method 77−21766
rock stress evolution rel. to compressive strengths and plate tectonics 77−9421
rock stress measurement, hydrofracturing method and recent field results 79−29885
rocks, inclined asymm. upward-moving gravity structs. 78−7637
rocks crenulation cleavage, mechanical significance investigations 80−21737
rocks drape folds, partially scaled models using folding under confining press. 79−58127
rocks jointing, distinguishing of regional directions from joint sets assoc. with individual structs. 77−86876
N.Rocky Mountains, British Columbia, Canada, structural interpretation 79−100835
Romanche fracture zone, equatorial Atlantic, Neogene crustal emersion and subsidence 78−11857
Rumania, geological models rel. to plate tectonics *(Rumanian)* 77−33040
Rumania, geothermal regimes of tectonic units 79−70768
Rumania, lithospheric microplates rel. to regional gravity anomalies *(Rumanian)* 78−20380
Russian platform, tectonic fluctuations determ. from geological records coding *(Russian)* 80−17383
Russian platform sedimentary basins development dynamics 77−21729
S-tectonites, finite and incremental deforms. recorded by planar subfabrics 77−21767
Sagatu Ridge dyke swarm, Ethiopian rift margin 77−37170
salt dome tectonics, seismic profile obs. interpretation *(Russian)* 77−44937
salt glaciers of Iran, seasonal movement obs. 80−104942
Salton Trough, California, deform. meas., 1973-77 period 79−84079
San Andreas and Calaveras fault region, crustal deformation, 1971-8 obs. 80−56428
San Andreas fault, California, bimodal distrib. of creep event amplitudes 77−78145
San Andreas Fault, California, in-situ stress meas. 79−79767
San Andreas fault, California, short-period nonseismic tilts rel. to episodic slip 77−29276
San Andreas fault, continuous strain meas. during and preceding episodic creep 78−36127
San Andreas Fault, crustal strain obs. site for earthquake prediction 80−81832
San Andreas Fault, cyclic displacements, viscoelastic relaxation 79−20799
San Andreas fault, fault creep obs. rel. to local mag. field meas. 80−85629
San Andreas Fault, geodetic tilt obs. 80−81800
San Andreas fault, local mag. field vars. and stress changes near slip discontinuity 80−26448
San Andreas fault, Rn emanation vars. meas. 78−32022
San Andreas fault, satellite laser ranging system 80−61984
San Andreas fault, slip assoc. with great 1857 earthquake 79−66633
San Andreas Fault, stress accumulation and release mechanisms 79−84194
San Andreas Fault, wire strainmeter data subject to meteorological noise 80−81831
San Andreas fault (central California), mag. field local vars., creep rate changes and local earthquakes 80−26450
San Andreas fault mechanical behaviour, influence of constitution at depth 79−12097
San Andreas fault movement determ. by artificial satellite laser ranging 77−64185
San Andreas fault strain accumulation 1964-1977 near 1976-7 earthquake swarm 80−36272
San Andreas fault system, stress field and aftershocks, theory 80−36249
San Andreas fault zone, central California, source processes of earthquake sequences 77−2111
San Andreas transform, geometry of subducted slab 80−98297
San Fernando earthquake, California (1971), dislocation fault model, tectonic significance *(Japanese)* 80−104923
San Francisco earthquake, 1906, kinematic viscoelastic model 77−73671
San Gregorio-Hosgri trend, evidence for 115 km of dexteral movement 78−53641
Sanbagawa Metamorphic Belt, Shikoku, Japan, evidence for recent tectonic uplift from crustal struct. anal. *(Japanese)* 80−94508
Sanriku, 1933 March 2, dislocation model rel. to tsunami waves and plate tectonics 80−31000
Sanriku-Oki region, Japan, 1965-1970 shallow earthquake source charcts. 80−12346
W.Santa Ynez fault system in S.California, struct. and neotectonics 79−79774
Santos Basin, Brazil, geology of bordering continental rifts system 77−21768
Sao Vicente, Mato Grosso, geology and geochronology of granite *(Spanish)* 77−70652
Sardinia, late Palaeozoic volcanics multivectorial mag., partial remag. and tectonic rot. 78−48960
S.Saskatchewan, seismotectonics 79−20757
N Saskatchewan, var. in lithology and tectonometamorphic relationships in Precambrian basement 77−91132
Saudi Arabia, late Proterozoic ophiolite complex at Jabal Ess, rel. to plate tectonics 79−70799
Scandinavia, Blue Road area, crustal model and isostatic state 77−64240
Scandinavian Caledonides, gabbro complex palaeomag., plate rot. or polar shift theories 80−21615
Scandinavian Caledonides, nappe displacement 78−81143
Scandinavian Caledonides, tectonic model, comments 77−66911
Scotia Arc evolution rel. to SW Gondwanaland reconstruction 77−33043
Scotland, Caledonian tectonics and crust elec. cond. 77−44920
N Scotland, Devonian John O'Groats Sandstone superimposed magnetisations rel. to tectonics 79−92481
Scotland, imbricate thrust model of Southern Uplands 77−53031
Scotland, magnetotelluric study, geophys. and tectonic implications 79−29706
NW Scotland, Palaeocene basalts, immobile trace elements rel. to palaeotectonic affinities 79−34816
sea floor depth anomalies, depend. on latitude and plate motion 78−28215

tectonics continued
sea floor spreading, deep subduction and plate motion 78−88810
sea level recorder for tectonic studies 77−45175
sea-floor topography, tectonic model using vol. expansion coeff. 80−90072
sea-mount loads affecting crust, isostatic compensation and geoid anomalies 80−109132
seafloor spreading, south of Agulhas Fracture Zone 78−24277
sedimentary basins, development and evolution 79−29719
sedimentary basins, development in Archaean rel. to lithosphere thickness 80−89986
sedimentary basins, form. with finite crustal extension rates 80−89987
sedimentary basins of continental margin and craton, conf., Durham, England (Apr. 1976) 77−21715
sedimentary basins subsidence mechanisms, review 77−21746
sedimentary rock faulting and folding, strain hardening theory 80−85628
seismic faulting, acoustic fluidisation theory 80−85653
seismic faulting mechanism, role of inhomogeneities 80−51342
seismic focal process, unexpected earthquakes occurrence *(German)* 79−66644
seismic fracture zones, effects of groundwater hydrostatic press. vars. on seismicity *(Russian)* 80−104913
seismic gap quiescence duration determ. method 80−26627
seismic refraction methods for tectonic dislocation detection *(Russian)* 78−12010
seismic sources with observable glut moments of spatial degree two 77−91039
seismology, implications of dilatancy-fluid diffusion theory for aftershock sequences 80−85604
seismotectonic microzoning for earthquake risk reduction 79−88290
serpentinites, Glenrock, New South Wales, foliation development 80−21738
shear deformation zones, along major transform faults and subducting slabs 78−73330
shear stress on base of lithospheric plate 77−91099
shear zone from Castell Odair, Scotland, quartz orientation re-investigation 78−77216
Shikoku Basin, off-ridge volcanism and seafloor spreading 78−65256
Shioya-Oki earthquakes, 1938 May and November, tectonic implications 77−81814
Shuswap Complex, S.Okanagan, British Columbia, recumbant folding, mechanism and geometry 80−4008
SE Siberia, crust struct. and role of Archean folded ovals 80−101349
NE.Siberia, pre-Cainozoic tectonic evolution 78−81132
E.Siberia, tectonic activity rel. to amethysts form. *(Russian)* 80−12393
Siberian platform, main structures development history and dynamics 77−21732
W Siberian platform development history and dynamics 77−21731
Sibley Group (Neohelikian), Ontario, stratigraphy and depositional setting rel. to Keweenawan rift failed arm 80−94517
Sierra Nevada, California, crustal movement anal. using repeated geodetic levelling data 79−79795
Sierra Nevada, California, regional deform. on conjugate microfault sets 80−21729
Sierra Nevada-Walker Lane region, recent crustal movements, rate and style of deform. 79−79838
Sigsbee Scarp, Gulf of Mexico, salt tectonism and evolution 77−73714
Sila nappes (Calabria), palaeomag. evidence for non-Apenninic origin 80−56369
Sinai subplate margins, Late Holocene tectonic activity 79−57907
single layer folds arc lengths, comparison between theory and obs. 79−53345
single-layer folds, shape at small but finite amplitude 80−56473
Sinkiang, China, earthquake swarm (1974), source mechanisms from surface waves anal. 78−81427
Sinkiang-Tibetan region, seismicity and tectonics 78−32030
S.Kivu, Zaire, basaltic flows on Idjwi Island *(French)* 77−64246
S.Kivu, Zaire, study of Tshibinda-Kalehe volcanic chain *(French)* 77−64245
slaty cleavage, development Fleurieu Peninsula 80−21735
Slave craton-Churchill craton collision tectonics, Canadian Shield 78−24278
slip faulting, far-field body waves generated by elliptically expanding rupture 77−81804
W.Slovenia, tectonic structures, rel. to macroseismic effects 78−24254
solid-body rotation in deformed rocks, natural indicators 79−79842
Solomon Islands, earthquake doublet mechanism in subduction zone 80−56410
source time function depend. on tectonic field 78−92799
source-span-sink thermal models of arcs and ridges 78−32040
Souss Basin, S.W. Morocco, mag. survey and crustal struct. 80−89958
South America, origin of compressional intraplate stresses 78−61385
W.South America, volcanism, seismicity and anelasticity interrelationships 77−33044
South China Sea basin, tectonics from profiler-sonobuoy meas. 80−8291
South Fork Mountain Schist (N Coast Ranges, California), early Cretaceous metamorphic age 78−81114
South Mayo Trough, W.Ireland, possible Ordovician marginal basin 78−36162
South Sandwich arc, moderate and large earthquakes, tectonic var. along subduction zone 80−26458
Southern Africa continental margin, sedimentary basin form. processes 77−21723
southern continents palaeopositions, revised reconstruction 78−92805
SE.Spain, Quaternary strike slip faults 79−79798
spreading centres, perpendicularity to transform faults questioned 78−24276
spreading ridge subduction, thermal effects 79−88321
spreading ridges, crests palaeobathymetry rel. to ocean basin ages and latit. 78−11869
spreading ridges in young oceans, model with thick oceanic crust at continental boundary 79−79781
St. Elias earthquake, Alaska, Feb. 1979, 1974-9 tilt obs. 80−81841
St. Vincent's Gulf, South Australia, regional tectonic setting rel. to geomag. vars. 80−72426
strain and rotation in a multilayered fold 78−88823
strain distribution across experimental single-layer fold 78−32076
strain variations of Skrino anticline, district of Kjustendil, deformed reduction spot meas. 77−37184
strains and stresses in seismically active regions, calc. 79−79744
strains and tilts on continental crustal blocks 79−79773

tectonics continued
stress accumulation in lithosphere 77−17071
stress concentration mechanism for intraplate earthquakes 78−81112
stress rel. to steady state flow of rocks 77−91120
stress release effect on P-wave signature of underground nuclear explosions 77−25642
strike slip fault, three dimens. viscoelastic model 77−56591
strike-slip failting, in crust of horizontally variable rigidity, model 80−56377
strike-slip fault in laterally inhomogeneous region 78−7591
strike-slip faults in continental crust, length and offset correl. 77−41011
structural geology, conf. (1978), Toronto, Canada 80−101666
structure development, new rotation hypothesis 77−81857
subducted lithosphere, correl. with positive geoid height anomalies 80−90056
subducting lithosphere, heat transfer with continental asthenosphere 80−94510
subducting lithosphere boundary determ. using ScS to P conversions 78−7572
subducting oceanic crust, thermodynamic consequences of minerals dehydration, high press. and temp. 78−69301
subducting slab creating deep-focus quakes, theory 80−51375
subducting slab undergoing upper surface melting, thermal field 80−85638
subduction, oceanic lithosphere age rel. to interarc spreading and cordilleran tectonics alternates 79−29732
subduction angle, in plate tectonics 78−11865
subduction beneath W.South America, evidence from converted phases 80−26484
subduction of young slabs, consequences 80−81862
subduction process of fracture zone and aseismic ridges, appl. to New Hebrides earthquake (1969, January 19) 78−73342
subduction process segmentation, evidence from Petatlan, Mexico, earthquake (1979 March 14) 80−76920
subduction rel. to geoid and lower mantle convection 80−31023
subduction shear zones in Tonga and Mariana systems, stress and temp. 79−8620
subduction zone, ascending flow between descending lithosphere and overlying asthenosphere 78−40531
subduction zone, thermal model with dehydration in downgoing slab 79−79784
subduction zone, thermal structs. evolution 80−56440
subduction zone dip angles and flow driven by plate motion 79−20801
subduction zone seismicity, Makran coast, Iran 80−85635
subduction zone topography, dynamics of subducting plate 80−51374
subduction zones, material transport within accretionary prisms and 'knocker' problem 80−101353
subduction zones, seismicity and seismic risk 79−88294
subduction zones, shallow seismicity and tectonics 79−16401
subduction zones, stresses due to phase changes, and empirical eqn. of state for mantle 77−73718
subduction zones, three-dimensional struct. from stereoviews of seismicity 80−72452
subduction zones, young lithosphere thrusting rel. to structs. in ophiolitic peridotites 80−56446
sublithospheric upwelling distrib. leading to mantle hot spots 80−109126
submarine geothermal resources, seafloor spreading centres and volcanic areas 77−37171
submarine lithosphere, geophys., geochem. and petrological model 80−3994
subregional models rel. to microzonation of offshore areas, overview 79−84182
Sudbury Basin, Ontario, mag. susceptibility anisotropy as rock strain indicator 77−78170
Suiko seamount, Emperor seamount chain, palaeomagnetism and relation to Hawaiian hot spot 78−57162
S.Sulaiman Range, Pakistan, struct. and seismicity rel. to tectonics 79−39715
Sulawesi, Indonesia, palaeomag. data rel. to palaeogeographic reconstructions 78−61330
Sulawesi, Indonesia, past and present geotectonic position 78−32056
Sulawesi (E Indonesia) western arc, palaeomag. studies and fission-track dating rel. to tectonic history 80−89957
Sumatra, late Cenozoic clockwise rot. 77−60363
Sunda Arc earthquake foci distrib. rel. to backarc area rotation 78−20381
Superior Geotraverse symposium (Toronto, 1978 October 23-26) 80−27029
Surkhob fault zone, crustal deformations rel. to tectonics 78−15979
Surkhob fault zone, USSR, tidal deform. determ. for crustal movement anal. 80−104944
suture zone complexities, review 77−66904
Sverdrup Basin, Arctic Canada, evolution, subsidence and uplift 77−25673
central Sverdrup Basin, crustal struct. and active intraplate tectonic feature 80−12355
Swabian Jura earthquakes, 1911 November 16, seismotectonic concepts 79−84176
symmetrical folds, simple derivation of straight limbs shortening/rot. relation 79−79841
Tabas-e-Golshan earthquake, Iran, Sept. 1978, faulting and bedding thrust 80−81826
Tajikistan, tectonomagnetic studies 80−26446
Tarbela reservoir, Pakistan Himalayas, seismicity during initial filling 80−56388
Tashkent Palaeozoic crystalline basement, tectonic struct., gravity survey *(Russian)* 78−53610
Tasman Fold Belt System in Victoria, evolution, tectonics, deform. 78−96212
Tasman Orogenic Zone, Thomson Orogen, tectonically active area 78−96213
Tasman Sea evolution, marine magnetic data 78−11870
Tauern eclogites, role of buoyancy in exotic eclogite blocks preservation 79−88350
tectonoelectricity, review 78−36095
tectonomagnetic anomaly due to lake ground loading, piezomagnetic effect 80−8346
tectonomagnetic events, detect. using empirical transfer functions 79−16374
tectonomagnetism and tectonoelectricity, symposium (Japan, 1975, September 5) 77−2084

tectonics continued
tectonomagnetism in western USA 77−2092
tectonomagnetism rel. to crustal seismic activity 77−2093
E.Tennessee, Ordovician polar wander from Moccasin, Bays and Chapman Ridge Forms. palaeomagnetism 79−57854
Tethyan oceanic crust evolution during Mesozoic, rel. to N.W.Syrian ophiolites 77−81896
Tethys early development, Iranian segment, Ar isotope age of ophiolites 80−46156
N.Thailand, hot springs and geothermal gradients extensional tectonic activity 80−94495
Thelon metamorphic front, cryptic suture in Canadian Shield 77−53023
thermal evolution of continental crust during magmatic accretion and metamorphism 80−46150
thermal evolution of ocean ridge, affected by spreading rate 80−56424
thermal structure of plates and mantle convection 79−2197
Three Forks Basin, Montana, USA, seismicity and tectonics 80−81829
thrust sheet deformation at ramp, mech. model 79−70779
Tibet, active tectonics, LANDSAT imagery 79−20794
Tibet earthquake, 14 July 1973, source mechanism and seismic wave attenuation 80−36252
Tibetan Plateau, late Cenozoic tectonics, LANDSAT imagery 79−20795
Tibetan Plateau underthrust by India, palaeomagnetic constraints 80−56449
tidal forces deforming crust, causing orogeny 80−85625
W.Tien Shan, crustal movements from geology of palaeomagnetic data 77−9392
Tien Shan region, contemporary tectonics 79−29733
Tierra del Fuego, tectonic and sedimentary significance of Cretaceous Tekenika Beds 77−44996
Timor and Australia relative positions in Upper Permian 77−29244
Tjornes Fracture Zone, N.Iceland, N.American-Eurasian plate boundary 78−3740
Tohoku district, Japan, crustal movements during 1900-1975 and tectonic implications 80−56453
Tonale line in Alps, strike-slip fault direction and extensions *(French)* 78−88811
N.Tonga region, Wadati-Benioff zone morphology and complicated subduction closure model 80−90010
Tonga-Lau system, deep collision of subducted lithospheric plates 79−29736
Torlesse Terrane, New Zealand, exceptionally large steeply plunging folds origin 80−12388
Transantartic Mountains, evidence to suggest uplift by Early Miocene 80−98287
Transdanubian Central Mountains, palaeomag. pole position, tectonic implications 78−48970
transform fault, quasistatic creep slippage inherent instability 79−84193
transversal bent fold, stress and strain rate, stress relax. effect 79−66651
Transverse Ranges, California, tectonics from recent seismicity in San Fernando region 79−66634
Triassic Hound Island Volcanics, Alaska, crustal movement from palaeomagnetic obs. 80−89945
Triassic Nikolai Greenstone, Alaska, palaeomag. 78−36166
triple junctions related to San Andreas transform, geometry 79−57904
Troodos Massif, Cyprus, preliminary tectonic results 77−17072
Turanian platform, regional struct. and development 77−21730
Turkey, seismotectonic implications of relocated aftershock sequences 79−44119
N.W. Turkey, tectonomagnetic effects rel. to earthquakes 77−2094
Turkey's rotation, palaeomagnetism of dykes and tuffs 80−31020
Turkish-Iranian Plateau, post-collisional tectonics, comparison with Tibet 80−3986
Tweeddale Granite batholith in Southern Uplands, rel. to Caledonian tectonics 79−92541
Twillingate Granite and Herring Neck Group, Notre Dame Bay, Newfoundland, geochronology 77−17049
two-dimensional strike-slip fault, static deform. of laterally inhomogeneous half-space 80−31012
Tyrrhenian Sea rifting, Rayleigh wave dispersion evidence 80−56445
Ukraine, recent vertical movement *(Russian)* 77−73699
NW Ukrainian Shield, abyssal fractures obs. from deep seismic sounding data *(Russian)* 79−96746
Ukrainian Shield, regularities in distrib. of dike complexes *(Russian)* 77−44995
Umbria, Italy, palaeomagnetism and tectonics 78−96129
Umfraville gabbro, Ontario, palaeomagnetism rel. to Grenvillian plate tectonics 78−92777
unit vectors, time series interpolation 79−92625
W.United States, collided Palaeozoic microplate (Sonomia) 80−41415
W United States, plate absolute motion and interaction constraints from Cenozoic igneous activity 79−2207
United States, tectonic obs. rel. to regional free air gravity anomalies 79−57906
United States, western region, strain accumulation rates, 1970-78 period 80−21607
United States east coast, recent vertical crustal movements 78−32052
Uordan-Dead Sea rift, crust and upper mantle seismic study, transition towards Mediterranean Sea 79−79766
uplift and erosion, transient heat flux with exponential heat source distrib. 79−57887
Upper Amur region USSR, seismicity, tectonic features and earthquake epicentre confinement 80−101343
upper mantle, dynamical processes rel. to seismic anisotropy of subcrustal lithosphere 77−49039
upper mantle, nonlinear stress propagation 77−17058
upper mantle thermomechanical models, plate vel. changes rel. to magnetic activity 78−65231
Upper Proterozoic apparent polar wander, analogous loops from Laurentia, Fennoscandia and Africa 80−56360
Urals, geodynamics 77−5175
Urals, geomag. secular var. anomalies rel. to aseismic geodynamics 80−26447
N.W.urope, gravity and height vars. meas. via gravity base network *(German)* 78−15948
USA, East-Central, geological perspectives of earthquake hazards 78−11834
N.E.USA, seismic risk analysis in rel. to nuclear plant siting 78−11835
W. interior USA, tectonics and late Cretaceous sedimentation 78−81134
W.USA, vertical crustal movement, anal. of levelling survey 80−72409
tectonics continued
W.USA Cenozoic geodynamics rel. to Columbia-Snake River-Yellowstone region magmatism 77−73738
USSR, tectonics and mineral resources *(Russian)* 78−40536
SW.Utah, two areas of probable Holocene deform. 79−79803
Ventura, California, high rates of vertical crustal movements 77−56614
vertical crustal movements, interpretation in time-space domain 79−80056
vertical crustal movements, solvability and multiquadric anal. appl. 79−79787
vertical crustal movements and regional tilt, precise levelling error propag. 77−44884
vertical crustal movements Carpathian area of Rumania *(Rumanian)* 80−8281
vertical crustal movements in Atlantic coastal plain, USA 79−79790
vertical crustal movements rel. to phase boundary motion in mantle 77−49040
vertical seismotectonic motions in Baykal rift zone 79−79783
Very Long Baseline Interferometry applications *(Russian)* 78−32357
Villalvernia-Varzi-Bobbio Line (N.Apennines), geomorphological evidence of neotectonic deform. *(Italian)* 79−8624
Virgin Islands, tectonic struct. and earthquake swarms, seismic network obs. 80−89973
visco-elastic modelling of tectonic systems, by finite element anal. 80−104930
viscous slab gravity flow, cumulative strain and boundary effects 77−81862
volcanic rocks, relation between major element chemistry and tectonic environment 78−16006
Walvis Ridge, heat flow profile rel. to mantle hot spot origin 77−86827
Walvis Ridge, S. Atlantic, gravity anomalies and origin 80−21682
Wellington region, New Zealand, seismicity within plate convergence zone 79−16398
Western Australia, pre-greenstone sialic basement, tectonic reactivation 77−17101
Western Australian Shield, struct. and tectonic style 80−3983
Western Minas Gerais State, Brazil, Phanerozoic tectonic evolution 77−70630
Wharton Basin near Investigator Fracture Zone, geophysical study 78−40532
White Mountain intrusives , NE United States, ages and relation to transform fault 77−78129
whole mantle convection rel. to plate tectonics 77−44957
Willaumez-Manus Rise, Papua New Guinea, origin 79−88329
Willimantic fault, Connecticut, pelitic lithologies 79−84245
Wisconsin reef on Daito Ridge, Philippine Sea, isotopic evidences, Late Quaternary tectonic history 79−84227
N.Wolverine Complex, British Columbia, geochronology and tectonics 80−3961
world distrib. of sutures, continental collision 77−66905
Xingtai earthquake, 1966 March, aftershock freq., possible tectonic stress monitor *(Chinese)* 80−76912
Xingtai earthquake series, 1966 March, hypocentral distrib. and tectonic stress field *(Chinese)* 77−91011
Xingyang metamorphic belt, existence of 3T-phengite and C-type ecologite, tectonic significance *(Chinese)* 79−84264
S.Yamanashi Prefecture, Central Japan, crustal movements changes rel. to microearthquake activity *(Japanese)* 80−67343
Yap arc-trench system, metamorphic rocks rel. to tectonic history 78−32093
Yellowstone caldera, Wyoming, USA, vertical crust movement 80−81859
Yellowstone hot spot, tectonics and crustal props., earthquake and aeromag. data 78−48996
Yellowstone Park hot spot, volcanic and tectonic evolution 80−56472
Yellowstone volcanic plateau, conf., USA (1974) 78−49004
Yong Shan-Da Guan, Yunnan earthquake (May 19, 1974), main shock source multiplicity *(Chinese)* 79−12075
coastal Zagros, Mountains near Bandar Abbas, Iran, Holocene folding rates 79−48445
Zagros collision orogeny, finite element modelling of lithosphere deformation 79−20803
Zagros Mountains, geological comparison with island arcs 79−2231
Zambia, gravity survey rel. to tectonics and struct. 77−40969
Zendan Fault region, Iran, struct. lineaments, interpretation of Landsat 1 obs. 80−104941
CO_2, release due to tectonic activity and earthquake prediction 80−94470

tektites *see meteorites*

telecommunication
see also biocommunications; carrier communication; communication channels; communication networks; communications applications of control; optical communication; radiocommunication; telemetering; telephony; television
conference, EUROCON, Venice, 1977, May 78−53552
conference, physics in industry, Dublin, Ireland (9-13 March 1976) 77−60887
conference on long distance neutrino detection, Washington, DC, USA (April 1978) 79−80217
extraterrestrial life, communication possibilities 79−35152
health service provision using telecommunication technology 79−74784
long distance communications, fibre optic developments *(Norwegian)* 80−1318
meteorology and telecommunications, special relationships 77−2236
microelectronics revolution, appl. in telecommunications, medicine, education 80−31446
neutrino telecommunication by high energy neutrino beams 79−76266
open universe, physics, biology and communication 79−97119
photovoltaic power systems, equipment performance and manufacturing techniques improvements and system design problems for telecommunication applications 80−55843
Polish conversion to SI system of units, technical aspects *(Polish)* 77−74346
remote site development, solar cell power supplies 80−26133
rural area primary health care delivery, telecommunication aspects 78−57122
rural telemedicine system planning, analysis 79−74785
search for extraterrestrial intelligence, implications for telecommunication 77−33361
solar power appl. in communications repeater stations 79−29450

telecommunication continued
teaching, developing countries, course content 78−3
teaching, underdeveloped countries, factors against learning 78−4
technical meteorology, technical and commercial appls. *(German)* 80−46231
teleprocessing innovation, role of US National Science Foundation 77−2504
underwater acoustic communications, swept carrier method for multipath interference suppression 79−3835
university teaching, course structure, Rio de Janeiro 78−2

telecommunication cables
see also coaxial cables; submarine cables; telephone lines; underground cables
coaxial telephone, resistivity measurements on Cu conductors *(French)* 79−69487
concatenated fibre-optic cable, cumulative baseband frequency response models 80−78983
conference on optical fibre communication, Washington, DC, USA (Mar. 1979) 79−46058
duplex fibre-optic cable interconnection system 78−46801
fibre optic undersea cables, small, recent experiences 80−14488
fibre-optic, construction and props. of 140 Mb/s trial system 80−23794
fibre-optic, measurement of baseband transfer function 80−1355
fibre-optic, monomode, fabrication, characterization and cabling for transmission in 1.2-1.6 μm range 80−10042
fibre-optic, single-mode evaluation of charact. *(Japanese)* 80−28316
fibre-optic, status of development 80−43485
fibre-optic cable and interconnection considerations and tradeoffs 79−94363
fibre-optic cable design and installation, environmental considerations 79−94362
fibre-optic cable selection considerations 77−54779
filled optical communication cable, viscous polyurethane appl. 79−72708
high quality optical fibre cable for telecommunication 79−37029
noise origins and control 77−42666
optical, attenuation and dispersion meas., and faults location *(German)* 79−14097
optical coated fibre and cable unit structure optimisation 80−53466
optical fibre, measurement of longitudinal internal stress 79−64350
optical fibre, metal-free, wide temperature range communications appl. 80−23795
optical fibre, modular, composite strain analysis 79−64351
optical fibre, origin of temp. dependence of attenuation 79−46073
optical fibre, single-mode, dependence of optical losses on bending effects 79−50417
optical fibre, stress-strain behaviour 80−69551
optical fibre cable, design, performance and development projections, review 79−46069
optical fibre cable attenuation and input and output efficiency 80−14469
optical fibre cable comprising 48 fibres, design and charact. *(Japanese)* 80−58688
optical fibre cable comprising 8 fibres, design and charact. *(Japanese)* 80−58689
optical fibre cable construction, installation, and testing 78−46797
optical fibre cable design, splicing and interconnection system developments 78−42431
optical fibre cable design and manufacture 77−54780
optical fibre cable developments *(Japanese)* 79−27405
optical fibre cable formats and construction techniques *(German)* 79−55206
optical fibre cable splice methods *(Japanese)* 80−58690
optical fibre cable transmission and strength improvement technology 80−28347
optical fibre cables, historical development *(Japanese)* 80−87494
optical fibre cables, structure design, compressive loads and internal stress determination 79−59829
optical fibre cables using reverse-lay unit-core struct., with attenuation <3 dB/km 79−46072
optical fibre cables with spacers, transmission charact. and mechanical props. 79−46070
optical fibre concatenated connectorized cables, transmission losses 79−46071
optical fibre splicing, connecting and sheath jointing *(Japanese)* 80−87497
optical fibre transmission, applications and cable techniques *(Japanese)* 80−87493
optical fibre unit, high density low-loss, cabling 80−53468
optical fibres, fabrication and construction of secondary coating for optimised design *(Japanese)* 80−87567
optical fibres, history and basic principles 80−69543
optical fibres, multicore, high density, design and manufacture, charact. *(Japanese)* 80−87501
optical fibres microbend charact. and mech. prop. for design, applicational examples *(Japanese)* 80−87500
optical single-mode fibre cabling for low-loss communication 80−53467
plastics, for transmission media, thermomech. reliability 80−40666
single fibre connectors and cable splice hardware, optical coupling theory 80−64187
submarine, dielec. loss measurements of polyethylene at high pressure and freq. 80−27316
superconducting, cryogenic envelope, determination of struct. and thermal insulation performance 79−58731
Pb sheathed, corrosion in plastic multiway ducts 80−7721

telecommunication equipment
see also multiplexing equipment; radio equipment; repeaters; television equipment
electronic devices, failure analysis of metal parts using fractography 79−61811
integrated optics manufacturing technology and appls. *(French)* 78−50946
parametric source for underwater acoustic communications 77−7247
petroluem industry, implementation guidelines for promotion of electronics in oil and gas sector 79−80039
SAW filters, design, construction, appl., book 80−1393
telex-communication system, subcarrier recovery ccts. optimisation and white noise effect reduction *(Rumanian)* 77−27427

telecommunication links
see also optical links; radio links; satellite links; space communication links
magnetic storm disruption effects, research progress report 79−101021

telecommunication systems
see also data communication systems; digital communication systems; radio systems; switching systems; telephone systems; television systems
fibre optics engineering techniques 78−50929
fibre-optic system components, status of development 80−43485
fibre-optic transmission systems, development progress 80−43482
hydrocom, underwater communications, non-acoustic long distance system appl. 79−5667
JROE II LIDAR, atmospheric measuring instruments *(Italian)* 78−3957
mankind's future needs and aspirations in space, conf., Washington USA, 1976 Oct. 78−4078
optical experimental loop system, field trial telephony, data, video appl. 79−72707
optical fibre applications, future trends 78−22214
small submersible, acoustic communications system design 79−5666
submersibles, acoustic navigation for precise underwater surveys 79−5683

telecommunication theory *see information theory*

telecontrol
see also alarm systems; telemetering
air sampling system, radio-controlled, for diffusion expts. 79−79440
Barnwell Nuclear Fuel Plant, remote handling systems, overview 80−68920
blood sampling system, radio controlled, for unrestrained monkeys 77−90967
Cary 14 spectrophotometer, remote control via digital interface 77−2697
fusion power plant, vacuum outer containment, safety, T control and monitoring 78−74498
fusion reactor, MFTF, exception handling control system 80−99325
fusion reactor, pulser system, air-driven fibre-optic coupled for Los Alamos ZT-40 expt. 78−54943
fusion reactor visible monochromator scanning drive 78−54940
gamma-ray spectrometer, remote computer-controlled, for nuclear power plant monitoring 79−9916
heart-lung machine two-circuit thermocontrol device 79−48374
HTGR, surveillance robot for fuel and reflector element inspection 80−68873
marine profiling system for shallow water 78−36328
micromanipulator for biological experiments, versatile remote control, economic construction 79−25163
mirror fusion reactors, remote servicing features 78−58448
nuclear fuel pellets, automated inspection 80−13766
nuclear power plant, instrumentation and control, remote multiplexing appl. 80−52752
optical shutter, electronic systems for remote control 77−3678
pellet fuels, γ-active, remotely operated plant for fabrication 80−32340
PWR irradiated fuel assemblies, remote operations 80−68918
remotely controlled computer-guided preparation facility for X-ray fluoresc. anal. at fuel reprocessing plant *(German, English)* 78−17399
sediment movement and associated hydraulic conditions in ocean 77−37421
selective digital voltmeter, electronic control of tuning frequency 77−10052
Space Shuttle orbiter, remote manipulator system 79−21150
teleoperator systems for reactor maintenance, technology assessment 80−68872
UK reactor fuel reprocessing plant remote handling experience 79−9839
underwater robot/manipulator, development and remote control 78−77356
US decontamination system for reactor fuel transfer pool, remotely operated 80−68916
UV spectrometers, on OSO-8, computer-controlled, mission operations 80−41723
Very Large Array waveguide transmission system for radiotelescope 77−5444
^{11}C-iodomethane remotely controlled synthesis 79−88192

telecontrol equipment
audio alarm system, using Doppler shift 79−64477
bidirectional optical-fibre transmission used for control appls. *(Japanese)* 78−66917
cation-exchange sorption microcalorimetry, automatic micro-injection system 78−24777
chart recorder timer control, pen overload protection systems, at. absorpt. appl. 77−73481
electrical stimulation remote control device for studying neural mechanism of monkey 77−86719
equipment and services, 1979 video yearbook 79−14197
fibre-optic remote control system for 1.5 MeV heavy-ion fusion preaccelerator 80−73993
fission reactor core, neutron detector telecontrol device with direct loading *(Russian)* 80−52770
fuel recycling remote manipulation systems design and performance 77−67854
gas flow rate meas. up to 2.8 m^3/sec, dynamic volumetric method 77−72380
GUPS-1 immersion follower gamma-level gauge 77−67412
headlight, light-operated remote-control device for handicapped persons 78−53571
hot cell manipulator remote decontamination facility and repair station 79−9911
inspection system for nuclear power plants, reduction of personnel radiation exposure 77−14275
LAMPF linac, Monitor remote-handling system, status, improvements and accomplishments 79−71997
lantern slide projector remote control using IR-60 infrared system *(German)* 80−95169
leaktight remote handling equipment for operations in an irradiating and contaminating environment 80−13951
light link coupled system for particle accelerator foil strippers 78−29670
master-slave manipulators and remote maintenance in nuclear research 77−71682
monochromator drive, using high-speed digital servo 78−36992
myocardial regional function and coronary blood flow study during ischaemia in baboons 78−44752
nuclear reactor pressure vessels, remote controlled US pre-service and in-service inspections 78−89955
remote handling system, fuel defect test loop 78−82436
satellite Yagi antenna, telecommand transmission, design 77−45286
US remote control circuit using US transducer 80−10097

telefilming
see also telerecording
colour film quality improvement, KT 116 M camera appl. *(Russian)* 78−29200
electronic masking techniques, colour film reproduction appl. 78−32902
equipment and services, 1979 video yearbook 79−14197
projection machines, Telekino-75, optical-mechanical systems *(Russian)* 79−76800
retrofocus lens system designs for film cameras *(German)* 77−54768
telecine, description of Thomson-CSF flying-spot twin format telecine *(French)* 80−37110

telegraph networks
meteorological information network in Europe, structure, operational facilities 77−70772

telemetering
ambulatory ECG monitoring problems 78−11763
animal biotelemetry studies, historical perspectives and recent applications 78−69266
ARAKS expt., EM wave meas. 79−21071
auto and cross-correlation analysis techniques on-board spacecraft *(French)* 79−70925
automation of information input and processing 77−78429
biological temperature in unrestrained domestic fowl, piezoelectric transducer, sampled data system 78−57152
biomedical appl., conf., Pacific Grove, Calif., USA, May 1976 77−86653
biomedical radionuclide tracers, semicond. memory systems for data storage 77−90877
biomedical signal processing and telemetry, digital bandpass analysis 78−57107
biomedical telemetry, transmission and reception with embedded antennae 78−77125
biotelemetry, conf., Garmisch-Partenkirchen, W.Germany (May, June 1978) 79−43980
biotelemetry, conf., Sapporo, Japan (June 1980) 80−90604
biotelemetry, literature survey 78−80996
biotelemetry based on small CdTe detectors, props., uses 77−44747
biotelemetry of glomerular filtration rate in man by external detection of DTPA-(Sn)-$^{99}Tc^{m}$ with CdTe 78−44591
broad-band wave meas. in ARAKS expt. 79−21072
cardiological, two channel storage cardioscope and multitrack video tape recorder, appl. 77−70561
cardiovascular changes with free-ranging and treadmill exercise in dogs 77−90821
cardiovascular emergency clinical assessment, use of ECG telemetry 78−44677
clinical ECG real-time telephone transmission usefulness and reliability 78−57108
deep body temperature measurement in rodents, inexpensive telemetry system 78−24185
drill-rod telemetry, calcs. for toroidal coil source 78−85710
dynamic bioradiotelemetry noise reduction methods 77−86672
EEG activity data from isolated olfactory bulb of rabbits 77−86516
electromechanical pressure transducer using acoustical resonance 78−77897
ELF/VLF goniometer receiver, remote, unmanned, in Antarctica, UHF telemetry link 80−21854
emergency medical telemetry standard development and implementation 78−3635
EMG and temporal information during gait, clinical telemetry 78−80994
environmental data from satellite system 80−56592
freely moving animals, cardiac frequency regulation by means of telestimulation 77−44859
frequency measurement methods using VHF/UHF receivers *(German)* 78−4631
fusion reactor, fibre optic telemetering for high voltage test stand 78−54939
groundwater resource detection *(French)* 79−96776
heart rate/respiratory freq. changes of ducks during submersion 77−86717
human motion three-dimensional monitoring by optoelectronic means, calibration 77−86658
identification of rice-growing land from teledetection data *(French)* 79−96775
implanted, unrestrained dogs, renal haemodynamics appl. 77−32927
intracranial pressure monitoring by passive radiosonde 79−57798
ion accelerator systems for ion implantation research 80−32540
Ionospheric Sounding Satellite, telemetry receiving system *(Japanese)* 77−78610
Ionospheric Sounding Satellite control, tracking system telemetry receiving antennas *(Japanese)* 77−78608
Ionospheric Sounding Satellite control centre, automated telemetry data acquisition *(Japanese)* 77−78606
irrigation detection in the Loire-Britanny river basin *(French)* 79−96774
Japanese weather satellite, on board equipment, geostationary orbit 78−4076
locomotion studies, technique for correlating film and EMG 78−24186
meteorology, GATE telecommunication data, computer processing 77−2251
multichannel biotelemetry, quality criteria and methods of measurements 77−48887
neurophysiological activity in olfactory system of rabbits, and pheromones 77−90816
nuclear fuel plant, remote solution meas., during cold checkout runs 79−85748
nuclear power plant, instrumentation and control, remote multiplexing appl. 80−52752
oceanographic data acquisition and processing system, microprocessor based, real-time 79−16676
oceanographic monitoring stations in Arabian Gulf, data telemetering and anal. 79−8728
patient heart condition monitoring during bath therapy using immersed electrodes 78−3665
PCM systems, air pollution detection/control appl. *(German)* 78−93003
pCM telemetry for physiological data 80−36059
perinatel radio telemetry 80−104722
Pioneer Venus Multiprobe entry phase, telemetry recovery 80−67493
radio pressure pills for back stress monitoring 77−73604
recent advances, space technology appl. *(German)* 78−93073

telemetering continued
respiratory flow meas. with mag. type flowmeter 77−86654
respiratory function telemetering by combined sensor 78−80995
RF EM exposure effects on biosystems, health hazards 77−86533
role of SAW oscillators and IR detectors in biotelemetry 77−90926
satellite pictures and teledetection methods used for snow measurement and forecasting *(French)* 79−96770
satellite solar cells radiation damage obs., GaAs and Si 79−48134
sector scanning sonar, use in fish heart rate telemetry 80−8225
sleep telemetry in rat, automatic identification and recording of vigilance states 78−48948
soil moisture surveys using microwaves and infrared heat measurement *(French)* 79−96772
soil water balance determination, hybrid model proposed *(French)* 79−96773
solar observatory, orbiting (OSO-8), solar panel design and in-orbit performance 79−48652
stress distribution meas. of patient sitting immobile, instrumented wheelchair 77−90930
surface water and moisture applications of teledetection *(French)* 79−96769
systalic blood pressure monitor, type SCS-501 *(Japanese)* 77−70565
total artificial hearts, pneumatic powered, telemetric monitoring system, in calves 77−90956
US inner planets exploration programme, data rate improvement 78−32317
Viking lander remote diagnostic techniques 78−57426
Viking Lander seismometer 78−16274
waverider buoy GOES satellite relay system reporting 79−5663
wildlife biotelemetry, reviews 80−30966
Mn nodules deposits, deep sea telemetry *(German)* 80−26623
$Na^{123}I$ tracer detection for biological rhythms in renal function study 77−86586

telemetering equipment
9-channel accelerometer for head crash impact accel. meas. 77−86655
acoustic miniature transmitter in fresh water, operating freq. choice for miniature transmitters 77−54826
biomedical temperature biotelemeter, modular, expandable, implantable 80−67191
biotelemetry and radiotracking receiver 77−48892
body temp./heat rate monitoring of hibernating/normothermic ground squirrels 78−3688
bone strain in-vivo telemetry in monkeys, method 78−3697
brain pressure, epidural, implantable LC cct. transducer, cat exp. results 77−32962
capacity-type pressure transducer, features, biomedical appl. 77−86671
cardio-telemeter, impedance *(Japanese)* 77−44790
cerebrospinal fluid pressure meas. by passive telemetry, improved instrument 78−31927
chronically implanted device, controlled transcutaneous powering 80−98152
coils for RF powered implant telemetry, design 78−31926
combined receptor for respiratory function meas. 77−86657
deep sea floor mapping instrumentation 77−5358
digital FM detector, multichannel, EEG appl. *(Danish)* 78−35980
digital frequency-to-temp. convertor for use in radio telemetry systems 80−8119
diving duck, heart rate and respiratory frequency monitoring by implantable transmitter 77−44858
Doppler flowmeters, directional, totally implantable, for animal research 80−67293
drifting buoys, appl. to ocean data collection 79−5668
dry hot rock hydraulic fracture characterisation acoustic instrumentation 77−33221
ECG apparatus, single-channel, PLL demodulator appl. *(German)* 78−57097
ECG telemetry, totally implantable multichannel system 78−44746
echo ultrasonometer, implantable, for organ dimension meas. 77−90866
EEG biotelemetry, multielectrode, for remote monitoring and stimulation of ambulatory subject 79−5386
EEG telemetry time-multiplex unit, ambulatory patients 79−44007
electrode, implantable stress-resist. design for biotelemetry 78−44629
electronic circuits implanted in freely moving animals, wireless power supply 79−29682
electronic tachymetry, ten years of Zeiss equipment *(German)* 79−34999
EM, perched water table detection appl. 80−26655
embedded bare and insulated receiving antennas, design for biotelemetry appls. 77−40947
EMG and temporal data monitoring during gait 78−3638
endogastric probe for telemetric pH meas. *(German)* 78−85452
fever alarm device using telemetry 80−21556
flowmeter, implantable Doppler design with phase-locked loop 78−31873
FM, foetal ECG and heart rate monitoring 78−3651
FM, for continuous foot vertical force meas. during walking *(Japanese)* 78−73273
FM, short-range, for skeletal muscle O_2 conc. meas., rabbit 77−86722
FM-AM miniaturised transmitter for EEG and EMG, for sleep telemetry in rat 78−48947
heart rate radio telemetry for rats, nonobtrusive system 77−90964
human hip prosthesis pressure radiotelemetering, design features 78−3671
human limb movement characterisation by accelerometry 77−86680
IC, generalised, Kitchip, for biotelemetry system design 77−86665
IC implantable systems for animal expts. 80−76887
IC pulse regenerator for digital telemetry signal wire transmission *(Russian)* 77−58503
implantable bidirectional blood flowmeter, micropower ICs 77−13038
implantable biotelemetry, multichannel, for recording physiological data of monkey 77−86660
implantable biotelemetry transmitter for 6 differential signals 77−48968
implantable SAW pressure transducer/transmitter 79−29575
implantable unit placed in thoracic cavity, effect on tissue 77−86663
indoor, 100 MHz tuned loop receiving antennas, biomedical appl. 77−90925
intracranial pressure monitoring, in vivo and in vitro, with capacitance transducer 78−7457
intracranial pressure telemetric meas. *(German)* 78−85403
medical research on animals, chronically implantable instrumentation 80−30834

telemetering equipment continued
micropowered IC modulator for implantable biomedical telemetry 77−78000
microprocessor based telemetry demodulation system 79−20738
multispectral camera, use on Soyuz 22 spacecraft 78−40794
oceanographic buoys, electronics and telemetry developments 79−5659
optical fibres as microphonic instrumentation transducers 77−17970
optical pulse receivers for distance meas., basic params. determ. 78−33843
orthotics parameter assessment based on telemetric heart rate monitoring, paediatric patient appl. 78−31974
PCM transmitter, implanted transmitters, stomach capsule, biomedical appl. *(German)* 77−29220
physiological measurements, integrated power controllers and RF data transmitters for totally implantable telemetry 80−67295
plasma double electric probe with VHF decoupling and telemetry, plasma parameter determ. *(Russian)* 79−7485
radiotelemetry pill for biomedical meas. of ionising radiation using HgI_2 detector 78−40318
radiotelemetry transmitter, for temp. meas. from unrestrained subjects 79−16356
remote ear canal temperature measurements in cattle 77−86714
RF powered cage system for implant telemetry 78−44745
RF powered cage system for implanted biotelemetry 79−20737
seismographic, PLL lock indicator and event alarm for multiplexed telemetry 79−62597
solid-state pressure transducers and transmitters 77−30175
spin-scan imaging photopolarimeter for Pioneer Jupiter missions 77−41303
temperature meas., inside furnace, radio transmitter design *(Czech)* 77−2659
temperature measurement, using an RF transmitter 78−205
temperature multiplexers, types of unit and configurations 80−82757
temperature telemeter with mag. core temp.-to-freq. convertor, cct. 79−199
temperature telemetry system for thermal monitoring 78−49837
temperature telemetry transmitter, crystal-controlled, surgically implantable, for animal expts. 80−72393
thermometer, electronic, using controlled hysteresis feedback comparator *(Spanish)* 78−16793
thermometer, transistorised, with remote indication, up to 150°C *(German)* 80−73356
transducer optimal signal correction with internal fluctuating white noise *(Russian)* 79−6107
transmitter for small animal temp. meas. 79−83888
transmitting antennas, body-mounted, design, radiation pattern, biomedical appl. 77−90927
two-element array of insulated antennas in relatively dense medium 77−25794
upper extremity function documentation in athetoid and spastic patients 77−40879
US implantable CW Doppler blood flowmeter, optimal system design 78−53460
US implantable IC CW Doppler flowmeter 78−31877
water supply monitoring, DIGI-way series, Japan 77−53877
YYB1-1 telemetering strain gauge, design and meas. accuracy *(Chinese)* 79−35699
Mn nodules deposits, deep sea telemetry *(German)* 80−26623
Si strain gauge for in vivo bone deformation meas. in monkey 77−86720

telemetering systems
acoustic, multifunctional seafloor instrumentation system development 79−53584
air quality data transmission, VHF transceiver thermoelectric plant installation *(Italian)* 77−82064
animal physiological research, totally implantable dimension meas. system 80−67294
atmospheric pollution centralised supervision system, computer station/capturing stations links 78−81410
Automated Meteorological Data Acquisition System 77−87077
automatic oceanographic profiling and transmission system 77−41231
avian ECG, radiotelemetry system 80−98202
avian heart rate meas. using autocorrel. techniques 78−31989
basal body temperature continuous monitoring in humans by radio telemetry 77−78015
bioelectric signal measurement and processing instrument trends *(Croatian)* 78−44665
biological tissue O_2 tension meas. multiple electrode system 77−56506
biomedical broadband communication network combining satellite link and TV broadcast techniques 77−64145
biotelemetry, cardiovascular monitoring, multichannel, implantable, single freq. RF powered 77−52897
biotelemetry antenna and propagation requirements for appl. for fresh water fish 77−78074
biotelemetry interference minimisation techniques *(Russian)* 79−29685
biotelemetry techniques for studies of brain elec. activity 77−60310
blood flow telemetering system using implantable CW Doppler US flowmeter, IC appls. 78−11749
brain unit and slow-wave field activity, telemetry with FM pulse subcarrier 77−25625
clinical paediatric gait biotelemetry 78−3652
coastal buoy data collection systems 78−36320
CW Doppler US vel. meter, implantable, IC, blood flow meas. appl. 77−86565
data buoy wideband wave directional spectra, real-time telemetry 80−46305
demodulation system, microprocessor based 78−44627
duoPIGatron ion source, optical telemetry and data transfer system 78−66443
ECG analogue and digital transmission 79−39564
ECG telemetry system Telecare *(Spanish)* 77−9296
EEG, automatic nocturnal sleep sampling 78−31916
EEG, cable telemetry computer seizure monitoring system 77−5090
EEG, including PWM multichannel system 78−31914
EEG olfactory bulb of salmon monitoring 77−86718
EEG physiological data teletransmission system 77−86687
EEG recording system, portable pulse-interval modulation telemetry/multiplexing system, home use 80−67261
EEG TDM telemetry unit for fifteen scalp electrodes 77−40822
electrophysiological research animal model, chronically instrumented 80−26323

telemetering systems continued
extracorporeal multichannel system for physiological meas. of small animals 77−86715
Finnish seismic array, data transmission, recording and handling 79−39917
flood prediction computer-operated telemetered gauge network 77−21818
FM, for extraluminal meas. of gastrointestinal motility 77−13043
FM, implanted CW Doppler flowmeters, renal/iliac blood flow meas. from exercising dogs 77−90822
FM/PWM, multichannel, for EEG recording from unrestrained psychiatric patients 78−3636
FN tandem accelerator, telemetry component tests 77−83156
four-channel, cardiovascular response to dynamic/static exercise monitoring 78−3633
GEOS, technical features 78−4071
heart rate activity of wild animal monitoring 77−86713
heat flux/temp. data telemetering for energy flow study of peccary 77−86716
high data rate acoustic telemetry system design 80−43573
human motion 3-dimens. monitoring by optoelectronic means, calibration and meas. 78−31913
human movement correction using computer and electrostimulating device 77−86656
implantable, for ureteral elec. activity in unrestrained dogs study, improved version 77−86664
implantable, multichannel, IC, for animal physiological data recording 77−86661
implantable, multichannel, inductively powered, for animal cardiovascular data recording 77−86662
implantable, single-freq., for monitoring body temp., blood pressure and ECG 77−86688
inductively powered system for animal monitoring 79−74796
integrated circuit approach to totally implantable telemetry systems 80−67291
intracranial pressure and temp. two-channel telemetry system 77−81619
intracranial pressure telemetric monitoring system 79−74736
intraocular pressure, telemetry monitoring 78−3632
Ionosphere sounding satellite, automated system for tracking, telemetering and commanding 77−60572
IR system for surgical patient monitoring 80−30836
Kawasaki City air pollution monitoring and telemetry system 77−37464
land seismic reflection exploration data acquisition systems 77−29444
Mars 6 descent vehicle radio signal parameters meas. by retranslation method 77−67020
medical research, chronic, appls. of totally implantable systems 80−67296
medical system, portable, multi-sensor, for rural health network 80−30835
meteorological observation system using telephone switching network 79−80031
meteorological rocket telemetry system *(German)* 77−64606
micropowered multichannel PAM/FM system for brain research 77−25618
multichannel, EEG monitoring for epiltogenic focus localisation 78−3653
multichannel cable system, for EEG seizure-monitoring 78−3640
multichannel telemetry system, design, seismic data processing *(Chinese)* 79−21033
multiterminal ECG processing system experiences 79−39573
myocardial regional function and coronary blood flow study during ischaemia in baboons 78−44752
ocean bottom refraction seismograph, data telemetry to surface vessel 79−39892
ocean bottom seismograph using digital telemetry and floating-point conversion 77−41197
ocean buoy testing, radiotelemetering meas. system *(Russian)* 78−16192
ocean sediment free-fall penetrometer with Doppler telemetry 80−46320
offshore oceanographic buoy, telemetering new mooring, design 79−5660
optical fibre data and telemetry links 79−27390
optical fibre link for EM probe, microwave radiation effects obs. appl. 78−15859
pacemaker patient routine monitoring by telephone 77−90957
pacemaker surveillance by telephone photoanalysis 77−81699
Parkinson tremor, long-term recording and evaluation 77−21639
passive, by modulated backscattered incident CW RF carrier beam, cattle temp. meas. appl. 77−90968
pathological gait assessment, foot force meas. device 79−20701
patient monitoring during surgery, 4-channel system 78−31961
pCM telemetry for physiological data 80−36059
Portable Automated Mesonet, design, performance and operation, for meteorology 77−78426
radio link, vibration measurements in steam turbine blades 77−68538
raingauge, automatic 79−21038
rat metabolism and energy balance continuous meas. 77−86712
real-time magnetometer data transmission via telephone lines 77−13126
remote automatic station on radio link for wind and temp. monitoring 78−85726
remote platform data acquisition and control by minicomputer 77−5330
RESMAC, Mexican microwave seismic array 77−5355
respiration monitor for children using belly-belt electronic sensor 77−56512
respiration remote meas. instruments, appl. to studies in centrifuge 77−77996
respirometer, flowmeter-polarographic electrode sensor, for respiratory function telemetering 78−80995
RF, for pressure/temp. monitoring of free swimming freshwater fish 77−90965
RF powered ECG telemetry system 79−48358
RF-powered cage system for implant biotelemetry 80−94422
SAS-3 X-ray astronomical satellite, programmable format telemetry system 77−2328
satellite solar cell panel monitoring by ground station telemetry 79−62003
satellite universal telemetering system for magnetospheric and ionospheric research *(German)* 77−73924
seafloor earthquake meas. system, acoustic telemetry 79−5689
seismological data collection and anal., detect. of possible violations of Nuclear Test Ban Treaty 79−39919
Seismological Service of Canada, instrumentation and data processing 79−39914
seven-channel, fully integrated, patient monitoring appl. 78−3634

telemetering systems continued
simultaneous telephone transmission of four ECG/EEG signals *(Spanish)* 79−62399
six-channel extracorporeal telemetry system 77−90931
Solar Maximum Mission GSTDN/TDRSS compatible RF system 78−45198
Spacelab data communication and acquisition system 79−84643
Spar Buoy Oceanographic Telemetry System 80−46307
Spar Buoy Oceanographic Telemetry System software engineering 80−46308
storage system for detection of radionuclide tracers in humans 77−12995
superconducting machine temperature telemetry via optical channel *(Russian)* 78−57966
surgery, scoliosis correction, noninvasive determ. of anterior spinal fusion following corrective surgery 77−44851
synchronisation of biotelemetry system, with time division of channels 80−94386
TDM, for biomedical data transmission using one carrier freq. 77−90928
telemedicine, diagnostic practice appl., technology 77−21649
telemetry, low power PAM/FM system for ventricular press. and cardiac dimension meas. 78−44747
telemetry system, implantable, multichannel, for physiological research 80−67292
temperature biotelemetry system for free-swimming fish 77−25624
temperature monitoring system using implantable thick film telemeter 77−40825
temperature telemetry system for small animals, miniature CMOS 4-channel PWM design 78−44751
temperature telemetry system with interference suppression, implantable, long-life, animal expts. appl. 80−101302
tide gauging network, automated, microcomputer interface and telemetry 79−5692
two-channel intracranial pressure temp. monitoring system, implantable 78−3637
US, for monitoring heart/respiration rate and body/skin temp. of scuba divers 77−90929
Van de Graaff, 10 MV, digital data telemetry system 77−83155
vertical automatic profiling system for lakes temp. and current meas. 78−36327
wideband EMG muscle activity monitoring for spastic gait anal. 77−90924

telemeters *see telemetering*

telemetry *see telemetering*

telephone calling equipment *see telephone station equipment*

telephone equipment
see also microphones; repeaters; telephone station equipment
ECG transmission, pacemaker, cardiac arrhythmias monitoring 77−52903
underwater sonar communication using type 2008 telephone equipment 78−94478

telephone exchanges
air pollution effects on reliability of contacts *(Polish)* 79−74573
noise abatement measures in PTT premises *(French)* 80−10079
solar-collection system for domestic hot water 80−66940

telephone interference
see also crosstalk
speech quality, deterioration by reverberation 78−94488

telephone lines
9 km fibre-optic telephone transmission system 78−42435
fibre-optic, interconnection using compound-lens devices 80−74493
glass fibre experimental cable, used between telephone exchanges by German Post Office *(German)* 79−64326
military local distribution systems, use of plastic clad/fused silica fibre 78−9457
multiterminal ECG processing system experiences 79−39573
optical fibre systems, developments 80−58678
optical fibre telephone carrier systems 78−42463
optical fibre test gear, BPO, view of likely requirements 79−64349
optical fibre utilization at 1300 nm wavelength *(Polish)* 79−76857
PCM 480 system for Deutsche Bundespost using fibre-optic link 80−38120
real-time magnetometer data transmission via telephone lines 77−13126
St. Margarets Bay-La Paune, submarine cable, sea bed measurements 78−15992
telemetry system for pacemaker patient routine monitoring by telephone 77−90957
tide gauging network, automated, with dial-up telephone line 79−5692
Cu conductors used in coaxial cables, resistivity measurements *(French)* 79−69487

telephone networks
ECG analysis by remote computer, data terminal with voice indication, general practitioner use 77−81613
optical fibre link, experimental system operating at 140 Mb/s 78−1321
simultaneous telephone transmission of four ECG/EEG signals *(Spanish)* 79−62399

telephone receivers
artificial ear for sensitivity/frequency meas. 78−63255
photoacoustic effect appl., optical links development *(Czech)* 78−77994
ring armature type, use of low Co ternary Cr-Co-Fe alloy 80−45318

telephone sets
aids for handicapped people 80−36196
optical fibre voice transmission using unmodulated transmission of AF, telephone terminal sets *(German)* 80−28314
Cr-Co-Fe cold formable mag. alloys for use in telephone receiver 79−52227

telephone station equipment
disabled persons employment using traffic operator position system 80−36197
single-channel electrocardiograph with telephone transmission attachment 78−88760
test acoustic chambers 78−87218

telephone switching equipment
microelectronic appls., conf., Calcutta, India (Jul. 79) 80−96755

telephone systems
see also telephone exchanges
9 km fibre-optic telephone transmission system 78−42435
140 Mb/s optical fibre transmission system 78−42436
telephone systems continued
ECG transmission, 3-lead, over Post Office telephone network, central computer analysis appl. 77−86698
FDM, optical fibre systems development in Australia 77−65630
fibre optics in telephone carrier systems 79−81528
Hermes, geostationary communications satellite, Canadian design 78−93068
Las Vegas, 4.5 km fibre optic cable 78−46822
light-wave telephone service in Chicago (USA) 78−5574
lightwave communications, Bell system evaluation in Chicago 78−46821
optical fibre links in Europe 78−46781
optical fibre trunk system, viscous polyurethane filled cable 79−72708
saturation diving communications system 80−43558

telephone transmitters
EL2, electret technology development 80−83723

telephones *see telephone sets*

telephony
see also carrier telephony; videotelephony
cables laying, underground, seismology appl., rocks location verification 80−72456
clinical ECG real-time telephone transmission usefulness and reliability 78−57108
ECG telephone transmission, analogue and digital, errors and noise 80−94398
optical fibre cables, design, manufacture, laying and jointing *(Italian)* 80−99838
optical fibre systems, worldwide development 80−43468
PARCOR analysis-synthesis telephony, improvement of speech quality 79−50534
PARCOR speech analysis-synthesis system 79−50533
speaker verification from actual telephone voice *(Japanese)* 79−81655
thickness meas. of Au and Ni layers on Cu substrates simultaneously 80−13041

telephotography *see facsimile*

telerecording
see also telefilming
colour image recording on monochrome film by carrier frequency photography *(Japanese)* 77−41711
image facsimile synthesized with Gaussian spot, fine structure 79−76604
interference images, spectral line contours, TV recording method 79−2833
telecine, description of Thomson-CSF flying-spot twin format telecine *(French)* 80−37110

telescopes
see also astronomical telescopes
aerial photographic equipment developments, aerial survey camera and navigation telescope 77−66997
alignment techniques by optical means 80−1341
anallactic (divergent lens), mounting and adjustment devices *(Hungarian)* 78−30038
angular tracking, annular apertures 77−83957
aplanatic two mirror telescope from near-normal to grazing incidence, comparative performance anal. 80−58654
aspheric reflecting systems, geometrical design 80−38083
auto-collimating, accuracy estimation, absolute calibration methods *(German)* 78−86239
auto-collimating, calibration methods, angular measurement appl. *(German)* 78−77848
autocollimating, angle measuring standards appl. *(German)* 78−77851
autocollimating, calibration by laser interferometer, angular measurement appl. *(German)* 78−77853
autocollimating, instrumental and other measurement errors *(German)* 78−77956
azimuth scan MTF techniques, for optical component and system evaluation 78−50900
binocular instrument collimation rel. to visual binocular summation 78−53417
binocular models, characts. and design features, review 80−74468
Cassegrainian type for lidar, for atm. meas. 77−37436
collimating system, laser radiation directivity pattern axis spatial location 80−102748
compensated levels, high-precision, geodetic appl. 80−101813
contrast telephotometer, multiwavelength, instrument design, data interpretation, atm. visibility determ. 79−66842
cryogenic, construction, appl. of C fibre reinforced epoxy 80−22414
design of instrument optics from basic elements 77−58418
gamma, of Kosmos-461 satellite 79−97480
grating detectability, aberration effect evaluation in visual instruments 79−55073
grazing incidence system, primary aberrations 77−88644
high-performance telescope aspheric mirror test error budget 80−48386
Hunt aberration generator 78−59119
image vergence variation with object distance change, general case 80−63934
infrared telescope, 6032 image conversion tube 80−42020
IR, image scanning systems, tilting plane mirrors 77−83944
IR Galilean telescope system, attachment for information scanning device, aberrations 78−46751
Keplerian, magnifying power meas. method 79−18497
laser beam expander, Galilean or Keplerian form telescope 78−50839
laser beam steerer-expander, two-mirror system design 79−18460
laser beam steerer-expander device, two-mirror afocal telescope design 78−46700
leak telescope for mol. flow direction detect. in large vacuum chamber 77−49735
lensless scanning telescope, MTF 80−58655
magnifying power, new method for determ. 79−14078
measuring, PPS 12, meas. of surfaces up to 30 m in extent, optical collimator appls. 78−94423
MTF curves, comparison of visual and photoelec. meas. imaging quality *(German)* 77−79763
multianode microchannel array photon-counting detectors 80−77869
on-axis reflective beam expanding telescope, for pulsed dye laser cavities 79−41398
OTF test standard, afocal system 79−36978
pancratic systems with linear and nonlinear relations between component motion, comparison 78−13782
parabolic telescope and spectrometer combination, optical props. 80−87455
parallax problems in telescopic systems 80−99818

telescopes continued
particle optics, telescope electrostatic system with removable spherical aberrations 77−6989
particle optics, telescope electrostatic system with removable spherical aberrations 77−6990
periscope telescope, mirror compensator of image surface curvature 77−72053
photomicrography appl., low-power, critical focusing 80−13165
primary mirror manufacture, monitored null corrector 80−78946
random image displacements in turbulent atm. *(Russian)* 78−20509
reflecting, with concave and flat mirrors *(Hungarian)* 78−32841
reflecting telescope design, appl. of plate diagram 79−94321
refraction-free direction meas., coincidence method *(German)* 78−87124
refraction-free directions, coincidence procedure 78−87125
resonator, unstable telescopic, precision of some methods of adjustment *(Russian)* 80−38040
search for objects in sector during viewing 77−87805
secondary mirror flexure, elasticity theory *(French)* 77−14789
segmented mirror control system optimality criterion choice *(Russian)* 77−34010
Shuttle Orbiter re-entry, remote IR imagery and tracking 80−82171
sighting, principles and designs *(Hungarian)* 78−21194
sighting accuracy on point and bisector indices 77−58421
sighting telescope and autocollimator, general-purpose optical string 79−81510
telescopic finder, PPS-11, alignment method 79−14081
testing of long-focus optical systems, vibr. insulation of equipment 78−90543
three-mirror telescope, design and optimisation 78−90476
time of flight telescope, compensated, for spaceborne cosmic ray measurements 77−67939
time of flight telescope for high energy gamma-ray astronomy 80−31210
trihedron optical system, for linear displacement meas., accuracy estimation 80−101780
triple-prism beam deflection compensation 79−75105
two-magnification system, using objective lens, prism erector and eyepiece 77−14790
two-mirror objective systems, field lens group corrector 80−78945
vision, light vergence and accommodation 78−24065
visual angle increase, optical devices, geometrical and physiological optics *(Hungarian)* 78−20312
visual instrument astigmatism, accommodation compensation 79−34563
visual instruments, optical component contamination, effect on visibility of extended objects 80−64137
visual search time rel. to field of view 79−27363
visual telescope light scatt. factor meas. apparatus 79−27365
wide field imaging, significance of optical transfer measure *(German)* 78−90374
wide-angle five-lens eyepiece 79−46027
CO_2 laser Helios fusion target positioning with orthogonal telescopes 80−74421
CO_2 laser Helios fusion system beam diagnostics 80−78882

teletypes *see interactive terminals*

television
see also colour television; video signals
black-and-white images, composition and decomposition 79−50233
holographic system signal frequency spectrum 77−7036
raster-scanned laser display using TeO_2 acousto-optical deflector 77−10930
real time optical sectioning using freq. interleaving, high S/N, 3-D TV 77−72062
schools and colleges, Tasmania, TV programme storage systems 79−80404
teaching demonstration using photographs or slides 77−49538
usable subject contrast range definition, TV colour films appl. *(German)* 80−57408

television antennas
equipment and services, 1979 video yearbook 79−14197

television applications
see also videotelephony
acoustic field schlieren visualization, using closed circuit TV system 78−46867
alignment system for large high-power pulsed CO_2 laser fusion system 78−59075
analytical video stereoscopy, extended images, real-time photogrammetry 78−88926
analyzer for material structure studies 78−27696
angiocardiographic image series storage improvement by digital signal processing *(German)* 78−92723
angiographic images of left ventricle, system for off-line anal. using minicomputer 78−80964
arc discharges, periodic processes, spectral emission characts., vidicon system investig. *(Russian)* 78−9848
artificial aurorae obs. in conjugate region during ARAKS expt. 79−21074
astronomical applications of IR TV imaging 79−92678
astronomical imaging tubes, utilisation *(French)* 78−40829
astronomical observations of faint objects, television detection techniques 80−82208
astronomical observatory, focal reducer for integrating TV system 80−67568
astronomical photometry with SEC TV camera at Loiano telescope 79−58272
astronomical spectrophotometry with TV-type detectors 77−78646
astronomical TV system, appl. to study of meteor bright line spectra 78−61817
astronomy, appl. of SIT vidicon detector system for Palomar 1.5 metre telescope 79−92674
astronomy, galaxy image picture processing system for colour 77−49303
astronomy, integrating vidicon systems at Cerro Tololo 79−66924
astronomy, SEC Vidicon photometry of ω Centauri main sequence 80−90491
astrophysical observations, image isocon appl. *(Russian)* 80−12671
atmospheric OTF degradation meas. by TV system 79−92590
atomic emission spectroscopy, multi-element, with C furnace and optical MCA 77−40607
auroral image monochromatic obs. with intensified TV camera 77−73859
automatic evaluation system, solid state nuclear track detectors 78−17496

television applications continued
biological micro-object geometric feature determination, TV set 80−85538
biological objects, electronic speckle pattern interferometry in vivo 80−109083
biomedical, X-ray intensifier viewing system 77−9251
biomedical broadband communication network combining satellite link and TV broadcast techniques 77−64145
biomedical display system for observing ground reaction forces during ambulation 79−96688
biomedical low light level video fluorimetry and microscopy 77−44874
bistable TV-optical feedback system using optical flip-flops 80−53354
blood analysis in vivo, noninvasive spectroscopic method 77−60234
body motion computer-aided tracking using CCD image sensor 78−61269
bubble chamber, projection graphic display for computer aided image anal. 80−27895
cardiac radiographic image sequence analysis and recording 78−57069
cell structure and function investigation by laser microirradiation 79 66599
checkerboard pattern generator for vision research 77−40801
Cherenkov light photograms, automatic scanning by TV digitiser 80−52822
chromosome classification system, banding technique 80−67320
cineangiocardiograms, automatic anal. using TV system on line with minicomputer 78−92699
cinematography, development and introduction of TV facilities *(Russian)* 80−22465
clinical seizure, long term time-lapse video monitoring system, synchronised with EEG 79−39461
clock synchronisation, in India through TV transmission, microsecond accuracy 77−87736
colour display of blood flow in brain, computerised picture processing technique *(Swedish)* 77−44780
communication aid for disabled, Telecad 80−17197
component inspection by speckle pattern interferometry 77−37975
computer augmented video education, project status report 80−22174
computerised tomographic image display by TV and photography 80−8129
computerised tomography, picture documentation and filing 79−66554
curved object shape description and recognition methodology 79−55077
cyclotron beam emittance measurements with a dispersion-matched magnetic spectrograph 79−54732
V1500 Cygni (Nova 1975), TV photometry 78−36602
cytology and chromosome analysis television data compression interface 77−86683
daily time comparisons long-term stability using TV method 79−75502
dendritic metal crystals, electrolytic growth, CCTV obs. 78−51863
diagnostic radiographic video system psychophysical evaluation 79−74751
digitising system for single shot oscillograms at sweep rate 0.1 ns/cm 77−406
display system using computer generated integral photograph, appl. to US images 78−87021
distance meas. of polyhedral objects from loci of vertices 80−42195
dynamic torsion-effusion pendulum, video obs. 77−61077
ECG display, direct conversion of real-time two-dimensional ECG images to standard TV format 77−60233
education, personalised system of instruction model use for TV 79−92912
education, vibrating string, tuning guitar by television 80−73134
education college, video technology uses 79−92913
educational applications 79−35491
educational display appl. *(Japanese)* 78−20924
EEG physiological data teletransmission system 77−86687
EEG real-time display of 2-dimens. fields 78−44651
electron microscopy, digital storage and processing system for aposteriori image accumulation 80−101901
electronic speckle pattern interferometry, phase modulated, principle 79−85167
electronic speckle pattern interferometry, vibrating object meas., use of chopped laser light 79−85165
EM, image recording system, detection quantum efficiency 80−99009
equipment and services, 1979 video yearbook 79−14197
eye tracking communication system feasibility for nonverbal cerebral palsy children 79−83981
eye tracking raster graphics device, picture processing computer appls. 80−41330
fibre index profiling by video analysis of interference fringes 78−55460
film copying for TV projection *(German)* 79−49311
flaw detector with automatic mechanical scanning, TV signal form. on basis of digital memory 80−71864
flow measurement, intact circulation, haemodynamics appl. 77−52822
fluoroscopic image recording using multiformat camera 80−51234
fluoroscopy, for X-ray diagnostics, persistence 79−8558
foot scale plantar pressures, meas. device 79−44004
frame recording method for intermittent X-ray TV to reduce exposure dose in fluoroscopy *(Japanese)* 78−89607
Fresnel holograms transmission 80−19009
garnet film, LPE, time resolved obs. system for domain dynamics, appl. to contracting motion of stripe domains *(Japanese)* 79−47312
gas proportional scintillation counter for use in large area detector systems without photomultipliers 79−59302
glass melting process, TV monitoring, equipment protection 79−58756
grain size determination and structural classification by visual comparative method using TV equipment *(German, English)* 80−35461
Hagerstown, MD, instructional TV system cost analysis 78−12501
heart, internal radiographical image display *(Dutch)* 79−70623
high detective quantum efficiency image detectors, review 77−71010
hologram reception and transmission by superorthicon television system 77−641
holograms transmission over TV channel, image distortion anal. 77−54684
holographic droplet image analysis by TV camera and table calculator via IEC-Bus 78−36337
holographic interferogram anal. with TV picture system 80−106489
holographic interferograms, interference anal. by analogue/digital video technique 79−86139
human eye movements recording using opto-television method *(Russian)* 77−12909
image counting and sizing using TV-microprocessor system 78−94377

television applications continued
image intensifier TV X-ray detector, high sensitivity, biological structure diffr. study appl. 78−89609
image processing, hybrid optical and TV system with feedback 77−61922
image processing, remote sensing imagery appl. 78−93005
imaging system, real time Doppler, colour TV display of particle size or density 77−62038
instantaneous spectra meas., TV camera and microcomputer appl. *(Japanese)* 80−31888
instruction by satellite, India, reception systems, overall appraisal 78−8185
intensified-Si intensity target vidicon application to IR astronomy 78−81544
interference microscope with electronic image formation *(Slovak)* 80−31862
interphase boundary analysis using TV 77−40483
intraoperative use of X-ray TV chain with video recorder 79−92334
Io interaction with environment, Jupiter Voyager imagery analysis 80−105197
IR imaging of superficial vasculature using Vidicon camera with Si target 77−21592
IR microscope linked with TV display, for optical material control 79−17483
IR TV system for building heat loss meas. 77−45837
Josephson video-detector, optimisation for mm wavelengths 80−4768
Jupiter colour pictures from Voyager space probes, 800 line scan TV system, land based receiver systems *(German)* 80−101549
LANDSAT image and digital terrain elevation data processing with parallax 77−29501
laser dot matrix space-coded surface topographical mapping 80−98885
laser intensity profile analysis using video equipment 78−59068
laser radiation TV analyser for intensity distrib. anal. 79−3702
laser scanning camera nuclear reactor surveys appl. 80−52748
laser single pulse spectral distrib. meas., using Fabry-Perot interferometer and CCTV system 79−3732
lecture demonstrations for general physics course using television 77−78939
LEED, photographic-vidicon camera method for intensity meas. 79−37596
LEED beam intensity measurement by photographic method, use of Vidicon camera 77−7638
LEED intensity measurement using modified CCTV system 80−31946
light velocity measurement using TV ghost, student expt. 77−13561
lip-opening area in speech, fast continuous meas. via. TV camera 78−3520
lunar occultation obs. using TV camera *(French)* 79−58263
lymphocyte sensitisation meas., electrophoretic mobility test improvements 79−25138
macromolecular structural studies, with synchrotron radiation, X-ray television area detectors 79−55610
marine life forms obs., using CCD colour TV camera 80−51301
materials science, use of closed circuit TV as teaching aid 79−71209
medical US diagnostic system, dynamic and still images display 78−65101
medical X-ray video images, enhancement 80−94353
metal sheet parity, pressed, X-ray TV system for automatic analysis *(German)* 77−90536
metallographic polished section, contour amplifier appl. using TV camera and monitor *(German, English)* 79−96261
meteor observations 77−87339
meteor spectra photography 77−67047
meteor trails televised spectra, photometry 78−20764
meteorology, thunderstorm development on colour TV display, of METEOSAT data 79−100936
meteors, prod. and study of television spectra 77−67076
meteors, television photographs photometry 78−96441
microcirculation flow dynamics meas. using video microscope 77−78009
microneurology, appl. of colour TV as surgery teaching aid 78−40396
microprocessor-based teleradiology system 80−26343
microprocessor-controlled hologram interferometry analysis using intelligent TV system 79−76648
microscopy, UV, with image intensification and TV image displays 77−5888
microscopy and cinephotomicrography with Zeiss Axiomat 80−27343
mobility aid for blind, passive optical system 77−25604
moire fringe biostereometry using parallel light beam 79−100701
motion online detection in digital video images, mice identification in labyrinth expts. *(German)* 78−92754
movement measurement, vidicon television camera appl. 80−41333
multichannel analogue detector system for star/planetary nebulae spectroscopic obs. 78−36461
neutron radiography with ^{252}Cf, use of TV imaging techniques 78−60922
noctilucent clouds, cine and television high-resolution obs. 79−39891
nonfilm method of high-speed process coords. meas., review 78−5093
nuclear emulsion tracks, detection and meas. by inexpensive microscope television 79−3290
nuclear reactor core instrumentation, approach based on IR television, on-line computing, pattern recognition 77−54310
object spatial location, TV meas. system accuracy 79−49200
ocean wave slope meter, fast response instrument, wind-wave moments meas. 78−45012
oceanography, slow-scan television camera for deeply towed vehicle 78−45045
ophthalmological research, training appl. *(German)* 78−24157
ophthalmoscope image processor/graphics system 77−81633
optical equipment for artificial aurora detection during ARAKS expt. 79−21075
optical feedback processing by TV-optical method 80−87335
optical fibre automatic refr. index profiling using video-based system 78−79104
optical fibre pattern display 78−33820
optical incoherent feedback using TV 80−87334
optical materials inspection, design of television projector 78−73006
optical multichannel spectrometric detectors, vidicon, online data handling capability 78−74077
optical operational amplifier 79−94327
optical spectra, direct encoding using computer interfaced vidicon TV camera 77−10114
television applications continued
p-n junction struct., X-ray topography visualisation during prep. *(Russian)* 78−26386
particle size distribution measurement apparatus, rel. time 79−17390
particle tracks, time digitiser in CAMAC format 80−14062
particle tracks in streamer chamber, recording technique 80−69023
Perseid meteor shower, television obs. 80−4309
photomicrography using planimeter and trinocular microscope 79−71523
photon counting and analogue TV systems, with digital real time image processing, astronomy appl. 78−96402
physics teaching, suggestion for teaching of physics, suggestions for demonstrations using TV 78−28895
picosecond exposure scanning camera, and associated recording system *(French)* 78−42429
PISCES submersible scientific equipment and data acquisition system 77−5381
planetary satellite Io, brightness increase after eclipse, colour TV obs. 77−87318
planimeter for meas. and displaying slide mounted samples 80−195
plasma, Princeton large torus, multi-channel TV-Thomson scatt., apparatus, mech. aspects 78−54932
plastic track detector, heavy ion tracks, automatic meas. device 78−17495
power plant stack emission vel. and SO_2 conc., IR TV appl. 77−49197
Prestel, as an information service 79−48979
Prestel, Post Office viewdata system, Meteorological Office participation 79−16675
PWR steam generators, remote controlled TV for detection of leaking tubes *(French)* 80−791
pyroelectric vidicon for thermal imaging *(Japanese)* 77−27359
pyroelectric vidicons for instrum. with IR lasers 78−59150
radiographic imaging, digital video acquisition system for extraction of subvisual information 78−69208
radiographic X-ray image intensifier video system, design characts. 78−69209
radiographic X-ray image intensifier video system, psychophys. evaluation rel. to system measures 78−73234
radiography, computerised tomography using video techniques 77−73568
radiography, diagnostic isocon imaging system 77−40760
radionuclide computer-assisted cardiology, off-line viewing using videotape 78−65119
radioscopic system, for 400 kV X-rays, using microchannel plate image intensifier *(French)* 77−38071
radioscopy, industrial, applied to solid propellant motors *(French)* 77−38072
real-time holographic viewing in moving fog 80−102676
retinal camera with infrared TV obs. *(German)* 79−2145
sapphire crystal float zone growth, meniscus angle meas., TV viewing system obs. 80−108347
scanning optical microscope 79−9242
seismic data colour TV display system 79−74995
sky brightness spatial var. obs. using intensified vidicon camera 77−70832
Skylab colour TV as primary data recording system 77−60569
slow-scan, Viking Orbiter visual imaging system appl., for Mars research 77−45282
software-based television image-analysis system 79−40559
solar EUV image, TV monitoring by Skylab Apollo Telescope Mount 77−60600
solar telescope, balloon-borne, narrow band TV system appl. as viewfinder *(Japanese)* 79−80228
solar XUV instantaneous images, obs. and recording on ATM television monitors 77−60605
solid state track detector, video electronic measuring system 78−17493
Spacelab image intensifying TV obs. of airglow and meteors 77−21966
speckle interferometry, double pulsed, television processing 78−65961
speckle pattern TV interferometer, principle and appl. 78−58014
Spectral Infrared Experiment equipment and objectives 78−81456
spectroanalytical information processing, television methods appls. 80−89568
spectrometer with attached vidicon, appl. to spectrochem. anal. 77−21453
sputnik Meteor series, TV communication system, optical-mechanical scanning devices *(Russian)* 77−64612
stable frequency standards comparison by TV carrier beat note transmission 78−57909
stellar objects monitoring using minicomputer-controlled photon counter *(Russian)* 80−31212
stellar occultation TV scanning, image freq. limitation *(French)* 79−58264
stellar radial velocities, determ. via TV detector and cross-correl. techniques 78−16305
stellar spectral classification calibration using TV multichannel system 77−67091
STEM image accumulation, storage and display system 80−37132
stereo SEM systems, design and performance 79−12906
streamer chamber track digitisation using standard 625 line TV camera 77−30715
stress/strain display on TV screen 80−21222
stroboscopic TV study, interaction of two high-velocity gas jets 78−42695
subliminal communication for behaviour therapy and education, audiovisual technique 78−73293
superficial vein imaging by infrared television 77−81546
surface dynamic representation by TV moire topography *(German)* 78−89430
teacher training, using closed circuit television 79−80388
teaching, closed-circuit system preparation and installation in colleges *(German)* 78−12521
teaching demonstration of diffr. and interference 77−5613
telemedicine technology development 77−21649
telescope, large azimuthal, search and guide system 78−57446
TEM image recording and processing TV system 79−58851
temperature meas. in polyorganosiloxane fluid friction zone *(Russian)* 80−7688
text TV display for visually handicapped *(German)* 79−2162
thermal imaging with pyroelectric vidicon camera 80−86288
three colour channel hybrid system to synthesize complex point spread functions 79−41347
time dissemination using TV signals from broadcasting satellite 77−60334

television applications continued
tracer particles detection and tracking, model packed-bed reactor 77−42012
TV lecturing system using frame multiplexing technique 78−28887
TV pupillometer, anal. of dynamic performance *(Japanese)* 79−39545
TV-computer interface system for human body sway study 77−81526
TV-optical analogue computer soln. of partial differential eqns. 79−76869
undersea stereoscopic television for offshore appls. 79−5677
underwater TV, wide angle correcting lens 80−91883
underwater viewing system, optical design 77−78459
US B-scan recording on video tape-recorder 78−77095
US fish finder display 78−38159
US video system *(German)* 78−94471
USSR and E.German time scale comparison by transportable atomic clocks and TV signals 77−79067
vapour pressure measurement, torsion-effusion method, automatic data acquisition 80−52188
Venera 9 and 10, TV surface expts. on Venus 77−78599
Venus cloud layer structure, determ. from Venera 9 televised pictures 80−67604
Venus cloudy layer observation in UV, violet regions, Venera station orbiter TV system appl. *(Russian)* 79−53747
vestibular postural control evaluation in humans using computer-TV interface system 77−44773
vibrating membrane speckle pattern analysis 80−106769
vibration measuring system using interf. fringes TV detect. and electronic image processing 80−103004
video correlating system for blood flow vel. meas. in microvessels 78−53543
video microscopy, review 79−58784
video-tracking of micro-circulation, appl. of bit-slice processors *(German)* 78−88749
videodensitometry in angiography 80−104745
videotape instruction in physics, low-cost systems 79−29
vidicon contrast sensitivity reduction for short pulse exposures 78−86254
vidicon tube appls. *(German)* 79−26050
viewfinder for balloon-borne solar telescope, narrowband TV appls. *(Japanese)* 78−24464
virtual image position determ., demonstration using TV camera 80−67992
wind speed remote meas. using video equipments *(French)* 80−7990
writing aid for motor handicapped, microprocessor-based device, LOGOS 78−81077
X-radiography TV of gas turbines, problems 78−95861
X-ray, medical, high-resolution TV system and video recorder 78−24120
X-ray colour TV system with soft X-ray preferred display 80−56186
X-ray diffraction topographic patterns, TV system for visualisation 77−58925
X-ray image projection installation, high-resolution *(German)* 79−57751
X-ray image transmission system response rel. to X-ray diagnosis 78−35941
X-ray images, quantitative anal. by TV image analyser 80−109008
X-ray intensifier TV picture transfer 77−5077
X-ray picture transmission *(Hungarian)* 78−21306
X-ray systems, flaw detection in welded joints, appl. and characteristics 77−81380
X-ray television system, based on vidicons, used for defectoscopy 78−72977
X-ray TV chain MTF and image quality determ. factors 80−36126
X-ray TV display systems, transmission characts. *(German)* 79−53215
X-ray TV system, EL-PC type image converting panel *(Japanese)* 77−67551
X-ray TV system for polymer deform. obs. 78−15610
X-ray TV-computer unit for measuring defect parameters in weld seams 79−67451
x-rays and vidicon TV combine for instant inspection of precision components 79−74321
^{4}He, superfluid, stationary vortex arrays, obs. with TV/photographic method 79−77851
Si vidicon optical detector, laser data acquisition/analysis system 78−58041
Si vidicon-image detector system, for atomic emission echelle spectrometer 78−61081

television broadcasting
biomedical broadband communication network combining satellite link and TV broadcast techniques 77−64145
cinefilm, role in TV broadcasting *(German)* 79−35866
cues for depth perception, visual sensitivities *(Japanese)* 78−48808
domestic time synchronisation method using TV broadcasting satellite *(Japanese)* 77−17956
educational programmes, problems encountered in Bulgarian People's Republic 79−17170
electronic colour reproduction correction during cine TV broadcasting *(Russian)* 79−49321
equipment and services, 1979 video yearbook 79−14197
interstellar communication via radio leakage, Earth model 78−57474
object-related colour reproduction in film scanning [TV broadcasting], matrix, electronic masking appl. *(German)* 80−105726
Open University, adoption of unorthodox TV practices 79−40332
psychophysics of vision, relation to TV 77−12923
RF radiation levels in urban areas 78−40351
satellite, tropospheric EM wave propag. meas. in 1978, eval. of long-term meas. *(German)* 79−84441
time and freq. meas., users' manual 80−94934
time dissemination using TV signals from broadcasting satellite 77−60334
USSR, educational TV and radio programme development *(French)* 78−89286
VHF and UHF, influence of polarisation on transmission quality *(German)* 78−61518
weather forecasting on radio and TV, development in America 77−49549

television camera tubes
see also image storage tubes
astronomical spectrophotometry using intensifier Si vidicon 78−32356
bubble chamber track extraction using single vidicon tube 78−82580
electron beam recording, film speed choice *(Russian)* 77−38049
image dissector tube design, with high resolution and large deflection angle 80−73475

television camera tubes continued
image-orthicon for spectral measurement of weak picosecond light pulses 79−93890
integrating vidicon systems at Cerro Tololo, astron. appl. 79−66924
Intensified Silicon Intensified Target (ISIT) tubes, medium speed gating 78−12766
interference fringe intensity distribution demonstration *(Polish)* 79−40340
IR imaging, imaging systems design, operation and performance, applications 80−47111
isocon plus image intensifier, appl. in astrophysical obs. *(Russian)* 80−12671
laser spatial profile meas. by pyroelectric vidicon camera 80−87425
low-level imaging, optical signal detection and meas. 79−94350
luminescence spectroscopy, image devices and photomultiplier detectors, signal-noise calcs. 77−81433
multichannel SIT image vidicon for mol. fluorescence meas. in soln. 77−79638
nuclear medicine appl., equipment improvements 77−44787
polyvinylidene fluoride, optimised target for IR vidicon camera tube 79−32050
Pyricon thermal imaging tube 78−9437
pyroelectric materials, limitations and improvements for vidicon performance 77−8519
pyroelectric vidicon, appls. 77−65635
pyroelectric vidicon, thermal props. of reticulated sensing layers, design parameters 78−49897
pyroelectric vidicon, ultrafast photography, with 10.6 μm radiation 78−38035
pyroelectric vidicon, use as medical thermograph 79−25060
pyroelectric vidicon for thermal imaging *(Japanese)* 77−27359
pyroelectric vidicon thermal imager principles and performance 77−39093
pyroelectric vidicons, CO_2 laser beam meas. 78−49907
pyroelectric vidicons, figures of merit, material parameters 80−77855
pyroelectric vidicons for thermal imaging 77−19449
resolution, monitor brightness, electronic speckle pattern interferometry, fringe contrast analysis 79−72506
return beam vidicon, high resolution, appls. 77−83988
SATICON return beam system 2-inch high resolution camera tube 79−5724
SEC vidicon, on Skylab Apollo Telescope Mount, solar EUV image monitoring 77−60600
SEC Vidicon photometer, appl. to photometry of ω Centauri main sequence 80−90491
secondary electron conduction vidicon digital TV camera, detection characts. 78−54457
SIT vidicon detector system, for Palomar 1.5 metre telescope 79−92674
Skylab ATM television monitors, obs. and recording of instantaneous solar XUV images 77−60605
slow scan SEC vidicon system coupled to telescope 77−25945
solid state imaging devices, comparison with TV camera tubes 77−83986
solid-state array and camera tube imagers compared 77−39090
streak camera, direct readout devices 78−38037
TGS vidicon tube, used with optical multichannel analyser as IR detector 78−86329
thermal TV camera, noise, synchronisation, spatial resolution and lifetime characts. 79−35833
three dimensional image transmission, real-time, using vol. scanning spatial modulation 77−72060
time resolved spectroscopy, picosecond mode-locked laser techniques for ultrafast mol. processes 77−75340
triglycine sulphate, deuterated, reticulated target for pyroelectric vidicon, IR imaging 80−77858
vidicon, Quantimet 720 system, video electronic image analyzing system, solid state track detector, automatic fission track counting 78−17494
vidicon, Si target, and minicomputer system, for laser intensity profiles meas. 79−27267
vidicon, Si target, as optical multichannel detection system for modulation spectroscopy 77−41693
vidicon, Si target, performance as multiwavelength detector for liq. chromatography 77−90658
vidicon based apparatus for spectral line contours investig. 79−93226
vidicon based rapid scan spectrometer, for anal. appls., design, evaluation 77−77827
vidicon contrast sensitivity reduction for short pulse exposures 78−86254
vidicon Raman spectrography detection system 80−37095
vidicon spectrograph for multichannel detection of Raman spectra 77−74518
vidicon spectrometer, appl. to spectrochem. anal. 77−21453
vidicon target, TGS-Ge contact, thermal resist. 77−4226
vidicon tube, video-electronic measuring system, nuclear track emulsions 78−17493
vidicon tube for low level X-ray and γ-ray imaging 77−81561
vidicon tubes, detect. sensitivity, at. spectrometry appls. 77−41695
vidicon tubes for use outside optical spectrum, X-ray, UV, IR appl. *(German)* 79−26050
vidicon varizonal target, resolution, internal elec. field effects *(Russian)* 77−7201
vidicon-camera parallel-detection system for angle-resolved electron spectroscopy 80−4817
vidicon-echelle spectrometer with random access, design and eval. for multielement determs. in atomic absorpt. spectrometery 77−90652
vidicons for X-ray diffraction topographic patterns, spectral sensitivity of TV system for visualisation *(Russian)* 80−62814
X-ray topographic images, direct display systems, review 77−68899
Si vidicon, performance at low signal levels, astronomical spectroscopy appl. 77−22085
Si vidicon-image detector system, for atomic emission echelle spectrometer 78−61081
Si:H, amorphous, image pickup devices 80−100481
Si:H film, amorphous, photocond. imaging 80−1300

television cameras
see also colour television cameras
astronomical photometry with SEC TV camera at Loiano telescope 79−58272
automatic focusing system, Visitronic, description *(German)* 79−6200
balloon-borne slow-scan TV camera performance test *(Japanese)* 80−12635

television cameras continued
C-CD, implantable, for continuous recording of sheep ovary images during reproductive cycle 78−40442
equipment and services, 1979 video yearbook 79−14197
Fabry-Perot-interferometer imaging system for thermospheric temp. and wind meas. 80−101441
imagery, 2-D sampled, aliasing and blurring effects 80−99635
IR heat camera component developments for night vision *(German)* 79−49287
IR video camera at 10 μm, using liq. cryst. thermooptical convertor and scanning polarimeter 79−94326
laser, with scanning head and photosensitive detector, nuclear reactor surveys appl. 80−52748
lens performance meas. system, routine checking appl. 80−277
lenses, zoom, glare characts. 79−10373
objective lenses testing by projection 80−9060
optical microscope combined with TV equipment for teaching and quality control 80−82817
planetary observation appls. 80−31197
polar camera, for optical space-variant pattern recognition 78−66767
precision image isocon X-ray TV camera 80−101263
pressure tolerant, small, oceanographic appl. 78−32243
pyroelectric vidicons for instrum. with IR lasers 78−59150
scanning nonlinearity cancellation, transmitting TV camera 80−52318
slow-scan television camera for deeply towed oceanographic vehicle 78−45045
thermal TV camera, noise, synchronisation, spatial resolution and lifetime characts. 79−35833
thermography, pyroelectric vidicon camera use 79−93143
TV 300 m lenses, modular construction method, Gaussian optics, Seidel aberrations 78−311
underwater viewing system, optical design 77−78459
video fluorometer, computer-controlled, multichannel, features 79−20495
video interferogram analysis by TV camera-microprocessor system 80−73440
vidicon camera, intensified, in pseudo real-time coded aperture imaging system 77−31133
Viking mission to Mars, optical equipment 77−29627
Viking visual imaging subsystem, inflight performance 78−36417
X-ray TV systems, parameter estimation 77−73404
zoom lenses, MTF meas., distortion influence, normal and inverse conjugate techniques 78−78008
zoom lenses for TV cameras, review *(Russian)* 78−90493

television equipment
16 mm Perfectone Comitor for sound dubbing, fast synchronisation and foreign language recording 78−59103
acousto-optic deflector for TV and oscillograph displays 77−39099
biological micro-object geometric feature determination, TV set 80−85538
camera spectrometer, for colour temperature meas. *(Russian)* 77−38050
dubbing suite for Anglia TV using Comitor projector and Sepmag machines 78−59104
electronic editing system *(Russian)* 79−89029
external synchronization of electric drive SA-120 when shooting combine pictures with TV images *(Russian)* 80−86484
films, 16 mm Fujicolor reversal film RT 500 and RT125 80−106585
geometrically correct stereo-TV observation of micro-objects *(Russian)* 79−26116
hardwired image analyser software control 78−57917
holographic TV, appl. of CRT with electro-optic crystal *(Russian)* 80−37974
Hungarian developments, BEAG activities 78−46860
large-screen virtual display, fabrication of parabolic mirror by rotational method 80−87465
laser, epitaxial waveguide type with distrib. second-order feedback, electron beam pumped *(Russian)* 78−29973
laser beam scanner, rotating mirror, development programme *(Japanese)* 80−74369
light modulator for laser image recording on cinefilm *(Russian)* 79−89027
optical microscope combined with TV equipment for teaching and quality control 80−82817
projection systems for large screen pictures *(German)* 79−80660
projection TV systems, sealed scanning semicond. laser with transverse electron-beam pumping 79−89936
projection TV using electron beam pumped semiconductor laser 77−88830
SAW filter appls. *(Italian)* 79−81642
SAW filter design for TV, CATV and radar appls. 80−53579
SAW TV intermediate-frequency filter, 58 MHz, using ZnO sputtered film 77−80022
scintigraphic TV displays, 4 standard types, comparative study 80−109005
screens, use of cholesteric-nematic phase transitions of liquid crystals *(Chinese)* 80−79922
semiconductor laser, electron beam pumped, for projection TV 77−72004
telecine FDL 60, CCD line scanning, digital frame store 80−278
X-ray image projection installation, high-resolution *(German)* 79−57751
X-ray picture examination TV equipment 77−21607
x-ray television using an image pick-up tube *(Chinese)* 79−54243
X-ray topography camera, high speed, semiconductor lattice defects exam. appl. 77−11443
X-ray TV display systems, transmission characts. *(German)* 79−53215
Si intensifier for Isocon low light level TV 79−37042

television interference
AC power line radio and TV interference control 77−75745
ghost images, used to locate offending building, for teachers 78−81764
monochrome flickering, subjective colours obs., using subjective modulation transfer functions *(Japanese)* 78−3490
windpower systems, TV interference aspects 80−61238

television picture tubes
see also cathode-ray tubes; colour television picture tubes; fluorescent screens
AC crest voltage superimposed on DC levels, measurement using static HV valve voltmeter *(German)* 79−58757
acoustooptic TV picture production, modulation of laser beam 79−55237
aperture distortion correction, optical method 80−95827
biocular magnifier design for display system viewing 79−27361

television picture tubes continued
cathodoluminescence of BeO with/without admixtures *(Polish)* 80−2869
electron beam pumped semiconductor laser as TV tube screen 78−29969
human picture distortion ratings compared with objective error measures 78−44510
kinescope spot size, relation to picture quality 77−44675

television receivers
see also colour television receivers
ceramic filters appl., using $Pb(Zn_{1/3}Nb_{2/3})O_3$-$PbTiO_3$-$PbZrO_3$ and $Pb(Mg_{1/3}Nb_{2/3})O_3$-$PbTiO_3$-$PbZrO_3$ *(Japanese)* 80−60507
equipment and services, 1979 video yearbook 79−14197
SAW bandpass filters, TV receiver appls. 78−51008
SAW filter appl. *(Japanese)* 78−71247
SAW ghost image cancelling circuit *(Japanese)* 77−27429
$LiTaO_3$ crystals for commercial SAW TV IF filters, fabrication 80−80961

television reception
ghost images, used to locate offending building, for teachers 78−81764

television reception quality *see television reception*

television signals *see video signals*

television standards
international, 1979 video yearbook 79−14197
precision TV demodulator using high-performance SAW transversal filters 79−49258

television studios
acoustic and other design factors for television and motion-picture stages 78−79169
acoustic design of talks studios and listening rooms 79−37091
acoustically optimal room proportions with regard to normal frequency spacing *(German)* 80−14522
equipment and services, 1979 video yearbook 79−14197
light sources, metal halogen, for colour rendition quality *(Russian)* 79−76785
rapid processing technique for colour reversal cinefilm *(Russian)* 80−3385
receiver for parallel operation of radiomicrophones *(German)* 80−4787
sound processing circuit diagrams *(German)* 80−18031
thyristor feeding device type TPU for light sources *(Russian)* 79−58816

television systems
see also cable television; closed circuit television; community antenna television
acoustooptic FM and freq. shifted heterodyne CO_2 laser system 78−5568
astronomical imaging tubes, utilisation *(French)* 78−40829
chromaticity anal. in 3 zonal objects registration processing *(Russian)* 79−89026
colour-rendering evaluation, extension of CIE colorimetric system, in film and television 78−310
data compression interface, for cytology and chromosome anal. 77−86683
digital system, for stellar radial vels. determ. using cross-correl. techniques 78−16305
fibre optic VSB-FDM CATV video trunking, transmission performance 77−62054
Hermes, geostationary communications satellite, Canadian design 78−93068
holographic, minimum frequency band evaluation *(Russian)* 77−54682
integrating vidicon systems at Cerro Tololo, astron. appl. 79−66924
large screen TV aspherical plastic lens optical design and evaluation 80−78937
low-light, military appl. of fibre optics, West German developments 1978 survey *(Swedish)* 79−55209
narrow band television system, appl. as balloon-borne solar telescope view-finder *(Japanese)* 79−80228
photon counting and analogue TV systems, with digital real time image processing, astronomy appl. 78−96402
three dimensional image transmission, real-time, using vol. scanning spatial modulation 77−72060
trichromatic acousto-optical laser-beam deflector for TV scanning *(Czech)* 79−98502
X-ray, parameter estimation 77−73404
X-ray diffraction topographic patterns, spectral sensitivity of TV system for visualisation *(Russian)* 80−62814
x-ray television using an image pick-up tube *(Chinese)* 79−54243

television transmitters
equipment and services, 1979 video yearbook 79−14197
SAW filter design applied to group-delay equaliser in TV rebroadcast transmitters 80−74676

tellurium
see also nuclei with .....
accumulation layer, surface states calc. 77−43692
acousto-optic modulator, props., for IR laser beam control *(Russian)* 77−72073
acousto-optic props. at 10.6 μm 79−91401
acousto-optical props. at wavelength of 10.6 μm 80−76001
acousto-optically phase-matched noncollinear optical SHG obs. 79−50353
acoustoelectric current flow, acoustic refraction effect 79−19637
acoustoelectric domain induced transparency at 11 μm 78−27182
acoustoelectric domain induced transparency near 11 micron 77−85727
acoustoelectric instability of current, mag. field influence 79−73547
adsorbed layer on Ni (111) surface, bonding geometry and electronic struct. 79−77909
adsorbed on Ni(001), core-level photoelectron diffraction 78−95659
adsorbed on Ni(001), photoelectron diffr. effects in core-level photoemission 80−76144
adsorbed on Ni (001), photoelectron diffr. obs. 80−40223
adsorbed on Ni (001), surface sensitivity of MeV He ion scatt. 79−56904
adsorption, on Ni, photoemission intensities from core states 78−95654
adsorption, on W, work function, field emission meas. surface film effects 78−19645
adsorption on Ni (100), orbital identification in INS and UPS spectra 77−43427
adsorption on Ni (111), angle-resolved photoemission 80−40230
adsorption on single cryst. faces of Mo and W field emitters 78−34714
adsorption on W and Mo field emitters 77−69177
adsorption on Zn (0001), UPS investigation 79−91563

tellurium continued
amorphous, electronic struct. and optical props., pseudopot. calc. 80−65428
amorphous, localised gap states, variable range hopping 77−72866
amorphous, obtained by splat cooling crystallisation 77−65949
amorphous, Rayleigh scatt. of Mossbauer radn., lattice dynamics 80−15845
amorphous, structure, random chain assembly model 78−6015
amorphous and liquid state, Raman spectra, crystn. processes 80−60608
amorphous film, vac. deposited, phonon-assisted hopping cond. 80−2392
anisotropic thermal motion of atoms, X-ray exam. 78−18730
atom, GTO basis sets, Hartree-Fock-Roothaan calcs. 79−97973
atom, $K\beta_3/K\beta_1$ and $K\beta_2/K\beta_1$ relative intensities 77−75088
atom, photoelectron spectra, strong many electron effects from core levels 77−18862
atom, photoionisation cross sections and ang. distribs., outer p subshell 80−9572
atom, XPS and XES, dynamical effects 80−52924
atomisation energy, mass spectrometric determ. 79−70361
Auger electron spectra, solid state effects 80−20739
band structure, laser-modulated photoemission expts. 77−28686
Bijvoet intensity differences, prediction in noncentrosymmetric structs. 79−7574
breakdown in high microwave impulse field, by impact ionisation 77−62957
carrier density nonlinearity of interacting acoustic fluxes 77−51781
carrier mobility, free, associated with dislocation strain fields 77−51738
carrier recombination at high optical excitation 77−72884
chemical bonding in group V and VI elements and compounds with tetradymite structure 80−15036
chemisorption on Ni, orbital energy spectrum of chemisorbed electrons 78−2542
circular photogalvanic effect in optically active crystal 79−73542
cluster superlattices in Na-type X zeolite matrix, N and S type volt-ampere characts. *(Russian)* 80−70665
coating of PbTe surfaces, struct. and junction characts. 80−50743
Compton profile, charge and momentum density 80−55220
conduction band parameters, interband magnetoabsorption meas. in Faraday configuration 77−89695
contact charge density, press. depend., trends for Ag-Te 78−39077
core level binding energies 80−71564
covalent solid, struct. props. and valence force fields, non-empirical calc. 77−1096
crystal growth by Czochrolski method 80−66423
crystallisation by hydrothermal method *(French)* 78−11096
crystallisation in constant electric field, thermoelectric parameters 77−44146
current induced optical activity, polarisation plane rotation rate *(Russian)* 79−65830
cyclotron resonance, transport and surface phenomena 77−40132
cyclotron resonance for holes with $B \perp c$ 78−10777
cyclotron resonance in pulsed high mag. fields, cond. band struct. 80−59867
Czochralski growth, etch pit orientation study 79−43133
Czochralski method of growth 79−4912
DC Bi:Te, elastic consts., electronic contrib. 77−84826
Debye temperature, using elastic consts. and Kopp-Neumann relations 78−2220
deformed and annealed crystal, elec. props , directional depend. 79−7847
detector for CO_2 pulsed laser radiation, using photon drag and optical rectification 78−21216
determination, in complex alloy, by at. absorpt. 77−40582
determination in inert gas, H_2 mixtures, oscillograph polarography method 78−61100
dielectric function in trigonal phase, model calc., local-field corrections 78−39045
diffusion and conduction properties, NMR investigation 79−78547
diffusion in $NaNO_3$, KNO_3 and $RbNO_3$ melts, high dilution 78−47546
diffusion into SnO_2 films *(Japanese)* 79−95218
dislocation density and config. effects on cyclotron reson. absorpt. 79−78526
dislocations influence on galvanomag. props. 80−54722
distribution equilibrium between FeO-Fe_2O_3-SiO_2-Al_2O_3-CuO/Cu slag/metal system 78−44111
doped, galvanomagnetic props. in fields up to 140 kOe 78−91707
double-beam photoemission, electronic structure 77−66576
electric field gradient and lattice location of Sn, TDPAC and Mossbauer effect meas. 78−52395
electrical conduction behaviour, 0-500 kbar 79−99589
electrical properties anisotropy, influence of deform. and annealing 77−15859
electron density at nucleus, press. depend., Hartree SCF calcs. 78−56411
electron irrad., mobility increase due to defect prod. 80−24501
electron irradiated, dose-depend. and recovery behaviour of transport props. 78−71761
electron mobility, elec. field depend., 77K 77−85233
electronic states, tight-binding model Hamiltonian for trigonal struct. 77−59250
electronic structure of cryst. phases, hydrostatic press. effects 80−59865
energy gap, laser emission study of press. depend. 79−82521
energy gap under press., elec. resist. and Hall effect meas. 78−30926
energy gap under press., photocond. and transmission spectra meas. 77−85267
enthalpy, heat capacity, 0 to 750°C 77−11705
evaporated film epitaxial and amorphous-crystalline phase transition growth and struct. 79−51449
facet coating, for side lobe suppression in far field of AlGaAs DH stripe laser 80−5744
Faraday-type microwave Kerr effect 79−23998
film, AES, LEED, XPS, energy loss spectra studies, oxidation effects 78−73086
film, annealing effect on elec. cond. and Hall effect 77−8213
film, atm. comp. influence on elec. surface props. 78−26980
film, elec. props., 77 to 450K, thermal width of band gap 79−51698
film, elec. props. effect of deposition rate 78−14844
film, electronic struct. charge on ordering, double beam photoemission 78−19634
film, evaporated, crystallinity and electronic props., annealing effect 77−85107
film, field effect meas. 77−43757

tellurium continued
film, gas-evaporated, selective absorpt. characts. and emissivity 80−50998
film, growth on (111) KBr films deposited on mica, TEM and electron diffr. obs. *(Japanese)* 78−64473
film, Hall consts., thickness depend. of mobility 79−87171
film, hole machining using (Ga,Al)As DH laser, high-density optical recording 79−89954
film, interference enhanced Raman scatt. 80−42273
film, microstructure 80−103598
film, on electron irrad. KBr, epitaxial growth and surface coverage 80−10825
film, on TGS substrate, ferroelec. field effect 79−42675
film, optical props. *(French)* 77−44076
film, piezoresistance 79−95524
film, polycrystalline, hole mobility, influence of tunnelling through barriers on grain boundaries 77−43748
film, stability in moist air, rel. to information storage capability, atmospheric corrosion model 80−71774
film, surface morphology depend. on vacuum deposition angle 80−103553
film, thermally evaporated, elec. cond., Hall voltage and thermoelec. power 77−47913
film, thin evaporated, 130 Å, temp. depend. of elec. props. 79−95529
film, vacuum deposited, growth and morphology of crysts. 80−96766
film, vacuum deposited on NaCl, crystallite growth and morphology, electron microscopy 80−65401
film, vacuum-evaporated at normal incidence, X-ray Fourier line shape anal. 79−99454
film and trilayer antireflection structure for optical recording 79−94329
film condensed on mica, struct. and electrophysical props. 80−39688
film deposition by electrolytic method 77−48355
film evaporation, predeposited Ag, Sn, Bi, Al and Se nucleation centres effect on grain growth 77−4739
film growth on KBr (111) on mica *(Japanese)* 78−79903
film nucleation on Au oriented islands, grain growth 78−2388
films, elec. and galvanomag. props., microstruct. 80−70859
films, elect. and galvanomag. characts. 79−33365
films, evaporated deposition, absorptivity and emissivity 80−25473
films, oriented, semiconducting props., Hall coeff., band structure 80−70854
n-GaAs:Te, interaction of positrons with dislocations 79−99974
GaAs:Te, radiative recomb. *(Russian)* 79−91499
galvano- and thermomagnetic effects 78−30939
galvanomagnetic props., surface layer effects reduced by etching 77−51769
Hall coefficient , magnetoresistance, two types of carriers 80−60013
Hall effect, mag. inversion *(Russian)* 77−4376
high pressure metallic phase, cryst. struct. 80−49161
high-pressure metallic, supercond. transition temp. press. depend. 80−80435
hole mobility anisotropy in edge dislocated cryst. 80−24936
imperfect pure cryst., thermomag. effects, dislocation effects and Auth model 77−85248
impurity in Nimonic 105, influence on creep and stress rupture props. 80−66602
impurity photoconductivity, Te in MIS structure 78−72203
impurity spectroscopy, magnetoresist. meas. under nonohmic conditions 78−30942
impurity spectroscopy 80−65499
impurity state and impurity cond., press. effect, pure and Sb doped crysts. 80−54723
interband photoconductivity at up to 10 kbar, 1.6-200K 77−47850
intervalence band absorption, press. and defects influence 80−55149
inversion layer, surface quantum levels, calc. from Shubnikov de Haas meas. and triangular surface pot. well 79−15207
inversion layers, surface quantum oscillations 77−89777
inversion layers, surface quantum transport 78−64088
inversion layers in mag. fields 80−44690
ion implanted in semiconductors, Mossbauer spectroscopy exam. of radiation damage 78−2176
IR optical absorption, 5-20 μm, for intrinsic Te 78−84562
isomer shift values of implanted $^{133}Xe/^{133}Cs$, Mossbauer spectra 80−7240
isotope shifts, odd-even staggering *(French)* 79−85936
isotopic composition in meteoritic and terrestrial materials 78−82856
J_1J_2 transition from LS, revised assignments for $d^9s^2p^2$, $d^9s^2p^3$ 79−45630
Kikuchi patterns, of non-centrosymmetrical crystal 80−100202
laser induced EMF, photon drag, optical rectification and spurious signals 78−19083
layer on TGS cleavage faces, oriented growth 79−38509
liquid, classical fluid model, neutralising negative background density 78−22621
liquid, compressibility 77−65997
liquid, diffusion of Hg and Cd 77−84955
liquid, elec. cond. at high temp. and press. 78−87959
liquid, elec. cond. in metallic region, calc. using modified Ziman theory *(Russian)* 77−66149
liquid, elec. resistivity up to 30 kbar 79−38070
liquid, electrotransfer of Se 77−11716
liquid, estimate of self-diffusion coeffs. from viscosity data 77−55370
liquid, localized impurity states, paramag. susceptibilities 78−64185
liquid, mag. susceptibility, temp. depend. 78−47943
liquid, meas. of viscosity, density and surface tension *(French)* 78−91371
liquid, semicond.-metal transition at high temp. and press. 77−51784
liquid, structure metallic constituent calcs. hard sphere model *(Russian)* 80−24349
liquid, surface tension isotherms, struct. changes 79−37904
liquid, thermal cond. meas., resistive probe method 77−15636
liquid, US rel. temp. depend., melting effects 78−38782
magnetic susceptibility meas. rel. to heat treatment 78−34952
magnetoacoustic effect 77−62963
magnetoresistance, Hall effect and elec. cond. meas., hydrostatic press. effect 77−47830
metallic state, press. induced, elec. cond. meas. 80−96949
MIS structure, photosensitivity spectrum 78−14834
mobility anisotropy in a-edge-dislocated crysts. 80−107781
molecular laser, optically pumped, review 80−58519
monoclinic, electronic states above high-press. phase transition 79−99476

tellurium continued
monolayer, adsorbed on Al (111), angle resolved UPS of 2-dimens. band struct. 80−60059
monolayer, on $Pb_xSn_{1-x}Te$, Raman scatt. meas. 77−48211
monomer in Ar matrix, formed by H_2Te photodissoc., Mossbauer spectra 77−20769
Mossbauer diffraction spectra, influence of nucl. reson. absorption 77−43922
Mossbauer spectra under press. up to 8000 MPa 80−80647
multilayer thin film struct. thermoelec. props. 80−92964
natural optical activity and features of struct. of electronic energy spectrum 79−8110
negative photoconductivity, intraband absorpt. *(Russian)* 80−107854
NMR chemical shift, tight-binding calc., trigonal Te 78−2759
NMR spectrum, electron paramagnetism and atomic self-diffusion mechanism 78−72426
$(np)^4\ ^1S_0$-level photoionisation via autoionising levels 79−76398
optical activity, de Haas-van Alphen oscillations and cond. band parameters 80−54605
optical activity rel. to band struct., 4 to 300K 77−77165
optical bleaching near fundamental absorpt. edge at 80K 80−28287
optical harmonic generation in crystal, second harmonic, IR irrad. *(German)* 79−50345
optical properties under high press., band struc. transform. 80−55112
optical props. in visible spectrum and microhardness meas. *(French)* 77−28590
optically active crystals, circular photogalvanic effect 80−54739
overlayer, c(2×2) on Ni surface, 4d levels, angle resolved photoemission cross section, atomic and solid-state effects 80−29853
overlayer, on Ni (100), bonding, photoemission expts. 77−35819
p-type, impact ionization rate of holes at 77K 80−10993
p-type, magneto-impurity effect, review 79−91081
p-type, photocond., 1.6-4.2K, spectral features 77−24591
p-type, photon-drag detectors for CO_2 lasers 77−5911
p-type, transverse and longit. Nernst-Ettingshausen effect, theory and expt. 78−76095
p-type Hall effect meas. at high elec. fields 77−66175
paramagnetic state (μ^+e^-) at high temp. 79−56676
phonon dispersion curves, scaling formalism 80−54326
photo-EMF obs., depend. on sign of circular polarisation of light *(Russian)* 78−80025
photo-excited carriers, far IR magneto-spectroscopy 80−50343
photoconductivity in strong mag. fields, doping effects, impurity levels 80−75602
photoconductivity spectrum in 1.6 to 4.2K band, nonequilibrium electron mobility *(Russian)* 77−11960
photoconductivity under pulse excitation conditions 80−2425
photocurrent generated by polarised light, direction depend. on polarisation *(Russian)* 78−64065
photoelasticity and acousto-optic diffr. in piezoelec. semiconds. 80−29715
photoionisation relax. energies 77−20988
photon drag effect 77−1443
photon drag effect theory 78−19084
photovoltaic effect in thin films, 10.6 μ, prep. methods 80−20252
physics, conf., Konigstein, Germany (May 1979) 80−51958
piezo-Hall effect from 4.2 to 77K 77−76848
piezoelectrical free-carrier scatt. by screw dislocations, Hall effect and cond. meas. 80−24926
polarographic prewave, photo-effect 77−36833
pure, prep. by combined method, vacuum distillation and double condensation 79−33956
quadrupole interaction for ^{129}I, ^{131}I, and ^{132}I, PAC expts. 78−48087
quadrupole interaction in Ni, β-γ TDPAC meas. 78−43730
quadrupole interaction of 81 keV state of ^{133}Cs and 247 keV state of ^{111}Cd, TDPAC expts. 78−48088
radiation damage expts. review, defect interactions 77−84800
relaxation of μ^+ meson spin, (μ^+e^-) paramag. state form. *(Russian)* 79−38424
ĉ-screw dislocation, induced acceptor levels and free carrier mobility 77−89730
screw dislocation substruct. studied by torsion expt. 79−10859
screw-dislocation-induced scatt. and acceptor states, galvanomag. and optical expts. 77−28142
self-defocusing of CO_2 laser radiation under phase matched SHG conditions 78−83043
shear deformation of single cryst. 77−81367
SHF, high efficiency, of 12.8 μm laser radiation 78−25923
SHG, 60% efficiency, 12.8 μm NH_3 laser pumping 80−83640
SHG, optical modulation 79−86212
SHG of ps pulses 79−45995
c-slips, asymmetry and orientation depend. 77−27888
solubility and cosolubility in InAs 77−16552
solubility in liquid Cu 77−21096
solvent, solution growth of ZnS, ZnSe, CdS and their mixed compounds 79−65993
space group $C3_12$-$C3_22$, habit variation 80−107090
spin-lattice relaxation and Knight shift of ^{125}Te in Te, high temp. behaviour 77−1614
steel, stainless, stabilised with Cr-Ni-Nb, reaction with Te vapour 77−8986
stimulated Brillouin scattering of CO_2 laser radiation 79−47469
stopping power nucl., in ferromag. Gd, transient mag. field 78−34555
strained and unstrained crystal, SHG and propag. of CO_2 laser radiation 80−58641
superconductor-semicond. device research, future prospects 79−28467
surface, (10$\bar{1}$0), struct., LEED intensities anal. 80−88411
surface, (1$\bar{1}$00), freq. depend. of surface cyclotron reson. 79−69724
surface, (1$\bar{2}$10) face, epitaxial growth of Se, LEED and AES meas. 77−1328
surface cyclotron resonance, freq. depend. 78−64084
thermal etch pits shape, on cleavage faces 80−107251
thermodynamic basis for generalisation of melting curves 78−2236
thin film, thermoelec. EMF, Seebeck coeff., elec. cond. structural depend. 79−78230
thin film selective absorber coatings, prod. using an oblique vacuum deposition technique 80−81488
thin films, textured, prep., high solar absorptivity by multiple refl. 80−11568
three-photon absorption, selection rules and exciton peak 78−43303
trigonal, ^{129}I Mossbauer obs. at high press. 80−55005
tellurium continued
trigonal, dielec. matrix calcs. 80−54630
trigonal, directional effects in double beam photoemission 79−74059
trigonal, electronic and optical props., press. depend., self consistent pseudopotential formalism 79−65838
trigonal, model of lattice dynamics using long and short range interactions 78−59893
trigonal, nucl. elec. field gradient ellipsoid, extended Huckel approx. calc., comparison with Mossbauer spectra 77−55736
trigonal, Raman scatt. at very high press. 80−60566
trigonal, self-consistent ground state, X_α calcs. 80−54604
trigonal, state-of-the-art review of model calcs. 80−54327
trigonal, surface lattice dynamics, mean square displacement spectra in long wavelength limit 80−54498
trigonal and amorphous, electronic struct. and nonempirical calc. of struct. props. 80−59866
trilayer for high-performance optical recording 79−50382
uniaxially stressed, cyclotron resonance 79−87319
uniaxially stressed, submm. cyclotron reson., deform. pots. and k.p coeffs. 80−54606
vacuum deposited film, effects of electron irradiation on surface coverage *(Japanese)* 79−82477
valence band struct., hydrostatic press. effect 77−47724
valence band struct. under press., spin-orbit splitting, intraband absorpt. spectra 80−2330
valence-band X-ray emission spectrum 78−84682
vapour laser, operation by dissoc. of metal complex 77−54702
VPE nucleation in submicroscopic holes, oriented film prep. 79−99443
warm hole conductivity 78−72160
X-ray photoemission, core level binding energy 78−2984
Ag/AgI/Te thin film galvanic cell, shelf life determ. 78−35702
Ag-Te thin film couple, room temp. interactions 80−2220
Al:Te, anodic oxidation, mobility of foreign atoms 77−90494
$Al_{0.3}Ga_{0.7}As$:Tl, impurity effects on interface morphology of LPE films on corrugated GaAs substrates 78−88435
$Al_{0.36}Ga_{0.64}As$, LPE films, Te-induced defects 78−43037
$Al_{0.4}Ga_{0.6}As$:Te, saturable optical absorpt. of deep Te-complex centre 79−99917
$Al_xGa_{1-x}As$: Te, persistent photocond., due to donor-related centres 80−15558
$Al_xGa_{1-x}As$:Ge(Te)(Zn), photo- and cathodolum., comp. depend. *(Russian)* 77−48215
$Al_xGa_{1-x}As$:Te, anneal-induced defects, photoluminesc. obs. 79−61422
$Al_xGa_{1-x}As$:Te, epitaxial film, elec. cond. and Hall coeff. rel. to donor levels 77−24630
$Al_xGa_{1-x}As$:Te, persistent photocond. trapping centre, donor complex model, photocapacitance meas. 79−65517
Al_2O_3-Si-Te-Al_2O_3 layered apertured facet reflector, for lateral mode stabilisation of diode lasers 80−23708
As:Te film, amorphous, chemical modification of props. 80−49250
As_2S_3:Te glasses, doping influence on AC conductivity, electron transport by hopping 79−78106
a-As_2Se_3:Tl, doped film, photoluminescence intensity and lineshape study 80−50448
Bi:Sn,Te, and undoped sample, low-temp. transport meas., electron scatt. 77−24551
Bi:Te, quenching and annealing of defects, elec. resist. meas. 78−87973
Bi:Te dilute alloy, elec. resist., 1.8 to 77K, electron-phonon scatt. mechanism 79−15144
Bi:Te neutron radiation defects 78−47430
Bi:Te polycrystal elastic constants for US velocity obs. 79−69180
Bi-Te, combination freq. in Shubnikov-de Haas and surface impedance oscillations *(Russian)* 78−10476
$Bi_{1-x}Sb_x$:Te, dispersion law of charge carriers *(Russian)* 79−87114
$Bi_{86}Sb_{14}$:Te, single crystal, dispersion of magnetoplasma waves *(Russian)* 80−70739
C_2O_3:$^{125}Te^{6+}$, mag. hyperfine interactions, Mossbauer study *(French)* 79−24247
n-CdS:Te, grown from Te soln., elec. props. 79−65475
CdS:Te-based photoelectrochem. cell, luminesc., thermal manipulation of deactivation processes 80−81479
CdS-Te, heterostructure, effect of low cond. CdTe interlayer on charact. 80−44721
CdS-Te-Ge heterojunction, prep. photosensitivity, and negative cond., 77K *(German)* 77−20413
CdSb:Te, p-n junction formation by laser radiation 80−96983
CdSb:Te, photoconductivity charact. 77−43653
CsI:Tl^+, Jahn-Teller split luminesc., high press. study 78−52565
Cu-Te thin film couples, room temperature interactions 80−96699
FaP:Te, nucl. relax. rel. to donor density 80−11284
Fe:Te, interaction of impurities with point defects, Mossbauer spectroscopy exam. 78−47414
Friedel's law, breakdown in Kikuchi patterns as obs. in TEM 79−69046
$Ga_{1-x}Al_xAs$:Te, plasmon-LO-phonon coupling, IR refl. obs. 80−50335
GaAs:Cr, Te, electron conc. and mobility profiles resulting from Te ion implantation 77−39607
GaAs:Cr (Cr-Te), and undoped, transverse-acoustoelec.-voltage spectroscopy 79−99586
GaAs:Cu, Te, photoelec. props. 80−92936
GaAs:Sn, Te, luminescence props. 79−52017
n-GaAs:Te, 0.93-0.99 eV luminesc. band charact. 78−19560
GaAs:Te, amorphous, ion implanted layers, optical refl., 1.5-7.0 eV 79−8152
GaAs:Te, dislocation-free, TEM study of microdefects 79−82213
GaAs:Te, dopant influence on hardness 77−84777
n-GaAs:Te, elec. cond. and Hall coeff. temp. depend. meas., three band model 79−33287
n-GaAs:Te, electron-irrad., absorpt. spectra *(Russian)* 78−15200
GaAs:Te, epitaxial film, influence of impurities on stacking fault energy 80−103371
GaAs:Te, Ge, compensated, activated cond. 77−76968
n-GaAs:Te, heavily doped, interband luminesc. intensity, heat treatment effect 78−72593
GaAs:Te, heavily doped degenerate semicond., Kondo effect 79−61053
GaAs:Te, heavily-doped, annealing-induced prismatic dislocation loops and elec. changes 78−51546
n-GaAs:Te, homogeneity, IR introscopy investig. 79−15446
GaAs:Te, implanted and laser annealed, surface crystallinity, refl. and channelling meas. 79−95036
GaAs:Te, ion implant depth distribs., AES and glow discharge optical spectroscopy meas. 80−65028

tellurium continued
GaAs:Te, ion implanted, abrupt dopant profile 77−1143
GaAs:Te, ion implanted, laser annealing 79−73192
GaAs:Te, ion implanted, laser annealing, ellipsometric and Hall meas. 79−73193
GaAs:Te, ion implanted, surface crystallinity and stoichiometry of laser annealed samples 79−73198
GaAs:Te, ion implanted, ohmic contacts produced by laser-annealing 79−73585
GaAs:Te, ion implanted optical transitions in modulated reflectivity spectrum 79−73972
GaAs:Te, LPE, Te induced defects, rel. to growth conditions 78−6067
GaAs:Te, laser annealed, donor implanted, elec. props. 79−4556
GaAs:Te, laser annealing of implanted Te 78−35400
GaAs:Te, microcathodoluminesc. of effect of struct. defects on radiative recomb. 79−11475
GaAs:Te, phonon-dislocation interactions, nonstoichiometry effect *(French)* 77−43298
GaAs:Te, powder, quadrupole interactions in NMR spectra 79−51880
GaAs:Te, preferential precipitation on dislocation loops 79−7612
n-GaAs:Te, pure and doped, diffusion of Sn, radiotracer profiles 79−23782
n-GaAs:Te, radiative transitions induced by modest annealing, photoluminesc. spectra 80−55158
GaAs:Te, recombination barrier, dark cond., photocond., and Hall mobility meas. 80−15559
GaAs:Te, solubility and point defect-dopant interactions 79−90687
GaAs:Te, superdilation and defects, lattice parameter meas. and carrier mobility 80−10569
n-GaAs:Te, vibr. props. of 1.0, 1.2 and 1.3 eV luminesc. centres 77−55823
GaAs:Te diffused LED, electron irrad. effect on characts. 80−39667
GaAs:Te influence of fluctuations of impurity pot. on Burstein-Moss effect 78−48240
GaAs:Te Schottky barrier solar cells, diffusion length determ. using minority carrier SEM 80−61359
GaAs:Te substrate, VPE growth, photoluminesc. and emission spectra 80−29774
GaAs:Te^+, ion implanted, laser annealing effect on elec. characts. 79−73195
GaAs:Te-implanted by laser-annealing, ohmic contacts 79−19658
GaAs-Cu:Tl, cathode luminescence spectra, Hall effect, cryst. defects 80−76087
$GaAs_{1-x}P_x$:Te, thermoelectric figure of merit 79−69538
$GaAs_{1-x}P_x$(Te), bound exciton stress depend., piezoluminescence, photoluminescence 80−80206
$GaAs_{1-x}Sb_x$:Te, LPE and elec. props. 77−55896
$Ga_xIn_{1-x}As_{1-y}P_y$:Te, epitaxial film, elec. and optical props. 79−11251
GaN-Te contact, using GaN made by oxidation and subsequent nitridation of GaAs, I-V characts. 77−20436
GaP, impurity behaviour during crystallisation from melt 77−84772
GaP:Ae,C(Mg), donor-acceptor pair luminesc., excitation spectroscopy 80−25440
GaP:N(Te), ion implanted at 40 keV, refl. spectra, 210-2000 nm, annealing *(Russian)* 78−80386
GaP:S, Se, Te, Si, shallow donors, excitation spectra 77−81128
GaP:Te, defects formed due to precipitation of Te, metallography and TEM exam. 77−84769
n-GaP:Te, doping parameters calc., by means of Hall data analysis 78−51925
GaP:Te, ENDOR meas., hyperfine interactions and elec. field gradient 79−42869
GaP:Te, Hall effect and elec. cond., 80-400K 78−91705
n-GaP:Te, IR absorpt. cross-section 79−38582
GaP:Te, IR lattice band profile, electron spin reversion in mag. field, Nf-R curve 79−28771
GaP:Te, IR photocond. response spectra 79−56257
n-GaP:Te, LPE layers, Hall effect 78−91704
GaP:Te, photostimulation spectra, bound electron phonon interactions *(Russian)* 77−1712
GaP:Te, pot.-depend. g-values and quenched diamag., props. of donor states 77−62861
GaP:Te, pot.-depend. g-values and quenched diamag., pseudoacceptors D^0, X 77−62862
GaP:Te, VPE grown layers, precision lattice parameter determination 80−24429
GaP:Te epitaxial layers, dopant distrib. obs. by amalgam polarography 77−39609
GaP:Te on GaAs, LPE growth fron Sn, exam. of impurity band conduction effects 79−11249
GaP:Zn, Te, epitaxial layers, determ. of Zn conc. 79−77614
GaSb:Te, carrier density dependence on impurity conc., rel. to solubility limit 77−8047
p-GaSb:Te, effective radiative recombination centre nature, photoluminescence spectra 79−90998
n-GaSb:Te, elec. transport mechanism in cond. band from Hall mobility and transverse mangetoresist. meas. 79−73531
n-GaSb:Te, epitaxial, IR refl. meas., carrier conc. and mobility determ. 80−80769
n-GaSb:Te, forbidden optical band gap, Moss-Burstein effect 78−88335
n-GaSb:Te, Hall coeff., carrier conc. and mobility, elec. cond., 290 to 550K *(Russian)* 79−19604
n-GaSb:Te, heavily doped, spontaneous radiative recomb. vel., photoluminesc. spectra 79−11458
GaSb:Te, indirect gap photolum. 80−29797
GaSb:Te, thermal sensitivity, −170 to +180°C, resist. meas. 77−39906
GaSb:Te,Zn(Te,Mn), prep. and electrophys. props. 79−87116
Ge:Te, ion-implanted, thermally assisted Xe-flash annealing, Rutherford backscatt. meas. 79−10881
Ge:Te^+, ion implanted, alignment of irrad. induced defects, TEM obs. 80−15168
Ge-Si:Te, solid solns., donor states energy spectrum 80−88516
InAS:Zn,Te, exam. of microhardness, Hall effect as function of dopant 79−95038
N-InAs, Moss-Burstein effect, S, Sn, Te dopants 78−64389
InAs:Cd,Te interaction between impurities, effect on elec. props., Hall effect. 80−19832
n-InAs:Te, heavily doped, cathodoluminescence, doping effect on luminesc. band position and spectral profile 80−45153
InAs:Te,Cd, donor-acceptor interaction, elec. cond. and Hall coeff. meas. 80−59988

tellurium continued
InAs:Te(Se)(S), intrinsic pt. struct. defects 80−33998
InGaAsP:Te, LPE growth, influence of growth-solution dopants on distrib. coeffs. 79−47640
$In_{1-x}Ga_xP$:Te, composition depend. of bound state luminesc. transitions 78−39595
$In_{1-x}Ga_xP$:Te,Zn, photolum. and electrolum., direct transition region 77−8659
InP:Te, dislocation-free, TEM study of microdefects 79−82213
InP:Te, mag. props. of conduction electrons 78−6510
InP:Te, powder, quadrupole interactions in NMR spectra 79−51880
InP:Te, quadrupole struct. of NMR line 80−20505
InP:Te(S), heavily doped, dislocation imaging using transmission cathodoluminesc. 80−29023
InSb:Te, anomalous impurity segregation Hall and mass spectrum meas. *(Chinese)* 80−59501
InSb:Te, cryst. growth from melt, pulling method, US effects on facet growth 80−76169
InSb:Te, Czochralski cryst. growth, strain configuration study using X-ray anomalous transmission topography 79−23552
n-InSb:Te, drift tunnel diode, prod., current ratio meas. *(Russian)* 77−8185
InSb:Te, heavily doped degenerate semicond., Kondo effect 79−61053
n-InSb:Te, Moss-Burstein effect, optical energy gap depend. on doping conc. 77−8581
InSb:Te, periodically laminated plasma, 56.5 GHz transmission, helicon diagrams *(German)* 77−20348
InSb:Te, reson. states and reson. scatt. 80−49738
InSb-NiSb, eutectic alloy, Te-doped, electrophys. props. 77−35955
KBr:Tl^-, Jahn-Teller split luminesc., high press. study 78−52565
Li ions stopping power and straggling 80−42908
liquid, elec. cond. at high temps. and press. 77−55592
Nb-Te-Pb Josephson junctions, prep. and props. 80−65754
Pb-Te-Pb Josephson junction, cavity resonances 78−84352
Pb-Te-Te oxide-Pb Josephson junctions, prep. and props. 80−65754
PbTe-Te, contact fusion in complex metallic systems 78−26664
Sb:Te, de Haas-van Alphen effect, effective mass, Fermi levels 78−75982
Sb:Te vapour saturation, diffusion zone struct. crystallisation orientation *(Russian)* 80−54438
Se, atom positions, effect of press. 78−34465
Se:Te, amorphous, conductivity and activation energy depend. on dopant conc. 77−69325
Se:Te, amorphous, negative magnetoresist., doping depend. 78−56161
Se:Te, amorphous, pure and doped, freq. depend. of elec. cond., 150 to 310K 79−42545
Se:Te, liq., viscosity, impurity effect, chain length role *(French)* 78−51717
Se:Te multilayer solar cell 79−43762
Se:Te(Ag), amorphous film, elec. cond., 300 to 350K, transition 77−4454
Si:P,Te, impurity implantation effect on CESR, spin-orbit interactions 77−36133
Si:Te, implanted impurity location, Mossbauer and channelling expts. 80−39128
Si:Te, ion implanted, annealing of heavy ion cascade damage, channelling meas. 80−89255
Si:Te, ion implanted, laser annealed, lattice location of Te 78−67725
Si:Te, laser melting, surface Te atom accumulation, profiles 80−100258
Si:Te, Mossbauer spectra of ^{119}Sn defect struct. 80−97175
Si:Te implanted, laser annealing, Mossbauer obs. 80−39127
Si-Te, laser and thermal annealing, Mossbauer resonance lines 79−99810
α-Sn:Te, implanted, impurity-defect structs., Mossbauer expts. 80−39129
Sn/Te/electrolyte system, interface processes 77−63923
SnTe-Te, contact fusion in complex metallic systems 78−26664
T-metal, thin film contact, time evolution of photovoltaic effect 80−65687
TE, small-ang. X-ray scatt., at. microgrouping depend. *(Russian)* 78−14271
Te, A1 type, supercond. destruction by mag. field 78−91825
Te and U/Te thin film junctions, combined electron, proton and X-ray beam obs. 77−85041
Te, elastic and piezoelec. consts., US phase vel. meas. 79−86834
Te, hole susceptibility anisotropy, spin contrib. and total 77−85413
Te I, UV line rel. oscill. strengths and unexcited atom conc., AAS meas. *(Russian)* 78−31749
Te II, vis. spectral lines, relative isotope shifts 78−37579
Te IV, radiative lifetimes, calcs. and beam-foil spectra 77−75223
Te lattice distortion and p-orbital bands 77−89405
Te, Te cpds., Auger spectra 78−58638
Te, trigonal, electronic struct., near metal transition, press. depend. 78−34758
Te VII, $4d^95d$ config., UV spectrosc. obs. 80−18817
Te VII, $4d^95s$-$4d^95p$ transitions, UV spectra 79−93942
Te VII, $4d^96s$ configuration spectrum obs., line identifications 80−106289
Te VII, spectra, ionisation limits 79−54794
Te VIII, $4d^85s$, $4d^85p$ and $4d^54d^{10}$ config. spectrum obs., line indentifications 80−106289
Te VIII, $4d^9$-$4d^85p$ transitions, spectra, least squares calcs., Hartree Fock calcs. 79−54794
Te^-, photodetachment cross-section meas., crossed beam expt. 77−61723
Te:^{111}Cd, quad. interac. temp. depend. 77−63324
Te:^{125}Te, PAC, quad. moment of $9/2^-$, 321 keV level of $_{52}{}^{125}Te_{73}$ 77−28488
Te:Cu films, elec. transport props. 80−60120
Te:I, semicond., elec. efficiency *(German)* 78−84166
Te:Sb, 96 to 500K, cond. Hall const., hole mobility, conc., dislocation effects *(Russian)* 78−64039
Te:Sb, impurity states and impurity conduction, hydrostatic pressure 80−39521
Te:Sb, surface carrier effects on Hall mobility at low temp. 77−80794
Te/Ag double films, interdiffusion and struct. modifications *(French)* 77−62682
Te-Ag thin film system, stress-relief appearance conditions 80−65416
Te-Au thin film interface, evolution, switching effects *(French)* 80−6660
Te-barium stearate-Te structs., internal voltage work function meas. 79−82684
Te-Bi, thin film system, stress-relief appearance conditions 80−65416

tellurium continued
Te-CdS-In contacts, ohmic nature, monitoring method 77−39935
Te-CdS-Te contacts, ohmic nature, monitoring method 77−39935
Te-Se-Cd, sandwich structure, fabrication and characteristics 80−60089
Te-Se-Cd rectifying sandwich structs., elec. forming action, Schottky junction form. 80−80371
Te-Se-CdO struct., fabrication and charact. 78−76106
Te+Cd, π^- capture, radioactivity meas. 80−47831
Te+H_2(HD)(D_2), intramultiplet transitions 77−54597
Te+LiH exothermic solid-state reaction, ion backscatt. obs. 78−20064
$Te^{24+}+I^{25+}$, correlation diagrams, inner-shell vacancy prod., characteristic X-rays 77−83503
Te_2, $B0_u^+-b^1\Sigma_g^+$ system, transition assignment, IR and visible spectra obs. 80−58298
Te_2, laser excited fluoresc. Fourier transform spectrosc. obs., isotope effects 79−59504
Te_2, laser induced fluoresc. in inert gas matrix 80−87161
Te_2, optically pumped CW dimer lasers 80−14322
Te_2, optically pumped continuous laser oscill., 550 to 660 nm 79−933
Te_{2s} yap., $M_{4,5}N_{4,5}N_{4,5}$ Auger electron spectra 79−50089
Te_4^{2+}, pseudopot. SCF-MO calcs., spectrum assignments 80−83269
Te_8 ring in zeolites, identification by Raman scatt. *(Russian)* 79−61378
Te_n, small aggregate, metallic character 78−86985
Te^- ($^2P_{1/2,3/2}$)+hν, Te electron affinity, Te^- fine struct. interval 77−79590
Te($^3P_1$)+inert gas, gas phase flash photolytic deexcitation obs., 1000K *(Russian)* 78−50626
Te($^3P_1$)+Te_2, gas phase flash photolytic deexcitation obs., 1000K *(Russian)* 78−50626
^{52}Te, L$\gamma_{2,3}$ X-ray emission spectra, line breadth 78−62760
^{122}Te on Au target fabrication for cyclotron isotope prod. 77−83406
^{125}Te, KLM- and KLN-Auger transitions 77−18884
^{132}Te, fission product, sequential cation-exchange separation from neutron irrad. U_3O_8 77−90898
^{132}Te in lower troposphere, airborne levels and lifetime 79−12242
^{132}Te, volatile fission product, diffusion in Mo, 1400-2000K *(Russian)* 78−91485
^{123m}Te-labelled adrenal-imaging agents, radiation dosimetry 80−101268
Tm^{3+}, in oxide glasses, multiphonon relax. rates and fluoresc. lifetimes 77−77266
Zn_3As_2:Te, single crysts., gas phase growth, elec. props. 79−15598
ZnS:Te, luminesc., exciton struct. 79−33801
ZnS:Te, single crysts. grown from Te soln., photolum. props. 79−52005
ZnS:Te phosphors, luminesc. excitation spectra and exciton struct. 80−55165

tellurium alloys
see also tellurium compounds
melting entropy and molar specific heat 79−29024
steel, low C, type AISI 1010, effect of Se, Te additions on fatigue props. 78−92359
steel, stainless, Cs enhanced corrosion, Te influence 78−23866
Ag-Te, liq., struct. and elec. props. 80−49083
Ag-Te, liquid alloys, Ag_2Te solid compound, calorimetric, investigation at high temp. 79−61893
Ag-Te amorphous films, effect of annealing on elec. resist., phase transitions 79−11241
Ag-Zn-Te(-Sn)(-In), internally oxidised, oxide particle size control *(Japanese)* 80−89480
Au-Te, charge-transfer and valence-band behaviour using ^{197}Au Mossbauer and X-ray photoemission spectra 79−60695
Au-Te, elec. field gradients and charge transfer, Mossbauer spectra 80−25268
Au-Te, liq. alloys, ΔG^E of mixing from ht. of melting of sp. ht. of cpds. 77−4920
Au-Te, thermodynamic props., calorimetric meas. 78−20051
$AuTe_2$, core-level binding energy shifts and charge transfer 80−25268
Bi-Sb-Te melt, Sb and Te distribution coeffs. during crystallisation *(Russian)* 80−93472
Bi-Te, dil., superconductivity, resist. obs. 78−64160
Bi-Te, dil. alloy, elec. cond. depend. on Te conc. *(Russian)* 78−76042
Bi-Te, dilute, oxidation kinetics 80−25914
Bi-Te, electron isoenergetic surface, variation of connectivity under press. *(Russian)* 78−60050
Bi_2Te_3 alloy thermocouples for solar thermoelectric conversion 80−94095
Cr_5Te_6, magnetoresist. in region of mag. phase transforms. *(Russian)* 77−66299
Cu-Ge-Te system, DTA, crystallographic and metallographic analysis *(French)* 77−25019
Cu-Sn-Te system, phase diagram exam. *(French)* 77−21107
Cu-Te, liq., struct. and elec. props. 80−49083
Fe, cast, fused metal solidification enhancement using Bi and Te *(Italian)* 80−7540
Fe-Ni-Te alloy system, first-order phase transformation obs. 78−64533
Fe-Ni-Te alloys, magnetisation 79−7975
FeNiTe alloys, disordered, polycrystalline, elec. resist., temp. depend. 80−49692
$FeTe_2$, Mossbauer spectroscopy and nonstoichiometry 78−31125
$Fe_{1.2}$Te-MnTe phase relations in presence of excess Fe 77−52292
Ga-Te, alloys, liq., thermodynamic functions, struct. 78−40075
Ga-Te, liq., compressibility and US velocity meas. 77−51426
Ga-Te, liq., mag. susceptibility 77−51881
Ga-Te, solid and liq., thermodynamic props. 80−35567
Ge-Te, As-Te, Ge-As-Te molten system, metal-semicond. transition, cond. obs. *(German)* 77−1457
Ge-Te, liq. alloy, heat of formation, 1030-1150K 77−1943
Ge-Te alloy, liq., magnetic susceptibility 79−87232
Hg-Cd-Te, partial vapour pressure, determ. for volatile component by static method 80−37150
In-Te, elec. field gradient, at ^{111}Cd probes, temp. depend. 79−28643
In-Te, liq., atomic struct., X-ray diffr. meas. 79−41934
In-Te, liq., mag. susceptibility 77−51881
In-Te, liq., nucl. spin relax. of ^{117}Sb 77−52004
In-Te, molten thermodynamic props. determ. by EMF method 77−51504
Li-Te alloys, liq., electrochem. investig. of thermodynamic props. 77−1244
Na-Te, liq., chemical pot. and resist. 77−55232
Na-Te system, liq., electrochem. determ. of thermodynamic props. rel. to temp. 77−1245
Ni-Te, liq., struct. and elec. props. 80−49083

tellurium alloys continued
$Ni_{3\pm x}Te_2$, long period superstructs. rel. to partial ordering, electron diffr. 79−51056
Pb-Sb-Te-Cu-Sn, influence of specimen and grain size on mech. props. *(Russian)* 77−81297
Pb-Sn-Te, liquidus meas. by DTA 79−95999
$Pb_{1-c}Te_c$, liquid alloys, local fluctuations and quadrupolar relaxation 80−66060
Pd-Te liquid alloys, thermodynamic activities *(German)* 79−29022
PdTe-Rh, dil, quadrupole interaction of ^{100}Rh 79−99520
$PdTe_2$, bandstructure, Fermi surface, LMTO method 78−6264
$Pd_{20}Te_7$, cryst. struct. determ. *(German)* 77−19905
$Pd_{75}Te_{25}$, ordered BCC phases at high temp. 79−32948
Pd_9Te_4, cryst. struct. and binding *(German)* 78−51471
Sb-Te, A1-type, superconductivity 80−29496
Sb-Te-Bi, miscibility limits, computer study 78−79773
Se-Te, liq., localised impurity states, mag. susceptibility of Co and Mn solutes 77−51882
Se-Te, new material for granule microphone 79−3878
SeTe liquid alloy, effect of branched chain polymers on bond equilib. 80−24348
Sn-In-Te system, SnTe based solid solns. formation 77−84929
Sn-Te, molten, elec. cond. and phase diagram 80−84454
Sn-Te alloy, liq., magnetic susceptibility 79−87232
Sn-Te liquid alloy, thermodynamic meas. 77−73271
Te-Ag, dil. liq. alloy, elec. cond. at high temp. and press. 78−87959
Te-Au, dil. liq. alloy, elec. cond. at high temp. and press. 78−87959
Te-Au film, metastable supercond. alloys, produced by low temp. ion implantation 80−88670
Te-Au film, supercond. by ion irrad. 80−34544
Te-Co, dil. liq. alloy, elec. cond. at high temp. and press. 78−87959
Te-Cr, dil. liq. alloy, elec. cond. at high temp. and press. 78−87959
Te-Ge eutectic alloy, glassy, crystn. mechanism 78−22836
Te-In alloys, direct reaction calorimetric study, 737 to 1340K *(French)* 80−49382
Te-In system, enthalpies of fusion, peritectic decomp. and allotropic transition, DTA *(French)* 80−76226
Te-Pb, amorphous, obtained by splat cooling, crystallisation, TEM obs. 77−66638
Te-Pb (20 at.%), amorphous, obtained by rapid cooling from liq. state, crystn. behaviour 78−26445
Te-Sb, liq., elec. cond. 78−84186
Te-Sb(Bi), liq., diamag. susceptibility, semicond./metal behaviour 78−14927
Te-Se liq. semicond., resist. meas. under high press. 77−51791
Te-Sn (20 at.%), amorphous, exam. of crystallisation by DTA, X-ray diffr. and TEM 78−47242
Te-Tl, eutectic liquid alloy, structural features, interatomic interaction *(Russian)* 79−77494
Te-Tl, liquid alloy, thermodynamic investigation, enthalpy of form. and phase diagram 77−59756
Te-Tl, thermodynamic investigation, equilibrium diagram calc. 79−34007
Te-Tl liq. systems, thermodiffusion of Tl 77−11717
Te-Tl system, thermodynamic investigation, enthalpy of form. at elev. temps. 78−52774
Te-transition metal, liq. semicond., elec. props. 80−96870
Te-transition metal, liquid, dil., elec. resist., cond. electron conc. 77−15814
TeSn, ^{115}Te elec. quadrupole interaction, temp. depend. 78−19399
Tl-Te, liq., atomic struct., X-ray diffr. meas. 79−41934
Tl-Te, liq. alloys, mag. susceptibility 77−51880
Tl-Te, liquid alloy, miscibility gap 79−10952
Tl-Te alloy, liq., bond equilib. theory for electronic props., thermochemistry 77−89365
Tl-Te liq. semicond., resist. meas. under high press. 77−51791
Tl-Te system melts, conc. depend. of surface tension 79−37904

tellurium compounds
see also tellurium alloys
antiferroelectrics with perovskite structure, synthesis and charact. 77−55758
binary, with non-transition elements, at. vol. and semicond. props. 77−20089
chalcogenides, ternary, glass transition temp. predictions 78−38823
chemical bonding in group V and VI elements and compounds with tetradymite structure 80−15036
dihalides, and organometallics, ^{125}Te, ^{13}C, ^{1}H NMR spectra, nucl. coupling, exchange processes 79−95658
electron spectroscopic studies *(French)* 80−108770
eutectics, Te-based, crystn. rate effect on electrophys. props. mutual solubility effect 80−60774
halides, UV photoelectron spectra of valence d shells, gas-phase 78−62845
halides, Wasastjerna pot. function, force consts., internuclear separations and binding energies 80−14187
inorganic, chemical bonds using Kα_1 line chem. shifts, Mossbauer isomer shifts 77−27089
NMR, orbital chemical shift of ^{125}Te, depend. on ionicity and local struct. 77−32273
tellurite glass, Cu^{2+} and Ni^{2+} doped, band-pass filters for 550 to 616 nm, transmission characts. 78−71166
tellurite glass film waveguide, Bragg electrostriction, power balance approach 77−75660
tellurite glasses: Ho^{3+}, nonradiative relax. 77−24881
tellurite glasses, binary, struct. and props. *(Japanese)* 79−32917
thiourea compounds, Mossbauer investig. of ^{129}I, quadrupole interactions and bonding 77−48111
X-ray photoemission, core level binding energy shifts rel. to Mossbauer isomer shifts 78−2984
Ag-As-Te glasses, elec. props. *(Russian)* 77−85211
Ag-As-Te system, vitrification region, physiochem. props. 79−41960
Ag-Ge-Te system, chalcogenide, phase equilibria and diagrams *(German)* 80−108418
Ag-Te-O, partial pressure diagrams 77−36681
$Ag_{19}Sb_{29}Te_{52}$, single-phase, thermoelectric efficiency 80−107826
$Al_{23}Te_{77}$ glasses, crystallization 79−51000
As-Ge-Te, chalcogenide glass, elec. cond. and dielec. const. 80−75567
As-Ge-Te glass, dielectric meas. 79−87382
As-S-Te, vitreous semiconductor, photoconductivity *(Russian)* 79−11172

tellurium compounds continued
As-S-Te, vitrification, density and elec. cond. measurements 79−7645
As-Se-Te, amorphous, electron and hole drift mobilities 80−34442
As-Se-Te glass, effect of Ag electrodiffusion on volt-ampere characteristics 79−7869
As-Se-Te glasses, electron transport props. 78−10439
As-Se-Te system glasses, AC cond. and permittivity, freq. and temp. depend. 77−76857
As-Se(Te)-Ge, fabrication of amorphous semicond. thin films with graded band struct. *(Japanese)* 77−55623
As-Te system glasses, DC and AC cond., thermo-EMF, 140 to 350K 79−42549
As-Te-Cu system glasses, DC and AC cond., thermo-EMF, freq. depend., 100 to 370K 77−76827
As-Te-Cu(Ag) system glasses, absorpt. coeff. and optical band gap 79−65829
As-Te-Ga, glass, elec. cond., 190-300K *(Russian)* 80−54702
As-Te-Ga system, glass-forming region and props. 80−25674
As-Te-Ge chalcogenide films, thermally induced transformations, TEM obs. 79−94917
As-Te-Ge system glasses, thin films, effect of S, Se, Sb, Bi, Tl on volt-ampere characts. 77−15976
As-Te-Ge/n-Si, film on cryst., heterojunction, elec. and photovolt. props. 80−100514
As-Te-Ge-Si, amorphous film, high-speed switching mechanism 77−8153
As-Te-Ge-Si sandwich type amorphous films with metal electrodes, space-charge-limited switching, pre-breakdown characts. *(Japanese)* 77−69385
As-Te-In, glass-forming, density and microhardness 80−103257
As-Te-Si-Ge amorphous chalcogenide semiconductor, thin film interface, electrical charact. *(Korean)* 80−97014
$As_{10}Ge_{15}Te_{75}$, glass, cond. and switching characts. 77−32054
$As_{10}Ge_{15}Te_{75}$:Ag glasses, elec. props. 79−91045
$As_{25}Ge_{10}Te_{65}$, chalcogenide glasses, dielectric relaxation 80−55027
$As_xGe_{10}Te_{90-x}$ glass, cond. and dielec. const. from 77 to 383K and from DC freq. to 5 MHz 79−23964
$As_{10}Ge_{15}Te_{75}Ag_x$ glass, elec. and dielec. props., Ag additions effect 80−65558
$AsS_{3.5}Te_{2.0}$ glass, gamma-irradiated, TSC meas. 77−66166
$As_2(Se,Te)_3$ glasses, X-ray absorption and photoelectron spectroscopy study 80−7463
$(As_2Se_3)_{1-x}(As_2Te_3)_x$ amorphous films, changes in optical props. under elec. fields and optical excitation 79−61455
$AsSe_{1.5-x}Te_x$ glasses, physical props. 78−68028
$As_2Se_xTe_{3-x}$ chalcogenide glasses, cond. meas., field strength and temp. depend. 78−84225
$As_{60}Se_xTe_{40-x}$ glasses, crystallisation 77−35488
$As_{25}Te_{75}$, and $As_{45}Te_{55}$, vitreous, local struct., elec. field gradient tensor asymmetry obs. 79−73847
$As_{50}Te_{50}$, amorphous films, metal and semicond. contacts, threshold switching, IR emission 80−49831
$As_{50}Te_{50}$ amorphous switches, light emission charact. 79−78139
$As_{50}Te_{50}$ glass, thermal cond., 100-500K, and sp. ht., 373-600K 77−20138
$AsTeCu_x$ ($0 \leq x \leq 0.4$) glass, effect of Cu on elec. cond. and thermoelectricity, 100 to 370K 78−87978
$As_{10}Te_{75}Ge_{15}$, dielec. props. 77−63355
$(As_2Te_3)_{1-x}Ge_x$, amorphous, AC cond. magnitude and variation *(French)* 79−47095
$As_{45}Te_{40}Ge_{15}$, amorphous, elec. cond. at room temp., contact effect 77−20354
$As_xTe_{90-x}Ge_{10}$, $As_{35}Te_{55}Ge_{10-x}Si_x$ glasses, elec. and optical props., comp. depend. 77−24555
$As_{35}Te_{28}Ge_{16}S_{21}$, chalcogenide semiconductor study of electric properties *(French)* 80−29414
$As_{0.3}Te_{0.48}Ge_{0.1}Si_{0.12}$, amorphous film, transient switching processes 78−84232
$As_4Te_5Ge(Si)$ glass, struct. changes, Mn^{2+} EPR expts. 78−79534
$As_xTe_xS_xSe_{100-3x}$ glasses, IR absorpt. spectra 77−12378
$AsTeS_x(Se_x)(Sb_x)(Bi_x)$, chalcogenide glass, thin film crystallisation 79−7758
$As_{30}Te_{48}Si_{12}Ge_{10}$, chalcogenide glass film, charge screening length 79−23974
Au-Ge-Te ternary system, solid soln. in vicinity of GeTe, phase diagram *(French)* 77−85994
AuTeI, cryst. struct. 78−51504
Ba-Te system, phase diagram 77−36472
$BaTe_2O_6$, X-ray cryst. struct., O_2 coordination no. of Te *(German)* 79−69075
$Bi_{88}Sb_{12}Te_{0.05}$, helicon dispersion, effect of slope of electron ellipsoids 79−28365
BiTeI-SbTeI solid solns., form., crystn., elec., thermal props. 78−44003
$Bi_{1-x}Te_xO_{3/2+x/2}$, solid solutions, phase transformations, dielectric and differential microcalorimetry *(French)* 79−55886
$Bi_2Te_{2.7}Se_{0.3}$, magnetoresistance and Hall EMF meas., using AM method 80−52278
n-$Bi_2Te_{2.88}Se_{0.12}$, extrusion deformed, powder dispersion degree influence on thermal and elec. props. *(Russian)* 80−39366
$Bi_2Te_{3-x}Se_x$ films, surface band struct. and scatt. mechanism 80−34535
$CaTe_3O_8$ (carlfriesite), cryst. struct., chemical formula revision, and synthesis 79−55709
Cd-Te-Ge system, CdTe-Ge cross section 77−52298
$CdO\text{-}TeO_2$ system, partial phase diagrams 78−84784
$CdTeMoO_6$, prep. and cryst. struct., X-ray diffr. obs. 79−1414
$CuIn_{1-y}Ga_ySe_{2(1-x)}Te_{2x}$ pentenary alloy compounds for photovoltaic solar energy conversion 80−93971
CuTeX (X=Cl, Br, I), solid ionic cond., props. 79−14963
$Er_2O_3\text{-}TiO_2\text{-}WO_3\text{-}PbO$, glass form., refr. indices and density meas. 77−90312
$FeBr_2$, transient species, He(I) photoelectron spectrosc. calcs., relativistic corrections 80−95677
Fe_2TeO_5, mag. struct. 78−27020
Ga-Ge-Te system, GaGeTe formation, peritectic decomp. and struct. *(French)* 77−85995
Ga-Te liquid alloys, mag. susceptibility 77−59383
$Ga_2As_{49}Te_{49}$ glassy film, nonlinear current voltage characts., Poole-Frenkel effect 80−7007
$Ga_2O_3\text{-}TeO_2$, phas diag. 77−81252
$Ga_{20}Te_{80}$, amorphous, splat cooled, thermoelectric props. 78−43426
Ge-As-Te, thin chalcogenide glass film, high-field switching effects 77−32052
Ge-As-Te glass, between metal electrodes, contact props. determ. 79−7908
Ge-As-Te glass, thermoelec. power and DC cond., temp. depend. 77−62955
Ge-As-Te system, glasses, magnetochemical exam. 78−88092
Ge-Se-Te amorphous alloys, prep. and calorimetric obs. 77−11675
Ge-Te, exam. of new compound, using light microscopy and X-ray diffr. exam. 78−48383
Ge-Te alloy films, amorphous, semicond. props., refr. index, struct. study 78−26978
Ge-Te and Ge-Te-As system glasses, local struct., ^{119}Sn Mossbauer obs. 79−41968
Ge-Te film, electrical switching 77−4411
Ge-Te system, phase equil. diagram, $GeTe_{1\pm x}$ region analysis by metallography, microhardness and DTA *(French)* 77−70034
Ge-Te-As-In quaternary compounds, elec. resist. of thin sheets, Mott's theory *(Spanish)* 77−69320
Ge-Te-As-In quaternary compounds, elec. props., Hall effect *(Spanish)* 77−69344
Ge-Te-As-In quaternary compounds, thin sheets elec. props., thermoelec. power *(Spanish)* 77−69358
Ge-Te-Se/Si amorphous film-cryst. heterojunction, electron-beam-induced current 79−24060
$Ge_{33}As_{27}S_{15}Te_{25}$ glass, switching, microstructural changes 79−65523
$Ge_{10}As_xTe_{90-x}$ glass, thermal cond., 100-500K, and sp. ht., 373-600K 77−20138
$Ge_{15}As_4Te_{81}$ glassy film, nonlinear current voltage characts., Poole-Frenkel effect 80−7007
$Ge_{10}As_{40}Te_{40}I_{10}$, chalcogenide glass film, switching delay time 78−26926
$Ge_{30}As_{17}Te_{30}Se_{23}$, antireflection coating for KCl, design, prep. and performance 79−14063
$Ge_{30}As_{17}Te_{30}Se_{23}\text{-}As_2S_3$, two-layer antirefl. coating, error considerations in design 80−74477
$Ge_xAs_xTe_xSe_{100-3x}$, glassy, IR absorpt. spectra 78−23448
$Ge_{20}Se_{40}Te_{40}$ amorphous alloys, thermal crystn. study 78−26789
$Ge_3Se_2Te_4$ film, chalcogenide glass, freq. depend. of Hall effect 77−1436
$(Ge_{0.32}Se_{0.32}Te_{0.32}As_{0.4})_{100-x}Ni_x$, ESR, rel. to elec. cond. 80−7155
$Ge_{10}Si_{12}As_{30}Te_{48}$, monostable chalcogenide glass threshold switch, temp. meas. *(German)* 77−4412
$Ge_7Si_9As_{39}Te_{35}Ga_{10}$, chalcogenide thin films, coupled carrier theory test, high field conditions 80−100466
$Ge_{0.5}Te_{0.5}$, heat capacity in solid and liq. phases, enthalpy of form. *(French)* 80−35565
$Ge_{1-x}Te_x$, amorphous, localised gap states, variable range hopping 77−72866
$Ge_{15}Te_{85}$, amorphous, splat cooled, thermoelectric props. 78−43426
Ge_xTe_{1-x}, amorphous, struct., quadrupole splitting of $^3/_2$ spin state of ^{125}Te calc. 77−65950
$Ge_{13.3}Te_{61.7}As_{19}$ film, amorphous, characts. of optical switching 78−18031
$Ge_{15}Te_{81}As_4$ film, amorphous, characts. of optical switching 78−18031
$Ge_{15}Te_{81}As_4$, influence of O_2 on phase separation of chalcogenide glasses 77−47354
$Ge_xTe_xS_xSe_{100-3x}$ glass, IR absorpt. spectra 77−12378
$Ge_{15}Te_{81}Sb_2S_2$ film, amorphous, characts. of optical switching 78−18031
$Ge_{15}Te_{81}Sb_2Se_2$, glassy and liq. states, elec. cond. freq. depend. 77−76856
$Ge_{20}Te_2Se_{80-x}Si$, amorphous-cryst. heterojunctions 79−65546
HgCdTe, ion implantation, junction form. 80−100260
$Hg_{1-x}Cd_xTe$ 0.1 eV, thermal conductivity meas. 77−24578
HgTe, Γ_8 symm. acceptor centre hole mag. props. *(Russian)* 80−88733
In-Te liquid alloys, mag. susceptibility 77−59383
In-Te system, thermodynamic props. 77−12821
$In_2O_3\text{-}TeO_2$, phase diag. 77−81252
$In_{20}Te_{80}$, amorphous, splat cooled, thermoelectric props. 78−43426
$MgTeMoO_6$, prep., cryst. struct., and catalytic props. 80−108709
$xMnO.(100-x)[19TeO_2.PbO]$, EPR studies of Mn^{2+} ion distribution 80−71167
Mn_2TeO_6, magnetic structure, stability of mag. modes, neutron diffraction study *(French)* 80−39744
$(NH_4)_2Te_2O_5.2H_2O$, crystal structure determination 78−91317
$Na_2O\text{-}TeO_2\text{:}Ho^{3+}(Er^{3+})(Yb^{3+})$ glass, luminesc. quenching by OH and OD *(Russian)* 79−28839
$Na_3Te_2Fe_3O_{12}$, neutron diffr. patterns, group theory approach for determ. of mag. struct. *(Russian)* 79−51749
P-Se-Te system glasses, mag. susceptibility and opt. props. 80−25079
Pb-Te-O, thermal stability 78−44104
PbO/TeO_2 system, central region of phase diagram, X-ray and thermal anal. 79−70046
$Pb_{1-x}Sn_xTe$, photoconduct., photoelectromag. effect, laser intensity depend., carrier lifetimes 77−15896
$Pb_{1-x}Sn_xTe$:Ge, anomalous behaviour of impurity centres under press. *(Russian)* 80−65491
PbTe N-type, TE figure of merit, integral form 77−24577
S-Se-Te semicond. glasses, mag. suscept. meas., refractive index 78−34952
S-Te, liquid semicond., bonding energies and entropies, mag. susceptibility meas. 80−49082
Sb-Te-Bi, computer study of miscibility limits, 273 to 300K 78−52781
Se-Ge-Te, chalcogenide glass, elec. cond. and dielec. const. 80−75567
Se-Ge-Te glass, dielectric meas. 79−87382
Se-Te, liq., electronic props., mag. susceptibility meas. 79−95567
Se-Te crystallised glasses, struct. transforms. and IR spectra 80−19712
Se-Te film, evaporated, drift mobility of holes, elec. field and comp. depend. 77−39977
Se-Te solid solutions, ordering, diffuse X-ray scatt. 77−65965
Se-Te whisker crystals, growth 79−99464
Se-Te-As-Ge glasses, absorpt. spectra, diffuse reflectivity loss correction 79−82995
Se-Te-As-Ge glasses, elec. transport 79−60833
Se-Te-Ge, amorphous, off-state thermal switching 79−65524
Se-Te-Ge system, amorphous, electrical transport, activation energy 79−95406
Se-Te-Sb glasses, electronic transport 80−88579
$Se_{90}\text{-}Te_{10}$ alloy crystals, growth and cleavage 78−88421
$Se_{0.95}Te_{0.05}$, glass crystallisation, effect of an alternating electric field 80−88054
$Se_{1-x1}Te_{x1}\text{-}Se_{1-x2}Te_{x2}$ heterostructure, amorphous, rectification phenomena and photovoltaic effects 79−99610
$Se_{1-x}Te_x$, amorphous, optical and elec. props. 80−84506

tellurium compounds continued
$Se_{1-x}Te_x$, amorphous film, photo-crystallisation 80−59839
$Se_{1-x}Te_x$ amorphous films, sublinear and superlinear I-V charact. 79−82695
$Se_{1-x}Te_x$, film, struct. and props. 79−99079
$Se_{1-x}Te_x$ systems, amorphous and liq. states, short range order, neutron scatt. study 80−49124
$Se_{90}Te_{10}$ whiskers, chem. and thermal etching 77−15417
Se_xTe_{1-x}, acoustoelectric current saturation 80−60053
Se_xTe_{1-x}, amorphous, structural relaxation and crystallisation kinetics study by DTA 80−59394
Se_xTe_{1-x}, growth of single crystals by Czochralski method 80−66423
Se_xTe_{1-x}, liq., thermoelec. transport at mobility edge 80−49787
Se_xTe_{1-x} melt, densities and surface tensions 79−86831
$Se_{12}Te_{49}As_{29}Ge_{10}$ semiconductor amorphous films, field effect, trapping 80−84472
$Se_{60}Te_{30}Ge_{10}$, amorphous, neg. magnetoresist. 79−51603
Si-As-Te glass, thermoelec. power and DC cond., temp. depend. 77−62955
Si-As-Te glasses, crystallisation kinetics under influence of water vapour 78−59762
Si-Te structural changes rel. to memory effect *(Russian)* 78−71679
Si-Te system, phase diagrams 80−89209
Si-Te system glasses, local struct., ^{119}Sn Mossbauer obs. 79−41968
$Si_{12}Ge_{10}As_{30}Te_{48}$, amorphous, energy controlled switching obs. *(Japanese)* 78−34867
$Si_{12}Ge_{10}As_{30}Te_{48}$, chalcogenide glasses, direct obs. of switching filaments 77−24595
$Si_{12}Ge_{10}As_{30}Te_{48}$, chalcogenide glass threshold switches, turn-on state maintenance *(Russian)* 77−85271
$Si_{12}Ge_{10}As_{30}Te_{48}$, chalcogenide glass film, switching delay time 78−26926
$Si_{12}Ge_{10}As_{30}Te_{48}$ chalcogenide glass threshold switch conductivity in high ohmic state *(Russian)* 78−43502
$Si_{12}Ge_{10}As_{30}Te_{48}$ chalcogenide glass, switching in thin layers with semicond. electrodes 79−4586
$Si_{12}Ge_{10}As_{30}Te_{48}$, conducting filaments and switching phenomena 79−87134
$Si_{12}Ge_{10}As_{30}Te_{48}$, dark cond. and thermoelec. power, thermal activation energies interpret. 78−23123
$Si_{12}Ge_{10}As_{30}Te_{48}$, energy-controlled switching obs. 77−35973
$Si_{12}Ge_{10}As_{30}Te_{48}$ glass, thermally stimulated depolarization current meas. *(Japanese)* 78−34875
$Si_{12}Ge_{10}As_{30}Te_{48}$ glass, nonlinear I-V charact. 79−99557
$Si_{12}Ge_{10}As_{30}Te_{48}$ surface, heat treatment and electron bombard. effects. SEM obs., rel. to switching filament form. 77−47700
$Si_{12}Te_{48}As_{30}Ge_{10}$ amorphous film, high-field transient conduction 78−43500
$Si_{12}Te_{48}As_{30}Ge_{10}$, amorphous film, elec. cond. mechanisms, temp. depend. *(Japanese)* 78−80078
$Si_{12}Te_{48}As_{30}Ge_{10}$ amorphous film, current-voltage charact. 79−87104
$Si_{12}Te_{48}As_{30}Ge_{10}$ film, temp.-depend. of non-ohmic current and switching charact. 77−8158
$Si_{12}Te_{48}As_{30}Ge_{10}$ film, amorphous, transient cond. charact. in preswitching regime 77−32055
$Si_{12}Te_{48}As_{30}Ge_{10}$ film, amorphous, Poole-Frenkel cond. for centres with screened Coulomb pot. 78−19044
$Si_{12}Te_{48}As_{30}Ge_{10}$-Au, Schottky barrier props. 79−7897
$Si_{10}Te_{40}As_{30}P_{20}$, amorphous films, optically assisted mono-stable switching 77−11968
Sr-Te-O system, amorphous thin film, vacuum deposited, elec. cond., current cut-off *(Japanese)* 77−24625
$TaSe_2$ (2H), broken hexagonal symm., incommensurate charge-density wave struct. 80−96646
Te (IV) compounds, Mossbauer spectra, direct population of solid-state bands 80−15905
Te complex, bis(pyridium) hexachlorotellurate(IV), cryst. struct. *(French)* 80−28965
Te complexes of thiourea, Mossbauer spectra 80−15914
Te, Te cpds., Auger spectra 78−58638
Te-$(Bi_xSb_{1-x})_2Te_3$ eutectic, electrophys. props., directed crystn. conditions influence and comp. depend. 80−107827
Te-As-Ge, RF sputtering, temp. and bias effects on comp. 77−40367
Te-Bi_2Te_3 oriented eutectic, microhardness, influence of size of phases *(Russian)* 78−92322
Te-Bi-Sb ternary system, phase drag. calc. 77−27980
Te-Ge-As-Si amoprhous film, voltage controlled negative resistance type charact. 79−69614
Te-Ge-Sn(Pb), Te rich, structural phase transformation concurrent with glass crystallisation, thermal evidence 79−4965
Te-I, A1-type, superconductivity 80−29496
Te-Sb_2Te_3 oriented eutectic, microhardness, influence of size of phases *(Russian)* 78−92322
Te-Se, Debye temp. calcs. using elastic consts. and Kopp-Neumann relation 78−2220
Te-Se liquid mixtures, sound vel. meas., adiabatic compressibility determ. 80−65161
Te-Se mixtures, liquid, electrical conductivity and thermoelectric power, high temps. and pressures 80−39639
Te-Si glassy alloys, IR transmission and sp. ht. changes in glass interval, vibr. modes, struct. models 78−23474
Te-$TeBr_4$ system, Gibbs free energy of reaction, electrochem. e.m.f. expts. 79−91991
Te-$TeCl_4$ system, Gibbs free energy of reaction, electrochem. e.m.f. expts. 79−91991
Te-TeI_4 system, Gibbs free energy of reaction, electrochem. e.m.f. expts. 79−91991
$Te_{40}As_{35}Ge_7Si_{18}$ film, threshold switching in relax. oscill. mode 77−69389
$Te_{40}As_{35}Ge_7Si_{18}$, amorphous, threshold switching, expt. 80−49830
a-$Te_{40}As_{35}Ge_7Si_{18}$, trapping, photo-stimulated and thermally-stimulated current obs. 77−28192
$Te_{40}As_{35}Ge_7Si_{18}$ with pyrolytic graphite electrodes, threshold switching charact. 77−24593
$Te_{48}As_{18}Ge_6Si_{28}$ amorphous film, I-V curve, memory switching 79−69615
a-TeAsSiGe film with Mo contacts, AC performance *(German)* 77−63012
$Te_{39}As_{36}Si_{17}Ge_7P_1$ amorphous film, electroluminescence from on state 79−8188
$TeBr_6^{2-}$, spectroscopic consts., environmental cation effects 79−56779

tellurium compounds continued
$TeCl_2$, transient species, He(I) photoelectron spectrosc. calcs., relativistic corrections 80−95677
$TeCl_4$, chem. transport with equilib. $NbO_{2.417}$ to $NbO_{2.5}$ 80−2934
$TeCl_4$ gas phase transport agent, chemical transport growth of NpO_2 single crystals *(French)* 80−60760
$TeCl_4$, vibr. anal., cubane-like T_d model 78−66537
$(TeCl_4)_4$, vibr. anal., cubane-like T_d model 78−66537
$TeCl_6^{2-}$, spectroscopic consts., environmental cation effects 79−56779
$TeCr_2O_6$, exchange interactions within binuclear entity $(Cr_2O_{10})^{14-}$ 80−60236
TeD_2+F_2 TeF radical form., chemiluminescence obs. 80−43058
TeF, chemiluminesc. from oxidation in $F_2+H_2Te(D_2Te)$ emission spectrum obs. 80−43058
TeF_6, electron affinities from collisional ionisation with alkali atoms 78−55226
TeF_6, electron affinity, MS Xα calc. 77−30778
TeF_6, gas phase electron diffr. patterns, mol. struct., three-at. scatt. 78−66662
TeF_6, molecular effects in F K-shell ionisation by 0.5 to 1.5 MeV protons 77−50515
$^{125}TeF_6^-$, radical, prep. and EPR comparison with other hexafluoride radicals 78−68381
$TeF_6+H^+ \rightarrow TeF_6^+ + e^- + H^+$, 0.3-1.8 MeV, electron energy and ang. distrib. 78−22015
$TeF_6+K(Cs)$, crossed beam reaction cross section 77−77740
$Te_{80}Ge_{20-x}A_x$ glasses, rapid melt cooled, glass transition and stability range 80−75170
$Te_{0.81}Ge_{0.15}As_{0.04}$, amorphous and cryst., sp. ht., 1-20K 78−22864
$Te_{81}Ge_{15}As_4$, Hall effect in electrically switched memory state 80−2403
$Te_{80}Ge_{15}Pb_5$, DSC sensitivity to controlled ageing in glass transition region 80−71673
$Te_{80}Ge_{20-x}Sb_x(Bi_x)$, DSC studies of struct. phase transformation 80−66505
TeH_2+F_2, TeF radical form., chemiluminescence obs. 80−43058
α-TeI, ^{129}I Mossbauer spectra, coupling consts. 78−62833
TeI_4, ^{129}I Mossbauer spectra, coupling consts. 78−62833
TeI_6^{2-}, spectroscopic consts., environmental cation effects 79−56779
$Te_3Nb_2O_{11}$, cryst. struct. 79−55715
TeO, pot. energy curves, dissoc. energies 78−50485
TeO-V_2O_5 glass system, X-ray diffr. study 79−10805
TeO_2, acoustic beam electronic steering 79−98569
TeO_2 acousto-optic laser deflector scanning 80−14486
TeO_2 acousto-optical broad bandwidth devices bonded with Sn 78−50910
TeO_2 acousto-optical tunable filter with microcomputer control 80−102833
α-TeO_2, anisotropy of atomic vibrations, Mossbauer absorption spectra 78−27147
TeO_2, band struct., tight-binding calc. 80−24796
TeO_2, cryst., acousto optical RF spectrum analyser, double diffr. *(Russian)* 77−7263
TeO_2 crystal, parametric excitation in an acoustic interferometer 79−64381
TeO_2, crystal gyrotropy, meas. in IR region 80−88957
TeO_2 crystal multichannel acousto-optic modulator 77−39100
TeO_2, Czochralski-grown oxide crystals, fluid-flow effect on gas-bubble entrapment 80−84121
TeO_2, elastic wave parametric instability kinetics in dielectrics *(Russian)* 80−45035
TeO_2, electronic struct. and densities of states, tight-binding calcs. 80−15447
TeO_2, ferroelectric glass, phase transition, permittivity, electrochromism, photochromism 80−80719
TeO_2, film, AES, LEED, XPS, energy loss spectra studies 78−73086
TeO_2, glass, phonon density of states, Raman spectra *(French)* 77−20841
TeO_2, glass, refractive index, effects of alkali oxide comp. changes *(Russian)* 78−22182
TeO_2, light diffr. by slow acoustic waves 80−29717
TeO_2, multifreq. acousto-optic diffraction 80−74300
TeO_2 noncollinear IR tunable acousto-optical filter 79−23086
TeO_2, nonlinear optical susceptibility, antisymm. components 78−13755
TeO_2, paratellurite, atomic motions corresponding to zone centre phonons 78−76461
TeO_2, paratellurite, lattice dynamics, IR refl. and Raman scatt. expts. 77−15518
TeO_2, paratellurite, optical absorpt. and refl. spectra, 80-500K, optical consts. determ. 80−50359
TeO_2, paratellurite, phase transition at high-press., Raman and far IR spectra 78−80328
TeO_2, paratellurite, refr. index, equal-deflection method, UV laser rad. 78−29145
TeO_2, paratellurite, single crysts., third-order elastic constants 80−88243
TeO_2, paratellurite, stress induced changes in Raman spectrum 78−39540
TeO_2, paratellurite acousto-optical deflectors, bandwidth and scanning linearity *(Chinese)* 78−90501
TeO_2, paratellurite cryst., polariton Raman scatt. 78−25928
TeO_2 paratellurite crystals, parametric excitation of sound, calc. 80−24537
TeO_2 piezoelec. powder, orientation depend. of memory echo 78−35094
TeO_2, press.-induced ferroelastic transition and internal displacement, soft effective elastic const. meas. 79−73240
TeO_2 shear wave acousto-optical device with polarisation filtering 80−106619
TeO_2, single crystals, acousto-optic props., optical information processing *(Russian)* 77−55768
TeO_2, structure simulation of some tellurite and chalcogenide glasses quasi-crystalline structural diffusion method *(Russian)* 80−54147
TeO_2 thin film, Al-TeO_2-Al, field-assisted cond. mechanism 80−11105
TeO_2 thin films, dielec. props. rel. to fabrication conditions 80−97199
TeO_2 time-integrating acousto-optical correlator for chirp spectrum analyses 80−106474
TeO_2, tunable acousto-optic filters 78−5570
TeO_2 two coord. deflector, anisotropic diffraction and wide band scatt. 80−91920
TeO_2, use in acousto-optical modulator, appl. to laser Doppler anemometers 78−83082
TeO_2, visible and UV refr. indices 78−19439

tellurium compounds continued
TeO_2 volume-acoustic-wave generator acousto-optical device, appl. in laser Doppler velocimeter 79−90030
TeO_2, zone centre optical phonons under uniaxial stress 78−79700
TeO_2:Gd^{3+}, mag. susceptibility, cryst. field calc. 78−76035
TeO_2:Se, Se determ. by neutron activation anal. 77−86400
TeO_2-Al_2O_3-WO_3 glass, rare earth doped, nonradiative decay and multiphonon relax. 77−85802
TeO_2-BaO, cryst. chem. study, X-ray diffr. powder data *(French)* 80−15080
TeO_2-CaO, cryst. chem. study, X-ray diffr. powder data *(French)* 80−15080
TeO_2-CdO, cryst. chem. study, X-ray diffr. powder data *(French)* 80−15080
TeO_2-CoO, phase diag. from thermographic analysis 78−23687
TeO_2-Cr_2O_3 system, phase diagram and vitrification 79−83182
TeO_2-Fe_2O_3 glass, atomic arrangement, neutron diffr. data 78−83743
TeO_2-Fe_2O_3 system, glass structure 79−90562
TeO_2-Fe_2O_3 system, mag. props. 78−27020
TeO_2-GeO_2 system, phase diagram, X-ray phase analysis, DTA and electron microscopy 77−15545
TeO_2-Li_2O glass:Nd^{3+}, highly doped, spectroscopic props. and CW laser action *(French)* 79−41385
TeO_2-Li_2O glassy system, struct. recomb. model 80−19707
TeO_2-MoO_3-M_nO_m, glass formation range 78−71680
TeO_2-MoO_3-V_2C_5, phase comp. determ. using X-ray diffr., electron microscopy and DTA *(German)* 80−88046
TeO_2-$Na_2O(Li_2O)(K_2O)$ glass, radiational EPR centres, struct. model *(Russian)* 77−28426
TeO_2-NaCl(-NaBr), condition diagram, thermographic obs. *(Russian)* 80−55377
TeO_2-NiO system, phase diagram and vitrification 79−83182
TeO_2-P_2O_5, electron microscope exam. of phase equilib. and immiscibility 78−52779
TeO_2-P_2O_5 system, glass struct., neutron diffr. study 80−70128
TeO_2-V_2O_5 glass threshold devices, reversible monopolar switching 80−2434
TeO_2-V_2O_5-Fe_2O_3 system, phase equilib. and analysis, primary crystn. fields 77−66628
TeO_2-V_2O_5-$Li_2O(Na_2O)(K_2O)(Cs_2O)(Ag_2O)$, glass, IR spectra of crystalline phases 79−38536
TeO_2-WO_2 glass, dipole correlations, capacitances and TSC meas. 79−28670
TeO_2-WO_3-R_nO_m, glass formation range 78−71680
TeO_2-ZnO, cryst. chem. study, X-ray diffr. powder data *(French)* 80−15080
TeO_2+$NiMoO_4(FeMoO_4)$, solid state reaction 80−108709
TeO_3^{2-}, TeO_4^{2-}, O K-emission spectra, electron struct. 80−87099
TeO_4^{2-}, normal vib. freq. and force const. calcs. *(Russian)* 78−46318
TeO_4^{2-}, normal vibr. freqs. calc. 79−54837
TeO_4^{2-}, vibr. props. calcs. *(German)* 79−3431
$Te^{VI}O_6$ ion in $A_2B^{II}B^{VI}O_6$ perovskites vibr. anal. using isotope shifts and perturbation theory 77−59073
$TeO_{11}Cl_2$ thermal decomposition, matrix isolation IR and mass spectra 80−81306
$Te(OH)_6$, $^1H/^2H$ quadrupole reson. freqs. detected by double reson. with level crossing 78−84497
$Te(OH)_6$, X-ray diffr. cryst. struct. refinement 78−95022
$Te(OH)_6.Cs_2HPO_4$, cryst. struct. 80−64975
$Te(OH)_6.Cs_2HPO_4.2CsH_2PO_4$, cryst. struct. 80−64975
$Te(OH)_6.Na_2HAsO_4.H_2O$, $Te(OH)_6 \rightarrow_4 6.Rb_2HAsO_4.Rb_2H_2AsO_4$ and $Te(OH)_6.2(NH_4)_2HAsO_4$, synthesis and cryst. data *(French)* 80−33948
$Te(OH)_6.Na_2HPO_4.H_2O$, X-ray cryst. struct. determ. *(French)* 79−69077
$Te(OH)_6.2(NH_4)_2HPO_4$, X-ray cryst. struct. determ. *(French)* 79−69077
$Te(OH)_6$.diurea complex, cryst. struct. determ. 80−28971
$(Te_2O_3)SO_4$, cryst. struct., X-ray diffr. meas. 77−4078
$Te_{1-x}S_x$, ^{125}I and ^{129}Te Mossbauer spectra obs. 77−90075
Te_xS_{1-x}, chemical bonding from ^{129}I and ^{125}Te Mossbauer spectra 79−73867
TeSe, valence fluctuation system, ground state and elementary excitations, Anderson lattice model Hamiltonian, dense Kondo problem 80−54656
$TeSe_{12.5}$, amorphous alloy, thermal and elec. cond. during devitrification 78−26922
$TeSe_{19}$ glass, crystallisation kinetics 77−35484
$TeSe_{19}$, glasses, crystallisation kinetics, elec. cond. meas. 77−43155
$TeSe_{20}$, vitreous alloy, elec. and thermal cond. during crystallisation 79−7550
$TeSe_{50}$, amorphous to cryst. transition, kinetics 79−73099
$Te_{1-x}Se_x$, ^{125}I and ^{129}Te Mossbauer spectra obs. 77−90075
Te_xSe_{1-x}, chemical bonding from ^{129}I and ^{125}Te Mossbauer spectra 79−73867
Te_xSe_{1-x}, localised gap states estimated by dielec. relax. 78−35087
$Te_{43}Se_{30}Sn_7$ in MSM struct., switching effects 78−19164
$Te_{50-x}Se_{50}Sn_x$, thin films, elec. cond. and thermoelectric power meas. *(French)* 80−80335
Te_xSi_y, (x=78,87, y=22,13), amorphous, struct., X-ray diffr. study 80−6362
$Te_{80}Si_{20-x}Pb_x$ glasses, phase separation, double T_g presence 80−88306
^{125}Te, Mossbauer isomer shifts, book contrib. 79−87360
TiO_2:$TeCl_4$ system, chem. vapour transport, matrix isolation IR studies 80−93755
$(Tl,Ag,Cd)NO_3$, mixed aq. solns., vapour press., 98.5°C, Brunauer-Emmett-Teller isotherms 78−51655
Tl-Ge-Te, glass formation 80−103255
Tl-Te, liq., reflectance, 0.65-3 eV, comp. depend. 78−72549
Tl-Te liquid alloys, mag. susceptibility 77−59383
TlCl-TlBr, single cryst., composition determ. by reflection spectrophotometry 77−1961
TlKr, low-lying electronic states, PE curves, transition moments, emission coeffs. 79−6894
Tl_2O-TeO_2, phase diag. 77−81252
Tl_5SbO_6, isomorphism with Tl_2SnO_3 *(French)* 78−10012
$Tl_2SeAs_2Te_3$, amorphous semicond., nuclear spin-lattice relaxation by localised electronic states, modification by spin diffusion 78−52372
$Tl_2SeAs_2Te_3$, glassy and liq. states, elec. cond. freq. depnd. 77−76856
$Tl_2SeAs_2Te_3$, molten chalcogenide semicond., temp. depend. of 10^{10} Hz elec. cond. 77−4388
Tl_2SnO_3, isomorphism with Tl_5SbO_6 *(French)* 78−10012
tellurium compounds continued
Tl_xTe_{1-x}, amorphous, bonding and electrical conduction 79−90951
Tl_xTe_{1-x}, liq. semicond. alloy, mag. susceptibility rel. to diffusive transport 77−20541
UF_6-TeF_6, dil. soln., liq.-vap. equilib. 77−62632
V-O-Te-Cl system, chem. transport of V_nO_{2n-1}, V_6O_{13}, V_2O_5 *(German)* 78−31343
V_2O_5-TeO_2 system, vitreous, struct. obs. using neutron scatt. 78−22667
Zn-As-Te system, phase diagram, As_2Te_3-ZnTe cross section investig. 77−36473
Zn-Te-O, partial pressure diagrams 77−36681

TEM *see transmission electron microscopy*

temper brittleness *see brittleness*

temperature
see also atmospheric temperature; boiling point; critical points; Debye temperature; ferroelectric Curie temperature; magnetic transition temperature; melting point; superconducting transition temperature; temperature scales
acoustical props. of laboratory sediments 80−96069
astronomical observatories, telescope and dome temps. rel. to dome seeing 80−12657
continuity of the temperature and derivation of the Gibbs canonical distribution in classical statistical mechanics 79−25965
continuum thermodynamics, existence of single temp., heat and entropy flux 77−13729
dew point temp. change with pressure, calc., nomogram 80−77607
Earth surface temperature, determ. of diurnal var. in mountainous terrain 80−82011
entropy increase principle, collection of thermally interacting systems, for teachers 77−33785
fibre-optic lightguides, temp. effects on transmission 79−76817
galaxies active nuclei, temp. and electron density in narrow line region 80−31364
giant stars in M3, M13, M92 and M67, IR photometry, bolometric magnitudes and effective temps. 78−57595
IC 4997, compact planetary nebula, electron temp. rel. to rapid emission-line vars. 79−92838
increase and skin sensation under strong lighting *(Japanese)* 78−44557
integral, approximative eqns., accuracy analysis 80−36834
intergalactic hot gas in clusters of galaxy, temp. and entropy 80−17660
intergalactic medium, temp. and ionisation struct., effect of UV stars 77−13455
intergalactic medium, temp. determ. from extended H I regions around spiral galaxies 78−12354
interstellar clouds, effects of temp. and activation energies on gas phase chemistry 80−105298
interstellar diffuse clouds temperatures, determ. from HD and OH column densities 78−93385
interstellar dust grains, temp. fluctuations 80−26938
interstellar Fe grains, temp. 77−71135
interstellar gas of solar neighbourhood, temp. and vel. determ. from interplanetary H I Lα emission profiles 80−105141
interstellar grains, max. temps. 77−49449
interstellar grains, temperatures in diffuse clouds rel. to interstellar Ar depletion 80−51848
interstellar graphite grains, effect of IR optical consts. 78−12324
interstellar medium, intercloud temp. from H_2 population distribs. 77−71136
interstellar medium, local, temp. from interstellar He I obs. 80−62234
interstellar medium, local, temp. rel. to ionisation state 80−90502
interstellar medium, temp. from Lyman α emission obs. 77−67120
late-type (K0 to M6) giant stars, effective temps. 80−46545
M-type giant stars, spectral energy distribs. and effective temp. scale 78−28678
Mars, longit. var. of thermal inertia and 2.8 cm brightness temp. 80−105191
Mars thermosphere, effects of energetically produced O_2^+ on ion temps. 79−96945
material with internal variables, condition equivalent to existence of non-equilibrium entropy and temp. 79−44890
microtemperature concept for heat conducting microfluids 79−72776
Moore County, eucrite meteorite, quench temp. and residence time on eucrite parent body 78−96444
nebulae central stars, temps. determ. from forbidden O III lines 78−41015
negative absolute temperature *(Chinese)* 79−30401
negative absolute temperature 79−63184
negative absolute temperatures 79−2742
Neptune, effective temp. from IR photometry 78−32394
neutron stars, effective temps. from search for pulsars thermal EUV radiation 77−22259
neutron stars, thermal/timing instability rel. to pulsar timing obs. and X-ray transients 79−92795
nonequilibrium temperature, definition 77−17934
nonequilibrium temperature, empirical foundation and axiomatic treatment 78−57882
Orion Nebula, H_2 emission extinction and excitation temps. 79−25668
E.Pacific Rise geothermal system, physical limits on geothermal fluid temp. and role of adiabatic expansion 80−101362
PHL 1092, narrow line quasar, Fe II emission region electron density and temp. 80−77508
planetary bodies, ancient, temps. rel. to lunar capture hypothesis 78−81570
planetary nebulae, electron density and temp. from absolute flux densities for emission lines in 6000-11000 Å range 80−51857
planetary nebulae, electron temps. from radio continuum obs. 78−41027
planetary nebulae central stars, comparison of Zanstra He II temps. and temps. from visual spectra 80−109434
planetary nebulae central stars, temps. determ. from nebulae ionic abundance ratios 79−2565
planetary nebulae central stars, temps. determ. rel. to nebulae evolution 80−67724
quasars, temp. and electron density in narrow line region 80−31364
red giant stars, effective temp. scale from TiO absorpt. bands 78−96480
relativistic radiation temperature of moving bodies 78−57775
river water temp. forecasting, Fourier series and communication theory techniques 77−25718
school physics, elementary presentation by theory of heat, thermodynamics, and thermometry *(Danish)* 80−4483

temperature continued
sea surface, temp. field rel. to poleward heat flux by oceanic gyre 80−85668
solar wind, α-particle/proton temps. in three-fluid model 78−57418
stars, early type, theoretical UBV colours and temperature scale 79−16933
stars, uvbyβ photometric system calibration in terms of temp. and gravity 78−4198
steady state plasma, electron temp. and density meas. system 78−87490
stellar effective temperatures, effect of atmospheres finite extent on colour indices 78−32450
Sun, radius and temp. vars. due to mag. buoyancy 79−92749
Talyvel electronic level, temp. effects *(German)* 78−45037
teaching, temp. concept without zeroth law 78−24607
Tieschitz, H3, chondritic meteorite, accretion temp. 79−75166
Uranus, microwave brightness temp. increase 78−93150
Venus upper mantle, temp. rel. to planet tectonics and comp. 80−72805
white dwarfs, hot, effective temps. 79−25602

temperature compensation *see compensation*

temperature control
see also thermostats
accuracy of on-off temp. regulators improvement 79−75527
AEG-Telefunken temp. controller for refrigerator system, IC *(German)* 79−26051
air, relative humidity control, error comparison for various sensors, accuracy 77−10034
air-conditioned laboratories, automatic temp. control and meas. *(Japanese)* 78−86245
amplifiers used for electrometer varactor-bridge 79−9219
annealing of electron field emitters and multiple multichannel analyser, precision temp. regulator 78−86384
Atmospheric Cloud Physics Laboratory 80−4090
atomic absorption spectroscopy with nonflame sample atomisation, thyristor thermostabiliser use 79−96388
automated vapour deposition apparatus based on programmable calculator 78−44022
automatic electric system 77−82501
baby incubator design for Ghanian manufacture and use 77−40900
biological media temperature stabilisation, electronic device 80−85539
biological preparation temp.-control system 79−57830
biological preparations, system with fast heating and cooling capability 77−40948
biological pressure meter, temperature and time stability 79−84059
biological specimen preparation, semi-automatic method, critical point drying for SEM 79−17406
'blackbody' IR sources 78−83059
body temp. regulation method for hyperthermia and hypothermia study 78−15778
body temperature humidification, effect on patient thermal regulation 78−85295
brain tumour therapy by RF field controlled temp. gradients 77−25522
calorimeter, automated, high precision, for 200K to 400K, temp. controller design 80−86310
calorimetric system, 3-300K, with on-line computer, adiabatic shield temp. control 78−4620
calorimetric water bath temp. control and temp. meas. devices 77−37893
capillary porous body, drying, X-ray absorption obs., radiometry, temp. control 78−67023
cell freeze conservation control unit *(German)* 79−5410
cell water permeability during freezing and thawing, cryomicroscope multiple nonlinear regression analysis 79−92197
cold-bath, precision, laboratory appl. construction 79−26048
combination light scattering spectrometer temp. regulating attachment *(Russian)* 77−53987
compensation for thermal drift in optical feedback stabilised photometer 77−2695
condenser system, submerged, buble pumped augmented natural convection 78−94535
constant temp. water bath using simple thermal/vapour barrier 80−86290
contact regulator, analytical and experimental study 79−185
contactless using radiometer with optical fibre as optical lens 78−49828
creep and long-term strength tests, system for automatic temp. regulation 77−63853
creep testing, at const. temp., humidity, appl. to nylon-6,6 78−95883
cryogenic, use of ICs 80−90856
cryogenic controller, simple, low cost, temps. 78 to 300K 77−22555
cryogenic temp. regulator for use with resistive and capacitive sensors 77−82534
cryostat, He immersion and gas-flow optical cryostat system 78−77923
cryostat, liq. N_2, for obtaining temps. −195 to 150°C and forced heating of specimens 77−74403
cryostat, temperature regulator for liquid ^{4}He bath near 4.2K 78−41319
cryostat controller, He, using digital voltmeter *(Czech)* 78−29120
cryostat for film vac. deposition onto low temp. substrate *(Japanese)* 78−27403
cryostat with optical high-pressure chamber 80−31767
crystal oven pilot-lamp stability controller 78−54374
crystal ovens using temp. gradient-free change of state for quartz cryst. standard *(Polish)* 79−30481
crystalline thermal treatment, control thermocouple *(Spanish)* 80−73362
crystallisation process, controlled, from binary melt *(Polish)* 79−14708
cytopherometer, reproducibility improvement 77−52954
DC proportional heater/cooler temperature controller for physiological research 78−7553
developing countries' architectural design for solar energy environmental control 79−57449
diamond turning, Honeywell Corporation facilities 80−5852
dipstick cryostat, with temp. controller for high thermal stability 80−37044
dynamic type temp. controller, 60 to 900K with 0.05K 77−10009
effective temperature criterion for exercise heat stress prescription 79−92159
electric cell sto... air thermostat 77−10058
electric furnace, muffle type, automation of temp. regime 77−61068
electric heating regulator using a FET amplifier and Schmitt trigger convertor *(French)* 79−58681
electric resistance high precision meas. and control in He II environment 78−54403

temperature control continued
electrochemical sensor for continuous transcutaneous meas. of PCO_2 77−13020
electron spectroscopies, low-energy, temp. controller 79−44987
electronic circuit, based on Wheatstone bridge and thermistor, high precision 78−86258
electronic temperature controller 80−86282
electronic thermostat, with 0.1°C accuracy and economical operation, photography appl. 80−77774
EM field cell culture exposure under controlled temp. and field strength conditions 78−40449
end-temperature in semi-infinite rod, distributed parameter optimal control problem 78−13886
EPR spectrometer, simple temp. controller, 85-400K *(German)* 78−45663
ESR and NMR spectrometers inexpensive temp. controller 79−35803
extracorporeal circulation apparatus using thermoelec. heat regulating systems 80−3870
extracorporeal circulation system, energy parameters of temp. stabilisation system 80−3867
filament, plate samples for gas adsorpt. heating controllers *(Japanese)* 77−51603
flash desorption spectroscopy, thermocouple-controlled temp. programmer 79−49224
float glass, heat transfer and temp. control in annealing, computer appl. 78−27543
furnace, temp.-rise controller up to 1000°C 77−17980
furnace thyristor temp. regulation circuits, for creep testing devices 80−25956
furnaces, elec. resist. 80−27307
gas chromatograph, self-monitoring high-performance instrument 77−36823
gas chromatograph system development *(Japanese)* 80−50922
glass balls production, drop feeders automation 79−61556
heart-lung machine two-circuit thermocontrol device 79−48374
heat pumps, energy and environmental considerations in extending appls. 77−17976
heat storage device, off-peak, ambient temp. observer/predictor control system 80−66950
high temp. furnace control methods in creep testing 80−30187
high-frequency heating of C, position regulator 79−80612
human thermoregulatory system structure and function maths. treatment 77−12888
humans, control theory model 78−35805
HV pulse controller and temp. monitor microcomputer-based, Kerr effect study appl. 79−6103
hyperthermia generator digital readout device 79−70697
IC temp. controller 77−67432
improved set-point setting temp. controller, construct. *(German)* 78−45606
incubator, portable, with radiant heating system and fine O_2 control 77−56511
incubators, portable, improvements 78−81055
induction salt baths, automatic temp. control 80−27300
inductive load temperature regulator, using IC zero voltage switch U 106 BS with triac. *(German)* 80−77779
industrial, thermocoupler and resistance thermometer 80−42221
injection laser system, using heat pump 77−19324
instrumentation, specialised, use of thermosensor indications 77−41599
IR cell, low temp. for use with hydrated films 79−6193
IR radiation thermometry, temp. monitoring and thermal inspection 78−45622
jacket, radiatively heated from side, rot., conical (spherical), condensable working fluid 77−42710
Knudsen effusion chamber with low axial temp. gradient for high temp. thermodynamic tests 77−71329
laboratory, modified window air conditioner, thermistor bridge circuit 80−68192
laboratory temperature regulation cct. 77−45836
laboratory thermostats, electronic device for precision temp. regulation 79−88931
lasers, injection, used for optical communications, Si bipolar transistor driver module 79−45971
light and water exposure apparatus 79−15914
liquid, dielectrophoretic heat transfer 78−94874
LMfBR, Na loop temp. control using 100 kW elect. heater *(Czech)* 80−5203
Lobar Wick heat pipe, 74 to 230K thermal control range 78−94532
low-temperature source to test for cold urticaria 78−61276
LPE, multi-layer, furnace design and fabrication *(Japanese)* 80−108366
LPE film property control, regression eqns. 79−33200
mass spectrometer, microcomputer-based controller for temp. programming direct inlet probe 78−16893
meter-controller for 1.5-300K range 77−45840
microprocessor triac interface, used to control kiln temperature 78−45632
microscope stage, for high-resolution optical microscope 79−17411
microwave thermography and local heating by same system, clinical applications 79−100695
mirror temperature effects on telescope seeing, compensation method 79−70961
modular control system for coupled-cavity structures in high duty factor accelerator 79−67992
multiple incubators, temp. drift elimination, for biological expts. 78−3696
multiplexers, temperature applications, types of unit and configurations 80−82757
multireflection absorption cell design and performance 77−18108
nitriding system for Si_3N_4 fabrication, automated 79−24468
optical glass melting in Pt crucibles, power supply freq. convertors 79−72728
optical modulator, temperature compensation by feedback control 77−42611
optical waveguide modulator for fibre transmission systems, temperature stabilized *(Japanese)* 79−27391
optoelectronic temperature profile recorder 80−105642
organ cryopreservation apparatus 77−37060
oven, reliable inexpensive design, for temp. stabilizing crystals 77−82503
ovens, electronic controller using TTL cct. *(German)* 79−67304
perspiration mass transfer coefficients and clothing models 79−92158

temperature control continued
photocompensation proportional temp. regulator with phase impulse control 77−82502
photographic developing bath, thermostatic control *(Spanish)* 80−77898
photographic developing solutions *(Russian)* 78−29202
photoresistor contactless temperature indicator *(Russian)* 77−10023
physicomechanical testing, low temperature, temp. control for tests in liquid coolant vapours 80−81260
plastic, extrusion cylinder and feed channel wall, US appl. 77−27448
plate heating, optimal fast response control under temp. field gradient constraints 80−38232
precision electronic controller, construction and operation 77−82504
programmed controlled temperature microscope stage 79−35821
proportional controller, using IC sensor diode and operational amplifiers 79−75515
proportional simple-precision regulator, for heating units and cryostats 77−37880
proportional temp. control scheme, ±0.002K for several hours, for student lab. 77−33806
proportional temperature controller, for teaching appls. 79−48997
radiation pyrometer, use in automatic control of molten glass temp. in feeders 77−49729
radiospectrometer, automatic thermostatic control, using Diapazon variator 80−47160
reference source radiation, temp. instability and compensation methods 79−14071
reflecting telescopes with zero expansion material mirrors, temp. control rel. to defocusing *(Russian)* 79−96912
refractory filament, method and its appl. to W 79−9215
regenerative refrigerators, closed-cycle, for cooling small supercond. devices, concept 78−93698
regulator and controller selection and specification 79−71439
regulator circuits, using thyristors and triacs *(Spanish)* 79−6115
regulator for 77 to 340K range, Ge transistors use as heating elements 77−67442
regulator for range 77-300K 77−33995
regulators using Darlington cct. as sensor and controller *(German)* 79−30467
residual resistivity specimens, temp. control during medium temp. electron irradiation 77−54016
resistance furnace programmed temperature regulator 78−86256
rotary tube photographic processor design 80−4795
rotating object, non-contact method with thermistor and pyrometric voltmeter 79−35742
rotating surface, contactless null method for controlling its temperature *(Russian)* 77−53899
sample heater, high vacuum, using Zener diode 78−12690
satellite, using In_2O_3 or In_2O_3-SnO_2 thin films 79−80187
semiconductor temp. detectors, control circuits for critical temp. machinery and fluid levels *(German)* 79−21747
semiconductor thermocamera, thermojunction method appl. *(Russian)* 78−45693
set-point of body temperature regulation *(Japanese)* 78−24032
shells of revolution, thin-walled, heated, temp. field, thermostatic control 78−67003
SHG, temperature tuned, Dewar design 77−62002
sintering uranium oxide, resistance furnace appl. and characteristics *(Italian)* 77−81239
solar cell maximum power output determ. 79−74527
solar central receiver plant, dynamic simulation of thermal-hydraulic charcts. of Na-cooled plant 80−30400
solar energy systems, modern control theory appl. reviews 80−66949
solar water heating systems, entering water control, by thermal operated mechanical device 79−62138
spacecraft heat rejection improvements using thermoelectric devices 80−108810
spectrometer, for surface barrier detectors study 77−83443
spectrophotometer, single beam, enlarged and thermostatted cuvette chamber 77−5925
SQUID magnetometer with temp. control, spontaneous magnetisation and mag. susceptibility meas. 80−68221
stabilizer for 77-340K range 77−74392
standard cell, temp. controlled enclosure with 25 μK stability 77−18027
superconducting thermometer, low temp. stabilisation appls. *(German)* 78−86250
superheated steam, control system using an adaptive regulator, synthesis *(Polish)* 79−75518
sustained thermodynamic equilib. used to control temp. of expt. chamber 77−33983
TEM specimen freeze drier, all-glass design 80−82854
tensile machines, temperature control of suspended electric furnaces 77−82523
thermal regenerator, with variable mass flow rate, computer model 78−75047
thermistors, PTC, appls. 79−71448
thermocouple reference junction box, used for vacuum chamber 80−90844
thermocouple temperature controller for field emitter 78−24898
thermodesorption, temp. control device *(German)* 78−86251
thermoelectric thermometer checking unit 77−22548
thermometers time constant influence obs. of resistance and thermoelectric types *(Czech)* 78−29114
thermophysical testing device, rate of change of temp. in time *(Russian)* 80−208
thermostat system, automatic, for high temps. 79−6112
thin specimens, temp. control for mech. meas. under light ion irrad. 78−86278
thyristor temp. regulator for pulsed NMR spectrometer 80−105687
thyristor temperature regulator 77−37881
thyristor thermostabiliser for at. absorpt., spectroscopy with non-flame atomisation, power supply *(Russian)* 78−76977
time-linear controllers used in analysis of thermoluminescence glow curves 79−63202
toroidal plasma, ion temp. control by neutral injection 79−37514
tumour microwave heating with automatic temperature control 77−77963
US tumour irradiation, closed-loop energy and temp. control 79−83874
vapour from solid N for temp. production in 20-63K range 78−221
variator coupling to EPR radiospectrometer 78−58003
varicap diode thermometer stabiliser, up to 150°C *(Czech)* 78−29115
temperature control continued
Varytemp NMR for pulse spectrometers, applic. to lineshape determ. 77−2674
Veritron AC power controllers, thermal equipment, automated manufacturing processes *(German)* 79−80598
viscometer system, semiautomatic meas. *(German)* 79−94561
viscosity meas., water bath with temp. control for glass capillary viscometers 78−59525
viscosity meas. device design 78−5834
water circulation type precision thermostat bath 79−49221
water thermostat, linear thyristor control and thermistor sensing *(Japanese)* 77−90264
weak signal detection, circuits for resistance meas. and temp. control *(Chinese)* 79−30451
whole-body hyperthermia with oesophageal temp. feedback control 79−92423
wide ribbon growth by multiple inert gas jet thermal profile control 78−64458
X-ray camera, 10 cm diam. back-reflexion focusing, design and fabrication 78−18489
X-ray small-angle scattering expts., temp. stabilisation of sample cell 77−13830
X-ray studies of phase transitions at low temp., automatic system 77−15281
$As_{10}Ge_{15}Te_{75}$, thermal memory switch development 78−89468
Cu-constantan cryogenic thermometer and temp. controller *(Czech)* 79−26056
GaAs-on-sapphire spatially distributed thermal light modulator 79−59839
H_2 bubble chamber, temp. and press. control 79−85860
He II, flow through porous plugs, space cooling system appl., plug charcts. 78−49842
He, liquid, manostat, thin film material utilized 79−35757
InGaAsP InP DH lasers, optical power and wavelength stabilisation 80−38036
Na system cold trap temperature control using resistance heater 77−57710
Ne+H_2 bubble chamber, heat exchange and temperature control system 77−6616
Si ribbon growth, high-meniscus, thermal balancing via distributed inert gas streams 78−31329
Si substrates during sputtering and sputter etching, thermal history of substrates 80−25562
Zn sherardising process development 79−78998

temperature distribution
30 T pulsed solenoid construction and life tests 79−31297
^{3}He-^{4}He dilution refrigerator process anal. 79−93150
^{3}He-^{4}He superfluid injection dilution refrigerator, process anal. 79−97394
ablation-stabilised arc temp. distrib. model 78−71585
absorbing-scattering infinite slab, combined conductive and radiative heat transfer 78−71269
accelerated temp. field, use in low-temp. investigation of multilayer insulation thermal conductivity 77−30162
adsorbent fixed bed, temp. profiles 79−23359
air, in wall cavity, slot filtration, temp. distrib. 77−65662
air, laser-evaporated microplasma radial glow and temp. distrib. 78−67387
air jet, heated, turbulent, discharged downward, temp. profiles 79−27677
air jet, vertical axisymmetric buoyant, profile meas. 78−90906
air-conditioned laboratories, automatic temp. control and meas. *(Japanese)* 78−86245
air-water interface, temp. waves 78−57213
Alboran Sea frontal system, XBT data for 1976 Nov. and 1977 March period 79−2256
altitudinal temp. gradients for N.Pennines in Britain 80−4094
analogies between electric and temperature fields, engineering calc. appl. *(Czech)* 79−68343
anisotropic medium homogeneous in cylindrical regions, steady-state anal. 77−58526
anisotropic sheet with insulated hole, temp. distrib. 79−32202
anisotropic solid, arbitrary shape, three-dimensional soln. 77−58527
annuli, spherical rot., stratified convection of viscous Boussinesq fluid 79−27635
annulus, spherical, rot., forced thermal convection of viscous fluid 79−27634
Antarctic Polar Front Zone, fine structure rel. to internal waves 79−2254
Antarctic Polar Frontal Zone from Australia from Drake Passage, thermal struct. 78−44850
aquifer, temp. field due to hydrothermal convection, numerical calcs. 80−90105
Arabian Sea, temp. and salinity fine struct. obs. 79−25257
Arabian Sea, upper layers temp. distrib., ISMEX-73 data 77−53065
aromatic hydrocarbons, heat transfer to ascending (descending) streams, near-crit. press. 77−65742
artesian wells drilled in permafrost, temp. field, efficiency of heaters for ice plugging prevention 77−78242
SW Atlantic, charcts. and circulation 77−64306
E. centralAtlantic, horizontal temp. in upper ocean layer *(Russian)* 80−17283
NW Atlantic, large scale variations in temp./salinity fine structure 77−56639
Atlantic, main thermocline props. 79−57960
N.Atlantic, sea surface temp. year to year changes, (1948 to 1974) 80−67367
NE tropicalAtlantic, thermohaline structure *(Russian)* 80−17281
central Atlantic, two-degree discontinuity 77−56633
S.Atlantic anticyclonic gyre, thermohaline structure and dynamics of upper layer *(Russian)* 79−100864
Atlantic mid-oceanic ridge, axial temp. profile and crustal struct. 80−26476
S.Atlantic Ocean, glacial and interglacial temp. conditions from $CaCO_3$ and radiolarian distribs. 80−72556
Atlantic Ocean, temp. fluctuations rel. to semidiurnal internal waves in Polygon-70 test area 80−31051
Atlantic Ocean surface temp., empirical orthogonal analysis 77−86934
Mid-Atlantic Ridge crest at 26°N, near bottom water temp. anomalies 79−34831

temperature distribution continued
Atlantic seasonal thermocline, turbulent mixing and vertical temp. structure *(Russian)* 78−85597
Atlantis II Deep geothermal system, temp. meas. rel. to changing hydrothermal activity 78−85532
atmosphere, boundary layer thermal structure at Cardington from acoustic sounding 77−53153
atmosphere, eddy temp. variances in weakly nonlinear theory 79−79928
atmosphere, ground-based inversion decay, analysis by direct and indirect meas. methods *(German)* 77−37310
atmosphere, Mason method for lidar temp. profiling, computer simulation 80−21827
atmosphere, spatial anal. of temp. field from weather satellite meas. 78−20488
atmosphere, temp. distrib. in stratified ground layer under coniferous forest canopy *(Russian)* 78−96266
atmosphere, temp. distrib. rel. to Earth global heat balance annual var. 78−73300
atmosphere, temp. profile retrieval with passive microwave sounder using Kalman-Bucy filters 79−21053
atmosphere, temp. profiles from Nimbus-6 soundings 78−53695
atmosphere, temperature profile retrieval from IR satellite data 79−48586
atmosphere, temperature profiles, ground-based microwave radiometric sensing 79−84392
atmosphere, thermal plumes and turbulence spectra in boundary layer 77−73793
atmosphere, thermal radiation obs. from ground *(Chinese)* 80−82041
atmosphere, thermodynamics of temp. inversion 79−57994
atmosphere, vertical temp. density from STRATCOM VII-A meas. 79−58079
atmosphere, vertical temp. profile estimation, system identification method 77−91342
atmosphere, vertical temp. profiles from microwave radiometers 79−58226
atmosphere, vertical temp. profiles using ground based IR spectroradiometer *(Japanese)* 77−29499
atmosphere and ocean surface, canonical correl. method study 80−26593
atmosphere boundary layer, diurnal temp. cycle 78−20434
atmosphere boundary layer temp. profile determ. from ground-based 60 GHz radiometry *(German)* 80−82097
atmosphere jet stream, fronts and wave disturbance compared with Gulf Stream 79−2268
atmosphere temp. profile, satellite determ. *(Hungarian)* 79−44218
atmosphere temp. profiling using IR heterodyne radiometer 77−49200
atmosphere temperature field over tropical Atlantic, statistical struct. and objective anal. *(Russian)* 77−64373
atmosphere temperature profile retrieval, generalized inverse theory appl. and spectral expansion method 80−17412
atmospheric temperature, vertical profile, from satellite data, information retrieval 78−3959
auroral arc, N_2^+ first negative (0-1) band temp. height profile 78−40725
Australian region forecasts using Nimbus 6 temp. sounding 79−5550
autocatalytic kinetic system, asymmetric multiple steady states 79−86527
Baltic Sea, estuary region, suspension distrib. under river drifts influence *(Russian)* 80−98345
Baltic Sea, small-scale temp. inhomogeneities 79−2275
Baltic Sea, water temp. stratification in offshore zone 78−3792
band, integral Fredholm eqn. appl. *(Polish)* 77−23860
Barents Sea, topographically controlled Oceanic Polar Front 79−2253
Benard problem, two dimens. nonlinear temp. and vel. distribs. 78−34134
benthic ocean, temp. distrib. and flow structs. 80−72532
binary star system accretion wake, temp. and density distrib. 79−21358
biological tissue, temp. distrib. with laser irrad., thermodynamic analysis 79−29562
biological tissue, transient temp. distribs. 79−96520
Black Sea upper layers, temp./salinity anal. of seasonal vars. *(Russian)* 78−77264
Blasius flow, horizontal, heated from below, longitudinal vortices onset 78−71342
blood perfusion rate determ. from temp. perturbation, unbiased minimum variance linear estimator 79−92283
body surface of warm-blooded animals, effect of tumours, math. model 78−64943
body temperature humidification, effect on patient thermal regulation 78−85295
borehole, obliquely bored, washing fluid temp. calc. method *(Russian)* 79−68555
borosilicate glass, Simax, internal and surface temp. during heating *(Czech)* 79−42285
boundary layer, dimensionless temp. profiles downstream from heat line source *(French)* 77−15008
boundary layer, thermal, thickness for Poiseuille flow past permeable bed 79−46299
boundary layer on rough surface, temp. distrib. 78−30279
boundary layer temperature fluctuation space correlation coeff. in turbulent core *(Russian)* 78−14001
Boussinesq fluids in turbulent convection, power spectra of temp. and vel. fluctuations 80−98543
buried convective heat source, in semiinfinite solid, steady temp. distrib., surface temp. 77−58534
buried cylindrical heat source, transient temp. distrib., upper and lower bounds 78−75048
burnt skin heat and water losses, thermal modelling 78−31790
BWR four-rod bundle burnout and heat removal intensification with water and freon-12 flows 80−18413
calorimetric sheath temp. distrib. for material selection criterion 78−77917
Caspian Sea, temp. fine struct. meas. *(Russian)* 78−73379
Caspian Sea, temp. vars. rel. to short internal waves in near-surface thermocline *(Russian)* 78−81231
Caspian Sea, thermocline depth determ. using sonar *(Russian)* 77−13132
casting, solidification and cooling in mold *(Russian)* 79−29038
U Cephei, eclipsing binary, hot/cool spots obs. in UV light curves 78−57577
ceramic, laser drilling and cutting, anal. of results using computer model 79−70180

temperature distribution continued
channel, axisymmetric, with axial press. gradient injection, turbulent boundary layer characts. 79−37304
channel, heat-insulated, laminar flow with nonuniform vel. and heat input distribs. *(Russian)* 79−64662
channel, rectangular, laminar forced convective heat transfer for 3rd kind temp. boundary conditions 78−87341
Chaudes-Aigues region, surface anomaly, aerial thermographs 77−21714
chemical reactor, falling-film gas-liq. type, mathematical model 79−86526
chemically hardening material cast in elastic cylindrical mold, transient thermal stresses 80−7589
chemically reactive flow characts., simultaneous heat-mass transfer *(Japanese)* 78−22431
chemically reactive flow in porous catalyst, conc. and temp. profiles, computation method 79−86523
chromosphere spicules, temp. struct. rel. to contrib. to solar EUV line emission 80−4325
chromosphere temperature rise, acoustic waves effects 79−16911
Chukchi Sea, temp. fine structure near sea ice margin 79−57961
circuit-breaking arc radiative transfer, magnetic stability, and turbulent heat exchange 78−75482
circular cylinder, local heat transfer by turbulence of free-stream flow of viscous liquid, theoretical determ. of influence *(Russian)* 80−96252
circumarctic ocean temp. linked with low level cloud, climatic change study 77−29415
clinical microwave focusing thermography 80−3771
closed cylindrical shell with insulated cross crack *(Ukrainian)* 78−90638
cloudy atm., long distance meas. by radiometry 80−90196
clusters of galaxies, OSO 8 X-ray spectra rel. to intracluster gas temp. distrib. 79−25734
coastal inlet water temp. change due to artificial heat input 79−16506
coastal submarine hydrothermal activity off northern Baja California 78−61431
coastal surface water temp., spatial var. during upwelling 80−36322
coastal waters of NW.Italy, oceanographic temp. and flow conditions during 1977 spring 79−34827
coastal zone thermal wedge dynamics *(Russian)* 78−81205
coaxial jet, Raman scattering diagnostics of turbulent flow field 78−18328
complex domain heat exchange, new soln. techniques 78−94509
complex structure, one-dimens. heat conduction eqn. 77−42690
composite cylinder, nonstationary temp. field 78−67014
composite cylinder, periodic heating *(Russian)* 77−42715
composite geometry reactor vessel, steady temp. distrib., thermal shock 77−54286
compound unbounded cones, temp. fields *(Ukrainian)* 78−54317
compressible laminar wall jet 80−28542
concrete creep under nonuniform temp. distrib., linear viscoelastic analysis 77−62172
condensed medium, semitransparent, plane layer radiative-conductive heat transfer 80−43590
conducting plate with temp. depend. resistivity and surface heat loss, temp., current and elec. field distribs. 77−42696
conductor in pulsed mag. field, influence of surface layer 79−31773
cone/plate system in fluid, friction heating and convection 78−87238
contact binary stars, temp. discontinuity maintenance 80−8655
contact binary stars structure, secular stability of stemp. inversion layer 80−109493
continental lithosphere, vertical temp. distrib. limits 78−65207
continuous heat source, sphere, boundary conditions of second kind, temp. field 77−23851
continuous logging of terrestrial temp. gradients 77−82052
convection, free laminar flow, between two parallel vertical walls 77−47010
convection, mixed forced/free, from horizontal plate, in porous medium 77−75908
convection, mixed free/forced, about inclined surfaces in porous medium 77−75973
convection, natural, in closed container, numerical simulation 78−46969
convection, natural, in porous medium, singular perturbation problem 79−94715
convection, natural, laminar, enclosure with heat source and sink on horiz. boundary 78−90882
convection, natural, transient and steady-state numerical solns. 80−10119
convection, past hot porous circ. cylinders, of 2nd-order liq. 79−14476
convection, unsteady combined forced and natural, from circular and elliptic cylinders *(Japanese)* 79−32510
converse problems, initial temp. distrib. determ. by optimal dynamic filtering 80−19208
cooled gas transport by pipelines, temp. and pressure distrib. determ. 79−23326
cooling bodies, thermal stresses and temps. determ. by finite elements 77−14881
R Coronae Austrinae interstellar molecular cloud, for IR study and dust temp. profiles 80−62237
coronal active region, temp. distrib. and exponential depend. of emission measure 78−53917
Cosserat medium subject to thermal stresses, plane contact problem *(Polish)* 78−22268
Couette flow, permeable wall layer, heat transfer and temp. distrib. 78−51165
countercurrently flowing fluids separated by thin wall, heat transfer 77−23949
cryostat, temperature field inhomogeneity in cooled screen, effect on efficiency 78−62204
cryosurgical applicator, temp. distrib. reproducibility 79−39589
crystal growing, electrical analogue model *(German)* 78−63688
crystal growing oven, temp. distrib. in working zone, heat transfer calc. 78−3016
crystal growth from melt, thermal conditions effect on stability 77−76343
cup ironing process, two-dimens. plastic flow prod. by temp. field *(Polish)* 78−26053
Cygnus Loop, supernova remnant, imaging X-ray obs., temp. struct. 80−41876
cylinder, circ., impulsively started from rest, heat transfer, numerical anal. 80−10248

temperature distribution continued
cylinder, hollow, unsteady axially nonsymmetric temp. distrib. *(Polish)* 80−10152
cylinder, hollow, with finite width ring heat source, temp. distrib. exact soln. 77−84124
cylinder, medium temp. control *(Russian)* 77−54856
cylinder, rotating, non-steady temp. distrib. *(Polish)* 78−13885
cylinder, solid, temp. prediction method for inverse heat cond. problem 79−94449
cylinder, solid circular, const. surface cooling, temp. fields, heat cond. *(German)* 77−39195
cylinder comprising homogeneous elements, calc. of temp. field *(Russian)* 77−84110
cylinder immersed in liq., correct boundary conditions 78−38171
cylinder in hot gas cross-flow, steady state temp. distrib. 78−30160
cylindric flow in tubes, temp. distrib. *(German)* 77−31391
cylindrical body heated by moving heat source, heat cond. and temp. distrib. Green's function derivation 77−42681
cylindrical plastic shell, nonstationary temp. field, contact press. calc. in cable pressing 78−63270
cylindrical shell of complex configuration, calc. of nonsteady thermal regime 78−1543
Czochralski crystal growth, temp. distrib. 79−60288
Czochralski method, thermal conditions effect in temp. distrib. 78−3019
deep ocean, bottom boundary layer short-term variability 79−2269
deep ocean, salinity and pot. temp. profiles rel. to boundary mixing 78−73388
deep ocean, temp. fine struct. rel. to internal gravity waves and wave breaking 78−85578
HR Delphini (Nova 1967), electron temps. in different regions of envelope 80−4369
Denmark Strait, upper layer temp. and salinity *(Russian)* 77−60413
E.Derbyshire, local temp. var. 77−64404
detonation wave front, heating of contained particles, residual cryst. defects anal. *(Russian)* 79−68749
Devon Island ice cap, Canada, theoretical and observed temp. profiles comparison 79−16524
DH lasers, thermal-gradient enhanced current spreading 79−18416
diatomic gas, transient flow, temp. and conc. profiles, by rot. Raman scatt. 77−75995
dielectric liquid, elec. stressed, motion due to Coulomb, electromech. forces, schlieren image obs. 80−100037
dielectric mirror, temp. field during laser radiation absorpt. 80−19063
diffusion furnace temp. profile meas. systematic errors, theoretical model *(German)* 80−8989
discharge, pulse, low voltage, radial temp. distrib., chem. composition determ. 79−50845
Drake Passage, Antarctic polar frontal zone variability during summer (1976-1977) 78−85579
drop, diffusional evap. in EM radiation field 78−43112
droplet, vaporising, internal temp. field 78−51042
duct, circ., laminar convective MHD heat transfer for 3rd kind temp. boundary conditions 78−87342
duct, narrow, plane, temp. distrib., heat flow to dense blown layer *(Russian)* 78−83402
duct, standing wave analysis with temp. gradients 77−62085
duct with axial temp. gradient, sound transmission and generation 77−62084
early universe, density-temp. fluctuations present observability 80−82554
Earth, extremal temperature bounds from surface gradient measurements 79−84189
Earth, geothermal effects of conducting zone formation 78−85519
Earth crust, temp. distrib. in Ukrainian Shield rel. to search for fracture waters *(Russian)* 80−104935
Earth crust press.-temp. conditions modelling, appl. of rocks elastic props. experimental studies *(Russian)* 78−96207
Earth upper mantle, palaeogeotherm from ultramafic xenoliths in Elwin Bay kimberlite 77−91078
earthquake slip, frictional heating on fault zone with finite thickness 78−36124
EBR-II primary system piping evaluation for safety research modification 79−9785
electrical contact, bridge transfer on electrodes with fibre struct. of heat-proof component 77−59325
electrically heated finite cylindrical coil, temp. distrib. calc. *(Polish)* 77−54865
electrode units in MHD channel, temp. distrib. 78−59258
electrosurgical dispersive electrode site temp. and current density distrib. model 79−92424
emission measure for UV spectra of RW Aurigae and RV Lupi 80−94788
SW.England heat flow anomaly 77−49041
equatorial Indian Ocean, seasonal temp. and density fields caused by monsoons *(Russian)* 78−44839
equatorial topside ionosphere, ion temp. troughs and interhemispheric plasma transport 78−96340
explosions, heat balance and reactant consumption 77−90601
face effect, with paraboloidal or ellipsoidal isotherm effect 80−107085
fatigue, thermal energy losses and steady state temp. field calc. 77−19571
fatigue specimen, nonsteady temp. field computation, rel. to thermal part of mech. hysteresis 79−3905
ferrofluid, helical flow with heat cond. between coaxial porous tubes 79−23371
fibre reinforced materials, therm. stresses in unit cell 80−10160
fibre-reinforced composite, quasi-one-dimens. thermal diffusion, mixture theory 78−71271
field distortion by thermocouple seal-in 78−81968
finite disc, thermal shock, finite integral transform method 77−3765
finned heat pipe latent thermal energy storage system performance 79−57487
fission reactor cylindrical fuel pins with gap and cladding *(Italian)* 79−13397
fission reactor evaporator, premature bend dryout phenomena, wall temps. 77−61499
fission reactor spent fuel bundle, analytical method of prediction 79−89472
fjord lake, thermal struct. rel. to internal Kelvin waves 78−73411
fjords, horizontal temp. and density gradients 78−24303
flame jet, premixed, impinging on plane surface, turbulent heat transfer 79−4054

temperature distribution continued
flame plume behind bluff body with fuel injection, elec. cond. mechanism 79−39150
flat layer of selective medium with semitransparent boundaries, radiative-conductive heat transfer 80−19227
flat plate solar collector thermal behaviour model and performance parameters 79−62045
flow, in channel, turbulent vel., press., and temp. fields, direct numerical simulation 80−19361
flow, nonequilib., two-phase, relation between thermal and flow characts. 78−55694
flow, periodic thermally developed regime in ducts with streamwise periodic wall temperature or heat flux 78−59484
flow-through reservoir, vel. and temp. fields, num. simulation 77−17152
fluid bed boilers, temp. profiles 79−32663
fluidised bed reactor, solid-circulation model, steady-state multiplicity 79−86524
forced convection flow and heat transfer of compressible fluid in porous medium *(French)* 78−30354
forward Monte Carlo heat conduction, known-temp. boundary condition treatment 79−158
Fourcault sheet glass, internal and surface temp. during heating *(Czech)* 79−42285
free burning arc characteristic formulae 80−70068
free convection flow past vertical porous plate set in impulsive motion 80−69818
free molecular vapour flow, mass transfer during condensation in channel 78−51198
frozen food, hydrostatic press. effect on phys. props. 78−26706
fuel element transient heat transfer, temp. distrib. 78−17280
fuel rod with cladding, time depend. temp. distribs. 78−17288
furnace heat transfer, 3-dimens. computer model predictions test 78−59504
gas, with variable physical props., pipe flow, turbulent momentum and heat transfer calc. 78−90869
gas centrifuge with insulated end walls, Stewartson layer struct., temp. distrib. 78−46973
gas jet, heat transfer to porous baffle 79−98776
gas layer, heat cond., radiation interaction in presence of band spectrum 79−55307
gas turbines, jet mixing, aspects and recommendations *(Russian)* 77−84292
gas turbines, temperature gradient along cooling channel surface, heat transfer in initial hydrodynamic section, effects 79−18892
gas-regulated heat pipe, anal. of operating temp. regimes 78−194
GCFR radial blanket velocity and temp. distrib., buoyancy effect 79−9678
geothermal reservoir, effect of magma dike intrusion on free convection 78−7599
giant planets, atmospheric thermal structs. 79−84735
glass container forming, mould surface temp. meas. 80−82767
glass melt, thermal inhomgeneity, method of determining 78−84756
glass plane layer, thermal radiation spatial distrib. rel. to temp. field, internal reflect. 79−59913
glass strip, surface temp. field during annealing in tower of vertical drawing system 78−11242
global sea surface temp. vars., atmospheric CO_2 long-term effects 78−73398
Graetz problem in horizontal isothermal tube, natural convection effects 77−75911
grey medium between concentric cylinders, 2 dimens. radiative equilib. 78−42523
ground surface temperature and moisture content, prediction with inclusion of vegetation layer 78−73373
Gulf of Alaska, ocean temp. distrib. 77−60393
W.Gulf of Maine, current, temp. and press. obs. rel. to winter circulation 80−51430
Gulf Stream, deflection by bottom feature off Charleston, S.Carolina 79−53365
Gulf Stream, fronts and wave disturbances compared with atmospheric jet stream 79−2268
Gulf Stream, vertical temp. gradient struct. 77−45007
Gulf Stream and the north east Atlantic temperature anomaly *(German)* 80−85684
Gulf Stream ring, temp. struct. during coalescence with Gulf Stream off Cape Hatteras 79−79872
Gulf stream ring frontal zone, asymmetric disturbances obs. 79−2267
half-space, plane Stefan problem soln., degenerate hypergeometric transformations method 79−86332
Hamels spiral flow, temp. and vel. distribs. *(German)* 80−87779
heat conduction, in monoclinic anisotropic system, various boundary conditions, temp. field soln. 77−58525
heat conduction, inverse nonlinear problems, simulation methods 78−94513
heat conduction, steady-state, soln. using heat balance integral method 77−14880
heat conduction, transient, one dimensional, early time, method of characts. numerical soln. 77−58524
heat conduction, unsteady, in quarter plane, appl. to bubble growth 78−75045
heat conduction in axisymmetric body-duct configuration 79−32185
heat conduction in cylinders of an anisotropic medium 79−94458
heat conduction in nonuniform media, boundary-value problems 78−63266
heat conduction problems, soln. method *(German)* 80−74705
heat exchanger, porous cylindrical board temp. field, heat transfer efficiency 78−5793
heat pipe, evaporator section, evap. and vap. flow between parallel planes 80−10115
heat pipe, gas-controlled, with wickless tank, steady-state and starting characts. 78−79187
heat pipe, high temp., subsonic vapour flux, heat exchange and friction 77−75779
heat pipes, rotating, temperature and heat load distrib. 80−64341
heat resistant monocrystal growth apparatus, heat regimes, crystallisation *(Russian)* 80−107071
heat sources method, appl. in temp. field anal. *(Russian)* 80−28410
heat transfer in semiinfinite region with variable physical parameters 79−90116
heat transfer problems, linear algebraic soln. method 78−59281

temperature distribution continued
heat-emitted pipe, with surface boiling, temp. fluctuations *(Russian)* 80−102962
heated grid, two-point turbulence meas. 77−19594
heating surface during boiling, temp. distrib. for a sudden increase in power *(Russian)* 77−84114
HZ Herculis, eclipsing binary, accretion disc. temp. distrib. from optical light curve 78−65658
HF heated cylindrical component temperature field computation for quench control 78−90632
high pressure chamber, temp. field distrib. determ. 78−82001
high temperature gas diagnostics by spectral remote sensing 78−74002
high-current free burning arcs, approximate model 80−70069
high-level radioactive waste storage, distribution calc. *(German)* 79−81014
high-level radioactive waste storage, temp. distribution simulation expts. *(German)* 79−81015
hollow cube, non-homogeneous, transient temp. distrib. 78−75035
hollow cylinder, internal one sided heating, nomogram construction, for computing temp. state 78−63271
holographic interferometry methods and applications *(French)* 79−7099
hot rolled T-section finite element anal. of temp. field *(Russian)* 79−29101
hot wall with impinging liq. droplet, transient temp. profile 78−75050
Hudson Estuary, salinity and temp. distrib. 77−17136
human body during hyperthermia therapy 77−16911
HWGCR, KS-150, in-core instrumentation, neutron flux, temp. distrib. 77−83050
hyperthermia, nonintrusive meas. by US temperature tomography 79−53282
hypervelocity particle impact, heating and vaporisation, temp. estimation 78−59290
IC 1396 interstellar molecular cloud, for IR study and dust temp. profiles 80−62237
ice-water interface, local temp. meas. and convective flow 79−73293
icy satellites, mass-radius relationships, density and temp. profiles 80−31222
III-V semiconductor, temp. distrib. around dislocations, due to Joule heating, calc. 78−71734
inclined surface, natural convection flow, transition, vortex system, meas. method 79−27632
incompressible viscous fluid, entrance region heat transfer in plane Couette flow, num. procedure 77−15020
Indian Ocean, modern and ice-age surface water zonal temp.-anomaly maps 80−77007
Indian Ocean, temp. meas. rel. to continuous spectrum of equatorial waves 80−98331
infinitely thick slab subject to random surface temps., frequency response function, temp. variations 77−19511
ingot, hollow cylindrical, temp. field and crystallisation front calc. *(Russian)* 78−63690
ingot, temp. field calc. approx. by equiv. cylinder *(German)* 78−84788
inhomogeneous rod in complex heat exchange conditions, temp. calcs., film sputtering evaporators *(Russian)* 80−38230
integral eqn. kernel approx. in axially symmetric temp. problem 79−35643
intense electric fields in needle/cylinder electrodes, space temp. and thermal model *(Rumanian)* 80−63885
interplanetary gas, radial temp. and flow vel. 79−96875
interplanetary-interstellar H, temp. meas., Prognoz-5 obs. 78−7922
interstellar dark clouds, grain surface reaction rel. to chemical and thermal equilib. 79−44593
interstellar giant molecular clouds, density inhomogeneities temps. rel. to gravit. field 80−62242
interstellar shocks, post-shock gas temp., density and vel. profiles, analytical results 80−56911
Intertropical Atlantic, sea temp. cycle in upper layers *(French)* 78−96227
intestine, exteriorised, influence of blood flow on temp. distrib. in the mouse 79−48219
inverse nonlinear heat cond. problem, thermal gas dynamic testing 80−23862
Io, surface temp. distrib. rel. to UV obs. of SO_2 80−36561
Ionian Sea, oceanic front obs. during early winter (1970) 77−45008
ionosphere, day-night terminator 80−4186
ionosphere and protonosphere, electron temp. profile over S.Atlantic geomag. anomaly *(Japanese)* 78−28368
IR streak camera, high speed, appls. 77−79093
irregular viscous fluid between rot. cylinders, temp. and press. distribs. 77−65769
irreversible transport processes, noncoupled, nonstationary, classical variational principles 78−4567
Japan, O_3 and air temp. distrib. rel. to pollutant profiles *(Japanese)* 77−70768
jet, cross stream injection boundary layer, flow and temp. field 79−1225
Jupiter, thermal profiles and NH_3 distribs. from IR spectral meas. 79−40126
Jupiter, thermal structure from IR spectral meas., filtered iterative inversion method 78−7918
Jupiter atmosphere, high resolution obs. between 30 and 50 μm rel. to temp. profiles 80−46462
Jupiter atmosphere, temp. struct. from inversion of IR spectral meas. 79−75141
Jupiter atmosphere and ionosphere, temp. struct. from Voyager 1 preliminary radio profiles 80−26791
KEMA Suspension Test Reactor neutron flux and Dodewaard BWR temp. noise 79−3193
Kirin meteorite, temp. gradient prod. in atm. passages, thermolum. obs. 80−67672
Kirishima volcanoes, Japan, surface temp. distrib. from geothermal survey *(Japanese)* 80−67357
Klamath Falls, Oregon, heat flow data and obs. geothermal phenomena 77−5158
Knudsen effusion chamber with low axial temp. gradient for high temp. thermodynamic tests 77−71329
kohlestein thermal insulation, temp. and heat flux distribs. meas. *(German)* 78−26023
labyrinth caloric test, estimation of stimulus strength 78−40210
Laccadive Sea (Lakshadweep), temp. and salinity charcts. 80−104966
Lake, Superior, LANDSAT-1 obs. of internal standing wave pattern 78−96244

temperature distribution continued
Lake Ontario thermocline, intermittent full upwelling 77−33110
lake sediment thermal diffusivity estimation from field obs. 77−2253
Lake Shlavantas, deep autumnal cooling and freezing *(Russian)* 78−36213
Lake Superior, Keweenaw Current, surface temp. structure 78−40597
Lake Tahoe, California-Nevada, effects of coastal front on temp. and chlorophyll distrib. 79−2301
lake upper layer mixing during heating cycle 77−29335
lake vertical temp. profile determ. by one-dimensional heat transfer eqn. soln. 78−77290
lakes, deep and shallow *(German)* 78−85618
lakes, stagnant, thermal stratification 80−36340
lakes, surface water temps. appl. to latent and sensible heat fluxes 80−72562
lakes, vertical automatic profiling system for temp. and current meas. 78−36327
lakes, winter season energy balance *(Polish)* 78−24315
lakes in Wyoming, bathymetry and temp. 80−94550
lamina, heat distrib., thermal conductivity 78−22246
lamina, porous, generalised boundary conditions, heat and moisture transfer Prudnikov problem soln. 78−1551
laminar boundary layer, heated, with nonuniform surface temp. distrib., stability 78−67175
laminar channel flow, heat transfer in entrance region 79−32518
laminar circular jets, friction heat effect on temp. distrib., anal., forced convection 80−10279
laminar flow around plate containing heat sources 77−23948
laminar forced convection to turbulent free convection transition over heated plate 79−32516
laser beam-surface impact, pulsed and CW modes, transient momentum transfer 77−89013
laser cylindrical resonator thermal distortion due to surface absorbed energy *(Russian)* 78−13729
laser light with time-varying intensity in optical medium, temp. field kinetics 78−59098
laser surface transformation hardening, heat flow model for cylinder 80−93700
layer, dense, large Biot no., heat exchange *(Russian)* 78−83400
Leiden dilution refrigerator, lowest temp. and temp. gradient in counterflow capillary calc. 77−2660
linear heat conductor, conduction anal. with heat flux branching at boundaries 77−11107
liquid, in vertical cylindrical cavity, sudden ambient temp. change *(French)* 77−47009
liquid crystal improved technique for thermal field measurements 80−216
liquid film, falling, laminar, evaporation model 79−46305
liquid film, viscous, between two nearly parallel walls, temp. distrib., convection effects 80−83801
liquid metal heat transfer in regular fuel element arrays, Nusselt no. calc. 78−89932
liquid metal MHD temp. pulsation cross correlation coeffs. *(Russian)* 77−65815
liquid vertical layers, convective flows with spatially modulated temp. distrib. at boundaries *(Russian)* 79−32496
liquid-filled closed volumes, temp. stratification at const. heat flux density 79−81871
liquids, throttling, temp. field near boundary 80−43757
Lithuanian lake water temperature rise (spring 1974) *(Russian)* 79−8644
living tissues, simulated, temp. distrib. in EM irrad. 80−85354
LMFBR, Clinch River Plant, pipe rupture simulation using DEMO code 78−8927
LMFBR, thermal profile development and inversion, analytic prediction for safety expt(s) 79−93754
LMFBR finite hexagonal bundles, laminar mixed-convection heat transfer 79−607
LMFBR safety application of US thermometry 79−45400
LMFBR wire wrapped fuel assemblies, temp. distrib., approx. method based on porous body model 77−18646
local heat flux distributions, highly inhomogeneous, auxiliary-wall meas. method 80−5917
local heating in layer with absorption *(Russian)* 77−42716
Loch Ness, Kelvin-Helmholtz billows, rel. to thermocline fine struct. 77−66935
long rod, direct-heating meas., interpretation 80−102964
louvres in thermal radiating panel 80−10124
low-flow vessels, temp. gradients, appl. to blood temp. distrib. 78−27990
LPE system, temp. gradient meas. using W-graphite thermocouple 80−25584
lunar boulder shadow temp. and duration from shaded soil sample thermoluminescence 77−33372
lunar surface layers, dielectric const. and temp. gradient from 2 and 6 cm brightness distrib. 78−81572
M17, Platt particles and spatial temp. fluctuations 78−61907
M8 electron temp. from radio recomb. line obs. at 5 and 10 GHz 79−84832
magnetic fluid, in current-carrying plate field, free vertical convection *(Russian)* 77−65806
on magnetosonic heating of semiinfinite body under periodic loading *(Russian)* 77−50855
mainstream acceleration effect on heat transfer and wall temp. downstream of gas injection 79−1251
mantle temp. from dunite-peridotite mixed-oxide compositional models 77−2124
marine thermocline evolution, study using Mellor-Durbin theory 80−4041
Mars, atmospheric thermal regime, long wavelength radiation fluxes 77−33385
Mars, tephigram of CO_2 atmosphere 78−73671
Mars, thermal and albedo mapping during Viking primary mission 78−20683
Mars atmosphere, scale height and temp. profiles from ε Geminorum occultation obs. 78−53853
Mars atmosphere thermal IR properties, 15 μm band meas. 79−84710
Mars atmosphere thermal IR properties, dust and ice clouds detect. from Viking IRTM spectral meas. 79−84712
Mars atmosphere thermal IR properties, global behaviour at 7, 9, 11 and 20 μm 79−84709

temperature distribution continued
Mars atmosphere thermal IR properties, local dust clouds effects 79−84711
Mars surface and atmosphere, IR thermal mapping by Viking 77−13264
Mars upper atmosphere, temp. struct. from ε Geminorum occultation obs. 79−53749
massive solids, temp. fields under mixed boundary conditions *(Russian)* 77−50869
medical thermographic system model parameter calc. 79−79477
melt, temp. field calc. by numerical implicit method 80−44342
melt adjoining solid phase, inhomogeneous temp. field influence on capillary phenomena *(Russian)* 80−20029
melting clad temperature distribution in fission reactor, Pekeris-Slichter series expansion method 77−88238
melting of semiinfinite solid, nonFourier heat cond. temp. distrib., interface location, small times 77−58542
melting semitransparent material, approx. temp. profile calc. emthod 77−75787
melting/freezing interface, annular region, perturbation soln. 78−59286
metal, US heating *(Russian)* 77−44258
metal plate transient temperature field in active thermal test methods, calc. 77−75775
metal rod, US heating to onset of plastic deform., temp. field calc. 77−69049
metallic heat carrier in loops, phase transition process, temp. field 79−55867
metals, plastically deforming at high strain rates, distrib. of temp., strain rate and strain 79−19311
metals, temp. distrib. during heating by electrolytic plasma *(Russian)* 79−1045
methane-air flame, Raman scattering diagnostics of turbulent flow field 78−18328
MHD, unsteady free convection flow past vertical porous plate 78−30361
MHD convective viscous flow past porous plate with suction, mass transfer effects 78−87398
MHD duct flow, H_2O_2, two-dimensional calc. 79−83605
MHD Ekman layer on porous flat plate, heat transfer, steady asymptotic soln. 78−79385
MHD flow between parallel plates, temp. field, vel. field, skin friction, heat transfer 77−68700
MHD forced convection in channel bounded by plate and permeable bed, Hall effects 80−69934
microcrystal, melting and solidification, temp. gradient, mol. dynamics model calc. *(German)* 77−76527
microwave brightness temp. distrib. over Bay of Bengal using SAMIR Satellite Microwave Radiometer data at 19 and 22 GHz 80−104980
microwave bulk biomaterial thawing, electric field uniformity requirements *(Russian)* 79−83852
microwave irradiated breast tumour thermal pattern calc. *(French)* 80−3759
microwave-irradiated cylinders simulating living tissues 80−3760
MIM cathode, radial temp. distrib. *(Russian)* 78−6833
Mississippi River delta, inner shelf temp. and salinity structure 77−37229
mobile powerful conc. heat source *(Russian)* 77−42718
moist porous material subject to sudden heating, mass transfer, press. rise 77−58787
molecular lasers with gas pumping, temp. field calc. 79−76673
momentum generation in high-current arc 78−71586
monitoring temp. uniformity in solid state reaction system 78−230
Monte Carlo heat conduction using transport eqn. approximation 79−159
Moon, electrical conductivity rel. to thermocline 77−60687
Moon, internal temp., solid state convection models 77−60688
MOS structure, with several heat sources, temp. distrib. 77−43730
moving heat source 79−27488
multidimensional body, radiant preheating *(Russian)* 77−42717
multilayer components, thermal quality control 78−85107
multilayered cylinders, nonstationary temp. fields with rotational symmetry *(German)* 78−79190
multispectral radiance method for temp. distribution meas. *(Japanese)* 78−77912
narrow zone heating of bodies *(Russian)* 77−72132
natural convection from vertical surface in thermally stratified fluid 77−15021
natural fluid circulation, horizontal pipe, closed at one end 77−47091
NDT, thermal flow method, calc. algorithm for object containing defect 78−72970
NDT of delamination and inclusion flaws, ID anal. 80−71820
nebulae, dusty, temp. profiles in non on-the-spot (OTS) models 78−85995
Neptune, atmospheric thermal profile, supersaturated stratospheric methane 79−40137
NGC 7027, planetary nebula, temps. from low excitation emission spectrum 77−64823
non-isothermal condensation, temp. distrib. 79−27501
nonlinear radiating linear absorbing rod of finite length, asymptotic temp. behaviour 77−50859
nonmetallic infinite plate exposed to laser pulses, temp. field calc. *(Russian)* 78−59061
nonstationary heat conduction process, optimisation, soln. 79−81686
nonstationary temperature field, in a crystal on a substrate, variational method *(Russian)* 78−18158
nontransparent medium, bounded flat layer effective temp. determ. 80−69638
W.North Atlantic Ocean, temp. meas. rel. to mesoscale motion space and time scales 78−49035
North Sea, sea surface temp. year to year changes, (1948 to 1974) 80−67367
Nova Scotia slope water, interleaving at subsurface front 78−85585
nuclear fuel pins with eccentric pellets, two-dimensional temp. profile calc. 79−9677
nuclear fuel rod gap conductance uncertainties deduced from fuel centreline temps. 77−46308
nuclear fuel thermocouple readings verification by transient response analysis 77−46309
nuclear power station thermal plume monitoring by drogues 77−3192
nuclear reactor, convection effects on temp. distribs. during emergency cooling in SNR-300 77−26839
temperature distribution continued
nuclear reactor, fuel element array, temp. distrib. for turbulent liq. metal flow 78−13203
nuclear reactor, press. and temp. loads on LWR containment after LOCA, scale model expts. 77−3134
nuclear reactor fuel pin behaviour, computer code FRUMP, stress, strain, temp. distribs., displacements 77−14235
ocean, bottom nepheloid layers and bottom mixed layers, on continental shelf off Oregon 78−16027
ocean, current vel. and temp. oscills. with periods to inertial oscills. *(Russian)* 77−33088
ocean, eddies and islands effects on temp. fine struct. and mixing 78−85572
ocean, energy dissipation meas. adjacent to island 78−85573
ocean, Loop Current winter intrusions 78−40569
ocean, low temp. skin-layer model *(Russian)* 78−36180
ocean, mesoscale synoptic eddy area, temp. field fine structure *(Russian)* 78−81195
ocean, model of annual temp. var. and appl. to study of climate 78−20433
ocean, radiothermal location, inverse problem soln. method *(Russian)* 78−16188
ocean, seasonal temp. var., model *(Russian)* 77−60402
ocean, seasonal thermocline, temp. field fine structure *(Russian)* 80−17278
ocean, seasonal thermocline, vertical structure of temp. field *(Russian)* 78−85596
ocean, temp. and salinity self-similar distrib. in upper thermocline *(Russian)* 79−16474
ocean, temp. fine struct. and banded salt finger struct. form. 78−85570
ocean, temp. oscills. rel. to small scale turbulence spectra *(Russian)* 79−88360
ocean, thermocline affecting vertical distrib. of oscills. *(Russian)* 80−21777
ocean, thermohaline circulation in two-dimens. dynamical model *(Russian)* 78−40557
ocean, vertical temp. gradients meas. via moored instrument 80−12561
ocean, water temp. rel. to irradiance in Norwegian and Barents Sea 80−31055
ocean abyssal shear zone, temp. and salinity distribs. 78−73386
ocean bottom mixed layer variability on Oregon shelf 79−74896
ocean colour and sea surface temp., remote meas. over Straits of Dover *(French)* 78−96238
ocean frontal regime, microstructure and fine structure 79−16487
ocean frontal zones light scatt. obs. rel. to temp. distrib. 79−2266
ocean fronts, Chapman conf. (New Orleans, 1977 October) 79−2246
ocean internal waves and temp. finestructure discrimination 77−60389
ocean shelf/slope water front, double diffusion, fine structure instabilities 79−16488
ocean surface, satellite data processing *(Russian)* 80−17417
ocean surface, temp. distrib. determ. via microwave radiometry 78−81415
ocean surface layer thermal struct. and atmospheric heat exchange *(Russian)* 77−73751
ocean surface temp., mid-latitude changes NCAR general circulation model response 78−16098
ocean surface temperature, meas. 200 km from land rel. to air-sea heat transfer coeffs. 80−72552
ocean synoptic eddy area, temp. disturbances, vertical structure *(Russian)* 78−85600
ocean temp. anomalies, 1966-74 period, NE. Pacific, gridded by objective anal. 78−92830
ocean temp. distrib. rel. to Earth global heat balance annual var. 78−73300
ocean temperature field, transformation after passage of tropical cyclone *(Russian)* 77−53069
ocean temperature field space/time struct. during NORPAX POLE expt. 78−3777
ocean thermal response to strong atm. forcing, events characts. 78−92827
ocean thermal response to strong atm. forcing, one-dimens. mixing processes 78−92828
ocean thermocline, small-scale turbulence *(Russian)* 80−61807
ocean thermocline, temp. fluctuations and internal waves rel. to wind field variability 80−31052
ocean thermocline and mixed layer, model of seasonal evolution 80−26546
ocean thermocline approx., discontinuity surface in active layer *(Russian)* 78−16037
ocean upper layer, small-scale temp. fluctuations statistical regularities *(Russian)* 80−94528
ocean upper layer temps. in Cayman Sea and Gulf of Mexico, rel. to local wind stress curl 79−48495
ocean vertical temperature gradients horizontal var. meas. by thermocouple arrays 78−61571
ocean-atmosphere system, interannual variability 79−2330
oceanic finestructure, wave-induced and intrusive structs. separation 79−48502
oceanic shallow thermocline onset determ. using acoustics 77−9523
oceanic thermal fronts off Korea, DMSP IR detection 77−21796
oceans, wideband temp. meas. rel. to kinetic energy dissipation field struct. *(Russian)* 77−13082
oil shale, transient temp. distrib. due to combustion flame in retort 79−37110
optical fibre drawing, neck-down shape prediction from furnace temp. distrib. 78−5594
optical fibre splicing using CO_2 laser, thermal conditions 78−13820
Oregon Inlet, N.Carolina, coastal upwelling, exchange through Barrier Is. Inlet 77−60401
Orion A, H II region, radio meas. of electron temp. distrib. at 22 GHz 77−87558
Orion Molecular Cloud, NH_3 emission obs. and rot. temps. distrib. 80−36687
Orion Nebula, temps. and abundances in outer part 79−53868
tropical N. Pacific, annual forcing of baroclinic long waves, bathythermograph obs. 77−60392
central N. Pacific, finestructure spectra from main thermocline 77−60390
central N.Pacific, frontogenesis and frontolysis rates, 1976-7 winter 79−2250
N Pacific, subsurface hydrography from radiolarian distribs. 77−33095

temperature distribution continued
tropical N.Pacific, temp. fine structure 79−16485
E.Pacific and equatorial Atlantic Oceans, hemispheric asymm. of heat budget 78−40570
N.Pacific mesoscale phenomena, oceanographic model and acoustic survey comparison 80−46195
Pacific Ocean, annual var. in slope of 14°C isotherm along equator 80−72537
tropical Pacific Ocean, climatological usefulness of satellite-determined sea-surface temps. 80−31044
Pacific Ocean, December sea surface temps. correl. with spring rains in California 80−77064
N. Pacific Ocean, interior midlatit., main thermocline seasonal cycle, wind driven model expt. 79−48499
N.Pacific Ocean, numerical simulation of anomalies, model and mean state 79−48494
E Pacific Ocean, surface temp. annual development in Panama Gulf and coast *(French)* 77−17109
N.Pacific Ocean, synoptic obs. of Kuroshio and Oyashio fronts 78−32113
N Pacific Ocean, temp. anomalies vertical struct. 78−73394
N.Pacific Ocean, west, depth, var. of temp., salinity and sound vel. meridional gradients 80−51429
equatorial Pacific Ocean, XBT sections and sea level meas. rel. to currents strength monitoring 78−73383
tropical Pacific Ocean thermocline displacement, simple Ekman-type model 79−48498
NW.Pacific subtropical front during 1954-74 period 79−2249
Pacific surface temps., empirical orthogonal function anal. 77−17127
packed bed, temperature profile for concurrent air-water downflow, latent ht. effect 79−50789
packed bed thermocline, anharmonic analysis 79−27494
parallelepiped with local energy source, approx. anal. of steady-state temp. field 77−11111
particles in nonisothermal plasma jet, trajectory and temp. calcs. *(Russian)* 80−7514
periodic system of narrow inclusions, effect on steady temp. field 78−63265
permafrost, two-dimens. temp. field with arbitrary temp. distrib. on subaerial surface 77−25703
permeable bed boundary layer flow, temp. distrib. and Nusselt no. 78−51166
Peru Current, sea surface temp. rel. to advection, satellite obs. 78−16029
phase changes subject to convection and radiation, perturbation solns. 79−76962
physicochemical processes, kinetic investigations by nonisothermal methods, inhomogeneous temp. field 78−59287
pipe, heated, straight, free-forced convection in entry region 78−90883
pipe, horizontal, with different end temps., fully developed natural counterflow, temp. distrib. 78−75137
pipe, laminar pulsating flow, heat transfer 79−94621
pipe, mean temp. and conc. profiles in turbulent liquid flow 77−47011
pipe, mean temp. and conc. profiles in turbulent liquid flow 77−47012
pipe, of variable thermal and elec. conds., elec.-heated, flow-cooled, temp. distrib. 78−90626
pipe, rotating, curved, convection heat transfer, appl. to spacecraft spin system 78−94737
pipe, with nonuniform heat source, convective heat transfer 77−31298
pipe entrance region boundary layer, turbulent temp. and vel. fluctuations *(Japanese)* 78−38301
pipe flow, laminar with nonlinear wall heat fluxes, axial cond. 79−27636
pipe outflow, turbulent, with wall suction, dynamic and thermal fields *(French)* 79−4082
pipe wall with radiative heating and working medium at supercritical pressure, temp. fields 77−7479
pipeline, nonstationary heat transfer to environment, soil temp. distrib. 77−84108
planar body, with circ. boundary and thermally insulated cracks, temp. distrib. 78−67002
plane channel of arbitrary shape, occupied by grid, heat and mass transfer, comput. method 77−7453
plane parallel layer with canonical boundary, temp. field determ. *(Russian)* 78−30148
plane stagnation flow, vel. and temp. profile determ. by variational method 77−72293
plane steady temp. field, effect of biperiodic system of plane inclusions 80−19224
plane thermal boundary layer, temp. distrib. determ. by var. formulation 77−23947
plane walls of variable thermal cond., transient temp. fields *(Polish)* 78−18155
plasma, inhomogeneous Alfven waves collisionless damping rel. to temp. profile shaping 79−64864
plasma ion temp. radial profile meas., neutron flux, Doppler broadening and charge exchange 78−79469
plasma spatial temp. distrib. meas., interference filter photographic method 78−67332
plasma-chemical reactor for AlN synthesis 77−59730
plasmatron spray, parameters meas. *(French)* 77−35402
plate, approx. soln. method for heat cond. problems 80−33415
plate, circular, thermally induced vibr. analysis 79−94524
plate, complex shape, temp. field during welding with moving heat source *(Russian)* 79−68553
plate, finite rectangular, superposition of boundary conditions in temp. distrib. eval. 77−14883
plate, heated, semiinfinite, vertical, with heat sources and sinks natural convection 80−59035
plate, heated equilateral triangular, large deflection, uniform load, temp. distrib. 78−83250
plate, heated thin annular circular, of variable thickness, buckling, thermoelasticity 78−9581
plate, mean temp. and conc. profiles in turbulent liquid flow 77−47011
plate, mean temp. and conc. profiles in turbulent liquid flow 77−47012
plate, steady-state temp. field calc. 77−58523
plate, thin, in gradient current flow, coupled heat exchange *(Russian)* 78−83398
plate, thin semiinfinite, mobile normally-distributed heat source on lateral surface *(Russian)* 80−23870
plate, vertical, with time depend. temp. or heat flux, unsteady natural convection 77−75777
temperature distribution continued
plate, volumetric heating and thermal stresses *(Russian)* 77−42714
plate, with discrete energy source, stationary temp. field, approx. soln. 77−46879
plate, with temp. and vel. profile nonuniformities, laminar flow and heat transfer 77−75913
plate with cylindrical heat generating inclusion, temp. field *(Ukrainian)* 78−55549
plate with steady state thermal boundary layer flow, appl. of governing principle of dissipative processes 79−50722
plume, above vert. heated plate, development of wall and free types 78−90881
plume, buoyant, turbulent, pl./line heat sources, temp. and vel. distribs. 77−84254
plume, turbulent, thermal, along vert. wall, struct. and heat transfer 78−90880
polar ice sheets, basal temps. 77−78250
polymer melting, during extrusion, integral energy-balance model 77−46899
polymer sheet, stretching, with suction and blowing, heat and mass transfer 78−34033
polymerisation, nonisothermal, in spherical reactor, temp. distrib., and reaction kinetics 79−87844
polymerisation in flow-through reactor, low-temp. conditions 80−61092
pore velocity, due to surface diffusion under temp. gradient, finite thermal conductivity correction 80−15428
porous annulus with fluid flow 77−15112
porous moist body, contact heating moulding, temp. distrib. heat/mass transfer 77−75784
post-arc column temp. variation obs. 78−71591
power-law fluids flowing between two rot. coaxial circular cylinders, heat transfer rates 77−58742
primary fluid heated by solar energy in linear collector, thermal regimes and appl. 78−75061
primordial background radiation, temp. fluctuations due to gravit. waves 78−65728
prismatic body for nonstationary thermal action, stress-state algorithm *(Russian)* 78−13905
pseudoplastic fluid, flowing upward in vert. heated tube, variable physical props. 78−90945
pyrolysis, of single solid particle accompanied by consecutive reactions, vol. reaction model 79−47896
radiating laminar boundary flow over flat plate at large free stream Mach no. 79−1270
radiation absorbing bodies, temp. fields Julich reactor expts., finite element calcs. *(German, English)* 77−82998
radioactive waste storage in crystalline rock *(German)* 78−86631
random heat stresses in elastic space with a cylindrical cavity *(Ukrainian)* 79−76971
reactor fuel cell temp. distrib., statistical variance 77−83021
rectangular jet distrib. in cross flow, expt. 80−19465
regenerative heater, high-temp., refined math. model 80−22365
reinforced organic composite, graphite, or C-C, ablation, mathematical modelling 79−41564
reservoirs, thermal stratification during winter season 79−5532
retina, primate, temp. rise and tissue damage due to Ar laser irrad. 78−44559
RF plasma torch, one dimensional analysis using finite element method 80−24264
rivers, thermal discharges, unsteady temp. distrib. modelling 77−5264
rivers thermal regime, influence of industrial effluents and sewage 79−29793
rock melting drills, thermal analysis 77−17258
rocks, metamorphic, joints temp. distrib. rel. to thermomechanical expts. using shear machine *(French)* 79−5474
rod, finite, insulated, unsteady heat cond. and temp. distrib., non-equilib. theory 78−67000
rod, two-layered, temp. distrib., 1D approx. applicability 78−1544
rod and attached wire system, time depend. temp. distrib. 78−18147
rod bundles, boiling crisis and press. drop, heat transfer enhancement devices 78−55638
rod pulled from melt, asymptotic calc. of thermoelastic stresses 78−2031
Ross Ice Shelf, circulation and melting 79−88363
Ross Ice Shelf sea temperatures 79−88362
Ross Ice Shelf temperature in bore holes, ice thickening history 80−31072
rotating body, axisymmetric, arbitrary surface temp. distrib., thermal boundary layer, exact solns. 78−75133
rotating channel with porous walls, heat transfer and temp. distrib. 78−30355
rotating cylindrical body, local heating and cooling on peripheral surface 78−67001
rotating disc with axisymmetric surface heat source distrib., in laminar flow, heat transfer 79−46314
rotating heat pipe, temp. distrib. and heat load characts. noncondensable gas effects 78−33992
rotating heated fluid annulus with semicond. walls, temp. gradients, lab. expt. 77−65744
rubber under cyclic compression, heat generation and thermal conduction 79−52283
S140 interstellar molecular cloud, for IR study and dust temp. profiles 80−62237
sapphire crystal grown by Stepanov's method, axial temp. distrib. 80−103280
sapphire growth and slicing developments 77−77371
NW.Sargasso Sea, effects of 1976 to 1977 winter cooling 78−28243
Sargasso Sea, narrow warm water tongue intrusion obs. using satellite and in situ data 78−73382
Saturn, South Pole temp. enhancement, spatially resolved IR obs. 79−25541
Saturn, stratospheric seasonal climate model 79−75150
Saturn atmosphere, temp. distrib. from spatially resolved IR obs. at 10 and 20 μm 79−84741
sea, temp. field fine structure influence on internal wave spectra *(Russian)* 78−36182
sea, thermal wedge, effects of tidal flow on position of upper surface *(Russian)* 78−16046
sea boundary layer, diurnal temp. cycle 78−20434
sea surface, SKYLAB 1.4 GHz radiometric meas. 78−65338
sea surface, tropical anomaly effect in ocean-atmosphere coupled model 80−12418

temperature distribution continued
sea surface temp., atmospheric effects elimination for remote sensing *(Russian)* 78−96311
sea surface temp. anomalies rel. to general circulation prediction 77−86963
sea surface temp. anomaly gradient in N.Pacific 80−85674
sea surface temp. fronts, environmental satellite survey 79−2247
sea surface temp. in N. Atlantic subtropical convergence, deep mesoscale eddies influence 77−41052
sea surface temp. obs. during 1952-65 period is N Pacific 77−41054
sea surface temperature, influence of mesoscale eddies *(Russian)* 78−81191
sea surface temperature, Noaa 4 satellite and Aries airborne radiometer meas. comparison 79−62517
sea surface temperature, response to vars. in atmospheric wind forcing 79−48505
sea surface temperature (SST), NOAA-4 data time series anal. 79−53364
sea surface temperature contouring, appls. of satellite ocean-related imagery programme 79−5681
sea surface temperatures, features enhancement on satellite IR pictures by digital techniques 79−5682
sea surface temperatures in shallow seas, 18.6 year cycle due to tidal mixing vars. 78−73387
sea temp. vertical distrib., modelling and prediction on expedition *(Russian)* 78−16190
sea upper layer, wind waves components of temp. fluctuations spectrum *(Russian)* 78−53655
seawater, Mangalore coast, India, 1976-7 nearshore water conditions 80−8315
seawater, salinity rel. to specific electrical conductivity and temp. *(Russian)* 78−16039
second order liquid porous parallel walled channel flow with free and forced convection 78−42635
sedimentary formations, bore hole drilling effect on thermal field *(Rumanian)* 78−20372
semi-infinite cylindrical rod, temp. gradient at conical end, radiation effects 77−11106
semi-infinite medium, transient thermal loadings, stress intensity factors 80−10193
semi-infinite solid, temp. distrib., variational formulation 79−55309
semi-transparent single cryst. temp. distrib. during Czochralski pulling, thermal emission 77−66584
semiconductor, inductively heated, computer simulation of temperature and EM fields 78−55961
semiconductor DH laser, thermal resistance and temp. distrib. calcs. and obs. 79−98368
semiconductors, laser annealing after ion implantation, temp. distrib. 80−54265
semigrey nondiffuse cone and V-groove, local temp. distribs. 77−65664
semitransparent shaped components, temp. and thermal stress patterns 78−2035
semitransparent single crystals, temp. distrib. during Czochralski pulling, thermal field anal. 77−66585
shallow lake heat balance, simple model, Lake Chad appl. 79−66716
shelf seas, temp. fronts adjustments revealed by satellite IR imagery 79−92545
shelf seas around British Isles, tidal fronts 79−2259
shell, nonaxisymmetrically heated thick cylindrical, thermoelastic anal. 79−10482
shell cooled by evaporating liq. drops, temp. fields 78−9546
shell enclosures, temp. distrib. calcs. under thermal radiation, numerical calcs. 80−38241
shells of revolution, thin-walled, heated, temp. field, thermostatic control 78−67003
shield, heat-absorbing, thermal vac. chamber, natural thermal radiation calc. 77−65666
Shinnecock Inlet, radiometric sea surface temp. distrib. 80−41454
shock layer, hypersonic, vibr. nonequilib., near stagnation streamline, low Reynolds no. flow 78−87417
shock wave, strong, piston struct. and gas distrib. 80−10265
shrouded parallel disc system, rot. and coolant throughflow effect on heat transfer and temp. field 77−15017
Shuttle Orbiter re-entry, remote IR imagery and tracking 80−82171
skeletal muscle undergoing rhythmic contractions 79−11901
skin temperature during sweating, estimation by graphical method and thermal cct. model 77−48757
slab, transient temp. distrib., differential operator method 77−31201
soil, periodic regression model for monthly mean temp. 78−73544
soil temp. differences and diurnal var. in Wales 77−64403
soil temperature profiles, theory for passive microwave remote sensing 77−87105
solar, water heater, low-temp., tubular heat receiver, temp. distribution, heat-balance differential equation solution 79−94464
solar active region coronal loops, temp. and density struct. 79−8890
solar chromosphere, C II reson. lines obs. by OSO 8 rel. to temp. struct. 78−53896
solar chromosphere plages, temp. profiles models based on Ca II and Mg II obs. 78−89153
solar collector, flat-plate, temp. distributions under actual unsteady insolation 80−97803
solar corona, EUV anal. of polar plumes 78−4178
solar corona, hydrostatic temps. in 1973 June 30 trans-polar coronal hole 77−53526
solar corona, temps., temp. gradients and comps. 77−53525
solar corona, temps. and Fe abundances from XUV emission lines 78−4180
solar corona, temps. and temp. gradients from OSO-7 spectroheliograms 77−17506
solar coronal holes, radio and EUV meas. *(Russian)* 78−16378
solar coronal loops, temp. and density struct. 78−89155
solar flares, heat transfer rel. to struct. 79−40168
solar flares, temp. min. region struct. and significance for flare heating 79−12458
solar inner corona, temp. gradients 79−25576
solar low photosphere, horizontal temp. var. 77−22163
solar photosphere, adiabatic cooling and mag. fields hydraulic conc. in downdraughts 78−45300
solar photosphere, north-south brightness and temp. asymmetry 78−45303
temperature distribution continued
solar photosphere, temp. depth relation in faculae and pores from line profile families 78−49408
solar photosphere, temp. distrib. in active regions and chromospheric network from Mg II line wings 78−57518
solar pond interaction with ground thermal storage 79−62093
solar power plant, transient temp. vars. in primary network 78−75062
solar power plant thermal storage unit analysis 79−57493
solar transition region and inner corona, temp. distrib. 79−75190
solar transition zone, nonresonant heating mechanism *(Chinese)* 80−85921
solar transition zone and corona, heating 77−29766
solar transition zone and corona, temp. profiles rel. to wave refl. and wave disorder 79−12453
solar water heater, natural circulation, with linear and nonlinear temp. distribs. 77−75778
solar wind, proton temp. correl. with thin layered field aligned currents 79−12375
solar wind, proton temp. heliocentric gradient from Pioneer 10 obs. 79−40052
solar X-ray flare, temp. distrib. models 79−35220
solar X-ray flares, temp. and thermal energy content profiles 80−17561
solid laser, active element temp. field calc. *(Russian)* 78−55359
solid laser thermo-optic lens temp. distrib. and focal length calc. 79−72575
solid propellent burning in three coord. systems, anal. 78−1558
solid pulsed laser cylindrical element, temp. distrib. anal. *(Russian)* 77−58332
solid transported by gas in pipe, heat output 78−63486
solidification, semiinfinite slab with const. boundary heat flux, transient interface position and temp. field 79−94481
solids of spherical symmetry with heat generation and radiation, time reversal problem 77−14873
Somali Current source region, temp. and current meas. during monsoon reversal 78−92833
specimen with bilateral electronic heating 78−26015
spent nuclear fuel elements, intermediary storage, stationary temp. level determ. calc. method 80−91223
sphere, approx. calc. of temp. and stress fields *(Russian)* 77−35034
sphere, arbitrary volume heat source, boundary conditions of third kind 77−68364
sphere in infinite medium, heat transfer problem, temp. profile 77−75783
spheres, almost touching, temp. field or elec. pot. 79−41268
spheres, concentric, cooling by forced convection, at low Reynolds no. 79−1183
spherical cone, generalised temp. fields *(Ukrainian)* 77−72141
spherical source in heterogeneous continuum, thermal field 77−84106
spouted bed, temp. distrib. meas., heat transfer characts. for appl. to PyC use *(Japanese)* 77−50275
stack of parallelograms, thin partition walls, steady temp. distrib. and heat flux 77−58535
stagnating thermal turbulent boundary layer mean and fluctuating characts., divergent flow heat transfer 78−83370
stationary boundary layer flow, plane heat balance eqn. asymptotic soln. *(German)* 78−63430
steel, alloy, nonsteady temp. fields during cooling, calc. 80−16346
steel, alloy, temp. profile, IR obs. during pull tests 77−44427
steel, boiler, determ. of temp. distribution in specimens with thermal fatigue *(Russian)* 79−68542
steel, CT specimens, irradiated in FRJ-1 research reactor, neutron flux densities, temp. fields meas. 77−83029
steel, platelike parts, quenching, temp. field calc. 80−60889
steel, structural, temp. increase during plastic deform. *(German)* 78−84903
STEM/SEM cold storage specimens, electron beam heating temp. profiles 79−5422
Stirling cycle numerical analysis, computerised, accuracy evaluation 79−48170
stochastic temperature fields in a solid spheric cone *(Ukrainian)* 79−50566
stomach tissues, canine, Ar and Nd laser damage 78−48831
stratified atmosphere, nonadiabatic heat dynamics with mass exchange and water phase transitions 79−58004
stratified lakes, temp. distrib. seasonal var., two-dimens. model, wind-induced currents effects 77−29327
stratocumulus cloud, finestructure of precipitation and temperature 79−88418
stratosphere, thermal structure and total O_3 obs., Nimbus 4 Iris expt. 77−21839
stratosphere and mesosphere, microwave limb sounding 77−21940
stream temp. modelling, 'dishonest' method 78−81454
streaming, of vel. and temp., in oscill. boundary layers 78−83358
stress in growing crystals, effects of radial and axial temp. gradients *(German)* 78−67672
stress pattern analysis by thermal emission 80−33552
structural elements, thin-walled, temp. fields calc., algorithm 79−37114
structural stress distrib. determ. by remote IR thermometry 80−87749
subarctic water mass intrusions at OWS November 79−2252
subducting oceanic crust, thermodynamic consequences of minerals dehydration, high press. and temp. 78−69301
subduction zone, thermal regime of descending lithosphere, effect of subduction angle 78−77206
subduction zone, thermal structs. evolution 80−56440
submerged jet closed vessel recirculation flow, temp. distrib. and buoyancy 78−90958
substrate heating by special lamp 78−59164
Sun, C_2 rotational temperatures, centre to limb behaviour 79−84758
Sun, chromosphere above sunspot umbrae, temperature and electron density 78−53908
Sun, coronal temp. distrib. 78−40908
Sun polar coronal hole, temp.-density model from EUV lines 79−5797
Sun under quiet conditions, SHF brightness temp. distrib., RATAN-600 obs. *(Russian)* 80−94776
superficial temperature testing, thermographic method *(Polish)* 79−67299
supersonic diffuser with surface cooling, flow and heat transfer meas. in pseudo-shock region 77−42868
supersonic flow, viscous, past corner, energy eqn., asymptotic solns., heat transfer 79−32564

temperature distribution continued
supersonic thermal boundary layer, effect of wall hollow-induced separated bubble *(French)* 78−5784
surface temperature of sea near Azores, thermal dispersion, math. model *(French)* 77−64290
Tarmanskii Marsh, influence of human activity on hydrological and thermal regimes 78−92864
temperate lakes, finite element analysis of one dimensional thermocline problem 78−49042
temperature stress-state of internal combustion engines finite element study 77−80073
thermal boundary layers in gradient flow around nonisothermal surfaces, temp. depend. of fluid thermophys., props. influence *(Ukrainian)* 77−51054
thermal conductivity, nonlinear problems, temp. fields with variable thermophys. props., calc. method 79−86324
thermal diffusion cloud chambers, wall linear temp. gradient rel. to supersaturation distrib. 80−56631
thermal diffusion in elastic layer, temp. and concentration fields distrib. 77−59137
thermal energy storage by latent heat of fusion *(French)* 79−3893
thermal energy storage tank, thermal stratification during charging 79−3890
thermal reistance minimisation, solid with heat-exchanging surfaces, variational method 78−94512
thermionic cathode, calculation of axial temp. distrib. 77−14889
thermoelastic anal. of finite orthotropic slab 79−1111
thermoelastic coupled field, spherical symmetric problems analysis 77−42737
thermoelastic half-space transient response 79−32253
thermoelectric cooling equipment, welded joints, heat emission effects on temp. distrib. *(Russian)* 80−69635
thermoelectric element, arbitrary shape, cooling efficency 78−67010
thermoelectric material, thermal cond. meas., 1100-2000K 78−24798
thermoelectricity, stationary interaction of temp. and elec. tension in 3-D body *(German)* 79−27497
thermogram enhancement by tissue-condition correction 79−39460
thermographic observability of tumours with microwave heating 78−73193
thermographic turnover detect., microwave enhancement with swept-freq. illum. 78−73194
thermohaline intrusions lie across isopycnals 79−84289
thermoluminescence glow curve anal., temp. inhomogeneity 78−27332
thermopile, harmonic temp. variations generation, analytic method 78−79193
thermotechnical equipment, radiant heat exchange modelling in rectangular chamber with attenuating medium 80−33433
thermoviscous fluid, steady flow through straight tubes 80−33636
thick-walled construction, 2-dimens. stationary heat cond. problem soln. *(Russian)* 79−64484
three-dimensional single-phase Stefan problem 77−7300
tissue, dynamic temp. distribs. in normal and neoplastic tissues during diathermy 78−31776
tissue, microwave heating, effect of surface cooling and blood flow 78−57038
tissue, perfused, macroscopic temp. distrib. 78−64944
tissue, soft, temp. distrib. monitoring by temp. depend. of US vel. 80−45994
tissue acoustic parameter characterisation by induced transient thermal gradient 77−64116
tissue heating by laser radiation, temp. profile and scatt. determ. *(German)* 79−2099
tissue microwave heating models, surface cooling and blood flow effects 78−7388
tissue microwave heating patterns in spherical models 77−86537
transient conduction, two dimensional finite solid, temp. depend. conductivity 77−58528
transient temperature field approx. in cylindrical and spherical bodies *(Polish)* 79−32192
transient thermal process calculation method, approx. polynomial representation *(Russian)* 78−83211
transparent medium with random absorbing inclusions, laser heating statistics *(Russian)* 77−28666
trapped flux removal by thermal gradient technique 80−75694
troposphere, temp. profiles from ground-based angular microwave meas. 80−51551
tube, elliptical, laminar liq. flow, nonsteady heat transfer 78−42598
tube, vertical, laminar and turbulent heat transfer, air and Ar 78−71332
tube, with heated inner eccentric rod, steady convective laminar heat transfer 78−38311
tube bundle in crossflow at low Reynolds nos., heat transfer 79−98712
tube entrance velocity and temp. distrib. with turbulent hot air flow *(Russian)* 78−14087
tube wall, gas film-cooled, turbulent heat exchange, coolant turbulence intensity influence *(German)* 79−18895
tube wall heating during steady state tube drawing *(German)* 78−84899
tube wall temperatures of an eccentrically located horizontal tube within a narrow annulus 79−32201
tumours in hyperthermia research, importance of good thermal dosimetry 78−64942
turbine blade, analogue simulation *(German)* 77−68551
turbulence, homogeneous vel. and temp. fields, statistical transfer coeffs. 77−7375
turbulence, nonisotropic, homogeneous, temp. distrib. degeneracy, statistical characts. 77−84232
turbulent boundary layer, nominally steady, two-dimens., vel. and temp. profile prediction method 80−1624
turbulent boundary layer, periodic intermittent model for wall region 78−87336
turbulent boundary layer, temp. fluctuations, diffusion *(French)* 77−62248
turbulent boundary layer, temperature fluctuations 77−75898
turbulent boundary layer, temperature profile and Reynolds analogy expressions 78−87337
turbulent boundary layer, viscous sublayer temp. fluctuation spatial correlations *(Russian)* 78−34114
turbulent boundary layer, wall suction and heating *(French)* 77−19595
turbulent boundary layer characterisation by velocity and temperature profiles *(Russian)* 78−34115
turbulent boundary layer downstream of step change in surface temp. 79−81862
temperature distribution continued
turbulent boundary layer in pipe, temp. distrib. 79−32668
turbulent boundary layer with wall suction, thermal and dynamic fields analogy *(French)* 79−1249
turbulent boundary layers near separation point, numerical prediction, heat transfer *(French)* 78−94657
turbulent flow around plate containing heat sources 77−23948
two semi-infinite rods, temp. field in system 77−68373
two-dimensional multiply connected regions of arbitrary shape and boundary conditions, temp. field calc. 79−86317
two-layer plate with separated suction, nonstationary temp. field 78−22255
two-layer thermal shielding, pulsed heat flow, temp. field 78−59260
two-phase medium, isotropic, heat distrib. eqns. *(Ukrainian)* 77−50863
two-phase medium, temp. field equalisation problem *(Ukrainian)* 77−50862
under-surface temp. pattern estimation by dynamic remote sensing *(Japanese)* 78−36315
underground cable system, convectively cooled, temp. distribs., heat transfer correlations 78−71262
underground channel, cylindrical, fluid flow and heat transfer 77−7455
underground railway tunnel microclimate, calc. method *(Russian)* 79−68548
underground temp. var. with depth and time 79−5463
unsteady forced convection heat transfer from impulsively started circ. cylinder 79−27633
upper ocean temperature and salinity structure, obs. during POLE expt. 80−72536
Uranus, thermal structure from IR meas. 78−36509
Uranus upper atmosphere, mean temp. and temp. vars. 80−46477
Uranus upper atmosphere, temp. struct. 79−62791
urban areas, land use, satellite temp. meas. appls. 78−65393
urban atmospheres, modelling of temp. and pollutant conc. distribs. 77−45143
urban temp. field dynamics in Calgary area 77−17168
US thermometers, nuclear fuel temp. profile meas., TRESON expts. 78−57955
Venus, atmosphere thermal contrast from Pioneer probe data 80−46229
Venus, electron temp. and densities, Pioneer Orbiter meas. of ionosphere 79−48705
Venus, IR brightness temp., daytime minima 80−77309
Venus, thermal radiance maps, anomalous features 79−101102
Venus, thermosphere, comp. meas., temp. profile and homopause altitude 79−48707
Venus atmosphere, height depend. of temp., 52-90 km altitude, model 79−8866
Venus atmosphere, struct., and light, heat and wind regimes from space vehicles 80−62062
Venus atmosphere, thermal anomalies persistence and size 78−85876
Venus atmosphere, thermal IR temperature maps anal. 78−89094
Venus atmosphere, thermal struct. during Pioneer Venus probe encounter from IR image 79−48714
Venus atmosphere structure up to 110 km, Pioneer Venus entry probes preliminary results 79−48715
Venus cloud-top, thermal asymmetry 77−53447
Venus middle atmosphere, temp. distrib. from Pioneer orbiter IR remote sounding 79−48712
Venus upper atmosphere, remote temp. soundings rel. to mean circulation diagnostic model 79−58287
vertical plate in free convection, temp. profiles meas. 77−915
vibrating thin rectangular plates, influence of thermal grad. on natural freq. 79−32353
Visakhapatnam coast, temp. and salinity of coastal waters 77−73757
viscoelastic fluid, Poiseuille flow and temp. distrib. 79−60039
viscous dissipation effect on heat transfer, circ. cylinder axisymmetric stagnation flow 78−51164
viscous fluid in channel, laminar steady forced convection flow 79−32505
viscous incompressible liquid between two coaxial cylinders, exponential rate of heat addition, temp. distrib. 77−68586
wall, with cylindrical cooling channels, steady-state temp. distrib. 77−65663
wall temperature distributions, in regions of deteriorated heat transfer 78−83377
water, convective heat transfer, free, with density inversion, in confined rectangular vessel *(German)* 79−18671
water, cooling, boundary layer thermal state during transition from free to forced convection *(Russian)* 78−81192
water, cooling from surface under free and forced convection regimes *(Russian)* 78−36179
water, fine struct. of thermal boundary layer near air-water interface *(Russian)* 78−22332
water, temp. field for surface boiling in round tube 77−42818
water adjacent to vertical uniform flux surface, buoyancy driven flow, transition and transport 79−27631
water bodies, wind effects on surface to bottom fronts 79−2261
water droplet aerosol interaction with EM radiation, temp. field and refractive index distrib. model 78−3899
water natural temp. and man-made variations *(Dutch)* 79−83642
Weddell Sea, bottom water temp. and salinity variability 80−67366
weldable butt joints, calc. of temp. field for nonideal thermal contact *(Russian)* 80−10121
welding, ultra pulse type, heat transfer characts. 79−1047
wide ribbon growth by multiple inert gas jet thermal profile control 78−64458
winter heat island formation over Milan city *(Italian)* 78−53709
World Ocean, waters heat and salt content 80−31054
X-ray sources, compact, temp. and ionisation struct. rel. to X-ray spectra form. 80−22115
X-ray tube rotating anodes, physical props. 78−29222
X-ray tube rotating anodes temp. distrib., compound anodes numerical anal. 78−62285
Zircaloy cladding, internally pressurized, effect of temp. nonuniformity on diametral expansion during transient heating in steam 79−30920
zonal ocean, narrow jets interaction with temp. fronts 79−2264
zone melting crystn. parameters optimisation using temp. distrib. calcs. *(German)* 79−43140
AgCl, temp. fields during plastic deform., cholesteric liq. cryst. technique 79−82278
Al billet, hot extrusion, nonsteady state temp. distrib., numerical method 80−60886

temperature distribution continued
Al, cutting, temp. effect on built-up edge behaviour *(Japanese)* 78−7083
Al, plastically deforming at high strain rates, distrib. of temp., strain rate and strain 79−19311
Al plates with air gap, temp. field for microplasma welding of edge joints *(Russian)* 80−7755
Al-Al_3Ni eutectic, temp. gradients, microstructural changes 80−84971
Al-SiC fibre reinforced materials, therm. stresses in unit cell 80−10160
Ar inductively coupled RF plasma, spatial distrib. of temperature 77−68873
Ar laser-evaporated microplasma radial glow and temp. distrib. 78−67387
CO_2 gas flow impinging on heating surface, heat transfer radiation 80−43710
CO_2, laminar free convection at supercrit. press. under cooling conditions, heat transfer analysis 79−86428
CO_2 laser, TEA, equilib. gas temp. and its distrib. 77−54691
CO_2 waveguide laser discharge, cooling, gas temp. meas. 78−17958
CdTe, laser annealing, surface layer temp. distrib. 79−74029
Fe melting and adiabatic temp. distribs. in outer Earth core 77−70626
GaAs laser, surface temp. distrib. *(Russian)* 78−74909
GaAs-$Al_{0.3}Ga_{0.7}As$ laser diode, spontaneous radiation transfer 80−91796
GaAs-$Ga_{1-x}Al_xAs$, single-heterostructure laser diode with short current pulses, heat spreading analysis 79−76690
n-GaSb, temp. distrib. around dislocations, due to Joule heating, calc. 78−71734
Ge ribbon single crysts. grown from melt, dislocation struct. form. under thermal stress 80−107082
Ge shaped single crystal, Stepanov method growth, temp. distri b. 78−2032
Ge single crystal of circular cross section, thermoelastic stresses 78−2033
Ge strips grown by Stepanov method, thermoelsatic stress calc. 78−2034
H II regions, effects of dust on thermal struct. 77−33588
H II regions, gradient of electron temps. and He abundance 79−21389
H II regions, temp. errors from radio emission improper anal. 78−54000
H II regions temperature structure, influence of star, gas density and chemical comp. 78−61911
H plasma plane and cylindrical layer emission field calc. *(Russian)* 80−33755
H_2-O_2 reaction boundary layer, numerical anal. *(German)* 77−35253
He flow in rot. cryostat, temp. distribs., thermodynamics 78−34666
He gas, temp. fluctuations 79−19414
He I liquid, temp. fluctuations 79−19414
He, liq., dewar, temp. profile 77−41621
^3He-^4He dilution refrigeration system, choice of tube lengths and diameters 80−57308
^4He superfluid, temp. fluctuations 79−19414
Hf electron field emitter, temp. drop meas., allotropic transform. temp. 80−2931
Hg, turbulent flow on stabilising thermal section, temp. fields and heat transfer 80−19366
InSb, Hall plates, temp. and pot. distribs. determ., temp. depend. cond. effect 79−60851
Li_2O pellets, neutron irradiated, temp. distrib. 80−86968
N_2, flow, cold gas, through porous-tube, heat-transfer, suction effect 78−59474
N_2, liq., in cryostat dewars, appl. to microwave thermal noise source 79−58700
Na, liquid, anal. of temp. fluctuations for local flow velocity determ. *(Spanish)* 79−46405
Na temperature fluctuation in single-pin-heated blocked annular channel 78−78439
Na vapour heat pipe performance rel. to nozzle discharge theory 78−75033
NaCl, Czochralski growth, temp. distrib. near crystn. front 78−2036
NaCl, temp. fields during plastic deform., cholesteric liq. cryst. technique 79−82278
NaCl:$MgCl_2$ (0.1 mol.%), thermoluminesc. glow curves, temp. distrib. and trapping centres 78−48241
Ne medium-pressure discharge, electron temp. radial profile meas. by electron-atom bremsstrahlung continuum 78−67497
Si, CVD growth, high- and low-temp. models 78−6244
Si crystals, temp. distrib. anal. in floating-zone method 79−74082
Si, laser annealing, surface layer temp. distrib. 79−74029
Si, p-n junction, ellipsometric method of temp. meas. rel. to secondary breakdown *(Russian)* 80−11074
Si ribbon crystal growth, 10 cm wide, temp. distrib. meas. in die 80−104059
Si, ribbon edge-defined film-fed growth control using C-CD imagers 78−68623
Si temperature field determ. under laser irradiation *(German)* 80−25496
Si wide ribbon, high speed edge-defined film-fed growth 80−104058
β-SiC, cryst. temp. variation during growth 77−40340
Si_3N_4 layers deposition, high-temperature, in resistance furnace, temperature gradient and nitrogen flow influence obs. *(Bulgarian)* 80−80981
Ti-Al-V (6, 4 wt.%), temp. distrib. for steady axisymmetric extrusion 80−11670
Ti-Al-V (6, 4 wt.%), temp. distrib. for steady axisymmetric extrusion numerical results 80−11671
UF_6, temp. and density profiles in freely expanding gas for laser enrichment 78−74458
ZnSe, Bridgman growth under Ar press., temp. distrib. in furnace 78−11100

temperature measurement
see also pyrometers; spectral methods of temperature measurement; temperature scales; thermocouples; thermometers
A/D convertors TL505/507 and microprocessor TMS1000 measurement system *(French)* 80−57290
absolute-reciprocal temp. convertor *(Polish)* 78−45626
AC calorimeter, construction and design *(Japanese)* 78−89481
AC circuits for low temperature measurement with semiconductor thermometers *(Polish)* 80−82766
accuracy, additive and multiplicative meas. errors influence *(German)* 80−8985
acoustic noise in electric arcs, arc temp. meas. appl. *(French)* 80−28865
acoustic pinger modification to transmit water temp. data 79−39895

temperature measurement continued
acoustic temp. indicator, consisting of temp. sensitive resistor and operational amplifiers *(Spanish)* 80−13061
air temperature sensors, aircraft borne, wetting in cloud rel. to entrainment overestimates 79−53483
air-conditioned laboratories, automatic temp. control and meas. *(Japanese)* 78−86245
airborne expendable bathythermograph, for upper ocean temp. meas. 77−2262
alloy, solidus temperature determ. by method of moving specimen boundary projected on screen 78−35353
analogue apparatus for determining average and difference of temps. given by two thermocouples *(French)* 77−57325
anemometer, hot wire technique for simultaneous nonisothermal flow vel. and temp. meas. *(Japanese)* 78−38421
anemometer, hot-wire, computerised, for vel.-and temp.-meas. in heat turbulent flow 78−91040
astrophysical plasma, use of a priori information in temp. structs. derivation from X-ray spectra 78−20778
N Atlantic, quasi-biennial cycles of water temp. fluctuations rel. to weather 79−53357
atmosphere, over ocean, salt spray contamination of atm. temp. sensors 78−69489
atmosphere, temperature profile retrieval from IR satellite data 79−48586
atmosphere temperature meas. in fog and stratus, shipboard use of low-level atmospheric thermograph 80−105073
atmospheric temperature meas., by IR method from Earth satellite *(French)* 77−9550
auroral ionosphere meas. in Antarctic by sounding rockets 79−8760
automatic oceanographic profiling and transmission system 77−41231
band radiation pyrometry for error reduction in transmission coeff. calc. of IR radiation energy depend. on atmospheric props. *(German)* 80−105649
basal body temperature continuous monitoring in humans by radio telemetry 77−78015
bathythermograph systems, new techniques 77−17221
bead thermistors in meteorology and oceanography *(German)* 77−21920
bench for metrological certification and testing of radiant-flux sensors (RFS) 80−98977
biological, deep body in unrestrained domestic fowl, piezoelectric transducer, sampled data system 78−57152
biological exposure chambers, automatic system for monitoring temp. and humidity, microprocessor controlled 79−49239
biomedical, implantable miniature transmitter *(Dutch)* 78−48908
biomedical electronic thermometers, review 78−69235
biomedical temp. measurements, radiation balance microwave thermograph, simultaneous independent temp. and emissivity measurements 79−100692
biomedical temperature biotelemeter, modular, expandable, implantable 80−67191
biomedical thermometry, use of salt-hydrate transition temps. as fixed points 80−104801
biotelemetry system for free-swimming fish .77−25624
biotite+apatite geothermometer, re-examination 78−85704
bipolar IC temperature transducer, intrinsic bandgap voltage as reference, Fahrenheit, Celsius or arbitrary scale operation 80−82761
blood temperature monitoring during extracorporeal circulation, noncontact transducer 80−85513
body, ATP-12M infrared imaging system (USSR) 80−67280
boiling point, uncertainty in thermistor ebullioscopes sensitivity 78−12695
borehole equipment for temp. and heat flow meas. in Ukraine *(Russian)* 77−91294
bridge circuit errors due to changes in resistance thermometer conductor resistance 79−30473
bridge circuits with thermistors and pulsed supplies, unbalanced, anal. 79−30474
bridge measuring circuit, linearisation *(Russian)* 80−90847
brightness temperature of atmosphere, by means of passive radar, humidity and clouds drop phase characts. determ. 79−74991
brightness temps. estimates from scanning radiometer data 78−85716
calibration standard, melting point of pure Ga 77−41611
calorimetric water bath temp. control and temp. meas. devices 77−37893
cancer detection by microwave thermography 78−24172
cancerous mouse hyperthermia meas., microwave, IR and thermocouple methods *(French)* 80−3768
capacitance thermometer for low-temp. measurements, bridge detector circuit 79−54132
cardiac output thermodilution meas., thermistor probe construction for use in small animals 77−64161
chart recorder, adaptor for converting single channel to multi-channel instrument 77−37874
cine-film, incandescent projector lamp performance obs., using thermocouple *(Russian)* 77−10129
clinopyroxene geothermometry of spinel-lherzolites 77−2126
cloud top heights determ. from satellite remote temp. sounding instruments 77−17256
combined radiation/contact thermometer, −10 to 600°C range, features *(German)* 78−32815
compact low-temperature fixed point device 79−35761
by compensated thermocouples *(German)* 78−41304
compensation-point Hall effect temperature sensor 78−93679
contact thermometer method, temp. field meas. by liquid crystals *(German)* 79−58686
contact thermosensor method for hot thin plates, heat loss elimination 77−74397
contactless, Hg-contact thermometer appl. *(Russian)* 77−65033
contactless, theory and practical aspects *(Dutch)* 77−67433
contactless temp. meas. in circular cyclic bending, using thermoelectric radiation sensors 78−57947
contactless using radiometer with optical fibre as optical lens 78−49828
coolants, thermistors method 79−85137
correlation at high press., belt apparatus temp. meas. *(Chinese)* 80−52200
cosmothermometry, appl. of Ti^{3+}/Ti^{4+} ratios in Allende meteorite 79−12437
cryogenic adjustable temperature system for radiation investigs. in 5-300K range 79−88960
cryogenic fluid in high magnetic field 77−30171
cryogenic resistance and diode thermometer appl. 77−26311

temperature measurement continued
cryogenic temp. sensors, for use in EM fields 77−2655
cryotron temperature-to-time interval convertor *(Russian)* 80−222
crystal maximum temperature measuring system using irradiated diamond powder, engineering applications 77−33991
with crystal resonator temp. sensor 77−82514
crystalline sample fusion temp. meas. automatic instrument 78−57945
cutaneous temperature of living human body 79−83976
Danish temp. transducer calibration at Riso, in −150 to 1100C range *(Danish)* 79−54129
data logger, YODAC-8, microprocessor controlled 78−49813
data logger for precision meas. of resistance temperature detectors 79−88925
decrepitation recording for gas-liquid inclusions in quartz powder 77−71325
deep body, thermistor, digital display, continuous recording, cardiac surgery appl. 77−29223
deep body thermometer testing and modelling 77−40816
deep ocean current meas. system 77−5382
deep sea temp. and pressure sensor for tidal meas. 77−37424
deep tissue temp. monitoring by ultraminiature thermistors 80−3761
degree-day measurements 80−77574
dielectric constant gas thermometry, 4-27K, and eqn. of state of He 79−63222
difference meas. by automatic thermistor bridges 77−22547
difference of temp., precision meas. in thermal conductivity measuring method 77−37878
differential temp. sensor with indicator system *(Spanish)* 79−54133
diffusion furnace temp. profile meas. systematic errors, theoretical model *(German)* 80−8989
diffusion furnaces, temp. profile meas., systematic errors *(German)* 80−37030
diffusion pump cooling water, temp. meas. by CMOS cct. 77−5855
digital level detector, using BCD adders 79−75528
digital measuring system for recording nonstationary temp. fields 77−53912
digital meter, using Wien-Robinson oscillator, and digital frequency divider *(German)* 78−29110
digital precision thermometer, using 3 ICs *(French)* 79−80616
digital quartz crystal thermometer principle and technical parameters *(Polish)* 78−24791
digital recorders, advantages over analogue instruments 80−210
digital thermocouple cold junction compensation methods *(Italian)* 78−37002
digital thermocouples, noise study 77−22544
digital thermometer, 35 to 40°C precision, biomedical appl. *(German)* 77−56499
digital thermometer, for 4 to 300K range 80−4709
digital thermometer, planar Si diode sensor long-term stability anal., 70-420K *(Czech)* 77−67435
digital thermometer, portable, liquid crystal display *(German)* 78−29112
digital thermometer, using a thermistor bead 79−21741
digital thermometer, using LSI ADC 79−44907
digital thermometer charact. *(Hungarian)* 78−54367
digital thermometer type AD2038 79−58684
digital thermometer types and technical data *(Russian)* 77−53911
digital thermometers, process meas. control appl. 78−49833
dilatometer for PVT meas. of liquids and plastic crystals at low temperature 80−68208
diode sensor based on const. leakage current with negative temp. coeff. 10 V analogue output *(German)* 80−47052
discharge, pulsed, inhomogeneous gas heating, acoustic wave temp. determ. 77−55175
disperse system with solid particles, temp. meas. from mag. props. variation near Curie pt. 78−9556
Drifting Oceanographic Profile Buoy with minimum vertical motion 80−46306
dual-channel ratio thermograph counteracting skin emissivity errors 77−40892
dynamic, results processing with aid of computer 77−5839
Earth, upper mantle, peridotite equilibration temp. from geochemical parameters 77−2130
Earth's atmosphere, remote meas. of 3-D temp. distrib. using TIROS-N microwave sounder unit 80−90265
Earth crust, continental geotherms during Archaean 79−34780
Earth surface temperature, remote sensing by Heat Capacity Mapping Mission 79−5640
EBR-II, comparison of XX08 steady-state temp. meas. with anal. predictions 80−579
eddy current temp. measurer, exam. of design 79−12803
eddy-current thin-film transducer appl. *(Russian)* 77−26294
elastic waveguide slow torsional wave sensors 79−46748
electric apparatus and power lines, temp. rise meas. by infrared radiometer *(Russian)* 78−89537
electric cell appl., using solid electrolytes *(Czech)* 77−77779
electric motors, ribbed frames with external fans, heat transfer coefficient measurements *(Hungarian)* 80−87709
electron beams, threshold temp. sensitivity of interelectrode gap determination 78−78890
electron microscopy, controlled-atmosphere, specimen temp. meas. using opt. pyrometry 78−93690
electron temperature meas. in ionosphere by high-freq. probe method 79−92632
electronic device, using a thermistor in a current bridge for clinical use 78−29109
electronic excitation and ionisation temp. meas. in ICP Ar source, H_2O vapour effects 80−75028
electronic instruments developments *(German)* 80−8986
electronic sensor, with 4-bit A/D convertor *(German)* 78−12693
electronic sensors for clinical replacement of metethmor 78−7473
electronic thermometer for telemetric link with direct reading *(Spanish)* 78−16793
electronic thermometry, accuracy improvements 77−41608
emissivity determination from thermal rad. spectrum and optimal methods of opt. pyrometry 78−24797
environment protection when siting power station, temp. and humidity meas. methods *(French)* 79−12318
error due to cond. along sensor leads, correction 77−13752
errors due to conduction along thermocouple leads 79−85136
evaporating surfaces, determination 77−89011
temperature measurement continued
expendable bathythermograph digital recording and display system 80−46318
exposure measured by thermolum. fading 78−24786
fast reactor boiling detection by noise analysis 79−13449
fatigued steel brittle transition temp. meas. by hardness testing *(Japanese)* 79−87797
ferrous metals, method to improve reliability/accuracy of immersion W-Re thermocouple 77−87767
fever alarm device using telemetry 80−21556
fibre optic Mach-Zehnder interferometer, sensing of press. and temp. 79−72671
fibre optic sensors appl. *(Norwegian)* 79−93121
fibre optic temperature probe 78−208
fibre optical interferometers for length, temp., pressure and force meas. 80−98971
fission reactor core monitoring, can thermocouple distribution procedure 78−54856
fission reactor steady-state fuel centreline thermocouple data confirmation from transient response 79−93767
flame, atm. press., temp. meas. using thermocouple of Ir/Ir-Rh alloy 77−86314
flame, swirling, temp. distrib. 80−61098
flames, corrections to local values of temp. meas. by suction pyrometer 77−22551
flames, temperature and conc. meas. by rot. Raman scatt. 79−31530
flow, heated grid flow, temp. derivative skewness, alleviation 78−46951
flow measurement, hot-wire calib., for vel. and temp. meas., low-freq. effects 79−50825
fluid, laser interferometry appl. 80−75018
fluidic capillary sensor appl. 78−24793
fluidic temperature sensors 80−73342
forests, Ge diodes for temp. and humidity profile meas. 77−64463
formaldehyde, molecular beam rotation temp. meas. *(French)* 80−78724
freeze-fracture specimen temp. changes during rapid quenching in liq. coolants 78−57140
frequency response of cold-wire thermometers used for atmospheric turbulence meas. in marine environment 80−56650
frequency thermoconvertor dynamic error electrical correction *(Russian)* 80−57242
fundamentals and techniques, book 78−81941
furnace, dipping depth effect of thermometer elements on accuracy *(Polish)* 77−53910
furnaces, industrial, measuring temp. of moving objects using pyrometer with sighting device 79−71455
furnaces, temp. distrib. measurement using thermocouples and wire bridge cct. 80−31758
fusion thermal tracers, thermophys. charact. investig. 77−5837
gas, 300-1200K, choice of informative parts of rot. spontaneous Raman spectrum *(Russian)* 77−31416
gas, high temp., numerical computation method for pulsed thermocouple measurements *(German)* 79−21749
gas, monatomic, perfect, thermodynamic state, confidence interval for temp. meas. *(Hungarian)* 77−41554
gas, nonstationary temp. meas. using sensors 79−80620
gas, thermal probe for high stationary temperatures 80−95101
gas discharges, temp. of heavy particles using contact methods 79−30476
gas flow dust content, temp. and speed meas. method 78−34216
gas flow study, temperature gradient meter for 79−86539
gas flow temp. meas. by two thermocouples 78−34218
gas temp. meas. by multiple-thermocouple method 77−49728
gas temp. meas. in glow discharge in capillary using thermocouples *(Russian)* 78−59694
gas thermometry, constant volume valve design 80−4711
gas thermometry by method of two containers 77−5838
gas thermometry scale from 2.6K to 27.1K, report 78−89480
gaseous mixtures, conc. fluctuation meas. using catalytic wire 77−26291
gases, dilute, temp. and thermophysical prep. meas., using acoustic resonators 80−53573
gases, noncorrosive, measurement using automatic microclimate testing and control system 79−67318
geothermal shallow-hole temp. meas. 78−11849
geothermal well logging, temp. meas. utilising melting props. of materials 80−56659
geothermometry, appl. of plagioclase-garnet-Al_2SiO_5-quartz assemblage 77−2147
geothermometry, electrochem. O_2 fugacity meas. appls. 77−2256
geothermometry, subsolidus phase relations of pyroxenes in CaO-MgO-Al_2O_3-SiO_2 system 79−16440
geothermometry and geobarometry, conf., University Park, Pennsylvania (October 1975) 77−2123
geothermometry and geobarometry for single pyroxene phase 77−2254
in Glaisher stand and Stevenson screen, max. summer temp. recording 77−81976
glass, IR thermometry, readings interpretation 80−82765
glass container forming, mould surface temp. meas. 80−82767
glass substrate, surface temperature measurement, heated through Ga 79−97390
glass track detectors, thermometry appl. 80−37031
glow discharge, gas temp. meas. by fluoresc. spectroscopy 78−18467
gradiometer for use in superfluid ^4He 78−57949
grinding, dynamic calibration of synthetic diamond thermoelectrodes 77−55985
heat filters for bolometers cooled to very low temperatures 80−52315
heated turbulent flows, cct. for instantaneous temp. meas. 78−21137
high sensitivity, thermocouple, microamplifier, galvanometer, teaching appls. 78−86085
high temperature, solid electrolytic cell, meas. at 700K and higher 80−31760
high temperature, using Mossbauer, noise and US thermometers 80−52202
high temperature inside furnace, by means of radio transmission *(Czech)* 77−2659
high temperature metrological cooperation between USSR and GDR *(German)* 78−4622
high temperature MOSFET characteristics for geothermal instrumentation, up to 300°C 78−73553
high-pressure liquid MP determ. centrifuge cell 80−31783
high-pressure temperature meas. in liquid He region 80−31748
holographic interferometry, 3-D temp. field meas. 78−37009

temperature measurement continued
hot cathode temperature, thermionic emission meas. method *(Czech)* 78−70121
hot turbulent flow, temp. fluctuations, hot-wire anemometer *(French)* 78−42684
hot two-phase flow, temp. meas. by absolute spectral line intensity method 79−94700
hot wire probes perpendicular to flow velocity vector, interaction 79−68825
hot-wire probe, simultaneous, instantaneous, temp. and vol. component meas. in turbulent flow 78−34236
human body-temp. sensor-environment system, analogue model of interaction 80−104783
hyperthermia, localised, thermometry considerations, review 78−53561
hyperthermia, nonintrusive meas. by US temperature tomography 79−53282
IC temperature sensors used in thermocouple cold junction compensation circuits 80−77777
implantation temperature meas. using impurity luminesc., for insulating materials 79−52012
in-reactor fuel temperature, transient response of centreline thermocouples, appl. to fuel modelling 80−95372
in-reactor performance of surface-mounted and embedded thermocouples 79−93704
in-reactor temp. meas. accuracy, thermometer construction effects 79−17969
induction salt baths, automatic temp. control 80−27300
industrial, thermocoupler and resistance thermometer 80−42221
industrial techniques, man/machine interface enhancement 77−22545
industrial type monochromatic pyrometer appl. *(French)* 77−5846
infrathermograms properties and evaluation in nonblack radiators *(Hungarian)* 78−65922
injection moulding, melt temp. meas., appl. of thermocouples or pyrometers 79−58694
instrument for temperature measurement using temperature-sensitive magnetic fluid 80−31745
instruments and techniques, industrial appls. 79−196
integral thermotome for water layer temp. meas. 79−29908
interferometer, Mach-Zehnder, test section misalignment errors for temp. and temp. gradient meas. 78−54447
interferometric technique for temp. field of axisymm. buoyant phenomena 78−89529
internal combustion engine, measurement of pulsating temp. and vel. using US flowmeter 80−1704
internal contraction engine, highly loaded, exhaust gases temp. and velocity meas. using two thermometer method *(German)* 80−31754
International Practical Temp. Scale, instrument interpolation, from 630.74 to 1064.43°C 79−40564
International Practical Temperature Scale revision, thermodynamic temperature in range 0 to 1064°C 80−62669
intracranial pressure and temp. two-channel telemetry system 77−81619
intracranial temp. monitoring, implantable two-channel telemetry system 78−3637
ion implantation, target heating, temp. measurement 80−34032
ionic sensors for nuclear reactor in-core temp. meas. *(Czech)* 78−32820
IPTS-68 values of secondary ref. pts. above 2000K 77−45819
IR battery operated portable thermometer *(German)* 80−57289
IR camera for contactless temp. meas., plastic processing industry appls. *(German)* 79−58685
IR detectors, temperature distribution in weld of thermoplastic foil *(Polish)* 80−22362
IR determ. of temp. increase in tension tests *(German)* 79−61806
IR device, minimum resolvable temp. difference charts 77−82509
IR pyrometry for measuring target temps. in solar furnace 77−41603
IR radiation thermometry, temp. monitoring and thermal inspection 78−45622
IR scanner, design, construction and anal. of continuous-temp. IR calibrator 79−75530
jet stagnation point heat transfer on plate, turbulence effects, liquid crystal meas. 78−18327
lakes, vertical automatic profiling system for temp. and current meas. 78−36327
laser beam propagation, thermal turbulence effects *(French)* 77−24038
laser components, fast thermal monitoring system 79−80614
laser diodes, junction temp. meas. method 79−36895
laser high power CW output meas. from temp. rise of Al slab power meter 79−59739
laser nozzle, chemical, temperature profiles meas. by thermal imaging system 80−14376
laser pulse heating, high speed pyrometry and spectroscopy, review of techniques 80−52225
lava temp. meas. techniques and apparatus on Etna 77−25800
leaf, infrared thermometer method in connection with plant physiology *(Japanese)* 78−31993
LED temperature display with integrated window discriminator TCA965 77−128
length standards, using thermocouples and Pt resistance thermometer *(Slovak)* 78−77907
linear meas. with double p-n junction diodes, cct. *(German)* 78−201
linear temp. and temp. difference sensor using ferroelectric sensitive element 78−21136
linear temperature-time period transducer *(German)* 79−40561
linear temperature-to-voltage convertor 78−32811
linearised NTC circuits with A/D convertor *(German)* 79−80619
liquefied natural gas, level, density and temperature measurement, prediction of roll-over 80−27269
liquid crystal improved technique for thermal field measurements 80−216
liquid crystal thermoindicators, colour-temp. characts., time depend. 79−40567
liquid crystal thermometry, optically active binary mixture 79−42952
liquid evaporation in circulating gas, porous channel temp. determ., obs. 79−72943
liquid metal, thermal conductivity meas. in Spacelab, temp. meas. device for control *(German)* 80−57303
liquid metal alloys solidification temp. range meas. technique 79−12799
liquid Na, thermocouple transfer function and flow velocity meas. by temp. noise 79−13394
liquid-crystal optical fibre temp. probe rel. to thermometry and dosimetry of heat 80−98204
temperature measurement continued
live connection temp. rise, portable IR pyrometer appl. *(Swedish)* 77−17981
LMFBR, Na liquid coolant, determ. of saturated temp. with automatic plugging indicator 79−97747
LMFBR coolant flow monitoring by balanced outlet temp. signals 79−13393
LMFBR coolant temp. meas. using high integrity coaxial thermocouples 80−32410
LMFBR fuel subassembly temp. noise prediction, Monte Carlo approach 79−13392
LMFBR Na-cooled 7-rod bundle acoustic and temp. noise obs. 79−13391
LMFBR safety application of US thermometry 79−45400
LMFBR steam generator tube thermal oscillation obs. 79−9672
LMFBR subassembly local boiling detection by outlet temp. fluctuation analysis 79−13390
LMFBR subchannel coolant flow behind blockage, temp. noise obs. 79−13389
LMFBR surveillance technique development 79−13448
LMFBR-subassembly outlet computerised temp. monitoring based on estimation theory 78−8948
LNG, automatic continuous level-gauging and temp. meas. system appl. 77−26272
long-term temp. recorder, geophys. appl. *(Japanese)* 77−82035
loudspeaker moving coil temp. meas. systems *(Hungarian)* 80−106698
low density supersonic gas flow, temp. meas. probe 80−74913
low frequency acoustic thermometry in the range 4.2-20K with implications for the value of the gas constant 79−30477
low temp. from 13.8K, IPTS 68 standard 77−26296
low temp. thermometry using semiconductor diodes *(German)* 79−35762
low temperature measurement in high mag. fields, instrumentation and methods, review 78−37003
low temperature rise heating of a field emission tip 80−52371
low temperatures, Pd+Cr+Ru/Au+Fe thermocouple for 2-200K range 77−26293
low temperatures, using GaAs semiconducting resistance thermometer, 0.3 to 350K range 79−58687
low temps, ~25 mK, using low-power Wien bridge oscillator 78−93680
low-temp. thermometers, magnetic-field-induced temp. error 79−80618
low-temperature fluids, meas. in guarded parallel plate thermal cond. apparatus 77−22553
low-temperature measurement, via Krion 1-2 instrument 78−222
low-temperature measurements between 0.5 and 30K 80−42225
low-temperature meter, digital, 4 to 300K, with Ge pickups 80−31747
lower troposphere, ground based radiometry 77−91330
magnetic core, temperature sensitive, appl. to new temperature telemeter 79−199
magnetically controlled reed switches, used for temp. meas. *(French)* 80−57291
marine air temp. sensor error analysis 77−78437
measuring bridge, using constant-current FET circuits 77−129
measuring cycle improvement, correction of measurement path *(Polish)* 80−22318
medical appls., radiation balance microwave thermograph 80−26315
medical temperature measurement, electrical measurement techniques *(Hungarian)* 80−30910
melting point standards, secondary, for temp. range 2000-3000°C, chemical aspects of choice 80−52226
metal, molten, digital device for determining temp. *(Russian)* 80−90846
metal fixed points, limitations caused by trace impurities 80−105644
metal forming, instrument for temp. determ. in deformed space 80−17938
metal objects, moving, temperature meas. by thermoelectrical thermometer *(Russian)* 80−90848
metal testing, thermoelec. thermometer error anal. 78−19975
metal-film temp. and vel. sensors and self-propelled research vehicle stability evaluation for ocean turbulence meas. 79−5672
metallic substrates during evap., thermocouple system 77−69997
metals, plastic deform., stored energy determ., temp. recording method 79−87775
metals, strain induced thermal signals, detection 79−1141
metals, working, method of applying fusion thermal indicators to surfaces, including heated surfaces 80−17937
metals and alloys, critical temperatures determination, elec. resist. method, IMASh-5S-69 installation 80−71827
meter-controller for 1.5-300K range 77−45840
MHD combustor and channel, microprocessor-based Na reversal instrument 80−73364
microprocessor based data acquisition and exptl. control system 78−36086
microprocessor-controlled system for precise meas. of temp. changes 80−22361
microscale sensing array for ocean meas. 78−85720
microthermometry, technique for local specimen temp. meas. in electron microscope 79−67297
microtransducer using fibre optics *(French)* 77−61084
microwave compatible MIC temperature electrode for use in biological dielectrics 79−88216
microwave radiometers, for atmos. temp. profile meas. *(Chinese)* 79−80188
microwave thermography: principles, methods and clinical applications 79−100691
microwave thermography, principle and biomedical appls. *(French)* 80−30957
microwave thermography and local heating by same system, clinical applications 79−100695
minerals, post-shock temp. meas. 79−92527
molecular torsional oscills., NQR freq. temp depend. electric field gradient asymmetry 80−18868
monitoring with remote indication, up to 150°C *(German)* 80−73356
monolithic temperature transducer, LX 5700 A, for −100 to +150 degree C temps., operation *(French)* 77−67431
monolithic two-terminal IC transducer, operation and characts. 77−10021
moving surfaces, contactless temp. meas. unit 78−4616
multichannel digital temp. recorder, TR-2711, measuring 100 channels in 10 s 78−65931
multichannel electric thermometer, 0-100°C, using transistor sensors 79−35741

temperature measurement continued
multichannel temperature measuring system, thermocouples multiplexing *(German)* 77−53902
multichannel temperature recorder, Thermodac II with 24 channels using thermocouples 78−65930
multiplexers, temperature applications, types of unit and configurations 80−82757
myocardial transmural heat gradient instantaneous meas. 78−44661
natural convection heat transfer rate, Moire pattern appl. *(Japanese)* 77−26295
NMR spectroscopy, low-temp. thermometer for ^{1}H, ^{19}F, and ^{13}C samples 78−65949
NMR thermometry at ultra-low temperatures, technique 77−17985
noise thermometry, theory and temp. determ. *(German)* 79−21748
noise thermometry, using conventional electronics 79−21751
noise thermometry, using Josephson junctions 79−21752
Noise thermometry in the range 630-962°C 78−73995
noise thermometry system, features, design aspects *(German)* 79−30478
NQR methods *(Russian)* 80−223
NQR precision thermometry, freq. meas. improvement 80−22356
NQR spectrometers, optimisation *(Russian)* 80−22412
NTC thermistor sensors, cct. designs and design calculation tables 80−68201
nuclear fuel thermocouple readings verification by transient response analysis 77−46309
nuclear power station thermal plume monitoring by drogues 77−3192
nuclear quadrupole resonance appl. 77−65031
nuclear reactor, press. and temp. loads on LWR containment after LOCA, scale model expts. 77−3134
nuclear reactor, pressure and temp. sensors, reactor time const. determ. by dynamic data system method 79−93750
nuclear reactor in-core meas., computerised *(Czech)* 78−86637
nuclear reactor safety qualification of class 1E transmitters 77−65287
nuclear reactor temperature sensors, response time testing by noise anal. 78−13300
nuclear reactor thermal mixer temp. fluctuation and pressure loss, scale model tests 79−9673
nuclear reactors automatic system using platinum resist. thermometers 79−89399
nuclear thermometry, possible appl. of brute-force nucl. orientation technique 77−59466
ocean, near-surface, distributed instrum. profiling sensors 77−82071
ocean internal wave obs. temperature measurement array 77−5380
ocean subsurface temp. remote sensing using laser Raman backscatter 77−78434
ocean surface layer remote sounding *(Russian)* 80−4138
ocean surface meteorological buoy and aircraft VHF link 80−46298
ocean temp. and salinity meas. by microwave radiometry 78−81416
ocean temperature, by coral skeletal aragonite Sr/Ca ratio 80−12568
ocean temperature measurements with Aanderaa thermistor chains, solar radiation effects *(French)* 79−62611
ocean temperature microscale studies, stable platform development 79−5669
ocean temperature microstructure low noise meas. with thermistors 79−58104
ocean vertical temperature gradients horizontal var. meas. by thermocouple arrays 78−61571
ocean water quality instrumentation system test 77−41066
oceanic temperature-depth profiles, recording via solid-state memories 78−24383
oesophageal multiprobe for temp., ECG and heart and lung sound meas. 78−77146
optical, based on fibre optics and phosphors 80−73360
optical system elements, steady temp. field meas. 77−50747
optoelectronic meas. methods appl., with twin diodes *(German)* 80−13064
optoelectronic temperature profile recorder 80−105642
p-n junction thermometer, using single quad op amp 77−45839
p-n series-connected junctions method *(Polish)* 80−13075
N.Pacific, sea surface temp. meas., 1976-77, from Nimbus 6 satellite 79−20841
palaeoclimatology, larval bivalve shell morphometry as temp. indicator 79−53510
particle temperature measurement, in a gas-solid fluidised bed 78−83464
particles in flight, temp. meas. by monochromatic photographic pyrometry *(French)* 80−27312
passive telemetry, by modulated backscattered incident CW RF carrier beam, cattle temp. meas. appl. 77−90968
Peltier effect appl. *(French)* 77−62908
perfusion blood temp. monitoring, zero-heat-flow transducer 80−8201
photochemical reaction temperature during laser photolysis, by use of cyclobutanone impurity 79−47944
photodetector, double layer As_2Se_3-HgSe system, thermometric charact. 79−88952
photoelectric micropyrometer, universal, for rapid var. meas. 77−41618
photoemission method, systematic error 79−93140
photographic developing bath, thermostatic control *(Spanish)* 80−77898
plasma, by meas. spectral density, for construction of 10000 to 15000K scale 79−30470
plasma, methods *(Hungarian)* 79−46477
plastic extrusion cylinder and feed channel wall, US appl. 77−27448
platinorhodium-Pt thermocouples, 1000-1300°C range, cold junction electrode compensation 78−216
platinum resistance thermometers, state of the art review *(Spanish)* 80−52212
polymer melts, thermocouple probe heat loss correction 77−65034
polyorganosiloxane fluids, temp. determ. in friction zone accompanying breakdown, using TV *(Russian)* 80−7688
poor thermal conductors, surface and contactless methods *(German)* 77−5832
portable instrument for thermal monitoring 78−49837
powders, in detonation deposition of coatings 80−11559
power, nonconducting, in detonation deposition 80−226
power plant cooling water, thermal IR scanner meas. technique 80−40947
practical scale between 1-273K, alternative to EPT-76 and IPTS-68 79−26052
pressure cell with temp. uniformity monitoring 78−230
pressure-volume and acoustic virial coeffs. for ^{4}He, temp. depend., quantum range 80−47056
probe, for use with digital multimeter, −10 to 100°C range 79−6125
pyroelectric vidicon, thermography appl. 77−54798
Pt thermometers for low temp. meas., AC circuits *(Polish)* 79−97389
PWR, Pt-resistance thermometers, in-pile response time testing 79−59219
PWR temp. sensor response time charact., estimation by noise anal. method 79−59216
pyrometer, fast wide ratio, construction and appl. *(Chinese)* 79−30483
pyrometer, for use in solar furnaces 80−86312
pyrometer, low-temp. total radiation, for 50°C to 150°C range 79−30471
pyrometer photoelectronic, using radiation invariant method, true temp. meas. of metals 80−52223
pyroxene geothermometry model with approx. soln. 77−2255
pyroxene solvus geothermometer in CaO-MgO-SiO_2 system 77−2144
quartz crystal with electrode-tab config., simultaneous mass and temp. determ. 78−54353
quartz microbalance, influence of tabs thickness on resonating props. of quartz cryst. 78−18140
quartz resonator, low-freq. heat-sensitive, charact. 79−30475
quartz thermometer with FET oscillator, −40 to 100°C range 78−77906
radiant heat flux portable direct reading measuring device, CERL flux-probe features 78−45633
radiation absorbing bodies, temp. fields Julich reactor expts., finite element calcs. *(German, English)* 77−82998
radiation balance microwave thermograph for industrial and medical appls. 78−45621
radiation pyrometer, use in automatic control of molten glass temp. in feeders 77−49729
radiation pyrometers, effect of aberrations on metrological charact. 78−77920
radiation thermometry, applied precision, current status 80−52224
radiometer, low-temperature, with conical light pipe, IC manufacture appl. 80−47105
radiometers, spherical-cavity, computation of errors 79−35829
radiometry of flat finite wave tank, three-dimensional vector modelling and restoration of meas. 77−22599
radiotelemetry, transmitter for small animal temp. meas. 79−83888
radiotelemetry transmitter, for temp. meas. from unrestrained subjects 79−16356
radiotelescope structure distortions determ., with aid of computer *(German)* 79−84669
rapid change measurement, computerised thermistor cct. 78−49829
rarefied gas flow, translational temp. determ. from mol. beam transverse density profiles 79−27726
recovery temperature data for cylinders in compressible flow 77−47036
reference standard for use below 0.5K, SRM 768 80−27303
reference temps. using triple points of Kr, Ar, N_2 and Ne 78−73997
remote circuit uses diodes as sensor 77−53901
remote ear canal temperature measurements in cattle 77−86714
remote sensing, selective radiant temp. mapping using layered classifier 77−56750
resistance bridge type thermometer, operational principles *(Polish)* 78−49834
resistance thermometer, GaAs p-type, for low temp. meas. under strong mag. fields *(Russian)* 78−89477
resistance thermometer, novel circuit *(German)* 77−74394
resistance thermometer, precision bridge using single inductive current divider 77−82517
resistance thermometer, Speer C, low-temp. magnetoresistance props. 78−49835
resistance thermometer, thin-wire, velocity-induced harmonics 79−49226
resistance thermometer and pyrometer methods and trends *(German)* 78−93681
resistance thermometer and thermocouple, rel. to radiation temp. scales 630-1064°C 78−37004
resistance thermometer based on thermal noise of sensors *(Russian)* 78−29113
resistance thermometer thermal inertia compensation *(Russian)* 80−62667
resistance thermometer transmission function approximation by Laplace transforms and Taylor series *(Russian)* 78−62197
resistance thermometers, thermojunctions and temperature sensitive ICs for automatic meas. *(German)* 80−77778
resistance thermometry, review 80−52206
resistive SQUID thermometer, theory 79−21753
resistive thermometric transducer appl. *(Russian)* 77−33987
respiratory phase detector system, battery operated cct., air temp. change meas. 79−100770
retinal photocoagulation by laser beam, temp. and bleaching dynamic meas. *(German)* 79−2098
review, techniques and instruments *(German)* 80−22358
review 80−86305
RF telemetry for temp. monitoring of free swimming freshwater fish 77−90965
rheogoniometer, Weissenberg-type, sample temp. meas. procedure 78−75113
rotating object, non-contact method with thermistor and pyrometric voltmeter 79−35742
rotating surface, contactless method of temp. monitoring 79−198
rotating systems, temp. meas., minimisation of contact drop error 78−73991
rotating-object surface temp. transducer test installation 78−4612
ruby, implantation temperature meas. using impurity luminesc. 79−52012
salinity/temperature sensor chain for estuarine meas. 79−5670
scale differences between IPTS-68 and thermodynamic temp. above 0°C 78−32814
sea ice age category differentiation through location and temp. observations using microwaves 80−67380
sea surface, multichannel scanning microwave radiometer, for Nimbus-G and SeaSat-A 77−29625
sea surface temp. meas., comparison of obs. in NE.Pacific Ocean 78−92837
sea surface temp. meas. from meteorological satellite images 79−100990
sea surface temp. obs. during 1952-65 period is N Pacific 77−41054
sea surface temperature, 8-13 μm satellite meas. interpretation 77−17145
sea surface temperature, meas. by meteorological drifting buoy 79−5661

temperature measurement continued
sea surface temperature contouring, appls. of satellite ocean-related imagery programme 79−5681
sea surface temperatures, features enhancement on satellite IR pictures by digital techniques 79−5682
sea temp. microwave radiometry, obs. at 2.65 GHz at Chesapeake Bay 77−29314
sea temperature gradient meas., anal. of two methods 80−31149
sea-surface, derivation from Meteosat image data 80−76985
seawater, microprocessor-based instrument 80−67440
seawater, using bathometer sonde 77−78480
seawater conductivity/temperature/pressure profiler errors 77−5377
secondary ref. stand., MP of Y_2O_3 77−45821
self-balancing nanovolt potentiometric system for thermometry and calorimetry 77−53903
SEM, stroboscopic, meas. of local temp. in specimen 79−9258
semiconducting transducers, up to 1000°C *(Croatian)* 79−40569
semiconductor temperature detectors, fundamental aspects and appls. *(German)* 79−21747
semiconductor temperature testing probes, accuracy and thermal characts. 80−52201
semiconductor thermometer, providing six point temp. meas. *(French)* 80−68200
semiconductor thermometry at low and very low temperatures 80−4713
semiconductors temperature dependences meas., of electric conductivity, Hall coeff. and magnetoresistance 80−31792
sensing element comprising GaAs thermionic diode (1 to 400 °C) 77−37886
sensing transducer with temp. sink chip on flexible dielectric cable 78−86264
sensors, determination of dynamic behaviour *(German)* 80−17940
sensors, Pt-100, stability and calibration 20-273K range *(German)* 77−79094
sensors, use of LEDs 78−4619
shear-band temp. meas., appl. to 4340 steel and 2014-T6 Al 80−48655
shipboard meteorological data system 80−46299
shock compression of solids, temp. meas. by optical means 80−86304
SI units fundamentals *(French)* 80−95059
simplified constant temperature electrolytic respirometer 79−12040
simultaneous mass and temperature determ. using single quartz wafer, optimized cryst. cut 79−49205
six-channel digital scanning thermometer type AD2036 operational principles 78−86269
skin, influence of cosmetics and ointments on spectral emissivity 77−9285
skin, thermographic image digitisation and anal. 77−16960
skin temperature, mean, simple meas. device using thermistors 79−2151
skin temperature measurements using a disc sensor, effect of press. 80−56259
sliding surfaces with lubrication, stationary and non-stationary meas. *(German)* 80−23975
small size plastic bearings, methods *(Polish)* 79−71449
small-animal microwave induced hyperthermia development system 78−11715
soft tissue temp. increases due to US Doppler blood flowmeters, thermographic meas. 79−62294
soil temp. differences and diurnal var. in Wales 77−64403
soil temp. prediction from winter period meteorological data 77−37418
soil temperature measuring system and data for Whiteshell Nuclear Resea-ch Establishment 79−48590
solar corona, temp. determ. from line breadths in electron scatt. continuum 77−22169
Spacelab optical techniques for liquid flow and temp. meas. 79−82007
Spar Buoy Oceanographic Telemetry System 80−46307
spectrophotometer, single beam, enlarged and thermostatted cuvette chamber 77−5925
specular reflection, use for radiation thermometry *(Japanese)* 80−101795
stagnation temp. meas. in hypersonic flow using fine W wire probe 77−79095
standard temperature lamps, with W ribbon filaments 80−95102
standards and thermometers in the USSR 80−62618
stars, absolute fluxes and temps. determ. from uvbyβ photometric system 77−64740
state of art and research appl. 80−31743
steady-state flow boiling curve, meas. using temp. controllers 79−32720
steel, mild, laser microspectral anal. 80−108769
steel forgings, expt.-calc. model of quenching, temp. meas. across cross section 80−16345
steel transition temp. determ. from fibrous structure in fracture, exam. of method 78−85080
still-shade-temperature meter for use in assessing personnel cold stress 80−81764
stopped flow temperature jump apparatus with spectrophotometric detection of fast chem. reactions 77−3892
stress anal. appl. 79−12796
subcutaneous, on living samples, microwaves non-conventional appl. survey *(Italian)* 80−13093
subcutaneous temperature meas., for thermoregulation obs., using passive microwave sensors 79−34721
subsurface, using Cu-constanton thermocouple rod 79−88954
subsurface water temperature and salinity remote sensing by Raman scatt. 79−80036
superconducting instruments for thermometry, future development in metrology 79−26020
superconducting machine temperature telemetry via optical channel *(Russian)* 78−57966
superconducting temperature sensor, NbTi monofilamentary wire in current sharing state 80−57288
superconducting transition temperature, dipstick cryostat 80−37044
superconductive device to provide reference temps. below 0.5K 79−63220
superconductive fixed points for temperatures above 0.5K 79−63221
superconductive temperature fixed point device, prep. and calibration 80−82770
superthermal electrons in laser-produced plasmas 80−1822
surface, automated zero-derivative method *(Japanese)* 78−210
surface, compensated contact thermometers appl. *(Polish)* 77−74401
surface, thin film resistance thermometers appl., Ti and Ge, design and fabrication 78−24792
surface, using Hg surface reflectance 77−2653

temperature measurement continued
surface temp., precision meas. w. contact thermometer 77−87761
surface temp. meas., temp. contact methods using thermistor and thermoindicators *(Russian)* 80−27295
surface temp. meas. at arbitrary heat flux *(Russian)* 78−45629
surface temp. meas. in continuous rating using separately applied detectors *(French)* 77−27466
surface temperature, pyrometer meas. errors limitation *(German)* 77−82522
surface temperature contactless meas. instrument 78−57946
surface temperature in fluidised beds, infrared photoresistors *(Russian)* 80−82763
surface temperature meas. through radiance temp. and emissivity, algorithm for calc. 80−52209
surface temperature meas. using radioactive kryptonates *(Czech)* 77−45842
surface temperature measurement using temperature indicating materials, crayons 80−86301
surface temperature measurement using thin film thermocouple 80−62668
surface-mounted beaded thermocouple transient response models 78−8405
surfaces, sliding, lubricated *(German)* 80−14643
surfaces in sliding contact, surface temp. effects 77−77594
target exposed to intense pulsed electron beam, kinetic temp. meas. method 77−82524
TCNQ salt, $Qn(TCNQ)_2$, Heisenberg antiferromag. chain for low temp. thermometry and cooling, EPR expts. 79−63217
techniques, sensor/instrument interface optimisation 77−5835
telemetric measurement, using an RF transmitter 78−205
telemetry system, implantable, single-freq., for monitoring body temp. 77−86688
telemetry system for measuring deep body temperature in rodents 78−24185
telemetry system for small animals, miniature CMOS 4-channel PWM design 78−44751
telemetry system with interference suppression, implantable, long-life, animal expts. appl. 80−101302
telemetry transmitter, crystal-controlled, surgically implantable, for animal expts. 80−72393
TEM, temperature calibration standards using graphite-halogens 80−86510
temperature contours, pulsating, using film structures, spatial resolution determ. *(Russian)* 77−74395
temperature drop parameter when testing with const. thermal flux 78−51049
temperature probe design, exptl. calibration results and numerical model predictions 80−56258
temperature scales above 0°C, evidence of IPTS-68 departures from thermodynamic temp. 78−32813
terrestrial surface temperature sensing, emissivity correction for thermal radiation interpretation 80−82092
thermal, temp. field meas., buoyant vortex bubbles and turbulent thermals 78−34232
thermal diffusivity determ. by temp. meas. at irregular operation stage 78−62199
thermal exchange between sensor and supports, temp. fluctuation meas. in turbulent airflow 78−21135
thermal imaging with pyroelectric vidicon camera 80−86288
thermal inertia mapping by IR imagery, mathematical model 80−109280
thermal interference from photolamps, reduction using Therm-O-lux 85 film 78−41302
thermal noise appl. *(German)* 78−4615
thermal relaxation oscillator using thermistor, temp. meas. appls. 78−73992
thermal sighter-radiometer, signal drift compensation unit 79−35830
thermal turbulence in plane airstream, temp. fluctuation meas., interferometric method 79−7432
thermistor, pulsed operation method 77−82510
thermistor appl. in potentiometer 78−207
thermistor multivibrator, temp. to freq. convertor and bridge 77−26289
thermistor probe, implantable, for continuous core temp. in rats 78−3686
thermistor selection guide 77−41607
thermistor temperature indication linearizing circuits 79−49230
thermistors, PTC, appls. 79−71448
thermo-electrical, lab. and industrial meas. using thermocouples, techniques 77−71324
thermo-sensors utilizing temperature-sensitive magnetic characteristics *(Japanese)* 79−12790
thermocouple automatic testing, base metal, temperature range 600 to 1300K 77−53908
thermocouple cavity in slab, transient temp. distortion 77−10016
thermocouple cold junction compensation method for portable instruments 79−2768
thermocouple network *(French)* 78−4613
thermocouple principles, ccts., and instrum. *(Dutch)* 78−198
thermocouple slip-ring assembly for measurement of temperature of rotating bodies 80−86294
thermocouple temperature transfer functions, theoretical and expt. determ. *(German)* 78−49827
thermocouple thermal inertia *(Russian)* 80−62665
thermocouple thermometry, accurate, review 80−52207
thermocouple thermometry, drift evaluation problem 77−53905
thermocouples, error due to time varying mag. field effects 78−4617
thermocouples, extension conductor connection provision 77−87762
thermocouples, modern design, avoiding errors 80−62664
thermocouples, temperature of oil in sliding friction bearings 80−31753
thermocouples, types and selection guidelines 79−194
thermocouples and resistance thermometer bridge networks, anal. *(German)* 77−71323
thermocouples and resistance thermometers meas. uncertainty estimation *(German)* 77−53909
thermocouples and resistance thermometers properties 78−199
thermodynamic method, using maximum entropy of electronic multiplets 77−74396
thermodynamic temperature, meas. techniques and concept. 80−52204
thermoelectric heat-flow meters, compensated, metrological charact. 79−37144

temperature measurement continued
thermoelectric needle probe for medical and biological temp. meas. 80−101299
thermoelectric thermometers cold junction thermo-EMF compensation, parameter optimisation *(Russian)* 78−86270
thermograph for soil temp. meas. 78−4005
thermogravimetric automatic temperature indicator 78−86257
thermometer with Si diode sensor, features, appls. *(Croatian)* 78−89479
thermometric AC bridge for temp. meas., 13.81-273.15K range *(Polish)* 78−93683
thermometric element for linear thermometer, using 5V reference power supply *(French)* 79−197
thermometric reference materials, purification and certification 77−67436
thermometry, use of anisotropic electrical conductivity in semiconducting crystals *(Russian)* 79−63211
thermometry below 1.5K 77−57332
thermometry range expansion 78−65927
thermophysical meas. above 2500K, apparatus 77−45845
thermophysical properties, conf., Dubrovnik, Yugoslavia (June 1978) 80−51944
thermophysical properties, temp. measurement methods at high temp. 80−52208
thermophysical properties, thermometric method determ., harmonic action of heat flow *(Russian)* 80−69642
thermophysical testing device, rate of change of temp. in time *(Russian)* 80−208
thermosensitive film coating, dispersed liq. cryst. microdroplets in gelatin matrix, exam. of preps. 80−42220
thermostatic air chamber, influence of radiation *(Japanese)* 78−37007
thin film temp. sensor with high temp.-resistivity 78−41308
three-dimens. fluid vel. vector and temp. fields from acoustic transmission meas. 78−30394
tissue, during microwave hyperthermia treatment of cancer 77−52859
tissue, noninvasive monitoring using temp. depend. of US vel. 78−40281
tissue, soft, temp. distrib. monitoring by temp. depend. of US vel. 80−45994
Tokamak, time resolved heat flux to wall meas., sheath model with secondary electron emission 78−79468
tolerated errors in determining transfer-function parameters of temperature transducers 78−73959
transducer, digital, solid-state, using automatically balanced Wheatstone bridge *(Rumanian)* 80−57287
transducer, temperature sensing, cct. and charact. *(Polish)* 78−29103
transducer with thermal feedback, operational principles *(Russian)* 80−86299
transducers, semiconductor diode junctions, variation of forward voltage with temp. 80−57293
transient gas flow, temp. meas. using hot wire anemometer 77−82508
transient heat transfer, temp. meas. with μs response time 78−71270
transistor, liquid or gas temperature meter, using separated readout 79−40563
transistor sensors for electrical temp. meas. *(German)* 79−30468
transistor temperature transducers, Motorola MTS IC series, appls. *(French)* 80−73357
transistor thermometer, precision, −50 to +125 deg. C at ±0.1 deg. C 78−21134
transition metal complexes, dimethylglyoxymate films, as temp. transducers 79−90923
transparent materials, laser irradiated, in-depth and surface temp. meas. by Moire-Schlieren technique 80−53392
triple point cells, Ar, O_2, comparison 78−73996
triple-point cell, diphenyl ether, for calibration of thermometers and thermistors 79−21750
TTF-chloranil visual pressure or temperature indicator 80−87443
turbine blade surface temperature meas. IR pyrometer 77−17983
turbulent boundary layer, temp. dissipation fluctuation component simultaneous meas. 78−26113
turbulent boundary layer, viscous sublayer temp. fluctuation spatial correlations *(Russian)* 78−34114
turbulent flow, hot wire meas., conduction error in probe 79−7423
turbulent temp. fluctuations recording, with detector dynamic response correction, dynamic errors determ. 80−77781
two-phase flow, nonequilibrium, phase temp. meas. 80−74950
ultra low temp. generation and meas. *(Japanese)* 78−45635
underwater temperature meas. thermistor chain 77−5379
unsteady gas stream temperature determ. using slow-response thermocouple 77−24046
US resonance method 78−16792
US thermometers, nuclear fuel temp. profile meas., TRESON expts. 78−57955
US thermometry, nuclear appls. 80−73365
vacuum coating, substrate and film surface temp. meas. 80−57297
vapour deposited coatings, precise meas. using combination of Pt resistor and Au-Pt thermocouple 79−49227
vapour pressure thermometry, appl. of equilibration of ortho-para H_2 using $KCr(SO_4)_2$ 78−62198
vapour-liquid equilibrium, T-x meas. by semi-micro method 78−87782
variation within ±0.0025°C, in BP studies of organic liqs. 77−15566
velocimeter for fluctuating temp. and vel. meas. in combustion field 80−14856
Venus ionosphere, electron temp. probe on Pioneer Venus Orbiter 80−67500
very low temp. physics and meas. *(Japanese)* 78−45636
viscosimeter solar radiation tracking sensor 80−86295
VMOS transistors used to give linear thermal response charact. 79−9216
voltage transfer standard SDET01, appl. *(French)* 78−236
W filament, appl. of noise thermometry, to specific heat meas. *(Russian)* 77−76573
water quality monitoring, modular system *(German)* 80−26186
welding arc, methods 78−55771
well temperature measurement, bottom-hole temperature stabilisation model 80−51356
West German metropolitan flat plate solar collectors, outdoor efficiency meas. 79−62048
Wheatstone bridge using thermistors for temp. meas. in calorimeter, optimisation *(German)* 78−86275
wide range pyrometer operational principle *(Russian)* 78−74004
wide range temperature/frequency convertor, expt. and cct. 77−17978

temperature measurement continued
wire sensors, frequency response meas. by internal and acoustic heating 80−31123
X-ray diagnostics of gas flow, temp. field determ. *(Russian)* 77−19648
X-ray diffractometer, PW1100, simple temp. monitor 78−67617
X-ray diffractometer furnace, temp. calibration using eutectic transitions of alloys *(Japanese)* 79−6128
X-ray thermographic installation, for temp. recording up to 1500°C 78−74003
Al_2O_3, temperature drop parameter when testing with const. thermal flux 78−51049
Ar, compressed gas, PVT meas. at high press. 80−98927
Ar, liq., magnetic field-induced temperature changes 78−57960
Au, heated thin film in liquid ^{4}He at 0.1K, temp. for large energy flux 79−55981
$BaTiO_3$, semiconducting ceramic, AC thermopower measurement 80−44624
$BaTiO_3$, temperature sensor using thick film techniques 79−93137
C powder magnetisation thermometry for very low temps. 79−63219
C resistors for low temp. thermometry 80−86308
CH_4 triplet point temp. meas. at 90.6861K 79−26060
$CePd_3$-Er, dil., low field mag. susceptibility, electro-nuclear effects, rel. to thermometry 80−60189
Cu, continuous casting, heat transfer and surface temp. meas. apparatus *(Russian)* 77−66631
Cu resistance temperature sensors *(Polish)* 79−97388
D_2, sticking and accommodation on low-temp. substrate, mol. beam expts. 80−84368
Ga triple point temp. determ. 80−42223
GaAs diode temperature sensors, charact. obs. at 4.2 to 393K 80−47054
H_2, sticking and accommodation on low-temp. substrate, mol. beam expts. 80−84368
^{3}He superfluid transitions, thermometry 77−65038
^{4}He, liq., magnetic field-induced temperature changes 78−57960
^{4}He, liquid, thermodynamic temp. meas. by noise thermometry at various vapour pressures 80−27298
Hg-in-glass thermostat 80−22359
$Li_2B_4O_7$, melt-crystal interface temp. meas. during crystallization of melts 79−44908
Mo-Mb, thermoelectric alloy for in pile temp. meas. *(French)* 79−67894
N_2 α-β transition, applicability as thermometric fixed point 80−13076
N_2, liq., magnetic field-induced temperature changes 78−57960
NQR absorption precision thermometer 77−5841
Na, liq., incipient superheat meas., expt. and physical parameter effects 78−18289
$Na_2B_4O_7$, melt-crystal interface temp. meas. during crystallization of melts 79−44908
NbTi-Cu, supercond. composite, use in temp. and heat transfer coeff. meas. 80−77780
Ni film, precise meas. using combination of Pt resistor and Au-Pt thermocouple 79−49227
Ni-NiCr probe for multichip component temp. meas. *(German)* 78−202
O_2, triple point, determination at low temp. *(Japanese)* 80−31749
Pt, freezing point determ. 77−26288
Pt resist. thermometers, 0-850°C range, principles and practice *(German)* 77−82512
Pt resistance elements 80−27296
Pt resistance temperature probes, constructional types and state of technique *(German)* 80−52213
Pt resistance thermometer, 0-850°C *(Dutch)* 77−127
Pt resistance thermometer, temp. meas. errors, 0 to 600°C 77−41605
Pt resistance thermometer, errors due to measuring-current heating in still air 79−30472
Pt resistance thermometer fast response meas., features 79−195
Pt resistance thermometers, thick film, resistance/temp. relationship 78−37008
Pt resistance thermometers, linearisation technique *(German)* 80−42224
Pt resistance thermometers, heat leaks effect anal. 80−57296
Si diodes as low temperature sensors *(German)* 80−31744
Si junction, charact. linearisation for temp. display 77−53904
Si, p-n junction, ellipsometric method of temp. meas. rel. to secondary breakdown *(Russian)* 80−11074
Si p-n junction local temp. meas. using pulsed SEM, induced-current mode 80−54775
Si, single cryst. growth, temp. gradient meas. by photoelec. pyrometer 77−40359
Si substrates during sputtering and sputter etching, thermal history of substrates 80−25562
Si whiskers, as basis for low-temp. sensors of temp. and deformation 79−5095
Sn, nuclear spin-lattice relax. time meas. using SQUID magnetometer, appl. to thermometry 79−63212
^{117}Sn, ^{119}Sn, low temp. NMR thermometry 80−82775
$SrTiO_3$, temperature sensor using thick film techniques 79−93137
W resistance temp. scale for field emission electron microscopy 77−45841
WC-Co based cutting tools, temperature meas. method based on amount of W in binder 79−96264
Xe discharge lamps, large, electrode temp. meas. by photographic method *(Russian)* 80−47057

temperature scales
0.5K to 30K, 1976 provisional scale 80−13034
0.5K to 30K, 1976 provisional scale derivation and development 80−13033
1337.58-2200K range representation by photoelec. comparator and W lamp *(German)* 78−4621
Celsius, Kelvin, Fahrenheit and Rankine, definitions and comparisons *(German)* 80−36972
comparison of scales in 1 to 30K range by Ge resistance thermometry 77−45854
contactless meas. using pyrometer, problems *(German)* 77−82507
cryogenic, 0.015 to 0.21K, based on superconducting phase transitions 80−17948
cryogenic temperatures, miniature sealed cells as temp. calibration device and precision thermostat 77−22559
education, elec. noise and Boltzmann's const. determ., absolute temp. scale noise thermometer 78−36767
fixed point, triple point of water 80−59626

temperature scales continued
gas thermometry, constant-volume, 2.6K to 27.1K (NPL-75) 80−13035
gas thermometry scale from 2.6K to 27.1K, report 78−89480
high-temperature, 10000 to 15000K, using plasma spectral density masurements 79−30470
high-temperature meas. and calibration, above 1000°C, based on Au melting point *(Rumanian)* 80−47061
International Consultative Committee on Thermometry recommendations 79−21693
International Practical Temp. Scale, instrument interpolation, from 630.74 to 1064.43°C 79−40564
international practical temp. scale of 1968 in region 90.188K to 903.89K 77−41609
International Practical Temperature Scale 1968, fixed point determination, amendment discussion 78−41270
International Practical Temperature Scale of 1968, density of Hg, −20 to 300°C 77−4139
International Practical Temperature Scale of 1968, future development 80−52205
international practical temperature variation from thermodynamic temps. in range 273.16 to 730K 77−65032
IPTS, β-γ transition in O_2 as reference temp. 77−103
IPTS, boiling points and triple points of O_2 and Ar 77−104
IPTS, O_2 boiling point and triple point realisation 77−105
IPTS, suitability of W strip lamps as secondary standard sources below 1064 degrees C 80−27297
IPTS realisation above 1337.58K using multiplicative comparator of spectral radiances *(Japanese)* 78−8407
IPTS-68 and thermodynamic temp. differences above 0°C 78−32814
IPTS-68 scales departures from thermodynamic temp. above 0°C, evidence 78−32813
Kelvin as standard temp. unit *(German)* 77−22520
low-temp. thermometry reference points based on H_2 and He 78−206
magnetic, based on susceptibility data for $Gd(PO_3)_3$ and Nd ethyl sulphate enneahydrate, 2.27K 79−63224
magnetic, for 2K to 30K range 77−5850
methane 80−95099
multiplicative comparator of spectral radiances, systematic errors *(Japanese)* 78−29139
neodymium ethyl sulphate, magnetothermodynamics, absolute temp. scale, mag. moment and magnetization , below 0.5K 78−34984
NQR methods of establishment *(Russian)* 80−223
practical scale between 1-273K, alternative to EPT-76 and IPTS-68 79−26052
primary thermometry, 2.5-27K, isotherm smoothing, ^4He 80−47056
provisional 1976 temperature scale between 0.5K and 30K *(French)* 79−63231
pulsed NMR thermometry below 0.1K 77−5852
pyrometer, wide spectral range, scale calc. 78−217
reference standards for radiation pyrometry, silver and copper freezing points 78−57888
resistance thermometer and thermocouple, rel. to 630-1064°C scales 78−37004
standards and thermometers in the USSR 80−62618
superconductive temperature fixed point device, prep. and calibration 80−82770
thermodynamic, gas thermometer reference standard 80−77782
thermodynamic temperature, meas. techniques and concept. 80−52204
thermometer calibration using Ga melting-point apparatus, enzymologic appl. 78−85460
thermometry, review 80−86305
thermometry below 1.5K 77−57332
thermophysical properties, conf., Dubrovnik, Yugoslavia (June 1978) 80−51944
triple point temp. of Ar and O_2 realised by calorimetry 79−12806
Ar triple point realisation cryostat for Pt resistance long stem thermometers 77−26307
Ar triple point sealed cells using stainless steel envelope 80−95099
CH_4, triple point, International Practical Temp. Scale, comparisons 79−40566
Ga melting point, thermometric standard 77−82516
Ga triple point temp. determ. 80−42223
Ge resist. thermometers, characts. from 1 to 35K, ISU mag. temp. scale 78−81970
H_2, thermometric fixed points determ. 77−82511
H_2 triple, boiling and 17K equilib. points realization, cryostat and method 80−27314
^3He, melting pressure temperature scale 77−22557
Nb, superconductive transition point as reference temp. 80−107943
O_2 solid-solid transition point, international practical temp. scale precision appl. 78−87786
Pd melting point, effect of surrounding O_2 80−27299
Pt freezing point determ. 77−26288
Pt, resistance thermometers and I_{68} calibrations, intercomparison 79−40565
Ta, superconductive transition point as reference temp. 80−107943
Y_2O_3, laser heated pellet, melting point determ., secondary melting point standard 78−37011

tempering
alloy steel, complex, X-ray diffr. determ. of fine struct. changes during quenching and tempering 77−56004
alloy steel, martensite structural singularities during tempering, electron diffr. study *(Russian)* 79−100177
alloys, temper embrittlement, impurities and alloying elements role, review 80−66649
austempered reinforcing wire, tempering under stress, effect on mech. props. and relaxation resistance 80−100861
austenite, quenched and tempered, effect of bainitic decomp. products on mech. props. 77−56007
brass LMtsSKA 58-2-2-1-1, heat treatment, struct. and props. 79−83239
butadiene nitrile, soot filled, thermal treatment influence on mech. props. *(German)* 80−30000
ceramics containing metastable tetragonal ZrO_2, grinding induced tempering 80−89260
crown glass impacted with sharp SiC particles, strength degradation of tempered surfaces 79−66183
diffusive release of gas from solid in presence of traps using linear tempering schedule 77−69187
dilatometric method for study of dimensional anomalies in metallic materials rel. to crystal struct. *(French)* 79−52563
tempering continued
embrittlement kinetics, computer simulation 78−84953
Ferrography, use of temper colours 78−3302
glass, annealed and tempered, impact damage, strength 80−85025
glass, chem. tempered, surface stress meas. using opt. waveguide effect *(Japanese)* 80−45473
glass, tempered, density and refractive index variation 78−64564
glass, tempered, spontaneous fracture due to NiS inclusions, exam. of behaviour mechanics 78−71294
glass, tempered, surface residual stresses from indentation fracture mechanics 77−90439
glass, tempered plate, stress state model and heat transfer rate determ. 78−60684
glass, tempering, stress and structural relaxation 78−64574
glass, thermal stresses, temporary and residual, monitoring by semiautomatic heating polariscope-polarimeter 78−16833
glass, thermally tempered sheet and plate, surface stress meas. using optical waveguide effect 80−25967
glass interferometer rod, inhomogeneity rel. to tempering 77−34919
glass plate, physically or chemically tempered, contact fracture resist., model 78−19895
glass plate with nonuniform temper, mottled pattern obs. 79−61750
glass plates, thermally tempered, strength degradation 78−48505
grain boundary segregation, T-t dependence of temper brittleness 77−36617
heat treatment apparatus 79−79005
high strength steels HT80, HY130, quenching and tempering effect on H_2 diffusion *(Japanese)* 78−64565
high-alloy die steel, heat resistance and crushing strength, low-temp. thermomech. treatment effects 77−52372
high-Si corrosion-resistant steel, 02Kh8N20S6, mech. props. and heat treatment 77−56003
isoprene rubber elastomers, thermal treatment influence on mech. props. *(German)* 80−30000
Kh20N40 alloys, phase composition after quenching, tempering 78−60650
lens, Schott S-1005, static fracture resist. rel. to thickness 78−81063
low-alloy cast steel, high-strength, fracture toughness 77−56109
martensite, microstresses associated with tempering 80−3111
martensitic steel, abrasive wear resistance, effect of tempering strain martensite 77−56116
martensitic steel, disloc. struct. obs. by amplitude independ. internal friction *(Bulgarian)* 77−19966
metal sheet, recovery strain during unloading in tensile test, roll-forming appl. *(Japanese)* 79−100182
optical glass, thermally tempered, surface stress meas. by crit. ray method 80−106766
products for nuclear power stations, research and development *(Russian)* 79−34080
PVC plastisols, thermally hardened, rheological props. *(German)* 79−29154
quenching-tempering apparatus with recirculation tempering furnace, thermal charact. 77−67438
reversible temper embrittlement, book contrib. 78−11334
semi-infinite solid, tempering induced diffusive release of gas in presence of traps 77−28045
soft-interlayer welded joint bending and torsion endurance, residual stress effects 79−83287
steel, 0.54% C, fatigue crack accel. and closure in rotating bending tests, in annealed or quenched/tempered state 79−43383
steel, 0Kh12G14N4Yu2, struct. after deformation under conditions of superplasticity 80−21031
steel, 18 Kh2N4MA, grain size effect on mech. props. 78−44207
steel, 24Kh2NMFA, crack resistance, yield strength, ductile-brittle transition temp., optimum tempering of 24Kh2NMFA 77−63787
steel, 30CH2GMT and 35CHG2SV, thermomechanical hardening *(Czechoslovakian)* 77−32602
steel, 30KhGSA, fracture toughness, tempering effects 77−90463
steel, 30N9K4, effects of Mo, V, and N on grain growth, tempering, hardenability, strength and toughness 78−44202
steel, 3.5% Ni neutron irrad. effects on tensile props., microstructure effects 77−69005
steel, 4140, fatigue crack initiation and microcrack growth 79−24617
steel, 4340, quenched, tempered, and austempered, effect of plastic strain followed by ageing on elastic limit 78−31446
steel, 45 and U7, deform. microheterogeneity and ductility 77−73309
steel, $\alpha \rightarrow \gamma$ transformation during rapid heating of N18K9M5T and N25 77−59788
steel, AISI 4340, positron lifetime and X-ray particle size meas. during high cycle fatigue 79−5053
steel, Al, quenched, tempered, orientation of precipitated Fe_xC particles, X-ray obs. *(Russian)* 79−29063
steel, alloy, 300M, fracture toughness and strength, effect of heat treatment on microstruct. 78−15436
steel, alloy, 30Kh2N2SMK5, temper brittleness of 79−96129
steel, alloy, austenitic, grain size, tempering effect on brittle fracture susceptibility 80−55534
steel, alloy, carburized case parameters, effect on props. of 20Kh3MVFA and 12Kh2N4A 78−52989
steel, alloy, cementite phase dispersion change during tempering *(Russian)* 80−93577
steel, alloy, Cr-Mo, alloy SCM3, hydrogen embrittlement, delayed fracture, exam. *(Japanese)* 78−64620
steel, alloy, Cr-Mo-V-P, quenched, temper brittleness in relation to V and P concs. 78−52986
steel, alloy, cyclic strength after strain hardening and tempering, precip. hardened 40FT and 40 78−52988
steel, alloy, embrittlement during tempering *(Russian)* 77−90436
steel, alloy, Fe-Ni-Cr-Sb-C effect of Ni, Sb, on temper embrittlement 78−60813
steel, alloy, fracture and fracture energy, subject to static, impact and repeated impact bending 77−63799
steel, alloy, heat-treated, crack resist. in seawater 80−104347
steel, alloy, high-speed, struct. changes investigation by hot hardness and quench dilatometry *(French)* 80−76249
steel, alloy, HY130, temper embrittlement due to Si intergranular segregation, effect on H_2 induced cracking 78−76735
steel, alloy, medium and low C, quenched and tempered, fracture resist., nonmartensitic transformation products effect 79−96054
steel, alloy, Ni-Cr-Mn, type 4340 intergranular brittle fracture, exam. by impact testing and Auger spectroscopy 78−52978

tempering continued
steel, alloy, Ni-Cr-Mo-V, exam. of temper embrittlement susceptibility 78−76737
steel, alloy, nonmartensitic decomposition of austenite, fracture strength of high tempered products *(Russian)* 78−11304
steel, alloy, type 52100, exam. of microstruct. and fracture, as function of austenitising in temp. range 800 to 1100°C 78−76673
steel, alloy, ultrahigh-strength, near threshold fatigue crack propag., microstructure effects 77−86168
steel, alloy, W-Mo-Cr-V, blanks welded to steel 45, optimal high temp. tempering 80−16351
steel, alloy low, Ni-Cr, tempered martensite embrittlement 80−7669
steel, alloy type 25KhN3MFA, tempering of bainitic structure 80−20983
steel, austenitic, 30KhGSA, grain size before quenching rel. to mech. props. 79−24553
steel, austenitic, 30KhGSA, heat treatment, preliminary, cold deform., elec. heating rel. to mech. props. 79−24554
steel, austenitic, CrNi, high Mo, corrosion, effect of struct. *(German)* 77−90481
steel, austenitic, phase composition of Kh14N16 with Zr, Ti, Nb and N additions after quenching and tempering 77−90378
steel, austenitic, strength, ductility and fracture toughness, N and Cr effects 80−100878
steel, austenitic, tempering cavity condensation *(French)* 80−55442
steel, austenitic, type of Kh15N27T3MR, exam. of elasticity props. 78−56687
steel, austenitic Mn, existence of carbide M_5C_2 phase, electron microdiffr. analysis *(Russian)* 78−23727
steel, austenitic stainless, supercond. magnets, mech. and phys. props. at 4K 80−86976
steel, austenitic stainless, temper embrittled, type 304, Auger spectroscopic exam. of grain boundary surface phases 78−76741
steel, austenitic type 110G13L, preliminary strengthening inheritance, exam. 78−44137
steel, austenitic type EI-69, carbide transformations on precipitation of C from austenite *(Russian)* 80−97487
steel, borided, 45, 20Kh, 30KhGSNA and Kh12F1, relative wear resistance 77−73351
steel, C, austempered, exam. of running in and wear 80−16485
steel, C, contact fatigue strength, effect of austenite grain size 79−100254
steel, C, diffusion of H_2, effect of quenching and tempering 77−7908
steel, C, diffusion of H_2, SCC via martensite form. cooling rate changes on Mn and Ni addition *(Russian)* 78−56813
steel, C, hard patch of rubbed surface, tempering effect *(Japanese)* 78−7054
steel, C, hypo-eutectoid naturally fibrous composites, strength analysis 78−3190
steel, C, quenched and tempered, ductility, effect of hydrostatic press. 78−44190
steel, C, rubbed surface, continuous hard layer *(Japanese)* 77−52501
steel, C, second stage of tempering 79−61627
steel, C, tempered martensite embrittlement, and retained austenite, exam. 78−56754
steel, C, type 1792AF 79−38966
steel, C and Co, carbide transitions during post-strain ageing and tempering *(Russian)* 78−95741
steel, C martensitic, tempering induced decomposition and segregation, atom probe study 80−3112
steel, C type 45, martensitic needle size, effect on mech. props. after induction hardening 80−11672
steel, C type U10A, X-ray diffr. investig. of carbide residues after deform. and tempering *(Russian)* 77−81275
steel, C-Mn and C-Mn-Nb, weldable, high temp. thermomechanical treatment 79−15709
steel, C-Mn-Cr-Mo (0.4, 0.8, 1.1, 0.25 wt.%) C, Ni, Mo, Cr addition effects on toughness of bainite 78−11327
steel, C-Mo-P, intergranular fracture and grain boundary segregation, P, H, Mo effects *(Japanese)* 79−15775
steel, C-Ni-Cr (0.6, 1, 1 wt.%), grain boundary segregation of S, N, P, As, Sb and Bi *(Japanese)* 78−15405
steel, carbide formation during tempering on martensite decomp. and ductility 78−23733
steel, carburised, alloying effect on props., mathematical-statistical determ. 78−19794
steel, casecarburized and hardened, relationship between fatigue strength and case hardness distrib. *(Japanese)* 79−61782
steel, CC Cr-Ni, soaking at forging temp., effect on struct. and mech. props. *(Czech)* 78−64628
steel, Co-Cr-Ni-Mo-Mn (39.65, 20.25, 15.33, 7.08, 1.9 wt.%) carbide formation during tempering after plastic deformation 80−16330
steel, cold rolling, effect of transformations during quench hardening and tempering 77−55989
steel, complex alloy, exam. of temper brittleness 78−44209
steel, constructional, impact strength/brittle fracture relationship in ductile-brittle transition zone 78−56740
steel, Cr, brittleness onset during high-temp. tempering *(Russian)* 77−81276
steel, Cr, corrosion resist., tempering after air-hardening in rolling heat *(German)* 80−45324
steel, Cr, high C, in situ transform. of cementite to M_7C_3 and internal defects of M_7C_3 by tempering 78−31412
steel, Cr, high-C hardened rolls, parameters for short tempering times 79−38865
steel, Cr, influence of ultrasound on tempering processes *(Russian)* 78−52827
steel, Cr, tempering resist., mech. props., Cu addition effect 79−79012
steel, Cr (12 wt.%), thermomechanical treatment, high temperature, effect on props. and struct. *(Czechoslovakian)* 77−32603
steel, Cr (12wt.%), mech. props, carbide phase struct. 79−15702
steel, Cr (13 wt.%), tempered, quenched, fatigue resistance in corrosive medium *(French)* 78−23870
steel, Cr (4 wt.%), Cr_7C_3 precipitate growth during tempering, effect of Cr diffusion *(Russian)* 79−52219
steel, Cr and Mn, softening during hardening, austenitising effect 79−96052
steel, Cr bearing, carbide phase precipitation during tempering, Mossbauer, X-ray diffr. studies *(Russian)* 79−87636
steel, Cr modified, heat resist. rel. to thermomech. treatment 79−20084
steel, Cr-C, (2.14, 1.08 at.%) tempered, resistance to small plastic deformation, strain relaxation *(Russian)* 78−56698

tempering continued
steel, Cr-C (13, 0.15 wt.%), bainitic transform. *(German)* 78−11218
steel, Cr-Mo, Mn-V, V, fracture toughness, pressure vessel appl. *(Czech)* 79−79094
steel, Cr-Mo (1.25, 0.5 wt.%), creep, fracture, Ti and Ti+B effects 77−36603
steel, Cr-Mo (2.25, 1.0 wt.%), temper embrittlement, effect of P, Sn, comp. and carbide precip. 80−85036
steel, Cr-Mo (2.25, 1.0 wt.%), temper embrittlement, effect of Mn, Si, comp. and carbide precip. 80−85037
steel, Cr-Mo (2.25, 1 wt.%), quenched and tempered, diffusion and solubility of H_2 *(Japanese)* 79−65255
steel, Cr-Mo (2.25, 1 wt.%), strain hardening shakedown load during bending 80−20958
steel, Cr-Mo (2.25, 1 wt.%), temper embrittlement trace elements, Mo, intercritical heat treatment effects 77−36634
steel, Cr-Mo (2.25, 1 wt.%), weld metal, high temp. crack growth, effect of tempering, prestrain and grain refinement 78−27622
steel, Cr-Mo (3 wt.%), temper embrittlement 77−36647
steel, Cr-Mo (9,1 wt.%), austenitized in $\gamma+\delta$ phase field, secondary hardening and tempering 78−11247
steel, Cr-Mo weld metal, trace element embrittlement suppression by creep strength effects 80−66656
steel, Cr-Mo-(Ni-V), temper embrittlement by P and Sn, effect of rare earth additives 79−61721
steel, Cr-Mo-Mn-Si-W (3, 1.95, 1.55, 1.45, 0.95 wt.%), struct. and props. 80−104175
steel, Cr-Mo-Ni-WV (6, 4, 3, 2 wt.%), tempering and secondary hardening, TEM obs. *(Chinese)* 80−104245
steel, Cr-Mo-V, 1% Cr, chem. comp. and struct. effect on deform. props. *(German)* 79−1888
steel, Cr-Mo-V, creep, effect of microstruct., heat treatment, transform. temp. 78−11248
steel, Cr-Mo-V, creep fracture, microstruct. effects 78−64668
steel, Cr-Mo-V, excessive temp. effect on creep behaviour, structure and hardness *(German)* 80−30054
steel, Cr-Mo-V, heat treated, mech. props. *(German)* 80−25724
steel, Cr-Mo-V, medium strength, correlation between crack initiation, propag. and microstruct. 78−60787
steel, Cr-Mo-V, normalised and tempered, size and geometry effect on creep cracking behaviour 78−64630
steel, Cr-Mo-V, press. vessel, fracture, effect of tempering 78−60799
steel, Cr-Mo-V (0.5, 0.5, 0.25 wt.%), bainitic and martensitic, tempered, creep crack growth 77−86136
steel, Cr-Mo-V pressure vessel, microstruct. parameters and yielding rel. to plastic deform. 80−89318
steel, Cr-Ni, effect of tempering under load on mech. props. 80−16354
steel, Cr-Ni, microstruct. effect on temper brittleness *(Korean)* 79−70092
steel, Cr-Ni (14, 5 wt.%), tempering resist., mech. props., Cu addition effect 79−79012
steel, Cr-Ni-Mo, handbook data for type 34KhN1M 79−78960
steel, Cr-Ni-Mo-Cu, ε phase particle precipitation from martensite, local internal stress relaxation *(Russian)* 79−78969
steel, Cr-Ni-Mo-V, austenite form. during heating, influence of recrystn. during tempering *(Russian)* 80−104188
steel, Cr-Si-Mn-Ni-Mo-C, resist. to deform. and fracture, C effect 80−71757
steel, Cr-W(Mo), quenched, carbide reactions during tempering 80−89229
steel, Cr-W-V-Mo (3.9 to 4.5, 1.5 to 2, 0.9 to 1.2, 3.9 to 4.4 wt.%), heat resistant, type 8Kh4M4V2F1-Sh, mech. props. 80−16464
steel, cracking resistance of high-strength 40Kh and 35KhGSA, tempering temp. influence *(Russian)* 79−52252
steel, CrMoV, creep resistant, quantitative struct. parameter use in props. prediction *(Czech)* 80−108481
steel, CVD coating temp. effect on hardness and dimens. stability 77−40470
steel, die, with high heat resist. and toughness 78−84989
steel, embrittlement control progress 78−72797
steel, eutectoid, U8, cold hydraulic press. forging effect on transform. and heat treatment *(Russian)* 79−52235
steel, eutectoid notch toughness, tempering at moderate temps., effect of quenching temp. 77−21193
steel, fatigue strength on combined surface strain-hardening and tempering *(Russian)* 77−59900
steel, Fe-Al-C alloy, redistribution of C during tempering *(Russian)* 77−90371
steel, ferritic martensitic, effect of ductility of second phase on ductile fracture 78−19847
steel, hardened and casecarburized, fatigue crack initiation, propag. and termination, notch depth effects *(Japanese)* 78−7022
steel, heat treated, alloying element distrib. effects, mech. props. 78−84876
steel, heat treated high strength, X-ray diffr. anal. of residual stress 80−3200
steel, high C, 80Kh5G5 and 120N12, austenite hot deform. effect on martensitic transform. *(Russian)* 77−48434
steel, high C, high Cr, rapidly quenched, in situ carbide reactions during tempering *(Japanese)* 78−84862
steel, high C, investigation of transformations during tempering by nuclear gamma resonance method *(Russian)* 80−76256
steel, high C, quenched and tempered, hydrostatic press. effect on brittle fracture stress 79−61727
steel, high C, type 7KhFNSh, plastic deform. influence of X-ray interference line breadth *(Russian)* 80−93599
steel, high purity, low S content, for tough semi-finished products in nuclear power plant *(German)* 80−45393
steel, high speed, anode potential determ. of tempering quality 78−53139
steel, high speed, hardened, for drills, mech. and cutting props. 79−43407
steel, high speed, microstruct. effect of splat cooling 79−61624
steel, high speed, tempered, etching reagents for austenite grain boundaries 78−80704
steel, high speed, type R6M5K5, secondary and red hardness of marquenching 80−16350
steel, high speed tool rapidly quenched, exam. of solidification struct. 78−39758
steel, high strength, 300-M, slow fatigue crack growth, threshold behaviour, temper embrittlement, impurity segregation effects 77−86152

tempering continued
steel, high strength, environmental effects on initiation and propag. of fatigue cracks 77−86216
steel, high strength, failure stress, structural relationships 80−81190
steel, high strength, fine grained, quenched and tempered, residual welding stresses, stress relieving temp. *(German)* 78−72793
steel, high strength, surface work hardening effect on life 77−70234
steel, high strength, treatment effect on ductility and strength 80−60880
steel, high strength weld metal, fractography, microstructure and reheated zone toughness effects *(Japanese)* 80−108543
steel, high-alloy die, electrothermal treatment 80−29996
steel, high-C martensite, struct. transforms. during low temp. tempering *(Russian)* 77−59737
steel, high-speed, low temp. mag. cycling effects on ferromag. struct. 80−100928
steel, high-speed, quenched and tempered notch toughness, ultimate and yield strength in tension and compression 78−95782
steel, high-speed cutting, struct. and props. Co addition effects *(Russian)* 77−21177
steel, high-speed tool, splat quenching, props. and struct. 80−76294
steel, high-temp. high temperature thermomechanically heat treated, fatigue strength improvement by cathodic polarisation *(Russian)* 77−25188
steel, homogenisation of sulphide inclusions 77−32605
steel, HSLA, V effect on mech. props. *(Korean)* 80−29987
steel, hypereutectoid, thermomech. treatment, Fe_3C distrib. and yield point *(German)* 79−52243
steel, hypoeutectoid, C22, recrystn., influence of carbides distrib., X-ray exam. *(German)* 79−38850
steel, hypoeutectoid, morphology and stability of Widmanstatten struct. *(Slovak)* 79−70094
steel, induction hardened, static bending strength and correlation between static strength and endurance limit *(Japanese)* 77−70108
steel, Kh17N2, endurance limit, effect of residual stresses caused by Cr plating and cyaniding 77−86184
steel, KhVG, quenched change in structure under influence of cyclic loads 78−56676
steel, lath martensite, elastic interaction of H_2 with precipitates 78−3129
steel, low alloy, 18KhMVTCh, corrosion cracking resistance in sulphide environments *(Russian)* 78−31571
steel, low alloy, acoustic emission during ductile fracture, isothermal tempering effect 79−83241
steel, low alloy, bainitic and martensitic transform., isothermal studies 77−36497
steel, low alloy, brittle fracture, quenched and tempered 80−11677
steel, low alloy, C-Ni-Cr-Mo (0.36 wt.%), impact toughness rel. to microstruct. *(Korean)* 77−21188
steel, low alloy, formation of stony fracture during forging 79−79059
steel, low alloy, hot deform. behaviour and modified ausforming *(Japanese)* 78−11244
steel, low alloy, impurity and strength effect on H_2 induced cracking 78−27625
steel, low alloy, isothermal tempering effect on acoustic emission during ductile fracture 80−85047
steel, low alloy, quenched, tempered martensite embrittlement, role of retained austenite and cementite 79−74251
steel, low alloy, radiation embrittlement, heat treatment effects 78−19893
steel, low alloy, SMCM 8, tempered, fractographic study of stress corrosion cracking *(Japanese)* 79−66214
steel, low alloy, SNCM 8, quenched, tempered, prior austenite grain size effect on stress corrosion cracks *(Japanese)* 79−66215
steel, low alloy, softening of heat affected zone under postweld tempering 77−21196
steel, low alloy, strengthening by strain tempering, deform. effects 78−15424
steel, low alloy, temper embrittlement, review 79−20154
steel, low alloy, temper embrittlement and ternary equilib. segregation 80−60958
steel, low alloy, tempered martensite embrittlement mechanisms 79−8351
steel, low alloy, toughness, effect of packet size and lath width 77−16677
steel, low alloy, type 4340, quenched and tempered, effect of plastic strain followed by ageing, on torsion fatigue resistance 78−92360
steel, low alloy and C, hardened and tempered parts, nondestructive magnetic inspection 78−95889
steel, low alloy and C, hardened and tempered parts, nondestructive magnetic inspection 79−1929
steel, low alloy and C, reversible temper brittleness kinetics *(French)* 78−35498
steel, low alloy Mn-Sb(2, 0.12 wt.%), reversibility of temper embrittlement, studied by XPS and AES 77−32667
steel, low alloy structural, heat treated, impurities effect on embrittlement susceptibility and temper brittleness 79−38955
steel, low alloy structural, type 30KhGSA, effect of thermomech. treatment on strength, fracture toughness and fatigue props. 80−11676
steel, low alloy type 14Kh2GMR, high strength, welded joint, impact toughness, welding thermal cycle and tempering effects 80−3157
steel, low and medium C, tempering 79−61629
steel, low C, and hardened and tempered, impact specimen fractures, stress concentrator sharpness effect on size of tough component 78−7015
steel, low C, effect of heat treatment on resistance to fatigue crack propag. 80−11675
steel, low C, high C, bainite transform. heat treatment effects *(Czech)* 77−63661
steel, low C, martensitic, fracture toughness variations during tempering 78−60812
steel, low C, Mb-Nb, reheated, quenched, tempered, microstruct. 77−36550
steel, low C, microalloyed, heat treatment, mech. props. 79−24551
steel, low C, Mn-Nb, quenched and tempered, microstruct. and props. 77−36549
steel, low C, quenched, struct. and props. after plastic deform: and tempering 78−23734
steel, low C, Si effect on gas nitriding, surface hardness *(Japanese)* 77−48582
steel, low C, tempered, lath martensite, Ni (5 wt.%), microstruct./yield strength relationship 77−21234
tempering continued
steel, low C Cr-Ni, temper embrittlement by antimony, Ti addition effects 77−32683
steel, low pearlite, low alloy, low temp. strength props., heat treatment 77−12658
steel, low S, ESR, overheating effect on toughness 78−52860
steel, low S, ESR and electric arc, notch toughness, interaction between overheating and tempering temp. effects 78−52970
steel, low S, overheating 77−21185
steel, low Si, martensite struct. and mech. props. *(Korean)* 80−93614
steel, low-alloy structural 16G2 and 16GFR, struct. and props. after quenching and tempering 80−76280
steel, low-tempered, corrosion cracking in NaCl soln. *(Russian)* 78−56801
steel, lower bainite, struct. changes during tempering *(Russian)* 77−21178
steel, magnetic field effect on retained austenite transformation 77−16580
steel, maraging, hardening mechanism of quenched samples, tempering *(Czech)* 79−78989
steel, maraging, Ni-Co-Mo (18, 8, 5 wt.%), fatigue strength charact. *(German)* 77−21241
steel, maraging stainless, phase transformation and mech. props. rel. to heat treatment *(Chinese)* 80−66501
steel, martensite, brittle fracture resistance, struct. after quenching effects, tempering effects 79−57104
steel, martensite, high C, tempering, nuclear gamma reson. meas. *(Russian)* 79−1883
steel, martensitic, age hardening with Cu, Nb additions, exam. of hardness 80−7681
steel, martensitic, ageing of 05kh3N2MD2, hardness depend. on tempering temp. *(Russian)* 79−24544
steel, martensitic, alloying element effect on coarsening behaviour of cementite particles in ferrite 80−66518
steel, martensitic, Cr (12 wt.%), temper embrittlement 79−87722
steel, martensitic, fatigue crack propag., effect of intercrystalline fracture associated with temper brittleness *(French)* 80−16463
steel, martensitic, high-C, formed from hot-worked austenite, struct. *(Russian)* 78−6950
steel, martensitic, impact bending failure resistance, initial crack length and tempering effects 78−31530
steel, martensitic, low C, nitriding, exam. of case props. 78−85045
steel, martensitic, low C wire, strain tempering by rapid heating *(Japanese)* 78−31428
steel, martensitic, medium alloy, quenched state, deform. hardened, ageing effects *(Russian)* 77−21179
steel, martensitic, modulated struct. form. by tempering, high resolution electron microscopy obs. 79−96042
steel, martensitic, retained austenite study by X-ray diffr. *(Korean)* 78−44143
steel, martensitic, tempered, C and low alloy, hardness, effect of alloying additions 78−27629
steel, martensitic transformation kinetics 79−87630
steel, medium alloy, constructional, strength-toughness relationship 77−70137
steel, medium C, tempered, normalised or quenched, statistical property of fatigue limit, press-fitted axles *(Japanese)* 77−12693
steel, medium C 80−11752
steel, medium C quenched, tempered, relation between wear and work surface layers *(Japanese)* 77−52499
steel, medium Cr, B effects on struct. and toughness 77−21265
steel, medium strength plate, quenched and tempered, fracture toughness in ductile-brittle range 78−7036
steel, middle and low C, clad plate, inhomogeneity and residual stresses, heat treatment effects *(Japanese)* 78−6955
steel, mild, semi-killed, tempering, effect of microstruct. and hardness 77−21184
steel, mild, tempered and quenched, dynamic fracture toughess 77−36665
steel, mild, yield strength and fracture toughness, microstruct. effect, heat treatment 78−27615
steel, Mn, influence of ultrasound on tempering processes *(Russian)* 78−52827
steel, Mn, tempered, sementite crystals, carbide phase segregation, X-ray study *(Russian)* 78−35391
steel, Mn, type 35SGM, magnetic, electrical, and mech. props. after tempering and hardening 79−66086
steel, Mn-B-V, low alloy, transform. singularities *(Russian)* 80−104116
steel, Mn-C-Si-Cu (0.95, 0.85, 0.25, 0.16 wt.%), fibrous-banded fracture mechanism 80−104280
steel, Mn-Cr, tempered, case hardened, shot peening effect on bending fatigue strength *(German)* 79−24645
steel, Mn-Cr-V, tool, quenched and tempered, fracture toughness *(German)* 80−25726
steel, Mn-Mo-Ni-Cr, bainitic, microstruct. and mech. props. *(French)* 80−16362
steel, Mn-Ni-Cr-C, supercooled austenite, influence of constant mag. field on diffusional decomp. *(Russian)* 79−4964
steel, Mn-Ni-Mo, PWR pressure vessel, irrad. induced embrittlement, chemical composition effect *(French)* 79−20195
steel, Mn-V and Cr-Mo, for pressure vessels, hydrogen embrittlement evaluation *(Czech)* 79−38950
steel, Mo-Cr (3 wt.%), CrC formation in isochronal tempering, electron microscope study 80−7584
steel, Ni, high-strength, impact fatigue strength, heat treatment conditions effect 80−76285
steel, Ni, martensite decomposition *(Russian)* 79−1841
steel, Ni(9 wt.%), isothermal bainitic transform., thermomechanical effects on mech. props. *(German)* 80−40383
steel, Ni (3.5 wt.%), heavy rotor forgings, temper embrittlement, metallurgical investigations *(German)* 80−16471
steel, Ni (9 wt.%), effect of repeated tempering on notch strength *(Japanese)* 79−43280
steel, Ni (9 wt.%), mech. props., effect of alloying 77−48462
steel, Ni (9 wt.%), tempered, mech. stability of retained austenite 79−24521
steel, Ni and W, recrystallisation mech. during laser treatment 80−50658
steel, Ni-B, B effect on temperability and microstructure 79−15710
steel, Ni-Co-Cr, high-strength medium C, Cr effect on props. 80−76339

tempering continued
steel, Ni-Cr, cast, tempering embrittlement due to impurities, Auger spectroscopy exam. 80−11683
steel, Ni-Cr, P doped, tempered martensite embrittlement 80−30089
steel, Ni-Cr, P induced temper embrittlement, Mo effect 77−86148
steel, Ni-Cr, temper embrittled, electron microscope and X-ray microstruct. obs. 79−38870
steel, Ni-Cr, temper embrittlement, intermediate tempering treatments 80−60944
steel, Ni-Cr, temper embrittlement by Sb, Ni, Cr effects 77−36628
steel, Ni-Cr, temper embrittlement by Sn 77−86149
steel, Ni-Cr low alloy, effect of Mo on tempered martensite embrittlement 80−3187
steel, Ni-Cr temper embrittlement by P 77−40448
steel, Ni-Cr-Mo, exam. of delayed fracture using fracture mechanics *(Japanese)* 78−52961
steel, Ni-Cr-Mo, quenched and tempered, nothced bar tensile tests *(German)* 80−35247
steel, Ni-Cr-Mo-V, temper embrittled, crack initiation strength *(Japanese)* 77−52474
steel, Ni-Cr-P (0.06 wt.%), influence of intercritical heat treatment on temper embrittlement susceptibility 78−52863
steel, Ni-Mo-C (5, 0.5, 0.5 wt.%), sintered, effects of powder and sintering variables on props. 80−104093
steel, Ni-Sn interaction during heat treatment in temper embrittlement temp. range 77−86176
steel, nuclear bolts, heat treatment for structural retraction prevention *(French)* 79−91713
steel, pearlitic, heat treatment effect on fracture resistance, microstruct. and mech. props. 80−104191
steel, pressure tank, heat-treatment effects and mech. props. *(German)* 80−40409
steel, prestressed concrete wire, strain tempering by rapid heating *(Japanese)* 79−70088
steel, quenched, exam. of phenomena taking place during tempering by positron annihilation *(Russian)* 79−24543
steel, quenched, martensite, tensile and compressive deform. resist. *(Russian)* 78−19819
steel, quenched, notch sensitivity, effect of tempering temp. 77−1846
steel, quenched, tempered, intergranular failure during fatigue crack growth 79−8357
steel, quenched, tempering treatment, ultimate tensile strength and yield point *(Russian)* 77−32599
steel, quenched and tempered, microstructure effect on cleavage fracture toughness 79−74252
steel, quenched and tempered 52100 bearing, plastic deform. in compression 77−40437
steel, quenched and tempered sheet, first operation cupping *(German)* 78−72788
steel, quenched-tempered, relationship between half value breadth and hardness *(Japanese)* 77−52366
steel, reactor construction material, He liberation 77−46290
steel, reinforcing, 20GS2, brittle fracture resistance in corrosive environment, tempering effects *(Russian)* 77−59974
steel, reinforcing bar, high-strength 20GS2 and 20KhGS2, corrosion cracking 80−55578
steel, retained austenite estimation during tempering, DTA *(German)* 77−28831
steel, rolls for cold-rolling mills, surface hardening, contact fatigue strength 79−24664
steel, rotor, Ni-Cr-Mo-V, reversible temper embrittlement 77−36656
steel, Si-Cr-Mo-W-V (2,4,1,3,2 wt.%), heat treatment and props. 80−16349
steel, Si-Mn, 27SG, heat treated sheets, underwater explosive forming *(Polish)* 79−34052
steel, Si-Mn-Cr-C (1.1, 0.9, 1.0, 0.29 wt.%) 30KhGSA, heat treatment effect on strength and toughness 78−15437
steel, silver, elastic limit, bending strength, and ductility rel. to tempering temp. after quenching 78−95764
steel, sintered type M2 high speed, heat treatment response and cutting props. 78−15336
steel, spring, 60C2A, tempered under stess, influence of tempering conditions on mech. props. *(Russian)* 79−47724
steel, spring wire and springs, type 60S2A and 50KhFA, stress tempering effect on mech. props. 79−66085
steel, stainless, martensitic 403, heat treated struct. effect on H_2 diffusion 77−63703
steel, stainless, sulphide stress corrosion cracking resistance, improvement by heat treatment 78−7076
steel, stainless, tempering after air hardening from rolling heat *(German)* 80−93571
steel, stainless ferritic, drawability, mech. props., and grain boundaries in 08Kh16AMT and 08Kh18T1 80−35270
steel, stainless Kh15N9Yu, elastic limit, effect of microstruct. and heat treatment 79−83251
steel, statistical distrib. of mech. props., and life characts. exam. 78−64606
steel, strengthened by surface plastic deform., tempering effect on physicomech. props. *(Russian)* 78−35409
steel, structural, 34KhN3M, heat treatment effect on magnetostriction 80−104306
steel, structural, addition of solid SiO, effect on ductile fracture 80−16465
steel, structural, austenite form. during heating *(Russian)* 77−32572
steel, structural, brittleness susceptibility rel. to heat treatment 79−24620
steel, structural, CrN-modified, tempering and quenching effects on struct. and props. 77−59835
steel, structural, effect of rare earth metals on cold temper brittleness 79−29202
steel, structural, strained in tension after tempering, compression effects on struct. changes *(Russian)* 80−66577
steel, structural 15Kh2NMFA, use of linear and nonlinear fracture mech. for crack propagation resist. determ. 79−5056
steel, structural 15KhNMFA, resist. to weakening during tempering, high purity effect 80−76279
steel, temper embrittled, grain boundary failure model for intergranular fracture modes 80−25825
steel, temper embrittlement, effect of sp-3d impurity interactions on resistivity 79−46696
steel, temper embrittlement, fracture mech. of grain boundary segregated phases 78−48531
steel, temper embrittlement and embrittling intergranular segregates, Mo effects *(French)* 79−91788
steel, tempered, kinetics of solution of Mn in precipitated cementite *(Russian)* 78−6891
steel, tempered, notched, impact bending tests, cold brittleness curves 80−71758
steel, tempered martensitic, type AISI 410, role of C in embrittlement phenomena 80−93652
steel, tempered or quenched, exam. of fracture toughness tests, for C shaped specimens 79−29215
steel, tempered StE70, water quenched, residual stress field in centrally welded plates *(German)* 78−72794
steel, tempering effect on fatigue strength 80−60891
steel, tempering effect on struct. and mech. props. of types 70, U8, and U12 *(Russian)* 80−50655
steel, Ti (0.1 to 0.55 wt.%), strengthening by carbide precipitation 77−25062
steel, tool, high-strength, mech. props. in compression, tempering temp. effect 79−83240
steel, tool, W-Mo, heat treatment effect on props. 80−50656
steel, TRIP, warm extrusion, process control and tensile props. 80−16338
steel, type 20 CND 10-10, temper brittleness and intercrystalline segregation *(French)* 77−81316
steel, type 20Kh deformed, austenite grain size, inheritance effect with quenching and tempering 80−60881
steel, type 27KhGSNL, castings, exam. of cracks due to treatment 78−44205
steel, type 28Kh3SNMVFA, strain hardened martensite, resist. to tempering, exam. 80−16348
steel, type 52100, heat treatment effect on microstruct. and mech. props. 80−29993
steel, types 15Kh2NMFA and 45, fatigue tests, low cycle, material variance distrib. law 79−91799
steel, types 60G, ShKh15, structural changes near holes and inclusions due to pulsed currents *(Russian)* 80−108459
steel, ultra high strength, historical 80−7609
steel, ultra high strength, P induced 350°C embrittlement 79−57099
steel, ultrahigh strength, monotonic and cyclic stress strain curves 80−35268
steel, ultrahigh strength, Si addition and retain austenite effect on SCC, quenched and tempered 78−48567
steel, V- or Cr- or Mn-, initial stages of carbide form., electron diffr. *(Russian)* 78−19760
steel, W and Mo, quantitative anal. of carbides formed during tempering 78−64571
steel, W-Co-Mo-Cr-V-C (8.5, 8.1, 4.5, 3.5, 2.2, 1.02 wt.%), phase composition, struct. and props. 80−104163
steel, W-Cr (3 wt.%), CrC formation in isochronal tempering, electron microscope study 80−7584
steel, W-Mo, tool, hydrostatic extrusion and tempering, wear resistance effect 80−50728
steel, wear resistance of 30KhGSA and 40 kHNMA after thermal and thermomech. treatment 77−70087
steel, wire, reinforced prestressed concrete, strain-tempering conductions and mech. props. *(Japanese)* 78−39816
steel *(French)* 80−66670
steel 14Kh2N3MA, brittle fracture susceptibility, heat treatment effects 77−21190
steel 18Kh2N4MA, phase transformations and props. 77−12614
steel 30khGSNA, low alloy, quenched, grain refinement influence on impact strength *(Russian)* 80−20974
steel 35KhGSA, resist. to fracture after low temp. temperating, P content and grain size effects *(Russian)* 78−48490
steel 40 G, coercimeters with attached electromagnets used for quality control 80−108672
steel 40 khNMS, high temp. thermomechanical treatment, Cr effects on props. 77−12651
steel 40Kh, notch sensitivity under cyclic impact loads 78−3220
steel 52100, compressive strain induced austenite transform. 77−86027
steel 65G, elastic props., effect of additional tempering temp. 77−21192
steel 80Kh5, thermomechanical treatment, high temp., effect of austenite deform. on martensite stability during low temp. tempering 79−57018
steel alloys, low and medium C content, relaxation phenomena in volume changes during tempering *(Russian)* 79−100176
steel bearing rings, optimisation of thermomechanical working parameters *(Russian)* 80−93579
steel Cr-Mo, Ni-Cr, Ni-Cr-Mo, Cr, quenched and tempered struct. effect on H diffusion coeff. and solubility *(Japanese)* 78−52857
steel fine structure after heat treatment, X-ray diffr. exam. 80−60890
steel high strength, Cr, Cr-Mo, Ni-Cr, and Ni-Cr-Mo, diffusion of H_2, effect of quenching and tempering 77−90384
steel JIS SNCM8, enhancement of delayed failure resistance by partial unloading method, environment effects 79−79146
steel Ni-Cr, Sb doped, temper embrittlement susceptibility, intercritical heat treatment effect 78−64570
steel nitride phase hardening, precipitation and solution kinetics after heat treatment 78−95756
steel R6M5, tempering after quenching with rapid heating 77−56002
steel tubes, square section, collapse in bending 80−25792
steel U8, hydrogenation effects on fatigue crack propag. *(Russian)* 78−56800
steel welded joint impact strength, preheating and tempering effects 79−24542
steel-cast Fe cam-roller pair, wear resistance after strengthening treatment *(Russian)* 78−31542
steels, austenitic, microdefect accumulation during creep, effects of heat treatment, hardening 79−24550
steels, C, quenched and tempered, struct.-prop. relationships 80−7599
steels, Cr and Cr-Ni-Mo refining effect on low cycle fatigue strength, resistance to hydrogen embrittlement 78−44208
steels, die, mech. props. high temp. thermomech. treatment 79−20086
steels, heat treatment of 30KhN2MFA and 40Kh, nondestructive mag. quality control method 80−108662
steels, high-purity and commercially based, containing 10 wt.%W or 5 wt.%Mo, tempering behaviour 80−7600
steels, low C S25C, medium C S45C, Cr-Mo SMC3, statistical fatigue props. eval., heat-to-heat variations 78−7048

tempering continued
steels, martensitic-ferritic, microdefect accumulation during creep, effects of heat treatment, hardening 79−24550
steels, secondary hardened, microstruct. rel. to mech. props. 80−25851
strain tempering by rapid heating and cooling of cold drawn wires *(Japanese)* 78−84863
structural steel, microstruct. and brittleness, rel. to austenizing and heat treatments 77−56091
surface stress meas. by optical waveguide effect 80−43681
thermal evolution of gas from solid following detrapping and diffusion during linear tempering schedule 78−75889
thin walled bearing races eddy current inspection of hardening and tempering quality 78−95892
ticonal, grindability improvement, thermomagnetic and heat treatments 77−16625
Ticonal with magnetic texture, struct. damages during ageing 77−16626
Al alloy, semifinished materials, fracture toughness determ. after tempering 78−7128
Al alloys, (5083, 6061, 2219), supercond. magnets, mech. and phys. props. at 4K 80−86976
Al film on single cryst. Si slices, long-term tests 79−33346
Al-Cr(Zr), dilute, vacancy-impurity interaction investig. by tempering method *(French)* 77−68995
Al-Cu(Si)(Mg) binary and ternary alloys, dimensional changes in heat treatment. 80−89271
Al-Mg-Si, type 6010, microstruct. characts. influence on formability, heat treatment 80−81090
Al-Mg-Zn alloys, liq./solid phase equilibria determ. *(German)* 80−50601
Al-Zn-Mg-Cu alloy 7075, SCC from T6 to overaged T7X 77−90487
Al_2O_3-SiO_2, fracture strength studies under dynamic conditions 79−96132
C steel, fatigue crack propagation, effect of mean stress on crack closure 77−73315
$Cd_{0.2}Hg_{0.8}Te$, annealing in saturated Hg vapour *(German)* 79−43447
Co-Fe, soft mag. props. rel. to metallurgical aspects 80−88810
Cr-Ni-Mo 40KhN2MA, magnetostriction used in inspection after heat treatment 80−108673
Cu, wire, recrystallisation *(German)* 77−86055
Cu-Al (10 wt.%), deformed and tempered transform. during heat treatment of β' martensite *(Rumanian)* 79−34031
Cu-Al (11.47 wt.%), high temp. phase transforms., effect of pre-exposure to neutrons 79−20045
Cu-Al (11.6 wt.%), mech. props., tempering temps. effects 78−76669
Cu-Al (21 at.%) transition state *(French)* 80−55392
Cu-Al martensite, temper hardening, study by TEM, DTA, microhardness and yield strength meas. 79−43260
Cu-Al(23.5 at.% and 25.3 at.%), martensitic transform., positron annihilation meas. 77−16578
Cu-Be-Co (2,0.3 wt.%) alloy, heat treatment, influence of tempering on hardness, tensile props. transform diagram *(French)* 78−31384
Cu-Fe alloy, cluster form., Fe solubility determ., 450 to 1000°C, Mossbauer spectra obs. *(German)* 79−29021
Cu-Ga alloys, massive phase ζ tempering, kinetics, order-disorder transform. *(French)* 78−44118
Cu-Ni-Fe, magnetic properties, heat treatment and compressive stress effects 80−60367
Cu-Zn-Al, reversible shape memory effect associated with $\beta_1 \rightleftarrows \beta_1' \rightleftarrows \alpha_1'$, transform. *(Japanese)* 79−43242
Fe alloy YuNDK35T5BA, thermomag. treatment, post-decomp. processes 79−87668
Fe, cast, steel cam-roller pair, wear resistance strengthening treatment *(Russian)* 78−31542
Fe cast with spheroidal graphite, fine cryst. struct. on tempering *(Russian)* 80−96476
Fe-Al (40 at.%) B_2 type ordered alloy, C migration, resistivity meas. *(French)* 78−52868
Fe-C (1.2 wt.%), Mossbauer study of early stages of tempering 80−16342
Fe-C single crystals, effect of heat treatment prior to cold rolling on recrystn. texture 79−83232
Fe-C-Ni-Cr(Cu), dynamically hot pressed, mech. props., additives effect 78−60620
Fe-Co based alloys (52KF, 35KKh, 35KFN), effect of heat treatment and mech. working, on sensitivity of mag. props. to mech. stresses *(Russian)* 79−34161
Fe-Co-V alloys, effect of V on struct., electron diffr. and Mossbauer meas. *(Russian)* 77−77507
Fe-Cr-Co ductile magnet alloys, phase diagram and mag. props., V or V+Ti addition effects 77−8959
Fe-Cr-Co-Mo, melted in open induction furnace, microstruct. and magnetic props. 79−61626
Fe-Cr-Co-Mo, microstruct., hardness, mag. props., influence of isothermal tempering and heat treatment 79−79129
Fe-Cr-N (5.9, 0.5 wt.%), martensitic, tempered, fine struct. 77−25079
Fe-Cu alloys, transform. substruct., lath microstructure after quenching 80−16298
Fe-Cu-C, fatigue behaviour for tempering at 500°C, precip. hardening 77−40442
Fe-Mn (2 to 8 wt.%) alloys, phase transformations, tempering influence *(Russian)* 80−25735
Fe-Mn (8.25 wt.%), irreversible temper embrittlement, Mossbauer spectra, impact strength depend. on interstitials *(German)* 79−74235
Fe-Mn alloys, high-purity, martensitic transform., heat treatment effect 79−56979
Fe-Ni, internal friction study, tempering effects *(French)* 77−81286
Fe-Ni austenitic, effect of Al and Ti on relaxation resist. 80−20993
Fe-Ni-Al-Co-Cu-Ti, 38 to 40 wt.% Co, 8 to 8.5 wt.% Ti, alloy YuNDKT tempering and thermomagnetic treatments 78−3154
Fe-Ni-C, intercrystalline embrittlement in tempered martensite, elimination by reaustenitization *(Slovak)* 80−108548
Fe-Ni-C, martensitic, internal friction 77−16633
Fe-Ni-C, martensitic, mech. charact., effect of ageing and tempering *(Slovak)* 78−19791
Fe-Ni-C, martensitic, mech. and fracture charact., effect of starting austenite heterogeneity *(Slovak)* 78−19792
Fe-Ni-C (9, 0.1 wt.%), effect of intercritical tempering on impact energy, exam. of mech. props. 78−52861
Fe-Ni-Cr, Elinvar, struct. and mag. props., singularities during tempering *(Russian)* 80−50627
Fe-Ni-P, segregation kinetics, theory, and temper brittleness 80−11649
Fe-Si (3 wt.%), breaking stress grain size and grain boundary energy during onset of reversible temper brittleness *(Russian)* 77−32673
Fe-Si cast alloy with spheroidal graphite, transform. investigation during tempering *(Russian)* 80−97479
Fe-V (10 to 50 at.%), solid soln., tempered, exam. of long and short range order, using Mossbauer effect *(Russian)* 79−29105
$Fe_{40}Ni_{40}P_{14}B_6$ amorphous alloy, temper embrittlement 80−76295
Mn-Cu-Zn system, optimum heat-treatment routine for max. damping 79−87670
Mo-Zr-Ti-C(0.1, 0.15, 0.004 wt.%), alloy TsM2A, cavitation failure mechanism 77−70169
Na_2O-CaO-SiO_2 glass, annealed and tempered, fracture strength studies under dynamic conditions 79−96132
Na_2O-SiO_2 glass, microcracking about NiS inclusions, fracture mech. description 80−89333
Ni, reactor construction material, He liberation 77−46290
Ni-Co-Al (1, 35.2 at.%), tempered martensite, new ordered phase 79−11560
Ni-Fe, soft mag. props. rel. to metallurgical aspects 80−88810
Ni-Fe-Nb-Mo-Al, head material for mag. recording, DC and AC mag. props. 80−88812
NiPt, quenched, ordering kinetics and domain struct. form. during isothermal tempering *(Russian)* 80−66502
$Sm(Co_{0.84}Cu_{0.16})_{6.9}$, microstruct. and domain struct., mag. reversal *(Russian)* 80−20429
steels, Cr-C-Mn(Ni), struct. prop. rel., design of struct. steels for high strength and toughness 80−97491
Ti-Al-Cr-Mo-V, alloy VT22M, exam. of ageing and phase transitions *(Russian)* 79−11641
Ti-Al-Mo-Cr alloy weldment containing orthorhombic martensite, autotempering behaviour and alpha precip. strengthening 80−84976
TiC-steel alloy, struct. form. during sintering, strength, rel. to heat treatments 77−59717
TiC-steel composite, effect of method of Cr additions on props. 78−15341
V_3Sn, ultrafast quenched and subsequently tempered, supercond. T_c 78−64162
Zr-CR (1.9 wt.%), β-quenched and tempered, tensile props. rel. to tempered conditions, SEM study 79−66109
Zr-Cr (1.9 wt.%), β-quenched and tempered, optical and TEM study 79−66061
Zr-Cr (1.9 wt.%), β-quenched and tempered, $ZrCr_2$ precipitation, TEM study 79−66062
Zr-Nb (2.3 and 5.5wt.%) martensite, precipitation 77−8836
Zr-Ta (5 wt.%), β-precipitation in martensitic struct., tempering temp. effect 79−34045
Zr-Ta (5 wt.%), martensitic transform. by rapid cooling, non-equilib. precipitation 79−34075
Zr-Ta (5 wt.%) martensite, β_1 precipitation, thermodynamics 79−74164

tenacity *see tensile strength*

tensile strength
see also fracture; yield strength
abdominal aorta wall, human, after endarterectomy, deform. and strength 77−25497
ABS mouldings, selective Cu plated in areas, effect on mech. props. 79−34182
ABS polymers, deposited in internal magnet magnetron sputtering system, adhesion of Cu films 79−83121
acrylic, denture base, tensile testing 80−16621
acrylic bone cement improvement by addition of fillers 77−37109
acrylic plastic, deform. of rigidly clamped specimens subject to one sided cyclic heating 77−59932
acrylourethane coatings, radiation curable, tensile, elongation and modulus props. appl. techniques 80−66847
adhesive materials 77−16638
Al alloy 6061, energy absorption during uniaxial tension and axial compression, geometric and heat treatment effects 77−73312
Al alloy blend 6061, isostatically computed powder, effect of heat treatment temp. on tensile strength and hardness 79−61720
Al-alloys, influence of strain path on mech. props., orthogonal tensile paths 80−30035
Al-graphite composite, mech. props., effect of thermal exposure 77−36629
alloy, heat resistance under one sided loading 77−1872
alloy, superplastic, anomalous response to notch under superplastic conditions 78−52930
alloy steels N30 and N29T, press. effect on reverse martensitic transform. and mech. props. *(Russian)* 79−38824
alloys, austenitic, neutron irradiation effect on tensile, creep-rupture, deform., fracture props. 79−65120
alloys for fission reactor components, mech. props. at high temp., failure prediction 80−5241
alumina, diametral compression test, parametric study 78−44282
angle ply laminate, fibre reinforced, interlaminar strength test for delamination 78−88523
anisotropic plasticity, theory development, expt. results 79−27553
anisotropic polycrystal, yield and tensile test meas. of plastic behaviour 77−32631
aorta, human, morphological and functional aspects of study of mech. props. 77−25499
aorta, strength variation with age in humans 78−48823
aramid fibre reinforced acrylic bone cement, tensile strength and fracture toughness, SEM study 79−29667
aramid/epoxy composite, tensile test 80−11778
articular cartilage in uniaxial tension, nonhomogeneous directional mech. props. meas. 77−29167
asbestos cement/glass reinforced plastics hybrid composites, tensile strength *(Italian)* 77−56024
asbestos fibre reinforced cement mortar, strength and fracture properties 79−100241
austenite, quenched and tempered, effect of bainitic decomp. products on mech. props. 77−56007
austenitic stainless steel, for cryogenic appl., tensile testing, room temp. and 4K 77−25119
automatic testing methods, process computer appl. *(German)* 78−35598
axially loaded butt joints, stress strain behaviour 79−74209
bagasse fibre reinforced phenol formaldehyde, tensile strength and Young's modulus, SEM study 80−60952

tensile strength continued
bainite, formed from deformed austenite, morphology and mech. props. 79−43345
bisphenol A polycarbonate, end-cap ratio and mech. props. of block copolymer 78−91266
bisphenol-A-diglycidyl ether epoxies, struct., fracture and mech. response, cure and crystallisation conditions effects 79−15779
Bohus granite, relation between uniaxial tensile strength and sample size 78−81153
bone, compact, fatigue damage, residual strength and stiffness 77−90834
bone, mechanical properties rel. to density and mineral phase orientation and particle size 80−16989
bone, rel. to strain rate, microstruct. and density 77−44703
bone china body, MgO effect on vitrification mech. props. *(Japanese)* 79−78922
bone/porous polyethylene interface, tensile strength 80−30737
bovine hip bone, compression tests, effect of specimen shape and size on mech. props. and fracture mode 78−69132
brass, adsorpt. of Hg, effect on mech. strength, creep, fatigue, embrittlement *(Russian)* 79−29267
brass, anisotropic bend ductility in single phase alloys 78−60726
brass, low-temperature testing, −196°C to +20°C 79−61692
brass, plastic props., room temp. to recrystallization temp., stress-strain relations, computer program 77−1865
α-brass, Portevin-LeChatelier effect *(Japanese)* 80−11724
brass, stress corrosion cracking, in ammoniacal atmosphere, surface stress change and crack growth *(Japanese)* 77−59986
brass, tensile curve and specific value of anisotropy coeff. *(French)* 77−28867
α-β brass, two phase bicrystal, deform. and fracture at 450K 80−16409
α-β-brass, two phase bicrysts., deform. and fracture at 150K 80−16388
β_1 brass containing α-precipitates, reversible shape memory effect *(Japanese)* 78−60711
brass LMtsSKA 58-2-2-1-1, heat treatment, struct. and props. 79−83239
brittle fibre reinforced composite, brittle reaction zones at interfaces, tensile strength 79−52306
brittle material, tensile strength determ., based on radial and compression tests 78−7156
brittle materials, diametral compression tests, tensile strength meas., appl. to biaxial stress fracture *(Japanese)* 78−72840
brittle materials, diametral compressive stress considering Hertzian contact, fracture and tensile strength meas. *(Japanese)* 78−72946
brittle materials, ultimate tensile strength determ. by radial compression testing 78−7132
brittle materials under complex loading systems, design parameters 79−38917
brittle rupture, strength time depend. *(Russian)* 78−46912
brittle solids, fracture prediction for short duration tensile stresses 77−70150
bronze, anisotropic bend ductility in single phase alloys 78−60726
bronze, sintered, mech. props. 77−28839
bronze P, heavily cold rolled, yield strength enhancement mech. 77−36539
butt joint, tensile bond strength, effect of aspect ratio 80−50823
carotid arteris, human, strength props., changes with age 80−16993
cast iron with lamellar graphite, reactor appl. 77−57718
celluloid, mech. props. under proportional load, time lapse, heating and isotropic props. effect *(Japanese)* 79−79043
celluloid, nonlinear viscoelastic deform. under superimposed hydrostatic pressure 79−34116
cellulose acetate films, light scatt., tensile creep, desalination 80−16050
cellulose acetate membranes, modified, tensile props., desalination performance 79−11818
cellulose fibres, from jute, crystallinity percentage, estimation by X-ray methods 79−7553
cellulose film, moisture effect on phys. and mech. props. 80−40450
cellulose nitrate, exam. of strength characts. 78−68748
cellulose triglycerl ether hexanitrate, exam. of strength characts. 78−68748
cellulose tripentaerythrityl ether nonanitrate, exam. of strength characts. 78−68748
cement, hot pressed, type III, role of admixtures on pastes and H_2O cured cement, exam. 78−44073
cement paste, direct tensile tests and tied crack model 78−11306
cement paste, direct tensile tests and tied crack model 78−11307
ceramic, proof testing 80−104207
ceramic, proof testing 80−108654
ceramic, tensile strengths, uniaxial and equibiaxial in bending statistical comparison 80−25775
ceramic implant/bone interface, tensile strength and bone form., effect of elec. stimulation 77−5108
ceramics, error sources in mech. testing of tensile and bend strength *(German)* 78−35421
ceramics, microstructure dependence of mechanical behaviour 78−88533
chamotte concrete, alumina-based cement, thermomech. props. 78−35455
chrysotile asbestos fibres, texture rel. to mech. props. 77−81300
circular cylinder, with straight crack, in grooved and ungrooved shafts, stress intensity factor calc. 77−56061
circular ring, inner boundary shapes, optimised, diametral compression 80−38369
circumferentially notched tensile specimen, finite element anal. 78−67150
coating struct., SEM study 80−97605
coke, metallurgical, industrial strength meas. methods, critique 80−85117
coke, metallurgical, strength and struct. relationship 80−84997
cokes, metallurgical, struct. and strength 80−93610
cold water, tensile strength expts. 79−10539
cold work in tension, strain rate effect on stored and dissipated energies 77−86111
compact bone, empirical strength theory, biaxial stress characts. 78−77081
composite, biaxial analogs of triaxial stresses 79−55345
composite, metal-based fibre-type, designing for structural integrity 79−83155
composite, physics of strength, kinetics of failure 78−3206
composite materials loaded in uniaxial tension under pressure 78−19828
composites, fibre reinforced, fatigue damage under pulsating tensile stress 79−100237
composites, single fibre-brittle zone model, fracture behaviour 80−97570
tensile strength continued
concrete, creep, elasticity and strength in tension and compression 78−11287
concrete, creep, time dependent behaviour under high tensile stress *(Japanese)* 78−31465
concrete, flowing, expt. studies *(Japanese)* 80−89298
concrete, high strength, made with a special cement admixture, mech. props. *(Japanese)* 80−89297
concrete, impact bending capacity *(Japanese)* 80−89341
concrete, prestressed, low-temp. tensile strength and linear expansion coeff. of reinforcing steel 80−30051
concrete, prestressed hollow beams in combined torsion and bending 79−96087
concrete, ribbed compression reinforcement, ultimate strength anal. of lapped joint 79−96086
concrete, strength, shrinkage strain and deterioration down to −160°C *(Japanese)* 80−100886
concrete, tensile strength determ. under impulse loading *(German)* 79−15919
concrete, tensile testing device, axial 80−61054
concrete sandwich composites, behaviour under compressive and tensile loads 77−8877
corneal wound holographic stress testing in postoperative patients, specular illum. arrangement 78−65102
Corson alloys, AE during tensile deform. *(Japanese)* 79−61654
corundum refractory ceramic deformation curve analysis *(Russian)* 79−90716
cotton fibres, specimen clamps for X-ray angle-tensile meas. 78−4603
crack, dislocation model of plastic zone 77−84837
crack growth, at rubber springs bonds, energy calc. and meas. 79−83316
creep in circular specimen subject to pure bend, ultimate tensile and compressive strength *(Russian)* 80−74768
CVD optical fibre, long length strength 80−58752
cylinder, plastic flow rules and Bauschinger effect parameters 78−6984
cylindrical specimen with external crack reaching surface of annular stress concentrator, tension and bending 79−14349
Dacron, vascular substitute, exam. of tensile fracture behaviour 78−77157
deformation strength props., simultaneous meas. of several samples, polymer films appl. 79−15896
determination, miniature test-pieces, multipurpose apparatus *(Russian)* 77−52558
diethyl ether, determ. using Brigg's method 77−62574
diffusion welded joints, creep deformation effect on characts. 80−25806
dislocation density depend. *(Russian)* 78−19820
dispersion hardened alloy, load type effect on yield stress 78−35458
double ligament tensile test in deformation processing 77−32753
dough moulding compound, exam. of tensile and fatigue props. 79−20152
ductile materials, tearing, fracture strength determ. 79−43385
ductile-brittle transition pressure, grain size effect *(Japanese)* 78−60745
Duralumin, adsorpt. of Hg, effect on mech. strength, creep, fatigue, embrittlement *(Russian)* 79−29267
Duralumin, lifetime after preliminary plastic deform., kinetic theory of strength 79−43395
Duraluminium rings, stress/strain relations, compression and tension tests, rigid plastic theory 79−34098
E-glass fibre reinforced epoxy, room temp. curable, mech. props. and thermal conductivity 78−68669
effect of pressurisation on acoustic emission characts. during tensile testing 78−92304
elastic springback in beams and plates, bending 80−38256
elastomer reinforcement, carbon black-polymer interaction, tensile strength 79−83171
elastomeric block copolymer properties obs. 78−27560
elastomers, rel. between relax. behaviour and tensile strength *(German)* 80−66604
ELN-1 alloy, prestrain effects on strength *(Russian)* 78−11267
EM tensile adhesion test method 80−50804
empirical determination, cleavage fracture in plane waves 80−96225
endopelvic fascia, human, stress/strain history relations in simple elongation 78−44539
epoxide resin cured with aliphatic dicarboxylic acids, fatigue behaviour *(Japanese)* 79−79092
epoxies, mechanical characterisation at low temps. 78−64611
epoxy Al bonded, adhesive joints under complex loading, development of failure criterion 78−92344
epoxy C plastics, under tensile stress, effect of whiskerization of polymer matrix on creep resist. 79−87699
epoxy impregnated superconducting composites, mech. props., strain effect at 4K 80−25822
epoxy laminate, glass-fibre reinforced, with circular holes, tensile fracture 80−25789
epoxy resin, low temp. fatigue, tensile strength, Young's modulus *(German)* 78−76748
epoxy resin, powder filled, exam. of mech. props., thermal contraction 80−25821
epoxy resin composite, powder-filled, of adjustable thermal contraction, mech. props., for construction of superconducting magnets 79−61691
epoxy resin EhDT-10, temp.-time rel. of strength 80−25798
epoxy resin systems, synthesis review, phys. and mech. props. at low temps. 80−25650
epoxy resins, correlation between valence energies and low temp. flexibility 80−25815
epoxy structural adhesives, tensile tests, stress/strain relations, stress relaxation 78−60702
equine long bone forces and moments, in vivo and anal. studies 78−40216
ethylene-base ionomers, impact tensile props. *(Japanese)* 79−96120
ethylene-Co copolymers and -SO_2 copolymers prep. by catalysis and ^{60}Co γ-radiation, mech. props. 80−66841
ethylene-propylene-diene terpolymer, sulphonated, ionically cross-linked, foam elastomer, thermo-mech. props. 78−48362
ethylene-vinyl acetate copolymers, extrusion and heavy duty films, radiation crosslinking, struct. effect 80−66844
FCC crystal, grip effect and bend gliding during uniaxial tensile deform. *(Japanese)* 79−52314
FCC crystal, transient effects during tensile tests in model of correlated dislocation motion 78−38715
Fe, pure AISI, flow stress, temp. and strain rate sensitivities 77−90421

tensile strength continued
Fe alloy YuNDK35, magnetic, brittle, strength in three axial stress state 79−66134
femoral cortical bone tensile props. instrumentation system 77−60025
ferrite-pearlitic grey Fe, tensile testing of mechanical props., from room temp. to liquidus *(Japanese)* 80−7728
ferritic grey Fe, tensile testing of mechanical props., from room temps. to liquidus *(Japanese)* 80−7728
ferromagnetic materials, fracture-induced magnetic effect 77−80986
fibre, single-mode, numerical aperture effects 80−69548
fibre bundles, stochastic strength and fatigue 78−79262
fibre composites impetus of composite mechanics on test methods 80−11868
fibre mechanical tensile test machine 77−40484
fibre reinforced cement, mech. and rheological props. *(German)* 79−20129
fibre reinforced composite, discontinuous, surface treatment effect analysis and obs. *(Japanese)* 77−77596
fibre reinforced composites, intralaminar-shear charact., 10 deg off axis test 78−35422
fibre reinforced composites, struct. parameters depend. 80−65134
fibre reinforced composites, transverse strength rel. to fracture mech., stress interactions 80−16421
fibre reinforced composites, unidirectional, tensile testing 80−40664
fibre reinforced laminated hybrid, tensile first cracking strain and strength 80−81175
fibre reinforced nonlinearly elastic matrix, unidirectionally reinforced, deform., strength, and failure 80−3134
fibre reinforced plastic, fracture mechanism study, cumulative failure model 78−92315
fibre reinforced plastic, tensile and compressive strengths, structural theory 77−52435
fibre reinforced plastics, spread of strength rel. to stress conc. *(Japanese)* 79−24610
fibre reinforced silicone rubber composites, interfacial slip and damping 79−5010
fibre-optic cable manufacture, testing, and installation *(German)* 78−33863
fibre-reinforced composite, unidirectional model for longit. tensile strength prediction 78−95778
fibres, optical, fatigue charact. improvement, using surface compression cladding 80−69549
fibrous composite materials, brittle interlayers influence on tensile strength *(Russian)* 80−21006
fibrous composite materials, models for composites with different props. in tension and compression 78−35417
fibrous laminated composite, tensile failure, quantitative fault tree anal. 77−59891
filament wound material, lamination theory for failure envelope prediction under biaxial loading 79−38931
filaments, elastic, tensile test method, and treatment of expt. data 80−85111
fission reactor irradiated cladding, in-cell facility for mechanical testing 80−21244
flat sheets, tensile deformation analysis 80−96198
fluorocarbon foil, Ftoroplast, homogeneity study *(Polish)* 80−35278
foil, thickness depend. *(Russian)* 77−59852
fracture toughness screening using sharp notch tension 77−56169
fusion-spliced optical fibres 78−87140
galvanic coatings, tensile testing device 80−100988
genesis problem, approx. soln. of initial states and properties 77−14927
GFRP laminate, damage assessment by stress wave emission and dynamic mech. meas. 78−11461
glass, fracture, by impulse loading, splitting method tests strength properties 79−57118
glass, inorganic, cylindrical shell, with initial geometric imperfections, precritical deform. under external hydrostatic press. 77−81306
glass, static fatigue, reexamination of limit 77−90458
glass, strength under linear tension, bending, torsion and compression of type K8 79−14062
glass, tensile and impact strength, effect of surface damaging and annealing *(Czech)* 79−74227
glass ceramic prep. by hot pressing and crystallisation of glass powder, mech. props. 78−15351
glass fabric reinforced plastic laminate, fatigue strength rel. to test frequency 79−8362
glass fibre, flaw generation and strength, dust particle effects 77−23741
glass fibre, tensile strength meas. using chain-loading fibre tensometer *(Japanese)* 80−55610
glass fibre composite, creep calc. in nonstationary temp. distrib., temp.-time analogy 77−70132
glass fibre for optical communications, statistics of tensile strength *(German)* 80−38121
glass fibre properties for information transmission *(German)* 78−9439
glass fibre reinforced Al alloy, formed by hot extrusion, mech. props. 77−24987
glass fibre reinforced cement, durability in wet and dry conditions, fibre length and content effect 80−71726
glass fibre reinforced composites, impact tensile strength obs. *(Japanese)* 78−23781
glass fibre reinforced composites, mechanical characterisation at low temps. 78−64611
glass fibre reinforced epoxy, as electrical insulation for Tokamak toroidal field coils, mech. props. 78−64610
glass fibre reinforced epoxy, wound, strength in twisting, stretching and transverse bending 80−11622
glass fibre reinforced epoxy laminate, internal moisture condition effect on strength 79−15736
glass fibre reinforced epoxy laminate, tensile testing, monitoring cond. effect on stress wave emission data 79−87814
glass fibre reinforced epoxy resin, cryogenic tensile, compressive and shear props. 78−6983
glass fibre reinforced Pb, production by infiltration, tensile strength 77−59720
glass fibre reinforced plastic, failure under compression, tension and bending 79−96142
glass fibre reinforced plastic, strengthening under biaxial tension 78−23797
glass fibre reinforced plastic laminate, mixture law of tensile and fracture strength and variation *(Japanese)* 79−43337
tensile strength continued
glass fibre reinforced plastics, cyclic strength in complex stressed state 80−3181
glass fibre reinforced plastics, laminated ring with extra steel pin radial reinforcement, mech. props. 80−11714
glass fibre reinforced plastics, stress conc. effect on spread of strength and fatigue life *(Japanese)* 79−96117
glass fibre reinforced plastics, stress luminescence, volume resistivity effects *(Japanese)* 78−43943
glass fibre reinforced plastics, temperature-force depend. of lifetime 78−23795
glass fibre reinforced plastics, under compressive load *(Japanese)* 78−92301
glass fibre reinforced polyester, behaviour under bending load *(Japanese)* 79−38904
glass fibre reinforced polyester, compressive fatigue tests at cryogenic temps. 80−25870
glass fibre reinforced polyester, epoxy-polyamide, single lap joint, tension-shear strength *(Japanese)* 78−11494
glass fibre reinforced polyester, filament wound pipe, winding angle effect on failure 79−43379
glass fibre reinforced polyester, single lap joint, tension-shear strength *(Japanese)* 78−11494
glass fibre reinforced polyester tube, strength under biaxial loading 79−38892
glass fibre reinforced thermoplastic, unidirectional short fibre reinforcement, tensile and impact strength 79−91734
glass fibre-reinforced polyester cross-ply laminates, effect of resin failure strain on tensile props. 78−3212
glass fibres, crack growth during dynamic fatigue and effect on strength loss for tensile loading 80−89334
glass fibres, epoxy-acrylate coated, static and dynamic fatigue, tensile strength 79−1906
glass fibres, tensile strength and fatigue 77−3662
glass optical fibre, epoxy-acrylate coated, strength and static fatigue 78−1386
glass optical fibres, tensile strength testing, Weibull statistics 78−59128
glass optical fibres, UV-cured, epoxy-acrylate coated, environmental effect on long-term strength 78−5582
glass opticalfibres 79−46062
glass reinforced epoxy resin laminator, strength tests *(Polish)* 77−12772
glass reinforced fabric, low-temperature testing, −196°C to +20°C 79−61692
glass reinforced plastics, strength in biaxial compression in three planes of symmetry 77−59874
glass-fibre reinforced cement, strength study by reliability concept, fibre concept and temp. depend. *(Japanese)* 80−66586
glass/epoxy composite, tensile test 80−11778
glued microplastic threads, tensile strength 79−61670
granite, exam. of fracture mech. under dynamic loading 79−29218
graphite, ATJS, oxidation effects up to 2500K 80−3209
graphite, deform. and fracture mech., high temp. effects 77−63763
graphite, diametral compressive strength, comparison with uniaxial tensile strength *(Japanese)* 78−72947
graphite, diametral compressive testing method 80−35495
graphite, fibre reinforced Sn-Pb investment castings, tensile strength 77−48487
graphite, fracture criterion 77−48552
graphite, irradiated ultimate tensile bending and compressive strength charact. 78−15479
graphite, pyrolytic, structural factor effect on strength 79−66135
graphite, pyrolytic commercial, high-temp. thermal and mech. props. 80−75372
graphite fibre epoxy composites, exposed to high temp., degradation of tensile and shear props. 80−81113
graphite fibre filled polyimide composite laminates, space environment, phys. and mech. response 80−81140
graphite fibre reinforced Al, mech. props., comparison with B-Al composite 77−52470
graphite fibre reinforced epoxy, correlation of tensile strength with US stress wave factor 79−87798
graphite fibre reinforced epoxy laminate tension-compression fatigue loading, fatigue residual strength degradation model, comparison with expt. results for 78−35491
graphite fibre reinforced epoxy laminates, expt. investigation of tensile moduli and strength 78−52870
graphite fibre reinforced epoxy resin, cryogenic tensile, compressive and shear props. 78−6983
graphite fibre/epoxy laminates, free edge induced failure 80−11775
graphite fibres, elec. resist., mech. props. after nitration 77−32698
graphite particle-Al alloy composite, prod. by pellet method, and mech. props. 78−27454
graphite reinforced epoxy laminate, fracture behaviour 79−83294
graphite reinforced epoxy steel scarf joint, adhesively bonded, exam. of failure 78−92350
graphite thermal shock resistance and fracture toughness meas. *(Japanese)* 79−91868
PAN graphite-Al composites, fracture characteristics and props. 80−11779
graphite-epoxy composites, Thornel 300/Fiberite 1034, effects of thermal spiking on moisture absorpt. charact., tensile strength and buckling modulus 79−43330
graphite/epoxy laminate containing holes, high temp. tensile strength 77−25105
graphites, reactor, strength and deformation under conditions of cyclic variation in load and temp. 79−43355
griseofulvin tablets, tensile strength and disintegration times 77−60027
gypsum casts, improvement in impregnation method, exam. of mech. props. 78−48503
hard metal, bend test-piece geometry appl. to tensile strength meas. 80−30184
Hastealloy X, relations between weld heat affected zone cracking and microstruct., Gleeble test *(Japanese)* 78−52858
Hastelloy C-4, loaded at high temp., useful life 80−40523
Hastelloy X, high temp. low cycle fatigue tests, ductility, fracture 77−90523
Hastelloy X, mech. props. effect of solidification substruct. 77−25040
heterogeneous composite materials, influence of prestress and limited deformations 78−38205
high-strength alloy filamentary crystal prep. from brittle high-strength mats., mech. props. *(Russian)* 77−59712

tensile strength continued
history Berthelot's first publication, 1850, subjection of liqs. to tension 78−32639
human soft tissues, tensile stress at const. elongation, temp. effects 77−32938
hybrid composites, statistical analysis 77−63624
hydraulic bulge test, use in biaxial tensile testing 80−1493
hydrogel of high water content as a material for the soft contact lens *(Japanese)* 80−12300
iliac arteries, human, strength props., changes with age 80−16993
impact tests with rupture diagram recording on pendulum machines, testing procedure 79−29313
Incoloy 800, and 800 H, low cycle fatigue behaviour comparison 79−43438
Incoloy 800, creep rupture, creep strength and tensile data, 500 to 800°C 79−43371
Incoloy 800, from KFA experimental duct at 700°C and 480 d in DRAGON reactor, mech. props. before and after contamination 79−47777
Incoloy 800, microstruct. effect on mech. props. 79−43367
Incoloy 800 and 802, influence of carburisation on mech. props. 79−20254
Inconel 600 and 601, influence of carburisation on mech. props. 79−20254
Inconel 706 and 718, relations between weld heat affected zone cracking and microstruct., Gleeble test *(Japanese)* 78−52858
IR determ. of temp. increase in tension tests *(German)* 79−61806
irradiation creep facility, materials testing for fast and fusion reactors 79−57192
izod polystyrene, influence of dimensions in mech. props. *(German)* 80−21039
Japanese red pine seedlings, tensile strength *(Japanese)* 77−77538
Kapron fibres, elongation and tensile strength rel. to UV irradiation 80−25796
Kevlar 49, fibre, mech. props., environmental effects incl. sunlight, ionising rad. 77−36560
Kevlar 49 fibre, poly p-phenylene terephthalate, Raman spectroscopy, heat, stress, radiation effects 79−65871
Kevlar aramid fibre reinforced composites, flexural strength 79−11671
Kevlav fibre reinforced cement composites, cement boards, exam. of mech. props. 78−48499
Kevler fibre, mech. props. in aq. H_2SO_4 soln. *(Japanese)* 79−47753
lactose powder coated with fatty acids, tensile strength 77−21304
laminated composite, tensor polynomial failure criterion 78−39886
laminates, damage zone failure analysis 80−85059
leucosapphire single cryst., W grid reinforced, growth 77−16530
ligaments of small animals, gripping device for tensile testing 80−81791
linear elastic incompressible solid, stability of void growth under uniaxial tension and shear 79−76972
liquids, Berthelot tube method, theory for tension before breaking 77−24341
LMFBR hexagonal ducts, cracking, effect on safety and fuel pin failure 78−17318
low-alloy steel, bending, effect of strain rate on dynamic stress factors 77−56046
marble, diametral compressive testing method 80−35495
marble, Italian Ondagata, diametral compressive strength, comparison with uniaxial tensile strength *(Japanese)* 78−72947
masonry units, splitting tensile test 78−53061
materials under complex stress, with local dynamic loading, strength 79−91768
mechanical anisotropy evaluation, using hardness test *(Polish)* 78−48575
metacarpi, equine, fracture toughness 80−3694
metal, deposition condition relationship with struct. and props. 78−11369
metal, electronic work function under tension, 20 to 1200°C 80−76448
metal, fracture and tensile props., effect of strain rate and temp. 77−36662
metal, hot deformability test methods, comparative evaluation *(German)* 77−36713
metal, plasticity under hydrostatic pressure *(Russian)* 78−68726
metal, relation to cohesive energy density, surface tension and butt joint strength 77−55431
metal, sheet, numerical anal. of tensile tests 77−86101
metal, thin sheet, tensile instability and limit strains, growth of surface roughness 77−86084
metal foil bulge-test samples, shape meas. by optical contouring 77−63843
metal matrix-fibre composites, brittle interface layers and tensile strength 79−79039
metal mechanical property effects on frictional behaviour 80−55548
metal powder, hot swaging test method for tensile testing 77−25235
metal rods, static mech. props. rel. to impulse stress 78−95779
metal specimen, semi-automatic universal test machine *(German)* 77−81346
metal-glass material, relation between struct. and props., prod. by hot densification 78−11145
metal-polymer splices, adhesive bond destruction and strength w.r.t. electrochem. interaction 79−20339
metallic glasses, structure and properties, review 78−47245
metallic materials, erosion resistance, eval. of role of mech. props. 79−83328
metals, deformation resistance, rel. between uniaxial stress state and breaking stresses in shear 80−3147
metals, in-situ deform., 200 kV STEM study 80−47155
metals, ionised gas effects 79−70252
metals and alloys, mech. props. electric current effect, test device for 4.2-300K 80−66719
metals and alloys, strength/ductility relation *(Japanese)* 79−29145
$Mg_{70}Zn_{30}$, amorphous alloy 77−27835
mineral wool fibre composites, mech. props., effects of thermally induced phys. and chem. changes 77−59884
multilayer plates, optimum design for cylindrical bending 79−87698
multimode fibres, recent advances in production 78−30096
natural rubber vulcanisate, network changes during physical testing 80−60936
natural rubber vulcanisates, creep under tension, O_3 effects 78−92302
necking, strain rate sensitivity under uniaxial tension 77−77525
neointimas developing on flocked surfaces of left ventricular assist device, mech. anal. 78−40431

tensile strength continued
Ni alloy KhN45Yu, strength properties, dispersity of struct. effect 80−55486
Ni-Cr-Mo-Ti-Al, quenching and ageing effects on props. of type 36NkhTYuM8 79−52275
Nimonic 115, superalloy, critical strain model for creep fracture 77−32648
Nimonic 80A, creep in tension and torsion 77−25113
Nimonic EhI437B, heat resistant, true breaking stress in rapid air stream 79−66163
Nimonic PE-16, damage in high energy fluence D plasma 77−34427
Nomex, fibre, mech. props., environmental effects, incl. sunlight and ionising rad. effs. 77−36560
nonmetallic material, mech. props., testing installation, +600 to −190°C 78−15633
notched fibre reinforced composites, tensile fracture 78−52991
notched flat tensile specimens, deform. zone *(German, English)* 78−64603
Nylon 6, fibre, crystallite dimensions, effect on struct., mech. and diffusive props. 78−11273
Nylon 6, unidirectionally reinforced, mech. props. and fracture 77−21252
nylon fibre reinforced polypropylene, enhanced fracture strain 78−15503
Nylons, morphology and crack propag. in inorganic salts 80−30118
optical, fibres with high tensile strength, furnace drawing method 78−68666
optical CVD fibres having surface compression, fatigue characts. 79−46064
optical fibre, furnace drawn, tensile strength 80−58751
optical fibre, long length for communications cable, proof testing 77−54818
optical fibre, mech. deform. meas. by light scatt. method 80−14452
optical fibre, modified CVD prep., optical and mechanical props. reproducibility 80−69535
optical fibre, rupture stress rel. to ageing *(German)* 78−38009
optical fibre cables with spacers, transmission characts. and mech. props. 79−46070
optical fibre coating concentricity improvement by tapered nozzles *(German)* 78−38095
optical fibre strength distribution description using upper and lower limits 80−53470
optical fibre strength tests, pulling machine construction 78−33931
optical fibre tensile and fatigue strength 77−7211
optical fibre tensile strength testing 78−42481
optical fibre waveguide testing, extrapolation of short length test results 78−9456
optical fibres, breaking strain estimation for long lengths of fibres 78−30060
optical fibres, GeO_2-$B_2O_3SiO_2$, ageing effects of moisture on fatigue and tensile strength 80−66539
optical fibres, mech. reliability 80−91909
optical fibres, packaged, tensile performance 79−55212
optical fibres, plastic primary coating materials, tensile strength and reliability tests *(Japanese)* 79−59818
optical fibres, preparation conditions influence 80−33205
optical fibres, strength and fracture behaviour 79−59828
optical fibres, tensile strength and static fatigue, analysis using Weibull distribution for optimum design 80−85011
optical fibres, tensile tester 78−83123
optical fibres and cables, tensile testing machine 77−3687
optical fibres pulled in graphite furnace, effect of drawing conditions on tensile strength 79−50469
optical fibres with high tensile strength prep. 78−63211
optical glass, reproducibility of symm. bending mech. strength values 78−46737
optical waveguides, dependence on sample length, Weibull distribution figures 78−30084
organoplastics, fracture characts., effect on strength 80−66642
Ozhennite, yield point, effect of ageing stress 77−21223
PAN fibres, neutron irradiated, struct. and props. *(Russian)* 80−25763
paper strip reinforced paraffin, model composite, optimum reinforced plates, tension/compression tests 77−86124
particle-filled polyurethane resin, tensile strength, particle size effect 77−73305
parylene polymers, synthesis, elec., phys., corrosion props. *(German)* 78−64521
PBI fibre, mech. props., environmental effects, incl. sunlight and ionising rad. effs. 77−36560
PCA, dehydration effect on carbonisation process, high temp. resistant materials *(Russian)* 79−8269
pentaplast, plasticised, thermal treatment effect on props. 80−40324
Permendur 49, ordered and disordered, clean mild wear 80−16508
PET, effect of liquid aliphatic compounds on mech. props. 80−55488
PET, fibre, crystallite dimensions, effect on struct., mech. and diffusive props. 78−11273
PET fibre reinforced polypropylene, enhanced fracture strain 78−15503
PET film, PET, transverse constriction and stresses accompanying uniaxial orientation 78−48475
phenol formaldehyde resin, (Novolak) with filler, mech. props. determ. *(German)* 78−84933
phenol formaldehyde resin (Novolak), with and without feldspar filler, mech. and thermal props. determ. *(German)* 78−84828
phenol resin (Resol), with and without feldspar filler, mech. and thermal props. determ. *(German)* 78−84828
photoelastic load meas. and testing *(German)* 80−19297
piezoceramic, polarisation method effect on mech. strength 78−39879
pivalolactone-α-methyl-α-propyl-β-propiolactone copolymers, struct., thermal and mech. props. 79−43582
plant fibres, fracture mechanism 80−35931
plastic, deformation speed in static tensile tests, machine rigidity effects *(German)* 78−48473
plastic, static strength determ. from elasticity and internal friction 77−70094
plastic composites 79−29162
plastic instability during tensile deform., numerical calc. 78−30203
plastics, high temperature 77−25092
plastics, tensile and flexural testing device, incorporating an impacter *(German)* 80−3276
plastics and reinforced plastics, tabulated data as design guide 77−21087
plastometer, electronically controlled, for tensile and compression tests *(German)* 80−3273

tensile strength continued
platilon UO1, use in artificial blood pumps, fatigue resist. and mech. props. 79−84026
plexiglas, strength in biaxial compression, testing machine 79−15899
PMMA, μs pulse tension loading, strength lifetime depend. on amplitude and temp. *(Russian)* 77−81303
PMMA, destruction kinetics of intense ms loading, laser differential interferometry obs. 79−24623
PMMA, effect of surface finish on strength, and craze reistance 78−76724
PMMA, porous, used as tooth replicas, phys. props. and biological acceptance 77−52926
PMMA glasses, crosslinked, strips, sheets, compression, tensile testing, mech. props., plasticiser effects *(Russian)* 77−32621
poly-p-phenylene terephthalate, high modulus fibre, struct. obs. 78−75564
polyacetylene films, tensile props. and partial alignment 80−104210
polyacrylamide solutions, dil., static and dynamic breaking tensions 79−23346
polyalkylene tetephthalates, amorphous and cryst., durability under stretching *(Russian)* 78−88511
polyamide, hydrogen bonding rel. to mech. props. 77−4053
polyamide, test pipes, static tensile strength, equipment effect on tension-extension diagram *(German)* 78−35453
polyamide-polyoxirane copolymers, mechanical properties evaluated 80−11700
polyamides, extended chain aromatic, fibres, tensile strength and moduli 80−81021
polyarylate, rupture mechanism 79−52372
polybutadiene, cross linked, deform. below T_g, radical form. and crazing 79−52307
polycaproamide, deformability props. in cyclic extension-compression 79−20183
polycarbonate, effect of rolling on mech. props. 78−52837
polycarbonate blends, yield and deform. behaviour, impact modification 77−36572
polycarbonate fibre, highly-oriented, drawing behaviour and mech. props. 78−76708
polychlorotrifluoroethylene, tensile deform. in He, N_2, Ar, O_2 and CO_2 gaseous environments 77−56040
polydimethyl siloxane-b-styrene-b-dimethyl siloxane block copolymer, morphology, mech. props. 80−64930
polydimethylsiloxane, end-cap ratio and mech. props. of block copolymer 78−91266
polydimethylsiloxane, rubber elasticity in uniaxial tension, compression 79−15714
polyester dough moulding compounds, fibre orientation and mech. props. 77−25116
polyester moulding compounds, cyclic loading and strength 77−81310
polyester resin, creep, temp. and humidity effects under shear and tensile strains 77−86105
polyester resin concrete, effects of styrene-unsaturated polyester ratio on props. *(Japanese)* 80−89299
polyester-polyurethane semi-interpenetrating networks, mech. props., morphology 80−45362
polyether sulphone, effect of rolling on mech. props. 78−52837
polyether-polyester elastomer, fine structure and mech. props. 77−59844
polyethyl acrylate modified mortars, inner struct. and flexural props., suspension and emulsion studies *(Japanese)* 77−86092
polyethylene: (Dy_2O_3), mech. props. and transfer to steel surfaces 80−16496
polyethylene, correlation between valence energies and low temp. flexibility 80−25815
polyethylene, cross linking by energy rich radiation, mech. and elec. props. *(German)* 78−20035
polyethylene, crystallised from oriented melt, mech. and thermomech. props., framework struct. 77−63756
polyethylene, deformation, Hartree-Fock SCF calcs. 80−18949
polyethylene, electric cables, anal. of breaking strength distrib. *(Japanese)* 78−84921
polyethylene, filled, linear, struct., strength 79−29149
polyethylene, filled, mech. props., cyclic heating effect 80−55526
polyethylene, high density, influence of dimensions in mech. props. *(German)* 80−21039
polyethylene, high density, injection moulding effect on strength props. *(Russian)* 79−34072
polyethylene, high density, plastic behaviour determ. at const. true strain rate 79−39073
polyethylene, high density, self-reinforced thermoplastic, extrusion 79−15699
polyethylene, high density, solid state coextrusion, geometric factors effect 80−71704
polyethylene, high density, solid state coextrusion, technique for ultradrawing thermoplastics 80−84979
polyethylene, high density, strength props. *(German)* 79−100219
polyethylene, high density extruded fibres, morphology effect on physical and mech. props. 79−83235
polyethylene, high-density, effect of fillers and moulding process parameters on strength *(Russian)* 78−60640
polyethylene, high-density, solid-state coextrusion, mol. wt. distrib. effect 80−104212
polyethylene, high-density, submicroscopic cracks form. and residual strength, hydrostatic press. influence 79−20185
polyethylene, high-density, tensile necking, specimen size and loading conditions effects 79−61672
polyethylene, high-density ultradrawn, extrusion ratio influence on tensile props. 79−61618
polyethylene, highly oriented fibre composite, self-hardening, tensile props. 77−55939
polyethylene, low and high density, tensile relaxation changes *(German)* 78−64599
polyethylene, low density, melt elongation, stress and recovery maxima 79−90209
polyethylene, modified with phosphonate ester pendant side group, thermal and mech. props. 78−11195
polyethylene, orientated, var. of yield stress with orientation, yield criteria exam. 78−52900
polyethylene, ultra-high-strength filaments, soln. spun/drawn, mech. and thermal props. 80−40440
polyethylene extruded melt, elongational viscosity, tensile props. 78−67163
polyethylene extruded melts, force-strain relation 79−77049
polyethylene fibre, high-strength high-modulus, morphology and tensile prop. relations 80−103264
polyethylene fibres, high density, ultra oriented, physical, mech. props. 80−25649
polyethylene filaments, ultrahigh-strength, from soln. spinning and hot drawing 80−45268
polyethylene implant-bone composite interfacial strength, porous high density polyethylene 78−31979
polyethylene oxide blends, thermal and mechanical props. 79−11679
polyethylene ribbons, flow-induced crystn. from melt, in dies fed by single screw extruder 80−84110
polyethylene stabilized with home-made antioxidants, thermal resistance *(Polish)* 79−52328
polyethylene surface-growth fibres, hot drawing 80−97517
polyethylene terephthalate, preoriented sheet, plastic deform., anisotropic behaviour 79−8335
polyethylenes, extrusion and heavy duty films struct. parameters influence on cross-linking by radiation 80−66844
polyhydroxyethyl methacrylate swollen network filled with polyhydroxyethyl methacrylate, viscoelastic and ultimate behaviour in rubbery region 79−83247
polyimide fibre reinforced polyamide-12 80−11754
polyimide film, heat treatment conditions effect on ultimate strength, expt. planning methods 78−6952
polyisobutylene-glass adhesion bond, macroscopic contact form. 79−39113
polyisocyanurate foams, strength, cellular struct. effect 80−40518
polymer, creep in tension under hydrostatic press. 77−70124
polymer, crystalline, in hydrostatic tension, plastic deform. of model 77−59870
polymer, filled, tensile strength calc., rel. to fracture *(German)* 80−25795
polymer, fluid high, ultimate strength in unixial extension 79−38920
polymer, hollow spherical particle filled, strength criterion 79−11682
polymer, lifetime, hydrostatic press. effect 77−70170
polymer, physical problem determ. problems, tensile strength, elastic moduli *(German)* 78−15470
polymer, relation to cohesive energy density, surface tension and butt joint strength 77−55431
polymer, rubber-like manipulator for placing ring shaped testpiece in cold chamber of tensile testing machine 77−63859
polymer, semicryst., and filled, elastic modulus, strength, rel. to crystallite shape 80−45335
polymer, specimen size effect on mech. behaviour associated with crazing 77−73337
polymer coated graphite fibre-epoxy resin composites, prep., adhesion 79−15644
polymer fibre, highly oriented, struct. and mech. props. 78−75563
polymer films and sheets 78−80590
polymer impregnated gypsum cast, mech. props. 79−100107
polymer-TiO_2 composite, dielec. props. *(Japanese)* 78−95540
polymeric foam, cell cracking 79−11701
polymers, mech. props., temp. dependence of polymers of different struct., 4.2 to 300K 78−68746
polymers, multicomponent, props. and struct., review 78−44076
polymers, nonlinear, under tension and torsion 79−52290
polyolefines, filled, struct.-mech. props. relation *(German)* 78−35451
polyphenylene sulphide, high mol. wt. soluble resin, prep., mech. props. 80−60828
polypropylene, flow-induced crystn. from melt, in dies fed by single screw extruder 80−84110
polypropylene, glass fibre reinforced, injection moulded discs, struct. and mech. props. 78−19706
polypropylene, mech. behaviour rel. to combined press.-temp. effects 77−16648
polypropylene, neutron irradiation effect on weldability and adhesion *(Japanese)* 79−60405
polypropylene, oriented, stress relaxation 77−44285
polypropylene, oriented, thermooxidative degradation kinetics, durability, influence of mech. initiated processes *(Russian)* 79−24591
polypropylene, thermal stabilizer content effect on props., processing and ageing *(Polish)* 79−70099
polypropylene fibres, homologue mixtures, props. 78−76709
polypropylene monofilaments, tensile props., orientation degree depend., IR dichroism obs. 78−3163
polypropylene nonfilaments, highly drawn, plastic deform. 78−44174
polypropylene powder, cold compaction, product strength, heat treatment effects 80−11621
polypropylene-bitumen mixture, thermomech. investigation changes in viscosity, ductility, elasticity, mol. wt. effects *(German)* 78−35454
polypropylene/peanut-hull flour composite, strength 79−8365
polystyrene, amorphous, fracture mechanism 77−8949
polystyrene, cryogenic foam insulators, low temp. props. 80−25818
polystyrene, impact resisting *(German)* 79−100219
polystyrene, nonisothermal rheology 77−32619
polystyrene, oriented amorphous, supermol. structures rel. to mech. behaviour 78−22673
polystyrene, props. changes upon photooxidation 80−30123
polystyrene, rupture mechanism 79−52372
polystyrene-ethylene propylene copolymer, strength and impact props. 78−52899
polystyrene-tetrachloroxylene(tetrachlorobenzene) glassy solns., additive morphology rel. to mech. props. 79−65007
polystyrenes, monodisperse, static and dynamic props., mol. wt. effect 78−84938
polystyrol, test pipes, static tensile strength, equipment effect on tension-extension diagram *(German)* 78−35453
polystyroles, filled, struct.-mech. props. relation *(German)* 78−35451
polysulphone, effect of rolling on mech. props. 78−52837
polytheylene, high density, under tension and torsion 79−52290
polytrifluoroethylene, dielectric relax. processes above and below glass trans. *(Japanese)* 80−55028
polyurethane, cryogenic foam insulators, low temp. props. 80−25818
polyurethane, tensile fracture stress eval. for prosthetic heart valve 77−56533
polyurethane foams, elastic, stability against organic solvents *(German)* 80−85074
polyurethane foams, strength, cellular struct. effect 80−40518
polyvinyl alcohol fibre reinforced epoxy resin, fracture kinetics 78−3222

tensile strength continued
polyvinyl nitrate, exam. of strength characts. 78−68748
polyvinylidene chloride co-polymer powder, cold compaction, product strength, heat treatment effects 80−11621
porcelain, elec., comparative assessment of methods of determ. strength 80−40429
porous materials, pore geometry effects on tensile strength 80−30048
porous sintered materials, mech. testing device for hydrostatic pressure conditions 80−40645
Portland cement, hydration mechanism, rel. to strength 78−35349
powder, temperature effect on flow and tensile strength 79−61668
powder, tensile and compressive strength meas. *(Japanese)* 80−25780
powder, tensile strength data and failure loci from Jenike shear cell tests 78−31476
powder-cushion gripping, tensile testing, for good alignment 78−92418
powders, modification of split plate tester 77−70255
power cables, HV, Rb coverings quality estimation using mechanical tests *(Polish)* 80−97525
prealloyed powder blending, composite materials fatigue and tensile props. *(French)* 80−20850
pressure vessel for tensile testing in high-pressure gases at high temps. 78−44303
prosthesis block copolymers, non-thrombogenic, struct. and mech. props. 77−52925
PVC, asbestos reinforced, CIR/Palram process preparation, mechanical and thermal properties measurements 79−66106
PVC, crosslinked, mech. and thermal props. with plasticisers *(Japanese)* 79−15741
PVC, filled, struct.-mech. props. relation *(German)* 78−35451
PVC, oriented mouldings, struct. order 80−60896
PVC, plastic behaviour determ. at const. true strain rate 79−39073
PVC, rigid, tertiary creep *(German)* 77−52433
PVC, rigid, viscoelastic props. rel. to thermal, mech. history 79−5016
PVC, tensile and indentation behaviour, durability tests, glass transition 79−5017
PVC, tensile test neck development theory 78−52897
PVC, tensile tests at low strain rate, secondary instability form. *(German)* 77−66727
PVC, test pipes, static tensile strength, equipment effect on tension-extension diagram *(German)* 78−35453
PVC, uniaxial tension, deep drawing, rigidity *(German)* 78−64556
PVC mixture with processing aids, mech. props. and morphology 79−57047
PVC powder, cold compaction, product strength, heat treatment effects 80−11621
PVC-g-butyl rubber grafted copolymer, tensile strength increased by S_2Cl_2 curing 79−95993
rare earths, elastic and mechanical properties, review 79−70132
refractories, thermal stress cracking resistance estimation 80−104288
refractory ceramic creep meas. in tension and compression 78−31486
refractory composites, fibre reinforced, directionally solidified tensile tests, in HVEM, deform. and fracture *(French)* 78−68785
refractory fibre, effect on high-temp. strength of refractory coatings *(Russian)* 77−52536
reinforced concrete deep beams, optimal force transmission 78−34009
reinforced plastics, subject to short-term tensioning, failure 79−61725
resin mortar, strength anal. by reliability concept *(Japanese)* 78−31466
resin-coated optical fibre, tensile strength tests *(German)* 78−33871
resins, thermoplastic, glass-fibre-reinforced, performance at elevated temperatures obs. 79−95067
rigid body collisions, spalling, tensile stresses on target, appls. 79−7324
ring samples, device for testing 77−25215
rings, circular optimal plastic, stress/strain relations for rigid plastic material 79−34098
rock, mech. props. rel. to cooling *(Japanese)* 80−31036
rock beam, laterally-constrained ultimate strength investigation with constrained beam test apparatus 79−29299
rock materials tensile strength determination, suggested methods 78−96314
rock parameters, drillability *(German)* 79−74888
rocks, rings, discs, under diametral compression, tensile strength calcs. *(French)* 77−70638
rocks tensile strength indirect measurements, new theoretical aspects 79−29883
rod, theory of resistance to failure of technical materials, tensile curve 79−10536
round bar, tensile deformation, mathematical description 79−10500
roving glass cloth fibre reinforced polyester resin cumulative damage fatigue *(Japanese)* 77−8941
rubber, crystallising, tensile test specimen prep. 80−71838
rubber, natural, tensile fracture strength eval. for prosthetic heart valve 77−56533
rubber, peeling initiation and propag. 78−76824
sand, resin-coated, curing effects on physicomech. props. *(Korean)* 78−60855
SAP 895 (Al-Al_2O_3) alloy containing ^4He and ^3H, tensile props. 80−34129
shaped strip, tension during rolling 78−84890
shear index, permissible values 78−63324
sheet material, method for strength meas. under biaxial tension 80−66717
sheet moulding compound, laminate, charge pattern influence on tensile strength *(Japanese)* 80−55513
shell buckling rigidity characts. *(German)* 80−48608
silica fibre, furnace drawn, tensile strengths >3.5 GN/m^2 in 1 km lengths 78−87135
silica fibre, laser drawn, coated, tensile strengths >3.5 GN/m^2 in 3 km lengths 78−87138
silica fibres, epoxy acrylate coated, tensile strength >500 ksi, km length prod. 77−11052
silica optical fibres, ageing polymer-coated fused specimens in pH solns., tensile strength and dynamic fatigue 79−46063
silica optical fibres, surface flaws obs., fracture strength 77−14793
silicone rubber, tensile fracture stress eval. for prosthetic heart valve 77−56533
silk, natural, elongation and tensile strength rel. to UV irradiation 80−25796
silk, spider, tensile, fracture strength, elongation and ageing effects 80−41072
simple tension test, appl. of hyperbolic theory of plasticity 77−39235
Sn coated Cu, fine struct. in diffusion zone and mech. props. 77−11739
tensile strength continued
solids weakened (strengthened) by inhomogeneity, tensile and compressive strength 78−42571
spheroplastic, spherical shells, supporting capacity 80−87723
stainless steel, bending, effect of strain rate on dynamic stress factors 77−56046
stainless steel wire reinforced Al sheet, prod. by explosive compaction, and mech. props. 77−32542
statistical study using small number of data *(Japanese)* 77−32736
steel, 0.2 to 0.8% C, ferrite-pearlite transformation, tensile strength, cooling rate effect 80−7549
steel, 10Kh11N20T3R, brittle fracture susceptibility rel. to grain size *(Russian)* 77−59901
steel, 12Kh18N9T-TiB_2, eutectic alloy, high temp. props. 78−84931
steel, 15NiCrMo 106, struct. changes, through simulated multiple layer welding, micro-tensile and shearing tests *(German)* 80−35215
steel, 20A, melt, tube blanks, mech. props., statistical determ. 79−29316
steel, 20Kh, warm extrusion effects on struct. and mech. props. 77−44311
steel, 3.5% Ni neutron irrad. effects on tensile props., microstructure effects 77−69005
steel, AISI 1010, low-cycle fatigue at temps. up to 1200°F 78−35516
steel, Al-killed, sheets, effect of strain path changes on formability 79−43347
steel, alloy, 08kp, denitriding annealing, affect on mech. props. 79−52461
steel, alloy, 16GNMA, stress conc. effect on endurance under repeated static loading conds. 79−43412
steel, alloy, 300M, fracture toughness and strength, effect of heat treatment on microstruct. 78−15436
steel, alloy, deformation, rapid dynamic, at −196°C 80−104220
steel, alloy, high C, amorphous, produced by rapid quenching from melt, hardness and strength 78−59764
steel, alloy, low, dual phase, high strength, exam. of energy absorption by structual collapse 80−7640
steel, alloy, low-temperature testing, −196°C to +20°C 79−61692
steel, alloy, mechanical properties, morphology, transform. kinetics and composition interrelations 77−86146
steel, alloy, static and fatigue strength, tension and compression test results 78−95810
steel, alloy, temp. profile, IR obs. during pull tests 77−44427
steel, alloy, tensile test, regulated, strength and deform. characteristic values, consistency *(German)* 80−93712
steel, alloy, tension test, computer simulation of deform. to fracture 79−11667
steel, alloy 18G2AV, residual stress distrib. effect on fatigue crack growth 79−57111
steel, alloy 4340, fracture and high temp. props., 533K to 1255K 78−60821
steel, annealed, limit stress, effect of specimen length 77−44357
steel, austenite decomposition, controlled rolling rel. to substruct., props. 79−29014
steel, austenitic, 30KhGSA, grain size before quenching rel. to mech. props. 79−24553
steel, austenitic, 30KhGSA, heat treatment, preliminary, cold deform., elec. heating rel. to mech. props. 79−24554
steel, austenitic, high tensile X 3 CrNiMoNbN 23 17, creep at room temp., effect of Bauschinger effect *(German)* 77−1852
steel, austenitic, Kh18N9T and EHI835, tension tests in high speed gaseous streams 77−63761
steel, austenitic, Mn-base, as LNG storage and transportation system material 79−70133
steel, austenitic, strength, ductility and fracture toughness, N and Cr effects 80−100878
steel, austenitic, tensile props. after corrosion by UO_{2+x} and fission products *(German)* 77−70216
steel, austenitic, tensile strength, elec. current impulse effect down to 4.2K 80−81131
steel, austenitic, types A533B and A508, acoustic emission and deformation processes during tensile tests 79−74212
steel, austenitic heat-resisting, deformation and fracture rel. to grain-boundary reaction nodules 78−80591
steel, austenitic Kh18N9T, porous fibres, oriented struct., strength props. 78−3199
steel, austenitic stainless, 304, solution annealed, tensile flow behaviour after exposure to flowing Na, in temp. range 550 to 700°C 78−35463
steel, austenitic stainless, 316, surgical implant ion beam textured, stress/strain relations, fatigue characts. 78−73297
steel, austenitic stainless, acoustic emission during tensile tests, H_2 assisted fracture 79−100257
steel, austenitic stainless, cathodically charged, H_2 embrittlement, α' martensite effect 80−71725
steel, austenitic stainless, Cr-Mn, austenite stability during deform. 77−70050
steel, austenitic stainless, Cr-Ni, Mn and Mo effect on mech. props. rel. to treatment 79−96039
steel, austenitic stainless, deformed plate, X-ray line profile anal. *(Japanese)* 78−7144
steel, austenitic stainless, electron beam welding effect, on mech. props. of steels 310L, 316, 21-6-9 78−48498
steel, austenitic stainless, martensitic transform. effect during static and fatigue loading 77−52325
steel, austenitic stainless, porous fibre, sintered and compacted, mech. props. 79−15623
steel, austenitic stainless, stressed state blistering 78−95085
steel, austenitic stainless, supercond. magnets, mech. and phys. props. at 4K 80−86976
steel, austenitic stainless, texture influence as through thickness strength 79−91771
steel, austenitic stainless, type 18-10, stress corrosion cracking in boiling solutions of $CaCl_2$, $MgCl_2$ and LiCl *(French)* 77−81342
steel, austenitic stainless, type 316, hydrogen embrittlement, tensile testing 80−7671
steel, austenitic stainless, types 304, 316, tensile props., effect of exposure to Li and LiH 80−35219
steel, austenitic stainless in liq. Na, mechanical props., review 79−20150
steel, austenitic stainless JIS type 304, tensile test at elevated temp., high velocity 77−73302
steel, austenitic stainless Kh18N10T, strength properties, dispersity of struct. effect 80−55486
steel, austenitic stainless tensile ductility in air and H_2 77−66687

tensile strength continued
steel, austenitic stainless type 304L, temp. depend. of acoustic emission accompanying plastic deform. 79−74217
steel, austenitic type 110G13L, preliminary strengthening inheritance, exam. 78−44137
steel, brass clad plate/roll bonded Ni clad, fatigue crack growth behaviour 80−40484
steel, brittle fracture, J-integral fracture criterion *(Japanese)* 77−48597
steel, C1020, dual phase, mech. behaviours and structs. *(Korean)* 80−25779
steel, C, accumulation of longitudinal strain under cyclic torsion 78−64615
steel, C, antifriction material, sintered, determination of elastic moduli 79−96070
steel, C, cumulative damage rule, based on reduction in fatigue limit, experimental confirmation 78−92358
steel, C, ductile fracture under cold forming conditions, press. effect 78−52938
steel, C, fatigue failure in type 45, strength charact. 79−52373
steel, C, low temperature strength, preliminary plastic deform. effect 80−81128
steel, C, mech. props. rel. to heat treatment, ferrite-pearlite transform. *(French)* 79−20043
steel, C, microduplex, ferritic-martensitic, struct. effect on tensile fracture *(Japanese)* 79−96113
steel, C, relax. resist. rel. to struct. 78−23788
steel, C, residual elements, effect on props. 80−66643
steel, C, rotating bending fatigue strength, high tensile load effect during stress cycling *(Japanese)* 77−52477
steel, C, rotating bending fatigue strength, periodic high tensile load effects *(Japanese)* 78−11313
steel, C, structural strength, increase by high temp. mech. treatment with austenite isothermal decomp. 79−24555
steel, C, tensile fracture surface in high press. H_2 at room temp. *(Japanese)* 80−108540
steel, C, tensile props. in high press. H_2 at room temp. *(Japanese)* 80−108501
steel, C, tensile strength, effect of specimen length *(Japanese)* 78−84920
steel, C, thermomechanically treated, in situ composite material description 80−7649
steel, C, type 1792AF 79−38966
steel, C and alloy, restricted durability, subject to pure bending with rotation 77−90431
steel, C and low alloy, mech. props. after warm extrusion 77−12668
steel, C-Cr (0.4, 1 wt.%), medium C, stress corrosion cracking, effect of H_2S, aggressive components of gas condensates and moisture *(Russian)* 77−16726
steel, C-Mn, pressure vessel usage, elevated temp. mech. beahviour 78−35462
steel, cast, 80 kg/mm^2, heat treatment 80−16358
steel, cast structural, heat treatment and mech. working influence on mech. props. *(Russian)* 80−40392
steel, CC Cr-Mo (2.25, 1 wt.%) effect of heat treatment on tensile props. 78−23745
steel, Co-Cr-Mo type HY-180M, mech. props. and SCC, overageing effect 80−108634
steel, cold rolled, deep drawing, continuous annealing effect on mech. props. *(German)* 77−90362
steel, cold rolled, high strength, mech. props. 77−36527
steel, cold rolled high strength sheet, with high drawability, fabrication process 77−73288
steel, comp. and processing effects on microstruct. and props. rel. to low temp. applic. 77−52365
steel, continuously cast, optimum conditions for annealing castings during dynamic working *(Russian)* 78−44134
steel, continuously cast, tensile strength and ductility above 800°C 80−55476
steel, Cr, corrosion resist., tempering after air-hardening in rolling heat *(German)* 80−45324
steel, Cr, previous deformation influence on strength, ductility, in biaxial tension, low temps. 79−90718
steel, Cr, type Kh, (GOST 5950-51), in biaxial tension, effect of charact. of preloading on low-temp. ductility and strength 79−15749
steel, Cr (13 wt.%), fatigue, effect of toughness *(Japanese)* 78−7025
steel, Cr (1.7 and 2.5 wt.%), segregation of S and P to prior austenite grain boundary, stress effect *(Japanese)* 77−55962
steel, Cr-Mn, annealing effect on mech. props. for cryogenic appl. *(Russian)* 78−19788
steel, Cr-Mn, unstable austenite, martensitic transform., effect of alloying, heat treatment, and deform. 78−19751
steel, Cr-Mo, cast and forged, difference in mech. props. 77−48465
steel, Cr-Mo, effect of Mo on high-temp. props. 80−85005
steel, Cr-Mo, high-temp. props. and constitutive equations 79−34146
steel, Cr-Mo, toughness of heat treated steels of equal tensile strength *(German)* 80−25727
steel, Cr-Mo (1.25, 0.5 wt.%), creep, fracture, Ti and Ti+B effects 77−36603
steel, Cr-Mo (2.25, 1.00 wt.%), bainitic, strain rate effects on elevated temp. tensile behaviour 78−35461
steel, Cr-Mo (2.25, 1 wt.%), annealed, heat treatment effect on tensile props. 78−11243
steel, Cr-Mo (2.25, 1 wt.%), temper embrittlement trace elements, Mo, intercritical heat treatment effects 77−36634
steel, Cr-Mo (2.25, 1 wt.%) annealing, high strain rate tensile props. 77−25117
steel, Cr-Mo (2.25, 1 wt.%) pipe, high temp. fatigue and creep strength 80−85060
steel, Cr-Mo-Ni-Nb, Nb effect on mech. props. *(German)* 80−30012
steel, Cr-Mo-V, press. vessel, fracture, effect of tempering 78−60799
steel, Cr-Mo-V (1.35, 1.0, 0.25 wt.%) exam. of mech props, comparison with mathematical model predictions *(Czech)* 79−91740
steel, Cr-Ni, hydrogen effect on strength, ductile and fracture charact. 79−38960
steel, Cr-Ni, tensile strength and cooling curve, regression anal. 79−57070
steel, Cr-Ni-(Mo), austenitic, strengthening by modified ausforming 78−76665
steel, Cr-Ni-Ti-B, grain size effect on mech. and struct. props. *(French)* 80−45361
tensile strength continued
steel, Cr-Si-Mn-ΔV-Ti-Nb-Mo, effect of V, Ti, Mo, Nb additions on substructure, mech. props. *(Russian)* 79−34108
steel, Cr-Si-Mn-Ni-Mo-C, resist. to deform. and fracture, C effect 80−71757
steel, cracking resistance of high-strength 40Kh and 35KhGSA, tempering temp. influence *(Russian)* 79−52252
steel, CrMoV, creep and creep strength under alternate tension/compression *(Czech)* 77−63728
steel, Cu-Zn, brass clad, fatigue crack growth behaviour 80−40484
steel, deformation ageing of 40Kh, effect of impact resistance and tensile strength *(Russian)* 78−31427
steel, diffusion coatings, carbide and boride, props. *(Russian)* 79−52443
steel, dispersion strengthened with Al_2O_3 or ZrO_2, by spray method into molten stream, exam. of mech. props. 79−11636
steel, duplex ferrite-martensite, microstructure resistance optimisation 80−40482
steel, energy absorption during uniaxial tension and axial compression, geometric and heat treatment effects 77−73312
steel, eutectoid, anisothermal strain with phase transform., effect on tensile strength *(Russian)* 80−40431
steel, eutectoid, mech. behaviour, thermomech. treatment effects 80−84970
steel, eutectoid and hypoeutectoid viscoelasticity under transformational superplasticity *(Japanese)* 77−52416
steel, extra mild, thin sheet, biaxial tensile deform., effect on crystallographic texture *(French)* 77−59814
steel, fatigue and tensile props., of heat resisting bars, type SUH 660-B and SUH 310-B at elevated temps. 79−38979
steel, fatigue life, structural parameters and chem. comp. effects, rel. to test parameters 77−59928
steel, fatigue reliability under random loads 79−79066
steel, fatigue strength, statistical prop. *(Japanese)* 79−20169
steel, Fe-Mn-C austenitic, deform. twinning and mech. props. 77−59868
steel, ferrite and dual phase, mech. props., effect of Si and P 79−57063
steel, ferritic martensitic, effect of ductility of second phase on ductile fracture 78−19847
steel, ferritic-pearlitic, fatigue crack development, load-cycle assymmetry coeff. effect 79−87710
steel, ferritic/austenitic high Cr, development, mech. props. and corrosion resist. 80−45422
steel, fibre reinforced Al, fracture mechanics under fatigue *(Czech)* 78−64629
steel, fibre reinforced Al composite, role of brittle layers at elevated temps. 79−96135
steel, for pressure tanks, yield point influence on brittle fracture, tensile strength *(German)* 80−40539
steel, fracture toughness eval. by equivalent energy method *(Slovak)* 79−43402
steel, free cutting, with MnS inclusions, tensile flow and fracture 78−11290
steel, H_2 effect on yield 78−15474
steel, hardness, rel. to tensile and impact strength 77−90428
steel, hardness, tensile and impact props. correlation, at low temps. *(Japanese)* 77−52413
steel, heat resistance, thermal stability, stress-rupture strength, and creep 80−81194
steel, heat resistant, tensile strain and endurance, normal and radiation conditions, linear load variation 80−81189
steel, high alloy Cr-Mo-W, splat quenched, formation of metastable austenite 80−84974
steel, high C, quenched and tempered, hydrostatic press. effect on brittle fracture stress 79−61727
steel, high C, tensile strength, working and heat treatment effects *(Japanese)* 80−104209
steel, high C, thermomech. treated, strengthening factors 77−8862
steel, high Mn, heat resistant, alloying additions, effect on mech. props. *(Korean)* 77−12631
steel, high Mn, mech. props., strain induced martensitic transform., effect of austenite predeformation 77−16649
steel, high speed, hardened, for drills, mech. and cutting props. 79−43407
steel, high speed type M-50 and 18-4-1, fracture and fatigue 80−16457
steel, high strength, failure stress, structural relationships 80−81190
steel, high strength, low alloy, fatigue crack growth from a surface flaw 78−68803
steel, high strength, low alloy, plate, impaired ductility in sheared edges 78−60727
steel, high strength, low alloy, splitting of tensile and impact specimens 77−63777
steel, high strength, plastic deform. and fracture under tensile stress *(Russian)* 77−70100
steel, high strength, press. depend. yield and plastic vol. change 78−19810
steel, high strength, sensitivity to stress concentration with various H content *(Russian)* 79−15724
steel, high strength sheet, absorbed energy during compression and crushing 77−36593
steel, high temperature strength, corrosion-erosion effect of gas metal mixtures stream *(Russian)* 78−35576
steel, high-speed, cast, mech. props. at high temps. 79−20135
steel, high-speed, N effects on struct. and props. 77−59799
steel, high-speed, quenched and tempered notch toughness, ultimate and yield strength in tension and compression 78−95782
steel, high-strength reinforcing, 20GS2, local microstresses on creep strength in hydrogenating media *(Russian)* 77−52462
steel, high-strength tool steel D7KhFN, remelting effect on mech. props. 80−76284
steel, hot forging die type, fractography *(Japanese)* 80−108547
steel, hot rolled, low C, low alloy, bainitic alloying addition effects on microstruct. and props. 77−36546
steel, hot rolled strip formability, mech. testing and mech. props. *(German)* 79−66089
steel, HSLA, V effect on mech. props. *(Korean)* 80−29987
steel, impact and tensile props., Si effects 79−24614
steel, intermediate class Kh16N6, structural aspects of work hardening 77−90369
steel, lamellar pearlite, containing proeutectoid cementite, brittle fracture study *(Japanese)* 80−93648
steel, laminar composite, crack extension, rising tensile load effect 77−36642

tensile strength continued
steel, laminated, tensile props. 77−52441
steel, large forging, mech. props. 77−4797
steel, lattice hardening and anomalous softening caused by electrolytic H_2 charging *(Japanese)* 79−43398
steel, low alloy, fracture strength investigation under various types of loading 78−7042
steel, low alloy, high strength, correlation between fracture toughness, tensile props., fracture morphology 78−60789
steel, low alloy, low C, double ligament tensile test in deformation processing 77−32753
steel, low alloy, reactor pressure vessel, effect of Mn and C content on irrad. response 79−20196
steel, low alloy, strength, Cr and N effects 80−104277
steel, low alloy, type 10KhN1M, heat-treated, struct. and resist. to thermal embrittlement 79−15788
steel, low alloy, type 3sp, effect of temp. at end of rolling on mech. props., and coercive force 78−72799
steel, low alloy, type 4340, quenched and tempered, effect of plastic strain followed by ageing, on torsion fatigue resistance 78−92360
steel, low alloy effect of grain size, and amount of pearlite on fracture resistance 79−100255
steel, low alloy press. vessel, fracture toughness determ. from invalid compact tension specimens 77−4848
steel, low C, brittle fracture susceptibility, low temp. deform. effects 77−56103
steel, low C, cold rolled sheet, strain rate effect on yield *(Japanese)* 79−96084
steel, low C, dual phase structures (martensite and ferrite), effect of martensite composition on content, mech. props. 78−76717
steel, low C, dual-phase, law of mixtures, applicability 80−89346
steel, low C, ductile-brittle transition behaviour, grain size effects 78−52942
steel, low C, impact and tensile props., effect of Si 77−36526
steel, low C, low endurance fatigue at low temps. 77−21274
steel, low C, mech. charact., specimen size and shape effects 80−66715
steel, low C, microalloyed, heat treatment, mech. props. 79−24551
steel, low C, Mn, strain hardening parameters, electron microscope obs. 77−63690
steel, low C, Mn-Nb, quenched and tempered, microstruct. and props. 77−36549
steel, low C, non-ductile transition temp., tensile speed, effect of prestrain *(Japanese)* 78−72839
steel, low C, notched sheet under tensile loading, notch tip opening/contraction, J-integral relationship *(Japanese)* 77−4840
steel, low C, plastic props., fracture, effect of strain rate in static tensile tests *(Czech)* 77−59866
steel, low C, relation between low yield behaviour and tensile speed, preloading and temp. effect *(Japanese)* 78−6982
steel, low C, rephosphorised static strain ageing 77−70079
steel, low C, rimmed, structural damage in sheet metal forming 78−64614
steel, low C, thermomechanically processed, martensitic fibre development, fatigue fracture 78−64572
steel, low C, type En3, high strain deform., struct. and props. 80−89301
steel, low pearlite, Nb microalloyed, ageing at 600°C, mech. props. *(German)* 77−36542
steel, low-alloy, bearing, mech. props., carbide behaviour effect *(Korean)* 80−93615
steel, low-alloy, plastic deform. mechanisms under dynamic loading 80−100883
steel, low-alloy, props. with nitride and Cu hardening at low temps. *(Russian)* 80−40372
steel, low-alloy, residual elements, effect on props. 80−66643
steel, low-C, fatigue strength, low-cycle, effect of shock wave press. 79−29205
steel, low-C, fully pearlitic, struct. and mech. charact. rel. to cooling conditions *(French)* 80−40425
steel, low-C, transformed by cooling in ferritic-pearlitic range, relations between cooling rate, struct. and mech. props. *(French)* 77−32570
steel, maraging, 18 wt.% Ni, tensile props., effect of aged struct. and austenite grain size 77−48511
steel, maraging, (18 wt.% Ni), solution annealed, exam. of cryogenic tensile, fatigue, and fracture props. 78−92311
steel, maraging, Ni-Co-Mo (18, 8, 5 wt.%), fatigue strength charact. *(German)* 77−21241
steel, maraging, notch strength 77−56056
steel, maraging, prior austenite grain size effect on tensile ductility and fracture toughness 79−100226
steel, maraging 350, produced by powder metallurgy, mech. props. 78−15334
steel, maraging Ni-Co-Mo, precipitation, elec. resist. meas. *(Japanese)* 78−11228
steel, maraging Ni-Co-Mo, strengthening by repeated strain ageing *(Japanese)* 79−100157
steel, martensitic, as LNG storage and transportation system material 79−70133
steel, martensitic, low C wire, strain tempering by rapid heating *(Japanese)* 78−31428
steel, martensitic low C, development and props. *(Russian)* 80−20933
steel, martensitic stainless, type 05Kh13N4m, strength and embrittlement, early stages of martensite decomp. effect 80−35227
steel, medium C, Nb addition, effect on transformation and strength 80−7607
steel, metastable austenitic, resistance to failure 77−4852
steel, Mg effect on precipitation of C and or N, and mech. props., during strain ageing *(German)* 78−35387
steel, microalloyed, fine grained, mech. props., effect of hot dip galvanising *(German)* 77−36679
steel, microalloyed, types V1599, V1600, V1286, NbCN precipitation in undeformed austenite 80−89230
steel, mild, AC effect on fatigue and static props. 80−45372
steel, mild, cold rolled sheets, microstruct. and strain path in deep-drawing 78−19775
steel, mild, fatigue crack growth from a surface flaw 78−68803
steel, mild, fatigue strength, effect of grinding surface *(Japanese)* 77−48533
steel, mild, fracture toughness meas. with reinforced-double-cantilever-beam specimen 77−4842
steel, mild, subject to three point bending and tensile load, acoustic emission 80−3154
tensile strength continued
steel, mild and HSLA, mech. behaviour, deform. rapidity influence *(French)* 79−57056
steel, Mn, acicular ferrite high-strength low-alloy, low temp. mech. props., pipe-line appl. 80−55472
steel, Mn, as rolled bainitic, tensile, impact and machinability props., transport appl. 78−88503
steel, Mn-Cr-Mo, Mn-V-Mo, high-strength heat-treatable sintered 80−50575
steel, Mn-Mo, castings, mech. props., Cu and Sn trace elements effect 80−66596
steel, Mn-V reinforcing type, strain ageing charact. rel. to mech. props. 80−84969
steel, Mo-bearing, intercritically annealed dual-phase strip, props. and appl. 78−84858
steel, natural gas environment effects on strength *(Russian)* 78−11401
steel, Ni, antifriction material, sintered, determination of elastic moduli 79−96070
steel, Ni, sintered, physical and mech. props. rel. to homogeneity 79−38762
steel, Ni, welded joints on LNG carriers mech. props. and fracture toughness 80−85017
steel, Ni-Cr-Mo, exam. of delayed fracture using fracture mechanics *(Japanese)* 78−52961
steel, Ni-Cr-Mo, quenched and tempered, nothced bar tensile tests *(German)* 80−35247
steel, Ni-Cr-Mo-U, ferritic, B segregation and high temp. embrittlement 78−7040
steel, nonmetallic inclusion, effect on hot ductility 80−29999
steel, nonmetallic inclusions effect on ductility 80−30042
steel, notched specimens, strength parameters and crack growth energy correl. 77−73334
steel, pearlitic, deform. microstruct. and cementite fracture, −196 to 700°C 78−27576
steel, pearlitic, heat treatment effects on mech. props. and microstruct. *(German)* 77−8857
steel, pearlitic or spheroidal plastic deform. and fracture *(French)* 78−35448
steel, plastic props., room temp. to recrystallisation temp., stress-strain relations, computer program 77−1865
steel, plasticity of grooved specimens at high temp., rel. to hot forming 78−23902
steel, powder forged, fatigue, surface treatment effect 80−85048
steel, powder forged, impact strength and fatigue strength, slag inclusion effects 77−21271
steel, prestressed concrete wire, strain tempering by rapid heating *(Japanese)* 79−70088
steel, quench ageing effect of Mn content on C and N precipitation and mech. props. *(German)* 78−31409
steel, quenched, tempered, intergranular failure during fatigue crack growth 79−8357
steel, quenched, tempering treatment, ultimate tensile strength and yield point *(Russian)* 77−32599
steel, rail, toughness, effect of Sn, SEM exam. 80−97569
steel, reinforcement, low, high temp. static strength testing 79−15902
steel, reinforcing wires, high strength, microstruct. obs. *(Czech)* 79−43342
steel, sheet, rapid test for props. assessment 80−40650
steel, silchrome, thermomech. hardening 78−23736
steel, sintered, mech. props. 77−40439
steel, spall investigations, pressures up to 100 kbar, failure and strength *(Ukrainian)* 77−73317
steel, spheroidised, H_2 embrittlement, fracture charact., electron probe anal. of inclusions 79−57109
steel, spring alloy, microstruct. and props. at low temps. 77−44286
steel, stainless, 10Kh18N9TL, S, Se, Te and Bi additions effect on mech. props. 79−83312
steel, stainless, 304, creep fracture propag., elongation, tensile strength, yield stress meas. applicability of fracture mechanics parameters 78−35508
steel, stainless, 304 and 316, evaluation of tensile and creep data 77−77552
steel, stainless, 316, 304, LMFBR primary piping materials, mech. props., review 77−25151
steel, stainless, 316, nuclear fuel cladding, crack nucleation 78−72864
steel, stainless, $\alpha+\gamma$ phase, tensile deform. induced α' martensite, morphology 78−44122
steel, stainless, AISI 304, dislocation struct., carbides, deform. mech. map 77−16650
steel, stainless, AISI 316, high-temp. mech. props. 80−66601
steel, stainless, austenite stability, deform. rel. to $\gamma \rightarrow \alpha$ transform. kinetics 79−24522
steel, stainless, austenitic, type 316, high velocity tensile test at elevated temp. 80−35194
steel, stainless, cold-worked, 316, chem. comp. effects on rupture life, tensile props. 77−25152
steel, stainless, Cr-Mn (21, 14 wt.%), grain boundary precipitation and fracture *(Japanese)* 79−100149
steel, stainless, Cr-Ni, low temp. plastic deformation, in mag. field 79−83256
steel, stainless, Cr-Ni-Nb stabilised, Te vapour effect on creep and tensile props. 79−24583
steel, stainless, deformation, rapid dynamic, at −196°C 80−104220
steel, stainless, embrittlement due to soldering with Cu alloy solder, effect of alloying additions 79−47773
steel, stainless, epoxide butt joints, effect of abraded and Ar ion bombarded surfaces on ultimate tensile strength 80−16638
steel, stainless, even elongation and relative hardening in martensitic, transition and austenitic 78−52926
steel, stainless, ferritic, anisotropic lamellar fracture mechanism 78−64639
steel, stainless, ferritic, mech. props., impurity effects *(Russian)* 77−52403
steel, stainless, ferritic, tensile strain direction and roping phenomena 77−36533
steel, stainless, fibre reinforced Al alloy, tensile props., cryogenic cooling effect 79−61623
steel, stainless, filament produced by glass-coated melt spinning, tensile strength 78−31488
steel, stainless, Kh18N10T, ionised gas effects 79−70252

tensile strength continued
steel, stainless, Kh18N10T, struct. and mechanical props., effect of previous deform. in rolling *(Russian)* 79−29099
steel, stainless, laminated with Cu interlayers, mech. props. 77−48506
steel, stainless, martensite nucleation and growth, expt. study 78−3125
steel, stainless, neutron irradiated, stress effects on microstruct. 77−47490
steel, stainless, neutron irradiation effect on low cycle fatigue and tensile props. at 298K 80−30059
steel, stainless, oxide dispersed, prod. by spray dispersion method, mech. props. exam. of mech. props. *(Japanese)* 78−48419
steel, stainless, tensile props. of GCFR ribbed claddings at 650°C 80−45364
steel, stainless, Ti modified 316, uniaxial tensile behaviour, Na environment effect 78−52916
steel, stainless, two phase, variation of tensile and impact strength with heat treatment 79−34085
steel, stainless, type 316, 20% cold worked, exam. of creep 78−72817
steel, stainless, Type 316, neutron irrad. effects on tensile props. and microstruct. 80−65059
steel, stainless, type AISI 316, effect on props. of Zn transfer from galvanised wire at 550°C 78−88527
steel, stainless 304, creep and fatigue crack propag. at elevated temps., fract. mech. and fractography 77−21279
steel, stainless 304, thermally exposed, tensile props. 77−25083
steel, stainless 316, controlled-porosity, mech. props. 79−96083
steel, stainless and ferritic, damping, logarithmic decrement meas. by torsion pendulum *(German)* 79−74195
steel, stainless type 304 L, mech. behaviour under constant stress associated with cyclic strain 80−25767
steel, stainless type SUS 304, diffusion welded joints, sound emission during tensile testing *(German)* 80−61062
steel, stainless type XM-19, influence of recrystn. behaviour on mech. props. 79−83213
steel, stainless/Al laminate, sandwich sheet materials, deform. in uniaxial tension 79−57061
steel, statistical distrib. of mech. props., and life characts. exam. 78−64606
steel, strengthening by rapid electrothermal treatment 78−84870
steel, structural, type St3S, hardness, random functions 80−76329
steel, structural, wide plate tensile testing eval. *(German)* 80−100969
steel, structural martensitic, corrosion resist. under stress effect of strain ageing with hydroextrusion *(Russian)* 79−38853
steel, tempered, high strength, internal stresses and mech. props. 80−3200
steel, tensile prestrained strength of anisotropic rolled steel, rot.-bending fatigue tests, slip bands 78−27590
steel, tensile test pieces, comparison of micro and standardised size *(German)* 79−83414
steel, tensile testing of ultra high tensile roping wire 77−44426
steel, Ti (0.1 to 0.55 wt.%), strengthening by carbide precipitation 77−25062
steel, toughness, review of joint tests *(German)* 80−65142
steel, TRIP, powder processing, tensile strength, ductility 78−64499
steel, TRIP, strengthened by hydrostatic extrusion, struct. and mechanical props. *(Russian)* 78−76647
steel, TRIP, warm extrusion, process control and tensile props. 80−16338
steel, two-phase austenitic-ferritic, plastic deformation under hot working conditions 77−48466
steel, type 28Kh3SNMVFA, strain hardened martensite, resist. to tempering, exam. 80−16348
steel, type 52100, heat treatment effect on microstruct. and mech. props. 80−29993
steel, type IN-787, for use in Arctic, low temp. effects on mech. props. 80−76310
steel, types A533B and KAS, fracture toughness meas. using elect. potential method *(Japanese)* 80−93722
steel, U8, diffusion coating protection for H_2 embrittlement, SCC and tensile tests *(Russian)* 78−31513
steel, ultrahigh strength, effects of strength and grain size on near-threshold fatigue crack growth 78−64704
steel, unalloyed, brittle fracture, effect of prestrain and ageing *(German)* 78−19857
steel, V high-strength low-alloy, for low temp. use, tensile and yield strength 79−70118
steel, V strengthened dual phase, deform. and fracture props. 78−48467
steel, yield point charact., grain size effect *(German)* 78−72810
steel 12Kh18N10T, struct. and mech. props. after prolonged working at −183°C 77−55988
steel 15Kh1M1F, temperature-time dependence of long-time structural strength 79−100232
steel 17G1S, magnetic method of mech. prop. determ. of thick sheet 78−48600
steel 23K2G2T, corrosion cracking susceptibility, C and Cr effects 78−19952
steel 45, fatigue strength determ. apparatus, in corrosive environment under complex stress *(Russian)* 77−77657
steel 45, fracture surface obs. during fatigue failure 77−86185
steel (0.45 and 0.8 wt.%), strength, fracture, effect of H_2 *(Russian)* 77−25129
steel A-106, yield point suppression by H_2 79−8368
steel AF1410, wear against stainless steel, repetitive impact, microstruct. effect 79−74263
steel alloy, type 30 KhGSA, expt. functions of resist. in tension and torsion 80−16397
steel bimetal, low-alloy austenitic ferritic stainless steel, fracture toughness *(Russian)* 78−35482
steel C, types AISI 1008, 1020, 1035, renitrogenized 1010 and 1522, dynamic strain ageing, tensile notch impact and fatigue props. 79−43288
steel fibre reinforced Al, fibre orientation effect on strength *(Korean)* 80−30027
steel fibre reinforced concrete, tensile strength and ultimate strain *(Polish)* 80−21027
steel fibre reinforced epoxy composite, static tensile behaviour *(Japanese)* 78−15482
steel fibre reinforced porous mat. prod., mat. props. 77−59723
steel H-beams, tensile samples shape influence on results of mech. props. determ. 77−52569
tensile strength continued
steel high strength X 3 CrNiMoNbN 2317, Bauschinger effect and creep at room temp., effect of heat treatment *(German)* 77−36543
steel intercrystalline stress corrosion cracking in a $Ca(NO_3)_2$ soln. *(German)* 80−30130
steel M16C, low C, natural discrete microlamellar composite *(Russian)* 78−39810
steel sheets, overlapped, glued with nonuniform epoxy resin layer, strength tests *(German)* 78−15647
steel tubes, square section, collapse in bending 80−25792
steel tubing, cold rolled, nondestructive mag. method for determ. of mech. props. 78−23903
steel U8, struct. and mech. props., effect of hydrostatic extrusion *(Russian)* 77−56022
steel wire, drawn, age hardening props. obs., mechanical and electrical props. relationship 80−50662
steel wire reinforced Al-Zn-Mg, tensile strength depend. on angle of reinforcement *(Russian)* 78−15452
steel wire rope, tensile testing, fastening method 79−87779
steel wires, drawn and annealed, tensile fatigue and tensile strength under cyclic stress *(Japanese)* 78−15507
steel/Cu bemetallic pipe, determ. of yield, tensile strength 80−25771
steel/SiO_2-Al_2O_3 glaze, adhesive behaviour of metallic cation glaze exchanged on acid site struct. *(Japanese)* 79−66216
steels, 45, Kh18N10T, and 30KhGSA, determining the relative elongation from a machine tensile curve 79−15927
steels, austenitic and type 316, neutron irradiation effect on tensile, creep-rupture, deform., fracture props. 79−65120
steels, dynamic material props. for FBR safety anal., testing devices 78−60966
steels, nitrided age-hardened, for blanking punches, chipping resist. props. *(Japanese)* 80−89340
steels, types SS41, SB42, SM50A, STK55, liq. Zn embrittlement *(Japanese)* 80−81164
steels, wide plate and V-notch bending tests evaluation on basis of materials mechanics *(German)* 80−66571
steels, with yield pt. of about 420 to 720 N/mm^2, correlation between yield pt./tensile strength ratio and toughness *(German)* 80−66615
steels 20Kh and 38Kh2N2VA, tensile testing, deform. rate effect 79−70115
stiffened panels with rectangular cut outs, stresses and deform. *(Japanese)* 79−3977
strain rate gradient development 79−46219
stress state of structural elements of vessels under external hydrostatic press. 77−14908
strip with semicircular notches, tensile load conditions at end, interf. effects obs. 80−64455
structural steel, microstruct. and brittleness, rel. to austenizing and heat treatments 77−56091
Stycast-1266, mechanical props. at low temps. 80−57286
styrene copolymer, props. rel to composition *(German)* 79−66291
styrene-butadiene-styrene block copolymer, with reinforcing resins, effect of styrene domain structure 79−83317
submarine cables, wire fracture modes and mech. props. correl. with fatigue life 78−35520
superalloy, microstructure resulting from alloying and heat treatment, effect on creep, fatigue, fracture strength 78−11246
superconductors, type II, review of mechanical behaviour and stress effects 77−86083
superplastic materials, flow and failure, review 80−50690
superplasticity, strain rate sensitivity of tensile flow curve *(German)* 77−63733
tensile stability, effect of crack and cavitation generation 77−16659
tensile test, alignment problems 77−16759
tensile test, uniaxial, for plastic deform. *(Hungarian)* 80−97657
tensile test piece, profile of contracted part after the beginning of necking *(German)* 77−86269
tensile test specimen contour, expt. and calc. comparison *(German)* 77−86233
tensile testing at const. true strain rates, test machine 79−34262
tensile/compressive strength test machine calibration *(German)* 77−77654
tension test instability *(German)* 77−52555
testing at high temp., self-locating grips design 79−52507
testing machine for up to 3000°C 79−87776
testing machine with automatic null-balancing load meas. instrument, dynamic behaviour and optimal adjustment *(German)* 77−60005
testing machine with automatic null-balancing load meas. instrument, dynamic behaviour investig. and control *(German)* 77−60006
tetrafluoroethylene-vinylidene fluoride copolymer, exporide-diphenylolpropane resin filled, viscoelastic and strength parameters 79−91730
tetraglycidyl 4,4′ diaminodiphenyl methane epoxy, diaminodiphenyl sulphone cured, struct., deform. mode, failure 79−29141
Tetron, vascular substitute, exam. of tensile fracture behaviour 78−77157
textile insulation tapes, low temp. testing, −196 to +20°C 79−61692
thermal fluctuation theory of durability of solids 77−4153
thermally sprayed coating adhesive strength testing method 79−83432
thermoplastic materials, flexure testing 77−86087
thermoplastics, 4.2-300K 77−25160
thermosetting polymers, fibre-reinforced, 4.2-300K 77−25160
Thornel 300/Fiberite 1034 graphite epoxy composite, elastic moduli, environmental effects 77−86068
Thornel 300/Fiberite 1034 graphite epoxy laminates, tensile strength, 200 to 422K, moisture effects 77−48486
thread, diameter depend. *(Russian)* 77−59852
β-III Ti alloy, powder compacted by hot swaging, tensile and toughness prop. 79−38764
β-Ti-Mo (15wt.%) metastable alloy, strength enhancement 77−66650
toluene sulphonate diacetylene polymer, vibr. modes, strain depend. using Raman spectra 80−20626
tubes, thin wall, long-time strength, steady creep conditions *(Russian)* 78−46900
tubular specimens, tensile testing with delayed necking 77−90522
two-axis tensile test machine, for static and dynamic tests *(French)* 78−15627
uniaxial tension, effect of material strain rate sensitivity and specimen heterogeneity *(Polish)* 78−84887
unidirectionally reinforced metal composite, complex torsional and tensile loading 79−61669
vertebrae, human, mech. props. 80−72206

tensile strength continued
viscoelastic material, failure and instability in tension 80−87720
viscoelastic non-Newtonian liquids, resist. to tensile stress 80−1505
VMP fibre reinforced epoxide binder, structure and strength, effect of fibrous filler tension 78−68751
VT3-1, HTMT effects on struct. and props. 78−23740
W, static deform., removal of surface layer effect on mech. props. in single crystal 79−43359
water, estimate of ultimate tensile strength 77−7779
water, free surface, metastable effects associated with press. pulse refl. 80−6463
water, tensile strength theoretical prediction 79−42131
water under tension monitoring, Berthelot-Bourdon tube method 80−88238
Weibull modulus estimation for brittle materials 79−55344
weld, heat affected zone extraction and testing of flat, microtensile specimens *(German)* 77−9017
wires in steel cables, tension measuring device and method of use *(Russian)* 80−68196
wood, stress distrib. in cell wall subject to tensile force in transverse direction *(Japanese)* 77−77539
wound healing, var. of mech. props. in different areas 78−27984
yarns, multi-filament, twisted, modified Platt's equation *(Japanese)* 80−5985
Zircaloy, annealed, neutron irradiated, inhomogeneous deform. behaviour 80−85014
Zircaloy, irradiated spent fuel cladding, annealing effects 79−89382
Zircaloy cladding, irrad., tensile props., effects of temp., strain rate and annealing 77−48463
Zircaloy-2, deformation instability and tensile elongation 77−32655
Zircaloy-2, effect of simulated fission products on elongation fractography and metallography 80−649
Zircaloy-2, effects of simulated fission products on mechanical props. 80−52740
Zircaloy-2, mech. props. after exposure to I_2-methanol solutions, SEM study 80−93689
Zircaloy-2, polycrystn., thermal history effect on tensile props. 79−74204
Zircaloy-2, polycrystn., thermal history effect on tensile props., comment 79−74205
β-Zircaloy-2, tensile creep and creep rupture props. under vacuum 78−52915
zircaloy-2 cladding tubes, post neutron irrad. ring-tensile props. prehydriding effect 77−42053
Zircaloy-4, H_2 effect on mech. props. *(Korean)* 79−70123
Zircaloy-4, load relaxation and tensile tests 79−20093
Zircaloy-4, strain rate dependent mech. response 77−21254
Zircaloy-4, strain rate sensitivity parameter measurement, from expt. load vs. time curves, superplastic range 79−8406
Zircaloy-4 spent fuel cladding, tensile props. and annealing characts. 79−22392
zirconosilicate glass fibre, effect of cement environment 77−44335
Ag, filament produced by glass coated melt spinning, mech. props. 77−86125
Ag films deposited from hot hollow-cathode source, adhesion, ion precleaning 77−8754
Ag, stacking fault energy meas. by tensile deform. of polycrystalline samples 78−95060
Ag-Cu, composite, fibre and layer structs., anomalous props. caused by internal phase boundaries 78−72754
Ag-Cu, highly deformed eutectic composite wire, anomalous props., fibre diameter and foreign atom effects *(German)* 77−36566
Ag-Cu alloy filaments, prod. by glass coated melt spinning, microstruct. and tensile strength 79−91667
Ag-Cu-Zn-(Cd)(Mn), solder, UTS, room temp. to 4.2K 79−57064
Ag-Ni, composite, fibre and layer structs., anomalous props. caused by internal phase boundaries 78−72754
Ag-Ni (10 wt.%) wire, plastically deformed, fracture struct. *(German)* 80−71744
Ag-Pd alloy, for use as wire-spring relay contact material 79−52278
Ag-Pd-Cu, contact-spring props., fatigue and spring limit *(Japanese)* 79−29117
Ag_3Sn, dental alloy, prod. by melt extraction technique, exam. of mech. props. 78−48349
Al alloy, 51S, modified by misch metal, for space appl. 80−55466
Al alloy, cast AL15V, brittle, strength in three axial stress state 79−66134
Al alloy, crack opening displacement, expt. and FEM study 78−68811
Al alloy, dispersion strengthened, made by mech. alloying 78−3136
Al alloy, mechanical properties, correlation with elect. cond. 79−34114
Al alloy, tensile test, double ligament, in deform. process 77−32753
Al alloy 2024-T3, fatigue crack propag., load interaction effects 77−56055
Al alloy 6061, thermomechanically treated elev. temp. mech. props. 79−8310
Al alloy 6061-T6, yielding of tubing under dynamic biaxial loading 80−16377
Al alloy 7001, ageing effect on hardness and tensile props. rel. to delay time till quenching 78−92286
Al alloy 7075, fracture toughness, hydrostatic press. depend., tensile ductility 78−3209
Al alloy 7075-T6, notched sheet under tensile loaded, notch tip opening/contraction, J-integral relationship *(Japanese)* 77−4840
Al alloy A356-T61, creep rupture props. 78−27612
Al alloy matrix, reinforced with fibrous and particulate nonmetals, wear, friction 77−4758
Al alloy V93, axial load, asymmetrically applied, sensitivity of strength 79−66126
Al alloy with different props. in tension and compression, creep 80−81129
Al alloy-mica particle composite, cast prep. and mech. props., bearing appl. 80−71613
Al alloys, (5083, 6061, 2219), supercond. magnets, mech. and phys. props. at 4K 80−86976
Al alloys, cryogenic, AMg5 and AMg6, mech. props. at −196°C 77−63748
Al alloys, pitting corrosion rel. to load-carrying capacity of sheets *(Russian)* 78−56806
Al alloys, stress-strain behaviour at large strains 77−52442
Al alloys, superplastic, tensile deform. behaviour *(Japanese)* 78−27558

tensile strength continued
Al, alloys, thermomechanical working effect on mech. props. *(Russian)* 77−21181
Al alloys AMg6M, AMg6, 5083, weld at cryogenic temps., mech. props. 79−66136
Al and Al alloy 5022, plastic anisotropy of textured sheet *(Japanese)* 79−34103
Al, Bauschinger effect, temp. influence, combined tension-torsion testing machine 80−45453
Al bronze, anisotropic bend ductility in single phase alloys 78−60726
Al bronze, G, Si additions, corrosion resistance 77−16714
Al, cast, strength and plasticity under hydrostatic pressure 78−56694
Al, deformed in tension, elec. cond. changes at 78 and 283K, grain boundary effect *(Japanese)* 80−30029
Al, dispersion hardening Al_4C_3 77−55978
Al, electroplastic effect 80−7647
Al foil, alloying additions (Si, Mg, Y, Se, Sc) effect, on tensile strength, weldability 80−55475
Al, oriented single crystal, plastic deform. *(Japanese)* 79−43336
Al, plane stress calc. with two dimensional elastic-plastic computer program 78−35465
Al, plastic props., room temp. to recrystallisation temp., stress/strain relations, computer program 77−1865
Al, plastic strain in tension, effect of strain rate 77−32654
Al, polycrystalline, deform. sub-struct., effect on tensile props. *(Japanese)* 78−11279
Al polycrystalline, exoelectron emission under tensile deform. and fracture *(Japanese)* 77−55870
Al sheet alloy, type 2036-T4, in-plane deformation, correlation with Hill's theory 79−83260
Al single crystals, liq. metal embrittlement by Ga, tensile tests 80−7675
Al single crystals, relation between axial orientation rotating and deform. banding 80−104206
Al single crysts., elastoplasticity, dislocation model, work hardening, tensile tests, stress/strain curves *(Japanese)* 77−52410
Al, stability and strength of FCC metal using Morse pot. 80−59430
Al, strength changes on US treatment in programmed loading *(Russian)* 77−32583
Al, tensile curve and specific value of anisotropy coefficient *(French)* 77−28867
Al, tensile flow stress at room temp., grain size and strain effect 77−77528
Al, ultimate tensile strength for brief impact 80−70309
Al/Cu laminates, vapour deposited, strength enhancement 79−24576
Al/Mg soldered samples, UTS and fracture surface comp., 20 to 500°C 79−38941
Al-Ag, nonhomogeneity of deform. 78−84888
Al-Al_3Ni, aligned, eutectic alloy, mech. behaviour at high strain rates 78−39855
Al-Al_3Ni directionally solidified eutectic alloy, struct. and mech. props. *(Korean)* 80−29944
Al-Al_4C_3, dispersion hardened physical props. meas. *(German)* 78−31415
Al-alloys, biaxial prestrain influence on tensile props. 80−30036
Al-C, dispersion hardened, effect of processing parameters on mech. props. 80−20826
Al-Ca-Zn (5,5 wt.%) superplastic sheet alloy, mechanical properties, superplastic forming behaviour 80−60920
Al-Cr (3 to 11 at.%), cooling rate effect on solidification struct. and mech. props. *(Japanese)* 78−39755
Al-Cu, single and two phase, superplastic behaviour 80−11709
Al-Cu (2.6 wt.%), sheets, effect of strain path changes on formability 79−43347
Al-Cu alloy, press-forming under coexisting state of liquid and solid, mech. props. 77−81240
Al-Cu-Mg, tube drawing, tensile forces, plastic deformation *(French)* 79−70130
Al-Cu-Mg alloy, extruded, press forming in liquid/solid coexisting state, mech. props., Mg effects 78−11151
Al-Cu-Mg type 2036, thermomech. treatment, flow stress anal., effect in mech. props. 80−93584
Al-Cu-Mg/mica particulate composite mech. props. 80−100919
Al-Cu-Mg-Mn-Fe-Si, alloy D16, effect of mechanisothermal treatment on mech. props. 78−56674
Al-Cu-Mg-Zn, Mg and Zn addition effects on dendrite struct. and mech. props. *(Korean)* 77−28796
Al-Cu-Mn-Mg-Fe-Si-Zn alloy D16, surface layers chem. composition rel. to fatigue resist., corrosion-fatigue resist. 79−29275
Al-$CuAl_2$, directionally solidified eutectic alloy, effect of heat treatment 77−55977
Al-$CuAl_2$, directionally solidified eutectic, structural changes during strength tests *(Russian)* 80−7543
Al-$CuAl_2$ aligned, fracture, effect of growth speed, orientation, environment 77−28907
Al-Cu(Ag), tensile ductility, effect of ageing and impact velocity *(Japanese)* 78−15465
Al-Cu(0-10 wt.%) sintered compacts, mech. props. rel. to sintering 80−76210
Al-$Fe_{78}Mo_2B_{20}$ wire composite, mech. props. 80−40441
Al-graphite particulate composite, exam. of friction, wear and tensile props. 78−72890
Al-Mg (7 wt.%), β-phase soln. behaviour and mech. props. *(Korean)* 78−11277
Al-Mg alloy AMg6, deform. in plane stress at low temps. 78−39873
Al-Mg_2Si (0.95 wt.%), excess Si effect on ductility 78−27580
Al-Mg-Cr, tube drawing, tensile forces, plastic deformation *(French)* 79−70130
Al-Mg-Cu-Si-Cr (1,2.7,0.6,0.2wt.%), laser shock hardening of weld zones 78−39800
Al-Mg-Mn alloy AMG-6M, endurance determ. by dimensionless damageability curves 79−96141
Al-Mg-Mn-Cr (4, 0.45, 0.15 wt.%), laser shock hardening of weld zones, exam. 78−39800
Al-Mg-Si, type 6061-T6, 6063-T6, effective stress range factor in fatigue 80−100924
Al-Mg-Si alloys, cast, precip.-rich zones on grain boundaries, soln. heat treatment conditions effect on mech. props. 80−104176
Al-Mg-Si-Cu, tube drawing, tensile forces, plastic deformation *(French)* 79−70130
Al-Mn, splat cooling and heat treatment effect on struct. and props. *(Russian)* 77−48456

tensile strength continued
Al-Mn alloys, study of solidification by rapid cooling *(Japanese)* 78−88459
Al-Mn profiled alloy components pulled from melt, physicomech. props. 78−3175
Al-Ni (6 wt.%), fine-grained, deform. in tension and torsion 80−85008
Al-Ni-Co(Si), directionally solidified eutectic, morphological and mech. props. *(Russian)* 80−30057
Al-rare earth alloys, granules, rolling to form foil, exam. 80−20825
Al-Si casting alloys, graphite-dispersed, mech. props. and wear resist. 77−4857
Al-Si eutectic, directionally solidified, tensile props. 78−64531
Al-Si eutectic alloy, hardness rel. to tensile and compressive strength 79−52354
Al-Si-Mg alloys, Si content and Mg addition effect on mech. props., Na treatment *(Korean)* 79−38901
Al-Si-Zn alloy, creep rates, pre-torsional deformation effect 79−96096
Al-Zn, nonhomogeneity of deform. 78−84888
Al-Zn (22 wt.%), superplastic strain rate sensitivity, rel. to ductility 78−31478
Al-Zn alloy, flow stress, Zn content effect 79−38913
Al-Zn alloy, type 7010, die-forged, tensile props. after heat treatment, stress corrosion 79−66103
Al-Zn-Mg, duplex ageing effect on tensile props. 79−91721
Al-Zn-Mg, plastic instability rel. to grain boundary failure at low temps. 78−56702
Al-Zn-Mg, type V-95, ultimate tensile strength for brief impact 80−70309
Al-Zn-Mg (4.5, 2.5 wt.%), composition effect on stress corrosion and mech. behaviour 78−27684
Al-Zn-Mg (6,1.5%), influence of ageing and cold work on tensile and fracture props. *(Japanese)* 78−52842
Al-Zn-Mg alloy, Ag addition and pre-precipitation treatment, influence on GP zone growth 80−71658
Al-Zn-Mg alloy V95, two-stage ageing kinetics, mech. props. effects 79−83238
Al-Zn-Mg plasma sputtered, mech. props. rel. to heat treatment *(Russian)* 80−40387
Al-Zn-Mg-Cu, age hardened, effect of strain rate, temp. and environment on ductility 80−45368
Al-Zn-Mg-Cu, optimum treatment combination for thermochemical processing 77−44278
Al-Zn-Mg-Cu alloys, heat treatment optimisation 80−60888
Al-Zn-Mg(3.2, 2.2 wt.%), deform. strengthened by Guinier Preston zones 77−52343
Al-Zn-Ti(Mn), mech. props., Ti or Mn addition effect *(Korean)* 80−93613
AlB_2 flake reinforced composites, prep., props. rel. to aspect ratio, book contrib. 78−48366
Al_2O_3, ceramic Sinoksal, strength variation dependence on type of loading and temperature 79−57080
α-Al_2O_3 fibre FP, manufacture, strength and modulus 80−81013
α-Al_2O_3 fibre FP reinforced Al and Mg composites, fabrication and props. 80−81004
Al_2O_3, polycrystalline, fracture probability under static bending and tensile loading at 800°C *(German)* 78−23806
Al_2O_3, unflawed polycryst., tensile failure, SEM and acoustic emission expts. 78−27598
Al_2O_3/Al soldered samples, UTS and fracture surface comp., 20 to 500°C 79−38941
Al_2O_3-Cu composite, dispersion-strengthened, hardness, tensile strength and struct. 77−70063
B fibre, prep. by closed CVD system, mech. props. and surface defects 79−52311
B fibre reinforced Al, fracture toughness 77−70157
B fibre reinforced Al, impact behaviour under fatigue 80−7661
B fibre reinforced Al, tensile and compressive strength, prior thermal treatment effect 78−11264
B fibre reinforced Al, tensile strength and brittle fracture 80−11707
B fibre reinforced Al, thermal degradation of tensile strength, due to fibre strength degradation 78−39861
B fibre reinforced Al, X-ray investigation of internal stresses *(Russian)* 77−73290
B fibre reinforced Al composite, strength of fibre-matrix interface and tensile strength *(Russian)* 80−21005
B fibre reinforced Al-Mg, heat treatment effect on struct., tensile strength 80−55487
B fibre reinforced epoxy, tensile anal. of edge notch 77−70159
B fibre reinforced epoxy and Al, cryogenic tensile, compressive and shear props. 78−6983
B fibre reinforced epoxy composites, notched, tensile strength and failure modes 80−81205
B fibres, surface morphologies rel. to mech. props. 80−11749
B fibres of various diameters, tensile strength, elasticity, elongation 78−3189
B filament, uncoated and SiC coated, high temp. physicomech. props. 79−20140
B thin wires, fatigue limit and tensile strength 80−25834
B-epoxy-Al sandwich laminate. influence of residual stresses on tensile strength 78−60703
B_4C fibres, yarn prep. from C fibres, mech., chem. props., struct., book contrib. 78−48365
BN fibres, prep., struct., thermal, mech. and elec. props., appls., book contrib. 78−48360
BaF_2:Y^{3+},Gd^{3+} production and mech. props. 79−72638
$BaFe_{12}O_{19}$, effect of impurity concentrations, and sintering conditions on grain size *(German)* 79−23630
$BaTiO_3$, ferroelec. ceramic, mech. strength, for single crysts. and Ca and Co modified specimens 78−64332
Be bronze, struct. and props. after ageing under load 78−84932
Be fibre reinforced Ti-Al-V (6.4 wt.%), synthesis and mech. props. 77−32544
Be, hot-extruded, fracture in impact, static tensile and fatigue tests *(Russian)* 77−52458
Be, low oxide, isostatically pressed block, factors affecting tensile strength, elongation, impact resistance 77−16610
Be, neutron irradiated, annealed, tensile props. and swelling, effect of He bubbles 78−22765
Be, sintered, physicomech. props. anisotropy, BeO inclusions effect 80−60804

tensile strength continued
Be-bronze BrB2, struct. and phase transform. during mechano-thermal treatment *(Russian)* 80−11667
α-brass, serrated yielding, tensile tests and TEM obs. 79−34110
β-epoxy composite, intermittently bonded, water and ice effects 77−12685
C fabric reinforced plastic laminates, tensile and compressive strength determ., 20-1500°C 80−100880
C fibre, high temp. obs. 79−20139
C fibre, Ni coated, high-temp. compatibility 78−19829
C fibre, physicomechanical props. stability, tensile strength versus fibre cross section 77−52387
C fibre, structural and mech. charact. 77−28737
C fibre, tensile strength, heat treatment and flaw effects 80−81173
C fibre composite, aligned, prep. and theoretical strength agreement 80−84906
C fibre derived from mesophase-pitch, Young's modulus and tensile strength, struct. flow elimination 80−80995
C fibre reinforced Al, formed by ion plating and vacuum hot pressing 78−11165
C fibre reinforced composite, unidirectional model for longit. tensile strength prediction 78−95778
C fibre reinforced composites for spacecraft use, prep., props. and struct. 80−71625
C fibre reinforced Cu, electrodeposited, tensile strength *(Japanese)* 79−43333
C fibre reinforced epoxy, fatigue strength 78−15495
C fibre reinforced epoxy, wound, strength in twisting, stretching and transverse bending 80−11622
C fibre reinforced epoxy and C fibre, elastic moduli 77−86069
C fibre reinforced epoxy phenol plastic, resistance to interlayer shear and elec. resistivity 78−68752
C fibre reinforced phenol resin, karbovoloknits, improving transverse tensile, interlaminar shear and compressive strengths 79−87691
C fibre reinforced plastic, laminate, non Hookean behaviour in fibre direction, effect of fibre waviness on tensile props. 78−19804
C fibre reinforced plastics, angle ply specimen, calc. of strength and elastic response 79−20108
C fibre reinforced plastic, tensile testing using ring specimens *(Japanese)* 79−29148
C fibre reinforced plastic, stress analysis of butt strap joint 79−43300
C fibre reinforced polymer, strength props., fibre surface treatment effects 78−27636
C fibre structure, recent advances 80−81069
C fibre-Kevlar 49 fibre epoxy laminate, impact props. 78−44164
C fibre-Mg matrix interaction, strength changes on heating 78−11164
C fibres, Al coated, effect of annealing on ultimate tensile strength and fracture 78−56744
C fibres, durability, elastic props. and struct., heat treatment temp. effect, US meas. methods 80−40446
C fibres, from mesophase pitch, resist. magnetoresist., EPR and mech. props. rel to struct. 79−78116
C fibres, from mesophase pitch, tensile strengths, Weibull parameters SEM study 79−79031
C fibres, oxidation by NO_2, struct., props. modification 78−44237
C fibres and C fibre reinforced epoxy phenol, oxidation, effect on props. 80−40574
C fibres with large breaking strain, prep., mech. props., struct., appl. 78−44077
C glass fibre hybrid plastics, review of mech. props 79−20107
C steel, bending, effect of strain rate on dynamic stress factors 77−56046
C, vitreous, oxidation effects up to 2500K 80−3209
C-fibre reinforced epoxy resin, laminated structs. mech. props. 80−50672
CU-Zr-(Cr), powder metallurgical alloys, thermomech. treatment effect on props. 80−50660
CaO-MgO-Al_2O_3-SiO_2, glass ceramic, prep. by hot pressing and crystallisation, mech. props. 78−15351
β-$Ca_3(PO_4)_2$, synthesis and fabrication, prosthetic appl. 79−24479
$Ca_{10}(PO_4)_6(OH)_2$, synthesis and characterisation in dense polycryst. form 77−4749
Cd, warm rolled, texture and grain size depend. of tensile props. 80−71720
Cd-Ge broken lamellar eutectic composite, tensile and compressive props. 80−71694
Co, influence of FCC phase retained at room temp. on mech. props. 79−47677
Co-Al-Nb, monovariant directionally solidified eutectics, struct. and mech. props. *(Russian)* 78−92254
Co-base superalloy, machine thixocast, mech. prop. deficiencies 79−74244
Co-Cr-Ni-TaC, directionally solidified eutectic, mech. props. and sruct., thermal cycling effects *(Russian)* 78−92282
Co-Cr(VC)((Ti,V)C)-(Al), eutectic alloy, unidirectional solidification, oxidation and tensile tests 78−52790
Co-Fe amorphous alloys, high permeability props. *(Japanese)* 77−51927
Co-Mo-B metallic glass ribbons, tensile strength, crystn. temp. 80−89173
Co-Mo-Cr-Si, plasma and detonation coatings, Laves- and carbide-strengthened, comparative props. 78−15562
Co-Ni-Cr (20,20 wt.%), internal oxidation, improvement of mech. props. *(French)* 77−16521
Co-Ni-Cr-Mo, mech. props., effect of twinning and FCC to HCP transform. 77−4779
Co-W-Cr (15,20 wt.%), surgical implant ion beam textured, stress/strain relations, fatigue charact. 78−73297
Co-WC dispersion hardened alloy, tensile deform., volume fraction of second phase effect, simulation *(Japanese)* 79−70122
Cr-Fe, with Si and Ta additions, metallurgical and mechanical characterisation *(Italian)* 77−66674
Cr-Ni-W(-Mo), heat resistant weld seam metal, tensile strength, thermophysical charact. 79−91769
Cu clad steel, bond strength through intermediate Zn layer *(Korean)* 79−66213
Cu, cold rolled sheet, anisotropy of elastic and strength props. 80−81077
Cu, cold worked, grain size effects on short-term strength *(Russian)* 78−56693
Cu, crystalline FCC, theoretical tensile strength, three separate first-principles calcs. 80−50683
Cu, deform. instability and tensile elongation 77−32655
Cu, deform. of ⟨100⟩ single crystal *(Japanese)* 77−59864

tensile strength continued
Cu, diffusion welding, tensile fracture strength *(Japanese)* 80−7663
Cu, filament produced by glass-coated melt spinning, tensile strength 77−48508
Cu high purity, grain boundaries as dislocation sources in premacroyield strain region 79−34096
Cu, high purity crystal, resistivity changes with deform., subsequent recovery 77−52397
Cu, low-temperature testing, −196°C to +20°C 79−61692
Cu, on thermally oxidised Si, EM tensile adhesion test method 80−50804
Cu, plastic deformation, steady state, transients due to strain rate changes 77−81302
Cu, plastic props., room temp. to recrystallisation temp., stress/strain relations, computer program 77−1865
Cu powder compacts sintering, depend. of neck form. on particle size and sintering temp. 79−28988
Cu, recrystallised, inhomogeneous deform. due to texture changes *(German)* 79−29158
Cu single cryst., drawing, deform. band form., tensile strength meas. *(Japanese)* 78−76710
Cu single cryst., drawing deform. band form., axial orientation force meas., X-ray pole figure determ. *(Japanese)* 78−76710
Cu, stress-strain behaviour over large strain range 79−15745
Cu, tensile curve and specific value of anisotropy coefficient *(French)* 77−28867
Cu, tension deformed single crystal, dynamic recrystallisation 79−47716
Cu, theoretical strength 80−104229
Cu, thin interlayer between high-strength alloy rods *(Russian)* 78−19821
Cu, whiskers, hardening during uniaxial extension, preliminary torsion deform. *(Russian)* 78−15420
Cu wire, electroplastic drawing X-ray diffr. anal. and mech. props. exam. *(Russian)* 79−29138
Cu wire rod, rolling temp. effects 77−70084
Cu-Al, internally oxidised, structural, elec. and mech. charact. 78−60761
Cu-Al (10 wt.%), annealed, tensile fatigue strength at high temp. in vacuum *(Japanese)* 78−35493
Cu-Al (10 wt.%) alloy, water-quenched, tensile fatigue strength at high temp. in vacuo *(Japanese)* 78−72837
Cu-Al (11.6 wt.%), mech. props., tempering temps. effects 78−76669
Cu-Al (15 at.%), single crystal, steady state deform. with ⟨001⟩ axis at high temp. *(Japanese)* 78−6980
Cu-Al (2.5 at.%), single crystal, steady state deform. at high temps. *(Japanese)* 77−52415
Cu-Al (7.5 at.%), single crystal, etched under load, slip bands 77−89446
Cu-Al composite, simulation of tensile behaviour and fracture void initiation *(Japanese)* 78−52948
Cu-Al solid soln., internally oxidised, mech. props. *(Japanese)* 77−52411
Cu-Al_2O_3, dispersion-strengthened, vapour-deposited, tensile creep 78−11115
Cu-Al_2O_3 dispersed system, electron beam evaporated thick film, struct./prop. relations 77−44198
Cu-Al_2O_3 extruded bars, strength anisotropy 77−16597
Cu-$Al_2O_3(SiO_2)$ dispersion hardening single crystal, cyclic deform. *(French)* 79−1893
Cu-Al-Fe, mech. props. rel. to heat treatment 80−50682
Cu-Al-Fe, strength increase from intermediate annealing determ. of annealing temp. by recrystallisation 78−44136
Cu-Al-Fe (11, 2 and 1 wt.%), Fe effects on microstruct. and mech. props. *(Korean)* 77−28807
Cu-Al-Ni, phase diagram associated with stress induced martensitic transform. 79−8272
Cu-Al-Si, Si effect on mech. props. and microstructure *(Korean)* 79−38903
Cu-based alloys, deposition condition relationship with struct. and props. 78−11369
Cu-Be (2 at.%), plastic deform. and dislocation substruct. 80−76307
Cu-Be-Co (2,0.3 wt.%) alloy, heat treatment, influence of tempering on hardness, tensile props. transform diagram *(French)* 78−31384
Cu-BeCo (1.85, 0.29 wt.%), type CA172 (TH04), strengthened by spinodal decomp., stress relax. in bending 80−7616
Cu-Fe, composite, fibre and layer structs., anomalous props. caused by internal phase boundaries 78−72754
Cu-Fe, composite, simulation of tensile behaviour and fracture void initiation *(Japanese)* 78−52948
Cu-$Fe_{78}Mo_2B_{20}$ wire composite, mech. props. 80−40441
Cu-Ge-La, Cu+Misch metal, eutectic alloy, internally oxidised, mech props. *(Japanese)* 77−52411
Cu-In, undirectionally transformed, mechanical props. 78−48492
Cu-Mn (3 to 20 at.%), high temp. steady state tensile deform. *(Japanese)* 78−52917
Cu-Nb multifilamentary composites, in situ formed, anomalous strength increase 79−43323
Cu-Nb multifilamentary composite, in situ formed, high temp. tensile strength 79−61602
Cu-Nb_3Sn, in situ formed multifilamentary composite, supercond. and mech. props. 78−39279
Cu-Nb-Sn, multifilamentary supercond. composite wires, fabrication on laboratory scale and mech. props. 80−29897
Cu-Ni cast alloy, effect of alloying and residual elements 78−85033
Cu-Ni diffusion couple, diffusion bonding process, fracture surface exam. *(German)* 77−35762
Cu-Ni-Cr (28, 2.8 wt.%), spinodal alloy, microstruct. and tensile props. 78−39858
Cu-Ni-Sn (4-15, 4-8 wt.%), strip strengthened by spinodal decomp., stress relax. in bending 80−7616
Cu-Ni-Sn spinodal substitute for Be-Cu alloy 80−35217
Cu-Ni-Zn, microduplex, superplastic deform., cavitation and fracture 78−64640
Cu-Si, stacking fault energy meas. by tensile deform. of polycrystalline samples 78−95060
Cu-$ThO_2(ZrO_2)$ alloys, dispersion hardened, electrical cond. and mech. props. 78−44133
Cu-Ti (Zr), strength improvement by thermomechanical treatment *(Japanese)* 78−48426
Cu-Zn-Be, precipitation hardening 77−16599
$Cu_{46}Zr_{54}$, devitrification effect on mech. props. 80−30082
tensile strength continued
$Cu_{56}Zr_{44}$ metallic glass, devitrification and its effect on mech. props. 80−33893
$(Fe,Ni,Co)_3V$, long-range ordered alloy for fusion reactor appl. 80−32481
Fe alloy MA-956E, oxide dispersion strengthened sheet, tensile and creep props. at 1365K 78−48470
Fe and alloys, softening effect *(French)* 77−63875
Fe and Fe alloys, fast neutron irradiated at high temps., mech. props. 79−51157
Fe and Fe-Cr, flow stress, effect of cathodic, H_2 charging *(Japanese)* 79−52313
Fe, appl. of KUR LINAC to radiation damage studies 78−71760
Fe, Armco, strength, fracture, effect of H_2 *(Russian)* 77−25129
Fe, Armco, struct. and mech. props., effect of hydrostatic extrusion *(Russian)* 77−56022
Fe atomised powder, sintering effect on recrystn., mech. props. 80−40292
Fe, cast, fracture mech. and fractography *(Japanese)* 78−7031
Fe, cast, grey, brittle, strength in three axial stress state 79−66134
Fe, cast, grey, tensile strength, surface area to volume ratio effect *(Japanese)* 80−45389
Fe, cast, mech. props., effect of repeated heating and cooling *(Japanese)* 77−59907
Fe, cast, spheroidal graphite, graphite size effect on mech. props. *(Korean)* 78−11278
Fe, cast, spheroidal graphite effects of Si and C on mechanical props. *(Korean)* 79−66114
Fe, cast, spheroidal graphite, degree of normalization effect on mech. props. *(Korean)* 79−87664
Fe, cast, tensile strength, Al addition effects *(Korean)* 80−71736
Fe, cast, thermal treatment influence on mechanical props. *(German)* 80−29980
Fe, cast flake and nodular, rupture strength, circumferential notch *(Japanese)* 80−93649
Fe, cast strength and plasticity under hydrostatic pressure 78−56694
Fe, cast with spherical graphite, SiC-Q apparatus for tensile strength meas. *(German)* 80−76450
α-Fe, cold rolled, hydrostatic press. effect on microstructural changes during creep 78−39871
Fe, commercial, deformability, containing H_2 77−90411
Fe, commercially pure, viscoelasticity under transformational superplasticity *(Japanese)* 77−52416
Fe, creep, effect of H_2 on struct. 77−16652
Fe, filament produced by glass-coated melt spinning, tensile strength 77−48508
Fe, grey cast, tensile testing of mechanical props., from room temp. to liquidus *(Japanese)* 80−7728
Fe, H_2 effect on yield 78−15474
α-Fe, high temp. deform. and substruct. *(Japanese)* 77−21226
Fe, intergranular brittleness, effect of O and S 77−36650
Fe, irradiation softening in single crystal, temp. and orientation depend. 77−86113
Fe, lattice hardening and anomalous softening caused by electrolytic H_2 charging *(Japanese)* 79−43398
Fe, low temperature deform., strain-rate cycling and stress relaxation tests *(Japanese)* 78−52876
Fe, plastic deform. of single crystal with shear tests in {110}⟨111⟩ and {112}⟨111⟩ slip system 77−48509
Fe, polycryst. whisker, microstruct. SEM and TEM 77−39755
Fe powder, ZhGr1.0, optimisation of heat treatment in salt bath 77−28756
Fe, powder forged, impact and fatigue strengths, slag inclusion effects 77−21271
Fe, powder preforms., hot consolidated rolled strip, mech. props. 78−15338
Fe, pure, mech. props. at low temps. 78−44219
Fe, pure, tensile deform., sources of acoustic emission 78−19814
Fe, sintered, fracture behaviour, microscopic obs. 79−47771
Fe, sintered, strength and elongation, rel. to density 80−30047
Fe, sintered and pressed, props., effect of atomised Fe powder particle size distrib. 80−11601
Fe static loading over wide deform. and temp. range, acoustic emission, plastic flow, fracture 77−90424
Fe, tensile strength and cyclic tensile fatigue strength at high temp. in vacuum, BCC and FCC phases *(Japanese)* 79−100251
Fe, whisker, H_2 effect on deform. 78−68755
Fe/zinc stearate, compacts, admixing, effect on mech. props. 80−45402
Fe-Al (0.069 and 0.158 wt.%), internally oxidised, low temp. deform. *(Japanese)* 78−52876
Fe-Al-(Nb), fatigue deform. 77−44350
Fe-B alloy reinforced polysulphone exam. of tensile and flexure props. 78−72823
Fe-B(-Si) alloy filaments produced by glass-coated melt spinning 80−76213
Fe-C, dil. alloys, softening, conventional and in situ expt. 79−47744
Fe-C, dilute alloys, softening, conventional and in situ expt., HVEM obs. 79−47743
Fe-C, softening of high purity Fe, by C, due to double kink nucleation *(French)* 78−84949
Fe-C-Mn (0.5, 0.6 wt.%), powder forged, mech. props. 80−21096
Fe-C-Ni-Cr(Cu), dynamically hot pressed, mech. props., additives effect 78−60620
Fe-C(0.001 to 0.44 wt.%), C effect on low temp. brittleness *(Japanese)* 80−50711
Fe-Co, damping capacity of Gentalloy, internal friction meas., mech. and mag. depend. *(Japanese)* 78−52875
Fe-Co (5 to 25 wt.%), exam. of damping capacity of Gentalloy 78−72800
Fe-Co heterogeneous alloys, fabrication by powder metallurgy, tensile strength 77−63600
Fe-Co-V(-Ni), annealing effect on microstruct. rel. to mag. and mech. props. 80−89267
Fe-Cr-Al (7, 5 wt.%), expt. stainless alloys, phys. and mech. props. 80−97637
Fe-Cr-Al-Ti-Y_2O_3 (20, 4.5, 0.5, 0.5) type MA956, strain rate effect on fracture behaviour at 1366K 80−16458
Fe-Cr-Al-Y (Y-Al_2O_3)(Y_2O_3), preparation and exam. of mech. props. 78−52720
Fe-Cr-Mn (11.5, 3 wt.%), microduplex ferritic-martensitic steel, exam. 78−39862

tensile strength continued
Fe-Cr-Mo sintered, damping capacity and mech. props. 78−44161
Fe-Cr-Ni, two-phase ($\alpha+\gamma$), and metastable austenitic, uniform elongation peak 77−77547
Fe-Cr-Ni (18,14 wt.%), γ to ε to α martensitic transform., external stress effect, double tensile deform. exam. 80−108438
Fe-Cu, precipitation hardening of α-Fe containing weak and strong particles 80−20946
Fe-Cu-Ti, improvement of irradiation-enhanced Cu embrittlement by Ti addition 79−43393
Fe-Mn-Cr-C (20, 4, 0.5 wt.%), hyperquenched and predeformed, mech. props. *(French)* 78−23786
Fe-Mn-Ni-V-C (0.5, 3.0, 1.0, 0.2 wt.%), austenite decomp., isothermal transform. characts. 80−97477
Fe-Mn-V-C (0.5, 1.0, 0.2 wt.%), austenite decomp., isothermal transform. characts. 80−97477
Fe-Mo, damping capacity 77−86082
Fe-Mo, damping capacity *(Japanese)* 78−11259
Fe-Mo (3 wt.%), substitutional solid soln. with cubic faced symmetry, Portevin-Le Chatelier effect *(French)* 78−23785
Fe-Mo-B metallic glass ribbons, tensile strength, crystn. temp. 80−89173
Fe-Mo-Ta, ternary Laves phase strengthening 80−108466
Fe-N, neutron irrad. effects on mech. props. 79−4338
Fe-Ni, fracture toughness at cryogenic temp. 78−72878
Fe-Ni base metallic glass, annealing embrittlement 78−64635
Fe-Ni-Al-(Cu) (12, 0.5, 0.5 to 3 wt.%), Cu addition strengthening at 77K, mech. props. 80−60875
Fe-Ni-Al(Ti)(V)(Nb), cryogenic toughness, strength, rel. to reactive metal addition 78−39885
Fe-Ni-Al(2.5, 7.5 at.%), fracture surface morphology, ageing temp. effects 77−16600
Fe-Ni-C, ausformed, ductility of martensite *(Japanese)* 77−48490
Fe-Ni-C, martensitic, mech. charact., effect of ageing and tempering *(Slovak)* 78−19791
Fe-Ni-C (21, 0.6 wt.%), stress assited and strain induced martensite morphologies 78−3187
Fe-Ni-C (31, 0.1 wt.%), pre-deformation and temp. effect on transformation-deformation behaviour 80−3127
Fe-Ni-C (9, 0.1 wt.%), effect of intercritical tempering on impact energy, exam. of mech. props. 78−52861
Fe-Ni-C alloy, austenitic, pre-deform. effects on TRIP *(Japanese)* 77−8890
Fe-Ni-Cr (23, 5 wt.%), martensite orientation formed under uniaxial stress alloy [001] 77−77475
Fe-Ni-Cr (35, 15 wt.%) superalloy, stress rupture and tensile props., C and B additions effect *(Chinese)* 80−104244
Fe-Ni-Cr-Si, superalloy, Cr and Si effect on mech. props. and microstruct. *(Chinese)* 79−100207
Fe-Ni-Cr-Ti, superalloy A286, powder, exam. of microstruct. and mech. properties 78−52979
Fe-Ni-Cr-Ti-Al, Ti and Al effect on microstruct. and mech. props. *(Chinese)* 79−74130
Fe-Ni-Cr-Ti-Mn-Mo, (25.8, 14.04, 2.17, 1.27, 1.30 wt.%), superalloy A-286, precipitation hardening, exam. of fracture toughness and mech. props. 78−92355
Fe-Ni-Mn, martensite, aged, grain boundary embrittlement 79−96144
Fe-Ni-Mo, ferrite plus martensite structures, exam. of mech. props. 78−56709
Fe-Ni-Mo alloy, high-strength ferritic, for cryogenic service, mech. characteris. 77−70143
Fe-Ni-Ti-(Cu) (12, 0.25, 2 wt.%), Cu addition strengthening at 77K, mech. props. 80−60875
Fe-Ni-V-C alloy, reverse α to γ transformation, previous deformation influence on struct. and props. *(Russian)* 79−100139
Fe-Ni-V-(Cu) (12, 2, 2 wt.%), Cu addition strengthening at 77K, mech. props. 80−60875
Fe-Ni-(Cu) (12, 0.5 to 3 wt.%), Cu addition strengthening at 77K, mech. props. 80−60875
Fe-Ni(Mn)-Al-C, form. of ductile Ni_3Al by split quenching, mech. props. 79−100197
α-Fe-P, static strain ageing 77−70079
Fe-Si, crack propag. kinetics, effect of current pulses 78−31531
Fe-Si (3 wt.%), Goss oriented, stress effects 78−91916
Fe-Si (3 wt.%), grain oriented, lowest core loss 78−91887
Fe-Si (3 wt.%), yielding phenomena at high temp. *(Japanese)* 77−48489
Fe-Si (3wt.%), notched sheet under tensile loading, notch tip opening/contraction, J-integral relationship *(Japanese)* 77−4840
Fe-Si (6.5 wt.%), Ni, Al and Mn additions effect on mech. and mag. props. 77−12667
Fe-Ti, precipitation hardening of α-Fe containing weak and strong particles 80−20946
Fe-TiB_2, eutectic alloy, high temp. props. 78−84931
Fe-Ti(Nb), internally nitrided, mech. props. 77−44307
Fe-W system, damping capacity of Gentalloy, internal friction, mech. and mag. props. 79−77679
Fe-W-Cr-Mo-Co with austenitic phase, magnetic and mech. props., cold working and ageing effects *(Japanese)* 78−60678
FeNi-Cu, composite fibre and layer structs., anomalous props. caused by internal phase boundaries 78−72754
$Fe_{29}Ni_{49}P_{14}B_6Si_{12}$, Metglas fibre reinforced mortar, fracture props. 79−70159
$Fe_{80}P_{16}C_3B_1$ amorphous filament, produced by glass coated melt spinning, mech. props. 78−15483
GeTe, stoichiometry deviations influence on mech. props., 25-500°C 80−103410
^4He, superfluid, tensile strength and visible US cavitation 77−7920
KH_2PO_4, filiform crystals at low temp., tensile strength determ. 80−100877
Li_2O-SiO_2-P_2O_5 glass ceramic fibres, heat treatment, crystn., tensile strength 80−84995
Mg, plastic anisotropy of extruded bars *(German)* 77−86126
Mg-Al single crystal growth, specimen for tensile testing in corrosive medium *(Russian)* 80−20774
Mg-Al-Zn (3, 1 wt.%), alloy AZ31, mech. props. of extruded and welded pipe and sheet, optical microscopy exam. 79−34065
Mg-Ce, workability, aging characts. and tensile strength 80−55416
Mg-La, workability, aging characts. and tensile strength 80−55416
Mg-Sm, phase diagram and mech. props. *(Russian)* 80−20892
Mg-Y-Nd-Zn-Zr (2,2,0.3, 0.7 wt.%), heat treatment effect on casting dimensional stability, alloy mech. props. 78−44146

tensile strength continued
Mg-Zn-Zr, cast, exam. of phase composition, mech. props. 79−100217
Mg-Zn-Zr rare earth alloy, mech. props., effect of microshrinkage during solidifaction 79−43234
MgF_2, single cryst., tensile strength and yield point, temp. depend. 77−14785
MgO, filamentary crysts., synthesis and props. 77−52267
MgO, filamentary crysts., mech. props. 77−52402
Mn-Ni-Ti (Zr) systems, and mech. props. thermal expansion for different heat treatments *(Japanese)* 79−29123
Mn-Ni-Ti(Zr), non-ferromagnetic Elinvar-type alloys 79−24566
Mo alloy, precipitation hardened, yield stress in tension and compression, SD-effect *(Ukrainian)* 77−56021
Mo alloy MT, strain hardening depend. on temp. and structural state *(Russian)* 79−91664
Mo and Mo alloy TZM, solid-state bonding, tensile strength of bond *(German)* 79−47756
Mo, C doped sheet, electron beam welded, low temp. ductility 79−87685
Mo, electron beam melted with C additions, mech. props. *(Japanese)* 77 48449
Mo, exam. of H_2 embrittlement mechanisms, effect on mech. props. 78−39891
Mo fibre reinforced Ni-Cr, effect of fibre coatings on composite strength 78−56710
Mo, high purity single crystal doped with C, low temp. mech. props. 77−77544
Mo, mech. props., influence of temp. on singularities of deform. *(Russian)* 78−6970
Mo, neutron irradiated, radiation softening and hardening 80−34083
Mo, polycrystalline, fracture and ductile-brittle transition, hydrostatic press. effects 78−60735
Mo powder, influence of powder reduction processes on props. 80−89175
Mo, strengthening by vacuum-deposited W film *(Russian)* 77−66714
Mo, surface oxide softening in single crystals 78−95860
Mo-C-Zr (0.03, 0.17 wt.%), thermal treatment effect on yield drop 77−90382
Mo-C-Zr-B (0.004, 0.12, 0.002 wt.%) effect of grain size, cellular dislocation structure, on mech. props. *(Russian)* 79−34105
Mo-Hf-C, superior powder metallurgy die alloys for isothermal forging mech. props. 79−74201
Mo-Ti-Zr (0.5, 0.7 wt.%) alloy TZM, props. and appl. *(German)* 80−21040
Mo-Ti-Zr alloys TZM and TZC, superior powder metallurgy die alloys for isothermal forging mech. props. 79−74201
$NH_4H_2PO_4$, filiform crystals at low temp., tensile strength determ. 80−100877
NaCl whiskers, plastification in elec. field *(Russian)* 80−21010
Na_2O-B_2O_3-SiO_2 glass fibre, plastic-coated, liq. N_2 strength 80−58707
Na_2O-CaO-SiO_2, glass, surface indentation effect on mech. strength, and thermal stress resistance 78−48463
Na_2O-CaO-SiO_2, proof testing 80−108654
Nb, effect of electron irradiation on low temp. deform., tensile stress-strain curves 79−55784
Nb, H_2 embrittlement, macroscopic behaviour at low temps. 77−32665
Nb, He implanted tensile specimens, TEM 77−51398
Nb, radiation damage from 16 MeV protons, effect on microstruct. and mech. props. 79−46721
Nb, stress differential in surface oxide softening of single crystals 77−86116
Nb wire, neutron irrad., tensile props. 79−70077
Nb:He, mech. props. and microstruct. 80−85003
Nb-Ti(Zr), type II superconductor, mech. behaviour and stress effects 77−86083
Nb-W-Mo-Zr-C(5,2,1,0.02 wt.%) alloy 5 BMTs, short-time tensile strength in liquid Bi and Li *(Russian)* 77−25186
Nb-Y, and Nb, mech. props., neutron irrad. and Y scavenging effects 77−90394
Nb-Zr-C, (1, 0.1 wt.%) alloy, mech. characts. structral sensitivity in strained state *(Russian)* 79−52301
Nb-ZrN alloy, high temp. hardness and short duration tensile strength *(Russian)* 77−44266
Nb_3Sn, filamentary, fatigue tests on small coils 78−64652
Nb_3Sn film, electron beam codeposited, growth morphology and tensile props. 78−10301
Nb_3Sn multifilamentary conductor production and testing 79−32809
Nb_3Sn superconducting wires, in situ multifilamentary, mech. props. 79−47746
Nb_3Sn superconductors, mech. behaviour, diffusion *(German)* 78−39880
Ni 200, static strain ageing, 373 to 473K 77−36558
Ni alloy, heat resistant, fatigue limit comparison in torsion and tension-compression 80−81181
Ni alloys, damping, logarithmic decrement meas. by torsion pendulum *(German)* 79−74195
Ni and FCC Ni-Fe, H_2 embrittlement *(Japanese)* 77−48526
Ni base alloys EhI607A and EhI929VD, fatigue strength, temp. depend. 79−15791
Ni films, adhesion on graphite 80−80141
Ni, Ni-Ti (1 wt.%), serrated yielding, 77 to 723K 77−32649
Ni, oxide dispersion strengthened, creep and tensile props. 77−86042
Ni, oxide dispersion strengthened materials, effect of prior creep at 1365K on room temp. tensile props. 78−39857
Ni powders, stereological appl. in study of compacting process, elec. and mech. props. *(French)* 80−40286
Ni, radiation damage from 16 MeV protons, effect on microstruct. and mech. props. 79−46721
Ni, shock loaded, work softening 78−27537
Ni/Ni_3Al-Ni_3Nb, directionally solidified lamellar eutectic alloy, deform. anisotropy and fracture 77−36604
Ni-Al (14 at.%), two stage ageing effect on spatial distrib. of γ'-phase particles *(Russian)* 78−39805
Ni-Al-Cr, precipitation-strengthened, mechanical props. 78−84968
γ/γ-Ni-Al-Nb, aligned eutectic alloy, H_2 embrittlement 77−8951
Ni-Cr, ERNiCr-3 weld metal, strain-rate effects on high temp. behaviour 79−93726
Ni-Cr, high temp. thermomech. treatment effect on tensile diagrams of KhN77TYuR *(Russian)* 80−60884
Ni-Cr alloy (20 wt.%), on steel, plasma-sprayed coating 79−96222
Ni-Cr alloys EHI437B and VZh98, tension tests in high speed gaseous streams 77−63761
Ni-Cr machine steel, austenite grain size effects on mech. props. *(Russian)* 77−44292

tensile strength continued
Ni-Cr-Al (20, 4 wt.%), tensile stress effect on high temp. oxidation *(Japanese)* 80−89393
Ni-Cr-Al sintered alloy, hot vac. pressure, fracture and mech. charact. 80−66667
Ni-Cr-Co alloys, relax. resist. exam. by bending and tension 79−24564
Ni-Cr-Co superalloy, σ-phase effect on mech. props. *(Chinese)* 79−74229
Ni-Cr-HfO_2, dispersion-strengthened, hot rolling effects on props. *(Russian)* 77−59797
Ni-Cr-Mn-Fe-Nb (20,3,3,2.5 wt.%), short-range order effects on tensile behaviour 80−25793
Ni-Cr-Ta-Ti-Si, EP557 precipitation hardening alloy, mech. props., heat treatment effect 80−60877
Ni-Cr-Ti-Al-Fe-Co (19.65, 2.40, 1.37, 0.78, 0.52 wt.%), strength of γ′ hardened alloy, ageing exam. 78−88501
Ni-Cr-W (20, 10 to 40 wt.%), phase composition, struct. and props. 80−21034
Ni-Cr-W-Mo-Al-Ti (15,6,3,2,2, wt.%), wrought, Si effect on transition brittleness *(Chinese)* 80−55491
Ni-Cr-(Al), oxide dispersion strengthened, creep and tensile props. 77−86042
Ni-Cr-(Al), oxide dispersion strengthened materials, effect of prior creep at 1365K on room temp. tensile props. 78−39857
Ni-Fe-Cr base superalloy, addition effect on mech. props. *(Chinese)* 80−20998
Ni-Mo-B metallic glass ribbons, tensile strength, crystn. temp. 80−89173
Ni-Mo-Cr-Si, plasma and detonation coatings, Laves- and carbide-strengthened, comparative props. 78−15562
Ni-Nb-Al, eutectic, thermal cycling effect on strength and ductility *(Russian)* 79−24601
Ni-Nb-Al (21,2.5 wt.%), eutectic aligned alloy, mech. behaviour at high strain rates 78−39855
Ni-Nb-Al-(Cr), eutectic, mech. props., high press. H_2 effects 77−63779
Ni-NbC eutectic, microstructure and strength depend. on composition and crystallisation conditions *(Russian)* 79−100128
Ni-Pd-P amorphous alloys, tensile deform. 77−32646
Ni-SiO_2 composite film, influence of hardening phase on yield stress *(Russian)* 79−5001
Ni-TaC, eutectic alloy, fibre reinforced, directionally solidified, anisotropic yielding behaviour 79−11675
Ni-Ti mech. memory alloys, tensile props. *(Korean)* 77−63724
Ni-W (45.5 wt.%), eutectic, mech. props., high press. H_2 effects 77−63779
Ni_3Al, ductility, tensile and compressive tests *(Japanese)* 77−52414
Ni_3Al, ductility in poly- and single crystals, compressive and tensile tests 78−56715
Ni_3Al, overshooting while testing in tension 78−44189
Ni_3Al-B, $L1_2$ type intermetallic cpd. room temp. ductility improvement by B addition *(Japanese)* 80−35263
$Ni_{36}Fe_{32}Cr_{14}P_{12}B_6$ metallic glass, mech. props. and thermal stability 80−76362
Ni_3Ge single crystals, orientation and temp. depend. of flow stress 79−5008
PVC-Cu, particulate composite, mech. props. effect of particle size 78−95799
Pb-Sb battery grids, ageing behaviour obs., effects of casting and cooling 79−100517
Pb-Sb-Te-Cu-Sn, influence of specimen and grain size on mech. props. *(Russian)* 77−81297
Pb-Sn, with brass insert, tensile flow and fracture 78−11290
Pb-Sn (62 wt.%), intercrystalline and interface boundary sliding, tensile tests, SEM obs. 79−38886
Pb-Sn-Ca alloy sheet, continuously cast, for battery grids, ageing behaviour 77−16603
$PbTiO_3$, ferroelec. ceramic, mech. strength 78−64332
$Pb(Zr,Ti)O_3$, ferroelec. ceramic, mech. strength 78−64332
Pd mechanical props., effect of H diffusion 79−65138
Pd-Cd eutectic, unidirectionally solidified, tensile and compressive props. 78−27567
Pd-H, mech. props., influence of dissolved H_2 *(Russian)* 80−81109
Pd-Si-Sb, mostly crystalline, rapidly quenched, mech. props. 79−61610
$Pd_{77.5}Cu_6Si_{16.5}$, cold drawn wires, surface markings, fracture stresses 79−56997
$Pd_{80}Si_{20}$, shear band form. 78−68756
Pt-Ni (42 wt.%) relationship between mag. saturation flux and tensile strength 79−15819
Pt-Rh-W (30, 8 wt.%), intergranular embrittlement by Se vapour 80−3185
α-Pu and δ-stabilised Pu-Ga alloy, strain rate effect on tensile props. 77−21284
$239PuO_2$, stoichiometric, high-temp. deformation 80−81111
Sc, strength and plasticity 77−90429
Si, stretched, lattice vibr. anharmonicity, influence of stress on elastic moduli, Raman spectra 80−80791
Si-Al, composite, simulation of tensile behaviour and fracture void initiation *(Japanese)* 78−52948
SiC coated B fibre Al-V-Ti, tensile and compressive strength, prior thermal treatment effect 78−11264
SiC, continuous fibre synthesis with high tensile strength and Young's modulus 79−15633
SiC continuous fibres, mech. props. depend. on testing conditions *(Russian)* 80−35297
SiC fibre reinforced Al-Si alloy, liq. phase process prep. effect on mech. props. 79−70020
SiC fibre reinforced Al-Mg, heat treatment effect on struct., tensile strength 80−55487
SiC fibre reinforced Al, synthesis by liquid pressing method 80−100816
SiC fibres, continuous, tensile strengths and Young's moduli, 600-1400°C 77−59885
SiC, tensile strength distrib. 80−40471
SiC-coated C fibre, compatibility with Al *(Japanese)* 80−71700
Si_3N_4, reaction bonded, bending strength meas., influence of loading conditions, proof testing and anal. methods *(German)* 78−31451
Si_3N_4, tensile strength distrib. 80−40471
Si_3N_4-MgO (2-5 wt.%) hot pressed, tensile creep testing 80−40423
Si_3N_4-SiC-Y_2O_3 (La_2O_3)(Ce_2O_3)(Eu_2O_3)(Gd_2O_3), reactively sintered, microstruct. and strength 80−25631
SiO_2, coated silica fibres, tensile strengths of 1 km lengths 78−1384
SiO_2 fibre lightguides, fused, zero stress strength reduction and transitions in static fatigue 80−87523
tensile strength continued
SiO_2 fibres, fused, load-elongation curves, elastic hysteresis, tensile testing machine 79−1891
SiO_2 fibres, reductions in static fatigue by hermetic jacketing with Al 79−43448
SiO_2 glass fibre, plastic-coated, liq. N_2 strength 80−58707
SiO_2, laser drawn fibers, tension rel. to drawing vel. and ultimate strength 78−74986
SiO_2, optical fibre, tensile strength distrib. and gauge length extrapolation 78−9434
$SiO_2B_2O_3$-K_2O-Al_2O_3-As_2O_3 glass fibres containing metallic granules, tensile strength, Young's modulus, DC conductivity 80−30023
Sn plate, rapid test for props. assessment 80−40650
Sn-Pb (38 wt.%), graphite fibre reinforced, effect of interface on fracture characts. 78−76723
steel, C, castability, in metal mould, mechanical props. *(Japanese)* 80−25681
steels, Cr-C-Mn(Ni), struct. prop. rel., design of struct. steels for high strength and toughness 80−97491
strengthened by lattice transformations, mech. props. study *(Japanese)* 79−43332
Ta, evidence for slow strain-rate embrittlement due to O_2, SEM study 79−79109
Ta, film, CVD on silica, struct. and mech. props. 77−24965
Ta single crystal, H_2 embrittlement *(Japanese)* 80−66636
Ti alloy, creep and long-term strength under cyclic loading 78−3191
Ti alloy, heat resistance, thermal stability, stress-rupture strength, and creep 80−81194
Ti alloy, microstruct. and mech. props., room and elevated temps. 77−36554
Ti alloy, microstructure resulting from heat treatment, alloying, effect on creep, fatigue, fracture strength 78−11246
Ti alloy, VT16, decomp. of α″ martensite during continuous heating *(Russian)* 78−48370
Ti alloy, VT23, ht. treatment effects on fracture *(Russian)* 78−80623
Ti alloy, VT3-1 mech. props. and low-temp. creep 77−44314
Ti alloy A-75, plastic instability in sheet deformed in uniaxial tension at 300 to 700K 79−47742
Ti alloy β III, precipitation of α and ω phase, evolution of mech. props. *(French)* 77−16591
Ti alloy RMI 38644, shock loaded, residual strength 78−27574
Ti alloy US meas., correlation with ductility and fracture detection 78−31601
Ti alloy VT20, phase composition and structure effect on mech. props. 79−38958
Ti alloys, AT3 and AT6, tensile props. prolonged oxidation effects 78−85050
Ti alloys, correl. with hardness 79−87707
Ti alloys, data handbook of low temp. mech. and phys. props. 80−22153
Ti alloys, heat-resistant, mech. props., alloying addition effects *(Russian)* 77−59861
α-βTi alloys, high strength, heat-treated weldments, intergranular fracture 80−21097
Ti alloys fracture toughness-mech. props. interrelations 77−86154
Ti alloys with eutectoid-forming elements, mech. props. 77−44313
Ti base alloys, melt-extracted polycryst., mech. props. 80−76360
Ti, high purity, data handbook of low temp. mech. and phys. props. 80−22153
Ti, high strength unsupported membrane fabrication 77−66589
Ti, IMI-125, strain rate effect on mech. behaviour 80−3153
Ti, mechanical props. and appls. 79−66104
Ti, plastic anisotropy of extruded bars *(German)* 77−86126
Ti, type 70A, containing 0-6000 ppm ^3He, sensitivity of tensile props. 80−39197
Ti-Al (14 at.%), with precipitate free zones, tensile props., grain size effects 77−16690
Ti-Al (4 wt.%), sintered, long-time strength 80−40529
Ti-Al-Cr-Mo-Fe(V)(Zr), effect of structure and heat treatment on tensile strength, ductility, fatigue limit and notch sensitivity 78−56711
Ti-Al-Mo alloy VT-14, spherical pressure vessel, correlation between fracture stresses and mech. laboratory characts. 80−25838
Ti-Al-Mo-Cr (4.5, 5, 1.5 wt.%), CORONA-5, effect of microstructure and heat treatment on fracture 78−60805
Ti-Al-Mo-Cr (4.5, 5, 1.5 wt.%), weld metal, α/β interace sliding 80−108512
Ti-Al-Mo-Zr, type VT-9, creep eqns. rel. to extension and compression props. 80−100875
Ti-Al-Sn (5, 2.5 wt.%) alloy, fatigue under combined alternating bending and torsional stresses 77−8923
Ti-Al-V, containing 0-6000 ppm ^3He, sensitivity of tensile props. 80−39197
Ti-Al-V (6, 4 wt.%), hot isostatically pressed casting, fatigue crack initiation 79−79078
Ti-Al-V (6, 4 wt.%), solution treatment temp. effect on fracture morphology 79−61620
Ti-Al-V (6, 4 wt.%) effect of high temp. oxidation on eddy current conductivity 78−76770
Ti-Al-V (6,4 wt.%), α/β interface phase influence on tensile props. 80−30034
Ti-Al-V (6,4 wt.%), strongly textured, influence of crystallographic orientation on tensile behaviour 80−7633
Ti-Al-V (6,4 wt.%), surgical implant ion beam textured, stress/strain relations, fatigue characts. 78−73297
Ti-Al-V (6,4 wt.%), to H effect on fracture props. and microstruct. 80−40512
Ti-Al-V (6.4 wt.%) cast alloy, with improved microstruct., mech. props. *(Japanese)* 80−71701
Ti-Al-V-Cr-Mo-Zr (3,8,6,4,4 wt.%), beta-C, microstruct. effect on mech. props. 78−27577
Ti-Al-V-Sn(Mo-Fe), heavy section extrusion, fabrication and mech. props. 78−6985
Ti-Al-Zr (3,3 wt.%), W alloying addition effects on mech. props. *(Russian)* 77−59860
Ti-Cu-Al(Zr)(Sn)(Nb)(Mo), heat treatable alloys, effect of alloying on strength, tensile props. 78−56671
Ti-Mo, fracture behaviour and tensile props. at elev. temp. 78−60822
Ti-Ni-Fe, plasticity, tensile stress-strain diagrams, ultimate tensile strength, elec. resist. depend. on temp. *(Russian)* 79−61652
Ti-Pd (0.15 wt.%), IMI-260, strain rate effect on mech. behaviour 80−3153
Ti-TiO_2-ZrO_2-Mo, sintered struct. and mech. props. 78−60618

tensile strength continued
Ti-V-Fe-Al (10, 2, 3 wt.%), fracture toughness and stress corrosion resistance 80−100904
Ti-V-Si, Si effects on precipitation and strengthening 77−55970
α-Ti-Zr-W, effect of W impurity on mech. preps. 80−16392
$Ti_{50}Be_{40}Zr_{10}$ glass, mech. props., X-ray diffr. exam. 78−11292
TiC coating on C fibre, by CVD TiC coated C fibre compatibility with Al *(Japanese)* 79−78898
TiNi-TiCu, exam. of shape memory effect, specific work 79−100216
U-Mo (1.5 wt.%), superplastic behaviour 450 to 720°C *(French)* 79−74203
U-Mo(2 wt.%), mech. props., effect of ageing 77−8914
U-Ti(0.75 wt.%), mech. props., effect of ageing 77−8914
U_3Si, tensile ductility from 25 to 320°C 79−74225
V,V-Zr (2 wt.%), internally oxidised, neutron irradiated, annealing effect on mech. props., elec. cond. and electron microscope obs. *(Japanese)* 79−15701
V and V-Mo, mechanical properties, O, N_2 and C addition effects 79−52356
V, hydrogenated, grain size depend. of tensile strength 77−36657
V, polycrystalline, strength, ductility, 4.2 to 400K, O_2 effect 77−36529
V-Fe (5.0 at.%), work softening at elevated temps. *(Japanese)* 77−52347
V-H, H effect on fatigue crack propag. 78−48516
V-H, H effect on tensile props. at moderate temps. *(Japanese)* 78−19831
V-Mo, effect of ion plated Mo on corrosion in liquid Na, mech. props. 78−53020
V-Nb-Mo(Cr), corrosion in liquid Na, O_2 effects 77−8987
V-Nb-Ti-N alloy, dispersion hardened, fracture characts. 79−15794
V-Ti (20wt.%), corrosion in liquid Na, O_2 effects 77−8987
W alloys, deformed, vacuum technology appl., mech. props. *(German)* 79−57046
W fibre, KSiAl doped, recrystallisation, Li diffusion effects, hardness, strength, microstructure meas. *(German)* 78−64644
W fibre reinforced Cu composites, correl. between thermal cycling-induced microstructural changes at interphase boundaries and tensile behaviour *(Japanese)* 80−71674
W fibre reinforced epoxy composite, static tensile behaviour *(Japanese)* 78−15482
W fibre reinforced Ni composites, high temp. tensile and creep props. 77−52444
W, metal-ceramic, mech. props. and structural nonuniformity 79−15705
W, sintered, brittle fracture, statistical anal. 80−11744
W sintered rods, hot rolling with four roll passes, effect on struct. and mech. props. 79−100195
W, strength, temp. depend. 77−1871
W, surface oxide softening in single crystals 78−95860
W wire from rolled rods, mech. props. and struct. 80−25743
W, with different microstructs., temp. depend. of yield strength 80−16404
W, with impurities, grain boundaries, effect on high temp. plasticity *(Russian)* 79−79057
W-C(0.01 to 0.2 wt.%), C effect on high temp. strength 77−16614
W-Ni-Fe (5(2), 5(2) wt.%) pore formation, effect on mech. props. 80−45396
W-Re, thin wires, fatigue limit and tensile strength 80−25834
W-reinforced Ni and Ni-Fe, fabrication, heat treatment, and mag. and mech. props. 77−40408
WC-Co, size factor effect on strength in complex stressed state 78−31483
$YH_{1.92}$, tensile strength and creep 80−55459
YH_x, mech. props. 77−44333
α-Zircaloy, strain ageing at 1000K 79−47725
Zircaloy-2, effect of simulated fission products on mech. props. 80−73922
Zircaloy-4, deformation behaviour between 77 and 900K 80−71686
Zn, compatible bicrystal, plastic deform. *(Japanese)* 78−31460
Zn, die pressed powder, green strength 77−59876
Zn, oriented polycrystals, tensile behaviour under hydrostatic press. *(Japanese)* 77−52417
Zn, plastic anisotropy of extruded bars *(German)* 77−86126
Zn-Al (10,22,50wt.%), low temp. mech. props. plastic deformation, glissile dislocation nucleation *(Russian)* 80−11695
Zn-Al (22 at.%), heat treatment and straining effect on fracture and corrosion 79−87672
Zn-Al-Cu (18, 4 wt.%), plastic deform. at room temp., superplastic props., tensile strength *(Czech)* 80−45360
Zn-Al-Cu casting alloys, mech. props. and dendritic morphology, Al content effect *(Korean)* 80−93612
Zn-Al(Cu), mech. and technological props. *(Polish)* 80−89286
Zr alloys, acoustic emission during tensile testing 77−90433
Zr and Zircaloy-4, tensile props., room temp. to 900K 77−70104
Zr, crept single crystal, nature of γ-hydride 77−21147
Zr, deformed at 77K, effect of fast-neutron irradiation on deformation twinning, TEM and optical microscopy obs. 79−37741
Zr, neutron irradiated, twinning deformation 79−14848
α-Zr, strain ageing at 1000K 79−47725
Zr TA6V6E2, tensile and toughness props. after isothermal quenching and continuous cooling *(French)* 77−59833
Zr-Al (8.0 wt.%), tensile props. and fracture toughness after fast neutron irradiation 80−3198
Zr-Al (8.6 wt.%), dimensional stability struct. and mech. props, effects of neutron irrad. 80−92563
Zr-Al (8.6 wt.%), neutron irradiation effect on tensile props., swelling 77−7768
Zr-Al(8.6 wt.%), mech. props., corrosion and fast neutron irrad. influence 78−84948
Zr-CR (1.9 wt.%), β-quenched and tempered, tensile props. rel. to tempered conditions, SEM study 79−66109
Zr-H, tensile strength and creep 80−55459
Zr-Nb (1 wt.%), tensile props., 295 to 773K 79−8318
Zr-Nb(2.5 wt.%), tensile props., strain rate and temp. effects 77−73307
Zr-Ru(Pd), heat treated, mech. props. and struct. 78−80571
Zr_3Al, cold worked, annealing effects 77−36535
Zr_3Al, hyperperitectoid, tensile strength, effect of fast neutron irrad. 77−52408
Zr_3Al, neutron irrad. effect on tensile props. 80−3156
Zr_3Al, ordered polycrystals, ductile fracture 78−64641
Zr_3Al, tensile props., surface preparation depend. 80−3155
ZrH_x, mech. props. 77−44333

tensimeters *see vapour pressure measurement*

tensors
almost contact manifold, generalised S-curvature like tensor field 80−36909
anisotropic media, piezomagnetoelectric effects 80−25174
associative algebra of tensor fields, duality and Dirac identities 79−71618
asymptotic eigensolutions of fourth and sixth rank octahedral tensor operators 79−93975
atom, coherent transients, spherical tensor treatment 79−26940
bi-recurrent Finsler space, basic props. 80−12958
bulk dispersion coefficient in bounded skewed shear flow, tensor form 78−73393
C*-algebras, tensor products 77−17764
Clebsch-Gordan coefficient, general expressions for group SO_5 77−13636
Clifford algebra and Dirac matrices in a tensor formulation *(Russian)* 80−12966
complex electron configurations, quasispin method, mixing configurations 80−42953
condensed matter, phys. props. description using irreducible tensors 79−2627
conformal invariant 2- and 3-point functions for tensor fields with arbitrary spin 78−49977
conformal space-time group, invariant tensors for maximal subgroups 79−85239
conharmonic curvature tensor, Kahler space 78−54146
Coulomb problem, symm. technique appls. 77−45731
crystal nonlinear electroacoustics, dynamical eqns. and constitutive relations 79−56734
crystal physics, multivector analysis, comparison with tensor algebra 80−100195
crystal physics, multivector analysis, comparison with vector anal. 80−100196
crystal rotational symmetry, and tensor props., 1-, 2- and 4-fold principal symmetry, trigonal, and hexagonal groups 80−100193
crystal rotational symmetry, and tensor props., method for group $3(3_z)$ 80−100192
crystal tensor components, unitary groups appl., and phase transition selection principles 79−46589
deformation function, construction for anisotropic medium 79−98633
dielectric tensor field determ. in weakly inhomogeneous anisotropic media 79−72492
differential geometry of deformed crystals 80−19867
differential geometry of phase transformations in solids 78−67805
divergence free tensor densities in 3-space 80−103
divergence free tensors, struct., Einstein field eqns. 79−17293
dynamic elasticity, tensor spherical harmonics appl. to Navier eqn. 80−98296
Einstein's field equations, Hilbert's metrical matter tensor, generalisation 78−21040
Einstein linearized tensor, massive spin two fields 78−36890
Einstein tensor in scalar curvature Finsler spaces 80−77655
elastic wave theory, phase velocity of longitudinal impact wave in solid elastic bar *(Japanese)* 77−72228
elasticity tensors of fourth order 79−97202
elastodynamic equations of motion 77−42766
elastodynamic Green's tensor for the 2D half-space 79−68581
electro-optical fourth-order effect, calc. of sixth-rank tensor 79−24291
EM beam self-focusing in semiconductor 79−18488
EM field energy-momentum tensor in phenomenological electrodynamics *(Czech)* 80−27146
EM transmission structures, relativistic foundation and network formalisms 80−58446
EM wave propagation, in moving anisotropic media, double ray refraction *(Russian)* 79−18329
EM waves in dispersive media, energy-momentum tensors 78−17842
energy momentum tensor, nominal source of the Kruskal metric 80−12956
energy-momentum tensor vac. expectation values, depend. on manifold geom. and topology 80−355
etergy-momentum tensors, characterization in gravitational field eqns. 79−88846
extended supergravity, SO_2 model, minimal set of auxiliary fields 79−58608
failure analysis of damage zone in laminates 80−85059
Feynman diagrams, dimensionally regularised, symbolic evaluation, quantum gravity application 80−13259
field dependent, solid state physics appl. 78−31055
fields, generalisation of theorem 78−49645
fluid Cosserat eqn., couple stree-tensor, associated with friction 79−7366
fractional-parentage coefficients, reduced in quasi-spin space, submatrix elements of tensor operators 80−4578
gauge-covariant conformal transformations 79−12946
general relativity, anisotropic interior soln. of Kerr metric tensor 79−63104
general relativity, EM polarisation tensors, calc. by Fokker's method *(French)* 78−24695
general relativity, spatial tensor anal. 78−93571
geodesic corrections to stochastic parallel displacement of tensors 80−8920
geodesy, telluroid definition and distortion tensor 78−65171
globally hyperbolic spacetimes, conformal deform., Ricci curvature and energy condition 79−9159
grade n material, tensor of effective elastic moduli 79−10473
gravitation scalar-tensor theory, plane-symmetry solns. 78−70035
gravitational field equations of fourth order and supersymmetry 79−12674
gravitational radiation and invariants of curvature tensor in general relativity 78−57836
Green's tensor for two elastic half-spaces with different moduli and frictionless sliding *(German)* 78−62083
Green tensor expansions for harmonic vector wave eqn. in spheroidal coord. systems 78−41171
Hilbert spaces, Gleason measures on infinite tensor product 77−26200
holonomic formulation of boundary layer eqns., use of tensors 79−1153
homothetic Killing trajectories, stationary limit surface geometry 79−40424
ionosphere, tensor conductivity 77−13172
irreducible isotropic tensors of rank six, complete set 80−91419
irreducible tensor operator methods in strong-field coupling 79−7811

tensors continued
Killing tensors, symmetric and skew symmetric 78−93573
Killing tensors and Killing-Yano tensors 77−33926
Laplace equations for binary star, partial separability Roche coordinates 79−44524
left Cauchy-Green tensor history, viscoelastic fluid theories 80−4534
Lie algebras, semi-simple, tensor operators and charact. identities 79−35956
ligand fields calcs., strong and intermediate fields, tensor algebra 80−42922
liquid-solid phase transition, dynamic Ginzburg-Landau theory 80−44292
magnetic point groups, simplified calc. and tabulation of tensorial covariants belonging to same Laue class 79−19174
many-body diagrams, tensor notation 77−57274
many-electron atom, tensorial props. of operators in quasi-spin space 80−42925
metric tensor components interpretation, astrophys. implications 78−93097
molecular energy level clustering, qualitative theory of irreducible tensor operators spectra 80−28001
molecular IR intensities of fundamental bands, polar tensor calcs. 79−13708
molecular light scattering, spherical tensor approach 79−72372
molecular rotationally inelastic collisions, tensorial factorisation 80−28096
molecular vibr. in solid hydrates, electric field gradient tensors at deuterons 77−71792
molecule, nuclear site symm. and nuclear mag. shielding in a uniform elec. field 79−41116
naked singularity in scalar-tensor gravit. theory 79−8826
non-linear model, constitutive equation testing with free. vol. relax. spectrum 80−6011
nonlinear viscoelastic media constitutive eqn. 78−81839
optical tensor operators, symm. props. 77−52033
photographic process, reaction tensor analytical treatment *(German)* 79−83481
plasticity, field theory, integral presentations of second-rank tensors 80−69690
plasticity problem soln. by symbolic computer processing of formulae 80−17803
polyatomic fluids, nonsymmetric pressure tensor 79−75350
polynomial irreducible tensors, generating functions 78−49633
polynomial tensors for double point groups 79−40681
quartz resonator, large mag. field effect on rate of time 80−27195
recurrence conditions in space-time, Riemann, Ricci and Weyl tensors 77−17883
reduced matrix elements for L-S coupled, N-electron configurations, tensor operators 79−13625
Riemann curvature tensor, expressed as third-order potential tensor with symmetry props. *(Italian)* 79−49129
Riemann curvature tensor and closed geodesic paths, for teachers 78−24600
Riemann spaces, conformal correspondence tensor *(Russian)* 77−53814
Riemannian manifold, harmonic forms of curvature type *(French)* 78−86124
Riemannian manifolds, separability structures, Killing 2-tensors 78−45470
S-PRF_n-space of first kind 79−17294
s-recurrent Finsler space, tensor field props. 80−12959
second order symm. tensors in compact Riemannian manifold, compatibility and orthogonal decomp. 77−57161
seismic sources moment tensors, discontinuous displacements 77−2110
spectral tensors $\Phi_{ij}(K, t)$ and $t_{ij}(K, t)$ for homogeneous turbulent field, direct modelling *(French)* 78−90813
spherical harmonics and multipoles in Euclidean space 77−2515
spherical harmonics on S^2 and S^3 as eigenvalue problems 79−17324
spherical tensors, cubic normal components *(French)* 77−41452
spin system, ABC type, matrix elements of tensor operators calc., transition probability matrix 80−25182
steady-state creep determ. eqns., microscopic stability restrictions *(Russian)* 79−10493
stellar magnetic configurations linear oscills., unrestricted second-order tensor virial eqns. 79−44461
strength-surface tensor components, determ. for anisotropic materials 79−98603
stress energy tensor symmetries, Einstein's equations, nonuniqueness of solutions 80−12953
stress tensors and creep-strain rates correl., correl. for isotropic stable media 80−87722
SU(5), Clebsch-Gordan series, quark model appl. 80−47256
superenergy tensors and supertensors 77−30081
supergravity, supersymmetric generalisation of differential geometry tensors 78−45546
surfaces with metric and curvature tensors 79−71252
symplectic groups, explicit decomp. of tensor products 79−17191
tensor harmonics in the helicity basis 79−49080
tensorial covariants for the 32 crystal point groups 79−19173
thermodynamics, irreversible, tensorial formulation of internal covariable theory, endochronic time spectrum 77−61036
twistors and multipole moments 78−16705
unified gauge field theory with torsion, symmetries 78−89386
vector multiplet coupled to supergravity, tensor calculus 78−86214
Warm nonuniform plasma, stress tensor for high freq. wave propag. 80−33764
wave mechanics, reciprocal mass tensor 79−12635
Weyl tensor in gravitational field, vector fields and ideal reference frames 80−36918
Wightman fields, algebra of test functions 77−18186

terbium
see also nuclei with .....
anisotropy energy in basal plane, temp. dependence 78−2673
atom, L-shell internal excitation accompanying L-capture 80−95726
atom, photoabsorpt. spectra 77−88417
conduction electron polarisation and high field magnetisation 78−72332
critical magnetic studies 80−15745
de Haas-van Alphen effect 77−15747
doped La-Al(Ag)(Sn)(Pb) superconductors, cryst. field transitions linewidths 80−24854

terbium continued
elastic constants, in paramag. temp. range, magnetoelastic contrib. 77−4538
elastic constants, magnetoelastic contrib. 80−15777
elastic constants, third order, and thermal expansion 77−80569
elastic modulus meas. using CdS US transducer, mag. field effect 77−11151
electrical resistivity, high-precision meas., 1-4K 77−15817
electroluminescence activator in La_2O_3, Y_2O_3, Y_2O_2S, comparison 77−20927
electron energy loss spectrum and surface electron states 77−85860
electron irradiated, defect annealing, recovery spectra 79−23648
electron-magnon interaction and elec. resist., 1.5 to 50K 79−60790
ferromagnet, field depend. of elastic const. c_{66} 80−15181
ferromagnetic, mag. dipole and elec. quadrupole hyperfine fields, NMR obs. 80−34791
ferromagnetic, spin wave resist., 1.5-50K 79−60813
ferromagnetic domain structures down to 95K 80−71080
ferromagnetic domains obs. by cryogenic X-ray topography 77−39507
film, GHz magnetoelastic wave excitation, field depend. 78−52334
film, O_2 and H_2 contamination effect on elec. resist. 77−80856
film, thermoreflectance dispersion curves at 315K and 97K 80−7332
film and powder, nuclear echo signals, crystal anisotropy consts. *(Russian)* 79−99790
fluoride, MF_2:Tb^{3+}, (M=Ba,Ca,Cd), far IR Stark and Zeeman splitting 77−48190
germanate glass: Tb^{3+}, luminesc. props. 79−33798
glass:Tb^{3+}, polarised, luminesc. 78−48224
glycerol-D_2O:Tb^{3+}, Nd^{3+} soln. and frozen glass, energy transfer 78−60509
high-pressure phase, mag. field effects *(Russian)* 77−66021
impurities in fluorophosphate glasses, magneto-opt. characts. 80−64126
impurity in metallic host, exchange interaction, electrical resistivity 80−84453
lanthanum ethyl sulphate nonahydrate: Tb^{3+}, ESR spectrum, spin lattice relax., effect of hydrostatic compression 78−88185
lattice dynamics, microscopic theory 77−43292
lattice dynamics, phonon freqs., calc. 80−15206
lattice dynamics of rare-earth HCP metals 77−7805
liquid, mag. susceptibility, elec. resistivity 80−20377
magnetic anisotropy energy, basal plane, meas. at low temps. 77−63166
magnetic characteristics in strong magnetic field 77−89936
magnetic domains, Lorentz microscopy obs. 78−84448
magnetic flux conc. in supercond. solenoids 78−49869
magnetic phase diagram, US meas. of elastic const. 80−15721
magnetisation, AC susceptibility and microwave absorption meas. 80−60221
magnetisation in basal plane, calc. 80−70969
magnetisation intensity in antiferromag. state and mag. field induced phase transforms. *(Russian)* 80−65811
magnetocaloric effect in high magnetic fields 80−25140
magnetocrystalline anisotropy, perturbation theory 78−2675
magnetoresistance, anisotropic electron spin wave scatt. 77−15831
magnon lifetimes at 4.2K 80−15710
metastable high-pressure phase, conversion into stable phase 77−55357
microcontact magnon spectra, electron-magnon interaction *(Russian)* 80−54768
neutron elastic scattering, high-angle, anal. 80−80480
particles, disappearance of mag. order, mag. susceptibility and magnetisation meas. 77−16117
phonon spectrum, obs. of one phonon transitions by nucl. reson. fluoresc. 79−38416
phosphate glass:Ce^{3+},Tm^{3+}(Tb^{3+}), temp. depend. of energy transfer $Ce^{3+}\rightarrow Tm^{3+}$, $Ce^{3+}\rightarrow Tb^{3+}$ 77−24882
phosphate glass:Tb^{3+}, luminesc. props. 79−33798
point defect production during electron irrad. at low temp. 80−49273
rare earth oxysulphide, R_2O_2S:Tb^{3+}, branching ratios for fluoresc. 79−33807
rare earth pentaphosphates:Ce^{3+},Tb^{3+}, energy transfer between dopants, excitation spectra, laser appls. 78−10961
silicate glass:Tb^{3+}, photoluminesc. and optical absorption spectra 79−19919
silicide thin film formation on (100) and (111)Si substrate, backscattering study 80−70542
single crystal flux concentrator for supercond. solenoids 78−57991
specific heat, using lattice dynamical model for HCP metals 79−51273
spin wave exam. 78−56306
spin wave theory in strongly anisotropic magnets 77−63151
structural transition, press. induced X-ray obs. 77−59113
surface ionisation on W (110) 79−87142
thermoelectric power anisotropy at high temp. 79−23952
transport props., anisotropy, high temp. obs. 78−26843
transverse magnetoresistance in single cryst. 77−66154
vapour, SiC cryst. growth from soln. in Si, temp. gradient method 78−35301
X-ray diffraction obs. of magnetostriction and phase transitions 77−73068
X-ray L_{III} absorption discontinuity, bidirectional orbital interpretation 77−16423
BaF_2:Tb^{3+}, cubic Tb^{3+} centres, energy level and cryst. field parameters 77−52181
BaF_2:Tb^{3+}, thermally, stimulated polarisation currents, 80 to 400K 79−51900
BaR_2O_4:Eu^{3+}-Tb^{3+}, luminesc. 77−52156
$BaTbO_3$:Tb^{4+}, perowskite struct., EPR, cryst. field parameters determ. *(Italian)* 78−52350
$Bi_2Al_4O_9$:Tb^{3+}, luminesc. expts. 80−60656
CaF:Tb, dimer reorientation activation volume 80−107285
CaF_2:Tb, EPR in new photoexcited centre 78−19319
CaF_2:Tb, spectra of radn.-induced defect form. 80−2801
CaF_2:Tb, V_k-centre recomb. kinetics, phosphoresc. 77−55817
CaF_2:Tb^{3+}, cubic Tb^{3+} centres, energy level and cryst. field parameters 77−52181
CaF_2:Tb^{3+}, one- and two-photon luminesc. excitation spectra 79−83023
CaO:Eu,Tb phosphor emission under X-ray excitation 79−52011
CaO:Tb, phosphor, isothermal decay 80−55156
CaO-Li_2O-B_2O_3 calibo glass, diffusion limited energy transfer from $Tb^{3+}\rightarrow Ho^{3+}$ 78−31235
CaS:Tb,Eu phosphors, fluoresc. spectra under X-ray excitation 80−16083
$CaWO_4$:Tb^{3+}(Tb^{4+}), new EPR centres *(Russian)* 79−1709

terbium continued
$CeBO_3$:Tb^{3+}, vacuum UV excitation spectra and quantum efficiencies 79−28811
$CeMgAl_{11}O_{19}$:Tb^{3+} phosphors, for low press. fluoresc. lamps, luminesc. characts. 78−10960
Cs_2NaYCl_6:Tb^{3+}, emission spectra, mag. dipole transitions assignments 78−23505
GaP:Tb, magnetic susceptibility, impurity states 79−61044
Gd:^{160}Tb, hyperfine interaction for ^{160}Tb *(Russian)* 77−63347
$GdBO_3$:Tb^{3+}, vacuum UV excitation spectra and quantum efficiencies 79−28811
GdB_3O_6:Bi^{3+}, Tb^{3+}, energy transfer from sensitiser to activator, intermediate role of Gd^{3+} 80−50389
Gd_2O_2S:Tb, recomb. processes and emission spectra *(Russian)* 78−6797
$Gd_xZr_{1-x}O_{2-x/2}$:Tb^{3+}(Eu^{3+}), energy transfer, luminesc. 79−51999
HfO_2:Tb^{n+}, impurity valence transitions 77−51694
K_2O-GeO_2:tb^{3+}, Yb^{3+} glass, luminesc, cooperative sensitization correlated with Rayleigh scatt. intensity 78−52573
$LaAlO_3$:Tb^{3+}, cathodo- and photoluminesc. 77−12448
$LaNbO_4$:Tb^{3+}, EPR and spin-lattice relax., Stark levels *(Russian)* 77−85563
LaOBr:Tb phosphor X-ray mottle reduction by multilayer screen construction 78−4756
La_2O_2S:Tb, cathodoluminesc., nonlinear depend. on activator concs. 79−8190
La_2O_2S:Tb, cathodoluminesc. efficiency changes due to processing, XPS meas. of surface changes 79−99951
La_2O_2S:Tb, recomb. processes and emission spectra *(Russian)* 78−6797
La_2O_2S:Tb based barrier layer phosphors, prep. and cathodum. props. in penetration phosphors 77−1738
Li_2O-Al_2O_3-SiO_2 glasses, Tb^{3+}($^5D_3$) luminesc., cross-relax. quenching *(Russian)* 79−33836
Mg, SiO_4:Th TLD phosphor, γ-ray induced sensitisation and photo-transfer 79−33851
Mg_2SiO_4:Tb, TLD material, UV induced thermolum. and phosphoresc. 78−92707
Mg_2SiO_4:Tb, TLD phosphor response, heating rate effect 80−26359
Mg_2SiO_4:Tb, thermolum. phosphor, photolum. and absorpt. spectra, thermolum. mechanisms 80−97321
Mg_2SiO_4:Tb TLD, response to X-ray and electron irrad. 79−3285
Mg_2SiO_4:Tb TLD, supralinearity of response to electrons and X-rays *(Japanese)* 78−78503
Mg_2SiO_4:Tb thermoluminescence phosphor, response to high energy electrons *(Japanese)* 78−78502
$NaGdO_2$:Tb^{3+}, obs. of efficient luminesc., UV excitation 78−43922
Na_2O-B_2O_3-SiO_2:Yb(Tb), luminesc. cooperative processes, glass struct. and comp. effect 80−16101
$POCl_3$-$SnCl_4$: Tb^{3+}, Sm^{3+}, lifetime and quantum yield of fluoresc. emission 77−20909
PbF_2:Tb^{3+}, cubic Tb^{3+} centres, energy level and cryst. field parameters 77−52181
PbF_2:Tb^{3+}, ESR spectrum of ions in cryst. field of cubic symmetry 79−38378
$ScBO_3$:Tb^{3+}, vacuum UV excitation spectra and quantum efficiencies 79−28811
SiC:Tb, various polytypes photolum. meas., identification of 4H and 6H polytypes 77−63459
SiC:Tb epitaxial layers, energy distrib. in photolum. spectra, influence of synthesis conditions 79−52009
SnO_2:Tb^{3+}, luminesc. and charge compensation 78−76532
SrF_2:Tb, and pure, UV induced processes 77−32452
SrF_2:Tb, far IR spectra 79−33736
SrF_2:Tb_3 V_k-centre recomb. kinetics, phosphoresc. 77−55817
SrF_2:Tb^{3+}, cubic Tb^{3+} centres, energy level and cryst. field parameters 77−52181
SrF_2:Tb^{3+}, mag., thermal and hyperfine props. 80−29368
SrO-Li_2O-Al_2O_3-SiO_2:Tb^{3+} glass, energy transfer, luminesc. efficiency under UV, neutron and charged-particle excitation 79−95822
SrR_2O_4:Eu^{3+}-Tb^{3+}, luminesc. 77−52156
Tb I, $4f^85d6s^2$ config., hyperfine struct. analysis 78−62732
Tb I, HFS laser fluoresc., unclassified lines anal. 79−81178
Tb II, Zeeman patterns, g-factors 79−22651
Tb^{3+} activated rare earth oxysulphides and oxyhalides 79−56849
Tb^{3+}, aqueous soln., radioluminescence intensity conc. depend. 80−87055
Tb^{3+}, bound to benzene-carboxylic acid derivatives, emission intensity 79−18230
Tb^{3+} in molten $LiNO_3$-KNO_3, transition probabilities in absorpt. and fluoresc. spectra 79−50085
Tb^{3+}, in $POCl_3$:$SnCl_4$, $^5D_3$→$^5D_4$ transition, solvent depend. 79−22644
Tb^{3+} in rare earth ion cryst. field in YF_3 struct., spectra 78−19563
Tb^{3+} in $TbCl_3(AlCl_3)_x$ complex, potential vapour laser system, fluoresc. obs. 78−66812
Tb^{3+}, luminesc. sensitisation by Yb^{3+}, in liq., efficiency *(Russian)* 78−90116
Tb^{3+}→Nd^{3+}(Ho^{3+}), diffusion limited energy transfer in DMSO soln., fluoresc. obs. 79−61428
Tb^{3+} soln., luminesc. quantum yield spectral depend. 80−2838
Tb^{3+}:Yb^{3+} in liq. media, luminesc. cooperative sensitisation 80−2827
Tb/Mo, point contact spectroscopy of magnons 79−38312
Tb^{3+}+$O_3(SO_3^{2-})(SO_2)$, in H_2SO_4 soln., electrochemiluminesc. emitters quenching by electrolysis products 79−1794
Tb^{3+}+UO_2^{3+} solution, nuclear pumped liq. lasers, LASL program 80−64011
^{160}Tb, hyperfine interaction parameters in Gd matrix 80−18240
ThO_2, pure and Tb^{3+} doped, impurities effect in absorboluminesc. and photoluminesc. 79−38597
$ThOF_2$:Ce,Tb, photolum. obs. 77−77270
Tm IV $4f^{12}$ configuration, spectra calcs. by configuration superposition *(Russian)* 80−14080
YAG:Tb, US attenuation 77−89500
YAG:Tb^{3+}, cathodolum. intensity, temp. depend., comparative study with other YAG:R^{3+} crysts. 79−99953
YAG:Tb^{3+}, recomb. processes, spectral, kinetic and relative quantum intensity meas. 79−61443
YAG-Tb^{3+}, cathodolum. efficiency rel. to activator conc. 80−11479
$Y_3Al_5O_{12}$:Tb^{3+}, mechanism of $^5D_3$-$^5D_4$ cross-relax. 77−4656
$Y_3Ga_5O_{12}$:Tb^{3+}, fluoresc. and absorption spectra 77−32422
$Y_3Ga_5O_{12}$:Tb^{3+}, luminesc. 77−48251
Y_2O_3:Tb^{3+}(Dy^{3+}), conc. quenching of X-ray and UV-excited luminesc. *(Russian)* 77−55829
terbium continued
YOF:Tb^{3+}, conc. quenching of X-ray and UV-excited luminesc. *(Russian)* 77−55829
$Y(OH)_3$:Tb^{3+}, excited state relax., ns time resolved spectroscopy 77−61140
$Y(OH)_3$:Tb^{3+}, spin-lattice relax. at high gap energies using pulsed tunable dye laser 77−48047
Y_2O_2S:Tb, cathodoluminesc. efficiency at low electron energy 78−6790
Y_2O_2S:Tb, cathodoluminesc. efficiency changes due to processing, XPS meas. of surface changes 79−99951
Y_2O_2S:Tb, recomb. processes and emission spectra *(Russian)* 78−6797
Y_2O_2S:Tb^{3+}, enhancement of cathodolum. efficiency 79−69891
Y_2O_2S:Tb^{3+}, temp. and viscosity depend. of colour coords. 80−40149
Y_2O_2S:Tb^{3+},Eu^{3+}, energy transfer mechanism 78−6793
YPO_4:Tb, luminesc. and optical spectra 79−65921
$Zn_4B_6O_{13}$:Tb^{3+}, fluoresc. and thermophosphoresc. spectra *(Spanish)* 77−90188
ZnO:Tb phosphor, electrolum. brightness, voltage and freq. depend. 80−60681
$Zn_4O(BO_2)_6$:Tb, phosphoresc. study *(Spanish)* 80−16105
ZnS:Tb_3 Cu(Ag) phosphors, luminesc. props. 80−100690
ZnS:Tb^{3+}, NdF_3 film, vac. deposited, electrolum. energy transfer 80−2861
ZnS:Tb^{3+}, sputtered film, DC electroluminesc. and host-excited photoluminesc., Tb^{3+} content depend. 77−85807
$ZrSiO_4$, isomorphous replacement of Zr^{4+} by Tb^{3+}, charge compensation 77−47424

terbium alloys
rare earth-Tb-Fe alloys, $R_xTb_{1-x}Fe_2$, Laves phase type, magnetostriction *(Russian)* 77−51932
Ag-Tb alloy, dil., magnetoresistance meas., contrib. from quadrupole and exchange scatt. 79−78078
Ag(Au)-Tb, dilute, thermoelec. power, crystal field and interaction effects 77−66158
Co-Tb film, magneto-optic coeff. and refr. index, ellipsometric determ. 80−71501
Dy-Er, Kaufman approach to calc. of intra-rare earth phase diagrams 80−25657
$Dy_{0.7}Tb_{0.3}Fe_2$, magnetostrictive material, liq. phase sintering 78−64493
$Dy_xTb_{1-x}Fe_2$, and $Ho_xTb_yDy_{1-x-y}Fe_2$, high magnetostriction cpd., mag. anisotropy origins 78−68217
$Dy_xTb_{1-x}Fe_2$, single cryst., torque meas. 80−65877
Er-Tb, elasticity modulus, ΔE-effect, internal friction, magnetic transformations *(Russian)* 79−91723
Fe-Tb, magnetoelastic hysteresis, elastic stress and mag. field depend. *(Russian)* 80−65982
Fe-Tb dilute alloy, amorphous, small angle mag. scatt. 78−27021
Fe-Tb film, magneto-optic coeff. and refr. index, ellipsometric determ. 80−71501
$Fe_2(Tb_{0.2}Dy_{0.22}Ho_{0.58})$, highly magnetostrictive alloy, vibrating-reed meas. of ΔE effect and internal friction 79−42819
Gd-Tb, elasticity modulus, ΔE-effect, internal friction, magnetic transformations *(Russian)* 79−91723
Gd-Tb, magnetic and electric hyperfine fields at Gd, NMR spin echo 77−77123
Gd-Tb (10 wt.%) film, nuclear echo signals, crystal anisotropy consts. *(Russian)* 79−99790
GdTb alloy, transport props., anisotropy, high temp. obs. 78−26843
GdTb, elec. resist. and thermal diffusivity anisotropy *(Russian)* 77−85192
GdTb, ferromag., magnetisation and microwave absorpt. 80−65816
$Gd_{70}Tb_{30}$, magnetisation, AC susceptibility and microwave absorption meas. 80−60221
Ho-Tb (50 wt.%) alloy, mag. phase diag. from anomalous US propag. 78−6526
$Ho_xDy_yTb_{1-x-y}Fe_2$, Laves phase cpds., anisotropy and magnetostriction 77−63167
$Ho_xTb_{1-x}Co_2$ lave phase compounds, elastic props., temp. and magnetic field dependence 80−60393
$Ho_{0.58}Tb_{0.20}Dy_{0.22}Fe_2$, magnetoelastic surface wave propagation, mag. field depend. 77−85535
$(Ho_{0.58}Tb_{0.2}Dy_{0.22})Fe_2$, microwave mag. props. 80−65860
$Ho_xTb_{1-x}Fe_2$, and $Ho_xTb_yDy_{1-x-y}Fe_2$, high magnetostriction cpd., mag. anisotropy origins 78−68217
$Ho_xTb_{1-x}Fe_2$, Laves phase, mag. anisotropy meas., cubic harmonic anal. 78−84410
$Ho_xTb_{1-x}Fe_2$, single cryst., spin orientations 78−84425
$Ho_xTb_{1-x}Fe_2$, single crystals, continuous spin orientations, magnetisation easy direction 78−84453
La alloys, supercond., Tb-doped, crystal field effects, tunnelling within mK range 80−70907
La-Tb/AlO_x/Al tunnel junctions, cond. meas., cryst. field effects 80−88694
$La_{1-x}Tb_xAg$, supercond., 0.6 meV cryst. field transitions, neutron spectroscopy 78−67991
$La_{1-y}Tb_yAg$, crystal field effects, normal and superconducting states 78−2621
$La_{1-y}Tb_yAg$, neutron spectroscopy of 0.6 meV cryst. field transitions 78−30894
$La_{1-x}Tb_xAg(Sn_3)(Al_2)$, paramag. anisotropy of Tb^{3+} in cubic cryst. field 80−15687
$La_{1-x}Tb_xAl_2$, competing paramag. anisotropy from cryst. field and indirect quadrupolar coupling 80−60180
$La_{1-x}Tb_xAl_2$, supercond., 0.6 meV cryst. field transitions, neutron spectroscopy 78−67991
$La_{1-y}Tb_yAl_2$, neutron spectroscopy of 0.6 meV cryst. field transitions 78−30894
$La_{1-x}Tb_xSn_3$, supercond., 0.6 meV cryst. field transitions, neutron spectroscopy 78−67991
$La_{1-y}Tb_ySn_3$, neutron spectroscopy of 0.6 meV cryst. field transitions 78−30894
Mg-Tb, (up to 45 wt.%), phase diagram, and mech. preps. 80−16277
Mg-Tb, dil., macroscopic shape effect due to quadrupole orientation, magnetostriction and thermal expansion meas. 80−60396
Mn-Tb, dil., hyperfine interactions, nuclear orientation 80−15929
Nd-Tb, HCP struct., mag. props. 77−63177
Pr-Tb, elec. resist. and magnetisation, spin glass behaviour 77−66367
Pr-Tb, elec. resist. temp. depend. 78−2462
Pr-Tb, HCP struct., mag. props. 77−63177

terbium alloys continued
rare earth-Tb-Fe alloys, $R_xTb_{1-x}Fe_2$, (R=Gd, Sm, Dy, He, Zr), props. of near magnetostrictive materials 77−51934
Sc-Tb, dil., high field magnetisation 78−56292
Sc-Tb, induced-moment spin glass, simple mean-field theory 80−29553
Sc-Tb, spin glasses low-field susceptibility, role of single-ion anisotropy 77−48000
$Sm_xTb_{1-x}Co_5$, temp. compensated magnetic material, mag. and struct. characterisation 78−68177
(Tb,Dy)-Fe amorphous films prep. by cosputtering, magnetoelastic props. 80−97429
(Tb,Dy)Fe_2 alloys, giant magnetostriction *(Chinese)* 79−51830
Tb-Al_2, cubic Laves phase compounds, exchange striction determ. 80−44895
Tb-Al(Ag), hyperfine field exam. by NMR spin echo 78−23365
Tb-Au, dil., Mossbauer exam. of mag. hyperfine field at ^{197}Au impurity 78−88244
Tb-Cd, dil., elec. field gradient, at ^{111}Cd impurities, temp. depend. 79−28642
Tb-Co(Fe)(Ni), amorphous film, Kerr and Hall effect meas. 77−24722
Tb-Cu-Ag, mag. props. *(Russian)* 77−51905
Tb-Cu-Zn(Al), mag. props. *(Russian)* 77−51905
Tb-Dy-Ho, phase diagram, alloy struct. *(Russian)* 77−25016
Tb-Er, Kaufman approach to calc. of intra-rare earth phase diagrams 80−25657
Tb-Er, magnetisation process of helical spin struct., neutron diffr. and magnetisation meas. 77−43850
Tb-Fe, amorphous, random anisotropy effects 78−68223
Tb-Fe, amorphous ferrimag. film, thermomag. writing using He-Ne laser 77−12163
Tb-Fe, amorphous ferrimag. film, mag. props. and Curie point writing 77−12164
Tb-Fe, amorphous film, Kerr readout charact. 79−15439
Tb-Fe, amorphous magnetism in bulk samples 77−66278
Tb-Fe, amorphous sputtered film, magnetostriction 79−47320
Tb-Fe amorphous film, sputtered, stress induced anisotropy 79−73706
Tb-Fe amorphous film, thermomag. contact printing 77−89986
Tb-Fe amorphous films of rare earth transition metal system, preparation by co-sputtering 79−56928
Tb-Fe amorphous magnetic films, domain wall obs. by Lorentz electron microscopy 77−80979
Tb-Fe amorphous thin films, magnetic after-effect, Kerr magneto-optic effect obs. 80−97123
Tb-Fe film, amorphous, contact printing 77−73061
Tb-Fe film, undoped and O-doped, amorphous, microstruct. and mag. props. 79−91273
Tb-Fe sputtered films, amorphous, mag. aftereffect due to domain well motion 79−73780
Tb-Fe-O system, O-stabilised intermetallic $Tb_{12}Fe_{32}O_2$, prep. and characterisation 77−8956
Tb-Gd, elec. resistivity and thermopower critical behaviour 80−15499
Tb-Gd, ferromag. monocrystalline, crit. behaviour of elec. resist. 77−62886
Tb-Gd, spontaneous striction and phonon contributions to thermal expansion *(Russian)* 79−90800
Tb-Gd alloy, spin orientation transition obs. 79−99714
Tb-Gd single cryst., mag., magnetoelastic and elec. props. *(Russian)* 78−2677
Tb-Ho, influence of internal strain on Neel temp., thermal expansion and elastic const. meas. 77−63176
Tb-Ho, Kaufman approach to calc. of intra-rare earth phase diagrams 80−25657
Tb-Ho, paramag., anomalous thermal expansion, up to 273K 79−7967
Tb-Ho, single cryst., annealed, thermal expansion 78−47541
Tb-Ho, thermal expansion in vicinity of Curie temp. 79−28524
Tb-Ho, US attenuation and elastic consts. in 3 mag. phases, 4.2 to 300K 77−72645
Tb-Ho (50%), antiferromag., hexagonal anisotropy effect on thermal expansion 79−51283
Tb-Ho (50%), antiferromagnetic, thermal expansion, US attenuation anomalies 79−47319
Tb-Ho dil. alloy, nucl. spin-lattice relax. of ^{165}Ho 78−48069
Tb-Ho film, helimag. order, surface deform., exchange and single-ion magnetocrystalline anisotropy energy 77−66390
Tb-Nd, antiferromag. state, decrease in stability 77−20556
Tb-Pr, antiferromag. state, decrease in stability 77−20556
Tb-Sc(Y)(La)(Lu)(Yb)(Mg)(Th), mag. ordering temps., susceptibility meas. 80−25136
Tb-Sm *(Russian)* 80−34608
Tb-Sn, effective field at diamag. Sn impurities, 4.2 to 235K *(Russian)* 77−69549
Tb-Ta(Cd), elec. quadrupole interaction, temp. and press. depend., TDPAC meas 80−60469
Tb-Tm alloys, mag. struct., neutron diffr. 77−8273
Tb-Y, Fermi surface topology var., mag. and elec. props. *(Russian)* 77−80723
Tb-Y, helicoid antiferromag. ferromag. transition, magnetostriction and magnetocaloric effect *(Russian)* 77−80937
Tb-Y, magnetostriction, mag. and elec. props. 78−27068
Tb-Y, single cryst., magnon component of elec. resist. 77−15827
Tb-Y, single crystal growth from melt, X-ray obs., props. *(Russian)* 78−95689
Tb-Y, spin wave dispersion, spiral mag. struct., neutron scatt. study 79−47268
Tb-Y alloy, mag. hysteresis in antiferromag.-ferromag. transition *(Russian)* 79−33508
Tb-Y solid solution, X-ray diffraction obs. of magnetostriction and phase transitions 77−73068
Tb-Y-Zn, magnetic props. conc. and temp. depend. *(Russian)* 77−47989
Tb-Y(Gd), mag. anisotropy, contrib. from single-ion cryst. anisotropy and anisotropic exchange *(Russian)* 80−29546
Tb-Y(Gd), mag. ordering temp. and indirect exchange integrals *(Russian)* 79−95590
TbAg, amorphous, bulk mag. props., field, time and temp. depends. 77−89932
$Tb_{52}Ag_{48}$, amorphous, bulk magnetic props., evidence of strong local anisotropy 77−43830
$Tb_{52}Ag_{48}$, amorphous, mag. after-effect meas. 79−24200
$Tb_{52}Ag_{48}$, amorphous, mag. aftereffect 80−20435
$TbAg_{1-x}In_x$, elec. and Hall resist. 80−96844

terbium alloys continued
$TbAg_{1-x}In_x$, mag. and transport props. 78−43572
$TbAg_{1-x}Zn_x$ solid solns., mag. props. *(Russian)* 77−77049
TbAl-NdAl, existence of high-temperature superconducting phase *(Russian)* 79−42685
$TbAl_2$, conduction electron spin and orbital polarisation effects 78−80228
$TbAl_2$, cryst. field volume magnetostriction calc. 79−8029
$TbAl_2$, ferromagnetic, extraordinary Hall effect 80−39560
$TbAl_2$, origin of magnetostriction 79−78499
$TbAl_3$, polytypism occurrence 80−44164
TbAlGa, mag. props. and struct. 78−39302
$TbAl_xGa_{2-x}$, mag. props. and phase transitions 80−25133
TbAu, amorphous, magnetisation characts., 5 to 300K, hysteresis cycle *(French)* 77−80965
$TbAu_3$, mag. phase diagram 80−75761
$TbAu_3$, mag. props. *(German)* 79−51761
$TbAu_{3.6}$, ordering temps. and effective moments 78−60283
$TbAu_6$, mag. props. temp. depend. *(French)* 77−51879
Tb_2Au, mag. props., 4.2-300K 79−7972
$TbAuNi_4$, mag. props. 77−20595
$Tb_3Au_3Sb_4$, mag. suscept. meas., 4 to 300K 79−51742
$TbBe_{13}$, mag. struct., neutron diffr. meas., 4.2K 78−47953
$TbBe_{13}$, magnetic structure at low temps., antiferromagnetic, neutron diffraction study *(French)* 80−39743
TbBi, electronic struct., LCAO calc. *(Russian)* 77−39777
TbBi, mag. transitions, quadrupolar interaction effects 80−80512
$TbCo_2$, elec. resistivity, thermopower, X-ray struct. meas. 80−24874
$TbCo_2$, magnetocryst. anisotropy props. by ^{57}Fe Mossbauer spectroscopy 77−63328
$TbCo_2$, magnetocrystalline anisotropy and spontaneous magnetostriction 80−75831
$TbCo_2$, origin of magnetostriction 79−78499
$TbCo_2$, polarised neutron diffr. exam. of mag. struct. 79−73681
$TbCo_2$, rhombohedral distortion at low temp. 80−34743
$TbCo_2$, spontaneous distortion, mag. props. due to cryst. field, exchange field, magnetoelastic energy 79−61096
$TbCo_2$, spontaneous vol. magnetostriction and thermal expansion meas. 77−12183
$TbCo_2$, sublattice magnetisation, powder neutron diffr. meas. 79−19725
$TbCo_2$, X-ray obs. of low temp. modifications of crystal struct. *(Russian)* 78−75632
$TbCo_3$, X-ray absorpt. edge shifts 80−25483
$TbCo_3$-H_2, phase equilibria, from dissociation isotherms 80−50591
$TbCo_5$, mag. moment orientation, anisotropic mol. field model 77−89950
$TbCo_5$, mag. state of Tb sublattice neutron diffr. meas. *(Russian)* 77−80915
$TbCo_{5.1}$, singularities of mag. transition *(Russian)* 77−77053
$TbCo_{5.1}$, sublattice magnetisation, temp. depend., neutron diffr. anal. *(Russian)* 80−103815
$Tb_{1-x}Co_x$, amorphous alloys, thermal stability, elec. cond. enthalpy 80−100172
Tb_2Co_{17}, magnetisation, magnetocryst. anisotropy and magnetostriction 77−8303
Tb_4Co_3, cryst. field effect on mag. moment direction, neutron diffr. meas. 78−80132
TbCoAl, mag. props. 78−2659
Tb_3Co_3Ga, crystal struct., X-ray determ. *(Russian)* 79−27951
$TbCu_2$, collinear mag. struct., neutron diffr. meas. 79−87242
Tb_xCu_{1-x}, amorphous film, magnetisation meas., local anisotropy effects 78−68309
$TbCu_4Ag$, mag. props. and cryst. struct. 77−20562
$Tb_{0.24}Dy_{0.73}Fe_{1.95}$, magnetostrictive underwater sound transducer 78−13881
$Tb_{0.26}Dy_{0.74}Fe_2$, temp. depend. of magnetomechanical coupling factor 77−90002
$Tb_{0.27}Dy_{0.13}Fe_{1.98}$, grain-oriented, permeability, magnetomechanical coupling and magnetostriction 79−78491
$Tb_{0.27}Dy_{0.73}Fe_2$, anomalous thermal expansion and magnetostriction 77−90003
$Tb_{0.27}Dy_{0.73}Fe_2$, domain configurations, obs. by Kerr effect and synchrotron radiation topographs 78−64215
$Tb_{0.27}Dy_{0.73}Fe_2$, LF magnetoelastic effects 78−68348
$Tb_{0.27}Dy_{0.73}Fe_2$, magnetisation and magnetic anisotropy 78−91862
$(Tb_{0.27}Dy_{0.73})Fe_2$, magnetisation, ferromag. domains 80−25162
$Tb_{0.27}Dy_{0.73}Fe_2$, perpendicular suscept., magnetomechanical coupling and shear modulus 78−91918
$Tb_{0.27}Dy_{0.73}Fe_2$, vertically zoned, magnetomechanical coupling and magnetostriction 80−65999
$Tb_{0.3}Dy_{0.7}Fe_2$, elastic vs. magnetoelastic anisotropy 78−68347
$Tb_{0.3}Dy_{0.7}Fe_2$, magnetoelastic coupling meas. by US method 77−69652
$Tb_{0.3}Dy_{0.7}Fe_2$, magnetostrictive, resonant coupling of shear waves 79−33517
$Tb_{0.3}Dy_{0.7}Fe_2$, prep. by powder metallurgy, magnetostrictive props. 80−75826
$Tb_{0.3}Dy_{0.7}Fe_2$, sound velocity mag. field and temp. depend. elastic moduli calcs. 80−39839
$Tb_{0.3}Dy_{0.7}Fe_2$, US velocity and attenuation obs. 77−28423
$Tb_{1-x}Dy_xFe_2$, pseudobinary Laves cpds., spin-orientation diagram, Mossbauer effect meas. 77−55739
$Tb_xDy_{1-x}Fe_2$, Laves phase alloy, magnetostriction depend. on powder orientation before sintering 78−76284
$Tb_xDy_yHo_zFe_2$, temp. depend. of magnetomechanical coupling factor 77−90002
$TbFe_2$, amorphous, mag. struct., US meas. 79−99683
$TbFe_2$, amorphous, Mossbauer spectra *(French)* 80−25261
$TbFe_2$, amorphous, struct. determ., EXAFS exam. 78−51421
$TbFe_2$, amorphous, temp. depend. of mag. hystersis props. 79−61186
$TbFe_2$, amorphous and crystalline, small angle neutron scatt. study of mag. order and mag. microstruct. 79−15283
$TbFe_2$, and $Tb(Co_{0.98}Fe_{0.02})$, magnetostrictive material, changes in vibr. modes near mag. phase transition 79−90736
$TbFe_2$, crit. phenomena, Mossbauer effect 78−52403
$TbFe_2$, domain configurations, obs. by Kerr effect and synchrotron radiation topographs 78−64215
$TbFe_2$, electronic heat capacity coeffs. 80−39787
$TbFe_2$, high field magnetostriction and magnetisation 78−84471
$TbFe_2$, highly magnetostrictive props. 77−12180
$TbFe_2$, magnetisation, ferromag. domains 80−25162
$TbFe_2$, magnetisation and magnetic anisotropy 78−91862

terbium alloys continued
- $TbFe_2$, magnetoelastic props., magnetostriction hysteresis *(Russian)* 80−29590
- $TbFe_2$ magnetostriction in polycryst. samples 77−73065
- $TbFe_2$ monocrystalline (111), under elastic compressive stresses, domain structure *(Russian)* 79−91247
- $TbFe_2$ powders, mag. and hysteresis props. *(Russian)* 79−42800
- $TbFe_2$, spontaneous magnetoelastic distortion, X-ray diffr. expts. 77−63253
- $TbFe_2$, X-ray obs. of low temp. modifications of crystal struct. *(Russian)* 78−75632
- $TbFe_3$ and Tb_6Fe_{23}, magnetostriction, room temp. to 80K 80−65993
- $TbFe_3$, ferrimag., mag. struct., powder neutron diffr. determ. 79−78328
- $Tb_{0.018}Fe_{0.982}$, amorphous, small angle neutron scatt. study of mag. order and mag. microstruct. 79−15283
- $Tb_{1-x}Fe_x$, amorphous film, cosputtered, struct. and mag. props. 78−60323
- Tb_xFe_{1-x} amorphous film, crystn., TEM obs. 79−87019
- Tb_xFe_{1-x} film, amorphous, magnetostriction and magnetisation 78−68305
- TbFeAl, scatter order cpd., mag. props. 77−51891
- $TbFe_{1.5}Al_{0.5}$, crystalline, small angle neutron scatt. study of mag. order and mag. microstruct. 79−15283
- $TbFe_4Al_8$, commensurate-incommensurate modulated mag. struct., neutron diffr. obs. 79−95576
- $TbFe_4Al_8$, mag. props. 78−52250
- $TbFe_4Al_8$, neutron diffr. exam., mag. struct. 78−10656
- $TbFe_2Ge_2$, magnetisation, 4.2-273K and Neel temp. 77−8310
- $Tb(Fe_{1-x}Mn_x)_2$, phase struct. mag. and Mossbauer meas. 77−20563
- $Tb(Fe_{1-x}Rh_x)_2$, Fe sublattice spin reorientation possibility, Mossbauer spectra *(Russian)* 79−78335
- $TbFe_2Si_2$, 5.5K T_N, mag. props. 4.2 to 950K 77−20544
- $Tb_2Fe_4Si_9$ and $TbFeSi_3$, cryst. struct. and mag. suscept., temp. depend. *(Russian)* 78−34957
- TbGa, ferromag., mag. props., 4.2 to 350K 77−63230
- $TbGa_2$, mag susceptibility, 1.5-300K and Neel temp. 78−68184
- $TbGa_2$, mag. props. and struct., neutron diffr. patterns at 4.2, 300K 77−63109
- $TbGa_2$, noncollinear magnetic order and spin wave spectrum in presence of competing exchange interactions 80−65834
- Tb_xGd_{1-x}, orientation phase transitions near Curie pt., magnetization and magnetocaloric effect meas. *(Russian)* 79−87261
- $Tb_{1-x}Gd_xAl_2$, effective mol. field at ^{159}Tb, NMR meas. 80−71197
- $Tb_xGd_{1-x}Al_2$, magnetic anisotropy, magnetostriction 78−56364
- $(Tb_{1-x}Gd_x)_3Co$, intermetallic cpd. mag. props., phase transform, and mag. hystersis *(Russian)* 80−93113
- Tb_5Ge_4, mag. struct. and mag. transitions, neutron diffr. expts. 78−43564
- $Tb_{0.5}Ho_{0.5}$, ferromag. and helical phase, spin wave dispersion relations 79−24149
- Tb_2In, mag. props., 4.2 to 270K 79−56512
- Tb_3In, mag. props. 80−108009
- Tb_5Ir_2, cryst. struct. 80−96473
- $(Tb_cLa_{1-c})Be_{13}$, mag. struct., cryst. field effects, neutron diffr. study 80−65789
- TbMg, mag. struct. and mag. props. 77−8275
- $TbMg_3$, antiferromagnetic struct. 78−14930
- $TbMg_3$, mag. props., Mg conc. depend. 78−84392
- $TbMn_{12}$, mag. interactions, mag. meas. and neutron diffr. 77−63103
- $Tb_{40}Nd_{60}$, mag. struct. and ordered moments, neutron diffr. data 77−66252
- $TbNi_5$, ferromag., magnetisation and paramag. susceptibility 80−25082
- Tb_2Ni_{17}, magnetic structure by neutron diffr. 77−73000
- $Tb_{69}Ni_{31}$, amorphous, Curie temp., mag. susceptibility and coercive force, 4.2 to 300K 80−93092
- $TbNi_{2-x}Cu_x$, elec. resist. and mag. props. 78−72348
- $TbNiSi_3$, mag. susceptibility, 80-1200K *(Russian)* 77−66281
- Tb_3Os, cryst. struct. 80−96474
- $TbPd_3$, specific heat at low temp. 80−20413
- Tb_5Pd_2, mag. props. 77−20547
- $Tb_{55}Pr_{45}$, mag. struct. and ordered moments, neutron diffr. data 77−66252
- $TbPt_5$, low temp. mag. susceptibility 80−93075
- Tb_2Pt, mag. susceptibility meas., mag. transitions obs. 80−60222
- Tb_3Pt_4, mag. props., 4.2 to 160K 79−78343
- Tb_5Pt_4, isotypic with Pu_5Rh_4, X-ray cryst. struct. refinement anal. 79−4271
- $TbRh_xSny$, crystallography X-ray powder diffr. study 80−100217
- TbSc, basal plane magnetocrystalline anisotropy and ferromag. ordering 79−1667
- TbSc, crit. scatt. of electrons near antiferromag. transition temp. 79−69505
- $TbSi_2$, γ-γ ang. correl. obs. of polymorphic transition, 200-900°C 80−29653
- $Tb_{1-x}Sm_xCo_2Ni_3$, giant intrinsic magnetic hardness 78−56347
- $Tb_{0.76}Y_{0.24}$, spin waves rel. to cond. electron susceptibility 78−68195
- $Tb_{1-x}Y_x$ alloy, helicoidal antiferromag. to ferromag. transition 78−10687
- $(Tb_{1-x}Y_x)_3Co$, mag. props. and transitions, conc. depend. *(Russian)* 78−10671
- $Tb_xY_{1-x}Co_{5+0.1x}$, exchange interactions and magnetocrystalline anisotropy 80−34618
- $Tb_cY_{1-c}P(As)$, singlet ground state systems, resistivities 77−62912
- $Tb_cY_{1-c}Sb$, elec. resist., cryst. field and exchange interaction contribs. 80−39556
- TbZn, elec. resist., behaviour at mag. crit. points 80−65901
- TbZn, ferromag., elec. resist., just below crit. temp., effect of mag.-domains 80−39557
- TbZn, ferromag., thermoelec. power, temp. depend. and crit. behaviour 80−96852
- TbZn, ferromag. transition, transport coeffs. critical behaviour 80−15498
- TbZn, mag. excitations meas. 80−70979
- TbZn, magnetoelastic consts. 78−15005
- Th-Tb (1 at.%), Heisenberg exchange, residual resist. meas. 80−75558
- Y-Tb, mag. susceptibility, 4.2 to 300K, Neel temps. 79−19735
- $Y_{1-x}Tb_xCo_5$, spontaneous magnetisation anisotropy, spin reorientation transforms. *(Russian)* 80−7082
- $Y_{1-x}Tb_xCo_{5+0.1x}$, ferrimag., magnetisation, exchange interactions, mag. anisotropy 80−80565

terbium alloys continued
- $Y_{1-x}Tb_xPd_3$, magnetisation, magnetostriction, and inelastic neutron spectra 80−65998
- $Zr_{40}Cu_{60-x}Tb_x$, amorphous, mag. ordering and local random anisotropy 78−68273
- $Zr_{40}Cu_{60-x}Tb_x$, amorphous alloy, mag. interactions 78−95432
- $Zr_{40}Cu_{60-x}Tb_x$, magnetically dil. glass, 4f moments, mag. susceptibility and magnetisation meas. 79−95575
- $Zr_xTb_{1-x}Fe_2$, Laves phase alloys, magnetostriction *(Russian)* 77−51932

terbium compounds
see also terbium alloys
- chelate solns., fluoresc. quenching by voltage appl. 79−87498
- ethyl sulphate, mag. and thermal props. 79−7971
- garnet and zircon structure compounds, anisotropic magnetoelastic props. 77−69660
- metaphosphate glasses, $n(M_2O.P_2O_5).(1-x)Y_2O_3.xTb_2O_3.3P_2O_5$, M=Li, Na, K, excitation and emission spectra 80−40150
- mixed valence compounds, charge dominated fluctuation props. comparison, mag. moments and ordering 80−54659
- salicylate, fast reactions, pulsed selective photoexcitation, rate determ., spectral method 77−86336
- CdF_2:TbF_3 films, electroluminesc. meas. *(French)* 79−11471
- $Cs_2NaTbCl_6$, Raman spectra 77−77205
- $Dy_xTb_{1-x}FeO_3$ orthoferrites, Dy^{3+} and Tb^{3+} contribs. to anisotropy const. *(Russian)* 77−89946
- $(Er,Tb,Gd_3)Fe_5O_{12}$ plate, pseudouniaxial, domain struct., magneto-optical obs. 80−11221
- GdF_3-TbF_3, stabilisation of rhombic β-YF_3 type struct. 78−67700
- $(Gd_{1-x}Tb_x)_2O_2S$ phosphor, concentration quenching of Tb^{3+} luminesc. 80−29785
- KF-TbF_3 system crysts., X-ray struct. investig. 77−43187
- $La_{1-x}Tb_xOBr$ phosphor, concentration quenching of Tb^{3+} luminesc. 80−29785
- $LiTbF_4$, magnetisation near crit. pt., temp. and field depend. 79−38337
- $LiTbF_4$, NMR shift tensors, temp. and field depend. 79−38391
- $LiTbF_4$, Tb^{3+} absorption spectra, 4000 to 25000 cm^{-1} 78−72550
- $LiTbF_4$, uniaxial dipolar ferromag., critical behaviour, mag. susceptibility meas. 80−80528
- $LiTbS_2$, long and short range order 78−38667
- $LiTb_{0.5}Y_{0.5}F_4$, mag. susceptibility, dilution effect on critical behaviour of dipolar uniaxial ferromagnet 80−34635
- $LiTb_{0.5}Y_{0.5}F_4$, uniaxial dipolar ferromag., critical behaviour, mag. susceptibility meas., effect of Y^{3+} dilution 80−80528
- $LiY_{1-x}Tb_xP_4O_{12}$ phosphor, prep. and fluoresc. 77−48219
- LuTb garnet film, scratch-modified mag. domain patterns 78−48007
- $Na_3La_{1-x-y}Ce_xTb_y(PO_4)_2$, optical props. *(French)* 80−103991
- Na_2O-P_2O_5-Y_2O_3-Tb_2O_3 glass, conc. quenching of luminesc. in disordered system with dipolar interaction 80−89059
- $Na_2O.SiO_2$-Tb_2O_3 glass magnetooptical study 80−88976
- $NaTb(MoO_4)_2$, lattice thermal expansion, rel. to temp., X-ray method 79−77782
- $Sm_{0.05}Tb_{0.45}FeO_3$, singularities of domain struct. in spin-flip region 78−19272
- $Sm_{0.55}Tb_{0.45}FeO_3$, orthoferrite cryst., domain memory effect *(Russian)* 77−55693
- $Sm_{0.55}Tb_{0.45}FeO_3$ orthoferrite, optical and magneto-optical props. 79−61396
- $Sm_xTb_{1-x}FeO_3$, gyrotropic props. and birefringence, in spin reorientation range 80−7324
- $Sm_xTb_{1-x}FeO_3$, mag. reorientation, temp. *(Russian)* 79−87263
- $Sm_xTb_{1-x}FeO_3$ orthoferrites, crystallo-optical props. 79−42027
- $Sm_xTb_{1-x}FeO_3$, rotation of polarisation plane, ang. depend. 77−43961
- $Sm_{0.8}Tb_{0.2}S$, resistivity and thermopower 80−20260
- SrF_2:TbF_3, absorpt. spectra of γ-irrad. cryst., 77K, 200-700 nm 78−84615
- $SrTb_2Fe_2O_7$, ferrite, Mossbauer effect study of hyperfine interactions, spin reorientation 78−19383
- $SrTb_2Fe_2O_7$, Mossbauer spectra, hyperfine parameters, ordering temp. 77−90079
- Ta-Ta_2O_5-ZnS:TbF_3-Au thin films, MIS struct., DC electrolum. obs., Poole-Frenkel effect 78−88038
- Tb complex, acetoacetic ether, luminesc. spectral band intensities, solvent effects *(Russian)* 78−84653
- Tb complex, in $Cs_2NaTbCl_6$, f-f transitions, mag. dipole intensities, vibronic coupling model 80−25404
- Tb complex, Tb(2,2,6,6-tetramethyl-3,5-heptanedione), vapours, excited-state kinetics and fusion laser media prospects 79−64243
- Tb complex, Tb(dipicolinic acid)$_3$ chelate, fluorescence energy transfer in the rapid-diffusion limit 79−92151
- Tb complex of L-histidine, influence of metal-to-ligand ratio on energy transfer to Eu complex of L-histidine 80−32763
- Tb complexes, intermol. energy transfer to Eu complexes in aq. soln. 80−25426
- Tb complexes, intermol. energy transfer to Eu complexes in aq. soln. 80−25427
- Tb-Al-Cl vapour complex, fusion laser gain medium 78−63073
- Tb-Sn-Se system, cross section Tb_2Se_3-$SnSe_2$ phase diagram, physicochem. anal. 79−87621
- TbAG, reson. electronic Raman effect, interferences, lifetime meas. 80−93294
- $TbAlO_3$:Nd^{3+}, absorpt. and luminesc. spectra 79−91470
- $TbAlO_3$:Yb^{3+}, Mossbauer relax. 80−15875
- $TbAl_3[BO_3]_4$, thermal stability, X-ray struct. anal., refractive indices 79−4297
- TbAs, mag. transitions, quadrupolar interaction effects 80−80512
- $TbAsO_4$, cryst. struct. by X-ray diffr. co-operative Jahn-Teller transition 77−89411
- $TbAsO_4$, cryst. struct. refinement at 77K and 5K by profile anal. from neutron diffr. powder data 79−37677
- $TbAsO_4$, ferromag., static and AC susceptibility meas. 80−29533
- $TbAsO_4$, mag. ordered, neutron diffr. study 79−47238
- $TbAsO_{...}$, ferroelectricity, dielec. meas. 80−60515
- TbB_{12}, nature of magnetism *(Russian)* 78−31049
- TbB_2, mag. props. and neutron diffr. 78−84401
- TbB_2, mag. struct., ferromag. ordering, neutron diffr. study 80−15692
- TbB_4, antiferromag. props. *(French)* 77−20566
- TbB_4, Czochralski crystal growth 79−95920
- TbB_4, ferromag. ordering, neutron scatt. meas. 78−10655
- TbB_4, mag. and elec. props., metallic character 80−20386
- TbBi, thermal expansion, thermal cond., 300-900K 78−91453

terbium compounds continued
TbBi, type II antiferromag., trigonal lattice distortion, temp. depend. 79−23732
$TbBiTe_3$, prep., elec. props., and crystallographic date 80−59981
$TbCl_3$, aquo complex form., in aq. chloride soln., coord., X-ray diffr. obs. 79−64975
$TbCl_3$, vapour press. and sublimation thermodynamics, mass loss effusion meas. 80−88313
$TbCl_3$-$AlCl_3$, vap., high-energy laser medium props., for fusion ignition 78−63075
$TbCl_3$-$AlCl_3$ complex, fluoresc. spectrum and gas-phase lasing 77−83861
$TbCl_3$-$AlCl_3$ vap. complex, kinetics and laser fusion pot. 79−98343
$TbCl_3(AlCl_3)_x$ complex, potential Tb^{3+} vapour laser system, fluoresc. obs. 78−66812
$TbCl_3.6H_2O$:Gd^{3+}, spin Hamiltonian parameters, EPR meas. 77−36128
$TbCl_3.6H_2O$-$PrCl_3.6H_2O$($ErCl_3.6H_2O$) in DMSO soln., $Tb^{3+}\rightarrow Pr^{3+}$($Er^{3+}$) energy transfer mechanism 80−5498
$TbCo_2Si_2$, mag. props. 80−107988
$TbCrO_4$, mag. susceptibility and magnetis. meas., 1.7-1000K, Curie pt. positron 77−66266
$TbCrO_4$, valence states of Cr, XPS obs. 80−40216
$TbCrSe_3$, prep., elec. and thermal props. 78−43390
TbD_2, mag. struct., neutron diffr. study 77−85421
TbD_2, sublattice magnetisation, cryst. elec. field effects 78−39295
TbD_{2-x}, mag. susceptibility conc. depend. 80−70968
TbD_x, non-stoichiometric, complex antiferromag. struct., neutron diffr. study 80−50061
$Tb_{0.7}Er_{1.3}Gd_{1.0}Al_{0.2}Fe_{4.8}O_{12}$, garnet plate, domain struct. 80−2602
TbF, absorption spectrum, vibr. and rot. anal. 78−55181
TbF_3, ^{19}F NMR, ligand hyperfine interaction, shift tensor determ. 78−48056
TbF_3, crystal growth by Bridgman-Stockbarger method 78−52660
TbF_3, crystal structure by powder neutron diffr. study 80−15077
TbF_3, mag. phase diagram, crit. and tricrit. behaviour 78−14959
TbF_3 thin films, AC conduction obs. 80−70868
TbF_3, transferred hyperfine interaction, NMR study 78−68393
TbF_3:Sm^{3+}, induced visible emission of Sm^{3+} 80−97330
TbF_3:Tb^{3+}, cryst. fields, luminesc. spectra 78−19563
$TbFe_2$, elastic modulus magnetic field dependence 80−87698
$TbFe_2B_2$, compounds with $CeAl_2Ga_2$ structure type *(Ukrainian)* 79−32970
$Tb^{57}Fe_{1-x}Cr_xO_3$ mag. props. from Mossbauer effect obs. *(Japanese)* 80−15933
$TbFeO_3$, mag. phase transitions, Van Vleck interaction and R-Fe exchange *(Russian)* 79−61105
$TbFeO_3$, mag. susceptibility, temp. depend., effective field at Tb ion sites 80−75742
$TbFeO_3$, magnetisation exam. 77−24681
$TbFeO_3$, metamag. phase transitions, mag. struct. instability *(Russian)* 79−61107
$TbFeO_3$, ortho-ferrite, electron spin relax. time temp. depend. 77−90026
$TbFeO_3$ static effective mag. field acting on ^{160}Dy nucleus 77−90074
$TbFeO_3$, thermodynamic props. 77−36078
$Tb_3Fe_5O_{12}$, Faraday rotation in high transient mag. fields 77−69810
$Tb_3Fe_5O_{12}$, quasiantiferromag. state magnetised along two-fold symmetry axis, mag. phase diagram 77−69564
$Tb_3Fe_5O_{12}$, weak field mag. transition, magneto-optical and magnetisation meas. 77−69551
TbG_3, uniaxial ferromagnet, logarthmic corrections to crit. behaviour 78−60294
TbGa garnet, mag. ordering induced by hyperfine interactions, neutron diffr. meas. 77−66265
TbGa garnet, Verdet const. meas. with pulsed mag. field 78−68486
$TbGa_3(BO_3)_4$, luminesc. spectra, local symmetry of rare earth ion determ. 80−16095
$Tb_3Ga_5O_{12}$, hyperfine interac. induced antiferromag. order *(French)* 77−59392
$Tb_cGd_{1-c}VO_4$, cooperative Jahn-Teller effect, linear birefringence 77−76550
$Tb_2Ge_2O_7$, flux-grown, X-ray topography 80−64939
TbH_{2-x}, mag. susceptibility conc. depend. 80−70968
TbIG, [111] magnetoelastic props., rel. to Cotton-Mouton birefringence, 90-500K 80−103876
TbIG, anisotropic forced magnetostriction meas. 78−64251
TbIG, anisotropic garnet, mag. struct., magnetisation and Faraday rotation obs. 78−68169
TbIG, anisotropic linear mag. birefr., light modulation 77−8548
TbIG, appl. of superposition model to cryst. field 78−68132
TbIG, Faraday rot., temp. and high mag. field depend. 79−95736
TbIG, Faraday rotation and transition of spin config. at high mag. fields 80−39776
TbIG, hyperfine interaction determ. from Mossbauer spectra in applied mag. field 77−28497
TbIG, mag. birefringence rel. to sublattices 79−28723
TbIG, mag. linear double refr., two-sublattice model *(Russian)* 79−28728
TbIG, magnetisation and mag. susceptibility meas. along (111) direction, 4.2-295K 77−80917
TbIG, mol. field coeffs., magnetisation and mag. susceptibility anal. 78−95406
TbIG, neutron depolarisation near mag. compensation point 77−24709
TbIG, refr. index, higher-order anisotropic mag. contrib. 77−69808
TbIG, spontaneous Faraday rot. rel. to sublattice magnetisation 80−66159
TbIG, X-ray topographic obs. of domain evolution in mag. field 77−69600
TbIG:Si magnetoresistance meas. 79−78120
Tb_3InO_6, high press. synthesis, cryst. struct. 77−68955
$Tb_3In_5S_{12}$, crystal struct. determ. *(French)* 77−43179
$Tb_xLa(Y,Gd)_{1-x}$.DAM.Sal_3, DAM=diantipyrylmethane, luminesc. *(Russian)* 77−55830
$Tb_2Lu_1Fe_5O_{12}$ film, magnetostriction meas. using double cryst. X-ray diffractometry 78−84468
$TbMnO_3$, mag. struct., ordering of Mn^{3+}, Tb^{3+} moments, neutron diffr. expt. 77−69500
$Tb(MoO_4)_3$ cryst. struct. in ferroelec., ferroelastic, antiferroelec. and paraelastic phases 80−75205
$Tb_2(MoO_4)_2$, ferroelectric-ferroelastic crystal, room temp. crystal struct., X-ray scatt. 80−28978
$Tb_2(MoO_4)_3$, crysts., elastic props. during domain switching under mech. loading 79−55809

terbium compounds continued
$Tb_2(MoO_4)_3$, elastic wave attenuation and velocity near ferroelec. transition 79−73257
$Tb_2(MoO_4)_3$, first-order to continuous phase transition, crossover induced by symmetry-breaking fields 79−82312
$Tb_2(MoO_4)_3$, hydrostatic press. effect on phase transition 78−27166
$Tb_2(MoO_4)_3$, improper ferroelectric, dielectric props., IR radiation pyroelectric detection 80−80711
$Tb_2(MoO_4)_3$, mode softening near ferroelec. transition, Raman and Brillouin spectra 79−33685
$Tb_2(MoO_4)_3$, nonlinear elastic props. near phase transition 79−73244
$Tb_2(MoO_4)_3$, nonlinear piezoelec. coeffs. near phase transition 79−95710
$Tb_2(MoO_4)_3$, proper and improper ferroelec., direct meas. of figure of merit 79−95711
$Tb_2(MoO_4)_3$, thermal expansivity and spontaneous strain temp. depend. 79−14943
Tb_2MoO_5, cryst. struct., IR spectra, elec. and mag. props. 80−33954
$TbMo_6S_8$, long range mag. order in supercond. state 79−65653
$TbMo_6S_8$, superconductor, neutron scatt. exam. of mag. phase 79−73680
$Tb_{1.2}Mo_6S_8$, long-range mag. order and supercond., neutron diffr. obs. 79−78320
$Tb_{1.2}Mo_6S_8$, low temp. heat capacity anomaly rel. to antiferromag. transition in supercond. state 80−25044
$Tb_{1.2}Mo_6S_8$, low temp. magnetisation meas., and supercond. props. 79−8018
$Tb_{1.2}Mo_6S_8$, mag. ordering in supercond. state, resist. and AC susceptibility meas. 78−19194
$Tb_{1.2}Mo_6Se_8$, crystal field excitations, inelastic neutron scatt. obs. 79−78321
$Tb(NO_3)_3$-$Fe(NO_3)_3$-$(NH_4)_2CO_3$-H_2O system, cpd. form., comp. and props. 80−100832
$TbNbO_4$-$CaWO_4$, phase transitions of fergusonite-scheelite *(French)* 80−19942
$TbNi_2Si_2$, mag. props., 4.2-200K 80−84602
TbO_2:Dy^{3+}, mag. hyperfine interaction, PAC expt. 78−35069
TbO_x, Mossbauer spectra of localised modes 79−73874
Tb_2O, Tb_2O_2, atomisation energies and stand. ht. of formation 77−54622
Tb_2O_3, 300 to 900K, mag. susceptibility and Curie temp. meas. 78−56288
Tb_2O_3, B-type monoclinic, DC(AC) elec. cond., thermoelectric power, dielectric const., temp. depends. 80−59980
Tb_2O_3, reaction with liq. Li and liq. Li-N 79−66276
Tb_2O_3-H_3PO_4-H_2O system, cpd. form., comp. and props. 80−100832
Tb_2O_3-P_2O_5-MO system glasses, (M=Mg, Ca, Sr, Ba or Pb), photoluminesc. under X-ray excitation 80−89060
Tb_4O_7, XPS, charging effects on core-level binding energies 79−24409
$Tb(OH)_3$, dynamical effects of interaction between 4f electrons and optical phonons 80−108196
$Tb(OH)_3$, exciton dynamics within an inhomogeneously broadened line, luminesc. spectra 80−50407
$Tb(OH)_3$, heat capacity from 10 to 350K, lattice and Schottky contribs. 80−84300
$Tb(OH)_3$, neutron diffr. struct. exam. 78−2077
$Tb(OH)_3$, powder and single crystal, mag. props. 80−2558
$Tb(OH)_3$, sign of energy dispersion of one dimens. excitons, time resolved spectroscopy 77−1377
$Tb(OH)_3$:Er^{3+}, ferromag., anisotropic exchange effects in optical spectra 78−80141
$Tb(OH)_3$:Er^{3+}, g-values and hyperfine interaction parameters, calc. for Er^{3+} 79−15123
Tb_2O_2S, tunnelling effect and mag.-cryst. transition, neutron diffr. expts. 77−63180
$Tb_2O_2SO_4$, antiferromag., mag. props. 1.6 to 40K 79−33464
$Tb_2O_2SO_4$, antiferromag., specific heat, 0.6 to 30K 79−33487
$Tb_2O_3.Si_3N_4$, prep. by sintering and X-ray diffr. data 79−77570
TbP, mag. excitations above antiferromag. ordering temp., inelastic neutron scatt. obs. 80−50112
TbP, mag. transitions, quadrupolar interaction effects 80−80512
TbP, magnetic Γ_1-Γ_4 exciton, inelastic neutron scatt. study 80−11159
TbP, magnetic low-frequency modes 78−88087
TbP, singlet-groundstate magnetism, static mag. props. 80−7109
$TbPO_4$, anomalous magnetostriction at low temp. 78−84470
$TbPO_4$, IR and Raman spectra 80−34904
$TbPO_4$, linear optical birefr. meas. near bicritical point 80−15719
$TbPO_4$, phase transitions at low temp. 80−15237
$TbPO_4$, sp. ht., 0.5-10K 78−52298
$TbPO_4$, specific heat from 1.2 to 6K 78−14475
$TbPO_4$, zircon struct., cryst. field analysis 80−80232
$TbPO_4$-$Pb_2P_2O_7$, solubility curves for high temp.-melts for growth of single crysts. 78−95687
TbP_5O_{14}, IR absorpt. and luminesc. spectra 80−55079
TbP_5O_{14}, luminesc. spectra 77−52155
TbP_5O_{14}, Raman scatt. at monoclinic to orthorhombic phase transition, soft mode behaviour 78−56486
$TbRh_4B_4$, cryst. struct., X-ray diffr. 77−89423
$TbRh_4B_4$, ferromag. Curie temp. 77−89893
$TbRh_4B_4$, NMR and sp. ht. in supercond. and mag. ordered phases 80−7037
TbS, type II antiferromag., trigonal lattice distortion, temp. depend. 79−23732
Tb_2S_3, polymorphic transforms. on impact compression 77−47575
Tb_xS, mag. ordering, neutron diffr. meas. 78−2649
TbSb, mag. transitions, quadrupolar interaction effects 80−80512
TbSe, formation and crystallographic charact. of thin film phase 78−91574
TbSe, type II antiferromag., trigonal lattice distortion, temp. depend. 79−23732
$Tb_2(SeO_4)_3.8H_2O$, thermal decomp. and IR spectra 80−3319
$Tb_4Si_2O_7N_2$, prop. and X-ray diffr. powder data 80−33944
TbTe, type II antiferromag., trigonal lattice distortion, temp. depend. 79−23732
Tb_xTe, mag. ordering, neutron diffr. meas. 78−2649
$TbTiO_3$, bulk mag. and struct. props., ferrimag. order 80−107993
$TbVO_4$, co-operative Jahn-Teller transition, low freq. dynamics, light scatt. study 80−88317
$TbVO_4$, cooperative Jahn-Teller effect, linear birefringence 77−76550
$TbVO_4$, dielec. meas. at Jahn-Teller transitions 77−24802
$TbVO_4$, Jahn-Teller distortion, mag. field depend. 78−79733
$TbVO_4$, Jahn-Teller phase transition, γ-ray diffractometry 78−91205
$Tb_2(WO_4)_3$, mag. props., 300 to 900K 79−28510

terbium compounds continued
Tb_2WO_6, growth from soln. in melt 77−1806
TbY ferrite garnet, Tb^{3+} energy level inversion, Faraday effect *(Russian)* 79−47418
$Tb_xY_{1-x}As$, anomalous resistivity maxima in metallic magnetic system 78−79977
$Tb_pY_{1-p}AsO_4$, crystallographic, mag. phase transition as function of temp. and Tb conc. 78−43334
$Tb_cY_{1-c}As(P)(Sb)$, singlet ground state systems, microwave resist. data 77−47843
$Tb_{0.2}Y_{2.8}Fe_5O_{12}$, Mossbauer investigation of spin-reorientation transition 78−88243
$Tb_{0.26}Y_{2.74}Fe_5O_{12}$, anomalous props., 200-250K 79−28527
$Tb_{0.26}Y_{2.74}Fe_5O_{12}$ garnet, mag. transition, mag. props. anomaly 80−93120
$Tb_xY_{3-x}Fe_5O_{12}$ hysteresis in spin-orientation phase transitions 79−73761
$Tb_xY_{3-x}Fe_5O_{12}$, spin reorientational phase transitions *(Russian)* 78−39349
$Tb_xY_{3-x}Fe_5O_{12}$, spin-reorientation phase transitions, neutron depolarisation factor 78−27037
$Tb_xY_{3-x}Fe_5O_{12}$, anomalies of magnetisation and magnetostriction obs. in strong fields, 4.2K 77−1581
$Tb_xY_{1-x}PO_4$, H_2 VUV laser excitation, fluoresc. decay characts. 78−60510
$Tb_{0.8}Yb_{0.2}(PO_3)_3$, cooperative sensitisation of luminesc., order-disorder transition effect 77−36283
Tb_2ZrS_5, mag. and sp. ht. meas. on polycrystalline samples 78−23253
$Tb_2[Pt(CN)_4]_3.21H_2O$, phase transitions, X-ray study and spectroscopic study 79−60506
$(YEuTm)_3(GaFe_5)O_{12}$ ferrite garnet films, mag. bubbles, translational motion, mechanism for inertial effects 80−100606
YIG:Tb garnet, Faraday effect in strong mag. field *(Russian)* 80−100651
$Y_{1-x}Tb_xAl_3B_4O_{12}$ phosphors, cathodoluminesc. 77−73177
$Y_{1.5}Tb_{1.5}Al_{0.65}Fe_{4.35}O_{12}$, garnet thin films, magnetisation orientation, temp. depend. 80−71125
$Y_{1-x}Tb_xP_3O_9$ phosphor, prep. and fluoresc. 77−48219
ZnS:TbF_3, photoelectroluminescence, effect of electron-hole pairs 78−27328
ZnS:TbF_3 film between semicond. Y_2O_3 layers, bright green electrolum. 80−2859

terminals, interactive *see interactive terminals*

ternary semiconductors
for pseudobinary semiconductors, see II-VI semiconductors, III-V semiconductors, III-VI semiconductors, IV-VI semiconductors and semiconductor materials
see also chalcogenide glasses
$A^{II}B_2^{III}C_4^{VI}$ semiconductor, crystal structure effects in electronic states 80−20085
adamantine family of semiconductors, props. and commercial appl. 79−42447
α-$AgSbS_2$ crystals, influence of external elec. field on elec. cond. 80−60056
average energy gap, calc. *(French)* 79−33228
$CdSiP_2$, one- and two-phonon Raman scatt. 79−78681
chalcogenide semiconductor amorphous-film comp. monitoring by EPR 77−51940
chalcogenide semiconductors, $ASbC_2$ type, thermal cond. 79−95224
chalcogenide spinels, thermal stability, thermochemical, thermodynamic and crystallochemical props. 77−51519
chalcopyrite, bibliography 78−38994
chalcopyrite, energy band struct. 78−34767
chalcopyrite compounds, $A^IB^{III}C_2^{VI}$, tetragonal distortion 79−32942
chalcopyrite compounds, ternary, review 79−70048
chalcopyrite crystals, refractive index, temp. depend., appl. to nonlinear devices 80−60555
chalcopyrite crystals, temp. depend. Sellmeier coeffs. and coherence lengths 79−76752
chalcopyrite ternary semiconductor, lattice thermal cond. and ionicity, dielectric model 79−77846
chalcopyrite type ternary crystals, IR dispersion *(Russian)* 78−76451
chalcopyrites, for electrolum. device appl., props. and technology, book contrib. 77−73175
chalcopyrites, sphaleritelike vibration mode, group theoretical anal. 79−7661
composition variation determ. using electrolyte electroreflectance 78−80809
computer prediction of system cpd. form., comp. and props. w.r.t. component electron struct. 80−103444
conference, Edinburgh, Scotland (Apr. 1977) 78−34736
covalent radii, tetrahedral and octahedral 77−31632
device applications, review 78−39207
diamond-like semiconductors, charact. features of electronic spectrum and stability 79−33230
energy band structure, structural effects 78−39021
glass, tetrahedral, disorder 78−51423
heteroepitaxial layer, measurement of lattice parameters, RHEED technique 80−15406
I_2-IV-VI_3 cpds., tetrahedral phase stability 77−48415
I_5-III-VI_4, synthesis and props. 77−52231
I-III-VI_2, optical and diamag. susceptibility, bond orbital theories 77−55761
I-III-VI_2 chalcopyrite compounds, d-level struct. and p-d coupling 79−42451
I-III-VI_2 epitaxial layers, lattice parameters meas. using RHEED 79−90913
I-III-VI_2 semiconductors, nucl. quadrupole coupling consts. and struct. parameters 79−42509
II-III_2-VI_4 compounds, electronic states, sensitivity to cryst. struct. 80−45209
II-IV-V_2, electronic band struct., general model pseudopot. 78−39020
II-IV-V_2, glassy, solid-state inductance, theory and expt. 78−56138
II-IV-V_2, optical and diamag. susceptibility, bond orbital theories 77−55761
II-IV-V_2 compounds, resist., possible use in thermistors 77−4343
II-IV-V_2 phosphides, cond. compensation by electron bombardment 79−15151
II-IV-V_2 semiconductor, electronic struct. determ. 77−76751
II-IV-V_2 semiconductors, amorphous, SRO 77−84653

ternary semiconductors continued
II-IV-V_2 semiconductors, equilib. between vapour phase and stoichiometric melt 77−11681
II-IV-V_2 semiconductors, heat of formation from spin-orbit splitting in valence bands 77−31985
II-IV-V_2-Cu, pseudo-straight-zone semiconductor, Schottky barriers, IR photosensitivity and photocond. *(Russian)* 77−8195
nonlinear optical materials, props. and device appls. 78−60131
nonlinear optical materials review 78−33782
photovoltaic devices, thin film heterojunction and homojunction, fabrication and performance 78−39208
practical applications, potential, review 79−10344
review of developments 78−34737
Schottky diodes with tunnel device characts. 78−39215
single crysts. and thin films, absorpt. edge temp. depend., gap energy changes 79−42991
solid solutions with nearly perfect sublattices, stoichiometry invariants 79−51270
thermal conductivity, theory and expt. data comparison 79−46851
V-VI-VII complex ferroelec. semiconductor monocrystalline film production 79−78905
α-$ZnIn_2S_4$, and related polytypes, electron band struct. 79−51485
Ag (112) chalcopyrite films, lattice mismatch with (0001)CdS substrates 79−87012
Ag-Ge-Te, phase equilib. from Ag_2Te-GeTe mixture meas. *(German)* 78−84782
Ag-Si-Te, phase equilib. from Ag_2Te-SiTe mixture meas. *(German)* 78−84782
Ag-Sn-Te, phase equilib. from AgTe-SnTe mixture meas. *(German)* 78−84782
$AgAsS_2$, $AgSbS_2$ and $AgBiS_2$, cryst. and vitreous, refl. spectra, energy spectrum 77−8596
$AgAsS_2$, cryst. and amorphous, band struct., photoemission and refl. spectra obs. 77−66581
Ag_3AsS_3, proustite, elec. cond. rel. to impurities, melt stoichiometry deviations 77−11914
Ag_3AsS_3, SHG, absorpt. coeffs. and temp. variation of refr. index difference 80−14390
$AgBiTe_2$-PbTe solid solution, prep. and thermoelec. props. 77−47839
$AgFeSe_2(S_2)(Te_2)$, elec. props., band gap *(Russian)* 79−11116
$AgFeTe_2$, Mossbauer parameters in phase-transition region 80−11308
$AgGaS_2$, up-conversion of 10.6 μm radiation into visible 78−33783
$AgGaS_2$, deep level obs. by TSC meas. 80−65590
$AgGaS_2$, elec. field influence on absorpt. spectrum, exciton parameters and energy of impurity levels *(Russian)* 77−69860
$AgGaS_2$, iso-index coupled-wave electrooptic filter 80−1324
$AgGaS_2$, optical quality, grown from melt, EPR characterisation 78−64260
$AgGaS_2$, Raman spectrum, degenerate mods, temp. depend. 78−35150
$AgGaS_2$:Fe, EPR of Fe-associated defect 80−60412
$AgGaS_2$-$AgGaSe_2$ system, phase diagram, lattice consts., and IR spectra 80−60841
$AgGaS_2(Se_2)$, ionic cond., galvanic cell meas. 77−47616
$AgGaS_2(Se_2)$, press. depend. of energy gap, absorption edge obs. 77−12401
AgGaSe, direct gap semicond., exciton energy at 300K from reabsorption of luminesc. 79−78728
AgGaSe, exciton energy determ., electron beam excited luminesc. 79−38680
$AgGaSe_2$, down-conversion of $LiNbO_3$ optical parametric oscillator output, 4 to 18 μm 79−86215
$AgGaSe_2$, growth by Bridgman method, optical characts. 77−69980
$AgGaSe_2$, polarised IR refl. spectra, optical phonon modes 77−16304
$AgGaSe_2$, reabsorpt. of excitonic luminesc. in direct band gap semiconds. 77−63469
$AgGaSe_2$, SHG, absorpt. coeffs. and temp. variation of refr. index difference 80−14390
$AgGaSe_2$, Schottky diodes with tunnel device characts. 78−39215
$AgGaSe_2$, seeded Bridgman growth of crack-free crysts., thermal expansion coeff. 78−11101
$AgGaSe_2$ single crysts., opt. quenching of photocond., temp. depend., slow centres activation energy *(Russian)* 77−69370
$AgGaSe_2$, two-photon absorpt. and short pulse stimulated recombination 80−89054
$AgGaSe_2$ wavelength-modulated reflectance, optical electronic transitions, 1.5-5.5 eV 78−35170
$AgGa(Se_{1-x}S_x)_2$, crystal growth, phase studies, optical props. 78−48305
$AgGaSe_2(Te_2)$, phonons, far IR refl. obs. 78−60459
$AgGaTe_2$, Debye temp., standard entropies and enthalpies, sp. ht. meas. 78−30769
Ag_8GeS_6, fundamental absorpt. edge changes due to polymorphic transitions 77−20240
$Ag_8GeS_6(Se_6)(Te_6)$, Ag_8SiSe_6, $Ag_8SnS_6(Se_6)$, absorpt. edge investigs. at phase transitions 78−35149
n-Ag_8GeSe_6, elec. cond. and photoelec. props. 77−69380
Ag_8GeSe_6, forbidden energy gap changes under high press., polymorphic transitions 77−51649
Ag_8GeSe_6, fundamental absorpt. edge changes due to polymorphic transitions 77−20240
Ag_8GeSe_6, polymorphic transition, absorpt. coeff. meas. 78−2257
$AgInS_2$, and $AgIn_5S_8$, spray pyrolysis, film struct., elec. and optical props. 80−71592
$AgIn_5S_8$, cryst. growth and props. 78−39677
$AgInS_2(Se_2)$-$SnS_2(Se_2)$, degree of solid solubility and phases characts. 78−35377
$AgInSe_2$, $AgInTe_2$, $AgGaSe_2$, pressure-induced phase transformations 78−30748
$AgInSe_2$, far IR refl. spectra, polarised light 78−43870
$AgInSe_2$, press. depend. of energy gap, absorption edge obs. 77−12401
n-$AgInSe_2$, press.-induced compensation, resist. expts. 78−30919
$AgInSe_2$, reflectvvity and XPS meas. 78−35165
$AgIn_5S_8$, optical gap and low temp. depend. 79−99907
$AgInS_2(Te_2)$, far IR refl. spectra, ionic bonds 79−55695
$AgInS_2(Te_2)$, phonons, far IR refl. obs. 78−60459
$AgInTe_2$, Debye temp., standard entropies and enthalpies, sp. ht. meas. 78−30769
$AgInTe_2$, far IR refl. spectra, polarised light 78−43870
Ag_2S-In_2S_3-SnS_2 system quaternary and ternary sulphide spinels, solid solubility and struct. 78−35376
α-$AgSbS_2$ crystals, photoelectric props. 80−107861
β-$AgSbS_2$, phase transitions, electrophysical props. 80−44316

ternary semiconductors continued
Ag_3SbS_3 film prep. 77−52250
Ag_3SbS_3, pyrargyrite, elec. cond. rel. to impurities, melt stoichiometry deviations 77−11914
$AgSbSe_2(Te_2)$, exam. of kinematic viscosity of melts, and short range ordering 79−1383
Ag_8SiSe_6, forbidden energy gap changes under high press., polymorphic transitions 77−51649
Ag_8SnS_6, fundamental absorpt. edge changes due to polymorphic transitions 77−20240
$Ag_2SnS_3(Se_3)(Te_3)$, Mossbauer effect, lattice dynamics obs. 77−43923
Ag_8SnSe_6, cryst., Hall effect investigation of polymorphic transform. 80−39605
Ag_8SnSe_6, forbidden energy gap changes under high press., polymorphic transitions 77−51649
Ag_8SnSe_6, fundamental absorpt. edge changes due to polymorphic transitions 77−20240
$AgTe_2I$, Fermi surface meas. by Shubnikov-de Haas effect 77−39767
$AgTlSe_2$ and AgTlSe, elec. cond. and thermoelectric power, doping effects, rel. to pseudogap model 78−2506
AsS(Se)I films, electrophys. and opt. props. 77−51741
$AuTe_2I$, Fermi surface determ. by Shubnikov de Haas effect 77−51639
$BaCuO_2$, prep. and props. *(French)* 77−43201
Bi-Sb-Te system, epitaxial film prep. in closed-crucible 77−52230
BiI_3-Bi_2Te_3, p-T-x phase diag. 77−36477
Bi_2Te_3-InTe, thermoelec. props. 77−85250
BiTeI, elec. props., crysts. grown from melt in excess iodine 79−4907
BiTeI, layered cryst., anisotropy and temp. depend. of mag. susceptibility 79−73673
BiTeI-SbTeI solid solns., form., crystn., elec., thermal props. 78−44003
$CaIr_xTi_{1-x}O_3$, semiconductor, struct., mag. and elec. props. 79−91046
CdA_2X_4 (A=Ga,In; X=S,Se), Fourier IR and Raman spectra, cryst. struct. and symm. *(German)* 79−24313
$CdB^4C^5_2$, chalcopyrite struct., surface energy and compressibility, rel. to glass form. 79−51417
$CdCr_2S_4$, $CdCr_2Se_4$, variation of elec. props. with chalcogen content of gas phase, 500-700°C 77−20310
$CdCr_2S_4$ crystal growth, structural defects, physical properties 80−60759
$CdCr_2S_4$, EPR line profiles in paramag. and ferromag. phases 79−28602
$CdCr_2S_4$ ferromag. semicond. film, props. 78−76175
$CdCr_2S_4$, ferromag. semicond., IR refl. spectra, phonon props. and dielec. function 80−66191
$CdCr_2S_4$, ferromagnetic semiconductor films, prep. and props. *(Japanese)* 79−47308
$CdCr_2S_4$, Heisenberg ferromag., obs. of dynamic dipolar crossover, ESR linewidths meas. 79−24209
$CdCr_2S_4$, hot-pressed, optical isolation appl. at 10.6 μm, intrinsic absorpt. props. 78−42368
$CdCr_2S_4$, phonon Raman scatt., mag. circular polarization effects 79−8134
$CdCr_2S_4$, polycrystalline films, mag. semicond., spinel-type, magneto-optical effects *(Japanese)* 79−47415
p-$CdCr_2S_4$, single cryst., elec. cond. 79−15148
$CdCr_2S_4$, single crystal ferromagnetic semiconductor, vapour-liquid transport growth method 77−21013
$CdCr_2S_4$:Gd, ferromag. reson. and electrical cond. 79−28626
$CdCr_2S_4(Se_4)$, ferromagnetic semiconductors, spinel-type, resonance Raman scattering and electronic structure *(Japanese)* 79−47421
$CdCr_2S_4(Se_4)$, pure and Ag doped, electronic struct., mixed valence 80−70612
$CdCr_2Se$, ferromag. semicond., high field effects, magnon carrier scatt. 78−87981
$CdCr_2Se_4$, crit. behaviour of optical absorption edge 78−35143
$CdCr_2Se_4$, crit. speeding-up of spin-relax. 78−48028
n-$CdCr_2Se_4$, current- and voltage-controlled negative resist. obs. 78−19041
$CdCr_2Se_4$, deviation from Kittel's mag. resonance formula near T_c 79−87322
$CdCr_2Se_4$, excitation of spin waves by current carriers, magnetisation and elec. cond. reduction *(Russian)* 79−7981
$CdCr_2Se_4$, ferromag. semicond., P-T phase diagram by annealing expts. between 600 and 964°C 77−63636
$CdCr_2Se_4$, ferromag. semiconductor, light scatt. from magnons under strong fields 78−84554
$CdCr_2Se_4$, ferromag. semicond., photoinduced mag. anisotropy 80−50086
$CdCr_2Se_4$, ferromag. semicond., conc. anomalies rel. to red shift of absorpt. edge 80−70732
$CdCr_2Se_4$, ferromagnetic semiconductor, P_{Se}-T phase diagram, where $Se=Se_2$, near peritectoid reaction temps. *(Japanese)* 77−52290
$CdCr_2Se_4$, ferromagnetic semiconductor, single cryst. growth *(Japanese)* 79−47612
$CdCr_2Se_4$ film, absorpt. and Faraday effect 78−2936
$CdCr_2Se_4$ film, electron irradiated, struct. 79−15032
$CdCr_2Se_4$, optical absorption due to transitions between bands and local levels 79−38537
$CdCr_2Se_4$, optical reflectivity, dielectric const. by expt. data Kramers-Kronig anal., spinel struct. 79−99903
$CdCr_2Se_4$, refr. index variation in strong alternating mag. field 80−23741
p-$CdCr_2Se_4$, resistivity anomalies at mag. transitions, sp.ht. 80−39785
$CdCr_2Se_4$ single cryst., photocond. in air, vacuum, mechanism 77−8138
$CdCr_2Se_4$, single crysts., mag. semicond., spinel-type, magneto-optical effects *(Japanese)* 79−47415
$CdCr_2Se_4$, single cryst. growth by chem. transport reactions 80−16163
$CdCr_2Se_4$, temp. depend. of resist. and magnetoresist., influence of Se vacancies 78−60130
$CdCr_2Se_4$, velocity-field characts., above T_c 78−64049
p-$CdCr_2Se_4$:Ag, electrical props., 100-300K 80−54692
$CdCr_2Se_4$:Ag, ferromag. linewidth and eddy current losses 79−33541
$CdCr_2Se_4$:Ag, impurity contrib. to low temp. ferromag. reson. linewidth 79−65743
$CdCr_2Se_4$:Ag, mag. anisotropy, effect of annealing in vacuum 77−80929
$CdCr_2Se_4$:Ag, magneto-electrical props. temp. behaviour depend. on dopant conc. *(Russian)* 80−11006
p-$CdCr_2Se_4$:Ag, oscillatory magnetoresist., temp. and mag. field depend. 78−52011
$CdCr_2Se_4$:Ag(Gd), doping effects on exchange interaction 78−43579
$CdCr_2Se_4$:Cu, elec. props., temp. depend. *(Russian)* 78−72181
$CdCr_2Se_4$:Cu(Ag), ferromag. reson. and ESR line widths 80−60413
$CdCr_2Se_4$:Ga, sp. elec. resist., temp. and mag. field depends. *(Russian)* 78−26893

ternary semiconductors continued
$CdCr_2Se_4$:Ga(Ag), and pure, photocond. and photomagnetoresist. spectra 77−80809
n-$CdCr_2Se_4$:In, electrical props., 93-168K 80−49713
$CdCr_2Se_4$:In, ferromag. semicond., carrier mobility, electron-two magnon scatt. Hall effect 78−51992
$CdCr_2Se_4$:In, influence of Se-deficiency on props. 78−30921
$CdCr_2Se_4$:In, nondegenerate ferromagnetic semiconductor, positive magnetoresistance 78−2505
$CdCr_2Se_4$:In (Ga)(Ag), and undoped, elec. prop., vac. heat treatment effect 80−15518
$CdCr_2Se_4$:In(Ga), temp. driven metal-semiconductor transition, temp. and mag. field depend. *(Russian)* 78−88003
$CdCr_2Se_4$-$ZnCr_2Se_4$, single cryst., mag. props. 79−28526
$CdCr_2Si_4$:Ga, negative magnetoresist. effects near Curie temp. 79−11152
$CdCr_2Sr_4$, press. depend. optical aborption edge shift and compressibility 79−28714
$Cd_{1-x}Cu_xCr_2Se_4$ solid solution, spinel struct., X-ray investigation 79−78940
$CdGaS_2$, single crysts., peculiarities of photocond. in strong elec. field 80−54736
$CdGa_2S_4$, direct excitons, refl. spectra 79−90972
$CdGa_2S_4$ double surface-barrier diodes, current-voltage characts. 80−92972
$CdGa_2S_4$, IR light transmission, IR refl. spectra and cryst. struct. 79−56777
$CdGa_2S_4$, IR refl. spectra 80−60604
$CdGa_2S_4$, interpretation of thermolum. and TSC meas. 78−27336
$CdGa_2S_4$, photoluminesc. and photocond. meas. 78−60159
$CdGa_2S_4$, Raman scatt. anal., optical phonons 79−73951
$CdGa_2S_4$, vibr. spectra, 33-400 cm^{-1}, symm. transform. *(Russian)* 78−23465
$CdGa_2S_4$:Ag(In), photoluminesc. and photocond. meas. 78−60159
$CdGaS_4(Se_4)$, absorption and refl. spectra anisotropy, band struct. 77−69840
$CdGa_2(S_{1-x}Se_x)_4$ solid solns., band struct. behaviour w.r.t. comp. *(French)* 80−107699
$CdGa_2S_4(Se_4)$, band struct., and optical spectra 78−19511
$CdGa_2S_4(Se_4)$, band struct., pseudopot. method 80−92816
$CdGa_2S_4(Se_4)$ film, optical absorpt., and energy gaps 78−11012
$CdGa_2S_{4(1-x)}Se_{4x}$, solid soln., crystallographic studies 78−15301
$CdGa_2Se_4$, electron traps, energy spectrum, photocurrent decay, TSC temp. depend. *(Russian)* 78−64057
$CdGa_2Se_4$, electrophotographic props. *(Russian)* 78−59100
$CdGa_2Se_4$, IR refl. spectra and cryst. struct. 79−56777
$CdGa_2Se_4$, IR refl. spectra, optical phonon dispersion 80−29746
$CdGa_2Se_4$, linear expansion anisotropy 79−86910
$CdGa_2Se_4$, ordered vacancy compound, Raman scatt. 79−95749
$CdGa_2Se_4$ ordered vacancy compound, Raman scatt. 79−99870
$CdGa_2Se_4$, struct. of valence band, photocond. and reflection spectra meas. 80−6719
$CdGa_2Se_4$, thermoreflectance and visible absorpt. spectra, energy gap, cryst. field splitting 80−34945
$CdGa_2Se_4$-$CdIn_2Se_4$ solid solutions, order-disorder transition 79−19181
$CdGa_2Te_4$ film, effect of thermal annealing on struct., optical absorpt. and photocond. 79−65342
$CdGa_2Te_4$, IR refl. spectra and cryst. struct. 79−56777
$Cd_{0.96}Ga_2Te_{4.1}$, amorphous film crystallisation and conductivity switching 77−4459
$Cd_{0.96}Ga_2Te_{4.1}$ film, switching effect 77−43753
$CdGeAs_2$, amorphous and cryst., short-range order, Mossbauer expts. 78−22648
$CdGeAs_2$, cryst. growth and elec. props. *(French)* 77−59682
$CdGeAs_2$ crystals, Bridgman grown, optical props. rel. to O_2 content of starting materials 80−81213
$CdGeAs_2$, develop. of tunable coherent radiation at 16 μm 78−90454
$CdGeAs_2$, elec. and optical props., acceptor levels and energy gap determ. 77−85218
$CdGeAs_2$, electron irradiated, change in electrical props. 79−7829
$CdGeAs_2$, glassy, structural model 77−35490
$CdGeAs_2$, optical and elec. props. 79−19590
$CdGeAs_2$, p-n junction form. by heat treatment, photosensitivity 77−28247
$CdGeAs_2$, phase matched fourth harmonic generation, cascade process contrib. 79−76761
$CdGeAs_2$, photosensitivity to linearly polarised radiation 77−55569
$CdGeAs_2$, polarised IR reflectivity, optical modes, optical phonons 77−69836
$CdGeAs_2$, SHG, absorpt. coeffs. and temp. variation of refr. index difference 80−14390
$CdGeAs_2$ tandem crystals, efficient freq. tripling of CO_2 laser radiation 79−45999
n-$CdGeAs_2$:In(Te), resist. and Hall coeff. meas., influence of press. 77−47810
$CdGeAs_2$-$ZnGeAs_2$, and $CdGeAs_2$-$GdGeP_2$, material distrib., possibility of heterostructure *(Russian)* 78−30979
$CdGe(As_{1-x}P_x)_2$, crystal growth, phase studies, optical props. 78−48305
$CdGe_{1-x}M_xAs_2$ (M=Si,Sn,Pb), (x=0.0,0.1,0.2), amorphous struct. 78−22651
Cd_2GeO_4 anode for H_2O photoelectrolysis 80−108716
n-Cd_2GeO_4, electronic and cond. props. rel. to prep. conditions and defect struct. 80−107787
$CdGeP_2$, cond. compensation by electron bombardment 79−15151
$CdGeP_2$, crysts., prep. by chem. vapour transport 80−55280
$CdGeP_2$, electronic struct. at cryst./vitreous transition, X-ray K-absorpt. and emission 78−15248
$CdGeP_2$, growth from melt solution in Cd, microhardness 77−44139
$CdGeP_2$, optically anisotropic, orientation, use of polarisation depend. of photo-EMF and photoconductivity 77−89807
$CdGeP_2$, polarisation of luminescence emitted 77−69909
$CdGeP_2$, pure and In-doped, polarisation of recombination radiation 78−19562
$CdGeP_2$ synthesis and cryst. growth 79−87577
$CdGeP_2$:Cu, impurity behaviour 77−15857
$CdGeP_2$:In, photolum. spectra and kinetic coeffs. 79−19927
$CdGeP_2$:In based surface barrier diode, photosensitivity 79−33330
n-$CdGeP_2$-p-$CdGeAs_2$ heterojunction photocells, polarisation-sensitive 80−11075
$CdGe_{1-x}Sn_xAs_2$, amorphous, radial distrib. anal. and mag. susceptibility meas. 77−43152

ternary semiconductors continued
$CdGu_2S_{4(1-x)}Se_{4x}$, opt. absorpt., elec. cond., spectral response, thermopower 77−72862
$Cd_{1-x}Hg_xCr_2Se_4$, photoferromag. effect and photocond. obs. 79−28376
$Cd_{1-x}Hg_xGa_2S_4$ solid solns., band struct. behaviour w.r.t. comp. *(French)* 80−107699
$CdIn_2$:Cr, photocond. and photoluminesc. spectra 77−28214
n-$Cd_{1-x}In_xCr_2Se_4$, effect of doping on elec. cond. and magnetoresist. 78−72174
$CdInGaS_4$, crystal, Raman scattering spectra, polarisation meas. *(Russian)* 80−71410
$CdInGaS_4$, far IR refl. and transmission spectra, lattice vibrs. 79−91439
$CdInGaS_4$, layered structure crystals, refractive index meas. method 80−98966
$CdInGaS_4$ plate in elec. field, photostimulated ocills. 79−65799
$CdInGaS_4$, pure and Cu-doped, electrophotography layers *(Russian)* 80−68282
$CdInGaS_4$, TSC and SCL cond. investig. of electron trap parameters, 120 to 350K 77−69341
$CdInGaS_4$:Au, single crystal, thermostimulated conductivity *(Russian)* 79−11142
$CdIn_2O_4$, anode for H_2O photoelectrolysis 80−108716
$CdIn_2O_4$, crystal growth from flux, elec. and struct. props. 77−81206
$CdIn_2S_4$, band edge study by photovoltaic effect 79−95444
$CdIn_2S_4$, Brillouin scatt., elastic and photoelastic consts. determ. 80−60619
$CdIn_2S_4$ cubic spinel, electronic band struct. and chem. bonds 78−34768
$CdIn_2S_4$, electronic states, sensitivity to cryst. struct., UPS study 80−45209
$CdIn_2S_4$ film, vac. deposited, growth, struct., optical and photoelectronic props. 80−10831
$CdIn_2S_4$ films, vac. deposited, struct. and photoelec. props. 79−87006
$CdIn_2S_4$, fund. reflectivity, 2 to 6 eV, band struct. implications 78−39574
$CdIn_2S_4$, fundamental optical constants 78−84549
$CdIn_2S_4$, impurity centres, photoluminesc. and photocapacitance data on config.-coordinate diagrams 78−10938
$CdIn_2S_4$, partial inverse spinel struct., detection by Fourier transform spectroscopy 80−108197
$CdIn_2S_4$, photocond. and trap. distrib. 78−39164
$CdIn_2S_4$, photocond. and electron trap distrib. 79−28373
$CdIn_2S_4$, photoconducting semiconductors, fundamental absorption edge 80−40130
$CdIn_2S_4$, photoluminesc. spectra anal. by method of moments 77−12433
$CdIn_2S_4$, photoluminesc., reson. Raman scatt. 78−48179
$CdIn_2S_4$, photoluminesc., thermal quenching and recomb. centres 79−24362
$CdIn_2S_4$, Raman and IR spectra 78−48181
$CdIn_2S_4$, single cryst., oscill. behaviour of photocurrent and luminesc. 78−10501
$CdIn_2S_4$ single crystal growth by two-zone horizontal Bridgman technique 78−27400
$CdIn_2S_4$ single crystals, recombination process and localised levels 80−93383
$CdIn_2S_4$, valence band densities of states, XPS meas. 79−28892
$CdIn_2S_4$:CO^{2+}, site symmetry, spectral meas. 79−78729
$CdIn_2S_4$:Co, optical absorption meas. 78−64384
$CdIn_2S_4$:Cr, absorpt. and photoluminesc, spectra, Cr conc. depend. 79−78712
$CdIn_2S_4$:Cr, thermal cond., 1.8 to 200K, phonon scatt. by impurity ions 77−76627
n-$CdIn_2S_4$/p-$CuInSe_2$ heterostructure, form. and photovolt. meas. 80−10831
$CdIn_2S_4$-Au surface-barrier diodes, mech. of current flow 78−56228
$CdIn_2S_{4-x}Se_x$, struct. types anal., X-ray diffr. exam. 79−86756
$CdIn_2Se_4$ defect tetrahedral crystals, band structure, charge density 77−11850
α-$CdIn_2Se_4$, defect zincblende struct., electronic props. 77−15767
$CdIn_2Se_4$, defect zincblende semicond., valence band, cryst. struct. effects 78−48278
$CdIn_2Se_4$, high resolution electron microscopic study of polytypism 80−88119
$CdIn_2Se_4$, needle-like cryst. X-ray exam. 79−42031
$CdIn_3Se_4$, cryst. growth, photoresponse and optical props. 78−39165
$CdIn_2Te_4$ defect tetrahedral crystals, band structure, charge density 77−11850
$Cd_{1-x}M_xS$ (M=Sr, Ca, Mg, Pb, Sn), solid soln., prep. and semicond. props. 80−2383
$Cd_4P_2Cl_3(Br_3)(I_3)$, elec. and photoelec. props. 80−34480
n-CdS/p-$ZnIn_2Se_4$ thin film solar cell, photovoltaic props. 80−89628
$CdSiAs_2$ chalcopyrite photovoltaic material 79−74526
$CdSiAs_2$, electron irrad., defects, elec. and optical props. 79−19282
p-$CdSiAs_2$, electron irrad. elec. props. annealing, lattice defects 80−100465
$CdSiAs_2$, polarisation of photoluminesc. 77−16389
$CdSiP_2$, birefringence meas. 78−56455
$CdSiP_2$, birefringence, effects on hydrostatic pressure and temp. 80−45033
$CdSiP_2$, bond strengths and bond lengths, thermal expansion coeff. meas. 78−87651
$CdSiP_2$, electronic struct., X-ray spectroscopic investigation 80−108300
$CdSiP_2$, optical activity near isotropic point, absorpt. spectra 79−69804
$CdSiP_2$, PAC examination of deuteron irrad. damage, annealing effects 78−47446
$CdSiP_2$, polarised Raman spectra 77−24853
$CdSiP_2$, pseudodirect bandgap semiconductor, natural birefringence 79−65834
$CdSiP_2$, pseudodirect chalcopyrite semicond., electronic band struct. 80−20079
$CdSiP_2$, reflectance spectra at 300K 80−25407
$CdSiP_2$, thermoreflectance spectra 77−81122
$CdSiP_2$:Fe, EPR and optical absorpt. of Fe^+, Fe^{2+}, Fe^{3+} and Fe^{4+} on tetragonal sites 77−8397
$CdSiP_2$:Na(Bi), single crystal, photocond. under laser excitation 80−44661
$CdSnAs_2$, electron induced defects, p- to n-type cond. inversion, Hall meas. 77−24557
p-$CdSnAs_2$, heavily doped, elec. transport props. under elastic deformation 80−96915
$CdSnAs_2$, hydrostatic press. effect on resist. and Hall coeff., band struct. 77−47808

ternary semiconductors continued
n-$CdSnAs_2$, optical absorption rel. to energy spectra *(Russian)* 78−75994
$CdSnAs_2$, solubility in Sn melt, temp. depend., enthalpy of melting 80−59658
$CdSnAs_2$-Au(Al), surface barrier junction, elec. props., temp. depend. 80−65686
$CdSnAs_2$-InP, n-p heterojunction, elec. props., electroluminesc., band struct. 80−75632
$CdSnAs_2$-$ZnSnAs_2$, and $CdSnAs_2$-$CdSnP_2$, material distrib., possibility of heterostructure *(Russian)* 78−30979
$CdSnAs_2(P_2)$ single crysts., refl. spectra, band struct., dielec. consts. 77−44022
$CdSn(Ge)As_2$, amorphous, SRO 77−84653
$CdSnO_3$ and Cd_2SnO_4, crystal growth by flux or high press. method, elec. and struct. props. 77−81206
$CdSnO_3$, single crysts., elec. props. 80−6978
Cd_2SnO_4, anode for H_2O photoelectrolysis 80−108716
Cd_2SnO_4, single crysts., elec. props. 80−6978
$CdSnP_2$ crystal growth, DTA obs. of Cd-Sn-$CdSnP_2$ phase diagram 80−24394
n- $CdSnP_2$, Hall mobility of electrons meas., 120-300K 77−4373
$CdSnP_2$, Hall mobility of holes 78−52015
$CdSnP_2$, luminescent props. *(Russian)* 78−35201
$CdSnP_2$, optical props., band struct. calcs., real space atomic potential parameters 79−95325
p-$CdSnP_2$, photocond. meas., polarisation depend. 78−39157
$CdSnP_2$:Cu, deep centres, emission transitions, polarisation *(Russian)* 78−84650
$CdSnP_2$-$CdSnAs_2$, and $CdSnP_2$-$CdGeP_2$, solid solution form. and elec. characterisation 78−43125
$CdSnP_2$-InP, n-n heterojunctions, growth, elec. characts. 77−11992
$CdTl_2Se_4$, single cryst., preparation, elec. cond. 77−24554
$CdTl_2Se_4$:Au, solubility meas. by microhardness method 80−96650
$CdTl_2Se_4(Te_4)$:Au, elec. cond., density, dielectric const., changes on fusion 80−88553
$CdTl_2Te_4$, Hall and thermo-EMF coeffs., in solid, liquid states 80−54704
$Cd_{1-x}Zn_xCr_2Se_4$, mag. semicond., neutronographic obs. *(Russian)* 79−11297
Co-Ge-Te system, phase equilib. 80−20908
$CoCr_2S_4$, CVD grown, surface microstruct. 79−4905
$CoCr_2S_4$ films, galvanomagnetic and thermoelec. props. 80−54717
$CoCr_2Te_4$, cryst. growth, struct., elec. props., Hall effect 78−43416
$CrPr_2S_4$, synthesis, single crystal growth, mag. and elec. props. 79−78857
$CrPr_2Se_4$, synthesis, single crystal growth, mag. and elec. props. 79−78857
$CsPbBr_3$, $CsPbCl_3$, ionic semiconductors, electronic and optical props. 79−38594
$CsPbBr_3$, electronic and optical props. 80−25414
$CsPbCl_3$, electronic and optical props. 80−25414
$CsPbCl_xBr_{3-x}$, optical meas., LCAO band scheme 80−25437
Cu, (112) chalcopyrite films, lattice mismatch with (0001)CdS substrates 79−87012
Cu-$CdSiP_2$ surface-barrier diode, photoelec. props. 77−4442
Cu-In-Se system cubic ordered phase existence and characts. 78−34495
$Cu_{1-y}Ag_yInS_{2-x}Se_{2x}$, for solar photovoltaic cells 80−10982
$Cu_{1-y}Ag_yInS_{2(1-x)}Se_{2x}$, lattice consts. and band gap variations 79−78000
$Cu_{1-y}Ag_yInS_{2(1-x)}Se_{2x}$ pentenary alloy system, appl. to photovoltaic solar-energy conversion 80−35680
$CuAl_{1-x}Fe_xS_2$ system, delocalisation of d-electrons, mag., elec. and optical obs. 78−34804
$CuAlS_2$, reflectvvity and XPS meas. 78−35165
$CuAlS_2$, X-ray spectroscopic study 78−39626
$CuAlS_{2x}Se_{2(1-x)}$, excitonic structure, phase-shift-difference spectra 78−2872
Cu_3AsS_4 and Cu_3SbS_4, thermal cond. in solid and liq. phases, 300 to 1100K, thermoelec. Q-factor 80−19997
$CuCrS_2$ single cryst., spectral study and phys. props. *(French)* 80−29002
$(CuCr_2S_4)_x$-$(Cu_{0.5}In_{0.5}Cr_2S_4)_{1-x}$ solid solution, piezoelectric effect, X-ray struct. anal. *(Russian)* 80−15978
$CuCr_2S_4(Se_4)$, electronic struct., mixed valence 80−70612
$CuCr_2Se_4$, cryst., preparation, elec. cond., thermo EMF 77−8125
$CuCr_2Se_4$, mag. reson. and valence state of Cu and Cr ions 80−60413
$CuCr_2Se_4(S_4)(Te_4)$, binary and ternary solid solns., mag. and elec. props. 80−2407
$CuFeS_2$, X-ray spectroscopic study 78−39626
$Cu(Ga_xIn_{1-x})(S_ySe_{1-y})_2$, spray pyrolysis 79−70004
$CuGa_xIn_{1-x}S_2$ solid soln., IR refl. spectra, comp. depend. 78−52498
$CuGa_xIn_{1-x}Se_2$, CVD, elec. and optical props., use as heterojunction solar cell absorber 79−52095
$CuGaS_2$, coloration, pure and Fe doped, EPR and optical absorpt. obs. 78−88336
$CuGaS_2$, crystal growth and luminesc. *(Japanese)* 78−23515
$CuGaS_2$, crystal growth by solid phase crystallisation 80−25556
$CuGaS_2$, direct gap semicond., exciton energy at 300K from reabsorption of luminesc. 79−78728
$CuGaS_2$, ESR assessment of S diffusion behaviour on annealing 78−35036
$CuGaS_2$, exciton absorption energies, appl. of modulated phase-shift-difference method 78−39565
$CuGaS_2$, exciton energy determ., electron beam excited luminesc. 79−38680
$CuGaS_2$, ionic. cond., galvanic cell meas. 77−47616
$CuGaS_2$, lattice vibr. modes, Fourier transform spectroscopy 79−33701
$CuGaS_2$, photoelectronic props., 77 to 300K 78−34865
$CuGaS_2$, press. depend. of energy gap, absorption edge obs. 77−12401
$CuGaS_2$, reabsorpt. of excitonic luminesc. in direct band gap semiconds. 77−63469
$CuGaS_2$, reflectvvity and XPS meas. 78−35165
$CuGaS_2$, single cryst., photocond. spectra 78−84252
$CuGaS_2$, tetragonal distortion, crystal field splitting, temp. depend. 79−47060
$CuGaS_2$, X-ray spectroscopic study 78−39626
$CuGaS_2$-$CuGaSe_2$ system, forbidden-band width 78−35280
$CuGaS_2$-ZnS heterodiodes, LPE, emission spectra 79−33335
$CuGaS_2$-ZnS p-n heterojunction, for LED appl., prep. and characterisation 79−1831

ternary semiconductors continued
$CuGaS_{2-2x}Se_{2x}$, mixed crysts., luminesc. spectra, lattice consts. and band gap energy 77−63454
$CuGaS_{2x}Se_{2(1-x)}$, excitonic structure, phase-shift-difference spectra 78−2872
$CuGa(S_xSe_{1-x})_2$, refl. spectra, comp. depend. 78−39570
CuGaSe, Schottky diodes with tunnel device characts. 78−39215
$CuGaSe_2$, cryst. struct., X-ray powder data 77−39565
$CuGaSe_2$ crystals, electron probe microanal., correction procedure 80−2171
$CuGaSe_2$ crystals, I_2 vapour transport grown, luminesc. spectra 78−88349
p-$CuGaSe_2$, electrolum. obs. 77−32444
$CuGaSe_2$, epitaxial layers, lattice parameters meas. using RHEED 79−90913
$CuGaSe_2$, evidence of donor-acceptor type transition 80−93375
$CuGaSe_2$ film, optical props. near and above fundamental absorption edge 78−35215
$CuGaSe_2$, film, spray pyrolysis prod. 79−95953
$CuGaSe_2$, obs. of energy transitions from lower valence band states 78−95576
$CuGaSe_2$, photoluminesc. spectra at 76K 79−38655
$CuGaSe_2$, single cryst. growth from melt, doping 77−12522
$CuGaSe_2$ single crysts., Hall effect and resist., acceptor states 80−10975
$CuGaSe_2$ single crystals, elect. and optical props. for solar cell appl. 80−10981
$CuGaSe_2$ single crystals, electrical and photovoltaic props. 80−92940
$CuGaSe_2$, temp. depend. of fundamental absorpt. edge 78−92090
$CuGaSe_2$, thermal expansion obs. 80−70432
$CuGaSe_2$ thin films, on GaAs substrates, structural and elec. props., photoluminesc. meas. 79−65564
$CuGaSe_2$/Cu Schottky-barrier cells, photovoltaic effect 79−96440
$CuGaTe_2$ and $CuInTe_2$, electroreflectance data, direct gap obs., cryst. field splitting and hybridisation degree 78−39557
$CuGaTe_2$, elec. and optical props. 80−6829
$CuGaTe_2$ epitaxial layers, elec. props. as function of growth temp. 79−65565
$CuGaTe_2$, exam. of kinematic viscosity of melts, and short range ordering 79−1383
$CuGaTe_2$ film, flash evaporated, growth and optical props. 79−95296
$CuGaTe_2$ films deposited on GaAs substrates by flash evaporation, struct. and elec. cond. 80−24755
$CuGaTe_2$, IR lattice vibr. spectra 79−28765
$CuGaTe_2$, refr. indices meas. 80−93259
$CuGdTe_2$, synthesis and elec. props. 78−26529
$Cu_{0.5}In_{0.5}Cr_2S_4$, piezoelectric effect, X-ray struct. anal. *(Russian)* 80−15978
$CuIn_{0.7}Ga_{0.3}Se_2$ epitaxial layers, on GaAs substrates, struct. and elec. props. 80−107670
$CuIn_{1-x}Ga_xSe_2$ mixed cryst., optical transmission spectrum and gap energy temp. depend. 79−65896
$CuInS_2$, cathodolum. spectra, heat treatment and electron irrad. effects 78−10996
$CuInS_2$, crystals and thin films, growth, struct., and elec. props. 79−38729
$CuInS_2$, epitaxial thin film on GaAs, exam. of growth, electrical props. 80−24754
$CuInS_2$ film, photoconductivity effects 77−43662
$CuInS_2$ film homojunction solar cell, fabrication, performance 77−80832
$CuInS_2$ films, RF sputtered, growth and props. 80−80124
$CuInS_2$ films prepared by spray pyrolysis, elec., optical and struct. props. 79−73609
$CuInS_2$ films prod. by RF sputtered Cu-In films exposure to H_2S 79−95926
$CuInS_2$, fund. reflectivity, 2 to 6 eV, band struct. implications 78−39574
$CuInS_2$, homogeneity region and intrinsic dopant mechanism 78−34630
n-$CuInS_2$, mag. props., obs. 80−70939
$CuInS_2$, minority carriers lifetime, photoelectromag. effect meas. 79−47125
$CuInS_2$, optical and elec. phenomena 78−39605
$CuInS_2$, p-n junction photovoltaic props. and detectors 79−99574
$CuInS_2$, region of existence, determ. by quenching and X-ray anal., phase transition 79−66054
$CuInS_2$, X-ray spectroscopic study 78−39626
$CuInS_2$:Cd(Zn), elec. props. 77−62927
$CuInS_2$-CdS photovoltaic heterojunctions, growth and characts. 77−39931
$CuIn_5S_8$, single crystn. phase, CVD prep., X-ray cryst. struct. determ. 79−65990
$CuInS_2(Se_2)$, film, spray pyrolysis prod. 79−95953
$CuInS_2(Se_2)$ film, vacuum deposited, absorpt. coeff. 78−72621
$CuInS_2(Se_2)$ films and heterojunctions, grain boundary and interdiffusion studies, AES and SIMS 79−77842
$CuInS_2(Se_2)$-$GeS_2(Se_2)$, degree of solid solubility and phases characts. 78−35377
$CuIn(S_xSe_{1-x})_2$, spray pyrolysis 79−70004
$CuInS_2(Se_2)(Te_2)$, film, electron and X-ray diffr. 77−11819
$CuInS_2(Se_2)(Te_2)$, thin films and photovoltaic devices, AES evaluation 78−67928
$CuInS_2(Se_2)(Te_2)$, thin film, bulk polycryst. and single cryst. samples, AES 78−72648
CuInSe, reflectvvity and XPS meas. 78−35165
$CuInSe_2$, acceptor levels, elec. props. study 80−39578
$CuInSe_2$ amorphous thin film, flash evaporation, struct., stoichiometry 80−89150
$CuInSe_2$ crystals, electron probe microanal., correction procedure 80−2171
$CuInSe_2$, dielectric const. from capacitance meas. 79−61292
n-$CuInSe_2$, effective electron mass, IR free-carrier Faraday rot. meas. 77−55783
$CuInSe_2$, energy gap, temp. depend., 15-300K, optical absorpt. obs. 77−36266
$CuInSe_2$ epitaxial growth on GaAs 78−84104
$CuInSe_2$ film, evaporation source temp. effect, on comp. 80−39478
$CuInSe_2$ film, MBE growth, AES and optical absorpt. obs. 79−78903
$CuInSe_2$ film, photoconductivity effects 77−43662
p-$CuInSe_2$ film, prep. from vac. evaporation of $CuInSe_2$, optical and elec. props. 79−82697
$CuInSe_2$, growth on CdS (0001) surface using MBE 79−56936
$CuInSe_2$, heteroepitaxy on {111} oriented Ge by flash evaporation, struct. 80−108333

ternary semiconductors continued
$CuInSe_2$, IR lattice vibr. spectra 79−28765
$CuInSe_2$, influence of impurities and free carriers on optical props. 80−108225
$CuInSe_2$, large single crystals growth by iodine transport and Bridgman methods 78−35300
$CuInSe_2$, melt-grown, EPR characts. 78−35030
p-$CuInSe_2$, minority carrier lifetime and surface recomb. velocity, photoelectromag. meas. 78−19085
$CuInSe_2$, n- and p-type, elec. resist. and Hall effect, 80 to 500K 79−87096
$CuInSe_2$ on GaAs, epitaxy grown RHEED exam. of epitaxial overgrowth *(German)* 79−11042
$CuInSe_2$, photovoltaic props. and p-n junction form. 77−69371
$CuInSe_2$ polycrystalline thin film anomalous photovoltaic effect *(German)* 78−68102
$CuInSe_2$, refr. indices meas. 80−93259
$CuInSe_2$, Schottky diodes with tunnel device characts. 78−39215
$CuInSe_2$ semicond. films, optical props., 1-3 eV 78−27346
n-$CuInSe_2$, single cryst., elec. props. 78−43397
$CuInSe_2$, spray pyrolysis 79−70004
p-$CuInSe_2$, thermal props. 80−96705
$CuInSe_2$ thin films for solar cells, radiofrequency sputtering technique, elec. props. 80−93487
$CuInSe_2$, Zn implantation profiles by AES 77−31692
$CuInSe_2$/CdS solar cell, grain boundary effects on performance 79−83603
$CuInSe_2$-CdS heterojunction, photovoltaic effect, rel. to optimum conditions for solar cell fabrication 77−51810
$CuInSe_2$-CdS photovoltaic heterojunctions, growth and charact. 77−39931
$CuInSe_2$-CdS solar cell, polycrystalline thin film, high photocurrent, characts. 80−61339
$CuInSe_2$-$CuInS_2$, melts, viscosity, elec. cond., density composition prop. graphs 79−14948
$CuIn_3Se_{3.5}$, cubic ordered compound, optical gap 78−48175
$Cu_{0.5}In_{2.5}Se_4$, transition state and domain struct. by electron microscopy and diffr. studies 80−15095
$CuInSe_{2-x}S_x$, phase equilibria 77−90328
$CuInSe_2(S_2)(Te_2)$, Debye temp., standard entropies and enthalpies, sp. ht. meas. 78−30769
$CuInSe_2(Te_2)$, far IR refl. spectra, ionic bonds 79−55695
$CuInTe_2$, direct energy band gap determ., electroreflectance meas. 78−2418
$CuInTe_2$ epitaxial layers, on GaAs, growth and props. 80−108359
$CuInTe_2$, exam. of kinematic viscosity of melts, and short range ordering 79−1383
$CuInTe_2$ film, photoconductivity effects 77−43662
$CuInTe_2$, grown from near stoichiometric comp., elec. and optical props. 78−68504
$CuInTe_2$, infrared optical properties 79−82974
$CuInTe_2$, optical transitions from valence band states 79−87416
$CuInTe_2$, pressure-induced phase transformations 78−30748
$CuInTe_2$, refr. indices meas. 80−93259
p-$CuInTe_2$, single cryst., IR study of lattice and free carrier effects 80−45074
$CuInTe_2$ single crystals, directional freezing growth and doping, resist. changes on annealing 80−60768
$CuInTe_2$, vac. deposited film, growth, struct. and elec. characts. 77−69995
$CuInTe_2$-CdS photovoltaic heterojunctions, growth and charact. 77−39931
$Cu_4Mn_2S_4(Se_4)(Te_4)$ spinel, prep. and elec. props., 100 to 650K 79−43127
$CuRTe_2$, R=Gd, Tb, Er, Tm, synthesis 78−26529
Cu_2S-GeS_2 and Cu_2S-SnS_2 systems dissoc. of ternary congruently melting cpds. 79−87832
$CuSbS_2$ crystals, growth and characterisation 80−60770
Cu_3SbSe_4, cathodoluminesc., 90-298K 77−40290
Cu_2Se-$GeSe_2$ and Cu_2Se-$SnSe_2$ systems, dissoc. of ternary congruently melting cpds. 79−87832
$Cu_2SnS_3(Se_3)(Te_3)$, Mossbauer effect, lattice dynamics obs. 77−43923
Cu_2SnSe_3, single cryst. growth and morphology 77−85908
Cu_2Te-Ge(Sn)Te_2, phase equilib., microstructural, DTA investigs. 77−16560
CuTlS, melting heat and melting entropy *(Russian)* 80−70374
Cu_3VS_4, mixed conductor, fast ion transport at room temp. 78−72214
$DyCrS_3(Se_3)$, prep., elec. and thermal props. 78−43390
$EuBi_2Te_4$, elec. cond., Hall, thermo-EMF coeffs. determ., 300-1100K 78−43386
$EuGa(In)_2X_4$, X=S,Se,Te, prep. and props. 77−85214
$EuSb_2S_4(Se_4)(Te_4)$ elec. cond., Hall, thermo-EMF coeffs. determ., 300-1100K 78−43386
$FeCr_2S_4$, pure and doped, CVD grown, surface struct., elec. props. and band struct. 79−4905
$FeCr_2S_{4-x}Se_x$ chalcospinels, ESR spectrum and paramag. susceptibility 80−15789
GaAs-$Al_xGa_{1-x}As$ epitaxial layer heterointerface, toroidal defect obs. 79−77933
$Ga_{0.67}Cr_2S_4$, semiconducting thiospinelide, spin glass type mag. ordering *(Russian)* 80−50123
$(Ga_xIn_{1-x})_2Se_3$, $1 \geq x \geq 0$, phases, lattice parameters and thermal expansion between room temp. and melting point 80−39031
GaTe-SnTe, phase equilib. 77−86006
Ga_2Te_3-Cu system solid solns., elec. cond. 78−51988
Ge-GaP system, phase analysis 78−23674
Ge-In-Ga system, microscopic and X-ray phase anal. 77−12606
Ge-In-Te system, region of solid soln. of In in GeTe 77−51499
Ge-InP system, phase analysis 78−23674
$GeBi_2Te_4$, Hall const., thermoelec. power, and elec. cond. 80−29407
$(Ge_{1-x}Ga_x)_{1-x}Te$, rhombohedral and cubic phases, transport effects 78−2481
$(Ge_{1-x}In_x)_{1-x}Te$, rhombohedral and cubic phases, transport effects 78−2481
GeTe-Ga_2Te_3, electrophys. props. 77−48403
$(GeTe)_x$-$(AgSbTe_2)_{1-x}$, thermoelectric props. of monolithic and pressed samples at 300K 78−80009
$Ge_{15}Te_{81}X_4$ amorphous semicond. switches, fabrication technology *(German)* 80−7493
HgA_2X_4 (A=Ga,In; X=S,Se), Fourier IR and Raman spectra, cryst. struct. and symm. *(German)* 79−24313

ternary semiconductors continued
$HgCr_2Se_4$, cryst., preparation, elec. cond., thermo EMF 77−8125
$HgCr_2Se_4$, ferromag. semicond., Raman spectra 78−52496
$HgCr_2Se_4$, ferromag. semicond., transport props. 78−68039
$HgCr_2Se_4$, initial mag. permeability freq. depend. near Curie temp. 78−10729
$HgCr_2Se_4$, initial mag. permeab., 77 to 300K, domain wall motion and damped ferromag. reson. 79−28562
$HgCr_2Se_4$-$CdIn_2S_4$ heterojunction, prep. and photovoltaic prop. *(Japanese)* 78−34889
$HgCr_2Se_4$-$CdIn_2S_4$ heterojunctions, prep. and photovoltaic prop. 78−34892
$HgCr_2Se_{4-x}S_x$, temp. depend. of EPR line intensity 78−27074
$HgGa_2S_4$, melt growth, optical props. and SHG, HgS-$HgGa_2S_4$ phase diagram 80−50548
$HgGa_2S_4$, energy band struct. calc., empirical pseudopot. method 80−24793
$HgGa_2Se_4$, anisotropic photocond., pleochroism, and band struct. 78−19094
$HgGa_2Se_4$, energy band struct. calc., empirical pseudopot. method 80−24793
$HgIn_2Se_4$, IR refl. spectra and cryst. struct. 79−56777
$Hg_3In_2Te_6$, complex ordered-vacancy cpd., struct. and lattice dynamics 78−34496
$Hg_{1-x}Mn_xTe$, mag. props., 4.2-300K 77−4508
$Hg_{1-x}Mn_xTe$, microwave helicon propag. and helicon excited EPR 77−43637
HgTe-MnTe, growth from two-phase melts, crystallisation characts. 77−36393
In-Sb-Te, region of In-Sb-based solid solutions 77−36466
In-Te-SnTe, phase equilib. 77−86006
$In_{1-x}Ga_xP$, epitaxial growth on GaAs substrate, formation of intermediate layers 80−2304
$In_xGa_{1-x}P$, TEM foil preparation, using polishing set 'Elypovist' *(German)* 79−9264
$In_{2/3}PSe_3$, cryst. growth and characterization 77−77357
In_2S_3, valence band densities of states, XPS meas. 79−28892
InSb-MnSb eutectic alloy, temp. depend. of conductivity and Hall effect, field depend. of Hall coeff. 77−24566
InSb-NiSb, eutectic alloy, Te-doped, electrophys. props. 77−35955
$InSbS_3(Se_3)$, prep., polymorphism, cryst. struct. 78−44002
$InSbSe_3$, cryst. prep. and props. 79−15601
$In_{1.8}Sb_{0.2}Se_3$, cryst. prep. and props. 79−15601
InSeI, X-ray cryst. struct. determ. *(German)* 80−100214
$(In_2Te_3)_x$-$(Hg_3Te_3)_{1-x}$, photoelec. and luminesc. props. 77−39889
$(In_2Te_3)_x(Hg_3Te_3)_{1-x}$, characts. of photocond. in strong absorption region 77−66184
InTeI, X-ray cryst. struct. determ. *(German)* 80−100214
In_2TeO_6, crystal growth by high press. method, elec. and struct. props. 77−81206
$(In_2Te_3)x$-$(Hg_3Te_3)_{1-x}$, $0.15 \leq x \leq 0.37$, E_g-comp. depend., spectral photo EMF meas. 77−47851
$LiInS_2$, single cryst. growth by directional solidification, photoluminescence meas. 79−61514
$MgSiP_2$, elec. props. and diode struct. exam. 79−51665
$MnCr_2Te_4$, elec. props., 100 to 650K *(Russian)* 79−11115
$Mn_{1-x}Cu_xCr_2S_4$, phase relationships and mag. phase diagram 79−78374
$MnGa_2S_4$, synthesis electrophys. props. 77−51747
MnS-$CuInS_2$, phase relations, 400 to 1300°C, X-ray and microscopic exam. 79−1853
$MnSb_2S_4$, synthesis, electrophys. props. 77−51747
$NaSbSe_2$ films, struct., photoelec. and opt. props. 78−51834
$Nb_3Se_5Cl_7$, preparation, struct. and props. 79−65040
$Nd_4In_5S_{13}$, chalcogenide cryst. struct., diffr. and Patterson function anal. 80−39056
$Pb_{1-x}Cd_xS$, metastable epitaxial films, elec. props. 78−26979
$Pb_{1-x}Cd_xS$ metastable epitaxial films, growth and physical props. 78−27417
$Pb_{1-x}Hg_xS$ film, IR detector material, struct. and IR props. 78−26775
$Pb_5Sb_8S_{17}$, dielectric props. 78−72452
p-$Pb_{0.8}Sn_{0.2}Te$/n-PbTe, multicolour photodetectors *(Czech)* 79−26126
$Pb_{1-x}Sn_xTe$ anodic oxide film form. conditions, IR absorpt. spectra 80−11494
PtGeSe, ferroelastic, cryst. struct. models 77−19927
SbSBr, electronic and optical props. 78−34763
SbSI, crystal growth from SbI_3 flux 79−66000
SbSI, electronic and optical props. 78−34763
SbSI ferroelectric, dielectric behaviour, particle-size dependence 78−2811
SbSeI, electronic and optical props. 78−34763
Se-Te-$Ge_{0.5}Sb_{0.5}$, DTA, critical cooling rates determ. *(French)* 77−72682
Sn-In-Te system, SnTe based solid solns. formation 77−84929
SnTe-Tl_2Te, phase and elec. props. 77−48406
$(SnTe)_{1-x}(PbSe)_x$ films on glass-ceramics, struct. and elec. props. 77−52251
$SrTiO_3$, electrode, photoelectrolysis of H_2O, solar energy conversion 79−52959
$SrTiO_3$ semicond. electrode, electrochem., photoelectrochem. props. 80−3352
$TbCrSe_3$, prep., elec. and thermal props. 78−43390
Tl $GaS_2(Se_2)$, optical and nonlinear optical props. *(Russian)* 79−51943
Tl-Bi-Sb-Te system, peritectic reactions in $TlBiTe_2$-$TlSbTe_2$ cross section, crystn. character 80−108406
Tl-Pb-Se system, quasibinary sections 77−86000
$TlAsSe_2$, diamag., thermal expansion rel. to temp. at cryst.-melt transition 78−34954
Tl_3AsSe noncollinear acousto-optic tunable filter, operation at 10 μm 79−41434
Tl_3AsSe_3, SHG, absorpt. coeffs. and temp. variation of refr. index difference 80−14390
$TlGaS_2$, layer ternary semicond., polarised Raman, IR reflect. spectra 78−68513
$TlGaS_2$, optical and photoelec. props. 77−55571
$TlGaS_2$-$TlGaSe_2$, phase and composition-property diagrams 80−55366
$TlGaS_2(Se_2)$, phase transforms. under hydrostatic press., Raman scatt. study 80−25366
$TlGaS_{2x}Se_{2(1-x)}$, layer solid soln., mixed one- and two-mode behaviour of optical phonons 79−47445
$TlGaS_{2x}Se_{2(1-x)}$, layer solid soln., long wave lattice vibrs., IR reflection spectra 80−11388
ternary semiconductors continued
$TlGaS_xSe_{2-x}$, optical and photoelectric props., composition depend. 79−15183
$TlGaSe_2$, impurity conductivity and TSC 78−23128
$TlGaSe_2$, layer ternary semicond., polarised Raman, IR reflect. spectra 78−68513
$TlGaSe_2$, monocrystal, processes of recombination and trapping levels, photocond. meas. *(Russian)* 80−70751
$TlGaSe_2$, Raman and IR spectra, zone centre optical phonons 78−76462
$TlGaTe_2$, IR refl. and Raman scatt. spectra, lattice vibrs. 80−40108
$TlGaTe_2$, $TlInTe_2$, and $TlInSe_2$, IR refl. spectra 80−60605
β-$TlInS_2$, layer ternary semicond., polarised Raman, IR reflect. spectra 78−68513
$TlInS_2$, optical phonons, IR and Raman spectra *(Russian)* 79−10903
$TlInS_2$ single crysts., three-dimensional exciton destruction, electroabsorpt. and transmission spectra 77−55803
$TlInS_2$-$TlInSe_2$, phase and composition-property diagrams 80−55366
$TlInS_2(Se_2)$, optical and nonlinear optical props. *(Russian)* 79−51943
$TlInS_{2x}Se_{2(1-x)}$, layer solid soln., mixed one- and two-mode behaviour of optical phonons 79−47445
$TlInS_{2x}Se_{2(1-x)}$ layer solid soln., long wave lattice vibrs., IR reflection spectra 80−11388
$TlInSe_2$, monocrystal, photoelec. props. *(Russian)* 80−70752
$TlInSe_2$, single cryst., elec. cond., photocond. and IR spectra absorpt. spectrum 79−47097
$TlInSe_2$, single crystals, optical phonons, Raman and infrared spectra studies 79−55842
$TlInSe_2$ single crystals, vibr. props. by light scatt. spectroscopy 79−56804
$TlInSe_2$-$TlPrSe_2$ system, struct., elec. cond., and thermoelec. props. 79−87119
$TlInTe_2(Se_2)$, IR refl. and Raman scatt. spectra, lattice vibrs. 80−40108
$TlSbS_2$, photocond. characts. 77−4407
Tl_2Te-Sb_2Te cross section of Tl-Sb-Te system, new $TlSbTe_2$ and Tl_9SbTe_6 cpds. 78−52778
VN-CrN system solid solns., electrophys. and galvanomag. props. 77−24567
$YbGa(In)_2X_4$, X=S,Se,Te, prep. and props. 77−85214
Zn-In-S thin layers, ternary phases, optical props. near long-wavelength intrinsic absorpt. edge 80−80887
ZnA_2X_4 (A=Ga,In; X=S,Se), Fourier IR and Raman spectra, cryst. struct. and symm. *(German)* 79−24313
$ZnAl_2S_4$-$ZnIn_2S_4$, phase relationships, 800 to 1050°C 79−1852
$ZnB^4C^2_2$, chalcopyrite struct., surface energy and compressibility, rel. to glass form. 79−51417
$ZnCr_2Se_4$, electroconductivity, thermoelectromotive force, Hall effect *(Russian)* 80−70694
$ZnCr_2Se_4$, screw spin struct., neutron diffr. exam. 78−27019
$ZnCr_2Se_4$, screw spin structure, method of controlling the sense, polarised neutron diffr. study 80−70944
$ZnGa_2S_4$, band struct., pseudopot. method 80−92816
$ZnGa_2S_4(Se_4)(Te_4)$, sp. ht., low temp. 77−35705
$ZnGeAs_2$, elec. cond. in solid and liq. state 77−11912
$ZnGeAs_2$, photoelectron spin polarisations, electron level struct. 79−87557
$ZnGeP_2$ bandgap absorption edge, spectra, electron transitions *(Russian)* 80−97305
$ZnGeP_2$, birefringence, effects on hydrostatic pressure and temp. 80−45033
$ZnGeP_2$, Br_2-methanol etching soln. for crystallographic axes determ. 78−35541
$ZnGeP_2$, cond. compensation by electron bombardment 79−15151
$ZnGeP_2$, cryst., electronic struct., X-ray K-absorpt. and emission 78−15248
$ZnGeP_2$, crystal, polarisation of recombination radiation 78−19562
$ZnGeP_2$ dissoc. press., vapour comp. and press., thermodynamic characts. 77−24934
$ZnGeP_2$, electron irrad., elec. and optical props. 79−33743
$ZnGeP_2$, IR radiation parametric conversion to visible range 79−94297
$ZnGeP_2$ layers, growth on Ge substrates, using chemical vapour deposition 79−52122
$ZnGeP_2$, one- and two-phonon Raman scatt. 79−78681
$ZnGeP_2$, P vacancies, lattice parameters, optical props. depend. on thermal treatment *(Russian)* 78−71729
$ZnGeP_2$ p-n homodiode, polarisation photosensitivity and photopleochroism spectra 80−107866
p-$ZnGeP_2$, photoluminescence of crystals with varying comp. and dopants 77−32431
$ZnGeP_2$, pseudodirect bandgap semiconductor, natural birefringence 79−65834
$ZnGeP_2$, synthesis, characts., applic. to laser windows *(French)* 78−80467
$ZnGeP_2$, temp. depend. phase-matched nonlinear optical devices 80−99794
$ZnGeP_2(As_2)$, reflectvvity and XPS meas. 78−35165
$ZnIn_2S_4$ (I) film, one-packed polytype, resist., photocond. and luminesc. 79−1608
$ZnIn_2S_4$, and $ZnIn_2S_4$-In_2S_3 alloys, SCL currents, trap distrib. 78−52000
$ZnIn_2S_4$, cond. and valence band states, photoemission study 80−35054
$ZnIn_2S_4$ crystals, switching effect, electric field distribution 80−107872
$ZnIn_2S_4$ diode struct., photoelec. props. *(Russian)* 77−43720
$ZnIn_2S_4$, electronic props. of polytypic forms, pseudopot. calc. 80−38997
$ZnIn_2S_4$ film, photoluminesc. and photocond. 78−52677
$ZnIn_2S_4$, fund. optical consts., Kramers-Kronig analysis, reflectivity spectra 78−39573
$ZnIn_2S_4$, fund. reflectivity, 2 to 6 eV, band struct. implications 78−39574
$ZnIn_2S_4$, III(a) polytype, absorpt. spectrum tail changes due to microstresses 80−2788
$ZnIn_2S_4$, IR refl. spectra and cryst. struct. 79−56777
$ZnIn_2S_4$, lattice dynamics, IR and Raman spectra 77−81106
$ZnIn_2S_4$ layered compound, phonon freqs., IR refl. and transmission spectra 77−77210
$ZnIn_2S_4$, layered semicond., wavelength modulated reflectivity spectra 79−8155
$ZnIn_2S_4$ layered semiconductor, fundamental optical constants, comparison with band structure calcs. and PES 79−56757
$ZnIn_2S_4$, photoluminesc., reson. Raman scatt. 78−48179
$ZnIn_2S_4$, Raman and IR spectra 78−48181
$ZnIn_2S_4$, Raman scatt., hydrostatic press. effect 80−84745

ternary semiconductors continued
$ZnIn_2S_4$, recomb. process of photoexcited carriers 77−44042
$ZnIn_2S_4$, S-type negative resist. and switching effects 80−65581
$ZnIn_2S_4$ single cryst., intense radiation effect on optical transmission, absorpt. saturation 80−53385
$ZnIn_2S_4$ switching investigation, negative resistance state instability, resistivity transitions 80−6920
$ZnIn_2S_4$, valence band photoemission spectroscopy 78−56569
$ZnIn_2S_4$, vibr. spectrum, Raman study 80−97278
$ZnIn_2S_4$-Ni diode, electric and photoelectric charact. 77−12005
$Zn_xIn_2S_{3+x}$, residual cond. 78−56185
$ZnIn_2Se_4$ defect tetrahedral crystals, band structure, charge density 77−11850
$ZnIn_2Se_4$, luminescence spectra, recomb. processes and energy level scheme 77−1726
$ZnIn_2Te_4$ defect tetrahedral crystals, band structure, charge density 77−11850
ZnS-$CuInS_2$, phase relations, 400 to 1300°C, X-ray and microscopic exam. 79−1853
$ZnSiAs_2$, birefringence, effects on hydrostatic pressure and temp. 80−45033
$ZnSiAs_2$, cryst. growth and elec. props. *(French)* 77−76815
$ZnSiAs_2$, electron irrad., defects, elec. and optical props. 79−19282
p-$ZnSiAs_2$, electron irrad. elec. props. annealing, lattice defects 80−100465
n-$ZnSiAs_2$ photodiode, fabrication and photoelec. props. 77−8146
$ZnSiAs_2$, photoelectron spin polarisations, electron level struct. 79−87557
$ZnSiAs_2$, pseudodirect bandgap semiconductor, natural birefringence 79−65834
$ZnSiAs_2$, synthesis and layer growth by CVD in open flow system 78−15312
p-$ZnSiAs_2$:Au(Tl)(S), photoluminesc., radiative recombination 77−24883
$ZnSiP_2$, 1 MeV proton bombardment, lattice deformation investigation by Kossel effect 78−22775
$ZnSiP_2$, band struct. calc., empirical pseudopotential method 77−1362
$ZnSiP_2$, birefringence, effects on hydrostatic pressure and temp. 80−45033
$ZnSiP_2$, chem. inhomogeneities, X-ray lattice parameter meas. *(German)* 77−72693
$ZnSiP_2$, conc. profiles during gas phase transport *(German)* 78−64452
$ZnSiP_2$ crystal growth, DTA obs. of Sn-Zn-$ZnSiP_2$ phase diagram 80−24394
$ZnSiP_2$, crystallisation from gas phase *(German)* 77−69977
n-$ZnSiP_2$, deep impurity levels, Schottky TSC meas. 79−95419
$ZnSiP_2$, effect of crystal growth method, on physical props., effect of doping on physical props. *(German)* 79−52094
$ZnSiP_2$, electronic struct., X-ray spectroscopic investigation 80−108300
$ZnSiP_2$, first- and second-order Raman scatt. 78−35151
$ZnSiP_2$, growth under nonstoichiometric conditions in gas phase, microanalytical investig. *(German)* 79−33909
n-$ZnSiP_2$, IR absorption 77−12377
n-$ZnSiP_2$, lattice limited Hall mobility, nonpolar optical scatt. mechanism 79−51579
$ZnSiP_2$ monocryst., impurity induced photoluminescence *(Russian)* 79−4850
$ZnSiP_2$, one- and two-phonon Raman scatt. 79−78681
$ZnSiP_2$, photocond. and photolum. spectra, optical anisotropy 78−72200
$ZnSiP_2$, photocond. under laser excitation *(Russian)* 78−84258
$ZnSiP_2$, pseudodirect bandgap semiconductor, natural birefringence 79−65834
$ZnSiP_2$, pseudodirect chalcopyrite semicond., electronic band struct. 80−20079
$ZnSiP_2$, reflectance spectra at 300K 80−25407
$ZnSiP_2$ Schottky diode, electrolum. under forward and reverse bias conditions 77−63466
p-$ZnSiP_2$, single cryst., recomb. processes, photoelec. props. *(Russian)* 78−68053
$ZnSiP_2$:Ga, effect of doping conc. on elec. cond. and Hall coeff. 78−76077
n-$ZnSiP_2$:Ga, elec. cond. and Hall meas., 77 to 1000K, scatt. mechanisms 79−11153
$ZnSiP_2$-Au(Ni) Schottky contact, production and props. 79−7901
$ZnSiP_2$-In Schottky diode, photovoltaic spectra 80−2423
$ZnSiP_2(As_2)$, thermal expansion coeffs. meas. *(Russian)* 80−65258
p-ZnSnAs, LPE, electronic struct. obs. by laser excited photolum. 80−60654
$ZnSnAs_2$, LPE in open tube system 78−92206
$ZnSnAs_2(P_2)$ single crysts., refl. spectra, band struct., dielec. consts. 77−44022
$ZnSnP_2$, characts. of Zn-Sn-P phase diag. 77−44225
p-$ZnSnP_2$, photolum. anisotropy, 77K 78−19557
$ZnSnP_2$-$ZnSiP_2$, heterocombination simultaneous crystallisation 78−60560
ZnTe-Ga_2Te_3, phase diagram 78−35360

terrestrial age *see geochronology*

terrestrial atmosphere
see also air; clouds; stratosphere; troposphere; upper atmosphere
acetonitrile, possible source of amino acids on primitive Earth 80−4112
acoustic gravity waves, generation mechanisms *(Russian)* 78−85621
active microwave sensing *(Japanese)* 78−16213
albedo change due to aerosol 80−56604
ancient atmosphere, fate of OH and O_2 origin 80−77116
angular momentum advection by axisymmetric motions 77−87039
barotropic Ekman layer over urban terrain 77−70733
biosphere, atmospheric effects, symposium (Mainz, Germany, 11-14 July 1977) 78−73461
biosphere and active solar processes link, role of Earth's natural electromag. field 78−61211
biota as modulator of atmosphere 78−73517
blunt body moving in atmosphere, heat protective coating destruction *(Russian)* 78−87251
boundary layer physics, conference (Smolenice, Czechoslvakia, 1974 February 18-21) 78−88873
Central Aerological Observatory, USSR, historical review 77−70798
circulation, by two-level quasi-geostrophic model 80−56546
circulation models of atmosphere 77−37348
climate variation throughout Earth's history, causal mechanisms 80−82048
clouds rel. to long-term stability of atm. and climate 79−74951

terrestrial atmosphere continued
comet impact, explanation of Cretaceous species extinction 80−76977
cometary nuclei or asteroids interaction with planetary atms., rel. to 1908 Tunguska event 78−49378
conference, New Delhi, India (Jan. 1979) 80−94912
cosmic ray penetration into atmos., calc. for energetic heavy nuclei 80−85826
Devonian atmosphere, Ar isotopic ratio determ. from Rhynie chert 77−66917
early atmosphere, NH_3 photochemically produced in small quantities 80−109208
early Earth, atmospheric comp. rel. to origin of life 78−69923
early Earth, pre-biotic atmosphere rel. to origin of life 78−69460
early evolutionary stages in atm. and climate 79−8696
Earth encounter with interstellar cloud, atmospheric and climatic effects 78−57292
Earth gravitational field, influence of atmospheric masses 79−57841
Earth optical horizon, height determ. from (Soyuz 9) 77−53186
Earth surface mechanical interaction, rel. to Earth rot. multiyear vars. excitation 79−96734
energy balance determ. methods *(French)* 77−33208
enhanced CO_2 greenhouse effect, compensation for reduced solar luminosity on early Earth 79−39865
environmental dispersion models, vertical averaging criteria 77−25725
environmental electromagnetic simulator 77−73894
escape of ions to space, ion chem. and low altitude accel. effects 80−85798
evolution, computer simulation, composition and surface temp. 78−28263
evolution implications for Earth's early atmosphere 78−36285
evolution of atmosphere, climatic changes 79−34962
evolution of interior, atm., ocean, Viking mission Mars information, appl. to Earth 77−78709
evolution of photosynthetic O_2, model 78−73516
evolution through geologic time, CO_2-HCO_3^--CO_3^{2-} system 78−73515
formation of atmosphere and sialic crust system from upper mantle 79−44153
gas body, low-density, entry motion in exponential atmosphere *(Russian)* 78−77376
gas exchange with magmas, determ. from mass fractionation of rare gas isotopes in volcanic rocks 80−98292
general circulation of 2-dimens. turbulent flow on β-plane 77−78317
geocoronal H conc. models, Hα emission rates and solar Lyman β flux 77−25808
global barotropic primitive eqns., Hough harmonics for spectral model 77−78442
global energy balance, environmental fluctuation effects 80−4084
global general circulation, 4th order model 78−11952
Hartmann boundary layer control of spin-up of stratified, conducting fluid 77−42923
ice clathrate as source of atmospheres on terrestrial planets 78−28557
inert gas composition, Earth's origin from solar nebula 80−61785
inert gases, accretion from protoplanetary nebula 80−109385
internally heated rotating annulus, axisymmetric states 77−45157
IR emission, Lambertian, of spherical surface, radiation press. on satellite *(French)* 78−81529
IR mosaic background obs. from balloon altitude expt. 80−90222
IR radiation absorpt. induced by press., mol. collision between CO_2, N_2, O_2 *(Russian)* 80−56600
IR remote sounding of atmosphere with multiple cloud formations 77−78319
IR remote sounding of cloudy atmosphere, CO_2 radiance data 77−78320
large scale process simulation, conf., Hamburg (30 Aug.-4 Sept. 1976) 77−86961
magnetosphere corotation lag, inertial limit, theory 80−41660
meteorites disintegration during atmospheric entry, appl. to Lost City, Grant and Pribram 77−67080
meteoroids atmospheric breakup, effects on crater field form. 80−94760
meteoroids ballistic shock waves and explosion, prod. of geomag. disturbances 77−13139
middle atmosphere, obs. from balloons, rockets and satellites, conference, London, England, (1978 December 12 to 13) 80−77540
monitoring techniques for neutral atmosphere *(Japanese)* 78−16126
motion of low-density gaseous bodies in the atmosphere, rel. to Tunguska catastrophe 79−84554
multilayer model, electrodynamic state, horiz. mag. field component influence *(Russian)* 78−73556
NASA solar terrestrial programme, planning 79−5731
near-space environmental structure, review 77−67002
nuclear, detonation waves, initiation and propagation conditions 79−93834
numerical and models of atmosphere, spectral-transform method 77−37342
numerical dynamic model atmosphere on a spherical Earth, used in forecasting 80−101416
optical parameters determ. by aerial photography at sunset 80−90219
optical studies from space, Soviet, review 78−85815
origin, implications of ^{36}Ar excess on Venus 80−12700
origin, of atmospheres of Earth and planets *(Chinese)* 79−16846
origin, rel. to Earth early history 79−20739
origin, role of shock degassing during accretion stage *(Russian)* 79−101099
origin, theory based on protoplanetary cloud history 80−12549
origin of atmosphere *(Russian)* 80−81857
palaeoatmosphere O_2 content, since Lower Carboniferous, fossil charcoal evidence 80−51542
palaeoatmospheric temp. struct. 78−28264
palaeoclimate of S.Hemisphere since 80 Myr BP, causes for change *(Russian)* 80−98440
palaeotemperature, O isotopes of mid-Wisconsin limestone cave deposits 80−82069
physics, book 80−51976
physics of atmosphere and ocean and weather prediction *(Russian)* 77−21774
physics of atmospheres, book 79−62568
planetary meteorology rel. to weather and climate on Earth 79−84697
plasma-neutral gas interaction in cosmic physics 78−69669
prebiotic model atmospheres, far UV irradiation effects 78−40668
primitive atmosphere and hydrosphere evolution *(Russian)* 77−53192
primitive equation models initialisation for alternating grid 77−45119
primordial dense atmosphere, blanketing effect rel. to Earth melting 79−57935

terrestrial atmosphere continued
radiation balance, sensitivity to cloud changes, zonal model 77−78419
radiation balance, zonally averaged model, improvements 78−61559
radiation budget at top of atmos., influence of cloud cover 80−98398
radiation problems, thermal struct. 80−82016
radiative balance, meas. by Cactus accelerometer on Castor satellite *(French)* 78−81530
rare gas fractionation rel. to Earth-atmosphere evolution model 77−13077
reducing to neutral biosphere, length of transition period 78−20519
remote sensing, conf. (Innsbruck, 1978 May 29-June 10) 80−31415
remote sensing *(Japanese)* 78−16205
response to heat sources and perturbations *(Chinese)* 80−85748
rotation rate from Cosmos 408 rocket orbit 78−73559
secular polar motion excitation function, low freq. spectrum anal. *(Chinese)* 80−104849
solar activity effects, surface press. maps during geomag. disturbances 77−78359
solar constant and the Earth's atmosphere, conference, Big Bear City, Calif. (1975, May 19 to 21) 77−2380
solar terminator, effect of slope on atmospheric disturbance prod. 77−91208
Spacelab, atmospheric physics, ESLAB Symposium (Frascati, Italy, 11-14 May 1976) 77−21775
Spacelab as orbiting atmospheric laboratory 77−21941
Standard Atmosphere, 1976, rel. to previous standards 78−11975
standard atmosphere, International and Soviet 80−26612
stratified, nonadiabatic heat dynamics with mass exchange and water phase transitions 79−58004
supernovae, nearby, effects on terrestrial atmosphere 80−94584
temperature regime, numerical model *(Russian)* 77−64368
thermal history, CO_2 content rel. to thermodynamic balance 79−29847
thermally driven rotating annulus, cyclic vars. of imposed temp. const. 79−7377
Tunguska catastrophe, computational modelling 80−41779
vacuum UV background, meas. 80−90221
vegetation-atmosphere interaction, one-dimens. model 77−37291
vertical temp. profile estimation method, system identification method 77−91342
VHF radar studies *(German)* 80−46294
windblown dust, threshold speeds and particle sizes 77−45083
Ar degassed from shungite, isotope composition of ancient atmos. 80−85749
CO_2 cycling in environment, non-proportionality between flux and reservoir content 80−46261
CO_2 model run in tandem with climate model, 1800-2100 AD 80−98381
C_3O_2 polymers in primitive atmosphere rel. to living systems genetic code 79−83690
H distribution and escape, charge exchange effects 77−29674
H_2 from water vapour photolysis in primitive prebiological atmosphere 78−73514
N_2 chemistry, history *(German)* 79−53415
NH_3 photolysis and greenhouse effect in primordial atmosphere 79−39864
$^{15}N/^{14}N$ ratio rel. to solar nebula differentiation 80−36519
O deficit consequences *(German)* 77−70799
O_2 and O_3 early history 79−84487
O_2 from water vapour photolysis in primitive prebiological atmosphere 78−73514
O_2 in early Precambrian atmosphere, photodissociation rather than photosynthesis 78−81409
O_2 levels in prebiological atmosphere, photochem. model 79−84486

terrestrial composition *see Earth composition*

terrestrial electricity
active hydrothermal systems, intrinsic fluid and rock resistivity anal. 78−40480
Adirondak mountains, deep crustal elec. cond. obs. 80−89946
S.Africa, resistivity soundings and continental crust 77−29252
air-Earth current density, rel. to ionosphere pot. and solar mag. sector struct. 77−33271
airborne EM mapping, aircraft altitude and displacement currents effects 77−52975
airborne EM meas., use of decay patterns in anomaly classification 77−17224
airborne wave tilt meas. for reconnaissance mapping at poorly cond. areas 77−78473
Alaska oil pipeline, elec. current induced by electrojet 80−61756
Alaska oil pipeline, induced elec. currents meas. by gradient fluxgate and SQUID magnetometers 80−98231
Alaska pipeline, auroral zone elec. currents induction 79−39645
alluvial aquifers, relation between resistivity meas. and hydraulic parameters *(Italian)* 77−53079
N America, cond. anomaly rel. to possible Proterozoic plate boundary 77−91079
N.America, E. coastal region, EM induction model 80−98235
Annamalainger, Tamilnadu, India, elec. resistivity meas. rel. to groundwater 79−92551
anomalous EM fields from different sources over polarized sections *(Russian)* 77−86776
apparent resistivities over layered Earth, transformation using digital filters 78−96304
apparent resistivity and Laterlog 7 sonde results 78−44759
apparent resistivity curve standardization 77−21675
apparent resistivity curves calculation, computer program *(Italian)* 78−40472
apparent resistivity curves for parallel layer Earth, difference algorithm 80−89937
apparent resistivity data interpretation, Apodi Valley, Brazil 78−3712
apparent resistivity for layered Earth *(Chinese)* 79−20746
apparent resistivity of perfectly cond. sphere buried in half-space, calc. 77−2269
apparent resistivity tensor appls. 78−28158
aquifers with horizontal and vertical fractures, elec. macroanisotropy coeff. calc. 77−52976
Arctic Ocean, magnetotelluric soundings rel. to sediment thicknesses and upper mantle temps. 79−48454
areal magnetovariation studies, Russian Platform 79−62432
arenaceous aquifers, matrix conduction props. 77−64347
Asama Volcano, Japan, amg. and elec. obs. *(Japanese)* 79−70736

terrestrial electricity continued
Middle Asia seismoactive regions, geomag. investigations rel. to rock cond. 80−26464
asthenosphere, elec. cond. and struct.-sensitive physical props. of partially melted rocks 79−12116
asthenosphere, electrical conductivity data and partial melt content 78−85518
asthenosphere under NE.Pacific, magnetotelluric sounding obs. 80−46123
NW Atlantic, lithospheric elec. resistivity struct. 77−2100
audiomagnetotelluric investigations in geothermal areas 79−84097
central Australia, elec. conc. profile from geomag. induction meas. 80−72424
Azov Sea, magnetotelluric soundings and dipole mag. profiling 80−3926
Baikal region, USSR, geoelectrical model 80−56365
Baikal rift zone, elec. anomalies rel. to continental rift form. *(Russian)* 80−12364
bay phenomena, theory of equivalent current systems including ground induction 80−41610
Bermudas, upper mantle conductivity 78−40482
bimodal Em induction in nonuniform thin sheets, N.Pyrenean induction anomaly appl. 78−11805
Black Sea branch of Carpathian electrical conductivity anomaly *(Russian)* 79−48394
British Isles region, EM induction by analogue model 80−56368
central California, self-potential vars. preceding earthquakes 77−52977
Canadian Cordillera geomag. transition anomaly, lateral cond. changes 77−64200
Canadian Shield, electrical resistivity structure, layer Earth models 79−48396
Carpathian region sedimentary cover, elec. conduction 80−89940
Carpathian regional lithosphere, geoelectric model from data along deep seismic sounding profile *(Russian)* 80−104934
Carpathians deep crustal struct., elec. cond. anomaly, numerical electromagnetic modelling 80−31008
Caspian Sea, Turkmenian sector, magnetotelluric sounding results 77−40980
Chaine des Puys, France, elec. cond. anomaly, struct., active magma chamber 79−2185
circular current loop as geomagnetic field representation 79−84105
coal, anisotropic elec. props. meas. 80−98312
coal fields of India, seam thickness by elec. and γ-logging 80−51394
coal seam depth determ. by elec. method *(Spanish)* 78−45031
coal seam thickness meas. using resonant loop as EM sensor 78−57366
coastal effect on geoelectrical soundings 80−46128
coastal zone, electric fields induced by sea currents *(Russian)* 79−39736
E.Colorado, electrical and seismic sounding of low-resistivity low-velocity materials 78−3711
conducting cylinder inside shell, EM response 77−64198
conducting slab response to source fields, EM analogue model and finite difference calcs. 78−61329
conducting sphere in mag. dipole field, general soln. 80−3921
conducting zone formation, geothermal effects 78−85519
conductive cylinder, anomalous mag. field, induced by elec. current *(Chinese)* 80−104858
conductive overburden effect on transient EM response of sphere 77−64197
conductivity, evidence for water 77−70593
conductivity, piecewise homogeneous ground models for sky-wave mixed-path loss and antenna elevation patterns 79−66774
conductivity anomalies, detect. from repeated high-accuracy geomag. field obs. *(Russian)* 79−96736
conductivity anomalies, Hokkaido, Japan 77−78098
conductivity anomalies, magnetotelluric calcs. 79−53299
conductivity anomalies 79−53303
conductivity anomaly, response to inducing source fields, lab. model 78−36100
conductivity anomaly near Exeter, effect on micropulsations 79−53305
conductivity determ. using single superconducting coil 77−41184
conductivity estimation using gradient data from magnetometer arrays 77−73867
conductivity in mantle, from heat transport processes 80−3929
conductivity inhomogeneities, alternating EM field perturbs. 79−39653
conductivity irregularities in layer, effect on variable EM field 78−20354
conductivity model, perturbation and induction arrow calc. 77−49004
conductivity model, three-dimens., perturb. and induction arrows calc. 77−73633
conductivity model and source fields, perturb. and induction arrows calc. 79−20751
conductivity modelling using finite element numerical technique 78−20357
conductivity of cracked solid 79−91117
conductivity of marine sediments from EM field of water currents 79−62480
conductivity of materials containing partial melt, simple model from Archie's law 79−100810
conductivity of upper mantle, interpretation of N.E.Japan Anomaly 77−78097
conductivity profile, meas. via geomag. D_{st} vars. anals. comparison 80−17419
conductivity rel. to random networks and mixing laws 77−44971
conductor depth estimation using EM transients 77−64195
continental shelf, possibility of geoelec. mapping 78−57341
core, monosulphide solid soln. in Fe-Ni-S system 80−90038
core-mantle EM interaction when elec. cond. concentrated near core boundary 77−91001
core-mantle system, conductivity profile 80−36238
Coso Range, California, reconnaissance electrical surveys 80−89944
cross-borehole EM probing, location of high-contrast anomaly 80−72639
crust, elec. cond. from spectral charact. of geomag. field vars. 77−87179
crust, nonparallel stratified models, scattered EM radiation field 78−44773
crust, nonparallel stratified models, scattered surface wave 78−40489
crustal resistivity, sounding data from South Africa, ridge regression inversion appl. 78−7561
crystalline foundation, anomalous high conductivity bands discovery *(Russian)* 78−96137
currents in bottom and shore of Barents Sea, EM field 80−104864

terrestrial electricity continued
DC apparent resistivity prospecting, topographic correction *(Chinese)* 78−24375
DC concentration on E.Sierran Front, shallow crustal conductors under Coso Range 80−89942
DC resistivity measurements, interpretation 79−5449
DC resistivity modelling for axially symmetric bodies, finite element method appl. 79−5445
DC resistivity sounding method, appl. to evaluation of non-uniform water-bearing formation 78−40474
deep electrical soundings, southern Africa, using Cabora Bassa power line 77−86770
deep EM sounding and profiling 77−9326
deep magnetic-variation sounding, geoelectric and geothermal interpretation of results 78−44765
deep magnetotelluric and magnetovariational sounding results in Ciscaucasian area 77−78096
deep magnetotelluric sounding, model of geoelectric section 78−44768
deep magnetovariation sounding curves, resolution of elec. cond. model parameters 79−53300
depth sounding by induction arrow representation, review 80−98486
detection of mineshafts by geoelectrical methods 77−64451
dielectric permittivity determ., water saturation effects *(Russian)* 79−62626
digital recording field system for geomagnetic telluric-array studies 79−62605
dipolar techniques, archaeological appl. 79−16687
dipole electrical soundings, perpendicular, numerical procedure for direct interpretation 79−34732
dipole soundings data obtained along crooked line, transform. 79−44259
dipole-dipole deep geoelectric soundings over geological structures 80−101449
direct current regimes, theorem proof 78−96131
direct interpretation of geoelectric soundings using filtered Bessel functions 79−74965
Dnieper-Donets depression, magnetotelluric sounding data rel. to deep struct. *(Russian)* 78−96170
E-polarisation, numerical soln., improved geomagnetic boundary conditions 78−77182
Earth's negative charge, supply mechanism 80−61758
Earth conductivities, mapping via multifreq. airborne EM system 79−5446
Earth conductivity, model for quantitative interpretation of towed-bird airborne EM system meas. 79−5447
Earth core, elec. cond. from geomag. field dynamics 79−12066
Earth core eldctric current and zonal mag. fields, theory 80−36240
Earth currents, short period oscills. rel. to AE and D_{st} indexes of mag. activity *(Russian)* 77−44914
Earth electrical parameters, determination from horizontal antennas input impedance meas. 80−90259
Earth induction, effects on vertical polarisation of Pc 5 pulsations recorded in auroral regions 79−12355
electrical sounding, elec. fields in random cond. layered Earth 80−77171
electrochemical glow discharge preceding earthquakes, rel. to aerosol anomalies 79−16407
electrode arrays comparison for induced polarization and apparent resistivity responses 79−58107
electrokinetic anomalies assoc. with dilatant regions in layered Earth, rel. to earthquake prediction 79−39658
electrokinetic props. of rocks, seismic wave propag. effects 80−76921
electromagnetic scale modelling, derivation of absolute units 77−14639
electromagnetic sounding, hybrid-ray approx. 80−72412
electromagnetic sounding transient pulse induction method, one-loop version 80−101448
electromechanical phenomena assoc. with earthquakes 78−36108
electrometry inverse problems, soln. via variational method *(Russian)* 77−44915
electroprospecting, direct problem soln. for ideally conducting hemisphere in space with point source *(Russian)* 79−34745
electroprospecting, inductive methods, resolving capabilities 79−84498
electrostatic field generation, Earth as unipolar generator 78−44771
elliptical borehole logging, resistivity tool response charcts. 77−87103
EM airborne profiles, sphere model for interpretation 77−45171
EM anomalies in Abitibi Clay Belt 77−81789
EM coupling in electrical prospecting systems 77−64193
EM depth sounding expt. in Tunisia 77−64192
EM depth sounding interpretation, master tables, book 80−86043
EM depth sounding systems, detectability analysis 77−91295
EM exploration, target near dipping contact, response modelling 79−8595
EM field above two-dimensional inhomogeneous struct., boundary conditions 80−85595
EM field build-up sounding method, resolution 78−16176
EM field eqns., transient time-domain EM method 80−98227
EM field formation method in conducting half space *(Russian)* 79−84110
EM field of infinitely long cable, diffr. over wedge-shaped conducting media *(Russian)* 78−40484
EM field short period variations, anal. for wave type and propag. direction determ. *(Russian)* 78−85474
EM field sounding, appl. of composite obs. patterns in near field *(Russian)* 79−44270
EM field variations assoc. with sea waves, possible origin 78−44834
EM fields, about horizontal electric wire source of abritrary length 79−27130
EM fields, topographic effect in three-dimensional cond. model 77−25639
EM fields in halfspace with ore body, local element transformation 79−66828
EM fields of vertical mag. dipole over thin conductive overburden 78−65183
EM frequency sounding, crustal struct. determ. 78−49167
EM frequency sounding in horizontal coils system, field test 77−49182
EM frequency soundings, exptl. study 79−58129
EM ground waves, elec./mag. field ratios in realistic terrain 78−88795
EM induction, freq. and transient responses of EM fields created by currents in confined conductors 79−29702
EM induction, H-polarisation problem soln. by wavenumbers integral eqn. method 77−44913
EM induction, in rot. conductive Earth 78−44764
EM induction, one-dimens. problem, Frechet derivative 77−48996
terrestrial electricity continued
EM induction, source field effects on transfer functions at mid-latits. 79−74831
e.m. induction, two-dimens., finite difference soln. 77−2101
EM induction, two-dimensional, in thin surface sheet of variable integrated cond. 79−16372
EM induction effects of ocean coast 80−76908
EM induction for island-continent ocean channels, analogue model 77−9336
EM induction for island-continent ocean channels, analogue model study for H-polarisation 77−81795
EM induction in conducting stratified medium, numerical analysis 79−34740
EM induction in Earth, by moving ionospheric current systems 79−16370
EM induction in Earth and Moon, workshop proc. (Murnau, W.Germany, 1978 September 7-13) 79−79741
EM induction in elongated structs., analogue model expts. *(German)* 79−25199
EM induction in layered Earth by surface loop, transient response 80−72410
EM induction in thin sheets, statistical theory 77−86769
EM induction in three-dimens. struct. for various source fields 79−66609
EM induction of laterally inhomogeneous anisotropic ground, VLF method 80−85754
EM induction one-dimensional problem, model refinement 79−44096
EM induction over perfectly conducting ocean edge, H-polarisation 77−44912
EM inverse interpretation, trend influence 78−81103
EM lateral waves, Earth-sounding radar obs. 77−44909
EM logging in inhomogeneous media, axisymm. problem 79−39877
EM methods with distant source, terrain relief effects 79−79735
EM modelling, finite element program package 77−73874
EM probing, expt. curves features due to seismoelec. effects *(Russian)* 79−39643
EM probing of permafrost terrain, theory 78−28323
EM propagation characteristics and interface aspects, Conf. Istanbul, Turkey (Oct. 1976) 78−22075
EM prospecting, harmonic and transient fields behaviour on surface of two-layer medium 79−92478
EM prospecting, inverse problem 79−53583
EM response of conductive inhomogeneity in layered Earth 77−40976
EM response of dipping half plane embedded in conducting rock 80−90236
EM response of Earth surface, aircraft remote sensing *(Chinese)* 80−104859
EM scattering from buried wires, fast Fourier transform 79−16369
EM shielding of sources within metal-cased borehole 77−40979
EM sounding, analogue model meas. for horizontal mag. dipole embedded in conducting medium 79−12068
EM sounding, appl. to shallow permafrost mapping 79−16694
EM sounding, computation of multilayer response 79−92618
EM sounding, detectability of intermediate layers, time domain anal. 80−72641
EM sounding, induced polarisation effect on near-field form. *(Russian)* 79−39641
EM sounding, interpretation of transients in Laplace space representation *(Russian)* 78−40483
EM sounding, iterative ray tracing between boreholes for underground image reconstruction 80−98466
EM sounding, multicoil II airborne system 80−51554
EM sounding, numerical modelling of new multi-freq. system 80−56623
EM sounding, of asthenosphere of E.European Platform 77−53021
EM sounding, VLF-EM profiles, topographic correction based on model studies 80−101452
EM sounding methods, theoretical principles 78−49166
EM sounding of buried axial conductor, time-domain response 80−105059
EM sounding of conductive circular cylinder, expt. and theoretical results 80−105058
EM sounding of glaciers and permafrost 79−62768
EM sounding of kimberlite pipes, prospecting techniques and EM signature 80−51393
EM sounding of ocean floor near Californian coast, interpretation 77−9383
EM sounding over permafrost region, computer-assisted anal. 77−2086
EM soundings, multifrequency, topographic and misorientation effects study 80−101451
EM subsurface profile from HF meas., reconstruction technique algorithms appl. 77−45199
EM surface impedance, N-layered half space theory 80−76909
EM time-domain sounding of multilayered Earth 79−57850
EM transient response of vertical elec. dipole in homogeneous anisotropic medium *(Polish)* 77−52970
EM transients over low-resist. polarisable Earth, formulae *(Russian)* 79−39644
EM wave excitation by dipole emitters buried in stratified media 78−48966
EM waves, lateral-wave propag. in oceanic lithosphere 79−92482
EM waves and antennas above and below Earth surface, theory 79−66620
energy propag. of EM field of dipole source on conducting halfspace 77−9330
Etna volcano, shallow geological struct. by elec. sounding 80−41419
central Europe, upper mantle conductivity anomaly rel. to geomagnetism and secular var. *(German)* 78−7565
E.European platform, peculiarities of geoelectrical section and zonation of Volyn-Podolian margin *(Russian)* 78−48964
N.Finland, magneto-telluric expts. 79−44093
Foredobrogen area, USSR abyssal elec. cond. 80−90000
galvanic prospecting effects, calc. via method of sub-areas 80−56348
gamma-ray pulse from nuclear explosion disturbing field 79−70852
geoelectric potentials and their derivatives, appl. to deep crustal sounding *(German)* 80−56626
geoelectric sounding, controlled-source DC pot. problem by self-pot. Green's function 80−77136
geoelectrical prospecting, thin-layer problem 79−44095
geomagnetic coast effect, review 80−94458
geomagnetic dynamo and secular variation, damping of Hide's mag. waves 80−98218
geomagnetic induction vectors, local time var. 78−85477

terrestrial electricity continued
geomagnetic transfer functions at pulsation periods 80−72417
geothermal energy resources in Oregon, USA, elec. and EM sounding obs. 80−97761
N.German sedimentary basin, cond. distrib. from widely spaced areal magnetotelluric meas. 79−74833
N.Germany, magnetotelluric meas. of nearly circular salt dome 77−64201
global electrical conductivity, qualitative character 80−17231
gradient magnetotelluric marine sounding method 79−62599
gradient media and equiv. sequences of layers *(German)* 78−69281
Gregory Rift Valley, Kenya, magnetotelluric study rel. to elec. cond. 77−91000
ground subsurface, EM transient response 78−57166
grounded structures, induced polarization effects 78−28157
groundwater resources in Kalahari Basin, geoelec. survey 78−3830
H-polarisation induction over ocean edge coupled to mantle by conducting crust 77−48994
Hawaii Island, mag. induction fields rel. to oceanic mantle elec. cond. struct. 78−40477
HF EM induction profiling, of boreholes in underground mines *(Polish)* 80−51547
HF EM logging in inhomogeneous media 77−81791
horizontally multilayered Earth models, recurrence formulae for layer eigenfunctions 80−90246
horizontally stratified media sounding, geophysical problems unification 80−56622
Iberian Peninsula, cond. anomalies, continuous cond. channel from Mediterranean to N.Morocco *(French)* 77−86756
NE.Iceland, elec. resist. model from magnetotelluric obs., correl. with temp. 80−89954
Iceland, magnetotelluric investigation of lower crust and upper mantle 79−66612
impedance determination, effect of field vertical components on magnetotelluric soundings results *(Russian)* 78−48963
impedance frequency sounding for multilayer geoelectric profile *(Russian)* 77−29517
Imperial Valley, California, quadrupole resistivity survey of geothermal fields 79−84096
Indian peninsula, induced currents at short periods rel. to horizontal mag. field vars. 77−86773
induced (galvanic) polarisation in solids with electrolyte pore filling, theory *(German)* 79−88344
induced currents during 23 October 1976 solar eclipse, mag. obs. in Australia 78−81498
induced polarisation, multifrequency, mineral discrimination and inductive coupling removal 79−5448
induced polarisation (IP) sounding, effects of EM coupling in electrode arrays over uniform half-space 80−101324
induced polarisation for geophysical exploration, book 77−41216
induced polarisation meas. using discharge transient recorder 78−65398
induced polarisation methods for ore body tracing *(German)* 80−82084
induced polarisation response of multilayered Earth with no resistivity contrast 77−64196
induced polarisation sounding, freq. depend. of measured parameters *(Russian)* 79−74836
induced polarisation sounding, response of polarisable inhomogeneous sphere 79−44092
induced polarisation soundings interpretation, freq.-effect transform function definition and appl. 80−56624
induced polarisation technique for prospecting 78−69473
induced polarisation theory, stochastic rock model appl. *(Russian)* 79−88250
induced polarisation vertical electric sounding curves, correl. analysis *(Russian)* 77−9565
induced polarization method, saturation effect *(Chinese)* 77−91280
induced polarization method, time domain and freq. domain comparative anal. 78−20351
induced polarization models, parametric study 78−7560
induced telluric current and power harmonic radiation enhancement during sudden storm commencement 79−2184
induced-polarisation data, inversion technique 79−16695
induction, in arbitrarily shaped ocean of finite conductivity 79−16371
induction effects, simulation on mid-latitude substorm data 78−15960
induction effects assoc. with equatorial electrojet 77−32992
induction effects in polar magnetic substorm modelling 77−9628
induction in arbitrarily shaped infinitely conducting oceans 78−61318
induction logging, longit. geometric factors *(Chinese)* 77−66998
induction logging, numerical soln. by transition process method 77−56751
induction model, for sea-floor coast effect in H-polarisation 77−2104
inductive dipole profiling, screening effect of surface deposits 77−81792
inductive dipole sounding anomaly, low-impedance overburden screening *(Russian)* 78−81106
inductive logging near single and multiple conductive bodies, scale model results 79−16696
inhomogeneities of geoelectric structure, position determination by variable geomag. field method 80−89956
central Israel, crustal structure for magnetotelluric data inversion 79−2196
Iturup Island, magnetotelluric soundings, geoelectric horizon and sedimentary layer 80−3925
Izu peninsula, Japan, elec. resistivity along Inatori-Omineyama fault *(Japanese)* 80−46121
Izu Peninsula, Japan, geoelectric survey near anomalous upheaval zone *(Japanese)* 80−46122
Izu Peninsula, Japan, geomag. variations rel. to earthquakes *(Japanese)* 80−41396
Izu Peninsula, Japan, resistivity meas. in crustal uplift area *(Japanese)* 78−96127
Izu-Hanto-Oki earthquake, May 1974, precursory resist. changes 80−51336
Izu-Oshima-kinkai earthquake, Jan. 1978, associated 73 Hz elec. resist. changes *(Japanese)* 80−46133
Izu-Oshima-kinkai earthquake, Jan. 1978, precursory elec. fields obs. *(Japanese)* 80−46131
Izu-Oshima-kinkai earthquake, Jan. 1978, precursory mag. variations and electricity *(Japanese)* 80−41397
central Japan, conductivity anomaly changes rel. to earthquake occurrences 77−2102

terrestrial electricity continued
Jharia Coalfield, India, coal seam mapping by elec. resist. methods 80−4133
S Karelia, elec. cond. anomalies from magnetovariation and magnetotelluric data *(Russian)* 79−96737
Kenya Rift, mapping of induced currents, comparison of techniques 77−73628
Kirovograd anomaly/Dnieper-Donets depression intersection, magnetotelluric sounding *(Russian)* 79−20748
Kokchetav mountain massif, magnetotelluric soundings 77−40981
NW.Kola Peninsula, near zone field development method testing *(Russian)* 80−85761
lateral induction logging, calibration of apparatus *(Russian)* 79−39941
lateral logging three-electrode probe, effective field model *(Russian)* 78−53762
lateral resistivity logging, effectiveness increase *(Russian)* 78−53760
Laterolog 7 resistivity logging, field tests 78−61574
layered Earth, negative-induced polarisation effects 77−44910
layered medium, anisotropy resolution by joint inversion 78−16173
line source DC apparent resistivity profiles, basement effect 77−78091
lower mantle conductivity, comments and reply 80−30988
magnetic induced polarisation techniques, effect of large cond. contrasts 80−98461
magnetic induced polarization method, theoretical problems *(Chinese)* 79−100962
magnetic secular variation, modelled on mantle elec. cond. inhomogeneity *(German)* 80−81806
magneto-telluric response dispersion relations, inversion problem theory 80−104861
magneto-telluric surface impedance, calcs. by layered Earth model 80−56349
magnetometric and electrometric methods for landslide dynamics investigation 77−87091
magnetometric resistivity anomalies, two-dimensional struct., mag. field determ. method 80−12334
magnetometric resistivity methods, theory 79−53531
magnetotelluric analysis for layered Earth, matrix relation 78−32008
magnetotelluric and geothermal surveys in NW Germany, comparisons 80−12336
magnetotelluric and magnetic variational sounding, 3-dim. modelling 78−7563
magnetotelluric and magnetovariation methods, elec. cond. functions 77−32982
magnetotelluric and telluric parameters, cross-correlation estimates 79−92484
magnetotelluric anisotropic data, inversion technique 77−60475
magnetotelluric apparent resistivity, effect of localised source 80−72429
magnetotelluric data analysis: removal of bias 79−53530
magnetotelluric diagrams 77−2087
magnetotelluric field in homogeneous layer with cylindrical inclusion *(Russian)* 78−53617
magnetotelluric field over gently sloping elongated structures *(Russian)* 79−84111
magnetotelluric field over graben *(Russian)* 77−91006
magnetotelluric field over graben containing high-resist. intercalation, calc. and anal. *(Russian)* 78−48965
magnetotelluric field variations due to atmospheric discharges and ionosphere elec. currents *(Darish)* 80−8250
magnetotelluric fields, calc. in horizontally-inhomogeneous media using finite differences method *(Russian)* 79−44102
magnetotelluric fields in E.Canada tectonically active region, time depend. 80−26451
magnetotelluric fields modelling above heterogeneities in conducting base 77−52979
magnetotelluric impedance function estimation 78−85731
magnetotelluric investigations, induction effects detect. methods appl. in Sakhalin and Yakutia *(Russian)* 79−39642
magnetotelluric meas. over horizontally stratified formations, stratigraphic interpretation method *(Russian)* 79−62620
magnetotelluric meas. using SQUID magnetometer, remote reference technique 79−29866
magnetotelluric measurements, using lock-in signal detect. 78−81104
magnetotelluric measurements, with remote mag. reference 79−88245
magnetotelluric method for investigation of media with monotonically changing cond. 77−78439
magnetotelluric probing, data interpretation, reliability estimate *(Russian)* 79−39949
magnetotelluric probing, input impedance determ. accuracy, noise effects *(Russian)* 79−39950
magnetotelluric probing in complex geoelec. conditions, data interpretation *(Russian)* 79−39932
magnetotelluric probing phase curves, horizontally inhomogeneous medium *(Russian)* 79−39931
magnetotelluric profiling of vertical conductors 77−52983
magnetotelluric prospecting methods, exact surface impedance for spherically concentric Earth model 80−46129
magnetotelluric rapid profiling across Berici-Euganean ridge eastern edge 77−48998
magnetotelluric resistivity and phase soundings interpretation, graphical procedure 78−40473
magnetotelluric signals digitization equipment *(French)* 77−87092
magnetotelluric sounding, affected by resistivity freq.-dispersion 80−41368
magnetotelluric sounding, audio-frequency, case history at Cavendish geophysical test range 80−51324
magnetotelluric sounding, effect of primary field inhomogeneity *(Russian)* 77−86774
magnetotelluric sounding, expt. study of edge effect 77−78441
magnetotelluric sounding, fields of vertical mag. dipole over vertically inhomogeneous Earth 79−34736
magnetotelluric sounding, fundamental model 80−77167
magnetotelluric sounding, high-resistance horizons in laminated medium *(Russian)* 78−69290
magnetotelluric sounding, interpretation method 77−44918
magnetotelluric sounding, inverse problems soln. 78−49162
magnetotelluric sounding, multiple-reflection method appl. to inverse problem soln. 78−61581
magnetotelluric sounding, natural source obs. one-dimensional inversion 79−92479
magnetotelluric sounding, plane EM field over polarized section *(Russian)* 77−86775

terrestrial electricity continued
magnetotelluric sounding curve distortion rel. to diurnal surface dip *(Russian)* 79−84109
magnetotelluric sounding curves in nonuniform field of linear sources, comparative anal. *(Russian)* 79−48395
magnetotelluric sounding localization and accuracy improvement *(Russian)* 78−53754
magnetotelluric sounding method development in USSR 78−49169
magnetotelluric sounding over models of continuously varying conductivity 78−32009
magnetotelluric soundings, analogue modelling 77−33197
magnetotelluric studies in Central Urals and Transurals 79−25194
magnetotelluric studies in USSR, review 78−49168
magnetotelluric study, S.Scotland, fieldwork, data anal. and results 79−29705
magnetotelluric study, S.Scotland, Monte-Carlo data inversion, geophys. and tectonic implications 79−29706
magnetotelluric tensor analysis, appl. to two-dimensional geological structs. 78−40471
magnetotelluric two-dimensional inversion 77−73629
magnetotelluric vars. in 10-1000 sec. range, processing *(Russian)* 79−84535
magnetotellurics, automatic data processing 79−80041
magnetotellurics, crustal resistivity and conductivity variations, thin sheet anal. 80−51329
mantle, conductivity in deep regions, geomagnetic impulses 78−28200
Mantle, elec. cond., effect of partial melting 80−76936
mantle, electrical conductivity rel. to geomag. field 60-year vars. 79−8596
mantle conductivity, constraints due to secular mag. variations 80−61754
mantle conductivity, distrib. rel. to core mag. field screening 79−12064
mantle conductivity anomaly interacting with ionosphere current to form geomag. variation 80−30985
mantle conductivity rel. to geomagnetic secular variation impulse 80−98236
marine electrical prospecting, EM field buildup by immersed dipole 77−70595
marine electrodynamics, magnetostatics problems and appl. to water masses movement *(Russian)* 78−77259
marine magnetotelluric investigations, tidal currents effects 77−78095
marine sediments, resistivity techniques validity for diffusion coeffs. determ. 79−92601
marine waves, nonstationary, theory of EM field 78−44833
Martinique, aeromag. survey, conductivity anomaly existence *(French)* 77−86754
Melendy Ranch, Calif., San Andreas fault, search for resistivity variations 78−28185
meltwater from glacier, elec. resist. obs. showing water origin 80−85689
metallic mineral deposits of Australia mag. induced polarisation survey results 80−98223
Mezen' Bay (White Sea), marine tides EM fields 78−73378
mineral exploration, effect of tropical weathering on elec. and EM meas. 79−88246
mineral ore/pore electrolyte phase boundary layer, excess voltage time depend. *(German)* 79−84233
mining tectonical forecast maps, geoelectric bed sounding method *(Hungarian)* 80−105075
N.Morocco, geomag. vars. recording, cond. anomaly existence *(French)* 77−86755
multilayer medium with periodic conductivity var., geomagnetic field *(Russian)* 77−44922
Nakaizu, Izu Peninsula, repeated resistivity meas. *(Japanese)* 80−41370
natural VLF antenna, Deception Island, impedance meas. 79−48399
New Brunswick, resistivity and induced polarisation (IP) survey for delineating saline water and fresh water zones 80−104867
nonharmonic EM induction in two-layer spherical Earth 79−100812
nonperiodic EM induction in conducting Earth 78−44761
ocean, baseless method of electric field meas. *(Russian)* 79−39900
ocean, EM field of wide current for arbitrary direction of permanent mag. field 79−57946
ocean bottom current formation by water movement 80−104863
ocean current induced EM fields, theory 80−61805
ocean current of finite width, EM field 79−53351
ocean electric current, induced in insulated oceans 80−51407
ocean electric current induced by Sq, around land masses 80−72413
ocean electric field measuring system equivalent base for rectangular fairing *(Russian)* 79−34988
ocean electric fields, EM phenomena accompanying movement of current fairing in sea water *(Russian)* 78−77361
ocean EM induction affecting Sq during IGY 80−72428
ocean water motion due to geomagnetic variation, theory 80−104962
ocean-coast model, EM response to E-polarisation induction 78−61321
oceanic asthenosphere off Californian coast, elec. cond. model 79−25193
oceanic crust, resistivity models, based on lab. meas. of basalts and gabbros 79−29703
oceanic dynamo, contrib. to O_1 tidal component of geomag. lunar daily var. at Alibag 80−56355
ohmic region effect on geomagnetic vars. *(German)* 79−29708
ore bodies, channel-type streaky conductivity model, polarisation 77−33063
orogenic regions deep crustal probing by natural EM fields surface impedance vars. 77−13060
Oshima Volcano, Japan, elec. resist. changes and 1978 Jan. 14 earthquake *(Japanese)* 80−46132
N. central Pacific, ocean floor magnetotelluric sounding 77−86772
E.Pacific Rise, active elec. sounding rel. to oceanic crust props. and origin 80−101360
Palmdale, California, crustal resist. changes 79−16373
peninsular loop current, ULF wave generation 80−90247
permafrost fossil patterns, S.W. Ontario, resistivity mapping 77−66991
permafrost mapping by audiofrequency magnetotellurics 79−58102
plasmasphere, magnetospheric and ionospheric elec. field simultaneous obs. 80−105110
polarisable half-space, current pulses, transient EM field 78−96130
potential field around subsurface electrically excited conductors, mathematical model 80−98230
probing of underground struct. *(German)* 80−82089
profiling technique for apparent pseudo-resistivity mapping *(French)* 78−69285
prospecting, kernel function for horizontally stratified Earth 77−21918
terrestrial electricity continued
prospecting equipment with focusing effect, detect. of cavity in lower half-space *(Russian)* 78−28336
prospecting in marine areas, dipole and unipole resistivity methods 80−56641
prospecting in marine areas, resistivity methods 78−65417
prospecting problems soln. for inhomogeneous media 79−88487
pulse excitation for EM freq. sounding 77−81793
quasi-static EM fields of horizontal electric dipole on polarisable half-space surfaces 78−69283
Quebec City, geomagnetic and telluric var. in seismic region 77−52974
SW.Queensland, telluric currents assoc. with anomalous geomag. vars. 80−109089
Raft River Valley, Idaho, surveys of geothermal system 79−84307
reciprocal geoelectric section appl. to vertical elec. sounding data 80−90237
region EM induction, inversion problem 78−7567
regularization method and uniqueness problems in study of regional flat-layered structs. 78−49161
Reis crater, struct. from geoelec. Schlumberger soundings *(German)* 77−64207
remote reference magnetotellurics, random error derivations relating to impedance 80−12335
resistance logging, continued fractions method appls. *(Russian)* 78−3971
resistance method, oil-gas field appl. *(Russian)* 79−20749
resistance vars., prior to earthquakes, appearance time rel. to earthquake energy 77−13061
resistive/conductive beds, limiting detection depth in line electrode systems 78−44760
resistivity, airborne survey using VLF plane waves, resolution studies 80−12333
resistivity and induced polarisation surveys, topographic effects 80−98224
resistivity and induced polarization, modified pseudosection 78−7562
resistivity and induced polarization modelling using buried electrodes 78−11802
resistivity anomalies over buried conducting dykes, model tank expts. 80−85582
resistivity anomaly detection, FORTRAN IV programs for statistical method appl. *(Rumanian)* 77−41214
resistivity changes as earthquake precursors 77−78121
resistivity changes in rocks during frictional sliding and fracture 79−16457
resistivity curves of horizontally multilayered models, calc. methods 80−46283
resistivity determination, by surface meas. 78−24393
resistivity distribution, in uppermost kilometres on continental areas 78−24219
resistivity finite-difference modelling, practical approach 79−29878
resistivity in layered structure with unconfined aquifer 79−79734
resistivity interp., application of rules of composition 77−64194
resistivity logging, direct problem soln. using graphic display *(Russian)* 78−69481
resistivity logging tool response, sonde position effect 77−86759
resistivity logging using ring probes *(Russian)* 77−86778
resistivity mapping using airborne multicoil EM survey system 78−77348
resistivity meas. for sandstone porosity determ. 77−9528
resistivity meas. in groundwater exploration in hard rock terrain 77−41075
resistivity method for geohydrological problems in geoelectrical prospecting 77−9527
resistivity method for geothermal reservoirs true temp. determ. 77−49043
resistivity methods for subterranean cavity research, theoretical and exptl. investigation 80−56625
resistivity modelling, arbitrary two-dimensional structures 79−92617
resistivity modelling for arbitrarily shaped three-dimens. structs. 80−3920
resistivity monitoring by magnetotellurics 77−2103
resistivity of frozen sandstones and shales 77−78157
resistivity probing of exponential Earth with homogeneous overburden 77−49180
resistivity profiles, electrode arrangement comparison 79−88486
resistivity prospecting, use of signal contrib. sections 80−21836
resistivity response of buried cables 79−92483
resistivity sounding, buried electrode data interpretation using layered Earth model 79−29701
resistivity sounding, computer program for related Hankel transforms numerical integration 79−92599
resistivity sounding, dipole to Schlumberger curve transformation by digital linear filters 78−45015
resistivity sounding, direct, interpretation by accumulation of layers 80−101322
resistivity sounding, direct interpretation, developments 77−9530
resistivity sounding, filter determination, Wiener-Hopf least squares method 79−92621
resistivity sounding, interpretation, descending and ascending methods 79−66810
resistivity sounding, technique for obs. crustal dilatancy prior to earthquakes 79−92609
resistivity sounding, variable resist. with depth Earth model 80−85583
resistivity sounding automatic interpretation 77−49192
resistivity sounding by bipole-dipole method, theory 80−101450
resistivity sounding curves, numerical interpretation *(Chinese)* 80−89934
resistivity sounding data, numerical anal., multi-vertical Earth model 77−70597
resistivity sounding for layered transitional Earth 80−85584
resistivity sounding interpretation, approx. method 77−41185
resistivity sounding interpretation without borehole control 77−9328
resistivity sounding master curves, rapid computation 80−51560
resistivity sounding on multi-layered Earth with transitional layers, theory 78−40475
resistivity sounding on multilayered Earth with transitional layers, examples 78−69282
resistivity soundings, detect. of underground cavities, rel. to hydrogeology *(Italian)* 77−86758
resistivity soundings over horizontal strata, man/computer interpretation system 78−45014

terrestrial electricity continued
resistivity survey, noise elimination, fluctuating Earth currents 79−92480
resistivity survey, VLF, effects of topography, flight altitude, wavetilt phase and amplitude 79−84093
resistivity surveying, apparatus, interpretation, undergrad. fieldwork 78−49623
resistivity surveys for study of coastal aquifers, Bahia, Brazil 79−57977
resistivity vars., short duration, before 1976 July 28 Tangshan earthquake *(Chinese)* 79−88235
resistivity vars. before earthquakes, negative result for 1977 Dec. 15, San Andreas Fault earthquake 79−57860
resistivity-logging measurements, formation anisotropy effects 79−92611
Rhinegraben, differential geomag. sounding rel. to anomalous currents channelling 79−74832
Rhinegraben mag. anomaly, responsible elec. currents 80−46124
Rio Grande rift, USA, deep crust struct., magnetotelluric interpretation 80−104878
rivers, telluric field increase near streams 78−65176
rock formation and penetration zone elec. parameters determ., probes number and type *(Russian)* 79−39969
rocks, complex resistivity meas. by freq. domain method *(German)* 80−4001
rocks, water-saturated, dynamic props. of seismoelec. effect 79−25233
rocks with fibrous dissemination, models 80−4002
Roosevelt Hot Springs, resistivity sounding, EM and Schlumberger 79−84095
rotating current dipole method, field test 77−87094
Rybachy peninsula, USSR, geoelectric freq. soundings *(Russian)* 80−36230
salt-bearing sections, vertical electric sounding *(Russian)* 78−11807
Schlumberger line sources and three-electrode anomalies, relative sensitivities 78−7564
Scotland, elec. cond. rel. to Caledonian tectonics 77−44920
Scotland, electrical model of crust and upper mantle 80−98234
sea, electric intensity vector direction determ. device *(Russian)* 77−60490
sea, induced currents effect on mag. bays observed at coastal observatory 78−65462
seawater-saturated ocean crust and oceanic island basalts, elec. props. freq. spectrum 79−25229
sedimentary rocks containing water and oil, dielectric constant and losses *(Russian)* 79−20747
seismo-magnetic induction, numerical theory of 3-dim. EM induction *(Chinese)* 77−64191
seismoelectric effect, intensification by steady elec. field 77−81790
seismoelectric effect in rocks, nature 77−44974
self-potential anomalies near vertical contacts 80−3919
self-potential method in geothermal exploration 80−4125
Senegal, telluric current variation obs. *(French)* 80−76903
W Sicily, Palermo-Sciacca vertical electric sounding profile 80−56344
Sierra Nevada batholith, elec. conductivity of crust 80−72411
simple bodies in half-space, elec. pots. *(Russian)* 79−34744
skywave field strengths, effect of proximity to discontinuity in Earth's elec. props. 77−40974
soil, resistivity meas., LF electromagnetic wave method *(French)* 78−24394
soil bulk resistivity, meas. method 78−24381
soils electrical properties, investigation of seasonal variations, in 10-1000 kHz band 78−88796
sounding methods, applied EM depth sounding 77−45173
sounding methods, statistical evaluation, expt. design 77−45172
South Novo-Tolbachinsky volcano, flowing lava elec. cond. 80−72498
specific resistivity of ground and water in high Tatra, Poland *(Polish)* 79−96735
St. Vincent's Gulf, South Australia, Island and coast effect in geomag. vars. 80−72426
stationary well quadrupole logging in layers of restricted thickness *(Polish)* 80−12556
Strait of Magellan, tidal currents monitoring by onshore elec. field recording 77−87107
subsurface electrical conductivity rel. to H amplitude of mag. storm sudden commencements 79−66889
subsurface EM field propagation from horizontal elec. dipoles, comprehensive study 80−98229
subsurface Em response of conducting-sphere in two-layer conductor 78−15961
subsurface line conductor, multiple EM scatt. 78−61317
sulphide minerals, induced polarisation, decay curves theory *(German)* 79−29709
sulphide ores, disseminated, electrochemical model of induced-polarisation phenomena 79−92526
sulphide ores, geoelectrical identification and location *(Rumanian)* 77−32997
sulphide prospect in California copper belt, broadband EM study 80−72503
Superior Province, Canada, shallow crustal sounding by audio freq. magnetotellurics 79−57882
surface geoelectric section effects on deep magnetotelluric sounding *(Russian)* 80−85588
surface geology sensed by ground mode radiowave propag., glaciated area of USA 80−76979
surface of Earth with variable conductance, 3D-model of EM induction 80−30983
Tangshan, China, elec. resisitivity anomaly in epicentral area prior to 1976 earthquake *(Chinese)* 79−20744
tectonoelectricity, review 78−36095
tectonoelectricity and tectonomagnetism symposium (Japn, 1975, September 5) 77−2084
telluric and magnetotelluric methods, comparison for sedimentary structures 78−3713
telluric anomalies caused by shallow structs., ellipsoidal approx. 77−56573
telluric current meas. in audio and subaudio freq. range, characts. 77−86760
telluric currents method for overhang bodies search *(Russian)* 79−88496
theoretical apparent resistivity over transition layer model, comments 77−40978
thickness var. detection, new geoelectrical method 79−2384
three-frequency computational method for two-layer CFS data 79−16688

terrestrial electricity continued
time-domain EM method, optimum pulse shape selection 77−45167
total field resistivity mapping, sounding over horizontally layered media 79−16693
transient EM field due to point source above surface of two-layered medium *(Polish)* 77−73627
transient EM fields about a grounded elec. dipole 80−56350
transient EM prospecting using interactive minicomputer 79−62604
transient EM response from irregular surface models 78−57165
transient EM response of anisotropic rock to vertical electric dipole *(Polish)* 80−41367
transient EM sounding in thin cond. layer with inhomogeneities *(Russian)* 79−84530
transient EM sounding records computer processing, meas. errors anal. *(Russian)* 79−44269
transient field curves in proximate zones, regularities *(Russian)* 79−62434
transients, from two horizontal thin conducting strata *(Russian)* 78−40485
Transverse Ranges, S.California, elec. struct. from magnetotelluric sounding 77−37127
Travale-Radicondoli geothermal area (Tuscany), dipole elec. sounding method appl. 80−97762
two dimensional inhomogeneity modelling, resistivity and induced polarisation response 77−17023
two-dimensional resistivity data, inversion technique 79−16695
two-fold resistivity mapping of lateral inhomogeneities 78−61573
two-layer polarizable Earth, transient EM fields 77−64199
Ukrainian shield rocks, correls. of electrical parameters at high temps. *(Russian)* 79−8628
ULF/ELF EM fields generated above finite depth sea by submerged vertical mag. dipole 79−48400
underground quarries, EM transmission meas. 78−57365
upper mantle, partial melting and electrical conductivity anomalies 78−28199
Urals, aseismic geodynamics rel. to rock cond. changes and geomag. secular var. anomalies 80−26447
Vancouver Island region, analogue model study of EM induction 80−56356
Vancouver Island region, electromagnetic induction model 80−56367
Vancouver Island region, terrestrial EM induction 80−104879
vertical component of field, propag. characts. 77−9331
vertical electric sounding curves, computer interpretation *(Russian)* 79−34741
vertical electric sounding for salt-bearing structures *(Russian)* 78−3714
vertical electrical sounding dipole-dipole filter coeffs. 78−12006
vertical frequency effect sounding in induced polarization and galvanic resistivity methods 78−69284
vertical intensity component meas. 77−91209
vertical tabular conductors, graphical interpretation method 77−41189
Victorio Peak, New Mexico, radar probing and resistivity meas. 79−84094
VLF-EM prospecting method, model study 77−49181
water detection in volcanic region of Armenia, elec. profiling and sounding 80−85753
wave dielectric log curves in formations of limited thickness, interpretation *(Russian)* 79−74990
wave tilt sounding of multilayered structures 80−61926
well logging, electric, geometrical factors determ. from electrostatic field successive approx. *(Chinese)* 80−105057
Wenner resistivity soundings, vertical contact effect 78−20541
Yerington mine, Nevada, in situ induced polarisation and mag. susceptibility meas. 80−51323
Yoshioka-Shikano Fault, seismically active fault along Japan Sea coast, geomag. induction study 80−26475

terrestrial heat
see also volcanology
active hydrothermal systems, intrinsic fluid and rock resistivity anal. 78−40480
Aegean region, heat flow rel. to dynamic model of Hellenic Arc 77−21734
Alae lava lake, Hawaii, numerical analysis of cooling 77−64248
Alpine fault, New Zealand, frictional metamorphism, Ar depletion and tectonic stress 80−41440
Alpine metamorphism, thermal budget 78−61373
alpine metamorphism study using fluid inclusions in quartz crystals *(German)* 77−25677
N.Apennine chain, heat flow meas. of folded continental arc 77−86841
aquifer fluid flow when charged with hot water from fault zone 79−74921
Archaean continental geothermal gradients 78−40525
Archaean crust, geothermal heating rel. to vertical tectonism in greenstone belts 80−81861
Archaean sialic crust, southern West Greenland, chemical and thermal evolution 80−31016
Archaean tectonics constraint from geothermal gradients and plate prod. rate 79−34770
Archean continental crust, magma genesis by crustal anatexis, garnet-pyroxene thermometry and barometry 78−65236
Arctic Ocean, sediment thicknesses and upper mantle temps. from magnetotelluric soundings 79−48454
Arctic regions, heat flow north of 60°N 79−48438
Argentina, heat flow meas. in San Juan and Mendoza 79−66653
E.Arizona, USA, heat flow rel. to subsurface struct. 80−21686
artificially disturbed strata, temp. distrib. during liq. filtration *(Russian)* 77−25667
artificially fractured rock, heat transfer agents flow patterns 80−17239
ascending andesitic magma, cooling model 78−65239
asthenosphere, frictionally heated shear flows stability 79−44164
asthenosphere thermal instability and tectonic plate motion 77−17073
asthenosphere thermal instability beneath moving plate 80−31007
E.Atlantic, Cretaceous black shale, thermal alteration by basaltic intrusions in E.Atlantic 78−61396
E.Atlantic, heat flow correl. with crustal age and tectonic province 77−86839
Atlantic mid-oceanic ridge, axial temp. profile and crustal struct. 80−26476
Atlantic Ocean, history of growth and topography of ocean bottom 80−3993

terrestrial heat continued
Mid Atlantic Ridge crest, geological and geophys. investigations 80−8284
Atlantis II Deep, geothermal brine system 80−94526
Atlantis II Deep geothermal system, changing hydrothermal activity 78−85532
Australia, geophysical profile along 29°S 80−72460
Australia, heat-flow data correction, glaciation effects 80−72457
Australia, regional heat flow maps 80−51351
Australian heat flow, regional variations 79−84203
back-arc basins, thermal effects of ridge crest migration rel. to asymmetric spreading 80−85636
Baikal region hot springs *(Russian)* 80−94551
Baikal rift zone, heat flow rel. to neotectonic activity 78−36135
Baikal rift zone, heat flux anomalies rel. to continental rift form. *(Russian)* 80−12364
basalt sheets, thermal effect on adjacent rock, heat flow model 80−46181
Basin and Range province, heat flow and thermal effects of tectonic extension 79−70763
Bering Sea, crustal heat flow and tectonic explanation 80−109123
biotite+apatite geothermometer, re-examination 78−85704
N Bohemia, heat flow meas. in Palaeogene, Cretaceous and Permo-Carboniferous sediments 77−44946
Bohemian Massif, heat flow pattern, rel. to tectonic struct. 77−64241
Bohemian Massif and W.Carpathians, geothermal models 77−81848
Bohus granite area, SW Sweden, geothermal investigations 80−85631
bore hole drilling effect on thermal field *(Rumanian)* 78−20372
borehole equipment for temp. and heat flow meas. in Ukraine *(Russian)* 77−91294
borehole meas., high temperature electronics for geothermal energy 80−11997
borehole temp. gradient logs and lithology correlation 78−61416
borehole temperature gradients, continuous logging, deconvolution 77−91288
Bournac, Haute-Loire, heat flow determ., geotherm proposal 80−8259
Brazilian Highlands, crustal heat flow obs. 80−109124
Broadlands geothermal field, New Zealand, boiling curves 78−85516
Broadlands geothermal field (NZ), DC resist. modelling via finite element method 79−5445
Bullaren lineament, SW.Sweden, heat extraction potential 80−76602
Caledonian granites in Britain, geochemical and geophysical evidence on geothermal pot. 79−74486
California, geothermal potential assoc. with crustal spreading along strike-slip faults 79−66645
Canada, P-wave residuals rel. to heat flow 77−91037
E. Canada, thermal struct. of upper crust 80−31013
Canada Maritime Provinces, heat flow 79−100819
Canadian hotspot under young submarine volcano J. Tuzo Wilson 77−37165
Canadian Shield, Superior Province lakes, heat flow meas. 80−31003
carbonate rocks, mineralogy rel. to metamorphism temp. 77−2128
E.Caribbean Sea floor, heat flow meas. 79−39683
Central Alps, Switzerland, heat flow, heat prod. and vertical crustal movements 77−81847
Cerro Prieto geothermal field, conf. at San Diego, (Sept. 1978) 80−94911
Cesano geothermal field, Italy, geological study 80−76975
Ceylon-Cocos Zone, thermal regime and nascent island arc 80−56418
charnockite series, form. temp. and press., evidence for geothermal gradients 78−40553
Chaudes-Aigues region, surface anomaly, aerial thermographs 77−21714
chemical and thermal struct. of deep interior, obs. constraints 79−53323
chemical geothermometers and mixing models 78−69503
chemical reactions in undifferentiated Earth, thermal effects 79−25218
Chile, heat flow meas. 79−66652
N.China, heat flow obs. *(Chinese)* 80−56416
clinopyroxene geothermometry of spinel-lherzolites 77−2126
Coast Plutonic Complex, British Columbia, geochronology and thermal history 80−12351
Coast Plutonic Complex of S.British Columbia, Canada, possible geothermal resources 79−70429
Coast Range Complex, British Columbia, heat generation 77−17050
coastal submarine hydrothermal activity off northern Baja California 78−61431
conductivity eqn. during formation 78−28196
conference, Nov. 1979, New Orleans, USA 80−81891
continental and regional heat meas., effects of climatically perturbed temp. gradient 77−81845
continental convergence zones, temp. modelling 77−81850
continental crust, heat flow rel. to lower crust model 77−81840
continental crust, heat-producing radioactive elements distrib. and redistrib. 78−65232
continental crust, thermal struct. and extension of oceanic heat flow-age relation 77−21696
continental crust and root zones, thickness and thermal history 79−88320
continental crust during magmatic accretion and metamorphism, thermal model 80−46150
continental crust heat production model 80−21690
continental crust thermal state and structure *(Italian)* 79−20769
continental geotherms during Archaean, upper limits 79−34780
continental heat flow, tectonic age and thermal evolution effects 80−72472
continental heat flow affected by erosion 80−89991
continental lithosphere, vertical temp. distrib. limits 78−65207
continental lithosphere thermal evolution 78−65234
continental mantle, heat flow var. with age, appl. to lithosphere thermal models discrimination 79−70764
continental shields, Curie temp. depth, compositional boundary 79−53330
continents, heat flow rel. to upper mantle lateral heterogeneity 77−29259
continuous logging of temp. gradients 77−82052
convection currents in cavernous aquifer rel. to geothermal activity 77−64340
convection fluid dynamics in a model of a fault zone in the Earth's crust 79−34778
convection in high Prandtl number fluid with strongly temp. depend. viscosity 77−3823
terrestrial heat continued
convective heat transfer model for lithospheric thinning and crustal uplift 79−84199
convective hydrothermal geothermal reservoirs, balance laws and constitutive relations 78−61379
convective instability of upper mantle models 79−88323
convective models and radiogenic heat production constraints 80−90006
cooling rate effects on texture and mineralogy of DSDP Leg 34 basalt 79−44148
cooling rate of Earth, reappraisal 80−76943
cordierite-garnet bearing assemblages as geothermometers in granulite facies terrains 78−44810
core, temp. distrib., using Gruneisen's parameter vol. depend. theory 80−90033
core ^{40}K decay as heat source 77−25663
core and mantle thermal eqn. of state 80−90029
core cooling by subsolidus mantle convection 80−36278
core formation effects, model 78−61368
core thermal evolution 80−21674
Coso, California, geothermal well water, chemical analyses 80−90104
Coso geothermal area, California, heat flow 80−90001
Coso geothermal area, underlying low-vel. body, teleseismic evidence 80−90005
Coso Hot Springs, Known Geothermal Resource Area, model 80−90004
Coso Range, California, geothermal system 80−90049
Coso Range, California, Quaternary rhyolite domes rel. to geothermal anomaly 80−90002
cratered terrain, thermal regimes and impact melt 77−2125
Crimea, heat flow meas. by temp. wave reduction method *(Russian)* 79−20774
crop rows, effect on thermal radiation from terrestrial surface 78−16016
crust and mantle, temperature-depth profiles, Poland, from geothermal and deep seismic sounding data 78−48988
crust hot spots, and sublithospheric upwelling distrib. 80−109126
crust radiogenic heat production, vertical distrib. 80−85619
crustal heat flow, global scale pattern *(Russian)* 80−98284
crustal heat loss of Earth, review 80−98286
crustal radiogenic heat production, depth depend. modelling by variational approach 80−72464
crustal rocks, critical thermal gradients for seismic low-vel. zones 80−41435
crustal rocks, exponential relationship between seismic vel. and radioactive heat prod. 79−70793
crustal rocks, lateral temp. vars. rel. to long-wavelength mag. anomalies over Canada 80−85594
Curie depth determination from aeromag. spectra, W.USA 77−60349
Cyprus ophiolitic sulphide ore deposits origin, hydrothermal convection model 79−29761
deep-sea hydrothermal site on strike-slip fault, discovery 80−21710
degassing and thermal history, simple calcs. 80−98282
desaturating geothermal reservoir, numerical modelling 80−12363
descending lithosphere thermal regime; effect of varying angle and rate of subduction 78−77206
dike burial depth estimation by mag. palaeogeobarometric method 80−98220
direct geothermal problem, numerical soln. 77−78138
diurnal surface temp. range sensitivity to changes in physical parameters 78−3875
drill holes, vertical, natural convection effect on temp. 77−78135
dynamothermal aureole of the Bay of Islands ophiolite suite 80−51355
early evolution and thermal history 77−44950
early evolution of Earth, model, thermal history 77−86845
early temperature and scale covariant cosmological models 78−57704
Earth, thermal history rel. to parametrised mantle convection 79−16429
Earth core, outward heat flow rel. to geomag. field origin 80−8251
Earth core, thermal consequences of gravitationally powered geomag. dynamo 79−39687
Earth crust press.-temp. conditions modelling, appl. of rocks elastic props. experimental studies *(Russian)* 78−96207
Earth interior, shear heating as explanation for lithosphere-mantle decoupling 79−20790
Earth interior, thermal model 78−15982
Earth mantle, infinite Prandtl number thermal convection in a spherical shell 80−59033
Earth thermal evolution, theory 80−89988
Earth thermal history, implications of Archaean sedimentary basins development 80−89986
Earth thermal structure, rel. to global sea-level changes 79−29743
Earth-atmosphere radiative heating effects on climate, NOAA radiometer meas. 80−8425
earthquake, elastic energy release, heat prod., and Earth inertia tensor changes 79−44106
East Pacific Rise at 21°N, hydrothermal activity and crestal struct. 78−28216
El Tatio geothermal field waters, N.Chile, isotopic comp. rel. to sources 79−16525
energy balance maps from remotely sensed imagery 77−37433
energy resources in Oregon, USA, elec. and EM sounding obs. 80−97761
energy resources in USA, National Exploration Program 80−72011
energy source possibility 79−35507
NE.England, granite plutons effecting surface heat flow 80−94490
SW.England heat flow anomaly 77−49041
enstatite-diopside solvus, En pressure depend. rel. to geothermometry 77−2141
Europe, heat flow, temp. distrib. and geothermal models, tectonic implications 77−81849
Central Europe, mantle heat flow and geotherms for major tectonic units 79−70767
Europe, preliminary heat flow map and tectonic and geophysical implications 79−70765
European territory, heat flow data review 79−96751
European USSR, heat flow map 79−70766
evolution of Earth's interior, heat generation and heat-mass transfer 80−90040
Explorer ridge, off W.Canada, marine geophys. survey 79−25224
extension behind island arcs and motions rel. to hot spots 79−20796
extraction by hydraulic fracturing of rock, growth rate of penny-shaped crack 77−29289
extraction from hot dry rock, fluid flow through large vertical crustal crack 77−33027

terrestrial heat continued
extremal temperature bounds from surface gradient measurements 79−84189
fault zone with finite thickness, frictional heating, comment 79−25215
Fennoscandian Shield and Danish Embayment, crust and upper mantle geothermal models 77−49044
flow/generation, linear relationship for exponential model of crustal heat production 79−66660
France, heat flow rel. to deep struct. and mantle convection 80−98291
free convection, about vertical flat plate in porous medium rel. to heat transfer from dike 77−64237
freezing soils, heat flux meas. *(Japanese)* 78−88835
frictional heating on fault zone with finite thickness 78−36124
Galapagos hotspot, spreading centre jumps and subaxial asthenosphere flow 77−33042
Galapagos hydrothermal mounds, sediment U content anomaly 80−56434
Galapagos Rift, hydrothermal plumes obs. 77−64258
Galapagos Rift, mantle He in hydrothermal plumes 77−64259
Galapagos Rift, submarine thermal springs 80−8295
Galapagos Rift hydrothermal fields, struct. and morphology of seafloor 80−72489
Galapagos Rift hydrothermal mounds, obs. with DSRV Alvin and detailed heat flow studies 80−51383
garnet and clinopyroxene solid solns., geothermometry based on Fe-Mg distrib. 80−46151
geoid major undulations, possible thermal nature 77−81784
geopressured geothermal wells production charact. 78−81223
Georgia Inner Piedmont, hornblende and biotite $^{40}Ar/^{39}Ar$ ages, rel. to tectonothermal history 78−48990
geosynclines, energy sources rel. to anomalous heat flow *(Russian)* 78−96182
geothermal and magnetotelluric surveys in NW Germany, comparisons 80−12336
geothermal aquifers, reservoir lifetime and heat recovery factor, for urban heating 79−74492
geothermal energy, heat extraction from hot dry rock masses 78−61378
geothermal energy, low grade, future uses in France *(French)* 77−53022
geothermal energy, review 79−29447
geothermal energy extraction, liq. flow pattern in system with three-dimens. filtration zone 77−49037
geothermal energy extraction, through hydraulically induced fracturesin hot dry rock 79−34424
geothermal energy extraction by two-loop systems 77−78134
geothermal energy extraction from penny-shaped reservoir made in hot dry rock 80−108784
geothermal energy extraction problem, thermal convection in shattered rock zones 77−78162
geothermal energy investigations in Sweden 79−74488
geothermal energy prospecting by geophys. methods, review 78−7803
geothermal energy prospects in Brazil 79−74487
geothermal energy recovery from hot dry rock, use of weighted brine 80−101076
geothermal energy resource exploitation, conf. Sept., Landerello, Italy 80−81418
geothermal energy resources, low enthalpy, in Denmark 79−74489
geothermal energy resources and storage, materials problems and research 78−86703
geothermal energy utilisation, rel. to nucl. energy *(German)* 79−52876
geothermal exploration in Iceland, volcanological methods 79−74877
geothermal field, approx. soln. for one-phase model, appl. to Wairakei 78−11853
geothermal field, pressure-temp. curves for CO_2-H_2O mixture 77−51488
geothermal field parameters, convection theory 79−66663
geothermal gradient at 1000 km depth 80−8260
geothermal heat, extraction by water circulation through crack in dry hot rock mass 79−57355
geothermal models development, Tikhonov's theory 78−48994
geothermal potential and heat flow meas. in Egypt 79−74490
geothermal power 79−70426
geothermal power plants flash cycle optimisation, analytical expression in terms of temp. only 80−40894
geothermal pressure transients, two-phase and single-phase 79−66664
geothermal prospecting, via field station GS-1 with thermoquartz resonators *(Russian)* 78−93000
geothermal region, thermal-convective instability through porous medium 80−53769
geothermal regions, seismic noise sources mapping 77−81828
geothermal research by IR scanning, image processing 77−64458
geothermal reservoir, effect of magma dike intrusion on free convection 78−7599
geothermal reservoir, liquid dominated, fault zone controlled charging model 80−81935
geothermal reservoir exploitation, finite difference modelling 80−55798
geothermal reservoir simulation, math. models 80−12446
geothermal reservoir simulation, numerical soln. techniques 80−12447
geothermal reservoirs, downhole meas. of thermal conductivity 78−61618
geothermal reservoirs true temp. determ. by resistivity method 77−49043
geothermal steam, ^{222}Rn emanations, rel. to seismic activity 78−11832
geothermal steam pipeline network, numerical simulation 80−40822
geothermal survey of Namekawa and Ubayu spas, Japan *(Japanese)* 77−70619
geothermal system, thermosyphon models for downhole heat exchanger appls. 79−57356
geothermal systems, natural convection in porous media, review 79−1194
geothermal technology, development into an exact science 80−61781
geothermal vapour dominated field, Larderello, Italy, gases and H_2O isotopes content of steam 79−74920
geothermal vapour dominated field, Larderello, Italy, noble gas concs. 79−74919
geothermal waste water, environmental effects on river system 79−29487
geothermal waters, fluorite solubility equilibria 77−60368
geothermal well logging instrumentation, hybrid microcircuit design, performance 79−96845
geothermal well logging using 300°C hybrid IC 77−73895
geothermal well logging using hybrid ICs operating up to 300°C 78−3976
geothermally active fault zone, water convection 80−19375
geothermometer using Na/Li ratio in geothermal waters *(French)* 79−53369
terrestrial heat continued
geothermometry, appl. of plagioclase-garnet-Al_2SiO_5-quartz assemblage 77−2147
geothermometry, chemical and isotopic techniques 78−69501
geothermometry and geobarometry, conf., University Park, Pennsylvania (October 1975) 77−2123
geothermometry and geobarometry in epizonal granites, comparison of feldspars and Fe-Ti oxides 77−5140
geothermometry of granulite facies rocks from Rogaland, Norway 78−96193
Geotraverse Rhenoherzynikum, crustal temp.-viscosity regime rel. to fault zones depth, seismic obs. 80−90046
German Democratic Republic, geomag. secular var. anomalies rel. to heat flow positive anomalies 80−26449
geyser vent, pre-boiling convection, mathematical model 80−31067
geysers, lab. models rel. to natural phenomena 78−69373
Geysers geothermal area, California, induced versus natural earthquakes 80−101332
Geysers geothermal field, California, explosions and microearthquakes study 80−3964
global geodynamics, Canadian contribs., 1971-79 period. 80−8262
global heat flow map and flow pattern, plate tectonics interpretation 78−7603
granite magmatism initiation and thermal diversity 78−65240
Grass Valley, Nevada, USA, microseisms in geothermal exploration 80−21647
Grassy granodiorite, Tasmania, thermal history meas. using garnet fluid inclusion data 80−4012
groundwater chemical geothermometer, Na-K-Ca temp. with Mg correction 80−51357
groundwater in Hawaiian geothermal areas, compositions 77−64331
groundwater temperatures in Athabasca Oil Sands area, Alberta 79−62465
Gruneisen parameter, melting curve and adiabatic gradient of core and mantle 80−90028
Guaymas Basin, Gulf of California, basaltic sill intrusion into sediments, hydrothermal activity 80−46154
Guaymas Basin, Gulf of California, heat flow at spreading centres 80−41411
central Gulf of California, heat flow meas. 80−3968
Gulf of California, temp., salinity and ^3He meas. rel. to geothermal heating and mantle volatiles 80−85640
Hakone volcano, Japan, thermal structure and energy balance 79−74878
halokinesis and thermal convection 78−65308
Hawaii, ground Rn survey of Puna geothermal area 80−85657
Hawaii Geothermal Project, groundwater geochem. study 80−72567
heat extraction from hot dry crustal rock via hydraulic fracture 79−74491
heat flow meas. in small lakes in N.W. Ontario, discussion and reply 77−53016
heat flow measurement, vertical groundwater movement correction 80−3969
heat flow palaeoclimatic and topographic corrections, erosion effects 79−34767
heat transfer with liquid filtration into shattered rocks 79−81962
heating by impact of accreted bodies 79−74868
Hele-Shaw cell, permeability determ., geothermal modelling appl. 78−59466
high Prandtl number convection, geophs. appl. 79−81875
Himalaya, asthenospheric heating rel. to intracontinental subduction initiation 79−16431
Himalaya, uplift and cooling rates from geochronological data 80−85627
Himalayan geothermal belt *(Chinese)* 79−79759
hot dry rock geothermal reservoir fracture mapping techniques 80−81419
hot dry rock project, Los Alamos Scientific Lab. *(German)* 77−91086
hot spring deposits of Roosevelt thermal area, hydrothermal alteration 80−76974
hot spring water chemical constituents, Mt. Akagi region (Japan) *(Japanese)* 78−16072
hotspot islands, Rodriguez, Darwin and Amsterdam Islands 79−20793
Hungary, image of geothermal energy for non-elec. purposes 80−76601
hydrothermal activity on Mid-Atlantic Ridge, ^3He excess in bottom waters 80−101383
hydrothermal alteration in active geothermal fields 79−5535
hydrothermal alteration mapping, airborne spectroradiometric data anal. and LANDSAT data appl. 79−34973
hydrothermal convection at slow-spreading mid-ocean ridges 79−88340
hydrothermal flows, two-phase, in permeable media, struct. 80−85693
hydrothermal system, temp. measurement scale based on chem. comp. of gas fraction 80−98277
hydrothermal systems, convective heat fluxes from cooling plutons 78−36206
ice sheets, continental, geothermal heating rel. to erosion and deposition 79−25276
Iceland, D tracing in hydrothermal systems 78−69386
NE Iceland, elec. resist. model from magnetotelluric obs., correl. with temp. 80−89954
Iceland, geothermal activity rel. to geological struct. 78−61376
Iceland, geothermal energy exploitation 78−57181
Iceland, H-water isotope thermometer appl. to geothermal areas 78−69384
Iceland high-temperature geothermal systems, aquifer chemistry 78−96245
Icelandic subglacial volcanisms, thermal and physical studies 80−101350
Icelandic thermal area rock stress implication for oceanic lithosphere 80−90012
Indian Ocean, heat transfer through floor 77−86833
Indian Ocean floor, geothermal convection through oceanic crust and sediments 79−79812
Indo-Australian plate, abnormally high heat flow rel. to plate internal deform. 80−109134
interior energy balance 77−81851
internal temperature distrib., geothermal interpretation of deep mag. var. sounding 78−44765
intraplate volcanism, geological and geophysical parameters 78−65243
Iowa, urban/rural radiances, seasonal and wavelength dependence 77−64384
isotope geothermometry in the Larderello geothermal field 78−69312
Italy, heat flow meas. rel. to tectonic features 79−70769
Japan, stable isotopic studies of geothermal systems 78−69385

terrestrial heat continued
Japanese Islands, compilation of eleven new heat flow meas. 80−67350
Japanese Islands region, heat flow data compilation *(Japanese)* 80−67332
Jharia Gondwana sedimentary basin, India, heat flow meas. and basement rocks heat prod. 80−98276
Jordan-Dead Sea Rift Valley warm springs, correl. between SiO_2 conc. and orifice temp. 80−41464
Juan de Fuca ridge, heat flow meas., evidence for hydrothermal circulation 78−28197
Juan de Fuca ridge system, heat flow meas., water circulation 80−72468
Kalapana, 1975 November 29, intra-plate earthquake rel. to geothermal processes 79−39664
Kamchatka, unsteady heat and mass transfer model of geothermal energy 77−64234
Keolu Hills, Oahu, Hawaii, hydrothermal mineralogy 77−73730
Kilauea 1977 lava flow, heat transfer meas. 80−85632
kimberlite nodules, upper mantle petrology and geotherms 78−65310
Kirishima volcanoes, Japan, geothermal survey *(Japanese)* 80−67357
Klamath Falls, Oregon, heat flow data and obs. geothermal phenomena 77−5158
komatiite generation and greenstone belt models, thermal aspects 79−70762
Kusatsu-shiran Volcano, Japan, geothermal survey *(Japanese)* 79−70760
Kusatsu-shirane Volcano, Japan, 1976 steam explosion, geophys. obs. *(Japanese)* 79−70773
Lake Assal (FTAI), geothermal zone, geochemical and expt. studies 78−69314
Lake Erie, heat storage and advection 77−41078
Lake Erie terrestrial radiation in 1952-1968 period 77−29343
lake sediment thermal diffusivity estimation from field obs. 77−2253
Lanzarote (Canary Islands) geothermal area, isotopic comp. of steam samples 77−49048
Larderello field, secondary changes in composition of geothermal fluids 78−69387
lava lake cooling model, numerical analysis method 77−64247
Lehmann discontinuity, mantle props. beneath continents 80−56425
Lepontine Alps, temporal changes in heat flow distrib. assoc. with metamorphism 80−101347
lithosphere, geothermics, Southwestern Germany and Switzerland *(German)* 78−53633
lithospheric downgoing slabs, temps. rel. to seismic zone lengths 79−25212
lithospheric formation, thermal boundary layer 77−73696
logging instrumentation, borehole measurements, developments 80−61909
Long Valley caldera, California, mag. model rel. to geothermal system 77−86846
Los Angeles basin (California) SW block, thermal subsidence and petroleum generation 80−3967
lower mantle, convection, composition and thermal state 80−21678
lower mantle, thermodynamically based eqn. of state 80−26473
lower mantle convection, inferred from low Q zone 80−76944
lower mantle Gruneisen parameter, evidence for approximation $\gamma\rho$=-const. 80−3970
magma, ascending, heat and mass transfer 79−34768
magma traps, lithostatic control theory 79−66669
magmas, thermal history, low press. reference point 78−65244
magmatic diapir folds, heat exchange with crustal materials rel. to evolution *(Russian)* 80−104957
magnetic and isotopic blocking temps. 78−65226
magnetic blocking temp. in cooling orogen 78−65227
Malaysia, heat flow estimation in exploration wells in offshore areas 80−67349
mantle, convection currents rel. to plate tectonics 77−29265
mantle, convective instability of multilayered and nonhomogeneous models 79−62476
mantle, geophysical constraints, on radial and lateral temp. vars. in upper regions 77−5141
mantle, melting point estimation using Uffen method, remarks 78−20367
mantle, radiogenic heating in convecting mantle rel. to oceanic bathymetry flattening 80−85642
mantle, thermal convection, time dependent simulation 80−101352
mantle, time dependent flow model 78−20369
mantle, two-dimensional flow beneath accreting lithosphere rel. to heat flow 79−12102
mantle, upper layer, heat convection rel. to viscoelastic instability 77−41010
mantle convection, Benard problem with viscosity depend. on temp. and press. 78−69317
mantle convection, seismic focal mechanisms and thermal boundary layer 77−17070
mantle convection, two-scale flow model rel. to plate tectonics 78−73348
mantle convection driven by radioactive energy, model for decaying source 80−72461
mantle convection model, finite element method 80−67354
mantle convection models, laboratory expt. 77−9396
mantle convective instability, thermomechanical 80−90063
mantle heat flow, map 77−37161
mantle hotspots, correl. with positive geoid height anomalies 80−90056
mantle melting, past and present, isotope and trace element evidence 78−65238
mantle of old platforms, heat flow 80−89996
mantle plume, fluid-dynamic model of ascending flow 80−12370
mantle radiative cond. from shock compressed Fe^{2+} bearing MgO absorpt. spectrum 80−90039
mantle structure peculiarities rel. to nature of excess quadrupole moment 78−73334
mantle subsolidus convection and cooling, lower mantle viscosity constraint 77−9384
mantle temp. from dunite-peridotite mixed-oxide compositional models 77−2124
mantle temperature implied from elec. cond. assumptions 80−61754
mantle thermal gradients estimation, geological problems 77−5138
mantle thermal struct., convective regime with moving plates 80−85634
mantle with differentiation, thermal evolution 80−98288
marginal seas, heat flow correl. with underlying mantle density inhomogeneities 80−21676
marine sediment heat flow, equatorial Indian Ocean 80−76958

terrestrial heat continued
Massif Central hot springs, France, alkaline earth ions acquisition, rel. to geothermometry *(French)* 79−29788
massive sulphide ores genesis, geothermal model from altered volcanic rocks geochemistry at Matagami, Quebec 78−77231
E.Mediterranean region, heat flow data review 79−70770
melt production in mantle, by viscous dissipation 80−72463
Mesa geothermal anomaly, Imperial Valley, California, assoc. microearthquake obs. 77−52992
Mesozoic and Cainozoic heat flow 80−76941
metamorphic rock temps., determ. from margarite stability and compatibility relations 77−5183
metamorphism temp. and press. determ. via garnets comp. and zoning 77−2148
N.Mexico, heat flow distrib. and radioactive heat generation 79−84198
Michigan Basin, heat flow meas. in deep borehole 79−39679
Michigan Basin, thermal and mechanical evolution, lithosphere elastic flexure 77−21719
Mid-Atlantic Ridge, geology of submarine hydrothermal field at 26°N latit. 80−85641
mid-ocean ridges, obs. and implications of ridge crest hot springs 80−98304
mid-plate hot-spot swells, thermal origin 79−8619
midocean ridge hydrothermal systems, hot water egress thermal constraints 79−39700
mineral cooling rates, implications of antiphase domains exptl. coarsening in pigeonite 80−81886
SW.Montana, Precambrian metamorphic rocks, mineral-pair geothermometers 80−81846
Montana de Fuego, Lanzarote, volcanic zone temp. distrib. *(Spanish)* 77−70627
multi-layered geothermal reservoir, natural convection 80−8347
Nain anorthositic complex, lower crust heating rel. to contrasted magmas commingling in plutonic environment 80−104959
Namafjall geothermal field, Iceland, volcanic eruption through borehole 79−53332
Naxos island, Greece regional metamorphism, petrology and geothermal gradients 77−44985
Nepal, geothermal springs 80−72476
Nevada, gravity surveys in Grass and Buena Vista Valleys rel. to geothermal resources 80−41365
New Zealand, geothermal systems, isotope techniques, appls. 78−69313
SW Newfoundland, Proterozoic-Palaeozoic thermal history from Grenville basement rocks $^{40}Ar/^{39}Ar$ ages 79−20771
Nigorikawa geothermal area, Japan, rare gas isotopic anomalies 79−88314
nonspherical thermoelastic deformations of nonuniformly heated Earth 79−74869
Norris Geyser, Yellowstone Park, USA, microseisms of geothermal area 80−104909
North Sea, Buchan and Witchground Grabens, seismology study 80−51364
Norwegian monzonitic rocks, heat generation versus crystallisation depth 78−65228
Norwegian-Greenland sea, thermal evolution in sea floor spreading model 80−56427
ocean crust heat flow from U abundance 80−8287
ocean floor bathymetry and heat flow vars. with age 77−33051
ocean floor hot spring created by drill hole 80−55951
ocean floor thermal cond. meas., pulse-probe method 79−53533
ocean ridge thermal evolution, affected by spreading rate 80−56424
ocean sedimentary basins, thermal and subsidence history 78−49010
ocean spreading centre processes, qualitative models including hydrothermal penetration 77−33045
ocean spreading centres, hydrothermal stress drops and convective patterns 79−88339
ocean spreading ridge crests, hydrothermal activity rel. to ocean major and minor elements balance 80−41459
oceanic crust, hydrothermal alteration age 79−34798
oceanic heat flow meas. over E Canada continental margins 77−5144
oceanic lithosphere thermal structure rel. to ridge-crest and transform earthquakes source parameters 79−88265
oceanic ridge crests, hydrothermal activity rel. to metal-rich deposits form. 80−41430
oceanic ridges, estimators for heat flow and deep rock props. 77−86843
oceanic spreading ridge subduction, thermal effects 79−88321
oil field heat flow determ. method 77−82021
Ontario, effect of Pleistocene climatic vars. on geothermal regime 79−57883
opaque minerals alteration states correl. with temp. in active geothermal system 78−40551
P-wave abnormal delays in The Geysers-Clear Lake geothermal area, California 79−74860
Pacific island and seamount ages rel. to volcanic chains origin 77−64242
Pacific plate, heat flow anomalies rel. to roll cell mantle convection 78−73345
E.Pacific Rise, hot springs and geophysical expts. 80−101360
E.Pacific Rise, hydrothermal heat flux of black smoker vents 80−94488
E.Pacific Rise−Galapagos Rise system, heat flow meas. rel. to sediment thickness 78−73331
E.Pacific Rise geothermal system, physical limits on geothermal fluid temp. and role of adiabatic expansion 80−101362
palaeo-geothermal gradients in Upper Rhine Graben, determ. from sedimentary organic matter metamorphism 79−70800
palaeogeotherms, implications of disequilib. in garnet lherzolite xenoliths 78−57179
palaeogeotherms, uncertainties due to Al_2O_3 low solubility in enstatite 78−65283
palaeogeotherms from xenolith suites in basalts and kimberlites 77−2127
passive continental margin, thermal evolution in sea floor spreading model 80−56427
peridotite equilibration conditions in upper mantle, exptl. determ. of geochemical parameters 77−2130
permafrost thermal behaviour, surface heat balance simulation 80−67385
plate tectonic driving forces, heat flow and tidal drag 78−32050
plate thermal structure and mantle convection 79−2197
plutons, thermal evolution, parameterised approach 80−90042
plutons undergoing hydrothermal cooling and thermal cracking, heat transfer 80−12362
Poland, heat flow map and Europe geothermal field *(Polish)* 77−21707

terrestrial heat continued
porous rocks, saturated with low cond. fluid, thermal cond. meas., systematic errors 77−86871
Precambrian shield of Liberia, heat flow 80−98279
Precambrian thermal regimes 78−65235
Proterozoic era, crustal temp. gradients rel. to tectonics and apparent polar wander loops 80−56360
proto-Earth, melting due to primordial dense atmosphere blanketing effect 79−57935
pyroxene geotherms, thermodynamics 78−65282
pyroxene solvus geothermometer in $CaO-MgO-SiO_2$ system 77−2144
Quebec, heat flow data anal., borehole obs. in small area 77−81846
Quottoon pluton, British Columbia, thermal effects of igneous intrusion and uplift 80−12352
radiation balance meas. as instrument design problem 77−41173
radiation budget expt., Nimbus-6 obs. 77−41106
radioactive heat generation, variation with depth 79−84202
radioactive heat sources rel. to convective stability of Earth interior 77−9381
radiogenic heat generation in old platform crusts 80−89996
radiogenic heat source content and whole planet cooling 80−90007
Raft River geothermal area, Idaho, seismic refr. study 80−3963
Raft River geothermal reservoir, Idaho, USA, borehole geophys. study 80−21672
Red Sea, heat flow map 77−91083
Red Sea geothermal system, ore transport and deposition 78−32096
reservoir temp. determ. using O isotopes in dissolved sulphate and water from hot springs and drill holes 78−69382
reservoir waters, sulphate-water O isotope thermometry 78−69383
Reykjanes Ridge, heat flow survey, age and heat flow relation 79−79768
Reykjanes Ridge, new heat flow obs. 80−90011
Rhinegraben area, gravity anomalies and geothermal implications 80−104852
Rhinegraben area, heat transfer and distrib. in upper mantle 80−104927
Rhinegraben geothermal anomaly at Landau oil-field, model 80−98281
Ries impact crater, thermal events, age and intensity 79−79760
rifted continental margins, thermal history and subsidence, Nova Scotian and Labrador Shelves 80−12353
Rio Grande rift, New Mexico, transient heat flow model 79−34771
Ririwai ring complex, Nigeria, heat flow meas. 79−57894
rock massif, nonstationary heat conduction near horizontal mine *(Russian)* 77−56620
rocks, crystalline, thermal cond., rel. to energy extraction from hot dry rock geothermal systems 79−70790
rocks, hot, dry, hydraulically fractured linearly expanding cracks, eqns. *(Japanese)* 79−34809
rocks, thermal cond. and diffusivity using modified Angstroem or impulse method 80−90085
Roosevelt hot springs, Utah, seismic noise study 80−56399
Roosevelt Hot Springs Thermal area, Utah, heat flow and hydrothermal alteration enthalpy 80−90008
Ross Ice Shelf project, geothermal heat flow 79−88366
Rumania, geothermal gradients rel. to hydrocarbon deposits *(Rumanian)* 77−29266
Rumania, geothermal regimes of tectonic units 79−70768
Salton Sea geothermal area, California, temp. gradients, onshore and offshore meas. 80−3962
San Miguel Island, Azores, heat flow and mid-Atlantic rift volcanism 77−86844
SW. Scottish Highlands, temporal changes in heat flow distrib. assoc. with metamorphism 80−101347
sea floor of Scotia, S.Atlantic and Weddell Seas, heat flow 80−94491
seafloor surface geothermal survey, techniques and results *(Russian)* 78−40527
sedimentary basins, heat flow and subsidence histories with finite crustal extension rates 80−89987
sedimentary basins development model, heat flow prediction 79−29719
self-potential anomalies near vertical contacts 80−3919
self-potential method in geothermal exploration 80−4125
shear deformation zones along major transform faults and subducting slabs thermal-mechanical struct. 78−73330
shear heating instability in upper mantle 79−20783
E.Siberia, amethysts form. temps. and history *(Russian)* 80−12393
S.E.Sicily, basalt thermomagnetic study 77−33056
simulation, digital and analogue techniques *(Rumanian)* 77−29510
Singhbhum thrust belt (India), results of geothermal studies 77−49050
Slovakia, W.Carpathians, heat flow meas. in deep boreholes 77−29258
Snake River Plain-Yellowstone region, geothermal significance of magnetotelluric sounding 77−70623
soil, thermal conduction flux in situ meas., methods *(French)* 78−96331
soil, unsaturated, coupled heat and water movement prediction, math. model 78−61446
soil temp. differences and diurnal var. in Wales 77−64403
soil temp. prediction from winter period meteorological data 77−37418
Soufriere Crater Lake, use as calorimeter, erupted lava heat loss rate calc. 78−28207
source-span-sink thermal models of arcs and ridges 78−32040
St. Lucia, Sulphur Springs geothermal field model 80−94494
standard geothermal provinces, heat flow-generation relation *(Polish)* 80−36271
steam reservoirs characts. determ. by ^{222}Rn meas. in geothermal fluid 79−74918
steam-water counterflow in porous media, model, geothermal systems appl. 79−79879
steamflow in geothermal reservoir, Kawah Kamojang, Java 80−77018
Stromboli, Italy, energy budget of volcano 79−70774
subducting lithosphere, heat transfer with continental asthenosphere 80−94510
subducting oceanic crust, thermodynamic consequences of minerals dehydration, high press. and temp. 78−69301
subducting slab undergoing upper surface melting, thermal field 80−85638
subduction zone, ascending flow between descending lithosphere and overlying asthenosphere 78−40531
subduction zone, thermal model with dehydration in downgoing slab 79−79784
subduction zone, thermal structs. evolution 80−56440
submarine geothermal resources, seafloor spreading centres and volcanic areas 77−37171
subsurface temperatures from surface heat flow data, theory of inverse problem 80−104928
terrestrial heat continued
sulphide deposits, heat flow anomalies due to groundwater flow *(Russian)* 78−15978
surface heat flow, geotherms and lithospheric thickness regional var. 77−53025
surface heat flow rel. to continental lithosphere thickening model 78−77200
surface heat flux, rel. to Earth core energetics and geomag. field generation 77−73638
surface temp. of early Earth 78−15981
Switzerland, siting criteria for heat extraction from hot dry rocks 79−39275
TAG hydrothermal field, ^3He excess in bottom waters as activity indicator 80−101383
Tasmania, two heat flow values 77−33018
tectonic unit heat flow, Romania *(Rumanian)* 80−8268
temp. gradient distrib. and geological struct. Izmir-Seferihisar geothermal area, Turkey, relation between temp. gradient distrib. and geological struct. 80−56441
temperature distrib. and electrically conducting zone formation 78−85519
temperature meas. in shallow holes, Salton Sea geothermal field test 78−11849
N.Thailand, hot springs and geothermal gradients, temp. obs. 80−94495
thermal balance, influence of human activity *(French)* 79−74553
thermal balance, natural conditions, quantitative estimates 1978 review *(French)* 79−57890
thermal conductivity measurements on saturated rocks at permafrost temperatures 79−84232
thermal convection, two-phase, in porous layer, flow visualisation study 79−72930
thermal domes, CO_2-rich mantle fluid heating possibility 79−66659
thermal effects on surface waves in stressed conducting media, theoretical study 80−8253
thermal fluids of Abano region, N.Italy, sources and circulation paths 79−20883
thermal gradient, from comp. of Cr-rich pyroxenes in peridotite xenoliths 77−5139
thermal history model of Earth with parameterized convection 80−26470
thermal inertia mapping rel. to surface composition and soil moisture 77−73740
thermal model of Earth's surface for geological mapping by remote sensing 77−53056
thermal state and evolution of Earth and terrestrial planets 77−64243
thermal water occurrences in Trans-Pecos, Texas 79−74923
thermoelastic deformations of half-space, strains and tilts, Green's functions 78−36092
thermomagnetoelastic model of earthquake source mechanism 79−70758
tidal heating and evolution of lunar orbit 77−29671
topographic corrections to geothermal obs., analytical method 80−46282
tracing with noble gases in meteoric water 78−69502
trans-Atlantic heat flow profile between 20°S and 35°S 77−86827
transient heat flux, during erosion and uplift with exponential heat source distrib. 79−57887
Travale-Radicondoli geothermal area (Tuscany), dipole elec. sounding method appl. 80−97762
Turkey-Iran, Moho temp. from 80−72462
Tuscany region, geothermal areas location via geochemical and isotopic methods 77−49049
two phase convection driven by phase change instability mechanism 77−86834
two-phase convection in a sandbox rel. to geological porblems 77−64238
UK mainland, heat flow field 80−26477
Ukraine, heat flow meas., radioactive elements distrib. in upper crust 77−86842
Ukraine, thermal props. of near-surface rocks *(Russian)* 77−91084
Ukrainian Shield, comparison of gravity and heat model with deep seismic survey profile *(Russian)* 78−48991
Ukrainian Shield, geothermal survey peculiarities rel. to search for fracture waters *(Russian)* 80−104935
Ukrainian Shield, thermal model from deep seismic sounding profile *(Russian)* 78−28190
under-surface temp. pattern estimation by dynamic remote sensing *(Japanese)* 78−36315
underground temp. var. with depth and time 79−5463
underground thermal wells, heat extraction with water 77−44949
United Kingdom, geothermal energy resources 79−17166
United States, geothermal resource assessment 79−70428
E.United States, low-temp. geothermal resources 80−85264
upper mantle, palaeogeotherm from ultramafic xenoliths in Elwin Bay kimberlite 77−91078
upper mantle, partial melting and electrical conductivity anomalies 78−28199
upper mantle partial melting under oceanic spreading ridges 78−65237
upper mantle thermomechanical models, plate vel. changes rel. to magnetic activity 78−65231
Urach region, Germany, very abnormal temp. field investigation at great depths 79−48440
SW USSR, heat flow determ. *(Russian)* 79−48430
USSR European section, heat flow rel. to crustal thickness *(Russian)* 79−20772
vertical orogenetic profile, relation between terrestrial heat flux and rocks mechanical characts. *(German)* 78−81123
western Virginia, heat flow rel. to origin of thermal springs in folded Appalachians 80−41414
volcanic processes and organic compound synthesis on primitive Earth 77−64434
Wairakei geothermal field, lifetime estimate 78−11854
Wairakei thermal region, thermal water transport of major rock constituents 77−81844
water convection, simple theoretical and expt. study, geophysical appl. and analogies 80−24018
wells, bottom-hole temperature stabilisation model 80−51356
White Mountain heat flow anomaly and geomagnetic sounding of NE. United States 79−8594
N.Wolverine Complex, British Columbia, geochronology rel. to thermal history and tectonics 80−3961
Wyoming, heat flow and radioactivity 80−72469
Yellowstone hot spot, tectonics and crustal props., earthquake and aeromag. data 78−48996

terrestrial heat continued
Yellowstone Lake, heat flow meas., Yellowstone caldera thermal struct. 78−48997
Yellowstone National Park as continental hot spot 80−3981
Yellowstone thermal waters, subsurface boiling and dilution effects on isotopic comp. 78−49048
Yellowstone volcanic plateau, conf., USA (1974) 78−49004
Yermak hot spot in Arctic Basin, magnetic and bathymetric evidence 79−88313
Zambia, heat flow and prod., evidence for lithospheric thinning 77−86840
Fe melting and adiabatic temp. distribs. in outer Earth core 77−70626
Hg emission rel. to Hg-sensitised UV photoreactions in abiogenetic organic synthesis on primitive Earth 77−37173
Rn in geothermal reservoirs 78−69381
SiO_2 geothermometer temp. of groundwater rel. to regional heat flow, United States 79−74876

terrestrial magnetic field *see geomagnetism*

terrestrial magnetism *see geomagnetism*

test equipment
see also automatic test equipment
abrasion test machine for refractories testing at high temp. 79−52505
abrasive and impact abrasive wear testing equipment for materials at elevated temps. 78−7136
abrasive impact wear test system 79−43513
abrasive wear resistance, rapid determ. using converted lathe 79−87780
acoustic filter components for ANSI standard psychoacoustic testing 78−83198
acoustic microscopy, nondestructive testing appl. 80−16612
acoustically active material, fatigue strength testing installation, electric and magnetic field effects 78−39995
amateur radiotelescope testing appl. 79−16830
angle tearing testing appliance for rubbers 78−7140
antimonic caesium vacuum photocell, test instrument for contactless circuits *(Russian)* 79−58676
artificial heart and assisted circulation apparatus, hydrodynamic test bench rigs 79−48372
atmospheric, standardisation and determ. of dynamic errors 79−8714
attachment for testing sheet materials during sign alternating loading 77−52579
austenitic steel, US test equipment and practice *(German)* 79−74316
autocollimation instrument for checking angles and pyramidicity of AR-90° prisms during manufacturing process 80−87570
batcher, portable universal, for testing air-pollution gas analyzers 79−8715
bending machine, four-point, assessment, steel bar deform. meas. by holographic interferometry 79−34266
biaxial testing machine, for flat specimens, study of specimen shape *(Japanese)* 77−70268
burn-test apparatus, for fibre reinforced composites 80−76441
calibration setup for gravimeter, based on inclination method 77−91313
calibrator using band-gap voltage reference, oscilloscope appl. 78−65941
capacitor loss-angle and capacitance checking cct. 77−61085
cardiac activity signal simulator 80−56230
centralised systems, with improved precision 77−79081
chemical indicator, for testing poisonous and explosive gases *(German)* 77−4950
clamp and strain gauge, for shear characts. determ. of glass reinforced plastic 80−85114
coated specimens, bearing capacity, testing under external and internal pressure 79−70254
complex dynamic Young's modulus measurement equipment for polymers 78−1615
component profile inspection equipment 80−105608
compression, biaxial, machine for testing brittle, plastic materials 79−15899
conductometric instruments metrological monitoring, for environmental contaminants control 80−55973
contact resist. in working media in static, dynamic loading, testing unit, appl. to steels 79−15900
controlled-current impedance meas. equipment design *(Spanish)* 78−8421
corona inception study on three-electrode systems *(German)* 77−7611
corrosion cell construction for metal SCC obs. in boiling $MgCl_2$ 78−39962
corrosion stability of metals under stress 79−70248
corrosion testing under stress, unit for producing biaxial tensile stresses 79−57174
creep curves, multicycle, device for recording at elevated temps. 79−43512
creep testing, device for producing constant stress 80−71835
CRT tester based on ohmmeter and adapter 79−35711
cryostat, He for prolonged low-cycle fatigue testing 79−52491
cylic load 18-position test unit for film and fabric materials 78−7120
cylinder, rectilinearity meas. using equal chromatic order fringes 80−27286
cylindrical part edge quality determ., acoustic method and equipment 80−35491
cylindrical surface linearity testing device 77−30129
defectoscope, portable, using Schmitt-trigger based annunciator, without hysteresis 77−90567
deflection measurement apparatus for bimetallic plates during high-temp. heating 78−7134
deformation processes in complex profile shells, installation UDM-1 80−81261
denture base materials, multi-station machine for fatigue testing 80−108648
diamond indentation and draw tester, for meas. of ultra-adherence in films 78−72944
digital cardiac defibrillator tester 80−41286
digital test instrument survey *(German)* 78−8394
digital time-interval meter test rack 77−74373
disperse materials, fine layers, autohesive strength, meas. installation 80−40644
driven member rotation uniformity test installation 80−92094
dynamic biaxial loading techniques and apparatus, cruciform specimen, elec. motor and hydropneumatic based devices 80−85129
ECG arrhythmia simulator for monitor testing 78−61270
ECG cable continuity tester 77−77997
ECG testing, digital simulator appl. *(Spanish)* 78−40359

test equipment continued
eddy current flaw detector, nuclear reactor fuel testing appl., electrically conducting inclusions detection 77−90560
eddy current probe, high saturation with internal reference, design and specifications 80−40658
elastic damping properties determ. unit for shock absorbers 78−5703
elastic yielding determ. 79−70251
electrodes, screening, discharge phenomena with UHV positive and negative lightning and switching pulses for dimensioning *(German)* 80−87963
electromanometric system frequency response visualisation device 77−48890
EM coating thickness meters, for NDT, standardisation, USSR 77−90561
endurance testing machine for plastics 77−52580
failure analysis tools comparison and selection 80−71865
fatigue crack generating and meas. device for use with cylindrical specimens 79−52508
fatigue cracking kinetics in pure bending *(Russian)* 79−52477
fatigue servo-hydraulic testing machines 80−108649
fatigue test machine, low-cycle, far sheet material bending to −196°C 80−55616
ferromagnetic probe coercimeter for inspecting the quality of parts with variable geometric dimensions 80−35488
ferromagnetic probe coercive force meter, different heads, for tubing inspection 78−60943
flow transducer testing appl. 78−18363
flowmeter and volume recorder checking system 77−72384
flowmeter checking, gas, using standard throttle system 77−80242
flowmeter time constant determining, using hydromechanical oscillatory system 77−76009
flowmeters metrological assurance, for petroleum-gas industry, Soviet standardisation 77−76004
fluoroscopic system, alignment checking device 77−86604
gamma radiation monitor testing, compact set-up with ^{60}Co reference gamma source 77−10494
gamma-gamma method, multibeam sonde, stand for adjusting 80−85103
geodesy, apparatus for testing bubble vials 79−29871
glass tubing dia. and wall thickness meas., P-329M instrum. 80−86262
hardness tester, portable, for determ. by Rockwell technique 77−63854
hazardous atmospheres, max. explosion press. affected by low ambient temp. 78−44380
hearing aid measurement system comparison 78−65151
heat and pressure chamber design, testing transducer for steam turbine flow-through clearance measurement appl. 77−53881
high and cryogenic temperature range mech. testing devices 78−7137
high-speed raster device for testing photoreceiver sensitivity nonlinearity 77−79150
holographic interferometer, piezoceramic radiators defects visualisation *(Russian)* 78−1530
hospital test instruments, scientific and medical instrumentation capability 78−69242
HTR plants components testing *(German)* 77−10482
HV instrument transformer calibration system based on LV inductive voltage divider 77−82567
hydraulic universal testing machine, K value determ. *(German)* 80−90836
hygrometers, precision salt standard, metrological support suite 79−17430
image analysis, semiautomatic quantitative system *(German, English)* 77−52602
impact fatigue test equipment for use at high-temp. 79−52492
impact testing equipment for small specimens 77−52578
impact testing of resilient materials 77−25223
installation for in-reactor study of creep and stress-to-rupture, plane stress mode 78−39996
installation for testing rotating-object surface temp. transducer 78−4612
instrumentation for impact, erosion and fracture studies 77−81383
insulation loss-angle and capacitance test trolley *(Russian)* 77−10041
interchangeable differential manometer test technique and equipment 77−57320
interleaved glass layer prism for semiconductor mask testing 80−43425
internal friction test unit for threadlike crysts. 78−36997
Josephson junction method, thin film tunnel, stability testing standard cell EMF appl. 77−67468
laboratory test instruments 79−30444
laser radiation pulse-length monitor testing, precision test system 78−45697
layer thickness uniformity meas. instrum. calibration *(German)* 77−74351
linearly varying pressure rate meas., instrument design 78−8395
LMFBR structure materials in liquid Na, capsule type creep tester *(Japanese)* 80−108653
low-cycle testing unit for use in vacuum and at high temp. 79−52503
LV short-circuit testing station, equipment and measurement methods *(Polish)* 80−77773
magnetic circuit loss meas. by warming/cooling method 77−57368
magnetic devices, constant magnetomotive force, testing and anal. using mag. potentiometer 78−62210
magnetic field simulation system for search coil magnetometer testing and calibration *(German)* 77−49754
magnetic permeability of ferrite meas. at 9.5 GHz 77−74465
magnetically hard materials testing instrument, pulse magnetiser design *(Russian)* 77−67481
mechanical properties testing, using Rayleigh surface waves 79−70249
metal crack depth meas. by potential probe method, principle *(German)* 77−86234
metals, for thermal cycling conditions 79−87778
metals, strength and ductility determ., pulsation attachment for TsDMU-30t test machine 79−52538
meter, for vibr. etching of rolled wire technical parameters meas. 79−14356
microammeter testing installation adaptation for <30 μA 78−45653
microhardness measurement, bicylindrical indentor 80−40642
microhardness tester recording the indentation diagram 79−57173
microscope testing, universal, set of attachments design 77−5907
microspecimens in strong mag. fields, device for tensile and creep tests 79−15903
mitral valve prosthesis in vitro tester, unique design 78−40426
mobile test laboratory for analyzing gases 79−71435
NDT laboratory and field equipment in India 80−108650

test equipment continued
negatoscope, 0D-10N, for scanning radiograph 80−35494
neutral beam high-voltage test stand, for fusion reactor 78−70632
noise generator, pseudo-random for sound absorption and buildings, insulation testing *(Spanish)* 78−13861
nomenclature, uniformity 79−6109
nondestructive, circuit for selecting signals in specified phase range 78−56863
nondestructive instrument for cutting steel testing, hardened by quenching 77−90559
nuclear fuel element, post irradiation testing in resistance furnaces *(German)* 78−29632
nuclear power stations, fission reactors testing using ultrasonic test apparatus *(German)* 80−13730
ocean buoy testing, radiotelemetering meas. system *(Russian)* 78−16192
optical fibre test gear, BPO, view of likely requirements 79−64349
pacemaker patient simulator 80−41322
particles, abrasive, mech. strength determ. 79−87781
passive solar building thermal performance modelling by passive solar test boxes, expt. 80−3494
passive solar building thermal performance modelling by passive solar test boxes, theory 80−7921
permanent magnets in instruments with partially closed mag. ccts., meas. errors *(Russian)* 77−67480
phase meters checking, by comparison with angular measure 77−10057
phasemeter test measuring transducers 78−77894
piezoelectric transducer parameters testing equipment 79−50555
plastometer, for determ. of deform. resist. of metals 78−7121
plastometer for multistage incremental compression testing of hot metals 80−85135
polyhedral prisms checking instrument, unit of plane angle transmission 77−7221
polymer films, vapour permeability determ., gravimetric test method 79−39066
polymer membranes, O_2 permeability, determ. with Zircon gas analyser 79−39195
polymer test apparatus for chem. resist. and penetrability in corrosive medium under hydrostatic pressure 79−39065
polymers, corrugated surface, Rayleigh wave excitation, modified wedge method 79−37261
polymers, deform., device for testing under hydrostatic pressure and anisotropic conditions 79−87783
potential-drop meas. system for fatigue crack detection of steel specimens 79−34225
potentiometric strip chart recorder calibrator/performance evaluator 77−87752
precise light pulser for testing surface barrier particle spectrometer 77−79508
precision DC and AC digital voltmeter tester *(Russian)* 79−26080
precision testing technique for intensive care instrumentation 79−70687
pressure-test apparatus for spirally welded tubes 77−52583
profile of components meas., using electro-optical instrument 79−21701
profilometer attachment for surface roughness parameter determ. 78−36967
prosthetic heart valve, disc-type, in vitro meas. of fluid stresses 77−52833
pulse dispersion test bench for optical fibre characterisation 77−50778
quartz crystal oscillator checking against standard frequencies in LF/VLF ranges 77−74372
radiography, test phantom for meas. of phys. parameters *(German)* 78−57068
random vibration simulator, practical realisation 80−53732
raster electron microscope test object 78−86393
reference manometer free-piston rotation with changes in tilt angle 77−57316
relaxation bending test device 79−70245
relaxometer, low temp. testing modification 79−43517
relaxometer for plastics testing *(German)* 79−39081
resistance thermometers, device for measurement of static characteristics 80−77784
resonant electromagnetic fatigue tester, features *(French)* 78−56870
respiration rate meter tester 80−81758
road construction nondestructive testing, appls. *(German)* 79−11742
rotatable sample holder with voltage readout, for low-temp. CW US expts. 78−13873
rotating body dynamic balancing, elec. meas. methods *(German)* 78−86261
rupture strength testing under cycic loading, AIMA-5 machine modification 79−52506
SEM specimen chamber use for dynamic expts., state-of-the-art review 78−23918
semi-automatic universal test machine for metal specimen tensile testing *(German)* 77−81346
servocontrolled hydraulic hot-torsion machine for hot working studies 78−27698
sinewave generator, simultaneous supply of fifty strain transducers, ship vibration testing 80−62652
solar concentrators, paraboloid type with reduced wind drag, design 77−23731
solar flat plate collector performance evaluation 79−62091
solar flat plate collector test apparatus 79−62100
space shuttle insulation coating, combined load testing at 1100°C 79−34261
spectral response, pulsed measurement, test set-up and apparatus, shortcomings and planned improvements 80−45695
split Hopkinson pressure bar use in obtaining dynamic stress/strain data at const. strain rates *(Japanese)* 80−16630
spot scan system for photodetector props. evaluation, 0.5-2 micron 79−2826
star simulator lightguide test instrument and method 79−27422
static bending testing device for samples at different temps. in aggressive media 78−39972
static tensile-compressive testing, smooth tubular specimens, grip for 80−66724
steel granular model material, equipment for shear deform. investigation *(German)* 80−35449
steel stress/deformation response meas. device *(German)* 78−3261
stochastic generator, theoretical fundamentals and applic. *(German)* 77−53956
strength, long term 79−70253
test equipment continued
strength and deformation testing, ceramics, wide temp. range, universal apparatus 79−57177
strength of metals, ionised gas effects, 20-900°C 79−70252
strength testing machine for use in mobile laboratories 79−15908
stress corrosion cracking, multisection plan for H_2 absorpt. of metals for tests under cathodic polarisation conditions 79−52504
stress corrosion testing device, lab. and autoclave testing 79−52502
stress relaxation test device, for variable temp. 80−85113
stretch testing of swollen rubbers, attachment to strength testing machine 79−15905
stretching strength of rubber, long term, testing apparatus 79−15907
stroboscopes appl. 78−55453
superconducting 7.5 Tesla segment test facility 78−54929
table top pulsed solar simulator, design and construction, for testing solar cell arrays powering artificial satellites 80−45696
tear resistance testing, instrument for controlled notching of rubber 79−70258
tensile tester, for long optical fibres 78−83123
tensile testing, fastening method for steel wire rope 79−87779
tensile testing at const. true strain rates, test machine 79−34262
tensile testing at high temp., self-locating grips design 79−52507
tensile testing machine by up to 3000°C 79−87776
tensile testing of reinforcement steel at high, low temps. 79−15902
tensile/compressive strength test machine calibration *(German)* 77−77654
tension-compression fatigue testing machines, characterisation of materials under cyclic loading at high temperature *(French)* 78−15628
thermal cycling apparatus for testing Ge thermometer stability 77−61066
thermal fatigue testing device, 180⇄1100°C, in inert medium 79−15904
thermal props. of metals at high temp., acoustic method, apparatus 79−14222
thermoanemometers for low air speeds, checking equipment 79−77311
thermometers testing, thermoelectric and resistance, using zero-setting and steam thermostats 77−74400
thickness gauges metrological provisions, 1979 status in USSR 80−77749
thickness testers, Kocour electronic models, for electroplated coatings, evaluation 79−21702
thin-walled tubes accelerated rate test system for two-dimensional stress states 79−43514
timer group testing installation 77−79083
Tokamak toroidal magnet supercond. cluster test design 79−31199
torsion bomb machine for dynamic stress/strain measurements under superimposed high press. 80−85130
torsion deformation test apparatus for 0-1150°C range in different gaseous atm. 78−7123
torsion pendulum oscillations recording equipment for internal friction meas. 78−36998
torsion rig, testpieces testing during variable torsion 79−52494
tubular sample testing unit with axial force, internal and external press. and torsional moment 78−39969
two-axis tensile test machine, for static and dynamic tests *(French)* 78−15627
ultra-microhardness tester, for expts. on vacuum deposited films 78−53161
uniaxial testing machine, Antarctic deep core ice under hydrostatic pressure *(Japanese)* 79−79890
US pulsed transducer effective directivity meas., semi-automatic method 77−84102
US pulsed-echo thickness meters calibration using liquid-thickness model 79−37102
US test unit for abrasive granular materials, failure characts. in US field 80−85112
US vel. propag. meter for NDT of polymers 78−19976
USSR flowmeter testing aggregate as basis for single metrological testing system 79−94752
vertical test machine for tension at speeds up to 25 m/sec 78−39968
video and audio, 1979 video yearbook 79−14197
viscoelastic tester with mech. drive *(Japanese)* 79−34232
volume stressed material under static or low-cycle load, testing device 80−71834
wear testing, specimen loading device 79−43516
wear testing of plastics, attachment to MI machine 79−87784
wear testing procedures, machine for joint prosthesis materials 79−20716
welding resistance of contacts in switching equipment, meas. apparatus 77−57353
wideband electronic voltmeter testing installation 77−79119
C materials, bend strength testing, bench assembly with strain recording 79−57176
Ni-Cd and maintenance-free Pb accumulator characteristics *(German)* 80−97782
Pt-alloy thermocouples, reference-standard testing apparatus 80−13077

test facilities
see also aerospace test facilities; anechoic chambers; reverberation chambers
5 MW Solar Thermal Test Facility 79−62113
acoustic facility for appliance sound power meas. 77−58507
acoustic intensity measurement standards, effect of reduction in measurement locations, household vacuum cleaner testing appl. 79−18647
acoustic test facility modification for ANS qualification 77−62121
Alpha-Gamma Hot Cell Facility at Argonne-East 80−68779
audiometric facility at West Middlesex Hospital, London for standardised hearing tests 80−76858
Babcock & Wilcox hot cell facility 80−68910
Battelle Hot Cell Laboratory 80−68913
Battery Energy Storage Test facility, test programs and data processing 80−30449
coal gasification, bituminous, in situ, linked vertical well concept 79−48051
coal gasification/combined cycle power generation test facility, preview 80−16773
conference on nuclear engineering remote systems technology, San Francisco, USA (Nov.-Dec. 1977) 79−45438
CRNL experimental fuel element postirradiation exam. hot cell facility 79−9749
Daresbury Laboratory automated magnet field meas. facility 79−30509
diesel engine noise research at Perkins Engines 79−32136

test facilities continued
Doublet III fusion testing 79−85763
far IR focal plane array testing, astronomical satellite telescope appl. 79−5755
fast reactor, commercial, sodium test rigs, in UK 78−732
fast reactors, Na components, test facility 77−46394
FBRs, testing full-scale components for sodium reactors 80−828
FFTF core component meas. system 79−9728
FFTF core component measuring system 79−45446
FFTF element measuring system 79−9729
FFTF fuel element measuring system 79−45447
FFTF Fuels & Materials Examination Facility design features and objectives 79−9746
FFTF Fuels & Materials Examination Facility equipment design and development 79−9747
FFTF Interim Examination & Maintenance cell equipment mock-up testing 79−9816
FFTF interim examination and maintenance cell, equipment testing program 79−45451
FFTF-type eddy-current flowmeter performance in SLSF P-series test trains 79−9669
fibre optic telemetering for high voltage test stand, Lawrence Livermore lab. 78−54939
flat plate solar water heater performance comparison 79−62062
flat-plate solar collector test facility to determine thermal performance characts. 80−45730
Fuels and Materials Examination facility, design and construction 80−73986
Fuels and Materials Examination Facility, design features and objectives 79−45448
Fuels and Materials Examination Facility, equipment design and development 79−45449
fusion energy, Engineering Test Facility work on magnetic confinement 80−52787
fusion hybrid blanket data and development, review, simulation test facilities 80−106170
Fusion Materials Irradiation Test Facility, Li liq., deuteron activated, shielding 80−99286
Fusion Materials Irradiation Test Facility 80−91361
fusion reactor, cluster test facility, design 80−90835
fusion reactor, Doublet III, neutral beam test tank design 80−99301
fusion reactor, Large Coil Test Facility test stand design description 80−102320
fusion reactor, TFTR, blanket module expts., engineering test station design 80−102338
fusion reactor, TFTR, neutral beam injector test facility construction 80−102336
fusion reactors, Large Coil Test Facility, liq. He cooling system 80−102321
fusion technology development, mirror fusion test facility 79−49856
General Atomic Hot Cell modification and refurbishment 80−68786
geothermal energy conversion, 10 MW, San Diego (USA) expt. facility performance 79−48085
handling equipment for neutron radiography facility 79−45443
Hanford hot cell facility 80−68911
heat exchanger fouling data analysis, for geothermal power plant appl., use of multivariate regression technique 79−52880
HFEF, irradiated fuel examination by eddy currents 79−45461
HFEF/N, equipment repair room modifications 79−45439
HFEF/N, Na loop safety facility expts., disassembly 79−45444
HFEF/N air sampling system 79−45441
HFEF/N irradiated fuel element eddy-current exam., cladding performance 79−9750
HFEF/S air cell, decontamination and refurbishment 79−45445
hot cell measurement and test equipment, calibration control 80−68787
hot fuel examination, neutron radiography facility 79−9725
hot fuel examination, neutron radiography facility handling equipment 79−9726
hot fuel examination, sodium loop safety facility, loop disassembly system 79−9727
hot fuel examination facility, air cell decontamination and refurbishment 79−9910
hot fuel examination facility, air sampling system 79−13541
Hot Fuel Examination Facility Complex, history and status 80−68909
hot fuel examination facility/north, equipment repair room modifications 79−9723
hot fuel examination facility/north, wall feedthrough removal, portable glove box system 79−9724
humidity chamber, convectively mixed, calibration appl. 78−54379
HVDC interrupter test facility, dual 30 kA systems 78−55035
installation for testing elec. contact transducer, using interferometer and photorecorder 78−12683
IR sensor test facilities 77−65647
IR sensors, long-wave, for astronomical obs., ground calibration 79−5749
irradiated reactor component fracture testing facility 79−79201
Large Coil Test Facility, instrumentation system design 80−95446
Lawrence Livermore Laboratory superconducting High Field Test Facility 80−90834
level gauge checking 77−22526
level gauge reference installation for calibration 77−71294
LMFBR secondary shutdown, absorber balls test 78−41821
LMFBR structural materials, development of an instrumented materials irradiation test for FFTF 80−57858
LMFBR structural materials, development of an instrumented materials irradiation test for FFTF 80−68797
low dielectric loss meas. apparatus for 0.1 to 200 MHz 80−15958
LV short-circuit testing station, equipment and measurement methods *(Polish)* 80−77773
marine environment test facility for electro-optical systems 80−45847
marine instrument testing, need for national programme 77−21924
measurement facility inspection, confidence and productivity improvement 78−77840
metal surfaces inspection, ground, light interferometry appl. 79−34216
MHD test facility safety analysis methodology and documentation system 80−61388
mirror fusion test facility, project scope and objectives 79−49848
Mirror Fusion Test Facility supercond. coil development 79−31202
moving material fault test rig *(German)* 80−11855
Neutral Beam System Test Facility, TFTR, neutral beam line final design 80−99309
test facilities continued
neutron production by neutral beam sources, shielding design criteria for fusion program 80−99387
neutron radiography at HFEF/N 79−45442
Nippon Nuclear Fuel Development Co. hot laboratory, present status 80−68781
noise measurements on domestic appliances, requirements for sound rooms 79−18604
nuclear fuel element postirradiation test facilities, Chalk River 79−45460
nuclear power station outages, turbine-generator reliability assurance through large scale test facilities 77−3151
nuclear power stations, fission reactors testing using ultrasonic test apparatus *(German)* 80−13730
nuclear reactor pump coolant tests, computerised monitoring 78−70585
nuclear reactor safety testing, at AEE, Winfrith, UK 77−6528
nuclear safety systems, periodic testing, time dependent unavailability anal., FRANTIC computer code 78−29588
nuclear safety testing, LOFT (loss-of-fluid) project at INEL 80−32386
O-arai Engineering Centre post irradiation examination facilities 80−68780
Oak Ridge, hot cell facilities, history 80−68784
Oak Ridge National Laboratory Ceramic Fuels Alpha Facility 80−68783
ocean test structure for wave force meas., improved platform design [Ocean Test Structure] 79−12306
ORNL Radioactive Materials Analytical Laboratory 80−68785
ORNL Transuranium Processing Plant, current status 80−68915
OTEC, design of seacoast test facility, Hawaii 80−55888
p-n junction, volt-farad characts. meas. with semiautomatic installation 77−41643
periodic inspection of meas. facilities, probabilistic confidence characteristic selection 78−77839
pulsed neutron, from spallation target, Rutherford Laboratory 78−29208
pulsed neutron physics facility, remote operation and maintenance 79−9934
pulsed neutron physics facility, remote operation and maintenance 79−45465
radiation damage test facility, LAMPF 79−45466
reactor emergency cooling model validation by Loss of Fluid Test Facility 79−80981
reactor fuels, post-irradiation examination, hot cell complex test facilities in Japan *(Japanese)* 80−63255
reactor testing, fast flux, research-type, neutron radiography facility 80−18371
relativity gyroscope expt., high accuracy test facility 77−30077
remote decontamination facility and repair station for hot-cell manipulators, Whiteshell, Canada 79−45453
solar, thermal, 400 kWth, Georgia Tech, preliminary (1979) results 79−61955
solar cells, testing using plane mirror heliostat 80−45668
solar collectors, standard test procedure and facility 79−61947
solar receiver convective losses determ., using cryogenic heat transfer tunnel 79−83636
solar simulator design for testing solar collectors 80−50996
solar standards and testing activities in developed and developing countries 80−55819
solar system, 32 kWe, total energy project 79−52912
solar thermal receiver, 5 MW, real-time computer control 80−72075
Solar Thermal Test Facility, 5 MW, heliostat focus and alignment system 78−50894
solar water-heating collector test procedure 79−62067
spectacle lens test facility complex 79−39603
superconducting high field test facility, and initial performance 79−30447
superconducting Tokamak toroidal magnet system development, cluster test facility 79−30495
telephone test acoustic chambers 78−87218
toroidal magnet coil design and testing 79−31195
total dynamic characteristics of meas. facilities, limit error estimation 78−77841
TREAT, neutron radiography equipment improvements 79−45462
Vallecitos Nuclear Center Hot Cells 80−68912
Whiteshell Nuclear Research Establishment Hot Cell facility 80−68914
wind energy conversion, diffuser augmented wind turbine concept 79−83556
Windscale AGR, high pressure fuel test loops design, installation, commissioning 77−6491
Winfrith Hot Cells−1964-1979 80−68782
worldwide flow meas. calibration facilities list 77−62322
Na boiling detection technique tests, FFTF capabilities 79−13395
Na ML-3 circuit for testing mech. props. of structural materials of LMFBRs *(Spanish)* 80−55595
SF_6 breakdown characts. in non-uniform field gaps, at 0.8-2 MV range 77−15269

testers *see test equipment*

testing
see also automatic testing; computer testing; electron device testing; electronic equipment testing; environmental testing; impulse testing; inspection; integrated circuit testing; logic testing; machine testing; materials testing; mechanical testing; nondestructive testing; optical testing; production testing; program testing; switchgear testing; transformer testing
60 kW experimental wind power plant in Sweden, test results 80−61253
1300 MW nuclear reactor steam isolating valve blowdown tests *(German)* 80−22967
acousto-optical correlator, with two-dimensional reference transparency 80−106485
analogue simulation of measuring equipment and testing means 79−80564
angular meas., testing instrument for errors 80−42186
artificial heart, bench test technique 79−48366
artificial heart, using miniature Stirling engine 79−53287
artificial heart valves, mock circulation system 77−52932
astronomical sites testing with balloon borne radiosondes, turbulence and seeing meas. 77−29645
atmosphere high acidity analysers, comparative tests near industrial installations in Fos-Etang de Berre region 78−81464
balances, general purposes, program of state acceptance testing 79−80581
basic metrological operations and methods 78−41263

testing continued
blood filter evaluation 78−69250
Calcutta variable energy cyclotron vacuum system design, testing and commissioning 78−86707
cloud condensation nuclei counters, comparison of two instruments 78−61598
computed tomography scanner, fourth-generation, performance evaluation 80−46035
computer tomography head scanner, translate-rotate type with Xe detectors, performance characts. 80−46036
conductometric instruments metrological monitoring, for environmental contaminants control 80−55973
dental instrument noise studies, canine evoked response audiometry system 77−29226
dielectric constant meas., test scheme design 80−13101
diffraction theory, spectral domain approach for testing Albertsen's corner diffr. coeff. 80−87304
Dobson spectrophotometer for atmospheric O_3 meas., pre-installation testing 77−17250
dosimetry, personnel monitoring performance standards 77−40783
dry cells, performance and life characts. 79−100508
edge operator evaluation test procedure 79−75646
effective intermittent shock testing *(German)* 78−77887
electromechanical balance type-test results *(German)* 77−79059
European Community solar collector test programme 79−62057
exponential distribution MTBF confidence limits determ. using Epstein and Harters methods 80−98790
FBR, sodium-cooled, blocking of cooling channels monitoring *(German)* 77−34372
FBR blanket, integral neutron reaction rate meas., in FBBF facility 80−22887
fission reactor containment structures, integrity and safety, isolating valve provision and testing aspects *(Spanish)* 79−93738
fission reactor cooling blockages, of LMFBR, simulation expts. *(German)* 78−94044
fission reactors, BWR, Enrico Fermi-2, system turnover, test and startup program 80−63338
fixed tilt solar collector with reversible vee-trough reflectors and vacuum tube receivers 79−100539
flow and volume meas. devices, laboratory practice *(German)* 78−32803
flowmeter, by comparison with standard instruments 77−76007
flowmeter, EM, without using liquids 77−80244
flowmeter, gas, using standard throttle system 77−80242
flowmeter, in working conditions, use of model EM flowmeter 77−76008
flowmeters, design principles for comparative testers 80−96319
fluoroscopic spot film system image quality evaluation and optimisation 78−69205
Fort St. Vrain HTGR rise-in-power test programme 79−9864
fusion reactor, neutral beam ion source, core snubber network design, fabrication and testing 80−102378
fusion reactor, TFTR, preoperational test plan, manpower loading and scheduling 80−102340
fusion reactors, Large Coil Program, Westinghouse coil stability testing, pulsed induction heating 80−106194
gas chromatograph oven testing 77−77835
GCFR fuel assembly testing in BR-2 helium loop, Mol 79−67924
geodesy, hypothesis tests for singular compensation problems *(German)* 78−44758
geodesy, hypothesis tests using adjustment in sections, linear test theory *(German)* 79−44083
heart assist energy convertors, using fluid controls logic 79−53286
heart valve prosthesis testing 77−56530
heat exchanger, liquid-fluidised bed, scale control and corrosion tests, geothermal power plant appl. 79−48090
hot-film anemometers, testing strategy for freq. optimisation 78−26218
hot-wire anemometer, dynamic characts. using shock tube and electronic testing 79−72974
HTR plants components *(German)* 77−10482
hydrometeorological meas. equipment, USSR state testing 79−70897
indentation hardness number conversion table analysis 79−11736
industrial ear protectors, standardisation of testing, current developments 78−22225
laboratory, test results, international acceptance *(Danish)* 80−8952
land-use map accuracy testing, sampling designs 80−17226
laparoscopic sterilisation techniques, preclinical and clinical testing 77−48929
lase coherence length, for holographic appl. 77−7100
laser techniques, state of art in Poland 77−5790
left ventricular assist device testing using calf model 78−73296
light sources, photometric laboratory equipment requirements and standards *(Slovak)* 80−17990
liquid heating flat plate solar collectors, testing consistency test program 79−74541
LMFBR secondary shutdown, absorber balls test 78−41821
long arc simulated lightning attachment testing using 150 kW Tesla coil 80−70074
lubricants, four-ball test specimens mag. orientation and effect on total test time 78−80700
magnetic containment testing for JET 78−54870
magnets, permanent, meas. errors determ. 80−52280
measuring instruments, determ. of valid interval between tests values 80−57284
microwave survey instrument evaluation and calibration 77−37946
monitoring system for pollution gases, performance tests and specifications 79−16659
motion picture film colour separation, computer appl. *(Russian)* 77−49796
neutron source calibration at NBS for calibration checks of neutron radiation instruments 77−38540
nuclear medicine measurements, quality assurance 77−40764
nuclear power stations, aseismic design and testing of equipment and components, Japan 80−52763
nuclear power stations, fission reactors testing using ultrasonic test apparatus *(German)* 80−13730
nuclear power stations safety, leakage tests, Spanish policies *(Spanish)* 80−5247
ocean bottom in-situ soil testing, direct and indirect methods, trends 79−12307
ocean current sensors, EM- and acoustic-types, performance assessment 79−25345

testing continued
oxygenator, bubble, blood damage test standardisation *(German)* 79−2158
oxygenator gas transfer performance test standardisation *(German)* 79−2159
pacemaker implantable lead performance evaluation, status report 78−57135
photodetection linearity, procedure *(Hungarian)* 79−89001
physical fitness test evaluation, bioenergetic model *(German)* 79−1992
poloidal field coil design and development of JT-60 Tokamak 79−31204
potentiometric displacement transducers, standards for specification and tests, book 79−2763
power transformers, fault diagnosis, dissolved gas analysis of insulating oils 80−26097
pulse-echo transducers, tone burst testing 79−27479
PWR reactor core barrel, vibrations, influence of boundary conditions and co-vibrating liquid obs., using model 79−36302
PWR reactors, commissioning and start-up procedures *(Slovak)* 79−36346
pyranometers for mesoscale solar irradiance network, test and calibration experience report 79−74499
PZT transducer manufacture and testing 79−23174
radiographic equipment acceptance testing, systems approach 78−69203
radiographic phantoms for testing X-ray imaging performance 80−51229
radiography, quality assurance meas. for diagnostic X-ray systems 77−40763
radioisotope thermoelectric generator shock and vibration test program for MB-M75(A) 80−35711
radiometer, neutron, testing techniques standardisation, in Soviet Union 80−99405
soft X-ray collimators, test procedures using laboratory X-ray sources 77−5436
solar collector thermal performance test procedures 79−62066
solar flat plate collector thermal performance testing 79−62061
solar materials research and collector thermal performance tests *(Japanese)* 78−46732
solar water heater, low-cost unit development *(Afrikaans)* 80−7925
solar water heating, flat plate system with thermosyphonic flow, investigation 79−70464
solar-electric heat pump for houses, design and tests *(German)* 80−7951
spacecraft systems, evaluation of acceptance testing 79−16797
spectral response, pulsed measurement, test set-up and apparatus, shortcomings and planned improvements 80−45695
speech and language prostheses evaluation 80−76864
standard cells, low resistance differential potentiometer appl. *(Polish)* 78−29127
tachometric flowmeters, volumetric dynamic flowmeter installation 80−96324
terrestrial solar modules, sandwich type glass encapsulation, climatic parameters effect, economic anal. 80−45673
theodolites, use of polyhedral prisms in testing 79−67370
thermal benchmark lattice expts., quantitative consistency testing 79−9700
toroidal field coil design and development for JT-60 Tokamak 79−31203
toroidal magnet coil design and testing 79−31195
transducers, using high-power DUMILOAD device 77−3707
unfolding codes for benchmark gamma spectrometry 80−47807
US diagnostic instrument performance evaluation, work of USA AAPM and AIUM 78−69170
US transducer characterization standards, tissue equivalent testing for hospital use 79−29651
vehicle noise, stationary test method 77−34998
vibration-acoustic diagnostics, random signal patterns recognition *(Slovak)* 79−18612
wave power convertor fully submerged model, design and experimental testing 79−92059
webermeter, using semiautomatic potentiometric apparatus 77−74464
weighing machines, reliability and performance testing 79−80579
West German metropolitan flat plate solar collectors, outdoor efficiency meas. 79−62048
wind turbine, variable pitch vertical axis, 2.4 m dia. prototype 80−61265
X-ray collimators, testing via parallel X-ray beam generation technique 78−28526
Ag-Zn cells, failure analysis, test methods evaluation 79−48105
Al electrolysis units, air washing tests *(French)* 79−29493
Ge resist. thermometers, stability test at 20K 78−81971
Li-I cell solid state, cardiac pacemaker power source 79−66584
NaI(Tl) long narrow rectangular polycrystalline scintillator performance testing 77−54418
Ni-Cd 6.0 Ah cells, accelerated testing of cell failure for life prediction 80−35670

testing apparatus *see test equipment*

testing equipment *see test equipment*

testing machines *see test equipment*

tetramethylammonium manganese chlorides *see organic compounds*

tetraneutrons *see neutrons*

tetrodes
fusion reactor, BBC CQK 200-4 modulator tube for sustaining neutral beam power supply 80−99290
fusion reactor, High Voltage Switch Tube, for Neutral Beam Power System 80−99291
high-power, switching and regulating elements for fusion research 79−54592
HV switch tube development, for Tokamak fusion test reactor 78−66385
inverse reflex tetrode, high power ion beam generation 80−68986
power capabilities for plasma heating *(French)* 78−9801
reflex tetrode, ion beam extraction anal. 80−48903
reflex tetrode ion-beam source, extracted ion beam anal. 80−23236
reflex tetrode with unidirectional ion flow, additional aluminised mylar anode 78−37473
two-dimensional, algorithm for solving space-charge problems with thermally-emitted electrons 80−100743

textile fibres *see fibres*

textile industry
agitating type polymerizer, synthetic resins and fibres manufacturing process 80−3341
colour distortion visual and objective assessment *(Hungarian)* 79−63291
colour uniformity meas., appl. of microdensitometry *(Czech)* 79−30524

textile industry continued
electrical resistance of textiles, meas. device using operational amplifiers 80−42240
fibre production, solid matter content radiometric meas. experience *(German)* 77−67488
lustre quality meas., recording and evaluation 80−98967
machine noise charact. meas. under production condition 78−5611
microtome, automatic for cutting 400 μ fibre snippets 77−9999
periodic structure defect detect. using optical processing 80−95829
polyesters, continuous production plants, technical details, polycondensation reaction stage analysis 79−100361
solar energy applications, hot water systems, dyeing, in textile industry, commercial aspects 79−83576
spectrophotometer head with small-spot fibre-optic viewer 79−30525
^{60}Co irradiation sterilisation processing, nonstandard double carton simulation 79−26760
^{60}Co irradiation sterilisation processing, unequal mass interchange model 79−26758
^{60}Co irradiation sterilisation processing unequal mass interchange model verification 79−26759

texture
see also recrystallisation texture; surface texture
Al alloys, influence of solid soln. elements and precipitation as correlation of formability parameters with texture 79−91696
Al thick probes, neutron transmission curves near Bragg-edge for grain size and texture eval. *(German)* 80−71667
4-4′-n-alkoxybenzylideneamino-biphenyls, central Schiff's base linkage reversal effect on liq. cryst. props. 80−79683
4′-n-alkoxybiphenyl-4-carboxylic acids, 4-(2′-methylbutyl)phenyl esters, smectic phases 79−86684
4′-n-alkylbiphenyl-4-carboxylic acids, 4-(2′-methylbutyl)phenyl esters, smectic phases 79−86684
alloy, two-phase, deform. struct. and recrystallisation, review 79−34061
alloys with twinned martensite, crystallog. singularities in reverse martensitic transform. *(Russian)* 77−32571
analysis, numerical calc. of generalised spherical harmonic function *(French)* 78−18484
analysis, vector method 79−83218
analysis by orientation distrib. functions 77−86282
analysis by vectorial method *(French)* 78−18483
Au film growth on Si(100), LEED and X-ray texture anal. 79−99452
BCC metals, influence of screw dislocations on cryst. lattice rotations during deform. *(Russian)* 78−6966
BCC metals, plastic deform., computer simulation 80−40456
benzene-hexa-n-alkanoates and benzene mixture, disc-like mesogens, thermotropic mesophases 79−86699
boundary conditions for textures and defects 78−26561
brass, 70:30, rolled, nucleation and annealing texture development 80−45320
α-brass, (211)[$\bar{1}$11] single crystal, rolling deform. 77−21174
brass, cold rolling, inhomogeneous texture 80−89251
α-β brass, cold-rolled, energy dispersive X-ray diffr. studies 80−40379
α-brass, drawability correlation with sheet metal texture 78−60683
α-βbrass, duplex, pole figures 79−87818
brass, FCC, rolling texture development 79−87657
brass, FCC rolling texture origin with rolling plane parallel to {111} 79−91674
brass, orientation distribution, texturised materials, Ghost effect demonstration 80−70080
α-brass, rolling texture development, dependent on relative stacking fault energy 79−52237
brass, rolling texture development and deform. struct., shear bands effect *(Japanese)* 80−84952
brass, simulation of rolling and shear texture, using an adapted Taylor theory 78−52835
α-brass, texture, recrystallised orientation distrib. function comparison with 40°⟨111⟩ rolling texture 80−25723
brass, textured thin specimens, fracture 78−60816
brass (70:30), cold rolled, optical, X-ray and TEM exam. of deformation struct., and textures 78−88500
α-brass sheet, shear bands and recrystallisation 79−91680
α-brass sheets, earing, R-values and 3-D orientation distrib. functions, comparisons 79−91702
bronze P, heavily cold rolled, yield strength enhancement mech. 77−36539
4-n-butyloxyphenyl-4′-nonyloxybenzoate, edge dislocations in smectic C mesophase 78−91231
calcite rocks, experimentally deformed, texture development 79−83230
calcite rocks, plastically deformed, texture transitions 79−83227
cellulose, fibres crystallised from hydrazine, texture by X-ray diffr. 79−69030
ceramic, one dimensional cooling, effect of particle orientation on frost damage *(Japanese)* 77−12701
cholesteric liquid crystal, struct. charact. from opt. circ. dichroism 77−62476
cholesteric liquid crystals, planar texture, field-induced square grid perturbation 79−90531
cholesteric liquid crystals, with course-pitch spirals, stable textures and EHD instability 79−90550
cholesteric mixture, solid phase, spherulite textures, optical effects and mol. ordering 79−1746
cholesteric planar texture, planar-finger print texture transform. around Cano disclinations 80−14999
cholesteric textures, confocal, optical and electro-optical props. *(Russian)* 77−80419
cholesteric-nematic mixture with negative dielec. anisotropy planar texture instability 78−59739
chrysotile asbestos fibres, texture rel. to mech. props. 77−81300
coatings, textured, crystallites faces determ. 80−64846
cold-drawn sheet, texture changes in stamping *(Russian)* 77−90365
composite alloys, two-phase systems, deformation textures 79−83219
composites, two phase, depend. of texture and microstruct. on yield stresses of components 79−91697
computer calc., library program, in FORTRAN IV 78−22598
computer simulation of errors in three dimensional anal. 78−64805
concrete, aggregate, shape and texture anal. by modified Fourier method, orientation effects 77−77691
copper phthalocyanin, thin film, thermal behaviour *(Japanese)* 80−24753

texture continued
Cosserat theory of crystal plasticity, appl. to anal. of lattice rotations under constrained deform. *(Japanese)* 78−2189
cross-rolling and compression textures, numerical prediction 80−40382
crystallite deformation in rolling, computer simulation *(French)* 78−31421
crystallite orientation distribution function, determ. from isolated axis density values 77−48612
crystallographic, meas. by X-ray diffr. 78−22604
crystallographic orientation distrib. function, use for texture study 79−52228
crystals, textural defects 80−49158
cubic polycryst. materials, texture determ. method, X-ray diffr. technique 77−68897
cubic polycrystal, anal. of orientation distribution plots obtained by vector method 80−29977
deformation texture calc. according to Taylor model 79−87652
deformation texture development and polycrystalline modelling 79−91671
deformation texture evolution 79−90721
deformation textures, eulerian simulation 80−3096
determination by magnetic texture gauge 79−66238
development in grain growth, computer simulation 79−96036
diamond, natural, polycryst., distinctive features of struct. 79−92530
diarylethanes, bromo- or cyano-substituted, mesomorphic props. 79−90535
earing behaviour, and formability limits prediction from texture data 79−91703
elastic properties, influence of texture 79−83224
elasticity, annealing and deformation effects, with and without texture 79−52274
electric steel, induction above magnetisation curve knee from pole density texture 77−12151
electron diffraction, orientation and position accuracy 78−22606
electron diffraction patterns, of textures, reflection sphere curvature influence on reflection location geometry 80−87996
energy dispersive diffractometry for quantitative determination of texture 79−87818
ethylene-propylene rubber, highly deformable, fracture surface roughness 78−44197
evaluation by X-ray and neutron diffr. anal., comparison *(French)* 79−91882
exploding wire unduloids, preferred grain orientations, lattice distortions, zonal texture 77−36568
f.c.c. alloy, rolling texture *(Russian)* 77−1843
FCC metal, polycrystalline, computer simulation of rolling texture *(Japanese)* 77−63686
FCC metal with cube orientation, texture variation during rolling 77−70065
FCC metals and alloys, macroscopic shear band contrib. to rolling texture 77−86056
FCC metals and alloys texture transitions, computer simulation 79−90666
ζ-Fe-Zn layer formed during hot dip galvanizing, texture 79−29287
ferroelectric, textured layered prep. by HF sputtering 77−85947
ferroelectric liquid crysts., chiral smectic C phase, phys. props., review 80−75150
ferromagnetic material, polycryst., magnetic texture anal. 80−108002
ferrous metals, banded structure determ., automatic structure analyser 78−39973
fibre, quantitative determ. of volume fraction, analytical method by pole figures 80−11863
fibrous, coincidence of bounds for some elastic moduli of polycrystals 79−28030
film, backscattering yield of 2 MeV ^{4}He, target texture influence 79−4875
films obtained by oblique mol. beams, texture formation *(Russian)* 77−66592
fir-tree textures, possible existence 80−76269
formation during anomalous grain growth *(Russian)* 77−55984
FORTRAN program for Fourier coeffs. of assoc. generalised Legendre polynomials of generalised spherical harmonics in texture analysis *(French)* 77−15279
glass porous, struct. and texture rel. to heat treatment effects *(German)* 78−44140
goniometer alignment of Schulz reflection technique, method for testing 80−81272
goniometer for analysis of rocks 80−26630
grain growth, computer simulation, taking account of texture 79−11546
grain orientation, of neighbours, disorientation description 80−79725
grain orientation nonuniformity across wire specimen sections, anal. of X-ray patterns 78−23886
grain volume meas. and topological parameters by serial section analysis 77−36705
graphite intercalation compound with SbF_5, texture 78−31355
haematite, neutron diffr. exam. of texture, comparison with magnetite 78−52849
haematite, textures and topotactical relationships, neutron diffr. study 79−83229
HCP metals, and alloys, anisotropy of phys. props. rel. to texture 79−91700
hybrid optical/digital texture analysis 80−78787
II-VI semiconductors, thin epitaxial layer, direct synthesis *(German)* 80−104070
image segmentation and texture unit cell size determ. 80−95817
in situ composites, crystallographic relation determ. by texture goniometry 79−86654
inverse pole figure construction using electron microscope *(Russian)* 77−60012
inverse pole figures, calc. method on digital computer 80−20950
ion beam texturing of surfaces 79−77876
isopermalloy, permeability stability calc. rel. to texture *(Chinese)* 80−65959
lattice period determ. by axial X-ray camera 79−68974
liquid crystal, cholesteric, long pitch type, with homeotropic boundary alignment, elongated and spherulitic domain struct. 80−107047
liquid crystal, field-induced nematic-cholesteric relax., hysteresis behaviour of texture 77−84900
liquid crystal with negative dielectric anisotropy, cholesteric planar texture EHD distortion 78−42894

texture continued
liquid crystals, nematic and cholesteric, surface and bulk configurations, topology 80−59381
liquid crystals, textures, deform. and struct. order, review 77−43135
Lucke goniometer with computer control, metal texture plotting appl. 78−18500
magnetic materials, anisotropy of magnetic and other props., crystallite orientation distrib. *(German)* 77−8307
magnetic properties, influence of texture 79−83224
magnetic texture analysis, generalisation of dispersion theory 80−80556
magnetite, neutron diffr. exam. of texture, comparison with haematite 78−52849
magnetite, textures and topotactical relationships, neutron diffr. study 79−83229
Magnico alloy, with Si, Nb, Ti and La, low-temp. thermomag. treatment 77−63812
materials, data acquisition and processing 80−64828
materials texture, conf., Aachen, Germany, (March 1978) 79−83217
MBBA, nematic phase, high freq. EHD instabilities, temp. depend. 79−94879
MBBA/CC mixtures, cholesteric phase, torsional shear flow in elec. and mag. fields 79−86697
measurement, expt. methods, review 79−87815
measurement by Schulz refl. technique, effect of X-ray linewidth on defocus correction 77−86255
mechanical anisotropy of texture effect on X-ray stress measurement *(German)* 79−29091
metal, BCC, rolling texture, effect of critical shear stress ratio of {112} and {110} 79−91673
metal, electrodeposited from molten salts, faceting rel. to texture axis direction 79−28969
metal, FCC, polycrystalline, quantitative anal. of cross-slip and twinning 79−90677
metal, FCC, with fibre texture, X-ray method of twin fault probability determ. 79−87817
metal, fibres, cubic struct., texture form. in uniaxial deform. theory 79−24532
metal, grain boundary groove migration at solid-liquid interface, simulation and with camphene 78−52789
metal, orientation distribution function determ. using one pole figure *(German)* 77−25242
metal, textured cubic, residual stress evaluation 80−89435
metal, textures and collective props. of lattice defects, external surfaces, grain boundaries 77−62543
metal, transversely isotropic plastic props., yield charact. 78−60707
metal Taylor wires, texture and metastable phases 77−8812
metals, BCC, predicted rolled textures, influence of slip system and deform. model *(French)* 79−43309
metals, cubic, crystallographic orientations distribution function, computer calc. 80−64827
metals, cubic, heavily deform., development of lattice curvature 80−81136
metals, cubic struct., numerical simulation of cross-rolling textures *(French)* 79−20061
metals, ellipsoidal model of textured specimens with uniaxial symm. *(Russian)* 80−80100
metals, FCC, 'brass to copper' transition in rolling textures 80−76246
metals, FCC, texture changes in running surface as result of frictional stress 79−91699
metals, FCC and CC, role of latent slip, computer simulation *(French)* 79−32998
metals, FCC nonhomogeneous sheet, orientational distrib. function calc. of mean texture 80−11659
metals, HCP exam. of texture and Young's modulus anisotropy, developed during deformation *(Russian)* 79−15694
microstructure alterations and texture form. in normal grain growth, computer simulation 79−90679
minerals, preferred orientation, review and outlook 79−83220
Mossbauer absorbers, deformation induced texture 79−8074
Mossbauer absorbers, deformation induced texture 80−7214
Mossbauer effect, crystallographic and spin texture determ. 77−69735
Mossbauer effect, texture problem and Goldanskii-Karagin effect, intensity matrix method 80−7215
mullite, quantitative X-ray anal., standardisation, texture *(German)* 78−11176
multicomponent axial, quantitative evaluation 80−85100
natural terrain scenes, segmentation-based boundary-modelling processor 80−99661
nematic phases of rigid macromolecules, texture *(French)* 79−1394
neutron diffraction anal., time of flight vs. conventional method on drawn steel wire 80−81078
Nimomic PE-16, equilibrium surface bombarded with high dose He^+ ions 78−95091
non-random orientation distribution functions with random pole figures 80−6320
nondestructive investigation by neutron diffr. 79−87795
4-n-octyl-4′-cyanobiphenyl, smectic A liq. cryst., shear-induced textures and rheology 78−91228
4-n-octyl-4′-cyanobiphenyl, smectic A phase, stimulation of EHD instability 79−78656
4-n-octyloxy-4′-cyanobiphenyl, smectic A liq. cryst., elastic modulus determ., stress/strain relationships 78−91229
orientation distrib. function from pole figures with reflection coincidences 78−68846
orientation distribution function analysis from incomplete pole figures normalised by iterative method 80−59344
orientation distribution function of texture samples, reproducibility from pole figures 79−55611
orientation distribution functions, rel. between recrystn. texture and deformation texture 79−83222
orientation distribution of texturised materials, demonstration of ghost effect 80−70080
oxide ceramics, dependence of props. on raw materials, exam. using ceramic magnets as model *(German)* 79−4936
oxide film texture on Zr, Zr-Sn and Zr-Ti following corrosion in air and water vapour 77−56163
4,4′-di-n-pentyloxyazoxybenzene, anomalous smectic mesomorphism, calorimetric and optical texture obs. 79−77505
peridotite xenoliths in S.African kimberlites, structurology, upper mantle constitution implications *(French)* 78−11889
texture continued
Perspex, adhesion of silicone rubber, surface topography effects 78−15644
petroleum feedstocks and cokes, graphitisability 80−93580
4-phenylbenzylidene-4′-n-alkoxyanilines, central Schiff's base linkage reversal effect on liq. cryst. props. 80−79683
phosphate bonded synthetic mica ceramics, form., physical props., texture 77−21063
picture segmentation by preprocessing and averaging 77−58272
plastic properties, influence of texture 79−83224
PNAOBA, type C smectic liq. crysts., electrohydrodynamic instability 80−1927
poly(azomethines), thermotropic mesophases *(French)* 79−77507
poly(L-glutamic acid), texture in conc. soln. and solid films *(Japanese)* 79−90534
poly(oxyethylene glycol), texture in conc. soln. and solid films *(Japanese)* 79−90534
poly-(p-alkoxy-phenyl-p-acryloylbenzoates), nematic polymer, struct. determ. 79−99064
poly-(phenyl-p-acryloyloxybenzoate), nematic polymer, struct. determ. 79−99064
polyamide, directionally solidified, morphology 79−10808
polyamide, directionally solidified, X-ray diffr. 79−10809
polyamide fibre, chain-segment orientation, US vel. meas., humidity effects *(German)* 78−75590
polybutene-1 film, tubular-extruded, light scatt. from crystn. superstruct. 77−55796
polycrystalline material, texture and anisotropy *(German)* 80−3097
polycrystalline materials, partial texture index and meaning of Williams approx. *(French)* 77−58919
polyethylene, chain-extended, oriented, microindentation hardness 78−76728
polyethylene, doubly oriented, low density, deformation and structure, exam. 80−11705
polyethylene, filled with glass particles, uniaxially drawn, elastic constants, filler addition effect *(Japanese)* 78−95780
polyethylene, high density, inorganic filled, calendered sheet, crystallisation in capillary viscometer *(Japanese)* 77−70112
polyethylene, high density, inorganic filler, calendered sheets, anisotropy of tear strength and crystalline texture *(Japanese)* 77−70110
polyethylene, high mol. wt., inorganic filler, calendered sheet, melt, flow props. *(Japanese)* 77−70111
polyethylene, linear, cold-deformed, texture and molecular chain mobility 78−19805
polyethylene, low density, highly deformable, fracture surface roughness 78−44197
polyethylene, Raman spectra, drawing effect on longit. acoustic mode *(French)* 77−24828
polyethylene, struct. transform. under tension in liqs. *(Russian)* 77−51492
polyethylene, uniaxially stretched, density fluctuations 78−75587
polyethylene melt, cryst. kinetics during cooling, nucleation density effect 80−100181
polyhexamethylene terephthalate/polyoxytetramethylene block copolymers, supramolecular texture 78−91261
trans-1,4-polyisoprene, crystalline morphology in thin films 78−6019
polymer, coorientation with low molecular organic substances *(Russian)* 77−21089
polymer, solid, orientation meas. and characterisation methods uing X-rays 78−75559
polymers, crystn., texture studies, review 79−83221
polyoxymethylene, rolled, prediction of yielding behaviour 77−73306
polypropylene, injection moulded, texture *(Japanese)* 80−25722
polypropylene, oriented fibre drawing *(Russian)* 77−21088
polypropylene-nylon 11 fibres, bimodal cryst. texture, X-ray diffr. and electron microscopy 78−75567
polystyrene filament, melt spun, struct. and mech. props., effect of drawing, twisting, annealing, untwisting 80−45331
polytetraoxane, polymerisation temp. effects, and NMR obs. of mol. motion in tetraoxane cryst. 77−84663
porcelain, conventional and rapid fired, comparison of texture and props. *(German)* 78−64510
powders, spray drying to minimize preferred orientation 80−3098
preferred orientation, quantitative determ. by energy-dispersive X-ray diffr. 77−25241
preferred orientation investigation by pole figures and mathematical technique 79−34227
PTFE, heat shrinkable tubing, crystallite orientation 77−4795
PTFE, oriented fibre drawing *(Russian)* 77−21088
PVC, highly deformable, fracture surface roughness 78−44197
quartzite, naturally deformed, textural and microstructural development, metallurgical approach 79−83228
rare earth alloys, RCo_5, sintered magnets, texture determ. 79−100085
rare earth cobaltide, RCo_2, 'as cast', neutron diffr. exam. 78−3117
recrystallisation, conf., Leeds, England (April 1978) 79−47706
refractories, fatigue, effect of texture/crack relationship *(German)* 80−25829
refractories, fatigue behavior, effect of texture and crack kinetics, AE anal. *(German)* 80−21061
rocks texture heterogeneity, study via dielectric const. and elec. resistance *(Russian)* 78−96195
rolling texture control, theoretical and practical study 79−87656
secondary recrystallisation, grain orientation 79−34063
shear band effect on development 79−91675
shear band formation models, in rolling and extrusion 80−11666
sheet, coeff. of anisotropy calc. from pole figure *(French)* 78−15621
sheet, cold rolled, texture form., model *(French)* 78−68705
sheet material, ideal texture determ., rapid method using colour slides 77−25226
sheet metal, texture heterogeneity, numerical simulation *(French)* 78−92274
sheet metals, strain-induced changes in mech. props. and press formabilities 78−19781
sheet metals, X-ray diffr. anal. 80−6316
side-scan sonar with selective textural enhancement 77−5371
silica gel, pore struct., effect of washing with aq. solns. containing Mg^{2+} Ca^{2+} ions 79−52786
single crystal deform., texture form. 79−87651
smectic A liquid crystal, scattering textures, appl. to display device 78−91236

texture continued
smectic liquid crystal, homeotropic to confocal texture transformation *(Russian)* 78−18548
steel, 08Yu, annealing effect on texture, microstruct., and mech. props. 78−44138
steel, alloy, corrugated texture perfection, mag. anal. 80−88745
steel, alloy, types CT40, CT40X, CT45, texture form. 80−25721
steel, austenitic, 16H2NMB, struct., texture and mech. props. of product of transform. 78−92273
steel, austenitic stainless, ferritic, single phase ferritic solidification in welds, exam. 80−7546
steel, austenitic stainless, texture effects in rods, in series tests, elastic props. *(German)* 78−15439
steel, austenitic stainless, texture influence as through thickness strength 79−91771
steel, austenitic stainless, welded explosively, induced martensites morphology 80−104153
steel, austenitic stainless sheet, texture anisotropy influence on deformation forming limits 79−91706
steel, bainitic, invariant plane strain theory, determ. of habit planes and orientation relationships 80−55388
steel, C, texture effect on mech. props./magnetic props. relationship, NDT appl. 79−96274
steel, C (0.01 and 0.06 wt.%), rephosphorised, mag. props. and texture 77−20634
steel, C content effect on annealing texture, plastic anisotropy and mechanical props. 80−29976
steel, C deep drawing sheets, influence of strain- and stress-ratios on preferred orientation change 79−91690
steel, C-Mn, corrosion in acidic soln., metallurgical factor effects 79−70206
steel, cold rolled high strength sheet, with high drawability, fabrication process 77−73288
steel, Cr (17 wt.%), stainless, hot-rolled texture, effect on cold-rolled and annealed textures 80−55425
steel, Cr-Ni (16,14 wt.%), Si effect on texture, grain growth after rolling or recrystallisation *(French)* 77−55986
steel, crystallographic texture perfection in sheet with S,Mn inhibitors *(Russian)* 79−91709
steel, deep-drawing, texture problem after processing through continuous annealing 79−87659
steel, electron microdiffr. determ. of orientational correls. between ferrite and cementite 77−52584
steel, eutectoid thermomechanically treated, textural studies 80−29978
steel, extra mild, thin sheet, biaxial tensile deform., effect on crystallographic texture *(French)* 77−59814
steel, grinding, effect of hardness, texture, and bond of grinding wheel, temp. effect *(German)* 79−43459
steel, hot rolled strip formability, mech. testing and mech. props. *(German)* 79−66089
steel, hypoeutectic, texture development from frictional stress *(German)* 78−53003
steel, ion plated Pb film covered, Hertzian contact expt. 77−52511
steel, low alloy, fatigue fractographs *(Japanese)* 78−92335
steel, low C, capped, cold rolled sheet, deep drawability, effect of carbide size, cold reduction annealing 78−64559
steel, low C, cold rolled and recrystallised, containing Nb(CN) dispersion, struct. and textural aspect of deform. 79−47712
steel, low C, cold rolled sheet, Cu effect on recrystallization texture *(Chinese)* 79−74173
steel, low C, containing P, Mg effect on annealing texture, mech. props. and plastic anisotropy 78−27536
steel, low C, deform. form effect on texture *(Russian)* 78−3141
steel, low C, fatigue fractographs *(Japanese)* 78−92335
steel, low C, Mn effect on recrystallisation and texture *(French)* 80−3110
steel, low C, orientation distribution function anal. in maximum shear planes 79−82172
steel, low C, P, plastic anisotropy and mech. prop. dynamic strain ageing effect 78−64608
steel, low C, texture hardening in maximum shear planes during expansion 79−91704
steel, low-alloy, BCC lattice, texture form. by drawing and pulling through nonpowered rolls *(Russian)* 77−25100
steel, low-C, phosphorus effect on annealing texture, plastic anisotropy and mech. props. 77−25069
steel, low-C, preliminary thermomech. treatment, cold deform. effect on struct. and props. 79−38847
steel, low-C sheet, texture anisotropy determ. using inverse pole figures *(German)* 77−44431
steel, microalloy V-Nb, V, Nb effects on strength and formability of cold rolled sheets 77−55979
steel, mild, deformation texture *(French)* 79−70082
steel, mild, orientation distribution function, representation of texture and slip directions 80−11665
steel, mild, rolled, texture, analysis, vector method 79−83218
steel, Mn-Ni-Cr-Mo, high tensile strength, control-rolled, transformation textures 79−83225
steel, Ni, ferrite, orientation in pearlite, rel. to austenite *(Russian)* 80−81072
steel, Ni-Mn directional martensitic transform expt. 79−11613
steel, non-oriented, texture and mag. props., effect of Mn and S content 77−86047
steel, nonoriented, mag. props. texture, Cr addition effect 77−1880
steel, P, deep-drawing, spatial orientation distrib. of crystallites in cold-rolled and in annealed sheets 80−81079
steel, plastic deformation and cryst. texture in equibiaxial expsn. 80−7653
steel, preferred orientation investigation by pole figures and mathematical technique 79−34227
steel, shear-spun tubes, texture inhomogeneity 79−91691
steel, Si, nonoriented sheet prod. with texture of {100} ⟨ovw⟩ 80−89246
steel, Si, textured, alloying addition inhibition effects on grain orientation and growth *(Japanese)* 79−43270
steel, Si (3 wt.%), hot rolled, effect of initial texture on secondary recrystallisation *(Czech)* 79−91711
steel, Si (3 wt.%), struct. and preferred orientation, annealing parameters influence *(Czech)* 80−89248
steel, Si (3 wt.%), textured, secondary recrystn., precip. annealing effect *(Japanese)* 80−71662
texture continued
steel, stainless, 316 and 304, equilibrium surface bombarded with high dose He^+ ions 78−95091
steel, stainless, Cr-Cu (17, 0.6 to 1.1 wt.%), texture 80−84957
steel, stainless, ferritic, anisotropic lamellar fracture mechanism 78−64639
steel, stainless, ferritic, tensile strain direction and roping phenomena 77−36533
steel, stainless, hot rolled texture, effect on cold rolled and annealed textures *(Japanese)* 78−48425
steel, stainless Cr (17 wt.%), hot rolled sheets, martensite distrib. effect on ridging phenomena 79−1887
steel, stainless sheet, texture effect on sputtering erosion by Ar^+, SEM-electron channelling study 79−91856
steel, texture sheet, mechanical anisotropy estimation using quantitive metallography *(German, English)* 77−77696
steel, textured, X-ray stress meas. 77−46975
steel, transformer, textural barriers to grain growth after cold rolling and annealing *(Russian)* 78−39796
steel, transformer, texture formation tendency *(Russian)* 77−59803
steel low C, rolled, analytical vectorial method for crystallographic texture *(French)* 80−20956
steel plate, rolling direction determ. with notched bend test specimen *(German)* 77−60003
steel plates, hot rolled, anisotropic texture, exam. of elastic deformation behaviour *(Japanese)* 78−64586
steel sheet, hot and cold rolled, cold formability, notched tensile test and stretch bend test *(German)* 80−61031
steel St 52, textured, rolled, REK and lattice strain distrib. *(German)* 79−29095
steel with micro-duplex structure, neutron diffraction analysis of rolling texture 80−16327
steels, hot forming property and struct. *(German)* 80−25730
steels, with micro-duplex struct., neutron diffr. anal. of texture and its development 79−91692
stress determination, by X-rays, texture effect 79−91701
styrene-butadiene rubber, highly deformable, fracture surface roughness 78−44197
Teflon foils, cryst. struct. and texture changes due to polarisation process *(Polish)* 80−35209
tetragonal powder, preferred orientation, X-ray intensity corrections 80−1880
textures materials, residual stress evaluation by X-rays *(German)* 80−40670
textures near $A \rightarrow A_1$ transition, NMR and current effects 78−59994
thermoelectric pressed powder specimens, elec. characts. anisotropy rel. to textural anisotropy 77−52515
three-dimensional texture analysis, data processing, subroutines 77−25240
tissue section electron microscope image texture discrimination and automated meas. 78−57099
transform., struct., texture conc. var. depend. on plastic deform. *(Russian)* 79−66050
transformation textures, calcs., misorientation distrib. function 79−83223
transverse section picture reconstruction, correction functions and statistical noise 77−12989
n-undecyl-p-azoxy-α-methylcinnamate, smectic C phase, domains, walls, and disclinations 79−86687
weld pool, preferred growth direction of cellular-dendritic crystallites *(Russian)* 77−44236
X-ray diffraction, energy-dispersive, preferred orientation influence 78−22603
X-ray diffraction topography, quantitative analysis *(German)* 77−48595
X-ray quantitative phase anal. *(Chinese)* 80−21195
X-ray topography *(German)* 80−1894
Zircaloy, micrograin superplasticity at 850°C 78−23758
Zircaloy, textural model for stress corrosion crack susceptibility 79−47825
Zircaloy, textured, interactive creep and growth, upper-bound evaluation 80−89293
Zircaloy tubes, grain struct., texture, dislocation density effect on irradiation creep, X-ray diffr. and optical microscopy anal. 79−74208
Zircaloy tubes, yield loci, evaluation based on texture data and mech. testing 79−91695
Zircaloy-2, anisotropic irradiation creep 79−8333
Zircaloy-2, irradiation growth, shape and volume changes 80−92562
Zircaloy-2, pressure tubes, irrad. creep and growth, anisotropy factors 80−97536
zircaloy-2 and 4, tubing, rel. between contractile strain ratio R and texture 79−61607
Zircaloy-2 cladding tubes, heat treatment influence on texture and mech. anisotropy 79−91694
Zircaloy-2 irradiation growth at 353 and 553K, texture and temp. cycling effect 79−46709
Zircaloy-2 tubing, quantitative charact. of crystallographic texture 78−21647
Zircaloy-4, plain strain ductility dependent of struct. and texture 77−8885
Zircaloy-4 cladding, irrad. growth prediction using crystallographic texture model 77−46300
Zircaloy-4 tubes, texture influence on anal. of thermoelastic/plastic anisotropy and initial yielding 80−35260
Ag, (211)[$\bar{1}$11] single crysts., shear band effects on rolling deformation 80−50651
Ag, cold rolling, inhomogeneous texture 80−89251
Ag electrodeposits, dendritic growth inhibition by tartaric acid and tartrates *(French)* 78−87894
Ag, filament produced by glass coated melt spinning, mech. props. 77−86125
Ag films, effect of Ar- and N-ion bombardment on texture *(Russian)* 80−107338
Ag vacuum-condensed films, on glass substrate, X-ray texture study 79−83226
Ag-Cu, directionally solidified, obs. of cutting deform. zone *(Japanese)* 78−15422
Ag-Cu alloy filaments, prod. by glass coated melt spinning, microstruct. and tensile strength 79−91667
Ag-Ge (4.5 at.%), FCC, vapour-deposited, lattice imperfections, X-ray diffr. 78−72032
Al alloys, inclusions, oriented distrib. metallography and effects on anisotropy *(Russian)* 78−80589

texture continued
Al and Al alloy 5022, plastic anisotropy of textured sheet *(Japanese)* 79−34103
Al, cold rolling, inhomogeneous texture 80−89251
Al, cyclic torsional deformation, final texture 80−7595
Al, defect structure after plastic deformation 78−31467
Al, dislocation substructure formation under hydrostatic extrusion 78−56696
Al foil, modification of texture by fatigue, X-ray diffr. exam. 78−88477
Al, high purity, development of rolling and recrystallisation textures 77−25070
Al, orientation distribution function determ. using one pole figure *(German)* 77−25242
Al, pure, hydroextrudates, incomplete axial orientation *(Russian)* 80−20949
Al, pure, texture influence on stress/strain curves, prestrain, solid soln. and particle hardening effect on inhomogeneous deform. *(German)* 80−30014
Al, rolled, analytical vectorial method for crystallographic texture *(French)* 80−20956
Al, rolled single crystal, annealing texture 79−91678
Al sheet, texture evolution, effect of rolling or tensile deform., rel. to strain ratio 79−91672
Al single crystals, relation between axial orientation rotating and deform. banding 80−104206
Al, tensile deformed single crystal, form. of recrystallisation textures 77−12647
Al, texture variation during rolling 77−70066
Al, uniform film, on Kapton laminates, prep. and characterisation 78−11373
Al, wire, determ. of incomplete axial texture by X-ray diffr. 78−23720
Al wire, torsion fatigue strength and fibre texture 77−48549
Al-Ag, nonhomogeneity of deform. 78−84888
Al-Cu, isothermal coarsening of liquid inclusions 77−21166
Al-Cu (0.5 to 4.6 wt.%), cathode foil for electrolytic capacitors, relationship between comp., struct., and etchability 79−74314
Al-Cu films, deposition rate, mol. beam incidence angle influence on struct., film props. *(Russian)* 79−60646
Al-Cu-Zr (6, 0.3 wt.%), superplastic, texture studies 79−83210
Al-Mg cold drawn wires with FCC lattice, texture and structure 77−70067
Al-Mg-Si, heavily rolled, electron microscope obs. of cube oriented region, rolling texture 79−29093
Al-Mg-Si rod, extruded and cold drawn, annealing *(German)* 78−39804
Al-Ni, solidification in mag. field, crystallite obs. *(Russian)* 77−4770
Al-Sn dil. alloy, cube orientation texture development 79−96040
Al-Zn, nonhomogeneity of deform. 78−84888
Al-Zn (40 wt.%), plastic deform. effect on discontinuous precipitation 80−3053
Al-Zn-Mg (9, 1 wt.%), superplastic flow, relative motion of grains 77−52426
Al_2O_3, fine grained, basal slip and nonaccommodated grain boundary sliding 80−60916
γ-Al_2O_3, heat treatment rel. to texture 78−72789
Al_2O_3, hot pressing, microstruct., texture 80−40299
Al_2O_3, translucent, fabrication by high press. sintering 78−11167
Al_2O_3-Cu composite, vapour deposition, microstruct., texture and surface topography 77−70001
β''-Al_2O_3-Na_2O, Li_2O stabilized, texture conductivity relationship 79−47788
β-$Al_2O_3.Na_2O$, ceramic tube fabrication, crystallite preferred orientation, ionic cond. 77−8781
AlZnMg alloy, precipitation hardened, strength 78−39786
B films, prep. by H reduction of BCl_3, struct. and hardness 80−54543
B-Al cast braid, crystallisation and structuring of Al matrix *(Russian)* 78−52725
BaO.n Fe_2O_3, magnet, effect of SiO_2 on texture and densification behaviour *(German)* 79−24631
Be bronze, struct. and props. after ageing under load 78−84932
Be bronze BrB2, quenched deformed, substruct. and props., effect of prerecrystallisation annealing *(Russian)* 78−60677
Be, deformation strengthening, microstruct. and impurity effects 77−4791
Be, rolled ingot, with duplex microstruct., basal texture of two grain size distrib. 77−36556
Be-diamond support, for high-pressure X-ray diamond-anvil cell 78−30515
$Be_4Ti_2O_{12}$ grain oriented ferroelectric ceramic, prep. by molten salt synthesis-tape casting method 80−40296
Bi film, ellipsoidal model of textured specimens with uniaxial symm. *(Russian)* 80−80100
Bi, film, evaporated, elect. and elastoresistance props. 79−33367
Bi foil, splat quenched, preferred orientation 80−40381
Bi, texture of deformed polycryst. 77−59809
Bi-Cd, solidification in mag. field, crystallite obs. *(Russian)* 77−4770
$Bi_{1-x}Sb_x$ film, evaporated, cross-sectional struct., electron microscopy and replica technique study *(German)* 78−22977
Bi_2WO_6 grain oriented ferroelectric ceramic, prep. by molten salt synthesis-tape casting method 80−40296
C fibre, as-processed, diamag. studies 77−25165
C, filamentous catalytic, rel. crystallographic orientations of C and metal 80−89240
C, texture change on ht. treatment under press. 78−60687
C, turbostratic, formed in phenolic resin C by catalytic graphitisation of dispersed Ni, TEM study 79−77466
$Ca_{10}(PO_4)_6X_2$ (where X is F, Cl, OH or Co), influence of mech. treatment on struct. and reactivity *(German)* 79−43272
β-$CaSiO_3$ fibre, continuous unidirectional crystallisation from melt 78−95739
Cd, cold rolling texture development 80−25720
Cd foil, splat quenched, preferred orientation 80−40381
Cd, warm rolled, texture and grain size depend. of tensile props. 80−71720
Cd-B(W) particulate composite, dispersion hardening, grain size and texture strengthening 77−8840
Cd-Zn, solidification in mag. field, crystallite obs. *(Russian)* 77−4770
Cd-Zn (Ag), annealed, work softened, exam. of crystallographic texture, hardness 78−80559
Cd-Zn (1.5 wt.%), warm worked, effect of grain size, texture, on mech. props. 79−4988
texture continued
CdS film, prep. by hot wall technique, morphology and semicond. props. 79−95292
CdS, film, X-ray diffr. and elec. cond. 78−64149
CdSe film, vacuum deposited, struct., resist. and Hall mobility 77−76974
Co evaporated film, X-ray diffr. study 80−6663
Co film, evaporated, columnar struct. depend. on degree of texture 80−54567
Co film, evaporated, texture and columnar struct. 80−54566
Co film, texture and adsorption of CO *(German)* 77−24485
Co, magnetic anisotropy induced by mag. annealing and cold rolling, expt. 80−7695
Co, magnetic anisotropy induced by mag. annealing and cold rolling, calc. 80−7696
Co-Cr mag. film, crystallographic texture formation effects on props. *(Russian)* 80−108471
Co-Fe, morphology and certain props. of α-and η-phase martensite *(Russian)* 77−1838
Co-Fe, soft mag. props. rel. to metallurgical aspects 80−88810
Co-Ni, magnetic anisotropy induced by mag. annealing and cold rolling, expt. 80−7695
Co-Ni, magnetic anisotropy induced by mag. annealing and cold rolling, calc. 80−7696
Co-Ni (32 wt.%), FCC, rolling texture development 79−87657
Cr electrodeposit, formation of axial texture (111) [hkl], math. model *(Russian)* 78−84082
Cr, electrodeposits, relation between preferred orientation and microstructure *(Korean)* 77−28733
Cr, hyperfine interactions on ^{111}Cd-probe nuclei, TDPAC meas. 80−75904
Cr, physically vapour deposited, struct., mech. props. 77−36400
Cr, sputtered, growth struct. influence of substrate surface topography and ang. of adatom incidence 80−20058
Cr-Sm-Pr, Sm and Pr additions and plastic deform. effects on texture *(Russian)* 77−55983
Cu and Cu alloys, deformed, texture development 79−87653
Cu and Cu-Cr (0.6 wt.%), electron microscope obs. of shear bands *(German)* 77−48454
Cu, cold rolled sheet, anisotropy of elastic and strength props. 80−81077
Cu, cold work, P effect on annealing 79−47707
Cu, contact, texture, rel. to manufacturing procedure 77−16611
Cu cyclic torsional deformation, final texture 80−7595
Cu, deformation in ultramicrotomy 77−8874
Cu, dislocation substructure formation under hydrostatic extrusion 78−56696
Cu, fibre texture of filament produced by glass coated melt spinning 77−85966
Cu film, effect of thermal strain on orientation 80−49294
Cu, heavily drawn ETP wire, secondary recrystallisation 77−36537
Cu, heavily rolled, electron microscope obs. of cube oriented region, rolling texture 79−29093
Cu, plane strain deformed, electron microscope obs. of morphology 78−31424
Cu, plastically deformed, lattice strain distrib. *(German)* 80−85012
Cu, recrystallised, inhomogeneous deform. due to texture changes *(German)* 79−29158
Cu, rolled sheet, texture transform. during primary recrystallisation as function of annealing time 79−91683
Cu, rolling textures and texture inhomogeneities, exam. of development in single- and poly-crystals 79−11637
Cu sheets, earing, R-values and 3-D orientation distrib. functions, comparisons 79−91702
Cu single crystals, influence of friction and geometry of deformation, on texture inhomogeneities during rolling 78−72792
Cu, tensile deformed ⟨110⟩ orientated single cryst., recrystn., high voltage electron microscopy study 80−84958
Cu, texture after rolling of single crystal at room temp. 77−25067
Cu thick probes, subthermal neutron transmission curves, for Bragg grain size and texture eval. *(German)* 80−71667
Cu, torsion deformation texture *(French)* 79−70082
Cu, wire, axial texture after electroplastic drawing, X-ray struct. investigation *(Russian)* 80−104177
Cu-Ag, solid soln., nonhomogeneity of deform. 78−84889
Cu-Ag (3 at.%), plastically deformed, lattice strain distrib. *(German)* 80−85012
Cu-Ag (8 wt.%), plastic deform. effect on discontinuous precipitation 80−3053
Cu-Al (10 at.%), single crystal, orientation depend. of work hardening near [111] axis 77−12646
Cu-Al (6.4 wt.%), rolled low stacking fault energy alloy, struct. and texture 78−52844
Cu-Al_2O_3 extruded bars, strength anisotropy 77−16597
Cu-based alloys, orientation dependence of mechanically induced transformations 79−87660
Cu-In eutectoid, directional eutectoid decomposition growth, crystallography 80−29874
Cu-Ni textured alloys, grain boundary effusion of Ni to surface 79−90680
Cu-Ti (4 wt.%), combined recrystallization and precipitation 79−29072
EuS, film, anisotropic growth on amorphous substrate 77−12547
Fe, (100) [001], texture development by recrystallisation and normal grain growth 78−27539
Fe alloy, (110) [001] texture development by recrystallization and normal grain growth 77−32594
Fe alloy, low, (110)[001] oriented, mag. charact. 77−1879
Fe alloys, elastic props., texture correction formulae *(German)* 78−15439
Fe, Armco, sleeve, deformed by cold drawing, exam. of surface and texture *(Russian)* 79−34057
Fe, Armco, texture role in prestrain embrittlement 78−60796
Fe, cold rolled, struct., transmission Kossel patterns obs. 77−48451
Fe, fibre texture of filaments produced by glass coated melt spinning 77−85966
Fe film, evaporated at oblique incidence, columnar and textural struct. *(Japanese)* 77−62776
Fe films, evaporated at oblique incidence, columnar struct. and texture 79−77967
Fe films, vacuum evaporated, exam. of texture for various vapour beam incidence angles *(Japanese)* 78−48318

texture continued
Fe, magnetic powder, particle deformation effects on mag. props. 77−63236
Fe polycrystals, grain misalignment, electron microscope determ. *(Russian)* 80−103358
Fe, pure, rolling texture *(German)* 77−86054
Fe, texture, recryst. annealing effect *(Czech)* 80−89249
Fe thick probes, subthermal neutron transmission curves, for Bragg grain size and texture eval. *(German)* 80−71667
Fe vacuum deposits on Ni(Cu)(Ag) (111) FCC substrates, orientation relationships 80−59836
Fe-Al, hot- and cold-rolled, texture form., pole figures method *(Russian)* 80−45317
Fe-Al (4 wt.%) single crystals, rolling induced mag. anisotropy and its removal by annealing treatment *(Russian)* 79−61746
α-Fe-Al(Zn), ⟨111⟩ fibre texture development through diffusion process without α-γ transform 79−100170
Fe-Co-Ni Perminvar, mag. props. singularities in region of mag. anisotropy *(Russian)* 80−84614
Fe-Co-Ni-Al (35, 14.5, 7.2 wt.%), high-coercivity, substructure and texture change during bending and upsetting 80−21037
Fe-Co-Ni-W alloy, 45KKhVN, plastic deform., electron microscope obs. *(Russian)* 78−80584
Fe-Cu (1.2 wt.%) effect of precipitation on recrystallisation, texture 78−88476
Fe-Cu-glass ternary multiphase composite, microstruct. and props. *(German)* 77−90314
Fe-Mn, ε-martensite, preferred orientation and constitution, reverse pole figures *(Russian)* 80−104178
Fe-Mn, warm rolled, rel. contribs. of texture and grain shape to props. 79−91705
Fe-Mn alloys, quantitative phase anal., correction factor for texture 79−52528
Fe-Ni (32.86, 30.65 wt.%), characts. of quenched struct. formed in textured sheets, TEM and optical microscopy study 79−34084
Fe-Ni (47 to 65 wt.%), soft magnetic alloy with crystallographic texture and field induced anisotropy, pulse permeability and excursion rate *(German)* 79−73779
Fe-Ni alloys, electrodeposit on Cu, texture investig. 77−11818
Fe-Ni alloys, graim growth texture 79−91687
Fe-Ni-Al-Co-Cu alloy, sintered single-crystal mag. prod., props. 77−66709
Fe-Ni-C alloy with single-component martensite texture, α→γ transform., changes in shape *(Russian)* 80−104152
Fe-Ni-Co, texture form. after cold working and annealing *(German)* 80−3089
Fe-Pd (47 at.%) alloy, powders and powder compacts, mag. props. rel. to heat treatment *(Russian)* 79−15816
Fe-Si, grain oriented, with unique inhibition system for texture development 77−90366
Fe-Si, non-oriented sheets, production and props. 80−88797
Fe-Si (3 wt.%), (110)[001] oriented single crystal, form. of rolling and annealing texture 77−16608
Fe-Si (3 wt.%), Al-bearing, grain-oriented, N_2-H_2 annealing effect on texture, mag. props. 77−12714
Fe-Si (3 wt.%), orientation development during secondary recrystallisation, primary matrix effect, magnetic props. *(Czech)* 78−60679
Fe-Si (3 wt.%), texture, Mossbauer expts. 80−71262
Fe-Si (3 wt.%), texture form., plastic strain effect, hot rolled 79−79002
Fe-Si (3 wt.%) (001) [100] single crystal, cold rolled texture *(Japanese)* 77−21169
Fe-Si (3wt.%), quantitative determ. of grain orientation and textile by etch figure method *(Chinese)* 78−11233
Fe-Si (6.5%) alloy, struct. and rolling texture 79−79006
Fe-Si-B-S, grain-oriented, high induction, B and S addition effect on magnetic props. *(Slovak)* 79−4697
Fe-Si-MnS-Al, Al effect on hot rolling struct., recrystallization, texture magnetic props. *(Chinese)* 78−11237
Fe-Zn, crystallographic relations by X-ray diffr. 80−24408
Fe_2O_3/Fe_3O_4 transformation matrices, higher-order orientation relationships 80−100846
Gd, texture formation during cold rolling *(Russian)* 78−92275
^{3}He, A phase, textures bearing surface singularities solns. 78−79841
^{3}He, A-phase slab, mag.-field-induced cellular superflow, periodic texture 80−24706
^{3}He, anisotropic superfluid phases, book contrib. 79−99387
^{3}He, B-phase, textures effect on sp. ht. 78−75900
^{3}He, superfluid, A-phase, generation of textural defects 79−60588
^{3}He, superfluid, A-phase, helical textures, NMR response 80−70496
^{3}He, superfluid, A-phase, mag. texture relax. 79−60581
^{3}He, superfluid, A-phase, order parameter singularities, confined to small cylinders, NMR 79−55994
^{3}He, superfluid, A-phase, slowly rotating, textures and free energy 79−60587
^{3}He, superfluid, A-phase, texture and supercurrents 79−65279
^{3}He, superfluid, B-phase, n-solitons, and NMR freq. calcs. 78−34670
^{3}He, superfluid, NMR, l-texture effects on satellite frequencies 79−60583
^{3}He, superfluid, planar textures, Ginzburg-Landau eqn. solns. 80−10729
^{3}He, superfluid, texture topology in planar phase 79−69310
^{3}He, superfluid, topology of non-singular textures using relative homotopy groups 78−84021
^{3}He, superfluid 79−82410
^{3}He, superfluid A phase, planar textures 78−79837
^{3}He, superfluid A-phase, current-driven textural transition 79−55993
^{3}He, superfluid A-phase, existence of helical texture around superflow 79−60586
^{3}He, superfluid A-phase, helical textures, hydrodynamic stability study 79−55990
^{3}He, superfluid A-phase, mag. resons. associated with linear textures 79−60585
^{3}He, superfluid A-phase, mag. field effect on texture 79−65276
^{3}He, superfluid A-phase, slab, nonplanar textures 78−51777
^{3}He, superfluid A-phase, small cylinders, evidence for textural transition from NMR expts. 78−56015
^{3}He, superfluid A-phase, superflow, topological aspects 79−60580
^{3}He, superfluid B-phase, textures and NMR, theory 77−39717
^{3}He-A, superfluid, first order current induced textural transition 79−95237
^{3}He-A, superfluid, helical texture stability, hydrodynamic free energy 79−95238

texture continued
KCl:RbCl, $SrCl_2$, laser window material, prep., grain boundary stability 77−46774
$LiNbO_3$ single crystals grown by automatic diameter control, power striations *(Chinese)* 80−81080
Mg alloy, texture of cladding tubes 79−87655
Mg cold rolling texture development 80−25720
Mg, HCP, computer simulation of rolling texture formation 80−3095
Mg, plastic anisotropy of extruded bars *(German)* 77−86126
Mg-Al-Zn (9wt.%Al), sand cast, preferred orientation and mechanical props. *(Japanese)* 80−20979
Mg-Mn-Ce (1.5%, 0.3%) alloy, dislocation slip during superplastic deform. *(Russian)* 77−21214
MgCd wire, elongation during disorder-order transform. *(Russian)* 80−104148
MgO brick, particle-size distrib. depend. of texture and struct. *(Japanese)* 78−84753
MgO-ZrO_2, dispersion hardened, fracture strength and texture, rel. to temp. *(German)* 79−43378
Mn-Al-C anisotropic permanent mag., cryst. orientation and form., X-ray diffr. anal. 79−82778
Mn_3Ge_2, textured, thermal expansion, 158K transformation *(Russian)* 77−32196
Mo, BCC lattice, texture form. by drawing and pulling through non-powered rolls *(Russian)* 77−25100
Mo, condensed layers, restricted growth texture formation singularities *(Russian)* 77−7982
Mo, deformed single crystal, correlation of textural and microstructural changes 77−32586
Mo, foil dislocation struct. of rolling texture *(Russian)* 78−59810
Mo, macroscopic heterogeneity of plastic deform., metallographic examination *(Russian)* 79−100210
Mo, orientation distrib. function depend. on deform. during cold rolling *(Russian)* 80−50647
Mo, orientation distribution function after longitudinal and cross cold rolling *(Russian)* 79−70076
Mo, plastic deformation during rolling at 293K, crystallography of slip *(Russian)* 77−32588
Mo polycrystals, grain misalignment, electron microscope determ. *(Russian)* 80−103358
MoS_2, $MoSe_2$, texture and lubricating props. 77−44368
$MoSe_2$ coating, on Mo, support annealing influence on orientation, texture and hardness *(Russian)* 80−20961
$MoSe_2$, lubricating coatings, texture, prep. by $Se_{(g)}$+Mo 78−53018
$MoSi_2$, ceramic additives effect on sintering, recrystallisation 80−40306
$MoSi_2$, diffusion grown layers, texture 79−74095
NaCl, halite, dynamic recrystn. during compression creep, geophys. appl. 80−25772
Na_2O-CaO-Al_2O_3-SiO_2 glass, crystn. for the purpose of obtaining vitroceramics *(French)* 80−75163
$Na_2O.11Al_2O_3$, polycrystalline with preferably orientated grains, preparation *(Japanese)* 80−81012
Nb, cold-rolled, deform. zone geometry and texture gradients 77−48452
Nb, mono- and polycrystn., crystallographic orientation, etching technique determ. 80−71814
Nb-Zr-C alloys, dispersion-hardened with carbide phase, influence of hydrostatic extrusion on struct. and props. *(Russian)* 77−52338
Nb_3Sn, diffusion-processed layer, texture meas. 79−82726
Nb_3Sn multifilamentary supercond. composites, crystallographic texturing 80−71669
NbTi films, effect of Ar- and N-ion bombardment on texture *(Russian)* 80−107338
$(Ni,Co)_3Ge$, single cryst., Co effects on temp. depend. of yield stress 77−4812
Ni alloy, rolled, annealing texture *(Russian)* 77−21159
Ni, alloying effect of magnetostriction and rolling texture *(Russian)* 77−32229
Ni, and Ni alloys, texture and magnetostriction 77−36671
Ni, dislocation substructure formation under hydrostatic extrusion 78−56696
Ni electrodeposit, crystallitemorphology *(French)* 77−32535
Ni electrodeposits, fibre textures before and after thermal treatment 79−91693
Ni, FCC, rolling texture development 79−87657
Ni, film deposit on (001)Fe substrate, misfit twin crystals 77−4273
Ni layers, fibre texture volume part determ. by quantitative X-ray diffr. *(German)* 77−48595
Ni, rolling texture, athermal softening *(Russian)* 77−66655
Ni, rolling texture development, dependent on relative stacking fault energy 79−52237
Ni, texture nonhomogeneity during rolling 79−91670
Ni, textured galvanic layers, grain size determ., matrix and twinning orientations *(Russian)* 77−43461
Ni wire, internal friction, influence of orientation of mag. field *(Russian)* 79−24559
Ni, yield point, effect of alloying elements *(Russian)* 80−50670
Ni-Co, rolling texture development, dependent on relative stacking fault energy 79−52237
Ni-Fe, soft mag. props. rel. to metallurgical aspects 80−88810
NiF_2, powder, preferred orientation, X-ray intensity corrections 80−1880
NiO, lattice parameters, microstrains, non-stoichiometry, comparison between mosaic microcrysts. and quasi-perfect single microcrysts. 80−24414
$PbBi_2Nb_2O_9$, bend strength, grain orientation effects 80−40375
PbO layers, crystal platelets orientation and thickness, X-ray diffr. obs. 78−87890
Pb_3O_4, phase transition, texture of tetragonal and orthorhombic phases *(French)* 79−23726
Pd particles formed by evaporation on alkali halide crystals, orientation and struct. 78−84108
Re, electrodeposited from fused salts, (10$\bar{1}$l) texture *(Russian)* 80−92791
Sb, film, evaporated crystallite struct., texturisation 77−7991
Se, red amorphous film, textural change, thermal and photo effects 78−63951
Si, compressed, polycrystalline, deform. and recrystallisation texture 78−27538
Si polycrystalline films, texture formation study 79−87662
Si_3N_4, hot-pressed with crystn. grain boundary phases, prep. 78−95715
Si_3N_4-Al_2O_3, hot-pressed with crystn. grain boundary phases, prep. 78−95715

texture continued
SiO_2 glasses surface textures and defects, exam. using liq. crysts. 80−6364
$SmCo_5$ alloy powders, orientability and texture, milling time effect 79−100168
Sn-Bi, eutectic, superplastic anisotropy *(German)* 80−25808
$(SnTe)_{1-x}(PbSe)_x$ films on glass-ceramics, struct. and elec. props. 77−52251
Ta, rolled single crystal, recovery and recrystallization 80−3093
TaS_2, texture and lubricating props. 77−44368
α-Ti alloy, crystallographic texture, importance in characterization 77−28821
Ti alloy TA6V, stress corrosion cracking in organic solvents, effect of microstruct. *(French)* 77−16745
Ti alloys, texture strengthening 78−23724
Ti, cold rolled, transcrystalline SCC in methanol-bromine soln., crystallographic texture effect 79−15872
Ti, commercial, texture depend. stress corrosion cracking 80−104334
Ti, crystalline orientation distribution analysis of texture development 79−91669
α-Ti, fatigue crack growth, influence of grain orientation, SEM study 80−108550
Ti, plastic anisotropy of extruded bars *(German)* 77−86126
α-Ti, plastically deformed by rolling, optical and electron microscope obs. 79−91666
Ti polycrystalline sheet, strain ratio prediction from the ODF, appl. of Taylor's model 79−91773
α-Ti, primary recrystallization study by three dimensional anal. of textures and annealing, HVEM obs. 79−91677
Ti, rolling and recrystallisation texture formation *(Russian)* 77−59802
Ti sheet, anisotropy and texture, effect of plastic deform., recovery and recrystallisation *(Russian)* 77−8850
α-Ti sheet, texture dependent stress corrosion cracking in Br_2-methanol soln. 80−71803
Ti, vacuum deposited, cryst. struct. and elec. props. 78−79908
Ti-Al-Sn (5, 2.5 wt.%), ductile fracture at low temps. 78−64659
Ti-Al-V (6, 4, wt.%), texture influence on fracture toughness and deformation 79−91801
Ti-Al-V (6, 4 wt.%), stress corrosion cracking, composition, microstruct. and texture effects 79−11725
Ti-Al-V (6, 4 wt.%), texture effect on fatigue crack path 78−27633
Ti-Al-V (6, 4 wt.%), textured, anisotropy of fracture toughness over various specimen orientations 79−8353
Ti-Al-V (6, 4 wt.%), texture depend. stress corrosion cracking 80−104334
Ti-Al-V (6,4 wt.%), heat treated and rolled, texture instability 77−63689
Ti-Al-V (6,4 wt.%), improved toughness from prior β-grains 78−15522
Ti-Al-V (6,4 wt.%), strongly textured, influence of cryst. orientation on fracture toughness 78−84951
Ti-Al-V (6,4 wt.%), strongly textured, influence of crystallographic orientation on tensile behaviour 80−7633
Ti-Al-V(Sn) alloys, plastic deformation and fracture characts. at low temps. *(Russian)* 80−7624
Ti-Al-V(6,4 wt.%), environmental fatigue crack propag. 77−36632
Ti-Al(Mo), swaged and recrystallized, grain growth 80−3092
Ti-Al(−V)(Mo), impact strength anisotropy, influence of texture *(Russian)* 80−20952
α-U, orthorhombic, computer simulation of rolling texture formation 80−3095
U-Nb-Zr (7.5, 2.5 wt.%), texture development role in shape memory effect 79−87661
V, polycryst., struct. changes during deform. *(Russian)* 78−48447
V_3Ga, diffusion-processed layer, texture meas. 79−82726
V_3Ga superconducting tape, diffusion-processed, cryst. textures, X-ray pole figures 79−11266
V_2O_5, amorphous semicond., solubility and fibrous texture 80−75162
W, heteroepitaxial deposits with (110) orientation by molten salt electrolysis 78−47683
W, recrystallisation of commercially pure and doped wire drawn to high strain 79−100165
W, texture and grain boundary struct., primary misorientation function 79−1877
W, texture and grain boundary struct., primary misorientation function, expt. deform. 79−1876
W, texture and grain boundary struct., primary misorientation function 79−1875
W, texture form. by drawing and pulling through nonpowered rolls, BCC lattice *(Russian)* 77−25100
W tube, CVD, study of preferred orientation *(Korean)* 77−8761
W, vapour deposited, dislocation struct., rel. to texture *(Russian)* 80−65394
W wire, cold drawn, dislocation processes occurring during tensile testing *(Hungarian)* 77−48450
W-Re film, obtained by electron beam volatilisation and vac. condensation, props. *(Russian)* 77−24490
WSi_2, diffusion grown layers, texture 79−74095
Y, texture formation during cold rolling *(Russian)* 78−92275
Zn, cold rolling texture development 80−25720
Zn foil, splat quenched, preferred orientation 80−40381
Zn, HCP, computer simulation of rolling texture formation 80−3095
Zn, oriented polycrystals, tensile behaviour under hydrostatic press. *(Japanese)* 77−52417
Zn, plastic anisotropy of extruded bars *(German)* 77−86126
Zn-Al, unidirectional eutectic, FCC phase, preferred orientation 80−29973
Zn-Al (0.4 wt.%), intergranular slip during in situ superplastic deform. 80−96538
Zn-Al (1.1 wt.%) superplastic alloy, grain size determ. *(Czech)* 80−81118
Zn-Al (22 wt.%), texture effect on superplasticity 79−20103
Zn-Al (22 wt.%) superplastic alloy, grain growth texture 80−81075
Zn-Al alloys, comp. effects on intergranular slip during superplastic deform. *(Russian)* 77−32633
ZnF_2 powder, preferred orientation, X-ray intensity corrections 80−1880
ZnO films, texture and grain size rel. to chem. spray deposition parameter 77−31921
Zr alloy, elastic props. of fuel cladding and press. tubing material 79−15711
Zr alloy, neutron irradiated, in-pile dimensional changes 77−24331

texture continued
Zr alloys, creep and growth, irradiation induced, rate theory approach 80−89294
Zr alloys, creep and growth, irradiation induced, microstruct. depend. 80−93602
Zr alloys, crystallographic texture, quantitative charact., review 78−21647
Zr alloys, factors affecting anisotropy of irradiation creep and growth, calcs. from crystallographic texture 79−83255
Zr, cold-rolled, textural transform. *(Russian)* 78−39790
Zr, deformation texture during rolling in sequential passes 79−11674
Zr, HCP, computer simulation of rolling texture formation 80−3095
Zr, rolling and recrystallisation texture formation *(Russian)* 77−59802
Zr-Nb (2.5 wt.%), annealed, irradiation growth at 353K 79−46710
Zr-Nb (2.5 wt.%), pressure tubes, irrad. creep and growth, anisotropy factors 80−97536
ZrO_2, hydrous, prep. from $ZrOCl_2$ soln. and cryst. texture determ. *(Japanese)* 77−89398
ZrO_2, hydrous particles, crystal texture *(Japanese)* 77−25002
ZrO_2-CaO-SiO_2, relationship between texture parameters, and sintering, elec. cond. and mech. strength props. *(German)* 79−24474

texture, surface *see surface texture*

thallium
see also nuclei with .....
alkali halide: Tl^+, charge transfer absorpt. band 79−73977
alkali halide:Tl^+, cryst. field effect on spectral characts. 77−24880
alkali halide:Tl^+, magneto-optical rot. dispersion anomaly near absorpt. bands 77−63400
alkali halide:Tl^+, struct. of Jahn-Teller induced B absorption band 77−12410
alkali halide:Tl^+-like ions, triplet state lifetime, hyperfine interaction 80−2844
alkali halide phosphors, Tl^+ doped, uniaxial stress effects 78−48202
alkyl ammonium halide:Tl phosphors, exciton absorpt. spectra 79−28782
anisotropic behaviour of Poisson's ratio, Young's modulus, shear modulus 77−11622
atom, 377.5 nm line, broadening by Xe 77−71781
atom, 535.0 nm line shift by H_2 perturber 80−91506
atom, $6^2P_{1/2}$-$7^2P_{1/2}$ M1 transition, parity violation detection in neutral weak interaction 77−30819
atom, $6^2P_{1/2}$-$7^2P_{1/2}$ transition, parity nonconservation obs. 79−31446
atom, $6^2P_{3/2}$-$6^2P_{1/2}$ transition, population inversion 80−950
atom, $6p_{1/2}$-$6p_{3/2}$, search for optical rot. induced by weak neutral currents 78−82710
atom, absorpt. and emission spectra, in inert gas matrix 77−57909
atom, and isoelectronic ions, excited-state energy level k-ordering, l-patterns 77−88406
atom, autoionisation reson. determ. from photoelectron polarisation meas. 80−58221
atom, diffusion coeff. in laminar flames 78−51272
atom, electron affinity, meas. by dissoc. ionisation of TlBr, TlI *(French)* 80−63849
atom, electron impact excitation, $7^2S_{1/2}$, $6^2D_{3/2,5/2}$, threshold to 1500 eV 77−54614
atom, electron impact excitation cross sections 79−54972
atom, electron impact excitation of vacuum UV spectral lines 77−3471
atom, g-factor anomalies and strongly forbidden M1 transitions 78−78825
atom, ground state, population 'freezing' effect in hyperfine structure *(Russian)* 78−937
atom, ground-state hyperfine struct. tensor polarisability 77−6708
atom, HF oscillator strength calculations, relativistic, $np^2P_{1/2,3/2}\rightarrow(n+1)^2S_{1/2}$ and $np^2P_{1/2,3/2}\rightarrow nd^2D_{3/2,5/2}$ transitions 79−89609
atom, hyperfine struct. optical pumping, O-O transition perturbation 80−949
atom, hyperfine structure 79−3375
atom, in gas discharge, optical self pumping, hyperfine struct., microwave-optical spectroscopy 80−32680
atom, L-shell X-ray photoelectric cross sections, fluorescence spectra 78−58636
atom, lowest S-state lifetime meas. 77−65436
atom, optical activity of vapour as indication of electron-nucleon weak interaction *(Russian)* 77−10618
atom, optical excitation, Landau-Ziner nonlinearity, fluoresc. obs. *(Russian)* 80−52948
atom, optical transitions, struct. of weak neutral currents *(Russian)* 77−88420
atom, optics activity near suppressed M1 transition *(Russian)* 78−46292
atom, oscill. strengths, Bates-Damgaard approx. calcs. 77−3311
atom, oscill. strengths, semiempirical relativistic one-electron central field, model pot. calcs. 80−78575
atom, parity non-conserving E1 matrix elements, many body calcs. 80−47924
atom, parity nonconservation in heavy atoms, weak electron-electron interaction *(Russian)* 78−55132
atom, parity nonconserving effects in $6^2P_{1/2}$-$7^2P_{1/2}$ transition 78−13458
atom, photodissociative pumping effect 80−58182
atom, photoionis. cross section, spin polaris. and ang. distrib. of photoelectrons, RPA calc. 78−13478
atom, photoionis. cross section and spin polarisation of photoelectrons 78−46307
atom, reson. lines, perturbing gas and self-broadening, temp. effects 80−42979
atom, sensitised fluoresc. in Hg-Fl vap., Doppler broadening 77−3314
atom, spectral line shape in Ar gas, collisional redistrib. of near-reson. rad. 79−31469
atom, spectral self-broadening of 377.6 reson. line 78−82692
atom, stimulated Raman scatt. and stimulated collision induced fluoresc. 78−87103
atom, strongly forbidden M_1 transitions, g-factor anomalies *(Russian)* 78−78648
atom, tensor polarisability calc. 79−76525
atom, Tl 5d XPS comparison with TlI 80−43099
atom, two-photon laser spectroscopy and ionisation 78−55153
atom, vacuum UV absorpt. spectra, at. consts. 77−57917
atom, valence orbitals, Dirac-Fock scheme, direct and indirect relativistic effects 78−41969

thallium continued
atom λ_{max}=251.3 nm absorption band, rel. to Tl atom conc., temp. and disturbing gases 80−42980
atomic, inverted populations, obs. of stimulated level shifting 80−58218
atomic beam tubes, freq. pulling effect with mag. double reson. 80−37802
atomic electron impact excitation cross sections calc. *(Russian)* 78−55240
atomic gas, Raman transitions, active reson. spectroscopy 77−27003
atomic HFS resonance lines anomalous intensity ratios 79−63961
atomic oscillator strengths and radiative lifetimes 79−54811
atomic polarisability, oscillator strength and radial integral, Dirac eqn. calc. 79−22620
atomic spectroscopy, search for parity-violating weak interaction of electrons with nuclei 79−36571
atomic spectrum, effect of intrinsic vapour pressure on shape of 258 nm line 77−46539
atomic vapour, optical difference freq. generation 77−27317
atoms, axial distrib. in unipolar arc discharge, influence of Li conc. 80−19656
atoms, ionisation limit and oscill. strength in VUV absorpt. spectra 80−74152
atoms, obs. of Dicke superradiance at 1.30 μm 77−441
atoms, VUV photoelectron spectra, pseudo-atomic beam technique 80−58225
atoms and ions, lifetimes, electron impact excitation 77−79581
atoms and ions, regularities within Stark widths of reson. lines 78−78662
Auger $N_{6,7}O_{4,5}O_{4,5}$ spectra, X-ray excited 77−85886
band structure, relativistic Green's function theory 79−82512
band structure and fermi surface using relativistic APW calc., optical spectra interpretation 77−20231
band structure by LMTO method 77−39773
borate laser glasses, Cl^- coordinated, Tl^+, Mn^{2+} and Nd^{3+} impurities, absorpt. and X-ray obs. 79−38575
cathodic deposition on Ag (111) and (100) surfaces, potentiostatic obs. *(German)* 79−15616
conduction-electron elec. field gradient, probe valence effects 78−47749
core level binding energies, UPS obs. 80−66388
determination, in complex alloy, by at. absorpt. 77−40582
determination with Pb in $ZnSO_4$ electrolyte by anodic stripping voltammetry 77−12844
diffusion in Al *(Japanese)* 79−19403
diffusion in liq. TlSe, Tl_2Se and Tl_2Se_3 *(Russian)* 77−28030
diffusion in liquid Cu *(Japanese)* 78−59962
DMSO-Tl^+, spin-lattice relax., chem. shift anisotropy 79−51870
electrical resistivity, 300-1050K 80−24868
electroreduction from $Ca(NO_3)_2.4H_2O$ soln. 77−77772
epitaxial growth on Ag (111) and Cu (111), LEED, RHEED, AES study 78−84090
film, Fuchs Sondheimer theory, size effect, elec. cond., Fermi surfaces 79−99637
films, supercond. amorphous, effective phonon spectrum and lattice sp. ht. 80−70895
green line superradiance, selective optical excitation and inversions via excimer channel using Tl-Hg and Tl-Cd-Ar systems 79−50281
HCP, lattice dynamics, local pseudopotential approach, dielectric functions 80−34151
hexagonal lattice equilibrium, electron gas model with noncentral forces, lattice dynamics 78−95123
impurity dopant incorporation and diffusion during MPE growth of IV-VI semiconductors 79−66012
impurity in Nimonic 105, influence on creep and stress rupture props. 80−66602
ion, HF calc. for ground and excited states, appl. to impurity centres 77−72835
ions in glass, thermal migration formed optical waveguides, props. 79−46031
laser, UF_6-TlF-F_2 nuclear-reaction laser, possible steady-state operation 77−42527
liquid, isothermal compressibility, harmonic pot. model calc. 79−14870
liquid, mag. relax. of excited ^{207}Bi 77−16217
liquid, O_2 activity from electrochemical meas. 80−104123
liquid, struct. factor, Percus-Yevick equation perturb. treatment, square-well pot. approx. 78−75530
liquid, thermal props. at high temp. 80−75536
liquid, thermoelectric power, pseudopotential calc. 80−59959
liquid, viscosity, comp. and temp. depend., up to 500°C 79−65233
liquid and solid, UPS, optical densities of states 80−2924
magnetic breakdown, electron energy spectrum 78−10335
metastable atoms quenching, diffusion and decay in buffer gases 79−54953
mitochondrial membrane monovalent Tl^+ ion transport 78−31787
muonic atom transition energy meas., tests of high-order vac. polarisation corrections 77−71895
Nernst-Ettingshausen effect in solid and liq. states *(Russian)* 78−6353
neutral atom production by pulsed laser heating 77−85848
neutron diffraction meas. of c/a ratio and vol. change at transition 77−15335
nonlinear helicon resonance due to open-orbit conduction 80−2324
normal atom conc. determ. by resonance line broadening with Hg press. 80−43883
parity non-conservation effect 80−68395
phase diagram and high press. phase transforms., DTA study *(Russian)* 80−66474
phase transformation in high-press. chamber *(Russian)* 77−76544
phonon spectrum from Krasko-Gurskii pseudopot. calc. 80−96608
photoelectronic spectra, UV incident, polycryst. film 78−2986
photoemission, transition from ordered solid to disordered liquid 80−45217
polymorphs α and β, stability range and supercooling, electron diffr. obs. *(French)* 77−84924
positron lifetime meas., comparison with theory 77−63483
quadrupole interaction of ^{69}Ge, TDPAD expts. 78−48089
Raman conversion of XeCl-laser radiation in metal vapours, up to 40% efficient 79−23025
superconducting crit. temp., functional derivative with electronic density of states, Eliashberg eqns. 79−56368
thermal and elastic props., lattice heat capacity, elastic constants and thermal expansion, model 80−39321

thallium continued
underpotential adsorption, cathodic deposition, on Ag(111) and (100) *(German)* 80−108363
underpotential adsorption on Ag (100), mean field theory and Monte Carlo simulation 79−60630
vapour, backward Raman amplifier, parasitic superfluoresc. suppression 80−69453
vapour, coherent anti-Stokes scatt. four-photon parametric oscill. 80−9959
vapour, electron drift vel., expt. 78−30403
vapour, electron drift vel., momentum cross-section, theory 78−30404
vapour, He-Ne laser radiation freq. conversion 1.15 μm to 377.6 nm 80−95948
vapour, Nd:glass laser output conversion from 1.06 micron to 388.1 nm 80−91850
vapour, optical SHG 78−50855
vapour, ruby laser third harmonic generation, focusing degree influence 80−48348
vapour impulsive production after discharge current pulses through halide vapours *(Russian)* 79−90491
X-ray M_5 absorpt. limits 78−6812
Ag halide emulsion props., Tl^+ ion influence 79−100413
As_2Se_3:Tl, hole transport, photoluminesc. and photoinduced ESR 79−8183
As_2Se_3:X (X=Cu, Ag, Tl, I, Ge), effect of doping, NMR meas. 80−11282
Ba-Tl laser optically pumped by pair-absorption transitions, 1.5 μm emission obs. 80−58517
Ba+Tl, atomic pair absorpt. obs. with white-light source 79−63944
Bi:Ti, microhardness anisotropy 80−21079
CdTe:Tl, growth by travelling heater method, elec. and optical characterisation 77−40356
CsBr:Th, absorpt., excitation, fluorescence spectra 79−43032
CsBr:Tl, emission bands, press. effect 79−33789
CsBr:Tl^+, ESR of [X_2^-] centres 79−33533
CsBr:Tl^+, impurity induced IR absorpt. spectrum, breathing-shell model 77−77256
CsBr:Tl^+, impurity induced Raman spectra, breathing shell model 78−39541
CsCl:Tl^+, ESR of [X_2^-] centres 79−33533
CsI:Tl, crystallophosphor, luminesc. characts., temp. and conc. depend. 80−55175
CsI:Tl, emission bands, press. effect 79−33789
CsI:Tl, gamma-scintillation growth front, external elec. field effect 80−34984
CsI:Tl, light yield under charged-particle bombardment 80−93409
CsI:Tl, luminescence yield depend. on orientation of fast electron beam *(Russian)* 77−8665
CsI:Tl, precipitation of Tl solid solns. 80−70419
CsI:Tl, X-ray phosphor, influence of different factors on emission intensity 79−8171
CsI:Tl, X-ray screens consisting of scintillating crystal fibers 79−6244
CsI:Tl phosphors and screens, possible appl. in X-ray radiography and fluorography 79−6245
CsI:Tl powdered phosphor screen for X-ray image intensifier 79−6246
CsI:Tl single crystal gamma-optical converting screens, factors influencing relative afterglow intensity 79−8173
CsI:Tl X-ray phosphor, spectral characts. 79−8172
CsI:Tl^+, far IR props. of lattice resonant modes, hydrostatic press. effects 77−28574
CsI:Tl^{3+}, cryst., influence of impurities on yield stress 79−15748
CsI-Tl, luminescence from bound excitons, UV absorpt. and EPR 77−77282
CsI(Br)(Cl):Tl, [X_2^-] centre dynamic props. 79−65730
CsI(Tl) thin film detectors, light output and resolution 78−9030
Cs_2O-B_2O_3:Tl^+ glass, optical basicity, variation with probe ion and comp. 80−2800
$CsSrCl_3$:Tl, absorpt. and luminesc. spectra 78−72586
Hg-Tl-I discharges, 50 H_z, Tl atoms axial segregation 80−38781
Hg-Tl-I discharges, 50 Hz, axial segregation effect on elec. field strength 80−59320
Hg+Tl, Tl sensitised fluorescence 78−70778
Hg+Tl vap., sensitised fluoresc. 77−88423
KBr:Tl, 480K thermal glow peak, Tl^+ centres 80−108284
KBr:Tl, A-band absorpt., sruct. high resolution spectroscopy 77−20896
KBr:Tl, A-emission, line shapes and relative efficiencies 79−83011
KBr:Tl, electroluminescence, spectra and quantum yield activator conc. depend., cond. changes 80−89070
KBr:Tl, impurity-induced first-order Raman scatt., critical-point and critical-line anal. 79−19884
KBr:Tl, luminesc., decay model for A_T and A_X emissions 80−93379
KBr:Tl, thermoluminesc. excited by UV radn. and X-rays 79−87513
KBr:Tl excitation in fund. absorpt. region, luminesc. and thermolum. 80−50433
KBr:Tl^+, quadratic Jahn-Teller effect, totally symm. vibr. mode effect, ang. overlap model 80−49680
KBr:Tl^+, thermally induced absorpt. transfer between impurity bands, electron-lattice interactions 77−77257
KBr:Tl^{2+}, relation between bonding and g-shift 80−39492
KBr-KI:Tl, spectral, polarisational and kinetic characts. 78−80385
KBr(Cl):Tl, visible emission, temp. depend. 78−60511
KBr(Cl)(I):Tl^+, recomb. luminesc. kinetics 77−16366
KCl:Ag,Tl, cryst. high-press. energy transfer, sensitised luminesc. 77−36281
KCl:Cu,Tl, plastic deform., charge exchange of hole centres *(Russian)* 77−11876
KCl:Tl, 375 nm emission band 79−95834
KCl:Tl, 475 nm emission, attributed to Tl^+ dimer 78−39611
KCl:Tl, ESR of trapped electron and hole centres 79−78516
KCl:Tl, effective cross sections ratio of charged and neutral centres for holes and electrons *(Russian)* 79−28319
KCl:Tl, electroluminescence, spectra and quantum yield activator conc. depend., cond. changes 80−89070
KCl:Tl, energy level scheme, mol. orbital model 80−10912
KCl:Tl, excitation in fund. absorpt. region, luminesc. and thermolum. 80−50433
KCl:Tl, F-centre formation efficiency 79−82203
KCl:Tl, formation of electron centres and self-localised holes, ESR exam. 78−91947
KCl:Tl, hole capture kinetics, influence of autolocalised and zone holes *(Russian)* 80−54714

thallium continued
KCl:Tl, impurity-induced first-order Raman scatt., critical-point and critical-line anal. 79−19884
KCl:Tl, low-temp ionisation of activator, photoexcitation, in region of interzone transitions *(Russian)* 79−28320
KCl:Tl, mixed phosphor, dimer absorption bands, 200-300 nm 79−73976
KCl:Tl, neutron scattering from localised electronic excitation, theory 79−4539
KCl:Tl, temp. depend. of cathodolum. *(Russian)* 80−80868
KCl:Tl, thermal glow of trapped electron and hole centres 79−78762
KCl:Tl, thermoemission of positive ions in simple gas atoms *(Russian)* 77−28676
KCl:Tl,Pb, X-irradiated, EPR spectra 79−28613
KCl:Tl (0.003 to 0.27 mol.%), electrolum. 80−71490
KCl:Tl and KCl, F-centre production by positive ions and X-rays 78−38760
KCl:Tl F-centre form. by electron irrad., efficiency penetration depth 77−51370
KCl:Tl phosphors, heavily doped, luminesc. obs. 77−32427
KCl:Tl^+, absorpt. spectra, electrolytic coloration, migration in electric field, heat treatment 78−23504
KCl:Tl^+, cryst., electron transfer, optical and thermal excitation 79−4833
KCl:Tl^+, decay modes of 3000 Å emission band 77−73168
KCl:Tl^+, optical absorpt. spectra following X-irrad., F- and V-centres 79−99912
KCl:Tl^+, quadratic Jahn-Teller effect, totally symm. vibr. mode effect, ang. overlap model 80−49680
KCl:Tl^+ cryst., A band, mag. field effect 80−34897
KCl:Tl^{2+}, hole mechanisms of H- can F-centre production, thermolum. obs. 77−16407
KCl:Tl^{2+}, Na, X-irrad., activator-impurity association *(Russian)* 77−85761
KCl:Tl^{2+}, optical absorpt. spectra interpretation mol. orbital scheme 80−20671
KCl:Tl^{2+}, relation between bonding and g-shift 80−39492
KCl-KBr:Tl^+, cryst., luminesc. and excitation spectra 77−66535
KCl-KI:Tl, spectral, polarisational and kinetic characts. 78−80385
KCl-Tl^+,Ca^{2+}(Sr^{2+}), electrolytic colouring, colour centre form., optical absorpt. spectra 79−15497
KCl(Br)(I):Tl, emission spectra, press. effects 78−23509
KCl(Br)(I):Tl, Jahn-Teller system, negative mag. circular polarisation in emission spectrum 80−20694
KD_2PO_4:Tl^{2+}, EPR of ferroelec. and paraelec. phases 80−66012
KH_2PO_4:Tl, 5.76 eV absorpt. band, temp. effects on doublet struct. 79−78713
KH_2PO_4:Tl^{2+}, EPR of ferroelec. and paraelec. phases 80−66012
KH_2PO_4:Tl, UV absorption bands obs. 78−27266
KI:Tl, activated crystal, induced recombination emission *(Russian)* 78−48214
KI:Tl^+, A_T emission, mag. circular polarisation, WKB approx. for non-radiative transition rate 80−55180
KI:Tl, $(Tl^+)_2$ centre luminesc. 78−84632
KI:Tl, A_T emission, linear polarisation, appl. of semi-classical WKB formalism 80−45134
KI:Tl, A-luminescence spectra and polarisation, Jahn-Teller minima 77−20914
KI:Tl, cryst., induced recomb. emission 79−4845
KI:Tl, crystallisation from melt by various methods, impurity distrib. 77−4733
KI:Tl, decay of fast component of impurity luminesc. excitation in A-absorption band *(Russian)* 80−84767
KI:Tl, electron-hole and V_k-Tl recomb., TSC and thermolum. study *(French)* 80−34461
KI:Tl, emission and excitation spectra, press. effects 79−83028
KI:Tl, emission bands, press. effect 79−33789
KI:Tl, nonradiative transitions in colour centres, WKB approximation 77−85803
KI:Tl, phosphor, press. effect on emission spectra at low temps. 77−85771
KI:Tl, polarised luminesc. of $(Tl^+)_2$ centres 80−71473
KI:Tl, triple decay-time in low-energy emission 78−43929
KI:Tl, type A long-wave luminesc., polarisation obs. 78−10944
KI:Tl^+, luminesc., time depend. polaris. 79−33810
KI:Tl^+, phosphor, anomalous stress-induced dichroism 79−4828
KI:Tl^+, pre-resonant enhancement of Raman scatt. 80−7354
KI:Tl^+ type phosphor, press. effects on triplet relaxed excited states, quadratic Jahn-Teller interaction 78−23510
KI-Tl^+, mag. circular dichroism meas. 79−42988
β-K_2SO_4:Tl^{2+}, ESR spectra theory 78−23323
KI:Tl, excitation in fund. absorpt. region, luminesc. and thermolum. 80−50433
KI:Tl^+, X-irrad., absorpt. spectra investig. of Tl_2^+ centres 77−20887
LiI:Tl, absorpt. spectrum obs. 80−50378
Li_2O-B_2O_3:Tl^+ glass, optical basicity, variation with probe ion and comp. 80−2800
NH_4Br:Tl, absorption, excitation and fluorescence spectra 79−33824
NH_4Br:Tl, and pure crystals, luminesc., VUV irradiated at 80K *(Russian)* 80−84763
NH_4Cl:Tl, phosphoresc. decay rates obs., pretreatment effects 79−4853
NaBr:Tl^+, absorption spectra meas. 78−15197
NaBr:Tl^+, emission spectra, excitation in A-band 78−15218
NaCl:Tl, deformed phosphors, thermoluminesc., impurity conc. effects 77−63473
NaCl:Tl, luminesc. yield, effect of fast electron channelling 78−84646
NaCl:Tl,Pb, X-irradiated, EPR spectra 79−28613
NaCl:Tl^+, γ-irrad., aquoluminesc. obs. 80−2856
NaCl(Br):Tl, emission spectra, press. effects 78−23509
NaI:Tl, fluoresc. excited by γ-rays, a student laboratory expt. 79−97143
NaI:Tl, scintillation excitation mechanism for γ-rays *(Russian)* 78−92126
NaI:Tl, scintillation excitation mechanism 80−2857
NaI:Tl, scintillation response to random and channelled ions 77−48255
NaI:Tl, triple-peaked scintillation pulse height spectra for MeV channelled ions 77−48254
NaI:Tl scintillation crysts., analytic calc. of photofractions to monoenergetic γ-rays 79−52038
NaI:Tl scintillator response, γ-ray, (X-ray) rel. $^1/_2$-width energy depend., undergrad. expt. 78−49600
NaI:Tl^+, luminescence, exciton diffusion 77−16367
NaI:Tl^+, luminescence spectrum, excited states of monomer centre 77−66536
NaI(Tl) detectors, response functions to terrestrial γ-radiation, computer program 80−83233
NaI(Tl) scintillation cameras, image artifacts and counting losses 80−94345
NaI(Tl) well-type detectors, photopeak efficiency values, expts. and calcs. 80−63454
NaX:Tl^{2+}, (X=Br, Cl, I), F-centres energy levels change 79−65075
Ne-Tl hollow-cathode discharge, CW laser generation on Tl II 594.9 nm line 79−76675
PbS:Tl, Hall and Seebeck coeffs., Hall mobility, impurity states 80−15545
PbS:Tl, self-compensation of acceptors by vacancies, Hall coeff. meas. 80−92913
PbSe:Tl, elec. props. and IR reflection 78−6686
PbSe:Tl, high temp. elec. and optical props., impurity states 79−60854
PbSe:Tl, impurity states, optical absorption and Hall effect meas. 78−18995
PbSe:Tl, scatt. of holes and phonons by impurities 78−19068
PbSe:Tl, self-compensation of acceptors by vacancies, Hall coeff. meas. 80−92913
PbTe:Tl, absorpt. coeff. spectral depend. 80−93370
PbTe:Tl, influence of Tl impurity states 80−20121
PbTe:Tl, thermoelectric power, elec. cond., Hall coeff. and optical absorpt. coeff. 80−39584
PbTl-oxide-PbIn thin film tunnel junction, subharmonic group struct., multiparticle tunnelling theory 79−56438
RbCl:Tl, absorpt. spectra, 210-300 nm 79−87473
RbCl:Tl, origin of 3.55 eV emission band 80−7401
RbI:Tl, emission and excitation spectra, press. effects 79−83028
RbI:Tl, emission bands, press. effect 79−33789
Se:Tl, and undoped material, dielec. losses and permittivity meas. 77−28518
Se:Tl, hole drift mobility meas. by light pulse technique 78−19086
Si:Tl, binding energy, excited state spectra, photolum., semi-empirical short range pot. 80−44534
Si:Tl, electron excited, recomb. radiation, high resolution investigation 78−15233
Si:Tl, energy level, deep level transient spectroscopy 79−19541
Si:Tl, IR excitation spectra 78−88289
Si:Tl, ion implantation, indirect doping method 80−10568
Si:Tl, optical absorption and photolum. of bound exciton 78−88359
Tl, elec. field gradient at ^{111}Cd, effects of high press., TDPAC meas. 80−25266
Tl I, $6s^26d^2D_{3/2}$ state, hyperfine struct. interaction const., mean lifetime 77−42286
Tl I, relativistic and cancellation effects in line strength ratios 78−82689
Tl I, Rydberg series, disctete levels and continua of finite bandwidth 78−74603
Tl single crystals, growth and polishing procedure for (0001) face 79−78870
Tl^-, photodetachment cross-sections, crossed beam meas. *(German)* 77−42298
Tl^+, adsorbed on Ag (111) or (100) surface, struct. *(German)* 78−68636
Tl^+ diffusion in molten (Li-K)NO_3, wave-front-shearing interferometry study 79−60535
Tl^+ in hollow-cathode Ne-TlCl discharge, 594.9, 695.1 nm CW laser oscill. 80−23674
Tl^+, in molten $TlNO_3$, self-diffusion coeff., 230-330°C 78−22878
Tl^+, in soln., luminesc., halide ion effects 78−35187
Tl^+ ions, diffusion coeff. in ion-exchanged glass 77−89583
Tl^+, radioactive and stable, diffusion in KCl, transmutation effect 77−89589
Tl:^{212}Fr, abs. mag. moment of $(h_{9/2})^n$ proton states from Knight shift obs. 77−82821
Tl:^{213}Fr, Knight shift, PAC 77−12275
Tl:Fe, impurity recoilless fraction calc. from mean square displacements 78−2216
Tl-Cs vapour mixture, CO_2 CW laser radiation freq. conversion 80−74438
Tl-Hg, excimer band emission from electron beam initiated discharge in Tll-Hg 80−78841
Tl-Hg, UV preionised discharge, possible excimer laser 79−55119
Tl-Hg excimer, emission pressure and temp. depend., blue band gain, RF excited discharge 79−22941
Tl-Li ion exchange effects on $LiNbO_3$ and $LiTaO_3$ optical waveguides 80−58791
Tl-Xe, electric discharge excitation of Tl in high-press. Xe 80−49025
Tl-Xe, excimer band emission from electron beam initiated discharge in Tll-Xe 80−78840
Tl+Ar, stimulated collision-induced fluoresc. and stimulated Raman scatt., simultaneous obs. 78−13463
Tl+Ba, dipole-quadrupole radiative collisional fluoresc. 80−83315
Tl+Ba, laser induced collisional and radiative energy transfer 80−53108
Tl+Ba, radiative collisional fluoresc. obs. from thermally excited atoms 80−102480
Tl+CO_2, relax. of $6^2P_{3/2}$ and $7^2S_{1/2}$ states 79−64094
Tl+Cs, Tl $6^2P_{3/2}$-state relax., NMR obs. 80−95653
Tl+H_2, Tl atomic fluorescence, pressure and Doppler broadening 80−5504
Tl+H_2(HD)(D_2), intramultiplet transitions 77−54597
Tl+H^+, L-shell ionis., 0.5-3.5 MeV, X-ray emission obs. 77−54528
Tl+Hg, excitation energy transfer, excitation rate consts. 80−37772
Tl+Hg, spectral-line contours in high-press. arcs 79−3412
Tl+inert gas, $6^2P_{1/2}$-$7^2S_{1/2}$ and $6^2P_{3/2}$-$7^2S_{1/2}$ line broadening 77−50475
Tl+inert gas atom, diffuse series head lines, hyperfine components, broadening calcs. 80−32632
Tl+N_2, Hg sensitised fluoresc., quenching 79−22643
Tl(Hg)/$TlClO_4$, aq. electrochem. system, kinetics, impedance *(German)* 77−32807
Tl($^7S_{1/2}$)+inert gas, long-range interaction, spectral line shifts and broadening 79−10174
Tl_2Te-Tl liquid system, conc. fluctuation, time-of-flight quasielastic neutron scatt. obs. 80−88324
Tl_2ZnBr_4, solid electrolytes, ion transport mechanism and polarisability role, comparison with Cu^+ and Ag^+ cond. 80−107531
^{199}Tl, production by ^{197}Au(α, 2n) reaction, medical appls. 80−51245

thallium continued
^{201}Tl abnormal myocardial rest image, significance in coronary artery disease 80−17060
^{201}Tl, coronary artery disease, sensitivity and specificity of perfusion scintigrams 79−25069
^{201}Tl dynamic analysis for regional myocardial blood flow determ. 79−70627
^{201}Tl, energy spectra and spectral resolution in Xe-filled multiwire chamber 79−49901
^{201}Tl, medical images, digital technique for accurate change detect. 79−48326
^{201}Tl myocardial images in coronary artery disease extent prediction 80−26336
^{201}Tl myocardial imaging, clinical usefulness analysis based on Bayes theorem 79−88170
^{201}Tl, myocardial imaging, collimator evaluation 79−34657
^{201}Tl myocardial imaging, redistrib. rel. to rest images 80−12225
^{201}Tl myocardial imaging, subtraction imaging using ^{201}TlCl and $^{99M}TcO_4^-$ 80−72318
^{201}Tl, myocardial imaging , characterization of ECG-synchronized images 79−39473
^{201}Tl, myocardial perfusion evaluation by coded aperture tomographic technique 80−21537
^{201}Tl, myocardial perfusion images, quantitative evaluation methods 79−39479
^{201}Tl myocardial perfusion imaging, computer processing 79−62356
^{201}Tl, myocardial perfusion imaging, algorithm for background activity calc. 80−56195
^{201}Tl, myocardial perfusion scintigrams, aorto-coronary saphenous bypass surgery 79−25068
^{201}Tl myocardial perfusion scintigrams in the evaluation of aortocoronary sapheneous bypass surgery 80−12235
^{201}Tl, myocardial uptake, correl. with local perfusion, dog expts. *(French)* 80−104740
^{201}Tl, production in neutron therapy cyclotron idle beam using Tl(d,xn) 79−20669
^{201}Tl scintigraphy of the myocardium, effect of gate width 80−41172
^{201}Tl stress myocardial scintography segmental anal. 77−66840
^{201}Tl stress scintigraphy of coronary artery disease, clinical value compared to ECG 79−29595
^{201}Tl, transverse computerised axial tomography of the myocardium 80−67222
^{201}Tl, tumour and organ affinity 80−67234
^{201}Tl, use in thyroid 'cold' areas scintigraphic evaluation 80−36078
^{204}Tl β-particle excitation of external bremsstrahlung spectra from thick targets 80−84797
^{204}Tl, effect of maximum β energy on colour quenching of Cherenkov radiation *(Spanish)* 79−76268
^{205}Tl, NMR of Tl borate, germanate and silicate glasses 77−59470
^{205}Tl, transitions, parity nonconservation due to neutral weak currents 77−13913
$^{205}Tl^+$ adsorbed on hydrated silica, NMR relax. chem. shift 78−72427
$^{205}Tl^+$ ion, solvent effects on spin-lattice relaxation time 77−48073
^{205}Tl(p,5n)^{201}Pb→^{201}Tl, yields and excitation functions for Pb radioactivities, medical appls. 80−67249
^{208}Tl photon measurement, in general phantom procedure for calibrating inhaled ^{212}Pb body burdens 77−64138
Tl(7^2P) states, isotopic forms, HFS, press. self-broadening, two-photon spectra 77−18879
ZnO:Tl^+, phosphors, emission spectra, impurity effects 77−32420
ZnS:Tl, UV spectra 77−12404
p-$ZnSiAs_2$:Au(Tl)(S), photoluminesc., radiative recombination 77−24883

thallium alloys
see also thallium compounds
liquid amalgams mixing, excess entropy, vibr. contrib. *(Russian)* 79−51263
Ag-Bi-Tl, system calculated from optimised binary boundary systems *(German)* 77−16545
Ag-Tl, eutectic liquid alloy, structural features, interatomic interaction *(Russian)* 79−77494
Al-Tl, enthalpy of mixing, 'const. vol. alloy' formulation 79−28111
Au-Tl (29 to 100 at.%), thermal analysis, exam. of phase diagram 78−88445
Bi-Tl, complex-regular eutectics, structural modification 78−23695
Bi-Tl, dilute, oxidation kinetics 80−25914
Bi-Tl, thermal cond., 1.5 to 50K, temp. depend. 78−26990
Bi-Tl film, superconductivity and phonon spectrum *(Russian)* 79−91190
Cd-Tl binary alloy system at high press. 80−97461
Ce-Tl, phase equilibrium and cryst. struct. 80−66483
$CeTl_3$, mag. susceptibility, magnetisation, neutron diffr., elec. resist., and sp. ht. meas. 80−75733
Cs-Tl, liq., elec. resist. meas. 77−51717
Ga-Tl, liq., mag. susceptibility *(Russian)* 78−6513
Hg-Tl, liq., positron annihilation meas. 78−43955
Hg-Tl, liq. alloys, struct. from thermodynamic props. *(German)* 77−1066
Hg-Tl, liq. alloys, struct. from elec. cond. 77−1067
Hg-Tl, liquid dilute amalgams, elec. cond. and thermoelec. power 78−51976
Hg-Tl, metastable system, prep. by quenching, phase struct. 78−52762
Hg-Tl, phase limits, determ. by enthalpy functions along liquidus *(French)* 80−84911
Hg-Tl alloys, compositional depend. of positron annihilation 79−99973
Hg-Tl amalgam, viscosity meas. 80−88349
Hg-Tl-Zn, liquid alloys, thermodynamic props., 25 to 75°C *(German)* 77−73259
In-Tl, BCC alloys, stability and elastic consts., US vel. 79−42133
In-Tl, crystallographic reversibility of martensitic transform. 78−6925
In-Tl, electrodeposition from aq. sulphate soln., X-ray struct. 78−84722
In-Tl, exam. of magnetic susceptibility in solid and liquid states, and X-ray data *(Russian)* 79−28503
In-Tl, first order displacive transformations, localized soft modes and US effects 79−73281
In-Tl, single crystal containing Li, X-ray study of FCC⇄FCT transform. *(Japanese)* 80−108435
In-Tl, small κ supercond., phase transitions higher than second order 80−88668
In-Tl, soft mode, latent heats and entropies of fusion 79−46786
In-Tl, supercond. transition in martensitic two phase region 77−72936
thallium alloys continued
In-Tl (up to 4.8 at.%) whisker, supercond. crit. temp., stress depend. 77−39988
In-Tl alloy, FCC→FCT martensitic transformation, on cooling, enthalpy meas. and X-ray exam. 78−39773
In-Tl alloy, superconducting transition temp., phonon mode softening 79−1637
In-Tl liquid alloy, thermodynamic props. and struct. *(German)* 77−48400
In-Tl single crystal, phase transform. X-ray topographic study *(Japanese)* 78−31405
$In_{0.69}Tl_{0.31}$, supercond. transition temp., specific heat, pseudopotential form factor 80−97026
K-Tl, liq., elec. resist. meas. 77−51717
$(La_{1-x}Pr_x)_3Tl$, mag. props., simple phenomenological model 77−16041
La_3Tl, mag. susceptibility and normal state NMR meas. 78−31118
Li-Tl, liq. semicond., electronic struct., resist. and thermoelectric power meas. 77−47712
Li-Tl, liquid alloys, calorimetry study *(German)* 80−25664
$LiCd_{1-x}Tl_x$, intermetallic, X-ray and Knight shift meas. of ^{205}Tl and ^{113}Cd 79−42851
LiTl, pseudopotential method and ordering problem 77−35500
Mg-Al-Tl system, phase diags., electrode pots. *(Russian)* 78−80516
Mg-In-Tl, phase diagrams and electrochem. props. *(Russian)* 80−40330
Mg-Li-Tl, phase diagram, isothermal cross section *(Russian)* 80−20900
Mg-Tl liq. systems, thermodiffusion of Tl 77−11717
β'-MgTl, energy bands and Fermi surface calc. 77−43481
MgTl, fermi surface exam. by de Haas-van Alphen effect 78−34752
Na-Tl, liq., elec. resist. meas. 77−51717
Na-Tl, liq., mag. susceptibility, diamagnetism 78−72326
NaTl, elastic moduli and Debye temp., US meas. 79−91724
NaTl, pseudopotential method and ordering problem 77−35500
Nd-Tl phase diagram, intermediate phases 78−60653
Pb and Pb-Tl (2.5 wt.%), grain boundary sliding, grain size and stress effects 78−27571
Pb-Bi-Tl, supercond., crit. mag. fields, influence of parameters 80−75691
Pb-Tl, liq., viscosity, comp. and temp. depend., up to 500°C 79−65233
Pb-Tl, low κ type II supercond., vortex motion anisotropy, intermediate-mixed state 78−47918
Pb-Tl, reversible surface superconducting magnetisation 78−43531
Pb-Tl, sliding and its accommodation during creep and superplasticity 77−40436
Pb-Tl, small κ type II supercond., flux line lattice, triangular/square transition 78−31025
Pb-Tl, supercond., crit. mag. fields, influence of parameters 80−75691
Pb-Tl, vacancies, positron capture, function of Tl concentration *(German)* 80−49213
Pb-Tl (20 wt.%) rod, supercond., critical current densities in surface pinning region 79−47216
Pb-Tl alloy, positron annihilation, evidence for microporosity and dislocations 79−78786
Pb-Tl alloys, pinning parameters 78−52173
Pb-Tl alloys, positron trapping in vacancies, varying concentration effects *(German)* 80−25477
Pb-Tl-Bi-In, localised phonons studies by supercond. tunnelling 79−87210
Pb-Tl-Cd(Sn) melt, short-range order struct. 80−49088
Pb-Tl-In, localised phonons studies by supercond. tunnelling 79−87210
Pb_xIn_{1-x}-Pb_yTl_{1-y} asymmetric supercond. tunnel junctions, subharmonic gap struct. 79−15260
PbTl-O-Pb, Josephson tunnel junction parameters, microwave freq., temp. depend. 80−34561
$Pb_{1-c}Tl_c$, liquid alloys, local fluctuations and quadrupolar relaxation 80−66060
Pr_3Tl, critical fluctuations temp. depend. 80−25160
Pr_3Tl, exchange-coupled singlet-groundstate system, central model 77−77060
Pr_3Tl, hyperfine interactions, sp. ht. and magnetisation meas. 79−28531
Pr_3Tl, induced ferromag., mag. props. under hydrostatic press. 78−56315
Pr_3Tl, linewidth of cryst. field excitations 78−67988
Pr_3Tl, magnetic low-frequency modes 78−88087
Pr_3Tl, microwave resist. meas., rel. to singlet ground state paramag. systems 77−20353
Pr_3Tl, resistivity and sp. ht. near threshold 79−78399
Pr_3Tl, thermal expansion and transverse elastic const. near mag. phase transition 80−60394
Pr_3Tl, transition temp. and magnetisation 80−25161
Rh_2MnTl, mag. and cryst. props. 77−20568
Sb_2Tl_7, single-cryst. struct., X-ray diffr. determ. 77−65963
$Sc_3TlC_{1-x}(B_{1-x})$, stabilising effect of C and B on alloying behaviour of Sc 77−36454
Se-Tl, liquid alloys, vapour phase effect on activity determ. *(German)* 79−43210
Se-Tl-S alloys, liq., dielectric relax. and elec. cond. 80−108150
Sn-Tl dilute alloys, thermo EMF *(Russian)* 79−33285
Te-Tl, eutectic liquid alloy, structural features, interatomic interaction *(Russian)* 79−77494
Te-Tl, liquid alloy, thermodynamic investigation, enthalpy of form. and phase diagram 77−59756
Te-Tl, thermodynamic investigation, equilibrium diagram calc. 79−34007
Te-Tl liq. systems, thermodiffusion of Tl 77−11717
Te-Tl system, thermodynamic investigation, enthalpy of form. at elev. temps. 78−52774
Th-T alloys, relationship between struct. and thermodynamic props. *(German)* 78−91307
Th_2Zn_{17}, constant axial ratio of the hexagonal cell 79−69056
Tl-Bi, liq., mag. susceptibility, MP to 1000°C, anomalies due to electron-ion interaction 77−20546
Tl-Bi system, phase transitions near Tl_3Bi, elec. props. meas. 80−35181
Tl-Bi-Hg alloys, phase diagrams and equilib. *(Russian)* 79−52166
Tl-Bi-Pb, phonon anomaly near Fermi surface topological transition, phonon softening at X point 78−95120
Tl-Cd, dil., quadrupole interaction, γ-γ ang. correl. meas. 79−56629
Tl-Cd-Sb, liq., Cd vapour pressure and thermodynamic functions *(Russian)* 79−51247
Tl-Li(Na), equiatomic, B-32 superstruct. instability in absence of many-particle interactions 77−58972
Tl-Pb, in solid and liquid state, specific electric resistance 80−103662
Tl-Pb-Bi, critical field and specific heat 79−73631

thallium alloys continued
Tl-Pb-Bi, supercond., electronic density of states from heat capacity meas. 79−56383
Tl-Pb-Hg system, thermodynamic props. *(Russian)* 77−25018
Tl-Sb, liq., mag. susceptibility, MP to 1000°C, anomalies due to electron-ion interaction 77−20546
Tl-Se, liquid mixtures, press. effect on two-phase region 80−75347
Tl-Sn-Bi, liquid alloy, thermodynamic props. *(Russian)* 79−10968
Tl-Te, liq., atomic struct., X-ray diffr. meas. 79−41934
Tl-Te, liq. alloys, mag. susceptibility 77−51880
Tl-Te, liquid alloy, miscibility gap 79−10952
Tl-Te alloy, liq., bond equilib. theory for electronic props., thermochemistry 77−89365
Tl-Te liq. semicond., resist. meas. under high press. 77−51791
Tl-Te system melts, conc. depend. of surface tension 79−37904
$TlBi_2$, cryst. struct. and density *(German)* 80−24407
Tl_xSe_{1-x}, liquid semiconductor, diamagnetism and paramagnetism, dangling bond paramag. centres, mag. susceptibility obs. 80−44797
Tm_5Ir_2, cryst. struct. 80−96473

thallium compounds
see also thallium alloys
chalcogenides, cryst. struct. types 77−15392
halide dimers, kinetic consts. method for vibr. analysis 79−26968
halide single crystals, spectral transmission meas. 77−59581
halides, anal. of cryst. binding and Anderson-Gruneisen parameters 80−15040
halides, cryst., van der Waals coeffs. calcs. 80−96459
halides, cryst. electronic polarisability and ion sizes 77−51341
halides, dielectric behaviour and optic mode Gruneisen parameters 79−10907
halides, polar semicond., binding energy of Wannier excitons 77−69232
halides, static dielec. constant, strain derivatives 80−100629
halides, strain derivatives of elastic and dielectric consts. 79−60421
halides, temp. and press. depend. of transverse-optic modes and anharmonic self-energies 77−11649
halides, van der Waals energy, cohesive energy calc. 77−51343
hexanoate, soliton conduction, elec. cond. field and temp. depend. anomaly *(Russian)* 80−103703
lithium thallium tartrate, single cryst., thermal cond. at low temps. 79−33125
lithium thallium tartrate, sp. ht., 0.3 to 25K, second-order ferroelec. transition 80−59674
lithium thallium tartrate monohydrate, paraelectric phase structure by neutron diffraction data 79−19238
organothallium (III) compounds, XPS study *(French)* 79−64047
thallous halides, electron-hole liquid theory, generalised RPA 78−87914
$Tl_{1+\alpha}(Ta_{1+\alpha}W_{1-\alpha})O_6$, exam. of ionic conductivity *(French)* 78−51729
Tl-Te melt system, semicond., Hall effect 78−56164
$^{205}TlF_6^{4-}$, radical, prep. and EPR comparison with other hexafluoride radicals 78−68381
(Ag, Tl, Ca)NO_3, aqueous solutions, vapour press. meas. 80−6504
$AgNO_3$-$TlNO_3$-$Cd(NO_3)_2$-H_2O mixtures, Henry's law, excess free energy 78−68908
Ag_2O-Tl_2O-B_2O_3, mixed-cation glass, electrical cond. 79−95210
Ag_2O-Tl_2O-B_2O_3 mixed cation glasses, elec. cond. 77−80644
$AgTlSe_2$ and AgTlSe, elec. cond. and thermoelectric power, doping effects, rel. to pseudogap model 78−2506
AgTlTe(S)(Se), cryst. struct. 80−107156
Al+TlF, rot. excitation, M-conserving approx. 79−3546
β-Al_2O_3-Tl_2O:Cu^{2+}, EPR of Cu^{2+} ions in conduction plane 77−69678
Ar+TlF, rot. excitation, body-fixed approx. 77−19015
Ar+TlF collisions, small angle scattering, calc. cross sections 78−70915
As-S-Tl, glass, viscosity and elastic props. 80−100180
As-Se-Tl system, chalcogenide glasses, NMR spin-lattice relax. time meas. 79−95671
As_2S_3-Tl_2S and As_2Se_3-Tl_2Se system glasses, comp. depend. of IR absorpt. props. 77−16292
As_2S_3-Tl_2S glass, phase relns. and crystallisation 78−23675
As_2Se_3-Tl_2Se (Tl_2Se_2) (Tl), glass, hot pressed, temp. dependence of optical absorption edge 78−88328
As_2Te_3-Tl_2Te system, phase diagram 77−16559
$As_2Te_3+Tl_x$, glassy system, composition depend. of activation energy, thermopower meas. 78−64052
B_2S_3-Tl_2S system, phase diagram and verification 80−35165
B_2Se_3-Tl_2Se_3 system, phase diagram 80−35165
$Ca_2TlTa_5O_{15}$, cryst. struct. *(French)* 79−86749
CdO-GeO_2:Tl_2O photochromic glass for optical information retention media 80−33108
CdTe-Tl, quasibinary cross section 78−3102
$CdTl_2Se_4$, single cryst., preparation, elec. cond. 77−24554
$CdTl_2Se_4$:Au(Ag)(Cu), doping effect on surface tension of melt and cryst. microhardness 80−49464
$CdTl_2Se_4(Te_4)$:Au, elec. cond., density, dielectric const., changes on fusion 80−88553
$CdTl_2Te_4$, single and polycryst. samples, linear expansion, heat capacity and thermodynamic props. 80−103489
CsBr-TlBr, phase diagram and pt. defect parameters 79−96017
CsCl-TlCl solid soln., point defect parameters 80−54224
Cu-Tl-S, phases, semiconductor and metallic behaviour *(French)* 79−96011
CuCl-TlCl system, phase diagram and high ionic cond. obs. 78−79802
$Cu_3MTl_2X_4$ (X=Se, Te, M=Fe, Ga, Al), struct. and phys. props. *(French)* 79−86758
Cu_2S-Tl_2S system, phase diagram 80−20906
CuTlS, melting heat and melting entropy *(Russian)* 80−70374
Cu_2TlX_2 (X=Se, Te), struct. and physical props. *(French)* 79−86758
GdTmGa garnet bubble film, ion implanted, pot. wells under charged wells 80−34717
HgTl optically excited excimers, upper state kinetics 80−37831
KBr:Tl, nonradiative transitions in colour centres, WKB approximation 77−85803
KCl:TlCl, lattice defects, X-ray line profile obs. 80−24455
KNO_3-TlBr, fused mixture, coexistence curve and elec. cond. 77−20071
KTl[Fe(CN)$_6$], isomer shift of Mossbauer spectra 80−29662
$LiTmF_4$, van-Vleck paramagnet, giant magnetostriction *(Russian)* 80−103872
NH_4Cl-TlCl, mixed phosphors, diffuse absorption spectrum 79−24342
$(NH_4)_xTl_{1-x}Al(SO_4)_2.12H_2O$:$Cr^{3+}$, zero field splitting, g-values, EPR spectra obs. 80−50169

thallium compounds continued
$(NH_4)_{1-x}Tl_xCl(Br)$, and $(ND_4)_{1-x}Tl_xCl(Br)$, phase diagrams, DTA and birefr. obs. *(German)* 79−83185
$NaNO_3$-$TlNO_3$-$Ca(NO_3)_2.4.09H_2O$ melt, mixed alkali effect 80−34219
Na_2O-Tl_2O-B_2O_3, mixed-cation glass, electrical cond. 79−95210
$NaTl_3(SO_3)_2$, heat capacity and thermodynamic functions, 10 to 300K 80−65244
Ne-TlCl hollow-cathode discharge, CW laser oscill. on 594.9, 695.1 nm Tl^+ transitions 80−23674
P-Se-Tl glasses, NMR of ^{31}P and ^{205}Tl 80−15812
Pb-Tl-Te, liquidus of ternary system 79−8285
PbF_2-TlI graded coatings on KCl laser windows, photoacoustic spectroscopy 80−33052
S-Tl, liquid semicond., bonding energies and entropies, mag. susceptibility meas. 80−49082
SiTe-TlTe, solid solns., mag. suscept. meas., defects 78−43552
SnSe-Tl_2Se, phase diagram, DTA and X-ray diffr. peritectic decomposition *(French)* 77−51471
SnSe-TlSe, phase diagram 100-900°C *(French)* 79−83180
$Th(C_8H_4F_3O_2S)_4$, X-ray cryst. struct. determ. 79−37689
$ThCdF_3$, cubic crystal, phase transitions with three-component order parameter, elastic anomalies *(Russian)* 79−37837
$(Tl,NH_4)_2Cd_2(SO_4)_3$, langbeinite type mixed cryst., ferroelec. transitions, dielec. and elastic meas. 78−2810
Tl (I)-O-M cpds., M=B,Tl,C,Si,Ti,Sn,Sb,P, lone pair position, electrostatic model *(French)* 78−34462
Tl atomic laser pumped by TlI photodissociation 79−18411
Tl complex of lasalocid (X-537A), ^{205}Tl NMR study 80−58288
Tl $GaS_2(Se_2)$, optical and nonlinear optical props. *(Russian)* 79−51943
Tl-B-Se system, vitrification region, primary crystallisation fields 77−15321
Tl-Bi-Sb-Te system, peritectic reactions in $TlBiTe_2$-$TlSbTe_2$ cross section, crystn. character 80−108406
Tl-Ge-S system, glass forming 80−19716
Tl-Ge-Te, glass formation 80−103255
Tl-halides, photoelastic const. calc. 77−76484
Tl-Pb-S system, phase diagram quasibinary Tl_2S-PbS section obs. 80−55372
Tl-Pb-Se system, quasibinary sections 77−86000
Tl-S melts, Hall effect 77−85239
Tl-Se liquid binary mixtures, phase separation under press. 80−34183
Tl-Se phase diagram, 73-100 at.% Se 79−96018
Tl-Se-$TlInSe_2$, isomorphic pairs, struct. and growth peculiarities 79−1421
Tl-Se-$TlInSe_2$, struct. and growth peculiarities, epitaxial heterojunctions *(Russian)* 79−11038
Tl-Sn-Te system equilibria, polythermal and isothermal cross sections obs., ternary cpd. form. 80−104128
Tl-Te, phase equilibrium exam., using DTA, X-ray diffraction, and hardness 79−1846
Tl-Te liquid alloys, mag. susceptibility 77−59383
Tl-V-S system, crystallographic data and phys. props of some phases *(French)* 79−99163
$TlAlF_4$, hydrothermal growth method in presence of hydrofluorhydric acid *(French)* 80−25543
$TlAlF_4$, single cryst., prep. and struct. *(French)* 80−79762
TlAs, possibility of existence with sphalerite struct. 80−33950
$TlAsS_2$, glass, crystallisation, effect of an alternating electric field 80−88054
$TlAsS_2$, Tl_3AsS_3, and Tl_3AsS_4, Raman and IR spectra *(Russian)* 77−66512
$TlAsS_4$, struct. and soft mode behaviour 78−91327
Tl_3AsS_4, crystal growth by Bridgman-Stockbarger method, exam. of props. 79−11506
Tl_3AsS_4, optical phonons, Raman and refl. spectra 80−11400
Tl_3AsS_4, prod. and acoustooptic props. *(Russian)* 78−63158
$Tl_xAs_{2-x}S_{3-x}$ glasses, opt. and mag. props., comp. influence 77−77225
$TlAsS_2(Se_2)(Te_2)$, elec. cond. and thermopower in solid and liquid states 77−89764
$TlAsS_2(Se_2)(Te_2)$, vitreous, crystn. kinetics 80−64918
$TlAsSe_2$, diamag., thermal expansion rel. to temp. at cryst.-melt transition 78−34954
Tl_3AsSe noncollinear acousto-optic tunable filter, operation at 10 μm 79−41434
Tl_3AsSe_3 10.6 μm tunable acousto-optic filters 79−55248
Tl_3AsSe_3, IR nonlinear material, laser induced surface damage 77−19266
Tl_3AsSe_3, refractive index, thermal expansion temp. depend. 80−97223
Tl_3AsSe_3, SHG, absorpt. coeffs. and temp. variation of refr. index difference 80−14390
$TlAsTe_2$, local struct. changes on crystal-glass transition, Mossbauer spectra 77−36157
$Tl_2B_{12}H_{12}$, cryst. growth from soln. and morphology 77−44145
$Tl_2BNi(NO_2)_6$, (B=Cd, Hg), single cryst. growth in gel *(German)* 79−74076
$TlBO_2$, mean geom. config., gas-phase electron diffr. 77−83759
$TlBO_2$, mol. struct. determ. by gas phase electron diffr. 79−10227
$TlBO_2$, photoelectron spectra of gaseous species 77−18974
$TlBO_2$, X-ray single cryst. struct. determ. *(French)* 79−32974
$Tl_2B_4O_7$, polymorphism *(French)* 78−6035
$TlBO_2.xH_2O$, x=0, 0.5, 1 and 2 cryst. chem. *(French)* 78−18606
Tl_2BRCL_6, B=Li,Ag,Na, systematic structs., X-ray Guinier-Simon method *(German)* 80−44186
TlBS, synthesis, struct., optical, spectral props. 79−15631
$Tl_2B[Co(NO_2)_6]$, (B=Pb, Ba), single cryst. growth in gel *(German)* 79−74076
TlBi, possibility of existence with sphalerite struct. 80−33950
$TlBiF_4$, anionic conductivity exam. *(French)* 77−35952
$TlBiF_4$, fast ionic conduction of F^- ions 79−99360
α-$TlBiF_4$, new solid electrolytes, conductivities and activation energies 79−28137
$(TlBiS_2)_{1-x}$-$(2PbS)_x$ system, phase diagram 77−36471
$Tl_4Bi_2S_5$, X-ray cryst. struct. determ. *(French)* 79−69063
$TlBiTe_2$, epitaxial film, struct. anomalies, TEM 77−11824
TlBr, and TlBr-TlI polycryst. fibre optical waveguides, for IR, fabrication and characts. 78−74974
TlBr, complex refr. index meas. in far IR, by dispersive Fourier transform spectroscopy 78−92042
TlBr, CsCl and NaCl phases, atomic interactions and lattice statics and dynamics 78−83889
TlBr, dielectric behaviour under hydrostatic press. 78−52420

thallium compounds continued
TlBr, electromodulation spectroscopy of excitons 79−73444
TlBr, electron impact dissoc. ionis., Tl electron affinity meas. *(French)* 80−63849
TlBr, electron-hole liquid, RPA calcs. 80−6743
TlBr, electronic state of excitations and their phonon coupling 79−60719
TlBr, exciton-phonon system, ground state energy in mag. field 77−11859
TlBr, He II photoelectron spectra 78−94285
TlBr, hot-exciton effects, luminesc. excitation spectra 77−32434
TlBr, light sensitive material, regularities in exciton states 77−20885
TlBr, mean Debye-Waller factors, vib. amplitudes and Debye temp. 78−75792
TlBr melts, Tl doped and pure, stoichiometric, nucl. spin relax. 80−25236
TlBr, phonon struct. of forbidden-indirect transitions 79−61393
TlBr, piezoreflectance of first exciton band obs. 78−64347
TlBr, polycryst. core fibre optical waveguides, IR transmission characts. 77−88936
TlBr, polymorphism, XPS obs. 80−97398
TlBr pseudodisplacive ferroelec., temp.-dependent dielectric response obs. 77−40247
TlBr, reson. Raman scatt., forbidden one phonon and intervalley scatt. at direct exciton 80−45073
TlBr, resonant polaron coupling and excitons under mag. field 80−71383
TlBr, second order Raman scatt., reson. behaviour rel. to phonon bands 80−40101
TlBr, selective photodissoc. branching ratios at 2660 Å, Raman up-convertor appl. 78−90243
TlBr, soft mode dielec., anomalous low temp. sp. ht. 78−14423
TlBr, two indirect excitons decay to direct and indirect excitons 77−44058
TlBr, Wannier exciton-ionised donor complexes, binding energy calc. 80−49609
TlBr, XPS, valence bands 78−76578
TlBr:I, isoelectronic donor, broad-band photoluminesc. meas. 77−8636
TlBr-$MgBr_2$ system, thermochem. and struct. investigation *(German)* 79−1423
TlBr-TlCl, photoelastic consts. dispersion 79−65136
TlBr-TlI, KRS-5, periodic strain anisotropy, optical and X-ray diffr. study 80−54167
TlBr-TlI, KRS-5 crystal, refr. index temp. increments meas. 80−33098
TlBr-TlI, polycryst. core fibre optical waveguides, IR transmission characts. 77−88936
TlBr-TlI, TlBr-TlCl, KRS-5 and KRS-6 crystals, optical losses, laser calorimetric meas. 80−9973
TlBr-TlI crystals, Pb halide impurity distribs. for various cryst. orientations 79−51135
TlBr-TlI KRS-5 fibre crystals floating zone growth, for IR optical waveguides 80−79019
TlBr-TlI KRS-5 single crystals, acousto-optical characts. 78−71165
TlBr-TlI(Cl) crystals, photoelastic moduli 80−97230
TlBr-VBr_2 system, cryst. struct., DTA investig. *(German)* 78−72766
$TlBr_3$-graphite intercalation *(German)* 79−43563
$TlBr_{0.42}I_{0.58}$, KRS-5 crystal, 10.6 μm absorption obs. by laser calorimetry 79−50360
$TlBrO_3$, polycryst., Raman and IR spectral assignments, room temp. 78−15156
Tl_2CO_3, phase diagram to 80 kbar 77−15576
Tl_2CO_3+8-hydroxyquinoline, solid state reaction 80−108708
$TlCdF_3$, elastic consts. near phase transition by Brillouin scatt. 78−38844
$TlCdF_3$, nonlinear elastic behaviour, US velocity, 1 bar-3 kbar 78−59851
$TlCdF_3$, thermal props. near phase transition 78−75850
$TlCdF_3$, third and fourth order elastic consts., press. depend. near phase transition *(French)* 80−34116
$TlCdF_3$, weakly discontinuous phase transition, linear birefringence obs. 80−11362
$TlCdF_3:Mn^{2+}$, zero-field splitting of Mn^{2+}, superposition model *(French)* 79−15267
$TlCdI_3$, X-ray cryst. struct. determ. and refinement 79−69070
Tl_4CdI_6, fast ionic cond. 79−99363
Tl_4CdI_6, ionic conductivity, Raman spectra 77−69113
$Tl_2Cd_2(SO_4)_3$, langbeinites, symmetry limitations on choice of hypothetical protophase 80−33916
$Tl_2Cd_2(SO_4)_3$, ferroelec. langbeinites, Raman scattering 80−34926
$Tl_2Cd_2(SO_4)_3$ single cryst., growth and phase transitions 79−33918
$Tl_2Cd_2(SO_4)_3$, structural phase transition, phenomenological theory 79−7693
TlCl, adsorption of water vapour, 273, 283 and 293K 78−56035
TlCl, band structure and optical spectra, local field and exchange effects 80−24798
TlCl component antireflection coating 79−27346
TlCl, Debye-Waller factors of Tl^+ and Cl^-, X-ray diffr. 77−31742
TlCl, Debye-Waller parameter by powder elastic neutron diffr. 80−29140
TlCl, dielectric behaviour under hydrostatic press. 78−52420
TlCl, electric fields generated in rapidly rotating crystal 78−46487
TlCl, electromodulation spectroscopy of excitons 79−73444
TlCl, electron-hole liquid, RPA calcs. 80−6743
TlCl, electronic state of excitations and their phonon coupling 79−60719
TlCl, exciton-phonon system, ground state energy in mag. field 77−11859
TlCl, ground-state props., Wannier functions, and electronic struct., ab initio self-consistent calc. 80−80178
TlCl, He II photoelectron spectra 78−94285
TlCl, hot-exciton effects, luminesc. excitation spectra 77−32434
TlCl, light sensitive material, regularities in exciton states 77−20885
TlCl, magnetoreflectance of $X_6^+ \times X_6^-$ exciton meas. 79−38525
TlCl, mean Debye-Waller factors, vib. amplitudes and Debye temp. 78−75792
TlCl, melts, stoichiometric, nucl. spin relax. 80−25236
TlCl, phonon difference band absorpt., far IR laser spectroscopy 80−93325
TlCl, phonon dispersion relations, neutron scatt. exam. 78−51628
TlCl, phonon struct. of forbidden-indirect transitions 79−61393
TlCl, piezoreflectance of first exciton band obs. 78−64347
TlCl, piezoreflectance spectra of first exciton band 77−12357
TlCl, polar semicond., exciton dispersion curves influence of optical phonons 79−15091
thallium compounds continued
TlCl, polymorphism, XPS obs. 80−97398
TlCl powder and solution, luminesc. obs. 77−32427
TlCl, Raman spectra in melting region 78−27224
TlCl, role of electron-hole interaction in optical spectra, review 80−45113
TlCl, second order Raman scatt., reson. behaviour rel. to phonon bands 80−40101
TlCl, self-consistent electronic struct. and ground state props. 80−15451
TlCl, surface polaron in mag. field 79−23912
TlCl, thermal vibr. amplitudes, 296-534K, X-ray obs. 77−35656
TlCl, two indirect excitons decay to direct and indirect excitons 77−44058
TlCl, UPS, valence band struct., dynamic hybridisation 77−20999
TlCl, Urbach rule at excitonic absorpt. edge, theoretical model tests 80−50299
TlCl, valence band electronic struct., XPS and UPS obs. 78−6826
TlCl, vap. press. and thermodynamics 80−6503
TlCl, Wannier exciton-ionised donor complexes, binding energy calc. 80−49609
TlCl, XPS, valence bands 78−76578
TlCl-CsCl solid soln., determ. and computation of phase diagram 80−55379
TlCl-Tl_2S system, molten, thermodynamic analysis of phase diagram 79−29031
TlCl-TlBr, internal damage threshold for CO_2 laser pulses rel. to absorption 77−75594
TlCl-TlBr, KRS-5, KRS-6 crystals, optical strength pulsed CO_2 laser radiation 79−27307
TlCl-TlBr, KRS-6, ultralow loss optical fibre material, loss mechanism 80−78920
TlCl-TlBr, KRS-6 crystal, refr. index temp. increments meas. 80−33098
TlCl-TlBr, KRS-6/GeSe, IR multilayer partial mirrors effective from 1.3 to 16 μm 80−9978
TlCl-TlBr mixed cryst., impurity-induced self-trapping of holes and minority-ion percolation 78−64398
TlCl-TlBr mixed crystal, reflectivity spectra meas. 77−85743
TlCl-TlBr single cryst., acousto-optic characts. 77−52039
TlCl-TlBr solid solution, photoelastic constants obs. *(Russian)* 78−39526
TlCl+KI, solid state displacement reaction, kinetics and mechanism 79−11788
$TlCl_2$, vap. press. and thermodynamics 80−6503
$TlCl_3$, intercalation with graphite *(German)* 79−43562
Tl_2Cl_2, mol. consts., IR and Raman freqs. assignments 78−17648
TlCl(Br), effective electron-hole interaction for intermediate and strong electron-phonon coupling 77−80735
$TlCl_{0.7}Br_{0.3}$, KRS-6 crystal, 10.6 μm absorption obs. by laser calorimetry 79−50360
$TlCl_xBr_{1-x}$, $TlBr_xI_{1-x}$, polymorphous mixed cryst. layers, opt. props. 78−23490
$Tl_2Cl_2Br_2$, excitation of luminesc. by AC elec. field 79−38670
TlCl(Br)(I), static polaris. and effective charge parameters, Born-Mayer pot. 77−31628
TlCl(Br)(I), van der Waal dipole-dipole and dipole-quadrupole energies, Born and Slater-Kirkwood models 79−27947
$TlClO_3$, polycryst., Raman and IR spectral assignments, room temp. 78−15156
$TlCl_3.(TlCl)_3$, labelled, exchange of Tl ats. rel. to γ-irrad., heat treatment, grinding 78−92470
$TlCoCl_3$, paramag., spin density, NMR study 78−88200
$TlCoCr_2(VO_4)_3$, synthesis and cryst. struct. 80−88114
$TlCoF_3$ paramagnetic, nonmagnetic atomic nuclei spin density, NMR study 80−29633
α-Tl_4CrI_6, prep. and cryst. struct. determ. 80−28957
Tl_2CrO_4, mean Debye-Waller factors, vib. amplitudes and Debye temp. 78−88326
$Tl_2Cr_2O_7$, $Tl_2Mn_2O_7$, pyrochlore type, synthesis and physical props. 80−33963
$TlCuCr_2(VO_4)_3$, synthesis and cryst. struct. 80−88114
Tl_2CuI_3, melting point, cryst. struct., DTA, X-ray diffr. *(French)* 77−84710
TlD_2PO_4, antiferroelectricity, permittivity, electric field double hysteresis loops 80−60512
TlD_2PO_4, dielectric props. under hydrostatic press. up to 7 kbar 80−29696
$TlEr(MoO_4)_2$, polymorphic transition characts., temp. regions of stability 79−14785
$TlEuO_3$, lattice parameters determ. *(French)* 78−95031
TlF, electric dipole hyperfine struct. calc. 80−53162
TlF, P- and T-violating interactions in hyperfine struct., mol. beam reson. expt. 80−53019
$TlF-F_2$ recombining plasma, light amplification possibility 78−17924
TlF+Ar, sudden approx. of Cross, computational tests, cross section factorisation, scatt. phenomena 80−58352
TlF+Kr(Xe), collision-induced ion-pair formation 78−17749
Tl_2F_2 (Cl_2), mols., assignment of vibr. Raman and IR spectra bands 80−58268
Tl_2F_2, mol. consts., IR and Raman freqs. assignments 78−17648
Tl_2F_2+Kr(Xe), collision-induced ion-pair formation 78−17749
$TlGaS_2$, IR refl. spectrum., LO phonons *(Russian)* 77−40221
$TlGaS_2$, IR refl. spectrum, Kramer-Kronig analysis, transverse optical phonons 78−19489
$TlGaS_2$, layer ternary semicond., polarised Raman, IR reflect. spectra 78−68513
$TlGaS_2$, mechanism of cond., AC cond. and permittivity meas. 78−14754
$TlGaS_2$, optical and photoelec. props. 77−55571
$TlGaS_2$, optical and photoelectric exam. 79−11180
$TlGaS_2$-$TlGaSe_2$, phase and composition-property diagrams 80−55366
$TlGaS_2(Se_2)$ film, elec. and photoelec. props. *(Russian)* 78−52109
$TlGaS_2(Se_2)$, IR reflection spectra, lattice vibrs. *(Russian)* 77−85701
$TlGaS_2(Se_2)$, optical phonons, IR and Raman scatt. meas. 78−59903
$TlGaS_2(Se_2)$, phase transforms. under hydrostatic press., Raman scatt. study 80−25366
$TlGaS_2(Se_2)$, Raman spectra, intralayer and interlayer modes 78−43876
$TlGaS_{2x}Se_{2(1-x)}$, layer solid soln., mixed one- and two-mode behaviour of optical phonons 79−47445
$TlGaS_{2x}Se_{2(1-x)}$, layer solid soln., long wave lattice vibrs., IR reflection spectra 80−11388

thallium compounds continued

$TlGaS_{2x}Se_{2(1-x)}$, solid soln., fundamental optical absorpt. edge 80−25408

$TlGaS_xSe_{2-x}$, optical and photoelectric props., composition depend. 79−15183

$TlGaSe_2$, electrooptic effect and refr. index anisotropy 77−16281

$TlGaSe_2$, impurity conductivity and TSC 78−23128

$TlGaSe_2$, layer ternary semicond., polarised Raman, IR reflect. spectra 78−68513

$TlGaSe_2$, mechanism of cond., AC cond. and permittivity meas. 78−14754

$TlGaSe_2$, monocrystal, processes of recombination and trapping levels, photocond. meas. *(Russian)* 80−70751

$TlGaSe_2$, Raman and IR spectra, zone centre optical phonons 78−76462

$TlGaTe_2$, IR refl. and Raman scatt. spectra, lattice vibrs. 80−40108

$TlGaTe_2$, IR refl. spectra 80−60605

$TlGaTe_2$, multilayer cryst., lattice vibr. symm., IR absorpt. and Raman scatt. selection rules 80−39231

$TlGdO_3$, lattice parameters determ. *(French)* 78−95031

$Tl_8Ge_5O_{14}$, X-ray cryst. struct. determ. and refinement *(French)* 79−46607

$Tl_4Ge_2S_6$, cryst. struct. determ. *(German)* 78−79577

$Tl_4Ge_4S_{10}$, cryst. struct., X-ray diffr. meas. *(German)* 77−4074

TlH_2AsO_4, proton spin-lattice relax. study of structural phase transition 79−19796

$TlHF_2$, ^1H and ^{19}F NMR 78−2753

$TlHF_2$, struct. and phase change 77−51996

TlH_2PO_4 and TlD_2PO_4, press. effect on dielec. props. 79−99832

TlH_2PO_4, dielectric props. under hydrostatic press. up to 7 kbar 80−29696

TlH_2PO_4, high resolution heat capacity meas. *(Japanese)* 80−52218

TlH_2PO_4, thermodynamics props. of solid phase transitions, heat capacity 79−10966

TlH_2PO_4, X-ray cryst. struct. refinement *(French)* 79−37666

$TlH_5(PO_4)_2$, X-ray cryst. struct. determ., Patterson and Fourier methods *(French)* 79−14741

Tl_2HPO_4, X-ray cryst. struct. determ. and refinement *(French)* 80−19756

TlH_2P0_4, calorimetric and dielectric exam. of phase transition, nearly crit. case. 77−40171

$TlH(SO_4)_2.4H_2O$, cryst. parameters and X-ray powder diffr. data *(French)* 79−14765

TlHg excimer, fluoresc. at 4590 and 6560 Å, possible laser action 77−6837

Tl(Hg)/$TlClO_4$, aq. electrochem. system, kinetics, impedance *(German)* 77−32807

TlI additives in Hg discharge, high-pressure, line broadening and radiative transport 80−74199

TlI, adsorption of water vapour, 273, 283 and 293K 78−56035

TlI, atomic fluorescence, D_2 pressure effect on width and shift 80−99475

TlI coatings on KCl laser windows, photoacoustic spectroscopy 80−33052

TlI, electron impact dissoc. ionis., Tl electron affinity meas. *(French)* 80−63849

TlI films, polymorphic, double epitaxy and growth on KCl, X-ray and optical obs. 79−77944

TlI, growth in silica hydrogels at 25°C, mechanism 78−35287

TlI, He II photoelectron spectra 78−94285

TlI, impurity in AC metal halide discharge, atomic plasma characts., a priori method 80−44034

TlI laser window films, stoichiometry, Rutherford backscatt. study 80−59831

TlI, linear thermal expansion coeff., capacitance method meas. 78−16772

TlI, mol. beam photodissoc., bond order and state symm. 77−34706

TlI multilayer film, intrinsic and thermal stress modelling and interferometry 79−14059

TlI, on KCl, epitaxial growth habit rel. to optical scatt. 77−50738

TlI, photodissoc., Tl 535.0 nm line shift by H_2 perturber 80−91506

TlI photodissociation, Tl atomic fluorescence, pressure and Doppler broadening 80−5504

TlI, photofragment spectroscopy 79−52718

TlI photographic layers, fogged with metals, spectral sensitivity and optical absorpt. *(Russian)* 77−30209

TlI powders, photoacoustic spectroscopy obs. 79−12855

TlI, Tl 5d XPS comparison with Tl 80−43099

TlI, UV photodissoc., time of flight spectra and ang. distrib., excited state assignment 79−64061

TlI, vapour, excited by photodissociation, fluoresc. yields 78−55138

TlI with CsCl struct., exciton magnetoabsorption 77−28593

TlI, XPS, valence bands 78−76578

TlI, XPS and UPS study of phase transforms. 80−45210

TlI:Cs, dielectric const. temp. and freq. depend. 77−32315

TlI/KCl/TlI low absorpt. antireflection coatings for KCl surfaces 80−38078

TlI-Hg, excimer band emission from electron beam initiated discharge 80−78841

TlI-Hg, lamp, chem. comp., temporal and spatial evolution 78−87532

TlI-PbF_2 graded-index film coating technique and results 80−33265

TlI-TlBr mixture, KRS-5, contamination by exposure to DC-704 silicone liq., IR refl. spectra anal. 77−59630

TlI-type atomic packing, swinging twinning as cryst. struct. building operation 77−31623

TlI-Xe, excimer band emission from electron beam initiated discharge 80−78840

Tl(III) compounds, XPS study *(French)* 79−64047

$Tl_6I_6M_{2/n}^{n+}(I_4)^{2-}$, (M=Pb, Ag, Au, $(Bi_{0.5}Tl_{0.5})$), struct., rel. to phonon spectra 80−71425

$TlIO_3$, polycryst., Raman and IR spectral assignments, room temp. 78−15156

$TlInS_2$, electrical cond. of single crysts. with symm. and asymm. Ag-In contacts 80−6835

β-$TlInS_2$, layer ternary semicond., polarised Raman, IR reflect. spectra 78−68513

$TlInS_2$, layered structure crystals, refractive index meas. method 80−98966

$TlInS_2$, optical phonons, IR and Raman scatt. meas. 78−59903

$TlInS_2$, optical phonons, IR and Raman spectra *(Russian)* 79−10903

β-$TlInS_2$, Raman spectra, intralayer and interlayer modes 78−43876

thallium compounds continued

$TlInS_2$ single crysts., three-dimensional exciton destruction, electroabsorpt. and transmission spectra 77−55803

$TlInS_2$-$TlInSe_2$, phase and composition-property diagrams 80−55366

$TlInS_2(Se_2)$, IR reflection spectra, lattice vibrs. *(Russian)* 77−85701

$TlInS_2(Se_2)$, optical and nonlinear optical props. *(Russian)* 79−51943

$TlInS_{2x}Se_{2(1-x)}$, layer solid soln., mixed one- and two-mode behaviour of optical phonons 79−47445

$TlInS_{2x}Se_{2(1-x)}$ layer solid soln., long wave lattice vibrs., IR reflection spectra 80−11388

$TlInS_xSe_{2-x}$ solid solution, optical and photoelectric props. 79−11179

p-TlInSe, piezoresist. effect 77−35942

$TlInSe_2$, electrical cond. of single crysts. with symm. and asymm. Ag-In contacts 80−6835

$TlInSe_2$, IR refl. and Raman scatt. spectra, lattice vibrs. 80−40108

$TlInSe_2$, IR refl. spectra 80−60605

$TlInSe_2$, monocrystal, photoelec. props. *(Russian)* 80−70752

$TlInSe_2$, single cryst., elec. cond., photocond. and IR spectra absorpt. spectrum 79−47097

$TlInSe_2$, single crystals, optical phonons, Raman and infrared spectra studies 79−55842

$TlInSe_2$ single crystals, vibr. props. by light scatt. spectroscopy 79−56804

$TlInSe_2$-$TlPrSe_2$ system, struct., elec. cond., and thermoelec. props. 79−87119

$TlInSe_2(Te_2)$, multilayer cryst., lattice vibr. symm., IR absorpt. and Raman scatt. selection rules 80−39231

$TlInTe_2$, IR refl. and Raman scatt. spectra, lattice vibrs. 80−40108

$TlInTe_2$, IR refl. spectra 80−60605

$TlLaO_3$, lattice parameters determ. *(French)* 78−95031

$TlLu(MoO_4)_2$, polymorphic transition characts., temp. regions of stability 79−14785

$Tl_{12}M_{13}O_{90}(.12H_2O)$, cation exchanger with intersecting tunnel struct. *(French)* 78−20014

$TlMgCr_2(VO_4)_3$, synthesis and cryst. struct. 80−88114

$TlMnCl_3$, antiferromag., absorpt. spectrum, excitation-magnon-phonon process 79−87461

$TlMnCl_3$, birefringence, twinning and structural phase transitions 79−38480

$TlMnCl_3$, optical props. 78−35111

$TlMnCl_3$, paramag., spin density, NMR study 78−88200

$TlMnCl_3$, refr. index and birefr., struct. transition effects 77−90126

$TlMnCl_3$, sp. ht. and latent heat, under press. 79−7694

$TlMnCl_3$, specific heat in region of struct. phase transition 77−7862

$TlMnCl_3$, specific heat near Neel temp. *(Russian)* 80−100340

$TlMnCl_3$, weak ferromag. and mag. struct., temp. depend. 78−19219

Tl_2MoO_4, prep., characterisation 78−63731

$Tl_2Mo_4O_{13}$, X-ray cryst. struct. determ. *(French)* 79−14748

$Tl_2Mo_8S_{11}$, X-ray cryst. struct. determ., Mo_{12} and Mo_6 isolated clusters *(French)* 80−92490

$Tl_2Mo_9S_{11}$, prep. and struct., Mo_{12} cluster in $Mo_{12}S_{14}$ unit 80−107168

$Tl_xMo_6S_8$ Chevrel phase, synthesis, stability and characts. 80−71608

$Tl_2Mo_{15}Se_{19}$, superconducting chalcogenides containing Mo_6 and Mo_9 clusters 80−103804

$Tl_2Mo_6Se_6$, one dimensional supercond. crystal struct., resist. and upper crit. field 80−50016

$Tl_2Mo_6Se_6$, X-ray cryst. struct. determ., monodimensional clusters $(Mo_{6/2})^1\infty$ *(French)* 80−96482

$TlMo_3Se_3(Te_3)$, synthesis and struct. 80−92498

TlN_3, diamag. susceptibility, rel. to cryst. struct. 79−24127

TlN_3, heat capacity from 5 to 350K 79−55901

TlN_3, lattice vibration Raman study, tetragonal-cubic phase transitions 79−77743

TlN_3, press. induced phase transition, Raman scatt. meas. 78−19468

TlN_3, press. induced transition dynamics, light scatt. 78−80362

$Tl_{0.33}(NH_4)_{0.67}H_2PO_4$, X-ray crystallographic investig. *(French)* 80−49192

$TlNO_3$, aq. solns., viscosities at 25°C 77−20104

$TlNO_3$, boiling and melting pts., heats of transformation, solid-solid transformation 78−91441

$TlNO_3$, electronic struct., relative energies, iterative EH calcs. 77−38615

$TlNO_3$, ion pair, in Ar matrix, solvation effects, IR spectra 77−46563

$TlNO_3$, melt, NO_3^- ion struct., pulsed neutron diffr. obs. 78−22631

$TlNO_3$, molten, Tl^+ self-diffusion coeff., 230-330°C 78−22878

$TlNO_3$, molten and aqueous soln., Raman spectra 79−78673

$TlNO_3$, photoelectron spectra of gaseous species 77−18974

$TlNO_3$-$Cd(NO_3)_2$ molten mixtures, electrical conductance, non-Arrhenian behaviour 78−43158

$TlNO_3$-$LiNO_3(KNO_3)$ mixtures, molten, surface tension, regular solution theory 78−71903

$TlNO_3$-$NaNO_3$, melt, cationic self-diffusion coeffs., temp. and conc. depends. 78−22879

$TlNO_3$-$RbNO_3$, melt, cationic self-diffusion coeffs., temp. and conc. depends. 78−22879

$Tl(NO_3)_3(H_2O)_3$, cryst. struct. determ. 78−59790

$Tl_3Na(SO_4)_2$, α-phase, IR and Raman spectra, order of cryst. struct. *(French)* 77−85718

$TlNbO_3$ and $Tl_3Nb_{16}O_{41}$, new phase of mixed oxide 78−59787

$TlNbO_3$, ceramics, hysteresis loops and dielec. props. 79−42885

$TlNb_{3+x}O_{9-y}$, cryst. struct., hexagonal bronze type with excess cations *(French)* 77−72591

$Tl_{7.7}Nb_{54+x}O_{146-y}$, single crysts., synthesis and X-ray cryst. struct. determ. 79−69065

$Tl_8Nb_{22}O_{59}$, synthesis and struct. *(French)* 77−24294

$Tl_xNbO_{2+x}F_{1-x}$ ($0.5 \leq x \leq 1$), heavy ion location Tl^+, and struct. refinement *(French)* 79−73144

$Tl_xNbO_{2+x}F_{1-x}$, pyrochlore phase, Tl^+ mobility 79−95209

$Tl_2Nb(Ta)_6TiO_{18}$, structs. with intersecting tunnels, Tl distrib. *(French)* 78−79586

$TlNbWO_6$, pyrochlore related structures, phases of type AM_2X_6, acentricity and phase transitions, X-ray diffr., DSC and NMR study 79−27943

$TlNdO_3$, lattice parameters determ. *(French)* 78−95031

$TlNd(PO_3)_4$, cryst. struct. determ. 79−19216

$TlNiCl_3$, paramag., spin density, NMR study 78−88200

$TlNiCr_2(VO_4)_3$, synthesis and cryst. struct. 80−88114

β-Tl_2O-Al_2O_3, cation distrib. 77−80487

Tl_2O-B_2O_3, glass, ^{205}Tl NMR 77−59470

Tl_2O-GeO_2, glass, ^{205}Tl NMR 77−59470

Tl_2O-GeO_2 system, structure of thallium I germanates *(French)* 80−79754

Tl_2O-SiO_2, glass, ^{205}Tl NMR 77−59470

thallium compounds continued
Tl_2O-TeO_2, phase diag. 77−81252
Tl_2O-TeO_2 glass, struct. and props. *(Japanese)* 79−32917
Tl_2O_3 single crystal, elec. cond., cryst. grown from vapour in air 77−85219
Tl_2O_3, single crystal, elec. cond., annealing at 923K in O_2 effects 77−85220
Tl_2O_3-V_2O_5, ceramic, elec. resist., dielec. props., porosity 77−8093
TlOH, aq. solns., viscosities at 25°C 77−20104
TlP, possibility of existence with sphalerite struct. 80−33950
TlP_3, elec. cond. temp. depend., 77-590K 77−51743
$TlPO_3$, vitreous and polycrystalline, NMR and IR exam. of cation motion 77−66041
Tl_3PO_4, heat capacity and thermodynamic functions, 5 to 320K 80−65245
Tl_3PS_4, optical phonons, Raman spectra study 80−80790
Tl_3PSe_4, phonon dispersion temp. depend. 80−96600
Tl_3PSe_4, struct. and soft mode behaviour 78−91327
$(Tl_{0.75}Pb_{0.25})_4Cl_5$, cation disordered phase, X-ray diffr. determ. of cryst. struct. 80−1985
$Tl_2PbCu(NO_2)_6$, incommensurate Jahn-Teller phase transitions 79−65185
$Tl_2PbCu(NO_2)_6$, incommensurate Jahn Teller phase transitions 79−95156
$Tl_2PbCu(NO_2)_6$, incommensurate Jahn-Teller transition, Huang scatt. 80−70401
$Tl_2PbX(NO_2)_6$, (X=Cu, Ni), single cryst. growth in gel *(German)* 79−74076
$TlR(MO_4)_2$, R=Eu, Dy, Er; M=Mo, W, luminesc. *(Russian)* 78−48229
$TlR(MoO_4)_2$, (R=Eu, Dy, Er), fluoresc. spectra at 77, 300K 79−56848
$TlR(MoO_4)_2$ (R=La to Ho), polymorphism, X-ray diffr., thermographic anal. 78−47269
$TlR(WO_4)_2$, (R=Eu, Dy, Er), fluoresc. spectra at 77, 300K 79−56848
$TlReO_4$, IR matrix-isolation spectra 80−87108
$TlReO_4$, photoelectron spectra of gaseous species 77−18974
TlS_2, amorphous, spectral depend. of absorpt. and refr. indices 77−77222
TlS_2, amorphous, struct. and origin of crystn. process 77−76322
TlS_2, amorphous semiconductor, optical consts. 79−11400
TlS_x, amorphous, struct. from radial electron density distrib. curves 79−23527
Tl_2S, liq., mag. susceptibility 79−24128
Tl_2S-Ag_2S system, phase equil., DTA, X-ray and microhardness obs. 79−38803
Tl_2S-SnS, phase equilibria exam. 80−55369
Tl_2S-Tl_2Se systems, melts, ion transfer, diffusion coeffs., elec. cond., density meas. 77−1253
Tl_2S-$Tl_2Se(Tl_2Te)$, exam. of phase equilibria, using DTA, X-ray phase analysis and microhardness 79−4953
$(Tl_2S)_{3x}$-$(Sb_2S_3)_{1-x}$, phase equilibria and struct. of cpds. 77−85996
Tl_2SO_4, aq. solns., viscosities at 25°C 77−20104
Tl_2SO_4, elec. cond. rel. to thermodynamic props. in phase transitions 77−39690
Tl_2SO_4, photoelectron spectra of gaseous species 77−18974
Tl_2SO_4, solid-solid transition temp. to 34 kbar *(French)* 77−20064
$Tl_2S(Se)$, molten III-VI semiconductors, SRO 77−65945
TlSb, possibility of existence with sphalerite struct. 80−33950
$TlSbF_6$, Raman spectra, at press. up to 25 kbar 78−6670
$TlSbS_2$, phase transitions under action of high press., elec. cond. meas. 77−4196
$TlSbS_2$, photocond. characts. 77−4407
$TlSbS_2$, single cryst., spectral transmission distrib., polaris. effect, refractivity, dispersion 77−59551
$Tl_{0.51}{}^{III}Sb_{0.71}{}^{III}Sb_2{}^{V}O_{6.32}$, X-ray cryst. struct. determ. *(French)* 79−69079
TlSe, heat capacity, at low temp. and Debye temp. *(Russian)* 79−10962
p-TlSe, monocrystal, temp. depend. of mechanical strength *(Russian)* 79−10892
TlSe, optical phonons, IR and Raman scatt. meas. 78−59903
TlSe, Raman spectra, phonon modes 80−40109
TlSe, refl. spectrum in 4.2 to 8.0 eV range 79−51984
TlSe, Tl_2Se, Tl_2Se_3, liq., diffusion coeff. of Sn, Ag and Tl *(Russian)* 77−28030
TlSe type crystals, possible second-order phase transitions, group-theoretical anal. 80−92672
TlSe, vibrational spectrum, IR spectra meas. 78−35146
$TlSe_x$ amorphous phase struct., rapid electron density distrib. curves 80−33896
$Tl_{1-x}Se_x$, amorhpous, IR spectra, structure 77−77194
Tl_2Se, diamag., thermal expansion rel. to temp. at cryst.-melt transition 78−34954
Tl_2Se, fused, diffusion of ^{204}Tl, ^{110}Ag, ^{112}Sn impurities 80−54415
Tl_2Se, liq., elec. cond. at high temps. and pressures 79−11119
Tl_2Se, liq., mag. susceptibility 79−24128
Tl_2Se-As_2Se_3-SnSe system alloys, covalent component of chem. bond effect in vitrification processes, Mossbauer obs. 77−36156
Tl_2Se-As_2Te_3 and Tl_2Te-As_2Te_3, vitreous, photo-EMF kinetics 77−76877
Tl_2Se-SnSe(PbSe) systems, phase equilib. 79−52181
Tl_2Se_3, diamag., thermal expansion rel. to temp. at cryst.-melt transition 78−34954
Tl_2Se_3, elec. cond. and thermoelectric power, doping effects, rel. to pseudogap model 78−2506
$(Tl_2Se)_{3x}$-$(Sb_2Se_3)_{1-x}$ system, phase diagram 77−16558
$Tl_{66}Se_{34}$, liquid, thermoelectric figure of merit meas. 77−28202
Tl_xSe_{1-x}, amorphous and cryst., IR transmission spectra and struct. interpret. 78−23471
p-Tl_xSe_y, IR bolometer detector performance 78−24856
$Tl_2SeAs_2Te_3$, amorphous semicond., nuclear spin-lattice relaxation by localised electronic states, modification by spin diffusion 78−52372
$Tl_2SeAs_2Te_3$, glassy and liq. states, elec. cond. freq. depnd. 77−76856
$Tl_2SeAs_2Te_3$, molten chalcogenide semicond., temp. depend. of 10^{10} Hz elec. cond. 77−4388
$Tl_2SeAs_2Te_3$, secondary electron emission, fluctuation state effect 80−40193
Tl_2SeO_4, structural transition, polarised Raman spectra 80−75349
TlSe.As_2Se_3, $Tl_2Se.As_2Se_3$, γ-irrad. effects on mech. props. 77−80567
$Tl_2Se.As_2Te_3$, vitreous, thermal switching process in high electric fields 80−2432
$TlSmO_3$, lattice parameters determ. *(French)* 78−95031
Tl_2SnF_6, thermal stability and thermolysis *(French)* 78−10011

thallium compounds continued
Tl_2SnSe_3, preparation, Mossbauer spectra 77−28489
Tl_2SnSe_3, X-ray cryst. struct. determ. *(French)* 80−107171
Tl_4SnSe_4, preparation, Mossbauer spectra 77−28489
$TlTaO_3$, ceramics, hysteresis loops and dielec. props. 79−42885
Tl_2TaO_6, Tl I lone pair stereochem. activity rel. to ferroelectricity 78−15131
$Tl_2Ta_2O_6$, localisation of Tll, electrostatic energy, calc. *(French)* 80−33926
$Tl_{4.62}Ta_{11.08}O_{30}$, cryst. struct. determ. *(French)* 79−69092
$Tl_{5-x}Ta_{11+x/5}O_{30}$, synthesis, non-stoichiometry, density and ionic cond. meas. *(French)* 78−52741
Tl_3TaS_4, optical phonons, Raman spectra study 80−80790
Tl_3TaS_4, piezoelec. semicond., acoustic wave generation, amplification material appl. *(Russian)* 78−72464
Tl_3TaSe_4, for SAW devices, temp. compensated cuts with zero power flow 77−12313
Tl_3TaSe_4, new SAW zero temp. cuts 78−2351
Tl_3TaSe_4 SAW coupling and temperature coefficients 79−51410
$Tl_{1+x}Ta_{1+x}W_{1-x}O_6$ pyrochlore system, comp. depend. of ionic cond. 80−107517
$Tl_{1+x}Ta_{1+x}W_{1-x}O_6.nH_2O$, pyrochlore type, stoichiometry and ionic cond. 80−24648
TlTe, elec. props., cryst. growth *(Japanese)* 79−33907
TlTe, empty lattice band struct. *(Japanese)* 77−51660
TlTe, melt, elec. cond., surface tension, microhardness, influence of impurities 80−88551
TlTe single crystal, resistivity, Hall coeff., magnetoresistance, thermoelec. power 78−43418
Tl_2Te, liq., elec. resistivity meas. up to 30 kbar 79−38070
Tl_2Te, liq., mag. susceptibility 79−24128
Tl_2Te, melt, resistivity, surface tension, microhardness, influence of impurities 80−88552
Tl_2Te-HgTe(HgSe) systems, phase diagrams 79−87620
Tl_2Te-Sb_2Te cross section of Tl-Sb-Te system, new $TlSbTe_2$ and Tl_9SbTe_6 cpds. 78−52778
Tl_2Te-Tl liquid system, conc. fluctuation, time-of-flight quasielastic neutron scatt. obs. 80−88324
Tl_2Te_3, exam. of electrical props., density and viscosity, for solid or liquid states 79−95431
Tl_2Te_3, exam. of electrical props., in solid, liquid state 80−54686
Tl_2Te_3 melt, impurities effect on surface tension polytherm and adsorption obs. 77−7947
Tl_2Te_3:Ag(Sn), effect of dopant on electrical props., density and viscosity, for solid or liquid states 79−95432
Tl_5Te_3-Tl_4SnTe_3-Tl_4PbTe_3, phase equilib., DTA, SPA and microhardness meas. 80−96628
Tl_xTe_{1-x}, amorphous, bonding and electrical conduction 79−90951
Tl_xTe_{1-x}, liq. semicond. alloy, mag. susceptibility rel. to diffusive transport 77−20541
Tl_xTe_{1-x}, thermodynamic evidence against large scale fluctuations in composition in heterogeneous transport models 77−28172
$Tl_2(TeCl_6)$, IR and Raman spectra, lattice and internal modes, phase transition 78−6659
Tl_2TeO_3, $Tl_2Te_3O_7$, $Tl_2Te_2O_5$, Tl_2TeO_6, Tl_6TeO_{12}, synthesis, thermal stability, crystallographic data *(French)* 78−51518
Tl_6TeO_6, solid, prep., thermal stability, cryst. parameters *(French)* 79−65037
$Tl_2(Te_xSe_{1-x})$ mixtures, liq., electrical conductivity, magnetic susceptibility 80−88715
$Tl_2Te.As_2Te_3$, vitreous, temp. depend. of cond. and thermopower, electron energy spectrum 77−76831
$TlTiMO_5$ (M=Ta, Nb), ion exchange props., synthesis and crystallographic props. *(French)* 80−28997
$Tl_{1-x}(Ti_{1-x}Nb_{1+x})O_5$, layer compound, cryst. struct., nonstoichiometry 80−64972
$Tl_2Ti_4O_9$ ceramics, hysteresis loops and dielec. props. 79−42885
$Tl^{I}Tl^{III}(SeO_4)_2$, $Tl_3{}^{I}Tl^{III}(SeO_4)_3$, and $Tl_5{}^{I}Tl^{III}(SeO_4)_4$, cryst. struct. *(French)* 80−84148
$TlTm(MoO_4)_2$, polymorphic transition characts., temp. regions of stability 79−14785
$TlUF_5$, X-ray cryst. struct. anal. *(French)* 80−54184
$Tl_2U_yF_{x+4y}$, cryst. growth from flux, crystallographic characts. *(French)* 77−77364
$Tl_{0.25}VF_3$, cryst. struct. examination by electron diffr. using TEM 79−23583
Tl_xVF_3, non-stoichiometric, struct. depend. on composition 79−99152
$TlVO_3$, cryst. struct. 78−6043
$TlVO_4$, synthesis and thermal props. *(French)* 80−97443
$Tl_{1.74}V_8O_{16}$, hollandite-type struct., synthesis and cryst. struct. 80−29003
TlV_5S_8, prep., props. and cryst. struct., metallic behaviour 77−27864
$Tl_2V_2S_6$ single crystal growth, Bridgman-Stockbarger technique 80−89132
Tl_3VS_4, acoustic surface wave propag., temp. coeffs., piezoelectric coupling *(French)* 78−35093
Tl_3VS_4, cryst. struct., X-ray diffr. obs. *(French)* 79−14763
Tl_3VS_4, for SAW devices, temp. compensated cuts with zero power flow 77−12313
Tl_3VS_4, growth of inclusion free crystals, for surface wave and bulk wave acoustic devices 80−25549
Tl_3VS_4 SAW coupling and temperature coefficients 79−51410
Tl_3VS_4, SAW zero freq.-temp.-coeff. configs. 77−43418
Tl_3VS_4 single-crystal substrate SAW filter performance 77−31186
$Tl_xV_6S_8$, prep., struct., props. 77−19935
$Tl_{0.3}WO_3$, struct. anal. *(French)* 78−59786
$Tl_{0.33}WO_3$ bronze, elec. resist. meas., anisotropy, supercond. 80−75569
$Tl_{0.33}WO_3$, supercond. and special phonons, neutron scatt. obs. 80−15643
Tl_2WO_4, solid-state prep., cryst. struct. and props. 78−38673
Tl_2WO_4, X-ray cryst. struct. determ. 79−99136
Tl_2WO_4-$In_2(WO_4)_3$, cpd. formation and single cryst. growth 77−86010
Tl_2WO_4-$Sc_2(WO_4)_3$, cpd. formation and single cryst. growth 77−86010
$Tl_2W_4O_{13}$, tunnel struct., related to hexagonal tungsten bronze 80−28988
Tl_2X_2(X=F,Cl), mol. force field and const. constraints from electron diffr. data 77−27197
$TlY(MoO_4)_2$, polymorphic transition characts., temp. regions of stability 79−14785
$TlYb(MoO_4)_2$, polymorphic transition characts., temp. regions of stability 79−14785
$Tl_2ZnBr_4(I_4)$, fast ionic cond. and order-disorder transition 79−99363

thallium compounds continued
Tl_2ZnI_4, ionic conductivity, Raman spectra 77−69113
Tl_2ZnI_4, solid electrolytes, ion transport mechanism and polarisability role, comparison with Cu^+ and Ag^+ cond. 80−107531
$Tl_2[Fe(CN)_5(NO)]$, X-ray cryst. struct. determ., heavy atom method 80−92495
$Tm_2Ge_2O_7$, flux growth 79−83113
$(YEuTmCa)_3(FeGe)_5$ bubble garnet films, ion-implanted, mag. susceptibility meas. 79−47311

thawing *see melting*

The Galaxy
2 μm radiation, mean intensity in solar neighbourhood 80−36744
5 GHz galactic plane radio sources, catalogue 80−4269
10 MHz radio emission, map of northern sky 77−13485
30 MHz all-sky map, galactic features study 79−21469
γ-ray sources, number intensity relation rel. to galactic disc emission 80−46702
abundance gradients, reassessment from spectrophotometry of Perseus arm H II regions 80−22055
abundance gradients derived from H II regions, spectrophotometry 78−41036
abundances of Ne, Ar and Cl rel. to O derived from planetary nebulae 79−5887
abundances of stable isotopes of common elements 79−44615
accretion of gas having specific heat ratio 4/3 by a moving gravitating body 79−70951
accretion of intergalactic matter in solar neighbourhood 80−67863
age, determ. from ^{187}Re-^{187}Os systematics in meteorites 80−41778
anticentre, 21 cm obs. of H I stream 80−90524
anticentre, space distrib. of stars and dust *(Russian)* 78−73754
anticentre anomalous-vel. streams, 21 cm. line obs. 79−40257
anticentre direction, radial vels. of early-type stars 78−7990
anticentre region, distance to low-latit., negative vel. clouds 77−45506
anticentre region, faint blue stars spectral types 79−71021
Ap and Am stars, space distrib. 77−71117
Aquila region, near IR mapping at balloon altitudes 79−12514
Australian Astronomical Society, conf. Melbourne, Australia (May-June '77) 78−69655
B5-A0 stars, local density and kinematics rel. to density-wave theory 77−56931
B-type stars at intermediate galactic latitude, space distrib. 77−91535
background radio emission fine struct. correl. with discrete radiosources 79−21457
Basle catalogue of 1906 blue objects at high galactic latitudes 78−32360
Be 94, UBV photometric obs. of young distant open cluster in Cepheus 78−61892
Be stars, photometric behaviour, UV excess, emission indices, galactic distrib. 80−36637
boundary layer circulation in disc-halo galaxies, appl. to Milky Way 78−57627
bright stars, XX LMC luminosity function 80−82499
broadcast strategies and source position for advanced civilizations 77−91449
bulge X-ray sources, radio continuum obs. at 2.7, 4.8 and 10.7 GHz 80−101619
bulge X-ray sources nature, implications of X-ray burst sources persistent emission 79−84871
carbonaceous material in Galaxy, origin and nature 78−24543
Carina arm region, OB stars, UBVβ photometry 80−85941
Carina spiral arm, galactic struct. and star formation, spectrographic and photometric obs. *(French)* 78−89256
Carina spiral arm, starlight as S.Celestial Pole nebulosity illumination source 79−92839
Carina spiral feature, distrib. of stars and interstellar dust along inner side 80−51871
Carina spiral feature, UBVβ photometry of young open cluster (NGC 3324) 77−22282
Carina-Crux-Centaurus region of Milky Way, interstellar extinction investigation 79−40242
Cassiopeia, photoelectric UBV photometry 77−37598
central IR surface brightness obs. by balloon *(Japanese)* 78−61925
central parsec, black hole 80−22089
central point radiosource size determ. *(Russian)* 79−58427
central region, 2.4 μm mapping 77−29934
central region, absolute surface photometry at 2.4 and 3.4 μm 77−57088
central region, formaldehyde and molecular clouds 80−94852
central region, formamide ^{13}C isotope detect. 79−25680
central region, gamma-ray line emission 79−44641
central region, gas, dust, high energy particles and star form. dust, high energy particles and star form. 80−36713
central region, IR profile at 2.47 μm 77−29935
central region, Prognoz-6 obs. of X-ray fluxes and energy spectra *(Russian)* 80−109562
central region, sources and obscuration 80−77487
central region, stellar bar rel. to distrib. of interstellar matter 77−45565
central region, variable extinction obs. 79−48909
central region gas distribution, barlike model based on improved H I data 80−67845
centre, 4 to 8 micron spectrum 79−48922
centre, ang. size for compact radio source 78−28779
centre, annihilation radiation due to positron prod. by evaporating black holes 80−46599
centre, as possible source of ultrahigh-energy cosmic rays 80−46351
centre, black hole mass from X-ray flux and radiation spectrum of accreted gas 80−90467
centre, distance from spatial struct. of globular cluster system 77−37625
centre, distrib. of stars and dust, black hole hypothesis 78−86010
centre, energy balance, star formation 78−81684
centre, extended thermal component, broad-line H94α emission 78−77598
centre, hard γ-rays and diffuse background, Kosmos 561 obs. 79−84597
centre, high resolution 8450 MHz obs. 79−44629
centre, IR obs., 1.25-12.5 μm interstellar extinction law 78−41039
centre, IR polarization due to silicate dust grains 77−9794
centre, IR source, radiating dust cloud 77−78863
centre, Ne II 12.8 micron emission obs. 78−32572
centre, nearest Cepheid, V1437 Sagittarii distance 80−82396
centre, radiation model, dust grains heating by O-stars and K-giants 78−36697

The Galaxy continued
centre, radio recomb. line emission from G 0.7−0.0 (Sagittarius B2) 77−17651
centre, radiosource size and struct., radiation scatt. and scintillation *(Russian)* 78−16535
centre, spectrum of compact radiosource 79−21422
centre, tidal disruption of stars and massive black hole evolution *(Russian)* 78−12371
centre, X-ray transients and burst sources 78−12425
centre direction, H200β line detect. 77−78868
centre direction, low-freq. radio recomb. lines studies 78−32589
centre field, planetary nebulae and Wolf-Rayet stars identifications 80−8674
centre region, 2.2 μ map 79−58424
centre region, 2.2 μm spectroscopy 78−36686
centre region, 252α recomb. line emission 77−45587
centre region, 5 GHz formaldehyde absorpt. obs. 79−84855
centre region, airborne far IR obs. 78−8110
centre region, compact radio continuum sources obs. 79−21430
centre region, compact radiosource interferometry 77−53686
centre region, eruptive phenomena 78−57647
centre region, forbidden O III 88 μm line emission obs. 78−49503
centre region, H I 21 cm line survey 78−12361
centre region, H I absorpt. obs. 77−45560
centre region, H radio recombination line obs. of arc-like source 80−82498
centre region, H recomb. lines obs. at decimetric wavelengths 77−82310
centre region, high energy gamma-ray emission 77−53704
centre region, high-energy X-ray detection 80−67854
centre region, ionising agent of extended thermal radio emission 79−97059
centre region, IR bright stars catalogue and photometry 80−77299
centre region, IR linear polarisation 77−91630
centre region, IR obs. and nature of compact IR sources 78−24551
centre region, IR polarisation obs. 78−8109
centre region, linear polarisation in near IR 78−96534
centre region, medium-energy gamma-ray emission obs. 79−9030
centre region, methylamine-d_1 detect. in Sagittarius A 77−33610
centre region, neutral H survey 79−88722
centre region, obs. of optical flashes from burst X-ray sources 77−41420
centre region, OH absorpt. struct. determ. using regularisation method 80−17505
centre region, OH maser sources systematic search at 1612 MHz 79−35415
centre region, polarisation obs. at 2.2 microns 77−64850
centre region, positron annihilation rel. to gamma radiation spectrum 79−44309
centre region, radio search for planetary nebulae, implications of flux density distrib. 80−56913
centre region, search for H_2 2.1 μ emission 80−22059
centre region, search for X-ray pulsations 79−44617
centre region, shock wave model of expanding ring 78−4365
centre region, shock wave model of kinematic features of H I and molecules 77−91629
centre region, star density rel. to nature of IR source IRS 16 80−46671
centre region, struct. from 2.4 μm obs. 78−81689
centre region, X-ray activity 79−58419
centre region, X-ray and gamma-ray lines prod. by nonthermal ions 78−36725
centre region far IR spectrometry 77−53668
Cepheid variables, intrinsic colours 79−84797
Cepheid variables, long-period, absence from Galaxy rel. to obs. of yellow variable supergiants 80−98672
Cepheid variables, period-amplitude diagram compared with Cepheids in other galaxies 78−53956
Cepheids, galactic distrib. between l∼294° and (331°) 79−48910
Cepheids between l=294° and 331°, UBV and 21 cm obs. 79−12478
chemical abundance gradient, determ. from open clusters H-R diagrams anal. 80−56938
chemical and dynamical evolution *(Polish)* 78−96542
chemical enrichment, effect of increasing He content and disc dwarfs evolution 79−88733
chemical evolution, effect of mass loss on chemical yields from massive stars 80−36614
chemical evolution, effect of stars mass loss by stellar wind 80−41814
chemical evolution, He enrichment 77−22208
chemical evolution, implications of C and N abundances in F- and G-type stars 77−91530
chemical evolution, Mg isotopic abundances in five G and K dwarf stars 80−51757
chemical evolution, review 77−26068
chemical evolution, role of planetary nebulae 80−109541
chemical evolution and nucleocosmochronology 77−29918
chemical evolution at initial rapid-collapse phase 78−69870
chemical evolution from main sequence disk star calcs. 80−109553
chemical evolution in solar neighbourhood, time scales and nucleochronology 78−8112
chemical evolution of galactic disc, inflow problem 80−62279
chemical evolution of two-component galaxies, numerical calcs. 79−25715
chemical evolution rel. to stellar evolution and nucleosynthesis 80−67847
chemical history in solar neighbourhood 77−91635
chemistry, workshop proc. (Frascati, Italy, 29 May-2 June 1978) *(Italian)* 80−12845
Circinus galactic window, early type star obs. 77−13342
Circinus-Norma region, faint OB star search 80−62121
clustering in S. Milky Way, UBV and uvby β photometry 79−44572
CO distrib. in central region 79−21416
comet orbital elements distrib., effect of galactic forces *(Russian)* 80−77353
communicative civilizations, formalism and numerical calc. 77−91448
core, H II obs. in near IR 79−53864
corona, ionisation struct. theory and absorpt. line spectrum 77−13448
corona, origin and props. 79−25709
corona, plasma parameters and heating mechanism 80−82492
coronal gas, interstellar O VI survey in OB star UV spectra 78−36679
coronal gas, statistical anal. of O VI absorpts. 78−36653
corrugation waves in differentially rotating gas layer, theory 77−5571
cosmic dust in central region and anomalous IR source 79−44588
cosmic gamma rays, origin rel. to galactic struct. 77−87213
cosmic ray acceleration by supernova shock waves 80−82154

The Galaxy continued
cosmic ray age distribs. in galactic convective halo 80−51625
cosmic ray confinement, effect of interstellar MHD turbulence 77−49246
cosmic ray confinement in dynamical halo, electrons 78−4044
cosmic ray confinement in dynamical halo, nuclei 78−4043
cosmic ray deuterons and antiprotons production mechanisms 79−29955
cosmic ray diffusion, evidence from nuclei charge comp. and energy spectra 78−93059
cosmic ray diffusion influence on gamma-ray flux from galactic plane 77−64854
cosmic ray diffusion model, age distrib. of interacting, decaying and secondary particles 77−5401
cosmic ray electron spectrum below 1000 MeV 79−5718
cosmic ray electrons, confinememt and radio emission 77−73910
cosmic ray electrons, energy spectrum and fundamental props. *(Chinese)* 80−105138
cosmic ray electrons, evidence for large-scale gradients 77−33299
cosmic ray electrons in galactic radio halo 77−9631
cosmic ray halo, origin 79−44314
cosmic ray nucleosynthesis, rel. to extragalactic matter local infall rate 79−17084
cosmic ray propagation, convective model 77−25890
cosmic ray propagation, diffusion model and electrons source spectrum 79−53677
cosmic rays, age derived from ^{10}Be abundance 78−12060
cosmic rays, energy dependent diffusion in dynamic halo model 80−82156
cosmic rays, evidence for short pathlengths deficiency and no-near-sources model 79−84596
cosmic rays, isotopic comp. rel. to origin and containment time 78−53781
cosmic rays, low energy, spatial inhomogeneities in diffusion model 77−5402
cosmic rays and magnetic field, distrib. from synchrotron radio and gamma-ray obs. 80−4207
cosmic rays electron component, diffusion model of propag. 79−53679
cosmic rays energy loss in expanding areas of Galaxy *(Russian)* 78−93055
cosmic rays history in dynamical halo, retrodictive probability approach 78−65467
cosmic rays origin, appl. of galactic models with halo to proton nucleon component 80−61971
cosmic rays propagation, diffusion model for nuclear component 79−53678
cosmic rays propagation, leaky-box model 78−57409
cosmic rays propagation and distribution in Galaxy 78−69621
Crux-Centaurus region, new Cepheid variable stars 79−12477
Cygnus direction, stars and dust space distrib. *(Russian)* 78−20893
Cygnus region, new optical supernovae remnant discovery 78−4330
Cygnus X region, gamma-ray flux prediction and nature of (CG 78+1) 79−92895
Cygnus-Vulpecula direction, stars and dust cloud space distrib. *(Russian)* 78−20892
dark dust clouds in southern hemisphere, kinematics rel. to galactic struct. 77−13434
dark nebulae and globules, star form. regions 78−12347
dense radio H II regions distrib. in inner Galaxy, kinematic models 80−12813
density wave evolution at unstable stage *(Chinese)* 78−28787
density wave propag. through disc 78−20894
density waves, maintenance and phase shifts between stellar and gaseous arms 79−44618
density waves amplification by nonadiabatic processes in gas 78−4364
density waves influence on star form. rate 79−88743
diffuse EUV flux, rel. to local interstellar medium ionisation state 80−90502
diffuse far IR emission detect. from galactic plane 77−33611
diffuse far IR emission from galactic plane, balloon obs. 79−35378
diffuse galactic emission in far IR 79−67092
diffuse galactic light, S2/68 sky-survey telescope UV obs. 79−12519
diffuse galactic light and Milky Way brightness fluctuations 78−61921
diffuse galactic light interpretation, models 78−8118
diffuse gamma radiation, galactic and isotropic components 78−65725
diffuse high-latitude UV light, average intensity rel. to interstellar grains phase function 79−97047
diffuse object, detect., in galactic centre direction *(French)* 79−8959
diffuse soft X-ray emission, brightness distrib. 79−53942
diffuse soft X-ray emission, distrib. and energy spectrum 78−28853
diffuse soft X-ray sky, astrophysics rel. to 0.1-2.0 keV cosmic X-rays 78−16581
diffuse soft X-rays from H I deficient region in Hercules, O VII emission line obs. 79−25759
Dirac cosmology, onset of galactic nucleosynthesis, and age of Universe 77−13514
disc, local K_z-force field rel. to interstellar matter z-distrib. 80−62271
disc, obs. between $-45° < l^{II} < 45°$ in 80 keV to 8 MeV energy range 80−82540
disc $\alpha\omega$ dynamo theory for mag. field generation 80−46663
disc anticentre direction, localised high-energy γ-ray emission, COS-B obs. 77−49495
disc chemical evolution and radial metallicity gradient 77−29937
disc direction, super-high energy cosmic rays anisotropy *(Russian)* 78−57410
disc emission at 4 cm wavelength, large-scale and small-scale cloud structs. 78−28795
disc evolution 77−29928
disc population stars, luminosity functions in SA 51, SA 57 and (SA 68) 80−98648
disc stars metallicity distrib. rel. to origin of galactic subsystems *(Russian)* 79−21441
disc thickness from H I 21 cm obs. rel. to mass models 79−75273
discrete gamma-ray sources rel. to galactic cosmic ray distrib. *(Russian)* 78−65719
disk and halo giant, CN strength differences 80−51750
distant satellite galaxies, spectra of giant stars 78−40926
distribution of matter in finite thickness disc model *(Chinese)* 79−80349
double structure and IR obs. of centre region 77−91633
dust clouds, far IR emission rel. to translational anisotropy of cosmic microwave background 77−33706

The Galaxy continued
dust grains distrib. in intercloud medium, from K-type giant stars colour excesses 79−40251
dust/molecular clouds in Galaxy, props. 80−26925
dwarf spheroidal satellite galaxies, H I content upper limits 78−57633
dwarf stars, K- and M-type, space motions rel. to stellar age 78−69846
dynamical halo model and cosmic ray path length var. with energy 79−53675
dynamics, appl. of generalised twice restricted three-body problem *(Russian)* 80−51643
dynamo action and ultra-high-energy cosmic ray propag. 77−74146
dynamo model, appl. to galactic mean mag. field 78−81685
early B-type stars in local spiral arm, var. of axial rot. vels. with galactocentric distance 77−56929
early-type stars, northern intermediate galactic latit., Hβ photometry, rel. to glactic struct. 80−36631
early-type stars in S. Milky Way, ubvyβ photometry 80−85942
early-type stars in S.Milky Way, photometry 79−62822
electron temperature gradients with distance from galactic centre 79−88744
equator region, H I recomb. line emission, 408 MHz obs. 77−13451
Equatorial stars, True Visual Magnitude Photographic Star Atlas 79−70967
EUV background, point source contribs. 80−62324
evolution, disk stars, metal abundance rel. to orbital elements *(Russian)* 79−25733
evolution, evidence of active phases, stellar populations statistical props. *(Russian)* 77−74141
evolution and abundance from obs. of globular clusters 80−90484
evolution and spiral structure of a spiral galaxy 80−17667
evolution from light-element abundances, models, cosmological constraints 80−31401
evolution rel. to star formation mechanisms 80−12811
evolutionary models, constraints from white dwarf data 80−46548
exchange collisions between binary and single stars 77−91563
expanding features 79−30132
expanding features of galactic centre 78−12365
expansion, evidence from stellar proper motions 77−5574
expansion, kinematics and struct. 77−5563
exponential disk, scale length 80−41901
extraterrestrial intelligent life 79−48692
faint blue stars in high galactic latits., search of PSS fields near South Galactic Pole 80−46415
faint blue stars near galactic anticentre, UBV photometry 78−40932
faint blue stars proper motions near galactic anticentre 77−87386
faint red dwarfs statistics, photometric obs. at intermediate galactic latit. 78−32457
far IR diffuse emission from galactic plane, longit. profile 79−88742
far IR scans of galactic plane 77−60823
far IR sources, large-beam sky survey at millimetre and submillimetre wavelengths 79−97045
far UV radiation background at high galactic latits., D2B-Aura satellite obs. 79−17143
FK4/FK4 Sup stars, three-dim. kinetics anal. 78−8060
for IR emission, balloon obs. *(Japanese)* 80−36714
force field normal to galactic plane, determ. from z-oscills. theory 80−46669
formation and chem. evolution rel. to stellar metallicity distrib. 77−91520
G0.7-0.0 (Sagittarius B2), struct. and He abundance 78−45380
G35.6−0.0 and G35.6−0.4, kinematic distance estimates 78−73769
G48.6+0.0, H II region, kinematic distance from H I, OH and H_2CO obs. 78−85996
galactic γ-ray lines, balloon investigation using Ge(Li) spectrometer 80−8677
galactic γ-rays from low energy cosmic ray interactions with interstellar medium 80−8678
galactic bulge, spectra of RR Lyrae stars 77−26012
galactic bulge wind, interaction with gas disc, hydrodynamic model 80−77476
galactic centre, 1415 MHz obs. of planetary nebulae 79−71096
galactic coordinate system, conversion to and from equatorial coordinate system 79−88569
galactic disc, dynamical friction theory 79−35367
galactic disc structure, theory of disc accretion in soft potential well 80−8532
galactic IR radiation, balloon borne obs. *(Japanese)* 79−80351
galactic plane, discontinuity near 140° longit. 77−9797
galactic plane, fine energy resolution gamma-ray survey using Ge spectrometer 77−53701
galactic plane, near IR photographic survey 79−62911
galactic plane, optical identification of five X-ray sources 77−87573
galactic plane, recomb. line and continuum emission obs. 77−13433
galactic plane, S hemisphere survey at 5 GHz 78−81686
galactic plane, warping by LMC 77−45540
galactic plane far IR emission, obs. at galactic longit. (l^{II}=27.5°) 80−62231
galactic plane towards PSR 1858+03, obs. rel. to pulsar distance 77−64785
S.Galactic Pole, astrometry of B<14 stars, UK Schmidt results 79−66929
N.Galactic Pole region, stellar polarisation meas. rel. to extinction 79−62814
galactic poles, Apollo 17 far UV obs. of cosmic background 78−93401
galactic research, effects of errors in uvby photometric standard stars 77−2347
gamma radiation, possible origin, data from COS-B and SAS-2 satellites *(French)* 78−85776
gamma radiation in 0.03-4.1 MeV range Kosmos 461 meas. 77−67144
gamma ray emission, discrete source component 79−35436
gamma-ray astronomy and cosmic ray origin 79−29951
gamma-ray burst origin, models review 80−82494
gamma-ray burst sources, galactic distrib. models 80−22117
gamma-ray burst sources, new limits on distrib. 78−93465
gamma-ray bursts, galactic origin 78−32303
gamma-ray bursts, galactic origin and chronological catalogue 77−37672
gamma-ray burts, distance limit for non-relativistic source models 78−32612
gamma-ray diffuse background from inverse Compton scatt. in halo 77−53711

The Galaxy continued
gamma-ray diffuse component from galactic centre and anticentre 79−62901
gamma-ray emission, discrete source contrib. 78−69907
gamma-ray emission, high-energy, from galactic disc, spectral characts. COS-B obs. 78−36695
gamma-ray emission, observational and physical review 79−80373
gamma-ray emission, observational results review 79−25763
gamma-ray emission, review of obs. *(Russian)* 78−41097
gamma-ray emissivity, large scale structure 79−71116
gamma-ray flux, 60 keV to 5 MeV range, from ensemble of point sources 79−53933
gamma-ray line at 1.2 MeV, search in galactic plane 78−93475
gamma-ray lines, balloon obs. with high resolution Ge(Li) spectrometer *(Japanese)* 79−80353
gamma-ray low-intensity anisotropic background *(Russian)* 77−33708
gamma-ray obs. with COS-B *(Danish)* 80−82544
gamma-ray observations, implications for galactic struct. studies 77−26083
gamma-ray observations *(German)* 77−60853
gamma-ray source distribution rel. to pulsars and SNRs 79−71152
gamma-ray sources, high-energy, obs. by COS-B satellite 77−91670
gamma-ray sources in anticentre region, final SAS-2 results 77−33688
gamma-ray spectra, rel. to cosmic ray electrons flux and cosmic ray gradients 78−40784
gamma-rays, galactic disc bremsstrahlung emissivity and local interstellar electron spectrum 79−25417
gamma-rays, prod. by non-thermal electron bremsstrahlung in galactic disc 78−24414
gamma-rays, ultrahigh energy, detect. by obs. of Cherenkov flashes of EAS 79−80368
gamma-rays from disk and inverse Compton effect of electrons on starlight 80−26702
gamma-rays from galactic disc, pulsar contrib. 77−67143
gamma-rays from galactic plane 79−71105
gas-to-dust ratio determ. from globular cluster obs. 79−88747
giant stars, late-type, semi-theoretical density profiles along galactic radius through Sun 79−35253
globular cluster age differences rel. to chemical evolution 79−80340
globular cluster distribs. 79−12513
globular cluster evolution and origin of galactic halo stars 79−58388
globular cluster populations uniformity 77−53654
globular cluster subsystem space distrib. and population 77−53689
globular cluster system, state of inferred fundamental knowledge about Galaxy 80−90488
globular cluster system flattening, interstellar extinction effects 79−48908
globular clusters, basic morphological data 79−92815
globular clusters, basic parameters 77−91593
globular clusters, expected number density near galactic centre 78−32535
globular clusters, integrated colours obs. 78−16469
globular clusters, kinematic and dynamical differences between two groups 78−8069
globular clusters, number *(Russian)* 79−17036
globular clusters, orbital eccentricities 77−71132
globular clusters, orbital evolution due to dynamical friction 78−24529
globular clusters, space distrib. 79−25o0
globular clusters colour excess ratio, rel. to interstellar absorpt. law 78−28797
globular clusters in Galaxy, tidal disruption 80−105294
globular clusters near galactic centre, IR studies 80−82434
globular clusters number correl. with spheroidal central bulge luminosity 77−91594
globular clusters radial motions rel. to galactic halo model 79−67068
globular clusters space distrib. 77−87481
globular star clusters, metal abundance and reddening from photometry obs. 80−67800
Gould's belt, anomalous extinction, grain growth 79−44603
Gould's Belt, structure 79−35368
Gould Belt, kinematics of Lesh's OB stars 79−67089
gravitating discs, models, phase description *(Russian)* 78−69887
gravitating spiral system, dispersion relation 77−87538
gravitational encounters with Local Group galaxies, numerical expts. 77−57098
gravitational instability in collisionless stellar disc, quasilinear saturation *(Russian)* 79−16824
gravitational potentials of spheroidal stellar systems, appl. to the Galaxy 77−53645
Great Debate of galactic astronomy, actual proceedings 77−29979
GX 1+4, galactic centre X-ray source, X-ray obs. periodicity 80−105399
H I subsystem, rot. curve *(Russian)* 80−36724
habitable planets number, conservative estimate 79−40221
halo, blue horizontal branch stars search on Schmidt plates 78−4362
halo, density gradients in SA 82 and SA 107 fields *(German)* 77−60825
halo, extent from props. of stellar images at faint magnitudes 80−82360
halo, metal-poor star distrib. *(German)* 80−94867
halo, new size constraints from galactic gamma-ray data 78−12353
halo, obs. of metal-rich distant globular cluster (Pal 12) 80−105290
halo, photometry and comp. of distant-globular cluster (NGC 5053) 77−74103
halo, radio obs. 78−96544
halo, regular magnetic field component *(Russian)* 80−67872
halo, rot. from subdwarf kinematics 80−22003
halo around Galaxy obs. and anal. 77−53687
halo formation and globular cluster compositions 79−5898
halo heavy element abundances, radial gradient 79−92857
halo low-frequency radio emission, diffusion models 78−12433
halo mass from high-velocity stars luminosity function 78−4368
halo population stars, luminosity functions in SA 51, SA 57 and (SA 68) 80−98648
halo stars and old disc population, orbits and kinematics, active phases in Galaxy evolutions 79−35394
halo to disc mass ratio, determ. from three-colour photometric obs. 77−45548
HD 27507 and escape vel. from Galaxy 78−85935
HD 84903 and 184711, differential anal. of extreme metal deficient stars rel. to halo star HD 122563 79−80302
The Galaxy continued
high latitude nebulosity, as source of enigmatic dark lines crossing (M81) 80−56947
high luminosity stars in Galaxy and Magellanic Clouds, UBV intrinsic colours 80−26855
high-latitude regions, balloon-borne UV survey 80−41891
hot gaseous corona, far UV spectral evidence 79−67097
hot halo as spherical plasma 79−58429
hot white dwarfs, EUV flux interstellar absorpt., local clumpiness factor determ. 80−36627
Houck atlas of Milky Way 77−37510
Hubble const. estimate from Galaxy rotation curves 77−33640
hydrostatic equilibrium for three unequal stellar vel. dispersions 77−57094
hypergalaxy, mass from Magellanic Stream kinematics 77−5573
inner Galaxy, stellar distrib. *(Japanese)* 79−80352
integrated starlight, synthetic spectrum between 3000 and 10000 Å, discussion 80−62200
interstellar $^{12}C/^{13}C$ ratio, rel. to ^{13}C enriched matter ejection from red giants 77−9788
interstellar absorption lines of Na I, K I, Ca II, in stellar spectra rel. to galactic gas distrib. 80−26963
interstellar absorption lines towards 30 Doradus central object (HD 38268), profiles 80−51839
interstellar absorption revealed by Rubin et al. Sc-type galaxies sample, anal. 78−49533
interstellar Ca II K-line profile in 30 Doradus direction, obs. 80−51850
interstellar CO, distrib. around (l=30°, b=0°) 80−41868
interstellar cosmic ray acceleration models, inconsistencies 80−82155
interstellar dense clouds encounters with stars 77−87497
interstellar dense molecular clouds, distrib., phys. conditions, origin *(Polish)* 79−101187
interstellar density fluctuations effect on pulsar scintillations 80−46649
interstellar diffuse EUV radiation field obs. 79−30099
interstellar dust, composition, origins *(French)* 79−30116
interstellar dust clouds above galactic plane, light scatt. detect. possibility 79−30124
interstellar dust clouds in AFCRL Survey, number and IR luminosity 77−87283
interstellar dust distrib. within 3 kpc in galactic plane 80−109512
interstellar electron density determ. from H I absorption in spectra of pulsars 79−92792
interstellar extinction, average model, from planetary nebulae obs. 80−62221
interstellar extinction and stellar space density in Ophiuchus region 77−64839
interstellar extinction law, vars. 78−85990
interstellar extinction laws from 13-colour photometry 78−81676
interstellar formaldehyde, obs. along galactic plane 79−48893
interstellar formyl ion ($HC^{18}O^+$), detect. in Sagittarius B2 79−35346
interstellar gas, dust and molecules, review 78−54006
interstellar gas, local, in southern sky, single 21 cm component study 79−84834
interstellar gas hydrostatic equilib. in solar neighbourhood 79−30098
interstellar gas hydrostatic equilibrium, rel. to cosmic ray confinement and Galaxy radio emission 77−29919
interstellar gaseous medium, small oscills. freqs. in cylindrically symmetrical gravit. field *(Russian)* 80−41883
interstellar giant molecular clouds, ^{13}CO emission distrib. in galactic plane 79−101183
interstellar giant molecular clouds, collisional growth 79−48877
interstellar HCN isotopic abundances in disc and centre region 77−53657
interstellar high-velocity clouds, fine struct., H I 21 cm obs. 79−30113
interstellar hot gas in Galaxy outer halo, evidence from IUE UV obs. of (3C 273) detailed UV obs. with IUE 80−94886
interstellar hot tunnels, simulation of interacting supernova remnants 77−17645
interstellar local electron spectrum determ. from galactic radio background 78−93056
interstellar local He I density from EUV obs. 78−4331
interstellar low-velocity molecular cloud obs. near Sagittarius A 79−53898
interstellar matter, far IR emission between l=36° and l=55° galactic longitudes 78−54014
interstellar medium, intragalactic factor in external objects apparent distrib. 78−96552
interstellar medium, radio emission at l=31.2° and (31.9°) 77−17724
interstellar molecules, galactochemistry and origin of life 78−12338
interstellar molecules, review 77−78856
interstellar NH_3, obs. in DR 21, NGC 1333 and NGC 6334 N 79−17044
interstellar NH_3 absorpt. in Sagittarius B2 direction 79−35341
interstellar OH clouds in direction of extragalactic radiosources, survey 77−64822
interstellar radiating dust clouds, review 77−78863
interstellar radioactivity, nuclear gamma-ray transition detection 77−2501
interstellar reddening and intercloud density in solar vicinity 79−88720
interstellar reddening in high-latit. field around ω Bootis 79−101185
interstellar reddening in solar neighbourhood, anal. 80−62239
interstellar reddening law derived using kinematically determined distances 77−45521
interstellar reddening material, distrib. in solar neighbourhood from stellar colour excesses 78−49502
interstellar southern molecular clouds, $^{12}C/^{13}C$ abundance ratio derived from H_2CO obs. 79−84838
interstellar UV extinction obs. in galactic plane from TD1 satellite 78−93382
interstellar UV radiation, role in interstellar gas heating 80−67839
interstellar UV radiation field, obs. from S2/68 sky-survey telescope 80−77523
intertial-coordinate frame rel. to celestial reference, for starship navigation 78−49346
ionized gas motion and distrib. in central parsec 79−25719
IR diffuse radiation obs. at 2.4 μ 77−33656
IR emission from galactic centre, maps at 10, 34, and 56 microns 78−41037
IR obs. at 2.4 μ wavelength by balloon *(Japanese)* 78−61924
IR obs. of centre region *(German)* 79−5906
IR photometric obs. using balloon-borne telescope 78−36453

The Galaxy continued
IR radiation, balloon obs. *(Japanese)* 79−80350
IR sources distrib. 77−64842
IR surface brightness, balloon obs. *(Japanese)* 77−82308
IR surface brightness obs. in anticentre direction 79−48935
isotopic species, stable, galactic distrib. from interstellar mol. obs. 80−109550
K-effect, linearised local vel. field in presence of density waves 77−33576
kinematics and local compression of O- and B-stars 79−8954
kinematics of old stars, rel. to Galaxy initial contraction 80−62204
late-type dwarf stars, orbital dynamics and photometric metal abundance index 77−60754
LF background radiation, spectra and absorpt. 77−33707
Lick proper motions referred to galaxies, precession and galactic rot. determ. 78−65487
light element abundances, galactic evolution and universal baryon density 79−40302
light extinction, A_B coeff. amplitude 80−17664
light metal synthesis, evidence from Al abundance in cool halo stars 80−105232
Lin's density-wave theory, observational possibilities *(German)* 78−73756
Lindblad's expanding H I ring, rel. to supernova hypothesis for extinctions at end of Cretaceous 78−32500
Local Group and the Galaxy, conf., Royal Greenwich Obs. (July 1975) 77−91631
local H I cloud, latit.-dependent line-shift field 77−74128
local mass density, mass defect rel. to undiscovered M-dwarfs 77−91632
local mass density from AF stars near N.Galactic Pole 79−40267
local missing, mass problem, undetected M3-M8 dwarfs 77−67123
local spiral arm, fine struct. 77−57091
local spiral arm, stellar velocity dispersion inhomogeneities 80−98653
local spiral structure model 77−22315
local structure, weak low-latitude X-ray source studies 79−84858
local structure-kinematic relation, appl. to OB-stars and variables *(Russian)* 78−77608
long period variable stars spatial distrib. *(Russian)* 77−45470
Loop III, linear polarization of 920 MHz galactic background 79−97087
luminous stars, props. of supergiants and O-type stars in Milky Way 79−40183
RR Lyrae star distrib. according to metal abundance, galactic evolution active phases *(Russian)* 77−74144
RR Lyrae stars, in Baade's window region, metal abundances 77−9749
RR Lyrae stars in Palomar-Groningen fields, rel. to Galaxy struct. and kinematics 78−93276
RR Lyrae variables in N.Galactic pole fields, metal abundances 79−88660
M33 direction, H I 21 cm emission/absorpt. obs. 80−62262
M39 region, low latit. galactic window and external galaxies pair discovery 78−96536
M dwarf distrib. at low z distances 78−12232
M-stars at $l^{II}=138°$, space density from objective prism spectral studies 77−9748
M-type dwarf stars near north galactic pole, scanner obs. rel. to ages 77−78789
M-type stars, in north galactic polar region, space motions 78−93235
Magellanic Clouds in binary state, galactic disc bending and Magellanic Stream 77−91620
Magellanic Plane 77−91649
Magellanic Stream, models and tidal origin 77−91647
Magellanic Stream, origin and dynamics 79−44594
Magellanic Stream, tidal origin 77−64834
Magellanic Stream, turbuelnt wake of Magellanic Clouds in galactic halo 78−69884
Magellanic Stream, vel. structure from H I obs. 79−97078
Magellanic Stream and adjacent HVCs, Jodreel Bank 21-cm obs. 77−91650
Magellanic Stream and gas concs. in Local Group 77−91646
Magellanic Stream from LMC close approaches 77−91648
magnetic features, large-scale 79−58418
magnetic field, review of obs. 80−73042
magnetic field components from pulsar rot. meas. 80−85966
magnetic field configurations, rel. to synchrotron radiation 78−20884
magnetic field dynamo, numerical models 79−40262
magnetic field fluctuations, correl. length and fluctuating angle from starlight polarisation theory 80−82442
magnetic field from Faraday rotation of extragalactic radiosources 79−58430
magnetic field from radioastronomy obs. 78−24548
magnetic field from radiopolarisation obs. 78−24547
magnetic field interaction with hot intergalactic gas, magnetosphere existence 80−67876
magnetic field scale and strength from pulsar data 78−28752
magnetic field structure and stellar polarisation 78−69869
magnetic field turbulent structure, determ. from extragalactic sources Faraday rot. 78−20885
magnetogasdynamic mechanism of rotation *(Russian)* 77−87536
mass, estimate from simulation of Magellanic Stream 77−91622
mass infall, rel. to cosmic ray accel. 77−78583
massive stars, evolution 79−101191
matter distrib., relation with cosmic ray dynamics and γ-ray production 78−4349
metal abundance vars. from young cluster photometry 80−101621
metallicity distribution in old stars and effect of dust accretion 77−29795
metallicity gradient across galactic disk 79−48905
MHD waves, propag. from galactic centre rel. to origin of 3 kpc arm and North Polar Spur 77−87547
Milky Way atlas using super-wide-angle photographs 77−74145
N. Milky Way fields, early-type stars photometry rel. to galactic struct. 77−2424
Milky Way northern region surface brightness, R photometry *(Russian)* 78−93388
Milky Way stars, five-channel photometric obs. 78−16398
Mira variables, discovery of 123 new stars in Palomar 10 globular cluster region 78−40837
Mira variables, statistical anal. of galactic concentration *(German)* 80−4390
Mira variables around globular clusters, freq. distrib., cluster membership 80−36676

The Galaxy continued
Mira variables kinematics towards galactic centre 80−46578
missing mass rel. to brown and black dwarfs 79−48800
molecular cloud complexes, origin, lifetimes and mass 80−82453
Monoceros region, interstellar extinction determ. 77−9777
N Monoceros region, late-type giants space density from two-micron objects survey 80−8555
morphology of H and trace gases, review 77−26070
motion of Galaxy and Andromeda nebula (M31); derivation from solar motion 77−91518
motion rel. to Sc I galaxy vel. anisotropy 77−91643
nearest stars, vel. components rel. to galactic plane 79−97088
neutron star binaries formation rel. to gravit. radiation 79−35291
neutron stars, form. rate estimated from stellar statistics 79−40208
neutron stars formation rate, upper limit 78−49471
NGC 1904 (M79), UBV photometry, colour-magnitude diagram of halo globular clusters 78−32528
NGC 2243, old open cluster, in halo, UBV photometry 77−78835
NGC 6200, loose young open cluster in Sagittarius arm extension 77−87493
non-stellar objects, data centre proposal 77−78905
non-thermal radio radiation from galactic polar regions, spectra 80−22082
nonejecting novae as EUV sources 78−12238
nonthermal emission in 0.25-9.18 MHz range, RAE 2 lunar satellite obs. 78−45398
Norma spiral arm structure, influence of projected dark cloud 78−16494
north galactic pole, A and F star radial vels. and MK classifications 77−22223
north galactic pole, A and F star uvbyβ photometry 77−22224
North Polar Spur, as remnant of supernova or galactic nucleus explosion *(Russian)* 78−41072
North Polar Spur, interplanetary scintillation and scintars 79−44579
North Polar Spur, radio continuum obs. at 1420 MHz 80−22100
North Polar Spur, X-ray features, supernova remnant 77−45554
north polar spur brightness distribution, interpretation *(German)* 78−12372
North Pole, NGC 4147 direction, halo density distrib. RGU photometry 77−37599
northern early-type stars at intermediate galactic latits., UBV photometry and MK spectral classification 77−82221
northern galactic plane, galaxies on POSS E prints obs. through transparent regions 80−62280
Northern stars, True Visual Magnitude Photographic Star Atlas 80−109376
novae, space density, recurrence rate and classification 78−53964
novae identified as Population II stars 79−30074
nuclear bulge, red giant star spectroscopy 77−26058
nuclear bulge, space distrib. of red giant stars, ellipsoidal density model 78−86009
nuclear bulge, spectral scans 79−21415
nuclear bulge, stellar UBV photometry 78−53926
nuclear radio emission, comparison with external galaxies active and normal nuclei 78−57646
nucleosynthesis history, chemical comp. of old halo stars 78−65616
nucleus, compact radiosource struct. 78−57669
nucleus, evidence for explosive activity 77−91634
nucleus, H I contour maps 79−35386
nucleus, limit on central black hole mass 79−25713
nucleus, radio source obs. 77−5572
nucleus, recurrent outbursts 79−21423
nucleus region, 6 cm recomb. line emission vels. 78−69885
O-stars, association with nebulosity in spiral arms 80−105236
OB stars, distrib. in Galaxy, comp. rel. to age and space motions *(Russian)* 78−93216
OB stars Local complex, kinematics 78−16396
OB-type southern stars, UBV, Hβ and polarisation meas. 77−26007
OB-type stars in vicinity of long period Cepheid VZ Puppis, UBV β photometry 78−45339
OH near galactic plane, 18 cm lines survey 79−75265
one-dimensional spiral shocks, stability 77−64849
open, places of form 78−8064
open cluster containing Wolf-Rayet and Of-stars 77−64810
open cluster distrib. in disk 80−101620
open cluster distrib. in Galactic plane *(Russian)* 78−32541
open clusters, formation positions rel. to galactic spiral arms 77−2457
open clusters with circular orbits, galactic rot. calc. 78−8068
open star clusters, space distrib. and age *(Russian)* 79−48871
Palomar 5, remote globular cluster in galactic halo, chem. comp. 77−87482
Parker instability with curved magnetic field lines 79−5889
particle dynamics in spheroidal mass distribs., third integral of motion 77−74101
peculiar motion, rel. to Hubble const. local value determ. from Sb galaxies luminosity classification 80−62339
periodic orbits near particle resonance, numerical appls. 78−49484
Perseus Arm, H II regions around l=111°, aperture synthesis obs. 77−64827
Perseus Arm H II regions, high-resolution radio maps 78−32549
Perseus arm member NGC 957, young open cluster, RGU photometry 80−85976
Perseus spiral arm, 21 cm obs. of assoc. nonplanar H I 78−16489
photographic four-colour sky atlas 78−24472
photometric disc model, direct starlight intensities and interstellar dust clumping effects 80−22077
photometric parameters, scale lengths and absolute magnitudes, two-component model 79−8995
planetary nebula and diffuse objects, detect. in galactic centre direction *(French)* 79−21434
planetary nebulae, birthrate in solar neighbourhood 77−13423
planetary nebulae, central stars masses rel. to galactic disc or halo membership 80−82344
planetary nebulae, chemical abundances rel. to galactic radial abundance gradient 78−36663
planetary nebulae, distances and galactic distrib. 80−67819
planetary nebulae, kinematics 80−26948
planetary nebulae, new synthetic distance scale 78−89240
planetary nebulae, Population II, origin rel. to CNO abundances and central stars masses 78−85992
planetary nebulae, spatial and vel. distrib. statistics 80−109518
planetary nebulae galactic centre distribution radio obs. 77−17667

The Galaxy continued
planetary nebulae kinematics, radial vel. meas. 80−46633
planetary nebulae near galactic centre, VLA and optical search 80−90506
planetary nebulae of galactic halo, photoionisation models and chemical abundances of K 648, 49+88.1° and (108−76.1°) 80−109507
planetary nebulae of overall field and galactic centre, physical charact. differences 78−54029
planetary nebulae spatial distrib. and luminosity function, evidence from obs. in (M31) 80−109520
point source at galactic centre, 1.4-2.7 μ spectrum 77−5569
polar regions, nonthermal radio spectrum rel. to cosmic ray electrons spectrum and γ-rays prod. 80−62257
Population I O-type runaway stars, nature and galactic distrib. 80−85938
Population I objects, location with respect to galactic plane 77−74127
Population I stars, chem. and physical props. 77−78782
Population I stars, kinematical trend of vel. residuals 79−48863
positron annihilation radiation at 511 keV from galactic centre 79−5902
positron production by pulsars, galactic 511 keV gamma-ray line from positron annihilation 80−46590
positrons, primary source, prod. rate, and escape probability 80−109319
pregalactic black holes in Galaxy, accretion of interstellar matter 78−8039
pregalactic halo objects, gravitational lens effect 80−17484
primary cosmic rays propag., evidence from antiprotons relative abundance 78−73594
primordial black holes, search for high energy gamma ray bursts 78−54084
primordial heavy lepton halo, annihilation contrib. to cosmic gamma-ray background 78−93479
pulsars, galactic distrib. 79−75231
pulsars, luminosity function and spatial density *(Russian)* 78−93290
pulsars, spatial distrib. and birth-rate 79−25624
pulsars birthrate and z-distribution from 2nd Molonglo Survey 79−8940
pulsars galactic distribution and evolution 78−4260
Puppis area, spiral arm struct. in third quadrant 80−85937
Puppis region (l=250°, b=0°), new UBV photoelectric sequences 77−45426
r-nuclei production sites 80−72932
radial vel. dispersion rel. to galactic longitude and distance 79−101142
radio and soft X-ray emissivity, anticorrelation, plasma cloud interpretation 80−82514
radio background, emission from energetic secondary electrons in interstellar clouds 77−33593
radio background, vars. in freq. spectrum along declination (+50° 30′) 77−17723
radio continuum emission, interpretation using new model of spiral struct. 77−13465
radio diffuse background, distrib. and model 77−5602
radio emission, 151.5 to 408 MHz, spectral index ang. and freq. var. 79−21446
radio emission, linearly polarised, bright spot obs. at 1 m wavelength 77−17709
radio emission spectrum, influence of primordial black holes 80−62179
radio emissivity, three-dimens. model 78−77604
radio halo shape and size 79−12521
radio loops and SNRs *(Hungarian)* 79−40263
radio sources, H110α line and formaldehyde absorpt. line obs., SHF obs. 80−77472
radio sources near l=333°, 8.87 GHz obs. 80−22102
radioastronomical obs. of galactic struct. *(Spanish)* 79−40275
radioemission, linear polarisation between 408 and 1411 MHz, reductions 77−2500
radiosource survey of galactic plane at 4.875 GHz, list of 1186 sources 79−21431
red dwarf stars in M15 field, photometry rel. to disk density gradient 77−78834
red dwarf stars near north galactic pole, vel. dispersion 78−7989
red dwarfs, systematic errors in evidence for high space density 77−5524
red stars at north galactic pole, proper motions 78−4214
reflection nebulosities, high latitude, as false companions of galaxy (NGC 772) *(Russian)* 80−36723
Reticulum globular cluster, structure, star counts 78−12309
RF synchrotron radiation, in inhomogeneous mag. field 77−67127
ring like structures, H II regions and OB associations distrib. *(Russian)* 78−93424
rotating stratified ellipsoids of revolution, effects on inertial frame dragging 79−2573
rotation, determ. from proper motions of AGK3 stars 77−45402
rotation, N-S asymmetry and fluctuations 79−17085
rotation and space velocity, determ. from solar motion rel. to Local Group centroid 78−12376
rotation and structure beyond solar circle, photometry and spectra of young stars towards galactic anticentre 80−22079
rotation constants and solar motion, from stellar proper motions 78−32440
rotation corrections to general catalogue for southern stars, proper motions in α *(Russian)* 79−92685
rotation curve, accounting for intersteller gas expansion *(Russian)* 79−48938
rotation curve, to R=16 kiloparsecs 79−97081
rotation curve from H I maps, mass distrib. 78−96529
rotation parameters from H I 21 cm data 79−97079
rotation parameters from O-type star radial vels. 79−12523
Rubin-152, possible massive O-type star on galactic fringe, spectroscopic obs. 80−98656
S106 and S235, aperture synthesis of H II regions, star form. regions 78−36672
s-process abundance evolution in galactic disc 77−13449
S-type stars, galactic distrib. and population-type charact. 79−88651
SA 133 field near galactic centre, three-colour stellar photometry *(German)* 80−36618
Sagittarius A, 540 μ obs. of galactic centre 78−36699
Sagittarius A, aperture synthesis obs. of H I absorpt. 77−26037
Sagittarius A, multifrequency radio image *(Russian)* 77−2478
Sagittarius A, radio emission scattering from compact object 78−54049
Sagittarius A region, 8.2 mm obs. 78−28794
Sagittarius A West, temp. and dynamics of ionized gas in nucleus 79−44595
Sagittarius A-west, IR obs. of Ne II forbidden line emission 78−36680
The Galaxy continued
Sagittarius B2, galactic centre H II region, He recombination line obs. interpretation 80−62300
Sagittarius B2, He abundance problem 78−49496
Sagittarius B2, weak maser action in cyanodiacetylene 77−5555
satellite galaxies and globular clusters, radial vels. and galactic mass 78−49522
Scorpius region, UBV surface brightness photometry of Milky Way from Helios 1 78−57634
Scutum Cloud direction, star field RGU photometry 79−35242
Selected Areas 82 and 107, electrographic extension of UBV magnitude sequences 79−44610
Sharpless H II regions, radial vels. and distances from radio obs. 77−87509
soft X-ray background, spatial struct., OSO-8 obs. 78−16580
soft X-ray background, three-band obs. rel. to thermal emission models 77−45604
soft X-ray diffuse background flux, southern galactic hemisphere 78−8170
solar absolute motion, rel. to discrete redshift 78−49530
solar motion relative to neighbouring galaxies *(Russian)* 78−24553
solar motion with respect to external galaxies 77−91619
solar neighbourhood, absolute magnitudes of F-, G-, and K-type stars 78−81632
solar neighbourhood, absolute magnitudes of M-type stars 78−81631
solar neighbourhood, initial mass function and stellar birthrate 80−62259
solar neighbourhood, integrated UBVRIJKL colours 79−44460
solar neighbourhood, star density curves and mass density 77−74134
solar neighbourhood electron density determ. from pulsar distance estimates by trigonometric parallax 79−88694
solar neighbourhood initial mass function determ. from upper H-R diagram study 80−36626
solar system encounter with nearby supernova, rel. to Earth ice ages and viological catastrophes 77−29662
South Galactic Cap stars, search for common-proper-motion pairs 78−73734
South Galactic Pole, K-type giant stars population CN anomalies and distances 80−8622
southern dark dust clouds, distrib. rel. to Gould's Belt 77−56844
southern galactic hemisphere, ultrasoft X-rays obs. 77−45615
southern galactic plane, near IR surface brightness 79−71128
southern H II regions, mapping at 1415 MHz 79−53899
southern high-velocity stars, kinematical and orbital props. 79−25600
southern Milky Way, loose stellar clusterings continued photometric studies 80−36679
Southern Milky Way, S-type stars catalogue 78−61754
southern sky, obs. in 2-20 MHz range 77−45563
Southern stars, True Visual Magnitude Photographic Star Atlas 79−75122
space motion, determ. from vel. anisotropy of distance Sc I galaxies, data 77−5560
space motion, determ. from vel. anisotropy of distance Sc I galaxies, anal. 77−9796
spectrophotometric survey of stars along Milky Way in Perseus 78−45403
spiral arm displacement from galactic plane 79−75275
spiral arms and terrestrial catastrophism, theoretical mechanism 80−31043
spiral density wave interaction with Sun and galactocentric radial motion 79−8998
spiral density waves, illustrated by periodic stellar orbits superposition 79−84828
spiral pattern speed, determ. from CO abundance distrib. 78−54036
spiral struct., peculiar solar motion and G giants kinematics influence on asymmetrical drift 77−13403
spiral struct. of inner parts from 21 cm line and stellar data 77−82304
spiral structure, accretion theory *(Russian)* 77−45568
spiral structure, cosmic rays and molecular clouds 77−87544
spiral structure, density wave theory, review *(German)* 79−17103
spiral structure, effect of sound wave propagation in hot gas 80−109511
spiral structure, gaseous theory of origin 80−82517
spiral structure, in vicinity of Sun *(Russian)* 80−62290
spiral structure, interstellar matter and star clusters, review 79−25723
spiral structure, mol. clouds as a tracer, 2.6 mm CO survey 80−105346
spiral structure, possible four-arm pattern 77−60821
spiral structure, tracing via young galactic clusters observed in three colours 79−40089
spiral structure *(Swedish)* 78−69876
spiral structure formation, role of Population II stars 77−13469
spiral structure from H I 21 cm obs., linear theory, nonreson. region 79−88738
spiral structure from obs. of H II regions and exciting stars 78−61900
spiral structure in Monoceros, photometry of luminous stars 77−9799
spiral structure parameters, derivation from stellar kinematics 80−17665
stability of galactic disk as rotating spheroidal stellar system 80−62203
star complexes in Galaxy, star form. regions *(Russian)* 78−69851
star density in solar neighbourhood 79−21447
star distribution perpendicular to galactic plane, fine struct. study *(Russian)* 80−73036
star formation, suppression rel. to delayed star form. problem 80−105349
star formation and interstellar gas density in Galaxy 78−86008
star formation and large-scale phenomena 78−32583
star formation by spiral density wave in disc of Galaxy 80−12812
star formation in inner regions, IR obs. 80−67704
star formation rate, rotational dynamics and interstellar gas density 80−51870
star formation rate and ionising Lyman continuum photon flux 80−67711
star formation rates calc. 78−61919
starlight, integrated, synthetic spectrum between 3000 and 10000 Å, calc. method and results 80−46536
starlight linear polarisation distrib., meas. catalogue and vector maps 77−13255
stars near South Galactic Pole, UBV photometry of 51 stars 78−4216
stars space densities derivation, new method 80−85932
stars unseen astrometric companions, mass density, rel. to local mass defect 77−91581
stellar age and metallicity distributions, effect of crossing times through solar neighbourhood 78−12362

The Galaxy continued
stellar associations, use as spiral arm tracers 78−57599
stellar birthrate constraints in solar neighbourhood based on kinematics and star counts 77−29930
stellar clusters NGC 2420 and 47 Tucanae comparison rel. to galactic evolution 77−45499
stellar collapse rate 77−71122
stellar collisions, by oscill. orbits of second kind 79−35312
stellar disc, central density min. 80−17663
stellar disc central hole, rel. to evolution 80−62268
stellar distrib. above galactic plane 78−12375
stellar dynamics, Hamilton-Jacobi eqn., velocity field gradient coeffs. *(Russian)* 79−88707
stellar dynamics, reson. orbits comparison 80−56889
stellar dynamics, work of Johann Georg Soldner (1776-1834) 78−81787
stellar kinematics and interstellar turbulence 79−35313
stellar kinematics and spiral structure *(Russian)* 79−21362
stellar nucleosynthesis, cosmochronology after Allende 80−4462
stellar populations, metals distrib. rel. to Galaxy chemical evolution 78−96545
stellar space density derivation methods, systematic comparison 78−61917
stellar spectral classification rel. to interstellar extinction and galactic struct. *(Russian)* 78−73701
stellar streaming motions and obs. determ. of structural consts. 78−96528
stellar velocity dispersion, age depend. in scale covariant gravit. 78−65661
structure, models and theories based on gamma astronomy *(French)* 77−60829
structure around $l=140°$, $b=0°$, from stellar photographic photometry 78−24555
structure from gamma ray obs., review 80−98743
structure from gamma-ray data 78−16538
structure from optical obs. *(German)* 79−17104
structure from star counts 80−82507
structure in S. Milky Way, stellar distrib. and colour excess obs. 80−85997
structure in solar neighbourhood, Aquila direction, RGU photometry 77−91621
substructure tidal and evaporative disruption 78−12366
Sun, distance from galactic centre determined from radial vels. of O and B stars 80−101584
supergiant stars, southern, late-type, chem. comp., solar neighbourhood metallicity distrib. 80−12758
supergiant stars intrinsic colours rel. to interstellar reddening material distrib. 79−8908
supergiants, comparison with Magellanic Clouds 80−67699
supernova explosions, heavy elements expulsion, accretion by Sun, rel. to terrestrial ice ages *(Polish)* 79−58310
supernova outbursts, frequency estimate 80−62168
supernova remnants, evolution of line intensity ratios in Galaxy and LMC 77−17656
supernova remnants, galactic distrib. rel. to radio evolution and population characts. 79−75254
supernova remnants, new catalogue corrected for distance from galactic plane 79−75120
supernova remnants, new optical obs. 80−17636
supernova remnants, radio brightness depend. on galactic height, implications 79−48894
supernova remnants interacting, rel. to galactic tunnel system 80−4409
supernova statistics 77−87460
supernovae, as main galactic energy source 77−87455
supernovae, historical and theoretical review *(Norwegian)* 79−80329
supernovae and SNR radial distrib., exponential law 77−45473
supernovae occurrence freq. and long-lived remnants prod. 77−64784
thin disc model of dynamo 78−73755
three-dimensional motion of dwarf stars and RR Lyrae variables rel. to primordial galaxy contraction 80−12754
tidal effects and mass distrib. in Hypergalaxy *(Russian)* 78−4367
tidal forces, rel. to truncation of dying globular cluster E3 (ESO-037-SC 01) 80−105291
transient X-ray sources in the galactic plane 78−93460
Trapezium type systems, statistical properties 79−44556
Trumpler 1, open cluster, UBV photometry 77−74105
turbulent interstellar medium rel. to planetary nebulae extinction 80−62220
turbulent magnetic field and cosmic ray diffusion 79−48627
UBV photoelectric standards in SA 1-115, final catalogue 80−41733
UV background radiation, TD-1 satellite obs. 77−13504
UV galactic light, rocket-borne photometry 79−35372
UV interstellar radiation field, galactic latit. depend. of 1530 Å radiation 77−33704
Vela, spatial distrib. of young stars, UBV obs. 77−37597
Vela region, search for faint OB stars, list of 166 objects 77−87280
Vela-Puppis, low-luminosity X-ray source obs. 78−93458
velocity dispersion of missing mass in solar neighbourhood, stability of N-component stellar disc 78−69886
velocity relative to cosmic background radiation, determ. from anisotropy meas. 78−4415
violent history and large-scale non-circular motion 78−81692
W49 direction, CH radio emission obs. rel. to galactic struct. 77−87511
white dwarfs, search at south galactic pole 79−21274
white dwarfs formation rate 78−28674
Wolf-Rayet, single-line Population I stars, distance from galactic plane 80−77415
Wolf-Rayet stars, galactic WN7/WN8 stars as massive O-stars in advanced evolution stage 79−92778
X-ray background, rel. to red dwarfs X-ray flares 77−9755
X-ray background radiation isotropy, 2-18 keV energy range 80−46709
X-ray burst sources, galactic distrib. rel. to accretion models 78−49566
X-ray burst sources, positions and relation to galactic bulge sources 78−12419
X-ray burst sources, review 78−41084
X-ray burst sources at galactic centre 77−13499
X-ray emission, contrib. to diffuse X-ray flux in 2 to 7 keV range 80−98745
X-ray emission from centre region 79−17102
X-ray source distrib. 78−93462
X-ray source distrib. 80−67905
X-ray sources, $320°<l^{II}<340°$, positions 78−28860
The Galaxy continued
X-ray sources, $-20°$ to $+6°$ galactic longit., positions 78−54094
X-ray sources, distrib. in Milky Way 78−28851
X-ray sources, large-scale distrib. 79−48954
X-ray sources, long-term variability 79−2579
X-ray sources, review 77−29962
X-ray sources, space distrib. and physical nature 80−62316
X-ray sources at galactic bulge, black hole and orbital disk model 80−17691
X-ray sources in galactic bulge, models, binary systems 78−81706
X-ray sources in nucleus, high-resolution 2-10 keV rocket obs. 78−65692
X-ray sources in the southern Milky Way, Ariel V obs. 77−2492
X-ray sources near galactic centre, positions meas. by Ariel-5 RMC expt. 78−4407
X-ray transient sources, galactic distrib. and physical nature 79−84867
zone stars, proper motions dispersion represented by vel. ellipsoids 79−8904
^{26}Al, in interstellar medium, source of γ-ray line emission 77−33692
Ar, galactic nucleosynthesis rel. to low Ar abundances in three halo planetary nebulae 80−82443
C and M-type giant stars distrib. 78−32460
C isotope ratio, in comets, stars, and interstellar matter 79−57656
CH stars in south galactic cap, radial vels., photometry 77−87396
CNO isotopes, origin and abundance ratios evolution 78−93201
CNO isotopes as probes of chem. evolution 77−91636
CNO isotopic abundances, interpretation of obs. 78−4356
CO and H comparative distrib. 78−16537
CO distribution in galactic equatorial plane, 115 GHz obs. 78−36689
CO in the inner Galaxy 78−8072
CO kinematics within 1° of galactic centre 77−33597
CO, radio emission rel. to cold mol. clouds in inner Milky Way 80−4425
D absorption line at 327 MHz, search towards galactic centre 78−77599
D abundance rel. to cosmology 78−69883
D distribution, radial gradient, from $DCN/H^{13}CN$ and $DCO^+/HC^{18}O^+$ ratios 79−40232
D/H ratio in galactic centre direction, 327 MHz obs. upper limit 80−26949
H I, column density as function of position in southern sky 80−4420
H I, emission-absorpt. obs. from Arecibo 78−57610
H I, high angular resolution emission spectra, self absorpt. and other characts. 79−35350
H I 21 cm absorption towards extragalactic radiosources, catalogues of 819 sources 78−57638
H I 21 cm emission-absorpt. survey, two component interstellar medium model 79−40256
H I 21 cm line, radial vel. contour maps 80−17626
H I 21 cm line obs. in $348°\leq l\leq 360°$, $-22°\leq b\leq -1°$ region 77−60824
H I 21 cm line survey, low latits. 20-42° galactic longit. 78−57637
H I 21 cm surveys and galactic structure 79−44611
H I absorpt. in seven low-latit. pulsars, meas. 80−101606
H I absorption, obs. of struct. on small ang. scales 80−22051
H I absorption at intermediate galactic latit., aperture synthesis obs. 79−12503
H I absorption in galactic centre direction 80−77465
H I absorption spectra in direction of extragalactic radiosources 78−24541
H I at high galactic latitudes, time variable 21 cm line profiles correction 80−51844
H I cloud struct. in interarm region 79−21445
H I clouds in solar vicinity, kinematics from Nancay 21 cm absorpt. survey 79−8971
H I cool clouds, kinematics and distrib. from 21 cm. obs. towards H II regions 79−44577
H I distrib. and diffuse gamma rays 80−41917
H I distrib. and kinematics in galactic centre, model 79−17079
H I distrib. outside solar circle 79−21421
H I distrib. small scale struct., obs. of 3C 10 and 3C 58 78−45383
H I emission and absorpt. towards extragalactic radio sources 80−94854
H I gas, pervasiveness of intercloud medium 80−51825
H I gas in centre region, vel. field, axisymmetric kinematic model 79−17101
H I high velocity clouds origin *(Russian)* 78−49492
H I in interarm region and gas layer parameters, 21 cm line obs. 79−9007
H I in region $348°\leq l\leq 12°$, $+3°\leq b\leq +17°$, 21 cm obs. 78−45377
H I longitude-velocity map 78−86023
H I regions, 21 cm spectra rel. to galactic shocks 78−54042
H I regions, N.galactic hemisphere 80−17643
H I regions, new feature discovery in Vulpecula-Delphinus *(Russian)* 80−46654
H I shells and supershells 79−53861
H I spectra analysis 79−44605
H I stream in galactic anticentre, 21 cm obs. 80−90524
H I survey, brightness temp. contour maps, 21 cm obs. 80−85986
H I survey, photographic presentation 80−62241
H I within 10° of galactic centre direction, broadband obs. 77−78853
H II large scale distrib., recomb. line surveys 78−16539
H II region, extended, low-density, rel. to star form. and diffuse IR emission 79−17047
H II regions, aperture synthesis obs., quick look survey 78−12329
H II regions, gas dynamics, galactic extended low density region components 80−36694
H II regions, H I and He I ratio recomb. line survey at 10.2 GHz 79−48874
H II regions, line intensity data compilation 79−88721
H II regions, origin from supernovae explosions 80−67877
H II regions in Perseus and local spiral arms, H166α line obs. 80−90512
H II regions near galactic centre, far IR obs. 78−41012
HCN emission detect. in Sagittarius A mol. cloud 78−73750
H_2O masers, 22 GHz galactic plane survey, 14 new sources 80−77464
H_2O vapour sources, maser phase duration galactic distrib. 79−35343
H56α radio recomb. line anomalous emission from galactic plane 79−80361
Hα background emission, high spatial and spectral resolution pictures 80−56897
Hα emission stars in Milky Way, catalogue of new discoveries 77−64665
He enrichment due to He shell flashes 77−45428

The Galaxy continued
high-velocity clouds, dynamic coronal gas flows 80−56928
^{7}Li enrichment, contrib. from nova explosions 78−57555
NH_3 emission obs. from galactic regions 78−28780
O enrichment of Galaxy, evidence from O/H ratios in planetary nebulae 80−105328
O/H abundance ratio determ. in Galaxy from H II regions radio obs. 80−36692
OH large-scale sky survey at 1612 MHz 78−32358
OH maser sources, search at 1612 MHz, large-scale survey 79−58395
OH/IR unidentified Type II stars, galactic distrib. and kinematics from 1612 MHz survey 78−49450

theorem proving
mechanical theorem-proving in elementary differential geometry *(Chinese)* 79−35535

theoretical mechanics *see mechanics*

thermal analysis
ablation of elastic solid, variational principle 78−90698
aerosol pollutant, in situ detection using thermal anal. 77−37364
air pollution monitoring, continuous in situ meas. of particulate S pollution 78−96296
aliphatic-aromatic block copolyamides, synthesis, struct. and dynamic viscoelasticity, DTA and X-ray anal. *(Japanese)* 78−31377
alite paste, mature, microstructure study by SEM, TG and X-ray diffr., corrosion 78−92381
alkali bromide-VBr_2 systems, cryst. struct., DTA investig. *(German)* 78−72766
alkali isoalkanoates, thermal behaviour, differential scanning calorimetry 78−34600
alkali metal alloy specimen preparation, for thermal analysis up to 1500°C 77−28948
alkali metal chloride melts and mixtures, thermogravimetric determ. of uranyl cation state 80−101050
alkali metal suboxides, thermal and struct. anal., elec. and optical props., photoelectron spectra 79−47587
alkali silicate glasses, secondary relax. transitions 80−88261
alkali silicate glasses, struct. and thermal props. 80−84075
alkaline earth ferricyanide hydrates, $M_3[Fe(CN)_6]_2.12H_2O$, Mossbauer spectra 79−99805
alkaline-earth-Os ternary oxide system, solid state prep. and reactions, cryst. struct., mag. and elec. props. 79−24739
alkanoate, Li, Na, K and Rb salt mixtures, DSC anal. 78−10192
n-alkoxy-α-methyl-p′-cyanophenyl cinnamate, orientational order, tricrit. behaviour 79−27907
p-alkoxy-phenyl-p-acryloyloxy benzoate polymers, mesomorphic struct. 80−38905
4″-n-alkoxyphenyl biphenyl-4-carboxylates, liq. cryst. props. 79−82150
alkylammonium zinc tetrachloride cpds., high temp. phase transitions 80−54372
N-4-n-alkyloxybenzylidene-4-n-alkylanilines, smectic polymorphism, calorimetric study 80−88307
2-4-n-alkylphenyl-5-(4-n-alkyloxyphenyl)-pyrimidines, smectic polymorphism, calorimetric study 80−88307
aluminas, surface modified, DTA and TGA exam., gas chromatographic eval. 77−36785
amorphous alloys, thermal stability, crystn., DSC and elec. resist. study 80−107060
anthracene-tetracyanobenzene, charge transfer complex, phase transitions, deuteration effect, mag. reson., spectral and thermal meas. 79−4412
application in electrical and electronics industries 79−75531
applications, review 80−26083
aqueous soln. reaction kinetics meas. microwave apparatus 80−3470
aragonite, polymorphic transition kinetics, differential thermal anal. meas. 79−14722
aromatic hydrocarbons, melting behavior and role of free radicals and molecular site in producing mesophase pitch 79−90523
Arrhenius equation, pre-exponential factor temp. depend., thermogravimetric data calcs. 78−15654
azobenzenes, p-acryloyl- and p-methacryloyl-oxy-p′-substituted, monomers and polymers, liq. cryst. props. 79−99065
azoxybenzenes, p-acryloyl- and p-methacryloyl-oxy-p′-substituted, monomers and polymers, liq. cryst. props. 79−99065
barium titanyl oxalate exam. of chemical production and thermal dissocation *(German)* 79−4935
basalt, naturally occurring, high-temperature quantitative DTA analysis 80−77144
BBB polybisbenzimidazobenzophenanthroline-dione, films, dynamic mechanical investig. at high temps. 77−4800
BBOA, polymorphism, radiothermoluminescence and differential scanning calorimetric study 80−24570
binary alloys, initial transient segregation during unidirectional solidification in a furnace with thermal damping 80−70146
4-biphenylyl 4″-n-alkoxybenzoates, smectic liq. crysts., transition temps., DTA 78−75815
bis-(4,4′-n-alkoxybenzylidene)-1,4-phenylenediamines, smectic polymorphism up to 3 kbars, differential thermal anal. 79−55873
bis-(4′-n-heptyloxybenzylidene)-1,4-phenylenediamines, smectic phases, previously unclassified 79−77508
bitumen salt mixtures for rad. waste containment, thermogravimetric anal. *(German)* 79−89391
bitumen-salt mixtures, radioactive, thermal stress. behaviour *(German, English)* 77−65290
brass leaded, effect of Al, Sn, Fe on solidification, differential thermal analysis exam. *(Russian)* 79−29041
bromoform, solid, phase transform., dielec. dispersion and differential scanning calorimetric obs. 80−24582
bronze P, heavily cold rolled, yield strength enhancement mech. 77−36539
butadiene-nitrile elastomers, high temp., and press. chem. transformations *(Russian)* 79−52659
N-tert-butylacrylamide-styrene copolymers, struct., composition, IR, DTA investigs. *(Polish)* 79−31751
calorimeter for differential thermal analysis, in temp. range 100-800°C, exam. of design 79−52514
carbon tetrachloride, emulsion dispersed, metastable phases at high press. *(French)* 77−56253
carbon tetrachloride, volume effect in metastability of crystalline phases on cooling 79−77716
carbon tetrafluoride+SiC(Si), reaction, metastable C phase prod. 79−29393

thermal analysis continued
cement, hot pressed, type III, role of admixtures on pastes and H_2O cured cement, exam. 78−44073
cement, hot-pressed paste, strength, X-ray diffr., DTA, Ir spectra, microstruct. exam. 77−8864
ceramic technology, DTA appl. 80−20913
p-chlorobenzylidene-p-n-pentylaniline, metastable phases formed by rapid cooling of mesophase, IR and Raman spectra and DSC obs. 80−34919
chloroform, volume effect in metastability of crystalline phases on cooling 79−77716
cholesteryl azo dyes, liq. cryst., prep. and struct. props. 78−51412
cholesteryl caprynate, liq. cryst., DTA *(Russian)* 79−77496
cholesteryl laurate, liq. cryst., DTA *(Russian)* 79−77496
cholesteryl myristate, smectic A-cholesteric transition, tricritical behaviour, DTA and DSC study 80−65206
cholesteryl propionate, liq. cryst., DTA *(Russian)* 79−77496
choline bromide, radiation sensitivity, cryst. struct. depend., calorimetric investig. 78−88647
choline chloride, radiation sensitivity, cryst. struct. depend., calorimetric investig. 78−88647
choline iodide, radiation sensitivity, cryst. struct. depend., calorimetric investig. 78−88647
Cl $(Co_{100-x}Fe_x)_{83}B_{17}$, $1 \leq x \leq 30$, annealing embrittlement and crystn. 80−45329
Cl ThO_2 glasses, thermal anal. *(French)* 78−14282
clay, thermobalance method of determ. and anal., modification 77−29073
coal gasification, in situ, diagnostic and remote monitoring instrumentation development 79−48055
coal tar and petroleum pitches, pyrolysis, press. effects on coke yield and microstruct. form. 77−70289
coaxial DTA cell for study of liquid crystalline transitions at elevated pressures 77−22564
combined photovoltaic/thermal flat plate collectors, extended Hottel-Whillier model 80−3520
complementary data, thermodynamic and kinetic parameters determ. 79−16080
composition obs. by thermogravimetry 79−16081
condensed systems, phase equilibria, 400-1100°C, DTA method 80−218
copoly(ethylene terephthalate/5-methoxyisophthalate), isothermal crystallisation, differential scanning calorimetry 78−30546
copoly(ethylene terephthalate/isophthalate), isothermal crystallisation, differential scanning calorimetry 78−30546
copolyazomethine, nematic mesophase, DSC study *(French)* 78−71672
copolyester, melting temperature changes due to heat treatment *(Japanese)* 79−70096
copper phthalocyanine α-β phase transform., heat of transform., DTA investig. *(German)* 78−30754
cryolite, hydrothermal synthesis of large synthetic single crystal, props. 78−19654
cyanomethylation process, investigation using bench scale calorimeter 79−97391
cyclohexane, differential thermal anal. under high press. 78−51669
cyclohexane, volume effect in metastability of crystalline phases on cooling 79−77716
trans-1,4-cyclohexane-di-4′-n-alkoxybenzenes, synthesis and mesomorphic props. 79−94887
cyclohexanone, solid, phase behaviour, at press. up to 3 kbar, DTA 78−43108
cyclopentanol, and cyclopentanone, solid, phase behaviour, at press. up to 3 kbar, DTA 78−43108
DL-cysteine, phase transition obs. at 10°C *(French)* 80−49355
data transfer to single recording instrument using multichannel commutator 79−52821
dekryptonation thermal anal. using flow type GM detector 77−66786
dekryptonisation thermal analysis, apparatus *(German)* 77−90699
dextran fractions, production, characterisation and solution properties 80−59368
DIA analogue processing system *(Russian)* 77−12849
dialkylammonium cupric chloride, calorimetric study of phase transitions 78−75804
1,2-dichlorobenzene, volume effect in metastability of crystalline phases on cooling 79−77716
dickite, unusual crystal habit, structural disorder 80−59445
dickite occurrence in Jamaica, DTA patterns rel. to ordered and disordered varieties 78−83786
diemthyl sulphoxide-H_2O-NaCl system, DTA exam. of primary ice phase field 78−48382
differential, twin-pen chart recorder appl. 79−12797
differential microcalorimetry for direct meas. of difference between two thermal effects *(French)* 78−57950
differential scanning calorimeter, thermochem. appls. 79−40578
differential scanning calorimetry, theoretical melting curves anal. 78−16799
2,2′-dimethylbutane, differential thermal anal. under high press. 78−51669
2,6-dioxaadamantane, plastic phase, transition and fusion thermodynamics, DSC meas. 78−75603
1,2-dipalmitoylglyceride, DTA and X-ray diffr., polymorphism *(French)* 78−43008
DNA, sorption and desorption of water, thermal-stimulated press. and thermogravimetric anal. 80−8008
DNA hydrate, stability studied by thermogravimetry 80−30650
DSC curves correction for thermal lag effects, sp. ht. determ. case 80−37035
DTA, thermal curve interpretation 80−45599
DTA, topological aspects, bond diagrams, heat transfer 77−16877
DTA and scanning calorimetry cell flow control system 79−67303
DTA apparatus, modelling, elec. analogue approach 80−3270
DTA apparatus for meas. in region 20 to 800°C 77−32864
DTA apparatus for use in martensitic transform. studies at low temp. 79−49237
DTA curves, kinetic evaluation *(German)* 79−79361
DTA development in US, (1887 to 1976) 77−33815
dunite-dolomite mixtures, sintering and minerogenesis 77−66613
EBBA, liq. cryst., rapid cooling and mag. field effects on NMR relax. and thermal behaviour 79−82321
EBBA, metastable phases formed by rapid cooling of mesophase, IR and Raman spectra and DSC obs. 80−34919
EBBA, polymorphism, radiothermoluminescence and differential scanning calorimetric study 80−24570

thermal analysis continued
emanation, solid state structure studied using radioactive inert gases 79−11834
energy conservation and thermal analytic methods 79−54128
enthalpimetric analysis and calibration, new instruments and methods 79−43615
enthalpimetry, direct injection, inverse technique 78−92569
enzyme-substrate reactions in differential scanning calorimeter, digital simulation 79−74794
epoxy-rubber glass transition rel. to filler, cooling rate 79−4403
ester-imide varnishes, electroinsulating, thermal resist. *(Polish)* 78−84014
ethanol, plural glass-transitions, thermodynamic functions 78−38820
ethanol-water system, metastable states, hydrates existence and props., low temp. 78−71835
ethyleneterephthalate-ethylene glycol copolyester/15% polyglycol, semicryst. melting and glass transitions 80−49346
experimental conditions and results 78−35757
exponential temperature change, appl. to nonisothermal kinetics systems 77−86404
FBR Sphere-Pac carbide fuels, SPECKLE-I, computer modelling of thermal aspects of fuel response 80−18427
ferrite, phase composition in magnetic field, use of DTA-TG-DTG *(Polish)* 78−31393
ferrocene, cryst., stable low-temp. phase 80−34185
ferrocene, orthorhombic low-temp. cryst. phase, characterisation 80−96507
finely divided solids, struct., thermal anal. methods *(French)* 78−14254
fission reactor materials, gamma heating-effects, meas. using calorimetric and dosimetric techniques 80−658
2-fluoronaphthalene-2-naphthol system, phase relations, X-ray diffr. and DTA study 80−45287
gas analyser, two-bridge, based on voltage ratios meas. 80−50907
gehlenite glass, crystallisation kinetics 79−4251
gelatin, aq., crystn. and melting 79−61914
glass, DTA, transformation range *(French)* 77−72562
glass fibre reinforced polymer, thermal expansion coeff. and glass transition temp., thermal stress effect 78−14484
glass-crystal transition energetics, Piloyan's method appl. 80−38916
glasses, aqueous soln., stabilising excess electrons, DTA at cryogenic temps. 78−76889
graphite fibre filled phthalocyanine composites, cure cycle investigation 80−81030
graphite fluorides, $(CF)_n$ and $(C_2F)_n$, prep., struct., discharge characts., electrode props. 80−89502
graphite-alkali metal-benzene ternary intercalation compounds thermal and X-ray anal. *(French)* 78−27434
graphite-halogen intercalation compound, calorimetric study of order disorder transform. 79−52206
graphite-HNO_3 intercalation compounds, differential scanning calorimetry investigation 79−42234
n-heptacosane, differential thermal anal. under high press. 78−51669
heterogeneous reaction kinetics, microcalorimetric and thermogravimetric curve comparison 77−21359
heterogeneous system, melting, enthalpy and phase relations *(Czech)* 80−45543
2,4-hexadiynyl-1,6-bis(p-toluenesulphonate), programmed temp. and DSC obs., cryst. forms and polymerisation kinetics 79−43583
hexamethylolmelamine, doped, and condensation resin, room temp. phosphoresc., thermal transforms. 80−45132
n-hexatriacontane, cryst. struct., γ-ray effects obs. 78−43048
p-n-hexyloxybenzylidene-p-aminobenzoic acid, liq. cryst. phase transitions, X-ray diffr. and DSC meas. 79−86877
high alumina cement concrete, quality, thermal anal. investig. 79−15912
high temperature, building, construction materials evaluation appl. 78−80687
high-temperature quantitative DTA analysis, appl. to basalt 80−77144
IC thermal analysis by IR microimager 78−45619
ice, melting, in porous solid, NMR and differential scanning calorimetry obs. 77−62621
Inconel 600, PWR primary corrosion products 80−13578
inorganic solids, high energy irradiation, energy storage meas. 78−51581
IR analyser, Infralyt 4, dynamic characts. *(German)* 78−88676
irradiated nuclear fuel transport flasks 80−5281
isopropyl ammonium chloroplatinate and chlorostannate, ferroelastic transition, thermal, optical, and elastic meas. 79−28096
laser beam heat flux and power profiling, using swept null point calorimetry 80−69439
liquid crystal eutectic mixtures, glassy transition, DTA obs. 79−4405
liquid crystal mixture phase equilibria and transition temperatures 78−63845
liquid crystals, phase transitions up to 3 kbar, transition enthalpy, entropy 77−20051
liquid crystals, solid state polymorphism, differential scanning calorimetry and IR and Raman spectra obs. 80−55094
lithium formate monohydrate, dehydration, kinetic parameters from thermogravimetric data 79−61859
lunar regolith samples from Lunar-24, X-ray diffr. and thermogravimetric obs. 80−67598
lysozyme, sorption and desorption of water, thermal-stimulated press. and thermogravimetric anal. 80−8008
lysozyme bound water, thermally-stimulated press. and current 78−15757
mass spectroscopic techniques, comparison 78−31742
MBBA, metastable phases formed by rapid cooling of mesophase, IR and Raman spectra and DSC obs. 80−34919
melting-pressure curves, press.-temp. analysis 79−23697
mercury carboxylates, phase transitions, DTA 79−90759
metallic glass, stability, hole theory of liquids appl. 80−100174
metallic glasses, crystn., thermosonimetric investigation 80−75180
metallurgical melts, vacuum thermogravimetric device for evaporation kinetics determination 77−37865
methanol, solid, phase behaviour up to 3 kbar by DTA 77−76528
5-methyl-1-thia-5-azacyclooctane-1-oxide perchlorate, single cryst. transform., evidence for intermediate state 80−88078
methylcyclohexane, differential thermal anal. under high press. 78−51669
microcomputer-controlled analyser, Du Pont 1090 system 80−16613
minerals, irradiated, differential thermal anal. 79−62484
montmorillonite, physicochemical and engineering props., k-fixation effect *(Japanese)* 78−31366

thermal analysis continued
multiple digital differential thermal analysis instrumentation, synthetic chemicals production appl. 78−77902
multiple methods, instrums. and appls., review 77−70363
naphthalene-tetracyanobenzene, charge transfer complex, phase transitions, deuteration effect, mag. reson., spectral and thermal meas. 79−4412
nematic liquid crystal, Merck 389, polymorphism, radiothermoluminescence and differential scanning calorimetric study 80−24570
nematic liquid crystal with lateral substituents, mol. struct. effect 78−51411
nickeliferous limonites, pressure leaching for Ni extraction, using H_2SO_4 78−39717
nitrocellulose-nitroglycerine propellant, glass transition temp., thermomech. anal. meas. 79−14917
non-stoichiometric, thermogravimetric anal. 79−23773
nonisothermal devitrification kinetics 80−92465
nonisothermal transformation kinetics, combined KEKAM eqn. appls. 79−14912
nonlinear temp.-time program using computers *(German)* 78−8406
p-n-nonyloxybenzylidene-p-aminobenzoic acid, liq. cryst. phase transitions, X-ray diffr. and DSC meas. 79−86877
nth-order reactions, reaction kinetics, DTA obs. 77−81386
nylon 6, oriented glassy, mol. wt. influence on cryst. rate 80−44156
nylons, glass transition temp., thermal, mech. meas. 77−31758
n-octadecanol, growth of high temp. α-phase crystals in γ phase single crystals 78−71700
n-octatriacontane 78−51669
OOBPD, smectic, DTA obs. of phase transitions to 3 kbar 79−23708
organic compounds, high-press. expansivity determ. by piezo-thermal anal. 77−72705
organic electrical insulating materials, thermal lifetime prediction, thermal anal. appl. 79−15913
2-oxa-6-thiaadamantane, plastic phase, transition and fusion thermodynamics, DSC meas. 78−75603
2-oxaadamantane, plastic phase, transition and fusion thermodynamics, DSC meas. 78−75603
oxide systems, exam. of techniques used to determine phase diagrams and equilibria, and effects on equilibria 79−8415
PAA, solid state polymorphism 78−42945
PAN fibres, heat treatment, structural changes *(Polish)* 77−28835
pentlandite, prep., H_2 reduction with lime, to yield Fe-Ni alloy 78−85018
4,4′-di-n-pentyloxyazoxybenzene, anomalous smectic mesomorphism, calorimetric and optical texture obs. 79−77505
phenolic, two-stage cured, molecular struct. of Novolac effect on thermal stability *(Japanese)* 78−3092
p-phenyl-benzylidene-p'-alkylaniline, ordered smectic B phase, mol. length, influence on characts. *(French)* 79−14671
p-phenylene bis (p-substituted benzoates), cryst.-nematic transition, mol. struct. effects, DTA 78−47504
phospholipid mixtures, phase transition anal. by high sensitivity differential scanning calorimetry 77−40637
photothermal radiometry, contact-free condensed matter anal., K_2SO_4 powder appl. 80−26088
phthalocyanides, thermal stability, DTA *(German)* 80−11945
physiological support medium+NaCl+cryoprotective agent, equilib. and nonequilib. behaviour 77−16561
pitch, coal-derived low-volatile residues, glass transition, rheological props., DSC anal. 80−39331
plastic crystal, solid-solid phase transitions at high-press., DTA obs. 79−23540
plastics, accelerated life testing, by thermal analysis 77−70261
plastics, thermosetting, characterisation by thermal anal. 80−61204
PMMA isotactic, syndiotactic stereocomplex formation in soln., composition, struct. 79−66292
Polimal 142, polyester moulding material, hardening *(Polish)* 80−66523
poly(1-butene), melting and annealing behaviour, X-ray diffr. and DTA 79−28083
poly(di-n-heptyl itaconate), alkyl side chain independent relax., double glass transition 80−59636
poly(trioxane), γ-irrad. effects on melting behaviour 77−62620
poly(vinylidene fluoride), melting and crystn. temps., press. depend., DTA meas. 79−90568
poly(vinylidene fluoride) films, poled, piezoelec. activity and field-induced cryst. struct. transitions 80−20592
poly(vinylidene fluoride) orientation, solid state deformation by coextrusion 80−40394
poly 2,6-dimethyl-1,4-phenylene ether, liquid-induced crystallisation 78−30551
poly-1-butene, annealing and melting behaviour 79−38871
poly-ε-caprolactone-PVC blends, morphology 79−69019
poly-ε-caprolactum, semicryst. melting and glass transitions 80−49346
polyamide single crysts., struct. *(Russian)* 77−43158
polyamide-Cu(Ni) oxalate, oxalate decomposition kinetics, in polymeric medium, thermogravimetry and DTA 78−52749
polyaryloxyphosphazene copolymers, thermal, morphological and rheological props. 80−103265
polybutadiene, carboxyl-terminated, glass transition temp., thermomech. anal. meas. 79−14917
polycarbonate, glassy state, enthalpy relax., thermal density fluctuations 80−59678
polycarbonate, glassy state, rel. between thermal pre-treatment and viscoelastic behaviour 79−79038
polycarbonate fibre, highly-oriented, drawing behaviour and mech. props. 78−76708
polycarbonates, glass transition pt., calorimetric determ. *(Polish)* 79−51241
polydioxolan, crystallisation, morphology and melting props. 78−14297
polydioxolan, crystn. kinetics, dilatometric analysis and microscopy obs. 80−79706
polydiphenylsiloxane, thermodynamics of fusion 80−84280
polyelectrolyte, plasticised, effect of ion placement and struct. on props. 79−7679
polyester, temp. index, rapid determ. by dynamic thermogravimetry 80−85101
polyester varnishes, electroinsulating, thermal resist. *(Polish)* 78−84014
polyester-organic solvent mixtures, phase diagrams, eutectic props., devitrification, crystn. *(French)* 80−3015
polyesteramides, glass transition temp. determ. by DTA 79−4402
polyesters, thermotropic, quiescent crystn. 80−38937

thermal analysis continued
polyether-polyester elastomers, differential scanning calorimetry, crit. points *(Japanese)* 80−75344
polyether-polyester elastomers, differential scanning calorimetry by using poly(oxy-1,4-butylene glycol) as soft segment *(Japanese)* 80−79916
polyethylene, crosslinked, from HV cables, differential scanning calorimetry 79−100466
polyethylene, crystallisation kinetics, use of DSC, comparison with dilatometry 77−31601
polyethylene, crystn. under high pressure 80−38946
polyethylene, drawn, ultrahigh modulus, linear, melting behaviour 80−19916
polyethylene, fibrillar, high mol. wt., oriented crystallisation, heat treatment effect *(Japanese)* 80−25738
polyethylene, high density, wear mechanism at steel surface, SEM, TEM and DTA 78−64727
polyethylene, high density extruded fibres, morphology effect on physical and mech. props. 79−83235
polyethylene, high press. phase, US, DTA, and X-ray diffr. study 80−75188
polyethylene, high- and low-density, crystallinity degree, comparative obs. *(Polish)* 80−1943
polyethylene, high-density, solid-state coextrusion, mol. wt. distrib. effect 80−104212
polyethylene, linear, glass transition temp. 80−15225
polyethylene, low density, melting and crystallisation, DSC characterisation 80−64927
polyethylene, low density, UV and heat treatment effects, DSC obs. 79−14915
polyethylene, modified with phosphonate ester pendant side group, thermal and mech. props. 78−11195
polyethylene, MP, heat of fusion, degree of crystn. determ. by differential scanning calorimetry *(Russian)* 77−62489
polyethylene, nascent, electron microscope study 80−38940
polyethylene, oriented, shear strain, effect on stuct., props. *(Russian)* 80−7656
polyethylene, prediction by isothermal differential scanning calorimetry 78−11485
polyethylene, single, polycryst., ^{60}Co-γ irrad., effect on melting behaviour 77−15548
polyethylene, stress crystallised, melting behaviour 77−47554
polyethylene, supermolecular structure, polymerisation at low pressure *(Russian)* 79−64126
polyethylene, ultraquenched, electron diffr., morphology and thermal anal. 79−15640
polyethylene crystal, longitudinal growth in flowing soln., melting of continuous fibrillar crystal 80−19917
polyethylene electrets, charge trapping mechanism, TSC, DTA and optical meas. 80−11322
polyethylene fibres, high density, ultra oriented, physical, mech. props. 80−25649
polyethylene fibril, high mol. wt., high melting point crystal *(Japanese)* 80−38954
polyethylene flow crystallisation, in extensional flow developed by convergent capillaries, props. 80−84111
polyethylene melt, cryst. kinetics during cooling, nucleation density effect 80−100181
polyethylene oxide, solid state relaxation, DSC study 78−9962
polyethylene oxide blends, thermal and mechanical props. 79−11679
polyethylene sulphide, thermal stability and stability against solvents *(Russian)* 78−51449
polyethylene terephthalate, amorphous material orientation determ. *(Polish)* 79−73111
polyethylene terephthalate, differential scanning calorimetry of melting, mosaic block struct. of cryst. layers 78−26452
polyethylene terephthalate, fibre, melting in crystn., intermediate and amorphous phases 77−84898
polyethylene terephthalate, glass conversion zone determ. from DTA *(German)* 77−20059
polyethylene terephthalate, nonisothermal crystallisation kinetics 79−32920
polyethylene terephthalate, oriented, amorphous, stress-induced crystn., shrinkage meas. 80−92466
polyimides, temp. index, rapid determ. by dynamic thermogravimetry 80−85101
polymer, degration, reaction product volatility effect on thermogravimetric anal. 80−104316
polymer, glass-like, DSC obs. of mol. interaction variations *(Russian)* 79−32924
polymer concretes, hydrothermally stable, hydraulic cement-type fillers 80−85144
polymer glasses, aged, enthalpic state determ. by scanning calorimetry 80−6528
polymer glasses, enthalpy relax., scanning calorimetry technique 80−90851
polymeric cryoprotectants in preservation of biological ultrastruct., aq. soln. low temp. states 78−65157
polymers, crystallinity determ. by thermal method *(Russian)* 80−38966
polymers, paints, testing, modern analytical methods appl. *(Polish)* 78−85253
polymers, thermal anal. methods, appls. 78−68845
polymethylene sulphide, thermal stability and stability against solvents *(Russian)* 78−51449
polyorganosiloxane, thermogravimetric assessment of stability at high temps. 77−52704
polyoxymethylene, wear mechanism at steel surface, SEM, TEM and DTA 78−64727
polyphenylacetylene cis-trans isomers, rel. mol. wt. distrib., heating effect 80−106409
polypropylene, Halen and Daplen, semicryst. melting and glass transitions 80−49346
polypropylene, isotactic, low temp. annealing, differential scanning calorimetry obs. 80−60895
polypropylene oxide, complex with metal salt, glass transition temp. 79−69234
polypropylene systems, elastomeric impact modifiers rel. to morphology 79−66154
polyquinazolones with N-phthalimide groups in side chain, prep., props. *(Japanese)* 79−15642
polystyrene, atactic, thermal behaviour above glass-rubber relax. temp. 77−39548
thermal analysis continued
polystyrene, extruded, glass transition temp., melting pt., DTA 78−2235
polystyrene, glass transition temp. meas. reproducibility using differential scanning calorimetry 77−15563
polystyrene, intermol. interaction, conform. *(Russian)* 79−23539
polystyrene, isotactic, isothermal crystn. using SiO_2 as nucleating agent 79−24807
polystyrene, isotactic and static cold-crystallised blends, thermal transitions 80−24381
polystyrene, plasticizer effect on electric strength 80−29688
polystyrene, ref. std. material testing, evaluation, glass transition temps., instrumental effects 79−4404
polystyrene, sp. ht. determ. by differential scanning calorimetry 79−33101
polystyrene, sp. ht. meas. by differential scanning calorimetry 77−51515
polystyrene, T_{11} relax. above glass transition 79−4259
polystyrene-polyisoprene block copolymers, low mol. wt., glass transition temp., DSC investig. 77−7854
polystyrene-polyolefin blends, mech. and swelling properties on heating 79−57053
polystyrene-SiO_2, glass transition rel. to filler, cooling rate 79−4403
polytetramethyl-p-silphenylene siloxane, morphology and mech. behaviour 78−84885
polytetramethyl-p-silphenylenesiloxane, degree of crystallinity determ. by DSC 78−26453
polythene-polystyrene blends, differential scanning calorimetry and swelling characterisation 79−57053
polyurethane, segmented, domain struct., deform. effect 80−93623
polyvinyl acetal, temp. index, rapid determ. by dynamic thermogravimetry 80−85101
polyvinyl acetate, struct. relax., enthalpy and elec. polarisation obs. 79−41978
polyvinyl alcohol, crystallisation from dil. soln. by stirring *(Japanese)* 77−89388
polyvinylidene fluoride, crystn. process and elec. cond., differential scanning calorimetry 79−24024
polyvinylidene fluoride-PMMA blends, differential scanning calorimetry of cryst. melting 78−26454
portland cement concrete, determination of hydrated cement content by differential thermal analysis 79−79335
portland cement paste, microstructure study by SEM, TG and X-ray diffr., corrosion 78−92381
Portland cement-fly ash, physico-mech. props., SEM and X-ray diffr. anal. 79−74239
potassium alkanoates, phase transitions, differential scanning calorimetry 77−43319
potassium n-alkanoates, thermal behaviour, differential scanning calorimetry obs. 80−92650
precise temperature programming using microprocessor 79−54127
propyl-1,3-diamino manganese chloride, structural phase transitions at 336 and 305K, NQR meas., DTA 78−63855
propylene-alkyl acrylates alternating copolymers characterisation 79−51950
PTFE, γ-ray effects on 19 and 30°C phase transitions, Fourier transform IR spectroscopy 80−103387
PTFE, annealing effect on melting and crystallisation *(Japanese)* 80−20980
PTFE, processing parameter effect on thermal props. and crystal struct. *(German)* 78−63679
PTFE, wear mechanism at steel surface, SEM, TEM and DTA 78−64727
PTFE+metal, fluoride prod., DSC and XPS anal., rel. to polymer wear 80−11889
PVC, enthalpy determ. of order 79−7556
PVC, influence of thermal history on physical props., DSC determ. 79−4984
PVC, plasticised, foam growth, thermomech. anal. 80−3416
PVC-ethoxymethylmelamine blends, dynamic mech. props. *(Japanese)* 79−96063
pyrazine, cryst. phases, entropy changes and struct. implications 80−54397
pyrene-tetracyanobenzene, charge transfer complex, phase transitions, deuteration effect, mag. reson., spectral and thermal meas. 79−4412
pyrochlore related structures, phases of type AM_2X_6, acentricity and phase transitions, X-ray diffr., DSC and NMR study 79−27943
quartz powdered, thermal effects of Fe contamination, adsorbed H_2O, annealing on DTA 79−100161
radiation effects on material determ., thermal defect meas. using total-absorption calorimeters 80−99427
radioactive waste, medium-level, sedimentation method of bituminisation, thermogravimetric charact. of products 77−61561
rare earth aluminium borates, thermal stability, X-ray struct. anal., refractive indices 79−4297
rare earth cpds., $R_3Fe_8O_x$-H, TGA-DTA meas., H absorption charact. 80−24600
rare earth oxide (R_2O_3)-M_xO_y glassy systems (M=Ti,Nb,Ta), rapid quenching by laser beam, exam. of composition and crystallization 78−52856
rare earth-Fe_2 Laves phase intermetallics, mag. ordering temps. by DTA 79−47283
rare earth-transition metal Laves phase, thermodynamic exam. of formation 77−1241
reaction kinetics, nonisothermal, studied by thermal anal. and DTA 79−40335
reactor spent fuel storage, thermal anal. of metal-encapsulated fuel 79−36359
reduced time plots for dynamic isothermal operations 79−57318
refractory materials quality control appl. *(German)* 78−35337
resins, prepregs and composites, charact. by differential scanning calorimetry 80−71869
review of developments over last 25 years 77−70369
rubidium n. alkanoates, long-chain, phase transformations, in melt, DTA obs. 77−76536
rutile structure fluorides, high temp. polymorphism and thermal props. 80−75199
satellite, gravity oriented, with thermally flexed appendages, librational dynamics 78−7868
Schiff's base compounds, double axis, Siamese Twin type liq. crysts., thermal and X-ray obs. 80−39312
semicarbazide hydrochloride, phase transition, IR spectra and thermal study 79−37833

thermal analysis continued
p-sexiphenyl, liq. cryst. phase transitions 79−82322
shell elements, thick curved, temperature load calc. 77−80066
silica gel, microporous amorphous toroidal, spectroscopic and thermal analysis, adsorption properties 79−57305
silica gel, skeletal struct. modification with alcohols and water vap., thermal analysis obs. 78−88659
silicate glass, hydration in steam atmosphere 80−85211
silicone rubber, RTV 560, diffusion of outgassing species, kinetics data 79−15010
silk fibroin films, conformational changes induced by water immersion 80−10498
solar furnace, focal spot thermal analysis 80−21383
solar power plant, transient thermal behaviour of primary circuit and thermal storage tank 80−85267
solar power satellite, power conversion concepts comparison 79−48094
solid material composition and structure determ. *(German)* 77−81437
solid state reaction, heterogeneous, Avrami parameter calc., modified Kissinger method 78−92239
sorbitol, crystallisation, thermal investig. 78−47257
β-spodumene-mica glass ceramics, phase evolution and TiO_2, MgF_2 additive effects, exam. 78−44089
static thermal analysis, equipment design, exam. 78−57943
steel, alloy, Fe-C-Zn (0.45, 1.56 wt.%), pearlite transformation during continuous cooling 78−80538
steel, alloy, high C, amorphous, produced by rapid quenching from melt, hardness and strength 78−59764
steel, austenitic types AISI 316, 347 and Esshete 1250, corrosion in molten SO_4 deposits 80−97625
steel, cold strained, defects interaction with carbide strengthening phases, carbide decomp. degree *(Russian)* 80−84955
steel, high-speed, solidification cycle, thermal anal. 80−29945
steel, maraging 18%Ni, calorimetric anal. of ageing *(Japanese)* 80−89264
steel, Ni-Co-C (9, 4, 0.2 wt.%) enthalpy, sp. ht. to 2000K 79−10960
steel, nitride inclusions, identification by differential thermal anal. and evolved gas anal. 78−48721
steel, retained austenite estimation during tempering, DTA *(German)* 77−28831
steel, second phases, appl. of DTA-evolved gas anal. 77−55971
steel, stainless, PWR primary corrosion products 80−13578
steel casting, calc. method of thermal and thermo-visco-elasto-plastic processes *(German)* 80−79859
steel continuous casting, thermal, thermo-visco-elasto-plastic processes *(German)* 80−81044
styrene-methacrylic acid copolymer, intermol. interaction, conform., composition depend. *(Russian)* 79−23539
symposium, Trondheim, Norway (Jun. 1977) 79−16079
TBBA, liq. cryst., metastable phase, thermodynamic props., differential scanning calorimetry meas. 78−94985
TBBA, new cryst. phase, calorimetric meas. 79−51254
TCNQ salt., $NMeQn(TCNQ)_2$, role of solvent in phase transition, thermal anal. and transport props. 79−33312
temperature integral, approximative eqns., accuracy analysis 80−36834
terephthalate copolyester, heat treatment effect on melting point *(Japanese)* 80−40400
terephthalylidene-bis-(4-n-alkylanilines), smectic polymorphism, calorimetric study 80−88307
tetraethylammonium iodide-Ag_nI_{n+1}, ionic conductors, electrochem., props. 77−31808
tetramethyl-p-silphenylene siloxane/dimethyl siloxane, block copolymer, morphology and mech. behaviour 78−84885
tetramethyl-p-silphenylenesiloxane-dimethyl siloxane copolymers, degree of crystallinity 78−26453
2,2,2,6-tetramethyl-piperidino-oxy, cryst. growth and polymorphism 80−96645
tetramethylsilane, phase rels. under press., DTA obs. 78−71850
thermobalance, high sensitivity for macro samples, construction, performance *(Japanese)* 80−47023
thermobalance for studying high-temp. sulphidation kinetics of metals 78−23876
thermogastitrimetric method using DERIVATOGRAPH-Q *(Hungarian)* 77−21449
thermogravimetric analyser, low cost design 78−20116
thermogravimetric apparatus, automatic device with digital output 78−7281
thermogravimetric automatic temperature indicator 78−86257
thermogravimetric data acquisition and reduction program 78−64901
thermogravimetric methods, review 78−3408
thermogravimetric system for investigating gas-metal reactions at elevated temps. 80−229
thermogravimetry, balance inclination and specimen temp. error sources 80−98887
thermogravimetry, development in United States, review 77−90668
thermoset and coating technology, torsional braid and thermal anal. 80−55622
2-thiaadamantane, plastic phase, transition and fusion thermodynamics, DSC meas. 78−75603
thiorhodites, $M_xRh_{3-x}S_4$ (M=Cu,Co,Fe), thermal stability and thermochem. props. 79−86904
TMMC phase behaviour, DTA using Ge-Ag thermocouple 79−65186
Tremolite, fibrous, high temp. phases, transformations, DTA 79−77742
s-triazine, sp.ht. 130-380K, melting enthalpy and solid-state transition 79−46812
1,1,1-trichloroethane, polymorphism under high pressure *(French)* 80−96644
trimethylammonium cadmium chloride, $(CH_3)_3NHCdCl_3$, struct. phase transitions 79−1502
two-component oxide systems, composition obs. by thermogravimetry 79−16081
unsteady heat conduction accompanied by an endothermic solid reaction *(Japanese)* 79−76939
urea-n-paraffin adducts, order-disorder transition, thermal anal., X-ray diffr., and NMR 79−33084
vanadyl phthalocyanine-copper phthalocyanine mixed crysts., α-β phase transform., heat of transform., DTA investig. *(German)* 78−30754
vaterite, polymorphic transition kinetics, differential thermal anal. meas. 79−14722
vermiculite, interlayer space struct. anal., by replacing exchange cations with NH_4^+ 77−7700
vinyl alcohol-vinyl acetate copolymers, mol. architecture and physicochem. props. 80−44103
vitreous state, thermal devitrification *(French)* 77−72563
water content determ., rapid thermal method 77−86258
o-xylene, volume effect in metastability of crystalline phases on cooling 79−77716
zeolite-bearing rocks, multicomponent, quantitative thermogravimetry 79−16082
zeolites, Na, Cs, Sr types, processing radioactive waste soln., thermal transform. 77−10477
Zircaloy, PWR primary corrosion products 80−13578
Zircaloy-2, hot-pressed, influence of diffused C on structure and oxidation 80−61016
- 78−18749
$3CaO.Al_2O_3$, hydration retardation by $CaSO_4$ 79−61856
Ag, vacuum deposited on Al substrate, recrystallisation 78−60044
Ag-Bi-S, ternary phase diagram, DTA and X-ray diffr. investigation 80−84917
Ag-Bi-Tl, system calculated from optimised binary boundary systems *(German)* 77−16545
Ag-CdO cermets, coprecipitated carbonates and hydroxides, physicomech. props. 80−25706
Ag-Pb-Hg system, DTA of phase diagram 77−12594
Ag-Sm system, phase diagram, eutectic temps., microstruct. *(German)* 80−104119
$AgAsS_2$-$AgSbS_2$ system, thermal, microstructural X-ray phase anal. 77−32565
$Ag_3Au_{1-x}Cu_x$, phase relations, X-ray diffr. and differential thermal anal. 80−108395
Ag_2CO_3, high press. phase relations, DTA 77−43329
$AgGaS_2$-$AgGaSe_2$ system, phase diagram, lattice consts., and IR spectra 80−60841
AgI solid electrolyte α-phase stabilisation 80−29209
AgI-Ag oxosalt systems, solid electrolytes with glass-like struct., thermodynamic and electrochem. props. 79−10978
AgI-$Ag_2Mo_2O_7$($Ag_2Mo_4O_{13}$), solid, intermediate compounds with fast ion transport 77−43371
AgI-Ag_2O-MoO_3 system, glass form. with high ionic conductivity 77−89379
AgI-$Ag_2O.B_2O_3$ system, ionic cond., struct., electrochem. prop. in galvanic cell 78−95181
AgI-Ag_3AsO_4, AgI-$Ag_2Cr_2(Mo_2)O_7$ systems, solid electrolyte stability 77−15619
AgI-BiI_3, phase equilib. study *(French)* 79−66047
AgI-RbI films, vacuum deposited, cond. determ. 77−39689
$AgInS_2(Se_2)$-$SnS_2(Se_2)$, degree of solid solubility and phases characts. 78−35377
$AgPO_3$-AgI glass system, solution calorimetry, enthalpy of formation *(French)* 78−64527
Ag_2S-(As)(Sb)(Bi), temp.-comp. diagram 78−44105
$Ag_2S+Ln_2S_3$, powdered mixtures, reaction rate, production of ionic semiconductors 80−93741
Ag_3SBr, ionic conductivity in temp. range 93-573K, X-ray diffr. and DTA 80−79988
Ag_3SI, ionic conductivity in temp. range 93-573K, X-ray diffr. and DTA 80−79988
Ag_2SO_4, enthalpies of transition and fusion 79−10925
$AgSbS_2$, synthetic crystals, DTA and cryst. struct., phase transitions *(German)* 78−42943
Ag_2Se-(As)(Sb)(Bi), temp.-comp. diagram 78−44105
Ag_2Se-Ga_2Se_3, pseudobinary phase diagram determ., DTA, X-ray diffr., cryst. growth investigs. 77−70036
Ag_2Te-(As)(Sb)(Bi), temp.-comp. diagram 78−44105
AgZn, $\beta' \rightarrow \zeta$ transformation, effect of additional elements 80−66507
AgZn-AgMg quasibinary alloy, phase relation and superlattice form. 78−3097
$AgZr_2(PO_4)_3$ system, phase charact. at different temps. 80−29936
Al alloy, calorimetric studies on 700 series, matrix precipitate charact. of 7075 77−86036
Al alloy, calorimetric studies of 7000 series, comparison of 7075, 7050 and RX720 77−86037
Al saponite, differential thermal anal., IR absorpt. spectra, chlorite-like mineral 78−88816
Al sheet, recrystallization, DSC eval. 80−3105
Al-Cu (2-5 wt.%), precipitation total surface influence on resistivity *(French)* 80−71650
Al-Cu hypoeutectic, solidification cycle, thermal anal. 80−29945
Al-Cu(Zn, Ag, Mg_2Si), intermediate precipitates, stability, X-ray, elec. resist. and hardness study 80−3063
Al-Li alloy, thermal anal. of precipitation 78−15417
Al-Mg-Si, DTA exam. after small and medium deform. 80−21002
Al-Mg-Si, Mg loss, mass spectrometry/thermogravimetry 77−16620
Al-Mg-Si alloys, DTA exam. of zone form. and other solid phase conversions 77−86057
Al-Mg-Si alloys, DTA meas. of struct. changes in zones after quenching and isothermal heat treatment 79−52248
Al-Mg-Zn-Cu, type 7050, calorimetric study of fatigue induced microstructural changes 80−85034
Al-Mn, cooling after recrystallisation, phase transform., X-ray and thermal anal. *(Russian)* 77−66663
Al-Si-Sr phase diagram *(Russian)* 78−15363
Al-Zn (10 wt.%), ageing behaviour, calorimetric study 80−45328
Al-Zn (15 wt.%), calorimetric ageing study 80−45330
Al-Zn-Mg, decomposition calorimetric study *(German)* 79−74165
Al-Zn-Mg, TEM and calorimetric study 80−76290
Al-Zn-Mg (4.5, 2 to 3 at.%) solid state reactions by interrupted continuous heating 80−25737
Al-Zn-Mg (4.5 at.%, 2 to 3 at.%), decomp. behaviour during continuous heating 80−29922
AlF_3 based glasses, chem., thermal and optical props. *(French)* 80−70139
α-AlH_3, prep., thermal decomposition, transform., struct. *(French)* 80−3326
Al_3Mg_2, diffusionless phase transformation 80−104150
AlO_2, corrosion resistance of phosphate bonded castable, and dense fired types in steam CO at 199°C 79−20222
Al_2O_3 hydrated gel synthesis by homogeneous precip. method using $NaAlO_2$, phase change by heating *(Japanese)* 78−68937
Al_2O_3 refractories, stability of refractory bond phases in steam-CO atmosphere 79−24634

thermal analysis continued
Al_2O_3 ultrafine gel particle form. from NH_3-$AlCl_3$ solution 80−93807
β-Al_2O_3-$H^+(H_2O)_n$, p-type conductor, stability *(French)* 79−38063
β-Al_2O_3-NH_4^+, p-type conductor, stability *(French)* 79−38063
β-Al_2O_3-NH_4^+, single cryst. characts. and AC cond. obs. 80−107514
Al_2O_3-SiO_2 glass powder, mullite crystallisation during hot pressing 78−60639
Al_2O_3-SiO_2 powder, plasma-prepared, glass form. and phase transforms 77−44208
Al_2O_3-Sm_2O_3, phase diagram at high temp. *(Japanese)* 78−92253
$Al(OOH)_3$, formed by reaction of methyl esters and $Na_2Al_2O_2$, exam. of props. 78−48346
$AlPO_4$, high temp. behaviour up to liq. state, phase relations, X-ray diffr. and therm. anal. study *(French)* 80−10660
$AlPO_4$, high-low cristobalite transitions, DTA meas. 79−82335
$Al_{23}Te_{77}$ glasses, crystallization 79−51000
Am metal, dilatometry and thermal anal., melting point, transformation regions 79−43241
Am, polymorphic transforms. obs. *(Russian)* 78−6153
Ar triple point determ. method *(Japanese)* 79−95123
As, condensed layers, low temp. allotropic phase transition *(Russian)* 80−54553
As-Sb-S-I system glasses, vitrification and volt-ampere characts. 77−31756
As-Te-In, glass-forming, density and microhardness 80−103257
As_2O_5-$Rb_2O(Rb_2CO_3)$ system, phase diagram, polymorphic transform. 79−83181
As_2S_3, amorphous film, photodissolution of Ag, struct. changes 77−11815
As_2S_3-HgS, phase diag., IR spectra 77−36479
As_2S_3-PbS glasses, structural props. 79−27925
As_xS_{100-x} amorphous films, optical props. and photoinduced changes 80−60700
As_2Se_3 glass, heat capacity and struct. relaxation of enthalpy 77−55360
As_2Se_3-based glasses, crystallization, DTA investig. 78−22658
$As_{60}Se_xTe_{40-x}$ glasses, crystallisation 77−35488
As_2Te_3-Tl_2Te system, phase diagram 77−16559
Au-Ge-Te ternary system, solid soln. in vicinity of GeTe, phase diagram *(French)* 77−85994
Au-In-Pb, $AuIn_2$-In-Pb portion of phase diagram 77−32562
Au-Pd-Zn system, quasibinary section phases investig. 77−12596
Au-Tl (29 to 100 at.%), thermal analysis, exam. of phase diagram 78−88445
$Au_3Cu_{1-x}Ag_x$, phase relations, X-ray diffr. and differential thermal anal. 80−108395
AuIn-Pb pseudobinary system, DTA 78−23667
B_2O_3-Li_2O-Fe_2O_3, prep. by quenching methods, exam. of microcrystalline precipitates of Li_2O-Fe_2O_3 *(French)* 79−20019
B_2S_3-Tl_2S system, phase diagram and verification 80−35165
B_2Se_3-Tl_2Se_3 system, phase diagram 80−35165
Ba-Al-Si system, phase diagrams construction by simplex designing method 78−6899
Ba-Se(Te) systems, phase diagrams 77−36472
$Ba_2Bi^{3+}Bi^{5+}O_6$, structure and elec., mag., thermal props. vs. temp. X-ray and neutron powder diffr. study 79−19189
$BaBr_2.H_2O$, dehydration, kinetic parameters from thermogravimetric data 79−61859
BaF_2-MnF_2-FeF_3 system, X-ray investigation, struct. relations, liquid-solid equilibria diagram, study by DTA *(French)* 79−34017
BaF_2-YF_3 system, phase diagram 78−35363
$BaMoO_4$-CdO(PbO)(ZnO) and $BaMoO_4$-$CdMoO_4(PbMoO_4)(ZnMoO_4)$ systems, phase diagrams 77−25034
$Ba(NO_3)_2$, low temp. struct. changes, elec. props. 79−87377
$BaNb_2O_6$, solid-phase formation reaction, thermographic, X-ray phase and chemical anal. 77−12783
BaO-Fe_2O_3-B_2O_3 glass, splat cooled, low temp. micromagnetism 80−34660
BaO-MoO_3, solid phase reaction, thermal analysis 80−55639
BaO-SiO_2 glass ceramic, growth and nucleation kinetics 80−7528
BaO-SiO_2-Fe_2O_3 permanent mag. ceramics, exam. of phase diagram, using X-ray analysis, optical microscopy, electron probe anal., and thermal analysis *(German)* 79−29012
BaO-WO_3, solid phase reaction, thermal anal. 80−55639
(BaTi) citrates, thermal decomp., thermal anal., IR and X-ray diffr. obs. 79−24735
$BaTiO_3$ ceramic, semiconductive sintering 77−36430
$BaTiO_3$, synthesis by solid-solid reactions 79−38776
$BaTiO_3$:C, solubility of C at low O_2 potentials, 800°C 80−100334
Be-Co (0-50 at.%) alloys, thermal, metallographic and X-ray anal., phase diagram *(Russian)* 78−56611
BeF_2 glass, glass transition temp. and thermal expansion 80−64902
BeO, heated on W, thermal anal. using mass spectrometric, technique, vaporisation behaviour 80−79932
BeO-Al_2O_3-SiO_2-MF_2 (MF) glasses, M=Mg, Ca, Sr, Ba, Li, Na, fluoride ion role during crystn. 79−65176
Bi-MnBi eutectic region, of Bi-Mn phase diagram 80−81034
$Bi_{24}CoO_{37}$, in Bi_2O_3-CoO system, X-ray diffr., thermal anal. and metallography obs. 80−24598
$BiH(PO_3)_4$, condensed, thermal behaviour and IR spectra 80−19912
Bi_2O_3, polymorphic transformation and elec. resistivity *(Japanese)* 80−93555
Bi_2O_3-$AlPO_4$, phase equilib. 80−35168
Bi_2O_3-CdO system, phase diagram 77−25032
Bi_2O_3-CoO system, X-ray diffr., thermal anal. and metallography obs. 80−24598
BiOI, synthesis, thermal decomposition in dry O_2 *(French)* 78−53205
$3Bi_2O_3.5B_2O_3$, viscosity, molar volume of melt and enthalpy of fusion 79−10924
BiP_5O_{14}, condensed, thermal behaviour and IR spectra 80−19912
$Bi_2Sn_2O_7$, polymorphic phase transition, X-ray, DSC, SHG, dielec. and optical obs. 80−44163
C, pyrolysis mechanism, electron microscopy, DTA, IR, ESR obs. 78−56593
$C_{12.6}AuCl_3$, intercalation compound, struct. *(French)* 78−42982
Ca-Sb, phase diag. 77−52284
$CaAl_2O_4$ compounds and cements, quantitative thermogravimetry after hydrothermal treatment 80−16737
$CaCO_3$, aragonite-calcite transformation, effect of impurities, DTA and IR studies 78−51662
$CaCO_3$, decomposition, formation of Ca_3SiO_5 79−52651

thermal analysis continued
$CaCO_3$+SiO_2, in presence of NaF, thermal decomposition of Ca_2SiO_4 formation 78−68889
$CaCl_2$-Ca phase diagram, DTA study *(French)* 80−25672
$CaCu_5$, γ-phase in Ca-Cu system, calorimetric determ. of enthalpy of form. *(French)* 80−84915
CaF_2-AlF_3, phase equilibria, DTA and X-ray diffr. study 78−27493
CaF_2-AlF_3-Na_3AlF_6(-Al_2O_3), phase equilibria, X-ray diffr. and DTA meas. 80−108409
CaF_2-LaF_3, solid soln. with fluorite struct., phase diagram 79−100119
Ca_2GeO_4-$Ca_4(PO_4)_2$ system, phase equil. 77−36469
CaO, heated on W, thermal anal. using mass spectrometric, technique, vaporisation behaviour 80−79932
CaO-Al_2O_3, molten binary slag, dissolved C study *(Japanese)* 78−60662
CaO-MgO-Al_2O_3-SiO_2, glass-ceramic prep. by hot pressing and crystallisation of powder 78−11192
$3CaO.Al_2O_3$+$CaSO_4.2H_2O$, effects of prehydration on liq. hydration 79−100354
$CaO.3B_2O_3$, form. by dehydration of hydrated calcium borates *(Japanese)* 79−74378
$Ca_5(PO_4)_3OH$, prep. from sulphate, X-ray diffr. and IR spectrosc. 80−29893
$CaSO_3.1/2H_2O$-$CaSO_4$ solid solution, prepared by coprecipitation from solns., exam. 79−20034
$CaSiO_3$ fibrous crystal reinforced matrix, unidirectional crystallization, anisotropic properties 79−56969
$CaWO_4$, crystn. from solns. in $NaWO_4$ melts, kinetics obs. by DTA 80−40246
$Ca[B_3O_4(OH)_3].H_2O$, differential thermal X-ray anal. of phase transitions in non isothermal conditions 79−52205
$Ca[B_3O_3(OH)_5].4H_2O$, differential thermal X-ray anal. of phase transitions in non isothermal conditions 79−52205
Cd-Ge-As system, quenched samples, phase diagram, DTA after annealing 79−69226
Cd_3As_2, amorphous to crystalline transform. 79−77519
$CdCl_2$-$PbCl_2$, thermodynamic quantity meas. by quantitative thermal anal. of heating process 78−19730
$CdGeAs_2$, amorphous, thermal gradient expts., recrystn. 80−55438
$CdGe_{1-x}Sb_xAs_2$ glass, DTA, microhardness meas. *(French)* 77−72564
$CdGe_{1-x}Sb_xAs_2$ system, amorphous and cryst. phases, DTA and microhardness obs. 78−22835
CdS, dry process formation from CdO and S *(Spanish)* 78−56607
CdSb:Au, solubility, thermal anal., microhardness, microstruct., elec. characts. 77−16557
$CdSnP_2$ crystal growth, DTA obs. of Cd-Sn-$CdSnP_2$ phase diagram 80−24394
CdTe-Au system, phase diagram rel. to doping 80−16282
CdTe-CdS solid solution phase diagram *(Russian)* 79−100120
CdTe-Co(Mn) systems, reaction of components, DTA, microstruct. and microhardness obs. 79−38804
CdTe-In system, equilib. phase diagram and liq. phase epitaxial growth of CdTe from In soln. *(Japanese)* 80−71634
CdTe-ZnS ternary mutual system, phase diagram 80−20904
Ce-Ga, phase diagram *(Russian)* 78−27478
Ce-Ga system, phase equilib. and cryst. struct. of phases 80−35159
Ce-In, phase equilibrium and cryst. struct. 80−66483
Ce-Pr powder, DHCP⇄FCC transition, X-ray, DTA and resistivity studies 80−50629
Ce-Tl, phase equilibrium and cryst. struct. 80−66483
$Ce(HPO_4)_2$×$1.33H_2O$, crystalline, thermoanal. meas. 79−91938
$CeNbO_{4+x}$, oxidation-reduction reactions 78−39930
CeO_{2-x} ($0<x<0.3$), oxidation-reduction study, Cahn electrobalance appl. 77−79084
CeO_n, redox reactions, quasiisothermal thermogravimetric obs. 79−15980
Ce_2O_5-P_2O_5 glass, crystallisation 77−51326
$CeTaO_{4+x}$, oxidation-reduction reactions, phase equilibrium, thermogravimetry and magnetic susceptibility meas. 78−39930
ClF_5-IF_5, determ. of phase diagram, using DTA 79−4955
Co-B-Si ternary system, partial phase diagram, Co rich region 77−52293
Co-Ga alloys, phase diagrams and cryst. struct., DTA, X-ray diffr. and microprobe anal. *(French)* 79−47660
Co-Ge binary system, phase diagram rel. to that of Ni-Ge *(French)* 80−97463
Co-P, electrodeposited alloys, heat-induced structural changes *(Japanese)* 80−89263
Co-Sb-Te ternary system, crystn., heat treatment and phase equilib. 79−52156
Co-Sm-Cu, phase diagram 79−91632
Co_2-rare earths, H_2 reaction, DTA and DTG anal. 79−100434
$Co_{1-x}Al_x$, ordered β-phase, enthalpy of formation are defect struct. descript. 80−89519
$CoCl_2$-KCl-NaCl system, melting diagram investigation by thermographic anal. *(Russian)* 78−3111
$(Co_yNi_{1-y})_{1-x}O$ and O_2 prep. props., and reactions 77−12569
CoNiZn ferrites, Fe excess, complex permeab. var. with annealing temp. 77−89979
$Co_{75}Si_{15}B_{10}$, amorphous, crystallisation study *(Japanese)* 78−9959
$CoTe_2$-GeTe, phase diagram, from thermal, X-ray, microstructural analyses 80−55367
$Co_{90}Zr_{10}$, ferromag. amorphous alloy, crystn. and domain struct. study 80−107056
Cr powder, thermogravimetric exam. of nitridation rate *(Japanese)* 79−20292
Cr-Ge system, phase diagram, thermal anal., X-ray diffr., microhardness, and electron probe anal. *(French)* 80−97462
$Cr_{1-x}Fe_xOOH$, thermogravimetric anal., thermal decomp. to obtain rutile type oxides 79−24740
$Cr_{1-x}Fe_xS$, metal-dielec. transition, X-ray, thermal anal., elec. cond. temp. depend. 78−67942
Cr_2N-CrN, thermogravimetric exam. of equilibrium *(Japanese)* 79−20292
Cr_2O_3-CrO_3-$ZrO_2.CrO_3H_2O$, exam. of thermal transitions 79−100116
CrS-FeS, sulphorspinel, struct. and elec. props. 80−49834
$CrSe_2$, layered, phys. and elec. props. 80−44594
Cs-SiO_2-Al_2O_3 system interactions, getter development for radiocaesium 80−83208
Cs-Sn alloy, peritectic reactions, phase diagram *(Russian)* 80−40784
CsCl-CuCl, phase transform. heats, DTA obs. *(Russian)* 80−55698

thermal analysis continued
CsF-EuF_3 system, thermal anal. and X-ray diffr., phase equilibria *(French)* 78−44107
$Cs_2Ni_3(P_2O_7)_2.nH_2O$, thermal dehydration 80−35513
$CsSrCl_3$, phase transitions, dilatometric and press. studies 77−15578
Cu, recrystallisation of cold rolled samples *(French)* 79−43269
Cu, vacuum deposited on Al substrate, recrystallisation 78−60044
Cu-Ag-Ge, Hume-Rothery glass form. 80−96449
Cu-Ag-P amorphous alloys, strain gauge factor and elec. props. *(Japanese)* 79−79130
Cu-Ag-P(6-14, 11-14 wt.%) amorphous, crystn. and elec. props., X-ray diffr., elec. resist. and DTA meas. *(Japanese)* 80−84088
Cu-Al martensite, temper hardening, study by TEM, DTA, microhardness and yield strength meas. 79−43260
Cu-Al-Fe-Mn (10,3,2 wt.%), phase comp. struct., continuous cooling from β-phase effect 79−24499
Cu-Al-Ni, mixed powder compacts, Ni content influence in sintering behaviour *(Japanese)* 80−35130
Cu-Al-Ni (13.8, 7.9 wt.%), cooling rates effect on internal friction *(Japanese)* 80−39217
Cu-Mn(Fe)(Ni)(Zn)(Ge), dilute solid soln., exam. of recrystallisation and stored energy 78−52836
Cu-Ni, adsorption of H_2+CO on (110) surface, TDS and UPS obs. 80−80052
Cu-Ni-Sn, liq. alloy, mixing enthalpies determ. using a SETARAM high temp. calorimeter *(German)* 80−44324
Cu-Sb (10-50 wt.%), thermal dilatometric anal. 79−56954
Cu-Si (up to 4.75 wt.%), exam. of high temp. oxidation in low O_2 and pure CO_2 atmospheres, by thermogravimetry 78−88574
Cu-Si-Te, phase equilib., DTA and metallographic anal. *(French)* 79−52182
Cu-W composite powder, prod. by H_2 reduction of $CuWO_4$ 79−20006
Cu-Zn-Al wire, made from pendant drop melt extraction technique from bulk material, X-ray diffr. and thermal anal. 79−43227
$Cu_3Ag_{1-x}Au_x$, phase relations, X-ray diffr. and differential thermal anal. 80−108395
CuCl-TlCl system, phase diagram and high ionic cond. obs. 78−79802
$CuFeO_2$, oxidation, thermogravimetric obs. 77−86203
$CuFe_2O_4$-$CuGa_2O_4$, physicochem. props. *(French)* 77−44233
CuI solid electrolyte α-phase stabilisation 80−29209
$CuInS_2$, region of existence, determ. by quenching and X-ray anal., phase transition 79−66054
$CuInS_2(Se_2)$-$GeS_2(Se_2)$, degree of solid solubility and phases characts. 78−35377
$(CuInTe_2)_{1-x}$-$(2ZnTe)_x$, phase diagram and cryst. growth of $CuZn_2InTe$ from $ZnCl_2$ flux 80−16287
$Cu_2Mn(Al_{1-y}Sn_y)$, Heusler alloys, thermal effects, saturation magnetisation 77−85499
Cu_2O-CuO-MoO_3, subsolidus phase diagram, mag. props. 80−50615
Cu_2S layer spray preparation and CuCl-thiourea complex formation 78−64471
Cu_2S-Tl_2S system, phase diagram 80−20906
$Cu_2S+Ln_2S_3$, powdered mixtures, reaction rate, production of ionic semiconductors 80−93741
Cu_2Te-Ge(Sn)Te_2, phase equilib., microstructural, DTA investigs. 77−16560
DyB_6, form. mechanism, reduction of Dy_2O_3 by B, DTA appl. 80−55643
Dy_xB_y, prep. and props., DTA study 80−20859
DyF_3-CsF, phase diagrams and ternary fluorides *(French)* 80−81040
DyF_3-KF, phase diagram, cryst. symmetry and lattice constants of phases *(French)* 79−65171
DyF_3-RbF, phase diagrams and ternary fluorides *(French)* 80−81040
$DyMnO_3$, thermogravimetric study of phase stability 79−100121
$ErMnO_3$, thermogravimetric study of phase stability 79−100121
Eu-Ga alloys, phase diagrams, struct. and comp. *(Russian)* 79−52163
Eu-Te, chalcogenides, exam. of crystal-chemical characts. 79−1407
EuTe, high-temperature evaporation and reactivity 80−103469
β-FEOOH, Mossbauer spectra obs., chemical and thermal anal., X-ray diffr., saturation magnetisation 80−88896
(Fe, Ni, Co)-Si-B, amorphous, compositional effect on struct. changes, after heating up to 700°C, exam. *(Japanese)* 78−48433
Fe, cast, spheroidizing effect of Mg and Ce modifiers 80−35193
Fe, cast, with spheroidal graphite, crystn. *(German, English)* 80−97473
Fe complex, $K_3[Fe(SCN)_6].4H_2O$, optical reflection spectrum, mag. suscept., permittivity, dehydration temp. 79−56809
Fe-(Co)-B and Fe-Ni-B(P), amorphous, crystn. 80−79704
Fe-Al (up to 7.2%), oxidation process 78−85022
Fe-B, metallic glasses and vapour deposited films, amorphous to cryst. transition 80−88048
Fe-B amorphous, crystallisation, activation energy conc. depend., DTA calcs. 79−60284
Fe-B metallic glasses, density, mech. and thermal props. 78−31432
Fe-B metallic glasses, struct., stability and crystn. 80−75173
Fe-B(−Ni), chemical ordering, crystallisation and glass transition temp. 79−90563
Fe-based metallic glasses, effect of metalloidal elements on thermal stability, crystn. temp. *(Japanese)* 79−94909
Fe-C eutectic, solidification cycle, thermal anal. 80−29945
Fe-C hypoperitectic, solidification cycle, thermal anal. 80−29945
Fe-Co-Ta for semipermanent magnets *(French)* 79−47675
Fe-Cr (20 wt.%), high temperature oxidation resistance, effect of rare earth and reactive element additions *(Japanese)* 79−20271
Fe-Cr-Al (0.3 wt.%), oxidation behaviour at high temps. *(Japanese)* 80−35404
Fe-Cr-Mo-Ti (13, 1.5, 3.5 wt.%), equilibrium studies on chi-phase strengthening 79−24496
Fe-Cr-Ni austenitic alloy, cold deformed, α-γ transition, calorimetric study *(Russian)* 80−55390
Fe-Cr-(C), oxidation, grain size and growth effects *(Japanese)* 77−48583
Fe-Cu-C, mixed powder compact, sintering mechanism 78−15343
Fe-Ga, constitution between 10 and 50 at.% Ga, heat treatment depend., BCC phases *(German)* 77−90325
Fe-Mo system, thermomech. props. 80−89208
Fe-MoS_2, exam. of props., using differential thermal analysis, and metallography *(Russian)* 79−15653
Fe-Ni, α to γ transformation, changes in Young's modulus and electrophysical props. *(Russian)* 79−20042
Fe-Ni (19wt.%) alloy, oxidation in CO_2, 700 to 1000°C, thermal and metallographic anal., EPMA 78−72931

thermal analysis continued
Fe-Ni (20 to 31 wt.%), exam. of martensitic transform. and reverse transform. using differential and thermomagnetic resistance analysis *(French)* 79−52214
Fe-Ni alloys, enthalpy change between $\alpha' \rightarrow \gamma$ and $\alpha \rightarrow \gamma$ transformations 80−93550
Fe-Ni based metallic glasses, nonisothermal crystallisation kinetics, DSC anal. 79−27927
Fe-Ni-Al alloys, phase diagram, miscibility gap, DTA meas. 78−92237
Fe-Ni-Al-Co-Ti base alloys, highly coercive, phase comp., Mossbauer meas. 80−39996
Fe-Ni-Cr-Si (35, 18, 2 wt.%), heating element wire, failure and oxidation 79−83378
Fe-Ni-Mn martensitic alloy, precipitation 77−12630
Fe-Ni-P-B, metallic glasses, struct. relax., annealing effects on mag. props. 80−89261
Fe-Ni-P-B metallic glass, crystallisation temperature values from isothermal transformation times 80−59397
Fe-P-C, amorphous alloy, crystallisation 79−100112
Fe-Si-B metallic glasses, crystn., differential scanning calorimetry obs. 79−82160
Fe-Ti-C, rapidly quenched by splat-cooling 80−84923
Fe-Zn, homogeneous intermetallic cpd., synthesis and charact., ξ-phase 79−83177
Fe-Zn, homogeneous intermetallic cpd., synthesis and charact., δ_1-phase 79−87616
Fe-Zn, phase diagram, DTA, EDAX, X-ray diffr. study 80−50602
Fe_2-rare earths, H_2 reaction, DTA and DTG anal. 79−100434
$Fe_{1-x}B_x$ metallic glasses, struct. and cryst., Mossbauer spectra, DSC, and magnetisation meas. 79−94906
$Fe_{84}B_{16-x}C_x$, amorphous alloys, short range order, Mossbauer and DSC study 80−39960
$FeBO_3$-MBO_3 solid soln., (M=Mn, Cr, Al, Ga, In), synthesis, crystal chem. and mag. props. 78−31058
$(Fe_{100-x}Ni_x)_{100-y}B_y$, metallic glass, embrittlement and crystn. 80−7685
$Fe_{40}Ni_{40}B_{20}$, amorphous, anomalous thermal dilatation 79−55668
$Fe_{32}Ni_{36}Cr_{14}P_{12}B_6$ metallic glass, crystn. kinetics by TEM 80−75186
$Fe_{40}Ni_{40}P_{14}$, glass transition, viscous flow and differential scanning calorimetry meas. 80−96635
FeO, wustite, invariant points between stable and metastable phases, T-P-X diagram *(French)* 80−29938
FeO_x, wustite field, thermodynamic props. and subphases, thermogravimetry, 1100-1300°C 80−76239
Fe_2O_3 based γ defective spinels, elec. cond. behaviour during transform. to α rhombohedral phases *(French)* 80−49354
α-Fe_2O_3 crystal flux growth, solubility and relative supersaturation in Fe_2O_3-PbO-V_2O_5 fluxed melt system 80−64934
α-Fe_2O_3, prep. by evaporative decomposition of $Fe(NO_3)_3.6H_2O$ soln. 79−20011
Fe_2O_3, reduction, double reaction, thermogravimetric curves, reaction kinetics exam. *(French)* 78−31705
Fe_2O_3, reduction by H_2, kinetics and mechanism 77−48619
Fe_2O_3:Mn, surface props. 79−65302
α-Fe_2O_3-Li_2O, structural and thermal phase behaviour from mag., spectral and thermal studies 80−2673
Fe_3O_4, finely dispersed, electronic phase transition, cond. and DTA meas. 78−91736
Fe_3O_4, magnetite, Verweg transition temp., isotope effect, elec. resist. and DTA meas. 80−24976
Fe_3O_4, reduction, double reaction, thermogravimetric curves, reaction kinetics exam. *(French)* 78−31705
$Fe(OH)_3$ thin films, Mossbauer spectra obs., chemical and thermal anal., X-ray diffr., saturation magnetisation 80−88896
β-FeOOH, dehydration 80−79767
$Fe_2O(OH)_4$, Mossbauer spectra obs., chemical and thermal anal., X-ray diffr., saturation magnetisation 80−88896
Fe_3Pt, off stoichiometric, austenite ordering and martensite tetragonality 77−36501
$Fe_{78}Si_{10}B_{12}$, amorphous alloy crystallisation study *(Japanese)* 78−9959
Fe_xVS_2 ($0.20<x<1.00$), phase diagram and order-disorder transition of vacancies 80−81039
Ga, vacuum deposited film characterisation *(French)* 79−51447
Ga-In-As-Sb quaternary system, phase equilib. and heterojunctions 79−34016
Ga-In-Sn, thermal analysis, determination of liquidus and reactions 78−88446
Ga+As reaction temp. determ. for GaAs synthesis 77−24978
GaP (100) thermal and vap. phase etching in H_2-HCl-PH_3, obs. 77−77612
$GaPO_4$, high-low cristobalite transitions, DTA meas. 79−82335
$(GaP)_x(ZnSe)_{1-x}$, solid solution, reaction of Zn with Se during Czochralski growth and LPE 79−8238
Ga_2Se_3-FeSe, phase diagram, elec. cond., mag. susceptibility 80−88301
Ga_2Se_3-MnSe system, crystallographic study, phase diagram, DTA and X-ray diffr. determ. *(French)* 79−24506
$GdCl_3.6H_2O$, X-ray emission luminesc. *(Japanese)* 80−55763
$Gd_3Ga_5O_{12}$, garnet-perovskite transform 80−15239
Gd_2O_3-Al_2O_3 glasses, crystallization 79−50998
Gd_2O_3-Ga_2O_3 system, phase diagram relationships of garnet-perovskite transform. 80−97460
Ge-As, p-T-x diagram 77−11669
Ge-GeO_2 mixtures, gasification kinetics and GeO form. mechanism *(Russian)* 80−21273
Ge-S glasses, Cu doped, thermal, structural and dielectric props. 79−60283
Ge-S-In, chalcogenide glass, determ. of glass phases, phys. props. meas. 79−23526
Ge-Se-Te glasses, form. region, elec. props. 79−94904
Ge-Sn-As system alloys, microstruct., X-ray phase and thermal anal. 77−32564
Ge-Te binary glass, eutectic, DSC obs., thermodynamic and thermokinetic characts. 80−39309
Ge-Te system, phase equil. diagram, $GeTe_{1\pm x}$ region analysis by metallography, microhardness and DTA *(French)* 77−70034
GeO_2 glass, nonisothermal devitrification kinetics 80−92465
GeO_2-CdO system, phase diagram anal. by differential thermal, X-ray anal. 77−8805
GeS, film on Ge, evaporation, thermogravimetric, electron microscopy investigs. 77−15715
GeS_{11} glass, neutron irrad., thermal and elec. props. 79−19286

thermal analysis continued
- $GeS(Se)_x$, x=1 or 2, ht. of transition determ. by thermography 78−22847
- $GeSe_2$ amorphous semicond., DC conductivity, calorimetric, and X-ray diffr. meas. 79−78107
- $GeSe_2$, single crysts., 3 polymorphic forms, DTA, photolum., IR and Raman sepctroscopy 80−33923
- $GeSe_2$-Te, phase diagram and vitrification region determ. by DTA, SEM, X-ray diffr. *(French)* 77−72565
- Ge_xSe_{1-x}, $0<x<0.2$, crystallisation in amorphous bulk and thin films 78−55813
- GeTe-As_2Te_3 system, phase diagram, eutectic comp., thermographic and X-ray anal. *(Russian)* 77−63646
- H_2O-NaCl-sucrose, phase diagram determ., appls. in cryobiology 78−15777
- β-$H_2O.11Al_2O_3$, conversion from β-$Na_2O.11Al_2O_3$ and characterization 78−3069
- $HUO_2AsO_4.4H_2O$ and $HUO_2PO_4.4H_2O$ layered cpds., struct. investigs. below antiferroelec. transition temps., H bond ordered structs. 80−107416
- ^4He, HCP-FCC transition, near triple point, thermal anal. 79−60596
- Hf-Ni(Co), amorphous, formation, decomposition and elec. transport props. 80−20143
- $Hf_{1-x}Fe_x$ amorphous alloys, formation, crystallisation and electrical resistivity 80−96838
- HfO_2-EuO_2 system, liquidus determ. from thermal anal. *(Ukrainian)* 79−96007
- HfO_2-PrO_x, phase equilibria and physicochem. props. in range 1000 to 1800°C 79−100117
- HfO_2-R_2O_3 solid solns., prep., crystn., R=Nd,Sm,Dy,Yb 78−42909
- HfO_2-TiO_2, phase relations and thermal expansion 77−21121
- HfO_2-TiO_2 system, liquidus determ. from thermal anal. *(Ukrainian)* 79−96007
- $Hg_{2.86}AsF_6$, anisotropic supercond. caused by Hg extrusion, DTA 78−55953
- $Hg_{2.91}SbF_6$, anisotropic supercond. caused by Hg extrusion, DTA 78−55953
- Ho-Ga, exam. of phase diagram, using differential thermal and X-ray phase anal. *(Russian)* 79−11555
- $HuO_2P(As)O_4.4H_2O$, water deficiency, enthalpy of dehydration, thermogravimetric anal. 80−65251
- In-Bi alloy system at high press. and temp. 78−92238
- In-Pb, thermal anal. solidus determ. 79−20030
- In-Pb-Sn system, thermal anal. 80−35162
- In-Sb, thermodynamic quantity meas. by quantitative thermal anal. of heating process 78−19730
- InAs-CdTe quasi-binary system, temp.-comp. diagram, physicochem. and thermodynamic analysis 80−104127
- $In_2O_3+Sb_2O_3(Sb_2O_5.H_2O)$ reacts., complex oxide form., struct. 77−16516
- $InSbS_3(Se_3)$, prep., polymorphism, cryst. struct. 78−44002
- InSe-SmSe system, microhardness and electrophys. props. 79−87093
- In_2Te_3-PbTe system, phase diagram, elec. props. 78−35361
- $KCaF_3$, struct. phase transitions, DSC, birefr., and neutron powder diffr. obs. 80−70149
- $K_2Ca(SO_4)_2.H_2O$, syngenite, thermal dehydration under nonisothermal conditions 80−3324
- $K_2Ca(SO_4)_2.H_2O$, thermal dehydration, isothermal kinetics 79−15982
- KCl-NaCl-K_2NaVF_6, phase diagram 77−48416
- $K_2CrO_4+La_2(NoO_4)_3$, $(Nd_2(NoO_4)_3)$, X-ray phase analysis, IR absorption spectra, and thermogravimetric anal. 79−1944
- $K_2Cr_2O_7$ melt, DTA and TGA curves 79−43131
- $K_2Cr_2O_7$, polymorphic behavior, depend. on thermal and prep. history 80−34184
- $K_2Cr_2O_7$, thermal props. thermal anal. and X-ray diffr. obs. 78−30752
- KD_2PO_4, transparent dielec., thermal analysis of laser-induced damage 80−66336
- $KEuHP_3O_{10}$ acid, exam. of thermal decomposition 80−55638
- KF-BeF_2-DyF_3 system, KBe_2F_5-DyF_3 cross section phase diagram, vitreous phases struct. 77−24383
- KF-ErF_3, phase diagram 80−92645
- KF-EuF_3 system, composition of phases determ. by DTA and X-ray crystallography *(French)* 77−68945
- KF-NaF-K_2NaVF_6, phase diagram 77−48416
- $KMg_2(AlSi_3O_{10})F_2$-$KMg_{2.5}Si_4O_{10}F_2$, solid soln., melting and crystn., quenching and DTA study 80−39263
- $KMg_2LiSi_4O_{10}F_2$-$NaMg_2LiSi_4O_{10}F_2$, solid soln., solid solubility and swelling characts. 80−59660
- $K_2Mg_4Mo_4O_{16}.(OH)_2(H_2O)_2$, dehydration processes rel. to stoichiometry *(French)* 79−24734
- $K_2Mg(S_2O_3)_2.6H_2O$, isolation, struct., decomposition *(French)* 78−52506
- $(K_xNa_{1-x})NbO_3$ single crystals, growth and phase transitions 79−33915
- $KNbO_3$ powder synthesis, unit cell determ. 78−11168
- $K_2Ni_3(P_2O_7)_2.nH_2O$, thermal dehydration 80−35513
- KO_2, non-isothermal decomp. kinetics 80−16649
- KO_2, thermal decomp. macrokinetics, differential thermal anal. 80−16650
- K_2O-MgO-SiO_2 glass, crystalline phase precipitation during crystallisation early stages, DTA *(Japanese)* 78−42919
- K_xO_y, thermodynamic props. 80−29184
- KOH-KO_2, phase diagram *(French)* 80−107177
- K_2SO_4, phase transform., mech. of thermal hysteresis, DTA, dilatometry and dielec. meas. 80−75353
- K_2SO_4-$ZnSO_4$ system, glass formation and phase diagram study, physical props. 78−27500
- $K_{1-x}Ta_{1-x}W_{1-x}O_6.nH_2O$, composition, struct. and ionic conductivity 80−49410
- $KX(MoO_4)_2$, X=Sm, Eu, Gd, polymorphism investig. by X-ray diffr. and DTA 77−4091
- $KYbHP_3O_{10}$, thermal decomp., thermogravimetric and X-ray obs. 80−101013
- $LaBO_3$ (B=V, Cr, Mn, Fe, Co, Ni), chem. stability X-ray and thermal anal. 79−79242
- $LaMn_{1-x}Cu_xO_{3+y}$, O_2 stoichiometry by thermogravimetry 77−36434
- La_3NbO_7, synthesis and cryst. growth 80−71590
- $La(OH)_3$, thermal decomposition, TGA, DTA, X-ray diffr. study *(Japanese)* 77−36436
- $La_2(SO_4)_3.9H_2O(D_2O)$, dynamic disorder of water mols., isotope effect obs. 80−55015

thermal analysis continued
- $(Li,Na,K)(Nb,Ta)O_3$, pseudo-binary and ternary systems quenched metastable glassy and cryst. phases 80−29935
- Li soaps, $n.C_{13}$-$n.C_{20}$, phase transition temps. and enthalpies, DSC obs. 80−45544
- Li/SO_2 cells, DTA, safety studies 80−81428
- Li/SO_2 cells, safety studies, DTA of constituents 80−16795
- Li-Pd, phase diagram and mag. props. 77−90321
- Li-Pt, phase diagram for comp. range 0-40 at.% Pt, mag. and elec. props. *(German)* 80−84912
- Li_5AlO_4, ionic cond., effects of Li_2SO_4 addition, moisture, and LiOH 79−99362
- Li_5AlO_4, ionic conduction, environment effects 77−76600
- $LiBO_2$-In_2O_3, phase composition, mag. props, elec. cond. 80−55365
- $LiCd_{1-x}Tl_x$, intermetallic, X-ray and Knight shift meas. of ^{205}Tl and ^{113}Cd 79−42851
- LiCl-$AlCl_3$, phase diagram determ. by DTA and X-ray anal. *(Japanese)* 78−92250
- LiCl-Li_2O-P_2O_5 glass system, vitreous domain, struct., elec. cond. *(French)* 80−70135
- Li_2CrO_4-K_2CrO_4, phase diagram determination by DTA and X-ray diffr. 78−31391
- LiF-AlF_3-Na_3AlF_6-Al_2O_3 system, phase equilibrium, X-ray diffr., DTA, quenching, optical microscopy study 80−50610
- $LiIO_3$, phase transitions obs. by DTA, heat treatment, X-ray diffr. *(Chinese)* 78−2249
- $Li_2K(IO_3)$ in $LiIO_3$-KIO_3 system, lattice parameter, equilib. and metastable phase diagram *(Chinese)* 80−7538
- Li_2MgSiO_4-Li_2ZnSiO_4, form. of solid soln. *(Japanese)* 77−25037
- $Li(Na,K)CO_3$, therm. anal. and X-ray diffr. study *(French)* 79−46630
- $LiNbO_3$-CdO, CdO addition effect on sintering 79−83157
- Li_2O-$2SiO_2$ glass, DTA study, Kissinger plot 80−84084
- Li_2O-$Al_2O_3(Ga_2O_3)(Bi_2O_3)$, quenched glasses, crystn. and ionic cond. 80−33899
- Li_2O-CaF_2 melts, component activities *(Russian)* 77−60104
- Li_2O-SiO_2 glass, water content effect on crystal nucleation and growth 79−55670
- Li_2O-SiO_2(-TiO_2) glass, crystn., kinetic study using differential scanning calorimetry 80−44138
- Li_2O-TiO_2, pseudobinary phase rotations, DTA and X-ray anal. 80−108411
- LiOH, ionic conduction, environment effects 77−76600
- $Li_{x+2}P_xO_{3x+1}$, polyphosphate, melting and crystallisation 80−70376
- $(LiPO_3)_x.H_2O$, existence of high- and low-temp. cryst. forms, X-ray diffr. data 79−19179
- $LiTaO_3$-$NaTaO_3$-$KTaO_3$, quenched metastable glassy and crystalline phases 79−61568
- Li_2TiO_3-MgO (20 to 40 at.%), order-disorder transitions, DTA and X-ray anal. 79−29050
- $LiVO_3$-$Li(Nb_{1-x}Ta_x)O_3$ systems, phase relations study using DTA, rel. to LPE of $Li(Nb,Ta)O_3$ 79−41467
- Mg-Cu(Ni), binary system, nonstoichiometry, of Laves phases, $MgCu_2$ and $MgNi_2$ *(French)* 78−52770
- Mg-Ga alloys, form. enthalpies and excess entropies, differential scanning calorimetry *(German)* 79−51278
- Mg-In liquid solns., EMF and calorimetric meas. 80−55359
- Mg-$MgNi_2$-Zn, diagram of state, Zn solubility, initial phase precipitation *(Russian)* 80−66478
- Mg-Y-Cd, phase equilibria and mech. props. *(Russian)* 80−20894
- $Mg(AlH_4)_2$, prep., thermal decomposition, molar heat capacity, heat of form. 80−3325
- $MgAl_2O_4$, powder effect of precursory sulphate solution anion on sintering 78−56605
- $MgBr_2$-ABr (A=Cs, Rb, K, Na, Tl), thermochemical and struct. investigation *(German)* 79−1423
- $Mg(IO_3)_2.4H_2O$, struct. and phase transition using X-ray diffr. and thermal anal. *(Chinese)* 79−51059
- $Mg(NO_3)_2$-RNO_3 (R=Li, Na, K), thermogravimetric anal. of dehydration processes *(Japanese)* 80−66791
- $Mg(NO_3)_2.6H_2O$, crystal structure changes due to substitution of Mg^{2+}, by Co^{2+} or Ni^{2+} *(German)* 80−24428
- MgO, heated on W, thermal anal. using mass spectrometric, technique, vaporisation behaviour 80−79932
- MgO-Cr_2O_3, composition obs. by thermogravimetry 79−16081
- $(MgO)_x$-$(Al_2O_3)_y$ formation of nonstoichiometric spinel on heating hydrous $MgAl_2O_4$ 78−76672
- $(MgO$-Fe_2O_3-Cr_2O_3-$TiO_2)$:Na_2O, powder, prep., heat treatment, Na_2O impurity effect on props. 77−16528
- $MgO.nAl_2O_3$, nonstoichiometric spinel, DTA 77−28791
- $Mg(PO_4)_2.xH_2O$, x=8, 22, dehydration and water bonding 77−44456
- Mn pyrophosphates, physicochem. charact. 77−39562
- Mn_2O_3, thermal decomposition, exam. by thermogravimetric methods 78−80743
- Mn_3O_4, reduction by C and CO, exam. by thermogravimetric methods 78−80743
- Mo oxides, low-grade, soda roasting study *(Korean)* 80−93508
- MoF_6-graphite intercalation cpd. 78−27441
- $(NH_4)_2Mg(S_2O_3)_2.6H_2O$, isolation, struct., decomposition *(French)* 78−52506
- NH_4NO_2, thermal anal. by energy-dispersive X-ray diffr. 78−91440
- $(NH_4)_2Ni_3(P_2O_7)_2.nH_2O$, thermal dehydration 80−35513
- $5(NH_4)_2O.12\ WO_3$, thermal decomp., 100-500°C, thermogravimetric, evolved gas, X-ray and SEM expts. 77−56223
- $NaCaPO_4$-Ca_2SiO_4 partial system, phase diagram 78−35364
- $NaCaPO_4$-Ca_3SiO_5 partial system, phase diagram 78−35365
- NaCl-$AlCl_3$, phase diagram determ. by DTA and X-ray anal. *(Japanese)* 78−92250
- NaCl-CsCl-$CrCl_3$ system, thermography *(Russian)* 77−63645
- NaCl-KCl-CuCl system diagram investig. *(Russian)* 79−96015
- NaCl-KCl-$NiCl_2$ system diagram investig. *(Russian)* 79−96014
- NaCl-NaBr-TeO_2, condition diagram, thermographic obs. *(Russian)* 80−55377
- NaF-Al_2O_3, β-Al_2O_3 form. *(Japanese)* 78−6912
- NaF-SrF_2-CrF_3, glass transition, crystn. and melting temps., optical transmission *(French)* 80−64910
- NaF-YF_3 system, fusibility diagram, quasibinary section of NaF-YF_3-YOF system characts. 80−55371
- $Na_3Fe_2(PO_4)_3$, polymorphism and ionic conduction *(French)* 78−67678
- $(Na_xKy)_2CO_3$, non-stoichiometric, cryst. struct. *(French)* 80−79761
- $NaNO_3$, low temp. struct. changes, elec. props. 79−87377
- $NaNbO_3$-$SrNb_2O_6$, phase diagram, props. meas. 79−11576

thermal analysis continued
$Na_2Ni_3(P_2O_7)_2.nH_2O$, thermal dehydration 80−35513
NaO_2, non-isothermal decomp. kinetics 80−16649
NaO_2, thermal decomp. macrokinetics, differential thermal anal. 80−16650
Na_2O-Al_2O_3-P_2O_5, exam. of subsolidus structure 79−4954
Na_2O-CaO-SiO_2 glass, water content effect on crystal nucleation and growth 79−55670
Na_2O-$GeO_2(TiO_2)(SnO_2)(ZrO_2)(ThO_2)$-$SiO_2$ glass, density, refractive index, thermal expansion, hardness IR spectra, DTA *(Japanese)* 78−15535
Na_2O-PbO-SiO_2 glass-ceramic composite, directionally crystallised 80−107058
NaOBr, solns., as reagents in enthalpimetric determs. 78−68954
$NaPO_3$-AlF_3(-NH_4HF_2) glasses, synthesis, chem. thermal and optical anal. *(French)* 79−100104
Na_3PO_4-$Ni_3(PO_4)_2$ system, phase equilibrium diagrams, crystallographic study, double orthophosphates *(French)* 80−93546
Na_2SO_4, high temp. phase, DTA and dielec. meas. 79−82333
Na_2SO_4, pure and K-doped, phase transforms., X-ray, DSC and elec. cond. obs. 79−33082
$Na_2[B_4O_6(OH_4)].8H_2O$, differential thermal X-ray anal. of phase transitions in non isothermal conditions 79−52205
Nb-Ge, superconductor, phase diagram determ. using various methods up to temp. of 2200°C 79−8414
Nb-Ge, thermal anal. of levitation-heated samples 79−2772
Nb-Si diagram of state, melting temp., polymorphic transform. temp. *(Russian)* 80−50594
Nb-Ti-O system, phase equilib., microstruct., thermal, and X-ray anal. 77−8806
NbH, internal friction 78−6962
$Nb_{12}O_{29}$-Nb_2O_5, oxide defect structures of stable and metastable phases, 800 to 1100°C 79−46651
$NbOAsO_4$ and $NbOAsO_4$ $4H_2O$, crystal growth, composition, struct. and crystallographic charact. 80−54198
Nd-Ga, phase diagram *(Russian)* 78−27478
Nd-Ga alloy, phase diagram, DTA, X-ray and metallographic obs. 79−24494
Nd-H, possibility of H ordering, DTA meas. 79−52174
$NdTlO_3$, physicochem. props. 80−25625
$Ni_{75}Si_8B_{17}$, amorphous alloy, crystallisation study *(Japanese)* 78−9959
Ni, electrodeposited film, thermal anal., occlusion of gases rel. to mag. props. 80−59823
Ni, preoxidised, reaction with SO_2 at high temp. 79−39047
Ni-B amorphous films, electronic transport and crystn. activation energies *(French)* 80−6807
Ni-Cr-Al-TaC, eutectic composite, microstructure, fatigue props. 80−85038
Ni-Ga alloys, phase diagrams and cryst. struct., DTA, X-ray diffr. and microprobe anal. *(French)* 79−47660
Ni-Ge binary system, phase diagram rel. to that of Co-Ge *(French)* 80−97463
Ni-P, amorphous electrodeposited alloys, phase-separation *(Japanese)* 80−54140
Ni-P, electrodeposited film, thermal anal., occlusion of gases rel. to mag. props. 80−59823
Ni-P alloy, electrodeposited, heat induced struct. changes *(Japanese)* 78−15433
Ni-P(B), amorphous, thermal anal. and X-ray diffr., solidification struct. development *(French)* 78−91253
Ni-S, electrodeposited film, thermal anal., occlusion of gases rel. to mag. props. 80−59823
Ni-Ta (70, 30 wt.%) metallic glass, struct. and crystn. *(Russian)* 80−70136
$Ni_{1-x}Cr_xS$, elec. transport, mag. susceptibility and DTA meas. 80−96954
$Ni_{36}Fe_{32}Cr_{14}P_{12}B_6$ metallic glass, mech. props. and thermal stability 80−76362
$(Ni_{1-x}Fe_x)S$, solid solns., electronic props., X-ray, thermal and Mossbauer study 79−78376
$Ni(H_2V)_2(H_2O)_2$, synthesis and characterisation *(French)* 80−45225
$(Ni_{0.5}Pd_{0.5})_{82}P_{18}$ amorphous alloy, liquid-quenched, crystn. kinetics, nucleation 80−100176
$(Ni_5Pd_5)_{82}P_{18}$, phase separated, exam. of crystallisation by differential thermal analysis 78−87623
$Ni_{1-x}S$, oxidation, TG/DTA/MS obs. 78−31745
$NiTiO_3$, synthesis from products of soln. spray drying, kinetics 77−16519
$Ni_{62}Ti_{29}Zr_9$, amorphous, H-sorption, X-ray and DSC obs. 80−49526
$Ni_{0.685}Zn_{0.177}Fe_{2.138}O_{4+\gamma}$, phase diagram, therm. anal. 79−78945
$Ni_{64}Zr_{36}$, amorphous and cryst., H-sorption, X-ray and DSC obs. 80−49526
PLZT ceramics, ferroelectric and struct. transitions, crystallographic, thermal, and dielec. anal. 80−29693
Pb bismuthate glass, IR transmission props., density 79−74127
Pb multicomponent glasses, alkali evaporation, mass spectrometry study, thermal anal. 79−74464
Pb, splat quench in vacuum 79−52268
Pb-In-Sn system, liquidus and solidus isotherms 78−44088
Pb-Rb, phase diagram *(Russian)* 78−19720
Pb-Sb, phase transform. at high press., DTA, eta, beta thermodynamic stable phases *(Russian)* 79−66051
Pb-Sb, thermal analysis in non-faceted/faceted eutectic systems 80−71637
Pb-Sn-Te, liquidus meas. by DTA 79−95999
Pb-Te-O, thermal stability 78−44104
Pb-Zn, liquid phase immiscibility determ., DTA 78−64523
$PbCl_2$-$ZnCl_2$, thermodynamic quantity meas. by quantitative thermal anal. of heating process 78−19730
PbF_2, polymorphic transition temps. under hydrostatic press., DTA study 80−2156
PbF_2-AlF_3 glass, optical props., crystn. and thermal expansion 80−48367
PbI_2, high press. phase diagram to 3.5 GPa 80−104126
$Pb(Mg_{1/3}Nb_{2/3})O_3$-$PbTiO_3$-$PbZrO_3$, piezoelec. PCM ceramic, formation process *(Japanese)* 77−85978
$Pb(NO_3)_2$, low temp. struct. changes, elec. props. 79−87377
Pb_2NbCoO_6, $Pb_3Nb_2CoO_9$, thermogravimetric and X-ray phase investig., synthesis by solid-phase reactions 77−21067
Pb_2NbFeO_6, form. reacts., thermogravimetric investig. 78−35340
$PbNb_2O_6$-$NaNbO_3$, DTA *(French)* 77−44234
thermal analysis continued
PbO/TeO_2 system, central region of phase diagram, X-ray and thermal anal. 79−70046
PbO-ZnO-B_2O_3, Corning 7575 seal glass, devitrification 78−79532
4PbO.GeO_2, X-ray phase and thermal anal., new antiferroelectric 79−1744
2PbO.SiO_2, glassy, DTA obs. of crystn. kinetics 77−89381
2PbO.SiO_2 melt, coding rate influence on constitution of silicate anions, crystn. kinetics 80−103248
$Pb_3(P_xV_{1-x}O_4)_2$, ferroelastic phase transition, DTA, dilatometric and Brillouin scatt. study 80−70398
$Pb_3(P_xV_{1-x}O_4)_2$, phase diagram and crystallography *(French)* 78−92252
PbS, oxidation, $PbSO_4$ distrib. in products *(Polish)* 80−25883
PbS-$CuS_{1.8}$-ZnS, phase equilib. *(Russian)* 77−28786
PbS-In_2S_3, phase investigation 80−66488
$Pb(SCN)_2$, thermal decomposition, kinetic parameters from thermogravimetric data 79−61859
$PbSnF_4$, allotropic transformations 80−84926
$PbSnF_4$, anionic conductor *(French)* 79−1523
Pb_2TaFeO_6, form. reacts., thermogravimetric investig. 78−35340
Pb_2TaMnO_6, reaction of form. from oxides, ferroder. props. 80−55326
PbTe-Ga_2Te_3, phase interaction, DTA, XPA and microstructural anal. 80−96625
PbTe-InTe system, phase interactions and solid soln. form., physicochem. and elec. characteris. 80−104129
PbTe-PbSe system, thermodynamic props. 80−11635
$PbTiO_3$, amorphous, crystallisation process, DTA and Raman spectroscopy meas. 80−75161
$Pb_3WFe_2O_9$, form. reacts., thermogravimetric investig. 78−35340
Pb_2WO_5, phase transformation study by high temp. X-ray diffr. and differential scanning calorimetry 79−43244
Pb(Zr, Ti)O_3, formation 79−43185
$PbZrO_3$, phase transitions, X-ray, dielec., and thermal anal. 80−45020
1-x$PbZrO_3$-x$PbSc_{0.5}Nb_{0.5}O_3$, $0 \leq x \leq 1$, phase transitions, X-ray, dielec., and thermal anal. 80−45020
Pd-Ag-H, alloys, 25-50% Ag, thermodynamic props., 555-700K 79−65216
Pd-Ag-Si alloys, amorphous, crystn. kinetics, DSC meas. 80−1933
Pd-Au-Si, amorphous films, RF sputter deposition, composition and thermal behaviour 80−55292
Pd-Cu-H(D) dilute alloy soln., thermodynamic props. at high-temp. 79−99334
Pd-Ni-Si amorphous alloys, crystn. process during isothermal ageing 80−89275
Pd-Si amorphous films, RF and DC sputter deposition, composition and thermal behaviour 80−55292
PdAl-Fe(Ni), phase diagrams, eutectic points and solubility *(Russian)* 80−40333
Pr-Ga (0 to 50 at.%), phase diagram and cryst. structs. of intermetallic cryst. 80−3002
$Pr(OH)_3$, thermal decomposition, exam. 80−55640
Pt-O, preanodised or passivated, DTA 77−16733
$PuC_{0.82(1.49)}$, high temp. enthalpies 80−49384
PuO_{2-x}, O_2 chem. diff., dilatometry and thermogravimetry study *(French)* 79−73339
Rb-Se system, phase equilibria 78−44079
Rb_2CO_3, high press. phase relations, DTA 77−43329
RbCl-CuCl, phase transform. heats, DTA obs. *(Russian)* 80−55698
$RbCrI_3$, radiocrystallographic and mag. study *(French)* 79−46632
RbF-EuF_3 system, thermal anal. and X-ray diffr., phase equilibria *(French)* 78−44107
$RbLiSO_4$, thermal and dielectric props., ferrielectricity 79−28688
$Rb_2Ni_3(P_2O_7)_2.nH_2O$, thermal dehydration 80−35513
$RbPO_3$-$AgPO_3$ system, phase diagram 77−25033
Re-Hg-O system, solid state synthesis of 5 crystn. compounds, thermal and X-ray anal. *(French)* 79−66281
Ru, oxidation resistance in Ar and air 77−25201
RuP_2, oxidation resistance in Ar and air 77−25201
α-S, monoclinic allotrope, thermal behaviour 78−67813
S_xSe_y, s=6-3, y=2-5, thermal behaviour 78−67813
Sb, liquid-quenched, stabilisation and transformation kinetics of metastable phases 80−3022
Sb, polymorphism at high press., temp. hysteresis, DTA *(Russian)* 79−82328
Sb-S-I glasses, activation energy of crystn. 80−64920
Sb_2O_3-Na_2O-B_2O_3-SiO_2 glass, elec. cond. meas., −160 to 200°C 80−20190
$Sb_4O_5Cl_2$, single crysts., prep. and props. 80−35067
Sb_2S_3 crystals, X-ray and DTA methods energy gap temp. dependence *(German)* 78−43119
Sc-Co(Ni)(Cu), phase diagram determination, using X-ray diffr., metallography and DTA techniques *(Russian)* 79−34004
Sc-H, p-T phase diagram and influence of H pressure, on decomposition temp., DTA exam. 80−29929
Se, amorphous, kinematic transform. study by DTA 79−27921
Se, amorphous films, evaporated, ageing and crystn., DTA 80−65413
Se film, amorphous, substrate effects on crystn. kinetics 77−1337
Se, liq., heat capacity and chem. equilib. 80−103486
α-Se, monoclinic allotrope, thermal behaviour 78−67813
Se, monoclinic to trigonal conversion, thermodynamic stability and associated investigs. 80−24592
Se-Bi bilayers chemical reactions, differential scanning calorimetry technique and obs. results 78−2398
Se-Te-$Ge_{0.5}Sb_{0.5}$, DTA, critical cooling rates determ. *(French)* 77−72682
$(Se)_x$, crystn. and melting 80−40241
Se_xTe_{1-x}, amorphous, structural relaxation and crystallisation kinetics study by DTA 80−59394
Si ribbon growth by EFG, thermal sensitivity and stability 80−107080
Si-B system, DTA, X-ray diffr. and metallographic study *(German)* 80−66484
Si-Na-B-O-N glass, synthesis and characterisation 80−108381
SiC fibres obtained from polycarbosilane fibre 80−50582
Si_2N_2O-Al_2O_3, solid soln., prep., effect of Si_3N_4 powder reactivity 80−45256
SiO_2, high-low cristobalite transitions, DTA meas. 79−82335
SiO_2-Al_2O_3-CaO-MgO-NaO-K_2O-B_2O_3-ZrO_2, glaze, exam. of zircon crystallisation 79−19155
SiO_2-Li_2O-K_2O-ZnO glass ceramic, prep., phase transformations and physical props. 80−45299

thermal analysis continued
SiO_2-Na_2O-K_2O water glass with polyethylene filler, thermogravimetric and thermomechanical anal. 79−20020
SiO_2-TiO_2 system, true solid soln. existence obs. 77−36475
SiO_2-water system, inorg. polymer struct. form., globular crystn. 80−101042
SiO_3-Na_2O-CaO-MgO-Al_2O_3 charge, silicate formation during heating 80−55342
Sm-Ga, phase diagram *(Russian)* 78−27478
$Sm_3Ga_5O_{12}$, garnet-perovskite transform 80−15239
$SmMnO_3$, thermogravimetric study of phase stability 79−100121
Sm_2O_3-Ga_2O_3 system, garnet-perovskite transform., phase diagram relationships 80−97460
Sn droplets, on Bi, Zn and Al, heterogeneous nucleation 80−44294
Sn-Bi, thermal analysis in non-faceted/faceted eutectic systems 80−71637
Sn-F system, partial phase diagram construct. in Sn-SnF_2 region *(French)* 80−50605
Sn-Ni electrodeposits, metastable, transform. kinetics 78−43262
Sn-Zn, thermodynamic quantity meas. by quantitative thermal anal. of heating process 78−19730
SnF_2, phase transitions, X-ray diffr., elec. cond. and thermal analysis 80−100329
SnI_2-SnF_2 system, phase diagram construct. *(French)* 80−50605
SnO_2-TiO_2 solid solns., X-ray diffr. and thermogravimetric meas. 79−90792
SnS-GeS_2, exam. of phase diagram using DTA *(German)* 79−11585
SnSe-Sb_2Se_3 system, phase diagram, differential thermal, microstruct., X-ray phase and microstructure anal. 77−16555
SnTe-Bi_2Te_3 system, phase diagram 77−36474
Sr Nb_2O_6, crystallography, polymorphism and isomerism, X-ray diffr. and DTA study 80−100216
Sr-Al-Nd phase diagrams *(Russian)* 78−27480
Sr-Al-Si system, phase diagrams construction by simplex designing method 78−6899
SrF_2, vaporisation and sublimation thermodynamics *(German)* 80−81355
$SrFe_{12}O_{19}$, exam. of factors affecting reaction kinetics, thermal analysis *(German)* 79−24471
$Sr(NO_3)_2$, low temp. struct. changes, elec. props. 79−87377
$SrNb_2O_6$-$NaNbO_3$-$LiNbO_3$ pseudo-ternary system, DTA, heat treatment and X-ray diffr. obs. *(Chinese)* 79−52175
SrO, heated on W, vaporisation behaviour, mass spectrometric thermal anal. 77−56277
SrO-SiO_2-Fe_2O_3, permanent mag. ceramics, exam. of phase diagram, using X-ray analysis, optical microscopy, electron probe anal., and thermal analysis *(German)* 79−29012
$SrTiO_3$, sintering kinetics rel. to added SrF_2, ZrO_2 78−44037
$Tb(NO_3)_3$-$Fe(NO_3)_3$-$(NH_4)_2CO_3$-H_2O system, cpd. form., comp. and props. 80−100832
Tb_2O_3-H_3PO_4-H_2O system, cpd. form., comp. and props. 80−100832
Te-Ge eutectic alloy, glassy, crystn. mechanism 78−22836
Te-In alloys, direct reaction calorimetric study, 737 to 1340K *(French)* 80−49382
Te-In system, enthalpies of fusion, peritectic decomp. and allotropic transition, DTA *(French)* 80−76226
Te-Sn (20 at.%), amorphous, exam. of crystallisation by DTA, X-ray diffr. and TEM 78−47242
Te-$TeBr_4$ system, Gibbs free energy of reaction, electrochem. e.m.f. expts. 79−91991
Te-$TeCl_4$ system, Gibbs free energy of reaction, electrochem. e.m.f. expts. 79−91991
Te-TeI_4 system, Gibbs free energy of reaction, electrochem. e.m.f. expts. 79−91991
$Te_{80}Ge_{12}Pb_{7.5}$, phase-separated system, overlapping effects of glass transition and crystn., DSC results 78−83739
$Te_{80}Ge_{15}Pb_5$, DSC sensitivity to controlled ageing in glass transition region 80−71673
$Te_{80}Ge_{20-x}Sb_x(Bi_x)$, DSC studies of struct. phase transformation 80−66505
TeO_2-CoO, phase diag. from thermographic analysis 78−23687
TeO_2-Cr_2O_3 system, phase diagram and vitrification 79−83182
TeO_2-MoO_3-V_2C_5, phase comp. determ. using X-ray diffr., electron microscopy and DTA *(German)* 80−88046
TeO_2-NiO system, phase diagram and vitrification 79−83182
$Te_{80}Si_{20-x}Pb_x$ glasses, phase separation, double T_g presence 80−88306
Ti, sulphurisation kinetics, 450-550°C, thermogravimetric determ. 77−25197
Ti-Al, phase diagram in Ti rich region *(Russian)* 77−25013
Ti-Mo-V-Al-Cr-Fe (4.8, 4.7, 5.2, 1.1, 1.0 wt.%), structural changes during heating up to 1000°C, DTA study *(Russian)* 80−93552
Ti-Nb-Si, amorphous alloy, supercond. props. and crystn. behaviour, TEM and DTA study *(Japanese)* 80−84536
Ti-O system, O/Ti<1, high-temp. thermodynamics using Tian-Calvet microcalorimetry 78−85190
Ti-Zr-W-(Al) alloys, phase struct. and props. *(Russian)* 80−16270
Ti_2AlN, prep. and props. 77−28745
TiB_2-Al_2O_3, thermal stability of composite materials 78−60638
TiB_2-CaO, thermal stability of composite materials 78−60638
TiB_2-MgO, thermal stability of composite materials 78−60638
TiB_2-Y_2O_3, thermal stability of composite materials 78−60638
$TiC_{0.93}$-$TiN_{0.818}$, structural parameters, and X-ray and pycnometric densities in homogeneity range 77−90311
Ti_2NiO_x (x=0 to 0.5), hydrogen characts., thermogravimetry/DTA meas. 79−52760
TiO_2, obtained ions $Ti_2OCl(HCOO)_3(OH)_2$, by thermohydrolysis, exam. of crystallisation 80−2173
TiO_{2-x}, comparison of photoelec. props. with system $TiO_{2-x}F_x$ 79−28371
$TiO_{2-x}F_x$, comparison of photoelec. props. with system TiO_{2-x} 79−28371
Tl, phase diagram and high press. phase transforms., DTA study *(Russian)* 80−66474
Tl-B-Se system, vitrification region, primary crystallisation fields 77−15321
Tl-Bi-Sb-Te system, peritectic reactions in $TlBiTe_2$-$TlSbTe_2$ cross section, crystn. character 80−108406
Tl-Sn-Te system equilibria, polythermal and isothermal cross sections obs., ternary cpd. form. 80−104128
Tl-Te, phase equilibrium exam., using DTA, X-ray diffraction, and hardness 79−1846
thermal analysis continued
TlBS, synthesis, struct., optical, spectral props. 79−15631
$(TlBiS_2)_{1-x}$-$(2PbS)_x$ system, phase diagram 77−36471
TlBr-VBr_2 system, cryst. struct., DTA investig. *(German)* 78−72766
Tl_2CuI_3, melting point, cryst. struct., DTA, X-ray diffr. *(French)* 77−84710
$TlGaS_2$-$TlGaSe_2$, phase and composition-property diagrams 80−55366
$TlInS_2$-$TlInSe_2$, phase and composition-property diagrams 80−55366
Tl_2MoO_4, prep., characterisation 78−63731
$TlNO_3$, boiling and melting pts., heats of transformation, solid-solid transformation 78−91441
$TlR(MoO_4)_2$ (where R=Er, Tm, Yb, Lu, Y), polymorphic transition characts., temp. regions of stability using DTA and X-ray diffr. anal. 79−14785
Tl_2S-Ag_2S system, phase equil., DTA, X-ray and microhardness obs. 79−38803
Tl_2S-SnS, phase equilibria exam. 80−55369
Tl_2S-$Tl_2Se(Tl_2Te)$, exam. of phase equilibria, using DTA, X-ray phase analysis and microhardness 79−4953
$(Tl_2Se)_{3x}$-$(Sb_2Se_3)_{1-x}$ system, phase diagram 77−16558
Tl_3Se-SnSe(PbSe) systems, phase equilib. 79−52181
$Tl_{1+x}Ta_{1+x}W_{1-x}O_6.nH_2O$, pyrochlore type, stoichiometry and ionic cond. 80−24648
Tl_2Te-HgTe(HgSe) systems, phase diagrams 79−87620
Tl_5Te_3-Tl_4SnTe_3-Tl_4PbTe_3, phase equilib., DTA, SPA and microhardness meas. 80−96628
Tl_2TeO_3, $Tl_2Te_3O_7$, $Tl_2Te_2O_5$, Tl_2TeO_6, Tl_6TeO_{12}, synthesis, thermal stability, crystallographic data *(French)* 78−51518
Tl_6TeO_6, solid, prep., thermal stability, cryst. parameters *(French)* 79−65037
Tl_2WO_4, DTA and TGA 78−38673
(U,Pu)-oxide nuclear fuel, near and non-stoichiometric, O_2 potential, thermogravimetric and galvanic cell meas. comparison 79−63744
$(U,Pu)O_2$ (30 wt.%), oxidation behaviour 79−66210
$(U,Pu)O_2$, close coupled O-to-metal ratio anal., rapid thermogravimetric method 79−11878
U-Co(Ce)(Fe)(Mn)(Ni)(V) metallic glasses, glass form. and thermal stability 80−75183
U-O system, phase equilibrium, thermal, X-ray and cond. meas. 78−35371
U-UNi_2-UCo_2, system, phase equilibria, lattice constants *(German)* 80−50598
UAl_2-UNi_2, phase relationships, thermal, microscopic and X-ray exam. *(German)* 78−88447
UC-PuC, carbothermal synthesis *(German)* 77−18661
$U(H_2P_2O_5)_2$, prep., identification, thermal stability 79−15970
$U(HPO_3)_4.2H_2O$, prep., identification, thermal stability 79−15970
$U(H_2PO_3)_4.2H_2O$, prep., identification, thermal stability 79−15970
UO_2 ceramic fuel fabrication, simulation of thermal processes by emanation thermal anal. 80−811
UO_2 nuclear fuel preparation, emanation thermal anal. for characterisation of uranyl gel microspheres 80−95391
UO_2, sintered, production by gel calcination and drying, thermal anal. *(Czech)* 80−45260
U_3O_8 preparation from ammonium diuranate, thermal anal. 79−81009
V-D, exam. of phase diagram, using DTA and calorimetry, isotope effect 78−80527
V-H system, DTA, phase diagrams, low temp. phase 78−6903
V-H(D), metallographic and thermal differential anal., potential for H energy storage appls. 80−45281
V-H(D), phase diagrams, struct. studies 80−66491
V-Ni-Mo, structure in alloy crystallisation region, peritectic equilibria *(Russian)* 80−50622
V-S system, quenched, order-disorder transition of metal vacancies, DTA and X-ray analysis 78−30576
V-Se system, quenched, order-disorder transition of metal vacancies, DTA and X-ray analysis 78−30576
V_2O_5, amorphous, hydration and fibrous texture, EPR study *(French)* 79−24826
V_2O_5, water in noncryst. solid, quenching of molten V_2O_5 *(French)* 78−42912
V_2O_5-CsV_2O_5 system, phase comp. and phase diagram for conditions of inert atmosphere 77−25030
V_2O_5-Fe_2O_3-LiO_2 system, physical properties 78−84503
V_2O_5-MoO_3, solid soln. thermogravimetric anal., ion formation on crystallisation 77−20076
V_2O_5-MoO_3 solid soln., number of V^{4+} ions, magnetic and thermogravimetric exam. 78−52199
V_2O_5-WO_5, solid soln. thermogravimetric anal., ion formation on crystallisation 77−20076
V_3O_5, electrical, thermodynamic and mag. props. at metal-semicond. transition, homogeneity range 77−4413
V_3O_5, high-temp. phase transition, resistivity, valence photoelectron spectra 80−49357
V_3O_5-Ti_3O_5, DTA, mag. susceptibility and X-ray diffr. study 80−70970
V_4O_7, metal-insulator phase transition temp. depend. on hydrostatic press., DTA meas. 79−73438
V_xO_y, film, preparation by calcining vanadium naphthenate, formation process exam. *(Japanese)* 78−30849
$V_{1-x}Re_xO_2$ ($0 \leq x \leq 0.15$), insulator-metal transition, DTA, X-ray, mag. and elec. meas. 78−10353
$V_xW_{1-x}O_2$, phase relations, vacuum seal study and DTA obs. 79−100122
WC, powder form. from WO_3-Co_3O_4-C powder mixture *(Japanese)* 78−92227
WC-Co powder, prep. by direct carburisation of WO_3 in presence of Co_3O_4 80−50573
WF_6-graphite intercalation cpd. 78−27441
YAG, melting behaviour and metastability determ. by optical DTA 80−92648
YAG, production of densely sintered ceramic, exam. of recrystallisation during sintering 80−11609
$YAlO_3$, with perovskite structure comparative assessment of methods of prep. 79−95980
YIG, nonstoichiometry and electronic defects, thermogravimetric expts. and anal. of elec. data 78−6050
$YMnO_3$, thermogravimetric study of phase stability 79−100121
Y_2O_3 hydroxy salt binder phase form., X-ray, thermal anal. obs. 79−28999
Y_2O_3, U, C interactions, thermal anal. 78−85154

thermal analysis continued
$Y(OH)_3$-α-FeOOH, physicochem. props. rel. to growth of $Y_3Fe_5O_{12}$ 77−40418
$Y(OH)CO_3$, ancylite like phase, hydrothermal cryst. growth *(French)* 80−108340
$Y_2Ti_2O_7$, precipitation from oxalates, carbonates, exam. 80−55641
Yb-Ga, phase diagram, differential thermal and X-ray analysis *(Russian)* 78−56615
Yb-Ga system, phase diagram, cryst. structs. of phases 79−52169
$YbMnO_3$, thermogravimetric study of phase stability 79−100121
YbTe, high-temperature evaporation and reactivity 80−103469
Zn ferrite, production by mechanochemical reactions by grinding in ball mill 79−20014
Zn-Cd alloys, liq. and solid, ultrasound speed and compressibility meas. 80−102941
$ZnCl_2$ glass, glass transition temp. and thermal expansion 80−64902
$ZnCl_2(NCR)_2$, R=CH_3 or C_2H_5, thermal decomp., thermogravimetric and differential thermal anal. *(Chinese)* 80−81291
$ZnFe_2O_4$-Fe_3O_4 solid solns., form. of α-Fe_2O_3 during oxidation 80−25889
ZnO, adsorpt. of H_2O vapour, annealing and grinding effects 78−68656
$Zn_3(PO_4)_2.4H_2O$, thermal transitions, thermographic investig. 77−9063
ZnSe+CeTe⇄CdSe+ZnTe ternary mutual system, phase equilib. 79−52179
$ZnSiP_2$ crystal growth, DTA obs. of Sn-Zn-$ZnSiP_2$ phase diagram 80−24394
$ZnSnP_2$-$ZnSiP_2$, heterocombination simultaneous crystallisation 78−60560
$Zn_2Ta_2O_6$, metastable orthorhombic variety, crystallographic characts. *(French)* 79−82185
ZnTe-Ga_2Te_3, phase diagram 78−35360
Zr-Ti-Be metallic glass, phase separation 80−97464
ZrF_4-BaF_2-NdF_3 glass, vitreous domain, prep. and optical props. 78−27304
$Zr(HPO_4)_2$, cryst., heat treated, acid strength distrib. 78−92377
ZrO_2, crystallisation from $Zr(OH)_4$, effect of water vapour, heat treatment and grain size *(Japanese)* 79−19170
ZrO_2 gels, calcination 80−11964
ZrO_2, stabilised, fabrication by hot petroleum drying method, X-ray diffr. and thermal anal. study 80−40297
ZrO_2-Cr_2O_3 system, react., phase diagram 1600-2400°C 79−11580
ZrO_2-R_2O_3 solid solns., prep., crystn., R=Nd,Sm,Dy,Yb 78−42909
ZrO_2-Sc_2O_3, phase system, X-ray and thermal anal. 78−27494
ZrO_2-Sc_2O_3 system, high-temp. phase transitions, elec. cond., thermal props. 77−16573
ZrO_2-ThO_2, high temp. study of phase diagram using X-ray and thermal anal. *(French)* 79−70049
ZrO_2-TiO_2 solid solns., X-ray diffr. and thermogravimetric meas. 79−90792
ZrO_2-TiO_2 system, Z *(Ukrainian)* 79−96007

thermal capacity *see specific heat*

thermal conductivity
see also Kapitza resistance; Lorenz number; thermal conductivity of gases; thermal conductivity of liquids; thermal conductivity of solids; thermal diffusivity; thermal insulating materials
Aerosil in cetane, suspension, thermal cond. rel. to elec. field, struct. form. 77−9138
air water downflow through packed beds, effective thermal conductivity 80−74952
analytic theory by integral transforms method 77−75773
bar, cylindrical, thermal cond. calc. using numerical soln. of Boltzmann eqn. 80−44373
Beuken model thermal conductivity nonlinear changes, hybrid simulation 77−42700
boson system, multicomponent, transport coeffs., crit. behaviour, kinetic theory 77−2611
boundary-value problems, numerical solutions *(Russian)* 78−55545
Boussinesq fluids, turbulent viscosity and conductivity in turbulent convection 80−98543
cavity packed with fibrous glass, effective thermal cond. 79−55317
chemical reaction, solid, endothermic, unsteady heat conduction, thermal conductivity change 80−76511
complex shape bodies, equivalent form factors for nonstationary problems 77−84107
composite bodies, nonstationary thermal conduction processes, numerical simulation *(Russian)* 80−92016
composite body, heat conductance, combined numerical method 78−63261
conference, Chicago, USA (Nov. 79) 80−31425
cosmological fluid, lepton era, transport coeffs., Weinberg-Salam model 78−32623
cylinders, perfectly conducting arrays, transport prop. investig. 80−13011
dispersed medium, effective viscosity and heat cond. coeffs. 80−89537
effective conductivity of systems with interpenetrating components, calc. methods 78−83209
electrical circuit analogue, for teachers 78−86089
electron gas, partially degenerate, thermal cond. 77−71266
entropy production minimum, rel. to thermal diffusion *(French)* 78−73943
equation, nonlinear physical parameter determ. 79−23196
ethyl chloride, thermal cond. meas. using thermal lens 79−12795
eutectics, HgTe-PbTe and Au-PbTe, prep. and thermoelectric behaviour characts. 80−107774
fibrosarcoma, para-7, hamster, local thermal conductivity obs. 80−104562
fins, nonlinear problems, 1-D conduction, initial value problem 80−83726
fluid, anisotropic, transport coeffs., perturbation theory 77−7497
fluid, turbulence models for heat transfer, review 79−4017
fluid flow in packed beds, effective heat transfer parameters, theoretical predictions 80−14802
fluid mixture, coeff. prediction 77−43361
fluidised glass ballotini-packed fixed bed, at low/intermediate Reynolds nos. 79−1244
fusion thermal tracers, thermophys. characts. investig. 77−5837
gas filled porous media, free convection heat transfer 79−98796
glass fibre reinforced epoxy resin composites, 2 to 290K 79−60528
glass fibre reinforced plastic, thermophysical props., 10-300K *(Russian)* 77−89390
glycerol, high press. heat capacity and thermal cond. meas. 77−41613

thermal conductivity continued
granular materials pneumatically transported, wall heat transfer coeff., effective thermal conductivity 78−87378
granular system, transport coeff., contacting particles in noncond. medium 78−59261
graphite foam, thermal props. 77−48689
hard-sphere mixtures, excess thermal cond. and viscosity 77−11292
heat filters for bolometers cooled to very low temperatures 80−52315
heat storage unit, finite conductivity effect 79−55316
heat-generating, transversely isotropic cylinder, transient thermal stresses and displacements 79−68584
heterogeneous mixture, thermal cond. prediction, digital simulation technique 78−87247
heterogeneous system with chaotic structure, generalized conductivity coefficients, review 77−87708
high-temperature reference standards, work of CODATA task group 77−45818
HTGR piping, heat transfer characts. of horizontal annular insulation layer *(Japanese)* 79−26520
hyperbolic equation application telegraph eqn. soln. 79−37122
hyperthermia, role of thermal conduction 80−104558
inhomogeneous body with source, temp. field determ. by integral transformations 77−42703
inhomogeneous thermal line, approx. by series connection of homogeneous thermal lines 77−7284
inhomogeneous thermal system, thermal cond. and boundary resistance at low temp., heat flow model calc. 80−10120
interfaces, pure, thermodynamics and dynamics rel. to Spacelab 79−28910
intermediate state, thermal conductivity giant fluctuations *(Russian)* 78−34922
inverse problems, numerical method *(Ukrainian)* 79−41560
inverse theral conductivity problem for one-dimensional rod., rel. to optimum filtration 78−5628
kinetic theory of dense fluids, generalised Chapman-Enskog soln. 79−54033
lamina, heat distrib., thermal conductivity 78−22246
laminar film boiling heat transfer, thermal conductivity and convection effects 80−74864
LMFBR, red. of two-phase thermal cond. and heat transfer by entrained inert gases 79−30897
low temp. heat pipe, metal-fibre wick thermal cond., heat transfer coeffs. 78−83217
LWR Sphere-Pac oxide fuel, eval. of thermal conductivity 80−102234
macroparticle capture by cryst. growing from melt, influence of particle thermal cond. 78−79543
membranes, phenomenological coeffs., frames of reference, isothermal systems 78−38862
membranes, phenomenological coeffs., frames of reference, nonisothermal systems 78−38884
metal, effects of large scale voids on thermal magnetoresist. 80−10946
metals, magnetic, Seebeck coefficient anomaly near spin ordering temp. 77−20302
methane, transport coeffs., statistical mech. calcs. 77−7494
MHD, thermodiffusive mixture flows, Hall and ion-slip effects, uniqueness theorem 78−87415
microinhomogeneous media, appl. of random functions theory *(Russian)* 78−63280
multiple-layer nonideally coupled spherical region, analyt. calcs. *(Russian)* 78−51037
neuroblastoma tumour, thermal conductivity and diffusivity meas. 79−5252
nonideal thermal contact, heat exchange between thin walled bodies *(Russian)* 80−14553
nonlinear, variational formulation, counter functional, exactness of soln. *(Russian)* 80−90800
nonlinear diffusion equation, general class of similar solns., laser interactions, thermal cond. 77−37827
nonlinear in semiinverse Stefan problems, calc. method 77−72136
nonlinear inverse, analytical investigation methods 77−75771
nonlinear inverse thermal cond., iterative soln. 80−23865
nonlinear problems, temp. fields with variable thermophys. props., calc. method 79−86324
nonlinear thermal conductivity boundary-values qualitative anal. 77−14879
nonlinear thermal diffusion equation, parameter calcs., numerical calcs. *(French)* 78−94584
nuclear matter, thermal conductivity calc. based on relativistic quantum field theory 79−75886
phase change problem, with temp. dependent thermal conductivity, noniterative soln. 79−27493
plane conductor, heated by current, effect of conductivity temp. depend. 77−42683
plasma transport, anomalous, electron temp. gradient instability 80−75034
plate, weakened by periodic system of sound orifices *(Russian)* 77−23880
plate heating by localised volume heat source with power-time depend. *(Russian)* 80−53608
porosity correction of conductivity using spherical pore geom. 77−42722
porous material, thermal cond. of gas and solid, separate determ. *(Polish)* 79−64486
heat-protective coating, temperature distrib., finite element anal. *(Russian)* 80−74701
quasilinear one-dimensional equation for pure and composite materials 77−7283
randomly-packed spherical particle bed, coord.-no. distrib., effective thermal cond., stat. thermodynamic theory 78−75028
silica (metallised) gels, thermal cond., 10-200K, cryogenic appls. 78−79828
silica gel for low temp. regenerator of cryogenic refrigerator 77−17994
solar flares, temp. struct. rel. to collisional heat cond. 79−40168
solar wind, thermally conductive flows in coronal holes 78−28614
solar wind, time-depend. two-fluid model with thermal cond. 79−92643
stack of thin layers, in high vac., thermal contact cond. correlation 77−58536
stars, rotating, secular instability from thermal cond. 80−21986
stationary nonlinear thermal conductivity problem, least squares approach *(Russian)* 78−38172
stellar atmospheres, thermal cond. without mag. field 77−87375
suspension, sheared, effective thermal conductivity 77−7436

thermal conductivity continued
suspension, sheared, macroscopic transport props. 77−32840
suspension effective thermal conductivity calc. *(Russian)* 78−76935
suspensions, averaged-equation approach 77−1949
suspensions, dilute, flow effects 77−1952
system with nonconserved order parameter, influence of heat cond. on relax. of unstable states 80−10637
system with variable heat transfer coeffs., conductivity determ. 77−75772
systems analysis method, to solve thermal cond. problems *(Russian)* 80−24685
temperature fields in space-connected regions with alternating contact thermal resistance *(Russian)* 80−53607
ternary semiconductors, thermal cond., theory and expt. data comparison 79−46851
thermal storage unit, sensible-heat, solid, transient response 79−3892
thermionic convertors, effect of electron thermal conductivity, theory 80−40892
thermoelectric energy conversion, heat losses compensation due to thermal cond. through Peltier heat 80−107773
thermophysical measurements, sample shape determ. 79−30457
thermophysical property research, metallurgical applications 80−97457
tissue, two-regime model of perfusion meas. heated thermocouple probe 77−5110
transient conduction, two dimensional finite solid, temp. depend. conductivity 77−58528
turbulent pipe flow, heat transfer, fluid props., var. calcs. 77−27527
two-dimensional transport coefficients, thermal cond., theory 78−32778
two-phase system, effective thermal cond. 79−30396
vapor-liquid energy transport in a porous medium 79−64762
variational principles *(Russian)* 78−59265
X-Y model, on linear chain in random fields, thermal props., appl. to praseodymium ethyl sulphate 79−65679
Al thin films, HF induction plasma treatment, effect on phys. props. *(Russian)* 80−24961
H_2, dissociated, viscosity, thermal cond., 1-1000 bars, 2000-10000K 77−39391
He, accurate empirical intermol. pot. 79−68291
^{3}He, boundary resistance of low temp., heat flow model calc. 80−10120
^{3}He, liquid, interface with antiferromagnet, anomalous thermal behaviour and nucl. spin relax. 79−56002
^{4}He, boundary resistance at low temp., heat flow model calc. 80−10120
^{4}He films, adsorbed on graphite substrate, layering and thermal cond., heat capacity and vapour press. meas. 79−51386
InSe-SmSe system, microhardness and electrophys. props. 79−87093
Pb-Cd lamellar eutectic composite, pair potential meas. 79−33396
SiC, 6H polytype, elec. and thermal cond., carrier concentrations 80−2223
V_3Si, low temp. sp. heat and thermal cond. 77−15995
Y_2O_3-Gd_2O_3-Nd_2O_3 solution *(Russian)* 78−88448

thermal conductivity measurement
anisotropic solid simultaneous transient meas. 78−94581
apparatus, thermophysical characts. by composite method, wide temp. range 77−26285
apparatus to meas. thermophysical props. at high temps. 80−37458
automatic gas/gaseous mixture thermal cond. analyser *(Spanish)* 78−76972
automatic thermal conductivity meter with digital readout 80−106714
Benard-Rayleigh problem, experimental system for measurement of equivalent thermal conductivity 80−33711
binary gas mixtures anal. cell using miniature thin film printed cct. 80−105640
biomaterial thermal conductivity and thermal diffusivity simultaneous meas. technique 78−57098
blast furnace blocks, carbon-containing, apparatus for thermal conductance determ. 77−57329
cast insulation materials measuring apparatus 80−86293
cerebral cortial blood flow transients in cat. meas. technique using tissue heat transfer 79−92457
comparative longit. ht. flux, use of generalised Bessel functions 78−26741
comparator for simple, rapid meas. 77−49722
comparison method using Si diode thermometry 79−72792
composite materials, metal reinforced, thermal activity, diffusivity, cond. meas. method 79−37141
constant power resistive probe for liq. semicond. thermal cond. meas. 77−15636
cryogenic equipment thermal insulation, porous multilayer, with diffraction shields 79−58732
cryogenic insulation, thermal cond. meas. 79−30484
cryostat, for meas. on plastically deformed specimens at liq. He temps. 78−81985
cryostat system, thermal transport in solids 80−52243
curve-fitting method based apparatus for thermal props. meas. at cryogenic temps., performance characts. 77−67441
cylindrical probe improvement 80−92033
detector, with a narrow packed column 80−22355
diamond, expt. device for thermal cond. meas. 78−65921
diamond, natural, thermal cond. with absorpt. at 3.22 μm 79−73353
diamond and other gemstones using thermal comparator 79−80613
differential, difference and integral methods of meas. of temp. depend. of cond. coeff. 77−5836
differential method, for low temp. meas. method and expts. on Al_2O_3:Mn 79−63227
diffusivity meas. apparatus. using low freq. sine wave generator and digital phase meter 78−94580
diffusivity meas. by laser-pulse technique, instrumental recording and data processing 77−45846
discs of arbitrary shape, method demonstrated on type II supercond. 79−63228
edge effects in diffusion and cond. meas. 78−32810
electrically insulating media, heat capacity and thermal cond. from pulsed wire probe meas. 77−41613
epoxies commercial powder filled, 1.5 to 15K 79−58729
epoxy, Stycast 1266, very low temp. thermal conductivity and optical props. 78−55992
Evanohm, meas. of Kapitza boundary layer conductance using supercond. current comparator 77−41645
film, device for compensating thermal stresses 79−18681

thermal conductivity measurement continued
film, thermal cond. meas. method, normal to layer, error anal. 78−90682
fluid, transient hot-wire method theory 77−58834
fluid thermal cond. meas. by transient line source method, radiation effects 78−94889
fluid thermal conductivity meas., transient hot-wire technique, theory 78−65933
fluids, absolute technique 80−101792
foam insulation material, unsteady probe method *(German)* 80−31740
frozen soil, thermal probe method *(Japanese)* 77−82034
gas, chemically reacting, temp. jump at gas-solid boundary 78−42701
gas, molecular, kinetic coeffs. calc. from ultrasonic data 78−42703
gas analyser, portable, 1920 to 1978 development 78−61124
gaseous mixtures, meas. theory of transient hot-wire cell 79−86328
gases, meas. in undergraduate physics lab. 80−82614
gases, thermal cond. by coaxial-cylinder method, Knudsen effect 80−42219
gases and vapours, thermal conduct. coeff. meas. up to 2500K by differential technique 77−33989
glass, thin layer thermal conductivity meas., radiometric method 79−94475
glass fibre reinforced plastic, thermal cond. meas. rel. to temp., heat cond. problem soln. 79−37887
granular material, simultaneous moisture content/thermal cond. meas. apparatus 78−53064
granular material, spherical probe meas. *(German)* 77−5830
harmonic temperature waves, thermoconductometer development and appl. 77−49720
heat flux measurement based on thermoelectric props. of thin electroplated foil 80−37026
heated filament method for thermal cond. meas. in gases at 600 to 2500K 77−35303
heated filament method incorporating null section, use in corrosive media 77−33990
high heat-conductance materials, method for determ. of thermophys. characts. on thin samples 77−61063
high-temperature US apparatus for elasticity characts. and thermal cond. meas. of materials 78−5705
hot wire method for gaseous CO_2 and Kr at elevated temps. 80−6199
hot wire method for gaseous CO_2 and Kr at elevated temps. 80−6200
hot wire method of meas., temp. drift effects *(Japanese)* 78−43191
hot wire techniques for refractories 80−37038
hot-plate meas., errors associated with imperfect surfaces 80−95098
hot-wire method, temp. depend. *(German)* 77−27464
hot-wire method for refractories, 20 to 900°C 80−31759
hot-wire method in nonstationary variation 78−32812
insulating materials for radioisotope thermoelectric generator appl. 79−48145
insulating mechanical supports, appl. to meas. thermal conductance 80−82772
insulating solids, transient hot-wire method 77−67428
inverse heat cond. problem soln. for thermal consts. determ. 79−37142
liquid, calorimetry at high state parameters 78−57953
liquid, superheated, thermal cond. meas. technique using shock heating 77−45834
liquid, weak IR absorbing, microtransient technique 78−22904
liquid metals, in Spacelab, design and terrestrial testing of measuring cell *(German)* 80−57303
liquids, coaxial cylinders method, investigation of meas. problems 78−81965
liquids, non-conducting, transient hot wire technique 77−10011
liquids, rapid meas. of cond. by transient hot wire method 77−30144
liquids, transient hot wire method, meas. at pressure 78−65920
liquids and solutions, spherically symmetric apparatus for transient conditions *(French)* 79−94477
low temperature thermal conductivity measurements under uniaxial compression 80−105653
low thermal cond. liquids, laser flash method 78−89476
low-temperature fluids, meas. using guarded parallel plate apparatus 77−22553
magnetothermal conductivity using frequency-crossing phonon spectrometer 80−31741
metallic thermal connectors for use in nuclear refrigeration, elec. resist. meas. 78−224
metals, residual resistivity and thermal conductivity coeff., comparison of max. values as parameter of metal purity 79−65431
method of coaxial cylinders for liquids, expt. problems 78−77903
multilayer insulation thermal cond., accel. temp. field method in low temp. investig. 77−30162
Nichrome, Kh20N80, varying porosity, effective thermal cond., 373-1400K, meas. method 78−75053
nonconducting solids, technique for thermal cond. and sp. ht. meas. 77−10015
nuclear reactor materials, thermophys. prop. meas. at RFL Springfields 77−14230
optical method for thermal cond. determ. of birefr. $Ba_2NaNb_5O_{15}$ 78−18851
organic liquid, layer, thermal cond. from IR absorption 77−89598
organic liquids, radiant heat exchange effect 80−19996
phonon heat conduction of single crysts. by quantum acoustic method 77−11748
plate apparatus, guard ring width effect on meas. accuracy *(German)* 80−90837
poor heat conductors, meas. under monotonic conditions 80−4706
porous cylindrical specimens, effective thermal cond. meas. method, 373-1400K 78−75053
porous material, thermal cond., diffusivity and water content meas., thermal shock transient *(French)* 78−94583
porous rocks, saturated with low cond. fluid, thermal cond. meas., systematic errors 77−86871
refractories, meas. above 1000°C 79−202
rock conductivity determ. from fragment meas. *(Rumanian)* 78−20563
rock sample, steady state plate method *(Chinese)* 80−56615
scanning temperature method for meas. of thermal cond. and diffusivity 77−45831
sedimentary rocks, semi-automatic apparatus using needle probe and microcomputer control 79−100970
sediments, using probes with semiconductor temp. sensors *(Russian)* 78−65431
semiconductor, rapid meas. method *(French)* 78−12689

thermal conductivity measurement continued
semiconductors, cryostat design for 90 to 450K 79−76957
semiconductors, thermophysical props. determ. from Ettingshausen effect meas. method 80−44376
simultaneous measurement method for thermal props. of plane-shaped solids using iterative calcs. 77−42713
soil, probe method, minimisation of errors 77−17259
soil, thermal conduction flux in situ meas., methods *(French)* 78−96331
solar collector thermal performance testing procedures *(Japanese)* 78−16795
solid thermal cond. and interface resistance meas. by radiation thermometry 80−86289
solidified gas constant-volume thermal conductivity meas. cell 80−31739
solids, 60 to 300K, USSR special standard 77−31205
solids, differential meas. method 78−57952
solids, thermal potentiometer method, 4-100K, 0.004-400 W/cm K 77−37878
solids and disperse materials, comparative method, 0.1-80 W m^{-1} K^{-1} 77−45835
standard reference mat., W, 4-3000K 77−45820
standard reference material, use of graphite 79−27496
steel, stainless, meas. method, precision 79−6121
steel, stainless, thin layer thermal conductivity meas., radiometric method 79−94475
superconductors with poor conductivity, measuring technique 79−58682
thermal insulation on metal backing, thermophys. characts., expt. determ. technique 80−4707
thermal lens, time-resolved geometrical optics 79−12795
thermal penetration property ρck meas. instrum. 78−70120
thermocouple probe, spherical heated, for perfusion meas. 79−92456
thermoelectric material, thermal cond. meas., 1100-2000K 78−24798
thermoelectric materials, thermal conductivity determ. heat losses, direct method 80−62662
thermoelectric method using Peltier effect for gases and liquids 78−45615
thermoelectric power and thermal conductivity, device for simultaneous meas., 100 to 300K *(French)* 78−77911
thermopower and thermal conductivity, simultaneous meas., method and apparatus 77−72854
thin films 80−68199
tissue, thermistor meas., influence of blood vessels using simulation model 77−40962
transient hot-strip method for simultaneously measuring thermal conductivity and thermal diffusivity of solids and fluids 80−1417
transient hot-wire technique, improvements, wire tension effect and elimination of stray electric pulses 80−48839
transient hot-wire technique 80−48838
transient line source techniques, thermal contact resistance 78−53744
transparent solids, non-steady-state method 79−50572
unsteady heat conduction accompanied by an endothermic solid reaction *(Japanese)* 79−76939
unsteady temperature data, calc. formulae 79−94476
viscometers, biconical and concentric spherical, heat transfer 79−55318
78 a/o Si-22 a/o Ge alloy 77−22543
BN_x refractories, thermal cond. determ. using IR laser heating 79−94479
H_2, gas, thermistor detector, ortho/para H_2 comp., temp.-jump region, 1-30 Torr 78−86263
He cryostat appl. *(Croatian)* 77−26302
$Hg_{1-x}Cd_xTe$, obs. 77−24578
MgO, thermal cond. up to 40 kbar 79−1533
NaCl, thermal cond. up to 40 kbar 79−1533
NbTi, supercond. measuring technique for thermal cond. 79−58682
Pt wire, automatic meas. device 78−54362
SF_6 at high pressures 78−67305
SiO_2, coesite, thermal cond. up to 40 kbar 79−1533
SiO_2 stishovite, thermal cond. up to 40 kbar 79−1533
W, sintered metal thermal cond. standard, high-temp. conductivity 78−89427

thermal conductivity of gases
acetic acid, thermal cond. meas. using Peltier effect 78−45615
acetone vapour, mol. assoc., monomer-dimer equilib., thermal cond. meas., MO calcs. 79−52647
aerosol particles, charged, effect on thermal and elec. conds. of ionised gas 80−28593
air, 400-1200K 78−75249
air, computation in 400 to 1600K range 78−5841
angular momentum polarisation contrib. 79−37435
aromatic hydrocarbons, thermal cond. at high press. and temp. 79−18988
benzene, benzene-d_6, thermal cond., 300-600K 78−63528
benzene, vapour, theoretical study 77−3904
benzene, vapour, thermal conductivity, 300-700K 78−38444
binary gas mixture, drop thermophoresis 80−93806
binary gas mixture, kinetic theory collision integrals, generalised phase shift approach 80−83874
binary gas mixtures, thermal cond. calc. method 80−79427
binary gas mixtures anal. cell using miniature thin film printed cct. 80−105640
binary mixtures of monatomic gases, Chapman-Enskog theory 80−24118
Boltzmann gas, heat transfer between parallel plates 77−87688
chemically reacting gas, temp. jump at gas-solid boundary 78−42701
corresponding states model 80−69964
cyclohexane, cyclohexane-d_{12}, thermal cond., 300-600K 78−63528
decane-air mixture, spontaneous ignition temp. limits determ. 77−52641
dense gas, logarithmic density dependence of viscosity and thermal cond. 77−51150
dense gas mixtures, thermal cond., composition dependence 78−51276
dense gases, viscosity and thermal cond. 79−46415
diatomic gas, thermal cond. in high temp. region, effect of vibr.-rot. collisions 77−42955
dilute gas transport props., logarithmic term in softness expansion 80−83872
ellipsoidal molecular models, transport props. determ. 77−68725
equation for calc. for gases and liqs. over wide parameter range 77−39395
ethane, viscosity and thermal cond. of liquid and gas, correl. eqns. 78−26715
ethylbenzole, thermal cond., 30-400°C, 1-10^3 kg cm^{-2} 78−26739
ethylene, and ethylene-d_4, 300-650K 77−11301

thermal conductivity of gases continued
ethylene, thermal cond., high temp. high press. meas. 79−68898
ethylene, thermal cond. meas. using thermal lens 79−12795
fission reactor thermal conduct. of gas mixture under fuel element jacket during burn-up 78−82478
fluid thermal cond. meas. by transient line source method, radiation effects 78−94889
fluidised bed, boiling layer, axial mixing of solid phase *(Russian)* 78−47035
FORTRAN appl. *(Japanese)* 77−27643
freon 113, 114 and 115, thermal cond., rot. relax., investigation *(Russian)* 77−89226
Freons 21, 22 and 23, thermal cond. 78−83513
gas-liquid cocurrent flow through packed beds, radial effective thermal conductivity 78−1723
global existence theorems for soln. of viscous heat-conducting perfect gas *(French)* 77−68363
homonuclear diatomics, dilute gas transport props. calcs. 77−72399
homothermal shock, prod. by instantaneous monochromatic radiation 80−59159
hydrocarbon, internal degrees of freedom, Eucken factor, effect on transfer props. 78−22445
inert gas, transport and equilib. props., using LJ (12-7) pot. 79−98849
inert gas binary mixture, unlike mol. force consts. from viscosity data, thermal cond. 78−33565
inert gas binary mixtures, thermal cond., 400-2500K 77−76020
inert gases, transient hot-wire technique 80−48838
interpolation formulae, extrapolatable, for data correlation *(Dutch)* 78−12661
kinetic theory, ideal monatomic gas, thermal cond. coeff., simple variational principle 77−968
Kr-Ag-N gas mixture, thermal conduction coefficient calculational methods *(Russian)* 80−96335
linear mol. gas thermal cond. Senftleben-Beenakker effect, effective collision cross section 80−24117
measurement, transient hot-wire method theory 77−58834
measurement, transient hot-wire technique, theory 78−65933
measurement in undergraduate physics lab. 80−82614
measurement using transient hot-wire technique 79−200
methane, and methane-d_4, 300-650K 77−11301
methane, thermal cond. meas. at room temp., and pressures up to 5 MPa 79−86551
methanol, gas thermal conductivity, H-bonds, tetramer form. 77−34776
methyl cyanide-Ar mixture, thermal cond. in mag. field 80−100058
mixtures, high temp., transport prop. calc. *(Russian)* 79−37432
mixtures, meas. theory of transient hot-wire cell 79−86328
mixtures, one-fluid approx. transport coeffs., critical region behaviour 79−14951
molecular gas, kinetic coeffs. calc. from ultrasonic data 78−42703
molecular gas, nonequilib., thermal conductivity 78−94885
monatomic gases, quantum corrections to transport coeffs. 77−15148
monatomic gases, transfer coeffs., 100-3000K 79−82021
multiphase flow, spherical particles, thermal conductivity determ. 78−71390
nonpolar binary mixtures, eqn. for calc., generalisation of expt. data 77−47135
olefin hydrocarbon vapour, thermal cond., 160 to 400°C 78−1783
optical lens, thermal pulse source 80−95968
polar gases in mag. field 80−1728
polyatomic, spin polarisation effect 78−71422
polyatomic gas, in external field, simplified expressions 80−6197
polyatomic gas, thermal cond., rel. to core form. in elec. arc 77−24241
propane, thermal cond., high temp. high press. meas. 79−68898
propane, viscosity and thermal cond. correl., liq. and gas 140-500K 79−77332
relativistic gas conducting heat, shock relns., and conservative form of hyperbolic eqns. 79−14498
Senftleben-Beenakker thermal conductivity effect apparatus 78−81989
sonic nozzle expansions, rot. relax. theory 80−43827
space environment, transport processes in fluids 79−46825
steam, thermal cond. equation, 0 to 800°C, triple pt. press. to 1000 bars, crit. region 80−39364
steam, thermal cond. in large Knudsen range, theory and expt. 78−94888
steam-air mixture, condensation, transport and thermodynamic props. *(Japanese)* 78−34251
symmetric top molecules, thermal cond., Senftleben-Beenakker effect 80−100049
symmetric top molecules, viscosity and thermal cond. under simultaneous elec. and mag. field 80−6188
teaching, relax. approx. to Boltzmann eqn. approach 78−73804
theory for wide press. variations 78−30402
thermal conductivity, vibr. energy diffusion coeff., 400-1600K 77−27644
transient hot-wire technique, improvements, wire tension effect and elimination of stray electric pulses 80−48839
water, vap., dimerization, from thermal cond. meas., 373K 78−44359
water, vapour, radiation absorption capacity 80−14873
water vapour, thermal cond., 375-600°C, 250 mPa 79−90367
water/steam systems, thermodynamic data tables 78−26679
Ar, at high press. 80−103099
Ar, conductivity coeff. meas. in 1100-2200K range by differential technique 77−33989
Ar, constant volume thermal conductivity *(Russian)* 77−76021
Ar, dense gas, thermal cond. and viscosity coeffs., irreversibility and Kirkwood superposition hypothesis *(French)* 78−94881
Ar, force constant props., 12-6 pot. model 78−13563
Ar, interatomic pot. and transport props. 77−14519
Ar, law of corresponding states *(Russian)* 78−87426
Ar, Lennard-Jones (12-6) pot. parameters calcs. 80−28591
Ar, thermal cond., 90-270K, 1 atm. press. 78−42700
Ar, thermal cond., 90-273K 80−48836
Ar, thermal cond., high temp. high press. meas. 79−68897
Ar, thermal cond. of gas and liq., eqn. verification 77−39395
Ar, thermal conductivity, near 300K, density depend., 0.8-35 MPa 78−67304
Ar, transport props. with Lennard-Jones (12-6) pot., distance parameter 79−55437
Ar-acetonitrile mixture, anomalous thermal cond. in const. elec. field 77−7505
Ar-He(Ne), thermal cond., composition dependence 78−51276
Ar-Kr, thermal cond., 90-270K, 1 atm. press. 78−42700

thermal conductivity of gases continued
Ar-Kr mixture, thermal cond., 120-273K 78−83514
Ar-Ne mixture, thermal conductivity, 400-1500K 79−18987
Ar_2, interatomic potential single parameter 80−48059
CO_2 thermal cond., simple relation, 1000-3000K 77−24048
CO_2, thermal cond. at 350 to 1300K 77−35304
CO_2, thermal cond. meas. at room temp., and pressures up to 35 MPa 79−86551
CO_2, thermal conductivity, 400 to 1500K, vibr. internal energy calc. 79−18986
CO_2, thermal conductivity meas. at elevated temps. by hot wire method 80−6199
CO_2, thermal conductivity meas. at elevated temps. by hot wire method 80−6200
CO_2, thermal diffusivity and cond. in crit. region meas. by holographic interferometry *(German)* 78−59942
$CO_2+O_2(NO)$, Senftleben-Beenakker effect, saturation field, Kohler-Raum theory and obs. 80−28596
Cs, thermal cond. coeff. meas., 600 to 2500K 77−35303
Cs vapour, thermal cond. in range 800 to 1100K 78−1782
D_2 gas, thermal cond. meas., 2-36 MPa 80−64668
$D_2+H_2(N_2O)(O_2)$, Wassiljewa coeffs., thermal conds., 50 and 100°C 79−37437
D_2O, thermal cond., 375-600°C 79−82026
D_2O, vapour, mol. association entropy and enthalpy, thermal cond. meas. 80−7777
H_2 gas, thermal cond. meas., 2-36 MPa 80−64668
H_2, p- and o- calc. 77−54587
H_2, thermal conductivity, quantum effects 79−14510
H_2, thermistor detector, ortho/para H_2 comp., temp.-jump region, 1-30 Torr 78−86263
H_2-D_2 gas, thermal cond. meas., 2-36 MPa 80−64668
H_2-He, thermal cond. meas., up to 14 MPa 80−64669
H_2-N_2(Ar), correl. between kinetic theory of thermal cond. and expt., 90 to 300K, 1 bar 79−81707
$H_2+D_2(O_2)(N_2O)$, Wassiljewa coeffs., thermal conds., 50 and 100°C 79−37437
H_2O, vapour, mol. association entropy and enthalpy, thermal cond. meas. 80−7777
He, at high press. 80−103099
He, thermal conductivity, near 300K, density depend., 0.8-35 MPa 78−67304
He, thermal conductivity, temp. depend. 78−59534
He, thermal conductivity determ., repulsive wall of interatomic pot. 77−54586
He-air, thermal cond. meas., conc. depend., 315K, 330K *(Russian)* 78−71421
He-Ar, gas mixtures, thermal cond. meas. in the range 0.5-15 MPa 80−14874
He-Ar mixture, thermal conductivity, 400-1500K 77−39394
He-N_2, correl. between kinetic theory of thermal cond. and expt., 90 to 300K, 1 bar 79−81707
He-Ne(Ar), thermal cond., composition dependence 78−51276
He-Xe mixtures, high temp. heat conduction 79−14509
^{3}He, thermal conductivity, quantum effects 79−14510
^{4}He, thermal cond., 3.3 to 20K, meas. in guarded parallel plate apparatus 77−22553
^{4}He, thermal conductivity, quantum effects 79−14510
^{4}He vapour, thermal cond. as function of density 78−55712
Hg, thermal cond. coeff. meas., 600 to 2500K 77−35303
Hg vapour, viscosity and thermal cond. meas., data anal., 694-1054K 80−19545
K vapour, 800-1050K 80−19546
Kr, at high press. 80−103099
Kr, conductivity coeff. meas. in 1100-2200K range by differential technique 77−33989
Kr, interatomic pot. and transport props. 77−14519
Kr, law of corresponding states *(Russian)* 78−87426
Kr, Lennard Jones (12,6) pot. distance parameter, transport props. calc. 80−79423
Kr, Lennard-Jones (12-6) pot. parameters calcs. 80−28591
Kr, meas. for 100-1200K 77−35305
Kr, reduced temp., atmospheric press. 77−84385
Kr, thermal cond., 90-270K, 1 atm. press. 78−42700
Kr, thermal conductivity, near 300K, density depend., 1.1-16 MPa 78−67304
Kr, thermal conductivity meas. at elevated temps. by hot wire method 80−6199
Kr, thermal conductivity meas. at elevated temps. by hot wire method 80−6200
N_2, dilute gas transport props. calcs. 77−72399
N_2, law of corresponding states *(Russian)* 78−87426
N_2, rotational collision number from thermal cond., 700-2500K 80−23526
N_2, thermal cond., simple relation, 1000-2000K 77−24048
N_2, thermal cond. meas. at room temp., and pressures up to 35 MPa 79−86551
N_2, thermal conductivity, 400 to 1500K, vibr. internal energy calc. 79−18986
N_2, thermomagnetic effect, Knudsen gas between Au surfaces, low temp. 78−30405
NF_3, thermal cond. in parallel const. and alternating elec., mag. fields, parametric reson. 78−83515
NH_3-Ar mixture, thermal cond., viscosity, Senftleben-Beenakker effect 80−100054
NO, thermal cond. Senftleben effect meas. 79−18985
NO-Ar(He), thermal cond. Senftleben effect meas. 79−18985
NO-$N_2(H_2)$ mixtures, thermal cond., mag. field effect 79−94764
NO_2, thermal cond. in parallel const. and alternating elec., mag. fields, parametric reson. 78−83515
N_2O, and mixtures with CO_2 viscosity and thermal cond. coeffs. predictions, 180-900K, ≤23 MPa 77−84383
$N_2O+O_2(D_2)(H_2)$, Wassiljewa coeffs., thermal conds., 50 and 100°C 79−37437
Na vapour, heat cond., temp. discontinuity for dissociating gas 78−94887
Na vapour, meas. in 900-1100K range by heated filament method 77−33990
Ne, at high press. 80−103099
Ne, conductivity coeff. meas. in 1100-2200K range by differential technique 77−33989
Ne, interatomic pot. and transport props. 77−14519
Ne, Lennard Jones (12,6) pot. distance parameter, transport props. calc. 80−79423
Ne, Lennard-Jones (12-6) pot. parameters calcs. 80−28591
Ne, low of corresponding states *(Russian)* 78−87426
Ne, reduced temp., atmospheric press. 77−84385
Ne, thermal cond., 90-273K 80−48836
Ne, thermal cond. meas. using Peltier effect 78−45615
Ne, thermal conductivity, 400-1500K 79−18987
Ne, thermal conductivity, near 300K, density depend., 0.8-35 MPa 78−67304
Ne-Ar, gas mixtures, thermal cond. meas. in the range 0.5-15 MPa 80−14874
Ne-Ar, thermal cond., 90-273K 80−48836
Ne-Ar (He), thermal cond., composition dependence 78−51276
Ne-Ar-Kr, gas mixtures, thermal cond. meas. in the range 0.5-15 MPa 80−14874
O_2 interacting with Au or Pt surface, thermomag. effect *(Russian)* 77−11302
O_2, rotational collision number, diffusion coeffs. 79−1281
O_2, thermal cond., mag. field effects 78−34255
O_2, thermal cond., simple relation, 1000-3000K 77−24048
O_2, thermal conductivity, 400 to 1500K, vibr. internal energy calc. 79−18986
O_2, thermal conductivity, calcs. 79−37434
O_2-Ar, gas, thermal cond., mag. field effects 78−34255
O_2-He, thermal cond. Senftleben effect meas. 79−18985
O_2-$N_2(H_2)$, gas mixture, mag. field effect on thermal conductivity 78−59533
Rb, vapour, thermal cond. meas. 80−14870
Rb vapour, viscosity rel. to thermal cond. 79−72982
Rn, law of corresponding states *(Russian)* 78−87426
SF_6 at high pressures, investigation 78−67305
SF_6, equilib. composition and transport props., 300 to 15000K 77−24051
SF_6 equivalent thermal conductivity determ. *(Czech)* 80−53911
SF_6 thermal cond., 230-350K, up to 50 MPa 79−33123
SF_6, thermal cond. at 350 to 1300K 77−35304
SF_6+H_2 mixture, equilib. composition and transport props., 300 to 15000K 77−24051
SO_2 on gas covered Pt surface, thermal conductivity and thermal accommodation coeff. 80−10346
$SiCl_4$ physical and thermodynamic properties, rel. to Si technology 79−65218
toluene, vapour, thermal conductivity, 300-700K 78−38444
UC, vapour, thermal conductivity, theoretical prediction 77−72402
UN, vapour, thermal conductivity, theoretical prediction 77−72401
UO_2 vapour, thermal conductivity prediction 77−68733
Xe, 170-1300K and press. to 200 Mpa 79−82025
Xe, at high press. 80−103099
Xe, conductivity coeff. meas. in 1100-2200K range by differential technique 77−33989
Xe, law of corresponding states *(Russian)* 78−87426
Xe, Lennard Jones (12,6) pot. distance parameter, transport props. calc. 80−79423
Xe, Lennard-Jones (12-6) pot. parameters calcs. 80−28591
Xe, thermal cond., 500 to 2400K, interatomic pots. 77−39393
Xe, thermal cond., 500 to 5000K 77−58833
Xe, thermal conductivity calc., law of corresponding states and interatomic pots. 79−7437
Xe+Ar(He)(Ne)(Kr), thermal cond., 800 to 2000K from Wassiljewa's expression 79−27736

thermal conductivity of liquids
alcohols, phonon MFP, H bond collisions 77−35655
aliphatic ethers, hot-wire meas. 78−63885
alkane-silicone oil mixtures, thermal cond. 79−42323
benzol, liq., thermal cond. coeffs. at high-press., 298-573K 79−73350
calculation method 78−67834
carbon tetrachloride, generalised transport coeffs., hydrodynamic eqn. 78−87803
carbon tetrachloride, thermal cond. and phase diagram under pressure 78−75893
carbon tetrachloride, thermal cond. meas. by transient hot wire method 77−30144
carbon tetrachloride, transport coefficients for a fluid of square-well rough spheres 79−55634
coolants and index matching media for Nd:glass laser systems 80−33015
cooling liquid for radiation absorption from flash tube, nonlinear hydrodynamics 77−11121
corresponding states correlation for dense fluids 77−59155
corresponding states model 80−69964
cyclohexanone(-polystyrene), thermal cond., appl. of spherically symmetric apparatus for liqs. and solns. *(French)* 79−94477
n-decane, thermal cond., meas. by transient hot-wire technique 80−103522
dense gas transport calcs., Rice Allnatt theory 77−76590
dielectric fluid, boiling on porous coating *(Russian)* 79−72788
dielectric fluid, Debye absorption at crit. liq.-vapour transition 80−100322
dielectrics, thermal performance estimation 80−88582
drop, boiling, rel. to gradient explosion, under conditions of bulk heat release 78−83226
dynamic viscosity and heat cond. coeffs., linear relationship 77−7884
equation for calc. for gases and liqs. over wide parameter range 77−39395
ethane, viscosity and thermal cond. of liquid and gas, correl. eqns. 78−26715
ethylbenzol, liq., thermal cond. coeffs. at high-press., 298-573K 79−73350
ethylbenzole, thermal cond., 30-400°C, $1\text{-}10^3$ kg cm^{-2} 78−26739
ferromagnetic suspension, mag. field effect on heat transfer, thermal cond. 78−59500
fluid thermal cond. meas. by transient line source method, radiation effects 78−94889
fluids, one and two dimensional, hydrodynamics, viscosity, heat conductivity, kinetics *(Russian)* 80−79972
fluids, simple, thermally induced surface fluctuations 80−88403
Freon, F-13V1 and F-23, thermal cond., −168 to 160°C, up to 6.10^7 Pa 77−47628
Freon F-113, boiling on porous Cu coating *(Russian)* 79−72788

thermal conductivity of liquids continued
Freons 21, 22 and 23, thermal cond. 78−83513
Freons of ethane series, thermal cond. meas. 78−63884
gas-liquid cocurrent flow through packed beds, radial effective thermal conductivity 78−1723
heavy water, 25-350°C, 0.1-245.3 mN/m^2 77−51556
homonuclear diatomics, dense fluids, transport props. 78−75519
hydrocarbons, saturated, thermal cond., rad. effect interferometry method 77−11745
inert gases, transport props. in mean spherical approx. 78−9927
inhomogeneous material, thermoelec. power and thermal cond. 78−10483
interpolation formulae, extrapolatable, for data correlation *(Dutch)* 78−12661
laminar convection in vertical tube, thermophysical prop. temp. depend., effects 78−90895
liquid crystals, thermal conductivity anistropy, forced Rayleigh light scatt. meas. 78−94991
lubricant, cond. and diffusivity joint meas., relative probe method 77−41600
measurement, laser flash method 78−89476
measurement, transient hot-wire technique, theory 78−65933
measurement by coaxial cylinders method, investigation of meas. problems 78−81965
measurement by method of coaxial cylinders 78−77903
measurement using transient hot-wire technique 79−200
measuring technique, weak IR absorbing fluids 78−22904
metal, Lorenz no. and thermal cond., apparatus for meas. 77−51716
metal, thermal cond. changes at melting point, vacancy model 79−33279
metals, in Spacelab, design and terrestrial testing of measuring cell *(German)* 80−57303
methane, dense gaseous and liq., thermal cond.-viscosity correlation, up to 500 atm., 95-500 K 77−80657
methanol, thermal cond. meas. by transient hot wire method 77−30144
mixtures, one-fluid approx. transport coeffs., critical region behaviour 79−14951
molecular liquids, corrected Enskog theory, transport props. 77−72538
nuclear reactor core melt from LOCA, viscosity, thermal cond., specific heat 77−14247
n-octane, meas. by transient hot-wire technique 80−103522
one-dimensional conditions departure in method of coaxial cylinders 77−85001
organic binary system, thermal cond. calc. 77−20135
organic compounds, comparison of predicted values with experimental results at different temps. 80−103523
organic liquid, layer, thermal cond. from IR absorption 77−89598
organic liquids, thermal conductivity meas., radiant heat exchange effect 80−19996
paraffin oil, thermal cond., appl. of spherically symmetric apparatus for liqs. and solns. *(French)* 79−94477
phenomenological coeffs., frames of reference, isothermal systems 78−38862
phenomenological coeffs., frames of reference, nonisothermal systems 78−38884
polyethyl siloxane, liqs., thermal cond. at high press., 20-200°C 78−79825
polymer melts, thermal conductivity, statistical mech. calcs. 78−34661
polymer solution, aqueous, meas. of thermal props. 77−51555
polymethyl siloxane liquids at high pressures 78−47609
Prandtl number, eqn. of state analogy and linear relations with transport props. 77−59156
principle of corresponding states, dynamic props. 77−89358
propane, viscosity and thermal cond. correl., liq. and gas 140-500K 79−77332
silicone oils 78−51752
simple fluids, order-parameter fluctuations near crit. point, Ornstein-Zernike theory 78−34416
space environment, transport processes in fluids 79−46825
Stepanov's method, of growing profiled optically transparent crysts., temp. fields 79−55688
supercooled liquid, thermal conductivity and viscosity, mode-mode coupling 80−88370
superheated, meas. technique using shock heating 77−45834
superheated liquid, rel. to effect of spinodal singularities on evaporation *(Russian)* 77−89533
superheated organic liquids, thermal cond. meas. 80−15316
tetraethoxysilane, −13.5 to +90°C 77−15637
tetraethyl tin, −13.5 to +90°C 77−15637
tetramethoxysilane, −13.5 to +90°C 77−15637
thermophysical properties rel. to compressibility 78−83964
toluene, high-precision meas. by obs. technique 80−101792
toluene, relationships between thermal cond., dynamic viscosity and density, high state parameters 78−83861
toluene, thermal cond. meas. by transient hot wire method 77−30144
toluol, liq., thermal cond. coeffs. at high-press., 298-573K 79−73350
transport coefficients for a fluid of square-well rough spheres 79−55634
transport properties, relationships between thermal cond., dynamic viscosity and density, high state parameters 78−83861
turbulent liquid, parametric method of integrating motion eqns. *(Russian)* 79−41672
two-phase system, effective thermal cond. 79−30396
water, 25-350°C, 0.1-245.3 mN/m^2 77−51556
water, mag. treatment affecting props., proposed mechanism 78−84827
water, relationships between thermal cond., dynamic viscosity and density, high state parameters 78−83861
water, thermal activity coeff., rel. to density, heat cond., sp. heat and viscosity meas. 77−7883
water, thermal cond. equation, 0 to 800°C, triple pt. press. to 1000 bars, crit. region 80−39364
water, thermal cond. in region of 4°C *(German)* 77−20136
water, thermal conductivity at high pressures, meas. with Ag co-axial cylinder cell *(Japanese)* 80−80007
water, transport and thermodynamic props. *(Japanese)* 78−34251
water in critical region, results analysis 77−89599
water meas. by transient hot wire method 77−30144
water/steam systems, thermodynamic data tables 78−26679
Widom-Rowlinson hard-sphere mixture model, transport props. 80−14981
xylol, liq., thermal cond. coeffs. at high-press., 298-573K 79−73350
Ar, at high press. 80−103099
Ar, thermal cond. of gas and liq., eqn. verification 77−39395

thermal conductivity of liquids continued
$As_2(Se_{1-x}Te_x)_3$ semiconducting glasses, solid and liquid, thermal cond. 80−6574
$As_2(Se_{1-x}Te_x)_3$, thermal cond. of solid solution and melt 78−67874
$As_2(Se_{1-x}Te_x)_3$, thermal cond., temp. and press. depend. 79−82396
B_2O_3-$Na_2O(K_2O)(V_2O_5)$, thermal cond. of melt in region 900 to 1100°C, effect of convection 78−2309
Bi_2Te_3, liq. semicond., thermal cond. meas., resistive probe method 77−15636
CO_2, thermal diffusivity and cond. in crit. region meas. by holographic interferometry *(German)* 78−59942
CsCl-$BaCl_2(LaCl_3)$ molten binary mixtures, thermal cond. 79−86931
Cu alloys, and elec. resistivity 80−103661
Cu, and elec. resistivity 80−103661
Cu_3AsS_4 and Cu_3SbS_4, thermal cond. in solid and liq. phases, 300 to 1100K, thermoelec. Q-factor 80−19997
Cu_3AsTe_4, elec. and thermal conds., thermo-EMF, solid and liq. states, temp. depends. 78−43384
$Cu_2S(Se)(Te)$, cond. changes on melting 77−7848
Cu_3SbTe_4, elec. and thermal conds., thermo-EMF, solid and liq. states, temp. depends. 78−43384
cyclopentane, plastic cryst. and liq. phases, thermal cond. and sp.ht., 100-300K, 0-2.1 GPa 78−34663
Fe_3O_4 in kerosene, thermal and electrical cond. in mag. field *(Russian)* 78−6188
Fr, properties from melting point to 7500K, prediction *(Russian)* 80−44296
Ga, liq., thermal props. at high temp. 80−75536
Gd, thermal diffusivity, conductivity and elec. cond. 110 to 2100K 79−42516
H_2O+HDO, isotope exchange in liq.-vapour system, r.i. and thermal cond. obs. *(German)* 77−4902
He, at high press. 80−103099
^{3}He, liq., hydrodynamic modes, macroscopic dispersion relations, two fluid model 78−10242
^{3}He, liq., hydrodynamic modes, microscopic dispersion relations, transport coeffs. 78−10243
^{3}He, liq., longitudinal zero-sound dispersion, thermal cond., and Landau F_2 78−2327
^{3}He, liquid, polarisation potentials, viscosity, thermal cond., spin diffusion 80−88389
^{3}He, liquid, shear viscosity and thermal cond., s- and p-wave approx. 79−1535
^{3}He, normal, diffusive heat flow and sum rules in the hydrodynamic limit 78−56012
^{3}He, normal, overdamped modes and transport 78−56011
^{3}He, superfluid, B-phase, transport processes at low temp. 77−55412
^{3}He, superfluid, B-phase, transport coeffs. 79−51342
^{3}He, superfluid, fountain press., sp. ht. and thermal cond. meas. 77−35782
^{3}He, superfluid, kinetic properties, model for calc. of helium-helium excitations cross-section *(Russian)* 78−56006
^{3}He, superfluid, nonequilib. processes, diffusive thermal cond. 77−66068
^{3}He, superfluid, spin relax., transport, spin fluctuation dominance model 77−66052
^{3}He, superfluid, transport and relaxation properties, viscosity, thermal, cond. and normal fluid density relax. 78−79839
^{3}He, superfluid, transport parameters, Kubo formulae and BCS-Green's functions 80−88382
^{3}He, thermal conductivity at very low temps., press. depend. 80−92742
^{3}He-^{4}He, superfluid solutions, second sound attenuation and dissipation processes, 1.3-2.0K *(Russian)* 79−42335
^{3}He-^{4}He mixture, dilute, diffusion const. and thermal cond. along λ line 77−47644
^{3}He-^{4}He mixture, dilute, thermal cond. conc. depend. on λ line 77−51567
^{3}He-^{4}He mixture, thermal transport properties near and below superfluid transition 79−60590
^{3}He-^{4}He mixture, transport props. near superfluid transition and tricritical point 80−29242
^{3}He-^{4}He mixtures, Benard instability and thermal meas. above and below T_λ 79−56009
^{3}He-^{4}He mixtures, thermal transport coeffs. near lambda line 78−22926
^{3}He-^{4}He mixtures, thermal transport near tricrit. point 79−51363
^{3}He-^{4}He mixtures, thermal transport near lambda line 79−56004
^{4}He film, heat cond. by ripplons 79−51375
^{4}He layered films on ZYX graphite, thermal resist. below 2K 80−70500
^{4}He, liq., critical thermal cond. near λ-point, light scatt. spectrum 80−24697
^{4}He, liq., dynamic scaling near T_λ 80−34264
^{4}He, liq., Kapitza heat-transfer model for boundary with solid 80−107591
^{4}He, superfluid, heat transport in restricted geometries, 0.8-2K 80−29237
^{4}He, superfluid, sound conversion phenomena at free surface, acoustic coeffs. 80−96709
^{4}He, superfluid, surface, ripplons, adsorbed ^{3}He and heat conduction meas. 80−49459
^{4}He, superfluid, transient heat transport 80−10715
^{4}He, superfluid, viscosity and thermal conductivity *(Russian)* 80−10720
^{4}He, thermal cond., 3.3 to 20K, meas. in guarded parallel plate apparatus 77−22553
Ho, thermophysical properties at high temps., exam. *(Russian)* 79−28105
In, liq., thermal props. at high temp. 80−75536
In, thermal cond. in solid and liq. phases, Wiedemann-Franz law 80−39554
In-Hg amalgam, thermal and electric cond., temp.-conc. depend. 78−43349
Kr, at high press. 80−103099
Ln, thermophysical properties at high temps., exam. *(Russian)* 79−28105
NH_3-metal, soln., thermophysical props., review 79−77758
N_2O, and mixtures with CO_2 viscosity and thermal cond. coeffs. predictions, 180-900K, ≤23 MPa 77−84383
N_2O_4, viscosity and thermal cond., approx. polynomials *(Russian)* 80−59739
Na-K alloys, liq., thermal conductivity, NaK_2 formation 78−10416
NaCl, aq. soln., thermal cond. meas., 20-330°C, 5, 10, 15, 20 and 25% solns. 77−47629
Ne, at high press. 80−103099

thermal conductivity of liquids continued
Pb-Bi alloy, liq., thermal cond. and elec. resistance up to 900°C 77−47785
SF_6 thermal cond., 230-350K, up to 50 MPa 79−33123
$SiCl_4$ physical and thermodynamic properties, rel. to Si technology 79−65218
Sn, liquid, thermal diffusivity and cond., 1000 to 1900°C, flash laser method *(French)* 79−99525
Sn, Lorenz number and thermal cond. meas. 77−51716
Tl, liq., thermal props. at high temp. 80−75536
UO_2, thermal and transport props., electronic contrib. 80−15432
Xe, at high press. 80−103099
Y, thermophysical properties at high temps., exam. *(Russian)* 79−28105

thermal conductivity of solids
see also thermal magnetoresistance
AC superconductor, uniform, behaviour of normal zones 80−11127
actinide, transport props. and sp. ht., role of optical and acoustic phonons 77−15821
actinide systems, nearly magnetic, thermoelectric power determ. 78−56133
actinide systems, spin fluctuations effect, model approach 77−28404
actinides, lattice vibrs. role in transport props. determ. 77−28158
actinides, spin fluctuation theory, for mag. and elec. props. 78−91869
adamantane, thermal cond. and heat capacity under press. 80−80008
adhesive layer, high viscosity thermal resistance 77−1269
alkali halides, strain defects, low temperature props., heuristic model 79−82245
alkali metal, electron-electron scatt. in terms of dielec. and vertex functions 79−95351
alkali metal, electron-phonon drag effects in elec. cond. and thermoelec. power 77−15824
alkali metals, electron-electron scatt., thermal and elec. resistivity 80−59956
alkali metals, ideal thermal resist. and Lorenz number due to conduction electron-phonon scatt. 80−29377
alkyl ammonium copper chloride, two-dimensional ferromag., low temp. lattice cond., phonon spectrum 77−4227
alloys, binary, lattice thermal cond. at low temps., solute at.-phonon scatt. 77−76512
alloys, binary, thermal cond. conc. depend., irreversible processes, thermodynamic calcs. *(Russian)* 80−39550
amorphous polymers, localised low-energy excitations 79−73322
amorphous solid, phonon scatt. by density fluctuations and thermal cond. 80−10626
amorphous solids, structure and low temp. props. 79−37631
amorphous systems, origin of thermal anomalies, struct. model 78−91256
anharmonic crystal, with isotopic impurities, lattice thermal cond. 77−59158
anisotropic composites, bounds and self consistent estimates for overall props. 78−5654
anisotropic solid simultaneous transient meas. 78−94581
anthracene, thermal cond. and heat capacity, meas. under press. 79−90796
antiferromagnetic insulator, magnetothermal resist. 77−35767
antiferromagnetic insulators, lattice thermal cond. 80−65319
Araldite AW106/Hardener HV953U epoxy resin, thermal props. at high press., glass transition 77−59160
articulated medium, elec. and thermal cond. anisotropy, crack density tensor 77−55505
austenitic stainless steel, heat conductivity, low temp. mag. susceptibility meas. *(Chinese)* 79−47080
baddeleyite-corundum refractories, thermophysical props. 79−82398
balsa wood, cryogenic insulation, exam. of strength specifications, props. 80−25819
benzene, thermal cond., heat capacity, 105-375K, up to 2.4 GPa 79−90839
benzene, thermal cond. and heat capacity, meas. under press. 79−90796
binary alloys, data anal. and synthesis 78−95284
binary disordered continuous solid solns., thermal cond. calc. method, struct. model 77−43394
Boltzmann eqn., phonon and electron transport in bounded systems 80−39545
borosiliate glasses, thermal conductivity meas. by laser flash method *(Japanese)* 77−69124
borosilicate glass containing simulated high level radioactive waste, characterization *(Japanese)* 79−93745
brass, electronic and lattice components, separation methods 80−29380
brass, lattice thermal cond. component, 30 to 300K, microscopic mechanisms 80−107758
brass, lattice thermal cond. component, 4.2 to 30K, microscopic mechanisms 80−107757
brass, thermal cond., effect of material on working parameters of cryosurgery instruments 78−36037
brass, thermal conductivity, 80 to 280K, depend. on Zn conc. 77−1405
brass alloys, thermal and elec. cond., 4 to 300K, Zn conc. depend. 80−29379
α-brass temp. dependence, rel. to heat-flux rectification at Sn-α brass interface 78−76048
brittle material, heat resistance criteria on surface during convective heat exchange 77−15642
Callaway eqn., phonon scatt. in highly disordered systems 80−20000
Callaway integral, contrib. of correction term to lattice thermal cond., low temps. 77−62693
carbon tetrachloride, thermal cond. and phase diagram under pressure 78−75893
cast insulation materials measuring apparatus 80−86293
cathode spots of the first kind, erosion rate resistivity and thermal cond. depend., explosive model 79−14630
ceramic fuels, effect of gas composition on thermal conductivity 79−93733
ceramics, thermal conductivity, temp. depend. with rarefaction of gas medium 77−7914
ceramics, thermal stress resistance, enhancement, for materials with thermal cond. gradient 78−48506
chalcogenide semiconductors, $ASbC_2$ type, thermal cond. 79−95224
chalcopyrite ternary semiconductor, lattice thermal cond. and ionicity, dielectric model 79−77846
charcoal, at room temp. 78−63889

thermal conductivity of solids continued
Clausius-Mossotti problem for cubic arrays of spheres 78−52422
coal, thermal diffusivity and cond. meas. for in situ coal gasification appls. 80−30360
coarse-grained soil, free thermal convection, effective thermal cond. 77−25705
composite, thermal conductivity range, knowing ranges for components 78−2313
composite, unidirectional, percolation in thin ply 79−42511
composite material, cubic arrangements of spherical particles in isotropic matrix, effective conductivities 78−55547
composite material, with spheroidal inclusions, calc. 77−28055
composite materials, effective thermal conductivity 80−54447
composite materials, phys. props. review 77−4720
composite materials, slender nearly-perfect conductors, dilute, bulk thermal properties 80−103525
composite materials, surface, flame propagation velocity rel. to thermal props. *(Russian)* 80−7797
composites, bounds for effective thermal conductivity and specific heat 79−23745
composites, short-fibre, unidirectional, effective thermal cond. bounds 80−92727
condensation heat transfer, effect of surface thermal conductivity 78−22252
constant power source method, for therm. charcts. 79−95222
contact bridges, electrolytic modelling *(Italian)* 77−24504
contact conductance, heat transfer between solid surfaces 78−46888
cryogens, porous solids, gradientless heat transfer, cryogenic liq. crystn. 79−59903
cryogens, porous solids, gradientless heat transfer, metallic thermal cond. theory 79−59902
crystal lattice low temperature thermal conducting, influence of dislocations 78−75769
crystals, track form., minimal energy loss rel. to thermal cond. 78−17525
curved beam, nonstationary heat conductivity and thermal elasticity 77−84109
cyclohexane, thermal cond. and sp. ht. under press. 78−22906
cylinder, hollow infinite, with temp. depend. thermal cond., thermal stress anal. 80−14575
deformation kinetics, Gibbs eqn. and nonequilibrium thermodynamic models *(Ukrainian)* 78−90720
degenerate semiconductor, film, with unlike surfaces, theory of kinetic effects *(Russian)* 79−51694
di(alkyl ammonium)copper tetrachloride, two-dimens. magnon and phonon thermal cond. in high mag. fields 77−69123
dialkylammonium copper chloride, two-dimens. ferromag., energy transport by paramag. magnons 77−80909
diamond, expt. device for thermal cond. meas. 78−65921
diamond, natural, thermal cond. with absorpt. at 3.22 μm 79−73353
diamond, natural type IB, thermal conductivity anomaly, defects obs. 77−85003
diamond, synthetic powder, thermal wave propagation delay method 80−96702
diamond, thermal cond. at low temp., correl. with IR absorpt. features 80−49435
diamond, thermal conductivity, high temp., electron irrad. effects 80−65318
diamond, type I_a, phonon scatt. by platelets, N-decorated stacking fault model 77−4173
diamond, type-II_a, electron irradiated, thermal cond. reduction at low-temps. 77−47631
diamond ceramic, elec. cond., thermal cond. rel. to temp. 79−15140
diamond type IIb, soft X-ray source for high resolution X-ray lithography 79−97481
diamonds, natural, thermal cond., 0.5 to 20K, anisotropic heat cond. in boundary scatt. regime 79−65267
diamonds, thermal conductivity, 320-450K *(French)* 78−43189
dielectric, kinetic eqn. for thermal phonons with finite mean free time, low-temp. thermal cond. theory *(Russian)* 77−62688
dielectric, thermal cond. at low conc. of phonon scatt. centre, freq. crossing signals 80−2224
dielectric crystal, small, size effect on thermal cond. 77−72724
dielectric crystal, thermal resist. due to four-phonon processes and optical modes 77−76632
dielectric material, phonon thermal conductivity, Umklapp process, comparison with LiF data 80−39367
dielectric phonon gas nonlocal hydrodynamics, second sound attenuation, thermal cond. *(Russian)* 78−47478
dielectrics, reduced conductivity, effect of boundary and dislocation scattering at low temps. 78−67872
dielectrics, temps. <1.5K, methods and apparatus *(French)* 77−1268
diffusion-reaction produced layer growth rate, heat release effects *(Russian)* 77−55397
dilute magnetic alloy, reverse Kondo effect, magneto-transport theory 80−15509
dilute magnetic alloys, transport props. from Suhl's dispersion relations 77−62891
dirty superconductor in mixed state, transverse thermal conductivity 77−32117
disordered two-phase materials, site percolation approach to transport props., effective medium theory 77−61032
dispersed materials, effective thermal conductivity *(German)* 80−33440
dispersed materials, effective thermal conductivity meas. *(Japanese)* 80−70485
doped crystal lattice, thermal cond. 78−71893
dye-polymer system, diffusion based direct marking process, laser induced, spectral thermal characteristics 79−76779
dynamic thermophysical charcts. of thermal receivers, nonlinear eqn. soln. with 3rd kind boundary conditions 77−43395
E-glass fibre reinforced epoxy, room temp. curable, mech. props. and thermal conductivity 78−68669
edge effects in diffusion and cond. meas. 78−32810
effect of boundary refl. and selectivity of optical charcts. on radiative-conductive heat transfer 78−1554
electrically conducting materials, at high temps., improved apparatus 79−86326
electronic contribution, mobility threshold effects 80−65570
energy transport, molecular dynamical calc. 78−95117
epoxy, Ag powder filled, props. below 3K 78−51757

thermal conductivity of solids continued
epoxy, Stycast 1266, very low temp. thermal conductivity and optical props. 78−55992
epoxy resin, low temp. thermal props., phonon states and crosslinked struct. *(German)* 78−75846
epoxy resin, mech. and thermal props., amine hardeners, added softeners and filter effects *(Polish)* 78−68741
epoxy resin DX210/$BF_3$400, reinforced with Morganite C-fibres, thermal cond. 79−65264
epoxy-Al composite, expt. obs. 77−76630
epoxy-Al composite, model 77−76629
epoxy-metal powder mixtures, cryo-tip refrigerator appl., heat transport 78−37013
epoxy-resins, sp. ht. and thermal cond., 0.1 to 80K, phonon scatt. 79−65215
ethylbenzole, thermal cond., 30-400°C, 1-10^3 kg cm^{-2} 78−26739
FBR sphere-pac fuel, prediction of thermal conductivity 79−59174
ferritic scales on steam generating tubes, thermophysical props., thermal conductivity 80−2221
ferroelectric, displacive type low-dimens. 79−61314
ferroelectric, H-bonded, central peak, thermal cond. 80−93250
ferroelectric crystal, displacive, effect of elec. field on thermal cond. 77−85002
ferroelectrics, displacive and order-disorder type, thermal cond. at low temps. 80−75391
ferromagnet, phonon thermal cond., crit. anomalies *(Russian)* 78−80159
fibre reinforced composite, effective transverse thermal cond. 78−18146
fibre reinforced composites, thermal and electrical conductivities *(German)* 77−28053
fibre-reinforced materials, slender, non-dilute, thermal and mechanical props. 80−103524
fibreglass composite, with complex spatial struct. 80−6571
fibreglass insulating materials, radiative heat transfer rel. to optical props. 80−100367
fibrous refractory, exam. of deform. behaviour and thermal cond. *(French)* 79−15719
film, galvano- and thermomag. phenomena, theory *(Russian)* 78−14743
fireproof material, effect of physicochemical processes 78−84012
fluidised bed, heat transfer in horizontal direction, thermal conduction coefficients determ. 79−60058
foils, surface scatt. data table 79−60907
food models, freeze-dried, apparent thermal cond. 79−1098
freeze dried food, thermal cond., var. calcs. of upper and lower bounds 78−9550
frozen food, hydrostatic press. effect on phys. props. 78−26706
frozen soil, thermal probe meas. method *(Japanese)* 77−82034
fuel rod, simulated, for HTGR, pre- and postirradiational thermal transport and thermal expansion 79−6742
glass, 1.5 to 30K *(French)* 77−39704
glass, acoustic phonons lifetime at low temps. 78−26650
glass, and sitalls, effective thermal cond. at various stages of heat treatment 79−60562
glass, localised acoustic phonons, effects on thermal cond. and Raman spectra 77−81092
glass, thermal conductivity effect of strain at 0.1K 77−89602
glass, thin layer thermal conductivity meas., radiometric method 79−94475
glass fibre reinforced epoxy, heat ageing effect on thermophys. props., 10-400K 77−59161
glass fibre reinforced epoxy, thermal cond., diffusivity and sp. ht., determ. 80−24613
glass fibre reinforced epoxy resins, thermal props., 80-300K *(German)* 79−10990
glass fibre reinforced plastic, temp. depend. 77−43393
glass fibre reinforced plastics, thermal cond. meas. rel. to temp., heat cond. problem soln. 79−37887
glass microscopic bead struct. material, thermal cond. and diffusivity, temp. depend. *(Russian)* 79−37885
glass reinforced plastic, thermal activity, prediction of struct. charact. and physicomech. props. 77−63872
glass-C fibre reinforced epoxy, thermal cond., diffusivity and sp. ht., determ. 80−24613
glass-fibre epoxy resin composite, thermal cond. and diffusivity, 2-15K 77−24457
glass-forming polymer, paramag. spin-lattice interactions 80−7149
glass-metal composite, heat conduction, memory switching 80−96703
glasses, thermal cond. rel. to diffusion process due to phonon-defect interaction 80−34259
granular material, simultaneous moisture content/thermal cond. meas. apparatus 78−53064
granular material, thermal conductivity, wetting effect 78−47611
granular materials, effective thermal cond., theoretical bounds 77−58541
granular materials, thermal and elec. cond. calcs. 77−50865
graphite, heat strength calc. for power reactors 79−36331
graphite, irradiated, thermal conductivity at elevated temps. by calc. 79−28163
graphite, near 100 mK, rel. to appl. in cryostat construction 77−82535
graphite, phonon thermal conductivity, rel. to elec. cond., possible supercond. 80−49434
graphite, Poco AXM-5Q1, thermal and elec. transport props., 4-3000K 78−6375
graphite, pyrolytic, neutron irrad. at low temp., thermal cond. recovery *(French)* 77−62566
graphite, pyrolytic commercial, high-temp. thermal and mech. props. 80−75372
graphite, recompressed expanded, thermal conductivity, elastic moduli, density effects *(French)* 78−26744
graphite, thermal conductivity, effect of porosity 80−65314
graphite structures in PBR, neutron radiation damage, mech. props., stress fields *(German)* 77−34387
Green River oil shales, anal. of depend. of thermal transport parameters on organic content 79−79817
gypsum, thermal conductivity thermal decomposition 78−2310
heat conduction in solid containing gas-liquid inclusions *(Russian)* 78−22908
heat flow rate, effect of asymmetry 80−102959
heat pulse technique, down to 25 mK, on poor thermal diffusivity and small sp. ht. samples 77−45850
heat-insulating material, simultaneous determ. of temp-depend. thermal cond., heat capacity 77−11120

thermal conductivity of solids continued
heat-pulse experiments, nonlinear effects, theory 80−96182
heterogeneous matrix system, generalised conductivity and loss, tangent 80−7289
heterogeneous matrix system, thermal cond. 78−9555
heterogeneous matrix systems, calc. of thermal cond. coeff. *(Russian)* 77−24455
heterogeneous systems with disordered structure, generalised cond. coeffs. 79−87075
hexamethylenetetramine, thermal cond. and heat capacity under press. 80−80008
high heat-conductance materials, method for determ. of thermophys. charcts. on thin samples 77−61063
hollow cube, non-homogeneous, transient temp. distrib. 78−75035
homogeneous isotropic solid body, variational principles *(Hungarian)* 78−22247
hot wire method of meas., temp. drift effects *(Japanese)* 78−43191
hot-wire method of determ., temp. depend. *(German)* 77−27464
hot-wire test, critical review and comparison with BS 1902 panel test 80−104409
HTGR multihole fuel, equivalent thermal conductivity calc. *(Japanese)* 79−45346
ice, Ih, thermal resist. near melting point meas. 80−44375
ice, thermal and electrical conductivity, 0 to −20°C 77−24450
ice, thermal conductivity of nine solid phases 78−30801
impure insulators, low temp. conduct. calc. 79−33128
inhomogeneous material, thermoelec. power and thermal cond. 78−10483
insulating mechanical supports, appl. to meas. thermal conductance 80−82772
insulator, lattice thermal cond., point defect scatt. relax. rate role 80−70478
insulator, lattice thermal resist. due to core dislocations 80−29231
insulator, low temperature, role of point defect scatt. in lattice thermal cond. 77−76631
insulator, with dislocations, lattice thermal cond. 77−59157
insulators, nonlocal hydrodynamic of phonon gas, thermal cond. and second attenuation coeff. 79−65158
intermediate state, Fermi surface shape and topology effects *(Russian)* 78−72314
intermediate state, reflectivity of S-N interface, application for Rowell-Tomasch oscills. amps. and thermal cond. 78−91822
intermediate state superconductor, kinetic props. of corrugated and thread struct., sound attenuation *(Russian)* 80−54843
ionic conductor, one-dimens., ion-ion interaction contrib. 78−55977
irreversible effects due to thermal perturbations, linear theory 77−22508
Ising model, randomly diluted two-dimensional kinetic, determ. of spin diffusion and thermal cond. by computer simulation 77−36039
isotopically disordered ferroelectric cryst. 77−76628
isotropic body with many cracks or intrusions, transport processes 77−11116
Jahn-Teller cooperative T−(e+t) systems, heat current operator 80−34405
Jahn-Teller cooperative T−(e+t) systems, pseudo spin thermal cond. 80−34406
Jahn-Teller cooperative T-(e+t) system, thermal cond. 80−70479
joint determ. of thermophysical charcts., quasilinear method 77−41601
Kondo superconductor, transport props. 79−65600
laser irradiation, solid surface, temp. rise calc. *(German)* 78−68580
lattice, anomalous temp. behaviour near structural phase transition *(Russian)* 80−75394
lattice thermal cond., variational bounds improvement by scaling and Ritz procedures 77−62689
lattice thermal conductivity, contrib. due to correction term, generalised Callaway integral 77−28056
lattice thermal conductivity, contrib. due to correction term, generalised Callaway integral 78−2318
lattice thermal conductivity, general transport theory, phonon Boltzmann eqn. 80−54446
lattice thermal conductivity, point defects effects at low temp. 79−90836
lattice thermal conductivity determ., hypercircle approach and complementary variational principles 77−47630
lattice thermal resist. due to bound state electrons in doped cryst. 79−46850
lattice thermal resistivity due to electrons 78−51756
layer material, local heating *(Russian)* 77−42716
layered material with through cracks, transverse conductivity 77−84122
layered orthogonally reinforced plastics, strength and stiffness prediction in interlaminar shear 77−9025
lithium thallium tartrate, single cryst., thermal cond. at low temps. 79−33125
low temperature thermal conductivity measurements under uniaxial compression 80−105653
low thermal conductivity material, solidification, dispersed high conductivity particles effects 77−80602
magnesite artifacts, roasted, props., filler porosity effect 80−104099
magnesite refractories, spinel bindal, with reduced thermal cond. 79−83162
magnetic crystals, models 77−47998
magnetic insulator, heat transport by magnons, effect of magnon-phonon thermal relax., calc. 77−39705
marine sediments containing gas hydrates, thermal cond. and acoustic wave vel. meas. 79−79819
measurement, 60 to 300K, USSR special standard 77−31205
measurement, calc. formulae for unsteady temp. data 79−94476
metal, deformed in pressing process, temp. field modelling *(Russian)* 80−53602
metal, electron Boltzmann eqn. solns., energy depend. 80−88537
metal, flow stress relation with thermal conductivity discontinuity at supercond. transition 78−60246
metal, heating by laser emission, spatial nonlinear problems *(Russian)* 80−7440
metal, kinetic eqn., iteration soln. 77−43564
metal, laser heating kinetics, influence of oxide film interf. effects 80−11841
metal, pseudoharmonic effects of phonons in heat cond., high temp. region 80−70326
metal, thermal cond. changes at melting point, vacancy model 79−33279
metal, thermal cond. size effect in normal and supercond. states, and supercond. radiometric effect 78−60245

thermal conductivity of solids continued
metal, thermal resist. calc., role of electron diffusion over Fermi surface 77−62894
metal cone, vaporisation, solution by wave front method 78−5640
metal fibre materials, thermal and elec. conductivities 78−10419
metal film, vaporisation kinetics on absorbing laser radiation *(Russian)* 77−43423
metal heating by laser radiation, calc. allowing for thermal props. temp. depend. 78−30770
metal wick, sintered, effective thermal cond. meas. 78−94582
metal wire, heated by electrical current, steady-state thermal cond. 78−59285
metal-filled polymers, thermal cond., var. calcs. of upper and lower bounds 78−9550
metal-H systems at high H press., physicochemical props., book contrib. 80−24535
metallic crystal, thermomechanical deform., analytical description 80−49391
metallic film, oscill. kinetic effects, boundary electron scatt. *(Russian)* 78−52104
metallic films, metal-dielectric boundary thermal resistance, nonlinear elec. resistance *(Russian)* 80−65530
metallic glass, phonon transport below 100K 78−14422
metallic glasses, elec. and thermal props. 78−72131
metallic thermal connectors for use in nuclear refrigeration, elec. resist. meas. 78−224
metallic thin films, thermal conductivity and thermal diffusivity, determ. method *(German)* 78−19165
metallic thin films, unlike surface properties, transport coeffs., diffuse surface scatt. 80−20331
metals, correl. between temp. depend. of elec. resist., resistivity, thermal cond. 77−8064
metals, electrical and thermal resistance, influence of static atomic displacements 80−103674
metals, electron-phonon interaction and lattice thermal conductivity 79−42189
metals, fracture during laser working, depend. on physico-chem. props., heat cond. *(Russian)* 80−55432
metals, frictionless heat motion at low temps. 79−69495
metals, nonstationary temperature fields due to moving heat sources, heat capacity, thermal cond. *(Russian)* 80−107448
metals, phonon-phonon scatt. role in lattice thermal cond., phonon drag, elec. cond. 80−70483
metals, radiation induced vaporisation, press. behaviour 80−84288
metals, residual resistivity and thermal conductivity coeff., comparison of max. values as parameter of metal purity 79−65431
metals, thermal conductivity models, during hot deseaming *(Russian)* 80−24869
methane and methane-d_4, solid, thermal cond. calc. 78−51753
mica, muscovite and phlogopite, anisotropic behaviour, 3-320K 77−43392
microscopic particles, heating by laser beams 78−50838
minerals, silicates and oxides, phonon cond. 77−73715
mixed-carbide, sphere-Pac fuel, thermal conductivity during initial stage reconstructuring 80−810
modified equations for wave number dependent relax. time 78−71259
moist disperse solids, thermal conductivity *(Russian)* 77−54864
moist porous solid, thermal cond., struct. model and computation method 78−2312
molecular dynamical studies of energy transport in crystalline solid 78−30803
molten salt, heat storage, review *(Japanese)* 80−6573
monatomic BCC lattice under intense excitation, energy transport 78−59922
monocarbides of subgroups IVa and Va, kinetic props., review 78−47613
Mott's formula for thermopower and for Wiedemann-Franz law 80−84462
Mott insulators, electronic contrib. to thermal cond. 77−69316
multilayer insulation, simple struct. insulating material props. for low temp. appl. 80−57307
multilayer thin film struct. thermoelec. props. 80−92964
multiphase material, average bulk props. calc., bounds 77−16237
naphthalene, thermal cond. and heat capacity, meas. under press. 79−90796
narrow band semiconductor, transport phenomena electron energy spectrum *(Russian)* 79−51616
Nichrome, Kh20N80, varying porosity, effective thermal cond., 373-1400K, meas. method 78−75053
noble metal, Matthiessen's rule deviations, var. calc. 77−43562
noble metal, thermal resistivity temp. depend., free electron approx., phonon spectrum 77−66152
noble metals, pure, low-temp. transport props. 77−8072
non-steady state thermal conductivity in multilayer sheets *(Russian)* 80−43596
nonlinear diffusion equations, identification of thermal cond. and sp. ht. *(French)* 77−47614
nonmetallic crystals, at high temps. 78−26740
nonsteady regimes, multilayer systems, applicability of additivity law anal. 77−42695
nonuniform systems, effective conductivity from percolation and conduction theory 80−62597
nuclear composite fuels, heat cond. parametric anal. 77−6523
nuclear reactor materials, thermal properties at elevated temps., determ. method 77−73402
nylon, near 100 mK, rel. to appl. on cryostat construction 77−82535
oil shales, review of thermophysical properties 79−100479
oligocarbonatemethacrylates, and their cross-linked polymers, thermophysical characts., temp. depend. anal. 80−19721
oxide ceramics, thermal conductivity and emissivity at high temp. 77−28051
paraffin wax, solar energy thermal storage, numerical simulation of energy transfer *(French)* 79−24916
penny shaped crack effects 79−10993
periodically nonuniform solids, effective thermal cond. 80−70486
phase transition, quasi-elastic scattering of phonons 79−82299
phonon conductivity correction due to three phonon normal processes in presence of dislocations 80−15318
phonon diffusion with freq. down-conversion 80−19886
phonon polarisation operator in one- and two-dimensional crystals *(Russian)* 78−79676
thermal conductivity of solids continued
phonon transport in bounded systems, influence of size effect and surface roughness 79−46849
phonon-phonon scattering, hydrostatic deformation effect 78−18721
plasma, nondegenerate, dense, electron transport *(Russian)* 79−98865
plastic, thermal cond. meas. rel. to temp., heat cond. problem soln. 79−37887
plastic insulating foam, thermal cond., var. calcs. of upper and lower bounds 78−9550
plate, calculation of unsteady temp. field and thermoelastic strain 77−19534
plate, transverse thermoelectric power effect of thermal conductivity anisotropy 77−72876
plate containing cracks, varying temp. cond. at edges, thermal conductivity and thermoelasticity *(Russian)* 77−23915
PMMA, amorphous, thermophysical props. depend. on hydrostatic press. 78−47612
PMMA, Gruneisen const. and thermal props., temp. depend., 4-300K, Brillouin scatt. obs. 80−100662
PMMA, thermophysical props. at high hydrostatic press. 78−2317
poly(alkyl methacrylate), vitreous state, thermal cond., hole theory of liqs., press. 78−84013
polyalkylmethacrylates, vitreous, thermal cond., press. and temp. depend. 78−2315
polyamide, Al_2O_3 filled, low temp. thermal and mech. props. 80−25816
polybutadiene, thermal cond. and sp. ht. 79−65265
polycarbonate, amorphous, thermophysical props. depend. on hydrostatic press. 78−47612
polyethylene, extruded, thermal cond. 220 to 360K 78−67873
polyethylene, extruded semicryst., thermal cond. and specific heat, <1K 80−59742
polyethylene, highly oriented 78−47614
polyethylene, irrad., thermophys. characts. of amorphous phase, effects on crystallinity 77−7870
polyethylene, low temp. thermal cond. 79−73351
polyethylene, ultrahigh-modulus, thermal cond. in region 2 to 100K 77−62690
polyethylene terephthalate, thermal diffusivity, conductivity meas., crystallisation rel. to glass transition 77−47632
polymer, amorphous, high temp. thermal transport, phonon modes 77−62691
polymer, amorphous, thermal conductivity and thermal diffusivity, press. and temp. depend. 77−7915
polymer, isotropic, oriented, 2-100K, crystallinity effect 77−20137
polymer, semicrystalline, model for thermal cond., orientation effects 77−85004
polymer, thermal conductivity as function of temp. 77−89603
polymer, thermal conductivity-pressure relationship *(German)* 77−20139
polymer foil, charge distrib. determ., thermal pulse technique, meas. accuracy 78−80287
polymer surface, flame propagation velocity rel. to thermal props. *(Russian)* 80−7797
polymers, amorphous, press. effect on thermal cond. *(German)* 79−95225
polymers, noncrystalline, thermal cond. rel. to temp. *(German)* 79−28159
polymers, thermal conductivity, temp. crystallinity and orientation depends., review 78−10234
polymers, thermal conductivity data, need and demand 77−72725
polymethylphenylsiloxanes, press. and 20-200°C temp. range 77−59162
polyolefines, filled, struct.-mech. props. relation *(German)* 78−35451
polyoxymethylene, low temp. thermal conductivity 78−38886
polyoxymethylene, thermal diffusivity, and cond. meas., two-phase model 77−47632
polystyrene, amorphous, thermophysical props. depend. on hydrostatic press. 78−47612
polystyroles, filled, struct.-mech. props. relation *(German)* 78−35451
polysulphur nitride, low temp. thermal cond. 80−24689
polyvinylidene fluoride thermal diffusivity and cond. meas., two-phase model 77−47632
pore velocity, due to surface diffusion under temp. gradient, finite thermal conductivity correction 80−15428
porosity correction to thermal conductivity based on analytical temperature solutions 79−59173
porous material, thermal cond., diffusivity and water content meas., thermal shock transient *(French)* 78−94583
porous material, thermal conductivity, theoretical models *(German)* 77−27462
porous metal, thermal conductivity meas. 78−18150
porous rocks, saturated with low cond. fluid, thermal cond. meas., systematic errors 77−86871
powder, particle size and porosity effects *(Japanese)* 78−6191
powder consisting of anisotropic grains, effective thermal and elec. cond. 77−89601
praseodymium ethyl sulphate, specific heat, electric suscept. and thermal cone., one-dimens. electric dipolar XY system 77−32148
proustite-pyrargyrite solid solns., thermal props. *(Russian)* 79−65227
PTFE, thermal cond., effect of material on working parameters of cryosurgery instruments 78−36037
pulse methods for investigating thermal diffusivity and conductivity in solids, theoretical models *(Polish)* 80−92728
PVC, filled, struct.-mech. props. relation *(German)* 78−35451
pyrographite, Si-containing, high-temp. treatment effects 77−40429
quantum crystal, role of defectons 77−35796
α-quartz:Al, γ-irrad., thermal cond. below 10K 79−51320
quartz, fused, thermal cond., temp. depend. at low temps. 80−65322
α-quartz, heat transfer at low temps., lattice thermal cond. 80−92729
quartz, phonon heat conduction of single crysts. by quantum acoustic method 77−11748
quartz ceramics, thermal and temp. cond. in range 500-1900K 80−39370
random two-phase material, thermal cond., var. calcs. of upper and lower bounds 78−9550
rare earth garnets, prep. and props. book contrib. 80−44193
rare earth monobismuthides, thermal expansion, thermal cond., 300-900K 78−91453
rare earth oxides, binary, struct. and props., book contrib. 80−45292
refractories, hot wire meas. technique 80−37038
refractories, hot-wire meas. method, 20-900°C 80−31759
refractories, microcracks contrib. 80−19999
refractories, temp. and press. depend. 78−43188

thermal conductivity of solids continued
refractories, thermal cond. rel. to gas phase mass transfer in pores and microcracks 79−73352
refractory, thermophysical props. in rarefied gaseous medium 78−34664
refractory, ultra-lightweight, thermophys. charcts., moisture effects *(Russian)* 77−55921
refractory materials, contrib. of segregation and diffusion to heat cond. 80−20001
refractory materials used in MHD generator channels, thermophysical props. 77−28054
refractory products, thermal conductivity, determ. standardisation 79−82397
refractory thermal insulation effective thermal cond., fibre diameter effects 80−104105
rocks, cond. and heat flow meas. in Singhbhum thrust belt (India) 77−49050
rocks, crystalline, thermal cond., rel. to energy extraction from hot dry rock geothermal systems 79−70790
rocks, thermal conductivity of granular media, results for greisen and granite *(French)* 78−11880
rocks and minerals, dry, water-saturated and petroleum-saturated specimens *(Russian)* 78−92817
rocks and minerals, lattice conds. at mantle press. and temp. 78−69338
rod, heating, thermal cycle, control, optimal conditions rel. to response speed *(Russian)* 77−19510
rubber, natural, thermal properties depend. on temp. and press. 79−95223
ruby, γ-irradiated low temp. UV bleaching 79−23646
ruby, phonon heat conduction of single crysts. by quantum acoustic method 77−11748
ruby, phonon spectrum, thermal pulses under diffuse phonon propagation conditions 80−103434
sapphire, heat transfer at low temps. 78−34665
sapphire, phonon cond. calc., 0.4-4K 78−18852
sapphire-Pb interface, heat transfer coeff. meas., 2-80K 80−88419
schist containing clay and sand, integrated normal emissivity with low heat conductivity coeffs. 80−103504
schist dust, integrated normal emissivity with low heat conductivity coeffs. 80−103504
selenide thermoelectric materials, thermal conductivity, long-term stability and other props. experimental anal. 80−107834
semiconductor, doped lattice thermal cond., role of electron-phonon interactions and peripheral phonons, appl. to Ge:P 78−79702
n-semiconductor, electron-phonon drag in longit. quantising mag. field 77−76805
semiconductor, exciton-phonon drag 77−15640
semiconductor, nonlinear thermal conductivity on pulse heating *(Russian)* 77−43391
semiconductor, p-type, with zincblende struct., internal strain on bound hole-phonon interaction 78−91492
semiconductor, phonon conduction and relaxation times 80−107585
semiconductor, rapid meas. method *(French)* 78−12689
semiconductor, temperature waves in nonequilib. conditions 77−43397
semiconductor, tetrahedral, lattice thermal cond., ionicity depend. 79−37884
semiconductor, thermal cond. calc. using numerical soln. of Boltzmann eqn. 80−44373
semiconductor injection lasers, output depend. on inhomogeneous bonding 80−64015
semiconductor thermal energy transformers, influence of anisotropy of thermal cond. 77−8127
semiconductor transport equations formulations 77−43585
semiconductors, disordered, elec. heat cond. calc. *(Russian)* 77−32009
semiconductors, lattice thermal conductivity, high temp., role of optical phonons 79−33129
semiconductors, thermal cond. theory *(Russian)* 79−37889
semiconductors, thermal conductivity meas., cryostat design for 90 to 450K 79−76957
semiconductors and insulators, phonon cond., three-phonon N- and U-processes 80−65313
semiconductors thermophysical props. determ. from Ettingshausen effect meas. method 80−44376
semiinfinite bar, boundary value inverse heat conduction problem, hyperbolic eqn. soln. 80−19210
semimetals, degenerate, heat conduction, thermal EMF, Lorenz number anisotropy at low temp. 80−75549
semimetals, exciton phase, transport effect in strong mag. fields 78−87977
semitransparent medium, effect of radiation heat transfer in thermal cond. meas. 77−23858
shells with asymmetric heating, thermal cond. and stresses 79−32182
silicate minerals, phonon cond. and mean sound vel., linear relationships 77−21761
silicate minerals, relationship between phonon cond. and seismic parameter Φ 79−39707
sintered porous materials, effective thermal conductivities 80−19998
sitalls, at various stages of heat treatment 79−60562
smoky quartz, thermal props. at very low temp. 80−24610
solid thermal cond. and interface resistance meas. by radiation thermometry 80−86289
solidified gas constant-volume thermal conductivity meas. cell 80−31739
soot, granulated, thermal and elec. cond. 80−24687
spatial distribution of temperature rise induced by Gaussian laser beam 79−69917
spectroscopy of high-frequency phonons, transport phenomena, review 80−49325
spherulite, two-phase, ht. cond. anisotropy 78−2316
spin glasses, elec. resist., thermal resist. and thermopower 80−65542
spin-lattice relaxation measurements, field depend., influence of thermal cond. 78−15013
steady-state heat conduction of solids with inclusions and cracks, analogy with longitudinal shear *(Russian)* 77−68371
steel, C, resistivity, thermal and elec., spin disorder scatt. anal. 78−76063
steel, Cr, hypereutectic, ShKh15, exam. of thermal props., 298 to 1173K *(Russian)* 79−28334
steel, N27Yu2T2B, elec. and thermal cond., 4.2 to 200K, Wiedemann-Franz law *(Russian)* 79−78076
steel, quenched, verification of change of props. in mag. field 78−52985
steel, stainless, meas. method, precision 79−6121
thermal conductivity of solids continued
steel, stainless, thermal cond., effect of material on working parameters of cryosurgery instruments 78−36037
steel, stainless, thin layer thermal conductivity meas., radiometric method 79−94475
steel, type 12X18H10T, strengthening based on intensifying heat exchange processes in martensitic transformation region *(Russian)* 79−70065
steel, type Kh23N18, integrated normal emissivity with low heat conductivity coeffs. 80−103504
steel 45, temp. depend. calc. *(Russian)* 77−55514
steel fibre reinforced Al, thermophys. props. 80−59745
steel forgings, expt.-calc. model of quenching, temp. meas. across cross section 80−16345
stochastic temperature field in cylinder, digital simulation algorithm *(Polish)* 79−71370
stochastic temperature field in cylinder, digital simulation algorithm *(Polish)* 80−17879
stycast 2850FT, low temp. thermal cond. 79−23790
superconducting materials, meas. from 4.2-300K 79−60970
superconducting tunnelling junctions, thermal conductivity meas. 77−36029
superconductor, carrying time-dependent current, normal zone propagation 78−84346
superconductor, composite, normal zone propag. calcs. 77−43778
superconductor, dirty, mixed state, thermal cond. anisotropy 80−7036
superconductor, electron-phonon thermal cond. *(Russian)* 78−26993
superconductor, type II, meas. for disc of arbitrary shape 79−63228
superconductors, long, thin-film, min. hotspot current 80−15656
superconductors at Lifshitz electronic transition point *(Russian)* 80−11135
surface roughness effects, low temp., including defect and boundary scatt. of phonons 77−28057
temperature dependence *(Russian)* 77−55514
tetrebromomethane, thermal resistivity, heat capacity and phase diagram under pressure 80−65316
TGS, nitroaniline admixture effect on thermal parameters 80−107580
TGS, X-irrad., thermal diffusivity, cooling const. and heat transmission coeff. 79−86935
thermal insulation on metal backing, thermophys. charcts., expt. determ. technique 80−4707
thermal penetration property ρck meas. instrum. 78−70120
thermal resistance decrease of pores and microcracks 78−75892
thermoelasticity in solid symmetrical bodies of revolution, thermal transients, finite element analysis *(Spanish)* 79−23208
thermoelectric material, thermal cond. meas., 1100-2000K 78−24798
thermophysical properties at high temp., conference, Moscow, USSR (May 1976) 77−28012
three-phonon resist. high-temp. comparison of different models 77−4171
tissue-equivalent plastic, A-150, thermal diffusivity, sp. ht., thermal cond. obs. 80−34258
transient temperature distribution in the reactor vessel wall after cooling system failure 79−54473
transition metal, thermal and electrical conductivity at high temperature, interpretation of temp. depend. 77−35912
transition metal compound refractories, electron and phonon behaviour 80−54624
transition metal oxides, dielec. and thermophys. props. 77−52009
transition metal silicides of groups IV-VI, thermal cond., 20-1000°C 79−10992
transition metals, electrnic sp. ht. and heat conduction, temp. depend. 78−71865
transparent dielectric with metallic inclusions, light pulse shape effect on optical breakdown threshold 80−20588
triglycine sulphate-Ge contact, thermal resist. 77−4226
$TSeTBr_{0.5}$, phase transition, mag. props., thermal capacity and cond. *(Russian)* 79−99537
TTF-TCNQ, thermal cond. above and below Peierls transition, electronic and lattice contribs. 79−95394
tube, transversely finned, in air flow, metal thermal cond. effect 78−75043
turbogenerator rotor and stator core thermal conductivity solution using integral representation method *(Russian)* 80−100451
two flat surfaces in contact, thermal conductance with applied load, variation, determination for elastic and plastic surface deformation 79−72782
two-component layered system, with interpenetrating components, thermoelec. and galvanomag. props. 78−79982
two-phase system, effective thermal cond. 79−30396
type I superconductor, thermal cond. in intermediate state, size effect in longitudinal lamellar struct. 78−52153
type II superconductor, clean, US attenuation and thermal cond. 78−91812
unsteady heat conduction accompanied by an endothermic solid reaction *(Japanese)* 79−76939
Wiedemann-Franz law in semiconductor and metal glasses 79−65422
YIG, thermal cond. at low temps. 80−2222
zeolite A, synthetic, with salt inclusions, elec. and thermal props. 79−55925
zinc blende semiconductors, small-gap, electron scatt. and transport props. 78−95294
zinc blende semiconductors, small-gap, electron scatt. and transport props. 78−95295
Zircaloy-2 and associated oxide layers, thermal property meas. 77−8063
Zircaloy-2 fuel tube, thermal conductivity of oxide deposit 79−63745
zircon bricks, meas. up to 1200°C, Eucken's eqn. anal. *(Japanese)* 78−95193
Ag alloys, dil., transport props. 78−76046
Ag, electrical contact material with liquid lubricant, prod. and appl. 78−10559
Ag, phonon-limited elec. and thermal resistivity 79−42517
Ag, thermal conductivity at high press. meas. 78−95283
Ag-Hg alloys, thermopower, thermal cond., elec. resistivity 79−65439
$(Ag_{x/2}Pb_{1-x}Bi_{x/2})Te$ solid solution, preparation and thermoelectric props. 77−47839
$(Ag_{x/2}Pb_{1-x}Sb_{x/2})Te$ solid solns., Hall coeff., thermoelec. power, and thermal cond., 100 to 500K 79−82614
$Ag_{19}Sb_{29}Te_{52}$, single-phase, thermoelectric efficiency 80−107826
Ag_2Te, low temp. thermal cond., thermoEMF 78−43423
Ag_2Te-Ag_2S system, elec. and thermal props. at 300K 78−64044
Al, annealed, coefficient temp. dependence, deformed and non deformed samples 78−76049

thermal conductivity of solids continued
Al, band struct. effects on electrical and thermal cond. 78−34820
Al, electron-phonon enhancement of electron-electron scatt., elec. and thermal cond. 80−49326
Al film, polycryst. heat conductivity depend. on thickness, block boundary density *(Russian)* 79−82689
Al, lattice thermal cond., 1.5-15K 78−30904
Al, lattice thermal cond. at low temps., Ashcroft pseudopotential method 80−19897
Al, low temp. electrical and thermal transport props., Matthiessen's rule breakdown 78−26847
Al, metal and dil. alloys, electronic thermal cond. calc. 78−47764
Al plates with air gap, temp. field for microplasma welding of edge joints *(Russian)* 80−7755
Al, polycrystalline, thermal cond. min. 78−76050
Al, simultaneous thermopower and thermal conductivity meas. 77−72854
Al, thermal cond. form diffusivity, press. depend. up to 2.5 GPa 77−85195
Al, thermal conductivity minimum, effect of lattice component 80−15500
Al, thin film, thermal cond. meas., size effect 80−65715
Al-2024-T351 alloy, precipitation hardening, thermal cond. 78−91661
Al-Ag(Cu), alloying effect on phonon spectrum and lattice heat cond. 77−62695
Al-Cu, lattice thermal cond. at low temps. 77−62889
Al-Mg-Si, DTA exam. after small and medium deform. 80−21002
Al-Mg-Zn solid solution, thermophysical props., 0-400°C *(Russian)* 77−89548
Al-Si alloys, eutectics and hypoeutectics, mech. props. and thermal cond., P impurity effect 79−83271
Al-Si-Cu-Ni alloy casting, thermal props. 78−95814
AlN powder, effect of O impurity on sintering and thermal cond. *(Japanese)* 79−20017
AlN, thermal cond. and stability at high temp. 78−47610
AlN-Al_2O_3 composites, hot-pressed 77−52275
Al_2O_3, alumina, meas. by scanning temperature method 77−45831
Al_2O_3 based catalysts, porous pellets 79−86936
Al_2O_3, fibrous, thermal diffusivity and conductivity 78−10232
Al_2O_3, phonon spectra using freq. crossing techniques 78−14415
Al_2O_3, therm. characts. using constant power source method 79−95222
Al_2O_3, transition metal ion doped, phonon spectroscopy using freq. crossing techniques 79−42193
Al_2O_3:Cr, Mg, stabilisation of Cr^{5+}, thermal cond. meas. 78−22905
Al_2O_3:Mn, appl. of differential method for low temp. thermal cond meas. 79−63227
Al_2O_3:Mn^{3+}, Jahn-Teller Mn^{3+} ions, phonon spectroscopy and thermal cond. meas. 80−88282
Al_2O_3:Ni, heat transfer at low temp. 78−38888
Al_2O_3:Ni^{3+}, heat transfer at low temperatures 78−91493
Al_2O_3:Ni^{3+}, phonon-spin interaction study by thermal cond. meas. 79−82395
Al_2O_3:V, valency changes of V ions, γ irradiation, thermal cond. optical absorption and EPR meas. 77−80541
Al_2O_3:V^{3+}, frequency crossing signals of V^{3+} ions, conc. depend. study using thermal phonons 78−95115
Al_2O_3:V^{3+}, $g_\perp/g_\parallel$ determ. by freq. crossing spectroscopy using thermal phonons 78−23055
Al_2O_3:V^{3+}, low temp. thermal cond., phonon scattering 78−95116
β-Al_2O_3-Ag_2O, thermal cond. below 300K 77−24454
Al_2O_3-Fe cermet, microstruct. and physical props. 79−42279
β-Al_2O_3-K_2O, thermal cond. below 300K 77−24454
β-Al_2O_3-Li_2O, thermal cond. below 300K 77−24454
Al_2O_3-Mo, dielectric cermet, thermophysical props. 77−51557
β-Al_2O_3-Na_2O, thermal cond. below 300K 77−24454
Al_2O_3-Nb, dielectric cermet, thermophysical props. 77−51557
Al_2O_3-SiO_2 heat insulating refractories, prep., physical, thermal, structural props. 78−68662
Al_2O_3-W, dielectric cermet, thermophysical props. 77−51557
Al_2O_3-ZrO_2, dispersion hardened, fracture toughness improvement by induced microcracking *(German)* 78−31501
Al_2O_3-ZrO_2 dispersed system, thermal diffusivity/conductivity, effect on microcracking resulting from phase transform. 78−10231
Ar, at high press. 80−103099
Ar lattice thermal cond. analysis, low temp. 77−35768
Ar solid, low temperature lattice thermal cond. 78−22910
As, amorphous, low temp. thermal cond. and sp. ht. 79−28161
As, amorphous, optical, vibr., transport and defect-related props., review 79−51935
As, amorphous, sp. ht. and thermal cond. at low temp. 79−65213
As, electrical and thermal props. 78−14747
As, electrical resist., thermal cond. and thermopower, low temp. transport props. 80−49708
As, thermopower and thermal cond. from 8K down to 0.3K 79−19610
$AsSe_{1.5-x}Te_x$ glasses, physical props. 78−68028
$As_2(Se_{1-x}Te_x)_3$ semiconducting glasses, solid and liquid, thermal cond. 80−6574
$As_2(Se_{1-x}Te_x)_3$, thermal cond. of solid solution and melt 78−67874
$As_2(Se_{1-x}Te_x)_3$, thermal cond., temp. and press. depend. 79−82396
Au, phonon-limited elec. and thermal resistivity 79−42517
Au, thermal conductivity at high press. meas. 78−95283
Au wire, thermal cond., 0.8-10K 77−89748
B fibre reinforced Al, thermophys. props. 80−59745
B_4C, mech. and thermal props. 80−21083
B_4C, thermal cond., nonstoichiometry effect 78−63887
B_4C, thermophysical props. and neutron absorpt. 80−103488
BN, hexagonal, parallel to basal planes, thermal conductivity 78−22907
BN-AlB, cubic phase solid soln., crystallographic and metallographic study, thermal resist. *(Russian)* 78−30599
BN_x refractories, thermal cond. determ. using IR laser heating 79−94479
B_2O_3-Na_2O-SiO_2-Al_2O_3, effect of alumina dispersions on the thermal cond./diffusivity/stress resist. 80−39368
B_6O, mech. and thermal props. 80−21083
Ba, transport properties, elec. resist., thermoelec. power, thermal cond. deviations from Matthiessen's rule 78−39086
BaF_2, single cryst., linear thermal resistance temp. depend. 77−66048
$Ba_2NaNb_5O_{15}$, birefr. material, thermal cond. determ. by optical method 78−18851
$BaTiO_3$, donor doped, exam. of heterogeneous microstructure *(German)* 79−24632
thermal conductivity of solids continued
Be, low temp. elec. and thermal cond. in mag. field, use as heat switch 77−35923
$BeAl_2O_4$, Czochralski grown single crystal, hardness, thermal expansion, concl., elastic const. 79−52353
Bi, deformed cryst., phonon scatt. by lattice defects, thermal cond. calc. 78−22802
Bi, electrical resist., thermal cond. and thermopower, low temp. transport props. 80−49708
Bi, thermal cond. under plastic deform., phonon scatt. by dislocations and twin boundaries 77−11746
Bi, thermal conductivity at ultralow temp. 79−1532
Bi, thermoelectric power, electronic thermal cond., in mag. field 80−60015
Bi-Sb alloys, thermomagnetic quality factor 77−15882
Bi-Sn, thermoelec. props. from 2 to 300K 80−24872
Bi-Tl alloy, 1.5 to 50K, temp. depend. 78−26990
$Bi_{12}GeO_{20}$, thermal cond. and absorptivity 80−70480
Bi_2O_3, thermoelec. props., 500-1500K 80−29423
Bi_2S_3-Bi_2Se_3 and Bi_2Te_3-Bi_2Se_3 systems, thermal cond. change during phase transitions 80−100368
BiSb (>20 wt.%), electronic band struct. 80−107698
$Bi_{0.5}Sb_{1.5}Te_3$ film, effect of struct. on thermal cond. 79−28257
Bi_2Te_3 film, effect of struct. on thermal cond. 79−28257
Bi_2Te_3-$SbTe_3$, ordered structure formation, heat treatment effect on thermal cond. 80−54448
BiTeI-SbTeI solid solns., form., crystn., elec., thermal props. 78−44003
n-$Bi_2Te_{2.88}Se_{0.12}$, extrusion deformed, powder dispersion degree influence on thermal and elec. props. *(Russian)* 80−39366
$Bi_2Te_{3-x}Se_x$ films, thermal cond. depend. on grain size, phonon-boundary scatt. 79−69304
C fibre reinforced Cu, temp. depend., 80 to 350K 77−24452
C fibre reinforced epoxy, thermal cond., diffusivity and sp. ht., determ. 80−24613
C fibre reinforced epoxy resin composites, 2 to 290K 79−60528
C, glassy reticulated struct., low temp. thermal cond. meas. 79−86938
C materials, thermal insulating props., furnace appls. *(French)* 78−44345
C, vitreous, low temp. sp. ht., thermal cond. and US vel. meas. 78−47533
C-C composites, existence diagram and properties *(French)* 78−64517
Ca, transport properties, elec. resist., thermoelec. power, thermal cond. deviations from Matthiessen's rule 78−39086
$CaBe_{13}$, thermal cond. coeff. determ. 79−1531
CaF_2, fluorite, use as standard specimen 80−96704
CaF_2, fluorite crysts., lattice O^{2-} effect on thermal, elec., and thermoelec. props. 77−76599
CaF_2, single cryst., linear thermal resistance temp. depend. 77−66048
CaF_2:NaF (YF_3) thermal conductivity of single crysts., 80-300K 77−11747
CaF_2:rare earth metal, thermal cond., 80 to 300K, defect centre struct. 77−15638
$10CaO.15Na_2O.75SiO_2$ glass, thermal cond., temp. depend. at low temps. 80−65322
$Ca_{10}(PO_4)_6(OH)_{2-2x}O_x\square_x$ polycryst. sintered bodies, prep. and thermal props. 80−25624
$CaSO_4$, cryst. growth kinetics at heated metal surfaces, thermal cond. morphology and crystn. 80−29867
n-$CdCr_2Se_4$, single crystal, transport props. near Curie temp. *(Japanese)* 78−6406
$Cd_xHg_{1-x}Te$, thermal cond. in mag. field, thermopower, and Nernst-Ettingshausen effect 77−31814
$CdIn_2S_4$:Cr, thermal cond., 1.8 to 200K, phonon scatt. by impurity ions 77−76627
CdTe, low temp. themal cond., growth parameter influence 80−92725
CdTe, phonon conductivity, 2 to 300K, scatt. mechanisms 79−4436
CdTe, thermal cond. and X-ray topography investig. of cryst. defects 77−39706
CdTe:Fe^{2+}, reson. relax. time for impurity electrons and localised phonons interaction, appl. to thermal cond. 80−59590
Ce, high temperature transport props., scatt. mechanisms, phase transitions 77−15825
$CeCu_2Si_2$, resistivity, thermal conductivity and thermopower between 1.5 and 300K 78−87963
$CeCu_2Si_2$, transport anomalies 80−20148
Ce_2Se_3-$SnSe_2$, solid-solution region, physical properties 78−43391
Co, impure, thermal cond., resistivity, total and spectral emissivity, linear expansion coeff., 300-1700K 77−47790
Co, thermal diffusivity meas., 300 to 1000K, Lorenz number determ. 80−29384
Co-Cr-C eutectic alloy, thermal conductivity and electric resist. at high temp. 80−103668
Co-P, metallic glass, phonon propagation at low temp. 78−87756
Cr, high purity, 280-1000K 77−39816
Cr-Al, abnormal thermal cond., 5 to 100K 79−19573
Cr-Si (1.37 at.%), thermal and elec. props. 79−78071
$Cr_2S_{3-x}Se_x$, elec. resist., thermal cond. and Seebeck coeff. meas. 80−24958
Cs, elec. and thermal resist. calc. using modified noncentral force model 79−91016
$CsMnCl_3.2H_2O$, thermal cond. in mag. field 80−70481
Cu alloys, dil., transport props. 78−76046
Cu, annealed coefficient temp. dependence, deformed and non deformed samples 78−76049
Cu, compressed powder, thermal cond. meas. *(German)* 80−70669
Cu, electronic contribution to thermal cond. at low temps. 79−95384
Cu, electronic transport properties, OPW calcs. 77−43553
Cu, grain boundaries effect on thermal cond. 79−51546
Cu, high purity, identification of imperfections by thermal resistivity meas. 80−59951
Cu, high-cond., high spt. ht., for cryogenic appl., prep. 78−76670
Cu, nonlinear diffusion eqns., identification of thermal cond. and sp. ht. *(French)* 77−47614
Cu, phonon-limited elec. and thermal resistivity 79−42517
Cu powder, sp. ht. cond. and sp. elec. cond. meas., Wiedemann Franz Lorenz law *(German)* 80−92872
Cu screw-fastened joints, low temp. thermal cond. and elec. resistance 79−95469
Cu, sintered, in contact with ^3He, thermal conductance, rel. to elec. resist., heat flow model calc. 80−10728

thermal conductivity of solids continued
Cu, thermal cond., effect of material on working parameters of cryosurgery instruments 78−36037
Cu, thermal conductivity, low temp., influence of plastic deform. 78−30899
Cu, thermal conductivity under high pressure 78−30901
Cu/Sn (Pb)(W) interface, thermal conductance at low temps. 80−49436
Cu-Al alloy, lattice thermal cond. meas., 0.06-2K 77−15822
Cu-Cr dilute alloys, thermal and elec. cond. deviations from Wiedemann-Franz law 77−66151
Cu-Ni alloys, alloying additions effect on thermal conductivity, 20-400°C *(Russian)* 77−59159
Cu_3AsS_4 and Cu_3SbS_4, thermal cond. in solid and liq. phases, 300 to 1100K, thermoelec. Q-factor 80−19997
Cu_3AsTe_4, elec. and thermal conds., thermo-EMF, solid and liq. states, temp. depends. 78−43384
CuCl, mech. vibrs. in piezoelec. solid, excitation by light pulses 80−75305
$CuCr_2Se_4$, temp. depend., 100 to 500K 77−24451
p-$CuInSe_2$, thermal props. 80−96705
Cu_2S, $Cu_{1.8}S$, $\alpha \rightarrow \beta$ transition, thermographic investigation of heats, entropies and activation energies 80−88314
$Cu_2S(Se)(Te)$, cond. changes on melting 77−7848
$Cu_2S_{1-x}Te_x$, comp. depend. 77−35765
Cu_3SbTe_4, elec. and thermal conds., thermo-EMF, solid and liq. states, temp. depends. 78−43384
cyclopentane, plastic cryst. and liq. phases, thermal cond. and sp.ht., 100-300K, 0-2.1 GPa 78−34663
D-T, estimated heat capacity, enthalpy, thermal cond. and diffusivity 77−4228
D_2, solid, thermal cond. *(Russian)* 78−38885
D_2-DT-T_2 mixture, solid and liq., props. for fusion reactor applications 78−66415
D_2O ice, thermal cond., H and D order effects 78−67871
D_2O-H_2O ice, thermal cond., H and D order effects 78−67871
Dy_2S_3, semimetallic, elec. and thermal transport meas. 78−10442
$Dy_2Ti_2O_7$, pressed powder, low temp. thermal cond., mag. field depend. 79−23789
$ErRh_4B_4$, supercond., thermal cond. between 0.05 and 4K 79−60967
ErS, heat carrier scatt., thermal and elec. cond. from 5-400K 79−14974
ErSb, cryst. field effects on transport props. 78−72133
$ErVO_4$, phonon resistivity mag. field depend. in paramag. phase 80−2226
Eu, antiferromag., thermal cond., elec. and thermal magnetoresist., at low temps. 77−69301
Eu, high temperature transport props., scatt. mechanisms, phase transitions 77−15825
Eu_2O_3, mech. and physical props. rel. to reactor control rod appl. 78−21641
Eu_2O_3, thermophysical props. and neutron absorpt. 80−103488
Fe, cast, thermal diffusivity meas. 293 to 873K, exam. of thermal cond. *(Japanese)* 78−47763
Fe, thermal cond., elec. resist., Lorenz number and magnetisation, crit. behaviour 77−4521
Fe-Cu-C alloy, sintered with added S, thermophys. props. 79−61541
Fe-Ni alloys, lit. review *(Russian)* 78−18805
Fe-P-Cu-SiO_2-$FeAl_3$-asbestos composite, thermal and elec. conds., temp. and composition depends. 77−66609
Fe-Ti (V)(W), dil., thermophysical props. and elec. cond., temp. depend. 80−96842
$FeCl_2$, antiferromag., magnon-phonon interactions in thermal cond. 80−65315
$Fe_{68}Co_{32}$, ferromagnet, magnon heat cond. and lifetimes, 1-2 to 4.5K 77−16066
$(Fe_2O_3)_x$-$(3B_2O_3.PbO)_{1-x}$ glass, thermal cond. and diffusivity obs. 79−60561
Fe_7S_8, pyrrhotite, thermocond. and thermoelec. power 80−96926
Fe_7Se_8 and Fe_3Se_4, temp. depend., 100 to 400K 77−35764
$Fe_{95}Si_5$, thermal and elec. cond., heat transport by spin waves 79−38047
GaAs, boundary scattering and phonon conductivity, 2-10K 78−63888
GaAs crystal growth, thermal and elastic const. evaluation 80−92586
GaAs, design and fabrication of cryostatic system 80−52243
GaAs, dislocation free, phonon-defect interaction 77−69061
GaAs, lattice thermal cond. from three phonon scatt. relax. rate 78−51755
GaAs, lattice thermal cond. at high temp. 79−90838
GaAs, lattice thermal cond., point defect scatt. relax. rate role 80−70478
GaAs, thermal cond. calc. using numerical soln. of Boltzmann eqn. 80−44373
GaAs:Mn, p-type semiconductors, internal strain on bound hole-phonon interaction 78−91492
GaAs:Te, phonon-dislocation interactions, nonstoichiometry effect *(French)* 77−43298
GaAs-$Ga_{1-x}Al_xAs$, single-heterostructure laser diode with short current pulses, heat spreading analysis 79−76690
$Ga_{1-x}Mn_xSb$ alloys, mag. phase transition obs. 78−52248
GaN, thermal conductivity, 25-360K 77−35766
GaSb based eutectics, thermal cond. and diffusivity, 300-700K, phonon mechanism 80−103526
Gd, thermal conductivity critical behaviour near Curie point 80−75540
Gd, thermal diffusivity, conductivity and elec. cond. 110 to 2100K 79−42516
Gd_2S_3, semimetallic, elec. and thermal transport meas. 78−10442
$Gd_2(SO_4)_3.8H_2O$, pressed powder and single crystal, low temp. thermal cond., mag. field depend. 79−23789
Ge, amorphous film, temp. thermal conductivity 78−22994
Ge, contrib. to lattice thermal cond. due to correction term in Callaway integral 77−62693
n-Ge, electron-phonon interaction, internal strain and impurity elec. field effect 78−14418
Ge, heavily doped; vacuum hot-pressing thermal and electrical props. 77−40400
n-Ge, internal stress effect on electron-phonon interaction, thermal cond. anal. 79−42468
Ge, laser interaction, multiple refls. contrib. to thermal runaway, heat cond. eqn. 80−33044
Ge, lattice thermal cond., contrib. due to correction term, generalised Callaway integral 77−28056
Ge, lattice thermal conductivity, contrib. due to correction term, generalised Callaway integral 78−2318

thermal conductivity of solids continued
Ge, lattice thermal conductivity, effect of Debye temp. var. 78−18850
Ge, lattice thermal conductivity three phonon processes 78−34662
Ge, low temp. calc. for impure insulators 79−33128
Ge, phonon boundary scatt., reduction of lattice thermal cond. 78−55921
Ge, phonon cond. correction term and electron-photon scatt. relax. rate, appl. to doped and undoped samples 80−39369
n-Ge, phonon conductivity and attenuation 77−4167
Ge, phonon scattering and dislocation effect on low temp. phonon cond. 78−51754
p-Ge, phonon thermal cond., 0.1-7K, Ziman model 77−35763
Ge, phonon-phonon scatt. strength, thermal cond. in low- and high-temp. regions 77−43296
Ge, phonons, directional depend. of boundary scatt. mean free path 79−73354
n-Ge, piezo-thermal cond. calc. 77−15639
Ge shaped single crystal, Stepanov method growth, temp. distri b. 78−2032
Ge, single crystal, meas. apparatus. using low freq. sine wave generator and digital phase meter 78−94580
Ge, thermal cond. calc. using numerical soln. of Boltzmann eqn. 80−44373
p-Ge, thermal conductivity, effect of uniaxial stress 79−23792
Ge, thermal conductivity at high temperature 79−55857
p-Ge, thermal conductivity meas. down to 50 mK, acceptor state exam. 77−80658
Ge, thermal conductivity of semiconductors, quantum acoustical method, thermal phonon lifetimes 80−65312
n-Ge, thermal phonon scatt., piezo-thermal cond. 80−70482
Ge:Al(B)(P), impurity ground state levels from photo-thermal cond. in mag. field 77−51699
Ge:As(Sb), phonon-bound donor resonance scatt., donor-electron radius mag. field depend. 79−77847
Ge:Ga, resonant scattering of phonons by bound holes in temp. range 1 to 5K 80−75393
Ge:Ga,Sb, compensated, low temp. props. rel. to appl. in bolometry 80−31867
Ge:Ga(In), shallow acceptor ground state, thermal cond. meas. 77−43540
Ge:Li, thermal cond., 0.4-20K, Li valley-orbit splitting 79−15111
Ge:P, charact. temp. and lattice thermal cond. 80−59743
Ge:P, lattice thermal cond., role of electron-phonon interactions and peripheral phonons 78−79702
Ge:P, lattice thermal resistivity due to electrons 78−51756
Ge:P, peripheral phonons and phonon cond. 79−14973
Ge:Sb, lattice thermal resist. due to bound state electrons 79−46850
Ge:Sb, phonon thermal cond. calc. 78−71893
Ge:Sb,In, lightly doped semicond., low temp., phonon cond., electron-phonon scatt. 79−60456
Ge:Sb semiconductors, inhomogeneously strained, phonon resonance scatt., Kwok's theory method 79−60455
Ge-Bi-Te system, thermal cond. change during phase transitions 80−100368
Ge-In-Te system, homogeneity region, struct., electrophysical props. 78−44091
Ge-In-Te system, region of solid soln. of In in GeTe 77−51499
Ge-Si alloy, phonon boundary scatt., reduction of lattice thermal cond. 78−55921
Ge-Si alloy, quenching from high temp., thermal electric parameters, obs. 77−28165
Ge-Si alloys, hot-pressed, fine-grained, boundary scatt. of phonons, lattice thermal cond. 80−107583
Ge-Si alloys, hot-pressed, fine-grained, boundary scatt. of phonons, theory 80−107584
GeS_x amorphous semiconductor, neutron irrad. effects on thermal parameters 77−11597
GeS_x, neutron irrad., thermal and elec. conductivity and heat capacity 78−2165
GeTe, high pressure effects on hole conc. and thermoelec. props. 78−26894
GeTe-Ga_2Te_3, electrophys. props. 77−48403
GeTe-MnTe-SnTe system, compds., GeTe phase transition temp., elec. props., thermal cond. 79−43220
$(GeTe)_x$-$(AgSbTe_2)_{(1-x)}$, thermoelectric characts., temp. depend. 300 to 750K 79−78123
H_2, solid, nonlinear conduction 79−69317
H_2, thermal cond. at varying o-H_2 conc. 78−51786
HD, lattice thermal cond., 0.2 to 4K 78−75903
He, at high press. 80−103099
^{3}He, BCC, Debye behaviour of thermal cond., 0.03-0.4K 79−56034
^{3}He, solid, low temp. thermal cond., structural crystalline defects 80−2240
^{4}He, single crystal, 0.4 to 1.8K *(Russian)* 80−103535
^{4}He, solid, boundary limited thermal cond., Poiseuille phonon flow 80−2241
Hf, thermal diffusivity meas., 300 to 1000K, Lorenz number determ. 80−29384
Hf, thermotransport and thermopower of O_2 78−76055
$Hf_xTa_{1-x}C$, thermal cond. and diffusivity, 1000-2200°C, elec. cond. 78−91491
$Hg_{1-x}Cd_xTe$ 0.1 eV, thermal conductivity meas. 77−24578
$Hg_{1-x}Cd_xTe$-type semimetals, kinetic props., local acceptor level effects 80−65557
$HgCr_2Se_4$, temp. depend., 100 to 500K 77−24451
HgI_2, single cryst. elec. and thermal props. 79−11111
Ho, thermophysical properties at high temps., exam. *(Russian)* 79−28105
HoF_3, monocrystal, thermal cond., temp. dependence 77−55402
In solder joints, thermal conductance at low temps. 77−30150
In, thermal cond. in solid and liq. phases, Wiedemann-Franz law 80−39554
In-Bi (2 at.%), supercond. film, in perpendicular mag. field 77−8229
In-Cr film, electronic thermal cond., 1.5 to 3K 77−47934
InP_xAs_{1-x} alloys, thermoelectric characts. 77−11947
InSb based eutectics, thermal cond. and diffusivity, 300-700K, phonon mechanism 80−103526
InSb, lattice thermal cond. from three phonon scatt. relax. rate 78−51755
InSb, phonon conductivity, temp. depend., 2-300K 77−31812
InSb, phonon conductivity, 2 to 300K, scatt. mechanisms 79−4436

thermal conductivity of solids continued
InSb, thermal cond., elec. cond., and thermoelec. power, press. depend. 80−59744
InSb:Cd, thermal conductivity down to 0.38K 80−107582
In_4Se_3, thermal cond., 2 to 30K, Umklapp processes and phonon boundary scatt. *(Russian)* 79−10991
$(In_2Te_3)_{1-x}(In_2Se_3)_x$, thermal cond. exam. 79−28160
K, electrical and thermal resistivity determ. from first principles 79−69493
K, electron-electron scattering, elec. resistivity, thermal cond., thermoelec. power and Lorenz function 79−95382
K, electronic contrib. to thermal cond., 1 to 330K 77−20291
K, free-electron approx., ideal thermal resist. 77−51724
K, high field Righi Leduc effect and lattice thermal cond. 80−10948
K, high field Righi-Leduc effect and lattice thermal cond., reply to comment 80−10949
K, high field thermomagnetic coeffs., 1.5-4.5K, lattice thermal cond. calc. 79−60800
K, high-field Righi-Leduc effect lattice thermal cond. 78−34825
K, high-field thermal magnetoresist., 2.5-8K 78−23072
K, low-temp. lattice cond., phonon drag thermopower 79−60789
K, Matthiessen's rule, low temp. deviations 78−14724
K-Cs, thermal conductivity determ. 80−107760
KCl, phonon-phonon scatt. strength, thermal cond. in low- and high-temp. regions 77−43296
KCl, pure cryst., thermal cond. meas., 50 mK to 50K 77−62692
KCl, thermal cond. press. depend. 77−15641
KCl, thermal cond. under press. meas. 78−30802
KCl, thermal conductivity at high temperature 79−55857
KCl:CN, reson. scatt. of phonons in thermal cond. 79−14972
KCl(:LiF), radiative Q-centres, opt. absorpt. and thermal conductivity 77−47450
KH_2PO_4 and KD_2PO_4, thermal cond., anomalous temp. behaviour near structural phase transition *(Russian)* 80−75394
KI, thermal cond. press. depend. 77−15641
KI, thermal cond. under press. meas. 78−30802
$KMnF_3$, phonon scatt., thermal cond. meas. 77−7916
Kh_2AsO_4, anomalous temp. behaviour near structural phase transition *(Russian)* 80−75394
Kr, at high press. 80−103099
$(La,Ce)Al_2$ and $(La,Gd)Al_2$, magnetic impurity effect on thermal cond., normal and supercond. states 77−63027
$(La,Gd)Al_2$, reverse Kondo alloy, transport props. at finite mag. field 80−6812
$LaAl_2$:Gd(Ce), supercond., electronic thermal cond. 77−12063
LaB_6 thermal and electrical conductivities, 1000-2100°C 77−69293
$LaCu_2Si_2$, resistivity, thermal conductivity and thermopower between 1.5 and 300K 78−87963
$La_xEu_{1-x}B_6$ solid solns., thermal cond., 300 to 2000K 80−59741
LaF_3, monocrystal, thermal cond., temp. dependence 77−55402
LaF_3, pre and Nd^{3+}-doped, thermal cond., 300-1450K 80−24686
$LaPt_5$, cryst. field effects on transport props. 78−72133
LaS, heat carrier scatt., thermal and elec. cond. from 5-400K 79−14974
LaSb, cryst. field effects on transport props. 78−72133
La_3Te_4, thermal cond., thermoelec. power abd elec. cond. meas., 80 to 750K 78−18853
La_3Te_4, thermoelectric material, thermal cond. meas., 1100-2000K 78−24798
Li, elec. and thermal resist. calc. using modified noncentral force model 79−91016
Li, free-electron approx., ideal thermal resist. 77−51724
Li, metal and dil. alloys, electronic thermal cond. calc. 78−47764
Li-Mg, Mathiessen's rule, elec. and thermal deviations, impurity scatt. 80−88536
LiF, γ-irrad. pure and Mg-doped, phonon scatt. and interstitial clusters 80−70254
LiF, thermal cond. press. depend. 77−15641
LiF, thermal cond. under press. meas. 78−30802
LiF, thermal phonon scatt. by low angle grain boundaries 78−67795
LiF, thermal phonon-dislocation interaction, thermal cond. and ballistic phonon propag. meas., 0.03-25K 79−95226
$LiNbO_3$, phonon heat conduction of single crysts. by quantum acoustic method 77−11748
LiO_2-Na_2O-MgO-TiO_2-Al_2O_3-SiO_2, exam. of specific heat and thermal conductivity *(Russian)* 79−55898
Li_2O, porosity, dependence on thermal diffusivity and thermal conductivity, 200-900°C 80−92726
Lu, thermophysical properties at high temps., exam. *(Russian)* 79−28105
$MgAl_2O_4$-Al_2O_3 powder prep., for plasma arc spraying, coating props. 77−66612
MgF_2, single cryst., linear thermal resistance temp. depend. 77−66048
Mg_2Ge, L, electron-phonon interaction and phonon cond. at low temp. L n-type semicond. 79−14903
Mg_2Ge, phonon cond. 4-1000K 78−79826
Mg_2Ge, three-phonon relaxation rate and phonon conductivity 78−14416
MgO, phonon spectra using freq. crossing techniques 78−14415
MgO, thermal characts. using constant power source method 79−95222
MgO, thermal cond. up to 40 kbar 79−1533
MgO, transition metal ion doped, phonon spectroscopy using freq. crossing techniques 79−42193
MgO:Cr^{2+}, reson. scatt. of phonons by ions 78−18716
MgO:Cr^{2+}(Fe^{2+}), reson. relax. time for impurity electrons and localised phonons interaction, appl. to thermal cond. 80−59590
MgO:Fe^{2+}, impurity electron-phonon reson. relax. time, thermal cond. 77−59085
MgO:Mn^{3+}, ground state exam., thermal conductivity meas. 79−42497
MgO-$MgAl_2O_4$($FeCr_2O_4$), thermoplastic and thermophys. props. for steel vacuuming installations 80−35281
Mg_2Si, phonon cond., 3-500K 78−79826
Mg_2Sn, L, electron-phonon interaction and phonon cond. at low temp. L n-type semicond. 79−14903
Mg_2Sn, phonon cond., 4-1000K 78−79826
$MnCl_2.4H_2O$, antiferromag., low temp. thermal cond. 80−65320
MnF_2, heat transport by magnons, effect of magnon-phonon thermal relax., calc. 77−39705
MnF_2, mag. field effects, magnon contrib. 78−38890
MnF_2, role of reson. scatt. of phonons by OH^- defects 78−38889
$MnGa_2S_4$, synthesis electrophys. props. 77−51747
MnS, thermal cond., temp. depend., paramag.-antiferromag. transition effects 80−65321
$MnSb_2S_4$, synthesis, electrophys. props. 77−51747
$MnSiF_6.6H_2O$, specific heat, thermal cond., simultaneous meas., method, 90-300K, near phase transition 77−37892
MnZn ferrite, thermal cond. of single crystals 77−36079
Mo and Mo superalloys high temperature properties 78−44173
Mo, high purity single crystals, thermal conduct. in temp. range 2-70K 80−75545
Mo, porous, high temp. props. 77−11894
Mo, sintered, thermal and elec. conds., 50-800°C, microstructure 78−43352
Mo, thermal conductivity and electrical resistivity, 300 to 2600K 77−35913
Mo, transverse galvanomag. and thermomag. coeffs. 77−20298
Mo_2B_5 and MoB_4, thermal, elec., and mag. props. 80−20187
$MoTe_2$, rapid meas. method *(French)* 78−12689
NH_4Cl, specific heat, thermal cond. simultaneous meas. method, 90-300K, near phase transition 77−37892
NH_4Cl, thermal cond. and heat capacity of solid phases under press. 80−2225
NH_4Cl, thermal conductivity, crystal transformation 78−2310
NH_4F, thermal cond. of four solid phases, rel. to H_2O 78−38887
Na, electrical and thermal resistivity determ. from first principles 79−69493
NaCl, doped by Ca^{++} and OH^-, thermal conductivity in 5-190K range 78−14520
NaCl, lattice thermal and optical phonon contrib. 79−14971
NaCl, thermal cond., meas. by pulse method, influence of press. 79−7701
NaCl thermal cond. press. depend. 77−15641
NaCl, thermal cond. under press. meas. 78−30802
NaCl, thermal cond. up to 40 kbar 79−1533
NaCl, thermal conductivity at high temperature 79−55857
NaCl, thermal phonon scatt. by low angle grain boundaries 78−67795
NaCl-NaBr, elastic wave damping, 300 to 1500 MHz, impurity effects 80−92602
NaF, lattice thermal cond., 2-10K 79−90834
NaF, lattice thermal conductivity, point defects effects at low temp. 79−90836
NaF, thermal cond. meas. at high press. 80−75392
$NaHCO_3$, thermal conductivity thermal decomposition 78−2310
Na_2O-CaO glass phlogopite mica powders, composite fabrication, cellular struct. 80−84902
Na_2O-Cs_2O-SiO_2 glasses, thermal diffusivity, heat capacity and thermal cond., laser flash method study 80−65310
$25Na_2O.75SiO_2$ glass, thermal cond., temp. depend. at low temps. 80−65322
$Na_2S_2O_3.5H_2O$, solidification, heat transfer processes *(Japanese)* 80−6372
Nb, 0.3-20K, temp. and impurities effects 78−14883
Nb alloys, supercond. and normal phases, electron scatt. and lattice thermal cond. 77−77001
Nb, cryst. and film, thermal and elec. cond., 9-50K 79−87078
Nb, plastically deformed single crystal, low temp. thermal cond. 79−28336
Nb, supercond. and normal state, thermal cond. meas., 0.05-23K 77−63025
Nb, thermal and elec. cond., temp. depend., 900-2100°C, additive effects *(Russian)* 77−15816
Nb:N,H(D), thermal cond., 0.07 to 1.5K, influence of N interstitials 79−65601
Nb-epoxy, interface, Kapitza resist. in supercond. and normal states 77−66085
Nb-Mo-Al-(Cr) eutectic directionally crystallised alloy, heat resistance, alloy struct. *(Russian)* 80−40481
Nb-Ti, thermal conductivity in low temp. range 78−39259
NbC_x, thermophys. props. 77−89600
NbC_x, thermophysical props. at high temp., thermal vacancies form. 78−43141
$Nb_{80}Mo_{20}$, $Nb_{75}Mo_{25}$, supercond., phonon cond. below 1k 78−14881
$NbSe_2$, supercond. and normal state, thermal cond., temp. and mag. field depend. 78−26992
Nb_3Sn superconducting wire, fabrication from Cu-Nb-Sn alloy using controlled high temp. gradient 80−25056
$Nb_{80}Ta_{20}$, supercond., phonon cond. below 1k 78−14881
NbTi, supercond., measurement of thermal conductivity 79−58682
Nd, antiferromag., thermal cond., elec. and thermal magnetoresist., at low temps. 77−69301
Nd, high temperature transport props., scatt. mechanisms, phase transitions 77−15825
Nd, thermal cond., 0.5-8K 78−34819
Nd, thermal cond. at low temps. *(Russian)* 79−11100
Nd, transport props., low temp., effect of mag. field 80−70679
Nd-Gd-Te alloys of R_2Te_3-T_3Te_4 region, physicochem. props. 78−52017
NdP_5O_{14}, thermal cond. and specific heat 79−42325
Nd_2S_3, semimetallic, elec. and thermal transport meas. 78−10442
Ne, 0.5-10K 77−43396
Ne, at high press. 80−103099
Ne, lattice thermal cond. 0.5 to 10K, dislocation densities, average grain sizes 78−79830
Ni, heat diffusivity and heat cond. near Curie point 77−24706
Ni, resistivity, thermal and elec., spin disorder scatt. anal. 78−76063
Ni-Cr-Co, Mo, Ti, Y and R alloying additions influence on oxidation *(Russian)* 80−40587
Ni-Cr-Mo-Mn alloy 02KhN40MB, corrosion-resist, heat-resist., phys. and mech. props. 80−35411
Ni-Ti (51.5 at.% Ni) metallide, thermal cond., elec. resistivity, 90-450K 78−68009
Ni_3Al-Ni_3Nb, directionally crystallised, thermal and electric cond., emissivity 77−43556
$NiFe_2Se_4$, temp. depend., 100 to 400K 77−35764
Os, elec. resist., thermal diffusivity, and thermal cond., 290 to 3300K 79−11101
Os; electrical resistivity and thermal diffusivity meas. 80−15495
$P_2Se_xS_y$ glass, thermophysical props., 303-413K, struct. interpretation 78−47615
Pb chalcogenide, solid solution, thermoelectric efficiency 79−95429
Pb, film, polycryst. or amorphous, thermal cond., 0.5-11K 78−39260
Pb, high-field thermal and elec. magnetoconductivities meas. 77−59279
Pb, intermediate state, thermal resist. of normal-supercond. interphase boundary 79−56384

thermal conductivity of solids continued
Pb, Pb-Bi, supercond., anomalous thermal cond., transition induced creep *(Russian)* 77−36020
Pb, perfect and deformed, phonon mean free path from thermal cond. meas., 0.6 to 7.5K 79−65166
Pb, phonon thermal conductivity of deformed cryst. below 2K *(Russian)* 78−60244
Pb, thermal cond. measurements below 1K *(German)* 80−49984
Pb, thermal conductivity, in normal and supercond. states, 0.6-7.5K *(Russian)* 80−6815
Pb, thermal conductivity in supercond. and normal states, press. effects 77−43779
Pb-Bi alloys, phonon-electron interaction, normal and supercond. state thermal cond. and elec. resist. meas. 79−60460
Pb-Cd eutectic composite, mag. flux entry in proximity effect regime 79−33418
Pb-In (21 at.%), dirty type II supercond., anisotropic thermal cond. 79−56385
Pb-Sn system, soft solder, elec. and thermal cond. at low temps., superconducting transition temp. 80−20150
PbCu film, amorphous supercond., phonon heat transport, thermal cond. meas. 78−19181
$Pb_{0.9}Cu_{0.1}$, film, polycryst. or amorphous, thermal cond., 0.5-11K 78−39260
PbI_2 layered cryst. under uniaixal compression, low temp. thermal cond. *(Russian)* 80−44374
PbI_2, low temp. thermal props. 79−95178
$Pb(Mn_{1/2}Ta_{1/2})O_3$, ceramic, for thermal and dielectric isolation at low temp. 80−39365
$Pb_{1-x}Mn_xTe$ (x=0.005, 0.001, 0.05), solid solns., exam. of electrical and thermal props. 79−1599
PbO, sintered, pure, prep. and props. 77−48361
PbS-Ni, phase diag., cpd. formation and electrophys. props. 77−85997
PbSe:Tl, scatt. of holes and phonons by impurities 78−19068
$Pb_{1-x}Sn_xTe$, effect of mag. field on thermal cond. 79−65263
PbTe film, electronic thermal cond. and thermoelec. power 80−93018
PbTe films, thermal cond. and elec. props., 4.2 to 300K 79−28162
PbTe:Bi(Sb)(Cr)(Ag), thermoelec. props., thermal and elec. cond. 79−82616
PbTe:Ga, location, behaviour of Ga, electrophysical props. meas. 79−38016
Pd, transport props. 40 mK-6K 78−51968
Pd-Fe, dil., transport props. at low temp. 0.05 to 5K 79−38046
Pd-H, low temp. transport props., heterogeneous-mixture model 80−24871
Pd-Ru, electron transport props., 50 mK-4.2K 78−14707
Pd-Ru-W(V)(Ti), elec. resist. and thermal cond. *(Russian)* 78−19017
Pd-Si, glass, 0.1-30K 77−20286
Pd-Si, metallic glass, phonon propagation at low temp. 78−87756
PdH_x, $x \simeq 1$, type I supercond. props. 79−56448
Pr, high temperature transport props., scatt. mechanisms, phase transitions 77−15825
Pr, transport props., low temp., effect of mag. field 80−70679
$PrCl_3$, cooperative Jahn-Teller ordering of elec. dipoles in non-Kramers doublets 78−15115
$PrCu_5(Pt_5)$, cryst. field effects on transport props. 78−72133
PrS, heat carrier scatt., thermal and elec. cond. from 5-400K 79−14974
$PrTe_{1.44}$, high-temp. thermal cond., 80 to 750K, lattice and photon components 79−33126
Pr_3Te_4-Pr_2Te_3 system, characts. of thermal cond. 77−7917
Pt, wire, thermal cond., 900-1800K, elec. cond., 800-1800K 78−26845
Pu-Ga (1 wt.%) alloy, delta-stabilised, heat transport props., room temp. to 500°C 77−20294
PuN, fabrication, high-temp. thermodynamic and transport props. 77−28774
Rb, free-electron approx., ideal thermal resist. 77−51724
Rb, transport props. and electron-electron scatt. 79−73490
RbBr, press. depend., up to 10 kbar, jump at phase transition 77−62694
RbBr, thermal cond. under press. meas. 78−30802
$RbCaF_3$, phonon scatt., thermal cond. meas. 77−7916
$RbMgF_3$, irradiated 78−22909
$RbMnF_3$, pure and Fe, Co or Ni doped, spin wave and mag. impurity contribs. 77−40046
Re, sintered, preparation, thermal cond., linear expansion up to 1000K 79−61533
Ru, kinetic and thermal props. at high temp., anisotropy 77−43563
RuO_2, thermal conductivity meas., rel. to elec. cond. 80−65317
S-based composite, engineering props. 77−86093
Sb, electrical resist., thermal cond. and thermopower, low temp. transport props. 80−49708
Sb, mutual drag effect in ideal elec. and thermal resist. 79−73507
p-$Sb_{1.48}Bi_{0.52}Te_3$, extrusion deformed, powder dispersion degree influence on thermal and elec. props. *(Russian)* 80−39366
$Sb_{1.5}Bi_{0.5}Te_3$ solid solution, temp. influence obs. *(Slovak)* 78−30946
Sb_2O_3, thermoelec. props., 500-1500K 80−29423
Sb_2Te_3, $Sb_{1.5}Bi_{0.5}Te_3$, Te- and Se-doped cryst. growth and elec. props. 77−48334
Sb_2Te_3-Bi_2Te_3 and Sb_2Te_3-Sb_2Se_3 systems, thermal cond. change during phase transitions 80−100368
Sb_2Te_3-Sb_2Se_3, ordered structure formation, heat treatment effect on thermal cond. 80−54448
Sc_3In, itinerant electron ferromagnet, spin fluctuations 77−73096
Se, trigonal and vitreous, sp. ht. and thermal cond., 3 to 300K 80−59676
Se-S, glassy alloy, order-disorder transition kinetics 78−67650
n-Si, electron-phonon interaction, internal strain and impurity elec. field effect 78−14418
n-Si, internal stress effect on electron-phonon interaction 79−42468
Si, ion-implanted, thermal cond. and free-carrier absorpt., temp. depend. 79−55757
Si, lattice thermal cond., 2-1400K, phonon scatt. calcs. 78−2311
Si, phonon boundary scatt., reduction of lattice thermal cond. 78−55921
p-Si, phonon conductivity and attenuation 77−4167
Si, phonons, directional depend. of boundary scatt. mean free path 79−73354
Si, powder heap, thermal cond., effect of temp., press., and atmospheric composition, sintering appls. 78−80487
Si, single crystal, meas. apparatus. using low freq. sine wave generator and digital phase meter 78−94580
Si, single crystals, thermal conductivity calculation *(Hungarian)* 80−65311
thermal conductivity of solids continued
n-Si, strained cryst., role of phonon reson. scatt. in phonon cond., appl. to Si:Li 79−19407
Si, temp. rise induced by laser beam, nonlinear heat cond. 79−11487
Si temperature field determ. under laser irradiation *(German)* 80−25496
Si, thermal cond. calc. using numerical soln. of Boltzmann eqn. 80−44373
Si, thermal conductivity at high temperature 79−55857
Si, variation of thermal conductivity with temperature 79−23793
Si:As laser annealing, heat and mass transport model 80−92546
Si:B, resonant scattering of phonons by bound holes in temp. range 1 to 5K 80−75393
Si:Li, electron-phonon scatt., in intermediate conc. region 80−65180
Si:Li, thermal cond., low temp. phonon scatt., internal strain effects 80−96706
Si:P, phonon cond., electron-phonon relax. rate 79−46771
Si:P, thermal cond., electron-phonon interaction at low temps. 80−92730
Si:Sn, thermal conductivity, Hall mobility depend. on Sn conc., phonon-defect scatt. 80−29232
Si-Al-O-N ceramics, elec. and therm. cond. 79−86934
p-Si-Ge, heavily doped, hot pressed, high temp. phonon thermal cond. *(French)* 78−43190
Si-Ge, heavily doped vacuum hot-pressing, thermal and electrical props. 77−40400
n-Si-Ge, phonon thermal cond. of hot-pressed alloy, 300-1100K 78−91494
Si-Ge alloy, hot-pressed, effect of grain size 77−31813
Si-Ge alloy, thermoelec. material, lattice thermal conductivity rel. to grain size and carrier conc. 78−91495
$Si_{6-x}Al_xO_xN_{8-x}$, x=1.5, 3, 4, Sialon ceramics, elec., thermal cond. 79−33124
SiB_{12-x}, thermam cond., temp. depend., up to 2000K *(French)* 80−70484
SiB_4, mech. and thermal props. 80−21083
SiC, chem. stability, mech. and thermal props. rel. to appls. 80−21103
SiC fibre reinforced Al, thermophys. props. 80−59745
SiC, pyrolitic coating for nuclear fuel particles 77−79465
β-SiC, thermoelectric material, thermal cond. meas., 1100-2000K 78−24798
Si_3N_4 amorphous films, CVD mech. and thermal props. *(Japanese)* 77−90280
Si_3N_4, hot-pressed, thermal cond. by laser flash method 79−69302
Si_3N_4, pyrolytic, crystn. and amorphous, thermal diffusivity, thermal cond., specific heat 79−69303
SiO, role of O in phonon conductivity 79−42326
SiO_2, coesite, thermal cond. up to 40 kbar 79−1533
SiO_2, fused, for sealed ampoule cryst. growth, thermal transmission function 80−84731
SiO_2 stishovite, thermal cond. up to 40 kbar 79−1533
SiO_2, vitreous, existence of gap in low-energy density of states 79−60769
SiO_2, vitreous, low temp. thermal props. and intrinsic defects 80−29057
SiO_2, vitreous, neutron irrad. effects on heat capacity, thermal cond., US velocity temp. depend. 78−83851
SiO_2, vitreous and neutron irrad., thermal cond., heat treatment effect 79−90837
$72SiO_2$ window glass, thermal cond., temp. depend. at low temps. 80−65322
SiO_2-Al_2O_3-Fe_2O_3-CaO-MgO-Na_2O-SO_3 glass, thermophysical props. 78−18849
Sm, transport props., low temp., effect of mag. field 80−70679
$SmRh_4B_4$, mag. ordered, persistence of supercond. 80−54834
SmS, semicond. phase, cond. band model, elec. and thermal cond. meas. 77−39854
Sn, Lorenz function and horizontal and vertical components of thermal resist. 79−65427
Sn, monocrystals, anisotropy of thermal cond. depending on chem. admixtures 77−85194
Sn, temp. dependence, rel. to heat-flux rectification at Sn-α brass interface 78−76048
Sn thin film, anomalous transmittance of metal-insulator interface for thermally radiated phonons *(Russian)* 80−103664
SnO_2 thermoelectrical properties, investigation 77−76852
Sn_xPg_{1-x}, thermal cond. and Lorenz function 78−51966
SnTe-In_2Te_3 system, thermoelec. props., phase diagram, transitions 78−43424
Sr, transport properties, elec. resist., thermoelec. power, thermal cond. deviations from Matthiessen's rule 78−39086
SrF_2, single cryst., linear thermal resistance temp. depend. 77−66048
SrT:O_3, anomalous temp. behaviour near structural phase transition *(Russian)* 80−75394
Ta, 0.3-20K, temp. and impurities effects 78−14883
Ta, 4.5 to 200K *(Russian)* 80−103665
Ta alloys, thermal conductivity at slow temps., temp. depend. *(Russian)* 79−91019
Ta, electrical and thermal resistance at low temp. *(Russian)* 78−68007
Ta, thermal cond. and emissivity meas. using imaging furnace 80−103667
Ta, thermophysical props. and neutron absorpt. 80−103488
TaC, thermal and electrical conductivity, 1500-3000K 78−43385
$Ta_{16}W_{18}O_{94}$, characterisation of thermally contracting tungstates 78−63869
Ta_2WO_8, characterisation of thermally contracting tungstates 78−63869
$Ta_{22}W_4O_{67}$, characterisation of thermally contracting tungstates 78−63869
$TbFeO_3$, thermodynamic props. 77−36078
TbZn, ferromag. transition, transport coeffs. critical behaviour 80−15498
Te-based chalcogenide glass, 100-500K 77−20138
$TeSe_{12.5}$, amorphous alloy, thermal and elec. cond. during devitrification 78−26922
$TeSe_{20}$, vitreous alloy, elec. and thermal cond. during crystallisation 79−7550
$(Th,U)O_2$, thermal conductivity model for temps. to melting 79−93732
ThO_2 compacts, thermal conductivity, dependence on porosity, mathematical anal. 79−4437
Ti alloys, data handbook of low temp. mech. and phys. props. 80−22153
Ti alloys, thermal conductivity at slow temps., temp. depend. *(Russian)* 79−91019
Ti and Ti-Nb, plastic deform. and thermal cond., 2.5 to 10K, dislocation pinning 77−35629

thermal conductivity of solids continued
Ti, high purity, data handbook of low temp. mech. and phys. props. 80−22153
Ti, powder heap, thermal cond., effect of temp., press., and atmospheric composition, sintering appls. 78−80487
Ti-Al-Sn alloy, VT5-1, solid solutions, heat cond. at low temps. *(Russian)* 79−82574
Ti-Al-alloy, VT5, solid solutions, heat cond. at low temps. *(Russian)* 79−82574
Ti-Fe alloys, elec. and thermal props. *(Russian)* 78−19020
Ti-Mn alloys, elec. and thermal props. *(Russian)* 78−19020
Ti-Zr-Hf disordered solid solns., thermal cond. 79−15132
Ti_2AlC, Ti_3AlC, TiC, phys. props. 77−43602
Ti_2AlN, prep. and props. 77−28745
TiC, high temp. thermal cond., ambipolar diffusion contrib. 78−26742
TiC-TiN system, electro- and thermo-phys. props. 80−34210
TiC-VC(ZrC) carbide alloys, thermophys. props., temp. depend., specific elec. resist. 79−86908
TiC_xN_y, thermal cond., elec. cond., and thermal expansion 80−10714
TiC_xO_y, thermal cond., elec. cond., and thermal expansion 80−10714
$TiN_{0.96}$, electronic component of thermal cond., inelastic electron-phonon scatt. 79−86937
$Ti_{55}Nb_{45}$, supercond., anomalous phonon thermal resist. 77−69451
TiO-MeO (Me=Ni, Co, Mn), solid soln., lattice thermal cond. 79−23791
TmSb, cryst. field effects on transport props. 78−72133
U, anomalous thermal prop. behaviour at low temp. 77−28018
UAl_2, transport props., susceptibility and sp. ht. 80−11174
UC_2, high temp. thermal diffusivity, thermal conductivity, spectral emissivity 77−28052
UO_2, by comparative longit. ht. flux, use of generalised Bessel functions 78−26741
UO_2 fuel, density, thermal conductivity, specific heat, thermal diffusivity, flash method 77−55362
UO_2, thermal and transport props., electronic contrib. 80−15432
UO_2, thermal cond. meas. under simulated in-reactor conditions 78−94079
UO_2-U_4O_9, thermal cond., effect of microstruct. and microcracking 79−97810
U_3O_{8-z}, therm. cond. from 200 to 750K using scanning temp. method 79−37886
U_4O_{9-y}, thermal conductivity and diffusivity, 250 to 415K 77−50234
V alloy, polycryst., thermal cond., 1200-1900K range 78−95282
V alloys, thermal conductivity at slow temps., temp. depend. *(Russian)* 79−91019
V, low-temperature thermal and elec. cond. 79−60792
V superconducting heat switches, effect of surface prep. 79−60966
V, thermal cond., 1200-1900K range 78−95282
V, thermal cond., elec. resist. and Seebeck coeff. meas., 6-300K 77−39818
V, thermal conductivity in ultrapure normal, mixed and supercond. states *(Russian)* 79−4617
V-Ti alloys, supercond., thermal cond. 77−89900
VN-CrN solid solutions, thermal cond., Lorentz number 80−15317
VO_2, thermal cond. meas., metal-dielectric phase transition, phonon scatt. mechanism 78−87831
V_2O_3, thermal cond. meas., metal-dielectric phase transition, phonon scatt. mechanism 78−87831
V_2O_5, thermoelec. props., 500-1500K 80−29423
V_2O_5-GeO_2 glass, effect of thermal processing on elec. and thermal props. *(Russian)* 77−63814
V_3O_5, thermal cond. meas., metal-dielectric phase transition, phonon scatt. mechanism 78−87831
V_xO-M_yO, (M=Ni, Co, Mn), solid solutions, exam. of thermal conductivity 78−79827
W crystalline samples, thermal contacts in high vac., low temp., press. and mag. field depend. *(German)* 77−11890
W, low temp. transport props., phonon and impurity scatt. 78−10418
W, porous, high temp. props. 77−11894
W, sintered metal thermal cond. standard, high-temp. conductivity 78−89427
W-Mo alloys, thermal conductivity and diffusivity, sp. ht., 100-2400°C 78−75842
W-Re alloys, sintered, preparation, thermal cond., linear expansion up to 1000K 79−61533
W_2B_5 and WB_4, thermal, elec., and mag. props. 80−20187
Xe, at high press. 80−103099
Y, thermophysical properties at high temps., exam. *(Russian)* 79−28105
YAG:Cr, optical detection of phonons 80−92630
YAG:Er, elastic wave damping, 300 to 1500 MHz, impurity effects 80−92602
YAG:rare earth, phonon impurity scatt., lattice thermal cond. and US attenuation meas. 78−87748
YIG, heat transport by magnons, effect of magnon-phonon thermal relax., calc. 77−39705
YIG, thermodynamic props. 77−36078
Y_2O_3 sintered bodies, thermal cond. and diffusivity *(Japanese)* 79−55944
YbS_x, thermo-EMF, elec. and thermal cond., 300 to 1000K, comp. depend. 79−38111
Zn, electrical and thermal resist. calc. 79−69489
Zn-Al-Cu-Mg (4.1, 3.1, 0.05 at.%), thermal cond. and sp. ht. meas. below 4.2K 77−20081
Zn-Mn, supercond., compared with Shiba's theory 77−8228
ZnS:Fe^{2+}, impurity electron-phonon reson. relax. time, thermal cond. 77−59085
ZnS:Fe^{2+}, reson. relax. time for impurity electrons and localised phonons interaction, appl. to thermal cond. 80−59590
Zr alloys, reactor fuel sheath mat., thermophys. props. 77−46280
Zr, powder heap, thermal cond., effect of temp., press., and atmospheric composition, sintering appls. 78−80487
Zr_xBe_{1-x} noncrystalline alloy, phonon-electron scatt., superconducting temp. 80−54330
ZrC-ZrN system, solid solns., elec. resist., thermo EMF, thermal cond., expansion coeffs. 78−60176
ZrC_x, thermophysical props. at high temp., thermal vacancies form. 78−43141
$ZrH_{1.9}$, neutron irrad. induced defects, nature and thermal stability 77−50246

thermal conductivity of solids continued
ZrO_2 coating on Zircaloy-2, thermal cond. meas. 80−80009
$Zr_{0.7}Pd_{0.3}$, amorphous supercond., sp. ht. and thermal cond., 0.1-10K 78−26991

thermal convection *see convection*

thermal decomposition *see pyrolysis*

thermal diffusion
see also thermal diffusion in gases; thermal diffusion in liquids
aerosol, photophoretic motion of nonvolatile particles, thermal diffusion effect 78−79364
aerosol, two-layer spherical liquid particle with solid core, thermophoresis 79−39211
aerosol particle capture by drops, thermodiffusionphoresis and Brownian motion effects *(Russian)* 79−39791
binary mixture theory for thermal diffusion in unidirectional fibrous composites 78−87230
Brownian motion in periodic potential, in presence of temp. and elec. potential gradients 80−4650
cloud chamber, continuous flow parallel plate type, analysis w.r.t. atm. water droplet growth 80−36416
convective heat transfer with diffusion, finite element anal. 79−4011
cooled electric probes in dense plasma, thermal diffusion effects 80−92384
cosmological fluid, lepton era, transport coeffs., Weinberg-Salam model 78−32623
deformable solids, variational theorems for thermodiffusion *(Russian)* 78−62169
elastic layer, temp. and concentration fields distrib. 77−59137
elastic micropolar material, constitutive eqns. 77−5667
elasticity with thermodiffusion, vibr. boundary value problems 78−41164
entropy production minimum theorem generalisation, thermal cond. coeff. depend. *(French)* 78−73943
integral equation method 77−17928
interferometrically recorded sedimentation, diffusion and thermal diffusion expts., reference marks arrangement 77−87813
laminar flame in tube, diffusion-thermal instability 79−86320
liquid inclusion migration in solid, nonequilib. morphology 78−38882
low-aberration focusing fibre, optimum diffusion exchange and heat treatment 78−1378
mass transport and assoc. failures 80−59694
nonlinear parameter identification by hybrid computation 77−53766
nuclear fuel, transport phenomena under severe temp. gradient 80−615
parasitic convection effects in thermal diffusion column in sampling mode 80−19386
porous materials, thermal diffusion based on electrokinetic effect, coefficient determ., calc. and obs. *(Russian)* 78−90641
protective coatings, thermodiffusional, form. kinetics and struct. on iron, steel, and cast iron 77−56158
reactor fuel cladding dilatation, influence of radial temp. gradient 77−46287
in rectangular cross-sectional area, equiv. time constant *(Polish)* 77−65008
relaxation theory of heat conduction and diffusion 77−35012
semiconductor doping, thermomigration method, using molten wires, nonequilib. morphology of migrating liq. inclusions 78−38882
soft mode coupling near struct. phase transition, hydrodynamical anal. 79−60468
thermomagnetophoresis of particles in magnetic suspensions 80−35581
thermosolutal convection rel. to stellar convection 78−89188
tissue perfusion measurements made with thermal diffusion probe, effect of probe geometry 80−104802
variational Lagrangian thermodynamics, nonisothermal finite strain mechanics of porous solids, thermomolecular diffusion 77−65668
viscous fluid mixture with thermomolecular diffusion, new variational-Lagrangian thermodynamics 79−49185
weakly conducting fluid, separation by thermal diffusion in elec. field *(Russian)* 79−16117
Al-Al_3Ni eutectic, temp. gradients, microstructural changes 80−84971
Al-Sc, dil., thermomigration of Sc 79−69280
$As_2S_3(Se_3)$:Ag glassy films, doped by photodiffusion and thermodiffusion, photocond. 80−29441
Co, thermomigration and electromigration in high-purity samples 79−55919
Ge, single cryst., ^{18}F penetration, charged particle activation anal. 80−93828
H thermal diffusion, apparatus 80−100358
H_2O, thermoosmosis through cellulose acetate membranes 79−52768
KCl, migration of brine inclusion, nonequilib. morphology 78−38882
KCl, thermotransport of ^{85}Sr and ^{54}Mn, Soret effect meas. 77−47624
Li_2O-SiO_2 glass, thermotransport props. 80−79985
Si, joining and recrystallisation using thermomigration process 80−65298
Si, monocryst. plates, purification by thermal diffusion, impurity migration anal. 80−25553
Si:Au, p^+-n junction, quantitative study of Au atoms by TSC method 80−2458
Si:B(P)(As)(Cu)(Fe), thermal and mass diffusion calcs. 79−69148
SiO_2-FeO_2 particulate mass transfer mechanism in modified CVD, thermophoresis 80−2955
$(U,Pu)O_2$ fuels, O distrib. during irradiation, calc. using CODIF program 78−70604
V, electro- and thermo-self-transport, 1480-1822°C 79−42297

thermal diffusion in gases
aerosol, spherical particle phoresis in multicomponent gas mixtures 78−22446
aerosol particles, theory of thermophoresis 79−55407
anthracene-He-Xe, gaseous mixture with one low conc. component, thermal diffusion calcs. 77−19661
binary gas mixture, drop thermophoresis 80−93806
binary gas systems, thermal diffusion factors meas. 80−10344
binary mixtures of monatomic gases, Chapman-Enskog theory, thermal cond. calc. 80−24118
chemically frozen multicomponent boundary layer, thermal diffusion effects behind strong shock 80−53772
combustion front thermal propagation and thermodiffusional instability 80−7796
concentration dependence, transient effect method determ. 77−11300
drop, thermodiffusiophoretic motion, weak solution in binary gas mixture 79−64744
drop dynamics in mixture with uniform temp., thermal diffusion effects 80−103097

thermal diffusion in gases continued
fluoromethane, molecular pumping, thermal lens phenomena 80−9708
hard sphere gas, binary mixture, diffusion coeffs., relativistic kinetic theory 77−3908
heat pipe, spectroscopic, operation 80−106708
hot film anemometer probe, wedge shaped, theoretical performance 77−31403
ice crystal morphology, vapour growth, influence of vapour diffusion and heat diffusion 80−64933
inert gas binary mixture, thermal diffusion factor meas. 80−79425
inert gas binary mixtures, expt. determ. of temp. depend. of thermal diffusion factors *(Russian)* 79−60095
intermolecular potential energy function determ. from thermal diffusion data 77−54590
meteor trails, effect of thermal diffusion on measured drift speed 77−21955
mixtures, marginal comp., thermal diffusion column performance evaluation *(German)* 80−59157
molecular pumping, thermal lens phenomena, time-resolved geom. optics approach 80−9708
non equilibrium light gas, heavy impurity thermal diffusion under laser irrad. 80−64667
optically active systems, transverse diffusion in electric field 80−6187
polyatomic-noble gas mixtures, mag. field effects 80−10345
porous material, thermal-diffusion couple appl. to gas compression and decompression 78−94882
spherical drop combustion, asymptotic, drop shrinkage and flame movement, heat and mass transfer 77−81405
thermal diffusion flame, two dimens. cellular struct. formation 80−69947
thermal diffusophoresis of droplets of a liquid solution in a binary gas mixture 80−43766
thermodiffusion separation column, theory according to Frazier scheme 78−5842
transient separation of thermal diffusion column, non-active end vol. influence 77−35300
velocity correlation functions, transport props. predictions, medium density 77−7500
Venus ionosphere, thermal diffusion calcs. 80−72806
wave propagation in viscous heat cond. gas, Gurtin type props. 77−27645
Ar binary mixtures, separation performance of Kr and Xe by thermal diffusion column 77−42192
Ar, intermolecular pot. energy function determ. from thermal diffusion data 77−54590
Ar, thermal diffusion factors, isotopic 78−22450
Ar-N_2(CO_2), thermal diffusion factors meas. 80−10344
Ar-Ne mixtures, thermal diffusion 80−1726
Ar_2, interatomic potential single parameter 80−48059
^{36}Ar, separation, calc. of thermal diffusion cascade *(Rumanian)* 78−58862
^{36}Ar-^{40}Ar, thermal diffusion column transport coefficients *(Rumanian)* 78−51274
BCl_3-N_2 mixtures, thermodiffusion props., effect of resonant excitation of mol. vibr. by laser, isotope separation 80−100047
^{13,14}C, thermal diffusion separation column, effective vol. calc. *(German)* 78−42235
H, spin-polarised, density, magnetisation, compression and thermal leakage 80−44391
H-Br systems, thermokinetic oscillations in flame propagation, stability diagram 79−79253
H_2 separation from HI-H_2-I_2 mixture in thermogravitational column 80−45561
H_2-He mixture, conc. depend. of thermodiffusion const. 77−7503
He-Ar, corresp. states law and thermal diffusion, two-bulb meas. 77−3910
He-Ar(Kr)(Ne), thermal diffusion, conc. depend. determ. 77−11300
He-Ar(Ne)(N_2)(CO_2) mixtures, thermal diffusion 80−1726
He-H_2(N_2O)(NH_3), thermal diffusion factors meas. 80−10344
He-Kr(Xe), scaling parameters for thermal diffusion factors, viscosity, mutual diffusion coeff. calcs. 77−35292
He-Ne, thermal diffusion factor, 65 to 300K 78−71418
I_2-He-Xe, gaseous mixture with one low conc. component, thermal diffusion calcs. 77−19661
Kr, intermolecular pot. energy function determ. from thermal diffusion data 77−54590
Kr, thermal diffusion factors, isotopic 78−22450
Kr, transient separation of thermal diffusion column, non-active end vol. influence 77−35300
Kr-Ar binary mixture, expt. determ. of temp. depend. of thermal diffusion factors *(Russian)* 79−60095
Kr-N_2O, thermal diffusion factors meas. 80−10344
Kr+Ar(He)(Ne), thermal diffusion, conc. depend. determ. 77−11300
^{78}Kr/^{86}Kr, isotope separation *(Rumanian)* 80−86988
N_2-Ar equimolar mixture, transverse Dufour effect 80−6194
N_2-Co_2 mixtures, marginal comp., thermal diffusion column performance evaluation *(German)* 80−59157
N_2-N_2O mixture, conc. depend. of thermodiffusion const. 77−7503
NH_3-CO_2 gas mixture, thermal diffusion const. 78−67300
Ne, transport properties, exponential 6-pot. model parameters 77−47130
Ne+Ar(He)(Kr), thermal diffusion, cond. depend. determ. 77−11300
Rn-CO_2 mixture, ^{222}Rn conc. monitoring by proportional counter 79−50839
^{222}Rn-CO_2, thermal diffusion, expt. method for study 80−5922
Xe isotope separation in HF discharge, thermodiffusion *(Russian)* 77−46649
Xe, thermal diffusion factors, isotopic 78−22450
Xe-Ar binary mixture, expt. determ. of temp. depend. of thermal diffusion factors *(Russian)* 79−60095
Xe-Kr binary mixture, expt. determ. of temp. depend. of thermal diffusion factors *(Russian)* 79−60095

thermal diffusion in liquids
alkali metal chlorides, thermal diffusion in H_2O, D_2O, potentiometric calcs. 78−18807
alkali metal-molten salt mixtures, thermal EMF calcs., Rice and Pitzer models 78−20057
aqueous electrolyte solutions, thermal diffusion, Soret coeffs. meas. 78−18811
binary fluid layer heated from below, thermal diffusion, instability 78−75860

thermal diffusion in liquids continued
binary fluid mixture, thermal diffusion ratio determ. by forced Rayleigh scatt. 78−75858
binary liq. layer, microgravity, thermoconvective stability 80−74866
binary liquid mixture, horizontal layer, surface tension driven instability in presence of Soret effect 80−10227
binary liquid mixture heated from above, convective instability, optical meas. 77−42823
Boussinesq fluid, Rayleigh-Benard instability in nonreactive binary fluids, results 79−90226
Boussinesq fluids, Rayleigh-Benard instability in nonreactive binary fluids, theory 79−90225
capillary mass transfer of porous solids based on pore distrib. curves 77−7443
carbon tetrachloride, Cl isotopes thermodifusion 79−90810
carbon tetrachloride-cyclohexane mixture, Dufour effect, Onsager heat-mass reciprocal relation 78−34638
column inclination, effect on thermal diffusion in binary solns. 79−86420
convective stability and thermal diffusion, role of rotating container 79−68725
coolants and index matching media for Nd:glass laser systems 80−33015
drop dynamics in mixture with uniform temp., thermal diffusion effects 80−103097
electrically conducting fluid, laminar flow mass transfer at high Peclet numbers 80−43784
ethanol-water mixture, Soret coeff. determ. 79−19386
ionic melts, thermal diffusion, thermoelectric power meas. 78−18810
isobutyric acid-water, mixture, heat of transport, crit. exponent 80−15277
lakes, stagnant, thermal stratification 80−36340
laminar boundary layer mass transfer with thermal diffusion 80−19323
laminar dispersion in rectangular conduits, side wall effects, convection 78−94636
linear convective stability, Soret effect, horizontal quiescent layer of two-component fluid 80−92144
linearly-stratified horizontal layer, onset of thermohaline convection 77−42897
macromolecular polydispersity by dynamic light scatt. and thermodiffusion 78−18816
macromolecules in solution, diffusion coeff. determ. by Soret effect, using optical method 77−28032
magnetoelectrolysis in steady Hartmann flow cells, hydrodynamics, mass transport 77−36759
metals, diffusion, electrotransport and thermotransport 77−55371
MHD generator, nonequilibrium channel, thermal diffusion of charge carriers, effect on electron density, obs. 79−68959
molten binary mixtures, in thermocell, Soret coeff., thermoelec. power 77−15614
moving liquid, numerical method for convective diffusion problem 77−89120
non-Newtonian liquid mixture separation by thermal diffusion in parasitic convection 80−64587
nonaqueous electrolyte solutions, thermal diffusion, Soret coeffs. meas. 78−18811
nonisothermal electrochemical system, thermal diffusion, thermodynamic theory 78−20056
overstability in horizontal layer of binary liq. mixture with Soret effect 80−106782
polymer solution, dil. buoyancy-driven instability 78−10206
Rayleigh scattering, forced appl. in method to determ. thermal diffusion ratio *(French)* 78−2271
singular perturbation problem with nearly resonant operator 78−22352
Soret coeff., nonstationary meas. method in diffusion column 77−89558
Soret coeff., packed thermal diffusion column expt. 77−89559
Soret coefficients, meas. methods 77−39685
Soret driven instability, secondary effects 80−6062
Soret effect, nonlinear two-dimens. Benard convection 77−19599
Soret-driven convective instability in two-component liq. layer heated from below, phase transition picture 79−77110
Soret-driven convective instability with rotation 78−46968
stability of flow between two rotating cylinders, effect of thermal diffusion 78−18308
tetrabutylammonium bromide, aq. soln., thermal diffusion, heat of transport *(French)* 78−18808
tetrachloromethane-cyclohexane liq. mixtures, heat of transport, Dufour effect 80−44344
tetraethylammonium bromide, aq. soln., thermal diffusion, heat of transport *(French)* 78−18808
tetramethylammonium bromide, aq. soln., thermal diffusion, heat of transport *(French)* 78−18808
thermodialysis of nonideal aq. solns. across non-isothermal partitions 79−96366
thermogravitation column, thermodiffusion and convection, flow distrib. and conc. profiles *(French)* 78−14493
transient-state Soret-coefficient determination for thermal diffusion column 77−89560
two-component fluid, laminar boundary layer, temp. and conc. field calcs. *(German)* 78−71386
two-component fluid layer, Soret effect on thermal instability 77−11185
viscous binary mixture in porous medium, thermal conc. instability 77−35231
volatile highly thermally conductive spherical drop, theory of diffusiophoresis 80−14784
water-oil microemulsion, thermal diffusion coeff. *(French)* 79−87880
wave equation for simultaneous heat and mass transfer in moving media 79−44747
CS_2-ethanol mixture, thermal diffusion ratio determ. by forced Rayleigh scatt. 78−75858
Cl isotope separation by liquid-phase thermal diffusion 79−89502
$CuSO_4$, aq. soln., Soret coeff. and heat of transport 78−18809
^{3}He-^{4}He, anomalous cooling power of dilution refrigerators 80−37045
^{3}He-^{4}He mixture, thermal diffusion ratio near λ transition, onset of heat flush 77−35787
^{3}He-^{4}He mixture, transport props. near superfluid transition and tricritical point 80−29242
^{3}He-^{4}He mixture near tricritical point, thermal diffusion ratio and thermal conc. gradients 77−76640
^{3}He-^{4}He mixtures, thermal transport coeffs. near lambda line 78−22926
^{4}He, dynamic structure factor near λ temp. 77−66049
^{4}He, liq., lambda transition, dynamic scaling correction 79−73357

thermal diffusion in liquids continued
^{4}He, superfluid, heat transport in restricted geometries, 0.8-2K 80−29237
^{4}He, superfluid, thermal counterflow at large heat currents, geometry effects 78−51763
^{4}He, superfluid, thermal counterflow, vortex line drift velocity effects on temp. diff. data anal. 78−51765
K isotope separation in solution by thermal diffusion 80−87236
Kr-methane, liq., Soret coeff. at low temp. 77−89565
Mg, diffusion and thermal diffusion of Fe, Si and Al, obs. using unidirectional solidification 78−30772
Mg-Tl liq. systems thermodiffusion of Tl 77−11717
$MgSO_4$ soln., thermal and Fickian diffusion 78−2272
Si, ion implanted, laser-annealed, theoretical anal. of thermal and mass transport in molten state 78−91364
Sn, thermotransport of solutes and NFE calc. of electronic heats of transport 77−55376
Te-Tl liq. systems, thermodiffusion of Tl 77−11717

thermal diffusivity
anisotropic body, nondestructive thermophysical checking methods 78−79196
apparatus for meas. thermophysical characts. by composite method, wide temp. range 77−26285
apparatus to meas. thermophysical props. at high temps. 80−37458
Araldite AW106/Hardener HV953U epoxy resin, thermal props. at high press., glass transition 77−59160
Armco Fe, meas. using new apparatus 77−67429
automatic meas. by pulse method using analogue computer *(Japanese)* 80−27294
automatic measuring method *(French)* 80−14559
baddeleyite-corundum refractories, thermophysical props. 79−82398
BBOA, forced Rayleigh scatt. 78−76483
benzoic acid, diffusivities in water 79−73328
biomaterial thermal conductivity and thermal diffusivity simultaneous meas. technique 78−57098
p-bis-octyloxyazoxybenzene, liq. cryst., thermal diffusivity, Rayleigh scatt. obs. 78−94977
borosiliate glasses, thermal conductivity meas. by laser flash method *(Japanese)* 77−69124
p-butyloxybenzylidene-p'-octylaniline, liq. cryst., thermal diffusivity, Rayleigh scatt. obs. 78−94977
calorimetry of low thermal diffusivity materials, advantages of spherical samples 79−54134
ceramics, sintered, thermal diffusivity meas. by flash with negative pulse, plasma jet heating 79−37888
coal, thermal diffusivity and cond. meas. for in situ coal gasification appls. 80−30360
composite materials, metal reinforced, thermal activity, diffusivity, cond. meas. method 79−37141
concrete, rich mix, thermal props., expt. study *(Japanese)* 77−77536
conference, Chicago, USA (Nov. 79) 80−31425
constant power source method, for therm. characts. 79−95222
cordierite glass-ceramic, effect of crystn. on thermal diffusivity 79−33127
curve-fitting method based apparatus for thermal props. meas. at cryogenic temps., performance characts. 77−67441
cyanobiphenyls, liq. cryst., thermal diffusivity, Rayleigh scatt. obs. 78−94977
dilatometric determination 77−41597
dispersed material, thermal diffusivity 79−55943
dynamic thermophysical characts. of thermal receivers, nonlinear eqn. soln. with 3rd kind boundary conditions 77−43395
elastic solid, difference and finite-element method for dynamical thermodiffusion problem 77−62154
electrically insulating media, high-press. diffusivity from pulsed wire probe meas. 77−41613
epoxies commercial powder filled, 1.5 to 15K 79−58729
evaporation, gas-side mass transfer coeff., diffusivity effect 79−18684
fluorophlogopite mica, glass-ceramic, thermal diffusivity, crystallisation effects 78−6190
fusion thermal tracers, thermophys. characts. investig. 77−5837
glass, meas. by constant-rate heating method *(Japanese)* 80−6570
glass fibre reinforced epoxy, heat ageing effect on thermophys. props., 10-400K 77−59161
glass fibre reinforced epoxy, thermal cond., diffusivity and sp. ht., determ. 80−24613
glass fibre reinforced epoxy resins, thermal props., 80-300K *(German)* 79−10990
glass microscopic bead struct. material, thermal cond. and diffusivity, temp. depend. *(Russian)* 79−37885
glass thermal diffusivity meas., calorimetric method 79−27349
glass-C fibre reinforced epoxy, thermal cond., diffusivity and sp. ht., determ. 80−24613
glass-fibre epoxy resin composite, thermal cond. and diffusivity, 2-15K 77−24457
glycerine, meas. by constant-rate heating method *(Japanese)* 80−6570
glycerol, liq. and glass, thermal diffusivity meas. 79−82394
granular matarials, thermal diffusivity measurement, constent rate heating method *(Japanese)* 80−6572
graphite, Poco AXM-5Q1, thermal and elec. transport props., 4-3000K 78−6375
graphite, thermal diffusivity, high temp., meas. by radial flash method 80−52227
graphite foam, thermal props. 77−48689
Green River oil shales, anal. of depend. of thermal transport parameters on organic content 79−79817
Green River oil shales, thermal diffusivity depend. on organic content 80−76965
heat diffusion process estimation methods comparison 77−3713
high heat-conductance materials, method for determ. of thermophys. characts. on thin samples 77−61063
Kapitza resistance, axiomatic acoustic mismatch theory, with loss 79−33132
laminate, effective thermal diffusivity 78−90643
laser-pulse meas., instrumental recording and data processing 77−45846
liquid, phenomenological coeffs., frames of reference, isothermal systems 78−38862
lubricant, cond. and diffusivity joint meas., relative probe method 77−41600
MBBA, forced Rayleigh scatt. 78−76483

thermal diffusivity continued
MBBA, nematic liq. cryst., thermal diffusivity, Rayleigh scatt. obs. 78−94977
meas. apparatus. using low freq. sine wave generator and digital phase meter 78−94580
measurement, calc. formulae for unsteady temp. data 79−94476
measurement, scanning temperature method 77−45831
measurement, transient hot-strip method for simultaneously measuring thermal conductivity and thermal diffusivity of solids and fluids 80−1417
measurement method, by pulse expt., error anal. 79−32208
measurement method, using wave packet soln. and microprocessor-controller 78−73989
measuring technique, weak IR absorbing fluids 78−22904
membranes, phenomenological coeffs., frames of reference, isothermal systems 78−38862
metallic powder, constant rate heating method *(Japanese)* 80−6572
metallic thin films, thermal conductivity and thermal diffusivity, determ. method *(German)* 78−19165
metals, thermal diffusivity determ., thermoelastic method 79−23940
methane, critical region, Rayleigh scatt. obs. 78−34607
methane, spontaneous thermal fluctuations, Rayleigh scatt. obs. 78−88317
methyl polymethacrylate, heat emission coeff. and cooling const., Angstrom periodic heat wave method 77−72706
MHD, thermodiffusive mixture flows, Hall and ion-slip effects, uniqueness theorem 78−87415
microfluids, linear theory of chemically reacting mixtures 80−14777
molecular dynamical studies of energy transport in crystalline solid 78−30803
molten salts, meas. by stepwise heating and improved apparatus, accuracy anal. 77−82525
monatomic BCC lattice under intense excitation, energy transport 78−59922
monocarbides of subgroups IVa and Va, kinetic props., review 78−47613
2-naphthol, diffusivities in water 79−73328
neuroblastoma tumour, thermal conductivity and diffusivity meas. 79−5252
nuclear reactor materials, thermal properties at elevated temps., determ. method 77−73402
nuclear reactor materials, thermophys. prop. meas. at RFL Springfields 77−14230
oil shales, review of thermophysical properties 79−100479
open channel thermally stratified flow, eddy diffusivity buoyancy effects, obs. 78−90904
packed beds, particle-to-fluid transfer coeffs., fluid diffusivities 77−31378
packed fluidised bed with horizontal flow, lateral thermal diffusivities 79−50788
parabolic free boundary problems, 1-D 77−23856
PMMA, amorphous, thermophysical props. depend. on hydrostatic press. 78−47612
PMMA, thermophysical props. at high hydrostatic press. 78−2317
polycarbonate, amorphous, thermophysical props. depend. on hydrostatic press. 78−47612
polycarbonate, thermal diffusivity meas., flash method 77−47632
polyethylene, partially crystalline, far IR absorption and thermal props. 79−33690
polyethylene terephthalate, thermal diffusivity, conductivity meas., crystallisation rel. to glass transition 77−47632
polyethylenes, thermal diffusivity anisotropy 78−75894
polymer, amorphous, thermal conductivity and thermal diffusivity, press. and temp. depend. 77−7915
polymers, thermal diffusivity, Fourier theory 80−31456
polyoxymethylene, thermal diffusivity, and cond. meas., two-phase model 77−47632
polystyrene, amorphous, thermophysical props. depend. on hydrostatic press. 78−47612
polyvinylidene fluoride films, pyroelectric current freq. depend., thermal diffusivity 79−78630
polyvinylidene fluoride thermal diffusivity and cond. meas., two-phase model 77−47632
porous material, thermal cond., diffusivity and water content meas., thermal shock transient *(French)* 78−94583
pulse methods for investigating thermal diffusivity and conductivity in solids, theoretical models *(Polish)* 80−92728
pulse propagation in coarse homogeneous large samples, model meas. method *(French)* 77−27465
pyroelectric target performance improvements 77−39103
radial flash method for high temp. thermal diffusivity meas. 80−52227
refractory, thermophysical props. in rarefied gaseous medium 78−34664
refractory, ultra-lightweight, thermophys. characts., moisture effects *(Russian)* 77−55921
refractory materials used in MHD generator channels, thermophysical props. 77−28054
rocks, meas. at high press. in cubic press. 78−69337
salicylic acid, diffusivities in water 79−73328
sand, constant rate heating method *(Japanese)* 80−6572
semiconductors thermophysical props. determ. from Ettingshausen effect meas. method 80−44376
semiinfinite region, variable coeff. of thermal diffusivity on boundary 77−46898
semimetal elements of group V, laser flash technique 78−6189
Sialon, reaction sintered, mech. props., effect of composition and X-phase 77−56013
silicate glass, thermal diffusivity in range 0-600°C, influence of TiO_2 80−29233
silicon oil, meas. by constant-rate heating method *(Japanese)* 80−6570
simultaneous measurement method for thermal props. of plane-shaped solids using iterative calcs. 77−42713
soil, Fourier anal. of temp.-depth profile 79−44264
solid, determ. by temp. meas. at irregular operation stage 78−62199
solid, iterative estimation method 80−43603
solid, ultrasonic method, and sp. ht. 77−89015
solid thermophysical properties at high temp., conference, Moscow, USSR (May 1976) 77−28012
solids, joint determ. of thermophysical characts., quasilinear method 77−41601
solids, meas. using modulated heating beam technique 80−52221
stainless steel, thermal diffusivity meas. using const. rate heating method *(Japanese)* 77−87759

thermal diffusivity continued
steel, C, thermal diffusivity meas., const.-rate heating method *(Japanese)* 78−79976
steel, Cr, hypereutectic, ShKh15, exam. of thermal props., 298 to 1173K *(Russian)* 79−28334
surface layers and thin films, thermal diffusivity of microsections, IR and X-ray electron-probe microanal. 78−2314
temperature dependence determ. from thermocouple meas. 77−42719
terphenyl, liq. cryst., thermal diffusivity, Rayleigh scatt. obs. 78−94977
TGS, deuterated and undeuterated, pyroelectric, dielectric and thermal props., temp. depend. 78−43809
TGS, nitroaniline admixture effect on thermal parameters 80−107580
TGS, pure and doped, thermal diffusivity, domain wall thickness determ. 79−42324
TGS, pure and Fe^{3+}-doped, thermal diffusivity, 25°C 79−90833
TGS, X-irrad., thermal diffusivity, cooling const. and heat transmission coeff. 79−86935
thermal conductivity, vibr. energy diffusion coeff., 400-1600K 77−27644
thermoelastic meas. method 80−107581
thermophysical measurements, sample shape determ. 79−30457
thermophysical property research, metallurgical applications 80−97457
tissue, thermistor meas., influence of blood vessels using simulation model 77−40962
tissue-equivalent plastic, A-150, thermal diffusivity, sp. ht., thermal cond. obs. 80−34258
transparent materials, laser irradiated, in-depth and surface temp. meas. by Moire-Schlieren technique 80−53392
transparent solids, measurement using non-steady-state method 79−50572
transport-diffusion interfaces in radiative transfer 79−98598
triglycine fluoberyllate, pyroelectric, dielectric and thermal props., temp. depend. 78−43809
tubular furnace for thermal diffusivity meas., design 80−30182
viscous liquid, acoustic and thermal props., phenomenological models 79−82393
viscous liquid, constant-rate heating method *(Japanese)* 80−6570
welding, ultra pulse type, heat transfer characts. 79−1047
Zircaloy-2 and associated oxide layers, thermal property meas. 77−8063
Zircaloy-2 fuel tube, thermal conductivity of oxide deposit 79−63745
Ag, expt. transient technique and theory for foils 78−43353
Al, expt. transient technique and theory for foils 78−43353
Al, thermal cond. form diffusivity, press. depend. up to 2.5 GPa 77−85195
Al, thermal diffusivity meas. by flash with negative pulse, plasma jet heating 79−37888
Al-Mg-Zn solid solution, thermophysical props., 0-400°C *(Russian)* 77−89548
$AlNbO_4$, polycrystalline, thermal diffusivity, effect of microcracking 78−26743
Al_2O_3, alumina, meas. by scanning temperature method 77−45831
Al_2O_3 dispersion hardened by Ba mica, thermal diffusivity 80−25713
Al_2O_3, fibrous, thermal diffusivity and conductivity 78−10232
Al_2O_3 plasma-sprayed, struct. and thermal diffusivity 79−86932
Al_2O_3, therm. characts. using constant power source method 79−95222
Al_2O_3-$4SiO_2$-H_2O, pyrophyllite, thermal diffusivity meas. using const. rate heating method *(Japanese)* 77−87759
Al_2O_3-ZrO_2 dispersed system, thermal diffusivity/conductivity, effect on microcracking resulting from phase transform. 78−10231
B_4C, thermophysical props. and neutron absorpt. 80−103488
BN thermal diffusivity meas. using ruby laser beam *(Spanish)* 79−90835
B_2O_3-Na_2O-SiO_2-Al_2O_3, effect of alumina dispersions on the thermal cond./diffusivity/stress resist. 80−39368
$BaMnF_4$, anisotropic order parameter phase fluctuations, light scatt. and thermal diffusivity meas. 80−80807
Bi-Bi_2O_3 black layer, on polyvinylidene fluoride film, pyroelec. camera tube for IR imaging 80−57369
C fibre reinforced epoxy, thermal cond., diffusivity and sp. ht., determ. 80−24613
C, glassy, thickness imposed gradients 78−14521
CO_2, thermal diffusivity and cond. in crit. region meas. by holographic interferometry *(German)* 78−59942
$Ca_{10}(PO_4)_6(OH)_{2-2x}O_x\square_x$ polycryst. sintered bodies, prep. and thermal props. 80−25624
Ce, high temperature transport props., scatt. mechanisms, phase transitions 77−15825
Co, thermal diffusivity meas., 300 to 1000K, Lorenz number determ. 80−29384
Cu, expt. transient technique and theory for foils 78−43353
Cu, thermal conductivity under high pressure 78−30901
Cu, thermal diffusivity meas. by flash with negative pulse, plasma jet heating 79−37888
D-T, solid, estimated heat capacity, enthalpy, thermal cond. and diffusivity 77−4228
Eu, high temperature transport props., scatt. mechanisms, phase transitions 77−15825
Eu_2O_3, mech. and physical props. rel. to reactor control rod appl. 78−21641
Eu_2O_3, thermophysical props. and neutron absorpt. 80−103488
Fe, cast, thermal diffusivity meas. 293 to 873K, exam. of thermal cond. *(Japanese)* 78−47763
Fe, expt. transient technique and theory for foils 78−43353
Fe, thermal diffusivity by pulse method 80−15497
Fe-Ni, thermal diffusivity during martensitic and austenitic transform. *(French)* 77−59781
Fe-Ni alloy, diffusivity, heat capacity and thermokinetic behaviour, simultaneous meas. *(French)* 77−1235
Fe-Ti (V)(W), dil., thermophysical props. and elec. cond., temp. depend. 80−96842
$(Fe_2O_3)_x$-$(3B_2O_3.PbO)_{1-x}$ glass, thermal cond. and diffusivity obs. 79−60561
Ga, liq., thermal props. at high temp. 80−75536
GaAs crystal growth, thermal and elastic const. evaluation 80−92586
GaSb based eutectics, thermal cond. and diffusivity, 300-700K, phonon mechanism 80−103526
Gd, T>1100K 77−24548
Gd, thermal diffusivity, conductivity and elec. cond. 110 to 2100K 79−42516
Gd, transport props., anisotropy, high temp. obs. 78−26843
GdB_6, thermophys. props., 700 to 1200K 79−37850
GdTb alloy, transport props., anisotropy, high temp. obs. 78−26843
thermal diffusivity continued
GdTb, elec. resist. and thermal diffusivity anisotropy *(Russian)* 77−85192
GeS_x glass, x=1.25 to 1.5, softening and crystallization kinetics 79−32906
^3He-^4He mixtures, thermal transport near lambda line 79−56004
Hf, thermal diffusivity meas., 300 to 1000K, Lorenz number determ. 80−29384
$Hf_xTa_{1-x}C$, thermal cond. and diffusivity, 1000-2200°C, elec. cond. 78−91491
Hg_2Cl_2, elec., dielec., and thermophysical props. 79−10989
Ho, thermophysical properties at high temps., exam. *(Russian)* 79−28105
In, liq., thermal props. at high temp. 80−75536
InSb based eutectics, thermal cond. and diffusivity, 300-700K, phonon mechanism 80−103526
$KTaO_3$:Gd semicond., temp. depend. of thermal diffusivity and Seebeck coeff. 78−10481
Li_2BeF_4, molten, meas. at 470-700°C 77−82525
$Li(N_2H_5)SO_4$, thermal diffusivity exam. 78−63886
Li_2O, porosity, dependence on thermal diffusivity and thermal conductivity, 200-900°C 80−92726
Lu, thermophysical properties at high temps., exam. *(Russian)* 79−28105
MgO, thermal characts. using constant power source method 79−95222
MgO-$MgAl_2O_4$($FeCr_2O_4$), thermoplastic and thermophys. props. for steel vacuuming installations 80−35281
$MgTi_2O_5$, thermal diffusivity, grain size and microcracking effects 78−10233
$NaNO_3$, molten, meas. at 320-80°C 77−82525
Na_2O-Cs_2O-SiO_2 glasses, thermal diffusivity, heat capacity and thermal cond., laser flash method study 80−65310
Nb-Ti, thermal conductivity in low temp. range 78−39259
NbC_x, thermophys. props. 77−89600
NbC_x, thermophysical props. at high temp., thermal vacancies form. 78−43141
Nd, high temperature transport props., scatt. mechanisms, phase transitions 77−15825
Ni, expt. transient technique and theory for foils 78−43353
Ni, heat diffusivity and heat cond. near Curie point 77−24706
Os, elec. resist., thermal diffusivity, and thermal cond., 290 to 3300K 79−11101
Os; electrical resistivity and thermal diffusivity meas. 80−15495
$Pb(Mn_{1/2}Ta_{1/2})O_3$, ceramic, for thermal and dielectric isolation at low temp. 80−39365
PbO, sintered, pure, prep. and props. 77−48361
Pd-Ag electrical resistivity, thermo-EMF and thermal diffusivity at high temps. *(Russian)* 80−6808
Pr, high temperature transport props., scatt. mechanisms, phase transitions 77−15825
Pu-Ga (1 wt.%) alloy, delta-stabilised, heat transport props., room temp. to 500°C 77−20294
PuN, fabrication, high-temp. thermodynamic and transport props. 77−28774
RbCl, thermal diffusivity, meas. by pulse method, influence of press. 79−7701
$RbNO_3$, single cryst., DC cond., dielec. and thermophys. props., temp. depend., transitions interpret. 78−26682
Ru, kinetic and thermal props. at high temp., anisotropy 77−43563
Ru, transport props., anisotropy, high temp. obs. 78−26843
Si, laser annealing, nonlinear dynamic transport processes 80−93437
SiB_{12-x}, thermam cond., temp. depend., up to 2000K *(French)* 80−70484
SiC, constant rate heating method *(Japanese)* 80−6572
Si_3N_4, hot-pressed, thermal cond. by laser flash method 79−69302
Si_3N_4, pyrolytic, crystn. and amorphous, thermal diffusivity, thermal cond., specific heat 79−69303
Si_3N_4, reaction-sintered, effect of oxidation on thermal diffusivity 79−86933
Si_3N_4-Al_2O_3(25.5, 37.0, 47.8 and 57.8 mol.%) thermal diffusivity 77−7913
SiO_2, stishovite, synthetic polycrystalline, thermal diffusivity meas. 79−39706
SiO_2, vitreous, Suprasil-W, thermal diffusivity, 16 mK-2.3K 79−60563
SiO_2-Al_2O_3-Fe_2O_3-CaO-MgO-Na_2O-SO_3 glass, thermophysical props. 78−18849
Si_2ON_2, thermal diffusivity meas. by flash with negative pulse, plasma jet heating 79−37888
SmB_6, thermophys. props., 700 to 1200K 79−37850
$SmCo_5$, specific heat and kinetic props. at elevated temp. *(Russian)* 79−28530
Sn, liquid, thermal diffusivity and cond., 1000 to 1900°C, flash laser method *(French)* 79−99525
Sn, thermal diffusivity by pulse method 80−15497
Ta, thermophysical props. and neutron absorpt. 80−103488
Tb, transport props., anisotropy, high temp. obs. 78−26843
$TbFeO_3$, thermodynamic props. 77−36078
Ti, thermal diffusivity determ., thermoelastic method 79−23940
Ti, thermal diffusivity meas., const.-rate heating method *(Japanese)* 78−79976
TiC-C composites, hot pressed, thermophys. props. at high temps. 80−59675
TiI_4, thermal diffusivity, near FCC to BCC transition 80−59740
Tl, liq., thermal props. at high temp. 80−75536
UC_2, high temp. thermal diffusivity, thermal conductivity, spectral emissivity 77−28052
UO_2 fuel, density, thermal conductivity, specific heat, thermal diffusivity, flash method 77−55362
U_4O_{9-y}, thermal conductivity and diffusivity, 250 to 415K 77−50234
W, sintered, Standard Reference Material, high temp. props. 78−89427
W-Mo alloys, thermal conductivity and diffusivity, sp. ht., 100-2400°C 78−75842
WC-Co, composition and oxidation resistance of coatings deposited by thermal diffusion, using TiB_2 *(Bulgarian)* 80−45430
Y, T>1100K 77−24548
Y, thermophysical properties at high temps., exam. *(Russian)* 79−28105
Y, transport props., anisotropy, high temp. obs. 78−26843
YAG:Nd, heat capacity and thermal diffusivity meas. 80−19956
YB_6, thermophys. props., 700 to 1200K 79−37850
YIG, thermodynamic props. 77−36078

thermal diffusivity continued
Y_2O_3 sintered bodies, thermal cond. and diffusivity *(Japanese)* 79−55944
Zr alloys, reactor fuel sheath mat., thermophys. props. 77−46280
ZrC-C composites, hot pressed, thermophys. props. at high temps. 80−59675
ZrC_x, thermophysical props. at high temp., thermal vacancies form. 78−43141
ZrN_x, thermal diffusivity in region of homogeneity, 1000-1800°C 78−71892
ZrO_2, Y_2O_3 stabilized, meas. by radial symmetry method 77−28021

thermal effects in magnetism *see magnetocaloric effects*

thermal expansion
see also Gruneisen coefficient
β-eucrypite, glass-ceramics, internal stresses 79−15770
β-spodumene, glass-ceramics, internal stresses 79−15770
A15 compound, superconducting transition depend. on non-hydrostatic stress 80−107948
adamantane, mol. cryst., thermal expansion coeff. and Gruneisen coeff. 77−84952
AGR fuel cladding, development of high strength, ductile stainless steel alloys 80−45367
alkali halides, doped, thermal expansion at low temps. 80−96672
alkali halides, thermal expansion, rapid increase near melting point 77−51521
alkali hydrides, bulk props. prediction from molecular behaviour 78−51468
alkali hydrides, thermodynamic props. calc. using ionic pots. 78−10155
alkali metal, thermal expansion, elastic constants, phonon freq. anisotropy *(Russian)* 79−1516
alkali metal, thermal expansion and Gruneisen parameters 78−38857
alkali metal halide mixed crystals, volume thermal coeff. of expansion, calc. 80−96671
alkali metals, anharmonic effects in thermodynamics *(Russian)* 78−43145
alkali metals, thermal properties and Gruneisen parameters, employing model pot. 78−71815
alkali metaphosphate, M_2O-R_2O_3-P_2O_5 (R=Y or rare earth), glass transition temps. and coeffs. of linear thermal expansion 80−88343
alkaline earth metaphosphate, MO-R_2O_3-P_2O_5 (R=Y or rare earth), glass transition temps. and coeffs. of linear thermal expansion 80−88343
alkaline earth oxides, cohesive and thermophysical props., role of three-body interactions 80−92477
alkaline earth silicate glasses, morphology effects on props. 80−49118
alkyl-cyano-biphenyls, nematic to isotropic phase transition, volumetric studies 79−86878
alloy, solidus temperature determ. by method of moving specimen boundary projected on screen 78−35353
alumina film, RF sputtered, stability 78−22993
anadalusite, thermal expansion and cell parameters 79−90801
and UO_2-Gd_2O_3 solid soln., high temp. thermal expansion, 298-1700K 78−83979
anharmonic crystal, thermal expansion contribution to free energy and heat capacity to order λ^4 78−6138
anharmonic crystals, Debye-Waller factor, specific heat thermal behaviour 80−54335
anthracene, birefr. changes due to thermal expansion 78−52468
anthracene crystals, dialometeric studies 80−34212
Araldite CT200/HT907, 263 to 343K, mechanical, physical and optical props. 78−56682
BCC crystal, elastic constants, thermal expansion and bulk modulus 80−6452
benzalazine, thermal expansion, lattice consts. meas. 78−47539
benzene, thermal expansion at high press., near melting 79−77777
benzene-toluene and benzene-o-xylene mixtures, US vels., compressibility, expsn. coeff. 79−33038
benzenechromium tricarbonyl, sp. ht. and thermal expansion tensor meas. *(French)* 78−79788
bicyclo[2.2.2]octane, thermal expansion coeff., Gruneisen parameter 77−76581
binary liquid mixtures, sp. ht., light scatt., two-scale-factor universality 79−42267
biocyclo[2.2.2]octane, mol. cryst., thermal expansion coeff. and Gruneisen coeff. 77−84952
blood and its constituents, coeff. of thermal expansion *(German)* 80−104556
bone china body, MgO effect on vitrification mech. props. *(Japanese)* 79−78922
borate glass melts, struct. determ. using graph theory 79−64980
Born model, electrostriction rel. to dielec. and thermoelastic props. 80−71322
borophosphate glasses, effect of F on props. 78−67657
borosilicate glasses, gamma irradiation effect on density, refractive index, thermal expansion 80−79838
braze alloys, low vapour press., binary eutectic, props., thermionic converter appls. 77−90236
brittle composite, local crack-driving force, elastic and thermal mismatch 78−7017
carbazole, birefr. meas., 20 to 190°C, crystal-to-crystal phase transform. 80−45031
carbon fibre reinforced composites, filament-wound, thermal residual stresses 80−49290
carbonmetalplastic, heating rate effect on thermal deform. in various atmos. 79−65226
ceramic composite, toughening by oriented nucleation of microcracks 77−8921
ceramic materials, fine-grained, cyclic plastic deform. as cuase for thermal expansion hysteresis 80−89290
chalcogenide glass, partial values and structure features 79−41969
close-packed materials, correl. with MP 77−47604
coefficient of thermal expansion of simple bodies, correl. with electromech., thermal and erosion charcts. *(Russian)* 80−49388
coke, shrinkage kinetics during calcination 80−93572
composite materials, phys. props. review 77−4720
composites, elastic modulus and expansion coeff., approx. method *(Russian)* 77−39681
concrete, prestressed, low-temp. tensile strength and linear expansion coeff. of reinforcing steel 80−30051
concrete, rich mix, thermal props., expt. study *(Japanese)* 77−77536
condensing steam, method for calculating expansion 77−27573

thermal expansion continued
conference, Chicago, USA (Nov. 79) 80−31425
Constantan single wire, thermal expansion +20 to −60°C, strain gauge use 77−67427
continuum model, appl. of mean-field state eqns. 77−20040
cordierite, thermal expansion 78−6165
cordierite electroceramic, thermal expansion coeff. meas., 80-300K 79−60526
crystal, anharmonic contribs. to sp. ht. and thermal expsn. 79−82354
crystal, statistical thermodynamics with collective vibrations 78−54289
crystallised solids, symm. of thermal expansion tensor, temp. variation *(French)* 78−34636
crystals, book 80−73115
crystals, theory *(Russian)* 78−26701
cubic crystal, phase transitions with three-component order parameter, elastic anomalies *(Russian)* 79−37837
cubic materials, correl. with MP 77−47604
cubic metal, elastic shear modulus, temp. depend. 78−10118
cubic pure metals, thermal expansion coeffs., Morse pot. calcs. 79−77775
cylindrical and plane parallel layered materials, thermographic determination of heat transfer coeff. 80−19221
density changes during melting by X-ray absorption 80−103462
deuteromethane, solid, thermal expansion *(Russian)* 78−26698
diamond, semiconducting, band gap temp. depend, dilation and vibr. contribs. determ. 80−10868
diamond, spectroscopic mode Gruneisen parameters rel. to low-temp. thermal expansion behaviour 77−7876
dicalcium lead propionate, ferroelec., piezoelec. and elastic props. 78−84528
dicalcium lead strontium propionate, mixed cryst., phase diagram, dielec. and dilatometric anomalies 77−11689
dicalcium strontium propionate, Landau theory breakdown in ferroelec. transition 77−12344
p-dichlorobenzene, expansivity, determ. by calorimetric compression from 0 to 400 MPa 80−44339
displacive type ferroelectric, thermal expansion and effect of press. on transition temp. 78−72471
Earth crust, anal. of thermoelastic strains and tilts 78−20346
electro-optic reflector, controlled, temp. fields, thermal distortions 80−96021
elliptic plate, heated, deflection under uniform load 77−35040
entropy change on melting of simple substances, thermal expansion, configurational entropy 80−59630
epoxy, thermomech. props., rel. to hardener type and conc. 79−1913
epoxy polymer, with low thermal expansion coeff. 78−3094
epoxy resin, glassy, thermoelastic effect, thermal expansion coeff. 79−14944
epoxy resin, low temp. thermal props., phonon states and crosslinked struct. *(German)* 78−75846
epoxy resin, meas. of glass transition temp., linear viscoelasticity 80−29157
epoxy resin, powder filled, exam. of mech. props., thermal contraction 80−25821
epoxy resin Araldite CT200/HT907, thermal expansion coeff. meas., −5 to 70°C 77−41598
epoxy resin systems, synthesis review, phys. and mech. props. at low temps. 80−25650
epoxy resin/particle composites, particle size effect in thermal expansion, filler effects on T_g 80−84305
epoxy/graphite composite and cured epoxy resin, thermal expansion and swelling 80−92450
ethanol-H_2O mixture, liq. US vel., −80 to 20°C, 1-5 MHz 78−59933
ethylene-propylene, synthetic rubber, mathematical simulation of kinetics of thermal expansion *(Russian)* 78−55958
extrudate swell, thermally induced, Galerkin method 80−79312
FCC lattice, uncorrelated-pairs approximation for anharmonic free energy, tests 78−59920
FCC metals, props. of vacancies and divacancies 80−10545
ferromagnet, metallic, correl. of temp. anomalies of hyperfine field and thermal expansion of lattice 80−20400
ferromagnetic amorphous alloys, thermal expansion anomaly near Curie temp. *(Japanese)* 77−85542
ferromagnetic metals, magneto-volume effect, Invar phenomena 80−66007
ferrous alloy, FCC, anomalous thermal expansion in paramagnetic temp. range 77−35724
fibre reinforced composites, thermophysical props. *(German)* 77−28053
fibre reinforced composites, transverse plane, elastic, failure behaviour *(Japanese)* 78−48510
fibre reinforced polymer matrix composites, space environmental effects 80−71721
fibreglass/epoxy composites, laminates, rings, tubes, thermal contraction at low temps., report 80−19968
filled polymer mechanical properties, particle shape effect, review 80−100864
fluid, heat capacity, thermal expansion, simultaneous meas., dilatometric meas. 77−84131
2-fluoronaphthalene, disordered form, thermal expansion, neutron and X-ray diffr. study 80−24621
fuel rod, simulated, for HTGR, pre- and postirradiational thermal transport and thermal expansion 79−6742
garnet:Fe^{3+}, spin Hamiltonian parameters, g-factors, temp. depend. EPR obs. 77−48038
garnet:Mn^{2+}, spin Hamiltonian parameters, g-factors, temp. depend. EPR obs. 77−48038
Gibbs equilibrium thermodynamic pot. second derivatives, discontinuity surfaces rel. to phase boundaries of q-component systems 79−82304
glass:Nd, laser material, linear expansion coeff. and r.i., temp. depend. 77−733
glass, low expansion types, ultraprecise meas. 77−1247
glass, ternary, composition-thermal expansion relationships 78−18801
glass, thermal expansion at low temps. 80−96672
glass, thermal expansion coeff. rel. to chem. composition *(Japanese)* 79−51285
glass bead-reinforced epoxy resin composite, bulk and shear elastic props. 78−6959
glass ceramic, variation with ratio of phases and comp. 77−35719
glass chip, reducing agent effect on crystn. 78−46736
glass fibre, thermal behaviour *(Japanese)* 79−77780
glass fibre preforms, elastic stresses 79−64343

thermal expansion continued
glass fibre reinforced epoxy resin, cryogenic tensile, compressive and shear props. 78−6983
glass fibre reinforced epoxy resin composites, 2 to 290K 79−60528
glass fibre reinforced polymer, thermal expansion coeff. and glass transition temp., thermal stress effect 78−14484
glass laser rod, mech. strength and heat resistance obs. 79−76776
glass narrow sandwich seal, correction factor for thermal expansion mismatch 78−75110
glass reinforced epoxide, winding in transverse direction, creep and thermal expansion 79−96093
glass substrate, rel. to thermal cycling stability of Pb film tunnel junction 79−87200
glass transition temperature, determ from expansion and elec. cond. temp. depend. 80−19967
glass-ceramic composite, internal stress effects on mech. props. 77−21250
glass-ceramic second-order microstresses 78−27468
glass-ceramics, transparent, microstruct. and props. 78−59960
glass-metal sealing, set point of glass 80−108423
glasses, thermal behaviour during heating or cooling, retardation kinetics 77−4049
glassy linear polymer, mol. model *(Russian)* 77−62610
glazes, thermal expansion coeff. rel. to chem. composition *(Japanese)* 79−51285
α-, β-, γ- glycine, thermal expansion tensor 79−95187
graphite, neutron irrad., microporosity, elec. resist., length, struct. changes 78−43051
graphite, nuclear, change in ratio of thermal expansion coeffs. at elevated temps. 79−42283
graphite, nuclear, prestressing effects 78−14482
graphite, Poco AXM-5Q1, thermal and elec. transport props., 4-3000K 78−6375
graphite, polygranular, flexural strength after heat treatment porosity correl. 80−84996
graphite, pyrolytic, thermal expansion coeff. rel. to temp. 78−43147
graphite, pyrolytic commercial, high-temp. thermal and mech. props. 80−75372
graphite fibre epoxy laminates, low thermal expansivity, design considerations 80−81031
graphite fibre reinforced epoxy resin, cryogenic tensile, compressive and shear props. 78−6983
graphite structures in PBR, neutron radiation damage, mech. props., stress fields *(German)* 77−34387
graphite-ICl residue compounds, struct., X-ray diffr. 78−47287
graphite-nitrate residue compounds, phys. props. 78−10199
graphite/epoxy, for ultra-low expansion mirror telescope, testing 77−78636
guanidinium aluminium sulphate hexahydrate:Mn^{2+}, NMR 78−91939
high temperature expansion of solids, calc. using extrapolated estimate 79−86909
ice Ih, polycryst., Raman spectra, OH stretching region 79−11410
ice IV, thermal expansion anomaly rel. to order/disorder transition at 115K, 10.54 kbar 79−46819
ice surface, liquidlike layer, thermal expansion meas. 79−19381
ice surface layer, viscosity, from thermal contraction meas., 0 to −50°C 80−49469
ideal gases, solns., basic props. kinetic derivation from elastic collision processes 78−91048
III-V crystals, thermally enhanced diffusion of point defects near dislocations during device operation 79−90820
inorganic crystals, glasses, thermal expansion coeff. rel. to phys. props. 80−49389
insulating materials, thermal expansion, Morse pot. model 80−107449
insulator, thermal expansion, empirical determ. with no exptl. input 80−107450
interferometric measurement 78−45676
intermediate valence compound, pressure-temperature phase diagram 79−28283
Invar, Fe-Ni (36 wt.%), alloy 36N, effect of melting conditions on thermal expansion coeff. 80−65256
Invar, local moment model 79−56505
Invar, mag. phase transitions, linear expansion coeff. and mag. susceptibility meas. 77−69553
Invar, magnetic structure, depend. on absorbed H, Stoner's band model calcs., Mossbauer spectra 80−65787
Invar, stainless, thermal expansion, elastic props. and Mossbauer effect 79−56502
Invar, ternary alloys based on Cr-Fe and 4d transition metals, magnetically insensitive 77−28026
Invar, thermal expansion coeff. relationship to magnetisation 80−15269
Invar, ultraprecise meas. 77−1247
Invar alloy, thermodynamic properties, effects of forced magnetostriction 79−11331
ionic crystal, defect formation volume, temp. and press. depend. 78−26563
isobutyric acid+water, thermal expansion near upper crit. soln. temp. 77−29031
isobutyric acid-H_2O, crit. mixture, partial molar vol., temp. depend. 78−18800
isotropic solids, size of thermal expansion coeffs. at low temps. 77−84954
itinerant electron ferromagnetism, press. effects on mag. props. 77−66241
itinerant ferromagnet, magneto-volume ext. 77−66404
ketone-paraffin solid soln., dielec. relax., temp. and lattice const. depend. *(German)* 78−76383
Kevlar/epoxy composites, elastic props. rel. to thermal expansion 80−24622
Kovar, effect of magnetic electrons on atomic interactions 77−43820
laser glass cladding composition and design criteria 79−18450
laser window materials, temp. and stress effects on refr. index 77−46771
lecithin bilayers, density and mol. interactions 78−80837
Lexan, optical and phys. parameters 79−32004
linear thermal expansion coeff. unit, 4.2 to 90K, USSR state standard 78−37001
$LiNO_3.3H_2O(3D_2O)$, density, thermal apansion coeff., isotope effect 78−87733
liquid, Rao's acoustical constant, temp. depend., from C_1-parameter 80−6462
liquid crystal, isotropic phase, compressibility and thermal expansion anomalies, appl. to MBBA 77−43138
liquid metal, thermophysical properties meas. by submicrosecond-pulse-heating method 80−52220
liquid metals, mixing volumes, pseudopotential method 79−37846
liquid surface deform. due to laser radiation thermal action, lens effect 80−33048
LMFBR, thermal expansion worths inferred from small sample reactivity meas. 78−29596
MBBA, nematic-isotropic transition, isothermal compressibility and thermal expansion coeff. meas. 79−99301
MBBA, volume meas. and phase transitions at high press. 79−90764
metal, allotropic transform., anharmonicity, effects due to thermal expansion and Gruneisen parameters 79−52207
metal, monovalent, low temp. eqn. of state 78−22820
metal, one component substances, surface energy, temp. depend. 77−72753
metal, thermal expansion and melting 77−69103
metal, thermal expansion coeff. of defect-entropy volume 78−26707
metal, thermodynamic properties, outer electron contributions *(French)* 78−43091
metal film, effect on temp. coeff. of resist. 78−43489
metal matrix composites, thermal expansion effects, fibre length depend. 78−51708
metallic elements, bond energy rel. to thermal expansion coeff. *(Chinese)* 79−14946
metallic glass, density and Young's modulus, struct. relax. effects 78−72804
metallic glasses, mats. props. review 77−4043
metallic thin films, thermoelectric power, thermal stress effects, theory 80−65714
metals, atomic interaction force characts., association with struct., mech. props. 80−49172
metals, Morse potential appl. in molecular-metallic framework 80−79742
metals, positron response to thermal expansion 80−84306
metals, rel. to temp. depend. of elec. resist. 80−51967
metals, simple, expansion coeff. rel. to heat capacity 77−43354
methane, solid, thermal expansion and conversion processes *(Russian)* 78−95163
methane, solid, thermal expansion coefficient and Gruneisen parameter 78−47540
methane, solid, with O_2 and N_2 impurities, thermal expansion, 2 to 14K, conversion processes 79−65228
methane-d_4, solid, lattice parameters and thermal expansion for different phases 78−51526
methane-d_4, solid, thermodynamic props. calc. using significant structures method, 6 to 87K 80−24616
methanol-cyclohexane, mixture, thermal expansion near crit. soln. point 78−71871
methanol-$d_3(d_1)$ in freon 11, self-associated, OH frequency temp. depend. 80−37809
microcline, maximum room temp. phase transition, unit cell parameters, thermal expansion 80−54208
microwave absorbing ferrite-dielectric composite 77−7880
microwave irradiated materials, rel. to acoustic-signal generation 78−24095
microwave resonant cavities, thermal expansion correction methods *(French)* 77−61087
minerals relevant to Earth interior geophysics, Hildebrand equation of state 80−56464
mixed valence compounds, anomalous thermal expansion 79−77783
mixed valence compounds, phase diagrams, lattice props., electron hole symmetry 79−91002
molecular solids, intermol. forces and eqn. of state, pseudoharmonic approx. calcs. 78−30731
mullite ceramic rollers, heat treatment effects 79−61616
mullite-corundum electroceramic, thermal expansion coeff. meas., 80-300K 79−60526
multilayer film, intrinsic and thermal stress modelling and interferometry 79−14059
Nafion, densities and expansion coeffs. as function of various parameters 80−79711
NASICON solid electrolyte, processing and phys. props. 80−60820
Nb, influence of plastic strain on thermal expansion *(Russian)* 79−65220
nematic planar liquid crystal, nonlinearities close to thermal threshold 79−99058
nitrocellulose-nitroglycerine propellant, glass transition temp., thermomech. anal. meas. 79−14917
nondeterministic thermal deformations of structures temp.-dependent material props. 77−65679
nylons, glass transition temp., thermal, mech. meas. 77−31758
oblate spheroidal inclusion, internal stress, misfit, inhomogeneity and plastic deform. 78−60701
oil shales, review of thermophysical properties 79−100479
optically uniaxial and biaxial crysts., thermal strain 78−46733
organic compounds, high-press. expansivity determ. by piezo-thermal anal. 77−72705
organic impurity crystals, press. effect on shift of zero-phonon lines 79−95824
oxamide, thermal expansion tensor, calc. from lattice constant changes with temp. 77−76582
oxide glasses, thermal expansion coeff. calc. from chem. comp. 77−11710
oxide minerals, characterisation technique 79−70795
oxide minerals, elastic constant systematics 79−69177
oxides, low expansion, common structural features 78−83981
paraffin, polymer modelling, mol. motion, thermal expansion and phase transitions 78−51436
paraffin crystals, molecular motion, thermal expansion and phase transitions *(German)* 78−67837
phase form. and relations, phys. props. 79−43218
phenanthrene birefr. changes due to thermal expansion 78−52468
phenol formaldehyde resin reinforced with chrysotile asbestos fibres 79−55908
phenol-formaldehyde resin, thermodynamic props. 78−91452
phosphate glass, thermal expansion and chem. durability 77−80636
phosphate glass-Al alloys seals, elec. and mech. props., glass transition 80−81018

thermal expansion continued
phosphate glasses, opt. and thermo-opt. props., calc. from chem. comp. 79−65826
plastics and reinforced plastics, tabulated data as design guide 77−21087
plate, thin, circ., quasistatic normal deflection due to time depend. heat-source distrib. 79−37145
plate temp. dependent props. under linear temp. distrib., thermoelastic problem for crack 80−48579
Plexiglas 55, optical and phys. parameters 79−32004
PMMA, amorphous, tunnelling models and thermal expansion below 4K 79−73326
PMMA, glassy, thermoelastic effect, thermal expansion coeff. 79−14944
PMMA, Gruneisen const. and thermal props., temp. depend., 4-300K, Brillouin scatt. obs. 80−100662
poly-1,6-di-N-carbazolyl-2,4-hexadiyne, synthesis, thermal expansion, photocond., optical transition 78−76858
polyalkaneimide, mech. and thermophys. props. at liq. He temps. 80−3117
polyamide, Al_2O_3 filled, low temp. thermal and mech. props. 80−25816
polyamides, 1,3-cyclohexanebis(methylamine) based, thermal props. and glass transition temp. 80−39264
polybutadiene, carboxyl-terminated, glass transition temp., thermomech. anal. meas. 79−14917
polycarbonate, bisphenol A, WAXS pattern, temp. effect and thermal history 80−93583
polycarbonate, glassy, thermoelastic effect, thermal expansion coeff. 79−14944
polycrystalline films, grain boundary reflection coeff. thermal expansion effect on resistivity temp. coeff. 79−91162
polycrystals with axial texture, heterogeneity of props. *(Russian)* 80−29192
polydiacetylene-bis(toluenesulphonate), single cryst., thermal expansion and optical band splitting 77−8594
polyethylene, high density, temp. change associated with adiabatic compression 77−66685
polyethylene, high density extruded fibres, morphology effect on physical and mech. props. 79−83235
polyethylene, hydrostatically extruded, linear, thermal expansion behaviour 79−77776
polyethylene, oriented, thermal expansion 77−7881
polyethylene, orthorhombic and triclinic lattices, eqns. of state 79−28069
polyethylene, transcrystalline, anisotropic thermal expansion 79−4420
polyethylene, ultraoriented high-density, annealing characts. 77−8852
polyethylene fibres, high density, ultra oriented, physical, mech. props. 80−25649
polyethylene spherulites, thermal expansion 78−2268
polyethylene terephthalate, glass-rubber transition determ., small-angle X-ray scatt. 78−95145
polyethylene terephthalate fibres, interdependence between struct. and thermal contraction *(Rumanian)* 78−91259
polymer, filled, thermal expansion, effect of particle shape at finite conc. 79−19384
polymer, oriented crystalline, anisotropic thermal expansion 80−39324
polymer, rigid, prefractured states study, elastic limit and strength 77−70092
polymer film, space charge, thermal expansion and pyroelectricity 77−4603
polymers, equation of state *(German)* 79−82309
polymethylsiloxane-2, liq., thermodynamic props. at high press., US propag. meas. *(Russian)* 80−65157
polyolefines, filled, struct.-mech. props. relation *(German)* 78−35451
polyoxymethylene, rel. to dielec. relax. in glass transition region *(Russian)* 77−69770
polypropylene, orientated, loose fitting tube for optical fibre packaging 78−1338
polystyrene, glassy, thermoelastic effect, thermal expansion coeff. 79−14944
polystyrene, microcryst. cellulose filled, glass transition temp. shifts 78−95144
polystyrene film formed by RF electrodeless excitation, dielec. props. 77−24795
polystyroles, filled, struct.-mech. props. relation *(German)* 78−35451
polyurethane foam, rigid, thermal expansion behaviour, mech. differential dilatometer method *(German)* 79−37859
polyvinylidene fluoride, elastocalorific effect and thermal expansion *(French)* 79−46818
polyvinylidene fluoride, film, piezoelec., pyroelec., thermal expansion, elastic consts. 78−84529
polyvinylidene fluoride, thermodynamical model, applications *(French)* 80−39315
porcelain wave, crazing resistance, glaze fitness *(Japanese)* 79−74278
porcelain-metal cermet, stress determ., meas. method *(German)* 80−76425
potassium acetate, thermal expansion 79−51280
proustite-pyrargyrite solid solns., thermal props. *(Russian)* 79−65227
PVA, microcryst. cellulose filled, glass transition temp. shifts 78−95144
PVC, filled, struct.-mech. props. relation *(German)* 78−35451
PVC, glass-rubber transition determ., small-angle X-ray scatt. 78−95145
pyrazine, thermal expansion tensor determ. 77−15600
pyrocarbon, lamellar material, thermal expansion meas. appl. of interlayer spacing X-ray diffr. technique *(French)* 77−20096
pyroceramic end gauge, high-precision stability 79−76778
PZT, polycrystn., thermal expansions, elasticity and internal friction 80−35238
quartz, electroded doubly-rotated thickness-mode resonators, temp.-induced frequency 79−55298
quartz, glassy, thermal expansion coeffs., represented by Gaussian spline polynomials 80−44341
quartz, thermal expansion near α-β transition under uniaxial stresses 80−70429
quartz tube, fused, in a dimensional stability test facility 79−58779
rare earth alloys, cryst. field effects on thermal props. 77−12072
rare earth alloys, RCo_2 and R_2Fe_{17}, Invar props. 79−56593
rare earth and transition metal oxides and fluorides, thermal expansion and MP correl. 77−47605
rare earth borides, higher types, phys. props. and electronic struct., group orbitals-LCAO calcs. 80−20077
rare earth compounds, binary, regression eqns., for calc. props. from electron struct. 80−39498
rare earth compounds, hexagonal, cryst. field effect in thermal expansion 80−49390
thermal expansion continued
rare earth dihydrides, lattice thermal expansion and point defect form. energy 77−51524
rare earth metal, electron interactions rel. to lattice props. *(Russian)* 77−35901
rare earth metals, preparation methods and properties, review 79−69969
rare earth monobismuthides, thermal expansion, thermal cond., 300-900K 78−91453
rare earth oxides, binary, struct. and props., book contrib. 80−45292
rare earth RNb_3O_9, synthesis and physicochem. props. 77−90304
rare earth systems, metallic, with unstable valence, model for thermodynamic props. 77−69487
rare earth-Al, RAl_2, spontaneous cell distortion due to cryst. field, magnetoelastic consts. 77−63255
rare earth-Al Laves phase intermetallics, RAl_2, R=Gd, Ho, Dy, Tb, cubic Laves phase compounds, exchange striction determ. 80−44895
rare earth-cobalt intermetallics, RCo_2, spontaneous vol. magnetostriction and thermal expansion meas. 77−12183
rare gas (111) adsorbate-substrate systems, stability, soft phonons 79−69352
rare-earth germanides, R_5Ge_3, thermal expansion, phase transition effects 80−70433
reactor fuel vapour expansion work energy calcs., effect of eqn. of state uncertainties 78−8940
reactor large-bundle LOCA expts., fuel rod ballooning probabilistic analysis 79−13462
reference data: 1-1000K 80−96669
refractories, graphitised and C-containing, thermal expansion 79−82362
refractories, thermal stress cracking resistance estimation 80−104288
refractory curvilinear lining, thermal stresses 78−5649
refractory material, with phosphate binder base, filler content and temp. influence on strain and thermal expansion *(Russian)* 80−19964
refractory materials used in MHD generator channels, thermophysical props. 77−28054
Rochelle salt, low temp. phase transition, dilatometric exam. 77−11691
Rochelle salt, thermal expansion and spontaneous strain meas., −40 to 40°C, electrostrictive consts. 77−16262
rock, thermal expansion expts. at high-press. 80−21719
rocks, compressional and shear wave velocities under high press., effect of high-low quartz transition 80−12380
rocks, effect of cracks on thermal expansion 78−28218
rod, expanding, conductive heat transfer computation, fast numerical technique 78−75029
rubber, natural, thermal properties depend. on temp. and press. 79−95223
semiconductor, diamond-like, adiabatic pot. in quasi mol. model 78−2063
semiconductor, tetrahedral, thermal expansion and MP, ionicity and bond length effects 77−47606
silicate glass, Li_2O and Na_2O effect on thermo-optic props. 78−18029
silicate glasses, longit. and transverse elastic wave vels., temp. and comp. variations 80−88258
silicate glasses, mixed-alkali, thermal expansion 77−4186
silicate minerals, characterisation technique 79−70795
silicate minerals, elastic constant systematics 79−69177
simple fluids, hard-core equations of state, C_p extrema loci 79−60474
simple liquids, thermodynamic props. and solubility parameters 78−2265
single phase system, microfracture from thermal expansion anisotropy 79−19314
slab, surface displacements for high speed rubs 80−83767
sliding contact seal, thermoelastic instabilities 78−18257
solid, difference and average temp. linear expn. coeffs. 80−24620
solid, thermal expansion at high temp. *(French)* 78−55960
solid state phase transformations, thermodynamic relations, appl. to K_2ReCl_6 80−29164
solids, equivalence of Gruneisen and Brillouin theories *(French)* 79−77773
specific heat, const. press., press. variation of vacancy contrib. 79−1510
β-spodumene-mica glass ceramic, thermal expansion thermal shock and moduli of rupture and elasticity 78−60736
squaric acid, hydrostatic press. effect on phase transition, dielec. and dilatometric meas. 78−55941
steatite electroceramic, thermal expansion coeff. meas., 80-300K 79−60526
steel, 12X2H4A, nonmetallic inclusion effect on plasticity and impact strength *(Ukrainian)* 78−92296
steel, austenitic, heavily doped, linear expansion meas. 80−103501
steel, austenitic, Mn and Mn-Cr *(German)* 77−59127
steel, austenitic stainless, ferrite volume fraction, high-speed determ. by XDXRD 78−76628
steel, die type 5KhNM, stressed state effect on softening 79−66168
steel, ferritic, underclad cracking mechanism, effects of residual strain and heat affected zone ductility 77−25158
steel, high heat resist., tool, density and extension coeff. *(Russian)* 79−51282
steel, martensitic, heavily doped, linear expansion meas. 80−103501
steel, Mo and Cr-Mo, X-ray elasticity constants at high specimen temp. *(German)* 80−35239
steel, Ni-Cr, 36NKh, thermal expansion under stress at −253°C 78−22871
steel, nonmetallic inclusion segregation during cooling *(Russian)* 80−100330
steel, solidification singularities in C and low-C steels *(Russian)* 78−80532
steel, stainless, type 1.4970, density, thermal expansion 79−65223
steel fibre reinforced Al, thermophys. props. 80−59745
steel finite life characteristics, temperature change effects, torsion cycle tests *(German)* 78−7004
stycast 1266 epoxy, thermal contraction, 4-300K 80−4724
styrene-sodium methacrylate copolymers, linear expansion coeffs., ionic groups conc. depend 79−42284
substitutional impurities in solids, entropy and volume of solution 80−15253
superconducting state, model for electronic contrib. to thermal expansion 78−80094
TBBA, smectic polymorphism *(French)* 77−35470
tellurite glasses, binary, struct. and props. *(Japanese)* 79−32917
TGS, crit. behaviour of thermal expansion, neutron diffr. study 80−75371
TGS, critical behaviour in thermal expsn. coeff. and dielectric const. 79−91334

thermal expansion continued
TGS, elastic vs. polarisation energy near transition 78−15118
TGS, ferroelec., thermal expansion 79−37855
TGS, thermal expansion and dielec. const. near ferroelec. crit. temp. 77−40188
TGS, thermal expsn. coeffs. log. anomaly 79−28112
thermal stress distribution associated with elastoplastic deform. 77−19549
thermobimetal, specific bending, effect of functional parameters and stabilizing heat treatment 77−89555
thermoelastic expansion flexible acoustic probe 80−16618
thiophenechromium tricarbonyl, sp. ht. and thermal expansion tensor meas., order-disorder phase transform. obs. *(French)* 78−79788
thiourea, expansion coeffs. in phase transition range 78−76407
TNT, creamed, expansion and contraction during thermal cycling 79−73316
transition metal alloys, AFe_2 and ACo_2, Invar effect, magnetovolume meas. 79−56592
transition metal alloys, magnetovolume effects near crit. conc. for ferromag. 79−56591
transition metal borides, higher types, phys. props. and electronic struct., group orbitals-LCAO calcs. 80−20077
transition metal carbides, Group IV-VI metals, thermal expansion coeff., rel. to bond energy 78−2266
transition metal silicides, group IV, thermal expansion, microhardness, Debye temp. meas. 77−35717
transition metal silicides, refractory for ICs, review 80−100820
transition metals, thermophysical data at high temps., submicrosecond-pulse-heating method 80−103459
trident seal, thermal expansion differential test 79−61815
tridymite, thermal expansion meas. 80−59682
triglycine sulphate, paraelec. phase, thermal expansion coeff. and dielec. constant 79−8100
TTF-TCNQ, metallic conductivity press. depend. thermal expansion effects 79−69502
undirectional fibre composites, anisotropic constituents, effect elastic moduli and other props. 80−58911
uniaxial crystals, third-order elastic consts., low temp. limit of thermal expansion 80−65119
unidirectional composites 78−67836
urea-oxalic acid (1:1), X-ray cryst. struct. determ. and thermal expansion 79−46645
vacancy effects, temp. depend. of thermal expansion coeff. 80−79962
vanadocene, order-disorder phase transition, sp. ht. and crystallographic study *(French)* 80−84131
Vespel SP-22 resin, thermal contraction, 4-300K 80−4724
Vicalloy 1, dilatometric anomalies and α to γ transform., effect of heating rates *(Russian)* 78−39762
vitreous china, crazing tendency, rel. to thermal expansion and quartz and cristobalite content *(Japanese)* 78−44243
water, liquid, physical props., two-state model approach 80−75144
water, temp. of maximum density, solute effects and partial molal expansibility 77−24256
window glass, temp. depend. of coeff. of thermal expansion rel. to const. fictive temp. 78−67839
Zerodur, glass-ceramic, thermoelastic props. 78−27550
Ag film, vacuum-deposited, removed from substrate, internal strain *(Japanese)* 78−22872
Ag, low temp. eqn. of state appl. to thermal expansivity 79−60476
Ag, simple eqn. of state appl. 77−27970
Ag, vacancy formation energy, thermal expansion meas. 79−14798
Ag-Au (50 at.%), thermal expansion and lattice parameters, temp. depend. 78−91456
Ag-Ge, thermal expansion, X-ray determ. 78−26697
Ag-Hg amalgam, lattice const., temp. depend., explained in terms of Hg evaporation 78−26704
α-Ag-In solid solutions, lattice dynamics parameters *(Russian)* 80−96477
Ag-Mn, dil., anomalous thermal expansion below 50K 78−51710
Ag-Zn (27-48 wt.%), interphase β'-ζ transform., thermal expansion exam. 77−63630
$AgClO_3$, NQR and thermal expansion investig. of phase transform. 77−12229
$AgGaSe_2$, seeded Bridgman growth of crack-free crysts., thermal expansion coeff. 78−11101
β-AgI, thermal expansion, 4 to 270K 80−79961
AgI, thermal expansion under press. 80−92690
Ag_2O, thermal expansion, lattice parameter determ., 150-250K 78−2267
Ag_8SnSe_6, phase transition, thermal expansion meas. 78−14466
Al, 5 to 320K, using dilatometer of parallel-plate capacitor type 77−51523
Al alloy, 51S, modified by misch metal, for space appl. 80−55466
Al, irradiation defects, intrinsic thermal expansion meas. 79−95186
Al, low temp. Gruneisen parameter 79−23694
Al, molten, thermal expansion meas. to 1300K 80−65254
Al, simple eqn. of state appl. 77−27970
Al, vacancy formation energy, thermal expansion meas. 79−14798
Al-Pb solid solution, 10-55K *(Russian)* 77−80635
Al-Si-Cu-Ni alloy casting, thermal props. 78−95814
Al_3Ce, thermal expsn. below 1K 79−90803
$Al_{10.4}Ga_{0.08}V$, low temp. thermal expansion 78−95167
AlN-Al_2O_3 composites, hot-pressed 77−52275
Al_2O_3, 20-100-1700°C, as standard samples for dilatometry 78−26699
Al_2O_3 based electroceramic, thermal expansion coeff. meas., 80-300K 79−60526
Al_2O_3 ceramic, thermal expansion coeffs., represented by Gaussian spline polynomials 80−44341
α-Al_2O_3, monocrysts., temp. depend., 28-800°C 79−82361
Al_2O_3-B_2O_3-P_2O_5 glasses, formation and props. 78−83737
Al_2O_3-Cr_2O_3, solid soln., thermal expansion anisotropy, lattice consts. 80−54411
Al_2O_3-Fe cermet, microstruct. and physical props. 79−42279
β-Al_2O_3-K_2O/K ferrite, interfaces and solid soln., thermal expansion and lattice parameter variations 78−55959
β-Al_2O_3-Na_2O, thermal expansion 79−55910
β''-Al_2O_3-Na_2O solid electrolyte, processing and phys. props. 80−60820
Al_2O_3-SiO_2-Cu_2O glasses, Grueneisen's constant of low expansion 79−77779
Al_2SiO_5 polymorphs (sillimanite-andalusite-kyanite), thermal expansion and high-temp. cryst. chemistry 80−39319

thermal expansion continued
Al_2TiO_5, grain size pseudobrookite oxide, microcracking relations 79−29194
$Al_{10}V$, low temp. thermal expansion 78−95167
Am metal, dilatometry and thermal anal., melting point, transformation regions 79−43241
Ar monolayer film adsorbed on graphite, thermal expansion and neutron diffr. study 78−34705
Ar, solid, equilib. props., uncorrel. pairs approx. 80−84303
Ar, solid, high-temp. thermal expansion characts. 80−59680
Ar, solid, self consistent field calcs. of isotherms and thermodynamic props. *(Russian)* 80−10633
Ar, solid, vol. depend. lattice dynamics, pseudo-harmonic approach 79−99260
As, Debye-Waller factors and thermal expansion 78−43089
As-S-Tl, glass, viscosity and elastic props. 80−100180
As-Se system glasses, free vol. at transition temp. *(Japanese)* 79−55876
As-Se-Te glasses, glass form., charact. temp., density, thermal expansion and dynamical viscosity, struct. model 78−26672
$AsO_{3/2}$-$BO_{3/2}$, glass, props. and struct. *(Japanese)* 77−27836
As_2S_3-PbS glasses, structural props. 79−27925
$As_2S_3(Se_3)$, thermal expansion at low temperatures 78−83982
Au, fine particles, gas evaporation technique for prep., X-ray diffr. study 80−75327
Au, low temp. eqn. of state appl. to thermal expansivity 79−60476
Au, simple eqn. of state appl. 77−27970
Au, thermal expansion coeffs., Morse pot. calcs. 79−77775
Au-Pd-Pt-Ag, composition-property diagrams, mathematical models for diagrams *(Russian)* 79−11554
B fibre reinforced Al, thermal expansion 77−51525
B fibre reinforced Al, thermophys. props. 80−59745
B fibre reinforced epoxy and Al, cryogenic tensile, compressive and shear props. 78−6983
B filament, uncoated and SiC coated, high temp. physicomech. props. 79−20140
B_4C, mech. and thermal props. 80−21083
B_4C, thermophysical props. and neutron absorpt. 80−103488
BN films, elastic stiffness and thermal expansion 80−49559
B_2O_3 and alkali borate glasses, Raman study at high temps. 80−93306
B_2O_3-V_2O_5-P_2O_5, glass, mech. and elec. props 80−84228
B_6O, mech. and thermal props. 80−21083
$(Ba,Sr)TiO_3$, ferroelec. props., press. depend., anharmonic oscillator model 80−80716
BaF_2, linear thermal expansion coeff., capacitance method meas. 78−16772
$BaGeO_3$-$(0.25MgF_2.0.75YF_3)$-Ga_2O_3 glass, synthesis and props. 80−25648
$Ba(NO_3)_2$, Born-Mayer interaction pot. and lattice props. 79−37858
$Ba_2NaNb_5O_{15}$, Gd substitution, effect on linear thermal expansion, possible BSN replacement 78−43153
BaO single crystal, temp. depend. of bulk modulus 78−27549
BaO, temp. depend. of thermal expansivity between 20-300K 79−77778
BaO-Al_2O_3-SiO_2-Ta_2O_5-Mo glass ceramic metal composites, cermet prep. 80−11618
BaO-Al_2O_3(PbO)-GeO_2-MF_2 (M=0.45CaF_2+0.55MgF_2), MgF_2 and CaF_2 effect on physicochem. props. 80−34876
BaO-B_2O_3-GeO_2, exam. of glass formation and physicochemical props. 79−4959
$BaPO_3F$-Al_2O_3-B_2O_3 glasses, phys. props. 78−63676
$BaR_2(MoO_4)_4$, (R=Nd,Eu), struct., optical, mech., spectral and physicochem. props. 80−84161
$Ba_2Si_2TiO_8$, elastic consts., thermal expansion and piezoelec. props. 77−85651
$BaSnF_4$, thermal expansion and phase transitions 79−77781
$BaTiO_3$, X-ray diffr. intensities, anomalous temp. depend. *(Russian)* 79−1484
$BaTiO_3$:Dy ceramic, sintering, grain size, characterisation and props. 77−55923
$Ba_2TiSi_2O_8$, fresnoite, Czochralski growth and phys. props. 78−3026
Be intermetallics, MBe_{13}, (M=Y, La, Ce, Lu, Th), lattice spacings and susceptibilities 80−65778
Be, sintered, physicomech. props. anisotropy, BeO inclusions effect 80−60804
Be-Cu, vibr. characteristics at low temp., effect of substitution impurities *(Russian)* 80−103439
$BeAl_2O_4$, Czochralski grown single crystal, hardness, thermal expansion, concl., elastic const. 79−52353
$Be_3Al_2(SiO_3)_6$, thermal expansion study 79−37857
BeF_2 glass, glass transition temp. and thermal expansion 80−64902
Bi, Debye-Waller factors and thermal expansion 78−43089
Bi, equilib. vacancy conc., thermal expansion meas. 77−59007
Bi, liq., US vel. and thermophysical props. meas., 500-1000K 78−38778
Bi, temp. depend. of positron annihilation parameters 78−76553
$Bi_{12}GeO_{20}$, elastic and piezoelectric consts., thermal expsn. 78−31157
$3Bi_2O_3.5B_2O_3$, thermal expansion coefficient 79−10924
C fibre reinforced Al, mech. props. 80−11708
C fibre reinforced C, processing, room temp. mech. props., and low temp. expansion 80−25820
C fibre reinforced C composites, exam. of thermal expansion 79−1513
C fibre reinforced composites for spacecraft use, prep., props. and struct. 80−71625
C fibre reinforced Cu, thermal expansion and thermal fatigue *(Russian)* 79−38936
C fibre reinforced CuO-H_3PO_4 effect of C fibre on props. 79−43192
C fibre reinforced epoxy resin, thermal expansion, influence of fibre type and orient. 77−35722
C fibre reinforced epoxy resin, in low temp. ranges 78−83978
C fibre reinforced epoxy resin composites, 2 to 290K 79−60528
C fibre reinforced plastic, epoxy resin DLS 351/$BF_3$400 90-500K, fibre vol. fraction effects 78−26703
C fibre reinforced plastic, influence of resin type 78−95164
C fibre reinforced plastics, ply multidirectional effects 78−95165
C fibre reinforced plastics, thermal expansion, matrix curing effects 79−55909
C fibre reinforced resin, optimisation of thermally stable structures using holographic interferometry *(German)* 79−90804
C fibres, coeff. of linear thermal expansion, sag method for determ. 79−77774
C, polygranular, flexural strength after heat treatment porosity correl. 80−84996
C reinforced plastic, degraded, study of strain, 20 to 1000°C 80−71680

thermal expansion continued
C-C composite material, syntactic-foam type properties 78−44169
$C_{12.6}AuCl_3$, intercalation compound, struct. *(French)* 78−42982
CO_2-N_2-H_2O mixture, unstable-oscillatory expansion *(Russian)* 78−1637
CaBr(Cl)(I), Gruneisen γ and other thermodynamic props. at zero and elevated press. 78−43142
$CaCeAl_3O_7$, melilite struct., prep. and props. 80−93524
$CaEuAl_3O_7$, mechanism of solid-phase reactions of formation and physicochem. props. 77−52622
CaF_2, fluorite, use as standard specimen 80−96704
CaF_2, linear thermal expansion coeffs. meas., room temp. to 250°C 78−55416
CaF_2, optical material, 60-300K 78−33791
$Ca_2Nb_2O_7$, ferroelectric phase transitions, dielec. constant and thermal expansion rel. to temp. 80−88934
CaO-B_2O_3-GeO_2 system glass, physicochem. props., alkaline earth oxides effect 79−65827
CaO-Fe_2O_3-B_2O_3 glasses, phys. props. rel. to struct. and comp. 78−23331
CaO-Ga_2O_3-Bi_2O_3, vitrification regions 77−15557
CaO-SiO_2-MnO system, melts, densities, molar vols., thermal expansivity *(French)* 79−51183
$CaO.Al_2O_3$, thermal expansion 77−84953
$CaSO_4$, thermal expsn., 22-1000°C 80−6530
$CaSiO_3$ fibrous crystal reinforced matrix, unidirectional crystallization, anisotropic properties 79−56969
$Ca_2V_2O_7$, $Ca(VO_3)_2$, and $Ca_3(VO_4)_2$, thermal expansion, lattice constants temp depend. 80−34211
Cd, anisotropic thermal expansion 79−23750
Cd, liq., US vel. and thermophysical props. meas., 500-1000K 78−38778
Cd, temp. depend. Knight shift 80−2655
Cd-Bi, liq., US vel. and thermophysical props. meas., 500-1000K 78−38778
Cd_3As_2 and $CdAs_2$, molten, thermal expansion and atomic bond strength parameters 80−65257
$CdCO_3$, thermal expansion temp. depend. 78−18803
$CdCr_2S_4$, thermodyn. props. 78−51703
$CdGa_2Se_4$, linear expansion anisotropy 79−86910
$Cd_{65}Hg_{35}$ and $Cd_{55}Hg_{45}$, X-ray study of cryst. struct. and thermal expansion 80−24405
$CdSiP_2$, bond strengths and bond lengths, thermal expansion coeff. meas. 78−87651
$CdTl_2Te_4$, single and polycryst. samples, linear expansion, heat capacity and thermodynamic props. 80−103489
Ce binary and pseudobinary intermetallics, struct. and mag. data 80−20129
Ce compounds, rocksalt type, low temp. thermal props. 78−84445
Ce, polymorphic $\gamma \rightleftarrows \alpha$ transform. and volume anomalies under press. 80−34189
$CeAl_2$, Anderson lattice system, thermal expansion meas. 1.5 to 10K 79−37860
$CeAl_2$, Anderson lattice system, ground state props. 80−20443
CeB_6, magnetostriction, US absorpt. and thermal expansion 80−66004
CeBi, thermal expansion, 20-800°C 79−14942
$CeIn_{3-x}Sn_x$, electrical resist. and thermal expansion meas., 1.5-300K 80−34400
CeP(As), single crystals, low temp. thermal, electrical and mag. props. meas. 78−27051
$Ce_{1-x}Pr_xAl_2$, mixed mag. phase at low temp. 78−68228
CeS, mag. props., sp. ht. and thermal expansion 78−60292
CeSb, crystal field effect in thermal expansion 78−19305
CeSe, mag. props., sp. ht. and thermal expansion 78−60292
CeTe, mag. props., sp. ht. and thermal expansion 78−60292
CfI_3, X-ray diffr., optical spectra, thermal expansion coeffs., 20 to 700°C 78−75645
Co, ferromagnetic, anomalies in thermal expansion and heat capacity 79−73744
Co, impure, thermal cond., resistivity, total and spectral emissivity, linear expansion coeff., 300-1700K 77−47790
Co, magneto-volume effects calc., rel. to itinerant electron model 78−43621
Co, thermal expansion and bulk modulus 77−31788
Co-Cr-Al-Y coatings, hot corrosion resist., thermal expansion coeffs. 79−24674
Co-Fe (2.92 to 30.05 wt.%), determination of phase equilibrium diagram *(Japanese)* 78−48374
Co-Fe alloy, Invar characts. 77−1550
Co-Sn, dil., ferromag., temp. anomalies of Sn mag. hyperfine field and thermal expansion 79−33270
Co-W-C system, η-carbide linear expansion coeff., X-ray diffr., 30-1500°C 77−25021
CoB, thermophysical props., 296-2000K 78−14477
$CoCr_2O_4$, thermal expansion 79−73327
$CoFe_2Se_4$, low-temp. thermal expansion anomalies and isothermal compressibility, mag. ordering and magnetorestriction 79−38363
CoS_2, ferromagnet, elec. resist. and thermal expansion anomalies 80−15542
CoSb alloys, sp. ht. and thermal expansion 77−47587
$CoSiF_6.6H_2O$, anomalous thermal expansion near transition temp. 78−47516
$Co_{2-y}Zn_yTiO_4$, cation distrib. and mag. props. 78−14939
Cr, linear expansion coefficient, at low temp. 78−83977
Cr-Co, phase transformations and magnetostriction *(Russian)* 80−103869
Cr-Fe alloys, polycrystalline, antiferromag., elastic moduli and thermal expansion meas. 77−43860
Cr-Fe-Co dilute alloys, Neel temp., thermal expansion rel. to Co content 79−47281
Cr-Ga alloys, dil., Neel temp., elec. resist. and thermal expansion meas. 79−51778
Cr-Ge, dilute alloy, phase diagram of spin density wave states 79−24158
Cr-Mn, order of mag. transitions in antiferromag. alloys 79−4677
Cr-Re, dil. alloy, mag. susceptibility temp. depend., thermal expansion coeff. *(Russian)* 78−76225
Cr-Re, phase transformations and magnetostriction *(Russian)* 80−103869
Cr-Re(Ru)(Os)(Ta)(V)(Nb), Invar alloys, thermal expansion, plasticity *(Russian)* 79−55907
Cr-Sb alloy, dil., mag. phase diagram, elec. resist. and thermal expansion obs. 79−1669

thermal expansion continued
Cr-Si, magnetically insensitive Invar-type alloys *(Japanese)* 79−8034
Cr-Si alloys, first order transition of spin density wave state, thermal expansivities meas. 77−85453
Cr_2O_3, magnetostriction anomalies near mag. field induced transitions 77−66315
$CrS_2(Se_2)$, physical props. 80−44179
$CrTe_{1+x}$, thermal expansion and spontaneous magnetostriction *(Russian)* 78−48017
CsBr, thermodynamic props., lattice dynamical calc. 77−20090
$CsCaCl_3$ crystal, sp. ht. and thermal expansion coeffs. 80−10681
CsCl, thermal expansivity determ. at high press. 78−79787
CsH_2PO_4, Raman scatt. and high temp. props. 80−16024
CsI, thermodynamic props., lattice dynamical calc. 77−20090
$CsMnCl_3.2H_2O$, diagonal elastic const., thermal expansion coeffs., ultrasonic velocity meas. 80−79853
$CsMnF_3$, mag. phase boundaries, XY to Ising crossover, virtual bicritical point 80−50095
$Cs_2NaM^{3+}Cl_6$ (M^{3+} = Bi,Nd,Pr), ferroelastic phase transitions, thermal expansion, elasticity, and X-ray anal. 80−70393
$CsNiCl_3$, linear-chain antiferromag., low temp. thermal expansion 80−39326
$CsPbCl_3$, elastic constants and thermal expansion, near struct. transitions 78−59849
$CsPbCl_3$, lattice thermal expansion, X-ray powder technique 80−19965
Cu, 300-700K, standard material 78−43152
Cu, 5 to 320K, using dilatometer of parallel-plate capacitor type 77−51523
Cu (001), surface relax. and thermal expansion calcs. 79−23820
Cu, foils and powder compacts, pulsed action of laser radiation, dimens. effect *(Russian)* 77−16437
Cu, thermal expansion coeff. meas. using strain gauges and thermocouple 78−53059
Cu, thermal expansion coeffs., Morse pot. calcs. 79−77775
Cu-Al, dil., thermal expansion *(French)* 79−95185
Cu-Ge, thermal expansion, X-ray determ. 78−26697
Cu-Mn, dil., anomalous thermal expansion below 50K 78−51710
Cu-Sb (24-45 wt.%), phase transform. exam. by thermal expansion 77−63629
CuCl, polycryst., meas. at low temps., Gruneisen parameters 77−55367
CuF_2, thermochemical props. 78−31674
$CuGaS_2$, tetragonal distortion, crystal field splitting, temp. depend. 79−47060
$CuGaSe_2$, thermal expansion obs. 80−70432
$Cu(NH_3)_n(ClO_4)_2$, (n=4 or 5), EPR parameters and dilatometry 80−39850
Cu_2O, thermal expansion at low temp. 78−59959
Cu_2O-Al_2O_3-SiO_2 glass, thermal expsn. coeff. 79−51284
Cu_xS, $1 \leq x \leq 2$, quantum temp. size effect and magnetism *(Russian)* 80−103764
Dy, anomalous thermal expansion, interferometric meas. 78−52333
Dy, antiferromagnetic, thermal expansion, US attenuation anomalies 79−47319
Dy, paramag., anomalous thermal expansion, up to 273K 79−7967
$DyCo_2$-$DyAl_2$ system, mag. and structural studies 80−108006
$DyFe_{1-x}Co_xO_3$, magnetostriction, thermal expansion and elastic moduli near Morin point 77−8383
Dy_2O_3-based ceramic, preparation, mech. props. 77−24998
Er, lattice dynamics, thermal expansion, bulk modulus calcs. 77−20022
Er_2O_3-ZrO_2, subsolidus phase relations, X-ray diffr. and thermal expansion exam. 78−31382
$ErRh_4B_4$, supercond. and mag. props. 79−4631
$ErRh_4B_4$, thermal expansion and magnetostriction meas. at low temp. 79−56374
ErSb, crystal field effect in thermal expansion 78−19305
ErZn, preferred mag. domain orientation, and microstructural defects, magnetostriction meas. 79−73769
EuB_6, X-ray method, room temp. to 1300 C 80−96670
Eu_2O_3, mech. and physical props. rel. to reactor control rod appl. 78−21641
Eu_2O_3, thermophysical props. and neutron absorpt. 80−103488
α-Fe, (001), surface relax. and thermal expansion calcs. 79−23820
Fe alloy, low at elev. temps. *(Chinese)* 77−72704
Fe, Doppler broadened positron annihilation lineshapes, prevacancy lattice expansion 78−27349
Fe, high-purity single crystals, X-ray topography and double-crystal diffraction 80−92534
Fe, magneto-volume effects calc., rel. to itinerant electron model 78−43621
Fe, pure and alloyed, density and thermal expansion in liq. and solid states 80−96668
Fe, thermal props. at high-press. (150 GPa), from shock-wave expts., Earth core struct. 80−21683
Fe-alloy, FCC, Invar, thermally excited electron transitions 79−56559
Fe-B, amorphous ferromag., Invar type, magnetisation, elec. resist. and thermal expansion meas. 78−2663
Fe-B(P) amorphous alloy, Invar effects, mag. props. meas. 79−56594
Fe-B(P) amorphous alloys, anomalous thermal expansion, ΔE effect, Invar and Elinvar characts., delay time 80−80589
Fe-Co-Mo-Nb(Ta) semihard mag. alloy, mag. props., thermal expansion, elec. resistivity and hardness *(Japanese)* 80−88789
Fe-Cr alloys, itinerant antiferromag., effect of mag. impurities, thermal expansion at Neel temp. calc. 77−32186
Fe-Cr-B, amorphous, Elinvar and Invar charact. *(Japanese)* 80−11832
Fe-Cr-B amorphous alloys, corrosion resistance, Invar and Elinvar characts. *(Japanese)* 79−96213
Fe-Cr-Ni alloys, linear expansion, 4.2-300K rel. to antiferromag. rearrangement 78−43146
Fe-Cr-Ni alloys, stable and metastable, 4.2-290K *(Russian)* 78−47537
Fe-Cu-C alloy, sintered with added S, thermophys. props. 79−61541
Fe-Mn alloy, magnetovolumetric anomaly *(Russian)* 78−64248
Fe-Nb(Ta)-Co, Recalloys, semihard mag. alloys, mag. and elec. props., hardness, thermal expansion *(Japanese)* 79−5066
Fe-Ni, FCC alloy, magnetovolume instability 79−8031
Fe-Ni, FCC and BCC lattices, X-ray characteristic temp. *(Russian)* 78−67797
Fe-Ni, Invar alloys, anomalous thermal expansion coeff. *(Japanese)* 79−65225
Fe-Ni, point defect form. at high temps. *(Russian)* 79−86787
Fe-Ni, quenched irreversible alloy, zero or negative thermal dilatation, para-process mag. susceptibility 79−4419

thermal expansion continued
Fe-Ni, thermal expansion, ferromagnetic-paramagnetic transition *(Russian)* 80−54412
Fe-Ni (308-44.1 at.%) Invar alloys, anomalous mag. anisotropy and thermal expansion 80−75755
Fe-Ni alloys, anomalous thermal expansion, Gruneisen eqn. 78−83980
Fe-Ni alloys, Invar effect explanation in localised moment model *(Russian)* 77−76580
Fe-Ni alloys, thermal expansion rel. to X-ray emission spectra *(Russian)* 77−32470
Fe-Ni alloys, thermal props., let. review *(Russian)* 78−18805
Fe-Ni FCC alloys, invar effect by local moment model 77−90006
Fe-Ni Invar alloy, thermal expansion coeff. at low temp. 79−86911
Fe-Ni Invar alloys, forced and spontaneous magnetostriction 78−48019
Fe-Ni Invar anomalies, explanation in terms of itinerant electron magnetism 80−75705
Fe-Ni Invar anomalies, low spin to high spin transition 79−56558
Fe-Ni-Mn alloy, temp. coeff. of linear expansion *(Russian)* 77−80634
Fe-Ni-Te alloy system, first-order phase transformation obs. 78−64533
Fe-Ni(41.3 at.%) Invar alloy, asymmetric Mossbauer spectra 77−63346
Fe-Pd Invar alloys, elec. and mag. props. and thermal expansion 80−75732
Fe-Pt, Invar alloy, strong ferromagnetism, magnetostriction and thermal expansion 79−8037
Fe-Pt, Invar type, charact. magnetovolume effects 79−82855
Fe-Pt Invar, magnetovolume effects 79−56597
Fe-Pt Invar alloy, homogeneous strong ferromagnet, thermal expansion and mag. props 79−91278
Fe-Si-B ferromagnetic amorphous alloys, Young's modulus and delay time characts. *(Japanese)* 77−85543
Fe-Sn, dil., ferromag., temp. anomalies of Sn mag. hyperfine field and thermal expansion 79−33270
Fe_3Al, ordered, magnetostriction and thermal expansion 80−39842
$Fe_{3-x}Al_xO_4$, cation distrib., mag. and other phys. props. 77−43818
FeB, thermophysical props., 296-2000K 78−14477
$(Fe_{1-x}Mn_x)_3Si$, mag. phase diagram determ. 77−24697
$Fe_{78}Mo_2B_{20}$ glass, thermal expansion, glass transform. and crystn. temps. 80−2183
$Fe_{1-x}Ni_x$, FCC, anomalies in sp. ht. and thermal expansion 79−19739
$Fe_{40}Ni_{40}B_{20}$, amorphous, anomalous thermal dilatation 79−55668
$Fe_{32}Ni_{36}Cr_{14}P_{12}B_6$ glass, thermal expansion, glass transform. and crystn. temps. 80−2183
$Fe_{0.5}(Ni_xMn_{1-x})_{0.5}$, FCC, anomalies in sp. ht. and thermal expansion in paramag. temp. range 79−19739
$Fe_{65}Ni_{28}Mn_1$, disordered, mag. struct. near ferro-antiferromagnetic transition 80−60211
$Fe_{40}Ni_{40}P_{14}B_6$ glass, thermal expansion, glass transform. and crystn. temps. 80−2183
$(Fe_xNi_{1-x})_{0.75}P_{0.16}B_{0.06}Al_{0.03}$, metallic glass, thermal expansion 78−43151
Fe_3O_4, magnetite, oxidation rate anomaly at Curie temp. 79−96298
FeP, mag. suscept., resistivity and thermal expansion meas. 78−2661
Fe_2P, magnetisation, susceptibility, thermal expansion and elec. resist. meas. 77−77037
Fe_2P, magnetisation, susceptibility, thermal expsn. 79−11302
Fe_3Pt Invar alloy, thermal expansion and spontaneous magnetisation, Invar anomalies, low spin model 80−71001
$Fe_{72}Pt_{28}$ Invar alloy, low temp. thermal expsn. 79−65221
Fe_3Se_4, thermal expansion, compressibility, magnetisation, susceptibility and magnetostriction 77−66318
η-Fe_5Si_3, thermal and mag. props. 77−36080
Fe_2TiO_5, grain size pseudobrookite oxide, microcracking relations 79−29194
Ga, positron annihilation lineshape factors, effect of thermal expansion 77−44084
GaAs crystal growth, thermal and elastic const. evaluation 80−92586
GaAs homojunction LED, mechanical stress induced degradation 80−2860
GaAs, lattice vibration, thermal expansion and pressure effect 80−39233
$GaBo_3$, coefficients of thermal expansions 80−39322
$Ga_{0.47}In_{0.53}As$, LPE growth and characterisation 80−10845
$Ga_xIn_{1-x}As_yP_{1-y}$, thermal expansion coefficients, 25-400°C 79−46817
$(Ga_xIn_{1-x})_2Se_3$, $1 \geq x \geq 0$, phases, lattice parameters and thermal expansion between room temp. and melting point 80−39031
β-Ga_2O_3-K_2O/K ferrite, interfaces and solid soln., thermal expansion and lattice parameter variations 78−55959
GaP, thermal expansion below room temp. 80−79963
n-GaP:S, elastic moduli and mode gammas 79−73242
GaP/Si heterostruct., differential thermal contraction, plastic deform., fracture 80−108494
GaS, lattice dynamics parameters, X-ray diffr. study *(Russian)* 80−29146
GaSb, lattice vibration, thermal expansion and pressure effect 80−39233
GaSe, lattice dynamics parameters, X-ray diffr. study *(Russian)* 80−29146
Gd, ferromagnetic, crit. sp. ht. and thermal expansion 80−60343
Gd, thermal expansion, near ferromag. transition 78−31084
Gd-Dy, magnetostriction contrib. exchange and magnetocryst. interactions *(Russian)* 77−12184
Gd-Y alloy, anomalous thermal expansion, interferometric meas. 78−52333
$GdAl_2$, thermal expansion and heat capacity Curie temp. determ. 77−1559
$Gd(Co_{1-x}Ni_x)_2$ compounds, NMR and thermal expansion 80−66070
$GdMn_2$-$GdAl_2$ system, mag. and structural studies 80−108006
Ge, linear thermal expansion coeffs. meas., room temp. to 250°C 78−55416
Ge, optical material, 60-300K 78−33791
Ge, thermal expansion coeff. and Gruneisen const. 77−59128
Ge, thermal expansion coeff., optical mode Gruneisen const. 79−46820
Ge-FeS, GeS-FeS, density of alloys, volume changes on melting 77−51473
Ge-GeO_2 boundary, electrophysical parameters *(Russian)* 77−85327
Ge-S system glasses, free vol. at transition temp. *(Japanese)* 79−55876
Ge-Se system glasses, free vol. at transition temp. *(Japanese)* 79−55876
GeO_2-PbO glasses, IR transmittance and thermal expansion, effect of oxides and fluorides 77−63405
$GeS_2(O_2)$, thermal expansion at low temperatures 78−83982
GeTe, quenched, phase transitions and electrophysical props. 79−51250
GeTe, thermal expansion meas. at phase transition 78−18771
H_2O, high-press. props. and struct., mixture model 77−84612

thermal expansion continued
He, second virial coeff., 0-500°C, two-temp. gas-expansion method 78−55711
^{4}He, liq., anharmonic effects in US propagation near λ transition 80−96707
^{4}He, liq., phonon dispersion relation 77−7924
^{4}He, superfluid, sound conversion phenomena at free surface, acoustic coeffs. 80−96709
^{4}He, superfluid, thermal expansion coeff. and phase transition 79−51333
^{4}He, superfluid, thermodynamic props. determ. from sound velocity data 77−15649
^{4}He, superfluid, thermodynamic properties, at very low temps., rel. to interacting boson systems 78−2320
^{4}He, thermal expansion coeff., scaling and universality near superfluid transition 77−7927
Hf, HCP, lattice dynamics, thermal and elastic props., model 80−34155
HfC_x, electron energy spectrum and phys. props. in homogeneous region *(Russian)* 77−31941
HfO_2, monoclinic, microcracking, elasticity, internal friction, thermal expansion meas. 79−29195
HfO_2, stabilised comps., elastic props. rel. to porosity and temp. 80−81096
HfO_2, zero and low coeff. of thermal expansion 80−39325
HfO_2-La_2O_3 system, phase form. and relations, phys. props. 79−43218
HfO_2-TiO_2, phase relations and thermal expansion 77−21121
HfO_2-TiO_2, thermal expansion coeff. and dynamic response to pulsed energy deposition 78−26705
HfO_2-TiO_2 system, zero and low coeff. of thermal expansion 80−39325
HfS_2, layer compound, expansivities and thermal degradation 77−89554
$HfSi_2$, work function rel. to phys. props. 77−47887
HfV_2, supercond. compound, low temp. obs. 78−76189
Hg, electrical and thermodynamic props. in metal-semicond. transition range 80−20144
Hg, expanded liquid, thermodynamic and electron transport props. 79−23938
Hg, P-V-T relations for temperatures of 40 to 240°C and press. up to 1400 kg cm^{-2} 78−6140
Hg, thermophys. props. rel. to clustering in liqs. 77−1065
Hg-In (3 at.%), amalgam, thermodynamic and electron transport props. 79−23938
Hg-Na (3 at.%), amalgam, thermodynamic and electron transport props. 79−23938
Hg_2Br_2, nonintrinsic ferroelastic, thermal expansion and thermodynamic potential 80−88344
Hg_2Cl_2, thermal expansion and ferroelastic $D^{17}_{4h} \rightarrow D^{17}_{2h}$ transition 79−99337
HgTe, 1.5 to 30K, thermal expansion and heat capacity meas. 80−59681
$(Ho,Y)Co_2$, mag. props., elec. resist. and thermal expansion 78−76246
Ho, bulk modulus, thermal expansion, third order elastic constants 77−84875
$HoRh_4B_4$, low temperature magnetic properties 80−88728
$InBO_3$, up to 610°C, X-ray determ. 77−43352
InSb, lattice vibration, thermal expansion and pressure effect 80−39233
α-In_2Te_3 single crysts., elec. and photocond., temp. depend., linear thermal expansion coeff. 79−42541
Ir, 440-2220°C, improved empirical formula 77−11709
Ir, thermophysical props. at temps. up to 7000K 80−103497
K, electrical and thermal resistivity determ. from first principles 79−69493
K, lattice parameter determ. by neutron scatt. 79−7576
K, liq., thermal expsn. coeff. for high temp. 78−75853
K, thermal expansion calc. 77−11711
$(K_{3/4}Bi_{1/4})(Zn_{1/6}Nb_{5/6})O_3$, cation disordered perovskite, elastic consts. and thermal expansion 80−96587
$KCaCl_3$, phase transitions, optical and dilatometric meas. 79−61394
$K_2Cd_2(SO_4)_3$, ferroelastic phase transition, X-ray diffr. and dielec. temp. depend. meas. 79−55882
$K_2Cd_2(SO_4)_3$, melt growth and ferroelastic transition, and K_2SO_4-$CdSO_4$ phase diagram 78−31335
KCl, electron-irrad., positron-capture centres, thermal annealing kinetics 79−95875
KCl, linear thermal expansion coeffs. meas., room temp. to 250°C 78−55416
KCl, optical material 60-300K 78−33791
KCl, thermal expansion, compressibility and melting calcs. 79−33069
KCl, thermal expansion coefficients temp. depend., anharmonic effects 79−99290
KCl, thermodynamic props., lattice-dynamical calc. 77−35715
KCl, X-ray irradiated, vacancy conc. determ., thermal expansion meas. 80−79782
$KCoF_3$, lattice parameter temp. depend., phase transitions and thermal expansion coeff. 80−1988
KDP monocrystal, expansion and contraction coeffs., tricritical point, Landau theory explanation *(Russian)* 80−44340
$K_2(F,O)$-B_2O_3-SiO_2, effect of replacing B_2O_3 by Al_2O_3 or Ga_2O_3 78−63677
KF, thermal expansion, higher-order anharmonic contrib. at high temps. 79−28113
KHF_2, nucl. spin-lattice relax. and anomalous thermal expansion meas. 77−8441
KH_2PO_4, crit. behaviour, dilatometric study 80−92689
KH_2PO_4, optical material, 60-300K 78−33791
$KH_3(SeO_3)_2$, ferroelastic, lattice consts. and thermal expansion tensors, X-ray diffr. meas. 79−37856
K_2IrCl_6, thermal expansion meas. near antiferromag. transition 77−20610
$KMnF_3$ lattice parameters, temp. depend., 21°C to MP 77−76583
$KMnF_3$, lattice parameter temp. depend., phase transitions and thermal expansion coeff. 80−1988
$KMn_{0.9}M_{0.1}F_3$, (M=Co,Ni), lattice parameter temp. depend., phase transitions and thermal expansion coeff. 80−1988
KNO_3, paraelec., precision lattice parameters meas. 77−11517
$KNiF_3$, lattice parameter temp. depend., phase transitions and thermal expansion coeff. 80−1988
$KNiF_3$, low anisotropy antiferromag., phase boundary crossover behaviour 79−38324
K_2O-Al_2O_3-SiO_2 system, crystallisation of glasses in primary phase field of leucite 78−67658
K_2OsCl_6, displacive phase transitions 78−10188
K_2ReCl_6, thermal expansion meas. near antiferromag. transition 77−20610

thermal expansion continued
K_2ReCl_6, thermal expansion transitions 78−10188
K_2ReCl_6, thermodynamic relations at solid state phase transitions 80−29164
$KReO_4$, NQR and thermal expansion 77−20745
K_2SO_4, phase transform., mech. of thermal hysteresis, DTA, dilatometry and dielec. meas. 80−75353
K_2SeO_4, paraelec., intermediate incommensurate and ferroelec. commensurate phases 77−16263
$K_2W_3O_{10}$, thermal expansion, X-ray diffr. obs. 77−43353
Kr, solid, high-temp. thermal expansion charact. 80−59680
La, $(SO_4)_3.9D_2O$, soln. growth, struct., props. 77−77363
LaB_6, X-ray method, room temp. to 1300 C 80−96670
LaBi, thermal expansion, 20-800°C 79−14942
$La_{1-x}Ce_xAl_2$, Kondo system, low temp. thermal expansion behaviour 79−19382
$La_{1-x}Ce_xSn_3$, electrical resist. and thermal expansion meas., 1.5-300K 80−34400
La_2O_3, thermal expansion, 100 to 300K, X-ray method 79−99335
LaP_5O_{14}, continuous ferroelastic transition elastic and mechanical props. 80−92668
LaP_5O_{14}, ferroelastic phase transition, thermal expansion and elastic consts. tensors 79−42236
Li, thermophys. props. rel. to clustering in liqs. 77−1065
$LiAl_{1-x}In_x$, comp. depend. 78−22869
LiF (001) surface, coeff. of thermal expansion (parallel to surface) 77−59129
LiF, high temp. depend. of thermal expansion coeff., interatomic pot. approach 78−95166
LiF, thermal expansivity determ. at high press. 78−79787
$Li_{0.5}Fe_{1.25}Ga_{1.25}O_4$, ferrimag. with local canted struct. thermal expansion anomalies 79−73762
$Li_{0.17}Fe_{2.17}Zn_{0.66}O_4$, ferrimag. with local canted struct. thermal expansion anomalies 79−73762
LiIn, electrical resist. and thermal expansion temp. depend., 30 to 400°C, vacancy form. 77−24547
$LiKSO_4$, uniaxial crystal, pyroelectric, thermal expansion, phase transition 80−19966
$LiNH_4SO_4$, ferroelectric phase transition, lattice parameters and thermal expansion coeffs. 80−40074
$LiNH_4SO_4$, temp. depend. of linear expansion coeffs. 78−76399
$LiNH_4SO_4$, thermal props. near high temp. phase transition 78−19428
$LiNO_3.3H_2O(D_2O)$, crysts. and melts, density, mol. vol., thermal coeff. of expansion, rel. to struct. 80−15270
$LiNbO_3$, linear thermal expansion coeffs. meas., room temp. to 250°C 78−55416
$LiNbO_3$, optical material, 60-300K 78−33791
$LiNb_{1-y}Ta_yO_3$, Czochralski growth and basic props. 77−63556
Li_2O-Al_2O_3-SiO_2 glasses, viscosity, thermal expansion, glass transform. temp., and refr. index 79−42282
Li_2O-B_2O_3-P_2O_5, glass, mech. and elec. props 80−84228
$Li_2O.2SiO_2$, ceramic, prep. of oriented microstructure by unidirectional solidification of melts 80−71614
$Li_2O.2SiO_2$, directionally solidified, thermal and mech. props. *(Japanese)* 80−16295
$100(Li_2O.2SiO_2).3B_2O_3(3Na_2O)(3MgO)(3Al_2O_3)(3SiO_2)(3P_2O_5)$, directionally solidified, thermal and mech. props. *(Japanese)* 80−16295
$Li_{1-x}Ti_{2-x}O_4$, struct. phase transition and thermal expansion 78−14465
Lu, lattice dynamics, heat capacity, thermal expsn. 79−86857
M_2O-MnO-B_2O_3 glasses, M=Li, Na, K, glass-forming region and physicochem. props. 78−63678
Mg $(Fe,In)_2O_4$:Pb,Pt film, LPE 77−77436
Mg, anisotropic thermal expansion 79−23750
Mg-Tb(Dy)(Ho)(Tm), dil., macroscopic shape effect due to quadrupole orientation, magnetostriction and thermal expansion meas. 80−60396
$MgAl_2O_4$ spinel, anomalous thermal expansion, second order transition 80−84307
$MgCr_2O_4$ spinel, exam. of expansion during synthesis 79−20012
MgF_2, optical material, 60-300K 78−33791
MgO, 500-1800°C, X-ray diffr. 77−35723
MgO:Cr^{3+} (Mn^{2+}), spin Hamiltonian parameters, lattice expansion and vibr. effects 80−24851
MgO-Al_2O_3-SiO_2, glass ceramic, structure and props. *(German)* 80−38927
MgO-CaO refractory ceramics, thermal expansion coeffs. 79−99336
Mg_2Si, charact. X-ray temp. and thermal expansion coeff. 77−15599
Mg_2Sn, third-order elastic constant, low temp. limit of Gruneisen parameter 79−73280
$MgTi_2O_5$, grain size pseudobrookite oxide, microcracking relations 79−29194
Mn complex, $[Mn(urea)_6](UO_4)_2$, thermal expansion coeff., crystal field parameters, phosphoresc., absorv., excitation spectra 78−43932
Mn-Ga, DO_{22} type alloys, magnetic props., crystal struct. *(Japanese)* 78−59784
Mn-Ga, Elinvar charact. *(Japanese)* 79−61638
Mn-Ga (19 to 30 at.%), phase equilib. diagrams, X-ray diffr., thermal expansion, and mag. meas. *(Japanese)* 78−39743
Mn-Ga (19.0 to 31.2 at.%), exam. of phase diagram, using X-ray diffr., thermal expansion and mag. meas. 78−76634
Mn-Ni, thermal expansion, mag. susceptibility, lattice consts. 80−100341
Mn-Ni alloys, antiferromag., Invar-like thermal expansion and spontaneous volume magnetostriction 77−69654
Mn-Ni-Ti (Zr) systems, and mech. props. thermal expansion for different heat treatments *(Japanese)* 79−29123
Mn-Ni-Ti(Zr), non-ferromagnetic Elinvar-type alloys 79−24566
Mn-Ni-V(Nb)(Ta), nonferromagnetic Elivar type, mech. props. meas. 77−48473
Mn-Pt, Elinvar props., −150 to 500°C *(Japanese)* 77−52385
Mn-Pt, exam. of Elinvar props., from −150 to 500°C 78−76684
$(Mn_{1-x}Cr_x(Fe_x))B$, Invar charact. 77−15602
MnF_2 lattice parameters, temp. depend., 21°C to MP 77−76583
$(Mn_{1-x}Fe_x)_5Si_3$, solid soln., mag. transitions sp. ht., magnetisation and thermal expansion meas. 77−16075
Mn_3Ge_2, textured, thermal expansion, 158K transformation *(Russian)* 77−32196
$Mn_2Sb_{1-x}Bi_x$ ($0 \leq x \leq 0.175$), mag. transition, thermal expansion, thermomag. effects and lattice constant changes *(Japanese)* 79−78375
MnSe, mag. suscept., thermal expansion and elec. resist. meas. 78−34964
$MnSe_2$, pyrite struct., mag. suscept. and thermal expansion 77−32176
Mn_2SiO_4, tephroite, thermal expsn., 25-850°C 79−60527

thermal expansion continued
Mo, 100-2000°C as standard samples for dilatometry 78−26699
Mo alloy VN-2M vac.-melted, 971-2153°C, impurity effect 78−26700
Mo and Mo superalloys high temperature properties 78−44173
Mo, linear coeff., 100-2546°C, cast and metal-ceramic, impurity depend. 77−66032
Mo, linear expansion coefficient, at low temp. 78−83977
Mo, liquid, thermal volume expansion, MP to BP 79−90802
Mo, liquid and solid, thermophysical props. 78−75808
Mo, MChVP, vac.-melted, 971-2153°C, impurity effect 78−26700
Mo, siliconised thermal stress and thermal expansion 77−21324
Mo, single crystal, thermal expansion in magnetically ordered phases 78−2269
Mo-Ti-Zr (0.5, 0.7 wt.%) alloy TZM, props. and appl. *(German)* 80−21040
2H-MoS_2, thermal expansion between 10 and 320K, cell dimensions meas. 79−65222
MoSCl, thermal expansion and thermal transform. 78−26696
MoS_2(2H), lattice dynamics, Coulomb and quasi-harmonic effects 80−39245
$MoSi_2$ film, elastic stiffness and thermal expansion coeffs. 80−107451
α-N_2, solid, thermal expansion and Gruneisen coeff. *(Russian)* 79−10969
NH_4HSO_4, volume expansion, spontaneous strain, second order phase transitions 79−65224
$(NH_4)_3H(SO_4)_2$, successive phase transitions, dilatometric and X-ray expts. 80−11348
α-NH_4HgCl_3, thermal expansion, lattice constants between 302 and 364K 80−15268
NH_4IO_3, effect of hydrostatic press. on ferroelec. phase transition 79−51917
NH_4IO_4, ^{127}I NQR rel. to thermal expansion 79−4742
NH_4LiSO_4, I-II phase transition in improper ferroelec., hydrostatic press. effects 78−84533
NH_4ReO_4, NQR and thermal expansion investig. 77−12229
NH_4ReO_4, NQR and thermal expansion 77−20745
$^{15}N_2$, solid struct., and thermodynamic props. *(Russian)* 80−88083
Na, electrical and thermal resistivity determ. from first principles 79−69493
Na, thermal expansion calc. 77−11711
Na, thermophys. props. rel. to clustering in liqs. 77−1065
Na, vacancy thermal expansion coeff., lattice statics calc. 79−37698
$NaBrO_3$, lattice parameters, thermal expansion, defect formation energy 78−79786
Na_2CO_3, single cryst. growth from melt, thermal expansion meas. 79−4913
NaCl, calc. of migration volume of vacancies from macroscopic parameters 78−75872
NaCl, Gruneisen γ and other thermodynamic props., vol. depend. 77−76577
NaCl, isothermal eqn. of state, length change meas. technique 77−1210
NaCl, thermal expansion, compressibility and melting calcs. 79−33069
NaCl, thermal expansion coefficients temp. depend., anharmonic effects 79−99290
NaCl, thermal expansion meas. after X-ray irrad., F-centre bleaching 80−44338
NaCl, thermodynamic props., lattice-dynamical calc. 77−35715
NaCl, X-ray irrad., vacancy conc., thermal expansion meas. 80−6431
NaF, thermal expansivity determ. at high press. 78−79787
$NaNH_4SO_4.2H_2O$, ferroelec. and thermal props. 78−83968
Na_2O-$2SiO_2$ high expansion glass, chemical durability improvement by ion exchnage 78−48361
Na_2O-B_2O_3 glass, negative thermal expansion, LF Guneisen parameter, numerical analysis 77−11707
Na_2O-B_2O_3-P_2O_5, glass, mech. and elec. props 80−84228
Na_2O-B_2O_3-SiO_2, two-phase, stresses arising during leaching 80−81086
Na_2O-CaO-SiO_2 glass, effect of phase on liquids and gas diffusion *(German)* 80−38931
Na_2O-$GeO_2(SiO_2)$, thermal expansion at low temperatures 78−83982
Na_2O-$GeO_2(TiO_2)(SnO_2)(ZrO_2)(ThO_2)$-$SiO_2$ glass, density, refractive index, thermal expansion, hardness IR spectra, DTA *(Japanese)* 78−15535
Na_2O-SiO_2 glass, 2-30K, comp. effects 77−20097
$NaReO_4$, NQR and thermal expansion investig. 77−12229
$Na_{1+x}Si_x\ Zr_2\ P_{3-x}\ O_{12}$; monoclinic to rhombohedral phase transformation 80−29950
$NaTb(MoO_4)_2$, lattice thermal expansion, rel. to temp., X-ray method 79−77782
$NaVO_3$, thermal expansion and ferroelec. phase transition 79−38482
Na_2WO_4 and $Na_2W_2O_7$, thermal expansion, X-ray diffr. obs. 77−43353
$NaYb(WO_4)_2$, thermal expansion, X-ray determ. 80−39323
Nb, thermal expansion, 1200-2000K 79−55905
Nb, thermal expsn., 1261-2289K 78−43150
Nb-H(D) system, incoherent phase transition 79−73304
Nb-Zr alloy, 5VMTs1, thermal expsn., 1261-2289K 78−43150
$NbBe_{12}$, by diffusion saturation in vacuum, resistance to heat 78−44259
NbC coating, vapour deposition, phys. and chem. props. 77−40456
NbC_xO_y, x+y=0.73 to 0.88, thermal expansion coefficients 80−103502
Nb_3Ge film, CVD, thermal expansivity, X-ray diffr. meas. 78−6166
NbH_2, harmonic and anharmonic elastic props. 80−10589
NbO_2, semicond., thermal expansivity 80−34213
$NbSe_2$, thermal expansion, lattice parameter meas. 78−18804
NdBi, thermal expansion, 20-800°C 79−14942
Ni, 300-1000K, and power law consts. near Curie temp. 78−38858
Ni, bulk modulus and thermal expansion coefficient, mag. contributions 79−8039
Ni, Doppler broadened positron annihilation lineshapes, prevacancy lattice expansion 78−27349
Ni, ferromagnetic, anomalies in thermal expansion and heat capacity 79−73744
Ni, low temp. Gruneisen parameter 79−23694
Ni, magneto-volume effects calc., rel. to itinerant electron model 78−43621
Ni, simple eqn. of state appl. 77−27970
Ni, thermal expansion anomaly near Curie temp. 77−85474
Ni/ZrO_2-Y_2O_3, sputtered multilayered ceramic/metal coatings, props. 80−40620
Ni-Al-Si, β-phase stability *(Russian)* 78−39738
Ni-Cr/ZrO_2-Y_2O_3 sputtered multilayered ceramic/metal coatings, props. 80−40620

thermal expansion continued
Ni-Cr-Mo-Mn alloy 02KhN40MB, corrosion-resist, heat-resist., phys. and mech. props. 80−35411
Ni-Cu-X (X=Sn, Nb, Ti), spinodal decomp. alloys, linear expansion coeff. influence on morphological anisotropy *(Japanese)* 80−70431
Ni-Fe Invar, thermal expansion and spontaneous magnetisation, Invar anomalies, low spin model 80−71001
Ni-P, amorphous, reversible effects of temp. on struct. 78−34442
Ni-Pt alloys, mag. props. under hydrostatic press. 78−6556
Ni-Pt alloys, thermal expansion, mag. contribs. 77−43355
Ni-Ti, heavily doped, linear expansion meas. 80−103501
Ni-Ti, Nitinol memory material heat engine, comment on efficiency 80−3529
Ni-Ti, Nitinol memory material heat engine, reply to comments on efficiency 80−3530
Ni_3Al, thermal expansion, mag. contribs. 77−43355
Ni_3B, linear thermal expansion 80−71639
$Ni_3B_7O_{13}I$, unit cell parameters and struct. transitions, 20 to 293K, X-ray diffr. study 80−24431
$NiCr_{0.5}Al_{1.5}O_4$, thermal expansion 79−73327
$NiCr_2O_4$, thermal expansion 79−73327
NiF_2, thermal expansion and magnetostriction, 55K to room temp. 80−80586
$Ni_{1-x}Fe_x$, short range order exam. allowing for formation of structural domains *(Russian)* 78−6888
$Ni_{1-x}Fe_2O_4$ ferrites, mag. thermal expansion anomaly 77−69595
$Ni(NH_3)_6(ClO_4)_2$, thermal expsn., phase transitions 79−60525
NiO, temp. depend. of thermal expansion and IR lattice vibrational mode 77−84950
NiO, thermal expansion, birefringence, AC susceptibility, temp. depend. 78−10664
NiO−CaF_2, hot-pressed, mech. props., thermal expansion rel. to CaF_2 additive 79−43321
NiS_2, cryst. distortion obs. below antiferromag. Neel and weak ferromag. Curie temps. 77−15579
NiS_2, high press. effect on mag. transition temps. 78−91866
O_2, solid, struct. elementary excitation spectrum and thermodynamic props. *(Russian)* 79−55696
Pa, lattice parameter variation at low temp., thermal expsn. 80−15046
(Pb,Sr)TiO_3, ferroelec. props., press. depend., anharmonic oscillator model 80−80716
Pb, film, deposited on Si substrate, residual strains 78−18915
Pb, Gruneisen parameters and thermal expansion coeff. 79−33103
Pb, molten, thermal expansion meas. to 1300K 80−65254
Pb, simple eqn. of state appl. 77−27970
Pb, thermophys. props. rel. to clustering in liqs. 77−1065
Pb-In-Au alloy, Josephson junction electrode materials, rel. to strain relax. 79−38255
Pb-Ta, appl. in thermal drive apparatus for direct vacuum tunnelling expts. 77−8175
PbF_2-AlF_3 glass, optical props., crystn. and thermal expansion 80−48367
$Pb(Fe_{2/3}U_{1/3})O_3$-$PbZrO_3$ solid solns., phase transition 77−48138
$Pb_3Ge_3O_{11}$, uniaxial ferroelec., thermal expansion and dielec. permittivity in vicinity of transition points 77−66459
$Pb_5(GeO_4)(VO_4)_2$, $Pb_5(SiO_4)(VO_4)_2$, and Pb_5GeO_{11}, elastic nonlinearity and acoustic losses 80−59554
$Pb(Mg_{1/3}Nb_{2/3})O_3$, cation disordered perovskite, elastic consts. and thermal expansion 80−96587
$Pb_3MgNb_2O_9$-$PbTiO_3$, relaxor ferroelectrics, electrostrictive effects 80−66112
$Pb(Mn_{1/2}Ta_{1/2})O_3$, ceramic, for thermal and dielectric isolation at low temp. 80−39365
$Pb(NO_3)_2$, thermal expansion study to test sensitivity of X-ray powder goniometer *(French)* 80−79631
PbO, sintered, pure, prep. and props. 77−48361
PbO/PbF_2/B_2O_3 solvent system, density, surface tension and expansivity data, effect of B_2O_3 conc. 79−19985
PbO-B_2O_3, solder glass, thermal reduction of Cu^{2+} and Cu^{+}:Cu^{2+} effect on thermal props. 78−15350
PbO-B_2O_3 glass-forming melt, specific volume and viscosity, temp. depend. 80−84073
PbO-B_2O_3-ZnO solder glass, with admixtures, crystallisation and thermal expansion 80−24364
$PbO_{1.57}$, thermal expansion tensor, phase transitions, X-ray diffr. obs. *(French)* 79−1515
$Pb_3(P_xV_{1-x}O_4)_2$, ferroelastic phase transition, DTA, dilatometric and Brillouin scatt. study 80−70398
$PbSbO_2Cl$, nadorite, thermal expansion, X-ray determ. 78−18802
$(PbSe)_{1-x}(SnTe)_x$, lattice dynamic props., Gruneisen parameters *(Russian)* 78−83984
$PbSnF_4$, thermal expansion and phase transitions 79−77781
$PbTiO_3$, anomalies in elec., photoelectric and mechanical props. 80−55051
$PbTiO_3$-$Pb(Ni_{1/2}W_{1/2})O_3$ system, solid soln. form., struct., dielec. props. and thermal expansion *(Japanese)* 78−27501
$PbWO_4$, thermal expansion tensor, phase transitions, X-ray diffr. obs. *(French)* 79−1515
$Pb(Zn_{1/3}Nb_{2/3})O_3$, cation disordered perovskite, elastic consts. and thermal expansion 80−96587
$Pb(Zn_{1/3}Nb_{2/3})O_3$, diffuse phase transition, electro-optical and dielec. obs. 79−82933
$Pb(Zr,Ti)O_3$, ceramic vibrator, resonant freq. temp. stability *(Chinese)* 79−47386
Pd, liq. and solid, thermophysical props. 78−75808
Pd, liquid, thermal volume expansion, MP to BP 79−90802
Pd-Ag-Au, lattice parameters and thermal expansion coeffs., X-ray diffr. meas. 79−99121
Pd-Ag-Au, temp. effect on lattice parameters and thermal expansion 78−51473
Pd-Fe-Mn, ferromagnet-spin glass, thermal expansion forced, magnetostriction and magnetisation under high press. 80−65255
Pd-H alloys, low and room temp., Gruneisen parameters 77−63026
Pd-H(D), thermal expansion and lattice anharmonicity 9 to 270K 80−39241
Pd-Ni, thermal expansion and magnetostriction meas. near crit. conc. for ferromagnetism 80−65881
Pd-Si, amorphous alloys, elastic props. and temp. coeff. of delay time, appl. to US delay lines *(Japanese)* 79−96069
phosphate glass, Li_2O and Na_2O effect on thermo-optic props. 78−18029
Pr, DHCP, cryst. field effect in thermal expansion 80−49390

thermal expansion continued
PrBi, thermal expansion, 20-800°C 79−14942
$PrCu_2$, Jahn-Teller transition, susceptibility, elec. resist., thermal expansion and acoustic meas. 77−20276
$PrNi_5$, crystal-field effects, comparison of calcs. with expts. 79−87071
$PrNi_5$, hexagonal, cryst. field effect in thermal expansion 80−49390
PrSb, crystal field effect in thermal expansion 78−19305
$PrSn_3$, thermal expansion and transverse elastic const. near mag. phase transition 80−60394
Pr_3Tl, thermal expansion and transverse elastic const. near mag. phase transition 80−60394
Pt, 100-1000°C, as standard samples for dilatometry 78−26699
Pt, liq., thermodynamic characterisation, by isobaric expansion meas. 80−103494
Pt, thermal expansion coeff. meas. using strain gauges and thermocouple 78−53059
Pu(C,N), lattice parameter variation, 50 to 300K 78−51709
Pu(C, N), PuC and PuN, lattice parameter variation at low temp., thermal expsn. 80−15046
PuC(N), lattice parameter variation, 50 to 300K 78−51709
PuN, fabrication, high-temp. thermodynamic and transport props. 77−28774
RbBr, sign of thermal expansion coeff. at low temps. 77−84954
$RbCaCl_3$, phase transitions, optical and dilatometric meas. 79−61394
RbCl, thermodynamic props., lattice-dynamical calc. 77−35715
$RbHSO_4$, volume expansion, spontaneous strain, second order phase transitions 79−65224
RbI, sign of thermal expansion coeff. at low temps. 77−84954
$RbMnF_3$, isotropic antiferromagnetic, T-H phase diagram as test of theory 77−32192
Rb_2ZnCl_4, phase transitions, thermal expansion coeff. 80−100638
Re, lattice dynamics, third order elastic consts. and thermal expansion 77−76505
Re, single crysts., 2-300K *(Russian)* 79−55904
Re, sintered, preparation, thermal cond., linear expansion up to 1000K 79−61533
Re, thermal expansion, 1200 to 2300K 80−103500
Re, X-ray determ., 113-1700K 78−67838
ReO_3, coeff. of linear thermal expansion, 100-500K 79−10972
ReO_3, lattice parameters, thermal expansion 291 to 464K, Bond technique meas. 78−75617
Ru, lattice dynamics, sp. ht., thermal expansion 79−82363
Ru, lattice dynamics, thermal expansion and bulk modulus 77−59079
S-based composite, engineering props. 77−86093
Sb, Debye-Waller factors and thermal expansion 78−43089
$SbGe_xSe_y$ glasses with const. Sb content, heat capacity, thermal expansion, US vel. and elastic moduli 77−76574
$SbO_{3/2}$-$BO_{3/2}$, glass, struct. and props. *(Japanese)* 77−27836
Sc, HCP, lattice heat capacity, third order elastic consts., thermal expansion 79−82352
Sc, thermal expansion anisotropy, 78-783K, X-ray determ. 78−83983
$Sc_2(WO_4)_3$:Er^{3+}, growth, solubility, absorption spectrum and thermal expansion meas. 77−36391
Se, trigonal or amorphous, thermal expansion and Gruneisen coeffs., 10-300K 78−22870
Se, vitreous, time dependent thermal expansion 78−14485
Si, 6 to 340K, using linear absolute capacitance dilatometer 77−47603
Si, lattice constants anomalous temp. depend. 79−46821
Si, pure and with adsorbed Al(Au), thermal expansion and at. vibr. singularities 77−89635
Si, temperature during CW laser heating, Raman scatt. meas. 80−76109
Si, thermal expansion coefficient and Gruneisen const. 77−59128
Si, thermal expansion coeff., optical mode Gruneisen const. 79−46820
Si wafers, process-induced in-plane distortion and wafer bowing 79−11048
Si-Al(Ti)C, sintered, exam. of props. 80−25644
SiB_4, mech. and thermal props. 80−21083
SiC fibre reinforced Al, thermophys. props. 80−59745
SiC-fibre reinforced glass, fabrication, thermal expansion, flexural and fracture toughness 80−40319
SiN film, elastic stiffness and thermal expansion coeffs. 80−107451
Si_3N_4 amorphous films, CVD mech. and thermal props. *(Japanese)* 77−90280
Si_3N_4 film, elastic stiffness and thermal expansion coeffs. 80−107451
Si_3N_4, reaction sintered, time depend. strength degradation 79−29235
Si_3N_4, synthesis and props. of shapes 79−47650
Si_3N_4:MgO, hot-pressed, linear thermal expansion rel. to MgO content 80−70430
SiO_2, amorphous, tunnelling models and thermal expansion below 4K 79−73326
SiO_2, cryst. and vitreous, struct. sensitive expansivity 78−22873
SiO_2, fused silica, KLR1, KLR2 and KU2, high-precision stability of end gauges 79−76778
SiO_2 glassy-amorphous system, struct. *(German)* 78−38626
SiO_2-B_2O_3 glass system, gel hot pressing synthesis and characterisation *(French)* 80−66468
SiO_2-base cores, for superalloys, high temp. characterisation 80−10640
SiO_2-K_2O-Na_2O-BaO-SrO-ZnO glass, props. optimisation 79−91611
SiO_2-Li_2O-K_2O-ZnO glass ceramic, prep., phase transformations and physical props. 80−45299
SiO_2-TiO_2 system, physicochem. props. of glasses with low thermal expansion coefficient 77−35718
α-Sm, low temp. phase transition *(Russian)* 79−32937
SmBi, thermal expansion, 20-800°C 79−14942
$SmCo_5$, sintered, anisotropic thermal expansion and fracture of radially oriented toroids *(Chinese)* 80−10686
SmS, intermediate valence compound, pressure-temperature phase diagram 79−28283
SmS, thermal expansion meas. using galvanomagnetic dilatometer 78−87797
SmSb, crystal field effect in thermal expansion 78−19305
Sn, liq., US vel. and thermophysical props. meas., 500-1000K 78−38778
Sn, molten, thermal expansion meas. to 1300K 80−65254
Sn, single cryst., equilib. vacancy conc., length and lattice parameter change meas. 79−60352
Sn-Bi, liq., US vel. and thermophysical props. meas., 500-1000K 78−38778
Sn-Pb alloy, dil., lattice dynamics, sp. ht., resist., thermal expansion and nuclear γ reson. expts. *(Russian)* 78−87749
Sn-Pb alloys, dil., low-freq. phonon spectrum peculiarities 79−60463
$SnCl_2.2H_2O$, Brillouin scatt. and thermal expansion 80−97289

thermal expansion continued
$SnS_2(Se_2)(SSe)$, layer compound, expansivities and thermal degradation 77−89554
SnTe, low-temp. sp. ht., thermal expansion and Gruneisen parameter 77−15601
SnTe, thermal expansion rel. to temp.-depend. ^{119}Sn isomer shift 77−8457
$Sr_{0.5}Ba_{0.5}Nb_2O_6$ crystals, ferroelec., dislocation free, pyroelec. props. 79−42907
SrF_2, linear thermal expansion coeff., capacitance method meas. 78−16772
SrF_2:La, type-I dipole reorientation, activation vol. determ. from dielec. const. 80−88916
$Sr(ND_2)_2$, neutron diffraction exam. 31 to 570K, temp. depend. of lattice parameters *(German)* 79−69085
$Sr(NO_3)_2$, 261-740K, X-ray diffr. obs. 77−35720
$Sr(NO_3)_2$, Born-Mayer interaction pot. and lattice props. 79−37858
$Sr_{1.8}Na_{0.1}Nd_{0.1}Ta_2O_7$, solid soln., ferroelectric phase transitions, dielec. constant and thermal expansion rel. to temp. 80−88934
$Sr_2Nb_2O_7$, ferroelectric phase transitions, dielec. constant and thermal expansion rel. to temp. 80−88934
$SrO-B_2O_3-GeO_2$ system glass, physicochem. props., alkaline earth oxides effect 79−65827
$SrSnF_4$, thermal expansion and phase transitions 79−77781
$Sr_2Ta_2O_7$, ferroelectric phase transitions, dielec. constant and thermal expansion rel. to temp. 80−88934
$SrTiO_3$, thermal expansion near displacive phase transition meas. 77−12345
$TABe_{12}$, by diffusion saturation in vacuum, resistance to heat 78−44259
Ta, liquid, thermophysical measurements up to 7500K 78−43136
Ta, melt, thermal expn., 1146-2288K 78−43148
Ta, thermophysical props. and neutron absorpt. 80−103488
Ta-W TV-10 alloy, thermal expn., 1146-2288K 78−43148
TaS_2, thermal expansion, lattice parameter meas. 78−18804
$TaSe_2$ (2H), first-order phase transition, thermal expansion meas. 79−51256
$TaSe_2$ (2H), thermal and elastic props., X-ray diffr. exam. 79−37754
$TaSi_2$ film, elastic stiffness and thermal expansion coeffs. 80−107451
$Ta_{16}W_{18}O_{94}$, characterisation of thermally contracting tungstates 78−63869
Ta_2WO_8, characterisation of thermally contracting tungstates 78−63869
$Ta_{22}W_4O_{67}$, characterisation of thermally contracting tungstates 78−63869
Tb, third order elastic consts. and thermal expansion 77−80569
Tb-Gd, spontaneous striction and phonon contributions to thermal expansion *(Russian)* 79−90800
Tb-Gd alloy, spin orientation transition obs. 79−99714
Tb-Ho, single cryst., annealed, thermal expansion 78−47541
Tb-Ho, thermal expansion in vicinity of Curie temp. 79−28524
Tb-Ho (50%), antiferromag., hexagonal anisotropy effect on thermal expansion 79−51283
Tb-Ho (50%), antiferromagnetic, thermal expansion, US attenuation anomalies 79−47319
Tb-Ho alloy, influence of internal strain on Neel temp., thermal expansion and elastic const. meas. 77−63176
Tb-Y, single crystal growth from melt, X-ray obs., props. *(Russian)* 78−95689
$Tb_{0.27}Dy_{0.73}Fe_2$, anomalous thermal expansion and magnetostriction 77−90003
$Tb_2(MoO_4)_3$, thermal expansivity and spontaneous strain temp. depend. 79−14943
$TbPO_4$, phase transitions at low temp. 80−15237
$Tb_{1-x}Y_x$ alloy, helicoidal antiferromag. to ferromag. transition 78−10687
Th, lattice parameter variation at low temp., thermal expsn. 80−15046
ThF_4, monoclinic, lattice parameters and thermal contraction coeff., 25 to 83°C 77−47607
ThO_2, 500-1800°C, X-ray diffr. 77−35723
ThO_2, cationic transport number determ., thermal expansion meas. *(French)* 78−84267
Ti alloys, data handbook of low temp. mech. and phys. props. 80−22153
Ti, high purity, data handbook of low temp. mech. and phys. props. 80−22153
Ti, lattice specific heat and thermal expansion 79−73318
Ti, liquid, thermal volume expansion, MP to BP 79−90802
Ti, specific heat and thermal expansion, 4-290K *(Russian)* 79−51276
Ti, thermal expansion coeff. and Gruneisen const., 6 to 300K *(Russian)* 79−51281
Ti:transition metal, linear expsn. temp. coeff., polymorphic transition temp. shift 78−6164
Ti-Al, Ti-Al-Sn, specific heat and thermal expansion, 4-290K *(Russian)* 79−51276
Ti-alloy, VT16, volume and phase changes during continuous heating *(Russian)* 77−77470
Ti-Mo-V-Al-Cr-Fe (4.8, 4.7, 5.2, 1.1, 1.0 wt.%), structural changes during heating up to 1000°C, DTA study *(Russian)* 80−93552
Ti_3Al, phase transitions and physical props. 77−25068
Ti_3Al-(Mo) (0.5 at.%), ordering, Mo effects 77−28841
Ti_2AlC, Ti_3AlC, TiC, phys. props. 77−43602
Ti_2AlN, prep. and props. 77−28745
TiC-TiN system, electro- and thermo-phys. props. 80−34210
TiC-VC(Nbc)(YaC), comp. depend. 77−28772
TiC-VC(ZrC) carbide alloys, thermophys. props., temp. depend., specific elec. resist. 79−86908
TiC_x, electron energy spectrum and phys. props. in homogeneous region *(Russian)* 77−31941
TiC_xN_y, thermal cond., elec. cond., and thermal expansion 80−10714
TiC_xN_z, thermal expsn. of cubic phases 79−1512
$TiC_xN_zH_m$, thermal expsn. of cubic phases 79−1512
TiC_xO_y, cubic phase, thermal expsn., lattice consts. 78−43149
TiC_xO_y, thermal cond., elec. cond., and thermal expansion 80−10714
TiC_xO_y, thermal expsn. coeffs. lattice spacing temp. depend. 77−69102
$TiC_xO_yH_m$, cubic phase, thermal expsn., lattice consts. 78−43149
$TiC_xO_y(H_m)$, cubic phases, thermal expansion, 77-300K 79−42281
$TiFe_xCo_{1-x}$, thermal expansion and magnetoelastic effects 80−80585
TiN_z-TiO_y, thermal expansion, 23-1000°C, X-ray obs. 78−91454
TiN_zO_y, cubic, thermal expansion coeffs., Ti-Ti bond screening 79−10970
TiO_2-Al_2O_3-SiO_2 system, ternary glass-forming region and phys. props. 80−84919

thermal expansion continued
TiO_y, thermal expansion of cubic phase at low temp. X-ray diffr. anal. 79−1514
TiO_y, thermal expsn. coeffs., lattice spacing temp. depend. 77−69102
TiO_yH_m, cubic phases, lattice consts. meas., thermal expansion coeffs. calc. 79−55906
TiO_yH_m, thermal expansion of cubic phase at low temp. X-ray diffr. anal. 79−1514
$TiO_yN_zH_m$, m=0, 0.31-0.34, thermal expansion, H at. ordering 79−10971
TiOy, annealed, lattice const. meas., thermal expansion coeffs. calc. 79−55906
TiS_2, layer compound, expansivities and thermal degradation 77−89554
$TiS_2(Se_2)$, physical props. 80−44179
$TiSi_2$, film, elastic stiffness and thermal expansion coeffs. 80−107451
Ti_xSi_y, work function rel. to phys. props. 77−47887
Tl, thermal and elastic props., lattice heat capacity, elastic constants and thermal expansion, model 80−39321
$TlAsSe_2$, diamag., thermal expansion rel. to temp. at cryst.-melt transition 78−34954
Tl_3AsSe_3, refractive index, thermal expansion temp. depend. 80−97223
TlI, linear thermal expansion coeff., capacitance method meas. 78−16772
Tl_2Se, diamag., thermal expansion rel. to temp. at cryst.-melt transition 78−34954
Tl_2Se_3, diamag., thermal expansion rel. to temp. at cryst.-melt transition 78−34954
Tm, lattice dynamics, thermal expansion, spt. ht., mag. contrib. 79−37778
TmSb, crystal field effect in thermal expansion 78−19305
TmSe, mixed valence cpd., thermal, mag., and transport props. 79−61074
Tm_xSe, $0.87<x<1.05$, mag., thermal and transport props., comp. depend. 78−68239
TmTe, crystal field effect in thermal expansion 78−19305
$(U,Pu)O_2$, vapour press. eqn. of state, VENUS-II code studies 78−8908
α-U, single crystal, thermal expansion coeff. and cones of zero expansion 78−34635
U, vacancy formation and phase transformation by positron annihilation 80−49215
α-U-Mo, dil., electronic properties depend. on $2^1/_2$-th order phase transition under high press. *(Russian)* 80−11128
UC 80−15046
UO_2 and UO_2-Gd_2O_3 solid soln., high temp. thermal expansion, 298-1700K 78−83979
U_3O_{8-z}, thermal expansion, phase transforms. rel. to temp. 77−35721
UP, vol. changes at mag. transitions 80−7107
$(UPu)O_{2-x}$, thermal expansion as a function of deviation from stoichiometry *(French)* 78−21645
US-UC-UC_2 system, potential nuclear fuels, phase solid soln. studies, prep. and props. exam. 79−40996
V, Doppler broadened positron annihilation lineshapes, prevacancy lattice expansion 78−27349
V, liquid, thermal volume expansion, MP to BP 79−90802
V, thermophysical props. at temps. up to 7000K 80−103497
V:transition metal, linear expsn. temp. coeff., polymorphic transition temp. shift 78−6164
$V_3Ge(Si)$, Gruneisen parameter and thermal expansion eval. at room temp. 80−70351
δ-VMn, ordering and disordering behaviours 77−48428
VO_2, X-ray determ. of lattice constants and thermal expansion coeffs. near transition temp. 79−86747
V_2O_3, thermal expansion tensor, phase transitions, X-ray diffr. obs. *(French)* 79−1515
V_2O_5, thermal expansion tensor, phase transitions, X-ray diffr. obs. *(French)* 79−1515
$VS_2(Se_2)$, physical props. 80−44179
V_3Si, martensitic transform., thermal expansion meas. in normal and supercond. states 79−56381
V_3Si, powdered, Debye-Waller factors and lattice consts., 25-1000K, X-ray diffr. obs. *(German)* 79−33060
V_3Si, thermal expansion, 20-300°C, using differential push-rod dilatometer 80−39320
V_3Si, thermal expansion meas., 4.2 to 293K 79−56382
W 79−42280
W, linear expansion coefficient, at low temp. 78−83977
W, liquid, thermal volume expansion, MP to BP 79−90802
W, thermal expansion coeff. meas. using strain gauges and thermocouple 78−53059
W-Nb (0-30 at.%), average thermal expansion coeff., 500-1200K 78−14483
W-Re alloys, sintered, preparation, thermal cond., linear expansion up to 1000K 79−61533
W-Zr (2.92, 7.42 and 10.02 wt.%), and W_2Zr, thermal expansion, elec. resistance, 100-900°C, crystallisation 78−91455
2H-WSe_2, thermal expansion between 10 and 320K, cell dimensions meas. 79−65222
WSi_2 film, elastic stiffness and thermal expansion coeffs. 80−107451
Xe adsorbed monolayers, thermodynamic props. and lattice const., quasi-harmonic theory 79−42380
Xe, monolayer adsorption on Ag (111), statistical mech. 80−34306
Y, thermal and elastic props. 79−33027
Y-Si-Al-O-N glass, prep. and props. 80−25647
YAG solutions, in $PbO/PbF_2/B_2O_3$ solvent systems, density, surface tension and expansivity data, effect of B_2O_3 conc. 79−19985
YAG:Nd, laser material, linear expansion coeff. and r.i., temp. depend. 77−733
$Y(Co_{1-x}Cu_x)_5$, neutron diffr., thermal expsn. *(French)* 80−19749
Y_2O_3, 500-1800°C, X-ray diffr. 77−35723
YbCuAl, mixed-valent cpd., thermal expansion and magneto-volume effects 80−66005
Yb_2O_3-based ceramic, preparation, mech. props. 77−24998
$YbSi_{1.8}$, valence fluctuation cpd., X-ray anal., mag. susceptibility and linear expansion coeffs. 79−77569
Yb_5Si_5, valence fluctuation cpd., X-ray anal., mag. susceptibility and linear expansion coeffs. 79−77569
$ZiSiO_4$, natural and synthetic, X-ray dilatometry 77−51522
Zn, anisotropic thermal expansion 79−23750
Zn, vacancy conc., lattice parameters meas. 78−10040
Zn, vacancy concentration meas., lattice parameter and length changes, form. parameters 79−37697

thermal expansion continued
Zn_3As_2 and $ZnAs_2$, molten, thermal expansion and atomic bond strength parameters 80−65257
ZnB_2O_4-MF_2 (M = Mg, Ca, Sr, Ba) glass system, physicochem. props. 80−34877
$Zn_2Ba_2Fe_{12}O_{22}$, phase transition, mag. props. *(Russian)* 79−51837
$ZnCl_2$ glass, glass transition temp. and thermal expansion 80−64902
$ZnCl_2$-LiCl(NaCl)(KCl)(CsCl), molten, density meas. *(Japanese)* 79−19383
ZnO, wurtzite structure, hydrothermally grown exam. of thermal expansion coefficient 78−75854
ZnO-Al_2O_3-SiO_2, transparent glass-ceramic, microstruct., physical props., crystallisation ht. treatment depend. 78−80506
α-ZnP_2, lattice parameters and thermal expansion, 80-320K, X-ray obs. 80−75373
ZnS, linear thermal expansion coeffs. meas., room temp. to 250°C 78−55416
ZnS:Fe^{2+}, thermal expansion and heat capacity, effect of Fe^{2+} 77−31782
ZnS(Se), optical material, 60-300K 78−33791
ZnS(Se)(Te), thermal expansion and lattice dynamics under press. 80−100316
ZnSb, X-ray diffr., 78-300K, dynamical props. and thermal expansion *(Russian)* 77−7833
ZnSe, 20 to 1100°C *(Russian)* 79−95188
ZnSe films, long wavelength IR polariton emission band thermal shift and broadening 80−92833
ZnSe, lattice vibration, thermal expansion and pressure effect 80−39233
ZnSe, linear thermal expansion coeffs. meas., room temp. to 250°C 78−55416
$ZnSiAs_2$, thermal expansion coeffs. meas. *(Russian)* 80−65258
$ZnSiP_2$, thermal expansion coeffs. meas. *(Russian)* 80−65258
ZnTe, 1.5 to 30K, thermal expansion and Gruneisen parameter meas. 80−59681
ZnTe, lattice vibration, thermal expansion and pressure effect 80−39233
Zr alloys, reactor fuel sheath mat., thermophys. props. 77−46280
ω-Zr, electric field gradients at substitutional Ta atoms, TDPAC high-pressure study 78−52384
α-Zr-H, volumetric changes, and thermal expansion, dilatometric and X-ray analysis exam. *(Russian)* 79−11665
Zr-Nb (1 and 2.5 wt.%), annealed, thermal expansion, α/β transition *(Russian)* 78−26702
Zr_3Al, ordered, exam. of Young's modulus and thermal expansion coeff. 78−72805
ZrC coating, vapour deposition, phys. and chem. props. 77−40456
ZrC-NbC-MoC_{1-x} system, thermal expansion coeff. up to 2500°C 79−69267
ZrC-ZrN system, solid solns., elec. resist., thermo EMF, thermal cond., expansion coeffs. 78−60176
$Zr(Fe_{1-x}Co_x)_2$, ferromag. and mictomag., thermal expansion and forced volume magnetostriction 80−75830
$Zr(Fe_{1-x}Co_x)_2$, magnetovolume effects, thermal expansion and forced vol. magnetostriction meas. 80−29595
ZrO_2, partially stabilized, props. and appl. to extrusion dies 80−97507
ZrO_2-HfO_2-CaO, cubic solid solutions, thermal expansion 77−15598
ZrO_2-Sc_2O_3 system, high-temp. phase transitions, elec. cond., thermal props. 77−16573
ZrS_2, layer compound, expansivities and thermal degradation 77−89554
$ZrSi_2$, work function rel. to phys. props. 77−47887
$ZrZn_2$, high purity, mag. props., pulsed fields up to 17 T 78−64198

thermal expansion measurement
absolute interferometric dilatometer 77−45832
alloys thermal expansion coefficient, and volume effect anomalies during transformations, review of differential dilatometric error sources *(Russian)* 79−34223
automatic linear expansion coefficient meter with digital readout 80−106713
bricks, extensometer for meas. of linear expansion due to freezing 78−53062
coefficient, steel gauge blocks, meas. in climatic chamber *(German)* 80−68171
contactless, by double Michelson interferometer 80−73317
diffractometer, Bond type, for precise meas. of single cryst. lattice parameters and thermal expansion 79−23498
dilatometer, absolute interference, for high-temp., high-precision testing installation 79−35677
dilatometer, alumina, for 25°C to 1600°C 78−36965
dilatometer, meas. thermal dilatation of metallic amorphous ribbons 80−86258
dilatometer based on mechanotron 80−105639
dilatometer for small linear expansion temp. coeffs. 78−77957
dilatometer of parallel-plate capacitor design, thermal expansion meas. 77−51523
dilatometric determ. of liquid specific heat and thermal expansivity 77−87758
dilatometric measurements, high temp. method accuracy 80−73308
dilatometric measurements, high-temp., systematic and fiducial error estimation 80−101796
dilatometry, photography appl. 79−15622
dilatometry and its versatility in metallurgical studies. I *(French)* 78−65919
electrophysical information collection, recording and processing system 78−8388
enamel, rapid method for determining thermal expansion coefficient 79−20308
fibres, determ. using optical dilatometer 80−45454
films, determ. using optical dilatometer 80−45454
flow microcalorimeter for direct continuous meas. of coefficients for liquids and solids 80−52164
gamma attenuation technique for thermal expansion meas. of solids. at high temperatures 80−31960
high temperature thermal expansion, meas. via laser interferometry of two fibres 77−26270
light interferometry, ultraprecise meas. 77−71290
linear expansion test rig 80−22324
low-temperature coeff. differences in 4 to 80K range, measurement using differential dilatometer 80−17922
metal pipe, thermal strain recording at elevated temp., photographic technique 77−66731

thermal expansion measurement continued
metals and alloys, thermal expansion charact. determ. using strain gauges 78−81942
metals and alloys, thermophysical charact., peculiarities of temp. depend., dimensional change meas. *(Russian)* 78−95868
mineral characterisation technique 79−70795
nuclear reactor materials, thermophys. prop. meas. at RFL Springfields 77−14230
paraffin waxes, melting point determ., automatic analyser, based on dilatometry 79−14223
plastics, technique for meas. of coeff. of linear thermal expansion 77−41598
polycrystalline materials, high temp. expansion coeffs. determ. via X-ray diffr. 77−39503
polymer, volume dilatometer design 78−5706
polymers, determ. using optical dilatometer 80−45454
quartz dilatometer with capacitance transducer 77−13736
reference vessel, He second virial coeff., 0-500°C, two-temp. gas-expansion method 78−55711
sag method for linear thermal expansion coeff. determ. 79−77774
single crystal, lattice parameters and thermal expansion coeffs. meas. by Bond's method 77−24243
solids, combined method of temp. coeff. determ. 78−167
solids, linear coeffs., capacitance meas. method 78−16772
solids at high temperature, simple differential dilatometer for reduced average coeff. of linear expansion meas. 78−193
speckle interferometric meas. apparatus 80−68170
standard samples for dilatometry 78−26699
strain gauge technique 78−53059
thermal diffusivity determ. by dilatometric technique 77−41597
thermostat metals, influence of specimen curvature on sensitivity *(German)* 80−27291
ultra-low thermal expansion materials, constant temp. over 170 day period 77−45824
vitreous SiO_2 tube dilatometer for thermal expansion meas. of solids, −195 to 1000°C 79−26026
Be rod, using holographic interferometry 77−31073
C fibres, thermal expansion coeff. meas. using TEM fitted with furnace 80−102966
Ir, empirical formula for 440-2220°C 77−11709
NaCl, capacitance determination of area thermal expansion 79−80573
NaCl, measurement using X-ray powder diffractometer with polythermal attachment 80−311
Si cell for precise measurement of thermal expansion at low temps., results for Cu, NaF 80−37027
WC, gauge blocks, using interferometric dilatometer 79−12767

thermal fatigue *see thermal stress cracking*

thermal insulating materials
see also thermal conductivity
ceramics, microcracking as mechanism to improve thermal shock resistance and insulating props. 77−28885
corrosion behaviour, in steel-sheathed pipe system *(German)* 78−31580
cryogenic, vacuum-powder insulation, radiative heat transfer determ. by IR spectroscopy 77−13759
cryogenic insulation, thermal cond. meas. 79−30484
cryogenic structural materials 77−17989
evacuated multilayer insulation, method for evaluation of normal heat flux 80−53610
foam thermal conductivity meas., unsteady probe method *(German)* 80−31740
graphite, thermal cond., near 100 mK, rel. to appl. in cryostat construction 77−82535
heat mirror on plastic sheet for radiation insulation of visible windows 80−95985
kohlestein insulation, material labelled as RUD-N *(German)* 78−26023
mechanical supports, app. to meas. thermal conductance 80−82772
multilayer insulation, simple struct. insulating material props. for low temp. appl. 80−57307
multilayer insulation materials, ambient temp. outgassing rate 80−84370
nylon, thermal cond. near 100 mK, rel. to appl. in cryostat construction 77−82535
phase change material wall thermal storage, design criteria 80−35759
phase charge material wall thermal storage, modelling 80−35758
plastic foam Dewar vessels for liq. N_2, manufacture, heat insulation test *(Japanese)* 78−37023
plastic foam thermal cond., var. calcs. of upper and lower bounds 78−9550
radioisotope thermoelectric generator, high-temperature insulations testing 79−48145
refractory, effective thermal cond., fibre diameter effects 80−104105
refractory nonmetallic materials, method of investigating in linear thermal loading 79−42327
Space Shuttle external insulation, acoustic emission inspection 78−16276
C materials, thermal insulating props., furnace appls. *(French)* 78−44345
$Pb(Mn_{1/2}Ta_{1/2})O_3$, ceramic, for thermal and dielectric isolation at low temp. 80−39365
SiO_2-Al_2O_3, refractory fibrous heat insulating material 78−6990

thermal insulation
aircrew protective equipment in event of accidental cold water immersion 79−88058
animal coats and human clothing, review 78−73139
buildings, heat conduction in disperse media, anal. *(Hungarian)* 79−1056
conference, nonmetallic materials and composites at low temps., Munich, Germany, July 1978 80−22139
cryogenic electrical cables, heat influx problem, calc. 78−81988
cryogenic electrical supply leads, cooled by vapour 79−75534
cryogenic equipment, porous multilayer thermal insulation with diffraction shields 79−58732
cryogenic insulation, porous gas-filled, configurational effects on heat transfer 79−58734
cryogenic liquid surface, floating insulation beads effect on evaporation rate 77−30164
deep body thermometer testing and modelling 77−40816
Dewar, for student expt. for meas. of heat of vaporisation of liq. N_2 77−9840
Dewar vessels for liq. N_2, foam plastic, manufacture, heat insulation test *(Japanese)* 78−37023

thermal insulation continued
foam plastics, crack inspection using dye solution or X-ray opaque solution 80−76440
gas flow in thermal insulation media, transient behaviour at rapid depressurisation 80−27701
glass-ball packing, thermal cond. props., low temp. appl. *(German)* 77−27463
hot water storage tank, heat loss rel. to thermal insulation *(Japanese)* 80−5918
house energy conservation measures obs. and evaluation, using minicomputer, Philips expt. house (West German project) 79−61951
insulants, thermophysical meas. by US method 77−45830
kohlestein insulation for use in HTR systems, further investigations *(German)* 78−66346
LMFBR, insulations 77−83068
on metal backing, thermophys. characts., expt. determ. technique 80−4707
metal foil insulation, ARGAS apparatus, depressuriser, report *(German)* 77−130
mineral fibre production with low dust and zero lubricant contents *(German)* 78−19678
multi-layer insulation with thermal cond. below 0.1 μW/cmK 77−30161
multilayer, simple struct. insulating material props. for low temp. appl. 80−57307
multilayer insulation, heat and mass transfer during evacuation 77−30167
multilayer insulation, heat flux, residual gas press. distrib. 77−30163
multilayer insulation thermal cond., accel. temp. field method in low temp. investig. 77−30162
optimal insulation calc., w.r.t. internal and solar gains 79−62147
periodic heat flux through a three layered slab exposed to solar radiation 80−43598
photolamps, thermal interference reduction using Therm-O-lux 85 film 78−41302
Pioneer Venus Programme stable quartz oscillator 77−41288
porous media filled enclosure, convective heat transfer, boundary layer 79−59908
radiation shield, for cryogenic apparatus, thermodynamic optimisation 78−81982
reactors, gas cooled, internal insulation 80−47537
reinforced organic composite, graphite, or C-C, ablation, mathematical modelling 79−41564
residential building heat loss estimation by aerial IR imaging 79−74586
solar energy collector design for low capital costs and least steady-state heat losses 80−104517
solar heating system components, optimal insulation, numerical sensitivity anal. 80−35745
solar water pump, for lift irrigation, modified design analysis 79−70440
space heating, energy utilisation improvements using new types of construction *(German)* 80−40903
thermal sensation evaluation, comfort chart *(Japanese)* 80−81545
thermocouples, lead temp. effect on accuracy of mineral insulated NiCr/NiAl thermocouples 78−54371
thickness meas., using easily calibrated eddy-current meter 80−73316
trunk pipeline systems, oil and gas, investigation and optimisation of thermal regimes 80−107579
two-phase porous cooling system, hydrodynamic and thermal characts. 77−10012
N_2 plasma jet anode root behaviour rel. to hollow-anode thermal insulation 78−71554

thermal magnetoresistance
alkali metals, elec. and thermal cond. in weak mag. fields 80−65535
magnetothermal conductivity measurement for selected metals, 4 to 20K 79−67317
metal, closed-orbit, uncompensated, elec. and thermal magnetoresist., quadratic field depend. 79−95388
metal, effects of large scale voids on thermal magnetoresist. 80−10946
metals, thermal magnetoresist. and cylindrical voids 78−91658
Al, cryst. and polycryst., inhomogeneity effects on galvanomagnetic props. 78−60109
Al_2O_3, conc. depend. of V^{3+} freq. crossing signals, thermal phonons study 78−95115
Be, low temp. elec. and thermal magnetocond., use as heat switch 77−35923
$Cd_xHg_{1-x}Te$, thermal magnetoresist. meas., 4 to 400K 77−31814
Cr_2O_3, thermal magnetoresist., 0.1 to 100K, magnon-phonon interactions 79−65266
$CsMnCl_3.2H_2O$, thermal cond. in mag. field 80−70481
Eu, low temp. thermal and elec. magnetocond. 77−69301
n-Ge, magnetothermal cond., 4.2K 80−24688
p-Ge, magnetothermal conductivity at low temp. 79−28158
K, high-field thermal magnetoresist., 2.5-8K 78−23072
K, magnetoresistance anomalies due to inhomogeneities, examination 78−56130
K, saturation of longitudinal thermal magnetoresist. obs. 80−88541
K, thermomagnetic and thermoelectric properties, phonon scatt. processes 80−29390
K, transverse and longitudinal thermal magnetoresist., 3 to 9K 79−95385
MgO:Cr^{2+}(Fe^{2+}), thermal magnetoresistance 79−10994
Nd, low temp. thermal and elec. magnetocond. 77−69301
Nd, transport props., low temp., effect of mag. field 80−70679
Pb, high-field thermal and elec. magnetocond. 77−59279
Pr, transport props., low temp., effect of mag. field 80−70679
Sm, transport props., low temp., effect of mag. field 80−70679

thermal noise
600 MHz to 1 GHz coaxial thermal noise standard 80−98875
artificial cold resistors, electronic feedback cct. 78−32750
balances, effect on meas. appls. 78−65906
bolometer, ^{3}He-cooled, low heat capacity, differentiated-structure, performance 79−30544
diamagnetic susceptibility meas., thermal, Nyquist and Barkhausen noise 77−13782
Dounreay Fast Reactor surveillance, noise analysis development 79−3215
education, capacitor complete discharge time, thermal noise 80−17727
equilibrium system, temp. fluctuations and 1/f noise 78−23143
fast reactor coolant blockages, detection by temp. noise tech. 79−30899
frequency standard, thermal noise effect meas. on amplitude of oscillation 80−98898

thermal noise continued
generating functions calc. from characteristic functions 79−914
gravitation radiation detection, active resonant antennas, sensitivity and noise 79−30346
gravitational constant, torsion balance, thermal noise limitation 78−16714
hot carrier effects, in p-Si and SCLC diodes 79−24036
hot carrier noise, exptl. and theoretical aspect, survey 79−28389
Johnson noise, variance, 1/f noise 78−68059
Josephson junction phase-locked loop analogue to study effects of thermal noise 77−47939
Josephson junctions, Fokker-Planck solution for thermal noise 77−89906
laser frequency measurement using supercond. point contacts 80−90824
light beam energy indirect meas. accuracy *(Russian)* 78−74046
linear quantum channel with thermal noise, quasiprobability distribs. 80−12984
measurement, zero point energy noise term presence 80−68213
metal, temp. fluctuations as 1/f noise origin, theory 80−11059
metal-oxide-metal photodetector, noise, ultimate sensitivity 77−5915
microwave hot/cryogenic noise standards, preliminary design 77−82563
noise thermometry, theory and temp. determ. *(German)* 79−21748
Noise thermometry in the range 630-962°C 78−73995
nondegenerate semiconductor, quantum correction of Einstein reln. at high freqs. 78−19072
nonlinear oscillator with fluctuating parameters, dynamics, thermal noise 80−101729
Nyquist noise in mag. and dielec. materials 77−1569
optical cavity, one-dimens., with output coupling, thermal radiation, fluctuation-dissipation theorem 79−978
optical fibre digital transmission error probability, quantum noise effects *(Italian)* 77−23623
optical fibre system, timing error tolerant waveforms 80−14293
photodiode sensor arrays, circuits and performance 77−39077
piezoelectric plate, thermal fluctuations *(Russian)* 78−76389
polymer solutions, aq., capillary flow, thermal noise, low freq. oscills. 80−48754
pyroelectric 80−82820
pyroelectric detector, temp. noise 78−89542
pyroelectric detector, temperature noise and dielec. loss 77−17975
pyroelectric detector materials, thermal noise and dielec. response 80−75952
pyrolusite powder, thermal noise *(German)* 78−64075
resistance fluctuations, anal. independ. of thermal voltage noise 80−84495
resistor, metallic, nonlinear current fluctuations, microscopic calc., heating, perturbation theory 79−69484
semiconductor, fluctuation spectra near the threshold of a current instability 79−24037
semispherical monopole, immersed in plasma electrons, input admittance *(Russian)* 77−76196
SQUID noise thermometer, future of superconducting instruments in metrology 79−26020
strain-dependent resistors, in force meas., noise limitations 78−16771
teaching, Campbell's theorem, use in elec. noise formulae derivation 78−24602
temp. meas. appl. *(German)* 78−4615
thermal fluctuations during amplification of magnetoacoustic surface waves 78−88158
thin films, substrate supported, temp. fluctuation noise 80−92949
Cu, Johnson noise, rel. to absolute temp. 77−47872
GaAs epilayer, for FET, hot carrier noise 79−24035
n-Ge, anisotropy of thermal and convective noise, in magnetic field 78−34873
Ge p-n junction, current filament form., fluctuations and thermal noise 77−69411
Ge:Ga,Sb, compensated, low temp. props. rel. to appl. in bolometry 80−31867
$Hg_{1-x}Cd_xTe$-CdTe photodiodes, backside-illum., LPE growth and thermal noise characts. 79−40610
n-InSb, hot electron noise temp., Monte Carlo calc. 80−107877
KH_2PO_4, initial dielec. const. in ferroelec. phase by thermal noise method 77−16267
$LiTaO_3$ pyroelectric detectors, temp. noise effects on performance 77−79156
Nb superconducting point contact, singularities of I-V curve and voltage fluctuations 80−93044
n-Si, bulk, hot electron noise in high fields *(Japanese)* 78−34837
Sn, film at supercond. transition temp. thermal noise fluctuations 78−47907

thermal properties of substances
see also magnetocaloric effects; Scott effect; specific heat; thermal conductivity; thermal diffusivity; thermal expansion; thermal variables measurement
air, heating by flashlamp radiation, ballistic and calorimetric meas. *(Russian)* 78−5843
alkaline earth difluorides, thermal props. *(German)* 80−81355
aqueous heterogeneous systems, thermal anomalies 77−32829
bitumen-salt mixtures, radioactive, thermal stress. behaviour *(German, English)* 77−65290
boride coatings on Ni alloy, thermal stability, exam. of coating 78−44271
cell nuclei and tissue denaturing process, cooperative charact. 79−57593
composite material, mechanical behaviour, book 80−94935
diethyl ether, field ionisation, thermal energy distribution and energy deposition 80−95732
dilatometric anal. of thermophysical props. 77−71316
ear, mouse, effect of prior heat treatment on thermal enhancement of radiation damage 79−48291
ear, mouse, induced thermal resistance 79−48220
EMF, semiconductors, thermal cell and copper blocks method, more accurate treatment of results 80−77812
fibre reinforced thermoelastic materials, nonlinear thermodynamic continuum theory 80−14579
fluctuations, driven nonlinear resistive system 79−25981
gas thermometry, constant volume valve design 80−4711
gases, thermophysical props. tabulated for mixture composition certification 78−80818
glass characteristics, electromagnetic, mechanical and thermal props. 80−106587
gradient index material models and exptl. verification 80−16002

thermal properties of substances continued
graphite fibre filled phthalocyanine composites, cure cycle investigation 80−81030
hexanes, isomeric, 80−95732
hollow cylinder, internal one sided heating, nomogram construction, for computing temp. state 78−63271
Mars, radar, visual and thermal characts. of rough planar surfaces 80−98589
materials, electronic, optical, magnetic and thermal props., rel. to energy technology 78−88412
metal, heat resistant charact. extrapolation by temp.-time methods, creep data 78−15477
metastable superheated water, specific vols. and P-V-T props. 80−92032
MgO-ZrO_2 ceramic reinforced with filamentary crystals, mech. and thermal props. 80−45262
minerals, post-shock temps. meas. 79−92527
nonmetallic plates, sensitivity of thermal inspection, mathematical model 78−72995
optical fibres, jacketed, thermal characts. of phase shift 80−58670
optical material physical props., seminar, San Diego, CA, USA (Aug. 79) 80−105423
oxide, solid electrolytes, thermal and mech. props. at steelmaking temps., review *(German)* 78−15418
PET fibre, aminolyzed, dynamic viscoelasticity and thermal behaviour *(Japanese)* 79−38880
polyamides, 1,3-cyclohexanebis(methylamine) based, thermal props. and glass transition temp. 80−39264
polyethylene, modified with phosphonate ester pendant side group, thermal and mech. props. 78−11195
polyethylene with asbestos and glass wool fillers, thermal props. determ. *(Russian)* 77−43340
polymer materials, NDT, rigidity and hardness from acoustic, thermal, optical and dielectric props. *(Russian)* 77−48601
PVC, rigid asbestos reinforced, stabilization and dynamic thermal stability 79−8270
quartzite, vitrified, and quartzite based refractory concretes, prep. and props. 80−89188
random heterogeneous materials, statistical theory of effective elec. thermal and mag. props. 77−48118
rare earth difluorides, thermal props. *(German)* 80−81355
refractories, strength and thermal properties, automated test system 80−100986
resins, thermoplastic, glass-fibre-reinforced, performance at elevated temperatures obs. 79−95067
rocks, metamorphic, thermomechanical expts. using shear machine *(French)* 79−5474
rocks and minerals, conf., Newcastle, England (April 1974) 77−37194
rocks in vertical orogenetic profile, mechanical and thermal props. rel. to terrestrial heat flux *(German)* 78−81123
skin burn thermal conditions, review of exptl. results for man and animals 77−48758
soils, transient measuring method *(German)* 78−61619
solid, thermophysical characts. temp. depend. determ. 77−42720
steel, first order phase transformations, in non-isothermal conditions, exam. of kinetic parameters *(Russian)* 79−34028
steel, heat resistant charact. extrapolation by temp.-time methods, creep data 78−15477
steel, thermal props. meas. *(French)* 80−25977
temperature rate dependent materials 79−90123
thermal-radiation absorption factor, temp. behaviour 77−51526
thermometric method determ., harmonic action of heat flow *(Russian)* 80−69642
thermophysical characts. determ. from inverse problem of nonlinear heat conduction 77−42721
thermophysical coefficients, integral characts. method *(Russian)* 80−69643
UV and IR instrument material mech. and thermal props. 80−106584
viscoelastic deformation, apparent activation energy, creep T-jump expt. 79−37264
water, transient heat transfer (0-220°C, 1-10 bars) *(Russian)* 78−38183
Al-reinforced plastic honeycomb structures, active thermal inspection 78−72994
Al_2O_3-Ln_2O_3, Ln=La,Ce,Pr,Nd,Sm,Gd,Tb, struct. and thermal characts. of amorphous phases *(French)* 77−72558
Ar, solid state props., statistical thermodynamic calc. using gas phase intermol. pair pot. *(German)* 77−20083
Be substrate for lightweight mirror, surface quality and thermal props. 80−23762
CdTe, physical props., review 77−39833
Cs_3CoI_5, cryst. struct. and thermal props. *(German)* 79−23578
Fe-Ni alloys, lit. review *(Russian)* 78−18805
Mn-H(D), ferromag., thermal, struct. mag. props. 78−88145
Mo-based metallic glass development 80−89172
Ni, black, solar collector selective coatings, optical and thermal props. 79−62028
Ni-base alloy, heat resistant charact. extrapolation by temp.-time methods, creep data 78−15477
Si_3N_4 reaction bonded, microstructure, formation, properties, phase composition 79−56947
ThO_2-UO_2 solid solns., props. of importance for use as nuclear fuels 79−54506
Ti-Ti joints, soldered, exam. of active thermal method of inspecting 78−72993
U-Co(Ce)(Fe)(Mn)(Ni)(V) metallic glasses, glass form. and thermal stability 80−75183
VH_x, temperature limits for stable existence of hydrides, ionic state *(Russian)* 77−7690
Zn, thermal recovery and stress-strain relations 78−11266
Zr gels, thermal and related studies 80−71937

thermal quenching *see quenching (thermal)*

thermal radiation *see heat radiation*

thermal resistance
bodies in contact, heat transmission, optimal control thermoelastic stress constraint 80−19223
brittle material, heat resistance criteria on surface during convective heat exchange 77−15642
composite materials, creation of matrices with operating temp. of 1100°C *(Russian)* 77−55913
contact between wavy surfaces in vacuum 77−7293
thermal resistance continued
contact resistance, determ. for solidifying metal and mould 78−39759
contact resistance, dimensionless relations 78−83221
contact resistance of rough surface junctions in gas. medium 77−35018
corundum-based refractory-lining material, heat resist. determ. by thermal softening assessment *(Russian)* 79−83237
ester-imide varnishes, electroinsulating, thermal resist. *(Polish)* 78−84014
fission reactor fuel rod pellet-clad gap thermal conductances, exptl. results, anal. correl. 78−70606
graphites, ARV, VPP, MPG-6, contact thermal resistance, surface finish and compression depends. 78−79829
heat pipe, low-temp., evaporator-condenser iterrelation effect 77−89003
heat pipe, low-temperature, efficiency calcs. 77−10030
heat pipes with metal fibre wicks, thermal resist. 80−43601
high-alloy bearing, LTMT effects on ht. resist. and contact fatigue resist. 77−44354
hybrid IC, calc. method 77−84104
metal, with high thermal cond., method for determ. of thermophysical characts. 77−45833
metal-dielectric boundary, role of cond. electrons in form. of thermal resist. *(Russian)* 78−19149
metallic contacts, directional effects of heat flow, thermal rectification 77−58532
minimisation of thermal resistance, solid with heat exchanging surfaces, variational method 78−94512
nonsteady regimes, multilayer systems, applicability of additivity law anal. 77−42695
particle layer deposition from gas dispersion turbulent flow in tubes, heat exchanger appl. 79−55409
plate-semi-infinite space, heat exchange process control, thermoelastic stresses *(Russian)* 80−53606
polyester varnishes, electroinsulating, thermal resist. *(Polish)* 78−84014
polyethylene stabilized with home-made antioxidants, thermal resistance *(Polish)* 79−52328
polymer electrophoretic coating, effect of silicone additive on electrophys. props. *(Russian)* 79−15615
pores and microcracks thermal resistance decrease, effect on thermal cond. 78−75892
refractory metal alloy, heat resistance and cold brittleness, achievements and trends 78−95718
refractory nonmetallic materials, method of investigating in linear thermal loading 79−42327
resistor, fluctuations in resistance and enthalpy, response to current changes 78−34871
semiconductor DH laser, thermal resistance and temp. distrib. calcs. and obs. 79−98368
steel, die, with high heat resist. and toughness 78−84989
stripe geometry proton-isolated DH lasers, thermal resistance models 78−37881
system of parallelepipeds, calc. method 77−84104
temperature fields in space-connected regions with alternating contact thermal resistance *(Russian)* 80−53607
thin-walled bodies, variable nonideal contact, coupled heat-conduction solutions 80−102961
transient thermal response of two bodies communicating through small contact area 77−39200
vapour-gas mixture, condensation, effect of thermal resist. of drops on heat and mass transfer 77−15015
wavy metallic surfaces in contact, thermal resistance 78−59262
Al alloy, AK4-1, dispersion-hardening, US effects on ductility and thermal resist. *(Russian)* 77−32582
Al mirrors, on metal substrates, resistance to heat and radiation 79−94319
Al, sintered powder, heat resistance increase method 77−90292
Al_2O_3-TiO_2 (1 wt.%), with and without α-Al_2O_3 laminar crystals, heat resistance 77−16532
Cu-epoxy-Cu sandwich, thermal boundary resist., 0.05-10K 78−14564
GaAlAs DH laser, In solder deterioration, Au diffusion in In 80−33019
$Ga_{1-y}Al_yAs$ laser diode, hetero-isolation stripe geometry for IR and visible radiation *(Japanese)* 80−83607
HoF_3, monocrystal, thermal cond., temp. dependence 77−55402
In solder joints, thermal conductance at low temps. 77−30150
LaF_3, monocrystal, thermal cond., temp. dependence 77−55402
Mo, ionic siliciding, diffusion layer prod. 78−23855
Ni-based eutectic alloys, struct. and props. *(Russian)* 77−21129
V-Zr-N quasi-binary section, long term hardness to compare heat resistance 78−3223
ZrO_2 coatings, prod. by low-temp. oxidation, props. 78−23856

thermal resistance measurement
contact resistance, prediction and measurement 79−37133
DH stripe-geometry lasers, thermal props., interpretation of thermal resistance measurements 80−64017
using forward characteristic temp. depend. of diode 77−47893
ground, theoretical basis and apparatus *(Rumanian)* 79−5461
injection lasers, meas. technique for impedance 78−13705
solid thermal cond. and interface resistance meas. by radiation thermometry 80−86289
specimens in transonic high temp. gas stream 79−63207
W wire reinforced Ni alloy, heat resist. testing, specimen gripping arrangement 79−15895

thermal resistivity *see thermal conductivity*

thermal shock
alloy, high temperature, mechanical, thermal and corrosion props. 78−95763
apparatus, for adherence, wear resist. and thermal shock meas. of thin films 78−72943
bench scale prebaked anode fracture, coke and formulation variables effect during Al smelting 79−52371
ceramic, thermal shock resistance determ., new heat flux method *(Japanese)* 79−39075
ceramics, high temp. props., conf., Baden-Baden (Feb. 1978) *(German)* 79−70135
ceramics, synthetic raw materials, sintered and fused, use in refractories industry, slagging, creep, thermal thick resistance *(German)* 79−4937
ceramics, thermal shock resistance meas. by AE *(German)* 79−70233
ceramics, thermal stress and thermal shock, review of test methods, thermal stress theory industrial problems 77−63805
coaxial plasmatron, Cu electrode degradation by arc spot, thermal shock and surface cracks 79−14629

thermal shock continued
concrete, heat resisting, exam. of deform. behaviour, description of testing rig and operation *(French)* 79−15720
corundum, subjected to thermal shock, study of substruct. and surface morpholoy 79−43292
corundum, thermal strength, effect of additives 78−19770
fast burst reactor, WSMR, thermal shock stress anal. for enlarged irradiation cavity 78−33242
fast burst reactors, thermal shock effects stress anal. 77−79428
finite disc, thermal shock, finite integral transform method 77−3765
fracture toughness testing by arc discharge heating 78−72835
fusion reactor materials, thermal shock resistance of limiter and first wall 79−3239
gases, thermal shock prod. with conc. solar energy *(French)* 78−91056
glass bodies, heat resistance, determ. 80−24690
graphite, neutron irradiation effects on thermal shock resist. and fracture toughness *(Japanese)* 80−66622
graphite, thermal shock on a finite orthotropic thin shell 79−68587
graphite, Tokamak reactor, mag. limiter plate, electron irrad. and thermal shock 78−66416
graphite shell, thin, cylindrical, orthotropic, thermal stresses and displacements due to instantaneous thermal shock 80−92060
graphite thermal shock resistance and fracture toughness meas. *(Japanese)* 79−91868
ice, heat and mass transfer during sublimation, thermal shock method 77−50864
Incoloy 800, clean and steam oxidised, T_2 permeation 80−88364
isotropic isoceles right-angled triangular plate on elastic foundation, thermal-shock induced vibr. 77−35070
laminated cermet coating on Cu, thermal shock performance 78−7081
liquid, superheated, thermal cond. meas. technique using shock heating 77−45834
magnetothermoelasticity, dynamic *(Russian)* 77−55995
metal sheet strength improvement by localised thermal shock 78−88483
metals, working, method of applying fusion thermal indicators to surfaces, including heated surfaces 80−17937
MHD generator duct wall, semi-hot, thermal stress design study *(Japanese)* 78−13890
microwave absorbing ferrite-dielectric composite 77−7880
mullite ceramic rollers, heat treatment effects 79−61616
nuclear reactor, LOCA, thermal shock in nuclear containment wall, computer code for safety anal. 77−3135
one-dimensional thermal shock problem of thermoelasticity in a non-simple medium 79−18794
optical long focal length aerial reconnaissance system response 80−78939
optical system response to thermal shock, meas. on long focal length reconnaissance lenses 80−77892
pellet fusion reactor, thermomech. dynamic behaviour of solid wall 80−95396
pressure vessel, strength analysis, by thermal shock 78−68819
reactor graphite, thermal shock fracture toughness eval. by arc discharge heating 78−72835
reactor pressure vessel, bimetallic, composite geometry, subjected to thermal shock, temp. decay, 2-D soln. 77−88209
refractories, classification according to brittleness and thermal shock resistance determ. 79−83321
refractories, fatigue behavior, effect of texture and crack kinetics, AE anal. *(German)* 80−21061
refractories, fracture toughness role in spalling resistance *(German)* 77−73316
refractories, role of fracture toughness in thermal shock resistance *(French)* 78−80618
refractories, thermal shock resist. criteria calc., rel. to deformability 79−29212
refractory, fracture under thermal shock, AE study 80−25865
refractory, thermal shock resistance by resonant frequency expt. *(German)* 77−9009
refractory, thermal shock resistance charact. by permeability variation meas. *(French)* 79−96108
refractory ceramic, heterogeneous, significance of non-elastic deform. in fracture 79−47765
refractory oxide, thermal shock resist. mechanisms 80−25860
rocks, fracture propagation by transient cooling 79−84236
Sanicro 31, T_2 permeation 80−88364
spherical body containing central inclusion, thermal stresses *(Russian)* 78−34018
β-spodumene-mica glass ceramic, thermal expansion thermal shock and moduli of rupture and elasticity 78−60736
steatite, ceramic, exam. of thermal damage by strength meas. 78−84997
steel, cast, equipment for thermal shock resistance determ. 80−55614
steel, nuclear pressure vessel time A533 grade B class 1, thermal shock fracture toughness at elev. temp. *(Japanese)* 79−83304
steel, thermal shock cracking, fracture mechanics and fractographic exam. *(Japanese)* 78−52964
UMFBR molten core debris and core containment material interactions 79−13469
Al_2O_3, coating on Cu, thermal shock performance 78−7081
Al_2O_3, crack detection caused by thermal shock, AE technique *(Japanese)* 80−21248
Al_2O_3, thermally shocked, strengthening kinetics 77−8920
Al_2O_3-TiO_2 (1 wt.%), with and without α-Al_2O_3 laminar crystals, heat resistance 77−16532
Be, plasma-sprayed coatings on Cu and stainless steel, fusion reactor appl. 80−18619
C fibre reinforced composite, space appls. rel. mech. and thermal props. 78−7016
$CeO_2La_2O_3$, ceramic, thermal stability, sintering, deform., effect of La_2O_3 79−11532
α-Cu-Ni-Zn-Pb, fire cracking and ordering *(German)* 78−60760
Fe-Cr-Al, HOS 875, oxidation, cyclic, role of thermal shock 80−97640
MgO and MgO-dolomite, crack detection caused by thermal shock, AE technique *(Japanese)* 80−21248
MgO, granular, first-order stresses due to thermal shock 77−40409
MgO, thermally shocked, strengthening kinetics 77−8920
MgO-Al_2O_3-SiO_2 based cordierite glass-ceramic, strength and thermal shock, surface treatment effect 80−25884
Mo, BCC, thermal shock resistance, original struct. effects 77−63803
Mo, Tokamak reactor, mag. limiter plate, electron irrad. and thermal shock 78−66416
thermal shock continued
Ni base alloys, IN-702, IN-601, TD-Ni-Cr-Al, B-1900+Hf, oxidation, cyclic, role of thermal shock 80−97640
Ni-Cr-Al coatings, corrosion and thermal shock resist. in diesel engines 79−24675
Ni-ThO_2, oxidation, cyclic, role of thermal shock 80−97640
SiC, subjected to thermal shock, study of substruct. and surface morpholoy 79−43292
SiC, Tokamak reactor, mag. limiter plate, electron irrad. and thermal shock 78−66416
Si_3N_4, reaction bonded and hot pressed. exam. of thermal shock behaviour *(German)* 78−64561
Si_2N_2O, elastic props. 79−29122
SiO_2-Al_2O_3 refractories, thermal shock props., fracture mech. appl. *(French)* 79−96109
TiB_2, plasma-sprayed coatings on Cu and stainless steel, fusion reactor appl. 80−18619
TiC, plasma-sprayed coatings on Cu and stainless steel, fusion reactor appl. 80−18619
TiC, tool carbide, thermal shock resistance and fracture strength 77−21257
TiO_2 based construction ceramics, fibre-like cryst. reinforced, mech. props. 80−55341
UO_2, isothermal crack healing and strength recovery, thermal shock effects 77−36625
V, BCC, thermal shock resistance, original struct. effects 77−63803
VBe_{12}, plasma-sprayed coatings on Cu and stainless steel, fusion reactor appl. 80−18619
W, BCC, thermal shock resistance, original struct. effects 77−63803
WC, tool carbide, thermal shock resistance, fracture strength 77−21257
Y_2O_3-Sc_2O_3 fused powders, production of ceramics of good thermal strength 77−63607
ZrO_2, coating on Cu, thermal shock performance 78−7081
ZrO_2, stabilized by Y_2O_3, corrosion and thermal shock resist. in diesel engines 79−24675
$ZrSiO_4$, plasma dissociated, improved thermal shock resistant refractories 79−52350
$ZrSiO_4$ zircon ceramic with glass-forming additives, sintering and mech. props. 80−60814

thermal shock failure *see thermal stress cracking*

thermal spikes *see crystal defects; radiation effects*

thermal stress cracking
accumulation of damage mechanism 77−44356
acrylic plastic, deform. of rigidly clamped specimens subject to one sided cyclic heating 77−59932
Al-graphite composite, mech. props., effect of thermal exposure 77−36629
alloy, coarsening by temp. cycling 79−29111
alloy, heat resistance under one sided loading 77−1872
alloy, high-temperature low-cycle fatigue strength at const. and variable temps., cycle period effect 78−7127
alloy, thermal cycling fracture 78−60839
alloys, heat-resist., evaluation method 80−3260
austenitic steel transformation temp. and crack prevention in weld cooling 79−83200
axially symmetric body, subject to cyclic heat loading elastoplastic strain 78−5672
bimetal, obtained by facing, static and fatigue strength, obtained by facing 77−90457
bimetal Nb-steel Kh18N10T with Cu interlayer, cyclic heating effect 77−16687
bimetallic tube, residual stress after thermal cycling 77−90465
brittle ceramics, effect of data scatter on apparent thermal stress failure mode 80−60949
brittle material, surface energy determ. from AE, automatic system 79−91899
brittle material, thermal stress resistance parameters when subject to thermal stress fatigue 78−90787
brittle solids, unstable growth of thermally induced interacting cracks 78−63374
brittle solids, unstable growth of thermally induced interacting cracks 79−23273
C Fe Armco, cumulative fatigue damage at US freqs., thermal activation 77−70181
central receiver solar power stations, solar receiver tube thermal stresses, fatigue aspects 80−40908
ceramic, failure prediction under thermal loading, Weibull eqn. 78−88534
ceramic, one dimensional cooling, effect of particle orientation on frost damage *(Japanese)* 77−12701
ceramic, structural integrity in severe thermal environments 77−36544
ceramic, thermal fatigue life prediction 78−19873
ceramic, thermal fatigue life prediction 79−38939
ceramics, fracture mech. appl. 79−43426
ceramics, microcracked brittle, thermal stress resistance anal. 80−40472
ceramics, microcracking as mechanism to improve thermal shock resistance and insulating props. 77−28885
ceramics, thermal stress and thermal shock, review of test methods, thermal stress theory industrial problems 77−63805
ceramics, thermal stress resistance, enhancement, for materials with thermal cond. gradient 78−48506
ceramics, thermal stress resistance, figures of merit, review 79−83290
coaxial plasmatron, Cu electrode degradation by arc spot, thermal shock and surface cracks 79−14629
composite fusion reactor liners, thermal fatigue tests 80−32460
composite medium, two-component residually stressed, elastoplastic crack model *(German)* 78−90790
concrete, reactor shielding thermal stress cracking anal. *(German)* 80−5232
concrete and mortars, containing S, durability study in temp. cycles and water resistance 78−27613
concrete dam construction elements, appl. of fracture mechanics to thermal stress cracking 78−76766
concrete walls, restrained stress and thermal cracking 79−100264
in corrosive-media, electrochem. polarisation applic. *(Russian)* 78−11356
corundum, subjected to thermal shock, study of substruct. and surface morpholoy 79−43292
corundum single crystals, stress relax., cracking during growth 78−47263

thermal stress cracking continued
Cr-Mo-V steel turbine rotor, fatigue tests 78−39912
crack growth at high-temp., fracture mech. appl., review 79−41628
crack propagation, brittle amorphous solids 78−75721
cylinder, transversely isotropic brittle elastic, stress and failure probability analysis for internal press. and thermal loading 77−50990
cylinder, weakened by penny-shaped cracks, thermoelastic stresses 80−10191
disc, subject to cyclic thermal effects, device to study strength 77−63880
disc, thermal cycling endurance, finite element method calc. 80−48646
edge-cracked plates subjected to transient thermal singularities, stress intensity factors 77−58612
ellipsoidal cavity, triaxial, collapse to crack, thermoelastic stresses 80−92061
elliptic slit in plate, thermal stress concentration 77−39262
extensometer design principles and props., thermal and thermomechanical cycle generation *(French)* 78−31598
fast reactor fuel pellets, crack pattern analysis 79−54497
fatigue of high-melting material sheets, testing device 80−25955
fatigue testing system for structural materials, metals 77−90525
fatigue testing under alternate force and thermal loading, installation 78−11481
Fe, cast, high Cr, hardfacing of roll, wear resistance and thermal durability 80−7686
fibre reinforced composites, exam. of thermal stress fracture 78−75103
fibre reinforced composites, thermal cycling, elastoplastic strain calc. under action of external stresses *(Russian)* 79−38896
fibre reinforced plastic/Al/adhesive laminate, interlaminar behaviour under thermal loading 77−81309
fusion reactor limiters; thermal and stress environment effects 80−32461
fusion welding of Al alloys, weld susceptibility to hot cracking 80−81143
garnet films, LPE, thermally induced substrate fracture 78−68639
gas turbine engine discs and blades design eval. of strength under thermocycling 77−70179
glass fabric reinforced phenol resin, effect of thermal loading on physicomech. props. 79−24622
glass fibre reinforced epoxy cross ply laminates, transverse cracking and long. splitting, strain effects 79−61723
graphite, fusion reactor liners, thermal fatigue tests 80−32460
graphite, thermal shock resistance and fracture toughness during graphitising heat treatment *(Japanese)* 80−71843
graphite-matrix pulsed reactor fuels, characteris. including thermal stress fracture 77−46294
graphites, reactor, strength and deformation under conditions of cyclic variation in load and temp. 79−43355
Haynes alloy 188, SEM exam. of fracture surface, due to low cycle fatigue at 700°C *(Japanese)* 78−52963
heat resistance testing, massive sample for mech. prop. changes obs. 78−7124
heat resistant material subject to asymmetric loading 77−48547
heat resisting, types EhI598, ZhS6KP, and 1, fatigue under mech. and thermal stress 79−66164
heat-resisting alloys, VM-1 and VX-4, thermal fatigue rel. to struct. changes *(Russian)* 78−11302
ice, thermal fracture 79−65141
irradiation reactor advanced fuels, effect of crack formation on fuel behaviour 80−650
J-integral appl. for stress intensity factors 79−81811
laser surface impact in air, optical breakdown threshold of air, reduced by cracks effects 79−69924
low-cycle nonisothermal loading, strain relations and failure criteria investig. method 79−52486
metals, test device for thermal cycling conditions 79−87778
metals and alloys, testing, installation for −180 to 1100°C 80−3266
meteors thermal fracture, detached particles mean dia. 80−62081
mullite-corundum ceramics, thread-like crystals reinforced, props. 80−108525
multipass welds, high temp. internal deformations development and effects on crack formation 80−81082
nuclear components, struct. integrity assessment mat. prop. variations 78−89953
nuclear power plants, structural materials and elements, thermal cycling strength calc. 78−31534
optical fibre, elliptically clad borosilicate single-mode, strain birefringence 80−33148
oxide crust thermal stress effect in LMFBR accident 79−13471
oxide films on $MoSi_2$, cracking under heat cycling, acoustic emission determ. *(Russian)* 80−30067
penny-shaped cracks, in elastic sphere embedding in infinite elastic space, thermal stresses 80−64460
periclase refractories, props. after testing at over 2000°C 80−104317
phase transformation, $\alpha \rightleftarrows \beta$, influence on mech. props. *(Russian)* 78−68681
porosity effect, on thermal stress resist. during steady-state heat flow 80−1488
Portland cement paste, hardened, creep under cyclic temp. 79−8320
PVC, tensile tests, post-yield phenomena 79−91752
quartz film, microcrack growth, electron microscope obs., electron beam induced thermal stress effects 77−69037
refractories, thermal shock resist. criteria calc., rel. to deformability 79−29212
refractories, thermal stress cracking resistance estimation 80−104288
refractory, thermal shock resistance charact. by permeability variation meas. *(French)* 79−96108
refractory, thermal strength, under program controlled thermal loads 78−11325
reinforced concrete containment model behaviour under thermal gradients and internal pressure 80−42837
rocks, igneous, thermal cycling cracks props. 79−29759
scale-resistant metallic materials, cyclic oxidation method for spalling and scale resist. determ. 77−77695
semi-infinite medium, transient thermal loadings, stress intensity factors 80−10193
sheet materials, heat stability, small automatic device for rapid testing 77−77672
slab containing annular crack, thermal stresses, integral transform techniques 80−96229
solid bodies, high-strength, thermodynamic determ. of safe stress *(Russian)* 79−50679
space-quality solder joints, resistance to thermal fatigue 80−25831

thermal stress cracking continued
steel, 12Cr1MoV, thermal fatigue and creep effect in fracture 80−104297
steel, 15Kh1M1F, thermal cycling and cyclic stress effects on strength and creep resist. *(Russian)* 79−52341
steel, acoustic emission associated with phase conversions 79−70275
steel, alloy, Cr-Cu-Mn-C, HT80, effect of grain size on sensitivity to reheat cracking *(German)* 78−72856
steel, austenitic, high-temp. crack resist., B and Mo influence *(Russian)* 80−16435
steel, austenitic, wire rod, austenite transform. kinetics accompanying interrupted cyclic cooling *(Russian)* 79−70064
steel, austenitic ferritic welded transition joint, type 316. thermal fatigue life *(Japanese)* 79−83307
steel, austenitic stainless, fatigue under static and cyclic heating fractographic peculiarities, electron microscope obs. *(Russian)* 77−52465
steel, austenitic stainless, thermal cycling, low temp., effect on principal mech. props. 77−81322
steel, austenitic stainless, thermal fatigue, fractographic features of failure 80−76349
steel, austenitic stainless, thermal fatigue of sodium mixer *(French)* 79−91789
steel, austenitic stainless, type 304, exam. of continuous cooling sensitization 79−29098
steel, austenitic stainless, types 304, 316, strain growth, due to thermal stress ratcheting, exam. 78−92354
steel, boiler, determ. of temp. distribution in specimens with thermal fatigue *(Russian)* 79−68542
steel, C, deformation peculiarities at high temp. under superplasticity with cyclic thermal load *(Russian)* 78−95776
steel, carbon, gas turbine disc, thermal fatigue 77−52452
steel, cast, thermal fatigue crack propag. *(Japanese)* 79−83305
steel, Cr, stress relaxation, superplasticity and thermal cycling *(Russian)* 80−21019
steel, Cr-Mo (2.25, 1 wt.%), thermal fatigue cracking caused by repeated quenching from high temps. 77−52469
steel, Cr-Mo (2.25, 1 wt.%) pipe, high temp. fatigue and creep strength 80−85060
steel, Cr-Mo-V, creep deform. under const. and cyclic temp. 79−38914
steel, Cr-Mo-V, creep fatigue interactions obs., strain controlled and load controlled tests 78−44214
steel, Cr-Mo-V, environmental crack growth during isothermal high strain fatigue and temp. cycling 79−5082
steel, creep and fatigue fracture prevention 78−60837
steel, die, thermal fatigue resistance, high temp. thermomech. treatment effect 80−50715
steel, eutectoid and hypoeutectoid stress relaxation during rapid heating transform. *(Japanese)* 78−11258
steel, ferritic, underclad cracking mechanism, effects of residual strain and heat affected zone ductility 77−25158
steel, finite life characteristics, notch effects *(German)* 77−90434
steel, G-Mo type, welded joints, thermal fatigue testing 78−3278
steel, heat resistance, thermal stability, stress-rupture strength, and creep 80−81194
steel, heat treated, deform. due to thermal gradient *(French)* 79−61631
steel, low alloy, thermally fatigued, fracture toughness 78−72872
steel, low alloy, welded joints, cracking during heat treatment 80−7724
steel, low alloy 10KhSND, thermal embrittlement when held for long periods at 340 to 450°C 77−70178
steel, low alloy Cr-Mo, heat fatigue, effect of technical factors 79−79058
steel, low alloy type 14Kh2GMR, high strength, welded joint, impact toughness, welding thermal cycle and tempering effects 80−3157
steel, low C, high temp. plastic flow under thermal cycling in superplasticity interval 77−70130
steel, low C, thermal fatigue, effect of temp. difference in fatigue tests on fatigue life *(Japanese)* 78−84978
steel, maraging, grain refinement due to cyclic heat treatment 78−52971
steel, microalloyed with Ce, La, Nd, effect on crystal structure and thermal fatigue and resistance *(Russian)* 79−34136
steel, Ni, cryogenic fracture toughness enhancement through grain refinement 77−36651
steel, Ni-Cr-Mo-U, ferritic, B segregation and high temp. embrittlement 78−7040
steel, rimming, shape change and pore form. during multiple polymorphic transform. *(Russian)* 77−25044
steel, rotor, thermal fatigue strength in presence of stress conc. 77−70180
steel, spalling and scale resist. determ. by cyclic oxidation method 77−77695
steel, stainless, 0Kh13N7, 0Kh13AN7, thermocyclic treatment effects, on struct. phase composition and mech. props. 78−44204
steel, stainless, 304, thermal fatigue and strength estimation, creep fatigue interaction 79−11708
steel, stainless, 304, thermal fatigue strength *(Japanese)* 79−83306
steel, stainless, 304, weld decay, precip. of $M_{23}C_6$ during thermal cycles *(Japanese)* 79−52468
steel, stainless, Cr-Ni-Nb (18, 10, 0.7 wt.%), type SUS 347-B, exam. of thermal fatigue props. 78−60755
steel, stainless, Cr-Ni-Ti, (18, 10, 0.4 wt.%), type SUS 321-B exam. of thermal fatigue props. 78−60755
steel, stainless, fatigue, high temp. under isothermal and thermal cycling conditions 78−60836
steel, stainless, high strength, influence of corrosive medium on low cycle fatigue, photography obs. *(Russian)* 79−34199
steel, stainless, LWR appl., US and AE testing of welds 79−36330
steel, stainless, notched, effect of stress hold time on high temp., low cycle fatigue fracture mode *(Japanese)* 78−52952
steel, stainless, stabilised, knife line attack phenomenon, dissoln. of carbides in thermal cycles *(Japanese)* 78−68701
steel, stainless, type 304, grain boundary sliding in isothermal and thermal fatigue *(Japanese)* 78−84979
steel, stainless, type 304, solution-annealed and thermally aged, correl. of high- and low-cycle fatigue data 78−15532
steel, stainless 316, cladding failure during thermal transients 79−8316
steel, stainless cold-worked austenitic, fatigue and creep crack growth at elevated temp. 78−48524
steel, stainless type 304, thermal fatigue, effect of temp. difference in fatigue tests on fatigue life *(Japanese)* 78−84978
steel, thermal cycling fracture 78−60839
steel, thermal fatigue, effects of inclusions 80−81183

thermal stress cracking continued
steel, thermal shock cracking, fracture mechanics and fractographic exam. *(Japanese)* 78−52964
steel, tool, material related model for thermal fatigue in hot work appl. 79−91791
steel moulds for die-casting Al alloys, thermal fatigue 79−24619
steel welded joints, resistance to cold cracking obs., C and H_2 content influence 77−21283
steels, Cr and Cr-Ni-Mo refining effect on low cycle fatigue strength, resistance to hydrogen embrittlement 78−44208
stress intensity factors calc. using contour integral method 79−37243
Superinvar alloy casting for optical instruments 79−81580
teeth, human, thermal stress effects and surface cracking assoc. with laser use 78−80915
testing at 200 to 430K 77−86248
testing device, 180⇄1100°C, in inert medium 79−15904
thermodynamics appl. in mathematical anal. 80−108530
Ti alloys, gas-saturated layer effect after welding 77−44359
Ticonal strength, effect of thermal stresses and phase transforms. 79−87721
transversely isotropic cylinder, thermal stresses for penny-shaped crack 77−89070
turbine blade, wedge-shape model 79−66169
turbine blade testing 77−63878
welded joints in dissimilar Al alloys, fishbone test piece axis of symmetry, residual stresses, cracking coefficient effects 80−7725
Zircaloy-2 irradiation growth at 353 and 553K, texture and temp. cycling effect 79−46709
Al alloy, weld metal structure and hot cracking susceptibility 79−24595
Al alloy welded joints, hot cracks in mutual solidification zone 79−24594
Al, thermal cycle annealing of single crystal, subboundary obs. 77−55992
Al, time-to-rupture and character of fracture, near MP *(Russian)* 77−21245
Al-Al_3Ni, eutectic composite, directionally solidified, thermal cycling induced distortion 78−39899
Al-Zn (40 wt.%), grain refinement by thermal cycling 78−3149
Al-Zn (40 wt.%), mechanical properties after thermal cycling 78−3150
Al_2O_3, crack detection caused by thermal shock, AE technique *(Japanese)* 80−21248
α-Al_2O_3, fusion cast refractory, effects of glassy phase on thermal cycling resist. 78−84956
Al_2O_3-Mo (20 wt.%) cermet, ZrO_2 crystal addition effect on thermal fatigue resistance 80−40528
Al_2O_3-Si_3N_4 preparation, compressive strength 80−25634
Al_2O_3-ZrO_2-SiO_2, fusion cast refractory, effects of glassy phase on thermal cycling resist. 78−84956
B fibre reinforced Al, thermal degradation of tensile strength, due to fibre strength degradation 78−39861
Bi-Sb, crack appearance in diffusion zones *(Russian)* 78−76727
C fibre reinforced composite, space appls. rel. mech. and thermal props. 78−7016
C fibre reinforced Cu, thermal expansion and thermal fatigue *(Russian)* 79−38936
C fibre reinforced epoxy cross ply laminates, transverse cracking and long. splitting, strain effects 79−61723
C, glassy, crack form. during prod., propag. by thermal stress 79−11700
Co base superalloy, rupture life, prior temperature cycling effect 78−60840
Co-Cr-Al-C eutectic alloy, thermal cyclic loading, exam. 78−48496
Co-Cr-Ni-W-Ta-C, alloy Mar M-509, TEM exam. of thermal fatigue crack propag. in cast alloy 78−76740
Co-Cr-Ni-W-TaC (15.7, 9.5, 3, 12.77 wt.%) alloy Co50B3W, temperature cycling effect on rupture strength 78−39898
CoCrAl-Y(HF), Y and HF effects on oxidative behaviour 78−44275
Cr effect on carbon steel weld metal hot cracking resistance 79−79061
Cr, on Nb, prior thermal working effect on coating quality *(Russian)* 78−23820
Cr-Ni alloy NK40, thermal fatigue life *(Japanese)* 78−19880
γ-γ'-Cr_3C_2-Y eutectic, Y addition effect on oxidation during thermal cycling 79−74310
Cu alloy, superplastic, activation energy of plastic flow 78−64584
Cu, foils and powder compacts, pulsed action of laser radiation, dimens. effect *(Russian)* 77−16437
Cu, time-to-rupture and character of fracture, near MP *(Russian)* 77−21245
Cu-In, thermally cycled, effect on mech. props. and microstruct. 79−4987
α-Cu-Ni-Zn-Pb, fire cracking, effect of pores and impurities 79−29207
Eu_2O_3-Ta_2O_5, microcracking, elastic props., internal friction 78−92326
Fe, cast, crazing with directionally arrayed flake graphite 77−59935
Fe, cast, mech. props., effect of repeated heating and cooling *(Japanese)* 77−59907
Fe, cast, US study of sections undergoing deform. or thermal cycling 80−104285
Fe, powder, sintering, effect of repeated allotropic transform. 77−40406
Fe-Cr-Al, scale and spalling resist. determ., appl. of cyclic oxidation method 77−77695
Fe-Cr-Al-TaC (13.5, 3.7, 9 wt.%) eutectic alloy, directionally solidified, thermal cycling effects on microstruct. 77−32686
GaAs, during deformation, acoustic emission rel. to cracks, dislocations 80−35441
GeTe, elec. cond. and microhardness, thermal cycling effect *(Russian)* 78−35485
HfO_2, monoclinic, microcracking, elasticity, internal friction, thermal expansion meas. 79−29195
LiF, thermocyclic stress effects in corrosive-media, electrochem. polarization applic. *(Russian)* 78−11356
MgO and MgO-dolomite, crack detection caused by thermal shock, AE technique *(Japanese)* 80−21248
MgO, sintered, refractories, props. after testing at over 2000°C 80−104317
Mn-Ga (24.1 wt.%), reversible memory of form, X-ray diffr. expts. *(Russian)* 79−5006
Mn-Ge (10.3 to 15.5 wt.%), reversible memory of form, X-ray diffr. expts. *(Russian)* 79−5006
Mo, candidate refractory for Tokamak, thermal fatigue failure testing 80−32454
Mo, cast, purification of C, O_2 and N_2 using thermal cycling *(Russian)* 79−70114
thermal stress cracking continued
Mo, fusion reactor appl., quick heating thermal fatigue test, ultra-high vac. environment *(Japanese)* 80−93716
Mo single crystal, thermocyclic strength of high temps. of single crystal 77−16685
Na_2O-CaO-SiO_2 glass rods, prediction of thermal fatigue resist. 78−84955
Nb thick layer vapour deposition by photoresist stripping 79−83135
Nb-stainless steel bimetallic strip Cu interlayer struct. during thermal fatigue *(Russian)* 78−15498
NbC, and NbC-ZrC solid soln., prep. by impregnation, strength, surface submicrocracks 77−16661
NbC, neutron radiation effects 79−77641
Ni alloy, Numonic 80A, grain boundary crack diffusional growth, high temp. rupture possibility 78−47471
Ni alloy EI617, creep, effect of preliminary heat treatment on struct. and props. 77−21195
Ni alloy EI617, cyclic temp. variation, loading parameter effect on laws governing distortion 77−16627
Ni alloys, welding crack resist. during welding, heating, stress reduction by hardening 79−24618
Ni base alloy VZhL-12U, heat resistance, thermal fatigue 79−20179
Ni base superalloy, directionally solidified, struct. and props. *(Chinese)* 80−20918
Ni base superalloy, rupture life, prior temperature cycling effect 78−60840
Ni, electrolessly deposited, structural comparison with electroplated films 79−23869
Ni/ZrO_2-Y_2O_3, sputtered multilayered ceramic/metal coatings, props. 80−40620
Ni-base superalloy IN713LC, hot corrosion, thermal cycling effects 77−70204
Ni-Co-Cr-Al-Y coating, electron beam deposited, for Ni-base superalloy, fatigue crack initiation and propag. 78−11438
Ni-Cr alloy, KhN70VMTYu, gas turbine blades, thermocyclic strength charact., exam. 78−60743
Ni-Cr alloy, structural changes, during thermal stress cracking, X-ray and microhardness meas. *(Russian)* 78−35496
Ni-Cr alloy EhI617, thermocyclic treatment effect on struct. and thermal fatigue resistance 78−7045
Ni-Cr/ZrO_2-Y_2O_3 sputtered multilayered ceramic/metal coatings, props. 80−40620
Ni-Cr-Al, resist. to cyclic oxidation at 1100 and 1200°C 77−77641
Ni-Cr-Al-Cr-Hf-Zr-C, directionally solidified eutectic with (Hf,Zr)C reinforcement, precipitation, and thermal cycling 78−44057
Ni-Cr-Al-Ti alloy type ZhS6U, effects of heat treatment in high vel. gas streams on props. 79−57025
Ni-Cr-Co, Nimocast alloy 738, γ'' precipitate morphology and creep rupture, thermal stress crack effect 78−11318
Ni-Cr-W-Co-Ti, thermal fatigue, effects of inclusions 80−81183
Ni-Nb-Al, eutectic, thermal cycling effect on strength and ductility *(Russian)* 79−24601
$NiCr_2O_4$, plasma-sprayed coatings, props. 77−59999
Si-B based CVD coating for gas turbine blading, props. 80−40615
SiC and Si_3N_4, hot pressed, comparison of high-temp. thermal fatigue resistance 77−36623
SiC coated fuel particles, failure during thermal excursion above 2000°C 79−36317
SiC, subjected to thermal shock, study of substruct. and surface morpholoy 79−43292
SiF_4, thermocyclic stress effects in corrosive-media, electrochem. polarization applic. *(Russian)* 78−11356
Si_3N_4, grain-boundary-crystallized, thermal shock resistance 78−11308
Si_3N_4, high temp. thermal fatigue, role of activation energy of slow crack growth 77−44340
Si_3N_4, reaction bonded, exam. of Na_2SO_4 induced heat corrosion 79−20224
Si_3N_4-Y_2O_3 ceramic, thermal degradation, C impurity effect 80−50708
Sn melt in contact with Fe, Fe distrib. on thermal cycling *(Russian)* 80−16562
steel, Cr-Mo-V, charact. investigation 78−72857
Tb-Ho alloy, influence of internal strain on Neel temp., thermal expansion and elastic const. meas. 77−63176
Ti alloy, cyclical heat treatment *(Russian)* 79−57009
Ti alloy, heat resistance, thermal stability, stress-rupture strength, and creep 80−81194
(U,Pu)C, fracture and crack healing, SEM study 79−79080
UO_2 minimum particle size to survive thermal stress fragmentation by fuel-coolant interaction 79−67886
UO_2+Na, fuel-coolant interaction, UO_2 fragmentation by thermal stress and pressurisation 77−88226
V-D alloys, low frequency internal friction study 78−48444
W, candidate refractory for Tokamak, thermal fatigue failure testing 80−32454
W, cast, purification of C, O_2, and N_2 using thermal cycling *(Russian)* 79−70114
W wire reinforced Cu, exam. of thermal cycling induced deformation 79−5050
W-ThO_2, candidate refractory for Tokamak, thermal fatigue failure testing 80−32454
Y_2O_3 ceramics, strength under mech. and thermal actions 80−97554
Zn, crack form. at grain and twin boundaries at low temp. *(Russian)* 80−66620
Zn, low-temp. thermal fatigue, causing fracture and plastic deform. 77−28837
Zr-Nb (2.5 wt.%), memory effect in hydride precipitation 78−11227
Zr-Nb (2.5 wt.%), seam welding tubing, microstruct. in weld region 79−61621
ZrC, and ZrC-NbC solid soln., prep. by impregnation, strength, surface submicrocracks 77−16661
ZrC, neutron radiation effects 79−77641
ZrC, rupture mechanism due to internal heat evolution 77−8922

thermal stresses
see also thermal stress cracking; thermoelasticity
after-effects in thermo-elasticity 80−106724
Araldite CT200/Hardener HT907 cylinder, thermal stresses and photoelastic fringe order 77−62219
arch, cylindrical, heat resistant material, exam. of thermoelastic stress problem 78−63306

thermal stresses continued
axisymmetric thermal stresses in transversely isotropic circular cylinder with spherical cavity 77—17824
beam, self-induced vibrations by thermal stress 78—75084
bimetallic plates, deflection meas. during high-temp. heating 78—7134
bimodulus thin plate stress anal. 77—19527
body with thermally insulated cracks, periodic thermoelastic situation 77—68417
bonded composite hollow circular cylinder, transient thermal stresses under symm. temp. distrib. 77—54887
brittle crystal grown from melt residual stress rel. to dislocation density 78—2042
brittle material, heat resistance criteria on surface during convective heat exchange 77—15642
brittle materials, grain size dependence of microcrack initiation 80—40505
carbon fibre reinforced composites, filament-wound, thermal residual stresses 80—49290
centre cracked plate under quadratic thermal gradient, stress intensity factors analysis 80—43665
ceramic, laser drilling and cutting, anal. of results using computer model 79—70180
ceramic elements in MHD generator channel walls 77—70075
ceramic powder, thermal stresses during spheroidisation process *(Russian)* 80—40386
ceramics, brittle, heat-transfer variables effect as thermal stress resist., meas. by quenching expts. 80—79871
ceramics, brittle, partially absorbing, thermal stress anal. subjected to symmetric radiation heating 80—59570
ceramics, brittle, post thermal buckling resistance, role of physical props. 78—64585
ceramics, thermal stress resistance, enhancement, for materials with thermal cond. gradient 78—48506
ceramics, thermal stress resistance, figures of merit, review 79—83290
circular cylinder under intermittently sudden heat generation, transient thermal stresses 77—3728
circular cylinder with circumferential edge crack under uniform heat flow, thermal stresses 80—48641
circular disc, axisymmetric, anal. by method of matched asymptotic expansions 77—14899
circular hollow porous cylinder with mass transfer through reflecting walls *(Russian)* 79—14220
circular-plates, effect of initial thermal stresses on large amplitude vibrs. 79—3949
clad-glass fibres, thermal stresses 80—107360
cladding, evaluation *(Russian)* 77—59952
cold sheet rolling, thermoviscoelastic problem, numerical soln. 77—39236
composite Cosserat elastic cylinders, thermal stress problem, soln. method 79—72812
composites, thermal stresses investigation, using polymer models 80—40639
concrete, bituminous, thermal stresses and brittle point, automatic installation for meas. 80—55605
constitutive equations of continuum creep damage mechanics 78—67054
contact, frictionally heated, thermoelastic deform. 80—83764
container wall, quasistatic stress distrib. due to internal press. and external temp. changing 77—84113
continuous elastic solids, foundations for coupled thermoelasticity 80—46807
cooling bodies, thermal stresses and temps. determ. by finite elements 77—14881
corundum, subjected to thermal shock, study of substruct. and surface morpholoy 79—43292
corundum-based refractory lining specimen, thermal softening assessment *(Russian)* 79—83237
Cosserat medium subject to thermal stresses, plane contact problem *(Polish)* 78—22268
crack, in semiinfinite thermoelastic solid with heated boundary 78—55610
crystal growth, effects of radial and axial temp. gradients *(German)* 78—67672
crystals pulled from melt, thermal stresses and struct. defects 78—2041
cyclic thermoplasticity, finite element analysis by subvolume technique 77—42749
cylinder, circular, thermal stress conc. determ. by integrated photoelasticity *(Russian)* 77—46925
cylinder, circular, three-dimensional transient thermal stresses under nonaxisymmetric temp. distrib. 80—92054
cylinder, composite circular, transient thermal stresses 78—79217
cylinder, hoilow, heated on outer surface, cooled on inner surface, temp. and thermal stresses *(Russian)* 80—74712
cylinder, hollow infinite, with temp. depend. thermal cond., thermal stress anal. 80—14575
cylinder, thermal displacements and stresses, determ. by computer-assisted classical methods *(Rumanian)* 80—92066
cylinder, thick orthotropic circular, bimodulus elasticity, thermal stress 77—23885
cylinder, thick walled, thermal stress calc. taking nonlinear creep into account 79—46184
cylinder, weakened by penny-shaped cracks, thermoelastic stresses 80—10191
cylinder elastic orthotropic brittle, under axisymmetric thermal and press. loading failure probability anal. 78—34078
cylinders, symmetric thermoelastic stress, Lanczos-Chebyshev method 80—33458
cylindrical plastic shell, nonstationary temp. field, contact press. calc. in cable pressing 78—63270
cylindrical shell, heated, large deflection 78—63289
cylindrical shell stresses by local heating, optimisation *(Russian)* 77—39225
cylindrical shell with circular hole or rigid inclusion 77—19518
cylindrical shell with longitudinal reinforcing ribs, thermal stability 79—98596
cylindrical shells, calc. of stresses *(German)* 80—33454
cylindrical shells, transient response to localised heat sources, thermal displacement and stresses 80—13538
decohesive carrying capacity in thermal stress problems 77—3741
diamond, laser beam drilling process mech., thermal stresses, elec. surface forces *(Dutch)* 77—7759
dielectrics, transparent solids, optical breakdown, role of thermal stresses *(Russian)* 78—95547
thermal stresses continued
diffusion effect, generation by heat stress variation in heat cond. 79—55309
distribution associated with elastoplastic deform. 77—19549
dynamic thermoelasticity, stress-temp. eqns., uniqueness theorem 79—72813
elastic circular cone, thermal stresses 78—90715
elastic cone, stress anal. 77—72159
elastic half-space, coupled thermoelastic problems 78—59300
elastic layer containing penny shaped crack, bonded to dissimilar half-spaces 77—58603
elastic medium, infinite homogeneous isotropic, with external crack, thermal stress anal. 77—42778
elastic stress analysis of an anisotropic compound rotating disc under thermal loading 78—67036
elastic strip with two coplanar Griffith cracks, stress distrib. 77—42779
elasto-viscoplastic thermal stress model, appl. to continuous casting of metals 79—18740
elastoplastic stress analysis based on initial strain method *(Japanese)* 80—77620
elastoplastic thermal stresses in axisymm. problems *(Japanese)* 78—51096
electric current pulse in conducting rod, skin 79—7287
elliptic plate, heated, deflection under uniform load 77—35040
epoxy EDT-10, rigid polymer, thermal stress isothermal relaxation 80—71683
epoxy models, thermoelastic strains and stresses using strain gauges *(Polish)* 79—64609
epoxy resin, thermoelastic stress creation and motion picture recording of interaction with dynamic crack 78—56697
epoxy resin composites, cooldown residual thermal stresses, viscoelastic response 80—60941
fibre reinforced composite, hygrothermal microstresses, in material exhibiting inelastic behaviour 77—84141
fibre reinforced composites, transverse plane, elastic, failure behaviour *(Japanese)* 78—48510
fibre reinforced composites, viscoelastic thermal shrinkage stresses 80—38287
fibre reinforced materials, therm. stresses in unit cell 80—10160
film, device for compensating thermal stresses during thermal conductivity meas. 79—18681
finite element thermal loading calcs., automatic mesh generation 77—3740
finite element variational anal. 77—7311
finite element variational technique 77—7310
finite short circular cylinder with arbitrary heat supply, unsteady thermal stress length effects 80—13541
fission reactor fuel can temp. and thermoelastic stress perturbations, conjugate heat transfer effects 77—54284
fluid filled porous medium, thermal behaviour, thermoconsolidation eqns. for elastic lattice 79—72933
fusion reactor, BBC CQK 200-4 modulator tube for sustaining neutral beam power supply 80—99290
fusion reactor limiters; thermal and stress environment effects 80—32461
fusion reactor solenoid, orthotropic, finite element stress anal. 78—55010
fusion-welded optical fibre splice loss expts. 79—37023
gases, new type of free convection 77—31419
glass, tempered, spontaneous fracture due to NiS inclusions, exam. of behaviour mechanics 78—71294
glass bodies, heat resistance, determ. 80—24690
glass fibre composite, shell, carrying capacity, heating effects 77—4865
glass fibre reinforced plastic, optimal reinforcement for cylindrical shell subject to temp. field. 77—84148
glass fibre reinforced polymer, thermal expansion coeff. and glass transition temp., thermal stress effect 78—14484
glassware, quenching, stress distrib. calc. using finite element anal. 79—66087
graphite, thermal shock on a finite orthotropic thin shell 79—68587
graphite shell, thin, cylindrical, orthotropic, thermal stresses and displacements due to instantaneous thermal shock 80—92060
graphite thermally stressed disc, nonlinear deformation 78—6964
heat exchanger, pebbles with periodically varying fluid temp., thermal stresses, heat storage capacity 78—26020
heat memory materials, dynamic thermoelasticity of infinite cylindrical rod *(Russian)* 80—74752
heat reflecting coatings, effect of thermal deformation depend. on heating rate 78—30169
heat-generating, transversely isotropic cylinder, transient thermal stresses and displacements 79—68584
heat-resistant alloys, fatigue under conds. of mech. and thermal stress loading 79—87726
heated cone, heat transfer and shear stress 79—46168
hollow cylinder, internal one sided heating, anal. of thermal state and thermal stress 79—98595
hollow cylinder with heat flux on inside surface, nonstationary thermal stresses 77—7308
infinite medium, thermal stress problem for ribbon-like inclusion 77—58554
infinite medium containing periodic ribbon-like inclusions, local intensification of thermal stresses *(Japanese)* 80—96195
ingots, cooling regime in conditions of minimal thermal stress, modelling *(Russian)* 80—65194
integrated retardation technique, rotationally symmetrical bodies 80—38362
intensity factors calc. using contour integral method 79—37243
laminate, edge effect on thermally induced stresses 77—84142
laminated active laser element, thermal stresses produced by longit. nonuniform pumping *(Russian)* 78—5474
laminated plates, symmetric, specially orthotropic, thermoelastic anal. 80—92058
layered system, thermal stresses and displacements 80—23891
linear elastic and post yield fracture mechs., thermal and residual stresses 77—89066
liquid-filled porous solid, first strain gradient theory of thermoelasticity 77—53783
LMFBR, finite element formulation for thin reactor struct. thermal stress anal. 78—70613
LMFBR steam generator tube thermal oscillation obs. 79—9672
loaded materials, thermal cycling, testing equipment, IMASh-9-66 machine attachment 77—77678
martensite, microstresses associated with tempering 80—3111

thermal stresses continued
metal, two-way polishing, thermal stresses and surface quality *(Russian)* 80−30151
metal film, effect on temp. coeff. of resist. 78−43489
metal-silicide coating system, thermal stresses *(Russian)* 78−13891
metallic thin films, thermoelectric power, thermal stress effects, theory 80−65714
MHD generator duct wall, semi-hot, thermal stress design study *(Japanese)* 78−13890
microelectronic component thermal stresses, photoelastic anal. 77−62217
microplanar elastic semi-space, axially-symmetric thermal contact stress 78−30179
micropolar layer, pertinent formulas for displacement vector components, force stress component distrib. 80−48581
microwave induced hazardous thermal stresses in ocular lens of human eye 78−80914
modelling using IFECS interactive software 79−80440
multilayer cylinder, exam. of stresses, considering layer contact charact. 78−63399
non-linear elastic thermal stress analysis with phase changes 78−79218
nuclear fuel can designs for Safety Test Facility, structural analysis 77−46310
nuclear fuel elements, control rods, transient thermal stress anal. 79−599
nuclear fuel pellets, cracked, finite element method anal. 78−82462
optical fibre, refractive index profile distortion, stress-induced 80−91889
optical fibre refractive index profile distortion due to thermal stresses 80−58726
optical fibres, piezo-optical effects due to thermal stresses 80−87519
optical glass, tolerancing of refr. index heterogeneity in objectives 80−78948
optical waveguide blanks, thermal and elastic stresses in a cylinder 80−14447
optical waveguides, inhomogeneous glass sintering, self stresses producing bulk flow 80−14448
optimal heating of solid body and stress relax. role *(Russian)* 78−22258
orthotropic elastic medium, plane stresses, analytic continuation 77−39232
oxide film, As doped, roughening during As diffusion into Si, stress effect 78−2389
oxide films, As doped, thermal stress effects on roughening 79−23813
permalloy films, thermoelastic stresses and magnetostriction effects during light recording *(Russian)* 79−97465
photoelastic cylinder with radial temp. gradient, integrated retardation fringe technique 77−62219
photoelastic investigation of thermal stress fields due to travelling heat source *(Japanese)* 77−42747
photothermoelastic technique, appraisal for transient 2D thermal stress analysis 80−79244
plane with heat-permeable curvilinear cut, limiting equilib. *(Russian)* 79−50576
plate, annular elliptic heated, const. thickness, buckling and stability criterion 80−28443
plate, cylinder, sphere, temperature (one-dimensional) and thermal stress fields, inverse problems 80−79134
plate, heated thin annular circular, of variable thickness, buckling, thermoelasticity 78−9581
plate, reinforced strip, 2-dimens. nonsteady temperature stresses 80−74734
plate, temp. bending, generalised eqns. WRT transversal mech. charact., stress conc. problems *(Ukrainian)* 77−54876
plate, two-stage circular with heat emission, thermoelasticity, force anal. 79−10481
plate, volumetric heating and thermal stresses *(Russian)* 77−42714
plate containing cracks, varying temp. cond. at edges, thermal conductivity and thermoelasticity *(Russian)* 77−23915
plate temp. dependent props. under linear temp. distrib., thermoelastic problem for crack 80−48579
plate with crack or ribbon like inclusion subjected to uniform heat flow, thermoelasticity 80−48578
plate-semi-infinite space, heat exchange process control, thermoelastic stresses *(Russian)* 80−53606
plates, piecewise-constant coeff. of heat transfer, thermoelasticity, method of integral charact. *(Russian)* 78−38188
plates, thermal stresses, temp. fields for butt-end narrow zone heating *(Russian)* 79−14248
PMMA, rigid polymer, thermal stress isothermal relaxation 80−71683
polycrystals of anisotropic substances under hydrostatic press., microstresses 79−25231
polymer rod, longit. oscills., continuous viscoelastic spectra *(Russian)* 77−19546
polymeric materials, stress meas., X-ray diffr. technique, review 78−5713
polymers, wear in thermally stressed state 80−3202
polystyrene, microcryst. cellulose filled, glass transition temp. shifts 78−95144
polyvinylidene fluoride, optimised target for IR vidicon camera tube, effect of thermal pre-stressing in sensitivity 79−32050
porosity effect, on thermal stress resist. during steady-state heat flow 80−1488
power plant pipelines under creep conditions, allowable thermal stresses *(Russian)* 78−13930
PVA, microcryst. cellulose filled, glass transition temp. shifts 78−95144
PVC, stress relaxation in macrodeformation range 80−16370
quartz resonators, thickness-mode, thermal stress effects on reson. freq., theory 80−50272
reactor cylinders, eigenload formulation of thermoelastic stress 79−46213
reactor cylindrical rods, anal. of self-equilibrating end stresses by Lanczos-Chebyshev method 79−46212
reactor graphite, stress and strain determ. depend. of mech. charact. on temp. and fluence 79−40998
rectangular plate with central hole, thermal stresses and buckling 77−3755
refractory, thermal stresses produced by temp. gradient, finite element anal. *(Japanese)* 80−33538
refractory composites, fibre reinforced, directionally solidified tensile tests, in HVEM, deform. and fracture *(French)* 78−68785
refractory curvilinear lining, thermal stresses 78−5649
reinforced plastics, load-bearing capacity, effect of one-sided heating 80−81135
reinforced polymer, thermal strain determ. 78−1560
thermal stresses continued
resin slab, stress response, fluctuating external moisture (temp.) effects 78−55620
resins, thermoplastic, glass-fibre-reinforced, performance at elevated temperatures obs. 79−95067
rock bodies, cooling, residual stress development 78−88819
rock salt, thermomech. impact due to storage of radioactive waste 80−5278
rod, expanding, conductive heat transfer computation, fast numerical technique 78−75029
rod, semi-infinite, temp. stresses 79−18714
rod pulled from melt, asymptotic calc. of thermoelastic stresses 78−2031
rollers, steel casting installation, effect of thermal stresses on fracture charact. 78−64650
rotating circular cylinder, stresses and displacements due to axially nonsymm. heating of lateral surface *(Polish)* 78−22248
rubber cylinder, circular, uniformly heated, combined extension and torsion 80−92057
rubber-modified glassy polymers, thermal stresses 77−77567
sandwich plate, modified Berger method, large thermal bending anal. 78−63297
satellite, gravity oriented, with thermally flexed appendages, librational dynamics 78−7868
SAW in layered media, thermal strain effects 79−19440
sea ice, surface layer induced thermal stress state meas. *(Japanese)* 77−81917
self stresses, expt. and numerical study *(German)* 79−90142
semi-infinite medium under uniform heat flow, thermal stresses around ribbon-like inclusion 78−59303
semicircular inclusion in semi infinite plane, experiment and analysis *(Japanese)* 77−65672
semiconductor single crystals, melt grown, dislocation creation by thermal stresses 78−83825
semiinfinite plate, heat transfer effect 80−96193
semitransparent shaped components, temp. and thermal stress patterns 78−2035
shell, cylindrical, nonuniform axial edge load, thermal load, linear buckling 78−63345
shell, finite circular cylindrical, rate formulation for elastic-plastic creep anal. 77−58568
shell, spherical, with conical nozzle, thermal stress anal. 78−79204
shell, thin spherical, axisymm. thermal stress by method of matched asymptotic expansions 77−72169
shell enclosures, temp. distrib. calcs. under thermal radiation, numerical calcs. 80−38241
shells, axisymmetric multilayer, finite element technique for thermal and press. loading, vibr. modes *(French)* 77−50973
shells, cylindrical, anisotropic, quasistatic thermoelastic eqns. 80−92059
shells, truncated conical, thermal buckling, axisymmetric initial deflections 78−79240
shells of revolution, thin, numerical anal. thermal stress relief 77−89041
shells of revolution, variable thickness, stress state determ. 80−38275
shells with asymmetric heating, thermal cond. and stresses 79−32182
simulation in continuous casting, finite element method 78−30170
simulation of inelastic material behaviour in struct. anal. 78−34041
solar collectors with multilayer cylinder heat exchangers, heat balance eqn. and thermal stress anal. 80−58977
solid bodies, high-strength, thermodynamic determ. of safe stress *(Russian)* 79−50679
solid hemisphere heated by distant source, thermal stresses 78−67045
solidifying semitransparent cylindrical medium, thermal stresses, radiation and conduction 79−46200
spherical shell with circular elastic inclusion, thermal stresses 77−3727
spherical thick-walled shell with filler thermal stresses 78−13909
stator windings, failure mechanisms under thermal cycling *(Japanese)* 80−104189
steatite, ceramic, exam. of thermal damage by strength meas. 78−84997
steel, alloy, 15KhM1 and 20KhM1, plastic deform. with thermal cycling 80−89310
steel, C, St.3, thermal stresses, spontaneous relaxation 79−1892
steel, C, thermal stresses in submerged arc welded joint, consideration of phase transformations 79−61683
steel, die type 5KhNM, stressed state effect on softening 79−66168
steel, medium, C, US attenuation, mag. field effect 80−89428
steel, platelike parts, quenching, temp. field calc. 80−60889
steel, plates, thin, welding residual stresses calc., elastoplastic thermal stress anal. 78−83262
steel, stainless, 316, fusion reactor first wall, thermal stress and creep fatigue limitations 79−76132
steel, stainless, type 316 20% cold worked fission reactor fuel cladding, axial stress effects on transient mech. response 80−71743
steel, welds obs. at high temperature, by moire photography 79−74336
steel bar, axially symmetrical residual stresses, with longitudinally nonuniform stress distrib. 78−51070
steel casting, calc. method of thermal and thermo-visco-elasto-plastic processes *(German)* 80−79859
steel continuous casting, thermal, thermo-visco-elasto-plastic processes *(German)* 80−81044
steels, alloy, surface plastic deform., effect of heating conditions, types 45, 40 Kh 78−53033
strain gauge, based on polyimide adhesive, effect of cyclic heat exchanges, 20 to 300°C 77−16775
substrate bending during thin film evaporation due to temp. difference between substrate faces 80−54571
substrates, instantaneous bending during thin film deposition, intrinsic stresses, cantilivered plate method anal. 80−54570
superconducting accelerator and beam-line mags., mech. and thermal stresses 77−83362
superconducting dipole magnets for high energy accelerators, stress and strain distribs. 79−31250
surfaces, Beilby layer generation, plate distortion by heat *(German)* 77−73370
thermal fluctuation theory of durability of solids 77−4153
thermal stresses in elastic plane with circular boundary and thermally isolated cracks *(Russian)* 78−55599
thermoelastic coupled field, spherical symmetric problems analysis 77−42737
thermoelastic half-space transient response 79−32253
thermoelastic interference, between two neighbouring ribbon-like inclusions *(Japanese)* 77−68423

thermal stresses continued
thermoelastic stress distribution in single cryst. pulling by Czochralski technique 78−63681
thermoelastic two-layer cylinder deform., rel. to microelectronic device manufacture 79−41561
thermoelasticity, distribution for stresses in half space, with moving boundary, influence of inertial effects *(Russian)* 79−55327
thermoelasticity theory computing, finite element method appl. *(Italian)* 79−18719
thermoelastoplasticity, doubly periodic, soln. 77−84165
thermoelectric cooler, single stage, finite element thermal stress anal. 80−108807
transient stresses in hardening and molding process 79−72817
transient thermal stress problems, numerical anal. method 79−72810
transversely isotropic finite circular cylinder, transient thermal stresses from internal heat generation 79−76974
tubular joints stress anal., finite element anal., computer programs 78−41808
two dimensions, comparison between mech. analogue and expt. meas. 77−46918
two joined plane strain sectors, stress and displacement relns. 77−58559
two-phase nodules, heat treatment, stressed state, connection with nodule size, cooling rate and phase ratio *(Russian)* 80−16334
unsteady thermal stress problems, numerical treatment based on Euler-Maclaurin summation formula 80−48580
unsteady thermal stress problems in a doubly connected domain by conformal mapping 80−69652
viscoelastic bodies, exam. of thermal stress state, for bodies with props. dependent on unsteady temp. 78−83229
viscoelastic bodies, residual stresses when cooling *(Russian)* 77−39234
viscoelastic materials, stress waves generated by internal heating in Voigt and Maxwell materials *(Japanese)* 80−69693
weakly absorbing solid medium, opacity fluctuations, heating by intense radiation and thermoelastic stresses problem 80−38048
welding, thermal stresses and metal movement, computer simulation 78−34002
wire, self-induced vibrations by thermal stress 78−75084
Ag films, hillock form. hole growth and agglomeration 80−44455
Ag, thin film, hillock growth due to thermal stress relax. of diffusion creep and surface diffusion 79−65345
Al alloy, residual stress relax. rel. to temp., load cycling, aircraft struct. appl. 78−7053
Al alloy cylindrical shells, buckling under combined axial preload, nonuniform heating and torque 80−53662
Al binary alloys, exam. of dislocation structure, using diffraction electron microscopy *(Russian)* 79−10857
Al-Si, thermal control of interphase microstresses and mech. props. 77−12654
Al-SiC fibre reinforced materials, therm. stresses in unit cell 80−10160
Al-SiO_2 interface, stress and microstruct. via TEM 78−26797
Al_2O_3, thermally stressed insulator surfaces, behaviour under vacuum 80−18652
B fibre reinforced Al, X-ray investigation of internal stresses *(Russian)* 77−73290
B_2O_3-Na_2O-SiO_2-Al_2O_3, effect of alumina dispersions on the thermal cond./diffusivity/stress resist. 80−39368
$Ba_xSr_{1-x}Nb_2O_6$ crystals, optical defects and edge dislocation distributions 80−19806
C reinforced plastic, degraded, study of strain, 20 to 1000°C 80−71680
CdS, dislocation motion due to heating by electron beam in TEM 80−79799
Cu, thermal stress role in dislocation form. during growth from melt 80−6374
Cu-Al-Ni alloy, thermoelastic transformation hysteresis loop width strain rate depend. *(Russian)* 79−100138
Cu-Zn (30 wt.%), single crysts., quantitative anal. of stress relax., obstacle strength and athermal stress variation 80−89277
Fe/Cu composite, prop. of fatigue crack crossing interface under residual thermal stress effect 80−45371
Fe-C-Mn-V, austenite microstruct. memory *(German)* 80−84977
Fe_2O_3 thin films, reactively sputtered, mechanical stresses rel. to deposition conditions 80−80146
GaAs crystal growth, thermal and elastic const. evaluation 80−92586
GaAs homojunction LED, mechanical stress induced degradation 80−2860
GaAs, pulled, dislocation generation, thermoelastic anal. 80−79787
GaAs-Si eutectic alloy, effect of crystallisation rate on microhardness 79−96110
GaP/Si heterostruct., differential thermal contraction, plastic deform., fracture 80−108494
GaS, elastic prop. anisotropy, Debye temp. *(Russian)* 80−88244
GaSb-Ge eutectic alloy, effect of crystallisation rate on microhardness 79−96110
$GaSb_{1-y}As_y$, MBE-grown, substrate effect on lattice consts. 79−77942
Ge ribbon single crysts. grown from melt, dislocation struct. form. under thermal stress 80−107082
Ge, shaped crystals, grown by Stepanov method, struct. perfection 78−2123
Ge single crystal of circular cross section, thermoelastic stresses 78−2033
Ge strips grown by Stepanov method, thermoelsatic stress calc. 78−2034
$In_{1-x}Ga_xAs$, MBE-grown, substrate effect on lattice consts. 79−77942
InSb, dislocations due to thermal stress, single and composite crysts. 78−2124
InSb-Ge eutectic alloy, effect of crystallisation rate on microhardness 79−96110
KBr-KCl, birefringence, annealing effects, photoelasticity 78−72483
KCl birefringence, annealing effects, photoelasticity 78−72483
$LiIO_3$ crystal, SHG, thermoelastic stresses and nonlinear refract. effect 80−74437
Mn coated BN powder particles, X-ray investig. of thermal stresses generated in vac. deposition 77−40455
Mo, deformed, dislocation-free channels prod. by heat pulses, electron microscope obs. and hardness meas. *(Russian)* 79−52251
Mo, siliconised thermal stress and thermal expansion 77−21324
NaCl type crystal, dislocations due to high temp. stress relax. 78−2126
Nb heteroepitaxial layers on sapphire, residual mechanical stress and strain influence on superconductivity 80−15644
Nd:glass, thermal distortion induced by optical pumping *(Chinese)* 78−50779
Nd:glass laser rod, pumped, thermal relaxation 80−69397
thermal stresses continued
Nd:YAG laser, thermal lens effect on emission stability 80−19064
Pb, film, hillock formation by grain boundary sliding 80−107673
Pb film, thermal strain, depend. on cryst. orientation 78−10311
Pb, film, thermal strain, strain relax. above room temp. 80−59841
Pb film, vac. deposited, thermal strain depend. on thickness and grain size 79−90926
Pb:O, thin film, microstruct. and thermal stress, doping effects 80−88458
Si on sapphire, stress-relieved regrowth by laser annealing 80−65389
Si, ribbon growth via RTR technique, process update and material characterisation 78−76597
Si ribbon parallel twinned structure development by shaped crystallisation 78−64465
Si single crystal growth, Czochralski method, small-angle dislocation boundary form. anal. 80−89136
Si thin ribbon grown at high speed, thermal stresses, reduced thermal buckling 80−107078
Si wafer, stresses generated by thermomigration of liquid inclusions 79−37875
p-Si-$In_{2-x}Sn_xO_{3-y}$ solar cells, thermal degradation mechanisms 80−55841
SiC, subjected to thermal shock, study of substruct. and surface morpholoy 79−43292
Si_3N_4, bending strength, deformability, elastic moduli and brittleness 80−81191
Ti coated BN powder particles, X-ray investig. of thermal stresses generated in vac. deposition 77−40455
Ti, TiN, thermal stress analysis *(Russian)* 77−59952
Ti-$TiSi_2$, metal-silicide coating system. thermal stresses *(Russian)* 78−13891
UO_2, molten, fragmentation in flowing Na under TOP accident conditions 79−30978
U_3Si, reversible twinning, in-situ obs. 80−104241
V alloy, fusion reactor first wall, thermal stress and creep fatigue limitations 79−76132
WC-Co hard alloy-steel welds, effect of intermediate layer composition on structural changes and mechanical properties 78−60616
WC-Co sintered hard alloy, yield stress, internal thermal stress effect 79−100230
ZrC, brittle mat. discs, ultimate thermal stresses 77−4210

thermal transformations *see phase transformations*

thermal variables control
see also temperature control
diffusivity measurement, using wave packet soln. and microprocessor-controller 78−73989
drying, heat and mass transfer, optimal control 78−67006
heat exchange rate in fluidisation, using magnetic field *(Russian)* 77−55083
microwave and HF thawing, of cryogenically preserved canine kidneys 77−5059
plate heating, two-step control *(Ukrainian)* 79−76958
porous surface, heat exchange optimal control 79−32661
production processes, nonstationary Doppler effect, freq.-phase methods of investig., control 80−45464
spray cooling, charact. and minicomputer control *(French)* 79−3889
stress compensation during thin-film meas., device 79−18681
thermal loading, automatic control system, quick-acting 77−48609
thermister ccts. two-point, thermostat appl. 77−41610
thermoelement cooling control by variation of geometric shape 78−62195

thermal variables measurement
see also bolometers; calorimeters; calorimetry; temperature measurement; thermal conductivity measurement; thermocouples; thermometers
AC calorimetry, small sample specific heat recording appl. *(German)* 77−82518
AC thermometry and DC heating circuitry in thermal props. meas. 78−74000
annular channels with turbulent gas flow, bilateral heating *(Russian)* 79−7375
annular channels with turbulent gas flow, unilateral heating *(Russian)* 79−10559
boiling, transition type, in forced convective flow, boundaries meas. 79−27499
boiling heat transfer crisis detect., sensitivity of bridge and thermocouple methods 77−61064
bolometer, for measurement channels of actinometric apparatus of Meteor Earth satellite 79−35828
calorimeter, BB2, for high-power CW laser energy meas. 78−54372
colour temperature charact. of cholesteric liquid crystals, using temperature wedge method 80−57359
complex heat exchange, radiant and convective components meas. method 78−32809
composite materials, metal reinforced, thermal activity, diffusivity, cond. meas. method 79−37141
composite method, apparatus for thermophysical charact. meas. over wide temp. range 77−26285
conducting thin films, covered with electrolytic deposit, thermoelec. props., appl. to thermal flux meas. *(French)* 80−59961
conference, Chicago, USA (Nov. 79) 80−31425
convection, natural, on inclined surface, transition, vortex system, meas. method 79−27632
convective heat transfer coeff. from gas to thermocouple 78−18149
convective heat transfer coefficient measurement using heat-flux sensor, error anal. 79−94463
convective heat transfer coeffs., interferometric meas. errors 77−71315
correlation anal. of temp. signals in presence of EM disturbances, current and voltage amplifiers appl. *(German)* 78−86267
cross-flow heat exchanger tube bank efficiency rel. to structure *(Russian)* 79−10448
cryogenic liquid, bubble population density meas. on immersed heated surface 77−30169
curve-fitting method based apparatus for thermal props. meas. at cryogenic temps., performance charact. 77−67441
diffusivity, automatic measuring method *(French)* 80−14559
diffusivity, calc. formulae for unsteady temp. data 79−94476
diffusivity, transient hot-strip method for simultaneously measuring thermal conductivity and thermal diffusivity of solids and fluids 80−1417
diffusivity automatic meas. by pulse method using analogue computer *(Japanese)* 80−27294

thermal variables measurement continued
diffusivity measurement, using wave packet soln. and microprocessor-controller 78−73989
diffusivity measurement method, by pulse expt., error anal. 79−32208
digital systems in thermal-testing laboratory 78−81966
DTA apparatus for meas. in region 20 to 800°C 77−32864
electrically conducting materials, at high temps., improved apparatus 79−86326
emissivity, thermal radiation of partially transparent materials, high speed spectrometric method 79−7280
emissivity meas., apparatus 77−45844
emissivity of solar absorber coatings, optical technique for meas. *(Spanish)* 80−16835
emissivity of solids and coatings at low temps., calorimetric technique 80−17941
evaporation rate of metal tip, by profile change meas. 77−24403
fibre optic probe for thermal profiling of liquids during crystal growth 79−68443
flames, radiation measurement techniques 78−94506
flow, in tube, of air, local heat exchange meas. using heat flux transducers *(Russian)* 78−83509
fluid, heat capacity, thermal expansion, simultaneous meas., dilatometric meas. 77−84131
fluid, thermoelasticity, near critical point, student apparatus 77−60881
fluxmeter, multiple thermoelectric junctions on thin conducting sheet *(French)* 80−86286
gas turbine stator, heat transfer rate meas. method 79−98731
gases, dilute, temp. and thermophysical prep. meas., using acoustic resonators 80−53573
gases, thermal activity coeff. meas., periodic-heating method, appls. 80−42218
granular matarials, thermal diffusivity measurement, constent rate heating method *(Japanese)* 80−6572
heat and thermal diffusivity of liquid and free-flowing materials, calorimeter appl. 77−87765
heat capacity, high temp., modulation method, thermal losses compensation 79−85144
heat capacity, true, of high-melting cpds., pulse method and meas. unit 80−19953
heat capacity meas. instrument for solid granular, fibrous and liquid materials *(Russian)* 78−29116
heat capacity of ferroelectrics, by dynamic method at high hydrostatic pressures 80−47059
heat detector, temps. close to absolute zero *(Russian)* 79−6130
heat flow in plasma jet, calorimetric probe for *(Russian)* 78−12698
heat flow meter dynamic properties *(Russian)* 78−86265
heat flux, local, high intensity, measurement pickup *(Russian)* 79−67296
heat flux, nonstationary component, using battery convertor 79−30466
heat flux, time depend., meas. method 78−81969
heat flux meas., nonstationary method using probe 77−42942
heat flux meas. by battery heat flowmeter using Kalman filter 79−37143
heat flux measuring devices, for radiant heat exchange investig. 78−94505
heat flux/temp. data telemetering for energy flow study of peccary 77−86716
heat loss from buildings, IR TV meas. system 77−45837
heat loss from heat receiver assembly, of fixed-mirror solar concentrator 79−52905
heat loss meas. from solid surface to airstream 79−37140
heat of adsorption, isosteric, determ. using contact pot. difference meas. 79−66347
heat of evaporation of liquids, quick method for determ. in region 30-95°C 78−21138
heat of vaporisation of liq. N_2, Dewar for student expt. 77−9840
heat of vaporisation spectrometer, multilayer desorption meas. 79−82453
heat pipe appls. in thermophysical props. meas. 80−23878
heat transfer gauge, thin film, use in shock tube *(Japanese)* 77−19654
heat transfer in aerodynamic tube, testing method 79−37147
heat transfer intensification processes, possible meas. using thermistors 77−57354
heat transfer of rough cylinder in transverse water flow *(Russian)* 79−10449
heat transfer rates, light fibre-photomultiplier combination 77−2658
heat transfer to air-water stream, expt. meas. unit 77−42941
heat-flux transducer, using artificially anisotropic thermoelec. materials 79−93136
heat-pulse experiments, nonlinear effects, theory 80−96182
heat-pulse technique for radiationless relax. meas. in solids 77−36277
high heat-conductance materials, method for determ. of thermophys. charcts. on thin samples 77−61063
high intensity local heat flow, meas. errors anal. *(Russian)* 80−74865
high pressure liquid, calorimeter design guidelines *(Russian)* 78−74001
high rate local heat flux meas. probe 80−47050
hot gases, convective heat transfer coeffs. to solid surface, moving thermocouple meas. 80−42230
induction heating, HF generators, calorimeter for power output investigation *(German)* 79−40571
insulants, thermophysical meas. by US method 77−45830
interferometric method for thermal expansion 78−45676
IR effective emissivity meas. by natural cooling *(Japanese)* 78−29117
isobaric specific heat of solids, for pressures up to 250 MPa and 150-350K temps., measuring installation 77−76572
joint determ. of thermophysical charcts., quasilinear method 77−41601
liquid, calorimetry at high state parameters 78−57953
liquid specific heat and thermal expansivity, simultaneous determ. by dilatometric method 77−87758
liquids, opaque and diathermanous, total normal emissivity meas. at high temp. 80−102965
liquids, thermophysical properties measurement *(Russian)* 80−77776
local thermal currents on boundary surface, meas. method 77−10014
long rod, direct-heating meas., interpretation 80−102964
magnetothermodynamic meas. using superconducting solenoid in persistent mode, error anal. 79−17454
melting point of paraffin waxes meas., automatic analyser 79−14223
metal, group V, thermophys. props. determ. at high temp. using deform. vibrs. of plates 79−85143
metal, with high thermal cond., method for determ. of thermophysical charcts. 77−45833
metal-hydrogen system, electronic sp. ht. meas. 80−49378

thermal variables measurement continued
metals, specific heat meas. method of low temperatures and high pressures 80−52246
metals, thermal props. at high temps. meas., acoustic method 79−14222
multichannel precision temperature measuring device, minicomputer, Pt 100 resistance thermometer appl. *(German)* 78−77914
nonstationary heat flux measurement by auxiliary wall sensors 80−86287
nonstationary heat fluxes meas. by heat meters using auxiliary wall method 78−59275
nonstationary thermal fluxes, in converter, meas. 80−74724
optimal estimates, Kalman filter appl. to accuracy improvement 77−10013
parallel tube banks in transverse viscous flow, heat transfer and hydraulic drag *(Russian)* 79−10450
pipes, local heat transfer using heat flux sensors 80−48709
prediction of thermophysical properties of fluid mixtures, generic procedure 80−48563
probe method for simultaneous determ. of cond. and diffusivity of lubricants 77−41600
production processes, nonstationary Doppler effect, freq.-phase methods of investig., control 80−45464
radiant-flux detectors, comparison 79−35831
radiating power, integral normal, high-temp. meas. technique, appl. to Nb 77−65667
radiation detectors, operating parameters *(German)* 78−57954
radiation shape factor integrator with oblique scale 77−42711
re-entry vehicle heat transfer meas. in separated laminar base flow 78−61708
reaction kinetics meas. using modified commercial stopped flow apparatus 80−86291
regular thermal regime method for heat transfer meas., nonideal sensor thermal simulation 77−57323
rotation ebulliometer, press. controlled, thermodynamic investig. of dilute solns. 78−18752
self-recording heat flux meter, mathematical model 78−93678
sheet materials, heat stability, small automatic device for rapid testing 77−77672
simultaneous evaluation of thermal properties, nonlinear estimation procedure 79−94478
simultaneous measurement method for thermal props. of plane-shaped solids using iterative calcs. 77−42713
soils, transient measuring method for thermal props. *(German)* 78−61619
solar radiation, automatic sun sighting system *(Italian)* 77−22062
solid, thermal diffusivity, iterative estimation method 80−43603
solid thermal diffusivity and sp. ht. meas., ultrasonic method 77−89015
solids near phase transition, simultaneous specific heat and thermal conductivity meas. 77−37892
specific heat, appl. of AC method to bulk samples 77−71317
specific heat, by elec. method 77−51513
specific heat, low temp., using $Ce_2Mg_3(NO_3)_{12}$ thermometry 79−88955
specific heat, precise meas. using analogue simulator 77−49721
specific heat, rapid pulse heating method for refractory metals near melting point 77−35704
specific heat capacity of NaCl soln., meas. at high press. by temp. jump method 77−69092
specific heat meas. at low temps. via adiabatic calorimeter 77−41614
specific heat of adsorbed gases, cryostat design 79−58695
specific heat of insulating solids, transient hot-wire method 77−67428
specific heat of $La_{1-x}Sr_xCoO_3$, using laser-flash method, at 80 to 950K, phase transitions obs. *(Japanese)* 80−54898
specific heat of liquids, quick method for determ. in region 30-95°C 78−21138
specific heat of solids, 4.2 to 90K, USSR special standard 77−31207
specific heat of solids, 90 to 273.15K, USSR special standard 77−31206
spectral emittance, meas. system for refractories at temp. up to 3000°C 77−22550
surface layers and thin films, thermal diffusivity of microsections, IR and X-ray electron-probe microanal. 78−2314
surface temperature meas. using radioactive kryptonates *(Czech)* 77−45842
temperature cond. meas. instrument for solid materials *(Russian)* 78−29116
temperature fluctuation measurement in turbulent channel, sensor wire-supports cond. influence *(French)* 79−94751
temperature gradients in liquid, using laser microrefractometer 80−57362
thermal diffusivity determ. by dilatometric technique 77−41597
thermal diffusivity determ. by temp. meas. at irregular operation stage 78−62199
thermal diffusivity in solids, meas. using modulated heating beam technique 80−52221
thermal diffusivity meas. by const. rate heating method *(Japanese)* 77−87759
thermal flux, high, using calorimeter probes 80−13080
thermistor ccts., two-point, thermometers and ice-point warning device 77−41610
thermistors, point matching of exchanged hot conductors *(German)* 78−77905
thermoelectric thermal flux meters, response time reduction 80−4719
thermoelectromotive force and temperature, study of kinetic phenomena of charge transfers 80−57330
thermographic instrument, types 78−86266
thermography, pyroelectric vidicon camera use 79−93143
thermophysical experiment, automatic information-processing system 78−196
thermophysical parameters, determ., temp. fields anal. 79−37118
thermophysical process ambiguous data gathering and processing optimisation *(Russian)* 80−73335
thermophysical properties, conf., Dubrovnik, Yugoslavia (June 1978) 80−51944
thermophysical properties, standardisation of meas. methods 80−52197
thermophysical properties dynamic meas. techniques 80−52219
thermophysical properties of liq. metals, submicrosecond-pulse-heating method 80−52220
transduction, thermoresistive, of nonelectric quantities with compensation for thermal inertia *(Russian)* 77−53885
transfer functions for thermal objects with internal sources 78−73960
transient heat flux, meas. using heat gauges 77−49723
tubular furnace for thermal diffusivity meas., design 80−30182
twin ampoules for thermophysical investigations 77−37895

thermal variables measurement continued
urea phenolic resins, long term thermal stability *(German)* 79−91943
US heating process parameter meas. and registration system *(Polish)* 79−12798
vapour-liquid equilibrium, ebulliometric determ. 78−18754
vertical wall heat transfer with combined forced and free convection *(Russian)* 79−94618
viscous liquid, thermal diffusivity meas., constant-rate heating method *(Japanese)* 80−6570
water heat transfer in calorimetric vessel and jacket *(Polish)* 77−54996
wet-bulb temp. and moist air heat content meas. 80−52211
Fe, sp. ht., electronic heating in modulation meas. method 80−24609
He, melting at room temp., high high-press. cell 80−80025
^{222}Rn-CO_2, thermal diffusion, expt. method for study 80−5922

thermally stimulated capacitor discharge *see thermally stimulated currents*

thermally stimulated currents
abietic acid glass, corona-charged, TSC curves 77−55744
Al-SiO_x-Al structure, maxima of TSC obs. 78−23178
alkali halides, thermally stimulated depolarisation of NCO centres 80−80678
alkaline earth glasses, $45RO.5Al_2O_3.50P_2O_5$, (R=alkali earths), electron beam irrad., exam. of charge accumulation and light-sum kinetics 79−4336
alkyl halide, amorphous, depolarisation thermocurrents and dielectric relaxation time distrib. *(French)* 80−60490
alkyl halides, depolarisation thermocurrent obs. of main relax. around glass transition 78−27158
amorphous materials, TSC calcs. 80−7284
amorphous semiconductor, trapping, photo-stimulated and thermally-stimulated current obs. 77−28192
anodic oxide films, space charge, TSC obs. 77−32326
anthracene, charge storage and trapping levels, TSC studies 80−6875
anthracene, laser excited single crystal, numerical anal. for TSC results *(Japanese)* 80−34464
anthracene, single cryst. with discrete shallow traps, computer simulation of TSC 79−99819
anthracene, single crystals, TSC excited by Q-switched ruby laser 80−29417
anthracene, thermally stimulated currents from shallow trapping centres *(Japanese)* 78−92015
anthracene, TSC and carrier retrapping 80−39599
anthracene, TSC meas. induced by Q-switched ruby laser 78−19087
anthracene crystals, carrier trapping in deformed surface region 78−47806
anthracene crystals, monomolecular glow peak 77−39869
anthracene crystals, monomolecular glow peak revealed by thermal cleaning 77−39870
apatites, dipolar reorientations, TSD study 80−107068
capacitor, thermally stimulated and isothermal discharges across semicond. with grain-boundary barriers 78−2582
carnauba wax and rosin thermal electret, elec. charge studied by TSC 80−7286
carnauba wax electret, electric charge studied by TSC *(Japanese)* 78−6626
carrier traps in polymeric insulating materials, investigation by X-ray induced thermally stimulated current method 80−93240
cellulose, dielec. relax. studies, TSD meas. 80−88907
cellulose, thermally stimulated discharge studies 80−11329
cellulose electrets, TSC and dielec. losses and relax. 80−25284
charge storage, charge transport and electrostatics conference, Kyoto, Japan (Oct. 78) 80−7252
chloranil pellets, thermally stimulated discharge current and dielectric studies 80−93236
cobalt naphthalate electret, thermally stimulated discharge, 55-75°C 80−25279
complex pattern analysis, appl. to Al anodic oxide 78−23104
computer simulation 78−39609
corona charged polyethylene thermally stimulated current and surface potential decay obs. 80−15945
p-cyanophenyl-p'-caproyloxybenzoate, charge carrier behaviour, thermal depolarisation current study 80−7283
data handling, organisation and evaluation of ITC meas. by on-line use of computer 78−10832
data processing of TSC/thermoluminescence ratio 78−10463
deep impurities role, book contrib. 78−10403
depolarisation current 78−10829
diamond:B, synthetic semicond., thermostimulated conductivity *(Russian)* 79−7834
diamond:B, thermoluminesc., TSC, correlation meas. 78−88369
dielectric, dipolar point defects, studied by ITC 80−6405
dielectric conduction and breakdown, conf., Gainesville, FL, USA (Oct.-Nov. 1979) 80−82564
dielectric response, TSC for nonexponential systems 79−47383
dielectrics, solid, dipolar relaxation time, trap levels and ionic space charge polarisation 80−84685
dielectrics, thermally stimulated depolarisation as method of studying charge trapping 80−11325
dielectrics, thermally stimulated dipolar processes, simulation 78−35080
diffusion traps for divalent ions, dielectric loss and ionic thermocurrent techniques 80−6566
dipolar relaxation study using thermally stimulated polarisation currents 80−7278
dosimetry after accidental exposure to ionising radiation using TSC in human nail 78−73253
electrets, thermally stimulated discharge 80−80683
electrets and dielectrics, conf., Sao Carlos, Brazil, Sept. (1975) 80−7251
epoxy resin composite containing mica flakes, 20-190°C 77−90091
epoxy-resin, Nomex-filled, space charge polarisation, thermal depolarisation current study 80−7282
ethylene-vinyl acetate copolymer, X-ray irrad., trapped carriers 77−69338
exoemission phenomena, TSC, thermionic emission, book contribution 80−80954
field induced thermally stimulated polarisation-depolarisation currents, relaxation, book contribution 80−80687
filling analysis, of thermally stimulated capacitance method 79−47107
glasses, electrical cond. meas. technique using thermally stimulated polarisation currents 79−99561
glasses, high-resistivity, uniform and space charge polarisation, thermally stimulated depolarisation anal. 78−15085

thermally stimulated currents continued
hexamethylcyclotrisilazane film, glow-discharge-polymerized, in MIM and MIS structs., elec. cond. mechanism 79−42680
p-hexyloxyphenyl-p-pentoxybenzoate, nematic liq. cryst., elec. discharge meas. of persistent internal polarisation 80−10488
hydrocarbon, long chain single cryst., carrier transport meas. 80−6874
hydroxyapatites, dipolar reorientations, TSC study 80−60491
ice, electrical effects during condensation and phase transitions 78−67821
insulators, trap struct. anal. by fractional glow techique 79−11078
ionic crystals, thermocurrents, review 78−60381
ionic electret behaviour, ionic thermoconductivity technique 80−7274
kinetic parameters of thermally stimulated processes 78−10460
lysozyme bound water, thermally-stimulated press. and current 78−15757
many-body model of universal dielec. response 80−75927
mathematical basis, logical anal. 78−10462
metal-polyethylene terephthalate-metal struct., electrochem. effects as source of EMF 78−72278
metal-polymer-metal systems, of PTFE, PVC, polystyrene and polyethylene 79−78201
methacrylic polymers, multiple dielectric relaxations, investigation by thermally stimulated current method 80−93238
methyl alcohol, adsorbed on silica, low temp. thermally stimulated depolarisation spectra fine struct. 79−78611
3-methylpentane, glassy insulator, γ-irrad., IR enhancement of carrier radiation yield 77−76870
MIM systems, TSC, space-charge layer model 80−93009
MIS capacitor, thermally stimulated discharge in differential regime 79−15214
MIS structure, mobile ions, TSIC meas. 78−68090
MNOS diode, trap distribution, memory characteristics 77−85326
MOS capacitor, neutralisation of Na^+ ions, TSIC method 79−38181
MOS capacitor, TSC meas., suppression of meas. interferences from interface states and mobile ions 80−29479
MOS structure, B ion implanted, form. and annealing of radiation damage 79−56321
naphthalene, electron trapping, one-carrier TSC and SCL currents 80−70715
non-polar dielectrics, TSC and carrier retrapping 80−39599
nonDebye dielectric solid, thermally stimulated depolarisation 78−10830
novolac and novolac allyl ether electrets, thermal depolarisation, chem. struct. effect 80−71297
nylon 6, transient elec. conduction at high temp. 79−69513
nylon 6, water effects 80−75925
p-octyloxyphenyl-p-pentoxybenzoate, nematic liq. cryst., elec. discharge meas. of persistent internal polarisation 80−10488
one-carrier TSC and isothermal decay currents, influence of blocking contacts 77−28182
organic semiconductor films, relax. currents, polarisation and depolarisation currents obs. 80−49764
p-n junctions, thermally assisted field emission near precipitates 78−14809
p-n junctions, TSC, impurity centre parameter determ. 78−47857
paper cellulose sandwiched between metal electrodes, thermo-induced elec. current 80−25021
PbI_2, trapping levels, TSC meas. 78−23107
perovskite oxides, single cryst., photocond. and TSC meas. 78−43436
Perspex magneto-electret, equiv. elec. field calc. from thermally stimulated discharge current 80−7259
Perspex pyramid electret, thermally stimulated discharge currents 80−2688
PET, ionic cond. current rel. to neutralisation at polymer-metal interface at elevated temps. 80−24664
PET, photoexcited, thermolum. and carrier detrapping mechanism 79−61445
photoresist, KTFR, thermally stimulated discharge current studies 80−75924
phthalocyanine metal free films, TSC, ferroelectric-semiconductor transition 80−66105
phthalocyanine thin layers, metal-free, mobility and thermally stimulated polarisation meas. 79−73527
PMMA, electret, dielectric meas. at ultralow freq. by reheating 80−4741
PMMA, thermoelectrets, γ-irrad., heterocharge stability, TSC spectra 78−72453
PMMA, thermorheologically simple material, thermostimulated depolarisation currents 77−90092
PMMA, tubular magnetoelectrets, TSC obs. 78−88250
polarisation currents in transient regime 78−43777
poly(alkyl methacrylate)s, corona charged, decay of surface charge and TSC *(Japanese)* 80−54712
poly(alkyl-methacrylates), surface charge decay and TSC 80−11328
poly(vinyl halides), surface charge decay and TSC 80−11328
poly-4-methylpent-1-ene, TPX, thermally stimulated conductivity 77−11905
poly-L-proline, TSC and dielec. study of multiple relaxations 77−55748
poly-p-xylylene films, carrier traps, X-ray induced TSC, thermolum. and dielec. loss study 80−88570
polyacrylonitrile, film, dielectric polarisation 78−52431
polyacrylonitrile, film, IR attenuated spectra determ. of chem. origin of TSC 77−55746
6-polyamide, dielec. relax. time, thermally stimulated current meas. 79−87381
polycarbonate, and charge-transfer complex modifications, TSC 80−88572
polycarbonate, effect of thermal treatment on strength, TSC meas. 77−52368
polycarbonate, TSC anal. by activation energy spectra 80−20579
polycarbonate thin films, solution-grown, dielectric relaxations 80−55029
polychlorotrifluoroethylene, electret, thermodepolarisation curves 80−7266
polychlorotrifluoroethylene electrets, TSC profiles, poling conditions depend. 78−10835
polyetheylene, charge carrier trapping phenomena *(Korean)* 77−89773
polyethylene, γ-irradiated, effect of elec. field on TSC 79−65790
polyethylene, carrier traps, photostimulated detrapping currents and TSC meas. 78−10458
polyethylene, dielectric props., investigation for morphology changes created by mechanical drawing and annealing 80−84697

thermally stimulated currents continued
polyethylene, elec. cond. of high and low density samples, oxidation effects 80−107784
polyethylene, elongated low density film, TSC 79−47106
polyethylene, high and low density, depolarisation thermocurrent study, relax. modes 80−7263
polyethylene, high density, carrier trapping, X-ray induced TSC 80−11005
polyethylene, high density, trapped carriers, thermally stimulated currents, influence of oxidation 77−80792
polyethylene, high density, treated in high elec. field *(Korean)* 79−28673
polyethylene, high density, TSC field depend. 78−76090
polyethylene, high density corona charged, TSC, oxidation effect 78−26882
polyethylene, oxidised and gamma-irradiated, carrier traps, thermally stimulated currents 78−19050
polyethylene, space-charge storage under high DC voltage condition, TSC meas. *(German)* 80−75576
polyethylene, surface charge release, crossover phenomenon, thermally stimulated discharge current study 80−50255
polyethylene, temp. depend. of elec. cond., isothermal current peak 79−51595
polyethylene, TSC due to trapped electrons, rate-determining process 77−59290
polyethylene, TSC study of deuteration 80−20581
polyethylene, X-ray irrad., trapped carriers 77−69338
polyethylene cables carrying DC current, TSC and space charge effects *(French)* 80−40042
polyethylene electrets, charge trapping mechanism, TSC, DTA and optical meas. 80−11322
polyethylene film, elongated, 20 to 60°C 78−10826
polyethylene film, high density, corona charged, thermally stimulated surface pot. 80−11327
polyethylene film electrets, polarisation obs. and influence of wax impurities, TSC obs. and analysis *(French)* 80−44999
polyethylene films, elongated, γ-irrad., TSC meas. 80−11324
polyethylene films, high density, corona-charged, surface pot. decay 79−24254
polyethylene terephthalate, amorphous, thermally stimulated creep and TSC expts., retardation modes 79−69768
polyethylene terephthalate, electret, due to injected charge 77−16242
polyethylene terephthalate, TSC and thermally stimulated creep, dielec. and mech. retardation modes 79−78613
polyethylene terephthalate, TSC and thermolum. due to electron detrapping by local mol. motions 80−96898
polyethylene terephthalate, TSC due to mobile ions and ionic conduction *(Japanese)* 80−54432
polyethylene terephthalate, TSC in high temp. region 78−38872
polyethylene terephthalate, TSC meas., space charge and injected surface charge effects 80−11320
polyethylene terephthalate, TSC spectrum from electron beam charging 77−77139
polyethylene terephthalate electrets, formed by electron injection, TSC meas., space charge drift 80−11321
polyethylene terephthalate electrets, TSC due to injected charges, electron trapping props. 79−4566
polyethylene terephthalate film, corona charged, surface voltage decay mechanism, TSC meas. 80−11326
polyethylene terephthalate film, elec. cond. and space charge accumulation 80−10998
polyethylene terephthalate film, TSC, depend. on heating rate 78−88249
polyethylene terephthalate photoelectret, TSC and photostimulated detrapping current obs. 78−10459
polyethylene TSC resulting from trapped carriers 78−6393
polyfluoroethylenepropylene, prepared for dosimetry, thermocurrents 77−52877
polyimide film, thermally stimulated depolarization anal. 79−69766
polymer, carrier trap study by X-ray induced TSC and thermoluminescence *(Japanese)* 80−54713
polymer, generation mechanism and characts. *(Japanese)* 80−60488
polymer, relaxation spectra determ. from electric discharge meas. with increasing temp. *(German)* 78−31151
polymer, secondary relaxation, TSC meas. 77−85643
polymer, thermal sampling technique for thermally stimulated discharge meas. 78−10831
polymer, thermally stimulated discharge, thermal sampling technique 77−85645
polymer, TSD and dielec. loss, comparison of activation energies 78−10834
polymer electret, thermally stimulated discharge, compatibility and impurity effects 77−4595
polymer films, carrier transport meas. 80−6874
polymers, electrical phenomena, nature and appl., book contrib. 80−50254
polymers, frictional electrification, temp. and friction speed dependence obs. 80−70798
polymers, transient current nature 78−80278
polymers powders, corona-charging props. 80−6946
polynaphthol film, semicond., trap depth and trapping cross section from TSC curves 79−51700
polyolefins, elec. cond., review 78−26867
p-polyphenyl, thin polycryst. layer 79−60946
polypropylene, electron bombarded electret, trapped charges ESR study 80−7170
polypropylene, TSC meas. of relax. modes, apparent double glass transition 80−11323
polypropylene electrets corona charged at high temp., TSC study 80−7261
polypropylene film, corona-charged, TSC and space charges 80−40041
polypropylene film, vac. evaporated, electron trap depth, TSC meas. for MIM struct. 79−95535
polypyromellitimide, thermal depolarisation current 78−52429
polystyrene:I films, thermally stimulated discharge, I conc. and polarisation temp. depend. 80−107937
polystyrene, charge injection during extrusion 78−60135
polystyrene, effect of doping on TSC 79−38085
polystyrene, thin film, TSC and dielectric props. *(Japanese)* 80−15632
polystyrene composite with mica flakes, TDC meas., interfacial polarisation 78−64316
polystyrene film, thermally stimulated discharge currents 80−71300
thermally stimulated currents continued
polystyrene film, thermally stimulated discharge currents of polarised film 79−78609
polystyrene film formed by RF electrodeless excitation, dielec. props. 77−24795
polystyrene films on metal substrates, electrode effect on carrier injection, TSC, I-V characts. 80−34463
polystyrene foils, breakdown-charged, surface charge densities and depths, TSC spectra 80−7260
polystyrene thin films, TSC and surface charge meas. 80−103769
polystyrene-chloranil molecular complex, glass-rubber and liquid-liquid transitions 80−45002
polystyrenes, anionic, TSC obs. of T_g and T_{II} transitions 80−84686
polystyrenes, comparison of head-to-head, head-to-tail, by thermally stimulated discharge 79−15396
polyurethane, TSD rel. to glass transition dipole relax. activation *(Russian)* 77−20793
polyvinyl acetate:Cu, and undoped, thermally stimulated currents exam. 78−35083
polyvinyl acetate film, charge retention, adsorbed water vapour effects, TSC obs. 77−32321
polyvinyl alcohol, bulk polarisation, thermally stimulated discharge current meas. 80−40039
polyvinyl butyral film, charge storage mechanism, TSC expts. 80−25280
polyvinyl cinnamate, and photocrosslinked form, low freq. dielec. loss evaluation 79−82919
polyvinyl difluoride, γ-irrad., low-temp. TSD obs. 77−63358
polyvinyl fluoride, pure and doped, self-activated centres 78−64315
polyvinyl fluoride film, electret effects 77−90094
polyvinylacetate film, effect of electrode metals on depolarisation current characts. 78−76387
polyvinylbutyral, elec. and dielec. props., mol. wt. effect on charge storage 80−97192
polyvinylcarbazole, Poole-Frenkel effect investigation by TSC 77−51755
polyvinylidene fluoride, γ-phase containing films, thermocurrent spectra 79−42555
polyvinylidene fluoride, ageing effects on thermally stimulated currents 77−1634
polyvinylidene fluoride, dielectric relax. mechanism 80−55023
polyvinylidene fluoride, piezoelectric effect formation due to injection process, TSC *(French)* 80−34856
polyvinylidene fluoride, TSC and thermoluminescence, reln. to molecular motion *(Japanese)* 80−55200
polyvinylidene fluoride, X-ray induced TSC 80−75578
polyvinylidene fluoride films, corona-charged, struct. changes, piezo- and pyroelec. props. 79−11389
Poole-Frenkel effect investigation by TSC 77−51755
PTFE, prepared for dosimetry, thermocurrents 77−52877
PTFE electrets corona charged at high temp., TSC study 80−7261
PVC:Cu films, electron transport and dielec. props. 79−82700
PVC, rigid, physical ageing effect on elec. props. 78−10836
PVC, rubbed, TSC meas. 80−55017
PVC electret, thermally stimulated depolarisation 78−48112
PVC-metal interface, ionic carriers behaviour 79−99622
pyrene picrate, charge transfer complex, thermally stimulated discharge current 79−78610
quartz, trapping levels 78−91703
radiation dosimetry and dating 78−11004
relaxation kinetics, transport phenomena in solids, book 80−77553
Schottky barrier, thermal emission from damage near interface, effect on TSC and transient current expts. 77−11982
semi-insulating material, elec. stressed, storage of charge caused by cond. gradient 80−25306
semiconductor, amorphous, dielec. relax. current meas. method and uses 77−77141
semiconductor, deep impurities, exptl. techniques *(Japanese)* 80−15476
semiconductor, deep level parameters, TSC meas., rel. to photocurrent techniques 78−72249
semiconductor, deep trapping levels, TSC meas. *(Polish)* 78−34797
semiconductor, interpretation of thermolum. and TSC, extensions of conventional model 78−27335
semiconductor, surface energy level determ., thermally stimulated contact pot. difference method 79−99601
semiconductor, thermolum. and TSC, evaluation of model, reliability of trap depth determ. 77−32451
semiconductor capacitor, parameters of local states using thermally stimulated discharge, allowance for strong field effects 79−51528
semiconductor materials and devices, high power, detection of deep levels 79−28318
semiconductors, deep level carrier trapping and emission, transient spectroscopy, book contribution 80−80216
semiconductors, local centre parameter determ. from thermally stimulated excitation curve derivative singularities 80−11004
semiconductors, thermally stimulated conductivity luminescence, defect levels, traps, book contribution 80−80296
semiconductors, thermally stimulated relaxation processes, book contribution 80−80295
semiinsulator, minority carrier injection effect 78−10466
silastic tubular electret, mag. polarised, thermal currents 80−40037
silicone resin electret, thermally stimulated discharge meas. 79−87378
sisal wax thermoelectrets, thermally stimulated discharge and internal polarisation 80−55016
solid, conf., Montpellier, France (June 1976) 78−10827
solid, thermally stimulated processes 78−10828
space charge effect on thermally stimulated currents 79−65793
styrene-acrylonitrile copolymer film, multiple relax. obs. using TSC 80−45000
Teflon, TSC, trap modulated electron and hole mobilities 78−10441
Teflon FEP, electron-beam-charged, population and temp. shift of TSC peaks 79−82914
Teflon FEP, N implanted, TSC spectra 80−88912
Teflon FEP film, thermoelectret 77−52012
Teflon FEP-A, corona and electron beam charged, TSC peak identification and surface-voltage stability 79−78614
Teflon film, TSC studies of carrier trapping and mobility 80−7016
tetracene, amorphous film, TSC meas., carrier traps 80−2496
tetracene, noncryst., localised valence states in forbidden gap 78−72113
TGS, conditions for electret state 78−43773
TGS, pyroelec. single cryst., elec. field meas., thermally stimulated charges 80−45012
thermoluminescence correlation, simultaneous meas. 77−81160

thermally stimulated currents continued
thermoplastic layers with fast heating, discharge process 78−49920
thin film transistor, quasi-equilibrium TSC process, model 77−36002
thiourea, thermally stimulated depolarisation currents, peaks interpreted in terms of molecular relaxations 78−19407
thiourea formaldehyde polymer, pyroelectricity and dielec. props. 79−91379
trap depth, determ. from TSC, theory 80−70716
trap depth determ. from TSC 80−59998
trap level spectroscopy by thermally stimulated release of trapped carriers 78−10461
trap modulated electron and hole mobility meas. in insulators 78−10441
trap parameters, calc. method from TSC under monomolecular recomb. conditions 77−8495
trapping, participation of two levels 79−56244
trapping levels, effect on TSC, calc. 80−60489
trapping parameters for thermally stimulated luminesc. and cond. 77−52190
TSCD meas. method and applic. 77−43615
urea, thermally stimulated depolarisation currents, peaks interpreted in terms of molecular relaxations 78−19407
vinyl chloride:vinyl acetate copolymer film dipole continuous relax. spectrum 78−91700
vinyl chloride-vinyl acetate copolymer film, dielec. relax. and thermally stimulated depolarisation current meas. 80−11336
vinyl chloride-vinyl acetate copolymer film between metal electrodes, depolarisation current studies 80−2691
viscoelastic materials, thermally stimulated processes 78−10829
water, adsorbed on silica, low temp. thermally stimulated depolarisation spectra fine struct. 79−78611
ALF_3 film, amorphous, AC elec. props. 78−2804
AgBr:I, refilling of recombination centres during thermal stimulation 78−10464
$AgGaS_2$, deep level obs. by TSC meas. 80−65590
Al-polymer-Au, short circuit current with temp. variation 77−32090
Al-SiO_2-Si, MIS diode, neutralisation of mobile ions in insulating film *(Japanese)* 79−73591
Al-SiO_2-Si, TSC due to trapped electrons, rate-determining process 77−59290
Al-SiO_2-Si MOS structures, charge motion, TSC meas. 80−100534
Al-SiO_2-Si struct., mobile ion neutralisation in SiO_2 layer, TSC and C-V characts. meas. 79−95503
Al-SiO_2-Si structure, ionic impurities motion in noncryst. SiO_2, trapping layers 78−30999
Al-SiO_2-Si:B ions, annealing effect on energy spectrum of radiation defects *(Russian)* 78−88488
Al-SiO_2Si, mobile ion kinetic behaviour 79−56315
AlF_3, localised electronic levels, thermoluminesc. and thermally stimulated current exam. 78−11001
AlH_3, photo-and thermochem. reactions, 200-350K, UV Induced local states 78−31667
Al_2O_3 anodic films, trapping levels study using TSC 80−103768
Al_2O_3, anodic oxide, complex TSC pattern analysis 78−23104
α-Al_2O_3, crystal defects from X-ray irradiation, F-centres, X-ray luminesc. obs. 80−55176
Al_2O_3, high purity, pot. for electrophotography in radiographic imaging 78−35936
Al_2O_3, X-irrad., electron and hole traps, TSC and optical bleaching meas. 79−28356
Al_2O_3:Cr, pure and doped, electron irrad. induced cond., TSC and EPR study 80−80277
α-Al_2O_3:Er(Cr), crystal defects from X-ray irradiation, F-centres, X-ray luminesc. obs. 80−55176
As_2S_3, glassy, thermally stimulated depolarisation 77−24782
As_2S_3 vitreous, Ag, Cu, Sn and Ge impurities influence on electrophys. props. 77−76826
As_xS_{100-x}, chalcogenide glass, hole trap levels *(Russian)* 79−91074
$AsS_{3.5}Te_{2.0}$ glass, gamma-irradiated, TSC meas. 77−66166
As_2Se_3 amorphous film, photocond., TSC, light-induced changes 80−49810
As_xSe_{100-x}, chalcogenide glass, hole trap levels *(Russian)* 79−91074
$BaF_2:K^+$, cryst., thermal depolarisation 79−82912
$BaF_2:La^{3+}$, relaxation processes, studies by ionic-thermocurrent techniques 79−69769
$BaF_2:R^{3+}$ (R=rare earth) dipole reorientation, ionic thermocurrents obs. 79−95705
$BaF_2:Tb^{3+}$, thermally, stimulated polarisation currents, 80 to 400K 79−51900
$Ba_{1-x}La_xF_{2+x}$, enhanced ionic motion in solid solutions 80−107491
$BaTiO_3$, unipolar cryst., topography of defect. and thermodepolarisation currents 77−43954
$BaWO_4$ crystals, X-irradiated, EPR, TSC and thermoluminescence spectra meas. 79−1791
Bi_2O_3-based glass, in ZnO-glass-ZnO struct., current-voltage characts. and TSC *(Russian)* 77−69404
BiTeI-SbTeI, solid solns., phase diagrams, photocond., elec. props. 79−38125
CaF_2, mixed cluster, doubly-doped with rare earths, elec. dipole relax. 79−82924
CaF_2 thin films, initial ionic thermocurrent meas. 80−97018
CaF_2:alkali metal cation, thermal depolarisation study 80−108147
CaF_2:Ce(Nd)(Dy)(Ho)(Yb), props. of ionic thermocurrents 77−7897
$CaF_2:Gd^{3+}$, ITC spectra of impurity aggregate 78−71883
$CaF_2:Na^+$, cryst., thermal depolarisation 79−82912
$CaF_2:O_x$ absorpt., ionic cond., and thermal depolarisation 79−14960
$CaF_2:O^{2-}$, $CaF_2:Na^+$, O^{2-} and $CaF_2:Y^{3+}$,O^{2-}, thermal depolarisation obs. of defect clusters 80−71299
$CaF_2:R^{3+}$, R=rare earth, dipole reorientation of charge compensation centres, ionic thermocurrents meas. 79−73880
$CaF_2:Y^{3+}$, ionic cond. and thermal depolarisation obs. of defect clustering 80−71298
$Ca(NbO_3)_2$, thermally stimulated currents exam. 77−69766
CaS:Pd phosphor, thermally stimulated elec. cond., kinetics, 300-413K 78−76088
$CaWO_4$:Gd, thermally stimulated depolarisation current, 100 to 300K 80−7280
CdF_2, electrical transport limitation by electrodes, polarisation effects 80−96689
CdF_2:Eu, role of solution and precipitation phenomena on ITC spectra 80−7265

thermally stimulated currents continued
CdF_2:NaF, formation and reorientation of Na^+-anion vacancy complexes, thermally stimulated polarisation and depolarisation 78−84516
$CdF_2:Sm^{3+}$, photoconverted, thermally stimulated relax. 80−84476
$CdGa_2Se_4$, electron traps, energy spectrum, photocurrent decay, TSC temp. depend. *(Russian)* 78−64057
$CdInGaS_4$, TSC and SCL cond. investig. of electron trap parameters, 120 to 350K 77−69341
$CdInGaS_4$:Au, single crystal, thermostimulated conductivity *(Russian)* 79−11142
CdO-B_2O_3-SiO_2, glass, dielec.-relax. currents 78−52004
CdS film, surface energy levels, thermally stimulated contact pot. difference method 79−99601
CdS films, photosensitive, growth by reactive RF sputtering, props. *(French)* 78−35308
CdS, neutron and fast electron irrad., local centre form., TSC and photoluminesc. meas. 78−87719
CdS polycrystalline layers, electron trapping depend. on preparation conditions 79−78232
CdS thin layers, recryst. from CdS-Cr_2O_3 mixtures, phys. and photoelec. props. 80−96935
CdS:$CuCl_2$($CdCl_2$) sintered layer, distrib. of energy levels of local centres 80−15568
CdS:Li, nature of recombination centres responsible for 0.95 μm luminesc. band 77−69908
CdS:Li, TSC and optical photocurrent quenching spectra, Auger excitation of recomb. centres 79−33294
CdS:Li(Cu), pure and doped, electrodiffusion of shallow donors, photocurrent, TSC, and exciton luminesc. meas. 80−79992
CdSe, deep dislocation levels, TSC and luminesc. obs. 77−8050
CdTe sputtered films, struct., photocond., and trap distrib. 80−29489
CdTe, thermostimulated capacitor discharge, trapping levels obs. *(Russian)* 78−10842
CdTe, undoped, high-resist.- characterisation, impurity level investig. 77−39801
CdTe:Cl, capacitance meas. and trapping, mol. centre model *(French)* 77−39872
p-CdTe:Cl, deep level characterisation, gamma-ray detector parameters 77−39802
CdTe:Cl, grown by travelling heater method, carrier homogeneity investig. 77−39848
CdTe:Cl(In), photoelectronic investig. of trap depths, TSC and SCL cond. 77−39893
CdTe:Ge, negative thermally stimulated cond. 79−19621
CdTe:Zn, TSC, carrier traps, depth and quenching by IR radiation 78−56420
$Cd_{1-x}Zn_xS$ films, thermal evaporation prep., phys. props. 80−84410
CsBr:Ca^{2+} (Pb^{2+})(Ba^{2+}) (MnO_4^{2-}), reorientation of dipolar complexes, ionic thermo currents meas. 77−80642
Cu-As-Se glass, localised states exam. *(Russian)* 78−34806
$Cu_{10}As_{31}Se_{38}O_{21}$, chalcogenide glass, exam. of electron mechanism of photo induced changes 78−87998
Cu_2O, defect levels, TSC 77−66138
FeF_3 thin film, polarisation mechanism, AC and TSC study 80−66104
FeO_x-P_2O_5 glass, semicond., dielec. props., thermally stimulated depolarisation meas. 79−95704
Ga chalcogenides, energy spectrum of local levels *(Russian)* 79−51517
n-GaAs, deep level traps, transient and thermally stimulated capacitance meas. *(Chinese)* 79−91072
GaAs on GaAs and Ge, epitaxy, mechanism, effect of substrate surface struct. 77−51614
GaAs, surface, distrib. of surface states 80−44692
GaAs, thermally stimulated relax. under internal field conditions 80−7279
GaAs:Cr, high resist., anomalously strong elec. field induced release of carriers from traps 78−6397
GaAs:Cr, semi-insulating, TSC, carrier recomb. and trapping 77−32014
p-GaAs:Cr, semi-insulating photoelectronic analysis 77−80804
n-GaAs:Cr, semi-insulating, contact effects, trapping levels 78−10465
GaAs:Cr, strong quenching of thermally stimulated conductivity by elec. field *(Russian)* 77−1434
GaAs:O, semi-insulating, excitation temp. effect on TSC 80−70717
GaP crystals, radiation defects, TSC obs. 80−65588
GaP diodes, TSCAP and admittance spectroscopy of gamma-ray induced defects 77−89472
GaP LED, red, efficiency degradation and deep level change obs. 77−81155
GaP, proton implanted, thermally stimulated current meas. 80−24943
GaP:Cu, thermally and optical excited cond., deep level centres 78−72190
GaP:Cu p^+-n junction, deep level parameters, TSC meas., rel. to photocurrent techniques 78−72249
GaP:Cu-Ni, Schottky barrier, TSC meas., trap levels 78−91709
GaP:O, multicharged state of O, TSC and photoinduced currents 79−7808
n-GaS, TSC, electron traps 80−11002
n-GaSe, photoconductivity and TSC investig. of trapping centres 77−20359
p^+-Ge-n-GaAs abrupt heterojunction, reverse currents *(Russian)* 78−10542
Ge-S glasses, Cu doped, thermal, structural and dielectric props. 79−60283
Ge-Si alloy p-n junction, Sb-diffused, TSC 80−20289
GeS, Si doped and undoped, elec. cond. and thermally stimulated currents 80−20194
GeS_{15} glass, TSD evidence for ionic cond. 77−76598
HgI_2 crystals, native defect compensation, doping, mobility-lifetime and TSC meas. 77−55492
HgI_2 crystals grown by soln. and vapour phase techniques 78−41896
HgI_2, photoelectronic props. 78−41897
HgI_2:Ag, trapping effects, TSC, photocond. and photolum. meas. 77−32023
α-HgS, trapping parameters determ. by TSC meas. 80−59997
HgSe-Se, photo-field model, rel. to anomalous photocond. in Se:Hg 77−43658
In-GaAs:Cu-In S-type diode, role of deep trapping levels in form. of current-volt. characts. 77−76948
InP:Fe shallow trap thermally stimulated cond. spectroscopy, photocond. spectrum under DC conditions 80−65585
In_6S_7, TSC at various cooling rates *(Russian)* 80−11000

thermally stimulated currents continued
KBr, proton irrad., divacancies, positron capture, ionic cond. and TSC study 80−54289
KBr, X-irrad. 78−72606
KBr:Cl^-, diffusion traps for divalent ions, dielectric loss and ionic thermocurrent techniques 80−6566
KBr:Se^{2-} single cryst., dielec. relax. of impurity-vacancy dipoles, ITC meas. 79−91349
KCl, low temp. space charge polarisation 78−43789
KCl, with divalent impurity, reorientation of impurity-vacancy complexes, thermally stimulated depolarisation 77−65977
KCl, X-ray irrad., thermoluminescence, TSC and thermal stability 79−95859
KCl:Ca(Pb)(Sr), structural state of impurities, hydrostatic press. effect, thermostimulated depolarisation exam. 77−39614
KCl:CrO_4^{2-}, reorientation of dipolar complexes, ionic thermo currents meas. 77−80642
KCl:Pb, light induced ionic polarisation 80−7264
KCl:Pb, photoluminesc. induced by Suzuki-like occlusions, ionic thermocond. 79−33808
KCl:Sn^{2+}, thermally stimulated space charge decay 78−48111
KCl:Sr^{2+}, polarisation-plastic effect 78−2794
KCl:$SrCl_2$, thermal depolarisation 77−28514
KCl:$SrCl_2$, Z_1-centres, dipolar relax., ITC meas. 78−75660
KCl-KF:Pb^{2+}, point defects, ionic thermal currents and optical meas. 80−6403
K_2FeF_4, charge transport and polarisation 80−80681
KH_2PO_4, single cryst., thermal depolarisation current 79−51303
KH_2PO_4:CrO_4^{2-} ($Cr_2O_7^{2-}$), electrical cond., thermal depolarisation studies 79−95212
KI:S^{2-}, impurity-vacancy dipole UV absorpt. and ionic thermocurrent, F-centre form. 77−36271
KI:S^{2-}, vacancy dipoles, photo-induced polarisation and depolarisation 80−2690
KI:Tl, electron-hole and V_k-Tl recomb., TSC and thermolum. study *(French)* 80−34461
KI-KCl:Cu^+ mixed cryst., off-centre Cu^+ 79−65112
$KNbO_3$, photoconductivity and TSC 78−2520
$KTaO_3$, photoconduction in ferroelectrics 78−91720
K_2ZnF_4, charge transport and polarisation 80−80681
$La_2(SO_4)_3.9H_2O(D_2O)$, dynamic disorder of water mols., isotope effect obs. 80−55015
$Li_2B_4O_7$, ferroelectric glass, phase transition, permittivity, electrochromism, photochromism 80−80719
$(Li_2B_4O_7)_{1-x}(WO_3)_x$ dipolar glass, space charge injection, thermally stimulated depolarisation currents 80−66103
$Li_2B_4O_7.xWO_3$ (x=0 to 1 mol.) glass, random elec. dipole, cooperative phenomena 79−28693
LiF:Be(Mg), Maxwell-Wagner relax. induced by impurity clouds around dislocations, ionic thermocond. meas. 80−7281
LiF:Mg, Z_2- and associated Z-centres, elec. cond., ionic thermocurrent, and optical absorpt. meas. 80−107229
LiF:Mg dosimetric cryst., light-sum storage during linear stage 79−8194
LiH, defect form. at low temp., EPR, thermolum. and TSC study 80−107222
$LiPO_3$-$Al(PO_3)_3$:Ag glass, ionic motions, thermally stimulated depolarisation study 79−65239
$MgAl_2O_4$, γ-irradiated crystal, TSC, thermoelec. power, thermolum. and afterglow 80−75583
MgF_2 film, crystn., AC elec. props. 78−2804
MgF_2, localised electronic levels, thermoluminesc. and thermally stimulated current exam. 78−11001
MgF_2:Mn(Co), thermoluminesc. and TSC in activator band 79−24359
MgO crystals, dipolar defects, thermally stimulated depolarisation 80−66101
MgO, evidence for field induced trapping of defect dipole, thermally stimulated depolarisation 79−99820
MgO single cryst., γ-irrad. in presence of O_2, H_2 and H_2O adsorbates, thermostimulated surface cond. 80−34499
MgO, single crystal, thermal and optical stimulation processes of V-centres *(Japanese)* 80−11485
NH_4Cl, pure and NH_3 and $NiCl_3$ doped, TSC obs. of polarisation 79−78618
NH_4ClO_4:SO_4^{2-} (CrO_4^{2-}), thermal depolarisation, relax. parameters 78−43779
$NH_4H_2PO_4$, single cryst., thermal depolarisation current 79−51303
$NH_4H_2PO_4$:CrO_4^{2-} ($Cr_2O_7^{2-}$), electrical cond., thermal depolarisation studies 79−95212
NaCl, evaluation of ionic thermocurrent technique in monitoring relaxation behaviour of impurity-vacancy dipoles 78−43778
NaCl, irradiated, at 80K, thermolum. processes 80−34990
NaCl, low temp. space charge polarisation 78−43789
NaCl:$(Mn^{2+}$-□$)_{Fanion}$, F^- assoc. complex, ionic thermocurrent and EPR 79−8086
NaCl:Cd^{2+}, superstructure obs. by ionic thermal current meas. 78−39499
NaCl:Mn^{++}, Mg^{++}, doubly doped, ionic thermocurrent study of linear dimer 80−79977
NaCl:Mn^{2+}, dimer detection, EPR and ITC expts. 78−59833
NaCl:Mn^{2+}, ionic thermocurrents, comparison between microscopic and phenomenological anal. 79−51302
NaCl:Sn^{2+}, thermally stimulated space charge decay 78−48111
NaCl:Sr^+, ionic thermocurrent exam. 78−10833
NaCl-NaF:Pb^{2+}(Eu^{2+})(Zn^{2+})(Mn^{2+})(Sn^{2+}), point defect ionic thermal current and optical meas. 80−6403
NaF:Ca_i migration enthalpy and entropy, TSC obs. 80−54716
NaI:Ca^{2+}, pure and doped, ionic thermocurrents meas. 80−80677
$NaMgF_3$, defects induced by X- and vacuum UV irrad., optical and elec. study 80−107319
$NaNbO_3$, photoconductivity and TSC 78−2520
Na_2O-Li_2O-NiO-Fe_2O_3-B_2O_3-SiO_2 glasses, thermally stimulated cond. studies of trapping centres 79−78113
Nb_2O_5, electron energy spectrum by optical and thermal methods 79−69418
p-n junction space charge region, thermally stimulated current, impurity centre parameters 77−85237
PbI_2, defect levels, TSC meas., photoconductor models, trap level capture cross section 79−69463
PbI_2, TSC meas., localised levels in energy gap, depend. on purity and history 77−15856
PbO-GeO system, pyroelec. and TSC props. 78−43798

thermally stimulated currents continued
3PbO.2GeO, TSC in thermoelectret state during ceramic synthesis, pyroelec. currents and energy struct. of capture centres 80−55014
PbSe, film, photoconductivity, temp. depend. 79−38200
PbTe film, residual conductivity 78−2595
$PbTiO_3$, photocond. and TSC meas. 77−15911
Pb(Zr,Ti)O_3 ceramics, space charge field meas. by ferroelec. domain switching current, piezoelec. reson. freq. ageing charcts. 80−7296
RbBr:Cu^+, off-centre ion position, ionic thermocurrent study 80−7271
RbCl, with divalent impurity, reorientation of impurity-vacancy complexes, thermally stimulated depolarisation 77−65977
RbCl:Cu^+, off-centre ion position, ionic thermocurrent study 80−7271
$RbCl_2$-$NiCl_2$, impurity ion and vacancy aggregation, thermally stimulated depolarisation investigation 78−18678
S magnetoelectret, thermally stimulated discharge current 79−91341
S:Si, implanted, defect signature by thermally stimulated meas. 78−91643
Sb-S-I system crystals and glasses, adhesion levels, TCE spectra 77−24529
Sb_2S_3, defect drift in elec. fields and bistable switching 80−92947
SbSI-BiSI, solid solns., phase diagrams, photocond., elec. props. 79−38125
Se, amorphous, TSC, dielec. relax. modes 77−90090
Se, epitaxial monocrystalline film, trapping 77−85349
Se layers, amorphous and partially crystallised, trap spectrum, TSC and I-V charcts. 77−76981
a-$Se_{97.5}As_{2.5}$, trapping, photo-stimulated and thermally-stimulated current obs. 77−28192
Si, amorphous, Schottky barrier solar cells, deep hole traps, spectral response and TSC meas. 80−50962
Si, amorphous film, TSC, density of localised states distrib. 80−65587
Si, amorphous layers, recrystallisation, pulsed laser annealing 80−65404
Si, deep centres, majority carrier thermal capture cross section 78−10468
Si, deep centres associated with plastic deform. and quenching *(French)* 77−28145
Si deep level determ. using deep depletion MOSFET test structure 78−10571
Si, defect prod. by GeV muons, thermally stimulated current technique 78−5099
p-Si, electron irrad. induced defects, thermally stimulated capacitance 77−11933
Si, high dislocation density crystals, photoelectret state investigation 80−97191
p-Si, high-resistivity, TSC and photo-EMF in p-n junction, deep levels 77−72913
Si, ion implantation, TSC meas. of coupled levels 78−84165
p-Si, low temp. defect prod., obs. by thermally stimulated capacitance technique 77−84801
Si p^+-n contaminated junction, precip.-induced and generation-recomb. currents 78−2555
Si:Al, thermally induced deep levels, TSC meas. 77−31974
Si:Au, p^+-n junction, quantitative study of Au atoms by TSC method 80−2458
Si:Au, thermally stimulated capacitance method fitting anal. 79−47107
Si:Au p^+-n junction, small area, acceptor level conc., determ. from TSC curves 80−75631
Si:Ni p^+n and n^+p diodes, thermally stimulated capacitance obs. of Ni acceptor levels 78−19137
Si:Pd, deep levels, conc., activation energies, thermal emission rate, thermally stimulated capacitance meas. 79−51524
Si:Pt, deep level, exam. by thermally stimulated current and capacitance techniques 79−1579
Si-SiO_2 interface, γ-ray irradiated thin oxide, MOS struct. *(Russian)* 78−84302
Si-SiO_2 structures, B ions implanted, energy spectra of shallow traps at various implantation energies 80−80392
$Si_{12}Ge_{10}As_{30}Te_{48}$ glass, thermally stimulated depolarization current meas. *(Japanese)* 78−34875
Si_3N_4 film in MNOS memory struct., distrib. and role of N-H and Si-H bonds 79−33358
Si_3N_4 films, thermally stimulated depolarisation current meas. 80−88643
SiO film, electrode effects in TSC and capacitance meas. 79−78203
SiO_2, evaporated film, Debye-type dielec. dispersion props. 78−56421
SiO_2 film, plasma grown, thermally stimulated depolarisation current meas. *(Russian)* 78−80082
SiO_2 film, thermally stimulated depolaris. current, model *(Russian)* 79−56342
SiO_2, HCl-grown oxides, characterisation of surface states using MOS transient currents 80−65696
SiO_2, in IGFET struct., thermal reemission of trapped electrons 79−42650
SiO_2, in MOS struct., charge transport, TSD obs. 77−89870
SiO_2, noncryst., in MOS struct., Na ion impurities motion 78−10223
SiO_2, trapping level exam. by thermally stimulated discharge of capacitor *(Russian)* 78−34845
SiO_2-Si in MIS, interface states, thermally stimulated charge decay 77−12009
SnO_2, correl. between simultaneous thermally stimulated cond. and thermlum. transients 79−91073
SnO_2-ZnO-Bi_2O_3, ceramic semiconductor, injection currents 79−11141
SrF:rare earth $^{3+}$, reorientation of dipoles 77−8494
SrF_2:Ce^{3+}, dipole reorientation, Ce^{3+} conc. effect 78−10841
SrF_2:Gd^{3+}, dipole relax. and equilib., ionic thermocurrent obs. 77−48121
SrF_2:Gd^{3+}, dipole strengths and conc. effects influenced by dipole-dipole interactions 79−69718
SrF_2:Na^+, cryst., thermal depolarisation 79−82912
SrF_2:rare earth, dipolar complex exam. 79−38435
SrF_2:rare earth, electric dipoles, relaxation parameters and dipole-dipole interaction 79−24255
SrO:Ni^{2+}, ionic thermocurrent meas. 80−108148
$SrTiO_3$, photoluminesc., thermoluminesc. and thermally stimulated currents 78−92121
a-$Te_{40}As_{35}Ge_7Si_{18}$, trapping, photo-stimulated and thermally-stimulated current obs. 77−28192
TeO_2, ferroelectric glass, phase transition, permittivity, electrochromism, photochromism 80−80719
TeO_2-WO_2 glass, dipole correlations, capacitances and TSC meas. 79−28670

thermally stimulated currents continued
ThO_2, ceramic oxide, thermally stimulated depolarisation currents, grain size and growth determ. 79−65792
TiO_2, plasma growth, photoelectronic props. 78−52662
TiO_2 sputtered film, photocond. and TSC meas. 80−15560
$TlGaSe_2$, impurity conductivity and TSC 78−23128
VO_2 pyrolytic film, phase transition and electrical cond. 77−89890
V_2O_5-P_2O_5 glass, dielec. relax. mechanism, SDRC investigation, Schottky barrier formation in metal-glass-metal systems 78−60388
V_2O_5-P_2O_5 glass, in metal-semicond.-metal struct., TSC of dielec. relax. *(Russian)* 77−35998
ZnO ceramic, with additives, nonohmic thermally stimulated current meas. 77−20325
ZnO non-ohmic ceramic, degradation props. under AC and DC bias 80−80262
ZnO, nonohmic ceramic, current creep 79−69514
ZnO, photoelectret, nonisothermal relax. 77−12306
ZnO photoelectret, TSC reversals 77−8493
ZnO-Bi_2O_3-ZnO structure, injection currents obs. *(Russian)* 77−32068
α-ZnP_2, local centre parameters, photoelectron transition scheme, recomb. process anal. 80−44654
ZnP_2, trapping levels, TSC and thermolum. meas. 79−15115
ZnS:Ag, Al(Cu), trap parameters, thermostimulated luminesc. and cond. meas. *(Russian)* 77−72868
ZnS:Ag, TSC and induced impurity photoconductivity, existence of two electron trapping centres 80−44655
ZnSe, heat-treated in controlled partial press. of Zn or Se, TSC 80−59910
ZnSe:Al, thermally stimulated transients, new approach 79−38086
n-$ZnSiP_2$, deep impurity levels, Schottky TSC meas. 79−95419
ZnTe, elec. field and impurity conc. effects on ionisation energy of impurities, appl. to acceptors 80−88514
p-ZnTe film, current-voltage characts. 77−66214

thermally stimulated depolarisation *see thermally stimulated currents*
thermally stimulated discharge *see thermally stimulated currents*
thermally stimulated ionic currents *see thermally stimulated currents*
thermally stimulated polarisation *see thermally stimulated currents*
thermally stimulated relaxation currents *see thermally stimulated currents*

thermionic cathodes
AES in SEM, high resolution, electron sources comparison 77−25330
arc cathode electron emission, individual ion fields effect 77−28677
coherence properties, correl. function 77−22622
convertor, surface serration development, influence on emission characts. *(Russian)* 77−81193
Davisson line retarded field data determ. of thermionic consts. 79−87555
design using heat flow optimisation 80−71558
electron beam from triode with explosive-emission cathode, variable current density 79−72475
electron gun employing spherical diode with plasma anode 77−591
field emission source for high resolution, high current e-beam microprobes 80−68297
graphite emitter, Cs-coated, for thermionic cell 79−11494
high-current multirod cathode, influence of absorption effects on characts. 80−20756
hybrid mode thermionic convertor, grooved emitter and flat collector 77−24214
impregnated and coated powder cathodes, reactivation following shelf-life poisoning, comparison 80−76128
impregnated W cathode, model based in Auger meas. of Ba-O-W system 79−43073
impregnated-cathode behaviour, emission, and lifetime, expt. study 80−84827
ionisation gauges, heated cathodes, emission characteristics, selection *(German)* 80−236
Knudsen converter low energy electron reflection from thermionic cathode, mag. field depend. 80−19627
negative surface ionisation on complex emitter 77−77335
plasmatron, emission cooling *(Russian)* 80−54052
porous metal thermionic cathode with sputtered metal films, emission operating characts. 80−100740
pulsed X-ray thermionic tube intensity and dose angular distrib. obs. 79−67450
rare earth oxide, work function, influence of surface and bulk effects 78−11065
semiconductor, fluctuations of velocity of emitted electrons 80−66380
temperature distribution, axial, calculation method 77−14889
thermionic diodes, planar low press. gas discharges, plasma regime, plasma characts. 79−77435
transition metal, 4d or 5d, work function of electropositive metal coadsorbed with O_2 78−11064
triode thermionic convertor, with W emitter and WO_2 collector, pulsed discharge characts. 77−24215
X-ray tube cathode heating transition processes *(Bulgarian)* 79−93264
BaO-Ba coated cathode, role of surface donor centres 78−11063
(BaSrCa)O, cathodes, thermionic emission characts., X-ray struct. obs. 78−48270
CeB_6, thermionic emission rel. to surface state 78−39654
Cs vapour thermionic diode, wall-to-wall theory, sheath anal. 77−24211
Cu, point emitter, surface microrelief under explosive electron emission 78−2973
Ge (100) with Cs and Cs+O_2 overlayers, negative electron affinity surface, thermal stability of work fn. 78−92167
LaB_5 gun, optimum brightness problem 78−21298
LaB_6 beam current stability in high vacuum 77−40321
LaB_6, brightness, cryst. orientation and purity effects 77−12483
LaB_6 cathode gun from transmission electron microscope appls. 80−18048
LaB_6 cathode poisoning, by residual gases, organic solvents, oils and greases 77−66568
LaB_6 cathodes, residual gas poisoning in vac. system, thermionic emission decay 78−27364
LaB_6, directly heated, for electron beam instruments, design and optimisation 78−93783
LaB_6 gun, Broers type, design, for SEM 78−21283
LaB_6, illumination system, for round beam electron probe systems 80−57436
LaB_6 mounting methods and operating characts. 80−57437
LaB_6, single crystal, of <100> and <110 orientations, brightness meas. from 1500 to 1950K 80−62808
LaB_6, single crystals, thermionic work function meas. 78−11067

thermionic cathodes continued
LaB_6, single-crystal thermionic electron emission anisotropy 77−24920
LaB_6, thermionic emission rel. to surface state 78−39654
LaB_6 three-electrode 250 A pulsed electron gun 78−82553
LaB_6-Ni-WC(TiC)(NbC)(TiB_2), thermionic emission 77−28678
Mo, (110) and (111) faces, joint adsorption of Cs and O, and emission props. 78−2364
Mo, point emitter, surface microrelief under explosive electron emission 78−2973
Mo-Mo_2C-La_2O_3-Pt cathode, Pt effect on work function *(German)* 79−74048
Mo-TiC(ZrC)(HfC), thermionic emission, surface structural characts. after prolonged use, work function variation 80−20758
Ni, Medicus matrix cathode, surface characts. 80−66378
Pd-Ba (1.5 wt.%), Auger spectrum fine struct. 78−2954
Pt-Ba, vaporisation expts., heat of adsorpt. and migration of Ba on Pt 78−10272
Pt-Ba alloy, elemental comp. and chem. state of surface during thermal activation, AES obs. 78−2345
Si (100) with Cs and Cs+O_2 overlayers, negative electron affinity surface, thermal stability of work fn. 78−92167
Ta, Cs adsorption, direct meas. of adsorpt. isobars 78−43235
TiC, cathode, thermionic emission, Ti and C admixtures, Os film covered, improved emission 79−28884
W dispenser cathodes, Ba-activated, surface characts., ion scatt. spectrometry and SIMS study 80−66377
W filaments, operated as cathodes in gas discharge characts. 79−50913
W high-current multicavity thermionic cathode, erosion mechanisms, sputtering 79−55570
W, impregnated, surface props. exam. using AES and work function meas. 77−8715
W, impregnated cathode, mechanism of operation, life-tests 79−78821
W plates, heating by DC electron bombardment 78−23578
W, struct. transforms. in BaO coating, LEED obs. 78−11061
W, tip electron gun, use of focused laser beam for cathode heating *(German)* 78−89591
W:Os coated dispenser cathode, chemical and physical process obs. 79−28885
W-Ba, type B impregnated cathode, operation mechanism 78−15278
W-ThO_2-B, thermocathodes diffusion mobility, based on deboronation kinetics 80−39349
W-Ti, Ti addition effect on heat resistance and radiative props. *(Russian)* 80−25515
W-TiC(ZrC)(HfC), thermionic emission, surface structural characts. after prolonged use, work function variation 80−20758
W-Zr, Zr addition effect on heat resistance and radiative props. *(Russian)* 80−25515
W-Zr-C, Zr and C addition effect on heat resistance and radiative props. *(Russian)* 80−25515
Y_2O_3 cathodes, thermionic emission, 1000-1800K 77−48302
Zr-O-W (100) thermal field emitters, operational experience 80−71576

thermionic conversion
advanced convertor, external ionis. mechanism for plasma 77−84541
advanced convertor with auxiliary ionisation, microwave heating 77−24216
advanced operating modes, arc drop elimination 77−24213
alkali metals, vapour states, laser spectroscopy and applic., review 80−68260
braze alloys, low vapour press., binary eutectic, props., thermionic converter appls. 77−90236
ceramic materials appl., fireproof *(Czech)* 79−70455
cermet electrode development for flame heated thermionic convertors 80−40891
combustion-heated diodes characts., ceramic and alloy materials suitability evaluation 79−48157
concentric electrode thermionic convertor, theoretical efficiency 79−48152
convertor, V-I characts., collector material depend. 77−7606
convertor in diffusion mode, V-I characts., Coulomb collisions effects 77−7604
Cs thermionic converter, auxiliary discharge to reduce voltage drop 79−10724
current density distribution in long cylindrical convertor 78−71552
cylindrical, low cost convertor for measuring lead efficiency 80−40889
electrical power density, optimisation of generating element 79−10723
electron beam, fast, relax. cross sections energy depend. 80−43939
electron thermal conductivity, effect on convertor performance, theory 80−40892
emitter and collector development 77−84539
enhanced mode converters, operation characts. 77−84538
flame-fired thermionic diode development 80−40890
fusion reactor topping cycles appl., preliminary assessment 79−48161
heat flux and electron reflectivity expts. for improved convertor efficiency 80−45719
heat pipes, spacecraft radiator elements, NEP thermionic system design 80−40887
heat pipes appl., using Li and K working fluids 79−48153
hybrid mode characts. 77−84536
hybrid mode thermionic convertor, developments 80−40888
hybrid mode thermionic convertor, grooved emitter and flat collector 77−24214
hybrid thermionic converter for 10 GW space power plant 79−92086
hybrid thermionic converter for space craft secondary energy source 79−92086
ideal convertor, output power optimisation 79−27841
ignited mode of convertor, electron energy distrib. meas. of Cs plasma *(Japanese)* 80−3528
ignited mode of convertor, internal phenomena and output characteristic *(Japanese)* 80−3527
ignited mode operation of thermionic diode, interelectrode space and sheath anal. 77−24212
instability of overneutralised thermionic plasma converter, simulation 79−14619
Knudsen converter low energy electron reflection from thermionic cathode, mag. field depend. 80−19627
Knudsen Cs-Ba converter performance optimisation 79−27840
low temperature thermionic convertor, with LaB_6 collector 79−27842
mathematical model of converter, plasma anal. 77−84540
multielectrode thermionic convertor 79−86622
NASA's program, 1978 status, objectives and plans 79−48159

thermionic conversion continued
NASA space power technology program 79−96883
nuclear reactor, ^{233}U fuel and Be moderator, neutron physics analysis 77−50281
plasmatron as thermionic energy converter 77−84537
power plant design point selection, economic impact 79−48155
power systems 1978 status and prospects 79−48162
pulsed operation, ionisation stage of thermionic convertor 79−64928
pulsed operation of thermionic converter, plasma decay effects 79−14620
R and D at US DOE 80−35715
ring triode, enhanced mode thermionic convertors, expts. 78−38553
sheath operating mechanism effects 80−30507
solar energy power generators with advanced thermionic converters for space craft applications 80−61389
solar thermionic power plant, central thermal receiver tower concept, geometric config. and design 80−61390
space nuclear propulsion, out-of-core thermionic power conversion system 79−48160
space vehicle thermionic convertor array, efficiency optimisation using heat transfer computer modelling 80−40886
space vehicle thermionic generators for solar energy conversion 80−35714
spacecraft, solar energy thermionic electricity generating plants 77−78603
steam power plant conceptual design, thermionic topped, using advanced boiler concept 79−48156
thermionic spacecraft reactors with ^{233}U as fuel, reflector drums as control mechanism 80−47686
thermionic triode, oscills. in low press. inert gas discharge 80−79590
transition metal carbide, behaviour in Cs or K plasma 77−20979
triode thermionic convertor, with W emitter and WO_2 collector, pulsed discharge characts. 77−24215
uniform-temperature thermionic generator, model 80−85296
USSR activity and 1978 status, comparison with USA status 79−48158
utilities topping cycle appl., Department of Energy (USA) development program 79−48154
Zepo−the world's largest thermionic converter, design and testing 80−40885
Cs convertor, pulsed, plasma parameters, operating characts. 80−6293
Cs plasma, in thermionic convertor, spectroscopic meas. of Cs I *(Japanese)* 77−58902
Cs plasma in thermionic converter, mass spectrometric study of positive and negative ions 79−19083
Cs, thermionic converter, ion species mass anal. 77−89344
Cs vapour source, thermionic energy convertor with Cs-He gas controlled heat pipe 80−64791
Cs vapour thermionic diode, wall-to-wall theory, sheath anal. 77−24211
Cs-Se thermionic converter, output power, vap. source depend. 80−44000
Mo, low-temperature thermionic converter with an expanded-area collector 80−70045
Ni alloy electrodes, thermionic electron emission into Cs vapour 78−60540
Ni alloy surfaces, electron emission in Cs vapour, pot. applic. in thermionic converters 77−90235
W, thermionic emitter, work function rel. to output characts., in arc regime 77−52213

thermionic electron emission
see also Schottky effect; thermionic cathodes
alkali halide, photo- and thermostimulated electron emission under ultrahigh vacuum conditions *(Russian)* 80−66383
alkaline earth electron thermoemission and tunnelling emission *(Russian)* 77−44113
alkaline earth oxide cathodes with In_2O_3 additions, effect on emissive props. 77−48298
angular distribution, cosine law theory 78−35233
arc cathode electron emission, individual ion fields effect 77−28677
arc-cathode emitting sites, effect of Cu-oxide thickness, obs. 77−55190
band induced anisotropy effects 77−32489
cadmium arachidate mixed with cyanine dyes, mol. layers, photoelec. props. 80−80401
cathode, oxide coated, emission local nonuniformities 77−20978
cathode, oxide type, conductivity model 79−15159
coherence properties, correl. function 77−22622
conduction electron retrapping probability, depend. of sums of thermally stimulated electron emission on heating rates *(Russian)* 80−84826
crystal, internal radiation spectral composition at high temp., energy transfer and thermionic emission 77−43359
Davisson line retarded field data determ. of thermionic consts. 79−87555
dielectric film transient thermal emission current model *(Russian)* 77−15982
distribution function, distortion 79−65970
electrode-insulator boundary, current injection in presence of space charge 79−1619
elliptic emission functions used in calc. of electron emission from surfaces 80−89124
exoemission phenomena, TSC, thermionic emission, book contribution 80−80954
exploding wires, electron emission 79−50914
flame plume behind bluff body with fuel injection, elec. cond. mechanism 79−39150
graphite emitter, Cs-coated, for thermionic cell 79−11494
high-current multirod cathode, influence of absorption effects on characts. 80−20756
hot cathode temperature, thermionic emission meas. method *(Czech)* 78−70121
III-V semiconductor-metal surface barrier structures, chem. precipitation and props. *(Russian)* 78−84298
laser spark in dense N_2 near metallic target *(Russian)* 80−38682
laser- or black-body radiation, strong electron coupling, limitation of Fermi-Dirac statistics 80−29843
liquid cathode arc, cathode sheath model, liquid K in Ar *(French)* 77−1032
local and integral emission meas., electron emission microscope adaptation 79−93258
magnetic modulation of thermionic emission between parallel cathodes 78−52615
magnetic multipole line-cusp plasma generator for neutral beam injectors 79−19056

thermionic electron emission continued
magnetron diode, cathode heating and back bombardment, calcs. 77−8713
metal, anisotropy 80−20757
metal, creep-electron emission relation 78−6994
metal, surface charge density prod. in satic electrification 78−14797
metal, thermoelectric effect in surface layer exposed to high-power heat flux 77−35926
metal surface, thermionic-field emission anal. 78−19642
metal whisker diode, thermal field emission, nonlinearity, response time and polarity reversal 78−2579
metal whisker diode, with thermally enhanced field emission, elec. fields, calc. by antenna theory 77−47889
metallic heated cathodes, physics of electron emission *(French)* 80−104033
metals and alloys, meas. instrument based on scanning electron beam 78−74025
orbitron device, optimum injection condition for electrons, influence of end effects 80−82784
plasma, highly-dispersed aerosol, nonisothermal, thermionic electron density function determ. 78−91066
point-contact junction, influence of mech. modulation elec. transport 80−2481
polymer film, in MSM struct., thermionic field emission from metal 79−1629
porous metal thermionic cathode with sputtered metal films, emission operating characts. 80−100740
radiographic X-ray tube current, effect of electron evaporation 78−69204
rare earth hexaborides, low work function thermionic electron emitters, props. 79−33884
rare earth hexaborides, thermoelectronic props. rel. to surface state *(French)* 79−69950
refractory metal, surface geometry and emission parameters, changes during directional mass transport 78−2344
Schottky, non-degenerate diode, current-voltage characts., analytical approx. 79−95494
semiconductor cathode thermionic emission, electron velocity and energy variance in elec. field 78−88402
semiconductor cathodes, fluctuations of velocity of emitted electrons 80−66380
T-F emitted electrons, energy spread *(Japanese)* 79−56916
tectrode system, two-dimens., algorithm for solving space-charge problems with thermally-emitted electrons 80−100743
TGS, emission of free charge carriers in vacuum as symptom of pyroelec. props. 79−42908
thermionic electron emission, from defect states at grain boundaries 79−91559
thermionic emission during stretching 79−95897
thermoautoelectronic emission into plasma, individual ionic field effects 79−69949
transition metal carbide, behaviour in Cs or K plasma 77−20979
transition metal carbide emitters, review *(Japanese)* 77−63521
transition metal nitrides, review *(Japanese)* 77−63522
ultrahigh vacuum setup for photo- and thermostimulated electron emission and luminesc. obs. *(Russian)* 80−66383
vacuum diode, laser produced cathode plasma, streaming, electron emission temp. determ. 78−91162
work function, local, surface with adsorbed atom islands 80−7462
n-Si, deep levels in p-n junctions or Schottky barriers determ., hybrid method 79−24067
Ag-Cs-O photocathode, operation mechanism involving Cs_2O_2 80−66384
Ag_3SbS_3, pyrargyrite, thermoelec. and photoelec. work functions, Fermi level and electron affinity *(Russian)* 77−15939
Al, laser irrad., charged particle emission from back side of target 78−2949
Al-GeS-Al structure, current-voltage characts., thermionic electron emission model 77−28260
AlGaAs-GaAs DH laser, carrier leakage, physical mechanisms 78−66824
Ar arc with hot W cathode, electron emission mechanisms 77−24224
Au-Al_2O_3-Al system, influence of mech. modulation on elec. transport 80−2481
Ba, adsorbed layers on W, Auger and work function meas., impregnated W cathode model 79−43073
Ba-O system, adsorbed layers on W, Auger and work function meas., impregnated W cathode model 79−43073
BaB_6, $(La,Ba)B_6$, $(Ea,Ba)B_6$, single crystal growth for thermionic emission 78−92183
BaB_6, O adsorption effects 77−8711
BaB_6 powder, surface struct. effects on thermionic emission characts. and vapour pressure *(Japanese)* 80−50506
BaB_6 powder prep., thermionic emission charact. *(Japanese)* 80−11610
BaB_6, work function, thermionic and field emission retarding pot. meas. 77−90233
BaB_6, work functions from thermionic and field emission retarding pot. methods 79−65537
BaO epitaxial films, cathode poisoning due to O_2, CO_2, and S, surface anal. 79−42600
BaO films on Ir, thermionic props., Auger, LEED, and emission microscopy 79−43089
$Ba_3Sc_4O_9$, $Ba_3Sc_2WO_9$ and Ba_2ScTaO_6, elec. cond. nature, depend. on comp. and medium thermodynamic parameters 80−70773
(BaSr)O on Ni, oxide thickness depend. of emission 77−48299
BeO, emission of free charge carriers in vacuum as symptom of pyroelec. props. 79−42908
CO_2 laser-heated electron emission from C-coated metal surface, appl. to emissive probe meas. 80−6270
$Cd_xHg_{1-x}Te$-metal contact, transport mechanism, thermionic and field emission processes 77−20425
CeB_6, single cryst. work function, thermionic emission, evaporation 77−24922
CeB_6, single crystal growth for thermionic emission 78−92183
CeB_6, thermionic emission rel. to surface state 78−39654
CeB_6, work functions from thermionic and field emission retarding pot. methods 79−65537
$CeBr_6$, work function, thermionic and field emission retarding pot. meas. 77−90233
Cs-Bi vapour saturated semiconducting film on collector, thermo-emission characts. *(Russian)* 78−23577

thermionic electron emission continued
Cs-O, low work function surface, prod. by Cs_2CO_3 decomp. and emission characts. 77−85882
Cs_2O-Al_2O_3-SiO_2, thermionic emission of ions and electrons 78−2969
Cu, point emitter, surface microrelief under explosive electron emission 78−2973
EuB_6, $(La,Eu)B_6$, $(Eu,Y)B_6$, $(Eu,Ba)B_6$, single crystal growth for thermionic emission 78−92183
GaAs, deep centres, collective thermal emission of electrons 80−10918
GaAs, temp. depend. of intervalley gap from Schottky diodes meas., thermionic emission theory generalization 79−73586
GaAs-$Al_xGa_{1-x}As$, negative differential resist., real-space electron transfer 80−6958
HfC coated emitters, thermionic emission props. *(Japanese)* 77−40322
Hg-Ar(Kr)(Xe) mixtures, prebreakdown discharges, discharge current depend. on electron mobility 79−77433
K_2O-Al_2O_3-$2SiO_2$-BaO plasma emitter 80−96368
$(La,Cs)B_6$, single crystal growth for thermionic emission 78−92183
(La, Y, Sc)B_6 solid solns. electron work function, thermal emission technique 80−20755
$(La,Y)B_6$, $(Eu,Y)B_6$, single crystal growth for thermionic emission 78−92183
LaB_6, $(La,Eu)_6$, $(La,Y)B_6$, $(La,Ba)B_6$, $(La,Cs)B_6$, single crystal growth for thermionic emission 78−92183
LaB_6, and related cpds., thermionic props. *(French)* 78−60541
LaB_6 cathode, beam current stability in high vacuum 77−40321
LaB_6 cathodes, residual gas poisoning in vac. system, thermionic emission decay 78−27364
LaB_6 cathodes, single crystal, of <100> and <110> orientations, brightness meas. from 1500 to 1950K 80−62808
LaB_6 emitters, thermionic emission *(Japanese)* 77−44114
LaB_6 single cryst. tips with [100], [110], [111] and [210] orientations, thermionic emission patterns 80−66379
LaB_6, single cryst. work function, thermionic emission, evaporation 77−24922
LaB_6, single crystals, thermionic work function meas. 78−11067
LaB_6, sintered, work function and Richardson const., Mo poisoning effects 79−52070
LaB_6 surface stoichiometry B conc. effects 79−87556
LaB_6, thermal field emitted electrons, total energy distrib. spread 77−52227
LaB_6, thermionic emission props. *(Japanese)* 77−63523
LaB_6, thermionic emission rel. to surface state 78−39654
LaB_6, work function, thermionic and field emission retarding pot. meas. 77−90233
LaB_6, work function 2.3 to 2.4 eV jellium model 77−8710
LaB_6, work functions from thermionic and field emission retarding pot. methods 79−65537
LaB_6:Y, Sc effects of impurities thermionic emission 78−60542
LaB_6-YB_6-ScB_6, thermionic emission 78−11068
LaB_x, phase relationships, chemical activity and work function obs., thermionic appls. 77−90234
LaB_x x=4.24 to 29.2, thermoelectric electron emission, work function, 1400-2100K 78−60539
$LaCrO_3$-MgO, LC20M electrode material in open cycle MHD systems, thermionic emission characts. 80−97394
LiF, cryst., laser irrad., electron emission 80−80948
$LiNbO_3$, effect of spontaneous polarisation on thermionic emission 78−35245
$LiNbO_3$, monocryst., thermoemission, anomalous zone bending *(Russian)* 77−55860
Mo, coadsorption of O_2 and Cs, electron emission props., thermal stability 80−66878
Mo, integral thermionic emission meas. using modified high vacuum electron emission microscope 79−9263
Mo, point emitter, surface microrelief under explosive electron emission 78−2973
Mo, thermionic emission, work function in atmospheric pressure gases 78−76575
NaCl, cryst., laser irrad., electron emission 80−80948
Nb (110), adsorption of O_2, variation in work function, retarding field and thermionic emission meas. *(French)* 79−78823
NbC coated emitters, thermionic emission props. *(Japanese)* 77−40322
$NbC_{0.86}$, single crystal work function, thermionic emission and contact pot., microhardness and binding 79−19649
Ni alloy surfaces, electron emission in Cs vapour, plasma anode meas. 77−90235
Ni alloys, work function for emission into Cs vap. 78−60540
Pd-Ba alloy emitter, thermionic emission props. and Auger spectrum 78−11066
Re, thermionic emission, work function in atmospheric pressure gases 78−76575
Re, thermionic work function of low index planes 80−55255
Rh film, work function rel. to degree of coverage of Th film *(Czech)* 78−80039
a-Si:H/Pt, Schottky diode, influence of prep. conditions on forward bias currents 79−78171
Si:Se, impurity states, A- and B-centres, electron, hole thermionic emission rates 80−96813
SmB_6, work function, thermionic and field emission retarding pot. meas. 77−90233
SmB_6, work functions from thermionic and field emission retarding pot. methods 79−65537
TGFB, emission of free charge carriers in vacuum as symptom of pyroelec. props. 79−42908
TGSe, emission of free charge carriers in vacuum as symptom of pyroelec. props. 79−42908
Ta autocathode, influence of electric field and heating on work 80−7478
Ta, thermoelectron emission, S impurity atom effects, electron spectra *(Russian)* 77−8712
TaC coated emitters, thermionic emission props. *(Japanese)* 77−40322
TaC surface, effect of C oxidation on work function, 1250-2000K, AES 79−24054
Th film, coating on Rh layer, work function rel. to degree of coverage *(Czech)* 78−80039
TiC, cathode, thermionic emission, Ti and C admixtures, Os film covered, improved emission 79−28884
TiC coated emitters, thermionic emission props. *(Japanese)* 77−40322
TiO_2, nonstoichiometry study, thermal emission of electrons 80−108317
W cathode, impregnated with Ba and BaO, AES and work function meas. 77−24921
thermionic electron emission continued
W filaments, operated as cathodes in gas discharge characts. 79−50913
W, hot electron emission using ruby laser pulses 79−28883
W, laser irrad., charged particle emission from back side of target 78−2949
W, regularly stepped single crystal surfaces, work function determ. by thermionic emission 77−59665
W single cryst., dislocation effects on thermionic emission and work function 80−76129
W, thermal field cathode emitters, end form changes, electron microscope obs. 77−4718
W, thermionic emission, work function in atmospheric pressure gases 78−76575
W, thermionic emitter, work function rel. to output characts., in arc regime 77−52213
W whisker, energy spread meas. of thermal field-emitted electron flow 78−92168
W:Os coated dispenser cathode, chemical and physical process obs. 79−28885
W-O-Cs system, 450-800K 78−2972
Y single crystal, thermionic emission work function 78−2971
Y_2O_3 cathodes, thermionic emission, 1000-1800K 77−48302
Y_2O_3, nonstoichiometry study, thermal emission of electrons 80−108317
Zn-GeS-Zn structure, current-voltage characts., thermionic electron emission model 77−28260
ZrC coated emitters, thermionic emission props. *(Japanese)* 77−40322
ZrC, in H_2, thermionic emission, residual gas effects 78−48269
ZrC, work function, effect of H_2 adsorpt., thermionic emission expts. 78−2970
ZrC work function, sorbed O_2 effect, thermionic emission and thermal desorption obs. 79−56285
ZrC-Re, in H_2, thermionic emission residual gas effects 78−48269
ZrC-W, thermionic emission current density, cathode operating time and comp. depend. 77−8714
$ZrC_{0.84}$, single crystal work function, thermionic emission and contact pot., microhardness and binding 79−19649
ZrN_x:Cs, thermionic emission, metallic sublattice vacancy effects 78−68597

thermionic emission
see also thermionic electron emission; thermionic ion emission
cathode emission theory using semiconductor theory, Ebers-Moll eqn. *(German)* 78−95646
convertor cathode surface serration development, influence on device characts. *(Russian)* 77−81193
dilute low-temperature plasma, ionisation in presence of solid phase and alkali metal component 77−42989
electron-black body radiation strong coupling at high temps. 78−52624
metal substrate, adsorption systems, relationship between work function and degree of adsorption coverage 79−83092
MIM structure, emission current density in second intermediate region of Christov 79−33360
MIS negative barrier contact for induced back surface field solar cell 80−101101
nonlinear electron and ion transport in thermionic diode 77−13717
plasma electron temp. control in double plasma device 77−35363
refractory metals, work function, ionising radiation effects meas. method 80−6951
Schottky barrier devices, edge current modelling, agreement with thermionic-field emission theories 78−56227
semiconductor, n-type, quasisteady noise effect on thermionic emission 78−2974
student experiment using phototube 77−24919
Ta film deposition and oxidation, form. of Ta_2O_5 79−61769
transition metal carbides, adsorption of Cs(K), adsorpt. energy, thermionic emission 77−7978
unified theory of electron emission, appl. 78−35256
wide-gap semiconductors, thermionic emission current, surface states effects 79−15581
CdS Schottky barrier diode with evaporated Au-Ti blocking contact, rectification props. 77−85319
CdS-Cu_2S junctions, carrier trap density, deep level defects 80−107801
GaAs-$Al_xGa_{1-x}As$ heterostructures, real-space electron transfer by thermionic emission, analytical model 80−100512
Ir, adsorption and condensation of Sm, thermal desorption mass spectra and thermionic emission meas. 79−69362
LaB_6 single crystal cathode, thermionic emission, surface struct. 80−97395
LaB_6, synthesis and props. *(Japanese)* 80−40255
LaB_6-Ni-WC(TiC)(NbC)(TiB_2), thermionic emission 77−28678
$LiNbO_3$, thermionic emission characts. 80−104034
MgO:Al(Li)(F)(Sn), hole processes in photostimulated luminesc., electron emission, X-ray irrad., ESR relaxation 79−69889
Mo-TiC(ZrC)(HfC), thermionic emission, surface structural characts. after prolonged use, work function variation 80−20758
Si, enhanced conductivity in plasma hydrogenated films, thermionic emission 80−70692
Ta hollow arc cathode, emission current density 78−76574
W cathode, hollow, cylindrical, heavy-current temp. condition 80−38763
W, high-current hollow cathode, energy balance *(Russian)* 77−58910
W, hot emitter, surface struct. change during baking above 2000K 79−65971
W-TiC(ZrC)(HfC), thermionic emission, surface structural characts. after prolonged use, work function variation 80−20758
W-ZrC (25 wt.%), eutectic alloy, thermionic emission and adsorption props. 79−69951
ZrC, pure and with Y additions, thermionic emission, hot pressed or CVD 77−12484

thermionic generators *see thermionic conversion*

thermionic ion emission
alkaline earth oxides, emission props. in CO_2 stream 80−100742
alkaline earth oxides, surface emission active centres 80−100741
arc, high current, anodes processes, plasma pot., probe meas. 77−19801
energy distribution, retarding field analyser-quadrupole mass filter *(Japanese)* 77−18130
exoemission phenomena, TSC, thermionic emission, book contribution 80−80954
II-VI semiconductors, thermoemission of positive ions in simple gas atoms *(Russian)* 77−28676
ion electric field effect calcs. 77−32490

thermionic ion emission continued
metal, thermal ion energy distrib. by retarding field modulation method *(Japanese)* 79−78822
polystyrene film, graft, positive-ion emission in thermal destruction 80−66381
Cs aluminosilicate, containing Mo, Cu, Re or W thermoelectronic emission characts. *(Russian)* 77−48301
Cs, ion source, thermionic emission in SF_6 mol. gas 80−71557
Cs_2O-Al_2O_3-SiO_2, thermionic emission of ions and electrons 78−2969
Ge, work function, meas. by thermionic emission 78−19628
KCl:Tl, thermoemission of positive ions in simple gas atoms *(Russian)* 77−28676
KF, positive ion emission from thick layers, effect of substrate metal 78−19627
KF/Pt thick layer/substrate system, thermal positive and negative ion emission, surface prop. non-uniformity effect 79−28882
K_2O-Al_2O_3-$2SiO_2$-BaO plasma emitter 80−96368
Mo (100), emission and work function, K adsorption effects 78−11060
$(Na_2O)(Al_2O_3)x(SiO_2)$, zeolites, thermonic emission of alkali ions, desorption mechanism 79−4887
Ta (112), oxidised, emission and work function, K adsorption effects 78−11060
W, emission of K ions anal. *(Hungarian)* 77−48300

thermionic power generation *see thermionic conversion*

thermionic tubes
see also cathode-ray tubes; electron-wave tubes; gas-discharge tubes; rectifier tubes; vacuum tubes
diode, non-Boltzmann distribution of free electrons under high space charge conditions 78−56555
flame-fired thermionic diode development 80−40890
plasma diode, cylindrical, current-density distrib. 78−79479
thermionic emission triode, with auxiliary discharge, rectifying parameters 79−64925
triode, oscills. in low press. inert gas discharge 80−79590

thermionic valves *see thermionic tubes*

thermistors
Aanderaa thermistor chains for ocean temp. meas., solar radiation effects *(French)* 79−62611
acoustic temp. indicator, consisting of temp. sensitive resistor and operational amplifiers *(Spanish)* 80−13061
anemometer application, thermally compensated, math. models *(French)* 80−90227
audible alarm system for liquid level detection 79−12764
bead, temp. meas. in meteorology and oceanography *(German)* 77−21920
Bermuda Eleuthera Acoustic Range environmental meas. buoy 77−41229
biological effects of US, use of thermistor probes to mean. energy distrib. 80−109075
bolometer with $Mn_xCo_yNi_2O_4$ spinel ceramic, current noise 77−51793
bridge circuits with thermistors and pulsed supplies, unbalanced, anal. 79−30474
cardiac output thermodilution meas., thermistor probe construction for use in small animals 77−64161
ceramic, microstructure and physical props. 78−72756
characteristic curve linearisation method *(German)* 78−77913
deep tissue temp. monitoring by ultraminiature thermistors 80−3761
digital ventilated psychrometer, direct reading relative humidity meter using thermistors 79−2777
dynamic behaviour determination *(German)* 80−17940
ebullioscopes, uncertainty in sensitivity 78−12695
electronic thermistor-type thermometer *(German)* 79−35740
electronic thermometer, current bridge appl., clinical use 78−29109
fluid anemometric microthermistor sensor sensitivity curves *(Russian)* 78−34219
fluidic capillary sensor 78−24793
heat transfer intensification effect in nonuniform elec. fields 77−57354
heat-pulse moisture meter for capillary-porous materials 77−82499
II-IV-V_2 semiconductors, resist., possible use in thermistors 77−4343
immersion thermistor bolometer use in radiometer 78−70188
laboratory temperature control, bridge cct., modified window air conditioner 80−68192
level sensing in elec. conducting liquids using PTC thermistors 80−42209
linear ohmmeter for resistors having negative temperature coefficient 79−21743
live connection temperature rise meas. *(Swedish)* 77−17981
low temperature measurement in high mag. fields, instrumentation and methods, review 78−37003
metals, strain induced thermal signals, detection 79−1141
microbe thermistor for metabolite anal. 77−78063
microbead, as atm. temp. sensor, response between 0-80 km altitude 77−53234
microwave compatible MIC temperature electrode for use in biological dielectrics 79−88216
molecular weight measurement using recording thermistor cryoscope based on standard components 77−50572
multiple thermistor unit for use with data loggers 78−41303
in multivibrator, temp. to freq. convertor and bridge for temp. meas. 77−26289
NTC sensors, cct. designs and design calculation tables 80−68201
ocean near-surface temp. meas., distributed instrum. profiling sensors 77−82071
ocean temperature microstructure low noise meas. with thermistors 79−58104
optical fibre absolute power meas. thermistor sensor 78−65971
Pirani gauge, constant resistance thermistor 78−45642
point matching of exchanged hot conductors *(German)* 78−77905
probe, for biomaterial thermal conductivity and thermal diffusivity simultaneous meas. technique 78−57098
probe, implantable, for continuous core temp. in rats 78−3686
probes for groundwater filtration rate meas. *(Polish)* 77−70872
PTC, operating modes for temp. meas. and control 79−71448
PTC thermistor P310-C11, level sensor for liq. N_2 80−52247
rapid temperature change measurement, computerised thermistor cct. 78−49829
recording temp. monitor using thermistor sensor 78−209
respiratory phase detector system, battery operated cct., air temp. change meas. 79−100770

thermistors continued
RF voltage standard, precision, using thermistor bridge, HF-UHF range 78−89504
RF voltage standard, precision, using thermistor bridge, HF-UHF range 79−21772
semiconductor thermometry at low and very low temperatures 80−4713
sensors properties and uses *(German)* 78−36991
sensors thermal sensitivity, physical mechanism and appl. *(Italian)* 79−80617
solar power measurement, microcomputer-controlled photodiode light meter and thermistors 80−50946
spectral response and sensitivity, comparison with other detectors 79−35832
spectral response characteristics, ocean temp. meas. 78−20533
stability, ageing in constant temp. baths 79−21745
static voltage/current characteristic calc. 77−26286
submillimetric-wave negative-feedback-loop thermistor bolometer 79−44931
surface temp. meas., temp. contact methods using thermistor and thermoindicators *(Russian)* 80−27295
surface temperature meas., poor thermal conductors *(German)* 77−5832
telemetry system, implantable, multichannel, IC, for animal physiological data recording 77−86661
temp. meas. of rotating object, non-contact method with thermistor and pyrometric voltmeter 79−35742
temp. measurement, review, techniques and instruments *(German)* 80−22358
temperature control system for biological preparations 79−57830
temperature detectors, fundamental aspects and appls. *(German)* 79−21747
temperature difference meas. by automatic thermistor bridges 77−22547
temperature indicating linearizing circuits 79−49230
temperature meas., clinical appl. 78−7473
temperature meas. appl., selection guide 77−41607
temperature measurement, pulsed thermistor operation method 77−82510
temperature measurement of coolants appl. 79−85137
temperature measuring bridge, using constant-current FET circuits 77−129
temperature measuring potentiometer appl. 78−207
temperature monitoring, deep body, cardiac surgery appl. 77−29223
temperature-time period transducer appl. *(German)* 79−40561
temperature/frequency wide range convertor, expt. and cct. 77−17978
ternary semiconductors, pot. practical appl., review 79−10344
thermal relaxation oscillator using thermistor, temp. meas. appls. 78−73992
thermochemical analyser, continuous flow, high sensitivity 79−92022
thermometer bridge network charact. linearisation *(German)* 78−86271
thermostat for aqueous solution, linear thyristor control and thermistor sensing *(Japanese)* 77−90264
thermostat for low-power semiconductor devices 79−71450
tissue stess state intensity measures, hospital patient pressure sore prevention appl. 77−48923
two-point, temperature sensing ccts., thermometer, thermostat appl. 77−41610
underwater temperature meas. thermistor chain 77−5379
Wheatstone bridge for temp. meas. in calorimeter, optimisation *(German)* 78−86275
AlB_{12}, α- and β-forms, elec. props. at high temps. and in strong elec. fields, thermistor appls. 80−92903
B, β-rhombohedral, elec. props. at high temps. and in strong elec. fields, thermistor appls. 80−92903
B, pyrolitic, preparation and properties 77−12536
$BaTiO_3$ based positive temp. coeff. of resist. thermistors, estimation of Al solubility by cond. meas. 79−69250
$Co_{3-x}Mn_xO_4$, solid soln., synthesis, effect of Bi_2O_3 admixture upon props., thermistor appl. 78−15325
CuB_{24}, elec. props. at high temps. and in strong elec. fields, thermistor appls. 80−92903
$MnCo_2O_4$ spinel, synthesis, effect of Bi_2O_3 admixture upon props., thermistor appl. 78−15325
Se photocells, temp. coeff. of sensitivity 78−82033
Si linear thermometer, superconducting transition temp. meas. 77−57330
Si whisker indirectly-heated thermoresistor 78−86255
SiC thin film, RF-sputtered, highly reliable temp. sensor 80−224
SiC thin-film thermistors with high thermal response *(Japanese)* 80−105629

thermo-optical effects
see also thermoreflectance
acoustic field excitation in liquid by periodic train of laser pulses 80−103945
acoustic pulses, short thermooptically excited, exptl. study of propagation 80−102891
alkali and alkali earth metal metaphosphate glasses exam. of temp. dependence of thermooptical const. 78−88286
alkali and alkaline earth metal metaphosphate glasses exam. of thermooptical and photoelastic props. 78−88287
alkali halides, thermo-optical props., 120-580K *(Russian)* 79−91414
alloy, electronic characts. from thermomodulation spectra 79−87421
anils, cryst., high-press. optical effects 78−31170
anils, polystyrene soln., high-press. optical effects 78−31171
anthracene, birefr. changes due to thermal expansion 78−52468
apochromat optical glass development status and prospects 79−27348
aqueous soln. reaction kinetics meas. microwave apparatus 80−3470
p-benzoquinone, mixed crysts., PMDR and thermal modulation spectroscopy, electron-phonon interaction 77−32297
cabled fibre, temp. effect on transmission loss and pulse delay distortion 78−1407
CBOOA, acoustic emission at liq. cryst. transitions prod. by thermooptically excited defects 79−95137
chalcopyrite crystals, refractive index, temp. depend., appl. to nonlinear devices 80−60555
N-5-chlorosalicylideneaniline, H^+-^{14}N double reson. NQR spectra temp. depend. thermochromism and tautomeric mech. 78−70849
N-5′-chlorosalicylideneaniline, photochromism and thermochromism, NQR spectra, temp. and UV irrad. depend. 80−54968
cholesteric liquid crystal, pseudoencapsulated film, selective light scatt. 77−16289
cholesteric liquid crystal thermo-optical monitor, for nonionising radiation 78−11742

thermo-optical effects continued
colour-centre lasers, thermal strains in active elements 80−91804
COOB, acoustic emission at liq. cryst. transitions prod. by thermo-optically excited defects 79−95137
crystal vibrational spectrum, inhomogeneous thermal broadening effect 80−55100
cylindrical waveguide optical modulator efficiency in thermal mode *(Russian)* 79−94345
diamond, refr. index, temp. and press. var. 78−27174
dye laser active medium, hydroacoustical perturbations *(Russian)* 78−82966
elastooptical constants and refractive index, thermo-optical method for meas. 80−7327
electrolyte, hydrothermal stability, thermochromism 79−39187
fluid, relaxing, thermally induced light scatt. 77−32388
glass:Nd, laser material, linear expansion coeff. and r.i., temp. depend. 77−733
glass, photochromatic, induced colour by optical/thermal treatment 80−34954
glass, photochromic, thermo-optic transitions 80−50307
glass, Schott BG20 and FG18, forced Rayleigh scatt. anomalies 79−82988
glass, small thermo-optical charact., stress coeffs. 77−31123
glass, TI-20, laser window material, IR thermooptic coeff. meas. 77−36208
glass active elements of pulse-periodic lasers, thermal lenses 79−89914
glass and single crystal production, special thermo-optic props. 79−94308
glass discs, thermal-optical distortions, rel. to solar obs. using 50 cm lens 79−72640
glass laser rods, silicate and phosphate, pumped in pseudoelliptic cavities, thermal effects 79−76692
glasses, activated, athermality criteria for laser appls. *(Russian)* 77−66485
image convertor, thermo-optical, with liq. modulating medium 80−91927
IR absorption measurement, interference calorimetric method, effect of crystal thermo-optic props. 80−47096
IR laser window material refractive props., temp. depend. 79−14052
laser glasses, figures of merit and physical/optical property correlations 79−13970
lasers for industrial chemistry, thermal lensing effect 80−87427
layered compounds, book contrib. 77−40267
Lexan, optical and phys. parameters 79−32004
liquid, thermal lens effect meas. by photomixing method, laser system 77−42577
liquid crystal electrothermo-optic effects, display appls. 77−11469
liquid crystal improved technique for thermal field measurements 80−216
liquid crystal thermometry, optically active binary mixture 79−42952
liquid crystals, thermooptical effects used to visualise EM fields 80−62723
long focal length aerial reconnaissance system response to thermal shock 80−78939
MBBA-PCB (41 wt.%)+pleochroic dye, electrothermo-optic effect, optical storage device appl. 78−87611
measurements at six European laboratories compared *(French)* 78−29107
metal, electronic charact. from thermomodulation spectra 79−87421
methanol, free O-H overtone absorpt. in vis. region, thermal lensing spectra 77−34644
military optical system temperature effects and counter-measures 80−78938
mirage effect spectroscopy 80−47116
molecular crystals, thermal modulation spectroscopy, electron-phonon interaction 77−32392
molecular vibrational states, visible region thermo-optical spectroscopy 79−50036
nonequilibrium harmonic chain, light scatt., temp. depend. 77−69827
nonlinear optical crystals, SHG, absorpt. coeffs. and temp. variation of refr. index difference 80−14390
optical glass, TI-20, IR transmitting semicond., dn/dT, wavelength depend. 77−77163
optical resonator, thermoelastically disturbed, mode calcs. 79−13992
optically thick sample, thermal lensing effect, revised model 80−34900
parametric effects anal., in optics 80−102619
phenanthrene birefr. changes due to thermal expansion 78−52468
phosphate glasses, depend. on chem. comp. 79−99861
phosphate glasses, laser props. under pulse-periodic pumping conditions 79−64236
phosphate glasses, non-alkaline, transition states, phys. effects of fluors, phase diagrams and optical effects *(German)* 80−88045
phosphate glasses, opt. and thermo-opt. props., calc. from chem. comp. 79−65826
phosphate laser glasses, review 80−9888
photothermal spectroscopy 78−32808
Plexiglas 55, optical and phys. parameters 79−32004
poly-1,2-bis 4-isopropylcarbamoyloxy-n-butyl-1-buten-3-ynylene, cryst., UV refl. spectra, 25-160°C 79−82991
polyethylene, mixing of high and low density, mixing ratio determ. by thermo-optical anal. *(German)* 78−53070
polyvinyl alcohol films activated, thermochromism *(Russian)* 79−91415
quartz, cryst., birefringence, temp. depend., intracavity method meas. 80−78931
repetitively pulsed dual beam thermo-optical absorption spectrometer 78−77999
rhodamine 6G laser with lamp excitation, cavity thermooptical distortions effect 79−55135
salicylidene-2-chloroaniline, photochromism and thermochromism, NQR spectra, temp. and UV irrad. depend. 80−54968
N-salicylideneanilines, thermochromic and photochromic, ^{14}N quadrupole coupling, NQR meas. 77−28480
semiconductor, appl. of two-ray methods of modulation spectroscopy *(Russian)* 78−54469
silicate glass, Li_2O and Na_2O effect on thermo-optic props. 78−18029
silicate glasses, depend. on chem. comp. 79−99861
single-mode fibre lightguide, phase of coherent signal, temp. and stress effects 80−33208
smectic A liquid crystals, thermooptical recording, echo images 80−91928
smectic liquid crystals, thermo-optic and elec. field effects *(French)* 78−91223
thermo-optical effects continued
solid laser thermo-optic lens temp. distrib. and focal length calc. 79−72575
sound generation, nonsteady acoustic fields 80−15193
sound generation problems, method of transfer functions 79−64478
thermal nonlinearity effects of thermooptical sound generation 80−38146
thermo-gasdynamic control in laser beam guidance, review of developments 78−74942
thermochromic materials, IR hologram recording 79−86135
thermosensitive film coating, dispersed liq. cryst. microdroplets in gelatin matrix, exam. of preps. 80−42220
TTF-chloranil visual pressure or temperature indicator 80−87443
uniaxial and biaxial optical crysts., thermal strain 78−46733
US generation due to moving laser thermoopt. source in liquid 80−102903
UV high-power laser material, refractive props. and optical constants 80−106555
Ag-containing glasses, colour adaptation, photoinduced optical anisotropy 79−61331
Al film, thermomodulation of Al $L_{2,3}$ absorption edge 79−91533
As-S chalcogenide glass holographic recording efficiency, photocond. and annealing effects *(Russian)* 80−15556
As_3Se_2 chalcogenide semicond. film, thermoptical transitions with photostructural transformations *(Russian)* 80−16016
Au film, self-supporting, thermotransmission meas. 1.8 to 3.5 eV 78−27343
BaF_2 crystal, refr. index temp. increments meas. 80−33098
BaF_2, polycryst., laser window material, IR thermooptic coeff. meas. 77−36208
$Ba_2Na(NbO_3)_5$, intracavity cryst., thermo-optical distortion, effect on freq. doubled Nd:YAG laser 77−71998
$Bi_{12}GeO_{20}$, piezo- and thermo-optical props., dispersion theories and models 79−56764
CO_2-N_2, kinetic cooling effect by CO_2 laser radiation, temp. dependence 80−10347
CaF_2, polycryst., laser window material, IR thermooptic coeff. meas. 77−36208
CaF_2, thermo-optic coeff., 95-175K 77−63403
$CaF_2:Ce^{3+}$, thermally modulated UV absorpt. spectra, 90K 77−28602
$CdGeP_2$ thermo-optic coefficient, dispersion 80−71396
CdS thermo-optic coefficient, dispersion 80−71396
CdSe thermo-optic coefficient, dispersion 80−71396
CdTe, IR transmitting semicond., dn/dT, wavelength depend. 77−77163
CdTe, polycryst., laser window material, IR thermooptic coeff. meas. 77−36208
Co enamel, vitreous, objective colour evaluation, rel. to firing parameters *(Czech)* 80−42252
$CoCl_2$-LiCl-glycerin-water system, Co^{2+} ion coordination transition, spectral investig. 79−42953
$Cs_3Cr_3Cl_9$, thermo-optical spectroscopy, detection by mirage effect 80−47116
CsH_2AsO_4, CsD_2AsO_4, SHG, laser heating effect 77−79891
$CuCl_2$, aqueous soln., nonlinear conversion of acoustic pulses with thermooptic excitation 80−14510
$CuGaS_2$ thermo-optic coefficient, dispersion 80−71396
Cu_2HgI_4, thermochromic material, IR hologram recording 79−86135
$CuSO_4$ solution, thermooptical excitation of sound by ns. laser pulses 80−79884
GaAs-on-sapphire spatially distributed thermal light modulator 79−59839
GaSe, refr. index meas., temp. variation 300 to 75K 80−25328
Hg vapour DRT-220 lamp temp. and Hg 253.7 line intensity relationship 79−2836
KBr:Tl^+, thermally induced absorpt. transfer between impurity bands, electron-lattice interactions 77−77257
KCl, single cryst., laser window material, IR thermooptic coeff. meas. 77−36208
KI, V-centres, optical and thermal bleaching of V_2 and V_3 bands 77−85751
K_2O-BaO-SiO_2-Ti(Ce)O_2 laser glasses, TiO_2 and CeO_2 antisolarisation additive effects 79−94309
LiF:Mg cryst., Mg electron colour centers 80−100229
$LiNbO_3$ crystal in laser resonator, thermo-optical effect *(Chinese)* 80−106546
$LiNbO_3$:Fe, optical damage depend. on temp., press., and applied elec. field *(Japanese)* 79−81498
MnF_2, magnetic, thermal, elastic refraction of light, mag. order influence on refractive index *(Russian)* 80−34880
NaCl:NaOH, $NaNO_3$, oxygen-colour centres, thermo-optical transform. 77−69862
Nd:glass, thermal distortion induced by optical pumping *(Chinese)* 78−50779
Nd^{3+}:YAG laser active element, linearly polarised light depolarisation due to thermally induced birefr. 80−106528
$Nd_2(MoO_4)_3$, thermo-optical spectroscopy, detection by mirage effect 80−47116
$POCl_3$,$SnCl_4$:Nd^{3+}, phosphor, laser parameters and physiochem. props. 77−14709
phosphate glass, Li_2O and Na_2O effect on thermo-optic props. 78−18029
SF_6, gas, heating effect on optical props., transmittance meas. 79−27737
Si amorphous films, laser beam annealing, optical information storage possibilities 79−87515
TiO_2-SiO_2, semicond. glass, optical props. 78−60412
TlBr-TlI, TlCl-TlBr, KRS-5 and KRS-6 crystals, refr. index temp. increments meas. 80−33098
VO_2, film, visualisation of microwave and IR radiation 80−5839
VO_2, thermochromic film, visualisation of microwave radiation using metal-semiconductor phase transition 79−65845
V_2O_5 amorphous film, photochromism and thermochromism 80−93254
V_xO_y, FTIROS thermochromic materials, colour and visual contrast 80−33100
WO_3-B_2O_3-ZnO semiconducting glasses, DC cond. and optical absorpt. 80−107783
YAG rods, thermally induced birefringence in (001) direction, transmission loss *(Chinese)* 77−77166
YAG:Nd, laser material, linear expansion coeff. and r.i., temp. depend. 77−733
YAG:Nd crystal, orientation influence on thermally induced birefringence *(Chinese)* 80−88958

thermo-optical effects continued
$Y_2O_2S:Tb^{3+}(Eu^{3+})$ temp. and viscosity depend. of colour coords. 80−40149
$ZnGeP_2$ thermo-optic coefficient, dispersion 80−71396
ZnS, CVD sample, refractive index var. with temp., 22° and 34°C 79−14053
ZnS(Se), IR transmitting semicond., dn/dT, wavelength depend. 77−77163
ZnS(Se), polycryst. laser window material, IR thermooptic coeff. meas. 77−36208
ZnSe crystal, refr. index temp. increments meas. 80−33098
ZnSe, refr. index meas. at 3.8 μm, 10.6 μm, 80 to 300K 79−82938

thermochemistry
see also chemical reactions
activation energy, bond energy-bond order method 78−60981
activation energy for diffusion in thermochemical treatment process *(Russian)* 79−77800
aliphatic perfluorocarbons, electron attachment, fragmentation 0-12 eV 80−5618
azide salts, univalent, lattice energy and enthalpy of form. of radical, direct minimisation eqns. 77−62501
cNRS solar program and thermochemistry *(French)* 79−100485
computer coupling of phase diagrams and thermochemistry, conf., Gaithersberg, USA (Aug. 1975) 77−77458
computer coupling of phase diagrams and thermochemistry 77−77460
condensed matter, orbital model, quantum mech. theory 78−31675
conference, 6th CALPHAD meeting, Harwell, England (18-21 Apr., 1977) 78−35350
data and calc. of phase diagrams, systems for storage and retrieval 78−31682
differential scanning calorimeter, thermochem. appls. 79−40578
gaseous ion thermochemistry, metastable ion kinetic energy spectrometry, review 77−44537
heat of adsorption determ., expt. methods 79−42370
heat pump/refrigerator thermodynamic analysis 80−35716
heteroazeotropic system, thermodynamics in Gibbs pot. metrics *(Russian)* 79−96355
heterogeneous reactions, modified entrainment method appls. 79−23551
hexahalometallate (IV) complexes, A_2MX_6, A=alkali metal or ammonium, M=lanthanide or actinide, X=F or Cl, lattice energies and thermochem. 79−60307
high temperature species, JANAF thermochemical tables, thermodynamic properties evaluation and compilation 80−41959
high temperature system characterisation, models, phys. and chem. reference data sources 80−41958
ion+molecule, entropy change, enthalpy of form., equilib. consts., thermochemistry 80−30233
ion-molecule, flames and diagnostic techniques 80−55664
metal oxide cycles for H_2 prod. using fusion energy 80−76658
metal sulphates, thermochem. approach to gas-phase reduction by H_2 79−5147
metals, FCC, under H_2 press., crit. phenomena and isomorphic transitions 80−49367
micellar systems, aqueous, thermochemistry 80−61133
multiphase solids under stress, equilibrium 79−1964
oxide systems, quasibinary and quasiternary, data base development for phase diagram calc. 79−96006
PMMA, thermochem. instability at Pt sphere inclusions caused by CW laser beam 80−29689
polyatomic molecule dissociation, thermochemical study of thermal negative ion production *(Japanese)* 80−50495
production by Westinghouse electrochem./thermochem. S-cycle process 80−45808
propane, radiative thermal cracking on porous glass *(Russian)* 79−39205
quasibinary and quasiternary ceramic oxide systems, calculation of phase diagrams 78−60660
reaction kinetics, temp. integral approximating eqns. accuracy 78−92445
refractory compounds heat of formation determ. using self-propagating high-temp. synthesis 80−3392
solar energy storage as hydrogen from bromine from hydrogen bromide 79−57470
solar energy storage by H_2 prod. using Mg(Al)(Fe)(Co)(Ni)(Cu)(Zn) sulphates *(French)* 80−55935
solar energy transfer, reversible reactions screening 79−87999
solar thermochemical cavity absorber based on NH_3 dissociation, design and cost anal. 80−81489
solar thermochemical electric power generation, reversible chemical reactions 80−61394
steel, plasma thermochemical treatment 79−94823
steel, surface hardened, luminescent-discharge optical emission spectrometry appl. to surface anal. *(French)* 79−79164
surface treatment of metals by ionic bombardment new technique *(French)* 77−77643
thermal stability and thermochem. props. 79−86904
thermochemical gas analyzer, porous flame barrier, reagents, reaction products, conc. diffusion *(Russian)* 79−29359
thermochemical properties of atoms and molecules in specific quantum states 78−68911
thermostimulated effects, correlations and invariants 78−31619
transition metal binary systems, couple phase diagrams and thermochemical data 79−66037
transition metal binary systems, coupled phase diagram and thermochemical data 79−95997
transition metal binary systems, coupled phase diagrams and thermochem. data 78−60647
transition metal binary systems, coupled phase diagrams and thermochem. data 78−60648
transition metal binary-systems, coupled phase diagrams and thermochemical data 79−66036
transition metal carbides, thermochemistry 79−43617
transition metal sulphides, liq. and solid thermochemistry 78−23962
transition metals, binary systems, coupled phase diagrams and thermochem. data 78−80511
turbulent diffusion, flames, high Reynolds number, rocket exhaust appl., chem. processes theory 80−45504
AlH_3, photographic processes, thermo- and electrochemical transformations 78−89576
Al_2O_2, thermochem. evidence rel. to mol. structure 77−38738
B_2O_2, thermochem. evidence rel. to mol. structure 77−38738

thermochemistry continued
$Bi_2(SO_4)_3$ thermochem. cycle, process engng. design for H prod. 80−30599
CO_2, thermochem. reduction using solar energy to provide C-based fuels 80−76610
CO_2-methane reforming-methanation cycle for Solchem thermochemical solar energy transport 80−94096
$CaCO_3$ decarbonation for solar energy thermochemical conversion 80−94097
$CaCl_2$-methanol thermochem. cycle for solar thermal energy storage 80−30587
CaO-$Ca(OH)_2$ reversible hydration-dehydration for solar energy storage 80−97810
Ca_3SiO_5, thermochem. effects on formation 80−16666
$ClCO_3NO_2$, synthesis by UV irrad. of Cl_2, NO_2, CO in air, decomp. kinetics 78−76880
$EuPO_2$, $EuPO_3$, gases, thermochem. props. 79−66334
$EuPO_4$ in Mo crucible, $EuMoO_4$ and $EuMoO_3$ atomisation energy 78−40073
Fe based ternary solutions, liquid, exam. of thermochemistry 78−80782
Fe, sintered, austenitic nitriding and bainitic hardening 80−85084
Fe-Mo system, thermomech. props. 80−89208
H, electro-/thermochemical prod. from H_2O by Westinghouse sulphur cycle 80−55940
H electrochemical/thermochem. prod. using S cycle, laboratory prod. model and electrolyser development 80−30602
H production, thermochemical or hybrid cycles of hydrogen production techno-economical comparison with water electrolysis 80−45796
H production using Ce-Cl cycle 80−35783
H production using hybrid electrochem./thermochem. cycles, search for electrochem. reactions 80−45807
H, thermochem. prod. by H_2O decomposition using Mg-I cycle 80−35786
H, thermochem. prod. using the Mark-13 process, status report 80−30606
H thermochemical prod., engineering impact on the validity of the Mark-16 thermochem. cycle 80−45806
H, thermochemical prod. by H_2O decomposition, impact of thermal burdens and kinetics 80−35787
H, thermochemical prod. from H_2O, noncorrosive two-reaction low temp. cycles based on mordenite-hosted redox reactions 80−55939
H thermochemical prod. using $Bi_2(SO_4)_3$ cycle, process engng. design 80−30599
H, thermochemical prod. using SO_2-I_2 water splitting cycle 80−30600
H, thermochemical prod. using Br-Ca-Fe H_2O-decomposition cycles 80−35784
H, thermochemical production using Hg-I ANL-4 cycle 80−35785
H, thermochemical production by coal gasification using steam 80−35789
H thermochemical production using air blown coal gasification, economics 80−35790
H, thermoelectrochemical prod. using NaCl 80−55946
H_2 and power production using thermoelectrochem. cycles 80−16820
H_2 production, engineering impact on the validity of the mark-16 thermochemical cycle 80−55931
H_2 production, process assessment and economics *(French, English)* 77−86309
H_2 production by polynaphthoquinone-SO_2-I_2 system for H_2O decomposition 80−16825
H_2 thermochemical compression for hydride thermosorption, theory *(Ukrainian)* 80−76657
H_2, thermochemical prep. by H_2O dissoc. using S-I cycle 80−16823
H_2 thermochemical prod. by H_2O dissoc. using Sb-I-Ca process 80−16824
H_2, thermochemical production, based on reactions of $CeTiO_2$ for water-splitting 80−55929
H_2 thermochemical production using open-loop cycles 80−55930
H_2 thermochemical production, plasmochemical H_2O decomposition using nuclear energy source 80−61436
H_2 thermochemical production by Mark-13 cycle, development of laboratory-scale plant 80−76659
H_2O, decomp., H prod. by thermochemical and thermoelectrochemical cycles 80−26029
H_2O thermochemical decomposition utilising solar heat for H_2 prod. 80−61451
Li_2O_2, gas, thermochem. props., mass spectra study 79−47957
Li_3O, gas, thermochem. props., mass spectra study 79−47957
$MgSO_4.7H_2O$, thermo-electrochemical H_2 prod. using solar energy *(French)* 79−24918
NH_4ClO_4, photothermochemical process 79−24769
NH_4ClO_4, photothermochemical process, influence of phase transition 79−24770
Np, ionisation potentials, 2nd-6th, thermochemical calcs. 79−98248
O_3^- +molecule reactions, thermochemistry, electron affinity and rate consts. 78−40040
OH, UV light absorpt. at 3080 Å, for Gibbs free energy of mol. 79−100425
PbO-Re_2O_7 system, gas phase components obs. using mass spectrometry *(Russian)* 79−96354
PbO_2, thermal decomposition, heating rate effect, kinetics, mechanism, struct. 78−92473
Pu, ionisation potentials, 2nd-6th, thermochemical calcs. 79−98248
S chemistry and thermodynamics on Venus .79−44391
$SO_3.H_2O$ and H_2SO_4, CNDO/2 calc. of thermal stability 78−76840
ScI_3, mass spectra and vapour press., and thermochemistry for dimerisation 78−27809
Te-$TeBr_4$ system, Gibbs free energy of reaction, electrochem. e.m.f. expts. 79−91991
Te-$TeCl_4$ system, Gibbs free energy of reaction, electrochem. e.m.f. expts. 79−91991
Te-TeI_4 system, Gibbs free energy of reaction, electrochem. e.m.f. expts. 79−91991
Th-U-C-O system, HTGR fuel system, thermodynamic assessment 78−70598
TiO_2:$TeCl_4$ system, chem. vapour transport, matrix isolation IR studies 80−93755
$TlNO_3$, boiling and melting pts., heats of transformation, solid-solid transformation 78−91441
U, ionisation potentials, 2nd-6th, thermochemical calcs. 79−98248
W-Br regenerative cycle of linear quartz lamps, metallic impurity effects, thermochemical interpretation 80−3312

thermochemistry continued
ZnO, thin Zn or O rich layers, thermolysis, photolysis, SEM, XPS 77−11821
ZnSe thermochem. cycle for H prod., chemical and process design studies 80−35782
Zr gels, thermal and related studies 80−71937

thermoclines *see temperature distribution*

thermocouples
see also thermopiles
anemometer, hot-wire, for boundary layer meas. with free convection in liquids *(German)* 80−10329
anemometer, mass flow meas. in shock tube 79−77300
arrays, for ocean vertical temp. gradients horizontal var. meas. 78−61571
automatic temperature measurement with thermojunctions, temperature sensitive ICs and resistance thermometers *(German)* 80−77778
base metals, automatic testing temperature range 600 to 1300K 77−53908
boiling heat transfer crisis detect., sensitivity of bridge and thermocouple methods 77−61064
calibrating apparatus, automatic, 4.2-300K range 78−45624
calibration and standards 79−85141
calibration on-site 80−90840
calibrations, comparison, fixed point and melting wire methods 80−86252
cancerous mouse hyperthermia meas., microwave, IR and thermocouple methods *(French)* 80−3768
cavity, minimisation of temp. distortion 77−82506
cavity enclosing thermocouple, transient temp. distortion 77−10016
ceramic, isolated, fault detection using computer-controlled capacitor discharging method *(German)* 80−13079
chromel and alumel, decalibration, quantitative SIMS anal. 80−4705
chromel-alumel, error statistical investigation 78−24794
Chromel-Alumel, in-reactor temp. meas. accuracy, thermometer construction effects 79−17969
chromel-alumel thermocouple readings, stability prediction 77−87760
Chromel-Copel, in-reactor temp. meas. accuracy, thermometer construction effects 79−17969
coaxial, high integrity thermocouple for LMFBR coolant temp. meas. 80−32410
coaxial thermoelectric discs, radial current flow, heat transport 79−2767
cold junction compensation circuits using IC temperature sensors 80−77777
cold junction compensation method for portable instruments 79−2768
comparator for testing gemstones 80−13070
conductor heating, similarity theory and dimensional anal. computional methods *(Rumanian)* 80−47053
construction method for miniature thermocouples with variable electrodes 78−24788
contactless temperature meas. methods *(Dutch)* 77−67433
convective heat transfer coeff. from gas to thermocouple meas. 78−18149
cooling, thermoelastic stress and Peltier coeff. calc. 77−71326
cooling device, rectangular monolithic infinite cascade thermojunctions 78−57944
crystal-melt interface temperature monitoring, thermoelec. method, appl. to Czochralski growth of InSb 78−31331
cylindrical, with plane frontal area, recovery factor in turbulent subsonic flow *(German)* 80−74882
DC thermocouple, with variable cross-section, thermoelec. cooling 78−24787
differential, effect of electrodes thermoelectric nonuniformity limitation 77−74398
differential, temp. drop meas. error determ. 79−21742
differential thermocouple transducer for electrically insulating liquid level 77−17969
digital, cold junction compensation methods *(Italian)* 78−37002
digital, noise study 77−22544
digital thermometer, type 2572, with temp. range 4K to 1760°C with 0.1°C resolution 78−65929
distributed thermocouple theory, electric pot. field, Green's function soln. 79−93138
dynamic error correction cct. 78−77909
dynamic errors, 3-channel corrector 80−17939
education, Joule heating, Peltier and Seebeck effects, Cu-Constantan thermocouple expt. 79−9056
electrical shunting and leakage errors in sheathed thermocouples, model 78−4618
electronic thermometer, microprocessor based linearisation of thermocouple temp. charact. 80−221
electronic thermometry, accuracy improvements 77−41608
EMF, macroscopic thermodynamic theory 78−91678
errors due to Nernst effect 77−67434
extension conductor connection provision 77−87762
ferromagnetic thermoelements, meas. error due to time varying mag. fields effects 78−4617
fission reactor core temp. monitoring, can thermocouple distribution procedure 78−54856
fission reactor fuel test rods, directly heated, influence of thermocouples in wall 79−93706
fission reactor loss of fluid test program, 2200°C fuel centerline thermocouples 80−57877
four-wire case thermocouple elements for gas and fluid flow meas. *(German)* 78−14111
furnace temperature meas., accuracy 77−5845
gas temp. meas. by multiple-thermocouple method 77−49728
gas temp. meas. in glow discharge in capillary using thermocouples *(Russian)* 78−59694
gas temperature meas., high, stationary, thermal probe 80−95101
glass container forming, mould surface temp. meas. 80−82767
heat pulse technique for bonding thermoelectric modules contacts 80−107904
heated probe, tissue perfusion meas., two-regime model 77−5110
high temperature in-fuel thermocouples for FBR fuel pin safety expts. 80−102283
high-pressure chamber thermocouple lead-ins for highly compressible media 78−86285
high-pressure temperature meas. in liquid He region 80−31748
hot gases, convective heat transfer coeffs. to solid surface, moving thermocouple meas. 80−42230

thermocouples continued
in-reactor fuel temperature, transient response of centreline thermocouples, appl. to fuel modelling 80−95372
in-reactor fuel-to-sheath heat transfer meas. 79−13408
in-reactor performance of surface-mounted and embedded thermocouples 79−93704
industrial appl., advantages 80−42221
injection moulding, melt temp. meas., appl. of thermocouples or pyrometers 79−58694
International Practical Temp. Scale, instrument interpolation, from 630.74 to 1064.43°C 79−40564
International Practical Temperature Scale 1968, fixed point determination 78−41270
IR windows, insertion of thermocouples for IR spectroscopy and reaction cells 80−57398
junction elec. field calc. 77−13751
laboratory and industrial meas. using thermocouples, techniques 77−71324
liquid metal alloys solidification temp. range meas. technique 79−12799
liquid Na, thermocouple transfer function and flow velocity meas. by temp. noise 79−13394
liquid-friction bearing temperature measurement, new bearing tester 80−64503
low temperature measurement in high mag. fields, instrumentation and methods, review 78−37003
meas. errors, due to windings heating *(German)* 80−95096
measurement error avoidance, temp. meas. 80−62664
measurement error due to cond. along sensor leads, correction 77−13752
measurement of temperature of oil in sliding friction bearing 80−31753
measurement uncertainty estimation *(German)* 77−53909
microcooler, threestage, with cascade thermocouples 79−2765
microprocessor-controlled, development trends 79−85135
mineral insulated NiCr/NiAl thermocouples, lead temp. effect on accuracy 78−54371
mounting method for thermocouple gauge tubes 80−77795
multichannel digital temp. recorder, TR-2711, measuring 100 channels in 10 s 78−65931
multichannel temperature measuring system, thermocouples multiplexing *(German)* 77−53902
multichannel temperature recorder, Thermodac II with 24 channels 78−65930
multiple thermoelectric junctions, thin conducting sheet, near heat fluxmeter *(French)* 80−86286
neutron irradiation effects *(Russian)* 77−82515
Nicrosil-Nisil, in production furnaces, 538°C to 1177°C 80−68198
Nicrosil-Nisil alloy usage, digital furnace control system appl. 78−49831
nonmetallic, differential-temp. probe for use in microwave fields 80−56320
photocompensation proportional temp. regulator with phase impulse control 77−82502
plated thermocouple in notched well, response time for LMFBR use 78−29546
platinorhodium-Pt type, 1000-1300°C range, cold junction electrode compensation 78−216
PR, simplified calibration *(Japanese)* 79−93139
psychrometer, bimetallic, bulb wetting by saturated $MgCl_2$ soln. *(Japanese)* 77−87772
psychrometers improvement for soil water potential meas. in temp. gradient 79−74974
pulsed, high temp. measurement of gases, numerical computation method *(German)* 79−21749
radiation temp. scales 630-1064°C relationship 78−37004
radiation thermocouple output signal calc. for cylindrical receiver *(German)* 78−41305
radioisotope thermoelectric generator, selenide, power degradation predictions, mathematical and computer models 79−48148
radiometry, far UV standards comparison 77−5912
readings stability in IVV-2 nuclear reactor 79−40568
reference junction box, used for vacuum chamber 80−90844
response time in melts 79−40570
RMS digital voltmeter, description and application *(German)* 77−18048
rotating bodies temperature measurement, thermocouple slip ring assembly 80−86294
Rysselberghe's contention in thermoelectricity 79−51555
Seebeck coefficient meas., 300 to 530K 78−91677
selecting semiconductor materials for thermocouples *(Russian)* 78−73990
semiconductor refrigerating thermojunctions with radial flow of current 79−2766
semiconductor resistance thermometers, for the interval 300K to 0.3K, thermoelectric charact. 80−73359
sensitive temperature measurement theory *(German)* 77−71323
spherical heated probe for perfusion meas. 79−92456
standard reference tables, polynomial representations, report 78−81973
standard reference tables, polynomial representations 77−74402
standards, GDR, testing *(German)* 80−90842
surface temp. meas. using automated zero-derivative method *(Japanese)* 78−210
surface temperature meas., poor thermal conductors *(German)* 77−5832
surface temperature measurement, of glass substrate heated through Ga 79−97390
surface temperature measurement using thin film thermocouple 80−62668
surface-mounted beaded thermocouple transient response models 78−8405
temp. measurement, review, techniques and instruments *(German)* 80−22358
temperature controller for field emitter 78−24898
temperature field distortion by thermocouple seal-in 78−81968
temperature meas. by compensated thermocouples *(German)* 78−41304
temperature meas. devices developments *(German)* 80−8986
temperature meas. in metal testing, error anal. 78−19975
temperature meas. principles, ccts., and instrum. *(Dutch)* 78−198
temperature measurement by means of thermocouple networks *(French)* 78−4613
temperature measurement in polymer melts, thermocouple heat loss correction 77−65034
temperature measurement of heavy particles in gas discharges 79−30476
temperature measurement of metallic substrates during evap. 77−69997
temperature programmer, thermocouple-controlled, for flash desorption spectroscopy 79−49224

thermocouples continued
temperature transfer functions, theoretical and expt. determ. *(German)* 78−49827
thermal inertia charact. determ. 78−73993
thermal inertia meas. *(Russian)* 80−62665
thermocouple probe, apparatus for testing under working conditions 80−22360
thermocouples and resistance thermometers properties 78−199
thermoelectric cooling devices, maximum refrigerating capacity determ. 80−86318
thermoelectric effects, reversibility, theory 77−59280
thermoelectric effects and contact pots., general theory for teachers 78−4440
thermoelectrode, synthetic diamond, dynamic calibration, grinding temp. measurement appl. 77−55985
thermoelectrode wire classification standard samples 77−5865
thermometer, constructed with a thermocouple, CMOS analogue and digital devices 77−33986
thermometers, voltage generation, calibration 80−57295
thermometry, accurate, review 80−52207
thermometry, drift evaluation problem 77−53905
thermostatic air chamber, influence of radiation *(Japanese)* 78−37007
thin film fission thermocouples for energy deposition meas. in FBR safety expts. 80−47658
thin-film fission thermocouple detectors for reactors safety expts. 80−22987
time constant measurement by cross power spectra 77−30145
tissue US absorption thermoelectric meas., beamwidth and thermocouple size effects 79−48306
transient EMF response under reactor conditions 77−71320
type T (Cu-constantan), simple conversion, formula for EMF to temp. 77−10022
types and selection guidelines 79−194
universal extension leads, geometry of connection 80−57294
unsteady gas stream temperature determ. using slow-response thermocouple 77−24046
vacuum gauge, gas analyser appl. 80−61183
vacuum gauge testing and calibration for low absolute pressure 77−57341
wideband current and voltage comparators 77−57356
Au/Fe vs. chromel, He cryostat temperature controller appl. *(Czech)* 78−29120
Bi_2Te_3 alloy thermocouples for solar thermoelectric conversion 80−94095
Bi_2Te_3-Bi_2Se_3 solid solns., single cryst. growth and thermocouple construct. 80−104056
Cr-Al thermocouple, temp. control system design *(Spanish)* 80−73362
Cu/Au+0.03 at.% Fe, thermocouple characteristics, in mag. field at low temps. *(Russian)* 78−54365
Cu/Cu+Fe low-temp. thermocouples thermo EMF, strong magnetic field effects 78−220
Cu-constantan cryogenic thermometer and temp. controller *(Czech)* 79−26056
Cu-constanton thermocouple rod for subsurface temp. meas. 79−88954
Fe-Ni film, fabrication and calibration 77−37885
Ge-Ag, DTA under hydrostatic behaviour, appl. to TMMC phase behaviour 79−65186
Ir/Ir-Rh alloy, appl. to temp. meas. in atm. press. flame 77−86314
Mo-Mb, thermoelectric alloy for in pile temp. meas. *(French)* 79−67894
Mo-Ni thin film junction, phys. vap. deposition parameters effect on thermoelec. power 77−39922
N, nonequilibrium plasma, thermocouple diagnostics 80−103188
Ni-Cr-Si thermocouple alloy, props. and thermoelec. reference data 79−26057
Ni-Fe thermocouple, appl. to surface temperature measurement 80−62668
Ni-Si-Mg thermocouple alloy, props. and thermoelec. reference data 79−26057
NiCr-Ni, statistical thermometer appl., with temperature regimes evaluation *(Czech)* 79−63208
Pd+Cr+Ru/Au+Fe thermocouple, for temp. meas. in 2-200K range 77−26293
Pt/30Rh vs Pt/6Rh (type B), HI BX extension wire, EMF characteristics 78−49832
Pt-alloy thermocouples, reference-standard testing apparatus 80−13077
Pt-Pt/13% Rh thermocouple testing in large creep lab. 77−37888
Pt-Rh thermocouple, Ta-sheathed, Al_2O_3-insulated, large decalibrations above 1330°C 78−24790
$Pt_{90}Rh_{10}$/Pt, Inconel sheathed, MgO-insulated, decalibrations during 1200°C use, ion microprobe obs. 78−57957
Sb_2Te_3-Bi_2Te_3 solid solns., single cryst. growth and thermocouple construct. 80−104056
Si ribbon-graphite in-situ thermocouple, calibration and meas. accuracies manufacture 79−97386
Si-Ge thermoelectric generators, approximation errors when using averaged properties solutions for required heat rates estimation 80−108808
W-graphite thin film thermocouple, temp. gradient meas. in LPE system 80−25584
W-Re, immersion, method to improve reliability/accuracy in ferrous metal temp. meas. 77−87767
W-Re alloy thermocouples, calibration, 77 to 290K 77−57324
W-Re thermocouple, thermal EMF var., stability 77−41604

thermodiffusion *see thermal diffusion*

thermodynamic changes of state *see phase transformations*

thermodynamic cooling *see cooling*

thermodynamic equations of state *see equations of state*

thermodynamic potential *see free energy*

thermodynamic properties
see also critical points; enthalpy; entropy; free energy; Gruneisen coefficient; latent heat; specific heat
^{3}He, solid, two parameter model of mag. and thermal props., spin exchange 80−49461
σ function, thermodynamics at nonequilib. steady states 79−6068
AB-type compounds, high-press. and high-temp. behaviour, review 78−22850
acetic, acid, ideal gas thermodynamic props. 78−51275
acetone-chloroform-methyl isobutyl ketone, ternary phase diagrams, interactive computer program 80−71629
acetone-methanol, acetone-CCl_4, methanol-CCl_4 and acetone-methanol-CCl_4 mixtures, acoustic and physicochem. obs. 79−96347

thermodynamic properties continued
acetone-toluene-tetrachloromethane, mol. interaction and thermodynamic props. 80−71935
acetonitrile binary liq. mixtures, excess thermodynamic functions, complex formation 79−52736
acetonitrile-toluene-benzene, mol. interaction and thermodynamic props. 80−71935
actinide aqueous ions, chemical thermodynamics, book 77−60108
actinide carbides, lattice defects and rel. to phys. props., review 77−27874
actinide elements, chemical thermodynamics, book 77−60107
actinide oxides, thermodynamic props. and high temp. chem. behaviour, comparison with lanthanide oxides 79−100127
actinide series, elements, ions in soln. 78−35716
actinides and alloys, metallurgical props. rel. to electronic struct., energies calc. method 77−20221
activity coefficient of nonmetallic solutes in liquid metals and binary alloys 78−52766
additives effect on deform. of solids, law of action 77−35628
adsorption isotherm and solute activities from spreading pressure-surface charge data 78−14576
air, electrostatic forces effect on thermodynamic props. and equilibrium composition 78−55710
alcohol-inert compounds mixtures, thermodynamic props. *(German)* 79−52748
alcohol-nonassociating active component mixtures, thermodynamic props. 78−64878
alcohol-unassociated active component liquid mixtures, associated soln. theory, thermodynamic parameters 80−7836
alcohols, vapour-liq. equilib. and heats of mixing, simplified group method anal. 80−96637
Alfven wave system, eqn. of state, thermodynamic props., Bose-Einstein statistics 78−87397
alkali halide crystals, heat of form. for high-conc. substitutional defects, model 78−10048
alkali halides, cryst., pot. parameters, Hellman function calcs. 80−2181
alkali halides, molten, crit. consts. calc., dense gas formulation 80−44100
alkali halides, V_k-centres, vibr. modes, calc. 80−84269
alkali halides aq. solns., interionic forces and thermodynamics *(German)* 79−52688
alkali metal, liquid, law of corresponding states, microscopic basis 77−47539
alkali metal actinide complex halides, thermochem. and struct. props. 80−7847
alkali metal hexachloroniobates and hexachlorotantalates, thermodynamic props. from VP meas. 79−34345
alkali metal liq. binary systems, thermodynamic props. at high temps. 80−15262
alkali metal salts, heat of melting and activities using cryoscopic data 77−40573
alkali metals and alloys, liq., internal energy, chem. pot., critical consts. 78−34422
alkaline earth halides, aq. solns., activity and osmotic coeffs. 78−53242
alkaline earth halides, thermodynamic and structural props., computer simulation 78−75849
alkaline earth molybdenates, electrophys. props., effects of thermophys. props. of medium in synthesis 77−48375
alkaline earth oxide based compounds, thermodynamic study using CaF_2 electrolyte 78−53241
n-alkane-cyclohexane, liq. mixture, excess vol. by density meas. *(German)* 79−73324
n-alkanes, liq. mixtures, thermodynamics 80−55700
alkanes, vapour-liq. equilib. and heats of mixing, simplified group method anal. 80−96637
alloy, activity coeffs. and short-range order, correl. *(Russian)* 78−56614
alloy, binary thermodynamic data 80−104121
alloy, dil., interstitial solute in multicomponent substitutional solvent, quasi-chemical approach to thermodynamics 77−28784
alloy, multicomponent, thermodynamic partial molar quantities, calc. from known quantity of one component 77−72703
alloy, super- and heat resisting, thermodynamic study of corrosion 79−57161
alloy melts, association, effect on thermodynamic behaviour *(German)* 78−20050
alloys, binary, thermal cond. conc. depend., irreversible processes, thermodynamic calcs. *(Russian)* 80−39550
alloys, DO_{22} and $L1_0$ superstructures, atomic ordering, multicluster approx., order-disorder transition 80−38990
alloys, gas solutions in alloys, due to impurity-deoxidising element interactions, thermodynamic analysis *(Russian)* 79−34347
alloys, structure at high temp., microscopic theory *(Japanese)* 80−29191
aluminates and aluminosilicates, thermodynamic props. determ. by Monte Carlo calc. 77−47597
amorphous magnetic metals and alloys, high temp. 77−16078
amorphous soft-core systems, low temp., mol. dynamic studies 80−6359
anharmonic crystals, unsymmetrised SCF approx. 78−63830
anisotropic multilayer solids, macroscopic fields anal. 77−89547
antiferromagnets, pseudo-one-dimens., thermodynamic variables 80−65935
apolar viscoelastic dielectrics, thermodynamic theory, linear effects 78−67059
aqueous non-electrolytes, solution structure, adiabatic compressibility studies 78−87605
aqueous nonelectrolyte solutions, thermodynamic excess functions at high press. 78−18793
aqueous solutions, naturally recurring, activity coeffs. rel. to ionic diffusion 78−57224
aqueous-organic mixed solvent structure, solvation, cation exchange *(Dutch)* 79−83500
arc plasma, stabilised by N_2 injection through porous wall, thermodynamic nonequilib., plasma parameters 79−86629
austenite, activity of C, computer simulation 79−37852
Becker-Doering high-temp. predictions of large polar mol. thermophysical props. 78−67820
bentonite, selective sorption props., thermodynamics of ion-exchange reactions 79−39203
benzaldehydes, para-halogenated, IR and Ramam spectra, vibr. assignments, thermodynamic functions 80−14139
benzene, benzene-d_6 soln. excess thermodynamic props. 78−53245

thermodynamic properties continued
benzene, in polar solvent, excess thermodynamic props., Rayleigh scatt. meas. 78−52523
benzene, mol. reorientationally disordered phases, thermodynamics 79−46782
benzene sulphonyl hydrazine, in nonpolar solvent, thermodynamics of dipolar relax. 79−91347
benzene-chlorobenzene, benzene-toluene, perfect binary liquid mixtures on silica gel, adsorption thermodynamics 80−44428
benzene-cyclohexane mixture, excess vol., indirect meas. 77−29032
benzene-tetrahydrofuran, soln., excess thermodynamic props. and interactions, US vel. and density meas. 80−39288
benzene-toluene, perfect binary liquid mixtures on silica gel, adsorption thermodynamics 80−44428
benzenes, trisubstituted, dil. solns., relax. mech., Debye relax. times 78−80744
benzenes chemisorpt. on α-Fe, π complex form., MO LCAO calcs., thermodynamics 77−52674
benzil-benzene, dil. soln., thermodynamic equilib., ebulliometric investig. 78−18752
binary aqueous electrolyte solutions, thermal props. 79−100429
binary dense gaseous mixtures, struct. and thermodynamic props., molecular dynamics study 80−64866
binary electrolyte solns. thermodynamics using US props. 78−73946
binary fluid, coexistence curve from refractive index obs. 77−32823
binary ionic highly dissymmetric mixtures, phase separation 79−46425
binary lattice gas, crit. phenomena, series anal. 80−4671
binary liquid mixture, glass transition temp., composition depend., theory 77−76531
binary liquid mixtures, cell mol. theory for calc. of thermodynamic props. *(Spanish)* 79−68991
binary liquid mixtures, nonassociated, thermodynamics 78−18797
binary liquid mixtures, viscosity rel. to thermodynamic excess functions *(German)* 77−35740
binary liquid solutions, struct. and thermodynamic props., molecular dynamics study 80−64866
binary oxide, cluster form., high temp. equilib. 79−60511
binary substitution solution, molten thermodynamics 79−11559
binary system, effect of mutual solubility of auxiliary solvent on liq.-liq. equilib. for activity coeff. 77−63945
binary systems, comparison Bale-Pelton and Redlich-Kister representations 77−47598
biopolymers, in helical and coiled state, 4 to 400K, calorimetry 78−20140
black hole, surface thermodynamics *(Russian)* 78−12270
boiling and cavitation, thermodynamic nondimensional parameters *(Italian)* 79−76959
boson magnetised ideal gas, effect of confinement, anal. 80−12987
boson system, phase transition in an exactly solvable nonpolynomial model 79−40455
branched polymer solutions, interaction function, thermodynamics, decomposition *(German)* 78−18531
brass, calorimetric investigation of thermodynamic props. 79−52172
brasses, thermodynamic anal. *(German)* 80−25663
brine, Dead Sea, KCl and H_2O activities 78−31673
t-butanol-CCl_4, excess thermodynamic functions, 15, 30 and 45°C, composition depend. *(Russian)* 78−31677
butanol-methylethyl ketone, soln., excess thermodynamic props. and interactions, US vel. and density meas. 80−39288
t-butyl alcohol, mixtures, assoc., thermodynamic study using 2-constant model 80−66789
caesium perfluorooctanate, thermodynamically independent nematic amphiphilic mesophase obs. 79−95126
caffeine in aq. electrolyte, adsorpt. isotherm and solute activities from spreading pressure-surface charge data 78−14576
carbon tetrachloride, liq. and plastic cryst. phases, thermodynamic props., light scatt., US propag. 78−2863
carbon tetrachloride-pyridine(anisole)(acrylontrile)(acetyl-acetone) mixtures, excess volume of mixing, mol. interactions 79−57281
cast iron-steel mixture, interaction of Zr, formation reaction thermodynamics *(Russian)* 80−55645
ceramic, calc. for solids and liqs. 77−43348
ceramic fission reactor fuels, high temperature chemistry, nonstoichiometry, review 77−14238
chain molecules in soln., thermodynamic props. related to chem. pot. 80−3394
chalcogenide glass, partial values and structure features 79−41969
chalcogenides of non-transition metals, at. vol. and semicond. props. 77−20089
characteristic vector analysis of solvent effects 77−21409
charged hard sphere fluids, meas. spherical model 78−18524
chemical durability, thermodyn. approach 78−7063
chemical potentials of structural elements of compounds and face or dislocation specificity, thermodynamic parameters 80−96514
chemical reactions, second-order, stochastic theory 78−73015
chemoepitaxial nucleation during reaction diffusion, thermodynamic anal. *(Russian)* 80−15394
chloroalkanes, vapour-liq. equilib. and heats of mixing, simplified group method anal. 80−96637
chlorobenzene-bromobenzene, perfect binary liquid mixtures on silica gel, adsorption thermodynamics 80−44428
chlorofluoromethanes, ideal gas thermodynamic props., mol. struct. 77−3912
o-chlorophenol-acetone (ethyl methyl ketone), thermodynamic and transport props. 80−92686
cis-1-cholobutadiene-1,3, microwave spectrum, struct., nuclear quadrupole coupling, distortion const., thermodynamic functions calc. 80−99500
classical and quantum spin models, functional integral method appl. 80−15676
Clausius eqn. of state, thermodynamic props. calc. 78−83909
clusters of atoms, phase transitions, thermodynamics calcs. 77−59096
collagen, helical and coiled, thermodynamic values, 4 to 300K 77−25379
colloid, excess press., calc. and expt. 77−86386
colloid stabilisation by polymers, excluded volume effects 77−60129
composite media, equivalence conditions from thermodynamical ratios *(Russian)* 79−9197
compressibility, isothermal, of hard-sphere liquids, equations of state 79−73285
compressibility factor calcs., extension of Pitzer correlation 79−86557
computation data bank, appl. to inorganic and metallurgical systems 77−59100

thermodynamic properties continued
condensed phase, lattice gas model 78−73931
conduction electrons, thermodynamic method for quantitative anal. 80−59946
coordination compounds, chemistry, electronic excitation, luminesc. methods 79−54880
copolyethylene terephthalate-p-oxybenzoate, nematic phase, thermodynamics 78−91427
corresponding states theory, thermodynamic props. 80−54338
Coulomb systems, thermodynamic functions, phase transitions 79−85108
creep and long-term strength 77−11139
critical behaviour, correction-to-scaling amplitudes, crit. exponents 80−57233
critical behaviour, correction-to-scaling amplitudes on coexistence curve 80−57234
critical maxima and minima of thermodynamic functions 77−27974
crystal growth spiral in chem. pot. varying in time and space 78−87631
crystal properties behaviour near structural transitions, thermodynamic theory *(German)* 78−38809
crystal-vapour interface, calc. using canonical and grand canonical ensembles 77−20180
crystalline solutions, binary, isostructural, mixing parameters computation, FORTRAN IV subroutines 77−86344
cyclopropane($-d_6$), centrifugal distortion const. and thermodynamic functions calc. 80−95582
cyclopropyl bromide, IR absorption, Raman scatt., assignments, thermodynamic functions 80−984
cylinder, perforated, radiated energy anal. 80−19228
Debye lattice, thermal props., WINIMAX approx. appl. 80−49333
n-decanol-CCl_4, excess thermodynamic functions, 15, 30 and 45°C, composition depend. *(Russian)* 78−31677
defect structure near phase transition pt., effect on solid props. *(Russian)* 79−37838
degree of dissociation of congruently melting compound, calc. from liquidus curve 77−84892
dense dipolar hard sphere fluid, integral eqn. theory 77−76278
dense electrolytes, thermodynamic props. as basis for pair correlation function 77−27800
dense fluids, equilib. props. semiclassical limit 77−49667
dense gases and liqs., three-body nonadditive interactions, thermodynamics props., mol. dynamics simulation 79−7435
dense liquid, integral eqn. with approximation of direct correl. function in pot. rigid core region 77−84611
dense plasma, atomic energy level deform. and eqn. of state 78−71435
dense simple fluid, equilib. props., 3-body forces effects 77−76273
dense stellar matter in asymptotically free gauge theories, high density limit 77−53421
diamond, 'melting' to solid metallic C phase above graphite triple point 80−15236
diatomic positive ions, partition functions and equilib. consts. 77−38626
dichloroanilines, vibr. assignments, Raman spectra obs., thermodynamic functions 80−52992
p-dichlorobenzene, lattice dynamics, thermodynamic functions and phase transitions 78−67777
Dicke model with classical spins, phase operator and phase transition 77−82448
dielectric and magnetic relaxation phenomena and thermodynamic vectorial internal degrees of freedom 77−77145
diffusion, activation enthalpy and entropy and defect form., basic thermodynamic relation, validity limit 78−47557
dilute solute-binary solvent activity coeffs., statistical mech. theory 80−59663
dilution dilatometer for excess vol. meas. 77−48678
dilutor method extension to meas. of high activity coeffs. at infinite dilution 79−19372
2,3-dimethylbuta-1,3-diene, IR, Raman spectra, torsional pot. function, thermodynamic function 80−43046
diphenyl-benzene, dil. soln., thermodynamic equilib., ebulliometric investig. 78−18752
dipolar fluids, equilib. statistical mechanics, struct., dielec. and thermodynamic props. 80−6345
dipolar hard sphere solvent with charged hard spheres, hypernetted chain approx. 80−61130
dipolar liquids, hypernetted-chain eqn., perturbation theory soln. 80−49072
divalent Sr, Ba, Ca, Zn, Cd iodates, complex salts, phase transitions, cryst. struct. *(Chinese)* 80−70171
DNA and polydeoxyribonucleotides, thermal properties in wide range of concs. of ions of neutral salts and of polymer 78−80833
DNA solution, thermodynamic props., phase transition, one-dimens. Ising model study 79−16125
dodecan-1-ol+n-hexane, vap. press. and thermodynamic props., 298.230 to 342.824K 78−47528
double oxides, thermodynamic obs. using galvanic cells with CaF_2 solid electrolyte *(French)* 80−85190
dynamic living polymers, thermodynamic enhancement of oligomers, end-group interactions 80−58423
Earth mantle elements compounds and modifications, high press. and temp. thermodynamics 80−81874
electrodes, adsorption isotherm equation, thermodynamic form 79−69369
electrolyte, free surface struct., single ion hydration energies 78−26752
electrolyte, solutions, 1-1 and 1-2, extended mean spherical approxs. 79−4216
electrolyte, strong, conc. solns., thermodynamic props. of mixed electrolytes and Harned rule basis 79−90506
electrolyte soln. grand canonical ensemble Monte Carlo method 80−54092
electrolyte solutions, multicomponent 79−16008
electrolyte solutions, thermodynamics, transport props., semi-phenomenological approach including short range forces 80−3353
electrolytes, aq. solns., ion-solvent interactions, transport props. *(German)* 78−79790
electrolytes, binary solns., nonideality, thermodynamics 79−39155
electrolytes, osmotic coeffs., mean spherical approx. refined model 79−1965
electrolytic solution, struct. factors and thermodynamic props. 78−18533
electron liquids, two-dimens., short-range order onset, thermodynamic props. 78−43454
electron system, two-dimensional, melting curve, phase diagram 80−57179
energy conversion, intuitive thermodynamics *(German)* 79−14225

thermodynamic properties continued
equation for liquidus line of narrow homogeneity range compound 77−35716
ethanoic, acid, ideal gas thermodynamic props. 78−51275
ethylebenzene, chem. thermodynamic props. 78−40074
ethylene copolymers, partially cryst. pseudoeutectoid, swelling, thermodynamics 80−39311
excess Gruneisen parameter in binary liq. mixtures, rel. to intermolecular interactions 77−20082
extended defect system, phase transform., critical props. 80−103455
extractive metallurgical processes, thermodynamic evaluations 80−11591
fatty acids in anhydrous solvents, partial molar volume from density meas. 79−43616
α-Fe alloy, ferromagnetic, thermodynamic analysis of solubility and miscibility gap 79−60508
Fermi liquid, normal, mag. ordering at absolute zero, ground-state props. 79−38344
ferrite systems, thermodynamic stability, dissociation and phase relations *(Japanese)* 80−55378
ferroelectric, order-disorder model, thermodynamic props. 78−10856
ferroelectric film, thermodynamics in vicinity of second order phase transitions 79−91381
ferroelectric semiconductors, props., book 80−82590
ferroelectric thin film, in neighbourhood of phase transition of second kind 80−45021
ferromagnet, high frequency, kinetic and thermodynamic props. *(Russian)* 78−19340
ferromagnet, uniaxial, with flat-parallel domain struct., classical phenomenological description 78−56316
ferromagnet, uniaxial two-sublattice, anisotropic, thermodynamic and mag. props. 80−65866
fibre reinforced composite, alloying effect on interphase interaction, thermodynamic calc. *(Russian)* 79−74134
fibre reinforced thermoelastic materials, nonlinear thermodynamic continuum theory 80−14579
film, spherical, van der Waals' forces contrib. to thermodynamic props. 77−15724
film on Si substrate, eutectic point displacement on annealing *(Russian)* 80−100850
fission product compounds in irradiated nucl. fuels *(Japanese)* 79−22387
fluid, (12-6-n), thermodynamic perturbation theory 78−26414
fluid, binary mixture, in centrifugal field, crit. dynamics 80−44310
fluid, dense of polarisable dipolar hard spheres, Monte Carlo study 79−86665
fluid, internal energy calcs. 77−28025
fluid systems, thermodynamic props., activity expansions 78−76901
fluids, low gravity expts. on phase transition and critical phenomena 77−39658
fluids, perturbation theory and thermodynamic props., CRIS model 80−92430
fluids, perturbation theory and thermodynamic props., inverse power and 6-12 pots. 80−92431
fluids, perturbation theory and thermodynamic props. 80−92429
fluids, thermoelastic, stability of motion anal. 80−10221
fluids interacting with Kihara potential, thermodynamic props. using cell theory with holes *(Spanish)* 77−72400
fluids with Lennard-Jones and soft sphere pots., thermodynamic props. using method of mol. dynamics *(Spanish)* 77−72533
fluids with Lennard-Jones pot., thermodynamic props. in terms of Lebowitz variables 79−7702
fluids with polar, quadrupolar, octupolar mols., thermodynamics, vapour-liq. equilibria 78−95127
fluoride-oxide-SiO_2 system, containing Mg^{2+}, Ca^{2+}, Ba^{2+}, Pb^{2+}, cryoscopy 77−28798
fluoride-oxide-SiO_2 system, containing Na^+, K^+, Li^+, cryoscopy 77−28797
fluoroanilines, isomers, thermodynamic functions and fundamental vibr. freqs. 80−9581
formic acid, ideal gas thermodynamic props. 78−51275
frozen food, hydrostatic press. effect on phys. props. 78−26706
furan, mol. reorientationally disordered phases, thermodynamics 79−46782
galvanic cell, reversible, thermodynamics, EMF rel. to temp. 77−1935
garnet-cordierite gneisses, geothermometry of granulite facies rocks from Rogaland, Norway 78−96193
gas, mass spectrometer, effusion cell surface evaporation effects and elimination 77−184
gas, Mayer theorem appl. to case of arbitrary interaction between gas particles 77−82478
gas, monatomic, perfect, thermodynamic state, confidence interval for temp. meas. *(Hungarian)* 77−41554
gas, multicomponent mixtures, thermodynamic equilib. 78−68909
gas mixtures, multicomponent thermodynamic equilib. 78−68909
gas mixtures, thermodynamic props. prediction 78−83512
gas mixtures containing common polar and nonpolar components 77−31417
gas-gas equilibrium, thermodynamics at high press. 78−18734
gaseous diffusion in stressed thermoelastic solid, thermodynamic struct. 78−51065
gaseous ions, thermodynamic props. calcs., dimens. model 80−96334
gaseous molecules, thermodynamic props. calcs., dimens. model 80−96334
gases, thermal activity coeff. meas., periodic-heating method, appls. 80−42218
gases, third virial coeff., nonadditive interactions effects calcs. 77−30122
gases and liquids, thermodynamic functions by computer simulation 79−86866
gases in compressed-atom model, macroscopic parameter calc. 77−47136
germylacetylene-d_0(-d_3), centrifugal distortion const. and thermodynamic functions calc. 80−95581
glass, refractive index during annealing, nonlinear structural relaxation model 78−44234
glass, ternary oxide systems, metastable two liquid tie line calc. 78−92246
glass melt, unified theory of chem. relaxation using light scattering or US absorption 79−16028
glasses, multicomponent, liquid phase separation 79−95173
grain boundary cohesion, segregation effects 78−15411
granular materials, localised internal heating, thermodynamic theory 80−19230
thermodynamic properties continued
graphite, adsorption of methane in first monolayer domain, thermodynamic props. *(French)* 80−29275
graphite, in HTGR core, accident anal. *(German)* 78−25315
graphite surface, adsorbed He, band struct. and thermodynamic props. 80−80349
graphitised carbon black, with adsorbed Ar (methane), surface excess isotherms, gravimetric determ. 78−51816
halomethanes, ideal gas thermodynamics props. 79−32733
hard heteronuclear dumb-bell fluid, thermodynamic props., eqn. of state 78−38599
hard rod system, improved lattice model, nematic and isotropic phases 80−33882
hard rods, attractive interactions, scaled particle theory 80−82735
hard sphere system in three dimens., thermodynamic props. 80−86226
hard spheres mixtures, equations of state for calc. thermodynamic props. 80−84301
hard spherocylinders and spheres mixtures, Monte Carlo study 80−49073
hard-core lattice gas with tricrit. point, phase transition behaviour 80−8926
hard-particle fluids, general scaled-particle-like descriptions 80−103231
hard-particle fluids, general y-expansion-like descriptions 80−107032
heat exchanger, indirect, air conditioning system appl., calc. *(German)* 77−23862
heat of transport in solids, computer simulation of a vacancy in FCC cryst. 79−14955
Heisenberg, ferromagnet, spin-one, uni- and biaxial anisotropy, RPA and mol. field approx. 78−34989
Heisenberg anisotropic linear chain, spectral density method 79−47222
Heisenberg ferromagnets, surface effect on thermodynamic props. and excitation spectra 79−11282
Heisenberg open finite chains, mag. and thermodyn. props. 77−72971
heterogeneous nonideal chemically reacting system, comp., thermodynamic props. calcs. 80−76492
heterogeneous surfaces, adsorpt. of atoms, monomol. adsorpt. thermodynamic functions *(German)* 79−90891
heterogeneous surfaces, multilayer BET adsorpt. of atoms, thermodynamic functions *(German)* 79−95267
hexafluorides, universal eqns. of state and thermodynamic similarity 77−35290
hexafluorocyclopropane, centrifugal distortion const. and thermodynamic functions calc. 80−95582
hexan-1-ol+n-hexane, vap. press. and thermodynamic props. 298.230 to 342.824K 78−43129
n-hexane, superheated, thermodynamic props. from ultrasound speed 80−92036
high pressure physics and technology, conf., Moscow, Russia (May 1975) 78−51611
high temperature species, JANAF thermochemical tables, thermodynamic properties evaluation and compilation 80−41959
high-temperature media, thermodynamic and thermophys. props. calcs. 79−47964
highly degenerate multicomponent plasma thermodynamic props. 80−33739
histones, H2a and H4, aggregation ionic strength effect *(Russian)* 80−55697
Hubbard Hamiltonian, coupled spin and charge fields 77−32147
Hubbard model, thermodynamic and correl. functions, field and temp. depend. 79−73666
Hubbard two-site model with orbital degeneracy, thermodynamic props. 80−2545
hydrocarbon liquid, residual energy and entropy, rel. to liq. and mol. structs. 78−71869
hydrocarbons, liq. mixtures, thermodynamics *(German)* 78−20047
hydrocarbons, mol. thermodynamics, information-theoretic aspects 78−13409
hydrocarbons, thermodynamic props., multiparameter conformal solution theory 78−18796
hydrogen, and isotopic forms, cryogenic data relevant to mag. fusion energy 80−8746
hydrophobic solutions molecular properties, one dimensional soluble models 79−46536
ideal elastic-plastic materials, constitutive eqns. and thermodynamics 78−71272
ideal type II superconductor, thermodynamics of inhomogeneous mixed phase 78−84365
III-V semiconductor phase diagram and thermodynamic data analysis 78−6913
III-V semiconductors, point defects and deep traps, thermodynamic history, model 80−59908
IIIiV semiconductor solid solutions, interaction parameters 78−51688
α-In_2Te_3. I phase, order-disorder transform. for DO_{22} struct., thermodynamic study 80−70155
individual ionic activity coefficients, determination, theory 78−20059
inert gas, thermodynamic properties, perturbation calcs., density depend. 77−7504
inert gas fluid, nucleation of freezing by positive ions 77−84893
inert gas small clusters, three body interaction effects on thermodynamic props., comparison bulk props. 80−28128
inert gas solid, calc., using model theory of free vol. and Lennard Jones potential 77−62653
inert gas solids, book contrib. 77−47522
inert gases in critical region, Ar, Kr, Xe, correlation experimental data 78−6139
inhomogeneous charged fluids, density functional theory, rel. to molten salts surfaces 80−79660
insoluble monolayers, thermodynamic eqn. of state for uncharged films 78−85195
intermetallic compounds, correl. between interstitial hole sizes and hydride thermodyn. props. 78−18798
interpenetrating EM structured continua, thermodynamic and mech. props. calcs. *(Russian)* 77−47580
interstitial ideal solution const. press. and vol. effect on nonideality 79−7697
interstitial-FCC soln., thermodynamics based on kinetic considerations 77−62651
interstitital ideal solution, const. press. and vol. effect on nonideality 79−7698
Invar alloy, effects of forced magnetostriction 79−11331

thermodynamic properties continued
iodide, charge transfer to solvent spectra, spectral shift data, Madelung const. determ. 80−85204
ionic clusters, struct., thermodynamic functions, energy surfaces and SIMS 80−63881
ionic crystal, thermodynamic props. calc., pot. energy function approach 80−54407
ionic molecules, vapours, thermodynamic properties, classical partition function, dimens. anal. 80−43829
ionic solute hydration, thermodynamic and transport props., review 78−27815
ionized gas, thermodynamic props., classical one-component Coulomb gas calcs. 77−5777
Ising lattice, thermal relaxation, nonideal behaviour, stochastic theory 80−22312
Ising magnet, random, with frustration, zero-temp. props. from series expansions 79−61129
Ising spin glass, random model, spins distrib. and thermodynamic props. 79−51786
Ising-Heisenberg linear ferromagnet, excitation spectrum and thermodynamic props. 80−50113
isotactic polypropylene/butene-1 copolymers, soln. grown crystals, props. 77−55247
isotopic isomers, solns. (one in another), excess thermodynamic props. 78−53245
isoxazolines, thermodynamics charact. of phase diagrams 78−23673
itinerant electron magnets, spin fluctuations and thermodynamic props. 79−65687
IV-VI compound layered materials, prep. and growth, book contrib. 78−19651
JANAF thermochemical tables, 1978 supplement 78−93637
kaolinite:C, high temp. reduction reactions, thermodynamic anal. 80−104426
laser, photon distrib. with 1st-order phase-transition analogy 80−23659
lattice gas, Ising-like, thermodynamic props., Monte Carlo calcs. 79−6054
lattice statistical models, series expansions of thermodynamic props. 78−57866
layered crystals, thermodynamic pot. in quantizing mag. field, conc. depend. *(Russian)* 79−15071
Lennard-Jones 12-6 fluid, liq.-vap. interface, density and surface tension 79−90772
Lennard-Jones fluid, hypernetted-chain eqn. of state 78−67800
Lennard-Jones fluid, thermodynamic props. calc. by modified Monte-Carlo method 77−35662
Lennard-Jones liquid mixtures, equimolar, mol. dynamics, struct. and thermodynamic props. 78−18517
Lennard-Jones liquid mixtures, mol. dynamics, particle mass and size depend. 78−22615
Lennard-Jones system, thermodynamic functions in liq. and vapour region 79−10910
leucite, phase diagram and thermodynamic props. 79−91985
linear Ising mixture, frozen system, thermodynamic props. 77−40064
lipid films, at fluid interfaces, phys. chem., review, book contrib. 77−39725
liquid, mean spherical approx. model 77−80401
liquid, modified cell theory appl. 79−19133
liquid, polar, computer simulation, thermodynamic props., diffusion coeffs. 79−90507
liquid, thermodynamic and struct. props., 2-Lennard-Jones centres pair pots. 77−58939
liquid alloy, rel. to struct. 77−1237
liquid alloys, thermodynamic properties, review *(German)* 78−18794
liquid and gas mixtures, thermodynamic props., conf., Braunschweig, Germany (May 1976) 78−20046
liquid binary acid+base mixtures, excess vol. and viscosity 77−21408
liquid binary mixtures theory in quasichem. approx., hole theory and thermodynamic functions *(Spanish)* 77−72534
liquid boundary layers, struct. and thermodynamic peculiarities 80−88408
liquid crystal, colloid and surface chemical aspects 78−9950
liquid crystal, nematic and thin film *(Russian)* 79−27903
liquid crystal, smectic-nematic phase boundary, elliptic, thermodynamic anal. 79−99300
liquid crystals, solid state polymorphism, differential scanning calorimetry and IR and Raman spectra obs. 80−55094
liquid metal, effective interionic pots. determ. from expt. data 77−47338
liquid metal, electronic theory of thermodynamics and struct., summer school lecture series 80−6353
liquid metal, perturbation theory extension to dense partially ionised plasmas 80−75500
liquid metal, phys. chem., conf., Konigstein, Germany (Mar. 1976) 77−1059
liquid metals, radial distrib. function and thermodynamic characts., inter-particle interaction pot. *(Russian)* 80−49086
liquid metals and alloys, book 78−51406
liquid metals and alloys, struct. and thermodynamic props., ab initio calcs. 77−84621
liquid mixture, crit. soln. point, sedimentation and density gradients in high gravit. field 77−59121
liquid mixtures, activity coeffs. calcs. using struct. group contribs. *(German)* 78−18777
liquid mixtures, intermol. forces effect on phase diagram and excess props., perturbation theory 80−39287
liquid mixtures, phase separation, umbrella sampling, Monte Carlo calcs. 77−35698
liquid mixtures, thermodynamic props., mol. theory 78−18515
liquid mixtures, thermodynamic props. for mixed fluid densities 78−18775
liquid solutions, activity coeffs. at infinite dilution, Wilson and UNIQUAC eqns. correl. 78−64875
liquid-liquid phase equilibria, theory, chem. models 78−18781
liquid-vapour equilibria calculation possibilities *(German)* 79−33067
liquid-vapour transition, non-Ising-like effects, eqn. of state, renormalisation group calc. 80−84286
liquids, kinetic theory, equilib. and non-equilib. props., book contrib. 79−60246
liquids, long-range dipolar interactions in computer simulations of polar liquids, Monte Carlo calc. 78−87603
liquids and solutions, group contribution mol. model, thermodynamic props. 77−58932
thermodynamic properties continued
liquidus in ternary system with small content of one component 77−4767
long chain paraffins, thermodynamic functions, Monte Carlo method appl. *(German)* 80−19962
LWR, HCDA, behaviour of concrete in contact with molten corium 80−13584
macromolecular liquids and solutions, statistical thermodynamics 78−18528
macromolecular multicomponent system, phase separation, thermodynamic perturbation theory, calculus 78−18778
macromolecular solutions trapped in small pores, statistics 77−39524
magnet, ordering temps. determ. by Bethe-Peierls-Weiss (BPW) method 80−54912
magnetic phase transitions, models 77−47998
magnets with two-sublattices, phase diagrams *(Russian)* 78−23268
marmem engines, martensitic transform. and shape memory effect 78−6920
materials interactions, stability, phase transformations, thermodynamics and corrosion 78−88444
Maxwellian materials, nonlinear dissipative, thermodynamics, constitutive eqns., stress relax. function 78−73950
MBBA-n-heptane, nematic soln., lattice model, thermodynamic functions *(Russian)* 80−64896
MBBA-n-heptane system, thermodynamic functions in lattice model *(Russian)* 80−33887
meniscus-film-vapour equilibrium, generalised Young equation at low or zero contact angle 79−65298
l-menthol, vap., homogeneous nucleation, high-temp. Becker-Doering theory predictions 78−67820
metabasites, geothermometry of granulite facies rocks from Rogaland, Norway 78−96193
metal, dislocations rel. to electron gas thermodynamics at $2^1/_2$th order transition *(Russian)* 78−51910
metal, interstitial soln., conversion of thermodynamic functions from const. press. to const. vol. 77−7877
metal, thermodynamic properties, outer electron contributions *(French)* 78−43091
metal calc. for solids and liqs. 77−43348
metal complexes, solns., activity correction in thermodynamic stepwise stability constant expression 78−56912
metal ethoxide ethanol system, thermodynamic anal. of ion-ion association, conductance meas. 79−29386
metal nitrates, molten mixtures, US vel., thermodynamic interpretation *(French)* 78−79670
metal oxides, diffusion activation process, interatomic bonding energy *(Russian)* 80−54428
metal systems, high-temp., conf., Helsinki, Finland, June 1975 77−52295
metal-H systems at high H press., physicochemical props., book contrib. 80−24535
metal-insulator transition, chemical mechanism, thermodynamics, vacancies 80−103626
metal-water systems at elevated temps. 78−76898
metallic alloy, liquid, binary, O_2 activity coeff. 77−4925
metallic soln., association 78−15373
metallic solution, α-parameter approach to thermodynamics 77−4207
metallic solution, thermodynamics of solutions, α-parameter approach 77−4208
metals, dislocations and shock compression, thermodynamics 80−100235
metals, enthalpy and average mass temp. on plasma-arc melting *(Russian)* 80−54405
metals, FCC, under H_2 press., crit. phenomena and isomorphic transitions 80−49367
metals, melting theory for small particles, Helmholtz free energy 80−59629
metals, structure at high temp., microscopic theory *(Japanese)* 80−29191
metals and alloys, thermodynamic props., evaporation, optical spectral method appls., review *(Russian)* 78−75822
metals diffusion thermodynamics, kinetics and mechanism 78−95179
metals under stress, thermally and radiation induced creep, constitutive relns. 77−90413
metastable superheated water, specific vols. and P-V-T props. 80−92032
methane, compressibility isotherms, thermodynamic props., 0 to 150°C 80−6196
methane, solid, thermodynamic props. from US velocity obs. 79−46753
methanoic, acid, ideal gas thermodynamic props. 78−51275
methanol, and $-d_{1,3,4}$, thermodynamic props. struct. and spectroscopic data 77−39396
methanol, boiling, on Cu surface, rel. to H_2O 78−90654
methanol-ethanol (n-propanol)(n-butanol) binary systems, excess vol. of mixing, dilatomitric meas. 80−59656
methylethyl ketone-butanol, soln., excess thermodynamic props. and interactions, US vel. and density meas. 80−39288
MHD generator, supersonic, working body thermodynamic props., chem. kinetics effect 78−91163
MHD generator current density and elec. field dependence on plasma thermodynamic pulsation *(Polish)* 77−80268
microfluids, heat conducting, theory 79−72776
microfluids, linear theory of chemically reacting mixtures 80−14777
minerals, dislocations and shock compression, thermodynamics 80−100235
mixed salt solutions, apparent and partial molal volumes, ternary systems 77−9114
mixing cell for indirect meas. of excess volume 77−29032
mixture, fluid, molecular basis of activity coeff., isobaric-isothermal ensemble approach 80−55690
mixture, large asymmetric mol. interaction with small mol., target factor 78−26225
mixtures, binary and ternary, activity coeffs. rel. to excess Gibbs free energies 80−96665
mixtures, binary interaction consts., thermodynamic props. 79−41917
mixtures, liquid-vapour equilibrium, thermodynamic props. using modified Redlich-Kwong eqn. of state 77−36775
mixtures, physical-chemical separation and thermodynamics, review *(German)* 78−18774
mixtures, simple, non-equilib. thermodynamics 80−76543
mixtures of interacting continua, thermodynamics and nature of 2nd law 79−26016

thermodynamic properties continued
model crystal, thermally activated glide in strain rate change and stress relaxation expt. 77−36615
molecular dynamics method in statistical physics, review 80−18895
molecular fluid, spherical harmonic formalism, thermodynamic props. 79−27886
molecular liquids, generalised mean field theory, thermodynamic props. 80−6332
molecule, nonrigid, sum of states, isometric group, symmetry no., thermodynamic functions 80−58186
molten metallic system, contribution to sign inversion of effective charge *(Czech)* 78−60656
molten salts, pure, theories of thermodynamic props., review 79−19380
monocarbide, cubic, calc. of surface energy, rupture energy, and theoretical strength 77−11775
monolayer, interfacial, thermodynamic treatment, excess quantities, adsorbed and spread layers 80−40732
monolayer films, films, partially mobile and partially localised, adsorpt. of single gases on solids 78−91550
monolayer films, partially mobile and partially localised adsorpt. of binary gas mixtures on solids 78−91551
Mott transition in Hubbard long range model, isostructural instability, thermodynamic props. *(Russian)* 80−65454
multicomponent electrolyte systems, velocity correl. coeffs. 78−85167
multicomponent systems, comput. techniques for thermodynamic data treatment and equil. calc. 78−10172
multicomponent systems, intensive parameters, thermodynamic props. depend., stability conditions *(Russian)* 80−65186
multicomponent systems, phase diagrams and thermodynamic data, electrochem. determ. 80−71922
multistage multicomponent separation, calc. using thermodynamic props. from SRK/PR eqn. of state 79−34346
muscle contraction, simulation of thermophysical processes 78−96063
1- and 2-naphthol, ideal gas thermodynamic props., vibr. fundamentals, rot. isomerism 79−24813
napthalene-m nitroaniline eutectic, excess thermodynamic functions 80−107445
narrow-band s-d magnetic materials, ground state and thermodynamic parameters, cond. electron density depend. 78−47934
natural gas, liq., thermodynamic props. for mixed fluid densities 78−18775
'nematic' amphiphilic liquid crystalline mesophases, thermodynamic stability 79−95126
nematic cholesteric liq. cryst. soln., thermodynamic props. 79−32903
nematic liquid crystal, surface tension, pre- and post-transitional effects 79−77511
nematic liquid crystal with lateral substituents, mol. struct. effect 78−51411
nematic liquid crystals, binary mixture, dil., thermodynamic props., statistical model 79−94882
nematic solution, hard rigid/flexible mols. mixture, unathermal, lattice model *(Russian)* 80−54129
nematic-isotropic phase equilibria, Flory-Huggins theory appl., heat of transition 77−4187
neutron star matter at high temp. and density, bulk props. 78−89812
NMR, double-quantum, cross-polarization, in solids, theory 80−100623
Noise thermometry in the range 630-962°C 78−73995
non-spherical molecule ensemble, background correl. in statistical thermodynamic calcs. 80−36958
non-stoichiometric compound with ionised punctual defects, Gibbs-Duhem eqn. 77−31786
nonelectrolyte aqueous solutions, lattice model approach 79−32876
nonelectrolyte aqueous solutions, temp. of max. density rel. to partial compressibility, struct. strengthening 80−30270
nonelectrolytic solns., unstirred, transient diffusion through membrane 78−92508
nonequilibrium temperature, definition 77−17934
nonideal gas, dissociating, composition and thermodynamic props., initial at. method 78−40034
nonideal gas in gravitational field, partition function, eqn. of state 80−6198
nonisothermal electrochemical system, thermal diffusion, thermodynamic theory 78−20056
nonisothermal systems, individual activity coeffs., electrochem. meas. method 78−20058
nonpolar binary mixture, partial molar vol. prediction from Lee-Kesler eqn. of state 80−10632
nonstoichiometric compounds preparation probability thermodynamic approach 77−31611
nonuniform fluid state, Van der Waals theory, thermodynamics, struct. and phase stability 79−77475
nucleation during precipitation, orientation relationship generation 77−73275
nucleation during precipitation, orientation relationship generation 77−77487
nucleation of new phase, role of fluctuations *(Russian)* 78−18563
nuclei, thermodynamic functions *(Russian)* 78−539
oligomeric liquid mixtures, transition to, polymer systems, thermodynamics 78−20048
one-dimensional magnets, thermodynamic behaviour, lattice compressibility effects 79−56482
organic binary liquid mixtures, excess free vol. calcs. 80−34202
organic binary mixtures, with weak charge transfer interactions, thermodynamic props. 80−54360
organic compounds, high-press. thermodynamics, review 79−24500
organic eutectic, heat of fusion and excess thermodynamic functions 78−3104
organic liquid mixtures, excess free vol. US vel. meas. 77−51294
osmotic pressure, teaching, solvent tension, dilution explanations 78−73803
oxalyl chloride (fluoride), centrifugal distortion consts. and thermodynamic functions, pot. energy calc. 79−22619
paracrystal theory, thermodynamic stability, statistical mechanics 78−75592
parchment-supported $AgPO_3$, determ. of thermodynamics of ionic diffusion processes 78−20068
partially dissociated gas, homonuclear diatomic mols., one-dimens. model 77−15157
permanent dipoles on lattice 78−88246
permeants, nonelectrolytic, stirred solns., transient diffusion through membrane 78−92507
thermodynamic properties continued
peroxyacetic acid, and isotopic forms, matrix IR spectra, force spectrum, force const., thermodynamic props. calc. 77−14427
petroleum gas, liq., thermodynamic props. for mixed fluid densities 78−18775
phase diagrams, review 79−91620
phase diagrams and synthesis of soln. thermodynamics, computer anal. 78−30739
phenol-formaldehyde resin, thermodynamic props. 78−91452
phospholipid bilayer melting transition, thermodynamic fluctuations, ion permeability, statistical mechanics model 78−73140
plasma, non-LTE, props. and at. processes, medium to high press. 80−59170
plasma, nonideal, elem. excitations and macroscopic props., review 80−43842
plasticized triblock copolymers, thermodynamic theory 78−15377
PMMA, glassy atactic, thermodynamic analysis of plastic deform. modes, 150 to 330K 80−84999
PMMA, solvent cast, surface characts., chromatographic study 80−20020
PMMA and brittle materials, slow crack propagation anal. thermodynamic model 78−35488
PMMA solution, diffusion coeffs. and thermodynamic props., conc. depend. 80−15274
pnictides of non-transition metals, at. vol. and semicond. props. 77−20089
polar fluid, translationally invariant correlation function, thermodynamic and dielectric props. 77−35457
polar fluids in elec. fields, statistical mechanics 80−54085
poly- and three-component systems *(Chinese)* 77−72698
poly-arylate-dimethyl siloxane, polyblock copolymers, struct., thermodynamic stability *(Russian)* 80−64931
poly-L-lysine, membrane phase, transport processes, helix-coil transition 78−77031
polyacrylamide, aq. soln., thermodynamic props., light scatt. obs. *(Russian)* 80−71439
polyatomic fluid mixtures, thermodynamics, phase equilib. calcs. 79−1485
polyelectrolyte solution, thermodynamic props. determ. from Donnon equil. obs. 80−7846
polyelectrolyte solutions, activity coeffs. and osmotic coeff., higher-order limiting laws 79−29387
polyethylene, low density, morphology and props. 80−64926
polyethylene, uncrosslinked amorphous matrix embedded cryst. orientation distrib., strain energy and hydrodynamic pot. effects 78−9968
polyethylene glycols, aq. solns., volumetic props. 79−20460
polyethylene oxide, aq. salt soln., meas.-based thermodynamic quantities 78−75525
polyethylene terephthalate, solid and molten, press. effects on compressibility and crystn., thermodynamic interpret. 80−84102
polyethylene-polyoxymethylene mixtures connection of melt thermodynamic props. with solid state struct. *(Russian)* 80−54152
polyheteroarylene-epoxy resin, thermodynamic stability and compatibility *(Russian)* 79−65204
polymer, adsorbed, conformation, excluded vol. effects 78−2372
polymer, dil. soln., light scattering charact. of thermodynamic props., solvent and mol. wt. effect 80−16717
polymer, glass transition, fluctuation theory and thermodynamics *(German)* 79−51242
polymer, glass transition thermodynamics, fluctuation theory approach *(German)* 79−33078
polymer, partially crystalline, sp. vol. press. depend. *(German)* 78−75852
polymer, single ring, Lennard-Jones model, eqn. of state calcs. 78−5379
polymer chain statics and dynamics, Lennard-Jones interaction, calcs. 80−58425
polymer crystal and melt, stat. thermodynamics using Midha-Nanda cryst. state theory 79−41979
polymer gels, thermodynamic props., review *(German)* 78−20073
polymer glasses, thermodynamics of densification process 78−95723
polymer melts, immiscible, surface and interfacial tension, thermodynamic theory *(German)* 78−26753
polymer mixtures, thermodynamics, review 79−1506
polymer solns., phase diagrams, pulse-induced critical scatt. 79−1490
polymer solution, excluded volume and intrinsic viscosity plots 77−89363
polymer solutions, dilute, regularly alternant, thermodynamic props. self avoiding random walk calcs. *(French)* 80−59369
polymer solutions, thermodynamic props. under high press., light scatt. obs. *(German)* 78−20049
polymer solutions, thermodynamics, review *(German)* 78−18530
polymer solutions, thermodynamics, scaling theories 79−10775
polymer spheres, colloidal suspension, steady state shear flow coupled to conc. fluctuations 80−61170
polymeric glasses, non-elastic deformation, thermodynamic and kinetic anal. 78−64604
polymeric liquid, entropic elasticity and time temp. superposition principle, thermodynamic eqn. of state 78−63406
polymethylpentene, press. effects on melting 78−56625
polypentenamer, thermodynamics *(Russian)* 77−21386
polystyrene, soln. in trans.-decalin, viscosity and thermodynamic props., press. depend. 79−69275
polystyrene hollow microspheres form., kinetic regularities *(Russian)* 79−57307
polystyrene melt, viscosity, thermodynamic props. *(Russian)* 79−51295
polystyrene-tetrahydrofuran-water system, thermodynamic and hydrodynamic props. 79−96353
polystyrenecobutadiene, vapour sorption isotherms for benzene and n-heptane 78−68912
polyvinylidene fluoride, thermodynamical model, applications *(French)* 80−39315
Prandtl number for liquids, eqn. of state analogy and linear relations with transport props. 77−59156
Prigogine-Defay ratio for inhomogeneous system with single internal parameter 77−76578
primitive model electrolytes, symmetrical, canonical Monte Carlo calcs. 80−92428
Principles of identification of the physical processes caused by variation of thermodynamic parameters in solids 78−22868
protein structure, areas, vols. and packing, review 77−86441
pure components, liq.-vapour equilib. and thermodynamic props. using modified Redlich-Kwong eqn. of state 77−36775

thermodynamic properties continued
pure material, in two-phase solid-liq. melt regime, eqns. 77−55342
PVC solution, diffusion coeffs. and thermodynamic props., conc. depend. 80−15274
pyroxene geotherms, thermodynamics 78−65282
pyroxenes in CaO-MgO-Al_2O_3-SiO_2 system, subsolidus phase relations rel. to geothermometry and geobarometry 79−16440
QED, thermodynamic potential, path integral methods 78−41459
quartic anharmonic oscillator, semiclassical and quasiclassical particle function 80−99434
quasi-perfect elasticity, adiabatic temp. variations 78−32675
quasilattice theory, complexation, thermodynamic parameters calcs., spectroscopic appls. *(Russian)* 78−76905
quasilattice theory of solutions, use in mol. spectroscopy, thermodynamic parameters determ. 79−96350
rare earth halides, prep. and props., book contrib. 80−54211
rare earth hydrides, props., book contrib. 80−45291
rare earth metals, thermodynamic props. determ. form US vel. meas. 78−55912
rare earth oxides, binary, struct. and props., book contrib. 80−45292
rare earth oxides thermodynamic props. and high temp. chem. behaviour, comparison with actinide oxides 79−100127
rare gas clusters, small, structure, thermodynamic properties 80−88341
real gases, thermodynamic props. and intermol. pots. *(German)* 78−17743
refractory carbides, thermodynamic evap. characts., cluster-component calcs. 78−51704
refractory oxide, high temp. props. conf., Odeillo, France (June/July 1977) 79−100125
relativistic electron beams, thermal equilibrium props. 79−86126
relativistic fluid, infinite thermal conductivity, Cauchy problem solutions, existence and uniqueness *(Italian)* 80−48821
relaxation functions of materials with memory 78−73949
rigid-rod fluid, thermodynamic props., crit. points and transitions 78−73919
rocket propellants, thermodynamic evolution, extension of Huff's method 78−75054
S activity in pyrrhotite at 1073K 77−72700
sanidine, phase diagram and thermodynamic props. 79−91985
scaled particle theory results for dense mixtures of convex shaped mols. 78−1969
seawater, thermodynamics at one atmosphere pressure 77−17108
seawater synthetic, solubilities and activity coeffs. of $CaSO_4$ and $SrSO_4$ 79−91986
semiclassical laser theory in the stochastic and thermodynamic frameworks 80−1178
semiconducting liquid alloys, anomalous thermodynamic props., theory 80−49287
semiconductor, interface form., initial steps, surface states and thermodynamics 80−49503
semiconductor materials, quantitative fitting of experimental phase lines, thermodynamic props. to model parameters 79−11593
semiconductors, chemical thermodynamics, review 80−55692
semiconductors, temp. depend. electronic cond. 80−59975
semiconductors, ternary and quaternary solid solutions with nearly perfect sublattices, stoichiometry invariants 79−51270
separation processes simulation in H_2SO_4-Br cycle 79−74413
shape memory alloys temperature entropy diagram of solid state engines and solid state heat pumping system 77−7785
shock wave propagation, in smoothly-varying density condensed medium 77−75844
silicate glass, hydration thermodynamics 80−81313
silicate glass, thermodynamic theory of structural relaxation *(German)* 80−38929
silicate minerals, thermodynamics and lattice vibrs. 79−100831
silicates, liquid, thermodynamic props., calc. model 79−34804
silicates and aluminosilicates, thermodynamic props. determ. by Monte Carlo calc. 77−47597
silylacetylene, centrifugal distortion consts., thermodynamic functions 80−47959
simple fluids, semiempirical calcs. using perturbation theory 80−28892
single phase liquids, thermodynamic stability limit and eqns. of state 80−92037
slag-metal equilibrium, thermodynamics 78−44108
slags, application of activity concept to physical chemistry 78−53243
small extended Hubbard rings, thermodynamic props. 80−2546
small metal particles, thermodynamic props. of electrons 80−59844
soft rods, one-dimensional, exact partition and thermodynamic functions 80−46953
solar energy storage by H_2 prod. using Mg(Al)(Fe)(Co)(Ni)(Cu)(Zn) sulphates *(French)* 80−55935
solar thermochemical energy transfer system, reversible reactions screening 79−87999
solid, high-density, quantum statistical model 79−55824
solid, non-hydrostatically stressed, thermodynamics 80−84304
solid electrolyte, transition temperature to high cond. state as function of press. 80−44365
solid electrolytes, phase transitions and thermodynamic states 77−84975
solid electrolytes, thermodynamic peculiarities 79−33114
solid electrolytes and mixed conductors, materials stability and chem. diffusion 80−65292
solid mechanics, continuum thermodynamics *(Japanese)* 79−75339
solid thermophysical properties at high temp., conference, Moscow, USSR (May 1976) 77−28012
solid under stress, nonlinear theory of thermochemical equilib. 78−18701
solute interaction energy, const. press. and const. vol. condition effects 78−38856
solute transfer between solutes, standard thermodynamics 78−76899
solutions of nonelectrolytes, structural, change characterisation 77−25301
solvation effects and Gurney cosphere overlaps, conductimetric approach 80−21354
spin glass-ferromagnetic phase, mean field theory 80−103841
spin one Heisenberg antiferromagnet, with uniaxial anisotropy, thermodynamic props. 79−56539
spin systems, dipolar interaction in solids, low mag. field, thermodynamic props. 78−76205
spin systems with truncated secular dipolar coupling 78−88130
spin wave damping, magnetic materials with canted mag. struct., thermodynamic and high freq. props. 80−11184

thermodynamic properties continued
spin-$^1/_2$ XY model, thermodynamic quantities, high-temp. series expansions anal. 80−7067
spin-phonon system, transition to self-trapping 80−10606
spinel, natural, solid soln., thermodynamic model *(French)* 78−32065
spinel structs., thermodynamic anal. of energy of cation octahedral sites 79−10827
spinodals and swallowtails, rel. to phase diagrams 77−7844
square-well fluid, eqn. of state and thermodynamic props. 77−7834
standards for single substances and mixtures 78−14481
star, cold, massive rest-mass density and redshift 80−56859
statistical models, variational calc. 77−85405
steam, numerical calc. programme *(French)* 77−69101
steam, saturated and superheated, up to 800°C, equation of state 79−14908
steam pressure and temp. in relation to enthalpy and entropy, approximation formulae in binary polynomial form *(German)* 78−59532
steel, alloy, thermodynamic aspects of gas-metal heat treating reactions 79−24547
steel, alloy with additions of Mn, Si, Ni, Cr, Mo, Cu, thermodynamic prediction of Ae_3 temp. 78−64524
steel, austenitic stainless, Cu-Mo substituted 18/8 type, austenitic stability 79−91716
steel, Cr, thermodynamic anal. of facing process using other metals 78−60878
steel, deoxidation by Ca-Si alloy, thermodynamics *(Russian)* 80−16268
steel, embrittlement by impurity segregation 79−8367
steel, maraging, solubility of Fe-Mo-Co (10, 0 to 20 wt.%) Laves phase, depend. on Co *(Russian)* 79−100145
steel, mild, laser microspectral anal. 80−108769
steel, stainless, clad oxide fuel pin, thermodynamic model for attack 79−97807
steel, stainless, intercrystalline corrosion, effect of alloying elements, thermodynamic anal. 77−90504
steel, stainless, nitriding charact. at low atmos. press. of NH_3, thermodynamic *(Russian)* 78−15573
steel, stainless, stabilised with Cr-Ni-Nb, reaction with Te vapour 77−8986
steel, thermodynamic props. of C in austenite, relationship with cryst. lattice anomalies of martensite *(Russian)* 78−59781
steels, austenitic-C steel diffusion couple, diffusion of C, 773-1373K 79−19392
stellar atmosphere, departure from LTE-radiative transfer 79−48777
Stockmayer fluid, mol. dynamics and thermodynamic perturbation theory, mol. polarisability effects 78−71419
strongly anharmonic crystals, improved unsymmetrised SCF approx. 78−75791
structural relaxation, order parameter model *(German)* 80−44146
sulphide melt, conc. EMF meas. using solid-electrolyte cell 77−40571
sulphides, direct leaching 77−29033
superconducting slab, type 1, first stage magnetisation and metastable migration field 80−15655
superconductivity, phenomenological parameters, thermodynamic and quantum mech. derivation 77−12054
supercooled steam, thermodynamic props., virial eqn. of state 80−14872
superheated binary solns., flashing kinetics, nucleation and critical bubble 80−92035
surface step, excess energy 78−47254
surface steps, solid on solid model 77−7683
surface tension, of liquid in equilib. with vapour, lattice model 77−43409
surface tension, review of theory 79−77866
surface tension computation in molecular dynamics experiments 78−30815
systems containing noninteracting mols., variational CI calcs. 77−67988
TCNQ anion radical salt, $[(C_6H_5)_3PCH_3]_{1-x}^{+}[(C_6H_5)_3AsCH_3]_x^{+}(TCNA)_2^{-}$, phase transition and phase diagram 77−76555
TCNQ complexes, disordered, thermodynamics of random exchange models 80−103826
TCNQ salt, quinolinium, electron spin location, elec., mag., and thermal props. 80−25189
temperature in range 0 to 1064°C, International Practical Temperature Scale revision 80−62669
temperature rate dependent materials 79−90123
ternary alloy of quasi-binary cross sections, thermodynamic functions calc. 80−16265
ternary alloy systems, calc. of phase equilibria using thermodynamic values from different models 78−60646
ternary and multicomponent systems, partial molal props. calc. 78−79784
ternary compounds, thermodynamic characterisation, case of extensive defect association 77−47445
ternary liquid mixtures, molecular interaction and thermodynamic props. 78−59861
ternary liquid mixtures, physical props., determ. by density and US vol. meas. 79−37751
ternary mixtures, eutectic point localisation, thermodynamic calcs. *(French)* 78−79742
ternary oxides, coulometric titration method for phase diagram and thermodynamic studies 79−47667
ternary phase diagrams, interactive computer program 80−71629
ternary solution phases, empirical methods of predicting and representing thermodynamic props. 80−70423
1,2,4,5-tetrachlorobenzene, lattice dynamics, thermodynamic functions and phase transitions 78−67777
tetrafluoromethane adsorbed on graphite, adsorption isotherms, crit. temps. *(French)* 80−34312
tetrahydrofuran-benzene, soln., excess thermodynamic props. and interactions, US vel. and density meas. 80−39288
tetramethylsilane, thermodynamic props. of polymorphic phases 77−84943
thermophysical properties, computer based determ. system *(German)* 78−18795
thiaalkanes pure crysts., thermal press. coeffs. and expansivity at 298.15K 80−49381
Thomas-Fermi screened Coulomb systems, thermodynamic props. calcs. 77−67399
toluene, in polar solvent, excess thermodynamic props., Rayleigh scatt. meas. 78−52523
toluene-bromobenzene, perfect binary liquid mixtures on silica gel, adsorption thermodynamics 80−44428

thermodynamic properties continued
toluene-chlorobenzene, benzene-toluene, perfect binary liquid mixtures on silica gel, adsorption thermodynamics 80−44428
trace elements, in acid solns., solvent extraction, chelation and thermodynamic activity *(French)* 78−27816
transition metal, Einstein temp. and vibr. entropy, semiquantitative calc. 78−2221
transition metal carbides, solid-phase reacts., effect of nonstoichiometry, thermodynamic evaluation 78−60632
transition metal diborides, C32-type, phys., chem. props., appls., review, book contrib. 78−47308
transition metals, liq., calc. *(Russian)* 80−15264
transition metals and alloys, metallurgical props. rel. to electronic struct., energies calc. method 77−20221
transuranium cpds. in aq. soln., electrochem. 77−29040
tricritical points and thermodynamic quantity singularities, renormalisation group method *(Russian)* 77−69071
two component classical Coulomb gas, equilib. props. 79−12709
two-component ionic mixture, eqn. of state and phase separation in uniform background 78−21058
two-phase fluid equilibrium, thermodynamic functions and surface tension 78−2262
unsaturated two-component associated vapour, press., comp., thermodynamic calcs. *(Russian)* 80−64671
uracil in aq. electrolyte, adsorpt. isotherm and solute activities from spreading pressure-surface charge data 78−14576
Van der Waals gas, thermodynamic props. review 80−31694
Van der Waals gases, adiabatic and isothermal spinodal curves 80−92034
van der Waals molecules, pot. functions, level spacings and thermodynamic props. 80−14185
vapour-liquid equilibrium, high press., quantitative description 79−14923
vessel cooling of HTR constructed of prestressed cast steel, with 3000 MW thermal power *(German)* 78−4982
VIII-IIIA, transition metal alloys, B2 struct., vacancy conc. and thermodynamic props. calc. 78−59801
viscoelastic materials with fading memory, thermodynamics of relaxation and creep processes 78−71282
volatile chlorides, adsorption isotherms meas. using radionuclides and chromatography 78−76902
water, appl. of polychromatic correlated site percolation 80−22296
water, compressed, thermodynamic props., evaluation by statistical error anal. 80−92685
water, free surface struct., single ion hydration energies 78−26752
water, LF sound velocity and related thermodynamic props. 79−73255
water, liq., internal press. isobars, anomaly short-range order influence 77−65944
water, liq., Monte Carlo-Metropolis computer simulation, convergence characts. 80−10485
water, Monte Carlo simulation of isothermal-isobaric ensemble 78−30530
water, Monte Carlo simulation of struct. and thermodynamic props. 80−88017
water, numerical calc. program *(French)* 77−69101
water, ordinary and heavy, US vels. thermodynamic props. calc. 80−65156
water, simulation, Monte-Carlo method, 1 g cm^{-3}, 300K, using Rahman Stillinger ST2 pot. 77−51290
water, struct. changes due to hydration of monat. ions, in stoichiometric mixtures, thermodynamic props. 78−7225
water, supercooled liq., high freq. sound vel. and absorpt., thermodynamic singularity, 228K 77−76489
water, temp. of maximum density, solute effects and partial molal expansibility 77−24256
water, thermodynamic props., computer programme calcs. *(French)* 80−54409
water, thermodynamic props. at high pressures from US vel. 79−94474
water condensation, thermodynamics of nucleation on charged centres 79−20955
water supercooled, hypersonic sound vel., thermodynamic interpretation 78−59860
water vapour, dissociating, composition and thermodynamic props., initial at. method 78−40034
water/steam systems, thermodynamic data tables 78−26679
weak-coupling superconductor, effect of electron-phonon renormalisation on thermodynamics 79−99655
$(X=H,D; n=1,2,3)$, thermodynamic function in ideal gas state 80−14871
X-Y model, one-dimens., with symmetry-breaking fields, thermodynamics and static props. 79−73742
Yukawa-tail fluid, semiclassical fluid struct. and thermodynamics props. 79−27895
Ag, activity determ. in molten Cu by two component method *(Japanese)* 78−11547
Ag-AgCl reference electrode, construction and thermodynamic props., high temp. aq. environment appl. 80−21288
Ag-Cu (6.2 at.%), tricrystalline specimen, discontinuous precipitation, thermodynamics *(German)* 79−34043
Ag-Ge alloys, liq., thermodynamics and short range order, mass spectra meas. 79−52740
Ag-Se mixture, activity of Se *(German)* 78−27492
Ag-Sn, liquid alloys, thermodynamic props. *(Japanese)* 80−108396
Ag-Zn, liquid, thermodynamic props. *(German)* 79−87615
AgBr NaBr, thermodynamic props., metastable states and demixing 80−96660
AgCl-KCl, solns., activity coeffs., surface tensions, 860 to 1000K 78−76897
AgCl-NaCl molten solns., activities and surface tension 80−10748
AgI, interfacial electrochem., review 78−80748
α-AgI, superionic cond., statistical thermodynamic description *(French)* 80−65281
AgI-PbI_2 molten mixtures, conductivity, thermodynamic excess props. 79−86914
$AgPO_3$-AgBr(Cl)(I) system glasses, soln. calorimetry obs., thermodynamic activity correl. with ionic cond. *(French)* 79−33102
$Ag_xV_2O_5$, thermodynamic, elec. and electrochem. props. 78−84265
Al, crystallisation thermokinetics calc. of pure cylindrical specimen *(Czech)* 77−63654
Al, monovacancy thermodynamic parameter calcs., temp. dependence 78−2114

thermodynamic properties continued
Al-Ga, face centred cubic struct. stability, melt equilib., α-Ga effects 78−18766
Al-Ga(-Ge), and Al-Ge, Al activity, EMF study, phase diagrams 79−83175
Al-La, thermodynamic interaction in liquid phase *(Russian)* 78−44080
Al-Mg, thermodynamic props. *(German)* 79−29027
Al-Mg-Si liquid alloy, exam. of thermodynamic props at 780-820°C *(Czech)* 79−91626
Al-Ni-Ti, calc. of phase equilibria using thermodynamic values from different models 78−60646
Al-Ni(Si), liquid, thermodynamic props. 79−91619
Al-Sn liquid alloys, heats of mixing and activities calcs. 79−42264
Al-Zn, liq. solutions, thermodynamic properties *(Polish)* 80−49380
Al-Zn-Si, thermodynamic props., meas. by EMF method *(Czech)* 77−59753
AlN, CVD from $AlCl_3/NH_3$, calc. of equilibrium yields 79−52121
Al_2O_3, thermodynamics 77−90595
Al_2TiO_5, activation energies for decomposition and nucleation *(Japanese)* 80−35156
Ar, liq., internal energy calcs. 77−28025
Ar, liq. nuclei, thermodynamic props. mol. dynamics calc. *(Russian)* 77−47325
Ar, liquid, velocity of second meas. and thermodynamic stability *(Russian)* 79−4374
Ar, solid, equilib. props., uncorrel. pairs approx. 80−84303
Ar, solid, thermodynamic props. under press., multiparametric pairwise and Lennard Jones potential calcs. 80−39316
Ar, solid state props., statistical thermodynamic calc. using gas phase intermol. pair pot. *(German)* 77−20083
Ar, thermodynamic behaviour, improved analytical representation 80−54339
Ar-Xe plasma, shock wave dynamic compression *(Russian)* 80−53931
ArHX, (X=F,Cl,Br,I) van der Waals mols. vibr. and thermodynamic props., WKB calcs. 77−71740
As_2S_3, thermodynamic of evaporation 77−47568
As_4S_4, VP and thermodynamic functions calc. 77−36470
$(AsSe)_{1-x}Te_x$ glasses, thermal props. and viscosity, temp. and conc. depend. 77−76324
Au-Cl system, high temp. vaporisation chemistry incl. form. of vapour complex species 79−47963
Au-Fe, liq., thermodynamic mixing effects, mass spectrometric meas. eval. *(German)* 77−59123
Au-M, liq. alloys., M=Ga, Bi, activities of Ga and Bi, ht. of mixing 77−4921
Au-Ni-Cu phase diagrams, thermodynamic calc. *(Korean)* 78−68672
Au-Si, melt, thermodynamic study of phase diagram *(French)* 78−27482
Au-Sn liquid alloys, Sn activity *(Japanese)* 78−6901
Au-Te, thermodynamic props., calorimetric meas. 78−20051
$AuGa_2$, supercond., press. depend., theor. *(Russian)* 77−51843
B, CVD from BCl_3-H_2 and BBr_3-H_2 gas mixtures onto inert substrate, thermodynamic approach *(French)* 78−44020
B fibre reinforced Al-Cr(Mg)(Mn)(Si), calc. of thermodynamic interaction potential between B fibre and matrix 80−11627
BBr_3-PCl_3-H_2, gas phase equilib. comp. 80−35166
BN, adsorpt. of Ar, thermodynamic values calc. from pot. parameters *(German)* 79−95268
BN, adsorption of methane in first monolayer domain, thermodynamic props. *(French)* 80−29275
BN, high temp. compatibility with insulating oxides 77−24995
B_2O_3 glass, nonlinear structural relaxation model for glassy state 78−26448
BaF_2-x$BaO.ySiO_2$, activities rel. to liquidus comp. 77−28798
$BaTiO_3$, thermodynamic props. 77−39680
$BaTiO_3$:C, solubility of C at low O_2 potentials, 800°C 80−100334
Be, containerless melts in terrestrial and space environment, thermodynamic props. calc. from solidification and cooling curves 79−70052
Bi-Cd-Sb, calc. of phase equilibria using thermodynamic values from different models 78−60646
Bi-Pb-Sn, molten metallic system, contribution to sign inversion of effective charge *(Czech)* 78−60656
Bi-S liquid soln., S activities meas. by EMF method *(Japanese)* 80−70425
BiLi, gas phase thermodynamics, Knudsen effusion mass spectrosc. 80−100057
Br_2, liq., entropy, computer simulation, Widom method 79−77486
C fibre reinforced composites, kinking as structural degradation mode 78−52893
C materials, thermodynamic props. rel. to struct. 77−80597
C_n aggregates in equilib. C vapour, MINDO/2 calc., isomerism 78−29873
CO_2, Joule-Thomson coeff. at 20-583°C 77−42956
CX_n radical, $(X=H,D; n=1,2,3)$, thermodynamic function in ideal gas state 80−14871
Ca-Mg, liq. alloys, thermodynamic activities determ. using modified Ruff method *(German)* 80−11631
Ca-S-O system, sulphide-sulphate equil., solid state EMF obs. 79−83492
Ca-Zn liquid alloys, thermodynamics 79−52173
$CaCl_2$, isopiestic studies of aqueous solns., 382 to 474K 79−24815
CaF_2, cond. meas. under controlled F_2 chem. pot. *(Japanese)* 78−59972
CaF_2-x$MgO.ySiO_2$, activities rel. to liquidus comp. 77−28798
CaO-SiO_2 glass, two phase region, expt. and thermodynamic data 80−16288
CaO-SiO_2-Al_2O_3, slag phase, activity of components at 1873K *(Polish)* 78−52775
$CaO.6Al_2O_3$, thermodynamic stability, reaction with Ti, Cr and Zr oxides 80−92687
$CaSO_2.2H_2O$, few thermodynamic invariants, proof from PMR 78−43657
$CaSO_4.2H_2O$, thermodynamic expression for crystal growth and dissolution affinity 80−24385
Cd-As, liq. alloys, thermodynamic props. and cpd. formation 77−1238
Cd-In-Sb, liq. alloys, thermodynamic activity of Cd between 833 and 953K *(German)* 80−45278
Cd-P, p-T-x phase diagram 80−88300
Cd-Pb-Bi-Sn system, ternary liq. alloys, thermodynamic props. 78−51701
Cd-Sn(-Pb) liquid (0.03 to 0.10 at.% Cd), Cd activity coeffs., interaction parameters, EMF depend. on temp. 80−49383

thermodynamic properties continued
Cd-Zn-Hg alloys, liq., comp. and temp. depend. of Hg VP, activity, free energy and enthalpy *(Russian)* 77−20087
$CdCl_2$-$PbCl_2$, thermodynamic quantity meas. by quantitative thermal anal. of heating process 78−19730
$CdCr_2S_4$, thermodyn. props. 78−51703
CdI_2-PbI_2-NaI, fusion diag. and thermodynamic calc. *(Russian)* 77−48417
Cd_3P_2, Cd_3As_2, sp. ht., thermodyn. props. 78−22863
CdSe, film, vacuum condensation thermodynamics, starting powder comp. effects 77−81220
CdX_2, CdXY, (X,Y=Cl,Br,I), matrix isolated, far IR spectra, thermodynamic props. 78−86869
Ce-Ga (Al)(In)(Sn)(Pb)(Bi)(Zn) liquid, solubility and thermodynamic props. *(Russian)* 78−19717
CeO_{2-x}, 1.5<O/Ce<2, physicochemical equilibria, statistical thermodynamics model *(French)* 78−38688
Cl_2, liq., entropy, computer simulation, Widom method 79−77486
Cl_2, mol. liquid, mean squared torque and mean squared force, interaction energy spherical harmonic expansion 80−54093
Cl^-Ar_{N-1} small ionic clusters, thermodynamic behaviour 79−77769
ClNO, phys. and chem. data 78−27727
$ClNO_2$, phys. and chem. data 78−27727
$ClNO_3$, phys. and chem. data 78−27727
Co alloy, dil., liquid, thermodynamics 77−20086
Co, liquid, N activity coeff. 77−72699
Co-Cr-Zr, thermodynamically calculated phase diagram 79−91617
Co-Fe(Ni)(Cr), liquid, N activity coefficient 77−72699
Co-S, thermodynamic anal., phase diagram 79−43226
Co-Zn melt, Zn activity determ. *(German)* 78−19715
$Co_{1-x}Al_x$, ordered β-phase, enthalpy of formation are defect struct. descript. 80−89519
$Co_xMg_{1-x}O$ system, thermodynamic investigation, 1100 to 1300K *(German)* 80−107430
Co_xS_y, exam. of thermodynamic activity, for several phases, using gas equilibration technique 78−52785
B-CoTe phase, thermodynamic study by Galvanic cell meas. 80−29190
CoZn β- and γ-intermetallic compounds, thermodynamics *(German)* 78−92242
Cr, liquid, N activity coeff. 77−72699
Cr-Fe-Ni, γ-solid soln., thermodynamic activity determ. at 1500K 80−108397
Cr-Fe-Ni alloys, interface with Th carbide fuels, basic chemical compatibility, thermodynamic calcs. 79−93727
Cr-Fe-V, calc. of phase equilibria using thermodynamic values from different models 78−60646
Cr-Ni-Fe, ternary phase diagrams, interactive computer program 80−71629
Cr-Ni(Co)(Fe), liquid, N activity coeff. 77−72699
Cr-rare earth alloys, liquid phase, topology in diagrams of state *(Russian)* 80−54121
Cr-W-O, phase relations, thermodynamic props. of $CrWO_4$ and Cr_2WO_6 80−104120
$Cr_{11}Ge_8$, Cr_3Ge, thermodynamic functions 77−84948
Cr_2O_3, vacuum vaporisation, porosity and thermodynamic treatment effects *(Japanese)* 77−43436
Cr_2O_3-Al_2O_3 solid solution, electrochemical determ. of activity 78−44391
CrO_2Cl_2, determ. of thermodynamic props. from vibrational freqs. and moments of inertia 77−31415
CrO_2F_2, determ. of thermodynamic props. from vibrational freqs. and moments of inertia 77−31415
Cs, absolute zero isotherms and polymorphic transition 79−73310
Cs halides, Gruneisen and Anderson-Gruneisen parameter determ. 80−59611
Cs, nonideal plasma press. ionisation, short range forces, thermodynamic props. 80−33733
Cs nonideal plasma thermodynamic props., shock wave obs. 78−71434
Cs vapour, thermodynamic props. calc. from Joule-Thomson data 78−94886
Cs-SiO_2-Al_2O_3 system interactions, getter development for radiocaesium 80−83208
$Cs_{1-x}Au_x$, liq., metal-nonmetal transition, electronic theory 78−79930
$CsPbBr_3$, critical thermodynamic props. around successive phase transitions 79−33627
$CsPbCl_3$, critical thermodynamic props. around successive phase transitions 79−33627
Cu alloy, binary liquid, activity meas. 77−20085
Cu alloys, ternary, phase diagrams and thermodynamic props. 79−8275
Cu bearing substitutional solutions, thermodynamics, Kapoor model applicability 79−77761
Cu, extraction by Kelex 100, meas. and correl. of solvent extraction equilibria 77−29034
Cu, matte, thermodynamics of converting, distrib. of Au, Ag, Pb, Zn, Ni, Se, Te, Bi, Sb, As, Noranda process 79−47648
Cu-Ag, dil. molten alloy, Ag activity determ. by two-component evap. *(Japanese)* 77−48395
Cu-Ag-O alloys, dil., O-metal interactions, activity coeff. meas. at 1423K 80−93792
Cu-Ag-Se, computation of component activities from ternary miscibility gap data 79−11591
Cu-Ag-X, X=metals, P, S, Se, phase diagrams and thermodynamic props., iso-activity coeff. curves 77−81249
Cu-Al-Ni, stress induced martensite 77−36500
Cu-Al-Ni (14, 2.5 wt.%). thermodynamics of thermoelastic martensitic transform. 79−61585
Cu-Au-O alloys, dil., O-metal interactions, activity coeff. meas. at 1423K 80−93792
Cu-Co-O, Cu-Fe-O and Cu-Ni-O systems, distrib. of Fe, Co and Ni between Cu and Cu_2O *(Russian)* 77−16540
Cu-Fe-O system, ternary phases, activities in spinel solid soln., phase equilibria and thermodynamic props. 78−6910
Cu-In(Sb), growth kinetics, of discontinuous precipitation, third element effects 77−36511
Cu-M-O ternary liquid alloys, thermochem. calcs. 80−85209
Cu-Ni-O, liquid alloy, thermodynamic study by EME method *(Japanese)* 78−15367
Cu-Ni-S, molten, thermodynamic props. 80−104122
Cu-Ni-Zn alloy, at 775 degrees C, diffusional and thermodynamic interactions 78−38883
Cu-O-Zn dilute liquid alloy, Zn-O interaction parameter 80−55694

thermodynamic properties continued
Cu-Pb (Fe), liq., thermodynamic props. *(Polish)* 80−89199
Cu-Pb-O, liquid, dil. alloy, O_2 activity, 1100 to 1200°C 80−25662
Cu-Pb-O system, ternary miscibility gap activity determ., thermodynamic method 77−28783
Cu-Pb-S system, at 1473K, thermodynamic anal. 78−39746
Cu-Pt-O alloys. dil., O-metal interactions, activity coeff. meas. at 1423K 80−93792
Cu-Se mixture, activity of Se *(German)* 78−27492
Cu-Sn alloy, thermodynamics of Cu and Sn solns. using copper β-alumina solid electrolyte, 800-1100K 80−107502
Cu-Sn system, thermodynamic study of gaseous molecules of $CuSn_2$ and Cu_2Sn 79−70360
$Cu_{1-x}Cr_2Se_4$, influence of excess Cu on physical props. 80−103836
$Cu_xMo_6S_{8-y}$, mixed conductor, equilib. partial thermodynamic props. 80−85270
Cu_2S-Ni_3S_2, melt viscosity 77−51536
CuZnAl single crystal, thermodynamic anal. of martensitic transform. under stress 79−87635
n-D_2, fluid, eqn. of state from P-V-T and US vel. meas. up to 20 kbar 78−63837
D_2O, appl. of polychromatic correlated site percolation 80−22296
D_2O+methanol-d_0(-d_2)(-d_4), D exchange reaction, thermodynamics 78−94328
Eu-W-O, reaction system, thermodynamics, mass spectrometric obs. 77−77748
EuF_2, thermodynamic data compared with SrF_2 *(German)* 80−81355
$Eu_3Fe_5O_{12}$, thermodyn. props. 77−84947
EuTe, high-temperature evaporation and reactivity 80−103469
(Fe, Mn)O_x, thermodynamic characts. deduced from Wustite reaction *(Italian)* 77−48401
Fe, Armco, nitriding charact. at low atmos. press. of NH_3, thermodynamic *(Russian)* 78−15573
Fe base ternary soln., containing interstitials and substitutional solutes, thermodynamic and kinetic props. 78−2297
Fe, cast, unalloyed and alloyed, addition effects on struct., thermodynamics of microsegregation 79−8305
Fe, heat capacity temp. depend. meas., internal energy and entropy, anharmonic theory calcs. *(Russian)* 80−54402
Fe, liquid, N activity coeff. 77−72699
Fe, powder, reduction annealing, thermodynamic anal. 78−60597
Fe-Al alloy, C saturated, at 1873K, activity meas. with Knudsen cell-mass spectrometer 78−39745
Fe-As-Su-Si (Cr)(Mn) melts, As and Sn distrib., Si, Cr, and Mn influence *(Russian)* 80−16274
Fe-bearing binary, substitutional liq. and solid solns., statistical thermodynamics 80−11630
Fe-C, exam. of phase equilbria, at high temp. and pressure 78−52759
Fe-C system, FCC, austenite field thermodynamics, re-anal. 80−89201
Fe-C system, mixing variables, activities and entropies calc., short range order model *(German)* 80−25655
Fe-C-Cr, pearlite reaction kinetics 80−3006
Fe-C-Cr, thermodynamics and phase equilibria near eutectoid temp. 80−3005
Fe-C-Cr(Al), electronic structure, thermodynamics of structure formation 79−99475
Fe-Co-Ni-C, activity coeff. of C at 1273K 80−96667
Fe-Co(Ni)(Cr), liquid, N activity coefficient 77−72699
Fe-Co(Si), determ. of chem. and magnetic interchange energies 77−80925
Fe-Cr, thermodynamics of chlorination *(Russian)* 79−52168
α-Fe-Cr solid soln., thermodynamic activity of components 79−38797
Fe-Cr-Al, thermodynamic predictions in coal gasifier environment 79−38799
Fe-Cr-Ni, thermodynamic prediction in coal gasifier environment 79−43206
Fe-Cr-Ni system, austenitic, energetic particle bombardment, thermodynamic and dimensional stability 77−27904
Fe-Cr-W-C, carbide/austenite equilibria, expt. and thermodynamic study 77−36459
Fe-Cu, thermodynamic analysis of phase relationships 77−73260
Fe-Ga-C melts, thermodynamics and C solubility *(Russian)* 80−39292
Fe-Mn-C, thermodynamic analysis 77−32563
Fe-Mn-S, thermodynamics, activity of FeS-MnS solid soln., 1100 to 1400°C 78−6902
Fe-Mn-S, thermodynamics, solid/liquid phase equilibria, 1100 to 1300°C 79−47663
Fe-Mn-S, thermodynamics, solubility of S and Mn in γ-Fe, 1100 to 1300°C 79−47662
Fe-Mo, ferritic, thermodynamics and solubility of C and ferrite 77−36456
Fe-Mo austenite, thermodynamics of C 77−36457
Fe-Mo system, thermomech. props. 80−89208
Fe-Ni, FCC alloy, magnetovolume instability 79−8031
Fe-Ni, liq. alloy, electrochem. meas. of O, thermodynamic props. at 1873K 80−30244
Fe-Ni, liquid and solid, thermochem. props. 77−59755
Fe-Ni, reference material for determ. of C activity, interaction parameter *(Czech)* 79−42278
Fe-Ni, solid and liquid, determ. of activities for temp. range 1500-1900K, using mass spectroscopy 79−11558
Fe-Ni, thermodynamic props., anomalous 80−39313
Fe-Ni Invar alloy, mag. phase mixing effect on thermodynamic props. 80−54891
Fe-Ni solid soln., thermodynamic study 78−6904
Fe-Ni-C, calc. of activity data, and exam. of phase equilibria 79−10912
Fe-Ni-C alloys, FCC, effect of two gamma states on C activity 78−6897
γ-Fe-Ni-Cr solid soln., thermodynamic activities determ. in Ni rich corner at 1500K 77−32561
Fe-Ni-Ge, liquid alloy, H_2 thermodynamic interaction, solubility *(Russian)* 78−11202
Fe-Ni(Co), liquid, activity meas. by transportation method *(Japanese)* 79−4949
Fe-O system, thermodynamics of viustite-haematite alloy melt *(Russian)* 80−65249
Fe-S phase diagram, thermodynamics 79−56966
Fe-S system, chemical transport of non-stoichiometric phase 79−69972
Fe-Si-C, liquid alloy, activity of Si and C *(Russian)* 78−11203
Fe-Si-C melt, Si and C activity *(Russian)* 77−55364
Fe-Sn, thermodynamic assessment, phase diagram 79−91618
$Fe(CO)_5$, chem. thermodynamics 78−18799

thermodynamic properties continued
$FeCl_3$, matrix isolation Raman spectra, mol. config., thermodynamic props. 78−46346
Fe_2Cl_6, matrix isolation Raman spectra, mol. config., thermodynamic props. 78−46346
FeH, partition function and equilib. const. 77−38626
Fe(II) complexes, high spin-low spin transition, phenomenological thermodynamic model 79−69675
FeO_x, wustite field, thermodynamic props. and subphases, thermogravimetry, 1100-1300°C 80−76239
$Fe_{1-x}O$, thermodynamic props. of wustite phase of iron-oxygen system, review 78−79780
Fe_2O_3-MgO-NiO, solid soln. spinel, activity-comp. relations at 1273K *(French)* 79−100124
Fe_3O_4-Co_3O_4 spinels, phase diagram anal., thermodynamic props. 80−3009
Fe_3O_4-$NiFe_2O_4$, solid soln., activities determ. from EMF of galvanic cell 80−16290
Fe_3O_4-$ZnFe_2O_4$, spinel type solid soln., thermodynamic study by EMF meas. 78−15379
FeS-Cu_2S, FeS-CoS, FeS-Ni_3S_2, melt viscosity 77−51536
$FeSb_2$, heat capacity and thermodynamic props. from 5 to 1021.2K, heat of decomposition 77−90636
Ga, FCC hypothetical struct., stability calcs. 78−18766
Ga-In, liq., O diffusion coeff., thermodynamic activity and solubility 78−38860
Ga-P-Bi(Sb), liquidus isotherms, GaP solubility in Sb, Bi, rel. to epitaxial growth 78−34721
Ga-Pb, liquid alloy, thermodynamic activity determ. using Knudsen method *(German)* 79−34008
GaAs, VPE, partial press. diagrams use for thermodynamic represent. 79−33201
GaAs, VPE, thermodynamic analysis of Si contamination 79−28932
$GaCl_3(I_3)$, gaseous, Raman spectra, struct., Fermi reson. and thermodynamic functions 77−18929
β-$Gd_2(MoO_4)_3$, antiferromag., polarised ferroelec., ferroelastic, magnetothermodynamics 79−7996
Ge-Ga liq. alloys, thermodyn. props. 78−26695
Ge-I_2, equilibrium study 700 to 1300K, vapour transport rate of Ge *(French)* 78−64476
Ge-Si system, solubility of Au, thermodynamic calcs. 79−86890
GeI_x, thermodyn. props. 78−23960
H, solid polarised spin system of H atoms metastable in mag. field 78−30812
H, spin-polarised, Bose-Einstein condensation 80−77698
H, thermodynamic props. and eqns. of state in stellar conditions 79−35241
H-He, metallic solid alloys, phase separation and thermodynamic functions calc. 77−43333
p-H_2, liq., equil. bulk props., perturbation theory approach and quantum effects *(Russian)* 77−89551
H_2, liquid, effect of ortho-para composition *(Russian)* 78−34419
H_2, liquid, perturbation theory and quantum effects, thermodynamic props. and quantum stat. corrections *(Russian)* 78−22867
H_2, metal phase, eqn. of state, thermodynamic pot. *(Hungarian)* 79−14909
H_2, solid, metallic, high density, thermodynamic props. 80−88337
H_2+O_2 fuel, equilib. compositions, 1000 to 6000K *(Ukrainian)* 79−50571
HCl, polar liqs. models, mol. polarisability effect 80−92444
HCl-$CoCl_2$-H_2O, activity coeffs., 298.15K, electrostatic terms effects 79−24812
HF, liquid, Monte Carlo simulations 79−64967
HF, polar liqs. models, mol. polarisability effect 80−92444
H_2O, acoustic relaxation in critical region *(Russian)* 80−92609
H_2O, boiling, on Cu surface, rel. to methanol 78−90654
H_2O, empirical potential model EPEN/2, parameterisation testing 79−54933
H_2O, n-state configurational excitation model, diagnostic thermodynamic props. 80−10481
H_2O-acetic acid, liq. mixture, thermodynamic excess functions, calorimetric meas. 77−52666
H_2O-HNO_x-NO_x clusters, gas phase, thermodynamic quantities, mass spectra obs. 80−50875
H_2O+methanol-d_0(-d_1)(-d_4), D exchange reaction, thermodynamics 78−94328
$(H_2O)_n$, n=8, 64, cluster thermodynamics calcs. using Monte Carlo method 77−58219
He, in HTGRs, accident anal. *(German)* 78−25315
He, liq. and vapour phases, thermodynamic and thermophys. props., HEPROP computer program 80−6529
He, solid, theory and thermodynamic props., book contrib. 77−47646
He, thermodynamic props. and eqns. of state in stellar conditions 79−35241
^{3}He, solid, phenomenological treatment of exchange effects in high-temp. limit 77−35795
^{3}He-^{4}He, dil. soln., grand partition function, ground state energy determ., ^{3}He conc. depend. 80−49455
^{3}He-^{4}He, liq. mixtures, molar volume meas. at pressures up to 100 atm., 1.5-4.2K *(Russian)* 77−35785
^{3}He-^{4}He, superfluid, osmotic and mag. props., review *(French)* 80−10733
^{3}He-^{4}He solutions, superfluid, ^{3}He supercritical states contrib. to thermodynamics *(Russian)* 79−65282
^{3}He-He II degenerate soln., kinetic coefficients, thermodynamic props., hydrodynamic, acoustic and spin wave propag. *(Russian)* 78−18867
^{4}He film, Bose-Einstein condensation, thermodynamic functions 79−82399
^{4}He, liq., quasiparticle model, finite temp. 77−39715
^{4}He, liq., thermodynamic props. at 0.7K, boson system anal. 77−4230
^{4}He, solid, thermodynamic props., Monte Carlo studies 79−65290
^{4}He, superfluid, continuum theory based on classical theory of irreversible processes 80−29236
^{4}He, superfluid, neutron scatt. and thermodynamic quantities, need for more precise data 78−22916
^{4}He, superfluid, quantum lattice gas model, thermodynamic props. 78−59986
^{4}He superfluid, thermodynamic props., review 77−39708
^{4}He, superfluid, thermodynamic props., appl. of theory of temp depend. energy levels 77−59163

thermodynamic properties continued
Hg-In(Tl)-Zn, liquid alloys, thermodynamic props., 25 to 75°C *(German)* 77−73259
Hg-Tl, liq. alloys, struct. from thermodynamic props. *(German)* 77−1066
Hg-U system, thermodynamic props., vap. press. and EMF expts. 79−91625
I_2 electrode, in $RbAg_4I_5$ electrolyte, thermodynamcis and electrochem. behaviour 79−70348
I_2-quinoline (pyridine) complexes, stability const. determ. by spectrophotometric methods 80−87056
$_xI_{1-x}$ mixtures, high-temp. solids and melts, struct., thermodynamic props., Raman spectra obs. 80−66174
In, liquid O_2 activity from electrochemical meas. 80−104123
In-As system, exam. of thermodynamic consistence of models, and QCE approx. for activity coeffs. *(German)* 80−24615
In-As system, p-T-x diagram 77−8801
In-Hg amalgam, EMF meas. of In/$InCl_3$/amalgam cell and thermodynamic quantities 79−33999
In-Hg liquid alloy, activities meas. 77−86351
In-Pb, liquid alloy, thermodynamic activity determ. using Knudsen method *(German)* 79−34008
In-Sb, metallic soln., association 78−15373
In-Sb, thermodynamic quantity meas. by quantitative thermal anal. of heating process 78−19730
In-Zn, liq., Zn activity meas. by Knudsen torsion-effusion method, thermodynamic props. of mixing 79−10950
InAs-InP, phase equilib. and dissoc. 80−35170
InI_x, x=1,2,3, thermodynamic props. 77−40572
InP, epitaxial growth, thermodynamic conditions 77−89661
InP, VPE, thermodynamics of transfer by water vapour 78−43260
InSb-Sn(Pb)(Bi), metallic soln., quasibinary alloy, association 78−15373
In_2Se_3, thermodynamic functions, 55 to 330K 77−24417
K-Cs solution, activity and saturated vapour press. of Cs, reson. line absorpt. obs. 77−51509
$KAlO_2$, phase diagram and thermodynamic props. 79−91985
$KAlSiO_4$, phase diagram and thermodynamic props. 79−91985
KCl, isopiestic studies of aqueous solns., 382 to 474K 79−24815
KCl molten salt, thermodynamic function, Brillouin spectroscopy, hypersonic vel. *(French)* 78−35161
KCl-$CaCl_2$-NaCl, ternary phase diagrams, interactive computer program 80−71629
KCl-KNO_3-H_2O, apparent and partial molal volumes in mixed salt solns. 77−9114
KD_2PO_4 type ferroelecs., distrib. functions and thermodynamic props. 78−76409
KF-$3K_2O.2SiO_2$, activities rel. to liquidus comp. 77−28797
$KO_{0.5}$-$AlO_{1.5}$-SiO_2 system, activities calc. from vapour press. meas. and known data 79−91985
K_2O-SiO_2, vap. press., thermodynamic props. and phase diagram at high temps. 78−83932
K_xO_y, mass spectrometric investigation 78−64873
$KReO_4$, heat capacity and thermodynamic props., 8 to 304K 80−100335
$K_2Si_4O_9$, phase diagram and thermodynamic props. 79−91985
Kr-Ar, mol. interactions, thermodynamic props., mol. dynamics calcs. 77−61044
La-B, phase and thermodynamic props., vaporisation 78−51660
La-Co-O system, stability of ternary phases, nonstoichiometry 80−24434
$LaNi_{5-y}Al_y$ alloys and related hydrides, thermodynamic and struct. props. for H_2 storage appl. 80−16847
$La_xNi_yH_z$, thermokinetics of H evolution 80−30593
Li-LiH liq.-vap. equilib., activity coeff. 80−103468
Li-LiH system, H isotope solubility thermodynamic singularities 80−81356
Li-Mg, liquid alloys, thermodynamic investigation *(German)* 79−91630
Li-ND_3, near liq.-liq. crit. point, conc. fluctuations, neutron diffr. long wavelength thermodynamic limit 79−10948
Li-Si alloys eval. as negative electrodes for Li-FeS_2 cells, thermodynamic props. 77−16547
Li-TiS_2 cell, electrochemical pot. spectroscopy, thermodynamic props. meas. 79−100426
Li_5B_4 form., thermodynamic considerations 79−56959
LiCl-$LiNO_3$-H_2O, mixed salt solutions, apparent and partial molal volumes 77−9114
LiF-AlF_3, mixture at 1293K, thermodynamic function 80−104134
LiF-$Li_2O.SiO_2$, activities rel. to liquidus comp. 77−28797
$LiH_2(LiD_2)(LiT_2)$, pot. surfaces, fundamental freqs. and thermodynamic functions 80−69205
$Li_2H(Li_2D)(Li_2T)$, pot. surfaces, fundamental freqs. and thermodynamic functions 80−69205
Li_2MoO_4, Li_2MoO_7, $Li_2Mo_3O_{10}$ and $Li_2Mo_4O_{13}$ 77−12822
Li_2O-CaF_2 melts, component activities *(Russian)* 77−60104
$Li_{1-x}Pb_x$, liq., metal-nonmetal transition, electronic theory 78−79930
$LiReO_4$, thermodynamic activity in $LiReO_4$-$CsReO_4$ system, mass spectra meas. 80−2174
β-$Li_xV_2O_5$ bronze, thermodynamics of ordering 80−84302
LuS_n, high-temp. vaporisation and thermodynamics 79−73325
Lu_3S_4, high-temp. vaporisation and thermodynamics 79−73325
Mg-Ca(Sr)(Ba), liquid, thermodynamic charact. *(German)* 77−59757
Mg-Cd, thermodynamic props., order-disorder transitions based on Helmholtz free energy 79−37853
$MgCl_2$, isopiestic studies of aqueous solns., 382 to 474K 79−24815
MgF_2-x$MgO.ySiO_2$, activities rel. to liquidus comp. 77−28798
$Mg_yU_{1-y}O_{2+x}$, thermodynamic props., EMF meas. 80−29187
MgZn ferrites and ZnO in MgO solid solns. 77−21116
Mn-(Fe)-Si-C, activity determ. by vapour press. meas. *(Japanese)* 77−63631
Mn-bearing binary substitutional alloy systems, props., applicability of statistical thermodynamic approach 80−88336
Mn-C(Si), activity determ. by vapour press. meas. *(Japanese)* 77−63631
Mn-Cu(Sn), liquid alloys, thermochemistry 79−56962
Mn-Ni(Cu)-S, solubility and activity of S *(Russian)* 77−25012
Mn-S-O system, sulphide-sulphate equil., solid state EMF obs. 79−83492
Mn-Si, liq. thermodynamic props., rel. to alloy form. 77−7875
Mn-Si(C), melt, activation determ. by vapour press. meas. 80−16279
Mn-Zn series, aqueous solutions, equilib. props. struct. 79−61894
α-$MnCl_2.4H_2O$, crossover from divergent to non-divergent nature of paramag. transition 79−73735
MnO-SiO_2 slag, SiO_2 solubility and MnO activity 79−52184

thermodynamic properties continued
MnO_2, activity in CaO-SiO_2-MnO ternary system, Gibbs-Schumann calc. *(Italian)* 79−20461
Mn_3O_4-Co_3O_4 spinels, phase diagram anal., thermodynamic props. 80−3009
Mo cpds., chemical structures, thermodynamic props., reactions 77−77750
Mo, strength and internal friction 77−63711
Mo-alkali earth oxides, multiple phase system calc. of phase equilibria using thermodynamic analysis *(Russian)* 79−56964
Mo-Fe-O-H system, thermodynamic equilib. 78−60657
Mo-N solid solution, thermodynamic props., 1618 to 1883K 80−65230
Mo_2C, free energy of form. and thermodynamic props. of C in solid Mo 80−15266
MoF_6, critical parameters determ. using thermodynamic and mol. similarities 77−43310
MoO_3-MO system, M=alkaline earth metal, eutectic coordinates on phase diag. 77−44227
N_2, liq., simulation of atomic and quadrupole interactions, predictions 77−11457
N_2, liq., thermodynamic props., perturbation theory with hard dumbbell reference system 80−14991
N_2, mol. liquid, mean squared torque and mean squared force, interaction energy spherical harmonic expansion 80−54093
N_2, thermodynamic and transport props., consistent correlation using Lennard-Jones (12-6) and Buckingham (exp-6) pots. 78−91045
N_2+methane, liquid mixture, press. effect on excess thermodynamic functions 78−47494
$ND_4D_2PO_4$ type ferroelecs., distrib. functions and thermodynamic props. 78−76409
NH_3, anal. of data tables 78−93636
NH_3-water system, vapour-liquid equilib., thermodynamics 79−42246
NH_4ReO_4, heat capacity and thermodynamic props., 8 to 304K 80−100335
$N_2O_4 \rightleftharpoons 2NO_2 \rightleftharpoons 2NO+O_2$, working fluid for power-producing thermodynamic cycles 80−13536
$NO_3^-.(HNO_3)_n$ clusters, form. studied by mass spectrometer, thermodynamic functions, sol. struct., 80−95754
$^{15}N_2$, solid struct., and thermodynamic props. *(Russian)* 80−88083
Na, liquid, eqn. of state and thermodynamic props. at high temp. and density 79−55902
Na, monovacancy thermodynamic parameter calcs., temp. dependence 78−2114
Na, thermodynamics of light interstitials, rel. to delocalised particles 79−46653
Na-Cs, liq., struct. factor, free energy of mixing, and electrochem. pot., thermodynamic calc. 80−96436
Na-In, dilute soln., thermodynamic props. 77−89553
Na-K liquid alloys, triplet correlation functions and thermodynamics, solute partial structure factor 80−64881
Na-NH_3, nonmetal-metal transition, thermodynamics 78−18964
Na-Se system, liq., thermodynamic props. 80−21319
$NaAl_2O_4$-$MgAl_2O_4$ spinel solid solns., activities rel. to cation distrib. 77−15377
$2NaBO_2$-B_2O_3 melt, mass spectra 80−65252
NaCl, activation energy for mass transfer, quantum theory calc. *(German)* 79−51031
NaCl, molten salt, thermodynamic function, Brillouin spectroscopy, hypersonic vel. *(French)* 78−35161
NaCl, supersaturated soln., H_2O activity prediction 79−23713
NaCl-KCl, aq. solns., isopiestic studies, 383 to 474K 80−21320
NaCl-$NaNO_3$-H_2O, apparent and partial molal volumes in mixed salt solns. 77−9114
NaF-$3Na_2O.2SiO_2$, activities rel. to liquidus comp. 77−28797
NaF-AlF_3 system, thermodynamics, solid soln. in cryolite 79−52183
Na_xMS_2 (M=Ta,Ti), Na chem. pot. and free energy of intercalation, electrochemical meas. 79−100396
$NaNO_3$-$RbNO_3$-$Pb(NO_3)_2$, crystn. heat of eutectic, thermodynamic anal. *(Russian)* 77−63644
Na_2O-B_2O_3 glass-forming melts, thermodynamic functions 80−25673
Na_2O-B_2O_3-GeO_2 glass-forming melts, thermodynamic props. and vaporisation processes, mass spectrometric study 80−79926
Na_2O-B_2O_3-GeO_2 vitreous melts, thermodynamic props. from mass spectra 80−65253
Na_2O-BaO-SiO_2, metastable two liquid tie line calc. 78−92246
Na_2O-MoO_3, melt, EMF meas., rel. partial molar thermodynamic props. 80−6526
Na_2O-PbO-SiO_2, activity of PbO, EMF meas. 77−47595
Na_2O-PbO-SiO_2, PbO activity 78−44112
Na_2O-SiO_2-Ga_2O_3-Al_2O_3 glasses in mixed $AgNO_3$-$NaNO_3$ melts, ion exchange 80−21282
Na_2SO_4 in aqueous soln., diffusion coeffs. and Onsager-Fuoss theory disagreement 80−40729
Na_2SO_4-$CoSO_4$-H_2O, phase equilib., activities, Pitzer eqn. calcs. *(Russian)* 80−65190
$NaTl_3(SO_3)_2$, heat capacity and thermodynamic functions, 10 to 300K 80−65244
Nb, H_2 embrittlement, microscopic obs. at low temps. 77−32666
Nb, superconducting, thermodynamic props. 80−107955
Nb-H interstitial alloy, props. and synthesis 79−69265
α-Nb-H solid soln., BCC, const. vol. thermodynamic functions 79−61561
Nb-K melts, thermodynamic characts., elec. resistivity, single parameter rigid sphere calcs. *(Russian)* 80−34410
Nb-Ta-O solid soln., thermodynamic props. 78−31386
Nb-V-O solid soln., thermodynamics of O_2 78−68673
Nb_3Ga, thermodynamic and expt. study of CVD 79−24441
Nb_3Ge, amorphous nongranular thin superconducting film, thermodynamic and resistive transitions 80−34571
$NbSe_x$, nonstoichiometric, thermodynamic props. and crystal struct. *(Japanese)* 78−11206
Nb_3Sn, supercond. thermodynamics 79−42693
Ne-H_2 mixture, liquid vapour phase equilib., sound vel., compressibility, thermodynamic perturbation theory obs. *(Russian)* 80−39306
Ni alloy, GAB 286, austenitic energetic particle bombardment, thermodynamic and dimensional stability 77−27904
Ni chemisorption of S on Al_2O_3-supported surface, thermodynamic parameters meas. 80−88424
Ni, heat capacity temp. depend. meas., internal energy and entropy, anharmonic theory calcs. *(Russian)* 80−54402
Ni, liquid, N activity coeff. 77−72699
Ni-Au-Fe alloy, liq., activity of iron at 1573K 77−70328
thermodynamic properties continued
Ni-Co, liquid, activity meas. by transportation method *(Japanese)* 79−4949
Ni-Co-Mo-Al-Cr, melt, effect of Al, Cr on O_2 activity, electrochemical determ. 79−11556
Ni-Cr solid soln., Ni rich, thermodynamic activity of components 79−70043
Ni-Cr(Co)(Fe), liquid, N activity coeff. 77−72699
Ni-Fe alloy, activity of iron at 1573K 77−70328
Ni-Fe-Cu, thermodynamic activities of components in pseudobinary section Ni_3Fe-Cu at 1520K 77−59752
Ni-Ge, liq. alloy, thermodynamic activity, mass spectrometric determ. *(German)* 78−20052
Ni-Nb (5 to 45 at.%) alloys, free energy and thermodynamic props. investigation using EMF method *(Russian)* 79−52160
Ni-S, phase diagram calc. and thermodynamic props. of liq. phase 80−108401
Ni-S, thermodynamics and phase relations 79−47666
Ni-S melt, three-suffix Margules equations with zero ternary interactions 80−19957
Ni-Si liquid alloys, thermodynamic props., enthalpy of mixing *(Russian)* 80−34207
Ni-V, solid soln., diffusion and thermodynamic props. 80−65278
Ni-W-C(Nb) system, γ to (γ+W) phase boundary calcs. using Wigner method *(Russian)* 80−54346
Ni-Zn liquid alloys, Zn activity obs., 1100 to 1300K 78−40072
Ni-Zn melt, Zn activity determ. *(German)* 78−19715
NiO-CuO, equilibrium relations 80−55375
NiTaC-13, directionally solidified eutectic alloy, chem. compatibility with ceramic materials 79−87623
NiZn β- and γ-intermetallic compounds, thermodynamics *(German)* 78−92242
$Np^{4+/3+}$ in fused salts, redox and chem. props. 77−29038
O_2 fugacity of basaltic magmas, role of gas forming elements 78−77218
O_2, solid, struct. elementary excitation spectrum and thermodynamic props. *(Russian)* 79−55696
O_2-N_2, gas mixtures, mass transfer, mag. field effects 78−63535
$Os(CO)_5$, chem. thermodynamics 78−18799
Pb liquid, O_2 activity from electrochem. meas. 80−55695
Pb, liquid, US wave velocity *(Japanese)* 79−60438
Pb melts, As and Sn distrib., Si, Cr, and Mn influence *(Russian)* 80−16274
Pb-Bi, thermodynamic props. 77−59743
Pb-Bi, transpiration method 78−3365
Pb-Bi alloy, vapour press., meas. using transpiration method, thermodynamic props. determ. 78−3365
Pb-Fe(Cu), liq., thermodynamic props. *(Polish)* 80−89199
Pb-Pd, liq. alloy activity by effusion method *(German)* 79−29023
Pb-Sb, liq. alloy, Pb thermodynamic props. *(Czech)* 80−29925
Pb-Sn-Hg amalgam, liq., thermodynamic props. *(Russian)* 77−66624
$PbCl_2$-$ZnCl_2$, thermodynamic quantity meas. by quantitative thermal anal. of heating process 78−19730
PbF_2-x$PbO.ySiO_2$, activities rel. to liquidus comp. 77−28798
$PbHPO_4$-type crystals, ferroelec. transition, statistical model 80−25321
β'PbIn, thermodynamic analysis 77−36455
PbLi, gas phase thermodynamics, Knudsen effusion mass spectrosc. 80−100057
PbO activity in ternary and binary silicates *(Japanese)* 78−6907
PbO, thermodynamic activity in liquid, PbO-$PbCl_2$ 78−7227
PbO-B_2O_3 melt, activity of PbO 77−11708
PbO-B_2O_3-$Li_2O(Na_2O)(K_2O)$ melt, activity of PbO 77−11708
PbO-Bi_2O_3, thermodynamic props. 77−59743
PbO-PbF_2 melt, thermodynamic study of solid-oxide galvanic cell 79−96013
PbO-SiO_2, molten, activity of PbO, effect of CaO, Al_2O_3, MgO and ZnO 78−60663
PbO-SiO_2 melt, behavior of MgO and NiO *(Japanese)* 79−52746
PbS, heat of entropy of fusion 77−72701
PbTe-PbSe system, thermodynamic props. 80−11635
$Pb(Zr,Ti)O_3$, absolute and relative vapour pressures, thermodynamic formation data 80−29939
Pd-Al alloys, Fermi level position rel. to mixing behaviour, Al activity, thermodynamic props. *(German)* 78−75835
Pd-Au:$H_2(D_2)$, thermodynamic props. at 555 and 700K, vibr. freqs. and excess entropies 80−29186
Pd-H, dil. soln., partial molar props., temp. depend. 78−68910
Pd-H and Pd alloy-H systems, review of props., book contrib. 80−24605
Pd-H system, thermodynamic aspects of atomic vibr. 78−59913
Pd-H system, thermodynamic props., 245-352°C, up to 34 atm. 79−23749
Pd-H_2, dilute soln., high temp. thermodynamics, partial molar props. 77−15597
Pd-In alloys, thermodynamic props., 800 to 1000°C 79−20454
Pd-noble metal solid solns., with dissolved H, thermodynamic props. 80−108402
Pd-Te liquid alloys, thermodynamic activities *(German)* 79−29022
Pd-Th, thermodynamic stability 79−55903
Pd-Ti liquid alloy, mass spectrometric study of high temp. thermodynamic stability 78−15369
Pd-Zr alloy, activity coeff. rel. to electronic props. *(German)* 77−20084
Pr-Al liquid alloys, atomic interactions, thermodynamic props. *(Russian)* 80−39307
Pt-Al(In)(Sn) alloys, Fermi energy influence on thermodynamic props. *(German)* 80−24619
Pt-Au, miscibility gap, thermodynamic anal. *(German)* 79−91629
Pt-Cd, thermodynamic props. 79−43207
Pt-Sn alloys, thermodynamic props. *(German)* 78−52769
Pt-Zr alloy, activity coeffs. rel. to electronic props. *(German)* 77−20084
Pt-Zr(Hf), high temp. thermodynamic props. 77−63633
β-PtZn nonstoichiometric Ll_0 phase, thermodynamic activity of Zn 77−90320
Pu and other actinides, conf., Baden-Baden, Germany (Sept. 1975) 77−19807
$Pu^{4+/3+}$ in fused salts, redox and chem. props. 77−29038
Pu-O system, substoichiometric phase range obs., high temp. thermodynamic parameters 77−21125
$PuFe_2(Os_2)(Ru_2)$ Laves phase cpds., stability correl. with unalloyed atomic radius ratio 77−20092
PuN, fabrication, high-temp. thermodynamic and transport props. 77−28774
PuO_2 nuclear fuel, eqn. of state and thermodynamic props. 80−13592

thermodynamic properties continued
PuO_2, substoichiometric, unified model for defects, thermodynamic functions 77−20094
rare earth oxide-Nb_2O_5 system, phase formation thermodynamics 77−86348
Rb, absolute zero isotherms and polymorphic transition 79−73310
$Ru(CO)_{5(g)}$, chem. thermodynamics 78−18799
Ru_4O_{16} clusters, thermodynamic props., exchange interactions effects 79−24180
S_8 rings, vibr. spectra and thermodynamic functions *(German)* 78−82742
S_n, (n=2-12), vibr. spectra and thermodynamic functions *(German)* 78−82742
SF_6, critical parameters determ. using thermodynamic and mol. similarities 77−43310
SF_6, equilibrium composition calc., in 20000 to 50000K range, in dependence on pressure 79−14511
SF_6 plasma thermodynamic props. at arc extinction temp. and pressures 80−79435
SF_4O, vibr. spectra, struct. and thermodynamic props. 77−63416
$S_{12}(S_{12}.CS_2)$, vibr. spectra and thermodynamic functions *(German)* 78−82742
Sb, liquid, diffusion of O_2, activity coeff. 80−65267
Sb, liquid, O_2 activity from electrochem. meas. 80−55695
ScI_3, mass spectra and vapour press., and thermochemistry for dimerisation 78−27809
ScI_3, vaporisation thermodynamics, sublimation and formation 80−54366
Sc_2O_3, reduction in Li vapour, 1800-2500K, thermodynamics 77−90595
Se-Tl(Bi)(Sb), liquid alloys, vapour phase effect on activity determ. *(German)* 79−43210
SeS gas, thermodynamic props., quadrupole mass filter study 80−16716
Si material processing, point defect thermodynamics 78−6054
Si:H, amorphous hydrogenated film, decomp. kinetics 79−100342
Si-Ge-Br, heterogeneous system, equilib. gas phase composition, Si-Ge cryst. growth appl. 79−10820
SiC:Be, gas-phase equilib. comp., thermodynamic analysis rel. to cryst. growth and doping 77−85909
SiC-H_2 system, thermodynamic analysis 77−86347
$SiCl_4$ physical and thermodynamic properties, rel. to Si technology 79−65218
Si_3N_4, and sp. ht. 77−80629
SiO_2-Al_2O_3, calculated thermodynamic data and metastable immiscibility 78−27495
SiO_2-K_2O, thermodynamic approach to ionic conds., statistical model of chem. potential 79−46833
SiO_2-water system, inorg. polymer struct. form., globular crystn. 80−101042
Si_2ON_2, and sp. ht. 77−80629
SiX_n radical, (X=H,D; n=1,2,3), thermodynamic function in ideal gas state 80−14871
Sn, liquid, US wave velocity *(Japanese)* 79−60438
Sn-Ag liquid alloys, thermodynamic study by solid-oxide galvanic cell 79−20031
Sn-Ge(Au), liquid alloy, exam. of activity and heat of mixing, using mass spectrometry 78−51706
Sn-Pb, liquid alloy, thermodynamic activity determ. using Knudsen method *(German)* 79−34008
Sn-Sb molten alloys, thermodynamic study *(Korean)* 78−31383
Sn-Zn, thermodynamic quantity meas. by quantitative thermal anal. of heating process 78−19730
SnO_2 film, deposition from vapour phase, thermodynamic anal. 80−15418
$SnSe_2$, rel. to p-T projection of phase diag. of SnSe-Se 78−27485
Sr, specific heat and thermodynamic props. 5-350K 78−47534
SrF_2, vaporisation and sublimation thermodynamics *(German)* 80−81355
$SrSO_4$, activation energies for mass transfer during crystallisation, surface active agent effects *(German)* 78−63689
$SrTiO_3$, thermodynamic props. 77−39680
Ta-D system, thermodynamic stability of Ta_2D, rel. to long-range order parameters *(Japanese)* 78−15376
Ta-Nb(Re)(W) (50,20,0 at.%), with N_2, spectral emissivity, N_2 absorption rate, N_2 solubility, thermodynamic data *(German)* 77−25026
Ta-Nb(W)(Re), kinetics and thermodynamics of reaction with N_2 *(German)* 79−74415
Te alloy, intermetallic, melting entropy and molar specific heat 79−29024
Te, atomisation energy, mass spectrometric determ. 79−70361
Te rich ternary chalcogenides, glass transition temp. predictions 78−38823
Te-In system, enthalpies of fusion, peritectic decomp. and allotropic transition, DTA *(French)* 80−76226
Te-Tl, thermodynamic investigation, equilibrium diagram calc. 79−34007
Te-Tl system, thermodynamic investigation, enthalpy of form. at elev. temps. 78−52774
TeO_2-NaCl(-NaBr), condition diagram, thermographic obs. *(Russian)* 80−55377
Th-Mo(Re), high temp. phase diagram, thermodynamic props. of refractory metal solutes in liquid Th 77−25022
Th-Pb, liquid alloy, thermodynamic props. *(Russian)* 77−25011
Th-U(Pu) fast breeder fuels, chemical, thermodynamic and selected transport props. 79−54505
$ThCl_4$, in LiCl-KCl and Na-K eutectic solns., thermodynamic props. 77−86345
ThO_2-UO_2 solid solns., props. of importance for use as nuclear fuels 79−54506
Ti-Ir system, high temp. thermodynamic investig. of Ir-rich portion by Knudsen cell mass spectrometry 77−12595
Ti-Mo-Al, determ. of interaction parameters from EPMA data 77−63635
α-Ti-O solid soln., hexagonal, thermodynamics 78−3098
$TiCl_3$ reduction to Ti by Mg, thermodynamics and heat physics *(Russian)* 78−15331
TiCo-H system, thermodynamic rels. and struct. transformations 80−49385
TiNi-H system, thermodynamic rels. and struct. transformations 80−49385
TiO, high temp. thermodynamics, vaporisation, and pressures over 80−10685
TiO, high temp. vaporisation and thermodynamics, stoichiometry, mass spectra 77−59109
TiO, high temp. vaporisation and thermodynamics, vapour press. temp. coeff. 77−59110
TiO_2-Ti-Cl_2 system, thermodynamic analysis, gas phase equilibrium composition 80−21317
TiO_{2-x}, nonstoichiometric and Nb_2O_5 doped rutile, defect struct. and thermodynamic props. 79−86790
TiO_{2-x}, nonstoichiometric and Nb_2O_5 doped, defect struct. and thermodynamic props. 79−90650
TiS_2-I_2 system, thermodynamic considerations for layered dichalcogenide growth by vapour transport process 79−4903
Tl halide dimers, kinetic consts. method for vibr. analysis 79−26968
Tl, liquid, O_2 activity from electrochemical meas. 80−104123
Tl-Pb-Hg system, thermodynamic props. *(Russian)* 77−25018
Tl-Sn-Bi, liquid alloy, thermodynamic props. *(Russian)* 79−10968
TlCl-Tl_2S system, molten, thermodynamic analysis of phase diagram 79−29031
Tl_3PO_4, heat capacity and thermodynamic functions, 5 to 320K 80−65245
(U,Pu)C, nuclear fuel, porosity and stability obs. 78−86629
(U,Pu)CN, nuclear fuel, porosity and stability obs. 78−86629
(U,Pu)N, nuclear fuel, porosity and stability obs. 78−86629
$(U,Pu)O_2$, hyperstoichiometric, oxygen potentials determ., 1500-1850K 77−20095
$(U,Pu)O_2$, substoichiometric, unified model for defects, thermodynamic functions 77−20094
$U^{4+/3+}$ in fused salts, redox and chem. props. 77−29038
U-H system, phase diagram and thermodynamic parameters 77−21124
U-Mo(Re), high temp. phase diagram, thermodynamic props. of refractory metal solutes in liquid U 77−25022
U-Pu-C system, segregation and v.p. obs. 77−28793
U-Pu-O system, substoichiometric phase range obs., high temp. thermodynamic parameters 77−21125
UC_x, x=1 to 2, high temp. thermodynamic props. 79−60524
UF_6, critical parameters determ. using thermodynamic and mol. similarities 77−43310
UFe_2, thermodynamic props., agreement with Campbell correlation of laves phase compounds 78−15370
UN, HTR fuel, X-ray phase anal. of thermodynamic stability 79−59165
UO_2 fuel rod, Zircaloy clad, chemical activity determ. of fission product 79−49682
UO_2 nuclear fuel eqn. of state and thermodynamic props. 80−13592
UO_2 phase, thermodynamic props. 80−13594
UO_2, thermodynamics, defect props. 77−67810
UO_2 vapour, saturated, thermodynamic state and gas kinetic relaxation to 5000K 80−13593
$UO_2^{2+}{}_{(aq)}+UO_2NO_3^{+}{}_{(aq)}$, ground and excited state interaction, struct., thermodynamic functions, photochemistry obs. 80−32779
$(U_{1-y}P_y)O_{2-x}$, thermodynamics 78−70594
$(U_{1-y}Pu_y)O_{2-x}$, thermodynamics 78−70593
$U_xPu_{1-x}O_2$, theoretical study of electronic thermodynamic and valence props. 79−37655
URu_3, sublimation thermodynamics 80−97722
V, electro- and thermotransport of O and N 77−28040
V-based ternary solutions, containing H, thermodynamics 80−19961
V-O solid soln., BCC, modelling of interstitial solute behaviour 79−77748
V-O solid solutions, solubility and thermodynamic props. 77−7866
V-O system, chemical transport of non-stoichiometric phase 79−69972
V-W-O system, phase diagram and thermodynamic props. at high temps., in region W-WO_2-VO_2-V_2O_3 80−104133
$VCl_4(Br_4)$, vibronic systems, degenerate ground states, statistical sums, thermodynamic func. calcs. 80−27997
V_2O_5-$AlNbO_4(GaNbO_4)(TiNb_2O_7)$ systems, interfacial reactions, efficient boundary conditions and solid state reactivity 80−76542
V_2O_{5-x}, O_2 equilib. press. above oxide system, thermodynamic props. 79−16029
VS through V_3S_4, nonstoichiometric, phase relations and thermodynamics 80−29188
V_3Si, normal, mixed and supercond. state, specific heat meas., thermodynamic and superconducting props. 80−49987
W, containerless melts in terrestrial and space environment, thermodynamic props. calc. from solidification and cooling curves 79−70052
W-alkali earth oxides, multiple phase systems, calc. of phase equilibria, using thermodynamic analysis *(Russian)* 79−56964
W-O system, surface elect. cond. of oxides in equilib. with gas phase 79−61791
WF_6, critical parameters determ. using thermodynamic and mol. similarities 77−43310
WO_2+NF_3, reaction product thermodynamic stability *(German)* 79−8449
XY_4Z molecules, assignment of fundamentals of vibr. spectra for 24 mol. with C_{4v} symmetry *(French)* 79−31504
Xe, modified equation of state, 161.36 to 800K and 0 to 350 MPa 77−51468
Xe, solid, elastic consts., thermodynamic props., Monte Carlo simulation 77−62575
Xe-Ar, mol. interactions, thermodynamic props., mol. dynamics calcs. 77−61044
XeO_2F_2, mean amplitudes of vibr. and molar thermodynamic functions 78−17649
Y-Fe-O, phase equilib. and thermodynamics, solid state high temp. electrochem. obs. 79−56967
$Y_3Fe_{5-z}Al_zO_{12}$, mixed garnet, cation distrib., temp. depend., magnetisation study 80−79831
$Y_3Fe_{5-z}Ga_zO_{12}$, mixed garnet, cation distrib., temp. depend., magnetisation study 80−79831
YbO, Yb_3O_4, form. at high press. from Yb+Yb_2O_3 78−85192
YbTe, high-temperature evaporation and reactivity 80−103469
Zn, liquid, US wave velocity *(Japanese)* 79−60438
Zn-Ca, liquid alloy, exam. of thermodynamic props., using EMF method *(Russian)* 79−34003
Zn-Cd liquid alloy, activity meas. by transportation method *(Japanese)* 78−35358
Zn-Ga liquid soln., thermodynamic props. determ., invariant method appl. 77−59742
Zn-In-Cd soln., liquid, thermodynamic props. 79−83176
Zn-In(Bi) interfacial tension and microstruct. 79−74132

thermodynamic properties continued
Zn-Sn-Bi, ternary phase diagrams, interactive computer program 80−71629
Zn-Sn-Hg amalgam, liq., thermodynamic props. *(Russian)* 77−66624
Zn-Y alloys, thermodynamic props. *(Russian)* 79−70041
$ZnCl_2$ in methanol-water mixtures, thermodynamic props. from EMF meas. 79−52735
$ZnCl_2$-LiCl(NaCl)(KCl)(CsCl), molten, density meas. *(Japanese)* 79−19383
$ZnCl_2$-LiCl(NaCl)(KCl)(CsCl), molten, US velocity, thermodynamic quantities and struct. *(Japanese)* 80−88270
$Zn(ClO_4)_2$, thermodynamic irreversible parameters, Onsager reciprocal relationship verification 79−47960
$ZnCl_2$; thermodynamic irreversible parameters, Onsager reciprocal relationship verification 79−47961
$ZnGa_2S_4(Se_4)(Te_4)$, thermodynamic parameters calc. using low temp. sp. ht. values 77−35705
$ZnGeP_2$ dissoc. press., vapour comp. and press., thermodynamic characts. 77−24934
ZnO single crysts. with stoichiometry deviations, intrinsic defects, thermodynamic analysis 79−42485
ZnP_2, sublimation 80−34181
Zn_3P_2, Zn_3As_2, sp. ht., thermodyn. props. 78−22863
$Zn_3(PS_4)_2$, synthesis, structural and thermodynamic props. 77−24304
ZnSe:Ag(In)(Cu), melt growth, dopant partition coeffs. 79−14837
ZnX_2, ZnXY, X and Y=halogen, matrix isolation IR and Raman spectra 78−55171
ZrN, thermodynamic props. of vacancies 77−11539

thermodynamics
see also atmospheric thermodynamics; critical phenomena; entropy; equations of state; Joule-Thomson effect; statistical mechanics
ϕ^4 lattice field theory, d-dimens., thermodynamic props. near Ising limit 80−82860
absolute temperature, a definition combining the classical method and Caratheodory's 79−49186
absolute temperature measurement, thermodynamic method, using maximum entropy of electronic multiplets 77−74396
absolute zero, vanishing of specific heat without invoking 3rd law, objections 80−8940
acceleration through random classical radiation, thermal effects 80−73191
activation of kinetic processes in condensed media 77−55368
activities on boundaries of two-phase region in ternary systems 79−34349
adsorbed layers, two dimensional incommensurate crystal theory, thermodynamics *(Russian)* 80−49524
adsorbed layers near λ-transition, thermodynamic relns. of Pippards type for dielectric and mag. props. 78−79881
adsorption, grand partition function and adsorption isotherm, statistical mech. calcs. 77−69162
adsorption, localised, on homogeneous solid surface, Berezin-Kiselev model 80−10780
adsorption and Gibbsian distance parameters in 2- and 3-phase systems 78−10282
adsorption excess quantities, comprehensive treatment 78−10281
adsorption isotherm shape, mol. theory 79−90867
adsorption of gas-mixtures on heterogeneous surfaces, stat. thermodyn. of localized monolayer adsorpt. 78−2371
adsorption on solid surface, surface stress and tension at gas-solid interface 79−60627
adsorption one-dimensional lattice model, thermodynamic functions calc., matrix method 79−37917
adsorption phenomena, thermodynamic theory 80−93794
air cooling cycle, expt. determ. of efficiency *(Russian)* 79−59917
aircraft jet noise reduction test facility 77−11096
alcohol-active soln., assoc. soln. thermodynamics, H^E, V^E curves 78−31671
n-alkane binary mixtures, infinite dilution activity coeffs. 78−15695
alloy, FCC closed packed, ordering-type transitions 80−2140
alloys, interstitial solid solns., HCP, ordering type transitions within thermodynamics theory framework 80−49162
ammonolysis of $AlCl_3$, thermodynamics of preparation of AlN 77−8758
amorphous Heisenberg and Ising chains, thermodynamics 80−108022
analogy with mechanics, symplectic struct. 79−71174
anharmonic oscillator, statistical thermodynamics 77−13724
aniline+cyclohexane critical mixture, gravity-induced concentration gradients 77−28004
anisotropic dissipative medium, σ-ε bond determ., scalar product maximum appl. *(Russian)* 79−12596
anisotropic micropolar fluid theory 80−31515
anisotropic simple materials, transport coeffs., reciprocal relations 77−72708
anisotropic spheres, adiabatic contraction in general relativity 80−36489
anisotropic viscoelastic ageing materials, linear irreversible thermodynamics and phenomenological consts. 77−14922
arbitrarily slow irreversibility, example 78−70083
arc electrode processes *(Russian)* 77−27755
arithmetic and geometric mean inequality, thermodynamic proof 78−73952
atomic statistical model thermodynamics in strong mag. field, pulsar crust condensed matter 79−2741
atomic system, two-level, collective behaviour in external field, thermodynamics 80−86236
autocatalytic reactions, symmetry breaking, spatial struct. striation theory 77−12778
axiomatic thermodynamics of open systems 79−12745
Ba-Mg, liq. alloys, thermodynamic activities determ. 80−50604
BBGKY system, irreversibility, velocity correlations and non-Hamiltonian dynamics 80−77686
Belusov-Zhabotinski reaction, nonlinear effects 80−3302
bifurcation and nonequilibrium phase transitions of limit cycles and multiperiodic flows in continuous media 78−81937
binary alloy freezing, non-equilibrium thermodynamic processes 80−34167
binary boson mixtures, thermodynamics ground state 79−35630
binary gas mixtures, excess pots., calc. method 78−45587
binary microcluster, struct. and thermodynamics, Monte Carlo simulation 79−7736
binary mixtures near critical state, gravitational distrib. of thermodynamic props. *(Russian)* 80−88241

thermodynamics continued
binary solutions of dense liquids and gases, isothermal eqn. of state calcs. *(Russian)* 80−88292
biochemical systems stability anal., practical guide 78−73135
biological longitudinal transport, electroosmotic model 80−45870
biological membranes, active transport, variational-Lagrangian thermodynamic theory 78−41255
biology, active transport rel. to second law of thermodynamics 77−9178
biomaterial growth phenomena and behaviour, math. theory 77−81458
black hole, quantum gravitational fluctuations, energy dissipation mechanism 78−57572
black hole, thermodynamic theory, phase transition, specific heat, stability criteria 77−33548
black hole+heat bath, thermal equilib. possibility, thermal Green functions 78−12275
black hole thermodynamics, second order phase transitions 80−46897
black hole thermodynamics and entropy 80−4613
black hole thermodynamics and time asymmetry 77−2451
black holes, irreverisble thermodynamics, fluctuation-dissipation theorem 77−60791
black holes, quantum processes, especially Hawking thermodynamic emission process 78−12284
black holes, thermodynamic mechanisms, review 78−93301
black holes, thermodynamics and space-time distortion 78−8041
black planet, surface Carnot interaction 80−85877
black-hole thermodynamics, general review 80−31696
blackbody cavities, directional emissivity calc., Monte Carlo method 80−83729
blackbody radiation between parallel plates, coherence props. 79−85107
Boltzmann H-theorem for gases in thermostat *(Russian)* 77−17927
bone functional adaptation model and thermodynamic consideration *(Japanese)* 78−7316
book, concepts and logic of classical thermodynamics, theory of heat engines 78−81938
book, fundamentals of classical thermodynamics 77−61046
book, statistical mechanics and foundations of thermodynamics 79−97294
Bose, imperfect gas, condensed state, limit Gibbs state 80−52124
Bose gas, weakly interacting in restricted geometries, low-temp. thermodynamics 80−34261
Bose-Einstein condensate dynamics, two-fluid hydrodynamics, Mori theory 77−28061
Bose-Einstein condensation of a relativistic gas in d dimensions 80−8902
Bose-Einstein ideal gas, review 77−87692
boson gas, interacting, approx. equilib. states 80−46962
boson quantum thermodynamical system in one space dimension, high-order perturbation expansion 80−4636
boundary conditions, spherical, for computer experiment 80−105597
Brusselator, two-box model, multiple stable steady states, chem. hysteresis 79−100428
C_p/C_v resonance apparatus for physics teaching laboratory 79−84885
canonical invariantly relaxing systems, props. 77−22505
capillarity, van der Waals' thermodynamic theory under hypothesis of continuous variation of density 79−56043
Caratheodory's integrating factor choice, for teaching 78−41110
carbide solid solns. decomposition temp. expression 80−55398
cardiac chemical power, derivation of chem. power eqn. and determ. of eqn. consts. 80−16911
cardiac work, anal. using general energy equation of thermodynamics 78−20207
Carnot's contributions to classical thermodynamics *(Czech)* 77−32
Carnot cycle, efficiency and irreversibility *(Spanish)* 80−176
Carnot cycle, systematics at positive and negative Kelvin temps. 80−42178
cast iron-steel mixture, interaction of Zr, formation reaction thermodynamics *(Russian)* 80−55645
chain molecular amorphous solids, stat. thermodynamics and mol. theory 78−26442
chain subduction criterion, continuous phase transform, Landau thermodynamic methods 80−62606
charge fluctuations in classical Coulomb systems 80−95027
charged black holes, phase transitions 77−74079
charged hard sphere fluid mixture, mean spherical approx., analytic soln., multicomponent plasma case 79−85057
chemical, consistency between kinetics and thermodynamics 77−44460
chemical, symbols and terminology 80−3296
chemical change kinetics, steady state approximation, validity 79−83439
chemical discontinuous systems, general inequality for irreversible processes 80−55676
chemical equilibrium, entropy differences and statistical effects, symmetry corrections and entropy of mixing 79−21480
for chemical equilibrium calcs., review for teachers 77−26108
chemical kinetics, connection to chemical thermodynamics *(Chinese)* 79−96352
chemical laser, mol. constraints implied by kinetic coupling schemes, maximal work 80−38010
chemical potential, computer simulation 78−31683
chemical potential and activity coeff., compositional depend., effect of const. press. or vol. conditions 77−63944
chemical power, appl. of power, work and efficiency eqns. to left ventricular energetics in man 80−16912
chemical reaction, Eckart barrier tunnelling, Arrhenium plot curvature 80−3298
chemical reaction system, nonequilibrium thermodynamics, stochastic approach 79−52749
chemical reactions, fluctuations, irreversible thermodynamics 77−52616
chemical reactions, nascent products, vibr. state distrib., statistical thermodynamics calcs. 77−5782
chemical reactions, phenomenological relations, linear network thermodynamics 78−95905
chemical system far from equilibrium, bifurcation and stability 77−73461
chemical thermodynamic equilibrium in strong elec. field, and field chem. consequences 78−7224
chemical thermodynamics, pseudothermodynamic activation parameters, empirical extended Arrhenius eqn. calcs. 78−85127
chemically assisted fracture, general reaction rate theory and thermodynamics 80−64465
chemically coupled equilibria, thermodynamic theory of solvent-jump relax. method 79−39186
chemically reacting fluid mixtures, phenomenological theory 79−1268

thermodynamics continued
chemically reacting nonequilibrium turbulent shear flow, prediction model *(German)* 79−18973
chemically reacting system, thermodynamic perturbation theory 77−70325
chemically reacting systems, sound wave attenuation, thermodynamic interpretation 80−43505
chemodynamics, far from equilibrium 77−32820
chemostress effect in ionic crysts. and metals 79−28193
classical equilibrium statistical mechanics, mathematical struct., book 79−26017
classical ferromagnet systems, partition functions zeros, correl. inequalities 78−27008
classical fluids, thermodynamic behaviour near crit. point, book contrib. 79−60479
classical thermodynamical fluid n-dimensional reductive perturbation method *(French)* 79−44891
Clausius' inequality, formulation using nonequilib. temp. 80−180
cluster expansion in statistical mechanics, S-matrix formulation *(German)* 78−41256
cluster expansion of partition function of Ising model 78−49759
coal conversion reactor environments, simulation 80−100831
coexistence of liquid and vapour, thermodynamic considerations, Van de Waals equation 79−35651
coexisting phases, interfacial profile near tricrit. points 80−19906
coexisting thermodynamic phase interface, Ginzburg-Landau-Wilson model, drumhead model derivation in low temp. limit 80−42180
cohomology of action differential forms 77−33832
collapsing shell, Schwarzschild-de Sitter space-time, thermodynamics and radiation 80−17607
collective open chemical systems, variational-Lagrangian thermodynamics of evolution 78−41255
colligative properties of simple solns. 77−21466
colloidal capillary-porous body, mass transfer parameters, adsorpt., osmotic moisture 78−11563
commensurability in one dimension at nonzero T 79−35655
complex solids, energy-momentum tensor, nonequilibrium relativistic dynamic eqns. *(Russian)* 80−57236
composite system approach to thermodynamic stability 79−12752
compressed gas, radial distrib. function hard sphere model 80−69961
compressible flow, steady, thermodynamic consistency, finite difference scheme 80−48732
compression of gas, fundamentals review 77−39390
condensers, parallel flat plate, thermodynamic anal. 79−6070
condensing systems, generalised theory 79−35653
conditional equilibrium and the equivalence of microcanonical and grand-canonical ensembles in the thermodynamic limit 78−93596
conductors, rigid, thermodynamic anal., hyperbolic heat conduction eqn. 80−64334
conference on nonlinear nonequilibrium statistical mechanics, Kyoto, Japan, (Jul. 78) 79−75441
conservation laws, convex extensions and Cauchy problem 77−17933
constitutive eqns. for ideal gas mixtures and solutions 77−33964
contact transformations and brackets in classical thermodynamics 80−95048
continuous elastic solids, foundations for coupled thermoelasticity 80−46807
continuous media, intrinsic parameters schematising shape and stress, Lagrangian formulation *(French)* 80−73173
continuous one-dimensional many-component Gibbs system with regular two-body interaction pot., transfer matrix 78−8342
continuous quantum systems, variational principle for pressure, entropy, free energy, convexity consequences 79−40453
continuum, interrelation between time rates of temp. and deformation 79−63179
continuum thermodynamics, entropy and hidden variables 77−33963
continuum thermodynamics, existence of single temp., heat and entropy flux 77−13729
continuum thermodynamics, functional form of eqns. 78−29075
continuum thermodynamics, objection to entropy as primitive concept 78−12659
continuum thermodynamics, subbodies additivity, flux props. 78−49783
continuum thermodynamics and nature of second law 77−79044
correlation function construction using generating functional *(Russian)* 77−41555
correlation function derivatives, averaged over equilib. grand canonical ensemble 78−32780
cosmological event horizons, thermodynamic quantities and props. 79−97113
Coulomb systems, thermodynamic function calc. in grand canonical ensemble calc. 77−35315
Coulomb systems and plasmas, nearest-neighbour approx. 77−41559
coupled heat and mass transfer, stability, inertial wave effects calcs. 80−105593
crack growth, quasistatic, nonlocal model, thermodynamics of irreversible processes basis 78−83324
critical molar volumes, empirical calc. method 77−21405
critical point hydrodynamics 78−59361
critical region fluctuations, Ginzburg-Landau systems *(Russian)* 79−75484
critical scattering theory, book 79−25913
critical thermodynamics, phase transition in transverse field with deform. depend., phonon anomaly separation 80−39258
cryogenic apparatus, Linde cycle, max. efficiency determ. *(Russian)* 77−17984
cryogenic He cycles, minimal losses due to thermodynamic irreversibility 80−86320
cryogenic refrigeration system, computer design and optimisation 79−71457
crystal growth, macroscopic equilib. and transport concepts, book 80−27054
crystal lattice stability and deform. phase transitions under press. 80−59624
crystal melting and glasses, dislocation theory 79−99298
crystal thermodynamics in statistical theory, density Fourier coeffs., stress tenser, internal energy 80−13025
crystallisation, activation energies of mass transfer at phase boundaries, quantum theoret. calcs. *(German)* 78−67671
crystallisation, activation energies of mass transfer at phase boundaries, quantum theoret. calcs. *(German)* 78−67673

thermodynamics continued
crystals, velocity autocorrelation function, long-time correlation tails 80−24541
crystals with dislocations, phase transitions of the second kind, dislocation superparamagnetism *(Russian)* 80−1957
Cu-Mn alloys, thermodynamics, suitability as electrodes 79−66339
cyanoacetylene, and isotopic forms, $^{13}C/^{12}C$ effects on partition function 79−29352
cycle operating between positive and negative absolute temps. *(Chinese)* 80−62610
cycling zone adsorption, travelling wave, continuous flow equilib. staged model 78−64874
cylindrical gas system, rotating and self gravitating, thermodynamic instability 80−82191
Davies model of heat cond., entropy prod. in open quantum systems 79−88899
dense fluids, kinetic theory, entropy abalance eqn. and irreversible thermodynamics 79−94758
diatomic molecules, binary mixture, thermodynamic description of vibr. relax. 77−34724
diatomic molecules, vibr. excited, in inert matrix, information theoretic anal. 78−91386
Dicke Hamiltonian, spin-spin interaction on super-radiant phase transition 78−16762
Dicke maser model-van der Waals spin system thermodynamic equivalence 80−83572
Dicke-maser model dynamics, phase transition to the spontaneous coherent state 78−66792
Dicke-type Hamiltonians with hidden variables 78−74874
dielectric fluid near critical point, effect of elec. field *(Russian)* 77−62647
dielectric negative static permittivity possibility *(Russian)* 80−50253
differential geometrical methods in phenomenological thermodynamics 78−45471
differential type media with internal variables, thermodynamic theory 80−99923
diffusing mixtures of continua, constitutive eqns. for fluid-fluid and solid-fluid mixtures 79−88898
diffusion limited and enzyme reactions, thermodynamics of chemical relaxation 79−43619
diffusion potential, concept. rel. to Maxwell's eqns. and irreversible thermodynamics 79−63171
diffusion thermodynamic coefficients in electrolyte in presence of mag. induction *(French)* 77−51533
diffusion with wave fronts, definition *(French)* 77−67386
dilute binary alloy monocrystal, thermodynamics of growth, model *(French)* 78−87635
diluted black body radiation, conversion thermodynamics 79−40507
dimensionless entropies, simplification of thermodynamic calcs. 80−13019
2,6-diphenyl-1,4-benzoquinone+aromatic amine, triplet exciplex quenching, H-transfer mechanism 79−79228
dipole relaxation in electric field, teaching 80−90625
discontinuity surface, nonequilib. thermodynamics, appl. to n-component viscoelastic mixture 78−93638
discontinuity surface model, balance eqn. and phase transition 78−73850
discrete systems, fundamentals of dissipation inequalities 80−27251
disequilibrium system, potential work, statistical mech. calcs. 77−5782
disequilibrium theory applied to two-spin Glauber model 80−31669
dislocations, thermodynamics and thermal activation, book contrib. 80−107241
dissipation inequality fundamentals, field formulation, continuous systems case 80−36960
dissipative dynamical systems of macroscopic phys., common formal struct. of kinetic theory, fluid mechs., nonequilibrium thermodynamics 79−140
dissipative flux and Onsager-Machlup function fluctuations 80−76544
dissipative processes, nonlinear theory *(Russian)* 79−30400
dissipative structures, non-equilibrium systems, self organisation *(Chinese)* 80−42168
dissipative structures, origins and perspectives *(French)* 80−151
dissipative structures in chemical systems, nonlinear effects 80−3302
dissipative systems, dynamical field theory, hierarchical struct. of field thermodynamics 78−73132
dissipative systems, stationary strata, nonlinear theory *(Russian)* 78−57884
dissipative systems with a Liapounov function, quantum rules 78−89611
distribution functions, high order, truncation procedure, compatibility problem 80−47004
distribution functions and Green functions *(Russian)* 78−65890
DNA, helix-coil transition, thermodynamics 79−11883
DNA-type macromolecule, melting, low mol. wt. impurity effect 80−12050
dolomite, $CaMg(CO_3)_2$, kinetics and thermodynamics of decomposition to metastable solid product 78−80740
DTA, topological aspects, bond diagrams, heat transfer 77−16877
dust formation in space medium thermodynamics and kinetics, workshop, Houston, Texas (1978 September 6 to 8) 80−22131
dynamical meteorology, relevant thermodynamic eqns. 78−73496
dynamical theory of irreversible processes and the microscopic interpretation of nonequilibrium entropy 79−30402
dynamics of molecules in contact with an external medium at equilibrium 79−9179
Earth global heat balance, annual var. 78−73300
Eckart's relativistic temp. gradient 80−103080
education, air conditioners, second law efficiency, energy efficiency ratio and performance coeff. 78−36742
education, energy conversion processes, performance standards, Atwood machine as example 78−62008
education, human body, live, thermodynamics of cooling for treatment purposes 80−73128
education, irreversible processes, linear coeff. calc., kinetic and Onsager reciprocity theorems, gas flow appl. 79−9053
education, thermodynamic work and harmonic oscill. 78−49598
education, zilch cycle and 1st law 77−82342
effective critical exponents in spherical limit 79−12749
efficiency and existence of entropy in classical thermodynamics 78−54324
Einstein action of Riemannian metrics, rel. to quantum gravity and thermodynamics 77−45778
elastic behaviour of elastic materials, thermodynamical bounds, thermoelasticity, deformation 79−41576

thermodynamics continued
elastic materials 77−14904
elastic micropolar material, constitutive eqns. 77−5667
elastic-plastic constitutive theory, thermodynamic treatment 80−64390
elastic-viscoplastic materials delayed behaviour of double shear perturbations 78−45483
elastically coupled systems at marginal dimensionalities, crit. dynamics and stability 80−101769
elastoplastic coupling within thermodynamic strain space formulation of plasticity 78−30189
elastoplastic materials, theory, thermodynamic restrictions 79−3924
electric current fluctuations in extended irreversible thermodynamics 80−42177
electrical circuit, power conversion of energy fluctuations, rel. to 2nd law of thermodynamics 80−17911
electrical contact phenomena, incorporation in electrodynamics eqns. 80−29374
electro-osmosis inversion point, Onsager coeff. transformation principles 79−74417
electrode-solution interfaces, role of water 78−40058
electrokinetic effects, phenomenological equations, fluxes and forces 77−5779
electrolyte transport, irreversible thermodynamics calcs. 80−3364
electrolytes, Wien dissociation, Gauss's divergence theorem in Onsager's theory 79−47934
electrolytic ion distribution near phase boundary *(German)* 78−56901
electrolytic solution, thermodynamics and correlation functions 80−24132
electron gas, thermodynamic properties, weak field expansions, in uniform mag. field at T=0K 79−85066
emulsion, thermodynamically stable 79−47993
endothermic solid-gas decompositions, activation energy, interpretation *(French)* 79−15981
energy considerations 78−88643
energy conversion, chemical to mechanical, reversible process, anal. 79−92087
energy conversion, intuitive thermodynamics *(German)* 79−14225
energy distribution, teaching aid *(Hungarian)* 77−64907
energy quality, principles of exergy *(German)* 78−12662
engine efficiency, operation around steady state at finite freqs. 79−21681
enthalpy-entropy compensation effect, separation of chemical from statistical effects 77−21412
enthalpy-entropy compensation effect, statistical analysis, van't Hoff and Arrhenius data 77−21411
entropy, definitions by Boltzmann and Clausius, reversible processes 77−10
entropy and Einstein's theory of gravitation 78−12638
entropy in quantum information theory, comments on recent studies 77−17851
entropy of thermodynamic processes induced by coherent radiation 78−32752
entropy prod. of extended irreversible thermodynamics, invariant transforms. 80−73293
entropy which does not increase, quantum logic 77−17850
enzyme-catalysed reactions, network thermodynamic modelling 80−89463
equation of state near critical point, thermodynamical scaling hypothesis 77−74341
equations of state, differential renormalisation-group generators, exact and approx. 78−77825
equations of state, very high press. and temp., Thomas-Fermi shell model 78−79738
equilibrium, teaching 80−46751
equilibrium and nonequilib. thermodynamics organised and unorganised systems, philosophy 79−40344
equilibrium chemistry in primitive solar nebula 80−82231
equilibrium phenomenological thermodynamics, geometrical formulation 79−54088
equilibrium state, teaching approach 79−27
eruptive gases, thermodynamic and isotopic studies 78−69316
ethane, pyrolysis, thermodynamics and kinetics 79−43577
ethane derivatives, diastereoselective form. and symm. props., semirigid mol. model 80−48099
ethylene-O_2 mixture, thermo-osmosis, heat of transport 79−43628
Ettingshausen refrigerator, longit., isothermal, nonstationary regimes, theory 78−18157
eutectoids(ic), lamellar, stability principles 80−89195
extended principle of corresponding states, rel. to pair interaction potential 78−51269
FCC crystal-melt interfaces, mol. dynamics simulation 80−79913
Fermi quantum crystals, melting curves low temp. anomalies rel. to neutron stars 78−24757
ferroactive thin films, physical prop. optimisation 80−80698
ferroelectrics, hydrostatic press. effect on phase transitions, thermodynamic considerations 79−15413
ferroelectrics, incommensurate polar phase form. 80−71344
ferromagnet, magnetic susceptibility, spin and charge density waves, Curie temp. *(Russian)* 80−100581
ferromagnet, magnetostriction is magnetic field, sound-spin wave coupling 79−15334
ferromagnetic crystal, spin subsystem thermodynamics, spin-phonon interactions, mag. order parameter 80−103848
fibre bundle struct. of thermodynamic states 78−8370
film, thermodynamic theory of clustering and percolation transitions 77−47697
finite system, order parameter and sp. ht. for epitaxial ordering renormalisation-group calc. 80−17862
finite time processes, generalised pots. 77−67401
finite time processes, step-Carnot cycle 77−67400
first law, formulation for nonuniform temp. processes 79−9200
first law deduction from microphysics, suggestion 77−87714
first principle of thermodynamics, for non-uniform temp. processes, mathematical formulation 79−71388
Fisher's droplet model for gas above T_c and the metastable phase 80−49348
fission reactor neutron gas, nonequilibrium thermodynamics *(Japanese)* 78−62595
fission reactors, thermodynamics and fluid dynamics, photographic techniques *(Spanish)* 77−71635
thermodynamics continued
flow equations for membrane transport, nonelectrolyte solute plus water case 80−26205
fluid, dipolar and ionic, electrically neutral, correl. condits. 78−4573
fluid dynamics, coarse mesh methods appl. *(German)* 77−88197
fluid mixture, unified theory of dynamics and thermodynamics *(Japanese)* 78−8244
fluid mixtures, thermophysical properties prediction 80−48563
fluid system, electric conduction in relativistic thermodynamics 80−105498
fluidised bed, surface to bed heat transfer intensification at controlled gas distrib. 79−1246
fluids, non-simple heat-conducting 77−80057
fluids, polarisable and magnetisable, theory in EM fields 77−57291
fluids with memory, simple, thermodynamics of linear flows 78−90812
Fokker-Planck eqn., kinetic effects due to detailed equilibrium violation, elastic scatt. *(Russian)* 80−31687
Fokker-Planck equation, manifolds of equivalent path integral solns. 80−4687
Fokker-Planck model, transport equation renormalisation 80−82732
foreign gas induced line shifts, thermodynamics 80−106295
formic acid anhydrides, valence force consts., IR spectra, isotope effects 79−93997
Frisch-Lloyd random system, low-lying electronic tail spectrum by path integral method and coherent state representation variational method 80−105580
fuel cells, nonequilibrium thermodynamics, heat release mechanisms and voltage 80−45660
fundamental Earth physics appls. 78−36125
fundamental laws of thermomechanics, constitutive eqns. *(German)* 78−24758
fundamental mechanics, thermodynamics and gravitation (book) 80−41964
G-varying cosmology, thermodynamic relations and 3K background radiation 80−56979
galaxy clustering and thermodynamics 80−51881
gas, alternant Takahashi nearest neighbour type, exactly soluble case rel. to soft rods 80−33718
gas, dilute, transient relativistic thermodynamics, kinetic theory 77−76014
gas, equilib. thermodynamic characts., compressed-atom model 77−7507
gas absorption by liquid, exothermicity altering solubility and reaction rate 79−74341
gas adsorption 79−73396
gas and solid particles suspensions energy balance 77−77812
gas flows, entropy prod. determ. using Boltzmann's H-theorem, Knudsen effusion 80−106867
gas in closed container, relativistic thermodynamics 77−45812
gas kinetic boundary value problem, non-equilibrium thermodynamics 80−19544
gas mixtures, third virial coeffs., nonadditive dispersion interactions effects 78−67299
gas thermometry scale from 2.6K to 27.1K, report 78−89480
gas-solid flow, nonreacting, heat and mass transfer, thermodynamic approach 78−51223
gaseous rotating cylinders, thermodynamic stability anal. by linear series 78−81618
Gaussian method, attempt to separate long and short range forces 79−63180
general physics and heat, book 79−25814
general relativity conformal groups, appl. *(French)* 80−101
generalised Kirchhoff law 80−17912
generalised mean suggested by equilib. temp. 80−86237
generalised one-dimens. oscillator, second order Wigner-Kirkwood semiclassical partition function and thermodynamic functions 80−62601
in geology, proc. of NATO Advanced Study Inst. (Oxford, 17-27 Sept. 1976) 78−32103
geometrical neoclassical thermodynamics 77−87711
geothermal power plant, energy conversion process, thermodynamic considerations 80−16779
geothermal power plants flash cycle optimisation, analytical expression in terms of temp. only 80−40894
geothermal technology, development into an exact science 80−61781
Gibbs (1839-1903), biography *(Czech)* 80−22180
Gibbs ensemble, approach to equilibrium 77−41553
Gibbs equation, generalised, heat fluctuations 79−76940
Gibbs formula for elementary quantum systems, thermodynamical proof 79−58628
Gibbs phase rule, history and development *(German)* 77−78943
Gibbs random fields described by generating functional method 80−31698
Gibbs space, group theoretic aspects 77−33971
Gibbs states, classical approximations 80−132
Gibbs-Duhem eqn. solns. 79−85106
Ginzburg-Landau model system, quenched, fluctuations growth 78−41260
glass, diffusion and relax. processes, nonequilib. thermodynamics *(German)* 78−83746
glass, equilib. thermodynamics, sp. ht., refr. index and glass transition *(German)* 78−83745
glass, internal parameters, ordering parameters, history function, rel. to glass transition 78−30738
glass transition, soft-sphere model, mol. dynamics study 80−49343
glass transition interval, theory, physical meaning *(German)* 78−22834
glass transition kinetics, linear nonequilib. thermodynamic theory 78−67815
glass transition temperature, domain size dependence 77−89525
glasses, dielectric relax., order parameter model appl. 80−108151
global mean value theorems in thermodynamics 80−31690
global thermodynanic stability and correlation inequalities 78−45560
grain boundary Gibbs thermodynamics anal., interaction with vacancies *(Russian)* 80−2034
grand canonical ensemble of MIT bags, thermdoynamics 77−79247
gravitating fermions, temp. inversion in Earth atmosphere 79−57994
gravitating fermions, thermodynamic functions 79−80552
gravitating fermions, thermodynamic potentials 79−80551
gravitating sphere in Lyra's geom., thermodynamic equilib. 78−65840
gravitational field, thermodynamic comments 79−2701
gravitism and new astrophysical school of thermodynamics 79−29986
gravothermal catastrophe 78−81536
gravothermal instability in two dimensions 78−89395

thermodynamics continued
Green's function, perturbation theory 77−26266
Griffith crack quasi-static growth, irreversible thermodynamics 79−18812
growth, self-reproduction and autoregulation model, anal. of reactions with stretchable semi-perm. walls 77−81460
H function, sign of d^2H/dt^2 78−29073
hadron matter, thermodynamic description, evolution, coupling const. depend., hot nucleon matter appl. *(Russian)* 79−3006
haemoglobin molecule from cybernetic and thermodynamic viewpoint *(German)* 79−1998
Hamilton's principle for thermodynamic systems 79−88896
hard sphere mixture, Ornstein-Zernike eqn. with Yukawa closure 78−18513
hard sphere mixtures, with negatively nonadditive diameters, scaled particle theory 78−71654
hard sphere system in equilibrium, two-dimens. hard disk system 80−107033
hard-particle fluids, series representation of eqn. of state 80−6337
harmonic oscillators, charged, interaction with transverse EM field mode 80−5712
heat and work, energy transfer fundamentals *(German)* 78−62171
heat conduction, interior algorithm for optimisation of forms *(French)* 77−72130
heat conduction, with finite wave speed, Lagrangian 78−94519
heat conduction in porous materials non-equilibrium processes *(Hungarian)* 80−178
heat conduction in relativistic extended thermodynamics 80−43803
heat engine, irreversible, optimal config., dynamical treatment 79−54086
heat engine, irreversible, optimal config. 79−54085
heat engine, quantum open system model 79−44894
heat engine theory, mathematical formulation including negative absolute temps. 80−27250
heat engine using clear night sky as heat sink for teaching 80−27082
heat engines, chemically driven, finite time thermodynamics 80−76541
heat engines, imperfect, extremals, time dependent thermodynamics 77−35025
heat engines and pumps at positive and negative absolute temps. 77−87712
heat engines using liquids, thermodynamic principles 80−83730
heat exchanger, recuperative, source/sink even model *(Hungarian)* 79−14226
heat flow in relativistic equilibrium thermodynamics 80−52017
heat flux fluctuations, Fokker Planck eqn. in extended irreversible thermodynamics 80−86205
heat pump operating principles and performance 78−71274
heat pumps, energy and environmental considerations in extending appls. 77−17976
heat theory, dynamical, of William Thomson, thermodynamics and natural philosophy 77−26122
heat transfer in direction of gravitational force *(German)* 77−80049
heat transfer in linear harmonic chain, nonequilib. steady states, information theoretic approach 80−19214
heater gas in cylinder with piston, maximum work production determ. 80−79129
n-heptadecane, short-chain mol. liq., statistical thermodynamics 79−73084
heterophase fluctuations in two component systems, distrib. function 79−80563
HF approximations, thermodynamic Fermi systems 80−4642
high density Bose model, low temp. thermodynamic props. 79−80502
high temperature system characterisation, models, phys. and chem. reference data sources 80−41958
high-pressure systems with liq. heat carrier, thermodynamic equil. approach to depressurisation calc. 80−17957
high-temperature chemical processes, review, book contrib. 77−40545
historical development effects *(French)* 77−26256
homogeneous perturbed classical states and equilibrium conditions 78−93595
homopolymer chain adsorption on homogeneous surface, theoretical model 77−70403
hydrodynamic contrib. to two-time correlation functions, using nonequilibrium distrib. function 77−49703
hydrophobic effect, dil. soln. struct. and thermodynamic props., semi-empirical model 78−20060
hydrophobic interaction, solubility and solvent struct. changes 78−83705
hyperbolic balance laws in continuum physics 80−4525
Il'iushin's postulate, thermodynamic conditions on elastoplastic coupling 78−18190
Il'iushin's postulate, thermodynamic conditions on elastoplastic coupling 78−18191
immiscible liquid binary cycle temp.-entropy diagrams 78−157
industrial gaseous environment characterisation, Brinkley method 80−93817
inelastic constitutive equation, irreversible thermodynamic treatment 77−82391
inequality between arithmetic and geometric mean, comment on thermodynamic proof 79−67241
infinite classical system, stability, equilib. and KMS 78−21055
infinite dilution activity coeffs. determ. from total press. VLE data, eqn. of state influence 80−40727
infinite particle two-dimens. systems, stochastic dynamics 79−80512
information contained in open systems by example of chemical reaction systems 79−91915
information theoretic approach, exptl. and inherent uncertainties 80−82733
inhomogeneous solid solutions with conc. expansion, thermodynamics, energy defect diffusion calcs. 80−24618
initially-stressed solids, variational-Lagrangian irreversible thermodynamics 78−29074
instabilities and fluctuations in systems far from thermodynamic equilibrium 79−21671
integro-differential type media, theory *(Ukrainian)* 79−49040
interface phenomena singular densities and currents at dividing surface 80−17907
interfaces, pure, thermodynamics and dynamics rel. to Spacelab 79−28910
interfacial statics differential eqn., micromech. derivation 79−46882
interfacial systems, nonequilib. thermodynamics 77−33966
intermolecular interaction thermodynamic parameters determ. from chem. shifts of functional groups 79−64068

thermodynamics continued
internal scalar pressure determ. in atom or molecule, density functional theory 80−47857
internal variables, internal forces concept 77−9971
interstellar space, disequilib. condensation environments as frontier in thermodynamics 80−26942
interstitial defects, migration kinetics and thermodynamics 80−107461
invariance of thermodynamic laws, contact transform. of variables 79−63181
ion clusters in heteromolecular nucleation, steady state thermodynamic model 78−48687
ion system, internal energy, Debye temp. function, Monte Carlo method data 77−35314
ion-molecule equilibrium constants, determ., rel. to thermodynamics 79−5154
ionic solution in molecular polar solvent, stat. mech. 78−30527
irradiation induced precipitation, thermodynamic approach 79−78975
irreversibility, evolution, process of local conc. 77−26257
irreversibility, time and anisotropies, cosmological origin 77−13510
irreversibility in strongly coupled system, Boltzmann H-functional 77−74342
irreversibility of thermodynamic processes, derivation from microscopic reversibility 79−71393
irreversibility postulates 78−24750
irreversible, and gas kinetic theory, boundary problems *(Russian)* 77−84382
irreversible, information-theoretic stability and evolution criteria 77−33965
irreversible, internal variable theory, Lagrangian formulation 80−73291
irreversible, near equilib., metric geometry 80−62604
irreversible, of steady state with disequilibrium 78−4576
irreversible, tensorial formulation of internal variable theory, endochronic time spectrum 77−61036
irreversible, vector forces and fluxes 78−24753
irreversible effects due to thermal perturbations, linear theory 77−22508
irreversible energy conversion processes, information model *(Ukrainian)* 78−89419
irreversible process thermodynamics, exergy representation 78−65892
irreversible processes, microscopic theory 78−49784
irreversible processes, nonlinear, memory function calc. 77−26265
irreversible processes, preferred choice of flows and forces *(Russian)* 78−4572
irreversible processes, thermodynamic flux structuring, dissipation inequality 79−44893
irreversible processes, thermodynamic in quality 77−61043
irreversible processes, time scaling 80−17906
irreversible processes, variational principles *(German)* 78−81936
irreversible processes and physical interpretation of rational thermodynamics, review 80−13020
irreversible thermodynamic treatment of particle diffusion among immovable particle system *(Russian)* 77−5778
irreversible thermodynamics, basic formulations of nonequilib. thermodynamics, review 79−35657
irreversible thermodynamics, corrections to linear transport laws, Onsager reciprocal relations 77−17938
irreversible thermodynamics, coupling and uncoupling of forces 79−58664
irreversible thermodynamics, extended, hydrodynamical fluctuations 80−86235
irreversible thermodynamics, minimum principle *(Japanese)* 77−41556
irreversible thermodynamics, review of foundations postulates and implications 78−12658
Ising chain, amorphous, finite, thermodynamic behaviour 79−61028
Ising model, S=1, violation of third law of thermodynamics 79−17372
isothermal chemical thermodynamics, equilib. and nonequilib., stochastic basis 79−83496
isotope transport in reversibly reacting species systems, isotopically labelled solvent and friction coeffs. 80−54420
isotropic elastic-plastic materials, thermodynamic theory, global entropy inequality 80−1436
itinerant electron magnetism, thermodynamic aspects 77−72992
Kac ring model, effect of irreversible microscopic dynamics on macroscopic behaviour of large system 79−49153
Kelvin's principle and the existence of a local integrating factor for the heat differential form *(Spanish)* 79−88897
Kerr black hole, spin thermodynamics 79−93015
Kirkwood-Salsburg eqns. for bounded stable Kac pot., instability and phase transitions 78−4553
Kirkwood-Salsburg eqns. for bounded stable Kac pot. 78−4552
Kramers rate theory, quantisation using Wigner representation 80−52054
Lagrangian for non dimensional non constant diffusion processes 80−31688
Lagrangian thermodynamics, rel. to governing principle of dissipative processes 78−65889
Landau theory for chem. instabilities 78−16763
laser pumping system, thermodynamic calc. method 80−58551
laser theory, statistical mechanics of open systems *(Japanese)* 79−76658
laser theory, statistical mechanics of open systems *(Japanese)* 79−76659
latent heat storage materials, high temp. corrosion resistance and thermodynamic stability 80−30582
lattice gas, phys. correl. factor in Nernst-Einstein relation 80−105591
lattice systems, metric space of interactions, grand canonical pressure, thermodynamic limit 78−12652
lattice systems, thermodynamic limitations, on interaction topologies 80−57217
law of mass action, first order phase transition, chemical instability 78−80778
Legendre transforms and thermodynamics, catastrophe theory 79−26012
Lennard-Jones liquid, mol. dynamics studies of glass form. 80−38896
life, pre-biotic energy sources rel. to origin 78−69460
Lifshits points for bidimensional representations *(Russian)* 79−93086
light elements formation, thermal cycle, isotopic abundances problem *(French)* 78−96574
light scattering in dynamical props. study, principles spectra derivation and applics. 80−53218
limit cycles and multiperiodic flow bifurcation and nonequilibrium phase transitions 78−24759

thermodynamics continued
linear interacting processes in nonequilibrium statistical mechanics, thermodynamic Lagrangian formulation 78−21087
linear microscopic equations in irreversible thermodynamics, eigenvalue problem 80−57227
linear Onsager relation, mol. kinetics basis 79−67242
linear relaxation theories, equations of motion, Green's functions, and thermodynamics relations 79−30352
linear thermoconsolidation, porous elastic solid containing compressible fluid 79−23186
lipid bilayers, planar systems, asymm. charge distribs. 77−29104
liquid, non-stoichiometric complex formation, thermodynamic equilib. consts. 77−21406
liquid, simple, equilib. theories, review 80−38887
liquid boiling wave processes at heat releasing surfaces 79−90773
liquid crystals, correlation in statistical theory 78−75536
liquid crystals, generalised Suzuki formula application *(Chinese)* 80−107045
liquid microclusters, thermodynamics, size effects, theory 78−22935
liquid mixture, adsorption on solid, equilib., thermodynamics correlations 78−84045
liquid mixture, binary, oscillatory convective instability, thermodynamic anal. 78−94753
liquid mixture, near tricrit. pt., thermodynamic model and sum rules, appl. to benzene-ethanol-water-$(NH_4)_2SO_4$ 80−34196
liquid mixtures, critical equilib., gravity effects 77−74340
liquid-gas phase transition, Percus-Yevick theory 78−38824
liquid-glass transition, free volume approach, thermodynamic behaviour 80−1940
liquid-liquid interfaces in isolation, and in interaction, review 77−47651
liquid-vapour equilibrium in system with chem. reaction, thermodynamics *(Russian)* 77−63947
liquid-vapour interface struct., Ar like fluid in equilib., thermodynamic states 78−10259
liquid-vapour interface struct. and thermodynamics, density fluctuations, grand ensemble formulation 78−22932
liquids, dielectric relax., order parameter model appl. 80−108151
liquids, low-press. evaporation, interface thermodynamic model 80−2252
liquids, simple, thermodynamically self-consistent theories, radial distrib. function, functional derivative 80−92435
liquids and mixtures, statistical thermodynamics, book 80−90616
local equilibrium hypothesis extension 80−27249
local thermodynamic equilibrium, possible relax.-time comparisons failure 78−81935
local thermodynamic stability and KMS conditions of quantum lattice systems 77−71275
locally equilibrium correlation function calc. method 80−36943
low-temperature bottoming cycles, thermodynamic analysis and optimum fluid props. prediction 77−33968
LWR, neutronic thermohydrodynamic interaction model *(French)* 79−89349
LWR fuel-cladding gap, Cs-U-Zr-H-I-O system, chemical thermodynamics 78−82440
macromolecualr thermodynamics and its possible relevance in physiology 80−53176
macromolecular decoding 79−31757
macroscopic system, reduction description method of nonequilib. states and fluctuations *(Russian)* 78−21089
macroscopic theory of statistical thermodynamics 80−105567
magnetic objects, current loops, thermodynamics, teaching 80−90633
magnetization equations based on laws of thermodynamics 77−89982
magneto-micropolar continua, spatial interaction 79−97198
mapping relations *(Chinese)* 80−27227
Markov processes, symmetry basis and generalised thermodynamic pots. 79−97304
Markovian processes and irreversibility, hydrodynamic equations, stress tensor and local eqn. 80−82720
Markovian processes and irreversibility, hydrodynamic equations from constitutive equations 80−82721
martensitic transform., thermodynamic anal. of work performance under stress, theory 79−74153
master equation, path integral solns., stationary Markov process 78−86233
master equation for time evolution of Markov process, network representation 77−5642
material with internal variables, condition equivalent to existence of nonequilibrium entropy and temp. 79−44890
materials with memory, thermodynamics 80−64356
mathematical inequality derivation from first and second laws 80−57229
matter plus radiation system with quadrupole interactions 79−49181
matter-antimatter accounting, thermodynamics, and black-hole radiation 79−49136
maximum likelihood test in estimation of exptl. inaccuracies, applic. to equilib. data 77−9867
mean field models, equilib. states 80−46961
mean molar functions, calc. using partial differential eqns. 79−21685
media with internal structure, thermodynamics 79−88901
membrane, parchment-supported, thermodynamic parameters, membrane and bi-ionic pot. theories testing 79−92168
membrane potentials, meas. in ionic environment, biological membrane simulation 80−3412
membrane potentials measurements 80−3411
membrane system, closed, vesicular, mechano-chemistry 77−60189
memory alloy engine, efficiency 80−71648
metabolism, energy conservation 77−81459
metal electrowinning, energy consumption reduction via anodic coal reaction 79−91965
metal-electrolyte interface, differential capacity, thermodynamic interpretation 78−27770
metals, chemisorption of gases, book 79−69370
metals, expansion, isentropic, vaporisation and condensation kinetics anal. 77−66623
metals, particle size depend. of melting temp., thermodynamic theory 77−89523
metastable state relaxation, critical point region nucleation in thermodynamic systems *(Russian)* 80−13026
metastable states close to instability, phase transition parameter eqn. of motion 80−57230
metastable states of quantum lattice systems 77−71276
meteors, nonequilibrium thermodynamic model 80−4308
methane, dil. aqueous soln., Monte Carlo calcs. on struct. 79−32874

thermodynamics continued
MHD convertor, phase transition in condenser *(Russian)* 79−1350
MHD generator, liquid-metal *(German)* 77−948
micellar aggregate, solubilisation parameters and dynamics, photoluminescence obs. 79−79297
microcanonical system, pressure anal. 79−40454
microcanonically distributed plasma, reduced distrib. functions 80−28604
microferroelectrics 77−59534
micropolar fluid, second order, fund. and constitutive eqns., thermodynamics and flow 78−20970
micropolar fluids, thermodynamical aspects, non-linear approach 80−105598
microstructural phenomena, physical chemistry 79−11550
miscible fluid mixtures, mechanics and thermodynamics, variational approach 79−93084
mixing character and irreversible processes in macroscopic systems 77−53845
mixing distance of set theory 78−77662
mixture, binary, off-critical, quenched, struct. functions and mobilities renormalisation 79−82343
mixtures, rational description, theory 78−20053
mixtures containing polar substances, corresponding states principle use in crit. states calc. 80−39196
mixtures of heavy and light gases, kinetics and thermodynamics *(Russian)* 77−76015
model systems, generalised theorems 79−21658
model systems in which particles interact with definite conservation laws 79−21659
modified Wilson equation, appl. to mixing, phase equilibra, thermodynamics *(Chinese)* 79−71390
mole, introduction in teaching of ideal and real gases 77−87611
molecular liquids and solids, dissipation functions, conservation laws 77−45817
molecular relax. phenomena, quantum statistical mechanical approach, irreversible thermodynamic theory for radiationless decay 80−48028
molecular relaxation in entropy and macroscopic disequilibrium, isothermal vibr. relax. 77−6896
molecular relaxation in entropy macroscopic disequilibrium, Markovian relax. 77−14539
molecular thermodynamics appl. to phase separation and critical phenomena *(German)* 78−14447
moleculear liquids and liq. crysts., theory of irreversible processes 80−54125
moving boundary problems, weak soln. 80−179
multi-molecular clusters, isomeric structures, weights and effective characts. 79−31759
multicomponent mixtures, vapour-liquid equilibria predictions, statistical thermodynamic approach 77−55335
multipulse NMR line narrowing in solids, thermodynamic theory *(Russian)* 79−19789
muscle, mechanochem. contractile system as thermodynamic machine 78−20201
muscle, skeletal, bond graph simulation of glucose metabolism 77−36894
muscle mechanics thermodynamic model 78−80908
muscle thermodynamic cycles, temp.-entropic relations 79−53049
muscle tissue, math. models 77−25358
N_2O refrigerator, thermodynamics and thermoelectric condenser design 80−108809
N particle system, quantum corrections for thermodynamics 78−70082
negative absolute temperature 79−63184
negative absolute temperature and Carnot cycle, for teachers 78−61996
negative ions, sputtered, characteristic electronic and vibrational temp., laser photoelectron spectral meas. 80−66346
negative Kelvin temp., discontinuous transitions 77−98
negative Kelvin temp. connections between regions of opposite temp. sign 77−97
negative Kelvin temperatures, anomalous behaviour anal. 77−99
negative Kelvin temperatures 77−100
negative specific heat paradox, astronomical and physical appls. 78−9557
nematic liquid crystal, extensible, micropolar continuum theory 79−4244
nematic-bilayer smectic A reentrant transition, thermodynamic model 79−95130
Nernst distribution law, use of thermodynamic excess functions 78−43123
nerve action potential, molecular events and energy changes 78−44497
network, complex system modelling 78−20955
network thermodynamic two-port element, representation of salt, current coupled flow 79−34505
network thermodynamics *(Czech)* 80−177
neutral gravitating fermion system, equilibrium states 80−31692
neutrino emission from blackbody, thermodynamic laws, teaching 80−105451
neutron gas, highly rarefied, non-equilibrium thermodynamics under creative and destructive reactions 79−12747
neutron stars thermal properties and detectability, cooling and heating processes 80−31323
Newtonian stellar dynamics, maximizing functionals, rel. to thermodynamic and dynamical stability 80−12782
nitrided Fe, thermodynamic considerations *(German)* 78−60874
non-conservative description of evolution in physics *(French)* 79−97328
non-equilibrium systems, statistical mechanics of steady states 79−54038
non-equilibrium temperature, concept 77−74339
non-equilibrium thermodynamic systems theory 80−105595
non-equilibrium thermodynamics, De Donder-Meixner transformations 80−8944
non-equilibrium thermodynamics of continuous media 80−8943
non-equilibrium thermodynamics of hydrodynamic instabilities 80−42184
non-equilibrium thermodynamics of two bulk interfaces including Em effects 80−13021
non-ionic reactions, temp. and press. effect on kinetic and thermodynamic parameters 80−3300
non-Newtonian third grade fluids, thermodynamics and stability 80−33638
non-stationary thermodynamics of polarisable and magnetisable dissipative fluid media 80−47002
nonclassical equations of state for critical and tricritical points 80−4683
nonconservative forces and internal degrees of freedom, exterior calculus 77−2631
nonequilbrium steady states, irreversible processes, Lyapunov functions 80−95049

thermodynamics continued
nonequilibrium, appl. to electrochem. and thermal diffusion 78−20056
nonequilibrium, derivation of evolution laws *(Spanish)* 77−30118
nonequilibrium, general antisymmetry prop. of the constitutive eqns. 79−58663
nonequilibrium, Onsager eqn., phenomenological coeffs. determ. 79−63183
nonequilibrium, with crit. fluctuations, Keizer's theory derivation from master eqn. 79−67240
nonequilibrium entropy and symmetry principle of transport coefficients 79−21683
nonequilibrium open systems, state variable contraction 80−105600
nonequilibrium phase transitions, synergetics study, recent trends and developments 79−75480
nonequilibrium processes, textbook 77−41560
nonequilibrium processes in open systems, fluctuation dissipation relations, p-n junction appl. *(Russian)* 79−58668
nonequilibrium states, variational approach to Fokker-Planck eqn. 77−87717
nonequilibrium states subject to Fokker-Planck eqns., thermodynamic props. 77−67396
nonequilibrium statistical mechanics, path integral formalism based on Onsager's principle 77−67373
nonequilibrium statistical mechanics, space-time coarse graining scaling, kinetic eqns. 79−75445
nonequilibrium statistical mechanics, validity of exact results 79−75444
nonequilibrium statistical thermodynamics, covariant formulation 77−41542
nonequilibrium steady states, distrib. functions and phase transitions 77−61041
nonequilibrium steady states, irreversible processes, Liapunov criterion 80−13023
nonequilibrium steady states 79−6068
nonequilibrium steady states of open systems, 2nd order type transitions and fluctuations 77−49680
nonequilibrium superconductor, normal component drag by condensate, tunnelling *(Russian)* 80−93051
nonequilibrium systems, existence of thermodynamic limit 79−54084
nonequilibrium systems, statistical mechanical theory from generalised phase space and damping theory 79−75481
nonequilibrium systems, with multiple stationary states, stability, thermodynamic anal. 78−27734
nonequilibrium systems with memory, vector-valued actions 80−86232
nonequilibrium temperature, empirical foundation and axiomatic treatment 78−57882
nonequilibrium thermodynamic Hamiltonian, contact transformations 79−17371
nonequilibrium thermodynamics, available energy theory 79−44669
nonequilibrium thermodynamics, macroscopic aspects of mixing distance 79−6064
nonequilibrium thermodynamics, statistical formulation by general Onsager Machlup formula 79−54089
nonequilibrium thermodynamics, steady state fluctuations 79−49187
nonequilibrium thermodynamics, stochastic measures 80−86240
nonequilibrium thermodynamics inequality conditions, stochastic laws 79−75482
nonequilibrium thermodynamics of luminescent processes in solids 80−50435
nonequilibrium transitions induced by external noise 80−152
nonideal system, thermodynamic variables, irreducible cluster integrals 77−67394
nonisothermal finite strain mechanics of porous solids, thermomolecular diffusion, variational Lagrangian thermodynamics 77−65668
nonisothermal rigid shell theory using fundamental laws of thermodynamics 80−87712
nonisothermal system, equilib. distribs. and detailed balance relations 79−36737
nonisotropic systems near liquid-vapour critical point, similarity hypothesis, gravitational effects 80−17913
nonlinear autonomous systems, charact. functions, transformation group symmetry 80−47007
nonlinear coupled dynamic physiological systems, network thermodynamic simulation 79−96504
nonlinear elastic dielectrics, thermodynamics and entropy flux 79−67164
nonlinear fields, one-dimens. 77−17830
nonlinear fluctuation-dissipation theory 80−36963
nonlinear irreversible processes, Fokker-Planck eqn. asymptotic solns., generalised Onsager-Machlup theory 78−36955
nonlinear irreversible thermodynamic processes, field anal. 78−156
nonlinear nonequilibrium statistical mechanics, Oji Seminar opening address 79−75442
nonlinear reaction diffusion systems, bifurcation anal., dissipative structs. in a sphere 79−11767
nonlinear relaxation and fluctuation 79−30373
nonlinear thermodynamic methods, parameters evaluation 78−41254
nonlinear thermodynamics of irreversible processes 78−54330
nonlinear thermoviscoelasticity theory for generalised thermorheologically simple material *(Russian)* 78−57785
nonpolar fluids, Hamaker consts. and principle of corresponding states 78−11543
nonrelativistic para-Fermi gas, thermodynamic and mag. props. 79−25974
normal modes in irreversible thermodynamics 80−52148
nuclear reactor, transient critical flow analysis in nodalised system 77−65258
nuclear shell correction, continuum, thermodynamical calc. *(Russian)* 78−29409
nuclear spin thermodynamics 80−54964
nuclear-spin subsystems, cross-relax., nonequilib. thermodynamics 79−58662
nucleation, theory for high and low supersaturations, review 80−49142
nucleation on charged centres 79−20955
nucleation theory, fundamentals *(Spanish)* 78−43101
oil-water interface, fatty alcohol adsorbed layer phase transition, high-press. effect 79−99395
one component classical charged particle gas, thermodynamic grand function using collective coordinates 80−73289
one dimensional fermion system, thermodynamics by cluster expansions 77−41535
one-dimensional fermion system, cluster expansion methods and thermodynamics 78−6289
thermodynamics continued
one-dimensional solitary-wave-bearing scalar fields, statistical mechanics, ideal-gas phenomenology 80−105792
one-dimensional system, with exponentially repulsive interactions, statistical mechanics 79−55629
one-ports, represented by eqn. involving two conjugated variables 79−85103
Onsager Casimir symmetry, Markovian processes and irreversibility. The Onsager-Casimir symmetry 80−62580
Onsager hypothesis calcs., crystal nonequilibrium thermodynamics, quasielastic light scatt., systematic anal. 79−61391
Onsager relations for non equilib. systems generalisations and sum rules 78−62153
Onsager thermodynamics, quasilinear generalisation 77−5780
Onsager-Casimir reciprocal relations, derivation from thermodynamic principles 77−37832
Onsager-Machlup Lagrangian for general diffusion processes, Fourier series anal. 79−6060
open BSC model, dynamics in weak coupling limit 79−2738
open quasi-free systems, time evolution 80−95030
open system, current-carrying states in quantum statistics 80−90802
open systems, definitions of heat, internal energy transfer by convection 80−69644
open systems, generalised master eqn. struct. 77−9972
open systems, generalised regression theorem for multitime correl. functions 77−9973
open systems, new thermodynamic theory, chem. appls. 77−63946
optimal control of ideal gas system 78−29071
order-disorder phase transitions, thermodynamics in mean field approx. 79−33633
oscillating reactions, thermal props. 80−7762
oscillator systems, nonlinear stochastic models 79−80525
Ott relativistic temperature variation, comment on derivation 80−86084
overvoltage theory, nonequilib. thermodynamics appls. 77−40550
Pade approximation method as renormalisation group method 80−17909
pair production in nondegenerate Fermi gas 79−44356
paragas, high temp. *(Russian)* 78−49754
paragas thermodynamics at intermediate temps. 80−46970
partial molar quantities, calc. from molar quantities *(German)* 78−85191
partition function, analytic props. of Lippman-Schwinger variational approx. *(German)* 78−36953
partition function, modified Lippmann-Schwinger variational principle 80−86233
partition function, semiclassical expansion 79−84993
passive states and KMS states for general quantum systems 78−41178
path-integral methods in nonequilibrium thermodynamics and statistics 79−26018
Percus-Yevick approximation, thermodynamically consistent analogue *(Russian)* 77−84603
permafrost on Mars 80−67621
phase equlibria, molecular thermodynamics calculations, practical appls. *(German)* 78−18733
phase separation, competitive statistical and chem. mixing effects *(German)* 77−52665
phase transitions, first order, matter transfer formalism *(French)* 79−6065
phase transitions, group theoretical methods rel. to problems of classical Landau theory 80−73292
phase transitions, induced by several order parameters, thermodynamic parameters 80−103457
phase transitions and critical phenomena, recent developments 77−87713
phase transitions in many identical thermodynamic spin-like systems 77−17906
phase transitions with two order parameters, Landau theory, mag. reorientation 80−103456
phenomenological eqns. for reacting fluids 78−3363
phenomenological thermodynamics to canonical ensemble 80−22269
phonon system, local cumulative excitation as transport phase transition 77−74336
phospholipid bilayer, hydrated, monoclinic (ripple) phase, thermodynamic model 79−70532
photography, sub-image and latent image Ag specks, formation 78−16874
photon emission from blackbody, thermodynamic laws, teaching 80−105451
photon-matter system, polariton instability and thermodynamic phase transition 79−86150
physical-chemical solids with finite deformation, variational irreversible thermodynamics 79−6067
pion gas, thermodynamical functions 77−64995
plane rotators, equilibrium state uniqueness 78−8369
plasma, classical two dimensional one-component, Monte Carlo simulation, solid-liquid phase study 79−94814
plasma, low-temp., with nonequilibrium ionisation, review 80−96343
plasma, one-component, two- and three-dimens., thermodynamic quantities lower bounds 79−68905
plasma, thermodynamics and correlation functions 80−24132
plasticity, constitutive equations derivation from Clausius-Duhem inequality 80−46804
plasticity theory, singular yield conditions 77−84162
plasticity theory governing relationships in stress and strain spaces 79−88812
Poincare cycle, general relativity, cosmology and thermodynamics 79−80378
point particle gas, grand partition function, zero distrib., logarithmic interaction 77−11296
Poisson-Boltzmann, continuum dielectric approx. 77−36762
polar fluids, continuum theory thermodynamics 80−31691
polarisation dynamics, fully relativistic kinetic model 78−62134
polydisperse solution of rodlike particles, isotropic-nematic phase transition, Onsager theory 80−100324
polydisperse systems of nonadditive hard particles, thermodynamics 80−7863
polyisobutylene melt, thermodynamic constitutive eqns., adiabatic deform. expts. 78−1620
polymer, high-modulus, behaviour in solid state, nonlinear irreversible thermodynamics approach 80−44154
polymer crystals, chain-folded, statistical mechs. in lattice model 78−47247
polymer science, conf., Pittsburgh, USA, (June, 1975) 77−38756

thermodynamics continued
polymer solution, intermolecular interaction phenomena *(Russian)* 77−21414
polymer solutions, thermodynamics, Flory-Huggins lattice theory appls. 77−40574
polymeric liquids, Hamaker consts. and principle of corresponding states 78−11543
polymers, stressed, thermodynamically controlled cryst. orientation 80−84112
polymers, thermodynamics and relaxation, memory and equilib., theory 78−76903
polyvinylacetate melt, thermodynamic constitutive eqns., adiabatic deform. expts. 78−1620
porous bodies, atom-atom interaction law *(Russian)* 80−19861
porous material, press. soln. thermodynamics, chem. and mech. forces interaction 77−60369
porous media models using thermodynamics of mixtures 80−96184
Potts model, first order phase transitions, Monte Carlo renormalisation group method 80−34645
pressure solution thermodynamics, interction between chemical and mechanical forces 78−57194
pressure unit, optimum metric, for thermodynamic standard state 80−8950
pressurised pipe guides, nonstationary discharge of boiling liq. in thermodynamic equil. approx. 79−81711
Prigogine-Defay ratio, macroscopic systems with more than one order parameter 77−20042
principle of maximum entropy and irreversible processes, review 80−86198
principles, book 80−73122
principles of max. entropy and min. energy, rel. to curvature of S,U,V and n 77−13537
pseudopotential in statistical thermodynamics 79−85109
PTFE grafted membranes, struct.-properties relationships, bifunctionality *(French)* 80−61137
pulmonary artery flow meas. after lung homograft in dogs, implantable directional Doppler flowmeter 77−90823
quadratic mass action system, irregular oscills. 80−62611
quantum amount of information and maximum work 79−63142
quantum channelling theory, channelled particle multiple scatt. by electrons, contrib. to dechannelling rate 80−107350
quantum coherence effects and the second law of thermodynamics 79−6025
quantum dynamics, generalised, two-level, irreversible conservative motion 78−36927
quantum fermion thermodynamic system, high-order perturbation expansion 80−4635
quantum harmonic oscill. chain, relaxation dynamics *(Russian)* 80−94992
quantum ideal gases, paradoxes associated with mixing 77−13728
quantum lattice system, local thermodynamic stability, KMS conditions 77−17902
quantum mechanical eqn. of Kadanoff and Baym, time reversal noninvariance 79−17332
quantum statistical mechanics, boundary-value problems *(Rumanian)* 78−86219
quantum statistical thermodynamics, rigorous information theoretic derivation 77−37837
quantum statistical thermodynamics, rigorous information theoretic derivation 77−74338
quantum statistical variational principles 79−75452
quantum theory and time asymmetry 30−22215
quantum thermodynamics and mech. unified theory, irreducible dispersions 77−60
quasi-Carnot cycles, negative Kelvin temps., theory 78−54111
quasi-perfect elasticity, theoretical foundations 78−63285
quenched magnetic system, statistical thermodynamics 77−66363
radiation temperature of moving bodies *(German)* 77−37830
radiative transfer, irreversible processes *(French)* 80−13002
radioactive material storage, thermodynamics of free-convection air-cooled storages 80−5282
randomly-packed spherical particle bed, coord.-no. distrib., effective thermal cond., stat. thermodynamic theory 78−75028
rare earth oxides, phase transition hysteresis, thermodynamic model 77−76570
rarefied shock wave existence near thermodynamic critical point of a substance *(Russian)* 80−88263
Rayleigh gas, irreversible processes, generalisation to non-equilib. systems *(Russian)* 78−54329
Rayleigh problem, exact transform soln. 77−53844
reaction kinetics and mechanisms by calorimetric methods, theory 78−27733
real gases, eqns. of state, limits of validity *(Italian)* 79−41781
reciprocating magnetic refrigerator for 2-4K operation 80−2577
refrigeration system, energy conservation estimates by second law anal. 80−45723
relations of continuum mechanics for irreversible processes 80−101715
relativistic, and temperature 79−63182
relativistic, collineation and motion, Cattneo's theory 78−51259
relativistic, density, momentum and energy laws 77−82424
relativistic, laws, macroscopic quantities 77−82423
relativistic, time conventions, effect on fundamental eqns. 77−67275
relativistic continuum thermodynamics, dynamical approach 79−58661
relativistic gas expansion, cosmology 77−64892
relativistic heat conducting inviscid fluid, exceptional waves *(French)* 77−53824
relativistic kinetic theory, thermodynamics, symmetry props. role 80−27117
relativistic quantum scalar plasma 78−75410
relativistic thermodynamics, entropy law 78−8373
relativistic thermodynamics, temp. transforms., invariance and meas. 79−92935
relativistic thermodynamics of chemically reacting fluids 79−64801
relativistic transformations 77−45813
relaxation functions of materials with memory 78−73949
relaxation phenomena, general treatment 78−44398
renormalisation group eqns. and thermodynamic anomalies near tricritical point *(Russian)* 80−13027
resonance phase transition in two-level lattice system, thermodynamics 80−69351
reversed causality illustration, Kac ring, expt. searches 77−49704

thermodynamics continued
reversible state space, geometric invariant representation *(Chinese)* 80−101771
review, non-equilib. systems 77−26255
Riemannian geometric model, appl. to pure fluid 80−17910
rigorous mean field theory derivation from many body interaction 77−26260
rotational like degrees of freedom system, phase transitions, thermodynamic props. 80−77737
rotationally symmetric fluid bodies in gravit. field, thermodynamic treatment of capillary phenomena 78−10262
running crack, cohesive fracture zone, thermodynamic laws 80−43676
running crack problem, thermodynamic calc. *(French)* 79−64582
safe stress of high-strength solid bodies, thermodynamic determ. *(Russian)* 79−50679
Saha equation, elementary derivation, rel. to mol. dissoc. 80−82599
scaling function for eqn. of state in 1/n and ϵ expansions 77−87718
school physics, elementary presentation by theory of heat, thermodynamics, and thermometry *(Danish)* 80−4483
sea ice, dynamic thermodynamic model 80−51432
second law, according to principle of max. entropy prod. *(German)* 77−65016
second law, classical derivation using Liouville theorem 79−21682
second law, entropy increase principle for collection of systems, for teachers 77−33785
second law, heat flow direction and Fourier inequality, comparative assessment 79−44896
second law, irreversible heat engines 77−101
second law, molecular teaching model *(Hungarian)* 77−64903
second law, perfect gas model *(Hungarian)* 77−64904
second law, rubber model teaching aid *(Hungarian)* 77−64905
second law and cyclic processes 79−30399
second law and thermally excited quantum oscillators 77−34863
second law from molecular viewpoint *(Hungarian)* 77−67393
second law limitations, Maxwell's demon 80−13015
second law of thermodynamics, crystal model teaching aid *(Hungarian)* 77−64906
second law of thermodynamics, time, struct. and fluctuations *(Czech)* 80−13016
second law of thermodynamics and stability in thermoelasticity theory 80−31689
second law rel. to time, structure, and fluctuations 79−30398
second principle, Clausius-Planck inequality as local formulation 78−45585
second-law analysis of solar-thermal processes 80−21378
second-order constitutive equations of hydrodynamics, dynamical interpret. 80−36860
selection game, fluctuation theory 77−26241
semi-systems, restrictions on accessibility of states 78−70080
semiclassical densities in phase space, Wigner's distrib. function for thermodynamic equilibs. 79−58565
semiconductor devices, theoretical foundations 77−39835
semiconductors, thermally stimulated relaxation processes, book contribution 80−80295
semiflexible macromolecule soln. liquid-crystalline phase determ. by Onsager method 78−94963
semimetal film, quantised, in high mag. field, thermodynamics of electrons *(Russian)* 79−56341
separation, partial condensation methods, thermodynamics *(German)* 78−20054
shock boiling, liq. discharge through short nozzles, flow blocking 79−86491
shock waves in incompressible elastic solids, thermodynamic theory 77−68508
short-range interparticle interaction potential, thermodynamic perturbation theory 77−43124
simple classical fluid, new theory 79−99051
simple fluid, struct. and thermodynamics, Monte Carlo calcs. 80−59365
simple systems, equilib. and the thermodynamic state surface *(Hungarian)* 79−26014
sine Gordon field, thermodynamics 77−87913
sintering, solid state, thermodynamic considerations 79−78912
size effect, model of dynamics, generalised thermodynamic forces 80−53627
size effect, thermodynamical model for constrained and unconstrained bodies 80−58900
slag equilibria Flood-Grjotheim treatment 78−39752
sliding bearings, effect of solid surface lubricant interaction on load carrying capacity 79−20206
small system in thermostat, reduced description 77−5783
soap films as analogue for minimum path and minimum area problems 77−17740
soil-water system, thermodynamic state functions *(German)* 80−4056
solar coronal loops, thermal equilibrium 80−94773
solar energy collector and task matching, thermodynamic aspect 79−57390
solar neutrino problem, limitations of energy transport by mechanical means 77−17461
solar stills, design and thermodynamic parameters, numerical anal. 80−55914
solar transition zone, energy balance and press. for network and active region features 80−21957
solar water pump for lift irrigation, thermodynamic anal. and simulation 80−61397
solid electrolytes with structural disorder, domain states, thermodynamic study 79−42307
solid lattice thermodynamics, two-temp. Debye approx. *(Russian)* 80−77728
solid solution, statistical treatment by first order approx. *(French)* 77−9117
solid-fluid interface, wetting and adhesion, thermodynamic aspects 80−89525
solid-fluid mixtures, thermostatics 77−856
solid-fuel mixture, incompressible, equilibrium theory 77−857
solid-solid reactions, analysis and reaction development, review 80−16648
solidifying melt, particle engulfment, thermodynamic aspects 77−4184
solids, large thermal fluctuations, kinetic eqns. for many-body treatment 79−54037
solids, polarisable and magnetisable, theory of in electromag. fields 77−57291

thermodynamics continued
soliton lattice melting, functional integral method 80−17883
solution, binary, ion solvation *(Russian)* 78−31676
solutions, thermodynamic functions, endostatic transformations 77−28022
some thermodynamical remarks on the theory of gravitational field 78−81899
sound propagation, influence of relaxation phenomenon, relativistic theory *(French)* 77−37754
spatially homogeneous simple reaction systems, indefinite second time derivatives of thermodynamic pots. 78−85126
special relativity, thermodynamic implication 80−47003
special relativity theory, thermodynamic quantities, Voigt-Palacios-Gordon transformations of thermodynamic quantities 77−9970
spectral distributions and subsystem density matrix *(Russian)* 78−65891
spherical limit for n-vector correls., spin correl. functions 78−24726
spherical multicomponent fluid, hydrostatic equilib., thermodynamic interpretation, 3-component neutron star 79−49135
spin glass, statistical thermodynamics 77−66363
spin glass theory and the third law of thermodynamics 77−55674
spin glasses, theory and third law of thermodynamics 77−89964
spin systems, Gibbs states, boundary condition equivalence 80−42159
spin systems, group theory anal. of thermodynamic limits 77−74343
spin systems in phase transition to superradiant state, dynamics and thermodynamics 79−22925
spin-systems, double-time Green functions method, thermodynamics 79−15313
spreading from binary surfaces, thermodynamics 78−6197
stability, constitutive inequalities and induced global bounds on thermodynamic states 79−166
stability and critical point, ferromagnets and simple fluids 78−16766
stability and relative stability in systems with multiple stationary states 79−79280
stability conditions, complete diagonalisation 80−17908
stability positive divisibility, exam. of necessary surface condition 78−73956
stability properties of equilibrium states, free Bose gas 78−8368
stars, self-gravitating systems, fluctuating hydrodynamics and thermodynamics 78−77485
stars containing mixed poloidal and toroidal mag. fields, adiabatic stability 80−67706
stationary states of systems with linear phenomenological relations and nonconstant coeffs., stability *(German)* 77−37831
statistical concepts, for teaching 79−35501
statistical equality connecting zero Fourier harmonics with average quantities 80−133
statistical information, information extent and information distance 78−77824
statistical mechanics, entropy, information theory *(French)* 79−63178
statistical mechanics, equilibrium distribution functions, thermodynamic derivation 79−71175
statistical mechanics, foundations 80−22271
statistical mechanics, relativistic formulation, appl. of bootstrap theory to thermodynamics and cosmology 79−40452
statistical mechanics, stability, equilib., and metastability 80−31659
statistical mechanics reln. with dynamics 78−49748
statistical thermodynamics from statistical theory of estimation 78−54328
steam drums in nuclear power plants, analogue simulation of dynamics 77−71645
steam-water mixtures, reversible adiabaticity equations 79−12751
steel powder, high speed, S and O reduction in a H_2 gas stream 80−61015
stellar atmosphere in statistical equilib., effects of deviations from LTE 80−31290
stellar equilibrium statistical mechanics of gravitating systems with energy cutoff 78−93326
stellar equilibrium statistical mechanics of relativistic systems with energy cutoff 78−93327
Stirling free piston heat engines, closed-form solns. for a coupled ideal anal. 80−35721
stochastic properties of the thermodynamic Hamiltonian 79−6069
stress corrosion cracking failure, predictive approaches 80−97611
stress energy finite temp. matrix elements in multiply connected spaces 80−4606
stretched dipoles, in applied elec. field, distrib. function 78−64851
structural phase transitions, applicability of thermodynamic theory 80−2139
subquantum thermodynamics 78−24751
subsystem interacting with thermal bath. kinetic eqn., Markov approx. 80−47006
superconductivity, general relativistic phenomenological theory 80−2518
superconductor nonequilibrium state stability with respect to finite fluctuations 80−103782
superionic crystal, domain formation, thermodynamic theory 77−84963
supernovae, thermodynamic of nucleon, lepton, photon mixture, quantum mechanical calcs. 80−77273
superradiance phase transition problem, applicability of Wang-Hion method 80−31695
surface, and surface waves 78−6207
surface films, thermodynamics of Volta effect 77−51604
surface reacting boundary layer, thermodynamic coupling theory 77−72369
surface thermodynamics, fundamental eqns. 80−107630
surfaces, equilib. and nonequilib. processes, review 77−44505
synergetics, introduction and appls. 79−26019
system with chemical reaction, thermodynamic stability, phase transitions 79−5174
systems far from thermodynamic equilib., dissipative structures, broken symm. equilib. phase transition theory 80−65827
teaching, 1st law, axiomatic vs. conventional formulation 78−24619
teaching, chemistry, applicability of $dE=TdS-PdV$ 77−87609
teaching, classroom example, free energy change during liq. vaporisation 80−42010
teaching, pressure-volume work exercises illustrating the first and second laws 80−22173
teaching, Spanish course based on Keller plan 79−58495
teaching, temp. concept without zeroth law 78−24607
temperature concept, meas. techniques 80−52204
temperature rate dependent materials 79−90123

thermodynamics continued
temperature scales, differences between IPTS-68 and thermodynamic temp. above 0°C 78−32814
temperature scales above 0°C, evidence of IPTS-68 departures from thermodynamic temp. 78−32813
ternary liquid-liquid systems, equilib. data correl. 77−4919
ternary systems with two component solid phases, eutectic, peritectic curve eqns. *(Russian)* 80−54344
tetraphersylanonium-tetraphenylborate assumption for single ion thermodynamics in amphiprotic and dipolar-aprotic solvents 80−55675
theory of constrained mixtures with multiple temperatures 80−62600
thermal cycling, thermodynamics appl. in mathematical anal. 80−108530
thermal equilibrium statistics, by fluctuation in thermodynamic theory of meas. 79−85074
thermal fluctuation of self oscillating reaction system under periodic external force 80−50828
thermal gas slip coeff., using Onsager symm. principle 77−58737
thermal mechanics: a quantum mechanical analogue of nonequilibrium statistical thermodynamics, stochastic processes 80−52125
thermal-caloric corresponding states one parameter model 79−44892
thermal-convective instability through porous medium 80−53769
thermo-kinematic constrants in the thermodynamics of elastic bodies 78−83255
thermo-osmosis, phenomenological equations, fluxes and forces 77−5779
thermochemical heat pump/refrigerator thermodynamic analysis 80−35716
thermodynamic energy conversion efficiencies 80−101081
thermodynamic fundamentals of continuum mechanics, equilibrium states 79−40373
thermodynamic limit for a classical system of particles with hard cores 79−71353
thermodynamic variable, nonlinear fluctuations, Onsager-Machlup function 78−36957
thermodynamics of internal variables, rel. to absolute reaction rate theory 78−18696
thermoelastic materials, constitutive functions 79−94488
thermoelasticity theory with appl., book 78−79219
thermoelectric convertor, generalised surface, quadratic form heat balance equations 79−83609
thermoelectric phenomena, irreversible homogeneous materials, single (double) bimetallic junctions *(French)* 78−95291
thermoelectricity, phenomenological equations, fluxes and forces 77−5779
thermoluminescence, nonequilibrium thermodynamics 78−68569
thermomechanic laws of gases and other substances *(Bulgarian)* 78−16767
thermomechanics, introduction, book 78−54187
thermoplasticity using thermodynamics of materials with internal state variables 78−18189
thermostatics, relativistic foundations 79−67239
thermoviscoelastic materials, thermodynamics of nonlinear single integral representations, appl. to one-dimensional wave propag. 77−68438
thermoviscoelastic-plastic materials, constitutive reln. 80−58
thermoviscous solids with microstructures, irreversible thermodynamics 78−34005
thin films, precipitation and nuclei form. in presence of condensation centres, thermodynamic model 80−103594
thin shells, thermomechanics by direct approach 79−18717
thiourea, incommensurable phase transitions. thermodynamic pot. 80−79941
time asymmetry for mixing system 78−12663
time-dependent Onsager problems, soln. 79−20457
transient relativistic thermodynamics and kinetic theory 79−17330
transient relativistic thermodynamics and kinetic theory 79−63177
transport relaxation equations, reciprocity, boundary conditions 77−13719
1,1,1-trichloroethane, in nonpolar solvents, permanent dipole moment determ. 77−43125
triple point, 180° rule violation criteria, thermodynamic stability 77−7841
two dimensional real matter, low density free energy in canonical thermodynamics plasmas 80−87852
two phase flow, constitutive laws determ. from irreversible thermodynamics 80−36861
two state approximation, for sp. ht. anomalies associated with phase transition 79−26013
two temperature theory of heat cond. fluids 78−26017
two thermodynamic phase interface and critical behaviour, surface fluctuation dynamical symmetry 79−97333
two-level quantum dynamics, representations of Kossakowski conditions 78−20989
two-level system in radiation field, dynamics, temp. depend. props. 78−66793
two-phase dispersion, size distrib. function of bubbles/droplets in thermodynamic equil. 80−7862
two-phase flows, transient, theoretical interfacial constitutive models 79−86497
two-phase system with interface, derivation of dynamical eqns. 79−49155
type I superconductor, magnetisation in thermodynamic and metastable phases 80−93027
unitary group representations, appl., book 79−30198
units, SI system *(Croatian)* 80−189
Universe, consequences of using concept of entropy 78−4418
unstable state decay of macroscopic system, deterministic description 79−17347
unstable systems, fluctuation dynamics in Ginzburg-Landau models 77−49685
vacuum bubble evaporation and thermodynamics, surface oscill. consideration 80−62608
vacuum system, rate of molecular impact on surface or orifice, possible conflict with second law of thermodynamics 80−46954
vanadate polystyrene based membranes, parameters, biionic pot. 79−57294
vapor-liquid energy transport in a porous medium 79−64762
vapour, associated, one-component unsaturated, press., composition changes, eqns. *(Russian)* 80−55696
vapour-liquid equilibrium, high-pressure, isothermal, meas. and correl. 78−18755
variational irreversible thermodynamics of heat and mass transfer in porous solids 79−4081

thermodynamics continued
variational Lagrangian irreversible thermodynamics of nonlinear thermorheology 77−27467
variational principle in nonequilibrium nonlinear statistical thermodynamics *(Russian)* 79−85058
variational thermodynamics of viscous compressible heat conducting fluids 77−50868
violation of second law, linear decompressive expansion followed by adiabatic compression, cyclic 80−42019
viscoelastic Cosserat, thermomechanical behaviour 77−19539
viscoelastic deformation kinetics, Gibbs eqn. and nonequilibrium thermodynamic models *(Ukrainian)* 78−90720
viscoelastic materials, restrictions on relaxation function 77−75821
viscoelastic matter cosmological evolution, causal thermodynamics *(Russian)* 79−101232
viscoelastic media, deform. theory with account of thermodiffusion *(Ukrainian)* 78−67052
viscous fluid mixture with thermomolecular diffusion, new variational-Lagrangian thermodynamics 79−49185
viscous fluids, nonstationary relativistic thermodynamics, hidden variable approach 80−68097
viscous interface theory and associated stability problems 79−95246
viscous liquid, glass transition, mol. mechanism for thermodynamic second order transition 78−2237
vitrification, thermodynamical and model-statistical treatment 78−26661
vortices, two dimensional, statistical mechanics 78−30304
water, Brillouin light scatt., temp. gradient induced 80−100663
water equation of state, between 350 and 1000°C (0 to 10 GPa) and between 100 to 350°C (200 MPa to melting curve) 80−15214
water pool nucleate boiling heat transfer thermodynamic investigation *(Chinese)* 79−72783
water solar photodecomposition, redox reaction thermodynamics 80−35697
water thermolysis, solar furnace, thermodynamic analysis 79−83625
weak second law of thermodynamics, classical gas in rectangular box 77−82442
weakly coupled non equilibrium systems, time asymptotics and reversibility 79−54049
Weinhold's length, significance 80−98866
wood, model for gasification process 79−61937
Yang Mills gas, contrib. of instantons to gas thermodynamics 79−12964
zeroth law and transitivity, empirical temp., for teaching 77−33790
$Ag(CN)_2$, adsorption on activated charcoal, kinetics and thermodynamics 79−82456
Al combustion in water vapour thermodynamic calc. 0.1 to 40 MPa *(Russian)* 79−39148
Ar, nucleation, thermodynamics 78−14454
B CVD from BBr_3-H_2 mixtures 79−47634
B_xP_y, gas phase deposition from B-P-U-H systems, thermodynamics 79−11518
BaO-B_2O_3-V_2O_5 glass, oxidation-reduction of V, thermodynamics 80−85169
$BaTiO_3$ type crystal, thermodynamic analysis of struct. phase transitions *(Russian)* 80−103473
C-C interaction energy, thermodynamics of steels 80−93793
C_3, linear, high temp., rot.-vibr., anharmonicity, thermodynamic function calcs. 80−43830
CO, vibr. excited, in Ar matrix, information theoretic anal. 78−91386
CO_2, linear, high temp., rot.-vibr., anharmonicity, thermodynamic function calcs. 80−43830
Cr binary substitutional solutions, thermodynamics 80−54410
Cr-rare earth alloy, calc. of phase diagrams, with immiscibility in liquid state, using thermodynamics *(Russian)* 79−20029
Cu liquid, thermodynamic study of O_2 80−88342
Cu matte converting, thermodynamics of process, Noranda process, exam. using computer model 78−80492
Cu-Cs diluted deuterated Tutton salts, electron non-Zeeman system, nuclear relaxation study 80−44951
Cu-Fe-S-O matte, appl. of Gibbs-Duhem eqn. 77−4923
Cu-O system, deposition by chem. transport, thermodynamic anal. *(German)* 78−31344
Cu-Sn (25 wt.%), liq., struct. from thermodynamic and diffr. studies 80−6350
$Cu_3(PO_4)_2$, polystyrene based membranes, parameters, biionic pot. 79−57294
Eu_2O_3+$EuPO_4$ in Mo crucible, $EuMoO_4$ and $EuMoO_3$ atomisation energy 78−40073
$EuPO_4$ in Mo crucible, $EuMoO_4$ and $EuMoO_3$ atomisation energy 78−40073
Fe-C, martensitic transformation, thermodynamical study *(Chinese)* 80−55395
Fe-Cr-Ti(Al) liquid alloys, thermodynamical anal. of O_2 solubility *(Russian)* 80−92676
Fe-SO_4-H_2O suspension system at 90°C, potential-pH diagram 78−61068
Ga-In-Sb, ternary phase diagram, thermodynamic models of solidus and liquidus isotherms 79−24504
GaAs, homogeneity region calc. 80−92681
GaAs-Sn-H_2-HCl, thermodynamic calcs., reduction of $SnCl_2$ by H_2 79−86903
$Ga_xIn_{1-x}As_yP_{1-y}$, CVD by Ga-In-P-H-Cl system, 80−54159
GaN, thermodynamic anal. of prep. methods 80−55328
GaSb, defect concentration determ. model, Hall effect 80−103385
Ge, high purity melt, stability of oxide second phases 79−47898
H plasma, pair correlations down to r=0 80−14883
H prod. by H_2O pyrolysis, computer thermodynamic anal. and optimisation 80−45766
H-like atom, spin-orbit interaction and single electron excitations rel. to mag. dielectrics 79−54780
H-like ions, departure coeffs. from thermodynamic equilib., rel. to radio-sources recomb. lines 79−76369
H_2 oxidation reaction kinetics, thermodynamic model appl. *(German)* 79−5130
H_2 production, engineering impact on the validity of the mark-16 thermochemical cycle 80−55931
HCl/membrane/NaCl+HCl isotonic osmotic systems, inversion 79−52775
HF chemical laser, pulsed, evolution, irreversible thermodynamic anal. 79−31887
HF-HCl, SCF energy hypersurface, stationary points, thermodynamics of form. 80−102436

thermodynamics continued
H_2O pyrolysis, solar-H_2 energy systems, theory 80−61448
He, superfluid, statistical thermodynamics of cubic system below 0.5K 79−86939
He, thermoacoustic oscillations in nonuniformly heated tubes 80−33441
He vapour, low-temp. positive ion mobility by absorptive model, WKB calcs. 79−77333
^{3}He, adsorbed on Grafoil surface, ground state, thermodynamic anal. 79−19421
^{3}He fluid-superfluid transition phase diagram, thermodynamic stability, fluctuations *(Russian)* 80−80023
^{3}He-B, superfluid, macroscopic parity nonconservation due to neutral currents 77−80671
^{4}He, liq., nucleation of freezing by positive ions 77−84893
^{4}He, superfluid, thermodynamics 77−69131
Hg-Cd cell, EMF rel. to temp., thermodynamics 77−12805
K, absolute zero isotherms and polymorphic transition 79−73310
$LiCrO_2$, evaporation, as a corrosion product in compatability experiment of Li_2O pellets with Fe-Ni-Cr alloys, mass spectrometric study 79−73301
$Li_{1.8}N_{0.4}Cl_{0.6}$, fast ionic Li conduction, elec. conductivity and thermodynamic stability 79−65247
Mg-Sr, liq. alloys, thermodynamic activities determ. 80−50604
N_2O_4, as working medium, thermodynamic cycle, approx. model *(Russian)* 77−73464
Nb, O_2 desorption in a vacuum, thermodynamic props. calcs. *(Russian)* 80−54501
NbN preparation, by precip. from gaseous NgF_5-N_2-H_2 mixture 80−20857
Ni-bearing substitutional binary solutions, thermodynamics 80−44336
Ni-C melts, reaction with Al_2O_3, activation energy 79−83448
NiF_2, antiferromag. reson., Lagrange and nonequilib. thermodynamics descriptions 79−15357
$Ni(OH_2)$ electrodes, charged, thermodynamic considerations of reversible potentials 80−55670
O_2 solubility in liquid Nb, exam. using thermodynamic anal. *(Russian)* 79−55889
Rb_2MnCl_4 antiferromagnet, spin flopping phase transition 79−69687
Si-Au system, ion implanted induced giant gettering, annealing effects 80−88221
SiC, vapour deposition, thermodynamics of Si-C-Cl-H system *(German)* 79−11520
Si_3N_4, low pressure CVD, thermochemical calcs. 80−108356
SiO_2, low pressure CVD, thermochemical calcs. 80−108356
Ta, O_2 desorption in vacuum, thermodynamic props. calcs. *(Russian)* 80−54501
α-Ti/Fe, retrograde solid solubility 80−79950
Ti-N-C-H-(O) system, thermodynamic anal. *(Russian)* 80−55325
Ti-Ni (50.4 wt.%), thermal conversion efficiency of ideal thermoelastic marmem cycle 79−66057
TiC, production from tetrachloride and hydrocarbon, thermodynamic analysis *(Russian)* 80−7523
TiO_2:$TeCl_4$ system, chem. vapour transport, matrix isolation IR studies 80−93755
(U,Pu)-oxide nuclear fuel, near and non-stoichiometric, O_2 potential, thermogravimetric and galvanic cell meas. comparison 79−63744
U compounds, reduced partition function ratio calculation 77−12819
UO_2 fission reactor fuel fragmentation gas thermodynamics 79−13458
$UO_2(NO_3)_2$ solutions, cryoscopy and activity coeffs. 78−11544
ZrI_4, thermodynamics of vaporisation from substoichiometric solid Zr iodides 80−3393

thermoelasticity
see also thermal stresses
acceleration waves in thermoelastic incompressible solids, propag., amplitude 77−19555
acoustic liquid, thermoelastic scatt. effect on wave processes in piecewise inhomogeneous space with plane interface *(Russian)* 77−55317
acoustic vibr. anal., finite heat propag. vel. soln. of coupled dynamic thermoelasticity problem 77−42770
acoustic wave generation at 20 MHz, from pulsed thermoelectric expansion of constrained surface 77−35007
after-effects in thermo-elasticity 80−106724
alkoxyphosphazene polymer, elastic and thermoelastic props. 77−56014
alloy, memory effects, props., phenomenological theory and appls. *(German)* 77−1864
anisotropic, at low reference temp., linear coupled theory 80−59
anisotropic 3-D problems, numerical projective method 77−68436
anisotropic bodies, generalised coupled thermoelasticity problem 77−89030
anisotropic media, uniqueness theorem for generalised thermoelasticity equations 80−92062
anisotropic shells, theorems *(Ukrainian)* 77−68403
anisotropic slab, thermoelastic crack problem 80−23960
anisotropic solids with magnetic symm., unified dynamic theory 78−77713
anisotropic thermoelastic shells dynamical coupled problem, variational theorem *(Russian)* 79−14255
annular plate of inhomogeneous material, varible loading and heated conditions 78−94594
Araldite CT200/HT907, 263 to 343K, mechanical, physical and optical props. 78−56682
arch, cylindrical, heat resistant material, exam. of thermoelastic stress problem 78−63306
aryloxyphosphazene polymer, elastic and thermoelastic props. 77−56014
asymmetric elastic medium, electrically conducting, magneto-thermoelastic waves anal. 80−15772
axisymmetric bodies, integrated photoelasticity, nondestructive anal. 79−18842
axisymmetric solids with rectangularly orthotropic props., asymmetric stress anal. 77−35031
axisymmetric thermoelasticity problem for two-temperature hollow cylinder 80−5941
axisymmetrical problems for media with transversal anisotropy *(Ukrainian)* 78−83246
Barber boundary conditions for thermoelastic contact, heat flows 80−69745
beam-like lattice trusses, numerical analysis 80−14566
bimodulus sphere, nonstationary thermal stresses 77−50902
bodies in contact, heat transmission, optimal control thermoelastic stress constraint 80−19223

thermoelasticity continued
bodies with wavy surfaces, thermoelastic contact, heat conduction 80−64492
body with thermally insulated cracks, periodic thermoelastic situation 77−68417
bonded composite hollow circular cylinder, asymmetrical transient thermoelastic problems 78−30181
book, theory of thermoelasticity with appl. 78−79219
Born model, electrostriction rel. to dielec. and thermoelastic props. 80−71322
boundary integral eqn. method for 3-D thermoelasticity 77−72175
boundary integral eqn. method for 3-D thermoelasticity 78−5657
boundary value problems, exterior, 2-D *(French)* 80−79144
α-brass, Gruneisen parameter determ. using thermoelastic effect 79−28068
brittle material, heat resistance criteria on surface during convective heat exchange 77−15642
brittle solids, unstable growth of thermally induced interacting cracks 78−63374
cavity, ellipsoidal, triaxial, thermoelastic stresses 80−92061
chemically hardening material cast in elastic cylindrical mold, transient thermal stresses 80−7589
circular cone, thermal stresses 78−90715
circular cylinder under intermittently sudden heat generation, transient thermal stresses 77−3728
circular cylinder with circumferential edge crack under uniform heat flow, thermal stresses 80−48641
circular hollow porous cylinder with mass transfer through reflecting walls *(Russian)* 79−14220
circular plate, quasi static thermal deflection 79−14259
circular plates, thermoviscoelastic anal. of a thermorheologically simple material 80−10161
circular plates with piecewise-constant thickness 80−99935
composite Cosserat elastic cylinders, thermal stress problem, soln. method 79−72812
composites, elastic modulus and expansion coeff., approx. method *(Russian)* 77−39681
concrete, unreinforced pavement slabs, environmentally induced stresses, computer experiments 78−35435
conductor, cylindrical, carrying elec. current, magnetothermoelastic interactions, mechanocaloric effects 79−72815
constitutive functions of thermoelastic materials, theory 79−94488
contact, frictionally heated, thermoelastic deform. 80−83764
contact, thermoelastic, involving a sharp corner 80−83766
continuous elastic solids, foundations for coupled thermoelasticity 80−46807
continuous media, energy rules 77−80074
corundum-based refractory lining specimen, thermal softening assessment *(Russian)* 79−83237
Cosserat composite elastic cylinders, thermal stresses 80−5937
Cosserat medium subject to thermal stresses, plane contact problem *(Polish)* 78−22268
coupled dynamic problems of thermoviscoelasticity quasilinearisation method 77−72188
coupled dynamic thermoelasticity problem for a half space with thermal 'memory', thermoelastic waves 80−83753
coupled field, spherical symmetric problems analysis 77−42737
coupled fields in solid mechanics 77−68391
coupled thermoelastic problem, formal soln. 80−4529
coupled thermoelastic problem, Green's function soln. 79−72818
coupled thermoviscoelastic structures, sustained periodic vibrs., finite element anal. 79−7315
crack, in semiinfinite thermoelastic solid with heated boundary 78−55610
crack problems in anisotropic thermoelasticity, temp., displacement, stress field 77−80105
cracked bodies, finite element anal. 77−3793
cracks, penny-shaped, in elastic sphere embedding in infinite elastic space, thermal stresses 80−64460
critical thermal load, for thermoelastic wave propag. 78−30228
crystal growth, creation of stress and dislocations *(Russian)* 80−103277
crystal growth from melt, stress form., dislocation density estimation *(German)* 80−15022
crystals, coupled hydrodynamic modes near structural phase transitions 77−1203
curved beam, nonstationary heat conductivity and thermal elasticity 77−84109
curved plates, subject to arbitrary temp. distrib., stresses and displacements 80−5938
curvilinear aeolotropic solids, 3-D thermoelasticity 80−56
cylinder, circular, thermal stress conc. determ. by integrated photoelasticity *(Russian)* 77−46925
cylinder, circular, three-dimensional transient thermal stresses under nonaxisymmetric temp. distrib. 80−92054
cylinder, dynamic thermal stresses due to heating *(Polish)* 78−18183
cylinder, elastic deform. due to heat sources 79−18713
cylinder, finite, of anisotropic material, thermal stresses due to thermal crack 77−39233
cylinder, hollow, unsteady axially nonsymmetric temp. distrib. *(Polish)* 80−10152
cylinder, short, visioelastic, expt. and theoretical investigation of heat evolution in cyclic compression 78−13929
cylinder, stresses due to plane temp. distrib. 80−5935
cylinder, subjected to heating and cooling, thermoelastoplastic soln. 79−72816
cylinder, thick orthotropic circular, bimodulus elasticity, thermal stress 77−23885
cylinder, thick walled with filler 77−84150
cylinder, transient thermal stresses due to arbitrary heat supply, 3-D anal. 79−46215
cylinder, weakened by penny-shaped cracks, thermoelastic stresses 80−10191
cylinder of short length, thermal stresses *(Russian)* 77−75798
cylinders, symmetric thermoelastic stress, Lanczos-Chebyshev method 80−33458
cylindrical plastic shell, nonstationary temp. field, contact press. calc. in cable pressing 78−63270
cylindrical shell, heated, large deflection 78−63289
cylindrical shells, calc. of stresses *(German)* 80−33454
decomposition theorem for thermoelasticity with finite wave speeds 80−57

thermoelasticity continued
deformable solids, singularities of dynamic processes, finite rate effect of heat propag. 80−19247
deformable solids with rough surface, stochastic problem of heat conduction and thermoelasticity *(Russian)* 78−38169
deformation, second order effects 80−92051
diatomic solids, thermoelastic, continuum theory 80−53635
dielectrics, constitutive eqns. determ. 78−18170
dielectrics, reciprocity theorem for dynamic problems 79−37165
diffraction problems in exterior domain, existence and uniqueness theorems, series expansion of potentials *(French)* 80−64366
direct anal. in 1-D 80−8797
dislocation motion, thermal and thermoelastic fields *(Russian)* 78−22731
dynamic contact problem, numerical anal. for thermoelastic half-space 77−62215
dynamic theory, based on causality principle 80−69657
dynamic thermoelasticity, stress-temp. eqns., uniqueness theorem 79−72813
dynamic thermoelasticity of body with crack, two- and three-dimensional *(Russian)* 77−68400
dynamical properties of thermoelasticity problems solutions *(Ukrainian)* 80−69663
Earth crust, anal. of thermoelastic strains and tilts 78−20346
elastic behaviour of elastic materials, thermodynamical bounds, thermoelasticity, deformation 79−41576
elastic dielectrics, Voigt's intramolecular force balance 77−60936
elastic heat conductors, second order response functions 77−68424
elastic medium, crack propag. in dynamic thermoelasticity *(French)* 80−38327
elastic solid, difference and finite-element method for dynamical thermodiffusion problem 77−62154
elastic solid, variational principle in ablation 78−90698
elastic stress analysis of an anisotropic compound rotating disc under thermal loading 78−67036
elastic viscoplastic body, differential rheological eqn. *(Ukrainian)* 78−55617
elastic wave excitation by laser beam, through thermoelastic effect 80−103503
elastically clamped variable-stiffness annular plate, thermostability 77−89052
elastohydrodynamic traction, non-Newtonian thermo-viscoelastic, from combined slip and spin 80−103043
electromagneto-thermoelastic plane wave propag. phase vel. and attenuation coeff. 80−48621
Elinvar, Cr addition effect on modulus of elasticity and thermoelastic coeff. 77−90387
elliptic plate, heated, deflection under uniform load 77−35040
energy of thermoelastic inclusions in a semi-infinite solid 79−37163
engineering materials, thermoelastic response, appl. to dynamic response of engineering structures 79−35724
epoxy models, thermoelastic strains and stresses using strain gauges *(Polish)* 79−64609
epoxy resin, glassy, thermoelastic effect, thermal expansion coeff. 79−14944
epoxy resin, thermoelastic stress creation and motion picture recording of interaction with dynamic crack 78−56697
epoxy resin (Araldite B), photothermoelasticity meas. by heating method 80−6000
epoxy resin and glass, thermoelastic phenomena *(Polish)* 80−93724
expansion flexible acoustic probe 80−16618
extensional rod, thermal initial post buckling 77−14931
eye lens, human, microwave-induced hazardous non linear thermoelastic vibrs. 79−83853
ferroelectric, anisotropic, ratios between critical indices of thermoelasticity *(Russian)* 77−1642
fibre reinforced composites, transverse plane, elastic, failure behaviour *(Japanese)* 78−48510
fibre reinforced materials, therm. stresses in unit cell 80−10160
fibre reinforced thermoelastic materials, nonlinear thermodynamic continuum theory 80−14579
fibreglass cross wound shell, thermoelastic consts. 80−14577
field-matter interactions, book 79−30270
finite disc, thermal shock, finite integral transform method 77−3765
finite elastic cylinders, Ritz solns. for axisymm. temp. and stress fields 78−38190
finite element analysis, numerical realization, appl. to two dimensional thermoelasticity problems 77−84132
finite element approximations in thermo-plasticity 80−1435
finite orthotropic slab anal. 79−1111
finite short circular cylinder with arbitrary heat supply, unsteady thermal stress length effects 80−13541
fission reactor fuel can temp. and thermoelastic stress perturbations, conjugate heat transfer effects 77−54284
fission reactor fuel pellet-cladding interaction, theoretical analysis 79−93699
fission reactor fuel rod hairline cracks, effect on thermoelastic stress in surrounding can, iterative method of determ. 77−54285
fluid, near critical point, student apparatus 77−60881
fluids, stability of motion anal. 80−10221
fracture of material through the action of an internal heat source 78−67025
fundamental solutions in thermoelasticity 79−68573
generalised thermomechanics, principle of least constraint *(Russian)* 78−59295
generalised thermorheologically simple porous materials, thermomechanical theory of viscoelasticity 80−33479
glass, tempered plate, stress state model and heat transfer rate determ. 78−60684
glass bodies, heat resistance, determ. 80−24690
glass ceramic, machinable, elastic moduli press. and temp. derivatives, specific heat 78−52873
glass fibre reinforced plastic cylindrical shells, temp. stresses developing during polymerisation 80−40326
granular materials, thermoelasticity theory 80−42066
graphite, thermal shock on a finite orthotropic thin shell 79−68587
graphite shell, thin, cylindrical, orthotropic, thermal stresses and displacements due to instantaneous thermal shock 80−92060
Griffith criterion for brittle fracture in nonlinear thermoelasticity 79−77020

thermoelasticity continued
Gruneisen parameter and thermal diffusivity, thermoelastic meas. method 80−107581
half plane with internal line crack 79−32259
half space subjected to a heat flux step, perturbation anal. *(French)* 79−90130
half-space, dynamic response to energy flux, stress wave evolution *(French)* 80−74795
halfspace with overlying liq. layer, Stoneley waves 79−1134
hard sphere crystal, thermoelasticity in relation to melting 80−107353
harmonic wave reflection, effect of thermoelastic scatt. 80−14613
hearing sensation induced by pulsed microwave radiation 77−60229
heat conduction, appl. of orthogonal projection methods 80−1403
heat conduction, formulation of field eqns. removing paradox of infinite signal propag. speed 77−35014
heat exchanger, pebbles with periodically varying fluid temp., thermal stresses, heat storage capacity 78−26020
heat instability in thermoviscoelastic coupled dynamic problems *(Russian)* 79−10489
heat memory materials, dynamic thermoelasticity of infinite cylindrical rod *(Russian)* 80−74752
heat-generating, transversely isotropic cylinder, transient thermal stresses and displacements 79−68584
heating of body with thermoelastic stress restrictions, optimal control *(Ukrainian)* 78−83245
hemitropic micropolar thermoelastic continuum, static and dynamic problems 78−22293
heterogeneous linear thermoelastic media, coupled mean fields 78−18171
hollow cylinder, temp. and stress fields under action of periodic heat flux to inside surface 77−35013
hollow cylinder with heat flux on inside surface, nonstationary thermal stresses 77−7308
hollow laminated cylinder *(Russian)* 77−68405
hollow sphere, time-optimal control of heating *(Russian)* 79−27491
hollow sphere exposed to radiation, thermoelastoplastic problem 77−14928
homogenization of static props. of media with periodic structs. *(French)* 79−41579
infinite hemitropic micropolar continuum, action of instantaneous heat sources 77−89025
infinite medium, thermal stress problem for ribbon-like inclusion 77−58554
infinite medium containing periodic ribbon-like inclusions, local intensification of thermal stresses *(Japanese)* 80−96195
infinite strip with two coplanar Griffith cracks, stress distrib. 77−42779
inhomogeneous anisotropic linear thermoviscoelastic medium, asymptotic stability proof 79−21554
internal state variables materials, thermomech. wave propag. 77−3760
isotropic medium, propag. crit. of accel. waves 77−62190
isotropic plane with cusped holes and cracks, thermoelastic state *(Russian)* 79−68577
isotropic semiinfinite plate heated by moving point source of heat, temperature stresses 80−43628
Kevlar/epoxy composites, elastic props. rel. to thermal expansion 80−24622
Lamb's thermoelastic plane problem with gravity 77−29241
laminated anisotropic shells, thermal stresses *(Ukrainian)* 77−68399
laminated plates, symmetric, specially orthotropic, thermoelastic anal. 80−92058
laminated thermoelastic media, aggregate response modelling 77−50897
laminates, residual thermoelastic stresses 80−106721
large deflection of a shallow spherical shell subjected to uniform normal pressure and heating 78−94593
large deflections of heated orthotropic plates 79−32262
laser materials with inclusions, thermal stresses 77−729
lattice dynamics and energy channelling in thermoelastic effect 78−22786
layered beams, interlaminar thermoelastic stresses 80−1432
linear, conservation laws, path independent integral generalisation 80−53626
linear, continuous depend. and instability 80−74783
linear, energy arguments 78−51067
linear coupled thermoelasticity with microstruct., existence and uniqueness theorems 80−60
linear generalized theory, stress-flux initial boundary value problem 80−61
linear micropolar, uniqueness, reciprocity and variational theorems 77−37760
linear thermoconsolidation, porous elastic solid containing compressible fluid 79−23186
linear thermoelasticity, domain of influence theorem 78−26042
linearised thermoviscoelasticity with high temperature variations and related periodic problems 78−89343
liquid, nonviscous, laser-induced acoustic waves 78−63808
liquid-filled porous solid, first strain gradient theory of thermoelasticity 77−53783
long flexible cylindrical panel deform., temp. field effect *(Ukrainian)* 79−90128
machining metals, thermoelastic distortion 80−5939
magnetothermoelastic continua, macroscopic nonlinear theory 77−83775
magnetothermoelastic interactions in cylindrical conductor, mechanocaloric effect 80−7139
magnetothermoelastic plane Lamb's problem in initially stressed conducting medium 78−67077
magnetothermoelastic Rayleigh waves with thermal relaxation in uniform magnetostatic field 80−2617
magnetothermoelasticity, dynamic *(Russian)* 77−55995
magnetothermoleastic waves, propag. in initially stressed conducting layer 79−63
martensite crystal, dislocation representations of development kinetics 80−39086
martensitic transform., thermoelastic, equilibrium temp. 77−63671
martensitic transform., thermoelastic, equilibrium temp. 77−66644
martensitic transformation, thermoelastic, factors affecting internal friction peak 77−28812
martensitic transformation, thermoelastic, hysteresis, exothermic and endothermic effects *(Russian)* 78−19749
media with internal structure, thermodynamics 79−88901
melting elastic solid, variational principle 77−84894
memory alloy engine, efficiency 80−71648
metal thermoelastic coeff. meas. by strain gauges 78−56853
thermoelasticity continued
metallic plate, subject to laser heating, nature of thermoelastic stresses *(Russian)* 77−21199
metals, thermal diffusivity determ., thermoelastic method 79−23940
metals and alloys, polycrystalline, LF viscosity meas. 78−80576
metals in nuclear reactors, thermo-elasto-visco-plasticity and neutron irradiation 77−3111
microplanar elastic semi-space, axially-symmetric thermal contact stress 78−30179
micropolar layer, pertinent formulas for displacement vector components, force stress component distrib. 80−48581
micropolar materials, thermodiffusion 77−5667
micropolar semispace, effect of heated boundary on normal stress distrib. 80−1433
micropolar thermoelastic solids, entropy inequality and accel. waves 78−47538
micropolar thermoelastic space, travelling discontinuities 80−92055
micropolar thermoelasticity, axial symmetric problems, stationary vibrations 79−68572
micropolar thermoelasticity, Green formula for infinite domain with cavity 79−30241
micropolar thermoelasticity, half-space problem 79−30237
micropolar thermoelasticity, radiation conditions, uniqueness theorems 79−12606
micropolar thermoelasticity, three dimens. theory, pot. method 77−68414
mixed boundary-value problems of steady-state thermoelasticity and electrostatics 80−55
molecular crystal, anomalous thermoelastic behaviour and orientational transition 77−76334
molecular crystals, anomalous thermoelastic behaviour, mol. reorientation, theory 77−84676
multilayer solids, soln. of heat conduction and thermoelasticity problems *(Russian)* 78−38177
multiply connected orthotropic body, plane thermoelastic problem 78−38199
noble metals, thermoelastic relax., interaction of thermal and acoustic phonons calcs. for US longitudinal waves 80−65165
non-Fourier solid, thermoelastic disturbances propag., integral transform. calc. 77−89024
non-local continuum mechanics, conservation laws 78−65770
non-negativity of specific heat, rel. to dynamic stability 77−42723
nonlinear, dynamical eqns. 77−39218
nonlinear, Hamilton type variational principles 78−54190
nonlinear, initial value prob. for dynamic eqns. 77−7304
nonlinear deform. wave propagation in dissipative medium, interaction and reverse problems 78−53
nonlinear elastic dielectrics, thermodynamics and entropy flux 79−67164
nonlinear orthotropic heated plates, prestressed, existence of solns. 78−63286
nonlinear theory, propagation of mechanical and temp. acceleration waves 79−75346
nonlinear thermal bending of shallow sandwich shells and flat plates, numerical anal. 80−5936
nonlinear thermoviscoelasticity theory for generalised thermorheologically simple material *(Russian)* 78−57785
nonlocal, closed system of eqns. 78−62081
nonlocal generalised thermoelasticity, thermal waves in rigid conductors 78−5656
nuclear fuel elements, control rods, transient thermal stress anal. 79−599
one-dimensional thermal shock problem of thermoelasticity in a non-simple medium 79−18794
optical resonator, thermoelastically disturbed, mode calcs. 79−13992
optimal heating of solid body and stress relax. role *(Russian)* 78−22258
orthotropic cylinder, nonuniform, thermoelastic stresses 77−7312
orthotropic elastic medium, plane stresses, analytic continuation 77−39232
orthotropic plate with square hole and convective heat exchange, plane static thermoelasticity *(Russian)* 80−33456
oxide single crystals, Czochralski grown, thermoelastic stresses 78−55822
patch contact problem for large Peclet number 79−14266
perforated plane, thermoelastic-plastic problem *(Russian)* 78−55571
periodic problems for infinite solid with disc shaped cracks, integral eqn. solns. *(Ukrainian)* 78−55559
permalloy films, thermoelastic stresses and magnetostriction effects during light recording *(Russian)* 79−97465
photoelastic investigation of thermal stress fields due to travelling heat source *(Japanese)* 77−42747
piecewise homogeneous bodies, thermoelast. eqns., generalised conjugation prob. *(Ukrainian)* 80−53629
piecewise homogeneous thermoelastic body, 3-dimens. quasi-static problem soln. *(Russian)* 79−80441
piecewise-uniform plane, curvilinear cracks, integral eqns. of heat conductivity and thermoelasticity *(Russian)* 78−38250
piezoelectric thermoelasticity, dynamic reciprocal theorem 78−83242
planar body, with circ. boundary and thermally insulated cracks, temp. distrib. 78−67002
planar thermoelastic contact problems, Green's function for exterior contact 80−38350
planar thermoelastic contact problems, Green's function for interior contact 80−38351
plane deformation states, stability 80−43634
plane harmonic waves in pre-stressed heat cond. elastic material 80−62
plane problem for solids with curvilinear hole and cracks, integral eqns. *(Ukrainian)* 77−31257
plane walls of variable thermal cond., transient temp. fields *(Polish)* 78−18155
plane wave propagation in thermoelastic solids with Tolotti's isothermal pot. 79−18786
plane weakened by infinite line of identical orifices, inverse problem *(Russian)* 77−23881
plane with curvilinear cuts, mixed thermoelasticity problem *(Ukrainian)* 78−90709
PLASTEF code, numerical simulation of thermoelastoplastic behaviour using finite element method 78−90731
plate, annular circular, thin, of variable thickness, thermal buckling 79−32312
plate, annular elliptic heated, const. thickness, buckling and stability criterion 80−28443
plate, calculation of unsteady temp. field and thermoelastic strain 77−19534

thermoelasticity continued
plate, circular, thermally induced vibr. analysis 79−94524
plate, heated thin annular circular, of variable thickness, buckling, thermoelasticity 78−9581
plate, multiply connected, convective heat exchange, small parameter method for thermoelastic equilib. problems. *(Russian)* 78−63301
plate, simply supported, stresses, displacements under arbitrary temp. distrib. 79−72814
plate, temp. bending, generalised eqns. WRT transversal mech. characts., stress conc. problems *(Ukrainian)* 77−54876
plate, thermoelastic, deflection under point heat source 79−32261
plate, thermoelastic deflection under point heat source 79−32260
plate, three layer, thermoelasticity problem, soln. method *(Ukrainian)* 80−48574
plate, two-stage circular with heat emission, thermoelasticity, force anal. 79−10481
plate, weakened by periodic system of sound orifices *(Russian)* 77−23880
plate containing cracks, varying temp. cond. at edges, thermal conductivity and thermoelasticity *(Russian)* 77−23915
plate temp. dependent props. under linear temp. distrib., thermoelastic problem for crack 80−48579
plate with crack or ribbon like inclusion subjected to uniform heat flow, thermoelasticity 80−48578
plate-semi-infinite space, heat exchange process control, thermoelastic stresses *(Russian)* 80−53606
plates, flat, stability of postbuckling behaviour 80−1453
plates, piecewise-constant coeff. of heat transfer, thermoelasticity, method of integral charact. *(Russian)* 78−38188
plates, thick, multiply connected, stressed-strain state under nonstationary heat conditions *(Russian)* 80−87714
plates, thick, thermally loaded, 3-D anal. 80−33459
PMMA, glassy, thermoelastic effect, thermal expansion coeff. 79−14944
poly-2-hydroxyethyl methacrylate gel, thermoelasticity 77−84205
polybutadiene networks, cis-trans, thermoelastic obs. 79−74220
polycarbonate, glassy, thermoelastic effect, thermal expansion coeff. 79−14944
polyethylene, high-density, gaseous environment effect on mech. relaxations, tensile and torsion tests 79−96068
polymeric material, temperature shear function and temp.-time analogy in linear thermoviscoelasticity region 79−18747
polymers, crystalline, thermoelastic effects 78−88491
polymers, glassy, Gruneisen const. calc. from thermoelastic meas. 79−14945
polystyrene, glassy, thermoelastic effect, thermal expansion coeff. 79−14944
polystyrene, shrinkability, orient. 79−11660
polyurethanes, crosslinked, thermoelastic props. 80−20991
polyvinyl alcohol, atactic, thermoelasticity of networks swollen in water, polymer-diluent interactions 80−29102
polyvinyl alcohol networks, swelling equil. with dil. salt solns., thermoelastic behaviour, hydroxyl group interact. 80−79667
polyvinyl alcohol swollen in aqueous glycol, network thermoelasticity, interactions 80−104201
porous elastic matrix, onset of convection, variable prop. effects 77−84321
prestressed thermoelastic media, seismic-dislocation theory 77−86811
prismatic body for nonstationary thermal action, stress-state algorithm *(Russian)* 78−13905
punch contact with elastic half-space, effect of heat flow on contact area 77−7294
punch problem for elastic layer overlying elastic half-space 77−42742
quartz, fused, elastic wave excitation by charged particle beam 77−89474
quartz resonator, nonlinear thermoelastic couplings *(French)* 80−34118
quasi-perfect elasticity, theoretical foundations 78−63285
random heat stresses in elastic space with a cylindrical cavity *(Ukrainian)* 79−76971
Rayleigh waves, magnetothermoelastic, with thermal relaxation, theory 79−62
Rayleigh waves in magneto-thermoelastic solids with thermal relaxation 79−28581
Rayleigh waves in thermoelastic half space under initial stresses 79−94545
Rayleigh-type surface waves, retrograde modes 79−77888
reactor cylinders, eigenload formulation of thermoelastic stress 79−46213
reactor cylindrical rods, anal. of self-equilibrating end stresses by Lanczos-Chebyshev method 79−46212
recrystallisation, induced, in thin metal plates *(German)* 78−19783
rectangular plate with central hole, thermal stresses and buckling 77−3755
rectangular viscoelastic prism exposed to repeated stretching and contraction, thermomech. anal. 77−54896
reinforced plates, heat conduction and thermoelasticity eqns. *(Russian)* 77−75795
residual stresses in shells of revolution, cut-out element method glass-plastic composite, thermoelastic residual stresses in shells of revolution, cut-out element method 80−38271
retardation time effects on heat pulse propagation 79−18725
retrospective problem, pot.-type singular integral approx. algorithm 80−27132
rocks, crack growth and thermoelastic behaviour 80−26502
rod, semi-infinite, temp. stresses 79−18714
rod of time hardening (softening) material, thermoelastic stresses 80−92046
rods, coupled thermoelastic wave propagation, asymptotic theory 79−12609
rods, thermomechanics, direct approach 80−10141
rotating circular cylinder, stresses and displacements due to axially nonsymm. heating of lateral surface *(Polish)* 78−22248
rotating disks, elastic and elasto-plastic, with temp. gradient, stress distrib. determ. *(Italian)* 79−41633
rubber cylinder, circular, uniformly heated, combined extension and torsion 80−92057
rubber elasticity, molecular aspects book contrib. 78−84886
rubber-like networks, thermoelasticity, rel. to rubber elasticity theory 77−31219
second law of thermodynamics and stability in thermoelasticity theory 80−31689
second order thermo-microelasticity 80−74742
thermoelasticity continued
second-order phase transitions in crystals, equilibrium configurations, thermoelasticity theory 80−70364
semi-infinite medium, transient thermal loadings, stress intensity factors 80−10193
semi-infinite medium under uniform heat flow, thermal stresses around ribbon-like inclusion 78−59303
semiconductor plate, light irradiation, heating and thermoelastic stress 80−25499
semiinfinite plate, thermal stresses, heat transfer effect 80−96193
shallow shell theory, series representation of fundamental solution 79−10468
shape memory effect, criteria for efficiency assessment *(Russian)* 80−21015
shell, cylindrical, inhomogeneous, thermoelastic torsional waves 79−92952
shell, nonaxisymmetrically heated thick cylindrical, thermoelastic anal. 79−10482
shell, thin spherical, axisymm. thermal stress by method of matched asymptotic expansions 77−72169
shell calcs. by sectioning stress state *(Russian)* 77−42745
shell of revolution, corrugated, thermoelastic plastic deform. at finite displacements 80−74772
shell of variable thickness, thermoelastic problem, perturbation method 79−32272
shells, cylindrical, anisotropic, quasistatic thermoelastic eqns. 80−92059
shells, cylindrical, asymptotic method 80−38273
shells of revolution, variable thickness, stress state determ. 80−38275
size effect, model of dynamics, generalised thermodynamic forces 80−53627
size effect, thermodynamical model for constrained and unconstrained bodies 80−58900
slab, flat, steady state thermoelastic boundary value problem 80−92052
slab containing annular crack, thermal stresses, integral transform techniques 80−96229
sliding contact seal, thermoelastic instabilities 78−18257
solid hemisphere heated by distant source, thermal stresses 78−67045
solid homogeneous spherical bodies, general temp. fields *(Ukrainian)* 78−90710
solid symmetrical bodies of revolution, thermal transients calc., finite element analysis *(Spanish)* 79−23208
solidifying sphere, thermal contraction and density change effects upon freezing 79−64517
sphere, approx. calc. of temp. and stress fields *(Russian)* 77−35034
sphere sliding on plane, transient thermoelastic contact 80−83765
spherical body containing central inclusion, thermal stresses *(Russian)* 78−34018
spherical shell with circular elastic inclusion, thermal stresses 77−3727
spherical thick-walled shell with filler thermal stresses 78−13909
stability, constitutive inequalities and induced global bounds on thermodynamic states 79−166
stability of first strain gradient solids 77−50893
state space approach to thermoelasticity 80−4527
state space formulation, connection to thermoelastic pot. 80−63
stationary vibrations in 2-dimensional micropolar thermoelasticity 80−74793
stationary wave process, finite heat propag. rate 79−94541
steady state response to moving load, effect of gravity and temp. 77−23871
steel, martensitic, Gruneisen parameter determ. using thermoelastic effect 79−28068
steel case hardened cylinders, heat treated, residual stress fields 80−3102
steels, thermal hardening stress determ. by thermoplasticity theory 79−29076
Stepanov method shaped cryst. growth, physical problems, thermoelastic stresses 80−103279
stored energy, and increment in heat capacity due to plastic deform. 80−54302
strain driven thermoelastic instability toward brittle fracture 80−103415
stress, thermal, anal. of infinite homogeneous isotropic elastic medium with external crack 77−42778
stress anal., axisymmetric, in thin circular disc by method of matched asymptotic expansions 77−14899
stress anal., finite element variational method 77−7310
stress anal. of solid elastic cone 77−72159
stress distribution for stresses in half space, with moving boundary, influence of inertial effects *(Russian)* 79−55327
stress variational finite element anal. 77−7311
stress-temp. eqns. of dynamic thermoelasticity, uniqueness theorem 80−4528
stressed solid, gaseous diffusion, thermodynamic struct., transport theory 78−51065
stressed solid, gaseous diffusion, thermomech. formulation 78−51064
stresses, two dimensions, comparison between mech. analogue and expt. meas. 77−46918
surface point source in a generalized thermoelastic half space 80−23893
surface thermoelastic waves in the regular layered half space *(Ukrainian)* 79−50625
surface waves in generalized thermoelasticity 78−87291
surface waves in micropolar elastic solid medium 77−72206
symmetry and stability 79−44743
system with variable heat transfer coefficients, thermal conductivity determ. 77−75772
TGS, paraelec. phase, elastic and thermoelastic consts. 77−47503
thermal deformation of a disk due to a moving heat source *(Japanese)* 79−14265
thermal flexure of an infinite plate with a doubly periodic array of holes 79−68586
thermal stress singularities at crack tips, effect of insulated circular hole 77−68525
thermal stresses due to moving heat sources *(Polish)* 78−18184
thermal stresses in conducting materials due to high current pulse 79−7287
thermal stresses in elastic plane with circular boundary and thermally isolated cracks *(Russian)* 78−55599
thermal stresses in rectangular plates, variational and finite element solns. 78−51082
thermally activated crack propagation 78−18247
thermally isolated sphere in an elastic half-space, Green's tensor solns. *(German)* 78−62083

thermoelasticity continued
thermo-elastic-plastic transition in rotating disks with steady state temperature 79−64528
thermo-kinematic constrants in the thermodynamics of elastic bodies 78−83255
thermo-piezoelectric material, time depend. harmonically changing plane wave propag. anal. 80−15977
thermodiffusion in elastic cylinder, quasistatic problem *(Polish)* 80−10150
thermodynamic theory, considering thermal vel. waves 77−62189
thermodynamics and nature of second law 77−79044
thermodynamics of non-simple elastic materials 77−14904
thermoelastic condition of a body containing a heat-evolving inclusion *(Russian)* 78−9563
thermoelastic cracks in plane, boundary integral eqn. method *(German)* 80−106761
thermoelastic dielectric, linear, wave propag., singular surfaces 77−72216
thermoelastic inclusion energy in semi-infinite solid 80−14565
thermoelastic interference, between two neighbouring ribbon-like inclusions *(Japanese)* 77−68423
thermoelastic-plastic coupled medium, accel. and shock wave propag. 77−58578
thermoelastodynamics mixed boundary value problem, algorithm *(French)* 77−50979
thermoelastoplastic 3-D problem formulation by integral eqns. 79−7292
thermoelastoplastic anal. for hollow sphere, incremental plasticity theory 77−62168
thermoelastoplastic medium, variables for universal deform. representation 78−49666
thermoelastoplastic solution for a circular solid cylinder subjected to heating and cooling 80−5952
thermoelastoplasticity, doubly periodic, soln. 77−84165
thermoelastoplasticity three-dimensional integral eqns. *(French)* 78−90718
thermomechanical constraint, internal, constitutive equations, material anisotropy 80−58897
thermomechanical interaction effect by finite-element method 80−42067
thermomechanics, introduction, book 78−54187
thermopiezoelectricity, general eqns. 80−7297
thermorheological problems, numerical soln. 78−13910
thermorigid dielectrics, nonlinear thermodynamic theory 80−10149
thermoviscoelastic laminate beam, stress anal. *(German)* 80−106727
thermoviscoelastic material, sensitivity of thermomechanical response to thermal boundary conditions and material constants 79−77001
thermoviscoelastic materials, thermodynamics of nonlinear single integral representations, appl. to one-dimensional wave propag. 77−68438
thermoviscoelastic media, dynamical problems, Volterra method generalisation 80−33481
thermoviscoelastic transient responses, stability and accuracy of finite element solns. 80−5951
thermoviscoelastic-plastic materials, constitutive reln. 80−58
thermoviscoelasticity, bound dynamical problems, approx. calc. methods for crit. thermal states *(Russian)* 78−28949
thermoviscoelasticity, heat liberation effect in deformable linear medium 80−33484
thermoviscoelasticity, linear bound, minimum principle *(Ukrainian)* 80−33468
thermoviscoelasticity, nonlinear universal functions, influence of temp. *(Russian)* 79−10495
thermoviscoelasticity, variational techniques *(Russian)* 78−13922
thermoviscoelasticity problems, numerical soln. processes, stability, convergence *(Russian)* 79−27536
thermoviscoelasticity theory, nonlinear, asymptotic soln. of problems 77−65695
thin shells, thermomechanics by direct approach 79−18717
thin walled elements, unbound quasistatic random thermoelastic fields, oscillations 80−69673
thin-walled box structures subjected to pure torsion, behaviour vs. temp. in 20-180 C range *(Italian)* 79−41572
third and fourth order elastic consts. *(French)* 80−34116
three-layer cylindrical shells, thermoplastic stress state 80−96204
Timoshenko beams, eigensolns. for coupled thermoelastic vibrations 79−64577
transient response of inhomogeneous thermoelastic media to a dynamic input 79−27532
transient response of thermoelastic half-space 79−32253
transition, thermoelastic, from line to point contact 80−83768
transparent dielectric, laser induced fracture *(Russian)* 77−51406
transversely isotropic finite circular cylinder, transient thermal stresses from internal heat generation 79−76974
tubes, thick-walled, thermoelastoplastic creep stress anal. 80−58922
two joined plane strain sectors, thermal stresses 77−58559
two-bar struct., creep problems with variable temp. 77−50935
two-component materials, thermo-viscoelastic theory 78−73854
two-dimensional wave propagation in a micropolar thermo-elastic layer with stretch 79−94527
two-layer cylinder deform., rel. to microelectronic device fabrication 79−41561
uncoupled, thermal stresses computing, finite element method appl. *(Italian)* 79−18719
uniqueness and domain of influence Zaremba-type theorems 77−37761
uniqueness theorem and variational principle 80−92056
unsteady thermal stress problems, numerical treatment based on Euler-Maclaurin summation formula 80−48580
variational Lagrangian irreversible thermodynamics of nonlinear thermorheology 77−27467
variational principle for thermoelasticity with finite wave speeds 78−65772
viscoelastic materials, thermodynamics and fracture, integral expansions 77−3736
viscoelastic media, deform. theory with account of thermodiffusion *(Ukrainian)* 78−67052
viscoelastic rod, dynamical behaviour, effect of thermomechanical conjugation under forced longitudinal oscillations *(Ukrainian)* 78−67074
viscoelastic rod driven by sinusoidal displacement, thermomechanical response 77−89056
water, vaporisation and thermoelastic press. due to CO_2 laser pulse 80−84227
wave propagation in micropolar thermo-elastic layer 77−35066
wave propagation in thermoelastic layer, gravity influence 79−94544

thermoelasticity continued
wave propagations in generalised thermoelasticity, effect of second order time derivatives 77−42772
weak nonlinear waves in homogeneously deformed heat-conducting elastic materials 80−48632
weak shock waves in thermoelastic solids 77−75849
weakly absorbing solid medium, opacity fluctuations, heating by intense radiation and thermoelastic stresses problem 80−38048
Zerodur, glass-ceramic, thermoelastic props. 78−27550
Ag-Zn (38 at.%), morphological and struct. studies of thermoelastic martensites 77−63669
Al alloy, retardation time effects on heat pulse propagation 79−18725
Al, Gruneisen parameter determ. using thermoelastic effect 79−28068
Al-Ni, thermoelastic phase transform., acoustic emission 80−3039
Al-SiC fibre reinforced materials, therm. stresses in unit cell 80−10160
$Au_{52.5}Ag_xCd_{47.5}$, pseudoelastic behaviour associated with thermoelastic martensitic transform. 80−16304
B, liq., thermoelastic props. near melting point 80−19862
$Ba(NO_2)_2.H_2O$, hexagonal, piezoelec., electro-optic, dielec., elastic, thermoelastic props., space groups 78−76388
$Ba_2TiSi_2O_8$, fresnoite, Czochralski growth and phys. props. 78−3026
CdTe, window material with absorbing inclusions, damage thresholds 77−38971
$Cs_2S_2O_6$, hexagonal, piezoelec., electro-optic, dielec., elastic, thermoelastic props., space groups 78−76388
Cu, Gruneisen parameter determ. using thermoelastic effect 79−28068
Cu-Al-Ni, elastic const. behaviour near Ms 77−12623
Cu-Al-Ni alloy, thermoelastic transformation hysteresis loop width strain rate depend. *(Russian)* 79−100138
Cu-Zn-Al, internally faulted martensite, TEM obs. 78−3124
Cu-Zn-Ga martensite, thermally produced large single crystals 77−12615
Cu_2O, single crystal, thermoelectric behaviour *(French)* 78−71786
Fe-Ni (31 wt.%), thermoelastic martensite obs. 80−3052
Fe-Ni system, constant modulus alloys for mech. oscillators 79−61641
Fe-Ni-Cr-Ti-Al, with thermoelastic control coeff., comp. and heat treatment influence on props. *(French)* 80−81074
Fe-Pd (31.2 wt.%), thermoelastic FCC-FCT martensitic transformation 80−104156
Fe-Pt, nearly thermoelastic, irreversible lattice defects formed by martensitic transform. cycles 78−60671
Fe-Pt (23,24,25 at.%), effect of austenite ordering on some thermoelastic transform. factors 78−88466
Fe_3Pt, martensitic transform., change from nonthermoelastic to thermoelastic type 78−19755
Ga, elastic moduli, temp. depend., anharmonic effects *(Russian)* 77−31708
GaAs, pulled, dislocation generation, thermoelastic anal. 80−79787
GaP, crystal, growth conditions rel. to dislocation struct. 80−88151
GaS, elastic prop. anisotropy, Debye temp. *(Russian)* 80−88244
GaS(Te)(Se), elastic characteristics, Debye temp., ultrasonic study *(Russian)* 80−79872
Ge ribbon single crysts. grown from melt, dislocation struct. form. under thermal stress 80−107082
$KBrO_3$, trigonal, elastic, thermoelastic and dynamic piezoelec. props., US vel. meas. 77−32328
$LiClO_4.3D_2O$, hexagonal, piezoelec., electro-optic, dielec., elastic, thermoelastic props., space groups 78−76388
$LiClO_4.3H_2O$, hexagonal, piezoelec., electro-optic, dielec., elastic, thermoelastic props., space groups 78−76388
$LiIO_3$ crystal, SHG, thermoelastic stresses and nonlinear refract. effect 80−74437
Mo film, constrained, 20 MHz thermoelastic wave generation 79−47880
NaCN, cubic, KCN-type anomalous thermoelastic behaviour 77−84823
NaN_3, struct. phase transform., microscopic model 79−65022
$Nd_3Ga_5O_{12}$, elastic and thermoelastic consts., US meas. *(German)* 77−59061
Ni-Ti, working medium in heat engine, rel. to engine efficiency *(Russian)* 78−48449
Ni-Ti alloys, shape memory effect materials, criteria for efficiency assessment *(Russian)* 80−21015
α'_2-Ni-Zn-Cu martensite, thermoelastic, microscope obs., TEM 77−55966
$Pb(Zr,Ti)O_3$, excitation of mechanical vibr. by ionising radiation beams 77−24799
$Sm_3Ga_5O_{12}$, elastic and thermoelastic consts., US meas. *(German)* 77−59061
α-Ti, strain driven thermoelastic instability toward brittle fracture 80−103415
Ti, thermal diffusivity determ., thermoelastic method 79−23940
Ti-Ni, thermoelastic phase transform., acoustic emission 80−3039
Ti-Ni (50.4 wt.%), thermal conversion efficiency of ideal thermoelastic marmem cycle 79−66057
Ti-Ni (51 at.%), martensitic transformation, thermoelastic, hysteresis, exothermic and endothermic effects *(Russian)* 78−19749
$TlCdF_3$, third and fourth order elastic consts., press. depend. near phase transition *(French)* 80−34116
U-Nb (14 at.%), exam. of shape memory effects 78−76694
YIG, elastic and thermoelastic consts., US meas. *(German)* 77−59061
Zn, growth from melt, conditions influencing dislocation struct. *(Russian)* 80−97424

thermoelectrets
alcohol, thermal electret, persistency of surface change *(Japanese)* 77−81048
carnauba wax, and rosin mixtures, hetero- to homocharge transition, temp. depend. *(Japanese)* 78−35082
carnauba wax, thermal electret, persistency of surface charge *(Japanese)* 77−81048
carnauba wax, thermoelectret, lattice parameter changes at elevated temps. 80−29674
carnauba wax, thermoelectret orientation parameters, solidification with different cooling rates 79−38444
carnauba wax and rosin thermal electret, elec. charge studied by TSC 80−7286
carnauba wax electret, electric charge studied by TSC *(Japanese)* 78−6626
carnauba wax thermoelectret, charge behaviour 80−7276
carnauba wax thermoelectret, mag. anisotropy evidence for dipolar orientation 77−16240

thermoelectrets continued
carnauba wax thermoelectrets crystallite orientation, X-ray diffr. obs. 78−43774
cellulose, dielec. relax. studies, TSD meas. 80−88907
diamagnetic anisotropy of thermoelectret and magnetoelectret states 80−97053
esters, thermal electret, persistency of surface charge *(Japanese)* 77−81048
fatty acids, thermal electret, persistency of surface charge *(Japanese)* 77−81048
Perspex pyramid electret, thermally stimulated discharge currents 80−2688
PMMA, thermoelectrets, γ-irrad., heterocharge stability, TSC spectra 78−72453
PMMA thermo-electrets, temp. and field effects 78−31148
polyelectrolyte membranes, persistent polarisation in aq. environment, neural model 78−48763
polypropylene, mag. polarisation, optical studies 80−55013
polyvinylidene fluoride-PTFE, thermoelectret, IR spectra, struct. modifications and dielec. props. 77−55785
polyvinylidene fluoride-PTFE copolymer, local electrostatic field determ. *(French)* 77−12305
PVC, thermally stimulated depolarisation 78−48112
rosin and carnauba wax mixtures, hetero- to homocharge transition, temp. depend. *(Japanese)* 78−35082
silicone resin electret, thermally stimulated discharge meas. 79−87378
sisal wax, space-charge-limited currents, thermoelectret state 79−51901
sisal wax, thermally stimulated discharge and internal polarisation 80−55016
surface charge density maximum during forming 77−36169
Teflon FEP film, TSC spectra 77−52012
thermo-ionic emission by electric field, electrets discharge, theory 79−33596
$AsSe_{10}$, stable thermoelectret, effects of anisotropic external perturbation *(Russian)* 77−63361
3PbO.2GeO, TSC in thermoelectret state during ceramic synthesis, pyroelec. currents and energy struct. of capture centres 80−55014
SSe_9, stable thermoelectret, effects of anisotropic external perturbation *(Russian)* 77−63361
$SrTiO_3$, impure, low temp. polarisation, thermoelectret state 77−12301

thermoelectric conversion
see also thermoelectric devices
alloys, thermoelectric, phase diagrams and imperfection chemistry 80−108422
alternating voltage unit, 20 Hz to 30 MHz, USSR special standard 77−30180
attainable efficiency values determ. 80−94094
battery convertor for measuring nonstationary component of heat flux 79−30466
biomedical implantable power sources, radioisotope thermoelectric generators appl., high reliability contacts using local heat pulses 79−52952
cassegrain solar collector with thermoelectric module, concentration efficiency 80−35709
eddy thermoelectric currents and eddy thermoelements 77−8126
efficiency, generalized for anisotropic material 79−56253
efficiency, in presence of small temp. drop 80−40878
efficiency of thermoelectric materials, new criteria 78−21130
error due to crystallographic misorientation anisotropy 78−77904
fast spectrum reactor space power system with thermoelec. conversion, baseline design 80−37441
ferroelectric materials, thermoelectric conversion during phase transitions *(French)* 78−76412
generator with permeable thermoelements, energy efficiency *(Russian)* 79−66414
generators, utilisation of amorphous semiconductors 80−35704
heat pumps, two-stage, design criteria anal. for cool-down speed maximisation 80−108812
heat pumps 80−35713
irreversible thermodynamics, minimum principle *(Japanese)* 77−41556
isotope power system, Brayton cycle, dynamic power convertor for space appl. 79−48167
isotopic and nonisotopic, 1978 state of art and development trends 79−43780
isotopic microgenerator design and construction optimisation due to min. power 80−108813
materials for thermoelectric conversion of solar energy *(French)* 80−89660
militarised power sources, technology improvements and 100 W and 500 W sources characts. 79−48151
multijunction thermal convectors for AC-DC transfer standards 80−98874
multijunction thermal convertor AC/DC transfer, Thomson effect error reduction 80−103679
NASA space power technology program 79−96883
OTEC; analysis of a heat exchanger−thermoelectric generator system 80−35710
Peltier effect, heat losses due to thermal cond. 80−107773
photovoltaic/thermoelectric refrigerator for medicine storage for developing countries 80−35712
polyacetylene, semiconducting and metallic, thermoelec. props. 80−40884
power conversion from energy fluctuations 79−100536
radioisotope, heat pipes design and testing, Cu/H_2O, axially-grooved 79−48144
radioisotope generator, high-temperature insulations testing 79−48145
radioisotope thermoelec. generators, design optimisation for Solar-Polar Mission 80−40880
radioisotope thermoelectric generator, selenide, power degradation predictions, mathematical and computer models 79−48148
radioisotope thermoelectric generator, selenide technology evaluation at JPL, for Galileo (NASA) spaceflight mission 79−48147
radioisotope thermoelectric generator cooling in spacecraft 80−40881
radioisotope thermoelectric generator shock and vibration test program for MB-M75(A) 80−35711
radioisotope thermoelectric generators, power degradation predictions using DEGRA code 80−40879
radioisotope thermoelectric generators, SNAP 19 performance update for Pioneer and Viking missions 80−40883
radioisotope thermoelectric generators, terrestrial and undersea appl. 79−48150
radiosotope thermoelectric generator cooling, in Shuttle 79−48142

thermoelectric conversion continued
selenide convertor technology, 156-couple ground demonstration system 79−48146
selenide thermoelectrics, analytical model for performance and degradation predictions 80−108805
semiconductor thermal energy transformers, influence of anisotropy of thermal cond. 77−8127
single-stage thermoelectric heat pumps, design, characterisation and optimisation 80−35735
solar, appls. to OTEC and agricultural irrigation 80−35708
solar, near-Sun missions appl. 79−48143
solar furnace type generator, high power density, with wedge-shaped electrodes 79−48100
solar thermoelectric generator panels, energy characts., estimation 80−101123
solar thermoelectric generator using tubular heat-pipe with concentrator 80−89658
solar thermoelectric generators, efficiency evaluation and improvement 79−62017
solar thermoelectric generators, metallic thermo-electric materials utilisation, economic characts. 80−101122
solar to electrical energy conversion anal. 79−43779
solid state energy conversion, appl. of solid state cooling to spaceborne IR focal planes 80−107772
solid state heat engine, experimental demonstration of heat-to-electricity conversion within a dielectric 80−35707
space nuclear power development, selenide isotope generator for Galileo mission 79−52951
space vehicle thermoelectric generators, Voyager and LES 8/9 flight performance 80−40882
thermal Albedo Energy Convertor, concept, design and testing for high altitude long endurance platforms 80−108789
thermal convertor with a synthetic anisotropy, response time 79−70454
thermoelectric convertor, generalised surface, quadratic form heat balance equations 79−83609
thermoelectric devices, design, construction and characteristics for high efficiency 80−108806
thermoelectric energy conversion, conf., Arlington, TX, USA 80−107779
thermoelectrochemical cycles for power and hydrogen production 80−45718
thermophotocell, design and calculations 80−97800
two-stage refrigeration and power producing arrangement, with cooling tube and thermoelectric stage 78−21142
Ag-AgCl/KCl/AgCl-Ag thermocell, and thermal liq. junction pot. for KCl solns. at high temp. 80−16819
AgI-Ag oxysalt ionic solids, power conversion determ. 78−30947
$B_{14}Si$ refractory thermoelectric material CVD and application 77−77411
Bi-Te thin thermoelectric films prep. by solid state reaction method 80−108361
δ-Bi_2O_3, thermoelectric power, heat of transport of O^2 ions 80−92713
Bi_2Te_3 alloy thermocouples for solar thermoelectric conversion 80−94095
$(Bi_2Te_3)_{0.9}(Sb_2Te_3)_{0.5}(Sb_2Se_3)_{0.05}$ n-type alloy for thermogenerators, thermo-EMF, elec. cond. and thermoelec. efficiency factor, 300-600K 80−70735
Cs plasma thermoelectronic laser energy convertor 78−90421
$(Cu,Ag)_2Se$ appl., p-type, vaporisation suppression, using inert and reactive coatings 79−48149
GaAs/Au-Ge-Ni alloy metal-semiconductor thermoelectric coolers, effects of contact resist. and dopant conc. 80−81481
H_2 and power production using thermoelectrochem. cycles 80−16820
$LaCr_3$ alloy development for thermoelec. appls. 80−35705
$LaCrSe_3$ alloy development for thermoelec. appls. 80−35705
Na heat engine, using β-alumina ionically conducting ceramic, principle and thermal efficiency 79−48179
Pt-Rh-W alloy corrosion by radioisotopic power system insulating and thermoelec. materials 78−7094
Si-Ge, high temperature thermoelectric materials 80−89659
Si-Ge alloys appl., figure-of-merit improvement by GaP additions 79−47115
Si-Ge thermoelectric generators, approximation errors when using averaged properties solutions for required heat rates estimation 80−108808
β-SiC, n-type, thermoelectric efficiency at high temps. 80−35706

thermoelectric devices
see also thermocouples; thermoelectric conversion; thermopiles
AC voltage standard, using thermoelectric convertors, 20 Hz to 1500 MHz 77−18036
AC/DC transfer measurements, wideband, automated 77−18035
anisotropic thermoelectric cooling unit, theory 78−47820
anisotropic thermoelements, transverse thermo-EMF, rectangular elements 78−56172
batteries, low-temp., stable life calculations 79−87998
battery convertor for measuring nonstationary component of heat flux 79−30466
calorimetry, applications of thermoelectric devices in various types of calorimeters 80−105648
contactless temp. meas. in circular cyclic bending, using thermoelectric radiation sensors 78−57947
cooler, single stage, finite element thermal stress anal. 80−108807
cooler for Si/Li spectrometer, using Peltier elements *(Czech)* 78−49947
coolers, fast transient response of novel Peltier junctions 78−21141
coolers, heat load estimation curves 78−45613
coolers, numerical anal. of transient behaviour 78−21140
coolers for micromodules 79−6120
cooling equipment, welded joints, heat emission effects on temp. distrib. *(Russian)* 80−69635
cooling module, for trapping gas chromatography fractions for vibr. spectroscopy 77−4960
cooling unit in mag. field 79−9218
current convertor, for accurate AC meas. 77−18032
design, construction and characteristics for high efficiency 80−108806
differential multijunction convertor, for AC/DC power transfer 77−18041
digital temp. meas. instrument with automatic error compensation of thermoelectric thermometer 79−75526
emissivity meas. by thermoreceiver/gas heat exchange 77−22552
expansion cloud chamber with thermoelectric cooling 78−90034
extracorporeal circulation apparatus using thermoelec. heat regulating systems 80−3870
extruded materials with tetradymite struct., primary and in situ recrystn. elec. props 79−43266

thermoelectric devices continued
Gipospast-1, thermoelec. apparatus for local hypothermia 80−104807
half-cells extruded from ceramic blanks, recrystn. and elec. props. 79−43267
heat flux, local, high intensity, measurement pickup *(Russian)* 79 67296
heat pumps, cross flow, anal. of operation and performance using mathematical model 80−107836
heat pumps, single-stage, simplified method for optimization 80−108811
heat pumps, two-stage, design criteria anal. for cool-down speed maximisation 80−108812
heat-flow meters, compensated, metrological charact. 79−37144
heat-flux transducer, using artificially anisotropic thermoelec. materials 79−93136
heater, miniature, for thermo-emf meas. using SiC heating element 79−2764
integrated direction sensitive flowmeter 77−7484
IR hot carrier diode mixer 78−29161
isotopic generators of multihundred watt design, integration with LES 8/9 spacecraft 77−46413
isotopic heat source of multihundred watt design 77−42194
laminated structure, thermal monitoring by near surface thermoelectric receivers 78−53107
laser/component cooling appl., development trends 78−22136
longitudinal thermomagnetic amplifier using Bi or InSb-NiSb 77−47838
metal-semiconductor thermoelectric coolers, effects of contact resist. and dopant conc. 80−81481
microrefrigerators, single stage and two-stage, limited heat transfer anal. *(Russian)* 78−70129
microwave transducer, using hot carrier semicond., reactive props. and equiv. cct. 77−10109
multijunction convertor, for AC voltage and current meas. 77−18033
N_2O refrigerator, thermodynamics and thermoelectric condenser design 80−108809
needle probe for medical and biological temp. meas. 80−101299
panel-type solar thermoelectric generator, water-lift appl., technical and economic eval. 79−83619
radioisotope thermoelectric generator, safety programme for LES 8/9 mission 77−46412
refrigerators, performance optimisation using asymptotic temp. distrib. 80−230
resistance thermometer *(Japanese)* 78−32816
semiconductor thermal transducer for elec. AC quantities meas. 77−45865
solar thermoelectric generator high temp., sintered Si-Ge, performance assessment 79−74534
spacecraft heat rejection improvements using thermoelectric devices 80−108810
thermal flux meters, response time reduction 80−4719
thermoelectric convertor, generalised surface, quadratic form heat balance equations 79−83609
thermoelectric energy conversion, conf., Arlington, TX, USA 80−107779
thermoelectric generators, utilisation of amorphous semiconductors 80−35704
thermoelement cooling control by variation of geometric shape 78−62195
thermometer, laboratory test equipment, using zero-setting and steam thermostats 77−74400
thermometer, Pt-Rh, 1300 to 1700°C, errors obs. and analysis 80−77783
thermometer, temperature meas. of moving metal objects *(Russian)* 80−90848
thermometer, time constant influence on temperature control circuits obs. *(Czech)* 78−29114
thermometers, automatic testing, structural method for improving precision 79−35744
thermometers, cold junction thermo-EMF compensation, parameter optimisation *(Russian)* 78−86270
thermometers, semiautomatic checking unit with programmed control 77−22548
thermometers, stability of readings 78−93682
transistor thermometer, thermoelec. *(Japanese)* 78−45625
type RTN (USSR), construction and charact. 80−57372
BiSb (>20 wt.%), electronic band struct. 80−107698
InP_xAs_{1-x} alloys, thermoelectric charact. 77−11947
$NiAl_2O_4$, entropy of form. determ. using solid electrolyte twin thermocell 78−27812

thermoelectric effect *see thermoelectricity*

thermoelectric effects in metals and alloys
actinide, transport props. and sp. ht., role of optical and acoustic phonons 77−15821
actinide metals and compounds, nearly magnetic, thermoelec. power 78−84197
actinide systems, nearly magnetic, thermoelectric power determ. 78−56133
actinides, lattice vibrs. role in phys. props. determ. 77−28158
actinides, spin fluctuation theory, for mag. and elec. props. 78−91869
alkali metal, electron-phonon drag effects in elec. cond. and thermoelec. power 77−15824
alkali metal-Au alloys, elec. props. 78−84187
alkali metals, liq., electrical resistivity and thermoelec. power, Harrison's method 79−78066
alkali metals, liq., Fermi energy, density of states, electronic props., exchange and correl. effects 80−96774
alkali metals, liq., optimised model pot. calcs. 78−2467
alkali metals, liquid, thermoelectric power, optimised model pot. calcs. 80−29391
alkali metals, thermopower and elec. cond., relationship at low temps. *(Russian)* 80−92882
alloy, dilute, thermoelectric effects, near cancellation of electron-phonon corrections 79−33283
alloys, thermoelectric props., effect of electron-impurity and electron-phonon interactions 79−33282
Alumel, thermocouple alloy, heat treatment effects on thermoEMF and mag. flux 77−63235
amorphous alloys, mag. and nonmag., thermoelec. power, 15 to 580K 80−80255
amorphous alloys, transport props., thermopower 80−34411
amorphous metals, electron-phonon interaction effect on thermopower 80−29393
anisotropic normal metal, thermopower calc. 80−24879

thermoelectric effects in metals and alloys continued
anomalies near mag. and order-disorder crit. points 79−65454
anomalous Thomson effect 79−65435
antiferromagnetic metal, thermoelec. power in mag. field 80−70686
binary alloy, thermal EMF, short-range order effects *(Russian)* 77−15835
binary alloys, charge transfer and transport props. in tight-binding model 79−82577
binary continuous solid solutions, elec. resist. and thermoelectric power behaviour 79−69492
Chromel, thermocouple alloy, heat treatment effects on thermo EMF and mag. flux 77−63235
composite materials, thermoelec. props. degraded by strengthening additive 79−47114
conduction current and generalised Einstein rels., from Boltzmann transport eqn. 77−15810
conference, East Lansing, MI, USA (Aug. 1977) 79−65433
cylindrical metal sample holder for thermoelec. power meas. 77−57309
diffusion thermpower, boundary scatt. effect 80−6817
dilute alloy, perturbation expansion for the asymmetric Anderson Hamiltonian 80−80202
dilute alloy, Seebeck coefficient, electron-phonon enhancement 80−70685
dilute alloy, thermoelectric coeff., vertex and other electron-phonon corrections to impurity scatt. 79−95390
dilute magnetic alloy, reverse Kondo effect, magneto-transport theory 80−15509
dilute magnetic alloys, transport props. from Suhl's dispersion relations 77−62891
eddy thermoelectric currents and eddy thermoelements 77−8126
electron-phonon interaction, many-body effect 79−69499
electron-phonon mass enhancement 79−65452
electroplated foil, appl. to measurement of heat flux 80−37026
eutectics, HgTe-PbTe and Au-PbTe, prep. and thermoelectric behaviour charact. 80−107774
ferromagnet, metallic, thermopower near crit. point, inelastic scatt. processes 77−15836
ferronickel, thermoelec. determ. of Ni content 78−40096
film, Mayadas-Shatzkes model appl. to thermoelec. power 77−47904
film, thermoelec. power and TCR, interrelationship 77−76957
film, with grain boundary scatt., thermoelec. power, Fuchs-Sondheimer eqns. 78−52108
film and bulk samples, thermoelec. power meas. apparatus 77−79092
group I metals, anomalous positive thermopower 79−65449
heat emission jump, in intense mag. field *(Russian)* 77−76796
high temperature thermoelec. props. of metals and metallic binary continuous solid soln. 78−91676
Invar, Nernst-Ettingshausen effect and galvanomagnetic effect anisotropy *(Russian)* 79−91030
irradiated metal, containing self-interstitials and vacancies, electronic transport props. 78−60105
Kondo alloy, dil., thermoelec. power in asymmetric single-orbital Anderson model, perturbation calc. 79−99534
liquid alkali metals, nonlocal harmonic model potential, appl. to elec. props. 80−6802
liquid metals, monovalent, divalent, and trivalent, resist. and thermoelec. power 79−19566
liquid metals, thermoelectricity, expt. methods review 79−65451
liquid metals and alloys, cond., Hall coeff. and thermoelec. power, tight-binding model 77−47798
liquid metals and alloys, thermoelectric power 79−65450
liquid metals in metallic containers, thermoelectric MHD 79−64787
liquid metals of groups IIB, IIIB, and IV, thermoelectric power, pseudopotential calc. 80−59959
liquid model, resistivity, thermoelectric power, Harrison nonlocal pseudopot. calcs. 78−23069
magnetic alloy, dil., thermopower, interconfig. fluctuations 79−65412
magnetic alloys, dil., in finite mag. field, Suhl's dispersion eqns. 77−24673
magnetic alloys, dilute, thermopower 79−65455
magnetic field, strong, effect on transport coeffs., Mott rule validity 77−69303
magnetothermoelectricity, phonon-drag, semiclassical theory 78−6354
many-body effects in thermoelec. in metals, observed and predicted, review 79−60803
measurement apparatus 79−40591
metal, electron transport properties 79−19565
metal, electron-phonon enhancement of thermoelectric power 77−72855
metal, ferromagnetic, Nernst-Ettingshausen effect, rel. to Hall effect and thermoelec. power 79−56199
metal, thermoelectric effect in surface layer exposed to high-power heat flux 77−35926
metal, thermoelectricity, electron-phonon enhancement 78−56135
metal film, laser induced transverse voltages, detector appl. 0.33 to 10.6 μm 77−39824
metal film, thermoelectric power and temp. coeff. of resistivity 78−91788
metal-H systems at high H press., physicochemical props., book contrib. 80−24535
metallic thermo-electric materials, charact. *(Russian)* 78−19023
metallic thin film, thermoelectric power 79−78210
metals, magnetic, Seebeck coefficient anomaly near spin ordering temp. 77−20302
milliKelvin temperature thermoelectric meas. 79−69500
Nernst-Ettingshauser effect based radiation detectors 79−58795
Ni-Cr, variation in absolute thermoelec. power under heat/treatment *(Ukrainian)* 79−38051
Ni-Mo, variation in absolute thermoelec. power under heat/treatment *(Ukrainian)* 79−38051
NK, thermocouple alloy, heat treatment effects on thermoEMF and mag. flux 77−63235
noble metal alloys, diffusion thermopower, phonon drag 79−65441
noble metal homovalent alloys, thermopower at low temp. 79−65437
noble metals, pure, low-temp. transport props. 77−8072
noble metals, pure, thermoelec. power at low temps. 77−76798
noble metals, TEP calc. 77−24549
noble metals, thermoelectric power, 290-560K 79−42522
noble metals, thermopower calc. using dHvA data 79−65448
noble metals, with transition metal impurities, thermoelectric power 78−91675
nonsimple metals, calc. of elec. resist. and thermoelec. power 78−19019

thermoelectric effects in metals and alloys continued
phonon drag influence in metals, coupled Boltzmann transport eqns. *(German)* 77−80766
polyacetylene, semiconducting and metallic, thermoelec. props. 80−40884
polycrystalline-thin metal films, thermoelectric power, mean free path model 80−107770
pseudopotential study of electronic props. 80−20149
rare earth alloys, RCo_2, elec. resistivity, thermopower, X-ray struct. meas. 80−24874
rare earth metal, conduction electron interactions, anisotropic 80−15492
rare earth metals, thermopower, 80-1000K 77−43572
rare earth orthocobaltites, $R_{1-x}Sr_xCoO_3$ and $La_{1-x}M_xCoO_3$, itinerant electron ferromagnetism obs. 78−10660
rare earth orthotitanates, $RTiO_3$, metallic and semicond. elec. and mag. props. 79−38068
rare earth systems, crystal field effects 78−67987
rare earth-Al_2, cubic Laves phases, prep. and phys. props. *(German)* 78−23075
review of general theory for teachers 78−4440
Rysselberghe's contention, appl. to thermocouples 79−51555
SA, thermocouple alloy, heat treatment effects on thermoEMF and mag. flux 77−63235
semimetals, degenerate, heat conduction, thermal EMF, Lorenz number anisotropy at low temp. 80−75549
Si-Ge alloy, time and temp. behaviour, meas. 77−22543
simple liquid metals, elec. resist. and thermoelec. power calc. 77−76788
spin glass, thermopower, rel. to spin glass freezing temp. 78−79983
spin glasses, elec. resist., thermal resist. and thermopower 80−65542
steel, ferrite-austenite transition, diffusion const. of C and carburisation rate consts., thermopower meas. 80−89216
steel, Mn, type 35SGM, magnetic, electrical, and mech. props. after tempering and hardening 79−66086
superconducting alloys with ordered magnetic moment distribution, thermoelec. effect 78−91811
superconducting loop, thermoelec. flux generation 79−65596
superconducting ring, thermoelectric effect 79−65597
superconducting state, possible existence of thermopower 78−23201
superconductor, nonequilib. 79−65594
superconductor, toroidal sample config. 79−65595
superconductors, thermoelectric effects 79−65593
TCNQ salt, $(DEPE)^{2+}(TCNQ)_4^{2-}$, elec. and mag. props. of two crystallographic form 77−28166
theory of thermoelectricity, electron-phonon interactions, and electron relax. time 79−69498
thermoelectric devices, design, construction and characteristics for high efficiency 80−108806
thermoelectric energy conversion, conf., Arlington, TX, USA 80−107779
thermoelectric materials, B_4C_x and $(B,Si)_4C_x$ P-type LaS_x N-type alloys, fabrication and thermoelectric props. 80−107771
thermoelectrode material nonuniformity data analysis 77−61065
thermoelectrode wire classification standard samples 77−5865
thermopower above 77K 79−65442
thin films, conductor covered with electrolytic deposit, thermoelectric props., thermal flux meas. *(French)* 80−59961
thin films, grain boundary and surface scatt., statistical model 80−103762
thin films, thermoelectric power, thermal stress effects, theory 80−65714
transition metals, liq., and their alloys. elec. resist. and thermoelec. power using t matrix 77−31988
transition metals, thermoelectricity 79−65443
transition metals and alloys, liq., thermoelectric power 78−91675
transport kinetic coeffs. quantum oscills. in mag. breakdown regime *(Russian)* 79−91035
TTT-$(I_3)_{0.5}$, one-dimens. metal, mag. susceptibility, elec. resist., thermopower meas. 78−87967
two-component layered system, with interpenetrating components, thermoelec. and galvanomag. props. 78−79982
Ag and Cu alloys, TE properties, research obs. 77−28163
Ag, Fermi surface and thermoelec. power, de Haas-van Alphen calc. 79−4503
Ag film, size effect in thermoelec. power, MFP and Fermi surface 77−69433
Ag, low temp. resist. and thermoelec. ratio, electron-electron scatt. contrib. 80−70670
Ag, thermopower temp. depend. 79−65436
Ag, transport props. meas., 20 mK-4.2K 77−20292
Ag, virtual bound states due to 4d- and 5d-transition metal impurities 80−70667
Ag-Cu(Zn)(Ga)(Ge)(As), α phase, thermopower at low temps. 78−84196
Ag-Gd(Tb)(Tm), dilute, thermopower, crystal field and interaction effects 77−66158
Ag-Ge alloy system, atomic struct. and electronic props. *(Russian)* 77−20289
Ag-Hg alloys, thermopower, thermal cond., elec. resistivity 79−65439
Ag-In(Sn)(Pb)(Bi)(Sb), liquid alloy, thermoelectric powder and magnetic susceptibility 77−8076
Ag-Mn, conc. spin glasses, thermopower 80−65538
Ag-Pd, thermoelectric force meas., test of virtual bound d-state model 77−32001
Ag-Sn(Sb), liquid alloys, anomalous behaviour of electrical resistivity and thermoelectric power 77−11901
Ag-Zn(Ga)(Ge)(As), thermopower at low temp., Fe impurities 79−65440
Ag-Zr(Nb)(Mo) film, dielec. const., optical props., DC resist. and thermoelec. power 77−85824
$Ag_{1-x}Au_xYb_y$, thermopower and resistivity 79−65457
Al, cold-worked, transport props., 1.5-8.5K 78−7059
Al, low temp. electrical and thermal transport props., Matthiessen's rule breakdown 78−26847
Al, low temp. resist. and thermoelec. ratio, electron-electron scatt. contrib. 80−70670
Al, low temp. thermopower of Frenkel defects 78−19024
Al, magnetic breakdown, quantum phenomena *(Russian)* 78−43290
Al, pure and dil. alloys, diffusion thermopower, inelastic electron-phonon interaction 80−96851
Al, simultaneous thermopower and thermal conductivity meas. 77−72854
Al, thermoelectric power and Nernst-Ettingshausen effect 78−56134
Al, thermoelectric props., giant quantum oscills. 79−65453
Al wire, hot and cold deformation drawing strengthened, thermal EMF study *(Russian)* 80−54674

thermoelectric effects in metals and alloys continued
Al, with dilute pt. defects, thermopower, Hall effect and magnetoresist. 79−65458
Al-3d transition metal, dil., transport props., sp. ht. and supercond. ant. temp. calcs. 77−1393
Al-Ag (up to 40 at.%), exam. of anelastic phenomena and structural state 78−76693
Al-Cu solid soln., supersaturated, plastic deform. effects *(French)* 79−91748
Al-Cu(Mg)(Zn), cold working causing preprecipitation, thermoelec. power *(French)* 79−8306
Al-Ge(Mg)(Zn)(Ga), dil., electronic transport coeffs. for point defect scatt., 4-OPW calc. 79−42531
Al-Mg alloys, cold-worked, transport props., 1.5-8.5K 78−7059
Al-Zn, Guinier-Preston zone reversion, thermoelectric power meas. *(French)* 79−20058
Al-Zn, solid soln., exam. of evolution by thermo EMF meas. *(French)* 78−52862
Al-Zn-Mg, zone composition change during ageing 79−29110
Au, Fermi surface and thermoelec. power, de Haas-van Alphen calc. 79−4503
Au, low temp. resist. and thermoelec. ratio, electron-electron scatt. contrib. 80−70670
Au, pure, thermoelec. power at low temps. 77−76798
Au, resistivity and thermoelectric ratio at low temp., 0.04 to 7K 79−73497
Au, thermopower temp. depend. 79−65436
Au, virtual bound states due to 4d- and 5d-transition metal impurities 80−70667
Au-Ag (13 at.%), thermopower standard in mag. field 79−78081
Au-Ag film, thermoelectric power and resist. meas., MFP and Fermi surface meas. 77−51826
Au-Ag(Cu), dilute, low temp. thermoelec. power, electron diffusion and phonon drag 77−20301
Au-Gd(Tb)(Tm), dilute, thermopower, crystal field and interaction effects 77−66158
Au-Mn(Cr)(Fe), conc. spin glasses, thermopower 80−65538
Ba, high-purity solid and liq. phases, elec. resist. and thermopower meas. 77−47799
Ba, transport properties, elec. resist., thermoelec. power, thermal cond. deviations from Matthiessen's rule 78−39086
$Be_{40}Ti_{50}Zr_{10}$, metallic glass, thermoelectric power and resist. 78−95289
Bi, metallic, thermopower meas., 9K-40 mK 78−91673
Bi, phonon-drag low temperature thermoelectric refrigeration 80−22366
Bi, thermal EMF giant quantum oscills. *(Russian)* 80−59960
Bi-Cd(Zn), alloy absolute thermoEMF temp. and conc. depend. *(Russian)* 80−39561
Bi-Sb, thermal EMF giant quantum oscills. *(Russian)* 80−59960
Bi-Sn, thermoelec. props. from 2 to 300K 80−24872
Bi-Sn, thermopower from 50 mK to 25K 80−24880
Ca, electrical resistivity and thermoelectric power 78−26846
Ca, transport properties, elec. resist., thermoelec. power, thermal cond. deviations from Matthiessen's rule 78−39086
CaSb, resist., susceptibility and thermopower rel. to electronic struct. 78−67935
Cd, thermo EMF oscills. on mag. breakdown *(Russian)* 79−60801
Cd, thermopower meas. in mag. field, 1.5-4K 80−54675
Cd-Sb, liq., thermoelec. power meas. 79−40591
$CdGu_2S_{4(1-x)}Se_{4x}$, opt. absorpt., elec. cond., spectral response, thermopower 77−72862
Ce impurity Kondo system, crystal field effects on thermopower and Kondo effect 77−66163
Ce, liquid, resist. and thermoelec. power, t-matrix calc. 78−26840
Ce, thermo-EMF up to 75 kbars 80−24882
Ce, thermoelec. power up to 6 GPa 79−51556
Ce, thermopower behaviour under press. up to 7500 MPa γ-α and α-α' transitions 79−47083
Ce-Co-Si, thermoelectromotive force and electrocond. *(Ukrainian)* 80−54670
Ce-Fe-Si, thermoelectromotive force and electrocond. *(Ukrainian)* 80−54670
Ce-Ni-Si, thermoelectromotive force and electrocond. *(Ukrainian)* 80−54670
$CeCu_2Si_2$, resistivity, thermal conductivity and thermopower between 1.5 and 300K 78−87963
$CeCu_2Si_2$, transport anomalies 80−20148
$Ce_{1-x}La_x$ alloy, thermoelectric power 79−78080
$Ce_{1-x}La_x$, thermoelectric power, mag. transition temps. 80−20154
Co, amorphous and liq., thermoelec. power, contrib. of d states 79−23881
Co, amorphous and liquid states, electronic states and transport 79−99474
Co, ferromagnetic, EMF generation by pulsed laser irrad. 78−68021
Co, liq., thermoelec. power meas. 77−35928
Co-Ni alloys, liq., thermoelec. power and elec. resist. meas. 77−51719
Co-Pd, transfer phenomena and association with electronic struct. *(Russian)* 79−91017
$Co_x(Ni_{0.5}Cu_{0.5})_{1-x}Fe_2O_4$ ferrite, relation between elec. cond. and mag. anisotropy 80−75548
Cr, high purity, 280-1000K, Seebeck coeff. 77−39816
Cr-Al, antiferromag., transport props., anomalous crit. behaviour 79−61108
Cr-Mo, elec. resist. and thermo-EMF, conc. depend., 4.2 to 1500K *(Russian)* 80−80247
Cr-V(Mo), thermopower composition depend. 79−65445
$Cr_{99.94}Al_{00.6}$, thermal and elec. transport coeffs. near Neel temp. 79−78075
Cs, saturation effect on thermo-EMF up to 1950°C and 140 atm. 77−51727
Cs-Au, electron diffusion thermoelectric power calc. 77−28161
Cs-Au, liq. ionic alloy, elec. props. 79−99338
Cs-Sb(Au) liq. alloys, metal-nonmetal transition and change in electronic and mag. props. 77−51790
$Cs_{1-x}Au_x$, liq., metal-nonmetal transition, electronic theory 78−79930
Cu, ageing effect of thermoelectric power 78−2584
Cu alloys, thermopower and resistivity, Nordheim-Gorter relation 79−65438
Cu, compressed powder, thermoelectric effects 80−20155
Cu, Fermi surface and thermoelec. power, de Haas-van Alphen calc. 79−4503
Cu film, electron transport props., struct. defects role 77−40117

thermoelectric effects in metals and alloys continued
Cu, film, thermoelec. power meas. 77−79092
Cu, low temp. resist. and thermoelec. ratio, electron-electron scatt. contrib. 80−70670
Cu, resistivity and thermoelectric ratio at low temp., 0.04 to 7K 79−73497
Cu, stranded and solid wire, rel. stability of thermal EMF in cryogenic environment 78−60111
Cu, thermopower temp. depend. 79−65436
Cu-Ag film, amorphous resistivity, Hall coeff., thermopower and annealing kinetics 77−43744
Cu-Al(Ge)(Sn) film, thermoelec. power, 80-350K 78−68096
Cu-Au(Zn)(Ga)(Ge) dilute alloys, thermopower and resistivities, validity of Nordheim-Gorter relation 78−91671
Cu-Be-Ni-Ti-Mg bronze, alloying element influence on minimum thermo EMF, cold working *(Russian)* 80−34426
Cu-Co, thermoelectric power, precipitation effects *(German)* 77−85200
Cu-concentration junctions with solder, shock-induced elec. response 80−75626
Cu-Cr, dil. alloys, Frenkel defects, effects on anomalous resistivity and thermopower 77−8084
Cu-Fe, dil., thermopower, interconfig. fluctuations 79−65412
Cu-Fe, dil. alloy, anomalous thermoelec. power, sensitivity to defects, annealing effect 77−51728
Cu-Fe, precipitation kinetics study by thermoelectric power measurement *(French)* 79−20050
Cu-Fe, thermal treatment effect on thermoelec. power *(French)* 77−32000
Cu-Fe (<4 wt.%), solubility determ. by thermoelectric power meas. *(French)* 77−62644
Cu-Ge codeposited film, elec. resist. and thermoelec. power, rel. to struct. 79−87168
Cu-Ge(Sb) alloy systems, atomic struct. and electronic props. *(Russian)* 77−20289
Cu-Ni, comp. modulated alloy films, transport props., 10 to 300K 79−95515
Cu-Ni film, struct. and mag. order effects on electron transport props. 78−6460
Cu-Sn, amorphous, electron-phonon interaction effect on thermopower 80−29393
Cu+3d alloying impurities, solid soln., exam. of thermoelectricity *(Russian)* 79−28339
Cu_5CdSb, electrophys. props. 78−27491
Eu, electrical resistivity of solid and liquid phases, thermopower, melting temp. 80−59955
Eu, liquid, resist. and thermoelec. power, t-matrix calc. 78−26840
$EuGd_2S_4$, nonstoichiometric, elec. transport props., semicond. and metallic cond. 80−107786
EuO(Se), complex elec. cond. anomalies 80−107812
$Eu_{1-x}Sm_xS$, ESR, exchange interaction, susceptibility, elec. cond., thermoelectric power 80−93174
Fe alloys, ferromagnetic, EMF generation by pulsed laser irrad. 78−68021
Fe base binary alloys, thermoelectric force caused by internal adsorption *(Russian)* 78−95288
Fe, cast thermoelec. method of Si, Mn, C content monitoring, thermo EMF meas. 77−73490
Fe, liq., thermoelec. power meas. 77−35928
Fe, liquid and amorphous states, electronic states and transport 79−99474
Fe-Al, variation in absolute thermoelec. power under heat/treatment *(Ukrainian)* 79−38051
Fe-B based alloys, amorphous, amorphous, thermopower meas., Nordheim-Gorter relations 79−99535
Fe-Cr-Al, Kanthal films, vac. deposited, evaporation characts., comp., struct. and elec. props. 80−88646
Fe-Ni, (35 wt.%), transport props. and Invar features *(Russian)* 78−51973
Fe-Ni, α to γ transformation, changes in Young's modulus and electrophysical props. *(Russian)* 79−20042
Fe-Ni, FCC alloy, thermoelec. power, anomalous conc. depend. at high temp. 79−4548
Fe-Ni, thermodynamic props., anomalous 80−39313
Fe-Ni alloys, thermal props., let. review *(Russian)* 78−18805
Fe-Ni based alloys, amorphous, amorphous, thermopower meas., Nordheim-Gorter relations 79−99535
Fe-Ni films, on glass substrate, thermoelec. effect 80−107769
Fe-Ni-Mo, pre-precipitation obs., small-angle X-ray scatt. and thermoresist. meas. *(French)* 78−19757
Fe-P-Si alloys, electrothermal-grade, thermoelec. characts. in region 273 to 573K 78−23834
Fe-Rh, mag. phase transitions, triple point 79−1672
Fe-Si alloy, Si content determ. from Seebeck coeff. 77−56269
$Fe_xNi_{80-x}B_{20}$ glass, resist., magnetoresist., and thermoelec. power 80−70681
$Fe_{20}Ni_{60}P_{14}B_6$, $Fe_{30}Ni_{50}P_{14}B_6$, amorphous ferromags., thermoelec. power and resistivity near Curie temp. 79−56200
$Fe_xNi_{80-x}P_{14}B_6$ glass, resist., magnetoresist., and thermoelec. power 80−70681
Ga, thermopower quantum oscillations 80−15505
Gd, liquid, resist. and thermoelec. power, t-matrix calc. 78−26840
Gd, temp. variation of absolute thermoelec. power 77−11900
Gd, thermoelectric power anisotropy at high temp. 79−23952
$Gd(Al_{1-x}Cu_x)_2$, thermoelec. power, exchange interactions 80−24881
Ge-Si alloy, quenching from high temp., thermal electric parameters, obs. 77−28165
Hf, thermotransport and thermopower of O_2 78−76055
Hf-Zr(Sc), thermopower composition depend. 79−65445
Hg, electrical and thermodynamic props. in metal-semicond. transition range 80−20144
Hg, electron density of states at 20 and 200°C 77−15754
Hg, expanded fluid, thermoelec. power near crit. point 79−23951
Hg, liq., elec. cond. and thermoelec. power meas. 77−59273
Hg, liq., themoelec. power from X-ray diffr. struct. at −30 to 290°C 79−46551
Hg, liq. and dil. liq. amalgams, elec. cond. and thermoelec. power 77−55511
Hg-Au(Tl)(Bi), liquid dilute amalgams, elec. cond. and thermoelec. power 78−51976
Hg-Cd liq. amalgam, elec. cond. and thermoelec. power meas. 77−59273
In dilute alloys, Nielsen-Taylor effect in thermopower meas. 77−66157

thermoelectric effects in metals and alloys continued
In, intermediate state, thermoelec. effects 79−65620
In, magnetothermopower giant oscills., mag. breakdown 77−8075
In, supercond., expt. study of thermoelectricity 80−60138
In, superconducting, thermoelec. transport effect 78−39257
In, transverse magnetothermoelec. props. 78−47768
In, type I superconductor, thermoelec. power in intermediate state 78−34935
InP, electrial props. at high temp. and in liquid state 77−11888
Ir-Fe, spin fluctuation alloy, thermopower peak diffusion origin 80−88542
K, electron-electron scattering, elec. resistivity, thermal cond., thermoelec. power and Lorenz function 79−95382
K, liquid, thermoelectric power, optimised model pot. calcs. 80−29391
K, low temp. resist. and thermoelec. ratio, electron-electron scatt. contrib. 80−70670
K, low-temp. lattice cond., phonon drag thermopower 79−60789
K, Righi-Leduc and Hall coeffs. meas., ^{4}He temp. range 77−66156
K, thermoelectric power, high-temp., first-principles calc. 78−91672
K, thermomagnetic and thermoelectric properties, phonon scatt. processes 80−29390
K, thermopower, high temp., first principles calc. 79−65447
K-Rb, dil., calc. of press. depend. of low-temp. transport props. 78−30905
K-Rb, liq., form factors and transport coeffs., pseudopot. perturb. theory 80−44561
$(La,Gd)Al_2$, reverse Kondo alloy, transport props. at finite mag. field 80−6812
La, liquid, resist. and thermoelec. power, t-matrix calc. 78−26840
$LaCu_2Si_2$, resistivity, thermal conductivity and thermopower between 1.5 and 300K 78−87963
LaS elec. cond. and diff. thermo-EMF in 77-300K range 77−24573
$La_{1-x}Sr_xCoO_{3-y}$, Seebeck coeff. meas., small polaron hole conduction model 80−20233
Li, liq., elec. resistivity and thermoelec. power, orthogonalisation hole pseudopotential calc. 80−29376
Li, Righi-Leduc and Hall coeffs. meas., 2 to 120K 77−66156
Li-Au, electron diffusion thermoelectric power calc. 77−28161
Li-Mg, liq., elec. transport props. and phase diagram 78−23070
Li-Mg, liq. alloy, thermoelec. power and elec. meas. 77−47788
Li-NH_3, conc. solns., elec. cond. and thermoelec. power 79−19640
Li-Na, liq. alloy, thermoelec. power and elec. resist. 77−47788
Li-Pt, phase diagram for comp. range 0-40 at.% Pt, mag. and elec. props. *(German)* 80−84912
$Li_{1-x}Pb_x$, liq., metal-nonmetal transition, electronic theory 78−79930
Mg, thermopower calc., 1-OPW model 79−38053
$Mg_2Si_xGe_ySn_{1-x-y}$ composite Te material with high figure of merit 77−28164
MnSb, resist., susceptibility and thermopower rel. to electronic struct. 78−67935
Mo, magnetothermopower meas. 77−76795
Mo, thermopower, 200-1600K 79−65446
Mo-Mb, thermoelectric alloy for in pile temp. meas. *(French)* 79−67894
Mo-Nb (Re), thermoelec. power, 4.2 to 300K 80−70683
Mo-Nb(V)(Cr), thermopower composition depend. 79−65445
Mo-Ni thin film junction, phys. vap. deposition parameters effect on thermoelec. power 77−39922
Mo-V, elec. resist. and thermo-EMF, conc. depend., 4.2 to 1500K *(Russian)* 80−80247
Na, liquid, thermoelectric power, optimised model pot. calcs. 80−29391
Na, thermopower, high temp., first principles calc. 79−65447
Na-Cs, liq., thermopower 78−23074
Na-Cs, liq. alloy, thermoelec. power and elec. resist. 77−47788
Na-K(Cs), liq., form factors and transport coeffs., pseudopot. perturb. theory 80−44561
Nb, thermopower, 200-1600K 79−65446
Nb-Ni, amorphous thin film, vapour quenched, elec. resistivity and thermoelectric power 79−33275
Nb-Ta bimetallic loop, supercond., thermoelec. flux effects due to penetration depth changes 77−24636
Nb-V(Mo), thermopower composition depend. 79−65445
Nb-Zr, thermoelec. power, 4.2 to 300K 80−70683
NbH_x, thermopower, role of phonon dynamics 79−33284
$Nd_{1-x}La_x$ alloy, thermoelectric power 79−78080
$Nd_{1-x}La_x$, thermoelectric power, mag. transition temps. 80−20154
Ni, amorphous and liquid states, electronic states and transport 79−99474
Ni, ferromagnetic, EMF generation by pulsed laser irrad. 78−68021
Ni foil, hydrogenated, thermoelectric and Hall effects 79−65559
Ni foils, hydrogenated, thermoelec. and Hall effect 78−43364
Ni, hydrogenated foil, surface states and thermo EMF 78−91674
Ni, liq., electronic density of d-states, hard-sphere model and tight-binding approx. calc., thermoelectric behaviour 79−15065
Ni, liq., thermoelec. power meas. 77−35928
Ni-Al (6.3 at.%), influence of localised order on thermo-EMF and Hall-EMF *(Russian)* 78−6951
Ni-Cr film, RF sputtered, Seebeck coeff. 77−63004
Ni-Cr-Si thermocouple alloy, props. and thermoelec. reference data 79−26057
Ni-Fe Invar alloy, thermoelectric power temp. and mag. field depend. 78−26849
Ni-Mn, low temp. kinetic props., 4.2-77.3K, thermoelec. power *(Russian)* 79−19568
Ni-Rh alloys, thermal EMF, elec. resist., mag. susceptibility, mag. moment and Curie temps., 18-500°C *(Russian)* 77−20288
Ni-Si-Mg thermocouple alloy, props. and thermoelec. reference data 79−26057
Ni(Fe,Cr) and Ni_3(Fe,Cr), electron states density model and mag. characts. calcs. *(Russian)* 80−92804
Ni_3(Fe,M), M=Cu, Cr, Mo, W, kinetic phenomena rel. to ordering and electron struct. *(Russian)* 78−76043
Ni_3Fe, effect of alloying with Cr, Mo, W or Cu *(Russian)* 78−39095
Ni_4Mo, ordered, electrical resistivity and thermal EMF, temp. depend. *(Russian)* 77−55513
$Ni_{76}P_{24}$, cryst. and amorphous, thermopower and resist. meas. 80−20145
NiSb, resist., susceptibility and thermopower rel. to electronic struct. 78−67935
Os, thermal EMF quantum oscills. *(Russian)* 80−88543
Pb, absolute thermoelectric power meas. between 10 and 350K 77−28162

thermoelectric effects in metals and alloys continued
Pb, absolute thermopower, Thomson heat expt. 79−65434
Pb, pure and dil. alloys, diffusion thermopower, inelastic electron-phonon interaction 80−96851
Pb, thermoelectric power below 17K 79−38052
Pb-Sn bimetallic loop, supercond., thermoelec. flux effects due to penetration depth changes 77−24636
Pd films, evaporated, and thermoelec. power, annealing effects 80−39684
Pd Ni, effect of hydrogenation on thermopower 80−39562
Pd, transport props. 40 mK-6K 78−51968
Pd-Ag electrical resistivity, thermo-EMF and thermal diffusivity at high temps. *(Russian)* 80−6808
Pd-Au, low temp. thermoelectric power 79−47084
Pd-Co (0.1-45.7 at.%), thermo EMF at 4.2-300K *(Russian)* 80−92881
Pd-Fe, dil., transport props. at low temp. 0.05 to 5K 79−38046
Pd-Fe (0.54-8.0 at.%), thermo EMF at 4.2-300K *(Russian)* 80−92881
Pd-H, low temp. transport props., heterogeneous-mixture model 80−24871
Pd-Ni, spin fluctuation alloy, thermopower peak diffusion origin 80−88542
Pd-Ni, thermopower and crit. conc., spin fluctuation system 78−30909
Pd-Ni (15-90 at.%), thermo EMF at 4.2-300K *(Russian)* 80−92881
Pd-Pt-Au alloys for low-temp. precision resistors 79−69490
Pd-Ru, electron transport props., 50 mK-4.2K 78−14707
PdCo, effect of hydrogenation on thermopower 80−39562
PdH_x, x=0.915 to 0.996, thermoelec. power, 10 to 170K, rel. to optical phonon spectra 79−56201
$(Pd_{99}Ni)_{1-x}Pt_x$, spin-fluctuation thermopower 79−60802
$(Pd_xPt_{1-x})_3Fe$ atomically ordered alloy, thermoelectric power, carrier energy spin shift, mag. props. 80−29394
Pt, air annealed, ultralow temp. transport anomalies 77−69297
Pt, thermoelectric power, 290-560K 79−42522
Pt-Co alloys, dil., thermopower and magnetothermopower 79−65456
PtCo, absolute thermopower meas., 4-300K 78−10421
Pt_3Fe, transport and mag. props. near Neel temp. 79−7976
Rb, liq., simultaneous meas. of density, elec. cond., absolute thermopower up to 1400°C and 400 bar 77−1402
Rb, liquid, expanded, eqn. of state, transport up to 1700°C, 400 bar 80−2136
Rb, Righi-Leduc and Hall coeffs. meas., 2 to 120K 77−66156
Rb, transport props. and electron-electron scatt. 79−73490
Rb-Au, electron diffusion thermoelectric power calc. 77−28161
Ru, giant thermopower oscillations due to magnetic breakdown trajectories 79−60688
Ru, magnetic breakdown trajectories, quantum oscillations of thermo EMF and Nernst effect *(Russian)* 78−95290
Ru, thermopower and magnetoresistance meas., mag. breakdown 78−47766
$(SN)_x$, thermoelec. power, 0.1 to 4.2K, phonon drag contrib. and supercond. transition 79−56356
Sb, liq., thermoelec. power meas. 79−40591
Sc-H, conc.-temp. depend. at room temp. of elec. resist. thermo-EMF, mag. susceptibility, and Hall coeff. 80−29382
Sc-Zr(Hf), thermopower composition depend. 79−65445
$ScAl_2$-Eu, intermediate valence on Eu ions, Mossbauer isomer shift 80−84587
Si-Au amorphous film, metal-nonmetal transition, elec. cond., thermoelectric power meas. 79−47132
Si-Ge thermoelectric generators, approximation errors when using averaged properties solutions for required heat rates estimation 80−108808
Sm, resistivity and thermopower anomalies at high temp. 78−64027
Sn film, thermoelec. power, 3.7-8K 78−39231
Sn, intermediate state, thermoelec. effects 79−65620
Sn-Cu(Au) films, amorphous and polycrystalline, thermopower meas. *(German)* 77−80857
Sn-Pb alloys, thermo-EMFs meas. 77−20300
Sn-Zn(Hg)(Tl)(Bi) dilute alloys, thermo EMF *(Russian)* 79−33285
Sr, electrical resistivity and thermoelectric power 78−26846
Sr, transport properties, elec. resist., thermoelec. power, thermal cond. deviations from Matthiessen's rule 78−39086
Ta film, RF sputtered, thermoelec. power, Hall coeff. and struct. props. 77−43743
Ta, thermo EMF, effect of H diffusion 79−23950
Ta-W, thermoelec. power, 4.2 to 300K 80−70684
Tb, thermoelectric power anisotropy at high temp. 79−23952
Tb-Gd, elec. resistivity and thermopower critical behaviour 80−15499
TbZn, ferromag., thermoelec. power, temp. depend. and crit. behaviour 80−96852
TbZn, ferromag. transition, transport coeffs. critical behaviour 80−15498
Th-Y alloys, absolute thermoelec. power values 77−20303
α-Ti alloy, VT1-1, cold rolled, recrystn. texture and prop. anisotropy 78−52846
Ti alloys, metallurgical characterisation using thermoelec. power meas. *(French)* 80−45462
α-Ti alloys VT1 and VT5, struct. and phys. props., H_2 effect 80−108576
Ti, film, elec. resist. Hall effect and absolute differential thermoEMF *(Russian)* 79−24083
Ti, thermo EMF, effect of H diffusion 79−23950
Ti-Al-Zr alloy system, room temp. elec. resist. and thermal EMF *(Russian)* 77−20290
Ti-Cu solid solution, determ. of Cu solubility, stability by thermoelec. power meas. 79−77753
Ti-Fe alloys, elec. and thermal props. *(Russian)* 78−19020
Ti-Mn alloys, elec. and thermal props. *(Russian)* 78−19020
Ti-Ru (0.05 to 90 wt.%) hardness, thermal EMF, electrical conductivity, in annealed or quenched state *(Russian)* 77−55998
Ti-Zr(Hf), thermopower composition depend. 79−65445
Ti_2AlN, prep. and props. 77−28745
$Ti_{50}Be_{40}Zr_{10}$, amorphous, thermopower meas., Nordheim-Gorter relations 79−99535
TiN, highly dispersed, metallic thermo-EMF 78−43363
Tl-Bi system, phase transitions near Tl_3Bi, elec. props. meas. 80−35181
TmS, metallic, thermoelec. power 80−6818
TmSe, metallic, thermoelec. power 80−6818
U-Cr(Mo)(Nb)(Zr) alloys, absolute thermoelec. power values 77−20303
U-Re system, γ-solid solns., thermo-EMF, temp. depend. *(Russian)* 79−73496
U-Ti system, γ-solid solns., thermo-EMF, temp. depend. *(Russian)* 79−73496

thermoelectric effects in metals and alloys continued
UAl_2, transport props., susceptibility and sp. ht. 80−11174
UMn_2, transport props., influence of lattice distortion 80−100452
$UNi_{5-x}Cu_x$, thermoelectric power, 5-300K 79−65444
UX_3, (X=Al,Ga,In,Si,Ge,Sn), thermoelectric power, 5-300K 79−65444
$(V,Nb)_3Ga$, $(V,Nb)_3Ge$ and $(V,Nb)_3Si$ solid solns., conc. depend. 77−36006
V, Fermi surface and magnetic breakdown, magnetoresistance and thermopower behaviour 79−33222
V, thermal cond., elec. resist. and Seebeck coeff. meas., 6-300K 77−39818
V-Cr, effect of alloying additive on thermoelectric props. 77−35927
V-Mo, effect of alloying additive on thermoelectric props. 77−35927
V-Re alloy, thermo-EMF and resistivity at 0 to 1500°C 77−43571
V-W, effect of alloying additive on thermoelectric props. 77−35927
V_3O_5, electrical, thermodynamic and mag. props. at metal-semicond. transition, homogeneity range 77−4413
V_3O_5, insulator-metal phase trnasition at 450K, properties 78−39023
W, electronic transport below 1K 80−2377
W, resistivity min., thermoelectric anomaly correlation 78−2468
W, thermopower meas. in mag. field, 1.5-4K 80−54675
W-Fe, electronic transport below 1K 80−2377
W-Re alloys, thermal EMF instability, heat treatment effects 80−75553
W-Re thermocouple, thermal EMF var., stability 77−41604
Y, electrical resistivity of solid and liquid phases, thermopower, melting temp. 80−59955
Y, magnetic and elec. props., 100 to 900K *(Russian)* 80−25077
Y, thermoelectric power anisotropy at high temp. 79−23952
YIG:Ca, oxidising effects of high temp. annealing in reducing atmosphere 80−66696
Yb impurity Kondo system, crystal field effects on thermopower and Kondo effect 77−66163
Yb, liquid, resist. and thermoelec. power, t-matrix calc. 78−26840
Zr, thermo EMF, effect of H diffusion 79−23950
Zr-Hf, mag. susceptibility, elec. cond., Hall conc. thermoEMF conc. depend. *(Russian)* 80−39551
Zr-Ti, alloy, mag. susceptibility, elec. cond., Hall conc. thermoEMF conc. depend. *(Russian)* 80−39551

thermoelectric effects in semiconductors and insulators
airtight cell for simultaneous conductivity and thermo-EMF meas. 78−21168
alkali metal-molten salt mixtures, thermal EMF calcs., Rice and Pitzer models 78−20057
alkali perchlorates, elec. transport during struct. transforms. 78−59971
ambipolar semiconductors, thermoelectric redistribution of carriers 80−107830
amorphous, thermoelectric power and transport models 78−10482
amorphous film junction, I-V and C-V characts. 77−85307
amorphous semiconductor, conductivity, thermopower and statistical shift 79−95434
amorphous semiconductor, substantially doped, electronic props., review 79−87175
amorphous semiconductor alloy, bonding and transport properties 79−90950
amorphous semiconductor thermoelec. power transport coeff. calc. by quasiclassical approx. 80−20230
amorphous semiconductors, appl. to thermoelec. generators 80−35704
amorphous semiconductors, classification into structurally 'soft' and 'hard', thermoelectrical approach 78−42908
amorphous semiconductors, doped, electronic props. 78−19030
amorphous semiconductors, electronic transport mechanisms and coeffs. 80−80282
amorphous semiconductors, thermopower, conductivity, statistical shift, doping effects 79−69537
anisotropic thermoelement, synthetic media, thermo-EMF 80−92918
anisotropic thermoelements, annular, thermo-EMF 79−15174
anisotropic thermoelements, theory 79−11162
anisotropic thermoelements, transverse thermo-EMF, rectangular elements 78−56172
anisotropy rel. to processing of specimens moulded from powders 77−52515
automatic meas. of semicond. thermoelectric properties *(Polish)* 77−69359
biopolymers, solid, apparatus for Seebeck coeff. meas. 78−21172
bipolymer, charge carriers origin and mobility, adsorbed water effects 79−92461
chalcogenide glasses, multicomponent, Hall-thermopower sign anomaly 77−35957
chalcogenide solid solutions, thermoelectric materials, physico-chemical study 78−30945
$CoCr_2S_4$ films, galvanomagnetic and thermoelec. props. 80−54717
composite materials, thermoelec. props. degraded by strengthening additive 79−47114
correlation effects in hopping transport theory, applic. to cond. and thermal EMF *(Russian)* 78−23079
DC thermocouple, with variable cross-section, thermoelec. cooling 78−24787
degenerate semiconductor, amplification of sound by temp. gradient 77−20366
degenerate semiconductor, conduction current and generalised Einstein rels., Boltzmann transport eqn. 77−15810
degenerate semiconductor, electron diffusion thermopower, oscillatory, mag. quantisation effects 79−91088
degenerate semiconductor, Sondheimer oscills., asymptotic behaviour 78−19059
degenerate semiconductors, longitudinal thermo-EMF in quantising mag. field, scatt. mechanism *(Russian)* 80−24960
diamond, natural, elec. cond. and thermoelec. power 78−39115
differential thermal EMF measurement device for solid fusion region and melt states 78−12716
eddy currents, thermoelec., mechs. 80−44626
eddy thermoelectric currents and eddy thermoelements 77−8126
electronic transport and photocond. 79−60834
EMF in semiconductors, thermal injection of electrons, obs. 79−23994
exciton, insulator, differential thermo EMF, temp. depend. *(Russian)* 78−72182
extruded materials with tetradymite struct., primary and in situ recrystn. elec. props 79−43266
ferroelectric ceramic, elec. and thermoelec. props. of grains and grain boundaries 78−43382

thermoelectric effects in semiconductors and insulators continued
ferromagnetic nondegenerate semiconductors, magnon drag thermoelec. power calcs. 78−80012
ferromagnetic semiconductor, thermoelec. amplification of magnons 78−14748
figure of merit measurement, appl. to $Tl_{66}Se_{34}$ 77−28202
film, cell for measuring electrophys. parameters over wide temp. meas. 77−51830
film, galvano- and thermomag. phenomena, theory *(Russian)* 78−14743
film, thermoelectricity, ageing differential efficiency *(German)* 78−60146
film and bulk samples, thermoelec. power meas. apparatus 77−79092
fuel rod, simulated, for HTGR, pre- and postirradiational thermal transport and thermal expansion 79−6742
graphite, cryst., thermoelec. power, anomalous phonon drag effect 78−19065
graphite, MPn-6, thermoelectric material, thermal cond. meas., 1100-2000K 78−24798
graphite, neutron irradiated, thermoelec. and thermomag. effects 77−59296
graphite, neutron irradiation, electron transport, annealing study 80−39165
graphite, thermoelec. and thermomag. props., cylindrical band model 80−39616
graphite, thermoelectric power, low temperature, anomaly rel. to phonon drag 80−65610
half-cells extruded from ceramic blanks, recrystn. and elec. props. 79−43267
heat pulse technique for bonding thermoelectric modules contacts 80−107904
heavily doped compensated semiconductor, phonon drag effect in disordered media 77−24576
heavily doped semicond., electronic sp. ht. and transport coeff., influence of band-tail parameters 79−14941
heavily doped semiconductors, materials science developments, appl. to thermoelectric heat pumps 80−35713
high temperature meas., solid electrolytic cell, meas. at 700K and higher 80−31760
hopping conduction, correl. effects 77−89762
hopping conductivity in ordered and disordered solids, review 77−15851
ionic melts, thermal diffusion, thermoelectric power meas. 78−18810
Kane semiconductor films, thermomag. and thermoelec. effects, theory 80−70864
lattice gas, thermoelectric power in half-filled bands 79−60859
liquid semiconductor, cell for thermo-EMF meas. 77−74439
liquid semiconductors, thermoelectric power 79−65450
longitudinal thermo-EMF in quantising mag. field *(Russian)* 77−28204
many-valley semiconductors, ellipsoidal energy surface, high field magnetoresist. and magnetothermal EMF 77−43621
many-valley semiconductors, thermoelectric power, depend. of longitudinal mag. field 80−39618
α-MnS, elec. props. meas. 78−87971
multilayer thin film struct. thermoelec. props. 80−92964
n^+-n linear-gradient junction, thermoelectric effects 79−73577
n-type semiconductor, thermo-EMF and thermocurrent 79−38112
naphthoxazole derivatives, elec. cond., thermoelec. power, energy gap, absorpt. spectra 77−32053
narrow- and zero-gap semicond., mag. impurity scatt. effect on transport props. 77−15852
narrow-band solids, elec. cond. and thermoelec. power, evaluation from effective one-electron representation 79−56112
negative effective mass carrier contribution to EMF, sign *(Russian)* 78−26886
nickel phthalocyanine, ohmic and space-charge-limited currents in vacuum ambient 77−20323
nonuniformity monitoring by relative thermoEMF meas., limits by applicability 77−36702
p-n junction with hot carriers, thermophotoelectric effects 79−73576
Peltier effect appl. *(French)* 77−62908
phase interface of semiconductor crystallisation in constant electric field 77−44146
phthalocyanine-halogen complex, influence of halogen on elec. and optical props. *(Japanese)* 79−51586
phthalocyanine-halogen complexes, elec. props. 80−29424
plate, transverse thermoelectric power effect of thermal conductivity anisotropy 77−72876
polyacene quinone radical polymers, elec. props. described by variable range hopping model 80−44588
polyacene quinone radical polymers, two-dimens. variable range hopping 79−51608
polyacetylene:AsF_5, heavily doped, transport props., evidence for metallic state 79−87121
polyacetylene:AsF_5, thermopower and transport props. 80−65611
polyacetylene:I, semiconductor-metal transition, thermoelec. power meas. 79−56271
polyacetylene, doped, elec. cond. and thermopower 80−96951
polyacetylene, semiconducting and metallic, thermoelec. props. 80−40884
polyacetylene, variable density, synthesis, elec. cond., thermopower 80−60016
polyethylene terephthalate, Mylar, thermoelectric power 78−80010
polypyrrole films, electrochemical prep., chem. and phys. characterisation 80−70708
proton semiconductors, with H-bonds, quantum theory of proton cond. 80−65641
rare earth chalcobismuthites, $RBiTe_3$, prep., elec. props., and crystallographic date 80−59981
rare earth chalcogenides, cond. mechanism and thermoelec. efficiency 79−38110
rare earth orthotitanates, $RTiO_3$, metallic and semicond. elec. and mag. props. 79−38068
rare earth tungstates, elec. cond. and thermoelec. power meas., band theory 80−20191
ruthenates, $ACu_3Ru_4O_{12}$, A=Na,Ca,Sr,Cd,La,Pr,Nd, synthesis, cryst. struct., mag. and elec. props. *(French)* 80−107151
second breakdown electro-thermal model, computer program 77−24561
Seebeck coefficient, AC method of meas. using laser beam 78−76096
selenide thermoelectric materials, thermal conductivity, long-term stability and other props. experimental anal. 80−107834
semiconducting glass, Anderson model, thermoelectric power 78−84241
semiconducting thermoelement as a medium containing hot electrons 80−107829
thermoelectric effects in semiconductors and insulators continued
semiconductor, amorphous, non-polaronic, cond. and thermopower near band edge 80−49719
semiconductor, bounded, transport effects when a current passes along an energy inhomogeneity 79−7845
semiconductor, disordered, hopping thermoelec. power, temp. depend. 79−23995
semiconductor, electron distribution function, temp. gradient effect 78−72145
n-semiconductor, electron-phonon drag in longit. quantising mag. field 77−76805
semiconductor, inertia of Benedicks effect in carrier heating by microwave field 79−15173
semiconductor, inhomogeneity effects on thermoelec. and photothermoelec. power meas. 80−54728
semiconductor, Kane, thermoelec. power and thermomag. effects of hot electrons 78−56174
semiconductor, longitudinal isothermal Nernst-Ettingshausen effect in a quantising magnetic field 79−51617
semiconductor, Nernst-Ettingshausen effect, thermopower, strong elec. field 78−23122
semiconductor, partly disordered, with mobility threshold, transport props. and thermoelec. parameters 80−34449
semiconductor, photostimulated transport effects 79−11182
semiconductor, photothermal cond., low temp. depend. 80−70756
semiconductor, polaronic hopping conduction at low temp. 78−51906
semiconductor, thermoelec. power, band edge temp. coeff. 77−89743
semiconductor, thermoelectric amplification of sound 80−2427
semiconductor, thermoelectric figure of merit, direct meas. in transverse mag. field 78−10485
semiconductor filament, phonon drag contribution 78−19069
semiconductor layered medium, electron dragging by spin wave *(Russian)* 79−78124
semiconductor thermal energy transformers, influence of anisotropy of thermal cond. 77−8127
semiconductor thermoelectric materials, thermal stability 79−19611
semiconductor thermoelectric power in high magnetic fields 79−60858
semiconductor transport equations formulations 77−43585
semiconductor transport props., effect of temp. depend. band shifts 77−55522
semiconductor-ferrite layer structure, EMF created by spin-wave, effect of current 80−11072
semiconductors, amorphous, doped, electronic props. 80−80283
semiconductors, thermoelectric and thermomagnetic effects, heat transfer due to quasi-particle subsystems *(Russian)* 80−24959
semiconductors, thermoelectric power meas. using analogue subtraction 78−244
semiconductors, thermoelectrically anisotropic, carrier kinetics at low temp. 80−92893
semiconductors, thermoelectrically anisotropic 80−92894
semimetal, phonon drag, role of surface in thermoEMF *(Russian)* 78−47819
semimetals, exciton phase, transport effect in strong mag. fields 78−87977
small-sample mag. semiconductor thermoelectric power meas. installation 80−31795
solar thermoelectric generators, efficiency evaluation and improvement 79−62017
spinel ferrites, thermoelectric power, effect of exchange interactions 78−43422
superionic conductor, ionic thermoelectric power, lattice gas model 78−26717
superionic conductor, model calcs. 77−39688
superionic conductor, thermoelec. power calc., nature of hopping process 78−51727
superionic conductors, ionic thermoelec. power 79−46835
superionic conductors, transport props., review 77−62671
TCNQ, salt, DBTTF-TCNQ, elec. resistivity and thermoelec. power meas. 80−20193
$(TCNQ)_2$ benzacridinium, small bandgap semicond., cond. and thermoelec. power meas. 77−35946
TCNQ complexes with N-methyl derivatives of pyridine, cond. and thermoelec. power meas., band model anal. 80−10952
TCNQ salt, $(DEPE)^{2+}(TCNQ)_4^{2-}$, elec. and mag. props. of two crystallographic form 77−28166
TCNQ salt, $(DEPE)(TCNQ)_4$, elec. props., semicond. behaviour obs., no stable metallic state 77−51772
TCNQ salt, $(NMP)_x(phen)_{1-x}(TCNQ)$, thermoelectric power temp. depend. 80−15548
TCNQ salt, dibenzo-TTF-$TCNQCl_2$, one-dimens. mag. semicond., mag. and elec. props. 80−88601
TCNQ salt, $MeDABCO(TCNQ)_2$, elec. cond. and IR and visible spectra meas. 79−42526
TCNQ salt, Rb-TCNQ-II, two carrier cond. 80−44625
TCNQ salts, direct current conductivity and thermo-electric force, 4-400K *(Hungarian)* 79−56251
TCNQ solt, $CS_2(TCNQ)_3$, cond. and thermopower meas., deep level acceptor model 79−42529
$TEA(TCNQ)_2$, elec. cond. and thermoelec. power under hydrostatic press. 80−11024
thermoelectric heat pumps, cross flow, anal. of operation and performance using mathematical model 80−107836
thermoelement with deliberately induced anisotropy, optimisation of figure of merit 79−95433
TTT-I_c, direct current conductivity and thermo-electric force, 4-400K *(Hungarian)* 79−56251
wurtzite structure semiconductor, transport in longit. quantizing mag. field 78−26891
zero gap semiconductors, electron scatt., thermoelec. power and Hall effect at low temp. 80−44628
zinc blende semiconductors, small-gap, electron scatt. and transport props. 78−95294
zinc blende semiconductors, small-gap, electron scatt. and transport props. 78−95295
Ag-As-Te glasses, elec. props. *(Russian)* 77−85211
AgI group superionic conductor, phase transition detection by thermoelectric power method 80−92669
AgI:Cd, polycrystalline, thermoelectric power meas. 80−59698
AgI-Ag oxysalt ionic solids, power conversion determ. 78−30947
$(Ag_{x/2}Pb_{1-x}Bi_{x/2})Te$ solid solution, preparation and thermoelectric props. 77−47839

thermoelectric effects in semiconductors and insulators continued
$(Ag_{x/2}Pb_{1-x}Sb_{x/2})Te$ solid solns., Hall coeff., thermoelec. power, and thermal cond., 100 to 500K 79−82614
Ag_2S, liquid, ionic and electronic cond., thermoelec. power 80−39329
Ag_2S, transport props., 700-1500K 78−47796
$Ag_2S(Se)(Te)$, changes in elec. cond. and thermoelec. power at melting point 79−15147
$Ag_{19}Sb_{29}Te_{52}$, single-phase, thermoelectric efficiency 80−107826
Ag_2Se, liquid, ionic and electronic cond., thermoelec. power 80−39329
$Ag(T_l)/AgI/Ag(T_2)$ cell, thermo-EMF of highly conducting solid electrolytes 80−24659
Ag_2Te, liquid, ionic and electronic cond., thermoelec. power 80−39329
Ag_2Te, low temp. thermal cond., thermoEMF 78−43423
Ag_2Te-Ag_2S system, elec. and thermal props. at 300K 78−64044
$AgTlSe_2$ and AgTlSe, elec. cond. and thermoelectric power, doping effects, rel. to pseudogap model 78−2506
α-AlB_{12}, heavily doped, elec. props. 78−10446
α-AlB_{12}, prep. and electrothermal props. 80−20863
AlH_3, thermo-EMF meas. 80−39617
$AlMgB_{14}$, prep. and electrothermal props. 80−20863
Al_2O_3-Al, disordered, energy diagram model 79−56110
ArO_2-ScO_3 solid electrolytes, thermoEMF 78−95184
As, electrical and thermal props. 78−14747
As, electrical resist., thermal cond. and thermopower, low temp. transport props. 80−49708
a-As, opt. and elec. props. 77−39894
As, thermopower and thermal cond. from 8K down to 0.3K 79−19610
As:Ni(Ge)(S)(Se)(Te) film, amorphous, chemical modification of props. 80−49250
As-Te system glasses, DC and AC cond., thermo-EMF, 140 to 350K 79−42549
As-Te-Cu system glasses, DC and AC cond., thermo-EMF, freq. depend., 100 to 370K 77−76827
As-Te-Cu system glasses, elec. cond. and thermo-EMF 79−42540
As_2S_3 glasses, DC elec. cond. and thermo-elec. power 80−96865
As_xSb_{1-x}, semimetal, thermopower, thermomagnetic power, 4.5 to 77K 80−107825
$As_4Sb_2Se_9$ glassy semiconductors, electronic props. 80−103712
As_2Se_3-As_2Te_3, molten semicond., thermoelec. power and elec. cond. near metallic cond. transition 78−10486
As_2Se_3-As_2Te_3 glass thermoelec. power, and transport mechanism 80−2408
As_2Te_3, molten semicond., thermoelec. power and elec. cond. near metallic cond. transition 78−10486
$As_2Te_3+Tl_x$, glassy system, composition depend. of activation energy, thermopower meas. 78−64052
As_xTe_{100-x}, glassy system, composition depend. of activation energy, thermopower meas. 78−64052
$AsTeCu_x$ ($0 \le x \le 0.4$) glass, effect of Cu on elec. cond. and thermoelectricity, 100 to 370K 78−87978
B, preparation and purification, physical characterisation *(French)* 80−16189
α-B, rhombohedral, elec. cond., thermoelec. power, and Hall coeff. 80−6843
B:Ni, zone-refined, conductivity type from thermo-EMF sign 77−31682
B-Si compounds, thermoelec. material, prep. by pyrolysis of BBr_3-$SiBr_4$ mixture 80−20862
B-Si materials for thermoelectric conversion of solar energy *(French)* 80−89660
$B_{12}C_x$, phonon energies and electronic props., x depend., refl. spectra and thermoelec. power meas. 80−16052
B_xCy, metal-insulator transition, elec. cond. and thermoelec. power, 80 to 700K 80−44673
BP film, high temp. thermoelec. power, scattering processes 80−80305
$B_{14}Si$, β rhombohedral, conduction mechanism, thermoelectric props. 80−24932
$B_{14}Si$ elec. props., medium range disorder model 80−15522
$BaCuO_{2+x}$ ($0 \le x \le 0.12$), study of mag. and elec. props. rel. to the non-stoichiometry *(French)* 78−95051
Ba_2MoO_5, Ba_3MoO_6, electrophys. props., effects of thermophys. props. of medium in synthesis 77−48375
BaO-B_2O_3-V_2O_5 glasses, polaron hopping cond., optical absorpt. and ESR spectra 79−23966
$Ba_{1-x}Sm_xB_6$, prep., elec. cond. and thermoelec. props. 80−49697
$BaTiO_3$, donor doped, exam. of heterogeneous microstructure *(German)* 79−24632
n-$BaTiO_3$, elec. transport props., theoretical discussion and expt. 78−84215
n-$BaTiO_3$, grain boundary resistivities 77−80782
$BaTiO_3$, H_2-reduced, elec. cond. mechanism, EPR, resist. and Seebeck coeff. meas. 80−10976
Bi, Bi-Pb and Bi-Sn, elec. cond. and thermal EMF at press. up to 12 kbar 77−47806
Bi bounded semimetals, phonon two-stage drag of electrons, thermoelectric power, scatt. mechanism 80−92919
Bi, diffusion thermoelectric power in mag. field, calcs. 78−56167
Bi, electrical resist., thermal cond. and thermopower, low temp. transport props. 80−49708
Bi film, carrier conc. and mobility, resist., galvanomag. and thermoelec. meas. 78−52111
Bi film, charge carrier scatt. *(Russian)* 78−80079
Bi, film, thermoelec. power in transverse mag. field *(French)* 78−23183
Bi film, transverse mag. field depend. of thermoelec. power *(French)* 78−2587
Bi, giant negative phonon drag thermopower, pure sample 77−76851
Bi, intervalley scatt. influence on mobilities, thermopower calc. 78−26866
Bi, intravalley electron-phonon scatt. non parabolicity, thermoelectric power 79−99539
Bi, magneto-thermopower, weak-field, implication for scatt. mech. 80−49790
Bi, thermoelec. power, influence of mag. field reversal, drift vel. method 77−69363
Bi, thermoelectric power, electronic thermal cond., in mag. field 80−60015
Bi whiskers, thermopower, temp. depend., 77 to 300K phonon drag effect 79−82615
Bi:Sn,Te, and undoped sample, low-temp. transport meas., electron scatt. 77−24551
Bi-Sb, solid solns., thermoEMF in transverse mag. field 77−47841
thermoelectric effects in semiconductors and insulators continued
Bi-Sb alloy, magnetothermoelec. quality factor of single crystals 77−51771
Bi-Sb interface, film, thermoelectricity, ageing differential efficiency *(German)* 78−60146
Bi-Sb solid soln., thermoelectric props., 80 to 300K *(Russian)* 78−43425
Bi(-Sn), hydrostatic press. effect on band struct., thermoelec. power meas. 79−69406
Bi_2O_3, thermoelec. props., 500-1500K 80−29423
δ-Bi_2O_3, thermoelectric power, heat of transport of O^{2-} ions 80−92713
δ-Bi_2O_3, thermoelectric power rel. to fast ionic conduction 80−107549
δ-$(Bi_2O_3)_{1-x}(Y_2O_3)_x$, thermoelectric power rel. to fast ionic conduction 80−107549
$Bi_{0.88}Sb_{0.12}$, semiconducting transport props., 2 to 100K 80−59989
$Bi_{0.52}Sb_{1.48}Te_3$, microstructure rel. to thermoelec. props. 77−85249
$Bi_{0.52}Sb_{1.48}Te_3$ thermoelec. solid soln., homogeneity, effects of prep. method 78−52698
n-$(Bi_{1-x}Sb_x)_2Te_3$, magneto-Seebeck and Shubnikov-de Haas effect, thermoelec. power saturation 79−42568
$Bi_{2-x}Sb_xTe_{3-y}Se_y$, elec. cond. and thermoelec. props., neutral defects influence 80−60017
$Bi_{2-x}Sb_xTe_{3-y}Se_y$ solid solution, density-of-states effective mass, carrier mobility temp. depend. 80−24931
ρ-BiSe, single crystal, synthesis and elec. props. 77−16490
p-Bi_2Se cryst. growth, elec. props. 77−8748
n-Bi_2Se_3, single cryst., new aspect of carrier scatt. 80−49707
$Bi_2TE_{3-x}Se_x$, solid solution films, prep. and props. 78−44013
Bi_2Te_3, bulk n- and p-type samples, thermoelec. power meas. 77−79092
Bi_2Te_3, galvanothermomag. props. up to 14 kbar 77−47829
n-Bi_2Te_3, galvonomagnetic props., influence of hydrostatic press. 79−73536
Bi_2Te_3 single crystal, thermoelec. power anisotropy 77−55554
Bi_2Te_3, thermoelectric p-n junction, pulse refrigeration 78−23156
Bi_2Te_3-Bi_2Se_3 solid solns., bladed cryst. growth, electrophysical props. 78−43387
Bi_2Te_3-Bi_2Se_3 solid solns., single cryst. growth and thermocouple construct. 80−104056
Bi_2Te_3-Bi_2Se_3 thermoelectric alloys, diffusion and evaporation of volatile component during prep. 80−35118
Bi_2Te_3-Bi_2Se_3-Sb_2Te_3, solid solution, single crystal, elec. cond., thermoelectric props. 80−88550
Bi_2Te_3-InTe, thermoelec. props. 77−85250
Bi_2Te_3-Sb_2Te_3, Bi:Sb=1:2, 2:1, solid soln. deviation from stoichiometric cross section 79−43221
Bi_2Te_3-Sb_2Te_3 film, cond., galvanomag. Seebeck and Nernst-Ettingshausen effects under press., band model 77−47907
Bi_2Te_3-Sb_2Te_3 solid soln., deviation from stoichiometric cross section 78−35362
Bi_2Te_3-Sb_2Te_3:Cu, electrical cond. and thermopower, disorder effects *(German)* 77−1422
Bi_2Te_3-$SbTe_3$, ordered structure formation, heat treatment effect on thermal cond. 80−54448
BiTeI-SbTeI solid solns., form., crystn., elec., thermal props. 78−44003
$(Bi_2Te_3)_{0.9}(Sb_2Te_3)_{0.5}(Sb_2Se_3)_{0.05}$ n-type alloy for thermogenerators, thermo-EMF, elec. cond. and thermoelec. efficiency factor, 300-600K 80−70735
n-$Bi_2Te_{2.88}Se_{0.12}$, extrusion deformed, powder dispersion degree influence on thermal and elec. props. *(Russian)* 80−39366
$Bi_2Te_{2.88}Se_{0.12}$, solid soln., single cryst. growth and doping, thermoelec. efficiency and Hall coeff. 79−33921
$Bi_2Te_{3-x}Se_x$, microstructure rel. to thermoelec. props. 77−85249
$Bi_2Te_{3-x}Se_x$ solid solution, Hall effect anisotropy parameter, thermoelectric power, depend. on carrier density 79−69536
$Bi_2Te_{3-x}Se_x$, thermoelec. mat., prep. effects on inhomogeneities 78−51576
C fibres prepared from benzene, thermoelec. power meas. 78−2507
$CaCO_3$, calcite, elec. cond., 300 to 1200°C at CO_2 pressure of 40 bars 80−20195
CaF_2, fluorite crysts., lattice O^{2-} effect on thermal, elec., and thermoelec. props. 77−76599
$CaMnO_3$, microstruct., elec. cond., thermoEMF 78−23084
CaO-B_2O_3-Fe_2O_3 glass, electronic and dielec. props. meas. 77−24574
$CaSO_4$:Dy, cryst. growth from soln., thermoelec. and thermoluminesc. props. 79−56923
$Ca_{0.15}VO_2$, electrical cond., thermo-EMF, and lattice consts. 80−54685
Cd-Sb thin film prep. by vacuum deposition, elec. props. 78−92194
$CdAs_2$, amorphous, elec. cond. and thermopower 80−49722
$CdAs_2$, synthesis, microstruct., hardness and elec. cond. 79−51268
$CdAs_2$, thermoelec. props., anisotropy 80−34470
Cd_3As_2, band structure, Kane model, magneto-Seebeck and Hall data 77−62821
Cd_3As_2, band structure, pressure dependence of galvano- and thermomagnetic effects 80−6722
Cd_3As_2, electron effective mass. temp. depend., Hall effect and thermoelec. power meas. 80−39613
Cd_3As_2, thermoelectric power and transverse Nernst Ettingshausen coefficent 79−38104
$Cd_3(As_xP_{1-x})_3$, thermoelectric power and Hall effect., mag. field depend. 78−10484
n-$CdCr_2Se_4$, single crystal, transport props. near Curie temp. *(Japanese)* 78−6406
$Cd_xHg_{1-x}Se$, 77-400K *(Russian)* 78−2485
p-$Cd_xHg_{1-x}Te$ solid soln., thermoelec. effects 79−73538
$Cd_xHg_{1-x}Te$, thermal cond. in mag. field, thermopower, and Nernst-Ettingshausen effect 77−31814
n-$Cd_xHg_{1-x}Te$, thermal EMF, in transverse quantised EM field *(Russian)* 79−23993
CdS, and CdS_xSe_{1-x}, thermoelec. and photothermoelec. power meas., inhomogeneity effects 80−54728
CdS, epitaxial film, structural and electron transport props. 79−82481
CdS film, chemically sprayed, carrier conc. and mobility, thermoelec. and photothermoelectric meas. 80−2503
a-CdS film, DC cond. Seebeck data 77−24626
CdS films, pure and Na doped, chemical bath deposited, photothermoelectric effect 80−6906
CdS:Li chemically deposited filter, elec. props. 80−11113
CdS-Al_2O_3-Al diodes fabricated by MBE, junction characts. 79−65550
CdSb-Ag, thermoelectric, thermal defect relax., elec. cond. and thermo-EMF effects *(Russian)* 78−14749

thermoelectric effects in semiconductors and insulators continued
Cd_2Se_3, elec. resist., thermoelectromotive force, temp. depend., 300 to 1400K *(Russian)* 78−84243
p-$CdSnAs_2$, Hall effect, thermo EMF, thermomagnetic effects 80−107822
CdTe-Te film, prep. by combined hot-wall-flash evaporation method, and characterisation 80−55296
$CdTl_2Te_4$, Hall and thermo-EMF coeffs., in solid, liquid states 80−54704
$Cd_xZn_{1-x}S$ films, chem. sprayed, carrier density and mobility 80−60121
CeO_2, nonstoichiometric, defect struct. and elec. props. 79−60827
CeO_2:S, influence of S on elec. props. *(Russian)* 79−51566
CeO_{2-x}, conductivity and Seebeck coeff., small polaron and hopping mechanisms 77−76812
$Ce_{3-x}S_4$, $Ce_{3-x}Sm_xS_4$, elec. cond. mechanism, thermoelec. power, Hall and absorpt. coeffs. 77−24559
Ce_2Se_3-$SnSe_2$, solid-solution region, physical properties 78−43391
CoB_{12}, growth from melt and phys. props. 80−20782
$CoCr_2Te_4$, cryst. growth, struct., elec. props., Hall effect 78−43416
$Co_{1-x}Fe_xSi$, elec. and optical props. 80−49740
$Co_2Ge_2Te_3$, struct., resist., and thermo-EMF 80−20908
$Co_{1-x}Mg_xO$ ceramics as O_2 sensors, phase stability, elec. cond. and thermoelec. power meas. 78−3420
$CoMoO_4$, mag. susceptibility and electrical transport props. 79−56511
$Co_{3-x}Ni_xO_4$, $0 \leq x \leq 1.1$, struct., semicond.-semimetal transition, Seebeck coeff. 78−87972
Co_3O_4:Li(Cr)(Al)(S), and pure Co_3O_4, elec. cond. and thermo-EMF 80−20231
Co_2RhS_4, mag. semicond., mag. and elec. props. 80−93121
CoSi, Mn_nSi_{2n-m}, thermoelectric and optical props. 78−91714
Cr-Ge system, phase anal. and physical props. 79−24160
$Cr_{1-x}Mn_xSi_z$, semicond. props. 78−79992
Cr_2O_3 carrier mobility temp. dependence 77−35958
$CrSe_2$, layered, phys. and elec. props. 80−44594
$CrSi_2$ based solid solns., prep., elec. cond. and thermoelec. props. 80−49697
$CrSi_2$, semicond. props. 78−79992
$(Cu,Ag)_2Se/(Bi,Sb)_2Te_3$, P type selenide segmented element fabrication, thermoelectric props. 80−107835
(Cu,Ag)X, (X=Cl, Br, I), molten, thermoelec. power determ. 78−26711
Cu-Ge codeposited film, elec. resist. and thermoelec. power, rel. to struct. 79−87168
Cu_3AsS_4 and Cu_3SbS_4, thermal cond. in solid and liq. phases, 300 to 1100K, thermoelec. Q-factor 80−19997
Cu_3AsTe_4, elec. and thermal conds., thermo-EMF, solid and liq. states, temp. depends. 78−43384
$CuCr_2Se_4$, cryst., preparation, elec. cond., thermo EMF 77−8125
$CuCr_2Se_4$, crystal growth from melt, exam. of props. 80−55283
$CuGdTe_2$, synthesis and elec. props. 78−26529
p-$CuInSe_2$, thermal props. 80−96705
$Cu_4Mn_2S_4(Se_4)(Te_4)$ spinel, prep. and elec. props., 100 to 650K 79−43127
Cu_2S, low temp. modification, elec. props. 77−8092
Cu_2S, thermoelectric props. 80−54726
$Cu_{2-\delta}S$, $Cu_{2-\delta}Se$ and $Cu_{2-\delta}(S,Se)$, ionic and electronic cond., thermopower and Hall coeff. 77−20117
$Cu_{2-x}S$ single crysts., thermo-EMF, comp. depend. 77−24302
$Cu_2S(Se)$-Ge(Sn)S, phase diagrams 78−44100
Cu_3SbTe_4, elec. and thermal conds., thermo-EMF, solid and liq. states, temp. depends. 78−43384
$Cu_{2-x}Se$, elec. props. and band struct. 79−73513
Cu_2Te-Ag_2S, kinetic props. of solid solutions 79−7827
$Cu_{2-x}Te$, x=0 to 0.3, elec. cond., Hall const., carrier mobility, conc., thermoelec., density, lattice parameter 77−11915
$CuWO_4$, elec. cond., thermoelectric power and dielectric constant temp. depend. 80−96886
$DyCrS_3(Se_3)$, prep., elec. and thermal props. 78−43390
DyIG, thermoelectric power, elec. cond. charge carrier conduction mechanism 80−34441
Dy_2S_3, semimetallic, elec. and thermal transport meas. 78−10442
Er_2Se_3, elec. resist., thermoelectromotive force, temp. depend., 300 to 1400K *(Russian)* 78−84243
Er_2Te_3, films, prep., elec. props. 78−43494
EuB_6, electronic struct., transport and mag. props. 80−96782
$EuBi_2Te_4$, elec. cond., Hall, thermo-EMF coeffs. determ., 300-1100K 78−43386
$EuGa(In)_2X_4$, X=S,Se,Te, prep. and props. 77−85214
$EuGd_2S_4$, nonstoichiometric, elec. transport props., semicond. and metallic cond. 80−107786
Eu_2O_3, elec. cond., thermoelec. power, dielectric const. 79−69763
$EuO_{1-x}N_x$, ferromag. semicond., elec. and mag. props. *(French)* 78−79993
$EuSb_2S_4(Se_4)(Te_4)$ elec. cond., Hall, thermo-EMF coeffs. determ., 300-1100K 78−43386
$Eu_2(WO_4)_3$, molar mag. susceptibility, DC elec. cond., thermopower meas. 79−15172
$Eu_{1-x}Yb_xO(S)$, solid soln., ferromag. semicond., increase of exchange interaction 78−88109
$FeCr_2S_4$, pure and doped, CVD grown, surface struct., elec. props. and band struct. 79−4905
$FeCr_2S_{4-x}Se_x$, elec. props. 78−23083
$FeNi_2S_4$, violarite, mag. and elec. props., struct. determ. 77−43633
$Fe_{1-x}O$, wustite, thermoelec. power coeff. rel. to O_2 press. at high temp. *(French)* 77−76850
Fe_2O_3, haematite, annealing of nonequil. defects 79−43283
Fe_3O_4, Coulomb gap and hopping cond., effects on thermopower and Verwey ordering 80−44583
Fe_3O_4, hopping conduction and the Coulomb gap 80−44605
$FeRh_2S_4$, mag. semicond., mag. and elec. props. 80−93121
Fe_7S_8, pyrrhotite, thermocond. and thermoelec. power 80−96926
$FeSb_xO_{4-y}$, defect struct. and mag. transition, elec. transport and Mossbauer expts. 78−59803
$Fe_{3-x}Ti_xO_4$, elec. transport near Verwey transition, thermoelec. power and cond. meas. 79−95455
GaAs, compensated, magnetoresist. and magnetothermoelec. power meas. 77−43627
GaAs, electrical conductivity and thermoelectric power charge due to melting 80−100490
n-GaAs, epitaxial, thermoelec. power, temp. depend. in mm wavelength range 79−23996
GaAs, H^+ irradiation, effect on electrical props. 80−65567

thermoelectric effects in semiconductors and insulators continued
GaAs, melted zone displacement by current *(Russian)* 78−26727
GaAs, surface photovoltage due to photo-thermo-ionization of surface states 78−14787
n-GaAs, thermoelec. power 79−60857
GaAs:Cu, Fe, Cr resistance thermometer expts., 0° to 200°C *(Russian)* 78−45627
GaAs-GaAlAs DH CW laser, growth by Peltier effect induced LPE 77−48357
GaAs-GaAlAs heterostructures, LPE growth, Peltier effect *(Polish)* 78−6861
$GaAs_{1-x}P_x$:Te, thermoelectric figure of merit 79−69538
$Ga_{1-x}Mn_xSb$, elec. cond., mag. susceptibility, Hall const., and thermo-EMF, 80 to 1000K *(Russian)* 80−88549
GaN film, thermoelec. power and Hall coeff. meas. 77−55627
GaSb films, amorphous and cryst., vac. evaporated, Elec. cond. thermoelec. power and optical absorpt. 80−2504
GaSb:Mn(Sm), struct., thermo EMF, galvanomag. props. rel. to dopants, eutectic $Mn_{0.6}Ga_{0.4}Sb$ form. 77−15869
GaSb-GaAs-Ge system, props. and struct. 80−20232
GaTe-SnTe, melt, temp. and composition dependence of elec. cond. and thermo EMF 79−95430
$Ga_{20}Te_{80}$, amorphous, splat cooled, thermoelectric props. 78−43426
Gd_2GeSe_5, elec. props., 300 to 1100K 79−51585
GdIG, thermoelec. power, elec. cond., 500-1200K, ferrimag. Curie temp. 79−99543
Gd_2O_3, B-type monoclinic, DC(AC) elec. cond., thermoelectric power, dielectric const., temp. depends. 80−59980
Gd_2O_3, elec. cond., thermoelec. power, dielectric const. 79−69763
Gd_2S_3, semimetallic, elec. and thermal transport meas. 78−10442
Gd_2Se_3/PbTe, N type selenide segmented element fabrication, thermoelectric props. 80−107835
$Gd_2(WO_4)_3$, molar mag. susceptibility, DC elec. cond., thermopower meas. 79−15172
Ge, amorphous, doping, Schottky barrier and p-n junction form. by RF sputtering 77−8187
Ge, amorphous, elec. and opt. props., review 78−23094
Ge, amorphous, substitutional doping, electronic props. 77−1418
Ge, amorphous, thermoelec. power in phonon-assisted hopping regime, Coulomb effects 78−76097
Ge, amorphous and polycryst. layers, sputtered, elec. cond. and thermoelec. power 78−2586
Ge, amorphous film, annealing, effect on localised states 79−4535
Ge, amorphous film, in situ meas. of thermal EMP, by ultrahigh vacuum electron microscopy 79−26184
Ge, amorphous film, variable range hopping 78−76176
n-Ge, elastically deformed, anisotropy of thermoelec. effect 78−19066
Ge film, amorphous, thermoelec. power and structural investigs. using in-situ electron microscopy 77−76983
p-Ge injecting contact, sign of developed hot-carrier thermo-EMF 77−55606
Ge, p-n junction with hot carriers, current-voltage characts. 79−91135
Ge, photothermal cond., low temp. depend. 80−70756
n-Ge, thermo-EMF drag, anisotropy parameter *(Russian)* 77−80799
n-Ge, thermoelec. power in quantising mag. field, phonon-phonon interactions 80−107832
n-Ge, vel. component of hot charge carriers' thermoelectromotive force 80−44630
Ge:metal, polycrystalline film, electron transport props. 79−99642
Ge:P, phonon drag thermoelectric power at low temp. 80−107828
Ge:Sb, amorphous, electronic transport props. 80−44589
Ge:Sb(Ga), amorphous, doping effects on Fermi level, electrical meas. 79−42546
Ge:Sb(In), film, electronic props. 78−84330
Ge-As-Te glass, thermoelec. power and DC cond., temp. depend. 77−62955
N-Ge-Bi-Se glass, elec. and optical props. 80−65550
Ge-In-Te system, homogeneity region, struct., electrophysical props. 78−44091
Ge-In-Te system, region of solid soln. of In in GeTe 77−51499
Ge-Mo amorphous semicond.-granular metal film system, elec. transport and thermopower 77−76984
Ge-Si single crystals, heat treated, hot carrier thermo-EMF 77−24575
Ge-Te-As-In quaternary compounds, thin sheets elec. props., thermoelec. power *(Spanish)* 77−69358
$Ge_{100-x}As_x$ glass, elec. props. 77−76966
n-$Ge_{20}Bi_{10}Se_{70}$ glass, preparation and elec. props. 79−74126
$Ge_{20}Bi_xSe_{80-x}$, semicond. glass, resist., thermoelec. power, optical absorpt. 80−88555
$Ge_{20}Bi_xSe_{70-x}Te_{10}$, n-type semiconducting glasses, resistivity and thermoelectric power meas. 80−54695
$Ge_{20}Bi_xSe_{70-x}Te_{10}$, semicond. glass, resist., thermoelec. power, optical absorpt. 80−88555
$GeBi_2Te_4$, Hall const., thermoelec. power, and elec. cond. 80−29407
$(Ge_{1-x}Ga_x)_{1-x}Te$, rhombohedral and cubic phases, transport effects 78−2481
$(Ge_{1-x}In_x)_{1-x}Te$, rhombohedral and cubic phases, transport effects 78−2481
γ-GeTe, anisotropy of elec. props. 79−73515
GeTe films, elec. props. and struct., influence of annealing and condensation conditions 80−15388
GeTe, high pressure effects on hole conc. and thermoelec. props. 78−26894
GeTe, machining effects on electrophys. props. 77−86199
GeTe, nonstoichiometric, homogenisation 78−44004
GeTe:Mn, thermoelec. power, 2.5-25K, magnon drag effect 78−56169
GeTe-Ga_2Te_3, electrophys. props. 77−48403
GeTe-In, solubility, thermo-EMF coeff. meas. 78−43124
GeTe-MnTe, heat treatment effect on struct., elec. props. 80−54725
GeTe-MnTe-SnTe system, compds., GeTe phase transition temp., elec. props., thermal cond. 79−43220
$(GeTe)_x$-$(AgSbTe_2)_{1-x}$, thermoelectric props. of monolithic and pressed samples at 300K 78−80009
$(GeTe)_x$-$(AgSbTe_2)_{(1-x)}$, thermoelectric characts., temp. depend. 300 to 750K 79−78123
α-$Ge_{1-x}Te_x$, anisotropy of elec. props. rel. to cubic phase transition and band struct. 77−76820
$Ge_{15}Te_{85}$, amorphous, splat cooled, thermoelectric props. 78−43426
HfS, equilibria, nonstoichiometry and elec. props. temp. depend. *(French)* 78−64053
$HfSi_2$, work function rel. to phys. props. 77−47887

thermoelectric effects in semiconductors and insulators continued
$Hg_{2.86}AsF_6$, thermoelectric power 78−34852
$Hg_{1-x}Cd_xTe$ 0.1 eV, thermal conductivity meas. 77−24578
$Hg_{1-x}Cd_xTe$, props. and appls., book contrib. 77−39834
$Hg_{1-x}Cd_xTe$-type semimetals, kinetic props., local acceptor level effects 80−65557
$HgCr_2Se_4$, cryst., preparation, elec. cond., thermo EMF 77−8125
n-$Hg_{1-x}Mn_xTe$, quantum transport phenomena, exchange interaction influence 78−76093
$Hg_{1-x}Mn_xTe$, Shubnikov de Haas effect and quantum oscills. of thermoelec. power 80−49781
HgSe, quantum oscills. in Seebeck effect in high mag. fields 77−72875
HgSe, thermoelec. power, spin split quantum oscills. 77−11948
HgSe-Se, photo-field model, rel. to anomalous photocond. in Se:Hg 77−43658
HgTe film, vac. deposited, elec. props., 78-420K 80−11119
HgTe, magnetophonon oscills. of thermoelec. power 80−49789
HgTe:Mn, impurity scatt. contrib. to electron mobility and thermoelec. power 77−15852
Ho_2Se_3, elec. resist., thermoelectromotive force, temp. depend., 300 to 1400K *(Russian)* 78−84243
InAs, electrical conductivity and thermoelectric power charge due to melting 80−100490
$(InAs)_{1-x}(CdSe)_x$ solid solution, elec. props. 79−15146
$In_{1-x}Ga_xSb$ films, elec. props., preparation 80−100473
In_2O_3, Seebeck coeff., density of states effective mass 78−56171
InP, electrial props. at high temp. and in liquid state 77−11888
InP, electron transport props., mag. field and temp. depend. 80−92888
InP, surface damage induced during SiO_2 deposition by RF sputtering 79−78879
InP_xAs_{1-x} alloys, thermoelectric characts. 77−11947
InSb, high-purity, electron irradiation effects on transport props. 79−23650
p-InSb, mobility, diffusion and thermoelectric power of hot holes 80−39595
InSb, periodically doped cryst. prod. by Peltier effect, helicon diagnostics *(German)* 77−48338
InSb, thermal cond., elec. cond., and thermoelec. power, press. depend. 80−59744
n-InSb, thermoelec. power in longit. quantising field, phonon drag component 78−19064
InSb, thermoelec. power and relative resist. at press. up to 35 kbar 79−65505
InSb:Cr,Zn, transport props. meas. 77−1424
InSb:S(Se)(Te), reson. states and reson. scatt., elec. props. 80−49738
n-InSb:Se(Te), heavily doped, anomalous press. depend. of thermoelec. power 77−47840
InSb-HgTe system solid solutions, elec. cond. and thermo-EMF 79−51570
In_6Se_7, single cryst. prep. and electrophys. props. 79−43129
InTe thin films, flash evaporation, electrical props. 80−65722
InTe-SnTe, melt temp. and composition dependence of elec. cond., and thermo EMF 79−95430
$In_{20}Te_{80}$, amorphous, splat cooled, thermoelectric props. 78−43426
In_2Te_3-PbTe system, phase diagram, elec. props. 78−35361
KCl:$SrCl_2$, effect of impurity on thermoelec. power 78−76098
$KNbO_3$, elec. and thermoelec. props., influence of O defects 80−29401
$KNbO_3$, thermoelec. effect and phase transitions 78−48123
$KTaO_3$, defect struct. and elec. props. 78−91695
$KTaO_3$, pure and Gd_2O_3 doped, elec. cond. and sp. ht. 79−78097
$La_{1-x}Ca_xVO_3$, struct., elec. and mag. props., temp. and conc. depend. *(French)* 77−4293
$LaCr_3$ alloy development for thermoelec. appls. 80−35705
$LaCrSe_3$ alloy development for thermoelec. appls. 80−35705
La_2GeSe_5, elec. props., 300 to 1100K 79−51585
$La_{0.65}Pb_{0.35}MnO_3$, transport props. near Curie points 78−88100
$LaS_{1.47}$ elec. cond. and diff. thermo-EMF in 77-300K range 77−24573
$La_{1-x}Sr_xCoO_{3-y}$, Seebeck coeff. meas., small polaron hole conduction model 80−20233
$La_{1-x}Sr_xCrO_3$, x=0-0.2, AC and DC cond., 77-1300K, hopping of polarons 78−2477
$La_{2-x}Sr_xNiO_4$, ($0 \leq x \leq 1$), cryst. struct. and elec. props. 78−2088
$La_{1-x}Sr_xVO_3$, high-temp. transport meas. 77−11917
La_3Te_4, thermal cond., thermoelec. power abd elec. cond. meas., 80 to 750K 78−18853
La_3Te_4, thermoelectric material, thermal cond. meas., 1100-2000K 78−24798
Li alloys, liq. semicond., electronic struct., resistivity and thermoelec. power 77−51753
Li-Au(Hg)(Tl)(Pb)(Bi), liq. semicond., electronic struct., resist. and thermoelec. power meas. 77−47712
Li-ferrites, hopping theory 78−19039
Li-NH_3, conc. solns., elec. cond. and thermoelec. power 79−19640
LiCr ferrite, elec. resist., thermoelec. power and Nernst-Ettingshausen meas. near compensation point 78−10487
LiH, ionic cond., thermocurrent and photocond., defect and electronic props. 77−15621
$LuRhO_3$, elec., mag. and photoelectrochemical props. 80−96925
Lu_2Se_3, elec. resist., thermoelectromotive force, temp. depend., 300 to 1400K *(Russian)* 78−84243
$MgAl_2O_4$, γ-irradiated crystal, TSC, thermoelec. power, thermolum. and afterglow 80−75583
MgO, $MgCl_2$ additions effect, ionic role 78−26895
MgO-Si_3N_4, hot-pressed, electrical props. 78−39136
$Mg_2V_2O_7$, elec. props. and EPR meas. 79−11114
Mn-Zn ferrospinels, carrier transfer phenomena 80−54727
$MnAs_{1-x}P_x$ whiskers, thermoelectric power, 5 to 350K, phonon drag effects and mag. transitions 79−28363
MnB_{12}, growth from melt and phys. props. 80−20782
$Mn_{1-x}Fe_xSi_{1.7}$, solid soln. system, temp. depend of conductivity and thermo-EMF, conc. depend of Hall const. 77−11913
$MnGa_2S_4$, synthesis electrophys. props. 77−51747
Mn_3O_4:Li(Cr)(Al)(S), and pure Mn_3O_4, elec. cond. and thermo-EMF 80−20231
$MnSb_2S_4$, synthesis, electrophys. props. 77−51747
MnTe film, elec. props. 78−43498
$(MnTe)_{1-x}-(As_2Te_3)_x$ solid solns., thermoelec. props. 79−42567
$Mn_{1.18}Zn_{0.06}Co_{0.01}Fe_{1.75}O_4$, transport props. near Curie points 78−88100
Mo_2B_5 and MoB_4, thermal, elec., and mag. props. 80−20187
MoO_3-P_2O_5 glass, thermoelec. power meas. 78−84242
$MoSe_{2-x}$, transport meas. and band structure 77−69361

thermoelectric effects in semiconductors and insulators continued
$MoTe_2$, elec. cond. and thermoelec. power 79−91047
$MoTe_{2-x}$, thermoelec. power and resist. meas., band struct. 77−1438
$Mo_{0.5}W_{0.5}Se_2$ single cryst. vapour growth, characterisation 80−93466
$NaNbO_3$, elec. and thermoelec. props., influence of O defects 80−29401
$NaNbO_3$, elec. cond., Hall mobility, thermoelec. coeff. 79−82584
$NaNbO_3$, elect. cond. mech., resist., Hall coeff. and thermoelec. power meas. 80−65603
$NaNbO_3$, ferroelec. semicond., thermoelec. power for small polaron 77−89784
$NaNbO_3$, thermoelec. effect and phase transitions 78−48123
$NaSbSe_2$ films, struct., photoelec. and opt. props. 78−51834
$Na_xVS_2(Se_2)$, mag. and elec. props. rel. to struct. transitions 78−91848
Nb-Al_2O_3 cermet-type film, thermoelec. power and annealing effects 77−47911
NbC, high-temp. plastic deform. effects on elec. props. 77−44370
$NbSe_3$, elec. field depend. thermopower 79−56204
$NbSe_3$, thermoelectric power 79−28362
Nd-Gd-Te alloys of R_2Te_3-T_3Te_4 region, physicochem. props. 78−52017
$Nd_{1-x}Ca_xVO_3$, solid solutions, elec. props. 80−96866
Nd_2GeSe_5, elec. props., 300 to 1100K 79−51585
$Nd_2(MoO_4)_3$, mag. susceptibility, elec. cond. and thermoelec. power 78−88091
Nd_2O_3, A-type, thermoelectric power, AC cond. 78−68044
Nd_2O_3, elec. cond., thermoelec. power, dielectric const. 79−69763
Nd_2S_3, semimetallic, elec. and thermal transport meas. 78−10442
$NdTlO_3$, physicochem. props. 80−25625
$Nd_2(WO_4)_3$, molar mag. susceptibility, DC elec. cond., thermopower meas. 79−15172
$Ni_{1-x}Co_xS_2$, anomalous elec. props., polaron transport in highly correl. narrow bands 77−85222
$Ni_{1-x}Co_xS_2$, elec. cond., thermoelec. power and optical meas. 80−59986
$Ni_{1-x}Co_xS_2$, elec. transport and semicond.-metal transition 80−10985
$(Ni_{1-x}Fe_x)_{1-y}S$, anomalous thermal hysteresis in metal-semicond. transition 80−39640
NiO, temp. and stoichiometry depend., antiferromag. T-domain influence 77−8332
$NiS_{2-x}Se_x$, elec. cond., thermoelec. power and Hall effect meas. 80−65561
$NiWO_4$, AC elec. conductivity, thermoelec. power and dielec. const. 80−70736
$Ni_{0.4}Zn_{0.6}Fe_2O_4$, conditions for max. resistivity 77−21065
Pb chalcogenide, solid solution, thermoelectric efficiency 79−95429
Pb-S melt, absolute thermo-emf obs. 77−85251
$PbCl_2$-MCl, (M=Li, Na, K, RB, Cs), molten systems, thermoelec. power 77−62658
$Pb_{1-x}Ge_xTe$ solid solns., phase transition influence on elec. props., 77 to 450K 80−103689
$Pb_{1-x}Ge_xTe$:Ga, Fermi level stabilization, transport props. meas., 77-400K 78−56065
$Pb_{1-x}Ge_xTe$:Ga, influence of hydrostatic compression on elec. props. 79−73516
$Pb_{1-x}In_xTe$, impurity-state conduction and temp. depend. of transport coeffs. 78−47795
$Pb_{1-x}Mn_xTe$ (x=0.005, 0.001, 0.05), solid solns., exam. of electrical and thermal props. 79−1599
PbS, low carrier conc., prep. and props. 77−39846
PbS, nonstoichiometric, increase of rest pot. with p-type semicond. character 78−56170
p-PbS, struct. of valence band, transport processes study 80−20081
PbS:Tl, Hall and Seebeck coeffs., Hall mobility, impurity states 80−15545
PbS-Ni, phase diag., cpd. formation and electrophys. props. 77−85997
PbS-PbSe(Te), thermoconductivity and thermoresistance 79−23992
PbS-Sb system alloys, phase diagram, composition depend. of microhardness and thermo-EMF 77−25028
PbSe film, influence of pot. barrier on thermoelec. props. 78−39239
PbSe:Tl, elec. props. and IR reflection 78−6686
PbSe:Tl, scatt. of holes and phonons by impurities 78−19068
$PbSe_{0.5}S_{0.5}$, valence band struct., absorpt. spectra, elec. props. 80−44505
$Pb_{0.65}Sn_{0.35}Se$, solid soln., elec. props. 78−39112
$Pb_{1-x}Sn_xSe$, band struct. parameters, thermoelectric power meas. in strong mag. fields 79−51474
$Pb_{1-x}Sn_xSe$, carrier effective mass determ. 77−24572
$Pb_{1-x}Sn_xSe$, n- and p-type, with band inversion, study of transport phenomena 80−49741
$Pb_{1-x}Sn_xSe$, transport phenomena in solid solutions with band inversion 80−107792
p-$Pb_{0.65}Sn_{0.35}Te$, transport coeffs. and dispersion law 80−44629
$Pb_{0.8}Sn_{0.2}Te$, hole conc. at 77K from room temp. thermoelec. meas. 78−56155
$Pb_{0.8}Sn_{0.2}Te$, LPE layers, carrier conc. variation with annealing and growth temp. 77−39878
$Pb_{0.82}Sn_{0.18}Te$, thermomagnetic, thermoelectric props., valence band struct. *(Russian)* 80−54724
$Pb_{1-x}Sn_xTe$, effective mass of holes, thermoelec. power, Hall coeff., carrier conc. 79−65371
$Pb_{1-x}Sn_xTe$, mag. and kinetic props. near ferroelec. transition 80−11160
$Pb_{1-x}Sn_xTe$ monocrystal and sinter thermoelec. inhomogeneity 78−91713
p-$Pb_{1-x}Sn_xTe$, thermoelec. power, carrier conc. and temp. depend., interband scatt. 80−24957
$Pb_{1-x}Sn_xTe$, thermoelectric effects, characteristics at low temps. 80−107831
$Pb_{1-x}Sn_xTe$: Mn, Mn mag. and elec. active states, mag. impurity behaviour 80−44627
$Pb_{1-x}Sn_xTe$:In, high temp. Fermi level position 79−90948
$(Pb_{0.95}Sr_{0.05})(Zr_{0.53}Ti_{0.47})O_3$+3% mol PbO, Seebeck effect, meas. and interpretation *(Polish)* 79−4574
p-PbTe based composite material thermoelec. props. degraded by strengthening additive 79−47114
PbTe, carrier conc. inhomogeneity 78−52019
n-PbTe, cold hydroextrusion, plastic deform. rel. to thermoelec. props., struct. 77−11945
p-PbTe, energy band struct. and scattering of holes 80−10874
PbTe film, electronic thermal cond. and thermoelec. power 80−93018
PbTe films, thermal cond. and elec. props., 4.2 to 300K 79−28162
PbTe N-type, TE figure of merit, integral form 77−24577
PbTe:As, hole conc. control, in LPE layers, plasma reflectivity and thermoelec. probe meas. 79−99640

thermoelectric effects in semiconductors and insulators continued
PbTe:Bi(Sb)(Cr)(Ag), thermoelec. props., thermal and elec. cond. 79−82616
PbTe:Ga, location, behaviour of Ga, electrophysical props. meas. 79−38016
PbTe:In based solid solutions, impurity states, elec. props. 79−87054
n-PbTe:Pb(Bi)(In), thermoelectric props., 300-750K 78−34851
PbTe:Ti, effect of impurities on transport props. 79−11158
PbTe:Tl, influence of Tl impurity states 80−20121
PbTe:Tl, thermoelectric power, elec. cond., Hall coeff. and optical absorpt. coeff. 80−39584
PbTe-based solid solns., 79−23990
$PbTe_{1-y}Se_y$:In, high temp. Fermi level position 79−90948
$PbTiO_3$, ferroelec. semicond. thermoelec. power for small polaron 77−89784
$PbTiO_3$, thermoelectric effect and ferroelectric transition 78−48123
$Pb(Ti_{0.47}ZrO_{.53})O_3$, small polaron cond. mechanism, elec. cond. and thermopower meas. point defects 78−43380
$Pb(Zr,Ti)O_3$ ceramic, solid solutions, props. appl. *(Polish)* 77−28203
$Pb(Zr,Ti)O_3$ solid soln., elec. cond. and Seebeck coeff. 79−51564
$PbZrO_3$, ferroelec. semicond., thermoelec. power for small polaron 77−89784
$PbZrO_3$, thermoelec. effect and phase transitions 78−48123
$Pb(Zr_xTi_{1-x})O_3$, elec. props. temp. and composition depend. 78−47817
Pr_2GeSe_5, elec. props., 300 to 1100K 79−51585
$RbAg_4I_5$, superionic conductor, phase transition detection by thermoelectric power method 80−92669
$Ru_xTi_{1-x}O_2$ films, elec. props. and IR spectra 79−38207
S-based amorphous semicond. film, prep. by plasma decomp. of H_2S-N_2-NH_3, and characterisation 80−80422
Sb, electrical resist., thermal cond. and thermopower, low temp. transport props. 80−49708
Sb, thermoelectric figure of merit, 1-12 kbar, 100K 78−80013
Sb, thermoelectric props., press. effects up to 90 kbar 78−47818
$(Sb_{1-x}Bi_x)_2Te_3$, δ phase, equilib. state, electrophysical props. 79−52178
p-$Sb_{1.48}Bi_{0.52}Te_3$, extrusion deformed, powder dispersion degree influence on thermal and elec. props. *(Russian)* 80−39366
$Sb_{1.48}Bi_{0.52}Te_3$, obtained by zone crystallisation, effect of extrusion and annealing on elec. props. 79−96038
$Sb_{1.5}Bi_{0.5}Te_3$ solid solution, temp. influence obs. *(Slovak)* 78−30946
p-$Sb_xBi_{2-x}Te_3$ *(German)* 79−51618
Sb_2O_3, thermoelec. props., 500-1500K 80−29423
Sb_2S_3, elec. and mag. props., carrier transport mechanism 78−47792
Sb_2Se_3 crystals, mag. and elec. props. 80−96873
$(Sb_2Se_3)_x$-$(Bi_2S_3)_{1-x}$ single crystals, elec. and photoelec. props., stoichiometry deviations influence 79−60870
Sb_2Te_3 epitaxial films, growing conditions effect on elec. cond., thermo-EMF 80−39687
Sb_2Te_3, mag. and elec. props., carrier excitation 78−43395
Sb_2Te_3, $Sb_{1.5}Bi_{0.5}Te_3$, Te- and Se-doped cryst. growth and elec. props. 77−48334
Sb_2Te_3, stoichiometric, Hall effect and thermoelec. power studies 80−100470
Sb_2Te_3, thermoelectric properties and phase transition, under hydrostatic pressure up to 9 GPa 80−65609
p-Sb_2Te_3, thermopower anisotropy, temp. depend. 77−15884
Sb_2Te_3-Bi_2Te_3, low-temp. thermoelectric mats., growth of microhomogeneous crysts. 77−48337
Sb_2Te_3-Bi_2Te_3 solid solns., bladed cryst. growth, electrophysical props. 78−43387
Sb_2Te_3-Bi_2Te_3 solid solns., single cryst. growth and thermocouple construct. 80−104056
Sb_2Te_3-Sb_2Se_3, ordered structure formation, heat treatment effect on thermal cond. 80−54448
ScN_x, region of homogeneity, physicochem. props. 78−52018
Sc_2Se_3, elec. resist., thermoelectromotive force, temp. depend., 300 to 1400K *(Russian)* 78−84243
$Sc_{2/3}\square_{1/3-y}Sc_yS$, elec. props. variation at high temps. *(French)* 79−82649
Se, liq., electronic transport props. at sub- and supercritical conditions 77−51788
Se, liq., electronic transport props., equation of state, to 1900K and 1800 bars 80−65574
Se, liq., pure and I doped, thermopower, temp. depend. *(French)* 77−69360
Se liquid, pure and I doped, DC cond. and thermoelectric power *(French)* 79−56223
Se-Te-As-Ge glasses, elec. transport 79−60833
Se-Te-Sb glasses, electronic transport 80−88579
$Se_{1-x1}Te_{x1}$-$Se_{1-x2}Te_{x2}$ heterostructure, amorphous, rectification phenomena and photovoltaic effects 79−99610
Se_xTe_{1-x}, liq., thermoelec. transport at mobility edge 80−49787
Si, amorphous, doped, density of states determ. from transport meas. 80−49720
Si, amorphous, doped, non-polaronic cond. and thermopower near band edge 80−49719
Si, amorphous, doping, Schottky barrier and p-n junction form. by RF sputtering 77−8187
Si, amorphous, elec. and opt. props., review 78−23094
Si, amorphous, electrical transport and photocond. 77−85355
Si, amorphous, hopping model for activated charge transport 79−87099
Si, amorphous, substantially doped, electronic props., review 79−87175
Si, amorphous, substitutional doping, electronic props. 77−1418
Si, amorphous, thermoelec. power in phonon-assisted hopping regime, Coulomb effects 78−76097
Si, amorphous, transport results, interpretation 80−80260
Si, amorphous film, variable range hopping 78−76176
Si, doped amorphous, transport props., conductivity, thermopower, temp. depend. 79−73512
n-Si, drag thermoelec. power, anisotropy parameter determ. 80−20235
Si, EMF appearance under action of thermal field pulses with high temp. gradients 79−56252
Si film, elec. props., effect of amorphous to polycryst. transition 79−28425
Si film, sputtered amorphous, P and B doped, elec. cond. and thermopower meas. *(French)* 78−47403
Si, $n\text{-}n^+$ point junctions 80−44719
Si, phonon-phonon relaxation investigation for conventional and neutron doped crystals 80−96927
n-Si, piezoresist. rel. to piezothermoelec. power, electron-phonon drag region 80−70737

thermoelectric effects in semiconductors and insulators continued
Si, transport phenomena in strong elec. fields, intervalley electron scatt. 79−56240
Si:As, amorphous, field effect and thermoelectric power 79−33289
Si:B, piezothermoelec. power 78−56173
p-Si:B, thermoelec. power, 20-300K 78−19067
Si:H,B, amorphous, field effect and thermoelec. power 80−96924
Si:Li, amorphous, elec. cond. and thermopower 79−73537
Si:Li, amorphous, interstitial doping by in-diffusion and implantation and elec. characterisation 78−26585
Si:Li, amorphous, thermopower and cond. meas. 79−69142
Si:Li(Na)(K)(F)(Cl), amorphous, implantation effects on elec. props. 80−49716
Si:Na(K)(Cs), amorphous, ion implanted, control of cond. 79−60835
Si:P, amorphous, elec. cond. and thermoelectric power 77−89783
Si:P, amorphous, thermoelectric power and conductivity 77−89782
Si:P, impurity cond., hopping conduction and the Coulomb gap 80−44605
n-Si:P, piezothermoelec. power in electron-phonon drag region, anisotropy 80−70738
Si:P film, amorphous, unusual temp. depend. of thermoelec. power 77−59343
Si:P(B), film, electronic props. 78−84330
Si:Sb, amorphous, electronic transport props. 80−44589
Si-As-Te glass, thermoelec. power and DC cond., temp. depend. 77−62955
Si-Au amorphous film, metal-nonmetal transition, elec. cond., thermoelectric power meas. 79−47132
p-Si-Ge, heavily doped, hot pressed, high temp. phonon thermal cond. *(French)* 78−43190
Si-Ge, heavily doped, reversal of precip. 80−2409
Si-Ge, high temperature thermoelectric materials 80−89659
Si-Ge (22 at.%) alloy, thermoelec. props., time and temp. dependence 78−91712
Si-Ge alloy, thermoelec. material, lattice thermal conductivity rel. to grain size and carrier conc. 78−91495
Si-Ge alloys, figure-of-merit improvement by GaP additions 79−47115
Si-Ge:Al, B, P, hot-pressed alloy, thermoelec. props. 78−91711
Si-Ge:As,P, heavily doped, electron scatt., Hall coeff., Seebeck coeff. and resist. meas., 4-300K 77−4379
Si-H amorphous film, reactively sputtered, prep. and props. 79−78889
n-Si-SiO_2 interface, hot carrier surface thermo EMF depend. on surface band bending 80−44734
$Si_{(6-Z)}Al_ZO_ZN_{(8-Z)}$ 78−39136
$Si_{1-x}B_x$:H, amorphous films, thermopower and cond. for mixed band and broad tail state cond. 80−49786
n-SiC (6H), anisotropy, of thermoelec. power and transverse Nernst-Ettingshausen effect 77−69362
n-SiC (6H), anisotropy of thermoelectric power *(Russian)* 78−91710
n-SiC (6H), density of states effective mass determ., high temp. meas. of elec. props. 79−15073
SiC (6H), phonon drag and phonon-electron interaction *(Russian)* 78−79701
β-SiC, n-type, thermoelectric efficiency at high temps. 80−35706
β-SiC, thermoelectric material, thermal cond. meas., 1100-2000K 78−24798
$Si_{12}Ge_{10}As_{30}Te_{48}$, dark cond. and thermoelec. power, thermal activation energies interpret. 78−23123
Si_3N_4, hot-pressed, electrical props. 78−39136
SiTe:Ge(Sn), substitution of Si, thermoelectric props. *(Russian)* 80−11023
SiTe-GaTe, thermo-EMF, elec. cond. and solubility 77−20346
Sm_2GeSe_5, elec. props., 300 to 1100K 79−51585
Sm_2O_3, B-type monoclinic, DC(AC) elec. cond., thermoelectric power, dielectric const., temp. depends. 80−59980
Sm_2O_3, elec. cond., thermoelec. power, dielectric const. 79−69763
SmS-based alloy, preparation and properties 78−44034
$Sm_2(WO_4)_3$, molar mag. susceptibility, DC elec. cond., thermopower meas. 79−15172
Sn-S melt, absolute thermo-emf obs. 77−85251
$Sn_{1-x}Mn_xTe$, degenerate mag. semicond., thermoelec. power meas. 80−29392
SnO, disproportionation, thermoEMF, Mossbauer spectroscopic, X-ray diffr. anals. 79−11776
SnO_2 thermoelectrical properties, investigation 77−76852
$Sn_{1-x}Pb_2Te$, elec. and struct. props. of epitaxial layers *(Russian)* 78−64147
SnS(Te):O, thermoelectric materials, Fe microtrace assoc. with O impurities 77−20763
SnTe, isothermal meas. of galvanomag. and thermomag. effects *(Russian)* 78−56160
SnTe-In, solubility, thermo-EMF coeff. meas. 78−43124
SnTe-In_2Te_3 system, thermoelec. props., phase diagram, transitions 78−43424
SnTe-PbSe, semicond. film, growth, phase composition, condensation temp. rel. to cond. type 77−28266
SnTe-Tl_2Te, phase and elec. props. 77−48406
SrF_2, thermo-EMF meas., ion transfer characts. 77−7892
Sr_3MoO_6, electrophys. props., effects of thermophys. props. of medium in synthesis 77−48375
$Sr_{0.15}VO_2$, electrical cond., thermo-EMF, and lattice consts. 80−54685
TCNQ salt, $TEA(TCNQ)_2$, Hall effect and thermopower sign anomaly 79−56205
$TbCrSe_3$, prep., elec. and thermal props. 78−43390
Tb_2O_3, B-type monoclinic, DC(AC) elec. cond., thermoelectric power, dielectric const., temp. depends. 80−59980
Te film, thermally evaporated, elec. cond., Hall voltage and thermoelec. power 77−47913
Te film condensed on mica, struct. and electrophysical props. 80−39688
Te thin film, thermoelec. EMF, Seebeck coeff., elec. cond. structural depend. 79−78230
Te-$(Bi_xSb_{1-x})_2Te_3$ eutectic, electrophys. props., directed crystn. conditions influence and comp. depend. 80−107827
Te-based eutectics, crystn. rate effect on electrophys. props. mutual solubility effect 80−60774
$Te_{50-x}Se_{50}Sn_x$, thin films, elec. cond. and thermoelectric power meas. *(French)* 80−80335
Th_3As_4, prep. and semicond. props. 78−23087
Th_3As_4-U_3As_4 solid soln., electronic props. 80−34469
Ti_2AlC, Ti_3AlC, TiC, phys. props. 77−43602
TiC-TiN system, electro- and thermo-phys. props. 80−34210

thermoelectric effects in semiconductors and insulators continued
TiC-VC, mag. susceptibility, elec. cond. and thermoelec. props. 80−50033
TiC-ZrC, mag. susceptibility, elec. cond. and thermoelec. props. 80−50033
TiC-ZrC, solid soln., conc. and temp. dependence of props. 80−39736
TiH_x, temp. depend. of thermo-EMF coeff., 100 to 350K 77−11944
TiI_4, temp. depend. of thermo-EMF coeff., 100 to 350K 77−11944
TiN-CrN system solid solns., electrophys. and galvanomag. props., energy spectra 77−15847
TiO_2:Nb, rutile, Seebeck effect, 90-300K 78−43427
TiO_2:Nb, Seebeck coeff., Fermi level temp. depend. 79−11161
TiO_2:Nb and TiO_2, reduced, thermoelec. power meas. at high temp., point defect model 77−32030
TiO_2:Zr, electronic conduction, temp. depend. 77−8099
TiO_2-P_2O_5 reduced glasses, prep., elec. transport, chem. anal., DC, AC cond., seebeck coeff. 78−30924
TiO_2-Ti_2O_3-P_2O_5, glass form., struct. and elec. props. 80−44592
Ti_2O_3, cryst. growth by chem. transport and tri-arc methods, and characterisation 78−3003
Ti_4O_7, hopping conduction and the Coulomb gap 80−44605
TiP_2, synthesis and charact. 77−85953
TiS_2, evidence for semicond. props., Hall coeff., refl., cond., thermoelec. power 80−20220
TiS_2, transport props. and semicond. nature 80−44598
$TiS_2(Se_2)$, modelling contrasting semimetallic characters 78−43393
$TiSe_2$, semimetal, electronic props., superlattice form. 77−15532
Ti_xSi_y, work function rel. to phys. props. 77−47887
$Ti_{1-x}Ta_xO_2$, solid soln. formed in TiO_2-Ta_2O_5-Ta at 1100°C *(French)* 78−35375
$TlAsS_2(Se_2)(Te_2)$, elec. cond. and thermopower in solid and liquid states 77−89764
$TlInSe_2$-$TlPrSe_2$ system, struct., elec. cond., and thermoelec. props. 79−87119
Tl_2Se_3, elec. cond. and thermoelectric power, doping effects, rel. to pseudogap model 78−2506
TlTe single crystal, resistivity, Hall coeff., magnetoresistance, thermoelec. power 78−43418
Tl_2Te_3, exam. of electrical props., density and viscosity, for solid or liquid states 79−95431
Tl_2Te_3, exam. of electrical props., in solid, liquid state 80−54686
Tl_2Te_3:Ag(Sn), effect of dopant on electrical props., density and viscosity, for solid or liquid states 79−95432
Tl_xTe_{1-x}, liq., rigid band behaviour, elec. cond. and thermopower 77−35845
$Tl_2Te.As_2Te_3$, vitreous, temp. depend. of cond. and thermopower, electron energy spectrum 77−76831
UO_{2+x}, elect. cond. and thermoelectric power 78−52020
$V_{1-x}Ga_xO_2$, phase transitions, semicond. metal transition, antiferromag. props. 77−11969
VN-CrN system solid solns., electrophys. and galvanomag. props., 77 to 1300K 77−24567
VO_2:M^{3+}, M=Al,Ga,Fe, anisotropy of thermoelec. power, hole conductivity 77−11946
V_2O_5, thermoelec. props., 500-1500K 80−29423
V_2O_5:Na(Li), pure and doped, elec. cond. and thermoelec. power meas. 80−10987
V_2O_5-As_2O_3-RO, R=Ba, Ca, Pb, semicond. glass, electronic props. 80−88557
V_2O_5-BaO-K_2O-ZnO glasses, elect. props. and struct. 80−15547
V_2O_5-MoO_3 solid solns., small polaron cond., elec. resist. and thermoelec. power meas. 80−34447
V_2O_5-P_2O_5 (70-30), electrical cond. and thermoelectric meas., Au-glass-Au sandwich 80−29403
V_2O_5-P_2O_5 glass, thermoelec. power meas. 78−84242
V_2O_5-V_2O_4-$BaZnO_2$ glass, V ion states, mag. and elec. props. 80−88556
V_3O_5, cond. transition at 154°C, effect on props. *(German)* 79−42594
V_3O_5, electrical, thermodynamic and mag. props. at metal-semicond. transition, homogeneity range 77−4413
V_3O_5, insulator-metal phase trnasition at 450K, properties 78−39023
V_3O_5, Mo,Ti, and Ga doping effects on conductivity transition 77−11971
$V_{2-x}Sb_xO_4$, defect struct. exam., temp. depend. 78−18635
VTe, mag. and elec. transport props. 80−92897
$(V_{1-x}Ti_x)_2O_3$, solid solution, phase transition exam. 77−15590
W, low temp. transport props., phonon and impurity scatt. 78−10418
WB_{12}, growth from melt and phys. props. 80−20782
W_2B_5 and WB_4, thermal, elec., and mag. props. 80−20187
WO_3 amoprhous film, sublimed under different conditions, elec. transport props. 80−7015
WO_3-P_2O_5 glass, thermoelec. power meas. 78−84242
WS_2-NbS_2 system, compds., elec., antifriction props. 79−38066
YH_x (x=1.92 to 1.98), magnetic and elec. props., 100 to 900K *(Russian)* 80−25077
YIG, nonstoichiometry and electronic defects, thermogravimetric expts. and anal. of elec. data 78−6050
YIG: Ca^{2+} epitaxial films, Fe^{4+} centres, MCD, optical absorpt., and thermoelectric power meas. 78−95595
Y_2S_3, elec. cond. and thermoelectric power, p-n transition *(French)* 78−84264
$YbGa(In)_2X_4$, X=S,Se,Te, prep. and props. 77−85214
YbS_x, thermo-EMF, elec. and thermal cond., 300 to 1000K, comp. depend. 79−38111
Yb_2Se_3, elec. resist., thermoelectromotive force, temp. depend., 300 to 1400K *(Russian)* 78−84243
Yb_2Te_3, films, prep., elec. props. 78−43494
$ZnAs_2$, homogeneity region and electrophys. props. 80−60833
$Zn_{30}Cd_{70}S$ ceramic, electroluminesc., stationary thermostimulated cond. 79−87120
$Zn_xCd_{1-x}S$ films, spray pyrolysis, elec. props. 80−75657
$Zn_{0.1}Cd_{0.9}Sb$, thermoelectrically isotropic semicond., carrier kinetics in intrinsic cond. range 80−92894
$ZnCr_2Se_4$, electroconductivity, thermoelectromotive force, Hall effect *(Russian)* 80−70694
$Zn_xHg_{1-x}Se$, band struct. and scattering mechanism, determ. from transport coeffs. 77−59254
$Zn_xHg_{1-x}Se$ semimetal-semicond. transition, thermo-EMF in mag. field and Hall expts. *(Russian)* 77−15881
ZnS, ion implantation effects on luminesc., thermo-EMF 80−88178
ZnSb, and p-$Zn_{0.1}Cd_{0.9}Sb$, thermoelec. anisotropic semicond., carrier kinetics at low temps. 80−92893

thermoelectric effects in semiconductors and insulators continued
ZnSb, epitaxial films, growing conditions effect on elec. cond., thermo-EMF 80−39687
a-ZnSe, elec. and optical meas., Mott-type model for amorphous semicond. 78−2414
ZnSe, thermoelec. power meas. 78−52021
ZnSe:In, heavily compensated, galvanomag. props. and thermopower 79−51600
ZrC high-temp. plastic deform. effects on elec. props. 77−44370
ZrN high-temp. plastic deform. effects on elec. props. 77−44370
ZrS, equilibria, nonstoichiometry and elec. props. temp. depend. *(French)* 78−64053
ZrS_3, quasi one-dimens. semicond., elec. transport props. 80−107790
$ZrSi_2$, work function rel. to phys. props. 77−47887

thermoelectric generators *see thermoelectric conversion*

thermoelectricity
see also Peltier effect; Seebeck effect; thermocouples; thermoelectrets; thermoelectric effects in metals and alloys; thermoelectric effects in semiconductors and insulators; thermomagnetic effects; thermopiles; Thomson effect
alkali metal-ammonia solns., elec.-cond. and thermopower 77−1370
alkaline earth halide crystals, thermal transport of charged point defects 80−15293
alloys, thermoelec. power meas. in studies of solid solns. *(French)* 79−69497
bulk differential thermo-EMF 77−4380
condensed systems, phase equilibria, 400-1100°C, DTA method 80−218
consolidation study by absolute thermoelectromotor force 77−73246
crystals of low symmetry and axially symmetric, Hall and thermoelec. effects *(Russian)* 79−95427
eddy thermoelectric currents in thermoelec. anisotropic inhomogeneous media 77−55555
efficiency of thermoelectric materials, new criteria 78−21130
electrical noise thermometer, novel circuit 78−54364
film and bulk samples, thermoelec. power meas. apparatus 77−79092
heat and electrical transfer differential eqns. 78−67004
heterophase material with artificial anisotropy of thermo EMF 77−89781
high pressure chamber designed according to opposed anvil principles, thermoelectric force meas. *(German)* 80−90863
HMTSF-TNAP, one-dimens. conductor, transport props. 80−20165
hopping conductivity and thermopower, percolation and effective medium theory 79−78103
Hubbard model, thermoelectric power near atomic line 79−47086
inhomogeneous material, thermoelec. power and thermal cond. 78−10483
linear crystal with thermal gradient, Green's function method 78−64019
measurement of thermoelectric power of solids up to 10 GPa 78−89495
measurement of thermoelectromotive force and resistance, study of kinetic phenomena of charge transfers 80−57330
measurement of thermopower, automatic *(Polish)* 77−41638
metal coating stability, thermoelectric method of assessment *(Russian)* 78−11459
MHD, thermoelec. appl. to fission and fusion reactors and metallurgy 79−50806
molten binary mixtures, in thermocell, Soret coeff., thermoelec. power 77−15614
Mott's formula for thermopower and for Wiedemann-Franz law 80−84462
naphthalene-I_2 soln., elec. cond., thermoelec. power, conc. depend., 120°C 77−39845
non-steady-state method, thermo-EMF coeff. determ. 79−85150
nonhomogeneous media, distrib. of external mag. field caused by thermoelec. currents *(Russian)* 78−76056
ohmic contact, hot minority carrier effects on thermoEMF and photovoltage 77−15956
ore, flotation extraction, thermoelectric power, extraction yield depdnd. 78−19686
phenomenological equations, fluxes and forces 77−5779
phonon inelastic interband scatt. in transport effects 77−43552
plane waves in generalised thermoelasticity, stability and propagation 79−50618
plate, DC-current-heated, vertical, natural convection 78−90873
polyacetylene film, doped, transport props. 80−24913
pyrene-I_2 soln., elec. cond., thermoelec. power, 155°C, conc. depend. 77−39845
pyridinium silver iodide, fast ion conductor, phase transitions, thermoelec. power meas. 80−107540
quasi-one-dimensional conductors, thermopower studies 79−65463
sample holder for thermoelec. power meas. 77−57309
semimetal, two-stage drag of electrons by phonons 77−15843
sisal wax, electronic conduction and persistent internal polarisation 78−80277
superconducting bimetallic ring, thermoelec. effect 79−4616
superconductor, charge inbalance generation by temperature gradient 79−95541
superconductor, quasiparticle charge imbalance induced by supercurrent with thermal gradient 80−34546
superconductor, surface thermoelectric effects *(Russian)* 78−34921
superconductor, tunnelling potentials, thermoelectric quasiparticle transport 79−47200
superconductor with low conc. of mag. impurities thermoelec. effect 77−69448
superconductor with mag. impurities, longit. elec. field penetration, thermoelec. energy flow *(Russian)* 79−19694
superconductors, difference between acoustoelec. and thermoelec. effects 79−38246
superconductors, general and theoretical anal., review 80−11133
superconductors, thermoelectric and acoustoelectric effects, influence of mutual drag of excitations and phonons 80−44761
superconductors, thermoelectric branch imbalance currents 79−56370
supercurrent-thermal gradient interaction, branch imbalance generation 79−99657
superionic conductor, model calcs. 77−39688
$(TCNQ)_5^{2-}(DBzPE)^{2+}$, cryst. struct., elec. cond. and thermoelec. power 77−72606
TCNQ complexes, elec. resist. and thermoelec. power meas. 80−107777
TCNQ salt, (N-methylphenazinium)$_x$(phenazine)$_{1-x}$, 1 band filling, carrier mogility and disorder effects 80−24904

thermoelectricity continued
TCNQ salt, $(NMe_3H)(I)(TCNQ)$, one-dimens. semicond. with metal-like cond. 80−24909
TCNQ salt, $(TSeF)_x(TTF)_{1-x}$-TCNQ, struct., elec. and mag. props., review 80−20158
TCNQ salt, HMTTF-TCNQ, structure, metallic cond. and thermopower 77−8080
TCNQ salt, MeDABCO$(TCNQ)_2$, optical, elec., and mag. props. 80−65539
TCNQ salt, Qn$(TCNQ)_2$, thermoelec. power and cond., large Coulomb repulsion model 80−24893
TCNQ salt, Qn $(TCNQ)_2$, configurational entropy, thermoelec. power meas. 80−34432
TCNQ salt, TMTSF-DMTCNQ, cond. and thermopower meas. 80−20165
TCNQ salt QCTCNO, strong Coulomb correlations 79−56203
TCNQ salts, ETPP $(TCNQ)_2$ and DEPE $(TCNQ)_4$, thermoelec. power 80−59966
TCNQ salts, thermoelec. power, two-band model 79−4551
TCNQ salts with asymmetric donors, transport props. 78−60115
TCNQ-TSeF:TCNQ-M, thermopower determ. 78−47772
temperature dependence of thermoelec. power *(French)* 77−57325
temperature distribution in 3-D current-carrying body *(German)* 79−27497
tetraphenyldithiapyranylidene triiodides, elec. cond. and thermoelec. power 79−56207
thermal conductivity determ. heat losses, direct method for thermoelectric materials 80−62662
thermo-piezoelectric material, time depend. harmonically changing plane wave propag. anal. 80−15977
thermo-piezoelectricity, of polarised annular disc, deformation due to prescribed temp. distrib. 80−2699
thermocouple EMF, macroscopic thermodynamic theory 78−91678
thermoelectric power, absolute scale 77−71288
thermoelectric power and thermal conductivity, device for simultaneous meas., 100 to 300K *(French)* 78−77911
thermoelectric refrigeration at low temp. 79−93147
thermoelectrode emissivity, test method 77−89556
thermopower and thermal conductivity, simultaneous meas., method and apparatus 77−72854
tight-binding model, non half-filled, Peierls transition props. in commensurate phase 77−31933
$(TMTSF)_2X$, (X=PF_6^-, AsF_6^-, SbF_6^-, BF_4^-, NO_3^-) highly conducting salts, props. 80−59969
TMTSF-DMTCNQ, metallic state, transport props. 80−24974
$(TTF)_{12}(SCN)_7$ and $(TTF)_{12}(SeCN)_7$, charge-transfer salts, elec., mag. and optical props. 77−43575
TTF-TCNQ:TCNQ-M, thermopower determ. 78−47772
TTF-TCNQ, phase transitions, thermoelec. power meas. 79−65464
TTF-TCNQ derivatives, transport props., reflectance spectra 78−91683
$TTT_{1.2}NiS_4C_4H_4$, quasi-one-dimensional cond., cryst., mag. and elec. props. 78−10424
$TTT_2I_{3+\delta}$, thermoelec. power and metal-semicond. transition 80−34431
TTT_2I_3, quasi one-dimens. organic metal, elec. cond. and thermoelec. power 80−24899
$(TTT)_2I_3$ quasi-one-dimensional organic metal, effects of disorder on cond. and thermoelec. power 79−56206
$TTT\text{-}I_{1.6}$, dimensionality and disorder 77−66160
wustite solid solns., props. connected with localised electron state 80−107734
α-AgI, fast ion conductor, phase transitions, thermoelec. power meas. 80−107540
$Al_{2+x}O_3$, sintered, elec. cond. temp. and comp. depend., thermoelec. power 80−2438
Al_2O_3-Nb, cermet thin film, electrical transport and thermoelectric power 77−20462
Ca, elec. resist. and thermopower, meas. at melting temp. 79−99524
Cs-Au alloy, liq., exptl. evidence for ionic elec. transport 77−51534
FeS, pressure effect on elec. resist. and thermoelec. power 80−70308
Ge-Al(Cu), alloying effects on elec. transport props. of amorphous and crystalline Ge films 79−51689
p-Ge-In injecting contact, sign of developed hot-carrier thermo-EMF 77−55606
$Hg_{2.86}AsF_6$, one-dimens. conductor, thermopower, temp. depend. 79−65465
$Hg_{3-x}AsF_6$, one-dimens. conductor, thermopower, phonon drag 79−65466
InSb-NiSb plate, transverse EMF due to modulated illumination 77−55572
$La_{0.71}Pb_{0.29}MnO_3$, metal-semicond. transition at Curie point, transport props. obs. 79−73554
$La_{1-x}Sr_xVO_3$, Anderson transition, elec. resist. and thermopower meas. 80−100488
$NbSe_3$ and $Nb_{1-x}Ta_xSe_3$, thermoelec. power meas., 10-300K 80−20177
$RbAg_4I_5$ film, thermopower meas. temp. depend., correl. effects role 80−107539
$(SN)_x$ films, electrical properties 78−91782
$(SN)_x$, thermopower from 0.15 to 4.2K 80−34427
Sb film, thermoelec. power, thickness depend. 77−1501
SmS, and $Sm_{0.8}Tb_{0.2}S$, resistivity and thermopower 80−20260
SmS, crit. point for isostructural black to metallic phase transition, thermoelec. power meas. 78−60174
Sr, elec. resist. and thermopower, meas. at melting temp. 79−99524
Te-Se mixtures, liquid, electrical conductivity and thermoelectric power, high temps. and pressures 80−39639
TiN-MnN, solid solns., electrophys. props. 77−35914
VN-Mn, solid solns., electrophys. props. 77−35914
ZrC-ZrN system, solid solns., elec. resist., thermo EMF, thermal cond., expansion coeffs. 78−60176

thermography *see infrared imaging*

thermogravimetry *see thermal analysis*

thermoluminescence
adamantane, plastic cryst., radio- and photothermoluminesc. *(Russian)* 79−11477
adamantane, plastic cryst., thermolum. curves 80−2876
L-alanine:Cr^{3+}, X-irrad., thermoluminesc., ESR, UV photobleaching 77−9104
albedo dosimeter response to monoenergetic neutrons 77−90905
alkali borate binary glass, energy storage behaviour studied by thermoluminesc. 80−50432
thermoluminescence continued
alkali halide:Eu^{2+} phosphor, explosive loading method form., spectra, luminesc. characts. *(Russian)* 78−35212
alkali halide, activated, luminesc. and stored light sum 78−6738
alkali halide, dynamics of nonrelaxed and self-trapped holes *(Russian)* 80−80607
alkali halide, F-centre, stabilisation process in first colouring stage 79−19246
alkali halide, rel. between thermoluminescence and X-ray induced luminesc. 79−28830
alkali halides, irradiated, formation of Z centre 80−103326
alkali halides, Z_1-centres, peculiarities of thermolum. 80−103999
alkali metal halides, X-ray induced colour centre and halogen aggregate form. 80−96565
alkaline earth fluorides, F-centre annealing and intrinsic luminesc. 79−65937
alkaline earth glasses, $45RO.5Al_2O_3.50P_2O_5$, (R=alkali earths), electron beam irrad., exam. of charge accumulation and light-sum kinetics 79−4336
alkaline earth glasses, RO-Al_2O_3, -P_2O_5, R=Mg, Ca, Sr, Ba, exam. of electron beam irradiation effects 79−4253
alkaline earth tetraborates, doped, radiothermoluminesc. detectors, dosimetric characts. 77−61665
aluminophosphate glass:Mn:Mg(Sr), optical props. H_2O effects 77−28600
archaeological applications, review 78−58104
Barwell meteorite, preatmospheric size, thermoluminescence studies 78−53893
BBOA, polymorphism, radiothermoluminescence and differential scanning calorimetric study 80−24570
benzophenone, vap., laser-excited long-lifetime luminesc. 79−54887
calcite, dating of Quaternary samples 79−84231
calcium halophosphate, thermostimulated luminesc., mech. milling effects *(Russian)* 78−76537
carrier traps in polymeric insulating materials, investigation by thermoluminescence method 80−93240
cavern, dating with ESR and thermolum. *(Japanese)* 77−44955
ceramic art objects, thermoluminescent dating 78−58503
ceramic materials, thermoluminesc. dating, comparison of results 80−84791
ceramic sculpture from Oaxaca, Mexico, authentication by thermolum. and style 78−70238
chert artifacts, thermolum. determ. of prehistoric heat treatment 78−24914
chloroplasts of higher plants, effect of medium redox. props. 79−57609
chondrites, thermoluminescence 80−51706
computer simulation 78−39609
cosmic muons, dose rate and flux density estimations 79−58208
data processing of TSC/thermoluminescence ratio 78−10463
dating, absorbed dose from ^{90}Sr-^{90}Y beta source, thermolum. dosimetry 77−90911
dating, effect of radioactivity within quartz 78−70241
dating, radiation dose-rate data 80−31964
dating, reassessment of fine grain dose-rate 77−34071
dating, revised dose-rate data 77−34072
dating, Udo Bronze Head 77−34069
dating archaeological specimens by thermoluminescence glow-curve simulation method 77−5973
dating methods using thermoluminescence *(German)* 80−105076
dating of aboriginal fireplaces rel. to archaeomagnetic polarity excursion 77−21679
dating of ancient kiln, mag. separation of quartz 77−34070
dating of burnt flint, appl. to lower Palaeoloithic site Terra Amata 78−345
dating of calcite and burnt flint, age relation for slices 77−34073
dating of pottery, ^{87}Rb dose-rate contrib. 78−70242
dating of sediments baked by Chaine des Puys lava flows 78−92808
deep-sea sediment core, thermoluminesc. dating 79−74871
defect recombination, diffusion-controlled, incorporating Coulomb interaction and annihilation 78−23044
diamond:B, thermoluminesc., TSC, correlation meas. 78−88369
diamond, electroluminescence, thermoluminesc., photocurrents 79−38675
diamond, N9 and ND1 energy levels, electron irrad. photocond. obs., thermolum. 78−6324
diamond, natural, thermoluminescence, phosphorescence, defects, low temp. 78−11000
dielectric, solid thermally stimulated characts., dipolar relaxation time, trap levels and ionic space charge polarisation 80−84685
differential, new instrument for glow curve meas. with blackbody radiation suppression 78−74080
dimethyl sulphoxide, UO_2^{2+} γ-irrad. frozen solns., radiothermolum. and temp. deactivation *(Russian)* 79−33854
dosimeter, energy and directional response of Harshaw TLD-100 in diagnostic X-ray range 78−11738
dosimeter, low dose meas. *(Japanese)* 78−86696
dosimeter, neutron damage, displacement and ionis. fractions of fast neutron kerma 78−30669
dosimeter, thermoluminesc., calibration, γ-ray irradiator *(Japanese)* 78−66452
dosimeter, thermoluminesc., reader, high sensitivity *(Japanese)* 78−66426
dosimeter, thermoluminesc., response, nonlinear behaviour 78−33293
dosimeter, thermoluminescence intensity depend. on heating rate, competing deep trap model 77−73590
dosimeter reader TLD-04B for research and routine dosimetry appls. 78−20291
dosimeters, thermolum., supralinearity 77−10495
dosimetry, appl. to radioactive minerals prospecting 78−32244
dosimetry, archaeologic ceramic samples age determining *(Czech)* 77−5972
EBBA, polymorphism, radiothermoluminescence and differential scanning calorimetric study 80−24570
electroceramics, thermoluminescent and dosimetric characts. 79−8196
entropy production 78−23539
entropy production in luminescent processes 79−28845
Estacado meteorite, thermoluminescence and 'terrestrial age' determ. 79−2535
exoskeletons of Magicicada sp., detect. of thermolum., possible use as TLDs 80−30896
feldspar, anomalous fading, thermolum. dating 78−10999
fluorides, glow-peak shapes 77−28639

thermoluminescence continued
fluorphlogopite, synthetic, luminesc. props. 78−19579
gamma ray analysis of K, U and Th for dose-rate estimation in thermoluminescent dating 79−79333
glass, colour centre form. by UV irrad., afterglow, thermolum. and EPR obs. 78−10047
glass, recording of pulsed EM radiation in RF band during heating *(Russian)* 77−55837
glow curve activation energy, Balarin-Zetzsche evaluation method 78−76022
glow curve anal., temp. inhomogeneity 78−27332
glow curve integral, computation technique 79−8199
glow curve theory, temp. depend. of pre-exponential factor, activation energy calc. 80−2878
glow curves, analysis using time-linear temperature controller 79−63202
glow curves, effect of temp. distrib. and trapping centre conc. 78−48241
glow curves, reflection of electron trap distrib. activation energy 79−43047
glow curves and desorption spectra anal. method 80−80053
halophosphate phosphors, radiation stability, recomb. processes effect *(Russian)* 80−7424
Hawaiian alkalic basalts, thermoluminescence dating 77−86832
hydrocarbon, long chain single cryst., carrier transport meas. 80−6874
insulators, trap struct. anal. by fractional glow techique 79−11078
9-iodoanthracene, picosecond fluoresc. lifetimes, thermally activated $S_1 \rightarrow T_n$ intersystem crossing 80−28045
ionic crystals, exposed to ultrasoft X-rays, thermal luminesc. and electron emission 79−8192
Jomon pattern pottery from Japanese Taishaku valley, thermoluminescent dating 79−26196
kinetic parameters of thermally stimulated processes 78−10460
latex films, surface struct., vulcanisation, radiothermoluminesc. obs., 100-230K 78−75575
Lexan polycarbonate, thermolum. radiation-induced EPR of free radicals and track etchability 79−76295
loess-formed quartz silt thermoluminescence and dating *(Chinese)* 78−57226
low level detection 77−61132
lunar boulder shadow temp. and duration from shaded soil sample thermoluminescence 77−33372
lunar samples, charged particle track anal., thermoluminesc. and microcratering studies 77−60665
lunar soil samples from Luna-24, radioactivity and cosmic ray dose rate, thermolum. obs. 80−67596
mathematical basis, logical anal. 78−10462
measurement, apparatus for study at ambient and liquid N_2 temp. 77−82614
measurement apparatus, lunar samples and meteorites appl. 77−13803
meteorites, stony, gamma-ray induced thermoluminesc. gradients 77−74020
meteorites, study of objects of known age 80−46498
meteorites, thermoluminesc. rel. to orbit, pre-impact history and Earth residence time 80−31262
meteorites, validity of irrad. history from thermoluminesc. 80−36584
meteorites from Jilin shower 80−90372
methylcyclohexane glass, γ-radiolysis, electron tunnelling from matrix trapped biphenyl ions 79−29379
3-methylpentane glass, γ-radiolysis, electron tunnelling from matrix trapped biphenyl ions 79−29379
microspecimens obs., with size ≥0.8 mm, installation for 300 to 1100 mm range 80−57381
minerals, physical theories for origin of colour 78−69323
minerals, thermoluminesc. dating, error sources 78−11006
naphthacene, thermoluminesc., exam. at liquid N_2 temp. 77−4692
nematic liquid crystal, Merck 389, polymorphism, radiothermoluminescence and differential scanning calorimetric study 80−24570
neutron detector, thermoluminescent detector for 14.7 MeV neutron-gamma mixed field 77−6625
nonequilibrium thermodynamics 78−68569
nonequilibrium thermodynamics of luminescent processes in solids 80−50435
nonlinear effects in yields, model 78−11007
numerical analysis of data for quasicontinuous activation energy distrib. 77−52189
obsidian source identification by thermoluminescence 79−26195
Oklo natural fission reactor materials, thermoluminesc. props., effect of radiation damage 80−21750
optical multichannel anal., data microprocessing of thermally stimulated luminescence 78−54347
organic compound, vap., laser-excited long-lifetime luminesc. 79−54887
paraffins, γ-ray irradiated samples 77−69922
PET, photoexcited, thermolum. and carrier detrapping mechanism 79−61445
phenanthrene, mol. cryst., thermolum. build-up 78−27334
phosphate glasses, fading mechanisms 79−95851
phosphor, stationary recombinatorial luminesc. without thermal transitions, model 79−8193
phosphors, thermoluminescence, UV dosimetry 80−853
phosphors, TLD, γ-induced sensitisation and residual thermolum. 79−28844
phototransfer technique for thermoluminesc. dating 78−11005
plagioclases, volcanic, thermoluminescence dating 80−98475
planetary satellite Io, bright dawn terminator due to thermoluminesc. 78−96425
PMMA, X-ray irrad., thermoluminescence emission, exam. of kinetic order 79−43046
PMMA, X-ray irradiated, thermolum. glow peaks 77−90204
PMMA crosslinked by dimethacryloxymethylanthracene, radiothermoluminesc. *(Russian)* 78−73068
poly-p-xylylene films, carrier traps, X-ray induced TSC, thermolum. and dielec. loss study 80−88570
cis-polybutadiene and butadiene-styrene copolymer mixture, effect of temp. on phase composition 79−96005
polyethylene, γ-irradiated, luminesc. in warming and cooling 77−32450
polyethylene, high density, thermolum. and its oxidation effects 77−77305
polyethylene, low-density, α-irrad., thermolum. mechanism biphenyl anions influence 80−2880
polyethylene, oxidised, origin of high temp. anomalous luminesc. 77−85812
polyethylene, thermoluminesc. spectrum *(German)* 78−76538

thermoluminescence continued
polyethylene terephthalate, photoexcited, thermoluminescence field quenching 78−43942
polyethylene terephthalate, TSC and thermolum. due to electron detrapping by local mol. motions 80−96898
polyethylene terephthalate sheeting, storage in aqueous media rel. to props. *(German)* 79−29250
polyethylene-terephthalate, field-controlled photogeneration and carrier trapping 80−25285
polymer, carrier trap study by X-ray induced TSC and thermoluminescence *(Japanese)* 80−54713
polymer, rel. to mol. relax. 78−11003
polymer films, carrier transport meas. 80−6874
polyoxymethylene, irrad., thermoluminesc. above room temp. 80−2871
polypropylene, thermoluminesc. spectrum *(German)* 78−76538
polystyre, irrad, thermoluminesc. 78−2931
polystyrene, electron trap depth distribs., thermolum. data 78−11002
polystyrene, thermoluminesc. spectrum *(German)* 78−76538
polystyrene, thermoluminescence glow curves, quenching and isothermal decay plots 77−48258
polystyrene, X-ray irrad., thermoluminescence emission, exam. of kinetic order 79−43046
polyvinylidene fluoride, melting and freezing obs. *(German)* 78−15389
polyvinylidene fluoride, relax., influence of monomeric unit conform. and supermol. struct. *(Russian)* 79−23537
polyvinylidene fluoride, TSC and thermoluminescence, reln. to molecular motion *(Japanese)* 80−55200
pottery dating by thermoluminesc. *(Japanese)* 79−15537
quartz:Mn, X-ray and thermally stimulated luminesc. *(Russian)* 78−84626
quartz, alpha particle induced radiation defects, EPR and thermoluminescence study 80−20461
quartz, crystalline, thermolum. sensitivity, proton and gamma induced 77−90205
quartz, defects growth, study by X-ray diffr. topography *(French)* 80−39095
quartz, electron capture by impurity ions, cross sections eval. using thermolum. data 79−95855
quartz, natural, gamma-irradiated, stress effect on thermolum. sensitivity 80−11482
quartz, natural, thermoluminesc. glow curves and spectral charcts., γ-ray effects 78−2927
quartz, natural, virgin (γ-irradiated), polarisation effect on thermolum. sensitivity 80−11483
quartz, thermally excited state relax., acoustic and EM pulse obs. *(Russian)* 77−40293
quartz, thermoluminesc., γ-irrad. sample, heat treatment 78−64418
quartz, thermoluminesc., sensitivity, heat treatment effects 77−59622
quartz, thermoluminescence, superlinear accumulation of light sum *(Russian)* 79−52030
quartz, thermoluminescence output intensity depend. on γ- and ξ-irrad. temp. 77−59623
quartz, thermoluminescence sensitivity change due to stress 77−59627
quartz grains, thermolum. dating, β-dose attenuation correction factors 79−75669
quartz inclusion morphology for thermolum. dating, effect of HF etching 78−70240
radiation crack detection, use of luminescent convertors 78−53125
radiation dosimetry and dating by thermostimulated processes 78−11004
radiography, thermoluminescent, improved resolution image storage panel 78−16898
rapid-scanning interference spectrometer appl. to low-level thermoluminesc., use in archaeological dating 78−12773
recombination interactions, unimolecular processes, diffusion-limited kinetics 78−6794
ruby, induced absorpt., radioluminesc., thermoluminesc., Cr^{3+} conc. depend. *(Russian)* 77−90206
ruby, radiation-induced optical processes, impurity effects 80−66310
ruby, red thermoluminesc. *(Russian)* 79−56868
sand, heated, appl. to radiation dosimetry 77−61613
sapphire, pure and doped, luminesc. centres 79−33791
semiconductor, Balarin-Zetzsche evaluation method 77−43535
semiconductor, interpretation of thermolum. and TSC, extensions of conventional model 78−27335
semiconductor, thermolum. and TSC, evaluation of model, reliability of trap depth determ. 77−32451
semiconductors, thermally stimulated conductivity luminescence, defect levels, traps, book contribution 80−80296
semiconductors, thermally stimulated relaxation processes, book contribution 80−80295
solid, thermally stimulated processes, conf., Montpellier, France (June 1976) 78−10827
solid, thermally stimulated processes 78−10828
spatial distribution determination, using image intensifier technique 80−47115
spectra estimation using colour transparency film 77−86646
styrene-methacrylic acid copolymer, ionomer radiothermoluminesc. 79−95856
superlinear filling of traps in crystals due to competition during irradiation 79−33850
supralinearity *(Japanese)* 78−31263
temperature exposure measured by thermolum. fading 78−24786
N,N,N′,N′-tetramethyl-p-phenylenediamine, TMPD, glassy soln., photoionisation, recombination isothermal luminesc. *(French)* 77−16404
TGS, thermoluminesc. near Curie temp., effect of DC elec. field 79−33848
thermally stimulated luminescence application, radiation dosimetry, book contribution 80−80882
thermally stimulated recombination, reaction order 79−95853
thermally stimulated relaxation in solids, transport phenomena, book 80−77553
thermally stimulated release of trapped carriers, trap level spectroscopy 78−10461
thermoluminescence, traps and emission centres 79−24373
thermostimulated recombination, reaction order *(Russian)* 78−76536
TLD, automatic readers for personnel monitoring 78−50408
TLD, clinical appls. *(German)* 78−15904
TLD, neutron dose monitoring using multiple LiF TLD badge 77−90907
TLD and film badge personnel dosimeters, appl. *(Russian)* 78−20293
TLD materials, kerma for monoenergetic neutrons, theory, expt. comparison 77−5086

thermoluminescence continued
TLD powders calibration for low expsoure rates 77−6632
TLD processing using desk-top computer 77−81580
TLD response to 14.7 MeV fast and thermal neutrons 77−66856
TLD-04B reader, meas. of TL materials for health phys. appls. *(Russian)* 77−86648
trap depth, method of determ. 80−80211
trapping parameters for thermally stimulated luminesc. and cond. 77−52190
triboinduced luminescence 78−19581
triethylenediamine, plastic cryst., thermolum. curves 80−2876
TSC correlation, simultaneous meas. 77−81160
tungstate phosphors, thermoluminesc. and afterglows 79−38681
ultrahigh vacuum setup for photo- and thermostimulated electron emission and luminesc. obs. *(Russian)* 80−66383
Vempalle dolomite, Andhra Pradesh, India, thermoluminesc. characts. 77−17088
xanthone, in n-pentane, heat pulse induced delayed phosphorescence 80−83404
zircon, natural and synthetic crysts. Hf and Tb activated, capture centres and luminescence mechanism *(Russian)* 77−28626
zircons, from gold-bearing region of Salsigne, France *(French)* 77−28637
AgBr:I, refilling of recombination centres during thermal stimulation 78−10464
AgCl-AgI, mixed cryst., trap distrib., thermolum. 78−68568
AlF_3, localised electronic levels, thermoluminesc. and thermally stimulated current exam. 78−11001
AlN:O, thermolum. mechanism, 80-420K 79−78761
α-Al_2O_3, complex glow spectra, improvement of fractional glow technique, thermally stimulated exoelectron emission 79−65984
α-Al_2O_3, crystal defects from X-ray irradiation, F-centres, X-ray luminesc. obs. 80−55176
Al_2O_3 dosimeter phosphor for gamma-rays 77−6637
Al_2O_3, effect of heat treatment following gamma irradiation 77−59624
Al_2O_3, γ-irrad., hole centres, luminesc. and EPR obs. 77−32256
Al_2O_3, thermoluminescence, in H_2O vap. atm., temp. depend., time decay *(Russian)* 77−44074
Al_2O_3, thermoluminescence, optical bleaching/stimulation effects following irrad. 78−43940
Al_2O_3, UV dosimetry grade, thermolum. glow curves and emission spectra, 90-500K 78−72615
Al_2O_3:Cr photoexcited crystals, cooperative thermoluminescence quenching *(Russian)* 80−80881
α-Al_2O_3:Cr(Ti)(V), impurities effect on thermoluminesc. 80−40170
α-Al_2O_3:Er(Cr), crystal defects from X-ray irradiation, F-centres, X-ray luminesc. obs. 80−55176
Al_2O_3:Mg, pure and doped, recombination luminesc. spectra 79−83021
Al_2O_3:Ni, γ-irrad., thermoluminesc. 78−2925
Al_2O_3:Si, Ti, pure and doped, luminescence, optical absorpt. and colour centres 79−87501
Al_2O_3:Si,Ti photostimulated thermolum., and appl. to UV dosimetry 78−53511
Al_2O_3:Si thermoluminescent phosphor, annealing characts. and nature of traps 77−85817
$Al_2SiO_4F_2$, topaz, dosimeter appl. 78−35957
Ar:N_2O(CO)(CO_2), fluoresc. and thermoluminesc. after photolysis 79−89700
α-Al_2O_3, thermoluminescent trap stability, 450 to 1400°C 79−24372
B_2O_3 glasses, additives effect 78−27337
BaF_2, thermoluminesc. and F-centre annealing, after neutron irrad. 80−7422
BaFBr, X- and γ-irrad., thermolum. and optical absorpt. spectra 79−95857
BaFCl crystals, F-centres, X- and γ-irradiation, thermoluminescence and optical absorption spectra 80−45155
$Ba_{1-x}Mg_xSO_4:Eu^{3+}$ phosphor, thermolum. characts. 77−90203
$Ba_2NaNb_5O_{15}$, ferroelec. phase, thermally stimulated light flashes, surface elec. props. effects 79−73885
$Ba_2NaNb_5O_{15}$, ferroelectric, local states, thermoluminesc. study 80−60690
$Ba_3(PO_4)_2$ phosphor, ionisation of capture centres, thermolum. spectra 80−11487
$Ba_3(PO_4)_2$, recomb. luminesc. mechanisms 80−2874
$Ba_3(PO_4)_2$:Eu, X-ray phosphor, study of emission and trapping centres 79−8197
BaS:Bi phosphors, polycrystalline, effect of grain size on thermolum. 79−61446
BaS:Cu, thermoluminesc. and decay 78−80426
$BaSO_4$, barytes, with large magnitude of emitted light, thermolum. curves 78−88368
$BaSO_4$ natural barite, glow curves after γ-ray irrad., low doses 77−63471
$BaSO_4$ natural barites, mech. of thermolum. 79−78763
$BaSO_4$, with small retrapping factor, thermolum. glow curve 77−52188
$BaTiO_3$, rare earth doped ceramics, thermolum. and microwave induced thermolum. fading 79−1792
$BaWO_4$ crystals, X-irradiated, EPR, TSC and thermoluminescence spectra meas. 79−1791
$BaWO_4$:Mo, P, thermoluminesc. traps, EPR meas. 77−90032
$BaZrO_3$, cryst. growth and thermoluminesc. *(Russian)* 78−23604
BeO, ceramic, sintered, thermoluminesc., EPR, emission spectra, energy level diagram 77−81163
BeO, ceramic, thermolum. glow curves 79−47527
BeO, ceramic and single cryst., EPR-ENDOR study of [Li]° centre 77−85569
BeO ceramic TLD, operational characts. and problems 77−42216
BeO discs, thermally stimulated exoelectron emission and thermolum. sensitisation 78−35277
BeO in TLD, for low exposure of personnel, sensitivity, accuracy 77−29209
CS_2, VUV photolysis in Ar matrix, thermoluminesc. 77−52659
Ca halophosphate luminophors, grinding influence on thermolum. 79−95854
Ca halophosphates, thermoluminesc., defects *(Russian)* 79−56869
$CaCO_3$, Akiyoshi stalactite, thermoluminescence and ESR dating comparison 78−88807
$CaCO_3$, luminesc. under N_2 laser excitation, and appl. to archaeological dating 80−60685
$CaCO_3$, thermoluminesc. spatial distrib. using image intensifier technique 80−47115

thermoluminescence continued
CaF_2, doped, colour centre form. by UV irrad., afterglow, thermolum. and EPR obs. 78−10047
CaF_2, doped and gamma irrad., high temp.-peak in thermoluminescence 80−50434
CaF_2, hot pressed, dielectric, optical props. 79−56720
CaF_2, kinetics of thermoluminesc. buildup 79−65936
CaF_2, phototransfer of thermoluminesc. peaks 79−83040
CaF_2, thermolum., F-centre annealing after neutron irrad. at 20K 79−55787
CaF_2, thermoluminesc. and F-centre annealing, after neutron irrad. 80−7422
CaF_2:Co, X-irrad., luminesc. spectra 79−28801
CaF_2:Dy, thermolum. induced by 254 nm UV photons 80−55204
CaF_2:Dy (TLD-200), practical UV dosimeter 77−60258
CaF_2:Dy dosimeter crystals, γ-irrad. dose effect on thermoluminesc. response 77−64135
$CaF_2:Dy^{3+}$, associated luminesc. centres and traps 77−28638
CaF_2:Dy(Mn), thermolum. induced by monoenergetic parallel beam 81 MeV diffr. neutrons 77−52883
CaF_2:Eu, thermolum. in presence of lanthanide impurities 80−2870
CaF_2:Mn TLD, internal background build-up 77−54399
CaF_2:Mn(Co)(Ni), X-irrad., thermolum. 80−60686
CaF_2:Na, single cryst., X-irrad., optical absorpt. and thermoluminesc. 80−34952
$CaF_2:Sm^{2+}$, phonon spectrum of thermal pulses by fluorescence 79−95860
CaO, doped, thermal stability of hole centres and hole recombination luminescence *(Russian)* 78−72614
CaO, Eu, Eu^{2+} to Eu^{3+} charge transformation *(Russian)* 78−72403
CaO:Cu(Ag)(Au), thermoluminesc., following UV excitation, 290-500K 77−40292
CaO:Dy, thermolum. induced by 254 nm UV photons 80−55204
CaO:Eu(Tb), phosphor, isothermal decay 80−55156
CaO:F(Cl)(Al), phosphon, luminesc., electron-hole recombination processes 79−65919
CaO:Y phosphor, chemical instability, thermoluminescence study 79−38682
$Ca_2P_2O_7$:Sb(,Mn), luminesc., colouration 80−2828
β-$Ca_3(PO_4)_2$:Sb(,Mn), luminesc., colouration 80−2828
$Ca_{10}(PO_4)_6(OH)_2$, UV induced thermolumin. glow peak obs. 80−29814
$Ca_{10}(PO_4)_6(OH)_2$:Mn, thermoluminesc. 77-500K, X-irrad. at 77K *(French)* 78−15234
$Ca_5(PO_4)_3OH$ prod. by hydrothermal synthesis, thermolum. props. 80−2877
$Ca_5(PO_4)_3OH$:Mn, synthesized by hydrothermal method in CaO-P_2O_5-H_2O, thermoluminescence study rel. to starting mixture 78−95612
CaS, phosphor, thermally stimulated luminescence expt. 78−10951
CaS:Bi,Dy phosphors, thermoluminesc. 77−69921
CaS:Bi phosphors, UV dosimetry by thermolum. 80−55199
CaS:Eu, Eu^{2+} to Eu^{3+} charge transformation *(Russian)* 78−72403
CaS:Pd phosphors, trap and luminescent centre location, photo-, thermo- and electroluminescence studies 80−71482
CaS:Zr, Gd phosphors, thermoluminesc., trap distrib., activator effects 78−2929
CaS-Bi, Mn, phosphors, thermoluminesc., phosphoresc. 78−2928
CaS-Pb,Mn, phosphors, thermoluminesc. and fluoresc. spectra 78−64396
$CaSO_4$, glow curves, X-irrad. effect 78−35210
$CaSO_4$ phosphors:Ce(Eu)(Dy)(Tm), gamma-irradiated valency conversions in rare-earth ions 80−55198
$CaSO_4$, TLD high-dose characteristics 77−40772
$CaSO_4$ with rare-earth and Y dopants, ESR, thermolum. correlation studies following gamma irradiation 77−59628
$CaSO_4$:Ce(Eu) phosphors, fluorescence spectra, thermolum. glow curve 80−2879
$CaSO_4$:Dy, Cd-covered TLD, thermal neutron dosimetry 77−90912
$CaSO_4$:Dy, competing deep trap model for thermoluminescence 79−83039
$CaSO_4$:Dy, cryst. growth from soln., thermoelec. and thermoluminesc. props. 79−56923
$CaSO_4$:Dy, γ-ray induced sensitization, competing trap model 80−2881
$CaSO_4$:Dy, high exposure UV response and sensitisation 79−91506
$CaSO_4$:Dy, phosphor, X-irrad., thermoluminesc., role of Na_2SO_4 as charge compensator 79−78764
$CaSO_4$:Dy, photo-stimulated thermolum., for high-exposure dosimetry 77−9262
$CaSO_4$:Dy, phototransferred TL studies 80−80875
$CaSO_4$:Dy, studies for dosimetry 79−29634
$CaSO_4$:Dy, TLD during irrad. by γ-rays, X-rays, electrons, ambient atm. effect 78−19578
$CaSO_4$:Dy, thermolum. origin, test of model on $CaSO_4$:Eu 77−85813
$CaSO_4$:Dy, thermoluminescent glow peaks, post γ-irrad. annealing study 80−89077
$CaSO_4$:Dy phosphor powder, effect of grinding on thermoluminescent sensitivity 79−33852
$CaSO_4$:Dy photostimulated luminesc. for dosimetry, effect on thermolum. 77−90910
$CaSO_4$:Dy ribbon, dosimetric props. study 80−63395
$CaSO_4$:Dy sintered pellets, thermolum. response 80−93411
$CaSO_4$:Dy Teflon TLD discs, graphite-mixed, for beta dosimetry 77−86639
$CaSO_4$:Dy-KBr thermolum. phosphor, thermal neutron detect. by activation 80−32581
$CaSO_4$:Dy(Tm), thermolum. induced by 254 nm UV photons 80−55204
$CaSO_4$:Dy(Tm) thermoluminescent props. of non-commercial phosphors 78−58550
$CaSO_4$:Mn, phosphor, thermoluminesc., low energy ion excitation 77−55838
$CaSO_4$:Sm phosphors, X-irrad., thermoluminesc., charge compensation effects 80−97351
$CaSO_4$:Tm, Li, mixed field TLD 77−9263
$CaSO_4$:Tm and nonluminous ^{6}LiF powders mixture, thermoluminesc. response to thermal neutrons 77−73588
$CaSO_4$:Tm composite TLD for γ-rays, X-rays, β-rays, and thermal neutrons 78−28076
$CaSO_4$:Tm/polythene mixture, thermoluminesc. response to fast neutrons 80−5340
$CaSo_4$:Mn trap depth, thermolum. meas. 77−36301
$CaWO_4$ phosphor, interaction between intrinsic and impurity emission 79−8198

thermoluminescence continued
$CaWO_4$, phosphors, energy storage, afterglow decay and thermolum. meas. 77−12422
$CaWO_4$:Mo, P, thermoluminesc. traps, EPR meas. 77−90032
$Cd_xCa_{1-x}MoO_4$, intrinsic hole centres EPR study, thermoluminescence and thermal decay 79−99957
CdF_2:Mn_3 recomb. processes 78−15237
CdF_2:Sm^{3+}, photoconverted, thermally stimulated relax. 80−84476
$CdGa_2S_4$, interpretation of thermolum. and TSC meas. 78−27336
CdI_2, thermoluminesc. of traps *(French)* 79−4856
CsBr, irradiated with ultrasoft X-rays, thermolum. meas., surface energy losses 77−16408
CsBr:Cu^+, X-ray irrad., thermoluminesc. 80−16107
CsBr(Cl):Cu^+, γ-irradiated, thermolum. emission 80−104001
$CsCaCl_3$:Pb, and undoped crystals, photolum. and thermolum. meas. *(Russian)* 77−85767
CsCl:Cu^+, X-ray irrad., thermoluminesc. 80−16107
CsI:Na, UV irrad., thermoluminesc. 79−28846
CsI(Br)(Cl):Tl, [X_2^-] centre dynamic props. 79−65730
Fe, ferromagnetic, partial circular polarisation of thermal emission in mag. field 80−71387
Fe, tribothermoluminescence of flakes in grinding wheel, rel. to solar coronal dust radiation 78−68570
Gd_2O_2S:Tb, recomb. processes and emission spectra *(Russian)* 78−6797
GeO_2, hexagonal and glassy, X and γ-irrad., thermolum. and paramag. centres 77−63472
KBr, cation defects creation mechanism 80−75224
KBr, excitation of thermolum. near liq. He temp. 80−40171
KBr, irrad., colour centres and thermolum. 77−85815
KBr, m-crocryst. powders coloured in electrodeless discharge, reflectance spectra, thermolum. 78−15238
KBr, self-trapped exciton form. via thermally induced defect reactions 80−60687
KBr, thermolum. and reactions of freed interstitial and trapped hole centres 78−23538
KBr whisker, X-irrad., defect form., thermolum. and ionic cond. obs. *(Russian)* 78−84666
KBr, with Frenkel cation defects, EPR and thermolum. of V_F, V_2-centres 78−10769
KBr, X-irrad., F-centre role in thermoluminescence 80−20720
KBr:Ca, X-ray re-irradiation effects on Z_1 centres 78−75664
KBr:NO_2, Na effect of Na^+ impurity on self-trapped hole *(Japanese)* 78−67982
KBr:Tl, 480K thermal glow peak, Tl^+ centres 80−108284
KBr:Tl, thermoluminesc. excited by UV radn. and X-rays 79−87513
KBr:Tl excitation in fund. absorpt. region, luminesc. and thermolum. 80−50433
KBr(Cl), X-ray irrad., tunnelling recomb. luminesc. 80−2873
KBr(Cl):Sr^{2+},Cu^+, thermolum. response, extension of two-step reaction model 80−89075
$K_{2(1-x)}Ca_xSO_4$:Tl^+ phosphor, thermolum. characts. 77−90203
KCl (Br) crystals, thermally stimulated luminescence accompanying recombination of V_F and F centres 80−55201
KCl, cryst., colour centres, ionic cond., X-ray effects, thermoluminesc. *(Russian)* 78−6056
KCl, gamma irrad. relationship between thermolum. and deform. luminesc. 79−19942
KCl, γ-irradiated, photo- and thermoluminesc., F-centre interstitial recomb. 77−44036
KCl, m-crocryst. powders coloured in electrodeless discharge, reflectance spectra, thermolum. 78−15238
KCl, pure and Pb^{2+}-doped, X-irrad., quenching effects on thermal glow curves 78−27333
KCl single crystals, F-band absorpt. and thermolum. under DC field and X-ray irrad. 79−65910
KCl, thermal annealing of F, V_2-, V_3-centres *(Russian)* 80−54229
KCl, thermoluminesc., halogen and alkali impurity effects 80−97352
KCl, with Frenkel cation defects, EPR and thermolum. of V_F, V_2-centres 78−10769
KCl, X-irradiated, formation of cation defects 78−91359
KCl, X-ray irrad., thermoluminescence, TSC and thermal stability 79−95859
KCl:Ag, thermoluminesc. meas. using high impedance DC amplifier 79−99955
KCl:Ag, X-irrad., thermoluminesc. study of Ag centres 80−80874
KCl:Ag(In)(Tl), excitation in fund. absorpt. region, luminesc. and thermolum. 80−50433
KCl:Ca, thermolum. and optical absorpt. spectra of Z_1 centres 79−52029
KCl:Ca^{2+}, Z_1-centre thermolum. 80−80879
KCl:Eu^{2+}, γ-irrad., photostimulated low temp. recomb. luminesc. 80−11435
KCl:H, migration and stabilisation of H atoms, ESR and thermolum. study 79−1430
KCl:Li, X-irrad., F_A centres, thermolum. studies 80−80878
KCl:Na, thermoluminescence peaks cleaning using optical bleaching 77−81162
KCl:Pb, thermoluminesc. meas. using high impedance DC amplifier 79−99955
KCl:Pb^{2+}, γ-irrad., rel. to props. 78−31262
KCl:Sn, pure and doped, thermoluminesc. and luminesc. decay 79−83041
KCl:Sr, thermally pre-treated, glow curves 80−25470
KCl:Sr^{2+}, X-irrad., thermolum., impurity aggregation, trapping centre form. 78−88367
KCl:Sr^{2+}, X-irradiated, thermolum. decay, effect of impurity aggregation 77−85814
KCl:Sr(Ca), thermoluminescence and colour centre thermal stability in irradiated sample 78−43941
KCl:Tl, 475 nm emission, attributed to Tl^+ dimer 78−39611
KCl:Tl, thermal glow of trapped electron and hole centres 79−78762
KCl:Tl^{2+}, hole mechanisms of H- can F-centre production, thermolum. obs. 77−16407
KCl-Ba, X-ray irrad. cryst., thermoluminescence spectra 80−20719
KCl-$BaTiO_3$, composite cryst., F-centres, thermoluminesc., DC field and X-irrad. effects 78−2926
KCl-KBr mixed crystals, thermolum. studies 80−11486
KCl-KBr:Mn mixed cryst. system for thermoluminescence dosimetry, glow curves, dose response 78−24150
KCl-Mg, thermolum. of Z-centre, optical absorpt. 80−55203
thermoluminescence continued
$KCl_{0.5}Br_{0.5}$:Ca, X-ray irrad., Z_1-centres, thermoluminesc. and optical absorpt. meas. 80−16108
KCl_xBr_{1-x}, mixed crystals, thermolum. and optical absorption studies 80−104000
KF, deformation coloration 77−76397
KI, self-trapped exciton form. via thermally induced defect reactions 80−60687
KI:Eu^{2+}(Sr^{2+})(Mn^{2+}), elec. field effect on mech. of recomb. 78−80397
KI:Tl, electron-hole and V_k-Tl recomb., TSC and thermolum. study *(French)* 80−34461
KI(Br), irradiated at room temp., thermolum. and F-centre thermal stability 78−84669
$(K_{1-x}Na_x)_2SO_4$:Tl^+ phosphor, thermolum. characts. 77−90203
K_2O-B_2O_3 glass, γ- and UV- irrad., thermodecolorisation and thermolum. 80−20721
KI:Tl, excitation in fund. absorpt. region, luminesc. and thermolum. 80−50433
LaCl-Pr(Dy)(Sm), mech. for X-ray luminesc. and thermolum. 79−8170
La_2O_2S:Tb, recomb. processes and emission spectra *(Russian)* 78−6797
Li disilicate glass, radiation induced centres, EPR exam. 78−35033
$Li_2B_4O_7$:Cu, Ag, as thermoluminescence dosimeter *(Japanese)* 78−31906
$Li_2Ba_4O_7$ non-universality of TL-LET response, effect of high-temp. TL 80−99348
LiCl single crysts., γ-irrad., thermolum. meas. 80−80880
LiCl, thermolum., order of kinetics 80−89074
LiF (TLD-100), behaviour for doses up to 10 Mrad 77−5084
LiF (TLD-100), pre-irradiated, non-irradiation induced TLD 78−48242
LiF (TLD-100), thermoluminescent glow peaks 78−35211
LiF (TLD-100), thermoluminescent response to 0.1-5 keV electrons 79−95852
LiF, annealing effects on thermoluminescence, dipoles and dimers 77−12452
LiF dosimeter, radiothermoluminescence dosimetry of 10 MeV electrons *(Italian)* 77−81582
LiF dosimeter, thermoluminescence glow curves and light absorption, thermal treatment effect *(Russian)* 77−32954
LiF, dosimeter material, thermolum. non-linear response to sequential irrad. at different dose rates 79−1793
LiF, effect of impurity traces on physical props. 77−12450
LiF, evaporated film, thermally stimulated exoelectron emission rel. to thermolum. 79−47602
LiF in TLD, energy response to neutrons 77−29210
LiF, irradiated and plastically deformed, thermoluminesc. defect centres 77−1740
LiF, non-universality of TL-LET response, effect of batch composition 80−16106
LiF, non-universality of TL-LET response, effect of high-temp. TL 80−99348
LiF, photostimulated thermolum. as UV radiation dosimeter 77−16984
LiF, prep. and dosimetric props. of new highly sensitive form 79−22483
LiF, response to gamma rays 77−59626
LiF, restored thermoluminescence mechanism 78−19580
LiF TLD, accuracy of megavolt. radiation dosimetry 77−81574
LiF TLD, anal. of energy response to high energy electrons 77−52882
LiF TLD, plastic deform. effects on thermolum. sensitivity, rel. to handling technique 77−16988
LiF TLD, press. deform. and recovery 77−8668
LiF TLD, re-estimation of absorbed doses below 1 rad using UV bleaching 77−16992
LiF, TLD 100, thermolum. peaks anal. 77−44073
LiF TLD and radiator, use with cellulose nitrate film in personnel neutron dosimetry 77−64132
LiF TLD materials, influence of composition on sensitivity to high energy electrons 77−40775
LiF TLD phosphor, γ-irrad. induced sensitisation, UV effects 80−108286
LiF TLD phosphor, incompatibility of sensitisation and dose re-estimation 78−40340
LiF TLD phosphor, residual thermoluminescence effect on sensitisation 80−108287
LiF, TLD phosphor, Z_3 centre, thermolum. and optical absorption spectra 79−24374
LiF TLD response to high-energy X-rays and electrons rel. to ^{60}Co photons 78−40332
LiF, TLD-100, glow curve kinetics 78−84668
LiF TLD-100, thermolum. response to 5 to 30 keV electrons effect of annealing atm. 77−86638
LiF, TLD-100, thermoluminesc. emission spectra meas. 78−84667
LiF TLD-100, thermoluminesc., kinetics and trapping parameters, dose depend. 80−2872
LiF, TLD-100, trapping centres, optical absorpt. spectra defect and thermolum. mechanism models 80−50436
LiF TLD-100 material, long term recycling characts. 78−11737
LiF TLD-100 phosphor, sensitisation mechanism study, thermolum. glow peak intensity obs. 80−55202
LiF TLD-700, Harshaw, effect of sample size and batch origin on thermal neutron sensitivity 78−40342
LiF, thermolum., formulation of sensitisation based on simple two-step reaction rate model 78−39610
LiF, thermolum., trapping mechanism based on Z-centres 80−76089
LiF, thermoluminescence, γ-radn.-induced sensitization and supralinearity 79−91507
LiF thermoluminescence induced by 13.8 and 81 meV diffr. neutrons 77−56481
LiF, thermoluminescence mechanisms following gamma irradiation 77−59625
LiF, thermoluminescence intensity depend. on heating rate and deep trap 78−56527
LiF, thermoluminescence mechanism, extension of Mayhugh-Christy model 78−80425
^{7}LiF TLD, efficiency for H^+ and Ar^{18+} detect. 78−53504
LiF:Mg, effects of grain size on thermolum. and thermally stimulated exoelectron emission 79−15536
LiF:Mg, role of impurity-vacancy pairs in thermolum. 79−8195
LiF:Mg, Ti TLD long-term annealing at 400°C, radiation and thermally induced damage, recovery 77−5085
LiF:Mg, X-irradiated, thermoluminesc. of Z_3-centres 78−15236
LiF:Mg,Ca detectors, variation of parameters of thermally stimulated luminesc. 79−6793

thermoluminescence continued
LiF:Mg,Ti, defect states, ESR and ionic cond. study 80−108058
LiF:Mg,Ti, thermolum. related Z-centres, optical absorpt. bands 78−23540
LiF:Mg,Ti, thermoluminesc. activation energies 79−74009
LiF:Mg,Ti crystals, Z_3-centres, correlation of thermoluminescence and optical absorption 80−45154
LiF:Mg,Ti TLD based passive neutron spectrometer and dosimeter 77−54394
LiF:Mg dosimetric cryst., light-sum storage during linear stage 79−8194
LiF:Mg^{2+}, TLD-100, precipitation reactions and ionic cond. 77−56479
LiF:Mg^{2+}, TLD-100, solution treatment temp. and ageing effects 77−56480
LiF:Ti, thermoluminesc. dosimetry appl. 79−38683
LiF:Ti, thermoluminesc., effect of plastic deform. 79−33853
LiF-PTFE TLD performance, influence of heating element design 78−25333
LiF-Teflon TLDs used in identification badges, fading 77−25556
LiH, defect form. at low temp., EPR, thermolum. and TSC study 80−107222
LiH, formation and annihilation of Li colloids and H bubbles 80−107228
LiH-LiF(Cl), mixed cryst., thermolum., appl. as X-ray detectors 79−6794
$LiNbO_3$, optically active centres, form. by electron and γ-irrad. 78−18642
Li_2O-B_2O_3, crystalline and glassy, thermolum. meas. 77−16406
$LuYScO_3$:Er^{3+}(Tm^{3+})(Ho^{3+}), thermolum. meas. 80−97354
$MgAl_2O_4$, γ-irradiated crystal, TSC, thermoelec. power, thermolum. and afterglow 80−75583
$MgAl_2O_4$, spinel, γ-irrad. effect on optical absorpt. and thermolum. spectra 77−85759
MgF_2, localised electronic levels, thermoluminesc. and thermally stimulated current exam. 78−11001
MgF_2:Mn(Co), thermoluminesc. and TSC in activator band 79−24359
MgO, defect centres, thermolum. examination 78−15235
MgO, deformation induced damage, effect on optical props. 77−77258
MgO, direct-response UV TLD 77−13010
MgO, doped, thermal stability of hole centres and hole recombination luminescence *(Russian)* 78−72614
MgO doped powder phosphors, photo- and thermostimulated luminesc. obs. *(Russian)* 80−66263
MgO, light emission during adsorpt. and desorpt. of O_2 78−38949
MgO, periclase, recording of pulsed EM radiation in RF band during heating *(Russian)* 77−55837
MgO powder, vacuum UV induced thermoluminesc. in Γ-irradiated and non-irradiated samples 77−36302
MgO, pure and doped crysts., X-ray stimulated luminesc. 79−28802
MgO, single cryst., thermolum. for UV dosimetry 77−16986
MgO, single crystal, thermolum. meas. *(Japanese)* 78−19577
MgO, single crystal, thermal and optical stimulation processes of V-centres *(Japanese)* 80−11485
MgO, thermoluminescence mechanism 79−15538
MgO:Al, and nominally pure single crystal, thermally stimulated luminesc. rel. to temp., and EPR *(Russian)* 80−84789
MgO:Sn(Al), V centres, destruction temp. 78−10998
MgO-Al_2O_3 spinel crysts., thermolum. spectra 79−65938
MgO-Al_2O_3-P_2O_5 system glass, heat treatment of aluminium metaphosphate influence on thermolum. 80−108285
MgO-P_2O_5-Al_2O_3-$3P_2O_5$ glass, absorpt. shift, electron and hole traps, thermolum. meas. 79−65897
$MgSiO_4$:Dy, thermolum. induced by 254 nm UV photons 80−55204
Mg_2SiO_4:Tb, TLD material, UV induced thermolum. and phosphoresc. 78−92707
Mg_2SiO_4:Tb TLD, response to high energy electrons *(Japanese)* 78−78502
Mg_2SiO_4:Tb TLD, supralinearity of response to electrons and X-rays *(Japanese)* 78−78503
Mo, oxidation, IR emission spectrosc. obs. 78−68942
N, active condensed, thermolum. meas. *(French)* 80−11484
NO+O, in Ar matrix, chemiluminesc. 78−35688
$Na_6Al_6Si_6O_{24}(NaX)_{2n}$, X=Cl, Br or I, sodalites, thermal destruction of colour centres *(Russian)* 80−84169
NaBr powder coloured in electrodeless discharge, reflectance spectra, thermoluminescence props. 78−6796
$NaBrO_3$, single crystals, thermolum., optical absorpt., X-ray effect 79−95858
NaCl, excitons at $L_{II,III}$ absorption edge of Cl^-, decay characts. thermolum. meas. 77−28121
NaCl, irradiated, at 80K, thermolum. processes 80−34990
NaCl, irradiation-induced energy transfer from bulk to surface, luminesc. meas. 78−92132
NaCl, m-crocryst. powders coloured in electrodeless discharge, reflectance spectra, thermolum. 78−15238
NaCl, microcryst. powder, isothermal stability of colour centres, thermolum. glow curve 79−15535
NaCl preirradiation effect on proton channelling, thermoluminescence study 80−19860
NaCl, pure and doped, 20K X-ray irradiation, thermolum. and recovery processes 80−93412
NaCl, self-trapped exciton form. via thermally induced defect reactions 80−60687
NaCl, thermoluminesc. and optical absorpt., simultaneous DC field and X-irrad. 79−99956
NaCl:Ag, diffusion parameters of hot holes created by ionising radiation 78−47800
NaCl:Ag, excitation in fund. absorpt. region, luminesc. and thermolum. 80−50433
NaCl:Ag, irrad. with synchrotron radiation, thermolum. light-sum spectrum of L absorpt. edge of Cl^- 79−15540
NaCl:Ag, thermolum. light sum storage by ultrasoft X-rays 77−20939
NaCl:Ca, microhardness and thermoluminescence, hardness-quenching temp. variation 80−29813
NaCl:Ca, X-irradiated, Z_1-centre form. kinetics, thermolum. investig. 77−4693
NaCl:Ca, Z_1 centre thermoluminescence study 80−16109
NaCl:Ca(Mg), X- and gamma-irrad., thermostimulated electrons and luminesc. 79−91505
NaCl:Cu, X-irrad., thermoluminesc., F-centres 79−33849
NaCl:Cu^+, X-irrad., thermoluminesc. centre, EPR anal. 79−43045
NaCl:Cu^+, X-ray irrad., role of Cu^+ in thermoluminesc. 78−56526
thermoluminescence continued
NaCl:$MgCl_2$ (0.1 mol.%), thermoluminesc. glow curves, temp. distrib. and trapping centres 78−48241
NaCl:Mn^{2+}, radiation-induced colouring, room temp. kinetics 79−55736
NaCl:Mn^{2+}, thermolum. spectra, mechanisms 80−80873
NaCl:Mn^{2+}, X-irrad., thermoluminesc. and EPR 79−61444
NaCl:Mn^{2+}, X-ray irradiated, thermolum. and EPR 77−81161
NaCl:Pb, γ-irrad., centres in thermoluminescent emission 77−85816
NaCl:Tl, deformed phosphors, thermoluminesc., impurity conc. effects 77−63473
NaCl(:Ca), irrad. at room temp., stored energy rel. to thermolum. 80−10574
NaCl(Br), X-ray or UV irradiated, cation defects creation mechanism 80−75224
NaCl(F), irradiated at room temp., thermolum. and F-centre thermal stability 78−84669
$NaClO_3$, X-irrad., thermal stability of radiation damage products 79−34324
NaF, X-irrad., colour centres and thermolum. 80−84790
NaF:LiF, γ-irrad., colour centre form., reflectance and thermolum. meas. 79−55739
NaF:Mn, role of Mn^{2+} in thermolum. 80−97353
$NaMgF_3$, defects induced by X- and vacuum UV irrad., optical and elec. study 80−107319
Na_2O-$3SiO_2$ glass, high-temp. thermolum., colour centre absorpt. 80−16110
Na_2O-GeO_2, glass, thermolum. rel. to coordination number 77−16405
Na_2O-SiO_2 glass, tunnelling recomb. luminesc. 80−2875
Na_2SiO_2-CaO glass, thermostimulated and tunnel luminesc. 80−45157
OCS, VUV photolysis in Ar matrix, thermoluminescence 77−52659
$PbMoO_4$, colour study from absorption, fluorescence and thermoluminesc. exam. 78−31245
$PbMoO_4$, defect electron centres after X-irrad. 79−55738
$Pb(WO_4)_{1-x}(MoO_4)_x$ mixed crystals, X-irrad., EPR and thermoluminesc. 79−15352
RbBr, suprapure, thermolum. glow and emission studies at room temp. 80−7423
RbCl, undoped and Sn doped, γ-irrad. crysts., thermolum. and emission, 300 to 560K 79−15539
RbCl:Ca^{2+}, thermolum. and optical absorption studies 80−104002
RbCl:Eu, γ-irrad., thermoluminesc., EPR meas. 78−84670
RbCl:Mg, γ-irrad., thermoluminesc. 79−47528
RbCl(Br), cation defects creation mechanism 80−75224
SO_2, chemiluminescence at ($c^1\Sigma^- \rightarrow a^1\Delta$) in Ar matrix, photolysis prod. and thermoluminesc. 79−5158
SO_2, in Ar:OCS:O_2 matrix, $S+O_2 \rightarrow SO_2$ chemiluminescence reaction 77−48647
α-SiC (6H) laser excited thermostimulated luminescence light sum dose depend. *(Russian)* 80−16111
SiC, thermolum. excited by light outside fundamental absorpt. region 79−24375
α-SiC(6H), two stage transitions, nonlinear absorpt., thermoluminesc. method 80−7425
SiO, doped, thermal stability of hole centres and hole recombination luminescence *(Russian)* 78−72614
SiO_2, thermoluminescence, in H_2O vap. atm., temp. depend., time decay *(Russian)* 77−44074
SiO_2, vitreous, grown from vapour, gamma ray irradiated, ESR and thermoluminescence exam. 78−88189
SiO_2:Ag, crystalline, fused, colour centres 78−10954
SnO_2, correl. between simultaneous thermally stimulated cond. and thermlum. transients 79−91073
SnO_2:Eu^{3+}, luminesc. and charge compensation 77−28618
SrF_2, neutron irrad., role of F-centres in thermoluminesc. 79−19941
SrF_2, thermoluminesc. and F-centre annealing, after neutron irrad. 80−7422
SrF_2:Tb, and pure, UV induced processes 77−32452
SrFCl, thermolum. and optical absorption spectra 80−66309
SrS:Hf phosphor, activation energy and freq. factor calcs. from glow curves 77−12451
SrS:Nd, phosphorescence decay, trapping levels 80−104003
$SrSO_4$, celestite, colouring mechanisms 79−82998
$SrTiO_3$, photoluminesc., thermoluminesc. and thermally stimulated currents 78−92121
Ta_2O_5, thermoluminesc., in H_2O vap. atm., temp. depend., time decay *(Russian)* 77−44074
YAG, transient colour centres caused by UV radiation 77−84744
YAG, traps, energy spectra, X-irrad. effects and thermoluminesc. *(Russian)* 77−20940
YAG:Cr^{3+}, radiation colour centres, absorpt. and thermolum. spectra 78−48206
$YAl_3(BO_3)_4$, thermolum. anal. 79−87514
$YAl_3[BO_3]_4$ crystals, capture centres, thermoluminesc. study 79−65935
Y_2O_3, formation and changes in point defects, EPR, optical transitions and thermolum. spectra 78−2118
Y_2O_3 sintered body, blackness study thermoluminescence anal. *(Japanese)* 78−23541
Y_2O_3, thermoluminesc., in H_2O vap. atm., temp. depend., time decay *(Russian)* 77−44074
Y_2O_3:Zr^{3+}, F-centre charge state, ESR and thermally stimulated luminesc. obs. 80−60418
Y_2O_2S:Tb, recomb. processes and emission spectra *(Russian)* 78−6797
YPO_4 phosphor, ionisation of capture centres, thermolum. spectra 80−11487
YVO_4 phosphor, ionisation of capture centres, thermolum. spectra 80−11487
(Zn, Cd, Hg)S:Cu,In, electroluminesc. temp. depend. 77−1732
$Zn_4B_6O_{13}$:Tb^{3+}, fluoresc. and thermophosphoresc. spectra *(Spanish)* 77−90188
ZnO, single cryst., photo- and thermoluminescence 80−66311
$Zn_4O(BO_2)_6$:Tb, phosphoresc. study *(Spanish)* 80−16105
ZnP_2, trapping levels, TSC and thermolum. meas. 79−15115
Zn_3P_2, thermoluminescence glow curve method for radiation induced traps 80−60689
$Zn_3(PO)_2$, thermoluminescence glow curve method for radiation induced traps 80−60689
ZnS crystals, luminescence kinetics, centre discrimination exam. 78−15215
ZnS, low-temp. trap anal. thermally stimulated luminesc. model extension 80−80877
ZnS, phosphor, thermally stimulated luminescence expt. 78−10951

thermoluminescence continued
ZnS, shallow traps, thermolum. glow curves obs. 79−91508
ZnS, thermoluminescence at different excitation levels 80−93413
ZnS:Ag, Al(Cu), trap parameters, thermostimulated luminesc. and cond. meas. *(Russian)* 77−72868
ZnS:Ag, cryst. struct., electron traps and glow curves 79−61437
ZnS:Ag, single crystal, ionisation mechanism of field trapping centres 80−45156
ZnS:Cl^-, $Cu^+(Ag^+)$, high press. effect 78−64419
ZnS:Cu, polycryst. phosphor, excitation storage, recombination barrier participation 78−27316
ZnS:Cu,Pt phosphors, photoluminesc., thermoluminesc. 78−43915
ZnS:Ne, implanted single crysts., photolum. and bombardment effect, thermolum. curve obs. 80−55166
ZnS:Pb phosphor, ionisation mechanism of field trapping centres 80−45156
ZnS:Pb phosphor mech. of elec. field liberation of electrons from traps 78−72616
ZnS:Tb, Cu(Ag) phosphors, luminesc. props. 80−100690
ZnS:Tm(Er)(Nd) phosphors, optical scintillation mechanism 79−56867
ZnS-CdS:Ag, Ni, Co, thermoluminesc. glow curves 78−95611
ZnS-CdS:Ag, Ni, Co phosphor, thermoluminesc. 77−66547
ZnS-CdS:Ag(Cu), cryst. struct., electron traps and glow curves 79−61437
ZnS_xSe_{1-x}, VPE, characterisation of defect centres by photoelectronic meas. 80−10914
ZnSe, donor-acceptor pair emissions charact. *(French)* 80−108249
ZnSe:Al, thermally stimulated transients, new approach 79−38086
Zn_2SiO_4:As,Mn, enhanced luminesc. stimulation, 20-320K *(German)* 77−20900
ZrO_2 TLD using stabilised single cryst., for high gamma doses 77−56476
ZrO_2, thermolum., UV and γ-ray effects 78−2930
ZrO_2, thermoluminesc., in H_2O vap. atm., temp. depend., time decay *(Russian)* 77−44074
ZrO_2, Y_2O_3-stabilised, X-irrad., thermoluminesc. 77−48259
$ZrSiO_4$, X-irradiated, trapping and emission centres, thermolum. meas. 80−89076
$ZrSiO_4$, X-irrad., trapping and emission centres, OH^- ion contribution 80−80876
$ZrSiO_4$, zircon, (sand), thermolum., UV and γ-ray effects 78−2930
$ZrSiO_4$, zircon, thermoluminesc. glow curve and spectrum 79−33847
$Zr(SiO_4)_{1-x}(OH)_{4x}$, synthetic hydroxyled zircon, influence of OH^- on thermoluminescent emission *(French)* 78−6795

thermoluminescent dosimeters
14.7 MeV neutron-gamma mixed field 77−6625
alkali borate binary glass, energy storage behaviour studied by thermoluminesc. 80−50432
aluminophosphate glass, improvement of fast neutron response 80−13932
archaeological dating, evaluation of internal beta-dose rate 80−98478
automated TLD processing and dose record keeping service 80−12267
calibration, source storage and irradiation device 80−5339
calibration procedures in the Studsvik standardized personnel dosimetry system, Sweden 80−9418
calibrator, for dosimeter element *(Japanese)* 80−23159
card reader design improvement 79−26757
cards, expected useful lifetime 80−86989
comparative investigation of charact. at low dose meas. 77−38558
composite X-ray and γ-ray detectors 79−9890
computerised system for automated radiological monitoring 80−27827
data analysis using a Texas instruments programmable calculator 80−36136
depth dose and off-axis charact. of TLD in therapeutic pion beams 80−101271
description 77−16990
differential calorimeter dosimeter for nonionising radiation 79−70649
dose distribution studies, partial body irradiation of small animals 79−20670
downward drift of IKS-A instrums. stored after irradiation 80−23157
electroceramics, thermoluminescent and dosimetric charact. 79−8196
element, effect of mounting condition on meas. *(Japanese)* 80−95471
energy and directional response of Harshaw TLD-100 in diagnostic X-ray range 78−11738
energy dependence of response, method for reducing using filters 80−106206
energy response of ^6LiF, ^7LiF to neutrons 77−29210
environmental meas. at nucl. facilities 80−42876
environmental monitoring methods and techniques at nuclear facilities 79−85819
exoskeletons of Magicicada sp., detect. of thermolum., possible use as TLDs 80−30896
exothermic model for thermolum. response 79−36424
fading characteristics, effect of post irradiation annealing 78−90029
fading characteristics, effect of post irradiation annealing 78−90030
fast neutron sensitivities 80−102413
fast-neutron TLD based on pellets of S-$CaSO_4$:Dy mixture 78−73251
gamma radiation monitoring, automated TLD system 80−57964
gamma-ray dosimetry errors with thermoluminescent dose meters 80−18705
graded-Z flash bremsstrahlung depth-dose spectrum 77−391
handling technique, rel. to LiF plastic deform. 77−16988
hardness dependence of glass dosimeters for photons with energy up to 6 MeV 80−846
heating rate effect on TLD phosphor response 80−26359
high current relativistic electron beam, X-ray emission, pulsed dosimetry 79−81099
high level photon dosimetry using various phosphors 78−74503
integrating detectors, error anal. of meas. 77−38428
ionisation chambers calibration in absorbed dose units 78−20274
LiF, TLD material, nonlinear response to mixed dose rates 79−5372
light conversion efficiency of TLD-700 for α particles rel. to ^{60}Co γ-rays 80−13935
lightning, thermoluminescent dosimetry measurement of radiation 80−36361
mammography, dose meas. with high-sensitivity coated-film system *(German)* 79−53257
mammography radiation dosage in different examination systems *(German)* 79−100750
materials, kerma for monoenergetic neutrons, theory, expt. comparison 77−5086

thermoluminescent dosimeters continued
medical and biological appls. of TLDs 79−74762
miniature, appl. to phosphate diffusion in sediments 78−20274
mixed-field dosimetry, appl. to personnel dosimeter badges 80−23170
monitoring post, concrete shielding to reduce background 78−817
neutron damage, displacement and ionis. fractions of fast neutron kerma 78−30669
neutron dosimetry, appl. of thermoluminescent materials 79−22497
neutron irrad., response to photon component of rad. field *(German)* 80−23176
neutron personnel dosimetry systems, TLD for albedo neutrons, single- and multi-element devices comparison 78−96099
nuclear accident dosimetry systems, comparison 79−22496
orientation effects, multivariate anal. 80−89862
orthovoltage X-ray therapy, TLD dose intercomparison 80−12272
paired LiF TLD 600, 700 technique, γ-dose in mixed n-γ radiation fields 79−45432
personal dosimetry service testing and evaluation in 1976 in Michigan 78−53498
personal monitoring, effect of environmental radiation *(Japanese)* 80−61707
personal monitoring, judgement of uncleanness in elements by residual value method *(Japanese)* 80−21546
personal monitoring, use of TLDs, judgement of abnormal value by glow curve *(Japanese)* 80−106208
personnel albedo, paired ^6LiF, ^7LiF, neutron dose precision for gamma-neutron irradiation 79−26755
personnel dosimeter TLD badge based on $CaSO_4$:Dy teflon TLD discs 80−57959
personnel dosimeters, Cd-capture γ-ray exposure 79−67963
personnel dosimetry methods introduced in the Czechoslovak National Laboratory *(Czech)* 79−36426
personnel monitoring, occupational radiation exposure in Austria *(German)* 80−26352
personnel neutron, combination TL-film 79−26756
personnel thermoluminescence dosimetry reader, microprocessor controlled 79−45428
phosphate glass, appl. in gamma dosimetry *(Slovenian)* 80−32521
phosphorescent detectors and X-ray convertors, Symposium, Riga, USSR (Oct. 1966) 79−6243
phosphors, thermoluminescence, UV dosimetry 80−853
phosphors, use for high-level gamma-ray dosimetry 80−13934
polyethersulphone, thin film TLD, skin dosimetry appl. 80−52790
powders calibration for low expsoure rates 77−6632
precision dosimetry, some problems 80−13936
quartz, natural, dosimetric props., possibility of thermolum. dating of geological objects 79−12288
reader, improved S/N ratio for low dose meas. 79−76153
reader, microcomputer controlled 80−69044
reader with photon counting and DC techniques for wide range dose meas. 80−42870
response, nonlinear behaviour 78−33293
review, characteristics and recent trends *(Korean)* 80−41253
self-shielding factors for TLD-600 and TLD-100 in isotropic flux of thermal neutrons 77−6638
sensitised TLD phosphors, photon energy dependence 80−78498
space research system for meas. of cosmic dose on board a spacecraft 80−109047
spectrometry of pulsed X-rays from hot plasma 79−7484
statistical errors of dose estimation in personnel neutron monitoring with albedo dosimeters 79−48344
supralinearity 77−10495
Teflon, phosphor embedded, fast neutron dosimetry using S activation 78−70648
thermal neutron self-shielding factors, Monte Carlo calc. for TLD probes 79−45431
thin film dosimeter based on polyethersulphone and LiF 80−23156
thin-layer TLDs based on high-temp. self-adhesive tape 80−13933
thyroid geometry influence on response of LiF and $CaSO_4$ TLD discs to ^{131}I and ^{125}I 78−73250
TLD 700, parameters affecting overall calibration accuracy 79−63821
TLD-600, activation and damage effects after neutron pre-exposure 79−13540
total radiation monitoring using liquid crystals and thermoluminescence 80−3819
transmitted information of TLD elements, entropy method 80−89860
ultra-thin bonded TLD for skin dose meas. complying with ICRP recommendation 78−92709
utilisation in field of atomic energy, review *(Japanese)* 79−26764
UV, thermolum. of MgO single cryst. 77−16986
UV, using LiF photostimulated thermolum. 77−16984
UV TLD, direct-response dosimeter using MgO 77−13010
X-ray luminescent dosimetry 79−8542
X-ray radiation, long wavelength, dosimetry by thermoluminescent method 79−6768
Al_2O_3 TLD for dosimetry after accidental gamma radiation release 78−57076
Al_2O_3 TLD phosphor for gamma-rays 77−6637
Al_2O_3:Si, Ti, pure and doped, luminescence, optical absorpt. and colour centres 79−87501
BeO ceramic TLD, gamma ray response 80−23153
BeO ceramic TLD, operational charact. and problems 77−42216
BeO compared with LiF 80−26357
BeO discs, thermally stimulated exoelectron emission and thermolum. sensitisation 78−35277
BeO, for low exposure of personnel, sensitivity, accuracy 77−29209
BeO, light influence 79−76293
BeO reactively evaporated film, appl. to nearly tissue-equivalent dosimeter 77−32512
BeO, solid state dosimeter 79−71981
CaF:Mn, annealing at low light levels 78−78508
CaF_2, calc. neutron sensititivies 79−22568
CaF_2, TLD, high-dose characteristics 77−40772
CaF_2:Dy, TLD-200, thermolum. phosphor, photolum. and absorpt. spectra, thermolum. mechanisms 80−97321
CaF_2:Dy sensitivity to UV and ionising radiations, temp. treatment effect 79−26763
CaF_2:Tm thermoluminescent dosimeters, response to 14 MeV neutrons 79−49867
$CaF_2+Dy_2O_3+KCl$, intermediate neutron detection by thermoluminescence 80−5444

thermoluminescent dosimeters continued
CaS:Bi as UV dosimeter 80−34991
$CaSO_4$, TLD high-dose characteristics 77−40772
$CaSO_4$:Dy, α and γ thermoluminescence response comparison 79−85814
$CaSO_4$:Dy, competing deep trap model for thermoluminescence 79−83039
$CaSO_4$:Dy, fast neutron dosimetry using S activation 78−70648
$CaSO_4$:Dy, high dose behaviour, comparison with trap depth model prediction 78−78588
$CaSO_4$:Dy, high exposure UV response and sensitisation 79−91506
$CaSO_4$:Dy, photo-stimulated thermolum., for high-exposure dosimetry 77−9262
$CaSO_4$:Dy, studies for dosimetry 79−29634
$CaSO_4$:Dy, TLD phosphor, gamma-ray induced sensitisation 78−74542
$CaSO_4$:Dy, TLD-900, thermolum. stability at low radiation doses 80−101272
$CaSO_4$:Dy, thermal neutron and γ-ray meas. in mixed radiation field, activation and capture gamma technique 79−738
$CaSO_4$:Dy embedded Teflon TLD phosphor photon energy dependence obs. 79−26761
$CaSO_4$:Dy phosphor, effect of Dy conc. on TL characteristics 79−93881
$CaSO_4$:Dy phosphor powder, effect of grinding on thermoluminescent sensitivity 79−33852
$CaSO_4$:Dy ribbon, dosimetric props. study 80−63395
$CaSO_4$:Dy TLD, fading in high γ-dose region 78−90027
$CaSO_4$:Dy TLD, glow curve behaviour in ^{60}Co γ-exposure 79−49903
$CaSO_4$:Dy TLD, low exposure rate depend. meas. 80−102408
$CaSO_4$:Dy TLD, monitoring of environmental radiation levels 79−93839
$CaSO_4$:Dy TLD, temp. effect during UV and gamma irradiation 79−38684
$CaSO_4$:Dy TLD, use in liq. contamination meas. 77−38574
$CaSO_4$:Dy TLD meas. of reactor thermal neutrons 78−78441
$CaSO_4$:Dy TLD phosphor, γ radiation changes in glow curve 80−60688
$CaSO_4$:Dy Teflon disc based TLD cards, annealing and repeated readout 80−3812
$CaSO_4$:Dy Teflon TL dosimeters, thin, development for β-dosimetry in personnel monitoring 80−63399
$CaSO_4$:Dy teflon TLD discs, effects of phosphor proportion and grain size on photon energy response 79−59304
$CaSO_4$:Dy Teflon TLD discs, thermal history and reusability 79−89507
$CaSO_4$:Dy Teflon TLD discs, metal filters for compnesation of photon energy depend. 80−30901
$CaSO_4$:Dy thermoluminescent dosimeters, low exposure rate depend. 78−20285
$CaSO_4$:Dy thermoluminescence sensitivity and glow curves, 700° to 1300°C 79−85815
$CaSO_4$:Dy thermoluminescent phosphor, effect of sensitisation on energy depend. 80−26358
$CaSO_4$:Dy+Dy_2O_3+KCl, intermediate neutron detection by thermoluminescence 80−5444
$CaSO_4$:Dy(Tm), thermoluminescent props. of non-commercial phosphors 78−58550
$CaSO_4$:Dy(Tm), thermolum. thermolum. phosphor, photolum. and absorpt. spectra, thermolum. mechanisms 80−97321
$CaSO_4$:Tm composite TLD for γ-rays, X-rays, β-rays, and thermal neutrons 78−28076
$CaSO_4$:Tm intrinsic thermoluminescence stability for UV dosimetry 80−12262
$CaSO_4$:Tm/polythene mixture, thermoluminesc. response to fast neutrons 80−5340
$CaSO_4$:Dy, multi-reading method 79−76154
^{60}Co total body irradiation, dose distrib. meas. using thermoluminescent dosimeters 80−41245
D-D neutron meas. on 40 kV, 60 A neutral beam test facility 80−37710
KCl-KBr:Mn mixed cryst. system for thermoluminescence dosimetry, glow curves, dose response 78−24150
$Li_2B_4O_7$, high dose characteristic 78−35966
$Li_2B_4O_7$ TLD, comparison of two commercially available types 79−81094
$Li_2B_4O_7$:Ag TLD, fast neutron dosimetry 78−94163
$Li_2B_4O_7$:Cu, Ag, as thermoluminescence dosimeter *(Japanese)* 78−31906
$Li_2B_4O_7$:MN bulb dosimeters, nonuniversality of TL linear energy transfer response 79−97948
$Li_2B_4O_7$:Mn, gamma ray response 80−23153
$Li_2B_4O_7$:Mn, thermolum. response to pions 80−101270
$Li_2B_4O_7$:Mn TLD phosphor, additivity of α and γ response 79−9891
$Li_2Ba_4O_7$, non-universality of TL-LET response, effect of high-temp. TL 80−99348
LiF (TLD-100), behaviour for doses up to 10 Mrad 77−5084
LiF (TLD-100), pre-irradiated, non-irradiation induced TLD 78−48242
LiF (TLD-100), thermoluminescent glow peaks 78−35211
LiF crystals, in pile irradiation, nucl. reactions 78−29463
LiF detectors, survey 80−68964
LiF, high and low temperature response to X-rays 79−22492
LiF, high dose characteristic 78−35966
LiF, high energy dependence in low Z media obs. 80−61700
LiF, high sensitivity, for low dose meas. 79−13538
LiF, non-universality of TL-LET response, effect of batch composition 80−16106
LiF, non-universality of TL-LET response, effect of high-temp. TL 80−99348
LiF, prep. and dosimetric props. of new highly sensitive form 79−22483
LiF, response to ^{99m}Tc γ-rays 80−89854
LiF, response to ground-level cosmic-ray background 79−59265
LiF TLD, Ne^{10+} beam profile and particle fluence meas. 77−3035
LiF TLD, press. deform. and recovery 77−8668
LiF TLD, re-estimation of absorbed doses below 1 rad using UV bleaching 77−16992
LiF TLD, use as thermal neutron detector 78−21821
LiF, TLD 100, thermolum. peaks anal. 77−44073
LiF TLD for radiotherapy dosimetry in accordance with section 13 of X-ray regulations *(German)* 78−20289
LiF TLD materials, influence of composition on sensitivity to high energy electrons 77−40775
LiF TLD meas. rel. to Burlin cavity theory 80−56220
LiF TLD phosphor, incompatibility of sensitisation and dose re-estimation 78−40340
LiF TLD response to high-energy X-rays and electrons rel. to ^{60}Co photons 78−40332
LiF, TLD-100, thermoluminesc. emission spectra meas. 78−84667

thermoluminescent dosimeters continued
LiF, TLD-100, thermolum., glow curve kinetics 78−84668
LiF, TLD-100, trapping centres, optical absorpt. spectra defect and thermolum. mechanism models 80−50436
LiF TLD-100 material, long term recycling characts. 78−11737
LiF TLD-700, Harshaw, effect of sample size and batch origin on thermal neutron sensitivity 78−40342
LiF, TLD-700, superlinearity of peak 5 and peak 6, C-hit trap struct. 80−99347
LiF, thermolum. light self absorpt. obs. 79−81097
LiF, thermolum. response to pions 80−101270
LiF, thermoluminescence, γ-radn.-induced sensitization and supralinearity 79−91507
LiF, thermoluminescence glow curves and light absorption, thermal treatment effect *(Russian)* 77−32954
LiF thin layers, effect of LET on thermolum. props. 78−73255
LiF:Mg, dependence of optical absorpt. on temp. during X-ray irrad. 80−66237
LiF:Mg, TLD-100, thermolum. phosphor, photolum. and absorpt. spectra, thermolum. mechanisms 80−97321
LiF:Mg, thermal annealing effects on sensitivity and fading of dosimeter 78−82522
LiF:Mg, Ti TLD long-term annealing at 400°C, radiation and thermally induced damage, recovery 77−5085
LiF:Mg,Ca detectors, variation of parameters of thermally stimulated luminesc. 79−6793
LiF:Mg,Ti, (TLD-100), optical bleaching of defect centres 79−19911
LiF:Ti, thermoluminesc. dosimetry appl. 79−38683
LiF-PTFE TLD performance, influence of heating element design 78−25333
LiF-polytetrafluorethane thermolumin. dosimeters, absorbed dose assessment 80−95470
LiF-Teflon TLDs used in identification badges, fading 77−25556
LiF(TLD-600), unannealed, fading for thermal neutrons and γ-rays 80−83225
^{3}Lif TLD, evaluation of γ-ray response calcs. 79−31229
^{6}LiF, response to neutrons, with thermoluminescent-LET dependency 79−13604
^{7}LiF, calc. neutron sensitivities 79−22568
^{7}LiF, response to neutrons, with thermoluminescent-LET dependency 79−13604
^{7}LiF, TLD, supralinearity meas. using ^{60}Co source 78−82534
^{7}LiF-Teflon disc TLD, determ. of neutron fluence and γ-dose distribs. 79−45434
Lif, nuclear reactor mixed radiation field, ambient atm. effect 79−13537
Mg, SiO_4:Th TLD phosphor, γ-ray induced sensitisation and photo-transfer 79−33851
MgB_4O_7:Dy, TLD phosphor development 79−79661
MgO, single crystal, thermolum. meas. *(Japanese)* 78−19577
Mg_2SiO_4:Tb, dosimeter response to e^- irrad. 79−13536
Mg_2SiO_4:Tb, TLD material, UV induced thermolum. and phosphoresc. 78−92707
Mg_2SiO_4:Tb, thermolum. phosphor, photolum. and absorpt. spectra, thermolum. mechanisms 80−97321
Mg_2SiO_4:Tb TLD, response to X-ray and electron irrad. 79−3285
N_2 hot gas TL reader incorporating post irradiation annealing facility 78−70649
Rn daughter time-integrating environmental TLD dosimeter 79−67962
Rn monitoring, TLD, passive detector, U mill field 80−57963

thermomagnetic effects
alkali metals, elec. and thermal cond. in weak mag. fields 80−65535
alumel, B versus H measurement from 25 to 180°C 78−23297
calorific galvanothermomagnetic phenomena, classification *(Russian)* 79−4573
deformed metal, kinetic eqn. *(Russian)* 77−35906
degenerate semiconductor, electron diffusion thermopower, oscillatory, mag. quantisation effects 79−91088
degenerate semiconductor, film, with unlike surfaces, theory of kinetic effects *(Russian)* 79−51694
degenerate semiconductor, Nernst-Ettingshausen effect, Sondheimer oscills., asymptotic behaviour 78−19059
degenerate semiconductor film, with different surfaces, transport effects in weak mag. fields 79−73607
Ettingshausen device, transient cooling effects, theory 80−80304
Ettingshausen refrigerator, longit., isothermal, nonstationary regimes, theory 78−18157
Ettingshausen-Nernst detectors with one- and two-phase detector layers *(German)* 80−27344
ferroliquid in annular channel, hydromag. stability, thermomagnetic effect 79−94593
ferromagnetic metal, dragging of domains by temp. gradient 80−34425
film, galvano- and thermomag. phenomena, theory *(Russian)* 78−14743
film, size quantised, thermomag. effects in strong mag. field *(Russian)* 77−63002
film, thermomagnetic effects in mag. field of arbitrary magnitude 78−47885
galvanothermomagnetic refrigerating element, cooling mechanism *(Russian)* 77−26308
gas analyser with internal convection, model simulation 77−56296
graphite, galvanomagnetic and thermomagnetic effects at low temp. 80−44618
graphite, neutron irradiated, thermoelec. and thermomag. effects 77−59296
graphite, thermoelec. and thermomag. props., cylindrical band model 80−39616
haematite-bearing rocks and concentrates, peaked thermomag. curves 79−79824
heat emission jump, in intense mag. field *(Russian)* 77−76796
heavily doped semiconductors, materials science developments, appl. to thermoelectric heat pumps 80−35713
intermediate state, thermal cond., Fermi surface shape and topology effects *(Russian)* 78−72314
Invar, elec. transport props. and Invar features *(Russian)* 78−14710
Invar, Nernst-Ettingshausen effect and galvanomagnetic effect anisotropy *(Russian)* 79−91030
magnetisable liquid, thermomagnetic convection between coaxial cylinders with distributed heat source 79−94622
metal, effects of large scale voids on thermal magnetoresist. 80−10946
metal, EMF appearance due to mag. field and laser pulse irrad. 77−76797

thermomagnetic effects continued
metal, ferromagnetic, Nernst-Ettingshausen effect, rel. to Hall effect and thermoelec. power 79−56199
metal, kinetic effects at high anisotropic strains, elec. transport props. meas. 78−54384
metal, magnetothermoelectricity, phonon drag contrib. 79−65432
metal, many-body effects of electron-phonon interaction on thermoelectricity 79−69499
metal, Nernst-Ettingshauser effect based radiation detectors 79−58795
metal, phonon drag magnetothermoelectricity, semiclassical theory 78−6354
metal, thermoelectricity, electron-phonon mass enhancement, Nernst-Ettinghausen coeff. meas. 79−65452
MHD convection, free, near plane and axisymmetric bodies 79−94728
motor, dynamic characts. and stable operation *(Japanese)* 80−16840
narrow band semiconductor, transport phenomena electron energy spectrum *(Russian)* 79−51616
Nernst amplifier, feasibility with heat sink and magnet winding at liq. N_2 temp. 77−53932
Nernst-Ettinghausen detector materials, criteria for selection 80−39615
nondegenerate semiconductor, thermomagnetic phenomena in quantising mag. field *(Russian)* 80−60014
Permalloy-Mn film, diffusion aftereffect causing mag. state change *(Russian)* 80−103860
phonon inelastic interband scatt., effect on Nernst-Ettingshausen coeff. 77−43552
polyatomic Knudsen gas, kinetic thermomag. phenomena 78−75246
power generation, appl. of spin reorientation phenomenon 77−4325
semiconducting or semimetallic film, size-quantised thermomagnetic coeffs. *(Russian)* 78−56249
semiconductor, Kane, thermoelec. power and thermomag. effects of hot electrons 78−56174
semiconductor, longitudinal isothermal Nernst-Ettingshausen effect in a quantising magnetic field 79−51617
semiconductor, longitudinal thermomagnetic effects odd in respect of mag. field 77−89780
semiconductor, Nernst-Ettingshausen effect, thermopower, strong elec. field 78−23122
semiconductor, thermomagnetic photoeffect 79−23991
semiconductor, total separation of galvano- and thermomagnetic effects 77−55545
semiconductor, type I zero-gap state, Nernst-Ettingshausen and Hall effects 80−44622
semiconductor film, cell for measuring electrophys. parameters over wide temp. range 77−51830
semiconductor films, Kane dispersion, thermomag. and thermoelec. effects, theory 80−70864
semiconductors, electrical properties calculated from thermophysical and thermomagnetic effects 79−73535
semiconductors, kinetic effects at high anisotropic strains, elec. transport props. meas. 78−54384
semiconductors, thermoelectric and thermomagnetic effects, heat transfer due to quasi-particle subsystems *(Russian)* 80−24959
semiconductors thermophysical props. determ. from Ettingshausen effect meas. method 80−44376
semimetal, two-stage drag of electrons by phonons 77−15843
single domain grain assembly, theory for magnetisation processes 80−88828
solid state energy conversion, appl. of solid state cooling to spaceborne IR focal planes 80−107772
solid with parabolic electron band, relaxation time oscillations in strong mag. field 79−60855
steel, C, decomposition of supercooled austenite, exam. of carbide formation *(Russian)* 78−35388
strong magnetic fields 77−62954
superconductor, hard, critical state stability and oscillations 80−107959
thermocouple errors due to Nernst effect 77−67434
thermoelectromagnetic waves in conductors in a mag. field *(Russian)* 80−49695
type II superconductor, thermomag. effects and crit. state stability 80−20353
weak magnetic fields, formulation of theory 77−62953
wurtzite structure semiconductor, transport in longit. quantizing mag. field 78−26891
AS_xSb_{1-x} thermomagnetic EMF, temp. and mag. flux density *(Russian)* 80−11022
Al low-temp. electron-diffusion magnetothermopower meas. 77−15834
Al, magnetic breakdown, quantum phenomena *(Russian)* 78−43290
Al, Nernst-Ettingshausen coeff., electron-phonon Umklapp scatt. 78−26848
Al, thermoelectric coeffs. in mag. field, giant quantum oscills. 79−65453
Al, thermoelectric power and Nernst-Ettingshausen effect 78−56134
Al-Ga, dil., low-temp. electron-diffusion magnetothermopower meas. 77−15833
As_xSb_{1-x}, semimetal, thermopower, thermomagnetic power, 4.5 to 77K 80−107825
Bi, diffusion thermoelectric power in mag. field, calcs. 78−56167
Bi, film, thermoelec. power in transverse mag. field *(French)* 78−23183
Bi, galvanothermomagnetic instability 80−49785
Bi, longit. thermomag. amplifier 77−47838
Bi, magnetothermal EMF, twinned layer effect 80−49784
Bi, magnetotransport props. in quantising mag. fields 77−20340
Bi, pulsed Ettingshausen cooling 78−91670
Bi, radioelectric effect in far IR 80−24967
Bi, thermomagnetic wave dispersion, propagation *(Russian)* 80−49696
Bi, thermomagnetic waves obs. *(Russian)* 78−80008
Bi, trigonal, weak field thermomagnetic coefficients 77−72874
Bi-Sb, dil., magnetothermal oscillation and spin splitting of electrons 78−43362
Bi-Sb alloys, thermomagnetic quality factor 77−15882
$Bi_{0.88}Sb_{0.12}$, semiconducting transport props., 2 to 100K 80−59989
$Bi_{0.91}Sb_{0.09}$, thermomag. power in strong mag. field, temp. and field depend. 78−43421
$Bi_{1-x}Sb_x$, narrow band gap semicond., photocond. and photomagnetic effect 79−51630
$Bi_{1-x}Sb_x$:Pb ($0.08 \leq x \leq 0.13$) Seebeck, magneto-Seebeck coeff., longitudinal Nernst coeffs. 78−56168
n-$(Bi_{1-x}Sb_x)_2Te_2$, magneto-Seebeck and Shubnikov-de Haas effect 79−42568
n-Bi_2Se_3, single cryst., new aspect of carrier scatt. 80−49707
Bi_2Te_3, galvanothermomag. props. up to 14 kbar 77−47829

thermomagnetic effects continued
n-Bi_2Te_3, galvonomagnetic props., influence of hydrostatic press. 79−73536
Bi_2Te_3-Sb_2Te_3 film, cond., galvanomag. Seebeck and Nernst-Ettingshausen effects under press., band model 77−47907
C fibres prepared from benzene, thermoelec. power, magneto-Seebeck effect 78−2507
CO, chemisorbed monolayer on Pt or Au, mag. phase transition, thermomagnetic study *(Russian)* 80−34319
$C_{12n}(SbCl_5)$, magnetothermal oscill. and electronic struct. 78−84129
Cd, thermopower meas. in mag. field, 1.5-4K 80−54675
Cd_3As_2, band structure, Kane model, magneto-Seebeck and Hall data 77−62821
Cd_3As_2, band structure, pressure dependence of galvano- and thermomagnetic effects 80−6722
Cd_3As_2, thermoelectric power and transverse Nernst Ettingshausen coefficent 79−38104
$Cd_{0.2}Hg_{0.8}Se$, longitudinal Nernst-Ettingshausen effect, effect of disorder scatt. 78−84240
$Cd_xHg_{1-x}Se$, 77-400K *(Russian)* 78−2485
$Cd_{0.15}Hg_{0.85}Te$, photothermomagnetic effect in mm range 80−92932
$Cd_xHg_{1-x}Te$, disorder scatt. 78−39137
$Cd_xHg_{1-x}Te$, photomag. and photothermomag. effects *(Russian)* 79−78137
$Cd_xHg_{1-x}Te$, photothermomag. effect and photocond. in millimetre wavelength range 80−44657
$Cd_xHg_{1-x}Te$, thermal cond. in mag. field, thermopower, and Nernst-Ettingshausen effect 77−31814
Cd_3P_2, free carrier and interband absorption 78−23446
Cd_3P_2, thermomagnetic transport effects obs. 77−15883
p-$CdSnAs_2$, Hall effect, thermo EMF, thermomagnetic effects 80−107822
Co-Mn alloys, Nernst-Ettinghausen effect and electrical resistivity *(Russian)* 78−14714
Co-Pd, transfer phenomena and association with electronic struct. *(Russian)* 79−91017
Cu-Mn spin glass, saturated thermoremanent magnetisation, time and temp. evolution 79−61167
Fe-Ni, (35 wt.%), transport props. and Invar features *(Russian)* 78−51973
Fe-Ni (20 to 31 wt.%), exam. of martensitic transform. and reverse transform. using differential and thermomagnetic resistance analysis *(French)* 79−52214
Fe-Si cast alloy with spheroidal graphite, transform. investigation during tempering *(Russian)* 80−97479
Fe_3Pd, quenched, or annealed exam. of magnetostriction, galvano- and thermomagnetic props. *(Russian)* 79−19757
Ga, thermopower quantum oscillations 80−15505
GaAs, compensated, magnetoresist. and magnetothermoelec. power meas. 77−43627
p-GaAs, influence of light holes on transport props. 77−4367
n-Ge, piezothermomagnetic analogue of Grabner effect 77−4378
n-Ge, thermoelec. power in quantising mag. field, phonon-phonon interactions 80−107832
n-Ge type semiconductor, thermomagnetic tensor struct. 77−62952
$(Ge_{1-x}Ga_x)_{1-x}Te$, rhombohedral and cubic phases, transport effects 78−2481
$(Ge_{1-x}In_x)_{1-x}Te$, rhombohedral and cubic phases, transport effects 78−2481
HgSe, quantum oscills. in Seebeck effect in high mag. fields 77−72875
In, magnetothermopower, phonon drag 79−69496
In, magnetothermopower giant oscills., mag. breakdown 77−8075
In, Nernst-Ettingshausen effect in solid and liq. states *(Russian)* 78−6353
In, transverse magnetothermoelec. props. 78−47768
InP, electron transport props., mag. field and temp. depend. 80−92888
InSb, Ettingshausen and Nernst-Ettingshausen effect meas. *(Russian)* 77−28201
InSb, Ettingshausen effect, influence of surfaces, narrow-gap semicond. characterisation 77−24571
InSb, longit. magneto-Seebeck coeff. in quantising mag. field 79−56250
n-InSb, thermoelec. power in longit. quantising field, phonon drag component 78−19064
InSb-NiSb, longit. thermomag. amplifier 77−47838
K, high field Righi Leduc effect and lattice thermal cond. 80−10948
K, high field Righi-Leduc effect and lattice thermal cond., reply to comment 80−10949
K, high field thermomagnetic coeffs., 1.5-4.5K, lattice thermal cond. calc. 79−60800
K, high-field Righi-Leduc effect lattice thermal cond. 78−34825
K, low-temp. lattice cond., phonon drag thermopower 79−60789
K, Righi-Leduc and Hall coeffs. meas., ^4He temp. range 77−66156
K, thermomagnetic and thermoelectric properties, phonon scatt. processes 80−29390
KNO_3, molten, thermomagnetoelec. effect *(French)* 77−76849
$La_{0.71}Pb_{0.29}MnO_3$, metal-semicond. transition at Curie point, transport props. obs. 79−73554
Li, Righi-Leduc and Hall coeffs. meas., 2 to 120K 77−66156
LiCr ferrite, elec. resist., thermoelec. power and Nernst-Ettingshausen meas. near compensation point 78−10487
$Mn_2Sb_{1-x}Bi_x$, temp. depend. of magnetisation *(Japanese)* 79−78375
Mo, magnetothermopower meas. 77−76795
Mo, transverse galvanomag. and thermomag. coeffs. 77−20298
N_2, thermomagnetic effect, Knudsen gas between Au surfaces, low temp. 78−30405
Nb, Hall and Nernst-Ettingshausen effects, temp. depend. *(Russian)* 77−85198
Ni-Fe, film, anomalous Hall and Nernst-Ettingshausen effect, contribution of phonon and impurity scatt. *(Russian)* 78−64145
Ni-Fe Invar alloy, thermoelectric power temp. and mag. field depend. 78−26849
Ni-Mn-Al-Si-Co, Alumel, Ettingshausen-Nernst coeff. and transport props. from 200 to 473K 80−44573
Ni_3(Fe,M), M=Cr,Mo,W, elec. resist., temp. depend. anomalies, Hall and Nernst-Ettinghausen effects *(Russian)* 80−10942
Ni_3Fe, Nernst-Ettingshausen effect, effect of alloying with Cr, Mo, W or Cu *(Russian)* 78−39095
Pb, superconductor, entropy transport effect *(French)* 77−63036
Pb-In (40-60 at.%), type II superconducting Ettingshausen effect, transport entropy of vortices 78−56272

thermomagnetic effects continued
$Pb_{1-x}Ge_xTe$ solid solns., phase transition influence on elec. props., 77 to 450K 80−103689
$Pb_{1-x}Ge_xTe$:Ga, Fermi level stabilization, transport props. meas., 77-400K 78−56065
$Pb_{40}In_{60}$, mixed state supercond., Hall and Ettingshausen effects, vortex entropy transport 80−44780
$Pb_{1-x}In_xTe$, impurity-state conduction and temp. depend. of transport coeffs. 78−47795
p-PbS, struct. of valence band, transport processes study 80−20081
PbSe film, influence of pot. barrier on thermoelec. props., elec. cond., Hall coeff. and Nernst-Ettingshausen coeff. 78−39239
PbSe, valence band struct., Hall and transverse Nernst-Ettingshausen effects, optical absorption 79−11064
PbSe:Tl, high temp. elec. and optical props., impurity states 79−60854
PbSe:Tl, scatt. of holes and phonons by impurities 78−19068
$PbSe_{0.5}S_{0.5}$, valence band struct., absorpt. spectra, elec. props. 80−44505
$Pb_{1-x}Sn_xSe$, carrier effective mass determ. 77−24572
$Pb_{1-x}Sn_xSe$, n- and p-type, with band inversion, study of transport phenomena 80−49741
$Pb_{1-x}Sn_xSe$, transport phenomena in solid solutions with band inversion 80−107792
p-$Pb_{0.65}Sn_{0.35}Te$, transport coeffs. and dispersion law 80−44629
$Pb_{0.82}Sn_{0.18}Te$, thermomagnetic, thermoelectric props., valence band struct. *(Russian)* 80−54724
$Pb_{1-x}Sn_xTe$:In, high temp. Fermi level position 79−90948
PbTe, radioelectric effect in far IR 80−24967
PbTe:Tl, influence of Tl impurity states 80−20121
$PbTe_{1-y}Se_y$:In, high temp. Fermi level position 79−90948
Pd-Ni alloy, dil., magnetothermopower meas. 79−78079
Pt-Co, dil, magnetopower, magnetoresistivity 78−68016
Pt-Co alloys, dil., thermopower and magnetothermopower 79−65456
Rb, Righi-Leduc and Hall coeffs. meas., 2 to 120K 77−66156
Ru, magnetic breakdown trajectories, quantum oscillations of thermo EMF and Nernst effect *(Russian)* 78−95290
Ru, thermo-EMF and Nernst effect under mag. breakdown conditions *(Russian)* 80−24878
Sb, effect of surface layer current, on transport coeffs., and meas. of Kapitza resist. 77−69348
n-SiC (6H), anisotropy, of thermoelec. power and transverse Nernst-Ettingshausen effect 77−69362
n-SiC (6H), density of states effective mass determ., high temp. meas. of elec. props. 79−15073
SiC (6H), phonon drag and phonon-electron interaction *(Russian)* 78−79701
SnTe, isothermal meas. of galvanomag. and thermomag. effects *(Russian)* 78−56160
TbMg, mag. struct. and mag. props. 77−8275
Te, galvano- and thermomagnetic effects 78−30939
Te, imperfect pure cryst., thermomag. effects, dislocation effects and Auth model 77−85248
p-Te, transverse and longit. Nernst-Ettingshausen effect, theory and expt. 78−76095
Tl, Nernst-Ettingshausen effect in solid and liq. states *(Russian)* 78−6353
W, low temp. transport props., phonon and impurity scatt. 78−10418
W, thermopower meas. in mag. field, 1.5-4K 80−54675
YIG, thermomag. anal. by electron diffr. 80−108035
$Zn_xHg_{1-x}Se$ semimetal-semicond. transition, thermo-EMF in mag. field and Hall expts. *(Russian)* 77−15881
$Zn_xHg_{1-x}Te$, impurity influence on thermomagnetic effects and elec. cond. 79−60856

thermomagnetic recording
amorphous metallic materials properties, Gd-Co ribbon for laser, electron beam thermal recording *(German)* 79−19744
Curie point, charact. of thermomag. recording *(Russian)* 78−23272
holographic recording materials and devices, book contrib. 78−25838
magnetic image formation on thin mag. films *(Russian)* 79−47286
Permalloy films with band domain struct., resolving power *(Russian)* 80−75769
rare earth-transition metal amorphous thin films for thermomag. recording 80−20403
semiconductor optical image transducers for increased sensitivity *(Russian)* 80−44833
singularities of optical information recording at Curie point, cylindrical domain form. *(Russian)* 77−8318
thin film nonselective media, threshold energy reduction method 77−54674
thin film thermomagnetic strip-domain type recorders, frequency-energy charact. *(Russian)* 77−67521
two-layer mag. structures, thermomag. recording 80−100588
Bi garnet-MnBi film structure, thermomag. information recording appls. *(Russian)* 78−23305
$Co_xFe_{3-x}O_4$, single cryst. mag. films, holograms recording and thermomagnetic writing 78−55324
Cr_7Te_8 film, optical and magneto-optical props., appl. as storage medium 78−23545
Dy-Fe, amorphous ferrimag. film, mag. props. and Curie point writing 77−12164
$(ErEu)_3(FeGa)_5O_{12}$ film, for mag. writing and magneto-optical displays 78−6549
EuO film, reversible holographic storage 77−34851
EuO film for thermomagnetic recording, anisotropy of resolving power 80−20404
EuO, resolution as hologram recording material 77−83834
Fe garnet epitaxial film, thermomag. data recording by electron beam heating 78−27066
FePd epitaxial film, vacuum-deposited, for thermomag. recording, mag. and magneto-optical props. *(Russian)* 78−60319
FePt epitaxial film, vacuum-deposited, for thermomag. recording, mag. and magneto-optical props. *(Russian)* 78−60319
$(Gd,Bi)_3(Fe,Al,Ga)_5O_{12}$ LPE film, 180° Bloch wall pinning at etched nucl. tracks 78−39376
$(Gd,Bi)_3(Fe,Ga)_5O_{12}$ magneto-optic film, ion irrad. effect on storage props. 78−52324
Gd-Co film, amorphous, stability of small bits to temp. and mag. field changes 78−68314
Gd-Fe, amorphous film, thermomagnetic writing 78−84428
Gd-Fe-Y, amorphous film, thermomagnetic writing 78−84428
thermomagnetic recording continued
GdCo, amorphous thin film, for thermomagnetic recording *(Japanese)* 80−11562
GdFe garnet, magnetised single cryst. plate 79−47285
GdFe homogeneous amorphous films, compensation point switching, magneto-optical Kerr signal anal. 80−15726
GdIG single crystal plates for magnetooptical information storage 79−7997
Mn-Bi magneto-optic memory system 77−85511
MnBi film for recording optical information, analogue charact. *(Russian)* 78−50716
MnBi films, prep. by ionised-cluster beam deposition technique, magnetooptical props. 80−100790
MnBi holographic film, reduction of thermomag. recording energy threshold *(Russian)* 80−43302
MnCuBi film, prep. by RF sputtering, and thermomag. writing expt. 77−8369
$Mn_{0.75}Ti_{0.25}Bi$ films as magnetooptic storage medium, mag. interferogram recording 78−19288
$NdCo_5$, ferromag., thermomag. charact. in mag. field *(Russian)* 78−23273
$(Sm,Er)(Ga,Fe)_5O_{12}$, LPE, non-grooved film, thermomag. writing 78−76278
Tb-Fe, amorphous ferrimag. film, thermomag. writing using He-Ne laser 77−12163
Tb-Fe, amorphous ferrimag. film, mag. props. and Curie point writing 77−12164
Tb-Fe amorphous film, thermomag. contact printing 77−89986
$YFeO_3$, thermomag. recording in surface layer of orthoferrite 79−24165
$Y_3Gd_3Bi_3(FeAlGa)_5O_{12}$, epitaxial film, thermomag. recording *(Russian)* 77−1571

thermomagnetic torque *see Scott effect*

thermomagnetic treatment
see also magnetic annealing; magnetocaloric effects
Alnico, interaction domains after heat treatment in mag. field *(Russian)* 78−68286
coal liquefaction residues, Mag. separability enhancement, thermomagnetic anal. and Mossbauer study 79−83544
composite superconductor, flux jumps and training 80−70911
Fe-Cr-Co-Si-Mo, plastic deform. influence on structure and mag. props. *(Russian)* 79−70176
magnetic materials, sintering, structure and props., external mag. and elec. field influence 80−50570
magnetothermoelasticity, dynamic *(Russian)* 77−55995
Magnico alloy, with Si, Nb, Ti and La, low-temp. thermomag. treatment 77−63812
permanent magnet magnetic texture form. in double pole gap of electromagnet 77−89985
PVC, magnetoelectret form., RF thermomagnetic treatment, dielectric aftereffects 78−6625
quenching liquids, cooling capacity in mag. field 79−38867
steel, carburised, transform. of residual austenite, mag. field effects *(Russian)* 80−29952
steel, induced anisotropy influence on mag. props., thermomagnetic working *(Russian)* 80−55549
steel, martensitic transformation kinetics 79−87630
steel, nitriding, mag. field effect 79−57153
ticonal, grindability improvement, thermomagnetic and heat treatments 77−16625
Ticonal, interaction domains after heat treatment in mag. field *(Russian)* 78−68286
Ticonal, two- and one-dimens. modulated struct. after thermomag. treatment and water quenching *(Russian)* 80−29983
Ticonal with magnetic texture, struct. damages during ageing 77−16626
Ticonal with Sm, magnetic props., phase transform. after thermomagnetic treatment 78−3155
Al-Ni, solidification in mag. field, crystallite obs. *(Russian)* 77−4770
Bi-Cd, solidification in mag. field, crystallite obs. *(Russian)* 77−4770
Cd-Zn, solidification in mag. field, crystallite obs. *(Russian)* 77−4770
Fe alloy YuNDK35T5BA, thermomag. treatment, post-decomp. processes 79−87668
Fe alloys, struct., appl. of mag., thermomag. methods *(French)* 79−20318
Fe-Cr-Co, magnetic domain walls, Lorentz microscopy 80−103854
Fe-Cr-Co (31 wt.%, 23 wt.%), microstruct. and mag. props., ageing and thermomag. treatment effects 78−76769
Fe-Cr-Co ductile magnet, with high $(BH)_{max}$, processing, mag. props., and microstruct. 77−8957
Fe-Cr-Co ductile magnet alloys, phase diagram and mag. props., V or V+Ti addition effects 77−8959
Fe-Cr-Co hard-mag. alloys, fine cryst. struct. *(Russian)* 77−66706
Fe-Cr-Co-Al (27.5, 17.5, 0.5 wt.%) alloy, induced anisotropy 78−76239
Fe-Cr-Co-Si alloy, interaction domains after heat treatment in mag. fields *(Russian)* 78−68286
Fe-Cr-Co-V-(Ti) hard magnets, V and V-Ti effects on mag. and mech. props. 79−91810
Fe-Mn base alloy, mag. preferred directions 78−39370
Fe-Ni alloy, in rotating field, effect on permeability and coercive force *(Russian)* 77−21294
Fe-Ni alloys, heat treatment variations effect on surface conditions and on Hg wetted switch behaviour 80−66547
Fe-Ni-Al, type YuN14DK25BA, thermomag. treatment 80−16512
Fe-Ni-Al-Co-Cu-Ti, 38 to 40 wt.% Co, 8 to 8.5 wt.% Ti, alloy YuNDKT tempering and thermomagnetic treatments 78−3154
Fe-Ni-Co-Mo-Ge alloy 40NKM, excess mag. noise after various thermomag. treatments *(Russian)* 80−29575
Fe-Pt, plastic deform. effect on struct. singularities and mag. props. *(Russian)* 80−44892
Fe-Si (3% wt.), increase in effectiveness of thermomagnetic treatment due to low temp. annealing *(Russian)* 79−51772
Fe-Si-Al-Ni alloy, Super Sendust, Ni content and thermomag. treatment effects 77−4861
Li-Co ferrite, mag. anisotropy induced by thermomag. treatment, ionic order effect, magnetostriction meas. 80−103830
TiO_2-Fe_2O_3-CaO-V_2O_5 system ferrites, TiO_2 content and thermomag. effects on dielec. props. 77−43927
YIG:Si, thermomagnetic processing and illum. effects on mag. props. *(Russian)* 77−8410

thermomechanical processing *see thermomechanical treatment*

thermomechanical treatment
see also hot pressing; hot working
alkali silicate glasses, secondary relax. transitions 80−88261
alloy, strengthening mechanism anal. by thermal activation theory 79−78987
austenite, hot-worked, subgrain struct., X-ray diffr. and electron microscope obs. *(Russian)* 79−15698
austenitic steel, mechanical properties, effect of high temp. thermomechanical treatment and post-deform. ageing *(Russian)* 78−39809
bainite substructure changes during HTMTI 78−23742
bronze, BrB2, thermostress treatment of thin rolled sheets 79−52273
bronze, sintered, mech. props. 77−28839
diamond, mechanical strength depend. on thermal working parameters, microcracks *(Russian)* 80−55501
diamond synthesis by graphitisation of carbon materials at high press. and temp., Ni influence 80−60795
dislocation substructure strengthening and thermomechanical processing, conf., Las Vegas, USA, Feb. (1976) 77−84760
elastic-plastic struct. cyclic thermomech. loading 79−7299
Elinvar, Cr addition effect on modulus of elasticity and thermoelastic coeff. 77−90387
epoxide resins, amine-hardened, heat distortion, glass transition temps., chem. cure 80−44302
epoxy resin, cure history effect on dynamic mech. props. 80−54356
eutectoid thermomechanically treated, textural studies 80−29978
extensometer design principles and props., thermal and thermomechanical cycle generation *(French)* 78−31598
ferromagnetic alloy, 35KFN10, X-ray diffr. investig. after thermomech. treatment *(Russian)* 77−48457
fission reactor materials, thermomechanical transient anal., strain-rate dependent plasticity 80−79864
glass-ceramic, dispersion strengthened glass matrix 77−40425
Incoloy 800, review of structural charact., heat treatment and comp. effects 79−43297
Incoloy MA956E, mechanical alloying for high temp. appl. 78−44046
Inconel MA754, mechanical alloying for high temp. appl. 78−44046
Kovar, thermostress treatment of thin-rolled sheets 79−52273
magnetic materials, high-energy, technology developments and props. *(Italian)* 80−54914
metal, and alloy, strain hardening criteria eval. 77−55982
metal, axisymmetric drawing simulation, numerical method development 78−30206
metallic crystal, thermomechanical deform., analytical description 80−49391
Nimonic EhI437B, heat resistant, true breaking stress in rapid air stream 79−66163
nylon 66, filament, heat setting and thermomechanical behaviour 78−15435
polyamidoimide film, thermomech. props. rel. to mol. struct. *(Russian)* 79−57029
polycaproamide, oriented filaments, mech. props. 80−66550
polyethylene, high density, injection moulding effect on strength props. *(Russian)* 79−34072
polyethylene, mech. retardation time spectrum, thermostimulated creep 79−5014
polyethylene terephthalate, filament, heat setting and thermomechanical behaviour 78−15435
polyethylene terephthalate, stretching, heat effects, struct. transforms. 79−15735
polymer, thermally stimulated creep 78−11245
polymer latex film composite, glass transition temp. determ. using thermomech. curves 80−75342
polyphenylene oxides, high temp. ageing effect on struct. and props. *(Japanese)* 77−70078
polystyrene, oriented amorphous, supermol. structures rel. to mech. behaviour 78−22673
press for hardening discs 79−57022
PVC, amorphous, orientation study by creep thermomechanical method, computer anal. 78−75561
PVC, plasticised, thermomechanical and dielec. relax. props. rel. to degree of processing 79−70124
PVC, thermal history and treatment effect on mech. props. 79−4986
rare earth magnetic materials, permanent magnets flux stability enhancement, gyroscope-based guidance systems performance improvement 80−50144
refractories, high-temp. installation for thermomech. testing 79−83425
refractories, subjected to severe thermomech. stress, behaviour *(French)* 80−81084
review 77−4796
stainless steel, thermomech. ageing compared with discontinuous precipitation mechanism *(Russian)* 77−70053
steel, 1Kh18N10T, corrosion fatigue during anodic polarisation after thermomech. treatment *(Russian)* 77−59976
steel, 20Kh, warm extrusion effects on struct. and mech. props. 77−44311
steel, 30CH2GMT and 35CHG2SV, thermomechanical hardening *(Czechoslovakian)* 77−32602
steel, 35Kh3MFS, strengthening involving austenite fine grain processing *(Russian)* 77−52358
steel, AISI 4340, sulphide inclusion behaviour during thermomechanical treatment 78−3151
steel, AISI 4340, thermomechanical treatment, sulphide inclusion behaviour 79−11647
steel, alloy, high-temp. combined ht. treatment and mech. working, C content effects *(Russian)* 78−52854
steel, alloy, surface quality improvement, thermomech. treatment 80−61020
steel, austenitic, 16H2NMB, struct., texture and mech. props. of product of transform. 78−92273
steel, austenitic, 30KhGSA, heat treatment, preliminary, cold deform., elec. heating rel. to mech. props. 79−24554
steel, austenitic, 45Kh2N12GS, post deformation holding at deform. temp. effect on struct. and strength of austenite and martensite *(Russian)* 79−1880
steel, austenitic, Cr-Ni (18,12 wt.%), containing coarse grain boundary precipitates, thermomechanical treatment 78−27545
steel, austenitic, mechanical strength, effect of mech. and heat treatment 77−12659
steel, austenitic, precipitation hardenable, friction and wear under abrasive conditions *(German)* 77−59951
steel, austenitic Cr-Mn, $M_{23}C_6$ carbide precipitates comp., heat and thermomech. treatment influence *(Russian)* 80−40361
steel, austenitic stainless, biphase, ferritic, ageing and thermomech. treatment effects on struct. and props. 80−35226
steel, austenitic stainless, blister initiation inclusion, heat treatment and thermomechanical treatment effects *(French)* 80−35224
steel, austenitic stainless, high N, plasma arc remelting, processing parameters and props. 80−16336
steel, C, structural strength, increase by high temp. mech. treatment with austenite isothermal decomp. 79−24555
steel, C, type 1792AF 79−38966
steel, C, U8A, struct. after low-temp. thermomech. treatment 79−79008
steel, C and HSLA, grain size and substruct. control by alloying and thermomech. treatment, review 80−3082
steel, coercive force measurement method of quality inspection of heat and thermomechanically treated parts 79−5113
steel, components, dimensional stabilisation, thermoplastic treatment *(Russian)* 80−20960
steel, constructional, struct., props., isothermal thermomechanical working *(Russian)* 77−25076
steel, Cr, phase transform., effect of high temp. plastic deform. *(Slovak)* 78−19837
steel, Cr (12 wt.%), thermomechanical treatment, high temperature, effect on props. and struct. *(Czechoslovakian)* 77−32603
steel, Cr modified, heat resist. rel. to thermomech. treatment 79−20084
steel, Cr-Mn type, martensite struct. after quenching and HTMT, X-ray diffr. obs. 80−84975
steel, Cr-Ni (32,8), two phase austenite-ferrite alloy, fatigue behaviour *(Japanese)* 79−79091
steel, diffusion of C after high-temp. thermomechanical treatment *(Russian)* 78−39813
steel, electric sheet, hot-rolled, recrystallization and texture formation during ht. treatment 77−44271
steel, eutectic 1080, fatigue life improvement by thermomech. processing 80−25732
steel, eutectoid, mech. behaviour, thermomech. treatment effects 80−84970
steel, high C, 80Kh5G5 and 120N12, austenite hot deform. effect on martensitic transform. *(Russian)* 77−48434
steel, high C, thermomech. treated, strengthening factors 77−8862
steel, high Mn, mech. props., strain induced martensitic transform., effect of austenite predeformation 77−16649
steel, high-temp. high temperature thermomechanically heat treated, fatigue strength improvement by cathodic polarisation *(Russian)* 77−25188
steel, high-temp. isothermic combined heat treatment and mech. working influence on struct. and mech. props. of 60S2 *(Russian)* 80−20969
steel, high-temperature thermomechanical treatment, holding after deform. effect on strengthening 79−38868
steel, hollow cylinder, thick walled, effect of thermomech. treatment 80−11674
steel, hypereutectoid, thermomech. treatment, Fe_3C distrib. and yield point *(German)* 79−52243
steel, hypoeutectoid, C22, recrystn., influence of carbides distrib., mech. props. meas. *(German)* 79−38850
steel, KhVG, deformation ht. treatment on carbide precip. in KhVG 77−63700
steel, low alloy, hot deform. behaviour and modified ausforming *(Japanese)* 78−11244
steel, low alloy structural, type 30KhGSA, effect of thermomech. treatment on strength, fracture toughness and fatigue props. 80−11676
steel, low alloyed (Mo,Cr,B) structural and mech. props., report *(French)* 80−25691
steel, low C, austenite transform., TTT diagrams 77−70031
steel, low C, bainitic, optimal struct., heat treatment effects 77−16624
steel, low C, high strength, thermomech. treatment, microstruct. 79−57015
steel, low C, high strength, thermomech. treatment, strengthening mech. 79−57014
steel, low C, thermomechanically processed, martensitic fibre development, fatigue fracture 78−64572
steel, low C (0.01-0.05 wt.%), structural and mech. props., report *(French)* 80−25691
steel, low C and alloy, serrated flow and thermomechanical treatment *(Korean)* 80−30026
steel, low-alloy, recrystallisation after hot deformation 77−44268
steel, low-C, preliminary thermomech. treatment, cold deform. effect on struct. and props. 79−38847
steel, maraging, crack resistance, effect of external stress during ageing *(Russian)* 77−59902
steel, maraging, N12K6M5TYu, fracture, influence of high-temp. thermomechanical treatment on charact. *(Russian)* 78−27591
steel, Mn-Cr-V, tool, quenched and tempered, fracture toughness *(German)* 80−25726
steel, Ni, struct. change of hot-worked austenite during post-deform. holding 80−35228
steel, Ni-(Cr)-Ti, thermomechanical and heat treatment effects on retained austenite *(Russian)* 77−66661
steel, precipitation hardening, strength and struct. *(German)* 79−47701
steel, sheet, thermomechanical bending, induction heating calc. 79−52280
steel, silchrome, thermomech. hardening 78−23736
steel, sintered, Ni-Cr-Mo additions, struct., props., thermomechanical treatment effects 77−12657
steel, stainless, 1Kh18N10T, solution annealed effect of cyclic stresses on corrosion rate in acid environments *(Russian)* 78−31577
steel, stainless, austenitic, CC Ni-Al, γ-phase, fracture mechanical aspects of abrasive friction, wear, chip formation 78−72865
steel, stainless, austenitic, Cr-Ni-Mn-Si-Mo-C alloy, 13Khi8N10G3S2M2, elastic moduli exam. after thermomechanical treatment *(Russian)* 79−24558
steel, stainless, fatigue, high temp. under isothermal and thermal cycling conditions 78−60836
steel, stainless, ferritic, Cr-Mo-Ni (29,4,2 wt.%) 77−44276
steel, stainless, Kh18N10T, substructure after high-temp. thermomechanical treatment with high deformation rates *(Russian)* 78−76657
steel, thermally and thermomechanically treated, struct. and decomposition of martensite 78−19784

thermomechanical treatment continued
steel, thermomechanical treatment effect on mech. props. and microstruct. *(French, German)* 79−66090
steel, TRIP, strength and plasticity rel. to thermomech. treatments 77−44281
steel, TRIP, warm extrusion, process control and tensile props. 80−16338
steel, type 12Kh1MF, dislocation struct. changes after thermomechanical treatment *(Russian)* 80−66545
steel, type 34Cr4, post-hotforming recrystallisation condition, use of NEOPHOT 2 and EPIQUANT 80−84949
steel, type 4052Kh, thermomechanical working influence on mech. props. *(Russian)* 80−93578
steel, type KVK, deform. strengthening of bayanite phase *(Russian)* 80−100851
steel, wear resist., mech. props. and struct. effects 80−35338
steel, wear resistance of 30KhGSA and 40 kHNMA after thermal and thermomech. treatment 77−70087
steel 77−4796
steel 120Kh3G3, lattice defects during $\gamma \rightarrow \alpha \rightarrow \gamma$ transform., electron microscopy obs. *(Russian)* 79−47681
steel 40 khNMS, high temp. thermomechanical treatment, Cr effects on props. 77−12651
steel 80Kh5, thermomechanical treatment, high temp., effect of austenite deform. on martensite stability during low temp. tempering 79−57018
steel austenite, recrystallisation diagrams, heating, plastic deform. rel. to struct. 79−20067
steel bearing rings, optimisation of thermomechanical working parameters *(Russian)* 80−93579
steel casting, calc. method of thermal and thermo-visco-elasto-plastic processes *(German)* 80−79859
steel continuous casting, thermal, thermo-visco-elasto-plastic processes *(German)* 80−81044
steel fine structure after heat treatment, X-ray diffr. exam. 80−60890
steel martensitic, high-C, formed from hot-worked austenite, struct. *(Russian)* 78−6950
steel susceptibility to H_2 embrittlement, fracture toughness *(Czech)* 77−59915
steel turbine casings, residual life determ. 80−93585
steels, die, mech. props. high temp. thermomech. treatment 79−20086
superalloy, microstructure resulting from alloying and heat treatment, effect on creep, fatigue, fracture strength 78−11246
technology, automobile industry 79−96048
thermoplastic elastomers, crosslinked by secondary valence interactions, elasticity and processing, crosslinking behaviour 80−40320
thermoplastic polymer, linear viscoelasticity, rel. to orientation, recoverable strain and mech. props. 77−56041
thin rolled sheets, thermostress treatment 79−52273
Ti alloy, VT22, hot deform., microstruct. form. and mech. props. *(Russian)* 77−28830
VT3-1, HTMT effects on struct. and props. 78−23740
Al alloy 2036, thermomechanical treatment on struct. and props. 79−29109
Al alloy 6061, thermomechanically treated elev. temp. mech. props. 79−8310
Al alloy 7050, fatigue, effect of intermediate thermomech. treatments 79−8352
Al alloy 7075, fracture props., effect of thermomechanical treatment 78−60793
Al alloy 7075, serrated flow and thermomechanical treatment *(Korean)* 80−30026
Al alloy RR58, low cycle fatigue at 423K, prior treatment effect 80−104254
Al alloys, thermomech. treatments, effects on microstruct. 80−100858
Al, alloys, thermomechanical working effect on mech. props. *(Russian)* 77−21181
Al conductor alloys, subgrain-strength relationship, effect of alloying and processing 77−32606
Al, high purity 6061, thermomechanical treatment 77−44277
Al wire, hot and cold deformation drawing strengthened, thermal EMF study *(Russian)* 80−54674
Al-Ag (15 wt.%), precipitation hardenend cyclic stress-strain response 78−35412
Al-Cu alloy 1201, thermomech. treatment effect on strength charact. and fracture toughness *(Russian)* 80−40391
Al-Cu alloy RR58, high strain fatigue life, prior treatment effect 78−60835
Al-Cu-Mg type 2036, thermomech. treatment, flow stress anal., effect in mech. props. 80−93584
Al-Cu-Mg-Ni-Fe alloy RR 58, creep resistance at elevated temps., thermomechanical treatment effects 77−59836
Al-Mg-Si, thermomechanically treated, age-hardening 78−11236
Al-Zn (6.5 at.%), fatigue props., effect of ageing and thermomech. treatment 78−27620
Al-Zn-Mg alloy, thermomechanically treated, precip. behaviour 78−84856
Al-Zn-Mg alloy 7075, effect of thermal and mechanical pretreatments, on Guinier-Preston zone 78−39817
Al-Zn-Mg-Cu, optimum treatment combination for thermochemical processing 77−44278
B fibre reinforced Al-Zn-Mg, packet rolling, thermodeform. process parameters *(Russian)* 80−55433
C fibre, morphological charact. rel. to fracture, SEM obs. 77−63791
C, pyrolytic, high-temp. deform. under mech. loads 77−16644
Ca_3SiO_5, thermomechanical effects on form. 79−15635
Cu, polycrystn., strain localisation during hot deform. 80−104195
Cu/Cu system, explosive cladding, TEM obs. and thermomech. model 79−96041
Cu-Al_2O_3 coatings, electrodeposited, dispersion hardened, exam. of props. 79−34181
Cu-Sn-Mg, precipitation, effect of thermomechanical treatment *(Japanese)* 79−4970
Cu-Sn-Ni alloys, mech. props. after thermomech. treatment 79−79009
Cu-Ti (Zr), strength improvement by thermomechanical treatment *(Japanese)* 78−48426
Fe, coercive force measurement method of quality inspection of heat and thermomechanically treated parts 79−5113
Fe, sintered PZh1M, fracture resistance subject to thermomechanical treatment 77−77517
Fe-BeO, dispersion hardened alloy, struct.-props. relationships 77−66652

thermomechanical treatment continued
Fe-Co (35 wt.% and 52 wt.%), heat treated, decrease in sensitivity of mag. props. to mech. stresses *(Russian)* 78−56363
Fe-Cr-Ni, solid soln. strengthened and precipitation hardened, in-reactor creep 79−43327
Fe-Mn, struct. and props., effect of Nb, C and Si alloying *(Russian)* 77−90360
Fe-Mn-Ni, fracture toughness, thermomechanical treatment effects 78−60794
Fe-Ni, reactive metal alloy, effects of thermomechanical processing on strength and toughness 79−70112
Fe-Ni-C (24, 0.5 wt.%), recovery and recrystallisation of stable austenite after hot rolling *(German)* 77−32591
Fe-Ni-Cr, austenitic, dispersion-hardened alloys, thermomechanical working *(Russian)* 77−66659
Fe-Ni-Mn, martensite, aged, grain boundary embrittlement 79−96144
γFe_2O_3, transform. to α-phase, effect of preliminary pressing or vibromilling 78−84798
GaAs:Si, hardening by solute-vacancy pairs 77−4794
$LiFe_5O_8$, hysteresis and other mag. props. rel. to microstruct., TEM investig. 77−20636
MgO-$MgAl_2O_4$($FeCr_2O_4$), thermoplastic and thermophys. props. for steel vacuuming installations 80−35281
Mo, fusion reactor appl., quick heating thermal fatigue test, ultra-high vac. environment *(Japanese)* 80−93716
Mo, high temp. creep and strength depend. *(Russian)* 79−79034
Mo-Zr-C (0.08, 0.02 wt.%), struct. and banding tendency, thermomechanical treatment effects 77−86063
Nb-W-Mo-Zr (5, 2, 1 wt.%), surface-layer struct. and mech. props., effect of O_2 diffusion saturation 79−5087
Ni, EP742 type alloys, variation in struct. during thermomechanical treatment *(Russian)* 79−52250
Ni-Cr, high temp. thermomech. treatment effect on tensile diagrams of KhN77TYuR *(Russian)* 80−60884
Ni-Cr alloy, EI 437B, vibrocreep at normal and high temps. 77−4824
Ni-Cr-Al-W-Ti alloy MA 6000E, mechanical alloying for high temp. appl. 78−44046
Ni-Cr-NbC eutectic composite, unidirectional solidification, thermal cycling, temp. range effect on microstructural degradation 80−89272
Ni-HfO_2 (3 wt.%), dispersion hardened alloy VDU-2, thermal and mech. treatment 77−90376
$NiFe_2O_4$, hysteresis and other mag. props. rel. to microstruct., TEM investig. 77−20636
PbO glass, mechanochemical reduction 77−52628
SiO_2-Al_2O_3, refractory fibrous heat insulating material 78−6990
SiO_2-Al_2O_3 refractories, thermal shock props., fracture mech. appl. *(French)* 79−96109
Sn-Pb eutectic, struct. and plasticity, thermomech. treatment effects *(Russian)* 78−60686
Ti alloy, microstructure resulting from heat treatment, alloying, effect on creep, fatigue, fracture strength 78−11246
Ti alloy, VT3-1 mech. props. and low-temp. creep 77−44314
Ti alloy TA6V, superplastic behaviour of welded specimens 77−86100
Ti alloy VT22, hardening during thermomechanical treatment, precipitate particle internal struct. *(Russian)* 79−91657
Ti alloy VT25, thermomechanical treatment effect on struct. and mech. props. 78−3152
$\alpha+\beta$Ti alloy VT3-1, drop forgings, grain orientation and props., combined mech. working, hardening and high-temp. heat treatment influence *(Russian)* 80−20973
Ti alloys VT23 and VT15, etching as a function of struct. *(Russian)* 78−15568
Ti-Al-Mo-(Cr), etching as a function of struct. *(Russian)* 78−15568
β-Ti-Mo-Cr-Al (8, 4.5, 2.5 wt.%), metastable, tensile ductility, α-phase morphology and distrib. effect 77−86098
TiNi alloys, structural transform., physical props. and memory effects *(Russian)* 79−1856
U-V (0.2 wt.%), mech. and struct. props., effect of internal H *(French)* 77−21253
W, high temp. creep and strength depend. *(Russian)* 79−79034
WC-Co and WC-Co-TaC-TiC-NbC cemented carbides, microstructure, high temp. deformation, uniaxial plastic compression 80−40451
Zr-Mo-Nb-V-Sn (1,2,2,2 wt.%), heat treatment, transform. reactions and mech. props. 79−24545
Zr-Mo-Sn (3,2 wt.%), heat treatment, transform. reactions and mech. props. 79−24545

thermometers
see also pyrometers; resistance thermometers; temperature measurement; thermocouples; thermopiles
absolute high-temperature Johnson noise thermometry 79−12800
acoustic, cct. and operation *(French)* 79−35739
acoustic thermometers with W resonators 79−32153
applications and types, review *(Japanese)* 77−71318
bimetal, design principles *(German)* 77−49724
bimetal strip based, contact, basic parameters *(Czech)* 78−12692
biofeedback, low-cost research-oriented, with digital readout 79−29673
biomedical digital thermometer, simple, inexpensive design 80−36178
biomedical electronic thermometers, review 78−69235
calcite crystal as radiation-stable thermometer 78−203
calibration, in liq. He range, dipstick cryostat 80−37044
calibration, sealed metal freezing point cell 78−12696
calibration, triple point cell of water prep. 78−204
calibration standard, melting point of pure Ga 77−41611
calibration using Ga melting-point apparatus, enzymologic appl. 78−85460
calorimeter with medical thermometer for X-ray pulse dose determ. 77−21628
capacitance thermometer for low-temp. measurements, bridge detector circuit 79−54132
cholesteric liquid crystal film, optical rotating power near cholesteric to smectic A transition, thermometry appls. 78−10865
combined radiation/contact thermometer, −10 to 600°C range, features *(German)* 78−32815
constant volume gas, for 4-300K *(French)* 77−133
contact thermometers, convertibility of dynamic characteristics to different operating conditions *(German)* 79−97387
contactless, 600 to 1200°C, using PbS detector *(Slovak)* 78−54366
cryogenic, using Si diode, 4.2-300K range 77−137
deep body thermometer testing and modelling 77−40816
demountable ^{3}He melting curve thermometer 78−54369

thermometers continued
differential thermometer, for teaching appls. 79−48997
differential thermometer, high sensitivity, calorimetric appls. 78−4614
digital, 300°C-1800°C range, features *(Russian)* 78−65926
digital, biomedical precision for 35 to 40°C operation *(German)* 77−56499
digital, characts. *(Hungarian)* 78−54367
digital, electronic, with two sensors, in kit form *(French)* 80−4712
digital, process meas. control appl. 78−49833
digital, six-channel scanning type AD2036 operational principles 78−86269
digital, type DTM 1, with LED display *(German)* 80−27302
digital, types and technical data *(Russian)* 77−53911
digital, using LSI for remote sensing 80−27301
digital, with crystal resonator temp. sensor 77−82514
digital, with quartz crystal oscillator, high accuracy achieved 78−65932
digital instruments, high precision using MPUs 79−54130
digital precision type, using 3 ICs *(French)* 79−80616
digital quartz crystal thermometer principle and technical parameters *(Polish)* 78−24791
digital quartz thermometer *(Russian)* 79−49229
digital readout, using LED display 77−37884
digital temp. meas. instrument with automatic error compensation of thermoelectric thermometer 79−75526
digital thermometer, linear, 0 to 99.9°C range *(German)* 78−93684
digital thermometer sensor nonlinearity correction *(Russian)* 79−26054
digital thermometer with seven-segment display 79−21746
digital time pulse thermometer, technical description and error anal. *(Russian)* 79−49228
digital type 2572, with temp. range 4K to 1760°C with 0.1°C resolution 78−65929
digital type AD2038, features 79−58684
diode, varicap, sensor, differential meter and stabiliser appl. *(Czech)* 78−29115
double grafted, operation *(Japanese)* 79−35746
education, elec. noise and Boltzmann's const. determ., absolute temp. scale noise thermometer 78−36767
electrical, expanding temp. ranges 78−65927
electrical thermometers, functional fault detect. using electronic devices, report *(German)* 78−81972
electronic, dual, relative humidity meas. appl. 78−65925
electronic, for 0 to 100°C, with transistor sensor *(German)* 79−6122
electronic, for telemetric link, with direct reading *(Spanish)* 78−16793
electronic, two-digit, LED, 0 to 99°F, remote monitoring outdoor temp. appl. 78−16794
electronic, with direct linear indication, 0-100°C range *(German)* 78−29111
electronic, with K° output, using AD 590 IC transducer 79−80615
electronic device, using a thermistor in a current bridge for clinical use 78−29109
electronic digital, for long-term patient monitoring 80−90849
electronic dual range thermometer 79−2769
electronic medical thermometer with digital display 79−25129
electronic sensors for clinical replacement of metethmor 78−7473
electronic thermistor-type thermometer *(German)* 79−35740
electronic thermometer circuit 79−54131
electronic thermometer with adjustable alarm setting *(French)* 79−63209
environmental type using ICs and a Si transistor 79−67300
ferroelectric thermometer *(Polish)* 80−31750
fluorescent decay thermometer with biological applications, using ruby sample 80−86306
furnace temp. meas., dipping depth effect of thermoelements on accuracy *(Polish)* 77−53910
gamma-ray thermometer and strain gauge for remote meas. 78−12694
gas, reference standard, 273.15 to 1337.58K range 80−77782
in Glaisher stand and Stevenson screen, max. summer temp. recording 77−81976
glass, IR thermometry, readings interpretation 80−82765
glass-ceramic capacitance thermometers, low temp., accuracy and stability 77−61074
grafted, for psychrometer *(Japanese)* 80−31771
graphite thin film low-temp. thermometer 77−49734
industrial IR thermometry using fibre-optic lightguides 80−86302
insulated plate thermometer, incompressible boundary layer flow 78−55626
internal contraction engine, highly loaded, exhaust gases temp. and velocity meas. using two thermometer method *(German)* 80−31754
ionic crystal, possible high-temp. thermometer using elec. cond. changes 80−52203
IR, calibration and standards 79−85141
IR, digital thermometer improvement *(Japanese)* 78−41306
IR battery operated portable thermometer *(German)* 80−57289
IR thermometer and pyrometer calibration methods and standards 79−88958
JFT-2 Tokamak, radiation loss meas. using thin-film thermometer 80−47698
Johnson noise power thermometer calibration using high-level noise source 78−82005
Josephson-effect absolute noise thermometer, resolution of unmodelled errors 78−62196
linear, using 5V reference power supply *(French)* 79−197
liquid crystal display, portable *(German)* 78−29112
low temp. meas., from 13.8K, calibration 77−26296
low temp. meas. in high magnetic field 77−30171
low temperature, cryostat for calibration *(German)* 77−37897
low temperature C-impregnated glass thermometer *(Chinese)* 79−30479
low temperature meas. using noise and nuclear orientation thermometers, comparison, 0.011-0.05K 79−63218
low-temp., magnetic-field-induced temp. error 79−80618
low-temp., reference points based on H_2 and He 78−206
low-temperature gas thermometer, parameter calc. allowing for actual state of He 80−105641
low-temperature thermometer characteristics in strong mag. fields 78−37005
LSI ADC used for digital thermometer 79−44907
magnetic, depend. of AC mag. susceptibility on magnitude of meas. field 80−241
magnetic, for 2K to 30K range 77−5850
magnetic, with La diluted $Ce_2Mg_3(NO_3)_{12}.24H_2O$, to below 1 mK 79−30469
medical temperature measurement, electrical *(Hungarian)* 80−30910
metal objects, moving, temperature meas. by thermoelectrical thermometer *(Russian)* 80−90848
microprobes, non-perturbing, based on cholesteric crystals 78−16791
monolithic transducer, LX 5700 A, for −100 to +150 degree C temps., operation *(French)* 77−67431
Motorola MTS 102 transistor temperature transducer, using LM10 IC op amp *(French)* 80−86298
multichannel electric thermometer, 0-100°C, using transistor sensors 79−35741
neodymium ethyl sulphate enneahydrate, mag. susceptibility, 2-27K, appl. as mag. thermometer 79−63224
noise thermometry, theory and temp. determ. *(German)* 79−21748
noise thermometry, using conventional electronics 79−21751
noise thermometry, using Josephson junctions 79−21752
non-contact thermometer based on infrared detector *(Polish)* 80−90845
nonperturbing dielectric microthermometer probes 78−11743
NQR, appl. of spin generator 77−10077
NQR, capture effect 77−10018
NQR, full automatic precision thermometer with 77 to 374K range 77−17979
NQR high-precision 77−10017
NQR impulse thermometer 77−37887
NQR system, pulsed, for temp. meas. and regulation 77−10020
NQR thermometer, calibration in 203-398K range 80−42222
NQR thermometer, pulsed for temps. up to 870K 77−13749
NQR thermometer circuit 77−10019
nuclear magnetic thermometry using SQUID magnetometer 77−26292
nuclear susceptibility thermometry using enriched ^{119}Sn 80−4710
optical meas. of semicond. temps. *(French)* 79−35743
p-n junction, with single quad op amp 77−45839
photoluminescent thermometer probes, temp. meas. in microwave fields 80−104721
psychrometer coeff. of wet bulb thermometers used in Met. Office large thermometer screen 77−70879
quartz, with FET oscillator, −40 to 100°C range 78−77906
quartz, with FET oscillator 78−81967
quartz crystal thermometer with 10^{-4}°C resolution *(Polish)* 79−40562
radiation thermometer with fibre-glass bundle, up to 1000°C *(German)* 79−35745
recording temp. monitor using thermistor sensor 78−209
resistive SQUID thermometer, theory 79−21753
resonant US thermometer for nuclear reactor appls. 78−57948
semiconductor diode sensor, for use in varying ambient conditions 80−73361
semiconductor instruments, providing six point temp. meas. *(French)* 80−68200
semiconductor temperature detectors, fundamental aspects and appls. *(German)* 79−21747
solid thermal cond. and interface resistance meas. by radiation thermometry 80−86289
sonic anemometer-thermometer, phase-locked loop CW system 80−41565
state of art and research appl. 80−31743
superconducting thermometer, low temp. stabilisation appls. *(German)* 78−86250
superconducting thermometer sensitivity, temp. and field depend. 80−4708
superconductive thermometer referenced by superconducting to normal transition point *(Japanese)* 80−77785
surface contact thermometers, dynamic behaviour *(German)* 80−90843
surface temp. meas., compensated static and dynamic methods *(Polish)* 77−74401
surface temp. meas. using contact thermometer, field meas. by liquid crystals *(German)* 79−58686
teaching apparatus using ballpoint pen case 77−49540
technical thermometer metrological characteristics, normalisation 78−77908
temp. meas. by thermal noise, appl. *(German)* 78−4615
temperature probe, −10 to 100°C range 79−6125
temperature sensors, Japanese and international standards 78−65928
temperature transducers, semiconductor diodes, variation of forward voltage with temp. 80−57293
temperature/frequency wide range convertor, expt. and cct. 77−17978
thermal noise thermometer with supercond. quantum magnetometer *(Czech)* 80−220
thermistor thermometer bridge network charact. linearisation *(German)* 78−86271
thermocouple, drift evaluation problem 77−53905
thermocouple, thermometers, voltage generation, calibration 80−57295
thermocouples used with CMOS analogue and digital devices 77−33986
thermoelectric, automatic compensation of thermal EMF of free ends 79−6123
thermoelectric, automatic testing, structural method for improving precision 79−35744
thermoelectric, cold junction thermo-EMF compensation parameter optimisation *(Russian)* 78−86270
thermoelectric, Pt-Rh, 1300 to 1700°C, errors obs. and analysis 80−77783
thermoelectric, semiautomatic checking unit with programmed control 77−22548
thermoelectric, stability of readings 78−93682
thermoelectric transistor thermometer *(Japanese)* 78−45625
thermographic camera, calibration, transmittance and emittance meas. 78−45628
thermometric AC bridge for temp. meas., 13.81-273.15K range *(Polish)* 78−93683
thin film, efficiency in meas. radiant flux density of pulsed lasers 77−38967
thin-film thermometer for meas. of transient plasma heat fluxes in divertor assembly 78−18447
time response calibration, concepts and model calcs. 78−54370
transistorised, with remote indication, up to 150°C *(German)* 80−73356
tympanic contactless membrane thermometer 79−34692
US temp. profiling system for critical heat flux meas. of nuclear reactor fuel assembly 80−37032
US thermometers, nuclear fuel temp. profile meas., TRESON expts. 78−57955
wet bulb, theory and comparison with expt. results *(Dutch)* 77−65039

thermometers continued
Al-Pb:Bi, tunnel-junction relax. oscillator, appl. to thermometry 79−85138
Au-Ho nuclear orientation thermometer for use from 1-30 mK 79−17419
C film resistor, high sensitivity temp. sensor, 1-10K 77−13757
CH_4, triple point, International Practical Temp. Scale, comparisons 79−40566
$(Ce_xLa_{1-x})_2Mg_3(NO_3)_{12}.24H_2O$, mag. susceptibility meas., AC method meas., appl. as thermometer in mK region 77−17999
$Ce_xLa_{2-x}Mg_3(NO_3)_{12}.24H_2O$, magnetically diluted thermometer 79−17420
$Ce_2Mg_3(NO_3)_{12}$ thermometry, for sp. ht. meas. below 10 mK 79−88955
Cu, nuclear susceptibility thermometer rel. to ^{199}Sn Mossbauer effect thermometer, 6 mk to 1K 79−35737
Cu-constantan cryogenic thermometer and temp. controller *(Czech)* 79−26056
$Gd(PO_3)_3$, mag. susceptibility, 2-27K, appl. as mag. thermometer 79−63224
Ge, doped thermometer for submillimetre wavelength composite bolometer 78−65964
He gas thermometer, small, const. vol., sensitivity and linearity at low temps. 79−63223
^3He gas thermometer secondary standard for 0.5 to 40K 80−82762
Hg-contact, contactless temp. meas., appl. *(Russian)* 77−65033
Hg-in-glass thermostat 80−22359
KCl:OH, mag. field-independent capacitance thermometers 78−4623
$KClO_3$, ^{35}Cl NQR appl. in thermometry below 77K 80−66067
$NaClO_3$, ^{35}Cl NQR appl. in thermometry below 77K 80−66067
NaF:OH, mag. field-independent capacitance thermometers 78−4623
Nb wire, Cu-clad, temp. sensor below 1K using proximity effect 79−85139
OH $A^2\Sigma^+$ state, laser excited, vibr. energy transfer, flame thermometry appls. 80−58349
Pt wire NMR thermometer for ultralow temp. down to 0.55 mK 78−89478
Si, commercial diodes, wide range temp. sensor, mag. field depend. 78−45623
Si diode, anomalous behaviour, 11 to 16K 79−35738
Si diode, thermometric characts., 15 to 300K 78−8403
Si diode thermometer, features, appl. *(Croatian)* 78−89479
Si switching diode, thermometric props. 77−37889
Si, temperature-resistance relations *(German)* 77−37897
Si transistor type, precision, −50 to +125 deg. C at ±0.1 deg. C 78−21134
n-Si:P, etched, high sensitivity temperature sensor, 1-10K 77−13757
^{117}Sn, ^{119}Sn, low temp. NMR thermometry 80−82775
^{199}Sn, Mossbauer effect thermometer, rel. to Cu nuclear susceptibility thermometer, 6 mk to 1K 79−35737

thermometric conductivity *see thermal diffusivity*

thermonuclear devices *see plasma devices*

thermonuclear reactions *see nuclear reactions and scattering*

thermopiles
contactless temperature measurement unit for moving surfaces 78−4616
fast-response thermoelectric radiation detector, construction and sensitivity 77−22597
film, thermoelectric characts. of combined branches of Bi and Sb 79−35826
IR detectors appl. 80−47104
low-temperature, diffusion process kinetics, $(Bi, Sb)_2 Te_3$-Co contact obs. 79−21739
multiple thermoelectric junctions, thin conducting sheet, near heat fluxmeter *(French)* 80−86286
multistage thermoelectric battery, extremal sequence of temps. and efficiency 77−17977
optical power meters for laser photometry 78−65953
pyranometer, accelerated response tests 77−10110
radioisotope thermoelectric generator, selenide technology evaluation at JPL, for Galileo (NASA) spaceflight mission 79−48147
radiometer for Earth radiation meas., fused silica filter performance 80−87473
radiometer/photometer appl., commercial devices survey and classification 78−16830
relative spectral detector response meas., 350 to 1200 nm using monochromator based spectral comparator 79−67374
selenide thermoelectric materials, thermal conductivity, long-term stability and other props. experimental anal. 80−107834
solar furnace type thermoelectric generator, high power density, with wedge-shaped electrodes 79−48100
solar thermoelectric generators, near-Sun missions appl. 79−48143
spectral response and sensitivity, comparison with other detectors 79−35832
temperature variation generation, harmonic, analytic method 78−79193
thin film, for elec. calibrated radiometer 79−6176
type RTN (USSR), construction and characts. 80−57372
Bi-Sb film for radiation pyrometry 78−214

thermoreflectance
alkali halides, thermoreflect. spectrum, 5 to 9 eV, electronic struct. 77−81123
anthracene, O-O exciton absorption bands, thermomodulation study 78−39563
group V transition metal dichalcogenides, layered, visible an IR spectra 77−52120
high-resolution spectroscopy in far UV 77−66484
metal, light refl., nonlinear thermo-optic effect at high intensity 80−93289
polydiacetylene, reflection spectra, thermochromism, temp. hysteresis and phase transformation 78−19452
semiconductors, modulation spectroscopy in far UV 77−66516
transition metal dichalcogenides, modulation spectroscopy obs. 78−80377
Ag, thermomodulation spectra of high-energy interband transitions 80−108226
Ag, thermorefl. spectrum at room temp. 77−8601
α-Ag-Cd, dil., electronic struct. determ. from thermoreflectance and XPS 78−39011
Ag-Cd dilute α-phase alloys, optical gaps, thermoreflectance meas. 77−66520
Au, high-resolution spectroscopy in far UV 77−66484
Au thermal modulation reflectance spectrum, temp.-dependent shift 77−81121
thermoreflectance continued
Au, thermomodulation spectra of high-energy interband transitions 80−108226
Cd_3As_2, thermoreflectance spectra 78−6702
$CdCr_2S_4$, thermoreflectance near Curie point 79−78659
$CdCr_2S_4(Se_4)$, thermoreflectance, photoconductance, Raman scatt. near mag. phase transition 80−97298
$CdGa_2Se_4$, thermoreflectance and visible absorpt. spectra, energy gap, cryst. field splitting 80−34945
$CdIn_3Se_4$, cryst. growth, photoresponse and optical props. 78−39165
CdS, $A_{n=1}$-exciton, reflectance and thermoreflectance spectra, spatial dispersion and angle of incidence effects 80−25409
CdS, thermoreflectance spectra, additional boundary conditions in terms of optical constants 79−15478
$CdSiP_2$, thermoreflectance spectra 77−81122
Co, HCP, low energy interband absorption, electronic struct. exam. 79−73930
$CrBr_3$, reflectance and thermoreflectance meas. 77−24866
$CrBr_3$, reflectance and thermoreflectance spectra in paramag. and ferromag. phases 79−56770
$CrCl_3$, reflectance and thermoreflectance meas. 77−24866
CsI(Br)(Cl), electronic struct. anal. by reflectance and thermoreflectance studies 79−69855
Cu, thermomodulation spectra of high-energy interband transitions 80−108226
CuBr(I), reflectance and thermoreflectance spectra, electronic struct. 80−71444
CuI, thermoreflectance spectrum, 4-7 eV region 79−19904
Dy, film, thermoreflectance dispersion curves at 315K and 97K 80−7332
EuO(S), ferromagnetic electronic structure, absorption, thermoreflection and thermotransmission spectra *(French)* 80−97300
EuO(S)(Se)(Te), phase transition spectroscopy 77−63426
EuS films, thermoreflectance spectra below Curie temp. 77−66550
EuS, thermo- and magnetorefl. spectra, dynamical spin fluctuation effect on exciton state 77−52126
EuSe(Te), magnetic phase transitions, thermal modulation spectroscopy study *(French)* 80−97301
Fe, BCC, low energy interband absorption, electronic struct. exam. 79−73930
Ga, optical properties in 0.3 to 5 eV range 78−31196
Ga, thermoreflectance, in near IR, down to 0.3 eV 77−85722
GaTe layer semiconductor, UV-visible wavelength derivative and thermorefl. spectra 78−6666
Gd, film, thermoreflectance dispersion curves at 315K and 97K 80−7332
Gd, thermoreflectance meas. 79−69816
p-GeTe, reflectance, and thermorefl. spectra 80−80814
$Hg_{0.75}Cd_{0.25}Te$, thermorefl. spectra, effect of excitons on E_1 and $E_1+\Delta_1$ structs. 80−16057
$HgCr_2Se_4$, thermorefl. near ferro- to paramagnetic transition 79−78660
$HgCr_2Se_4$, thermoreflectance, photoconductance, Raman scatt. near mag. phase transition 80−97298
LuH_2, electronic struct., optical studies, 0.2-5 eV, 4.2-340K 79−78005
Mo, thermoreflectance spectra, 0.3 to 6 eV, rel. to band struct. calcs. 77−66521
NH_4Br, thermorefl. spectra, band energy anal. 77−12402
NH_4Cl, thermorefl. spectra, band energy anal. 77−12402
NH_4I, thermorefl. spectra, band energy anal. 77−12402
Nb, electronic struct. 80−76047
Nb, optical spectroscopy, for investigation of electronic struct. 78−91611
Nb-Mo, electronic struct., thermoreflectance meas. 0.5-5.0 eV 80−45050
$Nb_3(AlSi)$ film, thermomodulation spectra, 1.1-2.8 eV 78−48250
β′-NiAl, electronic struct. and optical props. 80−97228
$NiBr_2$, thermoreflectance meas. 77−24866
$NiCl_2$, thermoreflectance meas. 77−24866
$Pb_xSn_{1-x}Te$, RF-sputtered epitaxial single-cryst. films, thermorefl. spectra 77−63476
p-PbTe, thermorefl., 1.0-4-6 eV 78−76492
Pd, thermomodulation spectra of high-energy interband transitions 80−108226
$PdH_{0.65}$ film, thermoreflectance spectra 78−56463
Pt, thermomodulation spectra of high-energy interband transitions 80−108226
Rb halides, high-resolution spectroscopy in far UV 77−66484
α-$RuCl_3$, reflectivity and absorpt. spectra, thermo-reflectance 79−47438
SbSI, energy band struct. from modulation spectra 78−43892
ScH_2, electronic struct., optical studies, 0.2-5 eV, 4.2-340K 79−78005
Si, electro- and thermo-reflectance spectra, line-shape anal. 79−24296
Si, thermoreflectance near $L_{2,3}$ soft X-ray threshold, temp. depend. 78−35224
Si:H, amorphous, refr. index, temp. depend., implications for thermoreflectance and electroreflectance 80−50290
SmS, metallic, thermal modulation of reflectivity, 1.2-3.8 eV 79−99909
Sn film, thermoreflectance meas. 77−28640
$SnSe_2$, Bridgman grown cryst., transition energies 77−90168
Ta, and α-TaH_x, electronic struct. 80−76047
Ta, optical spectroscopy, for investigation of electronic struct. 78−91611
TaS, (1T), effect of CDW on optical spectra 79−95738
$TaSe_2$ 2H, CDW effect on thermoreflectance spectra 77−52120
$TaSe_2$, 2H phase, CDW band struct. and IR and visible thermoreflectance meas. 77−28556
$TaSe_2$ (2H), effect of CDW on optical spectra 79−95738
$TaSe_2$ (2H), optical absorpt., band struct., plasmons, and CDW 80−45104
$TaSe_2$(2H), plasmon behaviour at charge density wave onset 80−10900
Tb, film, thermoreflectance dispersion curves at 315K and 97K 80−7332
Ti_2O_3, electronic structure from single crystal thermoreflectance spectroscopy 79−87420
$TiSe_2$ (1T), effect of CDW on optical spectra 79−95738
V, electronic struct. 80−76047
V_2O_3, metallic differential refl. spectra and band struct. 77−1699
W, thermoreflectance spectra, 0.3 to 6 eV, rel. to band struct. calcs. 77−66521
YH_2, electronic struct., optical studies, 0.2-5 eV, 4.2-340K 79−78005
YIG, pure and Ga-substituted diffuse refl. and thermorefl. spectra near Curie point 80−40131
YIG, thermoreflectance spectra 80−20616
ZnTe, free exciton refl., surface layer effects 78−76493
ZnTe, shape of reflectance and thermoreflectance spectra 79−11430
ZnTe, thermoreflectance spectra, at energies from absorption edges to 9 eV *(Japanese)* 79−11436
ZrS_3, thermomodulated reflectivity and transmission 80−50357

thermosphere
acoustic gravity waves, composition effects 77−21959
aeronomic parameters, rel. to nighttime F_2-layer height 79−8745
aeronomic parameters, selection for daytime F_2-layer simulation 78−45087
airglow diurnal var. and seasonal depend. rel. to solar semidiurnal tidal wind 77−21965
airglow in lower thermosphere, seasonal and long-term vars. and dynamics 77−33237
annual composition vars. from Aeros Nims data 80−12578
artificially-injected gases dispersal in night-time atm. 78−65460
auroral energy deposition and neutral comp. changes, simultaneous satellite obs. 77−53264
auroral energy input, effect on neutral and ion drifts 78−65446
auroral NO densities, horizontal winds effects 80−26656
auroral particle and Joule heating, global effects on undisturbed days 78−45069
auroral substorms, morphology of N and NO 79−48607
charge exchange of metastable ^{2}D O ions with N_2 78−20571
chemical processes 80−17431
circulation, seasonal and solar cycle variation 80−56661
circulation and comp., effects of magnetospheric elec. field and currents 80−17446
circulation systems, northern hemisphere, 80-100 km altitude 78−81481
composition, Esro 4 meas. rel. to upper atmosphere heating by solar wind energy 77−37471
composition, longitudinal vap. in geomagnetically quiet conditions 79−75001
composition, tidal vars. 78−96334
composition and temp., longitude/UT vap., global model 79−53591
composition changes during mag. storms, spherical asymm. 77−64501
composition changes inferred from twilight $O^+(^2P)$ airglow emission 79−62635
composition of middle atm., in situ meas. 80−17339
compositional modelling taking account of airglow tidal variation 80−109288
daytime neutral winds in lower thermosphere, trace constituents sounding rocket campaign results 78−45071
density, local time var., altitude depend. 78−61636
density, response to mag. storm, OGO 6 in situ meas. 77−9588
density, temp. and winds, review 79−75006
density correl. with charged particle precip. through magnetospheric cleft 77−87146
density enhancement and perturbations form. during geomag. storm, obs. in equatorial zone *(French)* 79−96846
density variations from AE-C accelerometer meas. 77−64500
diurnal and seasonal variations of O, H and N components 77−9586
diurnal tide excited by EUV and UV solar radiation absorpt. 77−53260
diurnal tide seasonal-latitudinal struct. 78−77377
diurnal variations in temp., comp. and winds 77−87141
diurnal winds, seasonal var. over Millstone Hill during solar cycle max. 77−53267
double photoionization and doubly charged ions 79−84559
dynamic model of lower thermosphere rel. to ALADDIN I program meas. 79−48592
dynamic processes from optical meas. of emissions 78−36342
dynamical processes in lower thermosphere, connections with processes in troposphere and stratosphere *(Russian)* 78−24401
dynamical properties 79−75005
dynamics, Fabry-Perot spectrometer obs. 80−12573
dynamics, incoherent scatt. radar technique appl. 79−8734
dynamics at high latits., magnetospheric convection effects 79−8733
dynamics calcs., Navier-Stokes eqns. validity 80−26659
dynamics of middle atmosphere, review 80−17338
eddy diffusion, models for mesosphere and lower thermosphere 80−109198
eddy diffusion coefficient, semi-theoretical global models based on satellite data 79−21086
eddy diffusion variations and assoc. transport processes 77−33226
electric field momentum coupling characts. 78−88958
electrodynamic and particle heating in disturbed polar regions 77−33231
electron density and ion comp. meas., X-ray and EUV solar flux estimation 77−87145
electron temperature and density relationship in daytime at solar minimum, model 78−61638
energy balance, importance of IR radiation 79−8729
energy transfer, estimate of O^+-O, reson. transfer charge cross-section 77−45231
equatorial, midnight temp. max. 79−84555
equatorial, neutral winds determ. from O I 6300 Å nightglow Doppler shifts 78−81473
W.Europe, atmos. temp. 20-110 km altitude, 1975/6 winter anomaly 80−36356
W.Europe, ion production obs., 50-120 km altitude, 1975/6 winter anomaly 80−36439
W.Europe, mesosphere and lower thermosphere temp. and density, 1975/6 winter anomaly 80−36357
W.Europe, mesosphere and lower thermosphere trace constituents, 1975/6 winter anomaly 80−36433
W.Europe, neutral atmosphere composition 1975/6 winter anomaly 80−36432
exosphere-thermosphere transition layer, structure, temps., H escape 79−66845
exosphere-thermosphere transition region, reduced H temp. 77−33225
F-region response to storm of June 1972, thermosphere-ionosphere coupling 80−41617
F-region thermosphere wind, southward midnight surge obs. by Chatanika radar 77−33233
field-aligned currents meas. by Spacelab incoherent scatter radar 77−21946
geomagnetic storm effects, OGO 6 obs. *(Japanese)* 78−85754
global comp. and temp. empirical models during quiet times compared with ESRO 4 data 79−8732
global composition and temp. during quiet times 77−33227
global model based on mass spectrometer and incoherent scatt. data, N_2 density and temp. 77−70897
global model based on mass spectrometer and incoherent scatt. data, composition 77−70898
global semiempirical models 79−66852
gravity wave activity effects on photochem. and comp. 80−41583

thermosphere continued
gravity wave assoc. with sudden commencement, ionospheric effects 78−57385
gravity wave ducting 78−77378
gravity wave generation, propag. and dissipation 79−2405
gravity wave propag. in diffusively separated atmosphere 80−12580
gravity waves, energy production and dissipation 79−74997
gravity waves, medium scale, generated by jet stream, vertical energy flux into thermosphere 78−81479
gravity waves, medium scale, sources in meteorological jet stream, exptl.-study 79−21088
gravity waves, minor species relative phase and amplitude response 79−58140
gravity waves, short periodic, propag. theory, plasma line meas. and Faraday rot. expt. appl. 78−49185
gravity waves, source in tropospheric jet stream *(French)* 78−69554
gravity waves, spectra propag. in thermosphere 79−66848
gravity waves and thermospheric winds *(French)* 77−53256
gravity waves correl. with tropospheric lightning 79−84557
gravity waves in lower thermosphere, detect. by French incoherent scatter facility 78−81478
gravity waves in lower thermosphere over S. Australia 78−36348
gravity waves propagation, dissipation and diffusion effects 77−13141
heating by solar UV, efficiency at mid-latitude 80−85780
heating during magnetic storm, dynamic energy transport from high to low latits. 80−26657
heating of lower thermosphere by acoustic waves dissipation 77−53266
heating rate parameterization, 15-120 km altitude, due to O_2 and O_3 absorpt. of solar radiation 79−39798
incoherent scatter meas. of thermospheric props. 79−53597
incoherent scatter radar studies of daytime middle thermosphere 80−72654
internal gravity waves, at mid-latits. in mesosphere and lower thermosphere 77−5298
internal gravity waves, rel. to tropospheric 77−91339
internal gravity waves thermal effects 77−25806
ion photochemistry, from Atmosphere Explorer C meas. 78−32261
ion-drag effects 80−17432
ionic reactions rate coeffs., AE satellite meas. 79−48594
ionisation caused by variable solar UV flux, 1974-9 obs. 80−17430
ionosphere sublayer origin in lower thermosphere 80−61956
Joule dissipation of elec. currents during equatorial spread-F events 78−45127
lower, data and models 79−84553
lower thermosphere, investigation by reflected natural infrasound obs. 79−21089
lower thermosphere gravity wave obs., 5-90 minute period 80−61930
Lyman-α absorber in winter, satellite occultation meas. 78−36349
macroturbulent scales estimation around 100 km altitude 78−61635
magnetic storm response, two-satellite study 77−9582
magnetic storms, thermosphere disturbances rel. to positive ionospheric storms worldwide distrib. 79−44290
mass density and seasonal-latitudinal tidal struct. of O and N_2 80−101467
meridional circulation and temp. latit. var. calc. for solstice conditions 77−56783
meridional wind and O depletion at high latitudes 78−28353
meridional wind divergences at midlatitudes 79−70901
meteor region, winter motions meas. in S. hemisphere 80−109287
middle atmosphere, obs. from balloons, rockets and satellites, conference, London, England, (1978 December 12 to 13) 80−77540
midlatitude F-region winds and temps. during 1976 March 26 magnetic storm 79−53594
midlatitude models seasonal vars. at solar max. and low geomag. activity 78−57376
midlatitude winds, simultaneous meas. at 105°W and 70°W longit. 79−16727
midlatitude winds rel. to storm time disturbance change rate 79−12323
minor constituents concentration profiles, Spacelab obs. 77−21967
minor neutral constituents, vars. due to solar EUV flux changes, calcs. 79−44293
model based on satellite drag data 78−69555
movements and electric currents in lower thermosphere, symposium, Seattle, Washington, 1977 August to September 80−62371
N densities at high altitudes 79−16729
neutral and ion winds in polar region 77−45209
neutral composition, meas. between 90 and 220 km by rocket-born mass spectrometer 78−77383
neutral composition intercomparison of satellite obs. 77−53261
neutral composition perturbations, momentum source signatures 78−77380
neutral composition vars. during 1974 Feb. mag. storm 77−87142
neutral gas temperature, in-situ meas. by Atmosphere Explorer 80−12576
neutral temperature and winds, geomag. disturbances effects 80−26658
neutral waves, direct meas. 77−9581
neutral wind, midlatitude meas. during ALADDIN programme 80−31153
neutral winds, tidal modes rel. to low latit. dynamo currents seasonal vars. 80−8479
neutral winds deduced above Millstone Hill, mathematical model, uncertainties and results 79−39995
neutral winds deduced above Millstone Hill, seasonal vars., (1970 to 1971) 79−39996
neutral winds in F-region, from ionosonde meas. of hmF2 at low latit. mag. conjugate regions 78−81477
nightglow, lower thermosphere emissions vars. rel. to thermal tides 77−78550
nightglow near IR continuum, implications for thermospheric physics 77−78551
nighttime, energy balance 79−35022
nighttime neutral conc. vars. meas., expt. method 77−45200
nighttime thermospheric winds at high latitudes 79−74999
nighttime winds and temps., monthly vars. during solar min. 78−32263
nighttime winds from Atmosphere Explorer C 78−28354
photoelectron daytime energy distrib. meas. by AE-E satellite 78−88953
photoelectron energy spectra, rocket borne meas. 78−77379
plate reduction study of stellar photographs rel. to thermospheric release expt. *(French)* 77−17330
polar airglow, mag. ordering obs. 78−57378
polar neutral temp. during solar cycle 79−53595

thermosphere continued
polar thermosphere, pressure gradients rel. to F-region drifts and winds 77−33274
predawn 630 nm airglow and conjugate photoelectrons, direct meas. 78−49196
quiet thermosphere dynamics, review 80−21866
radiative cooling, IR emission from NO 80−72656
radiative transfer in Doppler broadening atmospheres, stratosphere, mesosphere and thermosphere 77−78418
resonance radiation transport with varying Doppler width, thermosphere appl. 80−26737
response to 1969 November 8-9 magnetic disturbances 80−12574
responses during August 1972 mag. storms, review 77−25858
satellite observations of middle atmosphere processes 80−21803
seasonal and latitudinal variations in temp. and composition 77−45207
semi-annual temperature variations, rel. to atmospheric circulation and mesospheric clouds 78−45061
semiannual variations of n(O), 120-500 km heights 77−49214
solar radiation absorption change and wave generation by terminator 78−49191
solar X-rays, lower thermosphere attenuation meas. by rocket-borne proportional counters 78−45072
sonic boom propagation 80−33305
sonic booms from Concorde aircraft flight, atm. struct. information 79−66742
spectral absorption, Lyman-α extinction by O_2 80−77180
spectrally integrated transmittance in O_2 Schumann-Runge bands and O_2 column density, 76-102 km altitude 79−70902
storms, comp. and temp. meas., related ionosphere effects 77−9583
structure, composition, temperature and motion, general review 79−39997
structure and dynamics rel. to tides and diffusion waves 79−35026
structure and thermal regime, average daily closed model 77−17264
temperature, comparison of measured and inferred values from AEROS-B 77−21958
temperature, density, and comp. in disturbed thermosphere, global model from Esro 4 meas. 77−37468
temperature, density and comp., new models 77−64502
temperature, diurnal and semidiurnal components, solar cycle variability 79−75002
temperature, from incoherent scatt. radar and satellite meas. 77−33224
temperature, turbulence and N_2 composition, 95-150 km altitude, 1967-75 obs. 80−51588
temperature and composition, empirical model 80−77183
temperature and ion chemistry at nighttime, 400-450 km altitude, Ogo 6 data 80−90267
temperature and wind measurement Fabry-Perot-interferometer imaging system appl. 80−101441
temperature depend. of O I 6300 Å emission in twilight airglow 77−45215
temperature from O I 5577 Å nightglow line profiles, long-term vars. 77−9584
temperature-depend. model of odd N species 78−16226
temperatures, wind vels. and emission intensities from O I 630 nm airglow 79−58144
temperatures and winds from O I 630 nm line profiles in nightglow 79−58143
temperatures over Malvern, incoherent scatter data comparison with two global thermospheric models 80−8467
thermodynamic balance at middle latitudes *(French)* 78−12029
thermosphere wind causing ionosphere disturbance dynamo 80−82134
thin shear turbulent layers, induced by tides and gravity waves non-linear interaction 78−65444
tidal and planetary wave propag. 77−87147
tidal dynamics model with O-N_2 diffusion effects 80−101465
tidal var. in total mass density from AE-E Mesa expt. 79−53593
tidal winds in 100-200 km altitude region, Arecibo obs. 77−82074
tides, differential operator and integro-differential eqn. *(Chinese)* 80−56660
tides, simultaneous incoherent scatt. obs. 77−87135
tides and midnight temp. anomaly 79−84556
tides and planetary waves in lower thermosphere *(French)* 77−21962
tides in equatorial region, semidiurnal and terdiurnal 80−82119
tides in joint presence of friction and rot., f-plane approximation 79−66847
transport processes in diurnal tide, satellite meas. 78−88959
travelling neutral disturbances and minor constituent particle mass 78−49189
turbulence effects 79−88610
turbulent diffusion coefficient in mesosphere and lower thermosphere, seasonal vars. 79−53424
turbulent motions caused by temp. fluctuations, critical review of Boussinesq approx. *(German)* 77−45206
turbulent structure, spectral range *(Chinese)* 80−105092
UV spectrophotometric obs. from Spacelab 77−21964
vertical winds and turbulence from Ba cloud release over Thumba 78−49188
wave motions and daily neon winds, 52-110 km altitude, at midlatits. 79−5565
wave-induced diffusion effects on acoustic-gravity waves 78−61637
waves, large-scale, obs. during mag. storms 79−35021
waves, review 77−45211
waves generation in summer lower thermosphere, rel. to ionospheric absorpt. travelling disturbances 79−25392
waves rel. to dynamics of mesosphere and lower thermosphere 79−53464
wind, mass spectrometric meas. 78−28359
wind as cause of ionospheric disturbance dynamo 80−82134
wind enhanced thermal escape, collisional modifications 77−49204
wind flow directions from ionosphere nighttime total electron content meas. 77−25829
wind influences on F-region TIDs 80−109305
wind measurement at 60-120 km, radiowave drifts technique 80−31137
wind regime of lower thermosphere, rel. to stratospheric and mesospheric processes 78−4019
wind vel. meas. by using artificial luminous clouds, polar regions, disturbed and quiet times 79−62634
winds, excitation of transverse motions of ionospheric atomic and mol. ions 77−13155
winds, ionospheric model effects on thermospheric calcs. 78−36345
winds and temperatures, determ. from ionospheric obs. using numerical simulation 77−53268
thermosphere continued
winds and temps., nighttime meas. during mag. storms 77−9585
winds in mid-latit. lower thermosphere, meas. 79−53587
winds in mid-latitude lower thermosphere, meas. *(Russian)* 78−36340
winds in N.Polar Cap thermosphere 80−67445
zonal mean circulation, seasonal and solar cycle vars. 78−32262
zonal wind in F-region during Joule heating, computed bounds 79−21084
zonal winds in F-region, estimation during Joule heating using incoherent scatter techniques 78−36344
0 I, 63 μm emission as cooling mechanism in thermosphere and ionosphere 79−16732
Ar, global distrib., departures from hydrostatic equilib. 78−28358
CO_2, concs. in lower thermosphere 78−96336
H distribution, UV dayglow obs. 80−109290
He distrib., dynamical model 77−70896
He^+, Atmosphere Explorer-C abundances rel. to solar EUV flux 79−16919
N and NO conc. depend. on solar activity 80−77178
N and NO density in polar regions under auroral perturbs. 77−73897
N density, global empirical model 77−33232
N, in equatorial thermosphere, seasonal and diurnal variation 80−85782
N in upper thermosphere, impact of gas-surface reactions on mass spectrometric meas. 79−66849
N, NO concentrations, diurnal variability 77−78549
N number density meas., 180-450 km altitude 77−87143
N^+ photochemistry 79−96847
N^+ sources and sinks 79−96848
N_2 anharmonic molecules, vibr. relaxation and NO conc. in disturbed thermosphere 79−12322
N_2, rot. temp. meas., rocketborne electron beam fluoresc. meas., reflected mol. effects 77−29519
NO abundance meas. in equatorial region 77−78547
NO daytime conc. 79−2408
NO density, high-altitude rocket meas. 78−45068
NO, high-latit. airglow obs. in lower thermosphere 77−37467
NO in lower thermosphere, joint meas. by rocket borne UV photometer and mass spectrometer 78−40723
NO, latitudinal gradient 79−100991
NO, ultraviolet spectral absorpt. in lower thermosphere and density profile 80−85781
NO^+, daytime chemistry from Atmosphere Explorer-C meas. 77−33230
Na^+ and Na layers, meteor ablation-cluster ion theory 79−58138
Ne density in situ meas. by Ae-C satellite 77−21956
O and O_2 densities, photochemical deviations from diffusive equilib. 77−37470
O and O_2 density meas. by mass spectrometer technique 78−57348
O and O_2 distrib. in lower thermosphere assuming tidal effects, one dimens. nonstationary diffusion-photochemical model 80−4160
O atom corona, of fast atoms during solar max., airglow obs. 80−101469
O conc. at 400 km altitude, incoherent scatter obs., model construction *(French)* 78−12030
O concentrations, rel. to low-latit. NmF2 annual and semiannual periodicities 77−53306
O content of lower thermosphere, 100-160 km, new spectral method 80−41578
O global distrib., dynamical effects 79−74996
O I 5577 A emission rel. to lower thermosphere interaction with stratosphere 77−70899
O I 5577 Å, Na and OH nightglow emissions var. during stratospheric warmings 77−53270
O I 5577 Å green line, nighttime var. of 2-15 min fluctuations 78−49193
O I 5577 Å nightglow obs., evidence for vertical transport latit. var. near mesopause 79−70903
O I 63 μm emission spectrometric meas. 78−81474
O I airglow emission rate, midlatitude maximum characts. obs. 79−84561
O I(^{3}P) in lower thermosphere, nighttime conc. obs., using new rocket borne instrument 80−105066
O, O_2 distribution in lower thermosphere 80−4159
O profile of mesosphere and lower thermosphere 80−72660
O remote sensing in mesosphere and lower thermosphere, two-photon lidar technique 79−39869
O^+ energetic ions precip. during mag. storms and magnetosphere-thermosphere coupling 80−26665
O^+ reactions with N_2, O_2, and NO, nonthermal rate coeffs. 78−57375
O^{++}, concentrations and photochemistry 77−45226
O_2 and O distrib., effect of magnetospheric elec. fields 79−66850
O_2, concs. and absorpt. cross sections from EUV occultation profiles 78−28356
O_2 density, 110-170 km altitude, using 1450 Å photometer 77−87144
O_2 density, calc. and meas. values comparison 78−28357
O_2 density, solar flux var. 80−72659
O_2 density indirect determ. from AE-C satellite meas. 78−12032
O_2 density seasonal vars. near 100 km altitude 78−12034
O_2 thermal and wind induced var., AE-D meas. 79−53592
O_3, 9.6 μm band radiance calc., excitation processes 78−36350
O_3 meas. during Aladdin 74 program above Wallops Island 78−57247
$O^+(^2D)$ metastable ions, charge exchange with O_2 in thermosphere 79−58141
$O^+(^2D)$, quenching by electrons 80−94630
$O^+(^2D)$ quenching by O, Atmospheric Explorer data 78−28355
$O(^1D)$ formed by $N(^2D)+O_2$ reaction in thermosphere, 6300 Å dayglow implications 80−90270
$O^+(^2D)+N_2$, charge exchange rate coefficient, effect of N_2^+ recomb. on aeronomic determ. 78−88954
OH emissive layer, waves, near IR photographic studies 80−51545
$OH(X^2\pi)$ nightglow emissions, theory and meas. in (9-3) band 78−88960
$O^+(^2P)$ ionisation freq. determ. using satellite airglow and neutral comp. data 77−5384
$O(^3P)$ translationally hot, energy distrib. function 80−21811
$O(^1S)$ production in lower thermosphere, comparison of Chapman and Barth mechanisms 77−33235
$O_2(b^1\Sigma_g^+)$ quenching by $O(^3P)$ and O_3, rate coeffs. 79−70309

thermostats
see also cryostats; temperature control; thermistors
accurate to 1500°C, for precision measuring equipment 79−49225

thermostats continued
air, for reaction-solution rotating-bomb calorimeter 80−4717
automatic, using Diapazon temperature variator, radiospectrometer appl. 80−47160
Boltzmann H-theorem for gases in thermostat *(Russian)* 77−17927
cells storage appl., standard, saturated 77−10058
coil for liquid streams, prep. by Ag electroplating 78−8402
contact thermostat, regulation characts. 79−185
cosmic ray photon emission power spectra described by solns. of Kompanyets' kinetic eqn. *(Russian)* 78−152
cryogenic temperatures, miniature sealed cells as temp. calibration device and precision thermostat 77−22559
crystal oven pilot-lamp stability controller 78−54374
device for measurement of static characteristics of resistance thermometers 80−77784
electrocaloric refrigeration, for 4 to 15K 79−80624
electrometer ferroelectric modulator temperature stabilisation 77−82550
electron thermostat, ion prod. stationary nonequilibrium distrib. *(Russian)* 80−64684
electronic, with 0.1°C accuracy and economical operation, photography appl. 80−77774
electronic noise meas. passive thermostat 77−2654
fast reacting, for meas. below 1K, design and testing 77−33994
fuel saving by thermostat setback, teaching expt. 78−24626
general-purpose time-proportioning regulator for reliable thermostat 79−21740
IC temp. controller 77−67432
laboratory thermostats, electronic device for precision temp. regulation 79−88931
millidegree thermostat for optical studies of phase transitions, student lab. apparatus 77−33805
phase transition liberated heat used in laboratory thermostat 78−195
photographic developing bath, thermostatic control *(Spanish)* 80−77898
precision, capacitor enclosure, maintaining the unit of capacitance 80−95063
precision, elec. resist. meas. appl. 77−57355
precision automatic, 2700K max., vacuum furnace temp. control appl. 79−6112
precision thermostat, with stability of ±3.5 μK 78−21132
programmable temp. controller for crystal growth expts. 77−24944
reference source radiation, temp. instability and compensation methods 79−14071
sensitivity, influence of specimen curvature *(German)* 80−27291
solar water heating system, electronic differential thermostat, for teachers 78−81753
stabilization circuit based on industrial instruments 77−74407
stabilizer for 77-340K range 77−74392
static interrupt cct., triac, TDA 1024 *(Italian)* 78−73984
steady thermostat for optical and elec. expts. *(Chinese)* 79−80608
synchronous overheating equipment for air and liquid constant temp. baths 77−53898
test equipment for thermometers, thermoelectric and resistance, laboratory 77−74400
thermistor thermostat for low-power semiconductor devices 79−71450
thermostatic air chamber, influence of radiation *(Japanese)* 78−37007
vital microscopy, electronic thermostatic system 80−85537
water circulation type precision thermostat bath 79−49221
water thermostat, linear thyristor control and thermistor sensing *(Japanese)* 77−90264
$As_{10}Ge_{15}Te_{75}$, thermal memory switch development 78−89468
Be, low temp. elec. and thermal cond. in mag. field, use as heat switch 77−35923
Hg-in-glass thermostat 80−22359
W incandescent lamp, thermostatic control 79−36970

theta pinch *see pinch effect*

thick film circuits
adhesion testing, use of fracture mechanics concepts 80−50802
conductors, adhesion meas. 80−50808
hybrid, 300°C operation, for geothermal well logging 77−73895
hybrid ICs, geothermal well logging instrumentation appls. for 300°C operation 78−3976
optical waveguide integration with fibre-optic connectors 80−33246
rheological control of pastes to determine their suitability for serigraphy *(French)* 77−11154
Au conductor bonding performance and failure mechanisms 79−71436
Pt-Au, adherence meas. and evaluation 80−50813
VO_2 metal-insulator transition appls. *(German)* 79−99587

thick film devices
hybrid fabrication of pH-sensitive implantable bioelectrode *(German)* 78−40369
planar input/output couplers for multimode optical fibres features 79−72703
reed-type routeing switch for multimode optical fibres 80−53463
strain gauges and pressure transducers 80−57285
thermometers, C film for low-temp. meas., manufacture and performance 77−37883
$BaTiO_3$, temperature sensor using thick film techniques 79−93137
Pt resistance thermometers, resistance/temp. relationship 78−37008
$SrTiO_3$, temperature sensor using thick film techniques 79−93137

thick film resistors
drift free trimming for pacemakers 78−31977
CaB_6-SmB_6 system complex borides, prep. and props. 78−52703
Pt film resistance temperature detection 78−49830

thick films
adhesion, to ceramic, destructive and nondestructive meas. 80−50809
adhesion measurement, conf. Philadelphia, USA (Nov. 1976) 80−46729
adhesion measurement 80−50817
cermet layers deposited by silk-screen printing, microscopic struct. obs., cond. matrix form. mechanism *(Czech)* 77−48386
composite transparent film layer thickness meas. by Fourier transform spectroscopy 77−10093
concentrator solar cells, thick film conductive ink contacts 80−93957
conduction mechanism rel. to phase struct. 77−11972
conference, thin and thick film technology, Augsburg, Germany (1977) *(German)* 78−39685
diffusion experiment, introduction of weights to least squares anal. 80−49399
glass bonded Pt-Au thick film conductor, adherence fracture energy, Al_2O_3 substrate effects 77−56075

thick films continued
resistivity, struct. effects, determ. using statistical model of chain-like struct. 77−76891
solar cell fabrication, photovoltaic process based on thick film technique 80−94016
solar cell manufacture, thick film technology applic. 80−93903
soldered thick-film conductor, adhesion meas. technique 80−50811
solid films and surfaces, conference, Tokyo, Japan (Jul. 78) 80−10739
terminations on chip components, adhesion meas. methods 80−50810
vibration absorbing coating, cut constraining layer effectiveness 79−32130
BeO black tarnish film, on Cu-Be alloy, Auger electron spectroscopy anal. 80−97624
$Be(OH)_2$ black tarnish film, on Cu-Be alloy, Auger electron spectroscopy anal. 80−97624
CdS, films, photovoltaic effect in wedge shaped film 79−56331
CdTe, prep. by sintering and elec. props. 80−29451
Nb thick layer vapour deposition by photoresist stripping 79−83135
$Pb_3Rh_7O_{15}$ thick film, temp. coeff. of resist., cond. mech. 78−84315
Pt-Au glass-bonded printed thick-film conductor, adherence fracture energy 77−9037
Si solar cells with screen printed diffusion and metallisation 80−94015
SnO_2, glaze, high field cond., 4.2-470K 78−23100
V_2O_5-P_2O_5 (70-30), electrical cond. and thermoelectric meas., Au-glass-Au sandwich 80−29403

thickness control
automated vapour deposition apparatus based on programmable calculator 78−44022
cold light production by high vacuum deposition of multilayer interference coatings *(German)* 80−53486
constant-thickness film formation on axially symmetrical substrate 79−27453
electroplated coatings thickness test standards 79−8405
electrothinning, laser-monitored, for preparing ultrathin metal foils 78−53074
ferromagnetic films, electrodeposition, thickness control, magnetisation meas. 78−23306
film, thickness uniformity on rot. spherical substrate on planar wave holder 79−65351
film monitor, using preloaded quartz crystals 78−11116
freeze etching and related techniques, resist. monitor for automatic film thickness regulation 78−49810
galvanising process, digital control system for Zn coating distrib. 78−19960
glass fibre thickness meas. and control system in production *(German)* 80−10052
LPE 78−88432
multidielectric film, optical control by method of static ratios *(French)* 77−69993
multilayer interference film, mass production by roll coating *(Japanese)* 79−81577
optical fibre fabrication techniques using MCVD and refr. index profile control 79−59856
optical fibre substrate tube diameter-control system, for use during MCVD preform preparation 79−50463
optical fibres, control of diameter during drawing process 79−50468
optical film, optical thickness monitoring 78−5591
optical film, optical thickness monitoring using quartz cryst. monitor 78−5592
optical monitoring of nonquarterwave multilayer filter thickness 78−55476
optical thin film coating manufacture, automated deposition control system, design principles 80−64220
Schottky barrier solar cell, optimum thickness indicator for barrier metal 78−21120
self-shadowed replicas, controlled sputtering 77−26434
semiconductor epitaxial layers, resistivity and thickness monitoring, use of spreading-resistance method 80−47075
superconducting film, multisource deposition rate control using mass spectrometer as sensing element 78−72730
thin film composition gradient production 80−55295
thin film thickness monitor shutter 78−56583
vacuum deposited layers, thickness monitoring techniques *(Japanese)* 80−60783
vacuum deposited thin films, specific thickness profiles 78−95697
welds and castings, differential method of balancing out thickness-variation effects in radiography 80−66748
Zn sherardising process development 79−78998

thickness measurement
β thickness gauge, linearisation of curve of weakening of β particle beam intensity 78−89440
absorbent surface in differential digital radioisotope system, error anal. *(Polish)* 77−53860
absorption thickness gauges, effect of scattered γ radiation on sensitivity 79−71411
achromatic antireflection coatings, thin-layer, layer thickness calcs. 80−87468
acoustic pulse echo meas. of 200 MHz 77−23834
adsorbed polymer layer, on particles in suspension, thickness meas. by mag. birefringence 80−42191
alloy foils, X-ray microanal. technique 80−85256
amorphous layer thickness meas. by electron back scattering method 80−100721
annular liquid film meas. techniques 80−31439
antireflection coatings, thickness monitoring during deposition 80−19114
armour material, selection criterion 78−53063
arterial walls, human coronary, optical density determ. 80−12173
aspherising layer prod., monitoring by interf. fringes in periscopic microscope 77−14820
automatic US equipment for monitoring drill and casing tubes 78−53085
beta-ray source deposit uniformity, meas. techniques 79−26792
biological ultrathin section, electron probe microanalysis, local mass thickness meas. using STEM 79−62416
boride coatings on C and alloy steel, spectroscopic thickness determ. 80−85099
brass cylindrical shells, thickness determ. by inductive meas. 79−12760
broadband US spectroscopy, appl. to layered media study 79−14177
bubble film, ellipsometric meas. of thickness and refr. index 79−78463
ceramic and thin layer US pulse-echo meas. 77−28969

thickness measurement continued
chrome plating, nonmagnetic materials, model PINT-3 electromagnetic instrument 78−70162
coal layer thickness meas., EM technique 78−53740
coating, beta backscatter method, meas. uncertainty prediction 77−56206
coating, density meas. by monitoring by back scattering of single energy electrons 79−97362
coating, thin, on bulk materials, electron backscatt. w.r.t. thickness determ. *(German)* 77−10146
coating thickness gauges 77−63839
coating thickness measurement, optical monitoring 79−90041
coatings, methods and instruments for measuring the thickness, review 78−73000
coatings, nondestructive, by beta particles retro-dispersion *(Spanish)* 78−12672
coatings, X-ray fluorescence gamma-thickness meter based on NaI scintillation counters, improvement 79−35670
coatings, X-ray fluorescence thickness gauge, spectrometer channel with Si(li) detector 79−35671
coatings, Zn, colour, on steel products, thickness meas. by X-ray fluoresc. 77−54029
coatings industrial meas., 1979 status in USSR 80−77749
coatings of interference mirrors, meas. equipment 79−35676
coatings on small cylindrical samples, laser diffraction method 79−35674
coatings using bremsstrahlung radiation from monoenergetic fast electrons 77−77609
composite material, testing with fluctuating components using monoenergetic electrons, sensitivity 79−79209
composite transparent film layer thickness meas. by Fourier transform spectroscopy 77−10093
computerised tomographic scanner slice thickness meas. *(Japanese)* 79−92353
contact lens, soft, in-office meas. 78−7339
contact lens radii and thickness meas. by interferometry 80−8118
contact media for US thickness meas. and defect inspection over wide temp. range 80−104395
contactless, radioisotope appl. *(German)* 79−71414
contactless, with radioactive isotopes *(Bulgarian)* 79−80578
contactless transducer, for thickness meas. and metal flaw detection 78−44312
deposited film thickness and grain size determ. on non-conductive SEM specimens 78−77170
deposited thin film-resonating quartz crystal substrate interaction, energy transfer model 79−88914
dielectric film, refractive index and thickness meas. by optical method 80−82806
dielectric film, spectroscopy, using Lummer-Gehrcke interferometer 77−5898
dielectric film or membrane, optical thickness meas. using Fabry-Perot interferometer 77−71367
dielectric films, thickness and refractive index meas. by photoelectric scanning 80−105606
dielectric layers, ellipsometry for semicond. process control 78−49887
dielectric layers on semiconducting substrate, ellipsometric monitoring 79−49272
dielectric multilayers, optical and geometrical thickness monitoring using monochromatic maximeter, substrate effects *(French)* 80−38140
dielectric thin film, thickness measurements determ. using ellipsometer with nonmonochromatic source *(Russian)* 78−51862
dielectric thin film refractive index and thickness, algorithm for determ. on basis of ellipsometric meas. 80−34881
dielectric thin films, accurate meas. by symmetric prism wave couplers *(Chinese)* 80−2885
dielectric thin films, refractive index and thickness, spectrophotometric determ. 78−29144
diffused waveguide, effective thickness meas. 79−32070
dispersive device linear in wave-numbers, space-time optics appls. 77−72071
dye laser jet stream, thickness meas. in real time, by optical technique 78−82975
eddy current thickness gauge, total factor experiment exam., metrological characteristics determ. 78−39999
eddy current transducer part geometry effect on inspection 78−53078
eddy current transducers, for meas. thickness of lacquer coloured coating on mag. base 78−85101
eddy-current phase thickness gauge, automatic error corrections 79−9204
electrodeposits, multi-layer, using decade counter *(Czech)* 80−95071
electrodeposits, multilayer, instrument based on destructive coulombmetric method *(Czech)* 80−8980
electromagnetic instruments, interference factors on readings 78−48601
electromagnetic probe, of thickness gauges, linearisation of output signal 78−56862
electron beam, surface thickness monitoring, object accessible from one side 78−60944
electron beam evaporation rate automation by ion current meas. *(Hungarian)* 80−16198
electron beam evaporation source with integrated rate control *(Hungarian)* 80−20798
electron microscopy, wide-field, appls. in biology and medicine 77−56553
electron microscopy determ. of film thickness, electron backscatt. method 77−47703
electron-irradiated specimen, determ. by continuum integration 80−31713
electroplated coatings, Kocour electronic thickness testers, evaluation 79−21702
electroplated coatings thickness test standards 79−8405
ellipsometric, error estimation for water thin film on slightly rough quartz surface 78−32856
ellipsometry, in situ, compensator inaccuracy evaluation 79−54170
EM coating thickness gauge calibration using air gap 77−57300
EM coating thickness meter, for nondestructive testing, standardisation in Soviet Union 77−90561
epitaxial magnetic film thickness meas., interferometric method 79−35675
epoxy resin bond layer, prep. methods, ultimate thickness 80−71884
equipment for production line inspection 79−29320
falling liquid film, thickness meas., statistical props. 79−12708
thickness measurement continued
ferromagnetic film, domain wall width meas. with electron microscope, astigmatism effects 79−19753
ferromagnetic film thickness meas. by diffraction electron microscopy 78−86392
ferromagnetic films, electrodeposition, thickness control, magnetisation meas. 78−23306
ferromagnetic films of high conductivity, magnetic reluctance thickness gauge 80−68178
ferromagnetic material thickness determ., NDT technique 79−79187
film, 10^{-1} to 10^{3} nm, using laser microellipsometer *(Czech)* 77−61109
film, amorphous and cryst., thickness meas. in electron microscope 79−26186
film, backscattered electron intensities, ang. depend. 77−40317
film, dielectric, using varying gap immersion method, simultaneous determination with permittivity 78−6620
film, Fizeau method and surface deform. of opt. flats 78−77970
film, lattice absorption method *(Czech)* 77−172
film, low temp., quartz thickness monitor 77−79052
film, low temp., quartz thickness monitor 78−41275
film, optical charact., computer inversion method 78−11008
film, optical consts., thickness and surface roughness determ., technique and appl. to AlN *(German)* 77−41670
film, refr. index and thickness determ. using guided optical waves 78−74049
film, Talbot effect applic. 78−9321
film, thickness distrib. determ. by XPS 77−39743
film, unsupported, simultaneous meas. of refractive index and thickness *(French)* 77−55842
film, using excited fluorescence in dye solns., report 78−81945
film, X-ray fluoresc. technique, and its appl. to Cu, Ag and Cu-Ag 79−90911
film and slab-like materials, open transmission line UHF CW phase technique 79−35778
film on nonplanar substrates, light interferometry 78−29085
film refractive index and thickness meas., error anal. of SYNCANG and SYNCWANG methods 78−8439
film thickness and optical consts., spectrophotometer meas., computer program evaluation *(French)* 77−13808
film thickness meter, industrial appl. *(Russian)* 77−41566
film thickness monitor, quartz crystal, based on SAW oscillator 78−3036
films, electrically conducting, optical consts. and thickness meas. 79−67376
films, thin, on substrate, thickness meas., electron probe anal. technique *(French)* 78−41276
films, using calculator-coupled automated ellipsometer 77−82490
Fizeau interferometry, for refr. index and thickness meas. of nearly transparent films 79−17469
floating ice layer thickness meas. using nanosecond impulse X-band radar 78−62178
fluorescent film, method for refr. index and thickness determ. 80−40175
fluorocarbon foil, Ftoroplast, homogeneity study *(Polish)* 80−35278
foil, surface density meas. method using X-rays or backscattered γ-rays *(Czech)* 77−50323
galvanic coating thickness gauge performance characteristics 77−32746
galvanic coating thickness gauges using phase angle meas. 77−79114
galvanic coatings, profilography 80−85095
gamma-ray back scattering flaw detector and thickness gauge 78−44333
gamma-ray backscattering coefficients, Monte Carlo calcs. 77−61171
gamma-ray technique, spacecraft equipment thickness meas. appl. 78−66013
garnet-ferrite film thickness meas. with UM-2 monochromator interference attachment 78−3035
gauge for thin foil meas. *(Chinese)* 78−4584
glacier thickness meas. from helicopter in W.Spitzbergen *(Russian)* 77−29336
glaciers, thickness meas. rel. to gravity surveys in glacier-covered regions 79−16697
glass, layer, absolute thickness meas. of dielectric material 79−67253
glass fibre reinforced plastic 79−63189
glass fibre thickness meas. and control system in production *(German)* 80−10052
glass film and shell wall thickness meas., white light interferometric meas., dispersion effect 80−4757
glass industry, applications of gauges and optical projectors 80−21249
glass laser targets, microspherical, processing method in floating state 77−80337
glass surface, ellipsometric study of zone of optical contact 80−4754
glass surfaces, cracked layer thickness determ., chemical method 80−64226
glass thickness automatic measurement by laser beam 80−82744
glass tubing dia. and wall thickness meas., P-329M instrum. 80−86262
graphite, high temperature gauge calibration using Re+p cross section data 77−23054
graphite foil, thickness determ. by TEM using diffr. and energy loss anal. 78−29088
heat exchange tube thickness meas. by eddy current for corrosion testing, computer study 78−68852
human platelets, air-dried, topography and thickness measured by correlative TEM and SEM 79−84041
image spectrograms of three-dimensional objects, appl. thickness meas. appl. 79−7228
inductive sensors for coating thickness meas., correction for thermally produced errors *(Russian)* 77−13740
industrial thickness meas., destructive and nondestructive methods compared *(French)* 78−15611
inorganic nonmetallic building material with rough surface, abrasion test using pneumatic apparatus for thickness meas. *(German)* 79−52553
insulating thin film, thickness meas. by IR refl. spectroscopy *(German)* 79−58671
insulation, using easily calibrated eddy-current meter 80−73316
interferometric gauge system, white light 79−21807
IR ellipsometry of polySi-SiO_2-monoSi structure thickness 79−56287
isopachi fringe patterns using immersion method polarisation holography 77−19196
isotope radiometry, counting algorithm for information processing 78−44323
LAMBDA laser distance and thickness meas. system *(German)* 78−32792

thickness measurement continued
laser coupling, new technique for refr. index and thickness meas. 77−88965
laser fusion target microradiographs, wall thickness meas., 2D modelling 79−63804
laser interferometric method, solid state track detector thickness meas. 78−86735
latex suspension liquid film flow, local thickness meas. 79−4070
layer, principles and methods survey *(Dutch)* 78−29087
layer thickness uniformity meas., nondestructive, principle, instrums. *(German)* 77−74351
layered materials, in powder form, thickness meas. by XPS and ion sputtering 79−88913
left ventricular volume rel. to QRS voltage and Frank vectorcardiogram 79−44029
liquid films, conductometric method 80−77751
lubricant film thickness meas. using laser based fluorescence technique 79−49201
marble, layer, absolute thickness meas. of dielectric material 79−67253
marine sediment particles, surface organic layer containing U and Th, thickness meas. 78−40592
mass thickness of biological sections, determ. from electron micrographs 77−70573
measuring device fixture for gauging and calibration *(German)* 77−74353
membrane thickness distrib. determ. from orthogonal intercepts 79−74804
metal coating, foil thicknesses, X-ray fluoresc. meas. method, appls. *(Russian)* 78−56582
metal coatings, methods and apparatus *(Bulgarian)* 79−88906
metal films, methods and instruments *(German)* 78−32787
metal ultrathin foils, laser monitored electrothinner *(German)* 79−34219
metal whisker thickness meas. using MII-4 microinterferometer 78−166
metallic coatings, thickness meas., coulometric thickness gauge based on electrolysis laws 77−71293
metallic film, single layer and multilayer, thickness determ. by X-ray fluoresc. 80−68180
metallic film, using nondestructive radioisotopic technique 80−68179
metallic film thickness measurement by electron probe microanal. *(Czech)* 79−44899
metallic layer thickness measurement using X-ray fluorescence principle *(German)* 80−93705
metallic supported film, thickness determ. using ^{63}Ni radioactive source 78−22989
metallic thin films, discontinuous, electron mode microanalyser 79−2744
metallic thin films, pressure operated shutter for thickness control and monitoring 79−15607
metals, thickness meas. by backscatt. γ radiation 80−101781
microprocessor based film thickness measurement system *(German)* 80−57260
mild steel nuclear reactor structures, oxide thickness monitor 77−67806
multilayer Ni deposits, simultaneous thickness and electrochemical potential determination for individual layers 80−71813
multilayer optical film thickness analyser 78−32785
nonabsorbing film with randomly rough boundaries, refr. index and thickness meas. 77−82589
noncontact thickness testing by US and electromagnetic waves 78−48603
nonferromagnetic coating, stability and general serviceability of applied sensors 78−44326
nuclear powdered target, thickness determ. using α-ray and β-ray gauges 79−22519
nuclear resonance methods for metallic thin layers and film coatings 77−81334
nuclear target thickness meas. by photon induced X-ray fluorescence 77−18728
nuclear target thickness uniformity gauge using ^{147}Pm beta source 77−10512
nuclear targets, thin, techniques used in preparation 79−85201
oil films thickness meas. on polluted water from oil fluoresc. props. 79−79437
oil thickness on wavy water surface, light sensitive gauge 79−8720
optical, sheet metal, using dynascope visual projector *(French)* 80−82745
optical film, monitoring of props. during deposition, wide band monitoring system 79−81582
optical film deposition, thickness monitoring with optical time-domain reflectometer 79−55254
optical films, by light intensity ratios 77−2678
optical microscope nondestructive method of layer thickness meas. 78−77843
optical thin film, thickness monitoring 79−97358
optical waveguide, thin film, with emitting diffr. grating, inhomogeneity in thickness 80−48425
organic uniaxial films, optical consts. and thickness determ. by modified ellipsometry 79−91512
oxide film characterisation, using low energy electron induced X-ray spectroscopy *(French)* 78−41386
oxide layer, electron re-emission Mossbauer spectroscopy 77−16752
oxide thickness in shutdown fission reactor, abrading system appl. 79−63720
oxide thickness measurements up to 120 Å on silicon and aluminium using the chemically shifted Auger spectra 78−23586
oxides produced during Al anodisation, thickness meas. by ellipsometry 78−171
paint, non-magnetic, non-destructive measuring instrums. 79−52557
perfect crystal, disturbed surface layer, X-ray diffr. 77−85038
phase boundary, Fresnel refl. coeffs., optical thickness *(German)* 77−69794
piezoelectric transducer, aperiodic, for US radiation, design for testing applic. 78−36996
piezoelectric transducer, equivalent parameter study in resonance thickness meas. 78−54340
piezoelectric transducer, resonant, construction and delay line contract, US thickness meter 78−53100
pipe/boiler wall, US technique, test equipment *(German)* 78−18136
plastic films, using differential electronic circuit 80−73315
plating layers, using eddy-current probe linked to computer *(German)* 79−85112
polycrystalline Si film growth, underlying oxide layer thickness effect on in-process thickness monitoring 80−6679
polyethylene films 4 to 100 μm *(Japanese)* 80−52160
polymer films on metals, thickness determ. using profilograph-profilometer 79−70244
polymer powder layers, thickness distribution meas., by electrostatic method *(Russian)* 77−10042
portable digital US thickness gauge 78−92427
profile measurement of hot rolled strip during hot rolling *(German)* 80−25929
projected inertial confinement fusion reactor target evaluation by buoyancy analysis 80−78442
protective coating thickness meas. using radioisotope method 77−90520
quartz crystal thickness sensor isotope target preparation 80−17923
quartz film thickness monitors, effect of accumulated film layers on accuracy 78−72734
quartz mass/thickness detector using ICs, principle, design 79−17393
radioisotope gauge beta particles deflection by magnetic field 77−79054
radioisotope instrumentation, industrial appl. *(German)* 77−70245
radioisotope measuring convertor, parameter calc., thickness monitoring appl. *(Russian)* 78−25403
radioisotope thickness gauge standard sample certification 79−35672
radioisotope thickness meter, increasing speed of response by optimising detector parameters 79−75494
radioisotopic thickness gauges, errors due to fluctuation of source-detector spacing 79−67251
radioisotopic wall thickness gauge, description 78−44310
remote layers, CW phase comparison technique 79−35662
right ventricular wall thickness meas. by echocardiography, comparison with necropsy 78−40277
ring core flux-gate thickness transducer with permanent magnet 79−67280
rocks strained units, stratigraphic thickness determ. 79−21034
roughness evaluation from interference extremum amplitudes 79−78766
SEM appl. 78−29218
semiconductor detectors, determination of thickness of sensitive layer with aid of β and γ sources 80−22323
semiconductor epitaxial film optical constants meas. by far IR ellipsometry 78−93753
semiconductor film, heteroepitaxial, on insulating substrates, characterisation, book contrib. 79−82497
semiconductor materials, high-resistivity, using EM methods with capacitance sensing element, computer-aided evaluation 79−80647
semiconductor wafer thickness meas., contactless SHF method 79−67264
sheet material, beta gauge, optimal filter design 77−1904
shell target monitoring by X-ray Schlieren method 80−86263
simultaneous meas. of Au and Ni layers on Cu substrates, X-ray fluorescence 80−13041
skin friction meter using viscosity balance principle for metal surfaces 77−35266
slow-neutron monitoring of thin coatings 77−71297
spectrophotometer, Brewster's angle refined absolute refl. technique for film thickness meas. 79−21820
sputtered layer on metal collector, thickness distrib. meas. by electron backscatt. 78−18927
sputtering, new depth profile unit, Wehner 77−8753
steel, austenitic, nitrided layer depth meas. by eddy current instrument 79−34242
steel, galvanised coatings, thickness meas. using X-ray fluorescence radiation, apparatus design 80−21202
steel, neutron quasialbedo thickness meas. of single layer product, optimization 80−105611
steel, X-ray fluorescence thickness meas. for Zn and Sn coatings 77−55884
steel articles thickness and continuity monitoring by neutron radiometry 79−93100
surface and surface layer measurements, ellipsometric method 80−52295
surface film and bulk material, ellipsometric method 79−44926
surface layer thickness measurement by kinetic method 77−24503
surface layer thickness-composition monitoring by high energy electron backscattering 78−53146
target foils, using ^{14}C β-ray thickness gauge 79−26030
TEM, thin section uniform region quantitative meas. 78−58097
TEM energy loss anal. appl., local thickness meas. 77−44100
TEM foil thickness measurement for quantitative metallography 78−35632
thin coatings thickness monitoring using slow-neutrons 77−71297
thin conducting films, by skin impedance method 79−35673
thin film, by electron backscattering 80−101904
thin film, photoacoustic microscopy appl. 80−14525
thin film deposition control, thickness monitor using freq. demodulation technique 79−67249
thin film growth measurement using galvanically separated quartz monitor probe *(German)* 80−11576
thin film meas. tool calibration by cubic spline fitting 77−18063
thin film permittivity and thickness determ. using differential-gap varying method *(Japanese)* 80−4739
thin film thickness meas., automatic Brewster angle spectrophotometer 79−6078
thin film thickness meas. by in-depth-selective Mossbauer spectroscopy 79−63188
thin film thickness monitor, temp.-controlled, voltage readout 77−24953
thin films, calibration standards for surface profile monitors 80−17918
thin films, characterisation using proton-induced X-ray emission 80−35618
thin films, digital frequency meter and quartz crystal oscillator system 78−89436
thin films, step gauge, Ba stearate multilayer films on EDF glass, interference colours 77−5900
thin films, thickness determination, using backscattered electrons as tool 79−21704
thin films, uniformity, technique applied to polyimides 79−58672
thin films, X-ray interferometer based on small-angle scattering apparatus 80−27271
thin foil thickness meas. using ^{148}Gd and ^{241}Am alpha-particles 79−30417
thin layer thickness determ. from backscatt. ion spectrum 79−24399
thin layer thickness measurement, US waves, phase vel. and damping *(Russian)* 78−36969
thin liquid films on inaccessible surfaces, thickness meas. 79−30412

thickness measurement continued
thin pigment films, by perturbed total internal refl. spectroscopy *(Russian)* 77−52197
thin samples, mass thickness and chem. composition determ., by TEM and X-ray anal. 80−103227
thin surface layers, thickness and optical consts. using surface plasmon excitation 79−47533
thin tube wall in 1-5 mm range, US echo-pulse thickness gauge appl. *(Russian)* 78−49797
thyroid epithelial cell, methodology of thickness determ. 78−20330
time-interval meter for digital display pulse echo thickness gauges 78−48594
transparent film, from zero refl.-induced ellipticity angles of incidence 78−41345
transparent film on rough metal surface, ellipsometric data 79−88912
transparent film thickness and refr. index meas., polarisation-independ. reflectance matching 77−65052
transparent films, independent determ. of thickness and refractive index by MIS-11 microscope 77−49770
transparent films, on absorbing substrate, refr. index, thickness, ellipsometric meas. 77−52194
transparent layer refr. index and thickness determ., optical interf. method 78−89528
transparent plates, using interference method, 10 to 1000 μ 79−71406
tubing, pulse echo US thickness gauging 77−73392
ultrasonic thickness gauge, model ST-211, improved version, exam. 79−15941
ultrathin film thickness meas. by AES 79−35663
UNIPAN 545 US gauge, with digital readout 80−47019
universal β-backscatter thickness gauge calibration method 77−32747
US, of deep treated and corroded surface layers 79−34237
US echo pulse thickness gauge, portable, range 0.1 to 300 mm, digital readout 78−70108
US echo technique appl. *(French)* 78−29089
US echo-pulsed digital thickness gauge 77−74359
US gauge, pulse-echo, transistorised, with reduced dead zone 77−12766
US impulse thickness gauges, inspecting wall thickness of tapered profiles 78−72988
US inspection, variability of meas. 79−24704
US meter, digital *(Czech)* 78−49795
US pulsed thickness meter with digital readout 77−45823
US resonance method 78−48590
US resonance thickness gauge, improved readout device 78−95896
US spectrometry, physical basis *(German)* 79−7265
US testing, pulsed thickness gauge, inspection of tapered profiles, error anal. 78−40007
US thickness gauge, Kvarts-6, design of automatic control block 78−73005
US thickness gauge, resonant immersion-type, dynamic range of magnetic modulator 79−11756
US thickness gauge for continuous exam., instrument description 78−72981
US thickness gauges calibration, thickness standards 79−35669
US thickness gauging on hot surface, combination double transceiver probe 79−3882
UT-31MTs pulsed ultrasonic thickness gauge 78−24761
vacuum deposited films, quartz thickness monitor nonlinearity 78−29091
vacuum deposited layers, thickness monitoring techniques *(Japanese)* 80−60783
vacuum deposition, film thickness monitor 77−36401
vacuum deposits as calibration standards for X-ray fluoresc. anal., thickness meas. 77−60177
variable wavelength method for epitaxial garnet film 77−77309
various methods, critical assessment 80−47018
vertebrate cornea, transparent layered structure thickness monitor 78−92737
X-ray thickness gauge, factors affecting measurement errors 79−88911
Ag layers, thickness determ. by laser microprobe and flame atomic absorpt. 80−27355
Ag, thin film, thickness meas., Hall effect and interferometric methods 77−5802
Al coating on polyethylene terephthalate, using photometry 80−62626
Al, coating thickness determ. H_2 generating method *(German)* 79−35660
Al foils, thickness uniformity determ. from proton backscatt. yield 77−10510
AlN foil, thickness determ. by TEM using diffr. and energy loss anal. 78−29088
Al_2O_3 anodic film peak voltage rel. to ellipsometric thickness 77−77597
Al_2O_3 anodic layer formation in H_3PO_4 solns., surface charact. 78−15603
Al_2O_3, transparent films on Al refr. index, thickness, ellipsometric meas. 77−52195
Au, electroplated layer, beta-ray backscattering *(Slovene)* 78−6860
Au film on (100) Si, appl. of acoustic microscopy 80−53575
Au film on Si, SAW dispersion and film thickness meas. 80−10769
Au films, thickness meas. standards for Rutherford backscatt. 79−40529
Au layers, thickness determ. by laser microprobe and flame atomic absorpt. 80−27355
Au plated layer thickness meas., ^{195}Au nondestructive method 79−96244
Be coatings, α-radiation meas. of thickness 78−82600
Bi_2O_3 layer thermally grown on Bi film, thickness meas. by capacitance method 79−1554
C thin layers, thickness determ. by objective colorimetry 78−77844
^{252}Cf fission fragment implantation for wear meas. 79−87765
Cr, plating thickness meas. with MIP-10 78−53144
Cu coating on Ni and Zr, monitoring by back scattering of single energy electrons, density meas. 79−97362
Cu cylindrical shells, thickness determ. by inductive meas. 79−12760
Cu thin layers, thickness meas. by proton-induced X-ray emission 80−4690
Cu-Au-Cu, film, thickness meas. using quartz oscillator system 79−65968
Fe-Al, rate of form. and thickness of diffusion layer, 200 to 600°C 80−15315
Fe-Cr alloys, in acid and neutral solns., thickness and optical constants of passive and transpassive films 80−66698
GaAs, epitaxial growth and etching rate meas. method 77−35829
GaAs, layer growth by electroepitaxy, thickness profiles 79−4486
GaAs native oxide layer, determ. from C-V and photoresponse meas. on Schottky barrier 80−70821
thickness measurement continued
Ge X-ray detector, Au contact layer thickness meas. 80−62627
^{3}He profiling, depth resolution using ^{3}He(d,α)^{1}H reaction 78−58557
In_2O_3, elec. conducting film on glass substrate, measurement of optical constants and thickness 78−60525
Ni coating on mag. steel, thickness measurement of coating 78−76821
Ni, galvanic plating, stressed condition effect on magnetic thickness gauge reading 78−88611
Ni layers, thickness determ. by laser microprobe and flame atomic absorpt. 80−27355
Pb, parts, albedo thickness meas., neutron technique 79−29309
PbO layer vapour deposition, structure, and props. 80−65408
Pd-H thin film system, phase diagrams using quartz crystal thickness monitor 80−7537
Pt film, RF sputtered, thickness distribution function 78−11083
Se films, Ag diffusion, effect on interferometric thickness meas. 80−96695
Si, epitaxial layer thickness meas. using phase correction function of substrate resistivity *(Rumanian)* 80−90812
Si epitaxial layers during deposition using diffraction *(German)* 79−97355
Si epitaxial layers using IR laser ellipsometer expt. 78−62219
Si, film on Al-Cu, ellipsometric meas. technique, comparison to X-ray fluoresc. anal. 78−51840
Si film thickness meas. from visible refl. spectra 79−99960
Si, polycrystalline, film thickness meas., visible spectral reflectance analysis 78−32786
Si single-crystal, meas. using interference thickness gauges 79−97351
Si-Al devices, thickness meter for Al contacting layers *(Russian)* 80−36980
Si(Li) X-ray detector, Au contact layer thickness meas. 80−62627
Si_3N_4 ultra-thin film composites of FET wafers and devices, thickness determ. by micrprobe technique 77−36397
Si_3N_4-SiO_2, double dielec. layer on Si substrate, ellipsometric parameter meas. methodology 77−63474
SiNH films, thickness and refractive index meas., comparison of techniques 80−8957
SiO film, Au coated, thickness meas. using stereo technique, TEM 77−30220
SiO_2 films, thickness and refractive index meas., comparison of techniques 80−8957
SiO_2 HF plasma sputtered dielectric layer thickness and refractive index obs. 79−56931
SiO_2 layer, measurement by secondary electron emission 80−57435
SiO_2, oxide growth in HCl-O_2 mixture, ellipsometric meas. 78−7073
SiO_2 thickness in monolithic ICs, SEM technique 79−30619
SiO_2, transparent film on Al, refr. index, thickness, ellipsometric meas. 77−52195
SiO_2 ulra-thin film composites of FET wafers and devices, thickness determ. by microprobe technique 77−36397
SiO_x, SIPOS, O determ. using differential thickness meas. 79−28228
Sn mixed oxide film formation and meas. 77−77622
SnO_2, elec. conducting film on glass substrate, measurement of optical constants and thickness 78−60525
Ta, transmission channelling of MeV ions to study edge dislocations, expt. setup 80−29098
TiC coating thickness meas. using X-ray diffr. 80−21243
TiO_2 powder, $SiO_2(Al_2O_3)$ coated, thickness meas. of coating, XPS and ion sputtering 79−88913
V_2O_5 film, amorphous, thickness, density and refr. index determ. from reflectance interference spectra 80−55206
Zn, plating thickness meas. with MIP-10 78−53144
Zr foil, convergent beam thickness determ. 79−4215

thin film capacitors
breakdown counter for fission fragments 77−38563
complex permittivity in VLF range, meas. apparatus and method 79−21782
current pulse counter for fission fragments 77−38564
CVD, high temp. instrumentation fabrication 80−40266
humidity sensor appl., Finnish development of meteorological instruments 79−12310
ion current time const. 78−23390
ion polarisation meas., influence of electronic leakage current in evaporated SiO_x 77−63014
PTFE, electrometer, temp. effects 79−6141
SAW transducers, tap weight control via thin film capacitors 77−80041
stearic acid, vacuum evaporated film, for low-loss capacitors 80−71317
Al-Al_2O_3-Al, oxide film prod. by pulsed evap., capacitor prod. and characts. *(Russian)* 78−60584
Al-Al_2O_3-Al, thin film capacitors, dielec. losses 78−76382
Al-rare earth metal oxide dielectric-Al, charcts. and design considerations *(Russian)* 77−1638
Al-stearic acid-Al structure, dielectric behaviour 80−71317
Bi_2O_3, thin film capacitor elec. props. under reduced press. 80−80397
$Er_2M_3(BO_3)_4$, M=Ba,Cu, thin-film capacitor mats., synthesis and props. 77−48128
$La_xM_3(BO_3)_4$, M=Ba,Ca, thin-film capacitor mat. synthesis and props. 77−48128
Nb-Ta-N sputtered films and their anodic oxides, elec. props. of resist. and dielec. films 80−11126
Sb_2S_3, thin film, dielectric props. 79−15392
Si-SiO_2 MOS interface states density, transient capacitance meas. eval. 80−92989
SiO amorphous thin film capacitor, EPR, elec. cond. 78−68358
SiO-Al multilayer capacitors and inductors, heat treatment effect on elec. props. 77−32082
SiO_2, current pulse counter for fission fragments 77−38564
SnO_2-rare earth metal oxide dielectric-Al, charcts. and design considerations *(Russian)* 77−1638
$SrTiO_3$ film, polycrystn., dielec. props. and struct. 77−81057
Ta_2O_5, film on Al, Cu, Au, Ag electrode, electric strength of MIS system 80−96999
Ta_2O_5, sputtering conditions rel. to electronic cond. 77−40365
Y-Y_2O_3-Au, self-healing dielec. breakdown 80−11104
$Y_2M_3(BO_3)_4$, M=Ba,Ca, thin-film capacitor mat. synthesis and props. 77−48128

thin film circuits
fabrication, etch sputtering of Ge and InSb under controlled atmosphere 77−44397

thin film circuits continued
high temperature instrumentation, passive components fabrication 80−40266
hybrid IC monolithic crystal filter 77−39171
manufacture, using low-temperature radiometer, with conical light pipe 80−47105
preferential sputtering process *(German)* 78−39691
spark machining, with and without stencils *(Russian)* 78−27651
Cr films, on Al_2O_3, quartz and glass, electron-beam deposition techniques improvement 80−7496
Cr/Au metallisation system, corrosion inhibition using intermediary Pd layer 79−79155
Cu-based metallisation systems, in 85°C 78% RH SO_2 contaminated environment, performance 79−74304
Ti films on Al_2O_3, quartz and glass substrates, electron-beam deposition techniques improvement 80−7496
Ti-Cu, evaporated adhesion after electroplating 79−82475
Ti-Cu thin films, oxidation kinetics in air at 100 to 300°C, meas. 80−40590

thin film devices
see also magnetic thin film devices
acousto-optic devices, theory and experimental results 77−58472
amorphous materials appls. 80−107693
bolometers, charact. *(German)* 78−62226
captured nerve fibre multiple single-unit recording by tubular electrode array 77−60321
cathode, Al-Si_3N_4-Al struct., pulsed emission obs. 77−8728
chalcogenide glass threshold switch response to pulse burst waveforms 78−10523
eddy current transducer, for temp. meas. *(Russian)* 77−26294
embossed metallic film absorber for solar energy 79−29451
field ionisation source fabrication 80−52359
film preparation and practical device application *(Japanese)* 78−23609
fission thermocouple detectors for reactors safety expts. 80−22987
gas-sensitive sensor with ultrafine particle film deposited on monolithic IC chip *(Japanese)* 80−105630
graphite thin film low-temp. thermometer 77−49734
heat transfer gauge for use in shock tube *(Japanese)* 77−19654
image convertors, solid state, with integrated fixed-pattern noise suppression 80−14458
interdigital transducers for SAW devices at GHz freqs. form. by electron beam lithography 80−4702
IR frustrated-total-reflection polarising beam splitter 79−46047
materials engineering, electronics appl. *(Japanese)* 77−73229
MIM cold cathode emission density improvement, pinhole and compound insulator methods *(German)* 78−39670
MIM discontinuous metal film, fast detector for MM-wave through optical freq. range 77−18092
multielectrode for intracortical recordings prod. by thin-film technology 77−48959
optical disc for integrated optics 80−106641
p-i-n photodiode with internal reflection 78−37059
photovoltaic cell, grain boundary effects on performance 79−83603
PVF_2 film pyroelectric radiation detector sensitivity *(Japanese)* 79−93222
radiative heat transfer gauges, thin film prof. technique *(Chinese)* 79−38742
SAW, ZnO, for HF range *(Japanese)* 80−53598
SAW devices and filters *(Japanese)* 77−73116
semiconductor thin film struct., external circuit current calc. 77−39972
solar cell, comparison methodology 80−93920
solar cell, polycryst., chemical and structural defects 80−93919
solar cell, polycryst., research and develop. overview 80−93921
solar cells, Cu_2S/CdS, sputtered 79−43774
solar cells, degradation processes of electrophysical charact. during long-term operation 80−89617
solar cells, recent developments 78−80016
solar cells, thin film, technical and economical eval. 80−94012
solar cells, unified anal. of potential 80−81436
sputter-deposited thin-film pressure transducers 77−30139
strain gauge detectors, construction and appls. *(French)* 79−93130
superconducting thin film bridges, switching process depend. on control impulse ascent time *(German)* 78−2627
switches, electrooptic periodic waveguide switches and amplitude modulators anal. 78−22215
temperature sensor with high temp.-resistivity 78−41308
TGS thin film pyroelectric detectors, far IR absorption 77−38010
thermoelectric needle probe for medical and biological temp. meas. 80−101299
thermometer, efficiency in meas. radiant flux density of pulsed lasers 77−38967
thermometer, resistance, Ti and Ge, for surface temperature meas., design, fabrication and appl. 78−24792
thermopiles, thermoelectric charact. of combined branches of Bi and Sb 79−35826
TTF polymer thin film batteries 80−45709
Zn_3P_2, UV photoconductive detectors 80−4766
Al-Al_2O_3-Au thin-film cathode anomalous electron emission 79−8232
Al-Si_3N_4-Al thin-film cold cathode, electrical forming, expt. 78−76160
Al-$Si_xN_yO_z$-Al thin film cathode, physical model from expt. study 80−100535
As_2S_5, optical waveguide material for acoustooptic modulators 78−83051
Bi film photopot detector characteristics for adaptive optical systems 79−59741
C film bolometer detection system with <0.1 μs response time 79−63226
$Cd_xHg_{1-x}Te$ thin film Hall probes for high mag. fields 79−30452
CdS, piezoelectric transducers, testing via light diffr. by acoustic waves 77−23840
CdS thin-film Lamb wave delay line characteristics and strain effects 77−31185
CdS/Cu_2S thin film solar cells, design and fabrication, 9.15% conversion efficiency 80−81438
CdS-CdTe solar cells fabrication *(Japanese)* 79−87992
CdS-$CuInSe_2$, solar cell, grain boundary effects on performance 79−83603
CdSe solar cells 80−93970
CdTe thin film polycrystalline solar cells prepared by electrodeposition 80−93948
CdTe-CdS p-n film heterojunction, photoelectric props. 79−39298

thin film devices continued
$CuInS_2(Se_2)(Te_2)$, thin films and photovoltaic devices, AES evaluation 78−67928
$CuInSe_2$ thin films for solar cells, radiofrequency sputtering technique, elec. props. 80−93487
Cu_2S-CdS heterojunction solar cell 80−93922
Cu_2S-$Zn_xCd_{1-x}S$ and Cu_2S-CdS thin film solar cells by solid state reaction, comparison 80−101109
Cu_xS chalcocite solar cell fabrication, charact. 78−39240
Cu_xS/CdS solar cell, prep. by sequential evaporation 80−93902
Cu_xS-CdS heterojunction solar cell, reactively sputtered 79−11256
Cu_xS-CdS thin film solar cells, using all film vacuum deposited process 80−93977
GaAs polycrystalline thin film solar cells, fabrication 80−94066
GaAs thin film polycrystalline solar cells, props. and prep. 80−81437
GaAs thin film polycrystalline Schottky barrier solar cells, grain boundary chemistry 80−94067
GaAs thin film polycrystalline solar cells, grain boundary edge passivated 80−94069
Ge:Au film strain gauges, press. sensor *(Japanese)* 80−105631
GeO_2 films, memory switching phenomena 79−82650
$Ge_{15}Te_{81}X_4$ amorphous semicond. switches, fabrication technology *(German)* 80−7493
HgTe thin film Hall sensor fabrication 80−2951
InAs Hall element, CVD H_2O transport agent 77−40377
InP thin films for photovoltaic devices 80−93972
$NH_4Ag_4I_5$, thin film solid state battery 78−76876
Pt thin-film temp. sensor *(Japanese)* 80−105645
Pt-Pd discontinuous film MIM point-contact diode detector 77−5917
a-Si solar cells, current collection and electrical shorting problems 80−93969
Si surface barrier detectors, dE/dx thin detector technology, n^+ layer electrolytic removal *(Russian)* 77−57823
SiC thin-film thermistors with high thermal response *(Japanese)* 80−105629
Ta strain gauge, effects of Ar ion bombardment on elec. props. 80−80417
Ta_2O_5 film capacitative humidity sensor Panahume *(Japanese)* 80−105658
VO_2 thin film semiconductor-metal transition applications 80−49835
WO_3 film electrochemical colouration for displays 77−77170
ZnS:Mn, AC thin-film electrolum. devices, electrolum. efficiency profiles 79−65931
ZnS:Mn AC electrolum., memory effect 78−15228
ZnS:Mn AC electrolum. device, filament behaviour 80−20712
ZnS:Mn co-deposited electrolum. device, phys. and elec. characterisation 80−20713
ZnS:Mn film device, laser modulation of electrolum. 78−52576
ZnS:TbF_3, between semicond. Y_2O_3 layers, bright green electrolum. 80−2859
ZnSe-GaAs thin film DE electroluminescent cell with 20 V threshold voltage 78−76141

thin film resistors
CVD, high temp. instrumentation fabrication 80−40266
energy deposition measurement by thin film resistors 78−29719
ferroelectric-semiconductor structure, effect of potential relief of ferroelectric substrate on props. 79−11235
junction microresistor prepared by double ion implantation of ^{11}B and ^4He, ^{20}Ne, ^{40}Ar, ^1H 77−15432
metal, resistance fluctuations from spontaneous enthalpy fluctuations 78−72217
metallic layer, vapour deposited, struct., resist. component manufacture appl. *(German)* 77−55467
photoexcitation effects during laser trimming of restors on Si 80−64093
spatially distributed, AC and DC characteristics, current density and potential distributions, algorithm *(German)* 77−55618
thermal time constants, using pulse nonlinearity meas. 79−12815
Al, thin film resistor, rare earth alloying effects *(Russian)* 79−78211
C, high sensitivity temp. sensor, 1-10K 77−13757
CdS_xSe_{1-x} thin-film position-sensitive photoresistor prod. and props. *(Russian)* 78−43503
Cr, thin film resistor, rare earth alloying effects *(Russian)* 79−78211
Cr-Si, amorphous sputtered film, material for kilo-ohm sheet resistances, prep. and props 79−78227
Cr-SiO, sputtered, elec. and struct. props. 80−39694
Cr-SiO cermet thin films, thickness effect on density, resist., adhesion and annealing coeff. 77−69432
Cr-SiO film, elec. props., effect of P^+ and Ar^+ implantation 79−11239
Cu-Mn-Ti alloy, physical and electrical props. *(Russian)* 77−66208
Fe-Cr-Si, heat resistive films prepared by sputtering, lifetime meas. 80−80132
Nb-Ta-N sputtered films and their anodic oxides, elec. props. of resist. and dielec. films 80−11126
Ni, thin film resistor, rare earth alloying effects *(Russian)* 79−78211
Ni-Cr, alloy coating using jumping electron beam, expt. *(Hungarian)* 77−4738
Ni-Cr, props. prep. and appls., expt. *(Hungarian)* 77−4737
Ni-Cr, struct. transforms. induced during annealing, resist. obs. 79−77965
Ni-Cr, vac. deposition, elec. props. and comp. struct. 79−77966
Ni-Cr α-particle elastic scatt., and PIXE anal. 79−48022
Ni-Cr layers, ESCA meas., expt. *(Hungarian)* 77−4951
Ni-Cr pressure transducer for quickly varying pressure, expt. *(Polish)* 77−65041
Ni-Cr-P, deposited by electroless plating, resist. charact. 79−4607
NiCr deposition, 'clean vacuum' deposition equipment suitability obs. *(Polish)* 79−15611
NiCr, electron beam deposition, evaporation, gas phase analysis *(Polish)* 79−20492
Pt film resistance temperature detection 78−49830
Si-transition metal metastable films as temp. independent resistors 78−68097
Ta film, determ. of thickness and O, N content 78−80824
Ta, Ta_2N, sputtered layers, thermal oxidation, reaction kinetics 78−39959
Ta-Al-N thin film resistors with improved elec. props. 80−100544
Ta-Cr-Si-Al, heat resistive films, prepared by sputtering, lifetime meas. 80−80132
TaB_2-Cr-Si-Al, heat resistive films prepared by sputtering, lifetime meas. 80−80132

thin film resistors continued
TaN, film, triode sputtered, struct. and elec. props. 79−78242
Ta_2N, deposition by closed anode bias sputtering *(Japanese)* 80−93484
TiN films deposited by reactive sputtering, elec. props. 80−15638
TiN-Nb(Ta)N, microcomposite film prod. for radio resistors 78−3052

thin film transistors
CdTe thin film on ferroelectric TGS, influence of polarisation reversal on elec. cond. 80−65720
liquid crystal-fibre optic modulator for display 79−72718
MIMIM structure, photostimulated tunnelling, rel. to tunnel transistor fabrication 77−8204
MIMS tunnel triodes, hot electron transmission 78−6456
thin film transistor, quasi-equilibrium TSC process, model 77−36002
CdSe, sputter etching to improve adhesion, line definition and semicond. props. 79−43145
CdSe thin film transistor and MISM struct., effect of annealing on electron mobility and conc. 79−78198
CdSe thin film transistor on Cr substrate, cryst. struct., substrate defect effects 80−70563
CdSe-SiO_2 thin film transistors, fabrication and electronic characts. 79−33351
SiO_2 sputtered films in thin film transistors, trapping centres 80−7014
SiO_2-CdSe, slow states, trapping state densities and cross sections 80−15613

thin film triodes *see thin film transistors*

thin films
see also coatings; dielectric thin films; epitaxial layers; insulating thin films; magnetic thin films; metallic thin films; semiconductor thin films; semimetallic thin films; sputtered coatings; substrates; vapour deposited coatings
absorbing film, damage by high-power optical pulses, two-phase model 80−93438
absorbing films, laser-induced removal, two-phase mechanism 80−97384
absorbing films, laser-induced removal, two-phase mechanism 80−97385
absorption band studies using internal reflection spectroscopy, appl. 79−6194
adherence, locus of failure, implications for adhesion meas. 80−50818
adhesion, meas. device 80−66720
adhesion determination, electron and laser beam appls. 80−71833
adhesion meas., semiautomatic installation 79−96245
adhesion measurement, conf. Philadelphia, USA (Nov. 1976) 80−46729
adhesion measurement 80−50817
adhesion measurement 80−50819
adhesion stability and peeling off from substrate 77−24501
adhesion testing, simple real-time holographic interferometry method 78−92411
adhesive failure, rel. to interfacial structure 80−50820
AES, depth profile analysis, influence of impurity gases in UHV systems 78−76958
AES, digital anal. methods using computer controlled spectroscopy 77−56268
AES depth profiling with N_2^+ ion sputtering 77−16889
alkali chlorides, thin film, crystal-vacuum (100) surfaces, mol. dynamics computer simulation 80−34288
alkali halides, thin films, crystal-vacuum (110) interfaces, mol. dynamics computer simulation 80−34289
alloy, thickness depend. of CPA electronic densities of states 80−65644
American Vacuum Society National Symposium, Boston, USA (Nov 1977) 78−72718
amorphous, of hard spheres, digital simulation 78−22984
amorphous, tunnelling states, at low temps., thermal and acoustical props. 77−24500
amorphous film, anomalous scatt. of photoinjected electrons *(Russian)* 78−52642
amorphous film, surface phonon assisted tunnelling at low temp. 77−4421
amorphous film-crystalline substrate, relaxation process dislocation misfit theory *(Russian)* 80−39461
amorphous thin film, high resolution STEM 79−37597
amorphous thin film on crystalline substrate, computer simulation 79−15045
amorphous thin films, crack networks of voids 78−2399
analysis and characterisation, conf., Les Arcs, France (Jan. 1978) *(French)* 79−8466
analysis using alpha-induced X-ray emission 78−20132
analytical techniques, review 80−80120
anisotropic crystal films, surface polaritons 78−26822
anisotropy props., X-ray characterisation 79−23874
anthracene films, optical props., comparison between free and optical contact mounting 80−89079
apparatus, for adherence, wear resist. and thermal shock meas. of thin films 78−72943
aromatic organic macromolecules, energy-gain satellite in C(1s) XPS 79−1813
atomic composition depth distrib. by energetic ion anal. 80−35617
Auger electron APS, extended fine struct. analysis 79−28863
backscattering spectrum edge determ. theory, and expt. for Ag on Si 77−8702
band structure by linear APW method 78−87899
benzene film, on metal substrate, surface struct. using LEED 79−77879
bicrystals, dislocation interaction, with grain boundaries during plastic deform., electron microscopy technique 80−54281
binary compound thin films, A 15-struct., electron microprobe quantitative anal. *(German)* 77−16893
binary diffusion, effect of partial sink 78−43166
Brillouin scattering by Love waves, theory 80−66212
Brillouin scattering in absorbing film 79−65943
ceramic and thin layer US pulse-echo meas. 77−28969
characterisation and microanal. by STEM combined with other techniques 80−50901
characterisation using ion, electron and X-ray beams, combined, studies of surfaces and thin films 77−86412
chemical analysis, by energy loss spectroscopy 80−104493
chemical analysis, comparative survey of methods, book contrib. 79−66393
3-chloro-2-methylpentane, IR spectra of film, rot. isomerism 79−59595
2-chloro-4-methylpentane, IR spectra of film, rot. isomerism 79−59595
trans-1,4-chlorobromocyclohexane, liquid, crystalline and amorphous state, conformation and vibr. spectra, IR obs. 80−60568

thin films continued
trans-1,4-chloroiodocyclohexane, liquid, crystalline and amorphous state, conformation and vibr. spectra, IR obs. 80−60568
combinatorial-statistical topology of films with pores and islands 79−56096
composite (cermets and semiconductor-insulator), dielectric const. and selective solar absorption 78−2937
composition analysis, by ion beams *(French)* 79−8467
composition gradient production 80−55295
condensates coalescence, influence on morphological changes, modelling 80−107676
conducting, thickness meas. by skin impedance method 79−35673
conducting film in mag. field, dynamics 77−85539
conference, condensed matter physics, Sarajevo, Yugoslavia (Oct. 1976) 77−51629
conference, thin and thick film technology, Augsburg, Germany (1977) *(German)* 78−39685
conference on metallurgical coatings, San Francisco (1977) 78−2394
congress, Loughborough, England, (Sept. 1978) 79−77949
cooling by thin film coating on polymer substrate 78−197
CPA calc. of local density of electronic states, for 11-layered thin film 80−65643
crystal defects, obs. in SEM *(French)* 77−31662
crystal structure, influence of dynamic effects on height of pot. peaks in electron diffr. 77−39517
crystal symmetry, cubic and non-cubic, distinguished by weak field galvanomagnetic meas. 80−60009
crystalline, dispersion law and struct. transition, Fermi line geometry, acoustic spectrum, resist. min. *(Russian)* 79−7764
crystalline, investigation via low-energy proton beams, instrumentation aggregate 77−76266
defect growth and nucleation, electron microscopy and diffraction exam. *(French)* 80−59824
deposited thin film-resonating quartz crystal substrate interaction, energy transfer model 79−88914
deposition, adatom diffusion and capture by clusters, random-walk problem 78−2385
deposition and characterisation, book contrib. 79−1563
deposition control, thickness monitor using freq. demodulation technique 79−67249
deposition model, correlated percolation 80−107679
deposition techniques, review 80−80964
deposition technology, conf., Uppsala, Sweden (Aug-Sept. 1976) 77−90270
depth profiling techniques for thin film interdiffusion and interfacial reactions, book contrib. 79−1564
detection on surface by electron probe microanal., in depend. on substrate 80−35607
diamond indentation and draw tester, for meas. of ultra-adherence in films 78−72944
diatomic clusters, break-up in thin films, particle energy distrib., central peak nature 80−50490
diffusion, effect of surface condition at low temps. 78−91469
diffusion through surface film, into half-space, theory *(Russian)* 78−47553
direct ripening of crystallites on substrates 79−42417
domain size and internal strain, studied by electron diffraction line broadening 78−30840
dual source evaporation, rate control 80−40263
elastic moduli of film on cylinder, calc. *(Russian)* 78−63304
electrical conduction, appl. of Ziman approx. 77−59338
electrical conductivity, physical interpretation of specularity parameter 78−72282
electrically conducting on transparent ceramic, ellipsometry determ. of optical consts. 79−67376
electrochemical fused soft systems, solid films and interfaces, review 77−77783
electrode-electrolyte interface, solid film props., review of expt. techniques 77−77780
electrolyte, solid film, size-selective photochromism 79−99968
electrolyte systems, materials characts. and appls., review 77−77781
electron backscattering from supported films 77−20972
electron beam scatt. and energy loss during film processing 77−27930
electron energy loss spectra, keV, rel. to transition radiation, calcs. *(German)* 77−90213
electron energy loss spectrometry, thin specimen sections, electron microscopic chemical analysis, review *(French)* 79−8469
electron energy spectrum allowing for arbitrary one-dimens. internal field *(Russian)* 77−69212
electron interference effects, theory for film with arbitary lattice potential 79−90934
electron interference method for particle shape determ. in films, inner pot. determ. and external field determ. *(Russian)* 78−29209
electron microprobe analysis *(French)* 77−32856
electron microscopy technique for small voids obs. 78−34403
electron passage, linear transport theory in one-velocity approx. 79−14865
electron probe analysis, charact. fluoresc. effects calc. 80−81408
electron-induced X-ray spectrometry anal. *(French)* 79−43067
electron-probe microanalysis of thin coatings, charact. fluoresc. correction 80−7881
electronic properties in longit. mag. field 79−73603
electrophysical properties meas., using automatic recording and expt. data analysis 79−17446
electrophysical properties measurement apparatus 78−4654
ellipsometry of transparent films on transparent substrates, theory 80−104007
EM tensile adhesion test method 80−50804
ESCA, surface anal. and electronic structure *(French)* 80−7891
evaporation, unsteady 78−42519
EXAFS, fluorescence detection, sensitivity enhancement for dil. species and thin films 77−85843
film edge induced stress in substrates 79−94492
film-substrate bond strength, meas. by laser spallation 80−50821
film-substrate sysem characterisation by ellipsometry 78−8436
film-transition layer-substrate, theorem of electrical images *(Rumanian)* 79−74064
fluorocarbon polymer film, prep. by RF sputtering and plasma polymerisation, props. 77−55890
galvanomagnetic and thermomag. phenomena, theory *(Russian)* 78−14743

thin films continued
gelatin orientating action of solid substrates, on liq. cryst. layer exam. 80−44111
glass film, Brillouin scatt. from surface phonons, SAW vel. and attenuation 78−95587
grain boundary and surface diffusion 77−4276
grain boundary diffusion, analytical model 77−4275
grain boundary diffusion, book contrib. 79−1526
grain boundary electromigration, low temp. theory 77−31799
grain boundary migration, effect on thin film diffusion behaviour, simulation 80−88460
grain-boundary diffusion, analytic and numerical solns. 77−4274
graphite, low-temp. thermometer 77−49734
graphite, phase contrast electron microscopy of holes and steps 77−38063
graphite, relativistic excitations by inelastic electron scatt. 77−1463
graphite, thin support films, 2 nm, prep. for high resoln. electron microscopy 77−87880
growth, transition from island to layer growth, a Monte Carlo simulation 77−85104
growth due to crystallite surface migration, review 80−10810
growth measurement using galvanically separated quartz monitor probe *(German)* 80−11576
growth mode and growth kinetics of dislocation free interfaces 77−85103
growth modelling by computer, condensation coeff. influence evaluation *(Czech)* 79−77935
growth modes, determined by AES experiment *(Japanese)* 78−22975
growth parameters of isolated steps on vicinal faces, elementary rate anal. 80−10805
guided optical waves for refr. index and thickness determ. 78−74049
hard disc thin layer, solid-solid phase transformation 80−79908
hardness and adhesion meas., scratch technique 80−50805
harmonic generation of surface-plasmon nature, off-synchronous treatment 79−18475
HF density of states 80−6689
HF formalism for calc. of total energies and charge densities 80−49850
high purity materials for thin film technology *(Japanese)* 78−22974
high resolution phase contrast electron microscopy imaging 80−103224
holey film preparation by ion-etching method, electron microscopy appls. 80−105751
ice, film, on metal substrate, surface struct. using LEED 79−77879
ice, low-temp. diffusion of electrons, evidence for polaron bands 77−1380
impurity diffusion profiles, influence of limited solubility 78−55989
indandione-1,3 derivative, layer, electrooptical effect *(Russian)* 79−73900
inert gas refl., semiempirical analysis 78−6823
inhomogeneity characterisation by refl. and refractive index changes *(French)* 77−73180
inhomogeneous, galvanomagnetic props. 79−69608
interdiffusion and reactions, book 79−1561
interdiffusion and reactions, book contrib. 79−1562
interface reactions, $^{16}O^{2+}$ effect elimination in backscatt. 78−23575
interference colours produced by white light refl., teaching paper 80−8754
interference electron microscopy and electron interferometry in thin film studies 80−6328
interferometric meas. with laser beam, thickness on nonplanar substrates 78−29085
internal friction, measuring apparatus, during plastic deformation, 4.2 to 300K 79−71442
intrinsic stress determ., cantilivered plate method anal. 80−54570
ion beam uses in thin film analysis and technology *(Czech)* 77−47478
ion implanted 10 nm layer production method and apparatus 80−19818
ion implanted films, props. and appls. 78−71752
ion implanted layers, strain and damage distribs., X-ray diffr. model calcs. 79−69116
ion plating, evaporation source pellet or slug feeding system 79−69996
ion plating, inert gas handling 79−69994
ion plating, low-pressure, ion source design 80−35105
ion-bombarded, simple model of dose depend. of resist. 79−42669
island film, stresses and dislocations in substrate layers 79−87015
island film growth, cluster size distrib. 80−107665
island films, statistical model 80−92795
Kirlian-type images and transport in high-voltage corona discharges 79−55590
laser heating of thin films on absorbent supports *(Russian)* 80−7441
laser machining, projection method 77−26276
lens formation, appl. of alternating elec. field 80−12060
light reflection, transmission and scatt. effect of thin film *(French)* 78−33664
light scattering from surface polaritons 79−8202
localised elemental anal. of microphases and inclusions 78−85261
low energy ion scattering analysis of surface and thin film composition *(French)* 77−59663
magnetic depolarisation curve, influence of multiple re-emission *(Russian)* 77−28550
magnetic depolarisation curve, influence of multiple re-emission *(Russian)* 77−28551
magnetoresistance, specular reflectivity angular depend. *(Russian)* 80−100453
magnetoresistance, unified weak field, for (111) oriented thin films and surface layers 79−95514
magnetron ion sputtering, thin film layers depositon uniformity investigation *(Russian)* 80−20787
materials engineering, electronics appl. *(Japanese)* 77−73229
mechanical testing methods, review 80−40637
metal oxide film, optical and diffusion consts. meas., dynamic method *(Russian)* 78−43950
metallurgical coatings, conf., San Francisco, USA, April 1978 79−15052
metallurgical coatings, conf., San Francisco, USA (Apr 76) 77−31918
microchemical anal. by elastic scatt. of $^3He^+$ 79−1975
micromachining, by ion beam sputtering 77−55887
microporosity described in terms of vacancies and voids 80−24769
microporosity induced by nucleation and growth processes, TEM expts. 78−10303
microprocessing, laser microprobe mass analyser (LAMMA) appl. 80−18041
molecular films, detection by harmonic generation of SAW 77−80688
molecular solid, 0-15 eV electron transmission spectra 80−35023
thin films continued
morphology and morphological changes 78−72043
multi-scattering method for cryst. surface band struct. calc. 80−2439
multielement, on substrate, quantitative electron microprobe analysis 77−9150
multilayer neutron monochromator 77−84589
multilayers, periodic and near-periodic, small-angle interferences of reflected X-rays 79−94846
multilayers, ultrathin, optical charact. 80−104005
naphthalene, films, on metal substrate, surface struct. using LEED 79−77879
noble metal compounds, growth on dil. noble metal alloys in corrosive environment, model 79−24649
non-absorbing, with randomly rough boundaries, optical anal. by immersion spectrophotometry 79−75572
non-crystalline solid, surface and thin film chem. anal. techniques *(French)* 77−73495
nonabsorbing film with randomly rough boundaries, refr. index and thickness meas. 77−82589
nondestructive microhardness testing of near-surface layers 80−71829
normal-incidence Brillouin scattering by acoustic phonons 80−20648
nucleation, growth and transform. of amorphous and crystalline solids 80−24745
nucleation and growth at surfaces, kinetic studies, review 78−72046
nucleation kinetics, coalesc. of mobile nuclei 80−6671
nucleation kinetics, of thin films under complete condensation conditions 80−88453
object shape rel. to physical description 79−42422
on reinforcing fibres, morphological stability *(Russian)* 79−37928
optical absorption, lateral waves along interface, used in detecting surface absorption 78−4707
optical absorption meas. at air-film interface, within film and at film-substrate interface 79−80659
optical characterisation *(French)* 79−11402
optical const. determ. from meas. of normal incidence reflectance and transmittance 77−85825
optical constant volume and surface change separation, reflection, transmission *(Russian)* 80−66320
optical constants, film thickness, surface roughness determ., technique and appl. to AlN *(German)* 77−41670
optical constants, reflection spectra by Kramers Kronig method 80−76099
optical constants determ. 80−2883
optical constants measurement, Shamir-Graff method evaluation 80−11489
optical parameters meas. method, reevaluation 80−104004
optical properties, appl. of Ewald dynamical theory of diffr. *(Czech)* 79−46757
optical properties of film-substrate systems, reflectance-aided null ellipsometry 80−101827
optical transmittance and reflectance, bulk optical props. determ. 80−88954
organic, scanner laser marking 80−43385
organic films possible exptl. production in space 78−35304
organic uniaxial films, optical consts. and thickness determ. by modified ellipsometry 79−91512
orientation control, appl. of submicrometer struct., using STEM and X-ray lithography 79−15844
oxide, on Ti, optical consts. and thickness determ., ellipsometric method *(Russian)* 77−81164
oxide films, diffusing pt. defects recomb. 79−19475
perturbed total internal refl. spectroscopy for pigment film props. *(Russian)* 77−52197
phase and structure, X-ray diffr. rot. method *(Polish)* 79−55608
photoacoustic reflection-absorpt. spectroscopy for IR anal. of surface species 80−105723
photoemission of ultrathin films on nonphotosensitive cond. substrate 77−40325
photothermal deflection technique for absorpt. meas. in optically thin media, thermal lens effect comparison 80−105717
plastic deformation, internal friction meas. apparatus for 4.2-300K 79−5093
polycrystalline, nodule mechanism of diffusion-induced disintegration *(Russian)* 78−51829
polycrystalline film, singularities of recrystallisation *(Russian)* 78−2382
polycrystalline film couples, diffusion during recrystn., numerical simulation 79−77844
polycrystalline film gauge factor linearisation 79−78209
polycrystalline films, rate of mixing depend. on grain boundary struct. 80−107578
polycrystalline substances, use of Hall and Seebeck effects in phys. parameter determ. 77−12023
polymer, vacuum deposition device 77−77384
polymethine dye layer, vibr. spectrum anal., inelastic electron tunnelling spectroscopy 79−13716
polymorphic transformations and physical props. 77−43450
precision absolute thin film standard reference targets for nucl. reaction microanal., ^{16}O standards 79−2880
preparation and practical device application *(Japanese)* 78−23609
preparation and properties, symposium, Loughborough (1976) 77−77376
profiling using proton excited X-rays 79−4490
pseudobinary alloy, use of parallel and monochromatic beams for comp. determ. by X-ray fluorescence 79−48000
quantised, electronic energy spectrum *(Russian)* 80−44688
quantum resonance impedance oscillations *(Russian)* 78−91781
quartz, thin film deposition, by low pressure, high freq. induction plasma *(Russian)* 79−69992
rare earth hydrides and sesquioxides, prep., struct. and props., general review 80−54556
rare earth oxide, struct., electron microscope and diffr. obs. 79−11028
reduction in thickness D/λ, evaluated using XPS data *(German)* 79−1558
refractive index and thickness of unsupported film, simultaneous meas. *(French)* 77−55842
refractive index determ. by Nomarski differential interference contrast microscopy 78−24849
refractory, stability, high temp. and electron irrad. effects 77−39747
resonance fluorescence of thin crystal films, superradiance 78−68573
restricted geometry, thin film technology 78−72044
roller-plate technique, for thin film prep. from melt 80−71607
roughness evaluation from interference extremum amplitudes 79−78766

thin films continued
Rutherford backscattering spectrometry, signal overlap subtraction, surface struct. study 80−50486
Schumann UV spectrophotometer system for absorpt. and refl. meas. on thin films and solids 78−12772
segregation effects at surfaces and interfaces 80−39475
self-supporting films, method for coating substrate with parting agent 78−11112
separation from substrate using plasma etching *(Slovak)* 80−45405
silicide, radioactive ^{31}Si as marker in thin film form. 77−62681
sink strengths for thin film surfaces and grain boundaries 80−88207
size quantized, thermomag. effects in strong mag. field *(Russian)* 77−63002
size-quantised electron states, band theory 78−75976
size-quantised films, sound amplification under ESR conditions 80−70322
size-quantising film pulsed inversion of adsorbed molecules 79−90889
solar energy utilisation, deposition techniques 80−84847
solid films and surfaces, conference, Tokyo, Japan (Jul. 78) 80−10739
solid surface and thin film anal. methods, review 79−34410
solid surface and thin film analysis by SIMS and AES 78−80825
solid-phase reactions, laser annealing 79−51438
spectroscopy, using Lummer-Gehrcke interferometer 77−5898
spherical, van der Waals' forces contrib. to thermodynamic props. 77−15724
spontaneous mactrostress calculation, from substrate deform. 80−15412
sputter profiling, combined Auger-X-ray anal. 80−66909
standard reference targets for nuclear reaction microanal., precision absolute thin films for ^{18}O and ^{17}O 79−2881
steel, austenitic stainless oxide film morphology, irradiation effects in N_2O_4 *(Russian)* 79−33209
STEM antisymmetric phase function imaging 79−21861
stress measurement, X-ray technique for film on single cryst. substrate 78−51860
structure, X-ray and electron diffr. methods comparison *(Czech)* 77−47696
structures chemical anal. using Auger spectroscopy *(Russian)* 78−92581
substrate-thin film system with rough boundaries, ellipsometric obs. using equiv. film theory 80−2310
surface anal. and depth profiling by spark-source mass spectrography, discharge model 80−40781
surface analysis, modern methods 80−54486
surface analysis, survey of ESCA, AES, SIMS and ISS techniques, appls. *(Hungarian)* 80−70544
surface analysis techniques survey, for development and production *(Hungarian)* 80−54537
surface and surface layer measurements, ellipsometric method 80−52295
surface density of states calc. within tight-binding scheme 77−55594
surface films on solids, TEM study method 80−65409
surface layer selective erosion using ion etching, cathodic sputtering, overview *(Hungarian)* 80−66682
surface layers and (001)-oriented thin films, weak-field magnetoresist. anal. 79−56329
surface structure, ang. depend. of MeV H^+ backscatt. yield in glancing geometry 79−4874
surface structure and topological modification during depth profiling, FIM obs. 79−78816
symposium, American vacuum society, Chicago (Sep. 1976) 77−39722
TCNQ, energy loss spectra of low energy electrons 78−19116
TEM, X-ray anal., mass thickness and chem. composition determ. 80−103227
temperature control for mech. meas. under light ion irrad. 78−86278
tetramethylammonium silver iodide superionic film, electrocodeposition, electrochem. cells 80−107478
theory and appl. *(Japanese)* 78−10580
thermal conductivity measurement 80−68199
thermal diffusivity of microsections, IR and X-ray electron-probe microanal. 78−2314
thermal expansion coefficient, determ. using optical dilatometer 80−45454
thermionic deposition 77−48349
thermodynamic theory of clustering and percolation transitions 77−47697
thermomagnetic effects in mag. field of arbitrary magnitude 78−47885
thermosensitive film coating, dispersed liq. cryst. microdroplets in gelatin matrix, exam. of preps. 80−42220
thickness and optical consts. determ. using surface plasmon excitation 79−47533
thickness determination, using backscattered electrons as tool 79−21704
thickness determination from range for transmitted, reflected, and absorbed ions and electrons 79−68173
thickness determination in electron microscopy, electron backscatt. method 77−47703
thickness distribution determ. by XPS 77−39743
thickness meas., electron probe anal., Monte Carlo technique *(French)* 78−41276
thickness meas. by in-depth-selective Mossbauer spectroscopy 79−63188
thickness meas. tool calibration by cubic spline fitting 77−18063
thickness meas. using X-ray interferometer based on small-angle scattering apparatus 80−27271
thickness measurement, automatic Brewster angle spectrophotometer 79−6078
thickness measurement, by electron backscattering 80−101904
thickness measurement, lattice absorption method *(Czech)* 77−172
thickness measurement, of amorphous and crystalline thin films 79−26186
thickness measurement, US waves, phase vel. and damping *(Russian)* 78−36969
thickness measurement and characterisation using proton-induced X-ray emission 80−35618
thickness measurement using calculator-coupled automated ellipsometer 77−82490
thickness measurement using Talbot effect 78−9321
thickness monitor, temp.-controlled, voltage readout 77−24953
thickness uniformity on rot. spherical substrate on planar wave holder 79−65351
tight-binding Green's functions for surfaces, thin films, and solid interfaces using random-walk theory 80−54753
TTF, energy loss spectra of low energy electrons 78−19116
TTF-TCNQ, energy loss spectra of low energy electrons 78−19116
thin films continued
TTF-TCNQ, mag. field effects on IR spectra *(French)* 77−48260
TTF-TCNQ film on KBr, IR spectra in mag. field 77−16310
tunnelling currents through very thin films, temp. and space charge effects 80−70799
ultracold neutron scattering 78−9915
ultrathin film thickness meas. by AES 79−35663
unbacked, optical constants by transmission interferometry 79−78778
uniformity, thickness meas. technique, appl. to polyimides 79−58672
US reflection coefficient meas., substitution method 77−31189
Vacuum Society conf., San Francisco, USA (Nov. 1978) 79−77862
vacuum techniques applied to surface and thin film phenomena 78−86280
van der Waals interactions, dispersion depend., semiempirical anal. from Lifshitz theory 77−15728
Wannier excitons 79−69426
X-ray diffraction, $I \sim \sin^2 x/x^2$ intensity eqn. verification *(German)* 80−19668
X-ray diffraction, used for characterisation 78−22991
X-ray fluorescence analysis, simultaneous determ. of comp. and mass thickness 77−90655
X-ray standardless thin film analysis in electron microscope 78−24006
X-ray technique for struct. evaluation, device appls. 78−75949
Ag-AgCl films, photoinduced dichroism *(Russian)* 79−56878
Ag-AgI, photoinduced dichroism *(Russian)* 77−1743
Ag-Er film, stress-induced g-anisotropy, EPR of Er 77−85566
Ag-Zr(Nb)(Mo) film, dielec. const., optical props., DC resist. and thermoelec. power 77−85824
AgBr thin film interstitials, Frenkel and space-charge contributions 79−18494
β-AgI thin film, exciton spectrum 80−55216
$Ag_7I_4PO_4$ film formation from electrolysis of HI-H_3PO_4 soln., electrocodepositional method 80−55315
Ag_2S film, tetragonal to cubic phase transform. kinetics, kinematic electron diffr. 77−4269
Ag_2S, optical characterisation, inversion method 78−11008
Al-Al_2O_3 films, coincidence energy spectra for (e, 2e) reaction 79−69936
Al-paramagnet mixture, film, nonlinear elec. props. *(Russian)* 77−24624
Al_2O_3, refr. index determ. by Nomarski differential interference contrast microscopy 78−24849
Al_2O_3/CuO, thin film interaction, $CuAl_2O_4$ form. *(Russian)* 78−52697
Al_2O_3-Cr(Re)(Nb)(Ta)(Ti)(V) heterophase films, elec. props. rel. to Al_2O_3 content 77−15969
Al_2O_3-Nb, cermet thin film, electrical transport and thermoelectric power 77−20462
Ar:Xe, solid, competition between electronic energy transfer and relax., photoelectron spectra 77−24929
Au-Ag, thin film struct., Rutherford backscattering spectrometry, signal overlap subtraction 80−50486
AuBr, spectra and luminesc., 100 to 200K *(Russian)* 77−69911
B and borides, conference, Varna, Bulgaria (Oct. 1978) 80−12842
B:C,H amorphous film, IR absorpt. spectra 77−77312
$BaCl_2$, non-crystalline film, disorder-induced Raman scatt. 80−11387
BaFCl, non-crystalline film, disorder-induced Raman scatt. 80−11387
BaO film, depend. of struct. on thickness 78−2391
$BaTiO_3$, thin film, obtained by modified doctor blade method grain orientation *(Japanese)* 77−77455
BeO, free film and Au substrate, transmission spectra and photoemission characts. 77−24925
Bi-SiO_2 cermet films, elec. and optical props. 79−78775
BiI_3 exciton peaks, temp. depend. 90-270K, and press. depend., up to 3500 atm. 77−36265
Bi_2O_3, oxide film on polycrystalline Bi, exam. of oxide film growth rate using XPS *(German)* 79−11041
$Bi_{12}SiO_{20}$, film and single cryst., optical absorpt. edge and optical transitions 79−33730
$Bi_xSi_yO_z$ films on Si, form. kinetics and props. 80−35358
C, amorphous, catalytic crystallization by Ni particles 79−14683
C, amorphous, surface plasmon dispersion, electron energy loss spectra meas. *(French)* 77−63504
C, backscattered electron intensities, ang. depend. 77−40317
C, deposited on Pt, H sputtering 77−69951
C film, oxidation, IR spectroscopic study 79−96162
C, for STEM specimen support, prep. and observation 80−93496
C, orientating action of solid substrates, on liq. cryst. layer exam. 80−44111
C, secondary electron emission rel. to energy loss 77−16438
C/Pt-W (8 wt.%), desorption of K from C film surfaces 80−59784
CaF_2 film, ionic migration study by Rutherford scatt., defects, secondary emission *(French)* 78−55982
Cd_2SnO_4, optical transmission and reflection, evaluation for solar heat collectors 77−52191
Co-Ar, struct., electron diffr. meas., rel. to metal-nonmetal transition 77−51626
Cr-SiO, laser beam-treated, emission mode of SEM 79−28226
Cr-SiO cermet film, silicide form. during deposition 77−12535
Cr-SiO cermet thin films, thickness effect on density, resist., adhesion and annealing coeff. 77−69432
$Cr_{11}Ge_8$, CrGe and $Cr_{11}Ge_{19}$, amorphous *(Russian)* 78−56050
Cr_3Ge amorphous films, short range order struct. *(Russian)* 78−30841
Cu-Al_2O_3 cermet films, temp. depend. of AC and DC cond. 79−87166
Cu-Au film, short wavelength composition modulation, interdiffusion exam. 77−72723
Cu-Ni film, (001), in situ oxidation, TEM obs. 78−23874
Cu-Xe film, metal-nonmetal transition, optical and resist. meas. 77−89818
CuCl, photosensitive film formation on Cu 77−9105
DySe, formation and crystallographic charact. of thin film phase 78−91574
ErD_2 thin film, degradation during film processing, investigation 80−101047
ErO_x films, phase transforms. 77−62784
ErO_x, nonstoichiometric film, short-range order characts. and its effect on elec. behaviour 79−99435
Fe-Al, optical props., comp. and order-disorder transform. depend. *(Russian)* 79−28852
Fe-Al_2O_3 granular film, interface props., Mossbauer spectroscopy 80−34336

thin films continued
Fe-Cr alloy, sputter etching oxide film, comp. profile, quantitative AES 80−81383
Fe-Gd films, crystallisation, electron microscope obs. 79−15034
Fe-SiO_2 granular film, interface props., Mossbauer spectroscopy 80−34336
Fe-ZrO_2 granular film, interface props., Mossbauer spectroscopy 80−34336
FeB thin films, produced by ion bombardment on Fe and plain steel, X-ray struct. anal. *(French)* 79−73413
Fe_2B thin films, produced by ion bombardment on Fe and plain steel, X-ray struct. anal. *(French)* 79−73413
$FeSi_2$ films, Mossbauer investig. of struct. 79−87341
FeTe, on amorphous substrates, Mossbauer obs. of struct. 78−27142
Ga-Xe film, metal-nonmetal transition, optical and resist. meas. 77−89818
GdF_3, chemically reacted film on ferroelectric-ferroelastic $Gd_2(MoO_4)_3$, characterisation 79−15057
GdO film, new reduced variant due to annealing 77−89660
Gd_2O_3, 'monoxide' film reidentified as sesquioxide formed by oxidation by hydride 79−19474
Gd_2O_3 photoabsorpt. spectra, band struct., at ionisation mechanisms, electron energy loss spectra 77−24909
Ge-Al film, amorphous, EPR meas. 78−80212
Ge-Cu film, amorphous, EPR meas. 78−80212
$In_{2-x}Sn_xO_{3-y}$ thin films, optical transmission and elec. resist. 77−69926
IrO_2 film, A-C response 80−107926
KBr film, oblique incidence transmission spectra for polarised extreme UV radiation 78−39614
KCl film, oblique incidence transmission spectra for polarised extreme UV radiation 78−39614
KCl film, porous, injection mechanism for transmission secondary electron emission 78−19643
$KMnF_3$ film, photoelec. yield spectra, rel. to band struct. 78−43980
$KZnF_3$ film, photoelec. yield spectra, rel. to band struct. 78−43980
Kr, film, absorpt. in exciton region 78−52529
LiF, evaporated film, thermally stimulated exoelectron emission rel. to thermolum. 79−47602
LiF film, surface phonons and thickness variation, EELS meas. 80−92774
Li_3N thin film, vacuum evaporation on WO_3, retarded deposition 80−108351
MgO film, graphitic C detected by surface Raman spectra 80−2297
MgO, free film and Au substrate, transmission spectra and photoemission characts. 77−24925
MgO, with high secondary electron emission, growth on Al-Mg alloy 78−35590
MgO:Ni^{2+}, single crystal, thin film, near IR luminescence *(Russian)* 79−28807
Mn-MgF, cermet film, variation of resist. with deposition rate 77−43747
Mn-SiO cermet film, silicide form. during deposition 77−12535
Mn-Ti surface treatment on Al_2O_3 insulators 79−24261
MoS_2 film, adhesion to oxidised metal surfaces, XPS meas. 78−22972
MoS_2, growth in Mo(111) surface following chemisorption of H_2S 77−1329
$MoSi_2$ layer, formation kinetics on Mo, effect of direct elec. current 79−99436
Mo_5Si_3, electrotransfer of Si 80−92708
NH_3, film, on metal substrate, surface struct. using LEED 79−77879
NH_3 solid film, absorpt. coeffs. determ. 50 to 7000 cm^{-1} 80−97356
Na-Ar, metal-nonmetal transition 77−62966
$4NbO_{0.76}$ thin film, FCC cell struct. investigation 80−92796
Ne:Xe, solid, competition between electronic energy transfer and relax., photoelectron spectra 77−24929
Ni-SiO cermet film, elec. resist., percolation effects 77−76954
Ni_3C films, form. by carburisation, characterisation 80−34337
NiCo film, crit. angle meas., pinning mech. 79−1719
NiGe, and Ni_2Ge, amorphous film, electron diffr. exam. of struct. 77−35828
Ni_3Ge, amorphous film, electron diffr. exam. of struct. 77−35827
NiH_η thin film, X-ray phase analysis *(Russian)* 77−59124
Pb-Xe(Ar), struct., electron diffr. meas., rel. to metal-nonmetal transition 77−51626
$PbCl_{2-2x}I_{2x}$, orthorhombic, absorpt. spectra 77−59633
β-PbF_2 film, ionic migration study by Rutherford scatt., defects, secondary emission *(French)* 78−55982
PbI_2 film, photolyzed, refr. index change 78−11010
PbI_2, film intercalated with pyridine, UV absorpt. spectrum, Frenkel excitons 77−24864
PbI_2, fundamental absorption edge, complex dielec. const. *(Russian)* 77−40266
PbI_2, spectral depend. of optical consts. on fundamental absorption edge *(Russian)* 77−16415
PbO, on Na_2O-B_2O_3 glass, deep penetration of Pb^{2+} ions into glass 78−79535
PbO-SiO_2, glass on Si, emission mode of SEM 79−28226
PbO_x layer, ellipsometry, compensator inaccuracy evaluation 79−54170
$Pb_xSi_yO_z$ films on Si, form. kinetics and props. 80−35358
$PdH_{1.18}$, $PdH_{1.20}$, prep., cryst. struct., chem. comp. determ. by thermal decomp. 80−34334
PdO, optical props., 0.5-5.4 eV 79−56813
PtSi, growth under protective layers on Pt covered Si substrates, X-ray diffr. and Rutherford backscattering anal. 78−22965
PtSi thin film structures, preferential sputtering meas. Rutherford backscatt. 79−43087
$(SN)_x$, evaporated on low temp. substrate, elec. cond. 77−63003
$(SN)_x$, polycryst. films, single crysts., UPS, valence band struct. 77−69967
$(SN)_x$, reflectivity spectra meas. by synchrotron radn. 79−91513
S_2N_2, cryst. and partly polymerised films, Raman scatt., optical absorption 77−8673
SbI_3, exciton peaks, temp. depend. 90-270K, and press. depend. up to 3500 atm. 77−36265
$Sb_xSi_yO_z$ films on Si, form. kinetics and props. 80−35358
Sc_2O_3 photoabsorpt. spectra, at. ionisation, band struct. mechanisms, electron energy loss investig. 77−24909
Si-Al, silumin, crystn. of eutectic phases *(Russian)* 80−29942
Si-containing films, formed by reaction of Si with organic compounds of N, struct. investigation 79−87009
SiO_2-TiO_2(Al_2O_3)(ZrO_2), noncrystalline film form., IR study *(Japanese)* 77−59634
thin films continued
SmB_6, crystn., struct. and elec. resist. 77−63559
SmO film, new reduced variant due to annealing 77−89660
Sm_2O_3, 'monoxide' film reidentified as sesquioxide formed by oxidation by hydride 79−19474
SmSe, formation and crystallographic charact. of thin film phase 78−91574
SnI_2 film, absorpt. spectrum *(Russian)* 79−43056
SnI_2, single crysts. and film, optical props. 77−32437
$SrCl_2$, non-crystalline film, disorder-induced Raman scatt. 80−11387
SrF_2, optical props., spectral dependence, 460-1000 nm 80−76094
TaN, characteristics of Pirani type vacuum gauge *(Japanese)* 80−13086
TaN, in Pirani type vacuum gauge *(Japanese)* 80−52257
$2Ta_2O_3$ thin film, FCC cell struct. investigation 80−92796
TbSe, formation and crystallographic charact. of thin film phase 78−91574
Ti-Al_2O_3 system mixed films, prep., phase comp., struct. and elec. props. 79−37930
TiN-Nb(Ta)N, microcomposite film prod. for radio resistors 78−3052
TiO_x films, refl., 2-25 eV 80−55123
Ti_xO_y, AES, with and without simultaneous sputtering, beam effects 77−90224
UO_2-U_3O_8, sputtering under influence of fission fragments at low doses 77−48282
VO_2, optical and elec. props., 0.8 to 4.2 mm, near metal-semicond. transition 77−32473
VO_2-α-Fe_2O_3-Si, transverse elec. field effect on switching V-I charcts. *(Russian)* 77−55591
V_2O_5 film, electrochromism, X-ray electron spectra 78−48146
V_2O_5 film, optical absorption in 1.0 to 5.5 eV range 78−19586
V_xO_y, phase transformation interference reversible light reflector material, visualisation of CW EM radiation 79−71531
VSi_2 thin film growth rel. to annealing environment and interposed layers 78−2395
WO_3, amorphous, band struct. and colour-centre band, fast electron energy loss spectrum 77−55478
WO_3, amorphous, electrochromism and local order 77−59553
WO_3, amorphous coloured film, charge transfer, XPS 77−12491
WO_3 film, amorphous, struct. and crystallisation, high resolution electron microscopy 78−43268
WO_3 film, electrochromism, X-ray electron spectra 78−48146
WO_3M_x (M=H, Li, Na, K, Ag), bronzes, atom motion 78−75874
YH_2, struct. and elec. resist., electron diffr. meas. 78−87888
Y_2O_3, photoabsorpt. spectra, at ionisation, band struct. mechanisms, electron energy loss investig. 77−24909
Y_2O_3, thermoluminesc. in H_2O vap. atm., temp. depend., time decay *(Russian)* 77−44074
Y_2O_3:Eu sintered slice, DC electroluminesc., impact excitation 79−47522
YbSe, formation and crystallographic charact. of thin film phase 78−91574
ZrO_2, thermoluminesc. in H_2O vap. atm., temp. depend., time decay *(Russian)* 77−44074

third-order optical susceptibility *see nonlinear optical susceptibility*

thixotropy
blood, rheological parameters for viscosity, viscoelasticity and thixotropy 80−16963
butadiene-styrene block copolymer, viscoelastic props. 79−8336
clay suspensions, with negative thixotropy, hysteresis loops, deflocculant addition effect 79−52789
clays subject to vibr., influence of various electrolytes *(French)* 77−41024
coagulation kinetics, diffusion effects and rheological models for thixotropic fluids 80−43740
coal tar pitch, containing mesophase, thixotropic changes occurring on reheating 79−90205
colloids, nonlinear rheological behaviour and shear dependent struct. 79−7358
dispersions, mech. props., structural hysteresis, statistical thermodynamic anal. 77−46978
eye striated muscle, bovine, physico-chemical anal. of contractile proteins 77−90819
flow behaviour of disperse systems, the thixotropic compromise 79−77232
inelastic fluid, rheological characterisation 80−38373
liquid mixing, power requirement 77−15070
polyisobutylene, Aerosil-filled, solution, periodic and unidirectional deform. effects 77−42791
resin paste, characterisation by extrusion rheometer 77−63876
review 79−59959
rheological equations, for thixotropic-dilatant structs. 79−64616
skin, human forearm, rotary displacement obs. 79−39438
structure formation in dispersed media, rel. to phase transitions of second kind 77−7355
suspension, rheological thixotropy analogue simulation study with plane-cone Ferranti-Shirley viscometer *(French)* 77−65725
thixocasting, review 77−4757
AgI solid electrolyte plastic deformation and thixotropy obs. 78−79660
AlN, thermoplastic slips, viscosity, thixotropy, dilatance determs. 80−25633
Li_2SO_4 solid electrolyte plastic deformation and thixotropy obs. 78−79660
TiN, thermoplastic slips, viscosity, thixotropy, dilatance determs. 80−25633

Thomas-Fermi model
alkali metal diatomic ions, core-core interaction potential calc. 78−25645
alloy, binary, charge transfer and alloy binding, Thomas-Fermi-Dirac approx. 77−76775
analytical solution with Amaldi correction for ions *(Russian)* 77−18790
anomalous nuclei, crit. charge *(Russian)* 78−8736
atom, quasiclassical corrections to Thomas-Fermi model, electron density eqns. of state 78−25404
atom, spin waves and spin polarisability, Thomas-Fermi ground state 77−65538
atomic interaction energy calc., comparison with expt. 77−66131
atomic interaction energy calc. 77−66130
atomic scatt. factors and momentum densities, asymptotic form 80−74105
atoms, multistage ionisation in strong EM fields, Thomas-Fermi calcs. *(Russian)* 80−58226
atoms in strong mag. field 78−62724

Thomas-Fermi model continued
channelling and semistatistical model for interatomic pot. 79−33024
close-packed metals, elec. field gradients, vol. and struct. depend. 78−64014
contact exciton, screening and quenching 80−29334
covalent semiconductors, vacancy screening, dielec. const., exchange correl. pot., Thomas-Fermi description 80−44528
diatomic systems, correl. diagrams, Thomas-Fermi calcs. 80−23294
diatomic systems, Thomas-Fermi and Thomas-Fermi-Dirac-Weizsacker eqns., solns. 80−23293
diatomics, TFDW eqn., correlation diagrams 79−59355
Dirac exchange and relativistic corrections, effective EM potential 79−89614
donor-acceptor pair lines, broadening due to potentials of ionised impurities 79−51522
droplet of nucl. matter under rapid rot., anal. using Thomas-Fermi method 79−36179
electron plasma, impurity screening effects in intermediate degeneracy region 80−14882
electronic elementary excitations in far UV, core level exciton and core hole polarisation 78−39032
equations of state, very high press. and temp., Thomas-Fermi shell model 78−79738
graphite intercalation cpds., electrostatic interactions and staging, nonlinear Thomas-Fermi eqns. 80−107732
Hartree-Fock densities in Thomas-Fermi-Dirac formulas including inhomogeneity term 77−6680
image charge pot. at interface of two semi-infinite media, Thomas-Fermi soln. 79−87155
inert gas pairs, Thomas-Fermi-Dirac interaction pots. 77−75253
inhomogeneity correction for atom in strong mag. field 80−27947
interatomic potential for atomic pairs, Thomas Fermi model with quantum corrections 80−32797
ion, iterative soln. of Thomas-Fermi eqn. using nonlinear eigenvalue problem 78−909
ion, Thomas-Fermi-Dirac model for mag. susceptibility and binding energy 77−67981
iterative solns. to Thomas-Fermi eqn. 79−9185
lamellar graphite acceptor intercalation cpds., charge distrib. in c direction 78−87935
local density functional theory of atomic and mol. ground electronic states 80−23286
low energy heavy particles, total energy loss distribs. after penetration through matter 78−14385
many-valley semiconductor, metal-insulator transition at finite temp., calc. 80−49603
metal, core overlap interaction, interatomic forces 78−47724
metal, electron gas, local density functional for kinetic energy near defect, metal surface 80−20105
metal, single-particle density matrix, perturbation expansion 80−54635
metal surface electronic barrier, elec. field effect in presence of adsorbate 80−49864
metallic film, discontinuous, energy for electron transmission between two neutral islands, determ. 77−80852
metals, cohesive properties, energy density functional-pseudopotential method 79−73462
metals, simple, electrons around vacancy, Thoms-Fermi eqns. 77−15791
metals, simple, static props., Thomas-Fermi-pseudopotential approach 80−75514
modification, many-electron system in HF approx. 79−85899
neutral isolated atom, iterative soln. of Thomas-Fermi eqn. using nonlinear eigenvalue problem 78−909
neutral systems, positivity of pressure and compressibility 79−13639
nonlinear problem connected with Thomas-Fermi-Dirac eqn. 77−22483
nuclear collective motion, fluid dynamic approach 78−17121
nuclear kinetic energy density, extended Thomas-Fermi approx. 77−2919
nuclear matter and surface, relativistic calc. 78−25142
nuclei, finite, extensions of Thomas-Fermi approx. 77−6256
nuclei, static and dynamical Thomas Fermi theory 77−18599
nucleon, EM structure 80−9170
nucleon matter, Thomas-Fermi model rel. to eqn. of state at subnuclear densities 80−77278
p-n junctions, dielectric function calcs. of analytic charge distrib. 79−78161
plasma, dense, nondegenerate, electron transport, thermal cond. *(Russian)* 79−98865
positive ions, in extremely strong mag. field, 1/Z expansion for total energy 80−52855
positron annihilation enhancement effect, positron correl. with tightly bound electrons 77−73184
pseudopotentials and atomic core radius 78−95248
quantum-statistical eqn. of state *(Russian)* 77−9953
radiation damage cascade, time-energy distrib. of atoms 77−1159
relativistic generalisation for the atom, scaling and critical charge 80−63554
rotating nuclei in Thomas-Fermi approach 77−18442
screening in inhomogeneous systems 80−20106
semi-metals, layered, nonlinear screening 79−60746
semiconductor, dielectric screening, Thomas-Fermi model 80−49648
semiconductor, electronic properties, rel. to chem. bonding and lattice dynamics 80−44169
semiconductor, nonlinear impurity screening 78−67977
semiconductor, Thomas-Fermi dielectric screening eqn. 78−10388
semiconductor-metal transition, modified screened impurity pot. 79−99500
stability of matter, nonrelativistic quantum mechanics and Thomas-Fermi theory 77−5696
stability of matter, Thomas-Fermi theory 77−5678
statistical theory of matter, review 77−84
superconductors, polyvalent metals, Brillouin zone boundary influence on Coloumb interactions 80−24827
supercritical nuclei, Z>137, relativistic Thomas-Fermi eqn. soln. *(Russian)* 78−29748
surface properties from Thomas-Fermi calc. 80−13394
turning point in Thomas-Fermi approx. 77−71573
X-ray elastic scatt., electron density and ionisation pots., Thomas-Fermi and Hartree Fock anal. 79−52041
π^0 condensation in finite system, extended Thomas-Fermi model 78−41645
Al-Al, Thomas-Fermi-Dirac model, inhomogeneity corrections 80−23308
Ar, at. struct., with Fermi-Amaldi correction 79−81156

Thomas-Fermi model continued
Ar, incoherent X-ray scatt., statistical atom model 78−29747
Bi, film, quantum size effect, electric field effect, Thomas-Fermi approx. energy surfaces, cond. 78−47890
GaP, Thomas-Fermi theory, dielectric functions, screening, dielectric constants 79−99497
Ge, donor ion pot., small r behaviour of nonlinear Poisson eqns. 80−54652
He, thermodynamic props. and eqns. of state in stellar conditions 79−35241
Kr, at. struct., with Fermi-Amaldi correction 79−81156
N, elastic electron scatt., low energy, linear algebraic method 77−88562
N-N, correl. diagrams, Thomas-Fermi calcs. 80−23294
N_2, TFDW eqn., energies calc. 79−59355
Na, liquid, eqn. of state and thermodynamic props. at high temp. and density 79−55902
Na, self-consistent central field potential and physical quantities 78−79956
Ne, at. struct., with Fermi-Amaldi correction 79−81156
Ne, temp. perturbed Thomas Fermi eqn., variational principle 80−69074
Ne-Ne, correl. diagrams, Thomas-Fermi calcs. 80−23294
Ne-Ne, Thomas-Fermi-Dirac model, inhomogeneity corrections 80−23308
Pb, electronic thermal Gruneisen parameters 80−39242
Rn, at. struct., with Fermi-Amaldi correction 79−81156
SO_2, total electrostatic pot., Thomas-Fermi eqn. soln. 79−10034
Si, donor ion pot., small r behaviour of nonlinear Poisson eqns. 80−54652
Si, electronic properties, rel. to chem. bonding and lattice dynamics 80−44169
Si, electronic screening of lattice vibrs. 78−59875
Si, vacancy screening, dielec. const., exchange correl. pot., Thomas-Fermi description 80−44528
Sn^{4+}, electron density function, Thomas-Fermi calc. 80−6763
Th, electronic thermal Gruneisen parameters 80−39242
Tl-Te alloy, liq., bond equilib. theory for electronic props., thermochemistry 77−89365
Xe, at. struct., with Fermi-Amaldi correction 79−81156

Thomson effect
irreversible phenomena in homogeneous materials, and single and double bimetallic junctions *(French)* 78−95291
metals, anomalous Thomson effect 79−65435
multijunction thermal convertor AC/DC transfer, Thomson effect error reduction 80−103679
neutron stars, magnetic, Thomson scatt. rel. to radiative heat transfer in surface layers 80−94826
semiconductor, dumb-bell shaped specimen, vol. component determ. of Seebeck effect 80−49788
thermocouples, thermoelectric effects, reversibility, theory 77−59280
thermoelectric energy conversion, heat losses compensation due to thermal cond. through Peltier heat 80−107773
Thomson scatt. from thermal plasma, intensity depend. frequency shift 78−42770
Cu-Fe wire, low-temperature measurements, undergraduate lab. project 78−54119
Pb, absolute thermopower, Thomson heat expt. 79−65434
Pb, Thomson heat meas. and thermoelectricity absolute scale between 10 and 350K 77−28162
P-Si, highly doped, thermoelec. coeffs. meas. at semicond. solid-metallic liq. interface 77−39887

thorium
see also nuclei with .....
$^{232}Th/^{238}U$ comparative breeding potential in LMFBR blankets 80−22948
absorption coefficients, near O_{IV} O_V thresholds, 5d cross sections calc. 78−90134
abundance determ. for rocks using NaI detectors 79−80043
abundance in Archaean granites from NE.Minnesota 78−61356
abundance in Indian kimberlites 77−60376
abundance in Precambrian basement, W.Canada, petrologic and tectonic controls 80−17257
adsorption of O_2, and oxidation, electron-induced luminesc. expts. 78−38946
adsorption of O_2, XPS study 80−7473
adsorption on W film, work function, temp. depend. 77−28701
atom, Compton cross section, due to L-shell electrons, ang. variation 77−3322
atom, Compton scatt. of 1.12 MeV γ-rays by K-shell electrons 77−54539
atom, Compton spectrum due to L-shell electrons 77−34593
atom, incoherent scatt. of gamma rays 77−79585
atom, inelastic scatt. cross section of 279 keV photons by K-shell electrons 77−54537
atom, ion induced K-shell ionisation cross-sections determ. by comparison with nuclear Coulomb excitation 79−76500
atom, K-shell electrons, Compton scatt. of 1.12 MeV gamma-rays 77−68016
atom, K-shell electrons, Compton scatt. of 1.12 MeV gamma-rays, energy distrib. meas. 77−68017
atom, photon-bound-electron scatt. meas. 77−14394
atom, X-ray L shell emission spectra *(Spanish)* 79−98016
atom reson. localised 5,ef continuum state, giant reson. 80−91467
atom X-ray spectra, mass absorpt. coeffs. in ultrasoft region, spectral depend. 77−10622
automated Rn-Th monitor for earthquake prediction research 78−73532
BWR physics methods compared with ^{232}Th lattice benchmarks 79−9711
CANDU, Pu-topped Th fuel cycle characts. 79−36322
CANDU-PHW fuel cycle, study of running-in period 78−25313
Cerro Impacto, Venezuela, thermoluminescence radiation dosimetry appl. to Th prospecting 78−32244
chemical and isotopic anal. of U, Pu, and Th in nuclear fuel materials 79−81046
coadsorption with H on W surface 79−90869
content in natural samples, γ spectrometric determ. *(Russian)* 78−92562
correlation effect of crystal pot., RAPW calcs. 78−6265
denatured Th fuel cycle evaluation 79−13421
density functional theory 80−15442

thorium continued
determination, in natural waters, spectrophotometric method *(German)* 78−70952
determination in obsidian from northern New Zealand, archaeological sourcing method appl. 79−2239
diffusion and electrotransport of Fe, Co and Ni, 965-1625°C 79−90828
diffusion of fission products 77−4220
diffusion of Ni, Fe, Fe-Ni-Cr, at 500 to 800°C *(German)* 79−28157
dosimetry by plastic solid state nuclear track detectors 78−20556
elastic constants of single cryst., 4.2-300K, effect of C addition 77−90386
electronic states under press. 80−54600
electronic thermal Gruneisen parameters 80−39242
electrotransport of V, Nb and Ta, 1370-1665°C 78−59979
electrotransport purification under low press. 80−15303
fabrication of Th-based fuel pellets 78−86669
FBR, neutron/physical behaviour of thorium, expt. *(German)* 78−94109
FBR performance characteristics 79−9815
FBR Th-based metal alloy fuels, determ. of solidus temperature 80−104124
FCC, ground-state props. 78−75989
Fermi surface press. depend., de Haas van Alphen meas. 78−39006
field ion microscopy study of structure 80−59437
film, coating on Rh layer, work function rel. to degree of coverage *(Czech)* 78−80039
fission reactor fuel, U substitute, arguments against 77−54305
fission reactor fuel cycles for HWRs 77−34401
fission reactor fuel reprocessing, dibutyl phosphoric acid form. by degradation of TBP-n-paraffin extractant 77−70316
fission reactor fuel reprocessing, doses received by TBP-n-paraffin extractant 77−70315
fission reactors, integral experiments for testing Th and ^{233}U data 80−27707
fuel, resources and process technology 79−59170
fuel cycle, feasibility study, CANDU system 78−86619
fuel cycle, U cycle comparison use in LWRs *(Spanish)* 80−32420
fuel cycle for CANDU reactors 78−86620
fuel cycle for HTGR, merits 77−46385
fuel cycle performance in CANDU reactors and LMFBR 79−9742
fuel cycle role in thermal and fast reactors 79−13420
fuel cycles, Savannah River Plant processing experience 79−59243
fuel in power reactor systems, radioactive waste hazard anal. 79−30941
Funka Bay, Japan, ^{234}Th removal from seawater 80−61803
fusion hybrid reactor blanket, reaction rate calc., central DT neutron source, ENDF/B-IV cross sections 80−13792
gamma ray analysis of K, U and Th for dose-rate estimation in thermoluminescent dating 79−79333
GCFR lattice, Th reaction rate meas. 80−656
geochemical prospecting 80−72635
geological samples, f/α particle track anal. for U, Th and isotropic disequilibria 78−7799
graphite-Th assemblies for fusion blankets, neutronic calcs. using 14 MeV source 79−59262
ground state properties of f band metals 78−91607
groundwater in Grants Mineral Belt, New Mexico, effects of U mining and milling 77−56657
heat capacity, from 80 to 1000K of high purity metallic sample 80−34201
HTGR fuel, French, fabrication, irrad. performance *(French)* 79−30934
HTR fuel cycle program in the Federal Republic of Germany 80−544
HWR, Th advanced fuel cycle 77−67864
hydrochemical prospecting, APDC coprecipitation and X-ray spectrometry for trace element determ. 77−37445
interband, collective and atomic (p,d) excitations, Z-160 eV, fast EELS 80−93443
interband structure and role of 5f electronic states, optical reflectivity meas. 77−76744
ion irradiated, surface C and O, AES obs. 78−71775
isotope abundances in E.Pacific surface waters 78−96234
L-shell electrons, incoherent γ-photon scatt. cross-sections 78−62768
labile component, on marine sediment particle surfaces, surface layer thickness meas. 78−40592
lattice dynamics, crystal equilib. 78−47479
lattice dynamics, local model pseudopotential applic. 77−39646
lattice dynamics, unpaired forces 80−15201
lattice dynamics in reson. model pseudopot. theory 79−19334
lattice parameter variation at low temp., thermal expsn. 80−15046
LMFBR, effects of Th breeder material on Na-void reactivity 80−22982
LMFBR, heterogeneous, Th blanket zones study in ZPPR Assembly 8 80−22983
LMFBR performance of Th-based fuel cycles 79−9744
luminescence characteristics of pure surfaces acted on by flux of field emission electrons 80−100695
marine sediments from W Indian coast, geochem. of Th and daughter products 77−41019
metal rods, neutron capture, effective resonance integral meas. 77−71653
microdistribution in stony meteorites 79−75162
nondestructive assay reference materials 79−49702
nondestructive measurement of U and Th conc. and quantities using XFA and gamma spectrometry 80−71877
nuclear, fuel cycles, nonproliferation aspect of ^{232}U presence in ^{233}U-Th fuel cycle 80−57839
nuclear fuel, reprocessing, proliferation-resistant fuel cycles *(German)* 79−639
nuclear fuel appl., HTGR systems development 79−93717
nuclear fuel element reprocessing, avoidance of third phase *(German)* 79−6756
Oklo natural fission reactor, radioactive dating from Pb and Th meas. *(French)* 80−21762
optical reflectivity 80−16054
phonon dispersion, one parameter model pseudopotential calc. 78−26643
phonon dispersion curves, angular force electron gas model 77−7801
phonon dispersion relations, non-central electron fluid model 80−100312
phonon dispersion relations and lattice heat capacity, modified Bhatia model 77−20024
phonon dispersion relations and lattice heat capacity calc. 77−20023
phonon dispersion spectra from 5-parameter lattice dynamical model 78−10136
phosphate fertilizer, specific activity of U and Th rel. to particle size 80−106244
photoelectric cross section, total to K-shell ratios 78−5188
photoelectric cross sections of low energy photons 78−46309
photoelectric cross-section at K-edge measurements 78−2983
photoelectron spectra study, core and valence levels 80−66394
PIXE elemental anal. at $\mu g\ g^{-1}$ levels in ore samples 80−55758
power reactor fuel cycles, Pu, Th and U evaluation 79−26706
power station ashes, Th, U, and K conc. meas., dose rates in Poland 79−100754
prospecting, use of alpha sensitive plastic films 79−39980
prospecting method, using Ra accumulation in animal thyroid glands, anal. 78−27853
PWR, Th cycle, parametric anal. 79−26467
radioactivation analysis, of biological and geological materials, separation methods *(French)* 77−90700
rare metal ores, quantitative relns. between Ta, U, Th and Zr 77−56629
reactor fuel cycle, utilisation in light and heavy water reactors 79−26690
reactor fuel cycle in water moderated reactor systems 79−26691
reprocessing, continuous solvent extraction feed prep. 80−13773
reprocessing by Thorex solvent extraction process at Savannah River Plant 79−36381
resources and prospecting techniques and equipment development in India 79−30923
sand grains containing high ^{238}U and ^{232}Th concentrations, enhanced natural radiation exposure *(German)* 80−51018
sedimentary rocks, Th and U abundances rel. to crustal evolution and sedimentary recycling 80−85654
separation, by column extraction chromatography 78−44421
solar nebula, Th, U, Pu and Cm condensation and fractionation 79−35154
solid fuel utilisation in power reactors *(Japanese)* 78−74433
superconducting transition temperature calculation 79−7928
surface (111), struct., Debye temp., and oxidation, LEED and AES obs. 77−89625
surface structure, $He^+(Ne^+)(Ar^+)$ impact, appl. of double pass cylindrical mirror analyser 78−72658
thoron content in exhaled air, meas. apparatus 79−34672
tracer for atmospheric stability *(Spanish)* 80−51448
use in LMFBR blankets 79−9743
vacuum thermal reduction of Ho oxides *(Russian)* 80−16226
valence and 5f states, XPS and bremsstrahlung isochromat spectroscopy 80−66393
Venus surface rock, radioactive element concs., Venera 9 and 10 meas. 77−78691
X-ray emission following H and O ion impact, parameter depend. 80−66327
XPS of 5p level, screening and configuration interaction effects 80−54633
CaF_2:Th, electron irrad. defect aggregates, ordering, impurity effects 80−75216
CaF_2:Th electron microscopy study of lattice deformation due to electron irrad. 79−65077
$Ce_{1-x}Th_x$ solid mixture, isostructural phase transitions 77−84884
LMRBF, ^{233}U-Th fuelled pin diameter optimisation 79−9687
(La,Th)-Ce, dilute alloys, mag.-nonmag. transition of impurity moments, environment effects 77−40034
LiCl-KCl:Th^{n+}, fused eutectic, electrolytic behaviour *(Japanese)* 79−16009
(Th, U) fuel, burnup determ., using ^{148}Nd 78−82459
Th fuel cycle and technology 79−31114
Th II, oscillator strengths calc. 80−27982
Th, K-shell photoionisation, cross section meas. K X-ray-photoelectron coincidence method 79−72285
Th metal, diffusion and electrotransport of Th metal 78−86611
Th/^{233}U fuel cycle in FBR and thermal convertors 79−9745
Th-^{233}U fuel cycle, in molten-salt reactor, efficient fuel utilization without Pu separation 79−26499
Th-based fuel development for breeder reactor appl. 79−54502
Th-PuO_2 kernels, effect of fuel particle size on power excursions, Doppler feedback mechanism 79−30911
Th-W, TF electron emitters props. obs. 80−66403
Th+H^+, K-shell ionisation, 7-15 MeV, relativistic effects 78−82830
Th+H^+, L-shell ionis., 0.5-3.5 MeV, X-ray emission obs. 77−54528
Th+$H^+(D^+)$, L-subshell vacancy production, Coulomb deflection effects 80−9711
Th+Kr^{n+}, K-L level matching, X-ray obs. 79−63948
Th+O_3, assoc. ionis. cross sections, in crossed beams, mass spectra obs. 78−94317
Th+X^+, X=O, N, N_2, CO_2, charge transfer cross-section, 1-500 eV 78−82835
Th(IV), selective separation from rare earth elements on chelate ion exchangers 78−58861
$ThNi_{5-x}Al_x$, absorption of H, form. of hydride 77−84932
^{227}Th, short-lived α-emitter, late effects after incorporation in mice 78−96069
^{228}Th, exposure rates from gamma sources in dwelling room walls, Monte Carlo calc. 78−73260
^{228}Th-^{228}Ra radioactive disequilib. rel. to coastal pollution in New York Bight 79−29784
^{230}Th dating of fossil corals and shells 80−12434
^{230}Th determination in U ores, dusts and mill tailings 78−15736
^{232}Th, assay in phosphate containing materials by solvent extraction-liquid scintillation method 79−22447
^{232}Th, conc. in New Zealand soils 77−53057
^{232}Th cycle, review of low cost fuel cycles using two separate fuels 79−45389
^{232}Th, decay consts. for use in geochronology and cosmochronology 78−28189
^{232}Th enrichment by linear accelerator for LWR 79−13497
^{232}Th enrichment by proton accelerator 79−13498
^{232}Th, in aq. soln., assay by pulsed neutron interrogation 78−68966
^{232}Th irradiation in VVER reactors, relative accumulation of ^{232}U and ^{233}U 79−71923
^{232}Th, neutron spectra for fusion + hybrid reactor materials 80−23142
^{232}Th, radioactivity in Straits of Malacca marine environment 79−12135
^{232}Th, reevaluation of dose unit per unit intake 80−26356
^{232}Th, terrestrial beta radiation field in natural environment, numerical evaluation 78−81161
^{232}Th, Thorotrast kinetics and radiation dose 79−39523
^{232}Th utilisation in reactor fuel cycles, review 79−45390

thorium continued
^{232}Th-makrofol, solid state nuclear track detector, neutron response 80−27876
^{233}Th cycle for prod. of ^{233}U for thermal neutron reactors, review 79−45388
^{233}Th, role and importance in extension of nuclear fuel resources 79−45325
^{234}Th, isotope separation by extraction column chromatography using TnOA and filter paper 79−43659
^{233}U-^{232}Th fuel cycle alternatives to LMFBR 79−9741
^{233}U-^{232}Th reactor as burner of actinide wastes 77−23235
^{234}U→^{230}Th→^{226} Ra, superposition soln. of transport of decay chain through sorbing medium 80−37500
^{234}U→^{230}Th→^{226}Ra decay chain, hydrogeological migration anal. 80−37501
^{136}Xe+Th, 625 MeV, probability of forming 1sσ vacancies 78−25681
ZrO_2:Th, thermoluminescence, traps and emission centres 79−24373

thorium compounds
alternative fuel cycles, waste management aspects 79−59204
BWR Th cycles with improved performance 79−59138
CANDU reactor, Pu-topped Th cycle characts. 79−31101
ceramic fission reactor fuels, high temperature chemistry, nonstoichiometry, review 77−14238
ceramic recycle fuels, metal-clad, fabrication technology 79−59244
Cl ThO_2 glasses, thermal anal. *(French)* 78−14282
ESCA spectra, configuration interaction satellites 77−30923
fast molten chloride reactor on Th cycle 79−67839
HTGR fuel recycle technology 79−59246
monazite mineral, high-energy alpha emitters, E≥10.6 MeV 79−48467
orthovanadates:rare earth ions, spectroscopic props. 77−16363
phthalocyanine, phase contrast characteristics in STEM 80−100153
sulphito complex ion precipitation with hexammine Co(III) chloride cation 78−92495
ternary alloy, Al_4Ba-$ThCu_2Si_2$-type structure, geometrical characts. 77−58977
thoria effusion membrane, production techniques based on that of incandescent gas mantles 78−39724
$Ag_2Th(MoO_4)_3$, crystallographic data determ. *(French)* 78−10013
$CaThNb_2O_8$, monoclinic-quadratic phase transform. *(French)* 77−27998
$CdTh(MoO_4)_3$, struct., DTA and X-ray diffr. obs. *(French)* 78−95024
$CdThNb_2O_8$, monoclinic-quadratic phase transform. *(French)* 77−27998
$CdTh(WO_4)_3$, struct., DTA and X-ray diffr. obs. *(French)* 78−95024
$CrThS(Se)_3$, synthesis, cryst. characts. *(French)* 78−51517
Cu-ThO_2, dispersion hardened, electrical cond. and mech. props. 78−44133
$Cu_2Th_4(MoO_4)_9$, crystallographic data determ. *(French)* 78−10013
$FeTh_2S(Se)_5$, synthesis, cryst. characts. *(French)* 78−51517
$FeThSe_3$, synthesis, cryst. characts. *(French)* 78−51517
HfF_4-BaF_2-ThF_4-(ZrF_4) glass system, IR transmitting, synthesis and props. 80−71623
$Lu_{0.75}Th_{0.25}Rh_4B_4$, high supercond. transition temp. 77−89893
$MnThSe_3$, synthesis, cryst. characts. *(French)* 78−51517
Na_2O-ThO_2-SiO_2 glass, density, refractive index, thermal expansion, hardness, IR spectra, DTA *(Japanese)* 78−15535
Nb-Th, eutectic composition 80−100828
Ni-ThO_2, dispersion strengthened, high temperature cyclic deformation 80−16430
Ni-ThO_2 (2.51 wt.%), dispersion hardened, high temp.-strength, deform. method and annealing effects 79−1882
NiCr-MoAl-ThO_2 (13,3 wt.%), powder, mech. alloying 78−84744
$Pb_{1-x}Th_xF_{2+x}$, fast ionic conduction of F^- ions 79−99360
$Pb_{1-x}Th_xF_{2+2x}$, solid soln., anionic cond. *(French)* 78−91481
(Pu-Th)O_2, FBR fuel pellet fabrication, control of O_2-to-metal ratio 80−13760
$Sc_{0.65}Th_{0.35}Rh_4B_4$ and $Sc_{0.5}Th_{0.5}Rh_4B_4$, cryst. struct., X-ray diffr. 77−89423
$Sc_{0.75}Th_{0.25}Rh_4B_4$, high supercond. transition temp. 77−89893
$Sm_{1-x}Th_xS$, XPS, electronic struct. excitonic effects, insulator to metal transition 78−43988
SnO_2:ThO_2, exposed to CO gas, self-oscill. phenomenon 78−68032
SnO_2:ThO_2, exposed to H_2, temp. depend. of resistivity 79−56219
SnO_2:ThO_2, selective detection of CO, hydrophobic and hydrophilic silica effect 79−97372
$SrThNb_2O_8$, monoclinic-quadratic phase transform. *(French)* 77−27998
(Th,Pu)O_2 nuclear fuels, economic viability of Pu recycling in LWR 80−18576
$(Th,U)_2$, chemical form of solid fission product simulating high burnup 80−616
(Th,U)C advanced FBR fuels, radiological assessment of reprocessing 80−73983
(Th,U)O_2, burnup simulated, high O_2 pot., chem. state 80−91220
(Th,U)O_2, D_2O cooled, relative conversion ratio 78−29582
(Th,U)O_2 fuel conversion to (Th,U)C_2 for reprocessing 79−54579
(Th,U)O_2 fuel kernel prep. by external gelation of Th 79−93802
(Th,U)O_2 low burnup fuels, densification-related pellet diameter shrinkage 79−54510
(Th,U)O_2 microspheres, fabrication 80−801
(Th,U)O_2 reactor fuel, dissolution in HNO_3-HF mixtures, fuel reprocessing study 78−59951
(Th,U)O_2 recycled fuel elements, composition calc. 79−13504
(Th,U)O_2, thermal conductivity model for temps. to melting 79−93732
(Th,^{235}U)O_2 HTGR fuels, radiological implications of use 80−68777
Th complex, tetramethylethyl-cyclopentadienyl thorium trichloride, prep., NMR and IR spectra 79−76428
Th complexes, O-donor complexes of cyclopentadienyl Th (IV) halides, prep. and characterisation 79−15974
Th complexes, Th(IV) poly(pyrazol-1-yl)borate complexes, prep. and characterisation 79−15978
Th fuel cycle overview, DUTH fuels 79−59242
Th porphyrin complexes, luminescence 77−18958
Th-based fuel development for breeder reactor appl. 79−54502
Th-based fuel for LWR and LMFBR 78−86624
Th-C-N system, existence of new β'ThCN' phase, struct. and thermodynamic study *(French)* 80−92499
Th-Gd spin glass, low temp. sp. ht. 79−51795
Th-H system, supercond., book contrib. 80−25037
Th-Pb, liquid alloy, thermodynamic props. *(Russian)* 77−25011
Th-U non-oxide compounds, use as refractory breeder fuels 78−86612
Th-U-C-O system, HTGR fuel system, thermodynamic assessment 78−70598

thorium compounds continued
Th-U(Pu) fast breeder fuels, chemical, thermodynamic and selected transport props. 79−54505
Th-U(20 wt.%) alloy fuel, compatibility performance of candidate cladding alloys 79−54509
Th-Zr(Nb)(Ru)(Rh)-C, phase diagrams *(German)* 77−48413
Th_3As_4, heat capacity, 5-300K 80−88769
Th_3As_4, positron annihilation, mean ionic radius calc. 79−15550
Th_3As_4, prep. and semicond. props. 78−23087
Th_3As_4-U_3As_4, cryst. growth by chem. vap. transport 78−23588
Th_3As_4-U_3As_4 solid soln., electronic props. 80−34469
ThBC, crystal struct. 78−55853
ThBC, crystallographic relationship with with CrB, α MoB, UBC 79−42025
$Th_3B_2C_3$, crystal struct. 79−14772
$ThBe_{13}$:Er(Dy)(Gd), ESR, crystalline field single ion effects 78−84481
$ThBr_4$, crystal, self-induced α-spectra 77−67943
$ThBr_4$, inorganic scintillator, use in nucl. and accelerated particle detection 78−58540
$ThBr_4$, luminesc. conversion of efficiency on α- and β-particle irrad. *(French)* 77−77296
$ThBr_4$, new inorganic scintillators for nuclear particle detection, review of props. 79−45549
$ThBr_4$:U^{4+}, absorpt. spectrum, zero phonon line *(French)* 80−11443
$ThBr_4$:U^{4+}, IR luminesc., zero phonon lines 79−33769
$ThBr_4$:U^{4+}, single cryst., absorpt. and emission spectra 77−90174
$ThC_{0.063}$, cryst. struct. and lattice dynamics 80−88088
$ThC_{0.75}$, specific heat, Fermi level density of states 80−10680
ThC_2 reaction with Zn and $ZnCl_2$ in KCl-LiCl fused salt mixture in 500-800°C range 79−54580
ThC_3, atomisation energy, stability, mass spectrometric determ. 79−7037
ThC_x, 0≤x≤2.0, nonstoichiometric, statistical mechanical model for C activity 79−71892
ThC_x fuels, interface with Cr-Fe-Ni alloys, basic chemical compatibility, thermodynamic calcs. 79−93727
$ThC_{0.6}N_{0.4}$, specific heat, Fermi level density of states 80−10680
ThC_xN_y, NMR, Knight shift and spin-lattice relax. 80−100621
$Th(CO_3)_5^{6-}$, in Na and guanidinium salts, struct./props. correlation *(French)* 78−95032
$Th(C_2O_4)_2.6H_2O$, 4f level XPS shake-up satellites, assignments 78−1023
$ThCl_4$, 4f level XPS shake-up satellites, assignments 78−1023
$ThCl_4$, in LiCl-KCl and Na-K eutectic solns., thermodynamic props. 77−86345
$ThCl_4$, new inorganic scintillators for nuclear particle detection, review of props. 79−45549
$ThCl_4$, thermodynamics of vaporisation and melting 79−60492
ThC_n(n=1 to 6), Knudsen effusion mass spectrometric investigations, enthalpies and heat of formation calcs. 80−66858
$Th_{1-x}Co_x$, amorphous alloys, thermal stability, elec. cond. enthalpy 80−100172
$ThCo_{5-x}Mn_x$, struct. and magnetisation exam., temp. depend. 78−2662
$Th(CrO_4)_2$, 4f level XPS shake-up satellites, assignments 78−1023
$(ThCu_3)(Mn_2Fe_2)O_{12}$, synthesis, cryst. struct. and Mossbauer exam. 78−84505
$ThCu_3Mn_4O_{12}$, mag. structure, neutron diffr. powder data, 430K ferrimag. T_c 77−69502
$ThCu_3Mn_4O_{12}$, mag. struct. of new perovskite-type ferrimag. 78−52222
$ThCu_3Mn_4O_{12}$, synthesis, struct. and mag. props. of perovskite-like oxides 77−68960
ThC_{1-x}, nonstoichiometric, atomic short-range order obs. by diffuse neutron scatt. 77−24315
Th_4D_{15}, cryst. struct. meas. by neutron diffr. with spallation neutron source 77−43190
Th_4D_{15}, massive, prep. and characts., supercond. props. 77−43768
ThF_4, 4f level XPS shake-up satellites, assignments 78−1023
ThF_4, 5d X-ray spectra 78−88382
ThF_4, absorpt. spectrum of vapour, Th reson. localised 5,epsilon f state 80−91467
ThF_4, broadband dielectric mirror interference coatings, scatter losses 79−50365
ThF_4 coated CaF_2 trapezoid, IR characterisation by internal-refl. spectra 78−71161
ThF_4 film, 1064 nm 150 ps laser pulse damage rel. to OH^- content and refr. index 79−14016
ThF_4 film, IR absorpt. coeffs. meas. by laser calorimetry 78−25905
ThF_4 film, refr. index, 10.6 μm ellipsometric meas. 78−24847
ThF_4, inhomogeneous interface laser mirror coatings 80−1252
ThF_4, interband, collective and atomic (p,d) excitations, Z-160 eV, fast EELS 80−93443
ThF_4, interference filter, solar radiation resistance 77−39015
ThF_4, monoclinic, lattice parameters and thermal contraction coeff., 25 to 83°C 77−47607
ThF_4 multilayer film, intrinsic and thermal stress modelling and interferometry 79−14059
ThF_4, muon Coulomb capture ratio 78−62959
ThF_4, optical film cross sections, SEM and TEM 77−19387
ThF_4 single-layer film 2.8 μm, 3.8 μm absorpt. meas. 78−90463
ThF_4, spallation cross section and recoils, range calcs. computer code MARLOWE 79−93736
$ThF_4(Cl_4)$, electronic struct., MS-SCF-Xα calcs. and VUV photoelectron spectra 80−63710
$Th_6F_{24}.H_2O$, X-ray cryst. struct. determ. and refinement 79−90603
$Th_7Fe_3H_{14.2}$, Mossbauer spectra, mag. props. 80−15852
$ThGeO_4$, cryst. growth from PbO-GeO_2 flux 77−16484
ThH_2, electronic struct., photoelectron spectra meas. 77−85143
ThH_2, $ThH_{3.75}$, heat capacity and thermodynamic props. to 1000K 78−91451
ThH_2:Er^{3+}, EPR of Er localised electron mag. states, Kondo effect 80−25202
ThH_4, Dirac-Fock one-centre calcs. 79−6837
ThH_4, Dirac-Fock one-centre expsn. calc. 80−5485
Th_4H_{15}, and ThH_2, NMR relax. expts., diffusion processes and hyperfine fields 79−8066
Th_4H_{15}, electronic struct., photoelectron spectra meas. 77−85143
Th_4H_{15}, electronic struct., appl. of fast self-consistent cluster calc. for large systems 79−82513
Th_4H_{15}, H vibr. modes, neutron scatt. study, phonon density of states 79−42195
Th_4H_{15}, massive, prep. and characts., supercond. props. 77−43768
Th_4H_{15}, NMR investig. of proton environment and motion 77−48077
Th_4H_{15}, superconductivity and electron-phonon interaction 80−49975

thorium compounds continued
Th_4H_{15}, ThH_2, phonon densities of states rel. to supercond. props. 77−27960
Th_4H_{15}:Er^{3+}, EPR of Er localised electron mag. states, Kondo effect 80−25202
$Th_4H_{15}(D_{15})$ normal and supercond., low-temp. sp. ht., Debye temp. and supercond. props. 77−4466
$ThIr_3B_2$, supercond. and mag. props. 80−97028
ThN, photoelectron spectra study, core and valence levels 80−66394
$Th^{14}N$, $Th^{15}N$, matrix isolated IR spectra 79−59457
ThN-rare earth nitride mixed system, quasibinary existence *(German)* 80−91221
$Th(N_2)$ complex, IR matrix isolation spectrum 79−59457
$Th(NO_3)_4$, particle fuel prep., wet chem. process for LWR, FBR and HTR *(German, English)* 77−65314
$Th(NO_3)_4$-K_2HPO_3-H_2O, mixed phosphites formation and characterisation 77−52304
$Th(NO_3)_4.5H_2O$, 4f level XPS shake-up satellites, assignments 78−1023
$Th_{0.25}NbO_3$, cryst. struct., X-ray diffr. obs. *(French)* 79−1413
$Th_{0.25}NbO_3$-x$NaNbO_3$ solid soln., cryst. struct., perovskite-type phases, X-ray diffr. obs. *(French)* 79−1413
$ThNi_2$, Mossbauer effect of ^{57}Fe 77−69743
$ThNi_5$, Haucke compounds, low temp. heat capacity, Debye temp. 80−96663
$ThNi_{5-x}Mn_x$, struct. and magnetisation exam., temp. depend. 78−2662
ThO, HTGR coated-particle fuel performance charact. by fission gas pressure meas. 79−54584
ThO, $L^1\Pi$-$^1\Sigma^+$ and $N^1\Pi$-$X^1\Sigma^+$ systems, spectra, rot. anal. 80−23430
ThO, spectroscopic data rel. to thermodynamic functions 80−34208
ThO_2, ^{18}O self-diffusion, isotope exchange meas. 77−11725
ThO_2, ^{233}U/Th ratio determ. *(Spanish)* 77−70637
ThO_2, 4f level XPS shake-up satellites, assignments 78−1023
ThO_2, 5d X-ray spectra 78−88382
ThO_2 a once-through cycle for BWRs 80−18433
ThO_2 and $(Th,U)O_2$ fuel kernels, simplified preparation 78−86668
ThO_2 and $Th_{0.81}U_{0.19}O_2$, irradiated fuel particles, meas. and interpretation of CO and Kr-Xe content 78−25287
ThO_2 and ThO_2-UO_2 fuel, fission gas release 78−86651
ThO_2 based CANDU reactor fuels, review of potential for actinide redistrib. 78−66347
ThO_2, cationic transport number determ. *(French)* 78−84267
ThO_2 central zone is PROTEUS GCFR lattice 80−22984
ThO_2, ceramic oxide, thermally stimulated depolarisation currents, grain size and growth determ. 79−65792
ThO_2 ceramics, CaO and Y_2O_3 stabilised density, elec. cond., permittivity 78−47838
ThO_2 ceramics fireproof, direct energy conversion appl. *(Czech)* 79−70455
ThO_2 compacts, thermal conductivity, dependence on porosity, mathematical anal. 79−4437
ThO_2, core materials development for water cooled reactor systems 77−46296
ThO_2, correcting coatings, u.v. transmission cutoff 77−760
ThO_2, crucible material, Cu-Nb alloy prep. 80−84879
ThO_2 crystallite growth from oxide plasmas, growth morphology 80−59417
ThO_2, Danish thorotrast patients, malignancies 78−96074
ThO_2 dispersed Ni, recrystallisation during annealing, O_2 partial press. effects *(Russian)* 78−3140
ThO_2, electronic struct. and bonding, molecular cluster approx. 77−51657
ThO_2 electrophoretic coating for poisoning resistant Ir filament electron gun 78−54493
ThO_2, film, stability, high temp. and electron irrad. effects 77−39747
ThO_2, fuel cycles, Savannah River Plant processing experience 79−59243
ThO_2 fuel kernel prep. by external gelation of Th 79−93802
ThO_2 gel, morphology relations during bulk transport sintering 77−70015
ThO_2, German thorotrast patients, malignancies and estimated tissue dose 78−96072
ThO_2, Gruneisen coeff., lattice vibrational frequencies in range 298-2300K 78−79712
ThO_2, H_2^+, ion beam surface interaction, H^- formation by reson. electron capture 80−40691
ThO_2, HTR fuel elements, chem. prod. processes *(German, English)* 77−14256
ThO_2, HTR fuel particles, fission product behaviour anal. using gamma spectrometry 80−42778
ThO_2 in HTGR fuel design 78−86622
ThO_2, ionic conduction, doping effects and defect interactions 80−19978
ThO_2, isolated rod, exptl. and calculated resonance integrals 80−22986
ThO_2 kernel migration in HTGR 77−79440
ThO_2 Knudsen cells heated by radiation, emissivity *(Japanese)* 80−13073
ThO_2 laser coating, UV damage obs. 80−33056
ThO_2, lattice defects and irrad. effects, review 77−27873
ThO_2 low burnup fuels, densification-related pellet diameter shrinkage 79−54510
ThO_2 microspheres, coated, coating permeability meas. 80−95343
ThO_2, negative surface ionisation 77−77335
ThO_2, negative surface ionisation of H_2^+ ions 80−6280
ThO_2, nucl. Doppler effect in fast and intermediate spectra measured by direct flux depression in neutron beam expt. 77−50232
ThO_2 nuclear fuel production, economic and environmental anal. 80−18575
ThO_2, O_2 self-diffusion and intrinsic p-type electronic conduction 79−90821
ThO_2, particle size of crystallites in soln. by line-broadening meas. 78−18488
ThO_2, plasma deposition of crysts. and their characterisation 80−20800
ThO_2, Portuguese thorotrast patients, malignancies 78−96073
ThO_2, pure and Tb^{3+} doped, impurities effect in absorboluminesc. and photoluminesc. 79−38597
ThO_2 reactor fuel, in linear accelerator driven and regenerative reactors 79−81064
ThO_2, reactor fuel, neutron multiplication factors, temp. depend. 78−29557
ThO_2, satellites in XPS, cf UO_2 and La_2O_3 77−4711
ThO_2 single crystals, crystal growth, using crucibleless skull melting technique 78−39681

thorium compounds continued
ThO_2, sintered, fracture props. studied by Hertzian indentation technique 80−50703
ThO_2 sintered pellets, ^{131}I release at low temps. 78−21650
ThO_2, sol-gel, for nucl. applics., sorption of water, CO_2 and N_2 77−4940
ThO_2, sol-gel process for nucl. fuel fabrication 79−13503
ThO_2, spectroscopic data rel. to thermodynamic functions 80−34208
ThO_2, spherical pile, neutron spectrum meas. and analysis 78−17311
ThO_2, stabilised, ionic mech. of charge transport 79−10976
ThO_2, temp. programmed desorpt. and photoluminesc. of surface states 79−73399
ThO_2, thermal and transport props., electronic contrib. 80−15432
ThO_2, thermal expansion, 500-1800°C, X-ray diffr. 77−35723
ThO_2, thorotrast and ^{224}Ra radiobiological significance 78−96076
ThO_2, thorotrast biological effects, conf., Alta, USA (July 1974) 78−96068
ThO_2, thorotrast cases, bone irradiation meas. results 78−96092
ThO_2, thorotrast patients, α-ray tissue dose 78−96093
ThO_2, thorotrast patients, endosteal α-particle dose 78−96094
ThO_2:Ce^{3+}(Ce^{4+}), mixed ionic and electronic transport 80−107875
ThO_2:Gd^{3+}, ENDOR, nuclear mag. moment and HFS, stress-induced splitting 77−51990
ThO_2:Np^{4+}, cryst. field splittings, ab initio MO calcs. 77−20520
ThO_2:Pr^{3+}, luminesc., calcination temp. and excitation process depend. 79−33749
ThO_2:U^{4+}, paramag. acoustic reson. absorpt. in cubic field 77−20680
ThO_2:U^{4+}, spin-lattice relax. time calc., nearest neighbour point charge model 77−16146
ThO_2:Y_2O_3, electrochem. cell, complex impedance, temp. and freq. depends. 77−1458
ThO_2:Yb^{3+}, axial g-values of $4f^{13}$ ions with trigonal symmetry *(Korean)* 79−24135
ThO_2:Yb^{3+}, trigonal centres, point-charge approx. 78−39072
ThO_2:Yb^{3+}, trigonal sites of Yb^{3+}, ENDOR meas. 79−95677
ThO_2/Ni, adhesive energy, meas. techniques 80−50803
ThO_2/Ni-Cr, adhesive energy, meas. techniques 80−50803
ThO_2-^{233}U exponential expts. anal., cross section library sets, resonance integral correls. 77−23215
ThO_2-$^{233}UO_2$ fuelled core, spent fuel rod assay, reactivity perturbation method 77−18654
ThO_2-based ceramic impurity diffusion, electrotransport method 78−67869
ThO_2-Biso (mixgas), high temp. (2300-2500°C) treatment, metallographic cross sections, microradiographic anal. *(German)* 78−29586
ThO_2-Biso (propene), high temp. (2300-2500°C) treatment, metallographic cross sections, microradiographic anal. *(German)* 78−29586
ThO_2-CaO, and ThO_2-$YO_{1.5}$, solid solns., defective oxides, ionic cond. 80−107548
ThO_2-CaO electrolyte, mixed and ionic cond. regions 77−8156
ThO_2-UO_2 (0.1 wt.%), ^{133}Xe release after low dose irradiation 77−74919
ThO_2-UO_2 fuel performance after irradiation 78−86621
ThO_2-UO_2 in PWR fuel rod, LIFE-THERMAL computer code anal. 78−86623
ThO_2-UO_2 solid solns., props. of importance for use as nuclear fuels 79−54506
ThO_{2-x} phase, high temp. vaporisation behaviour 79−54508
ThO_4, prep., IR spectra and thermal exam. 77−89402
ThO_x:Y_2O_3 solid electrolyte high-temp. vaporisation obs. 78−14456
$ThOF_2$:Ce,Tb, photolum. obs. 77−77270
$Th(OH)_4$, 4f level XPS shake-up satellites, assignments 78−1023
$ThO(NO_3)_4.xH_2O$, satellites in XPS 77−4711
ThOS:Gd^{3+}, EPR study, g-factor and cryst. field parameters 80−25204
ThP, specific heat, Fermi level density of states 80−10680
Th_3P_4 compounds, lattice instabilities in non-A15 superconductors, struct. instability temp., 78−10591
Th_3P_4, cryst. growth by chem. vap. transport 78−23588
$Th(ReO_4)_4$-$M(KeO_4)$, (M=Na, K, Rb, Cs, Tl) crystallographic data for perrhenates of the actinides and their hydrates, thermal stability *(French)* 79−69091
$ThRh_4B_4$, cryst. struct., X-ray diffr. 77−89423
$ThRh_4B_4$, high supercond. transition temp. 77−89893
$Th(SO_4)_2.9H_2O$, 4f level XPS shake-up satellites, assignments 78−1023
$Th(S_2O_3)_2.nH_2O$, 4f level XPS shake-up satellites, assignments 78−1023
$ThSb_2$, Th_3Sb_4, cryst. growth by chem. vap. transport 78−23588
α-$ThSi_2$-AlB_2 series, struct., symm. and rel. to other linear structs. 77−11525
$ThSiO_2$, single crysts. prep. by vapour phase reaction 79−28905
$ThSiO_4$, cryst. growth from PbO-SiO_2 flux 77−16484
$ThSiO_4$, huttonite and thorite polymorphs, cryst. struct. 78−51478
$ThSiO_4$, synthetic, Raman spectrum and lattice vibrs. 77−48160
$ThSiO_4$:U^{4+}(U^{3+}), opt. spectra 78−88334
$Th(VO_3)_4$, crystallographic data *(French)* 78−63725
ThV_2O_7, V-O-V bridge stretching freq. correl. with bond angle 78−74636
$\{Th[(CH_3)_5C_5]_2H(\mu\text{-}H)\}_2.C_6H_4CH_3$, molecular structure by neutron diffraction 79−89801
Ti-Th, eutectic composition 80−100828
$(U,Th)O_2$ fuel pellet fabrication using gel microspheres 80−42844
$(U,Th)O_2$ fuel rods, analytical stressing in hot cell 80−18566
$(U,Th)O_2$, γ-active pellet fuels fabrication, conceptual design of remotely operated plant 80−32340
$(U,Th)O_2$ reactor fuel, annealing test up to 2500°C *(German)* 79−3228
U-Pu-Zr(-Th) LMFBR metal fuel elements, development and performance 80−57856
(U-Th) oxide, carbide, nitride and metal fueled LMFBR breeding performance 79−59175
(U-Th)C fueled reactor system, large plant, performance parameters 79−26500
UO_2-ThO_3, LWR and HWR fuel anal. of exponential expts. with WIMS-D code and data 79−81000
UO_{2+x}-ThO_2-MgO system, in air, phase rel., X-ray diffr., electron probe and metallography anal. 79−74137
$U_xTh_{1-x}As$ (Sb), electronic struct., relativistic KKR-averaged T-matrix approx. method 80−107702
$U_xTh_{1-x}As$, mag. phase diagram, magnetisation meas. 80−60271
$(U_xTh_{1-x})S$, mag. props. rel. to elec. struct., 1.5-300K 77−1557
$(U_xTh_{1-x})S$, metallic, 5f virtual bound states, elec. resist. and mag. susceptibility meas. 77−28363
$(U_xTh_{1-x})Sb$, magnetisation, U valence change 80−7089

thorium compounds continued
$U_xTh_{1-x}Sb$, valence change of U accompanied by singlet-ground-state ferromag. 80−70965
$(U_xTh_{1-x})Se$, metallic, 5f virtual bound states, elec. resist. and mag. susceptibility meas. 77−28363
$(U_xTh_{1-x})S(Te)$ solid solns., electronic struct., mag. susceptibility and elec. resist. obs. 77−20551
$(^{233}U, Th)O_2$ fuels for HTGR, remote fabrication 80−13752
$(^{233}U, Th)O_2$ pellet-type fuels for CANDU reactors, remote fabrication plant design 80−13751
$^{233}UO_2/ThO_2$ water-moderated lattice analysis with ENDF/B-IV data 79−9800
W:ThO_2, uncarburized filament activation by sputtering 78−52608
W-Th, field ion specimen, contrast bands in elec. field induced evaporation 79−50967
W-ThO_2, candidate refractory for Tokamak, thermal fatigue failure testing 80−32454
W-ThO_2 composite, struct., lamination tendency, effects of method of manuf. 78−68653
W-ThO_2 filament, W, TaC and HfC CVD coatings, effect on high temp. mech. props. 78−15347
W-ThO_2-B, thermocathodes diffusion mobility, based on deboronation kinetics 80−39349
Y_2O_3:ThO_2, IR absorpt., 2-4 μm 77−55805
$Y_{0.7}Th_{0.3}C_{1.55}$, superconducting crit. mag. field curve, initial slope 77−28318
$Y_{1-x}Th_xFe_3$ system, elec. resist. meas., 77-300K 80−34413
ZrF_4-BaF_2-ThF_4, vitreous phases, network formers, modifiers and stabilisers *(French)* 80−64909
ZrF_4-BaF_2-ThF_4 F^- ion cond. glasses, cond. process 80−107477
ZrF_4-BaF_2-ThF_4-NaF(RF_3) (R=rare-earth) glass system, anion cond. 80−70460
ZrF_4-THF_4-BaF_2 glass, IR-transparent, synthesis using reactive atm. processing technique 80−100826
ZrF_4-ThF_4-BaF_2:V^{3+}(Cr^{3+}) glasses, absorpt. spectra *(French)* 79−99918
ZrF_4-ThF_4-NdF_3(LaF_3), phase equilibrium, vitreous phase struct., charact. temp., optical props. *(French)* 79−11587
(ZrF_4-BaF_2-ThF_4)-EuF_2 system, glass forming region, prep. and props. 79−91633
ZrF_4ThF_4-BaF_2 system, new fluoride glass, optical props. *(French)* 77−36443
ZrO_2-ThO_2, high temp. study of phase diagram using X-ray and thermal anal. *(French)* 79−70049

three-phase flow *see multiphase flow*

three phase rectifiers *see rectifiers*

three-photon spectra *see multiphoton spectra*

three-term control
biological preparation temp.-control system 79−57830
dipstick cryostat, with temp. controller for high thermal stability 80−37044
radiation treatment of waste water, process control techniques appl. 79−96489
resistance furnace programmed temperature regulator 78−86256
X-ray studies of phase transitions at low temps., automatic system 77−15281

threshold elements
maximum periodic sequence realisable by autonomous threshold element network 78−44489
optical fibre laser plate for optical parallel processing 79−76695
random threshold element networks with absolute refractory period 77−29143
syneuristor discrete digital component design 79−96727
n-ZnSe−p-GaAs heterojunction high-detectivity threshold photodetectors 79−6181

threshold logic
EEG pattern classification using logic windows in time domain *(Japanese)* 77−70563

throat microphones *see microphones*

thulium
see also nuclei with .....
abundance in HD 18474 giant star *(Spanish)* 79−25605
atom, α-particle impact K-shell ionisation, 40 to 110 MeV 78−17752
atom, hyperfine struct. for various configs. 78−939
atom, intense 4d-f resons., cross-sections, spectra, calcs. 79−31426
atom, Kα line widths, precise meas. 78−62761
atom, nuclear K-X-ray satellites, Z=50-83, by α-bombard., 17.5-22.5 MeV 80−42984
atom, spectral line oscill. strengths determ. 77−3312
atom, tensor polarisabilities of levels, level crossing method 79−10223
atom, VUV emission spectra, 5p electron excitation by electron impact 77−68007
electroluminescence activator in La_2O_3, Y_2O_3, Y_2O_2S, comparison 77−20927
electron irradiated, defect annealing, recovery spectra 79−23648
electronic relaxation, Tm^{3+} Mossbauer spectroscopy 80−39914
energy transfer between 5d electronic states 80−2808
EXAFS, white lines, interatomic distances 77−40302
ferrogarnet film, cylindrical mag. domain motions, domain boundary oscills. *(Russian)* 80−71140
fluoride:Tm^{3+}, photon-cascade emission quantum yield calc. 77−4669
fluorite type crystal: Tm^{2+}, axial g-values of $4f^{13}$ ions with trigonal symmetry *(Korean)* 79−24135
glass:Tm^{3+}, nonradiative decay and multiphonon relax. 77−85802
glass:Tm^{3+}, polarised luminesc. 78−48224
Hall coefficient meas., 80 to 1000K 80−49694
impurity in metallic host, exchange interaction, electrical resistivity 80−84453
lattice dynamics, thermal expansion, spt. ht., mag. contrib. 79−37778
magnetic properties, para-, ferro- and ferrimag. and c-axis modulated phases 78−2660
magnetic transitions, effect of H_2 in solid solns., elec. resist. meas. 80−100585
Mossbauer effect, expt. in ^{3}He-^{4}He dilution refrigerator 78−27127
optical props., temp. depend., photocond., relaxation parameters 78−84603
phosphate glass:Ce^{3+},Tm^{3+}(Tb^{3+}), temp. depend. of energy transfer

thulium continued
phosphate glass:Tm^{3+}, eigenstates and radiative transition probabilities calcs. 77−77265
self-powered neutron detectors for power reactors 79−13607
tellurite glass:Tm^{3+}, eigenstates and radiative transition probabilities calcs. 77−77265
BaF_2:Tm^{2+}, EPR, optical recording in weak mag. field 78−68376
BaF_2:Tm^{2+}, EPR meas. of Tm^{2+} ion pair interactions 79−95641
BaF_2:Tm^{2+}, trigonal centres, point-charge approx. 78−39072
BaF_2:Tm^{2+}, vibronic spectra and dynamics of impurity-contaiing lattice 79−1787
$Ba_{0.54}Sr_{0.46}Nb_2O_6$:Tm, dielectric and electrooptic props. 78−68466
$Bi_4Ge_3O_{12}$:Tm^{3+} crystal growth, spectral and laser props. 80−45115
CaF_2:Tm, ^{19}F NMR studies 80−60429
CaF_2:Tm, cryst. fields, overlap and covalency contribs. 77−1397
CaF_2:Tm temperature dependence of V_k-centre generation efficiency *(Russian)* 78−48203
CaF_2:Tm^{2+}, EPR, optical recording in weak mag. field 78−68376
CaF_2:Tm^{2+}, EPR meas. of Tm^{2+} ion pair interactions 79−95641
CaF_2:Tm^{2+}, evidence for covalency 77−85180
CaF_2:Tm^{2+}, single cryst., ^{19}F nucl. spin cooling of Tm^{2+} electronic spin *(French)* 77−66440
CaF_2:Tm^{2+}, spin density parameters at ^{19}F nuclei 78−68001
CaF_2:Tm^{2+}, trigonal centres, point-charge approx. 78−39072
CaF_2:Tm^{2+}, ultra-low nuclear spin temp., low field behaviour, EPR study 80−100614
CaF_2:Tm^{2+}, vibronic spectra and dynamics of impurity-contaiing lattice 79−1787
CaF_2:Tm^{3+}, 8.2 keV excited state, mag. props., Schottky ht. capacity, nucl. quadrupole splitting 78−76037
CaS:Bi, Tm, phosphor sensitisation mechanism, energy transfer 78−60507
$CaSO_4$:Tm, gamma-irradiated valency conversions in rare-earth ions 80−55198
$CaSO_4$:Tm, Li, mixed field TLD 77−9263
$CaSO_4$:Tm, thermolum. phosphor, photolum. and absorpt. spectra, thermolum. mechanisms 80−97321
$CaSO_4$:Tm, thermoluminesc. props. of non-commercial phosphors 78−58550
$CaSO_4$:Tm and nonluminous ^{6}LiF powders mixture, thermoluminesc. response to thermal neutrons 77−73588
$CaSO_4$:Tm composite TLD for γ-rays, X-rays, β-rays, and thermal neutrons 78−28076
$CaSO_4$:Tm intrinsic thermoluminescence stability for UV dosimetry 80−12262
$CaSO_4Dy(Tm)$, thermolum. induced by 254 nm UV photons 80−55204
CdF_2:Er^{3+}, Tm^{3+}, evidence for $Er^{3+} \rightleftharpoons Tm^{3+}$ energy transfers, fluoresc. expts. 80−60655
Cs_2NaYCl_6:Re,Tm, fluorescence, two-step blue up-convertors 78−95603
ErAlG:Ho, Tm, Et$\rightleftarrows$Ho and Er$\rightleftarrows$Tm energy transfer, fluorescence meas. 78−27305
Fe:^{169}Tm(^{175}Lu), radiation-damage evolution influence on hyperfine interaction 80−6793
GaP:Tm, magnetic susceptibility, impurity states 79−61044
LaF_3:Tm, cryst. field anal. of triply ionised ion spectra 80−2796
LaOBr:Tm X-ray emission spectra and screen-film system design 78−11024
$LiYF_4$:Tm^{3+}, cryst. field parameters, appls. 77−20277
$LuYScO_3$:Tm^{3+}, thermolum. meas. 80−97354
SnO_2:Tm^{3+}, luminesc. and charge compensation 78−76532
SrF_2:Tm, far IR spectra 79−33736
SrF_2:Tm^{2+}, EPR, optical recording in weak mag. field 78−68376
SrF_2:Tm^{2+}, EPR meas. of Tm^{2+} ion pair interactions 79−95641
SrF_2:Tm^{2+}, modulation magnetooptic spectroscopy of cross-relaxation resonances 79−15381
SrF_2:Tm^{2+}, trigonal centres, point-charge approx. 78−39072
SrF_2:Tm^{2+}, vibronic spectra and dynamics of impurity-contaiing lattice 79−1787
Tm I, hyperfine struct., high resolution spectrosc. meas. 80−87238
Tm I, lifetimes of excited states, and oscill. strengths 79−3411
Tm II, lifetimes of excited states 79−3411
Tm IV, 3d and 4f energy level parametrisation, Slater parameters and correl. corrections 80−87041
Tm^{3+} rare earth oxysulphides and oxyhalides, thermochromatic luminophors, lumines. spectra rel. to temp. 79−56849
Tm^{3+}, Sternheimer valence shielding antishielding factor including exchange 77−85182
Tm:$LiYF_4$, XeF pumped, excimer excited storage laser 80−33003
Tm^{3+}:trifluoride, VUV fluorescence and tunable coherent sources from 1650 to 2600 Å 77−688
Tm^{3+}:YAG, 2.014 μm, stimulated emission, resonant pumping by Nd laser 78−17944
Tm^{3+}-doped trifluorides, vacuum-UV excitation spectra 78−80381
YAG:Tm, US attenuation 77−89500
YAG:Tm^{3+}, oscillator strengths of impurities, 5000 to 30000 cm^{-1} 79−4830
$YAlO_3$:Tm^{3+}, cryst. field parameter determ. 77−15800
YF_3:Tm, Nd, energy transfer between 5d electronic states 80−2808
YF_3:Yb^{3+}, Tm^{3+}, IR to blue up-converting phosphor 79−83004
YVO_4:Tm^{3+}, cryst. field parameters, appls. 77−20277
ZnS:Tm, cathodoluminesc. yield, calorimetric method determ. *(Russian)* 77−20938
ZnS:Tm phosphors, optical scintillation mechanism 79−56867
ZnS:Tm^{3+}, charge compensation and polytypism influences on fluorescence 80−89051
ZnS-CdS:Tm,Ni, recomb. centre interaction, luminesc. quenching 78−10946

thulium alloys
electronic relaxation, Tm^{3+} Mossbauer spectroscopy 80−39914
mixed valence compounds, mag. props. 79−78048
Ag-Tm, dil., high field magnetoresist. 80−15503
Ag(Au)-Tm dilute, thermoelec. power, crystal field and interaction effects 77−66158
Al-Tm, dil., transmission ESR expts. 77−20704
$Er_{1-x}Tm_xRh_4B_4$, mag. and supercond. transitions, cryst. field effects 80−107950
Ga-Ni-R, (R=Dy, Ho, Er, Tm, Lu), struct. determ. by X-ray powder method *(Ukrainian)* 80−39001
Gd-Tm, mag. anisotropy, from magnetisation meas. at 4.2K 78−68216

thulium alloys continued
Gd-Tm, magnetic and electric hyperfine fields at Gd, NMR spin echo 77−77123
Mg-Tm, dil., macroscopic shape effect due to quadrupole orientation, magnetostriction and thermal expansion meas. 80−60396
Mg-Tm, phase diagrams in Mg rich region *(Russian)* 77−52286
$Pd_{0.97}Tm_{0.03}$, dil. alloy, elec. resist. meas. 79−19583
Pr-Tm, mag. order onset, elec. resistivity 80−20416
Tb-Tm alloys, mag. struct., neutron diffr. 77−8273
Th-Tm (1 at.%), Heisenberg exchange, residual resist. meas. 80−75558
$ThFe_4Al_8$, mag. props. 78−52250
$(Tm,La)Al_2$ disordered alloys, cryst. field transitions, inelastic neutron scatt. obs. 80−50055
Tm-3d transition metal intermetallics, ^{169}Tm Mossbauer effect 80−71261
Tm-Ga, exam. of phase diagram, using differential thermal and X-ray phase anal. *(Russian)* 79−11555
Tm-H solid solution, struct., 20-500°C 79−90643
Tm-Zn, paramagnetism, mag. excitations, exchanges interactions 80−88718
$TmAl_2$, ferromagnetic structs., elastic neutron scatt. obs. 80−50055
$TmAu_3$, mag. props. *(German)* 79−51761
Tm_2Au, mag. props., 4.2-300K 79−7972
$TmAuNi_4$, mag. props. 77−20595
$Tm_3Au_3Sb_3$, mag. suscept. meas., 4 to 300K 79−51742
$TmBe_{13}$:Gd, Van Vleck paramagnet, exchange parameters, ESR determ. 77−4557
TmCd, parastriction, magnetoelastic and quadrupolar exchange coeffs. 79−19758
TmCd quadrupolar ordering and magnetic interactions 79−73676
TmCd, struct. phase transition driven by quadrupolar pair interaction 79−61583
TmCd(Zn), doublet-triplet mag. system, dipolar and quadrupolar ordering 79−8004
TmCd(Zn), quadrupolar phase transitions, magnetoelastic and quadrupolar coupling consts. 80−15744
$TmCo_2$, paramag. and ordered phases, Pauli type, Co susceptibility, polarised neutron diffr. obs. 77−63077
$TmCo_5$, covalent electron number, from chem. shift of Co X-ray absorption spectra 77−59641
$TmCo_5$, easy magnetisation direction 78−84415
Tm_2Co_{17}, single cryst., magnetostriction const. temp. depend., 78 to 300K 79−51836
Tm_4Co_3, cryst. field effect on mag. moment direction, neutron diffr. meas. 78−80132
TmCoAl, mag. props. 78−2659
$TmCu_5$, crystal field level scheme, neutron inelastic scatt. and specific heat meas. 79−51536
TmFe, Mossbauer expt. in ^3He-^4He dilution refrigerator 78−27127
$TmFe_2$, amorphous, neutron scatt. at transition, spin diffusion, magnetisation meas. 78−68174
$TmFe_2$, amorphous, small angle neutron scatt. study of mag. order and mag. microstruct. 79−15283
$TmFe_2$, electronic heat capacity coeffs. 80−39787
$TmFe_2$, low temp. magnetisation and magnetostriction 78−64249
$TmFe_2$, magnetisation and magnetic anisotropy 78−91862
$TmFe_2$, Mossbauer diffr., combination type maxima, hyperfine interactions on nuclei 80−25263
$TmFe_2$, spontaneous magnetoelastic distortion, X-ray diffr. expts. 77−63253
$TmFe_3$ and Tm_6Fe_{23}, magnetostriction, room temp. to 80K 80−65993
TmFeAl, scatter order cpd., mag. props. 77−51891
$TmFe_4Al_8$, mag. props. 78−52250
$Tm_2Fe_{17-x}Co_x$, and related cpds., easy magnetisation direction, Mossbauer spectra 77−63169
$TmFe_3H_{4.3}$, mag. props. and lattice consts., effect of hydrogen absorpt. 77−20561
$Tm_2Fe_4Si_9$ and $TmFeSi_3$, cryst. struct. and mag. suscept., temp. depend. *(Russian)* 78−34957
Tm_2In, mag. props., 4.2 to 270K 79−56512
$Tm_{1-x}Lu_xZn$, third-order mag. susceptibility, quadrupolar effects 79−99674
$TmMn_{12}$, mag. interactions, mag. meas. and neutron diffr. 77−63103
Tm_2Ni_{17}, magnetic structure by neutron diffr. 77−73000
$TmNiSi_3$, mag. susceptibility, 80-1200K *(Russian)* 77−66281
Tm_5Pd, mag. props. 77−20547
$TmPt_5$, low temp. mag. susceptibility 80−93075
Tm_3Pt_4, mag. props., 4.2 to 160K 79−78343
Tm_5Pt_4, isotypic with Pu_5Rh_4, X-ray cryst. struct. refinement anal. 79−4271
$TmRh_4B_4$, mag. and supercond. props., mag. susceptibility and sp. ht. meas. 79−78344
TmZn, cooperative Jahn-Teller effect 78−67998
TmZn, magnetic-ion-lattice interactions, cryst. elec. field 77−4540
TmZn, parastriction, magnetoelastic and quadrupolar exchange coeffs. 79−19758
TmZn, struct. phase transition driven by quadrupolar pair interaction 79−61583
TmZn, US attenuation in cooperative Jahn-Teller system 79−78053
$TmZn_2$, Mossbauer effect meas. in antiferromag. and paramag. states 80−71265
Y-Tm, mag. susceptibility, 4.2 to 300K, Neel temps. 79−19735

thulium compounds
see also thulium alloys
crystal field effects on EPR and NMR *(Japanese)* 77−43879
domain boundary mobility, effect of easy magnetization axis inclination 78−19293
mixed valence compounds, charge dominated fluctuation props. comparison, mag. moments and ordering 80−54659
mixed valence compounds, mag. props. 79−78048
neutron scatt. cross-section, mag. inelastic, rel. to cryst. field splitting 77−55659
phthalocyanine, mol. image in high resoluton electron microscopy, radiation damage effect 80−107203
pnictides, van Vleck paramag., relax., host exchange parameters 78−2735
thulium ethyl sulphate, Van Vleck paramag., mag. reson. on uniaxial and uniform compression *(Russian)* 79−61243
$Ba_{0.50}Sr_{0.50}Nb_2O_6$:$Tm_2O_3$, Raman spectra 79−78678

thulium compounds continued
BiTm ferrite garnet coating on $LiNbO_3$:Ti optical waveguide *(Russian)* 77−42623
$(BiTm)_3(FeGa)_5O_{12}$ ion implanted epitaxial garnet film, bubble domains, cryst. struct. disorder 80−93150
$(BiTm)_3(FeGa)_5O_{12}$, monocrystalline films, mag. anisotropy 80−2609
$CaSO_4$:Tm/polythene mixture, thermoluminesc. response to fast neutrons 80−5340
$CdTm_2Se_4$, mag. susceptibility meas. 4.2 to 300K cryst. field approx. 77−66246
$Cs_2KTmBr_6(Cl_6)(F_6)$, Cs_2NaTmF_6 and Cs_2RbTmF_6, mag. behaviour 2.9 to 251.3K, cryst. field levels, ang. overlap model *(German)* 80−29520
$Cs_2NaTmCl_6$, Raman spectra 77−77205
$Dy_xTm_{1-x}FeO_3$, transition to antiferromag. state, Dy^{3+} conc. effects 77−66319
$Er_{0.5}Tm_{0.5}FeO_3$, mixed orthoferrite crystals, ^{57}Fe NMR in spin reorientation range 78−15039
$EuTm_2Fe_5O_{12}$ film , CaGe substituted, LPE growth kinetics 78−31349
$(Gd,Tm,Y)_3(Fe,Ga)_5O_{12}$ film, magnetocrystalline anisotropy 79−78450
$(Gd,Tm,Y)_3(Fe,Ga)_5O_{12}$ LPE garnet thin films, magnetocrystalline anisotropy 80−93147
$(Gd,Tm,Y)_3(Ga,Fe)_5O_{12}$, bubble domain gradient propag., elliptical distortion and bias compensation 78−19292
$Gd_{0.9}YTm_{1.1}Ga_{0.44}Fe_{4.56}O_{12}$, ion implanted, ferromag. reson. meas. 78−68385
$K_{0.5}Tm_{0.5}Nb_2O_6$, ^{93}Nb NQR spectra, 77 to 450K 79−38401
$(LaTmCa)_3(FeGe)_5O_{12}$, mag. loss and domain wall mobility 80−65980
$(LaTmCa)_3(Fe_{5-x}Ge_x)O_{12}$ film, high g, for mag. bubble applics. 77−85529
$La_{0.9}Tm_{0.1}Se$, sp. ht. meas., 1.6 to 20K, mag. contrib. 80−65934
$LiTmF_4$, Van Vleck paramag., mag. reson. on uniaxial and uniform compression *(Russian)* 79−61243
$LiTmF_4$ Van Vleck paramagnet, electron and nuclear spin-lattice relaxation of Er^{3+} ions 79−95643
$LiY_{0.416}Er_{0.5}Tm_{0.067}Ho_{0.017}F_4$, Stockbarger single cryst., charact. of solidification behaviour 77−24948
$Sm_{0.3}Lu_{0.2}Tm_{0.2}Y_{1.45}Ca_{0.85}Fe_{4.15}Ge_{0.85}O_{12}$, LPE growth, saturation magnetisation, collapse field, bubble diameter 78−95703
$(SmTm)_3(FeGa)_5O_{12}$, small-bubble appl. 79−82845
SmTmIG, epitaxial layer with submicron bubbles, mag. props. 77−12172
$Sm_{1-x}Tm_xS$, optical investig. of substitution effects on metal-semicond. transition 77−63427
Tm monochalcogenides, valence related optical and other studies, review 78−31215
TmAG, XX 80−66082
$TmAlO_3$:Yb^{3+}, mag. relax., Mossbauer expts. 79−8078
$Tm_3Al_5O_{12}$:Yb^{3+}, g-shift meas., EPR 78−56376
$TmAl_3[BO_3]_4$, thermal stability, X-ray struct. anal., refractive indices 79−4297
TmAs:Dy^{3+}, singlet-ground-state paramagnets, EPR meas. 77−20695
$TmAsO_4$, optical side bands, absorpt. spectra in mag. fields 77−52123
$TmAsO_4$:Gd, cooperative Jahn-Teller system, dipolar and random strain effects 77−40124
TmB_2, nature of magnetism *(Russian)* 78−31049
TmB_4, mag. behaviour, in strong mag. field *(Russian)* 78−88119
$TmBO_3$, cryst. struct. reappraisal 77−47427
TmBi:ER(Dy), ESR of non S-state ions 77−43881
$Tm_{2.2}Bi_{0.8}Fe_{3.5}Ga_{1.5}O_{12}$ epitaxial film, Faraday effect and domain struct. near compensation point 77−20838
$Tm_{2.7}Bi_{0.3}Ga_{0.3}Co_xFe_{4.7-x}O_{12}$, Co ion concentration effect on mag. props. close to mag. compensation point *(Russian)* 79−73788
$TmBiTe_3$, prep., elec. props., and crystallographic date 80−59981
$TmCl_3$, aquo complex form., in aq. chloride soln., coord., X-ray diffr. obs. 79−64975
$Tm(ClO_4)_3$, osmotic coeffs. 80−45556
$TmCl_3.6H_2O$:Gd^{3+}, spin Hamiltonian parameters EPR meas. 77−36128
$TmCrO_3$, optical-absorption spectra of Tm^{3+} 80−20662
$TmCrO_3$, temp. and field-induced spin reorientation, magnetisation meas. 77−69588
$Tm_{1-x}Eu_xSe$, semicond. with valence instabilities, cryst. chem. considerations 80−100213
$Tm_{1-x}Eu_xSe$, valence changes, semicond.-metal transition 80−20086
TmF_2, thermal props. *(German)* 80−81355
TmF_3, thermodynamic props., galvanic cell meas. 80−21316
TmFX mixed halides, synthesis and lattice parameters 78−30594
$TmFe_2B_2$, compounds with $CeAl_2Ga_2$ structure type *(Ukrainian)* 79−32970
$TmFe_2H_x$, mag. props. 80−25095
$TmFeO_3$, acoustic vel. and attenuation shifts at spin reorientation phase transition 80−65986
$TmFeO_3$, domain struct. in spin reorientation region, Faraday effect obs. 77−20835
$TmFeO_3$, magnetoelastic props. at spin reorientation region 77−8382
$TmFeO_3$, orthoferrite, vel. of planar domain wall 78−72363
$TmFeO_3$, parameters of interaction between rare earth and Fe ions, theory and expt. 79−73705
$TmFeO_3$, temp. depend. of neutron depolarisation factor meas. near spin reorientation transition 77−16053
$Tm_3Fe_5O_{12}$, mol. field coeffs., mag. moment/temp. relations 80−50067
$Tm_3Ga_5O_{12}$, Mossbauer study of crystal field props. 80−66082
$Tm_3Ga_5O_{12}$:Cr^{3+}(Yb^{3+})(Gd^{3+}), Van Vleck paramagnet, EPR g-shifts and linewidths, temp. depend. 77−66419
TmH, $^1\Sigma$ state, Dirac-Fock one-centre calcs. 80−23301
TmH_2, lattice thermal expansion and point defect form. energy 77−51524
TmH_{2+x} ^{169}Tm Mossbauer studies 80−44975
TmH_3, ^{169}Tm Mossbauer study 80−44976
$Tm_y(La,Y)_{1-y}S$, microwave resistivity 77−11949
$Tm_y(La,Y)_{1-y}Te$, microwave resistivity 77−11949
$Tm_{0.82}Lu_{0.18}VO_4$, elastic consts. at 9 GHz 77−62576
$Tm_{1-x}Lu_xVO_4$, Jahn-Teller system, thermodynamic properties, internal stress effects 80−59679
TmN(P)(As)(Sb), singlet ground state paramag. system, microwave resist. meas. 77−20353
$TmNbO_4$-$CaWO_4$, phase transitions of fergusonite-scheelite *(French)* 80−19942
$TmNi_2Si_2$, mag. props., 4.2-200K 80−84602
Tm_2O_3, 300 to 900K, mag. susceptibility and Curie temp. meas. 78−56288
Tm_2O_3, EXAFS and chemical shift 77−81176

thulium compounds continued
Tm_2O_3 film, between Al electrodes, prep. and elec. props. 80−60103
Tm_2O_3 film, electron beam deposition, elec. props., and struct. 79−87580
Tm_2O_3, mineraliser effect on growth morphology 78−91283
Tm_2O_3, polycrystalline, elastic props., porosity depend. 77−52384
Tm_2O_3, susceptibility, 4.2-270K 77−12081
Tm_2O_3, XPS, charging effects on core-level binding energies 79−24409
$Tm(OH)_3$, cryst. struct. 80−24424
TmO_6S_8, low temp. Mossbauer study and mag. susceptibility 80−80656
$Tm_2O_2SO_4$, antiferromag., specific heat, 0.6 to 30K 79−33487
$Tm_2O_2SO_4$, antiferromag., mag. props. 1.6 to 40K 79−33464
$TmP:Dy^{3+}$, singlet-ground-state paramagnets, EPR meas. 77−20695
$TmPO_4$, IR and Raman spectra 80−34904
$TmPO_4$, Jahn-Teller induced elastic constant changes, 4.2 to 300K 78−79657
$TmPO_4:Gd^{3+}$, EPR spectrum and Jahn-Teller induced nonuniform dynamic strains 77−85565
$TmPO_4$-$Pb_2P_2O_7$, solubility curves for high temp.-melts for growth of single crysts. 78−95687
$TmRh_4B_4$, high supercond. transition temp. 77−89893
TmS, antiferromag. struct. below 8.9K, neutron diffr. obs. 79−78318
TmS, EPR studies of valence states of Tm 77−77095
TmS, metallic, thermoelec. power 80−6818
TmS(Se)(Te), far IR refl. and DC resist., 1-300K, interconfig. fluctuation effects 78−35136
TmS(Se)(Te), Mossbauer expt. in ^3He-^4He dilution refrigerator 78−27127
TmSb, cryst. field effects on elasticity, rot. and higher order interactions 77−63251
TmSb, cryst. field effects on transport props. 78−72133
TmSb, crystal field effect in thermal expansion 78−19305
TmSb, Gd ESR, Gd-Pr exchange, conduction electron effects 79−69719
TmSb, metallic, elec. resistivity, 4f-quadrupole charge distrib. 80−24873
TmSb, paramagnet, rotational invariance and magnetoelastic phenomena 77−48027
$TmScO_3$, synthesis and lattice const. 78−30593
TmSe and its mixed crysts., valence instabilities, phase diagram 80−70651
TmSe, Anderson lattice resist. for antiferromag. ordering 80−65556
TmSe, Curie constant rel. to valence bond strength 80−60251
TmSe, Debye temps., vibr. amplitudes, X-ray diffr. determ. 78−2222
TmSe, EPR studies of valence states of Tm 77−77095
TmSe, elec. resist. under press. at very low temp. 80−96878
TmSe, electron energy loss spectroscopy and UV photoemission meas. 78−31305
TmSe, first obs. of negative elastic const. 80−103409
TmSe, intermediate valence compound, mag. neutron scatt. 78−68164
TmSe, intermediate valence state, resistivity of magnetically ordered ground state 79−1683
TmSe, intermediate valent, Raman scatt. 80−16038
TmSe, intermediate valence cpd., susceptibility, single-ion approach 80−70935
TmSe, Kondo lattice model 80−97063
TmSe, Kondo lattice theory 80−20380
TmSe, mag. neutron scatt. 80−25096
TmSe, mag. ordering under press., neutron diffr. obs. 80−70947
TmSe, mag. props. 80−97086
TmSe, mag. props. and struct. 80−25109
TmSe, metal insulator transition, cond. processes 80−96787
TmSe, metallic, optical refl. investig. of valence fluctuations 77−63428
TmSe, metallic, thermoelec. power 80−6818
TmSe, mixed valence, X-ray absorption study 80−76102
TmSe, mixed valence behavior 79−78050
TmSe, mixed valence cpd., thermal, mag., and transport props. 79−61074
TmSe, mixed valence state, ferromag. alignment 80−20133
TmSe, mixed valence systems, spin dynamics and mag. ordering 78−68162
TmSe, mixed-valent, field-depend. mag. phase transitions 78−10657
TmSe, nonstoichiometry, high temp. chem. and valence instability *(German)* 79−23743
TmSe, paramag. intermediate valence cpd., single ion approach to susceptibility 79−61042
TmSe, spin dynamics, neutron scatt. study 79−24178
TmSe, susceptibility, Tm^{2+} and Tm^{3+} characts. 80−25110
TmSe, valence mixing, mag. props. obs. 80−70648
TmSe-TmTe(EuSe), semiconductor-metal transitions 80−96953
Tm_2Se_3, mag. susceptibility meas. 4.2 to 300K cryst. field approx. 77−66246
Tm_3Se_4, mag. susceptibility 77−40032
Tm_xSe, $0.87<x<1.05$, mag., thermal and transport props., comp. depend. 78−68239
Tm_xSe, low temp. props., effect of composition 77−80775
Tm_xSe, magnetoresist. and Hall effect, stoichiometry effects 80−65597
Tm_xSe, residual resistivity at very low temp., composition depend. 79−82588
Tm_xSe, valence instabilities, antiferromag. order 80−20128
$Tm_2(SeO_4)_3.8H_2O$, thermal decomp. and IR spectra 80−3319
$TmSe_{0.83}Te_{0.17}$, spontaneous magnetisation, mag. susceptibility, magnetostriction, elec. cond. 79−24146
$TmSe_{1-x}Te_3$, semicond. with valence instabilities, cryst. chem. considerations 80−100213
$TmSe_{1-x}Te_x$, mixed-valent cpd., spontaneous magnetisation 80−20392
$TmSe_{1-x}Te_x$, phase relationships and press. induced transitions 80−19771
$TmSe_{1-x}Te_x$, valence changes, semicond.-metal transition 80−20086
$Tm_xSe_yTe_{1-y}$, magnetic ordering studies *(German)* 80−54882
$Tm_2Si_2O_7$, crystal struct. of X form, polymorphism under press. *(French)* 77−47430
$Tm_2Si_2O_7$, polymorphism under press., cryst. struct. 77−35692
C-$Tm_2Si_2O_7$, single cryst. flux growth, morphology 79−52097
$Tm_4Si_2O_7N_2$, lattice consts., X-ray diffr. anal. 80−28986
TmTe, as example of fluctuating oxidation states 78−60089
TmTe, crystal field effect in thermal expansion 78−19305
TmTe, EPR studies of valence states of Tm 77−77095
TmTe, f^{12} and f^{13} config. photoemission fractional parentage coeffs., intermediate and LS coupling calc. 80−84829
TmTe, hyperfine struct. of Tm^{2+}, Mossbauer spectra 78−76368
TmTe, paramag., Faraday and Cotton-Mouton effects for acoustic phonons 78−52476

thulium compounds continued
$TmTiO_3$, bulk mag. and struct. props., ferrimag. order 80−107993
$TmVO_4$, centrosymmetric exhibiting cooperative Jahn-Teller effect, dielec. props. 79−28694
$TmVO_4$, dielec. meas. at Jahn-Teller transitions 77−24802
$TmVO_4$, elastic consts. at 9 GHz 77−62576
$TmVO_4$, enhanced nuclear cooling and spin-lattice relax. time 80−80632
$TmVO_4$, Jahn-Teller distortion, RF susceptibility and NMR meas. 80−44930
$TmVO_4$, Jahn-Teller system, critical dynamics and acoustic phonon coupling, Z-branch 77−84887
$TmVO_4$, type crystals with cooperative Jahn-Teller effect, acoustic NMR *(Russian)* 77−28460
$TmVO_4:Gd^{3+}$, EPR linewidth temp. var., random strains due to Jahn-Teller effect 77−12200
$TmVO_4$-type crystals, dipole nuclear spin-phonon coupling and US absorpt., theory 77−24753
$Tm_2V_2O_7$, physical props. 78−39320
$Tm_2V_2O_7$, prep., cryst. chem. and chem. anal. 79−41986
$Tm_2V_2O_7$, pyrochlore struct., mag. props. 78−72335
$Tm_2(WO_4)_3$, mag. props., 300 to 900K 79−28510
Tm_2WO_6, growth from soln. in melt 77−1806
$Tm_xY_{1-x}Se$, Kondo effect, Van Vleck behaviour 80−25085
$Tm_{1-x}Y_xTe$, $(0\leq x\leq 1)$, single cryst. growth and characts. 78−23603
$(Y,Eu,Tm,Ca)_3(Fe,Ge)_5O_{12}$, Ca, Ge substituted garnet LPE films, elec. props., charge imbalance, Seebeck effect 78−68101
$(Y,Eu,Tm,Ca)_3(Fe,Ge)_5O_{12}$ garnet film coercivity, new annealing method 78−84459
$(Y,Gd,Tm)(Fe,Ga)_5O_{12}$, cylindrical mag. domain behaviour in external mag. field *(Russian)* 78−6553
$(Y,Sm,Lu,Tm,Ca)_3(Fe,Ge)_5O_{12}$, epitaxial garnet film, temp. depend. mag. props. 80−39825
$(Y, Sm, Tm)_3(FeGa)_5O_{12}$ LPE films, factors affecting coercivity 79−91267
YEuTmCa garnet bubble films, domain wall transition 79−56584
$(YEuTmCa)_3(GeFe)_5O_{12}$ film, Bloch loop punch-through in mag. bubbles 77−59437
$Y_{1.52}Eu_{0.3}Tm_{0.3}Ca_{0.88}Ge_{0.88}Fe_{4.12}O_{12}$, bubble translation vel., ion-implantation effects 78−68327
$(YEuTm)_3(FeGa)_5O_{12}$ film, dynamic props. of bubble domains by high speed photography 80−15771
$(YEuTm)_3(FeGa)_5O_{12}$ garnet film, bubble domain steady state motion on a circle 80−29589
YEuTmGa garnet bubble film, dynamic diffuse wall deform. 80−54927
$Y_{1.57}Eu_{0.78}Tm_{0.65}Ga_{1.05}Fe_{3.95}O_{12}$ film, gradient propagation, overshoot and creep 78−19291
$YGdTmFe_{4.3}Ga_{0.7}O_{12}$ epitaxial films, bubble-domain lattices with specified parameters 80−60386
$(YGdTm)_3(FeGa)_5O_{12}$ epitaxial film, formation of lattice of cylindrical mag. domains from stripe domains *(Russian)* 80−80579
$(YSmTmCa)_3(GeFe)_5O_{12}$ film, YY pattern racetrack discrimination and state stability of S=1 and 0 bubbles 78−91908
$(YSmTm)_3(FeGa)_5O_{12}$, small-bubble appl. 79−82845
$Y_{1-x-y}Tm_xEr_yAlO_3$, $Y_{1-x-y}Tm_xEr_yScO_3$, stimulated emission of Er^{3+} ions 78−6705
$Y_{0.8}Tm_{0.2}Se$, sp. ht. meas., 1.6 to 20K, mag. contrib. 80−65934

thunderstorms
see also lightning
1975 July 9, elec. fields, electron precip. and VLF radiation during simultaneous substorm and thunderstorm 80−67392
activity index determ. technique, accuracy 78−61529
aircraft effects of thunderstorm-induced low-level wind variation 77−91217
aircraft EM environment meas. near thunderstorm cells 78−49180
Asia, thunderstorm location by single station techniques, improved method, radiowave propag. effects 80−67438
atmospheric electricity supply current, solar modulation 80−17329
Australia, thunderstorm, wind gusts 77−86996
Baghdogra, India, thunder occurrence over airport 78−20499
Baghdogra airport, India, probable thunder occurrence, climatological study 79−39802
Baikal-Amur region, USSR, thunderstorm activity 77−78379
Baltic area, activity in October-March period *(Russian)* 77−21850
birth zone, prediction by Explorer satellite *(Italian)* 77−81988
Bombay, growth and decay of thunderstorms during premonsoon season, radar study 79−48541
Bombay, unusual thunder activity during 1974 Sept.-Oct. 79−20918
charging by polarization-induction mechanism 78−32166
cloud drops collision efficiency, elec. charges and vertical external elec. field effects 77−25738
cloud elec. field meas. by balloon-borne coronasonde 78−61577
cloud electrification by precip. mechanism in presence of ion generation, model 79−84388
cloud growth and precipitation development, refined charge distrib. in stochastic elec. model 77−29374
cloud physics rel. to atm. electricity, review 79−70842
clouds, charge separation laboratory meas., associated with secondary ice crystal production 80−72623
clouds, elec. field inclination effect on inductive charging mechanism 77−78315
clouds electrification rel. to sudden increases in shower intensity 78−20491
NE.Colorado hailstorms and radar reflectivity of ground-level hail 79−53470
conjugate area of low-latit. whistlers, thunderclouds distrib. 77−2309
convective rainfall, storm life cycle, model 79−16589
convective rainfall, surface vel. fields, obs. in S.Florida 79−16588
corona from chaff, microwave radiometric detect. 78−16106
coronae effects on elec. fields beneath thunderstorms 79−79978
dangerous weather phenomena prediction, research prospects 79−34932
density currents, wind shear obs. 77−13109
distance determinations, calcs. and examples *(German)* 78−40680
Doppler weather radar, development of weather echo props. 80−26645
downbursts and aircraft accidents, analysis 78−53693
Earth-ionosphere cavity resonances, effect of thunderstorms on ELF radiowave props. 78−77416
electric charge build up, charging mechanisms 78−81320
electric charge generation and field parameter throughout storm 80−72595
electric charge separation, model 80−77076

thunderstorms continued
electric field and precipitation regions, airborne and ground obs. 80−85725
electric field and wind profile, balloon meas. 78−85636
electric field changes, rel. to ice particles orientation and alignment rapid changes 80−17330
electric field growth, field struct. and charge distrib. in thunderclouds 77−70777
electric field strength, study from mobile ground station 78−92943
electric fields, 10-year study of Minneapolis area 78−57253
electric fields, precip. elements charge and size, airborne obs. 78−73485
electric fields and charges, effects on aerosol particle collisions with cloud and rain drops 77−25748
electric fields over water, max. intensities meas. 77−33160
electric fields produced by Florida thunderstorms 78−40621
electrical conductivity, contrib. of cloud and precip. particles rel. to air relaxation time 80−17332
electrification, airborne expts. 77−66970
electrification, field expt. 80−72622
electrification process, charge separation laboratory meas., associated with secondary ice crystal production 80−72623
NWEurope, storm development on colour TV display of METEOSAT data 79−100936
Florida convective rainfall aspects 79−88455
forecasting, simple method 78−81304
forecasting at Srinagar, India 77−53128
forecasting hail, thunderstorms, and showers, book 77−73821
frontal, evolution studied by analysis of radar observations *(Russian)* 79−88405
generation linear model, heat addition 77−81973
global atmosphere electricity quasi-state model, role of thunderstorms as current sources 79−96799
gust front detection, sensitive pressure-jump sensor design 78−57357
gust front evolution and tornado genesis, Doppler radar obs. 77−91219
hail, cloud identification and suppression, lightning obs. *(Chinese)* 77−66968
hail probability rel. to radar echo heights, South African Highveld 79−20925
hail producing clouds, N.E.Colorado, observed and computed microstruct. 78−7716
Hampstead storm, London, numerical simulation of quasistationary cumulonimbus system 78−77308
Heatree, Devon, England, 1976 June 27 isolated heavy storm 78−57288
heavy rainstorms in Britain, diurnal var. in occurrence 77−64402
Hokuriku coast, Japan, anomalous winter thunderstorms obs. 78−73443
ice nuclei generation in surface outflow 80−90135
ice particle surface potential, laboratory study 80−51495
Indian monsoon rel. to equatorial stratospheric westerlies 77−29370
infrasonic pulses detect. from thunderclouds 77−29362
infrasonic signals from thunder 79−70846
intensity from satellite data 80−41518
Iraq, climatological and meteorological study 77−73796
isolated convective storm, three-dimens. numerical model, variable ambient wind shear 79−5574
Japanese winter thunderstorms hazard to aircraft, abnormal characts. 77−5309
lidar observations of high plains thunderstorm precipitation 78−32167
lightning, randomised modification expt., statistical anal. 77−2218
lightning, VHF direction finder studies 79−20928
lightning detection by satellite monitoring 79−92559
lightning location and ionospheric refl. heights from two-station mag. field meas. 79−70845
lightning peak current meas. and recording device results *(Japanese)* 80−46288
lightning radar echoes and simultaneous elec. field changes 79−84372
lightning study using thunder meas., thunder duration rel. to strike pt. *(Russian)* 80−56532
lightning suppression by chaff seeding, comments and reply 77−53139
lightning suppression by chaff seeding, further comments 77−53140
location errors anal., thunderstorms in Asia 80−101421
maximum precipitation, 1900-1977, Great Britain 78−85672
micrometeorological sink for stratospheric H_2O 79−84385
New Zealand, freq. distrib. 77−53160
nontropical storms initiation by solar activity 78−49096
outflow and hydraulic jump in assoc. cloud 77−91194
Oxford, 1682 May 31, point deluge and tornado 80−51521
Ozar airfield, India, thunderstorm occurrence 78−32159
photographic obs. from Space Shuttle 79−58078
photography and lightning recording with modified cine sound camera 79−21058
point discharge current, shift in diurnal variation compared with global thunderstorm activity 79−88409
point discharge current meas. during different types of rainfall 79−84379
point discharge from ground surface objects, annual charge change per km^2 80−77077
precipitation particle alignment by electrostatic fields, radar obs. 77−9464
prediction, automated 12 to 36 hour probability forecasts 80−77062
premonsoon thunderstorms, integrated field intensity of atmospherics, Calcutta 79−39792
pressure jump detector array, gust front detect. at Dulles Airport 78−32234
propagation of thunder through atmosphere, status of current research 80−87618
pulse Doppler radar obs. of severe thunderstorms 78−85651
radar and VHF emission obs. of three-dimens. motion 80−46218
radar information, automated acquisition and analysis 78−7772
radar obs., time-domain computation of mean and variance of Doppler spectra 79−100972
radar observation of precipitation related depolarisation 80−51453
radar precipitation maps as lightning indicators 78−85652
radiation fields, of multiple return stroke lightning 78−3885
radiowave propag. at 30 GHz during heavy thunderstorms, ATS-6 meas. 77−64377
radiowave propagation, depolarisation 78−3854
raindrop charge and assoc. electric field for different rain types 78−44933
riming electrification as a charge generation mechanism in thunderstorms 79−34917
thunderstorms continued
Schumann resonance noise generation, expt. data appl. to thunderstorms location and atmosphere cond. profiles 80−36360
severe local storm, Pennsylvania, predictibility of location and damage 77−66965
severe local storms, St. Louis region, urban effects 79−12199
severe storm warning using Doppler radar 78−49148
severe thunderstorms, nature and effects on society 79−5560
severe thunderstorms internal struct., dual-Doppler radar meas., tornado generation 78−61504
Sierra Leone, monsoon characts. 78−7693
solar corpuscular radiation effects 79−79982
South Africa, prefrontal squall line behaviour, radar obs. 78−3878
St. Mawgan, Cornwall, diurnal var. of thunder 78−24347
streamer velocities meas., positive, in quasi-uniform electric fields 80−72625
strokes to Earth per km^2 per year, CIGRE count (since 1962) *(German)* 78−40606
subcloud region, structure and interactions 77−45094
subsynoptic-scale energy transformations in severe storm situations 77−56673
summer thunderstorms, forecasting, use of wet bulb pot. temp. charts 77−91232
Sydney thunderstorms of 10 November 1976, descriptions 79−79995
tornado frequency correl. with thunderstorm days, seasonal and regional vars. 79−79957
tornadogenesis in rotating thunderstorm, numerical model 79−79970
TRIP-76 (Thunderstorm Research International Program) 77−45158
tropical, cloud to ground and intracloud discharge 80−85705
tropical convection in anvil clouds, hydrometeor precipitation, melting and evaporation 80−17323
tropical regions, atm. noise data 80−61875
updraft splitting and mesovortex couplet evolution, model 80−98395
urban pollutants scavenging by thunderstorm rainfall, numerical expt. 79−12261
vertical electric potential gradient profile under point discharge current and wind 77−53117
VLF atmospherics meas. at San Miguel, Argentina, rel. to thunderstorms 79−39799
VLF atmospherics over Calcutta rel. to local storms 79−88550
VLF atmospherics rel. to thunderstorms at sea, nighttime effect 80−26585
VLF radiometeorology for thunderstorm location *(German)* 77−17254
whistler, occurrence rate variation with geomagnetic latitude 79−40010
wind profile in subcloud layer of thunderstorm from lightning photographs 77−87013
Yakutskenergo, probability calcs., instrumental and visual registration 77−70797
N fixation by lightning 80−90147
NO_2 production, transport into stratosphere 80−8376
O_3 and N oxide production 77−37300

thyratrons
250 kV water Blumlein, off-resonance transformer charging 79−13564
dye laser, reliable thyratron switched flashlamp pumped 79−31930
extremal value indicator using glow-discharge thyratrons 77−17967
FX2508 for off-resonance transformer charging for 250-kV water Blumlein, Experimental Test Accelerator appl. 80−23183
high current discharge, in thyratron, nanosec. grid extinction time *(Russian)* 80−54057
high-power long-pulse thyratron modulator with small off-duty factor 78−86380
ignition of gas lasers *(German)* 79−64245
nanosecond discharge of H_2 plasma deionisation, spectroscopic study *(Slovak)* 77−47279
Pockels cell driver of fast rise time and high repetition rate using thyratron 80−69537
pulse generator, nanosecond pulses with sharp leading edge 78−4651
pulser, high-power, HF, for photo-impulse ionised lasers 79−18444
short pulse laser circuit thyratrons 79−18437
spark source, adjustable-waveform, thyratron-diode switch element, appl. emission spectrometry 77−63998
switch for high voltages and currents, thyratron-spark gap hybrid 80−54067
vacuum UV pulsed controlled source 78−87115
Cu halide laser driving ccts., parametric study 80−83610
H_2 thyratron switch for UV emitting N_2 laser 79−27290
N_2 laser, with discrete ceramic capacitors in Blumlein-type circuit 77−19330
Xe atom, electron inelastic interaction, two-grid thyratron expts. 77 83747
Xe atoms elastic scattering of electrons, expt. 79−857

thyristor applications
1 kV SCR pulse generator for US pulse echo excitation 79−70290
600 MW pulsed energy convertors for toroidal field coil, design philosophy 78−58496
arc ion source for cyclotrons, thyristor current modulator 77−46438
atomic absorption spectroscopy with nonflame sample atomisation, thyristor thermostabiliser use 79−96388
current pulse formation from pulse-gas-discharge lamp using thyristor keys *(Bulgarian)* 78−33795
current-supply stabiliser, adjustable, for magnetic lens β spectrometers 78−74528
drive control for machines for mechanical testing 77−25213
dual slide projector fader control cct., using a triac dimmer 80−69489
electrolysis voltage control *(Dutch)* 77−63925
electromagnet field control system 77−37950
electropolishing rectifier, thyristor current control, quick-acting electronic protection from short circuits 77−74377
film sound tracks, electronic cutting *(Russian)* 78−21252
frequency difference and ratio meters using thyristors 78−4649
furnace temp. regulation circuits, for creep testing devices 80−25956
fusion reactor, TEXT, motor-generator power supply system 80−99292
fusion reactor, TEXT, toroidal field coil power supply, thyristor controlled 80−91289
Geiger-Muller counter hodoscope, protection from spark chamber noise 77−18742
harmonic current AC filters at KEK accelerator 78−33333
injection laser pumping by thyristor oscillator 79−13982
KEK proton synchrotron, power supply 77−83245
laser pumping lamp ignition pulse semiconductor shaper 79−72585

thyristor applications continued
magnetic flaw detector, thyristor magnetising current switch, exam. 78−44311
magnetic flaw detector, using magnetic powder method 77−90571
microprocessor triac interface, used to control kiln temperature 78−45632
microtron voltage control system using thyristor convertors 77−14280
microtrons, thyristor modulator circuit and construction 80−63422
modulator using thyristor, microtron appl. 78−55061
optical glass melting in Pt crucibles, thyristor freq. convertor-fed power supply 77−50780
photo flood dimming, to reduce heating and extend life of lamps *(German)* 78−29193
photographic flash sequencer, using thyristor control 80−62749
power supply, transformerless, for laboratory furnace 77−65035
power supply for TV, cinematographic light sources, type TPU thyristor feeding device *(Russian)* 79−58816
resistance furnace programmed temperature regulator 78−86256
semiconductor heterostructures, elec. and optical phenomena, discrete devices, review 78−72250
semiconductor laser pumping thyristor current pulse generator 78−79024
semiconductor laser pumping thyristor nanosecond current pulse generator 78−79025
slide projector, dissolve control unit provides cross-fading and operational sequence recording 80−77833
sound-controlled flashlamp trigger circuit *(Spanish)* 80−13175
spark generator for dust explosion hazard assessment and gas ignition 78−57983
static interruptor cct., triac, thermostatic and lighting control appl. *(Italian)* 78−73984
superconducting coil energy storage power supply 79−34442
temperature regulator circuits, using thyristors and triacs *(Spanish)* 79−6115
temperature regulator for inductive loads using IC zero voltage switch U 106 BS with triac *(German)* 80−77779
temperature regulator for pulsed NMR spectrometer 80−105687
thermostat for aqueous solution, linear thyristor control and thermistor sensing *(Japanese)* 77−90264
thyristor thermostabiliser for at. absorpt., spectroscopy with non-flame atomisation, power supply *(Russian)* 78−76977
Tokamak equilibrium field coils, supply, pulsed 79−14622
two-phase servo master-slave manipulators, triac output control system 79−9213
voltage flicker suppression in KEK 12 GeV synchrotron 77−83230
X-ray pulse generator supply 80−57446
Ar laser, discharge current control using thyristor convertor 77−14747

thyristors
bevelled p-n junction in Si power device, elec. field in controlled region and blocking capabilities determ. 77−1474
dynamic electro-biased laser Q-switch with SCRs *(Chinese)* 79−45977
forced current pinching in p-n-p-n structure due to action of base current 79−95487
high-output, air cooling intensification design method *(Chinese)* 80−19229
lifetime profile measurements in heavily doped emitter structures using electron beams 80−15538
magnetothyristor with carrier recomb. on gate electrode 79−60918
p-n-p-n structure turnon parameter meas. by optical probe 77−57358
p-n-p-n structures, turn-on at high voltages and high currents 77−1475
power devices, book 77−78906
propagation of turned on state 79−11217
reversible thyristor convertors, in regulated current source 77−37921
solid-state device conference, Tokyo, Japan (Sept. 1976) 77−76901
temperature regulator 77−37881
thin-oxide MIS thyristor devices, interface state charge 79−38172
tunnel cathode, p-n-p-I-M struct., theory of switching effect 77−39930
GaAs-AlGaAs heterostructure thyristors, operation and elec. characts. 79−7891
Si monocrystals, neutron irradiation installation for power thyristor production 77−65993
Si-GaAs heterojunction photothyristor, spectral characts. 78−10546

ticking stars *see pulsars*

tidal power stations
Bay of Fundy, Canada, environmental aspects 79−92093
Bay of Fundy proposals 79−61944
Britain, proposals for Severn barrage 79−24888
Canadian reassessment of Bay of Fundy potential 79−43734
dams, flexible water barriers, energy conversion to compressed air energy 80−61273
dynamic dam utilising ocean and river currents and tidal power 79−20865
energy accounting study 80−76589
energy analysis 79−48083
energy from the sea [tidal and wave power], research in United Kingdom 79−79371
evaluation of alternative energy sources for the Guyana energy crisis 80−61270
feasibility, project selection and full project definition, French, Canadian and British developments 79−43731
future energy concepts, Conf. London, England (Jan.-Feb. 1979) 79−43709
immersed rotor ('tide mill') concept 79−43737
Korea, prefeasibility study 80−61271
pump-turbine, reversible, axial, with symmetrical double cambered profiles 79−43735
technical details and operating experience 80−72009
technological advances, influence on benefit/cost ratio 79−43733
United Kingdom potential 79−43729
West Bengal, siltation estimation 80−31059

tides
N.Adriatic Sea, Green's function of Laplace's tidal eqn. 80−17291
Adriatic Sea, meteorology contrib. to high tides prediction 77−86906
Aegean Sea, spectral anal. of tidal data 77−86905
amplitude factor, phase lag at Beijing, China *(Chinese)* 80−8246
anholonomic coords. and tidal gravitational field of planet 79−34723
antisymmetric tidal modes under equinoctial conditions induced by ozone heating 79−35024
aquifer response to tidal forcing and 1964 March 28 Alaskan earthquake 78−73407
aquifer storage capacity determ., well tide eqn. 80−21785

tides continued
artificial satellite laser ranging, oceanographic appls. 77−64484
N.Atlantic, energetics of baroclinic tides 77−86900
NW Atlantic, moored obs. of semidiurnal internal tide 77−60421
NW.Atlantic Ocean, oceanic geoid and tides derived from Geos 3 satellite data 80−3901
Atlantic Ocean, spatial characts. of semidiurnal internal waves in Polygon-70 test area 80−31051
Atlantic shelf-boundary tidal meas. between Ireland and Norway 77−37220
atmosphere, distrib. with altitude, wind field influence *(Russian)* 78−69402
atmosphere, electromagnetic force effect 77−87136
atmosphere, generated by differential heating between land and sea 78−65374
atmosphere, meteor zone, seasonal variations of solar and lunar tides 77−87134
atmosphere, rel. to O(^{1}S) excitation mechanism 80−41588
atmosphere, review 77−86957
atmosphere, simultaneous incoherent scatt. obs. 77−87135
atmosphere, solar modulation of lunar tide 80−94593
atmosphere, solar semidiurnal tide, zonal motion and meridional temp. gradient effects 80−98399
atmosphere, solar semidiurnal tide influenced by zonal wind, theory 80−61853
atmosphere, solar semidiurnal tide influenced by zonal wind, theory 80−61854
atmosphere, surface press. oscill. obs. 80−77054
atmosphere, surface tides, New Zealand 78−85665
atmosphere, synoptic object localisation, long-period tidal fluctuations *(Russian)* 78−81321
atmosphere, temp. tide in stratosphere due to Moon, NIMBUS 5 obs. 80−101405
atmosphere, theoretical work since 1970, review 80−94589
atmosphere, thermal exciting energy, numerical anal. 79−70833
atmosphere, thermotidal exciting function for water vapour absorption 78−28310
atmosphere, tidal dynamics model of thermosphere, with O-N_2 diffusion 80−101465
atmosphere, tidal obs. at Millstone Hill (1974 Aug.-1975 Oct.) 79−2414
atmosphere in 100-500 km range, Arecibo coord. tidal obs. 79−2410
atmosphere internal tidal waves, rate of energy transfer to upper atmosphere mean flow *(Russian)* 77−13101
atmosphere lunar O_1 tide, detect. in geomag. lunar daily var. at Alibag and contamination by M_2 component 80−56355
atmosphere lunar tide determination, data filtering method 80−46223
atmosphere Na layer, gravity waves and tidal oscills., lidar obs. 78−88955
atmosphere semi-diurnal tides, upward propag. rel. to ionospheric equatorial anomaly in E.Asia and India 80−109301
atmosphere tide at meteor altitude, CTOP radar obs. 80−77181
atmosphere tides in joint presence of friction and rot., f-plane approximation 79−66847
atmospheric and geomagnetic tides anal. method 77−87079
atmospheric high-latitude tidal forces, quasi-fortnightly rhythm, space-time characts. *(Russian)* 78−7726
atmospheric oscills. rel. to horizontal winds and temp. structure 78−20457
atmospheric tidal winds, meteor data, poleward momentum transport 80−12581
atmospheric tides and planetary waves *(French)* 77−21962
bay, tidal propag. equations, finite difference and analytical methods 79−12134
Bight of Abaco, Bahamas, algorithmic tidal study, expt. and harmonic anal. 80−8319
Bight of Abaco, Bahamas, tidal model comparison with data 80−4035
Bristol Channel, tidal regime by numerical model 80−85670
Bristol Channel tides, analytical wedge model 80−85671
S.California uplift area, tide-gauge records anal. for Recent vertical movements modelling 79−80055
Canaries Current eastern branch, tidal component *(Russian)* 78−77263
Caracas, gravity-tide meas. rel. to Pasadena magnitudes of earthquakes 80−51344
Chandler tides in atmosphere, calc. 78−69413
Chandler wobble affected by pole tide, theory 80−51318
S.China Sea, refr. of tidally forced internal waves, satellite obs. 77−64298
clinometric obs. at Khristoforov (1973-5 period) *(Russian)* 78−3704
Cochin Harbour mouth, India, hydrographic characts. and tidal prism 80−41452
Conference, Grenoble, France, 1975, Aug. 77−86898
connected basin natural oscillation, theory 80−61806
continental shelf, tidal model for N.W.Europe 77−37221
continental shelf width affecting tidal range 80−56483
Cook Inlet, Alaska, tidal currents meas. by two-site HF Doppler radar system 80−72533
Corio Bay, Victoria, tidal model, finite difference approach 79−12131
crust deformation by tidal forces, and orogeny 80−85625
crustal tilt obs. in N.Wales mine, strain-tilt coupling and Earth model 80−89926
current measurement from a surface following data buoy, major tidal constituent 79−84290
data processing, Tihany Observatory results 77−87097
day length and zonal tides, effect of core-mantle coupling 80−104850
deep sea temp. and pressure sensor for tidal meas. 77−37424
E-region luni-solar tides, electron density distortion meas. using group and phase height meas. 80−109299
E-region solar tides, electrodynamic effects, equatorial electrojet 77−9611
Earth, eastern USA, effect of ocean tides 77−81778
Earth, elastic tides and natural oscills. with Coriolis force included 77−37122
Earth, Europe, correction for M_2 freq. oceanic tides 77−9316
Earth, inhomogeneous tidal strain obs., USA 77−44881
Earth, mantle convection shaping by tidal bulge, rel. to global tectonics 78−32048
Earth, monitoring of seismic vel. variations 78−28183
Earth, ocean and atmospheric tides effects on artificial satellite orbits 77−87243
Earth, ocean loading effects on tidal gravity in Australia 78−28151

tides continued
Earth, oscillations of a gravitating and rotating uniform liquid sphere 79−44082
Earth, Phlegraean fields, Italy, intercrustal hydrodynamic correlation with geodynamics 77−2138
Earth, strain-tide spectroscopy 78−73301
Earth, tidal changes in force of gravity at Poltava (1973 to 1976) *(Russian)* 78−88782
Earth, Verbaandert-Melchior horizontal pendulum tidal anal. results *(French)* 77−17013
Earth's crust, tidal displacement, Geos-3 laser ranging obs. 80−3913
Earth anomalous gravity effects during 1976 April 29 annular eclipse *(Chinese)* 79−2174
Earth bodily tide and yielding due to tidal loading 78−36091
Earth gravity intensity variations, use of AChF-3 pendulum clock 80−104856
Earth gravity tide spectrum, 1 to 4 cycles/day 78−20345
Earth liquid core dynamical effects, nutations 77−86736
Earth rotation, periodical fluctuations due to lunar tides, calc. by Einstein *(German)* 77−67169
Earth rotation, tidal contribs. to Universal Time short-period terms *(Chinese)* 79−8589
Earth rotation, tidal irregularity rel. to study of forced nutation 77−52956
Earth rotation effects, Sun and Moon accels. rel. to origin of mountains 79−8592
Earth strain, topography, geology and cavity effects 77−44896
Earth strain meas. with laser interferometer *(Japanese)* 77−81783
Earth strain obs. with Cambridge laser strainmeter 77−44895
Earth strain tides in Great Britain, survey 79−44080
Earth surface tidal tilts, influence of atmospheric press. fluctuations *(Russian)* 78−88790
Earth tidal deformations and pot. vars., relation between Love numbers and load factors 78−61305
Earth tidal potential, multiple expansion 79−12062
Earth tide, dynamic shear modulus influence 80−76901
Earth tide, influence of mantle anelasticity 80−76900
Earth tide, review *(Chinese)* 80−89925
Earth tide and Arctic oceanic loading tide at Spitsbergen 77−9318
Earth tide effects on flows in horizontal permeable elastic layers connected to wells 78−7666
Earth tide gravity maps for W.Europe 77−9317
Earth tide information from counter-orbiting polar satellites 77−2083
Earth tide meas., non-linear effects in TRG-1 tide meter 78−45018
Earth tide obs., meteorological wave separation method *(Russian)* 78−4014
Earth tide obs., ocean tides effect in near zones 77−32974
Earth tide observations processing, individual monthly sets weightings *(Russian)* 78−88789
Earth tide recorder photoelec. compensation method to acquire data 80−77129
Earth tide recording equipment, phototransducers emission source light output ratio stabilisation *(Russian)* 78−88949
Earth tide registering stations, electronic time basis *(Rumanian)* 77−33216
Earth tides, anal. of obs., least squares methods *(French)* 77−87078
Earth tides, global interaction with ocean tides, model 80−51319
Earth tides, gravity and altitude vars. meas. via N.W.Europe gravity base network *(German)* 78−15948
Earth tides, meas. by borehole long-period seismometer (BELS type 79) with stable period *(Japanese)* 80−67417
Earth tides, planetary influence and rel. to earthquakes 79−100817
Earth tides, theoretical problems, conf., Aug. 1978, Caracas, Venezuela 80−51400
Earth tides, theoretical study assuming Earth viscoelastic body 80−67333
Earth tides, tilt meter obs. at Berezovaya Rudka station *(Russian)* 78−88783
Earth tides, tilts, parallel recording through digital print-out and photorecording channels *(Russian)* 78−88785
Earth tides anal. in Peking region before 1976 July 28 Tangshan earthquake *(Chinese)* 80−3892
Earth tides and core stability 77−9320
Earth tides in new USSR Universal Time system, 1955-74 period *(Russian)* 78−69279
Earth tides in time-service observations, effects of nutation errors 79−96733
Earth tides measurement, cavity effect in tunnels of various cross-sections *(Russian)* 78−88784
Earth tides measurement, influence of S_1 diurnal meteorological wave on tilt meter obts. *(Russian)* 78−88788
Earth tides observations, gravity screening effect assessment *(Russian)* 78−88787
Earth tides observations, monthly data set anal. *(Russian)* 78−88786
Earth tides studies using microcapacitive transducer *(Rumanian)* 79−58121
Earth tilt obs. corrected for rainfall as earthquake precursors 79−8609
Earth-Moon system, tidal evolution 80−82240
Earth-Moon system, tides rel. to evolution of lunar orbit 77−29671
Earth-Moon system tidal friction, changing Earth moment of inertia 80−81803
Earth-Moon system tidal friction theory 80−81802
earthquake prediction methods, solar-lunar tides *(Russian)* 79−84162
earthquakes, tidal triggering in Swabian Jura 80−12348
East River tidal strait, New York, hydrodynamic characts. 77−37222
elastic rotating Earth, elementary oscill., ordinary differential eqns. 79−39632
elastic spheroidal Earth, Green's function for deformation eqns. 77−81779
electrojet influenced by lunar tide, semimonthly variation 80−61937
energy dissipation by Antarctic ice shelf flexing 78−88845
energy dissipation in oceans, astronomical, geophys. and oceanographic consequences 78−20431
energy resources in late 1970s 79−57347
E England coast, storm surge (1978 January 11 to 12) 80−12419
English Channel, hydraulic model of nonlinear tidal deformations in shallow water 77−37218
English Channel M_4 tide derived from nonlinear numerial model of M_2 tide 78−49027
enhanced pole tide rel. to Chandler wobble period and damping 80−21778

tides continued
estuaries, explicit finite element formulation for tidal waves *(German)* 78−94755
estuaries, homogeneous, tidal currents calc. 78−7654
estuaries of variable breadth and depth tidally induced residual currents 80−72544
estuarine current meter data acquisition microcomputer system 80−46265
estuarine surface microlayer and trace metal cycling in salt marsh 79−57984
estuarine tidal front, trace metal enhancements in biotic and abiotic components 79−2265
estuary, tidal and thermal propag., numerical model 79−12133
estuary, tidal two-dimensional hydrodynamic digital simulation by finite element method 78−92846
estuary, well mixed, buoyancy effects on longitudinal dispersion 80−85681
estuary and river sited power plants, water discharge and chlorination, simulation 78−96250
estuary circulation (partially mixed), two-dimens. model 80−109161
estuary proportioning with sinusoidal tidal wave *(Italian)* 79−20839
estuary thermal impact of multiple power plant operations 78−96232
estuary water quality models, finite difference and finite element methods 78−77375
N.W.Europe, marine tides and crustal struct. interaction with Earth tide 77−86739
W.Europe, tilt and gravity obs. of Earth tides, spatial analysis 79−66602
F-region, equatorial, tidal modes rel. to motions deduction from Sq currents 78−96344
finite element analysis model, flow in rectangular channel example *(German)* 78−96233
finite element methods for flow anal., book contrib. 79−32522
fjord fronts, effects of winds and tides 79−57953
flood and tidal flows, network hydraulic model 79−12162
Florida Current, fluctuations in transport at periods between tidal and two weeks 80−72551
friction and Earth's rotation [conference, Bielefeld, Germany (Sep. 1977)] 79−88234
friction effect on tidal motion 79−44192
Galilean theory, reassessment 77−29980
gauge with fast-response characts. for shallow water 80−26639
gauging, automatic network 79−5692
geocentric position variation due to terrestrial fluid mass motion 80−76894
geomagnetic tide, ocean effects 77−86752
Ghana shelf fortnightly wave, characts. 80−26515
Gironde inlet and Pertuis of Maumusson, tidal effects on estuarine waters seaward dispersion *(French)* 80−8324
global dissipation and energy exchange between ocean and Earth tides *(Russian)* 77−73747
global Earth tides and upper mantle struct. 79−25182
global geodynamics, Canadian contribs., 1971-79 period. 80−8262
global hydrodynamic numerical 1° model, M_2 tide oscillation and energy dissipation 77−86899
global lunar semidiurnal geomagnetic var., seasonal changes 79−53598
global ocean tide, effects of loading and self attraction 77−70670
gravimetric observations, effect of the Honkasalo term in tidal corrections 80−21602
gravimetric tidal loading computed from integrated Green's functions 80−89928
gravity obs. of tides made in Gt. Britain 80−94446
gravity perturbation due to ocean tide, series computation 80−104857
Greater Cook Strait, New Zealand, M_2 tidal effects 80−90093
Gulf of Mexico and Caribbean Sea bottom press. obs. 78−36175
gulfs, tides and currents, math. models, finite difference techniques 79−12130
hemispherical ocean centred on equator, numerical model 80−72528
hydrodynamic numerical modelling, appl. to Lagoon of Venice 79−34832
hydrostatic tides, theory, Earth, planets and satellites appl. 79−84075
ice shelves, floating, tidal flexure cracks, fracture mechanics 78−69368
ice shelves tidal flexure, meas. by tiltmeter 80−31050
ice shelves tidal interaction 77−86902
inclination records, nontidal S_1 wave effects *(Russian)* 78−3707
inclinometric obs. at Peregonovka station *(Russian)* 78−3705
inclinometric tide, discrimination of barometric and oceanic effects *(French)* 77−86738
Indian equatorial region, lunar magnetic tides 77−87154
Indian Ocean, sea levels in western equatorial region rel. to tides, meteorology and ocean circulation 80−4018
N.Indian Ocean, tidal charts 78−32115
indirect mapping of ocean tides by solving inverse problem for tidal gravity obs. 77−86901
interlacing channels, nonlinear computer model 79−34828
internal solitary waves prod. by tidal flow over three-dimens. ridge, ocean appl. 79−46332
internal surface, two-layered basin *(Japanese)* 78−11912
internal wave formation, vertical diffusion driving mechanism in Oslofjord 80−26531
internal wave surface effects, LANDSAT and ship obs. 77−5215
ionosphere, F_2-layer, lunar tide over Japan 79−2436
ionosphere, lower, semidiurnal and diurnal tides rel. to wind obs. by Kyoto meteor radar 80−67444
ionosphere, lunar perturbations in columnar electron content, dynamo electrostatic fields interpretation 77−29570
ionosphere, lunar semi-diurnal elec. field rel. to total electron content lunar var. 79−21100
ionosphere, lunar tides rel. to monthly mean lunar daily geomag. vars. in Japan (1958-1973) 79−96739
ionosphere, lunar tides theory 78−77382
ionosphere, mid-latitude F_2-layer, electron density oscills. rel. to lunar tide 78−61655
ionosphere, mid-latitude F_2-layer, ion and neutral gas vel. oscills. rel. to lunar tide 78−61656
ionosphere, seasonally dependent tidal modes rel. to antisymmetric S_q vars. 78−81499
ionosphere, semidiurnal tide rel. to E_s-layer props. at Sodankyla, Finland 77−87183
ionosphere, solar tides and electrodynamic effects, polarisation elec. field 78−36391

tides continued
ionosphere, tidal wind elec. field rel. to F_2-layer global electron-density distrib. 77−64514
ionosphere, tides rel. to E_s-layer occurrence in Brazilian geomag. anomaly 77−78558
ionosphere tidal winds, mixing freq. components in electron content data 79−29929
ionospheric records over Shanghai, March 1953 to June 1955, influence of atmospheric tides *(Chinese)* 80−77192
Irish and Celtic Seas, tidal dynamics 79−25254
karst waters and karstic rocks tidal movements 77−86940
Knight Inlet, British Columbia, stratified flow tidal interaction with sill 80−101368
Kouchibouguac Bay, New Brunswick, tides rel. to barrier island breach morphology and dynamics 80−12371
lakes, circulation, seiches, tides and storm surges, finite element methods, book contrib. 79−34876
Laplace's tidal eqn. asymptotic eigensolns. 77−33166
Laplace's tidal eqn. soln. for standing semidiurnal oscills. 78−20456
Laplace tidal equation, perturbation methods, Ligurian Sea application 80−26533
large-scale hydrodynamic system simulation programs 77−21799
longshore sediment transport by tidal current, outside surf zone 80−76961
Love number changes during Earth model variations in static theory of tides 77−44951
Love numbers, tidal forces and surface loading 79−44081
lower thermosphere, compositional modelling taking account of airglow tidal variation 80−109288
lower thermosphere dynamics, connections with processes in troposphere and stratosphere *(Russian)* 78−24401
lunar and solar tide generating potentials, spectroscopy, rel. to ocean tide features 77−86904
lunar effects on earthquake periodicity 78−53844
lunar effects on periodicities of Alaskan and central American earthquakes 78−53621
lunar geomagnetic tidal variation in Indian region 77−60541
lunar geomagnetic tides and ocean dynamo 78−36099
lunar palaeotides and Earth-Moon system origin 79−62769
lunar semidiurnal oceanic and atmospheric tides, interfacial effects 79−100871
lunar semidiurnal tidal line width in geomag. spectrum, filtering methods 77−21678
lunar semidiurnal tides, effect on geomag. vertical intensity daily var. at Marion Island 78−81107
lunar tidal effect on spread F 79−80070
lunar tidal effects on OH and O I airglow intensities 77−60506
lunar tide, semidiurnal, basic physics 80−31449
lunar tides in equatorial ionospheric absorption 79−44286
M_2, stored energy of Kelvin wave in NE. Pacific, effects 79−79849
M_2 and S_2 tides calc. for world oceans from tidal potential 79−39752
M_2 ocean tide parameters and Moon's meas. longit. decel. from artificial satellite orbit data 80−31048
M_2 ocean tide parameters from satellite orbit perturbations 77−33093
M_2 ocean-tide corrections to tidal gravity observations in Western Europe 77−86737
M_2 tide eqn. deduced from artificial satellite obs. 77−41337
M_2-lunar tide, determ. from lunar daily geomag. vars. at Tucson 78−96136
Madras coastal zone, sea level, tides and waves 77−41038
magnetosphere, lunar and solar tidal effects 77−87184
old Mangalore port, tides effect on estuarine and oceanic waters hydrographic conditions 80−41451
mantle horizontal inhomogeneities influence on tidal oscill. amplitudes 78−57159
mareograph well type selection from charact. eqn. *(Polish)* 77−70871
Massachusetts Bay, tidally generated internal wave packets 79−44190
Mediterranean harbour tidal harmonic constants 80−41448
upper mesopause region, semidiurnal tidal wind meas. during winter/summer conditions transition 79−44220
mesosphere, equatorial tidal components of winds 78−36229
mesosphere, tides and gravity waves at mid and low latits. 78−36231
mesosphere vertical velocities, first VHF radar meas. at temperate latits. 79−16572
Messina Strait, tidal currents 80−81917
Messina Strait, tidal currents 80−81918
meteorological tide, energy transfer from atmos. to ocean *(Russian)* 80−76988
Mezen' Bay (White Sea), marine tides EM fields 78−73378
Middle Atlantic Bight, ocean tides and weather induced pressure fluctuations 77−81911
middle atmosphere dynamics, review 80−17338
Miramichi estuary, New Brunswick, tidal current control of submarine morphology 78−36174
Moon, tidal accel. calc. 79−16849
Msf propagation and sea temperature on Guinea Gulf northern coast 80−4033
Narara Bet, Gulf of Kutch, coastal currents, temp. and salinity 80−76990
natural vibration freqs. of Earth including ocean 79−62449
neutral atmospheric motions effects on two-stream irregularities in equatorial electrojet 79−16742
New Hebrides arc, tidal tilt from localized ocean loading 80−98211
nonlinear estuarine response to tidal action for potential hydroelectric power generation 77−70692
nonlinear mathematical model of the propagation of tides in interlacing channels 79−39720
North Sea, M_2 tidal elevations and currents, hydrodynamic model 80−104973
North Sea and River Thames, surge and tide interaction 78−96219
Nova Scotia crustal struct. and NW.Atlantic M_2 tide from tilt and gravity obs. 78−40464
Nova Scotia tidal loading, results from improved ocean tide models 78−92821
numerical model as aid to navigation 79−12121
numerical models of ocean tides 78−16049
numerical simulation of fluid motion, conf., Melbourne, Australia (1976) 79−9116
ocean, analysis methods 77−87080
ocean, barotropic and baroclinic tides over continental slope and shelf off Oregon 80−72543
tides continued
ocean, calc. using acoustic and vibr. techniques *(German)* 78−69366
ocean, effect on Earth gravity at Aburatsubo Crustal Movement Observatory 80−101316
ocean, model showing geometry effect 79−92546
ocean, modelling, shelf effects parameterisation, S. Atlantic appl. *(Russian)* 79−100843
ocean, oscillating three-dimensional tide generating currents struct. 80−72542
ocean, oscillatory tidal currents rel. to topographic generation of residual circulation 79−57954
ocean, periodic tidal flow, anal. by finite element perturb. method 78−24290
ocean, satellite-derived parameters, lunar tidal accel. determ. 78−73662
ocean, semidiurnal internal tide rel. to upper ocean temp. and salinity struct. 80−72536
ocean, tidal mixing and 18.6 year cycle of shallow seas surface temp. 78−73387
ocean, tidally varying sound speed and currents rel. to deep ocean acoustic propag. 77−79995
ocean, turbulent Ekman bottom boundary layer, effect of diurnal tidal currents 80−104977
ocean current regime in Gulf of Kutch, NW.India 78−36184
ocean currents, temperature and tides low freq. fluctuations near Peru coast 79−79858
ocean currents in synoptic eddy, periodic components *(Russian)* 78−85593
ocean global tides, geopotential effects 77−21787
ocean internal tidal oscills. spatial charact. from temp. meas. 78−61434
ocean internal tide rel. to underwater sound fluctuations, theory for parabolic vel. profile 77−31159
ocean lunar O_1 tide, contrib. to geomag. lunar daily var. at Alibag 80−56355
ocean palaeotides and nautiloid growth, rel. to Earth-Moon system dynamics 80−41713
ocean quarter-diurnal tides loading effects by Ligurian Sea 78−61308
ocean shelf edge tides, variable-depth Green's function 80−81915
ocean tidal currents, interaction with wind-generated sea waves 80−51428
ocean tidal flow in channel, modelling using turbulence energy closure scheme 79−79859
ocean tidal interactions in region of large bottom slope, NW Africa, JOINT-1 obs. 80−4016
ocean tide and solid Earth gravity tide interaction, Ross Sea area, Antarctica 77−86903
ocean tide effect on tidal deform. of sea floor and continents *(Russian)* 77−29308
ocean tide measurement, press. quartz qualification as deep sea gauge *(German)* 79−74980
ocean tide-induced residual current, numerical model verification 77−86920
ocean tides, energy balance and wind effects in shallow sound 79−2243
ocean tides, self-consistent equilib. model 78−96218
ocean tides, vol. to lunar orbit evolution 80−8565
ocean tides effect on tidal gravity vars. 79−53359
ocean tides effects on M_2 gravity tides in Japan 77−60342
ocean tides mapping with satellites, computer simulation 79−39880
oceanic and shallow water, spectral method of computation *(French)* 78−28321
oceanic loading on European laser-ranging sites 78−85462
oceanic tides, review 77−73762
oceanic tides, semidiurnal waves determ. via obs. of artificial satellites trajectories *(French)* 79−8634
Onslow Bay, eastern USA, existence of continental shelf waves 80−72529
open channel, two-dimensional tidal propagation model, difficulties 78−77272
orbital perturbations of satellite 1967-92A, tidal forces 78−61307
orthotides, appl. to sea level series 78−85565
Pacific, cotidal charts near Hawaii using f-plane solns. 77−60394
Par River estuary, India, effects of tides on pollution rel. to abatement methods 80−104521
Pentland Firth, anomalous tidal flow from cable voltage meas. 79−44191
periodic flow anal. by finite element perturbation method 77−70690
periodic Galerkin finite element method 78−28239
perturbations of satellite orbits rel. to Love number and phase lag 77−64187
planetary tidal potentials rel. to Maunder sunspot minimum 77−33376
plate tectonic driving forces, heat flow and tidal drag 78−32050
pole tide induced by Chandler wobble, tidal admittance 77−9443
pole-tide signal at low-latitude coastal station 78−61322
Polygon-70 in Atlantic Ocean, internal tidal structure *(Russian)* 80−51411
Port of Leba, Poland, reconstructed entrance, storm tides prediction, math. modelling *(Polish)* 78−40568
pure harmonic tide in canal, eqns. of motion quadratic resistance term linearisation 78−69369
quarter-diurnal in English Channel 78−61424
radar altimeter height and timing bias report 80−46326
radiowave wind obs. of waves during 1976 over Saskatoon 79−79935
residual motion, tidally-generated, in St. Lawrence estuary, numerical model 80−94541
review of tidal research 80−98349
river, tidal wave propag., nonlinear model 79−5512
river bore propagation theory based on classical hydraulic theory 79−84312
river tidal computations, explicit-implicit water level model 78−44886
rivers, shallow, diffusive model for tidal propag. 79−2303
rivers and estuaries, finite element models of tidal waves 79−53370
Ross Ice Shelf, ocean tides and waves 79−88364
S_3 atmospheric tide from surface wind field over ocean 78−44911
satellite laser tracking for polar motion, Earth tides and latitude determ. 77−56570
sea level extremes calc. using nonlinear programming method 77−78479
sea level recorder for tectonic studies 77−45175
Sea of Japan, tides rel. to seawater hydrochemical charact. and transparency distrib. 80−31057
secular variation of pole tide 78−88778
semiclosed water basin, eigenoscillations, hydrodynamic models, appl. to Ligurian Sea 78−3782

tides continued
semidiurnal internal tide var. along Oregon coast during coastal upwelling 77−37223
semidiurnal tide in the meridional wind at F region heights at low latitudes 79−53596
Seto Inland Sea hydraulic model tidal flow pattern anal. *(Japanese)* 78−36314
Severn estuary, seasonal and spring neap tidal depend. of axial dispersion coeffs. 80−94534
shallow sea, three-dimens. numerical model of tidal motion 77−37219
shallow water, three-dimens. nonlinear model *(Chinese)* 78−24309
shallow water areas, tidal wave spectrum structure, theoretical analysis 77−37217
shallow water equations, finite element finite difference method 79−34829
shallow water wave equation model, finite element tidal computations 79−84282
shallow water waves in rot. basin, integral formulation 80−81920
shelf sea fronts adjustments revealed by satellite IR imagery, tidal advection effects 79−92545
shelf seas around British Isles, tidal fronts 79−2259
simulation on sphere, geodesic finite-difference method for curved domains 80−109153
solar atmospheric tide in Barcelona, study for 1968-70 period *(Spanish)* 77−9479
solar system tidal interactions, consequences and inferences 77−87297
solar tides, electrodynamic effects, Sq current system 77−9610
solar tides effect on nightglow O I 5577 Å line, intensity var. *(Russian)* 80−12585
solar-lunar forces calc. accuracy *(Russian)* 80−61813
solid Earth tides, Fourier anal. applied to short data length 80−30972
South Pole gravity tides, long period, 1970 obs. 80−21611
spectral modelling, finite element method, appl. to M_2 tide in English channel 78−61579
spectral modelling by finite element method *(French)* 80−21782
St Kilda shelf, tidal regime, press. gradient obs. 80−85666
strain tide spectroscopy, interaction Earth mantle, liquid core appl. 79−5440
Strait of Magellan, tidal currents monitoring by onshore elec. field recording 77−87107
stratosphere, lower, wind tidal component meas. over Jicamaca 79−25308
stratosphere and mesosphere, wind and temp. diurnal and semidiurnal oscills., rocket meas. 79−5556
submarine cables voltage daily vars. at tidal freqs., due to induced oceanic elec. fields 77−86753
Sumy-Kherson profile, harmonic analysis of principal Earth tides *(Russian)* 78−3706
Sun-Moon-Earth system tidal stresses rel. to climate periods 77−33178
surge interaction in semi-infinite uniform channel, North Sea appl. 79−25251
Surkhob fault zone, USSR, tidal deform. determ. for crustal movement anal. 80−104944
Tagus Estuary, water quality study *(French)* 79−66706
thermal excitation of atmospheric tides due to insolation absorption by O_3 and H_2O 79−34890
thermal wedge, effects of tidal flow on position of upper surface *(Russian)* 78−16046
thermosphere, differential operator and integro-differential eqn. *(Chinese)* 80−56660
thermosphere, diurnal tide excited by EUV and UV solar radiation absorpt. 77−53260
thermosphere, diurnal tide seasonal-latitudinal struct. 78−77377
thermosphere, fundamental diurnal component of temp., comp. and wind fields 77−87141
thermosphere, lower, dynamics, incoherent scatt. radar technique appl. 79−8734
thermosphere, lower, thermal tides rel. to nightglow emissions vars 77−78550
thermosphere, lower, tidal effects investigation by reflected natural infrasound obs. 79−21089
thermosphere, lower, tides and gravity waves interaction rel. to thin shear turbulent layers 78−65444
thermosphere, midlatitude, tidal modes identification from neutral wind meas. during ALADDIN programme 80−31153
thermosphere, seasonal-latitudinal tidal struct. 80−101467
thermosphere, tidal struct. at equinox 78−81476
thermosphere, tidal var. in total mass density from AE-E Mesa expt. 79−53593
thermosphere, tidal vars. in composition 78−96334
thermosphere, tidal winds in 100-200 km altitude region, Arecibo obs. 77−82074
thermosphere, tides and midnight temp. anomaly 79−84556
thermosphere, transport processes in diurnal tide, satellite meas. 78−88959
thermosphere, winter semi-diurnal and diurnal tides in S.hemisphere meteor region 80−109287
thermosphere and mesosphere solar semidiurnal tidal wind rel. to airglow var. 77−21965
thermosphere neutral winds, tidal modes rel. to low latit. dynamo currents seasonal vars. 80−8479
thermosphere structure and dynamics rel. to tides and diffusion waves 79−35026
thermosphere tides, semidiurnal and terdiurnal 80−82119
tidal channel, energy dissipation due to bottom friction and eddy losses 80−31058
tidal wave profile distortion on entering river *(Russian)* 77−17115
transworld tidal gravity profile 78−57160
Trieste horizontal pendulum obs. of 1976 Friuli earthquake precursors 78−24216
tsunami wave propagation anal., 2-step explicit finite element method 78−40503
turbulent structure of bottom boundary layer in tidal current 79−84284
upper atmosphere, Cooperative Tidal Observations Program 79−2409
upper atmosphere, local winds rel. to ionospheric equatorial anomaly in E.Asia and India 80−109301
upper atmosphere, tides rel. to non-LTE radiative transfer in CO_2 15 μm band *(Russian)* 78−36341
upper atmosphere diurnal tide meas., 80-100 km altitude, Arecibo radar obs. 77−2290
tides continued
upper atmosphere tidal effects on geomagnetic and ionosphere variations 77−87137
upper atmosphere tidal wind variations, upper mesopause region, ionospheric reflection height *(German)* 77−87139
upper atmosphere tides and winds meas. from meteor radar obs. 79−66851
Urbana Meteor Radar observations during GRMWSP/CTOP periods 79−2412
Venice, sea-lagoon exchange in modified tide regime 80−12431
Venice historical centre, high water and sea defences, implications of altimetry surveys *(Italian)* 77−86740
Venice Lagoon, kinematic mathematical model of tidal wave *(Italian)* 79−16471
Virginia Beach, Virginia, coastal currents and assoc. sand stream 78−73392
VLBI, correction for effects of troposphere, ionosphere and Earth crustal tide *(Japanese)* 80−21926
waves in channel, bottom friction in perturbation method 80−98354
waves of tidal frequency, submerged elliptic ridge effects 78−69358
Weddell Sea, tidal currents in central region 78−44831
White Sea, study of tidal sand waves 79−2218
wind system in upper atmosphere rel. to ionospheric sporadic layer vertical motion 79−100993
O and O_2 distrib. in lower thermosphere assuming tidal effects, one dimens. nonstationary diffusion-photochemical model 80−4160

tight-binding calculations
A15 compounds, coherence length and phonon softening 78−34587
A15 compounds, high-temp. superconductors, martensitic transform., microscopic theory based on 3-dimens. band struct. 78−19752
A15 compounds, plasma energies, tight-binding energy-band model 78−84159
A15 ordered and disordered cpds., density of states calc. 79−87033
actinides and alloys, metallurgical props. rel. to electronic struct., energies calc. method 77−20221
adsorbed atoms, oscillatory indirect interaction, non-asymptotic behaviour in tight-binding models 78−72000
alkali metal chemisorbed layers, changes in work function due to charge transfer 78−18900
alloy, amorphous, electronic struct. 78−72062
alloy, cleaved, electronic theory, off-diagonal disorder 79−4596
alloy, disordered, bulk and surface density of states, effect of surface segregation 77−15729
alloy, one-dimensional, electronic struct. 79−69391
alloy thin film, thickness depend. of CPA electronic densities of states 80−65644
alloys, random binary, single-particle Hamiltonian and self-consistency 79−37953
alloys, substitutional, self consistent cluster theory for off diagonal disordered systems 80−84272
alloys, with off-diagonal disorder, density of states and cond., CPA calc. 80−24780
amorphous system, cluster effective lattice method, mag. and electron props. 77−66242
amorphous system, theory of electron localisation 77−1391
amorphous tetrahedrally bonded solid, theory of fluctuations and localized states 78−10405
Anderson localisation, study by continued-fraction method 79−4534
Anderson localisation problem, cond. numerical studies 80−49673
Anderson model, localisation edges and critical exponents 79−90986
auramine crystal, photocond. and intermol. electron interaction, tight binding approx. 77−15765
band tailing due to zero-point vibrs. in perfect cryst. 79−28267
BCC and simple cubic lattice, density of states of tight-binding s-bands using modified-moments method 80−15431
binary alloy, density of states, CPA with nonretracing paths 77−31924
binary alloy, model substitutionally disordered, electron momentum density 78−56061
binary alloy, ordered, electronic struct. in Bethe lattice, exact analytic treatment 80−49582
binary alloy, partially ordered, elec. resist., CPA calc. 78−43356
binary alloys, charge transfer and transport props. in tight-binding model 79−82577
binary alloys, density of states in CPA 77−51633
binary compound, Kohn anomaly in optical phonon branch 80−92626
binary linear chain, electronic props., short-range order effects 80−96769
Bloch electrons in uniform mag. and electric field, effective Hamiltonian 77−69207
borate glasses, effects of clusetring and transition metal ions on electronic struct. 78−10347
central peak in the density of states of a disordered linear chain 80−100428
chemisorbed atoms on transition metal surface, interaction energy calc. 80−54507
chemisorbed layer, depend. of work function in order-disorder phase transition 79−19460
chemisorption on model insulator 77−85072
clusters of arbitrary size, soln. of eigenvalue problem of simple tight binding model 77−43464
complex tight binding systems, surface density of states determ. 80−20272
Compton profiles, struct. depend. 78−35223
covalent elements, cohesion in condensed phases, corrections to simple Huckel approx. 78−59779
covalent elements, cohesion of σ and π bonds in condensed phases, simple Huckel approx. 78−59778
crystallites, finite SC and FCC, with (100) surfaces, tight binding eigenvalues 78−34745
deep impurities, large unit cell approach 78−23046
defect tetrahedral cpd. semiconductors, band struct. trends 79−90956
degenerate narrow bands, intraatomic Coulomb and exchange energies 80−84452
dense fluid, electronic struct., cluster effects 79−95305
diamond, (100) surface states, SCF extended tight-binding method 77−47881
diamond, nonlinear optical susceptibility, tight binding bonding orbital model 80−5784
diamond, phonon frequencies, model calc. using tight binding Hamiltonian 78−59894

tight-binding calculations continued
diamond, static dielectric function, local field correction, tight-binding model 79−95355
difluorides, rutile-type, upper valence band 77−55480
dimerized interrupted strand model, optical absorption 77−16271
dislocation scattering, new Hamiltonian for describing multivalued elastic displacement fields 80−24862
disorder at surfaces and interfaces, effect on electronic props. 78−26932
disordered chain, analytic behaviour of electronic density of states 77−76716
disordered electronic systems, spin interaction effects, loop expansion and exact relations among local gauge invariant modes 80−80221
disordered systems, electrical cond. in Kubo formalism 79−60778
disordered systems, systematic approach, averaged Green functions calc. 80−80150
disordered transition alloys, generalized perturbation calcs. of ordering energies 77−4282
electron-phonon coupling, Frohlich-Mitra modified tight-binding approx. 77−69253
electron-phonon quasi-one-dimensional system, fluctuations anal. 77−89703
energy band structure, nearly-free and tightly-bound electron approxs. 78−73792
(ethylene)$_x$, mol. crystals, quantum theory, mol. tight binding method calcs. 80−49572
excitons, tightly- and weakly-bound, unified treatment, Wannier representation 78−43301
excitons, Wannier and Frenkel, simple model for unified treatment 79−69422
FCC, BCC and SC crystals, struct. 78−84123
FCC clusters, size and shape depend., tight binding approximation 78−79920
ferromagnet, disordered itinerant-electron, spin waves 78−95427
ferromagnet, itinerant electron, surface spin waves, tight-binding Hubbard model 80−39763
ferromagnet, tight binding model, surface magnetisation 80−103807
ferromagnetic alloy, binary ordered, dynamic mag. susceptibility, spin wave stiffness constant 79−38307
film, surface density of states calc. within tight-binding scheme 77−55594
finite perturbed chains, g-factor, use of exact one electron solution *(French)* 80−59858
first principles method for electronic props. of surfaces, interfaces and bulk solids 80−49564
fluoride, perovskite- and tysonite-type, upper valence bands 77−80730
fluorite-type crystals, universal valence bands 77−35864
(formamide)$_x$, mol. crystals, quantum theory, mol. tight binding method calcs. 80−49572
glass, ionicity and coordination, tight binding calcs. 80−49129
glasses, defect reactions, ionicity dependence, negative-U states 80−88510
graphite, various modifications, electronic props. 80−49592
graphite intercalated with AsF_5, quantum oscillatory phenomena 80−107823
graphite intercalation compounds, band struct. model, dynamical dielec. function, reflectivity 80−34348
graphite intercalation cpds., mag. susceptibility, tight-binding model 80−44796
graphite-$FeCl_3$ intercalation cpd., electronic excitation spectrum, high resolution EELS meas. 80−45182
Green's functions for surfaces, thin films, and solid interfaces using random-walk theory 80−54753
HEED, many beam problem, use of Gauss-type orbitals and plane waves 78−83661
homopolar tetrahedral solids, Gaussian relaxation method of density of states calc., appl. to Ge 77−39760
ice, electronic struct. investig. and comparison with theory 77−16452
II-VI compounds with transition metal impurity, SCF LCAO MO formalism in CNDO and INDO approx. 79−38017
III-V semiconductor surfaces and interfaces, Green's function technique, tight binding approx. 80−49855
impurity electron states, linear chain, arbitrary number of impurities 78−2443
infinite crystal, surface states determ. by complex extension of tight binding 78−80032
insulators, tightly bound, collective excitations 79−51492
interfaces, empirical tight-binding method, critique 80−49854
ionic crystal, Compton profile interpretation to give ionic deform. and bonding 77−40301
ionic crystals, surface electron states in continuous spectrum 78−26931
itinerant electron ferromagnet, two magnon bound states 77−20537
itinerant magnets, band struct., mag. props. and local moments 80−70929
Leman-Weaire-Thorpe theorem generalisation 79−95308
liquid metal, electronic struct., similarity to spin wave excitations in amorphous ferromag. 77−12109
liquid metal, integrated density of states, expression in Roth's effective-medium approx., generalisation of Friedel formula 79−99467
liquid metal, tight-binding model, effective medium approx. 77−15756
liquid metals and alloys, cond., Hall coeff. and thermoelec. power, tight-binding model 77−47798
local impurity states, existence, levels, Green function, tight-binding calcs. 78−67981
local orbitals, optimisation for electronic struct. calc. 77−47711
localisation and off-diagonal disorder 77−20258
Lorentz-Lorenz formula, microscopical derivation 78−92014
matrix components, symmetry and analytical expressions 78−30862
metal, BCC, chemisorption of monolayer of atoms, charge in density of states determ. 77−47682
metal, electron-electron scatt. 79−38045
metal, FCC, (100) surface, chemisorption-induced interaction between electronic levels of two-level adsorbate 80−39644
metal, HCP, LCAO description of (0001) surface electron states, appl. to Sc 78−72232
metal, lattice stability, comparison of BCC and FCC struct. in tight-binding calc. 77−51632
metal, liq., tight binding theory of transport props., Ishida-Yonezawa approx. for single-band model 78−84190
metal, quasi one dimens., plasmon dispersion relations, RPA and HF calcs. 78−34789
tight-binding calculations continued
metal, tight-binding, electronic struct. and kinetic props. at high temp. 80−59848
metal, vacancy-dislocation interaction, tight-binding calc. 80−92554
metal surface, indirect long-range oscillatory interaction between adsorbed atoms 78−71997
metal surface, interaction between adatom and substitutional impurity atom 79−56076
metal surface, tight-binding, dissociative chemisorption of molecule 78−2368
metal surfaces, electronic spectrum of ordered monolayers 77−85293
metal-metal interface, simple, electronic props. 78−72234
metal-semiconductor interface, electronic structure 78−72261
metallic alloys, ordered and disordered, positron localisation 78−79962
metallic disordered systems, effect of nonorthogonality in density of states 77−59243
metallic state, one dimens. model, stability *(Russian)* 77−85171
metallic thin film, electronic props. and elec. cond. 79−78228
metals, electron waves, tight-binding description, appl. to heterogeneous catalysis 79−60700
metals, narrow-band, Auger line shape 80−60719
metals, non-simple liq., electronic props. 77−47721
metals, photoemission, theory, book contrib. 78−95670
microclusters, electric viewpoint of morphology, energy spectrum of single electron states 78−10327
MIM junction, tunnelling, tight-binding Green function calc., disorder effect 78−10577
mixed valence states, excitation mechanism in tight-binding approx., metal-insulator transition 80−10925
modified tight binding approximation, reexam. 78−43279
noncrystalline materials, optical props., lecture 78−31219
one dimensional electronic systems, instability due to electron-phonon interaction 79−99536
one-dimensional amorphous solid, short-range order effect on spectral density of excitations 77−76514
one-dimensional conductivity, with arbitrary bandfilling, Peierls instability 80−59968
one-dimensional conductor, lattice stability, phonon dispersion, Kohn anomaly 80−96603
one-dimensional electron system, distorted, dynamical elec. cond. calc. 80−59962
one-dimensional finite chain, boundary states and vibrs., tight-binding approx. 80−2317
one-dimensional molecular crystals, electronic struct., mol. orbital theory 80−54588
one-dimensional semiconductor, delocalisation and superalternation effects in nonlinear susceptibilities 77−11840
one-dimensional systems, exchange effects in plasmon dispersion 78−91628
one-dimensional systems, exchange effects in plasmon dispersion 79−60741
one-dimensional systems, optical props. 77−43472
one-dimensional tight-binding Hamiltonian, off-diagonal disorder, singular behaviour 78−88247
orbital effect on band calc., using one-electron Hartree-Fock pots. 77−15736
ordered adlayers, density of surface states, Green's function calc. method 77−85291
ordered adlayers, electronic struct. 79−38142
ordered overlayers, chemisorption energy, multiadatom effects 78−14581
orientational metal-insulator phase transitions in quadrupolar strands with itinerant electrons 80−15455
overlap and next-nearest-neighbour interaction effects 78−72059
overlapping potentials, tight-binding rel. to scatt. theory 80−10854
Peierls transition in non-half-filled tight-binding model, props. in commensurate phase 77−31933
polar semiconductor, conduction states, pseudopot. and tight-binding calcs. 80−24785
cis-polyacetylene, electronic struct. 79−47012
polyacetylene, pure and doped, electronic props. from one-dimens., tight-binding LCAO-SCF-MO calcs. 79−56123
polyacetylene, trans- and cis-isomer, electronic struct. calcs. 80−24788
polyacetylenes, fluorinated, electronic struct., tight-binding LCAO-SCF-MO calcs., prep. 80−70591
polyene, infinite, electronic states under local perturbation 77−57878
polyethylene, electronic band struct., tight-binding approx. with MNDO 77−89691
protein model chain, aperiodic, electronic spectra, hopping cond. 80−5641
α-quartz, electronic struct., local disorder influence 80−59870
quasi-one dimensional conductor, high temperature structural instability 77−8032
quasi-one-dimensional conductor, high temp. struct. instability, tight-binding approx. and fluctuation model 78−6292
quasi-one-dimensional metals, narrow-band, exchange-correlation effects on plasmons and on CDW instability 80−44525
quasione dimensional compound, commensurability effect 78−72095
random binary alloy with partial order, electronic struct., self-consistent approx. 77−62796
random binary alloys, quantum percolation 80−80156
random electronic models with spin-dependent hopping 80−70574
random lattice, with purely off-diagonal disorder, electron localisation 80−49672
random lattice with off-diagonal disorder, absence of Anderson's transition 78−30889
rare earth compounds, cooperative Jahn-Teller phase transition, theory of optical side-bands 77−1398
rare earth compounds, valence fluctuations, electron-phonon coupling effect 80−20134
rare-earth metal, semi-infinite surfaces with mag. struct., density of states calc. 80−10851
recursion method for the extended impurity problem 80−96814
Schottky barrier heights, semi-empirical tight-binding calc. 79−28408
screw dislocation, scattering of tight-binding electrons, numerical solution of Schrodinger equation 79−51540
screw dislocations, tight-binding electron scatt. 79−91012
semi-infinite solid, elementary excitations in surface region 79−60618
semiconductor, covalent, non-orthogonal tight-binding approach 80−2442
semiconductor, electron states at planar and stepped surfaces 78−10531
semiconductor, impurity band, first and second moments of density of states calc. 78−6329

tight-binding calculations continued
semiconductor, spin-orbit splitting, tight binding calc. 77−85184
semiconductor interface, scattering-theoretic approach and its appl. to Ge-GaAs 78−95340
semiconductor surface, chemisorption of mol. complexes, bond orbital model *(German)* 80−59807
semiconductor surface, clean and with chemisorbed species, atomic and electronic struct. 78−72223
semiconductor surface steps, electronic struct., Bethe-Peierls approx. 77−39911
semiconductor surfaces, empirical tight-binding method, critique 80−49854
semiconductor surfaces, review of electronic struct. calcs. 77−28226
semiconductors, covalent, tight binding analysis of step-depend. density of (111) surface states 77−59321
semiconductors, doping of amorphous tetrahedrally bonded cpds. 80−2361
semiconductors, EM wave interaction in weakly nonlinear medium with superlattice 80−93257
semiempirical method, relationship with HF method in band struct. calcs. 80−75495
semiinfinite crystal with surface substitutional disorder, electronic struct. 77−72903
simple cubic metal, defect states, nearest neighbour tight-binding model 79−7802
Slater-Koster tables for f electrons 80−44461
solid insulator, effective screening function 78−10383
squared electron-phonon coupling constant, tight-binding calc. in transition metals and alloys 79−1571
static macroscopic dielectric function, tight binding calcs., density response and local field effect 80−49644
superconductor, magnetic, Fermi surface nesting effect on mag. instability 80−54831
surface density of states in tight-binding formalism 78−10530
surface dielectric response in local representation, microscopic theory 77−85289
surface states, model calcs. using Koster-Slater type surface potential 79−7872
ternary semiconductor, struct. effects on energy band struct. 78−39021
tetrahedral semiconductor/oxide interface, continuous random network and tight-binding models 77−89866
tetrahedron method for evaluating spectral props. of solids 80−10855
thin film, 11-layered, CPA calc. of local density of electronic states 80−65643
total electronic energy, force consts., covalent systems appls. 79−60747
transition metal, 4d BCC, electron-phonon interactions 79−95107
transition metal, BCC, phonon dispersion curves and elastic, calc. using cohesive energy 78−59885
transition metal, chemisorption of ordered overlayers with C(2×2) and (2×1) structs. 79−46925
transition metal, dichalcogenide layer cpds., bonding and phase transitions 80−34186
transition metal, electron-phonon coupling, comparison of reson. and tight-binding description 77−15746
transition metal, FCC, semi-infinite, susceptibilities near (001) surface 80−15701
transition metal, nonmag., possibility of mag. monolayer formation 78−15009
transition metal, surface atom vibrations, self-consistent calc. 80−103560
transition metal, tight-binding theory of M adatoms interaction 77−1304
transition metal alloy, surface segregation, electronic theory 77−43414
transition metal alloy, tight binding theory of heat of formation 79−28110
transition metal alloys, binary, energy of formation 77−15341
transition metal alloys, disordered, formation energy of vacancies 77−27876
transition metal alloys, ferromag., effects of order on electronic struct. 79−90938
transition metal alloys, heat of formation theory, tight binding approx. 79−43618
transition metal alloys, heats of formation, tight binding theory, moments approach 79−61891
transition metal alloys, sigma phase occurrence from cluster model 77−59750
transition metal clusters, cohesive energy and level statistics 78−95267
transition metal dichalcogenides, electronic struct. and band theory 80−44497
transition metal interfaces, localised electron states 77−59313
transition metal layer compounds, Fermi surface anisotropy effect on struct. transitions 77−51661
transition metal surface electronic struct., influence of size and roughness 78−14785
transition metal surfaces, independent electron theory of atomic interactions 79−60903
transition metal-metalloid band structure, nonorthogonality and tight-binding fit 80−59852
transition metal-simple metal dil. alloys, electronic states, reson. model pot. method 79−77995
transition metals, amorphous, density of electronic states, effect of struct. variation due to interatomic pot. softness 80−54597
transition metals, atomic volumes 77−68943
transition metals, BCC, interaction energy between self-interstitial and screw dislocation, calc. 80−70248
transition metals, cohesive and elastic props. model *(Hungarian)* 80−34120
transition metals, FCC, surface relax. and force consts. 80−39404
transition metals, ferromag., dil. H electronic struct. 80−70638
transition metals, generalisation of modified tight-binding approximation 80−88288
transition metals, stacking fault and twin energies 79−82244
transition metals and alloys, metallurgical props. rel. to electronic struct., energies calc. method 77−20221
transition metals surface electronic structure, role of self-consistency in evaluation 77−39908
TTF-TCNQ, electron-electron interaction as source of metallic resist. 80−20162
TTF-TCNQ, enhancement of mag. susceptibility by Coulomb correlations 77−77023
TTF-TCNQ, plasmon spectrum, tight binding model 78−84158
Wigner condensation, localisation of electrons in a magnetic field 79−60752

tight-binding calculations continued
zinc blende type ionic semiconductors, vacancies, bound state energy level calcs., tight binding approx. 80−44694
zincblende compounds, (111) face, dangling bond surface state 78−84278
zincblende compounds, electronic struct. and atomic config. at cleavage surface 77−62974
zone structure in tight binding calc., program 79−42430
Ag halides, quadrupolar deformability theory by tight binding method 80−10614
Ag-Cu, surface segregation, electronic theory, density of states, cluster-Bethe-lattice approx. 80−49369
AgF(AgI,AgBr,AgCl), NMR chemical shifts 80−74180
AlAs-GaAs (001) interface and superlattice, electronic props., band struct. 79−95485
AlAs-GaAs (100) interface, tight binding calc. of electronic struct. 78−95342
AlAs-GaAs (100) superlattices, band struct. 78−30868
AlP(As)(Sb), APW calc. of electronic structure and optical props. 79−99479
As, amorphous, electronic struct. of defects using cluster-Bethe-lattice method 79−73471
As_2Se_3, glassy defect electron states, tight binding calc. 80−96818
As_2Se_3, polarised light reflectance spectra, band struct. 78−63979
Au-Ag(Cu), surface segregation, electronic theory, density of states, cluster-Bethe-lattice approx. 80−49369
BaF_2, width of upper valence band, tight-binding calc. 78−26814
$BaTiO_3$, band struct. calc., interpretation of XPS and UPS spectra 80−70597
$BaTiO_3$, photoelectron and optical spectra derived from self-consistent charge MO and band calcs. 80−96785
C, vacancy, tight-binding calc. 80−24844
C_8K, K-graphite intercalation compound, electronic struct. using semi-empirical tight-binding scheme 78−6255
CO_2, metallic, one-electron dispersion relations 77−62794
CaF_2, electronic band struct. determ., combined OPW and tight binding calc. 77−85145
CaF_2, electronic energy bands calc. 78−34762
CaF_2, width of upper valence band, tight-binding calc. 78−26814
CaO, electronic band struct., combined tight-binding and pseudopot. approach 77−47728
CdF_2, electronic band struct., combined tight-binding and pseudopotential calc. 77−43495
CdF_2, electronic energy bands calc. 78−34762
$Cd_xHg_{1-x}Te$, band struct. and optical props. 80−15450
CdI_2, band struct., tight binding calcs. and photoemission spectra 78−23018
CdI_2, electronic struct. 80−15446
CdS:In, impurity resist., Matsubara-Toyozawa theory extension 80−80264
CdTe, energy bands and optical props. calc., tight-binding model with spin-orbit interaction 80−65448
CdTe surface, nonpolar, electronic struct. 77−20383
CdTe-HgTe ideal superlattice, electronic props. calc. 80−49885
CdTe-HgTe superlattice on CdTE layers, evanescent states, tight binding calcs. 80−70611
Ce, Compton profile study of γ-α phase transition 80−11503
Co, amorphous and liquid, density of electronic states, hard sphere model and tight-binding calcs. 79−23881
Co, ferromag., HCP, electronic struct. calcs., band props. 78−39012
Co-Ni, selective catalytic surface behaviour, tight-binding approx. calcs. 78−76924
Cr, surface electronic struct., tight-binding approx. calcs. 78−64090
Cr, twin and stacking fault energies calc. 80−2038
$CrCl_3$, electronic struct. and struct. phase transition 80−59644
Cs-Au, liquid, metal-insulator transition, mag. susceptibility, Knight shift, theory 80−44672
Cu (001) surface electronic structure, self-consistency effects 77−39909
Cu (110) film, energy bands, tight binding calc. 77−15761
Cu (111) film, energy bands, tight binding calc. 77−15760
Cu, Brillouin zone integration special directions, electronic density of states calcs. application 80−49569
Cu, bulk and (001) films, extended tight-binding calcs. 80−70592
Cu film, electronic struct., self-consistent calc. 77−76959
Cu halides, reflection spectra, 4.5-7.5 eV bond struct. scheme 79−61402
Cu, $L_3M_{4,5}M_{4,5}$ and $M_{2,3}M_{4,5}M_{4,5}$ Auger line shapes, independent electron calc. 77−63500
Cu-Ni, density of states of d-electrons, tight binding approx. calcs. 80−59863
CuAu, order-disorder transform., band theory for internal energy, tight-binding Hartree Hamiltonian 79−19539
CuNi alloys, electronic theory of surface segregation 79−23819
Fe, energy bands, tight binding calc. *(Korean)* 79−51479
Fe, ferromag. nonrelativistic LCAO energy band calc. 78−10343
Fe, magnetism at high temps., total electronic band struct. energy calc. 80−75721
α-Fe, screw dislocation motion, orientation depend., tight-binding type electronic theory 79−51109
Fe, twin and stacking fault energies calc. 80−2038
Fe-Rh alloy, nonmag. and mag., band theory 79−37973
Fe_3O_4, electron energy band theory, thermodynamic functions *(Korean)* 79−7785
Ga-GaAs heterojunctions, electronic struct., tight-binding and pseudopot. models 79−42633
GaAS, O_2 chemisorption on (110) surface, bonding sites 78−38938
GaAs (110), adsorption of In, N, P, and As, UPS and EELS study, tight-binding calcs. 80−49496
GaAs (110), chemisorbed O_2, extrinsic surface states 78−91535
GaAs (110), chemisorption of Cl, photoemission spectra and tight-binding calcs. 80−6629
GaAs (110), chemisorption of Al, electronic struct., tight binding calc. 80−49842
GaAs (110), surface electronic struct., ang. resolved photoemission expts. and tight binding calcs. 78−91743
GaAs (110), surface states and matrix elements in angle-resolved photoemission 78−91741
GaAs (110) surface, electronic states near band gap 77−85290
GaAs (110) surface states, surface relax. models, tight-binding calcs. 79−4594
GaAs, electronic states associated with 60° dislocations, tight-binding calc. 79−15114

tight-binding calculations continued
GaAs, ideal vacancy, electronic struct., tight-binding calc. 79−4529
GaAs, surface, vacancies, bound state energy level calcs., tight binding approx. 80−44694
GaAs, surface structure and orbital symmetries of (110) surface state 78−72229
GaAs surfaces, electronic struct., tight-binding calc. 80−54755
GaAs-GaAlAs (100) abrupt interface, carrier transmission and refl. coeffs. 79−69588
GaAs-GaAlAs (100) interfaces, carrier transport coeffs., tight binding calc. 80−49889
GaAs(110), surface states, photoemission spectroscopy and tight binding calcs. 77−85888
GaP (110), surface bands in relaxed cleavage surface, tight binding model 78−91744
GaS, semiconductor layer cpds., band struct. calc. using tight-binding method 79−65376
GaS, XPS and valence band density of states, tight binding approx. 78−63974
GaS(Se)(Te), electronic struct. 80−15448
GaSb (110), chemisorption of Cl, photoemission spectra and tight-binding calcs. 80−6629
GaSb-InAs system, (110) surface and interface electronic struct. 80−100494
GaSe, band structure calc., semi-empirical tight-binding method 77−47726
GaSe, band. struct. determ. 77−80729
GaSe layers, band struct. and state density calc. by empirical tight-binding method 79−42443
GaSe polytypes, tight binding study of electronic states 79−60705
GaSe, semiconductor layer cpds., band struct. calc. using tight-binding method 79−65376
Ge, amorphous, ideal network struct., electronic struct., tight-binding model 80−44485
Ge, effective screening function 78−10383
Ge, electron states associated with core region of 60° dislocation 78−39057
Ge, ideal vacancy, electronic struct., tight-binding calc. 79−4529
Ge, microscopic screening of ion-ion interaction and phonon dispersion, tight-binding calc. 77−24528
Ge, nonlinear optical susceptibility, tight binding bonding orbital model 80−5784
Ge, phonon dispersion and microscopic screening, extreme tight-binding model 80−49324
Ge, static dielectric function, local field correction, tight-binding model 79−95355
Ge surfaces, electronic struct., tight-binding calc. 80−54755
Ge, vacancy, tight-binding calc. 80−24844
Ge, valence electrons, XPS, LCAO and OPW calc. 77−12496
Ge-GaAs (100) interface, electronic struct., scattering-theoretic approach 78−95340
Ge-GaAs interface, surface and interface states of (111) surfaces 79−15206
GeO_2, band struct., tight-binding calc. 80−24796
GeO_2, electronic struct., photoemission spectra calc. 77−35865
GeO_2, electronic struct. and densities of states 80−15447
GeS, density of valence states, tight binding calc. 79−77976
GeSe, density of valence states, tight binding calc. 79−77976
Ge_xSe_{1-x}, bonds and band struct. determ., tight-binding model 78−18959
GeTE, density of valence states, tight binding calc. 79−77976
Ge(100) surface electronic state localisation, layer density of states calcs. 80−6931
H atoms, chemisorbed on cluster, indirect interactions, Grimley-Pisani model and tight-binding calc. 80−65370
H, metallic, Hartree-Fock and correlation energies 78−34674
$(HCN)_x$, mol. crystals, quantum theory, mol. tight binding method calcs. 80−49572
He films, physisorbed low-density submonolayer thermodynamics, potential scatt. theory calcs. 79−95243
hexamethylphosphoramide:Li glass, metallic condensation of Wannier-Mott impurity states 78−2420
Hg, expanded liq., band model for electronic struct., Knight shift and electronic transport 77−89690
Hg, expanded liq., electronic props. 77−55477
HgTe, energy bands and optical props. calcs., tight-bonding model with spin-orbit interaction 80−65448
InAs-GaSb (001) superlattice, electronic struct., tight binding calc. 78−95350
InSb (110), chemisorption of Cl, photoemission spectra and tight-binding calcs. 80−6629
InSe, band structure, XPS, UPS and tight-binding calc. 77−47727
InSe, band structure calc., semi-empirical tight-binding method 77−47726
InSe, electronic struct. 80−15448
InSe, energy band structure, chem. bond polarity, photoemission, semiempirical tight binding method 80−44504
InSe, layer semicond., electronic props. 79−28275
InSe, semiconductor layer cpds., band struct. calc. using tight-binding method 79−65376
InSe, two-dimensional band struct., XPS meas. and tight-binding calc. 78−2419
$K_3Fe(CN)_6$, electronic struct., elec. field gradient tensor 80−15483
KI, mean free paths of 200-1500 eV electrons, XPS determ., model calc. 79−38715
$KNbO_3$, complex electronic dielectric const. from tight binding energy bands 78−60054
$KTaO_3$, complex electronic dielectric const. from tight binding energy bands 78−60054
Li, lattice stability, comparison of BCC and FCC struct. in tight-binding calc. 77−51632
LiC_6, and LiC_{12}, intercalation cpds., electronic struct. calcs. 80−70613
LiF, F-centre, excited state, optical absorption 77−20267
LiN_3, evidence for N_3^- from static and dynamic props. 78−60465
$LiSnS_2$, Li intercalation effects on electronic struct. 79−78004
$LiTiS_2$, intercalation complex, band struct., tight-binding calc. 79−95323
$MNbO_3$, tetragonal, electronic struct., optical anisotropy 80−70599
MgF_2, band struct., tight-binding calc. 80−24796
MgF_2, electronic struct. and densities of states 80−15447
MgO, electronic band struct., combined tight-binding and pseudopot. approach 77−47728
tight-binding calculations continued
Mo, (001) surface, electronic origin of reconstruction 80−11065
Mo (100) face, surface reson. 78−72226
Mo, Fermi surface, stress depend., hybridised nearly-free-electron tight-binding model 77−15757
Mo, twin and stacking fault energies calc. 80−2038
Mo(110) and (100) surface, surface reson. states and adsorption of 4d atoms 78−71982
Mo(110), surface densities of states for normal photoemission 78−35251
Nb, elastic constants, 0K to melting point 79−38882
Nb-Zr, elastic constants, 0K to melting point 79−38882
NbS_2, 2H layer cpd., electronic susceptibility and CDWs 78−39040
NbS_2, 2H layer cpd., tight-binding fit to bond struct. 78−39000
$NbSe_2$, 2H layer cpd., electronic susceptibility and CDWs 78−39040
$NbSe_2$, 2H layer cpd., tight-binding fit to bond struct. 78−39000
$NbSe_2$ (2H), electronic response function including electron-phonon matrix elements 79−28300
$NbSe_3$, electronic struct., chem. interpret. of geom. deform., oxidation state formalism 80−107690
Ni (100), electronic struct. of c(2×2) and p(2×2) O overlayers 79−47144
Ni (100) and (111) surface, chemisorption of CO, tight-binding theory 77−20395
Ni (111), adsorption of chalcogens, angle-resolved photoemission 80−40230
Ni (111) surface, with O_2, Se, S and Te adsorbed layers, bonding geometry and electronic struct. 79−77909
Ni clusters, FCC and icosahedral structs., relax. and stability, cohesive energy minimization 79−42479
Ni, H and O absorption, (001) surface, localised orbital approach 78−14587
Ni, liq., electronic density of d-states, hard-sphere model and tight-binding approx. calc. 79−15065
Ni, metallic particles, stability and electronic struct. *(French)* 80−80155
Ni, optical absorption in near IR 79−38539
Ni, surface electronic structure, rigid exchange splitting model 77−11977
PBI_2, electronic struct. 80−15446
Pb, surface density of electronic states 77−20397
PbI_2, tight binding band structure using scaled parameters 78−79927
PbO_2, electronic struct. and densities of states 80−15447
Pd (100), chemisorption of CO, adsorbate band formation, UPS expts. compared with calcs. 79−77916
Pd (100), with CO adlayer, band formation, calcs. and photoemission expts. 79−95463
Pd, g tensor of d holes near X point in Brillouin zone 79−23890
Pd, Lande g-tensor for d-holes 79−61221
Pd-H dilute alloy, impurity elec. struct. 80−103643
Pd-H system containing d impurities, chem. binding energies of point defects 80−107214
Pt, H and O adsorption, (001) surface, localised orbital approach 78−14587
γ-PtPc, Pc=phthalocyanine, single crystals, energy band structures and carrier mobilities 77−72817
Rh-Pd, mag. moment of Ni, Co, Fe, Mn and Cr impurities 78−95416
$(SN)_x$ and S_2N_2, electronic struct. calc. and comparison 77−76722
$(SN)_x$, tight-binding SCF MO calcs., interchain interaction 78−30859
$(SN)_x$, XPS calc. using photoionisation cross sections 78−72697
Sc, dielectric screening and lattice dynamics 77−35646
Se, amorphous, defect states, SCF pseudopot. and tight-binding calc. 79−65415
Se, bonding coordination defects 80−59927
Se, dielectric function in trigonal phase, model calc., local-field corrections 78−39045
Se, trigional semicond., electronic states, tight-binding model Hamiltonian 77−59250
Se, trigonal, NMR chem. shift 78−2759
Se, trigonal and amorphous, electronic struct. and nonempirical calc. of struct. props. 80−59866
Si (100), atomic and electronic structs., energy minimisation calcr. 80−49480
Si (111), chemisorbed O_2 electronic struct. tight-binding calc., XPS and UPS meas. 80−49845
Si (111)-Cl(7×7), angle resolved secondary emission and electron energy loss study of electronic struct. 79−61477
Si, amorphous, ideal network struct., electronic struct., tight-binding model 80−44485
Si, amorphous, topological and electronic struct. 77−28102
Si, atomic wave functions localisation and band struct., LCAO calcs. 77−51648
Si, deep level defects, struct. bonding, amphoteric centres 80−88506
Si, defects, divacancy and split 100 interstitial, electronic structure calc. 80−65494
Si, electron states associated with core region of 60° dislocation 78−39057
Si, ideal vacancy, electronic struct., tight-binding calc. 79−4529
Si, neutron irrad., EPR, ⟨100⟩ split di-interstitial, positive charge state 77−20698
Si, nonlinear optical susceptibility, tight binding bonding orbital model 80−5784
Si, phonon-mediated intervalley electron-electron interaction 78−95125
Si polymorphs, optical props., orthogonalized LCAO calc. 78−10345
Si, reconstructed surface (111)2×1, polarization depend. of optical absorpt. spectrum 79−28396
Si, SiO_2 electronic energy, structure calc. using tight binding approximation 77−69215
Si, static dielectric function, local field correction, tight-binding model 79−95355
Si surface, (111), energy states, computer renormalisation-group calc. 80−75617
Si surfaces, electronic struct., tight-binding calc. 80−54755
Si, vacancy, tight-binding calc. 80−24844
β-SiC, cubic, electronic props. of vacancies and divacancies 77−76767
$Si_{0.5}Ge_{0.5}O_2$, band struct., photoemission spectra calc. and meas. 77−35865
$Si_xGe_{1-x}O_2$, amorphous, electronic struct. in Bethe lattice approx. 80−44487
SiO_2, crystalline and amorphous density of states, bulk electronic struct., tight binding calcs. 80−44502

tight-binding calculations continued
SiO_2, electronic energy, structure calc. using tight binding approximation 77−69215
SiO_2, electronic struct., photoemission spectra calc. 77−35865
SiO_2, electronic structure, new interpretation 78−84120
SiO_2, ideal β-cristobalite struct., one-electron energy bands determ. 79−42452
SiO_x system, cluster plus effective medium tight-binding study 79−33216
Si(111) surfaces, H atoms chemisorption, monohydride and trihydride phases formation 79−15004
SmS type semiconductors, electronic struct., influence of point defects 80−70650
SnI_2 band struct., layer model 80−44501
SnO_2, band struct., tight-binding calc. 80−24796
SnO_2, electronic struct. and densities of states 80−15447
SnS, tight-binding calc. of density of valence states 78−34760
$SnS_2(Se_2)$, electronic struct. 80−15446
SnSe, tight-binding calc. of density of valence states 78−34760
SnTe, tight-binding calc. of density of valence states 78−34760
SrF_2, width of upper valence band, tight-binding calc. 78−26814
TaS_2 (1T) and (2H), bonding and charge density wave phase transitions 80−44282
Te, dielectric function in trigonal phase, model calc., local-field corrections 78−39045
Te, trigonal, NMR chem. shift 78−2759
Te, trigonal and amorphous, electronic struct. and nonempirical calc. of struct. props. 80−59866
Te, trigonal semicond., electronic states, tight-binding model Hamiltonian 77−59250
TeO_2, band struct., tight-binding calc. 80−24796
TeO_2, electronic struct. and densities of states 80−15447
$TiCl_3$, electronic band struct., tight-binding approx. 78−51872
$TiCl_3$, electronic struct. and struct. phase transition 80−59644
$TiCl_3$, lattice instability, d-electron-lattice interaction 80−44276
$TiCl_3$, layer compound, theoretical study of phase transition, energy bands calcs. 79−10945
$Ti_{1-x}Nb_xH_{1.94}$, electronic struct. MNR meas. 80−15439
TiO_2, cond. and valence band struct., gap anisotropy 77−47729
TiO_2 single cryst., refl. and electrorefl., energy levels 78−2871
$TmAsO_4$, optical side bands, absorpt. spectra in mag. fields 77−52123
V, twin and stacking fault energies calc. 80−2038
VC, energy band struct., chem. bonding 78−18958
VCl_3, electronic struct. and struct. phase transition 80−59644
VO_2, metallic, electronic struct., lattice instability 78−14664
VO_2, metallic phase, electronic props., plasma freq., Hall coeff. 78−84195
V_2O_5 and lower oxides, electronic, optical, structural and surface props., review 80−88120
V_2O_5, energy band structure, tight-binding method 80−70602
V_3Si, EFG and band struct. 77−35861
W (001) clean surface, spectral density of states 78−39181
W, (001) surface, electronic origin of reconstruction 80−11065
W (100) face, surface reson. 78−72226
W, electron-electron scatt. 79−38045
W, H and O adsorption, (001) surface, localised orbital approach 78−14587
W, screw dislocation motion, orientation depend., tight-binding type electronic theory 79−51109
W, twin and stacking fault energies calc. 80−2038
W(111), surface densities of states for normal photoemission 78−35251
Y, dielectric screening and lattice dynamics 77−35646
$YFe_2(Co_2)(Ni_2)$, density of states, mag. props. 79−90936
ZnS, F-centre and isoelectronic defects energy levels 77−20266
ZnS surface, nonpolar, electronic struct. 77−20383
ZnS, tight-binding model of F-centre 77−89729
ZnSe surface, nonpolar, electronic struct. 77−20383
ZnTe surface, nonpolar, electronic struct. 77−20383

tilting control *see attitude control*

timber *see wood*

time and latitude
see also Earth rotation; time measurement
1977 December 31, UTC positive leap second 78−7863
astrolabes concurrent obs., 1966-1975 period, Universal Time determ. *(Russian)* 78−73617
Astronomical Engelhardt Observatory, latitude obs. *(Russian)* 78−4080
astronomical latitude, azimuth and longitude, simultaneous determ. method 77−60339
astronomical refraction, general theory *(Russian)* 78−89045
astronomical time determs. rel. to continental drift 79−40063
astronomical time measurement, appl. to study of forced nutation 77−52956
atomic clock synchronisation via SIRIO satellite, expt., appls. *(Italian)* 79−2751
celestial navigation, with stereographic projection 77−60866
celestial pole, exact definition 79−53703
China, universal time service during 1966-75 period *(Chinese)* 78−28527
Chinese determinations during Yuan Dynasty *(Chinese)* 78−24631
chronometric system using punched tape for star transit obs. *(Russian)* 78−4110
clock (equatorial) stars, R.A. corrections to Pu 60 catalogue *(Russian)* 78−28643
clock synchronisation in rotating frame of Earth, time discontinuity obs. 77−60333
continental drift from time and latitude obs. 77−13072
continental movements and rotation determ. based on latitude meas. *(French)* 78−40529
corrections of clock and local latit., effect of light rays bending by Sun 78−7878
CTC right ascensions, synthetic catalogue for Chinese time service *(Chinese)* 78−28540
daily latitude variations anal. 80−21891
Danjon astrolabe, appl. to obs. of planets 77−64651
Danjon astrolabe, temp. effects on focal plane position *(Russian)* 78−4112
data acquisition and real time processing system for time service *(Italian)* 80−8549
day length irregular variations, core-mantle coupling 77−64186
decade fluctatons in Earth's rot. rate redeterm. for 1861-1978 period 79−84073
diurnal latitude vars. spectra based on obs. at Gor'kii 79−35100
domestic time synchronisation method using TV broadcasting satellite *(Japanese)* 77−17956
Earth daily free nutation parameters, determ. technique 78−96126
Earth rotation axis nearly-diurnal wobble effects in time and latit. obs. 77−56566
Ephemeris and Universal Time, empirical difference from polynomial approx. 80−17223
ephemeris time, correction determ. from photographic obs. of Sun annular eclipse (1976, April 29) *(German)* 79−44335
Ephemeris Time scale, effect of equinox and equator corrections *(Russian)* 79−21154
equinox and equator determ. using hypothetical asteroid obs. 80−94742
geodetic reference frames, polar motion effects 78−69272
geological time and tidal friction, evidence for Earth deceleration 80−3916
Gor'kii latitude observations, half-year nutation wave terms errors 79−62728
Gorky latitude, relativistic var. *(Russian)* 78−40462
Greenwich Obs., Time Report (1976, Jan.-March) 77−45293
Greenwich Obs. Time and Latitude Service, Time Report (April-June, 1977) 78−69661
Greenwich Obs. Time and Latitude Service, Time Report (January-March 1977) 78−57431
Greenwich Obs. Time and Latitude Service, Time Report (January-March 1978) 79−25453
Greenwich Obs. Time and Latitude Service, Time Report (January to March 1979) 80−72749
Greenwich Obs. Time and Latitude Service, Time Report (July-September 1976) 78−20624
Greenwich Obs. Time and Latitude Service, Time Report (July-September 1977) 78−73619
Greenwich Obs. Time and Latitude Service, Time Report (July-September 1978) 79−62729
Greenwich Obs. Time and Latitude Service, Time Report (October to December, 1977) 78−89046
Greenwich Obs. Time and Latitude Service Time Report (April-June 1979) 80−72750
Greenwich Obs. Time and Latitude Service Time Report (October-December 1976) 78−24443
Greenwich Obs. Time and Latitude Service Time Report (October-December 1978) 79−101053
Greenwich Observatory, 1976 April to June time report 77−70581
inertial rotation sensors for surveying and geophysical meas. 80−12571
International Latitude Service obs., errors 77−45324
Irkutsk prism astrolabe obs. programme *(Russian)* 78−4114
latitude obs. at Poltava, wind effects *(Russian)* 78−3915
latitude observations, props. of local non-polar terms *(Chinese)* 80−77266
latitude variation, polar motion and declination, effects of Oppolzer terms *(Chinese)* 80−76891
latitude vars. and diurnal polar motion *(Russian)* 80−51641
local non-polar terms determ. by Okuda's method, discussion *(Chinese)* 80−85842
local sidereal time determ. precision rel. to geographic latitude *(Russian)* 78−28647
longitude corrections for USSR Time Service observatories *(Russian)* 78−93077
longitude determ. using optical sensor array system 77−82023
Loran signal comparator at Kagoshima Space Center *(Japanese)* 77−73963
mean latitude, Chandler, annual and semiannual wobbles, anal. of 1957-77 data 80−30974
mean latitude non-polar var., techniques anal. *(Chinese)* 80−85841
mean solar time on Greenwich meridian, definitions and terminology 79−21155
Merate Observatory, Italy, time and latit. astrolabe obs. for (1976) 78−12078
Merate Observatory, time and latit. results of astrolabe obs. (1977) 79−40061
nonpolar latitude var. causes *(Russian)* 78−20637
Paris astrolabe, latit. from Saturn astrometric obs. (1975-1976) *(French)* 78−89115
Paris astrolabe observations, time and latitude (1976) *(French)* 77−78078
Paris astrolabe time and latitude obs. for 1977-8 period *(French)* 79−101051
phase photoelectric device for time service transit instrument *(Russian)* 78−73632
photoelectric astrolabe type II, accuracy, time and latit. obs. *(Chinese)* 77−22063
photoelectric transit instrument results *(Russian)* 78−73613
photographic zenith telescope, PZT 2, for time and latitude service 77−67036
photographic zenith tube obs. for time and latit. determ., meas. errors estimation 77−56816
polar latitude variations, VZT obs. at Cagliari *(Italian)* 79−21153
Poltava latitude differences from obs. of bright zenith stars 78−28488
positive leap second (1976, December 31) 77−2330
positive leap second on 1979 December 31, announcement 79−100808
Potsdam Observatory, long-term latitude determs. rel. to principal components var. 78−57158
PZT obs. reduction procedures *(Japanese)* 77−73972
quartz resonators, freq. instability rel. to time scales *(Italian)* 79−17400
radio interferometric systems, meas., appl. 79−25375
radio time signals, Tokyo reception accuracy 78−69606
reference frame for positional astronomy, appl. of lunar laser ranging 77−64618
residuals anomalies correl. with earthquakes *(Chinese)* 79−62725
rotation pole secular trend, consideration of motion of latit. observatories 77−86734
rotational pole annual motion, vars., 1846 to 1971, and period anal. *(Russian)* 78−40461
Santiago astrolabe, time, latit. and radius obs. (1968 to 1971) 78−12077
Santiago astrolabe observations from 1972 to 1976, results 80−46363
satellite laser tracking for polar motion, Earth tides and latitude determ. 77−56570

time and latitude continued
Shanghai astrolabe and diurnal latitude and longitude var. *(Chinese)* 77−67025
space geodesy, time synchronization requirements *(French)* 79−58233
star pair latitude obs. anal., mean pole position calc. 80−21892
star transits, photoelec. recording, grating inclination effect 77−91436
stellar transit times recording and errors *(Russian)* 78−73653
sunrise, sunset and eqn. of time 77−33326
systematic errors in astrometric obs., spectral anal. of obs. series *(Russian)* 78−73614
Talcott photoelectric micrometer for Bamberg zenith telescope latitude obs. *(Russian)* 78−4113
time adjustment on 1978 December 31, positive leap second 78−93079
time dissemination using TV signals from broadcasting satellite 77−60334
time obs., data smoothing method *(Japanese)* 77−73973
time observations, scientific problems and organization *(Russian)* 78−73616
time-service observations, tides and nutation effects 79−96733
Tokyo Astronomical Obs., Time and Latitude Bulletins (1976 April-June) 77−64619
Tokyo Astronomical Obs., Time and Latitude Bulletins (1976 Jul.-Sept.) 77−70982
Tokyo Astronomical Obs., Time and Latitude Bulletins (Apr.-June 1978) 79−101052
Tokyo Astronomical Obs., Time and Latitude Bulletins (April-June 1977) 78−45203
Tokyo Astronomical Obs., Time and Latitude Bulletins (April/June 1979) 80−72752
Tokyo Astronomical Obs., Time and Latitude Bulletins (December 1975) 77−2335
Tokyo Astronomical Obs., Time and Latitude Bulletins (Jan.-March 1976) 77−70983
Tokyo Astronomical Obs., Time and Latitude Bulletins (Jan-Mch. 1978) 80−17476
Tokyo Astronomical Obs., Time and Latitude Bulletins (January-March 1977) 78−45202
Tokyo Astronomical Obs., Time and Latitude Bulletins (Jul-Sep 1979) 80−82177
Tokyo Astronomical Obs., Time and Latitude Bulletins (July-September 1977) 78−73618
Tokyo Astronomical Obs., Time and Latitude Bulletins (July-Sept. 1978) 80−4239
Tokyo Astronomical Obs., Time and Latitude Bulletins (November 1975) 77−2334
Tokyo Astronomical Obs., Time and Latitude Bulletins (Oct.-Dec. 1976) 77−87242
Tokyo Astronomical Obs., Time and Latitude Bulletins (Oct.-Dec. 1978) 79−84646
Tokyo Astronomical Obs., Time and Latitude Bulletins (October 1975) 77−2333
Tokyo Astronomical Obs., Time and Latitude Bulletins (October-December 1977) 79−5736
Tokyo Astronomical Obs., Time and Latitude Bulletins (September 1976) 77−2332
Tokyo Astronomical Observatory Time and Latitude Service, Bulletin (January to March 1979) 80−72751
Tokyo PZT star catalogue, third improvement 77−91446
transit instrument automation *(Russian)* 78−73636
transit obs., external medium effect on accuracy of time meas. 77−87746
Universal Time, new scale for 1955-1974 period *(Russian)* 78−93076
universal time, random function determ. 80−46120
Universal Time, short period terms anal. *(Chinese)* 79−8589
Universal Time and polar motion determ. from lunar laser ranging and laser obs. of artificial satellites *(Polish)* 79−57844
Universal Time in China, short-period terms 80−12648
universal time measurement, results from lunar laser ranging 78−85854
universal time system (TU2), spectral anal. of differences 78−65174
USSR state time and frequency standards *(Russian)* 78−161
Valinhos astrolabe obs. (April 1974-December 1977) *(French)* 79−70944
variation of latitude, computation for national emphemerides calc. 78−88776
variations meas. at single laser tracking station 77−32976
Young Avestan and Babylonian calendars and the antecedents of precession 79−48693
Z-term of latitude variation, nutation amplitude calcs. *(Chinese)* 80−8244
zenith telescope, use as astrolabe for time and latitude meas. 80−98550

time bases
alternated double time base oscilloscope design and applications *(French)* 77−87784
CRO principles and appl. *(French)* 77−60884
digital high resolution time base for Cornell electron ring 79−76215
Earth tide registering stations, electronic time basis *(Rumanian)* 77−33216
frequency counter, precision 77−74432
high speed photometer of Asiago Observatory, data logger and time base 79−25505
oscilloscope double time multiplier *(Rumanian)* 78−86252
oscilloscope low repetition trigger cct., for high speed pulse observation *(Spanish)* 80−62657
oscilloscopes given dual delayed-sweep capability, low cost 77−18004
stellar occultation TV scanning time base, modification for image freq. limitation *(French)* 79−58264
tangent sweep circuit for recording of airborne IR line-scan data 77−9525

time delay circuits *see delay circuits*

time delays *see delays*

time division multiplexing
bidirectional fibre-optic data bus with T-couplers 77−19451
biomedical recording system, TDM multiplexing system for multichannel signal averaging of visually evoked responses 80−36165
biotelemetry, for data transmission using one carrier freq. 77−90928
ECG multichannel recording 80−101283
EEG TDM telemetry unit for fifteen scalp electrodes 77−40822
electro-optic multimode time division multiplex device 77−79958
electro-optic multiplexer system for multimode fibre data communications 79−18510

time division multiplexing continued
laser diode 1ns pseudo-random pulse modulation cct. 78−50836
morphognostic coil design for implanted nerve stimulator 79−84014
optical fibre data bus systems, on board appls. electrical control *(German)* 78−25968
optical fibre multiterminal data system for aircraft, based on time division multiplexing 78−46811
optical multiplexing of scintillation detector arrays 77−54438
SAW/CCD high-speed analogue programmable tapped delay line 77−39167
six-channel extracorporeal telemetry system 77−90931
telemetry system, implantable, single-freq., physiological parameter monitoring appl. 77−86688
telemetry system, seven-channel fully integrated, patient monitoring appl. 78−3634

time-domain analysis
200 to 500 MHz A-scan defect characterisation 79−47873
atomic reference frequency stability transfer to quartz crystal oscillator 79−54108
dielectric relaxation data representation by Havriliak-Negami formalism 80−15950
discrete-time Doppler frequency meter for blood flow imaging 79−57704
dominant noise process slope intersections, time/frequency-domain conversion 79−54107
EEG pattern classification using logic windows in time domain *(Japanese)* 77−70563
EEG quantification in normal children 79−96532
EEG slope descriptor computation, time and frequency domain comparison 78−57115
electromagnetics and its appl. 78−71010
EM field time domain reflection from inhomogeneous and dispersive slabs 78−62985
frequency response testing in noisy environment, time domain averaging 77−14856
frequency stability, characterisation and meas. 80−47025
glass fibre drawing process, characterization and control 80−58826
labial muscle EMG analysis and feature extraction by Hanning Cosine Modulated wave function 77−81605
LF dielectric measurements using time-domain technique, 20 Hz to 10 kHz 80−57329
multicomponent noise signal decomposition 79−3210
optical fibre frequency response meas., combined time/frequency domain technique 79−76809
optical receiver noise analysis, time-domain impulse response technique 77−68280
paediatric EEG reactivity, spectral and temporal analysis 77−9293
piping systems, gas, identification of standing wave parameters 79−18558
pressurised water reactor, fluctuation anal. of apparent malfunction, frequency and time domains 77−54313
rotating machine flaw detection, acoustic signature analysis and time-domain techniques 79−50525
space-time random speckle pattern optical analysis 80−102682
speech analysis by linear predictive coding, accuracy improvement 79−46133
structural damping constant evaluation by time series analysis 78−46902
transient field initial-boundary value problems, hybrid simulation 77−41469
US Doppler signal time-domain frequency analyser, numerical assessment 79−92314
US tissue characterisation by backscattered field space-time processing 79−48305
US transducer evaluation in exptl. and theoretical domains 79−46153
He speech unscrambling by nonlinear power spectrum conversion 79−46134

time-domain reflectometry
agricultural materials, determination of dielectric props. 79−71482
aqueous solutions, HF spectroscopy problems 77−74440
benzyl alcohol, dielectric time-domain spectrosc., short and refl. method 80−101805
n-butanol, dielectric response function, by lumped capacitance method 78−95539
1-butanol, permitt. meas. by transmission time domain spectroscopy 77−67462
N-t-butylformamide, in carbon tetrachloride, dielec. relax., time-domain reflectometric obs. 79−4762
chlorobenzene, dielectric time-domain spectrosc., short and refl. method 80−101805
chlorobenzene, permitt. meas. by transmission time domain spectroscopy 77−67462
circular waveguide, mm-wave, time-domain techniques for meas. and equalisation 77−18020
dielectric, reflection in terms of polarisation 79−82916
dielectric material, time-domain spectroscopy for permittivity and mag. permeability 77−18015
dielectric properties, time domain meas., multicomponent exponential decay curves, analysis method *(French)* 77−52007
dielectric time domain spectroscopy, transmission methods 77−67462
N-ethylacetamide, in carbon tetrachloride, dielec. relax., time-domain reflectometric obs. 79−4762
fast-rising pulse generating systems, development *(German)* 79−6148
fibre optic time domain reflectometer, high sensitivity fibre fault detection 79−54173
fibre-optic time domain reflectometer 79−37036
free-space, time-domain electromagnetics appl. 78−71010
HF, at high permittivity *(German)* 78−16816
high-sensitivity, picosecond 77−18016
index profile determ. 79−26075
lumped capacitance method, spectrosc. data treatment 80−82788
methods, appl. to dielectrics 80−52310
N-methylformamide, in carbon tetrachloride, dielec. relax., time-domain reflectometric obs. 79−4762
microprocessor-controlled TDR for dynamic shock position measurements 80−79248
N-methylpropionamide, in carbon tetrachloride, dielec. relax., time-domain reflectometric obs. 79−4762
optical fibre, attenuation meas. 77−84014
optical fibre connector loss evaluation by backscattering 80−58721
optical fibre joint loss measurements with OTDR 79−64354

time-domain reflectometry continued
optical fibre loss estimation using backscatter technique, time domain reflectometry theoretical assumptions 80−74508
optical fibre measurements, attenuation and fault location 79−64355
optical fibre parameter measurement using optical time domain reflectometer 80−58755
optical fibre splice insertion loss meas., backscattering method 80−58720
optical film deposition, thickness monitoring with optical time-domain reflectometer 79−55254
optical time domain reflectometry by photon counting 80−95122
polarisation optical time domain reflectometry, optical fibre technique 80−78959
precision time-domain measurement system 80−42236
review 78−37038
signal separation for overlapping time windows, homomorphic deconvolution 77−18019
travelling wave optical modulator using a directional coupler $LiNbO_3$ waveguide 80−96035

time interval measurement *see time measurement*

time measurement
see also clocks; frequency measurement; streak photography; time and latitude; time resolved spectroscopy
absolute motion, detection from atomic timekeeping data 80−13045
accelerating atomic clock synchronisation by radiowave propag., one-way Doppler effects 80−13044
acoustic chamber reverberation time, holographic meas. 79−68519
acoustic signals, freq. shift arrival time determ. 79−3875
adjustable exposure timer, circuit diagram and operation *(Hungarian)* 80−52169
Airy, G.B., Astronomer Royal 1835-81, contrib. to horology 80−86061
antimonic caesium vacuum photocell, test instrument for contactless circuits *(Russian)* 79−58676
astronomical laser ranging equipment, timing system *(Japanese)* 78−89077
atomic clock synchronisation via SIRIO satellite, expt., appls. *(Italian)* 79−2751
atomic time and frequency standards development at Shanghai observatory, China 80−105617
atomic time scale instability, contrib. of computation algorithm 80−98890
atomic time scales, construction and comparison with other time scales 80−82749
atomic- and molecular-beam spectroscopy, two-freq. separated oscillating fields technique 79−21715
automated time keeping system of Van Swinden Lab. 80−98891
automatic reverberation time meas. 79−68518
bifilar sundial, theory 78−93119
blood clotting timer, automatic 77−52896
blood coagulation time, US meas. 79−83870
calculator, used for measuring time, light digit, four function type 78−175
chart-recorder time markers, using digital clock module 79−30446
chemical reaction residence time measurement, magnetic recording and hybrid computers appl. 78−81953
chromosphere flares, effective time of observations *(Russian)* 78−40893
chronobiology in plants 80−56328
cinematography, EBU/IRT time codes with modified setting instrument *(German)* 80−18029
clock comparison by laser in the nanosecond range 80−47035
clock synchronisation, in India through TV transmission, microsecond accuracy 77−87736
clock synchronisation, India-W.Germany, relativistic corrections 80−95077
clock synchronisation in rotating frame of Earth, time discontinuity obs. 77−60333
clock synchronization, H-maser, using very-long-baseline interferometry 79−88920
clock synchronization using Symphonie satellite 80−68184
clocks, standard-freq. controlled, for high precision time meas. *(German)* 78−77871
comet telescope, timing system *(Japanese)* 78−89071
counter design 78−8385
counter timers, review 77−37913
counter-timer, Phillips PM 6610 and 6620 series, features *(Italian)* 77−26340
CRO signal time-interval measurement using digital meter 79−35702
CRO used for accurate time measurement *(German)* 79−30423
CROs used for time interval measurement 79−6098
crystal tuning fork development and biography of Jurgen Staudte *(German)* 79−30182
daily time comparisons long-term stability using TV method 79−75502
damped harmonic torsional oscill., period and logarithmic decrement meas. 77−30142
DCF 77 standard time and frequency receiver, display ccts. *(German)* 77−13737
decade counter for measuring thickness of multilayer electrodeposits *(Czech)* 80−95071
decimal time 79−9206
design principles and characteristics of freq. and time standards, radiation effects 77−22533
detector averaging time measurement, methods *(Croatian)* 77−37849
digital, 1024 channel apparatus for time interval distrib. meas. 78−81950
digital, microprocessor-controlled counter, Hewlett Packard (5315A) *(French)* 79−88938
digital, quartz controlled, techniques, problems 77−30133
digital counter and timer instruments, accurate meas. techniques 78−45605
digital event timer, liquid crystal display 77−5811
digital freq. counters and counter-timers, new range using MSI 80−27318
digital instrument for time interval meas.; with 2 nsec accuracy 78−77867
digital interval synthesiser, computer-controlled 78−8386
digital picosecond event timer, phase detection system 77−9988
digital time-interval meter test rack 77−74373
digital timer, IC, high accuracy and repeatability, photographic appl. 79−35683
digital timer for electroadsorption studies 77−90670

time measurement continued
digitiser for laser ranging, ps. resolution, built in CAMAC minicrate 78−36301
dissemination for public requirements and communication systems, Canada 78−41284
domestic time synchronisation method using TV broadcasting satellite *(Japanese)* 77−17956
drift chamber electronics for time and pulse height meas. 79−3326
dropping Hg electrodes, drop times determ. using digital drop timer 78−3394
duration subjective impression rel. to ambient noise 78−44554
education, electronic digital stopwatch for automatic time keeping, triggering ccts. 79−97158
education, mass and charge meas. using electronic time counter *(Japanese)* 78−41127
electrical stopwatch, testing using semiautomatic device 79−30424
electrolyte timing cell and coulometer 80−68216
electromagnetic meas., precision, conf., Braunschweig, Germany (Jun. 1980) 80−98903
electronic programmable timers for industrial lab., Xanadu up-timer 79−9207
electronic timer using TTL or CMOS ICs, for programmed delays 79−35684
electronic-based timing systems, time standards 79−85129
Ephemeris and Universal Time, empirical difference from polynomial approx. 80−17223
Ephemeris time, relativity and uniform time in astronomy 77−53402
errors, accuracy of watches and clocks, time standard 80−90821
exact time signal transmission using artificial satellites 77−79069
flow, automatic capillary, viscometer, accuracy one part in five million 80−87825
and frequency, timekeeping and dissemination 77−37851
frequency and time, conf., Helsinki, Finland (Aug. 1978) 80−46728
frequency stability, characterisation and meas. 80−47025
fundamental problems, frequency measurements, simple mathematical approach *(French)* 77−53865
GDR atomic time scale 80−98892
hebdomadal calendar, theory *(Danish)* 78−36440
HF time signal bilateral transmission propagation time error anal. 77−87740
high precision time comparison, via satellite, synchronisation discrepancy obs. 77−17953
Hoppler viscometer ball passage time meas. digital electronic circuit *(Polish)* 78−47075
Inca people (Peru), calendar system and astronomical knowledge *(Swedish)* 78−32640
instrumentation, standards, conf., Ottawa, Canada, 1978 79−21731
intercontinental laser synchronisation of high precision clocks via SIRIO geostationary satellite, nanosec. accuracy *(German)* 80−37000
intercontinental time comparison by spread-spectrum random-access geostationary satellite system 77−5815
International Atomic Time, role of primary standards 78−89459
International Atomic Time Scale, problems of generation, quality and availability 80−98889
International time and freq. comparison using Loran-C radio waves *(Japanese)* 78−81951
international time standard coordination *(German)* 80−52171
international time synchronisation, precision tracking package TEMPUS, NAVSTAR satellite network appl. 80−22332
interstellar rocket, relativistic navigation problem and ship's clock updating 79−21136
interval, counter design, 1 GHz, use of custom LSI 80−8973
interval, counter design technology 80−8974
interval, counter/timers, avoiding compromises in accuracy 80−8970
interval, counters and timers, var. in counting cct. techniques 80−8971
interval, universal timer-counter, design aspects 80−8972
interval analyzer for 10^{-10} to 10^{-2} sec range 78−24764
interval meter, broadband, with digital display 80−31729
laser Doppler microscope period meas. signal analyser *(Japanese)* 79−88998
laser radiation energy, spectral and time range meas., instruments 79−35687
LF meter used for measuring period between pulses 79−85128
LORAN-C type standard freq. signal, time and freq. calibration standard comparison *(Rumanian)* 79−40542
lunar occultations of point-like X-ray sources, time meas. accuracy 79−88567
magnetic tape recording, time reference signal, IRIG and NASA code formats 80−57262
mean solar time on Greenwich meridian, definitions and terminology 79−21155
mechanical start-stop gates for air tracks 80−101698
metrological Cs frequency standard MTs-1, description 77−79063
microchannel photomultiplier, with subnanosec. characts. 80−37001
microprocessor-based timer interval meter *(Russian)* 80−52172
microwave time and frequency standards 80−47026
monitoring unit for time-interval analyzers of nanosecond range 78−77868
multichannel high resolution time analyser scale instability *(Russian)* 80−73326
multistage parallel-serial time averaging filters to reduce time jitter in scintillation counter time meas. 80−102405
national time and frequency standards of Finland 80−47031
noninertial systems, synchronization of clocks 78−24665
optical fact directional coupler switch/modulators, novel ps optical pulse sampling method 80−58784
optoelectronic ps switch using pulsed lasers and photoresistive semiconductor *(German)* 77−72066
oscilloscope double time multiplier *(Rumanian)* 78−86252
period measurement by digital methods *(Rumanian)* 77−79120
periodic event timing in student expt., half-column method 78−12516
periodic source absolute timing, limiting standard deviation 77−45314
personal equation determ. method 78−89443
photocell pulse time resolution when optical pulse shorter than photoelectron transit time, theory *(German)* 80−9035
photosensor time characts. meas. meter 78−283
plane analemmic dials 79−16834
portable quartz clocks, accuracy in comparing time scales 80−101786
position location and navigation, conf., San Diego, CA, USA, Nov. (1978) 79−25374
positive leap second (1976, December 31) 77−2330

time measurement continued
precise time dissemination via OMA-50 kHz 80−47032
precise time recovery from Transit satellites 80−47037
precision clocks, synchronisation and time/frequency dissemination 78−49803
precision EM measurements conference, Boulder, Colorado (June 1976) 77−18010
primary Cs atomic clock, time standards and scales generation 78−41283
pulse duration below 1 μsec, frequency counter modification 77−10060
pulse picosecond waveform meas. 78−57923
quadrupole CAMAC universal timer 78−9040
quantum clocks, time meas., teaching 80−90632
quantum freq. standards, output signal sidebands/resonator detuning effects on accuracy 77−87743
quartz clock, accuracy, radio signal control *(French)* 80−95079
quartz electronic watch, past and possible future developments 79−93102
quartz resonators, freq. instability rel. to time scales *(Italian)* 79−17400
quasi-analogue display for electronic clocks *(German)* 79−49207
radiation detectors pulses, review of time position meas. methods 77−65410
radio time-signal codes in Italy *(Italian)* 80−98888
radiographic phototimers, acceptance testing and performance monitoring 77−5071
radionavigation, time deviation and prediction error for clock specification 79−21719
reaction timer cct., using bipolar transistors and LEDs 80−81781
recording on time-lapse cinemicrography, 16 mm film appl. 79−9252
regulating unit, synchronisation with atomic clock, TN DCF-77 *(German)* 77−74374
remote atomic clocks synchronisation using injection laser diodes 77−82493
remote site timescale intercomparison technology 77−37855
review *(French)* 78−49802
rubidium clock, portable, time scale generating clock coordination appl. 78−36973
satellite time system for utility companies 79−12774
satellite time transfer technology, review 80−47029
scale generation by international organizations 80−47028
second as standard time unit *(German)* 77−22534
secondary standard comparison, based on LF/VLF radio link synchronisation 77−87737
secondary standards, VLF radio station phase reception/processing convertor 77−87739
secondary standards automatic recording/processing system 77−87738
seismic events, radio broadcast signals appl. 80−90253
sidereal digital clock 78−36464
sidereal time source, electronic convertor for mean to sidereal time 79−84677
South African measuring standard, national and international role 80−36971
space geodesy, time synchronization requirements *(French)* 79−58233
spark gap breakdown, time-resolved resist. meas. 80−19639
square root of time mark generator using TTL digital ccts. for chronocoulometry 80−35588
standard, establishing common scale for COMECON member countries 80−42200
standard, precision and application *(Japanese)* 78−41282
standard differences and celestial mechanics *(Italian)* 78−93087
standard signals and applications *(German)* 77−71301
standard time/freq. service in East Germany *(German)* 78−93658
standards, electrically tuned far infrared lasers appl. 78−174
standards, time, freq. and physical measurement, unified standard 79−26038
standards comparison, improved accuracy 80−95062
standards of time and length 77−13734
star transit obs., external medium effect on accuracy 77−87746
statistical time interval analyser with visual display 77−37850
Sub-microsecond intercontinental time comparisons by satellite 77−82494
sundial, latitude-independent, theory and construction 78−81549
sundial, new device at Indiana Univ. 79−84678
sundials to atomic clocks for understanding time and freq., book 78−57904
Swedish measurements establishment for time and freq. standards *(Swedish)* 79−75503
Symphonie geostationary satellite, time transfer link for atomic clock synchronisation 80−47038
synchronisation by JJY signal reception via the E-region 78−65910
synchronisation using ATA standard time broadcast 80−47024
system adjustment and calibration signal generator 78−57903
systolic time interval meas. microprocessor system for heart malfunction detect 79−79681
techniques, book 79−176
teletherapy machine electronic dual timer 78−85358
time of signal passage over satellite link determination, for accurate time scale synchronisation 78−89444
time signal from Loran-S station, propagation path effect on locking error 77−87742
time signal multifreq. transmission ambiguity detection 77−87741
time signal transmission by radio, Einstein's theory 78−86154
time to amplitude converters, precision 1 GHz time calibration 80−27903
time-interval indicator *(Russian)* 80−105619
time-interval meter, reads digitally to 99.9 ms on a DVM IC 77−74429
time-interval series meter 78−176
time-to-number convertor, wide-range high-resolution 78−9039
timer group testing installation 77−79083
timing devices selection and appl. 77−82492
Transit satellite system for precise time dissemination 80−57263
transmission of exact time and freq., OMA 50 kHz Czechoslovak station *(Czech)* 79−30425
transmission times meas., in SW and VLW ranges, dynamics of seasonal variations obs. 77−79061
TV broadcasting satellite, use for precise real-time signal dissemination 80−47033
units, rel. to angle meas., history 78−20931
universal counted and dual-trace delayed-sweep oscilloscope used for precise timing measurements 78−24763
time measurement continued
universal time, random function determ. 80−46120
universal time interval counter, 5370A, 20 psec. resolution, features 79−26035
universal time measurement, results from lunar laser ranging 78−85854
US Naval Observatory, history, techniques 77−49714
US Naval Observatory clock time scale 78−89460
US transmission time meter, with digital readout 77−40485
USA Naval Observatory clock time scales, algorithm 79−21716
users' manual on time and freq. meas. 80−94934
using Nova satellite time signals 80−47036
USSR and E.German time scale comparison by transportable atomic clocks and TV signals 77−79067
USSR State Standard of time and frequency 77−79062
USSR state time and frequency standards *(Russian)* 78−161
USSR State Time and Frequency System data collection and processing automation 77−79074
USSR time and freq. state service 79−93103
USSR Time and Frequency Service collaboration with international organisations 78−41280
UV fluorescence lifetime determ., correction of instrumental time response var. with wavelength 78−5374
very short time interval measurements, using CRO 78−36975
very short time intervals, oscilloscope appl. 78−81948
VNG-derived frequency reference, adapting for astronomy 79−35139
wristwatch balance period/oscill. amplitude, photoelec. method *(German)* 77−87755
Cs beam deflection system for time and freq. primary standard 78−89453
Cs beam freq. standard research at PTB, beam optics, Majorana transitions 79−21709
Cs beam freq. standards, freq. offset due to spectral impurities 78−89455
Cs beam standard, Ramsey cavity and beam optics design, expt. 78−89456
Cs beam standard at Radio Research Lab., Japan 79−21714
Cs beam time/freq. standard, future prospects 77−74371
Cs clock, laser synchronisation between observatories of Paris and San Fernando *(French)* 78−89461
Cs freq. standard, angular distribution of atomic flux diffusing from rectangular channels 77−87744
Cs freq. standard, error due to second order Doppler shift 77−87745
Cs freq. standard, time scale unit duration estimation 77−74368
Cs long beam primary clock, accuracy, reliability 78−89454
Cs primary standard, TAI freq. estimation 77−17952
Cs primary standard of PTB, characts. 77−74369
CsV clock, long-beam, primary standard, continuous operation, concept 79−21711
CsV frequency standard, operation as primary clock 77−107
CsV primary clock performance of NRC 77−74370
H frequency standard undisturbed transition evaluation 77−79066
H maser, time-dependent freq. shift obs. 78−89457
H time and frequency standards with redundancy 77−79065
Rb portable clock transcontinental/intercontinental comparison 78−54345
Rb time standards, study review *(French)* 79−174

time of flight mass spectra
acetyl radical, photofragment spectroscopy, collision dynamics 78−25636
aliphatic perfluorocarbons, electron attachment, fragmentation 0-12 eV 80−5618
amino acid valine, heavy ion induced desorption, time-of-flight mass spectra anal. 80−54509
benzaldehyde molecules, photoionisation mass-spectrometry with excimer KrF laser 80−95691
benzene, multiphoton ionisation mass spectra 80−57420
benzene molecules, photoionisation mass-spectrometry with excimer KrF laser 80−95691
chlorobenzene ion fragmentation, kinetic shift and phenyl ion heat at formation, photoelectron-photoion coincidence meas. 80−25998
correlated events obs. method, appl. to fission fragment induced desorption 78−58089
dimethyl ether-trioxane mixtures, condensation-elimination ion-mol. reactions obs. 78−23939
ethane, H^+, H_2^+, and H_3^+ kinetic energy distribs., electron impact dissoc. ionisation, time of flight mass spectra 80−32843
ethanol, H^+, H_2^+, and H_3^+ kinetic energy distribs., electron impact dissoc. ionisation, time of flight mass spectra 80−32843
ethylene adsorbed on Ag, photon-induced field ionisation mass spectroscopy 80−6639
fission fragments with high KE, mass separation based on TOF spectra 78−46209
fission products of ^{252}Cf, masses, β decay energies, halflives, He jet TOF mass spectrometer 77−23355
fluorobenzene cations, fluoresc. quantum yields and lifetimes, electronic state relax. processes 80−48027
1,5-hexadiyne, time-depend. mass spectra, ionisation efficiency and breakdown curves 80−95747
ions, photon stimulated desorption obs. 79−82459
LAMMA mass analyser, laser microprobe *(German)* 79−29419
metal clusters, 2 to 500 atoms, nucleation, mass spectra 80−102596
methane, H^+, H_2^+, and H_3^+ kinetic energy distribs., electron impact dissoc. ionisation, time of flight mass spectra 80−32843
methanol and deuterates, H^+, H_2^+, and H_3^+ kinetic energy distribs., electron impact dissoc. ionisation, time of flight mass spectra 80−32843
microlocal analysis using laser mass spectrometer *(Russian)* 77−12862
molecule, multiphoton ionisation and fragmentation, UV laser induced, time of flight mass spectra 79−31625
nuclear materials analysis using plasma desorption mass spectrometry, isotope ratio determ. using TOF mass spectrometry 80−78375
particle identification at 2-400 keV/N 80−5435
pentafluoroethyl iodide, electron impact, time of flight mass spectrometry 77−42424
plasma barycentric velocity, time-of-flight, mass spectrometric meas. 77−43063
radionuclei prod. in heavy ion-nucleus reactions 79−6785
Rydberg state charge transfer reactions, time of flight mass spectrometric obs. 77−71867
steel, pearlitic atom probe microanal., computer controlled 77−66781
1,1,2,2-tetrafluorocyclobutane, ion-mol. reactions, reaction pathways, mass spectra 77−21368

time of flight mass spectra continued
Trichel corona negative ion transit times 79−19115
trifluoromethyl iodide, ion-molecule reactions, amongst radiolysis products, reaction rates, mechanisms, mass spectra 79−5136
Au, energy and mass spectra of scattered 8 keV Ar^+ ions and desorbed species 77−32487
CO_2, C $1s^{-1}$, π^*-state decay, fragment ion relative abundance by electron-ion coincidence technique 80−9743
$CsCl(Cs_2Cl_2)+Ar(Kr)(Xe)$, collision-induced ion-pair form., absolute cross sections 78−73029
Cu, polycryst., secondary ion energy spectra, ionisation mechanisms 79−38700
Fe, adsorption and condensation on W foil, meas. by thermal desorption in pulse time-of-flight mass spectra 79−15023
GaAs, time of flight atom-probe mass spectra 78−92584
GdS, vaporisation thermodynamics and dissoc. energy obs. 78−67822
H_2, rotational quantum excitation with protons 77−27154
$HD+D_2$, rot. inelastic differential cross sections, diffr. oscills. in elastic and inelastic scatt. 78−74743
HD+Ne, j=0 to 1 scatt. differential cross section, interaction pot. anisotropy 77−42382
$H_2(N_2)(NH_3)$ adsorbed on W, thermal desorption and pulsed time of flight mass spectra anal. 80−30285
$H(2S)+H_2(N_2)(NH_3)$(acetone)(methanol), collisional quenching, mass spectral obs. 78−25685
H(2S)+inert gas, collisional quenching, mass spectral obs. 78−25685
He*, Rydberg state charge transfer reactions, time of flight mass spectrometric obs. 77−71867
$I^-+COS(CS_2)(H_2S)$, endoergic reaction, time of flight mass spectral obs. 77−12786
I^-+SO_2, endoergic reaction, time-of-flight mass spectral obs. 77−12785
KBr(I), energy distribution of emitted alkali and halogen atoms 79−1804
LaB_6, time of flight atom-probe FIM study 80−6652
N_2O, N $1s^{-1}$, π^*-state decay, fragment ion relative abundance by electron-ion coincidence technique 80−9743
N_2O, vac. UV photodissoc., kinetic energy and ang. distribs. of fragments 77−30938
O_2, vac. UV photodissoc., kinetic energy and ang. distribs. of fragments 77−30938
PbO_2, thermal decomposition, heating rate effect, kinetics, mechanism, struct. 78−92473
Rb^+, ionic mobility in Ar, Kr and Xe, interaction pot. determ. 79−18991
RbBr(I), energy distribution of emitted alkali and halogen atoms 79−1804
S_2 polymerisation, kinetics obs. by pulsed field ionis. time-of-flight mass spectrometer 77−63890
SO_2, 193 nm photodissoc., photofragment translational energy distrib. 79−74402
SiO(g), enthalpy of formation and dissociation energy, time-of-flight mass spectra 77−16859
Sn-Ge(Au), liquid alloy, exam. of activity and heat of mixing, using mass spectrometry 78−51706
TlF+Kr(Xe), collision-induced ion-pair formation 78−17749
Tl_2F_2+Kr(Xe), collision-induced ion-pair formation 78−17749
^{235}U(n,f), fission fragments with high KE, mass separation based on TOF spectra 78−46209

time of flight spectra
see also atom probe field ion microscopy; time of flight mass spectra
alkali halides, energy distrib. of electron sputtered atoms 78−48263
alkali halides, exciton mechanisms of electron sputtering process 77−55857
alkali halides, sputtering of molecules, low-energy electron bombardment 80−35026
alkali metal chlorides, photofragment spectra, bond energies and excited state symmetries 80−87190
anthracene, scintillation decay time determ. using low energy spectra 79−9964
aryl halides, mol. beam photodissoc., fragment translational energy distrib. 77−50481
backscattered energy spectra of scattered ions and neutrals, anal. by TOF technique, surface anal. appl. 79−5236
benzene, total neutron cross sections for subthermal energies 78−74779
biphenyl, incoherent inelastic neutron scatt. time of flight spectra, vibr. spectra model calc. 78−63816
charged particle telescope TOF system, elemental assignments of reaction products 78−86720
1-chloropropyne cation, internal energy decay studied by photoelectron-photoion coincidence spectroscopy 80−69185
CO, electron drift velocity and longit. diffusion coeff. time of flight meas. 77−80264
collectively accelerated protons, nucl. activation, time-of-flight, and foil activation meas. 79−4195
correlation TOF technique, real modulation 79−49898
cyanoethylene, photofragment recoil, state selective time of flight- fluoresc. method 79−11809
cyclohexane, solid, neutron scatt. spectra using inverted geometry, white beam, t. of f. spectrometer 78−34395
cyclopentane, solid, neutron scatt. spectra using inverted geometry, white beam, t. of f. spectrometer 78−34395
desorption, fission-fragment induced mechanism, time of flight obs. 77−76674
difluoroethene, cis- and trans-, photoelectron-photoion coincidence study, fluoresc. obs. 80−95678
digital filtration in correlation time-of-flight spectrometry 79−49894
diphenyl, solid and liquid, total neutron cross sections for subthermal energies 78−74779
electron drift velocity in counter gas mixtures 80−28590
equilibrium K-shell excitation 79−22817
ethane, electron impact dissoc., high Rydberg fragments 77−83749
ethylene, CW CO_2-laser irrad., low-press., chem. relax. 79−74404
ethylene, electron impact dissoc., high Rydberg fragments 77−83749
fast projectile electron spectroscopy, autoionizing ion levels and lifetimes 77−38749
fibre optic waveguides 80−23767
fragments, produced via IR laser excitation 80−74257
gases, molecular, total scatt. cross sections for intermediate-energy positrons 80−91692
hydrocarbon, long chain single cryst., carrier transport meas. 80−6874

time of flight spectra continued
inert gas atom $+H^+$, electron capture, charge-state distrib. 80−32814
inert gas atom (metastable)+dichloroethylene (dichlorobenzene), mol. ionis., collisional energy depend. 79−54950
inert gas low energy electron elastic scatt. effective cross section, time of flight meas. 79−13823
inert gas-positron total cross-sections at intermediate energies meas. 77−3456
inert gases, multiple photoionisation, threshold to 280 eV, time of flight meas. 79−85939
iodomethane+Rb reaction cross section, translational energy depend. min. 77−66753
iodomethane$(-d_3)^+ \rightarrow CH_3^+(CD_3^+)+I$, kinetic energy release distrib. meas. 77−1922
ion photodissociation, kinetics meas. using time of flight mass spectrometer 77−75240
ions, thermal and very fast, from laser-prod. plasma 77−76190
leakage neutron spectrum meas. in light water using time of flight technique 78−62592
mass spectra, vel. distrib. effects, mol. beam inlet method 77−54627
metals, microwave transmission, time-of-flight effects in Fermi vel. determ., calc. 80−20238
methane, electron impact dissoc., high Rydberg fragments 77−83749
methane$+Li^+$, vibrational excitation time of flight measurements 79−45826
molecular beam, velocity distribution function, and moments, from TOF meas. 78−5371
molecular beam scattering, S/N ratio enhancement in time-of-flight anal. 78−86969
molecular beams, sources, gasdynamic, use of lasers, time-of-flight and detection techniques 80−69264
molecular bond energies from time-of-flight chemiluminesc. 78−40051
molecule+fast heavy ion, dissoc. ionisation obs. 79−47899
neopentane, plastic crysts., rot. correlation functions, neutron scatt. obs. 79−46578
neutron, effects of imperfect beam modulation using mechanical correlation choppers 77−57798
neutron detector for coincidence meas. *(German)* 79−18075
neutron diffraction for quantitative texture analysis, comparison with conventional method 80−81078
neutron diffractometry studies of time-depend. phenomena *(Japanese)* 80−70083
neutron meas. of direct react. spectra, resolution emprovement 80−18753
neutron polarisation expts., multiple scatt. effects 78−13052
neutron thermalisation in heavy water, meas. and calc. of spectra using TOF methods 79−85582
neutron time of flight anal., non-conventional methods, expt. capability study 79−44985
neutron time of flight meas., $\pi^-p \rightarrow \pi^0 n$ investigation 78−17045
neutron time-of-flight technique, for cryst. struct. investigation 79−19126
neutrons, dead time distortions in reverse Fourier TOF spectrometry 79−6789
one dimensional motion, statistics 77−85050
PANSI, polarisation anal. neutron scattering instrument, description and appls. 80−23280
parameter estimation of TOF spectrum, gain of correlation method 79−49895
photoion-photoelectron spectroscopy, ion internal energy and reaction 79−30616
plasma metastable at. sampling from hollow cathode arc, electron temp. probe 80−43967
polymer film, carrier transport meas. 80−6874
positive ions, photodissoc. spectra with time-of-flight anal. 79−50096
protein solutions, small-angle neutron scatt. using time of flight method, spectrometer 79−1371
quasi-elastic neutron scatt., direct model fitting of uncorrected TOF data 79−31309
rubrene, orthorhombic cryst. photogenerated carriers, transit time meas. 80−49811
spectral analysis, analytic approach 79−97929
surface structure, energy spectra of scattered ions, new method of surface struct. determ. 78−87854
terphenyl, ortho-, para-, meta-, total neutron cross sections for subthermal energies 78−74779
tribromomethane-methane, mass spectra, vel. distrib. effects 77−54627
trimethylammonium chloride, cation and CH_3 groups rot. diffusion, quasielastic neutron scatt. 77−27840
(d,n) diagnostic neutron spectra from deuterons 2.5, 3.0, 3.5 MeV on ^{12}C, ^{27}Al, ^{19}F, CH_2, CD_2, Teflon 79−40933
Ar, at. beam, scatt. from Ag(111), time of flight meas., 79−95894
Ar, high resoln. pulsed electron beam time-of-flight ejected electron spectra 77−3462
Ar total scattering cross sections for low-energy electrons 80−58417
Ar^{16+}, radiative decay from 2^3P_2 and 2^3P_0 levels, beam-foil time of flight meas. 77−68015
Ar^{17+}, Lamb shift, elec. field quenching time of flight method 79−13674
$Ar^+ + H_2(D_2)(N_2)$, small angle charge exchange, 0.5 to 1.0 keV, time of flight spectra 78−33604
$Ar^+ + H_2(N_2)(O_2)(CO)(NO)$, charge transfer cross sections 77−34751
$Ar^*(4s^3{}_{2,0}) + Kr(Xe)$, elastic and reactive scatt., ang. distribs. 77−6919
Au, 5 keV Ne ion scatt., energy spectra by TOF and electrostatic analyser methods, comparison 79−2895
Au cryst., ion bombarded, Ar^+ ions, time-of-flight spectra of sputtered atoms 80−89103
Au, ion bombardment by Ar^+, focused ejection 80−104028
Au, sputtering, by point defects 79−47573
B concentration profiling in solids by neutron TOF using $^{11}B(p,n)^{11}C$ 79−51131
$^{10}B(\alpha,n_0)^{13}N$, 18-20 MeV, neutron ang. distribs. multi-nucleon transfer mechanism 77−14144
$^{10}B(\alpha,n_1)^{13}N^*$, 18-20 MeV, neutron ang. distribs., multi-nucleon transfer mechanism 77−14144
$Ba+Br_2(I_2) \rightarrow BaBr(BaI)+Br(I)$, time-of-flight chemiluminesc., mol. bond energies determ. 78−40051
$Ba+N_2O$, crossed mol. beams, BaO recoil vel. spectra 78−7184
BaF_2+BCl_3, crossed beam metathesis, total cross sections 77−21354
$BaI_2+Cl_2(HCl)$(1,1-dichloroethane)(chloroethene), crossed beam metathesis, total cross sections 77−21354

time of flight spectra continued
BaO, recoil velocity spectra from crossed-beam spin-forbidden $Ba+SO_2$ reaction 79−74361
BaO, recoil velocity spectra from form. in crossed beam system 80−76500
Be, phonon spectrum from inelastic coherent scatt. of cold neutrons 80−10617
$C_4H_6^+$, fragmentation, kinetic energy release 77−77737
CO, dissociative excitation by electron impact, metastable fragment energy 78−66672
CO, electron scatt. at low energy, mechanisms *(Russian)* 78−90306
$CO+Li^+$, 4-7 eV, final rot. state distrib., small ang. depend. 79−68300
CO_2 electron drift velocity and longit. diffusion coeff. time-of-flight meas. 77−80264
CO_2-N_2-He gas mixtures, time-of-flight meas. of electron transport parameters 78−94387
CS_2, liq., struct. factor determ. by t.o.f. neutron scatt. 77−1060
$^{12}C(^{16}O, n)^{27}Si$, 12.8 MeV resonance investig. by time-of-flight spectra and n-γ coincidence 79−9627
Ca, forbidden transitions, radiative lifetimes, MCSCF and CI calcs., time of flight spectra for metastable state 80−91498
Ca, time-of-flight spectrum using pulsed tunable laser fluoresc. detect. 77−49804
CdI_2, photodissoc., spectroscopy and dynamics 79−98169
CdTe, charge carrier transport prop. meas. by time of flight technique 77−39850
CdTe, high-resistivity, carrier transport and trapping processes, growth parameter effects 77−39871
CdTe, high-resistivity, irradiation effects on carrier transport and trapping process 78−2164
CdTe, undoped, high-resist.- characterisation, impurity level investig. 77−39801
CdTe:Cl, grown by travelling heater method, carrier homogeneity investig. 77−39848
^{252}Cf spontaneous fission spectra, data anal. in TOF meas. 79−26811
Cl (IX-XV) allowed intra L-shell transitions, oscill. strengths and radiative lifetimes meas. 79−13676
Cl ions, multiply-charged, beam-foil obs. of allowed L-shell transitions 80−14113
Cl, metastable states, form. from Cl_2 dissoc. excitation, time of flight spectra 78−1094
Cl^++He(Ne)(Ar), highly charged low vel. recoil ion time of flight spectra, cross section energy depend. 80−14222
Cl_2, electron impact dissoc. excitation, metastable fragment form. translational spectra 78−1094
$Cr_4(OH)_6(NH_3)_{12}Cl_6.4H_2O$, exchange coupled mol. Cr^{3+} tetramers, inelastic neutron scatt. 80−65792
Cs^++Cs, mol. ion form. rate, from mobility meas. 79−34299
Cu surface, fast D_2 desorpt. mechanism, time-of-flight spectra 80−84379
Cu_{18}, total neutron cross-section meas. 77−74839
Cu^{18+}, Na-like, low-lying levels, radiative lifetimes, f-values obs. 78−25482
Cu_3Mn, atomic short-range order, TOF neutron diffraction 79−10831
$Cu_{0.57}Zr_{0.43}$, amorphous, partial struct. factor, TOF pulsed neutron 79−14684
$Cu_{46}Zr_{54}$, metallic glass, dynamical struct. factor and freq. distrib. meas. 80−54136
D_2^+, photodissoc. cross section, time of flight anal. of reaction products 77−83664
D_2O, collisionless multiphoton ionis. energy depend. by TEA-CO_2 laser 78−46405
DT fast neutrons in blankets and shields, neutrons, associated particle method 77−71690
D(2S), form. by electron impact from D_2(HD), time of flight obs. 79−86079
$Fe_{40}Ni_{40}P_{14}B_6$, amorphous ferromag., spin wave excitations 80−97079
H, beam, $2^2S_{1/2}$ metastabld ats., nonadiabatic transition in mag. field 78−55157
H beam, low temp., direct determ. of temp. and density 80−14875
H^++Ar, 5-1.5 MeV, ejected-electron energy and ang. distrib., differential cross sections 77−88547
H^++Kr(Xe), electron capture into 3s state, cross-section meas. 78−42209
H_2, dissociative photoionis. at 26.9 eV 77−3423
H_2, dissociative photoionisation, 19.8-40.8 eV, proton kinetic energy spectra 79−68273
H_2, electron drift velocity and longit. diffusion coeff. time of flight meas. 77−80264
H_2, electron impact dissociative excitation obs. 78−1090
H_2, solid collective excitations observed by incoherent neutron scatt. 79−23690
H_2, total cross sections meas. for electron scatt. at very low energies 80−58398
H_2+Cl^-, 4-11 eV, inelastic scatt. 79−98202
o-, p-H_2+Li^+, rot. excitation and ang. depend. transition probabilities, time of flight spectra 80−23517
H_2^++He, 10 keV, dissoc. excitation, ionis., energy distrib. 77−61849
H_{2n+1}^++Ar, $n \leq 7$, double differential fragmentation cross section 79−89821
H_3, electronically excited state obs., vibr. level struct. determ., predissoc. 79−41204
HD^+, photodissoc. cross section, time of flight anal. of reaction products 77−83664
HD+HD, state-resolved rot. excitation differential cross sections, crossed pulsed beams techniques 78−17766
H_2O, electron impact, inelastic scatt., 4-6 eV energy loss region 78−90277
H_2*, predissociation of vibr. excited mols. 78−42146
H(2S), form. by electron impact from H_2(HD), time of flight obs. 79−86079
He, 2^3S_1 and 2^1S_0 metastable states, static dipole polaris. meas. 78−1098
He, (2^3S_1) state excitation by electron impact, at. time of flight meas. 77−19083
He, high resoln. pulsed electron beam time-of-flight ejected-electron spectra 77−3462
He, positron inelastic scatt. at intermediate energies, time of flight spectra 80−18932
He, total scatt. cross sections for low-energy electrons 80−58417
He+HD collisions, single quantum rot. excitation by pulsed molecular beams 78−29840

time of flight spectra continued
He^++alkali metal, charge exchange, He metastable beam form., composition 79−89775
$He^+ + H_2(D_2)(N_2)$, small angle charge exchange, 0.5 to 1.0 keV, time of flight spectra 78−33604
$He^+ + O_2$, charge transfer product state distribs., time of flight obs. 80−87223
$^3He(^4He)$ clusters, metastable electronic states, electron impact excitation, time of flight spectra 80−106411
$He^*(2^1S)$+Ne, elastic and reactive scatt., ang. distribs. 77−6919
$He(2^3S)$+H(D), Penning and assoc. ionis. cross sections, vel. depend. 79−22815
$He(2^3S_1)$, metastable state electron impact excitation differential cross section meas. 79−10210
$He(2^3S$ and $2^1S)+H_2(D_2)$, Penning, rearrangement and total ionis. cross sections, vel. depend. 79−22816
H(t, n)^{3}He, appl. to H depth profile determ. in solids, pulsed T^+ beam 79−5198
I, state determ. following photodissoc. of KI, time of flight meas. 79−18105
I_2^+, fragmentation ang. distrib., energy disposal, branching, photoelectron-photoion coincidence spectra 79−68263
IBr^+, fragmentation ang. distrib., energy disposal, branching, photoelectron-photoion coincidence spectra 79−68263
ICl^+, fragmentation ang. distrib., energy disposal, branching, photoelectron-photoion coincidence spectra 79−68263
Ir, adsorbed gases, field desorption from field ion tips 80−59793
K, state determ. following photodissoc. of KI, time of flight meas. 79−18105
K+alkyl iodide, collisional electronic excitation, time-of-flight obs. 79−86049
$K+H_2S$(DS), collisional ionisation, positive and negative ion energy spectra obs. 80−63775
$K+NH_3$, rot. inelastic, time-of-flight spectra 78−5325
Kbr surface, residence times of Au atoms, time-of-flight meas. 80−10788
La_2O_3, fast ionic O_2 diffusion, neutron scatt. evidence 79−99357
Li, electron impact excited high-l Rydberg states 77−65535
$Li^+ + CO_2(N_2O)$, vibr. excitation, time of flight meas. 77−79682
LiF, laser-irrad., emitted electrons and positive ions delay 80−29830
Mg_δ energy distrib. of sputtered atoms 79−91549
Mg^{9+}, beam-foil excited, spin orbit-forbidden X-ray transition obs. 80−23537
MgI_2+Cl_2(HCl), crossed beam metathesis, total cross sections 77−21354
MnI, transition probability and solar abundance, beam foil TOF meas. 79−40154
Mo [110], metastable He impact, secondary electron spectra 78−95642
Mo surface, metastable He atom beam contamination by fast neutral atoms, effect on secondary emission 80−55253
N, high Rydberg states, radiative decay rates, TOF meas 78−46302
N_2, electron drift velocity and longit. diffusion coeff. time of flight meas. 77−80264
N_2, electron ionisation, N_2^{2+} form., decay to N^+, coincidence detect. 77−79695
N_2 electron scatt. cross sections, 0.04-3.7 eV 79−54978
$N_2+H^+(He^+)$, 1 MeV, dissoc. ionis., time-energy spectra 77−34744
N_2+K collision, electronic excitation and energy transfer, time of flight spectra 80−43151
NO^+, fragmentation ang. distrib., energy disposal, branching, photoelectron-photoion coincidence spectra 79−68263
NO^+, symmetric charge transfer reaction cross section, selected kinetic energies 77−16813
N_2O, electron impact, dissoc. patterns 79−7021
N_2O^+, photodissoc. cross section, time of flight anal. of reaction products 77−83664
$N_2(X^1\Sigma_g^+)+Ar(^3P_{2,0}) \rightarrow Ar(^1S)+N_2(C^3\Pi_u)$, sensitised fluoresc., vel. depend. 78−90204
Na_2, TOF spectra, molecular beam diagnostics with internal state selection 78−86968
NaCl beam thermal decomposition, Na time-of-flight spectrum using laser fluoresc. 77−49804
NaCl, sputtering of atoms by 540 eV electrons, delay times 80−35025
NaCl surface, residence times of Au atoms, time-of-flight meas. 80−10788
NaI, Xe^+ ion bombard., sputtering processes, time of flight meas. 78−88392
$(NbF_5)_4$ mass spectra, vel. distrib. effects, mol. beam inlet method, mol. dissoc. 77−54627
Ne, metastable electronic states, electron impact excitation, time of flight spectra 80−106411
Ne+HD, j=0 to 1 rot. excitation, differential cross sections, time of flight obs. 80−48104
Ni (001) surface, Ne^+ scattering and neutralisation on first and second layers 80−35045
$O+Cl_2(CS_2)$, reactive scatt. of beams, vel. distribs. 77−73443
O^-+Ne(Ar)(Kr), 0.2-1 keV, elastic and inelastic reduced differential cross-sections 80−32829
O_2, multiphoton ionisation, electron energy spectra 77−6865
O_2 photofragment, produced by O_3 photolysis at 266 nm 80−50865
O_2^+, fragmentation ang. distrib., energy disposal, branching, photoelectron-photoion coincidence spectra 79−68263
OH+Br_2, hydroxyl radicals reactive scatt. 80−85172
$O(^5S)$ metastable state, radiative lifetime determ. 78−74614
$O(^5S_2)$ metastable state g_J factor, TOF at. beam mag. reson. obs., rel. to $He(^3S)$ 79−3593
$O^+(^4S)(^2D)+Ar(H_2)(N_2)(O_2)(CO)(NO)(CO_2)$, charge transfer reactions, cross-sections meas. 78−92462
O** Rydberg state translational energy spectra in dissoc. electron impact excitation by CO_2 79−54979
P, black allotrope, orthorhombic bonding, up to 26.6 kbar, neutron diffr. obs. 79−99106
Pd, surface, fast D_2 desorpt. mechanism, time-of-flight spectra 80−84379
a-$Pd_{0.8}Si_{0.2}$ alloy, liq., struct. factor determ. by t.o.f. neutron scatt. 77−1060
$PrAl_3$, crystal field splitting of Pr^{3+}, inelastic thermal neutron scattering 78−67996
RbBr, sputtering of atoms by 540 eV electrons, delay times 80−35025
RbCl(Br)(I), Xe^+ ion bombard., sputtering processes, time of flight meas. 78−88392

time of flight spectra continued
RbI, sputtering of atoms by 540 eV electrons, delay times 80−35025
SF_6 electron scatt., total absolute cross sections, 0.5-100 eV, incl. reson. struct. 79−45843
SF_6, laser pumping in collisional region of nozzle beam, internal excitation, time-of-flight anal. 80−95719
SF_6 multiphoton dissoc. by mol. beam method, energy distribution meas. by time-of-flight spectra, dissoc. dynamics 80−78670
$SF_6+Li^+(H^+)$, mode selective vibr. excitation 80−58351
Se, appl. to xerography 80−57415
Se, liq., strict. factor determ. by t.o.f. neutron scatt. 77−1060
Se, liquid, chain molecule struct. exam. by time-of-flight pulsed neutron diffr. 77−55228
Se-As alloys, appl. to xerography 80−57415
Si, 5 KeV Ne ion scatt., energy spectra by TOF and electrostatic analyser methods, comparison 79−2895
Si, H^+, H_2^+ and He^+ backscattering, energy spectra and charge fractions 80−35046
$Sn+Cl_2(Br_2)$, reactive scatt., ang. distrib. and time-of-flight spectra 78−64842
$Sn+O_2$, crossed mol. beam kinetics, SnO time of flight recoil vel. spectra 78−68883
$SrBr_2(SrI_2)+Cl_2$, crossed beam metathesis, total cross sections 77−21354
Ti:T, depth profiling by neutron TOF spectroscopy 77−73500
TlI, UV photodissoc., time of flight spectra and ang. distrib., excited state assignment 79−64061
$UC_{0.60}N_{0.40}$ optical phonon splitting 78−71810
UF_6, photodissociation dynamics at 266 nm, recoil flight time 78−73062
W, adsorbed gases, field desorption from field ion tips 80−59793
W, direct inelastic and trapping-desorpt. scatt. of N_2, elementary steps in N_2 chemisorpt. 80−60737
$Xe^{\ddagger}$, symmetric charge transfer reaction cross section, selected kinetic energies 77−16813

time of flight spectrometers
aerosol particle time-of-flight spectrometry 77−37451
ASSIMOF, appl. to secondary ion energy spectroscopy of polycryst. Cu 79−38700
associated particle type, neutron elastic scatt. by ^{40}Ca and ^{32}S, 2 to 3 MeV 80−13468
Astacus, a time focussing neutron diffractometer based on the reverse Fourier principle 79−77457
atom probe, for metallurgical appl. 80−86498
atom probe field-ion microscope, computer-controlled, for metal defects study 77−82645
CERN OMEGA spectrom., slow proton trigger 78−17467
charged particle telescope TOF system, elemental assignments of reaction products 78−86720
cold neutron time of flight spectrometer at Studsvik, Sweden 80−63444
cold-neutron, resolution function determ. 78−78030
compact time-zero detector for heavy ions 79−76260
computer interaction through direct memory access and with buffer memory 78−70685
correlation chopper for TOF neutron scatt., deconvolution, triangular signal function 77−61158
correlation chopper for TOF neutron scatt., deconvolution theory 77−61157
correlation method, improvement by source pulsing 78−29699
cross-correlation time-of-flight analysis of molecular beam scattering 79−55000
detectors intrinsic time resolution 78−849
DIN-2K double slow neutron spectrometer *(Russian)* 79−45528
directional coincidence telescope for gamma ray telescopes 77−390
double-disc chopper with improved gating characts. 80−37120
dual beam fibre optic time-of-flight spectrometer 80−52347
electron vel. spectrometer using transverse elec. field deflectors 78−89584
electronic circuit, high resolution spectrometer 79−54997
electronic mass spectrometer with separator for metal cluster research 80−77907
fast neutron cross section facility for CTR program 77−26931
fast neutron time of flight spectroscopy, multi-angle detector system 80−52810
fission-fragment scattering kinematics multiparametric anal., TDF instrument with semiconductor detectors 78−78550
fission-fragment scattering kinematics multiparametric anal. electronic meas. system, semiconducting detectors 78−78551
Fourier time-of-flight spectroscopy, higher-harmonics contamination in slow-neutron spectra, theory 80−74072
gas-phase photoelectron spectrometer using synchrotron radiation 80−4818
gas-phase reactions, anal. using computer interfaced time-of-flight mass spectrometer 80−71967
heavy ion, apparatus principles *(Danish)* 79−31304
heavy ion detectors, review 79−72178
heavy ion identification, combined magnetic anal. time of flight and energy meas. 77−23359
heavy ion transmission detector, TOF appl. 78−46208
heavy-ion detector system, low-energy, A≤30, TOF spectrometer and ΔE-E telescope 77−65380
heavy-ion telescope, walk-free fast timing 77−404
heavy-ion timing with channel plates 77−14305
high energy ion analyser for laser produced plasma studies 77−51236
high pressure sample container for thermal neutron inelastic scattering on fluids 80−37681
high-resolution, using pulsed electron beam, performance 78−49939
inhomogeneous oscillatory elec. field mass spectrometer 77−13813
inverted geom. TOF spectrom. at ZING-P pulsed neutron source prototype 77−83448
ion energy and momentum spectrometer with high resolution 80−86495
ionisation chamber as start detector in TOF meas. of ^{252}Cf spontaneous fission spectrum 79−81128
linear mass-reflectron, non-magnetic time of flight mass spectrometer *(Russian)* 79−75652
low energy ion scattering, meas. of energy spectra of neutral particles, apparatus and expts. 80−55242
low-background detection system for neutron reaction expts. 77−54395
mass spectrom., for He-jet produced α-source recoil particle obs. 78−86717
mass spectrometer, 3-dimens., asymmetric quadrupole lens 80−4807

time of flight spectrometers continued
mass spectrometer, 3-dimens., quadrupole type, theory 80−4806
mass spectrometer, for studying, dynamics of fast chemical transforms. 77−74547
mass spectrometer, mag. energy analyser resolution 79−44980
mass spectrometer ion source, electron beam collimation, rel. to resolution and sensitivity 80−42294
multichannel counter for molecular beam time-of-flight experiments 80−37119
multiply charged ions, range-time-of-flight spectrometer 77−46447
NE213 liquid scintallator, light output for electrons and protons 80−32564
neutron, detector containing ^3He 80−63441
neutron, direct time to digital convertor with multi-stop facility 77−14317
neutron, high energy, TOF high efficiency detectors, subnanosec. time resolution 78−37481
neutron, historical review of developments 79−72179
neutron, large time compensated scintillation counters 78−55085
neutron, modular minicomputer multiparameter data system, neutron spectrometer 77−23396
neutron, nanosecond associated particles system for fast neutron scatt. expts. 77−6604
neutron, review of operation and circuitry 77−6605
neutron, use with 1 GeV proton synchrocyclotron 77−26927
neutron detectors for TOF meas. with very fast burst source *(French)* 80−14040
neutron diffraction data, multicomponent profile refinement 77−1047
neutron elastic scattering on powdered samples, TOF spectrometer 77 62447
neutron energy spectra at intermediate energy, measuring apparatus 79−54738
neutron facility at Manitoba cyclotron lab. 79−81114
neutron facility for 8UD Pelletron tandem accelerator 79−85856
neutron Fourier TOF spectroscopy, influence of higher harmonics in chopper modulation function 77−6609
neutron low-Q spectrom. appl. to small angle scatt. with pulsed neutron source 78−55083
neutron meas., rate depend. of counting losses 80−37692
neutron scattering, small-angle, using time of flight method, spectrometer, appl. 79−1371
neutron small angle scatt. on Harwell linac 80−19675
neutron spectra, multiple scatt. corrections and neutron attenuation 77−26928
neutron spectrom., Monte Carlo scatt. simulation 77−34509
neutron spectroscopy, pseudostatistical modulation method *(Russian)* 78−33360
neutron spin echo appl. on pulsed neutron sources 79−81115
neutron time of flight facility with mag. beam swinger, time, energy resolutions 77−57796
neutron time of flight single crystal diffractometer using a position sensitive detector 80−99404
neutron TOF expts., control and data processing system 78−25385
neutron totally absorbing TOF spectrom. 78−850
neutrons, reverse Fourier TOF anal. with mech. beam choppers 79−6788
neutrons, thermal, energy depend. detection efficiency of cylindrical counter, wall effect, calc. 77−57803
neutrons from extended source, meas. in spark chamber+time of flight detector 77−83447
parallel plate electrostatic analyser for positive ions 77−26428
particle guide, parameter anal. using radioactive recoil ions 78−33343
particle identification at 2-400 keV/N 80−5435
photoelectron-photoion coincidence spectrometer, with double field TOF mass anal. 79−54998
photoelectron-photoion coincidence spectrometer for the study of translational energy release distributions 80−11974
plastic scintillation counter with air light guide 78−29713
position sensitive transmission time detector, for heavy ions 80−63466
positron scattering experimental system, for meas. of angular distribs. of scattered slow positrons and electrons 80−86496
pulse shape discriminator for n,γ separation, appl. to TOF spectroscopy 79−6786
pulse-forming circuit, double step, for ion extraction in mass spectrometer 77−18124
pulsed accelerator for neutron travel time meas. *(German)* 78−17475
quadrupole, book contrib. 77−22615
quadrupole-focusing mass spectrometer 78−21804
radionuclei mass identification system, on-line experimental results 79−6785
reactor structural material transmission meas. using TOF spectrometer 80−18440
recoil, use with cryogenic He jet 78−17458
resonance ionization source for mass spectroscopy appl. isotope anal. and time of flight spectrometer 80−81380
reverse neutron time of flight method, slow neutron spectrometry with Fourier beam choppers 80−106230
reverse neutron TOF method, appl. to slow-neutron spectrometry with Fourier beam choppers 79−22534
scintillation associated particle TOF system for d(n,n) scatt. meas. 78−58535
scintillation liquid (NE 224) high-efficiency time-compensated neutron spectrom. 78−17468
scintillation spectrometers based on flight time 79−26818
scintillation time-of-flight telescope for cosmic γ-ray preselection 78−82572
scintillator thin films, ion discrimination in time of flight detectors 78−86718
secondary particle beams from accelerators, average momentum and comp. meas. 77−65382
shock tube, coupled to spectrometer via molecular beam sampling system 79−80717
slow electron production, design and operation of spectrometer 77−54391
static field spectrograph for laser induced plasma expts. 77−26427
surface barrier telescope, effects seen in fast timing 78−70683
surface investigfations, using spectrometry of low energy Ne atomic beam 77−28670
tachyon detection, using Cherenkov and ToF detectors, book contrib. 79−45125
tandem mass spectrometer, modified, for collision-induced dissoc. obs. 77−74545

time of flight spectrometers continued
telescope, compensated, for spaceborne cosmic ray measurements 77—67939
telescope for high energy gamma-ray astromony 80—31210
thin film plastic scintillator for light ions 78—29711
time zero detector using isochronous transport of secondary electrons 77—30700
TUNL fast neutron TOF facility, current status 77—34314
velocity selection, using pulsed tunable laser fluoresc. detect. 77—49804
$Z>5$ nuclides, methods of particle identification, review 77—23377
DD neutron experiments, time of flight spectrometer appls. 77—65383
He scintillation counter use in neutron time of flight spectrometer for 0.4-4 MeV range 79—68134
^{6}Li glass detector, threshold photoneutron spectra meas. 77—88334
NaI, meas. of fast neutron capture cross sections 78—74530
^{235}U foil, sputtered, energy spectrum, fission track technique using time of flight spectrometer 78—68593
Xe, gas, two-body time correls., Van Hove scatt. function meas. 80—100053

time resolved spectra
acetaldehyde photolysis products, time resolved Fourier transform spectrum 78—58071
acetylcholine, nonenzymatic hydrolysis, Raman obs. 79—29505
acetylene, He-Ne laser line, high temp. absorpt., anal. by high resolution IR spectra 80—91554
acetylene ($-d_2$), fluoresc., in matrix-isolated acetylene and ethylene photolysis 79—59505
acridine, excited state proton transfer reactions, ns fluorometry obs. 79—5132
acridine, singlet state absorption profile, time resolved spectra 79—45769
albumin, pulsed laser study of adsorbed aromatic mol. excited states 77—86448
aliphatic unsaturated normal hydrocarbons, positron annihilation time spectra, polarisability depend. 78—6806
alkyl aryl ketones, in homogeneous n-heptane solns., quasi-isoenergetic triplet energy migration, photolysis obs. 79—61878
alkyl benzenes, jet-cooled, intramol. vibr. relax., reson. fluoresc. and excitation obs. 80—14152
alkyl styrenes, fluoresc., ns time resolved emission spectra 77—6822
2-amino, 7-nitrofluorene, in 2-propanol, Stokes fluorescence shift time resolution 77—58060
2-amino-7-nitrofluorene, in binary solvent soln., time-resolved fluoresc. spectroscopy 79—36680
4-amino-N-methylphthalimide-decalin-n-propanol, translational relax. kinetics, luminesc. obs. 79—8180
1-aminopyrene, protonated, excited state proton dissoc., time-resolved spectrosc. obs. 79—50164
8-anilino-1-naphthalenesulfonic acid, fluoresc. probe mol. in mixed solvent 79—45746
1-(N-p-anisyl-N-methyl)-amino-3-anthryl-(9)-propane, intramol. exciplex formation 77—58059
anthracene, cryst., heat pulse propag., exciton condensation, time-resolved fluoresc. spectra 80—84771
anthracene, in cyclohexane soln., triplet state decay consts. by sampling flash apparatus 79—51998
anthracene, noncryst. solid, excimers, time resolved fluoresc. obs. 79—52006
anthracene crystals, α-particle induced scintillation, mag. field effects 80—40161
anthrone, intersystem crossing rates, ps time-resolved spectra 77—6821
apomyoglobin reconstituted with ^{111}In(III)mesoprotoporphyrin IX, rot. correl. time determ. 80—76698
aromatic hydrocarbon, quenched with Ag^+ in ethanol, triplet state form. 79—11801
aromatic hydrocarbon in soln., excited electronic state vibr. relax., time resolved fluoresc. 80—48024
atom, near-reson. scatt. with collisional perturbation, time and freq. depends. 79—72281
atomic beam reson. fluorescence, multiat. and transit-time effects on photon-correlation meas. 78—86812
atomic system, temporally limited EM radiation, time integrated spectrum *(German)* 80—37769
atoms, Raman scatt. in presence of two-photon reson., coherence effects 79—45679
atoms, two photon excitation, time depend. emitted light spectra, perturbation theory 80—63605
azobenzene, emission from $^1(n,\pi^*)$ state, spectrum and ultrashort decay time 77—30895
trans-azobenzene, $S_2 \rightarrow S_0$ fluoresc. 80—28044
azulene, picosecond dynamics 77—30896
azulene, soln., laser-excited $S_2 \rightarrow S_1$, $S_1 \rightarrow S_0$ emission and $S_2 \rightarrow S_n$ absorption 79—10131
bacterial photosynthesis, and model systems, electron transfer, ps studies 79—48214
bacteriochlorophyll, R. rubrum reaction centres, selective ps laser excitation in condensed phases 79—48217
bacteriorhodopsin, selective ps laser excitation in condensed phases 79—48217
bacteriorhodopsin, time-resolved resonance Raman spectroscopy 77—29103
benzene, nanosecond laser photolysis 80—66825
benzene($-d_6$), in Ar-Kr matrices, phosphorescence decay, external heavy atom effect 79—10132
benzene excimer, nanosecond laser photolysis 80—66825
benzene in dilute cyclohexane solution, fluoresc. quenching on pulsed proton irrad., temp. depend. 80—21307
benzil, excited electronic states; conformational relax., time resolved matrix isolation spectral obs. 80—32701
benzophenone, cryst., phosphoresc. spectra and decay time, temp. depend. 79—87479
benzophenone betyl radical, photochem. yield mag. field effect on spin rephasing, double-pulse technique 77—90615
benzophenone in isopropanol, submicrosecond time resolved EPR, lser photolysis, CIDEP polarisation mech. 78—80764
p-benzosemiquinone monoprotonated radical, submicrosecond time resolved EPR, lser photolysis, CIDEP polarisation mech. 78—80764
2-benzoylpyridine crystals, lowest triplet state, optically detected EPR 80—15827
biacetyl, multiphoton excitation of triplet state, fluoresc. decay 79—31632

time resolved spectra continued
biacetyl, single rovibronic state fluoresc., quantum beats 79—31570
9,9′-bianthryl, excited, proton-induced radiationless processes 77—88486
carbocyanine dye solns., photoisomerisation and internal conversion rates, time-resolved spectra 77—75201
carbon tetrachloride, liq., luminesc. on giant ps. pulse irrad., spectral and time charact. *(French)* 78—88348
charge-transfer, excited, ps. kinetics, geometrical and solvent polarity effects 77—30986
chlorella, delayed fluoresc., ns laser pulse excited, fast phase kinetic anal. 79—24951
chlorodifluoromethane, IR multiphoton dissoc., CF_2 form., time-resolved optical absorption obs. 80—16702
chlorophyll, -a and -b, fluoresc. fading curve of lowest triplet state 79—36691
chrysene, excited triplet state time-resolved vibr. Raman scatt. 80—58264
complex molecules, fluoresc. decay in nonhomogeneous level broadening conditions *(Russian)* 79—50073
coumarin 102, excited state interaction dynamics, picosec. time-resolved spectral shift obs. 80—78624
coumarin 102, excited state protonation kinetics, laser pH jump and picosecond spectroscopy 80—25992
coumarin dye molecules, CH stretching modes, population lifetime meas. 80—58185
cyclohexane, liq., ps time-resolved energy transfer, ultra-fast process, ps single pulse radiolysis 79—79267
cytochrome c, dilute soln., reson. Raman spectra, pulsed laser excitation; optical multichannel detection 78—76999
deactivation kinetics, Br($4^2P_{1/2}$) prod., time-resolved spectrosc. obs. 78—95917
1,4- dibromonaphthalene, highly disordered quasi-one-dimens., excitation transport 80—34961
1,4-dibromonaphthalene, k-k scatt., exciton dephasing time-resolved phosphoresc. obs. 80—11458
p-dichlorobenzene-p-dibromobenzene mixed crysts., triplet exciton migration, time resolved emission spectroscopy 80—89052
3,3′-diethyl-2,2′-thiatricarbocyanine iodide, solns., photoisomerisation and internal conversion rates, time-resolved spectra 77—75201
diethylamine, liq., Raman scatt. after optical excitation, vibr. relax. 79—26984
diethylamine-coumarin 6, soln., fluoresc. induced by laser vibr. relax. 79—26984
S_1p-difluorobenzene, time resolved fluoresc. spectra, direct view of intramolecular vibr. redistribution 80—83341
1,1-difluoroethane IR photolysis product, time-resolved fluoresc. obs. 79—57254
dihalogenoacetylene radical cations, $C_2X_2^+$, emission spectra, $A^2\Pi \rightarrow X^2\Pi$ band systems 78—17679
p-dimethylaminoacetophenone, ps reversible isomerisation kinetics, O_2 quenching obs. 79—5133
9,10-dimethylanthracene derivative, intramol. fluoresc. quenching, attached CBr_3 groups 78—42113
6,6′-dimethyloxyindigo, picosec. kinetics, and photostability, spectrosc. obs. 79—45748
2,6,dimethylpyrazine, PMMA soln., fluoresc. and phosphoresc. quantum yield and lifetime, 20-120 kbar 79—54902
2-(2′,4′-dinitrobenzyl)-pyridine, photochromism, ns laser absorption spectra 78—48138
9,10-dioxa-anti-bimanes, fast intersystem crossing, picosecond spectrosc. obs. 79—85998
2,6-diphenyl-1,4-benzoquinone+aromatic amine, triplet exciplex quenching, H-transfer mechanism 79—79228
direct semiconductors, picosecond absorption spectroscopy 79—47482
discharge, capillary pulse type, spectral chronographic-equidensitometric diagnostics 80—44055
DNA bases, selective ps laser excitation in condensed phases 79—48217
duro-semiquinone monoprotonated radical, submicrosecond time resolved EPR, lser photolysis, CIDEP polarisation mech. 78—80764
dye molecule relax. rates from intracavity spectroscopy *(Russian)* 78—25582
dye solutions, in micellar media, rot. diffusion, transient absorpt. meas. 79—92005
elastomer, segmented block, morphology, pulsed proton NMR study 80—33907
ethylene, excited with parametric oscillator, vibr. relax. obs. and interpret. 80—9702
ethylene, He-Ne laser line, high temp. absorpt., anal. by high resolution IR spectra 80—91554
ethylene oxide-d_0, -d_4, ion chemistry, photoionisation and ion cyclotron reson. obs. 77—21373
excited molecular systems, relax. processes, nanosecond time-resolved spectra 77—26992
excited single state kinetics on a subnanosecond time-scale 79—36677
extrinsic molecular crystal, luminesc. spectra, relax. of vibr. levels 79—87484
fibrinogen, bovine, high energy-induced aggregation, time resolved spectra 80—61655
firefly chemiluminescence emissions, time-resolved spectra 80—35822
fluoranthene, vapour, laser excited fluorescence 78—29807
fluorenone, intersystem crossing rates, ps time-resolved spectra 77—6821
fluoromethane, liq., transient stimulated vibr. Raman scatt. 78—71144
formaldehyde, four-level system, time-resolved microwave double reson. 79—59493
formaldehyde, T_2-relax., rot. transitions, time resolved spectra, microwave pulsed spectrometer study 80—18846
formaldehyde S_1 levels, collisionless single rot. level lifetimes, elec. field depend. 80—63566
germanate glass:Bi^{3+}, time-resolved spectra, radiative and nonradiative processes 79—47501
germanate glass:Bi^{3+},Eu^{3+}, time resolved spectra for Bi-Eu energy transfer 79—33748
glyoxal, radiationless transitions in weak mag. field, fluoresc. quenching 77—58062
glyoxal, relax. processes, single vibronic level fluoresc. spectroscopy 78—58789
glyoxal, selected state photodissoc., vibronic effects, CO quantum yield, 1-10 torr 78—37691
haemoglobin, nanosec. probe of dynamics using time resolved reson. Raman scatt. 80—94162
halogenoacetylene radical cations, C_2HX^+, emission spectra, $A^2\Pi \rightarrow X^2\Pi$ band systems 78—17678

time resolved spectra continued
heteroexcimers, intramolecular, picosecond time-resolved fluorescence studies 80−83401
hexamethyl-2,2′-indotricarbocyanine iodide, solns., photoisomerisation and internal conversion rate, time-resolved spectra 77−75201
1,3,3,1′,3′,3′-hexamethylindotricarbocyanine iodide, laser dye, ultra-fast excited state absorpt. spectroscopy 77−30876
hydrogenic and atomic observables, time resolved spectra, time reversal symm. 80−91418
2-hydroxy, 3-allyl, 4,4′-dimethoxybenzophenone, methyl methacrylate copolymer, excitation singlet, internal H^+ transfer, visible spectra 80−32728
2-hydroxybenzophenone, excitation singlet, internal H^+ transfer, visible spectra 80−32728
ortho-hydroxybenzophenone, soln., intramol. proton transfer and energy relax. photostability, transient absorption obs. 80−28032
III-V semiconductors, radiative recomb., optical evaluation review 80−60647
4,5-iminophenanthrene, polymorphism, X-ray diffr. and photoluminesc. obs., 77 to 300K 77−63449
immunoglobulin, human, high energy-induced aggregation, time resolved spectra 80−61655
indene, fluoresc., ns time resolved emission spectra 77−6822
indigo, picosec. kinetics, and photostability, spectrosc. obs. 79−45748
inert gas plasma, weakly ionised, photon echo relax. obs. in RF discharge 80−43986
inert gases in U hollow cathode tube, time resolved optogalvanic effect 79−37564
9-iodoanthracene, picosecond fluoresc. lifetimes, thermally activated $S_1 \rightarrow T_n$ intersystem crossing 80−28045
iodomethyl radical, vibr. excited, photofragmentation IR emission obs. 80−87162
ion-molecule reaction rate consts., time resolved meas. in mass spectrometry 78−48614
ions in solids, time resolved fluoresc. line narrowing 79−38611
kiton red S, mol. fluoresc. decay time, self-absorption 79−68255
lanthanides, Rydberg spectra and ionisation thresholds, time resolved resonant multistep technique 78−82701
lattice relaxation and time resolved polarization of emission from localized electron with level crossing 79−4840
malachite green, luminesc. decay kinetics on ps time scale 79−19916
matrix isolated molecules, vibr. relax. 78−46425
metal drilling with Nd lasers, absorption phenomena 78−30002
methane, energy transfer obs. using excitation of fund., overtone and combination bands 80−9704
methyl halide-inert gas mixtures, vibr. energy relax., opto-acoustic obs. 80−95711
methyl halides, vibr. energy relax., opto-acoustic obs. 80−95711
methyl nitrite, IR multiphoton dissoc., time resolved IR emission from prods. 78−29822
methyl radical, vibr. excited, photofragmentation IR emission obs. 80−87162
m-methyl-p-cyanodimethylaniline, ps reversible isomerisation kinetics, O_2 quenching obs. 79−5133
9-methylanthracene, in acetylcellulose foil, time-depend. fluoresc. anisotropy, crit. transfer distance *(German)* 78−21964
micelle solns., aq., pulse radiolysis, CIDEP in time-resolved EPR 77−30891
molecular rotational coherence, reson. collisional exchange, time-resolved microwave obs. 80−23525
molecular system, picosecond relax. processes, book contrib. 77−61788
molecule, ordinary Raman scatt., two-photon saturation effect 78−82738
molecule excited state lifetimes time-resolved spectra 78−17704
molecules, transition probability studies, review of recent advances 78−17655
molecules (molecular ions), lifetimes and branching ratios 78−17725
naphthalene:anthmacene, singlet exciton energy transfer dynamics, time resolved spectra 79−83032
naphthalene, triplet state time evolution after radiationless transition, initial vibronic distrib. effects 80−23450
naphthalene mixed crystal, time resolved excitation migration, triplet and singlet critical concs. 79−78010
naphthalene-d_8:naphthalene, betamethylnaphthalene, $^1B_{2u}$ naphthalene exciton percolation kinetics, exciton coherency 79−33750
β-naphtholate in methanol-methyltetrahydrofuran glasses, electron solvation, laser flash photoionis. compared with pulse radiolysis 79−74405
naphthyl, excited electronic states; conformational relax., time resolved matrix isolation spectral obs. 80−32701
1-naphthyl methacrylate-9-vinylanthracene copolymer, time-resolved fluoresc. spectra 78−80401
naphthylamines, excited state pK_a* values, proton-induced fluorescence quenching 78−21958
Nile Blue, subpicosecond spectroscopy, tunable probe, spectral dynamics 80−23429
NMR multiple-quantum coherence, selective excitation, appl. to benzene 80−23439
NMR multiple-quantum transition orders separation, using pulsed field gradients 80−50222
optical absorption spectrum dynamics using sub-ps. optical pulses 80−11431
optical Autler-Townes effect, time depend., finite bandwidth laser appl. theory 80−91499
optical precision spectroscopy, at. and mol. appls. 77−42444
oxazine dyes, orientation of $S_1 \rightarrow S_n$ transition moments, continuous ps photometry 79−10152
oxyhaemoglobin, dilute soln., reson. Raman spectra, pulsed laser excitation; optical multichannel detection 78−76999
oxypyrenetrisulphonate anion, aq. soln., ps time depend. fluoresc. depolaris. obs. rot. diffusion determ. 77−81139
pentacene, in naphthalene (p-terphenyl), picosec. coherent transients obs. 79−46013
pentacene−p-terphenyl, optical dephasing, optical mixing-detected ps photon echoes obs. 78−71155
pentacene in naphthalene crystal, relax. of vibronic states, photon-echo and ab absorpt. relax. expts. 79−95807
perylene, cryst., fluoresc. spectra, time-resolved, excimer and excitons 79−78724
perylene, organic soln., picosec. fluoresc. for rot. diffusion 79−56839
phase fluorometry as a probe of diffusion-controlled molecular encounters in dense fluids 80−32799
pheophytin-a, fluoresc. fading curve of lowest triplet state 79−36691

time resolved spectra continued
photodissociating small molecules in solid matrix, cage effect 79−52728
photosynthesis, fluoresc. and energy transfer, time resolved obs. 79−48216
photosynthesis, primary, selectively excited by tunable ps parametric oscillator 79−48163
photosynthetic membrane, in vivo, light collection and exciton dynamics 79−48215
photosynthetic reaction centre spectroscopy by tunable picosec. parametric oscillators 80−61513
photothermal radiometry, contact-free condensed matter anal., K_2SO_4 powder appl. 80−26088
phthalimide derivatives, solns., ultrafast mol. relax. 79−85984
picosecond transient spectroscopy of molecules in solution 79−36621
plasma formation dynamics of underexpanded supersonic erosive laser plasma flare, high speed techniques 80−48923
plasma-electrode contact processes, microplasma diagnostics 80−59325
PMMA film, doped, time resolved absorpt. spectra, decay kinetics of exciplex state 80−84098
poly-1-naphthyl methacrylate, time-resolved fluoresc. spectra 78−80401
poly-1-vinyl napthalene, excimer dissoc., time resolved fluoresc. spectra 78−33643
poly-1-vinylnaphthalene solution, time-resolved fluoresc. spectroscopy, excimer form. and dissoc. 79−38637
poly-2-vinylnaphthalene, soln., lowest triplet props., flash photolysis and radiolysis obs. 80−32861
poly-N-vinyl carbazole, pulsed laser excitation, time resolved fluoresc., 80−89041
poly-N-vinylcarbazole, soln., picosecond time-resolved fluoresc. by pulse radiolysis 80−28122
polyatomic molecules, intramolecular dephasing processes 78−74695
polyatomic molecules, vibr. energy transfer and relax., picosec. time-resolved spectra 79−50028
polymethine dyes, ultrafast absorpt. spectra 77−18934
polymethine pyrylium dye, IR saturable-absorbing, transient visible absorption 78−33784
polystyrene solution, time-resolved fluoresc. spectroscopy, excimer form. and dissoc. 79−38637
propylene, He-Ne laser line, high temp. absorpt., anal. by high resolution IR spectra 80−91554
propynal, energy dispersion and relax., laser IR-visible double reson. 80−48023
protochlorophyll, fluoresc. fading curve of lowest triplet state 79−36691
proton transfer photoreaction kinetics, in singlet excited state 78−48671
pseudocyanine, I aggregates, fluoresc. decay time 77−27105
pyrazine, PMMA soln., fluoresc. and phosphoresc. quantum yield and lifetime, 20-120 kbar 79−54902
pyrene, excimer form. process, ps laser fluoresc. obs. 79−11448
pyrene, in cyclohexane soln., triplet state decay consts. by sampling flash apparatus 79−51998
pyrene, mol. ionisation pot., two photon ionisation, micellar interface effects on ionisation threshold 80−91609
pyrene+N,N-dimethylaniline (deuterate)(3,5 dimethoxy-N,N-dimethylaniline), geminate recomb., solvent, isotope, mag. field effects 78−56888
pyrene excimer formation in micelle, time-resolved spectra 79−79298
pyrene vapour, laser excited fluorescence 78−29807
pyrene-DMA-methanol solution, photoinduced radical ion pair geminate recombination, triplet yield 78−76879
pyrene-N,N-diethylaniline exciplex, visible spectra obs., picosec. laser photolysis, solvent polarity depend. 77−38677
Quinacrine Mustard, time-resolved fluoresc. spectrum 80−87165
quinazoline, in n-pentane (isooctane) Shpolskii matrices, luminesc. props., vibr. struct. 79−22739
quinones, triplet quenching by organometal cpds., time resolved CIDEP and ESR obs. 80−95654
quinoxaline, in organic solvent, excited state absorpt. spectra, 422 and 533 nm, picosec. relax. 79−89683
Raman scattering, continuum, time-depend. excitation profile 79−41175
Raman spectroscopy, recent advances, reivew 78−41359
resonance fluorescence, saturation effects, coherent pulse calcs. 77−6785
resonance hyper-Raman effect induced by realistic coherent pulses, theory 77−58010
resonance Raman scattering and resonance fluoresc., time and freq. resolved 77−75624
resonance Raman spectra, saturation effects, coherent pulse calcs. 77−6785
rhodamine 640, subpicosecond spectroscopy, tunable probe, spectral dynamics 80−23429
rhodamine 6G, in ethanol, time-depend. fluoresc. spectrum, using synchrotron radiation 80−62736
rhodamine 6G, mol. fluoresc. decay time, self-absorption 79−68255
rhodamine 6G, rot. diffusion, fluoresc. spectra, solvent effects 77−75198
rhodamine 6G+BBOT donor-acceptor system, intermol. electronic energy transfer 78−17702
rhodamine 6G+malachite green, in low viscosity solvent, ps time resolved energy transfer 78−70910
rhodamine B, mol. fluoresc. decay time, self-absorption 79−68255
rhodamine dyes, phosphoresc. quantum yields determs. 79−8179
rotational diffusion and level kinetics separation in transient absorpt. spectroscopy 77−30877
ruby, excited state spin-phonon interaction, time resolved spectroscopic exam. 78−19549
ruby, radiative spectral transfer, time resolved fluoresc. 78−2900
sampling of rapidly reacting gases, mol. vel. distrib. effect on time resolved spectra 77−63888
second order transient scattering, stochastic theory of intermediate state interaction 78−13756
semiconductor, time resolved reflectivity of ps pulses 78−31217
serium albumin, bovine, high energy-induced aggregation, time resolved spectra 80−61655
solutions, highly dilute, picosecond reson. Raman spectroscopy, appl. to cytochrome c and β-carotene 79−98102
spiropyrans, photochromic transformation by electro-optical chronography 79−57264
steel, mild, laser microspectral anal. 80−108769
stilbene, cis→trans photoisomerisation rate const., direct meas. 80−30250
stilbene, cis and trans, transient spectra, radiative lifetimes and quantum yields 80−78640

time resolved spectra continued
stilbene, cis- and trans-, picosecond flash photolysis, intramol. charge-reson. transition obs. 80−7810
stilbene, direct photoisomerisation theory, from fluoresc. and absorption spectra 79−79262
trans-stilbene, fluoresc. decay, picosecond anal. 79−31569
stilbene, photo excitation kinetics 77−23525
stilbene, ps photoisomerisation, time-resolved spectra obs. 79−57252
trans-stilbene, time resolved fluoresc. in ps. regime 80−14164
stilbene, trans-, cis-forms, singlet excited state, picosecond dynamics 78−17677
trans-stilbene dianion, photolysis, intermediate struct., time-resolved reson. Raman spectra obs. 79−52695
trans-stilbene photoisomerisation, ps dynamics under collision-free conditions 79−91975
Stokes fluorescence shift time resolution, obs. of 2-amino, 7-nitrofluorene in 2-propanol 77−58060
styrene, fluoresc., ns time resolved emission spectra 77−6822
surfactant vesicles, low-ang. light scatt. and photon correlation spectroscopy 79−79484
symmetric top molecules, microwave transient phenomena, Bloch eqns. 79−26969
tetracene, fluoresc. fading curve of lowest triplet state 79−36691
tetracene, single cryst., exciton interactions, ps laser pulse intensity depend. 77−63448
tetrachlorotetraiodofluorescein, rot. diffusion, fluoresc. spectra, solvent effects 77−75198
tetramethyldioxetane, gas phase unimol. decomp. and chemiluminesc. initiated by TEA CO_2 laser 77−60068
tetramethylpyrazine, PMMA soln., fluoresc. and phosphoresc. quantum yield and lifetime, 20-120 kbar 79−54902
tetraphenylcyclobutane, in hexamethylphosphoric triamide soln., pulse radiolysis, optical absorption decay obs. 79−16019
s-tetrazine in n-hexane, picosecond time-resolved fluoresc., vibr. relax. 80−48025
thionine triplet+haloanilines, electron transfer reaction, radical yield meas. 80−3330
time and spatially resolved at. absorpt. anal. 80−40760
time-dependent spectra, alternative definition 79−89625
2,6 p-TNS fluorescence probe bound to apomyoglobin, nsec decay 77−29091
trans-stilbene, fluoresc. lifetimes, 77-295K 78−1029
transient radicals, EPR time profiles, CIDEP, electron spin-echo method 79−6953
trifluoroformamide, radiationless pathways, time-resolved fluoresc. obs. 78−66577
triphenylmethane dye soln., electronic relax., viscosity-depend., using picosec. flash photolysis 80−66258
unimolecular reactions induced by monochromatic IR radiation, intensity and laser energy fluence influence 80−11903
vinyl cyanide IR photolysis products, time-resolved fluoresc. obs. 79−57255
vinyl polymers quenched with electron donor (acceptor) in soln., ionic photodissoc. 79−11800
visual pigment solutions, flash photolysis, time resolved difference spectra, temp. var. 77−25434
visual pigments in solution, flash photolysis kinetics, effect of prep. 77−32892
water, liq., electron solvation dynamics 80−85205
xanthene dyes in n-alcohols (ethylene glycol) (glycerol), rot. relax., time-resolved fluoresc. depolaris. obs. 80−58300
xanthione in benzene, second excited singlet state, ps spectra 77−3399
Ag halide photochromic glass, darkening mechanisms under pulsed laser excitation 78−25938
Ag(II) protoporphyrin IX dimethyl ester, fluoresc. relax. after picosec. excitation 79−45751
Al alloys, time and spatially resolved at. absorpt. anal. 80−40760
Al I, $4s^2S_{1/2}$ reson. level, mean life 79−59400
Al^{3+} ion, plasma in fast evolution, time-resolved soft X-ray absorpt. transitions 77−18827
AlGaAs pulse modulate DH laser, oscillatory longitudinal mode competition 79−81427
Ar, 1s states deactivation by N_2 and SF_6, pulsed afterglow, kinetic absorption obs. 77−50398
Ar atoms in Ne matrix, radiative and nonradiative lifetimes in excited states 80−69106
Ar, excitation by pulsed electric discharge, luminescence obs., time resolved spectra meas. 80−102482
Ar, Paschen (1s) reson. state, decay mechanism and kinetics 79−27021
Ar-F_2, energy precursors, proton excited mixtures, energy transfer processes 78−66647
Ar-H_2, elec. breakdown, time and space resolved spectra 78−18470
Ar-Xe, energy precursors, proton excited mixtures, energy transfer processes 78−66647
Ar+Kr, $(4p^55p)$ and $(4p^55p')$ states, radiative lifetimes and two-body collisional deactivation rate consts. 80−95572
Ar+$N_2(SF_6)$, proton excited, time resolved VUV, UV and visible emission 77−14547
ArF*, Ar_2F^*, kinetics of proton-excited Ar-F_2 mixtures, time-resolved and time-integrated spectra 79−36883
$Ar(^3P_2)+N_2(C^3\Pi_u)$ excitation transfer cross section, radiative lifetimes, in N_2 laser transitions 79−27246
$Ar_2(^3\Sigma_u^+)+N_2$, quenching, fast absorption spectrophotometry 79−54940
$Ar^*+N_2(H_2)(D_2)$, de-excitation processes, by pulse radiolysis optical emission obs. 77−65529
Ar_2^* excimer, electron-beam excited, time-resolved fluoresc. spectra 79−813
$Ar^*(3p^54p)_i+Ar(^1S_0)$, collisional population transfer rate coeffs., 300K 79−10177
As, $(4^5S_{3/2})$ state, kinetic obs. using time resolved reson. fluoresc. 78−94211
As_2S_3, amorphous, time resolved spectroscopy of valence alternation pair luminesc. 80−50400
As_2S_3, amorphous, time resolved luminesc. 80−66288
As_2S_3, amorphous, time-resolved photolum., spectrosc. 79−24360
As_2Se_3, amorphous, photocond. and photoinduced optical absorpt. 79−82645
As_2Se_3, amorphous, time resolved meas. of photoinduced optical absorpt. and photocond. 80−49807
As_2Se_3, cryst. and amorphous, optically induced absorption in band gap, picosec. dynamics 79−87439

time resolved spectra continued
Ba II, $6p^2P$ fine struct. g-values, laser excitation of fast ion beam 77−10645
Ba, time-resolved saturated absorption expt., collisions effects 78−29758
BaCl($C^2\Pi$)+He(Ar)(N_2), collisional quenching, laser induced fluoresc. decay meas. 79−27075
BaO, spectra of fluorescence meas. using photon correlator 80−87250
$Ba[Pt(CN)_4].4H_2O$, polarised time-resolved emission spectra 79−33811
BeF_2, aq. glass, 76K, solvated electron spectrum evolution, following ns radiolysis 78−88295
$Bi_4Ge_3O_{12}:Er^{3+}$, host-sensitised energy transfer, laser time resolved spectroscopy 79−83013
$Bi(6^4S_{3/2})$+acetylene(ethylene), absolute rate consts., time-resolved reson. fluoresc. meas. 78−27731
Br, diffusion in Ar at 298K, time resolved mass spectrometric determ. 79−90365
Br II, visible spectrum, shock tube time-resolved photographic photometry, transition probabilities 77−23449
Br_2, diffusion in NO at 298K, time-resolved mass spectrometric determ. 79−90365
Br_2, laser-induced photodissoc. spectroscopy 77−90614
Br_2-Xe, UV transient absorption following flash photolysis 79−61879
BrCl, $^3\pi_0^+$ state, time-resolved fluoresc. 77−34679
BrCl, time-resolved fluoresc. of $a^3\Pi_0^+$ state 78−63093
$Br^*+I_2(Br_2)(Cl_2)(IBr)(ICl)(BrCl)$, deactivation rates of $Br^*(^2P_{1/2})$, collision complex form model 78−42179
Br^*+N_2O, electronic-vibr. energy transfer, time-resolved fluoresc. obs. 79−89753
$Br(4^2P_{1/2})+{}^{12}CO_2({}^{13}CO_2)$, electronic-vibr. energy transfer, temp. depend. meas. 79−10136
$Br(4^2P_{1/2})+N_2O$, electronic-vibr. energy transfer obs. 78−55220
CH, $B^2\Sigma^-$ state predissoc., calcs. and time resolved spectrosc. 80−23576
$CH_3C^{15}N$, rot. relax. time meas., self- and foreign-gas collisions, Stark-switched microwave, obs. 79−86048
CH_3O_2+NO, rate const., flash photolysis and kinetic spectroscopy 79−70305
CN, fluoresc. spectra, time resolved, radiative decay and radiationless deactivation in Ar 79−98142
CN monolayer on Ag, picosecond Raman gain spectroscopy 80−25351
CN, time resolved chemilum., in C_2+NO(vinyl cyanide)(ethylene), laser-generated radical kinetics 79−100352
$CN+O(^3P)(O_2)$ reacts., prod. energy distribs. meas., CO vibr. level population *(German)* 78−76833
CO, $A^1\Pi(v'=1)$, vibr. relax. by reversible intersystem crossing, fluoresc. obs. 80−14170
CO, collision-induced reorientation, direct meas. by IR double reson. 80−32800
CO, highly excited vibr. states, double quantum V-V transitions *(French)* 77−61837
CO^+, vibr.-excited $A^2\Pi$ state, radiative and radiationless vibronic deactivation rates with He 79−10134
CO-myoglobin, mol. tunnelling, isotope effect, time resolved IR Fourier transform obs. 80−72126
$CO+CO_2$, vibr. level depend. quenching of CO(v=1-16) 80−32808
$CO+O+M\rightarrow CO_2+M$, time-resolved and flame-band emissions in shock tube expts. 77−36729
CO_2, electron excitation-relax., time resolved Fourier spectra 78−58070
CO_2+deuteromethane, time resolved fluoresc. for vibr. relax 79−31659
CO_2+H_2, vibr. de-excitation of $CO_2^*(\nu_3)$, 200K 79−45802
CO_2+N_2, vibr. energy transfer, time-resolved laser induced fluorescence 78−29842
CS_2, laser excited fluoresc., time and freq. resolution, assignments 77−14476
CS_2, laser fluoresc., discrete and continuum, time and freq. resolved obs. 79−41195
$CaF_2:Eu^{2+}$, X-ray induced luminesc. kinetics, energy transfer processes 79−8181
$CaF_2:Pr^{3+}$, laser selective excitation and energy transfer 79−38612
CaF_2-$YF_3:Nd^{3+}$, spectral migration of electronic excitation, selective laser excitation *(Russian)* 78−80417
$Ca(PO_3)_2:Eu^{3+}$, amorphous, phonon-assisted site-to-site electronic energy transfer, fluoresc. line narrowing obs. 77−81140
$Cd(^1P_1)+N_2$(alkanes), laser excitation, absolute quenching cross sections and branching ratios 79−49979
CdS, time-resolved spectra of spontaneous luminesc. from high density electron-hole plasma 80−40156
CdS(Se), ps. spectra, high density exciton system 78−19553
CdS(Se), ps. spectra, high density exciton system 78−19554
CdTe, picosecond absorption spectroscopy 79−47482
CdTe, time-resolved spectra, carrier relax. time, phonon lifetime 80−11433
Ce, F states, radiative lifetime and g-factor determ. 79−41138
Cl_2, liq., transient stimulated vibr. Raman scatt. 78−71144
Cl_2-Kr(Xe), UV transient absorption following flash photolysis 79−61879
$Cl(3p^5(^2P_{1/2}))$+carbon tetrachloride (Cl_2)(He), VUV metastable state quenching, absolute rate const. 77−79641
Cr, pulse hollow cathode discharge, time resolved high resolution spectroscopy 80−38759
$Cr(CO)_6$, electronic spectra following flash photolysis, intracavity laser technique 79−31538
CrO_2Cl_2, collisionless IR multiphoton production of electronically excited parent mols. 79−41211
$CsMnF_3$, magnon absorption and luminesc. 80−7400
$Cs_2UO_2Cl_4$, fluoresc. decay rate of pure and impure cryst. 79−47487
CsXe+Xe, time resolved fluoresc. decay and collisional transition rates 77−27111
^{133}Cs, time-resolved fluoresc. spectra, collisional perturbation of Rydberg states 77−83529
Cu alloys, time and spatially resolved at. absorpt. anal. 80−40760
Cu^{18+}, $3^2P_{1/2}$ level decay, time-resolved obs., intensity modulations 77−61704
CuBr, emission spectra after two-photon excitation, Raman scatt. 79−47518
CuCl, biexciton luminesc., subnanosecond time resolved spectroscopy 77−73167
CuCl, emission spectra after two-photon excitation, Raman scatt. 79−47518
CuCl, excitonic mol. luminesc. spectra, picosecond time anal. 78−52548
CuCl, excitonic mols., ps time resolved luminesc. spectra 77−16383

time resolved spectra continued
CuCl, picosecond spectroscopy of secondary radiation from resonantly excited excitonic molecules 79−15461
CuCl, polariton vel. direct obs. 79−28297
CuCl, ps. luminesc. spectra, resonantly excited excitonic mols. 78−19555
CuCl, resonantly excited excitonic molecules, time resolved spectroscopy 78−92109
CuCl, time resolved exciton-biexciton transitions, UV excitation, luminescence spectra 79−69883
CuCl, time-resolved study of induced absorption due to exciton-biexciton transitions 79−38658
$CuGaSe_2$, evidence of donor-acceptor type transition 80−93375
Cu(II) protoporphyrin IX dimethyl ester, fluoresc. relax. after picosec. excitation 79−45751
D plasma, high current pulse discharge investig. *(Russian)* 78−47171
1,3-diphenylpropane, in isooctane soln., monomer phosphoresc., low binding energy triplet excimer not obs. 78−25597
Eu^{3+} fluoresc. lineshape in glass, temp., time and conc. depend., two-phonon Raman scatt. 78−64406
$F+H_2(D_2)$, absolute reaction rate coeffs., time resolved IR emission meas. 79−68258
$F+HCl \rightarrow HF+Cl$, time resolved vibr. chemiluminesc. and rate consts. 80−61069
GaAs, electron-spin relaxation and recomb. kinetics, time-resolved luminesc. study 80−108074
GaAs, photoexcited, band edge absorpt. dynamics 79−19879
GaAs, photoexcited, carrier relaxation determ. from time resolved transmission spectrum changes 79−99583
GaAs, picosecond absorption spectroscopy 79−47482
GaAs, Raman scattering from nonequilibrium LO phonons with picosecond resolution 80−80779
GaAs, time-resolved spectra, carrier relax. time, phonon lifetime 80−11433
GaAs, two photon absorpt., hot electron-hole plasma, relax. time depend., picosecond spectra 79−51979
GaAs:Te, implanted and laser annealed, surface crystallinity, refl. and channelling meas. 79−95036
GaSe, photolum. decay 79−15518
Ge, electron-hole droplet decay kinetics, microwave expts. 77−43517
Ge, recombination luminesc. spectra from hot and cold carriers in electron-hole drops 79−38608
Ge, stressed cryst., props. of strain-confined electron-hole liquid 79−7787
GeF, $A^2\Sigma^+$ state, time-resolved fluoresc. 78−58732
$Ge(3^3P_0)+O_2(Cl_2)(COS)(N_2O)(NO_2)(NO+Ar)$ oxidation reacts., gas phase, kinetics 78−92468
$H+PH_3$, abstraction rate consts., 209-495K, time-resolved fluoresc. 77−16807
H_2, electron impact excited singlet-g states, optical and time resolved spectra, radiative lifetimes, quenching rates for rovibronic levels 80−23564
p-H_2, solid, time-resolved CARS, disorder effects on coherent vibr. states 80−93342
$H_2+Ar^*(4s)$, H_2 continuum emission, kinetic studies in Ar-H_2 mixture, e-beam pumped 80−43153
$H_2+D(O)(Cl)(Br)$, relax. and chem. reaction, time resolved IR fluoresc. and mass spectrometry obs. 80−69177
H_n, 3s, 3p, 3d sublevels populations after dissoc. excitation of alkanes 77−75073
HBr, liq., transient stimulated vibr. Raman scatt. 78−71144
HCl, liq., transient stimulated vibr. Raman scatt. 78−71144
HCl-D_2, vibr. relax. time meas., by coherent Raman-induced IR fluoresc. 79−7038
$HCl+D(O)(Cl)(Br)$, relax. and chem. reaction, time resolved IR fluoresc. and mass spectrometry obs. 80−69177
HF, vibr. fluoresc. from SF_6H_2 collisionless multiple photon absorpt. photodissoc. 77−58099
$HF+HCl(CO_2)(N_2O)(CO)(N_2)(O_2)$, HF(v=3) relax. and rate consts. 80−61069
$H_2O+H(n=3)$, $O(3p^3P)$, radiation quenching in pulse radiolytically excited water vap. 79−89738
H_2S, liq., optical absorption transients produced by ns pulse radiolysis 79−11803
$HbBr(B^2\Sigma^+_{1/2})$, rate coeffs. for collisional quenching, time resolved emission obs. 79−89705
He and He^+, 3^3P and 4^2F levels excitation with electron beams, radiation decay obs. 80−43188
He, collisional excitation transfer for $3^{1,3}P$ and D states 80−106387
He, discharge, level populations, time resolved spectra 77−80391
He glow discharge, low press., excitation transfer and quenching of n=3 excited states 80−38743
He I 4^3D, ^3F-2^3P line struct., in low-press. linear discharge 79−14523
He II, plasma polaris. red shift, Stark profile, temp. depend. 77−18842
He, Lande g-factor determ. from free radn. beats 77−18880
He-N_2, de excitation rate consts., energy transfer, pulse radiolysis obs. 80−30303
He+Ne(Ar)(Kr)(Xe), energy transfer, time-resolved VUV spectra 77−19028
He^++C, beam-foil spectra, He atom orientation, ang. variation 78−86944
$He^+ + H_2(He)$, charge transfer, appl. of atom-photon coincidence meas. 79−45829
$He^+ + N_2$, charge exchange, time-resolved emission probe 78−86946
He_2, electronic and rot. energy relax., reactive collisions by isotope selective excitation 78−33541
He_2, form. in early afterglow of pulsed discharge, time-resolved spectra 78−63585
He^*+Ne, (3^1S, 3^3S, 3^1P, 3^3P) de-excitation cross section temp. depend., time resolved spectra 80−28100
$He(2^3S)$, quenching rates meas., in pure afterglow 77−75206
$He(3^3S)(3^3P)(3^3D)+He(1^1S)$, deactivation rate, 300-600K, time-resolved spectra 77−19037
$Hg+NH_3$, excited UV luminesc., low press., $HgNH_3^*$ form. 77−21388
Hg_2, excimer fluorescence, electron beam and optically produced systems 77−27107
Hg_2 excimer states, energy transfer kinetics 78−63090
$Hg_2(Hg_3)$, violet emission, formation and decay kinetics, luminesc. time resolved spectra 79−76464
$I(5^2P_{1/2})+HBr$, reactive and inelastic channels rate, temp. depend., AAS obs. 78−35657
I, produced in UV photodissoc. of alkyliodides, time-resolved obs. of $I(^2P_{1/2})$ reactions 80−11940

time resolved spectra continued
$I+HCl$, quenching of $I(5^2P_{1/2})$, temp. depend., time resolved at. absorpt. spectrophotometry 80−32655
I+methane $^-d_0(^-d_3)$,$(^-d_4)$, excited atoms, quenching, isotope effects, time resolved reson. fluoresc. 80−32656
I_2, effusive collisionless beam, optical Rabi coherent transient damping, time resolved obs. 77−75231
I_2, time-resolved reson. Raman and reson. fluoresc., hyperfine splitting effects 77−30874
I_2-Xe, UV transient absorption following flash photolysis 79−61879
$I_2(B^3\pi_{o^+u})$, ps excitation, in CCl_4 soln., ultrafast decay and spectrum 78−9184
$IBr(B^3\pi_{0^+})$, lifetimes determ. from time resolved fluoresc. 78−46385
$I(^2P_{1/2})$+n-iodopropane (iodoethane), quenching rate coeff., in UV photolysis of n-iodopropane (iodoethane) 79−11799
$I^*+H_2O(D_2O)(HDO)$, $5^2P_{1/2}$ electronic to vibr. energy transfer, quenching and time resolved IR fluoresc. 79−3537
$I^*+I_2(Br_2)(Cl_2)(IBr)(ICl)(BrCl)$, collisional deactivation and reaction rate consts., obs. 78−80738
$I(5^2P_{1/2})$, time-resolved reson. fluoresc., quenching rate coeffs. 78−25466
$I(5^2P_{1/2})+Br_2$, deactivation kinetics, time-resolved spectrosc. obs. 78−95916
$I(5^2P_{1/2})$+HBr(DBr)(methane)(propane), collisional deactivation, rate consts. meas. 77−86300
$I(5p^5(^2P_{1/2}))$, time-resolved kinetics, mean radiative lifetime, radiation trapping, HFS 78−5171
K, fine-struct. intervals, polarisabilities, highly excited d states 79−27100
K, s and d state radiative lifetimes, time and wavelength resolved fluoresc. spectra 80−14104
KBr:Br_2^-, triplet luminesc. kinetics, 0.4-4.2K 79−87482
KCl:Eu^{2+}, radiationless processes 78−80391
KCl:Eu^{2+}, zero phonon lines, time-resolved fluoresc. spectra 77−77269
KI:I_2^-, triplet luminesc. kinetics, 0.4-4.2K 79−87482
KI:In^+, luminesc. decay, excited state symm. and g-value 79−99922
KI:Sn^{2+} luminesc. decay, excited state symm. and g-value 79−99922
$KMnF_3$, exciton dynamics by time resolved emission spectroscopy 80−54615
$K_2UO_2Cl_4$, fluoresc. decay rate of pure and impure cryst. 79−47487
KXe, dye laser induced emission, excimer bands and uses 80−9650
Kr, $^3P_1$ state, reson. fluoresc., Zeeman beats, time-resolved VUV spectra using synchrotron radiation 78−33454
Kr, 6p levels, two-photon excitation, time resolved fluoresc., quenching, lifetimes and photoionisation cross section 80−78587
Kr atoms in Ne matrix, radiative and nonradiative lifetimes in excited states 80−69106
Kr, fluoresc. lifetimes, time resolved VUV spectra 78−17601
KrF^*, Kr_2F^*, kinetics of proton-excited KrF_2 mixtures, time-resolved and time-integrated spectra 79−36883
Kr_2^*, VUV time resolved spectra, formation and decay kinetics 79−31544
La I, lifetimes of $z^2F_{5/2}$, $z^2D_{3/2}$, $z^4G_{5/2}$ and $y^2D_{3/2}$ states 78−66489
LaF_3:Pr^{3+}, fluoresc., time resolved excitation technique 79−95820
Li, lifetime measurement of D-states, by time resolved resonance fluorescence 79−63965
$LiNbO_3$, exciton migration, laser time-resolved spectra obs. 79−69861
MgF_2, optical absortion following pulsed electron irrad., 100-500K 79−8164
MnF_2, biexciton decay, time resolved laser spectra 78−75999
Mo impurity flux, time resolved, in DITE Tokamak 80−63373
$Mo(CO)_6$, electronic spectra following flash photolysis, intracavity laser technique 79−31538
N_2, B-state collisional transfer, press. effects, oscillator strengths, time resolved spectra 79−36744
α-N_2, solid, coherent loss of vibr. and librational excitations 79−86852
α-N_2 solid, time-resolved CARS, disorder effects on coherent vibr. states 80−93342
N_2^+, A- and B-states interactions, time-resolved obs. 80−18862
N_2F_4, mol. photodissoc. using CO_2-laserradiation, rate const. meas., mol. fluoresc. and time-resolved UV spectra obs. *(German)* 80−83434
NH, ND, $X^3\sigma^-$ state vibr. relax. Ar matrix, energy gap law breakdown 77−30963
NH_3, laser saturation time-delayed IR spectroscopy 78−86976
NH_3, time-resolved four-level double-reson. signal, coherent transients effects 78−78732
NO, $3s\sigma(A^2\Sigma^+)$, in Ar Kr Xe matrices, Rydberg state 'bubbles', reson. fluoresc. obs. 77−83636
NO ($a^4\Pi$), condensed phase vibr. relax., isotope effect, time resolved obs. 78−94233
NO electronically excited photofragment of VUV photodissoc. methylnitrite, identification and quantum yield 80−99527
NO, measured lifetimes of $A\ ^2\Sigma^+$, $D\ ^2\Sigma^+$ and $C\ ^2\Pi$ states 78−90219
NO, predissoc. rates and pertrubations in certain electronic states, time resolved spectra 77−27131
NO_2, discrete reson. CARS emission, temporal and spectral props. 80−95630
NO_2, excited electronic states, time-resolved spectrosc. 79−45747
NO_2, inter and intramolecular radiationless transitions, relax., time resolved excitation and fluoresc. spectra 80−27966
NO_2, rot. cooled, vibronic band lifetimes, time resolved fluoresc. excitation spectra obs. 79−94025
N_2O+deuteromethane, time resolved fluoresc. for vibr. relax 79−31659
α-NPO, two-photon fluoresc. 77−30896
Na, anomalous emission in blue wings 77−46517
Na, diabatic field ionisation of highly excited at. states 80−43202
Na, reson. two-photon ionisation via $3p^2P_{3/2}$ state, photoelectron ang. distrib. 80−43016
Na, resonance fluorescence, photon antibunching obs. 77−83534
$Na(n^2D)+N_2(CO)$, collisional l-mixing, highly excited states, fluoresc. obs. 77−83686
Nb+Nb, selected MO X-ray coincidence with separated at. K X-rays 80−43148
NdP_5O_{14}, laser site-selection time-resolved spectroscopy 78−76524
$Nd_xY_{1-x}P_5O_{14}$, conc. quenching 79−61435
Ne, 2p-1s transition, time-resolved spectroscopy 78−90103
Ne pulsed transverse discharge, spectrosc. absorpt. investig with nanosec. time resolution *(Russian)* 80−64782
$Ne^+ + N_2$, charge exchange, time-resolved emission probe 78−86946
Ni (111), isothermal desorption of CO, UPS study, time-resolved approach 80−39440
$O+H_2O \rightarrow OH+OH$, energy partitioning 80−101009

time resolved spectra continued
O_2, $b^1\Sigma_g^+$ state excitation by 0.75-6 eV electrons 78−86958
$O(^1D)$+haloalkanes, deactivation reactions, absolute rate consts. determ. 79−11783
$OH+NO(NO_2)(O_2)$, $OH(\nu=1)$ relax., time resolved spectra 80−74240
$OH(C^2\Sigma^+)$, prod. by water radiolysis, time-resolved emission, quenching rate consts. 79−10138
$O(^3P)$+tetrafluoroethylene, time-resolved absorpt. spectra, triplet CF_2 formation 77−44472
$O(2^1D_2)+Cl_2$, reaction kinetics, vac. UV at. spectra 77−21365
$O(2^1D_2)+N_2(O_2)(N_2O)(CO_2)(H_2O)$(methane), collisional deactivation meas., 295K, rel. to atmospheric processes 80−16663
$O_2(c^1\Sigma_u^-)$, in Ar(Kr)(Ar-Kr) matrices, multiphonon vibr. relax. time-resolved emission obs. 80−18861
OsO_4, IR laser dissociation isotope separation appl. 77−18993
P, ground state $3p^3(^4S_{3/2})$, time-resolved reson. fluoresc. obs. 79−34333
PH, $(b^1\Sigma^+)$ state, radiative lifetime, time resolved spectra 78−78750
PH+He, collisional deactivation of $PH(b^1\Sigma^+)$, time resolved quenching 79−54948
$PH+N_2(CO)(NO)(H_2)$, collisional deactivation of $PH(b^1\Sigma^+)$, time resolved quenching 79−54948
$POCl_3:Pr^{3+}$, fluoresc. and lifetimes of excited states 80−71466
Pb alloys, time and spatially resolved at. absorpt. anal. 80−40760
Pb, chemiexcitation of ^3P metastable states, during combustion of acetylene and C_2H_2 78−3339
$PrCl_3$, spectral energy transfer 78−19550
PrF_3, spectral energy transfer 78−19550
Rb, anomalous emission in blue wings 77−46517
Rb, radiative lifetime, time resolved laser induced fluorescence 80−37781
$Rb_2UO_2Cl_4$, fluoresc. decay rate of pure and impure cryst. 79−47487
SF_6, collisionless intramol. vibr. relax., time-resolved spectra 78−82777
SF_6, collisionless intramolecular vibr. relax. obs. 79−45706
SF_6, highly excited, time-resolved IR absorpt. obs. 80−9666
SF_6, IR radiation induced mol. excitation and heating effects 77−75142
SF_6, time-resolved IR absorpt. meas. using injection-locked single mode TEA CO_2 laser 80−9665
SF_6+NO+O_3, laser sensitised reaction, time-resolved NO_2* emission obs. 78−20017
SO_2, T_2-relax., rot. transitions, time resolved spectra, microwave pulsed spectrometer study 80−18846
$SO_3^-+BrO_3^-$, fast oxidation in acid medium, laser Raman multichannel spectroscopy 78−27754
$SO_2(^3B_1)$, isolated mol., phosphoresc. decay efficiency 77−75194
$Sb(5^4S_{3/2})+NO(O_2)$, rate consts., time-resolved reson. fluoresc. meas. 78−27732
$Se(4^1D_2)$ atoms, electronically excited, direct obs., quenching by inert gases 78−25461
SF_6, IR-IR double reson. following IR laser excitation, ν_3 mode 79−54872
Si, amorphous, time resolved photoluminesc. near band gap 80−25445
Si, amorphous, time-resolved ODMR and luminesc. 80−25254
Si, excitonic molecules, thermodynamics, luminesc. 80−25442
Si:O,H amorphous, time resolved luminesc. 80−66288
SiC:Al(Ga)(B) (6H) LEDs, fabrication by rotation dipping technique, electrolum. mechanisms 80−50426
4H-SiC:Ga(Al), photoluminesc. spectra 77−66530
SiF, $A^2\Sigma(\nu'=0)$ state, radiative lifetime meas. 77−27110
$Si(3p^2(^1S_0))+He(SiCl_4)(O_2)(N_2O)$, attenuation of reson. radiation, time-resolved kinetic obs. 78−5329
$Sn(4^3P_0)+O_2(Cl_2)(COS)(N_2O)(NO_2)(NO+Ar)$ oxidation reacts., gas phase, kinetics 78−92468
$Tb(OH)_3$, exciton dynamics within an inhomogeneously broadened line, luminesc. spectra 80−50407
$Tb(OH)_3$, sign of energy dispersion of one dimens. excitons, time resolved spectroscopy 77−1377
Ti impurity flux, time resolved, in DITE Tokamak 80−63373
U, Rydberg levels, time-resolved stepwise laser photoionisation obs. 77−27038
UF_6, electronically excited, laser-induced time-resolved emission, self-quenching 78−42114
UF_6, electronically excited, emission quenching by organic mols. 78−42115
UF_6, electronically excited, emission quenching by inorganic mols. 78−42116
UF_6, multiphoton irradiation, spectra and modeling of laser induced emission 80−69160
UO_2^{2+} in aqueous solution, time resolved luminesc. for lifetime, $U_2O_4H^{4+}$ exciplex 79−61417
$W(CO)_6$, electronic spectra following flash photolysis, intracavity laser technique 79−31538
^{186}WO, electronic spectra following flash photolysis, intracavity laser technique, rot. consts. 79−31538
Xe, $^3P_1$ state, reson. fluoresc., Zeeman beats, time-resolved VUV spectra using synchrotron radiation 78−33454
Xe atoms in Ne matrix, radiative and nonradiative lifetimes in excited states 80−69106
Xe, cryst., X-ray and photoluminesc. 79−87480
Xe, fluoresc. lifetimes, time resolved VUV spectra 78−17601
Xe, time resolved spectra, UV and near UV continuums 78−78653
Xe_2, fluoresc. decay of O_u^+ and 1_u states, rad. decay consts. 79−86009
Xe_2, time-resolved excitation using synchrotron radiation *(French)* 77−88483
XeF fragment luminescence, during XeF_2 photodissoc. in solid Xe and Kr 80−3372
Xe_2(−Kr,He), time-resolved excitation spectra, 1500 Å region, fluoresc. lifetime 77−75195
Xe_2*, synchrotron radiation excited, time resolved spectroscopy 80−69092
YAG, transient colour centres caused by UV radiation 77−84744
$Y_3(Al_{1-x}Ga_x)_5O_{12}:Nd^{3+}$, time-resolved site-selection spectroscopy, energy transfer 80−2814
$Yb(6^3P_1)$, Zeeman splitting, high-resolution time-resolved quantum beat spectra 78−58640
Zn, excited states, collisional quenching cross sections and exit channels, fluoresc. quenching obs. 80−18919
ZnS, time resolved ODMR, electron-hole recombination 79−42872
ZnS:Cu,Cl(Br)(I), green luminesc., interimpurity phototransitions investig. *(Russian)* 77−66541

time resolved spectroscopy
see also streak photography
absorption measurements by time-resolved registration of difference between two laser pulses *(German)* 77−87841
acridine orange, fluoresc. decay meas. by high repetition rate gated photon counting 80−86402
anthracene dianions in dimethyl ether, rotational diffusion meas. 80−65262
atomic and molecular lifetimes, distortions of decay curves in delayed coincidence techniques 78−17620
benzene, ns time-resolved emission spectra, collisional processes 77−3490
benzophenone L in dibromodiphenylether, benzophenone triplet state, nanosecond resolved ODMR, freq.-agile techniques appl. 80−34825
biological picosecond relaxation meas., book contrib. 77−64166
biomembrane, apparatus for direct meas. of fluoresc. decay *(French)* 77−5116
biomembrane, apparatus for meas. of fluoresc. polarisation *(French)* 77−9307
Brownian motion, intensity fluctuation spectroscopy applics., review 80−52129
coherent optical transients, atom, mol. and solid spectroscopy using lasers 77−53986
coherent radiation sources for mol. spectroscopy, review 77−3343
coherent transients and optical pulse Fourier transform spectroscopy 78−86974
computers in optical systems conf. San Diego, CA, USA (Aug. 1978) 79−76356
cresyl violet, rot. diffusion, picosec. saturation spectrosc. obs. 80−5634
discharges, selfluminous, schlieren system for time and space resolved photography 80−87471
DODCI+malachite green (DQOCI), electronic energy transfer obs. 80−5633
dye CW mode-locked lasers for ultra-fast spectroscopic studies 79−31960
dye molecules, excited state lifetimes and lasing conditions 77−71983
electron beam produced plasma, fast photography, emission spectroscopy 77−39458
EPR, ns time-resolved, in pulse radiolysis, via spin echo method 80−43075
EPR spectroscopy, stopped flow EPR apparatus for biological appl. 80−36206
excitation spectroscopy, time-resolved photoluminescence emission and lifetime meas., synchrotron radiation use 78−66687
Fabry-Perot spectrometer, pulsed plasma emitted line profile meas. for vel. determ. 79−41869
fast fluorescence decay meas., appl. of curved microchannel plate photomultipliers 78−12743
fluorescence, apparatus for rapid recording of spectra of polymer solns. 79−38637
fluorescence lifetime meas., subnanosec. photon counting system 77−2699
fluorescence lifetime meas. by ps. single photon counting 77−5883
fluorescence spectroscopy using pulsed laser excitation source 80−9051
fluorescence spectroscopy using pulsed lasers 80−57393
fluorimetry, cross-correlation method 79−79331
fluorometric system, nanosec. time-resolved spectrometry with tunable dye laser and pulse-gated photon counter 80−11968
Fourier infrared spectroscopy of transient samples 77−75339
Fourier transform improvements 78−58070
Fourier transform spectrometer, double-pass rapid-scanning, for plasma diagnostics 80−103190
gated optical multichannel analyzer for tune resolved spectroscopy 77−74516
gating, subps, by optical wavefront conjugation 79−46004
glass microballoon, laser irradiated, time resolved spectroscopy of second harmonic emission 79−23457
Hartmann diaphragm device, for time resolution during selective volatilisation, spectroscopic anal. 77−49775
high resolution laser spectroscopy using fast ion beams 78−86975
highly transparent materials, relative dominance of bulk or surface absorption by transient methods 77−52031
instrumental advances in time- and space-resolved spectrometry, optical spectrometer *(Polish)* 80−90906
Intensified Silicon Intensified Target (ISIT) tubes, medium speed gating 78−12766
ion + molecule, elastic collision frequency, determ. by Fourier transform ICR spectroscopy 79−50105
ion cyclotron resonance, improved technique for absolute rate constants determ. 79−8462
IR, passive image dissection technique 77−41705
IR broadband absorption spectral photography of molecules 79−58808
IR photographic technique using freq. upconversion, methyl isocyanide isomerisation obs. 80−57400
IR time-resolved spectral photography, transient broadband absorption spectra 80−18024
iterative Rydberg-Klein-Dunham method calcs. and Weyl theory 80−23576
laser frequency switching technique, visible-UV spectra of ats., mols. and solids 78−86974
laser light source, intensity modulated, 0.01 Hz to 1.2 GHz 79−41400
laser monopulse energy meas. *(Russian)* 79−94272
laser near-reson. scatt. from collisionally perturbed mol. 78−1033
laser saturation molecular spectroscopy in time-delayed mode, appl. to NH_3 78−86976
laser saturation spectroscopy, time-resolved, free induction decay of two-level resonances 80−102775
laser saturation spectroscopy and coherent transients survey 80−9965
laser spectroscopy of primary energy conversion in photosynthesis 79−66461
laser spectroscopy of solutions, ultra-short time techniques *(German)* 78−82049
laser technique for gases, mol. beams and solids 77−79162
laser time resolved spectroscopy 78−303
laser-based methods for transient chem. events meas. 80−40801
laser-generated plasma, time-resolved spectroscopy and microanalysis 77−43015
laser-produced plasmas, time-resolved X-ray spectrosc. 80−84004
line profile recording with high time resolution 78−86351
linear accelerator with S-band subharmonic prebuncher for picosecond single electron pulse *(Japanese)* 80−78460

time resolved spectroscopy continued
liquid, electron spin echo phase memory decay, generalised cumulant expansions appl. 79−11334
low loss dielectric measurements using time domain spectroscopy 80−98983
luminescence investigations, improvement in resolution using phase spectra 79−54199
luminescence measuring setup with GDM 1000 grating double monochromator for semicond. 78−21226
luminescence spectroscopy, VUV time and energy resolved, system using synchrotron radiation excitation 78−65982
metal, laser initiated combustion, time-resolved spectroscopy 78−7207
metal combustion, laser-initiated, time-resolved spectroscopy 77−77765
molecular, astrophys. appls. 80−21913
molecular beam, collisionless, high-resolution laser spectroscopy, energy randomisation, optical phase relax. 79−3501
molecular fluorescence, self-absorpt. correction to decay time and quantum yield 79−68255
molecular fluorescence, subpicosecond singlet lifetimes, using two-photon gating 79−45769
molecular spectroscopy book 80−27052
multichannel time analyzers for luminescence spectroscopy 79−85185
Multipass optical cavities for laser spectroscopy 78−17982
nanosecond, emission, applic. to gas phase collisional processes 77−3490
nanosecond absorption spectroscopy equipment *(German)* 79−9244
nanosecond emission spectroscopy, developments 77−34037
nanosecond time resolved spectroscopy, pulsed tunable dye laser, single photon time correl. 77−61140
NMR pulsed, automatic trigger pulse logic for pulse programmer 80−47084
nuclear spectroscopy techniques in at. and mol. physics, review 78−22055
on-line computer-based system for performing time domain spectroscopy 80−271
optical fibres, subpicosecond response meas. 80−78961
optical picosecond spectroscopy using mode-locked lasers 78−58065
optical spectrometers, instrumental advances and new designs *(Polish)* 80 101847
opto-acoustic spectroscopy, nonradiative yields and rate consts. 78−58052
pentacene dianions in dimethyl ether, rotational diffusion meas. 80−65262
phenol, aq. soln., electron ejection, picosec. obs. 80−87187
phenolate, aq. soln., electron ejection, picosec. obs. 80−87187
phonon spectroscopy, high-energy monoenergetic pulsed source of phonons 77−31733
phosphoroscope, analogue switch type 78−45725
photoacoustic, applications 78−89550
photoacoustic, nonlinear signal, appl. to nsec. time resolution 77−74511
photoacoustic spectroscopy, time-domain, nonradiative lifetime meas. of condensed phases 80−55232
photoexcitation method, nanosecond pulsed laser apparatus 77−49787
photon echoes, ps, detection by optical mixing 78−71155
photon echoes in standing-wave fields: time separation of spatial harmonics 80−9759
picosecond chemistry, review 77−5933
picosecond excited state meas. using tunable laser induced grating 77−10786
picosecond fluorescence spectroscopy using CW laser and radio 77−27200
picosecond interactions in liquids and solids, book contrib. 77−65057
picosecond laser pulses absorpt., coherent coupling effects 79−72443
picosecond laser spectroscopy in physics, chemistry and biology using video systems 79−75615
picosecond laser techniques for obs. of vibr. modes in liqs. 80−5800
picosecond light pulse, meas. techniques *(Japanese)* 80−52291
picosecond light pulse techniques, historical overview of rapid phenomena meas., book contrib. 77−65026
picosecond light pulse techniques and applications, book 77−61137
picosecond luminescence detection using type II phase-matched freq. conversion 77−31024
picosecond mode-locked laser techniques for ultrafast mol. processes 77−75340
picosecond phase shift measurements at 358 MHz using synchrotron radiation 79−44949
picosecond pulse generation, book contrib. 77−61138
picosecond pulse measurement techniques, book contrib. 77−61139
picosecond pulse production, visible and IR, tunable, high-power, nearly bandwidth limited 79−46003
picosecond pulses, tunable, obtained using synchronously mode-locked dye lasers 77−41697
picosecond Raman techniques, vibr. dynamics in liqs. 80−52325
picosecond resonant spectroscopy, using nonlinear cryst. parametric excitation, stroboscopic method *(Russian)* 77−83930
picosecond spectroscopy, appl. to chem. and biological reactions 79−80697
picosecond spectroscopy, full synchronisation of optical multichannel analyser 77−38022
picosecond spectroscopy, methods and appls. 80−42263
picosecond spectroscopy, short time meas., kinetics of fast processes anal. 77−57411
picosecond spectroscopy of biological systems, exptl. system and rhodopsin example 80−56312
picosecond spectroscopy techniques *(Japanese)* 79−71541
picosecond spectroscopy using parametric amplification and generation 77−27320
picosecond time correl. pulse trains for rapid optical sampling of relax. phenomena 78−12771
picosecond time-resolved fluorescence techniques using mode-locked laser system 80−27359
plasma focus X-ray spectra meas. with time resolution 77−43064
polarisation relaxation of materials, meas. using synchronously mode-locked dye lasers 79−44952
polarized nanosecond time-resolved fluorometry 79−31738
polymethin cyanine dyes, vibronic energy relax., picosec. spectrosc. obs. 80−5526
polystyrene, in cyclohexane soln., mol. wt. distrib., photon correl. obs. 79−10239
ps relaxation rate determ. using ns pulses *(Russian)* 78−25582
pulsed channel plate exposure time meas. using N_2 laser 77−30205

time resolved spectroscopy continued
pulsed laser fluorescence spectroscopy for atomic and mol. excited states obs., review, book contrib. 80−9760
pyrene, in alcohol solns., polar fluid electrons optical absorption coeffs., ns laser ionis. obs. 78−84600
pyrimidine, vapour, phosphoresc. 80−83408
quantum beat high-resolution polarisation spectroscopy in transmission, technique 78−58640
Raman, sub-nanosecond, background rejection, fluoresc. enhancement 77−18109
Raman spectra, time-resolved, fluoresc. suppression using gated detect. 77−53984
rapid intramolecular radiationless transitions, decay rate by time resolved reson. Raman spectra 79−76434
rapid scanning Fourier transform time resolved spectroscopy, practical aspects 80−86464
relativistic electrons, focused beam energy determ. by time resolved energy analyser 77−34054
resonance Raman spectroscopy and vidicon Raman spectrography, vibr. spectra on nsec scale 80−37095
resonance scattering methods in atomic spectroscopy 80−53167
rhodopsin, picosecond spectroscopy obs. of primary events 80−56312
sampled photon counting with multilevel discrimination 79−6188
semiconductor, highly excited states, ps spectroscopy 77−48245
semiconductor submillimetric-wave spectroscopy 79−33221
single-photon counting fluorescnece decay-time spectrometer 77−82620
soft X-ray diagnostics, high efficiency CsI and CuI photocathode evaluation 80−57442
solids, time-domain photoacoustic spectroscopy, one-dimens. model 79−89010
spark BRV source, time resolved meas. of far UV output 79−98454
steel, impurity spectral lines, intensity, temp. and conc. effects 80−64774
streak camera, high-sensitivity, design *(Japanese)* 80−52327
streak camera, picosecond jitter 80−73486
streak camera system, picosec. operation 79−44945
streak spectroscopy, in ultrahigh mag. fields *(Japanese)* 80−18021
subnanosecond resolution using N_2 laser 78−17964
subpicosecond pulse spectroscopy advances 77−87842
subpicosecond spectroscopy, high intensity, broad wavelength tunability 79−44950
subpicosecond spectroscopy, tunable probe, spectral dynamics 80−23429
subpicosecond spectroscopy by passively modelocked continuously operated dye lasers 78−58066
surface potential on small fragile specimens, nanosec. time resolved meas. technique 78−12726
synchronized ultra-short pulse generation and streak-camera measurement with CW mode-locked lasers 79−44951
synchrotron radiation, appls. 78−74825
synchrotron radiation, props. and appls., review 79−36830
synchrotron radiation at storage rings 80−31902
synchrotron radiation used for fast fluoresc. obs. 80−62736
TAC-MCA systems, distortion of spectra by measuring process 79−63877
techniques with image detector (OMA 2) 79−75614
tetracene dianions in dimethyl ether, rotational diffusion meas. 80−65262
tetracene-Kr(Xe), intramol. intersystem crossing in supersonic beam, external heavy atom effect 80−14167
three-level coupled Doppler-broadened system, optical time-delayed laser saturation spectroscopy 78−54472
time resolved spectrofluorometry, appl. of synchrotron radiation 78−65978
time-frequency error product 77−173
time-resolved absorption spectra, with picosecond laser *(Japanese)* 80−22451
transient dispersion and absorption, bridge type superhet. microwave spectrometer investig. 80−91551
transient phenomena, multichannel detection of Raman spectra 77−74518
transient system, IR Fourier transform techniques 78−58071
tris(bipyridine)ruthenium(II)dichloride, fluoresc. decay meas. by high repetition rate gated photon counting 80−86402
two-photon Doppler free atomic excitation, optical transients 78−86977
unipolar pulsed LCD discharge, spectrum, time scanning 80−64774
vacuum, DC breakdown, electrode vap. reson. radiation emission 78−14234
velocity distrib. measurements using mass filter and focusing ion detector 80−4819
velocity-changing collisions, study by time resolved saturated absorption 80−82832
vibration relaxation time measurement, by coherent Raman-induced IR fluoresc. 79−7038
X-ray diffraction, time-resolved, using position sensitive counter 77−13831
X-ray diffraction counter and data acquisition system 78−45758
AgBr, cyclotron reson. of polarons at high density excitation 80−75859
AgBr excitonic mols., time-resolved luminesc. line obs. 77−69888
AgBr, highly excited, time resolved luminesc., recomb. of excitonic mols. 77−69889
^{13}C, 2D NMR spectra, off-resonance decoupling 80−74182
Cd, n^1S_0 and n^1D_2 levels lifetimes, time-resolved spectrosc. obs. *(French)* 80−102456
Cs-Xe molecular bands, time-resolved fluoresc., lifetimes 77−58068
^{57}Fe Mossbauer level excitation using synchrotron radiation 80−7204
KI, growth time of π emission in picosecond range 80−76067
Kr_2, prod. and decay of 0_u^+ and 1_u states, synchrotron excited 80−43109
N, $(2^4S_{3/2})$, kinetic study by time resolved atomic resonance fluorescence 80−95557
NH_3, IR-microwave double reson., rot. and vibr. relax., inversion layers 78−86902
^{22}Na, Rydberg states, fine struct. splitting, quantum beat and double reson. spectroscopy 78−86979

time series
adaptive adjustment of channel geometry 77−45027
air pollution appl 78−11982
air pollution level prediction 77−29428
algorithm for processing of observational series, ocean currents appl. *(Russian)* 78−65421
applied mechanics appl. 77−67232

time series continued
autoregressive-moving average models for Wolf sunspot data, new models 79−12442
bound and quasi-bound states in the continuum 77−14329
BWR dynamics, multivariable autoregressive identification 78−94107
BWR stability monitoring using time series anal. of neutron noise 80−47625
caustic junctions, fine structure 77−46683
chromospheric oscillations 79−62799
complete theoretical seismograms generation 77−45179
complete theoretical seismograms generation 77−45180
computation of complete theoretical seismograms for torsional waves 79−12289
conference, Nottingham, England (Mar. 1977) 80−82580
continuous noisy signal analysis by autoregression time-series model 79−3209
dosage population product in Venice, modelling and forecast 79−57546
Earth mean pole position from star pair latitude obs. anal. 80−21892
earth strain observations made with the Cambridge laser strainmeter 77−44895
eigenvector analysis for prediction of time series 77−56757
emergence and imbrication of levels of organization in complex systems *(French)* 77−9163
endocrine research, continuous blood sampling and time series anal. 78−77130
equatorial undercurrent 77−29306
extrapolation using multiparameter discounted least squares 77−17792
Fourier-autoregressive spectral estimation 79−59872
geomagnetic field reversals, correl. function anal. 80−21622
geophysical data, performance spectra estimation *(German)* 77−70852
geophysical sequences correlation 79−62509
geophysical time series alignment, new statistical approach 79−92623
geophysical unit vectors, time series interpolation 79−92625
geophysics, nonstationarity of mean and Hurst phenomenon 78−81253
groundwater, trend of hydrographs 80−85687
Hurst phenomenon in turbulent flows 78−59377
hydrology, Box-Jenkins models and rescaled adjusted range 79−16544
hydrology, fractional Gaussian noise algorithms and rescaled adjusted range 79−16545
hydrology, Hurst phenomenon and rescaled adjusted range appl. 79−16543
insolation stability characterisation by stochastic time series 79−57396
internal gravity wave instability 77−68663
liquid gas phase transitions 77−59092
machined surface time series modelling 80−36998
Markov chain model 78−7698
maximum entropy spectral estimation of frequency and arrival angle 80−96129
missing values in time series and the implications on autocorrelation analysis 79−17197
morphological characterisations of geomagnetic field components 77−91003
morphological properties and origin of the photospheric facular granules 77−78744
near inertial waves, vertical polarisation and energy flux observations 77−45015
nested variance power spectrum 77−87275
nonlinear autoregressive processes 78−24642
North Pacific sea surface temperatures distribution 79−20841
NRM in deep sea sediments, time series anal. 79−29757
nuclear reactor noise analysis, time series modelling methods, comparative eval. *(Japanese)* 80−13552
ocean current spectra interpretation, dynamical hypotheses testing 79−21045
ocean current spectra interpretation, three-dimens. vector time series kinematics 79−21044
ocean current velocities, spectral anal. of vector time series 79−39757
oceanic morphogenesis 77−5217
oceanic thermal response to strong atmospheric forcing 78−92827
parametric time series models for mutlivariate EEG analysis 77−40830
Peru coast currents and sea levels poleward perturbations 79−34841
Pi 2 geomagnetic pulsations, complex demodulation appl. 79−84588
predictability of vertical inhomogeneous atmospheric currents *(Russian)* 79−29809
prospecting, U quantitative determs. from gamma-ray logs, digital time series analysis 79−48580
PWR noise analysis using multivariate autoregressive time series modelling 80−23028
quasi-biennial geomagnetic variation caused by the sun 77−21677
radio-auroral signals maximum-entropy spectral anal. 78−93006
reactor malfunction detection by Dynamic Data System methodology 79−622
respiratory control system, time series cluster anal. 78−56959
rest frame fluctuation spectrums computed in moving frames 77−25795
running means and meteorological cycles 78−65378
sea level, orthotide appl. 78−85565
seismograms simulation 78−40498
shoreline run up spectra, universal form 77−78188
Si II, average phase spectra chromospheric oscillations 79−62801
Si II, average power spectra chromospheric oscillations 79−62800
solar activity cycle during classical antiquity, rel. to auroral cycle 79−92736
solar and geophysical parameters, power spectrum anal. 79−16705
solar cycle dependence of galactic ray flux 77−22026
solar wind speed power spectrum 79−2462
southern hemisphere mid-latitude stratospheric aerosol after the 1974 Fuego eruption 77−5276
space-time filtering of geomagnetic fields 77−49178
spectral analysis program *(Italian)* 77−70841
speech processing, parameter estimation of noisy all-pole process using pole-zero modelling 79−64419
stationarity and normality of EEG data during sleep stages 78−92610
statistical representation of joint roughness 79−48464
statistical structure of surface-wind time series 77−78370
stratosphere global-scale waves with zonal wave number zero 78−61515
sunspots, geomagnetic indices and the weather a cross-spectral analysis between sunspots, geomagnetic activity and global weather data 77−78313
sunspots Wolf numbers, rhythmic struct. amplitude-phase disturbances anal. 79−62806
thermocline velocity profiles 77−17135
time series continued
tidal records analysis 77−87080
upper extremity prosthesis online control based on EMG signal identification using microprocessor hardware 79−2166
upper-limb prostheses multifunctional control microprocessor system, myoelectric signal identification method 78−88766
vector wind meas., principal components anal. 79−39807
weather prediction, normalised variance anal. for meteorological time series, F-distribution *(Chinese)* 80−67388
wind, stochastic predictors, AR and ARMA models 80−67400
wind influence on stratified inlet 77−41050
wind influence on stratified inlet 77−41051
SO_2 concentrations of Venice air, time series anal. 79−57540
time sharing computer systems *see time-sharing systems*
time-sharing systems
mass spectra, continuous scan, low resolution data system 77−18127
multiuser facility, experimental data processing 79−88922
spectrometer for high resolution NMR of fluids, time sharing principles *(German)* 78−16822
^{13}C NMR probe for high resolution Fourier spectroscopy, cw time sharing appl. *(German)* 78−16823
time switches
electrochemical, using solid electrolyte *(Czech)* 77−77779
time varying parameters *see time-varying systems*
time-varying systems
articulation development, possible nonlinear time varying control in feedback path 78−35870
beam dynamic deflection under external force of time-dependent frequency 78−83289
conversion function of meas. facility, optimal value determ. 78−73958
gas stripping column, periodically cycled, feedback control, simulations 79−1231
geophysics, time series filtering with time variant operators, convolution and Fourier transform 77−87082
harmonic oscillator, Lewis invariant generalisation 78−93560
magnetic field problems, finite element formulations 79−41265
process dynamics investigation using time-varying models 77−41099
radiation of uniformly moving charge on nonstationary layer 80−32893
respiratory system, human, modelling and parameter identification 79−39444
signal coherent detection using multiple obs. 80−43553
stability anal. 78−37
two-dimensional nonstationary Euler eqn. solution in time-dependent bounded domain *(Italian)* 78−69986
vibrations of string with time-varying length 79−25870
water resource system, recursive estimation techniques appls. 79−5538
timing *see time measurement*
timing circuits
35 mm camera control cct. for automated time-lapse photography 78−58076
400 MHz SAW timing filter for optical fibre transmission 79−50415
adjustable exposure timer, circuit diagram and operation *(Hungarian)* 80−52169
astronomical laser ranging equipment, timing system *(Japanese)* 78−89077
automatic enlarger timer 79−67406
avalanche transistor discriminator for low energy radiations 80−5450
blind person's rocking motion sensor and recorder 77−52921
calculator, used for measuring time, light digit, four function type 78−175
CAMAC standard 160-MHz decade counter with digital readout 78−9041
camera character-forming display control, using LEDs array 79−9251
camera shutter control, use of photosensor with IC amplifier *(German)* 80−52341
chart recorder, multichannel sequential switcher, for teachers 78−81754
chart recorder timer control, pen overload protection systems, at. absorpt. appl. 77−73481
cinemicroscopic time-lapse unit circuit 79−67405
clock synchronisation circuit, digital clocks, using transmitted time code 79−67257
clock timer using thermal printer for time of day readings 80−42211
CMOS ICM 7216B multifunction counter used for time, frequency or period measurement *(German)* 80−74092
comet telescope, timing system *(Japanese)* 78−89071
constant fraction 100 MHz discriminator using hybrid microcircuit technology 78−33402
constant fraction timing discriminator for channel plate electron multipliers 79−59316
constant slope timing for nuclear semiconductor detectors 79−76305
counter-timer-frequency meter for teaching, evaluation 78−28901
darkroom timer, IC, DIY, photography appl. *(German)* 78−82065
delay line readout for drift chambers 79−3317
digital event timer, liquid crystal display 77−5811
digital IC capacitance meter *(German)* 79−67339
digital interval synthesiser, computer-controlled 78−8386
digital phasemeter with indicator using seven-segment luminescent vacuum lamps, counter scheme 78−4648
digital reaction timer cct., CMOS, LED, human reaction timing appl. 78−53600
digital timer with memory, appl. to dynamics experiments, principles of electronic circuitry 80−67994
digital verification timer for radiation therapy machines 77−21623
direct time to digital convertor with multi-stop facility, appl. to neutron TOF meas. 77−14317
dissector one-electron current pulse timing, delayed self-coincidence method 79−26846
drift chamber electronics for time and pulse height meas. 79−3326
education, mass and charge meas. using electronic time counter *(Japanese)* 78−41127
electron microscopy photographic exposure timer 77−41730
electronic timer for oceanological instruments, ±3 sec/day accuracy 77−49190
enlarger timer cct. without transformer 78−49924
exposure meter, enlarging, digital, using photodiode, for black-and-white photography 79−85190
exposure meter and development timer, used for photographic enlarger 80−101856
Farmer dosimeter type 2502/3, electronic timer for use with, in radiotherapy units 79−25114

timing circuits continued
flash counter and interval recorder 78−88928
frequency measurement, counting and timing circuits, optimum solution with Philips instruments 77−112
gas chromatograph radioactive effluent recycling timer 77−25326
gas flow calibrator fibre-optic timing system 77−31408
general-purpose timer compatible with transistor logic and auxiliary equipment 77−67420
graphite furnace anal., autosampling system, timing circuit for baseline absorbance monitoring 77−73482
gyrowave interaction experiment synchronising, triggering 77−45191
heavy-ion time-of-flight telescope, walk-free fast timing 77−404
illumination timer for hobby photography *(German)* 80−98992
injection diode modulated laser pulse generator and digital control cct. *(Russian)* 80−14372
internal friction in semicond., simple recording system using digital electronic counting timer 79−37260
irradiation timer for shutter of ^{60}Co teletherapy head 77−66836
laboratory timer based on electronic clock module 79−67282
least or greatest interval timer 78−62183
live, dead or clock time meas. in gamma-ray spectrometry 77−34524
logarithmic timer, for photographic dark room applications 78−8457
metronome, accentuated beat, ETI, using 555 timers 78−46864
miniature endplate potential amplitude online meas., programmable calculator conversion 79−84051
monolithic timers form capacitive transducer-to-recorder interfaces 77−87781
multifunctional programming unit for self-contained oceanographic instruments 79−2391
MWPC, drift time meas. electronics 79−3327
oscilloscope double time multiplier *(Rumanian)* 78−86252
photographic enlarger digitial timer, 0.1 second steps of 0.1 minute steps 80−77893
photographic flash sequencer, using thyristor control 80−62749
photographic print timer, using ring of LEDs 80−77899
photography with repeated exposures at varying intervals, filmspeed and illumination control *(Spanish)* 78−8459
programmable timer for pulsed NMR spectrometers 79−40598
pulse discriminator, timing distrib., effect of randomizing time 78−58555
pulsed beam time pickoff system for nanoampere beams 78−13393
pulses for adjustment of subnanosecond walk 79−76306
quadrupole CAMAC universal timer 78−9040
Random-Access Memory-Interval Timer and buffered storage system 79−84066
recovery circuit for fibre optical digital transmission, jitter invariance, timing extraction 79−10397
reference time interval reproduction device 78−77869
solid state laboratory timer for viscosity measurement 79−20690
spark timer circuit 80−67991
student laboratory apparatus three-digit or four-digit counter-timers 77−17743
student laboratory phototransistor timer adaptor for timing systems 78−8
subnanosecond lifetime measurements, system using microchannel plate photomultiplier 78−37520
synchroniser clock circuit, improves signal-to-noise quality of evoked response measurements 78−24155
tape and chart recorder timing waveform generator 79−17415
teaching apparatus, counter-timer cct. 78−28900
time counter design 78−8385
time interval digitiser *(French)* 79−76309
time stretcher with high resolution 77−6642
time to digital convertor in real time, low cost 78−55111
time-to-number convertor, wide-range high-resolution 78−9039
timer, touch controlled, photography appls. *(Spanish)* 80−86478
zero crossing discrimination technique for constant fraction timing 79−76308

tin
see also nuclei with .....
(100) surface, clean and O_2 exposed, slow positron studies, positronium formation 80−93429
acoustic emission generated during rapid heating of single crysts. 77−63659
acoustic wave drag, acousto-elec.-mag. effects *(Russian)* 79−19638
acoustomagnetic effect, temp. depend. acoustomag. effect. temp. depend. *(Russian)* 77−72941
adsorbed on W and Mo (001), struct., FIM obs. 80−103576
adsorption on Ni (100), effects on secondary electron spectra 80−50480
adsorption on P or C contaminated Ni, AES study 80−54521
adsorption on W, field emission, FIM 77−16470
aggregate film, resist., temp. depend. 78−39230
alkali halide: $Ge^{2+}(Sn^{2+})(Pb^{2+})$, T-centres, absorpt. spectra, energy level diagram 77−73157
alkali halide: Sn^{2+}, charge transfer absorpt. band 79−73977
alkali halide:Sn^{2+}, V_c^--centres, vacancy induced splitting of excited states, Sn^{2+} structure 78−51931
alkali halide:Sn, excited states producing polarised type A emission from Sn centres 78−10945
analysis in ^{99m}Tc radiopharmaceutical kits, rapid colour spot test 77−86630
anodic behaviour in neutral phosphate soln. 79−96187
anodically treated in borate buffer, passive film form., Mossbauer meas. 80−39990
anomalous diffusion in GaAs from doped oxides due to dopant depletion effects 77−89461
atom, γ-ray absorption cross-sections, 10-160 MeV 78−90136
atom, elastic scatt. of 145 keV gamma rays 79−13680
atom, excited states, quadrupole moments, Sternheimer shielding factors 78−82630
atom, gas phase reactions with oxidisers, visible chem. laser development 79−948
atom, GTO basis sets, Hartree-Fock-Roothaan calcs. 79−97973
atom, incoherent γ-ray scatt. by K-shell electrons 77−83560
atom, integral Compton scatt. cross sections, of γ-rays from K-shell electrons 78−58643
atom, integral K-shell Compton scattering, cross-section, for 1250 keV photons 78−90128
atom, $K\beta_3/K\beta_1$ and $K\beta_2/K\beta_1$ relative intensities 77−75088

tin continued
atom, K-shell electrons, Compton scatt. of 1.12 MeV gamma-rays 77−68016
atom, K-shell ionis. by electron impact, cross-sections, 300-600 keV 78−29853
atom, K-shell photoelectric cross section 79−22676
atom, $L\alpha_2$ X-ray fluoresc. spectra, natural linewidth meas. 79−85934
atom, $np^2 \rightarrow np(n+1)s$ transition array, relativistic oscill. strengths 79−31465
atom, nuclear K-X-ray satellites, Z=50-83, by α-bombard., 17.5-22.5 MeV 80−42984
atom, oscillator strengths and hyperfine splitting of $5^3D_1{}^0$ and $6^3P_2{}^0$ levels, line absorpt. meas. 80−18818
atom, photoelectric cross section, derived from total absorpt. cross sections 77−10646
atom, photoelectric cross sections for 323 keV gamma rays 77−88432
atom, photon-bound-electron scatt. meas. 77−14394
atom, Rayleigh scattering at 59.34 keV through 60° to 150° 77−83547
atom, reson. Raman X-ray scatt., K-vacancy excited state widths 79−45661
atom, total to K-shell photoelectric cross section ratios, 145 to 662 keV γ-rays 77−54545
atom, XPS and XES, dynamical effects 80−52924
atomic N-shell vacancy state widths, X-ray photoelectron, Auger spectra 77−18875
Auger electron spectra, solid state effects 80−20739
Auger spectra expt., fine structure anal. of clean and oxidised Sn 80−29831
band structure of diamond like crystals, cluster-Bethe lattice model calc. 80−6713
band structure using modified Vejkovic, Slavic pseudopot. form factor 79−56121
beta-ray backscattering variation with target thickness, self-absorpt. coeff., Z depend. 79−78801
binding state of atoms segregated at boundary of Fe and Fe alloys, Mossbauer study 80−7232
bombardment by Ar ions, impact-parameter depend. of K- and L-X-rays 79−76501
brass-Sn couple in souring substances, corrosion 79−87760
bremsstrahlung, β generated, spectral shape depend. on target thickness 78−56545
bulk modulus from local Heine-Abarenkov model potential, for α-Sn 78−42949
cathode, ion generation by O low pressure reactive sputtering *(Japanese)* 80−50494
chemisorption of O_2, AES and EELS study 79−46917
chemisorption of O_2, appl. of electron energy loss struct. in Auger anal. 79−47559
clean and oxidised, electron energy loss spectra at low primary beam energies 79−65963
coadsorbed with Pb on Al (100) surface, prep. and props. of monolayers 79−15018
coadsorption on Pb, P, or O contaminated Ni surface, AES study 80−88437
coating on Cu, fine struct. in diffusion zone and mech. props. 77−11739
coatings on Fe particles, in mag. liqs., effects on long term stability 77−29051
coatings on steel, Ni, Cu, polypropylene and ABS, autocatalytic deposition 80−100965
cold-rolling roll-force model 77−4788
complex with vacancy in Si, electron state calcs. 78−67980
concentration in a.c. arc, during interruption, time depend. *(Russian)* 78−22597
conduction-electron elec. field gradient, probe valence effects 78−47749
configuration of ^{57}Fe, Mossbauer effect measurements 78−47333
contact charge density, press. depend., trends for Ag-Te 78−39077
core level binding energies 80−71564
covalency of bonding, (202) almost forbidden reflection meas. for β-Sn 79−94953
crystallisation, mechanism of influence of soluble impurities 78−71692
CVD, onto GaAs surface, anal. of conditions 79−87584
DC reactive sputtering, glow discharge mass spectrometry and X-ray diffr. 79−38701
de Haas-von Alphen oscillations, torque snap effect 77−35850
determination, in beef extract, by NAA 78−27856
determination, in complex alloy, by at. absorpt. 77−40582
determination in rocks by thermal neutron activation anal. 77−44552
dielectric band structure calc. in α-phase 79−47034
diffusion along grain boundaries of Fe-Mn (3 wt.%), micro-Auger spectroscopy 77−11740
diffusion in β-Ti, isotope effect 77−76617
diffusion in bottom surface of float glass, synthesis 80−79993
diffusion in CdTe and intrinsic defects role 79−33116
diffusion in Cu via surface segregation 77−7905
diffusion in Fe-C, microprobe anal. of intermediate phases *(French)* 80−50596
diffusion in GaAs, effect of ambient As vapour press. on surface stability 80−2208
diffusion in liq. Sn and Pb, ^{113,117m,125}Sn diffusion coeff. meas. *(Ukrainian)* 80−10690
diffusion in liq. TlSe, Tl_2Se and Tl_2Se_3 *(Russian)* 77−28030
diffusion in liquid Cu *(Japanese)* 78−10204
diffusion in Pb, press. effect up to 30 kbar 78−10224
diffusion of ^{113}Sn in Cu 79−77828
discontinuous film, thermal hysteresis of phase transitions and mechanism of crystallisation 77−89679
dislocation superconductivity above crit. temp., diamag. moment meas. *(Russian)* 79−4619
dissociative diffusion of ^{57}Fe in β-Sn, Mossbauer expts., 90-462K 79−7714
distribution equilibrium between FeO-Fe_2O_3-SiO_2-Al_2O_3-CuO/Cu slag/metal system 78−44111
distribution function branch imbalance, relaxation in double tunnel junction 79−33401
Doppler effect meas. on solid and liquid metal 80−22933
droplets, on Bi, Zn and Al, heterogeneous nucleation 80−44294
Einstein force constants, harmonic and cubic, calc. 77−47515
electric field gradient, Debye model calc. 80−49682
electric field gradient, magnitude and sign 77−80755
electric field gradient and lattice location in Te, TDPAC and Mossbauer effect meas. 78−52395

tin continued
electric field gradient on Cd, press. depend., TDPAC expts. 78−48092
electric field gradients of recoil-implanted ^{19}F via $^{9}Be(^{12}C, np)^{19}F$ 77−8471
electrical resistivity and anisotropy coeff. at press. up to 80 kbar 77−43554
electrical resistivity anisotropy, single cryst. impurity effects 78−79975
electrochemical reactions in aqueous electrolytic solutions, review 77−86337
electrode, potentiostatic polarisation in NaOH soln., XPS 77−90608
electroless tinning onto Cu powder 80−25607
electromigration in Cu 80−6557
electron density at nucleus, press. depend., Hartree SCF calcs., Mossbauer shift press. depend. 78−56411
electron drag by sound waves obs. *(Russian)* 77−35968
electron stopping power, continuous slowing down approx., range difference for 0.2 to 10 MeV electrons 80−39187
electroplastic effect 79−24589
entropy of fusion, vibr. contrib. 77−47601
equation of state under press. for β-phase 79−33070
extractive metallurgy, developments, review 80−20820
Fermi surface, dilational strain depend., elastic moduli and torque obs. 80−70586
Fermi surface press. depend., surface impedance quantum oscills. in mag. field 77−47717
fibre reinforced Pb-Bi (12 at.%), type II superconductor, flux pinning *(German)* 77−85397
film, anomalous transmittance of metal-insulator interface for thermally radiated phonons *(Russian)* 80−103664
film, effect of rate of deposition on supercond. props. and struct. 80−2954
film, elec. resistivity and temp. coeff. of resistivity 77−63005
film, evaporated on cooled substrate, influence of annealing temp. on elec. resist. and struct. 79−65561
film, excess conductivity above supercond. transition temp. 77−32100
film, inelastic-elastic scatt. ratio of 80 keV electrons use for radiation damage monitoring 77−4127
film, limitation in microwave stimulation of supercond., crit. current meas. *(Russian)* 80−88695
film, melting and crystallisation kinetics, electron microscopy 77−15725
film, metastable supercond. alloys, produced by low temp. ion implantation 80−88670
film, on NaCl, preferential epitaxy induced by electron bombard. or elec. field 80−10824
film, oxidation mechanism, depth selective Mossbauer spectroscopy method 78−35549
film, polycrystalline, optical transitions from d core states 77−85827
film, reactively sputtered, discharge produce evaluation, mass spectrometer obs. 80−6668
film, substrate dependent excess electrical conductivity above superconducting transition temp. 78−84324
film, supercond., acoustic wave absorpt., quasiparticle distrib. 78−10603
film, supercond., energy gap reduction by quasiparticle injection 77−47941
film, superconducting, crit. currents in microwave EM fields, for long film 80−70898
film, superconducting, current-voltage characts. in microwave field 79−69631
film, superconducting fluctuations, transition temp. *(Russian)* 80−65740
film, superconducting transition curve stepped struct. due to microwave radiation *(Russian)* 78−2610
film, thermoelec. power, 3.7-8K 78−39231
film, thermoreflectance meas. 77−28640
film, ultrathin, quench-condensed, two-dimensional elec. cond. 78−39233
film, vac. deposited, influence of ion bombardment during condensation 79−82483
film, vacuum deposited, reflectance spectra, structural rearrangement effects 77−24905
film, vacuum deposited, substrate and substrate temp. effects on struct. 80−107677
film, vapour-deposited on NaCl single cryst., nucleation, growth, microstruct. 78−91561
film at supercond. transition temp. thermal noise fluctuations 78−47907
film epitaxially grown on KCl substrate 79−99441
film on Au, ultrathin, quantum size effect *(French)* 77−20466
film on Fe foil, EM excitation of sound, Mossbauer study *(Russian)* 79−99795
film polycrystn., elec. props., internal size effect rel. to annealing temp. 79−65560
film structure, cross-like, microwave irrad. stimulated superconductivity and Josephson effect 79−60988
fine powders, electrodeposition, effect of cathodic current density on structure 80−16238
foil, irradiated by laser beam, psec optical shutter 78−1350
foil, naturally passivated, ESCA, sputter etching 77−70218
foils, 1-3.5 GeV electron impact, transition X-ray emission, comparison with theory *(Russian)* 80−60704
galvanomagnetic props., temp. depend. meas. in single cryst. 80−96850
gamma-ray attenuation coeff. meas., 1115, 1173, 1332 keV 77−55303
gamma-ray elastic scatt. cross section at 279 keV 79−26421
gamma-ray impact, absolute pair production cross-section meas. 78−43958
gamma-ray scatt., incoherent 80−40179
gapless semiconductor, α-phase, effect of nonlocal pot. on hole energy spectrum in mag. field 78−39017
globular film, interf. and diffr., solar selective props. 79−4860
globular film, solar selective props., effect of dielec. layer addition 79−4861
grey, lattice dynamics, pseudopot. calc. 77−43295
grey, lattice dynamics 77−84865
grey, lattice dynamics 80−107389
grey, lattice energy, strong orthogonality, requirement in calcs. dealing with crysts. by geminal method 78−14307
grey, reson. first and second order Raman scatt. 78−35144
grey, sp. ht. at const. vol., leading anharmonic contribs. 77−89549
heat pipe meas. of corrosion and vapour press. 80−23878
heterodiffusion in n-PbSe 80−34245
hollow cathode, emission obs. from Sn II, I transitions 80−106509
homogeneous supercond., phase stratification in microwave field *(Russian)* 79−82711
impress creep of single crystal, β-phase 79−91743
tin continued
impurities in low alloy steels, effect on neutron irrad. embrittlement 80−85055
impurity in Cr-Mo-V low-alloy steel, effect on high-temp. ductility and crack growth 80−66652
impurity in Mn-Mo steel, effect on mech. props. 80−66596
impurity in Nimonic 105, influence on creep and stress rupture props. 80−66602
infiltrated Ti base composite sintered bearing materials, antifriction props. 80−60981
intercalated in NbS_2, lattice dynamics, hyperfine interactions 79−61273
intermediate state, US attenuation 79−42694
internal conversion coeffs. for inner shells of atomic ions and relativistic ionic potentials 80−68600
internal friction, time-dependent 80−7610
ion, HF calc. for ground and excited states 77−72835
ion bombardment-induced photon emission near melting point 80−100699
ion implanted in semiconductors, Mossbauer spectroscopy exam. of radiation damage 78−2176
ion implanted with Sn, Sb or Te, impurity-defect structs., Mossbauer expts. 80−39129
ion plated soft film, initial wear rate 80−11795
ion polarisation and point defect resistivity in metals 80−103672
ion recombination laser 78−17923
ions XVII to XXIII, relativistic Dirac-Fock-Slater orbital binding energies, one-electron transition energies 79−25778
island film, melting and crystn. kinetics, dark field electron microscopy 79−11026
isomer shift calibration const. of ^{119}Sn 77−28496
isotope separation by radical reaction of dissoc. of $(CH_3)_3SnH$ *(Russian)* 79−59604
J_1J_2 transition from LS, revised assignments for $d^9s^2p^2$, $d^9s^2p^3$ 79−45630
Josephson microbridge, I-V characts. microwave irradiation depend. 80−25051
Josephson tunnel junctions, high frequency losses 78−88083
L-shell fluorescence yield, L_3 subshell yield 80−47936
laser radiation absorption in craters on metal targets 80−97386
lattice dynamical calc. using extended Born-von Karman scheme for α-Sn 78−59889
lattice dynamics of diamond type crysts., Keating's valence force field 78−79687
lattice dynamics of group IV elements with the local Heine-Abarenkov model potential 78−63821
lattice stability, pseudopotential theory and problem of covalent bonding 77−55490
liquid, $^{113,117m,125}Sn$ diffusion coeff. meas. *(Ukrainian)* 80−10690
liquid, atomic self-motions *(Rumanian)* 78−47226
liquid, collective motions, struct. factors calc. 77−76295
liquid, contact angle with Nb and Zr substrates 79−77864
liquid, diffusion and electrotransport of impurities meas. 77−51535
liquid, diffusion coeff. of ^{113}Sn, ^{124}Sb, ^{110}Ag, and ^{195}Au 80−96676
liquid, distribution functions, 232 to 870°C 77−4035
liquid, elec. resist. calc., 232, 450 and 650°C, using calc. and expt. struct. factors *(Russian)* 78−56124
liquid, electrical resistivity and thermoelectric power using t matrix approach 77−31988
liquid, electrodiffusion conc. of impurities 80−54414
liquid, electron component of entropy *(Russian)* 79−23747
liquid, electron energy states calc. *(Russian)* 79−4506
liquid, electron transfer of rare earth impurities *(Russian)* 78−95278
liquid, environment for wear resistance testing of carbon steels and Armco iron *(Russian)* 77−59941
liquid, friction of C steels and Fe, Rebinder effect *(Russian)* 79−29269
liquid, impurity diffusion, shear cell assembly meas *(French)* 80−75375
liquid, interference function temp. depend. from X-ray diffr., elec. resist. calc. 77−47332
liquid, interference functions by double hard sphere model 80−49090
liquid, Lorenz number and thermal cond. meas. 77−51716
liquid, multiple scatt. calcs. of resist. 78−76039
liquid, optical props., 0.62-3.7 eV 80−75996
liquid, optical props. by spectroscopic ellipsometry, review 80−103929
liquid, pair interaction pot., struct. factor calcs. 77−51298
liquid, pure, surface tension meas. *(German)* 77−35799
liquid, quadrupole relax. of ^{114}Sb impurities 77−16215
liquid, second and fourth order moments temp. depend. 77−72545
liquid, small-ang. X-ray scatt., at. microgrouping depend. *(Russian)* 78−14271
liquid, soln. of InP, InAs, vapour phase partial press. 78−34610
liquid, structure factor meas. by X-ray diffr., interaction pot. *(Russian)* 77−7655
liquid, structure factor shoulders and interatomic pot. rel. to electron theory 77−7658
liquid, surface tension temp. depend. 77−4248
liquid, thermal diffusivity and cond., 1000 to 1900°C, flash laser method *(French)* 79−99525
liquid, US vel. and thermophysical props. meas., 500-1000K 78−38778
liquid, US wave velocity *(Japanese)* 79−60438
liquid, viscosity meas. *(Italian)* 79−19137
liquid, wetting of Ge surface rel. to cryst. orientation 78−43211
liquid, wetting of Si surface in H_2+HCl 78−43210
liquid, X-ray diffraction analysis 79−4232
liquid substrate for CVD of Si polycrystal 78−64479
liquid thermotransport of solutes and NFE calc. of electronic heats of transport 77−55376
Lorenz function and horizontal and vertical components of thermal resist. 79−65427
low-temp. specific heat meas. under pressure 78−77915
magnetic breakdown orbits 80−103615
magnetoresistance, anomalous, in high-purity wires 78−47765
melt, structural factors, tetrahedral concs., neutron diffr. study *(German)* 80−19688
melt fragmentation on quenching in n-pentadecane and water 79−15706
melt in contact with Fe, Fe distrib. on thermal cycling *(Russian)* 80−16562
metal: ^{119}Sn, impurity force const. changes from Mossbauer parameters 77−85630
MHD laminar flow, longitudinal dynamic effects determination for Sn *(Rumanian)* 80−64792
microstrip, optically illuminated, resistive transition and supercond. props. 80−54821

tin continued
mixed oxide film formation and meas. 77−77622
model pseudopotential, band struct. calcs., liquid semicond. resistivity calcs. 80−20075
molecular beam, modulated, for plasma diagnostics 77−27735
molten, struct. investig. by neutron diffr. 79−4233
molten, thermal expansion meas. to 1300K 80−65254
molten gas evolution on quenching 78−39818
molten reactor fuel-coolant interaction simulation, water-molten Sn reaction 78−58363
molten rotating stream, vortical filament generation during solidification *(Russian)* 78−88460
monitoring, in ^{113m}I eluates from ^{113}Sn generator 77−5078
monolayer, double layer wih Pb on Al (111), layer growth, struct. 80−70567
monolayer on Ge(111) surface, induced 7×7 superlattice struct. 78−91521
monolayers on W field ion image qualities and work function 78−35272
Mossbauer effect, filtered reson. radiation, time depend. 80−7216
Mossbauer effect anisotropy in β-Sn, quad. splitting 77−12268
Mossbauer isomer shift pseudopot.-Born-Oppenheimer theory development, β-phase 78−2775
Mossbauer spectra, 2nd-order Doppler shift, 1-100K 79−91317
Mossbauer spectra of Sn in $SnSO_4$ anodised Al 78−35582
muonic atom transition energy meas., tests of high-order vac. polarisation corrections 77−71895
muonium atoms, dimensions in α-phase 79−11374
narrow film, critical heat flux in He-II 79−23795
neutron activation analysis in biological samples at nanogram level by ^{121}Sn liq. scintillation counting 78−3693
neutron radiotherapy, 14 MeV, skin-sparing, effect of metal sheets 78−35923
nonequilibrium superconductivity in microwave field 79−42695
nonlinear conductivity of thin films in mixed state *(Russian)* 80−80464
nuclear quadrupole interaction, ^{119}Sn Mossbauer spectra 78−56412
nuclear spin-lattice relax. time meas. using SQUID magnetometer, appl. to thermometry 79−63212
nuclear susceptibility thermometry using enriched ^{119}Sn 80−4710
optical surface modes calc. in α-phase 77−59200
oxidation, exam. by ESCA 78−72920
oxidation kinetics, in high-temp. fast flow reactor, chemiluminesc. titration meas. 77−48623
oxidised surface, bonding of cadmium arachidate monolayers, XPS 79−15011
passivation films, on Sn-plate, TEM struct. obs. 80−45416
passive film formation in borate buffer polarisation curves, from Mossbauer studies 79−61778
penetration depth in float glass 77−76614
phonon dispersion relation, adiabatic bond charge model 77−69057
photoelectric cross sections, from total absorption cross sections, 5 to 130 keV 79−26947
photoelectric cross sections of low energy photons 78−46309
photoelectric cross-section at K-edge measurements 78−2983
photoelectric interaction around the K edge 78−5183
photoionisation cross section of d-core level synchrotron radiation study of spin-orbit branching ratio 79−74057
pitting corrosion in aq. solns., influence of Cl^-, ClO_4^-, SO_4^{2-}, and NO_3^- *(French)* 80−89389
pitting corrosion in aqn. soln. 79−52426
planar diffusion in GaAs, for planar junction fabrication 79−69289
plastic deformation, 1.6-300K, single crystal *(Russian)* 78−3179
plate, electron reemission Mossbauer spectra 79−19820
plate, lacquer adhesions of passivation films, adhesion, ESCA exam. of constitution and effects 80−40776
plate, passivated by cathodic dichromate treatment, nature of Cr 77−56139
plate, quality evaluation method using elasticity characts. 77−52582
plate, rapid test for props. assessment 80−40650
plate surface, ion-bombardment conditions effect on chem. profile 80−54287
polycrystalline films, elec. props. and crystallite size, 4.2K to room temp. *(Russian)* 80−93011
polymorphic transformation, β→α, mechanism of growth of cubic modification nuclei *(Russian)* 77−44239
polymorphic transformations (β→α), effect of impurities, exam. 80−7557
polymorphism, α→β transform., α-Sn nucleation and growth in β-Sn 78−38838
positron annihilation, Fermi momentum and core electron contribution 77−81173
positron annihilation in fine particles, surface trapped states 80−84800
positron annihilation parameters, temp. depend. 77−85832
positron annihilation rates, electron-electron and electron-positron correl. effects 78−76548
powder, incorporated into lacquers applied to tinplate containers 78−80671
powder production, interaction between N_2 jet and liq. Sn stream 79−43170
powders, fine, electrodeposition from choride-fluoride electrolytes 80−11598
power law creep, exam. of whether creep is diffusion controlled 78−52890
precursor adsorption of O_2, activation energy for chemisorption 78−71950
quadrupole coupling consts., search for isotopic mass effect, ^{69}Ge TDPAD expts. 78−43725
quadrupole interaction of ^{69}Ge, TDPAD expts. 78−48089
quench-condensed films, superconducting transition temp., elastic stress and strain effects 80−70883
radiation-induced migration in Si, Mossbauer obs. 77−15462
rare earth orthochromite, Sn^{4+}-doped, indirect Sn^{4+}-O_2^--Cr^{3+} interactions 77−11887
rare earth orthoferrite, Sn^{4+}-doped, indirect Sn^{4+}-O^{2-}-Fe^{3+} interactions 77−11887
recrystallisation textures, and deformation formed by dry sliding against steel 79−91698
ribbon, penetration depth of nonequilibrium elec. field, temp. depend. *(Russian)* 78−23202
rock samples, Sn determ. by neutron activation method 78−85258
saturated vapour pressure measurement by line absorpt. method in atomic absorpt. spectroscopy of SnI 80−55747

tin continued
segregation on Cu (111) and (100) surfaces 78−14554
segregation to Fe surface, AES obs. 77−20172
semiconducting α-phase, sound propag. RPA calc. 77−31721
slip band theory, model for creep based on dislocation climb at grain boundaries, comparison with expt. data 79−37756
small particles, electron level quantisation effects, Knight shift meas. of electron spin susceptibility 78−2624
β-Sn_n, cryst., fatigue crack propag. mechanism 80−25861
β-Sn, Fermi surface, electronic momentum densities, positron annihilation obs. 80−6696
solar abundance from Sn I line intensity profiles 78−20772
solubility and amphoteric behaviour in CdTe 79−33008
solubility in In_2O_3 cryst. grown from Sn-In melt 77−11697
solvent, LPE growth of GaP-GaS and Ga(AsP)-GaAs 78−88434
sound absorption giant resonance, produced by coherent mag. breakthrough *(Russian)* 80−6700
sound attenuation and velocity depend. on mag. field *(Russian)* 80−29446
specific heat, low temp., meas. under press. 78−81979
sputtered film, exam. of frictional props. 79−15814
steel, X-ray fluorescence thickness meas. for Zn and Sn coatings 77−55884
stopping power for 6.75 MeV protons 80−34107
supercond. crit. RF mag. field, rel. to superheating 78−2632
supercond. film, resistance, effective medium approach 78−60249
supercond. film, thermal processes *(Russian)* 77−55639
superconducting, bulk, ballistic propag. of near-gap phonons 77−85384
superconducting, EM detection and generation of US shear waves, theory and expt. 77−19468
superconducting, intermediate state, thermoelec. effects 79−65620
superconducting, mag. hysteresis meas. *(French)* 77−4463
superconducting, quasiparticle recomb. time and normal electronic density of states at Fermi surface from tunnel junction expts. 79−24108
superconducting, tunnelling-coupled fine particles, fluctuations of Josephson current 77−63031
superconducting, type I, temp. depend. of energy dissipation 78−76198
superconducting and normal phases, damping of dislocations and supercond. attenuation 78−52155
superconducting bridge microwave impedance anomalies 79−7942
superconducting crit. temp., functional derivative with electronic density of states, Eliashberg eqns. 79−56368
superconducting critical temp., shell model for clad particles *(Chinese)* 79−69623
superconducting current carrying film, resistive region boundary movement, ambient media depend. 80−44763
superconducting cylindrical and plane films, crit. current transverse distrib. 77−43795
superconducting film, A1-type, critical mag. field 78−31023
superconducting film, acoustic coupling and effective quasiparticle lifetime 77−20499
superconducting film, charge imbalance generation by supercurrent 79−95548
superconducting film, crit. current hysteresis prod. by electron overheating 79−56449
superconducting film, crit. mag. fields, temp. depend., penetration depth thickness depend. 80−70908
superconducting film, electron mean free path depend. of crit. currents and pair-breaking limit 77−20504
superconducting film, energy gap suppression and instability under strong quasiparticle injection 80−7042
superconducting film, intrinsic and expt. quasiparticle recomb. times 77−15999
superconducting film, long, order parameter relax. during flow of crit. current 77−59364
superconducting film, metastable current states, mean free path variation *(Russian)* 80−2538
superconducting film, paraconductivity 80−54845
superconducting film, phonon-injection-induced destruction of supercond. 80−6956
superconducting film, radiation induced critical temp. 79−87179
superconducting film bridge, obs. of operating conditions and shunting effects in small size supercond. 77−16005
superconducting fine particles, sp. ht., fluctuations, under mag. field, crit. field and transition temp. 77−80873
superconducting fine particles, specific heat exam., fluctuations in zero mag. field 77−28295
superconducting loops, thermally generated mag. flux 79−56452
superconducting microbridge, nonequilbrium enhanced supercurrents 78−43526
superconducting microbridges, non-equilibrium phenomena 79−56410
superconducting paramagnetic effect, threshold current *(Russian)* 79−87194
superconducting parameters, stress depend. 77−12045
superconducting small particles, Josephson-coupled, local fluctuation effects 78−72308
superconducting strips, nonequilibrium resistive state, penetration depth meas. 79−56377
superconducting thin film, crit. temp. enhancement *(Russian)* 80−93021
superconducting thin film, HF pair-breaking current *(Russian)* 77−32130
superconducting thin films covered by Ge, effect on excess elec. cond. 80−65741
superconducting thin-film bridge, IV curves, oscill. instability and quasiparticle recomb. *(Russian)* 80−44769
superconducting transition, chem. potential change 77−28301
superconducting transition, effect of AC EM field *(Russia)* 77−8232
superconducting tunnel junction, quasiparticle recomb. times and electronic density of states at Fermi level 79−56414
superconducting variable thickness microbridge, microwave response 79−82717
superconducting whiskers, current carrying 78−72304
superconducting whiskers, current induced phase transition 78−10600
superconducting whiskers, current-carrying, mutual influence of voltage steps in V-I characts. 78−10601
superconducting whiskers, HF radiation effects on current-voltage characts. 79−65619
superconducting-normal interface, boundary resist. 80−50006
superconductivity, stimulation and enhancement by external micropower irradiation *(Russian)* 78−95394

tin continued
superconductivity destruction by current in hollow cylindrical sample *(Russian)* 79−78278
superconductor, bulk non-equilib. quasiparticles probed by ballistic phonons 79−56391
superconductor, destruction in high amplitude LF varying field *(Russian)* 78−26999
superconductor, intermediate state structure, single and poly cryst. cylindrical samples *(Russian)* 78−43528
superconductor, paramagnetic effect fine struct., apparent mag. permeability *(Russian)* 79−95550
supercooled melt, dendrite growth *(Russian)* 77−81253
surface, isotope effects in ion-scattering double spectroscopy curves for He^+ 77−59658
surface, superconductivity suppression by microwave radiation *(Russian)* 79−24098
surface coating on W field emitter, stability 77−12500
surface impedance change, reflected RF EM wave interaction *(Russian)* 80−49867
surface melting of extremely fine crystals 77−62622
surface superconducting layer in high amplitude LF EM field *(Russian)* 79−78261
surface tension liquidus temp. to 550°C *(Korean)* 79−90848
target, microwave laser irrad., plasma form., inhibited electron thermal cond., laser intensity threshold Z-depend. 80−48928
tetragonal β-Sn, neutron-irradiated, Frenkel defect spontaneous recomb. volumes 79−60355
thermal conductivity anisotropy, 5 to 70K, chem. admixture depend. 77−85194
thermal diffusivity by pulse method 80−15497
thermally induced vacancies, positron trapping 80−89083
thin film, kinetics of agglomeration effects 77−15708
thin foil, 19.6 keV conversion e^- energy, ang. contrib., Monte Carlo calc. 79−11360
thin layers, EM field penetration, depend. on temp. in mixed and intermediate states 79−65598
ultrathin metallic filaments, appearance of dielec. instability, coexistence with supercond. 80−103784
undercooled, dendrite growth rate 77−90339
UPS electron distrib. curve 78−15282
US attenuation and dislocation damping 79−95086
u.s. surface generation, below 20K 78−2353
vacancy concentration, length and lattice parameter change meas. 79−60352
vacancy formation and activation volume, macroscopic model 80−54221
vacuum deposited metal film, elec. field effect on residual struct. 78−51836
vapour, Raman emission at 285 nm 79−3748
vapour laser, operation by dissoc. of metal complex 77−54702
vapour target for heavy-ion induced X-ray analysis 78−80822
variable thickness bridges on GaAs substrates, props. 79−28464
volume diffusion in Ni, activation energies, expt. and by Le Claire method *(Russian)* 79−99369
whisker, supercond. crit. temp., stress depend. 77−39988
white, anharmonicity in X-ray diffraction intensities 78−71626
white, band masses and deformation pots., OPW pseudopotential model 80−100430
white, configurations, formation and Burgers vector of coupled dislocations stradlling polygon wall 78−26569
white, cyclotron effective masses, US attenuation meas. 77−15753
white, edge dislocation walls with Burgers vector $1/2\langle 111\rangle$ 79−99202
white, elastic stiffness consts. calc. 78−39825
white, Fermi surface, dilational strain depend., OPW calcs. 80−84418
white, Fermi surface, electronic momentum densities, positron annihilation obs. 80−6696
white, film, optical props. between 2-15 eV 78−19584
white, lattice vibrations anharmonicity, X-ray meas. 78−51624
white, nuclear acoustic reson., Knight shift 80−71204
white, single crystal, dislocation movement in pre-yield region, etch hillock technique 79−60371
white, single crystal, dislocation walls consisting of double arrays 79−46664
white, US quantum oscillations exam. at 0.1K 78−47694
white crystals, dislocation reactions 79−86796
white crystals grown by Bridgman method, dislocation density, cryst. width 79−100045
wire, elastically bent, elec. resist. in mag. field 80−44568
X-ray attenuation, 5-40 MV, rel. sensitivities of materials for half-value-layer meas. 77−45927
X-ray cross sections, L-shell, proton induced, 1 to 3 MeV range 79−1799
X-ray diffraction, forbidden Bragg maxima 78−63638
X-ray diffraction, forbidden Bragg maxima 78−63639
X-ray diffraction, three and four wave, comparison of diamond type crysts. 78−67608
X-ray diffraction study of thermal motion of atoms in β-Sn 80−39243
XPS, electron inelastic MFP from photoionisation cross sections and ang. var. studies 77−66572
XPS, electronic struct. 80−7464
XPS, inelastic mean free path in 700 to 1200 eV range, bulk method 80−20763
XPS, outer core of level linewidths 77−44118
XPS, valence band spectrum, Mg Kα radiation excited, X-ray satellite line removal 77−77343
XPS and $M_{4,5}N_{4,5}N_{4,5}$ Auger spectra 79−61472
Young's modulus and internal friction, 20°C to melting point *(Russian)* 80−89278
Z dependence of thick target β-ray backscattering 80−76118
zero-gap semiconductor, α-phase props. rel. to Γ_8 symmetry 80−6717
zincblende structure group IVA covalent crystals, Murnaghan parameter estimates from Morse pot. 78−95014
SnTe-PbTe-GeTe, alloy semiconductor, phase transition *(Japanese)* 78−91443
Ag-Sn, supercond. proximity-effect bridge, thermal effects 79−78265
Ag-Sn double films, high-speed superconducting bolometer appl. 80−57368
Ag-Sn multilayers, vapour quenched, supercond. transition temp. 80−20346
Ag-Sn proximity effect bridge, crit. current anomaly 78−76194
Ag-Sn proximity effect bridges, long, voltage anomaly 79−51725

tin continued
Ag-Sn proximity effect bridges, nonequilibrium state, hysteresis of crit. current 79−56411
Ag-Sn proximity-effect bridges, crit. current hysteresis under phonon injection 79−87206
Ag-Sn proximity-effect bridges, T* anomaly under phonon injection 80−34566
Ag-Sn proximity-effect bridges, phonon-injection-induced first-order transition obs. 80−39718
Ag-Sn thin film couple, room temp. interactions 80−2220
Al, AES study of Sn diffusion and surface segregation in limit of small conc. 79−82384
Al/(Al_2O_3)-BaSt/Sn struct., internal voltage temp. variation 80−20326
Al/Sn, composite, kinetics of adsorption softening of solid interface *(Russian)* 79−61619
Al/Sn interface, effect of plastic deformation on structure and adhesion strength of interface *(Russian)* 79−28218
Al-Ba stearate-Sn struct., internal voltage, thickness depend. 77−72920
Al-Formvar-Sn coupled films, Ginzburg's excitonic supercond. model 80−97039
Al-formvar-Sn junction, supercond. order parameter fluctuations below T_c 77−66227
Al-Formvar-Sn tunnel junction, mode propag. in dirty type I supercond. 80−15662
$Al_{0.4}Ga_{0.7}As$:Sn, impurity effects on interface morphology of LPE films on corrugated GaAs substrates 78−88435
$Al_xGa_{1-x}As$: Sn, persistent photocond., due to donor-related centres, symmetry 80−15558
$Al_xGa_{1-x}As$:Sn, anneal-induced defects, photoluminesc. obs. 79−61422
$Al_xGa_{1-x}Sb$:Sn, doping of solid solns. during LPE *(Russian)* 77−85087
Ar bubbles injected into Sn, Pb and Cu melts, under laminar flow, charracts. 78−38394
As_2S_3, vitreous, Ag, Cu, Sn and Ge impurities effect on electrophys. props. 77−76826
Au/Sn evaporated film, interdiffusion, X-ray diffr. and ion backscatt. obs. 79−33121
Au/Sn films, evaporated, microstructure and texture, TEM obs. 80−39481
Au-Sn film, evaporated, interdiffusion and phase formation, in situ He ion backscattering meas. 78−22901
Au-Sn layer system, on glass, thin film interdiffusion 77−20134
Bi:Sn, carrier dispersion law, Shubnikov-de Haas meas. 77−20345
Bi:Sn, microhardness anisotropy 80−21079
Bi:Sn,Te, and undoped sample, low-temp. transport meas., electron scatt. 77−24551
Bi:Sn polycrystal elastic constants for US velocity obs. 79−69180
Bi-Sn, superconductive microsegregations, 3.7K resist. drop 79−69646
$Bi_{1-x}Sb_x$:Sn, dispersion law of charge carriers *(Russian)* 79−87114
Bi_2Se_3:Sn, dopant influence on elec. cond. 79−51569
$Bi_{12}SiO_{20}$:Sn, Raman scatt. spectra, impurity effect 80−80795
CaSe: Sn^{2+}, dimer centre, emission and excitation spectra, temperature quenching *(French)* 79−99937
CaSe:Sn^{3+}, EPR study of octahedral Sn^{3+} centres, 4 to 290K *(Russian)* 80−84637
Cd:^{116}Sn, quadrupole interaction, radiation damage effects 78−43752
Cr_2O_3:$^{119}Sn^{4+}$, Mossbauer spectra *(French)* 79−24248
Cu-Sn thin film couples, room temperature interactions 80−96699
Cu+Fe+Sn, nuclear target preparation by evaparation and rolling 80−23224
EuS:Sn^{2+}, Mossbauer spectra, Sn^{2+} transferred hyperfine fields 80−15887
EuTe:Sn^{2+}, Mossbauer spectra, Sn^{2+} transferred hyperfine fields 80−15887
Fe, pure, Sn and Cr diffusion, effect of boundary struct., autoradiography study *(Japanese)* 80−49419
$Fe_3Ge_{1-x}Sn_x$, ^{119}Sn mag. hyperfine interaction, Mossbauer spectra *(Russian)* 79−38420
α-Fe_2O_3:Sn, Mossbauer investig. of mag. hyperfine interactions 77−32306
α-Fe_2O_3:Sn^{4+}, antiferromag. reson. *(Russian)* 80−7175
Fe_3O_4:^{119}Sn, magnetic interactions, Mossbauer spectra 79−15301
Fe_3O_4:Sn, hyperfine field temp. depend., Mossbauer meas. near Verwey transition 77−69749
$Fe(OH)_3$, coprecipitation with Cu, Ag, Au; Ge, Sn, Pb; Mn and Ca 79−70415
Fe_3Pt:Sn Invar alloy, Mossbauer shift temp. depend. 80−100626
n-GaAlAs:Sn LED DH donor-level analysis, DLTS obs. 79−47040
$Ga_{1-x}Al_xAs$:Sn, layer Schottky barrier, deep level spectroscopy 80−49666
GaAs:$^{119}Sn^m$, Mossbauer spectra 80−29667
GaAs:Cr, Sn doped LPE layers, Au film deposition and annealing, Cr redistrib. 80−15312
GaAs:Ge MBE power FETs with Sn surface impurities 80−80374
GaAs:Sn, 1.39 eV luminescence, injection level depend., freq. response and thermal quenching 78−19529
GaAs:Sn, diamagnetism quenching 80−6782
GaAs:Sn, dopant segregation during liq. phase electroepitaxy 80−54384
GaAs:Sn, doping characts. during LPE 79−10866
GaAs:Sn, epitaxial film, influence of impurities on stacking fault energy 80−103371
n-GaAs:Sn, heavily doped, nonalloyed ohmic contact form. by MBE and metallisation 79−7895
GaAs:Sn, implantation, annealing, impurity-defect struct., Mossbauer study 80−54269
GaAs:Sn, influence of growth process in doping profile and mobility profile during LPE 79−70000
GaAs:Sn, ion implanted, laser annealed, high doping levels 80−88181
GaAs:Sn, LPE, growth rate and temp. depend. of impurity incorporation 78−3063
GaAs:Sn, LPE layer growth, impurity effect on terrace form. 79−95288
GaAs:Sn, LPE layers, electronic props., depend. on Sn incorporation 78−87883
GaAs:Sn, MBE layers, photoluminesc. 80−29803
GaAs:Sn, nature and conc. of point defects over conc. range 10^{17} to 6.10^{18} cm^{-3} 79−14802
n-GaAs:Sn, nonalloyed and in situ Ohmic contacts for FETs 79−56307
n-GaAs:Sn, photoluminesc. spectra 79−43031
GaAs:Sn, proton implantation and annealing behaviour *(Chinese)* 80−44224
n-GaAs:Sn, pure and doped, diffusion of Sn, radiotracer profiles 79−23782

tin continued
GaAs:Sn, selective LPE, orientation dependent growth, luminesc. 77−12551
GaAs:Sn, solubility and point defect-dopant interactions 79−90688
GaAs:Sn, surface segregation of Sn during MBE, SIMS and AES 78−72031
GaAs:Sn, Te, luminescence props. 79−52017
n-GaAs:Sn, VPE growth, reactor design 80−2956
GaAs:Sn diode, LPE grown, electron irrad. effect on characts. 80−39667
GaAs:Sn epitaxial layer, electronic props. and epilayer-substrate interface props. 77−89886
n-GaAs:Sn epitaxial layer, free carrier relax. time, transverse magneto-plasma refl. 77−90212
GaAs:Sn films, MBE grown, doping profiles, carrier mobilities, RHEED and AES obs. 79−1447
GaAs:Sn MBE films, elec. characterization 79−91168
GaAs:Sn thermal diffusion from spin-on SnO_2/SiO_2 source 80−96691
GaAs:Sn^+, impurity-defect complex from ^{119}In implantation, Mossbauer study 80−59486
GaAs:Sn^+, ion implanted, laser annealing effect on elec. characts. 79−73195
n-GaAs:Sn-p-GaAs:Ge-p-$Al_xGa_{1-x}As$:Ge heterostructure solar cells, LPE growth techniques 80−66977
$Ga_xIn_{1-x}As_{1-y}P_y$:Sn, epitaxial film, elec. and optical props. 79−11251
GaN-Sn contact, using GaN made by oxidation and subsequent nitridation of GaAs, I-V characts. 77−20436
GaP:Sn, complex impurity-defect, Mossbauer study 80−75898
GaP:Sn, lattice location of implanted atoms, ion backscatt. and ion-induced X-ray obs. 77−84785
GaP:Zn, Sn doped epitaxial layers, Hall const., hole mobility and conc. 80−15143
GaSb:Sn, p-n junction, electroluminesc. and photoluminesc. 80−66306
p-GaSe:Sn, majority carrier drift mobility meas. 80−92895
GaSe:Sn, single crystal, transient photoconductivity *(Russian)* 79−11171
GaTe:Sn, electroabsorption spectra 79−19901
Ga_2Te_3:Sn, impurity atom electron shell compression by matrix *(Russian)* 77−28146
Ge, pseudopotential method of band struct. anal. 78−51886
Ge:^{119m}Sn, impurity lattice dynamics, Mossbauer spectra, Debye temp. 80−84262
Ge:Sn, ion implantation of radioactive ^{119}Sn 80−59495
Ge:Sn, Mossbauer spectra of ^{119}Sn impurity atoms 80−15935
Ge-Sn friction pairs, elec. cond. of Ge tribolayers at He temp. 79−87140
H, and He, stopping powers meas. 80−42904
H^++U(Ni)(Au)(Sn), 4.88 GeV, K-vacancy production cross sections 77−19036
Ho:^{119}Sn, mag. hysteresis of hyperfine field, compensation in mag. field *(Russian)* 77−81039
IN_2O_3:Sn, RF magnetron sputtered film, elec. and optical props. 80−104065
In:Sn, phonon spectrum, electron-phonon interaction *(Russian)* 78−18722
N-InAs, Moss-Burstein effect, S, Sn, Te dopants 78−64389
n-InAs:Sn, heavily doped, cathodoluminescence, doping effect on luminesc. band position and spectral profile 80−45153
InAs:Sn, single crysts., defect formation 80−88606
InGaAsP:Sn, LPE growth, influence of growth-solution dopants on distrib. coeffs. 79−47640
InI:Sn, impurity behaviour during directional crystallisation, partition coeffs. 77−16491
InO_3:Sn transparent conducting films, homeotropic orientation of liquid crystals *(Russian)* 80−108181
In_2O_3:Sn, coating on polyester film, elec. and optical props. 79−99959
In_2O_3:Sn, film, HF sputtered, cond., Hall mobility, oxidation, charge carrier density 78−72287
In_2O_3:Sn, film, optical modulation effects in electroreflectance spectra 78−6800
In_2O_3:Sn, films, activated reactive evaporation technique of prep. 80−80989
In_2O_3:Sn, glass like thin film, electron evaporated, conductive transport *(Chinese)* 80−49960
In_2O_3:Sn, HF sputtered films, temp. depend. studies of the elec. transport props. 78−76170
In_2O_3:Sn, sputtered films for selective transparent films, prep., elec. and opt. props. *(Japanese)* 77−68247
In_2O_3:Sn, transparent conducting films, prep. by $InCl_3$ thermal decomp., transmittance, resistivity 79−33944
In_2O_3:Sn coated Si, temp. depend. of 10.6 μm refl., solar selective absorber appl. 77−58398
In_2O_3:Sn film, CVD and DC sputtered, electro-reflectance meas. 80−11496
In_2O_3:Sn film, electroreflectance effects 79−43055
In_2O_3:Sn film, RF sputtered, effect of O_2 press. during deposition on props. 78−19664
In_2O_3:Sn films, CVD prep. and elec. resist. meas. 79−52120
In_2O_3:Sn films, doping profiles and elec. props., appl. to optoelectronic devices 79−38203
In_2O_3:Sn films, elec. and optical props., solar energy conversion appl. 79−65945
In_2O_3:Sn films, prep. at low deposition temps. by ion-beam sputtering, elec. and optical props. 79−66004
In_2O_3:Sn films, prod. by ion plating, elec. and optical props. 80−2488
In_2O_3:Sn films, pure and doped, prod. by ion plating, elec. and optical props. 80−2488
In_2O_3:Sn films, RF reactive sputtered, optical props. rel. to band struct. 79−91515
In_2O_3:Sn films; vac. deposited, elec. props. 80−100542
In_2O_3:Sn solar collector selective coating resistivity obs. 79−62034
In_2O_3:Sn transparent cond. films, hydrolysis deposition, elec. and optical props. 79−43144
In_2O_3:Sn/n-Si heterojunction solar cell, fabrication and characts. 78−15314
In_2O_3:Sn-Si heterojunctions, current mechanisms and barrier height 80−11083
In_2O_3:Sn-Si solar cell, characterisation *(French)* 79−39306
InP:Sn, LPE growth from Sn soln., elec. props., 80 to 300K 79−11250
InP:Sn film, mol. beam epitaxial growth 77−16505
InP:Sn layers, VPE, growth kinetics 79−87569
InSb:Sn, equilibrium distribution coefficient of Sn 79−10872

tin continued
KCl:Sn, thermoluminesc. and luminesc. decay 79−83041
KCl:Sn^{2+}, EPR exam. of struct. and prod. of $Sn^-(5p^3,4S)$ defects 79−61215
KCl:Sn^{2+}, thermally stimulated space charge decay 78−48111
KCl:$SnCl_2$, electronic struct. of Sn^+ centres, model 77−43530
KI:Sn^+, magnetic circular dichroism of A- and B-absorption band region 77−12412
KI:Sn^{2+}, luminesc. 79−33817
KI:Sn^{2+}, red emission, mag. field effect on radiative decay time 79−33818
KI:Sn^{2+} luminesc. decay, excited state symm. and g-value 79−99922
$LaFe_{1-x}D_xO_3$:Sn, D=Al, Ga or Sc, Mossbauer effect, hyperfine mag. fields at Sn 77−24772
LiO_2-Al_2O_3-SiO_2-TiO_2:Sn^{3+}, ESR and X-ray phase anal. 79−99752
α-Sn, local field, microscopic electronic polarisation 80−25283
MgO:Sn, exciton, electron hole energy transfer 78−10998
MgO:Sn, hole processes in photostimulated luminesc., electron emission, X-ray irrad., ESR relaxation 79−69889
$MnFe_2O_4$:Sn, hyperfine mag. fields at ^{119}Sn and ^{57}Fe nuclei, influence of press. 79−99811
N_2^++Group IV elements and oxides, XPS and UPS prod. determ. 78−73084
NaCl:Sn^{2+}, electrolytically coloured, CESR 77−16174
NaCl:Sn^{2+}, thermally stimulated space charge decay 78−48111
NaCl-NaF:Sn^{2+}, point defects, ionic thermal current and optical meas. 80−6403
$_{28}{}^{58}Ni^{n+}$+$_{25}Mn(_{50}Sn)(_{82}Pb)$, 45, 94, and 138 MeV Ni inner shell vacancy production, impact parameter depend. 79−41130
Pb, effect of O ion irradiation on supercond. 78−52131
Pb, melting studies by temperature wave anal. method 80−15217
Pb-Sn bimetallic loop, supercond., thermoelec. flux effects due to penetration depth changes 77−24636
Pb-Sn Josephson junctions, small area high current density normal resistance, RC times 80−34555
PbTe:In, Shubnikov-de Haas oscillatory effects, quasilocal impurity level 80−92912
RbBr:Ba^{2+},Sn^{2+}, thermal depolarisation meas., relax. processes 78−23389
RbCl:Sn, γ-irrad. crysts., thermolum. and emission, 300 to 560K 79−15539
RbCl:Sn, Sn-centres study, X-ray and coloration effects 78−76500
Se:Sn, vitreous, crystallisation kinetics study by elec. cond. meas. 79−65526
Si:^{119m}Sn, impurity lattice dynamics, Mossbauer spectra, Debye temp. 80−84262
Si:Ge,Sn, role of interelectronic correl. in paramag. props. of impurity-vacancy complex 77−62858
Si:Sn, Mossbauer spectra of ^{119}Sn impurity atoms 80−15935
Si:Sn, Mossbauer study of defects due to ^{119}In implantation 80−80641
Si:Sn, thermal conductivity, Hall mobility depend. on Sn conc., phonon-defect scatt. 80−29232
Si-Sn tunnel structure, differential cond., density of states in heavily doped Si 79−15072
β-SiC_x wetting by fused Ge, Sn and Pb 77−85016
Sn $5p^2(^3P_0)$, kinetic studies of ground state atoms, by resonance line absorpt. 78−85128
α-Sn, compact prep., from β-Sn containing 0.1 at.% Ge 80−55320
α-Sn, dielectric polarisation calcs., microscopic local fields 80−20582
α-Sn, dielectric properties, mean point value calc. 78−87930
β-Sn, elec. field gradient at ^{111}Cd, effects of high press., TDPAC meas. 80−25266
α-Sn, electronic energy bands of diamond-type crysts., appl. of EHT method 78−87907
β-Sn, Fermi surface press. depend., de Haas-van Alphen meas. 79−73422
Sn I, absorption spectra of outermost d-subshell 77−75086
Sn I, absorption spectrum, 1580-2040 Å 77−71770
Sn I, Sn II, Sn III, atomic partition functions 77−26955
Sn I, Sn II, wall-stabilised arc, absolute transition probabilities, 5300-6850 Å 78−9105
Sn II, cool plasma, isolated lines, Stark broadening, semi-empirical impact approx. calcs. 80−59186
Sn II, oscillator strength meas. and trends in group IV homologous ions 80−42991
Sn II, radiative lifetimes, calcs. and beam-foil spectra 77−75223
Sn II homologous ions series, Stark broadening trends 80−105157
α-Sn, ion implanted, defect struct., Mossbauer spectra 80−80214
Sn, K-shell photoionisation, cross section meas. K X-ray-photoelectron coincidence method 79−72285
Sn Mossbauer isomer shifts, book contrib. 79−87359
Sn, powder particle nonequiaxiality effect on size distrib. meas. in pulse conductometeric anal. 80−20833
Sn, Sn^+, transition probabilities and Stark-broadening parameters, shock tube meas. 79−93956
Sn, sputtered film, exam. of frictional props. 79−15814
Sn, supercond. tunnel junction, quasiparticle excitation by α-particles 80−103791
β-Sn, transverse magnetoresist., temp. depend. in mag. field *(Russian)* 80−107765
Sn V, reson. lines, UV spectra 77−46515
Sn VI, $4d^85p$—$4d^85s$ transitions, near IR spectra 78−13449
Sn VI, $4d^9$—$4d^85p$ transitions, UV spectra 77−46515
Sn^-, photodetachment cross-section, crossed beam meas. *(German)* 77−42298
Sn^+, and isoelectronic ions, excited-state energy level k-ordering, l-patterns 77−88406
Sn^{4+}, electron density function, Thomas-Fermi calc. 80−6763
Sn:^{114}Sb, PAC, mag. moment of 8^-, 210 μs state of ^{114}Sn 77−26609
Sn:^{117}In, quadrupole interaction temp. depend. 77−8470
α-Sn:^{119m}Sn, impurity lattice dynamics, Mossbauer spectra, Debye temp. 80−84262
Sn:^{120}Sb, elec. qudrupole interaction, perturbed ang. distrib. method 79−99799
Sn:^{120}Sb (^{115}Te), nuclear alignment temp. depend. 78−41720
Sn:^{67}Ge, elec. quadrupole interaction temp. depend., PAC meas. 79−42877
Sn:^{67}Ge, quadrupole interaction temp. depend. 77−12264
Sn:^{99}Ru, quadrupole interaction temp. depend., PAC method, electric field gradients 77−73105

tin continued
Sn:I, α- and β-phases, isomer shift in Mossbauer spectra of implanted ^{129}I 78−15067
Sn/Au thin film couples, evaporated, TEM study 80−59832
Sn/Au thin film diffusion couples, Kirkendall void form. 80−96698
Sn/CU electroplated bimetallic films, interfacial reaction 80−96765
Sn/Cu interface, thermal conductance at low temps. 80−49436
Sn/Te/electrolyte system, interface processes 77−63923
Sn-Ag ohmic contacts, for InP, thin film epitaxy 79−38159
Sn-α brass interface, heat flux rectification, rectification coefficient 78−76048
Sn-barium stearate-Sn structs., internal voltage work function meas. 79−82684
Sn-Ge, amorphous, junction, current-voltage charact. 80−44725
Sn-GeS-Sn system, Schottky and Poole-Frenkel cond. mechanisms 80−54799
Sn-insulator-Sn, supercond. tunnel junction, phonon emission caused by subharmonic energy gap 79−56437
Sn-KCl granular superconductors, far IR absorpt. 80−84548
Sn-oxide-Sn Josephson tunnel junctions meas. temp. depend. of cos 0 conductance 78−10611
Sn-Pb proximity effect sandwich, mag. field depend. of tunnelling charcts. 77−20501
Sn-Pb supercond. loop, laser irrad. effects 79−56419
Sn-Si heterojunction, RHEED, Mossbauer spectroscopy and I-V charcts. 80−70828
Sn-Sn bridge, variable thickness, DC and AC Josephson effect 78−31016
Sn-Sn bridge, variable thickness, static mag. field effects, Josephson effects 78−31017
Sn-Sn_xO_y-Sn long Josephson tunnel junction, flux flow, crit. conditions 80−80452
Sn-SnO_2-Sn, supercond. tunnel junctions, energy gap suppression by quasiparticle self-injection 78−80102
Sn-SnO_4-Sn junctions, oxide growth, tunnelling charcts. 79−47173
Sn-SnO_x-SN tunnel contacts, spatially inhomogeneous state under strong injection conditions 80−80457
Sn-SnO_x-Sn long Josephson junctions, flux-flow voltage, dynamic vortex motion 79−4620
Sn-SnO_x-Sn tunnelling junctions, fabrication by modified RF plasma oxidation method 80−103787
Sn-SnO-Sn, supercond. junction, tunnel effect under laser irrad. *(Russian)* 77−43788
Sn-SnO-Sn Josephson tunnel junction, temp. depend. of cosϕ conductance, plasma reson. expt. 79−33405
Sn+Ar^{x+}(Cl^{x+}), vacancy sharing between K and L shells in 3dσ mol. orbital 79−22807
Sn+CH_3I(n-C_3H_7I)(CCl_4), crossed beam mol. kinetics, SnI and SnCl recoil vel. spectra 79−1947
Sn+Cl_2(Br_2), reactive scatt., ang. distrib. and time-of-flight spectra 78−64842
Sn+H^+(O^{5+}), L-shell X-ray prod. cross-section determ. 77−6913
Sn+He(C)(N)(O), inner-shell multiple ionisation systematics, X-ray obs. 80−63790
Sn+N_2O, chemiluminesc., high temp. fast flow reactor kinetics obs. 78−88636
Sn+N_2O, oxidation chemiluminesc., quenching kinetics 79−52672
Sn+N_2O→$SnO(a^3\Sigma)$+N_2, chemiluminesc. high temp. fast flow reactor obs. 80−45493
Sn+O_2, crossed mol. beam kinetics, SnO time of flight recoil vel. spectra 78−68883
Sn+O_2(NO_2), chemiluminescence and photon yields 77−29012
Sn_2, in Ar matrix, absorpt., fluoresc. and reson. Raman spectra 80−95640
Sn_2, low-lying states, energy curves, bonding 79−76367
Sn_2, matrix isolation Raman spectrum, overtone bands breadth 78−33515
^{50}Sn, L$\gamma_{2,3}$ X-ray emission spectra, line breadth 78−62760
^{113}Sn, diffusion coeff. in liq. Cu 79−95196
^{113}Sn, diffusion in Cu 80−65301
^{119}Sn conversion electron Mossbauer spectroscopy in β-Sn, $CaSnO_3$ and SnO_2 79−33575
^{119}Sn, hyperfine mag. fields in Cr_{1-x} Mn_xO_2 Mossbauer study 80−71260
^{119}Sn, isotope, fractionation during zone recrystn. 80−2946
^{119}Sn, Mossbauer isomer shift calibration scheme, matrix isolation of atoms and ions, book contrib. 79−85924
^{119}Sn resonance from inert gas matrix, Mossbauer isomer shift calibration 77−46530
^{119}Sn temp. depend. isomer shift, pseudopot. approach 80−84675
^{119}Sn$^{\prime}$, total mass absorpt. coeff. of gamma quanta, chem. binding influence, determ. using Mossbauer effect 80−99467
^{119m}Sn in FCC metals, isotope separator implanted, Mossbauer spectroscopy 79−24240
Sn(4^3P_0)+O_2(Cl_2)(COS)(N_2O)(NO_2)(NO+Ar) oxidation reacts., gas phase, kinetics 78−92468
Sn^+($5s5p^2$)$^4P_{1/2}$ level, lifetime and Lande g-factor *(French)* 80−52938
Tl_2Te_3:Sn, effect of dopant on electrical props., density and viscosity, for solid or liquid states 79−95432
$Y_{3-x}Ca_x[Fe_{2-x}Sn_x]Fe_3O_{12}$, Mossbauer spectra, Sn hyperfine mag. field 80−15893
YIG:Sn, IR absorpt. and MCD 78−19447
YIG:Sn, mag. circular dichroism orientation depend., optical absorpt. 79−99914
ZnS:Sn, melt grown cryst., impurity distrib. and ionicity 77−55298

tin alloys
see also tin compounds
admiralty brass, stress corrosion cracking, aqueous $CuSO_4$ 77−59961
admiralty brass, stress corrosion cracking, in nonammoniacal sulphate solns. 78−27592
Admiralty Metal, transgranular stress corrosion crack propag. 80−89402
alkaline earth-Sn, M_2Sn, occurrence, struct. 78−38663
Babbitt-steel bimetal, exam. of structure of transition layer 79−100293
bearing and frictional material, current state of prod. and development trends review 78−19902
brass leaded, effect of Al, Sn, Fe on solidification, differential thermal analysis exam. *(Russian)* 79−29041
Br.AZhNMts 7-2.5-1.5-9 bronze, Mg-Al, type, fatigue and stress corrosion cracking, welding effects 80−3233

tin alloys continued
bronze, air atomised, densification and pressure requirements during extrusion 77−59713
bronze, Al, electrode strip, short-time sintering 77−1824
bronze, Al, wear on 13% Cr steel in presence of aviation fuel 80−11781
bronze, Al and Ti, sintered frictional material, wear resistance, effect of matrix struct. 77−28911
bronze, anisotropic bend ductility in single phase alloys 78−60726
bronze, Be, elastic elements made from spring alloy bands 79−87678
bronze, BrB2, thin-rolled sheets, thermostress treatment 79−52273
bronze, deformability, quantitative determ. in drawing 79−52229
bronze, diffusion of Ga in V_3Ga layer, grain boundaries *(Russian)* 80−65297
bronze, effect on compression of Nb_3Sn multifilamentary conductors 79−61012
bronze, friction pair with Cu, Armco Fe or C steel, seizure centres on contacting surface *(Russian)* 77−70185
bronze, low-cycle fatigue, NH_3 effect 80−104348
bronze, P type, experimental analysis of junction growth with a junction model 79−47783
bronze, porous, PTFE impregnated, coeff. of friction, temp. effect 78−64737
bronze, powders, electric-pressure sintering onto cylindrical parts in fluidised bed 80−100960
bronze, shell, deposited in vacuum, elastic charcts. meas. by short time static extension *(Russian)* 78−39961
bronze, sintered, mech. props. 77−28839
bronze, sintered, Zr addition effects on struct., hardness, wear resistance *(Russian)* 77−70019
bronze, spherical powder, negative magnetic resistance changes 77−1410
bronze, spheroidal, equivalent sphere diameter calc., Saltykov method 78−31362
bronze, surface pretreatment effect on joint bond strength by cyanoacrylate adhesive Kanokonlit-E *(German)* 79−57202
bronze 905, partially solid, die thermal behaviour in machine casting 78−6917
bronze bearings, TEM exam. of wear debris 77−77595
bronze casting, graphite dispersed, graphite particle size effect on wear *(Japanese)* 79−15804
bronze layered-steel composite, water lubricated bearing mat., manuf. and props. 78−11341
bronze matrix, Be alloying addition effects on supercond. props. of Nb_3Sn monofilament wires 79−87222
bronze P, friction with steel, boundary lubrication conditions, element conc. anal. of films 78−85001
bronze P, friction with steel, lubricant friction boundary behaviour *(German)* 77−86190
bronze P, heavily cold rolled, yield strength enhancement mech. 77−36539
bronze powder, granulated, porosity of starting mat., zinc stearate additive, effects on sintering kinetics 77−63599
bronze powders preparation by electrodeposition 78−20026
bronze-on-steel contact, lubricated, effect of zinc di-n-butyl dithiophosphate on wear 79−20219
bronze-steel, phase composition and struct. of diffusional interlayer in fusion zone, X-ray analysis 78−56821
corrosion resist. depend. on mech. and heat treatments 80−653
dental amalgam, exam. of fracture toughness and critical strain energy release rate 78−48933
dental amalgams, Cu-rich, SEM and energy dispersive X-ray analysis 78−24184
Dilute, Fe-X-Sn, Mossbauer meas. of Sn interaction with solute atoms 80−15856
Dispersalloy, Sn-Hg amalgam, γ_2 precip. suppression and gettering kinetics 80−71651
electrospark machining, bronze, spreading and form. of surface layer, in solid-alloy-liquid-metal systems, kinetics *(Russian)* 78−27668
In-Cd-Sn, supercond. transition temp. and electronic props., Brillouin zone effect 79−56345
intermetallic ternary systems, new supercond./mag. cpds., X-ray powder diffr. data 80−100215
liquid amalgams mixing, excess entropy, vibr. contrib. *(Russian)* 79−51263
mag. props. from Mossbauer effect obs. *(Japanese)* 80−15933
Mossbauer isomer shifts, book contrib. 79−87359
phosphor bronze, beam, cylindrical, flexurally vibrating, Timoshenko's shear coeff. 78−83866
phosphor bronzes, surface Cs^+ impact, 5.5 keV negative secondary ion emission obs., rel. to Cu *(French)* 77−66562
rare earth alloy, RSn_3, ^{111}Cd quadrupole coupling consts. and valence states, PAC meas. 77−48102
rare earth rhodium tin intermetallic cpds., synthesis, supercond. and mag. props. 80−100547
rare earth-Sn-X, X=Rh, Ir, Ru, Co, cryst. growth and cryst.-chem. invest, supercond./mag. ternary cpds. 80−100777
slip band theory, model for creep based on dislocation climb at grain boundaries, comparison with expt. data 79−37756
steel, Ni-Cr, temper embrittlement by Sn 77−86149
steel, Ni-Sn temper embrittled, interaction detect. by Mossbauer spectroscopy 77−86176
steel, rail, toughness, effect of Sn, SEM exam. 80−97569
steel, Sn (1.5 wt.%), specimen fracturing device for ion microprobe analyser, appl. to grain boundary segregation 77−21341
steel-bronze bimetal mech. props., diffusional interlayer effects 79−29169
Wood's alloy, liq. enthalpy effects when solute is added 80−39314
Zircaloy, annealed, neutron irradiated, inhomogeneous deform. behaviour 80−85014
Zircaloy, breakaway mechanism, corrosion kinetics in steam 80−61030
Zircaloy, H absorption, Sn(Fe)(Cr)(Ni) effect 80−49527
zircaloy, nuclear microprobe methods for investigating oxidative corrosion 80−71787
Zircaloy cladding, stress corrosion cracking, inner surface texture effect 80−66695
Zircaloy-2, anodic oxidation kinetics, in 0.05M oxalic acid (aq. and alcoholic) 80−104331
zircaloy-2, plastic deform. generalised constitutive eqns. 80−104219
Zircaloy-2, reactor cladding, delta-wrinkly zone near crack edge obs. 79−3203
Zircaloy-2, tritium diffusion 80−32341
Zircaloy-2, yield pts. obtained by ageing at two stresses 80−81091

tin alloys continued
Zircaloy-4, creep rupture at superimposed non-stationary stress and temp. loading 80−66630
Zircaloy-4, elastic props., O additions effect 80−66565
Zircaloy-4, PWR tubes, ZrO_2 scales formed in steam, microstruct. 77−6524
Zircaloy-4, quenched and annealed, strain ageing 77−25071
Ag-Cu-Sn, effect of additions on eutectic and peritectic temp., of binary alloys 78−84801
Ag-Hg-Sn dental amalgams, non-γ_2 phase, transmission electron metallography 79−74162
Ag-In-Sn, internal oxidation, precipitation behaviour of oxide *(Japanese)* 80−66515
Ag-In-Sn, internal oxidation, solute element and O_2 behaviour *(Japanese)* 80−89479
Ag-Sn, dil., elec. quadrupole interactions on ^{111}Cd probe nuclei, time differential PAC meas. 78−15066
Ag-Sn, dil., electric quadrupole interaction of ^{111}Cd probe nuclei, time depend. PAC 77−16229
Ag-Sn, dil., high perfection single cryst. growth, strain-anneal technique 78−44010
Ag-Sn, dil., temp. depend. of elec. field gradient, impurity mass and conc. effects 78−48085
Ag-Sn, dil. alloys, single crystals, dynamic dislocation behaviour 77−4108
Ag-Sn, HCP ζ-phase, magnetic susceptibility 78−47946
Ag-Sn, liquid alloy, thermoelectric powder and magnetic susceptibility 77−8076
Ag-Sn, liquid alloys, thermodynamic props. *(Japanese)* 80−108396
Ag-Sn, single cryst. elastic consts. 77−1164
Ag-Sn, splat-quenched, X-ray diffr. study 80−81094
Ag-Sn, temp. depend. of elec. field gradient, TDPAC meas. 77−32304
Ag-Sn, UV photoelectron spectroscopy of valence bands 77−24924
Ag-Sn, Zener relaxation, valency and dimensional effects *(Russian)* 78−19802
Ag-Sn (0 to 6 wt.%) exam. of bulk diffusion of ^{113}Sn and ^{110}Ag 78−75864
Ag-Sn (0 to 6%), equilibrium intergranular segregation and diffusion 78−43130
Ag-Sn (6,11 at.%) alloy, splat-quenched, X-ray diffr. study of microstruct. 77−8860
Ag-Sn (6(8.2)(11) wt.%), splat-quenched, X-ray line broadening 80−40397
Ag-Sn alloys and amalgams, electrochem. considerations, corrosion in physiological soln. 80−93760
Ag-Sn alloys containing Au, splat cooled ribbons, electron microscope exam. 78−39987
Ag-Sn system intermetallic formation rate, H_2 adsorption effect 79−90819
Ag-Sn-Au, dental amalgams, effect of small additions of Au, struct. and corrosion study 79−20718
Ag-Sn-Cu-Hg, constitution of quaternary amalgam at 37°C *(German)* 77−81250
Ag-Zn-Te-Sn(-In), internally oxidised, oxide particle size control *(Japanese)* 80−89480
Ag_3Sn, containing Au, etching technique for alloys and amalgams 78−3291
Ag_3Sn-Hg, metallic powder-liquid system, correlation between hardness and evolution and sintering states 80−25614
Al bronze, anisotropic bend ductility in single phase alloys 78−60726
Al bronze, BA 1032, deformation at high temp. *(Polish)* 79−79023
Al bronze, creep forging 77−59848
Al bronze, duplex alloy, corrosion fatigue behaviour 79−70218
Al bronze, elastic limit after repeated transverse deformation *(Russian)* 77−66668
Al bronze, G, Si additions, corrosion resistance 77−16714
Al bronze, O free, annealing in photoemission electron microscope, twin density recrystallised grain size relation *(German)* 78−52850
Al bronze, plasticity of two-phase, coarse microstruct. material *(German)* 77−59882
Al bronze, superplastic low cycle fatigue 78−27632
Al-bronze, input energy, hysteresis, and fracture in low cycle buckling fatigue, superelastic range 78−31527
Al-bronze, single crystal rod, energy dissipation, deformed by cyclic buckling in superelastic range 78−31479
Al-Cu-Sn, ageing process, effect of Sn atoms, ^{119}Sn Mossbauer spectra obs. 80−7598
Al-Cu-Sn (3.4, 0.28 wt.%), Mossbauer anal. of Sn behaviour during ageing 78−31431
Al-Ga(In)(Sn), interpretation of metallic phase diagrams, entropy of mixing 79−42274
Al-Ge-Sn, thermodynamic props. of mixing of binary systems, phase diagram 80−45275
Al-Sn, (<0.28 wt.%) corrosion behaviour in 16% HCl 78−85054
Al-Sn, ab initio calcs. of partial enthalpy and result for enthalpy of mixing 79−43197
Al-Sn, binary metallic melt, deviation from the Kopp law, specific heat *(Russian)* 80−39305
Al-Sn, conc. profiles across solid-liq. interfaces 80−55382
Al-Sn, dil. alloy, vacancy-impurity interaction, exam. by electrical resistivity meas. at 77K *(German)* 78−83846
Al-Sn, discrete eutectic formation mechanism *(Russian)* 77−66634
Al-Sn, liq. alloy, chem. diff. coeff. determ. 77−1249
Al-Sn, liquid, surface tension, size effect *(French)* 80−15341
Al-Sn, liquid alloys, exam. of Si diffusion *(Russian)* 79−28118
Al-Sn, Sn effect on electrochemical behaviour in acetate buffer 78−19927
Al-Sn alloys, heat treatment effect on ^{119}Sn Mossbauer spectrum 80−7228
Al-Sn dil. alloy, cube orientation texture development 79−96040
Al-Sn liquid alloy, surface tension and surface adsorpt. determ. *(French)* 79−69325
Al-Sn liquid alloys, diffusion of Ge, mechanism *(Russian)* 80−15276
Al-Sn liquid alloys, heats of mixing and activities calcs. 79−42264
Al-Sn-U alloy, phase equilib. exam. by metallographic and X-ray anal. 77−21102
Au-Sn, charge-transfer and valence-band behaviour using ^{197}Au Mossbauer and X-ray photoemission spectra 79−60695
Au-Sn, dil., quenched, vacancy cluster form. 77−62546
Au-Sn, elec. resist. in liquid and solid state *(Russian)* 79−51549
Au-Sn, HCP ζ-phase, magnetic susceptibility 78−47946

tin alloys continued
Au-Sn, liq. alloys, ΔG^E of mixing from ht. of melting and sp. ht. of cpds. 77−4920
Au-Sn, zeta and AuSn phases, heats of form. and heat contents 80−60837
Au-Sn (100 ppm Sn), vacancy clusters, quenching and ageing, electron microscopy study 78−76671
Au-Sn alloys, surface comp. by Auger spectroscopy, sputter cleaning 77−59648
Au-Sn evaporated films, comp. and annealing behaviour, 20-400°C 77−76695
Au-Sn liquid alloys, Sn activity *(Japanese)* 78−6901
Au-SnNi-Au ohmic contacts on n-GaAs 78−35319
Au(Ag)(Cu)-Sn liquid, optical reflectivity spectra of virtual bound states 80−89021
AuSn, optical props., 0.5-5 eV 78−39522
AuSn, XPS, electronic struct. 80−7464
$AuSn_2$, core-level binding energy shifts and charge transfer 80−25268
$AuSn_4$-Sn, eutectic struct., faceting and morphological regularity 79−61573
$AuSn_4$-Sn, unidirectionally solidified, X-ray diffr. anal. of crystal struct. 78−91308
$BaNiSn_3$, cryst. struct. rel. to $ThCr_2Si_2$ type *(German)* 78−51470
BaPd Sn_3, prep. and crystal structure *(German)* 80−84138
$BaPtSn_3$, cryst. struct. rel. to $ThCr_2Si_2$ type *(German)* 78−51470
Be bronze, BrB2 grade, heat treatment quality evaluation, using eddy current device 77−90562
Be bronze, electrolytic polishing using cylindrical stationary electrode 78−64783
Be bronze, electropolishing using cylindrical electrode moving forwards 78−64784
Be bronze BrB2, quenched deformed, substruct. and props., effect of prerecrystallisation annealing *(Russian)* 78−60677
Bi:Sn elec. resist., 1.8 to 77K, electron-phonon scatt. mechanism 79−15144
Bi-Pb-Sn, eutectic alloys, struct. instability and absence of superplasticity *(Russian)* 77−8882
Bi-Pb-Sn, molten metallic system, contribution to sign inversion of effective charge *(Czech)* 78−60656
Bi-Sb-Sn, Sn and Sb partition coeffs. during crystallisation 77−48394
Bi-Sn, complex-regular eutectics, structural modification 78−23695
Bi-Sn, dil., superconductivity, resist. obs. 78−64160
Bi-Sn, dilute, electrical cond. and thermal EMF at press. up to 12 kbar 77−47806
Bi-Sn, dilute, oxidation kinetics 80−25914
Bi-Sn, eutectic, contact melting kinetics *(Russian)* 80−70377
Bi-Sn, hydrostatic press. effect on band struct., thermoelec. power meas. 79−69406
Bi-Sn, liq., conc. and temp. depend. nucl. relax. rates meas. 78−19357
Bi-Sn, liq., Hall coeffs. 78−14711
Bi-Sn, maximum diamagnetism rel. to electron density 80−54865
Bi-Sn, thermoelec. props. from 2 to 300K 80−24872
Bi-Sn, thermopower from 50 mK to 25K 80−24880
Bi-Sn melt structure, radial distrib. function of atoms, anal. *(Russian)* 80−14995
$Bi_{88}Sb_{12}$-Sn, current carrier energy spectrum *(Russian)* 78−60139
$CaSn_3$, powdered, de Haas-van Alphen effect 80−59857
$Ca_{31}Sn_{20}$, crystal struct. tetragonal phase 78−14310
(Cd-Bi)-Sn, eutectic alloy, directionally solidified, contact melting kinetics, mass transfer during solidification *(Russian)* 77−52310
Cd-Pb-Bi-Sn system, ternary liq. alloys, thermodynamic props. 78−51701
Cd-Pb-Sn melts, enthalpies of form. *(Russian)* 79−51277
Cd-Sb-Sn ternary system, phase equilib. 80−16266
Cd-Sn, binary metallic melt, deviation from the Kopp law, specific heat *(Russian)* 80−39305
Cd-Sn, eutectic alloys, struct. instability and absence of superplasticity *(Russian)* 77−8882
Cd-Sn, molten, EMF meas. of liquid separation 78−39747
Cd-Sn, spectral determ. of comp. using UHF plasmotron as source 79−52812
Cd-Sn alloy, superconductivity and microstructure 80−107949
Cd-Sn binary system, high press. study 80−93539
Cd-Sn-Bi, appl. of computational techniques for treatment of thermodynamic data, phase diagram calc. 78−10172
Cd-Sn(-Pb) liquid (0.03 to 0.10 at.% Cd), Cd activity coeffs., interaction parameters, EMF depend. on temp. 80−49383
Ce-Sn, liq., elec. resistivity negative temp. coeff., CPA calcs. 79−42515
Ce-Sn, liquid, solubility and thermodynamic props. *(Russian)* 78−19717
$Ce(In, Sn)_3$, heat capacity and elec. resist. 80−71049
$Ce(In, Sn)_3$, mag. susceptibility, temp. depend., intermediate valence 80−65779
$CeIn_{3-x}Sn_x$, conduction electrons role in valency fluctuations 78−47741
$CeIn_{3-x}Sn_x$ mixed valence system, low-temp. susceptibility, paramagnon study 80−97077
$CeIn_{3-x}Sn_x$, scaling behaviour near valence instability, mag. susceptibility and mag. transitions 80−25111
$CeIn_{3-y}Sn_y$, electrical resist. and thermal expansion meas., 1.5-300K 80−34400
$Ce_{1-x}La_xSn_3$ (x=0 to 1), mag. susceptibility and magnetisation, lattice parameters, X-ray and neutron diffr. meas. 80−49675
$CeSn_3$, crystalline elec. field parameters, exchange and Coulomb contrib. 77−20278
$CeSn_3$, field induced form factor, temp. depend. 79−78308
$CeSn_3$, induced magnetic form factor, polarised neutron studies 80−25078
$CeSn_3$, intermediate valence cpd., search for phonon anomalies, inelastic neutron scatt. 80−100317
$CeSn_3$, low temp. mag. behaviour, press. induced valence change 77−63078
$CeSn_3$, mag. susceptibility and magnetisation, lattice parameters, X-ray and neutron diffr. obs. 80−49675
$CeSn_3$, mixed valence cpd., electronic struct. and mag. props. 80−70649
$CeSn_3$, mode softening and elastic consts., acoustic vel. meas. 80−88242
$CeSn_3$, phase diagrams, lattice props., electron hole symmetry 79−91002
$CeSn_3$, polarised neutron study of induced magnetisation 80−34594
$CeSn_3$, valence instabilities 79−78546
Ce_5Sn_3, low temp. modification with tetrogonal struct. 80−1963
Co-Co_2Sn, directionally crystallised eutectic, influence of prolonged annealing on microstructs. and props. *(Russian)* 79−74182

tin alloys continued
β-Co-Mn-Sn Heusler alloy, constitution and magnetic props. *(German)* 79−34009
Co-Mn-Sn liquid alloy, magnetic props. *(German)* 79−87235
Co-Sm-Sn-$Co_{17}Sm_2$ eutectic fibre composite, coercive force 77−40084
Co-Sn, dil., ferromag., temp. anomalies of Sn mag. hyperfine field and thermal expansion 79−33270
Co-Sn, dil., hyperfine field, press. depend., Mossbauer spectra meas. 79−95375
Co-Sn, electroplated, oxide films, XPS/AES expts. 79−15862
Co-Sn system, phase Co_3Sn obtained by splat cooling *(German)* 80−104147
Co-Sn-M, n=Mg, Ca, Sr, Sc, Y, Zn, Cd, In or Th, cryst. growth and cryst.-chem. invest, supercond./mag. ternary cpds. 80−100777
Co_2HfSn, ferromag., hyperfine fields meas. by NMR 77−63315
Co_2MSn-Fe, (M=Ti, Zr, Hf), dil., Heusler alloy, Fe hyperfine fields, Mossbauer obs. 78−68424
$Co_2Mn_xFe_{1-x}Sn$ hyperfine fields of Fe impurities, Mossbauer effect meas. 78−31130
Co_2NbSn, ferromag., hyperfine fields meas. by NMR 77−63315
$Co_{2-x}(Ni,Fe)_xTiSn$, Heusler alloy, positive contribs. to hyperfine fields, magnetisation and NMR meas. 78−43654
$Co_{2-x}Ni_xTiSn$, mag. ordering, ^{119}Sn Mossbauer spectroscopy and magnetisation meas. 78−43753
$Co_2(Ti,Mn)Sn$, Heusler alloy, mag. meas. 79−47261
Co_2TiSn, ferromag., hyperfine fields meas. by NMR 77−63315
Co_2TiSn, Heusler alloy, positive contribs. to hyperfine fields, magnetisation and NMR meas. 78−43654
Co_2ZrSn, ferromag., hyperfine fields meas. by NMR 77−63315
Cr bronze Sn, recrystn. props., hot rolling, annealing, polygonisation *(Russian)* 80−55419
Cs-Sn, disordered, min. metallic cond. 79−95372
Cs-Sn alloy, peritectic reactions, phase diagram *(Russian)* 80−40784
Cu -Sn (0.05 at.%), grain boundary relax., misalignment angle effect *(Russian)* 78−3159
Cu/Sn-Ni/Au tricouples, electrodeposited, interdiffusion obs. 80−84331
Cu-Al-Sn system, coexistence of different and brass like phases 80−89206
Cu-Nb_2Sr, multifilamentary supercond. composites, in situ formed, critical currents 79−65625
Cu-Nb_3Sn, in situ formed multifilamentary composite, supercond. and mech. props. 78−39279
Cu-Nb_3Sn composite wires, powder metallurgically produced, supercond. props. 78−31026
Cu-Nb_3Sn composite wires, powder metallurgy prod., supercond. props. and annealing 79−33428
Cu-Nb_3Sn multifilamentary tapes, in situ formed, crit. current density anisotropy 80−84576
Cu-Nb_3Sn superconducting composite, crit. props., AC hysteretic losses 80−50014
Cu-Nb-Sn, multifilamentary supercond. composite wires, fabrication on laboratory scale and mech. props. 80−29897
Cu-Nb-Sn, phase relations and diffusion layer form. 77−36458
Cu-Nb-Sn composites, cold-powder-metallurgy processed, supercond. critical currents 79−78279
Cu-Nb-Sn dil. alloys containing Nb_3Sn precipitates, superconductivity 78−43507
Cu-Nb-Sn system, phase equilibria and supercond. props. *(Russian)* 80−50589
Cu-Ni-Sn, liq. alloy, calc. and anal. of mixing enthalpies *(German)* 80−44325
Cu-Ni-Sn, liq. alloy, mixing enthalpies determ. using a SETARAM high temp. calorimeter *(German)* 80−44324
Cu-Ni-Sn, thermal decomposition after prior cold work 78−15427
Cu-Ni-Sn (10, 6 wt.%), spinodal decomposition, X-ray and electron diffr. study 80−81063
Cu-Ni-Sn (10, 6 wt.%), temp. depend of yield stress and work hardening 80−21026
Cu-Ni-Sn (15, 8 wt.%), prior deform. effect on spinodal age hardening 80−108465
Cu-Ni-Sn (15, 9 wt.%), age hardening accompanying phase transition 78−64551
Cu-Ni-Sn (4,4 wt.%) resistance spot weld quality evaluation, using stress wave emission technique 78−53066
Cu-Ni-Sn (4-15, 4-8 wt.%), strip strengthened by spinodal decomp., stress relax. in bending 80−7616
Cu-Ni-Sn (9, 2 wt.%), surface comp., Auger electron spectroscopy study, manufacture and storage influence 80−65348
Cu-Ni-Sn (9, 6 wt.%), decomposition, initial stages, TEM study 80−2992
Cu-Ni-Sn spinodal substitute for Be-Cu alloy 80−35217
Cu-Ni-Su alloy, flat spring, mechanical props. in bending, stress relax. test, 23 to 232°C 78−72806
Cu-Sn, amorphous, electron-phonon interaction effect on thermopower 80−29393
α-Cu-Sn, cyclic work hardening frequency effects *(German)* 79−29090
A-Cu-Sn, cyclic work hardening during frequency change fatigue tests *(German)* 79−34068
Cu-Sn, deformed, martensitic transformation *(Russian)* 79−15668
Cu-Sn, diffusive redistrib. during friction *(Russian)* 78−52999
Cu-Sn, dil., optical props. and electronic struct. 78−35164
Cu-Sn, dil., oxide film form. in ammoniacal Cu(II) solns., AES obs. 80−45415
Cu-Sn, effect of Al on friction and wear 78−11348
Cu-Sn, exam. of surface segregation equilibrium and kinetics, by Auger spectroscopy *(Russian)* 79−56981
Cu-Sn, ε and η phases, surface struct. changes due to sputtering 77−73206
Cu-Sn, graphite dispersed, wear, effect of graphite content *(Japanese)* 77−56114
Cu-Sn, graphite fibre reinforced, high speed tribological props. against steel 79−15809
Cu-Sn, mean square strain, use of approx. methods for Fourier series coeffs. for X-ray diffr. lines *(French)* 77−31549
Cu-Sn, microconductors, cast, struct. and physical props. exam 78−44232
Cu-Sn, precipitating phase nuclei, diffuse X-ray scattering intensity determ. *(Russian)* 77−86031
Cu-Sn, self-diffusion of Sn, correl. with other props. *(Russian)* 79−23764

tin alloys continued
Cu-Sn, thermodynamics of Cu and Sn solns. using copper β-alumina solid electrolyte, 800-1100K 80−107502
Cu-Sn, vacuum condensed, reflecting surface absorpt. coeffs. at 10.6 μm 80−95984
Cu-Sn, wear, effect of Mn_5Si_3 content *(Japanese)* 78−35525
Cu-Sn (1 wt.%), stress removal during annealing after hydrostatic extrusion 79−83215
Cu-Sn (10 wt.%), wear, recrystallisation as controlling process, FCC metals 77−56117
Cu-Sn (15 at.%), temp. depend. of elastic consts. above martensitic transition temp., US exam. 78−76695
Cu-Sn (16.5 wt.%) alloy, stress induced martensite from γ phase 79−70066
Cu-Sn (2 wt.%), effect of undercooling on crystal multiplication 78−84866
Cu-Sn (25 wt.%), liq., struct. from thermodynamic and diffr. studies 80−6350
Cu-Sn (25 wt.%), struct. after ultrahigh-speed quenching *(Russian)* 78−80563
Cu-Sn (25 wt.%), struct. changes with ageing *(Russian)* 77−40421
Cu-Sn (4.9 wt.%), role of mech. twinning on stress/strain behaviour 80−85004
Cu-Sn (8 wt.%), supercooled melt, dendrite growth morphology *(Japanese)* 78−11216
Cu-Sn alloy chemical deposition process *(Russian)* 79−47642
Cu-Sn alloy components, photometric determ. *(Russian)* 79−11842
Cu-Sn alloy film, electron transport props. 77−76955
Cu-Sn binary system, wettability and interaction between solids and liqs. *(Japanese)* 80−92760
Cu-Sn film, thermoelec. power, 80-350K 78−68096
Cu-Sn industrial bronzes, Sn diffusion in deform. zone influence on wear resistance, friction *(Russian)* 80−108582
Cu-Sn liquid alloy, surface energy meas. by const. temp. method on solid alumina 78−6208
Cu-Sn liquid alloys, thermodynamic meas. 78−52765
Cu-Sn solid soln. steady state deform. *(Japanese)* 78−19832
Cu-Sn system, long period superlattice obs. and impurity effects 80−103297
Cu-Sn system, thermodynamic study of gaseous molecules of $CuSn_2$ and Cu_2Sn 79−70360
Cu-Sn system intermetallic formation rate, H_2 adsorption effect 79−90819
Cu-Sn warm pressed compact prep. 80−35136
Cu-Sn-Al, deform at high temps. *(Polish)* 80−89284
Cu-Sn-Mg, precipitation, effect of thermomechanical treatment *(Japanese)* 79−4970
Cu-Sn-Nb multifilamentary alloy, high field crit. current density 78−27004
Cu-Sn-Ni, mech. props. after thermomech. treatment 79−79009
Cu-Sn-P (5, 1-5 wt.%), effect of P on friction and wear charact. 80−16494
Cu-Sn-Pb-Fe-graphite, bronze-based, sintered alloy, silica additions effect 77−63807
Cu-Sn-Te system, phase diagram exam. *(French)* 77−21107
Cu-Sn-Ti, wetting of alumina and vitreous C 78−71904
Cu-Sn(-Ag-Se), Ag, Se, and Sn effects, singly and together, on recrystallisation 79−100164
Cu-Sn(-Al), quenched and aged, struct. of phases *(Russian)* 80−49184
Cu-Sn(5 wt.%), electrical resistivity, annealing, cold rolling 77−8070
Cu-Ti melts, wetting of SiC 78−68664
Cu-Zn-Sn (24-34, 1.0 wt.%), cold-worked microstruct., X-ray diffr. obs. 80−3088
Cu-Zn-Sn-Pb (5, 5, 5 wt.%) analysis in glow discharge lamp and in ion microprobe, sputtering processes 77−52730
$Cu_2Mn(Al_{1-x}Sn_x)$, Heusler alloys, thermal effects, saturation magnetisation 77−85499
$Cu_2MnAl_{1-x}Sn_x$, Mossbauer effect study 80−60473
$Cu_2MnIn_{1-x}Sn_x$ alloy, compositional SRO, hyperfine interactions 80−71065
Cu_2MnSn, Heusler alloy, hyperfine field at ^{111}Cd, TDPAC meas. 78−43705
$Cu_{1-x}Ni$, disordered muffin-tin, electron momentum density in average-t-matrix approx. 79−69390
Cu_2NiSn, Heusler alloy, elec. resist., 4.2 to 300K 80−75547
CuSn, amorphous, elec. resistivity temp. depend. comparison to Einstein oscillator model 78−6342
Cu(Sn)/Nb(Al), composite superconductor fabrication and charact. 77−81242
Cu_3Sn, modulated struct. phenomena, survey 79−95033
Cu_3Sn, one-dimens. long period superstructs. with Zn and Ni additions 78−83777
ε-(Cu_3Sn)-Cu diffusion couples, growth of intermediate phase layers *(Japanese)* 80−49431
CuSnMg, crystal struct. anal. 78−91306
Cu_4SnMg, crystal struct. anal. 78−91306
Dy-Sn, hyperfine fields acting on diamag. impurities and anisotropic exchange, Mossbauer spectra 77−1625
$DyRh_{1.1}Sn_{3.6}$, new supercond./mag. cpds., X-ray powder diffr. data 80−100215
$ErRh_{1.1}Sn_{3.6}$, new supercond./mag. cpds., X-ray powder diffr. data 80−100215
$ErRh_{1.1}Sn_{3.6}$, synthesis, supercond. and mag. props. 80−100547
$(Eu,Sn)Mo_6S_8$, ternary superconductor, mag. interactions 79−73613
$EuSn_3$, hyperfine interactions, high press. Mossbauer expts. 78−43714
Fe cast, Mg, austenite isothermal transform., Sn addition effect 79−87611
Fe, cast, Mg, despheroidising effect of Bi, Sn on graphite in alloy 78−56670
Fe, cast-Mg, 78−44149
Fe-As-Sn, Sn additions to Fe-As melts, influence on surface tension and density *(Russian)* 80−15337
Fe-As-Su-Si (Cr)(Mn) melts, As and Sn distrib., Si, Cr, and Mn influence *(Russian)* 80−16274
Fe-Co-Sn, mag. hyperfine field at Sn site, Mossbauer effect meas. 78−60363
Fe-Cr-Ni-Cu-Sn, Cu and Sn effect on Cr and Ni segregation *(German)* 78−72777
Fe-Fe_xSb, directionally crystallised eutectic, influence of prolonged annealing on microstructs. and props. *(Russian)* 79−74182

tin alloys continued
Fe-Ni (3 wt.%), grain boundary segregation of Sn and P embrittling additions, STEM microanal. 78−76654
Fe-Ni (6-8 at.%) 80−75888
Fe-Ni-Al-Co-Cu-Sn alloy YuNDK35T5, Sn addition effects on physicomechanical and magnetic props. and workability *(Russian)* 77−70101
Fe-Pd (1-2 wt.%), solution of ^{119}Sn, study by Mossbauer spectroscopy 80−75888
Fe-Sn, additive effect on eutectoid transformation of Fe 78−52799
Fe-Sn, dil., ferromag., temp. anomalies of Sn mag. hyperfine field and thermal expansion 79−33270
Fe-Sn, dil., mag. hyperfine fields, Curie temp. and Mossbauer meas. 77−63190
Fe-Sn, dil., size effects on mag. hyperfine fields at non-mag. impurities 78−43586
Fe-Sn, dil., spontaneous magnetoresistance anisotropy and deviations from Mattheissen's rule 79−51553
Fe-Sn, dil., XPS meas. 77−63538
Fe-Sn, grain boundary embrittlement by Sn segregation, Mossbauer study 80−7239
Fe-Sn, segregation of Sn, kinetics, theory 80−11649
Fe-Sn, thermodynamic assessment, phase diagram 79−91618
α-Fe-Sn alloy, grain boundary hardening and segregation 80−55417
Fe-Sn compounds, type of binding *(German)* 77−35503
Fe-Sn liquid alloy, conc. depend. of enthalpy of form., conc. depend. *(Russian)* 78−44081
Fe-Sn system, Sn binding state, using segregated ^{119m}Sn, Mossbauer anal. *(Japanese)* 80−20525
$Fe_{1-x}Co_xSn$, transferred hyperfine fields at ^{119}Sn, Mossbauer spectroscopy 79−33582
$Fe_{1-x}Mn_xSn$, spin reorientation, Mossbauer study, 77 to 400K 80−97172
$Fe_{1-x}Mn_xSn$, transferred hyperfine fields at ^{119}Sn, Mossbauer spectroscopy 79−33582
$Fe_{1-x}Ni_xSn$, transferred hyperfine fields at ^{119}Sn, Mossbauer spectroscopy 79−33582
$FeSn_2$, hyperfine mag. fields at ^{57}Fe, ^{119}Sn nuclei, under press. *(Russian)* 78−39486
Fe_3Sn_2, magnetic properties, ^{119}Sn Mossbauer study 79−91323
Fe_3Sn_2, Mossbauer effect and magnetisation meas. 78−31132
Fe_xSn_{1-x}, amorphous, mag. behaviour 78−95478
Fe_xSn_{1-x} amorphous alloy films, magnetisation meas. and Mossbauer spectra 78−95489
Fe_xSn_{1-x}, amorphous alloy stability, comp. and temp. depend. 79−19156
Fe_xSn_{1-x} amorphous alloy, elec. resistivity, Ziman's formula 79−15130
Fe_xSn_{1-x}, amorphous alloy, Mossbauer spectra, charge transfer and atomic vol. effects 80−39959
Fe_xSn_{1-x} amorphous alloy, elec. resist. 80−80246
Fe_xSn_{1-x}, amorphous film, struct. and mag. props. 80−65972
Ga-Cu-Sn solders, exam. of structural transformations due to hardening, heat treatment *(Russian)* 80−7578
Ga-Ge-Sn, thermodynamic props. of mixing of binary systems, phase diagram 80−45275
Ga-In-Sn, thermal analysis, determination of liquidus and reactions 78−88446
Ga-Sn, dil., elec. resist., temp. and impurity depend., deviation from Matthiessen's b-axis crystals 78−51970
Ga-Sn, liquid binary alloys, magnetic susceptibility *(Russian)* 77−24671
Ga-Sn alloys, compressibility, US velocity meas. *(Russian)* 77−59060
GaP-Sn, polythermal cross sections 77−52300
GdAuSn, mag. props. 77−85439
GdCuSn, mag. props. 77−85439
$GdSn_3$, Neel temp., hydrostatic press. depend. 80−29549
Ge-Sn, liq. alloys, thermodyn. props. 77−51518
Ge-Sn barrier Josephson tunnel junctions 78−68114
Ge-Sn barriers, Josephson tunnelling 79−28468
Ge-Sn melts, short-range order, radial atomic distrib. functions 79−86673
Ge-Sn solid solution, cooling rate effect on partition coeff. of Sn between liq. phase and crysts. 77−12510
Ge-Sn-M, M=Cu, As, Sb, formation of Ge-based solid solns. during crystallisation 77−80625
Hg-Ag-Sn, dental amalgams, corrosion penetration in crevices 80−3238
Ho-Sn, dil. alloy, hyperfine interaction of ^{119}Sn, Mossbauer meas. 78−91998
In-Pb-Sn system, thermal anal. 80−35162
In-Sn, binary metallic melt, deviation from the Kopp law, specific heat *(Russian)* 80−39305
In-Sn, dil., intermediate state, doping effect on US attenuation 80−2522
In-Sn, liq., conc. and temp. depend. nucl. relax. rates meas. 78−19357
In-Sn, phase diagram, and superconductivity of In_3Sn 79−38794
In-Sn, phonon spectra and superconductivity, single-particle electron-tunnelling expts. 77−40005
α-In-Sn, stress depend. of supercond. parameters 77−12045
In-Sn (up to 7.9 at.%) whisker, supercond. crit. temp., stress depend. 77−39988
In-Sn alloy, Lifshits transition, electron-phonon interaction 80−29502
In-Sn alloy crystals, phase changes and shape memory effect *(Japanese)* 80−108502
In-Sn film, supercond. transition temp. and crit. currents *(Russian)* 77−55632
In-Sn liquid alloy, 2-butanol vapour adsorption, effect on surface tension and surface comp. 79−14981
In-Sn-Sb, liquid state, structure of eutectic alloy 78−42890
InSb-Sn, metallic soln., quasibinary alloy, association 78−15373
In_3Sn, anisotropy of upper crit. field 80−20360
β-In_3Sn, band struct. and Fermi surface calc. using model pseudopot. 77−28103
β-In_3Sn, crystn., decomp. and superconductivity 79−91579
β-In_3Sn, decomposition, X-ray powder diffr. study 80−89196
In_3Sn, pulsed high field magnetoresist., 77K 79−73493
In_3Sn, tetragonal supercond., lower and upper crit. field, anisotropy and temp. depend. 80−97042
Ir-Sn-M, M=Mg, Ca, Sr, Sc, Y, Zn, Cd, In or Tl, cryst. growth and cryst.-chem. invest, supercond./mag. ternary cpds. 80−100777
$Ir_{1.07}Mn_{1.07}Sn_{0.88}$, ferromag. Heusler alloy, ^{193}Ir and ^{119}Sn hyperfine fields 79−78581
Ir_5Sn_7, cryst. struct. determ. *(German)* 79−27952
(La, Ce)Sn_3, dil. alloys, supercond. and normal state props. 78−76184
(La,Na)Sn alloys, supercond. transition temp. 79−78254

tin alloys continued
(La, Nd)Sn_3, cryst. field effects, normal and supercond. props. 79−60973
(La,Nd)Sn_3, reverse Kondo effect in presence of crystalline elec. field splitting 80−103684
(La, Nd)Sn_3, superconducting props. 79−60958
La-Sm-Sn, dil. alloy, Kondo effect obs., supercond. transition temp. meas. 77−51837
$La_{1-x}Pr_xSn_3$, Kondo effect from excited cryst. field levels, elec. resist. 78−14723
$La_{1-x}Ce_xSn_3$, electrical resist. and thermal expansion meas., 1.5-300K 80−34400
$La(Ce)Sn_{3-x}Pb_x$ system, mag. impurities in supercond., supercond. transition temp. and sp. ht. 78−39244
$La_3Co_2Sn_7$, prep. and crystal structure *(German)* 80−84138
(LaNd)Sn_3, containing Nd impurities, supercond. and normal state props. 80−49967
$LaNi_{4.6}Sn_{0.4}$, H_2 absorption props., desorpt. pressure calc., and decomp. pressures 79−24827
(LaPr)Sn_3, supercond., free energy and thermodynamical crit. field 77−32127
$La_{1-x}Pr_xSn_3$, singlet ground-state system, mag. susceptibility 78−19215
$La_{1-x}Pr_xSn_3$, supercond., 0.6 meV cryst. field transitions, neutron spectroscopy 78−67991
$La_{1-y}Pr_ySn_3$, neutron spectroscopy of 0.6 meV cryst. field transitions 78−30894
$La_{1-x}Sm_xSn_3$, Kondo scatt. from Sm ions 77−51734
$LaSn_3$, dilute alloy containing light rare earth impurities, press. depend. of supercond. transition temp. 79−47184
$LaSn_3$, doped with Tb, Nd, or Pr, crystal field effects, tunnelling within mK range 80−70907
$LaSn_3$, inelastic neutron scatt. 80−11165
$LaSn_3$, mag. susceptibility and magnetisation, lattice parameters, X-ray and neutron diffr. obs. 80−49675
$LaSn_3$, Tb and Pr substituted, superconductors, cryst. field transitions linewidths 80−24854
La_3Sn, cubic phase, high press. and high temp. synthesis, and characterisation 78−19687
La_5Sn_3, low temp. modification with tetrogonal struct. 80−1963
$La_{1-x}Tb_xSn_3$, paramag. anisotropy of Tb^{3+} in cubic cryst. field 80−15687
$La_{1-x}Tb_xSn_3$, supercond., 0.6 meV cryst. field transitions, neutron spectroscopy 78−67991
$La_{1-y}Tb_ySn_3$, neutron spectroscopy of 0.6 meV cryst. field transitions 78−30894
Li-Sn, phase relationships between Li_7Sn_2 and LiSn 79−78933
Mg-Li-Sn system in Mg-rich region *(Russian)* 77−52289
Mg-Li-Sn-Al, investigation in Mg rich region *(Russian)* 78−15364
Mg-Sn, melt, assoc., liquidus curve calcs. *(German)* 79−20352
Mg-Sn (21.4 wt.%), damping capacity 77−48474
Mg-Sn melt, density and free surface energy *(Russian)* 77−66074
Mg_2Sn, L, electron-phonon interaction and phonon cond. at low temp. L n-type semicond. 79−14903
Mg_2Sn, lattice dynamics, angular force model 77−4166
Mg_2Sn, Mossbauer effect exam. under press. up to 75 kbar 79−69759
Mg_2Sn, phase transition under hydrostatic pressure, Mossbauer effect and electric resistance 78−51665
Mg_2Sn, phase transitions under high hydrostatic press., Mossbauer spectra 79−87628
Mg_2Sn, semicond., electronic band struct., reson. Raman scatt. meas. 77−12384
Mg_2Sn, stress effects on Raman spectra 77−20851
Mg_2Sn, third-order elastic constant, low temp. limit of Gruneisen parameter 79−73280
Mg_2Sn, valence band, XPS meas. 77−8018
β-Mn-Fe-Sn, weak itinerant electron antiferromagnetism, Mossbauer spectra meas. 77−36158
Mn-Sn, liq., elec. resist. meas. 77−51721
Mn-Sn, liquid alloys, thermochemistry 79−56962
β-Mn-Sn, Mossbauer and neutron diffr. exam. 77−66253
MnSb-Mn_2Sn alloy system, continuous series of solid solns., homogeneity and ferromagnetic props. 79−52159
$MnSb_{1-x}Sn_x$ films, Faraday rotation, optical absorpt. coeffs. 80−97242
$MnSb_{1-x}Sn_x$, zero-field NMR investig. of domains and domain walls 77−32271
$Mn_{1+x}Sb_{1-x}Sn_x$, magnetisation and Curie temp., prep. and comp. depends. 78−64200
$Mn_{1+x}Sb_{1-x}Sn_x$, nuclear Zeeman effect, Mossbauer meas. 79−28654
$Mn_2Sb_{1-x}Sn_x$, mag. transitions, Mossbauer meas. 78−52406
$Mn_{1.77}Sn$, 170K transitions temp. in ferrimag. state, pressure and γ-irrad. effects 77−51902
Mn_3Sn, triangular spin ordering, weak ferromagnetism 79−47237
Mn_3SnN, perovskite type struct., mag. props., neutron and Mossbauer meas. 77−32159
Mo-Sn-Se system, supercond. crit. temp. and cryst. struct. *(Russian)* 80−107947
Mo_3Sn, thin films with A-15 struct., prep. 78−80478
Na-Sn, disordered, min. metallic cond. 79−95372
Na-Sn liq. alloys, thermodynamic props. by EMF meas. with β-Al_2O_3-Ba_2 electrolytes 79−19379
Nb/Cu-Sn-Mg, superconductor, effect of Mg addition to Cu-Sn matrix 80−25028
Nb-Cu-Sn, cast supercond. alloy, crit. current, degradation resistance 78−76203
Nb-Ge-Sn, A15 cpds. prod. by liq. quenching, phase stability and supercond. props. 79−95538
Nb-Ge-Sn A15 cpds., CVD, superconductivity 79−38222
Nb-Nb_3Sn supercond. point contacts, crit. currents, effect of laser radiation *(Russian)* 79−28484
Nb-PbSn, Josephson tunnel junction, 3rd yr undergrad. expt. 78−54126
Nb-Si-Sn, A15 cpds. prod. by liq. quenching, phase stability and supercond. props. 79−95538
Nb-Sn, A-15 compound formation by ion implantation 78−51572
Nb-Sn, A15 compounds, Hall coeffs. 79−33281
Nb-Sn, depend. of supercond. transition temp. on composition *(Russian)* 78−19173
Nb-Sn, diffusion couple, phase equilibria, effect on T_c and H_{c2} 79−56462
Nb-Sn, reactive diffusion *(Russian)* 77−20133
Nb-Sn, supercond. foils, phase anal. by Mossbauer spectra 78−64305

tin alloys continued
Nb-Sn alloys, stoichiometry and phase equilibria, X-ray diffr. study *(French)* 79−70040
Nb-Sn filamentary composite, supercond. crit. current and temp., as function of reaction conditions 77−28330
Nb-Sn sinter material, for superconducting tubes for magnetic shielding 79−67446
Nb-Sn-C, phase equilib. and supercond. 80−50593
Nb-Sn-Cu, Cu effect on Nb solubility and peritectic transform. temp. in Sn bath *(Czech)* 77−59754
Nb-Sn-Si(As), ternary A15 phase regions, solubility 77−44215
Nb-Sn(Ge), A-15 compound formation by ion implantation 78−51572
Nb_3/Sn-Cu composites, in situ processed, supercond. props. 80−75698
$Nb_3Ge_{1-x}Sn_x$, applicability of scaling laws for supercond. crit. currents 79−24118
$Nb_3Ge_{1-x}Sn_x$ CVD films, supercond. props., 4.2 to 19K 79−42713
NbSn multifilamentary superconducting composites, micromechanics 79−38878
$Nb_{1-x}Sn_x$, sp. ht., supercond. T_c and martensitic transform. *(French)* 78−43508
Nb_2Sn, filamentary segments, flux pinning, proximity effects, percolation thresholds 78−56269
Nb_3Sn, 2-MeV proton-irradiated, Mossbauer effect studies 79−69757
Nb_3Sn, [111] transverse acoustic phonon softening near martensitic transform. 79−73283
Nb_3Sn, A-15 compounds, interlattice displacements, elastic consts. 78−55906
Nb_3Sn, A-15 cubic phase, band calc. using APW method 79−56120
Nb_3Sn, A-15 struct. Nb based superconductors, irrad. type influence on radiation defects 80−15093
Nb_3Sn, A-15 struct. supercond., microhardness, bonding 78−76199
Nb_3Sn, A-15 supercond. cpd., martensitic transform. 79−60499
Nb_3Sn, A-15 superconductor, dHvA effect 78−75985
Nb_3Sn, AC losses, surface effects 78−64171
Nb_3Sn A15 composite superconductors, hydrostatic extrusion *(French)* 80−104090
Nb_3Sn, A15 compound, exam. of deformation processing, review 78−39864
Nb_3Sn, A15 cpd., normal state, low temp. resist., disorder effects 80−107762
Nb_3Sn, acoustic soft modes in high mag. fields, soft sound vel. meas. 77−43482
Nb_3Sn, alloying agent influence on struct. and supercond. props. *(Russian)* 80−39698
Nb_3Sn, anisotropic thermal parameters of Nb 79−99282
Nb_3Sn, annular superconductor, field replication and flux shielding 77−28286
Nb_3Sn, atomic displacements induced by radiation damage, X-ray study 80−2085
Nb_3Sn, α-particle irrad., relationship between density of states and supercond. transition temp. 79−42684
Nb_3Sn based multifilamentary superconductors, bronze process fabrication, voids growth obs., via hot stage SEM 80−70089
Nb_3Sn bronze process, flux pinning scaling law depend. on strain 80−75696
Nb_3Sn cable for TESPE superconducting toroidal coil used for Tokamak fusion plasma containment 79−54223
Nb_3Sn, cavities, quasiparticles in energy gap corresponding to weak spots 79−56386
Nb_3Sn, coherence parameter, nonlinear high temp. supercond. elements with A-15 lattice *(Russian)* 80−60127
Nb_3Sn composite, superconducting transition depend. on non-hydrostatic stress 80−107948
Nb_3Sn composite processes with Cu-Sn-Zn matrix, superconducting props. 78−84370
Nb_3Sn, composite superconductor, sp. ht., 4-24K, calorimetry 77−32116
Nb_3Sn composite supercond., current transfer, theory 78−72315
Nb_3Sn composite supercond., current transfer, expt. results 78−72316
Nb_3Sn, composite supercond., powder metallurgical prep. 80−2981
Nb_3Sn, composite superconducting wire, critical current-bend strain relationships 80−93063
Nb_3Sn, composite wire, boundary resistance and cryogenic stability 79−69629
Nb_3Sn composite wires, supercond., degradation mech. under tensile strain at 4.2K 79−38284
Nb_3Sn composites, crit. currents and microstruct. 79−38280
Nb_3Sn, composition effects on T_c 77−76993
Nb_3Sn conductor, bronze-process fine-filament, development and props. 79−33426
Nb_3Sn conductors for toroidal-field coils, forced-flow, flow characts. 79−58741
Nb_3Sn, crit. current ang. depend., prep. conditions effect 77−47949
Nb_3Sn, crit. current density, low dose fast neutron irrad. effect 78−14910
Nb_3Sn, crit. current enhancement by low temp. fast neutron irradiation 77−40014
Nb_3Sn, critical current density 78−52176
Nb_3Sn, critical current enhancement by low temp. fast neutron induced flux pinning centres 78−52177
Nb_3Sn, critical currents, ang. depend., prep. conditions effects 77−43793
Nb_3Sn, critical data, under hydrostatic pressure to 15 kbar 79−47217
Nb_3Sn, cryostabilised conductor cooling system for Large Coil Program 78−50393
Nb_3Sn cryotron, thermally controlled, used in transformer-rectifier flux pump for superconducting magnet 80−4727
Nb_3Sn, Cu admixture in Sn bath effect on critical current and stability temp. 80−7059
Nb_3Sn, current carrying capacity increase by Hf addition 80−7056
Nb_3Sn, de Haas van Alphen meas. of Fermi surface for $H \leq 40$ T 79−73424
Nb_3Sn, de Haas-van Alphen oscills. in normal state 79−56116
Nb_3Sn, Debye temp., determ. from elec. resist. meas. *(French)* 77−4322
Nb_3Sn, Debye-Waller factor temp. depend. 79−14907
Nb_3Sn, degradation mechanism of superconducting transition temp. under high energy neutron irradiation 78−52124
Nb_3Sn, delayed flux entry and surface barriers, tunnelling obs. 77−59355
Nb_3Sn, density of states from critical field meas. 79−42690
Nb_3Sn, dependence of max. trappable field on supercond. cylinder wall thickness 77−72952

tin alloys continued
Nb_3Sn diffusion layer material, characterisation 79−38213
Nb_3Sn, diffusion-processed layer, texture meas. 79−82726
Nb_3Sn, distrib. of mag. field of transport current in type II supercond. 79−51730
Nb_3Sn, effect of changes in $\alpha^2(\Omega)F(\Omega)$ on the zero-temp. energy gap 80−97025
Nb_3Sn, effect of diffusion couple Sn content on superconductivity 79−61009
Nb_3Sn, effect of O ion irradiation on supercond. 78−52131
Nb_3Sn, effect on critical temp. for supercond. of disorder, induced by α-particles 78−47897
Nb_3Sn, elastic instability in cubic to tetragonal phase transitions 78−39767
Nb_3Sn, electron beam deposited, microstruct., rel. to supercond. props. 79−37935
Nb_3Sn, electron energy loss spectra, AES and HEED investig. of surface 77−24635
Nb_3Sn, electron irradiation at cryogenic temps., effect on T_c and transport props. 78−52122
Nb_3Sn, electron-lifetime effects on props. 80−10951
Nb_3Sn, electron-phonon coupling and supercond. crit. temp. 79−33379
Nb_3Sn, electronic props. calc. 79−7780
Nb_3Sn, electronic struct., APW method 78−72066
Nb_3Sn, electronic struct. from three-dimens. k.p model 78−84139
Nb_3Sn, electronic struct. calcs. 79−47005
Nb_3Sn, electronic struct., electron-phonon interactions, and low temp. anomalies 79−60701
Nb_3Sn, fast neutron irradiation, effect on critical current density 78−19197
Nb_3Sn fatigue effects in unidirectional composites, computer simulated model 80−35289
Nb_3Sn filament, crit. current stress induced degradation 77−24658
Nb_3Sn, filamentary, fatigue tests on small coils 78−64652
Nb_3Sn, filamentary conductors, type-II, low temp. 30 GeV proton effects on critical props. 78−52178
Nb_3Sn, filamentary supercond., mech. props. and crit. current 77−24657
Nb_3Sn, filamentary superconducting composite, TEM 77−80887
Nb_3Sn filamentary superconducting composites, mechanical property variations between composites 79−57054
Nb_3Sn filamentary wires, fabricated by infiltration method, supercond. props. 77−28761
Nb_3Sn, filaments in Cu matrix, thermal strain effects on superconducting critical temp. 80−93032
Nb_3Sn film, electron beam evaporation, growth morphology 77−44167
Nb_3Sn film, electron beam codeposited, growth morphology and tensile props. 78−10301
Nb_3Sn film, growth by high-rate magnetron sputtering, transition temp. and crit. currents 77−28718
Nb_3Sn film, high T_c, high-rate magnetron sputtering, supercond. transition temp. meas. 77−43770
Nb_3Sn film, quasiamorphous, supercond. phase formation by heat pulse 77−63017
Nb_3Sn film, SQUIDs for operation above 14.5K 77−66226
Nb_3Sn film, T_c var. with ^4He irrad. induced defects 77−8220
Nb_3Sn film contacts, quantum interference at H_2 temp. *(Russian)* 77−12041
Nb_3Sn film formation, solubility, precipitating processes *(Russian)* 80−92792
Nb_3Sn film on insulating substrate, crit. mag. fields *(Russian)* 79−11277
Nb_3Sn films, deposition by quasi-closed vol. method, supercond. crit. temp. 80−15645
Nb_3Sn, flux density gradient determ. by Faraday effect 80−107969
Nb_3Sn, flux trapping and shielding capabilities in transverse fields 80−15667
Nb_3Sn, for supercond. microwave cavities, secondary electron emission and AES meas. 79−56895
Nb_3Sn forced flow superconductor design considerations for Large Coil Program 78−50394
Nb_3Sn forced flow superconducting test coil, Westinghouse design for fusion reactor large coil program 80−99337
Nb_3Sn, forced flow toroidal field coil, Westinghouse Electric conceptual design for test coil 78−50392
Nb_3Sn, gap anisotropy, electron irrad. effect on transition temp. 78−10599
Nb_3Sn, grain size in A15 reaction layers 78−14911
Nb_3Sn, helicon-phonon interaction for parallel wave propagation 78−64054
Nb_3Sn, high-T_c supercond., apparent T^2-depend. of normal-state resist. and lattice sp. ht. 77−47921
Nb_3Sn, high-current A-15 microcomposite material 80−44781
Nb_3Sn, high-rate sputter-deposited, effect of oxygen on microstruct. 80−20343
Nb_3Sn, high-temp. supercond., tunnelling spectra, electron pairing anal. 79−87205
Nb_3Sn, highly disordered, elec. resist. and supercond. T_c 78−52142
Nb_3Sn, hot isostatically pressed, plastic deform. 80−108510
Nb_3Sn in bronze, supercond. props. thermally induced matrix stresses 77−32134
Nb_3Sn in Cu matrix composite superconductor, cyclic stress effects on transport props. 77−28336
Nb_3Sn, inhomogeneity detection by penetration depth meas., proximity theory 77−28288
Nb_3Sn, irrad. effect on supercond. transition temp. 78−6472
Nb_3Sn, irradiated, critical current density 79−38293
Nb_3Sn, lattice dynamics at 300K 79−65155
Nb_3Sn, lattice microstrain induced metastable phase, low temp. struct. and props. 77−8482
Nb_3Sn, low field microwave props., H_{c1} 77−28317
Nb_3Sn, low fluence alpha irradiation, behaviour of supercond. transition temp. 78−43510
Nb_3Sn, low temp. irrad. with 20 MeV S ions, effect on supercond. props. 79−38223
Nb_3Sn, low temp. neutron irrad. expts., $E_n = 14$ MeV 79−33424
Nb_3Sn, martensitic transform. coupling with supercond. transition 78−44126
Nb_3Sn, martensitic transition, lattice anharmonicity 79−8300
Nb_3Sn microfilamentary superconducting composite, critical currents, fracture props. 80−107970

tin alloys continued
Nb_3Sn monofilament wires, supercond. props., effect of Be alloying additions to bronze matrix 79−87222
Nb_3Sn monofilamentary wires, supercond. crit. current density, bending effects 80−50018
Nb_3Sn, monofilaments, radiation-enhanced diffusion growth, crit. current density 80−65758
Nb_3Sn, multifilament composite technical superconductors, development and manufacture 79−19707
Nb_3Sn, multifilament conductors, strain-crit. current meas. 78−64174
Nb_3Sn multifilament conductors, strain effect on crit. props. 78−80108
Nb_3Sn multifilament conductors, fabrication and props. 79−33427
Nb_3Sn, multifilament conductors appl., production and props. *(German)* 80−3081
Nb_3Sn multifilament superconductors, designed for high B appl., losses 79−33414
Nb_3Sn multifilament supercond. wire, hydrostatic extrusion processing 79−33976
Nb_3Sn multifilament superconducting composites, alternative technologies for fabrication 79−38756
Nb_3Sn multifilament superconductors produced by ECN technique, prep. and props. 79−33975
Nb_3Sn, multifilament superconductor, metallurgical design 79−33434
Nb_3Sn multifilament superconductors, AC losses 79−60979
Nb_3Sn, multifilament superconductor, pulsed mag. field losses and critical current densities 80−54853
Nb_3Sn, multifilamentary, optimization of high field crit. current density 79−38288
Nb_3Sn, multifilamentary and cabled superconductors, cryogenic stability anal. 79−59260
Nb_3Sn, multifilamentary composite wires, critical current strain depend. 77−20511
Nb_3Sn multifilamentary conductor, crit. current, tensile stress effects 77−28329
Nb_3Sn multifilamentary conductor, for fusion research magnets, manufacture and props. 77−28760
Nb_3Sn multifilamentary conductors, crit. current under tensile stress 77−89912
Nb_3Sn multifilamentary conductors, enhancement of supercond. crit. current by tensile stress 78−6490
Nb_3Sn multifilamentary composite superconductor, reaction treatment, crit. current, transition temp. and bend props. 79−33430
Nb_3Sn multifilamentary composite superconductor, effect of heat treatment on supercond. props. 79−33376
Nb_3Sn multifilamentary conductors for large-scale magnets, crit. currents, stability, and stress effects 79−38291
Nb_3Sn multifilamentary composite wires, supercond. crit. current density, temp. and mag. field depend. 79−33425
Nb_3Sn multifilamentary conductor for fusion research 79−35797
Nb_3Sn, multifilamentary conductors, production using solid state diffusion technique 79−56454
Nb_3Sn multifilamentary composites, supercond. destruction by current, long N-S interfaces 79−56480
Nb_3Sn, multifilamentary conductors, effect of bronze on compression 79−61012
Nb_3Sn, multifilamentary conductors, stress-induced enhancement of critical currents 79−69644
Nb_3Sn multifilamentary composites, crit. currents, flux pinning, and crit. field 79−78280
Nb_3Sn, multifilamentary coils for Lawrence Livermore Laboratory superconducting High Field Test Facility 80−90834
Nb_3Sn multifilamentary composite supercond. wires, transverse sections prep., ion milling, TEM obs. of grain size 80−101000
Nb_3Sn multifilamentary dipole magnet, construction and performance 77−28758
Nb_3Sn multifilamentary dipole magnets, supercond. props., 4.2 to 15K 79−31275
Nb_3Sn multifilamentary hollow superconductor and magnet, fabrication and crit. currents 79−38289
Nb_3Sn, multifilamentary supercond., flexibility and elec. characts. 77−24990
Nb_3Sn, multifilamentary supercond., crit. current, bend tests 77−28335
Nb_3Sn multifilamentary supercond., Cu-stabilised, recent developments 77−28759
Nb_3Sn, multifilamentary supercond., prod. by ECN powder metallurgy method and props. 77−28762
Nb_3Sn, multifilamentary supercond., stress effects 77−32133
Nb_3Sn multifilamentary superconductors crit. current up to 18 T 77−47950
Nb_3Sn multifilamentary stranded compd. supercond., design, processing, mech., supercond. props. 77−76999
Nb_3Sn multifilamentary superconducting wires, crit. current density in high mag. field 79−38281
Nb_3Sn multifilamentary superconductor, stress induced normal⇄supercond. transition 79−33377
Nb_3Sn multifilamentary superconducting wires, improved high-field props. 79−47215
Nb_3Sn multifilamentary supercond. composites, crystallographic texturing 80−71669
Nb_3Sn, multifilamentary superconductor preparation by 'in situ' and cold powder methods, review 80−93522
Nb_3Sn multilayered supercond. power line conductors, elec. props. and growth morphology 77−28325
Nb_3Sn, NMR of ^{93}Nb and spin-lattice relax. time at low temp. 77−85388
Nb_3Sn, neutron irrad., crit. current change rel. to temp. and metallurgy 78−80109
Nb_3Sn, neutron irrad., elec. resist., temp. depend. 79−91024
Nb_3Sn, neutron irrad., X-ray scatt. theory 79−37740
Nb_3Sn, neutron irrad. effect on upper crit. field and crit. current 77−72954
Nb_3Sn, neutron irrad. effect on supercond. fusion magnet props. 78−52128
Nb_3Sn, neutron irrad. effects on transition temp. *(Japanese)* 79−82707
Nb_3Sn, neutron irradiated, A15 compound, recovery of T_c by annealing 78−52132
Nb_3Sn, neutron irradiation at 8K, supercond. crit. current and crit. temp. meas. 77−28334
Nb_3Sn neutron scatt. data, coupling between thermal and elastic variables 77−1203

tin alloys continued
Nb_3Sn, nonstationary Josephson effect, 13-18.3K, 9-10 GHz, 20 MW *(Russian)* 78−2631
Nb_3Sn, normal state, Fermi surface, APW band calc. and de Haas-van Alphen oscills. 79−65369
Nb_3Sn, O^{4+} bombarded, Mossbauer studies 80−2672
Nb_3Sn, on $LiNbO_3$ substrate, US attenuation of SAW in applied mag. field 80−75678
Nb_3Sn, phonon density of states, temp. depend. 79−42183
Nb_3Sn, phonon softening and T_c, strong electron-phonon coupling 78−31009
Nb_3Sn, phonon softening in [ζζζ] transverse modes, neutron scatt. obs. 79−33062
Nb_3Sn, plasma energies, tight-binding energy-band model 78−84159
Nb_3Sn, powder metallurgically produced, microstruct. characts. 80−89233
Nb_3Sn, produced by Sn implantation, supercond. and Mossbauer effect 79−4612
Nb_3Sn, proton and γ-irradiated, lattice dynamics from ^{119}Sn Mossbauer studies 78−39458
Nb_3Sn, proton irradiated, Mossbauer effect at 78K 78−19394
Nb_3Sn, quasi-one-dimensional supercond., giant enhancement of nucl. relax. rate near T_c 78−56257
Nb_3Sn, radiation damage effect on superconducting props. 78−52127
Nb_3Sn, resist. characts. in normal state 78−51963
Nb_3Sn, resistivity and T_c measurement after low temp. neutron irradiation 78−52123
Nb_3Sn, softening of surface phonons in (100) plane 80−107627
Nb_3Sn, stabilized multifilamentary superconductor, internal Sn diffusion process 79−61749
Nb_3Sn strip, made by diffusion method, crit. curent anisotropy, Zr alloying addition effects *(Russian)* 78−47921
Nb_3Sn, supercond., AC losses, low field behaviour morphology depend. 77−24655
Nb_3Sn, supercond., crit. fields Pauli paramag. limiting and material parameters 79−78277
Nb_3Sn, supercond., dielastic interaction of flux line lattice with internal stresses of cryst. imperfections 78−14906
Nb_3Sn, supercond., dielastic interaction of flux line lattice with internal stresses of cryst. imperfections 78−56270
Nb_3Sn, supercond., effect of trapped mag. flux on AC losses 79−33420
Nb_3Sn, supercond., elec. resist., phenomenological model 77−43775
Nb_3Sn, supercond., fast particle irradiation effects, using anti-site defect model, electronic state influences 79−56346
Nb_3Sn, supercond., production of high current carrying strip *(Russian)* 79−33435
Nb_3Sn, supercond., projected upper limits to crit. current density 77−36037
Nb_3Sn, supercond., thin film, US attenuation of SAWs 80−49988
Nb_3Sn, supercond. and high mag. fields 79−87215
Nb_3Sn, supercond. composite, residual stress state, crit. currents 80−80468
Nb_3Sn, supercond. crit. temp. and transition width, 25 MeV O ion irrad. effects 77−69439
Nb_3Sn, supercond. crit. temp., functional derivative with electronic density of states, Eliashberg eqns. 79−56368
Nb_3Sn, supercond. diffusion layer, Zr content and Nb cold working effects 77−16015
Nb_3Sn, supercond. film, electron beam codeposition, synthesis and props. 78−72296
Nb_3Sn, supercond. props., effect of neutron irrad. 80−80463
Nb_3Sn, supercond. props. and struct., neutron irrad. dose depend. 77−15985
Nb_3Sn, supercond. props. of cold worked core wires an basis of A15 phases 77−85369
Nb_3Sn, supercond. props. and appls., state-of-the-art 79−33413
Nb_3Sn, supercond. tape, crit. current, effect of Sn-Nb phase, annealing 79−24119
Nb_3Sn, supercond. thermodynamics 79−42693
Nb_3Sn, supercond. transition temp., deform. effects 77−12051
Nb_3Sn, supercond. transition temp., rel. to A15 phase stability 78−52137
Nb_3Sn superconducting, formed from Cu-Sn alloy, props. 79−42709
Nb_3Sn, superconducting, inelastic scattering of light 79−33390
Nb_3Sn, superconducting, optical props. and electron-phonon interactions 80−2510
Nb_3Sn, superconducting accelerating struct., high field exam. 79−36439
Nb_3Sn superconducting bridge junction, crit. current temp. depend. *(Russian)* 78−34938
Nb_3Sn superconducting composite, bronze process, metallurgy 80−3004
Nb_3Sn superconducting film, α-particle induced defects and stoichiometry 77−32101
Nb_3Sn, superconducting filament formation near edge dislocation *(Russian)* 79−4635
Nb_3Sn superconducting layers, crit. currents, struct. and prep. *(Slovak)* 78−56273
Nb_3Sn superconducting microwave resonator for measuring dielectric loss in polymeric solids 79−67316
Nb_3Sn superconducting multifilamentary wires, mechanisms for crit.current degradation 77−28324
Nb_3Sn superconducting multifilamentary conductors, localisation of defects by inductive procedure 79−33433
Nb_3Sn superconducting multifilamentary composites, strain depend. of crit. current and crit. field 79−33432
Nb_3Sn superconducting multifilamentary wire, stress effects 79−33431
Nb_3Sn superconducting multifilamentary conductors, AC losses 79−33394
Nb_3Sn superconducting props. and structural transition *(Russian)* 77−12052
Nb_3Sn, superconducting props., effect of radiation induced atomic disorder 78−52133
Nb_3Sn, superconducting thin films, energy gaps from tunnelling meas. 80−25050
Nb_3Sn, superconducting toroidal field coils for Tokamaks 78−50388
Nb_3Sn, superconducting transition temp., crit. parameters 77−28280
Nb_3Sn superconducting wires, in situ multifilamentary, mech. props. 79−47746
Nb_3Sn superconducting wire, fabrication from Cu-Nb-Sn alloy using controlled high temp. gradient 80−25056
Nb_3Sn, superconductive fixed points for temperatures above 0.5K 79−63221

tin alloys continued
Nb_3Sn, superconductive materials and magnet systems developed at Intermagnetics General Corp. 79−58699
Nb_3Sn superconductor, bronze processed, effect of third element additions 77−28333
Nb_3Sn superconductor, low temp. deuteron irradiation 78−52182
Nb_3Sn, superconductor for Large Coil Program, low temp. stability, joints, design method 80−106195
Nb_3Sn superconductors, bronze-processed, effect of Ta additions 78−95404
Nb_3Sn superconductors, Kirkendall voids, effects on mech. and supercond. props. 79−33429
Nb_3Sn superconductors, mech. behaviour, diffusion *(German)* 78−39880
Nb_3Sn, TEM of radiation damage 79−65122
Nb_3Sn tapes, appl. of method for continuous meas. of crit. current 77−24656
Nb_3Sn tapes, transition temp. meas. using Si linear thermometer 77−57330
Nb_3Sn, ternary additions effect on upper crit. field at 4.2K 77−28316
Nb_3Sn, thick walled tube, calc. of transverse dipole mag. field distributions *(French)* 79−47209
Nb_3Sn thin film bridges, AC Josephson effect 79−42702
Nb_3Sn, thin film weak-links SQUIDs, localised region radiation damage, fabrication and properties 78−47912
Nb_3Sn tunnel junctions, tunnelling density of states and electron-phonon spectral function 79−65618
Nb_3Sn, vap. deposited supercond. film, effect of N_2 and tape heating 78−34939
Nb_3Sn, vapour deposited, supercond., surface resist. and penetration depth 79−33392
Nb_3Sn, X-ray study of fission fragment induced structural damage 78−51589
Nb_3Sn, Young's modulus, 4.2-300K, behaviour near martensitic transition 80−66564
Nb_3Sn, Zr alloy element effect on growth kinetics *(Chinese)* 79−90579
Nb_3Sn-Al_2O_3 composite, electron beam deposited, microstruct., rel. to supercond. props. 79−37935
Nb_3Sn-Au, supercond. tunnel junction with microshort circuit, nonlinear phenomena 78−14898
Nb_3Sn-Cu, high-current A-15 microcomposite material 80−44781
Nb_3Sn-Cu composite superconductors, in-situ, AC losses 79−38283
Nb_3Sn-Cu multifilamentary wires, in situ prep., supercond. and mech. props. 79−38768
Nb_3Sn-Cu multifilamentary composite wire, Nb_3Sn filament morphology and grain size 80−100855
Nb_3Sn-Cu superconducting composite, electron beam co-evaporated, TEM study 79−28247
Nb_3Sn-Cu superconducting composites, produced by cold extrusion of fine powders 79−38767
Nb_3Sn-Cu superconducting composite with submicrometer filaments, fabrication and props. 79−38282
Nb_3Sn-Fe(Co)(Mn), mag. impurities effect on supercond. props. 77−1524
Nb_3Sn-Nb_3Sn supercond. point contacts, crit. currents, effect of laser radiation *(Russian)* 79−28484
Nb_3Sn-Pb tunnel junction, Josephson props. 79−7937
Nb_3Sn-V_3Ga concentric solenoid magnet system, 17.5 T operation 77−26353
Nb_3Sn-Zr (0.8%), supercond. tape, crit. current, two stage annealing effect *(Russian)* 77−63046
Nb_3Sn_4 film, critical currents due to microwave field 80−25058
Nb_3(Sn-Al) system, X-ray spectroscopic studies of electronic struct. of A15 cpds. 80−2900
Nb_3(SnGa), wire, neutron effect on T_c, I_c and flux pinning 79−38216
$Nb_3(Sn_{1-x}Ga_x)$, bronze processed wires, critical current densities in fields up to 23.5 T 78−47922
Nb_3(SnIn) tapes, diffusion processed, high field props. 79−38266
Nb_3(SnIn) wires, prep. by ductile fabrication process and props. 79−38265
NbSnSb, synthesis and struct. *(French)* 79−90596
Nb_3Su-Cu supercond. composites, fabrication, magnet appl. 80−11602
$(Nb_{1-x}Zr_x)_3$ Sn, bronze-processed tape, AC losses between 5 and 16K 79−82727
$(Nb_{0.99}Zr_{0.01})_3Sn$, AC power losses in parallel AC and DC mag. fields 80−97041
Nd-Sn (0 to 50 at.%), phase equilibria diagram *(Ukrainian)* 79−34001
$NdRh_{1.2}Sn_{4.1}$, new supercond./mag. cpds., X-ray powder diffr. data 80−100215
$NdSn_3$, crystalline elec. field parameters, exchange and Coulomb contrib. 77−20278
$NdSn_3$, elec. cond., cryst. field effect, spin disorder contrib. 80−65540
$NdSn_3$, magnetoresistance 80−24877
$NdSn_3$, Neel temp., hydrostatic press. depend. 80−29549
Ni-Be bronze, Fe and Si alloying addition effect on phase composition *(Russian)* 78−15360
Ni-Cu-X (X=Sn, Nb, Ti), spinodal decomp. alloys, linear expansion coeff. influence on morphological anisotropy *(Japanese)* 80−70431
Ni-Sn, dilute ferromagnetic alloy, resistivity and magnetoresist. anisotropy 79−11106
Ni-Sn, electrical cond. and magnetic susceptibility of B 8_2-compounds *(German)* 79−42520
Ni-Sn, spectral determ. of comp. using UHF plasmotron as source 79−52812
Ni-Sn intermetallic phase growth kinetics at liq. Sn-solid Ni interface 80−71638
Ni-Sn intermetallics, Ni_3Sn_4, Ni_3Sn_2 and Ni_3Sn, oxidation, AES obs. 77−48575
Ni-Sn ion implanted surface alloys, solid solubility and radiation-induced disorder, backscatt. obs. 79−46692
Ni-Sn system intermetallic formation rate, H_2 adsorption effect 79−90819
Ni-Ti, Nitinol memory material heat engine, comment on efficiency 80−3529
Ni-Ti, Nitinol memory material heat engine, reply to comments on efficiency 80−3530
$(Ni_xCu_{1-x})_2MnSn$, mag. props. and lattice parameter, composition depend. 77−80916
Ni_3Fe-Sn, dil., atomic order detection by ^{119}Sn spectroscopy 80−39993
$Ni_2Mn_{0.9}Fe_{0.1}Sn$, Fe site hyperfine field and mag. moment, Mossbauer effect meas. 78−76365

tin alloys continued
$Ni_2Mn_xM_{1-x}Sn$ (M=Ti,V) mag. hyperfine fields, ^{119}Sn Mossbauer spectra study 80−55003
$Ni_2Mn(Mn_xSn_{1-x})$, Heusler alloy, antiferromagnetic order, X-ray and neutron diff. 78−64189
Ni_2MnSn alloy, ionic spin distribution and RKKY interactions 78−27028
Ni_2MnSn and NiMnSn, Heusler alloy, hyperfine field at ^{111}Cd, TDPAC meas. 78−43705
Ni_2MnSn, ferromag. Heusler alloy, electronic struct., spin polarisations, theory 80−54598
Ni_2MnSn, Heusler alloy, mag. interactions and cond. electron polarisation, spin echo NMR meas. 77−77125
Ni_2MnSn, itinerant ferromagnet, neutron inelastic scatt. 79−7970
$Ni_2Mn_xTi_{1-x}Sn$, Mossbauer spectra, mag. hyperfine field 80−15857
NiSn, thermally prepared Mossbauer spectroscopy 79−61269
Ni_3Sn_2, single cryst. embrittlement and subboundary hardening via interstitial segregation *(Russian)* 77−12679
Ni_3Sn_2, thermally prepared Mossbauer spectroscopy 79−61269
Ni_3Sn_4, thermally prepared Mossbauer spectroscopy 79−61269
Ni_2(Ti,Mn)Sn, Heusler alloy, mag. meas. 79−47261
$NpSn_3$, band magnetism due to f-electrons, T_N 77−73039
$NpSn_3$, itinerant f-electron antiferromag. obs. 77−8315
Pb-Ca-Sn, chill cast and wrought, cyclic voltammetry and electrochemical meas. of anodic activity, PbO_2 form. 78−31582
Pb-Ca-Sn, effect of Sn additions on precipitation behaviour, of Pb-Ca alloys *(German)* 78−52821
Pb-Ca-Sn, for battery grids, proposed phase diagram, grain struct. development, corrosion phenomena 77−16546
Pb-In-Sn system, liquidus and solidus isotherms 78−44088
Pb-Sb-Te-Cu-Sn, influence of specimen and grain size on mech. props. *(Russian)* 77−81297
Pb-Sn, arc electrode processes, thermodynamic approach *(Russian)* 77−27755
Pb-Sn, controlled solidification, monograin growth, selection and struct. *(French)* 77−16568
Pb-Sn, DC arc plasma, meas. of conc. ratio of component atoms *(Russian)* 77−27754
Pb-Sn, dil., dislocation inertial effects, internal-friction meas. on normal and superconducting states 79−38883
Pb-Sn, dil., US oscillations and dislocation unpinning in supercond. and normal states *(Russian)* 79−11648
Pb-Sn, dil. alloys, dislocation motion and electron-dislocation interactions 77−7728
Pb-Sn, directionally solidified lamellar eutectic, deform. induced microstruct. instability 77−32623
Pb-Sn, dirty strong-coupling supercond., Ginzburg-Landau parameters, type II behaviour deviations 77−8249
Pb-Sn, eutectic, electron emission avalanche obs., during isothermal superplastic deform., *(Russian)* 77−48324
Pb-Sn, eutectic, superplastic behaviour, grain size effect 80−7635
Pb-Sn, eutectic alloy, plastic deform., work hardening *(German)* 78−92279
Pb-Sn, eutectic alloy, spiral growth phenomenon 77−48419
Pb-Sn, eutectic alloys, struct. instability and absence of superplasticity *(Russian)* 77−8882
Pb-Sn, ingots, solidified, formation of equiaxed eutectic grains *(Japanese)* 78−39756
Pb-Sn, lamellar eutectic alloy, proximity effect, entropies, free energies and transition temps. 77−51849
Pb-Sn, lamellar eutectic stability and growth struct., fault formation 79−96019
Pb-Sn, melt viscosity rel. to phase equilib. *(Russian)* 79−69272
Pb-Sn, off-eutectic alloy growth from stirred melt 77−8809
Pb-Sn, proximity and pinning effect up to 7K *(French)* 77−51858
Pb-Sn, solidification, predicted vol. change 77−28802
Pb-Sn, strength loss in supercond. transition, nonmag. and paramag. impurities influence *(Russian)* 80−70875
Pb-Sn, superplastic eutectic, roll load and torque necessary for rolling *(French)* 78−95761
Pb-Sn, undercooled eutectic, compositional variations at various gravity levels 77−52314
Pb-Sn, unidirectionally solidified eutectic, lamellar microstructure, influence of grain boundaries on thermal stability 78−72795
Pb-Sn, with brass insert, tensile flow and fracture 78−11290
Pb-Sn (20wt.%), eddy current study of solidification 80−104141
Pb-Sn (62 wt.%), activation energy for superplasticity 77−86112
Pb-Sn (62 wt.%), intercrystalline and interface boundary sliding, tensile tests, SEM obs. 79−38886
Pb-Sn (62 wt.%), superplastic eutectic, exceptional ductility 78−27579
Pb-Sn alloy, viscoplastic flow study, appl. of Moire fringe method *(Russian)* 77−35102
Pb-Sn binary alloy, unidirectional solidification, convective and interfacial instabilities 80−60851
Pb-Sn directionally solidified eutectic alloy, morphology and crystallography 77−90340
Pb-Sn eutectic, cavitation during superplastic flow, affecting factors 78−60728
Pb-Sn eutectic, directionally solidified, perfection and stability of lamellar struct. *(French)* 77−77468
Pb-Sn eutectic, directionally solidified, periodic array of supercond.-normal contacts, supercurrent and dynamic resist. 78−34928
Pb-Sn eutectic, strain rate sensitivity index, expt. comparison of different methods 80−3144
Pb-Sn eutectic, superplastic deform., appl. of SEM specimen holder for cold tensile deform. expts. *(French)* 77−36704
Pb-Sn eutectic, superplastic, anelasticity effect on stress relaxation 78−31443
Pb-Sn eutectic alloy, high temp. deform. 77−16637
Pb-Sn eutectic alloy, superplastic deform. of circular sheets *(French)* 77−28871
Pb-Sn eutectic alloy, superplastic deform. at relatively high strain rates 79−57042
Pb-Sn lamellar eutectic alloy, supercond. normal-supercond. junction arrays 77−24641
Pb-Sn microduplex eutectic, cavitation during superplastic flow due to hard particles 77−36575
Pb-Sn superplastic alloy, cutting, stress distrib. *(German)* 79−24682
Pb-Sn system, soft solder, elec. and thermal cond. at low temps., superconducting transition temp. 80−20150

tin alloys continued
Pb-Sn-Bi-Cd low melting point alloy block for organ shielding in radiotherapy *(Korean)* 80−36154
Pb-Sn-Ca sheet, continuously cast, for battery grids, ageing behaviour 77−16603
Pb-Sn-Cd, eutectic and monovariant eutectic, ingot struct. 78−15388
Pb-Sn-Cd, monovariant eutectic and eutectic alloys, ingot struct. 77−63656
Pb-Sn-Hg amalgam, liq., thermodynamic props. *(Russian)* 77−66624
Pb-Sn-Te, liquidus meas. by DTA 79−95999
Pb-Sn(-Sb), surface tension liquidus temp. to 550°C *(Korean)* 79−90848
Pb-Sn(Bi) alloys, dil., impurity effects on softening at T_c *(Russian)* 78−23220
Pb-Sn(20 wt.%), partially remelted interdendritic fluid flow 77−4771
Pb-Tl-Sn melt, short-range order struct. 80−49088
$Pb_2MnSb_{0.99}Sn_{0.01}$, ^{119}Sn Mossbauer study, compositional and heat treatment effects 79−42875
$Pb_{0.871}Sn_{0.129}$, supercond., hysteresis in flux flow charact., normal metal precipitates 78−80107
$Pb_{1-c}Sn_c$, liquid alloys, local fluctuations and quadrupolar relaxation 80−66060
Pd-Sn-Cd, non-unique stress/strain rate relations during superplastic flow 77−28855
$Pd_2MnIn_{1-x}Sn$, Heusler alloy, mag. order, disorder effects 80−88723
$Pd_2MnIn_{1-x}Sn_x$, Heusler alloy, Mossbauer effect exam., mag. coupling 79−69755
$Pd_2MnIn_{1-x}Sn_x$, Heusler alloy, Mossbauer effect exam., hyperfine interactions in ferromag. phase 79−69756
$Pd_2MnIn_{1-x}Sn_x$-Cd, dil., Heusler alloy, hyperfine mag. field on Cd, TDPAC obs. 79−8075
$Pd_2MnIn_{1-x}Sn_{1-x}$, mag. order exam. 77−40036
$Pd_2Mn_{1-x}Nb_xSn$, Heusler alloy, NMR and mag. coupling 78−43676
$Pd_2MnSb_{1-x}Sn_x$, Mossbauer meas. of ^{119}Sn mag. hyperfine struct. 77−12258
Pd_2MnSn alloy, ionic spin distribution and RKKY interactions 78−27028
Pd_2MnSn, Cd impurities, hyperfine field meas. 78−15074
Pd_2MnSn, ferromag. Heusler alloy, electronic struct., spin polarisations, theory 80−54598
Pd_2MnSn, Heusler alloy, interaction between local mag. moments 77−1540
Pd_2MnSn, Heusler alloy, mag. interactions and cond. electron polarisation, spin echo NMR meas. 77−77125
Pd_2MnSn, Heusler alloy, NMR and mag. coupling 78−43676
$Pd_2Mn_{0.95}Sn_{1.05}$, hyperfine mag. fields, Mossbauer spectra 80−15870
$Pd_2Mn_{0.98}Sn_1In_{0.02}$, Heusler alloy, hyperfine fields at sp elements, spin echo NMR meas. 78−84496
$Pd_2MnSn_{1-x}Sb_x$, Heusler alloy, Mossbauer effect exam., hyperfine interactions in ferromag. phase 79−69756
$Pd_2MnSn_{1-x}Sb_x$, mag. order exam. 77−40036
$Pd_2MnSn_{1-x}Sb_x$, Mossbauer spectra, mag. hyperfine field 80−15868
$Pd_2Mn_xV_{1-x}Sn$, Heusler alloy, structural disorder, Mossbauer study 80−80650
$Pd_{0.99}Sn_{0.01}$, lattice dynamics of ^{119}Sn impurities, Mossbauer meas. 77−76507
Pd_xSn_y (x=0.95, y=0.05; x=3, y=1), Mossbauer spectra, high press. effects, force consts. 80−84669
$Pr_xLa_{1-x}Sn_3$, anomalous resistivity maxima in metallic magnetic system 78−79977
$PrRh_xSny$, crystallography X-ray powder diffr. study 80−100217
$PrSn_3$, crystalline elec. field parameters, exchange and Coulomb contrib. 77−20278
$PrSn_3$, inelastic neutron scatt. spectra, cryst. elec. field effects 78−43336
$PrSn_3$, magnetoresistance 80−24877
$PrSn_3$, Neel temp., hydrostatic press. depend. 80−29549
$PrSn_3$, thermal expansion and transverse elastic const. near mag. phase transition 80−60394
Pr_5Sn_3, low temp. modification with tetrogonal struct. 80−1963
Pt-Mn-Sn alloy, mag. hyperfine fields 79−1737
Pt-Sn, Fermi energy influence on thermodynamic props. *(German)* 80−24619
Pt-Sn, solid soln., magnetic props. and lattice parameters *(German)* 79−87236
Pt-Sn alloys, thermodynamic props. *(German)* 78−52769
Pt-Sn melts, surface tension and density *(Russian)* 80−39388
Pt-Sn/Al_2O_3 catalyst, Mossbauer effect, reactivity 80−11298
PtMnSn, ^{197}Au and ^{119}Sn hyperfine fields, Mossbauer expt. 78−72439
PtMnSn, Cd impurities, hyperfine field meas. 78−15074
Pt_3Sn, electronic struct., calc. using linear-muffin-tin-orbitals method 77−24516
Pt_3Sn, Fermi surface, de Haas-van Alphen effect meas. 77−24514
Pt_3Sn, Ll_2 ordered alloy, positive temp. depend. on strength, phase destabilization 80−81203
Rh_2CoSn, ferromag., crit. exponent of ^{119}Sn hyperfine field, Mossbauer obs. 78−92008
Rh_2CoSn, ferromag., mag. hyperfine fields of ^{119}Sn, Mossbauer meas. 78−10816
Rh_2CoSn, ferromag. Heusler alloys, hyperfine fields, spin echo meas. 77−63314
Rh_2CoSn, hyperfine mag. fields at ^{119}Sn, under press., Mossbauer expts. 79−99812
Rh_2CoSn, metallic ferromagnet, hyperfine mag. field temp. depend. *(Russian)* 78−80265
Rh_2FeSn, ferromag., mag. hyperfine fields of ^{119}Sn, Mossbauer meas. 78−10816
Rh_2FeSn, ferromag. Heusler alloy, hyperfine fields, spin echo meas. 77−63314
Rh_2FeSn, Heusler alloy, Sn and Fe hyperfine field, Mossbauer exam. 77−43920
Rh_2FeSn, hyperfine mag. fields at ^{119}Sn and ^{57}Fe, under press., Mossbauer expts. 79−99812
Rh_2FeSn, metallic ferromagnet, hyperfine mag. field temp. depend. *(Russian)* 78−80265
$RhMn_2Sn$, mag. and cryst. props. 77−20568
Rh_2MnSn, and related cpds., with Heusler and Heusler-related struct., mag. props. 77−8311
Rh_2MnSn, ferromag., mag. hyperfine fields, time differential PAC meas. 77−81040
Rh_2MnSn, ferromag. Heusler alloy, hyperfine fields, spin echo meas. 77−63314

tin alloys continued
Rh_2MnSn, ferromag. Heusler alloy, hyperfine mag. field meas. by TDPAC technique 79−78580
Rh_2MnSn, Heusler alloy, Sn hyperfine field, Mossbauer exam. 77−43920
Rh_2MnSn, mag. hyperfine fields at Rh and Sn sites, and their temp. depend. 78−43708
Rh_2MnSn, Rh_2NiSn, Heusler alloys, hyperfine mag. field at Sn 78−39482
Ru-Sn compounds, type of binding *(German)* 77−35503
Ru-Sn-M, m=Mg, Ca, Sr, Sc, Y, Zn, Cd, In or Th 80−100777
Ru_2FeSn, ferromag. Heusler alloys, hyperfine fields at nonmagnetic atoms in various sites, Mossbauer effect and NMR meas. 80−66089
Ru_2FeSn, hyperfine mag. field, Mossbauer spectra 80−15865
Sb-Sn, dil., de Haas-van Alphen effect, effective mass, Fermi levels 78−75982
Sb-Sn, electronic work function, contact pot. difference meas. 77−85299
Sb-Sn (0.5 to 1.0 at.%), carrier transport, magnetoresistivity, field-dependent tensor study 80−39609
Sb-Sn (8 at.%), grain boundary-migration, intergrain liq. layer effects *(Russian)* 77−15633
Sb-Sn melt, electrotransfer *(Russian)* 77−66034
SbSn, ^{120}Sb elec. quadrupole interaction, temp. depend. 78−19399
$Sc_3SnC_{1-x}(B_{1-x})$, stabilising effect of C and B on alloying behaviour 77−36454
$SmSn_3$, NMR Knight shift, extension to low temp. 77−20735
Sn bronze, extruded atomized powders, struct. and props. 79−38763
Sn-Ag, liq., elec. resist. thermoelectric power using t matrix approach 77−31988
Sn-Ag liquid alloys, thermodynamic study by solid-oxide galvanic cell 79−20031
Sn-Al melt, reaction with Nb for protective coating prod. *(Russian)* 79−70221
Sn-Au, amorphous film, elec. resist., temp. depend. 79−91159
Sn-Au(Cu), amorphous film, optical props. 79−69895
Sn-Bi, atomic self-motions *(Rumanian)* 78−47226
Sn-Bi, crystal struct. and superconductivity after appl. of high press. and quenching 80−10531
Sn-Bi, crystallisation temp., overcooling temp. *(Russian)* 80−97472
Sn-Bi, eutectic, superplastic anisotropy *(German)* 80−25808
Sn-Bi, liq., US vel. and thermophysical props. meas., 500-1000K 78−38778
Sn-Bi, small κ supercond., phase transitions higher than second order 80−88668
Sn-Bi, supercooled, dendritic growth rates *(Russian)* 78−80533
Sn-Bi, thermal analysis in non-faceted/faceted eutectic systems 80−71637
Sn-Bi alloy, splat-quenched, energy dispersive X-ray diffr. 78−23728
Sn-Bi fine alloy powder, electrodeposition, electrolyte comp. effect 80−7519
Sn-Bi(Pb)(Ga), temp. regime of crystn. on rapid cooling *(Russian)* 80−66495
Sn-Cd, interface undercooling-growth vel. relationship, horizontal and vertical solidification 79−8294
Sn-Cd-Pb system, contacting layer struct. and phase composition *(Russian)* 80−66475
Sn-Co alloy plating from sulphate electrolyte 80−16597
Sn-Co liq., elec. resist. and thermoelec. power using t matrix approach 77−31988
Sn-Cu, strong coupling superconductor, LF EM response function 78−10605
Sn-Cu film, metastable supercond. alloys produced by low temp. ion implantation 80−88670
Sn-Cu film, spreading kinetics on Nb substrate in vacuum, 700 to 800°C *(Russian)* 77−80680
Sn-Cu(Au) films, amorphous and polycrystalline, thermopower meas. *(German)* 77−80857
Sn-Cu(Pb), effective atomic number from β-ray produced bremsstrahlung meas. 78−22046
Sn-Ge(Au), liquid alloy, exam. of activity and heat of mixing, using mass spectrometry 78−51706
Sn-In, dil., amplitude depend. US attenuation in normal and supercond. state 77−28299
Sn-In, dil., intermediate state, US attenuation 79−42694
Sn-In, dil. whisker, supercond., current-induced resistive state 79−51712
Sn-In, distribution function branch imbalance, relaxation 79−33401
Sn-In, nonlinear conductivity of thin films in mixed state *(Russian)* 80−80464
Sn-In, supercond. crit. RF mag. field, rel. to superheating 78−2632
Sn-In (50 wt.%), mech. state relations at low and high homologous temps. 77−63707
Sn-In dil. liq. alloy, electrodiffusion and electroconvection, effective diffusion coeff., apparent effective valence 78−87802
Sn-In multilayered superconducting film, critical currents 79−61017
Sn-In/Pb-In proximity sandwiches, crit. currents 79−60992
Sn-In-Te system, SnTe based solid solns. formation 77−84929
Sn-In(Cd)(Sb)(Bi) whisker, supercond. crit. temp., stress depend. 77−39988
Sn-La(Ce)(Y) systems, heats of form. 80−89517
Sn-Ni, electrodeposit, Mossbauer meas. 80−39990
Sn-Ni, electrodeposited, thermal stability 77−52319
Sn-Ni, electroplated, passive layer, ESCA study 78−23867
Sn-Ni, equiatomic, metastable, transformation kinetics, Avrami parameters calc. method 78−92239
Sn-Ni alloys, electrodeposited Mossbauer spectroscopy 79−61269
Sn-Ni electrodeposit, contact resist. corrosion effect 78−47847
Sn-Ni electrodeposit, metastable, transform. kinetics, X-ray and SEM meas. 78−38979
Sn-Ni electrodeposited equatonic alloy, cryst. struct., X-ray, electron diffr. anal. 80−79748
Sn-Ni electrodeposits, metastable, transform. kinetics 78−43262
Sn-Ni electrodeposits, worn, and Au coated, corrosion resist. 77−77628
Sn-Ni electroplated alloy, etch rates using quartz cryst. microbalance, contact resist. 77−59981
Sn-Ni equiatomic electrodeposited alloy, surface comp. 78−47649
Sn-Ni metastable alloy, surface film comp., time depend., XPS 78−60870
Sn-Ni metastable equiatomic alloy, sputter deposition 78−3043
Sn-Pb, binary liq. soln., surface cluster functions 78−67631
Sn-Pb, dil., lattice dynamics, sp. ht., resist., thermal expansion and nuclear γ reson. expts. *(Russian)* 78−87749

tin alloys continued
Sn-Pb, dil., undercooled alloy, solidification 78−3120
Sn-Pb, eutectic system, interlamellar spacing meas. 77−36492
Sn-Pb, liq. calc. of electromigration forces and resist. 79−82572
Sn-Pb, liquid alloy, thermodynamic activity determ. using Knudsen method *(German)* 79−34008
Sn-Pb, refining by fractional solidification 79−61536
Sn-Pb, supercooled, dendritic growth rates *(Russian)* 78−80533
Sn-Pb, thermo-EMFs meas. 77−20300
Sn-Pb (15 wt.%), forging of liquid and partially solid alloys 78−80569
Sn-Pb (15 wt.%), partially solidified slurry, exam. of structure, viscosity 78−84793
Sn-Pb (26%), liq. eutectic alloy Seebeck coeff. 80−84463
Sn-Pb (38 wt.%), graphite fibre reinforced, effect of interface on fracture characts. 78−76723
Sn-Pb (38.1 wt.%), liq., self-diffusion coeff. of Sn, 466 to 786K 77−69106
Sn-Pb (5 wt.%) ingots, quenching technique, for studying formation of macrosegregations 78−52793
Sn-Pb alloys, dil., low-freq. phonon spectrum peculiarities 79−60463
Sn-Pb alloys, electron work function determ., contact pot. difference method 77−39920
Sn-Pb alloys, inhibited electrocrystn. *(German)* 79−38753
Sn-Pb alloys, stress relaxation and activation enthalpy 79−74190
Sn-Pb alloys electroplating, comparison with Au *(French)* 80−89158
Sn-Pb composition anal. of PCBs using beta-backscatter gauge 80−16631
Sn-Pb eutectic, strain rate sensitivity of flow stresses, grain boundary sliding during superplastic, non-superplastic deform. 80−7645
Sn-Pb eutectic, struct. and plasticity, thermomech. treatment effects *(Russian)* 78−60686
Sn-Pb eutectic alloy, inelastic behaviour 77−48471
Sn-Pb investment castings, graphite fibre reinforced, tensile strength 77−48487
Sn-Pb solder, wettability on Cu and mild steel plates *(Japanese)* 80−89244
Sn-Pb solder on Cu plate, spreadability, effect of fluoride and iodide addition to $ZnCl_2$ flux *(Japanese)* 80−29251
Sn-Pb surfaces ageing, detrimental effect in PC fabrication 80−108625
Sn-Pb-Bi-(Cd) infiltrated Ti base composite sintered bearing material, antifriction props. 80−60981
Sn-Pb-(Bi) infiltrated Ti base composite sintered bearing material, antifriction props. 80−60981
Sn-Pb-(Bi)(Ag)(Sb) (Cu), microduplex eutectic, cavitation during superplastic flow 78−48457
Sn-rare earth , dil. liq., elec. resist. and mag. susceptibility 78−43350
Sn-Sb, A1-type, superconductivity 80−29496
Sn-Sb, small κ supercond., phase transitions higher than second order 80−88668
Sn-Sb (0.57 at.%) solid soln., yield point for cold-worked and annealed specimens *(Russian)* 78−48448
Sn-Sb (10 wt.%), decomposition of supersaturated solid soln. 80−29960
Sn-Sb alloys electrodeposition 80−25586
Sn-Sb dil. liq. alloy, electrodiffusion and electroconvection, effective diffusion coeff., apparent effective valence 78−87802
Sn-Sb molten alloys, thermodynamic study *(Korean)* 78−31383
Sn-Sb-Ag, splat cooled foils, TEM study 80−40344
Sn-Se, melt, density, kinematic viscosity, struct., 900-1400K 78−14395
Sn-Te, molten, elec. cond. and phase diagram 80−84454
Sn-Te alloy, liq., magnetic susceptibility 79−87232
Sn-Te liquid alloy, thermodynamic meas. 77−73271
Sn-Zn, ingots, solidified, formation of equiaxed eutectic grains *(Japanese)* 78−39756
Sn-Zn, molten, struct. investig. by neutron diffr. 79−4233
Sn-Zn, planar and cellular solidification interfaces, distrib. coeffs. and conc. profiles *(German)* 77−32568
Sn-Zn, thermodynamic quantity meas. by quantitative thermal anal. of heating process 78−19730
Sn-Zn, use as evaporant source for Zn bearing thin film alloy prep. 80−100789
Sn-Zn (0.4 at.%) solid soln., yield point for cold-worked and annealed specimens *(Russian)* 78−48448
Sn-Zn (9.8 wt.%), eutectic superplasticity 77−36582
Sn-Zn eutectic, liq., appl. to drilling of steel, cutting conditions rel. to tool parameters *(Russian)* 79−34187
Sn-Zn melts, plasticising action in deform. hardening of medium C steel 80−55415
Sn-Zn(Hg)(Tl)(Bi) dilute alloys, thermo EMF *(Russian)* 79−33285
$Sn_{11}Cu_{41}$, γ-brass struct., F-cells, X-ray diffr. 77−19903
$Sn_{90}Cu_{10}$, quench-condensed films, superconducting transition temp., elastic stress and strain effects 80−70883
Sn_3Cu_9Ni, γ-brass struct., F-cells, X-ray diffr. 77−19903
$Sn_{0.99}In_{0.01}$, superconducting-normal interface, boundary resist. 80−50006
$SnMg_2$, ^{119}Sn temp. depend. isomer shift, pseudopot. approach 80−84675
SnNi electroplate, anal. by SIMS, ion scatt. spectrometry, and Rutherford backscatt. 78−95979
SnNi, metastable, oxidation, AES obs. 77−48575
SnPb 38, superplasticity, effect of ageing *(Czechoslovakian)* 77−32644
SnPb eutectic alloy, Mossbauer spectra, isomer shifts 79−82903
Sn_xPg_{1-x}, thermal cond. and Lorenz function 78−51966
SnSb film, defect density variation with deposition rate, annealing, elec. resist. meas. 77−21027
$SrNiSn_3$, cryst. struct. rel. to $ThCr_2Si_2$ type *(German)* 78−51470
$SrPdSn_3$, prep. and crystal structure *(German)* 80−84138
Tb-Sn, effective field at diamag. Sn impurities, 4.2 to 235K *(Russian)* 77−69549
$TbRh_xSny$, crystallography X-ray powder diffr. study 80−100217
Te-Sn (20 at.%), amorphous, exam. of crystallisation by DTA, X-ray diffr. and TEM 78−47242
TeSn, ^{125}Te elec. quadrupole interaction, temp. depend. 78−19399
$ThSn_3$, inelastic neutron scatt. 80−11165
Ti-Al system, compact growth in liquid phase sintering 80−20835
Ti-Al-Mo-Cr-Fe, distrib. of Sn, Zr between phases, temp effect. 80−55357
Ti-Al-Mo-Sn, environmental effects in alloy fretting, effect on fatigue props. 78−56787
Ti-Al-Mo-Sn alloy, elastically and plastically deformed, positron annihilation meas. of deformation 80−21038

tin alloys continued
Ti-Al-Mo-Sn-Si (4,4,2,0.5 wt.%), fracture toughness and crack propag. 78−39892
Ti-Al-Sn, alloy 6242, dynamic effects of flow and fracture during isothermal forging 80−76343
α-Ti-Al-Sn, alloy Ti-679, electron diffr. anal. of Ti_3Si phase *(Chinese)* 80−64845
Ti-Al-Sn, electrochemical behaviour under tensile stress in boiling H_2SO_4 and acidic chloride solns. 78−95851
Ti-Al-Sn, specific heat and thermal expansion, 4-290K *(Russian)* 79−51276
Ti-Al-Sn, type Ti-5621S, irrad. induced creep 80−39163
Ti-Al-Sn, VT5-1, solid solutions, heat cond. at low temps. *(Russian)* 79−82574
Ti-Al-Sn (3.7, 0.8 at.%) alloy, specific heat, 4 to 290K *(Russian)* 79−14938
Ti-Al-Sn (5, 2.5 wt.%), annealing of near-basal hydrides 80−20989
Ti-Al-Sn (5, 2.5 wt.%), ductile fracture at low temps. 78−64659
Ti-Al-Sn (5, 2.5 wt.%), electron microscope and X-ray diffr. exam., of basal and near basal hydrides 78−80550
Ti-Al-Sn (5, 2.5 wt.%), fracture mechanism at cryogenic temps. 78−64642
Ti-Al-Sn (5, 2.5 wt.%) alloy, fatigue under combined alternating bending and torsional stresses 77−8923
Ti-Al-Sn (5, 2.5 wt.%). corrosion resist. in marine environments *(French)* 80−50767
Ti-Al-Sn (5, 2.5%) cryogenic constructing material, far IR spectral refl. 77−24855
Ti-Al-Sn-Zr, Ti-680, O contamination under high temp. *(Chinese)* 80−66688
Ti-Al-Sn-Zr (6.19, 1.92, 1.43 wt.%), fatigue cracking characteristics of β annealed microstruct. 79−5051
α-βTi-Al-Sn-Zr-Mo (6, 2, 4, 6 wt.%), interface struct. 77−44212
α-βTi-Al-Sn-Zr-Mo (6, 2, 4, 6 wt.%), deformation associated with surface cracks and α particles 79−79107
Ti-Al-Sn-Zr-Mo (6,2,4,6 wt.%), α-β type 6246, fusion zone fracture behaviour in weldments 80−30093
Ti-Al-Sn-Zr-Mo (6,2,4,6 wt.%) fusion weldment, substruct. characts. 80−84183
Ti-Al-Sn-Zr-Mo (6,2,45 wt.%), surface cracking under unidirectional loading 78−56753
Ti-Al-Sn-Zr-Mo alloy, Ti-6242, $\alpha+\beta$, creep property improvement by Pt ion plating 80−16408
$\alpha+\beta$-Ti-Al-Sn-Zr-Mo-Cr, low cycle fatigue crack nucleation and early growth 79−8354
Ti-Al-Sn-Zr-Mo-Si (6, 2, 4, 2, 0.1 wt.%), effect of elevated temperature and environment on fatigue crack growth 80−40486
Ti-Al-Sn-Zr-Mo-Si-O-H, Si, O, H effects on fatigue, fracture and creep charact. 79−11697
Ti-Al-V-Sn (5.5, 5.3, 2.3 wt.%) fatigue crack growth and fracture resistance enhancement, due to annealing 78−35510
Ti-Al-V-Sn (5.5, 5.5, 2 wt%), crack growth, slow, H-induced 80−104272
Ti-Al-V-Sn (6, 6, 2 wt.%), surface finishing effect on internal stresses, X-ray study *(German)* 79−34210
Ti-Al-V-Sn (6, 6, 2 wt.%) weldments, heat treated, transangular fracture 80−40524
Ti-Al-V-Sn (6, 6, 2 wt.%), fatigue crack growth, cyclic freq. and microstruct. influence 80−55515
Ti-Al-V-Sn (6,6,2 wt.%), heavy section extrusion, fabrication and mech. props. 78−6985
Ti-Al-V-Sn (6,6,2 wt.%), H_2 induced crack growth, in-situ scanning Auger anal. 79−8355
Ti-Al-V-Sn (6,6,2 wt.%), α-β type 662, fusion zone fracture behaviour in weldments 80−30093
Ti-Al-V-Sn (6,6,2 wt.%), depend. of K_{ISCC} on loading rate and crack orientation 80−45427
Ti-Al-V-Sn (6,6,2 wt.%) solid metal embrittlement by Cd, Ag and Au 80−16551
Ti-Al-V-Sn (6,6,2 wt.%) fusion weldment, substruct. characts. 80−84183
Ti-Al-V-Sn (6,6,4 wt.%), SCC, subcritical flow growth, comparison of aircraft alloys in NaCl soln. 78−53028
Ti-Al-V-Sn-Zr alloy TS5, annealing effect on ductility and strength *(Russian)* 78−35427
Ti-Al-V(Sn) alloys, plastic deformation and fracture characts. at low temps. *(Russian)* 80−7624
Ti-bronze, friction with diamond, characts. 78−48541
Ti-Cu-Sn, heat treatable alloys, effect of alloying on strength, tensile props. 78−56671
Ti-Mo-Zr-Sn, alloy, βIII, struct. transform. in thermally affected zones after electron beam welding 78−23919
β-Ti-Mo-Zr-Sn (10.2, 5.8, 4.7 wt.%) heat treated, tensile yield, fracture behaviour, primary deform. mode, exam. 78−60724
Ti-Mo-Zr-Sn (11.5, 6, 45 wt.%), plastically strained regions, decoration 77−28864
Ti-Mo-Zr-Sn (11.5, 6, 4.5 wt.%), metastable beta III phase, recrystallization and grain growth 80−3091
Ti-Mo-Zr-Sn (11.5, 6.0, 4.5 wt.%), mech. property, microstruct. relationships 80−84961
Ti-Mo-Zr-Sn (11.5, 6.0, 4.5 wt.%) alloy, struct. as affected by processing history 80−84972
Ti-Mo-Zr-Sn-Fe-C-Si alloy, β-III, cold deform. and annealing, effect on struct. and mech. props. *(Russian)* 79−24533
β-Ti-Mo-Zr-Sn(11.5, 6, 4.5 wt.%), metastable phase III, microstruct. and age hardening response 80−84945
α-Ti-Sn, Mossbauer spectra, metastable θ- and ω-phases 80−20556
Ti-Sn, porous, effect of Al and Sn on sintering 80−20830
Ti-Sn(0.5 to 2 at.%), thermal and athermal solid solution strengthening 77−4787
α-β TiAl-Sn-Zr-Mo (6,2,4,6 wt.%), age hardening 79−61604
Ti_3Al-Sn-Zr, alloy, Sn and Zr alloying influence on creep and scaling resist. *(Russian)* 79−52302
Ti_3Sn, oxidation *(Russian)* 78−19939
TiSnSb, synthesis and struct. *(French)* 79−90596
Tl-Sn-Bi, liquid alloy, thermodynamic props. *(Russian)* 79−10968
USn_3, crystalline elec. field studies using neutron inelastic scatt. at NRCN 80−10931
USn_3, inelastic neutron scatt. 80−11165
USn_3, thermoelectric power, 5-300K 79−65444
$V_3Ga_{1-x}Sn_x$, lattice props. supercond., ^{119}Sn Mossbauer shift meas., 5-300K 77−1627
V-Sn-C, phase equilib. and supercond. 80−50593

tin alloys continued
V-Sn-(Ti), corrosion resistance and some physicomechanical props. 77−70229
V(Nb)-Sn-Cu, rapidly quenched, comp. and phase equilib. 80−76235
V_3Sn, A-15 cpd., normal-state elec. resist. 80−75542
V_3Sn, elec. resist., temp. depend., T_c to 300K 79−65426
V_3Sn, electronic struct., electron-phonon interactions, and low temp. anomalies 79−60701
V_3Sn, electronic struct. calcs. 79−47005
V_3Sn, ultrafast quenched and subsequently tempered, supercond. T_c 78−64162
$V_3Sn_{0.5}Al_{0.5}$, elec. resist., temp. depend., T_c to 300K 79−65426
$V_{2.4}Ti_{0.6}Sn$, elec. resist., temp. depend., T_c to 300K 79−65426
$YbSn_3$, powdered, de Haas-van Alphen effect 80−59857
Zircaloy-4, deformation behaviour between 77 and 900K 80−71686
Zircaloy-4, vapour transport of Zr and Si 80−55437
Zn-Al-Cu-Mg-Pb-Sn, Cu, Mg, Pb, Sn effects on corrosion in wet steam 77−48585
Zn-Al-Cu-Mg-Pb-Sn (12, 1, 0.02, 0.01, 0.015, wt.%), combined effects of Pb and Sn additions on corrosion, in wet steam 78−39952
Zn-Cd-Bi-Sn phase diagram with liquid-liquid immiscibility, computer calc. 77−36463
Zn-Sn, binary metallic melt, deviation from the Kopp law, specific heat *(Russian)* 80−39305
Zn-Sn, discrete eutectic formation mechanism *(Russian)* 77−66634
Zn-Sn, specific elec. resist., temp. and conc. depend., 20-800°C 79−82571
Zn-Sn and Zn-Sn-Pb, intergranular and solid-liquid interfacial tensions 77−36452
Zn-Sn-Bi, ternary phase diagrams, interactive computer program 80−71629
Zn-Sn-Hg, diagram of state, melting temp., peritectic and eutectic phases *(Russian)* 80−55350
Zn-Sn-Hg amalgam, liq., thermodynamic props. *(Russian)* 77−66624
Zr-Mo-Nb-V-Sn (1,2,2,2 wt.%), heat treatment, transform. reactions and mech. props. 79−24545
Zr-Mo-Sn (3,2 wt.%), heat treatment, transform. reactions and mech. props. 79−24545
Zr-Nb-Sn (3.0, 1.0 wt.%), oxidation kinetics in flowing CO_2, 873 to 1173K 80−16596
Zr-Nb-Sn (3.0, 1.0 wt.%), high temp. oxidation in flowing O_2, 873-1173K 80−93687
Zr-Nb-Sn(3 wt.%, 1 wt.%), oxidation kinetics in flowing CO_2 at high temp. 80−47575
Zr-Sn, grain-boundary migration during fatigue at 600 to 775°C 80−16443
Zr-Sn, inelastic deformation, generalised strain rate dependent constitutive eqn., load relaxation tests 79−11655
β-Zr-Sn, zircaloy-2, exam. of grain boundary sliding 78−79616
Zr-Sn, Zircaloy-2 and 4, high temp. oxidation in steam 78−80676
Zr-Sn, Zr-Sn-Mo, creep characts., influence of Sn and Mo *(Czech)* 80−81119
Zr-Sn (1.5 wt.%), electron irradiation damage, direct obs. 80−84212
Zr-Sn (1.5 wt.%), martensitic transform. contrib. to strength and work hardening, and martensite flow props. 78−84842
Zr-Sn alloys, mathematical models for transient deform. 78−86616
Zr-Sn-Fe-Ni (1.5, 0.1, 0.15 wt.%), electron irradiation damage, direct obs. 80−84212
Zr-Sn-Mo (4.5,1 wt.%) and (4.5,2 wt.%), creep behaviour at room temp. *(Czech)* 79−24590
Zr-Sn-Mo (6, 1 wt.%), creep and creep rupture 78−23778
Zr-Sn-Mo-(Nb), creep and creep fract. at 623 to 823K *(Czechoslovakian)* 77−32643
Zr-Sn-Mo-(Nb), fracture in creep 77−36581
Zr-Sn-Mo(Nb), creep and creep fracture, 623 to 823K *(Czech)* 77−59916
Zr-Sn-No-(Nb), steady state creep 77−36580
Zr-Sn(Fe)(Ni) (0.15 wt.%), electron irradiation damage, direct obs. 80−84212

tin compounds
see also tin alloys
binary, with chalcogenides and pnictides, at. vol. and semicond. props. 77−20089
chalcogenides, multicolour photodetectors *(Czech)* 79−26126
chalcogenides, oxidation, thermal decomp., Mossbauer spectra 79−11713
chalcogenides, photoemission, book contrib. 77−44133
chalcogenides, screw dislocations in layer crystal growth from vapour *(Russian)* 80−1953
chloromethylstannane, polycryst., proton spin-lattice relax. times meas. 78−39430
n-dibutyl(ethylene-1,2-dithiol)stannane, cryst. data 77−15400
2,3-dihydroxybutanedioate, Sn(II) valency config., Mossbauer and X-ray electron determ. *(Russian)* 77−8483
dimethyl stannous chloride di(pyridine 1-oxide), ^{119}Sn Mossbauer spectra, elec. field gradient 80−15909
dimethyl tin diisothiocyanate, ^{119}Sn Mossbauer spectra, elec. field gradient 80−15909
dimethyltin difluoride, neutron scatt. exam. methyl group motion 78−59769
diphenyl tin sulphide trimer, cryst. data 77−15400
environmental pollution, separation and chem. anal. methods 79−79416
halides, effect on resin vulcanisation, IR spectra *(Bulgarian)* 79−33994
halides, matrix isolated, Mossbauer effect, isomer shift and quadrupole splittings obs. 78−46377
halides, mol. electronic struct., quadrupole-interaction-interaction consts., CNDO/2 calc. 77−10589
halides, UV photoelectron spectra of valence d shells, gas-phase 78−62845
halides, XY_4 molecules, force consts. by modified Redington and Aljibury method 80−69261
halomethylstannanes, internal torsion modes, inelastic neutron scatt. 77−19105
hexahalo ions, octahedral, mol. consts. calcs. 80−106317
inorganic and organometallic cpds., photoelectron spectra, valence bands, ligand field broadening 77−63525
$M^IM^{IV}IO_6$, vibr. spectra (M^I=Na,K,Rb,Cs,NH_4; M^{IV}=Ge,Sn,Pb) 77−42325
methyltin compounds, separation and determ. in environmental samples 79−79416
monochalcogenides, interaction of outer s states 79−10825

tin compounds continued
monochalcogenides interaction of internal s states 79−10826
Mossbauer effect, isomer shifts, quadrupole splitting, CNDO/II calcs. 77−24766
Mossbauer isomer shifts, book contrib. 79−87359
Mossbauer line intensity dependence on nonuniform electronic absorption 79−47372
organic compounds, $[R^IR^{II}R^{III}PO]_2SnR_nCl_{4-n}$, $[R^IR^{II}R^{III}PO]SnR_3Cl$, Mossbauer spectra, isomer shift and quadrupolar splitting *(Russian)* 79−61285
organo tin dichlorides, tetrahedral, dilute soln., dielec. and thermodynamic behaviour, microwave region 77−36170
organo tin polymers, glow discharge formed, interface composition and adhesion 79−82467
organotin compounds, with remote substitutions, ^{119}Sn NMR constants 79−65748
oxalate, Sn(II) valency config., Mossbauer and X-ray electron determ. *(Russian)* 77−8483
oxalate cryst. struct. determ. by X-ray crystallography, relations with $Na_2C_2O_4$, $Na_2Sn(C_2O_4)_2$ *(French)* 80−2004
n-propyl(n-butyl) tin dichloride, prep. and Lewis acid charact. 77−90597
silicones, fungicidal protection of optical components made of chem. unstable glass 78−59107
sodium tin oxalate, cryst. struct. rel. to those of $Na_2C_2O_4$, SnC_2O_4 *(French)* 80−2004
sulphide compounds of Si, Ge and Sn, struct. and chem. bonding *(French)* 78−30580
ternary compounds, $R_ySn_xMo_6S_8$ (R=La, Ce, Pr, Eu, Gd, Ho, Lu, Y, In, U), supercond. props. 80−97023
tetraethyl tin, thermal conductivity and density, −13.5 to +90°C 77−15637
tetrahalides, isotope shifts, Coriolis coupling and force consts., isotope substitution and matrix isolation 77−42322
tetrahalides, non-empirical valence electron MO calcs., ion states spin-orbit splitting 77−34544
tetrahalides of Gp.IV elements, M-X bond flexibility, by compliance scheme 80−37805
tetrahedral molecular solids, ^{119}Sn Mossbauer and Raman spectra 78−15070
tetramethyl tin, methyl reorient., lattice vibrs., neutron scatt. obs. 79−51016
trimethyl tin cyanide, ^{119}Sn Mossbauer spectra, elec. field gradient 80−15909
tris(trimethylstannyl)phosphine, gamma irrad., free radicals, struct. and EPR spectra 80−29623
Ag-Sn-Te phase equilib. 79−29033
$AgInS_2$-SnS_2, spinel phase $Ag_xIn_xSn_{1-x}S_2$ obs., stoichiometry *(French)* 80−44326
$AgInS_2(Se_2)$-$SnS_2(Se_2)$, degree of solid solubility and phases characts. 78−35377
Ag_2S-In_2S_3-SnS_2 system quaternary and ternary sulphide spinels, solid solubility and struct. 78−35376
$Ag_8SnS_6(Se_6)$, absorpt. edge investigs. at phase transitions 78−35149
$Ag_{1-x}Sn_{1+x}Se_2$ $_y$, supercond. and normal state props. 77−36008
β-Al_2O_3-$(K,Sn)_2O$, ionic cond. and Raman spectra 80−107509
As_2Se_3-$GeSe_x$-$SnSe_x$ (x=1,2), exam. of Sn valency and physical props. 79−4753
Au-$Pb_xSn_{1-x}Te$-Au structure, third harmonic variations at 77K and 300K 78−84313
BiTe-In(Gn,Sn)Te system, physicochemical anal., eutectic type phase diagram with solid soln. region 77−16556
$Ca_xGd_{2-x}Sn_{2-x}Sb_xO_7$, pyrochlorate struct. form. 80−92504
$CaO.SnO_2.SiO_2$, tin sphene, lattice parameters 77−7697
$Cd_2Nb_{2-2x}Sn_{2x}O_{7-2x}F_x$, solid soln., X-ray diffr. and Mossbauer study *(French)* 78−87659
CdO-SnO_2 DC reactively sputtered films, elec. and optical props. 80−103763
CdO-SnO_2 film, DC reactively sputtered, transparent electrode props., optimum sputtering conditions 80−11116
CdO-SnO_2 film, prep. by RF sputtering, elec. cond. and transparency 80−7492
p-$CdSnAs_2$, Hall effect, thermo EMF, thermomagnetic effects 80−107822
n-$CdSnAs_2$, optical absorption rel. to energy spectra *(Russian)* 78−75994
$CdSnAs_2$, solubility in Sn melt, temp. depend., enthalpy of melting 80−59658
$CdSn_xO_y$, DC reactively sputtered film, elec. and optical props. 79−87022
p-$CdSnP_2$, photocond. meas., polarisation depend. 78−39157
$CdSnP_2$-$CdSnAs_2$, and $CdSnP_2$-$CdGeP_2$, solid solution form. and elec. characterisation 78−43125
CdTe/$SnCl_2$/Pt, solar cell photoelectric props. *(Spanish)* 80−85290
CdTe-$SnCl_2$ electrolyte heterojunction photoelec. props., feasibility as solar energy convertors 77−76918
Ce_2Se_3-$SnSe_2$, solid-solution region, physical properties 78−43391
$Co(H_2O)_6[SnF_3]_2$, crystal structure *(French)* 80−59441
$CoSnTe_2$, thin films, metallic elec. props. 79−78212
$CuInS_2$-SnS_2, spinel phase $Cu_xIn_xSn_{1-x}S_2$ obs., stoichiometry *(French)* 80−44326
$Cu_2S(Se)$-SnS, phase diagrams 78−44100
Cu_2SnS_3-CdSe, diamond-type semiconductor, Mossbauer spectrum of ^{119}Sn 80−44991
$(Cu_2SnS_3)_x$-$(3CdS)_{1-x}$, diamond-type semiconductor, Mossbauer spectrum of ^{119}Sn 80−44991
$(Cu_2SnS_3)_x$-$(3ZnS)_{1-x}$, diamond-type semiconductor, Mossbauer spectrum of ^{119}Sn 80−44991
Cu_2SnSe_3-CdS, diamond-type semiconductor, Mossbauer spectrum of ^{119}Sn 80−44991
$(Cu_2SnSe_3)_x$-$(Cu_2SnS_3)_{1-x}$, diamond-type semiconductor, Mossbauer spectrum of ^{119}Sn 80−44991
Cu_2Te-$SnTe_2$, phase equilib., microstructural, DTA investigs. 77−16560
$Eu_xSn_{1-x}Mo_6S_8$, Chevrel phase supercond. cond. electron polarisation by Eu^{2+}, effect on supercond. props. 79−56650
$Eu_2Sn_{1-z}Mo_6S_y$, supercond., mag. props. 77−69447
$Eu_xSn_{1-x}Mo_6Sn_8$ (Se_8), ternary superconductor, paramagnetic relax. effects 78−68112
$(Eu_{1-x}Sn_x)S$, high press. Mossbauer exam. of Curie temp. and transferred hyperfine field 79−56643
Eu_2SnS_4, cryst. struct. *(French)* 79−86757
$Eu_3Sn_2S_7$, cryst. struct. *(French)* 78−18597

tin compounds continued
$Eu_1Sn_2S_7$, cryst. struct. *(French)* 79−86757
$Eu_4Sn_2S_9$, cryst. struct. *(French)* 79−86757
$Eu_5Sn_3S_{12}$, cryst. struct. determ. *(French)* 77−47388
$Eu_5Sn_3S_{12}$, cryst. struct. *(French)* 79−86757
$(Eu_{1-x}Sn_x)Se$, high press. Mossbauer exam. of Curie temp. and transferred hyperfine field 79−56643
Eu_xWO_3-Sn_yWO_3, prep. and struct. of mixed W bronzes 77−4085
$FeSnO_3$, Mossbauer spectral anal. *(German)* 79−19819
$Fe_2(SnO_3)_2$, Mossbauer spectral anal. *(German)* 79−19819
$Fe_{3-x}Sn_xO_4$, mag. hyperfine fields, ^{57}Fe and ^{119}Sn Mossbauer spectra 80−39944
$FeSn(OH)_6$, mag. props. 78−43574
$FeSnO(OH)_5$, mag. props. and cryst. struct. 78−43574
Fe_2SnS_4, cryst. struct. *(French)* 78−18595
GaSe-SnSe system, phase diagram and lattice consts. of solid solns. 79−34014
GaSe(Te)-SnO_2 spray heterojunction, electro-optical props. 78−64102
Ga_6SnTe_{10}, cryst. struct. *(French)* 79−78946
GaTe-SnTe, melt, temp. and composition dependence of elec. cond. and thermo EMF 79−95430
GaTe-SnTe, phase equilib. 77−86006
Ge-$Pb_{1-x}Sn_xTe$, amorphous/crystalline heterojunction, rectification props., IR detector appl. *(Japanese)* 78−60197
Ge-Sn-As system alloys, microstruct., X-ray phase and thermal anal. 77−32564
$GeSe_2$-$SnSe_2$-As_2Se_3, GeSe-SnSe-As_2Se_3, Mossbauer investigation 77−20052
$Ge_xSn_{1-x}S(Se)$, lattice parameters, optical energy gap and IR refl. 78−23021
$Ge_{0.5}Sn_{0.5}Te$ film, elec. and optical props. 77−12028
$Ge_{1-x}Sn_xTe$ film, amorphous, elec. cond. 80−93016
GeTe-MnTe-SnTe system, compds., GeTe phase transition temp., elec. props., thermal cond. 79−43220
Hg vapour high-pressure lamps with Sn halide additives, chemical transport obs. 78−71576
Hg-Sn halide arc, molecular optical absorption obs. 78−75457
n-(In,Sn)O_x-p-InP solar cell, growth, efficiency 77−72910
In-Te-SnTe, phase equilib. 77−86006
In_2O_3-SnO_2, magnetron RF sputtered electro-optical film for data storage and display 78−83047
In_2O_3-SnO_2, patterned thin films, strong electron emission obs. 77−8731
In_2O_3-SnO_2, thin films deposited on cold substrates, life stability 79−23867
In_2O_3-SnO_2, transparent thin films for satellite temp. control 79−80187
In_2O_3-SnO_2, X-ray and optical meas. of solubilities 79−55894
In_2O_3-SnO_2 electro-optical film, for data storage and display 78−71176
In_2O_3-SnO_2 film, reactive DC diode sputtering, using large scale system 78−72723
In_2O_3-SnO_2 film, stress, and elec. and optical props. 78−51861
In_2O_3-SnO_2 film, XPS expts., energy band model accounting for phys. props. 77−90241
In_2O_3-SnO_2 film on Si, heterojunction, photovoltaic effect, sunlight induced 77−1470
In_2O_3-SnO_2 sputtered film, appls. in displays, vidicon tube windows, dielec. window surfaces 79−59778
In_2O_3-SnO_2 thin film, effects of heat treatment on resist. and optical absorpt. 78−43495
In_2O_3-SnO_2 thin film, Hall mobility, temp. depend., grain boundary effects 80−75658
In_2O_3-SnO_2/GaAs, solar cell, fabrication, characts. and interfacial chemistry 80−21401
In_2O_3-SnO_2/InP, solar cell, fabrication, characts. and interfacial chemistry 80−21401
In_2O_3-SnO_2/InP junction, ion probe analysis of chemical nature 79−73411
In_2O_3-SnO_2/Si solar cells, antireflection props. of oxide film 80−3513
In_2O_3-SnO_2/SiO_x/Si diode solar cells, loss mechanisms, characts., band struct. 80−26135
In_2O_3-SnO_2/polySi, solar cell response exam. using electron-beam-induced current and scanning light spot tech. 80−81477
In_2O_3-SnO_2-CdTe:P, p-n homojunction solar cell, elec., photovoltaic props., photoluminescence 80−81463
In_2O_3-SnO_2-InP solar cell junctions, efficiency, InP surface props. 80−85288
In_2O_3-SnO_2-Si heterojunctions, elec. and photovoltaic characts. 78−52070
In_2O_3-SnO_2-Si SIS heterojunction solar cells 80−85281
In_2O_3-SnO_2-Si SIS solar cells, reverse current-voltage characts. under illumination 80−89622
InSe-SnSe system, phase diagram and lattice consts. of solid solns. 79−34014
In_xSe_{1-x}-SnO_2 amorphous film-SnO_2 system, photovoltic spectra, annealing effect *(Japanese)* 80−92926
In_xSe_{1-x}-SnO_2 heterostructure, anomalous temp. depend. obs. on photovoltage 78−56209
$In_xSi_yO_z$, thin film, sputter deposition form., optical and elec. props. 80−60123
$(In_{1-x}Sn_x)_2O_2$-Si-N solar cell efficiency and elec. props. 80−35676
$(In_{1-x}Sn_x)_2O_{3-y}$, pyrolytic selective coating, Sn additions effect 78−43499
$In_{1.9}Sn_{0.1}O_3$ laser-damage-resistant transparent conductive coatings, appl. in Pockels cells 79−50333
$In_{2-x}Sn_xO_3$, sputter deposited, electrical and optical props. 79−47181
$In_{2-x}Sn_xO_{3-x}$ film, deposition with sputter gun 77−44162
$In_{2-x}Sn_xO_{3-y}$ film, deposited from organometallic composition, transparent cond. appl. 78−91793
$In_{2-x}Sn_xO_{3-y}$ film, magnetron DC reactive sputtering, X-ray diffr. meas. 77−44160
$In_{2-x}Sn_xO_{3-y}$ solar cells, majority carrier conduction effects 80−97796
$In_{2-x}Sn_xO_{3-y}$ thin films, optical transmission and elec. resist. 77−69926
n-$In_{2-x}Sn_xO_{3-y}$/p-Si, semicond.-insulator-semicond. solar cell, performance and spectral response, fabrication 79−83596
$In_{2-x}Sn_xO_{3-y}$-CdTe(InP) photovoltaic heterojunctions, surface and interface studies, efficiency 80−45691
$In_{2-x}Sn_xO_{3-y}$-$Ga_xIn_{1-x}P$(-InP_yAs_{1-y}) heterojunction solar cells, chemistry and prep. 80−94073
$In_{2-x}Sn_xO_{3-y}$-Si solar cells, SiO_2 detection of interface, Auger anal. 79−87991
$In_{2-x}Sn_xO_{3-y}$-SiO_x-Si SIS solar cells, loss mechanisms study for improvement of efficiency to above 12% 80−94080

tin compounds continued
$In_{2-x}Sn_xO_3$-$_y$-ZnS:Mn thin film structure, surface morphology and electro-optical props. *(Russian)* 80−49554
$In_{2-x}Sn_yO_{3-y}$[SnO_2]-CdSe-CdS:Cd,Cl sandwich photoconductor injection obs. *(Russian)* 80−54773
$(In_2SnTe)_x$-$(2InSb)_{1-x}$ system, semicond., Mossbauer absorption line of ^{119}Sn 78−27146
InTe-SnTe, melt temp. and composition dependence of elec. cond., and thermo EMF 79−95430
$IrSn_{1.5}S_{1.5}$, new skutterudite relation compounds, prep. and charact. 78−52700
KCl:$SnCl_2$, action of ionising radiation on Sn aggregation processes 78−34543
KCl:$SnCl_2$, photostimulated hole recombination luminesc. *(Russian)* 80−80833
KCl:$SnCl_2$, Sn^+ centres, polarised luminesc. and EPR 79−65076
KCl:$SnCl_2$, X-ray irrad., polarised luminesc. and EPR study of Sn^{3+} centres 80−39868
K_2SnBr_6, transform. dynamics probed by Raman scatt. and microscopy 78−63832
K_2SnCl_6, structural phase transition exam. by neutron powder diffr. 78−55940
K_2SnF_6, Group IV hexafluoride anion radical γ-irrad., EPR spectra 78−72411
$K_2SnF_6.H_2O$, crystallographic characts. *(French)* 78−10011
$La_{0.98}Sn_{0.02}Mo_6Se_8$, Chevrel phase supercond., hyperfine interaction, microscopic study 79−56650
$La_{0.98}Sn_{0.02}Mo_6Se_8$, Mossbauer spectra 80−15926
$Mg_2Si_xGe_ySn_{1-x-y}$ composite Te material with high figure of merit 77−28164
$MnSnO_3$, ordered ilmenite phase, cryst. struct. 78−47288
Mo-Sn-S system, phase relationships, 500-800°C 79−24503
Mo_5SnS_6, supercond., at 2 to 25K, lattice and electron contrib. to sp. ht. 77−77003
$(N(CH_3)_3H)_2SnF_6$, phase transition and temp. effects, Mossbauer and NMR spectra 78−88236
$(NH_4)_2SnBr_6$, structural phase transitions study by Raman scatt. 80−93318
$(NH_4)_2SnCl_6$, ^1H spin-lattice relax., 100-500K 79−38398
$(NH_4)_2SnF_6$, thermal study and thermolysis *(French)* 78−10011
$Na_xIn_xSn_{1-x}S_2$ (1>x>0), intercalation-substitution system, NMR study *(French)* 79−69095
$Na_xIn_xSn_{1-x}S_2$, intercalation-substitution compounds, NMR study 80−44952
$Na_xIn_xSn_{1-x}S_2$, ionic conductors, ^{23}Na NMR and complex impedance meas. 79−91314
Na_2O-Al_2O_3-SnO_2-SiO_2 glass, chemical stability in NaOH and Na_2CO_3 solns. 80−16532
Na_2O-SiO_2-Ga_2O_3-Al_2O_3-B_2O_3-SnO_2 glasses, ion exchange reactions with $NaNO_3$ and KNO_3 melts 80−16673
Na_2O-SiO_2-SnO_2, exam. of Na^+ self diffusion, elec. conductivity, and viscosity 78−87819
Na_2O-SnO_2-SiO_2 glass, density, refractive index thermal expansion hardness, IR spectra, DTA *(Japanese)* 78−15535
Na_2O-SnO_2-ZrO_2-SiO_2 glass, chemical stability in NaOH and Na_2CO_3 solns. 80−16532
$NdCl_3$-$SnCl_4$-$POCl_3$, complex formation, struct. and comp. 77−89413
$NiSnCl_6.6H_2O$, ESR line shift at very low temps. 78−56375
$NiSnF_6.6H_2O$, probability anisotropy of Mossbauer effect 79−42874
PLZT, Sn substituted, antiferroelectric ceramics research and their applications *(Chinese)* 79−33617
$POCl_3$-$SnCl_4$, Sm^{3+} fluoresc. quenching temp. depend., near reson. interaction 79−65915
$POCl_3$-$SnCl_4$, splitting of Sm^{3+} near IR absorpt. bands 80−2750
$POCl_3$-$SnCl_4$: Tb^{3+}, Sm^{3+}, lifetime and quantum yield of fluoresc. emission 77−20909
$POCl_3$-$SnCl_4$:Nd^{3+} laser, relaxation oscillations with high power spikes obs. 78−42331
$POCl_3$-$SnCl_4$:Nd^{3+}, liquid laser material, luminesc. centres conc., temp. depend. 79−50287
$POCl_3$-$SnCl_4$:Nd^{3+}, liquid laser material, luminesc. centres changes, crystn. process effects 79−50288
$POCl_3$.$SnCl_4$:Nd^{3+}, phosphor, laser parameters and physiochem. props. 77−14709
(Pb,Sn)Se IR detector diode, junction resist. comparison with (Pb,Sn)Te 78−24858
(Pb,Sn)Te diode laser, grating coupled emission 77−79860
(Pb,Sn)Te IR detector diode, junction resist. comparison with (Pb,Sn)Se 78−24858
(Pb, Sn)Te-type semiconductors, displacive ferroelec. phase transitions, vibronic theory 80−11354
Pb-Sn-Te, microhardness meas. as function of applied load, elec. props. exam. 78−48493
Pb-Sn-Te, solid solution, scattering mechanism of carriers 80−49710
Pb-SnTe semiconductor, spectral response calcs. 77−87826
$Pb_{1-x}Sn_xTe$ film, possible applic. as mechanised stress transducers 77−58621
p-$Pb_{1-x}Sn_xTe$, carrier mobility, acoustical phonon and impurity scatt., deform. impurity const., conc. depend. 80−39570
$PbMo_{5.1}S_6$, high supercond. T_c, soft mode behaviour 78−14855
$Pb_{1-x}Sb_xTe$ DFB laser, CW operation 77−58338
p-$(PbSe)_{1-x}(SnTe)_x$, absorpt. edge temp. depend. *(Russian)* 78−34765
$(PbSe)_{1-x}(SnTe)_x$ solid solution, band struct. and some optical props. *(Russian)* 77−76752
$PbSnF_4$, anionic conductor *(French)* 79−1523
$PbSnF_4$, anionic conductor, thin films and ceramics 80−107556
$PbSnF_4$, high anionic cond. of new solid electrolytes 80−107546
$Pb_{0.9}Sn_{0.1}F_2$, NMR study of F atom motion *(French)* 80−100622
$Pb_{1-x}Sn_xF_2$, ionic cond. of F ion *(French)* 80−6547
$Pb_xSn_{1-x}F_2$ solid soln., struct. evolutions *(French)* 80−96488
$Pb_{1-x}Sn_xGe$:In, press.-induced transition to gapless state, galvanomag. effects 78−19108
$Pb_xSn_{1-x}I_2$, thin films, photosensitivity, ageing and annealing effects *(Russian)* 78−6804
$Pb_xSn_{1-x}O_2$ film, optical props. 78−39616
$Pb_xSn_{1-x}O_2$:Sb films, DC sputtered, elec. props. 80−80426
$Pb_{0.2}Sn_{0.8}S$, Mossbauer spectra, effect of optical emission *(Russian)* 78−60367
$Pb_{0.59}Sn_{0.41}Se$, struct. phase transition, temp and hydrostatic press. influence, Hall effect, resistivity *(Russian)* 78−51675
$Pb_{0.65}Sn_{0.35}Se$, solid soln., elec. props. 78−39112

tin compounds continued

n-$Pb_{0.83}Sn_{0.17}Se$, carrier mobility, 77-300K, scattering mechanism *(Russian)* 78−2486
$Pb_{0.91}Sn_{0.09}Se$ film, Bi and Tl impurity dopant incorporation and diffusion during MBE growth 79−66012
$Pb_{0.93}Sn_{0.07}Se$ crysts., sublimation growth, controlled carrier concs. for IR lasers and detectors 77−52237
n-$Pb_{0.94}Sn_{0.06}Se$ solid solns., Burstein-Moss effect and energy band struct. 80−40118
$Pb_{0.975}Sn_{0.025}Se$, film, acoustic wave modulation of electron current 78−64067
$Pb_{0.995}Sn_{0.045}Se$ pulsed laser for high-resolution NH_3 spectroscopy 79−64252
$Pb_{1-x}Sn_xSe$, (x=0.125), pressure induced band inversion, effect on energy spectrum *(Russian)* 78−39007
n-$Pb_{1-x}Sn_xSe$, absorption spectra investigation 80−2768
$Pb_{1-x}Sn_xSe$, band inversion effect on phonon spectra 78−79699
$Pb_{1-x}Sn_xSe$, band struct. parameters, thermoelectric power meas. in strong mag. fields 79−51474
$Pb_{1-x}Sn_xSe$, band struct. and transport props., hydrostatic press. effects 80−15452
$Pb_{1-x}Sn_xSe$, carrier density depend. of cyclotron mass, Shubnikov-de Haas effect 79−73533
$Pb_{1-x}Sn_xSe$, carrier effective mass, thermomag. effect meas. 77−24572
$Pb_{1-x}Sn_xSe$, determ. of anisotropy coeff. of Fermi surface, magnetoresist. meas. 78−51878
$Pb_{1-x}Sn_xSe$, displacive transition, temp. and press. depend., elec. meas. 80−10672
$Pb_{1-x}Sn_xSe$, energy band parameter determ. from Shubnikov-de Haas effect 77−69227
$Pb_{1-x}Sn_xSe$ epitaxial film, Hall mobility meas., surface charge transport 77−20473
$Pb_{1-x}Sn_xSe$ epitaxial layers, radiative and nonradiative recomb. processes 80−60670
$Pb_{1-x}Sn_xSe$ epitaxial layers obtained by LPE, growth conditions correl. with morphology 80−104079
$Pb_{1-x}Sn_xSe$, film struct. and elec. props. 77−80708
$Pb_{1-x}Sn_xSe$, gapless state and phonon spectrum *(Russian)* 78−30715
$Pb_{1-x}Sn_xSe$ laser, optical feedback effects on performance, external cavity modes 80−32981
$Pb_{1-x}Sn_xSe$, material props. and use in diode lasers, review 80−5732
$Pb_{1-x}Sn_xSe$, n- and p-type, with band inversion, study of transport phenomena 80−49741
$Pb_{1-x}Sn_xSe$, plasma reflection spectra, carrier effective masses and relax. times determ. 78−2858
$Pb_{1-x}Sn_xSe$, single crystal and film, X-ray spectral investigation of solid solution 77−16477
n-$Pb_{1-x}Sn_xSe$, single crysts. and diodes, elec. props. under high press. 77−47809
$Pb_{1-x}Sn_xSe$, single heterostruct. laser, wide tunability 77−79846
$Pb_{1-x}Sn_xSe$, small gap, band-edge parameters 80−49594
$Pb_{1-x}Sn_xSe$ solid solns., photoluminesc. spectra, energy band parameter determ. 80−71484
$Pb_{1-x}Sn_xSe$, thin film, opt. props. *(Japanese)* 77−1750
$Pb_{1-x}Sn_xSe$, transport phenomena in solid solutions with band inversion 80−107792
$Pb_{1-x}Sn_xSe$, valence zone struct. effect on mobility/inherent conc. ratio *(Russian)* 79−73437
$Pb_{1-x}Sn_xSe$, X=0.03-0.07, monocrystal film, edge of intrinsic absorpt. *(Russian)* 80−71368
$Pb_{1-y}Sn_ySe$, ($0 \leq y \leq 0.08$), spontaneous emission, temp. and carrier conc. depend., cathodoluminescence 78−10990
$Pb_{1-y}Sn_ySe$, characts. of IR absorption 77−1681
$Pb_{1-y}Sn_ySe$, electron-irradiated, elec. and recomb. props. 79−56227
$Pb_{1-y}Sn_ySe$-PbSe, ($0 \leq xy \leq 0.08$), semiconductor junction laser, lasing investigation 78−10990
$Pb_{1-y}Sn_ySe$-PbSe heterojunction laser, tunable 10.6-15 nm 77−58346
$Pb_{1-y}Sn_ySe$-PbSe pulse laser diode, temp. tuning of modes 78−50777
$Pb_xSn_{1-x}Se$ laser, electron-beam-pumped 77−50689
$Pb_xSn_{1-y}Se$, multispectral photovoltaic IR detectors 80−105710
$Pb_{1-x}Sn_xSe$(Te) epitaxial layers, growth, phase diagram, p-n junctions, optical, elec. props. 78−44029
$Pb_{1-x}Sn_xSe$(Te), single crystals, Bridgeman grown, X-ray exam. 79−56926
$Pb_{1-x}Sn_xSe$(Te):I epitaxial layers, photoelectric props., doping donor impurity behaviour 77−80810
$Pb_{1-x}Sn_xSe_{1-y}Te_y$ optically pumped heterojunction laser with matched gratings, photolum. obs. 79−89909
PbSnTe and PbSnTe, epitaxial-substrate system, far IR transmission and refl. 78−6802
PbSnTe DH laser, anodic oxide film to avoid degradation by thermal cycling 78−50809
PbSnTe detector and preamplifier modules for heterodyne detection of CO_2 laser radiation 78−32875
PbSnTe, electron irradiated, high temp. defects 79−78122
PbSnTe film epitaxial growth on BaF_2 substrates 78−11134
PbSnTe IR detectors, spectral response depend. on surface carrier concentration *(Japanese)* 79−44929
PbSnTe IR photovoltaic detectors for 8-14 μm range, review *(Italian)* 78−54451
PbSnTe laser diode, tunable emission, 5-15 μm 77−50686
PbSnTe, Magneto transport anomalies at low carrier densities, Wigner crystallisation 80−20222
PbSnTe, optical dielectric const. variation with carrier conc. 80−84709
PbSnTe/PbTe inverted heterostructure mosaics, long wavelength, energy gap-Fermi level temp. depend. 79−85182
PbSnTe-like semicond., Auger recomb., nonparabolic approx. 79−15161
PbSnTe-PbTe heterostructs., effect of electrical grounding on electron irrad. 78−60194
$Pb_{0.41}Sn_{0.59}Te$, Hall coeff., elec. cond. meas. 80−44615
$Pb_{0.56}Sn_{0.44}Te$, press. induced ferroelec. phase transition 79−65809
p-$Pb_{0.65}Sn_{0.35}Te$, transport coeffs. and dispersion law 80−44629
$Pb_{0.72}Sn_{0.28}Te$, Hall effect and elec. cond., 77 to 480K, energy band struct. 77−76817
$Pb_{0.72}Sn_{0.28}Te$, Hall mobility, temp. and carrier conc. depends. *(Russian)* 77−39877
$Pb_{0.76}Sn_{0.24}Te$ single crystals, current-voltage characts. at He temps. 80−20197
$Pb_{0.78}Sn_{0.22}Te$ film, Bi and Tl impurity dopant incorporation and diffusion during MBE growth 79−66012

tin compounds continued

$Pb_{0.78}Sn_{0.22}Te$, $Pb_{0.91}Sn_{0.09}Se$, radiative and nonradiative recombination 80−80849
$Pb_{0.78}Sn_{0.22}Te$:In, transport phenomena, below 20K *(Russian)* 79−38074
$Pb_{0.78}Sn_{0.22}Te$:In epitaxial layers, dislocation density, Hall effect, conductivity, photoeffects 80−25024
p-$Pb_{0.79}Sn_{0.21}Te$, free-carrier optical absorption 77−52101
$Pb_{0.8}Sn_{0.2}Te$ film, growth in quasi-closed space, single and polycryst. 79−33930
n-$Pb_{0.8}Sn_{0.2}Te$ film, magnetophonon reson., 55-90K 79−7913
$Pb_{0.8}Sn_{0.2}Te$, film photodiodes, quantum efficiency 79−75596
$Pb_{0.8}Sn_{0.2}Te$, hole conc. at 77K from room temp. thermoelec. meas. 78−56155
$Pb_{0.8}Sn_{0.2}Te$, implantation of S^+ and In^+ ions 77−19973
$Pb_{0.8}Sn_{0.2}Te$, LPE layers, carrier conc. variation with annealing and growth temp. 77−39878
$Pb_{0.8}Sn_{0.2}Te$, magnetophonon effect obs. 78−23115
$Pb_{0.8}Sn_{0.2}Te$, single cryst. and epitaxial film, far IR refl. spectra, carrier density, Hall const., and plasma freq. 80−20629
$Pb_{0.8}Sn_{0.2}Te$ surfaces, oxidation in air and thermal desorption, XPS and LEED meas. 79−47830
$Pb_{0.8}Sn_{0.2}Te$, susceptibility effective mass, carrier conc. depend. 80−20069
$Pb_{0.8}Sn_{0.2}Te$:Cd, defect struct., Hall effect and solubility meas. 77 11571
$Pb_{0.8}Sn_{0.2}Te$:Cd, influence of Cd doping on high field magnetoresist. and Hall effect 80−75590
$Pb_{0.8}Sn_{0.2}Te$:In, absorption spectra meas., 475-725K 77−4664
$Pb_{0.8}Sn_{0.2}Te$:In, implanted thin epitaxial films, laser annealing 79−65104
$Pb_{0.8}Sn_{0.2}Te$:La, evaporated thin films, low carrier conc. 80−65414
p-$Pb_{0.8}Sn_{0.2}Te$/n-PbTe, multicolour photodetectors *(Czech)* 79−26126
$Pb_{0.8}Sn_{0.2}Te$-Pb, Schottky barrier form., Auger depth profiling and I-V meas. 80−49903
$Pb_{0.8}Sn_{0.2}Te$-PbTe p-n heterojunction, prep., elec. and photoelec. props. 79−51664
n-$Pb_{0.82}Sn_{0.18}Te$, conduction band struct., determ. by Shubnikov-de Haas meas. 78−2504
$Pb_{0.82}Sn_{0.18}Te$ epitaxial films, surface transport of carriers at 77K 79−28419
$Pb_{0.82}Sn_{0.18}Te$, film, effect of hydrostatic pressure on props. 80−70862
$Pb_{0.82}Sn_{0.18}Te$ films, piezoresist. effect 79−38197
$Pb_{0.82}Sn_{0.18}Te$ films, VPE, hot wall technique, struct., elec. props. 79−37926
$Pb_{0.82}Sn_{0.18}Te$, Hall mobility, scatt. mechanisms, temp. and carrier conc. depend. 77−55548
$Pb_{0.82}Sn_{0.18}Te$, layers on mica substrate, Hall constant peculiarities 80−75588
p-$Pb_{0.82}Sn_{0.18}Te$, mag. susceptibility, inversion layers effect *(Russian)* 77−72996
$Pb_{0.82}Sn_{0.18}Te$, narrow band gap, relax. time for Shubnikov-de Haas effect 78−80006
$Pb_{0.82}Sn_{0.18}Te$, narrow gap semicond., mag. susceptibility meas. *(Russian)* 78−84397
$Pb_{0.82}Sn_{0.18}Te$, narrow-gap, Hall effect quantum oscillations *(Russian)* 77−4377
$Pb_{0.82}Sn_{0.18}Te$ solid solution, energy band spectrum characts., Hall effect meas. 77−76737
$Pb_{0.82}Sn_{0.18}Te$, thermomagnetic, thermoelectric props., valence band struct. *(Russian)* 80−54724
$Pb_{0.82}Sn_{0.18}Te$:Cd, effective distrib. coeff. of Cd *(Russian)* 79−73203
p-$Pb_{0.82}Sn_{1.8}Te$, Hall coeff. sign-inversion temp. 78−52010
$Pb_{0.83}Sn_{0.17}Te$, carrier tunnelling through potential barrier in p-n junctions *(Russian)* 78−52074
$Pb_{0.83}Sn_{0.17}Te$, recomb. at high levels of optical excitation 78−10503
$Pb_{0.85}Sn_{0.15}Te$ homostructure diode laser, LPE growth, with controlled carrier conc. 80−95903
$Pb_{0.86}Sn_{0.14}Te$/PbTe, interface recomb. velocity in DH laser diodes 79−64222
n-$Pb_{0.88}Sn_{0.12}Te$ spin flip Raman laser pumped by TE CO_2 laser, characts. 80−87397
$Pb_{0.92}Sn_{0.08}Te$, photoelec. props. 78−6415
$Pb_{0.93}Sn_{0.07}Te$ tunable diode laser for IR spectroscopy 78−33511
$Pb_{0.9}Sn_{0.1}Te$, situated in quantizing magnetic field, photolum. spectra 79−71461
$Pb_{1-x}Sn_xTe$ film, epitaxial, patterns of diffuse bands on electron diffr. patterns 79−11021
$Pb_{1-x}Sn_xTe$, ($0 \leq x \leq 0.2$), homogeneous, spontaneous emission, temp. and carrier conc. depend., cathodoluminescence 78−10990
$Pb_{1-x}Sn_xTe$ (x=0.15 to 0.20), SEM study, dislocation density, and carrier density and mobility 79−69107
$Pb_{1-x}Sn_xTe$, (x<0.35), permittivity and soft modes, carrier density and comp. effects 80−7256
$Pb_{1-x}Sn_xTe$, absorption edge shift, energy gap determ. 78−88308
$Pb_{1-x}Sn_xTe$ anodic oxide film form. conditions, IR absorpt. spectra 80−11494
$Pb_{1-x}Sn_xTe$, anomalous resist. near ferroelec. phase transition 80−20196
$Pb_{1-x}Sn_xTe$, band struct. and phonon energies, tunnelling spectroscopy 78−72070
$Pb_{1-x}Sn_xTe$, band struct. changes due to displacive phase transition, Hall coeff. meas. 80−10671
$Pb_{1-x}Sn_xTe$, basic electrons energy spectrum near mag. phase transition *(Russian)* 79−90955
$Pb_{1-x}Sn_xTe$, Cd-In diffusion, changes in elec. props. 78−91348
$Pb_{1-x}Sn_xTe$, charact. of photocond., 12-130K 78−26914
$Pb_{1-x}Sn_xTe$, characts. of IR absorption 77−1681
$Pb_{1-x}Sn_xTe$, continuously tunable electron beam pumped laser 78−50802
$Pb_{1-x}Sn_xTe$, correlation between elec. props. and crystalline environment 77−80773
$Pb_{1-x}Sn_xTe$, DH laser, gain-freq.-current relation, k.p band model 77−61951
$Pb_{1-x}Sn_xTe$ DH laser, minority carrier lifetimes and lasing thresholds 80−19031
$Pb_{1-x}Sn_xTe$, diffusion of Cd, Hall effect, cond. and solubility meas. 79−69292
$Pb_{1-x}Sn_xTe$ diode laser, contact degradation due to diffusion 80−102734
$Pb_{1-x}Sn_xTe$, displacive phase transition, effect of interband hybridisation 79−33233
$Pb_{1-x}Sn_xTe$, effect of mag. field on thermal cond. 79−65263
$Pb_{1-x}Sn_xTe$, effective mass of holes, thermoelec. power, Hall coeff., carrier conc. 79−65371

tin compounds continued
$Pb_{1-x}Sn_xTe$, electron-irradiated, elec. and recomb. props. 79−56227
$Pb_{1-x}Sn_xTe$, electron-phonon interaction 78−71819
$Pb_{1-x}Sn_xTe$, energy band parameters from IR Faraday rotation 78−48154
$Pb_{1-x}Sn_xTe$, energy band parameter determ. from photoluminescence. spectra in mag. field 79−11066
$Pb_{1-x}Sn_xTe$, energy gap of single crysts, comparison of indirect and direct determ. methods *(German)* 78−26812
$Pb_{1-x}Sn_xTe$, energy spectrum under hydrostatic pressure 79−65381
$Pb_{1-x}Sn_xTe$ epitaxial films, adsorption-induced accumulation layer form. on surface 80−60117
$Pb_{1-x}Sn_xTe$, epitaxial growth on $LiNbO_3$, electron diffr. and microscopy exam. 77−1331
$Pb_{1-x}Sn_xTe$, epitaxial layers, cond. *(Russian)* 77−24629
$Pb_{1-x}Sn_xTe$, epitaxial layers, In doping, donor impurity singularities, distrib. coeff. 77−80526
$Pb_{1-x}Sn_xTe$, epitaxial layers, carrier lifetime meas. 79−42559
$Pb_{1-x}Sn_xTe$, epitaxial layers, photolum. in mag. field 79−83033
$Pb_{1-x}Sn_xTe$, far IR magneto-optical meas. 79−61343
$Pb_{1-x}Sn_xTe$, Faraday effect and electron gas magnetisation, Kane two band model calcs. *(Russian)* 80−34899
$Pb_{1-x}Sn_xTe$, ferroelec. phase transition, hybridization effect *(Russian)* 79−61319
$Pb_{1-x}Sn_xTe$ film, Burstein-Moss effect, absorpt. and photocond. spectra 78−18961
$Pb_{1-x}Sn_xTe$ film, sputtered, for IR detector appl. elec. and optical props. 80−35084
$Pb_{1-x}Sn_xTe$ film on BaF_2, electron beam delineation effect on MBE growth, LEED and AES obs. 79−99434
$Pb_{1-x}Sn_xTe$ films, pure and Bi doped, polycryst., struct., elec., optical props. 79−42542
$Pb_{1-x}Sn_xTe$ films, size quantisation, optical orientation of free carriers 80−20725
n-$Pb_{1-x}Sn_xTe$, galvanomag. effects, alloy scatt., 4.2K 77−39880
$Pb_{1-x}Sn_xTe$, grown by LPE, solid-liquid tie line determ. 78−64526
$(Pb_{1-x}Sn_x)Te$, growth by sublimation technique *(German)* 77−73224
$Pb_{1-x}Sn_xTe$, growth of epitaxial layers, activation by UV and IR radiation 80−71598
$Pb_{1-x}Sn_xTe$, heteroepitaxial film, fundamental absorpt. edge and Shubnikov-de Haas effect 79−24381
$Pb_{1-x}Sn_xTe$ heterojunction lasers, instantaneous vacuum evaporation grown, threshold current density 80−5759
$Pb_{1-x}Sn_xTe$ heterostructure laser, fabrication and props. 79−10306
$Pb_{1-x}Sn_xTe$, hole effective mass near zero bandgap, IR refl. study 80−108205
$Pb_{1-x}Sn_xTe$ homojunction laser, increased freq. tuning range 77−75546
$Pb_{1-x}Sn_xTe$ IR detector, ESCA meas., surface leakage currents 77−20402
$Pb_{1-x}Sn_xTe$, impurity defused IR detector, spectral response depend. on impurity conc. *(Japanese)* 78−58036
$Pb_{1-x}Sn_xTe$, in MIS struct., tunnelling investig. of band gap and phonon energies 77−43733
$Pb_{1-x}Sn_xTe$, in MOS junction, phonon-assisted tunnelling 77−76928
$Pb_{1-x}Sn_xTe$, injection laser, use in high-resolution spectroscopy 79−76714
$Pb_{1-x}Sn_xTe$, inter- and intraband magneto-optical transitions 80−25346
$Pb_{1-x}Sn_xTe$, interband absorpt. edge for single cryst. epitaxial films 78−43948
$Pb_{1-x}Sn_xTe$ LPE film IR detector performance 80−86422
$Pb_{1-x}Sn_xTe$, LPE grown heterostructures, improved nucleation and planar interface 79−95949
$Pb_{1-x}Sn_xTe$ LPE grown heterostructures, dislocation etch pitch, interfaces 80−2023
p-$Pb_{1-x}Sn_xTe$, LPE layer, carrier conc. and mobility 79−99639
$Pb_{1-x}Sn_xTe$, large non-seeded single cryst. growth by sublimation method, and characterisation 79−78860
$Pb_{1-x}Sn_xTe$, large single crystal growth, on quartz surface, non-seeded 78−48293
$Pb_{1-x}Sn_xTe$, lattice and electronic props. and g-value 80−80161
$Pb_{1-x}Sn_xTe$, lattice instability and phonon lifetimes, neutron scatt. 78−55932
$Pb_{1-x}Sn_xTe$, lattice instability and phonon-width, comprehensive model 79−14906
$Pb_{1-x}Sn_xTe$ layers, LPE, phase diagram rel. to lattice const., distrib. coeffs. 79−37925
$Pb_{1-x}Sn_xTe$, MBE, O_2 uptake, AES, XPS and UPS expts. 78−95227
$Pb_{1-x}Sn_xTe$, MBE, state-of-the-art 79−24450
p-$Pb_{1-x}Sn_xTe$, mobility meas., impurity and phonon scatt. mechanisms 78−23091
$Pb_{1-x}Sn_xTe$ monocrystal and sinter thermoelec. inhomogeneity 78−91713
$Pb_{1-x}Sn_xTe$, Mossbauer investig. of phonon softening at semicond.-semimetal transition 77−43908
$Pb_{1-x}Sn_xTe$, narrow gap, many-body interaction effects, Bloch electron scatt. lifetimes, energy renormalisation 80−49637
$Pb_{1-x}Sn_xTe$ narrow gap solid alloys, hole Fermi surface, galvanomag. and oscill. effect obs. *(Russian)* 77−69345
$Pb_{1-x}Sn_xTe$, narrow gap solid solns., mag. susceptibility and energy band spectrum 79−28276
$Pb_{1-x}Sn_xTe$, narrow gap semicond., theory of mag. susceptibility 80−93070
$Pb_{1-x}Sn_xTe$ optically pumped lasers, power output and wavelength, 4 to 30K 78−79035
$Pb_{1-x}Sn_xTe$ p-n heterostructure, VPE, struct. and electrophysical characts. 78−10547
$Pb_{1-x}Sn_xTe$, photoconduct., photoelectromag. effect, laser intensity depend., carrier lifetimes 77−15896
$Pb_{1-x}Sn_xTe$, photoelec. props. 30 to 4.2K, temp. depend. of electron density 80−20246
$Pb_{1-x}Sn_xTe$, photomagnetic effect at low temps. 77−62960
p-$Pb_{1-x}Sn_xTe$ piezoresistance, temp. and conc. depend. *(Russian)* 79−1601
p-$Pb_{1-x}Sn_xTe$, pressure-induced transition to zero-gap state, changes in energy band parameters 79−69413
$Pb_{1-x}Sn_xTe$, properties and use for making devices, review 78−60131
$Pb_{1-x}Sn_xTe$, reststrahlen band, reflection spectra 79−8162
$Pb_{1-x}Sn_xTe$, segregation during solidification by Bridgman technique 79−38735
p-$Pb_{1-x}Sn_xTe$, single crysts. and diodes, elec. props. under high press. 77−47809
tin compounds continued
$Pb_{1-x}Sn_xTe$, single cryst. grown from vapour, photocond. meas. 79−24016
$Pb_{1-x}Sn_xTe$ single crystals, selection using travelling solvent method *(German)* 80−2936
$Pb_{1-x}Sn_xTe$, small gap, band-edge parameters 80−49594
$Pb_{1-x}Sn_xTe$, small-gap, recomb. mech. 79−38099
$Pb_{1-x}Sn_xTe$, soft mode, ferroelec. phase transition crit. temp. and dielec. const. calcs. 77−8530
$Pb_{1-x}Sn_xTe$, soft-phonon-induced Raman scatt. 77−77209
$Pb_{1-x}Sn_xTe$ solid solutions, EPR at Te vacancies *(Russian)* 77−48050
$Pb_{1-x}Sn_xTe$ solid solution, electron scatt. by charged Te vacancies 77−69328
$Pb_{1-x}Sn_xTe$ solid solution, radiative recombination 79−52016
$Pb_{1-x}Sn_xTe$, solid-liq. phase equilib. above 750°C 79−82316
$Pb_{1-x}Sn_xTe$, soliton modulation widths for TO-phonons 77−80588
$Pb_{1-x}Sn_xTe$, surface photo-EMF under laser excitation conditions 80−6897
$Pb_{1-x}Sn_xTe$, Te-rich growth by ingot nucleation method, laser fabrication 77−77362
$Pb_{1-x}Sn_xTe$, temperature gradient LPE, PbTe substrate 78−3066
p-$Pb_{1-x}Sn_xTe$, thermoelec. power, carrier conc. and temp. depend., interband scatt. 80−24957
$Pb_{1-x}Sn_xTe$, thermoelectric effects, characteristics at low temps. 80−107831
$Pb_{1-x}Sn_xTe$, VPE crystals, X-ray diffr. data interpretation 77−15712
$Pb_{1-x}Sn_xTe$, VPE growth control by EM irrad. *(Russian)* 80−34338
$Pb_{1-x}Sn_xTe$, valence band struct., Hall effect meas. 78−39016
$Pb_{1-x}Sn_xTe$, x=0.2, monocrystal, photoelectric props. of p-n structures *(Russian)* 80−70808
$Pb_{1-x}Sn_xTe$, X=0.2, monocrystal, edge of intrinsic absorpt. *(Russian)* 80−71368
$Pb_{1-x}Sn_xTe$: Mn, Mn mag. and elec. active states, mag. impurity behaviour 80−44627
$Pb_{1-x}Sn_xTe$:^{119}Sn, symm. breaking of Sn local environment, Mossbauer splitting obs. *(Russian)* 77−40166
$Pb_{1-x}Sn_xTe$:Cd, Cd diffusion obs. using Hall mobility and Cd solubility expts. 78−26584
$Pb_{1-x}Sn_xTe$:Cd, deep energy level, temp. depend. of elec. cond. 78−18994
$Pb_{1-x}Sn_xTe$:Cd, impurity photocond. spectra 80−6902
$Pb_{1-x}Sn_xTe$:Cd, long-wavelength photosensitivity shift on annealing, Cd influence 78−26912
$Pb_{1-x}Sn_xTe$:Cd, photocond., photomag. effect, carrier lifetimes 80−44658
$Pb_{1-x}Sn_xTe$:Cd, photoelec. props., surface recomb. effect 80−44659
$Pb_{1-x}Sn_xTe$:Cd(In), solid solutions, impurity states in photoluminescence spectra *(Russian)* 80−97333
$Pb_{1-x}Sn_xTe$:Ge, anomalous behaviour of impurity centres under press. *(Russian)* 80−65491
$Pb_{1-x}Sn_xTe$:In, carrier spectroscopic g-factors, magnetoresistance, temp. depend. 80−6705
$Pb_{1-x}Sn_xTe$:In, dielectric state, avalanche breakdown in strong elec. fields *(Russian)* 80−92901
$Pb_{1-x}Sn_xTe$:In, energy spectrum under combined effect of mag. field and hydrostatic press. 79−65382
$Pb_{1-x}Sn_xTe$:In, energy spectra modifications due to comp. changes and press. appl. 80−10915
$Pb_{1-x}Sn_xTe$:In, Hall const. depend. on temp., autocompensation, band gap temp. depend. explanation 79−69527
$Pb_{1-x}Sn_xTe$:In, Hall effect and photoconductivity *(Russian)* 80−103720
$Pb_{1-x}Sn_xTe$:In, high temp. Fermi level position 79−90948
$Pb_{1-x}Sn_xTe$:In, impurity influence on photoluminescence at large excitation levels *(Russian)* 80−93384
$Pb_{1-x}Sn_xTe$:In, nonequilib. metallic state *(Russian)* 79−33300
$Pb_{1-x}Sn_xTe$:In, semiconductor-metal-semiconductor transitions under press. 80−34491
$Pb_{1-x}Sn_xTe$:In, tunnelling impurity self-localisation, anomalous props. nature *(Russian)* 80−59915
$Pb_{1-x}Sn_xTe$:In, with low carrier conc., transport phenomena 80−49783
$Pb_{1-x}Sn_xTe$:In epitaxial layers, growth, elec. props., and luminesc. 80−54542
$Pb_{1-x}Sn_xTe$:In film, anomalous elec. props. 78−10477
$Pb_{1-x}Sn_xTe$:In(Ga)(Al), elec. props., dopant influence 79−51599
$Pb_{1-x}Sn_xTe/PbTe_{1-y}Se_y$ lattice-matched buried heterostructure lasers with CW single mode output 80−74386
$Pb_{1-x}Sn_xTe$-$Pb_{1-y}Sn_yTe$, p-n heterojunction, prep. and props. 79−51662
$Pb_{1-x}Sn_xTe$-PbTe, ($0 \leq x \leq 0.2$), semiconductor junction laser, lasing investigation 78−10990
$Pb_{1-x}Sn_xTe$-PbTe, amorphous/crystalline heterojunction, rectification props., IR detector appl. *(Japanese)* 78−60197
$Pb_{1-x}Sn_xTe$-PbTe heterojunction, Sn diffusion and elec. effects of dislocations, elec. and metallurgical expts. 77−89839
$Pb_{1-x}Sn_xTe$-PbTe heterojunction, Sn diffusion profile, X-ray diffr. data interpretation 78−51832
$Pb_{1-x}Sn_xTe$-PbTe heterojunctions, interface recombination velocity reduction with decreasing lattice parameter mismatch 79−98370
$Pb_{1-x}Sn_xTe$-PbTe heterostructures, MBE produced on mica and $LiNbO_3$, elec. props. study 80−88629
$Pb_{1-x}Sn_xTe$-PbTe pulse laser diode, temp. tuning of modes 78−50777
$(Pb_{1-x}Sn_x)_{1+y}Te_{1-y}$ system, VPE parameters influence on epitaxial film props. 79−28229
$Pb_{87}Sn_{13}Te$, phonon dispersion, mode softening 79−42175
$Pb_xSn_{1-x}Te$, for appl. in IR detector arrays, comp. control 80−31872
$Pb_xSn_{1-x}Te$, grown by vap. transport in closed system, quality improvement 77−40341
$Pb_xSn_{1-x}Te$, oxide and Te monolayer films, Raman backscattering spectra 77−48211
$Pb_xSn_{1-x}Te$, RF sputtered films, struct., lattice parameter, stoichiometric comp., RHEED 78−38975
$Pb_xSn_{1-x}Te$, RF sputtered film IR detector, photocond. response speed improvement by annealing 79−58790
$Pb_xSn_{1-x}Te$, RF-sputtered epitaxial single-cryst. films, thermorefl. spectra 77−63476
$Pb_xSn_{1-x}Te$, thin film, oxidation, appl. of Mossbauer method 80−45410
$Pb_xSn_{1-x}Te$-PbTe p-n junction, epitaxial, elec. props. and photoresponse 78−56225
PbSnTe(Se) Schottky barrier diode and n-p diffused junction IR detectors, comparison 80−9039
$Pb_{1-x}Sn_xTe_{1-y}Se_y$, narrow-gap solid soln., lattice parameter, energy gap and Hall mobility of carriers 79−73154

tin compounds continued
$Pb_{1-x}Sn_xTe_{1-y}Se_y$, quarternary solid solns. with const. lattice parameter, cryst. growth and characts. 80−108332
$Pb_{1-x}Sn_xTe_{1-y}Se_y$ solid solutions with constant lattice parameter, phase comp. 80−108417
$Pb_{1-x}Sn_xY$, Y=Te, Se, S, photocond. anisotropy rel. to lifetimes 78−52032
PbTe:Bi-PbSmTe-PbTe, epitaxial laser struct., growth, p-n junction position and lasing region 79−89908
n-PbTe-p-$Pb_{1-x}Sn_xTe$, heterojunctions, heavily doped, current-flow mechanisms 80−96974
PbTe-$Pb_{0.82}Sn_{0.18}Te$, p-n heterojunctions, electrical and photoelectrical properties 78−39193
PbTe-$Pb_{1-x}Sn_xTe$ n-p^+ heterojunction photodetector, hot wall evaporation technique 80−65673
PbTe-$Pb_{1-x}Sn_xTe$-PbTe DH, LPE and VPE, stimulated emission 77−75526
PbTe-SnTe, solid soln. single crysts., TSM growth and elec. characts. 78−68625
PbTe-SnTe, solid soln., enthalpy of formation *(Russian)* 80−15267
PbTe-SnTe compound semiconductors, lattice instability by mm-wave magnetoplasma refl. 80−54336
$PbySn_{1-x}Se$ epitaxial film narrow band photovoltaic detectors, detection at long wavelengths 78−8443
Rb_2SnF_6, thermal stability and thermolysis *(French)* 78−10011
Sb_2O_3-SnO_2 film vapour deposition in conveyor furnaces *(French)* 78−15311
Sb_2S_3-SbI_3, amorphous phase formation in vacuum condensates, TEM study 79−86712
Sb_2S_3-SnS, fused mixtures, resistivity 77−80815
a-Si/$In_{2-x}Sn_xO_{3-y}$, p-i-n heteroface solar cell, device physics and design 80−101113
Si/In_2O_3-SnO_2 thin film junctions, polarity dependent memory switching effects 80−70814
p-Si-$In_{2-x}Sn_xO_{3-y}$ solar cells, thermal degradation mechanisms 80−55841
Si-SiO_2-SnO_2 structure, switching props. 78−76138
n-Si-SiO_2-SnO_x SIS solar cell, transport props., 14% efficiency realisation 80−94079
Si-SnO_2, p-n heterojunction, prep., elec. and optical props., expt. *(Korean)* 77−4427
Si-SnO_2 heterojunction, barrier height meas. by HF capacitance method 77−69406
Si-SnO_2 highly photosensitive diodes, and their appl. 78−23152
SiO_2-CaO-Na_2O-SnO_2 system, water, alkali, acid resist., chem. durability 79−34162
$(SiTe)_{1-x}(SnTe)_x$, solid soln., mag. susceptibility meas. *(Russian)* 80−70933
$SmMn_3C$ noncolinear mag. struct., mag. transition *(French)* 77−69494
Sn (II) compounds, Mossbauer spectra, direct population of solid-state bands 80−15905
Sn (IV) in glassy aq. soln., Mossbauer spectra 80−15894
Sn borate glasses, IR and ^{119}Sn Mossbauer spectra 78−60438
Sn complex, $SnCl_4.L_2$ (L_2=organic phosphorus ligand), NQR of ^{35}Cl and ^{14}N 77−16201
Sn complex containing P, $L_2Sn(CH_3)_nCl_{4-n}$, Mossbauer parameters, quadrupole splittings *(Russian)* 78−76362
Sn complexes, $SnCl_4.L$ (L=organic radical), charge transfer and quadrupole-interaction consts. calc. 77−10590
Sn-Bi-Se, phase diagrams 79−87622
Sn-F system, partial phase diagram construct. in Sn-SnF_2 region *(French)* 80−50605
Sn-In-Te system, SnTe based solid solns. formation 77−84929
Sn-O system, amorphous, characterisation by appl. of Mossbauer effect 79−61283
Sn-S melt, absolute thermo-emf obs. 77−85251
Sn-S system, use of boiling points to investigate vapour pressure 80−54361
Sn-Sb-S-I, chalcogenide glass film, prep. by laser evaporation, and characterisation 77−12533
Sn-Se, liq., mag. susceptibility meas., electron localisation and chem. bonding 80−60178
Sn-Se-P system, glasses, comp. depend. 77−84658
Sn-Sn_xO_y-Sn long Josephson tunnel junction, flux flow, crit. conditions 80−80452
Sn-SnO_2-Sn, supercond. tunnel junctions, energy gap suppression by quasiparticle self-injection 78−80102
Sn-SnO_4-Sn junctions, oxide growth, tunnelling characts. 79−47173
Sn-SnO_x-SN tunnel contacts, spatially inhomogeneous state under strong injection conditions 80−80457
Sn-SnO_x-Sn tunnelling junctions, fabrication by modified RF plasma oxidation method 80−103787
Sn-SnO-Pb, supercond. tunnel struct., nonequilib. state, influence of illumination 79−15262
Sn-SnO-Sn, supercond. junction, tunnel effect under laser irrad. *(Russian)* 77−43788
Sn-Te, liq., mag. susceptibility meas., electron localisation and chem. bonding 80−60178
SnAs, Sn_3As_2, and Sn_4As_3, mag. susceptibility components 78−43551
$SnBaO_3$, resonantly scatt. gamma radiation from ^{119}Sn, energy spectrum with time parameters 80−108122
$SnBr_2$, ^{81}Br NQR line width obs. 80−50219
$SnBr_2$, UPS, 40.81 eV, valence band struct. 79−33891
$SnBr_4$, fine struct. resolution in Raman-active fundamentals 79−42967
$SnBr_4$, matrix-isolation and $^{79/81}Br$ and $^{116/124}Sn$ isotope shifts in IR spectra 77−46561
$SnBr_4$, vac. UV absorpt. spectra, 130-270 nm 77−75183
$SnBr_6^{2+}$, spectroscopic consts., environmental cation effects 79−56779
$Sn_2Br_{0.65}Cl_{3.35}.3H_2O$, X-ray cryst. struct. determ., Patterson synthesis *(French)* 80−28960
Sn_3BrF_5, cryst. struct. determ., environment of Sn (II) *(French)* 78−26508
$Sn_5Br_4F_6$, cryst. struct. determ. *(French)* 78−79591
SnCaV garnet polycrystal, ferrimag. resonance loss rel. to grain size 77−85581
$SnCl_2$, positron annihilation ang. correl., bonding depend. 77−20951
$SnCl_2$, UPS, 40.81 eV, valence band struct. 79−33891
$SnCl_2$, valence band electronic struct., XPS and UPS obs. 78−6826
$^{119m}SnCl_2$ adducts with O and N containing cpds., Mossbauer emission 80−15918
$SnCl_2$-AlkAlCl$_4$ melts (Alk=Li, Na or Cs) 79−99874
$SnCl_3^-$, harmonic approx., force consts., electro-optical parameters and normal vibrs 78−62790
$SnCl_4$, cationic polymerisation of styrene in presence of C black 78−68891
$SnCl_4$, He(II) photoelectron spectra, spectral intensity patterns 79−98152
$SnCl_4$, liq. struct., oscill. amp., neutron diffr. study 79−46544
$SnCl_4$, liq. struct. by neutron diffr. 79−73089
$SnCl_4$, vac. UV absorpt. spectra, 250 to 115 nm 77−79628
$SnCl_4$-PCl_4, mixtures, liq. and solid, Raman spectra study *(German)* 79−91451
$SnCl_4$-$TiCl_4$, liq. struct., oscill. amp., neutron diffr. study 79−46544
$SnCl_4$-$TiCl_4$ liq., beat effects, neutron diffr. studies 80−38897
$SnCl_4$+$K_2(Cs_2)$, ionisation reactions, absolute cross sections 80−99565
$SnCl_6^{2+}$, spectroscopic consts., environmental cation effects 79−56779
SnClF, cryst. struct. *(French)* 77−15349
$SnCl_2(H_2O)_x(D_2O)_{2-x}$, high resolution heat capacity meas. *(Japanese)* 80−52218
SnClI, X-ray cryst. struct. determ., Patterson synthesis *(French)* 80−96480
$SnCl_4N_2$ ions, force field calc., vibr. amplitude and rot. distortion consts. 79−98245
$SnCl_2.1.5H_2O$ single cryst., ^{35}Cl NQR, cryst. struct. 80−60449
$SnCl_2.2D_2O$, order-disorder transition, neutron diffr. study, lattice statistical model 80−24558
$SnCl_2.2H_2O$, Brillouin scatt. and thermal expansion 80−97289
$SnCl_2.2H_2O$, crit. dynamics, nuclear relax. 78−75805
$SnCl_2.2H_2O$, dielectric dispersion and absorpt. and proton spin-lattice relax. at phase transition 77−8437
$SnCl_2.2H_2O$, effect of hydrostatic press. on isomorphous phase transition, complex dielec. const. meas. 77−76551
$SnCl_2.2H_2O$, ferroelec., Cl NQR study 79−38467
$SnCl_2.2H_2O$, high temp. entropy of ionic model for phase transition 78−55949
$SnCl_2.2H_2O$, isomorphous transition, Landau type thermodynamic potential 80−107413
$SnCl_2.2H_2O$, layered, dielectric anomaly calc. using Ising model, possibility of antiferroelectricity 77−12341
$SnCl_2.2H_2O$ layered single cryst., protonic cond. and crit. behaviour 79−28136
$SnCl_2.2H_2O$, protonic order-disorder transition, H-bond vibr. Raman spectra temp. depend. 78−23437
$SnCl_2.2H_2O$, protonic order-disorder transition, inelastic light scatt. obs. 78−68497
$SnCl_2.2H_2O$, protonic cond. in layered single cryst. 80−19983
$SnCl_2.2H_2O$, quasi two-dimensional, DC protonic cond. 80−44362
$SnCl_2.2H_2O$, Sn(II) valency config., Mossbauer and X-ray electron determ. *(Russian)* 77−8483
$SnCl_2.2H_2O$-type layer cpds., two dimens. ferroelec. ordering sp. ht. obs. 78−92034
$SnCo_2O_4$ spinel, mag. props. 77−1543
$Sn_{0.5}Eu_{0.5}Mo_6S_8$, supercond., spin polarisation, NMR, Mossbauer effect and bulk magnetisation meas. 77−43782
$Sn_{0.75}Eu_{0.25}Mo_6S_8$, Chevrel phase supercond., spin-depairing interaction, Mossbauer obs. 80−25258
$Sn_{1-x}Eu_xMo_6S_8$, supercond., Mossbauer effect, struct. phase transition 77−12290
$Sn_{1.2(1-x)}Eu_xMo_{6.35}S_8$, supercond. transition temp., upper critical field, local spin fluctuations 79−38250
SnF, $A^2\Sigma^+$ state, radiative lifetime, quenching rates 79−98156
SnF, rotational struct. of UV (O,O) bands 77−34658
SnF, use in chemical lasers 80−64004
SnF_2, α and γ modifications, elec. cond., $\alpha\rightarrow\gamma$ phase transitions, structs. 78−75867
SnF_2, α- and γ-phases, elec. cond. characts. determ. *(French)* 79−47093
SnF_2, cryst. struct. of β- and γ-phases 80−92500
α-SnF_2, crystallochemistry 80−28990
SnF_2, phase transitions, X-ray diffr., elec. cond. and thermal anal. studies 80−100329
SnF_2, second order $\beta\rightleftarrows\gamma$ transition, neutron diffr. and NMR obs. 80−107095
SnF_2, SnFCl, ionic conductivity *(French)* 78−79806
SnF_2, solid electrolyte, conducting and activation energy 80−70464
SnF_2, valence bands, electronic struct., UPS 78−39656
SnF_2^{2-}, Mossbauer effect 77−85626
SnF_4, elec. field gradient at Sn^{4+} site, Mossbauer quadrupole splitting and anionic polarisability calc. *(French)* 79−15384
$SnF_2.AsF_5$, cryst. struct., X-ray diffr. 77−19921
$SnFe(CN)_6$, Mossbauer spectral anal. *(German)* 79−19819
$Sn_2Fe(CN)_6$, Mossbauer spectral anal. *(German)* 79−19819
$Sn_{0.225}Fe^{3+}_{0.575}Fe^{2+}_{1.465}Mg_{0.735}BO_3O_2$, hulsite, cation distrib., X-ray determ. 79−19225
$Sn_{1-x}Ga_xMo_5S_6$, heat capacity meas., singularities at low temp. 80−49985
$SnGa_6Te_{10}$, X-ray cryst. struct. determ. *(French)* 79−23580
$Sn_xGe_{1-x}Se$, ^{119}Sn Mossbauer and elec. conductivity study 79−19595
$Sn_{0.9}Ge_{0.1}Te$, Mossbauer spectra, soft modes 80−20550
$Sn_{1-x}Ge_xTe$, evaporated thin films, characts. 79−60944
$Sn_{1-x}Ge_xTe$, solid soln. series, Mossbauer study 80−39985
$Sn_xGe_{1-x}Te$ ($0.62<x<0.91$), specific heat anomaly at struct. phase transform. 77−69095
$Sn_xGe_{1-x}Te$, ferroelec. semicond. structural phase transition, X-ray study 79−37836
$Sn_xGe_{1-x}Te$, structural transitions 77−51497
SnH_2, struct. determ., restricted HF calcs. 80−87030
SnH_4,($SnCl_4$), mol. force consts., parametric representation method 78−25503
SnH_4, force consts. by modified Redington and Aljibury method 80−69261
SnH_4, relativistically parameterized extended Huckel theory 79−49924
SnH_4, tetrahedral mol., force field calcs. 78−29734
$Sn(HAsO_4)_2.H_2O$, cryst. struct. 78−26552
$SnHPO_4$, hydrogen-bonded dimers 77−15357
$Sn(HPO_4)_2.H_2O$ and its alkali metal salts, struct. and vibr. spectra 80−39030
$Sn(HPO_4)_2.H_2O$, cryst. struct. 78−26552
$Sn(HPO_4)_2.H_2O$, struct., vibr. spectra 79−15447
SnI, atomic absorpt. spectroscopy, line absorpt. method use for SVP meas. of Sn 80−55747
SnI_2, ^{127}I NQR freqs. meas. 80−58285

tin compounds continued
SnI_2 band struct., layer model 80−44501
SnI_2 film, absorpt. spectrum *(Russian)* 79−43056
SnI_2, layered cryst., photoluminesc., and reflection spectra obs. 78−6726
SnI_2 single crysts., Raman scatt. of light 79−73950
SnI_2, single crysts. and film, optical props. 77−32437
SnI_2-SnF_2 system, phase diagram construct. *(French)* 80−50605
SnI_3^-, harmonic approx., force consts., electro-optical parameters and normal vibrs 78−62790
SnI_3^-, vibr. intensities, forms and freqs. anal. SCF MO LCAO CNDO calcs. 78−9274
SnI_4, attachment energy as habit controlling factor 80−59421
SnI_4 in cyclohexane, far IR absorpt. using band shape absorpt. 77−71794
SnI_4, mol. solid, dynamics, press. and temp. depend. 78−79691
SnI_4, Raman spectra, temp. and press. meas. and lattice dynamical calcs. 78−56472
SnI_6^{2+}, spectroscopic consts., environmental cation effects 79−56779
SnI_7 crysts., dynamical props. of ^{119}Sn by Mossbauer spectroscopy 77−59495
Sn_2IF_3, X-ray cryst. struct. study using Patterson function *(French)* 79−4280
Sn(IV)-, Sn(II) halide mols., rare gas matrix-isolated ^{119} Sn spectra 77−48097
$Sn_{2.8}Li_{1.6}Mg_{1.6}O_8$, four layer close packing, cryst. struct. determ. *(French)* 80−28999
$Sn_{2.8}Li_{1.6}Zn_{1.6}O_8$, four layer hexagonal close packing, cryst. struct. determ. *(French)* 80−28999
$Sn_{1-x}Mn_xTe$, $0.02<x<0.08$, transport and magnetic properties, low magnetic field 79−99569
$Sn_{1-x}Mn_xTe$, degenerate mag. semicond., thermoelec. power meas. 80−29392
$Sn_{1-x}Mn_xTe$, electronic struct., transport props., mag. ordering effects 80−65441
$Sn_{1-x}Mn_xTe$, IR reflectivity, elec. susceptibility mag. order effects 79−47433
$Sn_{1-x}Mn_xTe$, magnetic behaviour of Mn 78−14938
$SnMo_5S_6$, high supercond. T_c, soft mode behaviour 78−14855
$SnMo_6S_8$, Chevrel phase supercond., phonon spectra, neutron scatt. meas. 79−42174
$SnMo_6S_8$, Chevrel phase, synthesis and supercond. *(German)* 80−25038
$SnMo_6S_8$, Chevrel phase, RE mag. isolation and supercond. 80−44470
$SnMo_6S_8$, Chevrel phase, mag. interactions, LMTO energy band studies 80−70606
$SnMo_6S_8$, crit. current density, effect of prep. technique and press. 78−14908
$SnMo_6S_8$, cryst. struct., superconducting characts. changes 79−86773
$SnMo_6S_8$, isotope effect props. *(Russian)* 80−37751
$SnMo_6S_8$, lattice softening, vibr. anisotropy 78−14428
$SnMo_6S_8$, mixed Chevrel phases, crystallography 80−39038
$SnMo_6S_8$, phonon density of states, mode softening correl. with supercond. transition temp. 79−51714
$SnMo_6S_8$, supercond., fast neutron irrad. effects on T_c 77−55633
$SnMo_6S_8$:Gd, EPR meas. *(French)* 80−54947
$SnMo_6S_8$:Gd^{3+}, powder EPR spectra, cryst. field, supercond. energy gap 80−34769
$Sn_{1.2}Mo_6S_8$, Chevrel phase supercond., compressibility and vol. depend. of Tc 78−31008
$Sn_xMo_3S_4$, chevrel phase, charge transfer and valence electron conc. 78−6029
$Sn_xMo_5S_6$, supercond. props., effect of W and Re alloying additions, Mossbauer and X-ray diffr. meas. *(Russian)* 79−15245
$Sn_xMo_6S_8$ and $(Sn\text{-}Al)_xMo_6S_8$, Chevrel phase supercond. prep. and supercond. props. 79−28434
$Sn_xMo_6S_8$, Chevrel phase, lattice instabilities, X-ray diffr. meas. 78−34491
$Sn_xMo_6S_8$, struct. anal. supercond. props. 80−97023
$SnMo_6S_8(Se_8)$ Chevrel phase supercond., hyperfine interaction, microscopic study 79−56650
$SnMo_6S_8(Se_8)$, Mossbauer spectra 80−15926
$Sn_xMo_6S_8(Se_8)$, prep., metallurgical and supercond. props. 77−32102
$Sn_xMo_6S_8(Se_8)(Te_8)$, Chevrel phase correlation between struct. and supercond. transition temp. 80−7023
$SnMo_6Se_8$, anisotropy of H_{c2} 78−39274
$SnMo_6Se_8$, Chevrel phase, RE mag. isolation and supercond. 80−44470
$SnMo_6Se_8$, high crit. field Chevrel phase 79−61003
$Sn_{1.2}Mo_6Se_8$, Chevrel phase supercond., compressibility and vol. depend. of Tc 78−31008
Sn(NCS)F, X-ray cryst. struct. anal. using Patterson functions *(French)* 79−4279
Sn(NCS)X, (X=F, Cl, Br or I), cryst. struct. *(French)* 79−51060
$SnNbS_2$, intercalate, cryst. struct. determ. 78−26534
SnNbS(Se), struct., X-ray powder diffr. meas 80−44175
SnO chlorination, Mossbauer and X-ray phase anal. 80−21266
SnO, $D^1\Pi$-$X^1\Sigma$ transition 79−41179
SnO, $D^1\Pi$-$X^1\sigma$ transition, electronic moment var. 79−41197
SnO, disproportionation, thermoEMF, Mossbauer spectroscopic, X-ray diffr. anals. 79−11776
SnO, population inversion of electronic levels by oxidation, visible emission 78−13697
SnO, prep. and growth, book contrib. 78−19651
SnO, produced in $Sn+N_2O(O_2)(O)$ reactions, kinetics of chemilum. emitter form. and quenching 78−63107
SnO, Sn(II) valency config., Mossbauer and X-ray electron determ. *(Russian)* 77−8483
SnO, under hydrostatic press. up to 41 kbar, Mossbauer study 79−51892
SnO-GeO_2 system, glass form., compound anal. 77−35486
SnO-SiO_2 glass, exam. of immiscibility 78−75837
SnO-SiO_2 glass, struct., X-ray density, IR obs. 79−46574
SnO_2, ^{119}Sn conversion electron Mossbauer 79−33575
SnO_2, ^{119}Sn-enriched, use as blackbody absorber in Mossbauer spectroscopy 80−2669
SnO_2, (cassiterite), crysts., vibr. spectra, approx. calc. method *(Russian)* 78−35148
SnO_2, activated sintering 77−36415
SnO_2, activated sintering, mechanism and kinetics, additives role 79−38771
SnO_2, adsorpt. of H_2O, isotherms 78−56038
SnO_2, adsorption anomaly of water, effects of cryst. growth of solid 80−10779
tin compounds continued
SnO_2, adsorption of water, adsorption anomaly rel. to pretreatment 79−28194
SnO_2 aerosols, Lamb-Mossbauer factor *(French)* 80−81375
SnO_2 and SnO, smoke particles prep. by burning metal in Ar-O_2 gas, electron microscope obs. 77−52238
SnO_2, anharmonicity effect, Debye temp. determ. from Mossbauer spectra 77−63335
SnO_2, band struct., tight-binding calc. 80−24796
SnO_2 based ceramics, sintering qualities 79−61547
SnO_2 CVD coating on glass, elec. resist. rel. to cryst. microstruct. 80−84520
SnO_2 CVD film form. mechanism 78−38977
SnO_2, CVD semicond. film, surface and bulk cond., process parameters effect 77−1502
SnO_2, cassiterite, appl. of cathodolum. microscopy and spectrometry 77−69919
SnO_2, catalyst particles, converger beam electron diffr. 78−83685
SnO_2 chemically sprayed antireflecting films on Si solar cells 79−72639
SnO_2 coated glass, surface elec. breakdown 80−25303
SnO_2 coating, scratch resistance and suitability for glass artificial heart valves *(German)* 79−12028
SnO_2, correl. between simultaneous thermally stimulated cond. and thermlum. transients 79−91073
SnO_2, cryst. growth by chem. transport method 78−3004
SnO_2, crystal growth habits, CVD method *(Japanese)* 78−95686
SnO_2, defect, resonance filter for Mossbauer spectroscopy 77−24767
SnO_2 defective crystals, exciton-impurity complex luminescence spectra *(Russian)* 79−65926
SnO_2 deposition, transparent, on glass plates, in tunnel furnace *(Hungarian)* 78−35303
SnO_2, doped, appl. as propane gas detector 79−29426
SnO_2 doped films for spectral-selective surfaces, refl. and elec. props. meas. 79−74013
SnO_2, ESR of adsorbed O species *(Japanese)* 78−10750
SnO_2, elec. conducting film on glass substrate, measurement of optical constants and thickness 78−60525
SnO_2, elec. field gradient at Sn^{4+} site, Mossbauer quadrupole splitting and anionic polarisability calc. *(French)* 79−15384
SnO_2, electro-conducting transparent film, props. rel. to production method *(Japanese)* 80−25557
SnO_2, electrochem. determ. of free energy 79−82360
SnO_2, electrochemical determination of free energy of formation 79−11797
SnO_2 electrode reactions with molten glass 80−85186
SnO_2 electrodes, dye-modified, erythrosin, attachment, X-ray photoelectron, photocond. investigs. 79−43600
SnO_2, electrodes, effect of DC on corrosion in lead glass melt 80−85075
SnO_2, electronic struct. and densities of states, tight-binding calcs. 80−15447
SnO_2, exciton luminescence spectra, absorpt. spectra 80−89064
SnO_2 far IR photoconductivity response obs. 77−38000
SnO_2 film, CVD using $SnCl_4$-H_2O and $SnCl_4$-H_2O_2 systems, elec. and optical props. 78−52686
SnO_2 film, deposition from vapour phase, thermodynamic anal. 80−15418
SnO_2, film, diffusion of impurities *(Japanese)* 79−95218
SnO_2 film, doped, electron effective mass and elec. props., carrier density depend. 77−43750
SnO_2, film, effects of Sb and In additions on struct. and resist. 77−20469
SnO_2 film, mobility limitation by intercrystalline potential barrier, tunnelling effect 77−66210
SnO_2 film, optical and elec. props., rel. to stoichiometric deviation and struct. 77−47701
SnO_2, film, optical characterisation, inversion method 78−11008
SnO_2 film, orientating action of solid substrates, on liq. cryst. layer exam. 80−44111
SnO_2 film, pure and Sb doped, transparent cond., prop., characts., stability, struct. *(Japanese)* 78−47889
SnO_2 film, RF plasma deposition on glass or $In_{2-x}Sn_xO_{3-y}$, and liq. cryst. aligning props. 77−48350
SnO_2 film, reactive ion-plasma sputtered, elec. and opt. props. 79−42677
SnO_2 film, reactor irrad. induced changes in elec. props. 77−28267
SnO_2 film, transparent cond. support for ZnS:Mn films, effect of morphology 79−56092
SnO_2 film growth at room temp. 79−91592
SnO_2 films, cohesive energy, free electron density effect 79−60655
SnO_2 films, selective, optical characterisation by thermodynamical method 80−84796
SnO_2, finely dispersed, Lamb-Mossbauer factor 80−39930
SnO_2 fluorite isotype, implications for Earth's lower mantle 78−61371
SnO_2, forbidden energy gap oxide semicond. crystals, review of spectroscopic props. 78−2876
SnO_2, from rocks, quantitative determination by Mossbauer effect *(Rumanian)* 78−49178
SnO_2, gas sensor, CO, H_2O vapour, surface temp. effect on cond. 78−76067
SnO_2 gas sensor, fast-detecting, prep. 80−61497
SnO_2, glaze, high field cond., 4.2-470K 78−23100
SnO_2, grown from Sn-In melt, In solubility 77−11697
SnO_2, heat treated film, electrical conductivity 77−8211
n-SnO_2, high resist., photoelectronic processes 78−60157
SnO_2, hydrous, gel, chemisorption of organic compounds, transmission IR spectroscopy 77−55465
SnO_2 layers, study using Mossbauer effect 78−31124
SnO_2, muonium and positronium form. 79−56679
SnO_2, nonstoichiometric crystal, free electron density anal. 79−99108
SnO_2, O chemisorption, elec. cond. and EPR meas. correlation 80−84369
SnO_2, optical props., review 77−1673
n-SnO_2 pigmented solar cell for electrolysis of water, two-photon process 80−93932
SnO_2, point lattice electrostatic pot. calcs. *(Russian)* 80−15044
SnO_2, powder, electron scatt. from ^{119}Sn, effective range, Mossbauer obs. 77−63345
SnO_2 powders, specific area, granulation and sintering *(Polish)* 79−52146
SnO_2, quantitative determ. by Mossbauer effect, using portable analyser 78−20131

tin compounds continued
SnO_2, rare earth ion doped, luminesc. and charge compensation 78−76532
SnO_2, reactive ion plating onto insulating substrates, and elec. and optical props. 79−87588
SnO_2, reduction by C 79−61901
SnO_2, rutile, band gap assignment by two-photon spectroscopy 79−19513
n-SnO_2, semicond. electrode, electrolum. due to wide injection from electrolytes 77−20926
SnO_2, semiconductor, photoluminescence, depend. on lattice temp. and excitation intensity 80−45137
SnO_2, single crystals, luminescence centres 78−80395
SnO_2, sintered, adsorption, of Ar, meas. and calcs. 77−69164
SnO_2, spray coated, reaction with Si, IR investig. 79−39197
SnO_2, sputtered film, thermal ageing, thickness dependent effects 78−6462
SnO_2 surface, interactions with O_2, H_2O and H_2, desorpt., ESR and cond. meas 80−10790
SnO_2, surface impurity in SiO_2-Na_2O-CaO-MgO float glass, ellipsometry and XPS study 80−84346
SnO_2 thermoelectrical properties, investigation 77−76852
SnO_2 thin film gas sensor, prep. 80−39691
SnO_2 thin films, analytical characterisation 80−20053
SnO_2 thin films, O_2 vacancy diffusion 80−107467
SnO_2 thin films, solid state gas sensor 80−40790
SnO_2, time-resolving high-intensity laser-light detectors 78−77982
SnO_2, transparent conducting coatings, book contrib. 78−10587
SnO_2, transparent conductive film, prep. by magnetron sputtering and elec., optical and structural props. *(Japanese)* 79−8247
SnO_2, transparent conducting film, prep. by CVD, and characterisation 80−11571
SnO_2, transparent electrode deposition on PLZT ceramic, elec. and opt. props. 78−74848
SnO_2, transparent films, state of art *(Chinese)* 79−73610
SnO_2, two-step deposition process using DC sputtering and oxidation, and characterisation 78−95691
SnO_2, VUV transparent electrode formation by chemical deposition and vacuum sputtering 79−56929
SnO_2:As film, prep. and elec. cond. 80−2959
SnO_2:Cr(Sb), cassiterite, gas phase growth on seed 77−24937
SnO_2:Eu film, RF cosputtering, cryst. site of Eu, cathodolum. obs. 77−7987
SnO_2:Eu powder phosphor, prep., low energy electron excitation 78−39608
SnO_2:Eu^{3+}, luminesc. and charge compensation 77−28618
SnO_2:F, thin films, prep. by pyrolitic method, charact. by SEM, electron diffr. and SIMS, solar energy appl. 79−43143
SnO_2:F films, elec. and optical props., solar energy conversion appl. 79−65945
SnO_2:Mo^{5+}, hyperfine and superhyperfine interactions, EPR 77−8398
SnO_2:P, CVD films, elec. props., cryst. to amorphous transition effects 80−107933
SnO_2:P, CVD growth and etching charact., doping effects 80−107667
SnO_2:SB,X, X=Fe,Cu,S, CVD thin film, resist. temp. coeff. 79−38198
SnO_2:Sb, and pure cryst., microstruct., X-ray diffr., optical and electron microscope studies 78−79619
SnO_2:Sb, prep. and material charact. for far IR detector 78−4697
SnO_2:Sb, transparent cond. film prep. by thermal decomp. of Sn salt of organic acid *(Japanese)* 77−90269
SnO_2:Sb, transparent cond. films, hydrolysis deposition, elec. and optical props. 79−43144
SnO_2:Sb film, amorphous, electrotransport phenomena obs., under DC electric field 80−59840
SnO_2:Sb film, DC sputtered, substrate temp. effect on cond. 77−39971
SnO_2:Sb film, DC sputtered, correspondence between Sb content and targets 79−23847
SnO_2:Sb film on glass substrates, elec. props. 80−88652
SnO_2:Sb sprayed film, growth mechanism and cryst. struct. 80−89143
SnO_2:Sb thin films DC sputtered, heat treatment effects, expt. 77−28719
SnO_2:Sb transparent conductive coatings for Cu_2S-CdS solar cells 79−61992
SnO_2:ThO_2, exposed to CO gas, self-oscill. phenomenon 78−68032
SnO_2:ThO_2, exposed to H_2, temp. depend. of resistivity 79−56219
SnO_2:ThO_2, selective detection of CO, hydrophobic and hydrophilic silica effect 79−97372
SnO_2:$V^{4+}(Cr^{3+})(Mo^{5+})(Nb^{4+})(Re^{4+})$, direct mechanism in supertransferred hyperfine interaction 79−23936
SnO_2:W^{5+}, EPR parameters, g hyperfine and superhyperfine tensors 77−85560
SnO_2/n-Si solar cells, fabrication and characterisation 79−79393
SnO_2/n-Si solar cells subjected to different weathering conditions, stability 79−52936
SnO_2/n-Si spray-deposited solar cells 80−12007
SnO_2/n^+-pSi heterojunction solar cells, fabrication by paint-on-diffusant method 80−94048
SnO_2/V_2O_5-P_2O_5/Si heterojunction, static optoelectronic charact. 79−87146
SnO_2-based gas sensors, resist. temp. depend. on exposure to CO, H_2, and propane 80−103694
SnO_2-CdO film, DC sputtering prep., visible and near IR transmission, resist. 78−88049
SnO_2-copper phthalocyanine-Ag systems, elec. and electroluminescent behaviour 80−80864
SnO_2-Cu_xS-ZnS:Mn,Cu-Al_2O_3-Al, light-emitting struct., cond. and electrolum., heat treatment 80−97345
SnO_2-fuchsin-Al MSM structure, field depend. of electroabsorption spectra 77−40263
SnO_2-$Ga_{1-x}Al_xAs$, rapid localised non-destructive optical charact., of ternary layer *(French)* 77−62725
SnO_2-Ga_xSe_{1-x} heterostruct., amorphous, photovoltaic effect 78−14803
SnO_2-GaAs heterojunctions, elec. and optical props., photovoltaic appls. 77−43714
SnO_2-GaSe heterojunction, elec. props. and electrolum. spectra 77−59328
SnO_2-GaSe heterojunction photocell, fine struct. of photo-EMF spectra 80−6967
SnO_2-GaSe(Te) heterojunction, electro-optical props. 78−64102
SnO_2-GaTe(GaSe)(InSe) heterojunctions, photoelec. props. 80−96945
SnO_2-InP heterojunctions, elec. and photovoltaic charact. 80−75628

tin compounds continued
SnO_2-InSe n-n heterostructures, photoelec. props., 80 to 300K 80−20297
SnO_2-$KInO_2(KScO_2)$, ionic cond., lamellar struct. *(French)* 77−1257
SnO_2-NiO(ZnO)(Nb_2O_5), activated sintering mechanism 80−60810
SnO_2-polySi solar cells, fabrication, grain size effects on device parameters 80−94045
SnO_2-$Sb_xS_{1-x}Sn$ structures, photovoltaic effects *(Korean)* 80−44647
SnO_2-Si, heterojunction solar cells, anomalous photocurrent 80−3515
SnO_2-Si, solar cell, max. theoretical efficiency 79−83598
SnO_2-Si heterojunction, elec. and photoelec. props. 77−1477
SnO_2-Si heterojunction, complementary Schottky barriers 79−78166
SnO_2-Si heterojunction solar cell, elec. props. *(Korean)* 80−45665
SnO_2-Si heterojunctions, elec. and photovoltaic props. 80−26141
SnO_2-Si n-n photodiode, 5.4 MeV electron irrad. effects 77−80806
SnO_2-Si solar cells, electron-beam-deposited, fabrication, angle-of-incidence effects 79−52931
SnO_2-Si solar cells, electron-beam deposited, struct., photovolt. props. 80−50956
SnO_2-SiO_2-n-Si heterojunction, cheap solar elements for ground-based appls. 80−40860
SnO_2-TiO_2 solid solns., X-ray diffr. and thermogravimetric meas. 79−90792
SnO_2-VO_x-PdO ceramic, switching and oscill. phenomena 78−6417
SnO_2-ZnO-Bi_2O_3, ceramic semiconductor, injection currents 79−11141
SnO_2-ZnS:Mn thin film structure, surface morphology and electro-optical props. *(Russian)* 80−49554
SnO_4^{4-}, normal vib. freq. and force const. calcs. *(Russian)* 78−46318
SnO_4^{4-}, normal vibr. freqs. calc. 79−54837
SnO_x films, non-stoichiometric, DC reactively sputtered, elec. props. 80−80415
SnO_x films, passivation effect on Si solar cells 80−61360
SnO_x films, phase composition, Mossbauer spectra 80−20051
SnO_x films reactive DC sputtering prep., phase comp., X-ray diffr. and Mossbauer meas. 79−90914
SnO_x thin-film conductance-modulation CO sensor, operation model 79−97371
SnO_x:Sb,F film CVD for bistable storage CRT 77−77410
Sn_xO_y films, semiconducting, equipment for deposition on cylindrical objects 77−40378
$(Sn_2O_2F_4)Sn_2$, synthesis and cryst. struct., X-ray diffr. meas. *(French)* 77−47411
$Sn_3(PO_4)_2$, cryst. struct. 77−58984
$Sn_2P_2S_6$, ferroelec., IR and Raman spectra, photocond., edge absorpt. spectra, spontaneous polarisation, forbidden gap 78−68514
$Sn_2P_2S_6$, ferroelec. and pyroelec. props. meas. 78−35107
$Sn_2P_2S_6$, ferroelec. semicond., phase transition and lattice dynamics 80−60526
$Sn_2P_2S_6$, ferroelectric semicond. polarisation Raman scatt. spectra, X-ray struct. study 79−95778
$Sn_2P_2S_6$, illumination effect on soft mode and dielectric props., luminesc. study *(Russian)* 80−50420
$Sn_2P_2S_6$, investigation of p-T diagram near a singular point *(Russian)* 80−88937
$Sn_2P_2S_6$, soft mode, interaction of modes and crit. Rayleigh scatt. 79−99836
$Sn_2P_2S_6$, soft mode, temp. depend. of Raman spectra near phase transition 78−88263
$Sn_2P_2S_6$, soft mode props., Raman scatt. study 80−60525
$Sn_2P_2(S_{1-x}Se_x)_6$, solid solutions, ferroelectric soft mode freq., displacive transformations 80−29701
$Sn_2P_2Se_6$, ferroelec. props. *(Russian)* 80−25313
$Sn_2P_2(Se_xS_{1-x})_6$, ferroelec. props. *(Russian)* 80−25313
$Sn_2P_2(Se_xS_{1-x})_6$, ferroelec. tricrit. phase transform., light transmission study 80−71355
$(Sn_{1-x}Pb_x)_2P_2S_6$, solid solutions, ferroelectric soft mode freq., displacive transformations 80−29701
$Sn_{1-x}Pb_xSe(Te)$ films, Mossbauer effect of ^{119}Sn, spectral charact., conc. depend. 80−103903
$Sn_{1-x}Pb_xSe(Te)$ films, oxidation rel. to annealing temp. and time, Mossbauer spectra, X-ray and microstruct. obs. 80−104311
$Sn_{1-x}Pb_xSe(Te)$ thin films, resistance to oxidation, Mossbauer study 80−39986
$Sn_{1-x}Pb_2Te$, elec. and struct. props. of epitaxial layers *(Russian)* 78−64147
$Sn_{1-x}Pb_xTe$, epitaxial layers synthesis, cryst. struct. perfection and elec. charact. 79−87587
$Sn_{1-x}Pb_xTe$, film, production under quasi-equilibrium conditions 80−45241
$Sn_xPb_{1-x}Te$ mixed cryst., cryst. growth and assessment 78−80463
SnS, coupling of plasma waves with optical phonons 78−31204
SnS, dielec. function, optical and electron energy loss spectroscopy 78−15189
SnS, electron-hole interaction in d-electron excitations, photoelectron and optical spectra 78−34776
SnS, electrorefl. spectra 77−16282
SnS, far IR optical props. 77−12375
p-SnS, IR photocond., direct and indirect gaps 78−2514
SnS, IR reflectivity and Raman spectra, phonon frequencies and dielec. const. 77−48166
SnS, photoconductivity 77−72888
SnS photoelectron spectra, rel. to ionicities and phase transitions 77−69960
SnS, Schottky barrier, photovoltaic props. 79−7854
SnS, single cryst. growth and struct. props. 79−52109
SnS, splitting and coupling of lattice modes 77−76503
SnS, tight-binding calc. of density of valence states 78−34760
SnS, valence level photoelectron spectra 77−27114
SnS, X-ray photoemission intensity, nearest-neighbour backscatter 79−65977
SnS, XPS investig. of valence band struct. 77−48311
$^{120}Sn^{32}S$, $^{120}Sn^{80}Se$, $^{120}Sn^{130}Te$, rot. g_J-factor meas., $^1\Sigma$ ground state *(German)* 77−30865
SnS:O, impurity assoc. with Fe microtraces, Mossbauer effect meas. 77−20763
SnS-GeS_2, exam. of phase diagram using DTA *(German)* 79−11585
SnS-PbS, phase diag. 77−36476
SnS-SnSe, solid soln. comp. calcs. 77−44230
SnS-SnTe, solid solns., synthesis, Mossbauer spectra 77−24768
SnS_2, 2H and 4H, effect of press. on optical absorpt. edge 77−77238
SnS_2 (2H), band struct. press. depend. 78−43292
SnS_2, band struct., effect of polytypism 78−43293

tin compounds continued
SnS_2 berndtite, cryst. struct. and compressibility at high press. 78−67685
SnS_2, conduction and valence band density of states 77−62817
SnS_2, cryst. growth, photoconductivity 77−85912
SnS_2, crystal growth and optical props. in visible and IR regions 77−52114
SnS_2, effect of powdering on polytypic cryst. struct. 80−1979
SnS_2, growth by I_2 vapour transport using temp. oscill. method 77−77355
SnS_2, Li intercalation effects on electronic struct. 79−78004
SnS_2, Mossbauer spectra, vibr. amplitudes anisotropy 80−15904
SnS_2, nonlinear susceptibility, SHG 78−30019
SnS_2, octahedrally coordinated, layer cpd., electronic struct. using synchrotron-radiation photoemission spectroscopy 79−74058
SnS_2, optical phonon anisotropies and intralayer bonding forces from IR refl. 77−59573
SnS_2, optical props., modulation spectroscopy, indirect absorpt. edge 77−52117
SnS_2, optical props. and band struct. 78−2880
SnS_2, optical transitions from d core levels 80−45105
SnS_2 polytypes, electronic bandgap meas. 80−34358
SnS_2, polytypism, and cryst. struct. by X-ray methods 79−77542
SnS_2, prep. and growth, book contrib. 78−19651
SnS_2 press. effects on optical absorpt. edge 77−52119
SnS_2, Raman active mode assignments 77−12387
SnS_2, refl. using Kramers-Kronig anal., optical functions 79−95798
SnS_2, single cryst., far IR reflectivity 79−56774
SnS_2, Sn4d photoionisation, second threshold 80−40222
SnS_2 thin layer, far IR refractive index 80−93421
SnS_2, UV reflectivity meas., band struct., LCAO calcs. 78−72545
SnS_2, X-ray photoemission intensity, nearest-neighbour backscatter 79−65977
SnS_2-Cu_2S, and GeS_2-Cu_2S systems, dissoc. of ternary congruently melting cpds. 79−87832
SnS_2-SnI_4, and SnS_2-I_2, systems, transport props. and thermodynamical calcs. 79−32928
SnS_2-SnI_4, T-x projection of phase diag. 78−23683
Sn_2S_3, mixed valence semicond., long wavelength phonons, full space group theoretical anal. 79−65873
Sn_2S_3 mixed valence semiconductor, far IR refl. spectra 80−108191
Sn_2S_3, resistivity, Mossbauer spectra, press. effects 79−73862
$SnSO_4$, Sn(II) valency config., Mossbauer and X-ray electron determ. *(Russian)* 77−8483
$SnS_{2(1-x)}S_{2x}$ solid soln. system, long-wavelength optical phonons, Raman scatt. study 80−80794
SnS(Se), electron diffr. struct. anal. 80−44449
SnSSe, electron mobility, elec. cond. and Hall effect meas. 78−80004
SnS(Se), layer crystals, optical phonons, Is and Raman spectra 77−73148
$SnS_{2-x}Se_x$, ($0 \le x \le 2$), ^{119}Sn Mossbauer spectrum, lattice dynamics 78−71809
$SnS_{2-x}Se_x$, electron mobility elec. resist. and Hall constants 79−28346
$SnS_{2-x}Se_x$, layer cryst., Raman active modes 80−80767
$SnS_{2-x}Se_x$, Raman spectra 79−28763
$SnS_{2-x}Se_x$ solid soln., resistivity, lattice parameter, comp. and temp. depend. 78−91693
$SnS_2(Se_2)$, electronic struct., tight-binding calcs. 80−15446
$Sn(S_xSe_{1-x})_2$, valence band states, composition depend., photoemission spectra study 80−100434
SnS_xSe_{2-x}, growth by I_2 vap. transport, cryst. struct. 77−73223
SnS_xSe_{2-x}, thermal changes in optical props. 78−19504
$SnS_2(Se_2)(SSe)$, layer compound, expansivities and thermal degradation 77−89554
SnS(Se)(Te), reaction with II-VI compounds, thermodynamic anal. 80−40728
SnS_2(2H and 4H), Raman scatt. and phonon frequencies 77−48159
$Sn_5Sb_2S_9$, cryst. struct. *(French)* 80−1991
SnSe, and $SnSe_2$, mag. susceptibility components 78−43551
SnSe, dielec. function, optical and electron energy loss spectroscopy 78−15189
SnSe, electron states anal. by pseudopotential method 77−66115
SnSe, electronic band struct. determ. 78−51890
SnSe, electronic props., region of existence *(French)* 77−35885
SnSe, electrorefl. spectra 77−16282
SnSe, far IR reflectivity spectra, lattice vibr. and dielec. const. 77−52068
SnSe, IR reflectivity and Raman spectra, phonon frequencies and dielec. const. 77−48166
SnSe, IR-active optical phonons, vibr. spectra 79−69848
SnSe, lattice refl. spectra in long-wavelength IR range 78−27236
SnSe, Mossbauer spectra, effect of optical emission *(Russian)* 78−60367
SnSe, orthorhombic, atomic pseudopots. 79−42453
SnSe, photoelectron spectra, rel. to ionicities and phase transitions 77−69960
SnSe, Raman scatt., zone centre optical phonons, layer-like struct. 78−48158
SnSe, single crysts., growth by Bridgeman technique, electron diffr. anal., lattice consts., carrier conc. 79−47616
SnSe, small gap, band-edge parameters 80−49594
SnSe, sublimation growth, deviation from stoichiometry, elec. props. 78−76594
SnSe, tight-binding calc. of density of valence states 78−34760
SnSe, XPS investig. of valence band struct. 77−48311
SnSe-$GeSe_2$-As_2Se_3 glasses, vitrification region and elec. cond. 80−15008
SnSe-Sb_2Se_3 system, phase diagram, differential thermal, microstruct., X-ray phase and microstructure anal. 77−16555
SnSe-Se, p-T projection of phase diag. 78−27485
SnSe-SnTe, solid solns., synthesis, Mossbauer spectra 77−24768
SnSe-Tl_2Se, phase diagram, DTA and X-ray diffr. peritectic decomposition *(French)* 77−51471
SnSe-TlSe, phase diagram 100-900°C *(French)* 79−83180
$SnSe_2$ (6Hb), Raman scatt. and phonon frequencies 77−48159
$SnSe_2$, band struct., angle resolved photoelectron spectra meas. 78−72680
$SnSe_2$, intercalated with cyclopropylamine, photoelectron spectra study of electronic struct. 78−84698
$SnSe_2$, layer struct., acoustic phonon dispersion curves, propag. modes 77−51462
$SnSe_2$, Mossbauer spectra, vibr. amplitudes anisotropy 80−15904
$SnSe_2$, optical phonon anisotropies and intralayer bonding forces from IR refl. 77−59573
$SnSe_2$, optical props., modulation spectroscopy, indirect absorpt. edge 77−52117
$SnSe_2$, optical props. and band struct. 78−2880
$SnSe_2$, optical transitions from d core levels 80−45105
$SnSe_2$, prep. and growth, book contrib. 78−19651
$SnSe_2$, press. effects on optical absorpt. edge 77−52119
$SnSe_2$, Raman active mode assignments 77−12387
$SnSe_2$, refl. using Kramers-Kronig anal., optical functions 79−95798
$SnSe_2$, single crystal, reflectivity, XPS, UPS, and band struct. 78−6701
$SnSe_2$ spatial symm. of valence band struct. by angularly resolved XPS 77−69961
$SnSe_2$, sublimation, temp. depend. of equilib. constants 80−88312
$SnSe_2$, thermorefl. spectra 77−90168
$SnSe_2$, UV reflectivity meas. 78−72545
$SnSe_2$-Cu_2Se, and $GeSe_2$-Cu_2Se systems, dissoc. of ternary congruently melting cpds. 79−87832
$SnSe_2$-$GeSe_2$, phase diag., electrophys. props. of solid solns. 77−52306
$SnSe_2$-$GeSe_2$-As_2Se_3 system glasses, vitrification and elec. cond. 79−50997
SnSeI film, growth, effect of artificial nucleation centres 79−11032
$SnSe_yTe_{1-y}$, semicond. chalcogen interdiffusion coeffs., antifrenkel defects, interstitials *(German)* 77−43375
$Sn(SnO_3)_2$, Mossbauer spectral anal. *(German)* 79−19818
$SnTaS_2$ intercalate, cryst. struct. determ. 78−26534
SnTaS(Se), struct., X-ray powder diffr. meas 80−44175
SnTe, ^{117}Sn diffusion coeff. meas., stoichiometric deviation, SIMS 80−34236
SnTe, ^{119}Sn temp. depend. isomer shift, pseudopot. approach 80−84675
SnTe, annealed, iodide method of prep., props. meas. 80−71591
SnTe, bond gap, phase transform., optical dielec. const. meas. 80−10630
SnTe, bond orbital model of band struct. 80−59853
SnTe, carrier density depend. of soft TO-phonon, Raman scatt. meas. 78−6684
p-SnTe, cathodoluminescence and Fermi level hole effective mass 80−25467
SnTe, complex-composition film production method from vapour *(Russian)* 78−95702
SnTe, crystal binding energy 79−37650
SnTe, crystallisation in constant electric field, thermoelectric parameters 77−44146
SnTe, cubic semicond. with ellipsoidal valleys, magnetoresist. 80−80300
SnTe, diffusion of ^{125}Te 80−84325
SnTe, displacive phase transition at 22K, Mossbauer spectra and elec. resist. meas. 80−6514
SnTe, displacive transform., interband electron-phonon interactions, phase diagram 80−93252
SnTe, donor impurities source for GaAs MBE 79−95035
p-SnTe, elec. resist. anomaly in vicinity of struct. phase transform. 79−19597
SnTe, electron-phonon interaction effect on ferroelec. transition 78−76416
SnTe, electron-phonon interactin induced phase transition 79−82338
SnTe, enthalpy of formation *(Russian)* 80−15267
SnTe, expitaxial film, early stages of growth, replication and TEM obs. 79−65348
SnTe, ferroelec. transition, quantising mag. field effect 79−87403
SnTe film, 50 μ, prep. in double quasiclosed volume 79−38745
SnTe film, amorphous, evaporated and annealed, variable range hopping cond. 78−80077
SnTe film, electroreflectance effects 79−43055
SnTe film, evaporated, electro-reflectance meas. 80−11496
SnTe, film, heat treatment in air, effect on struct., props. 79−11037
SnTe film, polycrystalline, anomalous resist. at struct. phase transition 80−29488
p-SnTe, film and bulk, weak-field magnetoresistance 78−84236
SnTe, Hall coeff., temp. depend., interpretation 78−87988
SnTe, isothermal meas. of galvanomag. and thermomag. effects *(Russian)* 78−56160
SnTe, LO phonons affected by dielec. screening 79−77697
SnTe, LPE, solvent choice, equilib. in Pb-Sn-Te system 79−87589
SnTe, light scatt. from soft modes, theory above and below displacive transform. temp. 79−95791
SnTe, low-temp. sp. ht., thermal expansion and Gruneisen parameter 77−15601
SnTe, mag-props., effect of structure transition 78−6158
SnTe, mechanochem. and thermal oxidation comparison, Mossbauer obs. 80−104310
SnTe, NMR of ^{119}Sn and ^{125}Te, low hole conc., 64-440K *(Russian)* 79−15365
SnTe, obs. of soft TO-phonon by Raman scatt. 77−69838
SnTe, phase transition at high hydrostatic pressure, Mossbauer study 79−95162
SnTe, phase transition obs. by Mossbauer spectroscopy 77−55740
SnTe, polymorphism, high press. and temp., X-ray diffr. study 80−54375
SnTe, press.-temp. phase diagram 77−51497
SnTe, Raman scatt. from soft TO-phonon modes 79−95773
SnTe, self-consistent relativistic energy bands 80−10870
SnTe, small gap, band-edge parameters 80−49594
SnTe, softening of TO phonon mode *(Japanese)* 78−2225
SnTe, solidus line anal., carrier conc. 78−75806
SnTe, sp. ht. mean field behaviour at phase transition 77−66023
SnTe, standard free energy of form. 79−57287
SnTe, strongly anisotropic polar semicond., electron-hole liq. in mag. field 80−59890
SnTe, structural phase transition threshold instability in strong EM field 80−103477
SnTe substrate, Ag epitaxial growth and topostactic exchanges 78−14640
SnTe, supercond., metal-insulator transition, electron pairing, effect on optical props. 80−60139
SnTe surfaces, oxidation in air and thermal desorption, XPS and LEED meas. 79−47830
SnTe, temp.-depend. ^{119}Sn isomer shift, calcs. 77−8457
SnTe, thermoelectric materials, physico-chemical study 78−30945
SnTe, tight-binding calc. of density of valence states 78−34760
SnTe, valence level photoelectron spectra 77−27114

tin compounds continued
SnTe, XPS investig. of valence band struct. 77−48311
SnTe:Mn, EPR as probe of phase transitions 80−15790
SnTe:Mn, ferromag.-ordering, transverse magnetoresist. and Hall effect meas. 77−85240
SnTe:Mn, NMR shift meas. 80−97154
SnTe:Mn, NMR study 4.2 to 300K *(French)* 80−54960
SnTe:O, impurity assoc. with Fe microtraces, Mossbauer effect meas. 77−20763
SnTe-Al_2O_3-Al junction, tunnelling, Fermi level depend. on carrier conc., influence of surface states 80−25016
SnTe-Al_2O_3-Al structure, tunnelling characts., model anal. 80−29480
SnTe-Bi_2Te_3 system, phase diagram 77−36474
SnTe-In, solubility, thermo-EMF coeff. meas. 78−43124
SnTe-In_2Te_3 system, thermoelec. props., phase diagram, transitions 78−43424
SnTe-InTe, SnTe-In_2Te_3, solid soln. region, lattice constant variation 77−35697
SnTe-InTe system, solid soln. films prep. under quasi-equilibrial conditions 79−33931
SnTe-MnTe, degenerate semicond., anomalous Hall effect 80−29420
SnTe-PbSe, semicond. film, growth, phase composition, condensation temp. rel. to cond. type 77−28266
SnTe-PbSe mixed system layers, struct. and props. *(Russian)* 77−28082
SnTe-PbTe solid solns., defects from susceptibility meas. 77−84737
SnTe-Sn epitaxial system, electron microscope contrast of misfit dislocations 77−85113
SnTe-Te, contact fusion in complex metallic systems 78−26664
SnTe-Tl_2Te, phase and elec. props. 77−48406
$(SnTe)_{1-x}(MnTe)_x$, ESR, effect of Mn ion conc. on line width and area 78−35026
$(SnTe)_{1-x}(PbSe)_x$ films on glass-ceramics, struct. and elec. props. 77−52251
$Sn_xTi_{(1-x)}O_2$, solid soln., thermal reaction with V(V), Cr(III), Cr(VI), Mn(II), Fe(III), Co(II), NI(II), Cu(II), Sb(III) 80−16674
$Sn_{10}W_{16}O_{46}$, cryst. struct. determ. 80−33934
$Sn_{10}W_{16}O_{46}$, struct. anal. and stereoactivity of Sn^{II} lone pair 80−33935
SnX_2 (X=Cl, Br, I), UV absorpt. cross-sections of vapour 78−25554
SnX_3^-, (X=F, Cl, Br, I), vibr. freqs. and intensities anal. *(Russian)* 77−23492
SnX_4 (X=Br, Cl, I) electron impact dissoc.-electron capture, ionis. efficiency curves 77−61865
$SnX_3^{\ominus}(SnX_2^{\ominus})$(X=Br,Cl,I), structs., electron affinities, formed by electron impact 77−61865
$SnX_3^-(SnX_2^-)$(X=Cl,Br,I), formed by electron impact from SnX_4, ionis. efficiency curves, structs. 77−61865
$Sn_xZr_{1-x}Se_2$, growth by I_2 vap. transport, cryst. struct. 77−73223
^{119}Sn free radicals, dynamic nucl. polarisation in solution 77−88475
^{119}Sn NMR by pulse Fourier transform, T_1, T_2 and chem. shifts 77−55715
^{119}Sn-^{117}Sn primary isotope effect on mag. shielding, NMR of Sn cpds. 79−72338
SrS-SnS_2 system, phase diagram *(French)* 79−34013
SrSn, Sr_2Sn, prep. by melting, characterisation *(French)* 77−70017
Sr_2SnS_4, $Sr_3Sn_2S_7$, prep., cryst. structs. *(French)* 79−34013
TaS_2.Sn, intercalated, Mossbauer effect, hyperfine interaction, lattice dynamics 77−8473
$Tb_{1-x}Sn_xTe$, ferroelectric transition calc., effect on carrier density 77−85673
Te-Ge-Sn, Te rich, structural phase transformation concurrent with glass crystallisation, thermal evidence 79−4965
$Te_{43}Se_{50}Sn_7$ in MSM struct., switching effects 78−19164
$Te_{50-x}Se_{50}Sn_x$, thin films, elec. cond. and thermoelectric power meas. *(French)* 80−80335
TiN, synthesis using enhanced reactive evaporation 80−2953
Tl-Sn-Te system equilibria, polythermal and isothermal cross sections obs., ternary cpd. form. 80−104128
Tl_2S-SnS, phase equilibria exam. 80−55369
Tl_2Se-As_2Se_3-SnSe system alloys, covalent component of chem. bond effect in vitrification processes, Mossbauer obs. 77−36156
Tl_2Se-SnSe system, phase equilib. 79−52181
Tl_2SnF_6, thermal stability and thermolysis *(French)* 78−10011
Tl_2SnSe_3, preparation, Mossbauer spectra 77−28489
Tl_4SnSe_4, preparation, Mossbauer spectra 77−28489
Tl_5Te_3-Tl_4SnTe_3-Tl_4PbTe_3, phase equilib., DTA, SPA and microhardness meas. 80−96628
W-Sn-S system, phase relationships, 500-800°C 79−24503
Zn-Sn-P, phase diag. rel. to $ZnSnP_2$ growth 77−44225
$ZnCl_2$-$SnCl_2$, molten, viscosity coeff. meas. *(Japanese)* 79−77662
ZnO-SnO_2-M_xO_y, M_xO_y=glass-forming additive, I-V characts., heat treatment effects 77−43595
$ZnSnCuO_4$, cryst., struct., mag. susceptibility obs. 78−2085
$ZnSnP_2$-$ZnSiP_2$, heterocombination simultaneous crystallisation 78−60560

titanium
see also nuclei with .....
$\alpha \rightarrow \beta$ phase transformation, elec. resistivity 79−15661
$\alpha \rightarrow \omega$ transform., pressure-induced, impurity effects and reaction kinetics 78−11220
α-titanium, plastic deformation, anharmonicity Gruneisen parameter 80−88246
abundance in stony meteorites 79−92731
acoustic harmonic generation by long-range dislocation motion 79−42150
adhesional reactions with refractory metals 79−29280
adhesive properties of melted Al, Ga and In, 300 to 1200K *(Russian)* 77−15663
adsorption, on (110), (121) and (111) faces of W 80−100411
adsorption and replacement of CH_4, CO and NO *(Japanese)* 78−22949
adsorption of CO, AES obs. 77−35818
adsorption of O_2, CO and CO_2, SIMS expts. using 500 eV primary Ar^+ ions 77−72785
adsorption of O on polycryst. film at room temp., UPS and XPS 77−89645
adsorption of Xe, electronically excited atoms coupling to cond. states 77−89642
AES meas. of soft X-ray emission threshold potential *(Russian)* 79−33866
air at Ti surface, optical breakdown, interferometric investigation 80−100064

titanium continued
annealed, high-temp., kinetics *(Russian)* 80−21166
anode, oxide growth, effect on breakdown voltage and efficiency 79−4766
anode, Pt-Ir coated, corrosion and passivation behaviour in Cu electrowinning appl. 80−55573
anode, with RuO_2-TiO_2 active film, Cl overvoltage, γ-irrad. effects 79−16005
anode and container for heart pacemaker 79−44052
anodic behaviour, steady-state, in conc. HCl 80−45515
anodic dissolution and passivation in acidic chloride solution 80−35541
anodic dissolution in electrolytic machining *(Russian)* 79−83463
anodic dissolution in SiO_2-Na_2O-K_2O-CaO-MgO-Al_2O_3 glass melt 80−19949
anodic film growth and crystn. *(French)* 78−76788
anodic film structure, intensiostatically formed, pH and current density influence, TEM study *(French)* 79−66217
anodic oxidation, ion implanted impurities effects 77−90502
anodic oxidation under high voltage, porous layers *(French)* 80−54574
anodic oxide film growth kinetics *(French)* 78−23864
anodic oxide film on TA6V alloy and Ti struct. and growth 78−23861
anodic oxide film struct., thick *(Russian)* 78−35577
anodic oxide films, space charge, TSC obs. 77−32326
anodic oxide superficial layer, X-ray emission spectrometry and ion backscattering *(French)* 80−49482
antifriction props. 77−90467
applications in aerospace and other industry, and properties 79−66104
Arabian Sea, DSDP Site 220, Fe, Mn and Ti distrib. 77−73708
atom, $4s3d^3$ and $3d^4$ states, HF descriptions, alternative orbital config. 80−63534
atom, Compton profile asymmetry obs., Al, Ti, Fe, Cu, using Kα fluoresc. 77−57937
atom, energy level data tables, Ti I to Ti XXII 79−59385
atom, fine struct. levels fitting, config. interaction effect, spin-orbit and electrostatic interaction parameters 80−69248
atom, ionisation potential, term value, correlation energy by vertical anal. 78−41964
atom, Kα^h hypersatellite spectra and double photoionisation cross-section 79−85922
atom, Kα and Kβ X-ray spectra induced by 84 MeV N^{4+} 77−50517
atom, Kβ/Kα ratio anomalies, K-capture rel. to bremsstrahlung excitation 77−18825
atom, K-shell hole production by light ions, hydrogenic and Hartree-Fock model of target 77−83715
atom, K-shell ionis., X-ray prod. cross section for incident H^+, ^{4}He and ^{14}N ions 78−70923
atom, K-shell ionisation cross sections, proton induced 77−23556
atom, Koopmans' ionis. pot., relax. correction 79−18308
atom, $O^{2+,3+,4+,5+}$ induced K-shell X-ray production cross section, 7 to 24 MeV 77−61850
atom, rel. at. transition probabilities, by flame at absorption spectroscopy 79−89642
atom, rel. oscillator strengths by combined absorption/emission meas., new method 80−37784
atom, reson. lines relative oscill. strengths, hook technique using wall-stabilised arc 78−13628
atom, X-ray production by protons by 0.5 to 2.0 MeV energy 78−66646
atoms, neutral and ion val. states, electron correlation, ab initio effective val. Hamiltonian calc. 80−99449
Auger electron appearance potential spectroscopy *(Japanese)* 80−50473
band struct., cryst. pot. anisotropy effect *(Russian)* 80−88474
band structure and X-ray emission spectra calcs. 77−28105
band structure correlation with TiC, APW calc. *(Japanese)* 78−23017
bar crystal, prep. by iodide process 77−55878
barrier metal for sintered Pt-GaAs contacts 77−8193
BCC β phase, anomalous diffusion behaviour 78−91474
beta III powder compact, fatigue origins 77−44351
biological implant, ion beam sputter of surface morphology, SEM exam. 77−44836
blister form. by He and H ion bombardment, target struct. effect 78−95087
bonding to Fe by vacuum rolling, corrosion protection appl. 79−29283
borosilicate glass, influence on absorption spectra of transition metals in glass 77−12403
borsic fibre reinforced Ti, unidirectional, K-calibration and compliance curves 78−88518
casting defects, NDT 78−27690
catalyst, BCl_3-H_2 photochem. with Ti, Pb catalysts, isotopic excitation by laser 78−64882
catalyst, for laser photochem. isotope separation of B 77−61612
cathodic alloying on surface, for increased passivation and corrosion resist. 80−100940
CESR, prediction of obs. 80−29369
charge state in titanates and titanosilicates, binding energy *(Ukrainian)* 77−68940
charged particle prod. cross sections for 14 MeV neutrons, Ti, V, Cr, Mn 80−42648
chemisorption, of N_2, O_2 and CO on polycryst. surfaces, secondary electron yield obs. 78−71971
chemisorption of CO, LEED struct. anal. 78−71964
chemisorption of H_2 and CO, flash desorpt. mass spectrometry obs. 77−89646
chemisorption of N_2, O_2 and CO, secondary electron yield spectrum obs., for polycryst. surface 78−38933
chemisorption of N_2-containing gases at high-press., XPS 77−20990
cladding, thermal stress analysis *(Russian)* 77−59952
coated Nb, reduction of void number density and size by ion irradiation 78−51600
coated system, Nb on Mo, Ti, evaporation, carburisation and diffusion behaviour 77−44410
coating on BN powder particles, thermal stresses generated in vac. deposition 77−40455
coating on steel, thickness meas. using radioisotope thickness gauge *(Russian)* 78−56582
coatings, electrolytically deposited, texture, anti-corrosional props. *(Russian)* 80−66532
cold rolled, transcrystalline SCC in methanol-bromine soln., crystallographic texture effect 79−15872
cold rolled α-phase, primary recrystn., in situ investig. in HVEM 80−104185

titanium continued
cold worked, annealed, internal friction meas. of H degassing *(French)* 79−43304
combustion, laser-initiated, time-resolved spectroscopy 77−77765
composite sintered bearing materials, metallic solid lubricant infiltrated, antifriction props. 80−60981
compression at high strain rate, deformation anal. 80−25769
concentration in atmospheric sedimentable powder, in Vizcaya, Spain *(Spanish)* 78−57265
conference, Rennes, France (Nov. 1976) 78−23857
contact reaction with BN at high pressures 80−61029
contact with SiC single crystal, friction and fracture of SiC 80−11780
cool stars, Ti isotopic abundance ratios 80−26840
corrosion, by hot perfluoropolyether 80−93684
corrosion, electrochemical behaviour under tensile stress in boiling H_2SO_4 and acidic chloride solns. 78−95851
corrosion by molten alkali metal hydroxides and liquid Li 77−44414
corrosion by O_2 containing H_2O and gaseous NaCl, volatile products 78−27674
corrosion in conc. H_2SO_4, effect of oxidation product coating on corrosion rate 79−74282
corrosion in H_2SO_4, estimated from weight loss meas. at 270°C and 56 bar *(French)* 80−85080
corrosion in seawater circulation plant, comparison with stainless steel *(German)* 80−25897
corrosion inhibition in acid medium, electrochem., Auger investigs. *(French)* 78−44430
corrosion resist. in marine environments *(French)* 80−50767
corrosion resistance in 1M $LiAsF_6$/THF, suitability for organic electrolyte Li secondary batteries 79−100387
corrosion resistance in HNO_3 *(French)* 77−59992
corrosion resistance increase by Pd electrospark coating *(Russian)* 78−27669
corrosion resistant pure metal, passivity and pitting in chloride solutions 78−44258
corrosion susceptibilities in synthetic geothermal brines 77−86223
Cr coating effect on mech. props. *(Russian)* 77−44290
crack growth under tensile loading, in-situ obs. of α-phase *(Chinese)* 79−96121
cracking in NH_3 at 600°C 79−70207
creep behaviour, 25 to 400°C, role of impurities and/or alloying elements of commercial grade specimens *(French)* 80−45354
crevice corrosion in NaCl soln., 100 to 250°C *(Japanese)* 78−72927
cryogenic constructing material, far IR spectral refl. 77−24855
crystalline orientation distribution analysis of texture development 79−91669
crystallisation, effect of SO_4^{2-} radical *(Chinese)* 79−51440
CVD layers on Fe substrate *(Japanese)* 78−27415
cyclic behaviour and delayed softening 77−36641
deformation, tension, torsion compression test exam. *(Russian)* 78−31455
deformation mechanism map 77−77546
degree of charging of surfaces polished by TiC and synthetic diamond micropowders 78−60880
determination, electron microprobe, VK_α X-ray interferences correction, graphical method 79−43707
determination, in laterite samples, using ^{55}Fe, energy dispersive X-ray fluoresc. 78−76955
deuteration, TiD_2 film fabrication 78−52600
diffusion, of Fe, under plastic deformation *(Russian)* 79−28146
diffusion bonding, low-pressure 80−11873
diffusion characteristics in Ag, 1051 to 1220K 80−15308
diffusion coated cast Fe, wear resistance 79−52459
diffusion in $LiNbO_3$, and characts. of graded-index lightguide 79−27433
diffusion in $LiNbO_3$, surface acoustic waveguide formation 77−79998
diffusion in $LiNbO_3$ low loss optical waveguide, XPS 77−11014
diffusion in $LiNbO_3$ waveguide, exam. by electron probe anal. and X-ray diffr. 78−47588
diffusion in p-Si, doping 78−18670
diffusion of Be, temp. depend., radioactive tracer method *(Russian)* 80−10703
diffusion of H_2, neutron radiography 77−24438
diffusion of H_2, nonisothermal, in temp. field of instantaneous plane heat source *(Russian)* 77−20123
diffusion of H_2 *(Korean)* 78−18838
diffusion of H, in β-phase, neutron radiography meas. 77−39696
diffusion of O_2, 700 to 950°C, lattice parameter and microhardness meas. *(French)* 79−86929
diffusion of O, atomic jumping model 80−44366
diffusion of S, C and Cl in α-phase, AES 78−51735
discontinuous electrical resistivity, low temp. active straining of polycrystal Ti *(Russian)* 80−103666
dislocation characterisation and obs. in recrystallised Ti by X-ray topography *(French)* 78−22722
dissolution in stainless steel, kinetics, steel component absorpt. *(Russian)* 80−34193
distribution in alloy steel welds, laser emission microanal. method 78−61110
ductility in vacuum, air and liq. metals at 700-900°C *(Russian)* 77−52537
dynamic annealing, effect on dynamic strain ageing phenomena 80−7594
efficient intensity modulator 78−22190
electrical resistivity high-temp. anisotropy 79−65429
electrochemical machining, electrolytes development, electrochem. in static solns. 80−85182
electrochemical machining, electrolytes development, electrochem. studies in flowing solns. 80−85183
electrodeposition from $TiCl_4$ nonaqueous solns. *(Russian)* 78−48339
electroless codeposition of Si and Ti on Ni superalloy 77−16513
electromigration effective charge for ^3H, H conc. depend. 77−51545
electromigration of H(D) 80−34247
electron fractography of α-phase 77−63778
electron microscope specimen prep. technique for dynamic straining expt. 78−88602
electron radiation damage, determ. of threshold displacement energy 78−59837
electronic structure, appl. of Auger and characteristic loss spectroscopies 77−77331
electronic structure calc. and obs., by APW method and X-ray photoelectron spectroscopy *(Japanese)* 79−15074
titanium continued
electronic structure of five and ten atom chains SCF-Xα-SW calcs. 80−5483
electronic structure of omega and alpha phases, nonrelativistic APW method 79−90952
electroplastic effect, effects of strain rate, temp., interstitial 79−83279
electroplastic effect 79−24589
electropolished, optical props. from 1.8 to 3 eV 80−85088
electropolishing, in perchloric acid-acetic acid soln., AES study of anodic films 79−5072
electropolishing in perchloric acid-acetic acid soln., polarisation behaviour, stoichiometry 79−5073
emittance, during nonstationary high temp. heating by Ar flow *(Russian)* 80−84308
emittance at 400 to 850K and normal spectral reflectance at room temp. 77−20813
energy loss of heavy nonrelativistic ions in matter, semiclassical theory 80−84224
energy loss spectra of C^{2+} ions in Ti targets 80−65114
erosion by coal ash particles 79−61745
erosion resistant boride coating 79−20290
evaporated film, adsorpt. of CS_2 and H_2S, 195 to 473K 79−33197
EXAFS from L edge, 200-1000 eV 79−69903
exam. of whether interstitial O can cause internal friction 78−48537
exploding wire, plasma prod., X-ray diagnostics 78−5909
extruded, continuum mech. anal. of flow curve anisotropy and plastic strain *(German)* 78−84947
fast reactor structural material, (n,p) cross section eval. from threshold to 20 meV 80−13623
fast reactor structural material, capture cross section eval. 10^{-5} eV to 200 keV 80−13622
fatigue crack closure mechanism 80−16434
fatigue crack closure mechanism 80−21107
fatigue crack growth, exam. of O transport 78−52981
fatigue crack growth, influence of grain orientation, SEM study 80−108550
fatigue crack growth micromechanisms at low stress intensities in α-phase 80−108570
fatigue cracking, initial stage under bending and torsion *(Japanese)* 79−20165
fatigue damage detection in notched sample, using optical correlation technique 78−35511
fatigue fracture surface microstruct., electron microscope obs. 78−60834
fibre reinforced with B, borsic, SiC, Al_2O_3, Be, W, Mo, prep. and mech. props. *(Russian)* 78−35335
film, chemisorption of N_2, O_2, CO and CO_2, changes in work function 77−59221
film, chemisorption of O_2 and CO, quartz cryst. microbalance obs. of O/Ti and CO/Ti atom ratios 79−4475
film, CO surface contamination effect on deuteriding 77−35814
film, deposited by cylindrical magnetron sputtering, internal stresses, optical reflectance and elec. resist. 77−43449
film, depth profiles of D and T from gas emission during sputtering by Ar ions 77−35581
film, EELS, anomalous L_3/L_2 white-line ratios 80−93444
film, effect of surface and bulk oxidation on charact. electron energy loss spectra *(French)* 78−39641
film, elec. resist. Hall effect and absolute differential thermoEMF *(Russian)* 79−24083
film, evap., CO effect on work function 78−39188
film, evaporated, adsorpt. of SO_2, corrosion 78−79897
film, evaporated, interaction with BCl_3, HCl, adsorpt. 78−75945
film, interaction with O_2 80−45431
film, interference enhanced Raman scatt. 80−40105
film, ion bombardment with N_2^+, Ar^+, struct. changes, chemical compound formation *(Russian)* 78−95084
film, ion plated, morphology exam. by SEM 79−28251
film, ion stimulated N_2 sorption, TiN_x form., sorption ratio, capture coeff. anal. 80−39411
film, on Be(Ag) substrate, range of primary electrons 77−4134
film, pumping $H_2(D_2)$, isotope effect on pumping speed 78−51819
film, reactive ion beam sputtering 78−19666
film, solid state reaction with Si or SiO_2 substrates, backscatt. anal. 80−34257
film, triode sputtering, for beam lead metallisation, reduction of contamination 78−72721
film, ultra-thin, AES and XPS anal. 78−91573
film, vacuum deposited, cryst. struct., elec. props. 78−79908
film, work function, effects of O_2 sorption 78−19125
film (0001), with adsorbed H (1×1) monolayer, electronic struct., surface geometry 80−54750
film (0001) electronic struct., Fermi level, surface states, GO calcs. 80−6927
film deposition on Si wafers, backscattering anal., of layer structure, silicide formation 79−69377
film electrode, oxidation, electrochem. and surface analytical characterisation 79−39034
film on Si, induced interface interaction by ion implantation, AES exam. 79−77625
film on Si, ion implanted, inert-gas-bubble form., TEM and Rutherford backscatt. anal. 79−90682
film pulse biased sputter deposited, Kr entrapment 79−28255
films, implanted inert gas desorption, reemission process 80−39453
flow stress during cutting 77−59881
flow stress relaxation *(French)* 77−86117
fluorite type crystal, Ti^{2+} doped, electronic struct. and EPR of Ti^{2+} 78−76034
foil, 150-400 keV electron transmission coeffs. Monte-Carlo calc. continuous deceleration model 77−50604
foil electrolytic perforation, surface film phase composition obs. *(Russian)* 80−61004
fracture mechanism at different temps. 77−63785
fracture mechanism maps 80−3188
friction surface structural investigation, O_2 surface diffusion *(Russian)* 80−96726
fusion reactor first wall material, thermal response 80−32456
fusion reactor material, 300 keV He^+ irrad., exfoliation, flaking, blistering, in-situ SEM obs. 77−35598
fusion reactor material, D profiles after D_3^+ implantation 80−37581
galvanic corrosion, electrochem. characts. rel. to Al alloys 80−21162

titanium continued
getter for TFTR Flexibility Modification, in-torus surface pumping 80−95451
getter pump, corrugated surface and pumping speed, fusion reactor application 78−74491
getter pump for economical sputtering with Xe 77−40371
gettering, excimer laser gas purification 78−46617
gettering of H, mass spectrometry and microgravimetry study, rel. to HTGR gas purification 80−73374
glass-ceramic protective coatings, synthesis and props. 80−25900
grain size effect on acoustic emission generated during plastic deformation 78−80609
grain size effect on yield stress and work hardening at 295 and 575K 78−64593
grinding of type VT1, abrasive props. of ZrB_{12} and diamond wheels 80−16489
HCP, elec. field gradient 78−14698
HCP, lattice dynamics exam. by inelastic neutron scatt. 79−60447
heat capacity and electric resistivity, pulse heating method, 1500 to 1900K 78−43139
heat capacity near polymorphic transition, temp. depend., vacancy mechanism 79−86884
heating and cooling rate effects on α to β phase transform. and recrystallisation 77−90379
heterogeneity of strain field in commercially pure alloy VTI-0 80−35286
high pressure gas target 78−70671
high temperature thermophysical properties 78−91404
hot-rolled, anisotropy of Young's modulus calc. *(Russian)* 78−23749
hydride precipitation in α-Ti, resistometric investigation, isothermal ageing effects *(Japanese)* 77−81265
hydriding, surface condition and environment influence 80−35380
implantation, biological props. and appls. 78−3678
implantation, of T, depth profiling by neutron TOF spectroscopy 77−73500
impurity, in Si n^+-p solar cell, associated degradation mechanism 80−81465
impurity flux, time resolved, in DITE Tokamak 80−63373
in-diffusion, in $LiNbO_3$ substrate, planar optical waveguides construction *(Czech)* 79−41452
integral composite joints, finite element and expt. eval. 79−11670
interface with molten glass, interactions and wetting, EPR anal. 78−14542
intergranular precipitation after annealing ion imaging microanalysis *(French)* 79−61594
internal friction, influence of H_2 *(French)* 78−75723
internal stress meas. by decremental unloading technique 78−64576
interstellar Ti II 3384 Å line, obs. rel. to Ti abundance 78−57611
ion bombardment, energy distrib. of positive secondary ions and sputtered atoms 77−32485
ion energy spectra, microlocal analysis using laser mass spectrometer *(Russian)* 77−12862
ion impact on C foil, energy loss 78−55902
ion implantation, comparison with thermal oxidation of Zr 77−8976
ion implantation, oxidation mechanisms study 77−8980
ion nitriding by a DC glow discharge method, surface anal. 78−80672
ion plating, on ceramic substrate, and coating struct. 78−11132
ion plating on steel, process parameters rel. to coating props. 77−70217
ions, beam-foil spectra from 20 to 238 MeV energy, 5 to 60 nm, lifetime meas. problems 80−9722
irradiated and cold worked, internal friction pdaks 77−86074
isotopic abundance ratios, in α Tauri (Aldebaran) 77−22212
isotopic anomaly from meteoritic materials study 79−53716
JAERI Tokamak. Ti coating for improved plasma characts. 80−24232
K shell prod. cross section of Ti, Cr, Fe, Ni, Cu, Zn for 75 to 150 keV p and e excitation 79−47552
K-shell X-ray prod. by $^{14}N^+$ bombardment 80−91482
lamellar single cryst. formation by heat treatment *(Russian)* 77−59800
laser generated stress waves, effect on microstruct. hardness and strength 79−69192
lattice specific heat and thermal expansion 79−73318
line fabrication, shadow deposition method using optical lithography for 0.15-0.3 μm widths 79−43148
liquid, density of states of d-band, heat of vaporisation 78−95253
liquid, elec. resist., melting pt. to boiling pt., temp. depend. 80−96839
liquid, sp. ht. eqn. for high temp. 77−51510
liquid, spectral emissivity and brightness-temp. meas. at MP 77−43356
liquid, thermal volume expansion, MP to BP 79−90802
liquid, viscosity at melting point, free energy *(Russian)* 80−92699
low friction wear-resistant surface form. by Al ion plating 78−11442
low temperature data, handbook of mech. and phys. props. 80−22153
lunar regolith, reduction of Fe, Ti, Si in H atom., X-ray photoelectron spectra 79−25527
lunar soil, Fe and Ti bands in glass fraction 77−49320
magnetic form factors, neutron diffr. study 79−47234
magnetic hyperfine field in Fe, TDPAD meas. 78−52389
martensitic transformation, strain energy minimisation 77−21140
mass transfer phenomena in aerated sulphuric solution, behaviour close to corrosion potential *(French)* 78−23862
mechanical, thermal and elec. props., data sheet 79−43317
mechanical deformation with superimposed insonation, volume effects 78−60723
mechanical properties, 20 to 300°C *(French)* 77−56018
mechanical props., electrochemistry, oxidation and corrosion resist., conference, Nantes, France (Nov. 1978) 80−41932
melting point, normal spectral emittance and elec. resistivity, pulse heating method 78−91423
membranes in pulsed electron beam, temp. and ultimate load calcs. 79−45484
metal-metal interface, adhesion energy, surface treatment and ion implantation effects 80−107660
metallic coated, produced by electrospark alloying, corrosion behaviour in Cl saturated NaCl solns. *(Russian)* 79−39026
metallographic specimen prep. for chem., mech., electrolytic polishing 78−80705
microflow parameters, determ. from compression tests for α-phase 80−66584
microparticle, 24 at. catalytic complex, electronic spectrum fluctuations 79−19501
molecular cluster approach to electronic struct. and bonding mech. for impurity C 77−20270
molten, reson. model calc. of elec. resist. 78−84189

titanium continued
monolayer, oxidation, quasisimultaneous SIMS, AES, XPS 78−72919
Moon, Fe and Ti surface distrib., orbital γ-ray spectra 80−94727
Moon, regolith Ti composition, orbiting γ-ray expt. 80−17510
Mossbauer fraction, press. depend. 77−59493
Mossbauer fraction for ^{57}Fe, press. depend. 77−16226
neutron effects on thermally activated tensile props. 77−62567
neutron irradiated, characterization of dislocation loops 80−88155
neutron irradiated, low temp. deform. studies 79−47757
neutron irradiated, relation between microstructure and recovery behaviour 77−15456
neutron irradiated, twinning deform. at room temp. 80−65061
neutron low energy interaction cross sections, gravitational spectrometer meas. 80−24521
nitridation to form Ti_xN_y 77−44200
nitriding, ESCA study *(Japanese)* 80−11833
nitriding, high temp., heat release kinetics *(Russian)* 77−66751
nitriding kinetics at 1230 to 1500°C, diffusion and struct. investig. *(French)* 77−36683
nitriding kinetics in RF discharge, surface hardening 77−36684
nuclear reactors, primary coolant purification by Ti gettering *(German)* 79−3204
O_2 diffusion from oxide surface layer, chem. anal. by nucl. reaction *(French)* 79−7710
O_2 getters for LMFBR fuel pins 78−74437
in oceanic phosphorites, Fe, Ti and Al behaviour during initial form. stages 80−31029
optical properties in radiative heating, O_2 diffusion and dissolution effects 79−65884
orthotropic compressible plastic yielding, derivation of elementary equation *(German)* 78−84902
oscillator strengths for hook method meas., lines from $^3F_{2,3,4}$ levels 78−70790
overlaid thin films, D pumping speed 78−33286
oxidation, ESCA *(French)* 77−36361
oxidation, ESCA and UPS meas., core levels 77−63542
oxidation, high temp., exam. and comparative study with Ti-Cu, Ti-Ni oxidation *(French)* 79−20285
oxidation, linear, O diffusion coeff. depend. on rutile layer struct. *(French)* 80−104328
oxidation, reaction mechanism 80−25912
oxidation, XPS exam. *(French)* 78−23858
oxidation behaviour in high temp. steam after heat treatments *(Japanese)* 78−48565
oxidation behaviour under pure O_2 atmos., temp. range 600-800°C 80−89415
oxidation by water vapour *(French)* 78−76787
oxidation in acid soln., electrochem. and optical props. 78−48560
oxidation in air, scanning electron microscope meas. 79−61794
oxidation in air, TiO_2 films X-ray diffr. meas. 79−11730
oxidation in O_2 atmosphere, role of oxide layer and mechanism of oxidation *(French)* 78−23859
oxidation kinetics, and oxide film structure, exam. 78−56822
oxidation kinetics, in water vapour, comparison Ti-6Al-4V 77−21321
oxidation kinetics in water vapour-Ar ambient mixtures 77−90498
oxidation under hydrothermal cond. to produce brookite *(Japanese)* 80−35433
oxide doped $BaO-B_2O_3-SiO_2$ glass system, electronic cond. of Ti ions 78−23095
oxide film characterisation, using low energy electron induced X-ray spectroscopy *(French)* 78−41386
oxide film form. during thermal treatment, morphological and struct. study *(French)* 80−50766
oxide layer growth by dry oxidation at 25°C, ESCA obs. *(French)* 80−45434
oxidised film electrode, AES, XPS and electrochem. characterisation 78−7086
pacemaker anode and container, passivation and muscle twitch 77−40934
partial densities of states, electron-phonon interaction 78−51869
passive oxide layer form. in H_2SO_4, ageing with and without photoexcitation *(French)* 80−45432
passive surface, anodic process kinetics 79−15861
permeation of H plasma through Ti reduced by layer of interstitially built ϵ-Ti_2N 80−16566
photoemission, primary and secondary yields using low-energy monochromatic X-rays 80−35053
photon emission due to Ar^+ ion bombard., adsorbed and recoil-implanted O effect 80−80872
physical props., implant surgery appl. 77−73615
physicomechanical and wear props., influence of ion implantation and overlay coatings 80−40603
pionic atom, Klein-Gordon eqn., relativistic fine struct. term, verification 79−22868
pionic atom, relativistic fine struct. splitting obs. 79−10237
pit nucleation in bromide media, ion beam anal. 80−93683
plasma, laser prod. study by UV spectroheliography 78−22529
plasma, laser produced, vac. UV emission 77−80372
plasma, laser-prod., space-resolved extreme UV emission 80−54015
plasma arc srapying, chem. reaction with plasma gases 80−66427
plasma chamber material for power generating Tokamak, suitability tests 80−32449
plasma etching, for appl. to patterning of Ti-Pd-Au metallisation 78−27677
plasma impurity, atom-electron collisions in inner discharge column *(Russian)* 80−38529
plasma produced by 250 ps laser pulse, X-ray spectra 77−19769
plasma-anodisation, surface film comp. determ. 77−48591
plastic anisotropy of extruded bars *(German)* 77−86126
plastic deform. dynamics, mech. characts. and phys. props., effect of O_2 *(French)* 80−45353
plastic deformation and thermal cond., 2.5 to 10K, dislocation pinning 77−35629
plastically deformed by rolling, optical and electron microscope obs. of α-phase 79−91666
plate, heat transfer to chemically reacting plate under unsteady state heating 79−81697
point defect estimation from specific heat and volume in plastically deformed pure metals *(Russian)* 80−54223
polycrystalline sheet, strain ratio prediction from the ODF, appl. of Taylor's model 79−91773

titanium continued
porous, infiltration kinetics of liquid Mg 78−60595
porous structure, change in presence of liq. phase *(Russian)* 80−16223
Portevin-Le Chatelier effect, mechanism 77−8886
positron annihilation γ-ray ang. correl. curves, effect of deform. and H_2 inclusions 78−31273
positron annihilation study of defects 80−3281
powder, electrolytic, rolling of porous sheets 77−63578
powder, exam. of mechanicochemical comminution, in the presence of epoxy resin or polysulphide rubber 80−16236
powder, physical props., effect of prep. methods *(Russian)* 77−66603
powder, resist.-sintability *(Japanese)* 80−16228
powder, vibratory densification in vibratory press 77−12576
powder heap, thermal cond., effect of temp., press., and atmospheric composition, sintering appls. 78−80487
powder metallurgy, developments 80−100801
preparation by electrolytic reduction of $TiCl_4$ *(French)* 78−23644
primary recrystallization study by three dimensional anal. of textures and annealing, HVEM obs. 79−91677
production methods, review of metallurgy methods, mathematical-physical considerations 79−95970
proton irradiated, K-shell ionisation probability, for 150 keV protons, impact-parameter depend. 79−10189
pump, sublimation type *(Japanese)* 78−24806
pure, rapid grain growth 80−16343
pure, type VT1-0, pool metal solidification kinetics in welding with electromag. stirring 80−71636
pure plate, shear band formation in ductile fracture process *(Japanese)* 80−16445
quantitative anal., for D, by ion microanalysis 78−56945
quartz:Ti^{3+}(Li), ENDOR 77−90067
quartz:Ti tube for I photodissoc. laser, C deposit elimination 77−10945
α-quartz, uncompensated Ti^{3+} centre, annealing, X-irrad., EPR meas. 79−65731
quartz glass, Ti-doped, acoustic props., thermal stability 77−24356
radionuclides prod. cross sections induced by 12-45 MeV protons 77−17310
range of $^{27}Al^+$ ions, meas. by (p,γ) reson. broadening 79−46729
rare earth orthoaluminates: Co, Ti, effects of Co and Ti ions on cryst. growth 77−28711
reaction with N_2 at elevated temp., kinetics and mechanism of reaction 77−12741
reaction with P, at high temp. 78−44260
reactive, trapping of energetic 18 keV deuterons 78−10096
reactive electro-erosion under pulse electric discharge 79−52686
reactive sputtering in Ar-O plasma, effect of target oxidation on sputtering rate 77−24955
reactive sputtering yield 77−66566
reactor structural material s-wave resonance parameters from capture cross section data 80−13629
reactor structural material transmission meas. using TOF spectrometer 80−18440
recrystallised α-phase of commercial purity, Fe-rich precipitates obs. *(French)* 80−50637
reflection of H, D and He ions 78−95640
repassivation and pitting corrosion 80−30143
RF sputter deposition, ion bombardment and ion implanation 80−25564
rolled foil preparation 80−18744
rolling and recrystallisation texture formation *(Russian)* 77−59802
rolling texture, determ. by three-dimens. anal. 77−86049
ruby:Ti^{3+}, cross-relax. 80−71163
sapphire:Ti^{4+}, plastically deformed, precipitation hardening, TEM study 80−7592
sapphire :Ti^{4+}, deformation history effects on precipitation hardening 79−83209
secondary ion emission, energy spectra, 0-55 eV, contamination levels 79−15573
self-diffusion in α- and β-phases *(Russian)* 79−86916
shear bands in cup and cone fracture in pure plate *(Japanese)* 79−15773
sheet, anisotropy and texture, effect of plastic deform., recovery and recrystallisation *(Russian)* 77−8850
sheet, plastic anisotropy, Bauschinger effect *(German)* 77−20006
sheet, texture and mechanism of primary recrystallisation 78−23721
sheets, porous, production and props. 78−60602
shell, explosive expansion, deform. and rupture modes and mechanisms 80−85064
sintered, fatigue strength, oxidation effect 79−96137
sintered, struct. stability, effect of dispersed refractory compound inclusions 77−28825
solar abundance from weak spectral lines obs. 77−29778
solar quiescent prominence spectra, meas. of Ca^+ 8542 and 8498 Å He 4471 Å and Ti^+ 4468 Å 80−90373
soldered joints, exam. of active thermal method of inspecting 78−72993
solid state phase transformation α→ω, exam. of phase transformation kinetics under static, and dynamic pressures 78−80541
solubility in β-Na_2O-Al_2O_3 rel. to isomorphous replacement of Al^{3+} 77−85926
solubility of H, neutron diffr. study 80−15254
solubility of V in α-Ti, 400-700°C 78−83959
sorption of H_2 and N_2, gas-discharge device appl. 80−10796
sorption pump for molecular beam detector 78−21150
spallogenic isotopes in Fe meteorites, radial distrib. 80−67488
specific heat, 4 to 290K for VT1-0 and 99.8% pure sample *(Russian)* 79−14938
specific heat and thermal expansion, 4-290K *(Russian)* 79−51276
specimen preparation for TEM, two-stage jet-stagnant electrolytic thinning, Ti, Mo appls. 77−71405
spongy metallic protective gettered coating for thermonuclear reactor walls *(Russian)* 80−106154
spray coating form. in pure Ar atm. 77−32709
sputter-erosion and impurity emission under low energy ion bombardment 78−95628
sputtered excited states, secondary photon emission, role of transition probability 80−102483
sputtered film, energetic neutrals rel. to impurities 79−69980
sputtered ion fraction meas. using matrix isolation spectroscopy 80−60738
sputtered particles from D bombardment, ion fraction and energy anal. 77−36345
sputtered Ti atoms, photon emission, nonradiative transition effects 80−58208
sputtering, low energy, H, D and He ions 80−100734
sputtering rate on Ar ion bombard. 80−55245
standard (11$\bar{2}$0) stereographic projection, computer generated, for α-Ti 79−37579
static strain ageing of α-phase commercial purity Ti 77−86061
steel, stainless, type 316 cladding, Ti-modified, performance in mixed-oxide fuel pins 79−67865
stopping of 3-7 MeV α-particles *(Russian)* 79−51181
stopping power for 0.3-1.5 MeV protons 79−55801
stopping power for 28 MeV α-particles, re-evaluation 78−79651
stopping power of 0.5-2.0 MeV ^4He ions, elastic backscatt. meas. 78−87730
stopping powers, projectile range for Z=8-20, 0.0125-12.0 MeV/nucleon 78−83856
stopping powers for 28.8 MeV α-particles 77−80556
strain ageing, initial stages in α-phase *(Russian)* 77−81278
strain ageing of α-solid soln. *(Japanese)* 78−6953
strain driven thermoelastic instability toward brittle fracture 80−103415
strain rate effect, upon mech. behaviour in type IMI-260 80−3153
stress corrosion cracking, texture dependence 80−104334
stress corrosion cracking in high temp. caustic soln. 77−59964
stress relaxation, in-reactor study at low temps. 80−93588
stress relaxation expt. 77−48472
strip prod. by powder rolling 78−80493
structural changes during polygonization *(Russian)* 78−19779
sublimation, pumping use in ISABELLE intersecting storage ring vaccum system for 1×10^{-11} Torr operation 79−81105
sublimation pump, behaviour in 10^{-11} Torr range 77−57336
sublimation pump, methane outgassing 80−77796
substrate, detonation deposition of Al_2O_3 coating, impact interaction parameters 80−40602
substrate for thin oxide film, optical consts. determ. by ellipsometric method *(Russian)* 77−81164
substrate for W-Al_2O_3 composite films, oxide evaporation deposited, struct., props. 80−25581
sulphurisation kinetics, 450-550°C, thermogravimetric determ. 77−25197
superconducting transition temp., perturbative corrections, direct and indirect ladder diagrams 80−49979
superconductiviy microwave cavity appl., secondary electron emission and AES meas. 79−56895
surface, (0001), oxidation, LEED and AES meas. 77−31851
surface, (0001), valence band struct. and chemisorption, XPS and UPS study 80−35062
surface, Ar^+ and e^- excited Ar Auger electron emission 79−47560
surface, Auger electron appearance potential spectrum, elastic and inelastic contribs. 78−35231
surface, newly generated, occurrence of salt films during repassivation 79−15860
surface (0001), H adsorption, geometric vs. electronic factor in surface electronic structure 80−70788
surface (0001), surface states 79−91120
surface (0001), with adsorbed N (1×1) layer, underlayer geometry, electronic struct. calcs. and UPS meas. 80−54751
surface (10$\bar{1}$1), chemisorption of CO, XPS, UPS, flash desorption mass spectra, and active ion bombard. obs. 79−11822
surface (10$\bar{1}$1), HCP→BCC transition He II UPS study 79−42345
surface analysis using digital scanning Auger electron microscope 78−12797
surface and grain boundary free energy, zero-creep determ. 79−4313
surface evaporation by Nd laser beam, spectral-line absorption 79−19951
surface impurity segregation, quantitative AES 78−19611
surface interaction with N_2, {0001}, at. under layer form. 77−15693
surface layer, study using vac. UV spectrograph *(French)* 80−71987
surface oxidation reaction, surface chemiluminesc. study 80−55708
surface sliding damage, no lubrication, materials depend. *(Japanese)* 78−56780
surface structure, HCP to BCC type struct. transition, FEM obs. *(Japanese)* 78−22938
surfaces, clean and oxidised, refl., 2-25 eV 80−55123
target, microwave laser irrad., plasma form., inhibited electron thermal cond., laser intensity threshold Z-depend. 80−48928
target impurity effect on laser produced expansion, ion spectrography 80−43945
technical, alloying effect on structure sensitivity of mech. props. *(Russian)* 79−47748
tensile properties and creep behaviour at high temp. 78−23773
thermal diffusivity determ., thermoelastic method 79−23940
thermal diffusivity meas., const.-rate heating method *(Japanese)* 78−79976
thermal expansion coeff. and Gruneisen const., 6 to 300K *(Russian)* 79−51281
thermally oxidised, ^{16}O conc. profiles anal., using (d,p) and (d,α) reactions 79−5215
thermo EMF, effect of H diffusion 79−23950
thin film, electron-beam deposition on Al_2O_3 quartz and glass 80−7496
thin films, H absorption and desorption, Tokamak gettering, Auger electron spectrosc. 80−75092
αTi, work hardened in tension, developed of internal strain *(French)* 78−76716
Ti recrystallisation texture from neutron diffr., cf X-ray diffr. *(French)* 77−84593
Tokamak fusion reactor first walls, hydrogen profiles 80−37578
Tokamak plasma, atomic struct., highly ionized Ti 80−75086
transport of H, study by neutron radiography, review of results 78−59961
trapping coeff. of energetic H at high doses 77−31699
tribological investigation using two-cylinder tribometer *(German)* 77−25164
tritiated self supported target prep. 80−23211
twin interfaces {10$\bar{1}$2}, serrated 80−84182
twinning deformation, neutron irradiation effects 80−75236
unsupported metal membrane fabrication, high strength 77−66589
uphill diffusion of H and progressive H embrittlement 77−90454
US interactions with thin gap discontinuities, resonance effects on energy flux coeff. 77−12761
US wave diffraction in penny-shaped cracks, theory and expt. 80−33267

titanium continued
US wave scatt. from ellipsoidal cavities, Born approx. theory comparison 79−100307
vacuum technology appl., melt processing and appl. *(Hungarian)* 80−55318
valence band electron distrib., photoelectron spectra obs. 77−44120
vapour-phase epitaxial growth *(Russian)* 77−59227
volume changes and defect healing due to plastic deform. *(Russian)* 80−81139
wear and corrosion resistance, effect of surface alloying with Nb and Si *(Russian)* 77−25191
wear at high sliding speed 78−3237
wear under conditions of rolling stress 79−20211
wire, polycrystn., electroplastic effect 79−57067
X-ray continua emission, proton and ^{14}N bombard. 78−23559
X-ray Debye characteristic temp., powder specimens of α-Ti 77−84876
X-ray emission, plasmon satellite 77−28662
X-ray emission spectra, $K\beta_{1,3}$ line width and $K\beta_5$ band 78−2946
X-ray emission spectra, rel. to TiNi alloy struct. 77−44091
X-ray emission spectra and electronic structure 77−20960
X-ray $K_{\beta 5}$ emission band, effect of struct. change on alloying *(Russian)* 77−59645
X-ray line profile anal. 77−47459
X-ray photoelectron appearance potential spectrum 79−65973
X-ray reflectivity, near $L_{2,3}$ absorpt. edge 80−71513
X-ray resonant Raman scatt. and fluoresc. near K-absorpt. edge 79−52042
X-ray topography, dislocations, recrystallised crystals 78−10054
XPS, valence bands 78−35249
yield points, obtained by ageing at two stresses 80−81091
α-Al_2O_3:Cr(Ti)(V), impurities effect on thermoluminesc. 80−40170
Al_2O_3:Si, Ti, pure and doped, luminescence, optical absorpt. and colour centres 79−87501
Al_2O_3:Si,Ti photostimulated thermolum., and appl. to UV dosimetry 78−53511
α-Al_2O_3:Ti, defect struct., electronic and ionic cond., optical absorption meas. 78−30603
Al_2O_3:Ti, gamma-irrad., low temp., induced absorpt. spectra 79−56820
Al_2O_3:Ti^{2+}, corundum, point defect diffusion and interaction with impurity, Ti^{3+} to Ti^{4+} reaction 79−10985
Al_2O_3:Ti^{3+}, dynamic Jahn Teller effect, role of nonadiabatic operators 77−59270
α-Al_2O_3:Ti^{3+}(Ti^{4+}), solid soln. hardening, yield stress conc. depend. 77−28823
Al_2O_3:Ti(Si), annealing, electron irrad., absorpt. spectra 77−20890
Al_2O_3-Cr cermet, Ti effect on sinterability 79−61552
β-Al_2O_3-Na_2O:Ti, dopant effect on ionic cond. and phase comp. 79−65242
Ar-Ti hollow cathode afterglow, energy transfer mechanisms and excited metallic ion prod. 80−43857
Au/Ti thin film, temp. and humidity effect on interdiffusion 79−51317
Au/Ti thin films, effect of Cl_2 on elec. resistance, Ti atom migration and preferred orientation 80−34530
Au-Ti/n-GaAs contacts, interdiffusion and Schottky barrier height variations 77−89849
B-Ti composite material, for loudspeaker's diaphragm, preparation by physical vapour deposition *(Japanese)* 80−58883
BaO-B_2O_3-SiO_2:Ti^{3+}, elec. cond., struct. 78−72148
BaO-B_2O_3-SiO_2:Ti^{3+}, optical absorpt. spectra 78−72564
BaO-B_2O_3-SiO_2:Ti^{3+}, Ti^{4+}, glass EPR spectra, variation of g-factor with temp. 79−99757
CdS:Ti^{2+}, linear electroabsorption due to Ti^{2+} centres 77−66525
CdS:Ti^{2+}, superhyperfine interact., ENDOR study at 4.2K 80−80639
CdSe:Ti, optical and elec. investig. of shallow donor levels, reson. states 77−63437
CdTe:Ti^{2+}, Jahn-Teller effect on $^3T_1(^3F)$ state, resonance on $^3T_1(^3P)$ state 78−27271
Cl^{5+}+Ca(Sc)(Ti) thick targets, 30 MeV, near symmetry collisions, double-K-vacancy sharing 79−3391
$ErFeO_3$:Co, Ti, effects of Co and Ti ions on cryst. growth 77−28711
EuIG:Sb(Ca)(Ti), growth from PbO-B_2O_3 based flux, prop. depend. on Pb content 80−39824
Fe:Ti, C induced amorphous surface layers 80−107287
Fe/Ti battery system, soluble, discharge charcts. 79−92070
Fe-Ni-Ti, cryogenic toughness, strength, rel. to reactive metal addition 78−39885
n-Fe_2O_3:Ti electrodes, characterisation and behaviour in acetonitrile solns. 80−25004
GaP:Ti, positron annihilation meas. rel. to deep levels study 80−60712
H impurity detection by $^1H(^{15}N,\alpha\gamma)$ reaction 80−55767
H_2 isotope release 80−37580
H_2-D_2-T_2 mixtures, mesic at. and mol. processes 80−23580
$KMgF_3$:Ti^{3+}, ESR and ENDOR spectra 77−40121
$KTaO_3$:Ti^{3+}, EPR meas. 78−35028
Kr+Ti, 200 MeV, collision, quasimol. bremsstrahlung, semiclassical calcs. 77−88530
$LiBaF_3$:Ti^{3+}, EPR, spin Hamiltonian parameters 79−65718
LiF:Mg, Ti, luminesc. increase by O implantation 78−64412
LiF:Mg,Ti, defect states, ESR and ionic cond. study 80−108058
LiF:Mg,Ti, optically induced dichroism of Z_2-centres 79−28710
LiF:Mg,Ti, thermolum. related Z-centres, optical absorpt. bands 78−23540
LiF:Mg,Ti, thermoluminesc. activation energies 79−74009
LiF:Mg,Ti crystals, Z_3-centres, correlation of thermoluminescence and optical absorption 80−45154
LiF:MgTi, (TLD-100), optical bleaching of defect centres 79−19911
LiF:Ti, EPR exam., superhyperfine interactions 78−31107
LiF:Ti, thermoluminesc., effect of plastic deform. 79−33853
LiF:Ti, thermoluminesc. dosimetry appl. 79−38683
$LiNbO_3$ planar waveguide, refractive index rel. to Ti diffusion *(Russian)* 78−59120
$LiNbO_3$, Ti diffused, mirror type optical branch and switch 78−33834
$LiNbO_3$, Ti diffused, optical directional couplers, charcts. 80−33145
$LiNbO_3$, Ti diffused optical waveguide, ferrolectric domain inversion 79−94338
$LiNbO_3$, Ti diffused slab waveguide, mode control by doping 77−88903
$LiNbO_3$ Ti diffused single-mode waveguide coupling to single-mode fibre 79−81547
$LiNbO_3$, Ti diffused waveguide, refr. index and thickness precise determ. 79−41446
titanium continued
$LiNbO_3$, Ti-diffused strip waveguide, appl. in balanced bridge modulator switch 78−63201
$LiNbO_3$:Ti, BiTm ferrite garnet coated, nonreciprocal optical waveguide system *(Russian)* 77−42623
$LiNbO_3$:Ti, coupled waveguided TE/TM mode splitter 80−64142
$LiNbO_3$:Ti, diffused, optical channel waveguides, Bragg switch 78−75002
$LiNbO_3$:Ti, diffused strip waveguide, refractive index changes, two-dimensional distrib. 79−86254
$LiNbO_3$:Ti, dopant conc., refr. index profile rel. to integrated optics 78−5583
$LiNbO_3$:Ti, electro-optic multichannel waveguide deflector 77−42607
$LiNbO_3$:Ti, graded-index optical waveguides, mode dispersion charcts. 79−3770
$LiNbO_3$:Ti, in-diffused waveguide, integrated bistable optical device development 78−75001
$LiNbO_3$:Ti, in-diffused waveguide, acousto-optical meas. of optical field profiles 79−23054
$LiNbO_3$:Ti, in-diffused waveguides, optical damage thresholds 79−46033
$LiNbO_3$:Ti, planar and channel optical waveguides, anisotropic diffusion expts. 80−64200
$LiNbO_3$:Ti, planar optical waveguides, processing and props. 80−78965
$LiNbO_3$:Ti, two mode waveguide coupler electrooptical switch 77−83961
$LiNbO_3$:Ti, Y-cut thin film waveguide, acousto-optical deflector, electro-optical modulator *(Russian)* 77−39115
$LiNbO_3$:Ti 3-dB optical waveguide mode convertor using chirped gratings, power transfer 80−79014
$LiNbO_3$:Ti active branching waveguide modulator 77−19392
$LiNbO_3$:Ti channel waveguide high-speed cutoff modulator 80−64195
$LiNbO_3$:Ti cleaved, waveguide, attenuation coefficient and coupling loss 78−74975
$LiNbO_3$:Ti diffused, optical waveguide, fabrication problems *(Japanese)* 80−33256
$LiNbO_3$:Ti diffused optical waveguide, guided light scatt. sources 80−78966
$LiNbO_3$:Ti diffused optical waveguide, efficient tapered gap prism coupling 80−78967
$LiNbO_3$:Ti diffused strip waveguide, optical insertion losses 78−74985
$LiNbO_3$:Ti diffused strip waveguide, optical propag. losses and coupling losses 80−58664
$LiNbO_3$:Ti electro-optic TE-TM mode convertor structure 80−64215
$LiNbO_3$:Ti electro-optic branching waveguide, charcts. 80−83681
$LiNbO_3$:Ti in-diffused optical waveguide fabrication 79−76892
$LiNbO_3$:Ti layers, detection by harmonic generation of SAW 77−80688
$LiNbO_3$:Ti narrow ridge optical waveguides and electro-optical, ion-bombardment-enhanced etching 80−38133
$LiNbO_3$:Ti optical waveguides, suppression of LiO_2 out-diffusion 77−50749
$LiNbO_3$:Ti optical waveguide, technique for suppressing Li_2O out-diffusion 78−18040
$LiNbO_3$:Ti optical waveguides, fabrication and waveguiding props. 78−30091
$LiNbO_3$:Ti optical waveguide diffusion profile, AES obs. *(German)* 78−33876
$LiNbO_3$:Ti optical waveguide, SHG with 25% conversion efficiency 78−94432
$LiNbO_3$:Ti optical waveguides, elec. field tuning of SHG, phase-matching condition 79−41412
$LiNbO_3$:Ti optical waveguides, Ti diffusion process and control, waveguide charcts. 80−58790
$LiNbO_3$:Ti phase-matched waveguide electro-optic TE⇄TM mode convertor 80−58749
$LiNbO_3$:Ti planar and channel waveguides, appl. of Li_2O compensation technique 78−74976
$LiNbO_3$:Ti planar and channel optical waveguides, Ti diffusion coeff. meas. 80−19096
$LiNbO_3$:Ti planar waveguide, edge coupling to GaAlAs DH laser diode 80−87559
$LiNbO_3$:Ti strip waveguide, SHG 80−102773
$LiNbO_3$:Ti waveguide, diffused, Mg diffusion effects on charcts. 78−66905
$LiNbO_3$:Ti waveguide, precise determ. of refr. index 78−94442
$LiNbO_3$:Ti waveguide, integrated bistable Fabry-Perot resonator fabrication 79−41459
$LiNbO_3$:Ti waveguide, in-plane scatt. obs. and countermeasures 80−33215
$LiNbO_3$:Ti waveguide laser diode end-fire coupling 79−94368
$LiNbO_3$:Ti waveguide thin film electrooptic Bragg modulator, bistable optical element 80−10034
$LiNbO_3$:Ti waveguide and cryst., absorpt. loss and photorefractive index changes 80−48368
$LiNbO_3$:Ti waveguide directional coupler switches, optically-induced cross-talk 80−48417
$LiNbO_3$:Ti waveguide electro-optic TE⇄TM mode converter-wavelength filter 80−64210
$LiNbO_3$:Ti Z-cut crystals, Ti diffusion process parameters 80−102849
$LiTaO_3$:Ti, diffused waveguide prep., parameters determ. 80−14465
$LiTaO_3$:Ti waveguide modulator structs., high optical power capabilities 77−39023
MgO-Ti^{3+}, orthorhombic distortion, Jahn-Teller effect 77−66140
MnZn ferrites, Ti substituted, mag. permeab. meas., grain boundary comp. AES obs. 78−95473
Mo, arc, steady, vac., plasma ion mass and energy diagnostics 78−51385
Na^++Ti(Ni)(Zn)(Fe), 0.2-3.0 MeV, united-at. limits, mol.-orbital continua 77−19030
Nb-Ti superconductor, for fusion facility, cold-pressure-welded joints 78−62630
Nb-Ti-O system, phase equilib., microstruct., thermal, and X-ray anal. 77−8806
Nb-Ti-Ta, superconductor optimisation for 12 Tesla toroidal field coils 80−91272
$NbSe_3$:Ti, elec. cond., anomalous, and microwave absorpt. 79−42527
Ni, electrolytic and carbonyl grades, sintered sheet material, stopping power and pore size relationship 78−19693
Ni-Cr (20wt.%), powder, nonspherical, mean pore size of sheet material 77−28757
Ni-Ti film system, interdiffusion, phase growth kinetics *(Russian)* 77−72722
Ni-Ti multilayers for monochromators and supermirrors, neutron reflectivities 80−22880

titanium continued
PbTe:Ti, effect of impurities on transport props. 79−11158
Pr covered Ti electrodes for cathodic protection for small plant *(German)* 80−100943
Ru complex, $[Ru(bpy)_3]^{2+}$-Ti (III), photochem. H_2 prod. from aq. soln. 80−85192
RuO_2 anodic coating on Ti, struct., electrochem. props. *(French)* 79−83385
Si:Ti, deep level impurity, Hall meas. 80−6768
Si:Ti, photoionisation cross-sections and energy levels 79−87060
Si:Ti contaminated solar cells, $POCl_3$ gettering 80−94010
Si:Ti substrate for epitaxial solar cells 80−61341
Si-Pd-Ti, silicide form. in evaporated films 80−80006
SiC:Ti (6H), absorpt. spectra of n- and p-type cryst. 79−38581
Ti (III), (IV), simultaneous photometric determ. 78−61102
Ti density, in DC sputtering discharge by atomic absorpt. spectroscopy 80−43973
β-Ti, dilute soln. of H and D 79−99322
α-Ti, effect of Pt ion plating on creep behaviour 79−66123
Ti electrodes, RuO_2 coated, corrosion during O evolution rel. to electrode prep. *(French)* 80−76420
Ti, fatigue damage, SEM, X-ray diffr. and surface trace anal. 80−85040
Ti film, deuteriding inhibition by surface contamination, rel. to Ti sublimation pump operation 77−57335
α-Ti, grain size independent viscous creep 80−40460
Ti I, hyperfine struct., far-config.-mixing effects 77−42240
Ti I, oscillator strengths, hook and emission meas. 78−42002
Ti I, solar lines oscillator strengths and Sun Ti abundance 78−45306
Ti I, transition probabilities rel. to solar Ti abundance 77−29743
Ti II, oscillator strengths from combined hook and emission expts. 80−87081
Ti II 3384 Å line obs. towards ζ Persei, interstellar Ti vel. distrib. 79−53877
Ti III, 3d and 4f energy level parametrisation, Slater parameters and correl. corrections 80−87041
Ti III, IV, V, radiative lifetime meas. using beam-foil technique, 700 to 1900 Å 80−78574
Ti, oxidation in monolayer range, SIMS, AES and XPS meas. 77−86215
Ti, pionic, pion mass high accuracy meas. from transitions 80−106406
α-Ti sheet, texture dependent stress corrosion cracking in Br_2-methanol soln. 80−71803
Ti, sputtering yields of D^+ and Ar^+ ions using matrix isolation spectroscopy 79−78809
Ti V, autoionising transitions $ns^2np^6-nsnp^6mp$ 77−88419
Ti XII, L-series satellite spectra 79−98012
Ti XII, wavelengths and energy levels, spectral obs. 77−428
Ti XIII, vacuum UV lasing action 78−1213
Ti XIX and XX resonance lines in Tokamak discharges 79−68941
Ti XX 80−100067
Ti XXI, He-like ion resonance line satellites 79−10064
Ti XXI, X-ray spectra from laser plasma 78−17596
Ti^+ excited config. position and level struct., review 80−32621
Ti^{2+}, doped ion in divalent metal cpds., correl. between Szigeti charge and hyperfine coupling consts. 80−96832
Ti^{4+} valence transition in fluorphlogopite, ESR and optical absorption data 77−16155
Ti:^{57}Fe, quadrupole interaction, Mossbauer and PAC meas. 77−48101
Ti:D, implanted, deuteride imaging using scanning Auger spectroscopy 80−89092
Ti:D, implanted, nucleation and growth of TiD_2 80−97717
Ti:D, ion implanted, depth profiles, temp. depend. 80−100270
Ti:O, channelled ions, flux peaking study using protons, H_2^+ and H_3^+ ions 79−1450
Ti:Pd, ion implanted, corrosion behaviour and Rutherford backscatt. anal. 80−71792
β-Ti:Sn, isotope effect for diffusion of Sn 77−76617
Ti:T, temp. depend. of effective electromigration charge 79−90826
Ti:transition metal, linear expsn. temp. coeff., polymorphic transition temp. shift 78−6164
Ti/Ag metallisation system, corrosion inhibition using intermediary Pd layer 79−79155
$Ti/RuO_2/MnO_2$ electrode, anode characts. 78−68897
Ti^{3+}/Ti^{4+} ratios in Allende meteorite, appl. as new cosmothermometer 79−12437
Ti-Al diffusion coatings on C steel, struct. and props. 79−57156
Ti-Al_2O_3 heterophase film, elec. props. rel. to Al_2O_3 content 77−15969
Ti-anodic oxide-Au(Al), electronic cond. *(French)* 79−95512
Ti-brass bilayer system, optical mechanical and corrosion properties 77−32707
Ti-C system, reaction diffusion analysis 77−28049
Ti-Co-Al(Ga), Th_6Mn_{23} type struct., mag. susceptibility *(Russian)* 79−42736
Ti-Cr_3C_2 composite, TiC and struct. form. during sintering 79−29011
Ti-H, H diffusion and phase consistution, V influence, proton spin-lattice relax. meas. 78−27484
Ti-MnO_2, porous anode for matrix-type electrochemical cell 77−81414
α-Ti-O system, exam. of static strain ageing 78−76675
Ti-O system, O/Ti<1, high-temp. thermodynamics using Tian-Calvet microcalorimetry 78−85190
Ti-oxide film electrode, photocurrents induced by subbandgap illumination 79−91094
Ti-Permalloy films, interdiffusion, Auger anal. and X-ray diffr. obs., degradation of mag. props. 80−34251
Ti-Permalloy thin film diffusion couples, low temp. interdiffusion interdiffusion 78−71889
Ti-Pt link on Si_3N_4-SiO_2-Si substrate, laser vaporisation, interference effects 77−69941
Ti-RuO_2 anode, electrochem. stability 79−70346
Ti-sapphire interface, solid-state reaction 78−72008
Ti-Si film thin film interaction, metallisation, X-ray diffr. and sheet resist. 80−54442
Ti-Si-Ti sandwich struct., elec. cond. processes and threshold switching in amorphous Si layer 79−78207
Ti-TiC-TiN system, phases 80−20905
Ti-TiN phase system, diffusion of N_2 77−39699
Ti-TiO_2-Au diode, spectral photoresponse and I-V characts. 80−15617
$Ti+^{28}Si^{n+}$, K-shell ionisation, projectile charge state depend., theory 78−17786
Ti+Al coating on steel 45, failure during high temp. creep in NH_3 79−11731

titanium continued
$Ti+Ar^+$, charge exchange obs. through spectral line enhancement 79−7005
Ti+C(B)(Si) self-propagating, high-temp. synthesis wave, radiating power 79−100377
$Ti+Cl^{n+}$, 35 MeV, K-shell vacancy sharing, impact parameter depend., X-ray obs. 77−71858
$Ti+Cl^{x+}$, K-shell ionization probability in energetic nearly symmetric heavy-ion collisions, 35 MeV 79−27078
$Ti+F^{q+}$, (q=6, 8, 9), target and projectile cross-sections, X-ray prod. yields 79−81269
$Ti+H^+$, K X-ray production, 0.2-0.5 MeV, ionis. cross-section 79−31459
$Ti+H^+$, K-shell ionisation cross sections for 15-65 keV protons 78−90284
$Ti+H^+$, K-shell ionisation calcs. 80−23534
$Ti+H^+$, K-shell ionisation cross-section determ. 80−48077
$Ti+H^+$(He ions), K-shell ionisation cross-section, 85 to 790 keV 80−106390
$Ti+He^{2+}(C^{4+})(O^{5+})(N^{4+})(N^{5+})$ atom-ion collisions, ratio of single K-shell ionisation cross section to double K-shell ionisation cross section 80−53119
$Ti+N^+$, X-ray production cross section, $K\beta/K\alpha$ ratio, 0.5-2.5 MeV/amu 77−54526
Ti+S ion, KL^n X-ray satellites, intensity distrib., photoabsorpt. effects 78−78657
Ti^{14+}+Ne highly charged very slow Ne recoil ions, K X-ray transition 80−91649
$Ti^{2+}+H(H_2)$, electron capture cross-sections, 0.5-14 keV 78−42205
$Ti^{q+}+O_2(Ar)(He)$, (q=8-19), K X-ray prod., charge-state depend. 80−106391
$Ti_{(S)}+P_{(V)}\rightarrow TiP$, direct two-temp. synthesis 77−81237
TiC-Ni-Mo sintered hard alloy TN-20, fracture surfaces 80−7684
$Ti(^3F)+N_2O(O_2)(NO_2)$, chemiluminesc., TiO dissoc. mechanisms, confirmation of $D^\circ_0(TiO)$ 77−40534
$TiH_{1.8}$, tritiated, NMR of ^3He formed by β-decay, radiation damage, ageing 77−24751
TiO_2-Ti-HCl, equilibrium composition of gaseous phase and TiO_x yield 78−27393
TiO_x-Ti selective solar absorber, optical props. and heat resist. 79−65951
$TiSi_2$, struct. refinement and bonding 77−72592
TiV, photoionisation, multichannel CI calcs. 79−93931
TiXIV (TiXV) (TiXVII), Tokamak discharge, ground state, mag. dipole transitions, UV spectra obs. 80−63575
^{A}Ti, A=46, 48, 50, pionic X-rays, strong interaction and isotope shifts, π-nuclear optical pot. 80−53169
^{47,48}Ti, precise atomic mass determ. 79−31718
U/Ti welded joints, mech. characts. determ. 20 to 750°C 79−29113
V-Ga-Ti, supercond. multifilamentary wire, crit. current props. 79−61013
W fibre reinforced, high temp. strength 79−70021
YAG:Ti, crysts., colour centres, optical absorpt. spectra 79−65080
YAG:Ti, growth conditions from melt 79−95924
YAG-Ti, polarised luminescence 79−95843
YIG:Ti^{4+}, X-ray induced change in initial permeability 78−19280
ZnO-Ti transparent type MIS solar cells 80−45662
ZnSe:Ti^{2+}, EPR meas. 80−80594
ZrO_2:Ti, thermoluminescence, traps and emission centres 79−24373
$(ZrO_2)_{0.9}(Y_2O_3)_{0.1}$:Ti, γ-irrad., ESR of trigonal centres, attributed to Ti^{3+} at cation sites 77−24740

titanium alloys
see also titanium compounds
$\alpha+\beta$ phases, interfacial precipitation 80−3068
Alnico 5 alloy, S and Ti additions effect rel. to non-metallic inclusions, coercive force and grindability 80−89375
Alnico alloys, effect of Ce addition on mag. props. 78−2699
anisotropy of magnetic and electric props. of α-Ti *(Russian)* 77−66292
annealed, faceted fracture in β-phase 79−57102
annealed, plastic deform. nonuniformity depend. on stressed state and test temp. 79−57071
anodic oxide film on TA6V alloy and Ti struct. and growth 78−23861
applications in aerospace and other industry, and properties 79−66104
beta processed alloy IMI 685, fatigue behaviour 77−90453
binary alloys, appl. to H storage as solid metal hydrides 80−45786
boronising, titanium alloys, effect on wear 78−19903
brittle fracture of compressive materials under impact loading 77−25137
bronze, Al and Ti, sintered frictional material, wear resistance, effect of matrix struct. 77−28911
BT3-1, fretting-corrosion in vacuum-chromized Ti alloy VT3-1 couple *(Russian)* 78−56804
butt strap reinforcement of fibre reinforced Al sheets, fatigue 79−100262
cast, welded joint mech. props., filler material and heat treatment effects, type VT9L 79−87671
colony size effect, in $\alpha+\beta$ alloys, on fatigue crack growth on Widmanstatten struct. 80−30094
combustion, laser-initiated, time-resolved spectroscopy 77−77765
compression at high strain rate, deformation anal. 80−25769
corrosion cracking resist. of type VT3-1 containing artificial defects *(Russian)* 79−52436
corrosion resistance in H_2S and NaCl, cracking tendency, strength *(Russian)* 78−31568
corrosion resistance in HNO_3 *(French)* 77−59992
crack development in air, H_2, aq. H_2SO_4, electrochem. charact. *(Russian)* 77−70209
crack initiation on planar shear bands, H_2 assisted 80−71749
crack resistance, J-integral approach, crack line wedge loaded specimen 78−35513
crack resistance, J-integral approach 77−66699
crack resistance limit, exam. in rotating discs containing cracks *(Russian)* 79−15766
creep, effect of environment and coating 78−31480
creep and long-term strength under cyclic loading 78−3191
creep resistance and thermal stability of Ti 685 and Ti 6242 in air and in vac. 80−30020
creep strain increments rel. to stresses, nonstationary loading 80−25776
creep strength rel. to diamond electrochem. cutting conditions *(Russian)* 79−96081

titanium alloys continued
cryogenic, VT5-1kt, fracture toughness and structural strength 77−59927
crystallographic texture, importance in characterization 77−28821
cyclic creep 77−81323
cyclic loading, at high temp. *(French)* 78−15628
cyclic strength under programmed loading of VT6 78−7043
cyclical heat treatment *(Russian)* 79−57009
data handbook of low temp. mech. and phys. props. 80−22153
decomposition of α'' martensite during continuous heating of alloy VT16 *(Russian)* 78−48370
decomposition of metastable β-phase in VT16 *(Russian)* 78−68710
decomposition of metastable phases during heating of quenched VT23 *(Russian)* 78−15432
decomposition of metastable phases of VTZ-1 and VT8, effect of plastic deform. *(Russian)* 78−39770
deformation and failure, microstructural, mechanism in biaxial stress state 79−66132
deformation field investigation in danger zone of sheet 77−16654
deformation twinning effect on mech. props. at low temps. *(Japanese)* 78−6979
deformation under biaxial stress at elevated temps. 77−12675
delayed brittle fracture, H_2 effect 80−100912
diffusion of H_2 at room temp. 79−51312
disc, rotating notched, strength in quasibrittle fracture 80−55533
dissolving in Al alloy melt, reaction zone formation, component interaction *(Russian)* 80−54377
domain struct. of diffuse ω-phase formed in quenching, 1D model 78−27523
drop forgings, grain orientation and props., combined mech. working, hardening and high-temp. heat treatment influence *(Russian)* 80−20973
ductile erosion, prediction, mechanistic model 77−12709
ductility, for different phase comps. at low temps. 80−35273
ductility enhancement by hydrogen in β-alloys *(Russian)* 77−52459
elastic modulus at low temps. of commercial alloys 79−66100
electrical resistance meas. at increased temp. under stress. 77−56147
electrochemical working, film form. and surface roughness *(Russian)* 80−76397
electrospark alloying of Ti substrate to transition metals and their carbides and aluminides, residual stresses obs. *(Russian)* 77−56145
elemental distribution, emission microspectral anal. *(Russian)* 78−35773
endurance in cyclic bending of alloy VT20 77−63798
etching as a function of struct. of VT23 and VT15 *(Russian)* 78−15568
with eutectoid-forming elements, mech. props. 77−44313
fatigue, low cycle, and microfractography *(French)* 77−70168
fatigue, low cycle, at 450°C *(French)* 79−70169
fatigue crack growth, exam. of some aspects 78−56772
fatigue crack initiation from notches 77−21259
fatigue crack propag. kinetics *(Russian)* 77−70146
fatigue crack propagation, kinetics 78−68804
fatigue crack propagation resistance, grain size effect, exam. 80−11765
fatigue failure of VT3-1, surface finishing influence 80−60972
fatigue life diagrams plotting, of type VT-20 79−70246
fatigue strength estimation after US hardening 77−12746
fatigue testing, low cycle, effect of testing method on fatigue on types VT5-1 and VT14 79−52515
$Fe_xCo_{1-x}Ti$, ferromag., high-field and high-press. mag. behaviour 78−91919
Fermi sphere limiting electronic capacitance, Brillouin zones *(Russian)* 80−92808
ferritic alloy DT02, oxidation behaviour in CO_2 or Ar with H_2O and H_2, 823-123K 80−3249
fracture, intergranular, high strength, heat-treated weldments, in α-β type 6246 80−21097
fracture mechanics, K_{Ic} values determ. in elastic-plastic material behaviour range 80−45376
fracture surface and metallographic features exam. by precision sectioning 77−36638
fracture toughness determ., rel. to mech. props. 77−21277
fracture toughness improvement by applying Pb-Sn-Cd coating to crack tip 79−43416
fracture toughness of alloy VT3-1, rel. to struct. 79−79105
fracture toughness testing with eddy current sensor 80−45459
fracture toughness-mech. props. interrelations 77−86154
fretting wear, role of adhesion and delamination 78−35533
friction with diamond characts. 78−48541
fusion reactor environment, first wall and blanket structure, impact of H_2, phase stability and solubility 80−32435
fusion reactor first-wall and blanket material, mech. props. 80−34074
fusion reactor materials, He and simultaneous damage production simulation 80−32480
fusion reactor radioactive structures, recycle time 78−58457
gas desorption coeffs., electron- and ion-induced, bakeout temp. effect 79−65329
grinding, effect on surface struct. of VT9 80−25878
hardening during thermomechanical treatment, precipitate particle internal struct., type VT22 *(Russian)* 79−91657
hardening heat treatment, alloying element effects development trends 78−95759
hardness, correl. with strength 79−87707
hardness measurement, peculiarities 79−87774
hardness testing, depth of impression meas., automated 79−15892
HCP-BCC binary systems, electronic struct. and supercond. *(Russian)* 79−33375
heat resistance, thermal stability, stress-rupture strength, and creep 80−81194
heat treatment, β-annealing and controlled rate quenching effects 78−80568
heat treatment, struct. and mech. props. of large forgings 78−52864
heat-resistant, mech. props., alloying addition effects *(Russian)* 77−59861
high plasticity effect in alloy OT4 80−35272
high strength structural mats., microstruct. influences on fatigue and fracture resist. 78−56728
high temperature, NaCl-induced accelerated oxidation 77−21322
hot deformation *(French)* 77−52371
hot salt stress corrosion cracking, electrochemical model 78−7078
hot salt stress corrosion cracking 79−47799
titanium alloys continued
hot salt stress corrosion cracking on type TA6V *(French)* 80−21185
hydrogen embrittlement, directional diffusion of H_2 *(Russian)* 79−15763
hydrogenation at 200-600°C and up to 10000 kPa 80−107435
hydrogenation during electrochemical treatment *(Russian)* 79−39024
impact strength, exam. with pulsed drop impact loading 78−84944
Inconel 750, volatilisation of oxides during oxidation at 1200°C 78−23873
Inconel X750, positron annihilation study of ageing and creep 80−29824
Inconel X750 springs, in-reactor stress relaxation 78−11256
Inconel X-750, deform. and fracture characts., 24-816°C 80−108551
ingots, produced by vacuum arc smelting, exam. of crystallisation process *(Russian)* 79−34019
intergranular precipitation after annealing ion imaging microanalysis *(French)* 79−61594
liquation in microdendrites, cells and macrovolumes *(Russian)* 77−76561
long-term strength criterion 77−44323
lubrication by chloroparaffins, friction and wear *(Russian)* 80−93657
Magnico alloy, with Si, Nb, Ti and La, low-temp. thermomag. treatment 77−63812
Magnico alloy, with Si, Nb, Ti effect of Ub on mag. props. and grindability 77−63811
martensitic transformations, reversibility *(Russian)* 80−108442
mathematical-physical considerations rel. to metal powder prod. 80−11595
mechanical, thermal and elec. props., data sheet 79−43317
mechanical props., electrochemistry, oxidation and corrosion resist., conference, Nantes, France (Nov. 1978) 80−41932
mechanical props. at high temp., effect of Pt ion plating 79−29156
metallurgical characterisation using thermoelec. power meas. *(French)* 80−45462
β-metastable, alloying element effects on phase equilib. 79−56975
microstruct. and mech. props., room and elevated temps. 77−36554
microstructure resulting from heat treatment, alloying, effect on creep, fatigue, fracture strength 78−11246
Ni-Cr-Mo-Ti-Al, quenching and ageing effects on props. of type 36NkhTYuM8 79−52275
Nichrome based dispersion hardened material, Ti, Y, Zr addition effects on crystallisation *(Russian)* 79−74143
Nimonic, IN100, γ' precipitates, casting conditions effect on morphology 80−7548
Nimonic 80A, rapidly solidified, struct. and initial precipitation, field-ion and TEM study 79−78982
Nimonic 90, creep rate stress exponents and friction stress, comparison with Lagneborg particle by-passing model 80−55481
Nimonic type, elastic interphase strains on ageing effects on extinction *(Russian)* 77−66646
Nitinol memory material for solid-state engine 78−59288
OT-4, creep, 800-1050°C *(Russian)* 77−59859
oxidation resist, 400 to 800°C 80−50768
phase composition and structure effect on mech. props. of VT20 alloy 79−38958
phase reflex calc. on theoretical roentgenograms of immobile monocrystals 79−23491
physical props., implant surgery appl. 77−73615
plastic deformation and rupture mechanisms, depend. on B additives for α-Ti alloys *(Russian)* 79−61650
plastic instability in sheet deformed in uniaxial tension at 300 to 700K 79−47742
plastic microstrain study during rolling under industrial conditions *(Russian)* 79−52263
plasticity, temp. and rate dependence for different rigidities of stressed state *(Russian)* 79−29139
plates with cut, stability loss critical stresses for VT-1-1 alloy 80−11690
powder compacted by hot swaging, tensile and toughness prop., β-III phase 79−38764
powder metallurgy technology innovations, 1978 status 79−47646
precipitate vol. fraction estimation from elastic modulus data 79−61595
precipitation of α and ω phase, evolution of mech. props. *(French)* 77−16591
prior β grains and α platelet morphology, exam. 78−76679
properties, medical equipment appl. 78−7456
quantitative anal., for D, by ion microanalysis 78−56945
recrystallization of β III type 80−108470
Rene 41, Ni-Cr-Co-Mo-Ti-Al-Fe (18.96, 11.09, 9.65, 3.06, 1.59, 0.89 wt.%) formation of Cr_2O_3 monocrystals on heat treatment 79−52455
Rene 41, volatilisation of oxides during oxidation at 1200°C 78−23873
residual strength of shock loaded RMI 38644 78−27574
rolled α-Ti alloy, elastic stiffness and Bauschinger effect accompanying anisotropic hardening *(Russian)* 80−40435
rolling orientation pattern form. *(Russian)* 77−21161
rotating discs, hysteresis losses and mag. phenomena 80−75695
salt-corrosion effects on long-term strength, vacuum annealing and stress concentrators effects *(Russian)* 78−11392
saturation with Al and Cr, powder method 77−21052
solidification, method for evaluating influence of each element on microsegregation *(French)* 79−74159
solution treated and aged, estimation of precipitate volume fraction using Young's modulus 78−39781
specific heat, 4 to 290K for VT5 and VT5-1 *(Russian)* 79−14938
sputtering, of type PT-7M in plasma, probe method obs. 79−55564
steel, 12Kh18N9T-TiB_2, eutectic alloy, high temp. props. 78−84931
steel, Al-Ti-(Mo), Al-Ti-V-(Mo), Al-Ti-Nb-(Mo) and Al-V-(Mo) low-alloy, toughness improvement through Ti additions 80−66525
steel, alloy, cyclic strength after strain hardening and tempering, precip. hardened 40FT 78−52988
steel, alloy, maraging 250 grade, hot isostatically pressed powder, Ti segregation embrittlement 78−52925
steel, alloy type N24M5, martensitic transform. microkinetics 78−56637
steel, austenitic, containing Ti, nitriding and nitride composition 79−20278
steel, austenitic, nitrided, creep, effect of N_2 and Ti and prior deform. 78−23789
steel, austenitic, phase composition of Kh14N16 with Zr, Ti, Nb and N additions after quenching and tempering 77−90378
steel, austenitic (03KH18N10T), heat treatment for fission reactor appls. 80−66454
steel, austenitic stainless, 08Kh18N10T, hot-worked precipitation kinetics and struct. of dispersed phases, Ti effect 80−29964

titanium alloys continued
steel, austenitic stainless, Cr-Ni-Ti, creep deform. effects on intergranular TiC dispersion stability 78−84912
steel, Cr-Mo (1.25, 0.5 wt.%), creep, fracture, Ti and Ti+B effects 77−36603
steel, Cr-Mo-Nb-Ti low alloy, material selection for nuclear steam generator tubes 78−54834
steel, Cr-Ni-Ti-B, grain size effect on mech. and struct. props. *(French)* 80−45361
steel, ledeburite, fracture during hot plastic deformation exam. 78−56755
steel, low C, Ti inclusion nucleation, effect on crack formation *(Czech)* 79−91782
steel, low C Cr-Ni, temper embrittlement by antimony, Ti addition effects 77−32683
steel, low pearlite, Ti addition effect on transform. behaviour *(German)* 77−90343
steel, maraging, Cr-Ni-Ti, effect of Ti addition on hardness and energy scatt. 79−15687
steel, maraging, grain refinement due to cyclic heat treatment 78−52971
steel, maraging 250-grade, fatigue crack growth model, notch analysis of fracture approach 78−52984
steel, martensitic, Cr-Ni-Co-Mo-Ti, Kh12N8K5M3TYu, ageing of C free martensite *(Russian)* 79−1884
steel, medium C, microalloying with V and Ti, effect on hardness and structure 80−11750
steel, microalloyed, structural, precipitation hardening, struct. and fracture *(German)* 79−61696
steel, Mn-Ti cryogenic mech. props. and intergranular brittleness *(Korean)* 79−70164
steel, Ni-Co-Mo-Ti, maraging, electron diffr. obs. of second phase *(Chinese)* 80−11655
steel, Ni-Cr-Ti, thin bands, cold working, props. and struct. of 36NKhTYu 79−78994
steel, Ni-Cr-Ti-P, Ti and P solubility effect on free surface segregation 79−11628
steel, Ni-Ti, high-alloy, precipitation hardening, fatigue strength 79−79103
steel, Ni-Ti-Al, 36NTYu, heavily deformed, subgrain struct. due to discontinuous precipitation of γ' phase *(Russian)* 79−52218
steel, R6M6, micro-alloying effect 78−6939
steel, sintered, high speed, with Ti(C,N) additions 78−11160
steel, sintered, maraging, N14K7M5T, mech. props., effect of Ti additions 77−25081
steel, solubility of W and Mo in $Ti(C,N)_x$ 80−16276
steel, stainless, Cr-Ni-Ti, metallographic detection of $(Ti,Ni)_6C$ 80−66721
steel, stainless, ferritic, corrosion resistance improvement by Mo and Ti additions 77−90505
steel, stainless, ferritic, Ni-free, effect of V, Ti addition on ductility 79−79048
steel, stainless, oxidation effect of Ti 80−35394
steel, stainless, recrystallisation texture, effect of Cu, Ti additions on development *(Japanese)* 78−80558
steel, stainless, Ti stabilised, creep props. rel. to B conc. *(French)* 79−20132
steel, stainless, type Kh17N13M2T, strengthening by plastic deformation and cold working *(Russian)* 78−52839
steel, Ti (0.1 to 0.55 wt.%), strengthening by carbide precipitation 77−25062
steel, Ti-V, Ti and V effects on precipitation, hardness and annealing *(German)* 77−55968
steel, X5CrNiTi26.6, ferrite-austenitic struct., optical and electron microscopy 78−84848
steel stainless, Ti stabilised, intercrystalline corrosion, repeated cold deform. effect 79−57000
steel W-Mo-V-TiC, powder, TiC effect on milling, pressing and sintering 78−60607
strain hardening, α- and $\alpha+\beta$ alloys of different stability, exponential law use for anal. of strain hardening process 79−15697
strength charact., elastoplasticity, creep 78−6976
strength in uniaxial dynamic extension, influence of α-ω transform. in alloy VT14 *(Russian)* 79−52200
strengthening heat treatment in vacuum, alloy VT16 79−79013
stress corrosion cracking, role of H_2, state of art review 80−61017
stress corrosion cracking control measures 77−90509
stress corrosion cracking in organic solvents, effect of microstruct. *(French)* 77−16745
structural materials for liquid metal radiation loops 78−72958
structure and physical properties, H_2 effect on α-VT5 and VT1 80−108576
structure sensitivity of mech. props., alloying influence *(Russian)* 79−47748
substrate Ni-Cr plasma spray coated, interface interaction 77−21323
superconductivity, deformation and solute-induced microstructural effects 79−7925
superplastic behaviour of welded specimens of TA6V 77−86100
superplastic state eqn. for sheet in biaxial tension 79−66131
surface layer alloying element distrib. *(Russian)* 78−19934
surface layers, cross-sectional struct., appl. of cryogenic fracturing technique 77−30219
surface layers examination using vacuum UV spectrograph *(French)* 80−71987
surface segregation, AES exam. in TA6V alloy *(French)* 78−22941
surgical implant materials, corrosion fatigue props. 79−39604
surgical implant materials, corrosion props. 79−39605
$TA6V_4$, oxidation mechanism determ. at high temp. *(French)* 77−21312
tensile props., prolonged oxidation effects 78−85050
tensile US meas., correlation with ductility and fracture detection 78−31601
texture strengthening 78−23724
Th_6Mn_{23} type struct., mag. susceptibility *(Russian)* 79−42736
thermal conductivity at slow temps., temp. depend. *(Russian)* 79−91019
thermal stability *(Chinese)* 77−73255
thermomechanical treatment, effects on struct. and props. of alloy VT22 *(Russian)* 78−19785
thermomechanical treatment effect on struct. and mech. props. of VT25 78−3152
β-Ti-Mo (15wt.%) metastable alloy, strength enhancement 77−66650
Ti-Ni, electron emission and shape memory effect 80−50687
Ti-Ta system, high-temp. oxidation *(Russian)* 79−74301

titanium alloys continued
Ticonal, effect of rare earth metals on mag. props., struct., and phase transformations 79−99732
ticonal, grindability improvement, thermomagnetic and heat treatments 77−16625
Ticonal, two- and one-dimens. modulated struct. after thermomag. treatment and water quenching *(Russian)* 80−29983
Ticonal strength, effect of thermal stresses and phase transforms. 79−87721
Ticonal with Sm, magnetic props., phase transform. after thermomagnetic treatment 78−3155
Ticonal-type alloys, struct. after quenching from 800-850°C *(Russian)* 77−59822
toughness and behaviour under dynamic loads *(French)* 80−45383
toughness and rate of fatigue cracking, structural morphology effects *(French)* 77−77579
tubing, heavy walled, US inspection 79−39107
twinned hexagonal α phase crystals, electron diffr. pattern analysis 78−56647
two-phase $\alpha+\beta$, singularities of decomposition of β solid solution, low temp. range *(Russian)* 79−1867
type 70A, containing 0-6000 ppm ^3He, sensitivity of tensile props. 80−39197
type OTCh-1, oxidation initial stages in Ni-O_2 mixture *(Russian)* 79−74302
type VT8, two phase, mechanism and kinetics of metastable β and α'' phases dissociation *(Russian)* 79−74152
type VTŽ-1, two phase, mechanism and kinetics of metastable β and α'' phases dissociation *(Russian)* 79−74152
TZM-Mo alloy, mech. props., effect of exposure to high temp. He containing O_2, room temp. study 80−93639
Udimet 520, Nicralloy-coated, microstruct. degradation, influence of corrosioin protective coating 80−40611
Udimet 700, Ni-Co-Cr-Al-Ti (18.8, 15.2, 4.5, 3.39 wt.%) exam. of high temp. creep 79−61684
Udimet 700, Ni-Co-Cr-Al-Ti (18.8, 15.2, 4.5, 3.39 wt.%) exam. of high temp. creep, viscoplastic flow 79−61685
Udimet 700, Ni-Co-Cr-Ti, hold time effects on high temp. fatigue crack growth 79−5036
universal diags. of cohesive strength *(Russian)* 78−56733
US flaw detection of ingots, struct. effect 80−66722
US wave propag. velocity, exam. 78−72982
VT16, volume and phase changes during continuous heating *(Russian)* 77−77470
VT22, hot deform., microstruct. form. and mech. props. *(Russian)* 77−28830
VT23, ht. treatment effects on fracture *(Russian)* 78−80623
VT3-1, HTMT effects on struct. and props. 78−23740
VT3-1, mech. props. and low-temp. creep 77−44314
VT3-1, vacuum-chromized, fretting-corrosion in couple with unprotected BT3-1 and steel 40KhNMA *(Russian)* 78−56804
VT6 Ti alloy, diffusion welding with constrained deformation 80−81104
VTO-1, high intensity US absorpt. 79−86845
wear resistant coated, metallic and intermetallic, electrospark applied *(Russian)* 79−1916
wear under conditions of rolling stress 79−20211
welding, gas-saturated layer effect on cracking 77−44359
Widmanstatten α-β alloy interfaces, elastic interact. stresses, effect plastic flow onset 80−104218
windmill blades materials and design 79−43719
X-ray diffr. anal. of hydrides 77−12628
X-ray phase analysis, quantitative, description of new method 79−52222
X-ray stress analysis of strongly fluorescing specimen 80−1499
yield, discontinuous, under tensile strain in liquid He, governing laws 77−63760
yield strength anisotropy and durability after cyclic loading *(Russian)* 78−27565
Al-Al_3Ti, directionally solidified, thermal stability during annealing, 435-660°C 80−108393
Al-Al_3Ti, peritectic transform. 77−16564
Al-Bi(Cd)(Pb)-Ti, containing low-melting pt. inclusions, mech. props. 80−93632
Al-Cu-Mg-Si-Fe-Mn-Ti, Si, Fe, Mn and Ti effect on precipitation in solid soln. *(Korean)* 79−66064
Al-Fe (0.5 wt.%)-Ti-Cr, Ti, Cr addition effects on toughness/microstruct. relationship *(Japanese)* 77−48525
Al-Mg-Ti, struct. and factors determining brittle intermediate compound form. 78−52817
Al-Mg-Ti-Zr alloy AL23-1, nucleating cellular dendritic crystallisation *(Russian)* 79−70055
Al-NbTi solenoid magnet for high energy particle detector, conductor and cryostat design 79−31319
Al-Ni-Ti, calc. of phase equilibria using thermodynamic values from different models 78−60646
Al-Ti, couple phase diagrams and thermochemical data 79−66037
Al-Ti, dil., electron irradiated, interaction of self interstitials with undersized solute atoms 78−63789
Al-Ti, dil., screening charge around 3d impurities, NQR meas. 77−32287
Al-Ti, dilute, morphological stabilities of planar solid-liquid interfaces during unidirectional solidification 79−4960
Al-Ti, liq., dissoln. and diffusion of alloying components, 700-1000°C *(Russian)* 80−15275
Al-Ti, manufacture, use of Na_2TiF_6, transfer of Ti 78−27453
Al-Ti, mechanical props. improvement, by work hardening *(French)* 80−97502
Al-Ti, molten, showering cryst. form. in mould cooled from top *(Japanese)* 80−66498
Al-Ti, solid soln., unidirectionally solidified, segregation patterns revealed by etching 79−47693
Al-Ti alloy spark alloying, cathode weight change and hardened layer obs. *(Russian)* 80−61005
Al-Ti alloy target in surface anal. by XPS 79−43682
Al-Ti alloys, growth crystallography and morphologies of Al_3Ti primary dendrites 79−43230
Al-Ti dilute alloys, solute distribs. during unidirectional solidification 79−4961
Al-Ti system, interdiffusion coeffs. determ. 80−70477
Al-Ti-B, liquidus surface at Al corner *(Japanese)* 77−55948
Al-Ti-B alloys, phase comp. and distrib. of components, X-ray obs. *(Russian)* 79−52164

titanium alloys continued
Al-Ti-B alloys, segregation of Ti, electron microscope exam. 78−52820
Al-Ti-C, grain refinements study using centrifugal force *(Japanese)* 79−20035
Al-Ti-Fe, ternary phase diagram, computer calculations 80−45274
Al-Ti-Si phase diagram, calc., interpretation of grain refinement results 78−84781
Al-TiB_2-Si, Si effect on grain refinement *(German)* 79−91656
Al-Ti(-Si), nucleation entropy and grain refinement 79−91627
Al-V-Ti, SiC coated B fibre reinforced, tensile and compressive strength, prior thermal treatment effect 78−11264
Al-V-Ti junction, spin-dependent electron tunnelling 79−19700
Al-Zn-Mg-Ti, TEM exam. of early stage ageing behaviour, exam. of precip. kinetics 78−56645
Al-Zn-Mg-Ti, Ti effect on microstructure during ageing 78−64568
Al-Zn-Ti, mech. props., Ti or Mn addition effect *(Korean)* 80−93613
Al_3Ti, effect on grain refinement in Al 78−52828
Al_3Ti, precipitate shape, and distribution in chill-cast Al-14 wt.% Ti alloy 80−16310
Au-Ti, dil., virtual bound states, optical absorption meas. 78−2891
Au-Ti/SiO_2/p-Si MOS struct., interface state distrib., DC tunnelling spectra determ. 80−75611
Au-Ti/n-InP Schottky diode, elec. characts. and barrier height 77−59329
B_4C-Ti, contact reaction with liq. Ni 80−55707
Ba-Ti, phase diag. *(Russian)* 78−80513
$Be_{40}Ti_{50}Zr_{10}$, metallic glass, thermoelectric power and resist. 78−95289
CC NbTi, pool cooling superconducting test coil, Japanese design for fusion reactor large coil task 80−99340
Ce-Co-Cu-Fe-Ti, sintered magnet, prep. and mag. props. 77−73043
Co-(Ti,V)C, eutectic alloy, unidirectional solidification, oxidation and tensile tests 78−52790
Co-Fe-Ti (12,6 wt.%), semihard permanent magnet, magnetic precipitation hardening 78−52830
Co-Fe-Ti alloy, precipitation hardened, rel. between struct. and mag. props. 78−95470
Co-Ti, cryst. struct. and stacking fault influence on mag. props. *(Russian)* 80−25164
Co-Ti, dendritic segregation 80−76260
Co-Ti, dilute, internal oxidation 77−31810
Co-Ti, multilayer and imperfect martensitic phases form. 78−19754
Co-Ti, neutron radiation stimulated diffusion, electrical resistivity exam. *(Russian)* 79−14959
Co-Ti (22 at.%), amorphous eutectic phase 80−55360
Co-Ti (9 at.%), decomp. kinetics, elec. resist., hardness, and saturation magnetisation during ageing *(Russian)* 80−50587
Co-Ti alloys, martensitic transformation depend. on ageing, cryst. struct. 79−91649
Co-Ti-C, secondary precipitation and allotropic transform., TEM obs. 80−108453
Co-Ti-Fe (3, 1 to 2 wt.%), spinodal decomposition 80−100839
Co-Ti-Si, directionally solidified eutectics 79−61575
Co(GaTiV) alloys, ferromag. onset, electron conc. depend. 80−60203
$Co_{2-x}(Ni,Fe)_xTiSn$, Heusler alloy, positive contribs. to hyperfine fields, magnetisation and NMR meas. 78−43654
$Co_{2-x}Ni_xTiSn$, mag. ordering, ^{119}Sn Mossbauer spectroscopy and magnetisation meas. 78−43753
$Co_2(Ti,Mn)Sn$, Heusler alloy, mag. meas. 79−47261
CoTi, dil., low temp. specific heat and magnetisation 80−65925
$Co_{1-x}Ti_x$, ferromag. props., Ti conc. effect 80−54872
Co_2Ti, Laves phase, elec. resist. rel. to mag. props. 77−59282
Co_2Ti, mag. susceptibility, 77-500K *(Russian)* 77−80911
Co_3Ti, electron energy spectrum calcs. by supplementary plane wave method 80−6711
$CoTi_{1-x}Al_x$, form. of mag. moment of Co atom, X-ray diffr., mag. meas. and NMR 77−43819
$CoTi_{1-x}Al_x$, mag. and electronic props., ferromag. and paramag. state 80−65814
Co_2TiAl, ^{59}Co NMR, above and below Curie temp. 78−2760
Co_2TiAl, Heusler alloy, paramag. state NMR and susceptibility meas. 79−65643
Co_2TiAl, hyperfine fields of Fe impurities, Mossbauer spectra 80−71255
Co_2TiSn, Heusler alloy, positive contribs. to hyperfine fields, magnetisation and NMR meas. 78−43654
Co_2TiSn-Fe, dil., Heusler alloy, Fe hyperfine fields, Mossbauer obs. 78−68424
Co_2TiSn(Al), ferromag., hyperfine fields meas. by NMR 77−63315
Cr-M, optimum alloying with rare earth metals, Ti, Zr, Hf, Nb, Ta 78−68651
Cr-Mo-Ni-Ti alloy A-286, stress-rupture data correlation 77−44346
Cr-Ni-Ti alloy and steel, emissitivty and reflectivity, oxide film thickness effect 79−82364
Cr-Ti, cast, B additions effect on struct. and props. *(Russian)* 78−19891
Cr-Ti/MgO-NbC(TaC) dispersion-strengthened, high temp. wear and oxidation resist. 80−25877
Cr-Ti/NbC(TaC) dispersion-strengthened, high temp. wear and oxidation resist. 80−25877
Cu-(Sn-)Ti melts, wetting of SiC 78−68664
Cu-Al-Ti, formation of modulated structure rel. to barrier nucleation of new phase *(Russian)* 77−32580
Cu-Al-Ti-Zr, internally oxidized, morphology of precipitates and dispersion hardening *(Russian)* 79−52217
Cu-Be-Ni-Ti-Mg (2, 0.3, 0.2, 0.02 to 0.4 wt.%), multiple step ageing *(Russian)* 78−19786
Cu-Be-Ni-Ti-Mg bronze, alloying element influence on minimum thermo EMF, cold working *(Russian)* 80−34426
Cu-Cr-Zr-Ti-B alloy system, solidification cracks formed during welding, reduction by microalloying with B 79−96148
Cu-Mn-Ti film, physical and electrical props. *(Russian)* 77−66208
Cu-Ni-Ti, ordering within precipitates, TEM obs. 80−108461
Cu-Ni-Ti system, phase equilibria in Cu rich-region and Cu-T quasi-binary constitution *(Japanese)* 80−89203
Cu-Ni-Ti system, reactions with melt in Cu-rich region *(Japanese)* 80−89202
Cu-Sn-Ti, wetting of alumina and vitreous C 78−71904
Cu-Ti, (1-1.3 at.%), elec. cond. exam. in solid and liquid phase *(Russian)* 77−62895
Cu-Ti, ageing effect on internal friction and elastic props. *(Russian)* 77−28842

titanium alloys continued
Cu-Ti, and Cu-Ti-Si(Fe), struct. and coalesc. of oxide particles during internal oxidation *(Russian)* 79−90781
Cu-Ti, deform. effect on precipitation and recrystallisation, electron microscope study 77−70115
Cu-Ti, dil., oxide film form. in ammoniacal Cu(II) solns., AES obs. 80−45415
Cu-Ti, dil. alloy, cellular precipitates, nucleation, TEM study 80−3069
β-Cu-Ti, dil. alloy, growth phenomena associated with precipitation, TEM study 80−3070
Cu-Ti, internally oxidised, morphology, struct., particle precipitation singularities *(Russian)* 79−70067
Cu-Ti, lattice parameter change during ageing *(Japanese)* 78−35411
Cu-Ti, liquid phase sintering, metallographic electron beam microanalytical investigation 78−95888
Cu-Ti, small-angle electron scattering in TEM, intensity meas. Grigson method 79−14658
Cu-Ti, solubility of Ti, exam. using NMR of ^{63}Cu *(French)* 80−7179
Cu-Ti, strengthened by modulated structs., anomalous age hardening effects 80−97497
Cu-Ti, study of internal oxidation using central diffusion of X-rays *(French)* 79−37839
Cu-Ti, Zr effects on cellular precipitation 77−16587
Cu-Ti (Zr), strength improvement by thermomechanical treatment *(Japanese)* 78−48426
Cu-Ti (0.9 at.%), age hardening effect on critical resolved shear stress 79−61603
Cu-Ti (1.07 wt.%), containing coherent precipitation, observations of flow and fracture 78−80643
Cu-Ti (3.5 wt.%), aged by US strain, struct. and props. *(Russian)* 80−21003
Cu-Ti (3.5 wt.%), internal friction in dissociating alloy following deform. by US *(Russian)* 78−35419
Cu-Ti (3.5%), coherent precipitates, US irrad. effect on struct. and hardness *(Russian)* 77−48446
Cu-Ti (4 wt.%), aged, stress corrosion cracking in Cu-NH_3 solutions, effect of pH, Cu and NHz conc. 78−88562
Cu-Ti (4 wt.%), ageing, X-ray study 77−56012
Cu-Ti (4 wt.%), combined recrystallization and precipitation 79−29072
Cu-Ti (4 wt.%), isothermal transformation, electron and optical microscopy obs. of microstructure 80−16307
Cu-Ti (4 wt.%), lamellar multiphase, struct. and spatial comp. variation, analytical STEM 78−24011
Cu-Ti (5 wt.%), effect of cold work on ageing behaviour, TEM study *(Japanese)* 79−78991
Cu-Ti (5.7 at.%), dil., β-phase struct. 79−55700
Cu-Ti alloys, activation vol. stress depend., single crysts. 77−48499
Cu-Ti alloys, CuTi, $CuTi_2$, solubility of H_2, decomp. reacts. 79−65197
Cu-Ti alloys (0.5 to 4.0 wt%) ageing charact. determ. 79−20089
Cu-Ti matrix of diamond composite, microstresses, X-ray diffr. exam. 78−56679
Cu-Ti system, diffusion obs. *(German)* 78−63881
Cu-Ti-Al(Ga)(Au)(In)(Ag)(Ni), wetting of Al_2O_3, alloying effects 80−107617
Cu-Ti-Cr(Fe), internally oxidised, morphology, struct., particle precipitation singularities *(Russian)* 79−70067
Cu-Ti-Fe (0.7, 0.9 wt.%) film, dispersion-strengthened, form. by high rate magnetron/plasmatron sputtering, and props. 80−25715
Cu-TiC precipitation hardened composite, struct. effect on friction 78−11337
Cu-Ti(0.7 at.%), plastic deform. and precip. hardened, annealing time 78−48446
$Cu_{40}Nb_{30}X_{30}$ (X=Ti, Zr, Hf), superconductors with metastable ordered structs. 80−108484
$Cu_{0.5}Pd_{0.5}Ti_2$, solubility of H_2, decomp. reacts. 79−65197
$Cu_{50}Ti_{50}$, amorphous and cryst. alloy, corrosion rates and anodic polarisation curves 79−24650
$Cu_{66}Ti_{34}$, metallic glass, neutron diffr. meas. of struct. factor 80−24367
Fe, cast, Ti effect on graphite nodularisation *(Japanese)* 77−55999
Fe-Al-Ni-Co-Cu alloys, Ti alloying and deoxidising addition *(Russian)* 78−80181
Fe-C-Mo-Nb-Al-Ti-B (0.015, 5.75, .7, 1.6, 2.5, 0.1 wt.%), TZM sheet, wear resistance, effect of surface hardening 77−59985
Fe-C-Ti (0.2 to 1.8, 0.1 to 1.7 wt.%), crystallisation and microstruct. *(Russian)* 77−66632
Fe-Co-Al-Cu-Ti (40, 14, 7.5, 4.5 wt.%), metastable equilibrium, high coercive state *(Russian)* 80−66476
Fe-Co-Ti, sp. ht. in ordered and disordered phases 80−71061
Fe-Co-Ti-Al alloy type YuNDK magnets, metallographic method of distinguishing cracks 80−85096
Fe-Cr-Al-Ti-Y_2O_3 (20, 4.5, 0.5, 0.5) type MA956, strain rate effect on fracture behaviour at 1366K 80−16458
Fe-Cr-Co ductile magnet alloys, phase diagram and mag. props., V or V+Ti addition effects 77−8959
Fe-Cr-Co-V-Ti, phase equilib., X-ray diffr. meas. *(Russian)* 79−47658
Fe-Cr-Co-V-Ti hard magnets, V and V-Ti addition effects on mag. and mech. props. 79−91810
Fe-Cr-Mo-Ti (13, 1.5, 3.5 wt.%), equilibrium studies on chi-phase strengthening 79−24496
Fe-Cr-Ni (12, 15 wt.%) austenitic alloy, Ni^{6+} irradiated, void swelling and phase stability, Si and Ti effects 80−65055
Fe-Cr-Ni-Ti-Al, superalloy, Ti, Ni, Al, H_2 variations effect on mech. props. 78−3188
Fe-Cr-Ti (18, 0.1-0.9 wt.%), high temp. oxidation *(Japanese)* 80−71806
Fe-Cr-Ti liquid alloy, thermodynamical anal. of O_2 solubility *(Russian)* 80−92676
Fe-Cr-Ti-Mo, sintered, mech. props. *(French)* 79−91726
Fe-Cr-Ti-Mo ferritic alloy, annealed, cold rolled, fast reactor material, mech. props. 78−21646
Fe-Cr-Ti-Mo-TiO_2 (13, 3.5, 1.5, 2 wt.%) dispersion hardened, void swelling 80−65046
Fe-Cr-Ti-TiO_2 (13, 2.5, 2 wt.%), dispersion hardened, ferritic alloy DT02, oxidation, 823 to 1123K 79−61803
Fe-Cu-Ti, improvement of irradiation-enhanced Cu embrittlement by Ti addition 79−43393
Fe-Hl (Si) (Ti) (V), molten, gaseous O_2 absorption 80−11836
Fe-Mn-Ti alloys, austenitic, precipitation strengthened 80−25714
Fe-Mn-Ti-Al, magnetic texture rel. to annealing temp., Mossbauer investig. 77−28499
Fe-Ni-Al-Co-Cr-Ti, YuNDK35T5BA, exam. of hypodissociation process *(Russian)* 79−11547

titanium alloys continued
Fe-Ni-Al-Co-Cu-Ti, 38 to 40 wt.% Co, 8 to 8.5 wt.% Ti, alloy YuNDKT tempering and thermomagnetic treatments 78−3154
Fe-Ni-Al-Co-Cu-Ti alloy YuNDKT, nature of X-phase heat treatment effect on microstruct. 77−90380
Fe-Ni-Al-Co-Cu-Ti magnetic alloy electrolytic treatment with programmed pulse current *(Russian)* 79−100282
Fe-Ni-Al-Co-Cu-Ti YuNDK type, S effect on mech. props. 80−60927
Fe-Ni-Al-Co-Ti base alloys, highly coercive, phase comp., Mossbauer meas. 80−39996
Fe-Ni-Al-Cu (25, 14, 4 wt.%), alloy YuND4, effect of Ti addition on structure, mag. props. 80−15714
Fe-Ni-Al-Ti, N27Yu2T2, aged austenite, diffuse electron scatt. distrib. during martensitic deform. *(Russian)* 78−60669
Fe-Ni-Co-Cu-Ti YuNDKT alloys, impaired mag. props. with C and S additions 80−60368
Fe-Ni-Co-Ti, coherent particles effect inherited by martensite on $\alpha \rightarrow \gamma$ transformation *(Russian)* 80−108443
Fe-Ni-Co-Ti, martensite cryst. lattice tetragonality, $\gamma \rightleftharpoons \alpha$ transform. *(Russian)* 79−61587
Fe-Ni-Co-Ti, shape memory effect after appl. of bending moment *(Russian)* 80−45305
Fe-Ni-Cr-Al-Ti-W-Mo (35, 15, 2.4, 2.3, 2.2 wt.%) wrought superalloy, freckles *(Chinese)* 80−104137
Fe-Ni-Cr-Mn-Al-Ti Incoloy 800, exam. of scale morphology, alloying element distrib. after oxidation 78−80677
Fe-Ni-Cr-Ti, superalloy A286, powder, exam. of microstruct. and mech. properties 78−52979
Fe-Ni-Cr-Ti based alloy, 36 NKhTYu, high temp. deform. characts., superplastic behaviour *(Russian)* 77−63719
Fe-Ni-Cr-Ti-Al, ausaging alloy, cellular precipitate indentification *(Chinese)* 78−11225
Fe-Ni-Cr-Ti-Al, Ti and Al effect on microstruct. and mech. props. *(Chinese)* 79−74130
Fe-Ni-Cr-Ti-Al, with thermoelastic control coeff., comp. and heat treatment influence on props. *(French)* 80−81074
Fe-Ni-Cr-Ti-Al Elinvar alloys, dispersion-hardened, structural transform. *(Russian)* 79−1872
Fe-Ni-Cr-Ti-Mn-Mo, (25.8, 14.04, 2.17, 1.27, 1.30 wt.%), superalloy A-286, precipitation hardening, exam. of fracture toughness and mech. props. 78−92355
Fe-Ni-Ti, ageing mechanism, neutron diffr. expts. *(Russian)* 78−48403
Fe-Ni-Ti, martensite, tetragonality, X-ray obs. 77−63665
Fe-Ni-Ti, ordered, low temp. $\alpha \rightarrow \gamma$ transform. *(Russian)* 78−19740
Fe-Ni-Ti, preaged martensite, shear strain magnitude, X-ray diffr. method 80−93592
Fe-Ni-Ti, shape recovery depend. on hardening *(Russian)* 79−83259
Fe-Ni-Ti, undeformed metastable alloy, cellular decomposition of austenite during ageing *(Russian)* 79−100178
Fe-Ni-Ti (25.9, 2.15 wt.%), exam. of effect of inhomogeneous solid soln., on martensitic transformation *(Russian)* 79−34034
Fe-Ni-Ti (27.4, 2 to 3 wt.%), aged, stress induced martensitic transform., mech. props. *(Russian)* 79−87632
Fe-Ni-Ti (30, 3 wt.%), reverse martensitic transform. and memory effect *(Russian)* 79−87627
Fe-Ni-Ti (30, 6 wt.%), austenitic, discontinuous coarsening of lamellar cellular precipitates, morphology 79−78967
Fe-Ni-Ti (30, 6 wt.%), austenitic, discontinuous coarsening of lamellar cellular precipitates, growth kinetics 79−78968
Fe-Ni-Ti (31.2, 5.3 wt.%), γ-phase ageing effect on martensitic transform. *(Russian)* 77−28814
Fe-Ni-Ti alloys, habit plane and morphology of lath martensites 77−8823
Fe-Ni-Ti alloys, high pressure effect on martensite crystal nucleation and growth *(Russian)* 78−39769
Fe-Ni-Ti austenite, high N content, cryst. struct. electron diffr. and electron miscroscope anal. *(Russian)* 79−24490
Fe-Ni-Ti martensitic alloy, γ' particle effect on crystallisation struct. *(Russian)* 78−44129
Fe-Ni-Ti-Al, martensite, nature of tetragonality 79−32936
Fe-Ni-Ti-Al-Nb, struct. mechanism for inverse $\alpha \rightarrow \gamma$ transform. *(Russian)* 80−40351
Fe-Ni-Ti-C (31, 4, 0-18 wt.%), coherent precipitates in austenite, effect on martensite substruct. 77−52327
Fe-Ni-Ti-(Cu) (12, 0.25, 2 wt.%), Cu addition strengthening at 77K, mech. props. 80−60875
Fe-Sb-Ti, dil., interactions and precip., Mossbauer study 80−39997
Fe-Sb-Ti, interactions and segregations, Mossbauer and X-ray diffr. study 80−70415
Fe-Si-Ti, eutectic alloy, exam. of eutectic temp., composition, and oxidation resistance 78−52767
Fe-Ti, BCC, mag. moment distrib. 79−47240
Fe-Ti, D storage, desorption isotherm and struct. study by neutron diffr. 79−1549
Fe-Ti, dislocation mobility and internal friction, effect of alloying in α-Fe *(Russian)* 77−31671
Fe-Ti, H_2 storage appl., alloy bonding theory approach 78−18786
Fe-Ti, hardness after nitriding, metallographic, electron microscopic and microprobe anal. 78−51608
Fe-Ti, industrial hydride reservoir, characts., technological aspects 80−45792
Fe-Ti, internally nitrided mech. props. 77−44307
α-Fe-Ti, ion implanted, microstruct., ion beam anal. and TEM study 80−107294
α-Fe-Ti, ion implanted, with C impurity, microstruct. of TiC precips. 80−66513
α-Fe-Ti, ion-implanted and annealed, microstruct. evolution 80−15132
Fe-Ti, mag. moment distrib. and environmental effects around Ti impurity 80−7092
Fe-Ti, mag. permeability disaccommodation rel. to dissolved N migration *(Polish)* 79−95611
Fe-Ti, magnetic aftereffects of H isotopes, book contrib. 79−82835
Fe-Ti, magnetic transition effect on alloying element solubility *(Japanese)* 79−42256
Fe-Ti, magnetism and H_2 storage 80−70941
Fe-Ti, multiphase binary diffusion couple, layer growth rate of intermediate phase, numerical calc. *(Japanese)* 78−14513
Fe-Ti, nitrided, struct. and props. 78−19950
Fe-Ti, O containing, mag. aftereffect and disaccommodation meas., time depend., activation energy, and ageing props. 80−88836

titanium alloys continued
Fe-Ti, precipitation hardening of α-Fe containing weak and strong particles 80−20946
Fe-Ti, solubility and diffusivity of H and D in mixed crystal phase, elec. cond. meas. *(German)* 80−107575
Fe-Ti, split bands evidence from sp. ht. and elec. transport data 77−24515
Fe-Ti, thermophysical props. and elec. cond., temp. depend. 80−96842
Fe-Ti, Ti as H trap for embrittlement control 80−66662
Fe-Ti (V)(W), dil., thermophysical props. and elec. cond., temp. depend. 80−96842
Fe-Ti (0.056 at.%), mobile dislocations during stress relaxation 78−68721
Fe-Ti (0.056 at.%), mobile dislocations during stress relaxation 78−68722
Fe-Ti (0.056 at.%), stress relaxation curves, anal. interpretation 77−59847
Fe-Ti (0.056 at.%) alloy, mobile dislocations during stress relax. 77−7729
Fe-Ti (0.056 wt.%), mobile dislocations during stress relaxation, comment 79−74193
Fe-Ti (0.056 wt.%), mobile dislocations during relaxation, reply to comment 79−74194
Fe-Ti (0.15 wt.%), H trapping obs. by high resolution autoradiography 79−73205
Fe-Ti (0.15 wt.%), Ti distrib., segregation, FIM anal. 80−84200
Fe-Ti alloys, kinetic trapping model for H_2-induced grain boundary cracking 79−29164
Fe-Ti metal hydrides, numerical physical property data for H storage 80−40929
Fe-Ti multiphase, binary diffusion couple, layer growth rate of intermediate phase *(Japanese)* 78−14514
Fe-Ti:H(D), isotope effects of diatomic TiH and TiD complexes 79−47259
Fe-Ti-C, quantitative anal. of H trapping 79−23622
Fe-Ti-C, rapidly quenched by splat-cooling 80−84923
Fe-Ti-D, ion implanted, D trapping, 90-500K 80−15131
α-Fe-Ti-N, mag. migrational relax., −60 to +200 degrees C 77−36099
Fe-Ti-S-(C), sulphide phases *(Russian)* 77−25017
Fe-Ti-Sb-C alloys, Sb trapping effect on temper embrittlement, ion beam study 78−92312
Fe-Ti-V-C-N, equilibrium comp. and solubility in steels, model of ideal solns. *(Russian)* 80−60832
Fe-Ti-(Mn)(O), exam. of interrelations between phase diagrams and hydriding props. 79−8277
Fe-TiB_2, eutectic alloy, high temp. props. 78−84931
Fe-TiB_2, phase composition, secondary ion-ion emission study *(Russian)* 80−20896
Fe-TiC pseudofused composite magnetoabrasive powders, props. 80−100926
Fe-TiC-WC(VC), sintering, densification 80−25615
Fe_3Al-Ti, ternary ordered solid soln., formation by substitution 77−43177
$Fe_xCo_{1-x}Ti$, high press. mag. props. 78−23271
$Fe_xCo_{1-x}Ti$, mag. props. 79−56532
$Fe_xCo_{1-x}Ti$, mag. props., sp. ht. and resist. meas. 79−61120
$Fe_{0.5}Co_{0.5}TiH_x$, transmission Mossbauer spectra 80−44964
$Fe_{36}Cr_{12}Ti_7Mo_3$, high temp. precipitation kinetics, internal friction study 79−43254
$Fe_{0.49}Mn_{0.01}Ti_{0.5}H_x$, localised vibrs., sp. ht. obs., room temp. 80−65248
FeNiCrAlLi alloy, γ' hardened, noncellular mech. for form of lamellar η phase morphology 77−28824
FeTi alloy, elec. and mag. props. near order-disorder transition 79−82576
ε-FeTi, Ce addition effect on H_2 absorption capacity 79−61899
FeTi crystals, use in storage and production of superpure H_2 *(German)* 78−53184
FeTi, dil., mag. hyperfine field, TDPAC meas. 78−43699
ε-FeTi, effect of Ce on H_2 absorption 79−73315
FeTi, H storage alloy, prep. for TEM *(German, English)* 80−30197
FeTi hydrides, struct., heat of soln., diffusion and hydriding kinetics for H storage 80−40930
FeTi, hydrogen energy storage, surface segregation *(German)* 79−77872
FeTi, hydrogen storage, annealing effects *(Japanese)* 79−100542
FeTi, hydrogenation, effect of surface segregation on mag. props. 78−84819
FeTi, positronium form. after hydrogenation-dehydrogenation cycling and annealing 80−18947
FeTi, surface and mag. props., heat treatment and hydrogenation effects 80−75447
FeTi, surface segregation and catalytic effect on hydrogenation, AES and XPS study 79−11626
FeTi, surface segregation, catalytic effect on hydrogenation 80−45814
$Fe_{1-x}Ti_{1+x}$, Mossbauer study, superparamag. clusters 77−85633
$Fe_{1-x}Ti_x$, ferromag. props., Ti conc. effect 80−54872
Fe_2Ti-Fe eutectic alloy, directional solidification singularities *(Russian)* 78−68678
FeTiB, corrosion-resistant amorphous mag. thin films 80−54923
β-FeTiD, neutron diffr. exam. of struct. 78−47282
α-$FeTiD_{0.057}$, solid soln., interstitial D, neutron diffr. study 80−39071
$FeTiD_x$ ($0 \leq x \leq 1.9$), structural phase transitions, absorpt. and desorpt. isotherms 80−19948
FeTiH, H storage material, H diffusion, neutron diffr. obs. 80−51013
FeTiH, solar energy storage by metal hydride 80−61455
Fe_2TiSi, Heusler type material, mag. props. 77−40042
$Fe_{3-x}Ti_xSi$, limits of solubility, mag. props. and electron conc. 78−10670
Gd-Ti amorphous films, spontaneous Hall effect and elec. resist. 80−80251
H assisted cracking, mechanisms, review 80−50721
Hf-Ti, binary continuous solid solution, elec. resist. and thermoelec. power behaviour 79−69492
IMI-685, unstable shear modes in fatigued β-annealed specimens 78−84984
LaB_6-Ni-TiC(TiBsd2), thermionic emission 77−28678
Mn-Cr-Ti layers on low C steel, composite, residual stresses rel. to arc-spraying parameters *(German)* 80−104077
Mn-Ni-Ti, and mech. props., thermal expansion, for different heat treatments *(Japanese)* 79−29123
Mn-Ni-Ti, non-ferromagnetic Elinvar-type alloys 79−24566
Mn-Ti surface treatment on Al_2O_3 insulators 79−24261
Mn-Ti-Al, phase stability 77−48397

titanium alloys continued
Mn-Ti-Fe, ternary phase diagram, computer calculations 80−45274
$Mn_{0.75}Ti_{0.25}Bi$ films as magnetooptic storage medium, mag. interferogram recording 78−19288
Mo-Nb-Ti-N alloy, with dispersed second phase, ductile-brittle transition 80−93653
Mo-Ti, electron beam melted, alloying addition effects on brittleness and ductility 79−61728
Mo-Ti, internally nitrided, lattice expansion by precipitation 78−68700
Mo-Ti, irrad. between 425 and 1000°C, ductility in bending 80−39164
Mo-Ti (1 wt.%), fast neutron irradiated, direct obs. of solute segregation to voids 79−78971
Mo-Ti (3.5 wt.%), load curves, structure states boundaries and strain hardening *(Russian)* 80−89241
Mo-Ti (3.6 wt.%), absorption of N_2 in induction and plasma-arc heating *(Russian)* 77−16732
Mo-Ti (up to 5.48 wt.%), internal nitriding, hardness, nitride type, precipitation *(Japanese)* 79−79157
Mo-Ti-La-C, influence of high pressure on mech. preps. after nitriding *(Russian)* 79−57137
Mo-Ti-N, exam. of phase equilibria *(Russian)* 79−29018
Mo-Ti-N alloy, with dispersed second phase, ductile-brittle transition 80−93653
Mo-Ti-Zr, alloy TZM, polycrystalline, anal. of elastic anisotropy and microyielding 80−30050
Mo-Ti-Zr, D trapping in fusion reactor materials, temp. dependence 80−37577
Mo-Ti-Zr, diffusion and solubility of C *(French)* 79−55932
Mo-Ti-Zr, fusion reactor first wall material, compatibility with impure He 80−32469
Mo-Ti-Zr, TZM, corrosion behaviour in high temp. impure He gas 80−76402
Mo-Ti-Zr (TZM), fusion reactor materials, radioactivity minimization by elemental substitution and isotopic tailoring 79−22463
Mo-Ti-Zr (0.5, 0.1 wt.%), neutron irradiated, void swelling and shrinkage, TEM study 80−34079
Mo-Ti-Zr (0.5, 0.7 wt.%) alloy TZM, props. and appl. *(German)* 80−21040
Mo-Ti-Zr alloy, neutron radiation-induced shrinkage of voids 79−51158
Mo-Ti-Zr alloy TZM, fatigue and plastic flow, irradiation effects 77−52466
Mo-Ti-Zr alloys TZM and TZC, superior powder metallurgy die alloys for isothermal forging mech. props. 79−74201
Mo-Ti-Zr-C, stress cycling at room temp. *(Russian)* 77−25148
Mo-TiC, eutectic formation of regular struct., crystn. *(Russian)* 80−66496
Mo-TiC-Ni phase equilibria, subsolidus temp., metallographic and X-ray anal. 80−16278
Mo-TiC(TiN), phase diagram *(Russian)* 78−27476
Mo-Zr-Ti-C(0.1, 0.15, 0.004 wt.%), alloy TsM2A, cavitation failure mechanism 77−70169
$(N_{1-y}Y_y)_3Al_{1-x}Ti_x$, quarternary γ' ($L1_2$) pseudobinary props., revealed by ionicity modified pair model 78−19725
Nb-Mo-Ti-Zr, influence of C content on creep charact. and creep-rupture strength *(Russian)* 77−48483
Nb-Mo-Ti-Zr-C, work function temp. and phase depend. *(Russian)* 80−2449
Nb-Mo-Zr-Ti, Zr and Ti effects on struct. and mech. props. 77−70061
Nb-Ti, AC loss minimum, pinning, flux distribution 80−84574
Nb-Ti, annular superconductor, field replication and flux shielding 77−28286
Nb-Ti, electrical resist. at low temp., enhancement due to short-range supercond. order 77−28157
Nb-Ti, film, composition determ. by ^3He elastic scatt. 78−76974
Nb-Ti, Helmholtz coils, optimisation, critical current rel. to mag. induction 79−67353
Nb-Ti, metallurgical treatment, effects on props. 79−38846
Nb-Ti, multi-filamentary superconducting wires, mag. field dependence of AC losses 78−60256
Nb-Ti, multifilament composite technical superconductors, development and manufacture 79−19707
Nb-Ti, multifilament superconductor, metallurgical design 79−33434
Nb-Ti, multifilament wire, superconducting magnet system, development for physical experiments 80−9008
Nb-Ti, multifilamentary, Mirror Fusion Test Facility, superconductor core manufacturing and quality 80−93521
Nb-Ti, nitriding, diffusive saturation, lattice spacing and activation coeffs. *(Russian)* 80−21168
Nb-Ti, pinning curves, high field J_c and scaling behaviour 80−93064
Nb-Ti, radiation effects on critical currents 78−52175
Nb-Ti, resistivity due to H incorporation 80−70666
Nb-Ti, sheet, flux trapping, appl. to mag. shielding and levitation 80−31806
Nb-Ti, single core conductor, carrying DC transport current, alternating field losses 80−34550
Nb-Ti, supercond., optimised pinning struct., crit. data 1.8-4.2K 77−89913
Nb-Ti, supercond. and mag. props., anisotropy *(Russian)* 77−59361
Nb-Ti, supercond. Helmholtz coils, optimisation 79−2795
Nb-Ti, supercond. low-temp. plasticity 77−15992
Nb-Ti, superconducting, pinning mechanism at high mag. fields 79−95555
Nb-Ti, superconductive materials and magnet systems developed at Intermagnetics General Corp. 79−58699
Nb-Ti, superconductivity after heavy ion irradiation at low temps. and high fluence 77−69437
Nb-Ti, superconductor optimisation for 12 Tesla toroidal field coils 80−91272
Nb-Ti, thermal conductivity in low temp. range 78−39259
Nb-Ti, type II supercond., hysteresis losses for round cross section with collective interaction 78−43513
Nb-Ti, type II superconductor, mech. behaviour and stress effects 77−86083
Nb-Ti, void volume fraction reduction, Ni^+ ion irradiation 79−51162
Nb-Ti, wire drawn and hydrostatically extruded supercond., crit. current density 79−38275
Nb-Ti 10 kA conductor development for Tokamak toroidal coil 79−31217
Nb-Ti (46%) composite superconductor, fabrication 77−24989
Nb-Ti (50%), supercond., cryostat design for magnetisation study *(Spanish)* 80−75673

titanium alloys continued
Nb-Ti (60 at.%), aged, TEM exam. of precipitation process *(Japanese)* 78−48409
Nb-Ti alloy, supercond. and high mag. fields 79−87215
Nb-Ti alloy strip, crit. current anisotropy 78−10624
Nb-Ti alloys, crit. current density, scaling law 78−31027
Nb-Ti alloys, oxidation, ESCA *(French)* 77−36361
Nb-Ti filamentary superconductor critical current density rel. to thermal treatment 79−33440
Nb-Ti films, ion beam sputtered, study by ^4He backscattering and nucl. reaction microanal. 79−42400
Nb-Ti in Cu, composite supercond. field replication and flux shielding 77−28286
Nb-Ti in Cu matrix composite superconductor, cyclic stress effects on transport props. 77−28336
Nb-Ti multifilamentary cable magnet, quench development 77−26351
Nb-Ti multifilamentary superconducting composite, subjected to rotating mag. induction, losses 79−33386
Nb-Ti multifilamentary supercond., AC losses, mag. field depend. of loss-freq. charact. 79−33384
Nb-Ti multifilamentary supercond., commercial, crit. current density 79−38274
Nb-Ti multifilaments, effect of mech. and thermal treatments of supercond. props. 80−104197
Nb-Ti superconducting alloy, critical current density, heat treatment effects *(Japanese)* 78−14909
Nb-Ti superconducting coils, for thermonuclear fusion *(French)* 80−95399
Nb-Ti superconducting composites, crit. current changes and fatigue damage after 4.2K strain cycling 77−28323
Nb-Ti superconducting cylinders, dynamically stabilised, differences in shielding versus trapping behaviour 77−47933
Nb-Ti superconducting magnet system, for short sample test on Tokamak superconductor 80−9010
Nb-Ti superconducting multifilamentary composites, high current, effect of matrix on losses 77−24649
Nb-Ti superconducting multifilamentary wires, high B losses 77−24650
Nb-Ti superconducting multifilamentary composites, high current, crit. current degradation 77−24659
Nb-Ti superconducting multifilamentary wires, mechanisms for crit. current degradation 77−28324
Nb-Ti superconducting single layered multifilamentary coil, eddy current loss depend. on demagnetisation 80−97040
Nb-Ti superconducting wire, Cu clad, Meissner effect in Cu meas. 78−64166
Nb-Ti wires, microplastic behaviour, acoustic emission, appl. to training effect in supercond. magnets 77−26356
Nb-Ti/Cu composite disc, crit. state model for crit. current determ. 79−99665
Nb-Ti/Cu sheet composite, flux trapping and shielding capabilities in transverse fields 80−15667
Nb-Ti-Al alloy, effect of heat treatment on strength and elastic props. 77−55976
Nb-Ti-C, phase comp. and precip. after heat treatment 79−57020
Nb-Ti-N, exam. of phase equilibrium using electron microscopy and X-ray analysis *(Russian)* 79−15654
Nb-Ti-Ta, pinning curves, high field J_c and scaling behaviour 80−93064
Nb-Ti-Ta alloys, metallurgical anal. and crit. current densities 79−38286
Nb-Ti-Zr, electrical resist. at low temp., enhancement due to short-range supercond. order 77−28157
Nb-Ti-Zr, supercond. wire, anomalous increments of AC losses due to flux jumps 77−28289
Nb-Ti-Zr, superconducting, ageing effect on critical current density *(Japanese)* 79−61747
Nb-Ti-Zr, superconducting, critical current density and microstruct. correlation *(Japanese)* 79−61748
Nb-Ti-Zr, superconducting wire, coil simulation, class and instability meas. 79−71487
Nb-Ti-Zr, superconducting wire, coil simulation meas. of losses and instabilities 80−37050
Nb-Ti-Zr, wire, anomalous crit. AC 77−16014
Nb-Ti-Zr ternary alloy wires, flux jumping 79−60965
Nb-Ti-Zr ternary system, high-field supercond. 80−97045
Nb-Ti-Zr wire, supercond., longit. critical currents in AC mag. field 77−72958
Nb-W-Ti-C, quenched from liquid state, formation of nonmetallic inclusions *(Russian)* 79−57007
Nb-Zr-Ti, needle field emitter, ion bombardment effects, field emission microscope obs. 77−55869
Nb-Zr-Ti alloys, scale formation 77−44229
Nb_3Ge-Ti, synthesis from thermalised sputtering and changes in Tc and depend. of H_{c2} on temp. 79−56350
NbTi, 7 T multipurpose split-coil superconducting magnet system for Mossbauer spectroscopy and susceptibility measurements, 2 to 300K 79−58746
NbTi cabled and soldered superconds. with low losses, for fusion research magnets, development 79−35796
NbTi, chemical comp., supercond. films and bulk surfaces 78−76973
NbTi composite supercond., current transfer, theory 78−72315
NbTi composite supercond., current transfer, expt. results 78−72316
NbTi, composite wire, boundary resistance and cryogenic stability 79−69629
NbTi composites, cryogenic stability due to boundary resistance between filament and matrix 79−58748
NbTi, dynamic stress effects, supercond. magnet training problems 78−49870
NbTi filament reinforced Cu, superconducting composite, elastic const., temp. depend. 78−68717
NbTi, filamentary conductors, type-II, low temp. 30 GeV proton effects on critical props. 78−52178
NbTi filaments for position-sensitive superconducting detector of ionizing particles 80−63460
NbTi films, effect of Ar- and N-ion bombardment on texture *(Russian)* 80−107338
NbTi, forced flow superconducting test coil, EURATOM design for fusion reactor Large Coil Task 80−99339
NbTi forced flow superconducting test coil, Swiss design for fusion reactor Large Coil Task 80−99341
NbTi, General Dynamics Convair conceptual design test coil 78−50389
NbTi, General Electric test coil conceptual design 78−50390

titanium alloys continued
NbTi in Al composite superconductor, AC losses and crit. current 77−28310
NbTi, monocore and filament conductors, crit. current densities and anisotropy factors, heat treatment effects 79−38285
NbTi monofilamentary wire in current sharing state, supercond. temp. sensor use 80−57288
NbTi multifilament superconductor, AC loss reduction by low twist rates 77 12057
NbTi multifilament supercond. wire, hydrostatic extrusion processing 79−33976
NbTi, multifilamentary composite wires, critical current strain depend. 77−20511
NbTi multifilamentary composite, appl. of method for continuous meas. of crit. current 77−24656
NbTi multifilamentary composite wires, supercond. crit. current density, temp. and mag. field depend. 79−33425
NbTi multifilamentary superconductor, production samples, performance 77−40012
NbTi multifilamentary wires, 30 GeV proton irradiated, effect on crit. currents 77−89911
NbTi, neutron irrad. effect on supercond. fusion magnet props. 78−52128
NbTi, RF magnetoresistance, flux flow resistivity 79−61002
NbTi solenoid, operating at 9 T in He gas 77−74461
NbTi, solid soln. supercond., crit. current anisotropy 79−38273
NbTi split coil superconducting magnet system, for Mossbauer spectroscopy and susceptibility meas. 79−71486
NbTi, supercond., measurement of thermal conductivity 79−58682
NbTi, supercond., processing parameter optimisation for high mag. field appls. 79−38290
NbTi, supercond., thermal cond. meas 79−60970
NbTi, supercond. critical temp., appl. of cryogenic calorimetry 79−40577
NbTi supercond. threads in Cu matrix, struct. composition and props. *(French)* 79−73649
NbTi, superconducting, orientation effects on magnetisation 77−28287
NbTi, superconducting, serrated yielding meas. via dynamic stress test facility 77−77698
NbTi, superconducting multifilamentary conductors, crit. current density, bending effects *(German)* 80−39727
NbTi superconducting state, stability under localised heat pulses 79−73611
NbTi superconducting tapes, mag. field profiles 77−28326
NbTi, superconducting test coil, General Dynamics Convair Division, Intermagnetics General Corp. design for fusion reactor Large Coil Program 80−99338
NbTi superconducting test coil, General Electric design and manufacture program, for fusion reactors 80−102319
NbTi, superconducting toroidal field coils for Tokamaks 78−50388
NbTi superconducting wire, Cu clad, proximity effect, Meissner screening length meas. 79−60996
NbTi, superconductor, acoustic emission during flux jump 80−39724
NbTi wire, supercond., magnetisation rel. to field orient. 78−52151
NbTi/Cu, room temp. elastic consts., US determ. 77−59839
NbTi/In composite superconductor, transport props. 80−88658
NbTi/In granular composite, resistivity mag. field depend. 80−15654
NbTi-Al-(Cu-Ni) multifilamentary composite supercond. wire, stability, AC losses 77−76998
NbTi-Cu, composite superconductor, acoustic emission 80−84546
NbTi-Cu, cryostatic influence of formvar coatings on sizing of stabilizer 79−61633
NbTi-Cu, supercond. composite, use in temp. and heat transfer coeff. meas. 80−77780
NbTi-In granular supercond. composites, mag. field-induced dissipation 80−84545
$(Nb_{0.99}Ti_{0.01})_{1-x}Ge_x$, high T_c, resist. meas. 80−88531
$(Nb_{0.99}Ti_{0.01})_{1-x}Ge_x$, supercond. transition temp. and crit. field 79−38220
$(Nb_{0.99}Ti_{0.01})_{1-x}Ge_x$, supercond., mag. field props. 80−54822
$(Nb_{1-y}Ti_y)_{1-x}Ge_x$, transition metal atom stabilised superconductivity 79−7924
$Nb_{1-y}Ti_ySe_2$, supercond. transition temp. and mag. susceptibility 77−12043
Ni base alloy IN792, carbide morphology 77−36508
Ni superalloy Mar-M200, slow fatigue crack propagation rate meas. using high freq. resonant technique 78−52983
Ni-A-Ti (6,1 wt.%), γ' phase precip., deform. effects *(Russian)* 78−48404
Ni-Al-Cr-Co-Ti, Waspaloy, exam. of dislocation-precipitate interaction, cyclic stress-strain behaviour 78−84925
Ni-Al-Cr-Mo-Ti-W-(Co) alloys EhI 826 and EhI 929, reverse elastic after effect under loading 78−39829
Ni-Al-Cr-Ti-W-Mo, US vibration applied during solidification, improved strength, corrosion resistance *(Russian)* 78−15382
Ni-Al-Ti, ageing kinetics and γ'-phase particles spatial distrib. under applied load *(Russian)* 77−32598
Ni-Al-Ti, heat resist., solidification range 80−35177
Ni-Al-Ti, heat-resisting dispersion-hardening alloys, props. and struct., γ'-phase comp. influence *(Russian)* 80−20943
Ni-Al-Ti, soln. temp. of hardening intermetallic phase in heat resistant alloys 78−52865
Ni-Al-Ti cast superalloy, eutectic transform. on ageing *(Chinese)* 79−100110
Ni-Al-Ti ferromagnetic non-homogeneous alloy, composition determination by Curie temp. meas. 80−11196
Ni-Al-Ti protective coating, on Ni-Al alloy IN 100, Ti content influence, oxidation behaviour *(French)* 78−3258
Ni-Al-Ti-Cr superalloys, estimation of conjugate γ and γ' compositions 79−8282
Ni-Al(Cr)-Ti, eutectic alloy charact. by melting temp., composition and oxidation resistance 78−52771
Ni-Ce-Fe-Ti (77, 20, 4, 2.5 wt.%), long-term strength in H at high pressure 80−55485
Ni-Co-Cr-Al-Ti-Mo superalloy IN738, casking porosity removal using hydrostatic press. sintering 80−55322
Ni-Co-Cr-Mo-Al-Ti (17.5, 15.1, 4.9, 4.15, 3.25 wt.%), creep and stress rupture behaviour in air and vacuum 80−60918
Ni-Co-Cr-Mo-Ti-Al Nimonic 105, loading frequency and environmental effects on high temp. fatigue crack growth 78−64675

titanium alloys continued
Ni-Co-Cr-Ta-Al-W-Mo-Ti, cast, phase volume fraction determ. using manual point count practice 78−53052
Ni-Cr-Al-Ti, KhN78TYu, heavily deformed, subgrain struct. due to discontinuous precipitation of γ' phase *(Russian)* 79−52218
Ni-Cr-Al-Ti, stress corrosion cracking, factors influencing susceptibility 80−97617
Ni-Cr-Al-Ti (Ti-Co), exam. of back stress role in creep behaviour of particle strengthened alloys 78−52889
Ni-Cr-Al-Ti alloy type ZhS6U, effects of heat treatment in high vel. gas streams on props. 79−57025
Ni-Cr-Al-Ti-Mo, low temp. mech. behaviour, precipitation 78−39860
Ni-Cr-Al-W-Ti alloy MA 6000E, mechanical alloying for high temp. appl. 78−44046
Ni-Cr-Co-Al-Ti-W-Ta-Mo, IN 738 LC, loading frequency and environmental effects on high temp. fatigue crack growth 78−64675
Ni-Cr-Co-Al-W-Mo-Ti-Ta, heat resist. and struct., Ta effect 80−76312
Ni-Cr-Co-Mo-Al-Ti (10, 15, 3, 5.5, 4.5 wt.%), superalloy, exam. of creep and fracture behaviour 78−48464
Ni-Cr-Co-Mo-Al-Ti alloys, Waspaloy, Astroloy, exam. of microstruct. effect on crack growth 78−52977
Ni-Cr-Co-Mo-Ti, oxidation depend. on alloying element, cohesion strength *(Russian)* 80−40587
Ni-Cr-Co-Mo-Ti-Al, powders, HCl surface treatment to prevent TiC precipitation, fracture props. 79−8397
Ni-Cr-Co-Ti, superalloy sintering thermochemical surface treatment 80−25617
Ni-Cr-Co-Ti-Mo-W-Al (14, 9.8, 5, 4, 3.9, 3 wt.%), low cycle fatigue, prior heat treatment effect 80−60962
Ni-Cr-Mo-Ti (19,11,3 wt.%) for TiC reactively sputtered coatings, adherence, XPES and wear study 80−25565
Ni-Cr-Mo-W-Al-Ti, heat-resist., phase comp. 80−76250
Ni-Cr-Ta-Ti-Si, EP557 precipitation hardening alloy, mech. props., heat treatment effect 80−60877
Ni-Cr-ThO_2 (20, 2 wt.%), dispersion hardened, model for high temp. deform. based on struct. obs. 78−19809
Ni-Cr-Ti, effect of ultrasound on crystallisation, dendritic structure, and plasticity *(Russian)* 80−11637
Ni-Cr-Ti, type EHI698, loading history effect on resist. to cyclic elastoplastic strain 80−16398
Ni-Cr-Ti (19.51, 4.2 wt.%), quench-ageing and fracture *(German)* 77−70088
Ni-Cr-Ti rapidly solidified superalloys, surface segregation 80−76263
Ni-Cr-Ti-Al, precipitation of γ' phase during single and combined ageing treatment *(Russian)* 77−52328
Ni-Cr-Ti-Al/Au-Ni brazed joint, high temp., AE under elev. temp. and loading *(German)* 78−31597
Ni-Cr-Ti-Al-Fe-Co (19.65, 2.40, 1.37, 0.78, 0.52 wt.%), strength of γ' hardened alloy, ageing exam. 78−88501
Ni-Cr-Ti-Al-Mo-Nb-Fe (13-16, 2.35-2.75, 1.3-1.7, 2.8-3.2, 1.8-2.2, 2.0 wt%), heat resistant props, mech props. struct., stepwise ageing effects *(Russian)* 78−76666
Ni-Cr-Ti-Co-W-Al-Mo alloys AF-115 and AF2 1DA, superalloy powder compacts, fatigue origins 78−48521
Ni-Cr-W-Co-Ti, high-temp. sulphide corrosion 80−76408
Ni-Cr-W-Co-Ti, thermal fatigue, effects of inclusions 80−81183
Ni-Cr-W-Co-Ti heat resistant alloy ZhS6K, fatigue resistance, heat treatment and protective coating effects 77−81320
Ni-Cr-W-Mo-Al-Ti (15,6,3,2,2, wt.%), wrought, Si effect on transition brittleness *(Chinese)* 80−55491
Ni-Cr-W-Mo-Ti-Al, heat-resist., recovery and recrystn. 80−76268
Ni-Cr-W-Mo-Ti-Al alloy KhN67MVTYu, heat treatment effect on mech. props. 77−70082
Ni-Cu-X (X=Sn, Nb, Ti), spinodal decomp. alloys, linear expansion coeff. influence on morphological anisotropy *(Japanese)* 80−70431
Ni-Fe-Co-Ti, electron microscopy and mag. meas. 80−71097
Ni-Fe-Cr-Mo-Ti-Al, PE 16, thermally activated domain wall motion 80−88777
$Ni-Ni_3Ti$ eutectic alloys, solidification 77−70042
Ni-Ti, Curie temp. determ. using deviation from Mattheisen's rule 79−15306
Ni-Ti, dil., optical absorpt., electronic struct. 80−108227
Ni-Ti, effect of solute misfit and temp. on irradiation induced segregation 78−72779
Ni-Ti, heavily doped, linear expansion meas. 80−103501
Ni-Ti, ion irradiation induced void swelling and defect microstructs., TEM obs. 79−51164
Ni-Ti, mag. moment distrib. and environmental effects around Ti impurity 80−7092
Ni-Ti, martensitic phase transformation effect on low cycle fatigue behaviour 80−7666
Ni-Ti, near equiatomic, pretransform. lattice instability, TEM and electron diffr. 79−11616
Ni-Ti, near equiatomic alloy, TEM exam. of austenite-martensite interface 78−51401
Ni-Ti, neutron irradiated, thermally activated deform. 80−6438
Ni-Ti, Ni-rich, temp. depend. resist. 80−10943
Ni-Ti, shape memory effect, criteria for efficiency assessment *(Russian)* 80−21015
Ni-Ti, shape-memory effect, intermetallic compounds 20-years research results 77−7843
Ni-Ti, spin polarised tunnelling expts. 78−39372
β-Ni-Ti, struct. changes during annealing, TEM and selected area diffr. 79−34081
Ni-Ti, structural instability, deform. effects on electron energy spectrum 80−39284
Ni-Ti, tunnelling electron spin polarisation 77−73058
Ni-Ti, wetting of AlN, effect of alloys exam. 78−80710
Ni-Ti, with shape memory effect, working medium in heat engine *(Russian)* 78−48449
Ni-Ti (0-1.5 at.%), elec. cond., mag. phase transition, 300-750K 78−2678
Ni-Ti (1 wt.%), serrated yield, 77 to 873K 77−32649
Ni-Ti (10 wt.%), X-ray study of ageing of plate and powder 77−1847
Ni-Ti (12 wt.%), dil. alloys, transform. early stages 78−3096
Ni-Ti (12 wt.%), early stages of transformation 80−76251
Ni-Ti (1.6, 7.64 wt.%), monophase high temp. scaling, metallography study 80−21159
Ni-Ti (2wt.%) alloy, polarised neutron diffuse scatt. 77−36057
Ni-Ti (3 wt.%), C precipitation 80−29958

titanium alloys continued
Ni-Ti (48 at.%), annealed and rolled electron microscope and probe analysis of structure 79−100189
Ni-Ti (51.5 at.% Ni) metallide, thermal cond., elec. resistivity, 90-450K 78−68009
Ni-Ti (60 at.%) alloy, high stress effects on struct. and props. *(Russian)* 78−19838
Ni-Ti (8 and 10 wt.%) alloy, aged, precipitation behaviour at 550 to 950°C, X-ray and electron microscopy exam. 78−39785
Ni-Ti (9.6 wt.%), mag. study on phase decomposition *(Japanese)* 80−15758
Ni-Ti alloy, shape memory effect mechanism 77−28865
Ni-Ti alloy, struct. and props., self-propagating high temp. synthesis *(Russian)* 78−26492
Ni-Ti dil., impurity effects on grain boundary mobility *(Polish)* 79−96073
Ni-Ti mech. memory alloys, tensile props. *(Korean)* 77−63724
Ni-Ti shape memory alloy processing and medical applications *(German)* 80−17203
Ni-Ti shape memory alloy trigger for space satellite boom latch and release mechanism 80−7575
Ni-Ti thin film, phase growth kinetics due to diffusive processes *(Russian)* 77−72722
Ni-Ti/Cu composite, plastic deform. influence on internal friction *(Russian)* 80−100871
Ni-Ti-Al, martensitic, coherent γ'-phase particles and influence on $\alpha \rightarrow \gamma$ transformation *(Russian)* 79−29056
Ni-Ti-Al superalloy, pendant drop melt extracted, struct. and props. 80−76242
Ni-Ti-Co, Co effect on martensitic transform. temp. and low temp. props. *(Korean)* 78−11224
Ni-Ti-P, amorphous, corrosion behaviour, immersion tests and electrochem. meas. *(Japanese)* 80−85085
Ni_3 (Al,Ti), flow stress and work hardening, exam. of temp. depend. by tensile tests 78−84839
Ni_3(Al,Ti), deformation characts., temp., strain rate and orientation depend. 77−44320
Ni_3(Al, Ti), S segregation to grain boundaries 78−48410
γ'-Ni_3(Al,Ti), single crystal, dislocation movement, HVEM obs. *(Japanese)* 80−108503
Ni_3Al-Ti, powder, X-ray spectral analysis exam. 80−16239
$(Ni_{1-x}Cu_x)Ti$, martensitic, shape memory effect kinetics and thermodynamics 80−3021
$Ni_2Mn_xTi_{1-x}Sn$, Heusler alloy, mag. moment exam. 77−24682
$Ni_2Mn_xTi_{1-x}Sn$, mag. hyperfine fields, ^{119}Sn Mossbauer spectra study 80−55003
$Ni_2Mn_xTi_{1-x}Sn$, Mossbauer spectra, mag. hyperfine field 80−15857
Ni_2(Ti,Mn)Sn, Heusler alloy, mag. meas. 79−47261
NiTi alloy single cryts., ferromag. reson., g-value and linewidth 80−71186
NiTi based alloys, plastic deform. mechanism 79−11676
NiTi equiatomic alloy, single cryst. elastic consts. near martensitic transform. 80−75283
NiTi martensite, shape memory effect, struct. characts., TEM $2^1/_2$ D imaging obs. 80−108446
NiTi, martensitic, shape memory effect kinetics and thermodynamics 80−3021
NiTi, martensitic transform. rel. to low frequency internal friction peaks 79−96024
NiTi, premartensitic transformation of B2 phase, shape memory 80−84931
NiTi, reversible martensitic transformations 78−27516
NiTi, search for electronic phase transition, soft X-ray appearance potential spectra 79−24391
NiTi shape memory alloys, mech. fatigue 79−29166
NiTi shape memory effects, substitution of Cu for Ni 79−61661
NiTi, stacking faults prod. by martensite transition, lattice imaging electron microscopy obs. 79−96026
$Ni_{1-x}Ti_x$, ferromag. props., Ti conc. effect 80−54872
Ni_3Ti, electronic struct., Xα calc., photoelectron and AES spectra 80−20769
Ni_3Ti-Ni eutectic alloy, directional solidification singularities *(Russian)* 78−68678
$Ni_{40}Ti_{60}$, amorphous, chem. short-range-order, X-ray and neutron scatt. obs. 80−96447
NiTiCu, shape memory alloys, electron microscope and X-ray diffr. study of struct. 79−82179
$Ni_3Ti_{0.5}Ta_{0.5}$, conservative domain struct., TEM study 80−79776
$Ni_{62}Ti_{29}Zr_9$, amorphous, H-sorption, X-ray and DSC obs. 80−49526
Pd-Ru-Ti, elec. resist. and thermal cond. *(Russian)* 78−19017
Pd-Ti, hydrogenation, lattice spacings, microhardness and mag. susceptibility meas. 79−77557
Pd-Ti, Matthiessen's rule breakdown 77−15823
Pd-Ti, hydrogenation, lattice spacings, microhardness and mag. susceptibility meas. 79−77557
Pd-Ti liquid alloy, mass spectrometric study of high temp. thermodynamic stability 78−15369
$PdTi_2$, solubility of H_2, decomp. reacts. 79−65197
Pd_4Ti, Ll_2 ordered alloy, positive temp. depend. on strength, phase destabilization 80−81203
Pt-Ti, Matthiessen's rule breakdown 77−15823
Pt-Ti bielectrode use as insoluble anode in electroplating 77−44490
Pt_3Ti, Ll_2 ordered alloy, positive temp. depend. on strength, phase destabilization 80−81203
Si-Ti-Cr system, plasma coating on Nb, alloy substrates, radiating power 79−60529
SiC fibre reinforced Ti, effect of Al, Zr and Mo alloying additions on reaction rate of Ti with fibres 80−16249
Sm-Co-Cu-Fe-Ti magnets, comp. and sintering effects on coercivity 79−15326
Sr-Ti, phase diag. *(Russian)* 78−80513
$Sr_2(Co_{1-x}Ti_x)_{17}$, powders, influence of substitutes on mag. props. 80−100601
TZM, D^+ impact, surface blistering, SEM study 78−71774
TZM, diffusion of Cs, AES, SIMS depth profile study *(German)* 78−84008
TZM, fatigue and threshold behaviour under high cycle fatigue 80−40487
(Ti,Al)Co, magnetovolume effects near crit. conc. for ferromag. 79−56591
$(Ti,Cr)B_2$, sintering kinetics and props. 80−100811
(Ti,V)C carbides, prep. and mech. props. 78−64518
α-β Ti alloy, fracture toughness rel. to microstruct. 77−16673

titanium alloys continued
α-β-Ti alloy, stress, H segregation, fracture 77−40450
α-Ti alloy, VT1-1, cold rolled, recrystn. texture and prop. anisotropy 78−52846
Ti alloy fatigue, stability of energy dissipative charact. 77−21209
Ti alloy VT30, H_2 effect on low temp. mech. props. *(Russian)* 78−35477
α-Ti alloys, anisotropy of phys. props. rel. to texture 79−91700
$\alpha+\beta$ Ti alloys, fracture, influence of phase comp. in VT16 and VT9, quenching effects *(Russian)* 78−56665
α-β-Ti alloys, stress anal. of strongly fluorescing specimen 80−1499
α,$\alpha+\beta$ Ti alloys, structural instability during prolonged periods of heating *(Russian)* 78−56664
Ti based alloy, type VT65, describing cyclic-creep processes with parametric eqn. 79−57074
Ti β III alloy, elastic and anelastic phenomena associated with α and ω phase isothermal precipitation *(French)* 79−52288
Ti powder metallurgy, developments 80−100801
α-Ti/Fe, retrograde solid solubility 80−79950
Ti-11, fatigue crack propag. under dwell time conditions 78−80639
Ti-11, unstable shear modes in fatigued β-annealed specimens 78−84984
Ti-50A and TiCode-12 80−104349
Ti-6Al-4V, oxidation kinetics, water vapour, comparison with pure Ti 77−21321
Ti-6Al-4V, stress distrib. for steady axisymmetric extrusion 80−3103
Ti-64, -811, 15333, fusion reactor structural alloys, dual-ion irrad, effects 79−45403
Ti-70A superalloy, fusion reactor blanket structures, radiation resistance 80−63379
Ti-(Al)-Zr-Si (5, 0.5 wt.%), creep 77−36595
Ti-A-V (6, 4 wt.%), castings, fatigue crack initiation 79−29186
Ti-Ag (10 to 17.5 wt.%), eutectoid system, $\beta \rightarrow \alpha_m$ transform., nucleation kinetics 80−97474
Ti-Ag(Au)(Si), existence of β to α_m phase transformation 78−44123
Ti-Ag(Au)(Si), thermodynamics and kinetics of β to α_m transformation 78−84795
Ti-Al, age-hardened, deform., order effects in Ti_3Al and temp. effects 77−25111
Ti-Al, Al effects on susceptibility to salt corrosion *(Russian)* 77−25185
Ti-Al, α_2 phase obs. using microscopy and X-ray diffr. 79−52497
Ti-Al, elec. spark Al doping of VT-18, surface struct. and props. *(Russian)* 80−76398
α-Ti-Al, H_2 diffusion *(Korean)* 78−30794
Ti-Al, H_2 diffusion at room temp. *(Japanese)* 80−19987
Ti-Al, hardening of Ti by addition of Al *(French)* 78−23715
Ti-Al, phase diagram in Ti rich region *(Russian)* 77−25013
α-Ti-Al, slip band spacing, correlation with β-Ti-Mn 79−99211
α-Ti-Al, stress/strain curves 77−63738
Ti-Al, structural and phase changes due to annealing *(Russian)* 80−55440
Ti-Al, surface segregation, AES exam. *(French)* 78−22941
Ti-Al, Ti-Al-Sn, specific heat and thermal expansion, 4-290K *(Russian)* 79−51276
Ti-Al, VT5-1, strength variation under influence of shock waves *(Russian)* 78−92299
Ti-Al (Sn), porous, effect of Al and Sn on sintering 80−20830
Ti-Al (14 at.%), with precipitate free zones, tensile props., grain size effects 77−16690
Ti-Al (14.4 at.%), void form. and solute segregation under Ni ion irradiation 79−42122
Ti-Al (14.7 wt.%), sintered, mech. props., effect of alloying and dispersed ZrO_2 phase 77−12636
Ti-Al (27.3 wt.%), arc melted, microstruct. 79−61577
Ti-Al (30 to 57 wt.%), phase equilibria from mag. susceptibility studies 79−60483
Ti-Al (4,6,9 wt.%), X-ray line profile anal. 77−47459
Ti-Al (4 to 5.5 wt.%), alloy VT5 with WC-Co coating appl. by detonation, antifriction props. 80−21188
Ti-Al (4 wt.%), sintered, long-time strength 80−40529
Ti-Al (40 wt.%), TiAl plate dissolution 79−66055
Ti-Al (6 wt.%), D profiles after D_3^+ implantation 80−37581
Ti-Al (6.1 wt.%), hot rolled sheet, ductile fracture nuclei, SEM obs. 78−64654
Ti-Al (6.6 wt.%), hydride habit planes, H_2 embrittlement, slip 77−36648
Ti-Al age-hardened alloys, fatigue crack propagation rel. to grain size in vac. and NaCl soln. 80−16538
Ti-Al alloys, Mossbauer effect, comp. depend. *(Russian)* 78−6611
Ti-Al film, evaporated, anodisation, anodic voltage-time dependence obs. *(Polish)* 80−55574
Ti-Al film, struct. and elec. props. 80−7002
Ti-Al system, quenched from β-region, struct. obs. *(Russian)* 77−21146
Ti-Al type VT5-1, describing cyclic-creep processes with parametric eqn. 79−57074
Ti-Al VT5, solid solutions, heat cond. at low temps. *(Russian)* 79−82574
Ti-Al_2O_3 system mixed films, prep., phase comp., struct. and elec. props. 79−37930
Ti-Al-C, ternary system, phase relationships 80−76230
Ti-Al-Cr-Fe-Si alloy AT6, and weldments, mech. and corrosion props. 77−90409
Ti-Al-Cr-Mo, type VTZ-1, machinability, using different abrasive materials *(Russian)* 80−97593
Ti-Al-Cr-Mo (6, 2.0, 2.5 wt.%), microstructural changes and mech. props. 77−25080
Ti-Al-Cr-Mo alloy VT3-1, reactions with some refractory compounds 80−16585
Ti-Al-Cr-Mo system, VTZ-1 alloy, microstruct. influence on fatigue charcts. 80−3195
Ti-Al-Cr-Mo-Fe(V)(Zr), effect of structure and heat treatment on tensile strength, ductility, fatigue limit and notch sensitivity 78−56711
Ti-Al-Cr-Mo-U, alloy VT22, phase composition and fatigue strength 78−3219
Ti-Al-Cr-Mo-V, alloy VT22M, exam. of ageing and phase transitions *(Russian)* 79−11641
Ti-Al-Cr-Mo-V, VT22 alloy, metastable β-phase decay under continuous heating, plastic strain effect *(Russian)* 80−71656
Ti-Al-Cr-Mo-V alloy VT-22, effect of heating rate on phase recrystallisation *(Russian)* 79−34077
Ti-Al-Cr-Mo-V(Fe), low cycle fatigue in repeated tension 80−76348
Ti-Al-Cr-Mo-Zr hard alloy VK15, shot blasting in strength improvement 77−81272

titanium alloys continued
Ti-Al-H, H effect on mech. props. and lattice constants 80−21036
Ti-Al-Kh18 steel, O_2 solubility thermodynamical anal. *(Russian)* 80−92676
Ti-Al-Mn, endurance with cyclic bending, effect of loading conditions 80−50724
Ti-Al-Mo, type BT22, phase transformations under step-by-step heat treatment *(Russian)* 80−108436
Ti-Al-Mo, type Ti-6242S, irrad. induced creep 80−39163
Ti-Al-Mo, type VT14, machinability, using different abrasive materials *(Russian)* 80−97593
Ti-Al-Mo (31, 13 wt.%), transform. microstruct. 78−48394
Ti-Al-Mo alloy VT-14, spherical pressure vessel, correlation between fracture stresses and mech. laboratory charact. 80−25838
Ti-Al-Mo alloy VT14, fracture anisotropy, with varying H_2 content, rel. to loading condition *(Russian)* 77−70148
Ti-Al-Mo-Cr, weldment containing orthorhombic martensite, autotempering behaviour and alpha precip. strengthening 80−84976
Ti-Al-Mo-Cr (4.5, 5, 1.5 wt.%), CORONA-5, effect of microstructure and heat treatment on fracture 78−60805
Ti-Al-Mo-Cr (4.5, 5, 1.5 wt.%), weld metal, α/β interace sliding 80−108512
Ti-Al-Mo-Cr (5.9, 2.5, 2.2 wt.%), heat capacity meas., 25-960°C *(Russian)* 77−66030
Ti-Al-Mo-Cr-Fe, distrib. of Sn, Zr between phases, temp effect. 80−55357
Ti-Al-Mo-Cr-Fe (6.4, 2.7, 1.6, 0.4 wt.%), quenched VT3-1, decomposition kinetics of α'' and β in annealing *(Russian)* 77−66662
$(\alpha+\beta)$-Ti-Al-Mo-Fe alloy VT-22, behaviour during creep testing, solid soln. dissoc. *(Russian)* 80−40346
Ti-Al-Mo-Sn alloy, elastically and plastically deformed, positron annihilation meas. of deformation 80−21038
Ti-Al-Mo-Sn-Si (2.25, 4, 11, 0.25 wt.%), type IMI 680, internal friction study of martensitic transformations 80−7573
Ti-Al-Mo-Sn-Si (2.25, 4, 11, 0.25 wt.%), type IMI 680, stability of martensitic phases 80−7574
Ti-Al-Mo-Sn-Si (4, 4, 4, 1/2 wt.%), type IMI 551, internal friction study of martensitic transformations 80−7573
Ti-Al-Mo-Sn-Si (4, 4, 4, 1/2 wt.%), type IMI 551, stability of martensitic phases 80−7574
Ti-Al-Mo-Sn-Si (4,4,2,0.5 wt.%), fracture toughness and crack propagation 78−39892
Ti-Al-Mo-V, crack resistance in chloride soln., electrochem. protection, polarization effect 80−55589
Ti-Al-Mo-V (8, 1, 1 wt. %), stress corrosion cracking and slow strain rate H_2 embrittlement 78−48569
Ti-Al-Mo-V (8, 1, 1 wt.%), environmental fatigue crack propag., texture influence 79−91802
Ti-Al-Mo-V (8, 1, 1 wt.%), Widmanstatten colonies, fracture toughness 80−85031
Ti-Al-Mo-V based alloy BT22 quenched from 850-1200°C, X-ray study of structure *(Ukrainian)* 80−24402
Ti-Al-Mo-Zr, compressor disk, surface plastic deform., optimal method 80−60924
Ti-Al-Mo-Zr, type VT-9, creep eqns. rel. to extension and compression props. 80−100875
Ti-Al-Mo-Zr (Cr-Fe), effect of heating on thermal stability of phases, lattice constants and chem. comp. 78−56672
Ti-Al-Mo-Zr alloy, VT9, decomp. kinetics of metastable β-phase, X-ray and mech. props. obs. *(Russian)* 78−48368
Ti-Al-Mo-Zr alloy VT9, Cu-Cr(Ni) coated, plastic deform. and diffusion annealing effect on props. *(Russian)* 78−35425
Ti-Al-Mo-Zr SiC fibre reinforced composites, matrix selection *(Russian)* 80−35192
Ti-Al-Mo-Zr-Si (6.6, 3.3, 1.8, 0.3 wt.%)-SiC fibrous composite, component interaction kinetics *(Russian)* 80−55364
Ti-Al-Mo-(Cr), etching as a function of struct. *(Russian)* 78−15568
Ti-Al-Mo(Cr)(Fe), thermomechanical treatment effect on mech. props., strengthening mechanisms 80−55441
Ti-Al-Nb-Ta-Mo (6, 2, 1, 0.8 wt.%), elevated temp. flow strength, creep resist., diffusion welding charact. 80−30033
Ti-Al-O, V effect on thermal stability and mech. props. 77−21171
Ti-Al-Sn, alloy 6242, dynamic effects of flow and fracture during isothermal forging 80−76343
α-Ti-Al-Sn, alloy Ti-679, electron diffr. anal. of Ti_3Si phase *(Chinese)* 80−64845
Ti-Al-Sn, type Ti-5621S, irrad. induced creep 80−39163
Ti-Al-Sn, VT5-1, solid solutions, heat cond. at low temps. *(Russian)* 79−82574
Ti-Al-Sn (3.7, 0.8 at.%) alloy, specific heat, 4 to 290K *(Russian)* 79−14938
Ti-Al-Sn (5, 2.5 wt.%), annealing of near-basal hydrides 80−20989
Ti-Al-Sn (5, 2.5 wt.%), ductile fracture at low temps. 78−64659
Ti-Al-Sn (5, 2.5 wt.%), electron microscope and X-ray diffr. exam., of basal and near basal hydrides 78−80550
Ti-Al-Sn (5, 2.5 wt.%), fracture mechanism at cryogenic temps. 78−64642
Ti-Al-Sn (5, 2.5 wt.%) alloy, fatigue under combined alternating bending and torsional stresses 77−8923
Ti-Al-Sn (5, 2.5%) cryogenic constructing material, far IR spectral refl. 77−24855
Ti-Al-Sn-Cu-Zn, (5, 2.5, 3, 1.5 wt.%), embrittlement after high temperature long-time exposure *(Chinese)* 78−95792
Ti-Al-Sn-Zr, Ti-680, O contamination under high temp. *(Chinese)* 80−66688
Ti-Al-Sn-Zr (6.19, 1.92, 1.43 wt.%), fatigue cracking characteristics of β annealed microstruct. 79−5051
Ti-Al-Sn-Zr (6.19, 1.92, 1.43 wt.%), fatigue fracture facet investigation by selected area electron channelling 80−89344
α-βTi-Al-Sn-Zr-Mo (6, 2, 4, 6 wt.%), interface struct. 77−44212
α-βTi-Al-Sn-Zr-Mo (6, 2, 4, 6 wt.%), deformation associated with surface cracks and α particles 79−79107
Ti-Al-Sn-Zr-Mo (6,2,4,6 wt.%), α-β type 6246, fusion zone fracture behaviour in weldments 80−30093
Ti-Al-Sn-Zr-Mo (6,2,4,6 wt.%) fusion weldment, substruct. charact. 80−84183
Ti-Al-Sn-Zr-Mo (6,2,45 wt.%), surface cracking under unidirectional loading 78−56753
Ti-Al-Sn-Zr-Mo alloy, Ti-6242, $\alpha+\beta$, creep property improvement by Pt ion plating 80−16408

titanium alloys continued
$\alpha+\beta$-Ti-Al-Sn-Zr-Mo-Cr, low cycle fatigue crack nucleation and early growth 79−8354
Ti-Al-Sn-Zr-Mo-Si (6, 2, 4, 2, 0.1 wt.%), effect of elevated temperature and environment on fatigue crack growth 80−40486
Ti-Al-Sn-Zr-Mo-Si-O-H, Si, O, H effects on fatigue, fracture and creep charact. 79−11697
Ti-Al-Sn(V), corrosion resist. in marine environments *(French)* 80−50767
Ti-Al-Sn(V)(V-Cr)(Mo-V), corrosion, electrochemical behaviour under tensile stress in boiling H_2SO_4 and acidic chloride solns. 78−95851
α-Ti-Al-Sn(5, 2.5 wt.%), effect of Pt ion plating on creep behaviour 79−66123
Ti-Al-U (6,4 wt.%), low and high cycle fatigue rupture at same load 78−3217
Ti-Al-V, (6,4 wt %), fracture mode, tearing topography surface fracture 80−7670
Ti-Al-V, (6,4 wt.%), history dependent steady state creep rate 78−39866
Ti-Al-V, (6,4 wt.%), single and dual ion irrad., microstruct. studies 80−29077
Ti-Al-V, (6.7, 4.3 wt.%), fatigue crack growth and fracture resistance enhancement, due to annealing 78−35510
Ti-Al-V, alloy 685, fatigue life, creep and dynamic strain ageing effect, 25 to 400°C *(French)* 80−45384
β-Ti-Al-V, annealed, differing interstitial O content, fatigue crack propag. resist. 79−11696
Ti-Al-V, containing 0-6000 ppm ^3He, sensitivity of tensile props. 80−39197
Ti-Al-V, erosion resistant boride coating 79−20290
Ti-Al-V, friction coeff. reduction on injection with TiC particles 80−85086
Ti-Al-V, fusion reactor blanket structures, radiation resistance 80−63379
Ti-Al-V, irrad. induced creep 80−39163
Ti-Al-V, long-term corrosion stability rel. to use in joint endoprostheses 78−36059
Ti-Al-V, oxidation by water vapour *(French)* 78−76787
Ti-Al-V, plane strain toughness and resistance to crack propagation *(French)* 78−23813
Ti-Al-V, rolled, elastic stiffness and Bauschinger effect accompanying anisotropic hardening *(Russian)* 80−40435
Ti-Al-V, VT6 alloy, butt welded joints, electron beam welding conditions effecting interstitial impurities distribution 80−39136
Ti-Al-V (Mo-Sn)(Zr), environmental effects in alloy fretting, effect on fatigue props. 78−56787
Ti-Al-V (4.7, 2 wt.%) pseudo alpha alloy, laminar struct. singularities, β to α transformation *(Russian)* 80−7552
Ti-Al-V (6, 4, wt.%), delayed retardation phenomena of fatigue crack growth, exam. 78−56745
Ti-Al-V (6, 4, wt.%), texture influence on fracture toughness and deformation 79−91801
Ti-Al-V (6, 4 wt.%), annealed and rolled plate, elevated temp. plastic anisotropy 79−61663
Ti-Al-V (6, 4 wt.%), α-β anneal, recrystn. anneal, β-anneal, room temp. creep 79−61662
Ti-Al-V (6, 4 wt.%), cavitation induced erosion, under mill annealed, soln. treated and aged, and beta annealed conditions 79−8371
Ti-Al-V (6, 4 wt.%), compliance calibration results 78−19798
Ti-Al-V (6, 4 wt.%), deform. charact. under isothermal forging conditions 77−36600
Ti-Al-V (6, 4 wt.%), dynamic crit. stress intensity vs. crack vel. 80−2115
Ti-Al-V (6, 4 wt.%), environmental fatigue crack propag., texture influence 79−91802
Ti-Al-V (6, 4 wt.%), fatigue crack growth data 77−73332
Ti-Al-V (6, 4 wt.%), fatigue crack propag. under dwell time conditions 78−80639
Ti-Al-V (6, 4 wt.%), fretting corrosion of orthopaedic implant materials by bone cement 80−104813
Ti-Al-V (6, 4 wt.%), friction charact. improvement by O_2 dissolution and controlled surface hardening *(French)* 80−45401
Ti-Al-V (6, 4 wt.%), gust spectrum fatigue crack propag. 80−21105
Ti-Al-V (6, 4 wt.%), high temp. cyclic oxidation, AE monitoring 79−83413
Ti-Al-V (6, 4 wt.%), hot isostatically pressed casting, fatigue crack initiation 79−79078
Ti-Al-V (6, 4 wt.%), improvement of props. by ion implantation 80−16601
Ti-Al-V (6, 4 wt.%), repassivation and pitting corrosion 80−30143
Ti-Al-V (6, 4 wt.%), ring test, evaluation for strain rate sensitive materials 78−39991
Ti-Al-V (6, 4 wt.%), solution treatment temp. effect on fracture morphology 79−61620
Ti-Al-V (6, 4 wt.%), stress corrosion cracking, composition, microstruct. and texture effects 79−11725
Ti-Al-V (6, 4 wt.%), superplastic, mech. behaviour and hardening charact. 79−83269
Ti-Al-V (6, 4 wt.%), targets, metallographic features after ballistic tests 79−79046
Ti-Al-V (6, 4 wt.%), temp. distrib. for steady axisymmetric extrusion 80−11670
Ti-Al-V (6, 4 wt.%), temp. distrib. for steady axisymmetric extrusion numerical results 80−11671
Ti-Al-V (6, 4 wt.%), texture effect on fatigue crack path 78−27633
Ti-Al-V (6, 4 wt.%), textured, anisotropy of fracture toughness over various specimen orientations 79−8353
Ti-Al-V (6, 4 wt.%), texture depend. stress corrosion cracking 80−104334
Ti-Al-V (6, 4 wt.%), type IMI 318, internal friction study of martensitic transformations 80−7573
Ti-Al-V (6, 4 wt.%), type IMI 318, stability of martensitic phases 80−7574
Ti-Al-V (6, 4 wt.%), void formation and growth, tensile fracture, exam. 78−80637
Ti-Al-V (6, 4 wt.%), Widmanstatten, microstructurally sensitive fatigue crack growth obs. 78−27627
Ti-Al-V (6, 4 wt.%) cylinders, residual stresses introduced by quenching elastoplastic anal. *(French)* 80−45355
Ti-Al-V (6, 4 wt.%) effect of high temp. oxidation on eddy current conductivity 78−76770
Ti-Al-V (6, 4 wt.%) slow crack growth in air and fracture toughness, H content effect *(French)* 80−45385

titanium alloys continued
Ti-Al-V (6,4 wt %), superplasticity, effect of temp. 80−7639
Ti-Al-V (6,4 wt%), cyclic temp. creep, transition effect 80−97539
Ti-Al-V (6,4 wt.%), age hardened, deform. charact. 77−36608
Ti-Al-V (6,4 wt.%), alloy plate, fatigue crack propag. under in-plane loading, expts. 79−52337
Ti-Al-V (6,4 wt.%), alloy plate, fatigue crack propag. under in-plane loading, anal. 79−52338
Ti-Al-V (6,4 wt.%), α/β interface phase, formation characteristics 79−52272
Ti-Al-V (6,4 wt.%), α/β interface phase influence on tensile props. 80−30034
Ti-Al-V (6,4 wt.%), β-annealed, subsurface fatigue crack initiation 80−108553
Ti-Al-V (6,4 wt.%), corrosion fatigue behaviour, surgical implant material 79−39027
Ti-Al-V (6,4 wt.%), cyclic stress-strain response 77−21170
Ti-Al-V (6,4 wt.%), D profiles after D_3^+ implantation 80−37581
Ti-Al-V (6,4 wt.%), D trapping in fusion reactor materials, temp. dependence 80−37577
Ti-Al-V (6,4 wt.%), effect of air exposure on fracture charact. 80−100890
Ti-Al-V (6,4 wt.%), fatigue crack growth, influence of dwell-time 79−43380
Ti-Al-V (6,4 wt.%), fretting fatigue resistant coating, for steel/Ti-Al-V mating surfaces 78−64721
Ti-Al-V (6,4 wt.%), fretting fatigue behaviour of temps. up to 600°C 80−21104
Ti-Al-V (6,4 wt.%), H related fatigue fracture 80−76344
Ti-Al-V (6,4 wt.%), heat treated and rolled, texture instability 77−63689
Ti-Al-V (6,4 wt.%), heavy ion irrad. effect on microstructure 79−10884
Ti-Al-V (6,4 wt.%), high temp. fretting fatigue, fatigue and fretting wear 80−3197
Ti-Al-V (6,4 wt.%), improved toughness from prior β-grains 78−15522
Ti-Al-V (6,4 wt.%), ion irradiated, microstruct. study using TEM 80−96572
Ti-Al-V (6,4 wt.%), laser surface melted, topographical charact. 79−70200
Ti-Al-V (6,4 wt.%), metallogaphically prepared, fracture surface, phase anal. by energy dispersive X-ray microanal. *(German, English)* 77−48606
Ti-Al-V (6,4 wt.%), microstruct. improvement by cyclic heating *(Japanese)* 79−100185
Ti-Al-V (6,4 wt.%), microstruct. effect of base metals on diffusion welding *(Japanese)* 80−89296
Ti-Al-V (6,4 wt.%), phase transformation after hydrogenation 80−7560
Ti-Al-V (6,4 wt.%), plastic flow instability and multiple necking during superplastic flow 77−8896
Ti-Al-V (6,4 wt.%), porous compacts, determ. of effective stress in hot pressing 80−100807
Ti-Al-V (6,4 wt.%), quenched, struct. and age hardening rel. to treatment temp. 80−11657
Ti-Al-V (6,4 wt.%), strongly textured, influence of cryst. orientation on fracture toughness 78−84951
Ti-Al-V (6,4 wt.%), strongly textured, influence of crystallographic orientation on tensile behaviour 80−7633
Ti-Al-V (6,4 wt.%), superplasticity microstructural influences 79−52323
Ti-Al-V (6,4 wt.%), surface cracking under unidirectional loading 78−56753
Ti-Al-V (6,4 wt.%), surface and grain boundary free energy, zero-creep determ. 79−4313
Ti-Al-V (6,4 wt.%), surface residual stresses, surface topography, fatigue behaviour 79−52366
Ti-Al-V (6,4 wt.%), surgical implant ion beam textured, stress/strain relations, fatigue charact. 78−73297
Ti-Al-V (6,4 wt.%), sustained loading charact. and H_2 effects 78−48515
Ti-Al-V (6,4 wt.%), to H effect on fracture props. and microstruct. 80−40512
Ti-Al-V (6,4 wt.%) alloy, fatigue crack closure eval. with electric potential method 79−50678
Ti-Al-V (6,4 wt.%) alloy foil, substrate temp. effect on struct. 80−7497
Ti-Al-V (6,4 wt.%) for TiC reactively sputtered coatings, adherence, XPES and wear study 80−25565
Ti-Al-V (6,4 wt.%) superplastic deform. 78−31471
Ti-Al-V (6,4 wt.%) superplastic alloy, maximum attainable ductility 80−60919
Ti-Al-V (6,4wt.%), galvanic couple with Al alloys, velocity effect on corrosion 78−35566
Ti-Al-V (6.4 wt.%), electron beam melting for scrap recycling 77−66604
Ti-Al-V (6.4 wt.%) cast alloy, with improved microstruct., mech. props. *(Japanese)* 80−71701
Ti-Al-V alloy, thermophysical meas. above 1450K, using subsecond transient technique 78−95161
Ti-Al-V alloys, 17.5 MeV Cu ion irradiation, resistance to void damage 79−55795
Ti-Al-V-Be-B, melt-extracted polycryst., mech. props. 80−76360
Ti-Al-V-Cr-Mo-Zr (3,8,6,4,4 wt.%), beta-C, microstruct. effect on mech. props. 78−27577
Ti-Al-V-Cr-Zr-Mo (3, 8, 6, 4, wt.%), phase transforms. 79−100113
Ti-Al-V-Cr-Zr-Mo-Fe (3.4, 8.3, 5.8, 3.9, 4.2, 0.06 wt.%), shock loaded, residual strength 77−36589
Ti-Al-V-Fe-Cu, melt-extracted polycryst., mech. props. 80−76360
Ti-Al-V-Fe-Si, alloy VT6, phase transform. kinetics and Young's modulus *(Russian)* 77−81258
Ti-Al-V-Sn (5.5, 5.3, 2.3 wt.%) fatigue crack growth and fracture resistance enhancement, due to annealing 78−35510
Ti-Al-V-Sn (5.5, 5.5, 2 wt%), crack growth, slow, H-induced 80−104272
Ti-Al-V-Sn (6, 6, 2 wt.%) weldments, heat treated, transangular fracture 80−40524
Ti-Al-V-Sn (6, 6, 2 wt.%), fatigue crack growth, cyclic freq. and microstruct. influence 80−55515
Ti-Al-V-Sn (6,6,2 wt.%), H_2 induced crack growth, in-situ scanning Auger anal. 79−8355
Ti-Al-V-Sn (6,6,2 wt.%), α-β type 662, fusion zone fracture behaviour in weldments 80−30093
Ti-Al-V-Sn (6,6,2 wt.%), depend. of K_{ISCC} on loading rate and crack orientation 80−45427
Ti-Al-V-Sn (6,6,2 wt.%) solid metal embrittlement by Cd, Ag and Au 80−16551
Ti-Al-V-Sn (6,6,2 wt.%) fusion weldment, substruct. charact. 80−84183

titanium alloys continued
Ti-Al-V-Sn-Zr (5.9, 2.0, 2.0, 2.0 wt.%), heat capacity meas., 25-960°C *(Russian)* 77−66030
Ti-Al-V-Sn-Zr alloy TS5, annealing effect on ductility and strength *(Russian)* 78−35427
Ti-Al-V-Sn(Mo-Fe), heavy section extrusion, fabrication and mech. props. 78−6985
Ti-Al-V-(Mo), Widmanstatten, quantitative anal. of microstruct. effect on fatigue crack growth 79−790/1
Ti-Al-V-(Sn), SCC, subcritical flow growth, comparison of aircraft alloys in NaCl soln. 78−53028
Ti-Al-V-(Sn), surface finishing effect on internal stresses, X-ray study *(German)* 79−34210
Ti-Al-V(Sn) alloys, plastic deformation and fracture charact. at low temps. *(Russian)* 80−7624
Ti-Al-V(6,4 wt.%), electrical potential method, unusual potential drop 77−16761
Ti-Al-V(6,4 wt.%), environmental fatigue crack propag. 77−36632
Ti-Al-V(6,4 wt.%), partially ordered, i.r. absorptance, 0-600°C 77−4632
Ti-Al-Zr, TA6Zr5D, oxidation at high temp. *(French)* 78−23860
Ti-Al-Zr (3,3 wt.%), W alloying addition effects on mech. props. *(Russian)* 77−59860
Ti-Al-Zr (6,5 wt.%), alloy IMI 685, SEM exam. of crack growth 78−72849
α-Ti-Al-Zr (6.16, 5.23 wt.%), alloy IMI 685, electron microscope observations of strain induced hydrides 78−72828
Ti-Al-Zr alloy, TA6Zr5D, structural evolution during continuous cooling at different rates *(French)* 80−45300
Ti-Al-Zr system, room temp. elec. resist. and thermal EMF *(Russian)* 77−20290
Ti-Al-Zr-Mo alloy 685, phase at α/β interface *(French)* 80−25661
Ti-Al-Zr-Mo-Si (5.97, 4.73, 0.49, 0.34 wt.%), fatigue fracture facet investigation by selected area electron channelling 80−89344
Ti-Al-Zr-Mo-Si (6, 5, 0.5, 0.25 wt.%), β-processed, fatigue props., hold time effect 80−60961
Ti-Al-Zr-Mo-Si (6,5,0.5,0.25 wt.%) fracture toughness and crack propag. 78−39892
Ti-Al-(Mo), phase relations 80−108398
Ti-Al-(V) (6,4 wt.%), hot salt stress corrosion susceptibility, microstruct. effects 77−36688
αTi-Al-(Zr), embrittlement due to ageing 78−56673
Ti-Al(Cr), interaction with N_2 at elevated temp., nitridation behaviour 77−12742
Ti-Al(Fe) microprobe anal. of alloying addition distrib. 80−55358
Ti-Al(Mo), swaged and recrystallized, grain growth 80−3092
Ti-Al(Sn) alloys, thermal and athermal solid solution strengthening 77−4787
Ti-Al(−V)(Mo), impact strength anisotropy, influence of texture *(Russian)* 80−20952
Ti-alloys, methods of studying effect of H on service behaviour 80−16478
Ti-Au, (9.9 wt.%), eutectoid system, $\beta \rightarrow \alpha_m$ transform., nucleation kinetics 80−97474
Ti-B, abrasive props. 80−16489
Ti-B, binary inclusions, interaction with diamond in polycryst. diamond sintering *(Chinese)* 78−80484
Ti-B-Mo system, phase equilibria at 1400°C 78−35354
Ti-B-W(Mo), annealed at 1400°C, exam. of phase diagram, using X-ray phase and metallographic analysis 79−1847
Ti-Be, coupled phase diagrams and thermochemical descriptions 80−25656
Ti-Be, metallic glass form. and props. 80−16219
Ti-Be-Si glass ribbons, physical and mech. props. 78−95767
Ti-Be-Zr, coupled phase diagrams and thermochemical descriptions 80−25656
Ti-Be-Zr base, glassy, temp. depend. of resist., rel. to resist. thermometer appl. 77−82532
Ti-Be-(Zr), struct. and form. of metastable phase m-TiBe 78−48375
Ti-Bi(Co)(Cr)(Cu)(Fe)(Mn)(Ni)(Pb)(Pd)(Pt), eutectoid decomposition 79−24491
Ti-C, coupled phase diagrams and thermochemical data 79−66036
Ti-$C_x(N_x)(O_x)$, solid soln. film prep. by reactive sputtering, solubility and effect on props. 79−28231
Ti-Co, radiation disorder model of phase stability 80−16297
Ti-Co, X-ray emission spectra investigation of electron struct. of Laves phases *(Russian)* 78−23554
Ti-Co alloys, absorpt. of H_2, press.-composition-temp. relationships, enthalpy, entropy 80−2267
Ti-Co alloys, absorpt. of H_2, thermodynamic parameters calc. 80−2268
Ti-Cr, diffuse electron scatt. *(Russian)* 80−103438
Ti-Cr, H_2 diffusion at room temp. *(Japanese)* 80−19987
Ti-Cr, phase transformation, appl. of Philips STEM400 system 80−25689
Ti-Cr, sintered, friction and wear, structural factors 78−60843
Ti-Cr (15 at.%), aged omega phase, electron microscope exam. 78−72783
Ti-Cr disordered alloy, gap nature of electron spectrum in region of struct. instability *(Russian)* 78−18947
Ti-Cr-B system, self-propagating high temp. synthesis, crystallochemical and mech. props. 80−20861
Ti-Cr-Zr, martensite formation, chemical composition effect 80−50634
Ti-Cr(Mo), alpha precipitation kinetics 78−68697
Ti-Cu, evaporated adhesion after electroplating 79−82475
Ti-Cu, struct. damage and internal fatigue cracks *(French)* 77−73341
Ti-Cu (Ni), oxidation, high temp., comparative study with Ti *(French)* 79−20285
Ti-Cu (2.5 wt.%), corrosion resist. in marine environments *(French)* 80−50767
Ti-Cu alloys, in acidic media, electrochemical behaviour *(French)* 78−23863
Ti-Cu alloys, mag. susceptibility meas., paramagnetic susceptibility meas. Curie temp. and mag. moments calc. *(Russian)* 78−34956
Ti-Cu dissolution mechanisms, photoelectron spectra study *(French)* 80−45198
Ti-Cu interdiffusion 77−89596
Ti-Cu metallisation systems, in 85°C 78% RH SO_2 contaminated environment, performance 79−74304
Ti-Cu solid solution, determ. of Cu solubility, stability by thermoelec. power meas. 79−77753
Ti-Cu system, appl. of metal-hydrogen equilibration determ. thermodynamic props. 79−77772

titanium alloys continued
Ti-Cu thin films, oxidation kinetics in air at 100 to 300°C, meas. 80−40590
Ti-Cu-Al(Zr)(Sn)(Nb)(Mo), heat treatable alloys, effect of alloying on strength, tensile props. 78−56671
Ti-Cu-Ni-Au metallisation systems, in 85°C 78% RH SO_2 contaminated environment, performance 79−74304
Ti-Cu-Si system, transforms. in Ti-Ti_5Si_3-TiCu region, 800-1600°C *(Russian)* 77−21099
Ti-Cu(Al,Si,Zr,Ni,Mo,W) powder based composite, high temp. strength of W reinforcing fibres 79−70021
Ti-Er(Y), effects of Er and Y additives on deformation behaviour 80−81121
β-Ti-Fe, (7.1 wt.%) exam. of ω phase formation, by X-ray diffr. and Mossbauer spectroscopy 78−52800
Ti-Fe, corrosion, effect of microstruct. caused by casting, annealing, beating *(Russian)* 79−57140
Ti-Fe, diffusion of H_2 *(Korean)* 78−18838
Ti-Fe, diffusion of stored H, Mossbauer study 80−34838
Ti-Fe, dil., phase analysis by Mossbauer spectra 80−15922
Ti-Fe, equiatomic, heats of form., influence of short-range order *(Russian)* 80−81354
Ti-Fe, force constant change with pressure, relative Mossbauer fraction 80−34163
Ti-Fe, H storage material, Mossbauer surface studies, Fe clusters 80−97167
Ti-Fe, magnetic susceptibility depend. on phase composition *(Russian)* 80−54875
αTi-Fe, plastically deformed, α→ω transform. 78−3095
α-Ti-Fe, solubility, resistivity variation rel. to quenching temp. 79−99324
β- Ti-Fe (1 to 6 wt.%) alloys, H diffusion *(Korean)* 79−42312
Ti-Fe (1.4 wt.%), polymorphic transform. due to plastic deform., positron annihilation 80−79939
Ti-Fe alloys, elec. and thermal props. *(Russian)* 78−19020
Ti-Fe corrosion resistant coating on Cu, obtained by contact eutectic fusion 80−50772
Ti-Fe-Al(Mn), homogeneity and lattice parameters, Mn and Al effect on hydriding cmpd. FeTi 80−108400
Ti-Fe-C, type 50A, pitting resist. in low salinity geothermal brines 80−93681
Ti-Fe-C-N, ion irradiated, microstruct. study using TEM 80−96572
Ti-Fe-H(D) system, struct. phase diagram, thermodynamics and diffusion *(German)* 79−56963
Ti-Fe-Ni (67, 30, 3 wt.%), reversible shape alteration *(Russian)* 80−71647
Ti-Fe(Co), oxidation of intermetallic phases 79−100298
α-Ti-Fe(0.22 wt.%), ω phase form. during ageing 77−52355
Ti-H, diffusion in hydride phase, exam. 80−29204
Ti-H, H diffusion and phase consistution, V influence, proton spin-lattice relax. meas. 78−27484
Ti-H, lattice strains, book contrib. 79−82202
Ti-H (Ni-H)(Cu-H), catalytic props. 80−30274
Ti-H system, cluster calc. of electronic struct. of interstitial H 78−43326
Ti-Hastelloy-N, homogenization 79−61606
Ti-Hf, dil., ^{178}Hf Mossbauer transition, electric quadrupole interaction 80−39928
Ti-Hf-O system, ω(0) phase form. 79−11553
Ti-Ir, dil., elec. field gradient at ^{193}Ir, Mossbauer meas. 80−66090
Ti-Ir, Ti-rich, thermodynamic study at high temp. using Knudsen cell mass spectrometry 80−45539
Ti-Ir system, high temp. thermodynamic investig. of Ir-rich portion by Knudsen cell mass spectrometry 77−12595
Ti-M-V-Cr-Mo, RMI 38644, shock loaded, age hardening 79−29112
Ti-Mg-ZrC(HfC)(TiC)(TiB_2) sintered, friction and wear props. 79−70019
β-Ti-Mn, exam. of reloading yield points 78−72822
Ti-Mn, fine cryst. struct. by diffuse X-ray and electron scatt. *(Russian)* 79−99329
Ti-Mn, hydride form. *(Japanese)* 77−52629
Ti-Mn, superplastic, microduplex grain struct. stabilisation 78−44058
Ti-Mn (0.4 and 12 wt.%), bonding between α-β interfaces, subsequent deform. 78−14517
Ti-Mn (15 wt.%), Baushchinger effect, grain boundary contrib. 79−47759
α-βTi-Mn (4.3 wt.%), interface phase struct. 77−44212
α-β Ti-Mn (8 wt.%), calc. of stress-strain curves by finite element method, comparison with expt. curve 78−84924
α-β Ti-Mn (8 wt.%), calcs. of stress-strain curve, stress and strain distribs., discussion 80−7637
α-β Ti-Mn (8 wt.%), stress-strain curve and stress and strain distrib. calcs., reply to discussion 80−7638
α, α+β, β-Ti-Mn alloys, Bauschinger effect during cyclic straining 79−43310
Ti-Mn alloys, elec. and thermal props. *(Russian)* 78−19020
α-β Ti-Mn alloys, etching and electropolishing to reveal α and β-grain size 78−3254
Ti-Mn base beta alloys, H effect on stability solid soln., hardness *(Japanese)* 77−81261
β-Ti-Mn slip band spacing, correlation with α-Ti-Al 79−99211
β-Ti-Mo, alloy, struct. changes during deformation and ageing *(Russian)* 78−39791
Ti-Mo, boronizing, reaction kinetics 79−61797
Ti-Mo, diffuse electron scatt. *(Russian)* 80−103438
Ti-Mo, fine cryst. struct. by diffuse X-ray and electron scatt. *(Russian)* 79−99329
Ti-Mo, fracture behaviour and tensile props. at elev. temp. 78−60822
Ti-Mo, lattice parameter and Debye temp., comp. depend. *(Russian)* 78−47280
Ti-Mo, martensitic alloy, decomposition by nucleation and growth and spinodal mechanisms 79−61590
Ti-Mo, martensitic transform., water quenched from β-region 79−38826
Ti-Mo, metastable β-phase, stress induced products formed by cold rolling *(Japanese)* 78−84843
Ti-Mo, phase diagram investigation *(Japanese)* 77−63632
Ti-Mo, structure associated with BCC to omega transform. *(Russian)* 80−108432
β−Ti-Mo, thermal instability, hardness and tensile deform. *(Japanese)* 80−71703
Ti-Mo (V), metastable diffusionless equilibria, high press. conditions 80−71627
Ti-Mo (Zr) (Nb), sintered, manufacture and exam. of props. 79−95975

titanium alloys continued
Ti-Mo (15 wt.%) alloy, metastable β-phase, deform. characts. 78−6975
Ti-Mo (16 at.%), effect of H impurities on lattice spacing, hardness, and plastic strain *(Russian)* 79−11664
Ti-Mo (20 at.%), incommensurate struct., stacking soliton 80−107109
Ti-Mo (3 to 35 wt.%), high pressure influence on transition temp. to supercond. 80−107952
Ti-Mo (5 at.%) based alloy, supercond. transition temp. enhancement by varying struct. state 77−20483
Ti-Mo alloy, thin anodic oxide, AES depth profile 80−71801
Ti-Mo alloys, elasticity moduli, 80-300°C *(Russian)* 78−80574
Ti-Mo alloys, structural stability under high-pressure soaking 80−104151
β-Ti-Mo alloys, thinning transformation 77−44438
Ti-Mo binary system, solid state phase transform. and miscibility gap, phase diagram 79−8298
Ti-Mo-Al, determ. of interaction parameters from EPMA data 77−63635
β-Ti-Mo-Cr-Al (8, 4.5, 2.5 wt.%), metastable, tensile ductility, α-phase morphology and distrib. effect 77−86098
Ti-Mo-Fe (3, 0.13 at.%), metastable phases, Mossbauer study 80−7243
Ti-Mo-Fe-Cr-Al, alloy VT3-1, influence of constitution on fracture toughness *(Russian)* 77−77559
Ti-Mo-V (8 wt.%, 8 wt.%), FCC phase, decay of β-solid soln., electron microdiffr. 79−15670
Ti-Mo-V-Al-Cr-Fe (4.8, 4.7, 5.2, 1.1, 1.0 wt.%), structural changes during heating up to 1000°C, DTA study *(Russian)* 80−93552
β-Ti-Mo-V-Fe-Al (8, 8, 2, 3, wt.%), exam. of stress induced H_2 migration 78−87823
Ti-Mo-V-Fe-Al (8,8,2,3, wt.%), exam. of stress controlled fatigue response 79−61734
β-Ti-Mo-V-Fe-Al (8,8,2,3 wt.%), metastable, high cycle fatigue crack initation, grain size effect 77−86145
β-Ti-Mo-V-Fe-Al (8,8,2,3 wt.%), metastable alloy, microstruct. and mech. props. ageing time and temp. effect 78−64569
β-Ti-Mo-V-Fe-Al(8,8,2,3 wt.%), metastable factors affecting stress corrosion cracking 77−28928
Ti-Mo-Zr-Al (15,5,3 wt.%), phase transform. kinetics study by X-ray diffr. 79−56960
Ti-Mo-Zr-Sn, alloy, βIII, struct. transform. in thermally affected zones after electron beam welding 78−23919
β-Ti-Mo-Zr-Sn (10.2, 5.8, 4.7 wt.%) heat treated, tensile yield, fracture behaviour, primary deform. mode, exam. 78−60724
Ti-Mo-Zr-Sn (11.5, 6, 45 wt.%), plastically strained regions, decoration 77−28864
Ti-Mo-Zr-Sn (11.5, 6, 4.5 wt.%), metastable beta III phase, recrystallization and grain growth 80−3091
Ti-Mo-Zr-Sn (11.5, 6.0, 4.5 wt.%), mech. property, microstruct. relationships 80−84961
Ti-Mo-Zr-Sn (11.5, 6.0, 4.5 wt.%) alloy, struct. as affected by processing history 80−84972
Ti-Mo-Zr-Sn-Fe-C-Si alloy, β-III, cold deform. and annealing, effect on struct. and mech. props. *(Russian)* 79−24533
β-Ti-Mo-Zr-Sn(11.5, 6, 4.5 wt.%), metastable phase III, microstruct. and age hardening response 80−84945
Ti-Mo-Zr(-Al) (15, 5 (3) wt.%), quenched and aged metastable β-phase, crystallography, morphology and decomposition 80−76262
Ti-Mo(Nb)(Ta), BCC struct., tetragonal phase form. by cold deform. *(Russian)* 78−88462
Ti-N system, phase relations, struct. rel. to heat treatment 79−11552
Ti-Nb, cold strained, exam. of ω and α phases, precipitated during ageing *(Russian)* 79−11620
Ti-Nb, diffuse electron scatt. *(Russian)* 80−103438
Ti-Nb, IR absorption peculiarities 79−65876
Ti-Nb, in Cu matrix, ductile failure at low temps. of superconducting composites 79−57119
Ti-Nb, phase transformation due to shock wave treatment *(Russian)* 79−91641
Ti-Nb, plastic deformation and thermal cond., 2.5 to 10K, dislocation pinning 77−35629
Ti-Nb (4.32 wt%), high temp. oxidation kinetics under 1 bar pressure, 1255-1471K 80−89410
Ti-Nb alloys, Fe, Mo, V, Ta alloying additions on microstruct. after combined treatment *(Russian)* 77−59826
Ti-Nb BCC alloys, diffusion coeffs. of Ti and Nb, 950 to 1511°C 79−73333
Ti-Nb superconducting alloys and cmpds. with A15 struct., H_2 effect on supercond. props 79−28438
Ti-Nb system, high-temp. oxidation *(Russian)* 79−74301
Ti-Nb-Al, decomposition during isothermal annealing 80−25653
Ti-Nb-Ge foils, β phase decomposition, electron microscopy struct. investigation *(Russian)* 79−83172
Ti-Nb-H, proton spin-lattice relax. time, conc. depend., diffusion effects 77−4576
Ti-Nb-H system, quadrupole interaction, ^{93}Nb NMR *(Russian)* 77−24761
Ti-Nb-Mo(V)(Ta)(Al)(Zr), BCC struct., tetragonal phase form. by cold deform. *(Russian)* 78−88462
Ti-Nb-Na (4 to 31, 8 to 38 at.%), with uniform distribution of refractory metal, prep. *(Russian)* 77−28747
Ti-Nb-Si, amorphous alloy, supercond. props. and crystn. behaviour, TEM and DTA study *(Japanese)* 80−84536
Ti-Nb-Ta-Ge (40,20,0.8 wt.%) foil, dispersion hardening, TEM and electron diffr. obs. *(Russian)* 79−1873
Ti-Nb-V-Zr, superconductor, struct. determ. by optical microscopy and electron diffraction *(Russian)* 77−16628
Ti-Nb-V(25 wt.%, 15 wt.%), precipitation of β and ω phases during ageing at 350°C 77−8838
Ti-Nb-W, 20 to 1000°C, isothermal section, X-ray anal., microstruct., hardness, cond., transform. *(Russian)* 77−55947
Ti-Nb-Zr (35, 3 wt.%), martensitic τ phase, X-ray diffr. obs. 80−16300
Ti-Nb-Zr-Fe, supercond. and paramag. props., effect of Fe additions *(Russian)* 80−65730
Ti-Nb-Zr-Fe-Mo-V, cold worked, struct. and phase transform. during ageing 78−3153
Ti-Nb-Zr-Ta, superconducting props. comp. depend., stress effects and precipitation behaviour, X-ray scatt. 80−93059
Ti-Nb(40 at.%), regions of maximum stability of β lattice 77−8838
Ti-Ni, effect of alloying on crit. points and martensitic transform. hysteresis 80−20935

titanium alloys continued
Ti-Ni, electron phase transition XPS, optical spectra and mag. susceptibility meas. 80−19943
Ti-Ni, energy band structures, X-ray spectra obs. *(Ukrainian)* 77−32469
Ti-Ni, eutectoid decomposition, effect of interphase boundary struct. on mech. 79−4952
Ti-Ni, first order displacive transformations, localized soft modes and US effects 79−73281
Ti-Ni, H_2 diffusion at room temp. *(Japanese)* 80−19987
Ti-Ni, hysteresis-free 'memory' effects 78−35385
Ti-Ni, internal friction and US props. *(Russian)* 80−84247
Ti-Ni, laser melting and splat quenching to form foils for TEM obs. 80−29986
Ti-Ni, martensite transform. B2-B19′, optical props. and electron struct. *(Russian)* 80−34878
Ti-Ni, martensitic transform., monoclinic to triclinic phase *(Russian)* 80−81058
Ti-Ni, multiplicity of structural transitions, phase diagrams, elec. cond. meas. 80−71649
Ti-Ni, passive surface, anodic process kinetics 79−15861
Ti-Ni, reversible shape changes during martensitic transform., dislocation struct. stability *(Russian)* 77−63666
Ti-Ni, thermoelastic phase transform., acoustic emission 80−3039
Ti-Ni, vacuum pressure seal with thermomechanical drive 80−31773
Ti-Ni (48 to 53 at.%), heat treatment and deviation from stoichiometry 80−104192
Ti-Ni (50.4 wt.%), thermal conversion efficiency of ideal thermoelastic marmem cycle 79−66057
Ti-Ni (51 at.%), martensitic transformation, thermoelastic, hysteresis, exothermic and endothermic effects *(Russian)* 78−19749
Ti-Ni (51 at.%), plastic deform., two reversible form change effects *(Russian)* 77−8881
Ti-Ni alloy, effect on $[Cu(NH_3)_4.(H_2O)]^{2+}$ solns. on drilling *(Russian)* 78−53017
Ti-Ni alloys, absorpt. of H_2, press.-composition-temp. relationships, enthalpy, entropy 80−2267
Ti-Ni alloys, absorpt. of H_2, thermodynamic parameters calc. 80−2268
Ti-Ni amorphous alloys, glass transition and ductility, O additions effect 80−75168
Ti-Ni-Al-(Ga), Th_6Mn_{23} type struct., mag. susceptibility *(Russian)* 79−42736
Ti-Ni-Co, constitution diagram, isothermal section, interdiffusion coeffs. *(Russian)* 80−89200
Ti-Ni-Co cubic B_2 alloys, phonon enhancement of electronic sp. ht. near martensitic transform. 79−60522
Ti-Ni-Co(Fe), shape memory temp., alloying effect 79−38912
Ti-Ni-Cu (44.5, 10 wt%), opposing stress effect on shape memory and martensitic reversion 78−44185
Ti-Ni-Cu system, phase relations at 800 and 870°C 78−27481
Ti-Ni-Fe, multiplicity of structural transitions, phase diagrams, elec. cond. meas. 80−71649
Ti-Ni-Fe, plasticity, tensile stress-strain diagrams, ultimate tensile strength, elec. resist. depend. on temp. *(Russian)* 79−61652
Ti-Ni-Mo, Ticode 12, pitting resist. in low salinity geothermal brines 80−93681
Ti-Ni-Mo (1.5, 2 wt.%), Mo effect on microstructure 77−36536
Ti-Ni-Si metallic glass, prep., thermal and mech. props. 78−64497
Ti-O, dil. HCP solid soln., O interstitial distrib. effect on lattice parameters 78−30588
Ti-O, stress corrosion crack propag. in aqueous and methanolic soln. 78−19919
Ti-O alloys+Li melt, ternary solid soln. formation *(Russian)* 78−11396
α-Ti-O solid soln., hexagonal, thermodynamics 78−3098
Ti-Pd, crevice corrosion in NaCl soln., 100 to 250°C *(Japanese)* 78−72927
Ti-Pd, dil., ion implanted, corrosion rate and electrochemical props. 79−43467
Ti-Pd (0.15 wt.%), IMI-260, strain rate effect on mech. behaviour 80−3153
Ti-Pd-Cu-Ni-Au metallisation systems, in 85°C 78% RH SO_2 contaminated environment, performance 79−74304
Ti-Pt, electrospark alloying for obtaining stable effective electrodes for electrochemical processing *(Russian)* 79−39157
Ti-Pt-Au, nonalloyed ohmic contacts to n-GaAs by pulse-electron beam annealed Se implants 80−2466
Ti-Ru, radiation disorder model of phase stability 80−16297
Ti-Ru (0.05 to 90 wt.%) hardness, thermal EMF, electrical conductivity, in annealed or quenched state *(Russian)* 77−55998
Ti-Si, binary inclusions, interaction with diamond in polycryst. diamond sintering *(Chinese)* 78−80484
Ti-Si amorphous alloy, melt-quenched, transform. studies and mech. props. 80−100838
Ti-Si cosputtered films, silicide form., X-ray diffr. and resist. study 80−54546
Ti-Si film thin film interaction, metallisation, X-ray diffr. and sheet resist. 80−54442
Ti-Ta (4.37 wt%), oxidation kinetics, 1258-1473K, and at pressure of 0.013, 0.133 and 1.0 bar 80−89411
Ti-Ta-Co system, phase stability, X-ray anal. 79−61580
Ti-Th, eutectic composition 80−100828
Ti-TiC composite, X-ray struct. anal. 77−28825
Ti-TiO_2-ZrO_2-Mo, sintered struct. and mech. props. 78−60618
Ti-$TiSi_2$, metal-silicide coating system. thermal stresses *(Russian)* 78−13891
Ti-transition metal, transition metal additives influence on struct., specific resistance, microhardness, mech. props. 79−29078
Ti-V, anomalous elec. resistivity, mag. susceptibility, soft-phonon induced structural inhomogeneities 78−60104
Ti-V, cyclic stress-strain response 78−60700
Ti-V, elastic moduli, comparison with paramagnetic Cr, V-Cr, rel. to bandstructure 80−7615
Ti-V, elastic moduli, electron conc., pulse echo overlap meas. 80−59550
Ti-V, IR absorption peculiarities 79−65876
Ti-V, metastable β-phase, stress induced products formed by cold rolling *(Japanese)* 78−84843
Ti-V, solubility of V in α-Ti, 400-700°C 78−83959
Ti-V (10 at.%), α→ω transformation, electron diffr. evidence of intermediate BCC phase 80−81051
Ti-V (15.5 wt.%), {332} deformation twins, optical microscopy study 79−79047

titanium alloys continued
Ti-V (19 at.%), aged ω-phase precipitation, incomplete proximity effect 78−60252
Ti-V (27 and 30 wt.%), fatigue crack propag., in single and poly. crystals 79−5048
β-Ti-V (40 at.%), BCC, flow stress asymmetry and cyclic stress-strain response 77−36583
Ti-V (40 at.%), BCC, single crystal, fatigue and slip 78−19854
Ti-V (40 at.%), microcracks intersecting fatigue crack, exam of origin 78−80638
Ti-V (40 wt.%), effects of H on anisotropic elastic props. 79−74192
β-Ti-V metastable alloys, fatigue crack propag. 80−60964
Ti-V-Cr, BCC, press. derivatives of elastic moduli, Fermi surface topological changes, band struct. 79−61639
Ti-V-Cr, electron-lifetime effects on props. 80−10951
Ti-V-Cr, type Ti-15-333, irrad. induced creep 80−39163
Ti-V-Cr-Al (13, 11, 3 wt.%) alloy spring wire, torsional fatigue props. 77−77649
Ti-V-Cr-Al (13, 11, 3 wt.%), stress corrosion cracking in methanolic solutions 80−50752
Ti-V-Cr-Mo, fracture resistance at low temps. 80−104284
Ti-V-Fe-Al (10, 2, 3 wt.%), fracture toughness and stress corrosion resistance 80−100904
Ti-V-H system, BCC, hydrogen effects on anisotropic elastic props. 79−24565
Ti-V-Mo alloy system, phase equilibria and interstitial effects, TEM and X-ray diffr. study 79−43204
Ti-V-Mo-Cr system, β-phase stability 80−55353
Ti-V-Ru system, metastable phases form. *(Russian)* 77−21098
Ti-V-Si, equlibrium silicide, X-ray and electron diffr. obs. 78−27483
Ti-V-Si, Si effects on precipitation and strengthening 77−55970
Ti-V-Si (30, 1 at%), quenched and aged, hardness, tensile behaviour and phase transform. 79−11646
βTi-V-Si (40, 1 at.%), Si effect of precipitation and age hardening 77−63676
α-Ti-V(Al)(Sn), Mossbauer spectra, metastable θ- and ω-phases 80−20556
Ti-V(Nb)(Ta), influence of different factors on supercond. transition width *(Russian)* 79−1636
Ti-W film, bias-sputtered, resist. and comp. 80−25023
Ti-W films, bias-sputtered, quantitative anal. 80−80114
Ti-W/Au metallisation on Al, temp. stability, barrier props. 79−23868
Ti-W(-Al), mech. props. and heat treatment 80−35274
α_m-Ti-X (X=Ag, Au, Si), precipitation mechanisms and Meyrick theory of cellular reaction initiation 79−74163
Ti-Y(Er), dispersoid effect on deform. 79−24530
Ti-Zr, binary continuous solid solution, elec. resist. and thermoelec. power behaviour 79−69492
Ti-Zr, equiatomic, allotropic transform., metal purity and N_2 effects *(French)* 77−59782
Ti-Zr, valence bands, X-ray M- and L-emission bands obs. *(Russian)* 78−19602
Ti-Zr-Cr-Mn/$LaNi_5$ hydriding alloy mixtures for H energy storage 80−45788
Ti-Zr-Hf disordered solid solns., thermal cond. 79−15132
Ti-Zr-Mo alloy, effect of O_2 on elec. resistivity, microhardness, mech. props. 77−56092
Ti-Zr-Mo-V, alloy VT20, exam. of plasticity in temp. range 20 to 1000°C 78−56712
Ti-Zr-Nb-Si, Nb and Si surface alloying effects on wear and corrosion resistance *(Russian)* 77−25191
α-Ti-Zr-W, effect of W impurity on mech. preps. 80−16392
Ti-Zr-W-(Al), phase struct. and props. *(Russian)* 80−16270
Ti-Zr(Hf), thermopower composition depend. 79−65445
TiAl, coatings, electrospark applied, friction and wear resistance obs. *(Russian)* 79−1916
TiAl, manufacture by extrusion of blended elemental powders 77−28750
TiAl, Mossbauer effect on impurity nuclei of ^{57}Fe *(Russian)* 77−1621
TiAl, Ti_3Al, ordered alloys, Fe impurity atoms distrib. *(Russian)* 77−35584
TiAl, Ti_3Al-(Nb) dynamic elastic moduli 77−86070
α-β TiAl-Sn-Zr-Mo (6,2,4,6 wt.%), age hardening 79−61604
$TiAl_3$ crystals dissolution in pure Al liq., grain refinement of α-Al solid-solution by Ti addition 80−35178
Ti_3Al, cyclic deform., dislocation struct. 78−7003
Ti_3Al, phase transitions and physical props. 77−25068
Ti_3Al-(Mo) (0.5 at.%), ordering, Mo effects 77−28841
Ti_3Al-(Nb), ordering transform. and mech. props. 78−31402
Ti_3Al-Sn-Zr, alloy, Sn and Zr alloying influence on creep and scaling resist. *(Russian)* 79−52302
$Ti(Al,B_{1-x})_2$ (B=Cr, Mn, Fe, Co), $0<x<0.4$, influence of Al on H sorption props. X-ray cryst. struct. determ. 79−28198
$Ti_{0.75}Al_{0.25}H_x$, $x<1.5$, metastable hydride form. 78−51682
Ti_3Al(Sn), oxidation *(Russian)* 78−19939
$TiAl_2V_4$, H impurity detection by $^1H(^{15}N,\alpha\gamma)$ reaction 80−55767
TiAu, dil., disordered, virtual bound states, reson. model pot. theory 79−23934
Ti_3Au, self-consistent LMTO band calcs. 79−37954
TiB_2, electrode, hot pressed, erosion resistance, struct. and porosity effects 78−3228
TiB_2 high temp. hardness of single crystals *(Japanese)* 77−48522
TiB_2, low temp. radiation damage, calorimetric investigation 77−27916
TiB_2-(Ni) (20 wt.%), initial stage sintering under high press., lattice strain 77−55905
TiB_2-$TiSi_2$ composites, high-temp. oxidation, scale comp. 78−15561
$TiBe_2$, de Haas-van Alphen effect, Fermi surface, theory 80−103614
$TiBe_2$, itinerant antiferromag., mag. susceptibility and elec. cond. meas. 79−19726
$TiBe_2$, neturon diffr. study of mag. ordering 80−44811
$TiBe_2$, weak itinerant magnetism as inhibited superconductivity 79−51715
$TiBe_{1.8}Cu_{0.2}$, ferromag., magnetisation density 80−103817
$TiBe_{2-x}Cu_x$, C-15 lower phase, itinerant ferromagnetism 80−15723
$TiBe_{2-x}Cu_x$, high press. study of Curie temp. and mag. susceptibility 80−84600
η-$Ti_3Be_3(O,N)_x$, formation and struct. 79−73151
$Ti_{50}Be_{40}Zr_{10}$, amorphous, thermopower meas., Nordheim-Gorter relations 79−99535
$Ti_{50}Be_{40}Zr_{10}$, amorphous, crystn. temp., press. and heating rate depend. 80−70132
$Ti_{50}Be_{40}Zr_{10}$ glass, mech. props., X-ray diffr. exam. 78−11292

titanium alloys continued
$Ti_{50}Be_{40}Zr_{10}$, Metglas 2204, stability, crystallisation, ductility meas. 78—47246
TiC base hard metals, N_2-containing surface wear resistant layers, struct. anal. *(German)* 78—92405
TiC, effect on grain refinement in Al 78—52828
TiC hard alloy prep., struct. during sintering 77—77448
TiC, X-ray diffraction study of struct. of ordered phase and phase transform. *(Ukrainian)* 79—37660
TiC-(Mo-Cr-Ni-Mn) steel alloy, optimum comp. and manufacture conditions, Mn effect 80—84896
TiC-alloy steel (30, 70 wt.%) composite, sintered, wear resist. 80—100815
TiC-Fe-Cr powder mixture, exam. of milling condition effects 80—16237
TiC-Kh6V3M steel alloy, reaction during sintering and heat treatment 78—60617
TiC-Ni, particle growth quantitative anal. by metallography and stereology 77—77684
TiC-Ni powder compact, wetting problems in sintering 80—11596
TiC-Ni-Co-Cr, sintered, mech. props. effect of processing factors 78—11159
TiC-Ni-Cr(Mo) hard alloy mixtures, pressing 77—63596
TiC-Ni-Mo hard alloy, wear resistance under end face friction cond. 78—60846
TiC-Ni-Mo hard alloys, use in hard layer prod. by electrospark alloying 77—59998
TiC-Ni-Mo(W), cemented carbides, grain growth, metallographic obs. 77—24982
TiC-steel alloys, structure formation during sintering 77—59732
TiC-steel cermet with Cu additions, precip. hardening and ht. treatment temp. 77—40414
TiC-TiB_2, friction characts., comp. depend., 20-1000°C 80—3203
TiC-TiB_2, preparation and high temp. antifriction props. 79—1918
TiC-TiB_2, wear in vacuum, role of boride phase 80—21113
TiC-TiB_2 alloys, composition effect on surface layer rupture at various temps. 80—25879
Ti_8C_5, X-ray order struct. determ. 80—103295
TiCo, and TiCoSi(Ge), electronic struct., X-ray K- and L-spectra obs. *(Russian)* 78—11022
TiCo-H system, thermodynamic rels. and struct. transformations 80—49385
$TiCo_{2+x}$ (x = −0.06, 0.0, 0.13), stacking faults in cubic Laves phase 80—19816
$Ti_{1-x}Co_x$, electronic struct. and anomalies of elec. and mag. props. 80—6710
$Ti_{70}Co_{20}B_{10}$, amorphous alloys, crystn. behaviour, TEM study *(Japanese)* 80—84087
$TiCo_{1-x}Mn_x$, H absorption-desorption characteristics 80—96735
$TiCr_{1.8}$, H and D soln., enthalpy, solubility and mol. vibr. determ., comparison with soln. in metals and binary alloys 80—79951
TiCu intermetallic compounds, decomposition reaction by H_2 absorption *(Japanese)* 78—23668
TiD_x, α- and β-phases, D-site occupancy, neutron diffr. study 79—42014
Ti(Fe,Co,Ni) cubic metal binary alloys for H energy storage 80—45787
Ti(Fe, Co), itinerant ferromagnet, magneto-volume expts. 77—66404
Ti(Fe,Co), magnetovolume effects near crit. conc. for ferromag. 79—56591
Ti(Fe, Co), off-stoichiometric alloy, inverse mag. susceptibility rel. to defect conc. 80—60216
$Ti(Fe,Co)H_y$, mag. and ^{57}Fe Mossbauer studies 80—71272
TiFe hydrides for bulk H_2 storage 80—61463
$TiFe_2$, mechanism of mixing and reactive diffusion 79—7706
$Ti_{1-x}Fe_x$ alloys, ($0<x\leq0.2$), nonmetallic resistivity and simultaneous superconductivity *(Russian)* 77—36005
$Ti(Fe\text{-}Co)_2$, itinerant electron ferromagnet, magnetovolume effects 80—60397
$Ti_{70}Fe_{20}B_{10}$, amorphous alloys, crystn. behaviour, TEM study *(Japanese)* 80—84087
$TiFe_{0.8}Be_{0.2}$ alloys for H_2 storage 80—97817
$Ti(Fe_{1-x}Co_x)$, density of states estimation from magnetisation and resistivity meas. 78—84119
$TiFe_{1-x}Co_x$, electronic struct. and mag. moment calcs. 80—65821
$Ti(Fe_{1-x}Co_x)$, ferro- to paramag. transition, press. depend. 77—73028
$TiFe_{1-x}Co_x$, mag. props., under high press. and in high mag. fields 78—95423
$TiFe_xCo_{1-x}$, thermal expansion and magnetoelastic effects 80—80585
TiFeD, cryst. struct., Mossbauer and neutron diffr. obs. 80—34839
$TiFeH_x$, metallurgical and electronic struct., Mossbauer effect meas. 77—16223
TiGa, $TiGa_2$, Ti_5Ga_3, X-ray K- and L-bands, electronic struct. *(Russian)* 79—1797
Ti_3Ga, lattice period and crystallographic struct., temp. depend. *(Russian)* 78—55835
TiGe, and TiCoGe, electronic struct., X-ray K- and L-spectra obs. *(Russian)* 78—11022
TiGe, $TiGe_2$, Ti_5Ge_3, X-ray K- and L-bands, electronic struct. *(Russian)* 79—1797
Ti_xGe_y, interrelationship of X-ray charact. with physical props. *(Russian)* 77—1765
$TiH_{1.8}$, tritiated, NMR of ^3He formed by β-decay, radiation damage, ageing 77—24751
TiH_x film electrode, oxidation, electrochem. and surface analytical characterisation 79—39034
TiMn, faceted parent martensite interface 80—6417
$TiMn_{1.5}$, hydrogen storage appl. *(Japanese)* 80—61443
$TiMn_2$, Curie-Weiss law depend. of susceptibility, mag. props. *(Russian)* 79—65655
Ti(N,C,O) coating for cemented carbides and high speed steels, by CVD 78—92406
TiN, hard coating on soft Al alloy, tribological anal. 80—108600
TiN-Ni mixed powder compact, phase relations and denitrification during sintering *(Japanese)* 79—43167
TiN-Ni powder compacts, sintering, gas atm. and vac., shrinkage, solid solubility *(Japanese)* 78—72750
TiN-VN alloys, synthesis in low-temp. plasma, phys.-chem. props. *(Russian)* 79—38761
$Ti_{55}Nb_{45}$, supercond., anomalous phonon thermal resist. 77—69451
$Ti_{1-x}Nb_xH_{1.94}$, electronic struct. MNR meas. 80—15439
$Ti_{1-x}Nb_xH_{1.94}$, x = 0.25, 0.50, low temp. specific heat meas. 80—2179
TiNi alloys, structural transform., physical props. and memory effects *(Russian)* 79—1856
titanium alloys continued
TiNi, imperfect elasticity, elastic after-effect on basis of martensitic transformation theory *(Russian)* 79—100198
TiNi, shape memory effect, spontaneous EMF generation 77—32637
TiNi, soft X-ray spectra, electronic struct. 77—44091
TiNi, strain recovery, memory effect, in martensite phase *(Russian)* 77—4806
TiNi-H system, thermodynamic rels. and struct. transformations 80—49385
TiNi-TiCu, exam. of shape memory effect, specific work 79—100216
$Ti_{0.60}Ni_{0.40}$ metallic glass, Young's modulus meas. by impulse induced resonance technique 80—40411
$Ti_{1-x}Ni_x$, electronic struct. and anomalies of elec. and mag. props. 80—6710
Ti_2Ni, determ. of H diffusion coeff., quasielastic neutron scatt. 78—30781
$Ti_{70}Ni_{20}B_{10}$, amorphous alloys, crystn. behaviour, TEM study *(Japanese)* 80—84087
$Ti_{50}Ni_{47}Fe_3$, premartensitic phases, neutron scatt., sp. ht. and electron microscopy obs. 79—96025
Ti_2NiH_2, H storage material, H diffusion, neutron diffr. obs. 80—51013
Ti_2NiO_x (x=0 to 0.5), hydrogen characts., thermogravimetry/DTA meas. 79—52760
TiO_x, interstitial alloy, electronic state, XPS, mag. susceptibility and elec. resist. 77—12486
$TiPd_3$, valence band struct., X-ray emission spectra *(Russian)* 77—40304
TiSi, and TiCoSi, electronic struct., X-ray K- and L-spectra obs. *(Russian)* 78—11022
$TiSi_2$, form. in Si-Pd-Ti evaporated films 80—80006
$TiSi_2$-Si interfaces, chemical state, AES expts. 78—91767
TiSnSb, synthesis and struct. *(French)* 79—90596
Ti(V,Ni)/Al bimetal film structure, macroscopic defects *(Russian)* 79—1555
Ti_xV_{1-x}-H_2 system, reaction and press.-composition isotherms meas. 80—108391
TiW-TiO_2-InP thin refractory MIS struct. deposition 80—75647
$Ti_{0.3}W_{0.7}$, thermal annealing study of metallisation on Si 80—80134
Ti(Zr,Hf)-Gd-B system, phase equilib. 80—11629
$Ti_{1-x}Zr_xCr_{2-y}Mn_y$, C14 type alloy, hydride form. *(Japanese)* 78—19944
$Ti_{1-x}Zr_xM1_{2-y-z}Cr_yV_z$, hydrogen storage appl. *(Japanese)* 80—61443
$Ti_{1-x}Zr_xMn_2$, hydride formation, hydriding characts. of reversible uptake 78—44402
$Ti_xZr_{1-x70}Nb_{30}$, ω phase precipitation 79—34042
Ti6A14V, superplastic deform. of circular sheets *(French)* 77—28871
U-Mo-Nb-Zr-Ti (0.75, 0.75, 0.75, 0.5 wt.%), heat treatment effect on microstruct. and mech. props. 78—23729
U-Ti (0.75 wt.%), quench rate sensitivity, effect on microstruct., mech. props., ageing 77—70077
U-Ti system, γ-solid solns., thermo-EMF, temp. depend. *(Russian)* 79—73496
U-Ti(Q^4)(Q^5), Q^4=quad, Q^5=quint, stress corrosion cracking in moist air, salt water, salted moist air 78—35562
U-Ti(0.75 wt.%), mech. props., effect of ageing 77—8914
(V,Ti)C+(Ni,Mo) cermet systems, effect or V/Ti ratio or Mo partitioning 79—79099
(V,Ti)C+Ni cermet, binder grain size 80—44401
V-Cr-Ti, fusion reactor first wall structural materials, prediction of life limiting props. 78—62605
V-Nb-Ti-N alloy, dispersion hardened, fracture characts. 79—15794
V-Nb-Ti-N alloy, with dispersed second phase, ductile-brittle transition 80—93653
V-Ti, and V-Ti-Be(Zr), 4 MeV Ni^{++} irrad., He gas bubble form. 80—29085
V-Ti, diffusion in H_2 *(Japanese)* 78—10221
V-Ti, exam. of intrinsic diffusion and vacancy flow effects 79—4430
V-Ti, vacuum deposited supercond. films, T_c chem. comp. depend. *(Russian)* 78—19174
V-Ti (20wt.%), corrosion in liquid Na, O_2 effects 77—8987
V-Ti (42 at.%), mixed state, US attenuation meas. at 4.14K 80—15657
V-Ti (42 at.%), ultrasonic vel. in mixed state 80—75689
V-Ti alloys, supercond., thermal cond. 77—89900
V-Ti amorphous films, supercond. transition temp. 79—60953
V-Ti superconducting film, electron spin effects 79—28488
V-Ti-C, elemental anal. by EELS 80—101069
V-Ti-C, elemental anal. of second phase carbides using electron loss spectroscopy 79—20500
V-Ti-C, high temp. carbide form., electron microscopy study 80—89228
V-Ti-O single crystal alloy, mech. props. 77—25112
V-Ti-(Sn), corrosion resistance and some physicomechanical props. 77—70229
V_3Si-Ti solid soln., supercond. T_c and paramag. susceptibility *(Russian)* 77—59348
V_3Ti, metastable supercond. phase, effects of rapid quenching on transition temp. 78—2611
$V_{3-x}Ti_xGa$, cryst. struct. and microhardness meas. 79—86740
$V_{75-x}Ti_xGa_{25}$, supercond. transition temp. and electron-phonon coupling parameter 79—60952
$V_{2.4}Ti_{0.6}Sn$, elec. resist., temp. depend., T_c to 300K 79—65426
W-Cu-Ti exam. of mech. props. as function of temp., composition, and oxidation props. 80—16472
W-Ti, Ti addition effect on heat resistance and radiative props. *(Russian)* 80—25515
W-Ti-C, cubic solid soln., form. and props. 78—48348
WC-Co-Ta-Ti-Nb, cemented carbide, deformation, high temp., stress relaxation, and strain rate depend. 78—39854
WC-Co-TaC-TiC-NbC cemented carbide, microstructure, high temp. deformation, uniaxial plastic compression 80—40451
WC-TiC, powder for plasma arc spray coating appl. 78—15591
WC-TiC-Co, powder compacts, effect of additional pressing at hydrostatic pressures on props. 78—56596
WC-TiC-Co, powder for plasma arc sprayed coating 78—15591
WC-TiC-Co alloys, microstresses in two- and three-phases, mag. investig. 77—63758
WC-TiC-TaC, powder for plasma arc spray coating appl. 78—15591
WC-TiC-TaC-Co cemented carbides, transverse-rupture strength at 600 to 1000°C obs. *(Japanese)* 79—43374
WC-TiC-Ta(Nb)C-Co, CVD and activated reactive evaporation of TiC, AES obs. of substrate-layer interactions 79—24679

titanium alloys continued
WC-TiC(TaC, NiC)-Co, hard, homogeneity and wear resistance estimation, by magnetic method 77−90558
Zn-Ti, environmental factors affecting pitting corrosion potential in NaOH solns. 80−45423
Zr-Cu-Ti (2.5, 0.15 wt.%), indentation irregularity at elastic limit after heat treatment *(French)* 79−79004
βZr-Mo-Ti, metastable, deform. induced transform. 78−52805
Zr-Ti, alloy, mag. susceptibility, elec. cond., Hall conc. thermoEMF conc. depend. *(Russian)* 80−39551
Zr-Ti martensites, furnace cooled and water quenched, strengh and deform. 79−20101
Zr-Ti-Be metallic glass, phase separation 80−97464

titanium compounds
see also titanium alloys
anatase fibres synthesis from K_2TiO_3 fibres, hydrothermal leaching *(Japanese)* 79−56949
bonding, struct., ligand field splitting, electron gas calcs. 78−17557
cabal glass:$SiO_2(TiO_2)$, microheterogeneity, and elec. cond. 78−83997
cordierite glass ceramics, effect of TiO_2 and ZrO_2 content on phase sequence during heat treatment 78−48381
bis-π-cyclopentadienyltitanium dichloride, struct. parameter refinement 78−87660
garnets, synthetic, IR spectra, Ti struct. role 80−7346
halides, XY_4 molecules, force consts. by modified Redington and Aljibury method 80−69261
hollandites, cryst. growth and structural props. 80−89129
hollandites, ionic cond., impedance, struct. 78−67856
homogeneity and struct. vacancies 77−84937
hydride, computer simulation of H reflection and scattering 79−1806
interstellar TiO^+, TiO, prod. by associative ionisation 77−29893
oxide films, anal. by AES *(French)* 80−44440
oxide reduction by electron cyclotron reson. plasma of H, model study on discharge cleaning 80−76548
oxides, hydrothermal crystallisation, review, book contrib. 79−69974
oxides, sputtered Ti atoms, photon emission, nonradiative transition effects 80−58208
oxides, XPS study, electron binding energies, spin orbit splittings, exchange splittings 79−78839
oxides on Ti film electrodes, AES, XPS and electrochem. charact. 78−7086
oxofluorotitanates, preparation and characterisation 79−99872
phosphate glasses: Ti^{3+}, $MO(M_2O)$-TiO_2-P_2O_5 M=K, Ca, Be, elec. resistivity *(Japanese)* 77−12719
phosphates, $MCrTi(PO_4)_3$, M=Mg, Mn, Co, Ni, Zn, Cd, Pb, Ca, Sr, Ba, cryst. struct. *(French)* 77−84708
phosphide precipitates, obs. in ferritic stainless and C steels *(Japanese)* 80−89221
photodecomposition over Pt/TiO_2 catalysts 80−81337
polymer-TiO_2 composite, dielec. props. *(Japanese)* 78−95540
pyrochlore, high temperature chlorination 78−11180
quartz ceramic, SiO_2-Cr_2O_3-TiO_2, creep and porosity, for ceramics with different structures 80−21011
rare earth oxide $(R_2O_3)TiO_2$ glassy systems, rapid quenching by laser beam, exam. of composition and crystallization 78−52856
refractory carbides, borides and nitrides, wetting by and interactions with liq. metals 80−54473
rutile: Ga, Mg, intersecting defect structures, TEM study 79−51123
rutile, model of charge injection, application to displacement of O^{2-} vacancies *(French)* 77−32079
rutile ceramic anomalous conductivity effect analysis 80−15512
rutile pigment-antioxidant interactions in polyethylene on photo-oxidation 77−63816
rutile type structures, rel. between β-gallia, ramsdellite psilomelane, hollandite and $Ga_4Ti_{x-4}O_{2x-2}$ type structs. 79−37664
β-spodumene solid solns., based glass-ceramics, dielec. const. calcs. 77−52008
tetrahalide-acetyl halide adducts, coordination, IR and Raman spectra 78−42050
tetrahalides, struct., force field and Coriolis const. calcs. 78−86843
tetrahalides of Gp.IV elements, M-X bond flexibility, by compliance scheme 80−37805
tienshanite, cryst. struct. determ. 78−83800
TiO_2, high temperature interactions with Re 80−16665
tiO_2 antireflection coatings by a low temperature spray process 78−90537
TiO, local density of states, X-ray spectra, Hartree-Fock and Xα calcs. discrepancies 79−77980
TiO, single cryst., short range ordering of vacancies, X-ray anal. 79−73163
TiO blanketing effect in stellar atmospheres *(Russian)* 79−30065
$TiSe_2$, anomalous behaviour and excitonic insulator mechanism 77−39782
titanates, isostruct. with $[CaCu_3](Mn_4)O_{12}$, synthesis and characterisation *(French)* 79−90615
titanates, Ti charge state, binding energy *(Ukrainian)* 77−68940
titanites, decomposition of N_2O, energy reson. in catalysis 78−95947
titanomagnetite, monodomain behaviour in multiphase oxidised material 77−60366
titanomagnetites, temp. depend. cation distrib., mag. prop. obs. 80−85647
titanosilicates, Ti charge state, binding energy *(Ukrainian)* 77−68940
vibr. anal., force fields and consts. *(German)* 79−45702
XPS, p-shell, multiplet struct. 78−76580
Zircon ceramic, exam. of development and fabrication 80−11608
zirconate-titanate ceramics, K_{IC} eval. by double torsion technique 77−90444
Ag_xTiS_2, intercalation cpd., Raman scatt. and electron diffr. meas. 79−24321
Al-SiO_2-TiO_2 interference mirror coatings, high mech. strength 78−30043
Al-$TiSi_2$-n-Si struct., elec. props., charge transfer mechanism across $TiSi_2$-Si interface *(Russian)* 80−34515
AlN, thermoplastic slips, viscosity, thixotropy, dilatance determs. 80−25633
Al_2O_3:Ti_2O_3, dopant influence on struct. and mech. props. 80−24471
Al_2O_3-SiO_2-Fe_2O_3-CaO-MgO-TiO_2, refractory, corrosion and mech. behaviour correlations 80−40563
Al_2O_3-SiO_2-TiO_2-B_2O_3-Fe_2O_3, exam. of porous structure, using a combinational method 79−29303

titanium compounds continued
Al_2O_3-SiO_2-TiO_2-RO system glass-crystal material, elec. cond. 79−60876
Al_2O_3-TiC, composite, fracture behaviour in three-point bending 80−60951
Al_2O_3-TiC, multiphase ceramics, mech. strengthening due to dispersion of non-metallic particles *(German)* 78−60674
Al_2O_3-TiO_2 (1 wt.%), with and without α-Al_2O_3 laminar crystals, bend tests 77−16531
Al_2O_3-TiO_2 (1 wt.%), with and without α-Al_2O_3 laminar crystals, heat resistance 77−16532
Al_2O_3-TiO_2 coating, prep. by plasma arc spraying and characterisation 79−23873
Al_2O_3-TiO_2 coatings, detonation deposited on steel, prep., wear resist., antifriction props. 78−60877
Al_2O_3-TiO_2 powder, plasma-prepared, morphology and phase constitution 80−100833
Al_2O_3-TiO_2 thermal-sprayed coating on steel, acoustic emission 80−21247
Al_2O_3-TiO_2-MgO.$2TiO_2$, exam. of solid solutions by X-ray phase analysis 79−95981
Al_2O_3-Y_2O_3-SiO_2 containing TiO_2, La_2O_3, exam. of elastic moduli and refractive indices 78−80502
Al_2O_3+TiC system, elastic and fracture charact. at elev. temp. *(German)* 79−43299
Al_2O_3+TiO_2, reaction on sintering in reducing media 78−27457
$AlTiTaO_6$, powder X-ray diffr. data 79−99155
B-C-Ti, paramagnetic centre struct. and defect form. 80−66034
$(B_{12})_4B_2Ti_{1.3-2.0}$, tetragonal, cryst. struct. 77−15360
$Ba_{3x}A_{2-2x}Ti_{6-x}O_{13}$, (A=Na, K, Rb), $0<x<0.2$, struct. evolution, tunnel struct. 79−65049
$BaCO_3$-BaF_2-$TiO(OH)_2$, coprecipitated, use in prep. of polycryst. $BaTiO_3$ 77−24996
$Ba_3(M_4Ti_4)O_{21}$, M=Nb, Ta, Sb, effects of Sb substit., synthesis and cryst. chemistry 77−76379
BaO-Al_2O_3-TiO_2-SiO_2, glass formation, structure of cations *(Russian)* 80−38933
BaO-Nd_2O_3-TiO_2-Bi_2O_3 system ceramics, high stability low loss dielectric preparation 80−81008
BaO-SiO_2-TiO_2, molten, ionic elec. cond., TiO_2 effects *(Japanese)* 77−51532
BaO-SrO-Al_2O_3-TiO-SiO_2 glass ceramics, cryst. phases form., BaO/SrO ratio influence 80−19705
BaO-TiO_2-Al_2O_3 system, subsolidus equilibria, X-ray powder diffr. 80−108413
BaO-TiO_2-Cr_2O_3, new compound, phase relations *(Japanese)* 78−6911
BaO-TiO_2-GeO_2, subsolidus equilibria 77−86014
BaO-TiO_2-Nd_2O_3, exam. of compositional and dielectric props. 79−33601
(BaTi) citrates, thermal decomp., thermal anal., IR and X-ray diffr. obs. 79−24735
$BaTiO_3$ ceramics, calcination effects, TiO_2 powder eval. *(Japanese)* 78−64516
$BaTiO_3$ crystals, octahedral TiO_6^{8-} cluster atomic population, ionisation energy, SCF MS Xα calcs. 79−72244
$BaTiO_3$-TiO_2 mixture, exam. of liquid phase sintering, densification 79−33979
$BaTi(PO_4)_2$, cryst., luminesc., struct. interpretation 79−47489
$Ba(V_{1-x}Ti_x)S_3$, synthesis and struct. phase transitions 80−107415
$(BaZnSr)TiO_3$ ferroelectric film, parameters at upper end of centimetre waveband *(Russian)* 77−40185
Bi_2O_3-TiO_2-Nb_2O_3, subsolidus phase equilibria 77−55954
$Bi_9Ti_3Fe_5O_{27}$, combined hyperfine interaction 79−28663
$BiTiNbO_6$, cryst. struct. determ. *(German)* 78−79570
CaO-Al_2O_3-TiO_2-SiO_2, glass formation, structure of cations *(Russian)* 80−38933
$Ca_2Ti_{2-2x}Fe_{2x}O_{6-x}$, antiferromag. phases, Neel temp. variation, vacancy long-range order *(French)* 78−34979
$CaTiO_3$-TiO_2, ceramic, phys. props. 78−43784
$Ca_3Ti_xV_{1.5-x}Fe_{3.5-x}O_{12}$, garnet, mag. and neutron diffraction investigation 77−16044
$CdFeTi(PO_4)_3$ cryst. struct., and prep., rhombohedral lattice *(French)* 77−27856
$Cd_2Ti_2O_5F_2$, single cryst. growth and props. 79−100046
CoO-MgO-Al_2O_3-Cr_2O_3-TiO_2, form. and colour of spinel solid soln. *(Japanese)* 77−32550
CoO-MgO-Cr_2O_3-Fe_2O_3-TiO_2, form. and colour of spinel solid soln. *(Japanese)* 80−16059
CoO-ZnO-Al_2O_3-Cr_2O_3-TiO_2 system, form. and colour of spinel solid soln. *(Japanese)* 77−25001
CrN-TiN, rhombic distortion of cryst. lattice at low temp. 78−2253
Cr_2O_3, influence of TiO_2 on sintering behaviour, densification as function of temp. 79−78919
Cr_2O_3-MgO-TiO_2, phase relations in air at 1400°C *(Japanese)* 77−77465
Cr_2O_3-TiO_2 system, phase relations 78−80523
$Cr_{1-x}Ti_xN$, cryst. and mag. struct., at low temps. *(French)* 80−29005
$(Cr_{1-x}Ti_x)_5S_6$, mag. props. 77−69548
Cs_2TiF_6, Raman spectra, internal and lattice vibrs. 77−8569
Cs_2TiF_6:Mn^{4+}, spin-orbit and field splitting, Jahn-Teller effect, Zeeman meas. 80−80234
Cu-coated TiO_2 particles, prep. for composites 80−89159
Cu-TiO_2 alloys, internally oxidised, plastically deformed, influence of particle form on primary loop nature *(French)* 80−103344
CuO-Cu_2O-TiO_2, phase equilibria, thermodynamics of Cu_3TiO_4 phase 80−55374
Dy_2O_3-TiO_2, high refractive index film growth by sputtering, waveguide appl. 77−48341
(Fe, Ti) silicate glasses, optical absorption and Mossbauer spectra 80−55136
$(Fe,Ti)O_4$, magnetostriction calcs. *(Dutch)* 80−2619
Fe-Cr-Ti-Mo-TiO_2 (13, 3.5, 1.5, 2 wt.%) dispersion hardened, void swelling 80−65046
Fe-Ti oxide minerals from Asama volcano, Japan, in 1973 eruption 77−17065
Fe-TiB_2, dispersion strengthened, thick vacuum condensate, control of struct. and mech. props. 80−16324
Fe-TiC, dispersion strengthened, thick vacuum condensate, control of struct. and mech. props. 80−16324
Fe-TiC condensate, struct. and mech. props., disperse particle content depend. *(Russian)* 78−19772

titanium compounds continued
$Fe_{0.394}$-$Ti_{0.606}$-O-S subsystem, equil. phase data under reducing conditions rel. to ilmenite upgrading 80−76240
$Fe^{2+}_{1+x}Cr_{2-2x}Ti_xO_4$ spinel, low temp. crystallographic transitions 77−15589
$Fe_{0.2}Mg_{1.9}Ti_{0.9}O_4$, Mossbauer parameters temp. depend. 78−23381
$Fe_{0.4}Mg_{1.8}Ti_{0.8}O_4$, Mossbauer parameters temp. depend. 78−23381
α-Fe_2O_3:TiO_2 electrode, water photooxidation appl. 78−15684
Fe_2O_3-TiO_2 system, high temp. intergrowth struct., metal atom ordering in intergrowth boundaries 78−79573
2.33FeO.TiO_2,2.33MnO-TiO_2 melt, free energy of mixing 79−61572
$Fe_{2.6-x}Ti_{0.4}Al_xO_4$, $Fe_{2.4-x}Ti_{0.6}Al_xO_4$, titanomagnetite, monodomain, mag. props. 78−56346
β-FeTiD, neutron diffr. exam. of struct. 78−47282
$FeTiD_x$ ($0 \le x \le 1.9$), structural phase transitions, absorpt. and desorpt. isotherms 80−19948
$FeTiD_x$, γ-phase struct., neutron diffr. study 79−51085
$FeTiH_x$, (x=0.65 to 1.03) diffusion of H, neutron scatt. exam. 79−65243
$FeTiO_3$, Fe_2TiO_4, influence of cryst. struct. on photoresponse of electrodes 78−43471
Fe_2TiO_4, ulvospinel, containing magnetized inclusions, mag. behaviour, cooling through Curie point 78−56314
Fe_2TiO_4-Fe_3O_4, titanomagnetite, prepared at different oxidation conditions, hysteresis props. 78−56352
$Fe_{2.4}Ti_{0.6}O_4$, titanomagnetite, single-crystal, mag. props. of multidomain TRM 78−56345
$Fe_{3-x}Ti_xO_4$, elec. transport near Verwey transition, thermoelec. power and cond. meas. 79−95455
$Fe_{3-x}Ti_xO_4$, IR transmission spectra 77−85714
$Fe_{3-x}Ti_xO_4$, Mossbauer study at low temp. 78−27133
$Fe_{3-x}Ti_xO_4$, Mossbauer spectra in paramag. phase 80−39943
$Fe_{3-x}Ti_xO_4$, spin glass behaviour, susceptibility and hysteresis meas. 80−65917
$Fe_{(1+x)}Ti_{2(1+x)}S_4$ non-stoichiometric cpds., vacancy-cation distrib., Mossbauer spectra 80−15900
Fe_xTiS_2, lattice dynamics and hyperfine interactions, Mossbauer spectra study 80−108135
HfC-TiC, pseudobinary systems, phase diagrams, computer calcs. 78−44092
HfO_2-TiO_2, phase relations and thermal expansion 77−21121
HfO_2-TiO_2, thermal expansion coeff. and dynamic response to pulsed energy deposition 78−26705
HfO_2-TiO_2 system, liquidus determ. from thermal anal. *(Ukrainian)* 79−96007
HfO_2-TiO_2 system, zero and low coeff. of thermal expansion 80−39325
$K_xAl_xTi_{8-x}O_{16}$, ionic cond., K mobility rel. to struct. and bonding *(French)* 77−76594
$K_2CrTi(PO_4)_3$, cryst. data 77−39564
$KLi_3Ca_7Ti_2(Si_6O_{18})_2F_2$, baratovite, cryst. struct. determ. by X-ray diffr. 77−76382
$K_{1.6}Mg_{0.8}Ti_{7.2}O_{16}$, solid electrolyte, dielec. response, 5.2-77K 79−56709
$K_xMg_{x/2}Ti_{8-x/2}O_{16}$, ionic cond., K mobility rel. to struct. and bonding *(French)* 77−76594
K_2O-Al_2O_3-P_2O_5-TiO_2, structural role of Ti, kinetic study of chem. destruction 80−88055
K_2O-BaO-SiO_2-Ti(Ce)O_2 laser glasses, TiO_2 and CeO_2 antisolarisation additive effects 79−94309
K_2O-TiO_2-SiO_2 glass, Si-O bonding, SiKβ X-ray fluorescence and IR spectra 80−10500
K_2O-TiO_2-SiO_2 system, vitreous, struct. obs. using neutron scatt. 78−22667
$K_xZn_{x/2}Ti_{8-x/2}O_{16}$, ionic cond., K mobility rel. to struct. and bonding *(French)* 77−76594
$LaCo_{1-x}Ti_xO_3$, cryst. struct., elec. and mag. props. 79−86748
$LaCrO_3$-TiO_2 photoactive anode, for photoelectrolytic production of H_2 and electricity 80−12024
Li/TiS_2 cell with solvate melt, discharge characts. and lack of rechargeability 80−72022
Li/TiS_2($TiSe_2$)($Ti_{1.1}S_2$), electrochem. obs. of Li intercalation 80−61216
Li-Ti ferrite, microwave props. 77−40082
Li-TiS_2 cell, electrochemical pot. spectroscopy, thermodynamic props. meas. 79−100426
Li-TiS_2 storage batteries *(German)* 80−12001
LiO_2-Al_2O_3-SiO_2-TiO_2:Sn^{3+}, ESR and X-ray phase anal. 79−99752
LiO_2-Na_2O-MgO-TiO_2-Al_2O_3-SiO_2, exam. of specific heat and thermal conductivity *(Russian)* 79−55898
Li_2O-Al_2O_3-SiO_2-TiO_2 glass, phase separation at initial stages of sitallization 80−88053
Li_2O-SiO_2-TiO_2 glass, crystn., kinetic study using differential scanning calorimetry 80−44138
Li_2O-TiO_2, pseudobinary phase rotations, DTA and X-ray anal. 80−108411
Li_2O-TiO_2-Al_2O_3-SiO_2 glass, γ-irrad., struct. position of Ti, EPR study 80−84644
$Li_2Si_2O_5$-TiO_2 glasses, struct. and crystn. investigation using Raman spectra 80−38918
LiTi ferrite, Mossbauer study, relax. and supertransferred hyperfine fields 80−39941
LiTi, substituted ferrite, cation distribution, Mossbauer, X-ray, neutron diffr. study 80−28975
$LiTiS_2$, intercalation complex, band struct., tight-binding calc. 79−95323
Li_xTiS_2, ($0 \le x \le 3$), intercalation in TiS_2, possible electrochem. cathode 80−19772
Li_xTiS_2, chem. diffusivity of Li at 30°C 80−59737
Li_xTiS_2, electrochemically intercalated, ion ordering, X-ray diffr. meas. 80−44177
Li_xTiS_2 electrodes, thermodynamic and transport props. 80−66963
Li_xTiS_2, intercalation cpd., Li ordering, electrochem. obs. 78−59795
Li_xTiS_2, struct. determ. by neutron diffraction 80−54196
LiTiZn ferrites, elec. resist., mag. props., effect of Bi addition 78−95474
LiTiZn microwave ferrites, effects of Mn and Bi additives, expt. *(German)* 77−28411
Li$xTiS_2$, mechanism of Li intercalation, optical and X-ray studies 79−100394
$MgCr_2O_4$-TiO_2, porous ceramics, humidity-sensitive electrical conduction 80−107782
MgO-Al_2O_3-SiO_2: ZrO_2, TiO_2, glass, phase separation *(German)* 80−38932
MgO-Al_2O_3-TiO_2-SiO_2, glass formation, structure of cations *(Russian)* 80−38933
titanium compounds continued
MgO-CaO-Al_2O_3-SiO_2-TiO_2 system, glass-ceramics, crystn. kinetics *(Russian)* 79−37626
MgO-TiO_2-Al_2O_3-SiO_2 glass, γ-irrad., struct. position of Ti, EPR study 80−84644
(MgO-Fe_2O_3-Cr_2O_3-TiO_2):Na_2O, powder, prep., heat treatment, Na_2O impurity effect on props. 77−16528
$Mn_{0.394}$-$Ti_{0.606}$-O-S system, 1380 and 1485K, phase equilib. study 80−50616
MnO-SiO_2-TiO_2 melt, electrical cond. meas. and electrolytic anal. *(Japanese)* 78−38861
$Mn_{1-x}Ti_xAs$, ferro- to paramag. transition, press. effect up to 7 kbar 77−89954
Mo-Nb-TiN, dispersion hardened with strong interface, fracture mechanism 79−5058
Mo-TiC lamellar eutectic composite, deformation and strength, room temp. to 2073K *(Japanese)* 80−71702
Mo-TiN (3.5 vol.%), failure characts. exam. 78−68788
MoO_3-TiO_2, reduction, Mo^{5+} and O_2^- form. 77−90590
$MoSi_2$/$TiGe_2$ mixed crystals, direct obs. of surface oxide form. *(German)* 77−12721
$MoSi_2$-$TiSi_2$, high-temp. oxidation 79−83341
$(N_2H_6)_2F_2[TiF_6]$, X-ray cryst. struct. determ. 80−54182
$(NH_4)_2TiF_6$, Raman spectra, internal and lattice vibrs. 77−8569
$Na_2Mg_2Ti_6O_{14}F_2$, α and β forms, ionic conductivities *(French)* 77−43373
Na_2O-Al_2O_3-SiO_2-TiO, effect of Cr_2O_3, NiO, and MgO additions on crystallisation 78−87626
Na_2O-Al_2O_3-SiO_2-TiO_2-NiO glass, paramagnetic centres, form. during crystn., ESR study 79−65710
Na_2O-BaO-TiO_2-SiO_2 glass, ion-bombarded, optical time intensities 80−35037
Na_2O-Bi_2O_3-TiO_2, subsolidus phase equilibrium at 1000 degrees C 78−48384
Na_2O-SiO_2-TiO_2, exam. of Na^+ self diffusion, elec. conductivity, and viscosity 78−87819
Na_2O-TiO_2-Al_2O_3-SiO_2 glass, γ-irrad., struct. position of Ti, EPR study 80−84644
Na_2O-TiO_2-SiO_2, phase relations 79−61567
Na_2O-TiO_2-SiO_2 glass, density, refractive index, thermal expansion hardness, IR spectra, DTA *(Japanese)* 78−15535
Na_2O-TiO_2-SiO_2 glass, elec. props. and energy gap 78−26921
Na_2O-TiO_2-SiO_2 glass, Si-O bonding, SiKβ X-ray fluorescence and IR spectra 80−10500
Na_2O-TiO_2-SiO_2 glass, co-ordination of Ti, X-ray emission spectra study 80−84072
$Na_2O.Al_2O_3.10TiO_2$, crystallized bronze, chem. comp., morphology, optical and thermal props. *(Japanese)* 80−16172
$Na_{0.9}Ti_{1.1}Fe_{0.9}O_4$, short period β-alumina type cpds., cryst. struct. and superionic cond. 80−107499
$Na_xTi_4O_8$ bronze, hydrothermal prep., Na ion arrangement 80−75209
$Na_xTi_4O_8$ type bronzes, synthesis in $NaBO_2$, growth conditions *(French)* 78−43998
$Na_3Ti_2(PO_4)_3$, synthesis and cryst. struct. *(French)* 79−32964
Na_xTiS_2, electrochemically intercalated, ion ordering, X-ray diffr. meas. 80−44177
Na_xTiS_2, Na chem. pot. and free energy of intercalation, electrochemical meas. 79−100396
Na_2TiSiO_5, cryst. struct. 78−42976
$Na_2TiZn_2[GeO_4]O_3$, cryst. struct. determ. 78−63734
(Nb,Ti)N_x, metastable supercond. phase, effects of rapid quenching on transition temp. 78−2611
Nb anodic oxide films, reversible optical changes 78−35580
Nb-Ti-Ti_3O system, phase analysis, struct. stabilization 77−90330
Nb-TiN, BCC solid soln., nitride solubility, alloying effects *(Russian)* 79−51262
Nb_2O_5-TiO_2, splat cooled, crystallization and ordering 77−68953
Nb_2O_5-TiO_2-ZrO_2, quasiternary system 77−44229
Nd:glass:TiO_2, lasing action, stabilisation *(Russian)* 78−13715
$Nd_2O_3.4TiO_2$, growth from soln., struct. 78−83794
Ni-TiO_2 electrochem. composite coating phase composition and microhardness factors *(Russian)* 79−91598
NiO-TiO_2, solid soln. series, between rocksalt and spinel structure 78−51513
$NiTiF_6.6H_2O$, mag. and struct. transitions 78−68257
PCl_5-$TiCl_4$, gas, melt, and solid, dimer-monomer conversion, Raman spectra obs. *(German)* 79−70320
$POCl_3$-$TiCl_4$, splitting of Sm^{3+} near IR absorpt. bands 80−2750
PZT, ferroelec. film, elec. props., composition anal., AES 78−84530
$PbFeTi(PO_4)_3$, cryst. struct. and prep., rhombohedral lattice *(French)* 77−27856
PbO-B_2O_3-SiO_2-LiO_2-TiO_2, glass enamel, chemical durability and microstruct., TiO_2 addition effect 79−29255
PbO-SiO_2-TiO_2, molten, viscosity *(Japanese)* 78−18819
PbO-TiO_2, phase equilib. determ. by mass-loss Knudsen effusion method 77−11668
PbO-TiO_2, solid phase reactions, thermodynamic anal. 77−12603
PbO-ZnO-B_2O_3:TiO_2 glass, circuit corrosion protection on alumina substrates 79−29236
Pb(Ti,Zr)O_3 solid solutions, phase coexistence discrepancies 80−96662
Pb(Zr,Ti)O_3 polycrystalline ceramic, fracture and strength, surface treatment effects 80−11704
Pt/TiO_2 catalyst for photoassisted decomposition at room temp. of H_2O and ethylene 80−55703
Rh-TiO_2 catalyst, adsorpt. of H_2, surface states, NMR spectrosc. investig. 80−103891
RuO_2-TiO_2 coatings for Ti anodes, microstructural investigations 79−43469
$Ru_{1-x}Ti_xO_2$ solid solns., metal-nonmetal transition 78−91735
$Ru_xTi_{1-x}O_2$ films, elec. props. and IR spectra 79−38207
$SbNbO_4$:TiO_2, growth, pyroelectric and ferroelectric props. 79−73886
$(Sc_xTi_{1-x})_2O_3$, semicond.-metal transition, sp. ht. meas., 300-600K 77−43347
Si-TiO_2-Al, current-voltage characts., oxide film effects 80−70841
Si-TiO_x-Ni, MIS amorphous solar cell, increase in open-circuit voltage and short-circuit current on addition of TiO_x layer 79−57425
$SiCl_4$-$TiCl_4$, liq. struct., oscill. amp., neutron diffr. study 79−46544
SiO_2:TiO_2, prep., amorphous struct., effect of roasting, bonds 78−44061
SiO_2-Al_2O_3-CaO-MgO-TiO_2 system glasses, phase separation and crystn. 77−24384

titanium compounds continued
SiO_2-Al_2O_3-Li_2O:TiO_2,Fe_2O_3, pyroceramic glass, coloration, absorpt. spectra obs. 77−8615
SiO_2-Al_2O_3-MgO-TiO_2 devitrificates, microstruct. and props. *(Polish)* 80−70141
SiO_2-Al_2O_3-Na_2O-BaO-TiO_2, glass ceramic interaction with Pb borosilicate glaze 80−84398
SiO_2-Al_2O_3-R_2O_3-MgO-TiO_2, T=rare earth of Ce group, glass-ceramic permittivity comp. depend. 77−43928
SiO_2-Al_2O_3-Y_2O_3-La_2O_3-TiO_2 glasses with high elastic moduli, alkaline durability 80−85071
SiO_2-CaO-Na_2O-TiO_2 system, water, alkali, acid resist., chem. durability 79−34162
SiO_2-TiO_2, noncrystalline film form., IR study *(Japanese)* 77−59634
SiO_2-TiO_2, vitreous, US velocity and absorption 80−107380
SiO_2-TiO_2 antireflection coatings, 1064 nm 150 ps laser pulse damage rel. to barrier layering and smoothness 79−14018
SiO_2-TiO_2 antireflection coating, 1.064 μm laser damage, barrier 80−33059
SiO_2-TiO_2 films, obtained from $Si(OC_2H_5)_4$ and $TiCl_4$, exam. of props. 79−95934
SiO_2-TiO_2 glass phonons, IR and Raman spectra meas. 79−91447
SiO_2-TiO_2 stack reflector and antireflection coating, 1064 nm 180 ps laser pulse damage 79−14017
SiO_2-TiO_2 system, physicochem. props. of glasses with low thermal expansion coefficient 77−35718
SiO_2-TiO_2 system, true solid soln. existence obs. 77−36475
SiO_2-TiO_2-Al_2O_3-SrO(BaO), glasses, ceramic form. rel. to Al_2O_3 content 77−25005
SiO_2-TiO_2-Na_2O glass, optical absorption coeff., 2.1-3.3 eV 77−77240
SiO_2-TiO_2-Na_2O(−CaO), thermal diffusivity in range 0-600°C, influence of TiO_2 80−29233
Si_2O_3-TiO_2 system, phase transform. at high temp. 77−84926
SiO_2(-TiO_2) glass prep., melting *(Polish)* 80−40316
$Sm_2Ti_2O_7$ form. kinetics rel. to TiO_2, Sm_2O_3 polymorphic transitions 79−11606
$SnCl_4$-$TiCl_4$, liq. struct., oscill. amp., neutron diffr. study 79−46544
SnO_2-TiO_2 solid solns., X-ray diffr. and thermogravimetric meas. 79−90792
SrO-Al_2O_3-TiO_2-SiO_2, glass formation, structure of cations *(Russian)* 80−38933
$Sr_nTi_{n-4}Nb_4O_{3n+2}$ layer ferroelectrics, physical props. 78−10854
$SrTiO_3$, chemisorpt. of O_2, phase investig. by UPS 78−72684
$SrTiO_3$, electrode, surface photovoltage expts. 78−72227
$SrTiO_3$ ferroelectric film, parameters at upper end of centimetre waveband *(Russian)* 77−40185
$SrTiO_3$:Fe, EPR, of Fe^{3+}-rhombic, Fe^{2+}-V_O and Fe^{1+}-V_O complexes 78−76302
T:O_2:Cr(Mo), anatase single cryst., ESR of Cr^{5+} and Mo^{5+} ions 79−28603
(Ta,Ti)B_2 on graphite, CVD coatings, hardness meas., SEM study 80−24760
Ta-Ti-N, reactive sputtered film, elec. props. 78−84336
Ta-Ti-O, reactive sputtered film, elec. props. 78−84336
Ta_2O_5-TiO_2, anodic film, Rutherford backscatt., capacitance 77−16734
$Ta_{1-x}Ti_xS_2$ (1T), magnetoresistance in the Anderson localized states near the metal-nonmetal transition 80−88479
$Ta_{1-x}Ti_xS_2$ (1T), magnetoresist. near metal-nonmetal transition at ultra low temps. 80−88600
$Ta_yTi_{1-y}S_2$, Li intercalation, electrochemical studies 80−39048
$Ta_xTi_{1-x}Se_2$, cryst. struct. and elec. props. 79−47133
(Ti, Cr)B_2-based alloys, densification of powder mixtures by hot-pressing, elec. and mech. props. 80−20812
$(Ti,Ni)_6C$, metallographic detection in 12Kh18N10T steels 80−66721
(Ti,V)C, activated reactive evaporation deposited films, annealing study, microstructure 80−24762
(Ti,V)C carbides, prep. and mech. props. 78−64518
$(Ti,V)_2O_3$, magnetisation, field and temp. depend., down to 1.6K 77−8284
(Ti,Zr)B_2 on graphite, CVD coatings, hardness meas., SEM study 80−24760
Ti complex, bis cyclopentadienyl Ti:N_2, liquid interactions, ab initio LCAO MO SCF calcs. 79−18256
Ti complex, dichloro bis-cyclopentadienyl titanium+dialkoxy bis chelated titanium compounds reaction, IR spectra 79−79239
Ti complex, $Ti_2Cl_8(CH_3NO_2)_2$, single cryst., struct., IR and Raman spectra, X-ray diffr. 78−43000
Ti complex, TiOCl[Co(cyclopentdienyl)$_2$]$_{0.16}$, sxnthesis and struct. 80−44176
Ti complex, Ti(IV)-H_2O_2, H_2SO_4-aq. soln., reson. Raman spectrum, vibr. assignments, molar absorptivity 77−65469
Ti complex with carboxylate, channel model in exchange theory 78−14950
Ti complexes, cryst., amorphous, coordinated H_2O, mol. force field ellipses, mol. force consts. 77−34609
Ti^{4+} hydroxide, coagulation struct. effects on particle size of TiO_2 78−52732
Ti-Al-C(N) system cpds., abrasive power, glass grinding 77−63820
Ti-anodic oxide-Au(Al), electronic cond. *(French)* 79−95512
Ti-B-C system, complex carbide phase synthesis by crystallisation from gas phase 77−16526
Ti-B-N, CVD, lattice const. 79−74097
Ti-C-N-O-H, solid solns. of H, exam. of props. 80−29172
Ti-Cr-TiC, sintered, friction and wear, structural factors 78−60843
Ti-H, deposited on carriers, synthesis, structure and catalytic props. 80−29890
Ti-H, diffusion in hydride phase, exam. 80−29204
Ti-H, proton spin-lattice relaxation time, band struct. 78−56395
Ti-H exam. of electron structure 80−29306
Ti-N_2, condensate formed by plasma flow precipitation in vacuum, cryst. and surface props. *(Russian)* 80−100788
Ti-N-C-H-(O) system, thermodynamic anal. *(Russian)* 80−55325
Ti-O system, intermediate oxide thermodynamics under equilibrium press. 80−55351
Ti-O system, nonstoichiometry between Ti_3O_5 and TiO_2 comps. at high temps. 77−15594
Ti-S, pressure-temp.-comp. phase diagram, TiS_2 growth by chem. vapour transport 77−59764
Ti-S, two novel polytype structs. in the system, 16H and 18H *(French)* 79−7582
26H Ti-S polytype, struct. determ. *(French)* 77−11509
titanium compounds continued
Ti-S system, nonstoichiometric, containing stacking faults, X-ray diffr. intensity distrib. calc. 80−28872
Ti-Si_3N_4 system, reactions under heating and plasma conditions 79−95988
Ti-Si-C system, complex carbide phase synthesis by crystallisation from gas phase 77−16526
Ti-TiC, sintered, friction and wear, structural factors 78−60843
Ti-TiC-TiN system, phases 80−20905
Ti-TiN phase system, diffusion of N_2 77−39699
Ti-TiO_2-Au diode, spectral photoresponse and I-V charact. 80−15617
Ti-V-C-N, solid solns., quasibinary cross sections 78−23676
Ti-Zr-B system, CVD 78−60581
$(Ti_{1-x}V_x)_2O_3$ spin glass, mag. props., metallic antiferromagnetism 79−82791
Ti_3Al, Cu, Fe, Mo (1 at.%) additions, oxidation resistance, 700 to 800 degrees C 77−12744
Ti_2AlC, Ti_3AlC, TiC, phys. props. 77−43602
Ti_2AlN, prep. and props. 77−28745
$(Ti_{1-x}Al_x)_2O_3$, crystal struct. determ., metal-metal distance, effect on electronic struct. 77−47431
Ti(B,N), CVD coating on cutting tool 79−61802
TiB form., kinetics investig., X-ray diffr. anal. using internal standard, dilution methods 77−70393
$TiB_{1.964}$, heat capacity thermodynamic properties from 5 to 350K 78−91446
TiB_2 based cermets, rel. to Ti-B-Mo phase equilibria 78−35354
TiB_2 CVD coating, surface damage and erosion under energetic D^+ and $^4He^+$ irrad. 80−39174
TiB_2, CVD from $TiCl_4$, BCl_3 and H_2, equilib. thermodynamic anal. 77−59694
TiB_2, CVD from $TiCl_4$, BCl_3 and H_2, deposition kinetics modelling 77−59695
TiB_2, cathode, production of D ion beam impurities 79−86592
TiB_2, chemical vapour growth by modified hot wire method 78−60555
TiB_2 coated limiters, first wall protection 80−32483
TiB_2, coating, D^+ and $^4He^+$ irrad. effects 80−20753
TiB_2 coating, erosion rates under H^+ ion bombard., fusion reactor appls. 80−39179
TiB_2 coating, on WC-Co alloy cutting plates, hardness and struct. 80−21175
TiB_2 coating on graphite by CVD 80−21131
TiB_2 coatings, CVD, electron microprobe, SEM, X-ray diffr. characterisation *(French)* 78−43271
TiB_2 coatings, prep. by CVD and interaction with substrate 79−24680
TiB_2 coatings for Tokamaks, H trapping and re-emission, annealing effects 80−37582
TiB_2, crystal growth by chem. vapour transport 80−16164
TiB_2, deposition of coating on WC-Co by thermal diffusion *(Bulgarian)* 80−45430
TiB_2 dispersion strengthened Fe condensates, struct., mech. props. 77−90361
TiB_2, electric arc melting prep. and oxidation props. 80−20860
TiB_2 electronic structure calc. and obs., by APW method and X-ray photoelectron spectroscopy *(Japanese)* 79−15074
TiB_2, first-wall coating for Tokamak, H retention and release 80−18620
TiB_2, fusion reactor first wall material, activation energies and populations of H traps 79−45409
TiB_2, fusion reactor material, low energy ion erosion expts., Kaufman source appl. 80−68942
TiB_2, hardness of sintered material 78−60636
TiB_2, ion microanalysis and implantation applied to fusion surface research 79−45405
TiB_2, low-temp. neutron irrad., electrical resistance and stored energy 78−67744
TiB_2, plasma-sprayed coatings on Cu and stainless steel, fusion reactor appl. 80−18619
TiB_2, preparation method rel. to compressive strength 80−55327
TiB_2, reactions with Ti-Al-Cr-Mo alloy VT3-1 80−16585
TiB_2, single crystal growth *(Japanese)* 79−65987
TiB_2, swelling, blistering, 140 keV p, d and He ion irrads., porosity effects 77−35603
TiB_2 thick film on low C steel substrate, CVD in US field, crystallite size 80−84854
TiB_2, TiB_2-ZrB_2, refractory compounds, direct evaporation deposition, struct. and props. 77−44392
TiB_2, TiC-TiB_2, and TiC-TiB_2-Co coatings, deposited by electron evaporation, struct. and props. 79−23871
TiB_2, vacuum condensate, struct. and mech. props., second phase effect *(Russian)* 80−71705
TiB_2-Al_2O_3 system-based composites 77−85979
TiB_2-MgO(CaO)(Al_2O_3)(Y_2O_3), thermal stability of composite materials 78−60638
TiB_2-TiC (BN), crucibles for vacuum evap. of Al 79−74094
TiB_2-TiC powder mixtures, hydrostatic pressing 79−100098
TiB_2-TiC(20 wt.%), sintered, US machining 77−21325
$TiBe_2$, cubic Laves compound, sp. ht. rel. to intinerant antiferromag. 79−82356
$TiBe_2$, itinerant antiferromagnetism, mag. susceptibility obs. 79−15288
$TiBr_4$, reson. Raman spectrum, vibr. analysis, Jahn-Teller coupling 79−85965
$TiBr_4$, X-ray photoelectron spectra 79−22759
Ti(C,N), hydrolysis 78−15713
TiC (001) surface, change in work function with chemisorption of O_2 and H_2O 80−29461
TiC abrasion-resistant coatings, glow discharge assisted CVD 79−83392
TiC, abrasive, effect on machinability of Ti alloys *(Russian)* 80−97593
TiC, abrasive action, X-ray investig. 77−52497
TiC, activated reactive evaporation deposited films, annealing study, microstructure 80−24762
TiC, additions, effects on binary, ternary and complex Ni-based alloys 78−92305
TiC, additions to sintered high-speed steel, effect on hardness and cutting performance 77−66608
TiC, adsorption of Cs(K), adsorpt. energy, thermionic emission 77−7978
TiC, ageing and ordering phenomena *(Russian)* 78−39807
TiC, band struct. correlation with Ti, APW calc. *(Japanese)* 78−23017
TiC, bond energy and ionization efficiencies from SIMS 79−24400
TiC, CVD, deposition rate meas., rel. to mass transport model 80−103599

titanium compounds continued
TiC, CVD and activated reactive evaporation on WC-TiC-Ta(Nb)C-Co, substrate-layer interactions, AES obs. 79−24679
TiC CVD coating, W_6Co_6C cemented carbide substrate, structure, composition and hardness exam. 78−11425
TiC, CVD coating on Co-bonded multicarbide substrate, SEM, RHEED, AES interface study 79−77927
TiC, CVD effect of cemented carbide substrated 79−74096
TiC, CVD layers on Fe substrate *(Japanese)* 78−27415
TiC, CVD on steel for wear resistance improvement 79−34196
TiC, CVD rate, depend. on gas composition 77−40386
TiC, calcs. of 2γ-ang. correlations and Compton profiles 78−39624
TiC, cathode, thermionic emission, Ti and C admixtures, Os film covered, improved emission 79−28884
TiC coated emitters, thermionic emission props. *(Japanese)* 77−40322
TiC coated high speed steel, machining of steel 4340, tool life 78−11435
TiC coated limiters, first wall protection 80−32483
TiC, coated WC cutting rools, frictional characts. 79−20218
TiC coated WC-Co cemented carbides, fracture toughness 80−85046
TiC coating, activated reactive evaporation and sputter deposition, wear characts. 77−44394
TiC coating, activated reactive evaporation and sputter deposition, ancillary props. 77−44395
TiC coating, erosion rates under H^+ ion bombard., fusion reactor appls. 80−39179
TiC, coating, wear characteristics, comparison or coated and uncoated WC hard metals 78−92365
TiC, coating for oxidation resistance 77−32704
TiC coating on C fibre, by CVD TiC coated C fibre compatibility with Al *(Japanese)* 79−78898
TiC coating on cemented carbide tools, machining evaluation 79−29253
TiC coating on steel Kh12, impact abrasive wear improvement 77−70187
TiC, coating on WC-Co, stoichiometry effect on mech. props. 77−66715
TiC coating on WC-NbC-Co, ion plating, and cutting tests 79−24678
TiC coating thickness meas. using X-ray diffr. 80−21243
TiC coatings, on cemented carbides, struct. and hardness 80−59771
TiC coatings, RF sputtered, on 440-C steel, adherence, friction, and wear props. 79−47823
TiC coatings on steels and hard alloys 80−76414
TiC, cpd. form. reaction in reactive evaporation, quadrupole mass analysis *(Japanese)* 78−23628
TiC, deform. at high temps. 80−104239
TiC, deformation behaviour during rubbing in wide temp. range 80−16486
TiC, deposited by activated reactive evaporation, TEM and hardness 79−23872
TiC, deposition from gas phase during pyrolysis of cyclopentadienyls 77−85944
TiC, determ. in cementite by annealing in moist H_2 *(German)* 79−39231
TiC, diffusion coating on steel electrode, effect on electric discharge sintering of metal powders 77−63598
TiC dispersion strengthened Fe condensates, struct., mech. props. 77−90361
TiC, electron irrad. damage, electron microsc. study 80−84210
TiC, electronic struct. and XPS, cluster method and band struct. 79−60710
TiC electronic structure calc. and obs., by APW method and X-ray photoelectron spectroscopy *(Japanese)* 79−15074
TiC, electronic structure, PES study 80−70594
TiC, energy schemes 77−39778
TiC, exam. of brittle fracture props., using Hertzian indentation 79−11686
TiC, field-emitted electron energy distrib., for single cryst., 77 and 290K 77−32510
TiC film, Au-dispersed, struct., hardness and wear rate 77−77493
TiC film, CVD, on WC, diffusion processes, ion beam anal. 80−49424
TiC, final-state effects in C Auger spectra 78−6818
TiC, fine powder form. by vapour phase reaction *(Japanese)* 79−70030
TiC, frictional characts. and contact-zone deform. in homogeneity range 80−66673
TiC hard coating on Co, effect of martensitic transform. in substrate causing cracks 79−29060
TiC, high temp. thermal cond., ambipolar diffusion contrib. 78−26742
TiC, ion plating and applics. *(Japanese)* 77−63565
TiC, LCAO band struct., Compton profile 77−85138
TiC, laser CVD, coating characterisation 80−93494
TiC, lattice dynamics, inelastic neutron scatt. 78−55918
TiC layers, on steel and cemented carbides, load-bearing capacities 80−40606
TiC, low-temp. reactor irrad., calorimetric investig. 77−80547
TiC, mag. suscept. rel. to temp. in homogeneity region 78−34953
TiC, magnetron-sputtered, solar selective absorbing surfaces 79−92079
TiC, mech. props., 1073 to 2273K *(Japanese)* 79−15732
TiC, micro-Vickers hardness, up to 1500°C 77−28890
TiC, microhardness and charact. hardness 79−52376
TiC, micropowder, abrasive props. 77−63821
TiC, micropowder, degree of charging of polished Ti and Fe surfaces 78−60880
TiC micropowder surface finishing of metals, surface struct. 80−11842
TiC micropowders, abrasive lapping of refractory metals 77−44391
TiC, molecular cluster approach to electronic struct. and bonding mech., for C 77−20270
TiC, nonstoichiometric, simple model for phonon dispersion, rel. to C vacancies 78−30718
TiC, one-centre exchange pot. superposition 77−15738
TiC, oxidation at various O_2 pressures 79−96172
TiC particles injection into Ti-Al-V alloy surface for wear resist. improvement 80−85086
TiC, plasma arc srapying, chem. reaction with plasma gases 80−66427
TiC plasma-chemical synthesis, depend. on geometric and flow rate parameters *(Russian)* 80−40677
TiC, plasma-sprayed coatings on Cu and stainless steel, fusion reactor appl. 80−18619
TiC, polycrystalline, elastic props. 78−27547
TiC, positron wavefunction calc. 79−99512
TiC powder, plastic strain of particles under vibratory milling 77−90423
TiC precipitate in austenitic stainless steel, grain boundary dislocation interaction, during creep 80−16384
TiC, precipitates in Ni-base superalloy, STEM microanal. 80−81067
titanium compounds continued
TiC precipitates in Ti-implanted Fe, microstruct. 80−66513
TiC precipitation, high temp. coarsening, of dispersions in ferrite 78−84874
TiC precipitation in alpha-radiated stainless steel, effect on He embrittlement 80−45399
TiC, precipitation in thermally embrittled maraging steel 77−25055
TiC, production from tetrachloride and hydrocarbon, thermodynamic analysis *(Russian)* 80−7523
TiC, pseudofused powder, abrasive props. 77−77589
TiC, RF sputtered, comp. by XPS 78−51839
TiC, RF sputtered film on steel, transition region 78−39956
TiC, Raman scatt., phonon density of states 78−52499
TiC, reactions with Ti-Al-Cr-Mo alloy VT3-1 80−16585
TiC, reactive RF sputtering in N_2, TiN film deposition 79−78886
TiC reactively sputtered coatings on Ni-Cr-Mo-Ti (19,11,3 wt.%), adherence, XPES and wear study 80−25565
TiC, refractory micropowder, geometric parameters of grains 77−16529
TiC, Shockley surface states and bonding 78−91739
TiC single crystal, deformation behaviour, operative slip systems 79−100211
TiC single crystal, micro-Vickers hardness meas. up to 1500°C *(Japanese)* 78−23804
TiC single crystal, prep. by floating zone technique *(Japanese)* 78−23607
TiC single crystal, vapour deposited on Mo and W wires, electron microscope study 77−1795
TiC single crystal, work function, field emission characts. *(Japanese)* 78−19641
TiC single crystals, growth from vapour by modified hot wire method, temp. effect on habit 79−61509
TiC single crystals, synthesis and impurities 80−55329
TiC, sintering and grain growth, metallographic anal. 80−25642
TiC, soft X-ray emission, excitation pot. spectra, excited level binding energy 80−35009
TiC, solid-phase reacts., effect of nonstoichiometry, thermodynamic evaluation 78−60632
TiC sputtered coatings on Ti-Al-V (6,4 wt.%), adherence, XPES and wear study 80−25565
TiC, sputtering, low energy, H, D and He ions 80−100734
TiC, sputtering yield, use as first wall material 78−95629
TiC substrate, TiB_2 coating prep. by CVD and interaction with substrate 79−24680
TiC, TiC_6^{20-} cluster electron state, MS Xα calculations 77−8037
TiC, TiC-TiB_2, and TiC-TiB_2-Co coatings, deposited by electron evaporation, struct. and props. 79−23871
TiC, TiN and VC, charge distrib. and bond ionicity 78−63961
TiC, TiVC, on steel, sputter deposited, adhesive quality 77−12531
TiC, tool carbide, thermal shock resistance and fracture strength 77−21257
TiC, ultrafine powder prep. by plasma jet *(Japanese)* 77−52273
TiC, VPE using $TiCl_4$-CCl_4-H_2 system *(German)* 77−24964
TiC, vacuum condensate, struct. and mech. props., second phase effect *(Russian)* 80−71705
TiC, valence band electron distrib., photoelectron spectra obs. 77−44120
TiC, valence X-ray photoelectron spectrum, density of states 77−81197
TiC, wear resistant film, activated reactive evaporation form. 77−44411
TiC, wetting by Cr-Ni-Mo-Mn alloy steel, expt. planning investigation 80−60822
TiC whisker, TF electron emitters, props. obs. 80−66403
TiC, whisker growth in CVD 80−59843
TiC whiskers, growth by CVD, catalytic effects of various metals and refractory oxides 79−33211
TiC whiskers, growth rate for CVD 77−47704
TiC, X-ray emission band exam. and electron struct. 77−8689
TiC, X-ray emission spectra and chem. bonding 77−20958
TiC-Au film, prep. by activated reactive evaporation, struct. and mech. props. *(Japanese)* 78−3252
TiC-Au multilayer struct., microhardness and elec. resist. 80−2950
TiC-B, struct. and mech. props. 80−55461
TiC-base alloys, anomalous phase flaky precipitation *(Japanese)* 78−48401
TiC-C composites, hot pressed, thermophys. props. at high temps. 80−59675
TiC-coated C fibres in Ni, diffusion barrier effectiveness 78−60624
TiC-Cr_3C_2(Cr_3C_2-WC), powder mixture, steel bonded, exam. of sintering behaviour 78−52712
TiC-HfC, phase diag. calc. 77−90329
TiC-Kh6V3M steel alloy, reaction during sintering and heat treatment 78−60617
TiC-Mo_2C-Ni cermets, influence of anomalous phases on strength 78−92228
TiC-Mo_2C-TiN-Co, fracture toughness, effect of microstructural defects *(Japanese)* 77−56087
TiC-Ni, reaction kinetics under simulated liq.-phase sintering 78−52746
TiC-Ni composite coating, activated reactive evaporation prep., structure 77−44393
TiC-Ni composite coatings, form. and wear resistant props. 77−63602
TiC-steel alloy, struct. form. during sintering, strength, rel. to heat treatments 77−59717
TiC-steel compact prod. by sintering in vacuum and in Ar or H_2 atmos. 77−63616
TiC-steel composite, effect of method of Cr additions on props. 78−15341
TiC-TiB_2, strength and antifriction props. over wider range of concs. 80−50673
TiC-TiN, hardness var. charact. in homogeneity field 80−3192
TiC-TiN, kinetic characteristics, review 78−47613
TiC-TiN, physicochem. props., comp. depend. 80−55370
TiC-TiN system, electro- and thermo-phys. props. 80−34210
TiC-VC, mag. susceptibility, elec. cond. and thermoelec. props. 80−50033
TiC-VC(NbC)(TaC), prod. and props. 77−28772
TiC-VC(ZrC) carbide alloys, thermophys. props., temp. depend., specific elec. resist. 79−86908
TiC-WC-TaC carbide mixture in plasma reactor *(German)* 77−1819
TiC-W(Mo), thermionic emission, surface structural characts. after prolonged use, work function variation 80−20758
TiC-ZrC, mag. susceptibility, elec. cond. and thermoelec. props. 80−50033
TiC-ZrC, phase diag. calc. 77−90329

titanium compounds continued
TiC-ZrC, pseudobinary systems, phase diagrams, computer calcs. 78−44092
TiC-ZrC, solid soln., conc. and temp. dependence of props. 80−39736
TiC-ZrC coatings, deposited by electron evaporation, struct. and props. 79−23871
$TiC_{0.93}$-$TiN_{0.818}$, structural parameters, and X-ray and pycnometric densities in homogeneity range 77−90311
TiC_{1-x}, substoichiometric, electronic density of states 80−2319
TiC_x (x=0.97, 0.90, 0.80), Raman scatt. induced by C vacancies 78−52500
TiC_x, comp. determ. by neutron diffr. 77−40411
TiC_x, complex phases with NaCl struct., microhardness rel. to electronic structure 77−90438
TiC_x, effect of structural vacancies on neutron radiation damage 77−35591
TiC_x, electron energy spectrum and phys. props. in homogeneous region *(Russian)* 77−31941
TiC_x film, form. by hollow cathode discharge reactive deposition process, on mild steel sheet 79−24451
TiC_x, fused material, microstruct. 78−44115
TiC_x, nonstoichiometric, densification during sintering 80−84895
TiC_x, phonon density of states and dispersion relations 79−42173
TiC_x refractory layers on steel surfaces, ESCA obs. 80−39471
TiC_x, single cryst., core level shifts, valence band struct., ESCA 77−32499
TiC_x single cryst. with homogeneous composition, preparation by floating zone technique 79−100049
TiC_x, static distortions and Debye temp. determ., neutron diffr. exam. *(Russian)* 77−80482
TiC_x^{n-}, nonstoichiometric, ESCA spectra, MO LCAO calcs. 79−59513
TiC_x-TiN double-layer films, on C steel, CVD in US field, X-ray and SEM characterisation 79−65338
Ti(CN) coating for steel, abrasion resist., CVD parameter depend. 77−40471
TiC(N) overlay coating on stainless steel, Ti or Al, effect on physicomechanical and wear props. 80−40603
$Ti(CN)_x$, reactively sputtered, erosion props. 79−47779
$TiC_{1-x}N_x$ formation in high temp. N flow, ultra disperse powder, thermodynamic anal. *(Russian)* 80−55325
$TiC_{1-x}N_x$, lattice distortion of ordered phase *(Ukrainian)* 78−68680
$TiC_{1-x}N_x$, VPE using $TiCl_4$-CCl_4-N_2-H_2 system *(German)* 77−24964
TiC_xN_{1-x}, electronic struct., theoretical approach 80−54584
TiC_xN_{1-x}, electronic struct., KKR-ATA method 80−65447
TiC_xN_y, fused material, microstruct. 78−44115
TiC_xN_y monolayer films, on C steel, CVD in US field, X-ray and SEM characterisation 79−65338
TiC_xN_y, neutron diffr. investig. 77−51355
TiC_xN_y, powder preparation, physical, chemical props. *(Russian)* 80−76212
TiC_xN_y, thermal cond., elec. cond., and thermal expansion 80−10714
TiC_xN_z, thermal expsn. of cubic phases 79−1512
$TiC_xN_zH_m$, thermal expsn. of cubic phases 79−1512
TiC_xNy, elastic props., 290K 77−52379
TiC_xO_{1-x}, electronic struct., theoretical approach 80−54584
TiC_xO_{1-x}, electronic struct., KKR-ATA method 80−65447
TiC_xO_y are $TiC_xO_yH_m$, cubic phases, mag. susceptibility 80−15680
TiC_xO_y, cubic phase, thermal expsn., lattice consts. 78−43149
TiC_xO_y, elastic characts. 77−80568
TiC_xO_y, lattice completeness and period 78−22706
TiC_xO_y, oxidation mechanism 77−86200
TiC_xO_y, structural mechanism of O inclusion into lattice 78−22707
TiC_xO_y, thermal cond., elec. cond., and thermal expansion 80−10714
TiC_xO_y, thermal expsn. coeffs. lattice spacing temp. depend. 77−69102
$TiC_xO_yH_m$, cubic phase, thermal expsn., lattice consts. 78−43149
$TiC_xO_y(H_m)$, cubic phases, thermal expansion, 77-300K 79−42281
$TiCl_3$, electronic band struct., tight-binding approx. 78−51872
$TiCl_3$, electronic struct. and struct. phase transition 80−59644
$TiCl_3$, lattice instability, d-electron-lattice interaction 80−44276
$TiCl_3$, layer compound, theoretical study of phase transition 79−10945
$TiCl_3$, phase transition, phonon dispersion curves 80−2130
$TiCl_3$ reduction to Ti by Mg, thermodynamics and heat physics *(Russian)* 78−15331
$TiCl_3$, vib. spectra 77−40231
$TiCl_4$, electrochemical behaviour in alkali chloride baths 80−30243
$TiCl_4$, electrolytic reduction *(French)* 78−23644
$TiCl_4$, IR absorpt. bands, absolute integrated intensities, obs. and calc. 78−78689
$TiCl_4$, liq. struct., oscill. amp., neutron diffr. study 79−46544
$TiCl_4$, liq. struct. by neutron diffr. 79−73089
$TiCl_4$, optical and Ti 2p core photoemission spectra, SCF Xα anal. 79−94032
$TiCl_4$, photoelectron and UV spectra, SINDO theory 77−50360
$TiCl_4$, reduction in steady beam-plasma discharge 80−100099
$TiCl_4$, sorption by H_2O-swollen PVA from benzene solns. *(Polish)* 79−4471
$TiCl_4$, $t_1 \rightarrow 2e(^1A_1 \rightarrow {}^1T_2)$ transition, bond props. and LCAO MO calcs. 80−18889
$TiCl_4$, X-ray photoelectron spectra 79−22759
$TiCl_4$-graphite intercalation compound 80−40675
$TiCl_4$-$MgCl_2$, high activity catalyst for polyethylene, struct. and mechanism investig. 80−11951
$TiCl_4$-$SiCl_4$($SnCl_4$) liq., beat effects, neutron diffr. studies 80−38897
$TiCl_5^-$, vib. anal., force fields and consts. *(German)* 79−45702
$Ti_2Cl_{10}^{2-}$, vib. anal., force fields and consts. *(German)* 79−45702
$TiCl_2(SO_3X)_2$.DMSO complex, X=F, Cl, IR spectra 78−42054
$TiCl_2(SO_3X)_2$.acetylacetone complex, X=F, Cl, IR spectra 78−42054
$TiCl_2(SO_3X)_2$.pyridine complex, X=F, Cl, IR spectra 78−42054
$TiCl_2(SO_3X)_2$.quinoline complex, X=F, Cl, IR spectra 78−42054
$(TiCl_4.POCl_3)_2$, normal coord. anal. and force consts. 79−22682
$(TiCl_4.POCl_3)_2$, solid, IR and Raman spectra, vibr. assignments 78−43868
$TiCl_4$.trimethylaluminium+ethylene, Zeigler-Natta reaction mechanism, restricted Hartree-Fock calcs. 77−73441
$TiCrB_2$-Ni(Ni-Mo) systems, interphase reactions, electron probe anal., metallography and hardness exam. 80−2990
$TiCuD_{0.90}$, neutron powder diffr. study for cryst. struct. refinement 78−95018
TiCuH, PMR obs. of H diffusion 78−91978
$TiD_{0.9}$, surface characts., AES, EELS, SIMS, and XPS study 80−65343
TiD_2, clean and contaminated films, fabrication and AES 78−52600

titanium compounds continued
TiD_2, film, AES detection of decomp. 79−91937
TiD_2, film formed during simulated Tokamak gettering cycles, desorption 80−34296
TiD_2, nucleation and growth in D_3^+ implanted Ti, TEM study 80−97717
TiD_x, α- and β-phases, D-site occupancy, neutron diffr. study 79−42014
TiF_2, force consts., mean amplitudes of vibr. 78−17647
TiF_2, TiF_4, X-ray emission, core level chem. shift calcs. 80−53010
TiF_2, vibr. anal., kinetic consts. method 80−18838
TiF_3, single crysts., vapour phase chem. transport prep. *(French)* 79−69971
TiF_4, equilib. config., force field, Coriolis consts., vibr. freqs. and amplitudes 80−32835
TiF_4, X-ray photoelectron spectra 79−22759
$(TiF_6)^{3-}$ complex, open-shell cluster calcs, semiempirical LCAO-MO method 80−54583
$TiF_2(TiF_3)$, ESR spectra in rare-gas matrices at 4K 77−88474
β-$TiFeH_{1.03}$, H diffusion, NMR meas. 80−10707
TiH, electronic structure of five and ten atom chains SCF-Xα-SW calcs. 80−5483
TiH, in M-tyre stars and sunspots 79−48789
$TiH_{1.45}$, PMR study of spin correl. and saturation effects 77−59477
$TiH_{1.92}$, thermal neutron inelastic scatt. phonon spectra determ. *(Chinese)* 79−10906
TiH_2, band model of martensitic phase transition 80−29953
γ-TiH_2, dissociation pressure, 20 to 70°C 78−85150
TiH_2, electronic density of states and tetragonal distortion, APW calc. 79−37986
TiH_2, H impurity detection by $^1H(^{15}N,\alpha\gamma)$ reaction 80−55767
TiH_2, nitridation to form Ti_xN_y 77−44200
TiH_4, Dirac-Fock one-centre calcs. 77−88380
TiH_4, electronic structure, ab initio calcs. 79−89601
TiH_4, X-ray emission, core level chem. shift calcs. 80−53010
TiH_x film, anomalous H_2 desorption at room temp. 80−29261
TiH_x film, kinetics of H_2 interaction 80−6620
TiH_x film electrode, oxidation, electrochem. and surface analytical characterisation 79−39034
TiH_x, H diffusion, NMR obs. 80−34813
γ-TiH_x, interstitial H diffusion mechanism, NMR spin-lattice relax. study 80−103515
γ-TiH_x, NMR spin-lattice relax., effect of correlated atomic diffusion 80−107495
TiH_x, surface characts., AES, EELS, SIMS, and XPS study 80−65343
TiH_x, temp. depend. of thermo-EMF coeff., 100 to 350K 77−11944
$TiH_x(D_x)$, electron-positron annihilation and X-ray K-spectra *(Russian)* 77−1761
$TiH_x(D_x)$ positron annihilation *(Russian)* 78−6807
TiH_3F, valence mol. orbital energy, nonempirical pseudopot. 79−22592
TiH_3F, valence-shell MO calc. with pseudopot. 78−907
TiH_3F, X-ray emission, core level chem. shift calcs. 80−53010
$Ti(HPO_4)_2 \times H_2O$, cryst. struct. 79−42023
$TiH(SO_4)_2.4H_2O$, cryst. parameters and X-ray powder diffr. data *(French)* 79−14765
$Ti_{1-x}Hf_xSe_2$ mixed cryst., elec. resist. and phase transition temp. 80−24928
TiI_4, pseudo exact force consts. 77−31022
TiI_4, temp. depend. of thermo-EMF coeff., 100 to 350K 77−11944
TiI_4, thermal diffusivity, near FCC to BCC transition 80−59740
TiI_4, X-ray photoelectron spectra 79−22759
TiI_4:C, deep doping during ion-beam welding, microhardness meas. 79−19294
Ti(IV)-Fe(II) oxide, U adsorption, U extraction from seawater 80−24730
TiN, appl. of quick survey method for CVD conditions 78−44019
TiN, CVD *(Japanese)* 77−63562
TiN, CVD growth in US field, effect on adherence and hardness 77−59696
TiN, CVD layers on Fe substrate *(Japanese)* 78−27415
TiN, cladding, thermal stress analysis *(Russian)* 77−59952
TiN coated WC cutting rools, frictional characts. 79−20218
TiN coating on refractory fibre, effect on high-temp. strength *(Russian)* 77−52536
TiN coating on steel for watch part finishing, ion plating *(French)* 78−23879
TiN coating on WC-NbC-Co, ion plating, and cutting tests 79−24678
TiN decorative coating, ion plating on steel and Stellite 78−11441
TiN diffusion barrier on Si device metallisation 80−65304
TiN, electronic absorpt. spectrum, rot. anal. 80−78601
TiN film, magnetron DC reactive sputtering, X-ray diffr. and SEM 77−44160
TiN film, struct. and elec. props. 78−26788
TiN film as protective coating for vacuum deposition chamber, Auger electron spectroscopy study 80−25922
TiN films, reactively RF sputtered, struct. and elec. props., substrate bias effects 80−96763
TiN films deposited by reactive sputtering, elec. props. 80−15638
TiN, for supercond. microwave cavities, secondary electron emission and AES meas. 79−56895
TiN formation, from TiO_2/Si_3N_4 reaction in N_2 atmosphere 80−71617
TiN, from high-temp. reaction of NH_3 and $TiCl_4$, physicochem. props. 80−55334
TiN, gaseous phase, crystallisation, effect of temp., vapour-gas mixture conc., and deposition time 79−33910
TiN, high dispersed superconductivity 78−43505
TiN, highly dispersed, metallic thermo-EMF 78−43363
TiN, influence on interaction between SiC fibres, reinforced complex alloy *(Russian)* 78−95820
TiN, interatomic interactions from XPS 80−49171
TiN layers formation, on steel substrate, microchardness and structure obs. *(Hungarian)* 80−2965
TiN layers investigation for solar-cell contacts 80−81461
TiN, low-energy ion-stimulated deposited, supercond. props. 80−88664
TiN, opt. consts. and physicochem. spectra 77−85677
TiN, optical props. at 300K 78−19466
TiN, phonon dispersion curves, soft-mode behaviour, inelastic neutron diffr. 78−43083
TiN, powder defect struct., thermal and elec. props. 77−59286
TiN, precipitation of ordered δ'-phase *(Russian)* 78−6929
TiN, RF sputter deposition, ion bombardment and ion implanation 80−25564

titanium compounds continued
TiN, Raman scatt. supercond. transition temp., phonon density of states, Debye temp. 78−52499
TiN, reactive ion plating with auxiliary discharge deposition conditions influence on film props. 80−20801
TiN, self-propag. high-temp. synthesis under high N_2 pressures 80−25630
TiN single crysts., supercond. T_c at high press. 79−38228
TiN, soft X-ray emission, excitation pot. spectra, excited level binding energy 80−35009
TiN, supercond. critical temp., neutron irrad. effect 80−80433
TiN, superconductivity 78−2605
TiN, synthesised in SHF discharge plasma, exam. of props. *(Russian)* 80−7524
TiN, TiC and VC, charge distrib. and bond ionicity 78−63961
TiN, ultra-fine powder prep. by reaction in N_2 plasma jet *(Japanese)* 78−72757
TiN, VPE, and superconductivity *(German)* 77−24964
TiN, vapour deposited coating on cemented carbide tools, deposition parameter effects on wear 77−63563
TiN, vibr. IR spectrum, mol. consts. 79−68230
TiN wear resistance coatings, reactive evaporation and activated reactive evaporation *(French)* 79−57126
TiN, wear resistant film, activated reactive evaporation form. 77−44411
TiN, whisker growth in CVD 80−59843
TiN, X-ray emission spectra and chem. bonding 77−20958
TiN-Al_2O_3, exam. of sintering and densification kinetics, and physical props. 79−95986
TiN-AlN, composite, erosion resist. in electron stream 78−11365
TiN-AlN composites, struct. and props. 77−40413
TiN-CrN system solid solns., electrophys. and galvanomag. props., energy spectra 77−15847
TiN-CrN systems, solid solns., mag. props. 77−12086
TiN-MgO (NiO), (FeO), solid-phase reactions 79−11774
TiN-MnN, solid solns., electrophys. props. 77−35914
TiN-Nb(Ta)N, microcomposite film prod. for radio resistors 78−3052
TiN-Ti_2N, activated reactive evaporation formed deposits, microstructure, transformation depend. on depositing conditions 80−24761
TiN-VN refractory powder composite, resistors, produced in low temp. 78−11182
$TiN_{0.91}$ plates, oxidation kinetics *(French)* 78−85199
$TiN_{0.96}$, electronic component of thermal cond., inelastic electron-phonon scatt. 79−86937
TiN_{1-x}, substoichiometric, electronic density of states, CPA method calcs. 80−88464
TiN_2, ultrafine synthesis in RF plasma, X-ray diffr. chem. and electron microscopy anal. 79−70026
TiN_n, effect of equilib. N_2 press, 10^{-2} to 100 atm, on MP 77−36465
TiN_x, cryst. and internal structs., electron diffr. and microscopy 77−27861
TiN_x, deposition by hollow cathode discharge process, and hardness 79−24452
TiN_x, film, non-stoichiometry rel. to optical charcts. 77−12456
TiN_x film, reactively sputtered in Ar-N_2 atm., elec. and struct. props. 80−15636
TiN_x, ion condensing metal plasma stream, coating microhardness, chemical reactions 79−42426
TiN_x, oxidation in oxygen, of plates 79−61766
TiN_x, oxidation mechanism 80−25912
TiN_x, phonon density of states and dispersion relations 79−42173
TiN_x spectral reflectance, selective solar absorber appl. 77−79954
TiN_x, synthesis by enhanced activated reactive evaporation 78−39705
TiN_y-TiO_y, thermal expansion, 23-1000°C, X-ray obs. 78−91454
ϵ-Ti_2N, interstitially built layer, reducing permeation of H plasma through Ti 80−16566
Ti_3N_4 plasma condensation on steel and carbide *(Russian)* 80−20796
Ti_xN_y, synthesis by nitriding Ti and TiH_2 77−44200
$TiN_{0.32}H_{0.19}$, cryst. struct., neutron diffr. anal. *(Russian)* 80−64965
TiN_xO_{1-x}, electronic struct., theoretical approach 80−54584
TiN_xO_{1-x}, electronic struct., KKR-ATA method 80−65447
TiN_xO_y, cubic, concentration dependence of the degree of filling of unit cell 78−44063
TiN_xO_y, cubic, thermal expansion coeffs., Ti-Ti bond screening 79−10970
TiN_xO_y, elec. cond., conc.-temp. depend., 25-1000°C 80−34439
TiN_xO_y, phase and structural features 77−48411
$Ti_{1-x}Nb_xH_{1.94}$, x=0.25, 0.50, low temp. specific heat meas. 80−2179
$(TiNbO_5)^-$ oxide layers, intercalation of alkylammonium ions 80−64985
$Ti_{0.5}NbSe_2$, cryst. struct., metallic cond., mag. and phys. props. *(French)* 80−33956
TiO, $(C^3\Delta\text{-}X^3\Delta)$ system, radiative lifetimes, oscillator strengths, flame spectroscopy 78−42136
TiO, (001) surface, spectral density of states 78−39187
TiO absorption and intrinsic amplitude of Mira variables 78−36580
TiO band absorption effect on stellar photometry with broadband filters 80−41811
TiO band in M-type stars, rotational excitation temp. 79−48790
TiO band strengths in metal-rich globular star clusters 78−49487
TiO bands in cool stars, polarization changes 79−97005
TiO β system, electronic transition moment and effective vibr. temp. 77−68078
TiO, β-system, radiative lifetime determ. 77−58086
TiO, $C^3\Delta$ term anomalous triplet splitting 78−13514
TiO, $C^3\Delta_3\text{-}X^3D_3$ α system, radiative lifetime meas. 78−55202
TiO, chemiluminesc., dissoc., heat of form., in metastable Ti collisions with O_2, N_2O, NO_2 77−40534
TiO, $e^1\Sigma^+\text{-}d^1\Sigma^+$ transition rel. to cool star spectra 77−67089
TiO, electron struct. calc. 80−49587
TiO, electronic excitations, electron energy loss spectra in 3 to 60 eV range *(French)* 78−80440
TiO, emission spectra in chemiluminesc. flames 77−38689
TiO, energy band struct. and density of states *(Russian)* 80−44493
TiO, Fermi surface and de Haas-van Alphen effect *(Russian)* 80−49573
TiO, Franck-Condon factors rot. depend. 80−58319
TiO, γ'-system, Franck-Condon factors, r-centroids and Einstein coefficients calcs. 80−74163
TiO, Hartree-Fock and local exchange energy bands, disagreement of results 77−76724
TiO, high temp. thermodynamics, vaporisation, and pressures over 80−10685
titanium compounds continued
TiO, high temp. vaporisation and thermodynamics, stoichiometry, mass spectra 77−59109
TiO, high temp. vaporisation and thermodynamics, vapour press. temp. coeff. 77−59110
TiO in Ar matrix, meas. of absorpt. and magnetic circular dichroism spectra 80−86356
TiO in M-type giant stars used for temp. sequence *(Russian)* 78−20831
TiO in sunspots, equiv. width meas. theoretical interpretation, line form. process 80−72902
TiO opacity in *o* Ceti (Mira) and R Leonis, effects on dia. meas. 78−16429
TiO, ordered phase, vacancy-strain coupling 78−79549
TiO, oxidation 77−90472
TiO, photoluminesc. of $\alpha(C^3\Delta\text{-}X^3\Delta)$ system in chemiluminesc. flames 77−38690
TiO, potential energy curves and dissociation energy 78−50531
TiO, powder solubility of H_2 77−11698
TiO Φ system, near IR emission spectrum 80−69131
TiO, rot. anal. of (0,0) (1,0) (0,1) (1,1) bands of $\gamma'(B^3\Pi\text{-}X^3\Delta)$ 79−22719
TiO, rot. lines in sunspot spectrum, temp. determ. 78−96451
TiO, rot. temp. in sunspots, rel. to photospheric and sunspot models 78−69766
TiO, soft X-ray spectra and XPS, Xα and Hartree-Fock calcs. discrepancies 79−77979
TiO, solar lines in 7100-7600 Å range, table 78−77495
TiO, X-ray diffraction, cubic and monoclinic phases of Kelley's sample 77−51356
TiO, X-ray emission spectra and chem. bonding 77−20958
TiO, $X(^3\Delta)$ state, vibrational IR spectrum using microwave powered molecular source, rotational analysis 80−9596
TiO-MeO (Me=Ni, Co, Mn), solid soln., lattice thermal cond. 79−23791
TiO-VO, solid soln. formation 77−89541
TiO-ZrO_2, pseudo binary system, effect of Ti addition on struct. and props. of zirconia 79−11583
TiO+Ar, collision cross-section meas. 78−55202
TiO+$BaCO_3$, react., mechanism, effect of polymorphic transitions 79−11605
$TiO_{0.3\text{-}0.5}$, O atom ordering, electron microscopy obs. 79−99150
$TiO_{0.42}$, diffuse X-ray and neutron scatt. due to out-of-step configurations of O atoms 77−62518
TiO_{1+x}, conduction band determ. 78−60055
TiO_2 (100), chemisorption of H_2, O_2, and H_2O, electron spectroscopy, evidence for Ti^{3+} photogeneration 78−38940
TiO_2, (100) surfaces, ionisation of sputtered-atomic particles 80−20750
TiO_2, (110) and (100) surfaces, LEED and electron spectra 77−72757
TiO_2 (rutile), (001) and (110) faces, UPS and LEED obs. 80−45206
TiO_2 (rutile), (001) and (110) surfaces, surface and bulk density of states calcs. 80−49858
TiO_2 (rutile) photoanode, corrosion suppression by high-energy redox reactions 78−23163
TiO_2 AR coating for Si solar cells by spray deposition, review 80−104511
TiO_2, absorbing film parameters determ. by ellipsometry 80−254
TiO_2, acoustic vel., absorpt. coeff. and photoelastic consts. rel. to acoustooptical parameters 79−56762
TiO_2, addition to Cr_2O_3 effect on sintering behaviour 80−66461
TiO_2, additive in ZnO sintering 78−80497
TiO_2, adsorpt. of water, IR spectra 78−14577
TiO_2, adsorption of electron acceptors, strength, and distrib. of electron donor sites, ESR meas. 78−84055
TiO_2, adsorption of neopentane, NMR pulsed field gradient method, diffusion coeff. meas. 80−15362
TiO_2, adsorption of O_2 and H_2O, UPS, LEED and AES studies 79−4480
TiO_2 amorphous film, alkali resistance, refractive index, IR spectra *(Japanese)* 78−23546
TiO_2, amorphous film, vac. deposited, struct. and crystn., TEM obs. 80−2291
TiO_2, anatase, effect of hydrostatic press. on Raman spectrum 79−61384
TiO_2, anatase, influence of Al_2O_3, Ga_2O_3 or In_2O_3 to polymorphic crysts. in vapour 79−78858
TiO_2, anatase, natural and synthetic crysts., Raman spectra and assignments 79−28752
TiO_2 anatase, Raman spectrum, temp. depend. 80−76027
TiO_2, anatase, single cryst. growth by chem. transport reactions 77−36384
TiO_2, anatase film, intermittent CVD conditions rel. to struct. 78−11119
TiO_2, anatase phase, lattice vibrs. calcs., rigid ion model 80−2125
TiO_2, anatase single crystals, switching, coloration and memory effect 78−72216
TiO_2, anatase-rutile transition, additives, mechanism of action *(Japanese)* 78−95744
TiO_2, anatase-rutile transform., inhibition by Nb_2O_5 addition 79−78948
TiO_2 anodes, corrosion suppression by high energy redox reactions 77−77599
TiO_2 anodic film, optical indices as function of crystallisation 77−66552
TiO_2, anodic films on Ti, struct. *(French)* 77−56154
TiO_2, anodically formed layers, film instability obs. 78−72916
n-TiO_2, appl. as cathode in stable photoelectrochemical cells for splitting of water 77−44484
TiO_2, aq. suspension, flocculation effect on dilatant flow 79−61916
TiO_2, arc-plasma-sprayed anodes, performance in photoelectrolysis of water 79−74407
TiO_2 based ceramic dielec. materials, medium permittivity, elect. charact. 78−35086
TiO_2 based ceramics, variation of dielectric constant and resistivity with temp. 80−2683
TiO_2 based construction ceramics, fibre-like cryst. reinforced, mech. props. 80−55341
TiO_2 brookite synthesis from Ti in NaF or Ti compounds, form. mechanism *(Japanese)* 80−93529
TiO_2, CW CO_2 laser deposited dielect. thin film, optical and struct. props. 80−7506
TiO_2, chemical effect, influence on stopping power 80−47830
TiO_2, chemical implantation of 10-keV H^+ and D^+, resist. and optical absorpt. expts. 77−59031
TiO_2, chemisorbed phases of water, UPS meas. 78−10285

titanium compounds continued
TiO_2, chemisorpt. of O_2, phase investig. by UPS 78−72684
TiO_2, chemisorption of H_2O, differential heat of chemisorption 78−84052
TiO_2, chemisorption of O_2 and H_2O, electron stimulated desorption, AES and charact. loss spectra 78−22963
TiO_2, clean and hydrated, surface sites, XPS 80−35052
TiO_2, cluster surface states, LCAO calc., electron energy loss peak interpretation 77−43686
TiO_2, clusters, surface electron struct. and defect states, DV-Xα calc. 80−20268
TiO_2, coincidence-site lattice interfaces 80−15381
TiO_2, cond. and valence band struct., gap anisotropy 77−47729
TiO_2 containing aluminosilicate glasses, paramagnetic defect formation, ESR study during crystn. 79−65739
TiO_2, core levels, cryst.-field splitting, X-ray emission study 80−66328
TiO_2, correcting coatings, u.v. transmission cutoff 77−760
TiO_2, Coulomb energy, pot., field and dipolar moments, self consistent calcs. 79−18323
n-TiO_2, crystal, in aqueous soln., electrochemistry and electrolum. meas. 78−48665
TiO_2, crystal dislocations, elastic parameters, elastic energy, stress field, anisotropic elasticity theory 79−95008
TiO_2, crystal growth from melts in Bi_2O_3-V_2O_5-TiO_2 system 78−19659
TiO_2, crystal structure, stability compared with CaF_2 *(Russian)* 80−64945
TiO_2, crystalline, photocurrent spectral distribution 79−56259
TiO_2, decomp. of $CaO.6Al_2O_3$ 80−92687
TiO_2, deform. pot. meas. of direct forbidden transition 79−95806
TiO_2 devitrified glass, Raman spectra 79−78677
TiO_2, dielec. dispersion and polarisation 78−2803
TiO_2, diffusivity of T and Raman scatt. meas. 79−86927
TiO_2, dispersive asymmetry of elasto-optical tensor 78−35112
TiO_2, distrib. over lunar surface from anal. of Mikhail's photometric catalogue *(Russian)* 78−73661
TiO_2 doped polycrystalline electrodes, for photo-assisted electrolysis of water, spectral response 79−29370
TiO_2, doping processes, influence on photoelectrochem behaviour 80−79822
TiO_2, ESCA, charge transfer satellite struct., hole state localisation intensity depend., MS-MO calc. 77−66139
TiO_2, effect of dynamical mechanical props. of polyester resin POLIMAL 190 *(Polish)* 79−96074
TiO_2, effect on oxidation of complex (Fe, Mn)-V spinels 79−43453
TiO_2, elastic const. C_{44}, depend. on temp. 79−73239
TiO_2, elec. cond., temp. depend. resistivity meas. at 77 to 600K, unwsitched samples 80−20262
TiO_2, electrochem. doping 77−76430
TiO_2 electrode, carrier density determ. by optical absorpt. and photoelectrolysis spectra 80−71462
TiO_2 electrode, chem. modification for dye sensitisation, rel. to H_2O oxidation 79−91964
TiO_2 electrode, doping density dependent attachment of rhodamine B 80−54777
n-TiO_2 electrode, flatband pot. determ. from differential stress meas. 80−75638
TiO_2 electrode, illuminated, Hg deposit from Hg(II) solns. *(French)* 79−52696
n-TiO_2 electrode, near UV photon efficiency, H_2 prod. from solar energy 77−11956
n-TiO_2 electrode, photo-oxidation of acetate and iodide 80−81331
TiO_2 electrode, photoelectrolysis of H_2O, solar energy conversion 79−52959
n-TiO_2, electrode, photogenerated free carriers and photocurrent relax. 77−15951
TiO_2 electrode, sensitised, photoelectrolysis of water in sunlight 78−19143
TiO_2 electrode, silanisation effects on semicond. props. 79−96364
TiO_2 electrode, surface comp. changes during photoelectrolysis, XPS obs. 79−7894
n-TiO_2 electrode in $AlCl_3$-NaCl melt, electrochem. and photoelec. props. 80−81328
n-TiO_2 electrode in photoelectrochem. cell, anomalous photoresponse 77−11998
TiO_2 electrodes, chemically modified, nature of surface states 80−107905
TiO_2 electrodes, electron transfer from rose bengal, photoelectrochem. meas. 77−66758
TiO_2 electrodes, in aq. electrolytes, surface states, photocurrent obs. 80−49895
TiO_2, electrodes, solar energy conversion, photocatalytic prod. of H_2 77−1932
TiO_2 electrodes in photoelectrochem. cell, photothermal effect 80−7947
TiO_2, electron energy loss spectra, 0.02-2 eV 78−39642
TiO_2, electronic energy levels, electrorefl. spectra 77−24870
TiO_2, electronic excitations, electron energy loss spectra in 3 to 60 eV range *(French)* 78−80440
TiO_2, electronic struct., XPS meas. 77−73217
TiO_2, electronic struct., XPES obs., rel. to RuO_2, IrO_2 78−52632
TiO_2, electronic structure, appl. of Auger and characteristic loss spectroscopies 77−77331
TiO_2, energy band struct., uniaxial stress depend. 80−2334
TiO_2, etching charact. by plasma reactive sputter etching 78−27661
TiO_2, exciton luminescence spectra, absorpt. spectra 80−89064
TiO_2 film, and TiO_2-SiO_2 film system, Rayleigh scatt., 441.6 nm, scatt. losses correl. with deposition parameters 79−78782
TiO_2 film, electron diffr. exam. 78−79906
TiO_2 film, ion plated, DC cond. study 80−100457
TiO_2 film, laser CVD 79−78897
TiO_2 film, optical inhomogeneity, rel. to struct. 79−83047
TiO_2 film, RF sputtering, dielec. props. and X-ray phase analysis 78−80288
TiO_2, film, reactive evap. of Ti-O phases, refr. index 77−19372
TiO_2 film, refr. index and struct., deposition temp. depend. 79−4857
TiO_2 film deposited on Si, SiO growth under film during postdeposition high temp. annealing 80−15400
TiO_2 film on Ti, simultaneous determ. of optical indices of film and substrate by statistical anal. 77−20946
TiO_2 films, deposition by electron beam evap. chem. comp., refr. index, struct. *(Japanese)* 77−62777
titanium compounds continued
TiO_2 films, in Ti-TiO_2-electrolyte system, electroreflectance response 79−42945
TiO_2 films as solar photocatalysts, preparation 79−74530
TiO_2, fine struct. in intrinsic absorpt. edge 79−42987
TiO_2, form. on Ti in acid soln., electrochem. and optical props. 78−48560
TiO_2, formation by pyrolysis of tetrabutoxytitanium 80−55311
TiO_2, H species characterisation by electron-stimulated desorption 80−34305
TiO_2, hexagonal, implications for Earth's lower mantle 78−61371
TiO_2, high refractive index film growth by sputtering, waveguide appl. 77−48341
TiO_2 high-frequency sputtered optical coatings 79−76900
TiO_2, IR spectra, up to 1635K 77−48155
TiO_2, in desert sand, photoreduction of N_2 to NH_3 79−83483
TiO_2 in non-aqueous liquids, effects of mol. architecture of long chain fatty acids on dispersion props. 80−40751
TiO_2, in silicate glass, thermal capacity 80−88335
TiO_2, indirect forbidden transitions, band struct. enhancement 80−44503
TiO_2, interionic repulsive short-range interaction pot., lattice energy calc. 80−96466
TiO_2, isothermal sintering, surface area reduction 77−8779
TiO_2, K^+ implantation, extended defects and precipitates 80−49251
TiO_2, lattice dynamics, unambiguous assignment of fund. absorpt. edge 78−71817
TiO_2 layer form. by anodic oxidation, characterisation using ^4He backscatt. *(French)* 80−45433
TiO_2 layers, activated reactive evaporation and absorpt. indices 80−97363
TiO_2 layers, obtained by cathode and HF sputtering, light scatt. and refr. index reduction 80−29877
TiO_2, liq., spreading over refractory metals 78−26749
TiO_2, long-wavelength lattice vibr. modes, symmetry coordinates 78−43081
TiO_2, metal-TiO_2-Si structure, I-V characteristics, deposition, post-deposition oxidation effects 78−80063
TiO_2, metal-insulator transition meas. by microcalorimetry *(French)* 77−47733
TiO_2, Mn^{3+} ion electron spin-lattice relaxation 80−108054
TiO_2, non-stoichiometric rutile, LO phonon-plasmon coupling, IR refl. spectrum 77−32376
TiO_2, nonstoichiometric rutile, dielec. props. 10 Hz to 30 kHz 77−28507
TiO_2, nonstoichiometric anodic films, O incorporation kinetics 80−97733
TiO_2, nonstoichiometry study, thermal emission of electrons 80−108317
TiO_2, OH^- adsorption on defect site, electronic struct. 79−47150
TiO_2, obtained ions $Ti_2OCl(HCOO)_3(OH)_2$, by thermohydrolysis, exam. of crystallisation 80−2173
TiO_2 on SiO_2, antireflection layer on Al mirrors, enhanced reflectance 77−42636
TiO_2, optical coating in liquid, laser damage 77−61994
TiO_2, optical coatings, laser damage resist., spectral depend. 77−62022
TiO_2 optical coatings, deposition, performance 77−88896
TiO_2, optical film cross sections, SEM and TEM 77−19387
TiO_2, paint type coating layer with spherical pigment, radiative transfer theory 80−61405
TiO_2 paper filler, quantitative determination, using radioisotope X-ray fluorescence anal. 78−56935
TiO_2, particle size, effects of coagulation struct. of Ti^{4+} hydroxide 78−52732
TiO_2 particles in hydrocarbon fluid, appl. of meas. method for particle charges and particle-substrate forces by optical transients 79−50218
TiO_2 particles in suspension, light scatt. phenomena and abs. *(German)* 77−10835
TiO_2, phonon spectroscopy, amorphous versus crystalline material 78−83898
n-TiO_2 photoanode, band bending at surface used to dissociate water under solar illumination 78−91765
TiO_2 photoanode, water photoelectrolysis at high current density 78−15679
n-TiO_2 photoanodes, corrosion suppression mechanism 80−2462
TiO_2, photodesorption of H_2O, pulsed-laser-dynamic-mass-spectrometer study 80−35568
TiO_2, photoelectrochemical systems, solar energy utilisation *(German)* 80−45713
n-TiO_2 photoelectrochemical electrodes, effect of Nb doping on quantum efficiency 80−101121
TiO_2 photoelectrode, stability 77−20422
TiO_2 photographic layers, sensitivity enhancement by addition of Ag^+ during cuprous development *(Russian)* 80−62780
TiO_2, photon-stimulated desorption of ions obs. 79−82459
TiO_2, photothermal spectroscopy 78−32808
TiO_2 pigments in commercial polyethylene, luminesc. props. and photoactivity 79−83008
TiO_2, planar defects, expt. and calc. images at high resolution 77−35575
TiO_2 planar optical waveguide preparation and props. 78−90524
TiO_2, plasma growth, photoelectronic props. 78−52662
TiO_2, plasma-sprayed coating against grey cast Fe, wear 79−34155
TiO_2, plasmochemical synthesis, oxidised from metals, exam. of props. 80−2984
TiO_2, polycryst., paramag. centres, illumination effects, ESR 77−48041
TiO_2, polycryst. film, threshold switching 78−14771
TiO_2 polymorphs, transform. enthalpy 79−100131
TiO_2, porosity-permittivity relations, depolarising factors determ. and pore effects *(Japanese)* 80−97189
TiO_2 powder, radiation induced defects 77−62562
TiO_2, powder, thickness meas. of SiO_2 and Al_2O_3 coating, XPS and ion sputtering 79−88913
TiO_2, prereduced surfaces, room temp. activity for oxygen isotopic exchange 79−91998
TiO_2, Raman spectra and struct. at high press. 79−87442
TiO_2 reaction with C/Cl_2, high temperature chlorination 79−83450
TiO_2 reaction with C/Cl_2, high temp. chlorination, volatile species 79−83451
TiO_2, reactive DC sputtering deposited films with magnetron-plasmatron, mechanical elec., optical props. 80−25566
TiO_2, reactive- and chemical-sputter deposition from Ti and TiC target 79−100051
TiO_2, reactively sputtered optical coating for inertial confinement fusion laser components 80−23705
TiO_2, reduction with CaH_2, preparation of rolled Ti foils 80−18744

titanium compounds continued
TiO_2, resolved quadrupolar transition, absorpt. spectra obs., 1.6K 78−27259
TiO_2, room temp. coloration by diffused Na and H from Na amalgam 78−84611
TiO_2, rutile, adsorption of acetic acid-d_4, IR obs. 78−30827
TiO_2, rutile, crystal growth by floating zone method using thermal imaging system 77−77373
TiO_2, rutile, defect struct. and elec. cond. at 1273K 80−44604
TiO_2, rutile, deuteron and alpha-particle implantation, chemical effects, optical and cond. meas. 78−67755
TiO_2 rutile, dielec. const., 10^2-10^7 Hz, DC bias effect 79−78603
TiO_2, rutile, electron diffr. patterns and extinction distances 77−76363
TiO_2, rutile, electron mean free path, four-step transition and Auger spectra investig. 80−97389
TiO_2, rutile, ferroelectric ceramic, dielec., piezoelec. and elastic props., orientational contrib. 78−68468
TiO_2, rutile, film, CVD in $TiCl_4$-H_2O system 77−12541
TiO_2, rutile, first order Raman spectrum, uniaxial stress effects 80−66196
TiO_2, rutile, first-order Raman spectrum, uniaxial-stress depend. 80−60586
TiO_2, rutile, isothermal compression under hydrostatic press. to 106 kbar 80−31035
TiO_2, rutile, K-edge X-ray absorpt., cond. band states 80−97382
TiO_2, rutile, mass transport mech. determ. by sinusoidal profile decay method 78−6178
TiO_2, rutile, mechanisms for H diffusion 79−73341
TiO_2, rutile, optoelectronic props., band struct., theory 80−80175
TiO_2, rutile, oscills. in elec. resist. induced by solid/gas interactions 79−91068
TiO_2, rutile, pure and SiO_2-coated, adsorption of N_2 and Ar, 77.4K, microcalorimetry obs. 80−80062
TiO_2, rutile, Raman study at high press. 80−89002
TiO_2, rutile, reduction by C, thermodynamic and struct. study, 1400 to 1600K 79−52650
TiO_2 rutile, single cryst., elec. cond. meas. rel. to O_2 press., temp. *(German)* 77−47823
TiO_2, rutile, single cryst., high temp. compression in O_2 atmosphere *(French)* 79−51194
TiO_2, rutile, superficial constitutive water, NMR study 80−88881
TiO_2, rutile, thin film CVD 77−77409
TiO_2, rutile, vol. depend. of refr. indices under hydrostatic press. 77−52036
TiO_2, rutile and anatase, periodic bond chains, computer determ. *(French)* 78−26474
n-TiO_2, rutile anode, water photolysis 78−2563
TiO_2, rutile ceramic, ageing in strong elec. field *(Polish)* 78−52869
TiO_2 rutile ceramics, capacitors, elec. cond. meas., anomalous conduction, ageing effects 78−14836
TiO_2, rutile ceramics, space charge effects 80−24945
TiO_2, rutile phase, shock induced phase transition anisotropic behaviour 80−103475
TiO_2 rutile single crystals, stoichiometric, dynamic strain ageing 80−50661
TiO_2, second order Raman spectrum 79−61364
TiO_2, semicond. anode in aq. electrolyte, electrolum. and electrochem. 80−76080
TiO_2, semicond. electrodes, defect doped, ageing effects, photocurrent meas. 79−69592
TiO_2 semicond. films for water photoelectrolysis 80−26146
TiO_2 single cryst., refl. and electrorefl. spectra 78−2870
TiO_2 single cryst., refl. and electrorefl., energy levels 78−2871
TiO_2, sintered ceramic, props. rel. to additives, impurities 78−35329
TiO_2, sintering, hardness, density, elec. cond. and colour *(Japanese)* 78−68659
TiO_2, sintering, struct., pressing, atm., and doping effects 80−20873
TiO_2, slightly reduced rutile, diffusion of Ti 78−79799
TiO_2, slightly vacuum-reduced, {312} planar defects, TEM obs. 78−22736
TiO_2 slips and castings, rheological and technical props., firing and sintering effects 79−87599
TiO_2, sol, mixtures with CuO and α-FeOOH sols, differential surface coagulation 79−79303
TiO_2, solubility in KF aq. solns. 80−34197
TiO_2, spray-on antireflection coatings for Si solar cells 80−80963
TiO_2, sputter-deposited, electrical and optical props. 79−47181
TiO_2 sputtered film, photocond. and TSC meas. 80−15560
TiO_2, sputtering defects, associated surface electron states, UPS, XPS and AES obs. 80−60755
TiO_2, stoichiometric single crysts., anisotropy of ion transport 80−2206
TiO_2, subsidiary valence band extrema, piezospectroscopic exam. 79−19516
TiO_2 surface, photocatalytic decomp. of H_2O 80−85194
TiO_2, surface coating constituent mat., adsorpt. of Cs^+ 78−23843
TiO_2 surface crystalline, mass transport mechanisms at high temperatures *(Japanese)* 80−54479
TiO_2, surface electronic struct. by discrete variational Xα cluster calc. 78−43449
TiO_2, suspended in highly insulated liq., photoelectrophoretic phenomenon, direct imaging system 77−54005
TiO_2 suspension, adsorption-desorption of IO_3^- 80−93804
TiO_2 suspension in glycerine, Bingham plastic flow through annuli 80−64521
TiO_2, thermal anal. using solar heating *(Ukrainian)* 79−77725
TiO_2, thermally stimulated exoelectron emission *(German)* 80−66404
n-TiO_2, thermodynamic pot. for anodic dissolution, rel. to photoelectrochem. cell efficiency 78−26948
TiO_2, third order nonlinear optical difference frequency generation 78−22176
TiO_2, Ti^{4+} XPS, band struct. investig. 79−38707
TiO_2, transition metal doped anodes for water photoelectrolysis, response to visible and UV 79−74531
TiO_2 transparent film photographic layers, props. *(Russian)* 80−43420
TiO_2 transparent film thickness and refractive index calc. 79−15547
TiO_2 treated with quinoline, photooxidation and effect of surface states, ESR obs. 79−66352
TiO_2 treatment with O_2, vacuum heat cleaned, O_2^- radical form., EPR 77−35806
TiO_2, two photon spectra, quantitative investigation, temp. depend. 80−50373

titanium compounds continued
TiO_2, two-photon absorption coefficient rel. to inverse Raman cross section 78−6678
TiO_2 type compounds, system of polymorphic transitions 78−47268
TiO_2 type noncubic structures, expansion of Madelung parameters as function of ratio of two lattice parameters 77−84693
TiO_2, UV photon induced secondary electron emission 79−52079
TiO_2, UV photon induced secondary electron emission 79−78835
TiO_2, uniaxial stress depend. of direct-forbidden and indirect-allowed transitions, absorpt. edge obs. 79−42990
TiO_2, vacuum deposited, destruction props. obs., suitability for integrated optics assessment *(Slovak)* 80−33224
TiO_2, wettability of single crysts. by liquid metals *(Russian)* 77−43408
TiO_2 wideband dielectric mirror production, spectral transmission 79−76897
TiO_2, X-irrad., adsorpt. of O_2, EPR meas. 78−80211
TiO_2, XPS satellite spectra, mol. orbital study 80−43100
TiO_2:^{44}Sc, gamma-gamma directional correlation 77−20775
TiO_2:Al(Y), polycrystalline photoanode, improved solar efficiency 79−96479
n-TiO_2:Be electrodes, photoassisted oxidation of water 80−30502
TiO_2:Cr^{3+}, maser, 8 mm, 15 MHz bandwidth, 15-18 dB gain at 4.2K *(Russian)* 78−25844
TiO_2:Cr(Ta), slightly doped, elec. cond. and defect struct., charge compensation and point defect model 80−75568
TiO_2:Cu, anodic, effect of Cu on optical props., rel. to possible appl. in solar energy conversion 80−16115
TiO_2:Fe, rutile, ESR meas. 80−54945
TiO_2:Fe^{3+}, low noise travelling wave maser, noise temp. 80−32945
TiO_2:Fe^{3+}, mag. susceptibility, cryst. field calc. 78−76035
TiO_2:Fe^{3+}, microwave second harmonic generation and freq. conversion 80−50166
TiO_2:Fe^{3+}, rutile, temp. depend. of spin Hamiltonian parameters, ESR meas. 77−32251
TiO_2:Fe^{3+}, uniaxial stress method for determ. of spin-lattice coeff. for Fe^{3+} 77−90018
TiO_2:Fe^{3+} 86-88 GHz low-noise TW maser 80−69354
TiO_2:Fe^{3+}. appl. of sensitive EPR spectrometer to zero field splitting determ. *(Russian)* 77−57372
TiO_2:Ga^{3+}, EPR spectra of trapped hole centre 78−80214
TiO_2:H photoanodes, diffusion and surface chemistry 80−35546
TiO_2:H(D)(T), IR spectra, 300, 77 and 8K 78−35175
TiO_2:Mg, high-resolution reflex images of crystal defects 78−6073
TiO_2:Mn, ESR spectrum anal. *(French)* 78−19309
TiO_2:Mn^{2+}(Mn^{4+}), anatase single cryst., ESR spectra at 77K, 300K 78−10764
TiO_2:Mn^{4+}(Cr^{3+}), rutile, temp. depend. of EPR 78−76299
TiO_2:Mo^{5+}, interstitial EPR, g-tensor and hyperfine tensor 80−84647
TiO_2:Nb, rutile, elec. cond., 1273-1623K, O_2 press. depend., charge compensation mechanism 77−85217
TiO_2:Nb, rutile, low temp. sp. ht. 78−55957
TiO_2:Nb, rutile, Seebeck effect, 90-300K 78−43427
TiO_2:Nb, Seebeck coeff., Fermi level temp. depend. 79−11161
TiO_2:Nb and TiO_2, reduced, thermoelec. power meas. at high temp., point defect model 77−32030
TiO_2:Nb semicond. electrodes, electroreduction process kinetics, cathodic dark current meas. 80−66807
TiO_2:Nb_2O_5, preparation method, effect on semiconductive props. and sintering temp. 77−16527
TiO_2:Nb_2O_5(Ta_2O_5), conduct. rel. to defect structure, obs. 77−76392
TiO_2:Ru^{4+}, rutile, EPR and cryst. field const. 80−60415
TiO_2:S, acceptor properties of S, free electron concentrations 80−34395
TiO_2:S, in O_2+CO_2+SO_2 atmosphere, elec. cond. study 80−39583
TiO_2:Sb(Fe), Mossbauer effect exam. of impurities 78−31140
TiO_2:Si(Fe)(Ni)(Mn)(Cr), anodes, performance in photoelectrolysis of water 79−74407
TiO_2:Ta, Ti^{3+}-Ti^{3+} exchange interaction *(French)* 77−89945
TiO_2:Ta_2O_5(Nb_2O_5), rutile, defect struct. and elec. cond. at 1273K 80−44604
TiO_2:$TeCl_4$ system, chem. vapour transport, matrix isolation IR studies 80−93755
TiO_2:V, localisation and migration of V^+ ions, ESR and ESCA study *(French)* 79−33529
TiO_2:V(Cr)(Mn)(Fe), impurity levels, photocurrent and ESR meas. 80−29346
TiO_2:Zn^{2+}, reduced by H_2, photoconductive props. 77−55558
TiO_2:Zr, electronic conduction, temp. depend. 77−8099
n-TiO_2/Au Schottky diodes, I-V and C-V characts. 80−96988
TiO_2/SiO_2 charge storage memory films fo IGFETs 80−11566
TiO_2-Ag-TiO_2 heat mirror on plastic sheet for radiation insulation of visible windows 80−95985
TiO_2-Al_2O_3-P_2O_5 glass, ESR of Ti^{3+}, exam. 78−88181
TiO_2-Al_2O_3-SiO_2 system, ternary glass-forming region and phys. props. 80−84919
TiO_2-aqueous electrolyte interface, pot. distrib., Mott-Schottky plots 80−11084
TiO_2-based ceramics, impurity atoms chem. state, Mossbauer spectra 80−15902
TiO_2-containing slag-glasses, phase separation and glass-ceramic formation 78−51424
TiO_2-electrolyte contact, electrolytic decomposition and photodecomposition 78−95357
n-TiO_2-electrolyte interface, electrolum. obs. 79−47520
n−TiO_2-electrolyte interface, equivalent circuit elements from impedance meas. 80−39669
n-TiO_2-electrolyte interface, charge-transfer-controlled photocurrent 80−50992
n-TiO_2-electrolyte interface, charge transfer via surface states, water photoelectrolysis anal. 80−75636
n-TiO_2-electrolyte interface impedance, freq. depend., equiv. cct. 80−100516
TiO_2-Fe_2O_3, comp. waves, Young's modulus minima rel. to crystallographic shear orientations 78−43034
TiO_2-Fe_2O_3-CaO-V_2O_5 system ferrites, TiO_2 content and thermomag. effects on dielec. props. 77−43927
TiO_2-Ga_2O_3, crystallographic shear planes and defect pair splitting, electron microscopy 77−76425
TiO_2-Ga_2O_3 system, phase relations and microstructs. 78−3107
TiO_2-Ge, elec. props., molecular deposition method 80−34525
n-TiO_2-KOH-Pt cell, water photolysis, H_2 partial press. 78−64858

titanium compounds continued
- TiO_2-$LaCrO_3$-GaP photoelectrochem. reactor for materials synthesis using solar energy 80−45712
- TiO_2-LiF film system, ATR, substrate surface polaritons reson. effect *(Russian)* 77−32384
- TiO_2-M_2O_3 (M is Al, Sc, Y or Er) system, dislocation mechanism of diffusion processes 79−77837
- TiO_2-NH_3 electrolyte interface, photo-assisted electron injection 79−87152
- TiO_2-Nb_2O_5 sputtered thin layer structure and optical props. 79−28851
- TiO_2-Ni (100) interface, electronic props., struct., comp., chemical bonding 80−84499
- TiO_2-NiO-Sb_2O_3 phase equilibria 78−44098
- TiO_2-O_2/OH^- photoelectrochemical cell, temp. effects on performance 79−92084
- TiO_2-opacified procelain enamel panels, quantitative X-ray diffr. anal. of anatase, rutile 79−32857
- TiO_2-P_2O_5 glasses, reduced, mag. susceptibility, 1 to 400K, mag. exchange between Ti^{3+} ions 79−73691
- TiO_2-P_2O_5 reduced glasses, prep., elec. transport, chem. anal., DC, AC cond., seebeck coeff. 78−30924
- TiO_2-PbO, acoustooptic props. from comp. and density 80−76000
- TiO_2-Pd Schottky barrier, work function depend. on adsorbed species 80−54782
- TiO_2-polycarbonate laminate, impulse surface flashover in vacuum, effect of normal elec. stress 79−4199
- TiO_2-RuO_2 anode, wear-resistant, use in applied electrochem. 80−40701
- TiO_2-RuO_2 surface, photocatalytic decomp. of H_2O 80−85194
- TiO_2-Sb_2O_3 system, phase comp. of roasted coprecipitates 78−23651
- TiO_2-Si, MIS capacitor, C-V charact. meas. 78−60208
- TiO_2-Si solar cell hybrid electrodes for photoelectrochem. H prod. 80−45775
- TiO_2-SiO_2, multilayer dielec. mirrors, laser-induced damage resist. 79−10335
- TiO_2-SiO_2, RF cosputtering optical film, prep. and props. 78−6849
- TiO_2-SiO_2, semicond. glass, small polaron hopping cond. 78−60126
- TiO_2-SiO_2, semicond. glass, optical props. 78−60412
- TiO_2-SiO_2, submicron dispersion of impurity, chem. diffusivity and elec. cond. 79−1528
- TiO_2-SiO_2 fibre, prep. from metal alcoholates, prep. of spinnable soln. *(Japanese)* 78−44071
- TiO_2-SiO_2 glass form. by low temp. chem. polymerisation 80−84899
- TiO_2-SiO_2 glass system, Raman and hyper-Raman light scatt. spectra 80−66187
- TiO_2-SiO_2 interference filters, narrow band, 0.7 to 1.5 μm spectral region, from cathodic sputtering 79−7221
- TiO_2-SiO_2 mirror, dielectric, Rayleigh scatt. at 441.6 nm 80−97367
- TiO_2-SiO_2 multilayer vacuum coatings, optical props. 80−97361
- TiO_2-SiO_2 multilayered film striped optical filters, optical props. and fabrication of RF sputtering 80−10030
- TiO_2-SiO_2 multilayers, laser damage, elec. field strength role 77−61993
- TiO_2-SiO_2 optical coatings, for Shiva laser optics 79−7135
- TiO_2-SiO_2 powders, anatase-rutile transition, mechanism investigation *(Japanese)* 78−95746
- TiO_2-SiO_2 reactive evaporation technique for multilayer coatings 77−10994
- TiO_2-SiO_2-Al_2O_3-MgO glasses, internal friction during crystn. 79−52285
- TiO_2-Ta_2O_5 system, surface microphases investigation by X-ray electron spectral anal. 79−51269
- TiO_2-Ti_2O_3-P_2O_5, glass form., struct. and elec. props. 80−44592
- TiO_2-Ti-Cl_2 system, thermodynamic analysis, gas phase equilibrium composition 80−21317
- TiO_2-Ti-HCl, equilibrium composition of gaseous phase and TiO_x yield 78−27393
- TiO_2-V_2O_5 interface, role of struct. props. in interfacial reactions 78−31688
- TiO_2-ZrO_2, submicron powders, vapour phase production from $TiCl_4$-$ZrCl_4$-O_2 system 80−40301
- TiO_2-ZrO_2 sputtered thin layer structure and optical props. 79−28851
- TiO_2-ZrO_2-SiO_2 amorphous film, alkali resistance, refractive index, IR spectra *(Japanese)* 78−23546
- TiO_2+C+N_2, high-temp. reaction 77−90299
- TiO_{2-x}, comparison of photoelec. props. with system $TiO_{2-x}F_x$ 79−28371
- TiO_{2-x}, nonstoichiometric and Nb_2O_5 doped rutile, defect struct. and thermodynamic props. 79−86790
- TiO_{2-x}, nonstoichiometric and Nb_2O_5 doped, defect struct. and thermodynamic props. 79−90650
- TiO_{2-x}, plasmon and polar optical phonons 77−39794
- TiO_{2-x}, reduced, cond. between elec. props. in equil. at 1100°C and after quenching, defects role *(French)* 80−44582
- TiO_{2-x} reduced, crystallographic shear planes, dislocation struct. 80−107175
- TiO_{2-x}, rutile, O chem. diffusivity, near stoichiometric ratio 77−11731
- TiO_{2-x}, slightly reduced rutile, Ti interstitials, proton channelling obs. 77−35551
- TiO_{2-x}, slightly reduced semiconducting, channelling expts. with 6 MeV protons, defect structs. 78−2117
- TiO_3 filled polycaprolactam, radiation effects *(Bulgarian)* 79−33015
- TiO_3, semicond.-metal transition, positron annihilation study 78−15246
- TiO_3:Cr_2O_3, dielec. consts., AC and DC resist. 80−20186
- TiO_3-Cl_2($SeCl_4$), equilibrium composition of gaseous phase and TiO_x yield 78−27393
- TiO_3-Dy_2O_3 sputtered film, optical waveguide with high refractive index 79−3797
- TiO_4^{4-}, normal vibr. freqs., force consts., calc. *(Russian)* 77−6759
- $TiO_{(g)}$, $TiO_{2(g)}$, thermochemistry, mass spectrometry 77−16857
- TiO_x, (x=0.88, 1.27), effect of heating at high press. on struct. 78−10190
- TiO_x, anomalous difference between theoretical and expt. densities, nonvacancy character 79−90630
- TiO_x antireflection coatings for solar cells, optical, struct., and compositional charact. 80−55852
- TiO_x evaporated films, epitaxial growth on NaCl, electron microscopy obs. 80−10822
- TiO_x film, durable optical, ion plating onto plastics, optical and mech. props. 80−38141
- TiO_x film, growth and struct. determ. 78−48328
- TiO_x, film and cryst., laser damage mechanisms 77−75592
- TiO_x films, refl., 2-25 eV 80−55123
- TiO_x, heat of form. of structural vacancies 79−14797
- TiO_x, interstitial alloy, electronic state, XPS, mag. susceptibility and elec. resist. 77−12486
- TiO_x melts, with differing valencies, density *(Russian)* 79−69173
- TiO_x, quenched and high temp. specimens, vacancy-vacancy and vacancy-electron interactions 78−79607
- TiO_x, reactive sputtering, film prep. conditions rel. to stoichiometry 77−40370
- TiO_x, struct. and coalescence of oxide particles, during internal oxidation of Cu-Ti, Cu-Ti-Si, and Cu-Ti-Fe *(Russian)* 79−90781
- TiO_x, struct. vacancies in unit cell 80−107213
- TiO_x, surface film on plasma anodised Ti, comp. determ. 77−48591
- TiO_x, UPS meas. of band struct., energy gap 78−72698
- TiO_x, vacancy ordering, transition state cluster model, electron diffr. 77−47547
- TiO_X, X-ray emission spectra, $K\beta_{1,3}$ line width and $K\beta_5$ band 78−2946
- TiO_x, X-ray Ti K spectra and band struct. 77−77320
- TiO_x-Ti selective solar absorber, optical props. and heat resist. 79−65951
- TiO_y, thermal expansion of cubic phase at low temp. X-ray diffr. anal. 79−1514
- TiO_y, thermal expsn. coeffs., lattice spacing temp. depend. 77−69102
- Ti_2O_3, 3d-T_{2g} band optical transitions near conductivity transitions, temp. depend. 79−19900
- Ti_2O_3, $(Ti_{0.98}V_{0.02})_2O_3$, lattice parameters, temp. depend. 77−11855
- Ti_2O_3 alloyed into V_2O_3, semicond. to semimetal electrical transition, lattice parameter changes 79−60714
- Ti_2O_3, cryst. growth by chem. transport and tri-arc methods, and characterisation 78−3003
- Ti_2O_3, crystal and band struct. calcs. 80−49858
- Ti_2O_3, electron density distrib., deform. density at 295K, X-ray anal. 80−107117
- Ti_2O_3, electron structures calc. using models, ESCA and X-ray spectral data 77−35863
- Ti_2O_3, electronic structure from single crystal thermoreflectance spectroscopy 79−87420
- Ti_2O_3, IR refl. spectra, IR active phonons, Ti 3d electronic effects 78−35145
- Ti_2O_3, metal-semicond. transition, refl. spectra study 80−10880
- Ti_2O_3, new synthesis method *(French)* 79−100095
- Ti_2O_3, optical consts., polarisation dependent reflectivity 78−52531
- Ti_2O_3, piezoresistivity and semiconductor-semimetal transition 79−42595
- Ti_2O_3, press. depend. of elastic consts. at 296K. 79−42134
- Ti_2O_3, semicond., effect of stress on elec. resist. 78−34832
- Ti_2O_3, semiconductor-metal transitions, photoelectron spectra meas. 78−84144
- Ti_2O_3, struct. changes at semicond.-metal transition 77−47397
- Ti_2O_3, structural changes associated with semicond.-metal transition 77−15583
- Ti_2O_3, XPS, band states 77−20986
- Ti_2O_3:Sc_2O_3(Al_2O_3), struct. changes on Sc(Al) substitution 77−55276
- Ti_2O_3:V_2O_3, XPS, band states 77−20986
- Ti_2O_3-$MgTiO_3$, phase analysis 78−3103
- Ti_3O_5, semiconductor-metal transitions, photoelectron spectra meas. 78−84144
- Ti_3O_5-Al_2TiO_5 ($MgTi_2O_5$), solid solubility, X-ray phase and optical microscopic exam. 80−59657
- Ti_3O_5-V; semicond.-metal transition, resist., enthalpy and mag. susceptibility changes obs. 77−62965
- Ti_4O_7, controlled growth by chem. transport reactions 77−90262
- Ti_4O_7, hopping conduction and the Coulomb gap 80−44605
- Ti_4O_7, metal-insulator transition, EPR elec. and mag. props. 80−2336
- Ti_4O_7, optical absorpt. and metal-insulator transitions 78−15165
- Ti_4O_7, semicond.-semicond. transition, lattice gas model 77−1364
- Ti_4O_7, Verwey transition, cond. processes 80−96787
- Ti_5O_9, phase transitions, elec. cond., mag. susceptibility, sp. ht., EPR and struct. aspects 78−10526
- Ti_6O_{11}, electron-optical imaging, at 1.6 Å point-to-point resolution 79−46531
- Ti_nO_{2n-1}, ^{18}O tracer diffusion coeff. determ. by continuous mass spectrometry 77−20124
- Ti_nO_{2n-1}, cryst. growth and characterisation 78−31311
- Ti_nO_{2n-1}, long-range strain and localised relax. energies of crystallographic shear structs. 79−94948
- Ti_nO_{2n-1}, reduced rutile, elastic strain energy due to crystallographic shear plane arrays 78−55880
- Ti_xO_y film, interference enhanced Raman scatt. 80−40105
- Ti_xO_y film, AES, with and without simultaneous sputtering, beam effects 77−90224
- TiO_2(-Cr_2O_3), rutile, Cr_2O_3 effects on O_2 tracer diffusivity, depth profile meas. by SIMS 80−24651
- $TiO_{2-x}F_x$, comparison of photoelec. props. with system TiO_{2-x} 79−28371
- $Ti(OH)_4$ in polyacrylamide gel, U(VI) extraction from seawater 78−54861
- $Ti(OH)_4$, polyacrylamide gel, adsorption of U (VI) from sea water *(Japanese)* 77−54347
- $Ti(OH)_x$, amorphous, dehydration and crystallisation 77−43150
- TiO_yH_m, cubic phases, lattice consts. meas., thermal expansion coeffs. calc. 79−55906
- TiO_yH_m, thermal expansion of cubic phase at low temp. X-ray diffr. anal. 79−1514
- $TiO_yN_zH_m$, m=0, 0.31-0.34, thermal expansion, H at. ordering 79−10971
- $(Ti_2O_3)_{1-x}(V_2O_3)_x$, lattice polarisability, electronic contribs. IR refl. obs. 78−59904
- TiO_2.$6Bi_2O_3$, IR and Raman spectra, vibr. anal. 78−76464
- TiO_2.nH_2O, U extraction from seawater by adsorption-exchange concentration 78−36198
- $TiO_{1.95}$iFe, quenched near melting point, transverse composition waves 79−99220
- TiOy, annealed, lattice const. meas., thermal expansion coeffs. calc. 79−55906
- TiP, and TiP_2, valence electron energy spectrum, deduced from X-ray spectra and XPS 79−99984
- TiP, direct two-temp. synthesis 77−81237
- TiP, form. by high temp. reaction of Ti with P 78−44260
- TiP, metallic, band struct., X-ray spectral obs. 78−11019
- TiP, TiP_2, electronic struct. of valence bands, X-ray spectra and XPS 78−92176
- TiP, TiP_2, iodide synthesis, and catalytic props. of TiP 80−55316

titanium compounds continued
TiP whiskers growth, on gold drops in VLS growth 79−4497
TiP-I_2, exam. of equilibrium gas-transport reaction 79−95911
TiP_2, synthesis and characts. 77−85953
Ti_3P-type structures, atomic coord. and bonding 79−60330
$Ti_x(PO_4)_y$, neutron activation determ. of macrocompounds *(Russian)* 77−32859
TiS, $C^1\Sigma_2$-$X^1\Sigma_2$, Franck-Condon factors and r-centroids 79−36700
TiS, disordered structures, two-dimensional, computer program for modelling *(French)* 80−59337
TiS, vaporisation chemistry and thermodynamics, computer-automated simultaneous Knudsen-torsion effusion 80−48837
$TiS_{1.46}$, $(4H)_2$-4C type superstruct., high resolution electron microscopy determ. 79−69060
$TiS_{1.5}$, $(4H)_3$-6C-type superstruct. revealed by high resolution microscopy 80−19755
$TiS_{1.7}$, hexagonal polytypes form. mechanism 78−9990
$TiS_{1.7}$, screw dislocs., X-ray topography 77−47460
TiS_2 (1T), electronic and vibronic struct. 80−44500
TiS_2, band struct., angle-resolved photoemission studies 80−70610
TiS_2, carrier-lattice coupling 78−63822
TiS_2, charge densities, X-ray form factors, and bonding props. 79−94950
TiS_2, chem. transport rate effects on stoichiometry 77−90263
TiS_2, core states, energy bands, and valence densities of states 79−95322
TiS_2, elect. resist. at room temp., press. depend. to 80 kbar 80−49730
TiS_2, electron energy loss spectra, dielectric function, reflectivity and absorption coefficient 79−69937
TiS_2, electronic struct. and props., self consistent numerical basis set LCAO calc. 77−89698
TiS_2, evidence for semicond. props., Hall coeff., refl., cond., thermoelec. power 80−20220
TiS_2, fast ion transport and electrochem. storage, Li reactions 80−61324
TiS_2, LEED, single-reflection layer scatt. theory 80−49059
TiS_2 layer compound, electronic ground state, band struct. calcs. 77−51651
TiS_2, layer compound, expansivities and thermal degradation 77−89554
TiS_2, layer cpd., metal-insulator transitions, energy gap calcs. 79−78009
TiS_2, nonstoichiometric, chem. transport reaction mechanism 77−8735
TiS_2, resistivity, Hall effect and mag. suscept. 78−79991
TiS_2, semicond. charact. under press., in-plane resist. and Hall coeff. meas. 78−23086
TiS_2, semimetallic charact. 77−62926
TiS_2, stoichiometric, heat capacity from 100 to 700K 80−10679
TiS_2, transport props. and semicond. nature 80−44598
TiS_2, transport props. under press. 79−95410
TiS_2, V addition effect on chemical transport 79−24419
TiS_2, vacuum UV reflectivity spectra, cond. band model 77−44012
TiS_2, valence density of states 80−44465
TiS_2, valence density of states, Gilat-Raubenheimer method 80−88465
TiS_2-I_2 system, thermodynamic considerations for layered dichalcogenide growth by vapour transport process 79−4903
TiS_2-Na_2S(K_2S) systems, synthesis of Na_2TiS_3, K_2TiS_3, K_4TiS_3 and K_8TiS_6 *(French)* 79−52636
TiS_2+Li, intercalation chemistry and electrochemical energy storage 79−100541
TiS_3, linear chain compound, lattice props., Raman spectral study 80−71421
TiS_3 synthesis 80−35141
TiS_x, cathodes in secondary Li batteries, operating characts. 77−86320
$Ti_{1+x}S_2$, polytypic struct., Ti ordering, two-dimensional model 79−14776
$Ti_{1+x}S_2$, short-range ordering, electron and X-ray diffuse scatt. 77−19936
$Ti_{1+x}S_2$, vacancy ordering, transition state cluster model, electron diffr. 77−47547
$TiS_2(ND_3)$, intercalation system, wideline NMR, temp. effects 77−16184
$TiS_2(NH_3)$, intercalation complex, wideline NMR obs., translational and reorientational effects 77−1602
$TiS_2(NH_3)_{1.0}$, NMR spectral densities and two-dimens. diffusion 80−50215
$TiS_2(Se_2)$, and alkali metal intercalates, phys. props. 80−44179
$TiS_2(Se_2)$, modelling contrasting semimetallic characters 78−43393
Ti_xSb_3, struct. study, space groups *(French)* 77−68949
$(Ti_{1-x}Sc_x)_2O_3$, crystal struct. determ., metal-metal distance, effect on electronic struct. 77−47431
$Ti_3Sc_4O_{12}$, cryst. struct. determ., powder X-ray diffr. exam. 77−4083
TiSe, optical phonon modes and localised effective charges, reflection spectra 78−76453
$TiSe_2$ (1T), structurally induced semimetal-to-semicond. transition, ab initio LCAO calc. 78−51896
$TiSe_2$ (1T), effect of CDW on optical spectra 79−95738
$TiSe_2$ (1T), electronic and vibronic struct. 80−44500
$TiSe_2$ (1T), lattice dynamics and phase transitions 78−79727
$TiSe_2$ (1T), phonons and CDWs, inelastic neutron scatt. meas. 79−28059
$TiSe_2$ (1T), Raman studies of lattice dynamics 80−103962
$TiSe_2$, band struct., angle-resolved photoemission studies 80−70610
$TiSe_2$, CDW and accompanying periodic structural distortions 78−72094
$TiSe_2$, CDW transition temp. and transport props. pressure depend. 79−99550
$TiSe_2$, carrier-lattice coupling 78−63822
$TiSe_2$, charge densities, X-ray form factors, and bonding props. 79−94950
$TiSe_2$, core states, energy bands, and valence densities of states 79−95322
$TiSe_2$, electronic instability, ^{77}Se NMR 78−10790
$TiSe_2$, IR reflectivity, phonons and free carriers 79−61379
$TiSe_2$ impurity effects on elec. props. 80−80263
$TiSe_2$, intercalation with Na and K, struct. and phase limits *(French)* 77−35536
$TiSe_2$, lattice dynamics, charge density waves transverse phonon dispersion curves, model 80−49322
$TiSe_2$ layer compound, electronic ground state, band struct. calcs. 77−51651
$TiSe_2$, layer cpd., metal-insulator transitions, energy gap calcs. 79−78009
$TiSe_2$, mechanism for 200K transition, sp. ht. meas. 78−22853
$TiSe_2$, optical refl. spectra obs., suppression of antiferroelectricity by excess carriers 77−59536
$TiSe_2$, quasi-two-dimens. layered struct., phonon dispersion surfaces 79−42180

titanium compounds continued
$TiSe_2$, semimetal, electronic props., superlattice form. 77−15532
$TiSe_2$, semimetal, IR props. 79−24318
$TiSe_2$, semimetallic behaviour band struct. from local-density functional approach 78−56070
$TiSe_2$, semimetallic charact. 77−62926
$TiSe_2$, semimetallic charact. under press., in-plane resist. and Hall coeff. meas. 78−23086
$TiSe_2$, structural distortion, band Jahn-Teller type mechanism 77−62875
$TiSe_2$, superlattice formation, Raman and far IR spectra 78−35135
$TiSe_2$, transport props. under press. 79−95410
$TiSe_2$, UPS, excitonic instability indicated from study of band struct. 78−56069
$TiSe_2$, vacuum UV reflectivity spectra, cond. band model 77−44012
$TiSe_2$, valence density of states, Gilat-Raubenheimer method 80−88465
$TiSe_2$ Young's modulus and internal friction obs., 1.3 to 300K 79−46750
$TiSe_2$:Ta(V), transport props. and phase transition 78−72149
$Ti_{1+x}Se_2$, superlattice form., phase transform., electron and X-ray diffr. meas. 77−15383
$Ti_{1+x}Se_2$, superlattice form. and phase transition, IR reflectivity meas. 79−24322
TiSi, thermal expansion, microhardness, Debye temp. meas. 77−35717
$TiSi_2$, crystal atomic struct., X-ray diffr. exam., lattice parameters and integrated intensities 78−75647
$TiSi_2$, film, elastic stiffness and thermal expansion coeffs. 80−107451
$TiSi_2$ RF sputtered wear-resistant coatings, XPS study of adherence 79−34191
$TiSi_2$, self-propag. high-temp. synthesis 80−2988
$TiSi_2$, thermal expansion, microhardness, Debye temp. meas. 77−35717
$TiSi_2$, TiSi, Ti_5Si_3, formed by solid state reaction of Ti film on Si, backscattering anal., of layer structure 79−69377
$TiSi_2$-$CrSi_2$, phase equilib., struct. and props. 80−50608
Ti_5Si_3, self-propag. high-temp. synthesis 80−2988
Ti_5Si_3, thermal expansion, microhardness, Debye temp. meas. 77−35717
Ti_xSi_y, work function rel. to phys. props. 77−47887
TiT targets, prod. of DT neutrons by d^+ beam irradiation analysed 77−18727
TiT$_{1.9}$, ^{3}He distrib. 78−30661
$Ti_{1-x}Ta_xO_2$, solid soln. formed in TiO_2-Ta_2O_5-Ta at 1100°C *(French)* 78−35375
$TiTe_2$, layer type cpd., reflectivity meas., 6-40 eV 77−55801
$TiTe_2$, struct. refinement by neutron diffr. 79−27967
TiU_4, intensity changes between He(I) and He(III) photoelectron spectra 78−21969
$Ti_xV_{1-x}C$, electronic struct. and X-ray emission spectra, cluster MO calc. 80−65444
$Ti_xV_{1-x}Cy$ solid solutions, mag. susceptibility and band struct. 79−51739
$Ti_{1-y}V_yH_x$, electronic props., H alloying effects, book contrib. 79−82522
$(Ti_{0.9}V_{0.1})_2O_3$, spin glass, dynamic mag. susceptibility meas. 80−39792
$(Ti_{0.99}V_{0.01})_2O_3$ spin glass, sp. ht. anomaly and entropy change 79−56546
$(Ti_{0.9975}V_{0.0025})_4O_7$, metal-insulator transition, struct. aspects 79−86752
$(Ti_{1-c}V_c)_4O_7$ order-disorder and metal-insulator transition theory 80−24802
$(Ti_{1-x}V_x)_2O_3$, crystal struct. determ., metal-metal distance, effect on electronic struct. 77−47431
$(Ti_{1-x}V_x)_2O_3$, nonlinear magnetisation at spin glass phase transition temp. 79−78403
$(Ti_{1-x}V_x)_2O_3$, $O<x<0.1$, magnetisation and mag. moments 80−65772
$(Ti_{1-x}V_x)_2O_3$, single crystal, anisotropic susceptibility 79−87228
$(Ti_{1-x}V_x)_2O_3$ solid soln., struct. changes comp. depend. 77−55275
$(Ti_{1-x}V_x)_2O_3$, spin glass, nonlinear susceptibility and sp. ht. 80−60304
$(Ti_{1-x}V_x)_2O_3$, spin glass props. and anisotropy, comp. depend. 77−66368
$(Ti_{1-x}V_x)_2O_3$, spin glass to antiferromag. regime 78−52276
$(Ti_{1-x}V_x)_2O_3$, spin glass and metallic antiferromagnetism 78−68268
$(Ti_{1-x}V_x)_2O_3$, spin-glass props., 0.05-300K 80−25149
$(Ti_{1-x}V_x)_2O_3$, susceptibility and ^{51}V NMR expts., spin glass behaviour 77−66369
$(Ti_{1-x}V_x)_2O_3$, US velocities in high mag. field 78−84262
$(Ti_{1-x}V_x)_4O_7$, elec. cond. and phase diagram near metal-insulator transition 80−11054
$(Ti_{1-x}V_x)_4O_7$, mag. susceptibility calcs. 78−91850
$(Ti_{1-x}V_x)_4O_7$, metal-insulator transition investig. by resist., sp. ht. and X-ray diffr. 77−43497
$(Ti_{1-x}V_x)_4O_7$, metal-insulator transition and mag. behaviour 78−51895
$(Ti_{1-x}V_x)_4O_7$, metal-insulator transitions, EPR, elec. and mag. props. 80−2336
$(Ti_{1-x}V_x)_4O_7$, order-disorder and metal-insulator transitions 80−39504
$(Ti_xV_{1-x})O_3$, impurity doping effects, elec. props. obs. 80−75609
$Ti_{1-x}V_xS_2$, resistivity, Hall effect and mag. suscept. 78−79991
$Ti_{0.99}V_{0.01}Se_2$, negative mgnetoresist. and nonlinear cond. 79−87105
$Ti_{0.99}V_{0.01}Se_2$, negative magnetoresist. and nonlinear cond. 80−44617
$Ti_{1-x}V_xSe_2$ ($0\leq x\leq 0.1$), elec. resist. and Hall effect 80−2386
$Ti_{1-x}V_xSe_2$, mag. susceptibility, 4.2-300K 80−60188
$(Ti_{1-x}V_x)_2O_3$, metallic antiferromag. struct., neutron studies 80−65797
TiW-TiO_2-InP thin refractory MIS struct. deposition 80−75647
TiX_4, (X=Cl,Br,I), He I and He II photoelectron spectra, ionis. energy, chem. bonding 78−46394
TiO, electronic polarisability of ions 77−40175
TiO_2 electrodes, effect of processing variables on photoelectrochem. props 80−6975
TiO_2 electrodes, room temp. diffusions, capacitance, spectral response and volt-ampere characts. 80−15294
TlF+Ar, scatt., l_2-conserving sudden approx. calcs. 78−66628
V-Ti-C precipitation, high temp. coarsening, of dispersions in ferrite 78−84874
VC-TiC, deposited by activated reactive evaporation, TEM and hardness 79−23872
VC-TiC coating, high rate deposition by activated reactive evaporation, and characterisation 78−11372
V_2O_3-Ti_2O_3, struct. and mag. props. 78−27041
V_2O_3-Ti_2O_3-TiO_2, phase equilib. at 1473K 77−16562
V_2O_5-$TiNb_2O_7$ system, interfacial reactions, efficient boundary conditions and solid state reactivity 80−76542
V_3O_5-Ti_3O_5, DTA, mag. susceptibility and X-ray diffr. study 80−70970
$(V_{1-x}Ti_x)Ge$, pseudobinary A15 compound, supercond. transition temp. 80−49970
$V_{1-x}Ti_xO_{1.75}$, synthesis and mag. susceptibility obs. 78−23243
$V_{1-x}Ti_xO_2$, metal-insulator transition, resist. meas. 78−14770

titanium compounds continued
$(V_{1-x}Ti_x)_2O_3$:Fe, metallic antiferromagnetism, Mossbauer spectra 80−15881
$V_xTi_{1-x}S_2$, elec. and mag. props. 79−65504
$V_xTi_{1-x}Se_2$, cryst. struct. and elec. props. 79−47133
Y_2O_3-TiB_2, ceramic, production by sintering in vacuo, or hot moulding at 1500°C 78−60629
Y_2O_3-TiO_2 system, elec. cond. at 700-1000°C 79−78100
$YTiTaO_6$, powder X-ray diffr. data 79−99155
Zn-Ti-Fe-O, spinel solid solns. 77−48409
ZnO-TiO_2 system, heat treated, X-ray anal. of phase form. sequence 79−1850
ZnTi ferrites, electron exchange between Fe^{2+} and Fe^{3+}, paramag., Mossbauer spectra and susceptibility meas. 77−63327
Zn_2TiO_4 crysts., grown by Bridgman techniques, as substrate for $(Mn_xZn_{1-x})Fe_2O_4$ growth 79−100065
ZrB_2-TiB_2 solid solns., prod., oxidation rate corrosion resist. 77−52274
ZrO_2-TiO_2 refractories, TiO_2 effect on props. and phase composition 79−38809
ZrO_2-TiO_2 solid solns., X-ray diffr. and thermogravimetric meas. 79−90792
ZrO_2-TiO_2 system, adsorption of electron acceptors, strength and distrib. of electron donor sites 78−84055
ZrO_2-TiO_2 system, Z *(Ukrainian)* 79−96007
$ZrSiO_4$-TiO_2, solid soln. formation, zircon stability 77−48377

Tokamak devices
34MW 120MJ pulsed DC supply for Divertor & Injection Tokamak Expt. 79−31214
200 kV Blumlein transmission line for Tokamak plasma heating, calc. and obs. 79−55521
600 MW pulsed energy convertors for toroidal field coil, design philosophy 78−58496
AC, design criterion 80−38726
acceleration system, two stage, in megawatt power ion source, numerical simulation for design 78−94941
accelerator technology in Tokamak plasma confinement devices 77−84527
adiabatic plasma compression, impurity spectra and Thomson scatt. *(Russian)* 77−76192
air-core Tokamak, optimisation of ohmic heating coil configurations 80−14914
Alcator, effect of wall temp. on O, N and C impurities, spectroscopic diagnostics 79−41840
Alcator, electron cyclotron emission, polarisation freq. depend. 80−33808
Alcator, geometrical and elec. props., rel. to THOR 79−98993
Alcator, reduced fusion neutron production 78−63577
Alcator C, design and discharge parameters, review 80−79533
Alcator C far IR emission diagnostics of electron temp. 80−59291
Alcator high density Tokamak, ion temp. profile reconstruction *(Russian)* 80−106959
Alcator tokamak, classical energy confinement 79−60172
Alcator tokamak, cyclotron radiation emission 79−60171
Alcator Tokamak, energy balance, MHD activity 80−28838
Alcator Tokamak, heat loss, mag. fluctuation mechanism 79−1292
Alcator Tokamak, high-density D_2 discharge parameters obs. 78−18438
Alcator tokamak, low q operations 79−60173
Alcator Tokamak, vacuum system, surface props. 78−71549
Alcator Tokamak submillimetric-wave emission obs. 79−32816
Alcator-C, mag. coil systems 78−50355
Alfven wave instability excitation by trapped α-particles 77−65855
ALVAND 2 diagnostic Tokamak construction 78−14217
arcing observations in ISX Tokamak 80−33836
Argonne/GA TNS Tokamak reactor supercond. ohmic heating coil design 79−31197
ASDEX, assembly and commissioning, review 80−102334
ASDEX, divertor expt., plasma-wall interaction 77−31504
ASDEX, extraction grid for high power ion source 80−102372
ASDEX, neutral beam injection, beam line design 80−99395
ASDEX, neutral beam injectors, HV power supply system, thyristor control 80−99332
ASDEX divertor Tokamak, toroidal and poloidal mag. field coils 78−50352
ASDEX fusion experiment, toroidal field coil construction features *(German)* 78−54877
axisymmetric equilib., flux surface shape and current profile optimization, resistive interchange stability 77−84480
axisymmetric Tokamak plasma MHD equilibria and Mercier local stability criterion 78−51333
back biasing for ISX Tokamak 78−71560
bakeable seals development for large noncircular ports on Tokamak fusion test reactor 80−82777
ballooning modes and pressure limits 80−28647
banana drift diffusion, Tokamak mag. field with ripples, model collision operator 77−65839
beam focusing, by aperture displacement, in two-stage acceleration system 79−46496
Berkeley multicusp ion source for use with TFTR neutral beam injector, characts. 80−54040
bifurcated equilibria, rel. to shrinking and disruption of current, kink mode 78−34359
blanket, liq. Li module stresses due to changing poloidal mag. field 80−95435
blanket and first wall design concept, thermal and hydraulic anal. 80−95460
bundle divertor, mag. config., wall impurity removal for Tokamak 77−65901
burn period plasma current maintenance, rectifying first wall, cct. anal. 80−102307
catalysed-D Tokamak reactors, direct energy converter attachment 77−88277
chopper system, UHV compatible, for meas. of energy spectrum of neutral D atoms 80−79587
cold plasma blanket for Tokamak, heat diffusion and temp. profile 77−65902
cold-banket systems, boundary layer analysis 80−28605
collisional divertor scrape-off layer in Tokamak, plasma transport 80−28614
collisional drift instability, shear stabilisation 78−59569
commercial fusion reactors, small Tokamak hybrid design 80−13797

Tokamak devices continued
commercial Tokamak fusion power reactor remote systems requirements 79−13525
commercial Tokamak hybrid reactor, blanket and shield design 80−106179
commercial Tokamak Hybrid Reactor, reference design 80−106171
commercial Tokamak reactor, 1000 MWe energy storage and transfer systems 79−76127
compact ignition test reactor, engineering design using Bitter type magnet 80−102310
compact Tokamak fusion reactor, conceptual design of commercial reactor 79−71970
compact Tokamak fusion reactor, nucleonic design for blanket and shield 79−81086
conference, New York, USA (Oct. 79) 80−73093
confinement and stability, effects of shaping and compression of plasma 80−28772
confinement time meas. 80−87945
construction, objectives and performance of future devices 77−34452
contacts for pulsed high currents, design and testing 80−70029
control coil optimum design, nonlinear optimisation 77−27744
control systems, construction and simulation study *(Japanese)* 80−100100
controlled fusion research and the Joint European Torus project 80−18593
controlled nuclear fusion, progress and problems review 79−36415
controlled Tokamak plasma, simulation 80−59269
cooling pattern of acceleration grids meas. by IR scanning 80−86303
corpuscular diagnostics by charge exchange of plasma ions at artificial target, in Tokamak T-4 *(Russian)* 80−83968
cryopumping, experimental system 79−58753
cryopumps for Tokamak reactors 77−30672
CT6B Tokamak, measurement of plasma column displacement 80−84001
CT-6 Tokamak device, development, test operation *(Chinese)* 80−87919
CT-6 Tokamak plasma props. *(Chinese)* 80−103159
CT-8, mag. field design *(Chinese)* 80−43995
CTR, nuclear energy strategy, Japan, possibility of FFHR 80−42868
CTR blanket design and associated problems *(Japanese)* 77−50286
CTR developments 77−67882
Culham Conceptual Tokamak Reactor Mk II, reactor costs and maintenance 77−74978
current disruption effects 80−74012
cyclotron radiation from Tokamak plasmas, diagnostic tool *(Dutch)* 78−30472
cylindrical plasma filament under axisymmetric perturbation, numerical anal. 80−106853
Demonstration Power Tokamak Reactor, vacuum outer containment and metal seals feasibility study 80−95458
Demonstration Tokamak Hybrid Reactor, design of advanced bundle divertor 80−13834
diagnostic Fourier transform spectrometer calibration by liquid N_2 cooled microwave absorber 80−59304
discharge cleaning in JFT-2 Tokamak, AES 78−51316
disruptions and turbulence in Tokamaks 80−28675
disruptions in Tokamaks and small scale turbulence 80−59266
dissipative trapped electron instability dispersion relation, ion-ion collisions 78−34290
DITE, arcing, time-resolved meas. 80−10436
DITE, arcing and surface damage, SEM obs. 78−59611
DITE, behaviour review including injection and bundle divertor 80−74021
DITE, low Q discharges 80−92374
DITE, neutral injection heating 80−92347
DITE Tokamak, beam driven current meas. 80−106940
DITE Tokamak, impurity ion concentrations and diffusion, spectroscopic measurement 80−28771
DITE Tokamak 80−28688
DITE Tokamak bundle divertor, Mk.II design 80−91268
DITE Tokamak re-cycling expts., interferometry, mass spectrometry and C thermal desorption probe 78−34356
DITE-II, neutral beam ion source particle beam identification 80−99397
DIVA, mag. divertor action for impurity control 79−4196
Diva, metal impurities origin, arcing ion sputtering, evap. 78−59691
DIVA, metal-impurity, confinement, discharges 80−28843
DIVA, methane pulsed injection into DIVA Tokamak, transport props. 78−79411
DIVA, scrape off layer, multigrid energy analyser applications 80−33818
DIVA, X-ray emission from Au impurities in H_2 plasma 79−32820
DIVA superthermal electron behaviour in scrape-off layer 78−30495
DIVA Tokamak, q=1 mag. surface noncircular cross-section, in low-q discharge 80−100090
divertor injection Tokamak experiment, plasma stability, energy and particle transport, and hydrogen recycling 80−28834
divertor mag. piston action, elec. AC power direct generation 80−102324
divertor Tokamaks, refuelling methods, pellet-plasma interaction 80−28841
divertorless Tokamaks, limiter pumping system 80−95463
Doublet IIA, doublet config. control, electron density, confinement time 77−80341
Doublet III, computer control system 80−99321
Doublet III, fusion reactor, noncirc. discharge, ohmic heating 80−52785
Doublet III, limiter performance, design and material selection 80−106162
Doublet III, neutral beam injection system, two-gap magnet design and performance 80−92379
Doublet III, neutral beam injection system 78−54970
Doublet III, neutral beam injector system, instrumentation and control 80−99322
Doublet III, neutral beam interlock system using IR detector 80−106228
Doublet III, neutral beam test tank design 80−99301
Doublet III, ohmic heating E-coil vacuum breaker system, function and operation 80−102323
Doublet III, plasma density, shaping and characteristics 80−74018
Doublet III, plasma shape control, 1.5 Megawatt DC chopper power supply 80−102333
Doublet III, possible Dee configs. 80−91269
Doublet III, toroidal field coils, Cu alloy plate defect size restrictions 80−91257

Tokamak devices continued
Doublet III, vacuum vessel neutral beam armour 80−95462
Doublet III beamline, review, component relation and config., design constraints 80−99382
Doublet III beamline calorimeter, three dimens. heat transfer anal. 80−99381
Doublet III neutral beam injector system, outgassing rate meas. and residual gas anal., coating props. 80−95457
Doublet Tokamak devices. TNS to demo, review 79−71968
Doublet-III, frequency generator-rectifier system performance 80−102326
driven magnetic fusion reactors, conf., Erice-Trapani, Italy (Sept. 1978) 80−41948
DTHR, advanced bundle divertor design 80−99281
eddy currents induced in vacuum vessel, anal. 80−1832
edge cooling during RF heating, high-Z impurity prevention 78−67400
EF coil energy transfer supercond. solenoids and phase-shifting bridge 79−31213
electrically isolated target, formation of arcing, role of runaway electrons 80−64764
electron beam driven Tokamaks, review 80−99317
electron cyclotron emission spectrometry by plasma-scanned Michelson interferometer 79−32814
electron cyclotron freq. absorpt. in finite density thermal plasma, optical thicknesses 79−64874
electron cyclotron heating, Bernstein modes, Vlasov dispersion relation 80−33809
electron density meas. in Tokamak plasma, far IR waveguides for interferometers 79−73034
electron temp. and spatial distrib., soft X-rays meas. *(Russian)* 77−47260
electron-cyclotron wave heating, cyclotronic attenuation energy loss calc. *(Russian)* 77−47225
energy confinement comparison of ohmically heated stellarators to Tokamaks 80−92360
energy confinement scaling, Frascati Torus results 80−79536
energy lifetime of plasma, T-3 scaling law 80−28635
energy loss determ., fast time resolution bolometer *(Russian)* 77−76193
energy storage for Tokamak reactor cycles 78−62661
enhanced plasma loss due to secondary currents, Tokamaks and non-Ohmic stellarators 77−65884
enhanced plasma-frequency radiation *(Chinese)* 80−59185
ERASMUS, low aspect ratio Tokamak, characts., RF expts. 79−99000
ETF, design considerations 80−95438
ETF, engineering challenges, review 80−95422
experimental fusion reactor preliminary design 77−74981
experimental power reactor, plasma position control and sensor requirements 78−62628
experimental power reactor, shielding of major penetrations 77−34455
Experimental Power Reactor remote maintenance considerations 79−9883
experimental Tokamak device, pulsed homopolar power supply 77−23286
far IR laser collective scatt. system 80−59300
fast electron intensive transverse migration *(Russian)* 78−18382
field coil design for fusion-driven actinide burner 77−27693
field line reconnection and disruptive instability 77−43045
filament ellipticity, energy lifetime in T-8 apparatus *(Russian)* 80−87930
finger ring Tokamak, plasma stability region *(Russian)* 77−51165
finger-ring Tokamak T-12, poloidal divertor mag. config. MHD and vertical stability effects *(Russian)* 78−59643
FINTOR-D, T breeding blanket, Monte Carlo calcs. 80−99283
first wall blanket, cylindrical module, reference design 80−106181
first wall materials, effect on Tokamak plasmas 80−38692
first-wall characterisation by in situ Auger electron spectroscopy 78−5022
FM-1 spherator, microwave scatt., drift wave turbulence 77−65912
force-cooled superconductor design for large fusion magnets 79−31216
formation of plasma in fusion devices, at. and plasma processes, diagnostic techniques 80−48915
Frascati high field Tokamak, technological aspects 78−50351
French Tokamak research *(Russian)* 80−38690
FT Tokamak, electron energy replacement time and total energy containment time 80−28836
FT Tokamak, non-thermal electron distrib. function 80−83891
FT tokamak, operation at cryogenic temperature 79−60170
FT Tokamak, status report 79−99004
FT Tokamaks, expt. results 80−74014
FT-1, lower-hybrid heating using decelerating system, neutrals diagnostics *(Russian)* 79−98927
FT-1 Tokamak, discharges in low density plasma *(Russian)* 80−106958
FT-1 Tokamak, electron cyclotron heating expt. 80−75071
FT-1 Tokamak, electron density and temp. radial distrib. laser scatt. obs. *(Russian)* 78−59666
FT-1 Tokamak, lower hybrid heating, energy balance 80−79523
FT-1 Tokamak, lower hybrid plasma heating 80−28700
FTR, equilib. field coils, electrical supply system, optimisation and computer aided performance anal. 80−91288
fueling and thermonuclear instability, cold plasma layer surface fueling source 80−59196
fusion devices, controlled, surface effects, conf., San Francisco, USA (Feb. 1976) 77−30659
fusion devices, development and testing of toroidal field superconductors 79−59263
fusion devices, secondary ion emission, appl. to impurity control 80−37584
fusion experimental power reactor, first-wall/limiter design 79−85797
fusion hybrid demonstration reactor, eval. of steam and boiling-water cooled blanket concepts 79−85789
fusion machine, boundary conditions for cryopumping 77−30671
fusion possibilities and plasma confinement and interactions in mag. config. Tokamak, review *(French)* 80−54017
fusion power generation 78−74472
fusion power plant economics, effect of major design parameters 79−76141
fusion power reactor conceptual designs 77−34453
fusion power stations, economic evaluation 79−76147
fusion power systems technology 78−50345
fusion reactor, advanced fuel type, bundle divertor design 77−38413
fusion reactor, Al low activity blanket 77−6560

Tokamak devices continued
fusion reactor, axisymmetric, slowing-down alpha particle loss, Monte-Carlo calc. 78−59653
fusion reactor, beam-driven, nucl. reactions among energetic ions 77−34469
fusion reactor, catalysed-D, startup investig. 77−34470
fusion reactor, commercial, plasma driving system requirements 78−54954
fusion reactor, compact high-density, system of field coils 77−34464
fusion reactor, design modifications to simplify remote maintenance 80−18613
fusion reactor, doublet Tokamak, parallel connected ohmic heating coil 78−54930
fusion reactor, efficient particle removal using liq. Li getter 77−38411
fusion reactor, flux-conserving, high power density, performance characts. 80−23124
fusion reactor, graphite blanket design concepts at BNL 77−3164
fusion reactor, high mode number ballooning instabilities, max. β-value 80−73995
fusion reactor, impacts of plasma perform. parameters on vacuum and T system design 79−76131
fusion reactor, magnet coil radius optimisation 77−42191
fusion reactor, material and design options for superconducting TF magnets 79−85801
fusion reactor, neutron flux and energy released in blanket 77−34447
fusion reactor, noncircular, blanket and shield design 77−3161
fusion reactor, superconducting heating coils and toroidal field coils design 79−6559
fusion reactor, T-20 installation, demonstration, characts. 77−38402
fusion reactor, thermal and dynamic flow props. of liq. Li falls 77−38412
fusion reactor, thermal stabilisation by controlled ejection of fusion α-particles 77−38408
fusion reactor, TNS, electrical design costing 78−55014
fusion reactor, Tokamak constant tension D-shaped coils, lateral support struct. 78−55013
fusion reactor and plasma physics magnets, USA development 79−31193
fusion reactor and plasma physics magnets, W.European development 79−31194
fusion reactor blanket and shield, nucleonic design 79−85803
fusion reactor design, considerations on the minimum size of a tritium burning, preferably self-sustaining Tokamak with a breeding blanket 79−76139
fusion reactor first wall, radiation damage simulation using fission reactor test facilities 80−57950
fusion reactor geometry, optimum plasma parameters rel. to reactor parameters 79−76140
fusion reactor homopolar motor-generator energy storage system 78−5044
fusion reactor maintainability considerations 79−9882
fusion reactor materials, surface anal. in Princeton Large Torus 77−57743
fusion reactor modelling, time-depend. computer codes 77−34468
fusion reactor prefabricated toroidal supercond. field magnet system 79−31211
fusion reactor RIGGATRON, neutronic anal. of two-dimensional models 80−13789
fusion reactor supercond. toroidal coil bending moment computation 79−41867
fusion reactor toroidal field magnet system utilizing normal metal trimming coils 78−54931
fusion reactor toroidal magnet system, technology-constrained scaling 79−76138
fusion reactor UWMAK II, thermal hydraulic and mechanical design of blanket 77−6556
fusion reactors, design consideration for maintenance access 77−3163
fusion reactors, design of Tokamak experimental power reactor 79−71967
fusion reactors, doublet research, plasma shape control, MHD stability 80−28837
fusion reactors, exptl. and demonstration, conceptual design studies 79−71964
fusion reactors, neutral beam driven, physical basis and engineering parameters 77−54360
fusion reactors, quasi-stationary, HF plasma heating methods 77−34445
fusion reactors, safety aspects 77−6562
fusion reactors, structural anal. 77−3162
fusion reactors, supercond. toroidal field magnets, large coil program 79−36400
fusion reactors, supercond. toroidal magnets, mag. and thermal loading 79−36407
fusion reactors, supercond. toroidal magnets, max. mag. fields, mech. stress calcs. 79−36405
fusion reactors, superconductor design considerations for poloidal field coils 79−63236
fusion reactors, superheating-diffusion instability, thermonuclear burn 80−32500
fusion research, philosophy 80−42854
fusion test reactor, cross section requirements 77−23294
fusion test reactor, engineering design 77−23265
fusion test reactor, in-vessel maintenance remote manipulator system 80−18611
fusion test reactor, neutron activation code REBATE 79−49852
Fusion Test Reactor remote handling and maintenance 79−9884
fusion test reactor vacuum vessel, flow-related heating/cooling problems 79−85798
fusion tokamak, development of superconducting magnet *(Japanese)* 79−73026
fusion-fission breeder, blanket fuel selection 79−22468
fusion-fission breeder reactor, supercond. poloidal field coil design 78−70640
fusion-fission demonstration hybrid reactor, blanket neutronics analysis 79−22469
fusion-fission demonstration hybrid reactor, fissile fuel breeding and blanket power prod. 79−22470
fusion-fission hybrid facility, multipurpose 79−85788
fusion-fission hybrid reactor, beam-driven, design parameters 77−34459
fusion-fission hybrid reactor energy research program 79−22471
heating in toroidal plasmas 80−24239
heavy-current cabled and soldered multifilament superconductor AC losses 79−32808

Tokamak devices continued
heavy-impurity control by light-impurity radiation, wall layer cooling 77−65879
HF gyrotrons appl. to tokamak plasma heating 79−60159
HF heating in Tokamaks, fast wave propag. at lower hybrid reson. *(Russian)* 77−7566
HFCTR, demonstration reactor conceptual design, high force density magnets and modularisation 80−95439
high field compact Tokamak reactor, conceptual design for operation at high power density 79−71971
high field tokamak, plasma energy balance and classical ion thermal cond., Joule heating *(Russian)* 79−27797
high field tokamak reactors 79−60176
high temperature stabilisation, heating *(Russian)* 79−82103
high-β skin current Tokamak, axially symmetric displacement stability 77−65899
high-β tokamak, ballooning mode instability theory *(Russian)* 79−27757
high-β Tokamak dynamics, reduced MHD eqns., linear, nonlinear stability 77−84479
high-β Tokamak equilibrium, second order effects 80−70024
high-beta, equilib. and stability, theory and expt. 77−43042
high-beta Tokamaks, MHD beta limits, dependence on current density and pressure profiles, num. calc. 80−28637
high-beta Tokamaks, MHD eqn., stability, transport calc. 80−28848
high-press. flux conserving Tokamak equilibria, theory 77−27695
homopolar generator, radially stacked drum type, for Tokamak Ohmic heating coils 78−13337
homopolar generator power source, Tokamak toroidal field coil system 77−23257
hybrid fusion reactor, Tokamak type, with fissioning matter, blanket parameters 77−34446
hybrid shielding, radiation heating rates, two-dimens. transport anal. 80−106178
hybrid Tokamak reactor, for prod. of Pu fuel and elec. energy, preliminary design 79−76122
hydromagnetic stability, ideal and resistive, review 78−34358
ignition test reactor with high field operation 79−71965
ignition TNS Tokamak reactor, engineering parameters 78−50359
impurity control in Tokamak *(Japanese)* 79−82085
impurity density distrib., energy loss and diffusion 77−65838
impurity effects and control, neutral beam injection, computational models 80−28773
impurity transport *(Russian)* 80−106957
induction coil system, superconducting for a doublet Tokamak reactor 77−30657
induction heating coils, 50 kA prototype superconducting cable, critical current 80−106196
instabilities, thermonuclear cone microinstabilities and anomalous alpha-particle losses 80−28636
internal resistive modes, (m=1, n=1) and (m=2, n=1) MHD eqns. linear anal., toroidal coupling 77−43048
ion-cyclotron instability, parametric depend., beam injection, Tokamak stability 78−47110
ISX, coil design and fabrication 78−50353
ISX, pneumatic H_2 pellet injection system 79−60202
ISX, Tokamak, assembly details 78−54883
ISX-A Tokamak, H pellet fuelling expts.. 79−22465
ISX-A Tokamak, plasma confinement and impurity flow reversal 80−28770
ISX-A Tokamak, plasma equilibrium position dynamics 79−77360
ISX-B, differentially pumped bellows 78−55025
ISX-B, electron cyclotron microwave heating 80−99329
ISX-B, high power neutral beam injection studies 80−79545
ISX-B, neutral beam power system 80−91283
ISX-B, neutral beam system 80−99388
ISX-B, with bundle divertor, structural anal. 80−91254
ISX-B fusion reactor design improvements for neutral particle heating 78−54881
ISX-B neutral beam injector expt. on prototype beam line 80−74039
ISX-B tokamak, design of bundle divertor expt. 80−102341
ISX-B Tokamak, expt. program, review 80−78435
ISX-B Tokamak, intense heating, plasma position and current, feedback control modeling 80−33802
ISX-B toroidal field coil finger joints, fatigue life, structural evaluation 80−91253
JAERI experimental fusion reactor, design problems 79−76126
JAERI large Tokamak, fast acting movable rail limiters, R and D programme *(Japanese)* 79−13524
JAERI large Tokamak, poloidal field coils, R and D program *(Japanese)* 79−7494
JAERI large Tokamak, toroidal field coils R and D program *(Japanese)* 79−7493
JAERI large Tokamak JT-60, vacuum vessel R and D programme *(Japanese)* 79−13523
JAERI Tokamak, Ti coating for improved plasma characts. 80−24232
Japanese Tokamak research, impurity control, low-q discharge, scaling law, RF heating 80−74015
JET, ballooning modes, MHD theory 80−28639
JET, cryopumps and cryogenic ancillary equipment 77−30670
JET, development of relevant technologies of vacuum vessel, toroidal field coils, and remote handling 79−71961
JET, extraction element design for long pulse multi-megawatt neutral beam 80−102373
JET, far IR interferometer design 80−59295
JET, neutral injector overvoltage injection system 80−99398
JET, periplasmatron ion source for intense neutral beam 80−99380
JET, toroidal field coil design and manufacture 78−50349
JET, vacuum vessel construction 78−55024
JET project, design proposals report 79−3241
JET project, scientific and technical developments 1976 79−3242
JET project description 78−58399
JET Tokamak inner poloidal field coil design 79−31209
JET Tokamak toroidal field coil design 79−31205
JET Tokamak toroidal field coil manufacture 79−31206
JFT-2, gross particle confinement characts. by boundary plasma, electrostatic probe diagnostics 79−32822
JFT-2, ohmically heated plasma, Thomson scatt. meas. 79−50890
JFT-2, origin of arcing 80−92414
JFT-2, scrape-off layer, particle and energy fluxes, probe and IR obs. 78−59690

Tokamak devices continued
JFT-2 Tokamak, impurity ion sputtering 80−79554
JFT-2 Tokamak, large scale fluctuation mode mixing, probe, interferometric obs., MHD anal. 78−67312
JFT-2 Tokamak, plasma heating near lower hybrid frequency 80−28698
JFT-2 tokamak radiation loss meas. with Ge film bolometer 80−95141
JFT-2a plasma behaviour with separatrix mag. surface 77−7581
JIPP T-II, electron cyclotron emission meas. using double-pass optical spectrometer 80−54035
JIPP T-II, electron temp. meas. using Thomson scatt. method 79−50891
JIPP T-II, horizontal plasma position control by feedforward-feedback system with digital computer 80−75093
JIPP T-II, neutral beam injection system, design and expt. test 80−106226
JIPP T-II plasma, soft X-ray spectrum meas. 79−55554
JIPP T-II torus, neutral gas injection and plasma current control, suppression of major disruption 80−28839
JT60 critical plasma testing device, status report 80−27801
JT-60, CAMAC system, microprocessor based 80−59309
JT-60, fault current anal. in grounding system 80−99307
JT-60, grounding system design 80−102313
JT-60, grounding system pot. rise during lightning strike, anal. 80−102314
JT-60, poloidal field DC power supply developments 80−102325
JT-60, poloidal field power supply system, AC voltage behaviour, simulation 80−91287
JT-60, prototype neutral beam injector unit 80−106225
JT-60, seismic anal., design changes 80−95425
JT-60 large Tokamak device, position and cross-section control 78−50366
JT-60 Tokamak, drive characts. of fast movable limiter 78−47193
JT-60 Tokamak vacuum vessel, stress anal. 78−66371
JXFR, superconducting mag. system conceptual design 80−99295
Large Coil Program, insulation system cryogenic elec. test 80−91263
Large Coil Program, Westinghouse superconducting mag. elec. design 80−91250
large magnetic field ripples, electric probe meas. 80−83976
large Tokamak, optimum config. of poloidal field coils 79−23464
LARTS, extended burn operation, physics, engineering and economics 80−95440
low power Tokamak experimental fusion power plant, scoping studies with empirical scaling, SISYFUS code 80−102309
low Z coating development program 80−106182
low-pass interference filters for Tokamak plasma diagnostics 80−64783
lower hybrid heating system for Tokamak fusion ignition 78−70636
lower hybrid wave propag. and damping in Tokamak plasma, numerical study 80−64698
LPTT, engineering design 80−102308
LT-3, stable discharge, ion temp. and energy balance, UV polychromator meas. 77−65914
LT-3 and LT-4, plasma physics research at the Australian National University 79−99003
machine with iron cct., flux mapping and current distrib. 79−41866
Macrotor, metallic impurity suppression by electron injection 79−32781
Macrotor Tokamak, laser-induced desorption of impurities from walls, spectral anal. 78−59681
magnet coil, finite element anal. 77−18058
magnetic confinement of plasmas, review 78−94928
magnetic diverters for experimental Tokamaks and fusion reactors 80−18621
magnetic field analysis, AC, three-dimensional, using finite element method 79−50191
magnetic field computation, conference, Grenoble (1978) 79−41262
magnetic field system for reactor 78−21761
magnetic island formation and evolution, MHD eqns. soln. *(Russian)* 77−47169
magnetic islands, feedback stabilisation 80−28638
magnetic islands, tearing modes 80−28846
maintenance design requirements and economics 80−99285
mathematical simulation of equilibrium plasma configurations and power supply operating conditions in Tokamak-type devices 79−76125
maximising beta with force-free current layer, diffuse MHD equilib. and sharp boundary model 77−43043
maximum toroidal mag. field value by core constraint 80−102349
metal surface cleaning, by electron cyclotron resonance plasma of H 79−47821
MHD equilib., var. method in Tokamak *(Russian)* 80−106960
MHD localised ballooning mode, kinetic anal. 78−75298
MHD processes, Kadomtsev-Pogutse eqns. numerical simulation, kink modes and internal disruption 77−43047
MHD stability limits of high-β Tokamaks 80−28643
MHD-mode stability, high wave number, in high-pressure Tokamaks 80−28644
Microtor Tokamak, LF microturbulence, far IR laser scatt. 80−96362
mobile diaphragm operation mode in Tokamak and CTR reactors *(Russian)* 80−83966
motion of relativistic charged particle in axisymmetric toroidal system 80−83991
multifluid Tokamak transport code, two dimens., time evolution 77−58880
near-future Tokamak power reactor remote servicing considerations 79−9887
neoclassical conductivity, numerical integration 77−65841
neutral beam injection in Tokamak, impurities and elec. field effects 77−65883
neutral beam injection reionisation power losses in duct, model 80−99385
neutral beam ion source, core snubber network design, fabrication and testing 80−102378
neutral injection kinetics, Monte Carlo anal., local liberation to wall 77−42992
neutral low energy transport, multigroup discrete ordinate methods, ANISN simulation code 78−34269
neutral-beam requirements for compression-boosted ignited Tokamak plasmas 78−78494
neutron source and toroidal geometry neutronics effects 77−34457
neutron transport problems, computational method 78−22538
non-circular Tokamak field shaping coils, current optimisation 80−95426
non-linear tearing mode, numerical code 77−43046
noncircular, reactor size plasma MHD equilib. calc. 77−24121

Tokamak devices continued
noncircular cross section, fast neutral atom injection, collective processes, Alfven waves *(Russian)* 77−47221
noncircular section construction with axisymmetric divertor JFT-2A, Japan 77−61605
noncircular Tokamak, time evolution of elongation ratio and Mirnov oscill. 80−64763
nonlinear perturbation in Tokamak, feedback effect *(Russian)* 80−83967
NOVA II, design and construction *(Japanese)* 78−87504
nuclear fusion, power supplies *(Dutch)* 78−741
nuclear power stations, combined heat and power, fusion reactor appls. *(German)* 79−67935
Oak Ridge ORMAK, energetic neutral-beam injection electron heating 77−80323
ohmic heating coil design and testing 79−32806
ohmic heating pulsed power supply digital simulation 78−8991
ohmic heating system for TFTR Tokamak 78−55017
operational principles and features 77−79473
ORMAK, contamination buildup on Tokamak liner anal., laser refl. technique 77−34436
ORMAK, first wall, surface impurities and cleaning techniques 77−34435
ORMAK, normal discharge energy loss to wall and limiter 78−34355
ORMAK, tearing mode mag. island struct. rot., diagnostics theory 80−48982
ORNL fusion power demonstration study, review 79−71969
ORNL/TNS and ETF, tokamak reactor poloidal field system study 80−95436
PDX, 6 MW Neutral Beam Project, overview 80−106223
PDX, assembly, description 80−99308
PDX, data acquisition systems, networking and distrib. processing improvements 80−99318
PDX, flexible work platform and balcony design 80−106161
PDX, initial operation 80−79555
PDX, large Tokamak, design and future use 80−79534
PDX, mech. design and assembly 78−50350
PDX, neutral beam elec. power system, ion source supply upgrade 80−102330
PDX, ORNL prototype neutral beam injection system, ion source development 80−99391
PDX, toroidal field coil and frame struct., anal., finite element anal. 80−106165
PDX neutral beam injector, ion accel. structural anal. 80−102375
PDX neutral beam injector, multi-aperture ion accel. electrodes thermal anal. 80−102371
PDX neutral beam injector development 80−99375
PDX power test results, struct. finite element anal. 80−91265
PDX Tokamak, finite element anal. using computer graphics 80−95424
PDX Tokamak, struct. anal. by finite element method 80−106166
PDX Tokamak, surface analysis station 80−79586
PDX toroidal field coil joint fatigue testing 80−91252
pellet refuelling of a divertor Tokamak 80−91247
PETULA, Al_2O_3-plasma interactions *(French)* 77−62372
Petula, vac. vessel and RF coils for compressional transit time mag. pumping heating 78−70634
PETULA Tokamak, lower hybrid heating expts. 80−83958
Petula Tokamak, lower hybrid waves, plasma heating and nonlinear effects 80−28697
PGFR seismic risk anal. 80−99298
PHIBEX, poloidal field power supply for ignition, computer based cct. anal. 80−102329
plasma boundary, particle energy meas., calibration method 79−98983
plasma column equilibrium in octopole Tokamak without conducting shell 79−41858
plasma confinement, series coupled power crowbar system *(Japanese)* 78−55755
plasma confinement in the TFR Tokamak 79−60169
plasma current profile meas. by neutral beam probe *(Japanese)* 80−96397
plasma diagnostic double-pass rapid-scanning Fourier transform spectrometer 80−59299
plasma diagnostics for large Tokamaks, particle and photon meas. 79−46479
plasma impurity diversion through ambient boundary layer flow 80−19603
plasma magnetic field meas. using laser light scattering 78−34370
plasma parameter improvement by Ti gettering in JFT-2 79−671
plasma startup system, for fusion reactor 78−62612
plasma surface interaction program of DITE Tokamak expt. 77−31503
plasma-surface interactions in Tokamaks, review 79−73017
PLT, coil stress and deflection analysis, ANSYS computer code appls. 78−50356
PLT, current profile evolution effect on plasma-limiter interaction and energy confinement time 80−10420
PLT, D_2 flux and energy incident on probe, power balance, impurity generation 80−79553
PLT, data acquisition systems, networking and distrib. processing improvements 80−99318
PLT, electron cyclotron radiation Fourier transform diagnostics 80−59292
PLT, Fe-charge state distrib. by Bragg cryst. X-ray spectroscopy 79−68956
PLT, first wall, surface modification, ion beam anal. 79−46457
PLT, fusion neutron yield during D neutral beam injection 80−79522
PLT, ICRF heating for two-ion regime 80−83959
PLT, ion temp. radial profile meas., neutron flux, Doppler broadening and charge exchange 78−79469
PLT, neutral beam duct reionisation losses, obs. and power loss model 80−99383
PLT, neutral beam heating 80−106950
PLT, neutral beam injection, power input and plasma temp. reconciliation 80−106224
PLT, neutral beam injection and ICRF heating, charge exchange meas. 80−83892
PLT, vacuum vessel residual gas and surface comp. changes with H_2 discharge cleaning 79−80631
PLT and ISX plasmas, field desorption and field ion surface studies of exposed stainless steel tips 80−34295
PLT discharges, resonance lines of highly ionized Ti, Cr, Fe and Ni 79−68941

Tokamak devices continued
PLT Tokamak, energy balance 80−28733
PLT Tokamak, neutral beam heating 80−28701
PLT Tokamak, ohmically heated plasmas, radiation, impurity effects, instability and particle transport 80−28833
PLT Tokamak, W ion soft X-ray emission effects 78−83537
PLT Tokamak, W XX to XXXV spectra and spatial distrib. 78−55747
PLT Tokamak cyclotron radiation Fourier transform spectral analysis 79−32815
polarization and millisecond spectral measurements of electron cyclotron emission from DITE Tokamak 80−92396
poloidal coil air-core system for experimental power reactor 77−26873
poloidal divertor for fusion reactor, reference design 78−54894
poloidal field coil design and development of JT-60 Tokamak 79−31204
poloidal field meas. by far IR polarimetry 79−32794
position instability analysis, effective mode approx. in Tokamak 80−103145
power reactor, burn cycle dynamics, confinement scaling laws and heating 77−23263
power reactor, electron cyclotron reson. heating by gyrotrons 80−99331
power reactor, interaction and protection of supercond. and pulsed coils 77−23262
power reactor supercond. coil design, experimental 79−31198
power reactor supercond. poloidal magnet system design, experimental 79−31207
power reactor toroidal field coil design and manufacture 79−31201
power reactors, initiation pulse prod. methods in ohmic heating circuits 78−55730
power supply, pulsed, based on thyristor switching circuit 79−14622
power supply by 500 V homopolar generator 78−5957
power supply by homopolar generator 78−5958
pressure upper limit 77−58884
PRETEXT, poloidal field coil code, expt. verification 80−92377
Princeton Large Tokamak, D electrodisintegration neutron spectrum 77−84521
Princeton Large Torus, engineering tests on toroidal and internal poloidal field coils 77−23264
Princeton Large Torus, unbalanced neutral beam injection, toroidal plasma rot., Doppler shift meas., confinement times 79−77400
probe diagnostics allowing for asymmetry 79−41881
Pulsator Tokamak, electron density limitation 80−96385
Pulsator Tokamak discharges with AC modulation 80−96386
Pulsator Tokamaks, modulated runaway losses and effects of helical dipole field 80−28845
pulsed fusion reactor, load-levelling considerations 79−85799
pulsed RF-trapped particle interaction stochastic effects in tokamak 80−59245
radial current distrib. meas. using neutral Li beam 78−30488
radial transport, computer model 77−65840
ray tracing for lower-hybrid waves 79−60139
ray tracing in axisymmetric toroidal coords. 77−84476
reactor, impurity control, divertor and gas blanket model 79−90445
reactor, short-pulse D-T, burn phase control 79−86604
reactor, turbulent plasma blanket generation *(Russian)* 79−55566
reactor shielding requirements, penetration size effects 79−9875
reactor Tokamak, heat transfer in wall region *(Russian)* 78−87501
reactors, demonstration and commercial prototype 79−49855
recycling and surface erosion processes 80−33805
refuelling by pellet injection, transport processes effects 80−38699
reversed ultra fast theta pinch, mag. wave heating of Tokamak 77−35364
review of recent progress in Tokamak expts. for fusion energy prod. 79−71948
RF heating, supplementary, in Tokamak installations *(Czech)* 80−24258
RINGBOOG II, toroidal discharges with cold blankets 80−83901
RST, RF driven steady state toroidal expt., design 80−91276
RST, support struct. 80−102342
scaling, empirical, energy confinement times and ignition temp. attainment 78−34354
second order effect of a high-β Tokamak equilibrium 79−68943
shaping and internal structure in non-circular Tokamaks 80−28842
shielding and maintainability in an experimental Tokamak 80−99287
simulation, equivalent cct. model and mag. field diffusion eqns. 77−84409
SLPX, Superconducting Long-Pulse Experiment, scoping study 80−91275
SLPX TF coil, stress anal. using COSMIC-NASTRAN 80−106168
small-aspect-ratio torus for demonstrating thermonuclear ignition 79−71966
small-scale, review 78−42831
solid breeding blanket for commercial Tokamak reactors, materials and design 80−95441
Soviet Tokamaks review *(Russian)* 79−4192
stability, two-fluid dissipative theory, shaped large-aspect ratio Tokamaks 80−28640
stability and beta limits in non-circular Tokamaks 80−28646
STARFIRE project, an overview 80−106183
STARFIRE project, design parameters 80−106184
STARFIRE project, first wall and blanket design 80−106188
STARFIRE project, impurity control system 80−102345
STARFIRE project, maintenance considerations 80−102346
STARFIRE project, superconducting poloidal coils design study 80−106185
STARFIRE project, T handling and vacuum requirements 80−106187
STARFIRE project, toroidal field coil system preliminary assessment 80−106186
static stability, equilibrium config., stray field effects in Tokamaks *(Chinese)* 77−76158
steady state resistive toroidal field coils 80−91264
steel, stainless, electron-bombardment surface prep. for Princeton Large Torus 77−59957
stellarator and Tokamak, progress in experiments 78−94122
stochastic orbits in Tokamak, statistical description, low freq. fluctuations 80−59265
superconducting coils, active energy transfer rate control using inductor-convertor bridges 78−13338
superconducting long-pulse expt., SLPX, design features 79−50898
superconducting mag. system sections for Tokamak-7, test results 77−27742
superconducting magnet systems, USSR designs 79−31192

Tokamak devices continued
superconducting material and device requirements for thermonucl. fusion *(French)* 78−13322
superconducting ohmic-heating coils for Tokamak fusion reactors, simulation expts. 79−36404
superconducting Tokamak design, TORUS II SUPRA 79−37527
superconducting Tokamak toroidal magnet system development, cluster test facility 79−30495
superconducting toroidal field coil concept 79−31200
superconducting toroidal field coils, pulsed field losses, expt. simulation 77−26871
superconducting toroidal field magnet 77−31496
superconducting toroidal system, force anal. for all fault conditions 80−91258
supra-thermal trapped electron quasi-linear diffusion, mag. drift reson. and Alfven wave excitation *(Russian)* 79−27748
surface and impurities studies 77−31531
surface conditioning and mass spectroscopy 79−672
T-10, discharge dynamics, calculations of plasma energy and particle balance 80−28847
T-10 Tokamak, electron cyclotron emission meas. 80−92375
T-10 Tokamak, plasma X-ray emission 80−28840
T-10 Tokamak, stainless steel limiter expts. in ohmic heating region *(Russian)* 80−83969
T-10M Tokamak, normal and supercond. inductive energy storage and switching 78−55018
T-11 Tokamak, neutral beam injection, plasma heating and stability 80−28702
T-12 Tokamak with two axisymmetric divertors, characteristics of divertor 80−28844
T-4, HF magnetoacoustic heating 77−76137
T-4 Tokamak, discharge chamber, AES anal. *(Russian)* 79−4163
T-4 Tokamak, impurity ion diagnosis, C nuclei absolute content *(Russian)* 79−14615
T-4 tokamak, ion cyclotron heating, obs. *(Russian)* 79−27796
T-6 Tokamak, disruptive instability growth, mag. field perturbation struct. and dynamics *(Russian)* 78−59560
T-7 Tokamak superconducting magnet test program, some results 79−37528
tearing mode, low-m, stabilization 77−65857
TETR Tokamak hybrid blanket design, breeding and power capabilities 78−62615
Texas experimental Tokamak, homopolar generator, eddy currents, EM forces (torques), due to misalignment 78−54953
Texas Experimental Torus, data acquisition and processing system 77−24217
Texas fusion plasma research Tokamak, power supply system 77−23258
Texas turbulent heating experiment, fast crowbar switching system 77−23260
TEXT, assembly plan 80−99305
TEXT, motor-generator power supply system 80−99292
TEXT, poloidal field power systems, design and anal. 80−102328
TEXT, pulsed homopolar generator power supply, engineering and design 78−55016
TEXT, regulating resistors and interrupters 78−55038
TEXT, Tokamak structural system 78−54882
TEXT, toroidal and poloidal field coil design 78−50354
TEXT, toroidal field coil fabrication 80−91267
TEXT, toroidal field coil power supply, thyristor controlled 80−91289
TEXT data acquisition, multichannel AD subsystem 78−54936
TEXT iron core Tokamak, design formalism for OH and VF coil system 77−23259
TEXT overview and status report 80−91273
TEXTOR, mag. diagnostics and monitoring systems data acquisition 80−99320
TEXTOR, poloidal coil system power distrib. system 80−102327
TEXTOR, toroidal field magnet design 78−50348
TEXTOR program at KFA, Julich 77−31505
TFR, extraction grid for high power ion source 80−102372
TFR, far IR Fourier transform spectroscopic Michelson interferometer 80−59294
TFR, high power neutral beam injection and ion power balance, anomalous heat conduction 78−82511
TFR, magnetosonic wave generation and damping near ion cyclotron freqs. 77−76058
TFR, reduced fusion neutron production 78−63577
TFR, runaway discharge, cyclotron radiation spectra interpretation 79−41805
TFR, variable-radius Mo and graphite limiters 78−63600
TFR 600, plasma equilib., numerical simulation of multitransformer eqns. 78−55760
TFR 600 Tokamak, electron heat transport anomaly 80−79449
TFR 600 Tokamak, plasma confinement, low effective plasma charge 80−28769
TFR 600 Tokamak, soft X-ray meas., mag. topology near q=1 surface 80−79580
TFTR, assembly 80−102335
TFTR, blanket module expts., engineering test station design 80−102338
TFTR, ceramic insulator rings 78−55022
TFTR, eddy current theory for structural materials 80−95427
TFTR, electrical power blanket module, conceptual design 80−102339
TFTR, energy conversion and storage systems, fault detection and protection 80−95431
TFTR, field coils cooling water system 80−106160
TFTR, gas injection assembly 80−99342
TFTR, general arrangement of diagnostics 80−95445
TFTR, high energy heat sink, ion beam dump and calorimeter 80−99394
TFTR, high power direct energy convertors for beams and plasma 80−99334
TFTR, High Voltage Switch Tube, for Neutral Beam Power System 80−99291
TFTR, hollow cathode mag. multipole ion source 80−102369
TFTR, large noncircular ports, development of bakeable seals 80−95454
TFTR, large section water cooled Cu conductor, brazing joints 80−91260
TFTR, neutral beam injector prototype, construction and performance 80−99390
TFTR, neutral beam injector test facility construction 80−102336
TFTR, neutral beam line cryopanels, cryogenic supply systems 78−55027

Tokamak devices continued
TFTR, neutral beam line final design 80−99309
TFTR, neutral beam line injectors, cryopumping system 78−55028
TFTR, neutral beam power system 80−91282
TFTR, neutral beam source, arc current modulator design 80−102379
TFTR, neutral beam sources overcurrent protection during spark down 80−102331
TFTR, neutral beam-torus connecting duct 80−99302
TFTR, neutron spectrometer mech. design 80−95498
TFTR, plasma generation and confinement 80−42864
TFTR, plasma position control, linear feedback optimal method 78−50365
TFTR, power line, variable freq. AC harmonic content 80−99293
TFTR, preoperational test plan, manpower loading and scheduling 80−102340
TFTR, T gas injection system transient response 80−102337
TFTR, tritium breeding test blanket module design 80−99304
TFTR, vacuum chamber for neutral beam injection system 78−55021
TFTR, vacuum pumping system 80−95447
TFTR, vacuum vessel bellows, strength and fatigue anal. 80−95455
TFTR energy conversion system simulation 80−99303
TFTR engineering developments in remote handling and maintenance vacuum vessel design 79−76129
TFTR Flexibility Modification, in-torus surface pumping, Ti and Zr/Al gettering 80−95451
TFTR mag. field coil electrical insulation system and test results 80−95429
TFTR neutral beam support system 80−102376
TFTR outer poloidal field coil insulation and mould design 80−91261
TFTR poloidal field coil system, charact. 80−95430
TFTR poloidal field coils, tooling and manufacture 80−91262
TFTR technology and Tokamak engineering 78−50344
TFTR toroidal field coil case design 78−50347
TFTR toroidal field coil design 78−50346
TFTR toroidal field coil support restraint struct. 80−95428
TFTR vacuum vessel, T permeation and wall loading 79−45412
TFTR-II, high density Tokamak design studies 79−71962
thermonuclear Alfven instabilities, toroidal effects, direct mag. field approx. *(Russian)* 77−51166
thermonuclear Alfven instability stabilisation in high press. tokamak, mag. surface distortion *(Russian)* 79−27758
thermonuclear fusion and the Tokamak, review *(Italian)* 79−31177
thermonuclear hybrid reactor for fissile fuel and electrical energy prod., preliminary evaluation 79−71954
thermonuclear reactor, first wall, conditions simulation, T+graphite reacts. 79−647
theta pinch pulse rapid heating 77−76132
Thomson scatt. diagnostics using optical multichannel analyser 78−67432
THOR, geometrical and elec. props., rel. to Alcator 79−98993
Thor Tokamak, wall conditioning by cleaning H discharges 80−78440
THOR Tokamak toroidal field system design and manufacture 79−32807
time resolved heat flux to wall meas., sheath model with secondary electron emission 78−79468
TM-1-MH Tokamak, HF heating expts. 80−79527
TM-3, near wall region, Langmuir probe obs. *(Russian)* 77−47261
TM-3, synchrotron emission from runaway electrons 77−15247
TM-3 Tokamak, multichannel atomic analyser with automatic data recording 78−67420
TNS, electron cyclotron heating startup system, design 80−99330
TNS fusion reactors, review of plasma engineering, design and program planning for future developments 79−71959
TO-1, plasma concentration control *(Russian)* 78−91160
TO-1 Tokamak, kink instability, feedback stabilisation 80−28634
Tokamak expts. survey, apparatus, techniques, containment times, plasma instabilities 78−59662
Tokamak fusion reactor vacuum vessel, eddy currents when plasma current is disrupted, calc. *(German)* 80−68937
Tokamak fusion test reactor, cross section sensitivity, uncertainty anal., design parameters 77−6554
Tokamak Fusion Test Reactor, elec. resistance bellows for vacuum vessel 78−50407
Tokamak fusion test reactor, thermal response of first wall limiters 80−79585
Tokamak fusion test reactor, transient getter scheme 80−79584
Tokamak Fusion Test Reactor diagnostic penetrations, neutron streaming calc. 79−9877
Tokamak Fusion Test Reactor neutron collimator design 79−9876
Tokamak microwave discharges, refraction losses, from measured plasma density profiles 78−22549
tokamak-10, ion energy balance, neutron flux and atom energy spectra, obs. and model *(Russian)* 79−27795
Tokamak-7, circulating superconducting magnet system, design and operational tests 79−89498
toroidal coil system, Oak Ridge Experimental Power Reactor 77−26872
toroidal field coil design and development for JT-60 Tokamak 79−31203
toroidal field coil finite element stress anal. 80−91256
toroidal field coil for Tokamak reactor, stress anal. compatibility calcs. 79−93824
toroidal field coil in-plane bending stress, struct. support design 80−106164
toroidal field coil shielding calc. 79−31212
toroidal field coils, bending-free, for Tokamak reactor 78−55012
toroidal field coils, EM parameters calcs. of current paths in homogeneous media *(Japanese)* 80−106155
toroidal field coils, high current superconductors 77−31530
toroidal field coils, reduction of bending moments 80−47697
toroidal inhomogeneity of vertical field 78−9816
toroidal magnet coil design and testing 79−31195
toroidal magnet design for Tokamak fusion reactor 79−76135
toroidal magnet supercond. cluster test design 79−31199
toroidal magnetic field strength requirements in Tokamak reactors, physical parameters, cost 77−19777
TORTUR toroidal device, plasma confinement and skin currents 77−76180
TOSCA, β optimisation studies 80−83990
TOSCA, small Tokamak, sawtooth oscills., X-ray diagnostics 79−41817
transport losses, computer modelling and scaling 80−28612
transport phenomena numerical computation codes 77−27691

Tokamak devices continued
trapped electron instability, mag. curvature drift driven, collision effects 77−55142
trapped particle instability in Tokamaks, book 78−83562
TTR, Thomson scattering system based on two-detector spectrometers 80−32426
TTT, turbulent heating model 79−37518
Tuman-2A, plasma compression particle diagnostics, density and temp. *(Russian)* 80−38677
Tuman-2A Tokamak, ohmic heating and compression of plasma 80−28703
turbomolecular pump vacuum system for the Princeton Large Torus 78−71521
turbulent heating current penetration, poloidal profiles and anomalous transport 77−55158
turbulent heating of plasma, small-scale apparatus *(Japanese)* 78−1914
two-component Tokamak, quality factor calcs. *(Russian)* 78−87500
ultrahigh vacuum sample transfer system, use in Tokamaks 79−80628
USA Tokamak fusion research 80−74017
UWMAK-III, non-circular, Tokamak, power reactor design 77−74979
vacuum monochromator, grazing-incidence, absolute calibration using Tokamak discharges 78−87492
Wega, HF heating at low hybrid freq. 77−76136
Wega Tokamak, lower hybrid heating 80−28699
X-ray emission of Tokamak plasma, reconstruction accuracy 79−77422
C bonding to Tokamak walls, XPS studies 80−80942
D, thermal desorption meas. of H-isotope retention in Alcator-A Tokamak 80−79588
D-T burning test facility for JT-60 79−71963
D-T steady state reactor, neoclassical diffusion 77−3159
D-T Tokamak reactor, costing and sizing using COAST code 79−76142
Fe cores of fusion reactors, design advantages 78−54897
Fe XV, line intensity and linewidths at high electron density, generalised population ratio 80−99481
H trapping studies in fusion first wall materials 79−45407
^{2}H-^{3}H fuel pellet electrostatic injection *(Japanese)* 80−78434
Nb-Ti 10 kA conductor development for Tokamak toroidal coil 79−31217
O bonding to Tokamak walls, XPS studies 80−80942
TiB_2, first wall material, activation energies and populations of H traps 79−45409
TiB_2 surfaces, ion microanalysis and implantation applied to fusion surface research 79−45405
W radiation generation in Tokamak, Ag I isoelectronic sequence identification 80−83981
Zr-Al getter pumping in beam driven Tokamaks 78−50401

tomography, computerised *see computerised tomography*

tool steel *see steel*

tools
see also hand tools; machine tools
cutting tool coating by cubic BN reactive vapour deposition 80−40545
disc-rod US tool, gain enhancement technique 77−35010
elastic tools for finishing optical components with noncircular cylindrical surfaces 80−28368
metal cutting, separation process tool tip, fracture detection, acoustic emission method *(Japanese)* 80−1388
optical fibre alignment tool 80−23814
optical fibre cutting tool 80−1360
optical fibre cutting tool and automatic splicing machine 80−87575
optical fibre ribbon cable cutting tool 80−19113
spherical diamond tool, durability 78−18075
US tool, radial mode, with statically loaded inner surface, anal. 78−183
US tools concentrators, wave propag. in curved rods of var. cross section 78−9484

topology
see also catastrophe theory; graph theory; network topology
A-topology for Minkowski space 79−92933
atom and mol. wavefunction nodal topology, quantised vortices and paramagnetism 77−46476
b-boundary of S^1 with const. connection 77−37802
bifurcation diagram and non-homogeneous steady states in a system of diffusion-coupled chemical reactors 80−16647
bifurcation into invariant tori at points of reson., use of Poincare maps 79−44707
biomedical surface mapping, interpolation methods 80−81750
black holes, exploding, instantaneous Cauchy surfaces topological change 78−12087
Bogolyubov axiomatic approach to nonlocal field theory, CSL topologization *(Russian)* 80−47202
boundary conditions for textures and defects 78−26561
bounded volume vector field topological theorem, nematic liq. cryst. appl. 79−67171
buckling, two-mode, asymptotic anal., reln. to catastrophe theory 78−34042
cardiotopological data reduction 79−39392
catalytic pellet, isothermal n-order decomposition reaction, steady state stability anal., topological degree and Lypunov method 80−30280
catastrophe theory, phase diagram classification 80−22313
catastrophe theory, rel. to global behaviour of μ, ρ and T-surfaces of real fluids 78−26226
catastrophe theory, singularities, examples, Thom 80−8785
catastrophe theory, symmetry and higher order cuspoids 78−62079
catastrophe theory as a bridge between mathematics and physics 80−8786
catastrophe theory as tool for physical scientists 78−41136
catastrophy theory appls., book 78−32665
categorical, pure and applied problems, conf., Mannheim, Germany, (July 1975) 77−9864
categorical, pure and applied problems, conf., Mannheim, Germany, (July 1975) 77−74200
Cauchy surface topology restriction in general relativity 77−9921
Cauchy surfaces, determ. from intrinsic props. 78−70023
chaos in simple nonlinear differential eqns. 77−13584
chemical bonding, topological resonance energy, appl. to benzene and cyclobutadiene 80−5462
chemical reaction potential energy surface, multidimens., topological stochastic approach 77−48638
chemical systems, topological model and orbital mapping 80−78512
compact spacelike submanifolds in Euclidean spaces 77−53750
comparability of structs., ordering 78−57754
topology continued
completely positive mappings on algebras of unbounded observables 77−45674
conjugated cpds., aromaticity determ. by topological reson. energy method 80−42915
conservation laws, dynamical topology for the space of states 80−27418
continuous neural networks with analogue neurons, properties 78−48783
crystal growth, topological modelling techniques 80−59418
crystal vacancy modelling, topological approach 80−10543
defect crossing in ordered media and topology of 3-manifolds 78−2108
density matrices convergence and entropy 77−30046
differential forms in mathematical physics, book 78−81810
diffraction catastrophe patterns, two dimens., caustics anal. 77−17827
DTA, topological aspects, bond diagrams, heat transfer 77−16877
education, knots, topology friction and strength 77−33769
eigenvalues of graphs with twofold symmetry (molecular configuration) 79−72437
elliptic space as unit sphere in Euclidean vector space *(German)* 77−60909
EM fields, basic equations 77−79723
equation solns. in given intervals, topological problem, physics appls. 77−60908
ferromagnets, ordered, nonsingular, topology appls. 78−10166
fibre bundles and topology 80−105793
finite-differential element nets, topological props. 77−67247
fixed point theorems involving radial compactness and angle conditions 79−71228
fixed points of continuous mapping, mathematical theory and appl. *(German)* 79−84943
flow fields and other vector field struct. and evolution 78−77733
fold field, evolving, structural stability 80−8802
four-colour theorem, proof 77−17784
fracture mechanics, conformal mappings to delete singularities, finite element anal. 77−72251
fuzzy spaces, direction and particle interactions 77−22395
general relativity, singularities and causality violation 77−87666
general three-body problem, M_8 manifold topology *(Chinese)* 79−16808
geodesy, Earth surface three-dimensional mapping onto telluroid 78−65171
Henon mapping, topological horseshoe, chaotic behaviour 80−73257
homotopy group theory of defects in ordered media 79−93072
homotopy theory for soliton solns. classification *(German)* 78−78062
hydrocarbons, mol. thermodynamics, information-theoretic aspects 78−13409
incompressible minimal surfaces, 3-dimens. manifolds with nonneg. scalar curvature, positive mass conjecture 79−30318
knot wormholes in quantum geometrodynamics 77−67612
Lagrange differential 77−53751
Lie groups, representation theory, topological methods *(Russian)* 78−54148
liquid, ideal incompressible flow, topological measuring of canonical Clebsch variables 80−69758
liquid crystal, singularities investig. by homotopic topology methods *(Russian)* 77−69140
liquid crystal, thin layer, symmetry defects and solitons, topological classif. 80−107044
Lorentz and Galilei group, condition from topology and Lie group methods 78−4462
Lorenz attractors, topological classification 78−77720
magnetic monopoles and topological lines 78−16907
Maxwell's eqns. for free fields on compact Lie group manifold 77−49608
measurable selection theorem, variational calculus appl. *(French)* 80−42045
mesonic topological amplitude products, an algebraic soln. 78−81884
minimal surface, asymptotic behaviour near corner 78−24641
molecular, π-electron total energy, approx. topological formulae 77−38603
molecular graph, topological resonance energy is real 79−81145
molecular structures, topological code, modified Morgan algorithm 80−58122
molecular topological spaces, structs. 80−91701
molecular topology description of molecular structure 78−46253
molecules, composite particle, vibr. amplitude and vibr.-rot. anal. 80−74158
n^+-n contact, electron transport, topological anal. 79−15209
near-rings theory and applics., book 77−37720
nematic liquid crystals, ordered, nonsingular, topology appls. 78−10166
nerve fields, topographic organisation 80−89742
nonintegral dimens. spaces, axioms, measures, topology, physical implications 77−64929
nuclear dense matter phase transitions, cusp catastrophe theory 77−22920
ocean surface pattern morphogenesis and catastrophe theory 77−5217
ordered nonsingular systems, topology appls. 78−10166
ordered systems, surface, topological singularities *(Russian)* 78−79847
patient topology, optical process for three dimensional assessment 79−20692
periods on manifolds, quantisation, gauge, topological props. of phys. theories 77−49826
phase transitions as catastrophes 80−8948
physics, algebras, manifolds and fibre bundles 79−44709
physics and topology, review *(Russian)* 80−8770
plasma, nonlinear mode coupling model eqns., topological struct. 78−75304
Polish groups, splitting and representation groups 78−36874
polymer network, Riemann's metric degeneration to graph metric demonstration, chain entanglement problems 80−38963
porous media topology rel. to percolation theory of residual fluid phases 77−75978
probability theory with essential analysis, book 77−37740
propagation of surfaces of weak discontinuity, broken extremals in classical field theory 78−93541
quantum mechanical model, Borel summation appl. 80−90718
quantum topology of mol. charge distribs., mol. struct. and its change 79−68175
quasi catastrophe theory, appl. to classical tachyon theory, imaginary units 77−22414
random moires processes, densities of Minkowski measures *(German)* 77−64932
relational theory of physical space 77−74184

topology continued
representation of groups, semigroups, and categories, book 80−57016
review of interferometry, including holographic interferometry 78−37050
RF SQUID structures, topology and theory 80−97036
S-matrix, planar, building of cylinder correction in topological expansion or dual unitarisation 78−62321
shock waves, global structure anal. 80−8800
soap films as analogue for minimum path and minimum area problems 77−17740
soap foam, arrangement of cells in a net rel. to grain sections of polycryst. 80−70225
Sobolev space mapping 80−12893
solitons, multidimens., additive topological laws of conservation *(Russian)* 77−74601
speckle photography and holographic interferometry, scatt. geometry, topology, vector fields, theory 80−87347
stability predictions through a succession of folds 79−76991
stream networks, distances determ. 77−91183
string-like topological excitations of the electromagnetic field 78−93835
strong topology on algebra of polynomials 77−45673
structural stability in physics (conference, Tubingen, Germany, May and Dec. 1978) 80−8739
surface topography as nonstationary random process 78−24739
surfaces with metric and curvature tensors 79−71252
symplectic manifolds, reduction through consts. of motion 79−49020
ternar semigroups of continued representation of metric spaces *(Russian)* 77−22372
tetrakaidecahedra as grain models 78−51458
thermal electrocyclic reactions, anal. using topological model 80−78512
thermodynamics, irreversible, near equilib., metric geometry 80−62604
Tokamak orbits, topology 80−28806
tops and d-functions in even spaces *(Russian)* 80−4508
transfer matrix of one-sided subshift of finite type with exponential interaction 77−33953
transitive dynamic systems, polhode concept generalisation *(French)* 78−62065
triatomic potential surfaces, global topology 77−50381
two-dimensional electrostatic field construction for energy analysis 80−9796
umbilic catastrophes, buckling mode 78−20945
unique structures, convention of assigning single name 79−41251
unstable modes of an equilibrium, number calc. 80−36493
variational principle for Z_+ action on compact space 77−53825
visual difference thresholds modelling, appl. of ordered topological vector spaces 80−104587
Yang-Mills fibre bundles, classification of monopoles and vortices 77−22635
Yang-Mills theory 78−78060
Yang-Mills-Einstein eqn. pseudoparticle solns., gravit. effect on Yang-Mills topology 77−82682
Cu, high purity, creep cavitation topology, high temperature region *(Czech)* 80−65138
^{3}He, superfluid, singularities investig. by homotopic topology methods *(Russian)* 77−69140
^{3}He, superfluid, texture topology in planar phase 79−69310
^{3}He, superfluid, topology of non-singular textures using relative homotopy groups 78−84021
^{3}He-A, superfluid, ordered, nonsingular, topology appls. 78−10166

torque
see also Scott effect
adhesion measurement, of thin evaporated films 80−50822
ankle joint, human, compliance 78−57034
arc discharge, electrodynamic anomalies, ion electron mutual action, torque 77−84549
bar magnets, torque theory 77−13527
black hole, charged rotating, mag. torque effects 79−17010
cilia and flagella, displacement and sliding of twisted filaments 77−32929
clamped heterogeneous circular cylinder, torsion problem, stresses and displacement 79−32278
eddy current torques, air torques, and spin decay of orbiting cylindrical rocket bodies 78−93074
electrostatic suspended gyroscopes, electrofield torque due to offset of envelope assembly *(Chinese)* 80−43225
fibres, biaxial rotation fatigue testing, torque development 80−71840
gait joint torque and energy patterns in normal humans 78−80897
galactic discs, torques and density waves excitation by external potential 80−22072
gyro, free tuned, expt. method for finding tuning speed 78−90701
induced torque magnetometer 77−13784
knee replacements, non-hinged, rot. characts. 77−44853
limit torsion problems, finite element method, failure torque 79−72820
magnetic anisotropy constant, determ. from torque curves 79−33474
magnetic stirrer, Lenz's law and induced current expts. 78−12485
magnetic thin films, saturation magnetisation and uniaxial anisotropy determ. using torque meas. 79−95614
magnetic torque on shielded supercond. gyroscope, for tests of gravit. theories 77−13678
molecular reorientation, dielec. friction theory 78−87599
muscle, rel. to weighted sum of EMG, human triceps surae 78−20203
nematic liquid crystal, effect of ultrasound on orientation *(French)* 77−59067
neutron star, magnetic, disc accretion torque 78−93294
neutron stars, rotating, magnetic, accretion torques rel. to pulsating X-ray sources period changes 80−31320
Newton's third law, teaching 78−12517
Nimonic 80A, creep rapture under non-proportional loading 80−108518
non-Newtonian creeping flow around rotating spheroidal spindle, torque calcs. 77−15073
penny-shaped crack, sudden twisting in a finite elastic cylinder, stress calcs. 78−67110
permeable spheres in incompressible fluid, hydrodynamic interaction vel. fluid, friction consts. 78−75202
polymer solution, semidilute, hydrodynamic interaction of two permeable spheres, method of reflections 78−71394
PVC, calendering, prediction of stress and torque 79−8266
rigid body orientation, rot. gradient operator and torque calcs. 77−67266
road vehicle stopping distance, weight transfer effect, for teaching 79−25800
rolling, torque calc., mechanical model 79−20078

torque continued
rotating disk, in liquid surface with adsorbed film, torque 78−32685
shaft, operating under torque, structural strength evaluation 79−83280
solid body first-order torques and spinning velocities in intense sound field 77−23798
steel, friction measuring test for use under conditions of high normal interfacial force 80−76454
student demonstration, use of modified beam-type torque wrench 77−41446
thermomagnetic motor, dynamic characts. and stable operation *(Japanese)* 80−16840
ventricular function quantitative meas. by torque ballistocardiography 78−44660
wind turbine, vertical axis, torque ripple analysis and obs. 79−48072
wood screw, effects of crest and pilot hole in withdrawal resist. *(Japanese)* 80−3290
X-ray sources, pulsating, torque vars. and stellar response rel. to period vars. 79−9029
Al alloy cylindrical shells, buckling under combined axial preload, nonuniform heating and torque 80−53662
Al, torque and length change during fracture in torsion test *(German)* 79−24611
Cr, antiferromag., magnetostriction and torque meas. below spin-flip transition 77−63186
Cr, antiferromagnetic, mixed state, mag. torque and magnetostriction meas. 77−89909
Fe-Si (3.25 wt.%) alloy, single cryst. with (007) planes, domain struct. influence on mag. torque 80−108034
^{4}He, superfluid, vortex-induced torque on porous disc, quantum calc. 78−51762
$NdCo_2$, magnetocrystalline anisotropic props., torque meas. 80−108003
Ni, magnetic anisotropy constants fitting to torque curves 79−7989
Pb-Sn, superplastic eutectic, roll load and torque necessary for rolling *(French)* 78−95761
W, Fermi surface, uniaxial strain depend., quantum oscills. in magnetostriction, US vel., with torque 77−28094

torque control
above-knee prosthesis simulator system in eval. of proposed damping torque control schemes 77−44854
wind energy conversion system control, on-line, performance in turbulent wind environment 79−48069

torque measurement
see also dynamometers
automatic torque magnetometer for vacuum-to-high-pressure H_2 environments 80−4746
automatic torque meters, electromechanical indicators application 77−87757
contactless coupling, construction and testing *(German)* 77−13744
dynamic methods, differentiation and direct transducer coupling *(German)* 78−73987
force transducer appls. 79−35720
inline, rotating transducer appl. 78−190
interfacial viscometers, surface shear viscosity determ. 79−23384
magnetic film, analysis method, saturation magnetisation and anisotropy const. determ. 77−8368
magnetic sensors for dynamic quantities *(Japanese)* 79−12776
magnetic suspension, simultaneous weight and torque meas. in controlled atmospheres 78−65907
magnetic torque acting on rotating sample, measurement using air turbine 80−31811
magnetocrystalline anisotropy torque in sheared crysts., meas. 78−24830
muscular effort monitoring, prototype instrument 77−5092
plastic screw-tip during extrusion process 77−27639
polarisation torque-measuring system error anal. *(Russian)* 80−52191
Al alloy cylindrical shells, buckling under combined axial preload, nonuniform heating and torque 80−53662

torque meters *see torquemeters*

torque motors
controllable force supply for human muscle voluntary reactions meas., design features 79−100801

torquemeters
automatic torque measurement, electromechanical indicators application 77−87757
calibration using rack with mobile primary transducer 79−80610
capacitance torquemeter, instrum. for meas. magnetocrystalline anisotropy energy of ferromagnetic materials 78−93743
capacitive, with digital display *(German)* 77−34006
magnetic torque curve analysis, online microprocessor system 78−254
plastic, fluid, charact. by torque rheometer 77−32751
pulse-phase, magnetically coupled pulse transducer with electronic phasemeter 80−74819
sensitive instrument for wind-tunnel appls. 77−53891
strip-support self-balancing, kinematic features 80−4704
with automatic feedback, appl. *(Polish)* 77−54940

Torrey oscillations (NMR) *see double nuclear magnetic resonance*

torsion
see also stress analysis
adhesive joint under combined stress, expt. study of strength 79−74339
aeolotropic cylindrical shell, nonhomog., hollow, thick-walled, torsional stresses, elastic deform. 78−75068
analogue, simplified numerical calc. *(German)* 79−32279
anisotropic composite cantilever, bending and torsion, mathematical formulation 79−18708
anodised Al rods, humidity and coating thickness effects on fatigue in reversed torsion 77−25205
axially symmetric, cylinder embedded in layered elastic half space 77−17822
axially symmetric twisted linear elastic body, numerical method for soln. 77−75802
axisymmetric butt joints, stress anal. in torsion and tension, response of adhesives 78−63397
bar, compressed and twisted, stability calc. *(Russian)* 78−63282
bar, nonlinear, multiply connected cross-section 77−50890
bar, prismatic, with rigid ends, lower and upper bounds for torsional rigidity 80−48568
bar, rectangular, torsion crack problem, harmonic function continuation technique soln. 80−99969
bar, thin-walled, effective torsional rigidity optimisation *(Russian)* 80−19245

torsion continued
bar (tube), compressible, combined loading, elastic-plastic problem 78−63311
bars, cylindrical, elastic-plastic torsion 80−33473
bars, cylindrical and prismatic, stochastic, holonomic, elastoplastic torsion *(German)* 79−37192
bars, prismatic, St. Venant's torsion problem, method of singularities *(German)* 80−73163
Bauschinger effect estimate from reverse torsion testing results 78−7133
beam, annular, torsional oscillations *(German)* 80−106752
beam, composite anisotropic, torsional vibration, torsional wave dispersion *(French)* 77−14934
beam, nonlinear viscoelastic, torsion creep 79−18745
beam, pretwisted, slender, coupled torsional and longitudinal vibr. 79−18770
beam (plate) pure bending, dynamic fracture, axial force effect 78−63385
beam torsional vibration frequency optimisation 78−83288
beams, heterogeneous anisotropic almost cylindrical, Saint-Venant problem 77−39220
beams, thin walled open section, free torsional oscills., secondary effects influence 79−32363
beams flexural-torsional problem by series expansion in eigenfunctions 80−83732
bending-free torsion condition to define centre of twist 80−79140
bluff structures, aerodynamic mechanism of torsional flutter 80−53689
bone, compact, deform. and strength 78−24087
bone, deformation capacity of compact tissue of human tibia subjected to torsion, age effect 77−52827
bones, long, struct. anal., appl. to human tibia 77−21551
box beams subject to torsion, stress anal., strain energy 79−30245
brass, cyclic strain induced creep, relation between modes of stress and strain superposition 78−60733
brass, hot ductility and torsional deform. *(Japanese)* 79−57069
brittle solids under hydrostatic press., statistical approach to torsional strength 77−84194
cantilever, lower bound for fundamental torsional frequencies 77−19565
cantilever (Timoshenko), elastically restrained, with attached masses, follower force stability 78−63347
cantilever beam, nonlinear bending and torsion deform. 77−58571
cantilever beam, pre-twisted, torsional vibr. 77−58583
cantilever minimum weight design with plural torsional frequency constraints 79−68629
castings, fracture toughness characteristics, using double torsion method 78−68863
celluloid, mech. props. under proportional load, time lapse, heating and isotropic props. effect *(Japanese)* 79−79043
celluloid, nonlinear viscoelastic deform. under superimposed hydrostatic pressure 79−34116
cellulose film, meas. of shear modulus and damping in a torsion pendulum 79−4989
cellulose nitrate, nonlinear viscoelastic deform., hydrostatic press. and third invariant of deviatoric stress tensor 80−93587
cilia and flagella, displacement and sliding of twisted filaments 77−32929
circular arches, lateral-torsional instability with motion-dependent loading 77−89049
circular cylinder, micropolar, elastic, flexure problem 78−51083
clamped heterogeneous circular cylinder, torsion problem, stresses and displacement 79−32278
colour geometrodynamics, eightfold way, review 80−95243
composite beams, effects of fibre orientations on free vibrations 80−87734
composite cylinders, St. Venant torsion warping and stress functions 79−32265
composite cylindrical shell, torsional vibr. in mag. field 80−48624
composite materials, fibre reinforced, rectangular rods, elastic wave propagation *(French)* 80−83749
composites, circular specimens, shear modulus determ. 80−25752
concrete, prestressed hollow beams in combined torsion and bending 79−96087
concrete reinforced rectangular membranes, torsional stiffness 80−65131
cone with spherical caps twisted by periodic terminal couples, forced torsional vibr. 77−27485
conic body torsion, double series method *(Russian)* 79−23206
conic section bounded by straight line, torsion problem, St. Venant semi-inverse method 80−54
conical rod, dynamic torsion, exact solns. *(Russian)* 80−1461
connected bars, torsion *(German)* 78−34024
cosmological ν sea, EM wave propagation, torsionic background 80−77283
coupled bending-torsion flutter in cascades, aeroelastic stability boundaries 80−64424
cracked hollow elastic solid, torsion anal. 78−51134
cracks, circular, forced torsional oscillations at low frequencies 80−53703
cracks, coplanar Griffith, in infinite elastic layer under torsion 78−1610
creep and relaxation curves for torsion-tension members at elevated temps. 78−83260
creep const. determ. from stress-relaxation meas. in bending and torsion 78−9572
creep fracture strength of precracked round bars under torsion, expt. and anal. investigation *(Japanese)* 77−59908
creep testing machine using torsion, in radiation zone of nuclear reactor 78−11480
curved box girders, coupled free vibrations 78−30217
curved structural members, large displacement theory, applic. to lateral-torsional buckling anal. of circular arches 80−23924
cylinder, clamped heterogeneous, stresses and displacement anal. 80−14571
cylinder, composite of compressible elastic materials, second order torsion 79−72808
cylinder, hollow, with external crack, axially symmetric torsion problem soln. 80−14614
cylinder, hollow with internal circular crack, axially symmetric torsion determ. 80−64456
cylinder, plastic flow rules and Bauschinger effect parameters 78−6984
cylinder, torsional vibr. superposed on finitely deformed state 80−19263
cylinder under torsion elastic, spherical cavity effect in stress-strain state 80−101717
torsion continued
cylinders, elastic doubly connected hollow, min. weight design for given torsional, flexural rigidities 78−18172
cylinders, stiffened, subjected to pure torsion, min. weight design 78−1582
cylinders, thin necked, thermoplastic deformations, stability analysis *(German)* 78−22281
cylindrical bar, elastoplastic, with linear hardening, simultaneous torsion and tension 80−53658
cylindrical elastic tube torsional oscillations under large internal and external press. 78−79249
cylindrical rod, periodic structure, torsional vibrations, interfacial elastic parameters 80−96215
cylindrical shell, stretching, bending, twisting and flexure 77−11125
cylindrical shell deform., effect of loading history on bifurcation *(Ukrainian)* 78−55578
cylindrical shell mixed boundary value problem, integral eqn. 77−35
cylindrical shell under torsion, stress conc. around elliptic hole 77−68422
cylindrical shell with elliptic cross section, subject to torsion, creep buckling 78−34040
cylindrical shell with strain depend. permeability, torsional response in radial and axial mag. fields 79−19754
cylindrical shells, fluid-filled, vibr. and buckling under torsion 78−79253
Dirac particles, creation in general relativity with torsion and electromagnetism, general formalism 79−88856
disc, axisymmetrically variable thickness, deflection by conc. lateral load *(Japanese)* 80−96194
disc, high freq. torsional oscills., Reissner Sagocci problem 78−26082
double torsion specimen, stress analysis 78−9567
ductile-brittle transition pressure, grain size effect *(Japanese)* 78−60745
dynamic stress/strain measurements under superimposed high press., torsion bomb machine 80−85130
Einstein-Cartan equations, solns., Kerr metric with torsion 78−8299
elastic bar under tension, torsion appl., 2nd order effects, energy method 80−79158
elastic bars, 2-D optimisation problem *(Russian)* 77−23877
elastic beams, 1-D, stability in torsional extension *(German)* 78−87270
elastic cylinder embedded in elastic half space, Reissner-Sagoci type problem 79−27524
elastic cylinder with holes, torsion problem, integral eqn. method soln. 80−36849
elastic cylinder with inserts and holes, torsion problem, integral eqn. soln. method 80−106717
elastic cylinders bonded to rigid end plates 79−76976
elastic half-space with rigid circular disc inclusion 77−72170
elastic inhomogeneous cylinders, torsional wave propagation 77−80104
elastic layer, by annular die, bonded to a semi infinite elastic medium 79−3969
of elastic layer by two circular discs 77−35037
elastic prisms, minimum energy, St. Venant's solns. 80−52027
elastic rod, nonlinear modulation of torsional waves 77−62195
elastic sphere torsion by elastic punches 80−99929
elastic torsion in open sets with holes, problem homogenisation *(French)* 77−67288
elastic-plastic problem, zone estimates 78−67058
elastic-plastic torsion, nonlinear boundary value problem 77−89043
elastic-plastic torsion, variational inequality concept, finite element anal. 80−23907
elastic-viscoplastic circular bar, tension and torsion 79−14285
elastoplastic bars, instability modes *(Russian)* 79−10514
electromechanical filter torsional mode transducer analysis 77−27436
electromechanical high-press. torsion apparatus, for polymer testing 77−51005
elliptical punch, elastic contact problems 78−9613
EM field in space with torsion, semi-minimal coupling principle 80−77675
epoxy resin, cure history effect on dynamic mech. props. 80−54356
epoxy resin, shear strength determ., anal. of methods 77−86107
epoxy resins, crack propag. stability, effects of water, temp., specimen geometry, hardener 78−11324
ethylene vinyl acetate copolymer, torsional rigidity testing *(German)* 77−52596
fatigue limit under combined stress 77−73314
fatigue strength criterion, of a round bar, subject to combined static and repeated bending and torsion 80−40496
Fe alloy YuNDK35, magnetic, brittle, strength in three axial stress state 79−66134
femur compact bone, adult human, relation between torsional props. and histology 79−16234
fibre reinforced composite, shear props., test method eval. 77−81353
flow induced by a torsionally oscillating wavy cylinder 79−64772
frameworks calc., composed of thin-walled open sections, with aid of computer 78−51059
friction welded joints, strain distrib. and fatigue cracks of joint's subjected to repeated torsion *(Japanese)* 79−8350
general relativity with torsion and non-metricity, variational principle 77−67347
glass, strength under linear tension, bending, torsion and compression of type K8 79−14062
glass fibre reinforced, thin walled cylinder, tangential stress charact. during twisting 78−13911
glass fibre reinforced composite, filament wound column, effect of end conditions on critical loads 77−59873
glass fibre reinforced composite, shear fatigue 78−15493
glass fibre reinforced epoxy, wound, strength in twisting, stretching and transverse bending 80−11622
glass fibre reinforced epoxy resin interlaminar shear strength determ., anal. of methods 77−86107
glass-plastic, unidirectional, torsion strength and shear modulus 80−99948
graphite fibre reinforced epoxy, notched, biaxial fatigue loading 78−19879
graphite reinforced epoxy laminate, cantilever shells and late, natural modes 79−91737
graphite reinforced epoxy/Al laminate, cantilever shells and late, natural modes 79−91737
gravitational energy, torsion of spacetime included in a quadratic Lagrangian 78−8316
helical springs, numerical soln. of dynamic response 78−67026
high-Si corrosion-resistant steel, 02Kh8N20S6, mech. props. and heat treatment 77−56003

torsion continued
hollow shaft with longitudinal slots, torsional stress state 78−30183
holographic interferometry, appl. to machine tool framework rigidity *(German)* 77−7040
homogeneous isotropic bar, torsional stress anal. for variously shaped cross sections *(Russian)* 79−32269
homogeneous isotropic compressible elastic media, circular concentric ring, second-order torsion problem 79−32276
hot strip rolling simulation, by hot torsion technique 80−29990
hot twisting, shearing stresses, anal. determ. 78−60900
hysteresis damping, continuum description 78−67078
impact torsional test accuracy determ. using simulation *(Japanese)* 77−56198
impact torsional test by means of dropped bar, appl. to low C steel 79−100304
infinite elastic solid, with flat annular crack, axisymm. stress distrib. under torsion 77−23913
infinite hollow cylinder with external crack, boundary value problem 78−90712
inhomogeneous elastic layer, torsion investigation by approx. methods 80−98799
internal friction test unit for threadlike crysts. 78−36997
isotropic circular cylinder, periodic shearing stress, torsional vibration 78−75087
Kevlar 49 fibre reinforced composite, shear fatigue 78−15493
kinematic hardening models, use in multi-axial cyclic plasticity 80−25717
knee joint, human, torsional load-displacement characts. in vitro 78−40235
laminated cylinder, imperfect, buckling under combined loading 80−7620
laminated cylindrical shell, coupling effect under internal press. *(Japanese)* 80−55449
large deform. three-dimens. anal. of thin walled beams 77−11126
lateral buckling by bending, and by torsion 77−42763
layer, double torsion method of crack propag. study 79−83412
layered shells of revolution, torsional vibrations 78−34053
life calc. under combined torsion and bending 77−11148
limestone tubes, dynamic torsional failure obs. 80−85648
limit torsion problems, finite element method, failure torque 79−72820
local buckling of twisted double-symmetric rectangular box girders *(German)* 78−13939
low-cycle testing unit for use in vacuum and at high temp. 79−52503
magnetosolid mechanics, semi-infinite cylindrical shell with strain depend. permeability, torsional response 79−94483
magnetostrictive cylinder, torsional deformation 80−53636
magnetostrictive viscoelastic cylinder, nonhomogeneous, torsional deformation 79−37169
matrix analysis of composed bar of open cross section 80−83736
metal, dynamic and static response to simple compression, tension and torsion 77−28858
metal, hot deformability test methods, comparative evaluation *(German)* 77−36713
metal, plastic props. investig. at elevated temps. by torsional method, review 79−43509
metal, plasticity under hydrostatic pressure *(Russian)* 78−68726
metal, Swift effect, rel. to stress/strain behaviour in simple compression, tension and torsion 77−28860
metal, thin-walled cylinder, elongation upon torsion 80−64386
metal, torsional creep under accelerator irradiation, meas. instrument 78−3262
metals and alloys, yield criterion, rheological interpretation *(Russian)* 80−21014
methyl torsion modes, vibrational optical activity, inertial contrib. 80−5524
micropolar elastic almost cylindrical beams, deformation 79−37177
mild, plastic flow under proportional and non-proportional straining at controlled rates 79−57084
minimum principle for the problem of torsional creep 79−75337
molecular crystal, unidimensional struct. instability charge under torsional force, liquid cryst. transition *(Russian)* 78−87776
multistage deformation simulation on torsion machine 77−40492
New Zealand plate boundary distortion *(German)* 78−20382
Nimonic 115, superalloy, critical strain model for creep fracture 77−32648
Nimonic 80A, creep in tension and torsion 77−25113
Nimonic 80A, creep rapture under non-proportional loading 80−108518
non-homogeneous circular cylinder 77−72152
non-homogeneous elastic medium, sudden twisting of penny shaped flow 78−87302
noncircular cross section, elastic torsion anal., simplified general method 79−90133
nonhomogeneous cylinders and cylindrical shells, torsional oscillations anal. 79−18768
nonhomogeneous elastic layer bonded to nonhomogeneous half-space, torsion by circular die 78−87263
nylon 6, relationship between morphology and dynamic mech. props. 79−4992
nylon-6, viscoelastic props., meas. with modified torsion pendulum *(Spanish)* 77−31264
nylons, glass transition temp., thermal, mech. meas. 77−31758
optical fibre, single-mode, for current meas. system, birefr. induced by bends and twists 80−99832
optical fibre end fracture torsion effects 79−76802
optical fibre tape twist induced stress estimation and reduction by pretwisting 80−53471
optical glass K8, torsional deform. above T_g under low stresses, temp. effect 80−21052
optical glass K8, torsional deform. above Tg under low stresses 80−25804
optimal anisotropy of elastic shafts under torsion *(Russian)* 79−23211
orthotropic laminates, torsion strength and shear modulus determ. 80−92587
oscillation of inhomogeneous elastic half space *(Russian)* 77−19559
oscillation test equipment with process computer control *(German)* 77−21344
oscillations, free and forced, methods of calc. *(Russian)* 77−35065
paper, meas. of shear modulus and damping in a torsion pendulum 79−4989
pendulum, automatically driven, for continuous meas. of amplitude and amplitude-independent damping 77−35099
torsion continued
pendulum, with anelastic solid of discrete relaxation spectra, resonant system 80−69687
pendulum for damping capacity meas. and related phenomena 77−77687
pendulum oscillations recording equipment for internal friction meas. 78−36998
pendulum with elastic wire element, free torsional vibr. anal. *(Spanish)* 79−68613
penny shaped crack in inhomogeneous medium high freq. torsional oscills., stress anal. 78−26086
phenol formaldehyde resin, (Novolak) with filler, mech. props. determ. *(German)* 78−84933
phenolic resin filled and unfilled, mech. relaxation behaviour, effects of temp. and time *(German)* 78−6963
phthalocyanine polymer, dynamic mech. props. and fracture energy 80−100866
piezoelectric cylindrical shell, finite, torsional wave propagation 78−56428
piezoelectric cylindrical shell, inhomogeneous, torsional wave motion 80−60506
piezoelectric plate, infinite, on elastic medium, transient response to pot. pulse 78−52442
piezoelectric thin plates, integer polynomial solns. *(Russian)* 78−52444
pipe elbow element, linear anal., bending axial and torsional displacements, ovalisation 80−79177
plastic, elongation due to Bauschinger effect and fibre rotation rotation *(German)* 77−72184
plastic, integral inequality anal. 80−10155
plastic, reactive, structurisation kinetics, torsion cord method *(Russian)* 79−34304
plastic, torsional rigidity testing instrument, used with strength testing instrument *(German)* 77−52596
plastic bending and torsion of simple geometries, subjected to cyclic loading, stress-strain analysis 78−90734
plastic bodies break-up *(Russian)* 77−80121
plastic flow of tube, under adiabatic torsion 77−62161
plastic material, impact-torsion test machine *(German)* 77−52595
plasticity diagram plotting by testing cylindrical samples in combined tensile tension 77−63879
plate, elastic, under uniform twisting, periodic collinear cracks *(Japanese)* 78−67097
plates with flows or cracks; twisting and bending theory 79−64545
PMMA, nonlinear viscoelastic behaviour in torsion 79−61640
PMMA, unstable crack propagation in liq. environment, fractographic study 80−30155
PMMA organic glass shell, circular, cylindrical, under combined twisting moment/axial load buckling 79−100220
Poisson's equation solution, using curvilinear finite differences 78−28923
polyamide, torsional rigidity testing *(German)* 77−52596
polycarbonate, rigid plastic, yield behaviour *(Japanese)* 80−93620
polycarbonate, yielding and crazing behaviour in torsion under superimposed hydrostatic press. 78−52898
polycrystalline material, plasticity analysis using stat. model *(Russian)* 78−26619
polyester, unsat., copolymers, crosslinking effect on viscoelastic props., free torsion oscill. study *(Russian)* 79−34093
polyester resin, creep, temp. and humidity effects under shear and tensile strains 77−86105
polyethylene, amorphous linear, glass transition temp. by torsion braid anal. 79−73296
polyethylene, high density, strength props. *(German)* 79−100219
polyethylene, low density, meas. of shear modulus and damping in a torsion pendulum 79−4989
polyethylene, low density, nonlinear variable temp. creep 79−38908
polyethylene, stress relaxation under tension and torsion 79−52290
polyethylene, torsional rigidity testing *(German)* 77−52596
polyethylene rod, high oriented, mech. behaviour 78−15446
polymer cyclic deformation amplitude, automatic meas., apparatus design 78−85082
polymer soft lossy, viscoelastic props. determ. from torsional vibr. of laminated bar 77−62218
polymers, nonlinear, stress relaxation under tension and torsion 79−52290
polymers, torsion pendulum dynamic mechanical testing 80−55620
polymethacrylic acid-polyethylene oxide polymer complex, H bond form., thermal behaviour *(Japanese)* 79−15454
polystyrene, impact resisting *(German)* 79−100219
polystyrene, impact-torsion testing *(German)* 77−52595
polystyrene, $T_{||}$ relax. above glass transition 79−4259
poroelastic cone, inhomogeneous, forced torsional vibrs. 79−32338
poroelastic hollow cylinders, torsional vibrs. 79−64557
poroelastic semi-infinite cylinder, torsional vibr. 79−32334
poroelastic semi-infinite solid, torsional loading 79−32335
porous sintered materials, mech. testing device for hydrostatic pressure conditions 80−40645
prism bending to helical form, formal perturbation scheme 78−55558
prismatic bar, finite element solution 80−38282
prismatic bar of linearly elastic material, maximum theorem appl. for complementary energy functional 80−83733
prismatic bar torsional rigidity estimation inequalities 79−88808
prismatic bars, elastoplastic torsion by quadratic programming, finite element scheme 79−32251
prismatic bars, torsional stiffness of heterogeneous material and solid cross section 79−27519
prismatic bars, torsional stiffness upper limit 79−32248
prismatic shaft, doubly connected cross section *(Russian)* 77−42744
prismatical beams, torsion and flexure 79−18711
Procopiu effect EMF in ferromag. material under torsion *(Rumanian)* 78−86986
PVC, rigid plastic, yield behaviour *(Japanese)* 80−93620
quantisation procedure for torsion and metric fields 79−35615
quartz, torsional vibration frequency temp. depend. 80−70294
rectangular bars, appl. of improved collocation techniques 77−68434
refractory, high-temp. stress relaxation during alternating torsional loading 77−16636
reinforced concrete, lower bound anal. for torsion 78−35436
reinforced concrete curved beam, expt. investigation of collapse 77−90404
relativistic quantum mechanics, role of wave fronts and torsion *(French)* 77−53795
relativistic theories involving torsion, variational principles 77−60990

torsion continued
rheological property meas. apparatus *(French)* 80−14644
rig, testpieces testing during variable torsion 79−52494
ring, homogeneous isotropic compressible elastic, second order torsion problem 80−14570
ring sector, plastic twisting *(Russian)* 77−50923
rod, thin elastic, non-conservative torsion *(German)* 80−106723
rod, twisted axially loaded, nonlinear anal. 79−72811
rod of rate-sensitive material, elastic-plastic tension-torsion analysis 80−83741
rod with helical anisotropy 77−62155
rod with nonlinear curvature, dynamic stability theory, lateral bending problem under torsion *(German)* 78−54
rods, prismatic, torsion with internal constraints *(Russian)* 80−69647
rods, prismatic, torsion with internal constraints *(Russian)* 80−69648
rods, second order theory for bending and torsion *(German)* 79−68598
rotor blades, flapwise and chordwise bending, and torsion 77−39251
round bars, endurance limit under combined tension and torsion 79−32387
rubber, natural, crosslinked by dicumyl peroxide, modulus, swelling relations 80−59551
rubber cylinder, circular, uniformly heated, combined extension and torsion 80−92057
rubber hydrochloride, meas. of shear modulus and damping in a torsion pendulum 79−4989
Saint-Venant's problem for micropolar elastic cylinder 77−3719
Saint-Venant torsion problem, classical, integral and functional eqns. 78−57780
sapphire rod, torsional waves at low freqs. 77−84053
scragged torsion bar, residual shear stress meas. 79−59954
servocontrolled hydraulic hot-torsion machine for hot working studies 78−27698
shaft, operating under torque, structural strength evaluation 79−83280
shaft with regular round polygon, stress state 80−35284
shaft-disk systems, lower bound for fundamental torsional frequencies 77−19565
shafts of varying cross section, bounds for torsional stiffness 78−87266
shallow groove, stress conc. factors 77−46919
sharply indented bodies, axially symmetric torsion, boundary integral eqn. method anal. *(German)* 79−90141
shell, conical, stress distrib. near hole, orthotropy effect 80−43630
shell, cylindrical, inhomogeneous, thermoelastic torsional waves 79−92952
shell, spherical, non-shallow, torsional axisymmetric deform. subprogram 80−43607
shell, stiffened, buckling under destabilizing loads including torsion 78−26062
shells of revolution, max. principles and pointwise error estimates for torsion 78−18180
shot peening residual stress effects on plastic microstrain in isotopic media *(French)* 79−77675
silicone oils, props. determ. by harmonical shear vibr. *(German)* 78−67164
soft-interlayer welded joint bending and torsion endurance, residual stress effects 79−83287
solid shaft, elliptic cross section, elastic torsion, polynomial soln. to approx. of any order *(Italian)* 78−13897
spacetime structure probed by spin 1/2 elementary particles, Riemann geometry with torsion 77−41517
spherical shell, torsional vibrs., numerical results 78−59322
spinning charge, torsion contrib. to magnetic field 80−77676
spinning particle in metric-torsion field, eqn. of motion 80−62543
spinor electrodynamics in Riemann-Cartan space, dynamical theory of axial vector torsion propag. in vac. 78−73889
springs, helical torsion, design for minimum weight 77−54881
steel, alloy, rectangular beam, stress-strain anal. of cyclic plastic bending and torsion 78−90734
steel, anisotropic rolled plate, torsional fatigue in middle and high cycle fatigue ranges *(Japanese)* 77−12691
steel, austenite hot deformation influence on phase transformations 80−7606
steel, austenitic, martensitic transform. during low temp. alternating torsion *(Russian)* 78−23706
steel, austenitic stainless, high temp. alternating torsion behaviour, saturation state phenomenology 79−70111
steel, C, accumulation of longitudinal strain under cyclic torsion 78−64615
steel, C, brazed butt joint, static torsional deform. 77−16657
steel, C, ductile fracture under cold forming conditions, press. effect 78−52938
steel, C, effect of pre-straining on torsional fracture strain *(Japanese)* 80−3183
steel, C, fatigue crack exam. using slip initiation phenomena *(Japanese)* 77−8930
steel, C, non-propagating microcrack, opening and closing behaviour in rotating bending and torsional fatigue *(Japanese)* 80−25846
steel, C, torsional prework effect on fatigue strength, crack propagation *(Japanese)* 80−55514
steel, C, unnotched, fatigue life estimation, under combined torsion and bending *(Japanese)* 80−93647
steel, C (0.54 wt.%), torsional fatigue process, obs. by electron microscope *(Japanese)* 77−12690
steel, C and alloy, restricted durability, subject to pure bending with rotation 77−90431
steel, C-Mn-Nb, Nb microalloying, weldable, structural, recrystallization and precipitation induced by high temp. deform. *(French)* 79−61632
steel, Cr (12 wt.%), thermomechanical treatment, high temperature, effect on props. and struct. *(Czechoslovakian)* 77−32603
steel, creep and fatigue fracture prevention 78−60837
steel, ductile fracture under cold metal forming conditions, metallurgical struct. influence 79−34125
steel, eutectoid, fatigue crack tip props. in rotary bending and cyclic torsion 77−32668
steel, eutectoid and hypoeutectoid viscoelasticity under transformational superplasticity *(Japanese)* 77−52416
steel, hardened, exoelectron emission from torsion fatigue damage 77−86142
steel, high C, piano wire, mean stress effect on low cycle torsional fatigue life *(Japanese)* 79−96114
steel, high-speed, cast, mech. props. at high temps. 79−20135
steel, low C, absolute dimensions effect on logarithmic decrement of torsional vibrs. 80−3150
steel, low C, corrosion, heat treatment and plastic deform. effects 77−63825
steel, low C, creep rupture strength, precracked round bars under torsion *(Japanese)* 77−59908
steel, low C, fatigue strength under rotating bending and torsion, understressing effects *(Japanese)* 78−44201
steel, low C, microplasticity at high and low loading freq. *(Slovak)* 79−38910
steel, low C, thin walled tube, fatigue behaviour, low endurance, under bending and torsion 77−86129
steel, low C, under rotating bending and torsion, overstressing effects *(Japanese)* 77−8935
steel, low C, unnotched specimens, brittle fracture beyond general yielding tensile-torsional stresses 77−56096
steel, medium C, S 45 C, influence of mean strain on low-cycle torsional fatigue life *(Japanese)* 79−8348
steel, medium C and austenic stainless, cyclic strain induced creep, relation between modes of stress and strain superposition 78−60733
steel, mild, plastic flow localisation under dynamic torsional loading, crit. variables 80−85015
steel, mild, plastically pretorsioned, dynamic props. 79−83267
steel, plasticity depend. on hydrostatic press. in low-angle fatigue, Manson-Coffin coeff. *(Russian)* 79−61651
steel, pressure vessel appl. 79−61690
steel, pressurised tubes under dynamic bending and torsional loading, inelastic deform. 77−77549
steel, rolled, effect of inclusions on torsional fatigue 78−92314
steel, rolled plates, anisotropic, fatigue behaviour under cyclic torsion 77−44326
steel, S45C, low-cycle torsional fatigue under multiple repeated loads *(Japanese)* 77−8925
steel, S45C and SS41 types, dynamic yield condition under dynamic torsion and static tension 79−34214
steel, spring, 60C2A, tempered under stess, influence of tempering conditions on mech. props. *(Russian)* 79−47724
steel, stainless, 304, deformed in torsion, annealed, static recrystallization and restoration after hot deform. 79−47735
steel, stainless, reinforced glass matrix, vibr. damping anal. rel. to internal friction 80−40413
steel, stainless, SUS 316, creep-fatigue interaction at 600°C 79−34123
steel, stainless, type 304, creep surface determ. from multiple integral representation 79−47761
steel, stainless type 304 L, mech. behaviour under constant stress associated with cyclic strain 80−25767
steel, stainless type 316, monotonic and cyclic biaxial loading at room temp. 78−52928
steel, tufftrided, fatigue strength under reversed torsion *(Japanese)* 79−61707
steel 15Kh1M1F, temperature-time dependence of long-time structural strength 79−100232
steel 2Kh13, damping props., effect of plastic deform. by torsion 77−70095
steel 45, fatigue strength determ. apparatus, in corrosive environment under complex stress *(Russian)* 77−77657
steel alloy, type 30 KhGSA, expt. functions of resist. in tension and torsion 80−16397
steel column design, I-section, braced multi-storey, torsional buckling at limit state of collapse 78−1586
steel finite life characteristics, temperature change effects, torsion cycle tests *(German)* 78−7004
steel JIS-SNCM8, fatigue under in-plane combined axial loading and torsion 79−96147
steel low C, notched, fatigue strength, crack propagation, plastic torsional prework depend. *(Japanese)* 79−15744
steel reinforced concrete beams, mech. strength determ. under combined bending and tension 78−60749
steel rolled, low-cycle torsional and push-pull fatigue anisotropy 78−27589
steels, C, cold worked and recrystallised, attenuation behaviour *(German)* 78−48445
stiffened cylinders under torsion with axial compression 78−26065
strain curves plotting 80−40638
strain diagram plotting from data obtained during elastoplastic bending or torsion 77−81371
stresses analysis in non-circular shafts, analogue simulation *(German)* 77−68551
structural anal., soln. by orthogonal collocation 78−51063
structural elements having 1- and 2-section; freedom, vibr. characts., optimum design 77−72207
tape cores carrying current, torsional stress effects 80−34742
Tennessee sandstone, Carrara marble, fracture toughness, double torsion testing method 79−84239
tension-torsion impact testing apparatus, instantaneous plastic property 79−52474
test apparatus for 0-1150°C range in different gaseous atms. 78−7123
test method, for plastic deform. *(Hungarian)* 80−97659
thick walled cylinder subject to torsion, stresses at offset oblique holes 79−32404
thick-walled tube, micropolar, generalised Lame problem and torsion *(Polish)* 77−54886
thin circular cylindrical shells, torsional stability *(Chinese)* 79−72833
thin shells of resolution, torsion and Saint-Venant's principle 77−50912
thin walled bar, subjected to bending, elastic-plastic behaviour, expt. *(Croatian)* 77−35060
thin walled tubular specimens, plotting hardening curves based on torsion tests 77−56180
thin-walled box structures subjected to pure torsion, behaviour vs. temp. in 20-180 C range *(Italian)* 79−41572
Timoshenko beam, coupled bending and twisting vibration 77−58584
torsional creep problem, appl. of maximum principle 78−71284
torsional damper using second order fluid *(German)* 79−68615
torsional vibration meas. with laser Doppler system 78−45612
transient elasto-dynamic response of circular crack in thick plate under torsion 80−5993
transversely isotropic plate with hole, edge supported, shear compliance in bending and torsion 77−2543
truncated elastic cone, mixed boundary value problem 77−46908

torsion continued
tube, plastically compressible material, length change *(German)* 77−23898
tube, porous, nonlinear viscoelastic materials, soln. using generalised correspondence principle 80−38288
tubular sample testing unit with axial force, internal and external press. and torsional moment 78−39969
tubular specimen, torsion stresses 78−63298
twisted bar, elliptic, stress and deform. states produced by axisymmetric elastic torsion *(Italian)* 78−22262
twisted elastic prismatic solid, torsion, Gohner-Giovannozzi stress anal. *(Italian)* 79−18766
twisting, differential geometry 77−84834
two channel drive dynamics with differential wave mechanism *(Russian)* 80−28449
two-layered circular cylinder with imperfect bonding, wave propag. 77−14948
unidirectionally reinforced metal composite, complex torsional and tensile loading 79−61669
unified theory of gravitation and electromag., Weyl-Dirac theory with torsion 80−52106
US vibrations in metals, measurement of absorpt. 80−58856
vibration on rotating machinery, measurement systems 79−23287
vibrational anal., iterative methods, accelerated automatic root search algorithm 78−59321
vibrations, optimal damping *(Russian)* 77−57179
viscoelastic beam, two-layer, dynamic torsion 77−7318
viscoelastic cylindrical rod, dynamic torsion 77−3739
viscoelastic layer, anisotropic, nonstationay torsional waves problem *(Russian)* 80−53678
viscoelastic rod, standard linear body, free torsional ascills. 80−99940
viscoelastic-plastic pendulum, prismatic, oscills. *(Spanish)* 77−3733
wedge-shaped straight elastic bars, new method for longitudinal and torsional vibration freq. calc. 78−59338
wind-induced bending torsional galloping vibration of rigid body, minimal wind velocity determ. 80−48623
wire, fatigue probability diagram plotting 79−52490
wire, locked coil rope, limiting moment calc. in torsion 79−10507
wire in torsion, installation for automated determination of yield strength 80−21221
wood, set, force induced from moisture recovery of drying set *(Japanese)* 77−77537
zirconate-titanate ceramics, K_{IC} eval. by double torsion technique 77−90444
Al alloy, cast AL15V, brittle, strength in three axial stress state 79−66134
Al alloy, yield surfaces, effect of preloading under combined axial load and torsion 77−25091
Al alloy 2618, creep and recovery under combined stress, viscous-viscoelastic model representation 79−34117
Al alloy fatigue crack growth, stage I, effect of liquid environment 77−86164
Al, annealed, subjected to torsional impact loading strain-rate effects 78−92303
Al, Bauschinger effect, temp. influence, combined tension-torsion testing machine 80−45453
Al, creep and rupture, in torsion, mech. *(Russian)* 79−5030
Al, fracture mechanism, plastic strain role 79−38977
Al, resistivity decrement under torsional deform., impurity segregation at moving dislocations 77−4321
Al, single crystal, superplasticity 79−1901
Al, tension-torsion impact testing, instantaneous plastic property 79−52474
Al, texture influence on stress/strain curves, prestrain, solid soln. and particle hardening effect on inhomogeneous deform. *(German)* 80−30014
Al, thermoactivation parameters of plastic flow in torsional deform. *(Russian)* 79−38926
Al, torque and length change during fracture in torsion test *(German)* 79−24611
Al, torsional fatigue and bending tests 79−43521
Al, transient creep, effect of pre-torsional deform., dislocation glide and density 77−4147
Al tube, thin-walled statically pre-tensioned, torsional impact loading 78−27557
Al wire, torsion fatigue strength and fibre texture 77−48549
Al-Ag (7.27 wt.%), peculiarities exhibited during fatigue loading *(Chinese)* 80−71723
Al-Cu, high temp. internal friction peaks 77−48470
Al-Cu-Mg-Mn-Si-Fe, torsional vibrations decrement, deformed vol. effect 80−76326
Al-Cu-Si-Mg, deform. simulation using torsional test, elastoplastic constitutive eqn. 80−93594
Al-Ni (6 wt.%), fine-grained, deform. in tension and torsion 80−85008
Al-Si-Zn alloy, creep rates, pre-torsional deformation effect 79−96096
Al-Zn eutectoid alloy, sensitivity analysis of torsion method in evaluating superplasticity indicators 77−56179
Al-Zn-Mg-Cu (6, 2.5, 1.5 wt.%), deform. simulation using torsional test, elastoplastic constitutive eqn. 80−93594
β-B, rhombohedral, sublimation, 1823 to 2253K, torsion-effusion and mass spectroscopic meas. 77−39673
B_2O_3, vitreous, torsional deform. above T_g under low stresses, temp. effect 80−21052
B_2O_3, vitreous, torsional deform. above Tg under low stresses 80−25804
B_2O_3-SiO_2 glass, crack front shape corrections for crack velocities in double torsion specimens 79−91778
C fibre reinforced composite, shear fatigue 78−15493
C fibre reinforced epoxide resin, torsion creep 78−44172
C fibre reinforced epoxy, wound, strength in twisting, stretching and transverse bending 80−11622
C fibre reinforced epoxy and C fibre, elastic moduli 77−86069
Cu, annealed polycryst., torsional vibrations decrement, deformed vol. effect 80−76326
Cu, brazed butt joint, static torsional deform. 77−16657
Cu, deformed by rolling and torsion, stored energy *(German)* 79−29160
Cu, grain refinement of dynamic recrystallisation during hot working *(Japanese)* 77−52345
Cu, hot ductility and torsional deform. *(Japanese)* 79−57069
Cu, recrystallised, inhomogeneous deform. due to texture changes *(German)* 79−29158
torsion continued
Cu, tension-torsion impact testing, instantaneous plastic property 79−52474
Cu, torsion deformation texture *(French)* 79−70082
Cu, whiskers, hardening during uniaxial extension, preliminary torsion deform. *(Russian)* 78−15420
Cu wire, creep rate, effect of pre-torsional deform. at room temp. or 350°C 77−84836
Cu-Al, single crystal, dislocation velocity meas. 78−3172
Cu-Al_2O_3 extruded bars, strength anisotropy 77−16597
Cu-Zn-Al (35.45, 1.72 wt.%), memory effect and martensitic transform. *(Russian)* 79−43320
Fe, cast, grey, brittle, strength in three axial stress state 79−66134
Fe, cast, rod, torsion, St. Venant's problem 77−70135
Fe, cast, white, fracture toughness testing by double torsion bend test 78−27705
Fe, commercially pure, viscoelasticity under transformational superplasticity *(Japanese)* 77−52416
α-Fe, polycrystalline, shear modulus, H_2 effects 77−36561
Fe whiskers, inverse Wiedemann effect, torsional strain and azimuthal mag. field influence 80−108045
Fe-C-Cu (0.21, 0.2 wt.%), neutron irradiated, torsional props. effect of Cu additions and annealing temp. 78−56699
Fe-Ni (15, 25 at.%), longitudinal forces in the hot torsion test *(German)* 79−38889
Fe-Ni (35 to 100%), magnetoelastic attenuation of torsional vibr. and shear modulus defect *(Russian)* 77−80982
Fe-Ni-C, N31, martensitic point lowering by microplastic deform. and room temp. ageing *(Russian)* 77−25049
Fe-Si (3 wt.%), internal friction, instantaneous, depend. on phase of torsional oscills. *(Russian)* 80−71142
$Fe_{40}Ni_{40}P_{14}B_6$, amorhpous ribbon, influence of torsion on mag. props. 80−7138
Mg alloys, strain rate effects during reverse torsional shear 77−4143
Mn-Cu-Al alloy under torsion, anomalous elasticity and transformation plasticity obs. *(Russian)* 78−75834
Na_2O-CaO_2-SiO_2 glass, stressed, chemical reaction in water vapour 79−91819
Na_2O-CaO-SiO_2, double torsion specimens, compliance and fracture load as crack length function 78−48508
Na_2O-CaO-SiO_2 glass, K_{IC} eval. by double torsion technique 77−90444
Na_2O-SiO_2, crack front shape corrections for crack velocities in double torsion specimens 79−91778
Na_2O-SiO_2(-B_2O_3) glass, torsional deform. above Tg under low stresses 80−25804
Nb, relaxation intensity due to interstitial O, temp. effect *(French)* 77−86080
Ni alloy, heat resistant, fatigue limit comparison in torsion and tension-compression 80−81181
Ni, ductility and fracture, nonmetallic inclusions effect 80−104221
Ni, internal friction, instantaneous, depend. on phase of torsional oscills. *(Russian)* 80−71142
Ni thin-walled cylinder, elongation upon torsion 80−64386
Ni wire, polycryst., inverse Wiedemann effect for low torsional stress 79−11332
Ni wire, polycryst., magnetoelastic hysteresis with torsion, inverse Wiedemann effect *(Spanish)* 77−73064
Pb, deformed by torsion, stored energy and recrystallization 79−34069
Pb(Zr,Ti)O_3, K_{IC} eval. by double torsion technique 77−90444
steel, C, annealed S45C, multiple repeated low cycle torsion fatigue under controlled strain *(Japanese)* 78−27610
Te, screw dislocation substruct. studied by torsion expt. 79−10859
Ti alloy, creep and long-term strength under cyclic loading 78−3191
Ti alloy, cyclic creep 77−81323
Ti, fatigue cracking, initial stage under bending and torsion *(Japanese)* 79−20165
Ti-Al-Sn (5, 2.5 wt.%) alloy, fatigue under combined alternating bending and torsional stresses 77−8923
Ti-V-Cr-Al (13, 11, 3 wt.%) alloy spring wire, torsional fatigue props. 77−77649
U-Mo (1.5 wt.%) metallurgical study of forging *(French)* 78−21737
V, internal friction α-peak origin 78−95773
V wire, deformed in torsion, internal friction, H effect 80−76300
V-H rods, twisting effect, anelastic deviations on thermal cycling 80−21043
W, cyclically deformed, electrical resistivity 77−52491
WC-Co, fracture toughness testing by double torsion bend test 78−27705
WC-Co, size factor effect on strength in complex stressed state 78−31483
Zn, line energy of basal screw dislocation, exptl. determ. 80−88154

torsion loading *see torsion*

total energy systems
25 kW Fresnel lens/photovoltaic concentrator application experiment at Dallas−Fort Worth Airport 80−89647
combined power and heat systems, waste heat utilisation, and heat pumps, economic aspects *(German)* 79−87981
diesel-driven chiller system simulation, with multi-tank thermal storage system, for large commercial buildings 79−48187
distributed microcomputer-based control system for a large scale solar total energy system 80−30396
energy cascading principles *(French)* 80−76621
free piston Stirling engines increase solar/thermal efficiency 79−96481
industrial solar total energy systems in United States 79−96426
integrated photovoltaic/thermal system with faceted-mirror sunlight concentrator 79−62010
optimal development strategies for a whole energy system based on hydrogen 80−45795
solar, 32 kWe, test facility 79−52912
solar, for US Army base buildings, conceptual design and large-scale expt. 79−52899
solar, preliminary design for large building supply 79−52898
solar building analysis and design, using Cal-ERDA programs 79−57456
solar concentrators, linear with fixed focal axis, appl. 78−9427
solar total energy system, Fort Hood, control system 80−30397
solar total energy system at Georgia, USA 80−35652
solar total energy system evaluation program 80−30402
Stirling engine powered total energy system for recreational vehicle appls. 80−30538

total energy systems continued
thermogravimetric reversible total energy system 80−55884
NaOH-8% $NaNO_3$ phase change thermal storage for solar total energy system 79−57481
touch *see mechanoception*
towers *see poles and towers*
town and country planning
agricultural land urbanisation hydrologic impact, distributed watershed model 77−37277
Bavarian surveying administration, centralised and decentralised data processing *(German)* 77−2288
cement works, implications for residential development 77−37403
coastal zone development pressure monitoring by remote sensing 78−78013
Iranian solar town conceptual development 80−35645
meteorological and climatic information rel. to urban planning 78−3916
Monarto new city, S.Australia, air pollution planning techniques 77−70818
multiobjective urban drainage and flood control project evaluation 77−37270
noise regulations in small cities, inexpensive community assessments 77−54841
traffic noise, model investigation on acoustical performance of courtyard houses 80−10077
traffic noise screening effect by buildings *(German)* 80−10076
urban erosion and sedimentation prediction and control 77−37282
urban flooding rel. to land use change, stormwater management model 77−37280
urban stormwater management, basinwide planning programme 77−37268
Townsend coefficient *see Townsend discharge*
Townsend discharge
acetone, Townsend coeffs. of avalanche counter gases 78−78582
air positive point corona current continuous component 78−67586
avalanche, vacuum UV spectra 80−64810
butene-1, Townsend primary and secondary ioniz. coeffs. and sparking voltages 78−51372
cyclohexane, Townsend coeffs. of avalanche counter gases 78−78582
electron back diffusion, Monte-Carlo calc. 77−68884
electron swarm develop., Boltzmann eqn. anal. 78−79487
ethane, positive-ion drift vels., Townsend primary ionis. coeffs. 79−55592
ethylene, Townsend primary and secondary ioniz. coeffs. and sparking voltages 78−51372
first Townsend coefficient, step ionisation effects, anal. 79−82117
flash tube discharge mechanism determ. from digitisation pulse output 78−17504
glass cell plasma production by pulsed discharge development, finite difference soln. 78−67559
n-heptane, Townsend primary and secondary ionisation coeffs. and sparking voltages 80−1732
n-heptene, Townsend coeffs. of avalanche counter gases 78−78582
n-hexane, Townsend primary and secondary ionisation coeffs. and sparking voltages 80−1732
inert gases, Townsend avalanches, gas scintillation counter obs. 80−38805
large-area nanosecond discharge breakdown 78−71614
mechanisms, of single-avalanche, Townsend and channel discharges *(Polish)* 80−79609
methyl alcohol, Townsend coeffs. of avalanche counter gases 78−78582
n-pentane, Townsend primary and secondary ionisation coeffs. and sparking voltages 80−1732
propylene, Townsend primary and secondary ioniz. coeffs. and sparking voltages 78−51372
Ramsauer-Townsend effect, partially ionised gas elec. cond. 78−67458
rod-to-plate system, initial corona voltage calculated according to Townsend's Theory *(Czech)* 80−87961
spark voltages, cathode surface state effects *(Korean)* 80−19643
stepped-sideways Townsend discharge movement in a crossed magnetic field 78−79489
Ar breakdown characts. obs. 78−87510
Ar discharge, optogalvanic and excited state photoionisation signals, space charge effects 80−14947
Ar, electron energy distrib. functions 77−58912
Ar, total electron impact excitation cross section, first Townsend coeffs. 77−536
H_2 plasma, electron transport coeffs. at high E/N values 79−94835
H_2, Townsend avalanches, gas scintillation counter obs. 80−38805
H_2, transverse diffusion and Townsend ionis. coeffs., photon flux meas. 79−1367
He, macroscopic quantities, Boltzmann eqn. and Monte Carlo calcs. 80−38848
He Townsend discharge field emission by higher-order ion clusters 78−67550
Hg, electron swarm props. Boltzmann eqn. anal. 80−19648
Kr, total electron impact excitation cross section, first Townsend coeffs. 77−536
N_2 breakdown characts. obs. 78−87510
N_2, electron energy distrib. and transport coeffs. in E×B fields 78−51277
N_2 plasma, electron transport coeffs. at high E/N values 79−94836
Ne afterglow, decay rate of metastable ats. 80−44011
Ne, electron energy distrib., relax. process 78−30507
Ne-He high press. flash tubes, digitisation pulse characteristics 80−9455
Ne-Kr Penning mixtures, Townsend ionisation coeffs. and breakdown pot. meas. 80−19641
Ne_2^+, formation and destruction in Townsend discharges 80−38747
O silent discharge, numerical simulation 78−63629
SF_6, electron beam irrad., delayed elec. breakdown 79−4200
SF_6, electron swarm development, Boltzmann eqn. anal. 80−6205
Xe, electron energy distrib. functions 79−4198
Xe Townsend discharge electron energy distrib. obs. 78−67549
tracers
see also radioactive tracers
aerosols, pyrotechnically produced, use as atmospheric tracers 77−41236
air pollutants dispersion and transport within coastal regions, tracer study of power plant emissions 79−62545
air pollutants dispersion and transport within coastal regions, tracer study of industrial emissions 79−62546
air pollution long-term dispersion studies, temporal sampling requirements 79−39325
tracers continued
air pollution transport and turbulent dispersion over rugged mountainous terrain 79−84349
air sampling system, radio-controlled, for diffusion expts. 79−79440
atmosphere, lateral diffusion parameters vars. 79−20931
atmospheric diffusion parameters on local scale, determ. by no-lift balloons 79−70853
atmospheric pollutants, molecular and isotopic tracers appl. to origins and residence times 78−69445
atmospheric precipitation systems, chem. tracer expts., review 78−24324
biological stochastic compartmental models, parameter estimation 78−40109
biosystems, tracer identification of time varying compartmental parameters 77−40960
blood flows and vols. in patients with transposition of great vessels, indicator-dilution meas. 78−61209
blood velocity, catheter meas., cross correl. technique 78−80943
capillary permeability determ. from multiple indicator data, effects of finite red cell permeab. 78−44483
cardiac output measurement, tracer transport model accounting for recirculation 77−36978
chemical analysis by proton excitation of X-rays *(German)* 77−25348
coastal currents and pollution, satellite, aircraft and drogue studies 77−37206
diffused substance kinetics in biological systems 78−53312
diffusion coefficients, capillary method determ. calcs. 78−91462
diffusion experiments in unstable conditions over inhomogeneous terrain 79−58059
diffusion obs., RF sputtering as microsectioning technique 78−14499
dye dilution method for large open and closed channel flows, validation 78−30395
electrically charged air tracking, for atm. diffusion meas., by ground level elec. field meas. 77−78450
fluorescent dyes, evaluation for water tracing 77−64493
fluorescent tracers in hydrology, conc. meas., synchronous excitation method *(French)* 77−77840
fusion thermal tracers, thermophys. characts. investig. 77−5837
galactic morphology of H and trace gases, review 77−26070
gas studies using automatic sequential sampler 79−83686
geophysical systems, tracer theory, nonsteady state 79−5646
groundwater recharge mechanism, Los Naranjos area, Mexico, using environmental isotope methods 80−12458
heart congenital defect evaluation from dynamic tracer meas. 78−40378
hydrodispersive transfer in aquifers 80−98374
hydrological system tracer, finite element method appl. 78−92881
impurity diffusion profiles, influence of limited solubility 78−55989
indicator dilution methods appl. to flow rate meas. 77−65825
ionized air as wind tunnel tracer 78−22435
isotopes for oceanographic investigations *(Russian)* 77−60486
medical applications in vitro using X-ray fluorescence 77−5063
nuclear microprobe anal. of stable isotope tracers spatial distrib. 80−50909
ocean circulation studies and use of tracers 78−16053
ocean surface currents charting by aerial tracking of dye emitting radio beacons 79−5675
offshore disposal of dredged material, sediment props. as tracers 77−5245
optoelectronic pattern tracer for laser plate cutting 79−55170
PIXE analysis of trace elements in environmental samples *(Chinese)* 79−61925
sand tracer dispersion under progressive water waves, laboratory and field obs. 80−46170
stratosphere tracer transport mechanisms, Lagrangian motion of air parcels in presence of planetary waves 80−109215
stream sediment sources, use of metals as tracers, field expt. 78−81227
trichlorofluoromethane, transport processes indicator in urban atmosphere 78−36264
3,3′,5′-triiodothyronine plasma to tissue transport rate estimation from 3-compartment model 78−31792
tumour in rat, concentration of Ga, Yb, Tl, anal. by proton induced X-ray spectroscopy 77−5122
turbulent diffusion from sources near obstacles with separated wakes, conc. meas. near cylinder 79−81866
turbulent free convection in fresh and salt water, characts., visualisation 79−18888
two-phase flow, local vels. of particles, using mag. markers *(German)* 77−42939
two-phase flow systems, tracer analysis 80−24073
underground water movement tracing using halogen tracers and NAA 79−88014
water, self-diffusion coeffs. in pure water and aq. electrolyte solns., ^{18}O and ^{2}H tracers 78−95169
^{48}Ca stable isotope tracer analysed by proton activation 77−21622
$Co_{1-x}O$, point defect struct., elec. cond. and Co tracer diffusion 79−10849
Fe aerosols in atmosphere, tracing techniques 77−41235
Fe-Cr (9 wt.%), oxidation studied using $C^{18}O_2$ and D_2O tracers 80−71784
He tracers for detection of gaseous atmos. pollutant emissions *(French)* 80−7987
N_2O, atmospheric, three-dimens. distrib. and variability, numerical simulation 79−58006
^{15}N, stable isotope tracer, anal. by proton scatt. 79−61926
Ni, oxidation transport processes using tracers in growing NiO scales 80−25913
^{18}O tracer diffusion coeff. determ. in Ti_nO_{2n-1}, continuous mass spectrometry 77−20124
SF_6 and atmospheric tracer gases, electron capture detection method 77−25785
SiO_2, dissolved, natural oceanic circulation tracer, Yucatan Strait 78−44830
^{31}Si tracer diffusivity in CaO-SiO_2 melt at 1600°C 80−54418
U atomic motion on thin C substrate, low-temp. obs., biomolecule marking appl. 79−25176
track visualisation, particle *see particle track visualisation*
tracking
see also radar
artificial satellite laser tracking, current status and future prospects of technology 79−66906

tracking continued
artificial satellite laser tracking, latit., time and height var. meas. at single station 77−32976
artificial satellite systems for Earth gravity field meas. 79−53298
binary image analysis, distance and region association algorithms 79−72523
coherent optical processor for vehicle tracking and identification using laser diode light sources 80−37957
conference on satellite Doppler tracking and geodetic appl., London, England (Oct. 1978) 80−77264
cumulus clouds, satellite tracking and derived mesoscale wind fields covariance anals. 80−82013
Deep Space Net, appl. of spacecraft tracking technology to experimental gravitation 80−8895
Doppler tracking of spacecraft, gravit. radiation detect. possibility 79−30345
Earth's rotation and Earth's crust movement by laser geodynamic satellite 77−41206
Earth survey satellites, orbit determination 79−25442
eye tracking as sequential input adaptive process 79−88074
Geos 3, calibration and evaluation of STDN S-band stations, using Doppler and laser ranging data 80−4228
Geos 3, satellite-satellite tracking data appl. to geocentric gravit. const. (GM) determ. 80−3911
Geos 3/ATS 6 satellite-to-satellite tracking for Geos 3 orbit determ., results 80−4225
geostationary satellites, optical observations 79−84627
high speed bodies, appl. of sub-tabulation 77−60915
ionospheric corrections for satellite tracking systems, total electron content model 78−69587
IR staring mosaic sensor background suppression and tracking 80−86415
Kuroshio Western Boundary Current, by Nimbus 6 satellite 78−36190
laser lunar ranging, scientific progress, 1969-77 period 78−36476
laser radar, image centroid, size and orientation estimation 77−88901
laser satellite-tracking, Ondrejov station site evaluation 78−36418
low power light sources, tracking via variable precision discrete photoelectric system *(Russian)* 78−57458
luminous pointlike object, three-dimensional trajectory recording 78−12671
magnetosphere plasma resonances, on-line tracking for electron density small-scale struct. 79−35073
Mars, dynamics obs. from Viking lander tracking data anal. 80−77314
methane gas plumes, in atmosphere, tracking via acoustic sounder 80−55968
mosaic IR image differencing for track assembly 80−86420
neurological function tracking-task instrument, portable, features 77−86678
ocean currents, results from satellite-tracked drifters between Africa and Antarctica 78−73376
ocean mooring monitoring, acoustic phase tracking technique 78−30138
ocean pollution, industrial waste dispersion meas. technique 78−44884
ocean surface currents charting by aerial tracking of dye emitting radio beacons 79−5675
optical angular tracking, annular apertures 77−83957
optical heterodyne receiver arrays, partial tracking, operating in turbulent atm. 79−41345
optical phase tracking, Fourier series and estimation appl. 78−25812
optical signals using SAW spectrum analyser in photon-counting mode 80−105712
pancreatic cell moving granules anal. by digital moving image processing 79−84063
planetary orbiters, tracking for planets gravit. spectra determ. 80−41744
projectiles, continuous-wave transmitting, passive array 80−94955
real-time moving objects, by optical correlation using liq. cryst. image transducer 79−32035
relativistic Doppler shift in satellite tracking 80−46951
satellite laser tracking data, horizontal refractivity gradient correction 77−91276
satellite photographic tracking, astronomical method *(Chinese)* 80−77254
satellite time transfer technology, review 80−47029
satellite to satellite tracking, appl. to geoid improvement in local areas 79−62423
solar power plant, direct tracking using two-mirror unit with plane and hyperboloidal counter-reflectors 80−91875
spatial pattern recognition by spectral feature classification and coherent optical correlation 80−99644
star tracker, utilising solid state image sensor *(Japanese)* 79−80227
station geocentric coordinate determination, artificial satellites, short arc station coordinate method 77−44902
strain measurement, 298 to 1477K, new optical technique 78−85063
stroke disability assessment by tracking task performance meas. 77−60280
target trajectory detection in multi-target environment, pattern recognition approach 79−26865
TRANSIT satellites' contribution to navigation and geodesy 78−57161
underwater construction teams tracking, appl. of portable acoustic system 79−3874
underwater Doppler tracking using optimization techniques 78−55526
Viking Lander tracking contributions to Mars mapping 80−12702

tracking (insulation) *see surface discharges*

tracking (sonar) *see sonar*

tracking systems
see also ground support systems; radar systems
3 m parabolic dish heliostat system design, fabrication and testing 79−62111
Air Droppable Random Access Measurement System buoy sea ice tracking 77−5363
airborne target tracking filter configurations compared 80−96130
aircraft wake vortices, tracking system based on acoustic refr. scatt. 77−46840
artificial satellite search systems, night sky model 77−73923
astronomical telescope, large azimuthal, search and guide system 78−57446
automatic centring system for bubble chamber film measuring and premeasuring tables 77−83455
automatic threshold following pacemaker concept and application 77−81671
biotelemetry and radiotracking receiver 77−48892
biotelemetry antenna and propagation requirements for appl. for fresh water fish 77−78074
Canadian satellite receiving station, Newfoundland, LANDSAT and weather satellite data monitoring 77−78600
charge injection device as stellar tracking sensor 80−85861
cloud motions, automatic tracking system using weather satellite picture sequences 78−45022
coherent monopulse tracking with 10.6 μm radar 77−88929
concentrator solar cell with tracking control information 79−29470
correlation receiver with feedback for radioastronomical interferometry 78−57445
direction finder with tracking receiver for whistler mode signals, initial results 78−77429
electro-optical detection of artificial satellites 79−62717
eye movement hierarchical control model 77−25429
eye tracking communication system feasibility for nonverbal cerebral palsy children 79−83981
fluidic element nonstationary flow meas. by laser Doppler velocimeter with frequency tracker *(Japanese)* 78−55707
Geos 3 tracking systems, intercomparison 80−4227
geostationary orbit determ., by single-ground-station tracking 80−109329
glint tracking by adaptive optical techniques 77−19458
Gulf Stream kinematics inferred from satellite tracked drifter 77−17246
HEAO-B X-ray telescope orbiting observatory, aspect system providing absolute referencing to celestial sphere 78−40791
hydraulic solar collector tracking device design and evaluation 79−62123
integrated photovoltaic/thermal system with faceted-mirror sunlight concentrator 79−62010
international time synchronisation, precision tracking package TEMPUS, NAVSTAR satellite network appl. 80−22332
Ionosphere sounding satellite, automated system for tracking, telemetering and commanding 77−60572
Ionospheric Sounding Satellite control, tracking system *(Japanese)* 77−78608
Ionospheric Sounding Satellite control centre, automated tracking and data acquisition *(Japanese)* 77−78606
IR imaging and missile-borne tracker optics, selection guidelines 79−23050
IR phase conjugation adaptive array 77−46790
IR scanning by SAW modulation 79−80687
IR tracking receiver with holographic information processing 78−78970
Jupiter probe-to-relay communication MFSK frequency acquisition and tracking 77−64613
laser beam turbulence compensating tracking system, lead angle effects 78−33763
laser designated target, simulation of low-level laser pulses 78−59074
laser pointing and tracking through air-sea interface 77−79776
laser pulse tracking position-sensitive photodetector characteristics 77−18098
laser tracker, target induced pointing noise 78−5519
laser tracking system testing by 1 m unobscured IR collimator 80−78991
LF coherent underwater acoustic transmission range meas. system, portable 77−88976
manual control operator performance, gain and vibration effects interaction 78−44756
Michelson interferometer stability improvement *(Russian)* 78−29149
microscope stage automatic white blood cells tracking appl. 77−78064
mitral valve velocity meas. by digital echocardiographic tracking system 77−21579
multidither coherent optical adaptive techniques 77−46793
near-millimetric wavelength military systems 80−86428
optical, turbulence induced tilt errors with shared and adjacent apertures 77−46792
optical beacon/tracker system simulation, turbulent atmospheric propag. 79−53525
optical tracking system for space laser communication 80−33068
optical tracking system properties and advantages 79−14080
passive tracking acoustic array evaluation, nonlinear filtering lower bound algorithms 80−96088
pendulum controlled solar tracking system and concentrator 79−62122
phase conjugate adaptive optics using perimeter phase meas. 77−46791
phase tracking meteor radar ambiguity elimination algorithm *(Russian)* 77−41311
phase-coherent dual-freq. link for high-precision Doppler tracking between spacecraft 77−60576
pulmonary parameter identification adaptive analogue tracker 77−48911
real-time and frequency-domain processor simulation 79−81643
satellite, low-orbiting, tracking errors estimation 80−36470
satellite to satellite tracking for orbit determination accuracies 79−25451
satellite-to-satellite statistical orbit determ. error analysis 78−65486
satellite-to-satellite tracking, ionospheric range-rate effects 79−58174
SEASAT-A satellite radar altimeter design 77−5415
semiautomatic Sun-tracking system for concentrated solar cells 79−62012
short range precision navigation and tracking system using PLL 78−53742
Shuttle Orbiter re-entry, remote IR imagery and tracking 80−82171
solar energy concentrator, heat transfer performance, parabolic collector 77−88892
solar flat plate collectors, fixed and fully tracking, useful energy gain comparison 79−3794
Solar Maximum Mission GSTDN/TDRSS compatible RF system 78−45198
solar thermal collector, line-focus Fresnel lens and secondary concentrator 79−62112
solar tracking electronic servo 79−57433
star tracker, microprocessor controlled CCD, STELLAR design 78−53792
star tracker error evaluation in optoelectronic direction finders 79−75075
step-stare spaceborne optical system smear compensation by focal plane manipulation 80−82172
Sun tracker, electronic, for clear or cloudy weather 80−76644
Sun-tracking concentrator for solar cells, solar eyeball for photovoltaic generators 78−66881
tracking by microprocessor-based coordinate calc. *(Spanish)* 80−89623
turbulence-induced wavefront tilt error tracking with shared apertures 77−19459
underwater acoustic tracking system for divers, PATS 80−91949

tracking systems continued
wideband optical disc data recorder systems 80−102751
wind profile determ. X-band solid-state radar system 78−12028
Woodhead seabed drifters, acoustic tracking 77−5366

tracks, particle *see particle tracks*

traction
electric traction units, driving axle oscillations damping using seismic dampers *(German)* 80−62458
motor, circuit fault detection by NDT method 79−39097
rail, Na/S cells appl., dimensions optimisation 79−48112
Saint-Venant's principle, elastic cylinder energy decay 79−14270
stress anal. in body under variable traction 80−8792
Na/S batteries, load levelling and traction 80−21391
Na/S traction batteries, development progress and problems, review 80−61326

traction current collection
high speed ground transportation vehicles gas-flow-controlled arcs for power collection 80−70054

tractive effort *see traction*

trade *see commerce*

trade fairs *see exhibitions*

trade shows *see exhibitions*

traffic
see also rail traffic; road traffic
1/f fluctuations *(Japanese)* 78−43448
noise measurement method and results *(Spanish)* 78−59219
nonlinear initial-value problem arising from kinetic theory of vehicular traffic 79−163

traffic computer control
surveillance system for anti-pollution programme *(Japanese)* 77−56726

traffic control
see also air traffic control; traffic computer control
energy and air pollution consequences of traffic systems management 79−52990
noise, traffic control effect on evaluation index 80−51024

traffic control systems
road, surveillance system for anti-pollution programme *(Japanese)* 77−56726

traffic restrictions *see traffic control*

training
see also education; teaching
accident investigation, advance prep. 78−57083
Ann Arbor school of astronomers, foundation, 1852-63 80−86062
behavioural objectives, classes of statements 79−92908
biofeedback therapy technique and application *(German)* 79−16341
biomedical engineering, hospital based, health care role fostering 77−41433
biomedical engineering, training experience at Ecole National Superieure des Telecommunications *(French)* 77−40817
biomedical engineers, W.Germany 78−41106
biomedical engineers and technicians in developing countries 80−62408
cooperative education programs in Omaha Public Power District 78−4429
deaf children training to comprehend passive voice 80−33372
deaf patients, tracking procedure for training and evaluating speech recognition 78−61204
dynamic electric and magnetic field evolutions, visualisation using computer graphics display 80−46776
electrical and electronic engineering design education and training conference, London, England 80−67971
electron microscopy, autotutorial methods utilizing sound-on-slide presentations 80−73534
energy option for undergraduates 80−31447
engineering education, importance of research and design for satisfying industrial needs 80−67974
engineering education, modern methods and instructional media roles 80−27064
fast breeder test reactor operator training simulator model development 80−91219
fibre optical communications, course status and effectiveness 80−62413
graduate laboratory teaching assistant course 78−41105
health physics technicians, uniform approach for on-site training and qualification 77−64900
heart model time-position mode scanning in obstetrics, heart model practice aid 78−24111
hybrid optical-digital radiography system for lung disease detection 78−11753
industrial internship programme in nuclear engineering education 78−4432
industrial radiography radiation exposures, causes, safety training program 80−17141
Jamaican solar energy training seminar programme 79−57395
maintenance of biomedical electronic equipment 79−96681
marksmanship training, moving target screen system with laser beam firing 78−54488
mathematical education development, M.Sc. course, for teachers 79−80384
medical electronics engineering, training in India 79−80390
medical physicists, training, survey of program directors 79−17159
NDT, use of US wave visualisation as teaching aid 77−57136
noise abatement, courses for non-specialists 79−23140
nuclear engineering, cooperative utility programs at North Carolina State University 78−4430
nuclear engineering, graduate cooperative program with industry, experience over 3 years 78−4434
nuclear engineering, process instrumentation meas. 78−17447
nuclear engineering, teaching project management as part of international technology transfer 78−4428
nuclear engineering, training of existing staff for new nuclear units at university 78−4431
nuclear engineering, undergraduate cooperative industrial program at Cincinnati University 78−4433
nuclear engineering education and training with JASON low power reactor 77−41431
nuclear fuel reprocessing, analytical procedure and training material development at ICPP 80−37569
nuclear material and facilities, physical protection at plant, IAEA first training course, report 79−76077

training continued
nuclear plants in developing country, development of local engineering capability 77−65350
nuclear power plant operator training, simulator 77−367
nuclear power station Czechoslovak Research Institute activities personnel *(Slovak)* 80−83188
nuclear reactors personnel, research reactors features and commercial types *(Czech)* 78−21745
objectives selection, four-step process 79−92909
ophthalmological instruments and eye models in teaching, training and education 80−51993
ophthalmology, research and training, TV appl. *(German)* 78−24157
optics, faculty of Inst. of Optics, profile 80−62422
optics, graduate education at Optical Sciences Centre, programmes 80−62418
physics and education, honours course at Loughborough University of Technology 79−35455
physics teachers, at Bremen University *(German)* 77−22349
physics teachers, German Phys. Society report *(German)* 78−24593
prosthetic equipment and functional training *(Japanese)* 78−44701
prosthetic/orthotic EMG control enhancement using predictor feedback technology 77−48952
pulmonary function testing, training course features 78−24169
pulmonary testing equipment, training and application techniques 78−24170
PWR, Spanish nuclear power program, technology transfer 77−65353
quality controllers in FDR, new regulations *(German)* 79−80391
quantum chemistry, analogue computer appls. *(German)* 78−28903
radiation therapy technology manpower needs, problems and potential in United States 77−86701
Radiological Emergency Response Planning and Preparedness Training Programmes, USA 78−57079
radiological emergency response training programme 78−57080
safety, hospital laboratories, general aspects 80−95089
scientists, role in modern society 79−80392
SEM, teaching methods for short courses 80−73533
Skylab simulator visual displays and training for joint obs. programmes 77−60566
slide preparation techniques for audio visual aids 78−54139
speech, intonation correction for hard of hearing children, trainer *(Japanese)* 77−25472
speech training system for deaf children *(Japanese)* 77−86515
storm spotting, National Weather Service's training programme 80−8382
suggestopaedia, training technique 79−17153
Swedish State Power Board nuclear power stations, training of emergency organisation 78−50412
Swiss Federal Institute for Reactor Research emergency organisation 78−55047
teacher, using closed circuit television 79−80388
teacher training with computers 77−33734
therapeutic radiologists, training in USA, 1978 survey 79−84878
University of London Institute of Education, Science Department, teacher training, curriculum devel. 80−27061
virtual image display using Fresnel lenses 80−1295
vowel articulation correction using trainer *(Japanese)* 77−25473
Yugoslav university training of biomedical engineers 79−35442
Zimdex audio indexing system, efficiency 79−92915
Pu-containing reactor fuel, safety training program 79−18053

tramcars *see road vehicles*

transceivers
CETI from Earth satellite orbit 78−61758
fibre optic link, LED as semicond. junction transceiver 78−42410
logic signal transmission system for spaced cosmic ray detectors 80−52837
optical, CO_2 waveguide laser development for space link transceiver 77−19322
US inspection unit receiver-transmitter 80−89458
US medical transceivers, gain transfer charact. 80−30814
VHF, portable, biological tissue heating by induction field, expt. using phantoms 78−57039

transducers
see also accelerometers; acoustic transducers; actuators; extensometers; Hall effect transducers; piezoelectric transducers; pressure transducers; strain gauges
1 MN combination load/bending moment transducer *(German)* 77−79080
AC voltage meas., analogue, checking and calibration methods in USSR 80−98872
AC voltage meas. transducer 78−74028
acceleration, design and characteristics *(Hungarian)* 78−29097
acoustic emission measurement transducers, comparison of piezoelec. and optical sensors 79−14192
acoustic emission transients meas. using capacitance transducer, crack propag. 79−8407
amplifier interconnection, analog signal processing, book 80−86047
amplitude phase methods of testing, design relationship for eddy current transducers 78−53152
analogue multilink linear-log. freq./current transducers, dynamic range and transduction error 79−40548
angle, gyroscope, for absolute angular velocity meas., precision increase, using structural redundancy *(Russian)* 78−49804
angle, vernier resolvers *(French)* 80−37022
angle-digital quantities, conversion error evaluation, using probability precision model 77−82498
angular and longitudinal displacement meas., magnetic scale recording system 77−2635
automated multichannel data and meas. system type MIIS-1, for transducer data 79−2754
automatic digital circuit for selecting information bearing components of output voltage of electromagnetic transducer 79−2760
automation in sugar industry, measuring transducers *(Polish)* 80−42212
biaxial laser-based displacement transducer 78−73967
biaxial strain transducer for appl. up to 1033K 79−80600
biological sensors of Medicor Works 79−100769
biomedical measurements and transducers, review *(Japanese)* 80−94393
bipolar IC temperature transducer, intrinsic bandgap voltage as reference, Fahrenheit, Celsius or arbitrary scale operation 80−82761
blood pressure measurement, noninvasive techniques 80−41298

transducers continued
blood temperature monitoring during extracorporeal circulation, noncontact transducer 80−85513
calibration, appl. of radiation coupling of disc to plane and back or to disc 77−46828
capacitance, effect of manufacturing errors on accuracy 78−89467
capacitance displacement transducers, effect of tilt and surface damage 78−54356
capacitive, for bulk material rigidity determ. 78−19977
capacitive, mechanical quantities meas. appl., based on frequency superposition principle *(German)* 77−53955
capacitive, of torsional oscills., for oscill. type viscometer 80−64656
capacitive, three-electrode, for permittivity of sheet materials meas. *(Russian)* 77−10047
capacitive contactless meas. transducer for impulsive displacement 79−6111
capacitive dispersion field transducers for granular material exam. 78−85078
capacitive displacement system for UHV operation 80−31737
capacitive displacement transducer, automatic calibration *(Russian)* 80−36981
capacitive hygrometers, HF, extension of range of applicability 79−75537
capacitive parametric, for displacements under dynamic damping 80−105626
capacitive transducer with superconducting resonator for mechanical vibration meas. 78−21127
capacitor type, capacitance meas. using noise-stable meas. cct. *(Russian)* 78−89493
carrying capacity safety factor, metrological characts., selection *(Russian)* 78−188
cavity transducer for subatomic mech. vibr. 77−82436
cellular elastomer selection for use in biomechanical capacitive force transducers, measuring device *(German)* 80−85545
chemotronic, liquid flow rate meas. appl., features 78−9739
circular plate, elastic moduli meas., appl. of contactless vibr. excitation and detection method *(Polish)* 79−94571
coercivity meter with portable display system 78−53135
complex dynamic Young's modulus measurement equipment for polymers 78−1615
complex shape product inspection, local eddy current transducer 80−108671
conductive paper transducer output signal fluidity reduction 77−57318
conductivity sensitive liquid level transducer for PWR coolant two-phase flow meas. 80−37550
contact-resistance transducers using electrically conductive paper 77−13747
contactless displacement/vibration meas. by fibre-optic and capacitive transducers 78−8400
contactless electropneumatic transducer parameter determ. *(Bulgarian)* 80−47045
contactless photoelectric fibre-optic vibration transducers 77−57319
corrosive liquid flowmeter with UHF heater *(Russian)* 78−59523
cryogenics, linear variable differential transformer displacement transducer optimisation 80−86323
current, for neutron flux density meas., use of self-powered detector *(Czech)* 77−50328
current transducer, electron beam ring type, appl. to current meas. by contactless method 77−26334
current-to-frequency transducer systematic error and sensitivity threshold 77−79117
DC voltage meas., HV, using solid-state sensors 79−44916
development trends, computers, control and industrial electronics appl. 77−10002
differential thermocouple transducer for electrically insulating liquid level 77−17969
differential-capacity transducers, improving metrological characts. for displacement measurements 79−75493
digital dynamometers, using period transducers, noise action *(Russian)* 79−88944
digital force transducer, design, features 78−21116
digital lineariser for nonlinear transducers 78−57931
displacement, diffraction grating imaging anal. 79−86258
displacement, for use below 50 mm, review 79−63200
displacement measurement, using linear variable differential transformer method 78−73978
displacement measuring fast precision capacitance transducer, design procedure *(Russian)* 80−98884
displacement transducer using second harmonic type magnetic modulator 78−21115
displacements below 50 mm meas., types available commercially, comparative survey 80−42214
double-ended eddy current transducers, signal calc. for nonferromag. cylindrical products 80−89443
drag disc turbine transducer calibration for mass flow rate meas. in PWR coolant two-phase flow 80−37552
drag disc turbine transducer for PWR coolant two-phase flow meas. 80−37550
driven-sweep generator scan velocity transducer 78−57925
dynamic damping effect in small force measurement *(Russian)* 78−12687
dynamic drag and lift co-eff. determ. in wind tunnel 79−40558
eddy current, calc. of EM field when inspecting conducting bodies of complex shape 78−72964
eddy current, higher harmonic signal analysis for nondestructive testing 78−70109
eddy current, impedance introduced by nonmagnetic plate 78−60939
eddy current through type transducer, operating condition simulation when inspecting ferromagnetic rods 78−53077
eddy current transducer, electrical conductivity meas. of coatings, tuning out of gap instability 78−36994
eddy current transducer of arbitrary form located parallel to multilayer medium, EMF 79−2762
eddy current transducer of complex geometry, calculating added resistance 79−97375
eddy current transducer part geometry effect on inspection 78−53078
eddy current transducer with electrical commutation of excitation field, NDT 80−105633
eddy current transducers, for meas. thickness of lacquer coloured coating on mag. base 78−85101
transducers continued
eddy current type, calc. of response, comparison with computer results 78−36995
eddy-current, mounted, correct. of errors in coating thickness inspection 80−77775
eddy-current, moving inspected plate, effect on transducer parameters 78−60938
eddy-current angle displacement type, in 213-473K temp. range, types *(Russian)* 77−33974
eddy-current feed-through transducer, approx. calc. of mag. field, nonferromag. media 80−78746
eddy-current flaw detect., suppression of interf. parameters 80−89442
eddy-current phase thickness gauge, for complex form inspection automatic error corrections 79−9204
EHD transducer, transient characts. anal. *(Russian)* 77−24031
EL2 electret telephone transmitter, technology development 80−83723
electric variables meas., third-generation, Czechoslovak (Metra Blansko) range *(Czech)* 80−73340
electrical, perfectly compensated, construction capabilities anal. *(Russian)* 78−89469
electrical conductivity, threshold sensitivity meas. 80−62688
electrical quantities meas. by analogue conversion, synthesis *(Polish)* 77−53882
electro-optical transceivers, optical analogue communication systems *(German)* 78−1333
electrocapillary acceleration meters, electrolyte composition selection 80−73331
electrocapillary acceleration meters with electrolyte in gel form 80−73330
electrochemical convertors, conc. type, for elec. signals, diffusion theory of conc. networks 78−61026
electrochemical convertors of mech. quantities, data readout 77−2287
electrochemical measurement transducers, actual distribution of errors 80−45605
electrodeless measurement of resist. and spherical curvature of semicond. struct. 79−49252
electrodiffusive flow and shear transducer electrical anal. 80−48824
electrodynamic convertor, ring-shaped, operation and appls. *(Polish)* 78−12685
electromagnetic, for nondestructive inspection of ferromag. materials 79−87771
electromagnetic, temp. error decrease 79−35710
electromagnetic flaw detector, differential eddy current transducer asymmetry effect on sensitivity 79−39092
electromagnetic flowmeters, effect of electrode processes on transmission coeff. 79−7426
electromagnetic inspection of electric and magnetic props. change with depth 79−52603
electromagnetic transducer for crack exam. 78−76816
electromagnetic with quartz resonator 79−2761
electromechanical, appl. to exposure control in pocket camera *(German)* 79−80708
electromechanical actuator, vibr. linearisation of mag. hysteresis charact. *(Russian)* 79−12789
electromechanical transducers in hostile environments, review 80−37019
electronic-micromechanical interactions, conference, Lausanne (1976) 77−30140
electronics-aided meas. transducers *(Dutch)* 80−105634
electrostatic field parameter measuring instruments, calibration of transducers 79−75551
electrostatic transducer, for Rayleigh waves detect. 77−19498
electrostrictive magnetic-field transducer design 77−57371
EM, for conducting liquid flow meas., testing 78−1768
EM, with periodic permanent magnets, horizontally polarised shear elastic wave excitation 79−76932
EM micrometers, dynamic characs., contactless displacement meas. appl. 78−41277
EM transducer for laser fine-tuning 77−79862
EM transducer with freq. output signal for ferromagnetic material inspection 78−53131
EM transducers for recording translations and vibrs. 77−67421
error analysis, dynamic, using conversion factor 80−77770
error-signal transducer, for precision ang. displacement control 78−186
feed through eddy current transducer, numerical anal. or operating mode during ferromagnetic rod inspection 80−108670
feeler probes for surface roughness meas., error source 78−169
ferrite magnetoelastic transducer, with increased mechanical strength *(Polish)* 79−40549
ferromagnetic contact ring for two-dimensional eye movement meas. 79−5387
ferromagnetic object inspection, method of higher harmonics, difference schemes 80−89444
ferromodulated, for magnetic field meas., local excitation *(Russian)* 78−86306
ferromodulation meas., with increased temp. stability 80−52281
FET, H^+, Ca^{++} and K^+-sensitive, biomedical appls. 78−28117
fibre optic lever displacement transducer 80−5816
fibre optic proximity transducer evaluation for surface texture meas. 80−36985
fibre optics sensors for measurement and control appls. 80−58780
fibre-optic force transducer for isometric muscle contraction meas. 79−79715
finger-tip transducer for meas. digital vol. pulse, skin-resist. response and ECG 77−86729
flaw detection systems based on semicond. detectors and scintillation crysts. for hard bremsstrahlung 79−11748
flow, with steady and pulsating flows, computerised flowmeter system 80−79416
flow measurement, electrolyte soln., transducer-electrode freq.-ampl. characts. 77−76001
flow rate transducer dynamic error determ. 77−72386
flow transducer test equipment 78−18363
footfall pattern transduction by foot or shoe cover 79−57799
force, acceleration compensation *(German)* 79−35733
force, calibration using theoretical calcs. 79−35719
force, designs and appls. 79−35720
force, digital, using multi-aperture ferrite core *(Japanese)* 79−93133
force, magnetically anisotropic, optimisation of mechanical and electric operating conditions 79−17412
force, using differential transformer, electric circuit analysis *(Russian)* 78−49824

transducers continued
force and meas. measurement, conf., Braunschweig, W.Germany (Sept. 1978) 79−35725
force transducer using amorphous ribbon core 78−93669
force/tension transducer for small muscle meas. 80−41281
frequency response measurement technique for press., vol. and flow transducers 80−41344
fuel elements, quality inspection by eddy currents, unit 79−100315
functional transducer, in microphotometer for intensity registration of spectra *(Russian)* 77−13244
galvanomagnetic semiconductor voltage and current transducers, Gauss effect compensation 78−77892
galvanomagnetic transducers, steady pressure effects 77−79129
gap transducer for contactless meas. of components of complex shape 78−93648
gas-gun projectile vel. meas., magnetoflyer method 78−49805
gel electrocapillary type for vibration meas. *(Polish)* 78−26094
general electromechanical reciprocity relations applied to the calculation of elastic wave scattering coefficients 79−56729
gravitational wave detector, resonant transducer matching between cryogenic antenna and low-noise amplifier 80−46949
haemocoagulometer 79−39541
heat and thermal diffusivity of liquid and free-flowing materials meas. 77−87765
heat flow transducers, in convective heat loss assessment from humans in cold water 78−81093
heat flux transducers for local heat exchange meas. of air flow in tube *(Russian)* 78−83509
heat-flux transducer, using artificially anisotropic thermoelec. materials 79−93136
high-temperature displacement meas. using capacitive transducers 78−172
humidity-sensing capacitance transducer, construction and charact. 80−4729
hyperbolic, for measuring systems, with piecewise-linear-approx. and memory capacity 79−6110
hysteresis-free magnetic transducer, features *(Russian)* 78−86305
incremental, for position measurement, analogue interpolation system *(German)* 80−17929
induction moving coil null offset compensation method *(Polish)* 77−49718
induction transducer displacement/voltage proportionality improvement *(Bulgarian)* 80−52183
inductive, for plasma jet reaction meters 77−11399
inductive, instrum. for meas. tension of threads 79−17414
inductive, selection, applications and technical specifications, output signals 80−101790
inductive, technique for computing basic charact. 80−4696
inductive bridge type, parameter anal., appl. 78−45608
inductive displacement-measuring system synthesis using CAD 78−73982
inductive force measuring transducer calibration charact., calc. and expt. *(Russian)* 77−10005
inductive magnetic transducer for ferromag./nonferromag. object displacement meas. 79−6154
inductive motion transducers, design for information measurement systems 79−67284
inductive rod gauge for measuring long hole diameter *(Polish)* 78−29086
inductive transducer summing circuit errors 77−18046
inductive using nonlinear bridge circuits, operation *(German)* 77−10007
inductive-capacitive, sensitivity of information conversion 79−6113
inline torque meas., rotating transducer appl. 78−190
integrated direction sensitive flowmeter 77−7484
integrated semicond. transducer suitable for colour distinction 77−10086
interfacing and analogue signal conditioning, book 80−86048
isotonic capacitive transducer for animal experiments 79−66585
length meas., capacitive transducer method, precision, procedure and instruments *(German)* 79−26024
line sensor used to monitor a distant transducer 79−6145
linear displacement transducer using vibrating string, pressure meas. appl. *(German)* 79−71441
linear meas. extension-nozzle ejector-transducer design 77−57313
linear movement transducers, magnetic amplifier principles 80−22341
linearisation, row switching and feedback methods, semiconductor strain gauge appl. *(German)* 77−37942
liquid level measurement 80−31709
liquid-crystal image transducer, normal incidence, on-state optical performance 80−99852
load cell transducers, shear force, mathematical modelling and design 79−35722
load cells, automatically controlled, method for digitizing measured values *(German)* 79−35721
load transducer parallel operation tests *(German)* 77−79079
logarithmic voltage transducers, optimisation of functional charact. *(Russian)* 79−75512
loudspeaker units, behaviour of damping materials *(Spanish)* 79−46146
low-reactive meas. of motion, trnasducer effects on body under investigation *(German)* 80−105621
magnetic amplifier linear movement transducer manufacture and static functioning 79−67279
magnetic core multivibrator, tensile stress measurement appl. 78−9615
magnetic field bipolar sensor using carrier domain rotation, proposed device design 77−2670
magnetic field bipolar sensor using carrier domain rotation, operation and performance 77−2671
magnetic search coil eye movement monitor, signal detection via phase-locked sampling 79−25124
magnetic sensors for dynamic quantities *(Japanese)* 79−12776
magneto-anisotropic type for force meas. *(Russian)* 77−65021
magnetoacoustic rod position monitoring transducer system for nuclear power plant 78−33262
magnetoelastic force convertor operation anal. using EM field theory in anisotropic medium *(Russian)* 78−70166
magnetoresistance, using InSb 79−67287
magnetoresistive, for strong mag. field meas. at 4.2-300K temp. range 78−45660
magnetostatic wave-current interaction, characterisation by coupling constant 78−84403
magnetostriction force transducer 79−2757
magnetostrictive, transducer in presence of eddy currents, mobility analogy equivalent cct. 80−48540
transducers continued
magnetostrictive transducer, electrical matching technique 77−35008
magnetostrictive transducer, wideband electrical matching 78−5626
magnetostrictive transducer at air-water surface, effect of spherical scatterer on radiation reactance 80−48531
magnetostrictive transducer terminated in arbitrary elec. impedance, elec. cct. anal. 78−5627
magnetostrictive type, accuracy study *(Bulgarian)* 77−53878
magnetotransistor, lateral with two meas. collectors, charact. 79−7887
maintenance-free water test stations, features and developments *(German)* 78−65403
matrix eddy-current, with magnetic circuit, design and construction 80−68228
measuring transducer testing, heat and pressure chamber design 77−53881
mechanical quantities meas., by electrical methods, using strain gauges or inductive transducers 77−33981
mechanical vibrators miniaturisation 78−18229
medical appl., design aspects *(Hungarian)* 79−92408
membrane pressure gauge with displacement sensor *(Hungarian)* 80−31733
membranes appl., silicone rubber, physical props. *(Slovak)* 80−61141
metal object in media, depth measurement instrument, eddy current transducer 79−39091
metallic cylinder in electromagnetic field of noncoaxial coil, AC current, field calc. 78−53153
metallic foil contact resistance, thermochemical method of oxide film formation 78−89466
metallic objects with complex shape, eddy-current inspection 80−89446
metals, NDT of hardness using applied EM transducer 77−56178
microcapacitive transducer for geophysical appls. *(Rumanian)* 79−58121
microdeformation transducer calibration for geodesy and instrumental geophysics *(French)* 78−12004
microinterferometer transducer, air-bearing, for use with universal inspection machines 78−57899
microtransducer using fibre optics for temperature and power density meas. *(French)* 77−61084
modular, third-generation, individual and group arrangements, NC series *(Czech)* 80−62645
moist porous materials, water content determ., rapid thermal method 77−86258
moisture measurement in porous ceramic components, equipment *(German)* 78−54378
monolithic timers form capacitive transducer-to-recorder interfaces 77−87781
monolithic two-terminal UC tranducers for temp. meas., operation and charact. 77−10021
motion transducer for use in intact in vitro human lumbar spine 78−57155
moving magnet transducer, dynamic props. 80−57276
multi-point meas. system average meas. time reduction anal. *(Russian)* 78−159
multilayer product, theory of laid-on shielded transducers for inspection 78−88610
multistage logarithmic freq.-current transducers, optimisation of time-constants *(Russian)* 79−75511
n-type InSb based low-temperature UHF detector, with low noise preamplifier 80−68230
nematic liquid crystal transducers, exam. of light absorption behaviour 79−40560
nematic liquid crystals, dynamic scatt., pre-excitation 80−88021
noise level calc. when registering hard γ-radiation 79−75517
noise suppression technique *(Polish)* 77−54837
noncontact optoelectronic position transducers 79−50406
nonelectric variables meas., current transformer error level calc. 77−13743
nonlinearity error minimisation method *(Polish)* 78−41298
nonmagnetic electrically conducting rod, section shape effect on eddy current transducer parameters with uniform field 78−53132
ohmic resistance, appl. in internal friction test device for thin-walled tubular specimens 80−71836
online sensor cleaning 78−77883
optic fibre light transmission, fibre production methods, transmission line structures details *(French)* 79−89998
optical, for use with windvane 79−39889
optical displacement type 78−24783
optical fibres as microphonic instrumentation transducers 77−17970
optical noncontacting transducer, for machined surface profile meas. 79−58765
optical path meas. using fibre optics, theoretical investigations of path transducers *(German)* 80−106608
optical profile transducer, for machined surfaces testing 79−85124
optical-fibre flowmeter using transducer 79−98830
optoelectronic vibration transducer based on coordinate photodetector 79−75495
optotransducers, electronic compensation for dirty lenses 80−68189
orientation system in screen methods of NDT 80−66745
oxide thickness in shutdown fission reactor meas., abrading system appl. 79−63720
parallel-connected transducer systems, integral parameters determ. 77−17939
passive optical rotation sensors using guided waves, developments 80−58781
passive value parameter transducer error correction method *(Russian)* 78−49819
perfusion blood temp. monitoring, zero-heat-flow transducer 80−8201
Permalloy proximity transducer 78−57929
phasemeter test measuring transducers 78−77894
photoelectric angular-displacement, accuracy 80−8977
photoelectric transducer for linear displacement meas. 79−50404
photometric, for relaxation props. determ. of polymers 80−3268
photoplethysmographic vaginal transdcuer, blood vol. change monitoring 78−92733
phototransducers in tide-recording equipment, emission source light output ratio stabilisation *(Russian)* 78−88949
physical to electrical value transformation devices *(French)* 77−30141
piezoelectric positioner three-axis coordinate convertor for optical scanners 79−63199
pneumatic force transducer, features 78−45611

transducers continued
pneumatic micrometer with positive feedback system *(Japanese)* 79−93101
point recording device realisable operations *(Polish)* 78−29099
polymer films, ultrathin, photochemical props., transducer appl. 80−37020
potentiometric displacement transducers, standards for specification and tests, book 79−2763
pressure transducer in silt-salinity-depth profiling instrument 79−88493
pressure-to-pulse frequency signal type, features and performance 78−16785
primary, relatively low accuracy, simultaneous use in automatic measurement, angular, linear displacements 79−6084
primary meas. transducer error twin-circuit correction *(Russian)* 79−71404
pulse generator, HF oscillator with single coil transducer, for NMR spectrometer 79−2802
pulsed frequency, continuous random signals errors evaluation, by means of computer simulation 77−74386
pylon transducer signal variability anal., below-knee amputees 79−74715
radioisotope meas. instruments, output transducer as intensimeter, sensitivity and scale parameters calc. 79−11747
reluctance, of small displacements, 'Polfer' ferrite cores appl. *(Polish)* 78−29100
remote transducer optimal signal correction with internal fluctuating white noise *(Russian)* 79−6107
resistance due to cracks, eddy current calc. and hodograph 78−53095
resistive, force and mass measuring, normalisation *(Rumanian)* 80−4699
resistive and potentiometric transducer connection line checking *(Bulgarian)* 79−93120
resistive thermometric, temp. meas. appl. *(Russian)* 77−33987
resistive transducers, percentage resist-duration meas. via wide-range ohmmeter 78−239
resonant EM transducer, two-circuit system for elec. cond. meas. *(Russian)* 79−213
respirometer, noncommercial respiratory transducer for EEG laboratory 78−65138
response linearisation using programmable multifunction module 78−45604
RF, linear, for joint angle of two dimensional limb movement meas. 77−90938
ring core flux-gate thickness transducer with permanent magnet 79−67280
rotating-object surface temp., test installation 78−4612
round specimen, tensile testing, at const. true strain rate simple beam diameter transducer 78−7162
selsyn rotor angle-to-digital code convertor, design *(Russian)* 78−65915
semiconducting, temp. meas. up to 1000°C *(Croatian)* 79−40569
semiconductor force transducer suitable for use with small muscles 80−72395
semiconductor thermal transducer for elec. AC quantities meas. 77−45865
servo force-balance instrum. for wall shear stress meas. 79−1273
sheet material, Lamb wave inspection, pulsed and impact excitation of transducer 79−34244
signal transmission, optical slip-ring 78−13814
single-channel optoelectronic raster-type displacement transducer 77−74384
skin recoil characteristics, human, in vivo meas. apparatus 79−57698
solid propellant stress transducer evaluation 80−81245
spring leaf mechanical type, dynamic anal. *(Polish)* 78−41297
steel, 45, case hardening quality control by ferromagnetic coercive force transducer probes 78−53151
steel, tube, mech. prop. testing by harmonic method using instrument type KAP with feedthrough transducer 78−53154
straight-through screened circular primary, between multilayer cylinder and tube, EM field 80−71856
strain gauge transducer compensation linearisation by shunt resistors 78−12688
string linear displacement transducer design *(German)* 77−79085
stroboscopic, dynamic characteristics determining, correlation method 77−5824
superconducting strain transducer 77−37877
surface mounting, reliability test system for accelerated tests 78−49820
surface roughness meas. *(French)* 79−170
surgical wound preoperative force meas. 78−36041
surround coil transducers, optimisation for eddy current testing 80−31728
telemetric system for extraluminal meas. of gastrointestinal motility 77−13043
telemetric temperature measurement, using an RF transmitter 78−205
temp. meas. of rotating object, non-contact method with thermistor and pyrometric voltmeter 79−35742
temperature, digital, solid-state, using automatically balanced Wheatstone bridge *(Rumanian)* 80−57287
temperature, monolithic transducer, LX 5700 A, for −100 to +150 degree C temps., operation *(French)* 77−67431
temperature, p-n junction diode as linear temp. transducer 80−57293
temperature gradient meter for gas flow study 79−86539
temperature sensing, cct. and characts. *(Polish)* 78−29103
temperature sensor with temp. sink chip on flexible dielectric cable 78−86264
temperature with thermal feedback, operational principles *(Russian)* 80−86299
temperature-time period, consists of astable multivibrator with thermistor and feedback loop *(German)* 79−40561
tensoresistive low meas. transducer for gas with low spontaneous comb. temp. *(Russian)* 77−11286
testing, using test installation with interferometer and photorecorder 78−12683
thermal, contact, dynamic characteristics normalisation *(Russian)* 77−13748
thermoresistive, compensating for thermal inertia in meas. nonelectric quantities *(Russian)* 77−53885
thickness meas., destructive and nondestructive methods compared *(French)* 78−15611
thin film eddy current transducer, for temp. meas. *(Russian)* 77−26294
thin film magnetic elements used in measurement transducers *(Polish)* 80−4700
three-needle magnetic induction convertor, practical problems *(Russian)* 78−70165
three-phase frequency meas. transducers with saturating transformers 78−77893
time-interval indicator *(Russian)* 80−105619
tissue parametric stimulation by inductive transducer and US phased array 79−92320
tolerated errors in determining transfer-function parameters of temperature transducers 78−73959
torque measuring contactless coupling, construction and testing *(German)* 77−13744
torsional vibration meas. appl. 78−57937
transformer-type for low rotational spaced meas. *(Polish)* 79−2752
transistor temperature transducers, Motorola MTS IC series, appls. *(French)* 80−73357
transition metal complexes, dimethylglyoxymate films, as temp. transducers 79−90923
uncalibrated, with nonlinear characts., physical quantity meas. appl. 78−73979
velocity meter for cond. flow, characts., freq. depend. calibration *(Russian)* 77−65819
velocity transducer for Mossbauer spectroms. 77−38544
vibrating capacitor displacement transducer, eqn. of state 80−57281
vibration, meas. errors due to surface compliance of vibrating body *(Japanese)* 80−79046
vibrational meas., dynamics *(Russian)* 80−105638
viscoelastic, in-situ, Duomorph, appl. to molymeric materials 79−30463
viscosity measurement using phase vibrations method 77−72375
visual prosthesis, processing and tactile stimulation of images *(French)* 79−100788
water content meas. capacitance transducer systematic error reduction 77−79082
weighing system, electronic, digital transducer instruments 80−95076
CdTe detectors, small, props. uses in biotelemetry 77−44747
Ge microconductor mag. field transducer, cast, galvanomag. recomb. effect 79−19609
HaO samples, meas. of small difference of density by elastic vibrator method *(Japanese)* 80−27272
$MgCr_2O_4$-TiO_2 porous ceramic humidity sensors 80−86325
Se photocell optical vibration transducer 80−77768
VO_2 film, negative resist. region, applic. as oscillator element and transducer *(Russian)* 77−85359
ZnO transducers for magnetoelastic Rayleigh waves, convolution on bulk YIG 79−64404

transductors *see saturable core reactors*

transfer functions
see also optical transfer function
12 m discus and NOMAD buoy hull transfer function computations 80−46303
AC voltmeter, transfer function, magnitude rel. to equivalent noise bandwidth approximation 78−4662
acoustic characteristics of flow through duct systems 79−18650
acoustic insulating material complex elastic modulus meas. and transfer function theory *(Hungarian)* 80−106765
acoustic motional source transfer function characts., ocean profile anal. appl. 78−66982
acoustic radiation coupling of disc to plane and back or to disc, exact soln. 77−46828
anemometer characts., hot-wire linearised type for turbulence research 77−55118
aorta, dog, simulation via adaptive model 79−11964
arbitrarily electroded piezoelec. plate acoustic spatial response determ. 80−99910
arterial haemodynamic transfer function calc. from Doppler US flowmeter waveforms 78−61235
artificial sensory feedback system, stimulation freq. discriminability 78−44714
band-pass filter synthesis, acoustic surface waves, transfer characts. *(Russian)* 77−58510
biomedical ultrasound system performance 79−25055
buoy wave data analyses noise correction functions and error sources 80−46302
circular waveguide, mm-wave, time-domain techniques for meas. and equalisation 77−18020
compensating circuit, system function of an acoustic transmission system *(Japanese)* 80−53566
cylindrical mirror analyser viewed in energy-angle space, transmission function 78−15745
ear, transform characts. of external human ear up to 15 kHz 77−86508
Earth EM induction, source field effects on transfer functions at midlatits. 79−74831
electron microscope, wave aberration, sign conventions 77−589
electron microscope transfer functions 77−87883
electron microscope transfer functions in closed form with tilted illumination 80−52368
eye, high-order aberrations, subjective meas. 77−1994
finite element-transfer matrix methods, appl. to structural anal. 77−62201
flaws, 2D, irregularly shaped, fracture mechanics transfer function 80−99970
flowmeters, determination using hydropulsator 80−103083
frequency-effect transform function for Earth induced polarisation soundings, definition and appl. 80−56624
gas analysis, by mass spectrometer, dynamic error determ. by transfer functions 80−61194
geomagnetic short-period variations, transfer function changes before 1972 Sitka, Alaska, earthquake 80−76923
geomagnetic variations empirical transfer functions for tectonomagnetic event detect. 79−16374
heart rate control in man, system anal. 77−25478
high-quality voltage follower input impedance and transfer factor meas. 77−13772
human motion bioelectric control 78−27926
human speech generating system, transmission behaviour in vowel articulation 78−15849
hydrophysical apparatus, channels with automatic transfer function correction *(Russian)* 78−16193
image tube lens, MTF 78−9428
in-duct acoustic props. meas., transfer function method, expt. 80−106688

transfer functions continued
in-duct acoustic props. meas., transfer function method, theory 80−106644
industrial chromatograph dynamic error estimation 77−77853
interdigital transducer design and component specification tradeoffs 77−27455
interdigital transducer design with spectral weighting frequency response 77−27454
ionospheric lossy channel, band limited impulse response 79−84569
liquid Na, thermocouple transfer function and flow velocity meas. by temp. noise 79−13394
lithosphere, isostasy in Australia and evolution of compensation mechanism 78−65252
lossless layered media state space models 77−91065
mechanical impulse testing techniques, computer evaluation, high-speed film recording 78−44343
middle ear systems simulation from physiological data 78−44514
model of with several inputs, math. methods of investigation identification 80−62451
MTF, radioisotope imaging, digital low-pass filtering 77−5065
MTF calculation in radioisotope scanning, improved FORTRAN II program 77−21612
multidelay system coherence function meas. 79−68530
multipass heat exchanger distributed temp. response *(Japanese)* 77−33985
narrowband matched SAW filters realisation *(Russian)* 80−23850
neuron models Volterra-like polynomial representation 77−90754
neuron populations as information processing system, stochastic properties 78−80860
nuclear reactor noise theory, adjoint space applic. 78−13202
ocanic aseismic ridges, gravity/bathymetry transfer functions rel. to isostasy 80−3971
ocean acoustic, impact on coherence of underwater acoustic propagations 79−59861
ocean acoustic transfer function impact on coherence of undersea propag. 80−58842
parallel-channel SAW filter bank transfer function synthesis 77−23828
photoacoustic spectroscopy, time-domain, nonradiative lifetime meas. of condensed phases 80−55232
photographic objective lens, testing, use of m.t.f. 77−181
physiological system, transfer function synthesis given magnitude or phase response 77−77864
physiological system transfer function synthesis, given magnitude or phase response 78−64919
plasma, stable and feedback-stabilised, anal. 77−51215
pneumatic micrometer with positive feedback system *(Japanese)* 79−93101
pressure regulator device, behaviour anal. 78−93668
propeller cavitation tunnel hydroacoustic transfer function, meas. and anal. *(Croatian)* 80−92002
radiative transfer in planetary atmosphere, transfer eqns. for scatt. a^m and b^m functions 77−56848
radiography, computerised tomography, MTF meas. method appl. to EMI head scanner 77−48864
radiography, focal spot meas. for quality control, using random object distrib. 77−2047
radiography, resolution, falling load principle, focal spot performance 77−2045
reciprocity calibration of acoustic emission transducers 80−28401
resistance furnace heat conduction, determ. for DDC *(German)* 77−3709
resistance thermometer, cold-wire, dynamic calibration in still air 77−5834
SAW delay line complex transfer coeff. calc., Shockley-Ramo induced current theorem 79−7264
SAW interdigital transducer transfer function rel. to fabrication tolerances 77−27452
SAW scattering by interdigital transducer, model and appl. to SAW track changer 79−59899
scintillation camera based on image intensifier tubes, for nucl. medicine appls. 77−5069
seismology, iterative identification of non-invertible autoregressive moving-average systems 78−81422
solar thermal systems long-term performance predictions using closed-form solutions 80−30556
space-variant EM transfer functions, for inhomogeneous scatt. media characterisation 78−71012
speckle interferometry application to partially-coherent sources 80−9032
STEM, partially coherent image form. 77−190
TEM, electronic prod. of hollow cone illum. 77−54026
terrestrial electricity, transfer functions rel. to induced currents mapping around Kenya Rift 77−73628
thermal objects with internal sources 78−73960
thermocouple dynamic error correction cct. 78−77909
thermogenesis, harmonic analysis and inverse filter 80−27304
thermooptical sound generation problems, method of transfer functions 79−64478
throat-wall, human, modelling and vocal tract study from input/output meas. 79−34577
tilt meters, photoelectric, with negative feedback, servo devices transfer functions *(Russian)* 78−88948
tolerated errors in determining transfer-function parameters of temperature transducers 78−73959
under-surface temp. pattern estimation by dynamic remote sensing *(Japanese)* 78−36315
US flowmeter data processing, transfer function modelling of arteries 78−61225
velocity meas. sonar system, transfer function model 77−7275
ventricular synchronous demand cardiac pacemaker advances 78−77152
wideband annular US imaging array response 79−55306
X-ray focal spots, characterisation of imaging props. 77−21596
C graphitic, high resolution electron microscopy imaging, phase contrast transfer functions in electron optical aberrations 79−77463
Si epitaxial reactor, doping system, transient steady state response, transfer function approach 79−42086

transferred electron devices *see Gunn devices*

transferred electron effects *see Gunn effect*

transferred electron oscillators *see Gunn oscillators*

transfluxors *see magnetic cores*

transformations, phase *see phase transformations*

transformer insulation
see also insulating oils
current transformers, oil insulated, parameters influencing heating assessment using sensibility matrix *(Hungarian)* 80−87708
gases in transformer oil, power transformer operating state determ. *(Czech)* 79−87894
liquid dielectrics, thermal performance estimation 80−88582
oil, optical obs. of pre-breakdown and breakdown 77−80386
oil diagnosis by chromatographic analysis, computerised evaluation of results *(Czech)* 80−97744
oil electrohydrodynamic flow, jet dynamic pressure obs. *(Russian)* 80−59117
oil immersed transformers, dissolved gas causes and phenomena, anal. *(German)* 80−76570
oil ion mobility and fluid motion, effect of additives and dissolved gases 78−47543
oils, under 60 Hz stress, elec. stress induced motion 79−90346
power transformers, electromagnetic testing of partial discharges for failure and breakdown prevention *(Russian)* 80−97743
Fe-Si (3 wt.%) cores with insulative coatings, morphological and struct. SEM characteris. 78−23881

transformer magnetic circuits
ferromagnetic, magnetisation characts. approximation *(Russian)* 78−31094
magnetism conference, Freudenstadt and Bad Nauheim, Germany (March and April 1978) 79−24121
vector potential of parallel conductors in rectangular metallic tunnel *(Polish)* 77−83778
Ar-air, transformer plasmatron, LF discharge, electrical and energy props. 80−103200

transformer protection
hum due to magnetostriction effects, insulation coatings appl. *(German)* 78−23311

transformer substations
audible noise, effect on urban environment 77−3701
audible noise reduction, means 77−23812

transformer testing
power transformers, electromagnetic testing of partial discharges for failure and breakdown prevention *(Russian)* 80−97743
preventive, by analysis of gases dissolved in transformer oil *(German)* 80−71969

transformers
see also autotransformers; current transformers; d.c. transformers; high-frequency transformers; potential transformers; power transformers; pulse transformers
active noise control 79−37085
arc snubber using transformer core, theory 80−59315
contactless EM transformer, floated density meter *(Russian)* 79−54099
contactless measurement apparatus for photomagnetoelectric effect, operation analysis using equiv. cct. 77−41655
core, mag. field distrib., graph-theoretic model appl. 80−87260
cores, use of high permeability Fe-Si materials 80−88793
electrotechnical steel, quality significance on energy and materials savings in magnetic circuits *(Czech)* 80−20947
energy transfer from low voltage capacitor bank to high inductance with air pulse transformer 78−49860
heart, human, elec. and mag. events, phase and amplitude relationship recording 80−104695
linear differential, profile meas. of two concentric round parts, concentricity errors *(German)* 80−57249
moving coil linear variable differential transformer for displacement meas. at liquid helium temps. in strong magnetic fields 78−54415
noise reduction by acoustical compensation 78−38134
off-resonance transformer charging for 250-kV water Blumlein, for Experimental Test Accelerator 80−23183
oil heat transfer efficiency from rough plate 80−48704
relativistic fluid eqns., hodograph transformations 77−955
sine cosine rotating transformer, angular displacement meas. apparatus *(Russian)* 79−97344
single-phase, calc. of inrush current 80−88787
steel, crystallographic texture perfection in sheet with S,Mn inhibitors *(Russian)* 79−91709
stray magnetic flux analysis, vector potential calc. method *(Polish)* 77−54645
strayvoltage elimination method, with respect to zero stability in magnetic flow measuring devices *(German)* 79−82018
Fe-Si (3 wt.%) grain-oriented transformer sheet, effect of phosphate coating containing Cr_2O_3 and CaO 77−16135

transforms
see also Fourier transforms; Laplace transforms; Z transforms
't Hooft transformation, explicit solns. 80−345
Abbe transform of Fraunhofer diffr. integral, Youngian boundary wave *(Czech)* 78−29893
Adamar, image shift analysis *(Russian)* 80−1134
Aitken δ^2 transformation, geometric approx. 77−10595
ambiguity group for classical canonical transforms, role in quantum mechanics 80−8839
artificial satellite motion eqns., time element for general time transform. 77−25928
artificial satellites, Kustaanheimo-Stiefel transform. rel. to Earth oblateness effects 77−60582
Backlund, and gravitational duality 80−12971
Backlund, local conservation laws of principal chiral fields (d=1) 80−4888
Backlund, symmetries of Yang eqns. 80−52393
Backlund problem for the equation $\partial^2 z/\partial x^1 \partial x^2 = f(z)$ 79−2597
Backlund transform. derivation in inverse scatt. formalism 80−8810
Backlund transformation in language of jet bundles *(French)* 78−28913
Backlund transformation in the classical massive Thirring model 80−57456
Backlund transformations as canonical transformations 78−81855
Backlund transformations as nonlinear Dirac eqns. or Cauchy Riemann eqns. 78−49965
Backlund transformations describing SU(2) mag. monopoles 79−2915
Backlund transformations in several variables, differential geometric anal. 80−86073

transforms continued
Backlund transformations of axially symmetric stationary gravitational fields 79−40421
Backlund transforms. for mag. monopoles in SU(2) gauge theory 79−2916
Bargmann-Segal, nuclear cluster norm determ. using SU(3) recoupling techniques for A=12 to 24 79−22214
Benjamin-Ono equation, meromorphic solutions 80−31980
Bessel, appl. to determ. of stellar rot. vels. 77−49369
Boltzmann equation, two-vector, analytical solns. in nonplanar geom. 77−65246
Bonnor transform. extension 80−31643
Borel summability, improvement on Watsons theorem, ϕ_2^4 appl. 80−52394
Borel transform and the renormalization group, review 79−26238
canonical transformations theory for nonlinear evolution eqns. 77−29993
cascade airfoil aerodynamic design, exact method based on conformal transformation *(Italian)* 79−41599
celestial mechanics, Kustaanheimo-Stiefel regularisation and nonclassical canonical transforms. 77−60586
celestial mechanics, Lagrangian eqns. generalization, KS transform. extension *(French)* 77−25922
celestial mechanics, numerical aspects of time elements for time transforms. 77−25929
chemical network, nonlinear pattern as transform. group symmetries 78−27878
chi-square transform, inversion 78−86122
classical nonconservative systems, appl. of time depend. canonical transforms 80−17792
closed time path Green's functions, transform. props. *(Chinese)* 80−105491
computer-aided seismic analysis and discrimination 78−20530
conference, nonlinear problems in theoretical physics, Jaca, Gain 1978 80−4478
conformal transformations combined with numerical techniques, with applications to coupled-bar problems 80−83538
constrained Hamiltonian systems, generators of symmetry transformations 80−57138
contact conformal transformations, finite, nonrelativistic 78−36815
contact Lie algebras, contraction 78−36816
coordinate transformation formulas for massive reference frame 80−90673
coordinate transformations and theory of meas. 78−36960
cracks, Griffith, at interface of two bonded dissimilar elastic wedges, stress field, inverse Mellin transforms 80−53718
cracks, Griffith-type, asymmetrically loaded in infinite anisotropic medium 79−50649
Delaunay-Zeipel transformation, use in reson. props. of celestial mechanics 80−46378
differential equations, generalization to transformation groups *(Russian)* 79−92991
differential transform technique in operational form, appl. to elastic point source problems 77−33865
diffraction integral transform, functional analysis 77−5635
diffraction integral transform, sampling theorem 77−45678
diffraction theory, table associated with integral transform 79−97185
dislocation scattering, new Hamiltonian for describing multivalued elastic displacement fields 80−24862
displacements produced in porous elastic half-space by impulsive line load, Laplace-Fourier transform 77−23908
distributed type associative memory model with quantised Hadamard transform 80−108867
Eckart Hamiltonian, transformation approach 80−101726
edge notches, conformal transformations 80−27128
education, extended Galilean transformation 79−25788
education, simplified relativistic force transformation equation 79−25791
elastic wedge, mixed boundary value problem, use of Mellin transforms 80−23884
elliptic systems and numerical transforms. 78−65780
EM field analysis, numerical techniques for conformal transformation 78−74816
ergodic nonsingular transformations, construction of factors 77−17780
ergodic properties of stopping-time transformations 78−89396
exchange kernels of nuclear cluster model 79−13228
fast convolution by finite ring arithmetics 80−36837
Fermat number transform for microwave holography data processing 80−43298
finite disc, thermal shock, finite integral transform method 77−3765
finite Haar, electrocardiogram waveform representation and recognition 78−3654
flows on sphere surfaces, comparison of spectral methods 79−72877
Foldy Wouthuysen transform. group content, nonrelativistic limit for arbitrary spin 79−75387
Foldy Wouthuysen transformations and Volkov states, unitary in 2-component forms 79−30688
for differential, partial and integral equations 77−75773
FREINT, an integration routine calculating Fresnel diffraction 79−30612
general affine transform, appl. to Landsat imagery planimetric restitution using Zeiss Stereotop 80−56648
generalised Legendre transforms, operational props. and appl. to heat transfer 78−59256
geophysical fields, props. of linear transform. characts. *(Russian)* 79−35007
Givens transformation techniques, appl. to Kalman filtering, orbit determ. 78−4473
gravity disturbance covariance functions, upward continuation, Legendre and Fourier transforms 78−85468
Hadamard and M-sequence transforms are permutationally similar 80−32921
Hadamard mass spectroscopy, H ion-He mass spectra 79−30601
Hadamard transform appl. to beam spectroscopy 80−62741
Hadamard transform optical instrument, systematic errors 78−94375
Hadamard transform spectroscopy with computation and superposition procedure for multielement analysis 77−70376
Hamilton-Jacobi problem and canonical transform., first order system from variational principle 79−17193
Hankel, computation using projections 80−96124
Hankel, inversion methods for integral transforms of class L_2 functions *(Russian)* 78−20940
Hankel, quasi fast, algorithm for evaluation 77−83826

transforms continued
Hankel transform, appl. to Earth dipole elec. soundings direct numerical interpretation 79−34732
Hankel transforms, related, of orders 0 and 1, numerical integration by adaptive digital filtering, FORTRAN IV algorithms 79−92599
heat cond. in truncated wedge of finite height 78−13884
heat exchange in complex domains, new soln. techniques 78−94509
hermitian matrix, large, eigenvectors determ., new approach 77−37717
Hippuran renograms, application of transform methods 79−8540
hodographic mapping, normalised, global anal. of two-terminal Keplerian trajectories 78−4085
homomorphic deconvolution, time domain reflectometry signal separation for overlapping time windows 77−18019
integral, calc. of resonating group kernals in nuclear cluster model 79−6446
integral, of generator coordinate method kernels 79−13227
integral, with non-standard kernals, uses, teaching appl. 80−31466
integral for neuronal ensemble principle and epileptic oscillation 79−83739
integral transform associated with Helmoltz eqn. in diffr. theory 77−67300
integral transforms, alternative forms using hyperdifferential operators 77−49570
inverse Gaussian transforms, general props., Slater type orbitals appl., coord. and momentum representation 78−37549
inverse scattering transforms, Zakharov-Shabat and Schrodinger-type, connection 78−21006
inverse spectral transforms, nonlinear evolution equations, soliton solutions 80−12919
Jansen-Byers Brown exchange perturbation theory, transformation operator 77−28380
Jaulent-Miodek transformation is canonical 80−36894
k-plane integral transforms, X-ray crystallography appl. 77−5633
K-transforms, theorems 77−17776
Karhunen-Loeve transformation, use in seismic data processing *(French)* 79−44258
Kinnersely-Chitre transforms for spinning mass solns. to Einstein eqns., integral eqn. method 79−97267
Kinnersley, soln. of Einstein-Maxwell eqns. 80−4617
Kinnersley-Chitre transformations, integral eqn. method 80−17844
Korteweg-de-Vries eqn., exact soln. via a generalisation spectral transform 78−65786
Kurskov-Ozernoi transformation, appl. to cosmic turbulence 77−5604
Kustaanheimo-Stiefel regularizing transformation derivation 78−93086
Kustanheimo-Stiefel transformation osculating variables, perturbed motion, differential eqns. 80−109344
Lagrangian coordinate transformations, in self-similar blast-wave models 77−57072
Landsat MSS points, coordinates linear lesat squares transforms for location on maps 79−2389
landscape multispectral data, Karhunen-Loove analysis 80−48164
Legendre, stochastic temperature fields in a solid spheric cone *(Ukrainian)* 79−50566
Legendre transform notation for critical point criteria 78−12657
Legendre transformation, geometric definition 78−24640
Lie series use in studying nonlinear Hamiltonian systems 79−8811
linear thermokinetics, transient conditions, resoln. using finite integral transform. method *(French)* 80−38218
M/M/S queueing system, finite discrete transform 79−67144
magnetogasdynamics, reciprocal type transformations 80−48804
many channel Marchenko transform. operator, upper bounds 79−63091
mass transfer eqn., integral transforms for boundary value calcs. *(French)* 77−13711
massive reference system, transform. of coords. *(Russian)* 78−65769
Mellin, anal. of point loaded circular disc with two diametrical cracks 79−27589
Mellin, appl. to edge crack pair in circular disc 78−46914
Mellin, numerical inversion 77−2514
Mellin transform technique, anal. of Griffith crack at interface of bonded wedges 79−40369
Melosh transformation, Eriksen like form, group theoretic interpretation 80−8859
Miura's transform. of modified Korteweg deVries eqn. 79−75356
Miura transformation of Kaup and Mikhailov eqns. 80−57103
modified Wiener-Khinstchine theorem, use in three-dimensional statistical gravity disturbance model 77−90991
multiband image spatial domain filtering by Karhunen-Loeve transform 78−78952
multidimensional convolution, efficient transforms 79−36846
multiple finite spheroidal transform and its application 80−12910
multispecies Tani transorm., kinematical props. 79−17333
neutron transport, two-group transport transforms, comput. merit in finite nonplanar media 77−65247
non-Fourier solid, thermoelastic disturbances propag., integral transform. calc. 77−89024
nonbijective canonical transformations, representation in quantum mechanics 78−45501
nonlinear continuum theories, generalised coordinate transformation 78−36828
nonlinear evolution equation, exact two-periodic wave soln. 80−12914
nonlinear optics, fast transform calcs., appl. to SHG with depletion and diffraction 80−53376
nonlinear transformation-operators, appl. in explicitly solving differential eqns. 79−12568
nonlinear transformations for accelerating convergence of infinite integrals and series 77−67260
nonlinear transformations for partial differential eqns. 80−42043
nonlinear transforms, quantitative universality, recursive mechanism 79−2604
nonseparable system semiclassical quantisation, invariant tori and energy levels calc. scheme 79−97225
notch analysis using conformal mapping, book contrib. 78−94620
nuclear n-body reaction calcs., integral transform applicability 78−4920
numerical Bessel transformation calc. program 79−49016
numerical Fourier and Bessel transforms in logarithmic variables 79−9089
numerical inversion, appl. 77−78967
numerical inversion, Mellin transform expressed as two sided Laplace transform 78−77694
numerical inversion of integral transforms 77−67259

transforms continued
numerical solution of problems in unbounded regions, use of coord. transforms 78−8219
optical processing, performance of generalised two-dimensional linear transforms 80−9824
optimum filter for image restoration *(Ukrainian)* 78−55308
orthonormalization, polar decomposition, and transformation to an effective Hamiltonian 79−6811
para-Bose states, generalised Bogoliubov transform. coeff. 80−27211
plane electrostatic fields in doubly connected polygonal domains, anal. using conformal mapping 77−58223
Poincare-Cartan integral invariant and canonical transformations for singular lagrangians 80−94956
pointlike and nonpointlike transforms of differential eqns. in cartesian coords., geometrical treatment 78−54159
polymer chain, self interacting, Legendre transformation 80−15018
post-Newtonian charged n-body problem, centre of inertia and coord. transforms. 79−93025
potential fields, accuracy of linear transformations in presence of interference 77−44900
projective symmetries of dynamical systems, infinitesimal symm. transforms of vector field 78−32650
radiation theory, transformation of a class of integrals 77−49285
radiative transfer, general integral transform of exponential integrals 79−88577
radiative transfer exponential integrals, Λ-transform determ. 79−35114
radioastronomy, aperture synthesis meas. processing, tangent-plane aberration, new transform 79−8847
Radon, for higher dimensions 79−5969
Radon, sampling with finite width beams 79−5968
Radon transform, Plancherel theorem extension to L_2 space 78−57807
Riccati transformations, invariant imbedding and eigenvalue problems for ordinary differential eqns. 77−37
Riccati transformations for eigenvalues of eqns. with separated boundary conditions 77−38
Riseman, modified integral transform method, appl. to radial size distrib. of parallel cylinders 78−83648
Schrodinger equation, discrete-time, Green functions, k-transforms 80−46859
seismic wavelets, transformation by optimal inverse filter, stability charcts. 78−81424
self-reciprocal functions, integral transforms 77−57154
sequential, appls. of quantitative image analysis 80−23627
sine-Gordon eqn., geom. prop. of Backlund transform. 79−12620
singularities of Borel transform in renormalisable theories, massive $g\phi^4$ theory 78−62304
smooth convex surface HF scatt., transform-domain Galerkin soln. 77−38783
sound synthesis by continuous spectral transformation *(French)* 80−79100
space vehicles, relative motion computation using time transformations 77−22050
space-time classical domain transformation groups and invariants *(Chinese)* 78−54162
space-time transformations leaving Einstein eqns. invariant *(French)* 78−62123
spectral transform, nonlinear discrete evolution equations 80−4553
spectral transform and nonlinear evolution equations 80−4551
spectral transform method extension for solving nonlinear differential difference eqns. 78−81804
spectral transform method for nonlinear evolution eqns. from Zakharov Shabat linear problem 78−65785
spectral transform method for solving evolution equations and conservation laws 80−62488
spectral transform method for solving nonlinear evolution equations 79−49019
spectral transforms, nonlinear evolution equations 80−4552
speech articulation rate and pitch modfication using constant-Q transform 79−68515
spin Hamiltonian diagonalisation, theory and appls. of generalised operator transforms 77−4546
steel CC types M6 and M3N, elastoplastic bending, insulating coating influence on magnetic losses *(Russian)* 79−100284
Stieltjes, inversion methods for integral transforms of class L_2 functions *(Russian)* 78−20940
still-picture real-time Hadamard transform coding quantiser design 77−27263
strong Backlund transformations, generalisation and existence in ≥ 4 dimens. 79−30316
superluminal and subluminal causal transformations through transformations of metrics 78−28943
supersymmetric Liouville and sine-Gordon eqns., method of inverse scatt. and Backlund transforms. 79−2951
tachyon solitons and their interactions, Backlund transformations in nonlinear systems 78−54181
teaching model using stored water, discrete transformations 79−23
thermal stresses in slab containing annular crack, integral transform techniques 80−96229
time transformations and Cowell's method 78−77466
transformation group techniques appl. to nonlinear fluid and plasma eqns. *(French)* 80−77623
two body problem, time transformations and local truncation errors 77−22053
two body problem, time transformations effect on local truncation errors 77−22052
two dimensional unitary transforms for image processing 78−58928
two-electron integral transformations for 2nd order multiconfig. Hartree-Fock method 80−87045
unified Radon inversion formula 79−2598
vitalism, nonlinear transforms in Hilbert space 78−73133
Walsh transform on standard microprocessor, use as EEG monitor 80−26399
weighted line-finding algorithm for digitised picture 80−99660
Weyl transform, semiclassical approx. by path summation 79−2644
Weyl transform inversion 79−99
X-ray structure determination, information theory aspects 77−51258
X-ray transform/computer tomography, math. aspects of divergent beam 78−96088
H, electron scatt. resons., coord. rot. method calcs. 77−83736

transient analysers
see also spectral analysers; wave analysers
anodic oxidation overvoltage, open-cct. technique 78−27776
exponential decays analogue anal. 78−86244
interictal epileptic EEG transient morphological discrimination algorithm 79−100758
recorders, transient, 1024-point, circuits, operation 77−53868

transient response
see also step response
accelerometer, induction generator type transient charcts. and Law-Novotny expression development *(Japanese)* 79−88921
acoustic half-space, transient response to rotating point load 79−3844
acoustic system matrix parameter determ., transient test principles 79−68527
acupuncture points Li-4 and Li-12 Laplace plane analysis of transient impedance 77−81772
aquifer, flow in fractured porous media 77−91173
baffled circular piston, radiation impedance deduced from transient state 77−79980
beam transient response prediction by Laplace transform techniques 78−1596
biological cell impedance transient response characterisation 79−53066
bistable optical device, transient response and applications 80−33214
BWR-II containment vessel, soil-struct. interaction for transient loads 78−29604
chemical reaction residence time measurement, magnetic recording and hybrid computers appl. 78−81953
cold lossy plasma half-space in transverse mag. field, transient response 79−77388
DH devices, interface recomb. effects on transient response anal. 78−22127
digital model anal. using transient excitation 77−84209
digital oscilloscope operation *(Danish)* 78−8392
discrete-time Doppler frequency meter for blood flow imaging 79−57704
dynamic loading of thick rectangular membrane, viscous damping effect 78−46906
Earth, low resistivity, polarisable, EM transients formulae *(Russian)* 79−39644
Earth, transients from two horizontal thin conducting strata *(Russian)* 78−40485
Earth EM sounding, interpretation of transients in Laplace space representation *(Russian)* 78−40483
Earth transient EM sounding, meas. errors anal. in computer processing *(Russian)* 79−44269
electrochemical reactor characterisation, marker pulse method improvements 80−76524
EM field response of dipole above ground surface 78−57166
EM fields created by currents in confined conductors, freq. and transient responses 79−29702
EM pulse response from irregular Earth's surface models 78−57165
ferrite pot core pressure transducer development and compensation 79−75519
fluid-filled porous media, response to transient input 77−31244
fusion reactor, TFTR, T gas injection system transient response 80−102337
gas flow generator transient process anal., controlled plunger movement method 77−72381
Gunn domain transient behaviour and associated equivalent circuits 78−19043
H-polarised EM wave by isotropic moving plasma 80−64731
hot-wire cell for liq. thermal cond. meas., transient response storage 77−30144
HWR reboiler hybrid computer dynamic simulation 78−8949
hybrid bistable optical devices, transient response 79−59803
injection lasers, phase-plane anal., effects of absorbing section 80−64022
ionosphere, topside, transient response to precip. 77−78566
ionosphere, uniform, transient response to geomag. storm sudden commencement rel. to preliminary reverse impulse 80−8477
ionosphere to solar flare, two-layer current model for geomag. crochet 79−44300
layered composite containing a crack, impact response 77−50991
linear elastic three layered rings, eqns. of motion 77−80075
linear system mean square response to nonstationary random excitation 80−57085
linear systems, response to square wave force, transients, teaching appl. 80−31467
3-lumped parameter vibrational mdoel, anal. for dynamic characteristics of materials of relaxation type 79−72827
magnetisation transient and steady-state charcts. with hysteresis, digital simulation 77−66385
minority carrier generation rate meas. using transient response of MOS capacitor with guard ring 78−2576
MOS inhomogeneous transmission lines, analytical solutions for charge transport 79−91153
neural adaptation and transient responses due to inhibitory feedback 79−92206
novel Peltier junctions, fast transient response 78−21141
nuclear research reactor ZED-2, two-phase control absorber development 79−85697
nuclear systems identification 77−88213
ohmic contact in two-carrier regime, avalanche injection model 77−55607
optical fibre, graded-index, minimum impulse response 77−68258
optical fibre, linear power response, impulse response 77−54790
p^+-n^--n^+ pulsed diodes, forward pulsed case, voltage transient response 80−60071
photomultiplier transient characteristics and intercascade time-of-flight dispersion 78−86333
photomultipliers, curved microchannel plate, impulse response 78−12743
piezoelectric plate, infinite, on elastic medium, transient response to pot. pulse 78−52442
plasma half-space, cold, lossless, transient response in presence of transverse static mag. field 78−67361
polymer solutions, dynamic compressibility study via press. transient technique 77−86256
preamplifier, wideband low-noise system, spectroscopy with Si surface barrier detectors 77−54467
radiation heat exchanger, temp. distribution, model, boiler appl. 77−39210

transient response continued
random threshold element networks with absolute refractory period 77−29143
receptive field types in lateral geniculate body and functional model 78−69046
renal tubule model injection transient response calc. 77−40700
resonator, transient process, excited by beam 79−81347
retina, frog, near IR transmission of rods rapid light-induced changes 79−74658
rivers downstream pollution, one-dimensional transient model for short-term prediction 80−81496
sea wave profile meas. by radar altimeter, computer simulation 77−5367
seawater conductivity/temperature/pressure profiler errors 77−5377
semiconductor, transient and alternating currents, influence of deep traps 79−73525
solar cell, p-n junction, photoinjected carrier lifetime meas. by reverse voltage pulse response 80−45664
solid with recombining space charge, small signal transient and AC response 77−51737
space frame transient analysis in large displacement 77−14955
surface-mounted beaded thermocouple transient response models 78−8405
system matrix parameter determ., transient test results 79−68528
temperature control system for biological preparations 79−57830
thermal regenerator, periodic flow type, transient performance 78−59389
thermocouple EMF response under reactor conditions 77−71320
thermoelectric coolers, numerical anal. of transient behaviour 78−21140
tsunami, island of Hawaii, 1979 November 25, numerical anal. by finite-element method 80−72449
UV fluorescence lifetime determ., correction of instrumental time response var. with wavelength 78−5374
vibrations, transient response of thin elastic spherical shells 80−96217
viscoelastic beam, continuous, dynamic response 78−9569
waves in fluid-filled porous media, refl. and refr. 77−49604
$Al_xGa_{1-x}As$-GaAs LED design and characterisation for fibre-optic communications 78−46796
CO_2 electrode, dynamic response 79−92025
GaAs, carrier diffusion in transient response regime 80−103688
GaAs, epitaxial multilayer, electron irrad. defect study by transient capacitance 79−99241
GaAs, self-scattering in Monte Carlo calcs. of transient dynamic response 80−103687
He cooled reactor turbine control experiences Fort St. Vrain HTGR *(German)* 80−57927
Mg_2SiO_4, pure forsterite, transient and steady-state creep at low stress 79−79827
Si epitaxial film dopant incorporation 77−76976
Si epitaxial reactor, doping system, transient steady state response, transfer function approach 79−42086
Si p-n junction radiation detector DC cct., performance anal. 77−70556

transient stability *see stability*

transient voltages *see transients*

transients
see also surges
aircraft EM environment meas. near thunderstorm cells 78−49180
arc channel transient characts. in air under impulse voltage *(Japanese)* 78−5973
arc plasma gun for metal cutting, transient performance, obs. 80−49017
arc quenching system for transient and statistical flashover, fusion reactor systems 78−75455
baffled piston wideband acoustic near- and far-field transients 79−46154
classic guitar quality correl. with opening transients 79−68516
compensated semiconductor, theory of transient processes 80−24930
CRO photographic recording status 79−93247
cryogenerator magnet field transient change calc. *(French)* 77−26303
currents and charges induced on wedges and strips 80−18974
Darrieus rotor, aerodynamic analyses comparison 80−61264
DC corona, transient regime determ. *(Russian)* 77−35412
deep level transient spectroscopy expts., high resolution anal. of exponentially decaying transients 80−10906
defect dielectrics containing electron trap centres, transient current model *(Russian)* 78−60134
dielectric loss, energy flow analysis 78−80282
diffusion of electric current and mag. fields in rect. cond., anal. *(Polish)* 77−65008
eddy current distribution in two insulated coils embedded in conducting medium *(German)* 79−41282
eddy current magnetic field time constant calc *(Polish)* 77−83779
eddy current method appl., distribution in plate of finite thickness calc., due to coil of arbitrary shape *(German)* 79−27129
electric breakdown, leader development and its mechanism in air under impulse voltages *(Japanese)* 77−80390
electric machines, automatic testing, of rotational speed, using digital measurement method, in steady or transient regimes *(Czech)* 79−71419
electro-optic signal representation by implicit sampling 79−76620
EM wave propagation in inhomogeneous media, polarisation rotation analysis by modified ray tracing 79−89831
ferromagnetic film with domain structure, transient state, mag. field calc. 77−4536
ferromagnetic material, magnetisation characts. approximation *(Russian)* 78−31094
field processes analysis, Bubnof-Galerkin method appl. *(Polish)* 77−54643
galvanic cell, electrochemical transient investigations 77−11930
Gunn diode, anode domain disappearance dynamics, computer simulation calcs. 80−6859
heat flow meter dynamic properties *(Russian)* 78−86265
HV nanosecond transient meas. from pulsed low inductance gas discharge, Kerr effect 78−51380
laser logic elements, transients during switching *(Russian)* 80−23697
lightning transient anal. for aircraft, flux induced voltage transients on low-loss transmission lines 79−36814
LMFBR thermal transients, impact of bypass flow 79−9680
logic latches, mag. approach to upset prediction 77−18710
meas. instruments random errors analysis, based on instantaneous frequency response 80−77741
MHD generator, electric power fluctuations due to Hall and ion slip currents 77−68879

transients continued
multiple lifetime measurements analysis modulation methods, excitation spectrophotometer 80−86449
nerve impulse local existence 78−96045
nuclear power plant, isolation and relief valve/piping transient force anal. program 78−50287
nuclear power station model validation and automatic control 77−88261
oil electric strength for switching surges and long flash-over distances, expt. *(Czech)* 78−56427
oscilloscope screen photography, shutter mechanism *(Danish)* 78−234
p-n junction temperature effect of forward current switching transients 77−62988
phase-change front propagation during reactor transients, appl. to LOCA in PWR 79−631
physiological system anal. using swept sine wave 78−28133
picosecond waveform meas. 78−57923
power supply, three-phase system, computer aided cct. design 78−54959
pressure transients, on fluid-filled porous media, response 77−31244
pulsed excitation of flexural modes in infinite plates 80−38167
recorders, multichannel *(German)* 78−235
recorders for natural and induced phenomena 80−27284
semiconductor, deep trap activation energy, effect of non-exponential transients, DLTs method 80−20115
semiconductor diode transient process calcs., minority nonequilibrium carriers, postinjection EMF 80−6971
signal recorder, Transcribe 10 uses A/D and D/A conversion 77−71340
skin effect transients on hollow sphere in plane field of system of conductors *(German)* 80−37927
superconducting cables for PF and TF coils, losses and transient field effect 78−62635
thermoelectric heat pumps, two-stage, design criteria anal. for cool-down speed maximisation 80−108812
time dependent heat conduction, partial differential equations solution 80−106707
transient input processes reconstruction, from output and dynamic props. 80−77742
two-dimensional steady-state and transient eddy current problem soln. 79−41289
voltage and current, fast digital technique *(Polish)* 80−86340
voltage transients, defect centres emission rates and density profile 78−10467
voltage wave propagation in mag. insulated line 80−5667
water-vapour velocity transient meas. by cross-correlation anal. *(German)* 77−62312
wire spark chamber with decoupling resistors, calc. 77−65396
Cu-CuI-graphite secondary cell, transient ionic current obs. 80−108790
GaAs MOS capacitor fabrication and transient response for minority carrier lifetime meas. 79−47103
GaAs MOS structures, props. of capacitance transient 80−25013
^3He-^4He mixture, optical pumping, transients theory 80−91509
N_2-O_2 gas mixtures, highly transient gas discharges, obs. 79−37562
SF_6 insulation, under impulse voltage stress, effects of pressure and vol. on firing delay *(German)* 80−87959
Si, transmutation doped, deep trap level analysis 78−10471

transistor circuits
Used for general papers and papers where the use of transistors is significant
see also bipolar transistor circuits; field effect transistor circuits
anemometer design using transistors, wind sensor for portable battery operated instrument 79−71420
avalanche transistor discriminator for low energy radiations 80−5450
avalanche transistor pulser for fast-gated operation of microchannel plate image intensifiers 78−37527
HV transistor nanosecond amplifier for unipolar pulse signals amplification 78−12720
linear convertor, for acoustic emission signals 78−9512
stabilised rectifier unit 78−4643

transistor-transistor logic
see also logic circuits
capacitance meter, linear direct reading, cct. *(French)* 78−237
digital universal counter, amateur constr. *(German)* 78−12727
event counter, with selectable time gate, for neurophysiological applic. 77−40944
ICs, dry cells appl. as power source 77−17745
spot exposure meter, for colour photography, techniques and description 78−12782
square root of time mark generator using TTL digital ccts. for chronocoulometry 80−35588
synchronous machine phase shift control cct. 78−22054
temperature-controlled ovens, electronic controller using TTL cct. *(German)* 79−67304

transistorised circuits *see transistor circuits*

transistors
see also bipolar transistors; phototransistors; power transistors; thin film transistors; unijunction transistors
1/f fluctuations *(Japanese)* 78−43448
injection field magnetotransistor, operation 79−7888
package, potential source of corrosion 79−70230
superconducting transistor, three-film three-terminal device, theory and construction 78−47908
Si, microwave Stark effect spectrometer, with electric molecular modulation *(Russian)* 80−9003
p-Si:P p-n junctions, dislocations investig. rel. to P diffusion, SEM, X-ray topography techniques 77−76433
Si-SiO_2 interface, Au conc., effective impurity doping 78−52094

transit time devices
see also BARITT diodes; IMPATT diodes
US volume flowmeter, in vivo validation 79−83872

transit time noise *see random noise*

transition metal alloys
see also alloys of individual transition metals e.g. nickel alloys
see also copper alloys; gold alloys; silver alloys; transition metal compounds
3d, Hall effect, electron scatt. processes 80−34419
3d, strong ferromagnet, electron correls. 77−40030
A15, band theory, semiself-consistent band calcs. 78−2406
A15 compounds as Jahn-Teller systems, multiple band electron-phonon transport theory 80−24902
A15 structure, nucl. quadrupole coupling const., at shear const., Born repulsion charge cloud 79−8070

transition metal alloys continued
absorption of H and mag. props. 80−60224
actinide impurity, in disordered host, occurrence of localised magnetism, CPA calc. 77−63096
aluminides, electrospark alloying to Ti, residual stresses obs. *(Russian)* 77−56145
aluminides of non-magnetic transition metals, atomic volumes deviation from additivity 79−82178
amorphous, and disordered, anomalous behaviour of resist., alternative mechanism to spin scatt. 78−91690
amorphous, elec. resist. 78−60103
amorphous, mag. props., chem. short-range order 80−75739
amorphous, mag. props., structure and preparation 80−75737
amorphous, mag. props. 80−29576
amorphous, reduced supercond. transition temps. 77−39991
amorphous, temp. stability 78−63948
amorphous alloys, at. order effects on mag. props. 77−73006
amorphous alloys, M-metalloid, elec. resist., 20 mK to 300K 79−73483
amorphous and liquid, elec. transport 77−51720
amorphous ferromagnets, itinerant electron model 79−73664
amorphous ferromagnets, mag. props., book contrib. 80−75743
amorphous ferromagnets, spatial fluctuations of magnetisation 79−19727
amorphous magnetic alloys, elec. field gradient 78−39475
amorphous superconductor, ratio of energy to transition temp. 78−10619
band structure, appl. of X-ray spectroscopy *(Polish)* 79−56887
BCC crystal struct. dependence on band struct. 78−83778
BCC magnetically ordered alloys, effects on at. ordering-spontaneous magnetisation reln. *(Russian)* 78−19261
BCC structure, elect. cond., electron lifetime affecting electronic props. 79−15134
binary, amorphous and crystalline, superconducting transition temp. correlation with solute conc. 78−52139
binary, conc., superconductivity and electron-phonon interactions, theory 78−14868
binary, energy of formation 77−15341
binary, ht. of formation, prediction model 77−56246
binary, lattice thermal cond. at low temps., solute at.-phonon scatt. 77−76512
binary, state density curves, relation between short-range order and Fermi level position, CPA calculations 80−107687
binary alloy with metalloids, glass forming ability 79−86714
binary intertransition metal compounds, hardness and oxidation resist. 77−63773
binary systems, couple phase diagrams and thermochemical data 79−66037
binary systems, coupled phase diagrams and thermochemical data 79−66036
binary systems with Si, coupled phase diagram and thermochemical data 79−95997
braze alloys, low vapour press., binary eutectic, props., thermionic converter appls. 77−90236
catalyst surface mag. field effect on mol. dissoc. rate 80−16721
charge transfer and heat of form. in intermetallic cpds. with CsCl struct. 78−22689
clusters, chemisorption, alloying effects, model calc. 77−62751
cohesive properties, and press.-vol. relation 80−92476
compensation-point Hall effect temperature sensor 78−93679
Curie temperature, high press. effects *(Japanese)* 80−20444
d electrons as current carriers and electron scatterers 78−91689
density of states and complex band struct. for one-dimens. model 78−79919
diffusion of H transition metal-H systems 80−29219
dilute, electronic cofiguration and vol. of formation 79−90991
dilute, magnetic ordering phenomena in high mag. fields 80−50075
dilute, spin fluctuation contribution to elec. resist., field depend. 77−1413
dilute, spin glasses, mag. ordering, book contrib. 80−75787
dilute, transitional and noble metal impurities in simple metals, electronic struct. 77−43528
dilute alloy, size effect 79−99508
dilute alloys, component segregation to interfaces 79−51398
dilute alloys, Einstein's temp. and vibrational entropy, rel. to electronic struct. 78−83900
dilute ferromagnetic, itinerant d-electron(hole) degenerate, spin stiffness constant 80−70930
dilute magnetic alloys, props., review of theory 79−15282
dilute transitional impurities in transition and noble metal hosts, electronic struct. 78−75990
disilicides, chem. linkage, enthalpy, above 1200K 77−90324
disordered, bulk electronic structure 80−44467
disordered, density of states, elec. cond., extended Hubbard model 79−37948
disordered, effect of electron correl. on elec. resist. 79−47076
disordered, elec. resist., force-force correlation function approach 79−51541
disordered, formation energy of vacancies 77−27876
disordered, generalised perturbation theory, appl. to self-consistent calc. of ordering energies 78−75975
disordered, local densities of states 77−59244
disordered ferromagnetic, spin wave stability 80−70994
disordered transition alloys, generalized perturbation calcs. of ordering energies 77−4282
disordered transition host, actinide impurity localised magnetism 77−51883
domain struct. of diffuse ω-phase formed in quenching, 1D model 78−27523
elastic properties, vol. depend. 78−95103
elastic-plastic transition behaviour model *(German)* 80−75295
electron factors in the occurrence of sigma and structurally related transition metal alloy phases 79−46602
electronegativities, d-band hybridisation, structural stability 79−42007
electronic specific heat, near and weak ferromagnetics 78−80158
electronic structure, mag. props. 78−95254
electrospark alloying of Ti substrate residual stresses obs. *(Russian)* 77−56145
energy band filling *(Russian)* 78−6263
failure, statistical model, in conditions of monotonous cyclic loading *(Bulgarian)* 80−70296
FCC, ordered, atomistic approach to ordering 79−94947
ferrimagnetic, magnetic torque near compensation point 79−33472
ferromagnetic, BCC, spin wave stiffness constant 78−91851
transition metal alloys continued
ferromagnetic, effects of order on electronic struct. 79−90938
ferromagnetic, high-field susceptibility 80−7083
ferromagnetic, interstitial or substitutional sp impurity doped, electronic struct. 80−34384
ferromagnetic, local environment effect on atomic moments, itinerant model 78−68188
ferromagnetic, local ordering effect on spin wave stiffness const. 77−66282
ferromagnetic, mag. props., review 80−44823
ferromagnetic, with atomic short range order, local environment effects on electronic struct., Fe-V appl. 78−67936
ferromagnetic amorphous alloys, mag. props. 77−55690
ferromagnetic transition metal alloys, CPA appls. 77−72983
germanides, X-ray emission, absorption and photoelectron spectra *(Russian)* 80−11509
glasses and amorphous films, supercond. and electronic props. 79−73612
group IV, electronic basis for ω-phase stability 79−91616
group VIII aluminides, NMR near equiatomic composition *(Russian)* 80−20479
group VIII solvent metals, relations involving max. or min. liquidus temps. 79−15651
HCP hosts energy splittings of transition metal ions 78−67989
heat of formation, model predictions 78−35351
heat of formation 80−7849
heat of formation theory, tight binding approx. 79−43618
heats of formation, quantum theory 79−86907
heats of formation, tight binding theory, moments approach 79−61891
Heusler alloys, hyperfine fields and mag. interactions, NMR spectra 78−88222
high-melting-point, fast cooling from melt, cooling rate influence on struct. *(German)* 79−43287
Hume-Rothery Phases, electronic struct., main features 79−23883
hydrides and deuterides, conc.-temp. depend. of mag. susceptibility 80−29523
hydrogen dilute solns., pair potential anal., unrelaxed lattice model 79−65070
III to V group p-element binary alloys, correlation between phase diagrams *(Russian)* 79−15649
inter-transition metal phase constitution 78−39749
intermetallic compounds, containing d-transition metal, hydrogenated, magnetism 80−34609
intermetallic compounds of rare-earth and 3d transition metals, struct., props., review 78−10668
intertransition metal phases, incidence and Fajan's rule 79−29026
ion polarisation and point defect resistivity in metals 80−103672
isomer shifts, vol. corrected, charge flow and electronegativity 78−39470
lattice dynamics calculations, superconductivity parameters 79−7655
liquid, elec. resist. using t matrix 77−31988
liquid, electron charge transfer 77−1388
liquid, electronic struct. and elec. resist. 77−51647
liquid, magnetic properties, review 79−51741
liquid, struct., review 77−51304
liquid, thermoelectric power 78−91675
liquidus temperatures, max. or min., for solid solutions 79−78934
local environment and mag. props., transition metal impurities 78−64187
local environment and mag. props. in binary alloys, effect of disorders 77−63085
local environment effect on magnetic states 79−56491
local moment formation 78−43562
localised magnetic states, origin, doubly degenerate orbitals 79−78311
magnetic alloys, dil., transition metal hosts, props. review 78−84417
magnetic moment distribution, asphericity, temp. depend. 77−20538
magnetic properties, alloying effects on ferro-, antiferromag. state, band theory *(Japanese)* 78−47935
magnetically hard materials, technology, development *(Polish)* 77−89973
magnetically ordered, effect of magnetic field on P-T diagram 78−52246
magnetoresistance, low temp., calc. for nearly mag. alloys 77−59278
magnetovolume effects near crit. conc. for ferromag. 79−56591
metal-H system, exam. of excitation spectra and diffusion mobility of H using neutrons 80−29203
metal-H system, thermal neutron scatt., general multisublattice jump diffusion model 77−66045
metal-H systems, anelastic and plastic props., review 80−49298
metal-H systems under high H pressure, phase diagrams., electrical cond., mag. props. 80−29923
metallic glass, micromag. calcs. and props. 80−80501
metallic glass, splat cooled, mag. props. 80−80491
metallic glass alloys, computer simulation of atomic struct. 77−31598
metallic glasses, short range order of dense-random-packing models 80−64907
metallic glasses, structural model 79−14690
metallic glasses, transition metal-metalloid glasses, struct., compositional effects *(Japanese)* 80−84086
metalloid cryst. and glassy alloys, electronic struct. from magnetisation and Mossbauer meas. 80−29363
metalloid-transition metal alloy, glass transition temp. 80−24371
metalloid-transition metal amorphous surface alloys formed by ion implantation, TEM study 78−67730
nearly magnetic, low-temp. magnetoresist. 78−39091
neutron spin wave scatt., itinerancy, 3d alloys 77−73018
noble metal, dil., solute segregation and subsequent film growth in corrosive environment, model 79−24649
noble metal, dilute, residual resist. calc. 77−28156
noble metal, electronic structure from optical spectroscopy 77−48168
noble metal, liquid, reversal of electromigration direction 77−55374
noble metal, neutron activation determ. of microcomponents Pt, Pd, Ir, Rh *(Russian)* 77−32858
noble metal alloys, diffusion thermopower, phonon drag 79−65441
noble metal alloys, superconductivity, correlations and predictions 78−23192
noble metal homovalent alloys, thermopower at low temp. 79−65437
noble metal-Gd(Eu), dil., hyperfine fields of rare earth impurity, calc. 80−15486
noble metal-rare earth, dil., magnetotransport props., theory 78−39097
noble metals and their dil. alloys, de Haas-van Alphen studies, book 79−37966
noble metals and their dil. alloys, electronic struct., de Haas-van Alphen studies, book contrib. 79−37967
noncrystalline, elec. resistivity, Hall coeff., mag. susceptibility 78−95280

transition metal alloys continued
nonstoichiometric compounds, physicochem. props. depend. on short-range order struct. 80−100227
ordered, ground state properties, self-consistent calc. 78−91587
ordered BCC phases at high temp. 79−32948
photoelectron energy distrib. curves, rel. to band struct., book contrib. 80−16156
rare earth alloy amorphous film, magnetostriction, dipolar mechanism 78−95502
rare earth alloys, amorphous, electronic and mag. props. 80−93093
rare earth alloys, amorphous, mag. props., mean field anal. 79−4701
rare earth alloys, amorphous, mag. props. 77−72985
rare earth alloys, amorphous, struct. and mag. props., book contrib. 80−39818
rare earth alloys, amorphous films, radiation damage of domain struct. 77−66398
rare earth alloys, amorphous mag. anisotropy 77−66295
rare earth alloys, CPA calc. of mag. moments and transition temps. 78−84423
rare earth alloys, cryst. and amorphous, mag. props. 77−73008
rare earth alloys, magnetic amorphous films for mag. bubble memories, materials review *(Polish)* 80−34715
rare earth alloys, RM_2, (M=Fe, Co, Ni), magnetism, review 80−20365
rare earth alloys, RM_2, magnetostriction and struct. distortion 77−63248
rare earth alloys, $RM_2Si_{2-x}Ge_x$ and $RM_{4+x}Al_{8-x}$, magnetism and hyperfine interactions, magnetisation and Mossbauer effect studies 80−75892
rare earth alloys, RM_5, intermetallic compound $CaCu_5$ struct. crystal field pots. 78−43339
rare earth and actinide alloys, binary system constitution diagram interrelations *(Russian)* 80−7535
rare earth impurities, hyperfine fields, theory 78−68226
rare earth impurity, dilute limit model of mixed-valence effect 77−47768
rare earth intermetallic permanent magnets, props. and technology, book contrib. 79−65696
rare earth intermetallics, H absorpt., Mossbauer studies 80−39987
rare earth-3d transition metal amorphous alloys, crystallisation behaviour 80−49116
rare earth-M_4Al_8 (M=Cr, Mn, Fe, Cu) intermetallic cpd., magnetism and hyperfine interactions 80−25256
rare earth-M, amorphous film, microstruct. 77−51619
rare earth-transition metal (4f-3d) intermetallic cpds., mag. moment and mag. anisotropy 80−25107
rare earth-transition metal alloy, disordered, saturation mag. moment using CPA 77−20515
rare earth-transition metal alloy, H_2 absorpt. 77−35812
rare earth-transition metal alloy, R_xT cryst. struct. 77−55265
rare earth-transition metal alloys, amorphous, anomalous low-temp. props. 78−91872
rare earth-transition metal alloys, amorphous, ferrimag., spin arrangements in large fields 80−75718
rare earth-transition metal alloys, CPA calcs., moments and transition temps. 78−52252
rare earth-transition metal alloys, disordered, magnetisation behaviour 80−71099
rare earth-transition metal alloys, H_2 absorption, effect on mag. props. 78−68231
rare earth-transition metal amorphous alloy film, magneto-elastic tensors, pair model calcs. 78−80185
rare earth-transition metal amorphous thin films, mag. potential distribution and wall velocity meas. 80−34725
rare earth-transition metal amorphous thin films for thermomag. recording 80−20403
rare earth-transition metal film, amorphous, microstruct., TEM obs. 78−72018
rare earth-transition metal film, amorphous, microstruct. and magnetism 78−64230
rare earth-transition metal intermetallics, two sublattice system with high competing single ion anisotropies, model 80−39767
rare earth-transition metal Laves phase, thermodynamic exam. of formation 77−1241
rare-earth-transition metal amorphous films, domain structure, technique for observation 78−91914
resistivity anomalies 78−19018
resistivity at low temp., disordered ferromag. alloys 80−24919
resistivity temperature dependence due to localised spin fluctuations 77−8083
s-d hybridisation in d-band metals and alloys 78−91644
sigma phase occurrence, cluster model in tight-binding calc. 77−59750
silicide, Schottky barrier to Si, effect of glassy membrane 77−85311
silicide formation at Si-metal interface, obs. using interface marker technique 80−59734
silicide interface with Si, chemical state, AES expts. 78−91767
silicides, atomic volume deviations and supercond. T_c 80−75203
solid solutions, diffusion equation, during a decomp. process, role of nonlinearised terms *(Japanese)* 80−92723
solid solutions, max. or min. liquidus temps. 78−39741
specific heat and electronic structure *(French)* 77−28400
specific heat at low temp. 79−61155
spin distribution in transition metal elements and alloys, neutron diffraction expts. 80−25097
spin fluctuations effect on temp. depend. of elec. resistivity 78−47776
spin glass behaviour, simple itinerant model 78−84436
squared electron-phonon coupling constant, tight-binding calc. in transition metals and alloys 79−1571
static magnetic suscept. calc. *(Russian)* 77−77036
structural and thermodynamic props. of transition metal-group IIIB alloys *(German)* 78−91307
superconducting, transition temp., effect of transition metal impurities, role of s-d Coulomb interaction 78−88061
superconducting critical temperature, influence of s-d Coulomb interactions 78−31012
superconducting transition temperature, empirical correl. with Hall coeff. 79−78247
superconductivity, deformation and solute-induced microstructural effects 79−7925
superconductivity, relevance of mag. interactions 80−100545
surface magnetism 78−48025
surface segregation, electronic theory 77−43414
surface segregation 79−34044
ternary, phase diagram computed, occurrence of sigma phase 77−48399
ternary germanides, $(M,Nb)_{11}Ge_8$, M=V, Cr, Mn *(French)* 78−38675
transition metal alloys continued
ternary silicides, (Cr, Nb or Ta)$_{11}Si_8$, $(Mn,Mo)_{11}Si_8$, cryst. struct. *(French)* 78−38675
tight binding theory of heat of formation 79−28110
transition metal alloys, Wolff model of origin of localised mag. moments 79−61049
transition metal-hydrogen systems, eqn. for multiplateau isotherm, lattice expansion role 80−39252
transition metal-metalloid amorphous alloys, mag. props. review 78−52300
transition metal-metalloid glasses, struct., elec., supercond., and mech. props. 80−6365
transition metal-metalloid glasses, struct. and plastic flow, review 80−84090
transition metal-metalloid glasses, struct. model 79−64997
transition metal-nonmetal glasses, with defined local coordination, struct. model 80−84092
vacancy concentration and thermodynamic props. calc. in VIII-IIIA intermetallic cpds., BZ struct. 78−59801
valence of transition metal atoms 77−4288
volume anomalies, Invar effect 79−56490
X-ray, K-absorpt. spectra *(Russian)* 79−1796
XPS asymmetry of core electrons and electronic struct. parameters 80−93460
Ag-transition metal, dil., mag. impurities, electronic struct., KKR-Green's function calc. 80−65783
Al-3d transition metal, dil. alloy, preasymptotic charge oscillations around 3d impurities 77−36055
Al-3d transition metal, dil., electronic states, reson. model pot. method 79−77995
Al-3d transition metal alloy, dil., electronic charge density around impurities 78−34799
Al-based 3d-transition metal alloys, soft X-ray absorpt., electronic struct. 79−38690
Al-Fe-X-Si (X=transition metal), struct. and comp. by electron microscopy 80−88093
Al-M, 3d impurities, transport props., sp. ht. and supercond. crit. temp. calc. 77−1393
Al-M, dil., localisation of additional screening charge 79−47051
Al-M, dil., pre-asymptotic charge oscills. 80−20099
Al-M, dil., residual resist. of 4d and 5d impurities 77−28155
Al-M, dil., residual resist., influence of multiple scatt. effects 79−19570
Al-M, impurity binding energies 79−42096
Al-transition metal, residual resistivity, effect of 4d and 5d transition metal impurities 79−60791
Au-transition metal, residual resistivity, effect of 4d and 5d transition metal impurities 79−60791
Au-transition metal alloys, ^{197}Au Mossbauer isomer shift cellular atomic model 80−84673
B-transition metal, amorphous thin film, crystallisation, TEM obs. 79−19483
B-transition metal thin films, amorphous to cryst. transformation 80−7563
CC Ni_3Al, refractory transition metal alloying effects on ht. capacity 78−26691
Ce-M intermetallic cpds., M=3d transition metal, sorption of H_2, structural charges 80−88429
Co-3d transition metal alloys, hyperfine field and mag. perturbation distrib., NMR spectra meas. 79−61263
Co-transition metal, transition metal additives influence on struct., specific resistance, microhardness, mech. props., magnetic props. 79−29078
Cu alloy, mobility of boundaries, transition metal addition effects *(Russian)* 77−21160
Cu-3d transition metal alloy, dil., electronic charge density around impurities 78−34799
Cu-M, dil., 3d, residual resist., Dingle temp. 77−1409
Cu-transition metal, alloys, satellite NMR study, lineshifts and splitting 80−34786
Cu-transition metal, dil., mag. impurities, electronic struct., KKR-Green's function calc. 80−65783
Cu-transition metal, residual resistivity, effect of 4d and 5d transition metal impurities 79−60791
Cu-transition metal alloy, internal adsorpt. and mag. susceptibility, grain size effects *(Russian)* 78−19759
Cu-transition metal dil. alloy, virtual bound states 79−37975
Eu-T intermetallics, valence fluctuations 78−91649
Fe group transition metal metalloid binary alloys, metallic glass form., eutectic composition 79−74133
Fe-M, dil., hyperfine fields for transition metal impurities 80−80237
Fe-M, dil., impurity electronic struct., multiple scatt. approach 80−92856
Fe-M, effect of transition impurities on structural stabilisation 77−76552
γ-Fe-transition metal alloy, mag. moment in FCC d-metal lattices *(Russian)* 78−72337
Ga-transition metal, phase diagrams and cryst. struct. *(French)* 79−47659
GdM_x, M=3d transition metal, hyperfine interactions 78−19401
H production on illuminated transition metal surfaces, tight binding model 80−45812
H_2SO_4 decomposition, corrosion tests on possible containment materials 80−45448
Ir-M, intermetallics, enthalpies of form. 77−12595
LaM_5H_4, and LaM_5H_6, H_2 storage appl., desorption isotherms dependence on d-bandfilling 78−18912
$LaNi_4M$ (M=Pd,Ni,Ag,Cu,Co,Fe,Cr), H_2 storage appl., desorption isotherms dependence on d-bandfilling 78−18912
M-actinides, nearly mag., low-temp. magnetoresist. 78−39091
M-Cr-Al-Y, M=Ni,Fe,Co, coating for oxidation protection of Ni base TaC eutectic 77−40475
M-Ge, RF cosputtered system, supercond. props. 77−51835
M-H, mag. suscept. and quasirigid model *(Russian)* 78−26805
M-H interstitial solid soln. H coordination 77−24289
M-N system, phase diagram, stable intermetallic nitride phases 79−91622
M-noble metal spin glass films, mag. props. 80−60306
M-rare earth, amorphous, mag. props. 77−16054
M-Sb, electronic struct. determ. 77−4290
M-simple metal, dil., electronic states, reson. model pot. method 79−77995
M-Yb(Ce), valence state of Yb and Ce 79−77545
$M_{1-x}B_x$ amorphous film, crystn., TEM obs. 79−87019

transition metal alloys continued
M_1Si, elec. struct., X-ray spectra *(Russian)* 77−28106
Mg-noble metal, sintered, superconducting for heat and H_2 gas generation, seawater reaction 78−15607
Mo-iron group metal, binary and ternary alloys, induced codeposition from aq. soln. 79−95954
β'-Ni-Al-M, effect of 3d impurities on elec. resist. 77−69295
Ni-M, dil., high field susceptibility 78−52230
Ni-transition metal, deviation from Matthiessen's rule in elec. resist. 77−4319
$(NiAl)_{1-x}M_x$, M=3d transition metal, elec. resist. and magnetoresist. 77−43580
NpM_2Ge_2 (M=Cr, Fe, Co, Ni, Cu), Mossbauer and magnetisation meas. 77−1555
Pd-noble metal solid solns., with dissolved H, thermodynamic props. 80−108402
Pd-transition metal, dil., itinerant versus localised magnetism 78−64188
Pt-M, dil., mag. susceptibility and NMR meas. 78−39290
Pt-transition metal, dil., impurity resist. 80−92875
Re-based HCP-BCC binary systems, electronic struct. and supercond. *(Russian)* 79−33375
Sc_2M_3Si, M=Fe, Co, Ni, struct. determ. by X-ray powder method *(Russian)* 77−55261
Si-transition metal systems, Si stabilised C14 Laves phases 78−84777
Sm_2M_{17}, sintered magnet, hard mag. props. optimisation 77−8340
Ta, sintering with transition metal additions 78−15335
Te-M, liq. semicond., elec. props. 80−96870
Te-M, liquid, dil., elec. resist., cond. electron conc. 77−15814
Ti-based HCP-BCC binary systems, electronic struct. and supercond. *(Russian)* 79−33375
Ti-transition metal, transition metal additives influence on struct., specific resistance, microhardness, mech. props. 79−29078
V_3Si-M, M=Hf, Nb, Mo, W, Ni, cryst. struct., supercond. T_c comp. depend. 78−51494
Y-M intermetallic cpds., M=3d transition metal, sorption of H_2, structural charges 80−88429
Zn-transition metal, residual resistivity, effect of 4d and 5d transition metal impurities 79−60791

transition metal compounds
see also compounds of individual transition metals e.g. nickel compounds
see also copper compounds; gold compounds; silver compounds; transition metal alloys
2H layer compounds, theory of superstructures 79−99291
3d-cation solids, insulators, mag. ordering at low temps., exchange perturbation theory 77−69529
alkaline earth precious metal hexahydroxides, prep. and characterisation 79−90610
alkaline earth transition metal ternary and quaternary oxides, ATO_3, $ATi_{1-x}T_xO_3$, and $AZr_{1-x}T_xO_3$, prep., mag. props. and struct. 79−15277
ammine complex, mol. force consts. and vibr. amplitude 79−31727
antiferromagnetic salts, ^{111}Cd hyperfine fields, PAC meas. 77−48104
antifluorite, 5d transition metal crystal, struct. props. and lattice dynamics, mag. struct. 80−44268
antimonides, Mossbauer spectra 79−91324
arsenides (Ti, V, Cr, Mn, Fe, Co, Ni, Cu), oxidation, hardness and electromechanical polishing response 80−71776
band structure calculation 78−18956
band structure of transition metal-metalloid compound, nonorthogonality and tight-binding fit 80−59852
binary melt, transition metal halide+alkali halide, spectra by cryst. field theory 79−4820
bond lengths in oxygen and halogen compounds of d and f elements 79−37653
bonds between metal and H, C and P 78−42947
boride, abrasive props. 77−63808
borides, binding energies from X-ray photoelectron spectra 80−49170
borides, charge state of B, core electron binding energies *(German)* 78−10391
borides, cryst. struct., prep. methods, chem., elec., mag. props., appls., book contrib. 78−47307
borides, d-band contraction upon metalloid formation, resolution of bonding controversy 79−87041
borides, higher types, phys. props. and electronic struct., group orbitals-LCAO calcs. 80−20077
borides, mag. props., book contrib. 78−47978
borides, narrow band types, electronic density of states, many-electron Hubbard model calcs. 80−20064
borides, refractory, single cryst. prep. methods and characterisation, book contrib. 78−48296
borides, secondary ion sputtering, ionisation, energy distrib. characts., atom binding energy *(Russian)* 79−69940
borides, superconductivity search below 1K 80−20342
borides, XPS meas. and chem. bond 80−20761
borides (Ti, V, Cr, Mn, Fe, Co, Ni), oxidation, hardness and electromechanical polishing response 80−71776
borides of group IV-VI transition metals, reaction with phosphoric acid 77−1946
borohydrides, formation by reaction of transition metals with $NaBH_4$ or $CaBH_4$ in organic solvents 80−30223
carbide, behaviour in Cs or K plasma 77−20979
carbide, d-band effects in lattice dynamics contrib. to acoustic phonon freqs. 78−2207
carbide, effect of mech. props. on erosion resist. under spark machining conditions 78−11421
carbide, reactively sputtered, solar absorbing surface, struct. and optical props. 79−79407
carbide, supercond. transition temp. and phonon softening 78−14848
carbide emitters, review *(Japanese)* 77−63521
carbide solid soln. formation, elastic lattice deform. energy 77−84927
carbide-nitride solid soln. formation, elastic lattice deform. energy 77−84927
carbides, 3d metal, interatomic interaction 79−1569
carbides, adsorption of Cs(K), adsorpt. energy, thermionic emission 77−7978
carbides, APW bands rel. to covalent bonding 77−59245
carbides, brittle materials, swelling, blistering, p, d, and He ion irrads. porosity effects 77−35603

transition metal compounds continued
carbides, charge transfer from XPS core level chem. shift anal. 77−72837
carbides, d-band contraction upon metalloid formation, resolution of bonding controversy 79−87041
carbides, elastic moduli, scratch geometry, micromech. tests 78−35416
carbides, electronically driven phonon anomalies and phase transforms. 78−63834
carbides, generalised susceptibilities, electronically driven phonon anomalies, APW calcs. 79−42208
carbides, influence of implanted ions on supercond. transition temp. 77−28276
carbides, nitridation in NH_3 stream *(German)* 78−68928
carbides, oxidation of H_2 80−104462
carbides, phonon dispersion, three-body-force shell model 77−1191
carbides, secondary ion sputtering, ionisation, energy distrib. characts., atom binding energy *(Russian)* 79−69940
carbides, separation layer in X-ray tubes, C diffusion from graphite to W coating prevention *(German)* 80−105759
carbides, surface energy for brittle fracture from phonon frequencies 78−67790
carbides, surface energy for brittle fracture from phonon freqs. 79−86837
carbides, thermochemistry 79−43617
carbides, Ti substrate electrospark alloying, residual stresses obs. *(Russian)* 77−56145
carbides, X-ray investig. of abrasive action 77−52497
carbides (Ti, V, Cr, Mn, Fe), oxidation, hardness and electromechanical polishing response 80−71776
carbides of d-metals, band struct. calc., Fermi level *(Russian)* 78−39019
carbonitrides, physicochem. props., comp. depend. 80−55370
carbonyl complexes UV and X-ray photoelectron spectra, effect of adsorbed CO 79−4897
carbonyls, photoelectron spectra, time depend. relax. effects 77−71829
carboxylates, exchange interaction mechanism 78−10411
chalcogenide, possible anionic clusters and mixed valence effects 78−43333
chalcogenide layer compounds, convergent beam electron microscopy obs. 80−108689
chalcogenides, diffuse intensity contours, electron diffraction patterns 79−23504
chalcogenides, layered structure metals, transport props., book contrib. 77−43566
chalcogenides, Mott metal-insulator and mag. phase diagrams 78−10354
chalcogenides, $MS_3(Se_3)$, present status of research *(Japanese)* 80−20100
chalcogenides, photoemission, book contrib. 77−44133
chalcogenides, quasi-one-dimens., elec. mag., and supercond. props., review *(Russian)* 80−93022
chalcogenides, reversible electrodes appls. 80−61112
chalcogenides, stability criterion between spinel- and defect NiAs-type structs. 77−84696
chalcogenides, struct. and mag. props., book contrib. 77−43808
chalcogenophosphates, intercalation with n butyl-lithium, possible appl. in Li batteries 80−71446
charge density waves, electron density periodic modulation 79−56148
Chevrel phase compounds, bonding and phys. props. rel. to struct., book contrib. 80−49209
chlorates, neutron activated, radiation annealing 80−93569
chlorides, 4d-series, electronic struct. and spectra, multiple scatt. calcs. 77−83486
chlorides, exchange interaction mechanism 78−10411
chlorides, origin of 'white' line in K absorption 77−8685
closed electron shell occurrence, at. vol. additivity deviations 77−31630
cluster carbonyls. fluxionality, collective oscills. and low energy spectra 80−78738
clusters, bonding capabilities, MO calcs. 79−22589
complex, CNDO method for study of electronic struct. and props., review 77−88392
complex, coord. polymer with tetrazaporphin, one-dimens. conductor, band struct., EHT theory 79−90941
complex, LCAO-HFS-STO calc., basis set effects 80−52882
complex, linear chain type, synthesis 78−6047
complex, MX_3.b(hexamethylenetetramine).nH_2O, optical reflection spectra, mag. suscept. 79−56810
complex, octahedral $(MeF_6)^4$, fluorine ion Sternheimer antishielding, PAC meas. 78−10818
complex, surfaces, and supported catalysts, analogies among active sites 78−56917
complex anion, vibr. spectra in solid and soln., struct. and fundamental mode assignment 78−62803
complex ions, charges in HCl aq. soln., electrophoretic meas. *(Japanese)* 78−35698
complex ions, in HCl aq. soln., electrophoretic behaviour *(Japanese)* 78−35697
complexes, acetylacetonates, mag. susceptibility and optical reflection spectra 77−59381
complexes, counterintuitive orbital mixing in semiempirical, ab initio MO calcs. 78−90078
complexes, discrete variational $X\alpha$ cluster calcs. 80−15444
complexes, electron densities, local orbital populations, polarised neutron diffraction 80−88725
complexes, electron energy transfer processes 79−10143
complexes, excited states geometrical parameters, Franck-Condon anal. 77−27047
complexes, isothiocyanates with pyridine, far IR spectra, vibr. bands 78−25535
complexes, lattice energies calc. methods 80−107099
complexes, LCAO Hartree-Fock-Slater method calcs. 79−31374
3d complexes, low spin-high spin paramag. transition, Ising model calc. 80−93073
complexes, mag. exchange in s=1/2 systems 78−43553
complexes, mol. dissymmetry, book 80−27057
complexes, octahedral, optical rot. dispersion theory 77−77164
complexes, of 4-methylpyridine, IR and Raman spectra, vibr. anal. 78−25536
complexes, proton NMR chem. shift, covalency parameters calcs. 78−42098
complexes, reaction mechanisms and solvent effects 80−26012

transition metal compounds continued
complexes, tetragonal, d^5 ions, ligand fields and electronic struct., theory 77−6666
complexes, theory of bonds *(Hungarian)* 79−3340
complexes, vibronic coupling and spin relax. NMR decay rate study 80−18870
complexes, with 1,2,4-triazole, mag. susceptibility, 2-300K, struct., antiferromag. props. 77−77045
conference, Stuttgart, Germany, 12-16 June 1979 80−57002
coordination compounds, electronic energy transfer process 78−56907
coordination polyhedra classification 77−4088
crystal field theory and mag. props. for amorphous compounds 78−72318
cubic crystal field, energy matrices for pd^N electron system *(Japanese)* 79−42504
cyanides, octahedral, electronic struct., multiple scatt., mol. orbitals calcs., ESCA satellites 77−14488
d-orbital occupancies refinement, from X-ray diffr. data 79−68971
diborides, 3d metal, interatomic interaction 79−1569
diborides, C32-type, phys., chem. props., appls., review, book contrib. 78−47308
diborides, heats of formation derived from theoretical bonding model 79−65027
dichalcogenide, deform. modulated superstruct., model explaining results for VSe_2 78−51515
dichalcogenide, physical props., reviews *(Japanese)* 80−33969
dichalcogenide layer compounds, bonding and phase transitions 80−34186
dichalcogenides: ^{57}Fe, Mossbauer spectra, isomer shift 80−15885
dichalcogenides, 2H polytype, Hall coeff. sign reversals 77−80795
dichalcogenides, electronic struct. and band theory 80−44497
dichalcogenides, layered, electronic band struct. and bonding by atomic orbitals methods 79−15077
dichalcogenides, layered, optical phonon anisotropies 77−59573
dichalcogenides, layered, surface Brillouin scatt. obs., surface ripple and elasto-optic mechanisms 80−16048
dichalcogenides, layered materials, struct. changes rel. to CDW, TEM, electron diffr. 80−39042
dichalcogenides, modulation spectroscopy obs. 78−80377
dichalcogenides, octahedral intercalate ordering study by electron diffr. 80−15076
dichalcogenides, of CdI_2-type, crystallographic parameters correlation to heats of formation and reduced length 79−27963
dichalcogenides, optical phonon modes and localised effective charges, reflection spectra 78−76453
dichalcogenides, periodic lattice distortions, charge density waves 79−82536
dichalcogenides, phenomenological theory of CDW state, trigonal-prismatically coordinated layers 80−80200
dichalcogenides, phys. props., review *(Japanese)* 77−69225
dichalcogenides, phys. props. and CDWs, review *(Japanese)* 80−49635
dichalcogenides, stacking layer study, appl. of convergent beam electron diffr. 80−39116
dichalcogenides, US characts. rel. to Fermi surface geometry *(Russian)* 78−34749
dichalcogenides, zone axis electron diffr. patterns 78−34497
dichalcogenides prep. and growth, book contrib. 78−19650
diffusion of H transition metal-H systems 80−29219
dihalide, high temp. vapour photoelectron spectra 79−36697
dihalides, crystal field stabilisation energies, lattice energies 80−38994
dihalides, layer struct., lattice dynamics, calc. 80−65177
dihalides, MS potential from a set of overlapping densities 80−52850
dihydrides, band struct. and electronic props., electron-phonon coupling 79−47011
dihydrides, gas phase geometrical struct. calcs. 80−42951
dioxides, elec. struct. props., two-band model calcs. 78−67934
dioxides, electronically conducting with rutile struct., electrode material behaviour 78−31656
direct exchange between $3d^n$ ions 79−69668
disilicides, powdered, determ. of free metals, oxides, photometric method 78−61101
divalent halides, Coordination equilibria in non-aqueous solvents. I 80−66860
electrical conductivity minimum near metal-insulator transition 78−30960
electrical resistivity, saturating contrib. from electron-phonon interactions 80−2376
electromechanical polishing method 78−53073
electronic excitation energy calc. correl. energy correction 78−17576
electronic spectrum calc. by GO-LCAO method *(Russian)* 79−73420
electronically driven lattice instabilities, role of p-d hybridisation 78−63835
electronically driven lattice instabilities, role of p-d hybridisation 79−7669
ESCA spectra, intense shake-up satellites, model 78−50589
ferrocyanide selective sorbents for alkali metals, sorptive props. w.r.t. struct. 80−101051
ferrocyanides, crystal structures and ion-exchange props. 77−15362
fluoride, antiferromag., magneto-optical effect in longitudinal mag. field *(Russian)* 77−85694
fluorides, electron affinities and ionis. pots. MS $X\alpha$ calcs. 79−10031
fluorides, flux growth 79−65991
fluorides, potential exchange theory in mag. insulators 78−19242
formation, Miedema's empirical theory, microscopic basis 80−45541
germanides, binding energies from X-ray photoelectron spectra 80−49170
germanides, Mossbauer spectra 79−91324
germanides, X-ray emission, absorption and photoelectron spectra *(Russian)* 80−11509
group VIa, layered dichalcogenides, hole reactions, electrochem. solar energy conversion appl. 79−7893
group VIb, oxides, oxysalts, reduction kinetics and mechanism 77−77733
halides, cryst. field stabilisation and lattice energy 80−75201
halides, electron spectroscopy of crystals, book 80−36786
hexaaquo ions, proton mag. relax., spin delocalisation effects 78−62827
hexafluorides, quadratic Jahn-Teller vibronic coupling calcs. 79−6881
hexahalide complex, polarised reson. vibr. Raman spectra, electronic degeneracy effects 78−78708
hexahalometallates IV, d-electron config., effects on phase transitions 77−35687

transition metal compounds continued
high spin compounds, X-ray and photoelectron spectra, one-config. approx. 78−92145
hopping among inequivalent octahedral sites in body-centred tetragonal lattice 79−1520
Hubbard model, two band, mag., orbital and charge ordered states 78−27012
hydrate complexes, first series, physicochem. props. CNDO calcs. 79−41110
hydrate complexes, first series, struct., bond energies, CNDO calcs. 79−41111
hydride complexes, struct. geometry bonding, neutron diffr. studies 79−46641
hydrides, binary, heats of form. 80−97725
hydrides, electron-phonon interaction const. calc. 79−65160
hydrides, electronic states calc. 79−7769
hydrides, electronic struct., heat of formation, single particle lifetimes, Dingle temp. meas. 78−51923
hydrides, H ordering, review 80−60850
hydrides, homoleptic, electronic structure, ab initio calcs. 79−89601
hydrides, IR spectra, vibr. levels, struct., H_2 chemisorpt. appl. 77−48686
hydrides, isotope effects on supercond. props. 79−65580
hydrides, magnetic props., book contrib. 79−82754
hydrides, Mossbauer studies, book contrib. 79−82906
hydrides, occurrence in slow field evaporation 77−85903
hydrides, proton diffusion mechanisms, NMR determ. 77−90060
hydrides, struct. change from metal struct., due to interaction of metal with H 80−49196
hydrides, supercond., isotope effects, depend. on cryst. field energies 79−56353
hydrides, synthesis and physicochemical props., conf., Moscow, USSR (Jan. 1978) 80−27032
hydrides (binary ternary systems with metallic cond.) review of research on catalytic props. 80−30273
hydrides and deuterides, conc.-temp. depend. of mag. susceptibility 80−29523
hydroxide layered materials, prep. and growth, book contrib. 78−19649
intercalation complexes with TaS_2, NbS_2, and $NbSe_2$, mag. and metallic transport props. 80−44814
interstitial compounds, electronic structure and useful phys. props. 77−89683
iron-transition metal oxinates, Mossbauer spectra 77−90082
Jahn-Teller effect in solid state chem. 79−47061
Jahn-Teller induced high spin-low spin transitions 79−69676
laser shaping, erosion resistance increase obs. *(Russian)* 77−53871
layer compounds, charge density wave transitions 77−59116
layer compounds, Fermi surface anisotropy effect on struct. transitions 77−51661
layer compounds, mag. model, 0K phase diagram, spin wave spectrum 79−87273
layer dichalcogenide, diffuse intensity contours in electron diffr. patterns, struct. interpretation 80−38878
layer materials, SXAPS interpret., cond. band self-convolution model, cryst. field splitting 78−23558
layered, superstruct., excitonic wave-phonon coupling 77−15775
layered compounds, book 77−39757
layered dichalcogenides and their intercalation compounds, physical props., review 78−27443
layered oxides, struct. classification and props. 80−39046
ligand field problems, group theory 80−42920
ligand field spectroscopy, selection rules, intensity enhancement of forbidden transitions 80−45049
ligand fields calcs., strong and intermediate fields, tensor algebra 80−42922
localisation of electrons, review 80−49650
lower carbides, Group IV-VI metals, thermal expansion coeff., rel. to bond energy 78−2266
magnetic clusters, neutron inelastic scatt., review 80−50083
magnetic ordering phenomena in high mag. fields 80−50075
magnetic oxide, polycryst., dynamic susceptibility of bulging domain wall model 78−23296
metal-H system, constitution diagrams and hydride struct. form. 79−24509
metal-H system, exam. of excitation spectra and diffusion mobility of H using neutrons 80−29203
metal-insulator transitions 80−59874
metal-rich compounds, struct. and props. 78−95045
metallic glass, mag. props., charge transfer model 78−39324
metalloid atom solubility and electronegativity difference correl. with phase stability and d-electron/atom ratio 78−6914
mixed halides, A_nCY_6, spectra by cryst. field theory 79−4820
mixed valence complexes, quasi-one-dimens., elec. props. at ultrahigh press. 78−2470
mixed valence compounds, charge-orbital ordering 78−39069
MO_4^{n-}, intramol. force fields 79−45693
molecule, SINDO/F theory of electronic struct. 80−69075
monoantimonides, 3d-states, optical evidence for analogy with transition metals 77−62816
monocarbides, Group IV-VI metals, thermal expansion coeff., rel. to bond energy 78−2266
monocarbides of subgroups IVa and Va, kinetic props., review 78−47613
mononitrides, 3d metal, interatomic interaction 79−1569
monosulphides of first-row metals, XPES and UV PES 80−20760
monoxides, 3d, ground state electronic struct., atomic sphere approx. 80−59855
monoxides, 3d metal, specific vol. and mag. moment calcs. 80−65822
monoxides of 3d elements, metallic and insulating, binding and stability 77−76760
Mulliken electronegativity scale, struct. stability 79−23562
niobates, columbite struct., IR and Raman spectra *(French)* 78−19485
niobates, columbite struct., normal coord. anal. 78−964
nitride, atomic struct. *(German)* 79−90622
nitride formation by N_2^+ ion beam reactions with first row transition metal surfaces 79−96363
nitride solid soln. formation, elastic lattice deform. energy 77−84927
nitrides, APW bands rel. to covalent bonding 77−59245
nitrides, d-band contraction upon metalloid formation, resolution of bonding controversy 79−87041
nitrides, lattice sp. ht. and phonon anomalies 78−63867
nitrides, liquid interactions, ab initio LCAO MO SCF calcs. 79−18256

transition metal compounds continued
nitrides, surface energy for brittle fracture from phonon frequencies 78−67790
nitrides, surface energy for brittle fracture from phonon freqs. 79−86837
nitrides, thermionic emission, review *(Japanese)* 77−63522
nitrides of group IV-V, laser irrad. action, erosion strength *(Russian)* 77−56112
nitroprussides, Mossbauer spectra, dehydration effects 79−24237
nitrosyls, ab initio HF calcs. 78−90082
nitrosyls, appl. of HF and CI calcs. 80−9513
noble metal complexes, hexafluoro, review of struct. obs., pseudorot., press. effects 78−6045
nonstoichiometric compounds preparation probability thermodynamic approach 77−31611
octahedral ions and molecules of 2nd and 3rd row metals, force consts. 77−54548
one-dimensional magnetic compounds, orbital interaction 78−6494
oxalate hydrates 77−44143
oxalato complexes, photochemical separation 77−60082
oxide, d-electron (hole) degenerate, Mott transition, electronic and mag. phase diagrams 78−51894
oxide, excitonic waves, role in distortive transform. 77−11861
oxide, extended defects, review 78−63753
oxide, tracer diffusion obs., RF sputtering as microsectioning technique 78−14499
oxide catalysts, reduction, cryst. defects influence, in-situ electron microscopy 80−81322
oxide perovskites, UPS, XPS, X-ray absorpt. spectra, band struct. study 79−56885
oxide reactions with phosphoric acid melts, form. and analysis of phosphates 77−12517
oxide surfaces, UPS, LEED and AES studies of mol. adsorption 79−4480
oxides, 3d metal, interatomic interaction 79−1569
oxides, 3d-, microwave cond. at high temp. *(Japanese)* 78−91715
oxides, ⟨100⟩ coincidence twist boundaries energy 80−107270
oxides, absorption spectra, in flame, optogalvanic spectrosc. obs. 79−18202
oxides, APW bands rel. to covalent bonding 77−59245
oxides, corrosion, defect. struct. and cation transport 79−100277
oxides, cryst. electronic polarisabilities and ion sizes, Madelung pot. effects 78−63693
oxides, cryst. field stabilisation and lattice energy 80−75201
oxides, crystal field effect on isothermal bulk moduli 78−61364
oxides, crystal field stabilisation energies, lattice energies 80−38994
oxides, d-band perovskites, concepts of surface states and chemisorption, book contrib. 80−107651
oxides, defect struct. review 79−42052
oxides, defects, coordination, topology, struct. 77−51367
oxides, determ. in powdered disilicides, photometric method 78−61101
oxides, dielec. and thermophys. props. 77−52009
oxides, dielec. behaviour 78−71703
oxides, doping of $LiNbO_3$, absorption spectra temp. depend. 77−90176
oxides, electronic polarisability of ions 77−40175
oxides, energy loss spectra, ion polarisability 78−68585
oxides, Li incorporated, topochem. reactions, chem. prep. and characterisation 80−61115
oxides, potential exchange theory in mag. insulators 78−19242
oxides, pressure-induced high-spin-low-spin transitions 78−85549
oxides, refractive index and extinction coeff. 79−78643
oxides, struct. transition, excitonic wave-phonon coupling 77−15775
oxides, surface oxidation, study by AES 80−45175
oxides, XPS, trapped electrons at F-centres and anion defects, photoionis. cross sections 77−90249
oxides+Li topochemical reactions in high energy batteries, solid state electrode materials 80−55836
oxides and fluorides, thermal expansion and MP correl. 77−47605
oxides cryst. growth, using $K_2S_2O_7$ as flux material 80−71582
oxides in binary tellurite systems, glass form. range 78−71680
oxyanions, tetrahedral, kinetic and pot. consts. calcs. 77−30951
oxygen-containing, X-ray Lα emission spectra, excited states calcs. 79−59488
paramagnetic complexes, nucl. spin-lattice relax., electron spin density matrix theory 78−13521
perovskitelike compounds, covalency effects, partial densities of p- and d-states, photoelectron spectra 79−38718
phonon anomalies due to d-band effects, electron-phonon matrix elements 78−30720
phonon anomalies rel. to superconductivity 77−12055
phosphides, NaCl struct., supercond. props. 79−4613
phosphides, valence electron energy spectrum, deduced from X-ray spectra and XPS 79−99984
phosphides, valence-level struct., X-ray spectra and X-ray photoelectron spectra calcs. 79−64044
photoelectron energy distrib. curves, rel. to band struct., book contrib. 80−16156
pnictides, Ab_2X_2, A=rare earth, B=Fe, Co, Ni, X=P, As, Sb, cryst. struct. 78−51502
pnictides, atomic volume, semicond. props. 78−59780
pnictides, displacive and mag. transitions 80−59616
polynary oxocompounds, struct. data, book 78−51521
porphyrins, quasiline absorpt. spectra, metal and substituent effects 77−34628
pyrite structured 3d-transition metal chalcogenide mag. props. from Mossbauer effect obs. *(Japanese)* 80−15933
pyrites, mag. and elec. props., review *(Japanese)* 78−47941
Q-switching transition-metal dithiene complex dyes for 0.9 to 1.4 μ lasers 80−1200
rare earth-transition metal garnets, $R_3M_5O_{12}$, amorphous films for mag. bubble memories, materials review *(Polish)* 80−34715
rare earth-transition metal hydrides, electronic and mag. props., Mossbauer study 80−34830
rare earth-transition metal hydrides, magnetic props., book contrib. 79−82754
reduced ionisation potentials as parameters in superconducting transition temp. calcs. 80−75671
refractories, electron and phonon behaviour 80−54624
refractory carbides, thermodynamic evap. characts., cluster-component calcs. 78−51704
refractory materials, slip and microhardness 78−3211
transition metal compounds continued
refractory metal compounds, electronic structure and chem. bonding 79−27948
refractory metals and oxides, reactions of liq. alkali metals, relevance to reactor technology 80−85173
rock salt struct., surface energy bands, Shockley surface states, bonding 80−92956
second row oxides, XPS 80−87170
selenide, d-electron (hole) degenerate, Mott transition, electronic and mag. phase diagrams 78−51894
selenides, NaCl struct., supercond. props. 79−4613
semiconducting glasses, containing transition metal ions, elec. props. *(Rumanian)* 78−47791
silicide, reactively sputtered, solar absorbing surface, struct. and optical props. 79−79407
silicides, 3d transition metals, photoelectric-yield spectrum of Si, complete energy diagrams 77−28680
silicides, atomic volume deviations and supercond. T_c 80−75203
silicides, binding energies from X-ray photoelectron spectra 80−49170
silicides, growth and characterisation 80−66408
silicides, Mossbauer spectra 79−91324
silicides, refractory for ICs, review 80−100820
silicides, self-propag. high-temp. synthesis 80−2988
silicides of groups IV-VI thermal cond., 20-1000°C 79−10992
SINDO theory 77−50359
specific heat and electronic structure *(French)* 77−28400
spectra, cryst. field least squares fitting interpretation 80−44548
spectral intensity, Laporte forbidden transitions, ligand polarisation model 78−64378
spinel solid solutions, $A_xB_{3-x}O_4$ type, quasichemical method of cluster components, electron exchange allowance 79−51475
spinels, MCr_2O_4 and MV_2O_4, valency and ionicity rel. to magnetism 78−52229
sulphate hydrates, systematic cryst. struct. differences *(German)* 77−84724
sulphates, exchange interaction mechanism 78−10411
sulphide, d-electron (hole) degenerate, Mott transition, electronic and mag. phase diagrams 78−51894
sulphides, displacive transitions, theory 80−59616
sulphides, ion bombardment damage, XPS obs. 80−97404
sulphides, liq. and solid, thermochemistry 78−23962
sulphides, NaCl struct., supercond. props. 79−4613
sulphides (Fe, Co, Ni, Cu), oxidation, hardness and electromechanical polishing response 80−71776
sulphides of nonmagnetic transition metals, semicond. props. rel. to at. vol. 78−64037
superconducting critical temperature, influence of s-d Coulomb interactions 78−31012
superconducting properties, lattice symm. and instability 77−8224
superconductors for strong magnetic fields *(Czech)* 78−23213
superexchange interaction, effective spin-orbital Hamiltonian 80−70998
superexchange interaction, multielectron theory 80−70997
surface properties, review 80−84349
TCNQ salt, alkali transition metal, elec. cond. and phase transition 78−43370
tetrahalogeno anions, ligand field spectra, MO model 78−17654
tetrahedral complex ions, F NMR chem. shifts, outer sphere cation effects 80−102527
tetrametaphosphates, cryst. struct., high press. effects *(French)* 77−15373
transition metal complexes, O containing, coordinate bonding, charge transfer electronic bands, complex struct. determ. 80−52977
transition metal complexes, octahedral substituted, ligand-fluid splittings, accidental degeneracy origin 80−10932
transition metal phosphate glasses, ohmic contact and dielectric. relax. 79−65795
transition metal precious metal hexahydroxides, prep. and characterisation 79−90610
transition metal systems, ESR studies, polarised absorption, ligand field model, group theory applications 80−43077
transition metal-carbonyl cluster molecules, electronic struct., localised orbital pseudopot. method 80−39653
transition metalloids, t-matrix theory of thermal and nonstoichiometric softening 79−86788
tricarbides, atomisation energy, stability, mass spectrometric determ. 79−7037
trifluorides, mol. and electronic structs., ab initio restricted Hartree-Fock calcs. 79−63900
trinuclear carbonyl complexes, electronic structures. and spectra 79−59480
valence band structure, X-ray spectroscopic study 80−29319
vanadates, elec. and mag. props., stoichiometry 78−51991
vanadates, elec. and mag. props. 79−78094
vibronic induced transitions, structural form of intensities vibronic intensities 78−90145
X-ray emission K-lines, of transition elements, free-atom approx. applic. 80−11513
X-ray photoelectron spectra, satellite lines *(French)* 77−36363
XPS, anal., approx. mol. orbital theories 77−18975
XPS, effects of electron transfer on shake-up satellites, model calc. 78−95650
XPS, satellite lines 77−12488
XPS asymmetry of core electrons and electronic struct. parameters 80−93460
zeolite of transition metal, CO adsorpt., ^{13}C NMR study 79−52751
AF_n^{x-} compounds, A-F nucl. spin-spin coupling, ligand influence 77−14454
Co^{3+} d^6-complexes and oxides, spin-state transitions, PES study 79−100014
double oxides, exam. of elec. cond. 78−51990
$KM^{II}M^{III}F_6$, (M=1st row transition metal, Zn, or Mg), divalent and trivalent ion distribs., Mossbauer obs. 78−2777
Li_xMO_2, M=Mo, W, Os, Ir, Ru, intercalation compounds, mag. props., decomposition effects 80−25075
$(M,M')_6Si_5$, M=V,Cr,Mn, M'=Ti,Nb,Ta, cryst. struct. *(French)* 77−43193
M ion photoemission spectra, multiplet and cryst. field splitting 77−66577
M-Ne compound ions, slow field evaporation 77−48322
M-O systems, exam. of phase diagrams and crystal structure 79−8291

transition metal compounds continued
M-R-B systems (R=rare earth), phase diagrams and struct. considerations 80−16286
MBr_2, 90° exchange interactions 79−69666
M_2C, struct. and phase transitions 79−70051
$M(CN)_5X^{n-}$ complexes, ^{13}C NMR, chem. shifts 79−51866
MCl_2, 90° exchange interactions 79−69666
MF_2, 90° exchange interactions 79−69666
MF_6 crysts., density of exciton states, two-particle and mixed cryst. spectra 78−2829
$M_xGe_yB_3$, metallic resist. mag. suscept. 79−42731
MI_2, 90° exchange interactions 79−69666
$M_{2-x}Mo_xAs(P)$, crystal struct. *(French)* 77−47429
$M_3Mo_3S_4(Se_4)$, prep. from $Mo_3S(Se_4)$ by topotactic reaction 77−90598
M_2N struct. and phase transitions 79−70051
MO, 90° exchange interactions 79−69666
MO, electronic polarisability of ions 77−19901
MO_2, defect struct., nonstoichiometry and elec. cond., pentavalent oxide dopant effect 80−24442
MRh_4B_4 (M=trivalent transition metal, usually rare earth) supercond. and ferromagnetism, role of Sc 78−95438
MU_8X_{14}, (X=S or Se), mag. susceptibilities 79−61073
$M_{2-x}W_xAs(P)$, crystal struct. *(French)* 77−47429
MY_4^{n-4}, MY_6^{n-6}, alkali metals and alkaline earth outer-sphere cations, spectroscopic splitting parameters 78−39075
Mn-Zn series, aqueous solutions, equilib. props. struct. 79−61894
$Sm_{1-x}M_xS$, valence charges, band struct. 80−20131
third row oxides, XPS 80−87170

transition metals
see also the individual transition metals e.g. nickel
see also copper; gold; silver
$3d^N$ ions, free and in crysts., Slater parameters and 3d-4s excitation energies 78−33433
3d, core electrons, Sternheimer shielding-antishielding factor 80−39534
3d, cryst., electron struct. 79−69455
3d, cryst. field potential calc. 77−59366
3d, electron-electron interaction, X-ray excited Auger spectra 78−91631
3d, electronic states, diluted in Al 78−64005
3d, energy parameter, Auger spectra, quasi-atomic behaviour 77−20966
3d, ESR for valency assessment, appl. to ceramics and glass industries *(German)* 80−34757
3d, Hall effect, electron scatt. processes 80−34419
3d, impurity in Cu, residual resistivity for electrons scatt. by spin-depend. potentials 77−39829
3d, M III excited states, radiative lifetimes, beam-foil obs. 77−30979
3d, paramag., energy band calcs. 78−91608
3d, superatomic relax. and positions of inner levels 78−11069
3d impurities in Al, self-consistent spin density functional calcs. 80−70635
3d metals, electron struct. plasmons 79−77996
3d system, configuration based quasi-particles 78−91648
3d-metal, ferromagnetic, spin-orbital interaction effect on NMR, g-factor anisotropy *(Russian)* 77−24752
3d-metal, X-ray emission and XPS broadening, many-body effects and intra-atomic exchange 77−44090
3d-metals, electron impact excited soft X-ray spectra, resonances and many body effects 80−50468
4d, adsorption on Mo (110) and (100), surface reson. states, tight-binding calc. 78−71982
4d, cathode, work function of electropositive metal coadsorbed with O_2, thermionic emission obs. 78−11064
4d, energy bands, s and d contribs. to eqns. of state 78−30865
4d, film, optical absorption meas. using synchroton radiation, 20-250 eK 77−12457
4d 78−92144
4d BCC, electron-phonon interactions 79−95107
4d BCC, phonon dispersion 79−95102
5d, cathode, work function of electropositive metal coadsorbed with O_2, thermionic emission obs. 78−11064
5d, single adatom on W (110), dipole moment, field emission meas. 77−47674
acoustic wave induced elec. field gradient 79−38034
adatom and substitutional impurity atom interaction at metal surface 79−56076
adatom surface diffusion characts., pair potential calcs. 80−39446
adhesion between two arbitrary metals, theory *(Russian)* 77−44455
adsorption, of alkali metals, valence electronic struct., wave-function matching calcs. 78−72235
adsorption of CO, AES obs. 77−35818
adsorption of CO, electronic struct., localised orbital pseudopot. method 80−39653
adsorption of rare-earth atoms, effects of changes in valence state 79−69367
adsorption of simple gases, phase transitions in adsorbed films 77−51606
adsorption systems, transition metal atoms interactions with PF_3 and CO ligands, MO calcs. 79−85896
AES, high resolution LMM, first row transition elements 78−15263
alkali lime germanosilicate glasses, optical absorpt. of transition metal impurities 80−2784
alloying and cpd. form. of later transition elements, graphical rep. 77−19895
amorphous, density of electronic states, effect of struct. variation due to interatomic pot. softness 80−54597
amorphous, elec. resist. 78−60103
amorphous, exhibiting Mossbauer spectra, mean mag. props. *(French)* 80−80489
amorphous, prep. and struct., rel. to liq. struct. 77−51323
amorphous, superconducting transition temp. *(Chinese)* 80−54817
amorphous and liquid states, simulated models 79−14733
Animalu transition-metal model potentials, nonlocality 78−6250
anomalous diffusion in omega forming systems 78−63873
APS, soft X-ray, 2p-shell, theory 79−87527
atom, 3-d, density functional theory 78−58578
atom, ion, solid, $M_{2,3}$ excitation spectra 78−91653
atom, ionisation pot., electron impact expts. 79−45849
atom, many-config. approx. in X-ray and electronic spectra interpret. 80−32615
atom, mixing of $3d^n4s^k$ configurations 79−63910
atom, Racah parameters, atomic screening parameter Slater and Clementi-Raimondi values 80−69071

transition metals continued
atom, Yb II, III to Bi XV, XVI isoelectronic sequences, wavelengths and ionisation energies 77−429
atom+O ion collisions, A=16, 18, K-X-ray production 77−23554
atomic and ionic hyperfine interactions, relativistic effects on core-polarisation contrib. 77−67990
atomic cluster total energy, diatomics-in-mol., LMTO calc. pot. curve, Lanczos eigenvalue method 78−9291
atomic correlation energies of 1st transition period, perturbation calc. 79−36508
atomic volumes 77−68943
atoms, CNDO/S method extension, parametrisation procedure *(French)* 80−9511
atoms, first-row, 3d orbital calcs. using Gaussian basis sets 77−65422
atoms, neutral and ion val. states, electron correlation, ab initio effective val. Hamiltonian calc. 80−99449
atoms, vertical analysis, third row atoms, ionisation pot., term value, correlation energy 78−41964
atoms and ions, electron affinities and ionis. pots. MS $X\alpha$ calcs. 79−10031
Auger effect, $K \rightarrow M^2$ radiative, low energy satellites meas. 80−45174
Auger relaxation energy theory 80−7446
Auger spectra, L_3MN, characterisation and electron delocalisation in 3d metals 77−48315
band model, mag. susceptibility of exchange-enhanced paramagnet 78−2644
band structure, appl. of X-ray spectroscopy *(Polish)* 79−56887
band structure, OPW and MOPW calcs. 79−90942
band structure, parametrisation via Hubbard's scheme 77−31938
band structure of 3d-, 4d-, and 5d-series from spectral data and theoret. calcs. *(Russian)* 77−8013
band theory, rel. to bulk props. and cryst. struct. trends 78−34757
BCC, 3d series, numerical calc. of orbital mag. susceptibility 79−82764
BCC, electronic struct., model Hamiltonian interpolation scheme 77−47723
BCC, films, optical props. 79−78781
BCC, interaction energy between self-interstitial and screw dislocation, calc. 80−70248
BCC, isothermal compression to 100 kbar 78−43069
BCC, lattice dynamics calc. 79−19329
BCC, neutron spectroscopy of fast H diffusion 80−59731
BCC, phonon dispersion curves and elastic, calc. using cohesive energy 78−59885
BCC, phonon dispersion relations, Fielek five-const. model calc. 80−34150
BCC, point defects chem. binding energy 79−82260
BCC, solubility, heat of solution calc. for H impurity 78−6160
BCC, solubility of C 78−71861
BCC, supercond. transition temp. and pressure effects 77−4461
BCC structure, elect. cond., electron lifetime affecting electronic props. 79−15134
BCC transition metals, screw dislocations, electronic theory, Peierls stress, core energy calc. 78−71737
bimetallic cluster, photoselective bimetallic aggregation, review 80−53182
binary systems, coupled phase diagrams and thermochem. data 78−60647
binary systems, coupled phase diagrams and thermochem. data 78−60648
binary systems, coupled phase diagrams and thermochem. data 78−80511
in borate glasses, electronic struct. 78−10347
borosilicate glass, influence of Ti on absorption spectra 77−12403
bulk modulus, correl. effects, equilib. lattice spacing 78−10115
bulk modulus, effect of correlations and ferromag. order 78−34564
catalyst surface mag. field effect on mol. dissoc. rate 80−16721
Cauchy discrepancy with supercond. transition temp. 80−84533
charge perturbation due to impurities, theory 79−23924
with chemisorbed layer, semiempirical model calcs., extended basis set 77−72793
chemisorbed layer of alkali metals, changes in work function due to charge transfer 78−18900
chemisorption, model Hamiltonian, specially parametrised 77−11785
chemisorption, of H, Hubbard-type surface mol. model binding energy calcs. 78−71990
chemisorption, of light gas atoms, on (100) surface, model calcs. 77−11797
chemisorption, theoretical model, formalism 80−6651
chemisorption of H_2, Anderson model, including correlation and overlap effects 77−76662
chemisorption of H_2 and O_2, chemisorpt. energy trends 80−107631
chemisorption of H, effect of surface spin fluctuations 80−75613
chemisorption of H, O and CO 78−2378
chemisorption of ordered atomic layers, HF Green's function formalism and phase shift technique 80−24733
chemisorption of ordered overlayers with C(2×2) and (2×1) structs. 79−46925
chemisorption of single atom, relax. shifts and singular broadening in spectra 77−59203
chemisorptive bonding of CO, photoemission investig. using synchrotron radiation 77−12498
cluster, cohesive energy and level statistics 78−95267
cluster, local densities of states and bonding props. 77−20401
clusters, chemisorption, alloying effects, model calc. 77−62751
clusters, particle size rel. to bulk metallic props. 80−44490
clusters, symmetric, higher order isotropic exchange, Schrodinger exchange model 79−7955
cohesion, local-density approx. to exchange and correlation effects 77−47749
cohesive and elastic props. model *(Hungarian)* 80−34120
cohesive energies, many-electron systems, self-interaction corrected approach, beyond local spin density approx. 80−92844
cohesive energy, lattice consts. and bulk modulus, renormalised atom method 77−43170
cohesive properties, correlation effects 77−69262
complex ion in aqn. soln. HCl, temp. effect on electrophoretic behaviour 79−24757
complex ions in aq. HCl, temp. gradient chromatography *(Japanese)* 78−61120
conduction electron behaviour and role of electron-ion and electron-electron interactions *(Japanese)* 77−66102

transition metals continued
conference, Toronto, Canada (Aug. 1977) 78−91577
core levels between surface and bulk atoms, variation of binding energy shifts 80−88615
core photoelectron spectra, of metal with incomplete shell, spin-depend. final-state interactions 77−69965
correlation effects, perturb. treatment within Hubbard model 80−70582
correlation effects, perturbation treatment 80−59897
corrosion due to V_2O_5 melts *(Japanese)* 80−93691
corrosion potential/time, and potentiostatic polarisation curves as a method of predicting corrosion 80−45419
covalence of atoms in heavier transition metals 78−47274
cubic, phonon dispersion, Fielek and extended Cheveau models 78−22801
d electrons as current carriers and electron scatterers 78−91689
d metal, distance separating dislocation, determ. by positron-electron annihilation method 79−14811
d-band metals, chemisorption, book contrib. 80−107649
d-d electron correlations in cohesion and ferromagnetism 77−62810
d-metals, electron Fermi liquid oscillations *(Russian)* 79−90979
deep impurities in semiconductors, SCF CNDO cluster calcs. 80−100442
determination, in geological samples, by X-ray microscopic chem. microanal. 78−20527
determination in estuarine and sea water by at. absorpt. spectra 79−74557
determination in powdered disilicides, photometric method 78−61101
diffusion in Si, anomalous behaviour 80−29044
diffusion into liq. Fe *(Russian)* 78−79791
diffusion mechanism for group IV metals, based on geometric configuration, analogous to chemical compound omega phase *(Russian)* 79−14956
diffusion of C, electronic state effect *(Russian)* 77−1264
diffusion of H 78−47596
diffusion of H 80−29219
dilute impurities in noble metal hosts, exact Green function treatment 77−62856
dilute impurities in transition metal hosts, exact Green function treatment 77−62856
direct exchange between $3d^n$ ions 79−69668
disordered, multiple scattering theory, optical theorem 78−95250
disordered, optical theorem and electronic states 77−76719
double d-band model, delocalisation of electrons 77−76743
double d-band model, dynamic susceptibilities calc. 77−1535
Einstein temp. and vibr. entropy, semiquantitative calc. 78−2221
elastic constants, temp. depend. rel. to conduction electron density of states *(Russian)* 78−38769
elastic-plastic transition behaviour model *(German)* 80−75295
electric field gradient at low temperature 79−78565
electrical properties, temp. depend. 80−15496
electrical resistivity, calc. using Animalu's model pot. 77−43558
electrical resistivity, ideal phonon limited and McMillan-Hopfield factor 78−64024
electrical transfer of O, N, exam., using heat transfer of interstitial atoms *(Russian)* 79−55931
electrnic sp. ht. and heat conduction, temp. depend. 78−71865
electromechanical polishing method 78−53073
electron-phonon coupling, comparison of reson. and tight-binding description 77−15746
electron-phonon coupling, electronic aspects 77−69255
electronic config. and nucl. quadrupole interaction, atomic SCF Hartree-Fock calcs. for higher elements 79−60777
electronic Gruneisen parameter 79−82297
electronic specific heat calculations 79−73323
electronic struct. and magnetism, review 80−70573
electronic structure and d-holes of films and surfaces 78−39180
electronic structure of interstitials 79−1583
emissivity, temp. depend. 80−10688
energy band and related props., theory, for 4d transition metals, rigid muffin tin approx. 77−62811
energy band filling *(Russian)* 78−6263
energy band structure and X-ray emission spectra, calc. *(Russian)* 77−1763
energy bands of 4d metals, band parameters and vol. depend. 77−39772
energy of cohesion calc., Hubbard Hamiltonian with exchange interaction 77−69261
EPR of ion complexes, mag. g-tensors, spin-orbit coupling 78−10752
equation of state, s- and d-contribs. 78−91633
erosion resistance, in intense laser radiation *(Russian)* 77−12702
even-even transitional nuclei, bunching of spin states in γ-band, asymm. rotor model 78−62485
exchange energy, 3d subshells *(Russian)* 77−72830
extraatomic relaxation energies *(Russian)* 78−31295
f^n-electron system, paramag. principal susceptibilities, calcs. using ang. overlap model 77−32158
failure, statistical model, in conditions of monotonous cyclic loading *(Bulgarian)* 80−70296
FCC, improved Fielek model 79−19335
FCC, surface relax. and force consts. 80−39404
FCC metals, lattice-dynamical model 79−51219
Fermi surface, stress depend., from quantum oscill. effects 78−91597
ferromagnetic, 3d, electron spin polarisation in field emission, state-of-the-art 77−69972
ferromagnetic, 3d, itinerant electron magnetism, magnetic excitation props., theory 80−34581
ferromagnetic, band theory of linear magnetostriction 80−71141
ferromagnetic, dil. H electronic struct. 80−70638
ferromagnetic, electron spin polarisation, review 78−76591
ferromagnetic, electron spin polarisation, review 78−76592
ferromagnetic, electronic struct. of interstitials 77−62867
ferromagnetic metal, Fano effect and hyperfine field of non-transition impurity 80−25128
ferromagnetic metals, dislocation drag by conduction electrons 80−24451
ferromagnetism, theory 80−2541
ferromagnetism, transition metal valence electron struct. explanation 78−47932
field emission, effect of model hybridized energy bands 77−77349
field emission and field ionisation, role in heterogeneous activation of gas molecules 78−35271
field emission spectroscopy 78−35257
field evaporation rate meas. 78−76590
transition metals continued
film, anomalous crystal structures 79−28222
film, calc. of tight-binding surface density of states 77−55594
film, chemical compound formation by ion bombardment 78−30846
film, electron beam evaporator for in situ deposition studies in UHV electron microscope 80−40264
film, energy band calc. by linear combination of muffin tin orbitals method 77−4283
film, on Si, silicide form. at interface, interface marker technique obs. 80−59734
first transition systems, survey of regular solution parameters 77−44220
first-row ions, core ionised states, ΔSCF MO calcs. 80−78523
flooded on noble metal surface, effect on sputtered negative ion yields 78−11056
fluorescence quenching mechanisms for organic compounds 79−56837
foil-electrolyte interface, optical and elec. expts. 78−88644
friction and transfer behaviour of various metals in contact with pyrolytic BN 78−88535
fusion entropy, electronic contrib. 79−42217
garnet, spin Hamiltonian and mag. anisotropy, appl. to $3d^4$ and $3d^6$ ions 79−99669
glass:M, photoacoustic spectrosc. 80−92611
group IV, diffusion mechanism *(Russian)* 79−73335
group IV, electronic basis for ω-phase stability 79−91616
group V, low temp. sp. ht. anomalies 77−77002
group V, thermophys. props. determ. at high temp. using deform. vibrs. of plates 79−85143
group VIII, O_2 chemisorption, UPS 79−7751
group VIII, O_2 chemisorption, UPS 79−7752
Hall coeff., force correlation function method 79−91028
HCP, electrical resistivity high-temp. anisotropy 79−65429
HCP, nonlocal effects in lattice dynamics 78−91397
heat of chemisorption of H_2 calc. 78−38959
high-melting-point, fast cooling from melt, cooling rate influence on struct. *(German)* 79−43287
hydrocarbon catalysis 78−11550
hydrogen embrittlement, model for metallic cohesion reduction mech. 80−7679
hyperfine field on nucleus, mag. moment and electron shock 77−62883
II-VI compounds with transition metal impurity, SCF LCAO MO formalism in CNDO and INDO approx. 79−38017
implantation of He^+, range profiles and thermal release 80−39138
impurities, as probes of critical points, in host band structure 78−91645
impurities, integration with large-angle grain boundaries 80−39148
impurities, volume-corrected Mossbauer isomer shifts 78−68434
impurities in Ba silicate and phosphate glasses, quenching of Nd^{3+} luminesc. 80−25449
impurities in ionic crystals, optical spectra *(Rumanian)* 79−87474
impurities in semiconductors, associated localised electron states 79−56164
impurity scattering and residual resistivity 79−56192
impurity screening, contrib. of d-electrons 77−62857
impurity states, multiple-charge, in semicond. 79−33259
impurity states in semiconductors, EPR linewidth calc. 80−80599
incomplete shell metal, spin-depend. final-state interactions in core photoelectron spectra 77−20981
incomplete shell metal, spin-depend. final-state interactions in core photoelectron spectra 77−20982
inner shell photoelectron and photoabsorpt. spectra 79−43091
interatomic forces, phonon spectra, from band structure charge densities 79−7662
interatomic potentials, from phonon spectra 80−33927
interface electron states 77−59313
interstellar grains, rel. to H_2 catalytic form. 78−54005
interstitial impurities, electron density of states 77−47766
interstitial impurities, energy in FCC transition metals 77−47765
interstitials, wave-packet motion in Eckart and quadratic pots. 80−52067
ion, 3d→4p transition, assignment from expts. on LiCl:Cu^+ 78−27272
ion, impurity levels in cryst. field of semicond. 78−23059
ion, in inert medium, electronic relax., coupling mechanism 79−76466
ion, in inert medium, electronic relax., theory 79−76465
ion, irreducible Raman scatt. tensor operator for 32 cryst. point groups 77−8572
ion, Jahn-Teller coupling consts., parametrisation method based on ang. overlap model 79−78052
ion, superposition of quasidegenerate configurations, principal quantum number N=3 80−14079
ion 3d→4s transitions in crystals, obs. and interpretation 78−6339
ion pairs, anisotropic exchange parameters 79−11093
ion pairs, simply reducible symmetry group crystal fields, kinetic exchange theory 80−39541
ion-induced photon emission spectroscopy, quantitative analysis appl. 77−48740
ionic associations with $eosine^{2-}$, in dimethylsulphoxide, fluoresc. quenching 77−73163
ionic crystal:transition metal, excitation and trapping at impurity sites 79−33776
ions, compressed D_{4h} cluster, g_{zz}-g_0 value 77−80756
ions, EPR in solids, review of 1973 literature 77−69675
ions, in complexes, vibronically allowed d-d transitions, band shape calcs. 77−50472
ions, in solid, nearly degenerate electronic levels, dynamical effects 78−68535
ions, photoredox reactions, for photochemical solar energy conversion 77−86334
3d-ions, s-doublet struct., appl. of exchange correlation mass operator approx. 80−106266
ions in solids, EPR 80−51968
itinerant and localised d-electrons, positron annihilation data 80−93428
itinerant electron magnets, neutron scatt. expts. 77−73002
itinerant ferromagnetism theory 79−78301
itinerant localised electron model for magnetism 78−14918
itinerant magnetism, quasispin model 77−66239
Jahn-Teller coupling constants calcs. in 3d transition metal ions in crystals 80−49679
laser shaping, erosion resistance increase obs. *(Russian)* 77−53871
lattice dynamics, microscopic theory 79−7664
lattice dynamics, seven parameter model 79−90739
lattice dynamics and scatt. reson. 78−59872
lattice dynamics calculations, superconductivity parameters 79−7655
lattice excitations, classical models 80−29132

transition metals continued
liquid, 3d, density of states of d-band, heat of vaporisation 78−95253
liquid, 3d, thermodynamic and electronic props., Percus-Yevick eqn. soln. *(Japanese)* 77−76579
liquid, density of states, effect of nonorthogonality 77−59243
liquid, electronic props. 77−47721
liquid, electronic struct. and elec. resist. 77−51647
liquid, electronic struct. and transport props. 80−29314
liquid, mag. susceptibility rel. to theories of electronic struct. 77−1536
liquid, muffin-tin pot. model, electronic density of states determ. 77−51645
liquid, multiple scatt. calcs. of resist. 78−76039
liquid, quasipolycryst. approx. for electronic states 79−77975
liquid, struct., review 77−51304
liquid, structure factors, calc. of temp. coeff. of resistivity, one component plasma model 79−32881
liquid, thermodynamic characts. calc. *(Russian)* 80−15264
liquid, thermoelectric power 78−91675
liquid, transition metal, electronic states densities from struct. and entropy data 77−1347
liquid 3d-metals, effect of d-band on heat of vaporisation and sp. ht. 77−76539
liquid and their alloys, elec. resist. using t matrix 77−31988
local density theory, mech. and mag. props. evaluation for 3d and 4d metals 78−91630
local pseudopotential theory 78−30863
Lorenz number and high-temp. interband transitions 78−26844
magnetic ground state props., simple one-electron theory 77−63063
magnetic moment near surface, one-electron band model 79−82747
magnetic properties, role of electron correlation 77−72974
magnetic surface anisotropy 77−1553
magnetic surface properties, review 77−73071
magnetic surface properties, review 80−44861
magnetic susceptibility, spin wave spectrum for improved itinerant-localised electron model 79−1654
magnetic susceptibility maximum and Fermi-liquid effect in 4d and 5d series 77−4480
magnetic susceptibility of 4d and 5d metals, susceptibility max. and grand Fermi-liq. effect 77−63082
magnetically ordered state, interacting virtual state approach 77−69464
magnetism, interacting virtual state approach 77−72987
magnetism of Fe group metals, mol. Jahn-Teller reson. states as possible antecedents 80−75701
magneto-optical Kerr effect spectra in UV region using synchrotron radiation 77−52127
many-body effects, role of density of states 77−15777
metal-H system, thermal neutron scatt., general multisublattice jump diffusion model 77−66045
metallic glass, short-range order, hyperfine field distrib. determ. by Mossbauer spectroscopy 80−39962
microscopic electronic theory 77−85112
model potential, generalised APW formulation 78−91579
model surface, with adatom monolayer, densities of states, chemisorption effects 78−26769
Mossbauer effect, change of charge radius for 2^+-0 transitions of ^{178}Hf, ^{182}W and ^{186}Os 78−25109
Mossbauer isomer shift, orbital electronegativity scale 77−73103
Mossbauer isomer shifts in 4d and 5d metals, book contrib. 79−87355
multiplet splittings of s-core levels, exchange correl. 78−10407
muons, positive, as light isotopes of H, book 79−82907
nitridation in NH_3 stream *(German)* 78−68928
noble metal, core overlap interactions 77−47759
noble metal, cubic close-packed struct. anal., interplanar interactions from degenerate perturbation theory 77−58971
noble metal, elec. resist. of dislocations, calc. *(Russian)* 78−60117
noble metal, electrical resistivity, calc. using Animalu's model pot. 77−43558
noble metal, electron-ion interaction, model pseudopot. 78−34785
noble metal, electronic properties, local model pot., form. factors, phonon freq. and elastic consts. 77−4168
noble metal, Gruneisen parameter temp. variation calc. 78−51638
noble metal, interfacial corrosion in metal to ceramic reaction welding 78−53035
noble metal, interstitials, displacement field calc. using discrete lattice model 77−1122
noble metal, lattice dynamics, central pair pot. calcs. 77−31736
noble metal, liquid, muffin-tin pot. model, electronic density of states determ. 77−51645
noble metal, positron annihilation data anal. by Mijnarends' method 77−20223
noble metal, thermal radiative properties at cryogenic temps., comparison with model predictions 77−15604
noble metal, thermal resistivity, Matthiessen's rule deviations, var. calc. 77−43562
noble metal, thermoemission, band induced anisotropy effects 77−32489
noble metal, transport properties, low-temp. 77−8072
noble metal, van der Waals energy estimation 78−91634
noble metal, van der Waals forces and their contrib. to vacancy form. energy and phonon dispersion 78−91635
noble metal, X-ray photoemission, many-body effects 77−28684
noble metal, XPS line shape asymmetry, simple model for quantitative evaluation 77−21002
noble metal, XPS of valance bands, ang. depend. 77−44122
noble metal aggregated film, light scatt. 78−64423
noble metal contact, substrate material diffusion and corrosion film formation, model 80−2312
noble metal point contacts, direct meas. of electron-phonon coupling 78−6433
noble metal whiskers in MIM diodes, freq. response, effect of d-electrons 77−47898
noble metals, anomalous positive thermopower 79−65449
noble metals, divacancy contrib. to impurity diffusion 78−79812
noble metals, impurity diffusion, electrostatic interaction theory, impurity-vacancy pair 78−43181
noble metals, Krasko-Gurskii model potential, test of validity for Cu 80−39485
noble metals, lattice dynamics, nonlocal effects 78−75754
noble metals, spectral detection limits, line increase cathode effect appls. *(Russian)* 79−11868
noble metals, thermoelectric power, 290-560K 79−42522
noble metals, thermopower calc. using dHvA data 79−65448
transition metals continued
noble metals, Van der Waals contribution to binding energy 78−2062
noble metals and their dil. alloys, de Haas-van Alphen studies, book 79−37966
noble metals and their dil. alloys, electronic struct., de Haas-van Alphen studies, book contrib. 79−37967
nohle metal, g-factor on the Fermi surface 78−18949
noncrystalline, elec. resistivity, Hall coeff., mag. susceptibility 78−95280
nonferromagnetic metal, two-component electron Fermi fluid, in mag. field *(Russian)* 77−20252
nonmagnetic, possibility of mag. monolayer formation 78−15009
one-electron theory, atomic sphere approx. to KKR and LMTO methods 78−91584
optical constants 12 to 24 μm, anomalous skin effect region 77−20842
optical emission, broadband, from Mo, Nb and W bombarded by heavy ions 77−28635
paramagnetic, dislocation magnetism *(Russian)* 78−39379
paramagnetic metal-NO· radical interactions, EPR spectra rel. to dipolar interactions 79−95647
paramagnetic metals, polarised neutron studies of field induced magnetisation 80−25084
paramagnetic state, itinerant electron model 80−65769
paramagnetic susceptibility, phonon instability, mixed localised-collective electron states 80−103811
partial resonance, Hubbard's theory of phase shifts 79−28264
penetration of interstitial elements during surface treatment 77−12737
phonon dispersion curves, extended de Launay model 77−4162
phonon dispersion relations, FCC transition metals, 5-parameter model calcs., appl. to Ni, Pt 78−75748
phonon dispersion using non-central force model 78−91392
photoelectron energy distrib. curves, rel. to band struct., book contrib. 80−16156
photoemission, metal surface and adsorbates, intermediate UPS/XPS synchrotron radiation study 78−52633
photoemission spectra, core-level satellite struct. 80−29855
PIXE anal. method 77−63973
projected surface energy bands, Shockley surface states 78−68061
radiochemical neutron activation anal. of environmental matrices for Hg and noble metals 80−16889
refractory, adhesional reactions with Ti 79−29280
refractory metals and oxides, reactions of liq. alkali metals, relevance to reactor technology 80−85173
refractory transition metal, abrasive polishing mechanism 77−12745
relativistic electron-phonon interaction 79−82532
resistivity and superconductivity 79−51550
resistivity anomalies 78−19018
s-d electron model, finite temp. diagram technique, perturbation theory 78−67932
s-d hybridisation in d-band metals and alloys 78−91644
SCF theory, orbital and pot. functions calc., eq. of state 80−44463
second series, electronic band Brillouin zone APW calc., electronic config. effects 78−51883
semi-infinite FCC metal, susceptibilities near (001) surface 80−15701
semiconductor:transition metal, Anderson model localised impurity states *(Russian)* 80−6788
Shockley surface states, projected surface energy bands 78−88009
slab, surface lattice dynamics and density response 78−71930
soft X-ray appearance potential spectra theory 79−78791
solubility of H_2 and bulk modulus 78−55950
spectral emissivity variation with temp. *(Japanese)* 79−1517
spin distribution in transition metal elements and alloys, neutron diffraction expts. 80−25097
spin fluctuation theory, for mag. and elec. props. 78−91869
spin Hamiltonian, higher order hyperfine terms, transition metal ion in octahedral symmetry field 78−79967
spin reduction in systems with orbital degeneracy 77−51873
spin-density-functional formalism 78−68140
Spreading of liquid TiO_2 over refractory metals under the influence of surface forces 78−26749
squared electron-phonon coupling constant, tight-binding calc. in transition metals and alloys 79−1571
stacking fault and twin energies 79−82244
steel, depth profiles of transition elements using (p,γ) react. 80−50910
stepped surface, electron states 78−95327
Stoner model in spin density functional formalism 77−72993
stopping power for 6.75 MeV protons 80−34107
substrates, catalytic effect on CVD of TiC whiskers 79−33211
superconducting alloy, transition metal impurities, described by Anderson model, Josephson tunnel effect 77−16000
superconducting transition temp. and phonon softening 78−14848
superconducting transition temperature, empirical correl. with Hall coeff. 79−78247
superconducting transition temperature, influence of implanted ions 77−28276
superconductive tunnel junctions, phonon struct., junction quality 79−11274
superconductivity, effect of s-, d-electron hybridisation *(Russian)* 78−39243
superconductivity, recent developments 79−11263
superconductivity, relevance of mag. interactions 80−100545
superconductivity, s-electron currents 77−47926
surface, (001), model, chemisorption, coverage depend. of adsorption behaviour 78−71976
surface, adatom vibr. model using pair interactions 80−15357
surface, adsorbed H, charge density oscills., LEED pattern anal. 79−42389
surface, continuous emission spectra of particles ejected by ion beams *(Russian)* 78−55140
surface, electron states at steps, cluster-Bethe lattice approx. 78−52045
surface, electronic perturbations 78−95334
surface, H_2 chemisorption, Hartree-Fock-Slater model cluster calc. 78−26929
surface, independent electron theory of atomic interactions 79−60903
surface, photoemission theory 78−95679
surface, reactions with O, 10^{-3} to 10^{-10} mbar, 77 to 370K, reactions 78−64889
surface, review of electronic struct. calcs. 77−28226
surface, spin fluctuations 78−95451
surface, spin orientation effect of shallow electrons by magnetization 79−65881

transition metals continued
surface, tight-binding theory of interactions between transition metal adatoms 77−1304
surface (100), chemisorption of acetylene and ethylene, molecular geometries determ., using SCF-LCAO calc. 79−19454
surface atom vibrations, self-consistent calc. in tight-binding model 80−103560
surface chemisorbed atoms, interaction energy calc. 80−54507
surface clusters, Hartree-Fock-Slater model calcs. 77−72899
surface density of states, continued fraction method 77−20388
surface density of states, d-electron 77−85296
surface electronic states, self-consistent model calcs. 79−42618
surface electronic struct., influence of size and roughness 78−14785
surface electronic structure, calc. method 77−89828
surface electronic structure, role of self-consistency in evaluation, tight-binding calcs. 77−39908
surface electronic structure calculations 78−95329
surface lattice dynamics 78−95224
surface magnetic order 78−95439
surface phonons and superstructures 77−62731
surface phonons calc., rel. to superstructures 77−1291
surface polycrystalline, tangential momentum accommodation coeffs. meas. of inert gases 79−95270
surface reaction with gases, exam. of mech. and kinetics *(Russian)* 79−57289
surface reactions with N, 10^{-3} to 10^{-10} mbar, 77 to 370K, reactions 78−64889
surface states, qualitative theory, Shockley model 80−6924
surface- or defect-induced magnetism, nearly half-filled bands 79−1671
thermal and electrical conductivity at high temperature, interpretation of temp. depend. 77−35912
thermoelectricity 79−65443
thermophysical data at high temps., submicrosecond-pulse-heating method 80−103459
third row atoms, contracted Gaussian type orbital basis set 80−23297
tight-binding approximations, modified, generalisation 80−88288
transition metal ions in crystals, thermal broadening and shift calcs. 77−48208
transition metal-O bond energy in O_2 glow discharge, mass spectrometry obs. 80−64808
transition metal-rare earth dil. alloy, hyperfine field of rare earth impurity 79−1588
transition metals ^{57}Fe study via conversion electron Mossbauer spectroscopy 77−55735
transport properties, modified tight binding approximation, reexam. 78−43279
two-centre exchange interactions between orbitally degenerate ions in crysts. 79−15126
universal LCAO parameters 80−75503
VA group, O and N determ. from internal friction meas.. 79−39246
valence, in metallic alloys 77−4288
wavevector-dependent spin susceptibility, variational principle 78−91586
whiskers in MIM diodes, freq. response, effect of d-electrons 77−47898
work functions and $2p_{3/2}$ core binding energies, APS meas. 78−15253
X-ray and ESCA spectra, effect of correl. interaction of electrons with core holes 78−92178
X-ray emission K-lines, free-atom approx. applic. 80−11513
X-ray photoelectron spectra struct., single and polycrysts., one-electron approx. 78−64445
X-ray scattering near K absorpt. edge, dispersion factors f′ and f″ 79−65954
XPS, asymmetric, due to electron-hole interactions, theoretical model *(Russian)* 79−33901
XPS asymmetry of core electrons and electronic struct. parameters 80−93460
zero-field splitting, $^6S(d^5)$ ions in tetragonal and rhombic symm. 77−1390
Al-3d transition metal, dil., localisation of additional screening charge 79−47051
Al_2O_3:M, phonon spectroscopy using freq. crossing techniques of transition metal ions 79−42193
CdTe:Fe-group metals, mag. susceptibility *(Russian)* 79−56496
Fe group, absolute oscillator strengths for second spectra, correction 77−3310
Fe group, BCC struct., X-ray absorption spectra, Mossbauer spectra, comparison *(Russian)* 78−64299
Fe group ions, spectra, calcs., allowance for d^n shell pair excitations 77−42261
Fe series, interstitial H, cluster model for bonding mechanism 79−60753
Fe-group, contact reactions with Al base melt 78−60879
Fe-group spectra, superposition configurations in semiempirical calc. 78−920
^{57}Fe, implanted in 3d, 4d and 5d metals, conversion electron Mossbauer spectra 77−12286
GaAS:M, electron struct. of deep centres 78−39060
GaAs, VPE, hole diffusion lengths, effect of transition metal diffusional doping 80−15628
GaAs(P):M, transition metal deep centres, model 79−78045
$GaAs_{0.6}P_{0.4}$, VPE, hole diffusion lengths, effect of transition metal diffusional doping 80−15628
H effect, on mech. props. review 80−50718
H_2 solubility rel. to electron density 79−51266
H_2SO_4 decomposition, corrosion tests on possible containment materials 80−45448
$LiNbO_3$:M, (M=Cr,Mn,Fe,Co,Ni,Cu), absorpt. spectra, 0.3-2.0 μm *(Russian)* 77−20898
$LiNbO_3$:M, photoferroelectric phenomena and optical storage 79−42577
$LiNbO_3$:transition metal, photorefr. effect, 1.5-4.0 eV 77−28213
M:^{129}I, calibration of Mossbauer isomer shift 80−20520
M-H, mag. suscept. and quasirigid model *(Russian)* 78−26805
MgO:M, phonon spectroscopy using freq. crossing techniques of transition metal ions 79−42193
MgO:transition metal, single cryst., grown with modified plasma torch furnace *(Japanese)* 79−95923
Mo-transition metal admixtures, equilib. distrib. coeff., functional dependence *(German)* 77−76566
N_2^+ + first row transition metal surface reactions 79−96363
Na_2O-WO_3:M glass, optical absorption 78−27254
Si:M, transition metal deep centres, model 79−78045
Si:M metastable films as temp. independent resistors 78−68097
Si-M system, interfacial reaction and Schottky barrier 80−39672

transition metals continued
Ti:transition metal, linear expsn. temp. coeff., polymorphic transition temp. shift 78−6164
V:transition metal, linear expsn. temp. coeff., polymorphic transition temp. shift 78−6164
ZnS:M, melt grown cryst., impurity distrib. and ionicity 77−55298
ZrO_2-Y_2O_3:M^{3+}, M=transition metal, X-ray luminesc. 77−44063

transition moments
achiral molecular system, elec. quadrupole transition moment, circ. polaris. spectroscopy 77−75219
alkali metal atom, perturbed by rare gases, dipole moments of S-P transitions 80−27979
alkali-rare gas atom systems, electronic collisionally induced transition dipole moments 79−98195
4-amino-4′-nitrostilbene, thermal motion of prolate luminescent molecules in solvents with different viscosities 79−83029
anthracene:2-aminoanthracene, polarised guest absorpt. spectra, transition dipole moment direction, cryst. packing 77−8610
atom, relativistic, level shifts, transition probabilities, perturbation theory 79−10067
atoms, electronic transition probabilities and lifetimes, expt. determ. 80−23369
atoms, monovalent, transition probabilities calcs. *(Russian)* 80−63594
bacteriochlorophyll electronic transition moment directions 79−100572
1,12-benzoperylene, in heptane, Stokes and anti-Stokes fluoresc., transition moment 77−61781
benzoxazole, polarisation of 274 nm absorpt. system, band contour analysis 79−27043
biphenyl, cryst., electronic absorpt. and refl. spectra 78−64377
charged particle scattering in homogeneous mag. field, transition amplitude 79−10218
conjugated molecules, resonance Raman spectra calc. 78−984
β-cyclodextrin-azulene complex, circular dichroism spectra 78−58713
diatomic molecule, electronic transition moment, internucl. separation depend., semiempirical calc. method 78−9199
diatomic molecule+diatomic molecule, collinear collision, anharmonicity effects 79−31656
1,6diazaspiro[4,4]nonane-2,7-dione, optical rot. strength calcs. 80−95793
2,5-dichloro-1,4-benzoquinone, mol. cryst., transition moment directions 78−64351
difluoramine, centrifugal distortion anal., microwave rot. spectrum 78−58650
4-dimethylamino-4′-nitrostilbene, thermal motion of prolate luminescent molecules in solvents with different viscosities 79−83029
DNA, Hg (II) and Ag (I) complexes in soln., theoret. interpret. of elec. dichroism obs. 80−85347
dyes, rot. diffusion of prolate, oblate mols. from absorpt. relax. 80−1008
elecronic excitation properties, RPA-CI calcs. using hypervirial relations as constraints 79−76413
EPR of $S=^1/_2$, $I=^3/_2$ system, quadrupole effects 79−42827
ethylene, transition moment closure tests of basis sets 79−6968
ρ-evaluation methods, for diatomics, f-centroid concept 79−31612
excimer laser, electronic structure, pot. energy curves, radiative transition probabilities, quantum mech. calcs. 79−10284
excitation of simple atomic and mol. systems, long-range force effects 79−10170
f^n systems, electron correl. effects on elec. dipole transition probabilities 80−23316
gauge invariance of transition probabilities 79−97487
haematoporphyrine, complexed with chloranil and tryptophane, energy spectra, transition moments and intermolecular distances 80−72127
heterocycles, five membered ring, MCD spectra dnd π-electron approx. calcs. 79−812
impurities in solids, absorption and emission spectra, bandshapes, moments 80−45122
indane, 271 nm spectrum, rot. band contour anal., puckering vibr. 78−1001
indoles, temp. effects on electronic transition moments in n-heptane and water 78−58744
inert gas dimer ions, $A^2\Sigma_{1/2u}^+ \rightarrow D^2\Sigma_{1/2g}^+$ system, theoretical absorption spectrum 80−32734
ions, electronic transition probabilities and lifetimes, expt. determ. 80−23369
IR radiation, interaction with molecular system, classical/semiclassical theory challenged 80−43117
K level X-ray lines, relative transition probability 80−935
light emission by mag. and elec. dipoles, radiation patterns 80−32886
liquid crystal display, with dichroic dye guest, field-induced colour switching 80−1327
local mode mols., normal mode spectra 80−95687
molecular collision, quasi-classical and quantum moments of distrib. of states, semiclassical comparison 80−23480
molecular electron-donor-acceptor complexes, solvent effect on charge transfer absorpt., thermodynamic props. 77−83615
molecular orientation, extensional effects, IR obs. 77−23591
molecule, vibr. problem in Cartesian displacement coords., Coriolis and transition moment calcs. 77−83573
molecules (molecular ions), excited state lifetime meas. 78−17725
multiconfiguration Hartree Fock method, appl. to at. energy levels and transition probabilities calcs. 80−23318
optical dipole transitions, first order model pot., appl. to Li isoelectronic sequence 78−25474
optical rotatory strength, gradient matrix eqn. of motion calcs. 80−95793
oxazine dyes, orientation of $S_1 \rightarrow S_n$ transition moments, continuous ps photometry 79−10152
pentacene, laser fluoresc. of mol., excitation bandwidth and optical dephasing 79−36679
phenyl isocyanate, electronic absorpt. spectrum, vibr. struct., f-values, spectroscopic moment and config. 78−58715
planar molecules in stretched polymer films, solute orientation, transition moment direction, dichroic spectra 78−58742
polarised electronic absorption spectrum at 300 and 77K, phys. chem. lab. expt. 80−17774
polarised photochromism in solid solutions 78−64859
polyatomic asymmetric top molecules, solns., IR spectra 78−58694
polymer film, stretched, orientation and transition moment directions of small planar molecules 78−1015
purple membrane fragment suspensions, elec. dichroism obs., chromophore transition moment 80−89728

transition moments continued
quantum transition probabilities, two-level approx. 80−9557
riboflavin, transition moments in 300 nm region 79−53042
semiclassical theory of mol. collisions in laser field 77−34718
solvated electrons, optical absorption spectra, temp. depend. moments, many-particle theory 79−72301
solvated excess electrons, optical absorpt. spectra, moment theory anal. 78−73072
thiosemicarbazide, mol. cryst., transition moment directions 78−64351
three-level system transition probabilites, molecular motion anisotropy by quadrupole relaxation 80−18867
triclinic crystals, polarized IR spectra, vibr. transition moments 77−85720
unlike molecules, in soln., electronic excitation energy transitions *(German)* 77−34749
vanishing electric dipole transition moment, appl. to fluoresc. 79−59397
vibrational, of diatomic and polyatomic mols., elec. and mech. anharmonicity influences 80−23459
γ-AlOOH, boehmite, lattice vibrs., evidence for $C_{2v}{}^1{}_2$ space group 79−28756
Ar I spectra, probabilities of $np^5n'p \rightarrow np^5n's$ dipole transitions, two-config. approx. calcs. 77−71779
Ar II, transition probabilities, lifetimes, intermediate coupling semiempirical calcs. 79−789
Ar_2^+ bound-free absorpt. cross section for Π and Σ states 78−5140
ArH^+, transition moments, perturbation calcs. 80−102542
BO, transition moment of diatom., ρ-evaluation 79−31612
BaO, excited electronic states, lifetimes and transition moments 80−87177
BaO, transition moment of diatom., ρ-evaluation 79−31612
Be, excitation energy and transition moment anal. of electronic transitions 78−25620
C_2, band system transition moment ab initio SCF and CI calcs. 79−13770
C_2, Swan bands, variation of electronic transition moment with internuclear separation 79−826
CH^+, $a^3\Pi$-$b^3\Sigma^-$ transition moment, ab initio calcs. 80−87047
CH^+, excitation energies and transition moments in a second order polarization propagator approach 79−10051
CH^+, excitation energy and transition moment anal. of electronic transitions 78−25620
CN, RKR Franck-Condon factors and r-centroids for $B^2\Sigma$-$A^2\pi$ transition 79−81195
CO, (4+) system, electronic transition probability 80−106332
CO, absolute intensity meas., 4-0 vibr.-rot band 77−6854
CO, high resolution lifetime meas., perturbation and collisional transfer correl. 78−78699
CO_2, $30^0 1_{II} \leftarrow 00^0 0$ band, meas. at different temps. of absolute intensities, line half-widths and broadening by Ar and N_2 78−86865
CO_2, $30^0 1_{II} \leftarrow 00^0 0$ and $30^0 1_{IV} \leftarrow 00^0 0$ bands, absolute intensity meas. at different temps. 78−86864
CO_2, combination and difference bands, IR intensities 77−466
CO_2, dipole moment functions 80−87094
CO_2, Π_u symmetry transition probabilities, dipole moment and electro-optical consts. calc. 80−43115
CO_2, transition calibration, rotational constants, absorption spectrum, 4.82-μm region 78−58868
CO_2, transition moment and probabilities of IR spectra 79−3498
CO_2, transition moment of IR band near 7740 cm^{-1} 78−90224
CO_2, transition moment of IR band near 7740 cm^{-1} 78−90225
CO_2, vibr.-rot. spectrum, absolute line intensity, vibr. transition moment 77−83655
Ca XV, transition probabilities, energy spectra calcs. 78−70791
DCN, electronic spectra, vibr. struct., ab initio calc. 78−9166
DCN, $\nu_1+\nu_3$ combination bands, transition moments, integrated intensities 77−79610
DT^+, HT^+, HD^+, accurate energy and transition moment calcs. 77−14412
$EuCl_3$, solns., $^7F_0 \rightarrow {}^5D_1$ and $^7F_1 \rightarrow {}^5D_0$ transitions, MCD 79−31566
Fe XXI, transition probabilities, energy spectra calcs. 78−70791
$^{74}GeH_4$, transition moment for ν_3, rel. to Jovian atmosphere 79−72363
H_2, excitation energy and transition moment anal. of electronic transitions 78−25620
HCN, electronic spectra, vibr. struct., ab initio calc. 78−9166
HCN, $\nu_1+\nu_3$ combination bands, transition moments, integrated intensities 77−79610
HD^+, HT^+, DT^+, accurate energy and transition moment calcs. 77−14412
H_2O_2, twisted mol., optical rot. strength calcs. 80−95793
H_20, vibr. transition moment and band intensity 79−27036
Hg_2, model calc. of electronic struct. and spectroscopy 79−3352
HgCl, photodissociation calcs., laser efficiency 80−48047
I+methane $^-d_0(^-d_3)$,$(^-d_4)$, excited atoms, quenching, isotope effects, time resolved reson. fluoresc. 80−32656
I_2, transition moment of BO_u^+-$X^1\Sigma_g^+$ system in I_2 laser 79−54917
$I^2P_{1/2} \rightarrow {}^2P_{3/2}$, collision induced emission (Ar)(Xe), dipole transition moment by perturbation theory 77−83528
Kr(-He) arc, wall-stabilised, atm. press. 79−46503
KrI, p-s lines, transition probabilities meas. 80−23366
$LaCl_3$:Pr^{3+}, dipole transition probabilities between states, electron correl. effects 80−23364
LaO, spectral intensity of $B^2\Sigma$-$X^2\Sigma$ bands, Rydberg-Klein-Rees pot. 79−31611
Li, two-photon ionis., many-body perturbation theory 79−22679
LiH, dipole moments and transition moments, semi-rigorous bounds, error limits 78−78635
^{7}LiH, $A^1\Sigma^+$-$X^1\Sigma^+$ bands, radiative transition probabilities calcs. 78−66603
MgH, X and $B'\ ^2\Sigma^+$ and $A\ ^2\Pi$ ab initio CI calc. 79−31415
MgO, $B^1\Sigma^+$-$X^1\Sigma^+$ and $B^1\Sigma^+$-$A^1\Pi$ fluoresc. 78−21963
N_2 ($C\ ^3\Pi_u$) vibr. levels radiative lifetime, transition moment internucl. distance depend. 78−1027
N_2, asymptotic expansion for Morse-Pekeris oscillators, band strength factors, electronic transition moment 78−78755
N_2, $B'^3\Sigma_u^- \rightarrow B^2\Pi_g$ (0,0) emission band 78−58690
N_2 $C^3\Pi_u$-$B^3\Pi_g$ second positive system, transition probabilities, transition moment 78−50593
N_2, energy levels, low lying triplet states, infrared emission analysis 78−58691
NF_2H, centrifugal distortion anal., microwave rot. spectrum 78−58650
NH, laser-excited A-X system fluoresc. 79−50060
transition moments continued
NO, γ and β system, electronic transition probability 80−106332
N_2O, combination and difference bands, IR intensities 77−466
N_2O, dipole moment functions 80−87094
N_2O+N_2, vibroluminesc., V-V transfer consts., quadrupolar transition moment, IR spectra 79−10112
$NO(A^2\Sigma^+, v'=0,1,2)$ lifetimes, $A^2\Sigma^+$-$X^2\Pi$ transition moment, oscill. strengths, internucl. separation depend. 78−82787
NaK, mol. transition dipole moment, from laser-induced fluoresc. spectra 79−94034
Ne I spectra, probabilities of $np^5n'p \rightarrow np^5n's$ dipole transitions, two-config. approx. calcs. 77−71779
Ne II, transition probabilities, lifetimes, intermediate coupling semiempirical calcs. 79−789
O_2, $b'\Sigma_g^+$-$X^3\Sigma_g^-$ electronic transition, absorpt. coeffs. and transition moments 80−43061
O_2, UV absorpt. into $^3\Pi_u$ state, calc., atmos. opacity 80−12582
O_2^+, $A^2\Pi_u \rightarrow X^2\pi_g$ and $b^4\Sigma_g^- \rightarrow a^4\Pi_u$ emissions by photoionis. of O_2 79−94041
O_3, line position and intensities of $2\nu_3$, $\nu_1+\nu_3$ bands 80−87181
OH, A-X system, rot. transition probabilities 80−43027
OH, $A^2\Sigma^+$-$X^2\Pi_i$ system, vibrational and rotational levels, transition probability determ. 80−43034
OH^+, rot.-vibr. bands, line positions, oscill. strengths transition probabilities 80−67828
OsO_4, and isotopic forms, stretching fundamental, 961 cm^{-1}, high resolution spectroscopy 78−90162
Pr^{3+}, anomalous hypersensitive $^3H_4 \rightarrow {}^3P_2$ transition 80−106296
SF_6, IR double reson. with tunable diode laser 80−14160
Sf_6, integrated IR band intensities and transition moments 80−95611
SiH, A state new predissociations, improved dissoc. energy value from rot. level lifetimes 79−3496
SiH, transition moments of $A^2\Delta$-$X^2\Pi$ band, 150-650 nm 79−45767
SiO, $E^1\Sigma^+$-$X^1\Sigma^+$ band system, transition moment 79−6970
SiO, transition moment of $A^1\Pi$-$X^1\Sigma^+$ band, 260-290 nm 78−13552
SnO, $D^1\Pi$-$X^1\sigma$ transition, electronic moment var. 79−41197
$TiCl_4$, IR absorpt. bands, absolute integrated intensities, obs. and calc. 78−78689
$TiCl_4$, $t_1 \rightarrow 2e(^1A_1 \rightarrow {}^1T_2)$ transition, bond props. and LCAO MO calcs. 80 18889
TiO β system, electronic transition moment and effective vibr. temp. 77−68078
XeCl, energy curves and transition moments 80−28210
XeF, energy curves and transition moments 80−28210
XeX, (X=F,Cl,Br,I), Ar matrix isolated, MCD, low temp. depend., spectroscopic parameters calc. 77−38682
ZrO, $C^3\Delta$-$X^3\Delta$ system, electronic transition moment depend. on internuclear dist. 77−68079

transition probability *see radiative lifetimes*

transition probability, nuclear *see nuclear energy level transitions*

transition radiation
channelling of electrons and positrons, radiation spectrum, complex and anomalous Doppler effect 77−84819
charged particle motion at vac.-medium interface, transient radiation emission spectral distrib. 80−63901
Cherenkov charge in nonstationary medium *(Russian)* 78−50694
classical theory 78−82896
cosmic ray apparatus, transition radiation detector system for high energy hadron interactions research 77−61651
cosmic ray electrons, meas. by transition-radiation detector and shower detector combination 77−57844
cosmic ray hadron interactions, 0.5-5 TeV, XTR-detector, Monte-Carlo simulation *(Russian)* 79−49564
detector, unconventional, data for X-rays, pions and protons 77−88341
dispersive medium of nucl. origin, nucl. levels and permittivity meas. *(Russian)* 77−59635
drift chamber, transition radiation detection 79−22546
electron and particle discrimination, transition and synchrotron radiation 77−10568
electron-photon cascades in homogeneous absorbers 77−61669
EM field excited medium, combination transition radiation from charged particle 77−19154
energy distribution of transition radiation, comparison with expt. data 79−63397
energy fluctuations, rel. to detector design 78−62681
energy flux generated in medium with nuclear dispersion, thin, thick plates *(Russian)* 78−68576
energy loss spectra of keV electrons exciting EM radiation in thin films, calcs. *(German)* 77−90213
ferrodielectric plate, entered by point charge particle with helical path 77−1757
gamma-ray generation of microwaves in Zn, possibly via transition radiation *(Russian)* 78−2939
gamma-ray resonance frequency range *(Russian)* 78−80432
gas proportional counter, relativistic electron ionisation loss, transition radiation effect 78−25389
hard transition radiation formation, effect of absorptivity *(Russian)* 77−8677
hybrid transition-Cherenkov radiation, props. 79−45897
immobile charge in nonstationary medium 78−31270
intensity derivation 80−106430
interference effects in transition radiation near Cherenkov radiation threshold 80−9454
metal surface plasmon light emission due to low energy electron irrad. 80−34997
microwave band, radio interferometer system 79−85181
mosaic crystal, ultrarelativistic charged particle-induced X-ray emission, theory *(Russian)* 78−39622
nonstationary media, radiation of uniformly moving charge 77−79738
optical, peculiarities of radiation from high-energy particles at inclined incidence 78−58893
optical pulse generation for optical receiver calibration, electron beam *(Russian)* 77−58409
perfect crystal, ultrarelativistic charged particle-induced X-ray emission, theory *(Russian)* 78−39622
piezocrystal, surface acoustic waves 78−43231
piezoelectric semiconductor plates, natural oscills. modulated by charged particle beam, energy losses *(Russian)* 80−2259
plasma, weakly inhomogeneous, charge density wave transform. *(Russian)* 77−3924

transition radiation continued
plasma sheath, modulated beam injection, transition radiation intensity calc. 77−11363
plate and stack of plates, hard transition radiation prod., absorbability depend. 78−19590
recoil force due to charged relativistic particle passing through plate *(Russian)* 78−72627
review 79−27143
soft X-ray transition radiation observation from medium energy electrons 80−76104
superheated superconducting suspension as transition radiation detector, electron meas. 77−6628
transitional radiation for magnetic charge *(Russian)* 79−22888
ultrarelativistic particle emission rel. to interface curvature 77−19153
uneven interface, transitional radiation emission *(Russian)* 77−6987
uniformly moving charge on nonstationary layer 80−32893
vacuum, transition radiation and scatt. in strong EM field *(Russian)* 78−58895
vacuum-metal boundary, role of Cherenkov radiation 79−99243
X-ray freq. spectrum from 5, 9 GeV electrons on multiple foils 77−27907
X-ray source, relativistic charged particles passing through periodic struct. 80−69303
X-ray spectrum and energy depend. meas. 78−68577
X-ray transition radiation, eikonal approx. 79−49422
X-ray transition radiation in stack of plates 78−9044
X-ray transition radiation spectra from relativistic electrons passing randomly spaced polyethylene interfaces 78−21805
Ag film, electron bombarded, transition radiation 77−85828
Ag rough surface, transition radiation for 77 keV electrons, surface plasmon light emission 78−60530
Ag, surface and volume plasmon light emission due to low energy electron scatt. 80−40177
$Ag+H^+$, X-ray emission, optical transition radn. 78−58618
Au, film, electron bombarded, transition radiation 77−85828
Au foil, optical transition radiation, bombardment by 29 MeV protons 78−2938
$Cu+H^+$, X-ray emission, optical transition radn. 78−58618
H isotopes, transition radiation from neutral beams, beam foil ionization 79−18299
Li radiators for electron identification at CERN ISR 77−30704
Sn foils, 1-3.5 GeV electron impact, transition X-ray emission, comparison with theory *(Russian)* 80−60704

translation (language) *see language translation*

translators (program) *see program interpreters*

translators (repeaters) *see repeaters*

transmission
see also acoustic wave transmission; light transmission; power transmission
double-pendulum vibration oscillator or seismograph, transmissibility curve 78−16200
elastic waves at frictional boundary, transmission (reflection), approx. anal. method 78−63371
electron beam, relativistic, refl. and transmission by strong mag. field *(Japanese)* 80−91737
Love waves in infinite strip with surface step, transmission, reflection and diffraction 79−88260
plane nonuniform waves of general form *(Russian)* 77−54668
quantal particle, inverted Morse pot. barrier, transmission, reflection coeffs., phase-integral approx. 77−53801
seismic wave attenuation, role of intrabed multiples 79−16393
seismic waves, refl. and transmission coeffs. in ellipsoidally anisotropic media 79−84136
spatially dispersive crystal, reflectivity and transmittivity 80−99604
vibration, transmissibility troughs in novel viscously damped dynamic absorbers 77−62096
Ag-Cu-Pb coin chem. anal. by low energy γ-rays and neutron transmission meas. 80−35591

transmission electron microscope examination of materials
see also transmission electron microscopy
A-15 compounds, radiation induced damage, TEM and heat capacity meas. 79−56349
adhesion, surface anal. techniques appl. 80−65381
adjacent crystals, appl. of meas. of relative translations 78−75675
afghanite, stacking variation, TEM study 79−99219
Ag, coincidence site lattice model, failure for grain boundaries 79−60384
β- and β''-Al_2O_3-Na_2O, fast ion conductors, TEM obs. 79−86920
β-Al_2O_3-Na_2O, geometrical aspects of breakdown, TEM study 79−79096
Al-Zn-Mg (5,1 wt.%), decomp. process, TEM study 80−71660
Al-Zn-Mg (6, 3 wt.%), water vapour embrittlement and H_2 bubble form 78−15564
alkali feldspar, deformation, plastic defects, TEM investig. 78−32066
alkali feldspars, TEM study of exsolutions, review *(French)* 78−28224
Allende meteorite, occurrence of Fe-Ni-Cr-S-O compounds *(French)* 78−32411
alloy lattice images using high resolution TEM 78−34399
alloy steel, austenitic, Ni free, TEM exam. of corrosion process 78−85029
alloys, industrial, stacking fault energy rel. to mech. props. *(French)* 79−43339
alloys, local composition determ., assessment of TEM direct lattice imaging technique 78−53294
alumina, prismatic slip dislocations in single crystals, obs. *(French)* 77−59016
amino acid block copolymers, morphology and mech. props. 78−91264
amorphous metal-metalloid alloys production by ion implantation 80−15128
amphibole fibre conc. in water, interlaboratory meas. by TEM 78−88590
anthracene, radiation-induced topotactic conversion from di-para-anthracene, low temp. TEM obs. 78−35710
anthracene, stable monoclinic phase, (001) planar faults 79−69115
9-anthraldehyde, struct. by TEM 80−79771
9-anthronitrile, struct. by TEM 80−79771
asbestos, fibre identification, selected area electron diffr. patterns in analytical TEM, optimum procedure using tilted specimens 78−24009
austenite solid soln., decomposition, effect of struct. of initial state *(Russian)* 77−48442

transmission electron microscope examination of materials continued
austenitic stainless steel, type 316, anelasticity and creep transients 78−84880
austenitic steel, solid solution decomposition at defects, TEM meas. 77−12656
austenitic steel, VN_x spherical misfitting particle precip. along dislocations, diffr. contrast 77−16595
automobile materials, appl. of microfractography 77−56199
bainite, formed from deformed austenite, morphology and mech. props. 79−43345
BCC crystals, atomic struct. of twin boundaries by electron microscopy 78−22735
BCC materials, small dislocation loop images 78−83823
BCC metals and alloys plastically deformed, electron microscopy *(French)* 77−44299
$Bi_7Ni_4NbO_{21}$, crystal point group determ. by high resolution electron microscope image 79−51036
biological specimen, high resolution obs. by incoherent illumination method 79−57820
biotite, disordered mica struct. high resolution electron microscopy exam. 78−91344
book 80−17726
α-brass, 70:30, cold-worked, recrystallised grains nucleation on heating 80−29998
brass, crystal structure and morphology of thin needle-like martensite 78−31425
brass, delamination effects during grinding 79−52470
brass, fatigue crack propagation, effect of stacking fault energy as deduced from dislocation patterns, TEM study 79−61719
α-βbrass, interface struct. of two-phase bicrysts. made by solid state diffusion couple method, X-ray Laue and TEM study 79−28214
brass, misfit dislocation struct. in interphase boundaries, electron microscope obs. 78−18649
brass, nondestructive determ. of in-depth profile 80−93836
α-brass, quenched, secondary defect form. during ageing, TEM obs. 78−88482
α-brass, with few inclusions, shear mode of ductile fracture 77−36652
brass (70:30), cold rolled, optical, X-ray and TEM exam. of deformation struct., and textures 78−88500
γ- brass type alloys, superstructures and defect obs. 80−107284
γ-brass type phases, inversion antiphase domains, formation and stabilisation, electron conc. effect 78−14363
bronze bearings, TEM exam. of wear debris 77−77595
bronze P, heavily cold rolled, yield strength enhancement mech. 77−36539
butanediol terephthalate-polytetramethylene oxide terephthalate copolymers, dielec. props. 78−95546
C GaP on GaAs substrate, heteroepitaxial layers, stuct. defects *(German)* 79−23865
carbonate minerals, deform. twinning mechanisms 80−79814
case hardened components, exam. of fracture surface by TEM. *(Japanese)* 78−52949
cavities observation, TEM techniques review 80−14974
cell membranes, at mol. resoln., introduction 80−104841
ceramic nuclear fuel, porosity characterization, optical and electron microscope exam. 78−44302
ceramic nuclear fuels, mech. props. at compressive deformation 80−651
ceramic oxide, TEM study of deform., review 79−87686
ceramic science application of high-resolution TEM 78−35397
ceramics, microcracks, and thin intergranular films obs. by TEM 80−68295
ceramics, TEM study of precipitation 79−87637
ceramics, TEM study of radiation damage, review 79−86816
chloritoid, topotactical dehydration, X-ray diffr. and TEM study 79−51057
chromate film, microporosity induced by nucleation and growth processes, TEM expt. 78−10303
chrysotile fibre conc. in water, interlaboratory meas. by TEM 78−88590
CMOS ICs electrically active stacking faults, anomalous leakage currents 79−78191
coatings, defects and their effect on props. 80−39474
collagen fibrils cholesteric analogue packing in Holothuria forskali 80−8035
compound eye of Cicindela tranquebarica herbst, fine struct. 80−85382
cordierite glass-ceramic, effect of crystn. on thermal diffusivity, crystallite morphology study 79−33127
corundum, subjected to thermal shock, study of substruct. and surface morpholoy, X-ray diffr. and TEM study 79−43292
crocidolite fibre fine structure rel. to pulmonary tissue immunoresponse 79−74824
crystal, accelerator irradiation, heavy ion irradiation damage 80−100291
crystals, particle irradiated, defect clusters identification 79−69108
decahecral, particles, high symmetry orientations, HEED and TEM study 79−86732
deep-drawing curves, cryst. microstruct. during deform. *(French)* 79−20066
diamond, accelerator irradiation, heavy ion irradiation damage 80−100291
diamond, natural, defect struct., recent obs. by new methods 78−30628
diamond, natural type IB, thermal conductivity anomaly, defects obs. 77−85003
diamond, planar defects, in {100} planes, electron microscopy 77−11569
diamond, type I, defects of platelet nature, TEM study 79−37719
diamond at room temperature 78−52927
discontinuous metal films, elec. and mag. field distrib., TEM obs. 79−95518
dislocation cell form. during plastic deform., TEM obs. 80−60935
dislocation core, thickness periodicity of atomic-resolution images 79−27995
dislocation loop obs. *(Japanese)* 79−82130
electrochemical displacement reactions, electron microscope obs. of nucleation and growth, comparison of Cu/Fe and Cu/Al cementation systems 79−47939
epitaxial growth, vapour phase, growth mode characterisation 78−87885
etched thin foils, comparative SEM, STEM and TEM analysis 80−100144
ethylene-vinyl acetate-vinyl chloride graft copolymers, rel. between morphology and toughness *(German)* 80−66665
faulted dislocation loops induced by elastic interaction, climbing motion 80−75227

transmission electron microscope examination of materials continued
FCC crystals, deform. faceting of large-angle grain boundaries TEM 77−65984
FCC materials, jogs on extended defects, weak-beam electron microscopy technique 78−38713
FCC metals and alloys, plastically deformed, electron microscopy *(French)* 77−44301
ferrite, transform. kinetics, grain size, alloying element effect, carbide precip. 80−93560
ferromagnetic materials, lens system with eucentric goniometer 77−72530
film, thermal strain, strain relax. above room temp. 80−59841
film/substrate interface, misfit dislocation obs. using electron microscopy 80−103605
films, elec. and galvanomag. props., microstruct. 80−70859
fission gas bubble distribs. in mixed oxide fast reactor fuel pin, anal. of TEM obs. 78−58358
foil, electron scatt., appl. of Monte Carlo type calc. *(French)* 77−7636
foil, recrystn. during heating in column of electron microscope *(Russian)* 78−48421
foil for TEM, preservation technique *(German, English)* 79−96263
franzinite, stacking variation, TEM study 79−99219
generalised routine for defect image simulation in TEM obs. 78−29220
glass, heat treated, thin foil prep. for TEM obs. 78−7154
glass-plumbite-treated cotton, form. of coating at interface 79−15058
glasses and ceramics, characterisation with analytical electron microscope 80−84068
grain boundaries, interfacial structure effects on high temp. mechanical behaviour 80−59480
grain boundary misfit dislocation, core structures, TEM obs. 79−90673
grain boundary misfit dislocation, core structures 79−90674
graphite, CTR material, the ion injection effect 78−34557
graphite, Fe-catalysed gasification, electron, microscopy 80−104358
graphite, ion bombarded, light gases, structural study using TEM 80−92570
graphite, sources of background X-radiation 80−101908
graphite, surface cleaning, air cleavage and UHV cleavage, obs. using Au decoration 78−80665
graphite, thin film, high resolution phase contrast imaging 80−103224
graphite, zone-axis pattern maps 80−100137
graphite foil, thickness determ. by TEM using diffr. and energy loss anal. 78−29088
guanidine aluminium sulphate hexahydrate, ferroelec. cryst., growth, domain struct., dielec., switching props. 77−43950
haemoglobin S, fibres, discs having six-fold symmetry, electron microscopy 78−76989
Hasteloy B, equilibrium surface bombarded with high dose He^+ ions 78−95091
Haynes Stellite 6B, particle erosion damage, TEM obs. 78−88546
HCP metals and alloys, plastically deformed, electron microscopy *(French)* 77−44300
hematite, multiple orientation relationships between magnetite, TEM study 79−60298
hereditary transfer of lattice defects at γ-α-γ transform. 79−96020
hexagonal networks in basal plane, TEM exam. 78−2132
hexamethylcyclotrisilazane film, plasma-polymerised, TEM study 80−44456
high resolution, high voltage, review 77−56189
humite, real structs., mixed layer characts. 78−79567
HV, appl. in sold-state physics 79−27882
II-VI semiconductors, lattice defects, X-ray diffr. and electron microscopic study 80−15088
II-VI semiconductors, struct. of thin foils 79−32864
III-V semiconductor, epitaxial layers, dislocations nature, origin and effects 79−28232
III-V semiconductor ternary alloys, VPE growth lattice mismatch effects 79−28220
image resolution and penetration in amorphous and polycrystalline materials, comparison with STEM 80−14976
implanted amorphous layer reordering 77−76435
Incoloy, alloy 800, $M_{23}C_6$/austenite phase boundary defect struct. resolution by weak beam microscopy 80−3046
Incoloy, oxide-dispersion-strengthened, pulsed YAG laser welding 79−70075
Incoloy 800, austenitic, fatigue at elevated temps., second phase form. effect 77−36637
Incoloy 800, cast, microstruct. evolution during creep, TEM obs. 79−43366
Incoloy 800H, high temp.-low cycle fatigue, ageing and cold working effect on initial stress/strain curve 79−47720
Incoloy 901, foil prep. for TEM exam. 80−88001
Incoloy 903, microstruct. and effect of H_2 charging 77−86143
Inconel, type 706, precipitation and creep rupture behaviour, optical and TEM study 79−74158
Inconel 600, equilibrium surface bombarded with high dose He^+ ions 78−95091
Inconel X750, positron annihilation study of ageing and creep 80−29824
Inconel X-750, deform. and fracture characts., 24-816°C 80−108551
insulating films, on Si, struct. stability 80−54564
ion bombardment, electron microscopical anal. of surface effects and volume defects, review *(Rumanian)* 80−29093
isocahedral particles, high symmetry orientations, HEED and TEM study 79−86732
Kevlar 29 and 49, aramid fibres, microvoid obs. 80−38960
layer structures, intercalation with N_2H_4, charge density waves or artefacts 80−100221
layered materials, struct. changes rel. to CDW, TEM, electron diffr., dichalcogenides appl. 80−39042
lipoprotein, low density, from human serum, STEM and FE-TEM obs. 79−100566
low-angle grain boundary dislocations, periodic clustering 79−46681
macroscopic metal catalysts, morphology and etching processes, review 80−7856
magnesioferrite spinels, noncubic, spinodal decomp. of Fe-rich chromites 78−72763
magnetite, multiple orientation relationships between hematite, TEM study 79−60298
materials failure and corrosion, microstructural aspects, obs. 79−52610
metal, atomic defect configuration from high resolution TEM 78−47324
metal, ductile fracture, crack initiation at dislocation cell boundaries 77−66692
transmission electron microscope examination of materials continued
metal, electron wave flux distrib. fine struct. near Bragg refl. 78−83670
metal, FCC, He ion irrad., He gas bubble lattice obs. 79−14858
metal, FCC, investigation of stage-I_E interstitial nature by TEM 78−47329
metal, plastic deform. mech., TEM appl. Mg, FCC metals *(French)* 77−1853
metal, point defect clusters, TEM obs., review 78−26564
metal coating, prep. by plasma arc spraying and characterisation 79−23873
metal crystallites, orientation and shape determ. by TEM 80−1907
metal crystallites characterisation by selected-zone and weak-beam dark field TEM 80−79654
metal film, microporosity induced by nucleation and growth processes, TEM expts. 78−10303
metal film, on pyrex, surface roughness meas. by ellipsometry and TEM 77−20205
metal films, on alkali halide substrates, nucleation and growth, surface study techniques, review 80−10809
metal oxide smoke particles, prep. by burning metal in Ar-O_2 gas, electron microscope obs. 77−52238
metal oxide smoke particles prepared by gas evap., morphology and coalescence growth 80−97738
metal particles, small, possible vibrations associated with twins 80−100253
metal powder, method for TEM study 80−84038
metal-C system, spheroidal graphite formation, role of high angle boundaries *(Russian)* 80−81065
metal-semiconductor contacts, new phases struct. 78−34899
metal-Si system, ion implanted, inert-gas-bubble form., TEM and Rutherford backscatt. anal. 79−90682
metallic epitaxial layers, TEM obs. *(Spanish)* 77−47308
metallic glasses, structure direct obs. by bright field TEM 80−10502
metallic systems, in-situ obs. of solidification interfaces with 1 MeV electron microscope 79−87574
metalloid-transition metal amorphous surface alloys formed by ion implantation, TEM study 78−67730
metallurgical and mineralogical specimens, electron beam microanalysis 77−60152
metallurgical problems, struct.-props. relation use of TEM and SEM and optical microscopy 77−56186
metals, deformation structure during cutting, investigation by TEM *(Japanese)* 80−70086
metals, metastable phases, ion implantation, review 80−49254
metals, stacking fault energy meas. by electron microscopy *(French)* 79−42079
methane-O_2, solid mixture, electron diffraction study *(Russian)* 78−83953
$Mg_{70}Zn_{30}$, amorphous alloy 77−27835
mica muscovite, iron latent tracks obs. by TEM 79−73235
micas, synthetic, polytypism and faulting, lattice imaging obs. *(French)* 78−79587
microcell for electrolytic polishing specimens 79−96248
micropipette electrode tips, beveled, non-destructive electron microscopic exam. 80−89915
microscope specimens, investigation of morphology of damage due to field corrosion 80−57425
microstructures digital simulation 80−19679
mineral, Burgers vector characterisation method using electron microscope contrast simulations 80−109141
mineral crystallographic defects, high-resolution TEM obs. 80−72517
mineral fibre characterisation using energy dispersive X-ray spectrometry in TEM *(French)* 80−82857
multiply twinned particles, with decahedral and icosahedral pt. group symm., twin cryst. struct. 79−86801
muskovite, disordered mica struct. high resolution electron microscopy exam. 78−91344
Nimomic PE-16, equilibrium surface bombarded with high dose He^+ ions 78−95091
Nimonic 80A, rapidly solidified, struct. and initial precipitation, field-ion and TEM study 79−78982
Nimonic PE16, neutron irradiated after heat treatment, solute segregation to pt.-defect sinks 79−78976
nylon 6,6, drawn fibre, selective degradation, gel permeation chromatography, TEM 78−71683
nylon 6,6, selective degradation, mol. wt. determ., gel permeation chromatography, TEM 78−71682
nylon-6, pressure-crystallised, morphology and structure 77−84669
optical multilayer film cross sections 77−19387
organic crystal, appl. of TEM 80−24327
organic molecular crystal, phase transforms. obs. using TEM, electron beam damage 78−34621
orthosilicate chloritoid, layered, disordered, electron microscopic and X-ray anal. 78−75511
oxides, plastic deform., TEM obs. *(French)* 77−44304
p-n junction with one-sided step model internal field topography, out-of-focus image interpretation 79−82129
particulates, quantitatives charact. by computerised high voltage, SEM 79−48036
PbO-Nb_2O_5 system, X-ray and electron microscopic phase and struct. determ. *(French)* 80−92508
Permalloy RF sputtered films, struct.-sensitive mag. props. 80−34705
Permalloy thin films, Neel wall transitions into cross-tie walls 79−95619
perovskite type oxides, long period structures *(French)* 78−26395
phyllosilicates, new types, in carbonaceous chondrite matrix 79−80285
piezoelectric material, fractographic features of fatigue 79−52374
pigeonite, antiphase domains exptl. coarsening 80−81886
pinned dislocation arrangements, TEM obs. 77−43217
plagioclase feldspar, deformed, elastic twinning, TEM obs. 77−62551
plagioclase feldspar, deformed in compression, dislocation substruct. and slip, TEM obs. 77−43221
plasma-wall interactions in Princeton Large Torus Tokamak, appl. of high-field surface and techniques 79−68942
plastically deformed, conf., Clermont-Ferrand, France (June 1976) *(French)* 77−44298
plasticised cellulose acetate sheet, post-yield fracture 80−25859
plessite structure in Carlton Fe meteorite, analytical study 78−32422
poly(4-methylpentene-1), permanganic etchant for TEM obs. 80−21132
poly(cis-isoprene), tagged, in untagged matrix, instantaneous shape, segmental density 78−62966

transmission electron microscope examination of materials continued
poly-γ-benzyl-L-glutamate, monolayers, struct. studies, IR, ATR, and TEM obs. 80−44396
poly-m-phenylene, isophthalamide-b-dimethyl siloxane, morphology and tensile deform. 78−91263
poly-m-phenylene isophthalamide-b-ethylene oxide, morphology and tensile deform. 78−91263
polyacetylene, nascent morphology obs. 80−24379
polyacrylonitrile, new model for structure, small-angle X-ray scattering and TEM study 79−77531
polyester-polyurethane semi-interpenetrating networks, mech. props., morphology 80−45362
polyethylene, high density, wear mechanism at steel surface, SEM, TEM and DTA 78−64727
polyethylene, high-density, lamellar sep. during deform. 78−23775
polyethylene, linear, injection moulded at high press. struct. 79−11640
polyethylene, obtained from heterogeneous Ziegler-Natta catalysts, cryst. morphology and growth 80−38941
polyethylene, single crystal, fold domain boundaries 80−107065
polyethylene crystals, plastic deformation, molecular mech., TEM obs. 80−21022
polyethylene single crystals, STEM advantage, specimen radiation damage 79−55620
polyethylene spherulites, thin melt-cast films, high density, deform. process in non-equatorial regions 80−81124
polyisobutylene, impurity distrib. of tagged poly-cis-isoprene, individual and aggregate 79−68339
polyisoprene, from guayule rubber, TEM exam. of crystallisation 80−10508
trans-1,4-polyisoprene crystals, press. effect on growth rate 80−88064
trans-1,4-polyisoprene crystals, press. effect on melting temp. and lamellar thickness, press. crystn. 80−88302
polymer, plastic deform., TEM obs. 77−44305
polymer blend morphology, methods for study and specimen prep. 78−75580
polymer blends, selective staining method for TEM obs. of morphology 80−84103
polymer crystal growth, during annealing 78−14300
polymers, defocus transmission electron microscopy 80−28927
polyoxymethylene, low-strain deform., transmission electron microscope exam. 79−5013
polyoxymethylene, wear mechanism at steel surface, SEM, TEM and DTA 78−64727
polypropylene, isotactic, epitaxial crystn. on alkali halide surface 78−26787
polypropylene, permanganic etchant for TEM obs. 80−21132
polysiloxane dizwitterionomers, mech. props., microstruct. 80−49131
polystyrene, compressed, TEM obs. of coarse shear bands 79−70117
polystyrene, craze density meas. by quantitative TEM 79−24701
polystyrene, crazed, orientation and struct., electron diffr. meas. 80−30122
polystyrene, isotactic, crystalline core of row structures, nucleation and growth 79−86718
polystyrene, isotactic crystals, plastic deformation, molecular mech., TEM obs. 80−21022
polystyrene, n-heptane and methanol crazes, structure 77−12681
polystyrene film, craze growth and fracture 79−83319
polystyrene-poly(styrene-b-butadiene-b-styrene) polyblends, electron micrographs for struct. 78−51442
polyvinylidene fluoride, chem. etching of fission tracks, growth of fine holes, TEM, SEM study 79−76297
Portland cement, HVEM and gas reaction cell for microstructural investigation 80−40649
protein adsorbed layers on field-emitter tips, removal by UV radiation 80−104836
PTFE, wear mechanism at steel surface, SEM, TEM and DTA 78−64727
PVC, rigid resin, TEM studies of morphology, processing effects 80−108385
PVC latex size determ. by TEM, vertical shadowing technique 77−53857
pyrene, low temp. phase transform., TEM obs. 78−22851
pyrocarbon, HTGR fuel particle coatings, struct. charact. 77−83034
pyrocarbon, microstructure of coatings on fuel particles, TEM study 78−25293
pyrocarbon coatings, deposition in fluidized bed, TEM, changes by irradiation 80−34084
pyrocarbon coatings, TEM anal. 77−79463
quantitative electron microscopy, recent developments, review 77−70250
quartz, Brazil twins, twinning prod. by successive shears 79−19263
quartz, dislocations, electron irrad. induced vitrification 80−107252
quartz, dissociated 'a' dislocations, TEM exam. 78−47379
quartz, dissociated a-dislocation, effect on plastic deformation 79−7610
α-quartz, electron irrad., defect struct. and radiolysis 80−107321
quartz, ion-etching of grooves for SAW devices 78−95822
quartz, naturally deformed, dynamic recrystn. during creep, dislocation substruct., Mg alloy comparison 80−109142
quartz, subgrain boundaries, theoret. predictions and microscopic obs. methods 80−84187
quartz, synthetic influence of hydrostatic pressure on precip. of structure-bound water in microinclusions 78−75838
quartz glass, ^{252}Cf fission fragment tracks 78−17526
quartz overgrowths, on quartz, high voltage transmission electron microscope exam. 79−25239
radioactive samples for TEM, jet electropolishing equipment 79−87766
rare earth oxide, lattice images *(French)* 78−26397
rare earth-3d transition metal amorphous alloys, crystallisation behaviour 80−49116
rare earth-Co alloy, electron microscopy exam. 78−67722
rare earth-Co permanent magnets, microstruct., TEM obs., magnetisation 78−91901
rare earth-iron alloy amorphous film, crystn., TEM obs. 79−87019
rare earth-transition metal alloys amorphous thin films, anisotropic mag. and microstruct. props. 78−95487
rare earth-transition metal film, amorphous, microstruct., TEM obs. 78−72018
rare earth-transition metal film, amorphous, microstruct. and magnetism 78−64230
rectorite, stacking and ordered interstratification, high-resolution TEM obs. 80−109140

transmission electron microscope examination of materials continued
refractory coatings, deposited by electron evaporation, struct. and props. 79−23871
refractory fusion reactor materials, neutron irrad., microstruct., voids, nucleation TEM study 80−29065
refractory metal films, evaporated, optical props., rel. to struct. 80−55211
refractory metal-H alloy prep. technique for TEM studies 77−90544
refractory oxide coating, prep. by plasma arc spraying and characterisation 79−23873
Rene 95, as hot isostatically pressed (HIP) and HIP+forged, low cycle fatigue 80−25854
Rene 95, Ni based superalloy, effect of grain size and gamma prime size, on fatigue crack propag. 78−64686
rutile: Ga, Mg, intersecting defect structures, TEM study 79−51123
SAP (Al_2O_3-Al) alloy, effect of high He^+ and H_2^+ conc. on microstruct. 80−34098
sapphire:Ti^{4+}, plastically deformed, precipitation hardening, TEM study 80−7592
sapphire, dislocation obs. by weak-beam TEM 77−47461
semiconductor, defects, electron microscopy study 79−95021
semiconductor, plastic deform., TEM obs. *(French)* 77−44303
semiconductors, ion-implanted, laser pulse annealing, TEM and channelling study 80−100264
n-Si:B, ion implanted, rapid identification of faulted loops 79−19254
silicates, layered, optical filtering of faulted areas in electron micrographs 80−84035
sodium acetate trihydrate, whisker growth on membrane in aq. soln. 78−30854
solid surfaces, TEM obs. appls. *(Spanish)* 77−47308
solid-solid interface chemistry, characterisation, theory 80−75448
SOS early growth 77−76703
specimen prep. methods for image processing, review 79−17405
specimen preparation for TEM, ultrasonic separation method 79−52561
specimen props., book 78−19989
sputtered coatings, metallurgical characterisation 79−15056
stacking faults, weak-beam contrast in TEM 80−75132
stained biological section, quantitative anal. of contrast 79−66596
stearic acid single crysts., electron micrographs of etch pits 77−89442
steel, 0Kh12G14N4Yu2, struct. after deformation under conditions of superplasticity 80−21031
steel, 10KhN1M, heat treated, TEM examination of dislocation arrays 79−15788
steel, 12Cr2MoWVTiB, transformation mechanism and fine structure of (M-A) phase, TEM study *(Chinese)* 80−66500
steel, 12Kh1MF, fracture in creep at temp. near 0.5 MP *(Russian)* 77−32675
steel, AISI 316, fast reactor irradiated, solution treated, struct. 77−69008
steel, alloy, high C, amorphous, produced by rapid quenching from melt, hardness and strength 78−59764
steel, alloy, type AISI 4340, martensitic transformation, TEM study 80−3043
steel, alloy, V-W-Mo-Cr, exam. of carbide transformation 80−16299
steel, alloy and C, ion nitrided and ion-softnitrided, comparison of compound layers *(Japanese)* 79−8386
steel, austenite decomposition, controlled rolling rel. to substruct., props. 79−29014
steel, austenite/ferrite interface, struct. and diffr. effects, TEM exam. 80−16308
steel, austenitic, alloyed with N, decomposition of solid solution 78−23712
steel, austenitic, Cr-Ni (20, 25 wt.%), containing B and Ti additions, splat quenching, X-ray and TEM study 79−74186
steel, austenitic, Cr-Ni (25, 20 wt.%) recrystallisation and sigma phase formation 80−35211
steel, austenitic, martensitic transform., mechanism and kinetics, TEM, X-ray and optical obs. *(Rumanian)* 78−19746
steel, austenitic, Mn-Cr-C(20, 4, 0.5 wt.%), intrinsic stacking fault energy, temperature variation 77−31679
steel, austenitic, Mn-V-C, discontinuous precipitation, grain boundary struct. effect 79−29068
steel, austenitic, Ni-Cr, neutron-irradiated solute segregation and void swelling 79−60407
steel, austenitic, type FV548, irradiated, Ni and Si rich phase, energy dispersive X-ray anal., voids and precipitation, TEM study 79−66063
steel, austenitic and duplex 308 stainless, mech. of intergranular corrosion and pitting corrosion 79−91846
steel, austenitic stainless, DIN 1.4970, influence of He on high temp. mech. props. 79−7636
steel, austenitic stainless, electron transmission microscopy, microstructural zones *(Spanish)* 79−39059
steel, austenitic stainless, embrittled by α-particle irrad. 77−69015
steel, austenitic stainless, grain boundary migration during high temp. creep, TEM exam. 78−88509
steel, austenitic stainless, He implanted 1.4970, high temp. fracture 77−86186
steel, austenitic stainless, matrix precipitation of Cr_2N, due to P addition, TEM exam. 79−4973
steel, austenitic stainless, microstructure and transient creep 79−61675
steel, austenitic stainless, NbC precipitate particle size distrib., TEM study of grain to grain variations 79−29066
steel, austenitic stainless, neutron-irradiated, gamma-alpha transformation 79−96027
steel, austenitic stainless, Ni-alloyed, Cr_2N precipitation, interface struct. and morphology 80−11644
steel, austenitic stainless, phase identification, $2^1/_2D$ imaging techniques 80−96424
steel, austenitic stainless, plastically deformed, TEM obs. *(French)* 77−44302
steel, austenitic stainless, recrystallisation, TEM obs. *(Japanese)* 79−52269
steel, austenitic stainless, stacking fault effect on martensitic transform. during plastic deform. *(Russian)* 80−25696
steel, austenitic stainless, stacking fault energy, effect of N 80−107279
steel, austenitic stainless, stress corrosion cracking in H_2SO_4-NaCl soln., Ni and N_2 effects *(Japanese)* 79−100289
steel, austenitic stainless, type 304 with He distrib., foil, effect of momentum transfer, damage energy gradient, on He distrib. 78−71773
steel, austenitic stainless, type 800, tensile creep props. rel. to intergranular microstruct. at 800°C, TEM study 79−38885

transmission electron microscope examination of materials continued
steel, austenitic stainless, unlubricated, friction, wear and microstruct. of types 304, 316 and Nitronic 60 80−108589
steel, austenitic stainless, V alloyed, creep inhibition at grain boundaries, dislocation struct., TEM study 79−43346
steel, austenitic stainless, V alloyed, creep mechanism 77−36591
steel, austenitic stainless, V alloyed, creep mechanism 77−48514
steel, austenitic stainless, welded explosively, induced martensites morphology 80−104153
steel, austenitic-ferritic Ni-Cr, 12Kh21N5T, phase and struct. transform. *(Russian)* 78−95748
steel, C content influence on brittle and tough fracture, heat treatment *(Russian)* 80−40500
steel, C martensitic, tempering induced decomposition and segregation, atom probe study 80−3112
steel, CC Cr-Mo-V, low alloy, creep fatigue interaction 78−64673
steel, cold worked, original struct. effect on softening during heating 80−60882
steel, cold-rolled, recovery of lattice defects in cementite 77−90370
steel, Cr, ferritic, N_2 effect on 475°C embrittlement 79−83313
steel, Cr, high C, in situ transform. of cementite to M_7C_3 and internal defects of M_7C_3 by tempering 78−31412
steel, Cr, lower bainite transform., significance of carbide precip. 80−97476
steel, Cr-Mo(-V), ductility and heat resistant prop. prediction rel. to fine struct. and solid soln. state 79−15751
steel, Cr-Mo (2.25, 1.0 wt.%), temper embrittlement, effect of P, Sn, comp. and carbide precip. 80−85036
steel, Cr-Mo (2.25, 1.0 wt.%), temper embrittlement, effect of Mn, Si, comp. and carbide precip. 80−85037
steel, Cr-Mo (2.25, 1 wt.%), damage accumulation and microstruct. changes during creep 80−3129
steel, Cr-Mo-Ni-WV (6, 4, 3, 2 wt.%), tempering and secondary hardening, TEM obs. *(Chinese)* 80−104245
steel, Cr-Mo-V, low alloy, V effect on creep *(Czech)* 77−86088
steel, Cr-Mo-V, press. vessel, fracture, effect of tempering 78−60799
steel, Cr-Ni (1.47, 1.48 wt.%), lath martensite microstruct. and props., cold rolling effect 80−55422
steel, Cr-Ni (2.25, 1 wt.%), role of Mo in P-induced temper embrittlement 80−35316
steel, Cr-W(Mo), quenched, carbide reactions during tempering 80−89229
steel, CrMoV, creep-resistant, quantitative struct. parameter *(Czech)* 80−35266
steel, Cu-Mo, tempered, cementite precipitation along twin boundaries 80−45309
steel, dual phase HSLA, compositional anal., TEM 80−85253
steel, duplex ferritic/ martensitic, design for improved mech. props., heat treatment, TEM obs. 77−63697
steel, electroless Ni plated, fatigue strength, effect of P content of Ni film *(Japanese)* 77−52478
steel, Fe-V-C (1, 0.2 wt.%), austenite formation 80−84927
steel, ferritic stainless, embrittlement 80−85041
steel, heat-resist., C replica method of investigating creep damage in TEM 80−21012
steel, high alloy Cr-Mo-W, splat quenched, formation of metastable austenite 80−84974
steel, high C, Burgers vector of dislocations in cementite crystal 77−27891
steel, high C, high alloy, $M_{23}C_6$ type carbides, effect of alloying elements on defect struct. and hardness 80−16481
steel, high C, high Cr, rapidly quenched, in situ carbide reactions during tempering *(Japanese)* 78−84862
steel, high Si dual-phase, mech. props and microstruct. anal. 80−40444
steel, hot rolled, low C, low alloy, bainitic alloying addition effects on microstruct. and props. 77−36546
steel, hot rolled, M1 tool type, microparticle distributions and mech. response 77−44279
steel, low alloy, cleavage fracture, fine scale precipitation dispersion effect, TEM obs. 78−60788
steel, low alloy, martensite twinning, direct anal. 80−2040
steel, low C, alloy, structural transform. during deform. and annealing *(Russian)* 79−91707
steel, low C, cold rolled sheet, Cu effect on recrystallization texture *(Chinese)* 79−74173
steel, low C, Mn-Nb, quenched and tempered, microstruct. and props. 77−36549
steel, low C, surface layer struct. under sliding friction 79−52393
steel, low C, tempered, lath martensite, Ni (5 wt.%), microstruct./yield strength relationship 77−21234
steel, low C, type En3, high strain deform., struct. and props. 80−89301
steel, marageing 300 grade, serrated flow in austenitic state 80−30041
steel, maraging, intermetallic phases precip. study by electron microscopy *(Polish)* 80−89217
steel, martensitic, tEM examination of microcracking in plate martensite *(German, English)* 79−91887
steel, medium C, fatigue behaviour of NiAl precipitation hardening 78−84983
steel, mild, AISI 1009 and 1018, corrosion incipient processes in hypersaline geothermal brine at 90°C 80−50753
steel, mild, cold rolled sheets, microstruct. and strain path in deep-drawing 78−19775
steel, mild, shear mode of ductile fracture 79−91785
steel, Mn-Cr-B (1.46, 1.03, 0.003 wt.%) 80−55422
steel, Mo, energy structure X-ray anal. using TEM 80−84036
steel, multicomponent duplex stainless, high temp. precipitation of α' 80−20939
steel, Ni (9 wt.%), tempered, mech. stability of retained austenite 79−24521
steel, Ni-B, B effect on temperability and microstructure 79−15710
steel, Ni-Co-Mo (17.55, 8.02, 4.92 wt.%) maraging, lath martensite microstruct. and props., cold rolling effect 80−55422
steel, Ni-Co-Mo-Ti, maraging, electron diffr. obs. of second phase *(Chinese)* 80−11655
steel, Ni-P plated, electroless, fatigue strength and plated layer microstruct. *(Japanese)* 80−93645
steel, Ni-Si-Nb (1.5,0.02,0.03 wt.%), fatigue crack growth under bending *(French)* 80−21089
steel, pearlitic, creep-induced micropore healing kinetics of 12MKh and 15Kh1M1F, TEM obs. *(Russian)* 80−71690
transmission electron microscope examination of materials continued
steel, pearlitic, deform. microstruct. and cementite fracture, −196 to 700°C 78−27576
steel, pearlitic eutectoid, cleavage fracture, grain size effect 78−60784
steel, pearlitic eutectoid, crack initiation and effective grain size for cleavage fracture 80−30085
steel, Si, bainite transform. 79−100134
steel, Si, metallography of bainitic transform., carbide precipitation 78−27527
steel, Si-Mn-Cr-C (1.1, 0.9, 1.0, 0.29 wt.%) 30KhGSA, heat treatment effect on strength and toughness 78−15437
steel, spheroidized, shear mode of ductile fracture 79−61714
steel, stainless, 18-8, stress corrosion cracking, in H_2SO_4-NaCl soln. *(Japanese)* 77−21315
steel, stainless, 18-8 type polycrystal, strain induced γ to α' transform. *(Japanese)* 78−11221
steel, stainless, 316 and 304, equilibrium surface bombarded with high dose He^+ ions 78−95091
steel, stainless, AISI 304, dislocation substruct. around fatigue cracks, SEM obs. 78−15516
steel, stainless, alloyed with C, magnetron-sputtered, microstruct., and cryst.-amorphous transition 80−19719
steel, stainless, annealed 310, deform. at erosion sites, TEM and SEM studies 78−64725
steel, stainless, austenitic, deform. substruct. and annealing, stacking fault tetrahedra form 80−107282
steel, stainless, austenitic, explosively welded, orientation relationship in martensitic transform. 80−104158
steel, stainless, austenitic Ni-Cr type, creep deformed, dislocation multipole obs. 80−107258
steel, stainless, depth distrib. of swelling, TEM exam. 80−15165
steel, stainless, dislocation struct. adjacent to fatigue crack tips 77−36643
steel, stainless, duplex, lattice-imaging technique 79−64965
steel, stainless, ferrite to austenite decomp. 80−93554
steel, stainless, ferritic and duplex, Mossbauer effect study of 475°C embrittlement 78−52933
steel, stainless, fracture and crack tip plastic zones, in situ obs. 80−108686
steel, stainless, grain boundary ledges, contrast phenomena identification 78−51555
steel, stainless, He ion irrad., fracture behaviour, in-situ HV electron microscopy 80−29089
steel, stainless, implantation of He ions, TEM exam. of He gas bubble lattice 79−46726
steel, stainless, Kh18N10T, substructure after high-temp. thermomechanical treatment with high deformation rates *(Russian)* 78−76657
steel, stainless, low energy D implanted, microstruct. 78−95073
steel, stainless, maraging, Cr-Co, effect of ageing on microstruct., TEM and neutron diffraction exam. 78−84867
steel, stainless, martensite nucleation mechanisms, HVEM obs. 80−104157
steel, stainless, microduplex, austenite/ferrite, recrystallisation, annealing and cold work effects 79−47713
steel, stainless, radiation-thermal treatment, N_2O_4 coolant action, intergranular corrosion *(Russian)* 78−58357
steel, stainless, shock loaded, peak press. and press. pulse duration effect on crystallographic transform. 78−67769
steel, stainless, shock loaded, residual martensite obs. 80−104414
steel, stainless, stress corrosion cracking, prestrain effect, stress relaxation study 80−35384
steel, stainless, TEM foils, white band contrast 80−75134
steel, stainless, type 304, TEM study of deformed and sensitized structs. 79−66071
steel, stainless, type 304, TEM study of dislocation emission from grain boundaries 79−66121
steel, stainless, type 304, void swelling, 200 KeV C^+ bombardment, dose and temp. depend 77−55309
steel, stainless, type 304 welded, low temp. sensitisation, nucleation of CR carbide nuclei along grain boundaries TEM, SEM study 79−38851
steel, stainless, type 304L, neutron irradiated, in-reactor precipitation and ferritic transformation 79−77644
steel, stainless, type 304L, neutron irradiated, TEM study of ferrite formation 79−42112
steel, stainless, type 316, microstruct. changes in creep ductility, SEM, TEM, optical microscopy and X-ray diffr. study 79−38927
steel, stainless, Type 316, neutron irrad. effects on tensile props. and microstruct. 80−65059
steel, stainless, type 316, neutron irradiated, ferrite formation, study by mag. meas. and TEM 79−37742
steel, stainless, Type 316 and 321, irradiation-induced creep following 4 MeV H^+ bombardment 78−14390
steel, stainless, type 430, Ni^+-implanted, struct., comp. and electrochem. anal. of surface alloy 80−16603
steel, stainless, voids, TEM, diffr. contrast 80−75218
steel, stainless 18-8, stress corrosion cracking in H_2SO_4-NaCl soln., martensite form. *(Japanese)* 78−92396
steel, stainless 304, cyclic deformation behaviour at elevated temps. 79−52322
steel, stainless 316, dislocation substruct. prod. by elev. temp. fatigue crack propag., TEM obs. 78−19863
steel, stainless 316, soln. annealed, cavity alignment and precipitation during dual ion bombardment 80−70273
steel, stainless AISI 304, low cycle fatigue at 649°C, substructural development 77−32664
steel, stainless M316, neutron irradiated, occurrence of ordered FCC phase 77−51411
steel, stainless type 304 attack morphology of stress corrosion cracking, TEM study *(French)* 79−83368
steel, stainless type 316, in-situ HVEM studies under ion beam irradiation 80−103396
steel, stainless type 316, neutron irradiated, or themally aged diamond-cubic η phase formation, TEM study 79−99249
steel, stainless type XM-19, influence of recrystn. behaviour on mech. props. 79−83213
steel, structural, second phase particle effects on impact strength 80−108581
steel, tempered martensitic, type AISI 410, role of C in embrittlement phenomena 80−93652
steel, thermally and thermomechanically treated, struct. and decomposition of martensite 78−19784

transmission electron microscope examination of materials continued
steel, tool, type M2, laser melting and heat treatment, microstruct. charact. 79−100188
steel, type 12Kh1Mf and 15Kh1M1F, damage accumulation during prolonged high-temp. creep fractography study 79−57026
steel, type 304, twinning and martensitic phases on hydrogen-charging, TEM 77−21222
steel, type 4340, deformation study, positron lifetime and hardness correlation 79−87649
steel, ultrahigh C, heat treated, mechanical properties and microstructure 79−57012
steel, V-C, as-quenched, struct. of lath martensite and occurrence of retained austenite 79−96033
steel, W, high C, amorphous, rapidly quenched from melt, mech. and thermal props. 79−38874
steel, weld metal, contrib. to mechanism of Nb(C,N) precip. *(Slovenian)* 78−84816
steel 15Kh1M1F, microstruct. changes rel. to creep and fracture *(Russian)* 79−24572
steel foil, microanalysis by energy dispersive X-ray spectrometry *(French)* 80−85250
steel hardness and ductility variations and micrographs rel. to heat treatment and phase diagram obs. 79−87609
steel mild, plastically deformed, X-ray meas. of stress and TEM 77−48496
steel SW7M, low-cycle fatigue at high hardness levels *(Polish)* 80−89323
steel-polymer wear mechanism during fretting corrosion 78−35522
step thickness determination, on crystal surfaces, use of defocus contrast of TEM 79−7531
stress corrosion cracking *(French)* 77−56153
stretched zone anal. by means of stereo matching method *(Japanese)* 80−108544
styrene-butadiene-styrene triblock copolymers, dielec. props. 78−95545
superconductor, magnetic flux quanta, TEM, SEM and STEM obs. 77−47945
surface films on solids, TEM study method 80−65409
taenite, cloudy, origin in meteorites, TEM study of Santa Catharina anomalous Fe meteorite 79−66968
tensile test specimen prep. for TEM *(German, English)* 78−60936
2,3,4,5-tetraacetoxymercurithiophene, dark-field TEM image simulation, rel. to S atom image 78−70229
TGS, cleavage surface, electron microscopy using shadow decoration technique 77−7955
thermoplastic, partially crystalline, microscopic methods of struct. anal. *(German, English)* 80−30198
thin crystal foil, large angle electron scattering by dependent Bloch wave model 79−99257
thin films, thickness determination, using backscattered electrons as tool 79−21704
thin foil, quantitative microanalysis, by energy loss spectroscopy *(French)* 80−50900
thin foils, electropolishing technique for transmission electron microscope specimen preparation 78−57919
thin metallic foil prep. for TEM obs. *(German, English)* 79−91885
thin section uniform region quantitative meas. 78−58097
thin specimen preparation by sputter-etching 78−24893
thin specimens, X-ray microanal. in TEM up to 1000 kV 80−101063
thinned semiconductor device, SEM, electron beam induced cond. of defects, rel. to TEM 80−107027
thulium phthalocyanine, mol. image in high resolution electron microscopy, radiation damage effect 80−107203
β-Ti-Mo (15wt.%) metastable alloy, strength enhancement 77−66650
titanomagnetite, single-domain particles identification by TEM 79−88342
titanomagnetites, exsolution microstructures, magnetic significance 80−98313
tooth enamel crystallites, contrast effects 80−85572
transition metal clusters, particle size rel. to bulk metallic props. 80−44490
transition metal-boron alloy amorphous film, crystn., TEM obs. 79−87019
transition metal-Si-B ternary and quaternary amorphous alloys, effect of comp. on crystn. *(Japanese)* 79−94910
turquoise, crystalline, Nogales Mexico, SEM and TEM study 79−29760
ultrathin section mounting on supported grid, wrinkleless, double grid method 79−34714
vacuum deposited metal film, elec. field effect on residual struct. 78−51836
vasopressin, dark field micrographs, image array filtering in reciprocal space 77−74557
vitrinite, in bituminous coal, microporosity and micromineralogy, small-angle X-ray scatt. study 79−12117
void contrast aid void vol. determ. 80−75217
void swelling depth distribution produced by 5 MeV Ni ions 77−7771
void volume, swelling, errors in determ. by TEM 80−84208
volcano eruption cloud particles, St. Augustine, Alaska 78−57186
weld, specimen prep. for TEM obs. 77−60029
wetting, exam. of accompanying size effect *(Russian)* 80−6596
zinc phthalocyanine film, between Au or Ag layers, microstruct. characterisation by TEM method 78−95241
Zircaloy, annealed, neutron irradiated, inhomogeneous deform. behaviour 80−85014
Zircaloy, deformed, positron annihilation and electron microscopy 77−8898
Zircaloy-2, electron irradiation damage, direct obs. 80−84212
Zircaloy-2, hydride precipitation and growth at crack tips, electron optical obs. 80−108449
Zircaloy-2, irradiation-induced creep following 4 MeV H^+ bombardment 78−14390
Zircaloy-2, neutron irrad. damage, TEM characts. 80−107332
Zircaloy-2, neutron irradiated, inhomogeneous deformation behaviour 80−50679
Zircaloy-2, neutron irradiation damage characterization by TEM 79−42110
Zircaloy-2, TEM and SEM of anodically formed oxides 77−21313
Zircaloy-2 and -4, ⟨c⟩ component dislocations from TEM contrast expts. 80−6412
Zircaloy-4, quenched and annealed, strain ageing 77−25071
Zircaloy-4, stress relaxation specimens, thermally induced strain recovery causing microstruct. changes 77−25057

transmission electron microscope examination of materials continued
Zircaloy-4-O alloys, rapidly heated and quenched, transform. charact. 79−20041
Ag, adsorbed on Si (111), electronic and cryst. struct., Schottky barrier form. obs. 78−84091
Ag, adsorption of O_2^-, catalytic oxidation mechanism 78−61046
Ag contacts on InP, TEM obs. of struct. 77−62765
Ag, deformed at room temp., glide on {001} planes, TEM obs. 79−19257
Ag, deformed bars, cold rolled, exam. of microstruct. by thin foil TEM 78−88502
Ag, dislocations gliding on (001) planes, bright field and weak-beam images 80−107266
Ag, electron beam plasma sputtered coatings on KCl substrate, islet struct. *(Russian)* 80−39460
Ag epitaxial growth, on W-ribbon substrate, in UHV, cryst. orientation determ. by etching *(German)* 79−65994
Ag, fatigued single crystal, annealing of deform. struct. 78−3204
Ag, film, chem. deposited, agglomeration, SEM and TEM obs. 80−59828
Ag film, elongated epitaxial (111) island growth on Cu(001), interface misfit, dislocations 79−82493
Ag film, epitaxial growth, characterisation of [001] tilt boundaries 78−84097
Ag film, epitaxial growth on O_2 conditioned (001)MgO film, TEM obs. 79−82489
Ag film, MBE deposited on InP(001), struct. using TEM and RHEED 79−82492
Ag film, vacuum deposited on NaCl, microstructure and orientation, surface condition influence 79−82486
Ag film, void growth, TEM obs. 80−59833
Ag films, hillock form. hole growth and agglomeration 80−44455
Ag, fine particles, adhesion and sintering, TEM exam. 78−44053
Ag formation on Ag-halide surface, flash photolysis expts. on Ag halide photochromic glasses 79−94310
Ag islands, on Al_2O_3 substrate, adsorption of ethanol, inelastic electron tunnelling spectra and TEM obs. 79−90884
Ag, small particles prep. by evaporation in clean Ar atm., cryst. morphology 77−62494
Ag, TEM exam. of ion damage in FCC metals 78−87727
Ag thin evaporated films, rel. between microstruct. and excess free energy, TEM 80−70427
Ag thin films, deposited by cathodic sputtering using high-resolution electron microscopy, voids obs. 80−49557
Ag, thin-film bicrystals, planar lattice defects and migrating grain boundaries interaction 80−79835
Ag, VPE on W (110), alignment of (111)FCC-(110)BCC epitaxial metal pairs 79−19488
Ag, vacuum deposited on Al substrate, recrystallisation 78−60044
Ag-Au, corrosion in HNO_3 80−85091
Ag-Cd (45 at.%), morphology and struct. of bainite plates in β' phase 79−52213
Ag-Cu (50 at.%), splat-cooled, struct. of γ' extended solid solution 78−3147
Ag-Cu metastable solid soln., form. by ion-beam mixing 80−75244
Ag-Hg-Sn dental amalgams, non-γ_2 phase, transmission electron metallography 79−74162
Ag-In alloys, rapidly quenched from melt, stacking faults, TEM and X-ray diffr. meas. 77−59768
Ag-SiO_2 film, elect. and struct. props., ion beam sputtering 78−80071
AgBrI photographic grains, TEM investig. of morphology and crystallography 77−57418
AgI aerosol particles, influence of particle size on cryst. struct., electron diffr. study 79−16048
Ag_3Mg, ordered alloy, projected pot. image of defect obs. 79−99176
Ag_3Mg, two different types of long-period ordered alloys, characterisation by high resoln. electron microscopy 80−49181
Al alloy, calorimetric studies on 700 series, matrix precipitate charact. of 7075 77−86036
Al alloy, calorimetric studies of 7000 series, comparison of 7075, 7050 and RX720 77−86037
Al alloy 6061, thermomechanically treated elev. temp. mech. props. 79−8310
Al alloys, age-hardenable, precipitation and dissolution processes, positron annihilation and X-ray small-angle scattering comparison 80−89238
Al alloys, rapid-quenched 80−76244
Al and Al alloys, quenched, multiple-faulted dislocation loop config., TEM 77−27887
Al, and Al-Cu(Pb) dil. alloys, pulsed ruby laser irrad., noncryst. phase form 80−35012
Al, anodic film formed in H_2SO_4, thin film TEM obs. by direct vertical sectioning 78−7106
Al anodic films, flaw obs. 80−93696
Al, anodic layers, coloured, prep. by ultramicrotome without embedding, for TEM and X-ray obs. 79−39074
Al, anodisation in H_2PO_4, irregular film formation obs. 80−30153
Al bicrystal, high resolution electron microscopy obs. of dislocations 80−103347
Al bicrystals, [011] low-angle tilt boundaries, high resolution electron microscopy 80−34012
Al, boundary dislocations gliding, on coincidence boundaries, TEM study 79−82224
Al cell structures produced by cycling and monotonic creep 80−55452
Al coating, plasma sprayed on steel substrate, microstructural investigation and oxidation effects 78−11426
Al, cold rolled, commercial purity, initial stages of recrystallisation, TEM obs. 79−56999
Al, cold rolling of 1100 plates, substruct. development 80−108476
Al, computer simulation of tilt grain boundaries compared with expt. 78−30642
Al, conversion coating formed in chromate/fluoride soln., TEM obs. 79−74289
Al crystals, TEM meas. of excess vol. of grain boundaries 80−15111
Al, deformed, thermal recovery, microstruct. and stress-strain relations 80−16325
Al, deformed in uniaxial and equibiaxial tension, dislocation arrangements 80−108516
Al, dislocation struct. change during cyclic straining at high temps. 78−44218
Al, electron beam plasma sputtered coating, islet struct. *(Russian)* 80−39460

transmission electron microscope examination of materials continued
Al epitaxial growth, on alkali halide substrates, role of phase interaction, TEM study 79−46979
Al, fatigue, effect of pre-existing subgrains 79−5041
Al, fatigue hardening at various test freqs. 79−24539
Al film, condensation from partially ionised vapour flow, peculiarities of form. and struct. 79−28252
Al film, deform. under He ion bombardment 80−65073
Al film, epitaxial growth on MgO, effect of weak interfacial interactions 77−1325
Al film, He^+ irrad., overpressurised bubble obs. 79−51165
Al, film, single cryst., defects, residual gas effects, TEM obs. 77−39587
Al film on GaAs, plasma oxidation, AES and TEM 77−77621
Al films, on calcite, electron diffr. using TEM, grain boundary scattering 79−65096
Al foil, α-particle irrad. under fusion reactor conditions, He bubble alignment during deform. 80−107345
Al, foil, influence of O_2-pressure on oxidation rate, TEM study 80−104355
Al, grain boundary migration, TEM obs. on mechanism 80−79812
Al, He injected, tracing bubble evolution by positron annihilation 77−19992
Al, high purity single cryst., etch pit morphology and their correl. with microstruct. *(French)* 79−69106
Al, high temp. creep, grain boundary dislocations 78−43065
Al, implanted Xe behaviour during anodic oxidation 80−71800
Al, ion-implanted, dechannelling by dislocations, backscatt. expts. 79−7642
Al, melting transition, TEM 77−80603
Al, oxidation, direct obs. in TEM 79−61789
Al, oxidation, in water, oxide growth rate and struct. 78−76783
Al, oxidation in hot water, electron microscope obs. of initial stages 79−11718
Al, periodic grain boundaries struct., computer simulation 77−89448
Al, periodic grain boundary struct., geometrical anal. 77−89449
Al, pipe diffusion along segment of faulted dislocation loops during annealing 80−107256
Al, plasmon-dislocation interactions, electron microscope investig. 77−15421
Al, polycryst. in annealed and creep conds., dislocation interactions with grain boundaries 79−42067
Al powder thin foil, prep. for TEM study 80−42310
Al, pure elec. cond. grade, substructural developments during recovery, Sandstrom's model validity 79−74187
Al, recovery features, TEM and positron lifetime meas. examination 78−80611
Al, recrystallisation nuclei form. and well defined deform. band struct. 79−20136
Al single crystal, high purity, unusual slip systems 78−47387
Al, small particles prep. by evaporation in clean Ar atm., cryst. morphology 77−62494
Al, specimen transfer device for combined AES/RHEED and TEM obs. 80−70093
Al, splat-cooled, grain-size distrib. function, TEM study 80−40396
Al, stationary creep in HVEM, cell struct. evolution 80−104242
Al, subgrain coalescence, grain boundary recrystallisation nucleation 80−3094
Al, surface deformation and wear track obs. using analytical electron microscope 80−108687
Al, surface film electronoptical exam., appl. of ultramicrotomy to specimen prep. 79−47847
Al, type Al6N and Al2N5, impurity influence on spreading temp. of grain boundary dislocations 79−77609
Al wire, specimen preparation for TEM by ion beam thinning *(German, English)* 80−11861
Al:Sb(Zn), ion implanted electron beam annealing, ion backscatt. and TEM meas. 80−59500
Al/Cu thin film couples, TEM study of intermetallic nucleation at interface 80−65305
Al/Pd thin film couples, thermal reactions 80−59830
Al-(Mg)(Fe), pure (dilute), large wire drawing plastic deform. 80−108508
Al-Ag, nonhomogeneity of deform. 78−84888
Al-Ag, precipitation kinetics and coarsening, effect of interfacial props. 79−91651
Al-Ag (15 wt.%), precipitation hardenend cyclic stress-strain response 78−35412
Al-Al_2Cu, aligned eutectic, precipitation, TEM and microhardness meas. 78−27529
Al-Al_2O_3, recrystallisation nucleation in drawn wires, optical and TEM obs. 79−47709
Al-Al_3Ni eutectic composite, substructural matrix hardening *(Russian)* 77−21162
Al-Al_6Fe, fibre reinforced eutectic, deformation behaviour by rolling, TEM and SEM study 79−29129
Al-Au (0.2 wt.%), precipitation mechanism and creep behaviour 80−3058
Al-Bi(Cd)(Pb)-Ti, containing low-melting pt. inclusions, mech. props. 80−93632
Al-Ce (0.06 at.%) alloy, rapidly quenched from melt, vacancy loops and precipitates, TEM 77−59769
Al-Cr (0.1 wt.%), exam. of pre precip. behaviour, by elec. resistivity meas. and TEM exam. 78−48406
Al-Cr(Mn), cold-worked and homogenised, precip. kinetics, impurity resist. and TEM meas. 77−16596
Al-Cr(Zr), simultaneous recrystallisation and precipitation *(French)* 80−16313
Al-Cu, intergranular morphology of θ′ precipitates, angle between grain boundary/precipitate plane 78−48413
Al-Cu, splat-quenched, microstruct. thickness and comp. depend., TEM 77−8863
Al-Cu (1 wt.%) alloy, plasmon dislocation interactions, electron microscope investig. 77−15421
Al-Cu (2.12 at.%), irradiated by 8J CO_2 laser pulses, metastable precipitate and amorphous phase *(French)* 78−80552
Al-Cu (33 wt.%) eutectic, superplasticity, in-situ obs. by TEM 77−28876
Al-Cu (3.97 wt.%) alloy containing Guinier-Preston zones, high resolution lattice images 80−107114
Al-Cu (4 wt.%), supersaturated and aged conditions, high strain deform. 80−60907
transmission electron microscope examination of materials continued
Al-Cu (4 wt.%), TEM obs. of intergranular corrosion 79−91835
Al-Cu (4 wt.%) alloy, high temp. cyclic deform., θ′ particle dissolution obs. 80−108515
Al-Cu (4 wt.%) alloy, neutron irrad., weak-beam dark-field obs. of dislocations near θ′ precipitates 80−107333
Al-Cu (4.3 wt.%) alloy, containing Guinier-Preston zones, high resolution lattice images 80−107115
Al-Cu (4.3 wt.%) alloy, lattice electron micrograph interpretation 79−86659
Al-Cu (4.6 wt.%), cold work and ageing influence on ductility and fracture behaviour *(Japanese)* 80−89295
Al-Cu samples (0.5, 2.0 and 4.0 wt.%) polycryst., precipitation, positron annihilation and TEM 80−50639
Al-Cu-Mg, dil. alloys, ageing response *(Korean)* 77−28832
Al-Cu-Mn-Zr, type 2219, particle, coarsening of disk shaped Θ′ particles 80−45315
Al-Cu-Mn-Zr-Fe-Si (6,0.3,0.18,0.3,0.1 wt.%) experimental evidence of Mn enrichment in Al_2Cu precipitates by EDS in TEM 78−15415
Al-Cu-Zn alloy, ageing, X-ray and electron diffr. meas. *(Russian)* 78−39806
Al-Cu-Zr (6, 0.4 wt.%), superplastic deformation charact. 80−16387
Al-$CuAl_2$ eutectic, heat treatment and interlamellar spacing effect on tensile deformation 80−29979
Al-Ge, directionally solidified lamellar eutectics, specimen prep. for TEM *(German, English)* 78−95885
Al-Ge (2 wt.%), averaged, plastic flow mechanism 77−48507
Al-Ge film, random percolation, elec. resist. meas. 79−28418
Al-Li, alloy, ageing, δ′-phase precip., effect of quenching conditions *(Russian)* 78−19761
Al-Li (2.8 wt.%), ageing in US field, precip. hardening *(Russian)* 80−29968
Al-Li alloy, annealing of vacancies and ageing, resist. and TEM obs. 77−21172
Al-Li alloys, cold worked and neutron irrad., He bubble behaviour, microstruct. changes 77−54359
Al-Li system, δ′ coherent miscibility gap determ. by small-angle X-ray scatt. 77−77483
Al-Li-Mn (2.8, 0.3 wt.%), recrystallised sheet, fracture behaviour, SEM and TEM study 80−97566
Al-Mg, foil, oxidation in O_2 atm., TEM study 80−104356
Al-Mg, grain boundary dislocation identification, TEM obs. 77−62534
Al-Mg, recrystallised, grain boundary dislocation identification by computer simulation of TEM image *(Japanese)* 77−47457
Al-Mg, Si alloy, void form. under different precip. conditions, after Al ion irrad. 80−59529
Al-Mg 0.1 at.%, neutron-irradiated, dislocation loop characterisation 79−23614
Al-Mg (3 and 7 at.%) alloys, plasmon-dislocation interactions, electron microscope investig. 77−15421
Al-Mg (5 wt.%) deformed bars, cold rolled, exam. of microstruct. by thin foil TEM 78−88502
Al-Mg (5.5 wt.%), effect of stress changes during creep on dislocation struct., TEM study 79−74214
Al-Mg solid solns., decomposition studied by ultrasonic meas. of elastic props. 80−35184
Al-Mg/Al_2O_3 composites, interface phase, Auger and electron diffr. study 80−25646
Al-Mg_2Si(1.42 wt.%), aged, dislocation structs. caused by plastic deformation 80−25786
Al-Mg-Si, influence of solid soln. elements and precipitation as correlation of formability parameters with texture 79−91696
Al-Mg-Si, precipitation of cube-shaped phases, electron diffr. study using TEM *(Japanese)* 79−43251
Al-Mg-Si, type 6010, microstruct. charact. influence on formability, heat treatment 80−81090
Al-Mg-Si alloys, cast, precip.-rich zones on grain boundaries, soln. heat treatment conditions effect on mech. props. 80−104176
Al-Mg-Si-Mn foil, planar defect spacing meas. by TEM 78−2135
Al-Mn, metastable Ll_0 phase, transformations, mag. struct., TEM study 80−3029
Al-Mn (0.35 wt.%), quenched exam. of Mn-vacancy interaction 78−76676
τ-Al-Mn-C, permanent magnetism and microstruct. 80−75811
Al-Mn-Si, recrystallisation and precipitation 78−52824
Al-Mn-Zr (0.9, 0.4%), strain induced continuous recrystn., rel. to superplastic behaviour 78−84915
Al-Ni (2 at.%) alloy, rapidly quenched from melt, vacancy loops and precipitates, TEM 77−59769
Al-Ni(Cd)(Fe)(Si), cold worked, struct. and props. 80−71666
Al-Sb, ion-implanted, precipitation form. and evolution TEM obs. 79−55766
Al-Si, deformed, local lattice rotations at second phase particles 80−25709
Al-SiO_2 interface, stress and microstruct. via TEM 78−26797
Al-silicide-Si systems with $CoSi_2$, $Pt_xNi_{1-x}Si$, and $MoSi_2$ as silicide, diffusion, compound form., and microstructure 80−34253
Al-Zn, metastable solvus curve, struct. changes 77−55950
Al-Zn, nonhomogeneity of deform. 78−84888
Al-Zn, precipitation struct. and phys. props. effect of miscibility gap *(German)* 78−92265
Al-Zn (10 wt.%), ageing at low temp., solute conc. fluctuation effects *(Japanese)* 79−4969
Al-Zn (15 at.%), supersaturated alloy, growth and decomposition kinetics 80−29965
Al-Zn (1.9 at.%), 1 MeV electron irradiated, induced homogeneous precipitation 79−77638
Al-Zn (30 wt.%), precipitation sequences and transformation kinetics, X-ray diffr. and TEM obs. 77−55959
Al-Zn alloy, metastable phases formed at 200°C, room temp. stability 80−16315
Al-Zn alloys, recrystallisation and superplasticity, HVEM straining 80−39207
Al-Zn alloys, room temp. decomp. of metastable phases precipitated at 200°C 78−84814
Al-Zn-Cu (22, 0-3 at.%) alloys, coherent spinodal curve 79−87605
Al-Zn-Fe-Si, Fe and Si effects on precip., TEM and X-ray diffr. obs., ageing at 90°C 77−48439
Al-Zn-Mg, polygonized struct. in extrusions, thermal stability and mech. props. 80−50659

transmission electron microscope examination of materials continued
Al-Zn-Mg, stress conversion cracking based on micromech. surface reactions 80−7716
Al-Zn-Mg, TEM and calorimetric study 80−76290
Al-Zn-Mg (3.87, 1.79 wt.%) TEM exam. of early stage precipitation, on dislocation lines 79−4972
Al-Zn-Mg (3.87, 1.79 wt.%), oriented growth of precipitates on dislocations, TEM obs. 80−108447
Al-Zn-Mg (4.5 at.%, 2 or 3 at.%), decomposition behaviour during continuous cooling, XSAS and TEM examination 80−16264
Al-Zn-Mg (4.5 at.%, 2 to 3 at.%), decomp. behaviour during continuous heating 80−29922
Al-Zn-Mg (5,2 wt.%), TEM of early stages of precipitation 77−40423
Al-Zn-Mg (5.9, 2.9 wt.%), ageing effects on microstruct. 80−16306
Al-Zn-Mg alloy, TEM characteris. of precipitates 80−104166
Al-Zn-Mg alloy, thermomechanically treated, precip. behaviour 78−84856
Al-Zn-Mg alloys, H_2 bubbles in embrittlement 78−19868
Al-Zn-Mg-Cu, age hardened, effect of strain rate, temp. and environment on ductility 80−45368
Al-Zn-Mg-Cu, optimum treatment combination for thermochemical processing 77−44278
Al-Zn-Mg(Mg-Ti), TEM exam. of early stage ageing behaviour, exam. of precip. kinetics 78−56645
Al-Zn-Mg(3.2, 2.2 wt.%), deform. strengthened by Guinier Preston zones 77−52343
Al_4C_3-Be_2C-SiC system, phase analysis and TEM struct. obs. 80−108420
$Al_4C_3.3Be_2C$, X-ray difr. and TEM study 80−14973
AlCu-NiCo (5 at.%), θ′ hardened, creep mechanism 80−85013
AlCuMgPb, microstruct. and flow stress during deform. at 573K 77−81307
(AlGa)As DH lasers, catastrophic optical damage generation mechanism, TEM obs. of dark line defects 80−100239
$Al_{0.36}Ga_{0.64}As$, LPE films, Te-induced defects 78−43037
n-$Al_xGa_{1-x}As$, Au-based ohmic contacts TEM obs. 80−34509
$Al_xGa_{1-x}As$ DH laser material, Ar laser induced catastrophic damage 79−86178
$Al_{45}Mn_{55}$, pure and C doped, phase transforms. 79−96022
AlN film, CVD, characterisation of film props. 78−43496
AlN foil, thickness determ. by TEM using diffr. and energy loss anal. 78−29088
AlN-Si_3N_4 mixture film, CVD, characterisation of film props. 78−43496
Al_2O_3, alumina, deformed by prismatic slip, HV TEM obs. of dislocations 80−108517
Al_2O_3 and Al_2O_3-Y_2O_3, plasma spraying, microstruct., porosity and adhesion 77−32710
Al_2O_3, atomically sharp cracks, TEM study 80−71729
Al_2O_3, β- and β″-phases, defect struct. obs. by high resolution TEM, battery ageing relevance 80−107501
Al_2O_3, defect microstructure due to ion bombardment, TEM study 80−34100
Al_2O_3 film, RF sputtered by planar magnetron, phys. props. 77−43448
Al_2O_3 film pore size distribution meas., adsorpt.-desorpt. vs. TEM methods 77−74357
Al_2O_3 films, DC reactively sputtered, struct. 80−96764
Al_2O_3, films, form., cross-sections, struct. obs. 78−67917
α-Al_2O_3, radiation damage in HVEM, at high temp. and high dose 79−46707
Al_2O_3, sapphire, edge dislocation loop obs. by high resolution lattice imaging 80−103346
Al_2O_3, sintered, TEM ons. of K containing β″′ precipitates 78−27522
Al_2O_3 substrates, grain growth during sintering 80−40302
Al_2O_3 substrates, tape-casted, fracture strength analysis 80−60948
Al_2O_3 void formation by fast neutron irradiation, TEM exam. 78−51591
Al_2O_3-Cu composite, dispersion-strengthened, hardness, tensile strength and struct. 77−70063
Al_2O_3-Cu composite, vapour deposition, microstruct., texture and surface topography 77−70001
β-Al_2O_3-Na_2O, grain boundaries and ionic cond. 79−23620
β-Al_2O_3-Na_2O, planar [00.l] disorder, TEM obs. 77−31680
β″-Al_2O_3-Na_2O, spinel formation, TEM obs. 77−76423
Al_2O_3-Na_2O, syntaxy between β and β″ structures, TEM 77−20075
Al_2O_3-Pt metal-ceramic reaction, micro/macro obs. 80−66467
Al_2O_3-SiO_2, sillimanite, lattice defects, crystallo-chemical model, TEM obs. *(French)* 78−26570
Al_2O_3-TiO_2 coating, prep. by plasma arc spraying and characterisation 79−23873
Al_2O_3-ZrO_2, dispersion hardened, fracture toughness improvement by induced microcracking *(German)* 78−31501
Al_2O_3-ZrO_2 cast refractories, nucleation processes reconstruction by SEM, TEM and STEM 78−35380
β-$Al_2O_3.Na_2O$ type compounds, struct. and stoichiometry by TEM 77−11521
Al_2O_3.Si kyanite, dislocation dissociation 77−76412
$3Al_2O_3.2SiO_2$-ZrO_2 composites, sintered, in situ-reacted, fracture props. 80−81158
As-Te-Ge chalcogenide films, thermally induced transformations, TEM obs. 79−94917
As_2S_3 thin films, vacuum deposited on Ge and PbS, sealing props. and TEM 80−35097
Au (111), anomalous surface superstruct., UHV electron microscope obs. 80−10760
Au, as deposited film prepared by vap. deposition, voids 77−69194
Au, atomic arrangements of defects, dynamic obs. of atom movement 80−39108
Au bicrystal, core structs. of misfit dislocations in grain boundaries, TEM 78−14360
Au bicrystal, dislocation networks in twin boundaries, TEM obs. 78−51556
Au, bicrystal, thin, tilt boundary migration and facet development 78−2379
Au bicrystalline film, lattice imaging of low angle tilt boundaries by TEM 78−79620
Au, bicrystalline thin films, faceting of [001] grain boundaries 80−70222
Au black solar absorbing film, particulate nature 77−39003
Au crystal, images of inner struct. of atoms 80−103229
Au crystallites, vacuum deposited on MgO (111) surface, in-situ TEM obs. of mobility 77−76686
Au, damage by ion implantation, spike threshold, TEM 79−90705

transmission electron microscope examination of materials continued
Au, deformed bars, cold rolled, exam. of microstruct. by thin foil TEM 78−88502
Au, discontinuous film, degradation under MeV heavy ion bombard., Rutherford scatt. and TEM obs. 79−24397
Au, dislocation free bicrystal, DSC dislocation network generation in coherent twin boundary 77−62544
Au, electroplated, microstruct. and hardness, effect of thickness and deposition conditions 80−20057
Au, epitaxial film, on NaCl substrate, electrotransport inferred from void growth rate *(German)* 80−10699
Au epitaxial growth, on alkali halide substrates, role of phase interaction, TEM study 79−46979
Au epitaxial particles, high resolution TEM topographical images 77−43439
Au, epitaxially grown bicrystalline thin films, preferred inclinations of ⟨100⟩ grain boundaries 80−103367
Au film, (001), vapour-deposited, surface struct. and lattice const., TEM obs. 77−1326
Au film, (001) surface atomic steps obs. using TEM 77−20173
Au film, deposition on polymer substrates, effects of glow discharge on nucleation characts. 79−77963
Au film, epitaxial growth, characterisation of [001] tilt boundaries 78−84097
Au film, ion bombarded, surface craters induced by displacement cascades 80−107344
Au film, low temp. void growth and resistivity decay 78−10302
Au, film, on sapphire substrate, nucleation, growth and postdeposition thermally induced epitaxy 79−77946
Au film, surface step structure imaging by dark field electron microscopy 80−15346
Au film, twin boundary struct. and migration, atomic scale electron microscopy obs. 80−107276
Au film, void growth in early stages of ageing and electromigration 78−38991
Au film (001), surface struct., high resolution TEM 80−100383
Au film (001) surface, computer modelling of high resolution TEM images 80−6330
Au film bicrystal, grain boundary dislocations in plane matching boundaries 80−39110
Au film sandwiches, recovery kinetics and early stages of diffusion, DC resist. expts., correl. with TEM 79−77971
Au films on Si substrate, solid-solid reactions 78−95369
Au, fine particles, adhesion and sintering, TEM exam. 78−44053
Au fine particles, adhesion, role of twinning and surface energy, TEM obs. 78−72009
Au fine particles, vacuum deposited, morphological features using TEM weak-beam dark-field technique 80−15410
Au, grain boundary struct. anal. by HVEM *(Japanese)* 80−15109
Au, grain boundary structure 80−100255
Au, growth on clean and contaminated GaAs (001) surfaces 78−26785
Au, hardening mechanisms, grain size effect 80−35302
Au, heavy ion irrad., cascade energy density effect on defect cluster type 80−107340
Au particles, small single cryst., habit plane characterisation 80−79733
Au particles, small vapour deposited multiply twinned, struct. anal. using TEM 79−82488
Au, quenched polycryst., vacancy loss at grain boundaries 80−59477
Au, serration and dissociation of edge dislocations in low-angle tilt boundaries 77−72621
Au, surface decoration, on (111) Ag surfaces, by electrodeposition *(French)* 80−44445
Au, TEM exam. of ion damage in FCC metals 78−87727
Au, thin disc prep. and electropolishing for TEM 78−88601
Au thin films, with nm-sized pores, prep. from Au-Ge eutectic films by etching 80−16227
Au, VPE on W (110), alignment of (111)FCC-(110)BCC epitaxial metal pairs 79−19488
Au vacuum deposited layer on KI, nucleation and growth 79−61516
Au vapour deposited particles, with pentagonal profiles struct. by TEM imaging techniques 79−77566
Au/AuPd, bicrysts., in situ relax. of interphase interfaces 80−39455
Au/Cu, bilayers, interdiffusion phenomena, lattice dislocations, TEM obs. 80−59736
Au/Cu, initial epitaxial growth at room temp. 80−59829
Au/Pd, bicrysts., in situ relax. of interphase interfaces 80−39455
Au/Sn films, evaporated, microstructure and texture, TEM obs. 80−39481
Au/Sn thin film couples, evaporated, TEM study 80−59832
Au-Ag, bicryst. thin film couples, interphase interfaces, TEM 80−70540
Au-Co electrodeposits, heating effect on microstruct. and surface topography 77−43456
Au-Cu-Ag dental alloy, age-hardened, struct. and morphology 78−92272
Au-Cu-Ag-Pd (35.4, 17.8, 9.7 at.%), dental alloy, age-hardenable, TEM obs. 77−21156
Au-Fe (17 at.%) alloy, fission fragment irrad., simulation of neutron effects 77−80549
Au-GaAs, film-substrate interface alloying behaviour, electron microscopic study 79−60652
Au-Ge contacts on GaAs, SEM and TEM obs. of struct. 80−100522
Au-Mg (18 at.%) alloy, superstruct. determ. 78−75630
Au-Mn alloy, ordered, coincidence sites in domain boundaries 78−71708
Au-Ni (15 at.%) film, evidence of modulated struct., TEM exam. 78−87887
Au-Pd, bicryst. thin film couples, interphase interfaces, TEM 80−70540
Au-Pd alloy, on rock salt, epitaxial growth and struct. 77−20211
Au-Si film, elec. resist. decay and struct. change on exposure to air 77−72924
Au-Si thin film double layer, silicide form., electron diffr. study 80−80005
Au-Sn evaporated films, comp. and annealing behaviour, 20-400°C 77−76695
Au-Zn(Cu) alloys, electrolytic thinning for use in transmission electron microscopy 78−57918
Au_3Cd, sputtered epitaxial films, order-disorder reaction obs. 78−84092
$Au_{11}Mn_4$, electron diffraction and microscopy obs. 78−75512
$Au_{11}Mn_4$, ordering obs. 78−71707
Au_3Zn, R_2-phase, long period domains, transmission, scanning and optical microscopy obs. 79−38801
B films, prep. by H reduction of BCl_3, struct. and hardness 80−54543

transmission electron microscope examination of materials continued
B-transition metal, amorphous thin film, crystallisation, TEM obs. 79−19483
B-transition metal thin films, amorphous to cryst. transformation 80−7563
BC, specimen preparation for TEM by ion beam thinning *(German, English)* 80−11861
B_4C, effect of fast neutron irradiation on struct. 78−26597
B_4C, morphology and struct. of vap. grown crysts. 79−7562
B_4C, TEM investigation using C replicas 80−61034
BN, TEM investigation using C replicas 80−61034
BN, wurtzite-type, prepared by static compression, struct. 77−35539
B_2O_3-Nb_2O_5 complexes, phase equilib. high resolution TEM obs. 78−35378
B_2O_3-Nb_2O_5 system, phase equil. and phase struct. obs. by high resolution TEM 80−108419
B_2O_3-TeO_2 glass, TEM obs. 78−9958
Ba ferrite compounds, microsyntactic intergrowth and cryst. defects, TEM obs. 79−10858
BaO-B_2O_3-V_2O_5 glass, oxidation-reduction of V, thermodynamics 80−85169
BaO-SiO_2 glass-ceramic, crystallisation mechanism 79−90559
$BaTiO_3$ ceramics, PTC-type, grain boundary study using TEM 80−107267
$BaTiO_3$, ferroelec. domain boundary struct. 77−24806
$BaTiO_3$, ferroelec. to paraelec. transform., influence of domain boundaries on interface struct. 79−95718
$BaTiO_3$, ferroelectric-paraelectric transform., basic struct. and characts. 79−95717
$BaTiO_3$, vacuum condensates, epitaxial growth on $SrTiO_3$ crysts., electron diffr. and TEM anal. 79−15051
Ba_2YbF_7 single crystals, electron diffr. cryst. struct. anal. *(French)* 80−92507
Be ingot, high-purity, TEM obs. of BeO dispersion 80−104165
Be, neutron irradiated, annealed, tensile props. and swelling, effect of He bubbles 78−22765
Be-Li-V, phase diagram, metallurgical aspects for fusion blanket use 80−32467
Be-Si-N system polytypes, struct. obs. using TEM 80−107192
Be-Si-O-N system, polytype periodicities, direct obs. 78−18662
Be_3N_2-$BeSiN_2$ system, crystallography and phase relationships, TEM and electron diffr. study 80−92502
$Be_9Si_3N_{10}$, TEM, direct obs. of cryst. struct. 79−60339
Bi film, initial stages of growth and orienation, TEM study 79−28237
Bi film, orientation on mica, effect of deposition parameters 77−28085
Bi film, structure and electronic props. 80−70562
Bi oxide film, struct. by electron diffr. and TEM obs. 80−6678
Bi oxides containing perovskite layers, ferroelec. cryst., electron microscopy, dislocation and domain boundaries 77−52030
BiOCl, exam. of crystal structure and morphology, as function of growth conditions, using electron microscopy 79−52103
BiTeI crystals, eutectic decomp. in transmission electron microscope 79−20024
α-brass, serrated yielding, tensile tests and TEM obs. 79−34110
C, amorphous, catalytic oxidation by Pd particles, TEM obs. 80−76555
C amorphous film struct., bright field hollow cone illum. advantages 78−22609
C characterisation, using dark-field electron microscopy 79−77464
C fibre, graphitisable, prepared by benzene decomp., stepwise heat treatment, TEM expts. 77−85950
C fibre layers on arc anodes props. and cooling behaviour 79−52245
C fibres, oxidation by NO_2, struct., props. modification 78−44237
C fibres, PAN-based type I, II and III, TEM study of structural heterogeneity 79−77465
C fibres, thermal expansion coeff. meas. using TEM fitted with furnace 80−102966
C fibres, treated with intercalating agents, lattice images 79−64993
C, filamentous catalytic, rel. crystallographic orientations of C and metal 80−89240
C films with high conductivity, prep. and props. 80−80983
C, foil, image restoration of TEM micrograph *(Japanese)* 79−71571
C, glassy, LMSC process prepared, exam. of props. by TEM and X-ray anal. 78−63675
C, glassy, prep. from liq. phenolformaldehyde resin, TEM obs. 79−83145
i-C, hard coating preparation by ion beam methods 80−25579
C, morphology and growth mechanism of carbons formed by Ni-catalysed decomp. of hydrocarbons 78−35679
C, pyrolytic, specimen preparation for TEM by ion beam thinning *(German, English)* 80−11861
C, turbostratic, formed in phenolic resin C by catalytic graphitisation of dispersed Ni, TEM study 79−77466
C vacuum deposited coatings for prosthetic devices 77−40374
CC Al-Zn-Mg (4.5,1(2)(3) at.%), decomposition during ageing, preageing and cooling rate influence 80−20938
CU-Zr-(Cr), powder metallurgical alloys, thermomech. treatment effect on props. 80−50660
Ca Mg $(CO_3)_2$ (dolomite), modulated struct. 79−100832
$Ca_2(Al,Fe,Cr)O_5$ solid soln., planar interfaces, TEM obs. 80−65008
$CaCO_3$, calcite, form of end of free elastic twin *(Russian)* 80−6416
$CaCO_3$, calcite, sputtering behaviour, optical and electron microscopy 78−43968
$CaCO_3$, plastic deformation in compression parallel to (111) 78−38709
$CaCO_3$, thermal decomp. in vacuo, ultrastruct. and crystallography 78−71864
CaF_2, plastic deform, work hardening regions, TEM obs. 80−3140
CaF_2, thin insulating film, lattice parameter meas. by electron microscope 77−65940
CaF_2:U single crystal, Czochralski-Kyropoulos grown, U ion localization 79−91580
$Ca_2(Mg,Fe)_5(Si_4O_{11})_2$-$(OH)_2$, amphibole nephrite, planar defects termination, high resoln. electron microscopy 80−79772
$CaMg(CO_3)_2$, dolomite, partial dislocations and stacking faults obs. 78−3761
$Ca_2NaHSi_3O_9$, pectolite, TEM obs., of microtwins and stacking faults 78−75677
$Ca_5OH(PO_4)_5$, powder, precise study of electron diffr. patterns, diffr. interpretation at high tension *(French)* 79−37594
$(CaO)_3SiO$ cement pastes, electron microsc. anal. 80−108761
$(CaO)_3SiO_2$, effects of polymorphism on hydration, X-ray and TEM obs. *(Japanese)* 79−20046

transmission electron microscope examination of materials continued
$Ca_x(PO_4)_y$, soln., coagulation effects on light scatt. obs., TEM, SEM 80−45090
$Ca_6Si_6O_{18}.4H_2O$, tobermorite synthetic crysts., hydrothermal growth, TEM and X-ray diffr. characterisation 79−43122
Cd chalcogenides, thin films, VPE, needle-like cryst. growth 80−80148
Cd, dislocation internal friction, orientation depend., for single crysts. 78−52882
Cd films, nucleation and growth, props. 80−29878
Cd-Zn, directionally solidified lamellar eutectics, specimen prep. for TEM *(German, English)* 78−95885
Cd-Zn alloys, splat-quenched, X-ray diffr., SEM and TEM study of struct. 79−66077
Cd_3As_2 films, nucleation processes, on NaCl substrates 80−59813
$CdBr_2(I_2)$, vapour growth crystals, decomposition, electron microscope study 78−92268
$Cd_xHg_{1-x}Te$ film, vacuum deposited, struct. and elec. props. 77−59344
$Cd_xHg_{1-x}Te$, vac. evap. film struct. rel. to carrier scatt. 77−85116
$Cd(OH)_2$ decomposition, martensitic character of struct. transition, CdO crystallite shape determ. *(French)* 78−10194
CdS, defect struct., dark-field microscopy, anal. of decoration patterns 79−23506
CdS, deformed, dislocation struct., TEM obs. 80−54250
CdS, dislocation motion, TEM obs. 80−79799
CdS film, crystallinity and optical props., effect of cation-anion ratio 77−76689
CdS smoke particle growth, prep. by evaporation in inert gases 77−24938
CdS/InP epitaxial thin films on NaCl, HEED and TEM study 80−88446
CdS(Se)(Te), evap. onto electron bombarded NaCl substrates, epitaxial growth and characts. 79−28948
CdSe evaporated films, struct. and epitaxy, TEM, RHEED, and X-ray diffr. obs. 79−77939
CdSe thin film transistor on Cr substrate, cryst. struct., substrate defect effects 80−70563
CdSe-Ge (111) heterojunctions, epitaxial, azimuthal rotation 78−84085
CdTe, aB glide dislocations, dissociated into two Shockley partials, stacking fault energy 78−43024
CdTe, laser window material, vap. deposition, mech. props. 77−46776
CdTe, single crystals, plastic deformation and dislocation struct. 79−8321
CdTe:P, annealing induced lattice defects, TEM obs. 80−2010
Ce_2O_5-P_2O_5 glass, crystallisation 77−51326
Co base alloy, FCC, twin-slip interaction 77−51379
Co, electrodeposited, influence of soln. pH on microstruct. 80−65399
Co ferrite film prep. by vac. evaporation and annealing 77−85939
Co film, electromigration exam. from structural changes and resistance increases 77−20213
Co film, on Si substrate, laser irrad., cellular struct. and silicide form. 80−10710
Co, glide ahead of terminating $\{10\bar{1}2\}$ twins 80−96545
Co, HCP, heavy-ion irrad., dislocation loops, TEM obs. 77−31667
Co, particle formation by evap., electron microscopy obs. of interaction processes 80−104053
Co, single crysts., $\{11\bar{2}1\}$ twins, accommodation and form. 80−96540
Co, superalloy, attritious wear in grinding 77−32696
Co vacuum deposited coatings on metal substrates, cryst. struct. and stability 80−75481
Co-Cr recording films, perpendicular mag. anisotropy, hysteresis loop, microstruct., TEM obs. 78−95491
Co-Cr-Ni-W-Ta-C, alloy Mar M-509, TEM exam. of thermal fatigue crack propag. in cast alloy 78−76740
Co-Cr-Nr-TaC eutectic alloys, fatigue, microstructure effects 78−23803
Co-Fe (6.25 wt.) FCC to HCP transform., model and expt. evidence 77−44243
Co-Fe alloys, transformation induced microstructs. extended total dislocations, TEM study 79−42073
Co-Fe-Nb, heavily cold worked, magnetic hardening 79−20073
Co-Fe-Nb alloys, effect of cold working on mag. props., and precipitation morphology 78−39803
Co-Fe-Ti (12,6 wt.%), semihard permanent magnet, magnetic precipitation hardening 78−52830
Co-Fe-Ti alloy, precipitation hardened, rel. between struct. and mag. props. 78−95470
Co-Ga β' quenched single crystals, annealing-out of point defects 80−55426
Co-Gd film, amorphous, prep. conditions influence on supernetwork struct. 77−76709
Co-Ni-Cr-Mo, mech. props., effect of twinning and FCC to HCP transform. 77−4779
Co-Ni-Cr-Mo (35, 20, 10 wt.%), MP35N, TEM study of phase transformations 80−81054
Co-P, electrodeposited alloys, heat-induced structural changes *(Japanese)* 80−89263
Co-Ti-C, secondary precipitation and allotropic transform., TEM obs. 80−108453
Co-Ti-Fe (3, 1 to 2 wt.%), spinodal decomposition 80−100839
Co-X-Co (X=Cr,Mo,W) systems, crystn. temp. and hardness, as quenched structures 79−77529
(Co-Ni)-$Cr_{23}C_6$ eutectic alloy, directionally soldified, microstruct. and crystallography 78−48390
Co(-Re) sputtered films, mag. props. and microstructures 79−82837
$CoFe_2O_4$ mag. fluid particles, comp., struct., and mag. props. 80−60374
CoO, polycrystalline, high temp. deform. 78−3174
CoO, pure and Li doped, dislocation spacing effect on high-temp. creep 78−35444
CoO, single crystal and polycryst., subgrain boundary form. and creep mechanism 77−39594
Co_3Pd epitaxial films, multiray dynamic theory of diffr. contrast to explain defects nature 79−64962
Co_3Pd film, ordered, stacking fault obs. by TEM and interpret. using many-beam theory 80−107680
$Co_{75}Si_{15}B_{10}$, amorphous, crystallisation study *(Japanese)* 78−9959
Co_5Sm crystals, microstruct., homogeneous precip. and nucleation 80−104160
$Co_{90}Zr_{10}$, ferromag. amorphous alloy, crystn. and domain struct. study 80−107056
Cr containing Cr_2O_3, film struct., oxide percentage determ. and temp. coeff. of resist. 80−103607
Cr, evap. film, refl. and struct. 78−72021

transmission electron microscope examination of materials continued
Cr film, on mild steel, hardness and protective props., rel. to grain size 78−11436
Cr film, size effects on spin density waves, struct. and elec. props. 77−80973
Cr film, vapour deposited on low temp. KCl substrates, struct. obs. 80−10826
Cr, oxidation in TEM 77−48593
Cr thin films, formation from $Cr(CO)_6$ dielec. breakdown 80−84881
Cr whisker cryst., growth incorporated with field electron emission 80−44458
Cr^{6+}/Cr^{3+} colloidal SiO_2 surface films on Al, TEM/XPS study 80−85090
Cr-C, hard coating preparation by ion beam methods 80−25579
Cr-Cr_2O_3, black chrome solar selective absorber, microstruct. 79−56875
Cr-Cr_2O_3 black solar absorber surfaces, microstruct. rel. to electroplating parameters 80−61418
Cr-Nb, dislocation cell growth kinetics by TEM during annealing *(Russian)* 79−65084
Cr-Si(GaAs) Schottky barriers, interfacial structural defects effect on avalanche breakdown 79−42644
Cr_5Al_8, γ-phase, microstruct., transform. strains, TEM obs. 79−11614
CrO_2 and CrO(OH), fine particle obs. of cryst. morphology and topotaxy 80−65969
$Cr_3Si_2(C_2)$, sputtered films, microstruct. and wear props. 78−64733
$Cr_{2.8}V_{0.7}Fe_{3.4}C_3$, stacking fault study, morphology, comp. and struct. 80−84190
Cs_xVF_3 (x=0.25,0.19), cryst. struct. examination by electron diffr. using TEM 79−23583
Cu, (111) surface atomic steps obs. using TEM 77−20173
Cu alloy, internally oxidised, FIM 77−20074
Cu and Cu-Al (8 wt.%) single crystal, surface dissolution effect on fatigue damage and crack nucleation 78−39936
Cu and Cu-Si, deformation and fracture under dynamic loading 78−35442
Cu, annealing twins, density, effect of recrystallisation temp. and electron microscope resolution *(French)* 78−31423
Cu, Ar^+ ion irradiated, defects study by electron microscopy *(German)* 80−2087
Cu, Ar^+ ion irradiated, small defect clusters, electron microscopy contrast *(German)* 79−99253
Cu, bright galvanic coatings, crystallite size determ. 79−66221
Cu, cementation, characterisation of nucleation and growth from aq. soln., TEM and SEM study 79−28972
Cu, cyclically deformed polycrystals, elastic limit, contribution of thermally active processes *(Spanish)* 79−91732
Cu, deformed at room temp., glide on {001} planes, TEM obs. 79−19257
Cu, dislocation structure, around tips of propagating fatigue cracks 79−29211
Cu, dislocations gliding on (001) planes, bright field and weak-beam images 80−107266
Cu, electrochem. nucleation and growth on Te and Al, TEM 80−104451
Cu, electrochem. overgrowths, role of substrate dislocations and grain boundaries in nucleation and growth 79−51454
Cu electrocrystallisation, multiple twin form. 77−39750
Cu electrodeposit, US agitation effect on hardness, porosity and grain size, work-hardening 77−60075
Cu electrolytic form. by electrodeposition, structural defects 77−39749
Cu, erosive wear mechanisms, combined TEM and SEM obs. 80−108601
Cu, fatigued single crysts., temp. depend. of saturation stress and dislocation substruct. 80−44211
Cu foils, near Σ9 grain boundary properties, boundary dissociation 80−100251
Cu, friction mechanism, HV TEM expts. 80−35341
Cu, friction surface structural investigation, O_2 surface diffusion *(Russian)* 80−96726
Cu, grain boundary anal. by TEM, CSL condition determ. 80−15117
Cu, grain boundary migration, TEM obs. on mechanism 80−79812
Cu HCP film, uniaxial, mag. domain struct. 80−60385
Cu high purity, grain boundaries as dislocation sources in premacroyield strain region 79−34096
Cu implantation of He ions, TEM exam. of He gas bubble lattice 79−46726
Cu, ion bombard. by 5 keV Ar^+, sub-surface damage 80−103399
Cu, ion irrad., Frank loops, electron microscope image contrast 80−6326
Cu, ion radiation damage 78−22773
Cu irradiation induced defects, electron microscope images 78−83854
Cu, layered cell structures and slip lines in deformed cryst., TEM obs. 79−99209
Cu metastable alloy layer, formed by Ag^+ and Ta^+ ion implantation 78−71709
Cu, near Σ9 grain boundary, structure and dislocation interactions 80−79808
Cu, near Σ9 grain boundary, props., identification by image matching of Burgers vectors 80−79810
Cu, neutron irradiation damage inhomogeneous clustering 79−73223
Cu, oxidation, electron scattering study 79−83377
Cu pin, heavily deformed surface layer after dry sliding against steel ring 77−60033
Cu, plane strain deformed, electron microscope obs. of morphology 78−31424
Cu polycrystal, fatigued, interior dislocation struct. 80−88147
Cu, proton-irradiated, H_2 gas-bubble struct., study at 300K 80−92569
Cu, pure, fatigue crack propagation, effect of stacking fault energy as deduced from dislocation patterns, TEM study 79−61719
Cu single crystal, large angle grain boundaries formed during cold work, TEM obs. of orientation relationships 79−90678
Cu single crystals, [100]- and [111], dislocation density meas. using TEM 80−79803
Cu single crystals, neutron irradiated, secondary slip 80−88161
Cu single crystals oriented along [100] and [111], exam. of slip line length 78−76664
Cu, single crysts., deformed in [001] and [111] axes, cell structs., TEM 80−70209
Cu spheres, on Cu single cryst. surface, grain boundary energy anisotropy using gravitational torques, TEM study 79−60385
Cu, TEM exam. of ion damage in FCC metals 78−87727
Cu, thick sputter deposit, microstruct., tensile props. 77−40461

transmission electron microscope examination of materials continued
Cu, VPE on W (110), alignment of (111)FCC-(110)BCC epitaxial metal pairs 79−19488
Cu, vacuum deposited on Al substrate, recrystallisation 78−60044
Cu/Cu single crystal, explosion clad bonding, TEM obs. 77−62763
Cu/Cu system, explosive cladding, TEM obs. and thermomech. model 79−96041
Cu/Ni double layer evaporated film, misfit dislocation effect on strength *(Japanese)* 79−42425
Cu-Ag, ion implantation as an ultrafast quenching technique for alloy production, ion channelling and TEM 77−55902
Cu-Ag, solid soln., nonhomogeneity of deform. 78−84889
Cu-Ag(Ta) metastable alloy form. by ion implantation, combined TEM and ion channelling obs. 78−34530
Cu-Al, gamma-2 phase intermetallic cpd., mech. props., effect of inversion domains 79−61599
Cu-Al, linear dislocation multipoles, weak-beam TEM 80−75233
Cu-Al (10 at.%) alloy, dislocation glide source obs. 77−19958
Cu-Al (12 wt.%), acoustic emission related to props. 79−34032
Cu-Al (15 at.%), rolled single crysts., metallographic study of deformation struct., orientational change, shear bonds *(Japanese)* 79−24582
Cu-Al alloy, irrad. in HVEM, climb of dissociated dislocations and point defect absorpt. 80−107257
Cu-Al alloy, planar faults, faint electron microscopic image contrast obs. 80−107283
Cu-Al martensite, temper hardening, study by TEM, DTA, microhardness and yield strength meas. 79−43260
Cu-Al_2O_3 thin film cermets, TEM study of composition and struct. 79−99437
Cu-Al-Co, precipitate-free zones near grain boundaries, growth kinetics, TEM obs. 80−40368
β-Cu-Al-Ni, nonradial diffuse streaks and complex diffuse scatt. patterns of electrons 79−7527
Cu-Al-Ni, quenched, complex martensite form. 79−56977
Cu-Al-Ni (14, 4.5 wt.%), premartensitic alterations 77−12655
β_1-Cu-Al-Ni (14.2, 4.3 wt.%), quenched, metastable 2H type phase charcts., TEM and electron diffr. study 79−74149
Cu-Al-Ni (14.5, 3 wt.%), fatigued, polycrystn., pseudoelastic, dislocation and martensite substructs. 79−82223
Cu-Al-Sn system, coexistence of different and brass like phases 80−89206
Cu-Au, corrosion in HNO_3 80−85091
Cu-Au-Cu thin film, diffusion induced grain boundary migration 79−77833
Cu-Be, dynamic strain age hardening 77−52375
Cu-Be (1.8 wt.%) alloy, discontinuous precip. form. and growth 80−104169
Cu-Be (2 at.%), plastic deform. and dislocation substruct. 80−76307
Cu-Be (2 wt.%), precipitation sequence, TEM obs. 80−108450
Cu-Be-Co, discontinuous reaction, analytical TEM 80−100842
Cu-Be-Co (1.8, 0.2 wt.%), TEM obs. of precipitates, ageing charact. *(Korean)* 77−66648
Cu-Bi (0.0115 wt.%), embrittled, grain boundary faceting, TEM study 79−27998
Cu-Cd (0.03 at.%), single cryst., deformed, dislocation arrangement 79−10856
Cu-Cr, age hardened, fine precipitates struct., TEM study 80−3066
Cu-Cr (0.75 wt.%), deformation charcts., fully reversed cyclic strain with fatigue cracks and dislocation struct. 80−81148
Cu-Cr-SiO_2 system, age and dispersion strengthened, dislocation struct. around SiO_2 particles 80−108468
Cu-Fe, growth kinetics and interfacial energy of coherent γ-Fe particles *(Japanese)* 78−19765
Cu-Fe, precipitation processes during aging, TEM, resistivity, hardness study *(Japanese)* 80−35221
Cu-Ga (17 wt.%), elec. resist. and TEM studies 80−108604
Cu-Mn-Al, constricted hysteresis loop rel. to microstruct. 78−19273
Cu-N, quenched, complex martensite form. 79−56977
Cu-Nb (0,4 at.%), splat quenched, aged, superconductivity *(Japanese)* 77−63018
Cu-Nb multifilamentary composites, in situ formed, anomalous strength increase 79−43323
Cu-Nb_2Sr, multifilamentary supercond. composites, in situ formed, critical currents 79−65625
Cu-Ni (10 wt.%), deformed bars, cold rolled, exam. of microstruct. by thin foil TEM 78−88502
Cu-Ni alloys, artefacts in thin foil images 80−3056
Cu-Ni bicrystal, misfit dislocation config., moire patterns, interdiffusion effects 78−84110
Cu-Ni bimetallic films, dislocation wall form. during interdiffusion, TEM obs. 78−51856
Cu-Ni-Al, ageing charact., optical TEM, X-ray, hardness obs. 79−29079
Cu-Ni-Cr, lattice imaging and optical microanalysis of spinodal decomp. 78−52754
Cu-Ni-Cr (28, 2.8 wt.%), spinodal alloy, microstruct. and tensile props. 78−39858
Cu-Ni-Fe, age hardenable, dislocation interactions with internal coherency stresses 77−36528
Cu-Ni-Fe, spinodal alloy, heat treatments for improved mech. props. 79−5024
Cu-Ni-Sn (15, 8 wt.%), prior deform. effect on spinodal age hardening 80−108465
Cu-Ni-Sn (9, 6 wt.%), decomposition, initial stages, TEM study 80−2992
Cu-Ni-Ti, ordering within precipitates, TEM obs. 80−108461
Cu-Pb thin film couple, interdiffusion and recrystallisation, grain size effects 77−76625
Cu-SiO_2, deformed, lattice rotations at second phase particles 80−25709
Cu-Sn alloy system, long period superlattice obs. and impurity effects 80−103297
Cu-Ti, dil. alloy, cellular precipitates, nucleation, TEM study 80−3069
β-Cu-Ti, dil. alloy, growth phenomena associated with precipitation, TEM study 80−3070
Cu-Ti, lattice parameter change during ageing *(Japanese)* 78−35411
Cu-Ti (4 wt.%), isothermal transformation, electron and optical microscopy obs. of microstructure 80−16307
Cu-Ti (5 wt.%), effect of cold work on ageing behaviour, TEM study *(Japanese)* 79−78991
Cu-Zn-Al, internally faulted martensite, TEM obs. 78−3124
β-Cu-Zn-Al, ordering, TEM obs. 78−39768

transmission electron microscope examination of materials continued
Cu-Zn-Al Marmem alloy, β_1 phase superstruct. obs., rel. to transform. mode 78−39776
Cu-Zn-Ga alloy, configs. of martensite variants, shape deform. matrices 77−12620
Cu-Zr (50 or 54 at.%), splat-quenched, glass transition and crystn. temps. determ. 78−22659
Cu_3Au, 5-100 keV Cu^+ ion bombardment, displacement cascades, TEM investig. 77−11601
Cu_3Au, disordered [001]-orientated single crysts., plastic deform., TEM and slip line studies 80−97541
Cu_3Au, displacement cascades prod. by Cu^+ bombardment 79−99251
Cu_3Au, fast neutron irrad., displacement cascades 78−83852
Cu_3Au, heavy-ion or neutron bombardment, disordered zone form., TEM diffr. contrast 77−11600
Cu_3Au, neutron irrad., displacement cascades, direct obs. method 80−107335
Cu_3Au, TEM diffr. contrast of dislocation loop 77−24253
Cu_3Au-Co, underaged, ordered and disordered single crystal, hardening mechanisms 78−3134
Cu_3Au-Ni, antiphase domains morphology 80−108460
Cu_2AuPd, struct., TEM and electron diffr. meas. 78−38666
CuCoNi ferrite magnetoacoustic oscills. rel. to microstruct. 77−85536
$CuCrS_2$, domain struct. and superstructure, TEM obs. 80−79779
$CuFeS_2$, natural chalcopyrite, defect struct., TEM 77−62535
CuI films, reactively sputtered, epitaxial growth on rocksalt substrates 79−4918
$CuInTe_2$, vac. deposited film, growth, struct. and elec. charcts. 77−69995
Cu_2MnAl, Heusler alloy, single crystal, plastic deform. 77−44308
Cu_xNbS_2, $0.8<x<1$, order-disorder transitions and incommensurate superstruct. 77−15587
$Cu_{40}Nb_{30}X_{30}$ (X=Ti, Zr, Hf), superconductors with metastable ordered structs. 80−108484
Cu_2NiZn, characterisation of superlattice dislocations by TEM 79−55748
Cu_2O, anodic form. on Cu electrodes immersed in NaOH, chronopotentiometry, SEM and TEM obs. 77−48573
Cu_2O, epitaxial, on Cu (111), misfit dislocations, TEM obs. 78−14629
Cu_2O, epitaxial, on Cu(111), misfit dislocation annealing, TEM obs. 79−82228
Cu_2O foils, electron microscope exam., Cu precipitates and CuO form. 79−1462
Cu_2O, laminar growth on (111) Cu single cryst. surface, microstruct. 78−72025
Cu_2O polycrystalline and single cryst. mech. behaviour 78−95777
Cu_2O(111) growth modes, on (111)Cu surfaces, UHV-RHEED and TEM study 79−19481
$Cu_{81}Pd_{19}$, Cu^+ (Au^-) ion-bombarded, displacement cascades and disordered zones, TEM studies 80−15167
Cu_3Pt, antiphase domains morphology 80−108460
Cu_2S, epitaxial overgrowths on Cu films, charcts., TEM and RHEED obs. 78−84101
Cu_2S, epitaxial overgrowths on Cu(111), struct. and morphology 79−82494
η-Cu_3Si precipitates in Si, cryst. struct. 78−91304
CuZn, planar faults, faint electron microscopic image contrast obs. 80−107283
CuZnAl, martensitic, ordering effect on yield stress 79−100133
depth distrib. of self-ion damage, TEM 77−51419
Dy_2Co_{17}, domain wall behaviour, TEM expts. 77−4524
Er, laser evaporation and condensation in H_2 and Ar atmospheres 79−10941
ErO_x films, phase transforms. 77−62784
Eu pellets, specimen preparation for TEM by ion beam thinning *(German, English)* 80−11861
EuS, defect struct., etch pitting and electron microscopic obs. 79−27989
(Fe, Ni, Co)-Si-B, amorphous, compositional effect on struct. changes, after heating up to 700°C, exam. *(Japanese)* 78−48433
Fe, [110] and [410] single crysts., push-pull fatigue, TEM fracture surface obs. 79−74257
Fe, Armco, cold-rolling cavity formation, TEM study 78−6947
Fe, Armco, dislocation struct. after hot and cold rolling *(Russian)* 77−8847
Fe based dispersion strengthened thick condensates, struct., mech. props. 77−90361
Fe, cast, flake and nodular, heterogeneous nuclei and graphite chemistry 79−55896
α-Fe, cold rolled, hydrostatic press. effect on microstructural changes during creep 78−39871
α-Fe, crack initiation study at low-cycle fatigue using slip bands *(Slovak)* 79−38949
α-Fe, creep life, meas. by microstruct. changes 78−35443
α-Fe, cyclically deformed, dislocation loops, TEM obs. 79−7608
Fe, defect trapping of ion implanted D, depth profile, diffusion eqn. calcs. 80−2047
Fe, dislocation dynamics, HVEM in situ obs. 78−83822
Fe, dislocation struct. at tip of fatigue crack 77−4107
Fe epitaxial growth, on alkali halide substrates, role of phase interaction, TEM study 79−46979
Fe, epitaxial growth on Au platelets, dislocations 80−96760
α-Fe film, deform. in electron microscope, dislocation mechanism 79−82227
Fe film, thermally evaporated, contamination effects obs. 80−49545
Fe, granular film, microstructure using X-ray, electron diffr. and TEM 79−65344
α-Fe, heavy ion irradiated, TEM exam. 79−7638
Fe, microcracks formed by H_2 precipitation, SEM and TEM obs. *(Japanese)* 79−70071
Fe, microhardness of single crysts. effect of temp. on dislocation structure *(German)* 79−52357
Fe, oxidation, under low O_2 partial press., wustite whisker form. obs. 79−77972
Fe, particle formation by evap., electron microscopy obs. of interaction processes 80−104053
Fe, polycryst. whisker, microstruct. SEM and TEM 77−39755
Fe powders, prep. by BH_4 process, comp. and stability 80−44878
Fe, relaxation process effect on initial stages of flow *(Russian)* 79−74189
α-Fe, TEM on struct. round fatigue cracks 77−12699

transmission electron microscope examination of materials continued
Fe vacuum deposits on Ni(Cu)(Ag) (111) FCC substrates, orientation relationships 80−59836
Fe, whiskers, high strength, polycrystalline, microstruct. obs. 79−33214
Fe, zone refined, strained, substructural changes during annealing *(Slovenian)* 78−84845
Fe-(Co)-B and Fe-Ni-B(P), amorphous, crystn. 80−79704
Fe-Al alloy, planar faults, faint electron microscopic image contrast obs. 80−107283
Fe-Al alloys with Fe_3Al order, phase separation 77−73258
Fe-Al-N alloy, precipitation and coarsening of AlN *(Korean)* 79−91652
Fe-As (0.22 to 1.68 wt.%), martensitic transform., struct. features 77−36499
Fe-B, metallic glasses and vapour deposited films, amorphous to cryst. transition 80−88048
Fe-B amorphous alloy, annealed, microstruct. and mag. domain changes 80−75790
Fe-B metastable alloys, Mossbauer spectroscopy and electron microscopy 79−28653
Fe-B(-Co), two amorphous phases form. and crystallisation 79−27924
Fe-C (1.2 wt.%), Mossbauer study of early stages of tempering 80−16342
Fe-C (1.6 wt.%) martensite habit plane poles, statistical TEM trace anal. 80−97494
Fe-C (4.3 wt.%), splat cooled, amorphous phase form. and crystn. 77−15323
Fe-C-Si (0.62, 2.0 wt.%), interfacial struct. of broad faces of ferrite plates 79−46660
Fe-C(C-B)(C-Si), splat cooled, formation of metastable crystalline phases and glasses 78−88461
Fe-Co alloy, V addition effect on atomic order parameters, dislocation struct., mechanical props. 79−91762
Fe-Co-Cr, magnetic, phase transform. obs. *(French)* 79−47676
Fe-Co-Cr-W-Ni-C, alloy KKhVN, transforms. during annealing and nature of hardening *(Russian)* 78−56653
Fe-Co-V, Vicalloy, $\alpha \rightarrow \gamma$ transform. under plastic deform., morphological singularities *(Russian)* 77−32576
Fe-Co-V alloy, Remendur, heat treatment effects on mech. and struct. props. 77−8846
Fe-Cr, high purity binary alloy, isothermal decomp. of austenite 78−64525
Fe-Cr, oxidation, in H_2/H_2O vapour mixtures, epitaxial oxide phase formation, effect on oxidation 78−88568
Fe-Cr (13 wt.%)+polycarbosilane, powder metallurgy, charcts. 77−85962
α-Fe-Cr alloys, recrystallised, C segreg. effects, TEM *(French)* 77−28828
Fe-Cr-C, austenite to ferrite+precipitate reaction, TEM/STEM study 80−3075
Fe-Cr-C, isothermal transformations 80−16302
Fe-Cr-Co, magnetic domain walls, Lorentz microscopy 80−103854
Fe-Cr-Co (31 wt.%, 23 wt.%), microstruct. and mag. props., ageing and thermomag. treatment effects 78−76769
Fe-Cr-Co alloy, spinodally decomposed, micro-twinning 80−92537
Fe-Cr-Co-Al (27.5, 17.5, 0.5) alloy, mag. props. and microstruct. obs. 78−72367
Fe-Cr-Co-Al (27.5, 17.5, 0.5 wt.%) alloy, induced anisotropy 78−76239
Fe-Cr-Co-V alloy, microstruct. and mag. props. 78−68221
Fe-Cr-Co-V-(Ti) hard magnets, V and V-Ti effects on mag. and mech. props. 79−91810
Fe-Cr-Ni, α-particle induced precip. and phase instability 79−1470
Fe-Cr-Ni (12, 15 wt.%) austenitic alloy, Ni^{6+} irradiated, void swelling and phase stability, Si and Ti effects 80−65055
Fe-Cr-Ni (18, 14 wt.%), single strain induced γ to α' cryst. transform. *(Japanese)* 78−11221
$\alpha+\beta$-Fe-Cr-Ni (23.19, 4.91 wt.%), orientation relationship between austenite and lath martensite 78−39775
Fe-Cr-Ni alloy 800, sensitization times for intergranular corrosion 77−16746
Fe-Cr-Ni based alloys, Ni^+ ion and neutron irradiated, γ' particle redistrib. and phase stability 79−78977
Fe-Cr-Ni-C (17.2, 7.34, 0.2 wt.%) alloy, twin related laths, fracture elongation, TEM study 79−29192
Fe-Cr-Ni-Nb-C, austenitic, splat quenching 78−72798
Fe-Cu, lath martensite habit planes, TEM study 80−84942
Fe-Cu (0.34 wt.%), neutron irradiated, field-ion microscope detection of ultra-fine defects 79−42116
Fe-Cu alloy, effect of ε-Cu phase on strain ageing *(Japanese)* 80−7582
Fe-Cu alloys, transform. substruct., lath microstructure after quenching 80−16298
Fe-Cu-Ni, austenite to ferrite+precipitate reaction, TEM/STEM study 80−3075
Fe-Cu-Ti, improvement of irradiation-enhanced Cu embrittlement by Ti addition 79−43393
Fe-Fe_2O_3 composite films, structural props., microhardness, 250 to 700K 78−84095
Fe-Mn, FCC to HDP transform. 79−61581
Fe-Mn (0.5 wt.%) alloy, Burgers vector of dislocation determ. by weak-beam image in HVEM 80−103351
Fe-Mn (1 at.%), strain age hardening 80−108472
Fe-Mn-C, austenitic, strain induced γ to ε transform., active slip systems 77−48427
Fe-Mn-C, martensitic transformations, electron microscopy and diffr. studies 79−68989
Fe-Mn-C (0.7, 0.9 wt.%), pearlitic, deform. 77−86095
Fe-Mn-Ni, fracture toughness, thermomechanical treatment effects 78−60794
Fe-Mn-Ni-V-C (0.5, 3.0, 1.0, 0.2 wt.%), austenite decomp., isothermal transform. charcts. 80−97477
Fe-Mn-V-C (0.5, 1.0, 0.2 wt.%) austenite decomp., isothermal transform. charcts. 80−97477
Fe-Mo (13-20 at.%) binary alloys, spinodal decomp. on ageing, TEM and X-ray diffr. study 80−97503
Fe-Mo (15.5 and 19.5 at.%), modulated struct., heat treatment effects, TEM obs. 79−100192
Fe-Mo (3at.%), internally nitrided, precipitate, morphology and chemistry 78−44128
Fe-Mo (4.1 wt.%), substructs. developed during steady state creep at 1100-1200K, TEM obs. *(Japanese)* 79−38900
Fe-Mo alloys, spinodal decomp. and modulated struct. form. on ageing *(Japanese)* 79−100184

transmission electron microscope examination of materials continued
Fe-Mo-Au, orienting of precipitating Au particles by external elastic stress 77−73279
Fe-Mo(4.1 wt.%), steady state creep at high temps. 80−89316
Fe-N, neutron irrad. effects on mech. props. 79−4338
Fe-N (0.022 wt.%), quenched, N precipitation during isothermal ageing 77−28820
Fe-N (0.03 at.%), single cryst., stress distrib. around sperical inclusion, TEM study 79−34038
Fe-N (10 at.%), structural transforms., expt. investig. *(Russian)* 77−12613
Fe-Ni, hardening by plastic deform. during polymorphic transform., struct. mechanics for γ-phase form. *(Russian)* 77−90344
Fe-Ni (23 wt.%), struct., composition changes during α to γ transform., martensite plastic deformation influence *(Russian)* 80−11642
Fe-Ni (3 wt.%), influence of temper embrittlement, on stress corrosion susceptibility 78−85023
α-Fe-Ni (3-12 wt.%), structure and γ→α polymorphic transform. kinetics 80−71645
Fe-Ni (32.86, 30.65 wt.%), characts. of quenched struct. formed in textured sheets, TEM and optical microscopy study 79−34084
Fe-Ni alloys, enthalpy change between α′→γ and α→γ transformations 80−93550
Fe-Ni base amorphous alloy, crystallisation 77−84660
Fe-Ni electrodeposited coatings, packing defects 79−60662
Fe-Ni film, amorphous, martensite form. time and struct. 80−104159
Fe-Ni martensite, TEM of passivity layer 77−36689
Fe-Ni-C, couplings of thin plate martensites 79−24492
Fe-Ni-C, model alloy, intercrystalline brittleness caused by segregation and precipitation in austenite *(Slovak)* 79−70073
Fe-Ni-C, thin foil, high voltage TEM exam. of martensitic form. 78−92264
Fe-Ni-C (19.5, 0.73 wt.%), banded struct. formed by deform., TEM and optical obs. 78−39869
Fe-Ni-C (24, 0.45 wt.%), martensites, TEM observation of double twinning 78−76651
Fe-Ni-C (31, 0.28 wt.%), crossings of thin plate martensites, TEM obs. 80−25756
Fe-Ni-C martensite, autoradiographic evidence of C clustering 79−83203
Fe-Ni-Cr (25, 15 wt.%), mobile dislocation density in steady state creep, strain transient dip test, TEM exam. 80−7650
Fe-Ni-Cr (40, 15.8 wt.%), precipitation and creep rupture behaviour, optical and TEM study 79−74158
Fe-Ni-Cr alloy, carbide form. by C diffusion, precip. distrib. and morphology 80−104164
Fe-Ni-Cr austenitic alloy, homogeneous and dispersion strengthened, internal stresses and high temp. creep 78−19841
Fe-Ni-Cr-C, effect of austenite yield strength, stacking fault energy, on martensite morphology 78−80546
Fe-Ni-Cr-P-B, Metglas 2826A, TEM of shear bands 78−48483
Fe-Ni-Mn (20, 5 wt.%), rel. orientation between adjacent martensite laths 80−76254
Fe-Ni-Ti-C (31, 4, 0-18 wt.%), coherent precipitates in austenite, effect on martensite substruct. 77−52327
Fe-Ni-V-C alloy, reverse α to γ transformation, previous deformation influence on struct. and props. *(Russian)* 79−100139
Fe-Ni-(Al) (Ti) (V)-(Cu), Cu addition strengthening at 77K, mech. props. 80−60875
Fe-Ni-(C), thin foil martensite, TEM obs. 77−51378
Fe-Ni(Mn)-Al-C, form. of ductile Ni_3Al by split quenching, mech. props. 79−100197
Fe-P film, amorphous, ion implanted, struct. and domain struct. obs. 79−91272
Fe-P-C, amorphous alloy, crystallisation 79−100112
Fe-Pt, nearly thermoelastic, irreversible lattice defects formed by martensitic transform. cycles 78−60671
Fe-rare earth, amorphous thin film, crystallisation, TEM obs. 79−19483
Fe-Si (3 wt.%), grain oriented, MnS-AlN-inhibited, precipitate morphology 77−12648
Fe-Si (3 wt.%), single crystals, cyclic deformation oriented for single glide 79−100224
Fe-Si (3.25 wt.%), dislocations in twin boundaries, electron microscopic images 80−34006
Fe-Si (3wt.%), grain-oriented, secondary recryst., grain growth inhibition 80−89245
Fe-Si amorphous film, conversion electron Mossbauer effect 78−72440
Fe-Si-Al (5,10 wt.%) struct. anal. by foil specimen techniques *(Chinese)* 79−11618
α-Fe-Ti, ion implanted, microstruct., ion beam anal. and TEM study 80−107294
α-Fe-Ti, ion implanted, with C impurity, microstruct. of TiC precips. 80−66513
α-Fe-Ti, ion-implanted and annealed, microstruct. evolution 80−15132
Fe-Ti-C, rapidly quenched by splat-cooling 80−84923
Fe-V-C, austenite to ferrite+precipitate reaction, TEM/STEM study 80−3075
Fe-V-C (0.3, 0.05 wt.%), interphase precipitation obs. in assoc. with Widmanstatten ferrite lateral growth 80−40365
Fe-X-C (X=Cr, Mo, W), quenched rapidly from melts, nonequilib. phases *(Japanese)* 80−71630
FeAl single crystal, compressed, dislocation arrangement 78−14354
Fe_3Al, Cu^+ (Au^+) ion-bombarded 80−15167
$Fe_{80}B_{20}$, crystallisation of amorphous alloys, TEM and X-ray diffr. exam. of struct., growth characts. 78−79539
$Fe_{83.4}B_{16.6}$, amorphous, mag. props. and microstruct., cooling rate and melt overheating effects 80−65965
$Fe_{80}(C_{1-x}B_x)_{20}$ amorphous alloy, α-Fe crystn., morphology 80−70129
FeCo, planar faults, faint electron microscopic image contrast obs. 80−107283
FeCoC, unidirectionally transformed eutectoid, crystallography of herringbone pearlite, TEM obs. 78−31399
FeNi amorphous films, fast phase transition investigation by TEM method 80−107029
$Fe_{50}Ni_{30}B_{20}$, crystallisation of amorphous alloys, TEM and X-ray diffr. exam. of struct., growth characts. 78−79539
FeNiCrAlLi alloy, γ′ hardened, noncellular mech. for form of lamellar η phase morphology 77−28824
$Fe_{32}Ni_{36}Cr_{14}P_{12}B_6$, METGLAS 2826A, metastable crystallization phases, TEM obs. 79−55671
$Fe_{32}Ni_{36}Cr_{14}P_{12}B_6$ metallic glass, crystn. kinetics by TEM 80−75186

transmission electron microscope examination of materials continued
$Fe_{40}Ni_{40}P_{14}B_6$ amorphous ribbon, mag. anisotropy distrib. near surface 78−95430
$Fe_{1-x}O$, precipitation of Fe_3O_4 during decomposition 78−84823
α-Fe_2O_3, crystalline grain growth during heat treatment 78−11252
γ- Fe_2O_3-Fe_3O_4, lodestone, microstructure and mag. props., source of mag. hardening 79−82828
Fe_3O_4 mag. fluid particles, comp., struct., and mag. props. 80−60374
Fe_xO_y film, thermally evaporated, contamination effects obs. 80−49545
δ-FeO(OH) and its solid solns. synthesis, X-ray diffr. and TEM studies 80−29891
δ-FeO(OH) crystallites, TEM imaging investigation 80−39096
β-FeOOH, lattice imaging and pore struct., high resolution electron microscopy obs. 80−103310
δ-FeO(OH), study of thermal decomp. by X-ray diffr., electron diffr. and TEM 80−66790
Fe_3Pt austenite, long range order parameter, temp. depend. discussion 80−97481
FeS_2, dislocations and stacking faults, TEM obs. *(French)* 79−99204
FeS_2, pyrite, stacking faults, TEM obs. *(French)* 79−28004
$Fe_{78}Si_{10}B_{12}$, amorphous alloy crystallisation study *(Japanese)* 78−9959
FeTi, H storage alloy, prep. for TEM *(German, English)* 80−30197
FeTi-H system, TEM study 79−58850
Fo-Fe-Nb, cold-worked and aged, mag. props. and microstruct. 80−34690
GaAlAs/GaAs heterostructures, ellipsometric assessment of epitaxial layer during growth in organometallic VPE system 79−37933
(GaAl)As-GaAs, double heterostructure laser, TEM study of dark line defect growth from dislocation clusters 79−33206
$Ga_{0.7}Al_{0.3}As$ epitaxial film, inclusion-generated dislocation clusters 77−89445
$Ga_{0.9}Al_{0.1}As$:Ge(Si) epitaxial layers, defect obs. by TEM 77−51618
$Ga_{1-x}Al_xAs$ DH injection laser diode, long-term-degraded, TEM obs. 78−71102
$Ga_{1-x}Al_xAs$ DH catastrophically degraded laser, TEM obs. of defects 80−32989
$Ga_{1-x}Al_xAs$, degraded DH LED, defect struct. by electrolum. topography and TEM obs. 79−60369
$Ga_{1-x}Al_xAs$ LPE crystals for DH laser, LEDs, TEM obs. of Ge, Si-doped epitaxial layers 79−1556
$Ga_{1-x}Al_xAs$, rapidly degraded LED, defect struct. of ⟨100⟩ dark lines 78−10052
$Ga_{1-x}Al_xAs$-GaAs, injection lasers, defects, TEM anal. 79−23866
$Ga_xAl_{1-x}As$-GaAs DH laser, degraded, nature of ⟨110⟩ dark-line defects, TEM 77−89439
GaAs degraded heterojunction lasers, TEM obs. of dark defects 78−14355
GaAs degraded lasers, climb asymmetry, TEM obs. 80−79802
GaAs, dislocation-free, point defects and rad. damage 80−88141
GaAs, epitaxial, polycryst., monocryst. layers and whiskers growth by CVD, SEM obs. electron diffr. study *(French)* 79−43150
GaAs epitaxial layers, non-doped, from Ga-$AsCl_3$-H_2 system, TEM and RHEED study of micromorphology and defects 79−65340
GaAs epitaxial multilayer photocathode structures, TEM obs. of dislocations generated 80−100241
GaAs heterojunction laser, origin of dislocation climb during laser operation 77−51380
GaAs, ion damage, TEM study of laser annealing 80−88215
GaAs, ion implantation damage, TEM exam. of variation with ion species and stoichiometry 78−59827
GaAs, ion implanted, laser annealing 80−107296
GaAs, ion-implanted, laser pulse annealing of amorphous surface layer, TEM 80−55436
GaAs, laser annealed, Ga precipitation, Rutherford backscattering and TEM study 79−79127
GaAs laser material, secondary dislocation climb during optical excitation 78−75672
GaAs MIS struct., elec. props., effect of interface As domains 78−88032
GaAs p-n junction formation, laser assisted, TEM and elec. props. 79−69138
GaAs, point defect generation by electron-hole recombination at dislocations 79−37699
GaAs, proton-bombarded, observation of radiation damage 80−75276
GaAs, surface segregation of implanted alkali metals, photoemitter prep. and characts. *(French)* 78−60544
GaAs, thermally oxidised, TEM obs. 78−72036
GaAs:Au, back surface gettering 80−10758
GaAs:Cr, gettering by back surface mech. damage 80−10759
GaAs:Cr pulsed electron beam induced recrystallisation and damage, amorphous layer formation 80−34052
GaAs:Cr substrates and LPE layers, Au film deposition, Cr redistrib., TEM and SIMS 80−15312
GaAs:Li diffused, lattice imperfections, TEM 77−80521
GaAs:p^+(N^+), struct. characts. of radiation damage produced by high energy ion implantation 79−4340
GaAs:S(Te)(Zn), dislocation-free, TEM study of microdefects 79−82213
GaAs:Se^+, TEM structural study, surface and interior damage 80−34025
GaAs:Si, faulted and prismatic loops obs. 77−51386
GaAs:Si, ion implantation, thermal annealing, Hall meas., SIMS atomic profile meas. 80−75243
GaAs:Si, Li, IR absorpt., microstruct., charge compensation 80−107565
GaAs:Si, pulsed laser annealing of implanted layers, defect structure and Hall effect meas. 79−69118
GaAs:Si defect density before and after Zn diffusion, SEM and TEM obs. 80−96529
GaAs:Te, heavily-doped, annealing-induced prismatic dislocation loops and elec. changes 78−51546
GaAs:Te, LPE, Te induced defects, rel. to growth conditions 78−6067
GaAs:Zn, implanted, furnace annealed, electrical, Rutherford backscattering and TEM meas. 80−100272
GaAs:Zn, ion implanted, TEM study after laser and furnace annealing 80−70234
GaAs:Zn(Cr), As precipitation at dislocations, TEM study 80−79820
GaAs:Zn(Se), recrystn. of implanted amorphous layers, TEM and channelling obs. 77−89459
GaAs-(GaAl)As, DH laser, injection enhanced dislocation glide under uniaxial stress 77−27885
GaAs-AlAs, alternate monolayer single cryst., optical waveguides 77−72065

transmission electron microscope examination of materials continued
GaAs-AlAs layered films, MBE prep., struct., rel. to optical props. 79−77950
GaAs-AlAs layered superlattices, deposited by MBE, exam. of crystal growth kinetics 78−72739
GaAs-$Ga_{1-x}Al_xAs$ LPE wafer stress-free dislocation generation 77−75527
GaAs-$Ga_xAl_{1-x}As$ laser, degradation obs. 77−51625
GaAs-GaAlAs, DH laser material, rapid optical degradation 77−7083
GaAs-GaAlAs DH lasers, optical studies of defects and degradation 78−18654
GaAs-GaAlAs DH material, dislocation glide and climb, electron diffr. 78−83824
GaAs-GaAlAs LPE layers, DH material, TEM obs. of crystal defects 78−6241
GaAs-GaAlAs planar stripe DH laser, origin of dark line defects 77−75510
GaAs-$GaAs_{0.5}P_{0.5}$ almost perfect epitaxial multilayers, TEM obs. 77−89668
GaAs-$GaAs_xSb_{1-x}$, heteroepitaxial structs., mismatch dislocation nets 79−10855
GaAs-GaInAs structure, dislocation struct., TEM anal., appl. as IR LED 80−70206
GaAs-ZnS p-n heterojunction, struct., multibeam electron microscopy obs. 79−11031
GaAs(-GaP) single cryst., defect distrib. near abraded surface 80−92533
$GaAsGa_{1-x}Al_xAs$ DH laser material, rapid optical degradation obs. 77−75528
GaAsP epitaxial film, TEM obs. of misfit dislocation arrays, nucleation and multiplication 77−39742
$GaAs_yP_{1-y}$ alloy, composition effects in growth by MBE 80−59816
$GaAs_{1-x}Px$, heteroepitaxial solid soln., defects of struct 79−28223
$Ga_{1-x}In_xAs$-GaAs epitaxial interface with small misfits, TEM image contrast 80−2275
$Ga_xIn_{1-x}P$, real struct. exam. by electron microscopy and channelling 78−2143
Ga_2O_3-Na_2O, syntaxy between β and β'' structures, TEM 77−20075
GaP, Be-Au and Si-Au ohmic contacts, metallurgical struct. 77−1485
GaP crystal, structure defect formation due to annealing and stress, dendrites, slip, dislocations 80−29026
GaP, electrical recomb. behaviour at dislocations 79−82606
GaP, epitaxial layer, carrier recomb. at dislocations 77−20932
GaP, green cathodolum. from cryst. defects, SEM, TEM study 80−80870
GaP, LEC growth of dislocation-free crysts., microdefects and striations 78−9974
GaP, preferential etching of dislocations and stacking faults 77−39589
GaP single cryst., defect distrib. near abraded surface 80−92533
GaP, VPE layer structures for LED's, SEM, and TEM obs. of dislocation density reduction expt. 80−100425
GaP:S, defect struct. and tetrahedral precipitates, TEM study 80−107246
GaP:Te, defects formed due to precipitation of Te, metallography and TEM exam. 77−84769
GaSb film, gamma-irradiated, struct., TEM and SEM obs. 79−15033
GaSb films, amorphous and cryst., vac. evaporated, Elec. cond. thermoelec. power and optical absorpt. 80−2504
GaSb, thin film prep. for TEM 77−9027
GaTe, cryst. struct., TEM and X-ray diffr. study 80−79757
Gd film, vac. deposited and VPE, deposition parameters effects on struct. 79−90912
Gd foil, domain and domain wall structure 77−69603
Gd-Co film, evaporated and sputtered, struct. and mag. anistoropy 79−56578
$GdAl_3$ thin films, polytypism 79−99446
GdCo amorphous film, O_2 contaminated, TEM obs. of source of perpendicular anisotropy 78−14993
$Gd_3Ga_5O_{12}$, garnet substrate surfaces, working damage, electron microscope investig. 77−77605
Ge amorphous film, effects of ion implantation on structure 78−55881
Ge, amorphous film, laser pulse annealing 80−15006
Ge, amorphous layer, comparison of laser and electron beam pulsed annealing 79−69374
Ge, amorphous thin films, fast crystn. and void precipitation in laser pulse annealing, TEM exam. 79−56086
Ge, atomically sharp cracks, TEM study 80−71729
Ge bicrystal, high resolution electron microscopy obs. of dislocations 80−103347
Ge bicrystals, high angle tilt boundaries, TEM *(French)* 80−70224
Ge, crystalline, high resolution image interpretation 78−14259
Ge, defect form. under radiation-accelerated diffusion conditions 80−19854
Ge, dislocations under high stress, stacking fault energies, TEM study 80−70202
Ge, dissociated dislocations, constriction correlation with jogs 80−79801
Ge, epitaxial film, crystallographic imperfections 77−35826
Ge epitaxial film, ion implantation and electron beam anneal effects on carrier conc. 80−75255
Ge, faulted dipoles, high-resolution TEM study 80−103345
Ge film, amorphous, prep. conditions influence on supernetwork struct. 77−76709
Ge, film, elec. resist. and struct., post-deposition heat treatment effects 79−78229
Ge, film, epitaxial growth on Si, interdiffusion, plasmon energy loss anal. 77−31916
Ge film, polycrystalline, structural and elec. props. 78−76173
Ge foil, [110] oriented, seven-beam lattice images of defects 80−107209
Ge foil, thinning for electron microscopy 79−49217
Ge, high-temp. radiation effects under HVEM obs. 77−89475
Ge, ion beam irrad., defects prod. by individual displacement cascades, TEM study 80−70265
Ge, lattice images of defects and radiation damage applics. 80−107210
Ge monocrystal, dynamic interaction of screw dislocations with flat clusters of dislocations on other slip planes *(Russian)* 79−86800
Ge:Te^+, ion implanted, alignment of irrad. induced defects, TEM obs. 80−15168
Ge-GaAs inter faces, heteroepitaxial, misfit dislocations, TEM obs. 79−23610
Ge-metal film, polycryst., struct. props. determ. 79−4494
Ge-metal films codeposited, amorphous and polycryst., struct. and elec. props. 80−24766

transmission electron microscope examination of materials continued
Ge-S glasses, Cu doped, thermal, structural and dielectric props. 79−60283
Ge-Si(GaAs) heterodiodes, interfacial structural defects effect on avalanche breakdown 79−42644
$Ge_{33}As_{27}S_{15}Te_{25}$ glass, switching, microstructural changes 79−65523
GeS, film on Ge, evaporation, thermogravimetric, electron microscopy investigs. 77−15715
$Ge_{20}Se_{40}Te_{40}$ amorphous alloys, thermal crystn. study 78−26789
α-GeTe, diffraction contrast between inversion domains and at boundaries in TEM 77−62457
Ge_xTe_{1-x} amorphous matrix with Te crystallites, effect of annealing 77−24274
HF with interstitial O, quantitative TEM obs. of small agglomerates 80−107227
He^+ implanted stainless steel, microstructure anal. 78−82516
$HfAl_3$, anomalous growth in thin films, AES, TEM and He backscatt. meas. 77−43462
HfO_2 film, CVD growth, struct., elec. and optical prop. characterisation 77−55891
HgS, RF sputtering on NaCl, growth and struct., electron diffr. and TEM obs. 77−90271
Ho-Co film, evaporated, struct. and mag. anistoropy 79−56578
In films, vacuum deposited, growth conditions effect on elec., optical, and structural props. 79−78215
In particles, grown in ultra-high vac. on KCl substrates, struct. and orientation 80−10814
In-Ge film, random percolation, elec. resist. meas. 79−28418
InAs films, MBE grown on GaAs, electron mobilities, lattice mismatch effect 80−80419
$InAs_yP_{1-y}$ alloy, composition effects in growth by MBE 80−59816
InGaAsP-InP DH LED, high temp. aged, dark-spot defects, TEM obs. 80−66300
In_2O_3 thin film on polyester substrate, struct. determ. by TEM 80−6674
InP, damage induced during handling for TEM obs. 80−2024
n-InP, defects in homoepitaxial layers, on p-type substrate, accurate lattice parameters 78−47675
InP film, electron-beam annealed, surface conduction 80−84500
InP single crystals, uniaxial compression deform. characts. 80−84991
InP, Zn diffused single-crystal, substitutional dopant and hole conc. meas. 80−75260
InP:Zn heavily doped X-ray topography, cathodolum., and TEM obs. 79−99197
$InP/In_{1-x}Ga_xAs_yP_{1-y}$ heterostruct., optically induced degradation 79−86791
InP-S(Te)(Zn), dislocation-free, TEM study of microdefects 79−82213
In_2S_3 destabilisation of stabilised γ-phase obs. 78−71853
InSb film, gamma-irradiated, struct., TEM and SEM obs. 79−15033
InSb, ion implanted, efficient void form., TEM obs. 80−44237
InSb:Se, exam. of defects in crystal 80−6423
InSb-GaSb superlattice, density of microtwins and dislocation boundaries, depend. on composition modulation 79−56930
In_2Te_3, low temp. ordered phase and transition state, TEM obs. 79−28095
Ir-W (0.3 wt.%), polycrystn., brittle fracture TEM study 79−61715
KCl, additively coloured, colloid nucleation and growth, TEM 77−62526
KCl, cryst. laser irrad. effects, electron microscopic obs. 77−73192
KCl:Ba, defect struct., dark-field microscopy, anal. of decoration patterns 79−23506
KNO_3 calcite-type crystals, topotaxial decomp. TEM obs. 80−108710
K_xVF_3 (x=0.25,0.19), cryst. struct. examination by electron diffr. using TEM 79−23583
$K_xWO_{(3+y)}$, direct imaging of ordering 77−11511
$LaAlO_3$, Pm3m to R3c or R3c phase transitions, TEM method for domain identification 80−14980
LaB_6 film, structure, stoichiometry, elec. properties 78−60043
$LaCoO_3$, reduction, direct obs. using high voltage TEM 77−63817
$(LaO)_2S$-$(LnO)_2S$ system (Ln=Y or Lu), TEM, X-ray diffr. and fluorescence spectroscopy 79−64957
$LaPO_4$ catalyst crysts., high resolution electron microscopy, morphological characts. rel. to catalytic activity 80−107193
Li electrode, in lithium perchlorate-propylene carbonate solution, surface anal. *(French)* 80−50859
Li electrode, passivation layer, in $LiClO_4$-propylene carbonate solution, composition *(French)* 80−11899
Li, temp. depend. of dislocation behaviour between 90 and 300K 80−88146
LiF, thin insulating film, lattice parameter meas. by electron microscope 77−65940
$LiFe_5O_8$, hysteresis and other mag. props. rel. to microstruct., TEM investig. 77−20636
$LiFe_5O_8$, vacuum annealed, tetragonal γ-phase obs. with TEM 80−11661
Li_2O-(Al_2O_3)-SiO_2 glass-ceramic, crystallisation mechanism 79−90559
$(Mg,Fe)_2SiO_4$, dislocation recovery rate affected by high-press. 80−94515
Mg alloy, dil., dynamic recrystn. during creep, dislocation substruct., quartz comparison 80−109142
Mg, cyclic hardening of single crystal 78−64552
Mg, deformed single crysts., stacking faults and dislocation dissoc. 77−31681
Mg, dislocation internal friction, orientation depend., for single crysts. 78−52882
Mg, dislocation loops induced by neutron irrad., TEM obs. 79−51113
Mg, neutron irrad. damage, TEM obs. 79−46713
Mg-Al spinel, non-stoichiometric, climb dissociation of network dislocations 80−2031
Mg-Al-Zn (94.3, 3.9, 1.8 wt.%), pricip. on dislocations, weak-beam TEM 80−76264
Mg-Mn-Ce (1.5, 0.3 wt%), superplasticity role of diffusional creep *(Russian)* 80−97528
$MgAl_2O_4$, faulted defect aggregates prod. by neutron-irrad. 80−107331
$MgAl_2O_4$, microplasticity at room temp., dislocations, TEM study 80−19805
$Mg_{1.86}Al_{1.67}Si_{2.47}O_{3.19}N_{3.81}$, 12H polytype, intergranular phases and compositional variations 80−79645
$Mg(Cu_{0.535}Al_{0.465})_2$, 2D lattice images of Friauf-Laves phase and defect type 80−24324
$(Mg_{0.88}Fe_{0.12})_2SiO_4$, natural peridot shock-prod. olivine glass 78−10178
MgO, a⟨100⟩ dislocation loops, TEM obs. 78−38710
MgO, boundary segregation of Ca, Fe, La and Si 79−70069

transmission electron microscope examination of materials continued
MgO, climb of a⟨100⟩ dislocations, TEM obs. 78−71741
MgO, crack tip dislocations and dislocation-free zones 80−96533
MgO, defect aggregation and thermal-electric breakdown, TEM obs. 79−42069
MgO, electron irradiation damage, cryst. defects 80−107320
MgO, fracture and crack tip plastic zones, in situ obs. 80−108686
MgO, melt-grown cryst., direct evidence for brucite precip. 77−28712
MgO, single cryst., order hardening by large precipitated vol. fraction of spinel particles 80−3085
MgO, single cryst., tensile creep, stress induced dislocation structs. 80−96539
MgO single crystal, dislocation struct. of slip lines, TEM 79−27990
MgO, smoke particles, size distrib. 80−104471
MgO, subgrain boundaries form. obs. by TEM, diffusion coeff. determ. 80−79817
MgO:K, implanted K aggregates, TEM and optical spectra obs. 78−83838
MgO:Li, formation of precipitates 79−29069
MgO:Li^+(Na^+), precipitation rel. to dislocations *(French)* 79−51163
MgO:Ni, heavily doped, defect characterisation, rel. to use as laser material 80−65000
MgO-Pd metal-ceramic reaction, micro/macro obs. 80−66467
$Mg(OH)_2$, and calcination product, relations between particle size, shape and surface area 78−48355
Mn film, variation of elec. resist. with deposition conditions, grain size determ. 77−43746
Mn film, variation of resist. with deposition rate, grain size determ. 77−43747
Mn-Al alloy, vacuum codeposited, disorder of $MnAl_6$ phase in recovery process 78−51854
Mn-Al permanent magnets, defect structure, mag. props. TEM obs. 78−91902
Mn-Bi film, amorphous, form. and crystn. 79−28923
Mn-Zn ferrites, grain boundary exam. using TEM and AES 80−107268
MnBi, Kerr effect and TEM obs. of mag. domains 77−89974
$Mn_{46}Co_{54}$, amorphous alloy prep. by high-rate sputtering, struct. and prop. characteris. 79−24462
$Mn_{1.15}Sb$, Kerr effect and TEM obs. of mag. domains 77−89974
MnZn soft ferrites, commercial grade, microstruct. rel. to mag. props. 80−34009
MnZn-ferroferrites, sintered, microstruct., TEM study *(Dutch)* 80−2036
Mo, 29 MeV α-particle irrad. in He, micropore and dislocation loops form. 79−14859
Mo, creep deformed single crysts., subboundary struct. obs., dislocation sets 80−103348
Mo, damage profile resulting from Ni^{2+} and He^+ ion bombardment 78−10100
Mo, defect struct. in plane strain deformed single crystal 77−63751
Mo, deformed single crystal, correlation of textural and microstructural changes 77−32586
Mo, dislocation dynamics, HVEM in situ obs. 78−83822
Mo, evap. film, refl. and struct. 78−72021
Mo film, deform. in electron microscope, dislocation mechanism 79−82227
Mo film, on Si substrates, laser irrad., cellular struct. and silicide form. 80−10710
Mo, fracture and crack tip plastic zones, in situ obs. 80−108686
Mo, fragmented struct. formed during plastic deform., TEM investig., dislocation model *(Russian)* 77−32634
Mo, He ion irradiated, TEM 77−19994
Mo, ion bombardment, damage profile, void size and density 78−47451
Mo, ion bombardment by Ni^{2+}, TEM study of damage depth distrib. 78−10101
Mo, ion irrad., defect anal., electron microscopy, appl. of theory of non-edge loop image contrast 80−70200
Mo, ion irrad., dislocation loops and stacking fault tetrahedra, electron microscope image contrast 80−6326
Mo, irradiation induced defects, electron microscope images 78−83854
Mo, mech. props., influence of temp. on singularities of deform. *(Russian)* 78−6970
Mo, microcrack formation, structural singularities, TEM obs. *(Russian)* 79−1905
Mo, neutron irradiated, small angle X-ray scatt. and TEM study of voids 79−14849
Mo, neutron irradiated, void swelling and shrinkage, TEM study 80−34079
Mo, recrystallised sintered sheet, C addition effect on ductility 79−8319
Mo, shock deformation twinning, shock press., pulse duration and grain size effects 79−5021
Mo, shock deformation twinning, shock loaded BCC and FCC metals comparison 80−104413
Mo, shock loaded, peak press. and press. pulse duration effect on crystallographic transform. 78−67769
Mo single cryst., oxidation, effect of high elec. fields, 1000-1200K, field emission and TEM obs. 77−90258
Mo, single crystals, recrystn. textures, effect of fine precipitates 78−88480
Mo, slip geometry, HVEM straining 80−39207
Mo, strain induced damping, micro- and macro-, and dislocation structures in single crystals 78−19797
Mo, structural singularities of plastic deform. at localised flow stage, TEM obs. *(Russian)* 78−6968
Mo, surface machined, struct., electron diffr., TEM *(German)* 77−73371
Mo, TEM exam. of Mo_2C precipitates, exam. of crystallographic relationships 78−52811
Mo whisker cryst., growth incorporated with field electron emission 80−44458
Mo wire, laser shock induced microstructural changes, rel. to explosive shock induced phenomena 78−67768
Mo-Al, thin film system, phase growth kinetics *(Russian)* 77−43390
Mo-Ni film system, diffusion reaction, phase form. 77−84999
Mo-Ni sputter deposited, amorphous and crystn., Ni^{++} ion irradiation effects, TEM study 79−65128
Mo-O crystals, electron microscopy study 80−28889
Mo-Ti, internally nitrided, lattice expansion by precipitation 78−68700
Mo-Ti (up to 5.48 wt.%), internal nitriding, hardness, nitride type, precipitation *(Japanese)* 79−79157

transmission electron microscope examination of materials continued
Mo-Ti-Zr (0.5, 0.1 wt.%), neutron irradiated, void swelling and shrinkage, TEM study 80−34079
Mo-Ti-Zr alloy TZM, fatigue and plastic flow, irradiation effects 77−52466
Mo-W bilayer films on Si substrates, silicides formation, marker expt. 79−99376
Mo_3CoSi, TEM study 79−51047
MoO_3, reduced crystals, planes of crystallographic shear, TEM study 79−46683
MoS_2 hydrotreating catalysts, Co, Fe and Ni effects on microstruct., TEM, SEM and EPMA obs. 79−52762
MoS_2, lattice images of defects and radiation damage applics. 80−107210
MoS_x RF reactively sputtered film, struct. and comp. 78−60038
$MoSe_2$ and other layer structs. containing hohlstellen, electron diffr. 77−80397
$MoSe_2$, imperfections from TEM study 80−79800
$MoSe_2$, single cryst., growth, struct. obs. 79−90607
$MoSe_2$, TEM exam. 77−35548
$MoSi_2$, sputtered films, microstruct. and wear props. 78−64733
NH_4Cl, submicron particles, density, morphology 80−61166
Na-rich plagioclase microstructure and exsolution 80−72501
$Na_8Al_6Si_6O_{24}Cl_2$, radiolytic radiation damage, TEM obs. 79−7628
NaCl cleavage step decoration, nucleation and growth of metallic thin films 77−69200
NaCl, deformed, dislocation densities, TEM 77−43219
NaCl, evaporation coeff. meas. by TEM 78−18909
NaCl, high resolution TEM and radiation sensitivity, dislocation obs. on deformed crysts. 80−107260
NaCl, plastically deformed [001] oriented single crystals, TEM 77−36579
NaCl, rocksalt (h10) faces, terrace like step trains, evaporation, TEM obs. 77−35801
NaCl:$MnCl_2$, Suzuki phase precip. obs. by TEM, misfit dislocations 77−31776
NaCl:NaBr crysts., dislocation motion under work hardening, transmission electron microscopy 77−51381
NaCl-gas reactions, atmospheric, in situ TEM studies 80−104544
NaF, thin insulating film, lattice parameter meas. by electron microscope 77−65940
$Na_2Ti_9O_{19}$, cryst. struct. anal. by 1 MV high-resolution electron microscopy 79−73137
Nb, 15 MeV and fission neutron displacement dqmage, TEM anal. 77−35592
Nb alloy SVMTs, high-temp. ageing, struct. and morphology of hardening phases *(Russian)* 80−40390
Nb film, deform. in electron microscope, dislocation mechanism 79−82227
Nb film, sputter-deposited on stainless steel, electron microscopy and ESCA 77−52554
Nb film sputtered onto Cu substrate, microstruct. and supercond. props. 77−85370
Nb, glissile dislocation interactions, TEM obs. 77−31666
Nb, He implanted tensile specimens, TEM 77−51398
Nb, ion bombard. by 5 keV Ar^+, sub-surface damage 80−103399
Nb, nanobridges Josephson effect, quasiparticle diffusion time, inelastic scatt. time 80−34556
Nb, neutron induced defect structs., TEM exam. 77−84802
Nb, neutron irrad., microvoid form., ang. correl. and yield strength meas., TEM obs. 78−88381
Nb, neutron irrad. effects on mech. props. 78−91361
Nb, neutron irradiated, TEM obs. of interstitial clusters 79−19288
Nb oxidation in H_2 atmospheres, TEM exam. of precipitated phase morphology and struct. 78−76790
Nb, plastic deformation effects on superconducting specific heat transition 80−20352
Nb, plastically deformed single crystal, low temp. thermal cond. 79−28336
Nb, plastically deformed single crystal, foil, damage free prep. for TEM and X-ray topography *(German, English)* 80−30200
Nb, proton irrad., dislocation loops and mag. flux pinning 79−56463
Nb, recovery and recrystallisation, fast neutron irradiation effects 77−70069
Nb, single crystal, surface oxide softening, TEM obs. 77−40462
Nb, voids, elastic side band imaging 80−75219
Nb:He, implant saturation and annealing, effect on struct. and supercond. props. *(Russian)*. 78−43538
Nb:He, mech. props. and microstruct. 80−85003
Nb-Ge, A15 struct. superconductor, high field transport props. TEM study 80−34574
Nb-Ge, compounds with A15 structure, films, TEM study *(French)* 80−80135
Nb-Ge film, coevaporated, supercond. critical temp. and struct. 77−28275
Nb-Ge film, phase transformations due to annealing, electron diffr. study 80−54551
Nb-Ge film, supercond., TEM expts., correl. of struct. and elec. props. 78−14628
Nb-Ge film, supercond., two-phase, tetragonal Nb_5Ge_3 phase identification by electron diffr. 77−89665
Nb-Ge-Si, A15 struct. superconductor, high field transport props. TEM study 80−34574
Nb-Ge-Si, compounds with A15 structure, films, TEM study *(French)* 80−80135
Nb-H, behaviour of H in Nb, relation to mech. props. 78−80572
Nb-H system, accommodation effects during hydride precipitation, TEM 80−89218
Nb-H system, phase diagram and transforms., struct. obs. of various phases 80−104125
Nb-Mo, BCC, struct. singularities rel. to solid solution behaviour *(Russian)* 77−11696
Nb-O, effect of neutron irradiation damage on low temp. deformation characts. TEM study 79−42117
Nb-Si, compounds with A15 structure, films, TEM study *(French)* 80−80135
Nb-Ti (60 at.%), aged, TEM exam. of precipitation process *(Japanese)* 78−48409
Nb-Y, and Nb, mech. props., neutron irrad. and Y scavenging effects 77−90394

transmission electron microscope examination of materials continued
Nb-Zr (1 at.%), annealed, TEM study of ion implanted irregular He bubbles 80−15164
Nb-Zr (1%), He bubbles and voids with ringed images SEM and TEM exam. 78−51529
Nb-Zr-C alloy, long term strength rel. to carbide precipitate geometry *(Ukrainian)* 78−92266
Nb-Zr-C alloy, long term loading at high temps. effect on struct. and morphology of carbide phase 79−15754
Nb-Zr-N, deformed and annealed, internal friction, rel. to structural state *(Russian)* 78−6957
Nb_3Al superconductors, sputter deposited, BCC to A15 transition, microstruct. investig. 78−27512
$Nb_3(Ge,Si)$ A15 film, supercond. and structural props. 79−87177
Nb_3Ge film, supercond., TEM obs. of microstruct. foil prep. method 77−55642
Nb_3Ge tape, prepared continuously by CVD, props. 78−60257
NbH, internal friction 78−6962
β $NbH_{0.82}$, fracture, TEM obs. 80−108519
NbH(D), ordered, TEM obs. of anisotropic lattice distortions 79−7579
$Nb_{40}Ni_{60}$, amorphous, produced by Ni^+ implantation, damage distrib. 80−107062
Nb_2O_5-WO_3 system, TEM study of intergrowth of ReO_3 and tetragonal-type structs. 79−7580
Nb_2O_5-WO_3 system complex cpds. with TTB type subcells, HV superhigh resolution electron microscopy obs. of struct. 80−103311
$4Nb_2O_5.9WO_3$, cryst. struct. determ. by 1 MV TEM 79−7581
NbS_3, Peierls distortion, chain polytypism and dislocation coupling 78−79589
Nb_3Sn composites, crit. currents and microstruct. 79−38280
Nb_3Sn, filamentary superconducting composite, TEM 77−80887
Nb_3Sn filamentary superconducting composites, mechanical properties and microstructure 79−57054
Nb_3Sn, grain size in A15 reaction layers 78−14911
Nb_3Sn, high-rate sputter-deposited, effect of oxygen on microstruct. 80−20343
Nb_3Sn multifilamentary composite supercond. wires, transverse sections prep., ion milling, TEM obs. of grain size 80−101000
Nb_3Sn, TEM of radiation damage 79−65122
Nb_3Sn, vap. deposited supercond. film, effect of N_2 and tape heating 78−34939
Nb_3Sn-Cu multifilamentary composite wire, Nb_3Sn filament morphology and grain size 80−100855
Nb_3Sn-Cu superconducting composite, electron beam co-evaporated, TEM study 79−28247
$Nd_{0.35}Co_{0.65}$ film, vac. evaporated, magnetisation ripple struct., TEM and defocused Lorentz microscopy 80−7136
$Ni_{75}Si_8B_{17}$, amorphous alloy, crystallisation study *(Japanese)* 78−9959
Ni and alloys, heavy ion irrad., defect cluster obs. 80−107341
Ni and Ni-Cr(Mo), wear tracks, TEM obs., tested in simulated face seal 77−52508
Ni, annealing twins, density, effect of recrystallisation temp. and electron microscope resolution *(French)* 78−31423
Ni, carbonyl powder, dislocation density sintering 80−108372
Ni, cavity evolution in 500 keV $^4He^+$ irrad. 80−29082
Ni, cold-worked, impurity-induced vacancy clustering 79−99972
Ni, deformed at room temp., glide on {001} planes, TEM obs. 79−19257
Ni, deformed bars, cold rolled, exam. of microstruct. by thin foil TEM 78−88502
Ni, dislocation dynamics, HVEM in situ obs. 78−83822
Ni, dislocations gliding on (001) planes, bright field and weak-beam images 80−107266
Ni, electrochem. overgrowths, role of substrate dislocations and grain boundaries in nucleation and growth 79−51454
Ni, electrodeposit, linear defect obs., TEM study 79−4304
Ni electrodeposited film, appl. of stereomicroscopic method for obs. of organic molecule incorporation 80−2288
Ni electrodeposition on Cu (001), three-dimens. epitaxial crystallites, TEM image contrast 80−88457
Ni, electroplated, fuchsin additive effect on low-temp. annealing characts., resist. meas. 77−32725
Ni, erosive wear mechanisms, combined TEM and SEM obs. 80−108601
Ni film, epitaxial growth on (001) diamond, TEM exam. 77−66098
Ni film, ion bombarded, porosity 77−66099
Ni, film deposit on (001)Fe substrate, misfit twin crystals 77−4273
Ni foils, 20 keV $^4He^+$ irrad., depth distrib. of bubbles 79−69166
Ni, grain boundary defect structure, hardening effects 80−103365
Ni, grain boundary ledge density, effect on flow stress 78−48465
Ni, grain boundary ledges, contrast phenomena identification 78−51555
Ni, implantation of He ions, TEM exam. of He gas bubble lattice 79−46726
Ni, implanted with Dy, annealing study by Rutherford backscatt., TEM, and total current spectroscopy 79−4343
Ni, in situ rare gas ion irrad., cluster creation obs. by electron microscopy 80−107343
Ni, ion irrad. with 20 and 500 keV $^4He^+$, depth distrib. of cavities and dislocation damage 80−107346
Ni, irradiated, with He^+ bubble depth distrib. meas. by TEM and blister form. mech. 78−95088
Ni, irradiation-induced creep following 4 MeV H^+ bombardment 78−14390
Ni monocrystals, struct., effect of stress applied during electrodeposition 78−26777
Ni, neutron irrad., slip bands, TEM and SEM obs. 78−51596
Ni, neutron irrad., void formation, C interstitial effects 77−76471
Ni, particle formation by evap., electron microscopy obs. of interaction processes 80−104053
Ni, pure, heavy ion irradiated, dendritic void growth 78−14386
Ni, self-ion irradiated, defect clusters, annealing 78−18687
Ni single crystal foil, H_2 induced deform. during thinning, electron-optical obs. 79−57059
Ni, structural singularities of plastic deform. at localised flow stage, TEM obs. *(Russian)* 78−6968
Ni superalloy, cast, microstruct. and microanalysis 78−35393
Ni, TEM exam. of ion damage in FCC metals 78−87727
Ni, thick sputter deposit, microstruct., tensile props. 77−40461
Ni, VPE on W (110), alignment of (111)FCC-(110)BCC epitaxial metal pairs 79−19488
Ni, void swelling caused by neutron and self-ion bombardment, 573 to 873K 78−14387

transmission electron microscope examination of materials continued
Ni/Ni_3Al-Ni_3Nb, directionally solidified lamellar eutectic alloy, deform. anisotropy and fracture 77−36604
Ni/Pt double layers on Si substrate, silicide formation 78−84010
Ni-Al, ion irradiated, dendritic growth of voids 77−11605
Ni-Al (12.8 at.%), irradiation enhanced coarsening 79−66060
Ni-Al (15 wt.%) single crystals, morphological changes of γ' precipitates during uniaxial stress-annealing 79−83236
Ni-Al (51 to 55 at.%), vacancy defective, TEM exam. of structure 78−76677
Ni-Al (6.35 wt.%) precipitate coarsening, redistribution and renucleation during ion irradiation 78−23709
Ni-Al alloys, effects of electron irradiation in precipitation, nucleation and dislocation loop growth, TEM study 79−42106
γ,γ'-Ni-Al alloys, irrad. effects on precip. 77−8829
Ni-Al film, co-evaporated, comp.-depend. struct. and morphological changes 79−87020
Ni-Al films, evaporated, grain size and microstruct. 80−15423
Ni-Al solid solns., N_2^+ irrad., void ordering 78−79644
Ni-Al-Mo (12.7, 21.6 wt.%), directionally solidified eutectic composite, precipitation 80−108454
Ni-Al(Cr)(Ti), ion irradiation induced void swelling and defect microstructs., TEM obs. 79−51164
Ni-Al(Si) foils, ion irrad., surface effects on precip. morphology 80 104168
Ni-base superalloy, IN-738, microstruct. changes during isochronal heat treatment, 773-1467K 78−27531
Ni-base superalloys, powder metallurgical, creep-rupture at intermediate temps. 80−97568
Ni-base wrought superalloy, creep and stress rupture behaviour in air and vacuum 80−60918
Ni-based superalloys, TEM obs. of cellular transformation products 80−3045
Ni-Be (2 wt.%), high-temp. radiation embrittlement, mechanical tests and TEM *(Russian)* 77−44331
Ni-C, quenched, struct. of graphite precipitates, TEM obs. *(Russian)* 78−68695
Ni-C (1.8 at.%), precipitation of graphite and NiC TEM obs. 77−52334
Ni-Co-Al alloys, continuous precip., SEM, TEM, X-ray diffr. study 80−89220
Ni-Co-Cr TEM foils, white band contrast 80−75134
Ni-Co-Cr-Mo-Al, Astroloy, extruded powder metallurgy superalloy, recrystallisation study 79−4976
Ni-Cr, movement and dislocations using SEM and diffr. contrast method *(Chinese)* 79−51110
Ni-Cr, partial dislocation, stacking fault TEM study *(Chinese)* 80−84174
Ni-Cr-Al (40, 4 wt.%), γ' and α-Cr duplex precipitation, TEM *(Japanese)* 77−25061
Ni-Cr-Co superalloy, combined TEM, FIM, atom probe microanalysis of precipitates and carbide phase comp. 80−100844
Ni-Cr-Co-Mo-Ti-Al, powders, HCl surface treatment to prevent TiC precipitation, fracture props. 79−8397
Ni-Cr-Fe alloys, radiation enhanced precip. and dissolution of precipitates, point defect kinetics and dislocation obs. 80−108467
Ni-Cr-TaC eutectic-like composite, obs. of interfacial diffusion by high resolution TEM 79−4432
Ni-Cr-ThO_2(20, 2 wt.%), dislocation struct. after high temp. deform. 77−52393
Ni-Cu-Si, Si effect on structural changes during ageing, TEM and X-ray obs. 78−15438
Ni-Dy, annealing behaviour of implantation damage, Dy outdiffusion, TEM obs. 77−77505
Ni-Fe alloys, electrodeposited, electron microscope investig. *(Russian)* 77−43442
Ni-Fe films, magnetisation reversal in narrow strips, TEM study 80−34720
Ni-Fe-Cr superalloy type 718, heat treatment effect on room temp. and elevated temp. fracture toughness response 80−100922
Ni-Fe-Nb (Mo), magnetic alloy, TEM and X-ray obs. *(Chinese)* 80−24401
Ni-Fe-Nb-Al (11.2, 8.09, 79.66 wt.%), modulated struct. growth process rel. to ageing *(Chinese)* 80−66541
Ni-Fe-Nb-Al(-Mo), wear resisting mag. head material, mag. props. and struct. 80−35350
Ni-Ge-Au evaporated contacts on GaAs, TEM obs 80−75449
Ni-Mo, off-stoichiometric, ordering 78−52752
Ni-Mo-Al and Ni-Mo-Al-V, high-resist., struct. transforms., TEM *(Russian)* 78−19762
Ni-Ni_4Mo system, deformation microstruct. 80−93591
Ni-P, amorphous electrodeposited alloys, phase-separation *(Japanese)* 80−54140
Ni-P alloy, electrodeposited, heat induced struct. changes *(Japanese)* 78−15433
Ni-p film, amorphous, ion implanted, struct. and domain struct. obs. 79−91272
Ni-S incongruently subliming system, SEM and TEM obs. of high temp. transitions, temp.-comp. diagrams 80−104136
Ni-Si (12.7 at.%), heterogeneous precipitation at internal and external surfaces during Ni ion irradiation 79−77647
Ni-ThO_2 dispersion strengthened, high temp. strength, grain size and shape effects 77−48447
Ni-Ti, near equiatomic alloy, TEM exam. of austenite-martensite interface 78−51401
β-Ni-Ti, struct. changes during annealing, TEM and selected area diffr. 79−34081
Ni-Ti (12 wt.%), dil. alloys, transform. early stages 78−3096
Ni-Ti (49.7 at.%) alloy, deform. behaviour and shape memory effect 77−32638
Ni-Ti (60 at.%) alloy, high stress effects on struct. and props. *(Russian)* 78−19838
Ni-Ti (8 and 10 wt.%) alloy, aged, precipitation behaviour at 550 to 950°C, X-ray and electron microscopy exam. 78−39785
Ni-Ti alloy, near equiatomic, pretransform. lattice instability, TEM and electron diffr. 79−11616
Ni-W directionally solidified eutectic composite, foil prep. for TEM 78−53072
α'_2-Ni-Zn-Cu martensite, thermoelastic, microscope obs., TEM 77−55966
Ni-ZrO_2, electron-beam-evaporated condensate, cold deform. and annealing effects on microstruct. 80−16331

transmission electron microscope examination of materials continued
β′-NiAl, dislocation climb, hot stage TEM 77−24318
NiAl, nonstoichiometric, interstital defect cluster obs. 80−107226
β-NiAl, oxidation, α-Al_2O_3 growth and microstruct. 80−108627
NiAl, quenched and annealed, void formation 79−46652
β′-NiAl, single cryst., quenched and annealed, ω-like diffr. effects, TEM and X-ray diffr. study 79−60216
NiAl-Cr, eutectic, directionally solidified, temp. behaviour of misfit dislocations *(German)* 78−3119
Ni_3C films, form. by carburisation, characterisation 80−34337
$Ni_{36}Fe_{32}Cr_{14}P_{12}B_6$, metallic glass, crystallisation 79−77520
$NiFe_2O_4$, hysteresis and other mag. props. rel. to microstruct., TEM investig. 77−20636
$NiFe_2O_4$ mag. fluid particles, comp., struct., and mag. props. 80−60374
$Ni_{0.33}Fe_{2.33}O_4$, {001} ⟨110⟩ glide system, room temp. TEM obs. 79−90660
$Ni_{2/3}Fe_{7/3}O_4$, precipitation of α-Fe_2O_3, optical microscopy, SEM and TEM studies *(French)* 80−11650
$Ni_{40}Fe_{40}P_{14}B_6$, amorphous alloy, microstruct. study of crystallisation 77−86062
Ni_3Ga, form. mech. of superlattice intrinsic stacking faults 77−27897
Ni_3Ga, with $L1_2$ struct., dissociated struct. of superlattice dislocations 79−37706
Ni_3Ge single crystal, yield stress, temp. and orientation depend. 77−90432
Ni_3Mn, dislocation struct. after heat treatments, TEM *(Russian)* 77−8848
Ni_3Mn, nonstoichiometric, order-disorder transition, A1 to $L1_2$ *(French)* 79−1861
Ni_3Mn, ordered at below Kurnakov temp. then deform., a/2⟨110⟩ dislocations and deform. antiphase boundaries *(French)* 77−51384
$Ni_3(Mo,Ta)$, quenched alloys, DO_{22} type ordered phase form. 78−95768
Ni_4Mo, antiphase domains growth kinetics, TEM and electron diffr. *(Russian)* 77−32557
NiO, polycrystalline, high temp. deform. 78−3174
NiO, single crysts., annealed, dislocation arrays in low angle tilt boundaries, TEM study 79−37707
NiO, single crysts., TEM of dislocations 79−4306
NiSb, dilute alloy, impurity-induced vacancy clustering 79−99972
NiSe film, vac. deposited, phase transformation, electron microscope studies 80−2302
NiSe, thin film phases, struct. and resist. 78−39236
NiTi martensite, shape memory effect, struct. characts., TEM $2^1/_2$ D imaging obs. 80−108446
$Ni_3Ti_{0.5}Ta_{0.5}$, conservative domain struct., TEM study 80−79776
Pb film, deposition using low-energy ion beam, Rutherford backscatt. and TEM anal. 77−59699
Pb film, deposition using low-energy ion beam, Rutherford backscatt. and TEM anal. 77−70003
Pb film, oxide form. on (111) surface, orthorhombic PbO 77−63835
Pb, polycrystalline film, electron diffr. evidence by off coincidence grain boundaries 77−47469
Pb:O, thin film, microstruct. and thermal stress, doping effects 80−88458
Pb-In(-Au) base electrode film Josephson junctions, tunnel barrier oxide struct. 80−65750
$Pb_{1-x}Cd_xS$ metastable epitaxial films, growth and physical props. 78−27417
PbSb foil production for TEM by electrolytic and ion beam thinning *(German, English)* 77−49812
$PbTiO_3$, ferroelec. domain boundaries, rigid body displacement of lattice 80−40079
Pd film, on Si substrate, laser irrad., cellular struct. and silicide form. 80−10710
Pd, two-dimens. nucleus form. on Ag (111), UHV electron microscope obs. 80−10760
Pd/Si interface, chem. and struct. props. during silicide form., AES and TEM obs. 80−49430
Pd-Ag-Cu (35,25 at.%), determ. of ageing transformations by resist. meas., metallography, TEM and X-ray diffr. 79−4967
Pd-Ce alloy, SRO determ. 77−7738
Pd-Cu-Si, laser melting and splat quenching to form foils for TEM obs. 80−29986
Pd+MgO, reaction and bonding below MP of starting materials, obs. in TEM 77−21419
Pd+SiO_2, reaction and bonding, below MP of starting materials, obs. in TEM 77−21419
$Pd_{781}Cu_{55}Si_{164}$, liquid quenched metallic glass, wear resistance 79−66079
Pd_2Si epitaxial islands on Si (001) substrate 80−96748
Pd_2Si film on Si, substrate temp. effect on microstruct., TEM obs. 78−14621
Pd_2Si films on Si, lattice imaging obs. of structural details 80−103604
Po-Ge film, random percolation, elec. resist. meas. 79−28418
polyethylene, permanganic etchant for TEM obs. 80−21132
Pt catalyst surface morphology, faceting induced by NH_3 and propane oxidation 77−52669
Pt, ion irrad. damage, temp. depend., electron microscopy obs. of defect kinetics 80−107339
Pt, quenched, coprecipitation of vacancies and C atoms 79−78978
Pt, TEM exam. of ion damage in FCC metals 78−87727
Pt-Au, amorphous struct. produced by Au implantation, spinodal decomp. TEM obs. 78−31379
Pt-Rh alloy, on rock salt, epitaxial growth and struct. 77−20211
Pt-Si contact, silicide layer struct., sputter etching and annealing ambient effects 77−62991
PtSi, Ar bubble formation after 20 to 160 keV sputtering, TEM and backscatt. spectrometry obs. 78−64435
PtSi surface, and interface with Si, impurity effects 80−80037
Rh, film, annealing effect on struct., TEM, electron diffr. study 78−76682
Rh film, evaporation onto single crystal Ag films and mica cleavages 77−40375
$Rh_{0.25}VF_c$, cryst. struct. examination by electron diffr. using TEM 79−23583
$(SN)_x$, deform. and defects, lattice strain, fibrillation 80−3139
$(SN)_x$, fibrous struct. study by electron diffr. using TEM 79−65004
$(SN)_x$, halogenated, struct. behaviour, TEM obs. 80−70126
$(SN)_x$, kink bands, deform. and defects 79−52308
Sb, electron microscope irradiation effects, agglomeration of point defects, dislocation climb and loops *(French)* 80−59518
Sb film, initial stages of growth and orienation, TEM study 79−28237

transmission electron microscope examination of materials continued
Sb, liquid-quenched, stabilisation and transformation kinetics of metastable phases 80−3022
$Sb_{0.2(0.4)}MoO_{3.1}$, synthesis, struct. and oxidation state *(French)* 80−64971
Sb_2S_3 spherolite crysts., direct lattice resolution obs. of defect struct. 80−107255
Sb_2S_3, spherulitic crysts., struct. revealed by direct resoln. of lattice by TEM 79−94982
Sb_2S_3-SbI_3, amorphous phase formation in vacuum condensates, TEM study 79−86712
Se-As film, evaporated, thickness, substrate temp. effects 79−15610
Si (001) wafer, pyramidal hillocks, TEM obs. during chemical etching 80−70508
Si (100), self-ion implanted, laser annealing, channelling and TEM meas. 80−24466
Si ⟨111⟩, self ion irradiated, study of defect structures in recrystallised amorphous layers 78−75688
Si, ambient effect of O precipitation, self interstitial mechanisms, IR spectra, TEM study 80−66510
Si, amorphous, small dia. laser beam annealed, temp. distrib. and microstructure 79−73098
Si amorphous film, crystallisation kinetics and morphology, TEM obs. 78−84093
Si amorphous film, crystn. on annealing at low temps. in contact with Al 80−24765
Si, amorphous layer, comparison of laser and electron beam pulsed annealing 79−69374
Si, As segregation, TEM obs. 77−63674
Si, atomically sharp cracks, TEM study 80−71729
Si, CVD epitaxial film, stacking fault nucleation and growth 78−10064
Si, coherent twin boundaries, struct. by TEM 80−75238
Si, containing stacking faults, MeV He ion irrad., TEM obs. of defect clusters 77−89483
Si, crystal defects and impurities interaction obs. by electron microscopic methods 80−65003
Si crystals, damage profiling after heavy ion implication, MeV region 78−75686
Si, Czochralski cryst., hillock etching of microdefects, TEM obs. 78−87678
Si, Czochralski crystal growth and charact., oxidation induced stacking faults 79−47621
Si, Czochralski grown, oxide precip. homogeneous nucleation 80−65221
Si, Czochralski grown, oxide precipitates, diffusion-limited growth 80−97484
Si, Czochralski grown crystal, O precip., nucleation behaviour and dislocation loop form. *(Japanese)* 80−59664
Si, Czochralski grown crystals, swirl-type defect obs. 80−100236
Si Czochralski wafer oxidation-induced stacking faults correl. with bulk defects 77−76428
Si, Czochralski wafers, oxidation induced stacking fault sources 77−7737
Si, Czochralski-grown crysts., thermally induced microdefects, annealing temp. and starting material effects 80−49141
Si, damage in electron bombardment, threshold voltage 77−27910
Si, deep amorphous layer implantation, laser effects, channelling diffr. study 80−25494
Si, defect form. under radiation-accelerated diffusion conditions 80−19854
Si, deformed, faulted dipole, TEM obs. 78−38712
Si, deformed crystal, Czochralski and float zone growth, Luder's bands 79−79025
Si, devices and starting material, high voltage TEM obs. 78−10037
Si, dislocation free, O_2 precipitation, stacking fault form. 78−38731
Si, dislocation generation, influence of film stress and thermal oxidation 79−23609
Si, dislocation generation in local oxidation 80−107245
Si, dislocation-free, O_2 precip., IR and TEM obs. 80−29173
Si dislocation-free crystal O precipitation obs. 78−6095
n-Si, edge dislocation and stacking fault defect electrical recombination efficiency 80−15106
Si, electrical recomb. behaviour at dislocations 79−82606
Si epitaxial film on sapphire, microtwins, TEM exam. 80−70555
Si, epitaxial layer on sapphire, shear strain, TEM 78−51835
Si, epitaxial layers, cryst. quality improvement by ion implantation, backscatt. and TEM obs. 79−42397
Si epitaxial layers, grown by sublimation in vacuum, TEM study of surface 79−46982
Si, epitaxial regrowth and grain struct. of Al metallisation on ⟨100⟩Si 78−79901
Si, epitaxial wafer, saucer pit microdefects reduction by intrinsic gettering 80−75450
Si epitaxial wafers, role of metallic contamination in formation of 'saucer' pit defects 77−39588
Si, extrinsic stacking faults, core struct., TEM obs. 78−55878
Si film, amorphous, formed by CVD, crystallisation 77−39746
Si, film, amorphous, prep. conditions influence on supernetwork struct. 77−76709
Si, film, CVD, low press., struct. and stability, X-ray diffr. and TEM obs. 78−91559
Si film, CVD or evaporated, covered with Al layer, solid-phase crystn. obs. 77−85100
Si film, epitaxial growth on Si, impurities, plasmon energy loss anal. 77−31916
Si film, low press. CVD prep., struct., elec. and optical props. 80−70548
Si film, on sapphire, defect struct., TEM obs. 77−47693
Si film, polycryst., grain struct. and surface roughness, TEM study 80−70556
Si films, polycryst., glow discharge deposited below 250°C, struct. and morphology 80−49535
Si, floating zone structural perfection changes by high temp. treatment, dendrites, dislocation interactions 80−29049
Si foil, computer simulation of high resolution images of defects 80−107208
Si, foil, thinning for electron microscopy 79−49217
Si, grain boundaries, high resolution TEM 80−103364
Si, heavily implanted, lattice defects and strains after high temp. annealing 78−10077
Si, high-dose implantation damage, reflectivity, Rutherford backscatt. and TEM obs. 77−7743
Si, identification of oxide precipitates 80−100723

transmission electron microscope examination of materials continued
Si, implanted and annealed, effect of twins on dechannelling charged particle beam 79−4315
Si, implanted annealed layers, amorphised structure formation mechanism and crystallographic nature 80−29091
Si, implanted with low solubility dopants, laser annealing, TEM study 80−70233
Si, interstitial swirl defect form. in dislocation free floating zone cryst. 77−7682
Si, ion beam irrad., defects prod. by individual displacement cascades, TEM study 80−70265
Si ion damage critical gettering microstructures 78−6098
Si, ion damage TEM study of laser annealing 80−88215
Si, ion implantation, high dose, solid phase epitaxial regrowth 80−103380
Si, ion implantation by laser annealing, characterisation, solar cell applications 80−70247
Si, ion implantation damage, annealing, role of stresses 78−75679
Si, ion implanted, complex annealing behaviour of amorphous layers, TEM obs. of defect struct. 80−107299
Si, ion implanted, damage struct. obs. using TEM and cross section specimens 80−107298
Si, ion implanted, defect struct., dislocation loops and elongated defects 80−107300
Si, ion implanted, extent of annealed or melted regions as function of pulsed laser irrad. energy 79−74025
Si, ion implanted, interstitial generation and loop form. during annealing in oxidising medium 80−107225
Si, ion implanted, laser annealed microstructure 79−74027
Si, ion implanted, structural and elec. profiles for double damage layers 78−2169
Si, ion implanted and laser annealed, characterisation 80−29043
Si ion implanted layers, pulsed electron beam annealing, TEM and particle backscatt. meas. 79−69134
Si, ion-implantation gettering effects, crit. microstructure 77−43229
Si, ion-implanted, defect struct., SEM, TEM and X-ray topography expts. 77−51399
n-Si, ion-implanted, elec. characts. after laser annealing 80−88562
Si, ion-implanted layers, crystn. by ns laser pulses, TEM and RHEED 80−100421
Si, ion-implanted layers, epitaxial regrowth by laser beam and flash annealing 80−100420
Si, lattice images of defects and radiation damage applics. 80−107210
Si layer, on buried SiO_2 layer formed by high-dose, O ion implantation, TEM, AES, and XPS obs. 80−88172
Si layers, ion implanted, pulsed electron beam annealing, He^+ backscatt. and TEM study 79−51152
Si layers, solid phase epitaxial growth, crystalline qualities, ^4He backscatt. and TEM exam. 78−10306
Si MOS device, electron optical identification of precipitations 80−16309
Si, morphology and electronic struct. 79−78194
Si n^+-p junction, microplasma sites, SEM and TEM characterisation 77−43702
Si n^+-p solar cells, degradation mechanisms associated with Ti impurities 80−81465
Si, new materials properties achievable by ion implantation doping and laser processing 79−69127
Si, nucleation of stacking faults at oxide precipi tate-dislocation complexes, TEM 77−19967
Si on sapphire, deposition kinetics and interface characteris. 79−28234
Si, on sapphire, early growth 77−24961
Si on sapphire, stacking faults and twins, TEM obs. at early stage of epitaxy 79−28233
Si, oxidation-induced Frank sessile dislocation loops, struct. change 80−75228
Si, oxidation-induced stacking faults, nucleation mechanism 80−15122
Si, oxidation-induced stacking faults, distinction between clean and decorated faults by etching 80−79818
Si, oxide scale microstruct. of oxidised single cryst. 80−108613
Si oxides, grown in Cl-containing ambients, correl. between elec. and material props. 80−39479
Si, P^+ implantation, induced disorders. 80−6422
Si p-n junction, charge carrier recomb. at dislocations, combined SEM and TEM study 80−15105
Si p-n junction formation, laser assisted, TEM and elec. props. 79−69138
Si, plastically deformed monocrystal, X-ray topographical study *(German)* 78−59813
Si, point defect clusters identification 77−43210
Si, polycryst., oxidation, morphological aspects 80−76388
Si, polycryst. film, ion plating on Al, growth from eutectic melt 77−8765
Si, polycryst. film on Si, disloc. config. obs. 78−10312
Si, polycryst. films, transport props. and grain boundary charact. by TEM 80−50980
Si, polycrystalline, grain boundary obs. by TEM, solar cell appl. 80−72057
Si polycrystalline films, texture formation study 79−87662
Si, porous, form. during anodic treatment in aq. HF 80−35369
Si porous layer, struct. and heat-treatment effect 79−1557
Si, postimplantation defect annealing in samples heavily damaged by 140 keV Si^{2+} ions 77−11602
Si, precipitation of O, 1000°C TEM, IR absorpt. and X-ray studies 80−34194
Si, residual stacking-fault-type contrast after unfaulting reactions 79−82243
Si, screw dislocation networks, TEM study 80−70204
Si, self-implanted, ⟨100⟩ and ⟨111⟩, crystallised layers by laser annealing, struct. 78−47644
Si, self-implanted layer, grain size, laser irrad. energy density depend. 78−72012
Si, sintered, grain boundaries, TEM obs. 80−15118
Si, slip, room temp., TEM obs. 80−79804
Si, small defects in Czochralski grown and zone-floated monocrystals, TEM identification 79−95001
Si, solar grade, directionally solidified using C crucibles, TEM study 79−47617
Si, sputter cleaning using Ar^+ ions, TEM and ion backscatt. investig. of damage 77−48558
Si, stacking fault energies, intrinsic and extrinsic, by TEM 80−10562
transmission electron microscope examination of materials continued
Si, stacking faults growth by Bardeen-Herring mechanism 79−99222
Si, surface, stacking fault generation due to mech. damage, preoxidation annealing influence 80−54261
Si, surface layer defects, influence of multiple oxidation *(Russian)* 78−47650
Si, thermally induced microdefects, effect of C, TEM obs. *(Japanese)* 80−54244
Si, wafer, suppression of oxidation stacking fault generation by preannealing in N_2 atm. 78−30648
Si wafers, saw damage reduction in lubricant environment 80−108585
Si:Ar, As, ion implanted, laser annealing, doping profiles, channelling 80−97506
Si:Ar, ion implanted, amorphous, epitaxial regrowth 79−10868
Si:Ar, ion-implanted, epitaxial regrowth by laser annealing, microstruct. 80−84404
Si:Ar^+(Si^+), implantation effect on carrier lifetime, damage obs. by TEM 79−65493
Si:As, implanted, residual defects after one- and two-step annealing 78−6083
Si:As, implanted through SiO_2 films, elec. props., defect struct. 80−54264
Si:As, ion implanted, amorphous-cryst. transition induced by multiple-pulsed ruby laser 79−90555
Si:As, ion implanted, laser annealed, lattice defects, epitaxial regrowth 80−103334
Si:As, ion implanted, pulsed laser annealing, partial solid-state regrowth 80−103591
Si:As, ion implanted, recrystallisation by free running ruby laser 79−73185
Si:As, ion implanted, two-step annealing 78−18664
Si:As, ion implanted, two-step annealing, TEM study 79−82249
Si:As, ion-implanted, CW IR laser annealing 80−34022
Si:As, ion-implanted, dislocation loops and etch pits, X-ray diffr. and TEM obs. 79−42068
Si:As, ion-implanted, laser recrystallisation by freq.-doubled Nd:YAG laser 79−77613
Si:As, ion-implanted and post-annealed, dislocation loops obs. 77−84776
Si:As wafers, laser annealing, Rutherford backscatt., optical, and TEM obs. 79−1445
Si:As^+(P^+) ion implanted, laser annealed, correlation of struct. and elec. props 80−70855
Si:As(B), ion-implanted, scanned laser and electron beam annealing 79−73182
Si:As(P), ion implanted, TEM study after laser and furnace annealing 80−70234
Si:As(Sb), implanted, pulsed ruby-laser annealing, Rutherford backscatt., TEM and ion channelling study 79−86805
Si:As(Sb), ion-implanted, CO_2 laser annealing 79−73183
Si:B, implanted, oxidation induced precipitate defects, TEM 78−31556
Si:B, implanted, oxidation-induced stacking faults, EBIC and TEM expts. 78−39923
Si:B, implanted, shrinkage of rod shaped defects 78−6061
Si:B, ion implanted, laser annealing 78−34525
Si:B, ion implanted, laser and thermal annealing compared, TEM obs. 78−75681
Si:B, ion implanted, laser annealed, thermal annealing effect 79−73191
Si:B, ion implanted, localised defects, TEM study 78−87699
Si:B, ion implanted, struct. of rod defects, TEM obs. 78−71744
Si:B, ion-implanted, dislocation climb, TEM obs. 78−6062
Si:B, ion-implanted, rod-like defects, TEM obs. 77−68975
Si:B, p-n junction form. by B deposition and laser-induced diffusion 78−87690
Si:B, polycryst., effect of laser annealing on struct. and elec. props. 79−11243
Si:B, solubility and precip., and supersat. resulting by thermal predeposition 78−11232
Si:B, TEM study of stacking fault form. and annealing 78−51566
Si:B film, sputter-deposited, elec. props., struct., SEM and TEM obs. 79−95298
Si:B^+, TEM of lateral implantation effects near mask edges in wafers 79−37724
Si:B(P), dislocations under high stress, stacking fault energies, TEM study 80−70202
Si:B(Sb)(P), microdefect formation depend on doping, Cu decoration, X-ray transmission topography, preferential etching 79−69120
n-Si:Cs, ion implanted, minority carrier lifetime and defect struct., annealing effect 78−6395
p-Si:Cu, Cn precipitation effects, for solar cells appl. 79−69249
Si:Cu, interaction between vacancy emitting absorbing precipitates and dislocations, TEM obs. 78−71755
Si:Fe(Cu), impurity segregation and microstructural changes by pulsed laser irrad. 79−82254
Si:Fe(Cu)(Pt), implant redistrib. and enhanced solubility following laser irrad. 79−69129
Si:Ga(Sb), epitaxial film, doping efficiency *(Japanese)* 79−73201
Si:Ge, recryst. after implantation using different temp. and energy sequences 80−84196
Si:H plasma deposited film, amorphous, microstruct., TEM and SEM obs. 80−10801
Si:Ne(Ar)(Kr), ion implantation damage, annealing, comparative study 79−10867
Si:Ne(Kr), ion implanted, amorphous, epitaxial regrowth 79−10869
Si:O, annealed, minority carrier lifetime 79−23985
Si:O, cryst., annealed, struct. defects 78−75673
Si:O film, thermally deposited, semi-insulating, crystallographic study 78−75954
Si:O wafer, annealed, surface- and inner-microdefects, TEM obs. 80−54236
Si:P, Au gettering, microstructure obs. 78−91346
Si:P, dislocation dissoc. mode obs. by weak-beam TEM 80−107259
Si:P, heavily doped, influence of impurities and crystalline defects on electron mobility 79−78095
Si:P, heavily ion implanted, polycrystalline, grain growth 79−19477
Si:P, high dose implantation, outside dislocation generation 78−87672
Si:P, implanted, two-stage laser annealing of lattice disorder 79−1452
Si:P, incoherent light flash annealing, elec. props., backscattering spectra 80−97504
Si:P, interstitial supersaturation near P-diffused emitter zones 79−65541
Si:P, ion implanted, regrowth of damage structs. by laser annealing 80−107289

transmission electron microscope examination of materials continued
Si:P, ion implanted, subsurface damage, TEM and channelled Rutherford backscatt. study 80−107337
p-Si:P, random and aligned implants, damage form. and annealing exam. 78−47454
Si:P, SiP precipitation concomitant with P predeposition 77−24326
Si:P bipolar transistors, interstitial supersaturation and misfit dislocation climb, TEM study 80−70203
Si:P polycrystalline layer, role in lattice defect reduction assoc. with P predeposition 80−70229
Si:P spherical defect cluster and dislocation loop analysis 78−14356
Si:P^+ ion implanted single crysts., secondary defects development during annealing 80−44228
Si:$P^+(As^+)(Sb^+)$, implantation damage removal by laser irrad. and its thermal stability, TEM study 79−74024
Si:Pb, He^+ Rutherford backscatt. and TEM exam., implant species effect on recrystn. 78−47452
Si:Pb, ion-implanted and annealed, dose depend. of residual lattice disorder 77−43228
Si:Pb implanted layers, recrystn. on annealing, backscatt. and TEM obs. 77−51421
Si:Sb, heavily doped, TEM obs. of impurity effects in dislocation motion 77−43220
Si:Sb, ion implanted, annealed, dislocation generation, channelling and Rutherford backscatt. meas. 80−88158
Si:Sb wafers, laser annealing, Rutherford backscatt., optical, and TEM obs. 79−1445
Si-Al-Al_2O_3 system, solid phase Si regrowth on sapphire 80−100413
Si-Al-O-N, high-temp. fracture and diffusional deform. mechanisms 80−40509
β'-Si-Al-O-N, Mg-containing phases, crystn. 80−39297
Si-Al-O-N, oxidation mechanisms 80−40570
Si-Al-O-N ceramic, single-phase, prep. by hot-pressing, microstruct. investig. 77−8792
Si-Al-O-N polytypes, hot-pressed, microstruct. 80−3023
Si-Al-O-N system, phase analysis and TEM struct. obs. 80−108420
Si-Al-O-N system, stable phase cryst. struct. and microstruct. obs. using TEM 80−108421
Si-Al-O-N system, TEM exam. of X phase structure 78−56606
Si-Au(Cr)(Pd), contact reactions between amorphous Si and metallic films, TEM, transmission electron diffr. obs. 79−23846
Si-Co interface metal-semiconductor transition, rel. to first compound nucleation 80−24771
Si-containing films, formed by reaction of Si with organic compounds of N, struct. investigation 79−87009
Si-Cr interfaces, metallurgical and electrical props. 80−60081
Si-Na-B-O-N glass, synthesis and characterisation 80−108381
Si-on-sapphire MOS devices, effects of planar defects near Si-SiO_2 interface on elec. props. 79−11231
Si-P, dislocation networks due to ion implantation, TEM exam. 77−35563
n-Si-Pd_2Si contact, interface struct. and Schottky barrier height, correl. obs. using TEM 80−100504
Si-$Pd_{80}Si_{20}$, amorphous, Pd_2Si layer form., shallow contact 80−103586
Si-Pd-Si structure, epitaxial growth, backscattering and transmission electron microscopy studies of layered structures 80−80123
Si-Pt(Ni)(Pd), laser-induced reactions of metal films with Si, surface struct. obs. by TEM 79−19471
Si-SiO_2, interface, morphology and electronic struct. 79−78194
Si-SiO_2 interface, thermal SiO_2 sputter induced roughness, Auger sputter profiling study 80−75424
Si-SiO_2 interface in MOS capacitors, lateral diffusion of Na^+, neutralisation 80−92986
Si-SiO_2 interface struct. by cross-sectional TEM, amorphous oxide layer 77−24487
Si-SiO_2 wafer thinning for TEM 77−89352
SiC, atomically sharp cracks, TEM study 80−71729
SiC, attritious wear in grinding 77−32696
SiC, CVD, microstruct. obs., optical and TEM 79−7560
SiC, cubic, atomic displacement energy determ. by bracketing technique 80−49272
SiC, engng. ceramic, lattice resolution studies 78−27510
SiC, extremely large-period polytypes, X-ray diffr. and TEM 77−31636
SiC film, growth on Si ribbon surface, TEM anal. 78−84094
SiC, HVEM obs. of various polytypes 80−76248
SiC, identation plasticity and microfracture 79−70158
SiC, microrelief of fracture failures *(Ukrainian)* 77−32729
SiC, oxide scale microstruct. of oxidised single cryst. 80−108613
SiC, polycryst., high resolution TEM study of $\beta \rightarrow \alpha$ transform. 80−84928
SiC polytypes, high-resolution observations 79−23621
SiC, polytypic transform., interface struct. exam. by TEM 80−15033
SiC, pyrolytic particles for high temp. reactor fuel, X-ray and SEM study *(French)* 78−22734
SiC, reaction bonded, microstruct. characterisation 78−48353
SiC, reaction sintered, TEM exam. of recrystallisation, phase transformation 78−80567
SiC single cryst., reaction-bonded and hot pressed, hardness and wear behaviour 79−38970
SiC, specimen preparation for TEM by ion beam thinning *(German, English)* 80−11861
SiC, subjected to thermal shock, study of substruct. and surface morpholoy, X-ray diffr. and TEM study 79−43292
SiC, TEM investigation using C replicas 80−61034
SiC, uncommon mode of morphological development among coherent phases, optical and electron microscope exam. 78−80544
β- SiC, undoped compact, microstruct. development during heating 80−25746
$Si_{0.92}Ge_{0.08}$ film on Si, elastic strain, misfit dislocation density 77−85119
Si_xGe_{1-x}-Si(GaAs) heterodiodes, interfacial structural defects effect on avalanche breakdown 79−42644
Si_3N_4 amorphous films, struct., short-range order, and crystn. kinetics 79−28240
Si_3N_4, α to β transform., TEM and electron diffr. obs. 78−27507
Si_3N_4, consolidation by hot isostatic pressing 80−11605
Si_3N_4, dielectric film, on Si. crysts. from amorphous state 79−28225
Si_3N_4, dielectric films made by NH_3-silane reaction, TEM study 80−84413
Si_3N_4, engng. ceramic, lattice resolution studies 78−27510
Si_3N_4, hot-pressed, impurity phases, TEM obs. 79−8260
transmission electron microscope examination of materials continued
Si_3N_4 layers, prep. by N_2 ion implantation into Si, TEM and IR absorpt. obs. 79−46974
Si_3N_4, reaction bonded, pore size and distrib. effect on strength 79−29165
Si_3N_4, reaction-bonded, microstructural analyses 77−8782
Si_3N_4, reaction-bonded and hot pressed, hardness and wear behaviour 79−38970
Si_3N_4, reaction-sintered, non-axial dislocs. 77−19956
Si_3N_4, Si rich, CVD film prep. and props. 78−76607
Si_3Ni_4, hot pressed MgO fluxed grain boundary impurity phases, lattice fringe imaging obs. 79−11540
SiO film, Au coated, thickness meas. using stereo technique, TEM 77−30220
SiO film, obliquely evaporated, topography rel. to liquid crystal orientation 77−69190
SiO, obliquely coated on In_2O_3 coated substrate, TEM exam. of surface topology 77−39726
SiO obliquely evaporated film topography, effect on liq. cryst. orientation 78−38987
SiO_2, dielectric film, on Si. crysts. from amorphous state 79−28225
SiO_2 film, from oxidation, in dry O_2 and H_2O ambients, initial oxidation regime obs. 79−29240
SiO_2 film, Ge substrate, structure investigation 78−10297
SiO_2 films, amorphous to cryst. transform. induced by diethyl ether vapour 79−55667
SiO_2 films, stabilised by ion bombardment and heat treatment, crystn. and phase separation 79−77931
SiO_2, Si rich, CVD film prep. and props. 78−76607
SiO_2, small amorphous particles, high resolution TEM 79−82157
SiO_2/GaAs, interface reaction during high-temp. heat-treatments 80−88439
SiO_2-Al_2O_3, calculated thermodynamic data and metastable immiscibility 78−27495
SiO_2-Al_2O_3 (36.6 wt.%) plasma prep. powder, metastable immiscibility and microstruct. during sintering 80−35143
SiO_2-Al_2O_3-Fe_2O_3-CaO, basalt glass ceramics, crystallite form. due to heat treatment 80−38917
SiO_2-Na_2O-CaO (13, 11 wt.%) glass, phase separation, SiO_2 purity effect 80−44144
SiO_2-Na_2O-CaO glass, phase separation characts., melting atmosphere effect 80−44141
SiO_2-Si interface, interaction of point defects, electron microscope exam. 77−7979
SiO_2-TiO_2 antireflection coating, 1.064 μm laser damage, barrier 80−33059
SiO_2-TiO_2-$(Al_2O_3)(ZrO_2)$, noncrystalline film form., IR study *(Japanese)* 77−59634
SiO_x, grown in HCl/O_2 ambients, phase separation and Na passivation 80−3219
SiO_x layers, grown in HCl/O_2 ambients, struct. and comp. 79−42404
SiO_x thin films, deposition and characterisation study 80−80133
$Si_xO_yN_2$, dielectric film, on Si. crysts. from amorphous state 79−28225
Sm-Co-Cu, with Sm_2Co_{17} struct., aged, TEM high coercivity material, TEM obs. of microstruct. 77−77073
Sm_2O_3, surface step thickness measurement 80−103555
SmS, defect struct., precipitate colonies, dislocation loops, TEM obs. 80−44214
Sn film, polycrystn., grain boundary scattering rel. to annealing temp., TEM study 79−65560
Sn film, vacuum deposited, substrate and substrate temp. effects on struct. 80−107677
Sn film, vapour-deposited on NaCl single cryst., nucleation, growth, microstruct. 78−91561
Sn film epitaxially grown on KCl substrate 79−99441
Sn/Au thin film diffusion couples, Kirkendall void form. 80−96698
Sn-Ni electrodeposited equatonic alloy, cryst. struct., X-ray, electron diffr. anal. 80−79748
Sn-plate passivation films TEM struct. obs. 80−45416
Sn-Sb (10 wt.%), decomposition of supersaturated solid soln. 80−29960
Sn-Sb-Ag, splat cooled foils, TEM study 80−40344
SnO-SiO_2 glass, exam. of immiscibility 78−75837
SnO_2 thin films, analytical characterisation 80−20053
SnTe, expitaxial film, early stages of growth, replication and TEM obs. 79−65348
$SrAl_2Si_2O_8$, TEM obs. of feldspar aand hexacelsian polymorphs 78−83827
$SrO.6Fe_2O_3$, ultrafine, microstruct. development during sintering, mag. props. 79−70022
steel, Cr-Ni, ferrite precip. *(Japanese)* 80−35187
steels, Cr-C-Mn(Ni), struct. prop. rel., design of struct. steels for high strength and toughness 80−97491
strengthened by lattice transformations, mech. props. study *(Japanese)* 79−43332
Ta and Ta alloys, electrolytic polishing, use of pure FSO_4H 78−85094
Ta, film, CVD on silica, struct. and mech. props. 77−24965
Ta film sputtered onto Cu substrate, microstruct. and supercond. props. 77−85370
Ta, Ta-Re, Ta-Re-N, deformed at 77K, dislocation substruct. 77−32647
Ta-H, phase diagram revision 77−63641
Ta-H system, phase diagram and transforms., struct. obs. of various phases 80−104125
Ta-N (4 at.%), TEM obs. of ordering 79−96021
Ta-O solid soln., interstitial ordering and precipitation at 100 to 270°C, exam. 78−52813
Ta_2O_5 doped systems, struct. and ordering, high resolution TEM obs. 78−35378
TaS_2, $1T_2$ polytype, incommensurate periodic lattice distortions, real space TEM 77−47432
TaS_2 polytypes, in situ intercalation in TEM, using N_2H_4 gas 79−8254
Te, amorphous, obtained by splat cooling crystallisation 77−65949
Te, breakdown of Friedel's law in Kikuchi patterns as obs. in TEM 79−69046
Te film, growth on (111) KBr films deposited on mica, TEM and electron diffr. obs. *(Japanese)* 78−64473
Te film, microstructure 80−103598
Te film, on electron irrad. KBr, epitaxial growth and surface coverage 80−10825
Te film, vacuum deposited, growth and morphology of crysts. 80−96766
Te film growth on KBr (111) on mica *(Japanese)* 78−79903
Te, screw dislocation substruct. studied by torsion expt. 79−10859

transmission electron microscope examination of materials continued
Te, vacuum deposited film, effects of electron irradiation on surface coverage *(Japanese)* 79−82477
Te, vacuum deposited on NaCl, crystallite growth and morphology, electron microscopy 80−65401
Te-Pb, amorphous, obtained by splat cooling, crystallisation, TEM obs. 77−66638
Te-Pb (20 at.%) alloy, amorphous, obtained by rapid cooling from liq. state, crystn. behaviour 78−26445
Te-Sn (20 at.%), amorphous, exam. of crystallisation by DTA, X-ray diffr. and TEM 78−47242
Th-pyromellitate, growth processes, TEM 80−103229
(Ti,V)C, activated reactive evaporation deposited films, annealing study, microstructure 80−24762
Ti, anodic film structure, intensiostatically formed, pH and current density influence, TEM study *(French)* 79−66217
α-Ti, cold rolled, primary recrystn., in situ investig. in HVEM 80−104185
Ti, corrosion in H_2SO_4, estimated from weight loss meas. at 270°C and 56 bar *(French)* 80−85080
Ti, friction surface structural investigation, O_2 surface diffusion *(Russian)* 80−96726
Ti, grain size effect on yield stress and work hardening at 295 and 575K 78−64593
Ti, neutron irradiated, characterization of dislocation loops 80−88155
Ti-11, unstable shear modes in fatigued β-annealed specimens 78−84984
Ti-(Al)-Zr-Si (5, 0.5 wt.%), creep 77−36595
Ti-Ag(Au)(Si), existence of β to α_m phase transformation 78−44123
Ti-Al (14.4 at.%), void form. and solute segregation under Ni ion irradiation 79−42122
Ti-Al (27.3 wt.%), arc melted, microstruct. 79−61577
Ti-Al (6.6 wt.%), hydride habit planes, H_2 embrittlement, slip 77−36648
Ti-Al_2O_3 system mixed films, prep., phase comp., struct. and elec. props. 79−37930
Ti-Al-Sn (5, 2.5 wt.%), annealing of near-basal hydrides 80−20989
Ti-Al-V (4.7, 2 wt.%) pseudo alpha alloy, laminar struct. singularities, β to α transformation *(Russian)* 80−7552
Ti-Al-V (6,4 wt.%), α/β interface phase influence on tensile props. 80−30034
Ti-Al-V (6,4 wt.%), ion irradiated, microstruct. study using TEM 80−96572
Ti-Al-V (6,4 wt.%), phase transformation after hydrogenation 80−7560
Ti-Al-V (6,4 wt.%), to H effect on fracture props. and microstruct. 80−40512
Ti-Al-V-Cr-Zr-Mo (3, 8, 6, 4, wt.%), phase transforms. 79−100113
Ti-alloy, IMI-685, unstable shear modes in fatigued β-annealed specimens 78−84984
Ti-Fe-C-N, ion irradiated, microstruct. study using TEM 80−96572
Ti-M-V-Cr-Mo, RMI 38644, shock loaded, age hardening 79−29112
α-βTi-Mn (4.3 wt.%), interface phase struct. 77−44212
β-Ti-Mo, alloy, struct. changes during deformation and ageing *(Russian)* 78−39791
Ti-Mo, metastable β-phase, stress induced products formed by cold rolling *(Japanese)* 78−84843
Ti-Mo, phase diagram investigation *(Japanese)* 77−63632
Ti-Mo alloys, structural stability under high-pressure soaking 80−104151
Ti-Mo binary system, solid state phase transform. and miscibility gap, phase diagram 79−8298
Ti-Mo-Zr-Sn (11.5, 6, 4.5 wt.%), β III, mech. props. rel. to heat treatment 80−84961
Ti-Mo-Zr(-Al) (15, 5 (3) wt.%), quenched and aged metastable β-phase, crystallography, morphology and decomposition 80−76262
Ti-Nb-Ge foils, β phase decomposition, electron microscopy struct. investigation *(Russian)* 79−83172
Ti-Nb-Si, amorphous alloy, supercond. props. and crystn. behaviour, TEM and DTA study *(Japanese)* 80−84536
Ti-Nb-Ta-Ge (40,20,0.8 wt.%) foil, dispersion hardening, TEM and electron diffr. obs. *(Russian)* 79−1873
Ti-Ni, laser melting and splat quenching to form foils for TEM obs. 80−29986
Ti-Ni-Mo (1.5, 2 wt.%), Mo effect on microstructure 77−36536
Ti-V, metastable β-phase, stress induced products formed by cold rolling *(Japanese)* 78−84843
Ti-V-Mo alloy system, phase equilibria and interstitial effects, TEM and X-ray diffr. study 79−43204
Ti-V-Mo-Cr system, β-phase stability 80−55353
βTi-V-Si (40, 1 at.%), Si effect of precipitation and age hardening 77−63676
Ti-Y(Er), dispersoid effect on deform. 79−24530
TiC, activated reactive evaporation deposited films, annealing study, microstructure 80−24762
TiC, deposited by activated reactive evaporation, TEM and hardness 79−23872
TiC, RF sputtered film on steel, transition region 78−39956
TiC whiskers, CVD growth on various metals and refractory oxides, TEM examination 79−33211
$Ti_{70}Co_{20}B_{10}$, amorphous alloys, crystn. behaviour, TEM study *(Japanese)* 80−84087
TiD_2, nucleation and growth in D_3^+ implanted Ti, TEM study 80−97717
$Ti_{70}Fe_{20}B_{10}$, amorphous alloys, crystn. behaviour, TEM study *(Japanese)* 80−84087
TiN-Ti_2N, activated reactive evaporation formed deposits, microstructure, transformation depend. on depositing conditions 80−24761
$Ti_{70}Ni_{20}B_{10}$, amorphous alloys, crystn. behaviour, TEM study *(Japanese)* 80−84087
TiO_2, amorphous film, vac. deposited, struct. and crystn., TEM obs. 80−2291
TiO_2, anodic films on Ti, struct. *(French)* 77−56154
TiO_2, K^+ implantation, extended defects and precipitates 80−49251
TiO_2 rutile single crystals, stoichiometric, dynamic strain ageing 80−50661
TiO_2, slightly vacuum-reduced, {312} planar defects, TEM obs. 78−22736
TiO_2-SiO_2, submicron dispersion of impurity, chem. diffusivity and elec. cond. 79−1528
TiO_{2-x} reduced, crystallographic shear planes, dislocation struct. 80−107175
$TiS_{1.46}$, $(4H)_2$-4C type superstruct., high resolution electron microscopy determ. 79−69060
transmission electron microscope examination of materials continued
$TiS_{1.5}$, $(4H)_3$-6C-type superstruct. revealed by high resolution microscopy 80−19755
$TlBiTe_2$, epitaxial film, struct. anomalies, TEM 77−11824
$Tl_{0.25}VF_3$, cryst. struct. examination by electron diffr. using TEM 79−23583
UC, MX-type LMFBR fuels, TEM exam. of microscopic swelling 78−70596
U_2C_3+UC, MX-type LMFBR fuels, TEM exam. of microscopic swelling 78−70596
UO_2, fission gas bubble distrib. from high temp. irradiated SGHWR fuel pins 77−46284
UO_2, intragranular fission gas bubbles, size and distrib. 80−57840
$U_{0.8}Pu_{0.2}C_xN_{1-x}(0\leq X\leq 1)$, MX-type LMFBR fuels, TEM exam. of microscopic swelling 78−70596
U_3Si, reversible twinning, in-situ obs. 80−104241
U_3Si, tensile ductility from 25 to 320°C 79−74225
(V,Ti)C+(Ni,Mo) cermets, carbide-binder interface ledges 80−29283
(V,Ti)C+Ni cermet, binder grain size 80−44401
V and V-Mo, mechanical properties, O, N_2 and C addition effects 79−52356
V, coherent twin boundary structure *(French)* 79−60379
V, electropolishing for TEM obs. 78−31605
V, He preinjected, void swelling on neutron irradiation 77−7765
V, ion implanted with 2 MeV He under pulsed conditions, microstructure obs. 80−29088
V, irradiation with 2 MeV He ions, low cycle at elev. temp. 78−95086
V, superconducting props., effect of voids 78−52168
V, void formation from 200 to 700°C following heavy-ion irradiation 78−10104
V/Cu-Ga, composite superconductor, V_3Ga phase form., TEM obs. *(Russian)* 80−84933
V-Al thin film system, phase growth kinetics, electrochemical anode etching 77−72805
V-H(D), phase diagrams, struct. studies 80−66491
V-N system, TEM of V-$V_{16}N$ precipitates 77−16590
V-Ti-O single crystal alloy, mech. props. 77−25112
V-Zr-C-Y alloy weld metal, hardening phase precipitates examination 80−7576
VC, precipitation in ferrite and pearlite. during C steel transformation, TEM exam. 78−52812
VC-TiC, deposited by activated reactive evaporation, TEM and hardness 79−23872
V_3Ga, grain size in A-15 reaction layers 78−14911
β-VH, precipitation crystallography, TEM obs. 77−77480
V_2O_3 film, reactively sputtered on sapphire, electron microscopy exam. 78−84106
V_2O_5, wedge shaped cryst., electron lattice image interpret. 80−103319
V_2O_5-based glasses, amorphous and crystallized electronic cond. and related props. 79−99547
V_nO_{2n-1}, microsyntactic intergrowth 79−1402
V_3Si, dislocations, obs. by TEM 77−59012
V_3Si, grain size in A-15 reaction layers 78−14911
V_3Si, grown-in dislocations, diffr. contrast behaviour 79−86794
V_3Si, lattice defect, high voltage electron microscopy *(French)* 79−27993
V_3Si, neutron irrad., grain boundary pinning, field-depend. change of crit. current density 80−65759
V_3Si, neutron irrad., volume pinning force, summation and saturation behaviour 79−95554
V_3Si, phase transition and transition temp., chemical comp. effects, defect struct. exam. 78−18651
W, BCC, struct. singularities rel. to solid soln. behaviour *(Russian)* 77−11696
W, drawn wire, microstruct. effect on fracture 80−3177
W, high resolution phase contrast imaging 80−103224
W, monocryst. particles and whiskers, reduction of vap. deposited WO_3 77−52249
W needles produced by $W(CO)_6$ decomp. 79−95302
W, polishing technique as prep. for TEM 80−71851
W, recrystallisation of commercially pure and doped wire drawn to high strain 79−100165
W, single and clusters of atoms obs. by bright field spectroscopy 77−62456
W, split crowdion interstitial, (111), computer simulation of TEM imaging 78−71723
W, strain induced damping, micro- and macro-, and dislocation structures in single crystals 78−19797
W, vacancies, quenching and recovery invest., resist. and TEM study 80−39074
W, vacancy-defect clustering, due to annealing and quenching, TEM and elec. cond. exam. 78−47344
W whisker cryst., growth incorporated with field electron emission 80−44458
W wire, AKS-doped, second phase particle obs. by TEM, SEM and atom probe microanalysis 80−108457
W, wire, doped, heavily drawn, recrystallisation 77−16609
W wire, laser shock induced microstructural changes, rel. to explosive shock induced phenomena 78−67768
W-K-Si-Al doped wires, heavily drawn, fibre struct., annealed 79−56993
W-Ni-Fe(Cu), liquid phase sintered, interfacial embrittlement 79−57101
WC grain, with grown-in stacking fault, contrast effects in electron micrographs 77−19959
WC-Co, sintered, obs. of spinel particles by TEM 78−95714
WC-Co and WC-Co-TaC-TiC-NbC cemented carbides, microstructure, high temp. deformation, uniaxial plastic compression 80−40451
W_2C, oxidation, oriented struct. transform. to W, FEM and TEM obs. 80−30124
W_2C, single cryst., decarburization, field emission microscopy and TEM 79−70368
$W_{50}Fe_{50}$ glassy alloy, refractory, triode sputtered 80−75185
WO_3, amorphous film, vac. deposited, struct. and crystn., TEM obs. 80−2291
WO_3 film, amorphous, struct. and crystn. 80−103606
WO_3 polymorph, hexagonal, cryst. struct. imaging by high-resolution electron microscopy 80−103309
YB_{68}, melt grown, props. meas. 77−11518
$Y_{2.3}Gd_{0.6}Fe_{4.7}Al_{0.4}O_{12}$ garnet, TEM examination of pretransformed nucleus contrast 79−11624
Y_2GdIG film, amorphous, mag. bubbles obs. and structural transformation 80−75824

transmission electron microscope examination of materials continued
YIG, deformed at high temp., subgrain boundaries and dissociations of dislocations, TEM obs. 79−90658
YIG, mag. domain walls, Lorentz microscopy 79−91249
YIG, plastically deformed, TEM, dislocation Burgers vectors 77−11557
YIG, substituted, magnetite nucleation in transitional zone, ionic process, lattice imaging 80−107424
Y_2O_3 film in Y-Y_2O_3-Au junction, defect struct. and local conduction 78−26970
Y_2O_3, plastically deformed, dislocations obs. by TEM *(French)* 78−51545
Y_2O_3, polycrystalline, high temp. O ion bombard., TEM microstruct. investig. 77−27923
$Yb_3Fe_4O_{10}$, struct. image by a 1 MeV high resolution electron microscope 79−37671
Yb_2O_3, merohedral twins, many beam diffr. contrast 78−83829
Zn chalcogenides, thin films, VPE, needle-like cryst. growth 80−80148
Zn, deformed single crysts., stacking faults and dislocation dissoc. 77−31681
Zn, dislocation interaction with 'forest' dislocation, TEM exam. 77−89440
Zn, dislocation internal friction, orientation depend., for single crysts. 78−52882
Zn film deposition on Al, TEM and electron diffr. obs. 80−75460
Zn, hot rolled, grain boundary fine structures, TEM exam. 78−76680
Zn, isothermal annealing effect at 400-410°C, on dislocation struct. in monocrystals *(Russian)* 79−20082
Zn-Al, splat quenched and bulk specimens, eutectoid decomposition 77−63628
Zn-Al (40 wt.%), superplastic deform., dislocation effects 77−48515
Zn-Al eutectoid alloy, straining at elev. temp., whisker crystal 79−29087
Zn-Ge, eutectic, stereomorphology using SEM, TEM and optical microscopy *(Russian)* 79−52187
ZnO, ceramic varistor, physical props. of elec. barriers by AES and electron microscopy 77−20326
ZnO ceramics, microstructural evaluation 79−55750
ZnO, crystallising in double HCP lattice, microstruct. 77−31655
ZnO, dislocation motion, in situ TEM obs. 77−19961
ZnO, irradiation in high voltage electron microscope dislocation loops study 80−88157
ZnO-Al_2O_3-SiO2, transparent glass ceramics, heat treatment effect on microstruct. 78−56667
ZnS, defect struct., dark-field microscopy, anal. of decoration patterns 79−23506
ZnS, laser evaporated film, microstruct. TEM obs. 79−82479
ZnS, twist boundary struct., atomic scale electron microscopy obs. 80−107276
ZnS, Zn(S,Se), large single crystals, vapour growth and defect characterisation 80−25540
ZnS-CdS:Ag(Ni)(Co), electron-irradiated phosphors, void formation mechanism 79−55780
ZnSe, electron irrad., dislocation climb, TEM obs. 79−1461
ZnSe epitaxial layers, organometallic CVD prop., growth kinetics and luminescent props. 79−51458
ZnSe, evap. onto electron bombarded NaCl substrates, epitaxial growth and characts. 79−28948
ZnTe, elec., SEM and TEM studies of impurity segregation during long annealing 80−30001
ZnTe, TEM obs. of precipitates, shape of Te solidus line 80−25703
ZnTe:B^+ native and implant-created defects 77−76446
ZnTe:Li, diffusion investigation by SEM and TEM 80−10706
ZnTe:Li, impurity segregation during short annealing and quenching, SEM, TEM and elec. meas. 80−10676
Zr alloy, neutron irradiated, in-pile dimensional changes 77−24331
Zr alloys, TEM obs. of irradiation damage, critical review 79−10879
Zr and alloys, neutron irrad. at 573 to 923K, damage struct. 80−107334
Zr, crept single crystal, nature of γ-hydride 77−21147
Zr, electron irradiation damage, direct obs. 80−84212
Zr foil, convergent beam thickness determ. 79−4215
Zr, hydride precipitation and growth at crack tips, electron optical obs. 80−108449
Zr, irradiation induced defects, electron microscope images 78−83854
Zr, neutron irradiated, dislocation loop nature 77−47489
Zr neutron irradiated, faulted loops 78−10094
Zr, thin film, sources of background X-radiation 80−101908
Zr-Al (14 at.%), martensitic, discontinuous precipitation, TEM obs. 79−34040
Zr-Al (4.6 wt.%) martensite, precipitation of Zr_3Al_2, TEM study 79−74156
Zr-Cr (1.9 wt.%), β-quenched and tempered, optical and TEM study 79−66061
Zr-Cr (1.9 wt.%), β-quenched and tempered, $ZrCr_2$ precipitation, TEM study 79−66062
Zr-Fe, amorphous alloy quenched by levitation method, crystallisation 79−55669
Zr-H formation, of δ→γ transformation 80−84929
Zr-H formation, the δ→ε transformation 80−84930
Zr-Nb, singularities of β→ω transform. in alloy, with high content of β-stabiliser *(Russian)* 78−76644
Zr-Nb (1 wt.%), static strain ageing between 295 to 773K, TEM obs. of plastic strain 79−38855
Zr-Nb (2.3 and 5.5wt.%) martensite, precipitation 77−8836
Zr-Nb (2.5 wt.%), cold-worked, pressure tubing, metallography and mech. props. 80−89269
Zr-Nb (2.5 wt.%), hydride TEM obs. in pressure tubing 79−8338
Zr-Nb (2.5 wt.%), hydride precipitation and growth at crack tips, electron optical obs. 80−108449
Zr-Nb (97.5, 2.5 wt.%) nuclear reactor pressure tube material, H embrittlement study by TEM 80−76363
Zr-Nb alloy, direct imaging of point defects using TEM 77−35453
Zr-Nb alloy, isothermal decomposition at elevated temp. 78−27470
Zr-Nb-Cr (0.5, 0.5 wt.%), TEM study on intermetallics in Zr alloys 79−11622
Zr-Nb-Ge, singularities of β→ω transform. in alloy, with high content of β-stabiliser *(Russian)* 78−76644
Zr-Sn-Mo (6, 1 wt.%), creep and creep rupture 78−23778
Zr-Sn(Fe)(Ni) (0.15 wt.%), electron irradiation damage, direct obs. 80−84212
Zr-Ti-Be metallic glass, phase separation 80−97464
Zr_3Al, deformed and irrad., lattice defects obs., superlattice dislocations and defect clusters 80−107261

transmission electron microscope examination of materials continued
Zr_3Al, ion beam prod. damaged regions 79−60409
Zr_3Al, irradiation 78−6111
Zr_3Al ordered alloy, ion bombardment damage, TEM 80−100287
Zr_3Al, ordered polycrystals, hardness and flow stress relationship 77−44309
ZrC CVD coated fuel particles, diffusion of ^{137}Cs, ^{90}Sr and ^{144}Ce 80−13582
$Zr_{50}Co_{50-x}Ni_x$, transform. and deform. studies 79−1864
ZrO corrosion layer, specimen preparation for TEM by ion beam thinning *(German, English)* 80−11861
ZrO_2 crystalline particles, TEM and electron diffr. meas. 77−21350
ZrO_2 film, CVD from organometallic cpds. and characterisation 78−23626
ZrO_2, MgO partially stabilized, microstruct. development during ageing 79−91710
ZrO_2-CaO (15 mol.%) precipitation and ordering 80−100837
ZrO_2-Y_2O_3 (9 mol.%), precipitation and ordering 80−100837

transmission electron microscopes
see also transmission electron microscopy
80 kV accelerating voltage transmission electron microscopes 80−27380
analytical, sources of background X-radiation 80−101908
cold trap assembly, liq. N_2, for contamination reduction in analytical microscopy 80−101056
coma-free alignment using optical diffractograms 79−21860
combined CTEM and STEM, using condenser objective lens and 100 kV LaB_6 gun 80−86516
development, refinements of lens correction, recording of individual electrons, holography, image quality monitoring *(German)* 80−57430
developments in instruments and techniques *(Hungarian)* 80−31949
diffraction patterns and bent contours visibility in thick composite amorphous-crystalline specimens 80−1906
electron probe X-ray microanalysis, quantitative investigation of thin specimens 80−101068
electron spectrometer for microchemical anal. in 100 kV TEM 79−39251
electronically controlled illumination appls. in conventional TEM 79−89046
electrostatic energy filter, telescopic, with cylindrical mirror analysers 80−87296
electrostatic high voltage generator for TEM, stability improvement *(French)* 78−62268
EM6G TEM, modification for X-ray microanalysis 79−74470
EM-14, design and operation 79−12886
energy filter, mag. prism design 80−86523
field emission electron gun, comparison of cold and thermal types used in the same electron microscope 80−101890
field emission gun use, phase contrast transfer improvement due to low energy spread 77−10145
half-plane and topographical contrast 78−32958
high resolution, 600 kV Cambridge Univ., condenser-objective lens design and construction 78−32938
high resolution, 600 kV Cambridge Univ., engng. design and construction features 78−32937
high resolution, combined with nanoPROBE anal. 80−4814
high resolution, electronic control systems 78−32939
instrumentation for direct obs. of frozen hydrated specimens 79−92454
lens system with eucentric goniometer for ferromag., material obs. 77−72530
liquid He cooled environmental cell 80−68323
low magnification with wide field, using HICOREX lens, features 79−17564
magnetic energy filter, without second-order aberrations 80−86524
magnetic energy filter optics 78−32944
magnetic imaging filter, electron optical experiments 80−87295
magnetic spectrometer for TEM energy analysis 79−26190
microdensitometer system for use in TEM 80−95197
microsecond pulse stroboscopic TEM, Mark I 79−71568
modifications allowing continuous failsafe pumping 77−22626
Mollenstedt-Duker electron biprism, use of Wollaston wire 78−54512
multilens imaging system design for minimum distortion at low magnifications 79−12897
objective lens, with compensated axial chromatic aberration 80−87293
on-line electron-optical correlation computing 80−99008
Philips EM400 TEM/STEM performance, with field emission gun and twin lens 80−57441
raster mode of image form. 80−101887
review, TEM, STEM, and SEM: microscopy to microfabrication 78−32936
rotation-free mag. electron lens 78−78042
sensitivity to AC mag. field meas. 79−75659
specimen grid holder 79−67436
specimen stage with combined top and side entry, for Hitachi H500 transmission electron microscope 77−67539
spectrometer attachment for energy-loss analysis, theory and instrum. 80−81405
spiral distortion correction 78−32942
stray X-rays from Cu and Mo components in JEM-100C microscope, reduction 80−73550
telescopic, with cylindrical mirror analysers 80−87296
tilting high temperature gas reaction chamber 80−101894
ultrasoft X-ray detection with variable geom. proportional counter fitted to TEM 77−48712
universal magnification curve 79−49340
vacuum pump system, simplified low-cost design for use with ZEISS microscope 80−99012
viewing arrangement improvements 78−32941
X-ray analysis in the TEM/STEM, review 78−24014
$In_xGa_{1-x}P$, TEM foil preparation, using polishing set 'Elypovist' *(German)* 79−9264
LaB_6 cathode gun 80−18048

transmission electron microscopy
see also transmission electron microscope examination of materials; transmission electron microscopes
1000 kV, appl. to metallurgy 78−8472
accelerating voltage measurement, non-electric methods 79−12896
adhesive energy, meas. techniques for metal/ceramic system 80−50803
amorphous materials, bright field hollow cone illum. advantages 78−22609

transmission electron microscopy continued
amorphous materials, tilting and defocus effects in high resolution dark field images 80−79652
amorphous objects, filtered electron image contrast for elastic scatt., calc. 80−107026
amorphous specimens, dose minimisation as criterion for imaging mode selection 77−55220
analytical, contamination reduction using liq. N_2 cold trap assembly 80−101056
anomalous transmission of high energy electrons *(Japanese)* 77−43117
application in modern science, review 79−26182
aromatic polyamide fibres, evidence of radial and tangential morphology 79−73107
asbestos aerosol electron microscopy and analysis *(French)* 77−37461
atmospheric interaction, between aerosols and gases 80−104544
atom, bright and shadow images 77−67544
atom images under dark field, STEM and TEM comparison 78−83696
bicrystals, grain boundary anal. using TEM 79−28003
biological high resolution microscopy, specimen damage and dehydration, struct. retrieval, instrumental limitations 79−20735
biological macromolecule observation using CTEM and STEM with negative staining 80−85561
biological materials, unmodified, transmission microscopy radiation dose with electrons vs. ultrasoft X-rays 78−11788
biological specimen-conductivity problem in electron microscopy, review 78−24206
biological specimens, high resolution obs. by incoherent illum. method 77−70571
biological specimens, low-temp. TEM, radiation damage, review 78−57147
bipolar transistors, emitter-push effect, analysis of isolated dislocation helices 80−70203
blistering by ion bombardment, ion energy, dose and target temp. depends., review 77−43261
book 80−17726
brass, interface boundaries, TEM procedures for struct. 80−19814
bright field hollow cone illumination advantages, appl. to amorphous C film 78−22609
bright field microscopy, obs. of single and clusters of atoms 77−62456
bright field TEM, partially coherent attenuation envelope shape 80−101885
bright-field image contrast and resolution 80−95200
buckled specimen, TEM bend-contour patterns 79−99040
Burgers vector characterisation method for minerals 80−109141
catalysis, advances in TEM obs. 80−85214
cathodoluminescence, bibliography of papers till 1977 79−21482
cell element observations in same sections by light microscopy, TEM and/or SEM 80−85556
cold-cathode ion gun for sputter etching of specimens 80−105748
computer aided indexing, of transmission electron diffr. patterns 78−38595
computer method for analysing TEM diffr. patterns 77−47309
computerised three-dimensional image reconstruction from projections under limited view angle 80−9078
contamination exam. and specimen cleaning methods 79−54232
contrast, fold domain boundaries and microsectors in polyethylene single crystals 80−107065
contrast enhancement hy changing objective lens focal length 77−41736
convergent beam patterns, 200-800 keV accelerating voltage 77−18142
correlative light microscopy, SEM and TEM of argentaffin cells 80−85557
correlative microscopy, comparison of SEM, TEM, STEM, scanning work on TEM, transmission work on SEM 79−17576
correlative SEM-TEM of primate infundibular recess 78−20336
craze density measurement by quantitative TEM 79−24701
critical voltage effect, influence of absorpt. 77−19853
critical voltage effect, many beam systems 78−14260
critical voltage effect, obs. in presence of non-systematic reflections 78−67626
critical voltage effect, qualitative influence of non-systematic reflections 77−47307
critical voltage effect in zone axis patterns, theory 80−59352
cryomicrotome attachment, modification to Reichert FC-2 device, improved sectioning reproducibility 80−47149
crystal atomic structure imaging technique and applications 80−105752
crystal defects, electron microscope diffr. contrast 78−83700
crystal orientation, determ. by zone axis method, appl. to grain boundaries 80−103226
crystal structure image computation for high-resolution TEM 78−71653
crystallographic applications, microscope modification to convergent-beam camera and shadow microscope 77−55215
CTEM image recording using CCD 80−68329
cubic crystal, image contrast of dislocation loops, elastic anisotropy depend. 80−103349
cultured cell preparation for electron microscopy, ethanol and chem. dehydration methods comparison 78−24208
dark field micrographs, image array filtering in reciprocal space, S/N enhancement 77−74557
dark-field image contrast and resolution improvement by subtraction anal. 78−338
dark-field microscopy, anal. of decoration patterns 79−23506
defect clusters, in particle-irradiated crysts., TEM identification 79−69108
defects, in semiconductors 79−95021
defects causing strain contrast and struct. factor contrast simultaneously 77−24253
defects in crystals, high-resolution imaging techniques 78−34400
defocus contrast, step thickness determination, on crystal surfaces 79−7531
defocus values, determ. using Fourier images 80−47148
deposited film thickness and grain size determ. on non-conductive SEM specimens 78−77170
depth of specimens meas. using stereo technique 77−30220
detects in materials, direct observation and characterisation 78−88617
diffraction crystallography appls. 77−58929
diffraction effect in TEM, violation of spatial invariance and appearance of pseudostructs. 79−6228
digital image enhancement 80−82852
digital scanning and recording system for spot electron diffr. patterns 77−13825
direct elemental analysis by electron energy loss spectroscopy 80−71998
transmission electron microscopy continued
disclocation structure, of sliplines, in single crystals 79−27990
dislocation core images, optical filtering for noise removal 80−107254
dislocation distribution, distances between parallel dislocations determ. 78−34514
dislocation image contrast, in TEM, dynamical analytical theory 79−95014
dislocation loop, image black-white contrast figure vector 79−7609
dislocation loop analysis and identification using black-white contrast images 80−103350
dislocation motion obs., work of Hirsch et al., (1946-56) 80−62445
EELS, chemical analysis, filtered images 80−101062
EELS, standard, implanted Si 80−99017
electric field effects 80−4823
electrocrystallisation, recent progress in electrochem. and physical methods *(French)* 80−7510
electron energy loss analysis, developments in instruments and techniques *(Hungarian)* 80−31949
electron energy loss spectrometry, thin specimen sections, electron microscopic chemical analysis, review *(French)* 79−8469
electron energy loss spectroscopy, in electron microscope, review 80−104025
electron energy-loss spectroscopy in context of TEM, review 80−31945
electron microscopy, diffr. and imaging techniques in material science [book] 79−67439
electron probe analysis of thin specimen, TEM attachment *(French)* 77−81445
energy anal. appls., image filtering, microanal., struct. determ., plasmon dispersion, thickness meas. 77−44100
energy dispersive X-ray analysis in TEM/STEM, sensitivity limits for thin specimen analysis 78−24007
energy filtering applied to thick objects *(French)* 77−27794
energy loss spectra, direct display using Si self scanned photodiode array 78−45753
energy loss spectrometry, use in microanalysis and errors involved 78−35785
energy loss spectrometry use in microanalysis 78−35784
energy loss spectroscopy, localised chemical characterisation *(French)* 77−77850
energy loss spectroscopy, quant. microanal. of thin foils *(French)* 80−50900
energy loss spectroscopy and microanalysis, instrumentation developments, review 78−35783
energy-loss analysis, single crysts., in TEM, diffr. conditions influence 80−81406
energy-loss spectral resolution optimisation wing electron lenses between TEM specimen and electron spectrometer 80−101886
epitaxially sandwiched macromolecules, contrast 80−85565
epitaxy, growth modes, exp. techniques, book contrib. 80−49558
evaporation coeff. meas. 78−18909
experience in TEM at the Univ. of California (Berkeley) 80−37130
extraction replica evaluation, Ashby-Ebeling model analysis *(Czech)* 80−49062
fatigue crack tip displacement visualis. and meas. using stereo viewer 79−24700
FCC materials, dissociated dislocation dipoles, weak-beam electron microscopy technique 78−34516
field electron source geometry determination by computer assisted shadowgraph technique 77−87882
field emission, sub-angstrom resolution 80−82851
field emission gun, appl. to TEM 77−54023
field emission gun use, phase contrast transfer improvement due to low energy spread 77−10145
fine fragmented crystals, complex struct. analysis by electron microscopy 80−104416
fine structure of images of atoms in crystals 77−31568
fixed beam, factors affecting 77−67545
foil, normalisation of ang. distrib. curves of transmitted electrons *(French)* 77−4026
foil thickness measurement for quantitative metallography 78−35632
foil thinning, monitoring by PP-8 radiometer (USSR) 80−73525
foils preparation, GaAs and CdTe, by ion sputtering *(Czech)* 80−16619
foundations of transmission electron microscopy *(Hungarian)* 79−54229
freeze drier, all-glass design 80−82854
grain boundaries, nearly transverse, weak-beam TEM imaging 77−19854
grain boundary anal., modified O-lattice for CSL and DSC lattice determ. 79−55752
grain boundary anal. by TEM, CSL condition determ. 80−15117
grain boundary dislocations, Burgers vectors, grain boundary dislocations 78−87680
half-plane apertures in TEM, ptychography 78−89603
heart muscle cells, paraffin-embedded, cryofracture, SEM and TEM obs. 78−57148
HEED atomic string approximation use in obtaining dispersion surfaces 80−100143
high resolution, combined with nanoPROBE anal. 80−4814
high resolution, low-noise B supports 80−8236
high resolution, role in structure research, C, W_xO_y and mineral examples *(Hungarian)* 77−76267
high resolution, use of Kodirex film 77−54025
high resolution, welding technique, grain boundaries in Si 80−103364
high resolution phase contrast, imaging of single atoms and amorphous state 80−103224
high-resolution electron microscopy, present state of instrumentation 79−2887
hollow cone illumination produced electronically 77−54026
holographic method for recording electron image 79−6224
human platelets, air-dried, topography and thickness measured by correlative TEM and SEM 79−84041
HV, appl. in sold-state physics 79−27882
HV electron microscopy, recent progress, book contrib. 79−67442
HV electron microscopy in biology and medicine *(German)* 79−57834
HVEM straining, optimum conditions 80−39207
II-VI semiconductors, struct. of thin foils 79−32864
III-V semiconductor compound structures, TEM analysis 77−89836
III-V semiconductors, film, sample preparation for TEM studies 78−14258
image analysis and beam damage, instrumental aspects 78−32954
image and electron energy loss spectrum display by self-scanned linear Si photodiode arrays 80−68330
image contrast, radiation damage, STEM and CTEM 77−49811

transmission electron microscopy continued
image contrast from single-electron excitation 80−59353
image enlargement and rotation *(Czech)* 80−73526
image reconstruction from projections, max. likelihood meth. 77−86690
image recording and processing TV system 79−58851
image resolution and penetration in amorphous and polycrystalline materials, comparison with STEM 80−14976
image theory, iconic approx., and its generalisation 78−79509
imaging code for long period struct. obs. in perovskite crysts. *(French)* 78−26395
implanted ion detection by X-ray emission anal. in TEM 78−51575
in situ experiments in the transmission electron microscope, review of principles and practice 79−71574
in-situ techniques, problems and appls. 80−76461
incoherent illumination method with conventional electron microscope, granular noise elimination 80−95201
inelastic scattering probabilities for fast electrons in single cryst., orientation depend. 80−2905
interphase boundaries, struct. anal. 80−19813
lattice defects, characterisation 80−103320
lattice defects, SEM, electron beam induced conductivity, thinned semiconductor devices 80−107027
lattice image formation, many-beam theory, TEM 80−38879
lattice images, effect of absorpt. 79−90497
lattice images of defects, aberration and cryst. misorientation effects, radiation damage applics. 80−107210
lattice images of defects, computer simulation of high resolution images 80−107208
limiting factors in specimen thickness in STEM and conventional TEM, expts. on Si 77−19852
Lorentz microscopy, thin film and bulk specimen, recent advances 78−35002
low-temperature, struct. determ. of frozen, hydrated, cryst. biological specimens 78−57146
martensitic transformations, electron microscopy and diffr. studies 79−68989
metal, plastic deform. mech., TEM appl. Mg, FCC metals *(French)* 77−1853
metal particles, 10-300 Å, high resolution TEM topographical images 77−43439
metal point defects, computer simulation of dark field electron micrographs 78−47219
metal specimen preparation for TEM, two-stage, jet-stagnant electrolytic thinning, Ti, Mo appls. 77−71405
metallurgy, review 80−76458
microanalysis, appl. to Nb_3Sn thin films 80−104491
micrograph image restoration, of weak-phase object using computer *(Japanese)* 79−71571
microscopic equipment, methods, appls. and related topics, bibliography 80−73124
microsurfaces, obs. using thermal desorption spectroscopy combined with TEM and transmission electron diffr. 79−90888
mineralogy, application of TEM, sample prep. methods *(French)* 79−5629
misfit dislocation observations at film/substrate interface 80−103605
molecular semiconductor/metal film junction, TEM method for cross-sectional exam. 78−95241
molecular solid, film, 0-15 eV electron transmission spectra 80−35023
multiphase polymers, morphology using electron microscopy 78−91271
multistrip components using computer graphics 79−30630
object reconstruction from real part of scatt. wave 79−93262
off-axis image electron holography, proposal 77−10151
optical filtering of faulted areas in layered silicate micrographs 80−84035
organic solid-sate chemistry, appl., review 79−60235
out-of-focus image interpretation, p-n junction with one-sided step model internal field topography 79−82129
p-n junction, image interpretation 79−51659
p-n junction, thinned, TEM image interpretation 77−20414
p-n junctions, defocused images, stationary field approx. 78−67628
particle track detectors, electron microscopy of etch pits 80−99424
particulate analysis, aspects of specimen prep. and a limitations of precision by SEM and TEM 79−17574
perfect crystal, distrib. of phonon scattered electrons 77−19846
phase contrast transfer with different imaging modes 78−70232
phase transformations, direct obs., using TEM 80−2997
phase transitions, appl. of TEM 79−68988
phosphatidylcholine vesicle sizing 79−70722
photograph simulations, on storage display, appls. to X-ray topography and TEM 79−14637
photomacrography and photomicrography, oblique transmitted light techniques 78−306
plural scattering, influence on image quality of thick amorphous objects 80−86533
point project electron microscope use in observing thickness extinction contours 77−82655
polymer materials, characterisation 80−103270
polymers, multicomponent-multiphase, bulk struct. by rheo-optical techniques 78−91267
pumping, 24 hr continuous fail-safe, TEM modifications for 77−22626
quantitative elemental analysis 80−101060
relative orientation of two crystals from analysis os spot diffr. patterns 77−47305
reproduction of electron micrographs and transparencies for publication and display 77−49817
resin slide technique for selection of fixed embedded cells 77−60316
review, TEM, STEM, and SEM: microscopy to microfabrication 78−32936
sample preparation, IBMA equipment for ion bombardment *(Czech)* 77−61161
scanning Auger microanalysis, charge buildup reduction technique 79−17569
semiconductor, TEM/SEM observations comparing diffr., elec. and luminesc. contrast from dislocations 78−38714
semiconductor crystal defect obs. by TEM *(Japanese)* 77−84752
semiconductor crystal growth and defects, appl. of analytical techniques 80−73546
semiconductor TEM 90° cross-section and 1° angle-lap specimen prep. 80−71881
single atoms, in molecules and crystals, TEM obs. 80−103229
small-angle scattering, selected area diffr. and long-camera-length methods, appl. to materials science 79−14658
specimen cup for X-ray anal. in a TEM 77−12851
specimen prep. methods for image processing, review 79−17405
specimen preparation, fine grained coatings, sputter source design 80−99015
specimen preparation, plasma etching use for foil thinning *(Slovak)* 80−45405
specimen preparation by chemical etching 77−52589
specimen preparation ion beam techniques 78−24778
specimen preparation using photochem. etching *(German, English)* 77−56202
specimen thinning, ion beam penetration switch 78−70228
specimen transfer device for combined AES/RHEED and TEM obs. 80−70093
stacking fault contrast using weak-beam imaging conditions 78−34401
stained biological section, quantitative anal. of contrast 79−66596
staining method using mercuric trifluoroacetate for polymer blend morphology obs. 80−84103
steel, austenitic stainless, phase identification, $2^1/_2$D imaging techniques 80−96424
stereo pair photography, freeze etch replicas examples 79−49345
stereo photo-micrographs, analysis using computerized graphical method 80−42304
stereomicroscopic method for obs. of organic molecule incorporation in electrodeposited films 80−2288
structure image high-speed calc. methods 79−55622
structure imaging, direct, in electron microscopy 79−68990
surface characterisation, physical methods, review *(French)* 80−7889
surface step thickness measurement 80−103555
temperature calibration standards using graphite-halogens 80−86510
temporal event representation by colour microphotography 79−17566
tensile specimen preparation, stress distrib. 78−73973
thin film, and surface anal., modern methods 80−54486
thin films, chem. anal. by energy loss spectroscopy 80−104493
thin metal films, for electron microscopy, production by jet polishing apparatus 78−86247
thin samples, mass thickness and chem. composition determ., by TEM and X-ray anal. 80−103227
thin specimens, X-ray spectra characteris. in TEM 78−35788
thin-foil technique for exam. of contact surface of worn Cu pin 77−60033
thinning of specimens for TEM 77−82644
three zone axis method, indexation of diffusion patterns, grain boundary characterisation *(French)* 79−99038
ultramicrotomy in corrosion and protection TEM 77−81358
ultrasoft X-rays, detection with variable geom. proportional counter fitted to TEM for microanalysis 77−48712
ultrathin cryo-section stabilization by freeze-drying 78−54349
void arrays in crysts., contrast 80−14975
wave aberration sign in electron optics 77−22623
X-ray analysis, energy selective, TEM appls. 80−84036
X-ray analysis in the TEM/STEM, review 78−24014
X-ray microanalysis, in TEM at high accelerating voltages 78−36078
X-ray microanalysis, in TEM up to 1000 kV 80−101063
X-ray microanalysis of thin foils, energy dispersive 77−60153
X-ray production, theoretical and exptl. 80−85258
X-ray standardless thin film analysis in electron microscope 78−24006
Al-Zn (38 at.%), precipitation process study 80−93561
Au decoration technique, TEM and SEM study of localisation of decorating crystallites *(French)* 80−10470
Fe, deformed single crystal, dislocation distrib. 77−59880
$Fe_{80}B_{20}$, absolute thermoelectric power between 300 and 1000K 79−19579
FeNi amorphous films, fast phase transition investigation by TEM method 80−107029
$LiNbO_3$, ion-bombardment erosion of single cryst., prep. for TEM exam. 79−38996
NiO, single crysts., TEM of dislocations 79−4306
S atom imaging, simulation of dark-field images of 2,3,4,5-tetraacetoxymercurithiophene 78−70229
Si wafers, preparation of preselected areas for TEM 78−24887
$SmCo_5$, single cryst., grown-in dislocations and stacking faults, TEM investigation 79−19253
W support film for high resoln. electron microscopy, phase contrast, computer modelling 78−1144
ZrO_2 foils, production for TEM 79−74087

transmission line theory
arterial velocity flow system, transmission-line model 77−44715
book *(French)* 78−13640
charged transmission line for pulsed high current accelerators, energy transfer 78−78519
concentric line with helical inner conductor, EM field and phase constants 79−86112
concentric line with helical inner conductor, wave impedance and attenuation consts. 79−86113
cruciform section optical fibre in single material 77−39046
Earth-ionosphere transmission line, ELF propag. rel. to ionospheric profiles 78−36234
elastic waves analysis appl. 77−62728
electromagnetic waves, transmission and propag., book 79−50198
EM field energy calc., using surface integral 78−5394
fields solution using transmission line matrix, Monte Carlo approach 79−53991
fireball plasma formation, transmission line model 78−59702
interacting SAW transducer equivalent circuits 77−27456
Josephson junction, long, oscills., exact solns. of sine-Gordon eqn. 78−68115
lightning return stroke, channel model, computer soln. 78−85644
lightning transient anal. for aircraft, flux induced voltage transients on low-loss transmission lines 79−36814
magnetic coated small dipole antenna. charact. using approx. surface wave transmission line theory *(Chinese)* 79−50193
Maxwell's equations, numerical soln. by transmission line and lumped network models 80−27147
mechnical coupled-transmission lines 78−52
modulational instability expt. using nonlinear transmission line 77−82397

transmission line theory continued
natural VLF antenna, Deception Island, impedance meas. and composite transmission line model 79−48399
ohmic contacts to semiconductor, meas. of contact resistance using transmission line model 80−70826
particle accelerator appl., nonidentical resonators with narrow coupling slits, dispersion and field distrib. characts. 79−41047
resistive gate MOS transmission line, charge propagation study *(Rumanian)* 79−11233
self-magnetic insulation in vacuum for coaxial geometry 78−78520
solitary waves in nonlinear transmission line 80−4543
Space Shuttle lightning current distrib., circuit modelling and exptl. verification 78−49293
superconducting phase slip centre, charge imbalance waves and nonequilib. dynamics 80−54830
US transducer evaluation in exptl. and theoretical domains 79−46153
wire antenna impedance in magnetoplasma transmission line theory 77−39429

transmission lines
see also cables (electric); communication transmission lines; high-frequency transmission lines; overhead lines; power transmission lines; waveguides
aeolian vibrations, effect of 4R dampers 79−23259
basilar membrane motion linear and nonlinear models 77−90800
cochlea model, for signal anal. 77−26281
Doppler frequency shift by fast moving boundary *(Japanese)* 80−18967
instantaneous frequency measurement of micro-wave range by two different point detected signals *(Japanese)* 80−73327
laser pulse display and shaping, subnanosecond electro-optic technique 77−19270
magnetically insulated, Compton scattering of photons from electrons 80−68982
metallic-conductor, far IR antenna appls., review 80−69553
MOS structure, resistive gate, charge propagation, model 77−85325
NMR probe coaxial transmission line, optimum charact. impedance 77−53967
optic fibre light transmission, fibre production methods, transmission line structures details *(French)* 79−89998
optical fibre cables, 10-fibre filled, 6-fibre, connector for field installation 80−43470
radial, use in pulsed electron accelerators 77−46425
radiotelescope transmission lines, antenna arrays and impedance transformation 78−96399
RF-biased SQUID, with half-wavelength transmission line 80−22342
side-plated piezoceramic bar, elec. and acoustic wave propag. 77−50847
TEM cell for electromag. interference investigations, large, based on rectangular coaxial transmission line 80−238
US transmission line of probe for hot metal inspection, spurious signals 80−66754
vibrational modes at high freqs. for cables with dampers 79−81773
vibrations, effects of Stockbridge type dampers 79−14323
N_2 laser, high-power, TE, UV, using Blumlein transmission line, construction characts. *(Korean)* 79−22971

transmission networks
see also communication networks
fast nuclear reactors, electrical supplies and Na pumping system 80−52723

transmission wavemeters *see wavemeters*

transmitters
see also radar transmitters; radio transmitters; television transmitters; transceivers; transponders
biotelemetering, industrial product survey *(German)* 77−29220
broadband transmit/receive circuit for NMR 78−89520
FM-AM miniaturised transmitter for EEG and EMG, for sleep telemetry in rat 78−48947
heavy ion linear accelerator, Munich, 50 kW transmitter, power stage design 77−83175
implantable, for monitoring diving duck heart rate and respiratory freq. 77−44858
laser-fibre transverse coupling and front-mirror monitoring for feedback control of laser transmitters 80−33151
linearised LED and laser transmitters, for analogue fibre optical systems 78−46818
optical communication, components development *(German)* 79−81563
optical fibre communication for military appls., review and assessment 78−42438
optical transmitter laser diode module description and performance 80−64069
optical transmitters, laser diode switching dynamics and noise *(German)* 79−89919
pulsed NMR transmitter, for relaxation time meas. in biological samples, construction and operational details 78−93745
GaAs-$Ga_{1-x}Al_xAs$ double heterostructure LED and injection laser transmitters 77−68282

transmitting *see transmission*

transonic flow
acoustic plane wave excitation by volume sources, nonlinear 80−38154
aerodynamic wind-tunnel testing, transonic flow simulation by tracking and blowing *(German)* 80−6081
aerodynamics, finite element method, book contrib. 79−32556
aerodynamics, variational formulation and finite element anal., book contrib. 79−32555
aerofoil, in transonic cascade, choking flutter 77−75885
aerofoil, thin, near-inviscid supercritical flow, numerical soln. 78−14038
aft-loaded airfoil, boundary layer displacement effect and wake near trailing edge 78−22366
aircraft design technology, fluid dynamics computer program assessment data base 80−1637
airfoil, finite-difference calc., computer code 78−26147
airfoil, wave drag in transonic flow, shear interferometry obs. 79−77165
airfoil flow, steady and unsteady, shock-induced separation 79−59999
airfoil optimisation, transonic flow finite element anal., book contrib. 80−1633
airfoil problem, variational principles 78−42626
airfoil section, boundary layer, laser velocimetry meas. 77−35274
airfoil vibration in transonic flow *(Russian)* 77−39308
airfoils, lifting, design procedure in transonic flow by integral method *(German)* 77−35163
airfoils, transonic testing at high Reynolds number in shock tube 80−14852

transonic flow continued
approximate solution using patched variational principles, appl. to elliptic and mixed elliptic and hyperbolic problems 77−89144
axial compressor rotor, transonic flow field, laser velocimetric obs. 79−4009
axisymmetric flow past slender body of revolution, integral equation method 80−74910
axisymmetric inlets and bodies at angle of attack, 3-D computation 78−9648
axisymmetric transonic flow around slender bodies, hybrid computation 77−42861
axisymmetric transonic turbulent base pressures 80−19425
backward facing step, viscid-inviscid interaction model 78−9649
blades in transonic flow, shocks and boundary layers, time marching method 79−4036
blunt cone-cylinder experimental study 78−87358
body of revolution, slender, nonlinear normal forces, Reynolds no. influence *(German)* 78−51191
body of revolution in flow, perturbation theory and numerical body 79−60000
boundary effects on transonic flow around bodies of revolution 79−90275
boundary layer, fluctuation anal. from hot-wire anemometry data 77−65817
boundary layer, two-dimens., viscous-inviscid flow matching, numerical method *(French)* 78−79334
boundary layers, freely interacting, compressive and expansive flow 77−89145
bow shocks comput. method 77−55027
cascade, high-deflection, transonic two-dimens. flow *(French)* 79−27664
cascade flow, transonic anal., by conformal mapping and relax. techniques 77−75934
cascade shock loss location and magnitude by high speed smoke visualisation 80−24051
cascade with slender profiles, transonic flow, numerical soln. 80−38436
cascades, supersonic and transonic compressor, unstarted choked regime calc. *(Chinese)* 80−43730
cascades with different trailing edge thicknesses, vortex shedding freq. determ. 78−75152
channel, anal. of unsteady transonic flow with shock waves 77−23991
channel flows, two-dimensional, shock-wave motion 79−60005
chemically active mixture, eqns. *(Russian)* 77−89208
chemically relaxing mixtures 79−64797
classical equivalence rule assessment for flows past nonaxisymmetric slender shapes 80−6079
compressed gas, nonsteady transonic flow, modified Khokhlov method study 80−79347
compressible and incompressible flows, recent theoretical and expt. developments, book 80−1620
compressible flow around an aerofoil or a cascade, up to shockfree transonic range 78−22365
compressible flow of perfect gas around uniformly expanding sphere 80−28528
compressible flow problems, modified FLIC method, finite element anal. 80−74911
compressor, prediction using characteristic method 80−96277
computational method for transonic aerodynamic flows 77−3842
cone, sharply pointed, press. distrib. at attack angle 0 to 10° 80−38434
conical supersonic flow around yawed circular cones in the transonic region *(German)* 79−77175
continuum source particle beam properties, comput. modelling 80−26062
converging bi-conical pipe, 3-dimensional internal blocking *(French)* 79−50751
curved wall, turbulent boundary layer detachment by perpendicular compressive thrust *(German)* 78−94661
cylinder in cross flow, skin friction and vortex shedding freqs. 78−94758
cylinders and airfoils, primitive variable least-squares finite element formulation 80−33623
density distribution in a non-stationary bow wave in a transonic flow, book contrib. 80−1631
detached bow waves around bodies at slightly greater than sonic speed, book contrib. 80−1630
detached flows past a cylinder with a flat end, subsonic and transonic vels. 80−92187
diffuser flow, shock wave oscillations 80−14729
diffusers, curved, performance, separation in subsonic, transonic channels *(French)* 78−94818
discontinuous, shock wave 78−38362
dispersive compressible fluid, transonic nozzle flows 80−69895
duct with abrupt enlargement, transonic flow, self-excited oscills., model calcs. 80−28522
Euler eqns., numerical soln., Lagrangian method 80−38435
European wind-tunnel project for testing at cryogenic temps. 79−58713
external flow problems soln. using method of decomp. 77−58725
far-field boundary conditions solution 77−55024
far-field matching method 78−26146
fast implicit solutn. procedure 80−19430
finite element anal., discontinuous trial functions 77−68619
finite element and finite difference calcs., book contrib. 79−32558
finite element formulation for subsonic and transonic flow 80−28526
finite element method 77−80135
finite element method appl., shock-fitting for transonic flow with shocks 80−14730
flow field computations, heuristic obs., book contrib. 80−1626
flow separation in transonic turbulent boundary layer, shock wave causing separation *(French)* 79−77186
gas, meas. by holographic interferometry appl. 79−86542
gas flow, optical excitation of intense acoustic waves 80−74564
gas mixture, binary, spherical expansion into flooded space, components separation 79−81948
gas mixtures with vibr. relax., nozzle flow 79−64727
gas plane flows in presence of weak supply of energy *(Russian)* 79−32498
Guderley's transonic small disturbance equation, exact solns. 80−19315
highly separated transonic flow, first vel. and RMS vel. fluctuation meas. 79−77166
hyperbolic Laval nozzles, transonic flow in throat region *(Chinese)* 80−6122
ideal radiating gas, sonic discontinuities, shock development 80−43802
implicit approximate-factorisation schemes 78−94759
integral eqn. formulation for lifting profiles and wings 78−38363

transonic flow continued
integral equation derivation, flow past thin two-dimensional airfoil 77−58721
inviscid free air flow simulation using perforated walls in wind tunnels 79−90276
inviscid hyperbolic flow, computational algorithms tests 80−27140
jet, free, overexpanded two-dimens., eqns. formulation and soln. method 80−6109
jet, sound power output, turbulent jet into gas with different sp. ht. 78−94789
laminar boundary layer flow near convex corners 79−64686
laser velocimetry appl. for unsteady transonic flow meas. 80−10341
Laval nozzles, subsonic, transonic, supersonic flow characts. calc. *(Chinese)* 79−32623
least squares approx. for partial differential eqns. of mixed type, indefinite problems 78−36807
lift correction to transonic equivalence rule 77−62273
lifting line theory for transonic flow 79−46338
lifting round-nosed airfoil, extended integral eqn. method 77−62271
lifting three-dimensional wings in transonic flow 80−19428
Mach line flow, two-dimens., equivalence conditions, physical interpretation *(German)* 80−1634
mixed compressible flow, type-independ. soln. 79−4035
mixed flows, numerical simulation using fast super-dashpot time-dependent technique 80−83813
multidimensional imbedded shocks in transonic flow 77−3841
nacelle flow fields, accelerated iterative calc. 78−26145
noise generation by transonic open rotors 80−69599
non-asymptotic shock-detachment distance of slender cones in transonic flow, book contrib. 80−1632
nonequilibrium flows with transonic vel., second approx. 80−33622
nonequilibrium two-phase flow in Laval nozzles 79−68820
nonlinear formulation for low-frequency transonic flow 78−94761
nonlinear near-sonic potential flow with viscosity, solns. *(German)* 80−1646
nonlinear wave propagation and unsteady transonic flow, variational formulations 78−55660
nonseparating normal shock-turbulent boundary layer interaction, approx. anal. theory 77−23992
nonstationary boundary layer with self-induced press. at transonic external stream vels. 78−83428
nonsteady two-dimens. transonic flow, numerical solns., shock waves 80−53808
normal shock-turbulent boundary layer interaction, Reynolds no. and mass transfer effects 79−37353
nose surface, press. distrib. of bodies of revolution, $\alpha=0$ to 10° 77−27549
not-so-slender wing theory 77−58717
nozzle, axisymmetric choked, transonic swirling flow analysis 77−58761
nozzle, heat transfer of transonic air flow 79−1230
nozzle, rotational, relaxation solution 78−30312
nozzle, square, transonic flow, 3-dimens. density field meas., holographic technique 78−47080
nozzle, supersonic, influence of transonic flow throat region for maximum thrust 79−41729
nozzle flow fields, quasi-one-dimens., time depend. calc. *(Japanese)* 77−58760
nozzle flow of gases with rate and nonuniform props. 77−62289
nozzle flow of vibr. relax. or chem. reacting gases 78−59506
nozzle gas blast flows with arc heating 79−46502
nozzles, gases with rate process 78−14058
nozzles, upstream-downstream speed transition 79−98779
numerical calculation methods and problems, review 77−58723
numerical design of transonic cascades 79−10585
numerical simulation by finite element method using optimal control theory 77−55025
numerical solution method using acceleration technique based on Wynn's ϵ-algorithm 77−58724
oblique wing as a lifting line problem in transonic flow 80−59065
ogive cylinder at high angle of attack, experimental investigation of support interference 80−10260
orthogonal finite element method 80−28529
oscillating profile, nonstationary transonic flow analysis by fractional step method *(French)* 77−51079
parabolic spindles, flow field determ. by method of characteristics 78−14039
perturbation potential for unsteady near-sonic flows *(German)* 80−1635
perturbation solution method, 2-and 3-dimens. flows 79−1208
perturbations, high and low freq., growth calc. for perfect inviscid gas *(Russian)* 78−46992
plane, exact shock-jump conditions, numerical solns. 79−41704
plane flows past oscillating airfoils, review, book contrib. 80−96278
plate, flat, attached subsonic and transonic turbulent boundary layers, press. fluctuations effect 79−94642
post shock expansion behind normal shock on curved wall, flow separation, book contrib. *(German)* 80−1628
potential axisymmetric around inlets, Cartesian mesh soln. 77−72323
potential flow partial differential equatn. solutn. by finite element method 80−24045
potential flows past cascades, in nozzles and channels, pseudo-unsteady method 80−14727
potential subsonic and transonic cascade flow, stability anal., finite area methods 80−48737
potential theory model for separation regions behind shock waves *(German)* 80−1636
pressure pulsations at cylinder at Mach 0.5-0.9, step effect 79−86453
profile flow at incidence with shock 79−4031
profile flow with shock, supercritical flow 77−15056
pseudo-shocks in cylindrical duct 77−58722
quantitative holographic interferometry *(French)* 77−65826
quasi axially symmetric bodies, series expansion and parabolic method 77−15057
quasi-linear initial value problems, variational formulation 77−13579
radial turbomachine, meridian plane characts. for subsonic and transonic flow, finite element calcs. *(French)* 80−38418
real gas effects in cryogenic wind tunnels 78−94760
real gas version of de Saint Venant and Wantzel gasdynamic formulae *(German)* 79−18974
recovery tube, turbulent boundary layer effect on press. variation 77−84238
transonic flow continued
relaxation solutions, convergence acceleration using cyclic iterative method 77−62272
relaxing gas, sonic discontinuities 80−28531
review of laser anemometry applications in France and Germany 77−35272
rotational transonic flow and inviscid potential computation by quasi-natural numerical methods 79−64666
shock free flow around a convex angle 80−1625
shock free profile flow at zero incidence, iterative computation 79−50750
shock motion effect on transonic indicial method 78−94769
shock wave interaction with turbulent boundary layer, pressure distrib. 80−74918
shock wave interaction with turbulent boundary layer, wall shear stress 80−74919
shock wave solns., weak 78−38364
shock wave-boundary layer interaction, dual-scatter laser velocimeter meas. 77−39376
shock-boundary layer interaction, shock obliquity effect 78−90933
shock-fitting, appl. to relax. solns. of small-disturbance eqns. 77−84275
shock-fitting scheme, implicit, for unsteady transonic flow computation 78−94763
similarity parameter, simple waves 77−23982
simulation, implicit finite-difference, of steady and LF transonic flow 80−19429
simulation by finite element method via optimal control, book contrib. 79−32557
singular aspects of three-dimens. flow 78−63445
sink-vortex flow in compressible medium, book contrib. *(German)* 80−1603
slender bodies, unsteady linearized formulation 77−89143
small disturbance theory, leading edge singularity 79−10586
small disturbance theory, self-consistant formulation, book contrib. 80−1629
small-disturbance theory, leading-edge singularity, num. integration methods eval. 80−6080
small-disturbance transonic flow, nonlinear mixed elliptic hyperbolic eqn., finite element anal. 80−83814
sphere drag coefficient in transonic flow at high Reynolds number 77−31323
spontaneously condensing and wet steam discontinuous flows in steam turbines, numerical investigation *(Russian)* 80−87800
static pressure hole meas. errors in transonic flow with pressure gradients 79−94645
steady potential flow, review 77−72324
steady three-dimensional, finite vol. soln. of Euler eqns. 77−55028
steady transonic Euler eqns., Newton's method soln., nozzle appl. 80−38437
steady transonic flow past aerofoil, viscous effects, prediction model 80−14732
steam turbine, meridional stream line calc. 77−23986
stellar atmospheres, spherical transonic flow, reson. line radiative transfer 80−94698
store configuration, critical Mach number 80−19427
strained coordinate method for transonic flows 80−69861
stream boundaries effect on flow around bodies of rotation *(Russian)* 78−87357
streamline shape, influence of nonconservative differencing 77−23983
sub and transonic flow over wing, flow separation, vortex struct., shock wave shape *(French)* 80−14733
subcritical flow, numerical soln. by integral eqn. method 77−65756
subcritical steady flow past swept semi-infinite elliptic cylinder 77−62275
supercritical compressor and turbine cascades, computation 80−96276
supercritical jet flapped airfoil, relax. soln. for transonic flow 77−23984
supercritical profile with oscill. control surface in transonic flow *(French)* 78−71357
supersonic to subsonic transition with local supersonic regions, book contrib. 80−1627
supersonic-transonic flow, thin airfoil in stratified atmosphere 78−5764
swept wing, finite volume method soln. 80−19431
symmetrical airfoil, transonic flow, inviscid and turbulent flow props., wake 80−48736
thick wing, two-dimens. aerofoil, boundary conditions 77−62274
thin finite wedge in parallel channel, drag and sonic line shape 78−26148
three-dimensional, flow analysis using STAR-100 computer 79−94644
three-dimensional, integral eqn. derivation 80−10259
torus, axially symmetric, transonic flow 80−28527
transonic flow around spheres, orthogonal collocation soln. 77−39307
transonic integral eqn. method with curved shock waves 79−68739
transonic shock/boundary-layer interaction subject to large pressure fluctuations 80−38433
turbine cascades, rotating annular, test facility of DFVLR, measurement and evaluation 80−14866
turblent boundary layer, shock penetration 78−14044
turbulence model development expts. with numerical simulations 77−27551
turbulence modelling, compression waves developing into shock wave 80−74909
turbulence spectrum, accuracy and space/time resolution of laser Doppler velocimetry *(French)* 77−35276
turbulent boundary layer, Mach 0.8, skin friction reduction by slot injection 77−39309
turbulent boundary layer-shock wave interaction *(French)* 78−34163
turbulent boundary layer-transonic shock wave interaction, integral computation method 79−1213
turbulent transonic flow about lifting aerofoil 79−4032
turbulent vel. profiles at transonic vels., local skin friction coeff. 78−67214
two-dimensional steady transonic flow, nonlinear wave propag. 77−75935
two-element airfoil, conformal mapping, including multiply connected regions 77−23981
two-element airfoil systems, num. comput. of inviscid irrot. flow eqns. 77−55026
two-phase flow in Laval nozzle, direct problem, numerical soln. 78−63475
two-phase flow in nozzles, subsonic and transonic 79−81950
two-phase vapour-drop flow in channel, stability singular point 77−55078

transonic flow continued
unsteady, flowfield computation by indicial method 78−51185
unsteady 3-dimens. compressible flow, implicit finite difference simulations, transonic appl. 80−64576
unsteady flow, similar solns. 78−94762
unsteady flow anal., mixed kernel function of approach 78−71360
unsteady flow in two-dimens. diffuser 78−71361
unsteady flow past airfoil 78−71359
unsteady flows, calc. using integral eqn. method, aerodynamics 79−32554
unsteady force and moment alleviation by control devices in airfoil 78−71362
unsteady inviscid, local linearisation soln. for pitching bodies of revolution, $M_\infty=1$, stability anal. 77−31322
unsteady local linearization solution for pulsating bodies in transonic flow 77−11219
unsteady perturbations, shock waves 79−4033
unsteady potential flow past oscillating flat plate airfoil 79−23337
unsteady transonic flow, freq. effects 80−14728
unsteady transonic flow about oscillating airfoil, perturbation soln. 77−23985
unsteady transonic flows with shock waves in an asymmetric channel 78−71366
unsteady transonic shock motions in two-dimens. flow 80−14731
unsteady two-dimensional flow over oscillating airfoil, Dowell's method 77−31321
unsteady two-dimensional subsonic, transonic and supersonic flow calcs. by method of characts. 77−55021
unsteady-state, of supersaturated vapour, in presence of condensation 77−35162
upwind second-order difference schemes for transonic flow with embedded supersonic and shock regions 77−23975
viscous effects, Navier-Stokes eqns. soln. method 77−55023
viscous flow, book contrib. 78−59416
viscous flow around 3D wings 79−37346
viscous transonic cascade flows around airfoil, coord. system for numerical calcs. 78−42627
viscous transonic eqn., algorithm for inviscid flow 79−4034
weak shock wave and sound wave refl. at shallow incidence, boundary layer effects 78−22373
wedge flow, parabolic series method, drag coeff., press. distrib. 77−89142
wind tunnel, cryogenic induction-driven, preliminary tests *(French)* 79−27730
wind tunnel, European transonic cryogenic, with high Reynolds number *(French)* 79−32714
wind tunnel, noise level effect on model characts. *(French)* 78−71411
wind tunnel laser velocimeter meas. interpretation 77−31324
wind tunnel testing, modern developments 77−31405
wind tunnel transonic test section wall interference minimisation *(French)* 77−27550
wind tunnel wall and viscous effects, numerical simulation 77−27552
wing, oscillating, in transonic flow, unsteady airloads and flow linearisation 80−19426
wing, unsteady lift and pitching moment at Mach no. 0.38-1.28 78−34151

transparence *see transparency*

transparency
see also light transmission; optical constants; self-induced transparency
absorption coefficients meas. of transparent materials, interf. effects 78−46699
acetate glasses, radiation effects on transparency 79−57261
aerosol, moving droplet, bleaching kinetics by CO_2 laser radiation 78−13743
aerosol particle size measuring device, using spectral transparency and small angle scatt. methods 80−95069
alkali halide thin films, photoacoustic determ. of optical absorptance of highly transparent solids 79−40632
alkali metal ternary chlorides, $ABCl_3$ type, optical props. 78−35111
alkoxybenzylidenaminobenzonitriles, elec. field and press. induced transitions, transparency and texture 77−43317
trans-4-alkylcyclohexane carboxylic acids, visible and UV spectroscopy transparent matrix 80−45102
atmosphere, absorpt. in 8-12 μm transparency window by fine aerosol particles *(Russian)* 78−16159
atmosphere, spectral transparency in 400-700 cm^{-1} range *(Russian)* 77−13121
atmosphere, transparency, meas. on Maidanak mountain during autumn and winter (1977 to 1978) *(Russian)* 80−72627
atmosphere, transparency effects on radial vel. meas. of solar pulsations 79−101130
atmosphere, transparency meas. in Uzhgorod *(Russian)* 78−40656
atmosphere 8 to 21 μm window, water vapour continuous absorpt. calc. *(Russian)* 78−96293
atmosphere extinction, monochromatic coeffs. determ. from spectrophotometric obs. on Terskol Peak *(Russian)* 79−44246
atmosphere of high-mountain regions, astronomical-climatic conditions evaluation for IR astron. obs. 79−62566
atmospheric multispectral analysis by NOAA and METEOR satellites 77−82009
benzene, liq., laser pulsation kinetics, optical damage effects 80−58614
ceramics, Rochelle-type, controllable transparency *(Russian)* 77−630
cholesterilcinamate, low press. phase transition temp. change, relative transparency *(Russian)* 78−2242
cholesteryl esters, liq. crysts., P-T diagrams up to 5000 kg/cm^2 78−2003
correlation reduction, spatial filtering and variation of resolution 80−102850
corundum, growth of large crystals of high opt. quality 77−34916
defect crystal structure determination, light interference, diffraction and scattering 80−103316
dense plasma layer, nonlinear transparency to EM field 78−87454
dental material transparency meas. device 78−31975
dielectric solids, role of thermal stresses in optical breakdown *(Russian)* 78−95547
dielectrics, highly transparent, refr. index dispersion 79−72635
disperse system, spectral transparency approx. by Legendre polynomials, distrib. density of particle size 80−95800
eclipsing binary stars atmospheres, light curve anal. with allowance for transparancy effects 80−82417

transparency continued
ellipsoidal particles orientation determ. by spectral transparency 79−98287
far IR transparent solid dispersive transmission meas., using Fourier spectrometer 79−30581
fibre material selection criteria for $\lambda>1.8$ μm 80−87554
flash lamp shell transparency changes and dynamic colour *(Russian)* 79−10370
four-colour reproduction, colorimetric anal. by photomechanical means 79−75635
glass, crystallisation and opacity, exam. by high temp. viscometry and X-ray diffr. *(Polish)* 78−84875
glass fibre reinforced polyester, photoelasticity, optical characts. 79−18709
glass fibres as optical waveguides 78−1332
heavily doped semiconductors as transparent heat reflectors *(German)* 78−79197
holographic grating, in spectrograph 80−57395
holographic memory with controlled transparency, associative access to data 79−31841
impact of transparent material by small particles, high speed photomicrographic recording 78−44342
intense radiation in a liquid, propag. instability 79−10346
interface between transparent media, *p* and *s* polarisation amplitude reflectances and phase shifts 79−76578
Iowa lakes, water transparency survey 79−2308
IR transparent materials, bulk and surface absorpt., calorimetric meas. method 79−27347
IR transparent materials and components 77−19374
laser window degradation interactions and impurity clustering effects 79−14050
liquid irradiated, dosimetry by holographic interferometry *(Rumanian)* 80−9412
liquids, laser pulsation kinetics, optical damage effects 80−58614
liquids for cooling and index matching of Nd:glass laser systems 80−33015
magnetic materials *(Japanese)* 80−11369
MBBA-EBBA, controllable liq. cryst. transparency, electrooptical characts. 80−78996
metal films on semicond. substrates 77−16411
mixed metal chloride acousto-optical props. *(Russian)* 78−60419
muscle, excitation-contraction coupling in voltage-clamped cut skeletal fibres, rel. to transparency 77−29138
nematic liquid cryst., ZhK-440, transparency, electrooptical characts. 80−78996
nematic liquid crystal, electrically controlled transparency based on frustrated total internal refl. 79−32074
ocean transparency field, statistical relationships with hydrological and biological characts. *(Russian)* 79−88361
optical interference filter, effect of harmonic variation of layer thickness 80−28326
optical thin film, thickness monitoring 79−97358
optical waveguide, conic and quasi-conic profile, calc. and construction *(Rumanian)* 80−28331
oxide, porous transparent films as antirefl. coatings for glass surfaces, low refr. index 80−74448
paradiheptyoxyazoxybenzol, low press. phase transition temp. change, relative transparency *(Russian)* 78−2242
particle size distribution, spectral transparency method, improvements 80−86254
paste, direct tensile tests and tied crack model 78−11178
plane-parallel absorbing layer, nonlinear optical props. 80−58631
plasma optical transparency evaluation, line broadening effect 80−79453
polaritons, molecular thin plate, with near-surface polariton transition layer, reflection and transmission spectra *(Russian)* 78−14677
polychromatic light diffr., transparency concept *(French)* 77−79746
polyethylene, high density, oriented extended chain crystals, transparency *(Japanese)* 80−38955
polyethylene, lightly crosslinked, processed under mol. orient., transparent film prep. 80−38957
polyethylene ribbons, flow-induced crystn. from melt, in dies fed by single screw extruder 80−84110
polymer system, two-phase, transparency conditions, interparticle interference effects 78−23428
polymers, mol. struct. rel. to bulk props. 77−32553
polypropylene, flow-induced crystn. from melt, in dies fed by single screw extruder 80−84110
porcelain, equipment for translucency testing *(Polish)* 78−19985
powder, particle size distrib. meas. by spectral transparency method 78−49876
quartz, synthetic, discoloration rel. to lattice deform. 77−24872
rare earth oxides, electron beam evap., optical and mech. props. 77−79907
sapphire, vacuum UV spectra, Cr^{3+} impurity and anion vacancy conc. 78−84605
seawater, transparency rel. to hydrochemical characts. distrib. 80−31057
seawater from Newfoundland Bank, seasonal var. of transparency *(Russian)* 79−100861
seawater in Pacific equatorial zone *(Russian)* 78−16043
seawater in Sargasso Sea, hydro-optical study *(Russian)* 78−85594
seawater inherent optical props. rel. to Secchi depth 79−16472
semiconductor background heating for laser annealing 79−96047
semitransparent structural materials, degree of blackness determ. *(Russian)* 79−27161
solar energy absorbers, thermokinetics of glass and semi-transparent materials *(French)* 80−61410
soot conglomerate destruction dynamics in pulsed laser radiation field 80−58617
transparency at 30 m depth in tropical Atlantic *(Russian)* 77−64307
UV visible absorption in highly transparent solids, laser component appl. 78−66876
water aerosol, propagation of intense radiation at 10.6 μm 80−5692
water transparency, in situ meas. 79−25355
weakly absorbing solid medium, opacity fluctuations, heating by intense radiation and thermoelastic stresses problem 80−38048
Weigert effect appl. to contrast reversal of black and white transparency 79−26165
Al foil, transparency, UV laser irrad. effects *(Russian)* 77−1768
Al_2O_3 porous transparent films as antirefl. coatings for glass surfaces, low refr. index 80−74448

transparency continued
Al_2O_3, transparent, evaluation of freeze drying and spray drying for prep. 77−4761
Al_2O_3, transparent hot-pressed, transparent and translucent properties 80−60533
As-S-Se-Ge semiconducting glasses, IR characts. *(Czech)* 80−25332
As_3Se, vitreous, optical transparency, photostimulated changes *(Russian)* 79−65941
$(As_2Se_3)_{1-x}(As_2Te_3)_x$ amorphous films, changes in optical props. under elec. fields and optical excitation 79−61455
Au, discontinuous film, optical transmittance 78−56529
BaF_2, ultralow loss optical fibre material, loss mechanism 80−78920
Bi film, transparency meas. in mag. field, electronic isoenergetic surface cross section *(Russian)* 79−47532
C film, amorphous, growth under ion impact in butane plasma, and IR transparency 78−52688
C, vapour-deposited, transparent and hard insulating layer, struct. and props. 80−10830
$CdCr_2S_4$, hot-pressed, optical isolation appl. at 10.6 μm, intrinsic absorpt. props. 78−42368
$CdGeAs_2$ crystals, Bridgman grown, optical props. rel. to O_2 content of starting materials 80−81213
CdS:In films, vacuum deposited, growth, elec. and optical props. 79−51460
$CdSn_xO_y$ films, transparent conducting, deposited by RF sputtering from CdO-SnO_2 target 80−76179
Cd_2SnO_4, $CdSnO_3$ electrodes, spray coatings, elec. sheet resist. and optical transparency 78−27401
$CsCuCl_3$, phys. props. 77−62511
CsI, ultralow loss optical fibre material, loss mechanism 80−78920
CuCl, propagation process of polaritons *(Japanese)* 80−24809
Fe_2O_3 films, DC reactively sputtered, for selectively semitransparent photomasks, deposition conditions and optical props. 80−60782
Fe_2SiO_4, fayalite, Czochralski growth under controlled O_2 fugacity conditions 80−84843
Ga-Sb-Te, props. of ternary solid solution based on GaSb 79−7826
GaAs MIS dynamic optically controlled transparencies 78−90523
GaAs oxide, anodic, heat treatment temp. effects, optical props. obs. 78−27658
$Ga_{1-x}Te_x$ amorphous films, elec. cond., optical absorpt. and transparency, band gap energy 79−56335
Ge, pressure tuning of picosecond pulse transmission, enhanced transparency 77−88871
Ge-S-Ga(In) system glasses, photoinduced changes 80−24365
$Ge_{0.3}As_{0.2}Se_{0.5}$, IR optic materials, characteristics *(German)* 80−38081
GeS_2, IR optic materials, characteristics *(German)* 80−38081
Hg_2Cl_2, cryst., birefringence and dichroism, 200-500 nm and far IR 78−27257
$HoAlO_3$, Czochralski growth and props. 77−48335
$In_xGa_{1-x}As$, epitaxial solid soln. film, spectral depend. of transparency, absorpt. spectra calcs. 80−45161
In_2O_3, electro-conducting transparent film, props. rel. to production method *(Japanese)* 80−25557
In_2O_3, films, activated reactive evaporation technique of prep. 80−80989
In_2O_3 films, reactively evaporated, elec. props. 80−84521
In_2O_3, In_2O_3-SnO_2, transparent thin films for satellite temp. control 79−80187
In_2O_3, transparent conducting film, prep. by CVD, and characterisation 80−11571
In_2O_3:Sn, films, activated reactive evaporation technique of prep. 80−80989
In_2O_3:Sn, sputtered films for selective transparent films, prep., elec. and opt. props. *(Japanese)* 77−68247
In_2O_3:Sn films, elec. and optical props., solar energy conversion appl. 79−65945
In_2O_3-SnO_2 sputtered film, appls. in displays, vidicon tube windows, dielec. window surfaces 79−59778
In_6S_7, absorpt. band edge investigation 79−69840
p-InSb, elec. instability and oscills. of transparency in transverse mag. field 78−6407
n-InSb, transparency, DC field induced enhancement 79−91407
$In_{1-x}Te_x$ amorphous films, elec. cond., optical absorpt. and transparency, band gap energy 79−56335
KBr extrinsic absorpt. near 9.6 μ, using CO_2 laser calorimetry 77−16341
KCl extrinsic absorpt. near 9.6 μ, using CO_2 laser calorimetry 77−16341
KCl, ultralow loss optical fibre material, loss mechanism 80−78920
KCl:OH, absorpt. in high-transparency region 80−89037
$K_xRb_{1-x}TiOPO_4$, new nonlinear optical material 77−14784
$K(Ta,Nb)O_3$ ceramic, prep. and electro-optical props. 80−25620
La_2S_3 single crystals, optical props. 79−87458
LiF mech. and optical props. rel. to forging conditions 80−33101
LiF, ultralow loss optical fibre material, loss mechanism 80−78920
$LiNbO_3$ transparency with vacuum-deposited electrodes *(Russian)* 78−60422
$LiTaO_3$-SiO_2-Al_2O_3, transparency in relation to microstruct. 78−53005
$Li_2Ti_3O_7$ growth by Bridgman-Stockbarger technique, optical transparency 80−25548
Mg-Al spinel, hot pressed ceramic, annealing effect on transparency and microstruct. *(Japanese)* 79−74188
$MgAl_2O_4$ transparent ceramic, transmittance, grain size and dopant effects *(Japanese)* 80−19083
$NaNbO_3$-$BaTiO_3$, unidirectionally solidified transparent ceramics 80−25677
Na_2O-B_2O_3-SiO_2:Fe_2O_3, effect of liquid phase separated structure on transparency in near UV and visible regions 79−4823
$Na_2O.SiO_2$-Tb_2O_3 glass magnetooptical study 80−88976
PLZT ceramic, transverse electro-optical effect, matrix-addressable transparency 79−27431
PLZT ceramics, transparent ferroelec., photorefraction and photocond. study 79−42581
PLZT ferroelectric thin films, epitaxial growth and optical props. 80−70543
PLZT porosity and transparency affected by vacuum hot pressing 77−12556
PLZT, transparent ferroelec., RF sputtering and film characterisation 78−72727
(PLZT)(PLZN) system, ferroelec. transparent, prep. and study 79−42911
$(Pb_{1-y}Ba_y)_{1-x}La_xNb_{2-x/5}O_6$, transparent ferroelec. ceramic, optical transmittance, electrooptic props. and Curie temp. 77−32395
transparency continued
$PbTiO_3$ ferroelectric thin films, fabrication by RF sputtering, characts. 80−40261
Pr tinted glasses, transparency, dichroism and colour effects *(Polish)* 80−71371
Si-In_2O_3:Sn heterojunctions for solar cells 78−64107
SiO_2, ultralow loss optical fibre material, loss mechanism 80−78920
SnO_2, electro-conducting transparent film, props. rel. to production method *(Japanese)* 80−25557
SnO_2 film, CVD using $SnCl_4$-H_2O and $SnCl_4$-H_2O_2 systems, elec. and optical props. 78−52686
SnO_2, transparent conductive film, prep. by magnetron sputtering and elec., optical and structural props. *(Japanese)* 79−8247
SnO_2, transparent conducting film, prep. by CVD, and characterisation 80−11571
SnO_2, two-step deposition process using DC sputtering and oxidation, and characterisation 78−95691
SnO_2:F films, elec. and optical props., solar energy conversion appl. 79−65945
SnO_2:Sb thin films DC sputtered, heat treatment effects, expt. 77−28719
Te, acoustoelec. domain induced transparency at 11 μm 78−27182
Te, acoustoelectric domain induced transparency near 11 micron 77−85727
TiO_2 and Dy_2O_3-TiO_2, high refractive index film growth by sputtering, waveguide appl. 77−48341
TiO_2 transparent film thickness and refractive index calc. 79−15547
Tl_3AsS_4, crystal growth by Bridgman-Stockbarger method, exam. of props. 79−11506
TlBr, and TlBr-TlI polycryst. fibre optical waveguides, for IR, fabrication and characts. 78−74974
TlCl-TlBr, KRS-6, ultralow loss optical fibre material, loss mechanism 80−78920
$TlMnCl_3$, optical props. 78−35111
Y_2O_3, prep. of transparent ceramic, exam. of light transmission preps. 79−20013
Y_2O_3 transparent ceramic, transmittance, grain size and dopant effects *(Japanese)* 80−19083
$Zn_xCd_{1-x}S$:In, low resist. film for solar cell window 78−71200
$ZnGeP_2$, single cryst., polarised light photocond., optical transparency anisotropy *(Russian)* 78−2518
ZnO-Al_2O_3-SiO2, transparent glass ceramics, heat treatment effect on microstruct. 78−56667
ZnTe:Cu films, high cond., elec. and optical props. 80−88651
ZrF_4-THF_4-BaF_2 glass, IR-transparent, synthesis using reactive atm. processing technique 80−100826
ZrF_4-ThF_4-NdF_3(LaF_3), phase equilibrium, vitreous phase struct., charact. temp., optical props. *(French)* 79−11587
ZrF_4ThF_4-BaF_2 system, new fluoride glass, optical props. *(French)* 77−36443
ZrO_2 transparent film thickness and refractive index calc. 79−15547

transpiration
see also flow through porous media
canopy interception, measure of loss from hydrologic budget 78−11928
canopy temp. thermal scanner meas. to estimate evapotranspiration 77−5324
climate, soil and vegetation, annual evapotranspiration value 79−79895
climate, soil and vegetation, annual water balance dynamics 79−79896
climate, soil and vegetation, water balance dynamics 79−79893
Douglas fir, evapotranspiration determ. using weighing lysimeter 77−64353
evapotranspiration, very dry seeded rangeland grass 79−88109
evapotranspiration meas. in Douglas fir forest, canopy resistance calc. 77−60432
gas-surface interaction effect on thermal transpiration, dusty gas theory 77−19634
hardwood trees transpiration differences, simulated streamflow response 79−84328
high-temperature, transpiration apparatus, viscous, incongruently vapourising melts 80−52231
mass spectrometry, of high temp. vapours 80−52356
MHD boundary layer flow on flat plate 77−24028
MHD boundary-layer flow on flat plate with uniform transpiration 79−55423
pine forest wet canopy evap. meas. 78−61460
skin water exchange measurement 77−81763
soil moisture deficit estimation from meteorological factors 79−20890
thermal transpiration, in circular capillary with small temp. difference 79−32191
thermal transpiration, theory and expt. comparison using He, Ar, CO_2 and air 79−32579
thermal transpiration effect, rarefied flow between parallel plates, polyatomic gas 79−86466
vegetation-atmosphere interaction, simplified one-dimens. theory 78−61479
Pb, vapour press., meas. using transpiration method, thermodynamic props. determ. 78−3365
Pb-Bi alloy, vapour press., meas. using transpiration method, thermodynamic props. determ. 78−3365
Sb, vaporisation behaviour, transpiration and boiling temp. studies 80−29161
ThO_{2-x} phase, high temp. vaporisation behaviour 79−54508

transponders
acoustic transponder navigation 79−59896
acoustic transponder navigation systems and ATNAV II system 77−70874
ATS-5 location by L-band trilateration 77−9652
biomedical telemetry, transmission and reception with embedded antennae 78−77125
undersea acoustic transponders, locations optimal estimation 79−5684
weather radar data transmission using VHF satellite links, expt. 78−20569

transport *see transportation*

transport equation *see Boltzmann equation*

transport phenomena *see transport processes*

transport processes
see also biotransport; Boltzmann equation; cellular transport and dynamics; cosmic ray propagation; diffusion; electrical conductivity; Liouville equation; master equation; neutron transport theory; photon

transport processes continued
transport theory; plasma transport processes; Senftleben-Beenakker effect; thermal conductivity; thermal diffusivity; viscosity
Abel integral function, numerical inversion using least-squares splines 78−16753
accretion discs in close binary systems, ang. momentum transport and tidal torques 78−12296
activation of kinetic processes in condensed media 77−55368
adjoint space in heat transport theory 80−58887
advection processes, finite difference method, balanced expansion technique 78−77719
aerosol dry deposition, filtration model rel. to trace metal deposition from atmosphere 78−73441
air pollution dispersion, modelling by smeared conc. approximation 78−81381
air pollution transport, air quality models development for limited wind fetch 80−104533
albumin, bovine serum, solutions, fluctuation transport theory 78−70057
alloys, random, equilib. and transport props., single-site approxs. 80−92801
analytic continuation of Wiener Hopf factorisation matrices, transport theory 77−96
anisotropic media transport theory, particle scatt., Boltzmann eqn. 79−26004
anisotropic simple materials, transport coeffs., reciprocal relations 77−72708
approximate method for solving the integral equation of transport theory 77−87707
array of spheres in dielectric matrix, exact solns. for transport props. 78−56120
artificial membranes, transport regulation by environmental H^+ conc. 80−89725
W.Atlantic Ocean, equatorial, subthermocline countercurrents mean geostrophic transport 80−51426
atmosphere, eddy diffusion models for mesosphere and lower thermosphere 80−109198
atmosphere, O_3 fluxes from zonal mean circulation model *(Russian)* 78−36224
atmosphere, obs. of O_3 flux by transient eddies in 0 to 30 km height range 80−109224
atmosphere, S dry deposition vels. over E United States and surrounding regions 80−56507
atmosphere, turbulent exchange coeffs. vars. rel. to zonal circulation model, numerical expts. *(Russian)* 78−81295
atmosphere charge transport, rel. to ion chamber response to particulate matter 78−88933
atmosphere eddies, transfer rate in air flow above sea surface *(Russian)* 79−16578
atmosphere large-scale eddy transports, linear parameterisation 80−17361
atmosphere O_3 production transport and distribution, numerical simulations with global general circulation model 80−56544
atmosphere pollutant dispersion during calm wind situations, analytical modelling 78−81385
atmosphere pollutants dispersion, completely Lagrangian random-walk model 78−81380
atmosphere turbulent boundary layer, finite-element numerical modelling 80−77061
atmosphere turbulent transport, Monte Carlo simulation and comparison with exptl. data 79−53479
atom-molecule anisotropic interaction pot. influence on transport cross sections, appl. to He-alkali dimer 80−9677
Baltic Sea, salt transports determ. from conservation calculations in natural coordinates 80−51433
barrier plastics, high nitride polymers, liq. transport, temp. effects 78−76921
binary gas mixtures, excess pots.; calc. method 78−45587
binary gas mixtures, thermal creep between parallel planes 79−14507
binary inert gas systems, determ. of (m,6,8) pot. parameters 79−46414
binomial redistribution process, Ehrenfest urn problem 80−52144
bistable potential model, renormalised transport eqns. 80−36957
black box approach to general systems theory 78−45583
black hole accretion discs, boundary-layer flow rel. to energy and ang. momentum transport 80−46598
Block equation, standard form, Markovian relaxation 79−58621
Boltzmann eqn., phonon and electron transport in bounded systems 80−39545
Boltzmann gas, moderately dense, momentum distrib., quantum corrections for smooth pots. 77−13692
Boltzmann gas, moderately dense, momentum distrib., quantum corrections for hard-sphere pots. 77−17903
Boltzmann-Enskog equation, nonlinear, acoustical approx. for elastic sphere system 78−41252
boundary-value problem, stationary transport, Laplace operator eigenfunction series soln. *(Russian)* 78−81931
branching asymptotic behaviour 80−175
bremsstrahlung distrib. in water, Al, Fe and Pb, 22 MeV electron bombardment 78−59840
bremsstrahlung in bulk media, shielding study, Monte Carlo anal. of thick target spectra 78−59839
Brownian particles interacting in periodic pot. 79−85083
calculation method 78−78767
carbon tetrachloride, transport coefficients for a fluid of square-well rough spheres 79−55634
carrier transport across heterojunction interfaces 79−47158
Chandrasekhar's X-function, reln. to eigenvalues of integral operators with difference kernels 77−71280
Chandrasekhar nonlinear H-eqn., iteration 79−58652
channelling, quantum theory, generated transport eqns. 78−10110
charged particle flux-at-a-point in complex geometries, numerical method 77−26249
charged particle transport, multigroup formalism to solve Fokker-Planck eqn. 80−68159
charged particle transport in one-dimensional finite system 77−61035
charged particles in thin solid layer, ang. deflection due to multiple scatt. 78−79650
Clausius-Mossotti problem for cubic arrays of spheres 78−52422
coefficients, Senftleben-Beenakker effects, transport-relaxation method 79−55436
collision probability integrals in annular geometry 78−29067

transport processes continued
collocation finite element method for potential problems in irregular domains 79−54072
colloidal systems, stochastic transport eqns. 78−93609
combustion, turbulent, implications of probability eqns. 78−14098
concentrated aqueous electrolyte solutions, transport props. *(German)* 78−80750
conference, radiation physics, Calcutta, India (30 Nov. to 4 Dec. 1974) 77−54128
continued fraction representation for time correlation functions 79−63174
continuity eqn., boundary conditions for integration 78−3342
convective heat transfer intensification and comparative heat transfer surface evaluation 78−30151
corrosion product transport, high temp. water loops in nuclear reactors 79−91840
cosmic ray particles propag. in interplanetary region, transport eqn. 79−44315
cosmic ray steady-state eqn., similarity solns. 78−16254
cosmic rays interplanetary transport, particle drift effects on solar modulation 77−45263
counting gas mixtures, calc. of electron transport coeffs. 79−32727
critical sphere problem 80−27245
crystal system, nonequilib. statistical operator method 77−33962
cylindrical critical problem for an extremely anisotropic kernel 80−27246
deep penetration shielding problems, calc. of contribution flux and current spatial distrib. 79−59283
dense fluid transport phenomena, generalised moment method 80−33866
dense gas, transport coeffs. density expsn., logarithmic terms 78−34250
dense hard core system, transport coeffs., entropy 77−62656
dense matter, transport props., neutron stars appl. 79−67236
dense one-component systems, low-temp., kinetic phenomena, shear viscosity *(Russian)* 80−10694
dielectric crystals, externally deformed, phonon transport eqn. 77−27956
diffusion equation model for kilovolt electron transport at X-irradiated interfaces 79−24388
diffusion of electron pencil beam, one-parameter model of spatial distrib. 79−54081
dilute gas, transport props., simple pair pot. model 80−87835
dilute gas mixtures, transport props., calc. prog. 80−10342
dilute gases, transport props., softness expansion for inverse power pot. 80−28589
direct inverse problems 78−77817
discontinuous trial functions, classical functionals 77−53842
discrete ordinates transport problems on large scale, numerical methods efficiency 79−85099
discrete random walk, differential equations for transport in two or more dimensions 79−85073
disordered systems, electronic energy processes 80−57221
dispersion corrected numerical schemes 78−36946
dissipative heavy ion collisions, transport equation for microscopic Wigner functions 79−13329
droplet transport in gases and liquids, gravitational and thermophoretic contribs. 80−100052
Duffing oscillator, damped, fluctuations, systematic expansion theory 77−13716
dust grains in solar nebula, dynamics rel. to role as isotopic anomalies carriers 80−26757
dynamical fluctuations in simple fluids, kinetic theory 77−7652
dynamical spherical model, transport coeff. kinetics near critical point 77−49695
effective, in suspension of interactive particles, method 79−50836
eigendistributions in linear transport theory 80−13523
eigenvalues of Fokker-Planck operators 80−98863
Einstein's contribution to twentieth century physics *(Chinese)* 80−17
electrolyte solutions, multicomponent 79−16008
electrolytes, aq. solns., ion-solvent interactions, transport props. *(German)* 78−79790
electron flux in slab geom., high-energy radiotherapeutic field 77−81585
electron gas, radiative interaction, with mag. field, distrib. function 79−60116
electron low-energy transport, validity of extended transport cross-section correction 79−71843
electron stream, diffusion in gas, elec. field effects near absorbing boundary 77−55127
electron swarms in gases with large inelastic cross sections, accuracy of numerical solns. of Boltzmann's eqn. 79−94756
electron transport, discrete ordinates calc. using standard S_n neutron tansport codes 80−46998
electron transport and small angle collisions 80−165
electron transport by the method of condensed collisions 80−47000
electron transport coeff. in gases used in proportional and drift chambers 78−58541
electron transport eqn., with random impurities 78−33654
electron transport in air and N_2, Monte Carlo calcs. 78−90042
electron transport in anhomogeneous anisotropically scatt. medium, medium Green's function 80−27244
electron transport in nonmonochromatic EM field 80−10937
electron transport in one-dimensional finite systems 79−54077
electron transport Monte Carlo calcs., orthogonal function expansion technique 77−26248
electrons, diffusion of pencil beam, ang. distrib. model 80−23273
energy dependent transport theory, exact solns. 80−32319
energy transfers across air-water interface at high wind speeds, effect of spray 78−85574
energy transport by waves without spatial damping, dissipative media 80−31531
energy transport equation, exact soln. for plane source in an infinite medium 80−82729
equilibrium states of continuous transforms on compact metric spaces 79−26000
estuarine particle dynamics, math. model, phys. and chem. processes 77−21793
evolution equations in fluid dynamics, soln. by second order backward difference method 79−92950
excitonic insulator, condensate flows in mag. field, charge and mass transport *(Russian)* 79−11108
extended Fermi-hypernetted chain scheme, Landau parameters calc., transport coeffs., Jastrow theory 77−41529

transport processes continued
F-region, interhemispheric ion transport induced by neutral zonal winds 80−98509
fast-electron transfer in lamellar materials 78−86230
Feller eqn., generalised, boundary condition solns. 78−62167
finite slabs, orders-of-scatt. anal. 77−22502
fission product ionisation by He jet rapid transport technique 79−63831
fission reactor materials, ion penetration distance calculations with multi-group transport computer codes 80−102246
Florida Current transport, fluctuations at periods between tidal and two weeks 80−72551
flow depend. expansion process, initial value problem, two step difference method *(German)* 78−57877
fluid, anisotropic, transport coeffs., perturbation theory 77−7497
fluid, classical, transport coeffs. computation by cell hydrodynamics 78−38600
fluid, dense, square-well pot. mols., struct. factor, transport props. 78−22620
fluid of square well rough spheres, transport coeff. 79−55634
fluid transport properties *(Japanese)* 78−21085
fluidised system, heterogeneous, aerodynamic aspects of transfer processes, crit. state 80−79394
fluids, low gravity expts. on phase transition and critical phenomena 77−39658
fluids, space environment 79−46825
flux-corrected transport algorithm, rezoning technique 80−31516
Fokker Planck eqn., system in periodic pot., 1-D, elec. field perturbed, mobility 78−32776
Fokker-Planck eqn. eigenfunction expansion soln. extension, first order system 80−31668
Fokker-Planck equation, for random process of nonlinear system, nonstationary soln. 77−88
Fokker-Planck equation, manifolds of equivalent path integral solns. 80−4687
Fokker-Planck equation, nonlinear drift, non-const. diffusion, stochastic quantisation, path integral formulation 78−86228
Fokker-Planck equatn. numerical solutn. 80−18622
Fokker-Planck-Coulomb systems, collective modes, 1-dimens. case 77−45809
force-free magnetic flux tubes, twist transport 78−40813
fusion reactor breeders, models for T_2 and ^4He transport 78−17424
fusion reactors, re-entrant boundary conditions for toroidal transport and diffusion 80−18592
gas, electron and hole drift velocity 80−57223
gas, electron and hole transport theory, free-path method, orders of approx. 80−62598
gas, moderately dense, transport coeffs. density expansion, 1st logarithmic term 78−94878
gas, weakly ionised, electron distrib. function, isotropic component, collision source 80−62599
gas, weakly ionised, electron distribution function, steady-state conditions and elastic collisions 80−57224
gas, weakly ionised, electron drift velocity and distrib. function 80−57225
gas, weakly ionised, electron transport quantities, divergences 80−57222
gas flow, vibrationally relaxing, eqns. and transport coeffs. 77−89084
gas in porous medium, continuity of soln. in n space dimensions 78−95130
gas mixture in Knudsen layer, transport eqns. 77−47045
gas of nonspherical mols., transport processes, kinetic cross sections, temp. depend. 77−80259
gas transport, in synthetic polymer membranes, history 78−76912
gas transport coeff. data inversion iterative procedure, pot. energy function determ. 78−91051
gas transport in magma, determ. from mass fractionation of rare gas isotopes 80−98292
gaseous transport coeff. data inversion, intermol. pot. energy functions determ. 77−35293
gaseous transport coefficients, rot. inelastic collisions effects 79−82020
gases, electron motion, Boltzmann eqn. soln. two-term approx., validity 77−35309
gases weakly ionised, electron motion, stochastic theory of homogeneous systems, review 80−77735
generalised hydrodynamics construction by nonequilibrium statistical operator method 77−30116
generalised Langevin eqn. with Gaussian fluctuations 78−32760
geochemistry, transport models rel. to mantle and crustal reservoirs mean age 80−51359
H-functions in multiplying media, remodelled representations 78−53808
hard sphere gas, temp. depend., relativistic kinetic theory 77−3907
hard sphere gas, three-particle collision effects 78−38442
hard sphere relativistic gas transport coeffs. 78−30401
hard-sphere fluid, modified nonlinear Enskog eqn., entropy function 78−63526
harmonic chain with random masses, transmission coeff. and heat conduction 79−80547
heat and mass transfer bibliography−Soviet works 79−23318
heat propagation, finite vel. problem, kinetic theory anal. 77−46881
heat storage, periodic, heat-carrying fluid and storage material transport kinetics 79−3901
heavy ion radiation transport computer codes for thick targets 80−39180
Helmholtz eqn., 1-dimens., refined Maslov-WKB technique appl. 80−90795
Helmholtz eqn., transmission problems 78−62168
heterogeneous media, random dispersed phase model 78−65885
heterogeneous system with chaotic structure, generalized conductivity coefficients, review 77−87708
high-temperature media, thermodynamic and thermophys. props. calcs. 79−47964
higher order parabolic differential eqn., probabilistic soln. from heat eqn., with Brownian motion 79−97322
Hilbert asymptotic expansion method for evolution equations in Banach spaces 79−17368
Hilbert space decomposition and W-A determinant factorisation in linear transport theory 77−67189
homogenisation and approximation *(French)* 80−31684
homonuclear diatomics, dilute gas transport props. calcs. 77−72399
hopping model, exact solns. for neutral particles 80−98865
hopping transport theory, master eqn. approach *(German)* 80−27237
hot matter, conductive opacities and free-free Gaunt factors 80−3361

transport processes continued
hybrid shielding, radiation heating rates, two-dimens. transport anal. 80−106178
hydrodynamic contrib. to two-time correlation functions, using nonequilibrium distrib. function 77−49703
hydrodynamics, equations of motion and transport coefficients, using discrete formulation 79−90504
hydrology, anal. of numerical soln. of transport eqn. 77−64358
hydrothermal systems, nature of porosity rel. to transport phenomena 78−36205
hydrothermal systems, transport phenomena assoc. with cooling plutons 78−36206
hygroscopic particle size, air humidity depend., applic. to lung dynamics 77−90841
infinite dimensional Riccati eqns. from transport theory, strong solns. 80−73287
inhomogeneous medium with cavity, transport operator spectrum *(Chinese)* 78−16756
integral transport eqn., asymptotic props. near curved material interface 79−63175
integral transport theory for charged particles in electric and magnetic fields 79−26006
intermolecular pair pot. energy function from gaseous transport coeffs. 78−62870
intermolecular pair pot. energy function from gaseous transport coeffs., unlike monatomic interactions 78−62871
interphase mass flux and mass fluxes within phases 80−48561
interstellar charged dust grains, motion in interplanetary space 80−4300
intramolecular energy transfer, quantum effects 80−42964
invariant imbedding eqns. in general geometries 79−76050
inverse albedo problem for finite medium 79−17366
inverse problem soln. for finite slab 79−17365
inverse scattering problem for single-speed transport equation 79−88895
ionic crystals, lattice defects, conference, Canterbury, England (Sept. 1979) 80−105420
ionic solute hydration, thermodynamic and transport props., review 78−27815
ionosphere, ionisation transport effects on total electron content 78−45089
irreversible thermodynamics, corrections to linear transport laws, Onsager reciprocal relations 77−17938
irreversible transport processes, noncoupled, nonstationary, classical variational principles 78−4567
Jourdains variational principle, use in nonlinear mechanics and transport phenomena 79−9093
Jupiter, ang. momentum outward transfer rel. to atmosphere differential rot. 80−46467
Jupiter magnetodisc, plasma transport into outer magnetosphere 79−58297
K-distributed noise, statistics 80−27220
kinetic theory of dense fluids, derivation, transport coeffs., soln. of kinetic eqn. by moment method 79−54032
Kubo formula derivation of Boltzmann equation, resolvent method 78−95277
laminar blood flow, gas and heat transport, platelet and protein diffusion 78−92669
Landau-Lifshitz hydrodynamic fluctuations in nonequilib. systems, Boltzmann eqn. reduction 78−81929
Landau-Zener problem, random nature of motion role in intersecting terms problem 80−8937
lattice conducting sites, energy migration dynamics, percolation concept 79−85085
lattices, finite, with traps, random walks, Monte Carlo simulations 80−52131
layered media, modified modal theory of transient response 79−71255
light scattering in dynamical props. study, principles spectra derivation and applics. 80−53218
linear Boltzmann equation, transport and scatt. props. and solns. 78−93628
linear filter matrix, variational principle, functional max. value 80−27243
linear partial differential eqns. describing transport phenomena, soln. technique 80−13004
linear response theory, macroscopic vs. microscopic, appl. to electron in periodic pot. 78−65813
linear response theory, many-body van Hove limit 78−62156
linear transport eqn., asymptotic theory for small mean free paths 78−70078
linear transport equation, continuously varying spatial media, elementary solns. 80−86229
linear transport equation, degenerate case, full range theory, appl. to Milne problem 78−57874
linear transport equation, degenerate case, half-range theory, appl. to Milne problem 78−57875
linear transport operator, spectrum with diffuse reflection 77−17930
linear transport operator spectrum, semi-infinite medium 77−2626
linear transport operator with periodic boundary conditions, spectral decompositions 77−33961
linear transport theory, point spectrum, generalisation 78−41251
linearised hydrodynamics, derivation from kinetic theory 79−21679
linearised reaction diffusion equations solutions 77−74331
Liouville problem, quasi-particle dynamics from a given kinetic eqn., inverse 80−101749
liquid mixture, crit. soln. point, sedimentation and density gradients in high gravit. field 77−59121
liquids, momentum transfer, cooperative effects 80−68160
LMFBR materials, electron transport method, expt. verification, energy deposition 79−22386
LMFBR safety, collocation method soln. of radiation-conduction problems 80−13720
Lorentz model, simplest limit cycle analytic form 79−86405
Lorentz process, convergence to random flight process 78−73941
Lorenz model, transient behaviour in periodic regions 79−17346
lunar soil electrostatic transport, terminator configuration model 79−35157
LWR lattices, Monte Carlo radiation transport program for reactor bundle gamma transport and energy deposition analysis 80−22915
magnetic semiconductors, conference, Montpellier, France (Sept. 79) 80−94916
magnetotail, distant, anomalous transport props. due to lower-hybrid-drift wave turbulence 79−25399

transport processes continued
main-sequence stars envelopes, macroscopic and microscopic transport, implications of Li, Be and B obs. 78−93202
many body problems, coarse grained variables, dynamics exact results 79−80500
marine atmosphere stratocumulus convection, turbulent fluxes in horizontally inhomogeneous solns. 80−56543
marine pollution, dynamically passive impurity propag. in sea surface layer 80−31063
Markovian processes and irreversibility. The Onsager-Casimir symmetry, Onsager Casimir symmetry 80−62580
matrix Riccati eqn., quasi-linearisation, iterative approx. 78−57871
maximal variational principle for transport theory 78−62166
Mediterranean Sea, hydrological regime during glacial periods *(French)* 80−4040
membrane transport, active, for anions, synthetic membrane synthesis 80−61142
membrane transport matrix, relation between conc. depend., matrix transformation and flux representation 78−20069
membranes, artificial, light-driven carrier-mediated electron transfer 77−29110
memory functions for transport fluxes 80−42172
methane, gas, electron transport, kinetic theory 77−84391
mode-mode coupling equations, microscopic derivations 79−54073
model transport equation, with inelastic scatt. of electrons, exact soln. 77−59272
molecular dynamics method in statistical physics, review 80−18895
molten salt, hydrodynamic correlation functions 77−31577
molten salt mixtures, transport props. *(German)* 78−80750
molten salts, transport processes by ionic dynamics, mass depend. 78−22616
momentum balance of continuous media, correction based on Ott's transformation 78−41249
monatomic gas, boundary conditions for distrib. functions and moments 79−44887
Monte Carlo biased transport calcs. optimisation, prediction of statistical error 79−58654
Monte Carlo calcs., variance anal. 79−93079
Monte Carlo exponential biasing method, optimal choice of parameters 79−40498
Monte Carlo game, variance versus efficiency 80−27238
Monte Carlo importance sampling with parametric depend. 80−13013
Monte Carlo recursive methods, optimal strategies for appl. 80−13014
Monte Carlo transport calcs., error anal. 79−80548
Monte Carlo transport calcs., second moment functionals for last event and collision estimators 80−13012
moving fluids, transport eqns. and accoustic motion 80−53523
multicomponent gas mixture, transport eqns. and distrib. functions 80−64581
multidimensional diffusion equation, class of general boundary conditions 80−90796
multidimensional inverse problem in transport theory 80−174
multigroup electron transfer cross-section method 80−46999
multigroup Monte Carlo computer codes, bounded flux-at-a-point estimators 79−40499
multigroup transport eqn. in L^p spaces, soln. using resolvent integration techniques 77−5775
multiple band electron-phonon transport eqn. derivation 80−100318
multiple integrals of transfer theory 78−4568
multispecies gas flows, transport eqns. mathematical struct. 78−47084
multistate trapping model, rel. to continuous-time random walk model 78−93624
multitemperature gas mixtures, Maxwell-Grad moment method calcs. 77−47134
neutrino chemical potential and heat cond. with allowance for scatt., collapsing stars appl. 79−84657
neutrino component of $e\bar{e}\nu_e\bar{\nu}_e$ mixture, transport eqn. 77−33941
neutrino Comptonisation in high-temp. nuclear matter, neutral current theory 80−21905
neutrino system, relativistic transport eqn. 77−33940
neutrino thermalisation in stars, contribs. of conservative scatt. and electron scatt. 79−92659
neutrino transport, direct simulation and aspects of equilibration 78−89050
neutrino transport, weak neutral currents; supernova model 78−62391
neutrino transport calcs. using neutron transport methods 77−87377
neutrino-antineutrino gas, transport coeff. values *(French)* 79−30388
neutrino-antineutrino mixture, transport props. 78−93625
neutrinos+antineutrinos gas, transport coeff., thermal diffusion *(French)* 78−86217
neutron pulse, P_N approximation in spherical geometry, time depend. 79−80967
nonequilibrium entropy and symmetry principle of transport coefficients 79−21683
nonequilibrium statistical mechanics, kinetic eqns. derived 77−57269
nonlinear coefficients, generalised Nernst-Einstein relations 80−52145
nonlinear convective problems, stable explicit finite difference scheme 78−151
nonlinear distribution processes with drift, one-dimens., conservative solns. 79−49179
nonlinear electron and ion transport in thermionic diode 77−13717
nonlinear evolution eqn., family of H-theorems 80−31685
nonlinear initial-value problem arising from kinetic theory of vehicular traffic 79−163
nonlinear integral equations arising in transport theory 79−30393
nonlinear Markovian system, fluctuations 79−75460
nonlinear master equation, asymptotic expansion 77−49682
nonlinear simultaneous transport processes, complimentary form of variational principle *(Russian)* 79−54076
nonlinear simultaneous transport processes, variational principle *(Russian)* 79−58653
nonlinear transfer processes, optimisation *(Russian)* 80−8934
nonlinear transport, in Burnett order, theory 78−49778
nonlinear transport and dynamics of fluctuations 79−44884
nonlinear transport equations from statistical mechanics 79−75478
nonlinear transport in the Boltzmann limit 79−63173
nonlinear transport processes, hydrodynamics 80−22310
novel Monte Carlo binning technique 79−160
nuclear plant cooling, effluent dispersion, thermal and radioactive, math. model *(Spanish)* 77−74908
transport processes continued
nuclear power stations, transport process models for dissociative cooling *(Russian)* 79−13410
nuclear power stations, unsteady state processes for dissociative coolant *(Russian)* 79−13411
nucleus-nucleus and nucleon-nucleus collision model, Glauber's theory, classical transport eqn. 79−6522
numerical simulation of transport coeff. meas. by correlation method 78−8364
numerical soln., estimation of moments 77−71281
numerical solution of transfer theory problems by the direct reduction method 80−22309
objective and regular differentiation and integration, constitutive law and transport *(French)* 80−57090
observability for regular processes 77−67211
ocean, advective mixed-layer model with imposed surface heating and wind stress 80−12395
ocean, barotropic transport in wind-driven zonal channel with stratification and bottom topography 80−51402
ocean, low-freq. momentum, heat, salt and nutrients fluxes at Scotian Shelf edge 79−2242
ocean, realistically stratified, nonlinear energy and enstrophy transfers 80−101370
ocean, vorticity topographic transfer from oscillatory tidal currents to residual circulation 79−57954
ocean circulation, northward transport in modelling expts. 79−57952
ocean synoptical eddies, numerical scheme *(Russian)* 78−81190
oceanography, time depend. of scalar undergoing advection 79−48507
oceans in Southern Hemisphere, mean annual poleward energy transports 80−51406
one speed linear transport theory, fundamental relns. in 1-D geom. 79−35644
one velocity transport theory, scatt. function, specified density distrib. 78−24749
one-dimensional chain of harmonically coupled Brownian particles, Smoluchowski eqn. 80−17878
one-dimensional conductor, phenomenclogical eqns. of motion for electrons, phonons and librons 80−10955
Onsager Machlup formula for 1-D nonlinear diffusion processes 78−77816
Onsager-Machlup function, Lagrangian for diffusion process most probable path 78−73940
open quantum systems with time-dependent Hamiltonians and their linear response 79−44852
optimal control adaptive criterion study 77−17931
optimization method for exponential biasing in Monte Carlo calculations 79−54080
optimum biasing of integral equations in Monte Carlo calculations 79−54078
Pacific Ocean, T transport models source function 78−32122
PALLAS discrete ordinates transport code, improvement 79−76052
parallelepiped, linear transport generalised boundary conditions 78−16757
particle collision inclusion in extended time dependent HF approx. 78−49780
particle kinetics on one-dimensional lattice with inequivalent sites, stochastic model 77−41546
particle mobility in Gaussian pot. at high temp. *(Russian)* 79−30364
particle motion through matter, fluctuations in cascade processes 80−5456
particle transport in absorbing media with anisotropic scatt., synthetic scatt. kernel 79−21678
particle transport in finite slabs, orders-of-scatt. anal. 77−22502
particle transport phenomena, theory, book 79−63176
particle transport theory, fluctuation problem, probability balance eqn. 77−37829
particle transport theory, fluctuation problem 78−8363
particle transport theory, integro-differential eqn. soln. 80−36955
particle transport with multiplication, math. expectation of symm. functionals *(Russian)* 77−82469
particles transport by turbulence, meas. of small sphere motion in rot. vel. field 77−58771
Peierls-Boltzmann equations, generalised, for phonons and local excitation kinetics 77−47518
percolation in one-dimension, finite size and scaling theory 79−54064
phonon system, local cumulative excitation as transport phase transition 77−74336
phosphate fertilizers, leaching from agricultural soils to groundwater 79−20901
photophoresis, stable orbits, circular, cycloidal and oscillating *(German)* 79−80545
plane steady solutions for stress-assisted diffusion 79−90136
Poisson equation for relativistic streams of charged particles, analytical soln. *(Russian)* 79−9319
polarised radiation transport theory, charact. eqn. 80−4678
polarized radiation, transport process in optically isotropic media 79−13899
pollutant advection eqn. integration 77−13118
polyatomic fluids, generalised hydrodynamics 77−1055
polyatomic gases, transport props., Monte Carlo method 77−89223
polymer solutions, concentrated, transport properties, hydrodynamic mean field theory of voscisity of sphere suspension 79−4422
potential scatt., classical and quantum transport theories 78−16603
probabilistic methods for stationary problems of linear transport theory 80−167
Purex kinetics, U extraction with tributylphosphate *(German)* 80−57937
pyrene:rubicen(coronen), exciton migration and energy transfer, temp. depend., model 78−79932
quadratic finite element schemes for 2-D convective transport 78−21084
quantum mechanical Brownian particle, tunnelling and transport problems 80−4644
quantum transport effects in DC elec. resistance of solids, review 79−40500
quasi-particle transport eqns., statistical T-matrix approx. 77−65011
radiation problem simplified boundary elements 78−86226
radiation problems transport eqns., using Wigner distribution 80−168
Radiation Shielding Information Centre, available computer codes and data 77−65343
radiation transport, integral equation methods 77−53843

transport processes continued
radiation transport, multiple scattering of waves by particle ensembles 77−95
radiation transport in absorbing medium, analytic solns. 77−14886
radiation transport theory, characteristic eqn. 77−82473
radiation transport theory, tracklength biasing in Monte Carlo methods 80−5335
radiative flux local characteristics calculation using Monte Carlo method modification *(Russian)* 79−35648
radiative transfer multiple nonstationary scatt. with curved surfaces 77−29641
radioactive waste, low-level solute and gas transport from burial site 79−85628
radioactivity waste, low-level, shallow land disposal, microbiological aspects 79−85630
radionuclide chain transport through heterogeneous media 80−99250
radionuclide geospheric transport eqn., boundary conditions 80−47611
radionuclide transport through heterogeneous media 80−32382
rare earths, physics and chemistry (book) 79−69384
rarefied gas, nonisothermal flow in cylindrical capillary, calc. of vel. profile and flux 80−6098
reaction-diffusion system, global branching theorem 80−4677
reaction-diffusion systems, periodic solns. and multiple steady states 79−54082
reduced equations of motion for generalized fluxes and forces in the continued-fraction expansion 80−105594
relativistic continuum physics, transformation laws *(Hungarian)* 78−89383
relativistic kinetic theory of $e\nu_e$ and $e\nu_\mu$ systems, transport coeffs. 79−21680
relativistic multicomponent systems, transport coeffs., variational calcs. 77−15151
relaxation time approximation in the presence of capture processes involving real probability depletion 79−58656
resolvent integration techniques for generalized transport equations 79−76051
resonance transfer rate of electron excitation, model of convergent terms, effect of diffusional motion of particles 80−8936
retardation of electrolytic mass transport in collinear electric-magnetic fields 80−104443
reverse osmosis, mechanisms, membranes, transport and appls. 79−29396
Saturn, ang. momentum outward transfer rel. to atmosphere differential rot. 80−46467
scalar wave propagation, coherent scalar field in pair correlated random distribs. of aligned scatterers 78−32690
scattering expansion truncation error correction program 80−47001
scattering medium description by number of particles scattered 78−93623
Schottky, non-degenerate diode, current-voltage characts., analytical approx. 79−95494
sediment transport in W. Hellenic Trench, high sedimentation rates and variable dispersal patterns 78−57193
sediment transport modes in channelised water flows, appl. to Martian outflow channels erosion 80−98363
semiconductor, electron and hole drift velocity 80−57223
semiconductor, electron and hole transport theory, free-path method, orders of approx. 80−62598
semiconductor, intrinsic, electron distribution function, steady-state conditions and elastic collisions 80−57224
semiconductor, intrinsic, electron drift velocity and distrib. function 80−57225
semiconductors, Fermi-Dirac integral, approx. by 12th order polynomial *(French)* 79−11109
shearing flow over wavy boundary, heat, mass, momentum transfer, turbulence model 78−87335
slab geom., transmission and reflection coefficients in the slowing down region 80−13005
soil gases, long distance migration detect. via Rn integrated emanation mapping 78−85560
in soils, convective-dispersive solute transport with combined equilib. and kinetic adsorption model 77−64356
solar nebula/giant gaseous protoplanets ang. momentum transfer rel. to protoplanet evolution 80−56727
solid film, passage of electrons, linear transport theory in one-velocity approx. 79−14865
solid particle systems, high Reynolds number, momentum trasfer. Karman-Pohlhausen method 80−74947
solids, kinks, solitons, and nonlinear transport 80−65421
solutes, movement through aqueous fissures in porous rock 80−94553
solutions, fluctuation transport theory 78−70057
source biasing optimisation technique using Monte Carlo calc. 79−26005
Spencer-Lewis eqn., orders of scatt. soln. 79−85098
spherical particle in slightly rarefied gas, forces calcs. 79−94672
spray drying, of highly viscous conc. solns., heat and mass transport *(Russian)* 78−83230
square well fluid, viscosity 79−98847
square-well potential liquid, struct., transport props. 77−7643
stability investigation, transport problems *(Russian)* 78−57880
static conductivity of 1-D disordered systems 77−49697
statistical mechanics, continued fraction error bounds, for complex transport coeffs. and spectral functions 79−12744
statistical mechanics, nonequilib., perturbation theory, memory function formalism 77−26234
statistical mechanics nonequilib., perturbation theory, time-displacement operator 77−26233
statistical mechanics of quantum stochastic transport processes 77−5749
steady state one dimensional transport in prism with partially absorptive walls and fixed scatt. centres 78−41248
steady two-dimens. viscous boundary layer, transport physics and math. characts. 80−14673
Stefan one-phase quasilinear problem *(Ukrainian)* 78−65884
stochastic systems, Bubnov-Galerkin method appl. *(Russian)* 77−49578
stochastic theory of particle transport, appl. to radiation damage cascades 78−153
stratosphere tracer transport mechanisms, Lagrangian motion of air parcels in presence of planetary waves 80−109215
stratosphere turbulent transport estimates, implications of wave spectra resembling turbulence 79−79981
strong quantised EM field, statistical description 78−16961
superfluid Bose liquid, hydrodynamics allowing for dissipative processes 79−23796
transport processes continued
surface transport and reaction, stochastic calcs. 80−108736
suspended sediment transport theory, elliptic boundary value problem 79−14466
test particle slowing down, rarefied gas added to host, with external conservative force 79−97326
theory of constrained mixtures with multiple temperatures 80−62600
thermophoresis, slightly rarefied flow over specularly reflecting body 77−55040
thermosphere, middle, incoherent scatter radar studies rel. to energy and mass transport 80−72654
three-body contribs. to transport coeffs. 77−5776
TIGERP, 1-D multilayer electron/photon Monte Carlo transport code 79−54079
time dependent Poisson queue and moving boundary problems for the heat and wave equation 79−63172
time-dependent transport by some order-of-scattering methods 78−77814
track distribution through spherical shell 78−8365
transfer coefficients, behaviour at relativistic temps., dissipative effects *(Russian)* 79−6062
transport calculations in cylindrical geometry 79−58655
transport coeff., elimination of t-explicit divergence 79−26008
transport properties, hydrodynamic screening theory of viscous friction in suspension of spheres 79−4421
transport relaxation equations, reciprocity, boundary conditions 77−13719
transport scattering coefficients from reflection and transmission measurements 79−93078
transuranic transport from environment to man modelling 79−96669
turbulence, two-layer quasi-geostrophic, baroclinic energy transport and conversion 78−81186
two-dimensional transport coefficients, self-diffusion, theory 78−32777
two-dimensional transport coefficients, thermal cond., theory 78−32778
two-group integral transport equation, variational method 80−68156
two-group problems with anisotropic scatt., closed-form solns. 78−4569
ultracold neutrons, lifetime in traps, film-substrate model calcs. 80−106098
Van der Waals fluid near critical pt., transport props. 79−46537
variational principle, time-depend., and reciprocity theorem for transport-relax. eqns. 78−12655
variational techniques application 78−89415
velocity distrib. function of light ions in heavy gas in elec. field 78−83526
Venus upper atmosphere, momentum and mass fluxes from mean circulation diagnostic model 79−58287
Voigt and complex error functions, rapid computation 78−57873
water, turbulence vertical transport by controlled Langmuir circulations 79−23330
water pollution in Par River estuary, India, transport and abatement methods 80−104521
Winfree meandering, in 2-dimens. 2-variable excitation medium 79−58660
zodiacal dust cloud, charged dust particles motion in interplanetary space 80−4299
$e\bar{e}\nu_e\bar{\nu}_e$ mixture, covariant transport eqns., collision terms from Weinberg Salam theory 77−74315
$\nu\bar{\nu}$ system, transport coeffs. 78−93871
Ar, electron mobility and lateral diffusion coeff. 77−35307
Ar, electron momentum transfer cross-sections 0.4 eV 77−35308
Ar, low-energy electron drift vel. at 293 and 90K 77−35306
Au foil, relativistic electron beam deposition, field-enhanced, bremsstrahlung prod. 78−29677
C, excited electronic states contrib. to transport props. 80−23326
C, monatomic, transport properties, rel. to spacecraft entry into planetary atms. 78−87424
H^+, atmospheric, transport behaviour rel. to concs. in E United States precip. 78−92962
H-He fluid planets, phase diagram and transport props. 78−28554
H_2, electron swarm transport coeffs. determ. by Boltzmann and Monte Carlo methods 79−90359
H_2, electron swarms, motion, Monte Carlo simulation 77−39398
^{3}He, liquid, shear viscosity and thermal and s- and p-wave approx. 79−1535
I deposition velocity rel. to environmental transport of radioiodine from air to milk 77−66866
K^+ mobilities in gases *(Japanese)* 79−60101
Li^+ mobilities in gases *(Japanese)* 79−60101
LiBr, liq., transport processes by ionic dynamics, isotope substitution, mass enhancement 78−22616
LiCl aqueous solns., dynamical props. by ultrasonic propag. meas. 80−76517
N_2, dilute gas transport props. calcs. 77−72399
N_2, electron energy distrib. and transport coeffs. in E×B fields 78−51277
NO_3^-, atmospheric, transport behaviour rel. to concs. in E United States precip. 78−92962
N_2O in agricultural soil, losses in solution in drainage water 79−43797
Na^+ mobilities in gases *(Japanese)* 79−60101
Ne, exponential-six pot., new parameters 78−55217
O_3, atmospheric, sources and transport in NE. United States 79−92110
O_3, of stratospheric origin, measured over Pacific Ocean, source and large-scale wave transport 80−72600
O_3, tropospheric, long-range transport 78−61514
P_i through sandy soils, experimental and simulated transport 77−66940
^{226}Ra leaching from contaminated soils, investigation of Ra bearing soils from Port Hope, Ontario 79−20900
Rn, long-distance migration in Earth, subterrestrial fluid convection hypothesis 77−37246
^{222}Rn in Hudson River estuary, distrib. and transport across sediment-water interface 78−16064
S compounds, atmospheric, meso-scale transport obs. in rurual East Midlands, England 80−94124
SO_2 transfer resistance of European soils, laboratory meas. 77−37384
SO_4^{2-}, atmospheric, transport behaviour rel. to concs. in E United States precip. 78−92962
^{90}Sr, leaching behaviour in cement composites 78−37416
Th-U(Pu) fast breeder fuels, chemical, thermodynamic and selected transport props. 79−54505
ThO_2-UO_2 solid solns., props. of importance for use as nuclear fuels 79−54506

transport processes continued
W-O-F system, gas phase, comp. and chem. transport reactions in discharge lamp *(German)* 77−32826
Xe, thermal cond. and other transport props., 500 to 2400K 77−39393
$Zn(ClO_4)_2$, thermodynamic irreversible parameters, Onsager reciprocal relationship verification 79−47960
$ZnCl_2$; thermodynamic irreversible parameters, Onsager reciprocal relationship verification 79−47961

transport properties *see transport processes*

transport theory *see transport processes*

transport theory of neutrons *see neutron transport theory*

transport through biomembranes *see biomembrane transport*

transportation
see also aircraft; lifts; marine systems; rail traffic; rapid transit systems; road traffic
algae aqueous suspension, fragile nonspherical solid particle hydraulic transport investigation 77−73618
applied mechanics computing, conference, New York (1976) 77−67285
batteries development, large-scale energy storage 79−43756
British Government transport policy criticised 78−55512
criticality aspects of fuel storage and transport in UK 79−63791
dosimeters, exposure during air and ground transit 77−16987
environmental noise, importance in France 80−48510
fission reactor fuel, mixed oxide, suitability of spent fuel shipping casks 80−27757
hydraulic coal trunk pipeline transport systems, methods of improving economic effectiveness 80−106837
Iranian solar town conceptual development 80−35645
irradiated LWR fuel, European transport experience 80−63309
irradiated nuclear fuel, transport, packaging, UK experience 79−26782
irradiated nuclear fuel transport, European experience 79−31235
irradiated nuclear fuel transport and handling, French nuclear power plants *(French)* 79−31233
LF noise, effects on human performance tests 77−19483
liquefied natural gas, nonsteady-state flow calculations in horizontal pipeline systems 80−106838
LNG, transport and storage hazards 80−45620
metals in road transportation, review 78−88622
mobile incubator transport for premature and newborn babies *(German)* 79−16336
noise and vibration, ride quality criteria 79−90076
nuclear fuel, irradiated, shipping cask design 77−79483
nuclear fuel cycle, transportation status and problems 79−59236
nuclear fuel transport by air, feasibility and economics 78−94154
nuclear materials, SABRE II combat simulation model 80−37542
nuclear materials transportation and safeguards 77−67837
nuclear spent fuel shipping cask licensing 80−37545
nuclear vessels, probabilistic model for assessment of collision likelihood 78−5063
nuclear waste material, risk anal. 78−17357
nuclear waste transportation, DOE transportation technology centre 80−37537
passenger compartments, modal synthesis of LF props. 77−88980
pipeline systems, problems in fluid mechanics for hydraulic transport of solid materials 80−106836
public, fuel conservation, environmental, economic and social aspects 80−35621
radioactive, low- and intermediate-level waste, risk anal. of road transport in Netherlands 78−17359
radioactive calcined waste solid spillage, recovery of U, erosion in solids transport system 78−13264
radioactive contact-handled transuranic waste transportation 80−37538
radioactive low-level waste transport and disposal, logical 80−23044
radioactive material transport, USA experience 79−31236
radioactive materials, IAEA transport regulations, underlying radiation protection principles 80−63414
radioactive materials, international regulatory control for safe transportation 80−63411
radioactive materials, package design, construction and testing for safe transportation 80−63412
radioactive materials, reactor fuel transport requirements, Poland 79−31232
radioactive materials, transportation, safety aspects 79−67968
radioactive waste, from nuclear power station to reprocessing plant and final storage *(German)* 77−34403
radioactive waste, low level, transport regulations, proposed changes 80−68896
radioactive waste, new SF, HLW and CW shipping systems 79−59205
Radiological Emergency Response Planning and Preparedness Training Programmes, USA 78−57079
reactor fuel element disposal 80−13707
reactor used fuel shipment, risk assessment 79−81013
reprocessed nuclear fuel transportation 79−30918
shipment, computerised transportation model 79−85743
solar town in Iran, conceptual development 79−57408
space, Space Shuttle reusable orbiter vehicle development 79−84640
spent fuel transportation, commercial experience in US 80−63310
spent nuclear fuel shipment, appl. of ALARA principles 80−37541
spent nuclear fuel shipping casks, R and D sea going vessel requirements 79−31083
spent nuclear fuel transport problems *(Russian)* 79−31084
technical meteorology, technical and commercial appls. *(German)* 80−46231
transportation of irradiated nuclear fuel, in Canada, emergency planning 78−50411
TRIGA reactor fuel, long-distance transfer 79−67929
vibration prevention approaches 78−55506
vitrified high-level radioactive waste, rail transportation, fault tree anal. and accidental release 78−17358
Pu compounds 18B packagings for transportation 80−37544
Pu, transportation, effect on environment, evaluation study *(French)* 80−27785

transportation networks *see transportation*

transportation services *see transportation*

transportation systems *see transportation*

transverse rupture strength *see bending strength*

trapped electron centres *see F-centres*

trapped free radicals *see free radicals*

trapped hole centres *see V-centres*

traps, electron *see electron traps*

travelling-wave-tubes
see also backward-wave tubes
beam-plasma system, trapped particle oscillations, destruction, simulation by TWT 77−31462
diamond turning, optics and TWT components manufacture 79−81584
electron cyclotron maser as high power travelling wave amp. of MM waves 80−1176
EM waves generation and amplification based on Doppler effect 80−63902
gate valve, bakeable, for UHV microwave tube expt. 77−5854
microwave spectrometer using TWT prior to crystal detection for sensitivity increase 80−82822
nonlinear theoretical problems *(Chinese)* 78−74824
power capabilities for plasma heating *(French)* 78−9801
$Sm_{2-x}Gd_xCo_{17-y}Mn_y$, saturation magnetisation and anisotropy field temp. depend., suitability for microwave/millimetre wave TWT 79−82824

treatment, heat *see heat treatment*

treatment, patient *see patient treatment*

treatment, surface *see surface treatment*

treatment, water *see water treatment*

trees (mathematics)
see also network topology
Bethe lattice, random ordered phase and glasslike phase 78−29060
binary tree-based image processor architecture 79−72524
cactus tree, Ising model, ferromagnetic and antiferromagnetic interactions 77−9964
computer program for availability and reliability evaluation, Karlsruhe nuclear centre, complex repairable systems 77−88249
decision tree classifier, design and pot. for remote sensing 77−56745
dielectric breakdown tracks in polymethylmethacrylate 80−100633
diffusion in random networks near percolation threshold, ant in labyrinth problem 80−77732
event tree construction by AUTOET I computer code 78−17379
fault conditions diagnosis based on tree logic and probabilistic importance, appl. to nuclear power plant 77−6549
fault tree analysis, development of DICOMICS-TWIN self-adaptive algorithm for minimal cut sets determ. 78−17380
fault tree analysis, vital area identification in nuclear facility 79−85691
fault tree analysis for fission reactor risk assessment 80−63330
fault tree analysis of fission reactor auxiliary feedwater systems 80−63332
fault tree analysis of fission reactor cooling system *(Spanish)* 80−57870
fault tree analysis of fission reactor decay heat removal system 80−63333
fault tree analysis of fission reactor shutdown heat removal system failure 80−63334
fault tree and reliability analysis, modular decomp., PL/1 program 78−17381
fault trees, methodology for computer-aided construction, nuclear system appl. 78−37412
fission reactor, criticality safety, fault tree logic anal. of violations 79−22445
gauge symmetry hierarchies, tree approx. 77−2758
gauge theories, U-gauge Green's functions construction, with spontaneous symmetry breaking and Slavnov identities 79−235
Hilhorst model, generalised, statistics of trees and branched polymers 79−3604
Ising model on Cayley tree, phase transition of continuous order 79−40488
Ising spin systems on Cayley tree-like lattices, spontaneous magnetisation, correlation function far from boundary 78−68137
lattice vibration of Cayley tree type system, modes, densities 78−71813
nuclear facility safety assessment, material control and accounting system 79−85673
phase transitions in tree like percolation 79−75473
QCD_2, fermionic Green function and functional determinant, closed representation 80−13269
random Ising model, variational principle for distrib. function in the Bethe approx. 80−15674
random lattices, bond percolation and cluster form. 77−45798
risk tree analysis in criticality control of nuclear reactors 79−85632
rotation matrix, finite, in space of trees 78−36792
safety assessment of radioactive waste disposal into salt deposits, fault tree anal. appl. 78−55046
scattering processes, Penrose graph representation 78−49983
spanning trees, number on large square, triangular or honeycomb lattice 77−57282
supergraph anal., gauge supersymmetry, S-matrix 80−27422
time-dependent Ising model and Cayley trees 79−75472
topological indices for branching of tree-like graphs 80−57076
undirected multigraph conversion for tree-finding *(Russian)* 77−57150

triboelectric emission *see electron emission*

triboelectricity
see also static electrification
acetone, electrification during laminar flow in metal pipe 80−6954
alkanes, low press. triboelectric discharge, decomposition products *(French)* 77−48622
benzene, electrification during laminar flow in metal pipe 80−6954
charging process, surface chemistry 79−78157
charging technique for surface contamination analysis 80−11966
electron spectroscopy for chemical anal., appls. to materials for electrophotography 78−92565
electrophotographic developer neutralisation mechanisms 78−16863
electrophotography, electrostatic aspects, review 78−25768
electrophotography, triboelectrical properties of toner and carrier 80−18039
ethyl alcohol, electrification during laminar flow in metal pipe 80−6954
granular bed, aerosol filtration efficiency, triboelec. effects 80−38487
n-heptane, electrification during laminar flow in metal pipe 80−6954
metal-polymer friction pairs, triboelec. effects 80−11784
nylon 6, frictional electrification between metal and polymer, depend. on temp. and friction speed, contrib. of mol. motion of polymer to electrification 80−6953
particle charging against conducting wall in DC field 77−10808
polymer films, electronic cond., electro-, photoresponsive effects, review 79−56261

triboelectricity continued
polymer films, frictional electrification, temp. and friction speed depend. 78−60190
polymer films, frictional electrification, temp. depend. at various friction speeds 77−11985
polymeric electrophotographic developer, triboelec. two-step decay scheme 79−80711
polyolefins, triboelectric charging, linear free energy relationships 78−6431
polystyrene, frictional electrification between metal and polymer, depend. on temp. and friction speed, contrib. of mol. motion of polymer to electrification 80−6953
polystyrene-nylon 6 films, frictional electrification, temp. and friction speed depend. 78−60190
polystyrene-polycarbonate films, frictional electrification, temp. and friction speed depend. 78−60190
powder-bead mixture, triboelec. charging, incremental charge-mass characterisation 78−17833
PVC-polycarbonate films, frictional electrification, temp. and friction speed depend. 78−60190
semiconductor coatings space charge effects on triboelec. charge exchange 80−54763
silicone, electrification during laminar flow in metal pipe 80−6954
toner-carrier pair, surface interaction model for triboelectrification 79−17524
triboelectric discharge in N_2O, methane, propane, Hg rolling on glass, chem. effect *(French)* 79−77438
in vacuum, high-energy electron emission phenomena 79−11197
water, electrification during laminar flow in metal pipe 80−6954
Fe, triboelectric charging, effects of fluorinated compounds 78−60188
LiF, crystal fracture induced surface charge, elec. signal meas., double elec. layer approx. 80−44254
NaCl-metal system, sliding and rolling electrification 78−14796
ZnO:Li_2O single crystal, triboelectric charge and photodischarge obs. 79−82663

tribology
see also friction; lubrication; mechanical contact; wear
abrasion and erosion, superficial plastic deformations by particles *(French)* 80−40540
ball bearings, surface comp., AES and ion sputter profiling 77−40465
ceramic endoprostheses (total hips), mech. and tribological props. *(German)* 79−84005
CVD application 78−64743
elastohydrodynamic contacts, ellipsoidal solids subjected to Hertzian contact stress, surface deform. 77−35097
electron interactions with solids, conf., Southampton, England (Apr. 1976) 77−44570
fatigue life, contact, equations relating to material, lubricant and operating variables 79−96107
friction, lubrication and wear, review of papers published 1974 to 1976 79−15806
friction surfaces microstructure, during tribotechnical processes *(German)* 78−15540
friction test simulation in lubricated condition *(French)* 79−57189
general theory 78−11345
high-alloy bearing, LTMT effects on ht. resist. and contact fatigue resist. 77−44354
ion implantation studies, review 77−43236
metals, surface sliding damage, no lubrication, materials depend. *(Japanese)* 78−56780
metrological provisions, Soviet installations and instruments development 80−23974
parameter prediction, for evaluation of surfaces 80−64496
poly-1,1-dihydropentadecafluorooctyl methacrylate barrier films, props. 79−51197
polyamides, carborane-containing, antifrictional props., chem. struct. effect *(Russian)* 79−57123
prosthetic total knee joints, tribological investigation *(German)* 79−84004
review of current understanding 77−59066
rough surfaces, exam. of functional filtering concept 78−95106
shear press apparatus with roller bearing 77−41592
sliding contact, stress conc. on rough surfaces determ. by polarisation-optical method *(Russian)* 78−30244
solid body, reduced by mechanical vibrations, piezoelectric drive *(German)* 77−35101
spheres and rough planes, in contact with normal load, numerical analysis and expt. verification *(Japanese)* 77−19575
steel/Al sliding system, tribological behaviour, effect of temp., atmos., load and geometry *(German)* 79−34158
Stellite-6 in liquid Na, tribology 79−26525
technical systems reliability 78−39918
TiO_2, reactive- and chemical-sputter deposition from Ti and TiC target 79−100051

triboluminescence
alkali halide crystals, X-ray irradiated, luminescence during release of pressure 79−65939
alkali halide crysts., photoemission on mech. stimulation, mechanism *(German)* 77−85819
alkali halide crysts., triboluminesc. spectra 80−66312
alkali halides, cryst., optical emission following pulsed 10.6 μ irrad. 79−28847
ammonium tartrate, triboluminescence and cryst. fracture dynamics 80−50437
benzil crystals, mol. triboluminesc. meas. 80−40172
bony tissue, human, mechanoluminesc. during rupture 79−20572
citric acid monohydrate, triboluminescence and cryst. fracture dynamics 80−50437
crushing and high stress appl. device, for triboluminesc. meas. 78−27338
crystals, fracture in air and liq. anhydrous diethylether, triboluminescent intensity 78−19582
crystals, kinetics 77−77306
erosivity and mechanoluminescence *(German)* 80−25873
ferroelectrics, triboluminescence on piezo-electrification of surfaces during fracture 80−29815
glass fibre reinforced plastics, stress luminescence, volume resistivity effects *(Japanese)* 78−43943
hexaphenylcarbodiphosphorane, cryst. struct., triboluminesc., polymorphism effects 79−61447

triboluminescence continued
image intensifier spectroscope appl. for low intensity spectroscopy 78−58061
metal, visible region emission associated with deformation and destruction *(Russian)* 77−12453
orthorhombic crystals, triboluminescence and piezoelectric behaviour 79−95861
polymethyl methacrylate, subthreshold luminesc. 80−93414
review 78−19581
review 79−11478
Rochelle salt, depend. on mechanoluminescence on charge prod. during fracture 78−88370
small crystals, fracture strength and triboluminesc. 78−64420
stress depend. 77−44075
student experiment using common candies 80−17778
sugar, cryst., triboluminesc. kinetics 77−8669
sugar, fracture in air and liq. anhydrous diethylether, triboluminescent intensity 78−19582
sugar, mechanical relax. time, determ. from tribolum. 77−1173
sugar, mechanoluminesc., cryst. size depend. 79−38685
sugar, triboluminesc. kinetics 77−77306
sugar, triboluminescence and cryst. fracture dynamics 80−50437
sugar crystal, triboluminesc. kinetics and mech. relax. 77−73178
sugar crystals under stress, fracture-initiation time from triboluminesc. 77−59065
tartaric acid, fracture in air and liq. anhydrous diethylether, triboluminescent intensity 78−19582
tartaric acid, triboluminescence and cryst. fracture dynamics 80−50437
transparent dielectrics, with inclusions, laser-induced stresses 79−28012
Ag halide microcrystals, low-temp triboluminescence 77−87861
Al, oxide covered, tensile deform. in high vac., particle and photon emission 78−39672
B, filament, light emission during fracture 77−28896
CaO, single cryst., tribolum. obs. 79−52031
Cu, dislocation mechanism of luminescence during fracture 79−24376
Fe, burning particles, flashes, spectrographic obs. 80−89078
Fe flakes, light flashes, tribo-induced discharge luminesc. rel. to astrophys. 80−25471
Fe, tribothermoluminescence of flakes in grinding wheel, rel. to solar coronal dust radiation 78−68570
KCl, gamma irrad. relationship between thermolum. and deform. luminesc. 79−19942
KI(Br), X-irradiated cryst., luminesc. during press. release 80−20722
LiF, cryst., triboluminesc. spectra 80−66312
LiF, mech. excitation, luminesc. electron emission, friction, static electrification, meas. method *(German)* 77−24904
LiF, prep. and dosimetric props. of new highly sensitive form 79−22483
LiF, X-irradiated cryst., luminesc. during press. release 80−20722
Li_2SO_4, triboluminescence and cryst. fracture dynamics 80−50437
MgO, single cryst., tribolum. obs. 79−52031
$NaBrO_3$, cryst., mechanoluminesc. spectra 80−97355
NaCl, cryst., triboluminesc. spectra 80−66312
NaCl, mechanoluminesc. peaks, microbreakdown mechanism, generation of ionisation waves 79−33032
$NaClO_3$, cryst., mechanoluminesc. spectra 80−97355
Ni, oxide covered, tensile deform. in high vac., particle and photon emission 78−39672
SiC, grey, green and black, Mn impurities role 78−39612
SrO, single cryst., tribolum. obs. 79−52031
$UO_2(NO_3)_2$, mechanoluminesc., cryst. size depend. 79−38685

trigger circuits
see also flip flops; multivibrators
analogue, for MWPC 79−13605
annunciator for portable defectoscope, Schmitt circuit based, without hysteresis 77−90567
auto-increment circuit for digital pulse programmer 77−79134
carotid artery pressure, noise-resistant trigger cct. 77−48889
delay, for N_2 pulsed laser interfacing with higher freq. electro-optic instrumentation 77−50698
delay unit for automatic variable-path-length US meas. 77−11095
direct-reading phase meter with Schmitt trigger *(Spanish)* 77−37935
electric heating regulator using a FET amplifier and Schmitt trigger convertor *(French)* 79−58681
electrostimulator three-mode control unit 79−20693
flash chambers as 'active' detectors and a special processor for fast decision making 79−26832
flashgun slave trigger, using Si solar cell 80−47125
HV pulser development for CS_2 laser cavity 80−23707
IEEE 488-1975 interface bus, high speed ADC and addressable trigger generation 80−41283
noninvasive His bundle and sinoatrial node activity recording system 79−39560
nuclear event simulation, green LED, trigger circuit, wavelength matched to photomultiplier 77−3238
optically isolated trigger system for pulsed high voltage plasma expt. 77−41650
particle detectors, combinatorial logic trigger system 77−54465
photographic flash unit, sound operated trigger 77−41717
photographic flashlamp trigger circuit 80−62750
photographic multimode flash trigger cct. 78−21248
picosecond trigger system for mode-locked laser pulse meas. 77−26406
programmable combinatorial logic trigger system for high energy particle physics expts. 77−38589
programmable trigger logic 78−17533
Q-switched laser pumping lamp trigger circuit 79−68403
reliability and precision of QRS trigger circuits, synthetic ECG test signals *(German)* 78−92716
Schmidtt, for timing control appl. 78−8
Schmitt trigger used in controlled-delay marker circuit for oscillographs 79−35703
sound triggered electronic photo flash unit, using variable time delay 80−57407
sound-controlled flashlamp trigger circuit *(Spanish)* 80−13175
track-finding trigger processor for mag. detector 78−46244
triggered calibrated sweep for AC oscilloscope 80−67987
triggered vac. gap, Pb(Zr,Ti)O_3, dielec., low-voltage firing characts. 77−80381
X-ray tube, part of installation for rapid process frame-by-frame registration 80−47159
Nd^{3+}:$YAlO_3$ laser double-pulse flashlamp trigger cct. 78−55378

triode sputtering
amorphous alloys, prep. by high rate sputter deposition *(Japanese)* 79−95971
coating techniques, for SEM and X-ray microanalysis 79−12783
euglenoid flagellates, sputter and vacuum evap. coating, comparative effects on delicate features 78−24205
glass, dense crown, HF sputtering prep. of thin-film waveguides 79−10415
high-rate vapour quenching techniques and use in amorphous phase prep. 80−80977
ion sputtering pumps, power supply, press. control *(Spanish)* 77−37902
Au, polycryst., RF bias-diode and triode sputtered, resist. and microstruct. 78−80072
CdS, sputtered film, Rayleigh wave propag. *(French)* 77−62727
CdS_xSe_{1-x} photosensitive films, prep., props., and use for photodetectors 80−55298
CdS_xSe_{1-x} semiconductor film, electrophysical props. *(Russian)* 79−42642
$CdSe_yTe_{1-y}$ semiconductor films, electrophysical props. *(Russian)* 79−42642
In, reactive sputtering in DC triode config. 78−23618
$Mn_{46}Co_{54}$, amorphous alloy prep. by high-rate sputtering, struct. and prop. characteris. 79−24462
Nb film, bias sputtering prep. 79−1826
Nb film, props. control, bias sputtering model 78−72720
$Pb_{1-x}Sn_xTe$, for IR detector appl. elec. and optical props. 80−35084
Pt, for beam lead metallisation, reduction of contamination 78−72721
Ta film deposition by sputtering, influence of Ar plasma 77−69988
Ti, for beam lead metallisation, reduction of contamination 78−72721
$W_{50}Fe_{50}$ glassy alloy, refractory, triode sputtered 80−75185
ZnO low-loss optical waveguides on amorphous substrates 80−58793

triodes
activation efficiency of single crystal whisker field effect cathodes, improvement methods 78−27377
electron beam from triode with explosive-emission cathode, variable current density 79−72475
electron gun, keV anode-controlled telefocus, focusing props. 78−342
grid controlled switching element, stationary conducting state 79−77430
grid controlled switching element, stationary conducting state, arc conditions 79−77431
injection system of Elektronika linear accelerator, triode gun anode modulation 79−67978
ion beam prod., high current 80−99372
MIMIM, photoresponse 77−39963
nonisochronic reflecting electron system, high power microwave emission 78−1140
plasma, reflex, anode design for ion beam impedance collapse 78−9862
plasma triode distributed coupling cable propagation 79−55515
power capabilities for plasma heating *(French)* 78−9801
reflection triode, prod. of high current ion beams *(Russian)* 80−83230
reflex triode, unidirectional ion generation and geometric focusing 79−76235
reflex triode system, generation of intense microwave radiation by relativistic electron beam 80−14887
reflex triode with uniform ion flow 79−98928
ring triode, enhanced mode thermionic convertors, expts. 78−38553
spherical reflex triode, extraction and bunching of ion beam 80−18727
spherical reflex triode, ion beam extraction and bunching 79−97471
superconductor-semicond. device research, future prospects 79−28467
thermionic convertor, ignited noble gas triode, arc drop elimination 77−24213
thermionic convertor, with W emitter and WO_2 collector, pulsed discharge characts. 77−24215
thermionic emission triode, with auxiliary discharge, rectifying parameters 79−64925
thermionic triode, oscills. in low press. inert gas discharge 80−79590
Cs-Ba triode arc switch, high-current, low-voltage, pulsed control 78−71551

triple point *see critical points*

triplet absorption detection of magnetic resonance *see microwave-optical double resonance*

triplet state
^3P isoelectronic series, Sternheimer valence shielding and antishielding factors 80−18807
acetaldehyde, first triplet state geometry, fragmentation into free radicals 80−47915
acetaldehyde+CO_2, vibr. relax., search for unquenchable species, room temp., 5-2200 torr 78−9229
acetone, mol., radiative lifetime of phosphoresc. state, influence of high lying triplet states 79−86006
acetophenone, triplet-triplet energy transfer, naphthalene-d_8, in EPA rigid soln., donor phorphoresc. decay 78−10971
acetophenone in toluene glass, quasi-line phosphoresc. spectra 77−69883
acetylene, electron impact energy loss spectra, mol. configuration 77−68128
acetylene, ground and triplet states, electronic and geom. struct. 78−94184
cis-acetylene, triplet state, near IR electronic absorption spectrum, and form. 79−63997
acetylene, triplet state quenching by foreign gases 80−91596
acridine, Ar matrix-isolated, lowest triplet state IR and visible absorption spectra 79−68228
acridine, T-T absorpt. build-up, following picosec. pulse singlet excitation, in gas phase 78−9161
acridine dyes in methanol-water glasses, EPR spectra of triplet state 79−18212
acridine in fluorene matrix, RF induced mag, reson. transitions, triplet state, optical nucl. polarisation 79−31561
acrolein, triplet state vertical and adiabatic excitation energies, CI calcs. 78−9083
albumin, human serum, assoc. solns., excited state deactivation, flash photolysis obs. 79−54895
alicyclic ketones, triplet state behaviour, non-RRKM photochemical decay, vibr. relax. 78−61030
alkali bromides and iodides, self-trapped exciton and F-centre form. by picosecond laser pulses 80−10546
alkali cyanides, mol. excitons, X-ray excited emission spectra obs. 80−66287
alkali halide:Tl^+-like ions, triplet state lifetime, hyperfine interaction 80−2844

triplet state continued
alkali halides, ^{14}N impurities, molecular point defects, EPR isotropic hyperfine triplets 80−2636
alkali halides, self trapped exciton, optical detection of spin relax. processes 78−60358
alkaline earth fluoride, EPR of triplet state of self-trapped excitons 78−43684
n-alkanes, mol. Rydberg S_n←S and S_n←T transitions, semi-empirical SCF MO calc. 80−91453
alkyl aryl ketones, in homogeneous n-heptane solns., quasi-isoenergetic triplet energy migration, photolysis obs. 79−61878
alloys, dilute mag., local moment formation, nonequivalent orbitals model 80−11164
alternant hydrocarbons, approx. calc. by spin-extended HF method 79−26889
amino acids, positron annihilation in D and L isomers 77−12887
2-aminopurine, triplet state, electric dipole moments 79−22742
5-aminopyrimidine triplet state, electric dipole moments 79−22742
aniline, in p-xylene host cryst., phosphoresc. triplet state, ESR and MIDP obs. 80−66077
anilinium ion, $C_6H_5\dot{N}H_3^+$, fluoresc. and phosphoresc., pKa values 79−13755
anthracene: phenazine, optical nuclear polarisation, 1.4 to 300K *(German)* 77−63321
anthracene: tetracene, singlet exciton trapping mechanism, fluoresc. mag. field modulation obs. 77−77267
anthracene:rhodamine, triplet exciton density, isotope substitution effect, in weak mag. field 77−90184
anthracene:tetracene, crysts., triplet kinetics model *(German)* 79−4518
anthracene:tetracene crysts., mag. field modulation of scintillation under α-irrad. 77−48256
anthracene, α-particle tracks, excited states, creation and evolution 78−43934
anthracene, carbonyl derivatives, triplet state population, picosec. laser obs. 78−13544
anthracene, cryst., triplet exciton pair kinematics, diffusion model 78−79931
anthracene, diacetyl-sensitised delayed fluoresc. 79−54888
anthracene, electron irrad., creation and evolution of excited states, scintillation obs. 78−92128
anthracene, EPR of triplet excitons, source of residual linewidth 79−15338
anthracene, exciton sounding of α-particle induced radiation defects 77−12423
anthracene, in cyclohexane soln., triplet state decay consts. by sampling flash apparatus 79−51998
anthracene, luminesc. spectra, exciton-phonon interaction, triplet exciton bands 79−65387
anthracene, pulsed electron excitation, triplet excitons, spectral and electrical investigations 80−92828
anthracene, pure and d_n, PMMA soln., triplet lifetimes, 77-300K 78−25594
anthracene, single cryst., X-radiation damage recovery, using triplet state exciton probe 78−75694
anthracene, single cryst., X-ray radiation damage, delayed fluoresc. meas. *(Japanese)* 79−37736
anthracene, single cryst. triplet excitation form. 79−69437
anthracene, singlet and triplet excitons as probes for photochem. reactivity 79−74406
anthracene, singlet-triplet absorpt. spectra, 2-300K, photoexcitation spectra 78−43890
anthracene, theory of fission of singlet Frenkel exciton into two localised triplet excitons 79−23901
anthracene, triplet exciton absorpt. lines 79−47475
anthracene, triplet excitons, phosphoresc. and delayed fluoresc. excitation spectra 78−63986
anthracene, triplet-exciton fine struct., high resolution optical meas. 80−45099
anthracene in glassy matrix, triplet state spin relax. time, anisotropy *(French)* 77−65492
anthracene-amine cation radicals, electron transfer with heterocyclic and carbonyl anion radicals, triplet state electrogeneration 80−63803
anthracene-d_{10}-s-tetracyanobenzene, rotational mode coupling in phase transition 78−71827
anthracene-dimethylpyromellite-imide, CT complex, reaction yield detect. double reson., delayed fluoresc. quenching *(Russian)* 78−88230
anthracene-dimethylpyromellitimide, cryst., triplet exciton pairs, EPR spectra 77−43906
anthracene-dimethylpyromellitimide CCT crystals, mutual annihilation of triplet excitons 78−19543
anthracene-dimethylpyromellitimide charge-transfer complex, photoconductivity mechanism 77−47860
anthracene-PMDA crysts., phosphorescence blue shift of charge transfer config. 77−36278
anthracene-TCNB charge transfer crystal, EPR spectra of triplet excitons, and Raman spectra 78−26817
anthracene-tetracenebenzene, triplet excitons annihilation, mag. reson. sign reversal 79−65769
anthracene-tetracyanobenzene, triplet exciton annihilation, mag. double reson. *(Russian)* 78−19380
anthracene-tetracyanobenzene cryst., triplet exciton annihilation, time correlated delay fluoresc., ODMR 80−39895
anthracene-tetracyanobenzene cryst., triplet excitons, zero-field EPR splitting temp. depend. 78−10748
anthracene-tetracyanobenzene crysts., deuteration effect on phase transition, triplet state EPR study 80−50163
anthracene/TCNB, charge-transfer cryst., fluoresc., 1.2-300K, mobile triplet excitons 78−43913
anthracenes, in soln., triplet-triplet fluoresc. 79−59501
anthracenes, nonradiative relax. of higher excited triplet states, double excitation obs. 78−29805
anthraquinone, in Shpolskii matrices, triplet state spin-lattice relax. rates 78−21952
9,10anthraquinone, lower triplet states, interactions and position, matrix isolation spectra 80−63634
anthraquinone, site selective sublevel phosphoresc. spectra in octane or hectane soln. 79−69878
anthrone, 533 nm excited state absorpt. kinetic, triplet quenching solvent, internal conversion, vibr. relax. 78−21935
p-(9-anthryl)-N,N-dimethylaniline derivatives, excited emitting states in polar solvents, fluoresc. 78−5263

triplet state continued
arene, photophysics, functionalised micellar assembly, phosphoresc. and triplet Ag^+ enhancement 78−95598
aromatic aldehyde, phosphorescence spectra of mol., intensity and vibronic coupling 79−76461
aromatic aldehyde, triplet state dipole moments, vibronic coupling effects 79−31493
aromatic compounds in benzene polycrystalline host, active N_2 induced chemilum., 77K 80−60691
aromatic hydrocarbon, quenched with Ag^+ in ethanol, triplet state form. 79−11801
aromatic hydrocarbon crystals, model for fission of singlet excitons into triplet-exciton pairs 78−14672
aromatic hydrocarbon soln., delayed fluoresc., mag. field effect, excimer form. 77−14479
aromatic hydrocarbons, aqueous micellar soln., triplet state room temp. phosphoresc., hydrophillic quenchers 78−9181
aromatic hydrocarbons, ethanol-KI solns., fluoresc. affected by I^- 79−13749
aromatic hydrocarbons, nitroxyl radicals, energy transfer, quenching 78−35651
aromatic hydrocarbons, oxygen quenching of triplet states, charge-transfer interactions 77−23516
aromatic hydrocarbons, singlet-triplet conversion at low temp. 80−43094
aromatic hydrocarbons in Shpolskii matrices, $S_0 \rightarrow T_1$ absorpt. spectra 79−85995
aromatic isolated mol. nonradiative conversion, internal and S-T conversion, vibr. excitation and fluoresc. quantum yield 80−43095
aromatic molecular crystals, optical nuclear polarization by optically excited triplet states 79−19804
aromatic molecule, electronic excitation energy degradation, electronic-vibr. spectrum 77−488
aromatic molecule, in aromatic (aliphatic) solvent, 77K, triplet-triplet absorption spectra, anomalous broadening 77−88502
aromatic molecules, energy transfer from upper triplet states 79−10142
aromatic molecules, phosphoresc. triplet spins phase coherence, ESR 79−31559
aromatic molecules in cryst. lattice, phosphoresc. intensity and optical nuclear polarisation, level anticrossing effects 78−91992
aromatic solutions, triplet-triplet absorption, anomalous broadening 79−54842
aromatic systems, alternant, sign-alternation rule for triplet state 80−102420
aromatics in stretched PVA films, ESR of phosphorescent triplet state 77−30908
aryl cations, triplet state, multiple site splitting, ESR obs. 80−97126
aza-aromatic molecules, intersystem crossing, quantum interference effects 80−53037
9-aza-bicyclo (3,3,1)nonan-3-one-9-oxyl, dimerisation, ESR, NO radical pair exchange 78−19330
azaaromatics, neutral and protonated, excited singlet and triplet states, charge densities, INDO calcs. 80−58152
azaphenanthrenes, lowest triplet state zero field splitting parameters calcs. 80−83391
azulene-fluoranthene, soln., triplet energy transfer, delayed fluoresc. study of $S_2 \rightarrow S_0$ 80−23331
bacteria, photosynthetic, triplet-state EPR spin polaris., intramol. model 78−44469
bacteriochlorophyll a, triplet state energy and lifetime 80−30682
bacteriopheophytin a, triplet state energy and lifetime 80−30682
benzaldehyde, and deuterated forms, in p-xylene, 4.2K, $n\pi^*$ phosphoresc. assignments 78−9197
benzaldehyde, and substitution products, spectral props. 79−27007
benzaldehyde, electronic spectra, Cl and F substitution effects 80−23456
benzaldehyde, $n\pi^*$ and pi pi* triplet states, props., SCF calcs. 77−6695
benzaldehyde in toluene glass, quasi-line phosphoresc. spectra 77−69883
benzaldehyde-biacetyl system, self-quenching and electronic energy transfer obs. 80−5571
1,2-benzanthracene, monomer and excimer fluoresc. in soln., triplet-triplet annihilation and mag. field depend. 78−78738
1,2-benzanthracene in polystyrene films, delayed luminesc. decay kinetics 80−43088
benzene, $-d_0-d_8$ vapour at low press., intersytem crossing and internal conversion, press. depend. of triplet form. 77−30918
benzene, and derivatives, Jahn-Teller instability 79−47062
benzene, deuterated mixed crysts., phonon assisted trap-trap triplet energy migration, 0K limit, phosphoresc. obs. 77−48218
benzene, excitation spectra, cluster configuration method appl. 80−78546
benzene, fluoresc., triplet state and isomerisation yields, photochem. 77−1942
benzene, fluoresc. triplet state and isomerisation yields, low vibr. levels 79−64035
benzene, ground, singlet and triplet states, ab initio VB STO, GTO calcs. 77−75060
benzene, isotopic mixed crysts., triplet excitation energy transfer theory 77−28611
benzene, isotropically mixed crysts., singlet and triplet exciton percolation theory 78−26818
benzene, lowest triplet state, pulse radiolysis obs. 79−39168
benzene, photoexcitation, triplet factor group states assignment 77−85741
benzene($-d_6$), in Ar-Kr matrices, phosphorescence decay, external heavy atom effect 79−10132
benzene in 3-methylpentane glass, phosphoresc. polarisation and intensity, 77K 77−46588
benzene triplet state, self quenching, effect on naphthalene internal conversion rate estimate 78−25586
benzene-d_0($-d_6$), radiationless triplet decay, non-Condon effects 80−83405
benzene-deuterate benzene cryst., triplet migration, cluster method 79−73510
benzene/benzene-d_6, cryst., X-trap phosphoresc., ODMR, 1.3K, triplet state struct. 77−20902
benzenes, lowest triplet states, instability rel. to environmental effects 77−57893
benzenoid aromatics, triplet zero field splitting parameters, ODMR obs., struct. effects 80−78636
benzenoid hydrocarbons, triplet state decay, kinetic spectroscopy, 220-250 nm 78−62820
benzil, cryst., excited triplet state spin-lattice relax. probabilities, temp. depend. *(Russian)* 80−88860
triplet state continued
benzil, ENDOR study of geom. struct. of lowest triplet state 79−89696
benzil, excited electronic states; conformational relax., time resolved matrix isolation spectral obs. 80−32701
benzil, high temp. ODMR obs. of cryst. phases 79−38407
benzil triplet-anisole, reversible exciplex form., phosphorescence, photostationary and transient obs., simulation 78−9182
benzil X-trap, ODMR, near planarity in triplet state 77−32295
1,2-benzocoronene, phosphoresc. and ODMR meas. 79−18220
benzophenone, and d_{10}, ODMR and phosphorescence spectra in organic matrix 79−36671
benzophenone, cryst., phosphoresc. spectra and decay time, temp. depend. 79−87479
benzophenone, high resolution ODMR and optically detected ENDOR 79−19811
benzophenone, lowest triplet state, ODMR spectra, D- and g-tensors 77−75191
benzophenone, metastable triplet state, SCF CI calcs. 79−54776
benzophenone, migration of triplet excitons, EPR profiles and phosphoresc. decay data 80−84641
benzophenone, triplet, optically detected EPR, ENDOR and ODMR, HFS, isotope and spin-orbit effects 78−86898
benzophenone, triplet exciton absorpt. lines 79−38563
benzophenone, triplet state in organic cryst., ENDOR spectra for spin density 79−64021
benzophenone, triplet state zero-field ODMR, ^{17}O HFS 79−18216
benzophenone $^3(n,\pi^*)$, and isotopic forms, in 4,4′-dibromodiphenylether, level anticrossings, ODMR obs. 78−2772
benzophenone betyl radical, photochem. yield mag. field effect on spin rephasing, double-pulse technique 77−90615
benzophenone in toluene glass, quasi-line phosphoresc. spectra 77−69883
benzophenone L in dibromodiphenylether, benzophenone triplet state, nanosecond resolved ODMR, freq.-agile techniques appl. 80−34825
benzophenone vapour, fluoresc. and phosphoresc., nonradiative transitions between triplet and singlet state obs. 80−99516
benzophenone-d_{10}, $^3(n,\pi^*)$ state, containing ^{13}C, in 4,4′-dibromodiphenylether, hyperfine ENDOR spectrum 78−42102
benzophenone-Eu complex, triplet-triplet energy transfer, viscosity and temp. depend. 79−87847
benzophenones, in host crysts., triplet state PMDR, phosphoresc. spectra, transitions mechanisms 77−46585
benzophenones, triplet state fine struct. parameters and phosphoresc. spectra 79−50065
$^3(n,\pi^*)$benzophenones in 4,4-dibromodiphenylether, oriented triplet state, LAC and cross relax., phosphoresc. 77−81143
p-benzoquinone, second order Stark shift of zero-field transitions, isotope effects 77−24860
p-benzoquinone($-d_4$), n-π^* excited states, distant intramol. interaction between identical chromophores 78−90203
2,1,3-benzothiadiazole, EPR of phosphorescent state 77−8405
2-benzoylpyridine, mol. cryst. triplet state selective photoexcitation, phosphoresc. spectra and microwave-optical double reson. 79−15507
2-benzoylpyridine, triplet states, phosphoresc. and ODMR 79−38603
2-benzoylpyridine crystals, lowest triplet state, optically detected EPR 80−15827
2-benzoylpyridine crystals, optical spectra of lowest triplet state 80−16081
benzo[α]pyrene-DNA complex, triplet state props., optically detected zero-field mag. reson. obs. 77−79636
benzo[α]pyrene-DNA complex, triplet state props., optically detected zero-field mag. reson. obs. 79−18222
1,2-benzpyrene, butyl bromide solid soln., phosphoresc. line struct. obs., vibr. assignments 77−58075
3,4-benzpyrene, monomer and excimer fluoresc. in soln., triplet-triplet annihilation and mag. field depend. 78−78738
biacetyl, multiphoton excitation of triplet state, fluoresc. decay 79−31632
biacetyl, single rovibronic state fluoresc., quantum beats 79−31570
biacetyl, triplet kinetics, EPR fine struct., ODMR 77−71824
biacetyl, triplet $n \rightarrow \pi^*$ and $\pi \rightarrow \pi^*$ transitions studied by low-energy electron diffr. 80−83502
bilirubin, anomalous solvent shift effect and phosphoresc. 77−30899
1,1′-binaphthyl, $T_n \leftarrow T_1$ absorption spectrum in rigid and fluid media, CNDO/A study 79−76355
biphenyl:fluoranthene(pyrene)(chrysene), triplet and singlet transport rate ratio 79−56832
biphenyl, carbonyl derivatives, absorpt. and luminesc. spectra, solvent effects and triplet lifetimes 77−24889
biphenyl gluterate diacetylene, monomer, single cryst., stable and metastable UV photoexcited states, EPR obs. 79−78522
biradical, photogenerated in Norrish type II reaction, solvent effects on lifetime 79−11804
biradical, triplet state, S-T_0 CIDNP, biradical scavenging rate const. from mag. field depend. CIDNP 79−3461
borazine, triplet instability, RPA calculations 80−27938
Born-Oppenheimer and true eigenstate prep. by coherent light, large mol. nonradiative relax. 77−88490
broadening, inhomogeneous and homogeneous, of optical and ODMR transitions in solids 80−32750
butadiene, excitation spectra, cluster configuration method appl. 80−78546
trans-1,3-butadiene, valence electronic excited states, SCF ab initio GVB and CI calcs. 79−31423
1,3-butadienes, methyl substituted, singlet-triplet transitions, energies, relative cross-sections, $He^+(H_2^+)$ impact spectra 78−86942
1-butyne, and propyne, electron impact spectra, comparison with acetylene 79−3585
calorimetric techniques for excited states detection 78−32847
carbazole, crystalline, room temp. afterglow 78−27314
carbazole, in presence of KI, decay functions of triplet state of fluoresc. and phosphoresc. 78−66590
carbazole, triplet state of X-traps, ODMR 79−24231
carbazolyl substituted diacetylene monomer cryst., ODMR and triplet state kinetics 78−76355
carbene in polydiacetylene, zero field splitting parameter 78−27075
carbenes, bond angles, inversion barriers, singlet-triplet energy differences, struct. fragments method 77−10782
carbenes, core ionised states, singlet and triplet state binding energy, struct. changes, LCAO-SCF calc. 79−97982
carbenes, triplet state g-tensors and hyperfine coupling tensors 80−52895

triplet state continued
carbocyanine dyes, triplet state quenching by nitroxyl radical, charge transfer complexing 78−25585
carbonyl anion radicals, electron transfer with anthracene-amine cation radicals, triplet state electrogeneration 80−63803
carbonyl compounds, metastable triplet states, var. and perturbational calcs. 77−61680
carbonyls, electric polarisability, in excited singlet and triplet states *(Bulgarian)* 80−52897
cell surface component rotational diffusion, time-resolved phosphoresc. anisotropy 80−97885
charge ordered crystals, mag. props., energy spectrum, triplet excitations 78−18979
charge-transfer crystals, long lived emission 79−33752
chemically induced magnetic polarization by S-$T_{\pm 1}$ mixing in strong mag. field 80−83515
Chichibabin's hydrocarbon, ESR spectra, electron exchange integral 78−50562
p-chloranil+tetrachlorohydroquinone, H atom abstraction by p-chloranil triplet 78−80720
chlorin, ab initio CI calcs. on ground, singlet and excited states, visible spectrum 79−16139
1-chloro-9,10-anthraquinone crystal, electronic structure of lowest triplet state *(Japanese)* 79−8158
p-chlorobenzaldehyde, p-dibromobenzene and p-dimethoxybenzene hosts, dipole moments, lowest electronic states 77−18954
p-chlorobenzene, and deuterated forms, in p-dibromobenzene and p-dimethoxybenzene, 4.2K, $\pi\pi^*$ phosphoresc. assignments 78−9197
chlorophyll, -a and -b, fluoresc. fading curve of lowest triplet state 79−36691
chlorophyll, enhancement of fluorescent mag. resonance detection, under intense laser excitation *(Russian)* 78−91995
chlorophyll, fluoresc. detection of triplet state kinetics 77−30903
chlorophyll, photooxidation, triplet state mechanism 78−27791
chlorophyll, photosynthesis mechanism, upconversion, EPR and O_2 evolution data anal. 78−35811
chlorophyll, singlet-triplet optical resonance in solid soln. 77−52741
chlorophyll a, phosphoresc., triplet state, photochem. reacts. *(Czech)* 78−78842
chlorophyll a, photo-oxidation by p-benzoquinone, nature of electron-excited state 78−76991
chlorophyll a and analogues, triplet state, phosphoresc. polaris. 79−39358
chlorophyll a and b, assoc. solns., excited state deactivation, flash photolysis obs. 79−54895
chlorophyll a and b, triplet state level positions 79−89706
chlorophyll b derivatives, metal substitution effect on triplet state, intersystem crossing 77−88476
chlorophyll photo-oxidation, role of singlet-excited and triplet states 80−51156
chlorophyll photo-oxidation, spectral detect. of exciplex in triplet state 77−25368
chlorophyll photo-oxidation mechanism, effect of spectral composition of light 77−25369
chlorophyll solutions, triplet state props., ODMR meas. 79−20517
chlorophyll-a, triplet and excited singlet optical absorpt. spectra 79−59477
chlorophylls, luminesc. analysis of triplet states *(Russian)* 78−27288
chlorophylls, mag. reson., site selected fluoresc. detection 80−69164
chlorophylls, triplet state ESR, fine struct. and rate consts. determ. 78−25574
chlorophylls, triplet state ESR, fine structs. and rate consts. determ. 78−25575
chlorophylls, zero field triplet spin sublevel ordering, magnetophotoselection obs. 77−42342
chlorophylls and pheophytins, phosphorescence and fluorescence polarisation spectra 79−70522
chloroplast photosystems, exciton annihilation at 100K 77−25371
chloroquinolines, photophys. behaviour, substituent and solvent effects 80−106342
chrysene, butyl bromide solid soln., phosphoresc. line struct. obs., vibr. assignments 77−58075
chrysene, excited singlet and triplet state, CARS obs. 80−83374
CIDEP, triplet mechanism, vector model 80−48020
coherently coupled ensemble, energy exchange, density matrix calcs. 78−64298
collision free triplets, spectrum, temporal evolution 78−33441
complex compounds, calc. of probability of electronic excitation energy transfer 79−69478
complex molecules, photoinstability and quenching effect on laser generation kinetics 80−3390
complex molecules, triplet state, photoinstability and quenching effects on lasing kinetics *(Russian)* 79−13778
condensation in magnetic field 80−2341
conference on optical techniques in mag. reson. spectroscopy, Dublin, Ireland (Aug. 1977). 78−43683
configuration interaction method formulation for triplet states 78−37536
conjugated molecules, electronic transitions, Σ-Π separability 80−58124
copper phthalocyanine-iodine, amorphous cpd. prep. by I_2 diffusion in polycrysts., triplet EPR signals obs. *(Russian)* 80−66016
copper porphin, Zeeman expt. on phosphoresc. triplet and quartet states 79−33786
coronene, butyl bromide solid soln., phosphoresc. line struct. obs., vibr. assignments 77−58075
coronene, fluorescence spectra, zero field line splitting *(Russian)* 78−17604
coronene, in ethanol soln., external heavy atom effect on triplet state, phosphorescence meas. 79−18231
coronene, triplet mol. in n-heptane Shpol'skii sites, distortion and orientation meas. by MIDP 78−37668
coronene, triplet state, photomagnetism 80−97125
cubic crystal, multimode Jahn-Teller coupling, orbital triplet 78−23062
cyanine dyes in methanol-water glasses, EPR spectra of triplet state 79−18212
cyanobenzenes, weak triplet-triplet absorpt. spectra 77−58027
cyclic polyphenylacetylene, thermally excited paramag. props. 77−88614
cyclobutadiene(-d_1), singlet and triplet ground states, vibr. freqs., MINDO/3 and ab initio SCF calcs. 78−13429
1,3,5-cycloheptatriene, singlet→singlet (triplet) excitation, electron impact energy loss spectra 78−46451
triplet state continued
1,3,5,7-cyclooctatetraene, electron impact energy loss spectrum 79−10214
cyclopentanone, excited triplet state, intramolecular tunnelling, optically detected electron spin coherence 77−61774
cyclophanes, double and triple-layered, triplet state zero field splitting parameters, HMO calc. 77−50366
cyclopropane, triplet states, electron impact and photosensitised dissoc., chem. effects 77−14592
cytochrome b_5 rotational diffusion, triplet absorbance anisotropy decay obs. 79−83693
deoxyhaemoglobin, porphin-Fe-imidazole system, SCF-LCAO-ASMO and CI calcs. of low-lying multiplets and excited states 80−94155
1,4-di(triphenyl lead)diacetylene, phosphoresc. spectra, triplet state 79−47490
1,4-di(triphenyl tin)diacetylene, phosphoresc. spectra, triplet state 79−47490
diacetyl vapour, fluoresc. and phosphoresc., nonradiative transitions between triplet and singlet state obs. 80−99516
diacetylene, low temp. photochemical polymenisation, decay kinetics, ESR spectra obs. 80−100616
diacetylene, luminesc. and ODMR spectra 79−38604
diacetylene, single cryst., EPR of low-temp. photoproducts, photopolymerisation 78−85175
diacetylene, single cryst., photopolymerisation, intermediate states, struct. changes 80−30235
3,6-diaminophthalimide vapour, mol. electronic excitation energy degradation path depend. on pentane 80−74195
diarylalkane, in isooctane soln. triplet excimer form., phosphoresc., delayed fluoresc., triplet-triplet absorption 78−25597
diatomic molecule, singlet-triplet perturbations, spin-orbit interaction, matrix elements 77−10653
1,4-diazaphenanthrene, zero-field splitting, basic triplet states, H bond effects 78−5366
1,4-diazatriphenylene, zero field splitting, basic triplet states, H bond effects 78−5366
diazonium salts in aqueous solns. and polymer matrices, IR absorpt. spectra 80−76030
1,2,5,6-dibenzocoronene, phosphoresc. and ODMR meas. 79−18220
dibenzofuran, cryst., phosphoresc. spectra and ODMR meas. 80−11470
dibenzofuran, triplet state of X-traps, ODMR 79−24231
dibenzofuran-fluorene, mixed cryst., phosphoresc. spectra and ODMR meas. 80−11470
dibenzothiophene, triplet state of X-traps, ODMR 79−24231
dibenzoylperoxide, triplet sensitized photolysis, mag. isotope effect 77−60081
4,4′-dibromobenzophenone, ODMR and phosphorescence spectra in organic matrix 79−36671
4,4′-dibromodiphenylether:benzophenone-d_{10}, optical decay constants, photoexcited triplet state near level anticrossing field 78−80250
1,4-dibromonaphthalene:octafluoronaphthalene, absorpt. and phosphoresc. spectra, intermol. reson. 79−33764
1,4-dibromonaphthalene, phosphorescence microwave photoexcitation spectrum (PMPS) 77−32294
1,4-dibromonaphthalene, proton spin relaxation by optically excited triplet states 79−19810
1,4-dibromonaphthalene, substitutionally disordered, energy localisation, optical and ODMR spectra of triplet Frenkel excitons 80−54996
(1,4)-dibromonaphthalene, triplet exciton scatt., absorpt. spectra 78−6696
1,4-dibromonaphthalene, triplet-triplet exciton annihilation in quasi-1-dimens. cryst. 78−27297
9,10-dichloroanthracene, cryst., singlet-triplet absorpt. spectra, delayed fluoresc. 77−8619
p-dichlorobenzene, in p-dibromobenzene, optical detection of Cl NQR in mag. field 80−50228
p-dichlorobenzene, optically detected X-band ENDOR of excited triplet state 79−18221
p-dichlorobenzene, triplet state symmetry, geometry, ODMR, ENDOR obs. 79−18214
p-dichlorobenzene-p-dibromobenzene, solid soln., local struct. and triplet energy migration 78−60489
p-dichlorobenzene-p-dibromobenzene mixed crysts., triplet exciton migration, time resolved emission spectroscopy 80−89052
4,4′-dichlorobenzophenone, cryst., $T_1 \leftarrow S_0$ singlet-triplet absorption profiles, temp. depend., phonon-exciton anal. 78−60436
4,4′-dichlorobenzophenone, cryst., X-traps, rel. populations, elec. field effect 77−12414
4, 4′-dichlorobenzophenone, triplet exciton absorpt. band, zero phonon line *(French)* 79−33726
4-4' dichlorobenzophenone, triplet exciton absorpt. lines 79−38563
4,4′-dichlorobenzophenone single crysts., mutual annihilation of triplet excitons, 1.5 and 4.2K, phosphoresc. obs. 80−80850
dichloronaphthalenes, heavy atom effects on subrates of lowest triplet states, MIDP obs. 80−91594
6,6′-diethoxy-thioindigo, cis⇌trans isomerisation, nanosecond flash photolysis and steady state methods, triplet state 78−35648
1,1′-diethyl-2,2′-cyanine iodide, neat and mixed crysts., visible absorption and emission spectra assignments 77−1692
difluoromethane, triplet state emission spectra, phosphoresc. and energy transfer 78−53196
diformamide, excited singlet and triplet states, CNDO-CI calcs. 77−26990
4,4'-dihalobenzophenone, lowest triplet state, ODMR spectra, D- and g-tensors 77−75191
dihydroporphin free base, in n-octane cryst., zero-field optically detected mag. reson., triplet state kinetics 78−42103
dihydroxycarbene, singlet and triplet state rot. pot. surfaces 80−32627
dimer triplet state line shape, small excitons, appl. to phenazine, naphthalene, tetrachlorobenzene 80−48041
dimers, singlet-triplet energy gap, temp. depend. 79−7809
9,10-dimethyl anthracene, excited singlet state quenching by nitroxyl radical, triplet form. 77−88487
dinaphtho-(2′.3′:1.2);(2″3″:6.7)-pyrene, triplet state, phosphoresc. and ODMR obs. 79−27013
α,α-dinaphthylalkanes, absorpt. spectra and phosphoresc. in soln., triplet excimers 78−62816
dinaphthylalkanes, triplet-triplet annihilation of excimers in soln. 78−86904
diphenyl:(benzophenone, naphthalene), triplet exciton diffusion, phosphoresc. obs. 78−10964

triplet state continued
diphenyl:naphthalene, benzophenone, phosphoresc., triplet diffusion excitons 78−63985
9,10-diphenyl anthracene, excited singlet state quenching by nitroxyl radical, triplet form. 77−88487
2,6-diphenyl-1,4-benzoquinone+aromatic amine, triplet exciplex quenching, H-transfer mechanism 79−79228
diphenyl-d_{10}: diphenyl, triplet state EPR and ENDOR, 1.9K, mol. struct. implications 79−94021
9,10-diphenylanthracene, electrogenerated chemiluminescence, T_2 state emission 78−60524
diphenylmethylene, triplet state, ENDOR in $P2_1$ benzophenone, conformation and spin distrib. 77−483
diphenylmethylene-d_0,-d_{10}, in benzophenone, ground triplet state, electron spin echo expts. 77−16144
2,5-diphenyloxazole, phosphoresc., 77K, solvent effect 78−42118
DNA, triplet state excited by X-rays 77−9174
durene:fluoranthene(pyrene)(chrysene), triplet and singlet transport rate ratio 79−56832
durene:naphthalene, spin-lattice relax. in photo-excited triplet states, spin axes rot. on thermal excitation 78−76294
durene:quinoline-d_0,(-d_n), phosphorescent triplet spins, phase coherence, spectral diffusion effects 79−87334
durene-naphthalene melt, exciton diffusion, percolation approach 80−2390
dye laser, triplet losses, six level model 77−14711
dye laser, triplet state, rel. to chem. stability and H-bonding 77−75508
dye laser, tunable, flashlamp excited, triplet quenching effect 79−31892
dye laser materials, PPP calcs., ground and excited states, triplet yields and efficiency 80−37743
dye lasers, metastable state relaxation time determ. 80−102719
dye lasers, triplet loss influence on relaxation oscills. 80−23680
dye vapour, fluoresc. meas., buffer gases effect 77−75503
dyes for tunable lasers, intersystem crossing rates and saturation parameters in triplet state 77−36280
education, two-electron atom, 1snl excited levels, ionisation energy calc., perturbation, Schrodinger eqn. methods 80−17728
EEDOR triplet state zerofield transition energy, spectral diffusion 80−88893
electrogenerated chemiluminescence, estimation of triplet energies, possibilites and restrictions 80−34992
electron spin coherence in nonphosphoresc. triplet states, optical detect. meas., TADMR and FMDR 78−25578
electron-atom inelastic collision, singlet-triplet transition, polarisation effects *(Russian)* 77−46645
electronic correlation, n-AO in ground state, $n\pi^*$-excited states *(Bulgarian)* 80−32614
EPR line shape of pairs of differently oriented molecules, effect of coupled coherent and incoherent motion of triplet excitons 79−69427
EPR spin Hamiltonian, perturbation treatment, M=0 electronic state, HFS of triplet state EPR 80−25185
ethylbenzocarbazole, soln., luminesc., effect of electronic excitation energy vibr. 80−55174
ethylene, $\pi\rightarrow\pi^*$, electron energy loss spectroscopy 79−72432
ethylene, diatomics-in-mols., semiempirical valence bond π-electron theory 80−99461
ethylene(−d_4), Rydberg states assignments, electron energy loss specta 80−53153
N-ethylphthalimide+olefins, photochemical reaction, absorpt., fluoresc., phosphoresc. and triplet-triplet absorpt. spectra 80−85197
ethyltoluenes, fluoresc. and triplet state quantum yields, biacetyl method 78−37671
excimer, fluorescence, relative yield following triplet-triplet annihilation, re-encounter effects 78−33538
excitons, quasi-coherent, in pairs of differently oriented mols., EPR line shape 78−43631
ferrous porphyrin, intermediate spin, reson. Raman spectra 79−69820
flavins, phosphoresc. props., solvent effects 77−12885
fluorene: acridene, radical pair form. from excited states, optical nucl. polarisation obs. 80−14155
fluorene: pyrene-d_{10}, triplet state energy transfer, EPR 79−15354
fluorene:acridine, EPR of excited triplet state complex 79−19767
fluorene:acridine (phenazine)(anthracene), optical nuclear polarisation, non-crossing rule, guest-host complex 77−42339
fluorene:pyrene-d_{10}, exciton-guest, triplet-triplet annihilation, impurity traps effects 80−25433
fluorene:pyrene-d_{10}, single cryst., host-guest triplet pairs, mag. field effect 80−60649
fluorene, cryst., phosphoresc. spectra and ODMR meas. 80−11470
fluorene, in ethanol soln., external heavy atom effect on triplet state, phosphorescence meas. 79−18231
fluorene, optical polarisation of H nuclei, 4.2K *(Russian)* 77−12255
fluorene, triplet state of X-traps, ODMR 79−24231
fluorescein dye(-Yb^{3+}), triplet state energy transfer, fluoresc. quenching obs. 79−54897
fluorocarbonyl compounds, triplet state, trapped electron ICR spectrosc. 79−59373
formaldehyde, and cation, vertical proton affinity in singlet and triplet states 78−90079
formaldehyde, excited state photodecomp., rotationally resolved spectra 77−60088
formaldehyde, mag. rot. spectrum, A^1A_2 state, singlet-triplet perturbations 79−98126
formaldehyde, mol. Rydberg S←S and S←T transitions, semi-empirical SCF MO calc. 80−91453
formaldehyde, triplet instability, RPA calculations triplet instability, RPA calculations 80−27938
formaldehyde, triplet state g-tensors and hyperfine coupling tensors 80−52895
formamide, ab initio calcs. on ground and excited states 77−83494
formamide, low-lying triplet states, relative energies and conformational preferences 77−3266
formic acid, and dimer, ab initio MO calcs., ground and excited states 77−83492
formylstyrene copolymers, luminesc. *(Russian)* 79−56861
free electron pair, possible ferromagnetism of triplet state 79−30272
fulvene, ground and excited states, electronic correl. and struct. 79−26898
glyoxal, lowest triplet state, excitation energies, electron correl. effects 78−5147
glyoxal, singlet-triplet radiationless processes in mag. field 80−106347
triplet state continued
glyoxal, triplet $n\rightarrow\pi^*$ and $\pi\rightarrow\pi^*$ transitions studied by low-energy electron diffr. 80−83502
glyoxal, triplet state excitation energy calc., modifed CI method 78−37536
glyoxal-d_0, -d_2, triplet kinetics, microwave-saturation recovery and MIDP obs. 77−71823
halonaphthalenes, heavy atom effect on radiative and nonradiative decays 79−31584
1-halonaphthalenes, lowest triplet state, spin sublevels decay, internal heavy atom effects 79−95819
heterocyclic anion radicals, electron transfer with anthracene-amine cation radicals, triplet state electrogeneration 80−63803
heterocyclic aromatic molecules, nonradiative transitions activated by external fields 77−65501
hexacyanobenzene-naphthalene, charge transfer triplet states, electron distrib., ESR 77−3388
1,3,5-hexatriene, electron scatt. at low-energy, vibronic struct. of triplet state 79−3574
hexatriene, excitation spectra, cluster configuration method appl. 80−78546
trans,trans-1,3,5-hexatriene, valence electronic excited states, SCF ab initio GVB and CI calcs. 79−31423
hole burning, photophysical and photochemical theories 80−58322
homogeneous linewidths in ODMR and optical transitions, connection 79−91316
hydrocarbons, associated, Electric dipole polarizability of molecules in excited electronic states 78−70966
hydrocarbons, conjugated, effect of semi-empirical parameters on simple RPA calcs. 79−10037
hydrocarbons, electric polarisability, in excited singlet and triplet states *(Bulgarian)* 80−52897
ortho-hydroxybenzophenone, soln., intramol. proton transfer and energy relax. photostability, transient absorption obs. 80−28032
II-VI compounds, Jahn-Teller effect, average phonon energy 79−15122
impurity molecules, population kinetics *(Russian)* 78−56519
2-indanone, single cryst., ODMR and phosphoresc. of $^3n\pi^*$ state 79−78570
indigo dyes, triplet state config., laser flash absorpt. spectrosc. obs. 80−5557
indoles, laser flash spectroscopy in presence of nitroxide radicals, protein-membrane interaction probing 79−87855
intermolecular triplet excitation transfer in diffusive limit 80−28046
intersystem crossing rates from ODMR 78−78735
1-iodonaphthalene-perfluorated naphthalene solid soln., sensitised phosphoresc., site selection method, Dexter's theory 79−4836
isoquinoline, radiationless transition branching ratio, temp. effects 79−54900
isotope separation, microwave reson., triplet state photochem. technique 77−32818
Jahn-Teller effect, intermediate, in orbital triplet, effect on EPR 80−34756
Jahn-Teller effect of triplet on trigonally distorted site 77−89739
Josephson effect between superconductors in singlet and triplet spin-pairing states 78−14896
ketones, mol. cryst., interband transitions, triplet-triplet absorptions 79−11452
ketones, triplet-triplet absorption carbonyl group role 77−83641
Knight shift, triplet exciton contrib. 77−59472
lambda coupling in II states of triplet or higher multiplicity 79−59429
large molecules, nonradiative transitions activated by external fields 77−65501
lowest triplet state zero field splitting parameters calcs. 80−83391
magnesium chlorin, ab initio CI calcs. on ground, singlet and excited states, visible spectrum 79−16139
magnesium porphin, ESR study of metastable triplet state, in n-octane matrix, 1.3K 79−72340
magnesium porphin, lowest triplet state, zero-field ODMR 79−31562
magnesium porphine, ab initio CI calcs., electronic absorpt. spectra 78−78639
magnesium porphin.ethanol, in n-octane cryst., triplet state splitting, fluoresc. intensity microwave-induced changes 77−6820
magnesium tetraphenylchlorin, lowest triplet state, zero-field ODMR 79−31562
metal porphin, triplet state, spin density and zero-field splitting, PPP-SCF-CI calc. 79−68200
metal porphyrins, Jahn-Teller instability 79−47062
metalloporphyrin triplet state quenching by Fe II- and Fe III-porphyrins 78−76992
metals, triplet supercond. transition in strong mag. field 80−25040
N-methyl diformamide, excited singlet and triplet states, CNDO-CI calcs. 77−26990
N-methyl-2-N-phenylamino-6-naphthalene sulphonates, triplet excitation, multiple fluoresc. 77−71826
p-methylbenzaldehyde, p-dimethoxybenzene host, dipole moments, lowest electronic states 77−18954
methylene, photoelectron spectra, singlet and triplet state calcs. 78−42127
methylene, singlet-triplet separation, ab initio calcs. 78−74582
methylene, singlet-triplet separation, relativistic corrections 80−32618
methylene, singlet-triplet splitting, ab initio calc. 78−5128
methylene, triplet ground state, var. and perturbational calcs. 77−61680
methylene, zero-field splitting, absolute sign, EPR determ. 77−10692
methylene+$H_2\rightarrow CH_3+H$, triplet methylene abstraction, partial open shell FSGO calc. 78−80719
methylenimine, lowest excited state, singly excited config. interaction calcs. 79−59361
N-methylphthalimide in ethanol soln., gain and induced absorpt., struct. props. 77−24890
5-methylpyrimidine, singlet-triplet intersystem crossing, ODMR and MIDP in matrix at 1.6K 79−50055
methylsilylene, isomerisation, lowest triplet state reaction surface studies 79−15963
β-methylumbelliferone, amplification spectra, triplet-triplet absorpt. 77−31101
mixed crystal, intermolecular host deuteration effects on guest relaxation rates, phosphoresc. charact. 79−43010
mixed organic solids, Anderson transition, electronic energy transfer in impurity bands 79−99502
mixed organic solids, triplet exciton transport at crit. conc., Anderson localization or delocalization 79−15087

triplet state continued
molecular $\pi\pi^*$ and $n\pi^*$ states, rel. positions, single-triplet conversion probability, low temp. 79−816
molecular $\pi\pi^*$ and $n\pi^*$ states relative position, optical props., singlet-triplet conversion processes 79−3484
molecular aggregates, triplet, ESR line shape in solid matrix, fine and HFS 78−58878
molecular cryst., triplet exciton annihilation and triplet exciton quenching by free radicals, analytical form of mag. field depend. of rate consts. 79−15094
molecular crystal, Frenkel exciton, coupled coherent and incoherent motion 77−35870
molecular crystal, light absorpt. with excitation of singlet and double triplet excitons *(Russian)* 77−15773
molecular crystal, singlet and triplet biexciton spectra 78−10366
molecular crystal, triplet exciton excess EPR linewidth, orientational order effect 78−72389
molecular crystal, triplet spin-lattice relax. rate anisotrpy at low temp. and high mag. fields 79−42822
molecular crystals, charge-transfer electron-exciton bound states 77−43543
molecular crystals, diffusion mediated exciton processes, mag. field depend. of fission and fusion 79−37998
molecular crystals, exciton annihilation at high exciton densities, Suna equation calcs. 79−78016
molecular crystals, shallow traps, spin triplet population temp. depend. 77−1371
molecular one-dimensional systems, electronic collective excitons, EPR response 77−31960
molecular solid, triplet exciton system, motional correlation effects, model 78−75997
molecular solids, substitutionally disordered, Anderson localisation of mol. excitons 77−89733
molecular triplet states under optical spin orientation conditions, microwave energy transfer 80−74187
molecule, oriented, in solid matrix, slow mol. motion, ESR spectra 77−90014
MTPA(TCNQ)$_2$ radical salt, triplet exciton system, motional correlation effects, model 78−75997
1,2-naphthacoronene, phosphoresc. and ODMR meas. 79−18220
naphthalene:2-fluoronaphthalene, photoexcited triplet state X-traps, ENDOR meas. 78−39444
naphthalene:2-fluoronaphthalene(2-chloronaphthalene), triplet state X-traps, ENDOR obs. 79−33561
naphthalene:β-chloronaphthalene, reaction rate constants of triplet excitons 78−80407
naphthalene: quinoxaline, anisotropic spin lattice relax. of triplet mols. in high mag. field 77−81141
naphthalene: quinoxaline, isolated triplet mol. direct spin-lattice relax., librational model 79−11444
naphthalene:quinoxaline, spin-lattice relax. of triplet states of high mag. fields 79−19933
naphthalene, anion, cation and triplet, GO LCAO MO calcs. of electronic struct. 78−25416
naphthalene, fluoresc. and phosphoresc., singlet/triplet excimers conform. difference 77−14469
naphthalene, in durene, photoexcited triplet state spin-lattice relax., local phonons effects 78−6605
naphthalene, isotopic mixed cryst., phospheresc., photoselection of pure initial triplet states 78−35189
naphthalene, mag. effects on delayed fluoresc. at high and low triplet exciton density 77−8634
naphthalene, multiphoton excitation 79−61414
naphthalene, phosphorescence spectra in rare gas matrices, multiplet struct. and pot. energy functions 80−106341
naphthalene, singlet and triplet excimer interactions, exciton resons. 80−95535
naphthalene, singlet and triplet exciton percolation, tunnelling and thermalisation 80−84432
naphthalene, theory of fission of singlet Frenkel exciton into two localised triplet excitons 79−23901
naphthalene, triplet excimer conformation, σ-π interaction transitions 77−6701
naphthalene, triplet exciton annihilation and triplet spin relax. 80−29792
naphthalene, triplet exciton annihilation at high triplet densities 79−37996
naphthalene, triplet exciton tunnelling, crit. concs. 79−15086
naphthalene, triplet excitons, phosphoresc. and delayed fluoresc. excitation spectra 78−63986
naphthalene, triplet pairs in naphthalene-d_8, ESR, nonreson. 78−64257
naphthalene, triplet state time evolution after radiationless transition, initial vibronic distrib. effects 80−23450
naphthalene β-chloronaphthalene, optically induced detrapping of triplet excitons 79−28828
naphthalene in durene matrix, spin-lattice relax. of phosphoresc. triplet state, PMDR study 79−27012
naphthalene mixed crystal, time resolved excitation migration, triplet and singlet critical concs. 79−78010
naphthalene pair ($C_{10}H_8$) in $C_{10}D_8$ host, mini-exciton obs., electron spin echo and ODMR 77−4559
naphthalene vapour, fast obs. of primary triplets with tandem laser pulse absorption 77−58056
naphthalene-betamethylnaphthalene, mixed cryst. ($C_{10}H_8/C_{10}D_8$), luminesc., test of excitation transport model 79−65914
naphthalene-d_0(-d_8), radiationless triplet decay, non-Condon effects 80−83405
naphthalene-d_8:naphthalene-h_8 cryst., triplet excitons in A-B pairs, origin of inhomogen. broadened ESR lines 78−91623
naphthalene-d_8, metastable triplet states, spin-lattice relax. at high mag. fields, phosphoresc. meas. 78−15063
naphthalene-h_8 and -d_8 mixed crystal, two-dimens. lattice, cluster-cluster interactions, model inhomogeneous distribs. 79−23922
naphthalene-TCNB, charge-transfer cryst., donor mol. orient. and dynamics 79−32926
naphthalene-TCPA charge transfer triplet states, electron-phonon coupling 79−38601
naphthalene-tetrabromophthalic anhydride, complex cryst., visible spectra, singlet-triplet absorpt. 79−19897
naphthalene-tetrachlorophthalic anhydride, complex cryst., visible spectra, singlet-triplet absorpt. 79−19897
triplet state continued
naphthalene-tetrachlorophthalic anhydride charge-transfer cryst., electronic states 77−32415
naphthalene-tetracyanobenzene, doped cryst., EPR of triplet state for mol. reorientation 79−38368
naphthalenes, heavy atom effects on phosphorescent triplet states 78−70858
1,2-naphthalocyanine-rare earth ion complexes, electronic excitation deactivation mechanism 79−85986
β-naphtholate in methanol-methyltetrahydrofuran glasses, electron solvation, laser flash photoionis. compared with pulse radiolysis 79−74405
1,4-naphthoquinone, $T_1 \leftarrow S_0$ transition, elec. and mag. field spectra 78−88322
naphthyl, excited electronic states; conformational relax., time resolved matrix isolation spectral obs. 80−32701
nicotinamide co-enzymes, reduced, phosphorescence obs. at −196°C 79−79471
3-nitropyrene, triplet state, absorption spectra in soln. 78−33440
nitrosodisulphonate ion salt dimerisation, ESR of dimers in triplet state *(French)* 77−12791
nucleic acid components, pyrimidine and purine, electronic struct. 80−30654
nucleic acids bases, excited state dipole moments and geometries 80−95738
octafluoronaphthalene crystalline complexes with naphthalene and durene, triplet exciton emissions 80−84760
ODMR, spin-lattice relax. and triplet-triplet. absorpt. effects 79−19807
olefin triplet lifetime measurement by electron transfer interception 79−79269
one-dimensional solids, energy transfer processes, optically detected electron spin coherence meas. 79−19808
open shells, RHF treatment without Lagrange multipliers 80−32589
optical nuclear polarisation, field and orientation depend., non-crossing rule, perturbation anal. 77−42337
optical nuclear polarisation, the non-crossing rule, electronic relax. perturbation anal. 77−42338
organic charge transfer crystals, transport props., phase transitions, mol. dynamic *(German)* 80−39507
organic compound, fluoresc. quenching by transition metal, mechanism 79−56837
organic compound, vap., laser-excited long-lifetime luminesc. 79−54887
organic crystals, kinetic model of triplet exciton dynamics 78−67948
organic donor-acceptor solns., triplet-triplet energy transfer under Shpolskii effect conditions 79−64031
organic gases, kinetics of intermolecular triplet-triplet electron energy transfer 79−10141
organic molecular cryst., singlet-triplet-triplet triexciton bound states 78−2426
organic molecular crystals, optical spin alignment, phosphoresc. *(Russian)* 78−84652
organic molecular crystals, phosphoresc., optical spin alignment 79−95827
organic molecular solid, space group C_{2h}^5, triplet excitons energy band struct. 78−6276
organic molecule, triplet-triplet annihilation, delayed fluoresc. in soln. *(Russian)* 79−6962
organic molecule complex mixtures in solid-state matrices, dip shape saturation effects on nonuniformly broadened spectra 79−95799
organic molecule concentration after excitation by different forms of impulses 77−18809
organic molecules, triplet state electronic energy delocalisation 77−3478
organic molecules, triplet state quenching by ruthenocene 77−83630
organic molecules in Shpolskii matrices, phosphoresc. site selection spectrosc., ODMR 79−36687
organic scintillators, vap. phase dye laser media, photophysical parameters 80−95884
organic solid, exciton motion effect on proton relax. 78−14671
organic solid, motion of localised excitations 77−31961
α-oxalic acid dihydrate, low-lying excited states, ODMR and optical obs. 79−41188
oxides, excited states of F-centres 78−64006
oxirane, triplet state, torsional motion relax. 79−49959
palladium porphin, optically detected EPR and Zeeman meas. 79−19809
palladium porphin, Zeeman expt. on phosphoresc. triplet and quartet states 79−33786
palladium-octaethylporphyrin, gas phase delayed fluoresc. and phosphoresc., triplet excimer formation 80−18884
palladiumporphin in n-octane cryst., lowest triplet state, ESR-optical detect. 77−58050
paramagnet singlet-triplet, collective excitations 77−72995
pentacene in naphthalene, triplet state, EPR study by electron spin-echo and laser flash excitation 80−58172
pentamethylbenzene-TCNB, charge transfer triplet states, electron distrib., ESR 77−3388
perdeuterobenzophenone, in 4,4'-dibromodiphenylether, cross-relax., microwave pulse obs. 80−53031
perylene, excited singlet state quenching by nitroxyl radical, triplet form. 77−88487
[2.2]phanes in glass matrices, transanular π-electron interaction, emission spectra 79−36682
phenanthrene:anthracene, cryst., triplet-triplet annihilation, shallow traps effect, 77-293K 79−11446
phenanthrene:anthracene, delayed fluores. of cryst. in mag. field 79−52023
phenanthrene, lowest triplet state zero field splitting parameters calcs. 80−83391
phenanthrene, triplet state conc. quenching in propan-1,2-diol 77−75196
phenanthrene-d_{10}, oriented in biphenyl, triplet zero-field splittings, conc. depend. 78−2773
phenanthrene-PMDA, cryst., triplet charge transfer state symmetry 77−72836
phenanthrene-PMDA, spin polarization of charge-transfer excitons, EPR meas. 79−19766
phenanthrene-pyromellitic acid dianhydride, single cryst., EPR, delocalised and localised charge transfer excitons 77−85545
phenanthrene-pyromellitic dianhydride, single cryst., charge-transfer triplet excitons, spin polaris. 79−11069
phenazine: azulene, EPR, azulene triplet state 78−35024
phenazine, ^{14}N quadrupole tensor, optical detection of NQR 79−18218
phenazine, first excited state ^{14}N quadrupole tensor by ODNQR 78−50561

triplet state continued
phenazine, substitutionally disordered, energy localisation, optical and ODMR spectra of triplet Frenkel excitons 80−54996
phenazine, T-T absorpt. build-up, following picosec. pulse singlet excitation, in gas phase 78−9161
phenazine, triplet formation kinetics temp. depend., analogue computer anlaysis 77−58058
phenazine, triplet state intersystem crossing, picosec. singlet excitation 77 6824
phenazine, zero field studies of spin lattice relaxation in excited triplet states 79−18219
phenyl cation, singlet, triplet state mol. geometries, energies, ab initio UHF STO calcs. 77−6672
phenylcarbene, singlet and triplet ground states, rearrangement to cycloheptatrienacarbene, MINDO/3 calc. 78−13430
p-phenylphenol in stretched polyvinyl alcohol film, phosphorescent triplet states, ESR spectra obs. 80−83393
p-phenylphenolate ion in stretched polyvinyl alcohol film, phosphorescent triplet states, ESR spectra obs. 80−83393
pheophytin a and b, assoc. solns., excited state deactivation, flash photolysis obs. 79−54895
pheophytin-a, fluoresc. fading curve of lowest triplet state 79−36691
pheophytins, lowest triplet state, zero field splitting consts., decay rate consts., EPR determ. 78−27896
phosphorescent triplet spins, phase coherence, spectral diffusion effects 79−87334
phosphorescent triplet state, spin-lattice relax. mechanism *(Russian)* 78−68542
photoexcited, coherent averaging of electron spins by rotary echoes 79−42823
photoexcited molecule, exchange between triplet states with nonparallel eigenvectors 79−59374
photoexcited triplet state molecules, in cryst., cross-relax., variable freq. ODMR obs. 80−53031
photosynthetic membrane, in vivo, light collection and exciton dynamics 79−48215
photosynthetic reaction centre chromophore organisation, high-resolution magnetophotoselection 80−97880
photosynthetic reaction centres, triplet population, mag. field and g-factor differences effect 80−97879
photosynthetic systems, reaction centre struct., triplet state ODMR 77−29093
photosynthetically relevant mols., electronic structural props. 80−16902
photosystem I of spinach chloroplasts and subchloroplast particles, EPR obs. 80−85344
phthalic anhydride and halogen derivatives, phosphorescence spectra *(Japanese)* 78−48217
phthalimide, soln., triplet state accumulation and deactivation depend. on solvent polarity 79−85982
phthalocyanine, metal-free, singlet-triplet fusion rel. to carrier photogeneration 77−36276
picene, EPR in p-terphenyl cryst., triplet state 79−36668
pigment soln., luminesc. of singlet state O_2 in energy transfer 79−54886
platinum phthalocyanine single cryst., triplet state Zeeman effect, phosphoresc. 78−6747
polar crystal, biexciton, lowest triplet state 79−56137
polar dielectrics, triplet two electron states 80−24810
polar molecule, Stark effect in electron spin transition in zero-field 77−27099
poly(N-vinylcarbazole) film, fluoresc. and phosphoresc., energy transfer mechanism 80−16112
poly(vinyl cinnamate), excited state, low-energy EELS and INDO/S calcs. 80−106407
poly riboadenylic acid, time dependence of triplet-singlet excitation transfer 79−57586
poly-2-vinylnaphthalene, soln., lowest triplet props., flash photolysis and radiolysis obs. 80−32861
poly-N-vinylbenzocarbazole, soln., luminesc., effect of electronic excitation energy vibr. 80−55174
poly-N-vinylcarbazole film, triplet-triplet energy transfer, chemiluminesc. 78−43944
poly-N-vinylcarbazole-biacetyl, triplet exciton quenching, exciton trapping model 80−66267
polyarylenealkyls, colour, EPR, electron density delocalisation degree determ. *(Russian)* 80−7152
polyatomic molecules, triplet states, var. and perturbational calcs. 77−61680
polyatomic molecules in solid matrices, ODMR in triplet states, appl. of spin echoes 79−18217
polycyclic monoazines, temperature dependence, triplet formation, radiationless transitions 79−54900
polyene chain, collective excitations and optical absorpt. 79−47019
polyenes, photoisomerisation, triplet pot. energy surfaces and normal mode anal. 80−108700
polymethine dye behaviour in lasers, efficiency and photoisomer generation 80−14335
polynitramines, solid cyclic, luminesc. meas. 77−32424
polypeptide hormones, conformations, ODMR investig. 78−76356
polypeptide hormones, folding, ODMR and phosphoresc. 79−20518
polyvinylbenzocarbazole, weak solution, intramolecular energy transfer by singlet and triplet excitons 80−34971
polyvinylcarbazole, weak solutions, intramolecular energy transfer by singlet and triplet excitons 80−34971
POPOP, vap., electron energy loss spectra rel. to lasing 78−29947
POPOP laser, bleaching of vapour 80−19027
porphin ($-d_2$,d_4,d_6,d_8,d_{10},d_{12},d_{14}), nonradiative transition probabilities, deuteration effects 79−3485
porphin free base, triplet state electron spin echoes, fluoresc. detection 78−70856
porphyrin, triplet-state EPR spin polaris., intramol. model for photosynthetic bacteria 78−44469
porphyrin free base, spin-dependent D isotope effect in triplet state decay, N-H vibrs. 77−30909
porphyrin free lasers, radiationless decay of triplet state, position dependent D effect 77−30902
porphyrin singlet and triplet states, quenching of O_2 79−92141
porphyrin solns., quenching of excited states by nitro-cpds., donor-acceptor interactions 78−2899
porphyrins, non-radiative deactivation of lower excited states, effect of mol. struct. 78−68987
triplet state continued
porphyrins, solid solns., phosphoresc. rel. to solvent heavy ats. *(Russian)* 77−40286
porphyrins in liquid crystal, oriented photoexcited triplets, EPR study 80−84636
propene, triplet states, electron impact and photosensitised dissoc., chem. effects 77−14592
propylene, mol. dissoc. on bombardment by low energy electrons 80−43845
propynal, IR photochem. in electronically excited state 80−11923
propyne, and 1-butyne, electron impact spectra, comparison with acetylene 79−3585
proteins, adsorbed at interfaces, fluoresc. spectroscopy study 80−12315
proteins, triplet state energy transfer 78−20143
protochlorophyl, mag. reson., site selected fluoresc. detection 80−69164
protochlorophyll, fluoresc. fading curve of lowest triplet state 79−36691
protoporphyrin IX, triplet states, flash photolysis, obs. 80−95555
protoporphyrin IX dimethyl ester, triplet states, flash photolysis, obs. 80−95555
pyrazine, in pyrazine-d_4, p-dioxane, X-trap, p-xylene, benzene(-d_6), cryst., MIDP, PMDR, low temp., assignments 77−36154
pyrazine, intensity of intercombination transitions, influence of n-σ-type complex form. *(Russian)* 77−26980
pyrazine, lowest triplet state, phosphoresc., intersystem crossing 78−5269
pyrazine, mol., radiative lifetime of phosphoresc. state, influence of high lying triplet states 79−86006
pyrazine, zero field studies of spin lattice relaxation in excited triplet states 79−18219
pyrazine triplet state, mol. distortion, MIDP using polarised light 79−10137
pyrazine-d_4, in p-dioxane, p-xylene, benzene, cryst., MIDP, PMDR, low temp., assignments 77−36154
pyrene, crystalline, EPR spectrum of triplet excitons 78−27076
pyrene, distinction of delayed fluorescences $S_1 \rightarrow S_0$ and $S_2 \rightarrow S_0$ by selective quenching of $S_1 \rightarrow S_0$ 80−69175
pyrene, emission from triplet state in electrochemical at low temps. 77−77307
pyrene, fluoresc. quenching by 1,4-diazabicyclo[2-2-2]octane in cyclohexane soln. 79−31575
pyrene, in cyclohexane soln., triplet state decay consts. by sampling flash apparatus 79−51998
pyrene, monomer and excimer fluoresc. in soln., triplet-triplet annihilation and mag. field depend. 78−78738
pyrene, triplet exciton absorpt. lines 79−47475
pyrene, triplet state, excitonic energy transfer, phosphoresc. and delayed fluoresc., 2 to 300K 80−84776
pyrene in glassy matrix, triplet state spin relax. time, anisotropy *(French)* 77−65492
pyrene-d_{10}, EPR line shape of photo-excited triplet state, in cryst. and glass 79−24210
pyrene-diethyl aniline in acetonitrile-toluene, triplet exciplex state in pulsed laser photolysis 77−16836
pyrene-DMA-methanol solution, photoinduced radical ion pair geminate recombination, triplet yield 78−76879
[2.2](2,7)pyrenophane, emission spectra, transannular interaction 77−489
pyridinium(-d_5) ion, triplet state obs. by ODMR, rel. to CNDO/2 STO calcs. 77−18951
pyrimidine, and derivatives, intersystem crossing rates, triplet sublevel decay, vibronic coupling 78−5271
pyrimidine, singlet-triplet intersystem crossing, ODMR and MIDP in matrix at 1.6K 79−50055
pyrimidine, zero field studies of spin lattice relaxation in excited triplet states 79−18219
quinoline, radiationless transition branching ratio, temp. effects 79−54900
quinoline complexes with proton donors in triplet state, phosphorescence spectra 77−48230
quinolines, heavy atom effects on phosphorescent triplet states 78−70858
quinones, triplet quenching by organometal cpds., time resolved CIDEP and ESR obs. 80−95654
quinoxaline$^+$, (singly protonated), struct. and kinetics of fluoresc. and phosphoresc. states 77−30906
quinoxaline, in naphthalene-d_8, sublevel phosphorescence spectra, radiative mechanisms 77−75203
quinoxaline, in p-dibromobenzene, triplet state NQR, nucl. spin polarisation effects 79−18208
quinoxaline, optically detected X-band ENDOR of excited triplet state 79−18221
quinoxaline, triplet state symmetry, geometry, ODMR, ENDOR obs. 79−18214
quinoxaline, zero field studies of spin lattice relaxation in excited triplet states 79−18219
quinoxaline, zero-field splitting, basic triplet states, H bond effects 78−5366
quinoxaline guest molecule in p-dibromobenzene, crystal nucl. spin polarisation cross relax. study 80−29647
R. spheroides, triplet state electron spin echoes, fluoresc. detection 78−70856
rare earth phthalocyanine solutions, rel. to bleaching by ruby laser beam 78−30030
reaction yield detected mag. reson. spectra, evolution, degenerate energy levels, triplet excitons 78−19378
refractive index transients, laser-induced, low-temp. solns., excited triplet state polarisabilities role 79−87411
11-cis-retinal, donor energy effects on triplet-sensitized isomerization 78−3353
retinal, isomeric triplets, low temp. spectrosc. and kinetic flash photolysis obs. 79−85972
RF saturation spectroscopy, optical nucl. polarisation detect., excited state NMR and ESR transition mechanisms 80−54995
rhodamine, soln., triplet state accumulation and deactivation depend. on solvent polarity 79−85982
rhodamine 101, quenching of emission in methanol and latex particle suspensions 80−3374
rhodamine 6G, aqueous soln., absorpt. spectra, ground and triplet state photoprotonation pH depend. 80−42961
rhodamine 6G, associated, in polyvinyl alcohol film and soln., emission, room temp. 79−54896
rhodamine 6G, delayed fluoresc. of simple associates in polar and nonpolar solvent mixtures *(Russian)* 78−48185

triplet state continued
rhodamine 6G, soln., triplet state lifetime determ., solvent effect 78−1225
rhodamine 6G, solns., delayed fluoresc. of simple associates 79−56847
rhodamine 6G and 4B, amplification spectra, triplet-triplet absorpt. 77−31101
rhodamine 6G soln., delayed annihilation fluoresc., external heavy at. effect 79−99931
rhodamine dye, intercombination conversion rate consts. from triple quenching by 1,4-diphenylbutadiene 79−956
rhodamine dye solutions, additional heavy atom effects on triplet state transitions *(Russian)* 77−85800
rhodamine dyes, methanol-water solns., triplet state EPR spectra, aggregation, mol. orientation 77−48031
rhodamine dyes, phosphoresc. quantum yields determs. 79−8179
rhodamine dyes, triplet state, role in intermediate prod. 77−29018
rhodamine dyes in methanol-water glasses, EPR spectra of triplet state 79−18212
rhodamines in ethanol soln., gain and induced absorpt., struct. props. 77−24890
rhodopseudomonas sphaeroides, reaction centre triplet state fluoresc. mag. field depend. 78−53358
rubrene, electrogenerated chemilum., production of excited states by direct heterogeneous electron transfer 79−20371
rubrene radical cation reduction at n-ZnO electrode, triplet state formation, luminesc. 77−16825
rubrene-in-benzene, excited state migration and charge transfer 77−55559
Rydberg INDO method, mol. Rydberg S←S and T←S transitions and oscill. strengths 78−17572
sapphire, luminesc. of F centre, forbidden triplet-to-singlet transition 79−73990
scandium octaethylporphyrin, μ-oxo bridged dimer, triplet states and geometrys, ODMR obs. 80−9625
scandium octaethylporphyrin, triplet states and geometrys, ODMR obs. 80−9625
Schiff's base, thin layer samples, mechanism of change carrier photogeneration *(Russian)* 77−32045
Shpolskii system, 77K, sensitised phosphoresc. spectra 79−815
Shpolskii systems, sensitised phosphoresc., triplet-triplet energy transfer *(Russian)* 78−76527
silaethylene, isomerisation, lowest triplet state reaction surface studies 79−15963
silaethylene, singlet-triplet energy separation 78−58594
silaethylene, singlet-triplet energy separations 77−57866
silaethylene, triplet carbenoid isomers, thermodynamic stability 78−90076
silylcarbene, isomerisation, lowest triplet state reaction surface studies 79−15963
singlet-triplet energy difference and singlet generalised oscillator strength, Lassettre-Dillon relation 80−63508
six-level model, triplet-triplet pumping 78−25870
spherical top molecule, triply degenerate fundamentals, line freq. expression for lage ang. momentum 79−36614
spin relaxation in photo-excited triplet states via vibronic excitation: rotation of spin axes 79−78503
spin-dependent magneto-optical rotation for free radicals and for singlet-triplet transitions 79−10129
spiropyrane, triplet-triplet absorpt. by laser photoexcitation 77−10685
spiropyron solutions, nitro-substituted, electronic state participation in photochromy 80−81347
trans-stilbene, cryst., triplet excitons, $S_0 \rightarrow T_1$ transition 78−76518
stilbene, direct photoisomerisation theory, from fluoresc. and absorption spectra 79−79262
stilbene, pulsed electron excitation, triplet excitons, spectral and electrical investigations 80−92828
stilbene, single cryst. under pulsed electron excitation, triplet exciton, optical absorpt. spectrum 79−7838
trans-stilbenes, triplet energy, substituents effect, singlet-triplet absorpt. and electrochemilum. obs. 79−81225
substitutionally disordered material, impurity band triplet energy transfer 79−51513
superconductor, triplet pairing, strong Kohn anomaly *(Russian)* 78−19179
TCNB, electron donor-acceptor complex, triplet state phophoresc. kinetics, MIDP obs. 78−62839
TCNQ compounds, electron-proton couplings, dimensionality 78−91974
TCNQ salt, MEM$(TCNQ)_2$, phase transition electronic struct. interpretation 80−24781
TCNQ salt, N-n-butyl-quinolinium $(TCNQ)_2$, ESR spectrum fine struct. splitting 80−44904
TCNQ salt, N-propyl-quinolinium$(TCNQ)_2$, defect conc. depend. phase transition 80−44577
TCNQ salts, Rb^+TCNQ^-, and TMB^+TCNQ^-, triplet exciton dipolar splitting tensors rel. to mag. susceptibility 77−62839
TCNQ salts, simple, triplet exciton obs. by ESR 78−10373
TCNQ salts, spin density distribs., estimation from EPR fine struct. and cryst. data 79−11347
p-terphenyl, cryst., highly excited states decay, mag. field effects 78−10962
p-terphenyl, triplet exciton annihilation and triplet spin relax. 80−29792
p-terphenyl, vap., electron energy loss spectra rel. to lasing 78−29947
p-terphenyl in benzene, triplet state resonance Raman spectroscopy 79−6944
tetracene:pentacene, thermally activated heterofission, fluoresc. 77−85787
tetracene, cryst., prompt fluoresc., mag. field depend. 77−85788
tetracene, cryst., triplet exciton pair kinematics, diffusion model, prompt fluoresc. decay 78−79931
tetracene, cryst., triplet exciton pairs, EPR spectra 77−43906
tetracene, fluoresc. fading curve of lowest triplet state 79−36691
tetracene, theory of fission of singlet Frenkel exciton into two localised triplet excitons 79−23901
tetracene, triplet exciton diffusion and double photon absorpt., delayed fluoresc. obs. 77−36287
tetracene/aq. electrolyte contact, illuminated, space charge behaviour 78−84290
2,3,4,4-tetrachloro-1-keto-1,4-dihydronaphthalene, photochromic single cryst., triplet photochem. 79−39164
1,2,4,5-tetrachlorobenzene, excited triplet state dimer, intermol. exchange integral, isotope effect 80−15826
triplet state continued
1,2,4,5-tetrachlorobenzene, exciton migration and trapping, X-trap phosphoresc. 79−1780
1,2,4,5-tetrachlorobenzene, exciton states in crystals and dimers 80−70620
1,2,4,5-tetrachlorobenzene, impurity induced states, spin dephasing, spin coherence expts. 78−84498
1,2,4,5-tetrachlorobenzene, in durene host, phosphoresc., cross-relax. between spin levels 78−9186
1,2,4,5-tetrachlorobenzene, mol. solid, heat pulses, phonon-induced delocalisation of trapped excited triplet states 80−89053
1,2,4,5-tetrachlorobenzene, proton spin relaxation by optically excited triplet states 79−19810
tetrachlorobenzene, pure and doped crysts., triplet exciton trapping, phosphoresc. spectra 77−85766
1,2,4,5-tetrachlorobenzene, triplet energy transfer in substitutionally disordered system 79−52000
tetrachlorobenzene, triplet exciton spectral line shape, 2-45K 78−19498
1,2,4,5-tetrachlorobenzene, triplet excitons, ESR and ODMR 78−43681
1,2,4,5 tetrachlorobenzene, triplet excitons, high. mag. field, spin-lattice relax. study 80−20517
1,2,4,5-tetrachlorobenzene, triplet excitons, zero field ODMR 80−88891
1,2,4,5-tetrachlorobenzene, triplet state spin-lattice relax. in cryst. and matrix isolated mol. 79−11449
tetramethyl pyrazine in durene, phosphorescent mols., quantum beats in triplet states 80−58312
tetramethylphenylenediamine chlorate, EPR investig. of exchange interaction 77−40114
tetramethylpyrazine-d_{12}, in durene matrix, intersystem crossing of 859.5 MHz transition 79−27015
tetramethylpyrazine-d_{12}, photoexcited triplet state, in durene, phosphoresc., spin coherence and quantum beats 78−76517
tetramethylpyrazine-d_{12}, photoexcited triplet state, phosphoresc., quantum beats 77−71827
thieno(3,2-b)thiophene, electronic and vibr. spectra, vapour phase and cryst. 77−34654
thioindigo, cis⇌trans isomerisation, nanosecond flash photolysis and steady state methods, triplet state 78−35648
thioindigo dyes, triplet state config., laser flash absorpt. spectrosc. obs. 80−5557
thionine triplet+haloanilines, electron transfer reaction, radical yield meas. 80−3330
thionine-monohaloaniline triplet exciplex, quenching position dependent heavy atom effect, intersystem crossing 78−53197
thiophosgene, triplet state, detected by electron energy-loss spectra 78−78808
thiourea, ground and first excited triplet state configs., ab initio SCF calcs. 79−89597
time-resolved, opto-acoustic spectroscopy, nonradiative yields and rate consts. 78−58052
$[TMPD^+]_2[Cu_xNi_{1-x}(mnt)_2]$, ESR obs. of triplet excitons and Cu(II) ions, mag. interactions 79−95633
TOPOT, 1,4-bi[2-(5-p-tolyloxazolyl)]benzene laser, bleaching of vapour 80−19027
s-triazine, triplet instability, RPA calculations 80−27938
2,4,5-trimethylbenzaldehyde, durene host, dipole moments in lowest electronic states 77−18954
N-trimethylborazine, triplet state, ICR trapped electron spectra obs. 79−6884
trimethylenemethane, ground state triplet, HFS, EPR obs. 80−50188
triphenylene, trapped in n-heptane single cryst., ESR and orientation *(French)* 78−91928
triphenylene, triplet state, MIDP and T-S excitation spectrosc. 79−81233
triphenylene(-d_{12}), lowest $T_1[^3A_2'(\pi\pi^*)]$ state vibronic coupling 80−47955
triphenylene-d_{12}, in ethanol soln., external heavy atom effect on triplet state, phosphorescence meas. 79−18231
triphenylmethylphosphonium-TCNQ, paramag. echo from triplet excitons obs. 77−28130
triplet exciplexes, rapid rot., spin-selective depopulation of sublevels, heavy atom-induced mag. field effect 80−95552
triplet exciton annihilation rate, magnetic field depend. effect of spin-lattice relaxation 80−65459
tryptophan, laser flash spectroscopy in presence of nitroxide radicals, protein-membrane interaction probing 79−87855
tryptophan, triplet state, zero-field splittings, wavelength depend. 78−43680
two-level atomic system, triplet state with separated side-bands 79−49981
uranine, intercombination conversion rate consts. from triplet quenching by 1,4-diphenylbutadiene 79−956
vanadates, closed-shell tetroxo-complex triplet levels, luminesc. meas. 79−69874
N-vinylcarbazole-1-vinylnaphthalene copolymer, triplet-triplet annihilation carrier photocurrent, delay fluoresc. 78−2513
xanthene dyes, internal heavy atom effect on radiative and non-radiative rate consts. 80−32765
xanthene dyes, phosphoresc. spectra of T_1 state in ethyl alcohol soln. 79−85981
xanthene dyes, phosphorescence and orbital nature of triplet state *(Russian)* 77−85797
xanthione, large zero-field splitting of lowest triplet state 80−58171
xanthione, optically detected mag. reson. study of lowest excited triplet state of aromatic thioketones 78−86901
xanthione, solns., triplet state quenching by ground state xanthione 78−42180
xanthone in host crysts., triplet state PMDR, phosphoresc. spectra, transition mechanisms 77−46585
xanthone in n-hexane, 77 and 4.2K, phosphoresc. spectra, triplet lifetime 78−21957
p-xylene, isotopically mixed cryst., phosphoresc. triplet state, ESR and MIDP obs. 77−58071
xylenes, fluoresc. and triplet state quantum yields, biacetyl method 78−37671
ytterbium etiophorphyrin, electronic energy transfer with porphines and metalloporphyrins, luminesc. 77−474
zinc chlorophyll b, triplet state population at 4.2K, magnetic field effects 77−30915
zinc porphin, ESR study of metastable triplet state, in n-octane matrix, 1.3K 79−72340

triplet state continued
zinc porphin in n-octane, population hole-burning using triplet reservoir 79−87491
zinc pyrochlorophyllide in nematic liquid crystals, oriented photoexcited triplets, EPR study 80−84636
$(\mu p)_{1S}$ muonic atoms in gaseous H, triplet state lifetime 80−23579
$\mu p + p$, elastic scattering cross section of muonic H atoms 80−69278
Ag complexes, Ag(II) porphyrins, picosec. flash photolysis, transient absorpt. 80−52976
Ag halide, EPR of triplet state of self-trapped excitons 78−43684
AgBr, Bose-Einstein condensation of triplet excitons 77−44057
AgBr, decay of proposed Bose-Einstein condensed excitons 78−15221
AgBr, luminesc. band shape of free excitons, at high exciton density, calc. 77−81148
AgBr, new shoulder in luminesc. spectra, triplet excitons 80−20706
AgBr, radiative recomb. of indirect excitons at high concs. 78−6732
AgBr, shoulder in luminesc. spectra due to triplet excitons 79−15525
$AgNa(NO_2)_2$, triplet absorpt. polarised spectra, near ferroelec. phase transition 79−47473
AlH, (1,1)-band emission of $b^3\Sigma$-$a^3\Pi$ system 78−42092
α-Al_2O_3, additively coloured single crystal, luminescence *(Russian)* 80−55169
Ar, excitation by pulsed electric discharge, luminescence obs., time resolved spectra meas. 80−102482
Ar, liquid, triplet state of self-trapped exciton states, evidence of existence, luminescence meas. 78−72608
Ar, liquid and solid, absorpt. and luminesc. spectra of self-trapped excitons 79−65893
$Ar(^3P_{0,2}) + H(^2S)$, energy transfer collisions, Lyman-α emission profile obs., in microwave discharge and reaction cell 80−58359
$B^+(^3P_u) + D_2$, reactive scatt., 1-40 eV, ion products ang. and energy distrib. 79−98214
BaO, lowest triplet state, photoluminesc. optical-optical double reson. obs. 79−68254
Be, excitation energies and transition moments in a second order polarization propagator approach 79−10051
C_3, matrix isolated, vibr. relax. 78−66637
$CF_2(^3B_1)$ triplet-triplet annihilation, CF_2, $CF_2(^1B_1)$ energy distrib. 80−50861
CH_2, photoprod. from ketene, singlet-triplet energy separation and rovibronic level obs. 80−11936
C_2N_2, triplet state electronic energy delocalisation 77−3478
CO, $A^1\Pi(v'=1)$, vibr. relax. by reversible intersystem crossing, fluoresc. obs. 80−14170
CO, $b^3\Sigma^+$ state excitation, low-energy electron impact, $v'=3$ level lifetime 80−1072
CO, form. from spin transfer reaction with Ar *(French)* 79−34289
CO, triplet state electronic energy delocalisation 77−3478
CO_2 lowest triplet state, Ar matrix isolation spectra 80−91569
$C(^3P) + O_2(^3\Sigma_g^-) \rightarrow CO(^3\Sigma^+) + O(^1D)$, pot. energy surface, vibr. population inversion, classical dynamics 77−52630
CS, spin-orbit and spin-spin parameter calcs. 77−27044
CS_2, $^3A_2$ state, triplet bands, MCD spectrum, near UV absorpt. spectrum 80−48010
CaF_2:PrF_3, EPR of cubic Pr^{3+} 79−28607
CaO, ODMR and spin coherences in phosphorescent state of exchange-coupled F^+-centre pairs 79−87336
CaO, triplet state of F_A centres, ODMR obs. 79−28639
CaO:V^{3+} orbital triplet, intermediate Jahn-Teller effect, APR 80−34758
$C_2(a^3\Pi_u)$ + methane(acetylene)(ethylene)(ethane)(O_2), reaction rate consts. and quenching, multiphoton UV photolysis, fluoresc. obs. 79−74355
Cd, triplet states, hyperfine struct. obs., project expt. 77−33737
$Cd + N_2$, vap., creation of inverse population of atomic Cd 6^3S and 5^3P_2 levels 80−58219
$Cd(^3P_{0,1}) + CO(CO_2)(NO)$, absolute quenching cross section, phase-shift method 80−58340
$Cd(^3P_1)$ radiation imprisonment lifetime, inert gas effect, phase-shift method 80−58213
$Cd(^3P_1) + H_2(HD)(D_2)$ react., CdH(CdD) yields, quenching cross sections 79−1948
CdS, spatial diffusion of excitons under intense excitation 77−44061
CdTe:Ti^{2+}, Jahn-Teller effect on $^3T_1(^3F)$ state, resonance on $^3T_1(^3P)$ state 78−27271
$Cd(5^3P_{0,1}) +$ methane $(H_2)(D_2)(N_2)$, absolute quenching cross sections 80−5604
Cl_2CS, excitation, singlet and triplet states, two photon absorpt., singlet-singlet energy pooling, fluoresc. obs. 80−48032
Cs_2, $\tilde{a}^3A_2$-state detect. by reson. enhanced multiphoton ionis. spectrosc. 80−95551
Cs_2, dimer and higher polymer IR absorpt. bands, triplet state 80−63629
CsI, self-trapped exciton electronic struct., semi-empirical mol. orbital method 80−49605
CsI:Na, self-trapped exciton emission polarisation 80−49607
Cs_2MX_6(M=Se, Te, X=Cl, Br), $\Gamma_4^-(^3T_{1u})$ state, Jahn-Teller effect, luminesc. obs. 80−60650
Cu complex, bis(triphenylphosphine) phenanthroline copper (I), luminesc. spectra, decay times 80−60648
Cu complex, Cu(II) dimers. temp. depend. PMR relax., singlet-triplet separation determ. 80−43073
Cu complexes, spin coupled ion pair, singlet-triplet splitting 77−85552
CuBr, 1S exciton triplet state, magneto-optical props. 80−25345
D_2, $G(3d)^1\Sigma_g^+$ and $g(3d)^3\Sigma_g^+$ singlet-triplet anticrossing 78−42138
1,6-di-(N-carbazolyl)-2,4 hexadiin, cryst. struct., luminesc., γ-ray polymerisation 78−18629
9,10-dichloroanthracene, mag. field effect on exciton processes and photodetrapping 77−4668
EuO:Eu, paramag. triplet state, mag. susceptibility 77−72820
$F^+ + H_2$, empirical and ab initio correlation diagrams, pot. energy surfaces 78−40041
F_2CS, pot. surfaces, X^1A_1, a^3A_2 and $a^3A_2(b_1)$ states, ab initio SCF calcs. 78−86795
GaP:O^-, two-electron O state evidence, ODMR, IR emission, phonon replicas 80−15828
GaS, optical detection of triplet excitons 80−29650
GaSe excitonic spectra fine struct., reflection and transmission spectra *(Russian)* 80−55126
GaSe, magnetoluminesc. at 4.2K 79−61345
GaSe, optical detection of triplet exciton reson. 79−33567
GaSe, triplet excitons ODMR 80−25252
triplet state continued
GaSe, triplet indirect bound exciton, level anticrossing effect on magnetolum. 79−47513
GaSe, type II crysts., triplet exciton resonances 79−47359
Ge:As, far IR transmission spectra, singlet-triplet optical transitions in ground states of donors 78−2887
H^-, bound states in mag. field, binding anal., variational calcs. 80−42940
H_2, $^1\pi_u$ and $^3\pi_u$ states, singlet-triplet energy difference, Hund's rule, inequality formulation 78−66482
H_2, $^3\Sigma_g^+$ state, improved adiabatic energy, dissoc. energy 79−10011
H_2, 3d-triplet complex, Zeeman effect, eigenvectors and g-factors, rovibronic states 79−72353
H_2 3s, 3d: $^3\Sigma$, $^3\Pi$, $^3\Delta$ complex, fine struct., Doppler-free laser spectroscopy 80−1087
H_2, lowest singlet and triplet states, interactions, electronic force calcs. 80−63742
H_2, triplet state, molecular polarisability, ab initio calcs. 80−63860
H_2, triplet state, pot. curve van der Waals region, MS-MA calcs. 77−79551
H_2, triplet state, screening and susceptibility 79−41117
H_3, interat. pot. energy matrix elements, generalised DIM calc., ZDO approx. 80−52864
H_3, dissociating states, lowest singlet and triplet PE surfaces, HF calcs. 79−81160
H_4 excimer, electronic and geom. struct., ab initio CI calc. 79−76348
H_4, triplet state, instability of restricted Hartree-Fock, orbital degeneracy 78−25457
HCN, intravalence triplet-triplet electronic transition, geometrical struct. and rel. energies determ. 80−99586
H_2O, mol. Rydberg $S \leftarrow S$ and $S \leftarrow T$ transitions, semi-empirical SCF MO calc. 80−91453
H_2O^- in γ-irrad. Y-type zeolite, alternative EPR triplet assignment to NO_3^{2-} 78−11534
H_2O^-, trapped in γ-irrad., Y-type zeolites, ESR obs. 77−9099
H_2S, valence and Rydberg excited states, SCF-Xα-SW mol. oribtal study 79−36550
$H_2^* + H_2$, depolarisation cross-section of (1s 3p) $^3\Pi_u$ (N=1) level 77−61829
He, 1s3d config., Zeeman sublevel energies, anticrossing and degeneracy 77−23417
He, 2S metastable states, singlet and triplet; two and three photon ionisation cross section, absolute determ. 80−83329
He, bound states in mag. field, binding anal., variational calcs. 80−42940
He, elastic electron scatt. phaseshifts, 2s2p ^3P autoionisation, 1s2s $^3S \rightarrow$ 1sep ^3P triplet continuum photoionisation 79−31480
He, fine structure, 2nd order contribs. from all intermediate states 79−3354
He I, fine struct. of triplet term of 1s3d config. 79−3595
He I, triplet state, excitation energy transfer among upper levels 79−26901
He like atoms, dipole transitions, transition integral cancellation 80−69052
He, triplet P state splittings, higher order corrections of theoretical calc., book contrib. 78−82632
He triplet states, doubly excited, spectrum and polarisation 80−99472
He-Cd hollow cathode laser, He singlet and triplet metastable number densities 78−29938
He-like ions, triplet-state, electron impact excitation cross sections obtained by Coulomb Ochkur Rudge approx. 80−102576
He+He, Rydberg states ang. momentum transfer, singlet-triplet anticrossing 77−88543
$He + He^+$, triplet excitation cross-section, Ochkur-Rudge approx. calcs. 80−28101
$He^+ +$ Ne, 10-150 keV, Rydberg-state total cross section, oscillatory behaviour 77−83716
He_2, spectra, struct., triplet states, $4p\pi$, $5p\pi$ UAO's 77−34647
HeH^+, spectroscopic characts. in ground and first excited triplet states, Dunham pot. approach 77−42234
HeH^+, triplet Σ, Π and Δ states, config. interactions 78−78633
$^3He(^4He)$ clusters, metastable electronic states, electron impact excitation, time of flight spectra 80−106411
^4He, 3p ^3P state alignment and orientation as function of foil tilt angle, quantum heat spectra 79−94071
He*, collisional transfer rates between excited levels 79−22793
He*(1s2s,^{3}S) + Ar, Penning ionis., discrete-continuum states coupling 79−10193
$He_2(1\sigma_g)^2(1\sigma_u)np\lambda$ triplet levels, multichannel quantum defect anal. 80−91542
He(2^1S, 2^3S), threshold to 0.10 eV, energy-integrated total cross section ratio 80−37885
He(2^1S,2^3S) + Ne(Ar)(Kr)(Xe), Van der Waals forces, one-electron model pot. calcs. 80−14094
He(2^3S,2^1S) + H, Penning ions. 79−64089
He($2^{1,3}$S), inelastic scatt., RPA and 1st Born approx. calcs. 80−53148
He(2^3S), electron impact ionis. to 1s, 2s, and 2p state, autoionis. 80−1068
He(2^3S) + H(D), Penning and assoc. ionis. cross sections, vel. depend. 79−22815
He(2^3S_1) in alkali-He quantum magnetometer 80−17965
He(2^3S_1) + Ca(Sr)(Ba), coherent $^2P_{3/2}$ levels excitation by Penning ionis., Hanle effect 80−5520
He(2^3S and 2^1S) + $H_2(D_2)$, Penning, rearrangement and total ionis. cross sections, vel. depend. 79−22816
He($2s^3S_1$) + Sr, alignment of ions in Penning collisions, polarised emission obs. 80−23533
He(3^3P) electron beam-excitation 80−43188
He(3^3S) decay rates in high-press. afterglow 79−41898
He(3^3S)(3^3P)(3^3D) + He(1^1S), deactivation rate, 300-600K, time-resolved spectra 77−19037
$Hg(6^3P_1)$, slow electron scatt. stepwise excitation function to 6^3P_2 state 79−858
I_2, $(B^3\pi_{0+u})$, dissoc. reaction, computer simulation 78−48639
$ICl(A^3\Pi_1)$, zero-press. lifetimes, fluoresc. quenching 79−68266
KBr, F_2 centres triplet state, radiative and nonradiative decay 79−11438
KBr, spectral distrib. of triplet to singlet luminesc. of F_2 centre 77−59601
KBr:Br_2^-, triplet luminesc. kinetics, 0.4-4.2K 79−87482
KBr:PO_2^-, phosphorescence, triplet state sublevels, mixing 80−25446

triplet state continued
KBr(Cl)PO_2^-, spin-lattice relax. in triplet state of PO_2^- centres, pulsed photoexcitation 79−95644
KCl, F_2-centre triplet-triplet transition at 685 nm, MCD obs. *(French)* 77−63433
KCl, F-centre formation at highly excited triplet states of self-trapped excitons 80−76066
KCl, perturbed M-centre triplet state, M-F centre exchange mechanisms 79−69884
KCl, self-trapped exciton luminesc. 77−48225
KCl, spectral distrib. of triplet to singlet luminesc. of F_2 centre 77−59601
KCl, Z_2 centres in triplet state, EPR study 80−108068
KCl:Ca, Z_2-centres, optical absorpt. and ESR spectra 79−91480
KCl:PO_2^-, phosphoresc. and PMDR spectra, electronic and vibr. states 79−65768
KCl:PO_2^-, triplet state pseudonuclear Zeeman effect, optical detections *(Russian)* 79−78571
KCl:PO_2^-, triplet state, level anticrossing and pseudonuclear Zeeman effect, microwave ODIMR 80−39896
KCl:Sr, triplet state of F_2-centres, ESR spectra 80−29616
KCl:Yb, Z_2-centres, optical absorpt. and ESR spectra 79−91481
KCl(Br), triplet state lifetime of F_2 centre, mag. field effect 78−35177
KCl(Br)(I), electronic struct. of self-trapped excitons calc. 77−39784
$K_2Cr_2O_7$, closed-shell tetroxo-complex triplet levels, luminesc. meas. 79−69874
KF, self-trapped exciton, ODMR spectra 79−28286
KI, spectral distrib. of triplet to singlet luminesc. of F_2 centre 77−59601
KI:I_2^-, triplet luminesc. kinetics, 0.4-4.2K 79−87482
KI:Tl, phosphor, press. effect on emission spectra at low temps. 77−85771
KI:Tl^+ type phosphor, press. effects on triplet relaxed excited states, quadratic Jahn-Teller interaction 78−23510
$KMgF_3:Fe^{2+}$, Jahn-Teller quenched spin-orbit, splitting of $^5T_{2g}$ state 77−63442
Kr, liquid, triplet state of self-trapped exciton states, evidence of existence, luminescence meas. 78−72608
Kr, liquid and solid, absorpt. and luminesc. spectra of self-trapped excitons 79−65893
$Kr(^3P_2)+F_2(NF_3)(CF_3OF)$, KrF* bound-free oscill. emission spectra calc. 80−7799
$LaPd_3$, Γ_5 and Γ_2, states at Pr^{3+} site, creation by cryst. field 79−28547
Li^+, ^2P and ^2S states, fine (hyperfine) struct., dye laser saturation spectroscopy, beam expt. 80−58169
Li_2, pot. energy surface, half-projected HF model 79−36564
Li_2, second virial coeffs., Konowalow MCSCF potential calcs. 80−23312
Li_2, spectroscopy and structure, triplet excimer continuum emission 80−32769
Li_2, triplet absorpt. bands, 6215-5875 Å, after two-photon excitation 79−50035
Li_2Cl^+, triplet polarisability, ab initio MO calc. 79−98244
LiF, self-trapped exciton, ODMR spectra 79−28286
$Li^+(2^3P)$, electron impact excitation, absolute 548.5 nm emission cross-section 79−10209
Mg, hollow cathode discharge, excitation mechanisms of triplet state atoms and decay obs. 80−44015
Mg porphyrins, additional ligands deuteration effect on luminesc. charcts. 79−99932
Mo complex, μ-oxo bridged oxomolybdenum(V) dimers, conform. anal. by ang. overlap method, triplet ground states 78−5119
N_2 ($C\ ^3\Pi_u$) vibr. levels radiative lifetime, transition moment internucl. distance depend. 78−1027
N_2, $B'^3\Sigma_u^- \rightarrow B^3\Pi_g$ (0,0) emission band 78−58690
N_2, diffuse plasma, population densities of triplet states, correl. with electron impact processes 80−43966
N_2, energy levels, low lying triplet states, infrared emission analysis 78−58691
N_2, solid, self-localisation of high frequency triplet excitations *(Russian)* 79−8176
N_2, solid and matrix isolated mol., triplet state spectra *(Russian)* 80−5574
N_2, triplet state electronic energy delocalisation 77−3478
N_2 triplet-triplet transitions, Einstein-A coeffs., oscill. strengths, lifetimes, theory and experiment comparison 80−47876
N_2+Ar, triplet state excitation *(French)* 77−83704
N_3^-, low-lying excited states 79−31425
$N_2(A^3\Sigma_u^+, v_i)+N(^4S) \rightarrow N(^2P \text{ or } ^2D)+N_2(X^1\Sigma_g^+, v_f)$, energy partitioning 78−66636
NH_2^+, triplet state ab inito CI pot. energy surfaces 78−74729
NH_3, first triplet state, photodissoc. and Rydbergisation investig. 80−53067
NH_3 low lying states, generalised VB and CI calcs., vertical excitation energies 77−30789
NH_3, lowest triplet excitation, electron energy loss spectra 77−71880
NH_3, lowest triplet state geometry, SCF and CEPA-PNO calc. 80−914
NH_3, mol. Rydberg S←S and S←T transitions, semi-empirical SCF MO calc. 80−91453
NH_3+2H_2, triplet n3S Rydberg state, ab initio UHF CI SCF calc. 80−53095
$NH(A^3\Pi, b^1\Sigma)$, two-photon generation in NH_3 UV laser photodissoc. 80−11901
NO_2^-, heavy cation effect on singlet-triplet intercombination 79−85946
NO_2^-, microwave transition probability in zero field, spin-orbit interaction 78−25518
NO_2^- triplet state lifetimes and fine structs., CNDO-CI calcs. 77−57897
NO_3^-, triplet state lifetimes and fine structs., CNDO-CI calcs. 77−57897
NO_3^{2-}, in γ-irrad. Y-type zeolite, EPR triplet assignment, instead of H_2O^- 78−11534
Na_2, spectroscopy and structure, triplet excimer continuum emission 80−32769
Na_2, triplet satellite band obs. in self-broadened D-line very far blue wing 80−95688
NaBr(:I), exciton ionisation and decay, photoluminesc. in elec. field 77−44046
NaBr(I), optically activated F→F′ centre conversion in mag. field 80−108253
NaCl, luminesc. singlet from triplet self-trapped excitons 79−99936
NaCl, search for IR absorption by triplet self-trapped excitons 78−56473
NaF, self-trapped exciton, ODMR spectra 79−28286
NaK dimer formed in supersonic beam, laser-induced emission 80−9636
$NaNO_2$, cryst., delayed fluoresc., triplet excitons, dopant effects 78−10963
$NaNO_2$, cryst., Stark shift of visible absorpt. of NO_2^- 78−19499
$NaNO_2$, cryst., triplet excitons, localised states, zero-field ODMR, dopant effects 78−15062
$NaNO_2$, phonon side bands of triplet absorption 78−76488
$NaNO_3$, pure cryst., NO_3^- singlet-triplet absorption, Stark effect obs. 79−8153
Ne ($^3P_2$) metastable state decay in Townsend discharge afterglow 80−44011
Ne I to Ne IV, excitation in ion-atom collisions, 100 keV region, emission spectra obs. 80−14205
Ne, liquid and solid, absorpt. and luminesc. spectra of self-trapped excitons 79−65893
Ne, metastable electronic states, electron impact excitation, time of flight spectra 80−106411
Ne^++He, 10-150 keV, Rydberg-state total cross section, oscillatory behaviour 77−83716
$Ne(^3P_{0,2})$+Ne, differential cross sections 80−58370
$Ne(^3P_2)$ elastically scattered, metastable, ang. distrib., conventional rel. to Doppler shift methods 80−58418
$Ne^{2+}(2s2p^5\ ^1P,^3P)$, singlet/triplet population ratio, in 100 keV ion impact excitation, ion Z depend. 78−37733
O+H_2, trajectory calcs., fitted ab initio pot. energy surface 79−74358
O_3, approximate spin extended HF calcs., singlet and triplet states 78−78621
$O_2{}^1\Delta_g$, singlet and triplet precursors of photosensitised addition to organic acceptor 79−52714
$O(^3P,^1D)+H_2(^1\Sigma_g^+) \rightarrow H_2O$, potential energy surfaces, extended basis first-order CI study 80−7776
$O(^3P)$ translationally hot, energy distrib. function 80−21811
$O(^3P)$+benzene (toluene), absolute reaction rate consts., 299-440K 79−70304
$O_2(^3\Sigma^-)$, geometry optimisation, using bond function augmented basis sets 78−905
Pd, phonon mediated interaction for triplet pouring 79−23911
Pd, triplet pairing, spin fluctuation contrib. 78−10711
$PrPd_3$, Γ_5 and Γ_2 states at Pr^{3+} site, creation by cryst. field 79−28547
PrSb, mag. excitations, press. depend., inelastic neutron scatt. meas. 78−10699
Pt porphin in n-alkane single cryst. ^3E_u-$^1A_{1g}$ transition, Zeeman expts. at 4.2K 80−78645
$RbMnF_3$, triplet states, piezospectroscopy 79−38562
rhodamine 6Zh, quantum efficiency of intercombination conversion to triplet state by sensitised phosphoresc. *(Russian)* 77−85798
Ru complex, electrogenerated chemiluminesc., production of excited states by direct heterogeneous electron transfer 79−20371
Ru complex, ruthenium(II) tris(2,2′-bipyridine), absorption spectrum and quantum yield of formation *(French)* 80−5554
S_2, matrix-isolated, $B^3\Sigma_u^-$ predissoc., relax. processes 80−58329
S_2N_2, $(SN)_x$, (x=2 or 3), minimal STO-3G basis HF ab initio LCAO SCF MOC, geometry 78−903
S_2N_2, polymerisation, mol. struct., INDO calcs. 77−70301
SO, and isotopic forms, $X^3\Sigma^-$ state, CO_2 laser mag. reson. spectroscopy 80−9602
$S^{16}O_2$,$S^{18}O_2$, (0,0) band rot. anal., a^3B_1 state electron spin fine struct. consts. 77−10687
SO_2 ($^3B_1$), phosphorescent lifetimes, press. saturation effect on quenching by CO_2, CO, N_2 78−1017
SO_2, triplet state electronic energy delocalisation 77−3478
SO_2, UV absorpt. spectrum, triplet states, phosphoresc. lifetime 79−50042
Si:Al, bound-exciton absorption 78−56507
Si:Cr, spin-lattice relax. of Jahn-Teller Cr^0 centre *(Russian)* 78−72402
Si:Ga, bound-exciton absorption 78−56507
Si:In, bound-exciton absorption 78−56507
SiO emission, $A^1\Pi$, $b^3\Pi$ and $a^3\Sigma$ states, Si+N_2O flame chemiluminesc. 77−77767
Sr atomic beam, time correlations between two sidebands of reson. fluoresc. triplet, multiphoton processes 80−95570
$TiF_2(TiF_3)$, ESR spectra in rare-gas matrices at 4K 77−88474
TiO, $C^3\Delta$ term anomalous triplet splitting 78−13514
$Ti(y\ ^3D_2{}^0)$ lifetime, in rel. oscill. strengths determ. by combined absorption/emission meas. 80−37784
Xe ($^3P_1$), in afterglow 80−38742
Xe, liquid, triplet state of self-trapped exciton states, evidence of existence, luminescence meas. 78−72608
$Xe(6s,^3P_2)+Cl_2(PCl_3)(CCl_4)(COCl_2)$, vibr. energy disposal from XCl* spectrum 79−100345
$Xe(6s,^3P_2)+RCl$, reactive quenching, XCl* emission spectrum obs. 79−100344
YF, $^3\Phi-^3\Delta$ system, rot. anal. 78−9149
YH, YD, 3800-9000 Å negative glow spectra, triplet and singlet systems 77−79608
Yb, highly excited levels, odd and even parity spectra, multichannel quantum defect anal. 80−58133
Zn complexes, pheophytins a and b, dual phosphorescence molecular splitting 79−89706
Zn etioporphyrin, excited triplet states absolute rate consts., ODMR meas. 78−33533
Zn, triplet state lifetimes, (4s6s), (4s5d), (4s6d) configs. *(French)* 78−5175
Zn-porphin($-d_4,d_8,d_{12}$), nonradiative transition probabilities, deuteration effects 79−3485
Zn-tetraphenylporphine/metal electrode, photocurrent generation mechanism 78−76868
ZnO electrode, role of triplet states in xanthene dye sensitisation 78−76869
ZnS:Cu^{2+}, motional averaging in excited state 77−66137

tritium
activity meas., in exhaust gases from nuclear power stations *(German)* 77 25322
adsorbed on Ni sheet determ. by autoradiography 77−63989
adsorption by type 304 stainless steel container, surface treatment effects 77−59984
air contamination monitoring using centralized control *(French)* 80−63407

tritium continued
airborne short-lived radionuclides of unknown origin in Sweden (1976) 78−32219
amino acid sequence determination of proteins labeled in tritium gas by microwave discharge 79−12057
aqueous tritiated waste management from fuel reprocessing 80−5272
assay, liq. scintillation counting, use of Aquasol in plastic Mini-Vials 77−26934
N.Atlantic Ocean, deep western boundary current core, ^3H conc. obs. 80−101380
atom, hyperfine quadratic shift in electric field, pressure dependence 78−13442
behaviour in advanced nuclear fuel systems 80−18633
behaviour in pebble bed reactors, numerical calc. *(German)* 80−9387
biological effects, mouse liver chromosomes, effect of continuous intake of HTO 77−25518
breeding costs in critical fission reactor 78−58456
breeding fusion blanket with boiling water coolant 80−99274
breeding in TFTR, tritium breeding test blanket module design 80−99304
breeding performance of Tokamak blankets, comparative eval. of Li, Li_2O, Li_7Pb_2 80−95398
breeding ratio maximisation by geometric programming 79−9879
buildup in D_2O of CANDU reactors, due to $^3He(n,p)^3H$ reaction 79−22389
CANDU, energy, water, tritium budgets for Perch Lake 1975 78−29563
CANDU heavy water reactors, storage and monitoring of tritium 80−5291
Caspian Sea, T content 79−34858
cells exposed to HTO, T distrib. obs. 80−72142
chemical behavior associated with tritium decay *(Japanese)* 79−20452
cholesterol, T-labelled, prod. by catalysed exchange with T_2 *(German)* 77−90599
concentration and distrib. in N.Atlantic surface water 78−65345
concentration in atmospheric precip., rivers, and seas, USSR 79−74560
concentration in water, meas. with electrolytic enrichment cell and reduction systems 78−20128
concentration meas., scintillation detector appl., bremsstrahlung from β-rays 78−55042
concentration meas. by portable gas radiometer 80−32570
control by glove box containment at fusion reactor plant 78−46169
control strategies in PWRs, cost effectiveness 77−38360
counting efficiencies and sample time stabilities in a Triton X-100/toluene scintillant 80−52813
cryogenic data relevant to mag. fusion energy 80−8746
CTR blanket model with graphite reflector, tritium prod. anal. 77−61609
CTR Monsanto-Mound Laboratory eng. development of T handling systems 77−50295
cyclic purging for low-temperature solid fusion reactor blanket operation 79−59256
D-T filled cryogenic spherical shell targets, laser implosion 77−74977
dating using cyclotron as mass spectrometer 77−64489
decay in solid H_2 matrix to produce H atoms 77−29028
depth profile in Ti film from gas emission during sputtering by Ar ions 77−35581
detection, absolute efficiency of phosphate glass channel electron multiplier 77−67945
detection in gases and liquids, state of art *(Czech)* 77−86403
determination in biological and botanical samples, field instrument 77−9306
determination in organic cpds. and biological samples by combustion method with isotope exchange 79−57333
deuterium-tritium thermonuclear ignition, high current density approach, expt. 78−54874
diffusion coeff. in Zr foil 80−15306
diffusion coefficients in pyrolytic C 80−37443
diffusion in Al_2O_3 and BeO 77−55391
diffusion in BCC metals, phonon-assisted quantum-mechanical tunnelling of interstitials 80−59730
diffusion in niobium 78−6182
diffusion in Pd-Pt (Cu), effect on freq. factor and activation energy 78−63880
diffusion in reactor graphite *(German)* 77−24442
diffusion in SiC, exam. of coeffs. 78−79816
diffusion in TiO_2, Raman scatt. meas. 79−86927
diffusion in Zircaloy-2 80−32341
distribution, Ross Ice Shelf Project ice hole 79−88371
distribution in glycogen, haemoglobin and chromatin of mice drinking tritiated water 78−31910
distribution in irrad. UO_2 pellets, radiochem. anal. *(German)* 77−16880
distribution in Weddell Sea water masses 79−39728
DT self-propelling pellets for fusion-reactor refueling 79−677
E. coli, damage induced by T decay, secondary lethality under nongrowth conditions 80−104654
electrolytic enrichment in environmental samples, using controlled power supply 78−21173
electromigration effective charge for ^3H in Zr and Ti, H conc. depend. 77−51545
electromigration in Ti, temp. depend. of effective electromigration charge 79−90826
enrichment in water by electrolysis for low-level T activity meas. 78−17536
environmental analysis by mass spectrometric meas. of ^3He 77−9447
environmental concentration, meas. using gas-filled proportional counters 78−86699
environmental control of use and release at TFTR 80−13829
environmental levels, detection with liquid scintillation spectrometers 77−9489
environmental transport from atm. release of mol. ^3H 78−11987
equations of state deduced from P-V-T and US meas. of up to 20 kbar 79−23696
fallout in S.Australia rainfall and wine samples 78−11960
fast fission yields of ^{238}U and ^{232}Th, implications for FBRs 77−46195
fluid-wall inertial confinement fusion reactor concept, tritium breeding control 79−85773
formation and elimination in LWRs *(French)* 79−31164
formation by solar flare particles in terrestrial atmosphere 78−92886
freshwater marsh, simulation model of freshwater kinetics 78−24318
fuel handling, safety and control systems for TFTR 78−50364
fuel handling systems, for TNS Tokamak 78−50363

tritium continued
fusion, inertially confined, high thermonucl. gain with low T inventory 78−58403
fusion blanket models, calc. of T breeding per source neutron 79−67934
fusion fuel exchange between fusion hybrid, fission, and T producer reactors 80−13811
fusion power plant, vacuum outer containment, safety, T control and monitoring 78−74498
fusion reactor, D-T to catalysed-D operation, trapped ion scaling law 78−66419
fusion reactor, FINTOR-D, T breeding blanket, Monte Carlo calcs. 80−99283
fusion reactor, limitations on T transport 78−70628
fusion reactor, mirror hybrid type, T handling systems 78−62617
fusion reactor, PLT, fusion-produced T confinement 79−98955
fusion reactor, T_2 valve, pulsed gas feed into Tokamak reactor 78−66412
fusion reactor, T inventory associated with metal-getter recovery systems 77−38415
fusion reactor air detritiation operations, computer modelling and bench-scale testing 79−85784
fusion reactor blanket design, effect of module size on T breeding 80−102295
fusion reactor breeders, models for T_2 and ^4He transport 78−17424
fusion reactor direct-cycle steam generating blanket design 80−37615
fusion reactor fuel streams, impurity removal and recovery processes 79−85783
fusion reactor Li sphere, neutron spectra and T prod. meas. 78−62604
fusion reactor solid breeder blankets for D-T reactors, operating temp. limits for T release and recovery 80−102294
fusion reactor steam generator permeation and content in CTR coolants 77−50293
fusion reactor T breeding, comparative evaluation for Li, LiO_2, Li_7Pb_2 80−13831
fusion reactor T systems test assembly, containment and cleanup technology 78−767
fusion reactor with injection of deuterium and tritium ions, calc. of characts. 78−37447
fusion reactors, air detritiation operation, computer model and scale expt. 78−66413
fusion reactors, scoping studies on T permeation 78−769
fusion reactors, T release control and environmental monitoring *(Japanese)* 79−81078
fusion reactors, UWMAK II and III, T handling breeding and containment 77−6557
fusion research, Lawrence Livermore Laboratory, quality assurance of systems 77−50297
fusion research, T high-pressure equipment 77−50294
fusion-fission Tokamak, T breeding, optimisation with geom. program 78−74477
gas, container prep. effect on growth of protium and methane impurities 80−78436
gas escape, into forest ecosystem, potential radiation dose to man, calcs. 78−96101
gas injection system transient response in TFTR 80−102337
gas target as intense 14 MeV neutron source 77−83429
gaseous effluents from LWR and reprocessing plants, treatment and control 77−61589
gettering from fusion reactors breeder blankets using La binary alloys 79−67946
glass microspheres, T-filled, assay by liquid scintillation counting 80−63481
goose barnacle, effects of tritiated seawater on development 79−66486
graphite, tritium effects, first wall controlled thermonuclear reactor conditions, simulation 79−647
handling facilities in US and Europe *(Japanese)* 79−9895
handling systems for fusion reactors, materials considerations 80−32463
HTGR, T contamination of product gas 80−13590
human intake during various processes in industrial, academic and medical institutions 77−73600
hybrid fusion reactor, Tokamak type, with fissioning matter, blanket parameters 77−34446
hybrid fusion reactors, problems 77−38403
isotope separation by H_2-Pd system, effect of isotopic conc. on separation coeff. of H-T, H-D and D-T mixtures 79−71979
isotope separation in Ti-fluidised bed 80−18676
labelled biologically active compounds obtained using at. ^3H bundles, appls. 80−30888
laser fusion microsphere targets, nondestructive anal. using rot. Raman spectroscopy 80−50896
laser fusion reactor targets, energy partition and neutron spectra 78−58451
levels in urine of occupational exposed persons, working environment effects 79−83947
liquid and solid, collision induced infrared spectra 79−45717
liver, mouse, effects of tritiated water rel. to age 79−43967
LMFBR, computer model for ^3H transport and release 79−36371
LMFBRs, tritium control, sources and removal 79−36335
losses in primary and steam circuits in FINTOR-D, control system 80−18634
low-dose β-ray relative biological effectiveness 80−12190
measurement, in aqueous samples, single solvent cocktail for liq. scintillation counting 78−856
E.Mediterranean Sea, T and O_2 profiles 80−17298
meter for Na coolant systems 79−9690
methane+tritium reaction, reaction ergodography 77−21371
migration from low-level waste burial site 78−21671
molecule, ortho-para transistion, catalytic-, radiation-, and self-induced conversion, review 77−90633
molecule, pure rot. and rot.-vibr. Raman spectrum 78−94253
monitoring at nuclear power stations 80−18691
monitoring methodology using SiO_2 desiccant, appl. to research reactor facility 80−21434
monitoring using scintillation chamber 79−89519
nervous activity monitoring in Drosophila by [^3H]deoxyglucose 80−56024
Norwegian Sea pycnocline, T vertical distrib. rel. to apparent vertical eddy diffusion rates 78−81185
nuclear fusion research, review of T chemistry *(Japanese)* 79−63806
nuclear production complex released, detection and meas. of chem. forms 77−54372

tritium continued
nuclear reactor radioactive gaseous effluents, abatement techniques 79−3221
Pacific Ocean, T transport models source function 78−32122
permeability of heat exchange material, oxide protective layer formation meas. 78−8895
permeation eccentricities of He, Ne, and D-T, from SiO_2-CaO-Na_2O glass microbubbles 78−47598
permeation in high temp. nuclear reactors *(German)* 79−3204
permeation in stainless steel 80−34241
permeation test facility at Julich, safety measures and monitoring 79−36428
permeation through 304 stainless steel at ultra-low press. 79−19402
permeation through Croloy steel for LMFBR steam generator 80−68775
permeation through He heated tube walls in HTR 77−50250
permeation through Incoloy 800 and Sanicro 31 80−88364
permeation through steam generator alloys 80−34250
personnel exposure, rapid evaluation using surface monitor 77−56485
phase composition examination by tritiation system 79−39068
pollution in liquid media and working area air at nuclear power stations 77−71699
pollution in N.Pacific surface water during 1974, conc. meas. 80−26181
production and distrib. in Peach Bottom HTGR 80−47581
production in advanced stellar evolution, reaction cross sections 80−56815
production in fission and fusion reactors 79−71874
production in fission research reactors to fuel CTR expts., feasibility 80−18632
production in toroidal fusion reactor, cross section sensitivity calc. using SENSETWO code 80−835
production meas. in Li metal sphere, using new methods of neutron source strength determ. 78−74470
proportional counters, multielement, anticoincidence techniques for measuring low T activities 80−27874
proteins, ^3H-labelled, fluorography in immunoelectrophoresis 80−17220
PWR, T sources, releases, monitoring, management and environmental impact 80−18690
rabbit tritium obs. after ingestion of contaminated food and water 80−21549
radiation induced exchange reaction kinetics of H_2, D_2 and T_2, review 78−61005
radiation safety in nucl. fuel cycle *(Russian)* 80−56227
radioactive effluent gases from nuclear power industry, ambient contamination *(Spanish)* 78−61540
radioactive fallout at South Pole, 1954-1978 T content of snow 80−16867
radioactive fallout damping coefficients 78−92961
radioactive liquid waste with T contamination, packaging 77−6538
radioactive pollution from nuclear facilities, T population dose in the Northern Hemisphere 80−104779
radioactive target preparation and characterisation 80−18734
radioactive waste, leaching behaviour from hardened cement paste 80−18443
radioactive waste, low-level, radionuclide migration in soil 79−54610
radioactive waste, tritiated, gas generation by autoradiolysis 80−32384
radioactive waste immobilisation, possible solid mats. 80−27755
radioactive waste transport, storage and disposal, characts. of metal tritides 77−54343
rats, T content in organs, and DNA of rat liver cells, after doses of tritiated food, protein or water 80−56226
rats, T radiation dose absorbed in rat organs, after feeding with organically bound T 80−51262
reactor fuel reprocessing liquid waste concentration determ. by vacuum freeze distillation 77−14255
reactor loop, experimental, hazard and protection from tritium 79−36420
reactor waste, removal from air streams of reactors by catalytic oxidation and water adsorption 77−50292
recoil atom reaction with methyl chloride, methyl abstraction to substitution ratio 78−85187
recoil atoms+H_2O, neutron effects, apparent phase effect 77−63935
recoil replacement reactions in alkane systems moderated with inert gases 78−68906
recoil tritium reactions with cis- and trans-1, 2-dichloroethylene 78−3360
recovery from liq. Li blanket by Y 80−95434
recovery from molten Li by Y getters 80−32470
recovery from solid Li-Al and sintered Al product blanket materials 78−58455
reflection from amorphous Be, Fe, Mo, W, Monte Carlo study 80−40197
release behaviour and chem. forms on heating neutron irradiated UO_2(Li) pellets 78−40071
release from nuclear power stations 80−23032
removal from flowing Ar, U and Ce as hydriding materials 78−17438
removal from fusion reactor molten breeder blanket, sorption from K and Li onto Y 78−66411
removal from irradiated UO_2 in fuel reprocessing 77−67850
removal from solid Li compounds in fusion reactor blanket 80−32513
research animals, monitoring of airborne tritium evolution 79−39526
RFPR, T transport in packed bed Li_2O fusion blanket 80−37612
scintillation meas. of T in air using liquid adsorbent 79−76291
seawater, ^3H vertical profile meas. in North Sea *(German)* 78−3814
self-diffusion in ZrH_x, autoradiographic study, energy of soln. in H sublattice *(Russian)* 80−2194
separation from Li at low conc. using Y for fusion reactor appls. 80−83219
soil moisture movement and groundwater recharge by T tagging technique 78−61438
soil plant system ^3H persistance, compartmental model 77−90919
in solar wind, $^3H/^1H$ ratio 77−5407
SOLASE, tritium pathways and handling problems in a laser fusion reactor 79−36411
solid, radiation-catalyses ortho-para transition 79−73832
solid breeding blanket for commercial Tokamak reactors, materials and design 80−95441
solubility in Pd, isotherms at low equilib. press. 79−14935
solubility in Y, 250-400°C, rel. to possible appl. for T recovery from molten Li blanket in fusion reactor 79−90784
sorption in Li-Bi(Al), for appl. in thermonuclear reactor 77−1301
sources and reactions of T species 80−21432
spin-aligned, ground-state energy and finite temp. props. 77−61014
sputter cone ion source for Minnesota MP Tandem, installation 78−29683
STARFIRE project, T handling and vacuum requirements 80−106187
steel, stainless, 304L, T grainboundary diffusion and trapping, autoradiographic exam. 78−51738
thermonuclear fusion plasmas, elem. processses and role of atomic, ionic and mol. data 80−14916
thymocyte, calf, tritiation by catalytic hydrogenation 79−88152
TNS fusion reactor, T handling system design 78−62616
Tokamak reactors impacts of plasma perform. parameters on vacuum and T system design 79−76131
tracer for aquifer interconnection investigs. in Turtz mine *(Rumanian)* 77−53251
tritiated waste materials, gas generation by self-radiolysis, container suitability 79−26579
tritiated water intake, calc. of committed dose equiv. 79−16311
troposphere, in water vapour, rel. to reactor release detect. 78−11988
troposphere, tritiated water vapour natural fluctuation rel. to environmental radiation surveillance 77−88287
vapour pressures, 4 to 30K, isotope effects 77−72674
visual pigment regeneration studies, use of [15^3-H]all-trans-retinal tracer 80−41357
VVER, T buildup estimation with allowance for ^6Li conc. 79−97833
VVER fuel elements, T and ^{85}Kr content obs. 77−54349
water, deep electrolytical enrichment for T meas. behaviour of phosphate pickled mild steel electrodes 80−93764
water, low-level meas., inter-laboratory comparison 78−44888
water cooled, water moderated reactor, coolant tritium content in first loop 80−32334
water pollution, T concentration in natural waters of N.Italy *(Italian)* 80−40933
wells of Greater Chicago area, dead water, ^3H anal. 78−16062
yeast, ^3H induced lethal and genetic changes 78−28015
D-T pellet, ideal gas treatment, implosion and shock waves 78−55735
$\bar{p}$ radiative atomic recombination, antiprotonic atoms 80−83527
CO_2-T_2-F_2 chemical laser using energy transfer from TF to CO_2 77−58322
Ce adsorption, getter beds, T removal from inert gases, CTR appl. 78−41861
D-T, liq., dielectric constant and elec. cond. 80−84680
D-T, solid, estimated heat capacity, enthalpy, thermal cond. and diffusivity 77−4228
D-T, steady-state thermonuclear reaction in Tokamak *(Russian)* 77−18693
D-T ball, compressive plasma fusion using CO_2 lasers 78−82507
D-T ball, explosion compression of plasma up to critical values of thermonuclear microfusion 77−67873
D-T ball, laser driven compression with profiled explosion induced precompression 77−68838
D-T charges, explosion-induced compression for thermonuclear microfusion, power station parameters 78−82508
D-T compression, explosion-induced, thermonuclear avalanche reaction 78−47144
D-T cylinder with plexiglass envelope, profiled cylindrical explosion-laser compression 77−68837
D-T filled glass microshell, laser-irrad., plasma electron energy profile steepening, polarimetry obs. 78−34349
D-T filled laser fusion microballoon targets, fuel content characterisation and press. retention meas. 79−54594
D-T fusion fuel, liquid-vapour equilib., Raoult's law 79−67947
D-T fusion plasma, parametric noise effect on temp. stability 77−39439
D-T fusion reactor, tritium recovery using Zr, Y *(Japanese)* 78−29646
D-T fusion reactor core plasma, α-particle heating, dynamic characts. 77−74985
D-T fusion sources, light water hybrid breeding reactors, source driven 79−13518
D-T laser fusion target, fabrication using cold-gas jets 79−49833
D-T layer implosion through nonhomogeneous transition layer 78−74465
D-T linear mag. fusion device, particle end loss reduction 78−33289
D-T magnetoplasma, fusion effects on diffusion and thermal cond. 77−67883
D-T microsphere, concentric cumulation of laser generated fast ions 78−30456
D-T miniball in heavy envelope, explosion compression of plasma up to critical values of thermonuclear microfusion 77−67872
D-T pellet neutron moderation on blanket neutronics of inertially-confined fusion reactors 80−836
D-T pellets surrounded by high density shells, implosion characts. 77−3969
D-T plasma, adiabatic heating and fusion energy production by compressible fast liner 79−31182
D-T plasma, EM field induced resultant drift inwards from boundary 80−38577
D-T plasma, fast-wave ion-cyclotron and 1st harmonic heating, in large Tokamak 77−51204
D-T plasma, hot, dense, alpha-particle transport calc., moment method 78−22458
D-T plasma, ion-cyclotron wave spectra dispersion eqn. numerical soln. *(Russian)* 78−59561
D-T plasma, kinetics of compression induced fusion chain reaction 78−50297
D-T plasma ball, critical continuously shaped concentric explosive compression, approx. estimate 78−87473
D-T shell, thin, hollow, laser-driven implosion, ignition problem 79−31183
D-T target, laser pulse compression, thermonucl. reaction initiation *(Russian)* 77−23249
D-T thermonuclear plasma, neutron collision diagnostics *(Russian)* 77−34471
D_2-DT-T_2, three-phase region, temp.-press.-composition correlations 77−84889
D_2-DT-T_2 mixture, solid and liq., props. for fusion reactor applications 78−66415
D_2-T_2-H_2, fusion reactor fuel, isotopic exchanges, equilib. consts., 4.2-300K 77−70331
DT, condensation in laser fusion targets 77−42190
DT fusion microballoon, Ne seeded, compression by CO_2 laser 79−22466
DT fusion reactors, environmental aspects, review *(German)* 79−54599

tritium continued
DT laser-driven plasma, thermonuclear burn wave with electron- and α-conductivities 77−18698
DT, liquid and solid, collision induced infrared spectra 79−45717
DT near critical explosion compression, neutron output 77−67867
DT plasma in glass shell, laser-induced fusion, spectrum and absolute yield of α-particles 77−79482
DT, solid and liq., fusion reactor applications 78−66415
DT sphere compression, neutron yield, self-similar hydrodynamic model 77−18703
DT thermonuclear miniexplosion produced by explosion compression, energy output minimisation 77−67896
$F+T_2 \rightarrow TF+T$, rate meas. using TF-molecule chemical laser 77−86291
H:T solid, collision induced IR lines caused by T_2 radioactivity 80−84756
H-T fusion fuel, liquid-vapour equilib., Raoult's law 79−67947
H_2, solid, T-impregnated, storable conc. of atomic H 80−30594
HF+T hot atoms, energy loss 78−15691
HT, interhemispheric transport, atm. H_2 residence time estimation 78−32182
HT single release in a room, radiation dose 78−74513
HT-HTO in air meas. system 80−21433
HTO incorporation in maize and barley 79−25107
^{2}H-^{3}H fuel pellet electrostatic injection *(Japanese)* 80−78434
^{2}H-^{3}H ionised plasma, fast α particle energy deposition, transport eqn. 80−100071
$^2H^3H\mu \rightarrow {}^4He+n+\mu^- +17.6$ MeV, muonic catalysis in synthesis reactions *(Russian)* 80−52706
^{3}H β-spectrum in valine molecule, νe mass 80−91158
^{3}H calibration of photomultipliers on liquid scintillator *(Czech)* 79−31324
^{3}H distribution between gas and liquid in isotope equilibrium in H_2O-H_2S and D_2O-D_2S systems 79−45376
^{3}H paint, effect of occupational exposure, chromosomal aberrations in lymphocytes 77−37011
^{3}H/^{3}He dating as meas. of O_2 utilisation rates, appl. to Sargasso Sea 77−56654
^{3}H-TdR effect on division in Chinese hamster cells 77−29179
^{3}H-methyl acetimidate preparation for protein labelling 79−53246
$^3H \rightarrow {}^3$He, in $TiH_{1.8}$, NMR investig. of radiation damage, ageing 77−24751
^{6}LiD sphere, T prod. under 14 MeV neutron irradiation 79−59254
T in solid H_2, equilib. stability 77−81396
T^+ ions, 20 keV, trapping efficiency of molten Li 77−50290
T^+, sputtering yields 77−36343
T+chloroethane(cyclobutane), recoil reaction, 5×10^{-2} torr 78−44389
T+D, guiding centre distrib. spatial separation, reaction rate enhancement 80−33737
$T+F_2$, exothermic triatomic exchange reactions, dynamics, anal. theory 78−3322
$T+F_2$, impulsive triatomic reaction, vibr. state distrib., impulsive energy release model 78−92456
$T+F_2 \rightarrow TF+F$, exchange reaction, quasiclassical dynamics calcs. 79−91942
$T+F_2 \rightarrow TF+F$, isotope effects, quantum mech. and information theoretic calcs. 78−44360
T+fluoroform, 4.5 to 6.0 eV, substitution reactions 78−85146
T+H, excitation transfer, thermal energy, dipole-dipole interaction 79−31666
$T+H_2$ reactions, accurate pot. energy surface, isotope effects, quasiclassical trajectory study 80−97698
$T+H_2O$, energetic reactions, hard sphere excitation functions 79−1963
T+HD, variational transition field theory and unified statistical model 80−97700
T+HD hot atom exchange reactions, trajectory calcs. 80−26037
$T+HT \rightarrow TH+T$, collinear reactivity bands 78−85143
$T+O_2$ high energy reaction, excitation function 78−68907
T_2, condensation in laser fusion targets 77−42190
T_2, cryocondensation pumping, smooth surface at 4.2K, fusion reactor application 78−74492
T_2 impurity control in EBR-II sodium systems 79−93696
T_2, quadrupole mass filter sensitivities and β-particle induced exchange kinetics 78−58090
T_2-HT(HD), liq. and solid, vibr.-rot. IR spectra 80−50313
T_2+Cl, atom transfer reaction in gas phase, reaction rate computing, tunnelling corrections 79−79237
T_2+H reactions, accurate pot. energy surface, isotope effects, quasiclassical trajectory study 80−97698
T_2+H(D), H-exchange studied by crossed molecular beam experiments 80−93747
T_2+He, vibr.-rot. transitions, optical potential approach 78−62885
T_2+NF_3, chem. laser, TF spontaneous emission, Einstein coeffs. determ. 77−58073
T_2+Y, high temp. equilib. meas. 80−66780
$T_2^+ + T_2$, charge transfer reactions rel. to vibr. states 77−9070
Ti, tritiated self supported target prep. 80−23211
Ti:T, depth profiling by neutron TOF spectroscopy 77−73500
TiO_2:T, IR spectra, 300, 77, and 8K 78−35175
UO_2, irradiated, T loss during oxidative processing in air 79−97831

tritium compounds
beta decay, transition probabilities, ab initio calcs. 77−61387
metal tritides characteristics for transport, storage and disposal of tritium 77−54343
nuclear production complex released, detection and meas. of chem. forms 77−54372
sum rules for connecting vibr. freq. parameters of H_2O, D_2O and T_2O 79−36615
tritides, He behaviour 79−17981
water, tritiated, inhalation hazard from open containers 80−8240
β decay in labelled compounds, potential energy curves 78−56910
HT, dissociation by T beta-decay 77−63941
HT-HTO in air meas. system 80−21433
HT_2, storable conc. of atomic H in T-impregnated crystalline solid H_2 80−30594
H_2T, storable conc. of atomic H in T-impregnated crystalline solid H_2 80−30594
HTO, atmospheric condensation-evaporation model 77−29326
^3H_2O, yeast cell mutagenesis by storage in tritiated water 80−17017
^{3}HOH, effects of chronic ingestion on prenatal brain development, rat expts. 80−36004

tritium compounds continued
T compounds, beta-decay, transition probabilities, ab initio calcs. 77−61387
TBr, mol. consts., calcs., rel. to HBr, DBr *(French)* 77−57855
TF, energy transfer to CO_2 for chem. laser 77−58322
TF, spontaneous emission, Einstein coeffs. determ. using chem. laser 77−58073
TF-CO_2, chem. laser, rate const. of energy transfer from TF(v=1) to CO_2(00°0) 77−675
THO, prediction of flux from air to plant leaves 80−26381
THO, release from CTR, radiological dose calc. 78−78511
T_2O, charge spectrometer studies of chem. effects of nucl. transforms. *(Japanese)* 77−57420
T_2O, inertia defects and dipole moments by kinetic consts. method 80−928
T_2O, injectable soln., radionuclidic purity using liquid scintillation counter *(French)* 78−73118
TOT, vibr. intensities, ab initio and empirical calcs. 80−78592
TOT, vibr. intensities, ab initio and empirical calcs., band strengths 80−78593

triton interactions *see triton-nucleus reactions*

triton-nucleus reactions
for inelastic triton-nucleus scattering, see "triton-nucleus scattering" see also nuclear fusion
exact finite range calculations of light-ion induced two-neutron transfer reactions 79−63639
form factors for two-nucleon stripping process wth Skyrme potentials, DWBA 78−58287
multi-nucleon transfer and direct reactions, nuclear struct., review 78−50060
Pt(t,α), A=194, 196, population of Ir, A=193, 195, proton states 78−33123
(t,α) reaction, 17 MeV, proton hole states in ^{187,189,191}Re 77−88025
(t,d), absolute normalisation, comparative DWBA anal. of nucleon-transfer reactions 77−14143
(t,p), double stripping core independ. 2-nucleon transfer, Tang-Herndon effective interactions 80−73836
(t,p), even actinides, lowest 0^+ state excitation, collective phonon state, spectroscopic factors 80−13410
(t,p), radioactive targets, for study of nuclei far from stability 77−22990
(t,p) ground state cross section systematics in 2s-1d shell 80−5148
(t,p) stripping reactions, repulsive-core effects, Tabakin potential 77−30607
(t,p) two-nucleon stripping reactions with Tabakin pot. 78−21570
^{10}B(t, α)^{9}Be*($2s_{1/2}$), resonant spectra 80−22691
^{10}B(t,α)^{10}B, 0.5 to 1.25 MeV, excitation functions and ang. distribs. 78−17216
^{10}B(t,α)^{9}Be, 0.5 to 1.25 MeV, excitation functions and ang. distribs. 78−17216
^{10}B(t,p) 23 MeV, ^{12}B state excitation energies and widths, DWBA ang. distribs. 78−70544
^{10}B(t,p)^{12}B, 0.5 to 1.25 MeV, excitation functions and ang. distribs. 78−13109
^{11}B(t,p), 23 MeV, ^{13}B state excitation energies and widths, DWBA ang. distribs. 78−70544
^{9}Be(t,^{6}Li), polarised t, 17 MeV, ^{6}He mass six supermultiplet system anal. power 79−45244
^{9}Be(t,n), 1.1-1.7 MeV, neutron spectra and ang. distribs. meas. *(Russian)* 77−50140
^{9}Be(t,p) 23 MeV, ^{11}Be state excitation energies and widths, DWBA ang. distribs. 78−70544
^{10}Be(t,p), 12 MeV, ^{12}Be core excited T=2 levels, spin, half life 78−66210
^{10}Be(t,p), 17 MeV, ^{12}Be mass excess and excited states 79−22183
^{210m}Bi(t,α)^{209}Pb, 20 MeV, cross-section meas., ^{209}Pb levels 77−34320
^{12}C(t,γ_0)^{15}N, 1-3.4 MeV, giant reson. excit., J^π,Γ assignments 77−34277
^{12}C(t,p), 18 MeV, ^{14}C energy levels, spins, parities 78−70542
^{12}C(t,p) 23 MeV, ^{14}C energy states 78−78392
^{12}C(t,p) 23 MeV, ^{14}C state excitation energies and widths, DWBA ang. distribs. 78−70544
^{12}C(t,p)^{14}C, spin and parity of states near 10 MeV excitation in ^{14}C 78−37263
^{14}C(t,^{3}He), 23 MeV, proton shell closure, spectroscopic factors 79−80871
^{14}C(t,p) 23 MeV, ^{16}C mass excess and final states, DWBA anal. 78−78392
^{14}C(t,p)^{16}C, 3.02-6.1 MeV, spectroscopy of ^{16}C 78−613
^{14}C(t,pγ), 12 MeV, ang. correls., ^{16}C levels, spin assignments 78−8830
^{40}Ca(t,p), centre of mass corrections to DWBA overlap factors 80−18319
^{40}Ca(t,p)^{42}Ca, form factors for two-nucleon stripping process wth Skyrme potentials, DWBA 78−58287
^{40}Ca(t,p)^{42}Ca, two-nucleon stripping process with effective interactions 78−610
^{48}Ca(t,d)^{49}Ca(g.s.), 2.5-3.5 MeV, sub-Coulomb reaction calibration 77−79387
^{48}Ca(t,p), exact finite range DWBA calcs., realistic triton and nuclear wave functions 80−63191
^{254}Cf(t,p), ^{256}Cf spontaneous fission, mass and kinetic energy distribs. 80−47518
^{246}Cm(t,p)^{248}Cm, 17 MeV, shell gap obs. 77−46174
^{54}Cr(t,^{3}He), 23 MeV, ^{54}V energy levels, mass excess 77−54230
^{54}Cr(t,pγ)^{56}Cr, 2.9 MeV, γ-ray spectroscopy of low-lying states in ^{56}Cr 77−10358
^{166}Er(t,α), 17 MeV polarised tritons, ^{165}Ho levels, analysing powers, spins 78−78390
^{170}Er(t,p) 15 MeV, ^{172}Er levels, bands, J^π and transitions 80−83038
Er(t,α), polarised t, 17 MeV, ^{A}Ho, A=167,169, energy levels 79−36155
^{254}Es fission coincidence data from d, t, and ^{3}He induced reactions 80−42720
^{254}Es(t,p), 16 MeV, prod. and discovery of ^{256}Es 7.6 hr β-decaying high-spin isomer 77−22964
^{153}Eu(t,α)^{152}Sm, level population 77−67755
^{19}F(t,p)^{21}F, 0.9 and 1.1 MeV, proton ang. distribs., possible compound nucl. form. 78−17218
^{54}Fe(t,d), 2.5-3.5 MeV, ^{55}Fe $Zp_{3/2}$ neutron orbit radius isotone shift from DWBA anal. 80−32172
^{56}Fe(t,p)^{58}Fe, 17 MeV, polarised triton, meas. and two-step calcs. 77−54204

triton-nucleus reactions continued
^{56}Fe(t,p)pol.t, 17 MeV, ^{58}Fe levels, J^{π}, anal. powers and cross sections 80−68539
^{58}Fe(t,^{3}He), 23 MeV, ^{58}Mn energy levels, mass excess, spin-parity assignments 77−54230
^{58}Fe(t,p) 17 MeV, ^{60}Fe, level struct., spin and parity assignments, mass excess 78−82288
^{257}Fm(t,p), 16 MeV, ^{259}Fm detection from spontaneous fission activity 77−26795
^{257}Fm(t,p), 16 MeV, cross section, ^{259}Fm spontaneous fission, $T_{1/2}$ and kinetic energies 80−47517
^{257}Fm(t,p), prod. of ^{259}Fm, half-life and fission mass distrib. meas. 77−26776
Ga(t,p), 17 MeV, ^{A}Ga, A=71,73, levels, ang. distribs., spin assignments and deformation transition 79−54392
Gd(T,α), 17 MeV, polarised t, ^{A}Eu, A=157, 159, single proton states, rot. bands, J^{π} assignments and mass 79−45132
^{152}Gd(t,p), 15 MeV, ^{154}Gd levels, bands, J^{π}, DWBA anal. 80−78110
^{156}Gd(t,α), 17 MeV, pol. t., ^{155}Eu single proton states, spins and parity, rot. bands 79−30766
^{A}Ge(t,p), pol.t, A=70,72, octupole oscillations modes from anal. powers, 3_1^- octupole transition 80−102142
^{70}Ge(t,p)^{72}Ge, 15 MeV, spin, parity assignments, new O^+ states for ^{72}Ge 79−63594
^{72}Ge(t,p)^{74}Ge, 15 MeV, ^{74}Ge struct. study 78−93945
^{74}Ge(t,p), 15 MeV, ^{76}Ge levels, J^{π} assignments, shape transition DWBA anal. 79−17815
^{76}Ge(t,p), 15 MeV, ^{78}Ge level struct., proposed nuclear shape transition, DWBA anal. 78−78266
^{76}Ge(t,p), 17 MeV, ^{78}Ge level struct., J^{π} values from DWBA anal. 79−6417
Ge(t,p), 17 MeV, ^{A}Ge, A=72,74,76,78, ang. distribs., levels and spin assignments, deformation transition 79−54390
Ge(t,p), shape transition obs. 78−25190
^{1}H(t,dn), 2.5 GeV/c, 4π geometry, pole approx. description 80−68678
^{1}H(t,n), signal to background ratio for 10 to 14 MeV neutron prod. 77−30683
^{2}H(t,n)^{4}He, 10.5 MeV polarised tritons, analysing power, polarisation function and transfer coeff. 77−10413
^{2}H(t,n)^{4}He, 20 MeV, neutron spectra normalisation, differential cross-section meas. 77−88106
^{2}H(t,n)^{4}He, 7-17 MeV, absolute differential cross sections meas. 77−26780
^{2}H(tμ,nμ)^{4}He, muon catalysed fusion, neutron yield, muonic molecules 80−106095
^{3}H(t,2n)^{4}He, 30-160 keV, differential cross section measurement 78−17223
^{3}H(t,de$^-$)4He, 1.4 MeV, cross-section meas. 77−74861
^{3}H(t,π$^-$), π$^-$ production by nucleons on light nuclei, estimate of energy consumption *(Russian)* 79−80943
^{3}He(t,d)^{4}He, 9-17 MeV, polarised tritons, analysing-power ang. distrib. meas. 78−29481
^{3}He(t,d)^{4}He, charge asymmetry effects 79−3159
^{3}He(t,d)^{4}He, symmetry breakdown as cluster spatial effect 79−6619
^{3}He(t,d)^{4}He asymmetry, cluster model anal., isobaric analogue states 78−78389
^{4}He(t,n), 10-11 MeV, multichannel R-matrix anal. of polarisation effects 77−2968
^{4}He(t,n)^{6}Li, cross section using var. calcs. in generator coordinate method 78−13122
^{4}He(t,n)^{6}Li, meas. review, differential, angle integrated and neutron total cross sections 79−9582
^{4}He(t,p), 23 MeV, ^{6}He state excitation energies and widths, DWBA ang. distribs. 78−70544
^{4}He(t,t), 10-11 MeV, multichannel R-matrix anal. of polarisation effects 77−2968
^{204}Hg(t,p), 17 MeV, neutron pairing vibr. in ^{206}Hg 78−62549
H(t, n)^{3}He reaction, H depth profiling in solids by neutron time of flight, pulsed T^+ beam 79−5198
Ir(t,α), 15 MeV, ^{A}Os, A=190,192, two-quasiproton states, level struct., DWBA anal. 79−89237
Ir(t,α)Os, A=191,193, 15 MeV, possible excit. of hexadecapole vibrs. 77−26560
^{6}Li(t,d)^{7}Li, 0.35 to 1 MeV, resonance struct. in compound nucl. excitation curves 78−17217
^{6}Li(t,γ)^{9}Be, 0.35 to 1 MeV, resonance struct. in compound nucl. excitation curves 78−17217
^{6}Li(t,p), 23 MeV, ^{8}Li state excitation energies and widths, DWBA ang. distribs. 78−70544
^{6}Li(t,p)^{8}Li, 0.35 to 1 MeV, resonance struct. in compound nucl. excitation curves 78−17217
^{7}Li(t, ^{9}Li)^{1}H, near threshold anomaly, S-matrix formalism, ^{10}Li neutron binding energy *(Russian)* 80−105961
^{7}Li(t,^{9}Li), 5.43-5.95 MeV, near threshold anomaly, ^{10}Be near threshold state *(Russian)* 80−13484
^{7}Li(t,α)^{6}He, possible resonant struct. in excitation functions 78−13110
^{7}Li(t,γ)^{10}Be, excitation functions and resonant struct. for 17.79 MeV state 78−13110
^{7}Li(t,p), 23 MeV, ^{9}Li, state excitation energies and widths, DWBA ang. distribs. 78−70544
^{24}Mg(t,^{3}He) giant dipole reson. excitation 77−6338
^{24}Mg(t,^{3}He)^{24}Na, 2.46 MeV state absence in ^{24}Na 77−34229
^{55}Mn(t,p)^{57}Mn, exciting ^{57}Mn low lying level struct. 77−74769
^{96}Mo(t,p), pol.t, cross section and anal. powers, struct. depend., DWBA anal. 80−78272
^{100}Mo(t,^{3}He), 23 MeV, ^{100}Nb mass and excited states 79−63581
Mo(t,p), pol.t, 17 MeV, ^{A}Mo, A=98,102, anal. powers, transitions, shape coexistence states, DWBA anal. 80−86895
^{14}N(t,γ), 0.8-3.3 MeV, ^{17}O levels, resonances, J^{π} and radiative width 80−47389
^{14}N(t,p), 15 MeV, ^{16}N ground state quadruplet, DWBA anal. 79−22200
^{14}N(t,p), 15 MeV, ^{16}O T-mixed analogue states, (^{3}He,p)/(t,p) cross section ratio 79−9478
^{14}N(t,p), levels in ^{16}N from 5.5-8.5 MeV 78−66207
^{15}N(t,p), 15 MeV, ^{17}N levels and ang. distribs. meas., shell model calcs. 80−9233
^{15}N(t,p), 15 MeV, 2p-1h states in ^{17}N, spins parities, cross sections 78−62548
^{23}Na(t,p), ^{25}Na J^{π} assignments 79−6381
Nd(t,α), ^{A}Pm, A=143-153, odd-A, spectroscopic factors, shell model anal. 80−78137

triton-nucleus reactions continued
^{21}Ne(t,p)^{23}Ne, energy levels, spin, parity 77−2917
^{58}Ni(t,p), high excitation region of ^{58,60}Ni, two- and four-nucleon transfer spectra 79−6675
^{58}Ni(t,p)^{60}Ni, 17 MeV, polarised triton, meas. and two-step calcs. 77−54204
^{59}Ni(t,p), 17 MeV, ^{61}Ni level ang. distribs., DWBA anal. 79−17816
^{60}Ni(t,d), sub-Coulomb region, neutron orbit radius determ. 77−38217
Ni(t,d), 16 MeV, polarised t, ^{58,64}Ni level ang. momentum and spin values, DWBA anal. 79−36163
Ni(t,p)pol.t, 17 MeV, ^{60,62,66}Ni levels, J^{π}, anal. powers and cross sections 80−68539
^{16}O(t,γ)^{19}F, energy levels from α-^{15}N and t-^{16}O coupled channel orthogonality condition model 80−37326
^{16}O(t,n)^{18}F, 1.6 to 3.7 MeV, cross-section meas., O_2 dose meas. appl. *(French)* 77−29077
^{16}O(t,n)^{18}F, 2.73 MeV, triton recoil and ^{18}F yields 80−68677
^{16}O(t,p), centre of mass corrections to DWBA overlap factors 80−18319
^{16}O(t,p)^{18}O, excitation curve meas., 500-1250 keV 78−37359
^{18}O(t,αγ), α-γ angular correlation using Plurimat 20 data acquisition system *(French)* 77−41579
^{18}O(t,αγ)^{17}N, study of ^{17}N excited states *(French)* 77−14031
^{18}O(t,p), 15 MeV, ^{20}Ne, levels, J^{π} and ang. distribs. 80−18204
^{18}O(t,p), 15 MeV, ^{20}O states below 6 MeV, J^{π} assingments, DWBA anal. 79−22201
^{18}O(t,p) reaction, location of 4p and 6p-2h states in ^{20}O 79−40849
^{A}Os(t,p), 15 MeV, A=188,190,192, cross section meas., DWBA calcs. 78−50181
^{189}Os(t, α)^{188}Re, 15.1 MeV, ^{188}Re energy level obs. 80−47487
Os(t,p), 17 MeV, two neutron transfer strength, O(6) limiting symmetry in IBA, Pt comparison 80−32287
^{205}Pb(t,p)^{207}Pb preliminary results using reactor produced ^{205}Pb 77−22990
^{208}Pb(t,p), centre of mass corrections to DWBA overlap factors 80−18319
^{210}Pb(t,d), Pauli principle effects in ^{211}Pb levels 78−17108
Pb(t,α), polarised t, proton hole states in ^{203,205,207}Tl obs. 77−41978
Pb(t,p), pairing vibr. band, microscopic struct. and wave functions 80−91126
^{106}Pd(t,p), pol.t, cross section and anal. powers, struct. depend., DWBA anal. 80−78272
Pt(t,p), 17 MeV, two neutron transfer strength, O(6) limiting symmetry in IBA, Os comparison 80−32287
^{244}Pu(t,α), polarised t, 17 MeV, ^{243}Np energy level spin assignments and anal. power 79−36165
^{244}Pu(t,p), 17 MeV, ^{246}Pu excited states, mass excess and shell gap, L=0 transition 80−9236
^{32}S(t,p), 10 MeV, DWBA anal., ^{34}S levels 78−50180
^{34}S(t,^{3}He)^{34}P, 23.0 MeV, populating ^{34}P excited states 77−34229
Sb(t,α), A=121, 123, α-particle ang. distrib. at 12 MeV, DWBA anal. 78−62546
^{A}Se(t,^{3}He)^{A}As, A=78,80,82, ground state mass meas. and excited state energies of ^{A}As 79−63595
^{148}Sm(t,α), 17 MeV, ^{147}Pm proton states and transitions shell model anal. 79−30781
^{150}Sm(t,α), pol. t, 17 MeV, ^{149}Pm single proton states, spin assignments, spectroscopic factors 80−18170
^{152}Sm(t,α) 17 MeV, polarised t, ^{151}Pm single proton states, rot. bands, level J^{π} assignments, spectroscopic strengths 79−67626
^{154}Sm(t,α), ^{153}Pm $5/2^-$ $h_{11/2}$ dominated band, anomalous ang. distribs., CCBA calcs. 80−86788
^{154}Sm(t,α), 17 MeV, polarised t, ^{153}Pm struct., spin and parity assignments, Nilsson model interpretation 79−469
Sm(t,p), SU(6) boson model for two-nucleon transfer intensities 78−25206
^{A}Sn (t,α), 4.75-5.25 MeV, A=112, 116, 118, 120, 124, single proton states RMS radius 80−13350
^{A}Sn(t,d), A=112,114,116,117,118,119, rms neutron orbit sizes, DWBA anal. 79−36145
^{122}Sn(t,^{3}He), ^{122}In states and masses determ. from (t,^{3}He) 78−66290
^{124}Sn(t,^{3}He), ^{124}In states and masses determ. from (t,^{3}He) 78−66290
^{126}Te(t,p), pol.t, cross section and anal. powers, struct. depend., DWBA anal. 80−78272
Te(t,α), 16 MeV, ^{A}Sb, A=123,125,127,129, cross-sections, ang. distribs., spectroscopic factors, DWBA anal. 80−52572
Te(t,p), SU(6) boson model for two-nucleon transfer intensities 78−25206
^{50}Ti(t,d), 2.25-3.00 MeV, ^{51}Ti $2p_{3/2}$ neutron orbit radius isotone shift from DWBA anal. 80−32172
T(t,2n)^{4}He, fusion cross sections and thermonuclear reaction rates 80−533
^{234}U(t,α), polarised t, 17 MeV, ^{233}Pa anal. power for spin states 79−36165
^{238}U(t,pf), fission probability, fragment ang. distrib. meas. *(Russian)* 77−46199
^{184}W(t,p)^{186}W, 15 MeV, study of levels, spin-parity assignments 77−18572
^{186}W(t,α), pol.t, 17 MeV, ^{185}Ta single proton states and rot. bands, J^{π} 80−91130
^{186}W(t,p)^{188}W, 15 MeV, study of levels, spin-parity assignments 77−18572
W(t,p), pairing excitations in even nuclei, anal. 79−93532
^{172}Yb(t,p)^{174}Yb, 15 MeV, pairing vibr. character of 1494 keV 0^+ state in ^{174}Yb 77−18572
^{176}Yb(t,α), pol. t, 17 MeV, ^{175}Tm single proton states, rot. bands, J^{π} assignments 80−452
^{90}Zr(t,p), centre of mass corrections to DWBA overlap factors 80−18319
^{90}Zr(t,p), exact finite range DWBA calcs., realistic triton and nuclear wave functions 80−63191
^{96}Zr(t,p), 20 MeV, short range correlations with Tabakin pot. 78−13115

triton-nucleus scattering
elast. scatt. on heavy nuclei, anal. with molecular type pots. 77−18502
elastic scatt., optical spin-orbit pot., spin-orbit strength 79−85480
internal structure influence on elastic scatt. at intermediate energies *(Russian)* 79−30844
optical model spin-orbit pot. for spin $^1/_2$ particles 79−97686
R-matrix anal. of reactions in ^{7}Li system below 10.5 MeV 77−26751
(t,t), A=40-208, 17 MeV, pol. t, cross sections and anal. powers, optical anal. 80−47462

triton-nucleus scattering continued
^{8}Be(t,t)^{8}Be elastic scatt. generalised optical potentials, three-body approximation *(Russian)* 79−13313
^{9}Be(t,t)^{9}Be, 15, 17 MeV, polarised t, differential cross sections and optical model fits 78−41730
^{12}C(t,t)^{12}C, 15, 17 MeV, polarised t, differential cross sections and optical model fits 78−41730
^{1}H(t,t)^{1}H, 1.26-3.71 MeV polarised t, spin depend. N-N forces 79−6634
^{2}H(t,t)^{2}H, 10.5 MeV polarised tritons, analysing power meas. 77−10413
^{3}H(t,t)H, 0.6-3.4 MeV, differential cross-sections, ^{3}He energy levels deduced 80−47488
(^{3}H,^{3}H), polarised scatt., optical model parameters 78−70540
^{3}H doublet scatt. length, Phillips plot, N/D input parametrisation 80−42672
^{3}H(t,t)^{3}H, up to 14 MeV, elastic and inelastic cross sections, phase shift anal. 77−22996
^{3}He(t_{pol},t)^{3}He, 9-17 MeV, analysing power, differential cross sections 77−74829
^{4}He(t,t)^{4}He, cross section using var. calcs. in generator coordinate method 78−13122
^{4}He(t,t)^{4}He, elastic cross section from two-centre generator coordinate model functions 78−12994
^{4}He(t,t)^{4}He, meas. review, differential, angle integrated and neutron total cross sections 79−9582
^{4}He(t,t)^{4}He, R-matrix anal. of ^{7}Li system 79−9585
^{4}He(t,t)^{4}He cross section, exptl. data base for ^{7}Li system 79−9584
^{16}O+light ion scatt., exchange Coulomb kernel in resonating group formulation 79−6531

triton scattering *see triton-nucleus scattering*

tritons
binding energy, D-state percentage of deuteron, wave function shape 77−2902
binding energy *(Russian)* 78−29376
bombardment of human blood cells, morphological detail of radiation damage 77−60230
coupling constants of dN and d*N three-body vertices, spectator functions 78−46011
D-state asymptotic normalisation const., Faddeev eqn. with Reid soft core pot. 79−59017
fast stable particles from light emulsions nuclei following 1.5 GeV/c K^- interactions 78−17245
hyperspherical approach to simple model, basis expansion 78−54693
ion medium energy beam from α-particle fragmentation 80−27847
momentum space calculations, Faddeev bound-state eqns., binding energy 78−25122
nonlocal separable interactions in the study of nucl. props. *(French)* 78−33115
partly non-local potentials model 77−54157
production in Br,Ag+p in 24 GeV/c reacts., role of pick-up processes 80−27632
relativistic bound state calcs., off shell depend., binding energy 78−82295
relativistic nuclear collisions, p, d, and t inclusive energy spectra 80−63199
three-particle bound states for partly nonlocal interactions with continuum bound states 80−32206
unitary scheme model anal. with Gogny, Pires and de Tourreil interaction 79−59016
virtual dissociation into deuteron and neutron, mean square radius *(Russian)* 79−3092
wave function, asymptotic normalisation 77−10384
wave functions, unnatural parity transitions in (p,t) reactions 77−67750
t and ṫ prod. by 200 GeV protons 79−9563
HT, triton-proton mag. moment ratio determ. by NMR method with 10^{-6}% accuracy *(Russian)* 77−61773
$^{3}H_{\Lambda}$, binding energy, Fadeev equation in coord. space, Lambda-nucleon potential 80−63120
$^{3}H_{\Lambda}$, decay rates and two-body (π^{-}^{3}He) decay mode branching ratio 79−63620
^{3}H-^{3}He charge asymm., neutron-proton mass difference 78−70464
^{3}H→n+d, s-wave asymptotic normalisation consts. in one-boson exchange model 80−37334

trolleybuses *see road vehicles*

troposphere
see also atmospheric boundary layer; tropospheric electromagnetic wave propagation
acetylene, tropospheric and lower stratospheric vertical profiles 80−4073
acoustic sounding with balloonborne instrument, scatt. structs. vertical profile 78−57353
aerosol global distribution, 162-238 millibar altitude 80−56591
aerodynamic roughness as function of wind direction over asymm. surface elements 78−92890
aerosol, particle size distribs. evolution via Brownian coagulation, num. simulation 80−41513
aerosol climatology in Europe, Project OPAQUE 79−66784
aerosol conc. statistics for N. tropical Atlantic region 78−32188
aerosol concentration, Antarctica, seasonal and frontal vars. 79−70855
aerosol concentration above South Polar Plateau, rel. to meteorological transport of particulate material 80−51481
aerosol in lower troposphere, seasonal vars. in vertical profiles *(Russian)* 78−16092
aerosol measurement problems 79−66839
aerosol monitoring using Spacelab lidar system 77−21876
aerosol particles physico-chemical property models 78−92898
aerosol properties at S.Pole, 1978 obs. 80−41484
aerosol size and comp. at Mauna Loa Obs., Hawaii 77−78333
aerosols, characts. over India, role in warm rain process 79−92573
aerosols, chem. comp. of particles with diameters >1 μm over Tasmania 77−87014
aerosols, chemical components of particles in lower troposphere above central Europe 77−29354
aerosols, effect on surface and surface-atmosphere radiation budgets 80−17375
aerosols, from dust storms, SW United States 79−20932
aerosols, trace gases in summer, background levels in Greenland 80−72609
aerosols with soil-derived component, commonalities in measured size distribs. 77−60454
W.Africa, mean tropospheric conditions for 11-year period, climatological features 77−2221

troposphere continued
E.African low level jet stream, theory 78−40632
E.African low-level jet stream, five-day oscill. 78−53705
air collection and analysis techniques, troposphere and stratosphere 80−26566
air modification due to step change in surface temp. 77−78294
air pollution effects on urban-rural complex, two-dimens. numerical simulation 78−81369
air-Earth current density latit. var., aircraft meas. 77−53141
airborne pollen and spores, long distance transport 78−73466
airflow, diffusion and momentum flux patterns in high mountain valley 79−5544
n-alkane pollutants, N.Atlantic gas and particle concs. 80−7969
anisotropic multiple scatt. effects on solar radiation 79−80016
annual zonally averaged climatic model with diffuse cloudiness feedback 77−29416
Antarctica, surface O_3 meas., annual variations 77−9465
Antarctica, winter, Nimbus-5 atmospheric temp. fields deviation from radiosonde data 78−32138
Antarctica and equatorial India, atm. struct. during southern summer 77−53121
artificial clouds form. possibilities and methods 79−29823
S.Asia, monsoon circulation, role of mountains 77−49121
Asian summer monsoon, simulation by general circulation models 78−40637
Asiatic monsoon, synoptic aspects of droughts 77−56703
Assam valley, low press. area intensification into mesoscale depression 77−53125
N.Atlantic, equatorial tropospheric dust conc. rel. to Sahelian drought 77−78356
Atmosat balloon for tropospheric research, flight history and appls. 78−7775
atmosphere, radiation modulation of aerosol state by moving clouds *(Russian)* 78−88916
atmosphere, surface tides, New Zealand 78−85665
atmosphere-ocean, penetrative convection regime, entrainment rate *(Russian)* 78−69401
auroral zone neutral wind vels. near tropopause using Chatanika UHF Doppler radar 77−5274
Australia, east coast, radioactivity seasonal and latit. vars. 77−64400
background pollution characteristics 79−57531
Baltic Sea region, aerological climatology rel. to atmospheric heat and moisture balance 77−87057
baroclinic boundary layer structure 78−81326
baroclinic instability, critical temp. gradient, eddies, climate model 79−5562
baroclinic instability, model with realistic tropopause 77−78307
baroclinic instability at long wavelengths on β-plane 77−66953
baroclinic instability max., wavelength, quasigeostrophic model 78−44926
baroclinic models, growth rate and vertical propag. of initial error 79−16620
baroclinic unstable wave vertical scale, rel. to eddy heat flux parameterisation 79−5563
baroclinic waves growth rates and phase speeds, multilevel models 79−58022
barotropic and baroclinic instability in tropics, model study 79−58023
barotropic atmosphere eqns., boundary problem soln. *(Russian)* 77−45072
barotropic-baroclinic instability of mean zonal wind during summer monsoon 78−40638
biogeochemical cycles, role of atmosphere 79−79427
buoyancy waves, Doppler radar obs. and theoretical model 79−84367
chemical modelling of lower troposphere, conference, Reston, Virginia (1978 May 15 to 17) 80−62383
chemical-diffusive model 77−21873
chemistry, recent advances, review 79−12204
chlorofluorocarbons, photodecomposition under simulated tropospheric conditions *(German)* 79−53408
chlorofluorocarbons 11 and 12, observability of possible atmospheric removal processes 77−25773
chlorofluoromethane negative ion products, in 0-10 eV near-monoenergetic electron impact 79−41245
chlorofluoromethanes CCl_2F_2 and CCl_3F in Wuppertal-Dusseldorf region, ground level meas. 78−73478
chlorofluoromethanes effect on atm. surface temp. 79−70832
chlorofluoromethanes in upper troposphere and lower stratosphere, vertical distrib. 78−73477
circulation, forced by heating, transient mass flow adjustment 79−53455
circulation, linear theory of response to sea surface temp. anomalies 77−78308
circulation, quasigeostrophic model, mountain barrier effects 77−66974
circulation, solar cycle influences 79−34919
circulation associated with cold front, moist case 79−2334
circulation charge rel. to solar wind proton boundary transits 79−53491
circulation in equatorial latits., contrib. to theory 79−29821
circulation in N.Pacific rel. to sea surface temp. anomaly gradient 80−85674
circulation intensity assoc. with solar mag. sector boundary transits 79−74936
circulation over Antarctica, seasonal vars. 77−21829
circulation over oceans in equatorial latits., numerical calc. 78−92949
circulation patterns, affected by stratosphere wind spring reversal date 80−82021
circulation patterns, influenced by stratosphere winter strength 80−82021
circulation type over N.Atlantic, effect on Gulf Stream channel line oscills. 78−92841
cirrus clouds, influence on IR cooling rate 78−73455
classification of pollutants and pathways in atmosphere 79−70489
clear air turbulence and in cumulus clouds, vertical gust vels. and normal gravity vars. 79−48543
clear radiance estimates from truncated observations 79−80025
climate and climatic change, numerical simulation 79−16643
cloud condensation initiation by gravity waves 80−90159
cloud field over Transcaucasia, statistical struct. 78−92942
cloud microphysics anal. 79−16853
clouds influence on atm. dynamics *(Russian)* 79−8653
cold easterly circulations over Canadian Western Plains, mesoscale boundary layer model 77−78295

troposphere continued
composition, interhemispheric gradients of CF_2Cl_2, $CFCl_3$, CCl_4 and N_2O 78−81289
composition, natural and effects of pollution 78−28262
condensation nuclei vertical profiles 79−79956
conduction current, direct meas. 78−85637
convection initiation and development in temperate latits. 78−20480
convective clouds and rain showers form. over Indian Ocean 78−7735
convective instability and thermodynamic parameters of tropical atm., GATE obs. 79−39827
convective plumes detect. by Doppler acoustic sounding *(French)* 78−40603
convective scale precipitation downdraughts in cumulus and synoptic scale interactions 77−33145
coronae effects on elec. fields beneath thunderstorms 79−79978
coupling with stratosphere rel. to vacillations in general circulation model 79−79926
cumulonimbus anvils, protrusion into stratosphere, lifting of tropopause *(French)* 77−29357
cumulonimbus cloud top heights over Bombay, radar meas. 77−53127
cumulonimbus motion and splitting, role of downdraught, numerical simulation 79−44227
daytime urban moisture field struct. 79−57998
desert region, surface albedo and vertical vel. relations 78−11953
dichlorodifluoromethane+OH reaction, rate const. and tropospheric lifetime 77−64366
dichlorofluoromethane pollution, conc. obs. in background troposphere air 80−97843
difference equations, generalized vertical coordinate, total energy conservation 79−84363
diffusion props. over urban site, anal. using radioactive tracers, effect of air masses 79−84347
diffusion props. over urban site, anal. using radioactive tracers, effect of meteorological variables 79−84348
difluorodichloromethane, spectral data evaluation for atm. sensing 79−62582
downslope severe windstorm and aircraft turbulence event induced by mountain wave 78−73431
dry penetrative convection 78−92889
dust, planetary radiation balance, climatological consequences 78−36242
dynamical meteorology, trough-ridge systems as slantwise convection 79−79993
dynamical motion, spectral representation of primitive eqns. 77−78314
dynamics, Nimbus 4 THIR obs. at 6.7 microns 77−17164
EAS, upper troposphere, balloon obs., nuclear reactions, 10^{15} eV energy particles 79−80161
eddy and turbulent diffusion at 0-65 km altitude, model simulation 79−84438
eddy flux measurements over ocean, related transfer coeffs. 78−81265
eddy transport of sensible heat and momentum, time spectral anal. 78−92899
Ekman boundary layer pumping and topography interaction in stratified atm. 78−73486
electric fields and currents, origin and structure *(German)* 78−32196
electric potential gradient, slow vars. and short-period pulsations of magnetospheric origin 79−12188
empirical orthogonal functions of 500 mb height, truncation of series 80−56581
empirical orthogonal functions of 500 mb level, N.hemisphere 80−56580
energetic O atoms distrib. functions 77−41127
energetics, superposed epoch anal. rel. to Sun-weather relation 78−81285
energetics of entrainment across density interface 77−5283
energy balance, diurnal variation 80−56548
energy dispersion in barotropic atm. 78−20473
energy dissipation, statistical props. 78−81267
energy parameters, hemispheric-scale, vacillation during winter season 77−53132
energy transfer in tropical subcloud layer, aircraft meas. during GATE 79−79989
S.England 1968, September 14-16, mesoscale and small scale motions during outstanding rainfall event 77−45122
entraining convection at upper limit of convection 80−26568
equatorial, response to heat sources 79−29832
equatorial trough zone occurrence and struct. in Venezuela 79−79974
equatorial vortices over South China Sea and Malaysia during winter monsoon 78−40633
ethane, tropospheric and lower stratospheric vertical profiles 80−4073
evaporating downdraught model comparison with obs. behind squall lines 78−92913
fallout fluxes of Pb, Cd, Cu, Zn, Ag in Antarctica and Greenland 79−58007
fluorocarbon mixing and photolysis, eddy diffusion, tropospheric lifetime 79−62551
fluorocarbon mixing and photolysis, tropospheric mixing ratios 79−12181
fluorocarbon-11, estimated future atmos. concs. for various tropospheric removal rates 77−21892
fluorocarbons conc. meas., model validation 77−45138
fluorotrichloromethane, spectral data evaluation for atm. sensing 79−62582
fluorotrichloromethane in N.American troposphere and stratosphere 79−79430
fog and clouds, liq. water content rel. to atm. visibility 78−81404
forecasting method for weather assoc. with western disturbances 79−100903
forecasting of sharp temp. drops in Ararat Valley using circulation indices 79−25317
formaldehyde, concs. in rain water and on atmospheric aerosol 78−57243
formaldehyde, in marine air and rainwater, wet season obs. 80−85703
formaldehyde, meas. by high resolution IR absorpt. spectroscopy 79−84371
formaldehyde, meas. in atm. by ground based IR absorpt. obs. *(French)* 79−66764
formaldehyde, photodecomposition in tropospheric clean air *(German)* 79−53405
formaldehyde composition of air over N.Germany coast, obs. 80−26584
freons, tropospheric photodissoc. rates from solar 1950-2150 Å radiation ground level meas. 79−2345
frictional and orographic effects on precip. in coastal areas 77−60442
frictional effects in strongly divergent flows 79−53434
front formation over central Europe, internal processes 80−81979
troposphere continued
frontal passage, VHF radar obs. 79−53482
frontal waves development, numerical simulation accounting for mountain ridges effect *(Russian)* 78−53701
frontogenesis, 3-dim. study using stream axis coords. 77−87001
fronts and depressions at middle latitudes, mesoscale struct. 80−26604
frost point meas. systematic error using Meteorological Office Mk3 hygrometer 78−73538
gaeous and particulate pollutants transport, interconversion and removal, model, urban plume appl. 78−44984
gaseous halogens in the atmosphere during 1975 77−56681
gaseous pollutants mesoscale transport, math. modelling 78−44986
general circulation, anal. of rocket soundings on Kerguelen Island (February-May, 1973) 78−20489
general circulation model, space-time spectral anal. of midlatit. disturbance 77−66951
general circulation model of atm. without clouds 78−49110
general circulation of midlatitude troposphere, NCAR and GFDL models 80−61856
geomagnetic disturbances effect on atm. processes 77−29361
geopotential height data over ocean areas, supplementary method 80−26647
geopotential height fluctuations, geographic variation of vertical struct. 80−90132
geostrophic large-scale drag coefficient estimation 78−61488
global energy budget, annual cycle of available pot. energy, variability 79−20909
global January and July climate, numerical simulation with two-layer circulation model 77−56722
global vorticity budget over tropics and subtropics at 200 mb during northern summer 78−40640
gravity wave-meanflow interaction, indication in upper atmosphere radar obs. 78−81282
gravity waves, ground level, in SE.Australia, microbarographs obs. 78−73439
gravity waves and LF oscillations, tropical lower atmos., theory 80−12496
gravity waves generated by shear flow instability 80−31098
gravity waves generated by shear layers 77−2195
gravity waves nature and role 79−92575
N.Greenland summer tropospheric aerosol, ground level meas. and elemental anal. 78−85645
ground based radiometric measurement, lower troposphere 77−91330
growth and decay of large-scale waves in tropics during northern summer 79−88428
hailstones, free-fall kinematics near ground 80−12519
halocarbon and N_2O destruction by siliceous land surfaces 79−12168
halocarbon conc. meas. in southern hemisphere 79−5602
halocarbon decomp. by natural ionisation 77−33139
halocarbon lifetimes and conc. distrib. using two-dimens. model 79−12180
halocarbon meas. in Alaska troposphere and lower stratosphere 77−70719
halocarbon sinks, photooxidation, $O(^1D)$ atom and OH radical reactions 77−17165
halocarbons, decomp. by natural tropospheric ions 77−21889
halocarbons, identification and meas. 78−32186
halocarbons, SF_6 and N_2O concs., rel. to tropospheric OH conc. 77−45069
halogenated compounds, meas. in air over Europe 77−37351
halomethanes, electron impact dissoc., tropospheric lifetimes *(German)* 79−50141
heat and humidity exchange laws, model approach 77−66948
heating and cooling due to aerosol IR radiation scatt., calc. 80−72630
S Hemisphere, 200 mbar flow determ. from satellite data 77−33158
N.hemisphere, press. distrib. assoc. with poor summers in British Isles 80−109241
hemispheric mean surface temp., nonequilib. model, pollution effects 77−49150
high-pressure systems in E.United States, ^7Be distrib. 80−4072
humidity distribution, new insight with Meteosat water vapour channel 79−25292
hurricane rainbands, possible form. mechanism 79−8658
hurricane rainbands, vertical struct., interaction with mean vortex 79−8659
hurricanes, forced secondary circulations 79−84387
hydrostatic mountain waves numerical simulation 78−73432
ice particles, depolarisation of 19 and 28 GHz Earth-space signals 78−73492
impact ejecta trajectories, drag and gravity effects, analytic solns. 78−40854
inclinations of atmospheric layers, determ. from sounding data *(Russian)* 80−72569
W.Indian Ocean, low-level cross-equatorial jet stream 78−44959
Indian summer monsoon cyclogenesis and variability 78−81319
Indian summer monsoon rel. to tropospheric flow patterns over southern hemisphere 78−81334
inhomogeneous troposphere model, microwave ducting anal. 79−39818
instability following solar corpuscular stream arrivals 80−109416
interhemisphere transphere in troposphere, CO content study 80−31106
interlatitudinal angular momentum exchange 79−39834
internal gravity waves generated by jet streams 77−25737
internal gravity waves generated by penetrative convection 77−2196
internal gravity waves momentum flux and orographic scatt. 79−8663
intertropical convergence zone, air circulation 78−92948
intertropical convergence zone, interaction with upper westerly waves rel. to Zambian weather during rainy season 80−90175
intrusion of stratosphere air mass, explanation for ^7Be var. 80−98525
intrusive density flows, soliton source 80−12499
inversions, time dependent behaviour in different climatic regions 79−20908
ion concentration, elec. parameters and space charge density correls. 77−13104
ionosphere-troposphere coupling during 1973 November 20 isolated tornadoes 79−70851
IR attenuation *(Italian)* 79−48567
IR fluxes meas. by radiometric soundings, parametric law derivation *(French)* 79−25358
IR high resolution spectra, ground based obs. 77−41167
IR high resolution spectra, numerical simulation 77−41166
IR radiation, cloud height, thickness and overlap effects 78−57252

troposphere continued
IR radiative energy exchange from six-layer general circulation model 80−101432
isentropic and sigma coord. hybrid numerical model 80−12485
isentropic coordinate models, boundary problems soln. 77−29372
jet stream, different, theory 80−46242
jet stream, fronts and wave disturbances compared with Gulf Stream 79−2268
jet stream, influence on evolution of environmental radioactive pollution *(Spanish)* 79−100549
jet stream, medium scale gravity waves generation and vertical energy flux into thermosphere 78−81479
jet stream, source of thermospheric gravity waves *(French)* 78−69554
jet stream, VHF radar obs. 80−90187
jet stream and associated O_3 enhancement *(Russian)* 80−94568
jet stream as source of medium scale thermospheric gravity waves, exptl. study 79−21088
jet stream-frontal systems, pot. vorticity, role of turbulence 80−77044
jet streams cold fronts, waves generation rel. to upper atmosphere irregular motions *(Russian)* 78−96333
Kelvin-Helmholtz instability, jet stream generated, radar obs. and model 80−90165
kinetic energy balance of large-scale motion over British Isles 80−56578
kinetic energy maintenance in tropical disturbances over E.Atlantic, GATE data 78−77307
kinetic photochemistry downwind over water from urban areas 78−28278
Lamb waves originating in nongeostrophic disturbances, a case study 77−45085
lapse rate and climatic sensitivity, two-level atmospheric model 79−80004
lapse rate depiction for clear-air convection 77−53145
lapse rate parameterization in terms of surface temp. 77−86999
large-amplitude standing planetary waves, induced in troposphere by Sun 78−36236
lee waves, models, limiting cases *(Russian)* 80−12480
Lee waves classical theory, asymptotic approx., upper boundary condition role 80−12472
light attenuation, experimental profiles in visible and near IR regions *(Russian)* 78−61558
lightning correl. with thermospheric gravity waves 79−84557
linear lee waves reson. characts. in three-layer atm. 79−44228
local circulation in Rome area, surface obs. 78−81264
low vortex over S.E. Chinghai-Tibetan Plateau, annulus expt. simulation *(Chinese)* 77−70787
low-level jet, struct. investigations *(German)* 78−69422
lower, solar flare effects on temp. and press. 78−40615
lower troposphere, mean thermodynamic instability in N tropics 77−25751
lunar tide in atmosphere, influence of local weather on solar modulation 80−94593
marine aerosols, organic and inorganic Cl gas concs. and particulate Cl size distrib. 78−32187
mass vertical transport across temp. inversion 77−87015
mean zonal velocities determ. by detection of radioactive clouds *(Spanish)* 77−73782
mean zonal wind in upper troposphere, determ. with allowance for turbulent heat fluxes *(German)* 78−32137
meridional and zonal cells, rel. to drought forecasting in Indian subcontinent 77−56710
mesoscale cellular convection rel. to seagull flight behaviour 78−81269
mesoscale divergence of horizontal vel. field and press. gradient force, rel. to momentum transport 78−11954
mesoscale flow over complex terrain during Eastern Tennessee Trajectory Expt. (ETTEX) 78−49101
mesoscale turbulence in upper troposphere, experimental studies *(Russian)* 78−16090
meteorological elements diurnal var. in GATE region 79−29826
methane, atmospheric circulation, destruction through photochemical oxidation *(German)* 79−84424
methane, conc. over ocean, var. with latit. 78−81372
methane, troposphere vertical profile, eastern USA in winter 80−77035
methane, tropospheric abundance and flux from Earth surface *(Russian)* 78−36223
methane and ethane conc. meas. in nonurban area 78−32184
methane atmospheric sources and sinks 78−73472
methane conc. meas., geographical and altitude distrib. *(Russian)* 77−60449
methane concentration in surface air layer from IR absorpt. meas. *(Russian)* 77−29366
methane variations, transport and photochemistry 77−53138
methyl chloroform as indicator of OH radical abundance 77−49134
methylhydroperoxide, UV absorpt. spectra of vap. 80−69159
microbarograph, sodar, FM-CW radar studies, review 77−91332
midlatitude, large-scale fluctuations zonal propag. 77−2194
midlatitude synoptic scale disturbances, energy sources 78−32162
minimum precipitable H_2O above Skibotn, N.Norway, rel. to IR astron. obs. 79−92572
minor constituents transport between troposphere and stratosphere 80−105034
mixed layer depth model based on turbulent energetics 77−5284
mixing depth and stability regional patterns, sodar network meas. 79−100965
moist circulation maintenance and available energy 78−57281
moist convection, six-component spectral model 80−61859
moist penetrative convection and incipient cloud form. 79−66755
moisture, temp., IR soundings anal. by statistical struct. and correl. functions 80−8398
moisture distrib. and H_2O vapour flux over Arabian Sea during S.W. monsoon 77−53111
momentum flux by standing eddies 78−81314
momentum flux maintenance by transient eddies 78−73435
momentum horizontal transport, cumulus-scale, in monsoon depression over India 78−44961
SW.monsoon, orographic effects, review 78−44962
monsoon circulation and rainfall S.Asia 78−44958
monsoon circulation dynamics 79−5559
monsoon depression, Bay of Bengal, tropospheric vertical wind shear 79−8670
monsoon depressions, life history, struct. and movements 78−44963
monsoon system oscillations, spectral anal. of obs. records 77−33148
troposphere continued
monsoon trough typical config. at 850 mbar, assoc. rainfall patterns 79−96795
monsoonal mid-tropospheric cyclone formation mechanism 79−34913
monsoonal quasistationary ultralong waves, real data numerical prediction over global tropical belt 78−40631
morning and evening temp. differences of cloud tops over tropical continents and oceans 79−12219
mountains affecting geopotential, Coriolis force variability 80−26602
negative ions evolution times 79−70829
neutral wind profile following surface roughness change, calc. 78−73483
neutrally stable atmospheric layer, mass and energy transport 79−74927
non-frictional equations of motion validity *(Flemish)* 77−17184
nonurban, oxidation of NH_3, H_2S and methane 78−32183
nonurban composition, conf., Hollywood, Florida (Nov. 1976) 78−32174
northern hemisphere circulation, quasibiennial oscill. and southern oscill. effects 77−78386
O_3 distrib., evidence for higher background values, comment 79−39801
O_3 distrib. and origin 78−85663
OH and peroxy radicals in polluted air 79−62560
N.Pacific, South China Sea and Indonesian Seas, regional energetics during winter 78−44960
particle size distrib. skewness and mode radius relationships 77−45121
particle sources over Australia 79−20907
particulate nitrate in marine air of equatorial Pacific 80−85702
particulate pollution, climatological effects 78−85678
particulate thermal coagulation and downstream transport from urban area source, math. model 78−44985
penetrative cumulus convection, assoc. with travelling disturbances in equatorial ionosphere 78−36361
photochemical and physical transformations, obs. by tunable lasers 77−60460
photochemical mechanisms, computational methods 78−49084
photochemical tropospheric O_3 transport, effect on pollution at rural site 80−61481
planetary pressure waves, transient coupling with D-region short wave absorpt. vars. 77−33162
planetary standing waves in northern hemisphere in July, model 78−61487
planetary waves, effect on eddy momentum and heat fluxes 80−85720
planetary waves in middle troposphere, nonlinear interaction, theory 80−36385
planetary waves of N.Hemisphere, space time anal. 80−51468
planetary-scale waves, effect on polar surface energy budget and circulation 77−66957
planetary-scale waves, vertical energy flux, obs. results 77−2193
point discharge current meas. during different types of rainfall 79−84379
pollutant aerosols, mass density function multimodality 77−70807
pollutant gases, monitoring from space using passive microwave techniques 80−76690
pollutant transport and struct., in lower troposphere 80−85319
pollutants, Gaussian diffusion-deposition model for elevated point sources 77−49156
pollutants dispersion near roadways, simple line-source model 79−5600
pollutants dry deposition from point source, pseudospectral simulation 79−2362
pollutants from industry, domestic coal burning and vehicles *(German)* 79−52973
pollution, remote meas. by aircraft 77−49195
pollution remote sensing from space 78−61621
precipitable water, computation from upper air data 79−34886
precipitable water vapour in atm. with temp. inversion 77−78330
pressure and temp. meas. by lidar differential absorpt., influence of laser emission spectral width *(French)* 80−41554
pressure at high altitudes, correl. with interplanetary mag. field struct. and solar wind 80−56515
pressure fluctuations, time spectra 77−78367
pressure sensor for constant-level balloon expt., boundary layer to 100 mbar level 79−21047
radar echo mechanisms, returns from clear air 80−90181
radar facility, MST radar at Poker Flat, Alaska 80−90254
radar observation of fine struct., pulsed VHF radar method 80−51566
radar observations during clear air conditions, review 80−90178
radar observations of velocities and irregularities, spaced antenna VHF method 80−90185
radar signal reflection and scatt. from refr. index structs. 80−90182
radar techniques (VHF and UHF) for dynamic struct. 80−105078
radiation budget affected by N_2O and methane 80−90211
radiative cooling rate and flux, theory 80−85711
radiative divergence in GATE, results 80−17320
radiative energy balance, affected by stratospheric O_3 content 80−51466
radiative flux divergence effect on entrainment of saturated convective boundary layer 79−79979
radiative heating model from GATE multispectral scanning radiometer expt. 77−91221
radiative transfer, simplified radiative-convective model 77−5320
radio-acoustic sounder, metric radio wave device 80−46276
radio-acoustic sounding methods for tropospheric temp. meas. 78−53728
radiometry, ground-based, atmospheric variables spectra deduction 79−92567
reactive N in unpolluted troposphere, stratospheric source 80−94561
relative diffusion observations 77−78337
remote monitoring using discretely-tunable IR gas lasers and heterodyne detect. techniques 78−61605
remote sensing by VHF radar expts. 78−88938
Rn series disequilib. in S. California coastal air 79−58041
Sahara dust cont. over N.Atlantic from air cond. meas. 78−92897
scattered solar radiation field meas. *(Russian)* 79−16667
scattering of middle UV radiation from an internal source, Monte Carlo model 79−12263
sea breezes of Alaskan Beaufort Sea Coast 80−41485
sea salt quantitative meas. over N.Atlantic 79−16624
sea-air CO_2 flux meas., eddy correl. method 78−32191
seasonal temperature variations, subsurface energy storage influence 77−49122
semi-arid region radio climate and tropospheric model 77−21844
severe cyclonic storm, 1975 October, over India 78−85626
shear instabilities in presence of jump in Brunt-Vaisala freq. 79−53451
shortwave spectral characts. over desert, calc. from CAENEX-70 data 79−100956

troposphere continued
smog episode, Los Angeles, pollutant transport in daytime sea breeze regime 79−5605
solar magnetic field daily changes and tropospheric response 78−88888
solar radiation absorption, cloud and aerosol effects on heating rate 78−57319
solar radiation absorption by water vapour, thermotidal exciting function 78−28310
solar radiation and temp. fluctuations rel. to stratospheric aerosol vars. 78−81327
solar radiation budget in cloudy atm., modified two-stream approx. 79−58090
solar radiation distribution in cloudy atmosphere 78−3955
solar radiation input in tropical ocean regions, influence of clouds 78−3956
solar radiative heating, in presence of aerosols 79−16665
solar UV flux meas., $O(^1D)$ photoprod. rate determ. 79−12197
source height dependence of lateral and vertical dispersion characts. 79−70823
spectral transfer of turbulent energy and temp. variance 78−61489
spherical model, zero-gravity, thermo/hydrodynamic characts. 78−24351
stability class determ. on 481 m tower in Oklahoma 79−58000
stable layers obs. by vertical pointing VHF radar 80−90189
stably stratified layer, resonant parallel shear instability 77−2200
standing planetary waves induced by Sun, comment, statistics reanal. 79−74935
stationary planetary waves and zonal wind, southern hemisphere 78−28276
stationary waves, vorticity and heat balance calcs. 80−51460
steady perturbations, two-level primitive eqn. model 77−25755
storm turbulence zones prediction at 400 and 300 mb levels 77−70789
stratified flow around three-dimens. barrier 80−48769
stratosphere air intrusion near tropopause break, O_3 vertical distrib. study 80−94582
stratosphere warming event of January-February 1979, tropospheric-stratospheric interaction 80−4074
stratosphere-troposphere coupling, implications of zonal mean winds vars. and planetary waves 80−109225
stratosphere-troposphere exchange at polar latits. in summer, from O_3 concs. meas. 80−72599
stratospheric-tropospheric polar vortex breakdown 1977 January 77−53107
structure over Bay of Bengal, during Aug. 1977 active and break monsoon 80−56570
sulphate and nitrate mixing ratios obs. near tropopause 80−61835
summer large scale convective system over Tsinghai-Tibetan plateau, annulus simulation meas. 79−16616
summer monsoon, mid-tropospheric cyclones 78−40636
summer monsoon over S. Asia, break and active phases 78−3912
Sun-weather relation, vorticity area index to interplanetary mag. sector struct. 80−46222
Sun-weather relations, solar mag. sector crossings effect on troposphere 78−88876
supergradient flows, divergence and pressure patterns 77−45076
surface contamination, air conc. and horizontal fluxes estimation 79−5599
surface flow in statistical climate model, parameterization of large-scale momentum fluxes 77−45104
surface layer, accuracy of moments of vel., temp. and humidity vars. 78−92891
surface layer, structural turbulence coeff. depend. on height *(Russian)* 78−69400
surface layer press. perturbs. due to ocean swell waves *(Russian)* 78−65362
surface layer temperature extremes, probability determ. method 78−45020
surface pressure, instability connected with solar activity 79−92580
surface winds, small-scale, vars. over water surface, computation model 78−61480
surface winds, topographic influence 78−81266
synoptic windfinding using tropical constant-level balloon system 80−17395
synoptic-scale vertical motion calcs. in Atmospheric Variability Experiment (AVE) IV 77−21831
temperature, aerosols from Mount Agung eruption as test of global climatic perturbation 78−69440
temperature, annual and semiannual oscills. in northern hemisphere 79−48545
temperature and humdidity structure of subcloud layer over land 77−91200
temperature anomalies, conjugate functions appl. in anal. and forecasting 79−39829
temperature anomaly over European USSR, monthly forecasting 79−39830
temperature corrections for Menaka-II meteorological rocket payload 79−5558
temperature determ. by satellite, sensitivity due to water vapour estimates 78−3874
temperature fields variability in Calgary, Alberta 79−5545
temperature lapse rate, rel. to refr. effects on satellite range meas. 78−73609
temperature lapse rate effect on pilot balloon ascent rate, further comments 77−17175
temperature lapse rate effects on pilot balloons ascent rates 77−2204
temperature mean, rel. to sea surface temps. and volcanic aerosols 77−33168
temperature profiles from ground-based angular microwave meas. 80−51551
temperature profiles meas. using Raman lidar 79−100974
temperature remote sensing by O_2 60 GHz absorpt. 80−77172
temperature variance spectrum in inertial and dissipation range of isotropic turbulence 78−61490
temperature-pressure profile meas. by microwave remote sensing *(Chinese)* 80−4116
terpenes, conc. meas. in Adirondack Mountains pine forest 78−32185
tethersonde system for remote meas. of wind and temp. 79−80038
thermal balance in low latits. in zonal circulation model 79−25316
thermal stability diurnal and seasonal var. at Poona, rel. to pollution 77−53130
thermal structure, acoustic sounding technique appl. to siting studies 78−81467
thermal structure, sodar obs. at Delhi, India 79−53428
thermal structure, sodar obs. at Delhi 78−32151
thunderstorm production of O_3 and N oxides 77−37300
trace gases and free radicals, chemistry, two-dimens. model 78−32214
trace gases vertical conc. from solar radiation absorpt. spectra *(Russian)* 78−69442
transient eddy statistics of northern hemisphere winter circulation 79−58027
trichlorofluoromethane, tropospheric lifetime 78−3920
trichlorofluoromethane, tropospheric lifetime 79−53497
tritiated water vapour natural fluctuation rel. to environmental radiation surveillance 77−88287
tropic winds meas. by Arecibo 430 Mhz radar 79−100975
tropical, Fourier component eigenvalue anal. of CISK-induced disturbances 77−2199
tropical, struct. and energy fluxes 77−2203
tropical, thermally driven motion, influence of stable stratification 77−2201
tropical, three-dimens. wind struct. around cumulus clouds over island 79−5588
tropical atmosphere, combined IR cooling of two absorbing gases in same spectral region 78−81405
tropical coastal region, lower troposphere features during rainfall 78−81332
tropical cumuli, props. and bulk thermodynamic effects 79−8657
tropical cyclone, intensity inferred from troposphere temp. 80−67416
tropical easterly waves over Pacific during sea surface temp. anomaly periods 77−78309
tropical iridescent cloud occurrence rel. to tropopause temp. 78−85675
tropical lower troposphere, geopotential response to tropical forcing 77−21860
tropopause, ^7Be, ^{137}Cs and shortlived fission product concs. *(German)* 77−29408
tropopause, detect. by partial specular refl. with VHF radar 80−8411
tropopause, O_3 vertical and horizontal fluxes, GASP data 78−7720
tropopause, position identification by VHF radar, vertical pointing 80−90189
tropopause gap, generation of mesoscale travelling ionospheric disturbances *(French)* 79−84346
tropopause height estimation from nonlinear functions of satellite meas. spectral radiance 77−78335
tropopause height from spacecraft obs. of atm. refr. of starlight 77−2280
tropopause height rel to sunspot activity 80−77090
troposphere and stratosphere sounding by pulsed VHF radar 80−51566
Tsinghai-Tibetan high movement, annulus simulation, summer flow pattern forecast of high troposphere 78−32211
Tunguska meteorite explosion, shock wave propag. calc. 77−66973
turbidity of Barcelona's air, anal. of 1971-7 obs. *(Spanish)* 80−36375
turbulence, influence on radio-interferometric differential meas. of astronomical coordinates 80−67581
turbulence, optical remote sensing and comparison with simultaneous thermal meas. 79−34965
turbulence effects on meas. accuracy in radioastrometry *(Russian)* 77−22092
turbulence effects on target irrad. by laser beam 77−58254
turbulence kinetic energy budget in convective conditions 79−79975
turbulence simultaneous meas. using sodar and aircraft 79−20923
turbulence small-scale struct., airborne hot-film meas. during GATE 77−29373
turbulence struct. near tropopause, review of radar obs. 80−90179
turbulent diffusion in boundary layer with Rossby number similarity 78−92896
turbulent velocity components in surface layer under convective conditions 77−78297
two-layer atmosphere, orographic perturbations *(Russian)* 78−16136
typhoon characteristics over South China Sea 79−25309
Typhoon Della, weather conditions in eye of storm 79−29828
typhoons, transform in northern latits. 78−92947
ultralong waves, β-effect influence on baroclinic instability *(Chinese)* 80−4062
upper air meteorological data, rel. to regional evpotranspiration determ. 77−91171
upper air pressure field anal. using surface-derived data 78−61523
upper troposphere easterlies, waves rel. to monsoon over Kerala 77−56706
urban, photochemistry, kinetic study 77−45058
urban photochemistry, computer simulation 78−49085
urban pollutants scavenging by thunderstorm rainfall, numerical expt. 79−12261
urban ultragiant aerosol particles conc. meas., St. Louis, Missouri, USA 77−49159
urbanisation and pollutant effects on thermal struct. in various climatic regimes 78−61500
UV flux calcs. and photolysis rates 80−12465
vacillations in general circulation model, large-scale energy cycle 79−53430
Van der Waals molecules comp. of lower atmos. 80−85699
vertical mass diffusion coeff., Rn tracer determ. *(Spanish)* 77−70717
vertical sounder radiances rel. to midlatit. 300 mb flow patterns 78−92983
vertical structure from ground-based IR radiometry 78−57273
vertical temp. profiles, meas. using ground based IR spectroradiometer *(Japanese)* 77−29499
vertical velocities, organised, in middle troposphere, correl. with clouds 78−92939
VHF coherent radar sounding, wind and refractivity turbulence struct. 78−28281
virtual temperature rel. to height of isobaric surface, theory *(French)* 80−21806
viscous internal gravity waves and low freq. oscills. in tropics 77−87003
volcanoes airborne particle and gas emissions, meas. 79−2203
vortex cloud street during AMTEX 75 79−79988
vorticity and vertical motions over E.Asia, AMTEX 75 78−20492
warmings in stratosphere, effect on troposphere 80−105031
water vapour, in situ meas. with new moisture sensor 79−74930
water vapour in troposphere under stable anticyclonal conditions, CO_2 laser radiation absorpt 78−20515
wave generation and frontal collapse 78−77300

troposphere continued
wave motion, balloon obs. using data storage system on balloon 80−46263
wave processes rel. to wind vel. fluctuations in 95-100 km altitude region *(Russian)* 77−29523
waves in tropical upper troposphere, dynamical anal. 80−98388
waves of long- and synoptic-scale, growth and decay in mid-troposphere 79−39793
waves of short-period, 13-25 km altitude, Doppler radar obs. 80−90192
weather conditions for long gliding flights over England 79−58048
westerly upper air troughs, rel. to western disturbances development over India 80−90173
western disturbance intensification moving from central Iran to NW India 78−81302
western hemisphere, rocketsonde-derived temperature vars. 79−58018
wind, radar obs. made at Kwajalein Atoll, equatorial Pacific 80−90188
wind, rel. to near-surface internal gravity waves *(Russian)* 77−33141
wind, strong shear obs. using pulse compression radar 78−32193
wind at 300 mb, scale-interaction study with horiz. filtering method 80−98423
wind flow periodicities during NE monsoon season 79−20917
wind meas. with clear air Doppler radar, vertical component 80−72642
wind measurement by radar, method for reducing backscatt. data 80−90257
wind measurements by radar in Arctic region 78−49172
wind profile in subcloud layer of thunderstorm from lightning photographs 77−87013
wind profile in troposphere and stratosphere, using Poker Flat MST radar 80−72579
wind shear fluctuations downwind of surface roughness elements 78−92918
wind structure over Antarctica 80−81992
wind velocity indicated by cumulus motion across sky 80−98418
wind vertical profile, high-altitude meas. with IR radar 79−70865
wind vertical velocity, acoustic Doppler power spectra comparison with direct meas. 79−57999
wind-height data for tropical cyclone recurvature forecast 77−64380
winds and turbulence continuous meas. using VHF Doppler radar, preliminary results 80−8444
winds in troposphere and stratosphere, connections with dynamical processes in lower thermosphere *(Russian)* 78−24401
winds in upper troposphere/lower stratosphere rel. to satellite-derived radiance gradient 80−98447
winds variance spectrum over E.Europe 80−8397
winter lower atmosphere, influence of interplanetary mag. field sector struct. 80−8510
zonal and meridional large scale flow over British Isles 80−56579
As, conc. determ. over marine and continental regions 79−70486
As, enrichment, sources and flux 79−70487
^{7}Be aerosols content increase over Pacific Ocean during strong jet stream 77−78373
^{7}Be bearing aerosols mean residence time 77−87018
^{7}Be, cosmic-ray-produced, mean tropospheric residence time at north temperate latits. 78−85633
C, non-methane organic, in global troposphere 78−73462
CO, condensation nuclei and O_3, meas. on aircraft flight 79−58010
CO, content observed on circumpolar airliner flight 80−51475
CO, troposphere vertical profile, eastern USA in winter 80−77035
CO, tropospheric latitude distrib., model involving production and transport 80−41483
CO-OH-CH_4 cycle, implications of anthropogenic CO emissions 77−49160
CO_2 conc. meas., comparability 78−20495
CO_2, in troposphere under stable anticyclonal conditions, CO_2 laser radiation absorpt. 78−20515
COS and CS_2 pollution conc. meas. 77−73830
Cs_2, precursor for atm. COS 79−53490
H_2, CO, N_2O, methane, chlorofluoromethanes, vertical profiles meas. 79−84384
H_2 latitudinal and vertical distrib. 78−49089
H_2 mixing ratio over N.Atlantic 80−77057
H_2 mixing ratio vertical profiles 78−32181
H_2 residence time from interhemispheric HT transport meas. 78−32182
H_2 sources and sinks, anthropogenic activity influence 77−64394
HNO_3 in marine air of equatorial Pacific 80−85702
HNO_3 vapour and particulate NO_3^-, global meas. 78−88904
HO, average tropospheric concs. in northern and southern hemispheres 78−32140
$HO_2+NO \rightarrow OH+NO_2$, kinetics temp. depend. 80−3313
H_2O isotopic sampling apparatus for troposphere *(French)* 80−94614
H_2O vapour large-scale irregularities, effects on radioastronomical seeing 78−24339
H_2O vapour mixing ratio and influence on tropopause over India 77−53123
H_2O vapour total content rel. to surface layer humidity characts. 79−39836
H_2O_2 vapour, UV absorpt. cross sections, photodissoc. rate 78−32222
H_2S in troposphere, photochem. production reactions 80−90112
H_2S role in S cycle 78−49123
H_2SO_4 aerosols, heterogeneous atmospheric reactions and role as tropospheric sinks 80−72612
H_2SO_4 secondary aerosol form. in urban atmosphere 77−33137
^{3}H in water vapour, rel. to reactor release detect. 78−11988
Hg conc. determ. *(German)* 79−53406
N fixation by lightning 80−90147
N fixation in instantaneous linear discharges, variable energy input effect 79−20952
N fixation in lightning channels, theory 80−90148
N oxides, photochemistry 78−44914
NH_2+NO_2, reaction rate const. meas. 80−7772
NH_3 fluxes into free atmosphere over W.Germany evaluation 80−94132
NH_3, vertical distrib. by photochem. model 80−85701
NH_3 vertical profile, daily and seasonal variation 80−85700
NH_4^+, mutual neutralisation, with simple and clustered positive (negative) ions 78−44372
NO emission effects on O_3 and OH 77−86992
NO, NO_2, O_3 conc. meas. at ground level at unpolluted maritime site 78−3951
NO production by lightning discharges 77−17189
NO, surface mixing ratios meas. in equatorial Pacific region 79−100893

troposphere continued
NO, troposphere content, 0-7 km altitude over clean and polluted areas 80−51478
NO_2 composition of air over N.Germany coast, obs. 80−26584
NO_2 photodissociation rate constant depend. on altitude 78−11949
NO_2 vertical column abundance, optical absorpt. meas. 78−85632
NO_3, detect. in polluted troposphere by differential optical absorpt. 80−77036
NO_3 in troposphere, obs. of content in mountain air 80−72582
NO_x chemistry, significance of HO_2NO_2 78−11971
NO_x concentrations, predicted CO-OH-CH_4 perturb., sensitivity 79−58043
N_2O altitude profiles at five latitudes 77−78318
N_2O, conc. meas. using electron capture-gas chromatography technique 77−9531
N_2O continuous meas. 78−81318
N_2O cycle, sources and sinks 79−70871
N_2O, decomposition over particulate matter 79−16014
N_2O, distrib., mixing ratio 78−32175
N_2O, global atmos. composition and residence time 80−51519
N_2O, greenhouse effect and climatic implications 77−9460
N_2O in N.American troposphere and stratosphere 79−79430
N_2O in troposphere, absence of photolysis 79−53493
N_2O measurements, laboratory intercalibration 78−81277
N_2O mixing ratio meas. and residence time 78−49088
N_2O, sources and sinks, review 77−37374
N_2O, three-dimens. distrib. and variability, numerical simulation three-dimens. distrib. and variability, numerical simulation 79−58006
O_3 and mass transport, stratosphere to troposphere, Project Dustorm, tropopause folding 78−32177
O_3 background mean. conc., balloon obs. 78−32189
O_3 budget, effect of lower stratosphere O_3 net vertical flux 80−101402
O_3 budget, one-dimens. photochem. model 78−32180
O_3 column, increase rel. to NO_x emission from SST and subsonic aircraft 78−11979
O_3, composition observed on circumpolar flight 80−51475
O_3 composition of air over N.Germany coast, obs. 80−26584
O_3 conc., effects of NO_x emissions of high-altitude aircraft 78−32176
O_3 conc. and vars. in clean remote atm. 79−62554
O_3 conc. rel. to general weather situation 80−101397
O_3 depletion by halomethanes 80−16866
O_3, differential absorption lidar meas. 80−12554
O_3 distributions, distribs. meas. with airborne laser absorpt. spectrometer 79−2344
O_3 elevated levels from natural sources 79−62552
O_3, evidence for significant in situ photochemical source 80−72619
O_3, ground level conc., rel. to regional transport of pollutants 78−44990
O_3, long-range transport 78−61514
O_3 meas. in Boston metropolitan area, mesoscale anal. 78−32178
O_3 meas. in rural areas 78−32179
O_3 meas. using microprocessor controlled lidar 79−58137
O_3, meridional distrib. and seasonal vars. 77−60453
O_3 monitoring with IR heterodyne radiometer 78−16216
O_3, near surface meas. at Hohenpeissenberg, historical review *(German)* 78−65369
O_3 obs. and atm. physics research at Belsk, Poland *(Polish)* 77−21825
O_3, obs. of meridional flux by transient eddies in 0 to 30 km height range 80−109224
O_3, partial press. profile over Uccle, Belgium, April-June 1979 obs. *(French, Flemish)* 80−98385
O_3, partial pressure profile over Uccle, Belgium, 1979 obs. *(French, Flemish)* 80−94571
O_3, photochemical prod. and influence on climate 80−36365
O_3 photochemical production, W.Europe, rel. to meteorology 77−78292
O_3 photochemistry 77−81968
O_3 profiles rel. to solar mag. activity 78−65373
O_3, radiation attenuation, aureole around UV source at finite distance 78−77320
O_3, stratospheric determ. at ground level using ^{7}Be/O_3 ratios 79−58011
O_3 total content determ. using remote spectroscopy 78−65437
O_3 total content estimation from UV radiance meas., aerosol effects 79−8662
O_3 tranpsort mechanisms, general circulation model 80−109196
O_3, transport and photochemistry 77−53137
O_3 transport from stratosphere to troposphere 78−7687
O_3 variations along meridional band 78−32190
O_3, variations rel. to general atmospheric circulation over Middle East in summer *(Russian)* 77−53156
O_3 vars. from Gasp meas. 79−100905
O_3 vertical distrib. over Aspendale, Australia, climatology 78−20475
OCS, atmospheric concs. in S.W. and E.United States 78−20466
$O(^1D)$ formation by O_3 photolysis, tropospheric meas. 78−73536
$O(^1D)$ quantum yield from O_3 photolysis 79−53492
$O(^1D)+H_2O$, rate coeff., atm. OH prod. 79−58009
OH budget, reaction kinetics of OH+trichloroethanes 80−16657
OH concs. rel. to CH_4, CO, H_2 and CH_3CCl_3 budgets 77−86991
OH radical concentration, determ. method using atmospheric ^{14}CO meas. *(German)* 80−8419
OH, vibr. energy distrib., atm. chem. modification 77−25735
OH+gaseous S compounds, lower atmos. chem. 80−61870
OH+halocarbons rate consts., appl. to tropospheric degradation 79−52622
OH+methane+M, absolute rate consts., 296K, flash-photolysis reson. absorpt. technique 77−86290
$OH+NO_2+M \rightarrow HNO_3+M$, N_xO_y, removal from polluted atmospheres 80−50846
OH+trichloroethane$\rightarrow H_2O+CH_2CCl_3$, rate const. and tropospheric chem. 80−16658
OH+CO(N_2O), rate consts. 77−16781
Pb baseline, anthropogenic sources effects 78−7757
^{210}Pb tropospheric residence time 78−85396
^{226}Ra background levels in lower troposphere from coal burning 77−37361
S aerosol, of S. American troposphere 80−67401
S budget over Europe, residence times 79−70475
S compounds, homogeneous chemistry 78−49119
S compounds, large-scale spatial and temporal distrib. 79−20981
S compounds homogeneous oxidation in atmosphere 78−96258
S compounds wet removal from atmosphere 79−2363
S, linear eight-box model for tropospheric global cycle 80−56506
SO_2 and SO_4^{2-}, dry and wet removal from atmosphere 79−2361

troposphere continued
SO_2 and SO_4^{2-} conc. relationship in urban and industrial air 79−2360
SO_2, homogeneous oxidation mechanism in troposphere 78−96257
SO_2 in marine troposphere, sources in CS_2 and COS oxidation 80−4085
SO_2 oxidation to sulphate in troposphere, model predictions 80−81963
SO_2, reversible washout by rain, improved model 79−2364
SO_2, SO_4^{2-}, vertical distrib. in lower troposphere 79−79428
SO_2 to SO_4 transformation rate from atm. conc. data, aircraft meas. 77−73829
SO_4^{2-} aerosol layer, form. and evolution model 80−21801
SO_4^{2-} aerosols chem. props. 78−96254
^{90}Sr tropospheric residence time 78−85396
^{132}Te in lower troposphere, airborne levels and lifetime 79−12242

tropospheric electromagnetic wave propagation
11 GHz forward scattering due to rain, 9 km line of sight link 77−86995
11 GHz rain attenuation distribution, from 5-min. rain rate statistics, calc. 78−24326
12 GHz statistical propag. params. meas., effect of rain *(German)* 77−17183
15 GHz, losses on long-range air-to-ground transmission, statistics 77−17218
18 GHz path attenuation statistics influenced by rain cell orientation 77−5278
20 GHz multi relay links, simultaneous probability of rain attenuation 78−3898
35 GHz short-range pulse radar, effects of precipitation *(German)* 77−49147
50 GHz band, atmospheric attenuation, meas. 78−73494
140 GHz atmospheric attenuation by rain, obs. 78−3914
absorption altitude profile determ., at 2.53 mm by zenith brightness radiometry 77−81979
aerosol concentration deduction from 1.06 μm lidar meas. 79−25323
aerosol light scattering, obs. of polarisation and intensity 80−51541
amplitude scintillation temporal spectra at 10 and 36 GHz 79−12192
amplitude scintillations of mm waves, wind vel. effects 78−61496
angular scattering of water drops and ice particles [electromagnetic interference], freq. above 10 GHz appl. 80−109183
anomalous propagation, meteorological aspects 78−57277
antenna temp. and horizontal path attenuation due to 320 GHz water vapour absorption line, calc. 77−41139
antennas and interferometers, troposphere random inhomogeneities, effect on operation, statistical anal. 77−13111
attenuation, at microwave freq. due to rain, comparison results from radar, distrometer recordings with radiometer meas. 79−62542
attenuation and cross polarisation meas. at 20 GHz, ATS-6 satellite and radar system caused by hydrometeors 79−20912
attenuation and rainfall rates dual-polarisation radar meas. technique, precision 79−25371
attenuation at 230 GHz, meas. 78−73425
attenuation by aerosols in absorpt. bands of moistened particles *(Russian)* 78−65384
attenuation caused by rain above 10 GHz freq. *(French)* 78−53686
attenuation meas. for radio delay system design *(French)* 78−53685
attenuation of 1.25 and 2.0 mm waves, radiotelescopic obs. 79−34897
aureole around UV source at finite distance 78−77320
aureole radiance field about point source in scatt.-absorbing medium 78−77319
beyond-the-horizon propagation, in tropospheric ducting environments 77−41132
clear air radar returns, review of obs. 80−90178
cloud or rain layer, microwave thermal emission, scattering effect 77−91211
clouds, radar reflectivity rel. to cloud dynamics and microphysics 80−61877
communication channel, energy spectrum of delays 79−84442
Comstar beacon cumulative slant path rain attenuation statistics, 28.56 GHz 80−26582
copolar and cross-polar signals rain attenuation meas. at 30 GHz using ATS-6 satellite *(French)* 78−49064
correlation bandwidth, empirical evaluation over troposcatter paths *(French)* 80−41527
cross-polarisation comparison with circular and linear polarisation at 11.6 GHz 79−16633
decametric radiowaves emitted by dipole, propag. problem 78−69399
degradation of cross-polarization isolation due to rain 78−69417
delays energy spectrum *(Russian)* 79−2329
depolarisation by rain, thermal emission Stokes spectral vector 77−66976
depolarisation due to snow at 11.6 GHz 78−57239
depolarization at 11.6 GHz on a terrestrial radio link *(French)* 78−53687
differential attenuation and phase shift meas. for 36.5 GHz polarised waves rel. to raindrops 78−3856
differential attenuation at 13 GHz and 20 GHz on 53 km link *(French)* 78−53684
differential rain attenuation prediction, adjacent microwave and mm-wave links 77−87048
diffuse solar radiation field in cloud layer *(Russian)* 79−29851
diffusively evaporating water aerosol 77−728
direct attenuation function and field strength calc., computer aided anal. 79−25373
distortion characterisation of tropospherical channel for digital transmission *(French)* 79−58065
dual-polarisation radar for rain targets, rel. of diff. reflectivity to correl. 79−62556
ducted EM wave propagation, roots of modal eqn. 80−72607
ducting of HF radiowaves, numerical study 80−36378
Earth-ionosphere duct, radiowave propag. parameters at ELF 77−45067
Earth-space path rain attenuation at 11 and 14 GHz, Darwin, Australia, satellite communications appl. 79−62541
Earth-space paths, rel. between rain depolarisation and attenuation 78−3858
Earth-space paths, tropical rain attenuation at 11 GHz, radiometric meas. in Australia 77−33165
Earth-space signals, at 19 and 28 GHz, depolarisation by ice particles 78−73492
EHF clear air refractivity calc. procedure 78−57266
EMF air refractivity, variability w.r.t. temp. pressure and freq. 77−41112

tropospheric electromagnetic wave propagation continued
EMF properties of air 77−17182
extinction at 10.6 μm CO_2 laser wavelength, from meteorological records 79−39848
extinction cross section for single particles at 100 GHz 80−82116
fading at low elevation angles, meas. of satellite signals *(French)* 78−49069
fog, IR extinction and absorption, linear relation to water content 80−56603
forward scatter and cross-polarisation from spheroidal ice particles 77−25733
forward/backward scattering from liquid/solid hydrometeors, Rayleigh approx. 79−25321
frequency scaling of attenuation above 10 GHz due to rain, use of COMSAT satellites 79−5595
global model for rain attenuation prediction 79−5594
guiding of radio waves using ducting refr. gradients, review 79−84374
hail, Doppler radar spectra at vertical incidence 78−65368
hail, ice samples backscatter matrix rel. to identification by radar 79−58046
hail, radio emission characts. in cm waves 79−96802
hailstorm, finger radar echoes, form. mechanism *(Chinese)* 80−109234
HF and VHF emissions temporal struct. during lightning return strokes 77−33136
HF Doppler ground-wave radar for off-shore wind meas. 78−77295
HF fading ionospheric reflection channel, delay and Doppler power spectra 79−8765
HF ground wave propag. over seawater, basic transmission loss meas. 77−78353
HF radio obs. of wave height, surface winds and currents 78−77241
hurricane sea surface wind speed, L-band radar backscatt. obs. 80−56561
IEE antennas and propag. international conf., London, England, 1978, Nov. 79−12342
inhomogeneity transfer velocity meas. by 10 cm radiowave propagation correlation *(Russian)* 78−77297
inhomogeneous stratified atmosphere, normal-wave soln. 78−53710
integral eqn. soln. to EM scattering by dielectric spheroid and ellipsoidal raindrops 78−85622
IR and microwave propagation, atm. humidity meas., optimization of conditions *(Russian)* 79−34898
IR attenuation by atm. H_2O, lab. study of role of mol. and aerosol contribs. *(Russian)* 79−34945
IR cloud opacities averaging for climate modelling 79−8692
IR propag. over long atm. paths, instrumentation 79−39875
IR radiative transfer, absorpt. in partial cloud cover model 80−12544
IR transmission rel. to precipitable H_2O at Gornergrat Obs., Switzerland 79−34941
IR transparency window, 10-13 μm, H_2O and aerosol effects in winter and summer *(Russian)* 80−105048
irregularities, effects on lunisolar precession determ. via extragalactic radiosources obs. 77−5129
jet stream winds, mesoscale var., Sunset 40 MHz Doppler radar obs. 79−53477
joint Gaussian statistics 78−42265
Kanpur-Nainital troposcatter link, Doppler crosswind relations 77−5303
Kanpur-Nainital troposcatter link, radio signal characts., simulation and obs. 78−40614
laser beam attenuation by snowfall, characts. 80−26611
laser beam vertical propagation through troposphere 79−39851
laser radiation absorpt. by water vapour and CO_2, stable anticyclonal conditions 78−20515
in laterally nonuniform troposphere 78−57267
lidar observations of altostratus mixed-phase cloud 77−91220
lidar returns depolarization, scatt. from virga and source cloud 77−49169
line-of-sight radio link, experimental investigation by direct meas. of impulse response *(Italian)* 79−70867
line-of-sight radio link propag. characts. eval. using impulse analysis *(Italian)* 79−70868
long-distance propag., multiple scatt. effect 80−109229
medium scale broadcasting satellite for experimental purposes, rain-scatter interference 79−8668
meteorological radar performance as device for propagation studies at Spino d'Adda 79−84342
MF broadcasting waves, long-distance propag. characts., round-Pacific mobile expt. *(Japanese)* 77−21997
microwave, rain attenuation study on terrestrial link, weather radar appl. 77−41130
microwave attenuation, in rain, UK rainfall data 78−11965
microwave attenuation by salt water droplets 78−7725
microwave attenuation due to precip. of water vapour in atmosphere, meteorological data, raindrop spectral distrib. *(German)* 80−90176
microwave attenuation from rainfall rates, 10-40 GHz 78−40607
microwave attenuation through rain, Earth satellite path 77−5279
microwave cross-polarization due to precipitation in atmosphere *(French)* 78−53674
microwave depolarisation, rain and imperfect antennas combined effects 78−92936
microwave diffraction around Earth, bilinear model of troposphere *(Russian)* 77−64367
microwave ducting in inhomogeneous troposphere, anal. 79−39818
microwave link, cross-polarisation on terrestrial path, wind, raindrop size and canting angle effects 79−66736
microwave link, rain attenuation on terrestrial path 79−66734
microwave link, scintillation fading meas. at 100 and 36 GHz, wavelength depend. 77−41110
microwave link at 19 GHz over 35 km, attenuation meas., effects of rain and multipath propag. 79−88453
microwave link rain attenuation, year and worst-month rain rate distrib. estimation method 79−5648
microwave link rain attenuation on parallel, series, and convergent terrestrial paths 79−66735
microwave links, 11 GHz, fading due to rain, snow and multipath propag. 77−91206
microwave links, rain attenuation estimation in UK at freqs. 10 to 100 GHz 78−73426
microwave links, short and long term rainfall rates, link design implications *(German)* 78−49082
microwave measurement of absolute values of H_2O vapour absorpt. 79−66773

tropospheric electromagnetic wave propagation continued
microwave propag. during 1974, Dec. 17-21 disturbance 77−70736
microwave propag. through rain, numerical calcs. *(French)* 78−53675
microwave propagation, path attenuation during sandstorms 79−70834
microwave propagation at 10, 11 GHz, radiometric measurement of rain attenuation 80−67397
microwave propagation in standard atmosphere, ducting, subrefraction effects, radio links appl. *(Norwegian)* 79−29835
microwave radiation from clouds meas. by Nimbus 6 for rainfall distrib. determ. 78−3981
microwave radio links, data meas. over 10 years rel. to radiowave propag. 78−3857
microwave radio refractometer, expendable, lightweight, construction and performance 79−8708
microwave radiometry in O_2 5 mm absorpt. band, appl. to temp. inversion detect. *(Russian)* 78−11963
microwave rain attenuation, 11.6 GHz, diversity meas. at Etam and Lenox, West Virginia 79−79922
microwave rain attenuation distributions on Earth-satellite paths, empirical calc. 79−5592
microwave rain attenuation terrestrial link, freq. range 10 to 40 GHz, calcs., meas. 77−70771
microwave rainfall attenuation, 680 m vertically polarized link invest. 78−36238
microwave refraction coeff. rel. to humidity 78−69398
microwave scatter and sea state estimation, ocean wave models 78−77244
microwave signals cross-polarisation rel. to atm. elec. field strength 77−49132
microwave slant-path attenuation prediction from rainfall rate meas. 77−70741
microwave transmission networks appl. *(Norwegian)* 79−29834
microwave wave amplitude/phase fluctuations, statistical characts. 79−12225
microwaves, satellite-borne monitoring of atmospheric and surface characteristics 78−24353
microwaves absorpt. by water vapour at 0.869 mm *(Russian)* 77−5277
microwaves anomalous depolarisation on 19 and 12 GHz Earth-space paths 77−78354
microwaves at 11 GHz, rain outage performance of tandem and route diversity systems 77−41131
microwaves near horizon meas. over water at 30 GHz, ATS-6 to ground link 78−24345
mm wave propag., rain attenuation meas. at 35 GHz over two sites at different altitudes 79−8667
mm wave propagation and atmospheric influences 79−84466
mm wave radar, measurements of effective sea reflectivity and attenuation due to rain at 81 GHz 79−80001
MM wave radiometry for atmospheric sounding 79−84551
mm wave slant path propag., 15 to 40 GHz, survey of expts. 79−84465
mm waves, attenuation due to rain at 74 GHz 79−80002
MM waves, influence of atmosphere on passive radiometric measurements in 10 to 1000 GHz range 79−88465
mm waves, rain attenuation measurements at 94 GHz 79−80000
multipath fading and radio refractivity meas. at 11, 19 and 36 GHz on 7.5 km path 77−41111
multipath fading and rain attenuation on terrestrial radio links, 7 to 15 GHz 79−16630
multiple atmospheric parameter meas. laser radar system 78−4009
multiple scatt. effects from stochastic medium 78−44941
non-spherical hydrometeors scattering properties *(French)* 78−53676
nonuniform radio wave guide, coupled mode anal. 80−94587
numerical comparison of ray method and normal wave method 80−21858
ocean surface, radar backscatter rel. to wind speed and fetch 78−77247
ocean wave detection by microwave radar, gravity-capillary wave modulation 78−77333
ocean wave scattering theories, review 78−77243
ocean waves travelling against wind, HF radar obs. 78−77242
photodissociation fluxes, tropospheric and stratospheric, Mie scatt. contrib. improved model 80−77103
polluted boundary layer, radiation model 77−49168
precipitation, attenuation and cross-polarisation due to various drop size distribution functions 79−84373
precipitation attenuation studies from meas. of ATS-6 20/30 GHz beacon signals 79−20911
precipitation detection by radar *(German)* 80−46227
precipitation parameter meas. method using radar reflectivity and optical extinction *(French)* 78−53729
precipitation properties using radar polarisation techniques 80−61925
propagation meas. at 94 GHz, expt. and theoretical rain attenuation results 79−16632
pulse propagation over smooth irregular terrain 78−20458
radar attenuation in rain, iterative correction 78−92923
radar backscatter from ocean surface, friction vel. depend. 78−77246
radar cloud meas., comparison of simultaneous studies by satellite 79−58077
radar echo mechanisms, returns from clear air 80−90181
radar echoes from distributed targets, averaging of time, angle and range 80−109264
radar measurement of clouds and precipitation, correl. and spectral anal. 80−12529
radar observation of cloud and precipitation particles, X- and K_a-band method 80−46273
radar observation of hydrometeors 80−46219
radar reflection from cloud and clutter targets, broad-band noise techniques 80−51454
radar reflection from rain, differential refl. method 80−46221
radar reflectivity calibration using ground return targets 79−53471
radar reflectivity of ground-level hail in Colorado hailstorms 79−53470
radar reflectivity profile classified by rain types 80−101420
radar reflectivity variations with height due to wind shear on rain cells *(French)* 78−53682
radar reflectivity/precipitation relation variations *(German)* 77−17180
radar reflectivity/rainfall rate relation, effect of vertical air motions 77−45098
radar reflectivity/rainfall rate relation for seeded and nonseeded clouds 77−45099
radar scatter from waves of short-period, 13-25 km altitude 80−90192
radar signal reflection and scatt. from refr. index structs. 80−90182

tropospheric electromagnetic wave propagation continued
radiances in absorpt. bands, calc. methods including multiple scatt. 78−61554
radio and optical waves refraction in atmospheric boundary layers 80−36400
radio beam curvature effect on phase meas. 78−49118
radio communication, book 80−62400
radio links, refractive index gradient layers effects 77−13107
radio propag. characts. prediction using FORTRAN computer programs *(Italian)* 78−85666
radio refractive index, calc. from temp., press. and humidity data *(Czech)* 80−36351
radio refractive index and potential refractive index, lower troposphere, S.England 79−34928
radio refractive index structure in transitional boundary layer 78−57268
radio refractivity diurnal variation up to 3 km over India 78−40627
radio wave absorpt. by water vapour in atmosphere, 0.8-20 mm range 80−4086
radio waves, propag. rel to radio-interferometric differential meas. of astrometric coordinates 80−67581
radioastrometry, limitations on meas. accuracy *(Russian)* 77−22092
radiointerferometric frequency and coordinate meas. accuracy, tropospheric fluctuation constraints 79−8848
radiosonde meas. and spectral anal. of LOS fading 80−56568
radiothermal sounding of press. and geopotential *(Russian)* 80−77038
radiowave, broadband communication, tropospheric scatt. mechanisms and channel characterization 79−29837
radiowave, investigation using modelling technique 79−29838
radiowave above uneven Earth's surface, field calc. 78−57275
radiowave attenuation at 225 GHz meas., correlation with surface water vapour density 78−85624
radiowave attenuation by rain, calc. 78−44919
radiowave attenuation statistics at 15 and 35 GHz for very low elevation angles 79−8674
radiowave ducting by stratified troposphere 79−29842
radiowave phase fluctuations in anisotropic turbulent atmosphere when emitted by moving source 80−17352
radiowave propag., angular depend. of rain scatt. at freqs. below 30 GHz 80−8416
radiowave propag., crosspolarisation and attenuation meas. at 11.6 GHz using theoretical rain model, canting angle distrib. 80−4070
radiowave propag., rain-induced attenuation, expt. results and calcs. *(French)* 79−12164
radiowave propag., scattering amplitudes and crosspolarisation of spheroidal ice particles, calc. 77−70740
radiowave propag. errors during geomag. storms 80−4077
radiowave propag. expts. in 19 and 28 GHz range using COMSTAR beacon 78−73420
radiowave propag. over S.England, 6-year study of RRI and PRI 79−39823
radiowave propag. problems, URSI and CCIR collaboration 78−57322
radiowave propag. studies by International Radio Consultative Committee 78−77311
radiowave propagation, refr. theories review 78−69425
radiowave propagation, tropospheric and precipitation scatter, rel. importance in interference and coordination calcs. 78−73423
radiowave propagation above 30 MHz, role of sporadic-E layer and troposphere 80−41636
radiowave propagation in troposphere waveguide, effect of elevated M-inversion 80−90195
radiowave propagation research, using radiosonde data 79−2350
radiowave propagation studied by FM-CW radar 80−90186
radiowave refractive index meas. using digital refractometer 78−86321
radiowave scatter communications, review 79−34935
radiowave scattering by rain, COMSTAR beacon receiver diversity experiment 78−73421
radiowaves, delay fluctuations with scale sizes >1 km, obs. with radio interferometer array 79−8675
radiowaves, effects on communication systems 78−92954
radiowaves, propag. in ducts used for line-of-sight links *(French)* 80−17303
radiowaves, quasioptical approx. isotropic absorbing medium 77−75377
radiowaves, refr. rel. to oblique-incidence sporadic-E propag. 78−73578
radiowaves, troposcatter channels and appls. of adaptive equalization techniques, statistical anal. 79−29841
radiowaves, troposcatter developments in North Sea 80−46246
radiowaves, tropospheric reflection of differently polarized transient signals 79−29839
radiowaves, vertical distribs. of Radio Refractive Index and Potential Refractive Index 79−12228
rain, radar attenuation at 3.2 cm and 5.4 cm rel. to surface precip. meas. *(German)* 77−82038
rain, radar attenuation rel. to rain-rate estimates 78−73540
rain, radar reflectivity data rel. to attenuation on terrestrial and Earth-space propag. paths 78−73490
rain, specific attenuation and phase shift in 10 to 30 GHz range *(Italian)* 78−96261
rain attenation at 11 GHz *(French)* 78−77292
rain attenuation, frequency scaling 77−45071
rain attenuation, radiometric determ. at millimetre wavelengths, multiple-scatt. effects metric determ. at millimetre wavelengths, multiple-scatt. effect 80−90260
rain attenuation above 10 GHz, regression curves for tropical areas, telecommunication, broadcasting systems appl. 80−90111
rain attenuation above 11 GHz, radio links appl. 80−98410
rain attenuation at 11 GHz on radio links *(French)* 78−53683
rain attenuation at 13 GHz on Earth-space paths, depend. on elevation angle 77−70742
rain attenuation data, appl. to path engineering 78−24327
rain attenuation distribution estimation *(French)* 78−53688
rain attenuation effect on Earth to satellite radio link, statistical study *(Japanese)* 79−5555
rain attenuation effects on multiple access transmission of data via satellite 78−77313
rain attenuation for Earth-space links, comparison between radar- and radiometer-derived data 78−24343
rain attenuation meas. on Earth-space paths at 37 GHz by passive radiometry 77−41109
rain attenuation model for Earth-satellite paths 79−62561
rain attenuation of radiowaves meas., microwave radio link projected design appls. *(Slovenian)* 80−46217

tropospheric electromagnetic wave propagation continued
rain attenuation on microwave link slant path 79−66737
rain attenuation on satellite-Earth path at 11.4 and 14 GHz by radiometric meas. *(French)* 78−49066
rain attenuation on terrestrial and Earth-space propag. paths, joint statistics 78−73490
rain attenuation prediction methods comparative analysis, radiowave propagation appl. 80−109182
rain attenuation prediction on terrestrial radio links from rainfall data 79−16636
rain attenuation prediction using radar and in situ meas., 28 GHz Comstar beacon signal 79−70839
rain attenuation ratios and path diversity gains of mm waves at 11, 20 and 36 GHz 79−16631
rain attenuation study at 11 GHz, statistical properties, single attenuative events 79−34885
rain cells, path diversity and baseline orientation [rain cell effects] in Earth-satellite links 79−20913
rain depolarisation and attenuation meas. at 11.7, 19.04 and 28.56 GHz *(French)* 78−49067
rain depolarisation using INTELSAT-IV satellite in 4 GHz band at low elevation angle *(French)* 78−49068
rain depolarization statistical distribution for microwave signal propag. *(French)* 78−53673
rain effects on 18 GHz dual-polarised propagation link 77−29404
rain induced attenuation and cross-polarization calcs. *(French)* 78−53677
rain induced signal fluctuations, incoherent effects investigation *(French)* 78−53679
rain rate distrib. study, Japan, attenuation in telecommun. systems 78−92934
rain rate statistics, approx. method for use in signal attenuation estimating 79−70840
rain scattering of microwaves, drop-size and temp. effects on forward and backward scattering 80−17317
rain slant path attenuation statistics prediction at various locations 78−24344
rain-cell modelling for earth-space links using SIRIO satellite radiowave propagation data 80−36352
rain-induced polarization, theoretical model of wind gust effects *(French)* 78−53678
raindrop induced forward and backward scattering amplitudes, tabulations 79−34884
raindrop sizes in mm radio attenuation, lognormal distribution 79−16635
raindrops, spreading of ellipsoidal raindrops orientation during intense rainfall, expt. results 79−16634
rainfall characteristics across Europe 79−66733
rainfall intensity data for radio-relay system design above 10 GHz *(French)* 78−53690
rainfall meas. by microwave attenuation in 1-3 cm band 78−65414
rainfall over land, microwave radiometry by Nimbus 6 ESMR 80−56635
rainfall prediction for attenuation prediction in Earth-space paths *(French)* 78−49062
range correction algorithm 78−61591
range instrumentation for the measurement of the effects of a marine environment on electro-optical radiation 79−8726
reflectivity meas. by radar and disdrometer, comparison for rain 79−53546
refraction values of radiowaves in troposphere in air temp. inversion 80−4087
refractive index gradients study, new approach 79−25322
refractive index structure parameter, height distrib. in atmosphere with lower boundary spatial transition 78−73491
refractive index variance, height distrib. in different air masses 77−41133
refractive struct. using Rake probing 77−91231
refractivity turbulence struct. const., Sunset Radar obs. comparison with theoretical model 79−8673
remote probing for wind and struct. const., line-of-sight method 80−36426
remote sensing by two satellites, radio illumination method 80−51550
remote sensing progress and implications for local weather services 77−81990
RF propag. in turbulent atmosphere, temporal freq. spectra of multifreq. waves 77−21834
RF refractive index, synthetic properties, over Japan 77−87047
satellite beacon signals attenuation by rain at 19 GHz 79−5593
satellite communication systems, rain effects on propag. 77−41126
satellite communications above 10 GHz, rain effects 80−8410
satellite links, seasonal var. of attenuation statistics due to bright-band height 79−100889
satellite links at 20 and 30 GHz, crosspolar phase variations on satellite-Earth path, meas. 77−81957
satellite links rain attenuation and site diversity effect, statistical studies 78−88892
satellite loss angle transmission effects, VHF and UHF 78−7747
satellite range measurements, formula for refr. effects computation 78−73609
satellite TV broadcasting, long-term propag. meas. in 1978 eval. *(German)* 79−84441
scanning beams for UHF/SHF tropospheric scatter radio links 78−81276
scatter channel for ELOS optical communications system, scattering from marine aerosols 79−29862
scatter transmission path loss, new formulas 79−48556
scattering from large dielec. spheres, lidar signal analysis from rainfall 78−66754
scintillation effects at 30 GHz on ATS-6 geostationary satellite *(French)* 78−49065
semi-arid region radio climate and tropospheric model 77−21844
semi-empirical theory 80−90220
shadow mapping to study rain attenuation on satellite microwave links 77−29505
SHF, ATS-6 satellite 20 GHz carrier, attenuation and depopolarisation meas. *(French)* 78−49063
SHF, scatt, props. of Pruppacher-Pitter form raindrops and cross polarisation due to rain 77−41129
SHF beyond-the-horizon signals, evaporation duct influences 78−92935
SHF line-of-sight propag. 79−48555

tropospheric electromagnetic wave propagation continued
SHF meas. using 12 GHz Communications Technology Satellite beacon 78−73422
SHF signal attenuation by rain, monitored by radar 80−51567
SHF slant-path rain attenuation, satellite broadcast paths 77−86988
SHF-EHF scintillation, refr. scatt. explanation 79−48615
SIRIO satellite, 11.6 and 17.8 GHz cumulative attenuation statistics 79−84339
SIRIO satellite down link propagation expts. in Finland 79−84338
SIRIO satellite link, 11.6 and 17.8 GHz attenuations relationship 79−84340
SIRIO satellite link, 11.6 GHz, propag. meas. in Munich 79−84337
SIRIO satellite link, propag. meas. in Eastern USA 79−84343
SIRIO satellite reception, atten. meas. during first year at Deutsche Bundespost Earth station at Leeheim 79−84335
SIRIO satellite signal propag. meas. by Netherlands PTT ground station, and equipment 79−84344
SIRIO satellite to Earth propagation path, precipitation scatter meas. 79−84336
SIRIO satellite transmissions near 11.6 GHz at Slough UK, meas. 79−84333
skywave field strength prediction, MF propag. in North America 77−78350
skywave field strengths, effect of proximity to discontinuity in Earth's elec. props. 77−40974
slant path rain attenuation characteristics in 20 and 30 GHz bands 79−8678
snow penetration and backscatter of millimetric waves 77−21877
solar radiation absorpt. by H_2O vapour, including multiple scatt. 78−61553
solar radiation absorption by aerosol, spectrophone meas. 79−80027
space sciences, conf., Waltair, India (Jan. 1978) 79−101000
space sources, tropospheric limitations on astronomical co-ordinate meas. using phase and fringe freq. 79−44375
space-time distribution of refractive index of air in Mongolia 78−81335
spot dancing in inhomogeneous random media 78−46496
stochastic dynamic model of rain attenuation 79−53506
storm precipitation observed with radar 80−46220
submillimetric wave noise interaction with rainy atmospheres 77−41138
surface layer, over sea, refr. index statistical charact. *(Russian)* 78−65363
surface radio refractivity and signal strength, sea breeze circulation effects 79−20919
thunderstorm, radar and VHF emission obs. of three-dimens. motion 80−46218
thunderstrom observed by radar, depolarisation rel. to precipitation 80−51453
trans-horizon propagation path over sea, transmission loss due to ducting at 1.8 GHz 80−105041
transhorizon propag. at freqs. >1 GHz on transmission paths set up in CSSR and GDR *(German)* 80−17364
transhorizon propag. paths in Indian subcontinent, transmission loss prediction 77−13105
transhorizon radiowave propag. in lower troposphere, refractivity effects 77−70747
transhorizon radiowave propag. rel. to remote sensing 78−44921
turbulence and wavelength effect on scintillation fading at mm. wavelengths 78−85623
ultrashort radio waves, refr. index vertical struct. at subfreezing temps. 78−16128
ultrashort wave, long-range propagation, climate effects 77−56716
ultrashort wave diffraction field, mountain ridge snow cover effect 77−64395
USA rainfall variability rel. to microwave attenuation 79−62562
vertical profiles of rain rates rel. to Earth-satellite radio attenuation modelling 79−70841
VHF, meas. in Rajasthan area, India, rel. to climate 77−13106
VHF and UHF, influence of polarisation on transmission quality *(German)* 78−61518
VHF coherent radar sounding, wind and refractivity turbulence struct. 78−28281
VHF propag. over diffr. paths 77−13108
VHF radar echoes, appl. to velocities and irregularities study 79−16701
VHF radar signals, partial refl. and scatt. from clear atmosphere 78−81278
VHF radar signals partial refl. 78−85656
VHF technique for space-time mapping of lightning discharge processes 78−85721
VLBI, correction for effects of troposphere, ionosphere and Earth crustal tide *(Japanese)* 80−21926
VLF radiometeorology for thunderstorm location *(German)* 77−17254
VLF sferics from Union City, Oklahoma tornadic storm 78−85639
water vapour absorption 10 cm-0.27 mm wavelength, temp. dependence 77−2235
water vapour absorption at CO laser wavelengths, 5 μm region 77−2241
water vapour absorption of mm- and sub-mm-waves, calc. method 77−49144
water vapour dielectric constant, rotational part, engineering method of calc. 78−40717
water vapour studies at 22.235 GHz using microwave radiometer 80−72610
waveguide propagation over sea, theory for atmosphere radiothermal radiation *(Russian)* 79−88406
weather radar, Doppler, estimation of echo spectral moment 80−51563
weather radar echo, receiver bandwidth effect on refl. and Doppler vel. estimates 79−53549
wind shear detection radar, for airport use 80−51565
zero cross-polarisation mode for orthogonally polarised signals in rain 77−81991
H_2O vapour, refr. index calc. and dispersive Fourier transform spectrometry 79−32736
H_2O vapour absorpt. in 10-12 μm atm. window 78−20513

truth tables *see logic design*

TSC *see thermally stimulated currents*

TSCD *see thermally stimulated currents*

TSD *see thermally stimulated currents*

TTL *see transistor-transistor logic*

tubes (electronic) *see electron tubes*

tuners *see tuning*

tungsten
see also nuclei with .....
(100), H adsorbate low energy electron vibrational excitation 80−84375
(110) surface, conduction electron interaction with diffracting electrons *(Russian)* 80−79643
acoustic emission under action of single elec. pulse discharge *(Russian)* 77−59071
acoustic NMR line shape, effect of demagnetisation 79−95654
activated sintering, diffusion mech. *(Korean)* 77−73248
adatom, on W (110), dipole moment, field emission meas. 77−47674
adatoms, on Ir(110), surface diffusion by atomic exchange mech. 80−49508
adatoms on (110), substrate strain induced interaction 80−96744
adion-surface interaction energy, density formalism calcs. for alkali metal ions 78−68069
adsorbed Be layers on W(110) and (100), work function and loss spectra meas. 80−6638
adsorbed H_2, LCAO calc. of band struct. 77−8168
adsorbed H, nondipole electron impact vibr. excitations obs. 78−63922
adsorbed H on (100) surface, angle-resolved and variable impact energy electron vibr. excitation spectroscopy 80−76119
adsorbed H on W (001), atomic nature of β-states, electron energy loss spectra 77−76664
adsorbed K layer on (112) planes, temp. depend. of noise spectral density functions 78−2992
adsorbed La atoms on W (112), strongly anisotropic interaction *(Russian)* 77−11798
adsorbed layers of K on (112) planes, flicker noise field emission obs. 78−26774
adsorbed monolayer of CO on (110) surface, LEED meas. 77−59213
adsorbed O, electron stimulated desorption ion energy distrib. and surface struct. 78−75940
adsorbed O, surface diffusion, secondary electron emission study 80−76117
adsorbed O on stepped (100) surface, electron stimulated desorption ion ang. distribs. 80−20035
adsorbed on W(001), struct., FIM obs. 80−103576
adsorbed on W (110), long range interatomic interactions with coadsorbed Pd 80−59789
adsorbed Xe on (110) plane, mobility and two-dimens. compressibility, field emission current fluctuation method 80−80089
adsorped He layer, accommodation coeffs. calcs. 80−66866
adsorption, of Ba and Ti, work function meas. 80−100411
adsorption, of CO, on (110) surface, adsorbate characterisation by UPS, XPS and X-ray AES 77−15683
adsorption, of Na, on (110) plane, ordering, theoretical anal. 78−18892
adsorption, of O_2, electron stimulated desorpt. study, 300K, kinetics, order-disorder transition 78−71985
adsorption, of O, order-disorder transition, theory 78−38811
adsorption, potential of He atom above field adsorbed He or Ne atoms 78−35267
adsorption and decomposition of methanol 77−31887
adsorption and desorption of Ag, mass spectra obs. *(German)* 79−46951
adsorption and early stages of condensation of Ag and Au on single cryst. surface 78−6212
adsorption and replacement of CH_4, CO and NO *(Japanese)* 78−22949
adsorption of 0_2 and CO, angle resolved electron stimulated desorption, LEED and AES 80−6645
adsorption of Ag, substrate temp. effect on relation between work function and coverage, FEM obs. 80−2272
adsorption of Ag on (001), (011) and (111), work function changes 77−62757
adsorption of Ag on (011) surface, LEED, AES, and work function meas. 79−86990
adsorption of Au, field emission microscopy exam. of work function, correlation with LEED and RHEED meas. 78−35276
adsorption of B and La, field emission meas. 78−47662
adsorption of Be, work function changes and scatt. electron energy losses 79−46947
adsorption of Be on (110) surface, film growth and struct. 80−75477
adsorption of benzene, isothermal ramped field desorption technique 79−82450
adsorption of C, Auger signal intensity in differential and energy distrib. mode spectra 79−78799
adsorption of C(O), Auger signal comparison using differential and integral Auger spectra 78−76561
adsorption of Cl_2 on (100) surface, LEED and AES study 79−90878
adsorption of CO, adsorption state at 300 to 80K *(Japanese)* 77−85057
adsorption of CO, AES obs. 77−35818
adsorption of CO, electron energy loss spectral study of surface vibrs. 77−69160
adsorption of CO, FEM expt., pseudoclean pattern *(Japanese)* 78−34701
adsorption of CO, FEM obs. of adsorption state *(Japanese)* 77−62738
adsorption of CO, mol. orientation, ion scatt. 78−71949
adsorption of $CO(H_2)(O_2)$, surface reflectance spectroscopy on low index planes 78−71965
adsorption of CO and N_2 on surface (210), surface struct., LEED obs. 79−82449
adsorption of CO on (001) surface, electron energy loss spectra 78−71999
adsorption of CO on (100), surface vibrs., EELS 77−62745
adsorption of CO on (100) plane, thermal desorption and work function meas. 80−29273
adsorption of CO on (110) plane, electron impact desorption, thermal desorption and work function meas. 77−85064
adsorption of CO on polycryst., SIMS 78−14585
adsorption of Cs and O_2, work function and thermal stability 80−44427
adsorption of Cs on oxygenated and oxidised (110) 80−44424
adsorption of Cu, Ag and Pb, pairwise interaction approach to adsorpt. of oriented overgrowths 77−62759
adsorption of Cu, FIM and FEM obs. of nucleation, epitaxial growth and interface form. 78−26800
adsorption of Cu and Pd, adsorpt. energies 79−51464
adsorption of Cu on single crysts. 78−14612
adsorption of Dy, Ho, Er, field emission electron study 80−100393
adsorption of Fe, work function and field emission obs. *(Japanese)* 78−91536

tungsten continued
adsorption of Ga, In and Sn, field emission, FIM 77−16470
adsorption of Gd in field ion microscope *(Russian)* 77−47662
adsorption of H_2, D_2 and C_2H_2 on (111), EELS 77−66090
adsorption of H_2, FEM study of binding states *(Japanese)* 78−2370
adsorption of $H_2(N_2)(NH_3)$, thermal desorption and pulsed time of flight mass spectra anal. 80−30285
adsorption of H_2 in presence of adsorbed H 77−51594
adsorption of H, PMR meas. of adsorption state, surface migration 78−10275
adsorption of I on (100) at room temp., LEED and AES study 80−84389
adsorption of K, field emission flicker noise, coverage depend. 78−35262
adsorption of La, specific charcts. *(Russian)* 79−1543
adsorption of La monolayer, LEED and contact pot. difference meas. *(Russian)* 77−1316
adsorption of Li, Na, Cs, Sr and La on (011) face, disordering of submonolayer film, LEED obs. *(Russian)* 77−89655
adsorption of methane, on (100) and (111), work function meas. 78−38963
adsorption of Mo on (211) planes, direct obs. of atomic processes by field ion microscopy 77−59219
adsorption of N_2, CO, and O_2, total current spectrum interpretation 77−85857
adsorption of N_2, effect of SIMS, sputtering induced recomb. anal. 80−55243
adsorption of N_2 on (001) surface, effect on LEED electron spin polarisation and intensity profiles 80−65377
adsorption of N_2 on (110) plane, thermal desorpt. and work function meas. 77−1294
adsorption of N_2 on W(110) vicinals, step sites as dissoc. centres 80−6642
adsorption of Ni, effect on surface self-diffusion, FEM charcts. *(French)* 77−1296
adsorption of NO, dissociative, FEM obs. 77−4258
adsorption of NO and NO_2, FEM obs. 80−84390
adsorption of NO on (110) surface, chemical changes detected by AES 80−10787
adsorption of O_2, (110), electron impact and thermal desorption at high temp. 78−30821
adsorption of O_2, H_2, N_2, CO, NO and water on (100) surface, adsorbate densities determ. 77−1320
adsorption of O_2, N_2 and Co, on (100) planes LEED-AES obs. 77−69186
adsorption of O_2, surface struct. and thermally stimulated reaction 77−55451
adsorption of O on (110), adatom interaction energies, Monte Carlo calc. 78−71948
adsorption of Pb, on low-index planes, probe-hole field emission microscopy obs. 77−47677
adsorption of Pb on W(100), W(110) substrates, pairwise interaction model using Morse pot. 80−6657
adsorption of Re_2, on (211) surface, dissoc., thermodynamics 78−87861
adsorption of Sm, conc. depend. of lifetime and heat of adsorption of Sm atoms 79−69364
adsorption of Sr and La on (011) face, influence of substrate electronic struct. on props. 78−60032
adsorption of V, effect on work function 77−51607
adsorption of W single atoms on (111), (211), and (311), surface site geometry determ. by FIM 80−39447
adsorption of Xe and coadsorption with O on (110) and (100), work function and thermal desorption meas. 80−39448
adsorption of Zr, low-temp. mobility, surface struct. 77−20197
adsorption of Zr on (100) surface, AES, LEED, thermal desorption, and work function meas. 80−39444
adsorption on Mo (100), effect on surface reson. 79−65983
adsorption surface migration and thermal desorpt. of LaB_6 79−56075
adsorption-desorption behaviour of KCl on (110) and (111) surfaces 80−75442
alloy systematics, rel. to the long periodic table, β-W phases systematics 79−37649
amorphous, reflection of D and T, Monte Carlo study 80−40197
annealed wire, analytical determ. of K content of single bubbles 78−64909
anode, dendritic growths during prebreakdown conditions in organic residual gas, electron microscope obs. 78−44383
anode, of end-fire plasma accelerator, high-current discharge effects, anode damage 79−27839
anodic behaviour in methanolic solns. 77−73368
anodic dissolution macrokinetics, in alkaline solutions *(Russian)* 77−12804
anodic oxidation, effect of electrostriction, ellipsometry meas. 78−92394
anodic oxidation, open circuit transient anal., dielec. and elec. props. of oxide film 80−3245
anodic oxidation in aq. base 77−77627
anodisation, oxide struct., electronic current, and const. current efficiency 78−15575
anodisation in acidic chloride solns., formation and breakup of anodic oxide films 77−16719
anodised layer, structure and stoichiometry, thickness effects 77−77634
arc welds, fatigue crack growth behaviour in air and high-C liquid Na, carburization studies 80−40625
atom, α-particle impact K-shell ionisation, 40 to 110 MeV 78−17752
atom, even config., parametric calcs. 78−82631
atom, fast electron beam scatt. calcs. 77−65534
atom, first-principles pseudopotential in the local-density-functional formalism 79−59328
atom, high resolution phase contrast electron microscopy imaging 80−103224
atom, ion induced K-shell ionisation cross-sections determ. by comparison with nuclear Coulomb excitation 79−76500
atom, $K\alpha_1$ X-ray line wavelength determ. 79−41132
atom, L-shell X-ray photoelectric cross sections, fluorescence spectra 78−58636
atom, magnetic hyperfine struct. 78−934
atom, multiphoton ionisation and absorpt. 80−95575
atom, N-shell ionisation by proton impact 78−78800
atom, photon-bound-electron scatt. meas. 77−14394
atom-probe field ion microscopy obs. *(French)* 78−86389
atomic absorption analysis, using electrically dispersed sample 79−74459

tungsten continued
atomic beam magnetic resonance, HFS and contact interaction 79−68207
atomic density, effect on proton energy loss and dechannelling 80−65088
atomic masses and mass differences, mass spectrometric obs. 77−42433
atomic spectra, isotope shifts in visible region and HFS 78−82694
atomic X-ray spectra, parity violation, from electron-nucleus weak currents *(Russian)* 79−22642
Auger spectrum, 150 to 200 eV 80−35022
backscattered energy spectra, charged particles energy losses 79−83086
backscattering energy spectra, channelling proton energy loss determ. 78−2181
barrier metal for sintered Pt-GaAs contacts 77−8193
BCC, interaction energy between self-interstitial and screw dislocation, calc. 80−70248
BCC, neutron-irradiated, Frenkel defect spontaneous recomb. volumes 79−60355
BCC, structural singularities rel. to solid soln. behaviour *(Russian)* 77−11696
binding energy, lattice parameters bulk modulus, self-consistent pseudopot. calc. 79−60748
block boundary dislocation struct. singularities under high temp. steady state creep conditions *(Russian)* 79−90670
bombardment by 1 to 30 keV ions, emitted radiation spectral comp. *(Russian)* 77−81159
bombardment with Na and K ions, neutral component of scatt. 78−11047
boriding, Cu influence 80−21165
borosilicate cladding compatibility *(Russian)* 77−66741
bremsstrahlung spectra, 10 to 30 keV, thick target expts. 77−8687
candidate refractory for Tokamak, thermal fatigue failure testing 80−32454
carburisation by methane, initial kinetics 79−47824
carburization, catalytic Co effect 80−3255
carburizing rate, Co effects *(Japanese)* 79−52453
catalytic activity during adsorption of HD 79−69358
catalytic decomposition of NH_3 single pulses, mol. beam relax. spectrometry 80−21321
cathode, BaO-coated, struct. transforms. in coating, LEED obs. 78−11061
cathode, electron emission mechanisms in Ar arc 77−24224
cathode, explosive emission charact., microscopic surface effects 77−7624
cathode, high-current, multicavity, thermionic, erosion mechanisms, sputtering 79−55570
cathode, high-current hollow, energy balance *(Russian)* 77−58910
cathode, hollow, cylindrical, heavy-current temp. condition 80−38763
cathode, impregnated with Ba and BaO, AES and work function meas. 77−24921
cathode, motion of cathode spot of vacuum arc 80−54069
cathode, multicavity, Ar discharge, V-I and power charact. 78−26360
cathode spots on vac. arc discharge electrodes, model 78−91179
cathodes, heating by DC electron bombardment 78−23578
cathodes, micro-size, change in shape and electron field emission 79−74067
cathodes arced in vacuum, erosion structs. 80−1872
channelled particles, quantum oscills. of spatial density 77−39620
channelled proton energy losses 77−1161
channelling, axial to planar transition, proton induced X-ray yield meas. 77−31704
channelling of H^+ and He ions, backscatt. particles ang. distrib. 79−51174
channelling of He atoms, calc. 80−34108
chemically activated sintering 77−1826
chemically driven grain growth during sintering in liquid Ni 79−61532
chemisorbed CO and acetylene, IR vibration spectroscopy using refl. inelastic electron scatt. 78−14603
chemisorbed H_2, on (100) surface, vibr. excitation of hydrogenic modes, angle dependent electron energy loss meas. 79−46914
chemisorbed H_2, vibr. spectra charact., adsorption sites 80−70535
chemisorbed H, surface cond. and intrinsic surface states, surface refl. spectra 80−15378
chemisorbed H monolayer on (001), surface phonons, lattice dynamical model 80−39405
chemisorbed O on (110), island form. and condensation 80−49517
chemisorption, of N_2 and H_2, on perfect surfaces 79−86979
chemisorption, of $NH_3(ND_3)$, decomposition mechanism, isotope effect 79−29409
chemisorption, of O, on (110) surface, adatom-adatom interaction energies determ. 78−67904
chemisorption, of O, on (110) surface, phase transitions, coverage effects 78−79879
chemisorption of β-N_2 on {110} surface, underlayer mechanism 80−39432
chemisorption of acetylene, rehybridization, electron energy loss spectra 78−31289
chemisorption of Ba, inelastic tunnelling spectra 78−47664
chemisorption of C, N and O, SXAPS obs. 79−52048
chemisorption of CO_2, NO, on (100) surface, UPS studies 79−23841
chemisorption of CO and N_2, α and β states, AES and electron energy loss spectra 77−1313
chemisorption of CO on (100) surface, mol. orbital study 78−71995
chemisorption of CO on (110) plane, LEED, XPS and Auger meas. 77−89647
chemisorption of cyclic hydrocarbons on (100) surface 80−59782
chemisorption of ethane on W(111), AES and LEED pattern exam. 79−15005
chemisorption of ethylene, reaction with atomic H 77−36789
chemisorption of H_2, HFS model cluster calcs. 77−51795
chemisorption of H_2, on (100) surface, adsorbate-induced surface reconstruction 79−4472
chemisorption of H_2 and halogens on (100) surface, adatom charge and binding energy, self-consistent calc. 77−62734
chemisorption of H, angled resolved UPS exam. 77−55865
chemisorption of H and O, (001) surface, localised orbital approach 78−14587
chemisorption of H on (001) surface, HF Green's function formalism and phase shift technique 80−24733
chemisorption of H on (100) surface, localised orbital approach 77−69165
tungsten continued
chemisorption of H on (100) surface, struct. determ. by surface vibr. modes anal., EELS obs. 80−39435
chemisorption of H on surface (100), phase changes, LEED obs. 79−77911
chemisorption of halogens on (100) surface, UV photoelectron spectrosc. study 80−7854
chemisorption of N, surface diffusion, scanning Auger spectroscopy exam. 77−55452
chemisorption of NO, 80K, FEM obs. 77−39733
chemisorption of O_2, initial oxidation, reaction probability 78−15700
chemisorption of O_2, island form., adatom interactions 79−46922
chemisorption of O_2, SIMS, hysteresis effect 77−72771
chemisorption of O_2 on (110) surface, low temp. precursor state 77−11794
chemisorption of O_2 on surface (100), SIMS spectrum 78−34712
chemisorption of O, island dissolution phase transition 77−80698
chemisorption of O atoms, atom interactions, Monte Carlo simulation 77−52667
chemisorption of O on (110) surface, three-adatom non-pairwise interaction, Monte Carlo simulations 79−82466
in chondritic meteorites abundance and distrib. 78−32412
Clebsch-Gordan coeff. for X×X and R×R irreducible representations 79−14732
Clebsch-Gordan coeffs. in β-struct. 79−37645
clustering of adsorbed Kr, He desorption spectrometry 80−77908
coadsorption, of Cs and O_2, on (110) surface 77−89656
coadsorption of Ba and Cu atoms, work function changes 80−65378
coadsorption of Cs and Ba, work function of surface under equilibrium conditions 79−15025
coadsorption of H and CO on (100) face, photoemission and thermal desorpt. investig. 77−28079
coadsorption of La and B, field emission and field ion microscopy 80−104049
coadsorption of Ni and K, average work function change 79−28190
coadsorption of Th and H, FEM exam. 79−90869
coadsorption of Zr and O_2 at high temp. on (100) surface 80−6653
coated graphite, substrate for CVD of GaAs, film prep., props. and solar cell charact. 79−28930
codeposition of Cs and O on (110), Cs_2O form. 80−44425
collective field evaporation from (110) face, field ion microscopy *(Russian)* 79−61504
combustion under CW CO_2 laser radiation action 80−30241
composite W-PVC material, fabrication and performance, acoustic properties 80−76218
condensation of Cu and Ag on (100), early stage comparison with Mo(100) 80−80072
conduction electron g-factor, US vel. quantum oscills. 77−28100
conduction electron mirror refl. from cryst. surface *(Russian)* 77−35985
conduction electron spin waves, Larmor wave 79−33543
contact with BN, barrier layers for good high-temp. stability 79−70194
containerless melts in terrestrial and space environment, thermodynamic props. calc. from solidification and cooling curves 79−70052
corrosion protective coating for Al_2O_3-Y_2O_3 ceramics 80−35367
creep, high temp., influence of thermomechanical treatment *(Russian)* 79−79034
creep in monocrystal at 0.57 T_m *(Russian)* 77−1856
crystallisation by containerless levitation 77−36394
CVD, by reaction of WF_6 and H_2, kinetics 79−19995
CVD, high temp. strength and ductility 77−52406
CVD, on Si, properties and kinetic parameters for deposition 78−91570
CVD coating, on W-ThO_2 and SiC filaments, effect on high temp. mech. props. 78−15347
CVD hardfacing of coal gasification unit components 77−40472
cyclically deformed, electrical resistivity 77−52491
D electro-fission on relativistic channelling *(Russian)* 80−54294
de Haas van Alphen signal anal. by linearly recursive approx. 78−91603
Debye-Waller exponents, modified ang. force model 77−76515
Debye-Waller factor, temp. variation, lattice dynamical calc. 78−55925
defect recovery following neutron irrad., annealing effect 79−77642
deformed, surface layer struct. effect on polygonisation and recryst., X-ray diffr. anal. and metallographic exam. *(Russian)* 80−84948
dendritic surface anodisation for solar absorptance enhancement 79−34440
dendritic surfaces, antireflection coated, reflectance geometrical study 79−91511
desorption, electron stimulated, of O^+ ion on (100) surface, hysteresis and ion yield minimum 77−59218
desorption, of Cs-O_2, activation energy 80−103562
desorption, of Ga from oxidised polycryst. surface, kinetics 78−75939
desorption, of O^+ and O, electron-stimulated, cross-section temp. depend. 77−31908
desorption, photon-stimulated, angle-resolved, of O^+ from (111) surface 80−88434
desorption by electron impact of CO and O_2, isotope effects 77−76658
desorption dynamics of Cs, surface ionisation voltage modulation method 80−44426
desorption kinetics of halogens, pulsed ion beam method 80−34300
desorption of Cl(Br)(I), field ion microscope exam. 78−35270
desorption of CO, thermal desorption and conversion kinetics, AES study 78−71959
desorption of CO from (100) surface, electron and photon stimulations 79−99414
desorption of D_2, meas. of fast desorption kinetics by laser heating technique 79−23837
desorption of F and Ba, from polycryst. ribbon, electron stimulated 77−11793
desorption of H^-, electron stimulated, from chemisrobed H_2 79−86999
desorption of O_2, electron desorption cross sections 79−46944
desorption of O_2, electron-induced *(French)* 77−85853
desorption of O^+ and O^-, electron stimulated, from chemisorbed O_2 79−90875
desorption of O^+ bonding and kinetics 77−62746
determ. by atomic absorption, using low temp. flames 80−30307
determination, in Mg alloy, emission spectrographic DC arc-powder technique 78−48713
diatomic cluster migration on W {100} plane, elementary displacement steps 80−88436
diffusion anomalies, vacancy model *(French)* 77−43366

tungsten continued
diffusion barrier between Ni-Cr-Al coatings and Ni eutectic alloys in gas turbines 79−24673
diffusion in Mn steel, electron probe microanalysis *(Czech)* 77−59149
diffusion in Ni, to Co diffusion, 1050 to 1400°C *(Russian)* 79−28147
diffusion in semicond., B, temp. depend. of coeffs., mechanism 77−7898
diffusion in ZrC and TaC, correl. with self-diffusion 77−24437
diffusion interaction with liquid Al *(Russian)* 78−26735
diffusion into liquid Al, under low gravity *(Russian)* 78−22875
diffusion of Li, Cs, vacancy and divacancy mechanisms *(Russian)* 80−70472
diffusion of P, 1880-2180°C *(Russian)* 78−43182
diffusion of U at high temp., determ. by neutron fission tracks meas. 77−89587
dislocation structure of block boundaries in single crystals *(Russian)* 79−77603
dispenser cathodes, Ba-activated, surface characts., ion scatt. spectrometry and SIMS study 80−66377
dissociative adsorption of O_2, energy accommodation and reactivity 77−86352
distribution of C, effect of grain boundary free energy *(Russian)* 77−90351
divacancy binding energy, appl. stress effect, computer simulation 77−15408
doped, Ni activated recrystallisation, ion probe mass spectrometer obs. 77−44280
doped wire, secondary recrystallisation temp., bubble parameter effects 77−32596
doped wire, textural aspects of recrystallization 78−11239
Doppler-shifted cyclotron reson. along nonprincipal cryst. directions *(Russian)* 79−4725
drawn wire, microstruct. effect on fracture 80−3177
edge dislocation interaction with interstitial atoms, influence on Peierls stress 78−34537
elastic wave scatt. from oblate spheroidal WC inclusion 80−65151
electrical resistivity, quadratic contrib., 2 to 40K *(Russian)* 80−92874
electrical resistivity -temperature scale and vacancy parameters 78−71727
electrical resistivity below 1K meas. 77−15820
electrnic sp. ht. and heat conduction, temp. depend. 78−71865
electrochemical treatment, current distrib. and metal throughput *(Russian)* 79−15849
electrode, method for sealing into quartz 79−71463
electrode material, influence on electric breakdown in dielectric liquids *(Russian)* 80−50265
electrode reactions with molten glass 80−85186
electrodes, C segregation and arc damage 80−64795
electrolytic anodisation, production of WO_3 electrochromic elements 80−25921
electron backscatter fractions 78−87717
electron channelling in (111) direction, 1000 to 2000 eV energy range 78−38763
electron channelling in (111) direction, 200 to 1000 keV 78−2182
electron channelling map *(Chinese)* 79−73229
electron emission spectra, transmission induced struct. 78−43965
electron energy loss mechanism, surface and volume losses, anal. 79−91547
electron energy loss spectra, vol. and surface plasmon excitation 77−52207
electron field emission statistics 77−1791
electron gun cathode heating using focused laser beam *(German)* 78−89591
electron impact ionisation, L-subshell cross-sections, X-ray obs. 79−76519
electron induced Auger spectrum, double ionisation satellite 79−87532
electron irradiated, or ion irrad., stage II, point defect struct., FIM 77−80542
electron irradiated, recovery of resistivity, 4.5-380K *(German)* 78−87714
electron irradiation, 1200 MeV, ang. distrib. of emitted particles *(Russian)* 79−33025
electron loss spectrum, (001) surface, momentum transfer effects 77−85858
electron stimulated desorption of O_2, CO, and H_2, threshold behaviour 77−47678
electron stimulated desorption of O^- and O^+ ions from adsorbed CO 80−2270
electron stimulated desorption of O from (100) and (110) surfaces, combined LEED and AES method 79−33181
electron stimulated desorption of O from (110) stepped surface, atomic steps and defects influence 80−80091
electron stimulated desorption patterns from O_2 on (100) and (111), computer simulations 80−75443
electron stimulated H^+ desorption, (100) face 77−66091
electron-channelling patterns, crit. voltage effects 80−79647
electron-electron scatt. 78−68025
electron-electron scatt. 79−60822
electronic and struct. props., nonlocal pseudopot. calc. 80−34349
electronic density of states, optical mass and DC elec. resist., Slater-Koster interpolation 77−15731
electronic transport below 1K 80−2377
electroplastic drawing, deformation zone current delivery schemes 79−91761
EM showers produced by electrons, positron spectral distribution *(Russian)* 80−55218
emissivity, integral hemispherical degree of blackness, 1200-3000K 78−43154
emissivity, total hemispherical, of W (100), sensitivity to O_2 adsorption 80−79964
emissivity, total hemispherical 79−10973
emissivity angular dependence, meas. in IR spectral region 80−34214
emittance, calc. from spectral radiative and reflecting props. 77−35730
emitter, surface struct. change during baking above 2000K 79−65971
emitter characts. for field desorption mass spectrometry of salts 77−63980
emitter tip, surface shape changes, field ion microscopy meas. 78−26754
enhanced penetration of low energy He along ⟨100⟩ channel 80−65093
enthalpy, relative, 273 to 1173K, electronic heat capacity coeff. 80−103496
epitaxial film CVD growth, inelastic light scatt. as in situ probe of chem. reaction 77−40383

tungsten continued
epitaxial growth of Fe, FIM obs. 78−79904
epitaxial growth of Rh, Ir, Pd and Pt on (001) surface 79−99450
epitaxy of Au on (110), LEED and AES 77−69198
epitaxy of Ni, Cu, Au, Ag on (001) 78−60041
epitaxy on W(110) substrate, work function meas., LEED investigation 80−80103
erosion by laser beam, in self-consistent mode *(Russian)* 77−69945
evaporated coatings produced by carbonyl method, struct. *(Russian)* 77−43441
evaporated film production, notched wire flashing method 78−35309
excess edge and screw dislocation density calc. *(Russian)* 78−34519
exploding wire, peripheral arc initiation 78−87559
Fermi surface, uniaxial strain depend., quantum oscills. in magnetostriction, US vel., with torque 77−28094
Fermi surface press. depend., surface impedance and US attenuation oscills. in mag. field 77−43476
Fermi velocity calc. 79−4504
fibers, dependence of fine struct., on processing parameters 79−34082
fibre, brittle to tough transition, impact strength meas. 80−40527
fibre, deposition of ZrC coating acting as diffusion barrier in composite 77−4759
fibre, KAl, KSi, KSiAl and KSiGa, addition effects on workability *(German)* 78−64557
fibre, KSiAl doped, recrystallisation, Li diffusion effects, hardness, strength, microstructure meas. *(German)* 78−64644
fibre, spiral, brittle, densification of particulate materials, general law 78−19692
fibre reinforced Al, alloying element effect on interface form. *(Czech)* 77−85963
fibre reinforced Co powder alloys, reactions and recryst. 80−11603
fibre reinforced Cr alloy composites, reactivity of Y_2O_3 protective film 79−100297
fibre reinforced Cu composite, hardening in two-phase material 77−52448
fibre reinforced Cu composite, temp.-load depend. of time-to-rupture *(Russian)* 78−11299
fibre reinforced Cu composite, work hardening 77−52341
fibre reinforced Cu composites, correl. between thermal cycling-induced microstructural changes at interphase boundaries and tensile behaviour *(Japanese)* 80−71674
fibre reinforced epoxy composite, static tensile behaviour *(Japanese)* 78−15482
fibre reinforced leucosapphire single cryst., growth 77−16530
fibre reinforced Nb, plastic deform. and fracture 77−40438
fibre reinforced Ni, high temp. stability 77−48372
fibre reinforced Ni, produced by liquid infiltration 77−48371
fibre reinforced Ni, work hardening tendency, at elevated temps. 77−52353
fibre reinforced Ni alloy, high temp. composite development 77−48370
fibre reinforced Ni and Ni-Fe alloys, fabrication, heat treatment, and mag. and mech. props. 77−40408
fibre reinforced Ni composite, prep. by hot isotactic pressing, mech. props. *(Slovak)* 78−19694
fibre reinforced Ni composite, study at high temp. in O_2 and combustion gases 77−48567
fibre reinforced Ni composites, high temp. tensile and creep props. 77−52444
fibre reinforced Ni-Cr (20 wt.%), hot pressing kinetics 78−35334
fibre reinforced Ni-Cr steel, TiN coated fibre, protective props. *(Russian)* 79−66201
fibre reinforced Ni-Cu composite, liquid phase sintering under press. 78−19695
fibre reinforced powder metal and alloy based composites, high temp. strength of W wire 79−70021
field cathode with (001) orientation preparation technique 80−15241
field desorption of Ba atoms, conc. depend. 80−25533
field desorption of K, from (001), (011) and (112) planes 78−34715
field electron energy distrib., surface density of states, surface pot. effects 77−16471
field emission, absolute tunnelling current density 79−38724
field emission, mag. field effects 80−93463
field emission, spin filter effect of EuS 80−45221
field emission anomalies in mag. field *(Russian)* 80−93462
field emission cathode, oxygen processing method 78−64448
field emission current instability, freq. spectrum, effect of H_2 and CO adsorption 77−32509
field emission currents, modified by external mag. fields 78−88408
field emission energy distrib., adsorbate overlayer geometry effects 77−8730
field emission tip, (310)-oriented with high brightness, appls. 78−27382
field emission tip, microscopic protuberance formation, min. elec. field and temp. 78−6835
field emitter, adsorption of Cu, field emission energy distribs. 77−59677
field emitter, adsorption of Se, field emission meas. 77−31889
field emitter, adsorption of Te on single cryst. faces 78−34714
field emitter, covered with Ga, In and Sn, tip stability, alloy form. 77−12500
field emitter, Cs VPE, FEM obs. 80−70552
field emitter, current fluctuations from cryst. faces 78−35263
field emitter, effect on Au adsorption on (110) and (211) planes 77−12503
field emitter, field-induced stresses, numerical analysis 78−35274
field emitter, imperfect, In epitaxial layer formation 78−60037
field emitter, periodic field-dependent photocurrent 78−35260
field emitter, strong polarisation effect in photoinduced field emission 78−95684
field emitter, substrate for K, emission from individual K planes 78−27385
field emitter, surface migration and overgrowth of LaB_6 77−85902
field emitter, Te adsorption 77−69177
field emitter, work function determ. for Bi and Bi_2S_3 78−6834
field emitter tip, condensation remoulding, field emission microscopy 78−2995
field evaporation, gas-surface interaction in atom-probe FIM 77−40336
field evaporation end form at 4.2K 77−1790
field evaporation in FIM, computer simulation 77−69973
field evaporation patterns, multilayer 77−59675
field ion (emission) microscope tip prep. from sheet and block metal 78−7155

tungsten continued
field ion emitter, calibration using energy distrib. of free space field ionisation 77−69971
field ion image, stripe contrast form., dislocations role 78−18652
field ionisation, photon assisted 78−3000
field-emitted electron energy spectrum, microprojection effects 77−1789
field-ion emitter, determ. of precise geometry from field-ion image 80−2930
filament, adsorpt. of CO, temp. controller for filament heating appl. *(Japanese)* 77−51603
filament, coated with thin Ni film, creep and recrystn. *(Russian)* 78−19822
filament, enhancement of field ionisation efficiency by carbide particle nucleation 77−90256
filament, hot, adsorpt. and decomp. of formaldehyde 77−90641
filament, incandescent, light flux fluctuations, limiting factors in photoelectric meas. 80−13136
filament, incandescent lamps, creep, failure, life prediction 78−84927
filament, resist. heated, for metal vapour deposition 78−52689
filament, temp. control 79−9215
filament lamp, polarization characteristics 80−95970
filament lamp, Stefan's law demonstration, student expt. 78−54125
filament-metallised MOS capacitor, effect of K contamination 79−51679
filaments, as electrothermal atomisers in at. absorpt. spectrophotometry 78−44432
filaments, as electrothermal atomisers in at. absorpt. spectrophotometry 78−44433
filaments, operated as cathodes in gas discharge, characts. 79−50913
filaments as electrothermal atomisers, atomic absorption spectrophotometry appl. 78−86346
filaments as electrothermal atomisers in at. absorpt. spectrophotometry 78−27860
film, band struct., appl. of extended rigorous cellular method 78−52055
film, BCC, optical props. 79−78781
film, CVD, optical props., solar absorber appl. 77−55844
film, electron beam deposition on Si, X-ray obs. of silicide form., diffusion processes *(German)* 77−1341
film, electron beam evaporator for in situ deposition studies in UHV electron microscope 80−40264
film, evaporated, optical props., rel. to struct. 80−55211
film, ion plating deposition system using electron beam evaporation *(French)* 80−20802
film, optical absorption meas. using synchrotron radiation, 20-250 eK 77−12457
film, silicide formation during growth by electron beam evaporation *(German)* 78−84717
film, specularity coefficient of conduction electrons, angular dependence *(Russian)* 79−87167
film, sputtered, physical props. 79−77938
film, support, for electron microscopy, Fourier spectrum analysis of phase contrast 80−95199
film, surface RF impedance in strong mag. fields *(Russian)* 80−92920
film and foil, surface IR wave propag. distance 77−28641
film deposited by low temp. carbonyl pyrolysis, struct. 78−72039
film production 77−21029
film sputtered on Si crysts., annealing response, strain distrib. characterisation 77−70140
films, (010), energy band calc. including spin-orbit interactions 80−20274
films, vac. evaporated, optical cond. 80−76100
FIM study of lattice damage caused by low-energy He ion bombardment 78−95090
fine particles formed by gas-evap. technique, cryst. struct. and habit 79−27935
fine tip cathode, field emission stability, rel. to passivation 80−100760
fine tip microcrystal, microscopic protuberance form., crit. remoulding obs. 78−27380
fine tip microcrystal, thermal smoothing after critical remoulding 78−27381
fine tip microcrystal, vertex remoulding, effects on field emission 78−27379
flow stress temp. depend., effect of interstitial atom clustering and embrittlement *(Russian)* 78−34538
foil, adsorption and condensation of Fe, meas. by thermal desorption in pulse time-of-flight mass spectra 79−15023
foil, adsorption of Sm, kinetics meas. by flux modulation method 79−69363
foil, electron diffr. effects and images from inclined grain boundaries 79−82241
foil, integral heating by msec laser pulses *(Russian)* 77−59824
foil, rolling procedures 80−23225
fractional charge on W particles, Millikan method search 77−74349
fracture, semi-brittle, of (100) oriented cryst., plastic relax. effects 77−69036
Frenkel pair creation and stage I recovery of electron irrad. cryst. near threshold 79−1463
friction in contact with polycrystalline elbor and diamond, temp. depend. *(Russian)* 77−73350
gamma-ray scattering, incoherent, total at. cross section 79−13679
grain boundary migration initiated by high hydrostatic press. 78−51554
grain boundary migration obs. using FIM 78−79617
grain boundary segregation, competition between interstitial atoms, AES obs. *(Russian)* 77−25008
grids of fine W wire, production, use in IR spectroscopy, polarization interferometry 80−9052
growth and desorption of In epitaxial layers on W tips, high field microscopy obs. 79−69380
Hall effect, alternating sign, and doppleron spectrum 78−79981
Hall effect, temperature dependence 78−91666
heat resistant particles in low temp. Ar plasma, heating, melting, vaporisation *(Russian)* 80−40384
heater for leucosapphire synthesis, recrystallisation 78−2151
heteroepitaxial deposits with (110) orientation by molten salt electrolysis 78−47683
high purity, zone-refining growth, radial distrib. of structural defects *(Russian)* 79−19250
hole ellipsoid scatt. rate temp. dependence, magnetoacoustic obs. 79−51472
hot electron emission using ruby laser pulses 79−28883
hydrometallurgical plant effluent waters, Mo and W determ. by activation analysis with low-power neutron sources 78−7279

tungsten continued
impedance oscillations in mag. field 78−39140
implantation effects of ^{133}Xe, annealing behaviour, Mossbauer study 80−40011
impregnated cathode, mechanism of operation, life-tests 79−78821
impurity interactions with C, N, and O, struct., mech. props. and purification 79−52277
interaction with gases, H_2, N_2, O_2, CO, water vapour and hydrocarbons *(German)* 79−74296
interatomic pair potential, phonon spectra 80−33927
internal friction and elastic constants, reson. vibrs. of metal spheres 78−15443
ion, spectra from beam-foil excitation and Tokamak produced plasmas 79−54828
ion backscattering, H^+ and He^+, from W and WO_3 79−43081
ion bombardment, energy distrib. of positive secondary ions and sputtered atoms 77−32485
ion emission from PLT Tokamak, W ion soft X-ray emission effects 78−83537
ion impact desorption of atoms and molecules by low energy ion scattering 79−4883
ion implantation, $^4He^+$ range profile and ^4He diffusivity meas. 79−33022
ion induced secondary electron emission, probe for adsorbed O 80−55251
ion irradiated, defect clusters obs. 80−2089
ion scattering from clean surface in 1 to 10 eV range, trapping probability model 77−12479
ion scattering from single crysts., MeV He^+ ions 77−69952
ion sputtering yield reduction by special surface microtopography 77−36330
ion-irradiated, recovery behaviour studied by field ion microscope 80−29074
ions, beam-foil spectra from 20 to 238 MeV energy, 5 to 60 nm, lifetime meas. problems 80−9722
ions, fractionally charged, search 78−29083
isomer shift values of implanted $^{133}Xe/^{133}Cs$, Mossbauer spectra 80−7240
isotopically enriched target preparation using electron gun 80−23226
ISSEC selection for fusion reactor 80−57950
Knight shifts obs. with 6.2 keV ^{181}Ta Mossbauer resonance 79−11369
Knudsen cells heated by radiation, emissivity *(Japanese)* 80−13073
L-subshell ionisation cross section, branching ratios, fluoresc. yield, Coster-Kronig factors 80−43166
laser damage threshold at 10.6 μm, up to 10^{10} W/cm^2 77−50707
laser heating in air by obliquely incident radiation 80−71815
laser induced desorption, mirror electron microscopy 78−84067
laser irradiated, charged particle emission from back side of target 78−2949
laser irradiation, negatively charged particle emission 77−8690
laser shock induced microstructural changes, rel. to explosive shock induced phenomena 78−67768
lattice dynamics, model incorporating second neighbour shell-shell interactions 77−59082
lattice frequency spectra, sp. ht., Debye temp. 78−22799
lattice linear and surface defects, math. modelling 77−89450
lattice wave dispersion, lattice consts., elastic consts. 80−24545
LEED, low index surfaces, spin polarisation, intensity profiles 77−62722
LEED and electron microscopic investigs., review *(Hungarian)* 77−47654
linear expansion coefficient, at low temp. 78−83977
liquid, elec. resist., melting pt. to boiling pt., temp. depend. 80−96839
liquid, thermal volume expansion, MP to BP 79−90802
liquid density at onset of sharp fall in elec. cond. 79−33026
longwave dopplerons, nonlocal Hall effect, surface impedance, size effect *(Russian)* 80−80253
luminescence characteristics of pure surfaces acted on by flux of field emission electrons 80−100695
magnetoacoustic effect shear wave selectivity 79−47131
magnetoacoustic studies for longit. and shear waves 78−91604
magnetoresistance, linear, semiclassical transport theory 77−35925
magnetoresistance, temp. depend. in single cryst. plates *(Russian)* 79−7820
magnetoresistance of size influenced samples, temp. depend. 79−28338
mechanical properties and structural nonuniformity 79−15705
metal, optical props., high-temp., from emissivity ang. depend. data 78−39519
metallic coated, produced by electrospark alloying, corrosion behaviour in Cl saturated NaCl solns. *(Russian)* 79−39026
microelectrode potential and small-signal impedances 79−34715
microhardness and charact. hardness 79−52376
microhardness anisotropy determ. by scratching, single crysts. 77−77669
microneedles, field electron emission, suitability for electron source investigation 78−52644
microscopy, signal-to-noise enhancement by superposition of bright-field images obtained under different illumination tilts 80−6329
molten, expansion, upon rapid elec. current-heating 79−42280
molten drop break up in gas flow, surface drag, capillary excitation *(Russian)* 80−100024
monocrystals in alkaline electrolyte, surface orientation, effect on anode current *(Russian)* 80−75360
monolayer gas adsorption, relax., electron contrib. to chemisorption, Auger shift study 80−20738
monolayer of Ga(In)(Sn), field ion image qualities and work function 78−35272
Mossbauer effect, Debye temp. *(Russian)* 78−23383
Mossbauer recoilless fractions, temp. depend. 78−15076
Mossbauer spectra, 2nd-order Doppler shift, 1-100K 79−91317
multiple field ion emitters, props., ionisation efficiency improvement 78−76588
needle crystal growth, discharge-induced decomp. of hexacarbonyltungsten mols. 80−84414
needle field emitter, ion bombardment effects, field emission microscope obs. 77−55869
needles, mechanism of cathodic growth, decomp. of $W(CO)_6$ under high field conditions 80−76162
needles produced by $W(CO)_6$ decomp. 79−95302
neutron activation analysis using low energy accelerator 77−73499
neutron irrad., at thermal energies, annealing exam. of recovery 78−47355
neutron irradiated, FIM obs. of radiation damage 79−7632

tungsten continued
neutron irradiated, recovery of defects, isochronal and isothermal annealing 79−46712
neutron irradiation temp. determ. by electrical resistivity meas. 78−58354
neutron low energy interaction cross sections, gravitational spectrometer meas. 80−24521
neutron sources with 10 MeV electron beams 80−83231
neutron yield calcs., electron beam incidence 78−95622
optical constants, dispersion, temp. depend., Kramers-Kronig calcs. *(Russian)* 77−69796
optical emission, broadband, due to heavy ion bombardment 77−28635
optically polarised conduction-band electrons, spin-polarised photoemission obs. 79−74055
oxidation, staged flow of O_2 interaction process, secondary ion emission obs. 78−11386
oxidation, WO_3 amorphous anodic film growth in acidic soln. 80−81232
oxidation during energetic particle irrad., influence of reactive gases on sputtering and secondary ion emission 78−72656
oxidation in flow conditions at 1000 to 6000K 78−11445
oxidation mechanism, 773 to 973K 80−108644
oxide film, contact interaction with graphite, exam. of interference effect *(Russian)* 79−11721
oxidised surface, adsorbed amines and hydrazines identification by surface ionis. 77−21456
P-V meas., 5 to 45 kb *(Chinese)* 79−23676
particle formation, ultrafine, via pulsed laser breakdown of $W(CO)_6$ 80−84881
phase transition on (100) surface, LEED exam. 77−55433
phonon density of states determ. from heat capacity *(Russian)* 80−29131
phonon dispersion, Debye temp. and Debye-Waller factors, lattice dynamical model 78−55920
phonon dispersion curves, extended de Launay model 77−4162
phonon dispersion relations, modified tensor force model 80−103428
photo field emission spectra of optical transitions, band struct. 77−16467
photo field-emission, periodic current deviation, wavelength depend. *(German)* 78−23579
photo-stimulated field emission, effect of light polarisation, pure and Ba covered W *(French)* 80−7480
photocathode, for windowless XUV photodiode, photoefficiency 20 to 250 eV 78−65963
photodesorption of CO forming CO_2 79−52777
photoemission, angle-resolved, from clean surface 78−15294
photoemission, four-photon, incident angle and polarisation depend. 80−40221
photoemission, two-photon, induced by picosecond laser pulses 77−77347
photoemission anisotropy from core levels, W (100) surface with adsorbed Cs 78−11076
photoemission efficiency of Cs and O_2 coadsorbed W (100) 77−55862
photoemission from clean and H_2 chemisorbed surfaces, symmetry-related polarisation effects 78−56566
photoemission of polarised electrons, W (001) adsorbate system 77−36374
photoemission of spin polarised electrons 78−35248
photoemission spectroscopy, angle-resolved, of (001) surface, polarisation expt. anal. 77−40332
photon absorption and photoelectric cross-sections calcs. 79−31486
photon and electron stimulated desorption ion energy and angular distributions for O^+ 80−96734
photoneutron yields released by incident electrons, improved calc. 80−27630
physisorption of Xe on (100) surface, Lennard-Jones model, mol. dynamics study 80−34308
plane {123}, clean and H saturated, surface diffusion of single W atoms 80−80081
plasma, high temp., opacity calcs. 78−79414
plasma, Saha's ionisation eqn. soln., input for opacity calcs. 77−39412
plasma, Tokamak-produced, W radiation obs. 78−9835
plasma arc srapying, chem. reaction with plasma gases 80−66427
plasma coating, thick, struct. and mech. props. 77−28716
plasma impurity, radiation loss effects on Tokamak expts. 78−22465
plasma spray coatings, relaxation phenomena 80−19876
plasma sprayed coating, effect of Si substrate surface conditions and impact velocity of sprayed particles 80−21145
plasma sputtering of Ni wire, coagulation, struct. and particle size *(Russian)* 80−40260
plastic deformation, flow of crystalline mat. *(Russian)* 78−76705
plastic working of wires, high-density current appl. 79−57002
plastically deformed single cryst., mag. susceptibility *(Russian)* 80−93074
plasticity, high temp., effect of structural state of grain boundaries, on W with impurities *(Russian)* 79−79057
plate, oscillations of surface impedance in circularly polarised RF fields *(Russian)* 78−39144
plates, magnetoresistivity, multiple Sondheimer oscills. *(Russian)* 79−60796
PLEED results for W (100) using appl. of GaAs spin-polarized electron source 80−69000
point target, temp. depend. of electron emission caused by laser illumination 79−43107
polarisation-dependent angle-resolved photoemission for band structure studies 78−95678
polarised neutron, scatt., nucl. and mag., on single cryst. enriched with ^{186}W 79−87234
polishing technique as prep. for TEM 80−71851
polycrystalline, loss of shear strength under shock compression 77−11635
polygonisation critical stage in single crystals deformed in compression 79−4979
porous, chromising 80−100959
porous, high temp. props. 77−11894
porous, physicomechanical props. sintering effects 77−12575
porous, thick-plate technique for measuring ejecta from shocked surfaces 79−37760
porous, variation of open and closed porosity during sintering 78−15342
porous room temp. shock compression expts., Hugoniot states, 0.6-7.6 GPa 77−84842
positron annihilation and vacancy formation 80−16119
positron lifetime meas., comparison with theory 77−63483
positron trapping and annihilation at vacancies 80−29823
tungsten continued
powder, cold isostatic compaction effect on thermophysical props. 78−52717
powder, effect of prep. temp. on fine structure, X-ray diffr. anal. 79−33971
powder, gas adsorption and desorption *(Russian)* 80−75429
powder, hydrostatic pressing 78−11161
powder, pressing with dispersed strengthening phase additions using flexible bags 79−70016
powder, produced by plasma regeneration *(Russian)* 78−31360
powder, subjected to vibratory milling, exam. of plastic deformation, recrystallisation, sintering 80−16234
powder, sulphiding with H_2S 79−5071
powder metallurgy prep. 80−29904
powder preparation by WO_3 reduction in H plasma jet *(Russian)* 80−76211
powder production, H reduction of WO_3, staring specific surface effect on kinetics 80−11599
powders, defective structure and activated sintering, exam. 80−16240
powders, influence of geometrical props. on compaction *(Russian)* 80−20818
proton bombard., radiation damage, proton backscatt. obs. *(Russian)* 79−46720
proton integral dechannelling functions for single cryst. *(Russian)* 78−10111
proton-induced L-shell ionisation cross-sections 80−100707
quarks, fractional charge search using a Millikan type apparatus 78−54334
radiation generation in Tokamak, Ag I isoelectronic sequence identification 80−83981
range of $^{27}Al^+$ ions, meas. by (p,γ) reson. broadening 79−46729
reactive sputtering yield 77−66566
recrystallisation of commercially pure and doped wire drawn to high strain 79−100165
refractory fibre, effect on high-temp. strength of refractory coatings *(Russian)* 77−52536
reinforced Al, melting under weightlessness *(Russian)* 78−23691
resistivity min., thermoelectric anomaly correlation 78−2468
resonant and nonresonant conduction-electron-spin transmission 80−75857
RF size effect, surface electron scatt. influence *(Russian)* 80−2414
RF surface impedance, new type of oscills. 79−15070
RF surface impedance at different sample surface states 79−60911
ribbon, with adsorbed CO, CO_2 or methane, electron beam induced C deposition, AES obs. 77−89651
ribbon-filament temperature lamps, radiation error estimation 80−64128
rigid collar, for sensitivity enhancement in flameless atomisation systems 78−35770
SAW, excitation using wedge-shaped transducers 79−69334
scattering rate temp. depend. from magnetoacoustic expts. 79−65522
screw dislocation motion, orientation depend., tight-binding type electronic theory 79−51109
secondary electron emission, electronic struct. of semi-infinite cryst. obs. 79−33871
secondary electron emission, theory, rel. to expt. data 78−76564
secondary electron emission 2-12 MeV electron impact, Monte Carlo calc. 79−28868
secondary electron emission spectra, angular depend. and phenomenology 79−43076
secondary electron yields from ion impacts, stopping power calcs. 78−11053
secondary emission and photoemission props., effect of one-electron density of states 80−16152
secondary ion emission, energy spectra, 0-55 eV, contamination levels 79−15573
self-diffusion, high temp. bulk modulus determ. 80−79976
self-diffusion, vol., temp. depend. from radiometric anal. *(Russian)* 77−66040
self-diffusion 78−47565
self-diffusion in range 1700 to 3400K 79−42296
self-diffusion parameters, depend. on degree of purity *(Russian)* 79−19391
self-interstitial diffusion, fully dynamic computer simulation 77−39687
self-weldability in high temp Na *(Japanese)* 80−89392
SEM expts., anomalous patterns *(Chinese)* 80−59349
shock compression, 1223K, re-exam. of expt. data 77−55320
Shockley surface states, projected surface energy bands 78−88009
siliciding in vacuum, diffusion saturation, effect of NaCl, kinetics 79−15859
single cryst., high temp. creep and dislocation struct. 80−71715
single crystal, coated with ferromagnetic layer, longit. cond. electron spin wave 79−11307
single crystal growth by plasma heating 78−60569
single crystal wire fabrication using electron beam zone-refining system modification 78−6845
sintered, brittle fracture, statistical anal. 80−11744
sintered, porous struct. rel. to powder props. 79−61540
sintered rods, hot rolling with four roll passes, effect on struct. and mech. props. 79−100195
sintering, enhanced low temp. process using transition metal activators 77−36418
sintering, Ni activated, grain boundary diffusion mechanism 79−91606
sintering of W-spheres in liquid Ni, computer simulation of chemically driven grain growth 80−55427
slip system geometry *(Hungarian)* 77−47463
solar absorbing surfaces, dendritic, anodised interference coatings 78−13815
solid particle concentration profiles in turbulent jet, laser Doppler anemometer meas. and theoret. calcs. 79−27686
sorption, of He, gas-solid interaction dynamics, energy transfer and sticking calcs. 77−51593
space group of {001}($\sqrt{2}\times\sqrt{2}$)R45° surface struct., LEED patterns 77−85037
specific heat, from calorimeter meas. of enthalpy in 1500-2800K range *(French)* 77−13754
specific heat at high temp. 2300-3600K, meas. of wire cooling in vacuum 77−35703
specific heat near melting point, rapid pulsed heating method 77−35704
spectral emissivity, 4.2-2800K 78−2874
spectral emissivity in 1-10 μm range at 100 to 400°C 77−11713
spectral emittance, meas. system at temp. up to 3000°C 77−22550

tungsten continued
spin polarised LEED, energy and ang. distrib. *(German)* 80−49468
split crowdion interstitial, (111), computer simulation of TEM imaging 78−71723
spray coating form. in pure Ar atm. 77−32709
sputtered atom angular distrib., mass effects in Mg plasma 79−87538
sputtered film, compressive stress transition 78−10310
sputtering, low energy, H, D and He ions 80−100734
sputtering damage due to low-energy ion bombardment, depth of damage, FIM obs. 80−60734
sputtering yields, ang. distrib. and differential, for low-energy light-ion irrad. 80−71527
stacking fault stability determ. 80−96548
stacking faults, microstress relax. effects, field ion images 77−89453
standard ref. mat., thermal. cond. and elec. resist., 4-3000K 77−45820
Standard Reference Materials, electrical resist. and thermal props. at high temps. 78−89427
static deform., removal of surface layer effect on mech. props. in single crystal 79−43359
steel, W content, rapid anal., scattered radiation recording using γ-absorpt. method 77−73489
steels, high-purity and commercially based, containing 10 wt.%W or 5 wt.%Mo, tempering behaviour 80−7600
stepped surface, adsorption and desorption of O, LEED, AES and work function obs. 77−47675
stepped surface, edge atom dipole moments 78−14791
sticking coefficients of CO, O_2, and Xe on (110) and (100) planes 79−82464
stopping power for 0.3-1.5 MeV protons 79−55801
strain induced damping, micro- and macro-, and dislocation structures in single crystals 78−19797
strength, temp. depend. 77−1871
strip lamp temp.-measurement using multiwavelength radiation pyrometry 80−31757
strip production, flattening mill employing US and electroplastic effect 78−84941
structural defect recovery after irradiation and cold work 78−47429
substrate, deposition of Au film, interface struct., FIM obs. 80−65384
substrate, TiB_2 coating prep. by CVD and interaction with substrate 79−24680
substrate, WSi_2 based silicide and borosilicide coatings, serviceability at elevated temps. 79−87751
substrate for Ag, UHV-SEM studies of Stranski-Krastanov growth 80−79722
substrate for Cu cementation, field ion microscopy of cementation vs. substrate dissolution, pH effect 80−16206
substrate for electrodeposition of Nb 77−59704
substrate-oxide film system with rough boundaries, ellipsometric obs. using equiv. film theory 80−2310
substructure stability of single crysts. on high temp. annealing *(Russian)* 77−66666
superconducting transition temperature, ab initio calc. 80−25036
superconductive device to provide reference temps. below 0.5K 79−63220
support film for high resoln. electron microscopy, phase contrast, computer modelling 78−1144
surface, {001}, clean, reconstructed, field-ion microsc. obs., 15-400K 80−15348
surface, {001}, displacive surface phases formed by H_2 chemisorption LEED study 80−49520
surface, {100}, co-adsorption of Cu and O_2, AES, thermal desorption, LEED and work function meas. 78−38950
surface, {411} and {320}, sticking probability and coverage determ. of N_2 80−54528
surface, (001), anal. of surface barrier struct. using LEED data 78−84037
surface, (001), and crystal-atom, energy positron diffraction, theoretical study 80−84034
surface, (001), electronic origin of reconstruction 80−11065
surface, (001), electronic surface reson. and thermally induced struct. transition 80−88614
surface, (001), high resolution LEED, threshold effects 77−51581
surface, (001), LEED spectra, expt. rel. to theory 78−84039
surface, (001), long-wavelength surface phonon spectrum 78−75921
surface, (001), low-energy electron double diffr., spin polaris. effects 79−64963
surface, (001), reconstruction and reordering by H adsorption, MeV ion scatt. 79−23835
surface, (001), reconstruction and reordering by H adsorption, MeV ion scatt. studies 79−82443
surface, (001), relax. determ. using LEED rot. diagrams 78−38917
surface, (001), spin polarisation and temp. effects in refl. diffr. 78−18881
surface, (001), spin polarisation in LEED, theoretical predictions 77−31855
surface, (001), surface CDW phase transitions 78−43455
surface, (001), surface phase transition, electronic contribs., surface susceptibility, ab initio self-consistent thin-film energy band calc. 80−29255
surface, (001), thermal desorption kinetics of Cs atoms and ions 79−28210
surface, (001) clean, long-range inhibition by N of displacive phase 80−2266
surface, (001) electron loss spectra 79−33872
surface, (100), adsorbed H induced lattice reconstruction, surface vibr. obs. 79−19445
surface, (100), adsorbed Pb and Fe, field emission microscopy study 79−15015
surface, (100), angle-resolved photoemission from surface states, refraction effects 78−48279
surface, (100), chemisorbed H, ν, vibrational mode, IR study 80−60582
surface, (100), dynamic props. of adsorbed Si, LEED 77−89634
surface, (100), energy loss mechanisms in low energy electron scatt., use as surface sensitive spectroscopy 77−85859
surface, (100), fluctuation, thermal impurity depinning and commensurate-incommensurate transition of CDWs 79−42611
surface, (100), instability, distortion and dynamics 80−84360
surface, (100), LEED data anal., Fourier transform-deconvolution procedure, multiple scatt. effects 79−41913
surface, (100), LEED data anal., Fourier transform-deconvolution procedure, multiple scatt. effects 79−41914
tungsten continued
surface, (100), photon and electron stimulated desorpt. of O 80−100397
surface, (100), reconstruction in presence of O half monolayer, struct. props. 80−44421
surface, (100), scatt. of mol. and atomic H ions 79−69943
surface, (100), Si film, struct. and work function, LEED meas. 77−66096
surface, (100), surface reson. 78−72226
surface, (100) adsorbed N_2, vibr. spectra, bonding struct., LEED study 80−84387
surface, (100) and (110), theoretical Debye-Waller factors 80−92773
surface, (110), adsorpt. of Xe, 77 to 90K, LEED study 79−42382
surface, (110), adsorption of CO, mobility of CO 79−46955
surface, (110), adsorption of O_2, LEED, AES and thermal desorption meas. 78−38957
surface, (110), chemisorpt. effects on dielec. function, refl. spectra 80−75616
surface, (110), low energy ion scatt. features, inelastic loss and surface crystallography 80−66371
surface, (110), Ne scatt., sudden approximation accuracy, coupled channel calcs. 79−4873
surface, (110), O overlayer, surface struct. refinement via reliability factors for surface crystallography 77−59193
surface, (110), overlayer covered systems, angle-resolved UPS, substrate effects 78−84694
surface, (110), Pd coadsorbed with Re, W, long range interatomic interactions 80−59789
surface, (110), surface diffusion of O_2, contact pot. difference meas. 77 39921
surface, (110), trapping of K and Na atoms, trajectory calcs. 77−48295
surface, (110), trapping probabilities and desorption kinetics of alkali atoms 77−62754
surface, (110), X-ray photo emission spectra, bulk atom 4f splitting 79−100020
surface, (110) Ba monolayer, struct. transformation stages 77−47681
surface, (110) plane, tunnelling of H in surface diffusion 80−75416
surface, (111), surface densities of states for normal photoemission 78−35251
surface, (111), surface site geometry and diffusion characts. of Ni atoms 78−71953
surface, (112), adsorption of La, coating growth and struct. obs. *(Russian)* 78−14618
surface, (112), diffr. intensities in He scatt., topographic curves 78−15274
surface, (210), surface struct. for adsorbed CO and N_2 79−15009
surface, adsorbed CO, electron-stimulated desorption, photoemission, relax. energy 80−100401
surface, adsorbed CO, electron-stimulated ion desorption 80−59797
surface, adsorbed formaldehyde, XPS obs. of decomp. 77−4927
surface, adsorbed gases, field desorption from field ion tips 80−59793
surface, adsorbed H_2, energy spectra for electron stimulated desorption of H^+ calc. 78−79892
surface, adsorbed H_2 on (011) face, bidimensional lattice *(Russian)* 79−7744
surface, adsorbed Hg, thermal desorption kinetics, theory 80−59792
surface, adsorbed K layer, field emission flicker noise power 80−59795
surface, adsorbed layers of Ba and Ba-O, Auger and work function meas., impregnated W cathode model 79−43073
surface, angled resolved UPS exam. 77−55865
surface, Ar and Ne impact, generalised Langevin theory 77−8701
surface, Ar beam direct inelastic scatt., vel. distrib. meas. 80−66351
surface, atom zigzag chains obs. by field ion microscopy 78−84036
surface, atomic struct. using FIM 79−73384
surface, atomically conduction electron reflection, skin effect, transverse electron focusing, simultaneous meas. 78−76131
surface, Br_2+O_2 reaction, rate of reaction meas., gas flow experiment 78−92510
surface, charged-particle emission caused by laser beam scanning 80−11518
surface, chemisorbed H layer, modulation spectroscopy, anal. of Kramers-Kronig relations 78−23423
surface, clean and CO covered, He metastable atom bombard., secondary electron emission 79−47581
surface, clean and H_2-covered, Cl_2 scatt. 80−20743
surface, clean and oxidised, mol. binding states of SiO 79−7750
surface, Cs coated, survival probabilities of emerging H^- ions 80−45187
surface, Cs ion evap. isotherms from single cryst. faces 79−24829
surface, Cu covered, field ion microscopy study 78−23587
surface, direct inelastic and trapping-desorpt. scatt. of N_2, elementary steps in N_2 chemisorpt. 80−60737
surface, elastic refl. of slow electrons 79−28869
surface, electronic surface resonances of crystals, W(001) 79−95464
surface, field depend. of spectral line energy of He-H_2 adsorbate 79−78853
surface, gas-covered, K atom beam inpact, K^+ ion current peculiar decay 79−74045
surface, glancing scatt. of light ions from single cryst. 77−36347
surface, He, Ne, tangential momentum accommodation coeff. meas. by acoustic vel. and absorpt. obs. 80−66867
surface, He ion bombardment damage, field ion microscope obs. 77−31701
surface, impact determ. of inert gas ion beam metastable fractions, secondary electrons obs. 79−28873
surface, influence of alkali films on props., calc. *(Russian)* 80−2273
surface, interaction with F_2 and fluorides at low temp. and high press. 78−39700
surface, interaction with He metastable atoms 79−91558
surface, isothermal ramped field-desorption of benzene 79−90870
surface, K atom beam impact, mean residence time of K^+ and ionisation efficiency 77−73208
surface, methane dissoc. by adsorption-desorption process 78−92511
surface, mirror electron microscopy for total electron refl. coeff. determ. 78−5994
surface, Ne elastic scatt., high-energy approx. 79−65965
surface, optical magnetisation from spin polarised photoemission 79−78830
surface, physisorbed O_2 layer, $Ar^+(Ar^{+,m})(Ar^{2+})$ impact, electron emission obs. 80−60740
surface, polycryst., heat of desorption of Cs 80−75430
surface, polycryst., N_2 adsorption states 80−100404
surface, pulsed laser atom-probe FIM, expts. 80−66402

tungsten continued
surface, reaction with CO_2 and D_2O at high temps. and low press. 77−86379
surface, regularly stepped, work function determ. by thermionic emission 77−59665
surface, resonant absorpt. of sound *(Russian)* 78−95216
surface, secondary electron emission rel. to LEED 78−84689
surface, self-diffusion coeff., determ. from van der Mast's expt. data between 3000-3600K 79−11011
surface, SiO_2 supported, adsorbed O_2, EPR evidence for surface mobility of O_2^- 78−84046
surface, spectral density of states 78−39181
surface, static skin effect and transverse electron focusing *(Russian)* 79−91036
surface, struct. anal., trajectory focusing in surface scatt. of channelled ions 78−68594
surface, thermal accommodation of He, two-phonon contribs., DWBA calcs. 79−95893
surface, tight-binding theory of interactions between W adatoms 77−1304
surface, with adsorbed Pd, field emission obs. of adsorpt., diffusion and self-diffusion 78−38945
surface {001}-(1×1), struct. determ., dynamical and exptl. LEED results 78−14560
surface {100}, anisotropy of inelastic electron refl., energy loss effects 80−79642
surface {100}, coadsorption of N_2 with O_2 or C, AES obs. 77−35821
surface {100}, N_2 adsorption, disorder effects on work function change 77−20192
surface {100}, with chemisorbed CO, electron beam effects, AES obs. 77−31897
surface (001), disordered CO and O_2 overlayer effect on electron spin polarisation in LEED 79−60632
surface (001), displacive transition, H adsorpt. effects, theoretical model 80−65352
surface (001), dynamics of H atom collisions with adsorbed H atom 77−10726
surface (001), electron spin polarisation and intensity in LEED, temp. depend., 1000-300°C 79−14989
surface (001), electronic reson. band struct. and lineshape, LEED meas. 79−82655
surface (001), electronic struct. of Au monolayer 78−72236
surface (001), LEED, 20 to 150 eV, electron-spin polarisation 78−51400
surface (001), ordered CO overlayer effect on electron spin polarisation in LEED 79−60633
surface (001), spin-depend. features in LEED intensity curves, model calcs. 78−34685
surface (001), surface relax., LEED rotation diagrams 79−28180
surface (001) states and surface resonances, self-consistent electronic struct. 80−96960
surface (100), adsorbed Na atom, binding props. calc. 80−49522
surface (100), adsorpt. of acetylene, room temp., electron spectroscopy obs. 79−7749
surface (100), adsorption of ethylene at 80K and decomposition to acetylene, AES obs. 79−66353
surface (100), adsorption of La, depend. of work function, heat of adsorpt. on surface coverage, contact potential study 78−67912
surface (100), adsorption of O_2, AES, description, LEED and work function obs. 77−1317
surface (100), chemisorbed, H, D, ^{16}O, and ^{18}O, isotope effects obs. by SIMS 79−5234
surface (100), chemisorpt. of O_2, low-energy SIMS, ion yields depend. on surface chem. and primary ion energy 78−73105
surface (100), chemisorption of Hg, AES, LEED, work function and thermal desorption expts. 78−34709
surface (100), CO/H_2 surface complex, flash desorption and AES obs. 78−73083
surface (100), coadsorption of CO and H_2, CO/H surface complex obs. 79−4478
surface (100), desorption of Hg, fractional and zero order kinetics 79−60634
surface (100), electron-stimulated desorpt. of O 78−2363
surface (100), formic acid decomp., flash desorption obs. 79−29402
surface (100), LEED intensities, temp. depend., surface struct. phases and surface Debye temp. 80−39395
surface (100), MeV He scatt. expt. 79−4455
surface (100), NVV Auger spectra, $O_2(H_2)$ adsorption effects, comp. to band struct. calcs. 78−72643
surface (100), O covered, ion scatt. spectroscopy 77−73205
surface (100), specular scattering of polarised low energy electrons 79−60233
surface (100), surface resonances, photoemission and field emission meas. 79−4593
surface (100), with ordered C overlayer, adsorption of O_2 and CO, UPS meas. 79−77907
surface (100) and polycryst, electron stimulated desorption of O^+ ions from adsorbed O 79−99428
surface (100) reconstruction kinetics in presence of O half-monolayer 80−65375
surface (110), adsorpt. of N_2, N_2O, and NO_2/N_2O_4, 300K and 100K, XPS, UPS, and XAES 79−28203
surface (110), adsorpt. of NO, 300K and 100K, XPS, UPS and XAES 79−28204
surface (110), alignment of VPE Ni, Cu, Au and Ag 79−19488
surface (110), chemisorpt. of CO and O_2, absolute coverage and work function meas. 100 and 300K 78−71986
surface (110), chemisorption of O, displacement reconstruction model 79−46949
surface (110), chemisorption of O, Monte Carlo modelling of phase changes 78−71969
surface (110), D depth profiles using imaging field desorption 77−59038
surface (110), density of extended defects, LEED obs. 79−82421
surface (110), dipole moments of single 5d metal adatoms, field emission meas. 77−47674
surface (110), H adsorption, band struct. and adsorbate geometry, surface-reflectance-spectroscopy 80−44416
surface (110), ionisation of hyperthermal Na atoms, temp. depend. 80−50504
surface (110), mobility of adsorbed O, 300 to 800K, field emission current meas. 79−33187
surface (110), O_2 and WO_2 adsorption, LEED and AES obs. 80−34317
tungsten continued
surface (110), order-disorder transform. in chemisorbed O, theory compared with LEED data 79−7748
surface (110), Pd adsorbed layer, growth, struct., stability, desorption 80−59794
surface (110), relaxation determ. from LEED Fourier transform-convolution method 79−4459
surface (110), scatt. of Ne, coupled channel calcs., symmetry appls. 78−92156
surface (110), work function, Fowler-Nordheim studies 80−34501
surface (111), adsorption of Ni, surface site geometry, diffusion charact. 78−75944
surface (111), adsorption of O_2, AES, LEED and electron stimulated desorption obs. 79−46935
surface (111), field adsorption of He, array model 80−59800
surface (112), He atom scatt., theory for stationary sinusoidal hard wall surface with one-dimens. periodicity 78−92161
surface (112), He scattering, theoretical interpretation of data 78−35241
surface (121), Ba atom desorption in strong elec. fields 80−29280
surface (310), field emission current instability induced by migrating atoms 78−35254
surface adsorbed W, Ga, Sn, struct., FIM obs. 80−103576
surface adsorption processes following electron excitation, cathodeluminescence studies 80−100390
surface bands dispersion (001) 77−15930
surface chemical effects in electron loss spectrum of W(100) 77−4705
surface cleanness control using secondary electron spectroscopy *(Russian)* 79−90858
surface contraction of (001) (1×1) using LEED intensity anal 80−6606
surface contraction of (001) face, LEED exam. 77−43412
surface density of states for directional photoemission spectroscopy 77−20396
surface diffusion 79−56048
surface diffusion of adsorbed Pd and Au layers, spreading behaviour 79−99421
surface diffusion of adsorbed Re atoms and dimers along (211) 77−20183
surface diffusion of O_2 on (110), coverage-distance plots, diffusion coeff. 77−62755
surface diffusion of Pd, anisotropy effects due to substrate struct. 79−99422
surface dipole moment calc. 80−60060
surface electron density crimping, Ashcroft potential, density functional calcs. *(Russian)* 79−82653
surface electronic structure and spectral densities 77−80824
surface energies and vacancy-surface interactions calc. 79−19448
surface energy anisotropy and faceting behaviour in vac. and in H_2 77−7961
surface finish of single cryst. cylindrical component, electroerosion polishing *(Russian)* 79−15847
surface geometry and emission parameters, changes during directional mass transport 78−2344
surface impedance and HF cond. in strong mag. field, thin single cryst. plates *(Russian)* 77−89831
surface ionisation of Gd, Tb, and Dy on (110) surface 79−87142
surface ionisation of SF_6, laser irrad. effects 80−93440
surface layer struct. during milling, plastic deform., failure *(Russian)* 80−40586
surface oxide softening in single crystals 78−95860
surface periodic struct. development, under conditions of thermal mass transfer *(Russian)* 77−59187
surface pot. barrier effect on photofield emission 78−60551
surface reconstruction, physical realisation of two-dimensional Ising and X-Y model 80−15351
surface reflection of conduction electrons *(Russian)* 78−43373
surface relaxation and electronic structure of (100) surface 79−73561
surface relaxation determ. from LEED via transform method 77−43419
surface resonance, (100), effect of Cu adsorption 77−59201
surface resonance band fine struct. in LEED 78−47844
surface resonance bands, dispersion relations, (001) surface 77−51797
surface resonance bands 78−47843
surface self-diffusion, anisotropy 78−34689
surface self-diffusion, ion impact induced, FIM study 80−103549
surface self-diffusion by ion impact, protrusion formation 78−75938
surface state resonance exam. above vacuum level 78−30965
surface structure, LEED anal. 78−38919
surface structure, pseudo-relativistic LEED calcs. and R-factor anal. 80−70510
surface structure, thermally induced 77−62714
surface structure and topological modification during depth profiling, FIM obs. 79−78816
surface structure by MeV ion backscattering, channelling 80−6605
surface structure changes due to ionic bombardment, LEED and AES obs. *(Russian)* 77−1775
surface structure transition, {001}(1×1)→($\sqrt{2}\times\sqrt{2}$)R45°, LEED, AES, and work function meas. 79−42348
surface thermoelectrotransport of atoms 80−2448
surface wetting by liquid Cu depend. on preliminary surface treatment *(Russian)* 80−35388
surface-atom polarisability derivation from field-ion energy deficits 80−76155
surface-electron beam interaction, 0.4-5 mA ion beam extraction 77−84456
surfaces, (100) and (110), chemical effects in N_7 VV Auger spectra 77−32474
TEM, single and clusters of atoms obs. by bright field microscopy 77−62456
texture and grain boundary struct., primary misorientation function, expt. deform. 79−1876
texture and grain boundary struct., primary misorientation function 79−1877
texture and grain boundary struct., primary misorientation function 79−1875
texture form. by drawing and pulling through nonpowered rolls, BCC lattice *(Russian)* 77−25100
thermal accommodation coeffs. for N_2 and CO_2, gas saturated system 77−70335
thermal accommodation of alkali metal vap. 80−24729
thermal capacity meas. using noise thermometry *(Russian)* 77−76573
thermal contacts between crystalline samples, high vac., low temp., press. and mag. field depend. *(German)* 77−11890

tungsten continued
thermal expansion coeff. meas. using strain gauges and thermocouple 78−53059
thermal expansion reference data: 1-1000K 80−96669
thermal field cathode emitters, end form changes, electron microscope obs. 77−4718
thermal ion energy distrib. by retarding field modulation method *(Japanese)* 79−78822
thermal neutron irradiated, radiation damage and stage III defect annealing 78−51586
thermal neutron irradiated, recovery processes 80−19848
thermal shock resistance, original struct. effects 77−63803
thermionic emission, work function in atmospheric pressure gases 78−76575
thermionic emission and work function, dislocation effects, for single crysts. 80−76129
thermionic emission of K ions from W *(Hungarian)* 77−48300
thermionic emitter, work function rel. to output characts. in arc regime 77−52213
thermophysical data at high temps., submicrosecond-pulse-heating method 80−103459
thermophysical meas. above 2500K, apparatus 77−45845
thermopower meas. in mag. field, 1.5-4K 80−54675
thermoreflectance spectra, 0.3 to 6 eV, rel. to band struct. calcs. 77−66521
thin crystal, anomalous transmission of high energy electrons *(Japanese)* 77−43117
thin wire, negative longit. magnetoresist., kinetic theory 78−34821
thin wires, electron emission into gases under strong elec. fields 79−83108
thoriated hairpin filament electron source for high brightness appl. 78−341
threshold atomic displacement energy, temp. depend., computer simulation 77−1148
tip, pure and Ba coated, photoemission in electric field *(French)* 78−80458
tip, [310], prep. from rolled sheet 80−97447
Tokamak limiter, plasma interaction, current profile evolution effect 80−10420
Tokamak reactor ISSEC 78−41860
transport properties at low temp., electron and impurity scatt. 78−10418
trapping and desorption of alkali atoms on clean and O_2 covered (110) surface 77−11786
trapping of He at Xe atoms, attachment of mobile particles to non-saturable traps 80−39418
tube, CVD, study of preferred orientation *(Korean)* 77−8761
twin and stacking fault energies calc. 80−2038
twin boundary and twinning dislocation struct., computer simulation 78−30644
twin boundary microfaceting on annealing, field ion microscope determ. 79−77608
twin lamellae shape of single crystal *(Russian)* 80−19812
twinning dislocation, math. model 77−59024
twins, fan shaped of type II, struct. 79−90676
unipolar arc damage in hot, dense D plasma 79−3235
UPS, angle-resolved, surface resonances on (100) face 78−2987
US absorption, temp. depend. *(Russian)* 79−51203
US attenuation due to electron-phonon interaction 79−77687
US attenuation meas. of mean free path temp. dependence 77−39825
US waves, rot. of polarisation plane and ellipticity near doppleron-phonon reson. *(Russian)* 79−19325
US working effect on single cryst. during deform., strengthening effect, plasticity resource *(Russian)* 79−34107
vacancies, quenching and recovery invest., resist. and TEM study 80−39074
vacancy annealing stage after heavy ion implantation, Mossbauer meas. 78−39463
vacancy diffusion along single edge dislocations, computer modelling *(Russian)* 77−47612
vacancy recovery stage, radiation doping, elec. resistivity meas. 79−51102
vacancy struct. of depleted zones after ion irrad. 79−73224
vacancy structure in near surface depleted zone following ion bombard. 80−70267
vacancy-defect clustering, due to annealing and quenching, TEM and elec. cond. exam. 78−47344
vacuum-deposited coating on Mo, strengthening effect *(Russian)* 77−66714
vaporisation, influence of inert gases on losses *(Russian)* 79−55878
vapour deposited, dislocation struct., rel. to texture *(Russian)* 80−65394
vapour press. above different crystallographic planes *(Russian)* 78−18762
viscoelastic wave propagation model at near-melt conditions, electron-photon impact energy deposition 79−77002
volcanic rocks, W abundances 79−16468
volt ampere characteristics during electron melting process *(Russian)* 80−75336
whisker crystal growth incorporated with field electron emission 80−44458
whisker fabrication, AC and DC electrochem. etching 78−43278
whiskers, energy spread meas. of thermal field-emitted electron flow 78−92168
whiskers and particles, monocryst., reduction of vapour deposited WO_3 77−52249
wire, AKS-doped, second phase particle obs. by TEM, SEM and atom probe microanalysis 80−108457
wire, cold drawn, dislocation processes occurring during tensile testing *(Hungarian)* 77−48450
wire, doped, heavily drawn, recrystallisation 77−16609
wire, doped, high temp. creep behaviour 78−88499
wire, doped, high temp. tensile behaviour, bubble dispersion effect 79−74237
wire, elec. resistance, low-temp. continuous and cyclic heating effects, compared with W-Re 78−92370
wire, exam. of grain boundary segregation, using Auger spectroscopy, new technique 78−80551
wire, incandescent, motion and growth of K bubbles *(Hungarian)* 77−48460
wire, increasing plasticity, by electroplastic rolling *(Russian)* 79−29103
wire, microparticle trigger discharges and impact damage in HV vacuum insulated gap 77−24227
wire, organic microneedle growth under intense elec. fields, X-ray diffr. and AES 80−54580
wire, struct. and high-temp. creep, dopant elements influence 80−66603
wire, US inspection, immersion method 80−66757
wire for high-speed matrix printers *(Japanese)* 80−55540
wire from rolled rods, mech. props. and struct. 80−25743
wire grids, FIR performance and appl. 80−10012
wire reinforced Cu, exam. of thermal cycling induced deformation 79−5050
wire reinforced Cu, microfield, flow stress 78−27575
wire reinforced Cu, notched, analytical method for predicting plastic flow 77−70114
wires, KSiAl doped cavity formation *(German)* 78−31524
work function, field emission meas., Te and Cs surface film effects 78−19645
work function, nonideal terraced surface, calc. 80−6950
work function, self-consistent calcs. 78−76135
work function changes due to La and O surface layers *(Russian)* 77−35816
work function measurement in SEM 80−80918
X-ray $L_{\alpha 1}$ line width meas. *(French)* 77−50393
XPS, angle-resolved, from valence bands, obs. of strong temp. depend. and direct-transition effects 80−60752
yield strength, temp. depend., of W with different microstructs. 80−16404
Z dependence of thick target β-ray backscattering 80−76118
zonal electronic purification, mass spectra of contaminants *(Polish)* 80−25552
$\bar{p}$ prod. in W+p, 25 GeV, flux optimisation using hadron cascade calcs. 77−83411
Ag epitaxial growth, on W-ribbon substrate, in UHV, cryst. orientation determ. by etching *(German)* 79−65994
Al_2O_3-W cermet, phase bonding 78−52745
Al_2O_3-W cermet, sintered pressed compact, compressive and transverse rupture strength 78−19850
Al_2O_3+W interaction, 2200 to 3200°C *(Russian)* 79−39194
Al_2O_3+W(WO_2) reacts. in H_2, vacuum, high temps., reduction, oxidation conditions 77−16518
Au-W/n-GaAs contacts, interdiffusion and Schottky barrier height variations 77−89849
Au-W-GaAs Schottky barrier, elec. and chem. props., AES 80−96973
B fibre reinforced W double coaxial composition rod, waveguide, normal mode US propag. 79−100317
BaO thin films, on (110) face of W, struct. study by LEED 79−60659
Bi adsorption, and condensation on W 79−73394
C content determ., isotope-spectral method *(Russian)* 80−55766
CaV_2O_6:W^{6+},Mo^{5+}, g-factors and hyperfine coupling parameters of V^{4+}, ESR 77−12196
Cs/W, work function measurement in SEM 80−80918
Cu-W composite powder, prod. by H_2 reduction of $CuWO_4$ 79−20006
D^+ depth distrib., effect of surface impurities, channelling model 79−1451
Eu-W-O, reaction system, thermodynamics, mass spectrometric obs. 77−77748
Fe meteorites, W concs. 79−35200
Fe, surface phonon spectra 78−71934
GaAs:W, deep trapping centre exam. by thermally stimulated capacitor discharge method and luminesc. 77−55495
GaAs:W^{2+}, radiative transitions, photoluminesc. obs. 80−108271
Ge-W contacts, surface electron state spectrum surface treatment effects *(Russian)* 80−34497
Mo, film on sapphire substrate, orientational growth, epitaxial textures, nucleation textures *(Russian)* 80−75454
Nb_2O_5:W^{5+}, ESR obs. on B-form single crysts. 80−54946
Ni-W surfaces in contact, deform. and adhesion at very low loads 80−39457
Pb(Zr,Ti)O_3:Cd,W, electro-optical ferroelec. ceramic, secondary electron emission yield 79−91546
Pt-W interface, contaminated, contact adhesion, deform. and interfacial energy 78−22306
SiO_2:W film electron trapping characts., obs. by avalanche injection techniques 77−89862
SnO_2:W^{5+}, EPR parameters, g hyperfine and superhyperfine tensors 77−85560
VO_2:W, thin layer prep. by reactive DC sputtering, doping effectiveness *(German)* 78−6847
VO_2:W layers, liq. phase prep., resist.-temp. behaviour *(German)* 77−77435
W (110), scatt. of He(Ne), sudden decoupling approxs. 78−64437
W (110) surface states, characterisation and transferability obs. 79−33319
W (110)-O chemisorbed layer, island size determ., response function and substrate struct., LEED meas. 79−42414
W bicrysts., crack propag. across grain boundaries, crack speed meas. technique appl. 80−108575
W, cast state, interaction nature between C, O_2 and N_2 *(Russian)* 79−70114
W, electron irradiated, or quenched, point-defect mechanism for Stage III recovery, field ion microscope study 79−60403
W, electron-electron scatt. 79−38045
W film, adsorbed Th layer, work function, temp. depend. 77−28701
W glass, laser-irrad., plasma electron energy profile steepening, polarimetry obs. 78−34349
W, ion prod. in hollow cathode source 78−74525
W layers on Mo, exam. of epitaxial orientation, and deposition *(Russian)* 79−11039
W, RF size effect signal, anomalous behaviour 77−89788
W, reflection of H, D and He ions 78−95640
W spheres, in liq. Ni, sintered, coalescing, crystallographic orientation, SEM study 80−45249
W, surface state transferability, UPS meas. for (011) states 80−39650
W, thermal and anodic oxidation, production of WO_3 layer semiconductor electrode 80−35544
W VI, one-electron spectra energy levels and line lists 79−49953
W XLVII X-ray spectra from laser produced plasmas 80−42981
W XX to XXXV spectra and spatial distrib. in PLT Tokamak 78−55747
W^+, relative ion sputtering yield, integration of secondary ion energy distribution, retarding dispersive ion energy analyser 79−33875

tungsten continued
W^{3+} field ion evaporated from ionic bonding states, appearance energies 80−89125
W^{71+}, electron impact excitation, relativistic Coulomb-Born approx. 79−68318
W:^{3}He, implanted ion positions, determ. using mol. deuteron beam 80−70240
W:H, correlations between elastic energy transferred by implanted H ions and H trapping 78−14370
W:K-Al-Si, state of bonding, distribution of impurities 78−92212
W:Kr, He trapping at substitutional Kr, vacancy creation 77−43258
W:La, B coadsorption and work function, FEM and FIM obs. 79−52087
W:Ni compacts, optimum conc. of Ni for activated sintering, optical microscopy obs. 79−38758
W:Os coated dispenser cathode, chemical and physical process obs. 79−28885
W:Re, polygonisation in diffusion process, glide dislocation interactions 80−38998
W:ThO_2, uncarburized filament activation by sputtering 78−52608
W:Xe, BCC, heavy ion implanted, vacancy recovery, Mossbauer spectroscopy 79−82896
W/α-Al_2O_3, heteroepitaxial structs., refined formulation of relative orientation criterias 80−44448
W/α-Al_2O_3 heteroepitaxy, orientation relationships, X-ray diffr. study 79−60661
W/Cu, Stoneley waves at (001) interface between cubic symm. cryst. 80−100388
W/Cu interface, thermal conductance at low temps. 80−49436
W/Cu powders, liq. phase sintering, particle rearrangement 80−45253
W/EuS field emitters, electron emission current depend. on annealing temp., mag. props. 80−16160
W/K(Na), superthermal neutral beams impact, stimulated chemical reaction 77−9123
W-Al fibrous heat treated composites, thermal stress anal. 77−46943
W-Al_2O_3, vaporis. at elevated temp., mass spectrometric obs. 79−29388
W-Al_2O_3 cermet films, oxide evaporation deposited on Mo, Ti, Al_2O_3 substrates, struct., props. 80−25581
W-Al_2O_3 granular film, percolation conductivity 78−84319
W-Ba, type B impregnated cathode, operation mechanism 78−15278
W-Br regenerative cycle of linear quartz lamps, metallic impurity effects, thermochemical interpretation 80−3312
W-C point contact, compared with TGS pyroelec. detector, appl. to temporal coherence meas. of HCN laser 80−31871
W-Cu composite materials, vel. dispersion and scatt. of transverse US waves 78−91383
W-dimethyl terephthalate contacts, effect of elec. field on contact electrification 79−19660
W-EuS, amorphous, memory effect in field emission 80−89126
W-EuS field emitter, field emission of monoenergetic spin-polarised electrons 77−85899
W-EuS interface, electron spin polarisation in field emission 78−35265
W-GaAs contact, Schottky barrier 78−39213
W-Ge whisker diode, 337 μm IR detector *(French)* 78−8445
W-MgO cermet film, dielectric const. and selective solar absorption 78−2937
W-Mo-Co high-speed cutting steels, Co determ. 78−3416
W-Ni point contact diode, IR antenna characts. 77−49772
W-Ni point contact diode, rectifying props. in CO_2 laser radiation 77−76942
W-Ni point contact diode detectors at 10.6 μm, mech. and props. 78−24861
W-Ni point contact diode fast acting detect. for modulated CO_2 laser beams 79−3730
W-O-Cs system, thermionic emission, 450-800K 78−2972
W-O-F system, gas phase, comp. and chem. transport reactions in discharge lamp *(German)* 77−32826
W-oxide-Ni high speed submicron junction, electron tunnelling spectra 79−99635
W-Pt mechanical contact, FIM obs. of contact area 78−35527
W-Re immersion thermocouples for ferrous metal temp. meas., reliability/accuracy improvement 77−87767
W-SiO_2 cermet film, deposition by RF sputtering of powder target, elec. resist. and TCR 79−78890
W-ThO_2, candidate refractory for Tokamak, thermal fatigue failure testing 80−32454
W-ThO_2 filament, W, TaC and HfC CVD coatings, effect on high temp. mech. props. 78−15347
W-ThO_2-B, thermocathodes diffusion mobility, based on deboronation kinetics 80−39349
W-Zr field emitter, time-of-flight atom-probe study 80−80949
W+H^+, 4 MeV beam-foil X-ray production cross-section 79−7003
W+Kr^{n+}, K-L level matching, X-ray obs. 79−63948
W+SO_2, reaction kinetics, 1600-2100K 79−20266
W^{n+}+H, single electron capture cross-section 79−59560
W^{n+}+H_2, single electron capture cross-section 79−59560
W_2, dissoc. energy, estimated from LaIr(g) thermal decomp. obs. 80−7781
W_6 clusters, electronic struct., scattered wave-Xα calc. 79−11053
W_9 cluster, Hartree-Fock-Slater model calcs. 77−72899
(W-Au)-SiO_2-Si:B MOS transistor, ion implantation effect on threshold voltage 78−34903
WC-Co particle-matrix composite, fracture and cleavage strength 77−73342
WI lines, relative oscill. strengths 79−63962
WO_2+NF_3, reaction product thermodynamic stability *(German)* 79−8449
WSi_2 based silicide and borosilicide coatings on W substrate, serviceability at elevated temps. 79−87751
^{74}W, L-emission spectrum, forbidden lines 77−3295
^{178}W, production of, parent of ^{178}Ta used in nuclear medicine 79−16300
^{178}W, productions in ^{181}Ta(p,4n), purification procedure 80−12252
^{187}W, absorpt., distrib. and milk secretion by dairy cow 77−9281
W(100) TF electron emitters props. obs. 80−66403
Zr-O-W (100) thermal field emitters, operational experience 80−71576
ZrN+W reaction, high-temp. compatibility 79−39132
ZrO_2-W, eutectic microstruct. 78−27499

tungsten alloys
see also tungsten compounds
brittle alloy rolling, contact stresses *(Russian)* 80−93576
cast alloy, shape, size, distrib. of carbides and oxides 79−24528

tungsten alloys continued
deformed, vacuum technology appl., mech. props. *(German)* 79−57046
dilute, effect of grain boundaries on high temp. plasticity *(Russian)* 79−79057
fibre reinforced Co powder alloys, reactions and recryst. 80−11603
Gentalloy, in Fe-W system, damping capacity *(Japanese)* 79−20094
Hastelloy, C-276, H-induced crack growth 80−71747
Hayes alloy no.716, Fe-Cr-Ni-Co-W-Mo-Si-C-B (26, 22, 12, 3.5, 3, 1.2, 1.1, 0.4 wt.%), hardfacing alloy 80−100802.
Haynes alloy 188, H_2 permeability 77−46399
Haynes alloy 188, SEM exam. of fracture surface, due to low cycle fatigue at 700°C *(Japanese)* 78−52963
ion-irradiated, recovery behaviour studied by field ion microscope 80−29074
multimaterial impact, dynamic yield point 77−32731
neutron activation analysis using low energy accelerator 77−73499
nonlinear compliance curves, caused by crack closure and fracture tests 77−56064
phase anal., electrochem. separation of carbides 78−60651
recrystallisation, alloying effects of ThO_2, Mo-Re, HfC, NbC 77−70083
Relite-base alloy compositions wear caused by sliding abrasive material stream 78−95813
sintered relation between density and sound velocity 78−53173
sintering, physical and chemical phenomena *(Italian)* 79−83147
steel, 12% W, eutectic carbides struct. and comp. during heating 80−76283
steel, alloy, V-W-Mo-Cr, exam. of carbide transformation 80−16299
steel, alloy, W-Mo-Cr-V, blanks welded to steel 45, optimal high temp. tempering 80−16351
steel, austenitic, high-speed, austenite grain growth, W addition effects 79−20085
steel, Cr-Mn-W, W addition effect on carbide form. in type 30 KhG *(Russian)* 79−87638
steel, Cr-Mo-V-W, crack-growth and thermal-mech. fatigue 80−21072
steel, Cr-Mo-W-V, long term creep rupture props., turbine blade *(Japanese)* 77−59909
steel, Cr-Mo-W-V, long time stress relaxation props. *(Japanese)* 77−59841
steel, Cr-Mu-W, carbide form., W effect 80−76259
steel, Cr-Ni-W, W addition effect on carbide form., X-ray obs. *(Russian)* 79−87639
steel, Cr-W-Mo-Co, high-speed, from atomised powders, mech. and cutting props. 80−66556
steel, Cr-W-V-Mo (3.9 to 4.5, 1.5 to 2, 0.9 to 1.2, 3.9 to 4.4 wt.%), heat resistant, type 8Kh4M4V2F1-Sh, mech. props. 80−16464
steel, high speed, W-Mo-Cr-V, production by powder metallurgy 77−12574
steel, high V-W-Mo, high speed, phase composition and struct. of atomized powders 77−90323
steel, microstruct. and hardness, splat quenching effect 80−76293
steel, Si-Cr-Mo-W-V (2,4,1,3,2 wt.%), heat treatment and props. 80−16349
steel, solubility of W and Mo in $Ti(C,N)_x$ 80−16276
steel, stainless, Ni-Cr-Mo-W (29, 13, 3, 2 wt.%), long-term strength in H at high pressure 80−55485
steel, tool, W-Mo, heat treatment effect on props. 80−50656
steel, W and W-Mo, sintered high-speed, naphthalenelike grain form., quenching effect on fracture toughness 80−30103
steel, W-Cr (3 wt.%), CrC formation in isochronal tempering, electron microscope study 80−7584
steel, W-Mo, high speed, hot deform. and heat treatment effect on props. 77−90372
steel, W-Mo, tool, hydrostatic extrusion and tempering, wear resistance effect 80−50728
steel, W-Mo-Co, high-speed tool, struct. and props., cooling rate effect at primary crystn. temp. 80−76241
steel, W-Mo-Cr-V tool, laser surface melted, struct., heat treatment effect 80−76424
steel, WC reinforced surface layer, serviceability improvement by Ni, Cu-Ni, V alloying additions 77−21290
steel electrode, erosion resist., influence of C and carbide-forming elements *(Russian)* 78−11389
steel turbine casings, residual life determ. 80−93585
steel W-Mo-V-TiC, powder, TiC effect on milling, pressing and sintering 78−60607
Stellite, friction behavior in high temp. Na environment *(Japanese)* 80−40546
Stellite, self-weldability in high temp Na *(Japanese)* 80−89392
Stellite 6B, volatilisation of oxides during oxidation at 1200°C 78−23873
stellite hardfacing materials, friction characts. in high temp. Na *(Japanese)* 80−89356
Stellite-6, XPS obs. of aqueous oxidation, surface comp. and gaseous oxidation effect 80−81238
VK6 grade, mean grain size by acoustic method 78−72961
W-Al, phase formation in diffusion layers between solid and liquid metals *(Russian)* 79−69257
wire, increasing plasticity, by electroplastic rolling *(Russian)* 79−29103
wire reinforced stainless steel, fibre/matrix interaction, fabrication and heat treatment effect 79−91607
Al-W, struct. and props. of alloys obtained from granules 80−50717
C/Pt-W (8 wt.%), desorption of K from C film surfaces 80−59784
Cd-W particulate composite, dispersion hardening, grain size and texture strengthening 77−8840
Co-Cr-Ni-W-Ta-C, alloy Mar M-509, TEM exam. of thermal fatigue crack propag. in cast alloy 78−76740
Co-Cr-Ni-W-TaC (15.7, 9.5, 3, 12.77 wt.%) alloy Co50B3W, temperature cycling effect on rupture strength 78−39898
Co-Cr-W-C, hardfaced coating for high temp. liquid Na service, deposition and wear 77−32724
Co-Cr-W-C, wear-resistant coating alloy, carbide form. and decomp. 77−32711
Co-Cr-WC, corrosion and corrosive wear in sea water 78−92408
Co-W (36 wt.%), magnetic alloys for high temp. appl. 77−85503
Co-W alloy electrodeposition, influence of $MgSO_4$ and gum arabic additives *(Russian)* 80−80991
Co-W alloy electrolytic coatings, heat treatment effects on coercivity, hysteresis and structure *(Russian)* 80−60381
Co-W-C system, η-carbide linear expansion coeff., X-ray diffr., 30-1500°C 77−25021

tungsten alloys continued
Co-W-C system at 1150°C, phase equilibria, isothermal reactions and thermodynamic study 78−31385
Co-W-Cr (15,20 wt.%), surgical implant ion beam textured, stress/strain relations, fatigue characts. 78−73297
Co-W-Si, directionally solidified eutectics 79−61575
Co-WC, corrosion and corrosive wear in sea water 78−92408
Co-WC, levitation quenching 77−59711
Co-WC, protective coatings by B diffusion, microstruct. and mech. props. 78−11427
Co-WC dispersion hardened alloy, tensile deform., volume fraction of second phase effect, simulation *(Japanese)* 79−70122
Co-WC hard alloys, rapidly quenched struct. 80−76233
Co-W(25 wt.%), cellular decomposition, third element effects *(Russian)* 77−1837
Cr-Mi-W-(-Mo), heat resistant weld seam metal, tensile strength, thermophysical characts. 79−91769
Cr-W, anodic dissoln. at high current densities *(Russian)* 80−76395
Cr-W-O, phase relations, thermodynamic props. of $CrWO_4$ and Cr_2WO_6 80−104120
Cr_3C_2-WC-Ni (40, 15 wt.%), sintered, cavitation erosion resistance *(Japanese)* 77−52500
$Cr_{1-x}W_x$, neutron scatt., selection rules for phonon mass operator 79−28065
Cu-Ni-W melt, solubility of W, primary solidification 78−19726
Cu-W, biphase material X-ray stress determ. *(Russian)* 79−5097
Cu-W, powder, prod. by controlled reduction in H_2O/H_2 mixture of $CuWO_4$ 79−24458
Cu-W sintered materials, porous, mech. and X-ray elastic const. *(German)* 77−81288
Fe-Co-Ni-W alloy, 45KKhVN, plastic deform., electron microscope obs. *(Russian)* 78−80584
Fe-Co-W-C steel, M_6C carbide behaviour during ht. treatment *(Russian)* 77−66658
Fe-Cr-W-C, carbide/austenite equilibria, expt. and thermodynamic study 77−36459
Fe-Ni-Co-W (18.65, 8.99, 4.87 wt.%), ageing characts., 380-530°C 80−60876
Fe-Ni-Cr-Al-Ti-W-Mo (35, 15, 2.4, 2.3, 2.2 wt.%) wrought superalloy, freckles *(Chinese)* 80−104137
Fe-Ni-Mo (16.4, 8.1 wt.%), effect of substituting Mo by W during ageing 80−29991
Fe-Ni-WC hard alloy, struct. and props. 79−79007
Fe-W, dil., high freq. induction melting and centrifugal casting, working curve sample prep. photoemission anal. *(Japanese)* 78−53050
Fe-W, dislocation mobility and internal friction, effect of alloying in α-Fe *(Russian)* 77−31671
Fe-W, Gibbs energy of form. of phases *(German)* 80−97724
Fe-W, recrystallisation under laser irradiation *(Russian)* 78−35396
Fe-W, semihard magnetic alloys, magnetic, elec. mech. props. *(Japanese)* 79−70078
Fe-W, split bands evidence from sp. ht. and elec. transport data 77−24515
Fe-W, thermophysical props. and elec. cond., temp. depend. 80−96842
Fe-W (5%), internal friction, mag. and nonmag. components *(Russian)* 78−48018
Fe-W system, damping capacity of Gentalloy, internal friction, mech. and mag. props. 79−77679
Fe-W-C, eta carbides at 1250°C 77−36506
Fe-W-C-Cr, eta carbides at 1250°C 77−32581
Fe-W-Co, solubility anomaly due to magnetic transition, Co effects *(Japanese)* 79−42257
Fe-W-Cr-Mo system, mag. and mech. props. rel. to production methods *(Japanese)* 80−71107
Fe-W-Cr-Mo-Co (18,12,3,x wt.%) magnetisation and hardness, cold working effect obs. *(Japanese)* 77−40428
Fe-W-Cr-Mo-Co with austenitic phase, magnetic and mech. props., cold working and ageing effects *(Japanese)* 78−60678
Fe-W-P-C, amorphous, corrosion resist. in 1N HCl 78−80678
Fe-WC-VC(TiC), sintering, densification 80−25615
Ir-W (0.3 wt.%), grain growth, temp. and time effects 79−100186
Ir-W (0.3 wt.%), P segregation to grain boundaries, effect on high temp. ductility 78−95754
Ir-W (0.3 wt.%), polycrystn., brittle fracture TEM study 79−61715
Ir-W (0.3 wt.%): Al(Fe)(Th)(Ni)(Rh), effect of additions on grain boundary composition 79−83309
Ir-W (0.3%), grain boundary comp., trace element additions effect 80−66661
LaB_6-Ni-WC, thermionic emission 77−28678
Mg-Ni-W-Co-Al-Cr alloy KhN56VMKYu, Al effect on excess Mg phase 80−29926
Mn cast Fe, W effect on transform. in thin surface layers during dry sliding friction 77−21289
$(Mo,W)C$-$(Mo,W)_2C$, hard facing alloys 79−24667
Mo-W, calibration line introduction for comp. determ. by AES 79−56892
Mo-W, fatigue and threshold behaviour under high cycle fatigue 80−40487
Mo-W, integral hemispherical degree of blackness, 1200-3000K 78−43154
Mo-W, oxidation 77−70227
Mo-W (30 wt.%), wrought, fracture, characteristic features 80−104278
Mo-W (50 wt.%), emissivity, 1200-3000K, effects of annealing and surface treatment 78−43154
Mo-W alloy type MW25N, crystallisation form, globular dendrites, grain boundaries *(Russian)* 80−66494
Mo-W solid soln., joint solubility of C and Zr 77−25025
Mo-W system, short-range order calc. *(Russian)* 79−23566
Mo-W-C, phase equilibria calc., line compounds 80−10638
Mo-W-Mo (4.74, 2.17 wt.%), creep resistance in ultrahigh vacuum 79−5027
Mo-W-N system, nitrided annealed samples, W replacement of Mo 80−76227
Nb-W, cold plastic deform., oriented microdistortions *(Russian)* 78−39840
Nb-W, diffusion of N, effect of W and struct. defects 79−55938
Nb-W, dil., neutron irradiation at 4.6K, influence of impurities on defect prod. 79−55790
Nb-W, single cryst. elastic consts. 77-298K 78−84879
Nb-W-Mo-Zr, long-term strength props., vac. level effect 80−55484

tungsten alloys continued
Nb-W-Mo-Zr (5, 2, 1 wt.%), surface-layer struct. and mech. props., effect of O_2 diffusion saturation 79−5087
Nb-W-Mo-Zr (5, 2.1, 0.92 wt.%), creep resist., high temp. ageing in vacuum 80−71716
Nb-W-Mo-Zr-C, strength and ductility, prolonged high-temp. soaking effect 80−55483
Nb-W-Mo-Zr-C(5,2,1,0.02 wt.%) alloy 5 BMTs, short-time tensile strength in liquid Bi and Li *(Russian)* 77−25186
Nb-W-Si, ductile amorphous, superconductivity 80−60131
Nb-W-X-C, X=Ti, Zr, Hf, quenched from liquid state, formation of nonmetallic inclusions *(Russian)* 79−57007
Nb-W-Zr-N alloy, with dispersed second phase, ductile-brittle transition 80−93653
Nb-W-Zr-Ta, long-term strength props., vac. level effect 80−55484
Nb-W-Zr-Ta (90, 4.5, 3.5, 2 wt.%) creep and creep limit in super vac. at 1100°C, heat treatment effect 80−81133
Ni base alloy IN792, carbide morphology 77−36508
Ni plated WC powder, detonation spray deposited hard alloy coating, electrical conductivity 77−12025
Ni superalloy Mar-M200, slow fatigue crack propagation rate meas. using high freq. resonant technique 78−52983
Ni-(W,Cr)C, corrosion and corrosive wear in sea water 78−92408
Ni-Al-Cr-Mo-Ti-W-(Co) alloys EhI 826 and EhI 929, reverse elastic after effect under loading 78−39829
Ni-Al-Cr-Ti-W-Mo, US vibration applied during solidification, improved strength, corrosion resistance *(Russian)* 78−15382
Ni-Al-W, heat resist., solidification range 80−35177
Ni-C-W-Cr(-Mo), Vickers hardness and crystallisation temp. 80−16361
Ni-Co-Cr-Mb-W-Ta, Cr, Mb, W, Ta effects on σ phase occurrence 77−36507
Ni-Co-Cr-Ta-Al-W-Mo-Ti, cast, phase volume fraction determ. using manual point count practice 78−53052
Ni-Co-W, electrodeposition, surface morphology and cryst. struct. 80−71602
Ni-Cr-Al-W-Ti alloy MA 6000E, mechanical alloying for high temp. appl. 78−44046
Ni-Cr-Co-Al-Ti-W-Ta-Mo, IN 738 LC, loading frequency and environmental effects on high temp. fatigue crack growth 78−64675
Ni-Cr-Co-Al-W-Mo-Ti-Ta, heat resist. and struct., Ta effect 80−76312
Ni-Cr-Co-Ti-Mo-W-Al (14, 9.8, 5, 4, 3.9, 3 wt.%), low cycle fatigue, prior heat treatment effect 80−60962
Ni-Cr-Co-W (47.5, 25, 12, 8.75 wt.%), vaporization of IN-643, high-temp. mass spectrometry 79−7685
Ni-Cr-Fe-W, type EHI868, loading history effect on resist. to cyclic elastoplastic strain 80−16398
Ni-Cr-Mo-W-Al-Ti, heat-resist., phase comp. 80−76250
Ni-Cr-Ti-Co-W-Al-Mo alloys AF-115 and AF2 1DA, superalloy powder compacts, fatigue origins 78−48521
Ni-Cr-W, heat-resistant, integrated hemispherical degree of blackness, specific elec. resist., oxidised surfaces 79−86912
Ni-Cr-W, oxidation behaviour in air at 1000-1250°C 80−89407
Ni-Cr-W (20, 10 to 40 wt.%), phase composition, struct. and props. 80−21034
Ni-Cr-W (20, 3 wt.%), high temp. creep, atmospheric effect on anomalous behaviour 78−80617
Ni-Cr-W-C(-Si), struct. and props. of corrosion and wear resistant alloys 79−24627
Ni-Cr-W-C(Si) hardness, corrosion resistance, wear resistance tests in 10% HCl *(German)* 78−92368
Ni-Cr-W-Co granules type ZhS6U, EP741, hot hydrostatic pressing 80−60796
Ni-Cr-W-Co-Ti, thermal fatigue, effects of inclusions 80−81183
Ni-Cr-W-Co-Ti heat resistant alloy ZhS6K, fatigue resistance, heat treatment and protective coating effects 77−81320
Ni-Cr-W-Co-(Al)(Ti)(Mo), high-temp. sulphide corrosion 80−76408
Ni-Cr-W-Mo-Al-Ti (15,6,3,2,2, wt.%), wrought, Si effect on transition brittleness *(Chinese)* 80−55491
Ni-Cr-W-Mo-Ti-Al, heat-resist., recovery and recrystn. 80−76268
Ni-Cr-W-Mo-Ti-Al alloy KhN67MVTYu, heat treatment effect on mech. props. 77−70082
Ni-Fe-Nb(Ta)-W, high magnetic permeability alloys, Hardperm 77−48012
Ni-Fe-W alloy, electrodeposition, SEM and optical obs. 79−66018
Ni-Mo-C-W, Vickers hardness and crystallisation temp. 80−16361
Ni-Mo-W, diagram of state, W solubility, dispersion hardening *(Russian)* 80−66477
Ni-Mo-W, type N55M20V25, quenched at various cooling rates, phase transformations *(Russian)* 79−66052
Ni-W, eutectic form., struct. and mech. props. *(Russian)* 77−21129
Ni-W (2%), Mg diffusion meas., 970-1330K, appl. of vapour collect and AES method 78−75876
Ni-W (20 to 50 at.%), phase distrib. var. with annealing time, metastability of hexagonal phase *(Russian)* 77−8851
Ni-W (45.5 wt.%), eutectic, mech. props., high press. H_2 effects 77−63779
Ni-W directionally solidified eutectic composite, foil prep. for TEM 78−53072
Ni-W melt, N_2 diffusion *(Russian)* 78−18812
Ni-W sintered powder pressings, intermetallic phases *(Russian)* 80−55349
Ni-W-B, superalloy, M_5B_3 type boride 78−44131
Ni-W-C, X-800 centrifugally cast cylinder lining alloy, compatibility with hardfacing alloys 77−32726
Ni-W-C(Nb) system, γ to (γ+W) phase boundary calcs. using Wigner method *(Russian)* 80−54346
Ni-W-Co-Cr, superalloy MAR 200, with Hf, cellular composite prod. by isothermal dendrite ripening 78−44150
Ni-WC, dispersion hardened, centrifugally cast metallurgical coatings for wear resistance in plastics molding machines 79−29285
$Ni_3(Al,W)$, yield strength, temp. and orientation depend. 77−28857
$Ni_3(Al,W)$, yield stress, orientation depend. 78−39830
Ni_3Al-W, powder, X-ray spectral analysis exam. 80−16239
$Ni_3(Fe,W)$, elec. resist., temp. depend. anomalies, Hall and Nernst-Ettinghausen effects *(Russian)* 80−10942
$Ni_3(Fe,W)$, kinetic phenomena rel. to ordering and electron struct. *(Russian)* 78−76043
Ni_3Fe-W, transport props. and magnetisation, effect of W alloying *(Russian)* 78−39095
Ni_4W, order-disorder phase transition, X-ray struct. exam. *(Russian)* 78−64532

tungsten alloys continued
Ni_4W_9 ionisation states of field evaporated ions 77−81200
Pd-Ru-W, elec. resist. and thermal cond. *(Russian)* 78−19017
Pd-W, elect. resist., mag. susceptibility, Hall coeffs., in plastically deformed state and after annealing *(Russian)* 79−66174
Pd-W, substrate temp. influence on shallow contact formation on Si 80−96963
Pd-W (20 wt.%), permeability, diffusion, and solubility of H_2, elec. resist., heat treatment effects *(Russian)* 79−51307
Pd-W/Si, contact reactions, backscattering, X-ray diffr. meas. 80−20040
$Pd_{1-x}W_x$, calc. of short-range order parameters from X-ray scatt. data *(Russian)* 80−75367
Pt-Rh-W (30, 8 wt.%), intergranular embrittlement by Se vapour 80−3185
Pt-Rh-W alloy corrosion by radioisotopic power system insulating and thermoelec. materials 78−7094
Pt-W, substrate temp. influence on shallow contact formation on Si 80−96963
Pt-W, surface segregation, appl. of quantification of atom-probe FIM data 78−62263
Pt-W (92-8%), UF_6 mol. negative surface ionisation 78−56913
Re-W (up to 6.1 wt.%), X-ray diffr. study of conc. and temp. depend. of lattice parameters 79−94965
Re-W alloy, mag. suscept. of HCP transition metal alloys *(Russian)* 78−80138
Re-W/C multilayer films for X-ray mirrors 79−44992
Rh-W disc bonded to graphite, for X-ray tube rotary anodes *(German)* 80−105760
Si-Fe-W, dil. alloy, compositional changes on sputtering, projectile energy depend. 80−66362
TC-Co, nearest-neighbour size correlation with grain size *(French)* 77−8843
Ta-N, kinetics and thermodynamics of reaction with N_2 *(German)* 79−74415
Ta-W, electronic density of states, temp. depend. of elec. resist. and mag. susceptibility 77−11891
Ta-W, thermoelec. power, 4.2 to 300K 80−70684
Ta-W (10 at.%), with N_2, spectral emissivity, N_2 absorption rate, N_2 solubility, thermodynamic data *(German)* 77−25026
Ta-W BCC, press. derivatives of elastic moduli, Fermi surface topological changes, band struct. 79−61639
Ta-W film, amorphous, temp. stability 78−63948
Ta-W optical props., temp. depend., 4.2-1100K 78−2874
Ta-W TV-10 alloy, thermal expn., 1146-2288K 78−43148
Ta-W-Hf, embrittlement, effect of composition 77−21247
Ta-W-Hf, small-angle electron scattering in TEM from lattice strains accompanying precipitation 79−14658
Ta-W-Hf (8,2 wt.%), T-111, O_2 absorption, effect on lattice parameter and specimen dilation 78−83958
TaC-Ni-W alloys, oxidation resist. 77−60000
Th-W, TF electron emitters props. obs. 80−66403
Ti-Al-Zr (3,3 wt.%), W alloying addition effects on mech. props. *(Russian)* 77−59860
Ti-B-W, annealed at 1400°C, exam. of phase diagram, using X-ray phase and metallographic analysis 79−1847
Ti-Nb-W, 20 to 1000°C, isothermal section, X-ray anal., microstruct., hardness, cond., transform. *(Russian)* 77−55947
Ti-W, dilute, superconducting transition temp. and mag. susceptibility 78−47899
Ti-W film, bias-sputtered, resist. and comp. 80−25023
Ti-W films, bias-sputtered, quantitative anal. 80−80114
Ti-W/Au metallisation on Al, temp. stability, barrier props. 79−23868
Ti-W(-Al), mech. props. and heat treatment 80−35274
α-Ti-Zr-W, effect of W impurity on mech. preps. 80−16392
Ti-Zr-W-(Al), phase struct. and props. *(Russian)* 80−16270
TiC coated WC-Co cemented carbides, fracture toughness 80−85046
TiC-Ni-W, cemented carbides, grain growth, metallographic obs. 77−24982
TiW-TiO_2-InP thin refractory MIS struct. deposition 80−75647
$Ti_{0.3}W_{0.7}$, thermal annealing study of metallisation on Si 80−80134
V-W, effect of alloying additive on thermoelectric props. 77−35927
V-W, X-ray K-emission spectra *(Russian)* 77−55851
V_3Si-W solid soln., supercond. T_c and paramag. susceptibility *(Russian)* 77−59348
W/Cu powder with varying W particle size, burning behaviour and crack form. tests *(German)* 78−7005
W-Al, couple phase diagrams and thermochemical data 79−66037
W-C, coupled phase diagrams and thermochemical data 79−66036
W-C-(Zr)(Hf)(Nb)(Ta)(Re) alloys, vacuum melted, phase composition, struct. and props. 78−31403
W-C(0.01 to 0.2 wt.%), C effect on high temp. strength 77−16614
W-Co, carburizing rate, Co effects *(Japanese)* 79−52453
W-Co, dil., excess resistivity, temp. depend., Kondo effect 78−68011
W-Co mixed powder, carburizing *(Japanese)* 79−52454
W-Cr alloys, segregation of Cr to gain boundaries, field ion microscope investigation 77−8816
W-Cr powder alloys, sintering in presence of Cu-Ni liq. phase 80−16246
W-Cr solid solution, precipitation behaviour, reaction front motion, lattice parameters *(German)* 80−55401
W-Cr-Pd, Pd effects on diffusion 77−24445
W-Cu, electrical erosion resistance during electrospark machining 78−35531
W-Cu, porous material, skeletal type, produced by liquid phase sintering, exam. of mech. strength, determ. resistance 80−16245
W-Cu (92.8, 7.2 wt.%), liq.-phase sintered, embrittlement and interfacial impurity segregation 80−66647
W-Cu amorphous metal films, struct. and elec. characterisation 79−87017
W-Cu composite materials, vel. dispersion and scatt. of transverse US waves 78−91383
W-Cu contact materials with Ni and Co dopants, sintering 77−55908
W-Cu fibre reinforced composites, interface shear strength, critical aspect ratio 77−4826
W-Cu permeable materials, development 77−28755
W-Cu powder, liquid phase sintering, stabilisation of porous structure and control of volume changes 79−95974
W-Cu pseudoalloy, porous, chromising 80−100959
W-Cu sintered alloy, produced from coreduced powders, densification 78−11154
W-Cu-Co(Ni) electrical contact material, comparison of Co and Ni effects *(Korean)* 78−10539

tungsten alloys continued
W-Cu-Ni powder, liquid phase sintering, stabilisation of porous structure and control of volume changes 79−95974
W-Cu-Ni(6), contact materials, activated sintering, Ni and Co effects 79−95967
W-Cu-(Ti)(Zr), exam. of mech. props. as function of temp., composition, and oxidation props. 80−16472
W-Fe, dil., excess resistivity, temp. depend. 78−68011
W-Fe, dil., spin glass props., DC mag. susceptibility meas. 78−68283
W-Fe, electronic transport below 1K 80−2377
W-Fe, spin glass props., DC susceptibility and remanence meas., 1.6 to 295K 80−29560
W-Fe spin glass, optical props. and electronic states 80−20412
W-Fe-Co, sintering and mechanical props. *(Japanese)* 80−21086
W-Ge-B, phase diag. 77−52285
W-Hf-C, phase equilib. 80−55348
W-Ir (1 wt.%), positron annihilation, photon ang. distrib. meas. effect of deformation, annealing temp. *(Russian)* 78−35220
W-K-Si-Al doped wires, heavily drawn, fibre struct., annealed 79−56993
W-Mo, powder mixture, electric discharge sintering, struct. changes 77−77446
W-Mo, refractory, surface investigation by FIM and atom probe *(German)* 79−55623
W-Mo, vapour deposited, long-term strength and thermocyclic creep 80−16405
W-Mo alloys, positron interactions with component atoms *(Russian)* 77−63486
W-Mo alloys, thermal conductivity and diffusivity, sp. ht., 100-2400°C 78−75842
W-Mo powder mixture, activated sintering 77−21058
W-Mo powder mixtures, form. using electric discharge sintering 77−12563
W-Mo-Re heat resisting alloy MVR-27-VP2, high-temp. emissivity and resistivity 77−35727
W-N amorphous metal films, struct. and elec. characterisation 79−87017
W-Nb (0-30 at.%), average thermal expansion coeff., 500-1200K 78−14483
W-Ni, liquid phase sintering, microstruct. meas. 78−44054
W-Ni, liquid phase sintering 80−16232
W-Ni, liquid phase sintering 80−25613
W-Ni, MBM diode, resist. depend. of detected signals 80−2482
W-Ni, MOM diode, breakdown effect in visible and near-IR regions 80−6999
W-Ni, surface barrier influence on C diffusion in stainless steel type 1Kh18N9T *(Russian)* 80−54434
W-Ni (0.5, 2 and 5 wt.%), Ni effect on shrinkage anisotropy during sintering 77−21056
W-Ni compact, sintering behaviour and workability *(Japanese)* 80−20822
W-Ni liquid alloys, sintered, coarsening of W grains, exam. 78−56598
W-Ni powder compacts and wires, recrystallisation, influence of omni-directional press. *(Russian)* 77−8849
W-Ni sintered alloy, etching 79−29323
W-Ni system, grain growth and densification during liquid phase sintering 79−38760
W-Ni system, liq. phase sintering, 1640°C, solubility and vol. diffusion of Ni in W 79−86895
W-Ni-Cr, high-temp. phase diag. *(French)* 77−48393
W-Ni-Cu(4, 2 wt%), radionuclide calorimeter for liquid He range 4.2 to 8K 79−18093
W-Ni-Fe, W-Ni-Fe-Mo (Mn), sintering and mechanical props. *(Japanese)* 80−21086
W-Ni-Fe (5(2), 5(2) wt.%) pore formation, effect on mech. props. 80−45396
W-Ni-Fe system, reduction kinetics and alloy form. 80−60801
W-Ni-Fe(Co)(Cr), structural characterisation *(French)* 77−56074
W-Ni-Fe(Cu), liquid phase sintered, interfacial embrittlement 79−57101
W-Ni(Co) point-contact diodes as harmonic generators and mixers, DC bias dependence 80−75653
W-Ni(Fe,Co,Cr,Ti) powder based composite, high temp. strength of W reinforcing fibres 79−70021
W-Os system films, condensation temp., conc., and phase comp. effect on struct. and props. *(Russian)* 80−24749
W-Re, amorphous wire, elec. resist., 2-20K, dimens. and mag. field depend., quantum localisation 80−39547
W-Re, dil., excess resistivity, temp. depend. 78−68011
W-Re, integral hemispherical degree of blackness, 1200-3000K 78−43154
W-Re, ion irradiated, recovery behaviour studied by field ion microscope 80−29074
W-Re, neutron irrad. effects on phase stability free energy changes 79−11566
W-Re, optical props., temp. depend., 4.2-300K 78−2874
W-Re, phase form. and diffusion interaction with liquid Al, under weightlessness *(Russian)* 78−22876
W-Re, sigma phase stability and irrad. effect 78−11200
W-Re, substruct. stability of single crysts. on high temp. annealing *(Russian)* 77−66666
W-Re, surface diffusion 79−56048
W-Re, thin wires, fatigue limit and tensile strength 80−25834
W-Re, wire, elec. resistance, low-temp. continuous and cyclic heating effects, compared with W 78−92370
W-Re (3%), W adatom-substitutional Re atom interaction, FIM obs. 77−89626
W-Re alloy, effect of thermal prehistory on resistivity meas. 78−3241
W-Re alloy, elec. resistivity meas. near conc. anomaly, 300 to 1200K 77−35911
W-Re alloy, prep. by powder metallurgy technique, appl. in lighting industry 80−29904
W-Re alloy thermocouples, calibration, 77 to 290K 77−57324
W-Re alloys, anomalous conc. depend. of elec. resistivity 77−35917
W-Re alloys, polarographic determ. of Re 79−16071
W-Re alloys, Re determ., electrochem. method 79−16073
W-Re alloys, sintered, preparation, thermal cond., linear expansion up to 1000K 79−61533
W-Re alloys, thermal EMF instability, heat treatment effects 80−75553
W-Re amorphous alloys, phase-slip and localisation diffusion lengths 80−107747
W-Re fibre-reinforced Ni-base refractory alloy, struct. and props. *(Russian)* 77−59721

tungsten alloys continued
W-Re film, amorphous, temp. stability 78−63948
W-Re film, obtained by electron beam volatilisation and vac. condensation, props. *(Russian)* 77−24490
W-Re films, amorphous, one-dimensional quantum localisation 80−80413
W-Re thermocouple, thermal EMF var., stability 77−41604
W-Re wire, CVD coatings of SiO_2 and Mo, for neurological electrode, elec. cond. and bending props. 78−11752
W-Re/C multilayer, periodic and near-periodic, small-angle interferences of reflected X-rays 79−94846
W-Re(Mo)(Cr), powder mixture, activating effect of Group VIII metals on alloy form. during sintering 77−59728
W-Ru based refractory transition metal-metalloid glass, struct. 80−1938
W-Si-Cu, struct. and supercond., Cu influence 80−50592
W-Th, atomic structure of grain boundaries 79−33003
W-Th, field ion specimen, contrast bands in elec. field induced evaporation 79−50967
W-Th, mean square strain, use of approx. methods for Fourier series coeffs. for X-ray diffr. lines *(French)* 77−31549
W-ThO_2, sintering for fabrication of ionisers for electric propulsion *(French)* 79−56946
W-ThO_2 composite, struct., lamination tendency, effects of method of manuf. 78−68653
W-ThO_2 fibre reinforced Ni base alloys, powdered matrices, fibre/matrix interaction above 1300°C, alloying effects *(Russian)* 78−95755
W-Ti, Ti addition effect on heat resistance and radiative props. *(Russian)* 80−25515
W-TiC(ZrC)(HfC), thermionic emission, surface structural characts. after prolonged use, work function variation 80−20758
W-Ti(Zr)(Hf)-C, cubic solid soln., form. and props. 78−48348
W-W_2C, directional crystn. using plasma heating 78−60569
W-WC, activated sintering, mech. props. *(Korean)* 78−60622
W-Zr, Zr addition effect on heat resistance and radiative props. *(Russian)* 80−25515
W-Zr (2.92, 7.42 and 10.02 wt.%), and W_2Zr, thermal expansion, elec. resistance, 100-900°C, crystallisation 78−91455
W-Zr system, kinetics of interdiffusion process *(Russian)* 79−69298
W-Zr-C, Zr and C addition effect on heat resistance and radiative props. *(Russian)* 80−25515
W-ZrC (25 wt.%), eutectic alloy, thermionic emission and adsorption props. 79−69951
W-ZrC(-Re) eutectic alloy, Re effect on breaking stress, lattice parameters, electron struct. *(Russian)* 79−1845
W_2B_5-based alloys, mech. props., rel. to appl. as electrodes in electrospark machining 80−21174
WC base alloys, uncoated and TiC or Al_2O_3 coated, wear charact. 78−92365
WC, cemented carbide, deformation, high temp., stress relaxation, and strain rate depend. 78−39854
WC, plasma sprayed coating 78−35592
WC powder, chemical plating with Co and Co-P 80−25593
WC powder, effect of prep. temp. on fine structure, X-ray diffr. anal. 79−33971
WC, roughness and wear characteristic of spark-eroded surfaces 79−52390
WC/Co cemented carbides, fracture toughness testing 80−104410
WC-Co, (3%), meas. of yield stress by compressive loading 79−54150
WC-Co, calc. of weakest link in struct. 80−11730
WC-Co, cemented carbide sintered, appl. of dihedral angle meas. to microstruct. 78−39716
WC-Co, cemented carbide, deformation, high temp., stress relaxation, and strain rate depend. 78−39854
WC-Co, comparison of indentation crack resistance, and fracture toughness 78−76739
WC-Co, composition and oxidation resistance of coatings deposited by thermal diffusion, using TiB_2 *(Bulgarian)* 80−45430
WC-Co, conditioned metal electrode, effect on electrical strength of vacuum gap 79−90489
WC-Co, contact reaction with BN at high pressures 80−61029
WC-Co, creep rupture strength meas. 78−31475
WC-Co, developments, properties and fabrication processes *(Dutch)* 77−70021
WC-Co, elastic and plastic charact. 80−35280
WC-Co, elastic moduli and their press. derivatives 79−83248
WC-Co, elemental and phase comp. of diffusion-deposited boride coatings 80−15402
WC-Co, evidence for H embrittlement 78−48530
WC-Co, exam. of effect of continuous carbide phase, on hardness, and deformation 78−52974
WC-Co, fracture toughness testing by double torsion bend test 78−27705
WC-Co, nearest-neighbour size correlation with grain size *(French)* 77−8843
WC-Co, on-line computer anal. of SEM obs. 79−87807
WC-Co, phase comp. and oxidation resist. of coatings deposited by thermal diffusion using TiB_2 80−21173
WC-Co, precursor derived powder, prep. 77−32541
WC-Co, prep. temp. effect on fine struct. of WC phase, X-ray obs. 79−33971
WC-Co, quantitative charact. of surface damage by electrochemical grinding 79−47836
WC-Co, rupture of bending specimens, use of quantitative metallography and stereology *(French)* 77−28899
WC-Co, rupture stress, microstructure and other effects 77−73343
WC-Co, STEM anal. of grain boundaries 80−79644
WC-Co, sintered, obs. of spinel particles by TEM 78−95714
WC-Co, sintered hard alloy, mechanism of penetration of liquid metals 78−60619
WC-Co, size factor effect on strength in complex stressed state 78−31483
WC-Co, TiC coated, TiC stoichiometry effects on mech. props. 77−66715
WC-Co, time-depend. strength params. 78−31516
WC-Co, VK type hard alloy, influence of residual stresses on static strength 77−1862
WC-Co, various combinations, fracture characts. in bending, compression, and toughness tests 78−60808
WC-Co (10 to 30 wt.%) transverse rupture strength, residual stresses due to surface grinding effects 77−63789

tungsten alloys continued
WC-Co (10 wt.%), elevated temp. bend deform. and fracture, effect of C 77−59877
WC-Co (10 wt.%), high temp. transverse rupture strength 77−63790
WC-Co (10 wt.%), vacuum sintered, short-time bending creep rupture strength *(Japanese)* 78−15508
WC-Co (10%), cycle fatigue, optical microscopy and SEM obs. 77−52494
WC-Co (12 wt.%), sintering with various binding phases *(German)* 79−28984
WC-Co (15 wt.%), alloy VK15 coating on Ti-Al, detonation sprayed, antifriction props. 80−21188
WC-Co (15 wt.%), detonation spray deposited hard alloy coating, electrical conductivity 77−12025
WC-Co (15 wt.%) detonation spraying on to Cr-Ni steel with automatic powder feed 80−25558
WC-Co (5wt.%) hardmetal, η-phase precipitation effect on struct. and mech. props. 79−47696
WC-Co (6 to 20 wt.%), bend deform. and fracture up to 1000°C 77−48510
WC-Co alloy, hard metal, resistance of cavitation erosion *(Japanese)* 80−16575
WC-Co alloy, short-time creep rupture strength, C content effect 400° to 900°C *(Japanese)* 78−48487
WC-Co alloy, transverse rupture strength rel. to grain size and strain rate, 400° to 900°C *(Japanese)* 78−48486
WC-Co alloys, brittle fracture, precision matching of mating fracture surfaces, by SEM fractographs 78−60807
WC-Co alloys, fracture toughness model 80−84243
WC-Co alloys, microstresses in two phases, mag. investig. 77−59879
WC-Co alloys, P additions, effect on hot pressing, hardness and wear resist. 78−11162
WC-Co alloys, single edge notched beams, exam. of fracture toughness 78−52975
WC-Co alloys fracture, spatially constrained crack tip opening displacement 77−77580
WC-Co and WC-Co-TaC-TiC-NbC cemented carbides, microstructure, high temp. deformation, uniaxial plastic compression 80−40451
WC-Co based cutting tools, temperature meas. method based on amount of W in binder 79−96264
WC-Co carbide, crack paths, SEM study *(Japanese)* 80−50710
WC-Co cemented carbide, bending strength, surface roughness effects *(German)* 77−8947
WC-Co cemented carbide, carbide grain size effect on strength rel. to structural defects 77−32689
WC-Co cemented carbide, relation between transverse rupture and tensile rupture *(Japanese)* 77−52473
WC-Co cemented carbide, indentation fracture, operative fracture mode survey 77−70183
WC-Co cemented carbide, fracture toughness meas., model for variation with microstruct. 78−60806
WC-Co cemented carbide, stress-strain curves using ultrahigh-pressure apparatus 79−43322
WC-Co cemented carbides, effect of Co form and distrib. in prep. starting mixture 78−44072
WC-Co cemented carbides, high temp. transverse rupture strength, effect of domain size of binder phase *(Japanese)* 78−92329
WC-Co cemented carbides, rel. between Palmqvist indentation toughness and fracture toughness 79−70155
WC-Co cemented carbides, transverse-rupture strength obs., w.r.t. domain size of binder phase *(Japanese)* 80−11741
WC-Co cemented composites, abrasion by quartz 80−16495
WC-Co cermet, dynamic SEM wear obs. 77−36667
WC-Co compacts and sintered alloy, fine struct. of carbide phases, preforms re-pressing under high press. effect 79−28987
WC-Co composite, ion scatt. spectrometry and AES 77−60150
WC-Co cutting plates, hardness and struct. of TiB_2 coatings 80−21175
WC-Co from directionally carburized WO_3-C-Co_3O_4 mixtures, sinking *(Japanese)* 80−11589
WC-Co hard alloy, preheating influence on explosive shock hardening *(Russian)* 79−29083
WC-Co hard alloys, hot pressed, mech. props. 79−100260
WC-Co hard alloys, hot-pressed, wear resist. under abrasive friction, heat treatment effect 80−66555
WC-Co hard alloys, machined with polycryst. superhard materials, surface struct. using X-ray photoelectron spectroscopy 80−25919
WC-Co hard metal, binder phase charact. by magnetic props. 79−29439
WC-Co hard metal, stress conc. factor and stress intensity factor, rel. to wear *(German)* 78−11335
WC-Co hard-alloy cermets, strength, fatigue, static tests 79−29314
WC-Co hardmetal, defect initiated fracture and bond strength 78−11319
WC-Co hardmetals, β-SiC to turbostratic graphite transformation 79−74150
WC-Co mixed powder prod. by rotary kiln, new continuous process 78−64502
WC-Co molten Zn reaction, lamellar struct. form. 79−33964
WC-Co powder, prep. by direct carburisation of WO_3 in presence of Co_3O_4 80−50573
WC-Co powder form. from Wo_3 and Co_3O_4 carburization, C behaviour *(Japanese)* 80−7517
WC-Co sintered carbide tips, microscopic stress anal. 78−5663
WC-Co sintered hard alloy, yield stress, internal thermal stress effect 79−100230
WC-Co sphere, erosion of Al by solid particle impingement at normal incidence 80−104304
WC-Co substrate, load-bearing capacities of TiC layers 80−40606
WC-Co-C, densification kinetics, in hot pressing of VK6 hard alloy 80−11600
WC-Co-Cu, interdiffusion up to 1120°C 78−11492
WC-Co-Ta(Ta-Ti-Nb), cemented carbide, deformation, high temp., stress relaxation, and strain rate depend. 78−39854
WC-Co(TiC-Co), powder compacts, effect of additional pressing at hydrostatic pressures on props. 78−56596
WC-NbC-Co, TiC and TiN coating by ion plating, and cutting tests 79−24678
WC-Ni (10 wt.%), room temp. transverse rupture strength *(Japanese)* 77−63774
WC-Ni detonation sprayed coating, wear resistant 78−35594
WC-Ni hard alloy composite, sintered, void healing 80−60821

tungsten alloys continued
WC-Ni hard alloys, sintered, with uneven binder metal distrib., molten Ni migration 78−35336
WC-TaC-Co, cemented carbide, strength improvement by hot isostatic pressing 78−84969
WC-TiC, powder for plasma arc spray coating appl. 78−15591
WC-TiC-Co, powder for plasma arc sprayed coating 78−15591
WC-TiC-Co alloys, microstresses in two- and three-phases, mag. investig. 77−63758
WC-TiC-TaC, powder for plasma arc spray coating appl. 78−15591
WC-TiC-TaC-Co cemented carbides, transverse-rupture strength at 600 to 1000°C obs. *(Japanese)* 79−43374
WC-TiC-Ta(Nb)C-Co, CVD and activated reactive evaporation of TiC, AES obs. of substrate-layer interactions 79−24679
WC-TiC(TaC, NiC)-Co, hard, homogeneity and wear resistance estimation, by magnetic method 77−90558
W_6Co_6C cemented carbide substrate, TiC CVD coating, structure, composition and hardness exam. 78−11425
WCuB prep. by infiltration of W skeleton by CuB, hardness meas. *(German)* 78−64508
$W_{50}Fe_{50}$ glassy alloy, refractory, triode sputtered 80−75185
$W_{0.65}Re_{0.35}$, search for strong coupling superconductivity 79−28441
WSi_2, diffusion grown layers, texture 79−74095
WSi_2 film, FET gate electrode, oxidation mechanism, SiO_2 overlayer formation 78−76773
$W_{70}Si_{20}B_{10}$, amorphous alloys obtained by liq. quenching, superconductivity 80−75670
Zr-Fe-Cu-W, Mossbauer spectra parameters of Zr_2Fe particles *(Russian)* 80−29654
Zr-W-Cr, Zr-rich corner of phase diag. *(Russian)* 78−80517
ZrC-W, thermionic emission current density, cathode operating time and comp. depend. 77−8714
ZrC-W (75 wt.%) eutectic refractory alloys, smelting in suspended states, components distrib. *(Russian)* 80−19913

tungsten compounds
see also tungsten alloys
alkali metal tungsten bronzes, enhanced supercond. T_c, possible explanation 78−14850
alkali metal tungsten bronzes, superconductivity at press. up to 20 kbar 79−38226
anodised layer, structure and stoichiometry, thickness effects 77−77634
borides, chemical vapour deposition *(French)* 77−36406
bronzes, hexagonal, supercond. and special phonons, neutron scatt. obs. 80−15643
chalcogenides, layered, soln. mechanism of metals 79−42249
complex, $WOCl_4.Ph_3SO$, prep. and characterisation 78−30592
dichalcogenide, valence band nature, elec. and mag. props. 78−39014
ESCA using Au M_α X-rays (2123 eV) 78−72683
metatungstate mixed valence anions, XPS spectra, oxidation states 78−6824
phosphate-tungstate semicond. glass, W (V) complex, EPR and electronic spectra interpretation 77−69682
rare earth tungsten bronzes, search for coexistence of superconductivity and long range mag. order 79−38226
refractory carbides, borides and nitrides, wetting by and interactions with liq. metals 80−54473
ternary oxides, with Mo_5O_{14} struct., occurrence and struct. stabilisation 77−4084
transition metal compounds, $M_{2-x}W_xAs(P)$, crystal struct. *(French)* 77−47429
triphenylphosphine compounds, $(C_6H_5)_3PM_xM'_{1-x}(CO)_5$, M,M'=Cr, Mo, W, mixed cryst., CO vibr. spectra, modal anal. 78−35128
tungstate phosphors, thermoluminesc. and afterglows 79−38681
tungstates, $A(B_1W)O_3$, $A(B_1C_1W)O_3$, perovskite struct. 77−51352
tungstates, alkaline earth, U activated, scheelite struct. luminesc. props. vibr. modes and quenching temp. 80−60651
tungstates, $Me^{II}WO_4$ (Me^{II}=Cd, Cz, Sr, Ba, Pb), refr. index, single crystals having scheelite struct. 78−79082
tungstates, U-doped, perovskite struct., luminesc. quenching, QMSCC calcs. 80−71470
tungstates (double), of mono- and tri-valent metals, polymorphism, X-ray diffr. obs. 78−87642
α-W_2C, polycryst., plastic behaviour at ambient temp. *(French)* 79−1435
WO_3 reduction with H, starting specific surface effect on kinetics 80−11599
Al:WO_3 films, resistive state, effect of UHF rad. on dynamic cond. *(Russian)* 78−52154
Al_2O_3-W, dielectric cermet, thermophysical props. 77−51557
Au-WO_3, electrochromic cermet, optical and electrical props. 79−33674
Au-WO_3 cermets, electrochromism 77−90129
Au-WO_3 electrochromic cermets, resist. and optical density meas. 79−8201
BaO-WO_3, solid phase reaction, thermal anal. 80−55639
BaO-WO_3-P_2O_5 glass, struct. and IR spectra 80−64914
$Ba(PO_3)_2$-WO_3, electron-absorpt. spectra and structure of W centres 80−88873
$CaO+WO_3 \rightarrow CaWO_4$, solid-state reaction mechanisms 77−36750
$CaWO_4$, scheelite struct., intrinsic hole centres, EPR study 78−64274
CdO-WO_3 phase diagram and prep. of $CdWO_4$ single crysts. 80−29933
CdO-WO_3-H_2O, interconnection between kinetics of structure formation and chem. reactions 78−53198
$CoWO_4$, reduction in H_2 77−4931
$CoWO_4$, reduction in H_2 77−4932
Cr_2O_3-WO_3, phase relations 78−92249
$Cr_{12-x}W_xP_7$, solid solns., prep., cryst. struct. *(French)* 78−63723
Er_2O_3-TiO_2-WO_3-PbO, glass form., refr. indices and density meas. 77−90312
Fe-W-O(C), Gibbs energy of form. of phases *(German)* 80−97724
Fe-WC-MoS_2, self lubricating coatings, exam. of props. 79−96217
Fe-WO_3 system, struct. phase exam. by optical microscopy and X-ray diffr. 78−31389
Fe_2O_3-WO_3, phase relations 78−92249
Ga-In-WSe_2 eutectic alloy, self-lubricating, struct. and props. 79−100267
$(H_5O_2^+)_3(PW_{12}O_{40}^{3-})$, struct., X-ray and neutron diffr. study 79−42037
$(H_3PO_4)(WO_3)_{12}29H_2O$, electrochromic solid-state cells 80−2724
$H_{0.4}WO_3$, inelastic neutron spectra 77−15287

tungsten compounds continued
H_xWO_3, amorphous, Anderson transition, disorder depend. and optical detection 78−47840
H_xWO_3, amorphous film, electronic transport meas., insulator-metal transition 77−72923
H_xWO_3 films, proton diffusion coeffs. 80−6548
H_xWO_3 film, effect of struct. on optical and electrical props. 78−84671
$In_{0.30}WO_3$, struct. anal. *(French)* 78−59786
KBr:WO_4^{2-}, IR absorpt. spectra, vibr. splitting *(Russian)* 79−51995
KCl:WO_4^{2-}, IR absorpt. spectra, vibr. splitting *(Russian)* 79−51995
$K_2O.2WO_3$ glasses, X-ray diffr. study of struct. *(Japanese)* 77−11489
$K_3O.nWO_3$, n=4-20, X-ray diffr. 77−84726
$K_{0.33}WO_3$, hexagonal, phonon dispersion curves, neutron scatt. obs. 78−14411
$LaCrO_3$-W eutectics, prep. and microstruct. 80−108380
$La_{10}W_2O_{21}$, enthalpy and heat capacity at high temp. 80−70424
α-La_2WO_6, enthalpy and heat capacity at high temp. 80−70424
$La_6W_2O_{15}$, enthalpy and heat capacity at high temp. 80−70424
$Li_2B_4O_7.xWO_3$ (x=0 to 1 mol.) glass, random elec. dipole, cooperative phenomena 79−28693
Li_2O-B_2O_3-WO_3 glass, photochromic and electrochromic props. 79−28787
Li_xWO_3, electrochem. and chem. Li incorporation, cryst. struct. 80−88131
Li_xWO_3, Vegard relationships, lattice parameter versus composition, X-ray and chem. anal. 79−23582
$Mn_{12-x}W_xP_7$, solid solns., prep., cryst. struct. *(French)* 78−63723
Mo-W-S system, phase relationships, 500-800°C 79−24503
$Mo_{0.5}W_{0.5}Se_2$ single cryst. vapour growth, characterisation 80−93466
Na_2O-WO_3 glass containing transition metal ions optical absorption 78−27254
$Na_xTa_yW_{1-y}O_3$, substitution of W with Ta, Anderson type transition *(French)* 79−60879
Na_2WO_4-$CsWO_4$-WO_3, system form., melting point 79−43222
Na_2WO_4-K_2WO_4-WO_3 ternary system, phase diagram investig. 77−12608
Na_2WO_4-Pb_2WO_4-WO_3 system investigation, crystn. from melt, coordination compounds form. 79−52189
Na_xWO_3, ($0.22 \leq x \leq 0.84$), ^{183}W NMR, electronic struct. near metal-semicond. transition, Knight shift 78−48063
Na_xWO_3, bronze, composition-dependent microhardness, rel. to bonding 79−24606
Na_xWO_3 bronze, XPS of W 4f levels 78−95648
Na_xWO_3 bronzes ($0.4<x<1$), domain, surface and substrate structs. 80−34281
Na_xWO_3, cubic single cryst., LEED/Auger obs. 78−19614
Na_xWO_3 enhanced T_c, interband coupling 78−91804
Na_xWO_3, intra- and interband plasmons, inelastic electron scatt. exam. 78−72098
Na_xWO_3, metallic, XPS, initial and final states, WO_3 binding energy 79−95898
Na_xWO_3, supercond. crit. temp., semiempirical model lor lattice instabilities in nonstoichiometric materials 78−14442
Na_xWO_3, vacuum UPS exam. 78−84700
Nb_2O_5-WO_3, solid-state reactions, electron microscopic obs. 77−16818
Nb_2O_5-WO_3 system, TEM study of intergrowth of ReO_3 and tetragonal-type structs. 79−7580
Nb_2O_5-WO_3 system complex cpds. with TTB type subcells, HV superhigh resolution electron microscopy obs. of struct. 80−103311
$Nb_nW_{6-n}O^{(n+2)-}$, config., IR and Raman spectra 77−42324
$Nb_{1-x}W_xSe_2$ x=0 to 0.15, elec. resist., mag. suscept., heat capacity, structural, supercond. transition *(Russian)* 78−31006
Ni-W-O system, phase relns. and Gibbs' free energy of formation of $NiWO_4$ 77−73262
Ni-WC, dispersion hardened coating, chemically deposited using electroless baths, protection props. 79−34208
NiO-WO_3, phase relns. 78−3106
P_2O_5-WO_3:CuO glass, EPR, Cu impurity effect on elec. props. 79−51849
$Pb(Mg_{0.5}W_{0.5})O_3$-$BiFeO_3$, dielec. props., cryst. struct. 78−84534
PbO-WO_3-MO system, M=Ca, Ba, Mg, Sr, perovskite type cpds. detection 80−108404
Pb_xWO_3 ($0.01 \leq x \leq 0.28$), tetragonal and orthorhombic bronzes, cryst. chem. data 78−42997
Pb(Z,Ti,Mg,W)O_3, low-Q ceramics, props. and transducer appl. 80−75944
$PbZrO_3$-$PbCd_{0.5}W_{0.5}O_3$, phase transitions 78−43817
Pt-WO_3, electrochromic cermet, optical and electrical props. 79−33674
$Rb_{0.30}WO_3$, struct. anal. *(French)* 78−59786
TeO_2-WO_2 glass, dipole correlations, capacitances and TSC meas. 79−28670
TeO_2-WO_3-R_nO_m, glass formation range 78−71680
TiC-Co(Ni), grain growth kinetics *(French)* 77−44252
TiC-Cr_3C_2WC, powder mixture, steel bonded, exam. of sintering behaviour 78−52712
TiC-WC-TaC carbide mixture in plasma reactor *(German)* 77−1819
TiO_2, iron bearing, exsolution of Fe_2O_3 79−61597
TlR$(MO_4)_2$, R=Eu, Dy, Er; M=Mo, W, luminesc. *(Russian)* 78−48229
$Tl_{0.3}WO_3$, struct. anal. *(French)* 78−59786
UF_6-WF_6, dil. sol., liq.-vap. equilib. 77−62632
V-W-O system, phase diagram and thermodynamic props. at high temps., in region W-WO_2-VO_2-V_2O_3 80−104133
V_2O_5-WO_5, solid soln. thermogravimetric anal., ion formation on crystallisation 77−20076
V_2WO_6, magnetic structure, stability of mag. modes, neutron diffraction study *(French)* 80−39744
(W, Mo)C, hard-facing applications, effect of Mo on struct and hardness of WC 80−108474
W complex, $Li_4W_2(CH_3)_{8-x}Cl_x.4THF$, quadrupole bond stability, crystallographic investig. 77−58193
W complex, W(acac) (CO_3) (C_5H_7O), atom assignment problems, alternative to Hamilton's R-factor ratio test 79−7506
W-alkali earth oxides, multiple phase systems, calc. of phase equilibria, using thermodynamic analysis *(Russian)* 79−56964
W-O system, surface elect. cond. of oxides in equilib. with gas phase 79−61791
W-O-Br system, appl. of mass transfer model of halogen doped incandescent lamps 77−32832
W-Sn-S system, phase relationships, 500-800°C 79−24503
W-Y(La)(Ce)-B, phase equilib., struct. of crysts. 77−21122

tungsten compounds continued
W_2As_3, decomp. press. and enthalpy of decomposition 79−66042
$W_5(B,Si)_3$, stability of heatproof coating 77−86201
WB, abrasive, effect on machinability of Ti alloys *(Russian)* 80−97593
WB_{12}, growth from melt and phys. props. 80−20782
WB_4 and W_2B_5, core of B filaments, elec. resist. 80−15523
W_2B_5, abrasive, effect on machinability of Ti alloys *(Russian)* 80−97593
W_2B_5 and WB_4, thermal, elec., and mag. props. 80−20187
W_2B_5, monocryst., grain size, abrasive and strength props. 80−11787
W_2B_5, reactions with Ti-Al-Cr-Mo alloy VT3-1 80−16585
W_2B_5, sintering rel. to prod. by boron carbide process 78−11184
W_aBr_b, enthalpy determ. by mass spectroscopy 78−11584
WC anode, performance in fuel cells with H_2SO_4 electrolyte 80−21293
WC anvil, truncated, compressive strength, high press. apparatus appl. 78−84906
WC, balls, appl. in simple high press. apparatus 77−5856
WC, bond energy and ionization efficiencies from SIMS 79−24400
WC, charge transfer from XPS core level chem. shift anal. 77−72837
WC, crystallite size distrib. of powder, SEM method *(German)* 78−47218
WC cutting tools, TiN, TiC coated, frictional characts. 79−20218
WC, deformation behaviour during rubbing in wide temp. range 80−16486
WC, effect on cordierite synthesis 77−8787
WC, electrochemical grinding, effect of mag. field 77−86214
WC electrode, catalytic activity for hydrogen oxidation in acid obs., effect of starting material 79−100500
WC, exam. of brittle fracture props., using Hertzian indentation 79−11686
WC, explosive plasma sputtered coatings, struct. and props. *(Russian)* 80−100783
WC, fine powder prod. from $WO_3+C+Co_3O_4$ *(Japanese)* 78−92226
WC, friction against FeO compacted powder, effect of wall groove orientation and wall lubricants 78−23831
WC, friction between WC ball and ice single cryst., slider size effect *(Japanese)* 78−88538
WC, friction between WC ball and ice single cryst., anisotropy *(Japanese)* 78−88539
WC, gauge blocks, determ. of thermal expansivity using interferometric dilatometer 79−12767
WC grain, with grown-in stacking fault, contrast effects in electron micrographs 77−19959
WC, hexagonal, meas. of mean square shift of atoms in micron powders *(German)* 78−47313
WC, liquid phase sintering 77−4751
WC, MP depend. on press. up to 80 kbar, optical meas. *(Russian)* 77−80604
WC, microcrystalline, mol. dynamics, motion of H_2O and H_2 mols. adsorbed on surface, catalytic activity 78−71941
WC, micropowder, abrasive props. 77−63821
WC micropowder surface finishing of metals, surface struct. 80−11842
WC micropowders, abrasive lapping of refractory metals 77−44391
WC, plasma sprayed coating 78−68835
WC powder, sintering processing conditions 80−11614
WC, powder form. from WO_3-Co_3O_4-C powder mixture *(Japanese)* 78−92227
WC, powder prod. by vapour phase reaction in WCl_6-CH_4-H_2 system 78−60626
WC powder production from vapour phase 77−21077
WC, reactions with Ti-Al-Cr-Mo alloy VT3-1 80−16585
WC recoil implantation damage, PAC obs. 77−85620
WC, refractory micropowder, geometric parameters of grains 77−16529
WC, rolling bearing materials, effects of high temp. operation 80−21124
WC, single cryst. elastic constants from mech. and X-ray elastic constants of polycryst. *(German)* 80−10591
WC, sinterability of ultrafine powders obtained by CVD method 80−108378
WC, small clusters, one-electron energy levels and charge densities determ. 77−59253
WC, sputter deposited coatings, elec. resist., mag. susceptibility and adhesion meas. 77−44395
WC, sputtering, low energy, H, D and He ions 80−100734
WC substrate, TiB_2 coating prep. by CVD and interaction with substrate 79−24680
WC, tool carbide, thermal shock resistance, fracture strength 77−21257
WC, ultrafine powder, prod. by cryochemical, freeze drying, spray drying or soln. techniques 80−55336
WC vacuum sintering furnace systems 78−84737
WC-Co, fracture mode determination, using Auger electron spectroscopy 80−7680
WC-Co, grain growth kinetics *(French)* 77−44252
WC-Co cemented carbides, irreversible deformation, yield stress, SEM study 79−70110
WC-Co coating, sputter deposition, friction and wear characts. 77−44394
WC-Co composite, surface anal. by quantitative AES 78−76622
WC-Co composite chemical characterisation by AES and ISS 78−76621
WC-Co DC and RF sputtered coatings, bias effect, struct., X-ray-Auger study 80−70565
WC-Co hardmetals, heat-treated, single domain obs. 79−73771
WC-Co particles electrophoretic deposition, on metal surfaces, wear resistant coatings preparation *(German)* 80−2969
WC-Co sputter deposited film, struct. and comp. 78−72023
WC-Co sputter deposited film, friction and wear 78−72918
WC_x, (3×5) struct. on W (110) surface, at. beam diffr. and scatt., surface characteris. 79−78819
WC_x, electrochem. separation from W alloys, phase anal. 78−60651
WC_x formation during pyrolysis of WCl_6 and toluene, coating props. 77−36682
W_2C, ^{14}C self-diffusion *(French)* 79−60542
W_2C and WC, plastic deform. under bending, 800-2200°C *(French)* 80−55482
W_2C, oxidation, oriented struct. transform. to W, FEM and TEM obs. 80−30124
W_2C, single cryst., decarburization, field emission microscopy and TEM 79−70368
W_2C, slip systems, at ambient temp. *(French)* 78−84926
W_2C, W_3C, wear resistant coatings, chemical vapour deposited, low temp. form., on steel substrate 78−92404
$W(CO)_6$, bonding, IR intensity anal. 78−25526
tungsten compounds continued
$W(CO)_6$, decomp. under high field conditions, cathodic growth of W needles 80−76162
$W(CO)_6$ decomposition, W needles growth 79−95302
$W(CO)_6$ dissolved in oriented compensated nematic mixture, distortion of cubic mol., linear dichroism obs. 79−95797
$W(CO)_6$, electronic spectra following flash photolysis, intracavity laser technique 79−31538
$W(CO)_6$, in nematic matrix, linear dichroism, distortion and local field contribs. 79−87415
$W(CO)_6$, MCD spectra, charge transfer transitions 80−95658
$W(CO)_6$, mol. vibrs. and reaction pathways, min. energy coords. and compliance consts. 77−57966
$W(CO)_6$, photodissoc., W prod. 80−95575
$W(CO)_6$, relative intensities of ν(CO) and ν(MC) Raman bands 78−55176
WCl_5, crystal structure determination 78−91318
WCl_5, intensity changes between He(I) and He(III) photoelectron spectra 78−21969
WCl_5, photoelectron spectra 79−821
WCl_6, dissoc. in discharge, WI lines oscill. strengths 79−63962
WCl_6, force fields, IR spectra, isotope shifts 77−14432
WCl_6^-, n=1,2, vibr. IR meas., Raman spectra obs. 79−68234
WCr_2O_6, exchange interactions within binuclear entity $(Cr_2O_{10})^{14-}$ 80−60236
WCs, preparation method effects on catalytic activity for H_2 evolution 80−101024
WF_5, dissoc. electron capture, electron impact mass spectra, electron affinities 77−88579
WF_6 addition to chem. pumped Br_2-CO_2 laser, output energy increase 79−45939
WF_6, CW CO_2 laser spectroscopy 80−83367
WF_6, critical parameters determ. using thermodynamic and mol. similarities 77−43310
WF_6, cryst., overall vibr. band struct., excitons 77−90136
WF_6 crysts., density of exciton states, two-particle and mixed cryst. spectra 78−2829
WF_6, dissoc. electron capture, electron impact mass spectra, electron affinities 77−88579
WF_6, effect of high hydrostatic press. in reorientation and internal motion, ^{19}F NMR spectra 79−15364
WF_6, electron affinities from collisional ionisation with alkali atoms 78−55226
WF_6, electron and fluoride affinities, ICR spectra 79−39130
WF_6, electron impact, negative ion form., mass spectra *(German)* 77−88586
WF_6, electronic structure, SCF-Xα-SW calcs. 77−26974
WF_6, excitation spectra after electron impact, 30-75 eV impact energy 79−45854
WF_6 gas acoustic dispersion obs. by double-crystal US interferometry *(Japanese)* 79−4100
WF_6, ionis. energies, optical spectra, Dirac-Slater model 77−83488
WF_6, mechanism of heterogeneous reduction by H_2 *(Russian)* 80−21265
WF_6, mol. vibrs. and reaction pathways, min. energy coords. and compliance consts. 77−57966
WF_6, orthorhombic crysts., Raman spectra, int./external mode separation and factor group anal. 77−90135
WF_6, second virial coeff. meas., Lennard-Jones pot. determ. *(German)* 77−19658
WF_6, supercooled, IR absorpt. spectrum 77−23574
WF_6, universal eqns. of state and thermodynamic similarity 77−35290
WF_6, valence electron spectra, vibr. band struct. 77−23520
WF_6, vapour press., phase transform. enthalpy *(German)* 78−51654
WF_6-graphite intercalation cpd. 78−27441
WF_6-graphite intercalation cpds., prep. and props. 80−40686
WF_6+alkali atom(dimer), ionis. reactions, electron affinity 77−81398
WF_6+Cs, collisional ionisation, crossed beam obs. 79−68299
WF_6+K(Cs), crossed beam reaction cross sections 77−77740
WF_6+Na(K) electron transfer, WF_6^- form., dissoc. energies, electron affinity 77−19071
W_3Fe_3C, pyrochlore struct. and its relatives 79−14773
W_5GE_3, synthesis at high press. and struct. 79−77565
WGe_2, synthesis at high press. and struct. 79−77565
WH_6, Dirac-Fock one-centre calcs. 79−6837
$W_xMo_{1-x}O_3$, absorpt. spectra and optical gap energies 79−91464
$W_xMo_{1-x}O_3$, mixed cryst., structural phase transition, Raman and IR spectra 78−79766
$W_xMo_{1-x}O_3$, reduction and temp. effect on electronic core levels, XPES 79−91564
$W_9Nb_8O_{47-x}$ polycrystalline film as electrochromic material 79−65949
$W_xNb_yO_z$ ordering of atom string, cluster model 77−68959
$W_{1-x}Nb_xSe_2$, packing defects, correl. with diffr. pattern changes 77−15429
WO_2 and O_2 adsorption on W (110) LEED and AES obs. 80−34317
WO_2, cryst. growth, chem. transport conditions influence on morphology and quality 79−43114
WO_2, effect of pressure on Fermi surface *(Russian)* 79−77988
WO_2, Fermi surface calcs. 78−67934
WO_2 film characterisation technique, APFIM, time-of-flight spectroscopy 80−75138
WO_2 film coatings for Mo tips, film characterisation by atom probe FIM atomic clusters, voids 80−33863
WO_2, optical conductivities and dielec. functions in 0.2-6 eV range, rel. to band struct. 79−42938
WO_2, struct. refinement by powder neutron diffr., profile anal. 79−99139
$WO_2+Al_2O_3$ react., high temps., vacuum, $AlWO_4$ form., struct. 77−16518
$WO_{2.96}$, reduction to W 77−28744
WO_3, (100) and (111) layers, electron stimulated desorption of O^+, LEED obs. 79−23840
WO_3, acoustic instability near monoclinic orthorhombic phase transition, X-ray scatt. 80−65215
WO_3 addition to WC powder, sintering processing conditions 80−11614
WO_3 amorphous anodic film growth on W in acidic soln. 80−81232
WO_3, amorphous coloured film, charge transfer, XPS 77−12491
WO_3 amorphous film, elec. cond. and dielec. const. 78−60238
WO_3 amorphous film, sublimed under different conditions, elec. transport props. 80−7015

tungsten compounds continued
WO_3, amorphous film, vac. deposited, struct. and crystn., TEM obs. 80−2291
WO_3, amorphous film, vac. evaporated, density meas., microcrystalline model of struct. 80−2313
WO_3 amorphous layers, electrochromic absorpt. depend. on crystallinity and electron localisation 77−59589
WO_3 anode, props. and appl. to photoelectrolysis of water 77−66757
WO_3, antirefl. coating on textured W surface, for solar absorber appl., props. 78−63157
WO_3, antireflection coating on W dendritic surfaces, reflectance, geometrical study 79−91511
WO_3, band struct., XPS meas. 77−59667
WO_3, ceramic, Raman spectra, 80-300K, inhibited ferroelectric phase transition 77−32378
WO_3, chem. transport, thermodynamic investigations *(Russian)* 79−69990
WO_3, close-spaced chem. transport rates *(Russian)* 80−11570
WO_3, condensed modes represented by normal modes in space group D_{4h}^1 79−90747
WO_3, condensed phonon modes in successive phases 79−46765
WO_3 electrochromic absorption dependence on crystallinity 77−77314
WO_3 electrochromic amorphous films, colouring and bleaching, expt. and anal. 77−20829
WO_3 electrochromic cell, deposited Cr_2O_3 as barrier 78−15147
WO_3 electrochromic elements, prod. by electrolytic anodisation of W, and characterisation 80−25921
WO_3 electrochromic film in liq. electrolyte, chem. and electrochem. stability 78−73054
WO_3 electrochromic films, bleaching by electric fields 79−99852
WO_3 electrochromic reaction kinetics 77−77176
WO_3 electrochromics in nonaqueous acid soln. 80−2722
WO_3, electrochromism for student lab. expt. 80−17738
WO_3 electrode, surface growth of ternary compds., in electrolyte containing redox couples 78−61016
WO_3 electrodes, electrochem. and photoelectrochem. behaviour 78−26949
WO_3 electrodes, electrochromic processes, digital simulation model 80−76518
WO_3 electrodes, vac. evaporation and anodic oxidation prep., electrochromic process kinetics 79−100390
WO_3 electron density map of W^{5+} polarons, EPR and optical absorpt. obs. 80−44912
WO_3, electron spectroscopic exam. of reduction 77−4714
WO_3, electronically induced lattice distortion, screening effect on vibrs. 80−75356
WO_3 evaporated film composition and chem. structure rel. to electrocoloration 77−77175
WO_3 film, amorphous, electrochromism and local order 77−59553
WO_3 film, amorphous, struct. and crystallisation, high resolution electron microscopy 78−43268
WO_3 film, amorphous, struct. and crystn., TEM obs. 80−103606
WO_3 film, anodically formed, electrochromism 79−1752
WO_3 film, Au surface layer effect on electrochromic behaviour 80−76004
WO_3, film, electrochem. injection kinetics of Li, LF AC meas. 80−57339
WO_3 film, electrochromism, X-ray electron spectra 78−48146
WO_3 film, evaporated, electrochromism *(Japanese)* 79−38686
WO_3 film, evaporated, mech. of elec. cond. 80−44747
WO_3 film, intra- and interband plasmons, inelastic electron scatt. exam. 78−72098
WO_3 film, optical absorpt. after ion irrad., appl. to ion beam profile monitoring 79−26181
WO_3 film electrochemical colouration for displays 77−77170
WO_3 films, ESR study after colouring by H_2 injection and after bleaching in air 80−39867
WO_3 films, electron struct. changes during electrocoloration, XPS obs. 80−40217
WO_3 films on Si, sapphire, glass and metal substrates, colour intensity dependence obs. *(Russian)* 80−2430
WO_3, force field, normal coord. anal., kinetic consts. method, thermodynamic props. 78−25504
WO_3, hexagonal form, struct. study, X-ray powder diffr., electron diffr., and electron microscopy meas. 79−99157
WO_3, IR spectra, normal coord. anal. 78−58682
WO_3 in binary oxide systems, exam. of phase relations 79−8290
WO_3 layers, semiconductor electrodes, electrochromism and photoelectrochemistry 80−35544
WO_3, light induced W^{5+} ESR 77−36126
WO_3, metal-insulator transition meas. by microcalorimetry *(French)* 77−47733
WO_3, nonstoichiometric, elec. investig. of correl. between defects and O chem. pot. *(French)* 77−47817
WO_3, on glass substrate, electrochromism of glass film compositions 80−29720
WO_3, optical props. 79−38515
WO_3, orthorhombic phase struct. 77−24297
WO_3, oxide film on W, contact interaction with graphite, exam. of interferences effect *(Russian)* 79−11721
WO_3, oxidised W foil, electron bombardment effects on surface composition, Auger spectroscopy, electron desorption measurements 79−77874
WO_3, polar, electrochromic absorpt. bands, small polaron theory 78−39528
WO_3 polymorph, hexagonal, cryst. struct. imaging by high-resolution electron microscopy 80−103309
WO_3 powder, electron bombardment effects on surface composition, Auger spectroscopy, electron desorption measurements 79−77874
WO_3 powders, hopping mechanism and Poole-Frenkel effect, elec. props. determ. 80−49734
WO_3, recoil implantation damage PAC obs. 77−85620
WO_3, reduced, elastic strain energy of crystallographic shear planes 77−69026
WO_3, reduced, elastic strain energy in cryst. shear planes 80−75239
WO_3, reduced, electrostatic interaction energy between crystallographic shear planes 77−47471
WO_3, reduction, defect role, in situ HVEM obs. 80−81323
WO_3 reduction, in H plasma jet, W powder prep. *(Russian)* 80−76211
WO_3, reduction and temp. effect on electronic core levels, XPES 79−91564
tungsten compounds continued
WO_3 reduction in hydrogen, electron microscopic obs. of solid phases formed *(Hungarian)* 77−48635
WO_3, semicond. anode in aq. electrolyte, electrolum. and electrochem. 80−76080
WO_3 semiconducting electrode, influence of surface states, impedance meas. *(French)* 77−1468
WO_3, semiconductor-metal transition, structural phase transition 80−107870
WO_3, single cryst. and amorphous film, ESR of defects 78−10770
WO_3, slightly reduced, interaction between non-parallel {102} crystallographic shear planes 77−80517
WO_3, smoke particles, coalescence growth by gas-evaporation 78−47256
WO_3, smoke particles prep. by burning metal in Ar-O_2 gas, electron microscope obs. 77−52238
WO_3 smoke particles prepared by gas evap., morphology and coalescence growth 80−97738
WO_3 solar absorber surface spectral selectivity rel. to temp. and UV ageing 79−62027
WO_3, solid state electrochromism and electrochromic cell deterioration 79−78655
WO_3, strain energy, between parallel {001} shear planes 78−34523
WO_3, struct. transforms. during crystallisation from P_2O_5-WO_3-CaO 77−40343
WO_3 substrate, Li_3N film, vacuum evaporation, retarded deposition 80−108351
WO_3, surface pot. between ferroelec. domains 78−15132
WO_3 thin film, Li diffusion, appl. of AC techniques 80−70468
WO_3, thin films, electrochem. coloration, optical and elec. props. 77−85345
WO_3, triclinic, condensed modes 80−15211
WO_3, trigonal, cryst. struct. 78−51483
WO_3, vibr. anal., mol. consts., kinetic consts. method 80−23393
WO_3:H^+, optical and elec. props., suggested band struct. model 77−4654
WO_3-alkali tungstates liq. mixtures, mixing enthalpies at 801, 950°C 79−10949
WO_3-B_2O_3-ZnO semiconducting glasses, DC cond. and optical absorpt. 80−107783
WO_3-BaO film, electrochromic coloration and decoloration, BaO additive effects 78−72620
a-WO_3-Cr_2O_3, electrochromic layer device, characts. 79−90009
WO_3-electrolyte electrochromic cells, proton injection phenomena 80−71448
WO_3-LiF system, on glass substrate, electrochromism of glass film compositions 80−29720
WO_3-LiF(MgF_2), electrochromic display struct., efficiency and humidity depend. 79−81540
WO_3-LiI, solid-state electrochromic cell, fabrication and characts. *(Japanese)* 80−84717
WO_3-MnO-P_2O_5 system, glass form. and memory effects 77−76888
WO_3-MoO_3, film, evaporated, electrochromism *(Japanese)* 79−38686
WO_3-MoO_3 film, amorphous, electrochromic optical absorpt., expt. results and model 78−27341
WO_3-MoO_3 system, on glass substrate, electrochromism of glass film compositions 80−29720
WO_3-$N6_2O_5$ system, strain energy due to {001} crystallographic shear planes 79−99223
WO_3-$NiCO_3$-Fe_2O_3, reduction alloy form. 80−60801
WO_3-P_2O_5, glass, DC cond. meas. high temp. range 78−6376
WO_3-P_2O_5 alkali glasses, electrochromic, electron-ion processes 80−25341
WO_3-P_2O_5 glass, AC cond. and dielec. props. 80−92717
WO_3-P_2O_5 glass, DC elec. cond., 100-400K 78−39106
WO_3-P_2O_5 glass, thermoelec. power meas. 78−84242
WO_3-P_2O_5 glasses, electrochromic effect 79−95735
WO_3-R_2O_3 (R=La, Ce, Pr, Nd) system, X-ray characterisation and thermal props. of $3R_2O_3.2WO_3$ cpds. 77−43194
WO_3+CuO− solid state reaction kinetics, $CuWO_{4-x}$ formation study 80−66796
WO_{3-y} thin films, charge storage and types of colour centre, expt. 77−20830
$(WO_3)_3$, identification of polymer species by vapour phase electron diffraction 80−53135
WO_4^{2-}, valence level electron struct. by XPS 77−4712
WO_5 film, amorphous, band structure and colour-centre band, fast electron energy loss spectrum 77−55478
WO_6^{6-}, electronic struct., discrete variation and scatt. wave X_α methods 80−917
WO_6^{6-}, in lattice electronic struct., luminesc. ab initio calcs. 78−6337
WO_n, (n=2-3), adsorption of O_2 (propene), struct., rel. to catalysis 78−51826
WO_x, anodic oxide films, quadratic electro-optic and electrostrictive effects, ellipsometry 80−108184
WO_x, nonstoichiometric, XPS meas. 77−48307
WO_x, powders, coarseness meas. using powder surface reflectance 79−96246
WO_x-MO_y system, (M=Mn, Fe, Co, Ni), phase relations in dioxide-trioxide region, 1373K 78−11212
W_2O-P_2O_5, glass, 1.06 μm laser radiation interaction 78−91132
W_2O_{5-x} current noise due to adsorption of water 78−6421
W_xO_y, carburisation/reduction with CO, morphological study 79−47977
W_xO_y microstructure, example of high resolution TEM application *(Hungarian)* 77−76267
WO_aBr_b, enthalpy determ. by mass spectroscopy 78−11584
WOF_4, dissoc. electron capture, electron impact mass spectra, electron affinities 77−88579
WOF_4, gas phase electron diffr., mol. struct. 77−34775
WOF_4 statistical thermodynamic functions calcs., force consts., vibr. amplitudes, between 250-1000K *(French)* 79−31504
WO_2F_2, thermodynamic stability *(German)* 79−8449
$WO_{2.7}H_x$ film, colouring, comp. depend. 78−15239
WO_3M_x (M=H, Li, Na, K, Ag), bronzes, atom motion 78−75874
WO_3(WO_3-UF)(WO_3-MoO_3) glass film compositions, electrochromism *(Russian)* 79−28721
W_2OsB_2, cryst. chem. and struct. 78−42995
WS_2 (2H), layered cpd., Raman scatt. 80−103960
WS_2, effect of uniaxial stress on excitonic optical spectra 78−84606
WS_2, excitons, mag. circular dichroism and wavelength modulated reflectance meas. 79−23900

tungsten compounds continued
WS_2 films, exciton peaks in absorpt. spectra, press. and temp. depend. 79−51496
WS_2, optical phonon modes and localised effective charges, reflection spectra 78−76453
WS_2, self-propag. high-temp. synthesis, wear props. 80−2975
WS_2, single crysts., growth by direct vapour transport method, X-ray and electron diffr. study 79−28904
WS_2 solid lubricant, antifriction and elec. props. depend. on oxidation temp., dopant influence 80−108584
WS_2 unsupported hydrosulphurization catalyst promoted by group VIII metals, catalytic, structural and textural props. 79−79289
WS_2-NbS_2 system, compds., elec., antifriction props. 79−38066
WS_2-oxide layer formation and props. 79−50359
WS_3, amorphous struct., X-ray radial distrib. anal. and XPS 80−49115
$WSCl_3$, prep. and characterisation 77−59705
WSE_2, Raman spectrum, long wavelength optical phonons 77−40218
$WS_2(Se_2)$ and Ga alloys, mixing powders using US treatment 79−24454
WSe_2 (2H), elec. cond. press. depend. 78−43394
WSe_2, chem. vapour transport growth, microstruct. develop. 80−103278
WSe_2 d-band semicond., photoelectrochem. props., electrochem. solar cell appl. 79−66411
WSe_2, effect of uniaxial stress on excitonic optical spectra 78−84606
WSe_2, elec. cond. and Hall coefficient temp. depend. 77−28180
n-WSe_2 electrode in aq. iodide medium, high efficiency photoelectrochemical solar cell 80−72069
WSe_2, excitons, mag. circular dichroism and wavelength modulated reflectance meas. 79−23900
2H-WSe_2, layered cpd., anisotropic X-ray absorption 78−39629
WSe_2, lubricant, prep. by self-propagating high-temp. synthesis, technological characts. 78−35338
WSe_2, optical phonon modes and localised effective charges, reflection spectra 78−76453
WSe_2, refl. spectra and photovoltaic effect, 1.5-3.2 eV, 4.1-300K 79−47470
WSe_2, Schottky barrier, photovoltaic props. 79−7854
WSe_2, single cryst. growth by sublimation method 78−11091
2H-WSe_2, thermal expansion between 10 and 320K, cell dimensions meas. 79−65222
WSe_2-$MoSe_2$, cryst. struct. parameters and growth conditions 79−86759
WSe_2-oxide layer formation and props. 79−50359
WSe_4^{2-}, anharmonicity consts., reson. Raman spectra 77−61754
$WSeF_4$, cryst. struct., and preparation 78−63730
WSi_2, amorphous, crystallisation by energy beam annealing 79−69012
WSi_2, diffusion marker for backscatt. studies of W+Mo bilayer film 78−87828
WSi_2 film, elastic stiffness and thermal expansion coeffs. 80−107451
WSi_2 on W, coating by local heating 77−81335
WSi_2, oxidation in CO_2, 1200-1700°C 77−40454
WSi_2 refractory formation by As^+ ion beam bombardment 80−107286
WSi_2, silicides formation in Mo-W bilayer films on Si substrates 79−99376
WSi_2, sputtered, props. for MOS IC appl. 80−70831
WSi_2 sputtered film on Si and SiO_2 substrate, thermal oxidation kinetics 80−3208
WSi_2, steam-oxidized, Auger sputter profiling studies 80−107663
WV_2O_6, exchange interactions within binuclear entity $(V_2O_{10})^{14-}$ 80−60236
WV_2O_6, magnetic susceptibility, behaviour in terms of quasi-isolated binuclear units 80−97073
WV_2O_6, X-ray cryst. struct. refinement at 298 and 383K *(French)* 79−14747
α-$W_xV_2O_5$, paramag. defect study by ESR 80−103881
$W(ZrO_2.La_2O_3)$, structural changes during reduction and sintering 80−25636
^{186}WO, electronic spectra following flash photolysis, intracavity laser technique, rot. consts. 79−31538
WO_3, H^+ and He^+ ion backscattering reflection coeff. 79−43081
Xe-MF_6, M=W, Mo, U, Re, Ir, charge transfer interactions, VUV and IR obs. 78−50664
$YCrO_3$-W eutectics, prep. and microstruct. 80−108380

tuning
see also laser tuning; receivers; resonance
accelerating resonators, for proton synchrotrons with short accel. time 77−46429
acousto-optical noncollinear UV tunable filter 80−102832
birefringent filter mechanical tuning techniques 80−102834
clavier, tuning, freq. matching using pocket calculator 78−81728
dye laser, using tilted birefringent Fabry-Perot etalon *(Japanese)* 77−54735
education, vibrating string, tuning guitar by television 80−73134
electro-optical polarisation conversion and interference tunable filters 80−102829
electro-optical tunable filters, programmable 80−102830
extensional trapped energy mode transducer bandwidth, influence of tuning inductor 79−55303
Fabry-Perot interferometer length stabilisation using He-Ne laser radiation 77−79141
flexible band-pass filtering using coherent optical feedback 79−94166
helical resonant cavities, technique for broadband tuning, MHz to GHz range 78−94502
holographic grating monochromator for 5 to 1000 eV synchrotron radiation 78−18049
microtrons, nondimensional tuning of coupled-cavity structs. 80−32546
mm-wave Fabry-Perot tuning and freq. modulation by electrically variable external reactance 79−68409
multicavity IR electro-optical tunable filter 80−102831
NMR at high freqs., matching and tuning network for slotted tube resonator 77−30192
nuclear magnetic double resonance probe circuit with transmission-line tuning 77−26375
optical directional coupler phase tuning by chalcogenide glass film loading 78−1373
proton storage ring NAP-M freq. tuning of accelerating system 77−65364
quartz SAW resonator tuning by shorted reflector opening 78−59246
resonator of H_2 generator, methods 77−88294
resonators of H masers, automatic 80−95859
SAW in-line chirp filter applications 78−59207
SAW oscillator with two acoustic paths 77−23846

tuning continued
selective digital voltmeter, electronic control of tuning frequency 77−10052
semiconductor Fabry-Perot interferometer retuning by optical excitation *(Russian)* 80−98970
string instruments, electronic method of tuning to overtones 77−50839
submillimetric heterodyne receiver with laser local oscillator 77−38042
superconducting cavities for heavy ion LINAC, freq. tuning 77−26896
swept-frequency heterodyne receiver with CRT display for spectral analysis *(Spanish)* 77−37875
thickness mode piezoelec. US probe design factors 79−68540
tunable variable bandwidth/frequency SAW resonator 78−59247
unidirectional transducers, group type 79−68535
US transducers array, transducer elements tuning 80−87684
waveguide reflection maser, 9 to 10 GHz tuning 78−5443
wideband carcinotron tunable submillimetric source 77−41304
GaAlAs DH laser, broadband single mode tuning system 79−27256
H maser autotuning system analysis 79−55101
H maser autotuning systems, theoretical anal. based on freq. or phase method 80−83575
H maser cavity, tuning using variable capacitance diode 79−72545
H_2 four-wave interactions for tunable IR generation 77−54759
H_2 maser, amplifiers and limiters with level independ. phase shifts 77−19223
HF resonantly enhanced stimulated Raman scatt. for tunable IR generation 77−54759
He-Ne laser frequency stabilisation using mag. field tuning dip 79−55153
$LiNbO_3$ computer-controlled Nd:YAG-pumped parametric oscillator 77−54758
$LiNbO_3$ crystal acousto-optical tunable filter 77−19434
$LiNbO_3$ crystal acousto-optic tunable filter 79−55245
$LiNbO_3$, IR parametric oscillator source for remote air pollution monitoring 77−21936
$LiNbO_3$ optical waveguide, tuning characts. of parametric interactions 79−3779
$LiTaO_3$ platelet, electro-optical tunable filter, birefr. electro-optic cryst., light energy coupling 79−59804
TeO_2 acousto-optical tunable filter with microcomputer control 80−102833
TeO_2 noncollinear IR tunable acousto-optical filter 79−23086
Tl_3AsSe_3 10.6 μm tunable acousto-optic filters 79−55248

tuning forks *see vibrating bodies*

tunnel diode oscillators
^3He gas thermometer secondary standard for 0.5 to 40K 80−82762

tunnel diode storage devices *see semiconductor storage devices; tunnel diodes*

tunnel diodes
see also tunnelling
coincidence selection element appl. 77−18755
comparison circuit for betatron energy varying and stabilisation 77−6581
Esaki junctions, tunnelling and negative resistance phenomena, book 78−26947
MIM tunnelling diode, detector performance, IR and microwave freqs. 79−12844
MIS, photoionisation of states 80−11099
MIS solar cell, on amorphous hydrogenated Si *(French)* 79−24897
MIS structures, photovoltaic energy conversion, band struct. 80−92995
MIS tunnel diode, minority-carrier, pot. barrier height 80−96998
MIS tunnel structure, injection and extraction effects, self-consistent model 80−92996
MOS tunnel diodes characterisation, solar cell appls. 77−32089
multistable system, dissipative steady state, stability 79−9187
phototransitions accompanied by impurity scatt. 80−107901
piezojunction tunnel transducers for hydrostatic pressure *(Polish)* 78−89470
quantum noise at low temperature 80−103733
ternary semiconductor based Schottky diodes with tunnel device characts. 78−39215
AlGaAs p-n diodes, I-V characts., tunnelling 80−100510
AlGaAs tunnel diode, fabrication and appl. in cascade solar cell struct. 80−35682
Cr-SiO_2-n-Si tunnel diodes elec. characts. meas. and modelling 77−39955
GaAs, electron beam bombard. induced defects, influence on excess current *(Russian)* 77−4424
GaAs epitaxial tunnel diode pressure sensors 78−57975
GaAs, interband tunnel current, influence of press. 77−76910
GaAs, pressure sensitivity of peak current *(Russian)* 77−4423
p-$(GaAs)_x(ZnSe)_{1-x}$-nn^+.GaAs, avalanche heterojunctions, inverse branch of volt ampere characts. *(Russian)* 80−6974
InSb, tunnel diode, V-I characts., hydrostatic press. effects 79−38157
n-InSb, tunnel diode, with high reverse bias, V-I characts. 79−38158
InSb, tunnel diodes, abnormal V-I characts. *(Russian)* 77−8184
InSb:Se p-n tunnel diodes, influence of doping on characts. 79−73575
n-InSb:Se(Te), drift tunnel diode, prod., current ratio meas. *(Russian)* 77−8185

tunnel effect *see tunnelling*

tunnel triodes *see thin film transistors*

tunnelling
see also superconductive tunnelling; tunnelling spectra; tunnelling spectroscopy
ϕ^4 system, metastable state, decay rate calc. 80−22301
acetone, solid, effects of tunnelling on spin-lattice relax. of methyl protons 77−12216
acoustic tunnel effect for linearised quantum eqns. of elasticity 77−26188
adatoms, electron state at high coverages 79−28400
alcohol galsses, tunnelling reactions of trapped electrons with electron acceptors 78−76887
alcohol glasses, X-irradiated, electron scavenging mechanism 77−56235
alkali halide:NH_2^-, dipole centre paraelectric alignment, phonon-assisted tunnelling 77−12413
alkali halide:NH_4^+, hindered rot. energy levels calc. 80−10514
alkali halide, electric-dipole ordering of tunnelling impurity centres 80−2215
alkali halide, with oppositely charged defect centres, autoionisation-tunnel relax. of electron excitation 78−72112
alkali halides, doped, thermal expansion at low temps. 80−96672
alkali halides, off to on centre defect transitions under hydrostatic press. 78−15199

tunnelling continued
alkali halides, positive colour centres, long-lived excited states and spontaneous tunnel transitions 79−82552
alkaline earth electron thermoemission and tunnelling emission *(Russian)* 77−44113
ammonium compounds, rotational tunnelling, temp. dependence 80−38970
ammonium ions, tunnelling, model of spin-lattice relax. time 77−63305
ammonium salts, proton spin relax. and phonons 78−84493
amorphous film, surface phonon assisted tunnelling at low temp. 77−4421
amorphous film, tunnelling states, at low temps., thermal and acoustical props. 77−24500
amorphous materials, dielec. and US dispersion at low temps. freq. and temp. depend. 79−95092
amorphous polymers, localised low-energy excitations 79−73322
amorphous solid, surface phonons, tunnelling states and propagation charcts., low temps. 79−69337
amorphous solids, optical absorption tail, shape 80−34946
amorphous systems, origin of thermal anomalies, struct. model 78−91256
associated liquids, mechanism of structural dielectric relaxation 80−107034
atom, bound state decay in external field in semiclassical approx. 80−12941
atom, chemisorbed on solid, diffusional motion, microscopic anal. 79−4467
atom+diatom reactions, semiclassical tunnelling probabilities, trajectory calc. 80−71886
atom transfer processes, Franck-Condon vibr. overlap factors and Gamov formula 79−66263
atom transfer reaction in gas phase, reaction rate computing, tunnelling corrections 79−79237
atom-surface impact, electron tunnelling in external electric field, atomic resonant ionis. and field ionis. 77−52208
band theory, cryst. with arbitrary band widths ratio *(Russian)* 78−14650
barium stearate single-layer Langmuir films, elastic and inelastic tunnelling 80−80403
barrier penetration theory in more than one dimension *(Russian)* 77−33879
benzene, deuterated mixed crysts., phonon assisted trap-trap triplet energy migration, 0K limit, phosphoresc. obs. 77−48218
benzene, isotopic mixed crysts., triplet excitation energy transfer theory 77−28611
benzene, isotropically mixed crysts., singlet and triplet exciton percolation theory 78−26818
benzene, polymerised, barrier in MIM tunnel junction, zero-bias anomalies 77−43739
benzene glow discharge, junction barrier, inelastic electron tunnelling 77−72916
biological photo-induced charge transfer, mechanism and range 77−60182
borosilicate glass, new dielec. props. at 5 mK 77−63354
calcium copper acetate hexahydrate, and deuterated cpd., tunnelling reson. effects in nonreson. spin-lattice relax. 79−86726
CDW condensates, soliton pair creation by elec. fields 77−69309
cermet, cond., temp. depend. 77−20467
chemical reaction, Eckart barrier tunnelling, Arrhenium plot curvature 80−3298
chemical relaxation, tunnelling, Mossbauer emission spectroscopy studies 80−40683
chlorophyll-a, microcryst., trapped-electron doping in photovoltaic sandwich cells 78−53334
CL Al_2O_3, film, dielec. const. and resist., thickness depend. 78−39502
classically stable state, local potential minimum, decay 78−16693
clathrate deuterohydrates, ^1H NMR lineshape of tunnelling methyl group, <5K 78−46370
complex molecules, π-electron pair correl. of supercond. type, appl. to optical and mag. props. 79−54778
computer experiments and their applications *(Polish)* 78−89420
conductance vs. voltage characteristics, M-I-Al junctions, tunnelling conductance of asymm. barrier 78−72279
cubic crystals, Raman scatt. from tunnelling of substitutional molecules 80−40107
cyanine dye monolayer assemblies with Al and Ba electrodes, photovolt., dark cond. and photocond. 80−80400
cyclopentanone, excited triplet state, intramolecular tunnelling, optically detected electron spin coherence 77−61774
cytochrome c, electron tunnelling to cytochrome c peroxidase 79−20507
cytochrome c-$Fe(CN)_6$ electron transfer, verification of vibronically coupled electron tunnelling 78−48750
cytochrome c-$Fe(CN)_6$ electron transfer, vibronically coupled tunnelling description 77−52737
decaying states, using Kapur-Peierls and Siegert resonant states and extended Hellmann-Feynman theorem 78−4503
defect tunnelling, phonon assisted, in-band defect-induced phonon reson. modes effect 78−14419
density matrix, semiclassical phase space representation, appl. to pot. barrier tunnelling correction 79−9135
diamagnetic glassy semiconductors, at. tunnelling states, dielec. and elastic losses 79−87385
diatomic molecule, neutron scatt. induced electronic transitions, tunnelling 80−63844
p-dichlorobenzene-p-dibromobenzene mixed crysts., triplet exciton migration, time resolved emission spectroscopy 80−89052
diffusion-controlled defect recombination, incorporating Coulomb interaction and annihilation 78−23044
diffusion-controlled defect recombination, quasi-steady radius, tunnelling and elastic interaction *(Russian)* 80−10908
dimethylacetylene, tunnel splitting, rot. pot., μeV neutron scatt. study 79−41993
dipolar centres, tunnelling to electron release 79−95420
dipolar impurity tunnelling model, elastic interaction and const. 78−71826
dipole pseudo-spin glasses, collective excitations 80−59617
discontinuous metal film, cond., temp. depend. 77−20467
discontinuous metal film millimetric-wave and IR detectors *(Japanese)* 77−49771
discontinuous metal films, elec. cond., review 78−19167
tunnelling continued
discontinuous metal films, resist. and strain gauge factors expressions, quantitative formulation 79−95521
discontinuous metallic film, field effect of electrical conductance 77−39964
disordered materials, fluctuation-induced tunnelling cond. 80−65516
disordered semiconductor, possibility of density of state determ. by tunnel spectroscopy *(Russian)* 77−47713
disordered systems, spontaneous echoes, spectral diffusion decay 80−84270
disordered systems, tunnel transparency, random scattering centres *(Russian)* 80−2454
DNA, mutations, quantum theory, proton transfer by dynamic interactions 77−77868
doped electrode junction, tunnelling, Kondo scatt., coherence distance 78−31001
double oscillatory tunnelling, soln. by effective Hamiltonian method 77−20109
double potential wells, tunnelling and over-barrier decay rates, method of beats calcs. 78−44363
double well anharmonic oscillator, 1-d system, effect of fermions upon tunnelling 78−16689
double well damped motion, proton tunnelling, transfer rate temp. depend. *(German)* 80−87058
double-well potential, transmission function vs energy splitting methods 79−25883
double-well potentials, symmetric and asymmetric, periodic orbit theory 80−23488
dynamic Jahn-Teller effect, existence of tunnelling splitting 77−69275
dynamic potential barrier and tunneling, perturbation theory 78−62740
eight-site order-disorder model, influence of tunnelling 80−2709
electrode-insulator boundary, current injection in presence of space charge 79−1619
electroluminescence excitation, tunnelling theory 78−43936
electron, in real layer structures, theory 77−66196
electron scattering, influence on current-voltage charcts. of tunnel contacts 78−14798
electron tunnelling, thermal and photoassisted, theory, fast charge separation in photosynthesis 80−89730
electron tunnelling, two band calcs., Gamow formula applications 80−54665
electronic energy distrib., Schrodinger wave eqn. solutions 80−103743
elimination reaction, D kinetic isotope effects, tunnelling, zero-point energy effects 78−56889
ethanol-d_0, -d_1, -d_5, γ-irrad., trapped electron spin-lattice relax. 77−60089
ethylene, glow discharge, junction barrier, inelastic electron tunnelling 77−72916
ethyliodide-d_2, NMR, spin-torsional spectra 79−15363
excess electrons in condensed media, migration in dilute mol. solns. 77−81457
exciplex gas lasers, pumping by barrier tunnelling 78−17908
exciton insulator, coherence factors and transport props. 79−28291
excitonic insulator, tunnel breakdown theory *(Russian)* 80−29686
fatty acid monolayers, electron tunnelling 77−69428
fatty acid-cyanine dye mixed monolayer, on metal electrodes, photocond. 78−68050
ferroelectric, H-bonded, central peak, thermal cond. 80−93250
ferroelectric crystal, hydrogen-bonded, partially-deuterated, coupled tunnelling-lattice modes 77−63372
ferroelectric H bonded crystals, linear response function for tunnelling systems in polariton region 78−43799
ferroelectric transition, tunnelling concept in general theory 77−63375
ferroelectricity, unified theory including active atom tunnelling motion 77−63373
ferroelectrics, order-disorder, displacive transformations, tunnelling, phonons 80−75975
ferromagnetic transition metals, electron spin polarisation, review 78−76591
ferromagnetic transition metals, electron spin polarisation, review 78−76592
ferromagnets, transfer matrix and WKB models 77−11986
field emitted electrons, effects of band struct. on energy distrib. 77−24932
field-evaporated ions, post-ionisation by tunnelling into substrate 80−80951
fluorene, electroluminesc. *(Russian)* 78−92129
glass, thermal expansion at low temps. 80−96672
glass, time depend. sp. ht. rel. to US props., at low temps. 78−59957
glass, tunnelling systems, intrinsic elec. dipole moment, coherent elec. echo obs. 80−29705
glass, ultrasonic spectral diffusion, low temp. 78−18709
glass, US propagation at ultralow temperatures 77−39635
glass density fluctuations from elastic dipoles at low temps. 78−79709
glasses, non-radiative recombination at valence-alternation pairs 80−89048
glasses, time-dependent sp. ht. at low temps. 79−60520
glasses, US properties and short-time sp. ht. relationship 79−60440
glassy matrices, electron tunnelling in radiation chem. 79−91980
glassy organic matrices, electron spin-lattice relax. of radiation-produced Ag atoms, temp. depend., tunnelling relax. 79−34331
Heisenberg spin 1 system assembly with tunneling, phase transitions, thermodynamic behavior 80−4667
heterojunction, composite barrier, thermally assisted tunnelling 78−19136
2,4-hexadiyne, solid, methyl group tunnelling and torsion, neutron scatt. 78−18560
HF characteristics at low temps., multiphoton absorpt., tunnelling under dimensional quantisation effect *(Russian)* 78−68073
hindered rotational energy levels of a linear ion in octahedral and tetrahedral crystalline fields 78−59767
hindered rotator in mag. field, mag. moment due to orientational tunnelling 77−68931
hydrocarbons, saturated open-chain, transport behaviour of excess electrons and props. 80−39643
hydrogen bond, quantum tunnelling of proton and activated complex theory 78−17586
hydrogen-bonded ferroelectric, Ising model in transverse tunnelling field and proton-lattice interaction 80−7307
ice, H_2O:D_2O, I_c phase cryst., IR spectra, H exchange activation energy 79−99866

tunnelling continued
ice, quantum mechanical approach to velocity of dislocations 78−91339
ice Ih, NQR of ^{17}O, double NMR for ^{1}H tunnelling, 1.3 and 4.2K 79−47353
ice matrices, polycryst., electron spin-lattice relax. of radiation-produced Ag atoms, temp. depend., tunnelling relax. 79−34331
II-IV p-n amorphous heterojunction, phenomenological model 80−54769
impurity centre repulsive barrier, anisotropy in electon penetration 79−65497
impurity molecules in crystals, exclusion rules for librational-tunnelling states 78−84174
instanton applications in statistical mechanics 79−75450
instantons, relationship to confinement, one-dimens. quantum mech. model anal. 79−12962
insulator, Coulomb interaction effects 77−8051
insulator, in inhomogeneous elec. field, localized states in forbidden band 77−8060
interimpurity tunnelling of electrons in solids, theory 78−88019
IR interaction with mols., classical/semiclassical theory 78−90164
IR point-contact diode tunnelling and rectification rel. to electrode geometry 80−57378
Ising model, central peak with transverse field 80−7306
Jahn-Teller problem, $T\times\varepsilon_g$, spin-orbit allowed tunnelling splitting, zero-phonon line splitting 78−19006
Jahn-Teller $T\times(\varepsilon_g+\tau_{2g})$ problem, tunnelling splitting 77−8059
junction mixers, quantum limited detection 80−18015
junctions generating burst noise, existence of tunnel-effects *(Rumanian)* 80−6960
kinetic model for electron tunnelling in frozen irradiation systems 77−52655
layered crystal, three-dimens. ordering of CDWs *(Russian)* 78−2439
liquid He-solid interface, tunnelling as mechanism of anomalous Kapitza resist. 79−55982
magnetic materials, spin polarised electron emission, review 77−73215
MAOS capacitor, cond. and charging behaviour 78−26963
MAS capacitor, cond. and charging behaviour 78−26963
metal, electron field emission, energy distrib. 77−1788
metal, H(D) diffusion, role of tunnelling, reson./nonreson. approaches 80−59718
metal, Lifshitz transitions and tunnelling effect 78−91591
metal films, quench-condensed, two-dimensional elec. cond. 78−39233
metal surface, dynamic image pot. for tunnelling electrons 80−49874
metal whisker diode, thermal field emission, nonlinearity, response time and polarity reversal 78−2579
metal whisker point contact junctions, tunnelling and rectification charcts. 80−6955
metal-barrier-metal diodes, I-V charcts., nonlinear mechanism in low voltage region 80−88618
metal-barrier-metal structures, coherent coupling of radiation by surface plasmons 77−89877
metal-barrier-metal structures, stimulated emission of surface plasmons by electron tunnelling 78−56236
metal-insulator, photon assisted tunnelling and internal photoemission 78−60202
metal-insulator contact, electron tunnelling and its role in contact electrification 80−2453
metal-insulator-metal junction, hopping model of zero-bias tunnelling anomalies, mag. field effect 79−60936
metal-insulator-metal structure, oscillatory effects connected with electromagnetic radiation in inelastic electron tunnelling *(Russian)* 78−91777
metal-metal contact, electron tunnelling stimulated by surface plasmons *(Russian)* 78−30974
metal-NH_3 mixture, attractive electron-electron interaction from molecular tunnelling mode 79−37793
metal-polymer-Si structure, elec. props., tunnel current 77−28256
metal-semiconductor interface, photoelectron injection, quantum mech. transmission and optical phonon scatt. 80−84511
metal-semiconductor-metal junction, tunnelling phenomena in terms of exact method and WKBJ approx. 80−20329
metal-solution interface with adsorbed molecules, enhanced light scatt. 79−82989
metal-tunnel oxide-Si junctions, processing condition depend. 80−80380
metal-vacuum-metal point contact junction charcts., Green's function calc. 80−103744
metal/PbI_2/metal struct. reson. and inelastic tunnelling 80−44739
metallic filaments, Tomonaga-Luttinger model, quasi-1D generalisation *(Russian)* 79−51560
metallic fine particles, tunnelling effects on props. 78−14704
metallic glass, conduction electrons interacting with tunnelling states 79−15137
metallic glass, tunnelling states, struct. model 80−70137
metallic glasses, conduction electron and tunnelling level interaction 79−60817
metallic glasses, tunnelling two-level system, Kondo-like state 80−88547
metallic particle tunnel junctions, light emission 78−80066
metallic point contact diodes, tunnelling props., geometrical asymmetry effects 78−10576
metals, BCC, diffusion of H_2 and its isotopes, phonon-assisted quantum-mechanical tunnelling of interstitials 80−59730
metals, chemisorption of gases, book 79−69370
metals, diffusion of H, theory, book contrib. 79−82389
metals, proper EM radiation on inelastic electron tunnelling with photon emission, cond. *(Russian)* 80−54765
metals, surface positronium formation, stopping distance, positron-phonon interactions 80−96582
metastable state, quantum kinetics of phase transitions *(Russian)* 79−51235
methane, solid, orientational order of molecules in phase III 79−51042
methane-d_1, tunnelling states and nuclear spin conversion 79−10944
methane-d_2, orientational ordering and tunnelling states meas. 79−10963
methane-d_4, solid, rot. tunnelling, neutron scatt. obs., isotope effect 80−92468
methane-d_4, solid, tunnel splittings, heat capacity meas. 80−96451
methanol glass, H atom abstraction by methyl radicals, 15-100K, limiting rate const. rel. to tunnelling 77−60037
4-methyl 2,6 di-tertiary butyl phenol, gamma-irradiated, electron-methyl group dynamical interactions 77−43161
methyl (CH_3D) group tunnelling in solids, quantum model rel. to two T_1 temp. depend. minima 78−2028
methyl compounds, rotational tunnelling, temp. dependence 80−38970
tunnelling continued
methyl group internal rot., pot. barrier and activation energy, absolute rate theory 79−79220
methyl group nuclear spin symmetry species, torsional relax. 79−60287
methyl group tunnelling and coupling to internal vibrations 78−79675
methyl groups, detection of proton NMR at arbitrary temps. of tunnelling system 78−39432
methyl groups, flip-flop motion and spin symmetry conversion 77−15326
methyl groups, spin symmetry species, neutron scatt. transitions 80−92470
methyl groups, tunnelling, proton second moment, signal-to-noise ratio effects 78−70766
methyl groups in solids, reorienting and tunnelling, spin-lattice relax. 80−50217
methyl groups in solids, tunnelling freq. for internal rotation in pot. function 80−49134
methyl radical in sodium acetate, EPR spectra, anisotropic hyperfine interaction, rot. tunnelling 80−34775
4-methyl-2,6-ditert-butylphenol, temp. depend. of methyl tunnelling spectrum by inelastic neutron scatt. 79−51015
4-methyl-2,6-ditertiarybutylphenol, methyl group reorientation, classical dynamics, NMR relax. and inelastic neutron scatt. 80−88066
4-methyl-2,6-ditertiarybutylphenol, proton spin-lattice relax. and activation energies of tunnelling CH_3 groups 77−48071
4-methyl-2,6-ditertiarybutylphenol, tunnelling methyl groups, EPR 79−4723
4-methyl-2,6-t-butylphenol, γ-irrad., electron-methyl group spin-spin interaction 77−85572
4-methyl-2, 6-ditertiarybutylphenol, tunnelling methyl group, inelastic neutron scatt. study 79−46580
methyl-containing mol. solids, proton NMR line shape, methyl group tunnelling 78−6588
methyl-d groups, reorienting or tunnelling spin-lattice relax. 80−97156
3,5-methyl-pyridine, rot. pot., proton spin-lattice relax., inelastic neutron scatt. study 79−47351
methylcyclohexane glass, γ-radiolysis, electron tunnelling from matrix trapped biphenyl ions 79−29379
methylcyclohexane glasses, γ-irradiated in presence of naphthalene, isothermal luminesc. 80−93388
3-methylpentane, γ-irradiated, isothermal luminescence in presence of aromatic solutes at 77K 78−76519
3-methylpentane glass, γ-radiolysis, electron tunnelling from matrix trapped biphenyl ions 79−29379
3-methylpentane glasses, γ-irradiated in presence of naphthalene, isothermal luminesc. 80−93388
methylpyridines, rot. tunnelling, NMR relax. and inelastic neutron scatt. 79−4733
MIM, open system normal tunnelling Hamiltonian, stationary state 78−39190
MIM, structure, resonant tunnelling, IV characteristics, comments 80−70847
MIM, thin film, use as non-heated source of electrons, review 80−84516
MIM diode, elastic tunnelling current, phenomenological theory 78−19159
MIM diode, US effect on tunnel current for normal and supercond. metals 77−16006
MIM diodes, negative differential resistance, stimulated inelastic tunnelling theory 80−49951
MIM heterojunction, theory of reson. tunnelling through insulator cond. band. 77−59336
MIM junction, tight-binding Green function calc., disorder effect 78−10577
MIM structure, elastic tunnelling spectroscopy of single-particle excitations 78−56260
MIM structure, electron tunnelling through insulating layer 79−24082
MIM structure, eqns. for potential barrier height determ. 77−47899
m.i.m. structure, light emission, by inelastic electron tunnelling 77−1734
MIM structure, nonequilibrium states, kinetic eqns. *(Russian)* 80−11101
MIM structure, quantum size effect in normal metal tunnelling 79−73601
MIM structure, tunnelling current vs. voltage charcts. calc. 77−12020
MIM structure, zero-bias anomalies due to Kondo scatt., hopping model, mag. field effect 77−59334
MIM structures, analytical expressions for tunnel currents 80−60064
MIM structures, zero bias anomaly due to elastic tunnelling, calc. 80−2483
MIM structures nonlinear properties, EM signals detect. appl. *(Russian)* 78−34912
MIM tunnel junction, conductance-voltage charact., analytic expression for zero-bias offset 78−52102
MIM tunnel junction, direct calc. of resonance tunnelling 78−14837
MIM tunnel junction, magnetically doped, hopping model of zero-bias tunnelling anomalies, comparison with expt. 80−65703
MIM tunnel junction, surface plasmon excitation by electron tunnelling 78−91779
MIM tunnel junctions, enhancement of light emission 77−51824
MIM tunnel junctions, roughened, photon emission, calc. 80−44738
MIMIM structure, photostimulated tunnelling 77−8204
MIS devices, large-amplitude hysteresis, model 79−19665
MIS structure, band to band tunnelling *(French)* 77−1487
MIS structure, photocurrent flow mechanism, carrier tunnelling 77−28258
MIS structures, analytical expressions for tunnel currents 80−60064
MIS structures, photovoltaic energy conversion, band struct. 80−92995
MIS tunnel diodes, photoionisation of states 80−11099
MIS tunnelling spectra, interaction of holes with local modes and one and two optical phonons 77−20457
mixed organic solids, triplet exciton transport at crit. conc., Anderson localization or delocalization 79−15087
mixed valence system, far IR intervalence tunnelling transition, vibronic coupling model 78−58646
MNOS devices, switching charcts. at low fields 79−56311
MNOS diode, trap distribution, memory characteristics 77−85326
MNOS structures, discharge behaviour 79−38174
molecular chain, 1-D electron motion, electron-phonon interaction, acoustic solitons 80−70628
molecular crystals, rot. excitations and tunnelling, review 79−46579
molecular rotational spectra, doublet splittings caused by tunnelling. perturbation treatment 80−91541

tunnelling continued
molecular solid, electron tunnelling, long-range electron transfer processes, orbital overlap model 80−7813
molecular tunnelling in chemical reactions *(Russian)* 77−52615
molecule, asymmetric double-min. pots., tunnelling 77−6660
molecule, tetrahedral, in cryst. field, torsional ground state splitting, appl. to methane and $(NH_4^+)_2SnCl_6^{2-}$ 80−15019
MOS capacitors, establishment of inversion layer in Si substrate under high oxide field conditions 77−66202
MOS devices, inversion layer, pot. and carrier distrib., quantum mechanical determ. 80−29483
MOS diodes, tunnel-assisted transport at room temp. 80−92975
MOS elements in depletion, interfacial tunnel interaction anal. 78−64121
MOS structure, negative bias stress at high elec. field, rel. to MNOS device degradation 77−62996
MOS structure, photon-assisted tunnelling at Al/SiO_2 and Si/SiO_2 interfaces 77−89865
MOS tunnel structure, $Si\text{-}SiO_2$ barrier height, SiO_2 thickness depend. 78−14831
MOSFET, n-type inverted surface channel, reproducibility of electronic props. 79−99628
Multiphonon effects in the theory of electron tunelling between deep impurity levels and the conduction band in strong electric fields 78−2447
multiphoton processes, in homogeneous electric field *(Russian)* 78−39607
multipolar superconductive tunnelling device, theory and technical feasibility *(Chinese)* 79−38253
muon spin rotation method, review *(Polish)* 80−88901
muonium reactions, tunnelling effect 79−57276
naphthalene, long range exciton percolation, superexchange, energy denominator 77−28609
naphthalene, singlet and triplet exciton percolation, tunnelling and thermalisation 80−84432
naphthalene, triplet exciton tunnelling, crit. concs. 79−15086
negative ion formation, by sputtering, work function depend. 78−39645
nitromethane, 1-dimens. reorientation and tunnel splitting in solid 79−99086
nitromethane, solid, tunnel states investig. 80−103274
NMR field cycling method for obs. of low temp. tunnelling in molecular solids 79−65755
non-redundant spectral tunnelling through periodic struct. at total refl. 78−78906
nonadiabatic leakage of particles from mag. mirror trap, multiple lifetimes 80−106968
nonadiabatic properties of tunnelling centres 78−79705
nonlinear tunnelling of soliton pulse 78−57811
nuclear relaxation in symm. groups, phonon-induced transition model 78−38635
nuclear spin-lattice relaxation of identical nuclei, rotational tunnelling induced *(Russian)* 78−60353
one-dimensional substitutionally disordered system, energy transfer, coherence, tunnelling, thermal promotion 78−56078
one-sided abrupt junctions, distinction between avalanche and tunnelling breakdown 78−56211
optical fibre, elliptical step-index, tunnelling-radiating effect 80−58714
organic glass, electron-cation recombination; charge distrib. simulation and luminesc. kinetics 80−2855
oxide electrodes, electron transfer reactions, tunnelling through a space charge barrier 78−80050
oxide film on metal electrode, nonadiabatic theory of electron transfer 77−28237
oxide glasses with Bi or Se granules, elec. props. and microstructure 78−2490
oxide-covered metal electrodes, direct elastic electron tunnelling, calcs. 78−52085
p-n tunnel junctions, photoinduced transitions, theory 80−65669
p-n tunnel junctions, phototransitions accompanied by impurity scatt. 80−107901
paraelastic tunnelling system dynamics, intermediate coupling regime 77−55489
paraelectric defect relaxation process, quantum interference and multilevel aspects 79−95109
paraelectric resonance of nonstationary tunnelling states *(Russian)* 80−34869
paraelectric tunnelling systems, broadening mech. 79−28701
passive layer, on Fe electrode, semiconductor model, appl. to electrochem. reactions, review 80−26022
phonon scattering at multilevel impurities, dispersion, damping, Green's function calc. 79−14892
phonon-assisted defect tunnelling with quadratic defect-lattice coupling, small polaron theory 79−73274
photon detection in nonlinear tunneling devices, theory 79−6177
plasma, stratified, obliquely propag. extraordinary microwave Budden tunnelling 80−48895
PMMA, amorphous, tunnelling models and thermal expansion below 4K 79−73326
point contact IR detector tunnelling and rectification characteristics, geometrical and multiple image interactions 80−57376
point-contact junction, influence of mech. modulation elec. transport 80−2481
poly-α-methyl styrene, viscoelastic relaxation and methyl group tunnelling 79−57038
polyacetylene, doped, fluctuation-induced tunnelling cond. in metallic regime 80−65516
polyatomic mols., dissoc. reaction path Hamiltonian 80−45486
polyethylene, dielec., cryogenic tunnelling losses at microwave frequencies 77−52016
polyethylene, dielec. loss below 4.2K arising from proton tunnelling 77−52015
polyethylene, oxidised, paraelectricity, dielec. relax. obs. 77−48123
polyethylene, thermally oxidised, low-temp. dielec. relax., dipolar tunnel states 78−2797
polyethylene dielectric losses, at very low temperatures *(Japanese)* 80−11331
polymer electret, charge dissipation, transport mechanisms 80−7268
polymer formation, interstellar molecules and prebiological evolution 79−92842
polyphenylacetylene films, phys. struct., AC and DC cond. 80−44750
tunnelling continued
polytetrahydrofuran films, electrochemically prepared between metal electrodes, DC elec. props. 80−39695
potential barrier, axially symmetric, tunnelling calc., appl. to energy level splitting and well broadening *(Russian)* 79−58588
potential barrier, electron tunnelling, with allowance for electron incidence angle *(Russian)* 77−15940
potential barrier, tunnelling probability spectrum and tunnelling time 78−79
potential models, tunnelling and quark leakage through the confining pot. 79−6317
prelumirhodopsin, psec. kinetics, primary photochem. event in vision, proton translocation 78−44508
propane mol. ion, competing slow metastable processes, tunnelling mechanism, tandem-ICR obs. 77−28976
1-propanol, electron traps, prestabilised electron relax. model 78−27803
proteins, electron transfer mechanism 79−96510
proton spin-lattice relax. and activation energies of tunnelling, CH_3 groups 77−48071
PVC films, soln. grown, DC cond. mechanisms, field and temp. depend. 80−97021
PVC-C composite, fluctuation-induced tunnelling cond. 80−65516
QCD phase transitions, chiral symmetry breaking, confinement, as tunnelling through singular barriers 78−82145
quantal particle, inverted Morse pot. barrier, transmission, reflection coeffs., phase-integral approx. 77−53801
quantal tunneling through a rectangular barrier using $|\psi|^2$ and flux, education 80−105457
quantum crystal, model of tunnelling point defect at finite temp. 78−38907
quantum fluid, Kapitza thermal resistance and tunnelling states of atoms, theory 77−85046
quantum mechanical barrier penetration, rel. to classical escape over pot. barrier 78−57819
quantum mechanical tunnelling, historical survey 78−54141
quantum solid, Kapitza thermal resistance and tunnelling states of atoms, theory 77−85046
quantum tunnelling, reaction coord. method 80−62500
quasi one-dimensional metal, crit. temp. for phase transition *(Russian)* 79−78253
quasi-one-dimensional conductors, order in coupled metallic chains problem 78−6358
quasi-one-dimensional cryst., three-dimens. ordering of CDWs *(Russian)* 78−2439
quasistationary state decomposition, effect of transient excitation *(Russian)* 78−77769
radiation-induced trapped electron yields, close effects, tunnelling processes 79−39161
Raman spectra line polarisations, impurity mol. orientational tunnelling effect 77−77208
rare earth ferromagnets, spin polarised electron tunnelling 78−68094
real-time approach to instanton phenomena, multidimensional pots. with degenerate absolute minima 78−78067
recombination kinetics controlled simultaneously by diffusion and tunnel effect, transient case 77−8120
reflected and transmitted beam, trajectories, in oblique tunnel effect 78−78903
Reggeon field theory, tunnelling at zero transverse dimens., path integral formulation 79−12986
relaxation, competing models, paramagnetic defects 79−37787
reorientation and spin-lattice relaxation due to a tunnel-controlled mechanism 79−28585
resonance differential negative resistance in the Fredkin-Wannier inhomogeneous field model 80−80355
resonance tunnelling of electrons in Bloch wave representation 78−11088
resonant optical orientation, tunnel centres, kinetic eqn. *(Russian)* 78−43911
resonant tunnelling current for general junction pot. barrier 79−51656
resonant tunnelling in film optical waveguides 79−27430
rigid rotor, asymmetric, semiclassical energy levels determ., tunnelling 78−37624
rotational tunnelling and diffusion in condensed mol. systems, neutron scatt. 78−63658
scattering resonances, tunnelling decay, absorbing boundary layer 80−57121
Schottky, barrier height modification by interfacial oxides 79−47163
Schottky barrier, optically biased tunnelling MIS device 77−85334
Schottky barrier, tunnel effect theory, random field contrib. 77−43727
Schottky barrier, tunnelling current assisted by deep traps, theoretical evaluation 77−43722
Schottky barrier field, exciton reflection band burning *(Russian)* 79−47479
Schottky barriers, resonant tunnelling through traps, theory 78−10553
self-trapping of electrons or Frenkel excitons, theory *(Russian)* 78−60192
semiconductor, bound levels and band struct., rel. to inelastic electron tunnelling spectroscopy 79−4597
semiconductor, low temp. field ionisation of localised impurity levels 79−47600
semiconductor, polycrystalline, elec. cond. model 77−11908
semiconductor in constant elec. and mag. fields, interband tunnelling 78−43405
semiconductor superlattice with cond.-valence band interactions 77−72815
semiconductor tunnelling and negative resistance phenomena, book 78−26947
semiconductor-electrolyte boundary, hot carrier injection, tunnelling from semiconductor states in depletion region 80−75637
semiconductor-oxide-semiconductor diodes, tunnel-assisted transport at room temp. 80−92975
semiconductors, temp. depend. electronic cond. 80−59975
semiconductors, Zener tunnelling in mag. and elec. fields 79−91082
slow neutron scatt. by rotating systems of identical nuclei *(Russian)* 80−14968
small polaron tunnelling, thermally assisted, computer anal. 80−2391
small-particle tunnel junction, light emission, local plasmon modes 79−19676
sodium acetate trihydrate, press. depend. of methyl tunnelling motion 80−10603
solid-state redox reaction, electron tunnelling rate, transfer model 78−76844

tunnelling continued
solitons and CDWs through impurities 78−51913
squaric acid, $C_4H_2O_4$ and $C_4D_2O_4$, struct. transitions, theory 77−15585
stearic acid layers, charge transport processes 78−84316
stochastic quantisation theory of time dependent tunnelling effects 78−41197
structural phase transitions, de Gennes pseudospin model, lattice phonons tunnelling effects 79−73290
structural phase transitions, tunnelling effects 79−55858
styrene glow-polymer in MIM sandwich, tunnelling and interface barriers 77−63001
SU(2) Yang Mills multi-instanton paths, tunnelling pots. and WKB wave functionals 79−248
superlattice, plasma oscillations 77−72878
surface channel tunnel junctions, subband spectroscopy 78−64104
synaptic and ephaptic transmission, quantum mech. tunnelling model 77−52772
TCNQ, salt, $Me\phi_3As(TCNQ)_2$, nonOhmic elec. cond., tunnelling model and expt. 79−99558
TCNQ salt films, textured TCNQ and NMP-TCNQ, cond. and dielec. props. 77−51733
TCNQ salts, electron tunnelling 78−47769
temperature Green's function for tunnelling model, new contraction method 79−35635
1,2,4,5-tetrachlorobenzene, localised excitations thermal promotion to exciton band, impurity states effect 78−52539
1,2,4,5-tetrachlorobenzene, triplet energy transfer in substitutionally disordered system 79−52000
tetrahedral four spin $^1/_2$ systems, Zeeman and tunnel system reson., coupled and uncoupled relax. 80−50214
tetrahedral molecule, in torsional ground state, total neutron scatt. cross section 79−50954
tetramethylgermanium, Zeeman spin-lattice relaxation rate maxima 80−84666
tetramethyllead, tunnel splitting, rot. pot., μeV neutron scatt. study 79−41993
meso-tetraphenylporphine, NH H^+ tunnelling rate 80−97158
meso-tetraphenylporphine, potential parameters of H migration tunnel rates calcs. 80−5600
TGS, eqn. of state near ferroelec. Curie temp., including tunnel effect 77−12342
TGS, vacuum-cleaved cryst., rel. to charge compensation 78−95556
TGS deuterated, X-irrad., negative ENDOR, collective motion 79−47357
thermal neutrons, inelastic scattering by one-dimens. defecton *(Russian)* 78−84169
thermally degenerated Schottky diodes, resonant tunnelling 80−100503
thin disordered film, electronic energy spectrum calcs. extended Halpern Green's function technique 80−20066
thin-oxide MIS thyristor devices, interface state charge 79−38172
transmission coeff. for 1-D potential barrier, discretisation of Schrodinger eqn. 80−57123
trapped electron two-step tunnelling to scavengers 79−96288
2,2,5-trimethyl-1,3-dioxane-4,6-dione, cryst., X-irradiated, methyl group hindered rot. tunnelling, EPR, ENDOR, and ELDOR 79−68328
tropolone, π-π^* singlet state, H^+ tunnelling dynamics and equilib. geometry 80−102539
tropolone vibr. spectra and proton tunneling 80−28014
TTF-TCNQ, interchain tunnelling effect on nucl. spin-lattice relax. time, interchain coupling of CDW 80−20163
two loop calculation about quantum mech. instanton, test of tunnelling 78−58126
two-level system, phonon interaction theory 77−15525
ubiquinone-Fe complex, bacterial photosynthesis primary electron transfer processes, psec. dynamics 78−80841
vacuum tunnelling expts., thermal drive apparatus 77−8175
vacuum tunnelling of gauge theory in Minkowski space 78−41425
very thin films, tunnelling currents, temp. and space charge effects 80−70799
vibrational adiabaticity, quantum mechanical derivation of transition state theory 79−74350
vibronic ferroelectric semiconductor, tunnel effect 78−10853
wave mechanics and tunnel effect, internal energy storage 78−36857
weakly coupled 1-D metallic chains, phase transition *(Russian)* 77−31946
Wigner distribution function, temporal positivity conservation 79−9183
zero bias anomaly in tunnel resistance and electron-electron interaction 79−65539
η or η' meson, tunnelling effects, phase coherence and mass in non-Abelian gauge theory 79−93287
Ag:Al_2O_3:Al tunnel-junction struct., surface polariton mean free path, roughness 80−93008
Al tunnel junctions, superconductivity enhancement by microwaves 80−107956
Al-adsorbed monolayer-Al junction, elec. cond. mech. 78−95386
Al-Al_2O_3 electron transport in very thin multilayers 79−4602
Al-Al_2O_3 triple-barrier structure, negative resist. caused by resonant tunnelling 78−14819
Al-Al_2O_3-Ag tunnel junction, 4-pyridine carboxaldehyde-doped, surface enhanced Raman spectra, surface plasmons 79−98111
Al-Al_2O_3-Al, tunnelling junctions *(Russian)* 78−60232
Al-Al_2O_3-Al junctions, Dy doped at Al_2O_3-Al interface, electron transport mechanisms and barrier height 78−91778
Al-Al_2O_3-Al structure, tunnel I-V characts., transmission coeffs. 78−80068
Al-Al_2O_3-Au thin-film cathode anomalous electron emission 79−8232
Al-Al_2O_3-Dy junctions, steady state and nonsteady state behaviour 79−78205
Al-Al_2O_3-Hg structure, I-V characts. at room temp. for different thicknesses 79−47172
Al-Al_2O_3-Pd diodes, resonant tunnelling via localized inpurity states 79−28416
Al-Al_2O_3-SnTe, junction, tunnelling, Fermi level depend. on carrier conc., influence of surface states 80−25016
Al-Al_2O_3-SnTe structure, tunnelling characts., model anal. 80−29480
Al-Al_2O_3-(a-Ge)-Al, electron tunnelling into a-Ge, press. effect 80−49938
Al-Al_2O-Al tunnel junction, Fe doped, Kondo-type zero-bias conductance 78−56237
Al-Al_xO_y-Pb tunnel junction, thermal annealing effects 80−49952

tunnelling continued
Al-I-Pb tunnel junction, clean and doped, tunnelling conductance 79−15232
Al-insulator-Al(Au) diodes, elastic tunnelling current 79−42666
Al-insulator-$In_{1-x}Mg_x$ film tunnel junction, resistance zero-bias anomalies 80−107925
Al-Mn, dil., coherent propag. and strain-induced localisation of muons 78−95537
Al-oxide-Pb tunnel junction, clean and doped, cond. 77−59335
Al-Si, contact resist. response surface of sintered Al film on Si (100) 79−78175
Al-SiO_2 interface, internal photoemission and photon-assisted tunnelling 80−6982
Al-SiO_x-Au, MIM struct., electroformed, struct. and elec. props., 4-300K 79−78206
Al-SiO-Al structure, tunnel I-V characts., transmission coeffs. 78−80068
AlAs-GaAs LEDs, Ge or Zn-doped, mechanism of degradation 77−76911
AlGaAs p-n diodes, I-V characts., tunnelling 80−100510
$Al_xGa_{1-x}As$-GaAs, p-*n* heterostruct. laser, tunnel injection and phonon-assisted recomb. 80−5733
β-Al_2O_3-Ag_2O, thermal cond. below 300K 77−24454
β-Al_2O_3-K_2O, thermal cond. below 300K 77−24454
β-Al_2O_3-Li_2O, thermal cond. below 300K 77−24454
β-Al_2O_3-NH_4^+, NH_4^+ jump diffusion and rotational tunnelling, proton NMR, spin isomerism theory 79−99778
β-Al_2O_3-Na_2O, colour centre ESR by localised tunnelling states 80−108073
β-Al_2O_3-Na_2O, microwave absorpt., low-temp. dielectric props. anomalies, ion tunnelling states 78−92013
β-Al_2O_3-Na_2O, thermal cond. below 300K 77−24454
β-Al_2O_3-Na_2O, tunnelling states, electron spin relax. 79−78518
β-Al_2O_3.$Li_2O(Na_2O)(K_2O)(Rb_2O)(Ag_2O)$, low temp. sp. ht., tunnelling states and diffusion theory 77−43345
Al|chlorophyll-a|Hg/In, sandwich cell, photovoltaic, rectifying and tunnelling effects 79−1628
As, amorphous and cryst., NQR for tunnelling modes and local struct. order 79−61261
As_2S_3, amorphous, temp. below 1K, props., tunnelling 80−49576
Au, electron tunnelling from particle, polarised light emission and plasmons 79−51685
Au/oxide/n-GaAs struct., photocurrent relax. 80−92978
Au-Al_2O_3-Al system, influence of mech. modulation on elec. transport 80−2481
Au-InS Schottky-barrier diode, tunnelling current due to thermionic-field emission 79−33340
Au-SiO_2-Si system, oxide film 16-36 Å thick, tunnel currents 80−70842
B amorphous film, elec. cond. in strong elec. field 77−11928
$Ba_3(PO_4)_2$, recomb. luminesc. mechanisms 80−2874
Bi, electron tunnelling and band struct., mag. field effect 79−37979
Bi film, quantum size effect and band struct. Bi-dielec.-metal system obs. 80−54811
Bi-Bi_2S_3 superlattice, elec. props. 78−10558
C-PVC composite, fluctuation induced tunnelling conduction 78−52044
C-PVC composite, transport props. 79−38073
CH_3PF_4, nonrigid mol., tunnelling mechanisms, spectrosc. theory 80−78605
CO-myoglobin, mol. tunnelling, isotope effect, time resolved IR Fourier transform obs. 80−72126
CSI:Na cryst., V_K-Na^0 centre pairs, tunnelling recomb. 78−91952
$CaCO_3$, calcite, tunnelling afterglows and retrapping 77−69902
CaF_2, ionic clusters, struct., thermodynamic functions, energy surfaces and SIMS 80−63881
CaS, phosphor, tunnel luminescence *(Russian)* 78−72577
$CaWO_4$ phosphor, interaction between intrinsic and impurity emission 79−8198
$Cd_xHg_{1-x}Te$, tunnelling effect in p-n junctions 80−75630
CdS-Cu_2S, thin film heterojunctions, tunnelling current, depend. on heat treatment 79−56294
CdS-InP(CdTe)(GaAs)(Ge), solar cell heterojunctions, CVD fabrication, photovoltaic response 80−93878
CdS-Te, heterostructure, effect of low cond. CdTe interlayer on charact. 80−44721
CdSe-Mo Schottky barrier, tunnelling and majority carrier density 79−51673
CdTe diode, generation-recomb. and ionisation processes, temp. depend. *(Russian)* 77−39942
$Cd_zZn_{1-z}S$/Cu_2S, heterojunction interface double layer, potential spike, electron tunnelling 79−7855
$CeCu_2Si_2$, tunnelling anomalies due to intermediate valence phenomenon 77−62873
$CePd_3$, tunnelling anomalies due to intermediate valence phenomenon 77−62873
$ClPF_4$, nonrigid mol., tunnelling mechanisms, spectrosc. theory 80−78605
Co, tunnelling electron spin polarisation rel. to band struct. 78−68095
Cr, antiferromagnetic, muon diffusion, spin relax. and coherent motion 80−71281
Cr-SiO films, sputtered, elec. and struct. props. 80−39694
Cr-SiO_x-Si MIS solar cell, current cond. 80−7936
CrOOH(D), barrier to proton or deuteron tunnelling 80−70156
CsH_2PO_4, ferroelec. transition, deuteration and press. effects 78−35101
CsI:Na, tunnelling recomb. of electron-hole pair, optical detection of ESR and circ. dichroism 79−47360
CuCl film tunnel conductivity *(Russian)* 79−51726
Cu_2S-CdS heterojunctions, role of deep levels in controlling photovoltaic props. 80−92941
Cu_2S-CdS solar cells, interface recombination phenomena and tunnel effect 80−66978
Cu(ethylenediamine)$_2^{2+}$, electron tunnelling probability as function of distance for chem. reactions 78−80759
D_2O, isolated in glassy H_2O, IR spectrum, deuteron tunnelling 78−27207
$Dy(Co,Ni)_2$, rel. to intrinsic mag. aftereffect 77−63237
Fe, electron tunnelling 80−60104
Fe, field-emitted electron spin polarisation by tunnelling through surface pot. 80−29861
Fe microsphere impact on electrode, charge reversal, oxidation effect 77−12042
Fe, quantum diffusion of positive muons, 3 to 300K 80−75909
Fe, spin polarised electron tunnelling results 79−28417

tunnelling continued
Fe, tunnelling electron spin polarisation rel. to band struct. 78−68095
FeF_3 film, elec. cond. mechanisms 79−99649
Ga, supercond. thin film, tunnelling meas. in high mag. field 78−68120
$Ga_xAl_{1-x}As_x$ photodetector diode on GaAs substrate dark currents, tunnelling, energy gaps, effective masses 80−70805
GaAs epitaxial layers, structural defect and conc. inhomogeneities influence on barrier diode I-V characts. 80−15602
GaAs, heavily doped, fluctuation-induced tunnelling cond. 80−65516
GaAs, hole effective mass, press. depend., theory and tunnelling expts. 78−75986
GaAs, interband tunnel current, influence of press. 77−76910
n-GaAs, nature of low temp. field generation of carriers, liberation from surface states 80−92960
GaAs, p-n junction, piezotunnel current *(Russian)* 77−47890
GaAs, phonon assisted tunnel emission of electrons from deep levels 80−25532
GaAs, tunnel MIS structures, surface states 77−85336
GaAs:Co^{2+}, piezoabsorption meas. tunnel splitting and Jahn Teller effect in $^4T_1(P)$ state 79−15494
GaAs:Cr^{2+}, dynamic Jahn-Teller effect, relaxation time for reorientation 80−6798
GaAs:Si p-n junction LED, electroluminesc. efficiency 80−71491
p-GaAs/rare earth metal contacts, surface pot. barrier 80−60086
n-GaAs-Au Schottky barrier diode, thermally assisted tunnelling currents 77−20412
$GaAs-Ga_{1-x}Al_xGaAs$ heterostructure, electron tunnelling theory 78−47861
$GaAs-Ga_{1-x}In_xAs$ heterojunction, thermally assisted tunnelling 78−19136
p^+-GaAs-n-(Ga,In)As heterostructure, thermally assisted tunnelling currents 77−20412
$Ga_{0.47}In_{0.53}As$ p-n junctions, band-to-band tunnelling current 80−107895
GaP:N, temp.-modulated photoluminesc., phonon assisted tunnelling process 78−23511
GaSb-Pb junction, Ar ion bombard. effect on tunnelling props. 80−54783
Ge, acceptor complex spectra, tunnelling H systems 80−89036
Ge, amorphous, tunnelling states simulation and sp. ht. 79−37791
Ge amorphous film, high freq. phonon scatt. 80−49328
Ge:Li-O, donor complex EPR and photoelectron piezoelectric spectra, dynamic tunnelling 79−1711
n-Ge:Ni, recombination of hot electrons on Ni impurity centres 80−44612
Ge-GeO_2, MIS struct., electrophysical characts. 79−82680
Ge-SiO_2, MIS struct., electrophysical characts. 79−82680
Ge-SiO_2-Si_3N_4, MIS struct., electrophysical characts. 79−82680
Ge-SiO_2-p^+Si tunnel junctions, for determ. of AC cond. of amorphous Ge 77−24608
H atom lattice impurity, H atom confined to spherical box with penetrable walls, Schrodinger eqn. 79−84987
H^+ transfer reaction tunnelling probability 80−26032
H-bonding, strong, stochastic model and IR spectra temp. effects 78−62805
H_2^+ system, quantum oscillations in tunnelling, oscill. freq., tunnelling currents *(Russian)* 80−60065
H_2+H_2, van der Waals pot., electron tunnelling, charge transfer 77−54588
HN_4^+, in crystalline cpds., tunnelling, PMR, generalised line shape, theory 79−73827
$(H_2O)_2$, tunnelling-rotational energy levels, group theoretical classification 77−54549
$HTaWO_6$, and $HTaWO_6.H_2O$ defect pyrochlores, NMR study of proton motion 79−82889
He, adsorbed on graphite, band struct. effects in heat capacity 80−59788
He, laser induced tunnelling, avalanche initiating electron prod. 77−39441
He, liquid, electron bubble tunnelling below surface 79−86945
He, solid, vacancy tunnelling freq. calc. 77−80678
^{3}He film, theory of motional inhibition of interlayer quantum tunnelling 80−54466
^{3}He monolayers, quantum tunnelling, NMR linewidth 77−39720
^{3}He-^{4}He solid mixture, ^{3}He-^{3}He and ^{3}He-^{4}He tunnelling motions, NMR meas. 78−38908
^{4}He film, superflow onset, 2-dimens. XY model 78−47623
^{4}He, solid, phase transition 80−15333
^{4}He, solid BCC, vacancy tunnelling at finite temp. 78−38907
^{4}He, superfluid, tunnelling effect and vacancy wave 78−47618
$Hg_{1-x}Cd_xTe$ photodiodes, long cutoff wavelength, effect of trap tunnelling on IR detector performance 80−73451
HgCdTe(Se) MIS junction, phonon-assisted tunnelling 79−47170
In:Sn, phonon spectrum, electron-phonon interaction *(Russian)* 78−18722
In-Ge:As, Schottky barrier tunnel junction, zero bias resistance, temp. depend. 78−72258
$In_{0.53}Ga_{0.47}As$ photodiodes with dark current limited by generation-recombination and tunneling 80−107893
$In_xGa_{1-x}As_yP_{1-y}$ photodetector diode on InP substrate dark currents, tunnelling, energy gaps, effective masses 80−70805
$In_{1-x}Ga_xP_{1-z}As_z$ DH laser diode, defect and phonon assisted tunnelling 78−13708
$In_{1-x}Ga_xP_{1-z}As_z$ well in InP, tunnel injection into confined particle states 78−19130
$In_{1-x}Ga_xP_{1-z}As_z$:Zn, x∼0.12, z∼0.26, LPE, DH lasers, tunnelling involving defects 77−65594
In_2O_3:Sn-Si heterojunctions, current mechanisms and barrier height 80−11083
InP, exciton localisation at impurity pairs 79−37999
InP inversion-type MISFET with SiO_2 gate insulation interface props., elec. drift 80−93002
n-InSb based MIS struct., carrier generation under nonequilibrium conditions 80−88640
InSb, Zener tunnelling in mag. and elec. fields 79−91082
KBr, diffusion-controlled defect recombination, quasi-steady radius, tunnelling and elastic interaction *(Russian)* 80−10908
KBr, electron irrad. at 4K, role of V_K centres in equilib. among centres 78−67712
KBr, recomb. in ionic crysts., defect interaction 80−84206
KBr:CN^-, neutron scatt. studies of $(CN)^-$ defects 80−92620
tunnelling continued
KBr:CN^- tunnelling motion of dipolar impurities, absorption spectra 80−66239
KBr(Cl), X-ray irrad., tunnelling recomb. luminesc. 80−2873
KCl, luminescence induced by tunnelling recombination between neutral Ag atoms and V_k centres 79−61442
KCl, positive colour centres, long-lived excited states and spontaneous tunnel transitions 79−82552
KCl, pure cryst., residual OH^- impurities, thermal cond. meas., zero field tunnelling splitting determ. 77−62692
KCl, radiative tunnel transitions in negatively charged colour centre systems 80−49655
KCl:AgCl, tunnelling-recombination luminesc. 78−88354
KCl:CN^-, paraelectric reson. study, tunnelling parameters and elec. dipole moment 80−25326
KCl:Eu^{2+} crystals, photostimulated afterglow investigation at room temp. 80−108259
KCl:Li, ⟨111⟩ off centre Li^+ under biaxial stress, bistable tunnelling 78−15090
KCl:Li^+, defect induced tunnelling states, depend. on strain, pot. model calcs. 79−69865
KCl:OH^-, paraelec. system, acoustic susceptibility in strong phonon-coupling approx. 78−71801
KD_2PO_4, deuteron tunnelling, barrier height and energy level calc. 80−6482
KD_2PO_4, H-bonded phase transitions, SCF approach 78−92030
KD_2PO_4-type ferroelectrics, parametric tunnelling-like reson. 80−66119
KH_2AsO_4, ferroelectric phase transition under high hydrostatic press., mol. dynamics, NQR study 80−75880
$KH_{2(1-x)}D_{2x}PO_4$, Raman spectra, effects of deuteration on proton tunnelling modes and coupled optic modes 77−59570
KH_2PO_4, H-bonded phase transitions, SCF approach 78−92030
KH_2PO_4, proton tunnelling, barrier height and energy level calc. 80−6482
KH_2PO_4 type ferroelectrics, Raman spectra, coupled tunnel-phonon modes, isotope effect 79−69205
KH_2PO_4, variational treatment of proton-photon system 78−88261
KH_2PO_4-KD_2PO_4 mixed cryst., dielec. polarisation, Green's function anal. 77−52011
KH_2PO_4-type crystal, LF dynamics 80−10602
KH_2PO_4-type ferroelectrics, inelastic neutron scatt. theory 78−48122
KH_2PO_4-type ferroelectrics, tunnelling integral 80−70156
KI, luminesc. lines due to n=2 free exciton state of Wannier series 80−29776
KI:OH^-, paraelec. reson. at 1.5 and 4.2K from 12 to 150 GHz 79−38512
KI:Tl, A_T emission, linear polarisation, appl. of semi-classical WKB formalism 80−45134
KI:Tl, electron-hole and V_k-Tl recomb., TSC and thermolum. study *(French)* 80−34461
KNO_3-$Ca(NO_3)_2$ glasses, radiation products and recombination 79−57261
$K_2Pt(CN)_4Br_{0.3}.3.2H_2O$, motion of Br^- ions, NMR 77−90051
$KTaO_3$, electromech. props. and electron tunnelling 78−23403
$LiH_3(SeO_3)_2$, IR and Raman spectra, internal modes, intra- and inter-H-bond tunnelling 78−43853
$LiIO_3$, US wave tunnelling across piezoelectric gap 78−87857
LiO_2-$2SiO_2$ glass, alkali motion ionic thermocurrent study, polarised impurity-vacancy dipole relaxation study 79−77806
$(LiO_{1/2}$-$NaO_{1/2})$-$2SiO_2$ glass, alkali motion ionic thermocurrent study, polarised impurity-vacancy dipole relaxation study 79−77806
methane, solid, librational tunnelling and proton relax. temp. 80−38969
Mg-MgO-Ag, tunnel junction, potential barrier, equivalent rectangular shape 79−7906
MgO, electron irradiated, luminescence, radiative recombination kinetics 80−7421
MgO:Fe^{2+}, Jahn-Teller effect in ^5E_g state, tunnelling splitting obs. 78−19517
Mn-Zn ferrospinels, carrier transfer phenomena 80−54727
MnF_2, thermal cond., temp. depend., role of reson. scatt. of phonons by OH^- defects 78−38889
$Mu+F_2 \rightarrow MuF+F$, 300 to 400K in N_2 moderator, reaction rate determ., tunnelling 78−48682
N_2, laser induced tunnelling, avalanche initiating electron prod. 77−39441
ND_4^+ ion, tunnelling, deuteron NMR lineshape computations, first order quadrupolar interactions 79−15362
ND_4ClO_4, level-crossing relax. study of MD_4^+ ion tunnelling freq. 80−7185
ND_4ClO_4, librational tunnelling and proton relax. temp. 80−38969
$(ND_4)_2PtCl_6$, level-crossing relax. study of MD_4^+ ion tunnelling freq. 80−7185
NH_4 Br single cryst., low temp. PMR lineshapes of tunnelling NH_4^+ ions 80−25223
NH_4 compounds, tunnelling frequency of NH_4 ion in crystals, cubic and noncubic 78−38633
NH_4^+, in crystal lattice, tunnelling effect on proton spin-lattice relax. time 79−61252
NH_4^+ ions undergoing slow tunnelling rotations, proton NMR line shapes 79−90576
NH_4^+, libration and tunnelling freq. rot. heat capacity, hindered rot. energy level calcs. 79−98058
NH_4^+ motion in solids, nucl. spin-lattice relax. exam. 78−56388
NH_4^+, NMR line shapes at low temp., composite tunnelling, reorientation 78−48054
NH_4^+, tetrahedrally coordinated four-spin-$^1/_2$ system, PMR absorpt., semiclassical anal. 77−8425
NH_4BF_4, H^+ relax. and tunnelling, nucl. spin-lattice relax. obs. 79−51876
$(NH_4)_2Ce(NO_3)_6$, proton relax. by tunnelling at low temp. 78−43666
NH_4ClO_4, NH_4 ion rot. tunnelling splitting, inelastic neutron scatt. 77−15325
NH_4ClO_4, proton relax. by tunnelling at low temp. 78−43666
$(NH_4)_2GeF_6$, H^+ relax. and tunnelling, nucl. spin-lattice relax. obs. 79−51876
NH_4I, NMR, spin-torsional spectra 79−15363
$(NH_4)_2MCl_6$, (M=Pd, Pt, Te, Ru, Ti, Ir and Re), proton relaxation and tunnelling 79−4737
NH_4PF_6, H^+ relax. and tunnelling, nucl. spin-lattice relax. obs. 79−51876
$(NH_4)_2PbCl_6$, librational tunnelling and proton relax. temp. 80−38969

tunnelling continued
$(NH_4)_2PbCl_6$, temp. depend. of tunnel freq. 80−1947
$(NH_4)_2ReCl_6(IrCl_6)$, proton relaxation near antiferromagnetic phase transitions 80−80640
NH_4ReO_4, PMR, NH_4^+ tunnelling, ground torsional level struct. 78−27097
$(NH_4)_2SiF_6$, proton relax. by tunnelling at low temp. 78−43666
$(NH_4)_2SnCl_6$, proton relax. by tunnelling at low temp. 78−43666
$(NH_4)_2TiF_6$, H^+ relax. and tunnelling, nucl. spin-lattice relax. obs. 79−51876
^{15}N, spin-lattice relax. time, quantum effect of NH_4-ion rot. 80−75875
Na-NaO-Na struct., inelastic tunnel effect, spectra, potential barrier parameters 79−95511
Na-zeolite, matrix, Te cluster superlattices, N and S type volt-ampere characts., elec. cond. *(Russian)* 80−70665
$Na_8Al_6Si_6O_{24}.Cl(Br)(I)$, cathodochromic sodalites, coloured crysts., tunnel and recomb. luminesc., temp. depend. *(Russian)* 80−66261
NaCl, absorpt. spectra, influence of elec. field 80−2794
NaCl, luminescence induced by tunnelling recombination between neutral Ag atoms and V_k centres 79−61442
NaCl:Ag, absorpt. spectra, influence of elec. field 80−2794
$NaH_3(SeO_3)_2$, IR and Raman spectra, internal modes, intra- and inter-H-bond tunnelling 78−43853
Na_2O-$2SiO_2$ glass, alkali motion ionic thermocurrent study, polarised impurity-vacancy dipole relaxation study 79−77806
Na_2O-B_2O_3-SiO_2-$As_2O_3(As_2O_5)$ glasses, DC and AC resist., bipolaronic hopping cond. 80−88558
Na_2O-SiO_2 glass, tunnelling recomb. luminesc. 80−2875
NaOH, electron tunnelling to NO_3^- scavenger sites 77−52655
NaOH:CrO_4^{2-}(NO_2^-), electron tunnelling, pulse radiolysis 80−108722
NaOH:$Fe(Cn)_6^{3-}$, electron tunnelling, pulse radiolysis 80−108722
Na_2SiO_2-CaO glass, thermostimulated and tunnel luminesc. 80−45157
Nb single crystals, for tunnel meas., annealing in ultra high vac. device *(German)* 80−89169
Nb:N, H, atomic tunnelling of interstitial pair, specific heat meas. 78−47600
Nb-Al_2O_3 composite, semicond. films, cond. on localised states 77−24628
$NbSe_3$, non-Ohmic conduction, depinning of charge density waves 79−65459
Ni (100), electron field emission, positive spin polarisation and band model of magnetism 77−52226
Ni, and its alloys, spin polarised tunnelling expts. 78−39372
Ni and Ni alloys, tunnelling electron spin polarisation rel. to band struct. 78−68095
Ni complex, $[Ni(OCH_3)(acac)(CH_3OH)]_4$, sp. ht., 0.4-285K, methyl group internal rotation 78−47531
Ni, electron tunnelling 80−60104
Ni, field-emitted electron spin polarisation by tunnelling through surface pot. 80−29861
Ni film, granular, tunnelling of spin-polarised electrons and magnetoresist., exchange effects 77−12024
Ni-alloys, spin polarised tunnelling 78−95494
Ni-SiO_2, granular film, hopping cond., magnetoresist. 78−56240
Ni-Ti(Mn)(Cu), electron spin polarisation 77−73058
NiFe, grain oriented, mag. domain wall slow motion, tunnelling mechanism 77−32210
$Ni(NH_3)_6I_2$, phase transition and rot. excitation 80−96642
$Ni(NH_3)_6X_2$, X=Cl,Br,I, rotational tunnelling by inelastic neutron scatt. 78−30553
O_2^+, $c^4\Sigma_{u^-}$ state predissoc. calcs. 79−50095
OH, $A^2\Sigma^+$ state, predissociation and tunnelling 78−29823
OH, $A^2\Sigma^+$ state, predissociation, tunnelling 78−29824
Pb films, conduction electron surface scatt. phase shift, tunnelling meas. 79−51648
Pb-Al_2O_3-HgSe junction, asymmetry of tunnelling characts. 79−47169
Pb-SiO_2-Au tunnel junction, obs. of conductance anomalies 78−26968
$Pb_{1-x}Ge_xTe$, band struct., tunnelling obs. in MIS struct. 80−54795
$PbHAsO_4$, ($PbDAsO_4$), Raman spectra of ferroelec. transition proton tunnelling 78−23410
$PbHAsO_4$, hydrostatic press. effect on ferroelec. transition 78−35102
$PbHPO_4$, hydrostatic press. effect on ferroelec. transition 78−35102
$PbHPO_4$, Raman spectra study of ferroelec. transition, proton tunnelling 78−23410
$Pb_{0.83}Sn_{0.17}Te$, carrier tunnelling through potential barrier in p-n junctions *(Russian)* 78−52074
$Pb_{1-x}Sn_xTe$, in MIS struct., tunnelling investig. of band gap and phonon energies 77−43733
$Pb_{1-x}Sn_xTe$, in MOS junction, phonon-assisted tunnelling 77−76928
PbTe surfaces, tunnelling spectroscopy in MOS and Schottky barrier junctions 80−49945
PdSiCu, amorphous, US attenuation and vel. studies at low temps. 80−88278
$Pd_{0.775}Si_{0.165}Cu_{0.06}$, metallic glass, 0.01-10K, relax of tunnelling systems by conduction electrons, US expts. 79−14889
Pt film, quantum size effect, and its temp., tunnelling obs. 79−91160
Pt tips, glass-coated, field emission microscopy Fowler-Nordheim emission regime and periodic current oscills. 79−95907
Pt-Si thermally degenerated Schottky diodes, resonant tunnelling 80−100503
RbCl:Ag^+, off-centre system, quadratic-coupling phonon-assisted defect-tunnelling theory 79−55849
RbCl:Li^+, new off-centre defect system, studied with dielec. techniques under hydrostatic press. 79−19834
$(SN)_x$, electron tunnelling, absence of supercond. energy gap 78−47769
$(SN)_x$, epitaxial film, elec. resist., 0.03-8.9K, possible supercond. 77−15970
$Sb_{35}Se_{65}$, polycrystalline, elec. cond. mech. 80−49705
Se, amorphous, electrical transport, activation energy 79−95406
Se-Te-Ge and Se-Sb systems, amorphous, electrical transport, activation energy 79−95406
Si, amorphous, mag. field depend. of luminesc. 79−43034
Si, amorphous, radiative and non-radiative tunnelling, photoluminesc. decay meas. 79−83026
Si, amorphous, tunnelling states simulation and sp. ht. 79−37791
Si, amorphous presence of acceptor states around Fermi level 78−2445
Si gas-sensitive microtransducer, cond. variation with pulsed ethanol adsorption *(Russian)* 80−50915
Si, heavily doped, doping density striation effects in studies of metal-nonmetal transition 79−28383
Si n^+-p solar cell, forward and reverse bias tunnelling 80−85274

tunnelling continued
Si:H, amorphous, geminate recombination model for photoluminescence decay 80−71481
Si:H, amorphous, radiative recomb. by diffusion and tunnelling, photocond. quantum efficiency 80−50394
Si:H, amorphous, surface states distribution using MOS tunnel junctions 80−103735
Si:H,P, amorphous, in MOS tunnel junction, electron tunnelling characts. 79−73592
a-Si:H MIS junction, electronic struct. study by tunnelling 80−44729
Si:O, O rich polycryst. film, carrier transport 78−80076
p-Si/rare earth metal contacts, surface pot. barrier 80−60086
Si-SiC p-n and n-n heterojunctions, prep. by ion implantation, tunnelling cond. 77−43710
Si-SiO_2 double barriers, reson. tunnelling 77−80846
Si-SiO_2 interface, barrier height in MOS tunnelling structures 80−88644
Si-SiO_2 interface, electron tunnelling meas. 77−12018
Si-SiO_2 interface, electron injection into oxide due to mobile ion induced internal field 77−15963
Si-SiO_2 MIS systems, dynamic props. of switching, appl. to charge transfer devices 80−92997
Si-SiO_2-Al, interface barrier energies for tunnel oxides, internal photoemission meas. 80−84512
Si-SiO_2-Al MOS surface channel influence on channel-to-contact diode charact. 80−92994
Si-SiO_2-Mo-Si_3N_4-Al MNOS structures with metal grains, charge transport at SiO_2-Si_3N_4 interface 80−65693
Si-SiO_2-metal structures, tunnelling probabilities for electrons and holes in ultrathin SiO_2 79−99631
Si-SiO_s interfaces, carrier transport processes, electron states, conference, Durham, England (July 1979) 80−90612
SiC LEDs prepared by overcompensation method, photon assisted tunnelling 80−97341
SiH_3 radical, in Ar(Kr)(N_2) matrix, anisotropic ESR spectroscopic parameters 80−63687
SiH_4, appl. of NMR field cycling method for obs. of low temp. tunnelling in molecular solids 79−65755
SiH_4, solid, NMR direct detection of tunnel splittings 78−56396
Si_3N_4, amorphous, in MIS struct., high field conductivity 78−23101
SiO amorphous film, high freq. phonon scatt. 80−49328
SiO_2, amorphous, sp. ht., time-dependent, 0.1 to 1K 80−100338
SiO_2, amorphous, temp. below 1K, props., tunnelling 80−49576
SiO_2, amorphous, tunnelling models and thermal expansion below 4K 79−73326
SiO_2, and $SiO_{0.7}$, amorphous sputtered thin film, US anomalies, 0.5-300K 80−34145
SiO_2 based glasses, highly absorbing anomalous IR absorption at low temps. 78−43871
SiO_2, Fowler-Nordheim tunnel injection, Si surface pot. effect 79−91151
SiO_2, glass, HF phonon phase vel. meas., below 1K, tunnelling model 77−7818
SiO_2 layers, DC current-voltage behaviour 77−85333
SiO_2 sputtered films in thin film transistors, trapping centres, electron tunnelling 80−7014
SiO_2 tunnelling barrier asymmetry to electrons and holes in MOS struct., photocurrent 80−75645
SiO_2, vitreous, existence of gap in low-energy density of states 79−60769
SiO_2:Cs(B) film, implanted electronic cond. mechanism in MOS struct. 77−15983
SiO_2-layers, charge transport induced by electron beam, simulation *(German)* 79−51702
SiO_2-Si, P ion implantation, electrical transport props. 80−39130
$SiO_2B_2O_3$-K_2O-Al_2O_3-As_2O_3 glass fibres containing metallic granules, tensile strength, Young's modulus, DC conductivity 80−30023
Sn-SnO_4-Sn junctions, oxide growth, tunnelling characts. 79−47173
SnO_2 film, mobility limitation by intercrystalline potential barrier, tunnelling effect 77−66210
SnO_2, glaze, high field cond., 4.2-470K 78−23100
$Sr(NH_3)_6$, PMR linewidth, proton tunnelling and NH_3 rot., rapid NH_3 diffusion 78−35045
SrO:Cu^{2+}, phonon-induced tunnel hopping, ESR obs. 79−69714
Ta-Ta_2O_5-Ag junctions, polarity-depend. tunnelling cond. 80−70846
Ta_xO_y on Ta, anodic film, electrochem. reactions by tunnel current 77−81340
Te film, polycryst., hole mobility, influence of tunnelling through barriers on grain boundaries 77−43748
TiO_2:Si(Fe)(Mn)(Cr)(Ni), anodes, low breakdown voltage due to electron tunnelling via grain boundaries 79−74407
n-TiO_2-electrolyte interface, electrolum. obs. 79−47520
TlH_2PO_4 and TlD_2PO_4, dielec. props. under hydrostatic press. up to 7 kbar 80−29696
V, phonon assisted tunnelling in impurity induced lattice strains 78−47601
V_2O_5, elec. cond. in strong fields, tunnelling mechanism 78−91699
V_2O_5-P_2O_5 glasses containing metallic particles, elec. props. 79−42547
W (110) plane, tunnelling of H in surface diffusion 80−75416
W field emitter, effect of Au adsorption on (110) and (211) planes 77−12503
W, point target, temp. depend. of electron emission caused by laser illumination 79−43107
W-oxide-Ni high speed submicron junction, electron tunnelling spectra 79−99635
W(110), field emission, absolute tunnelling current density 79−38724
$YbCu_2Si_2$, tunnelling anomalies due to intermediate valence phenomenon 77−62873
ZnO based varistors, nonlinear cond. theory 79−78192
ZnS, phosphor, voltage and temp. dependence of pre-breakdown electroluminescence 80−45147
ZnS, phosphor, voltage depend. of electrolum. brightness 80−45148
ZnS phosphors, Gudden-Pohl effect, field ionis. of trapping centres 77−73170
ZnS, single crystal, effect of elec. field on cond. 78−84228
ZnS:Pb current pulses due to elec. field liberation of electrons from trapping centres by tunnel processes 79−28378
ZnSe, Gudden-Pohl effect, release of electrons from traps 80−45149
ZnSe-electrolyte junction, current photoresponse 79−82669
ZnTe, elec. field and impurity conc. effects on ionisation energy of impurities, appl. to acceptors 80−88514
ZnTe, exciton localisation at impurity pairs 79−37999

tunnelling spectra
adsorbate concentration dependence of IETS intensity 79−68284
aromatic ring compounds, single, nitro-substituted, inelastic electron tunnelling spectroscopy 77−42367
aromatic ring ompounds adsorbed on Al-AlO_x-Pb and Mg-MgO-Pb, inelastic electron tunnelling 79−59521
benzoic acid, and p-deuterobenzoic acid, sensitivity of inelastic electron tunnelling spectroscopy 77−88605
chemisorbed atoms, inelastic tunnelling spectra 78−47664
m-cresol, vibr. spectrum determ. using Al-insulator-Pb tunnel junction 77−6782
dimethyl sulphoxide-d_6, intensities in inelastic electron tunnelling, IR, and Raman spectroscopy *(French)* 79−822
electron beam damage in chemisorbed layers, tunnelling spectra 77−76672
epoxy system, inelastic electron tunnelling spectroscopy appl. 79−15952
ethanol, adsorbed on Al_2O_3, inelastic electron tunnelling spectra, surface vibr. struct. determ. 80−35572
ethanol, adsorption on Ag islands on Al_2O_3 substrate, inelastic electron tunnelling spectra and TEM obs. 79−90884
Formvar, phonon spectrum from Al-Formvar-Pb junction electron tunnelling 77−59080
β-D-fructose, film, electron irrad., struct. changes, tunnelling spectra 77−10781
inelastic electron tunnelling structure, cover electrode metal effects 78−19127
MIM junctions, theory of vibr. mode intensities in inelastic electron tunnelling spectroscopy 77−14510
MIS tunnel junction, light emission via inelastic tunnelling effect 79−24076
molecular chemical tunnelling, facts and hypotheses 79−59520
molecular film, electron irrad., struct. changes, tunnelling spectra 77−10781
monocarboxylic acids, chemisorbed on Al_2O_3 78−91545
MOS structures *(Japanese)* 77−39953
nitrobenzene, intensities in inelastic electron tunnelling, IR, and Raman spectroscopy *(French)* 79−822
organic materials, inelastic electron tunnelling peak intensities 78−76139
organic molecular electronic transitions, obs. by inelastic tunnelling spectroscopy 77−38704
organic molecular monolayer in MIM tunnel junction, anomalous surface 79−72324
phenol, adsorbed layer, inelastic electron tunnelling spectral lineshapes below 100 mK 78−31000
phthalocyanine films, electronic transitions, 0.5 to 2.5 eV, inelastic electron tunnelling spectra 79−41214
polymethine dye layer, vibr. spectrum anal., inelastic electron tunnelling spectroscopy 79−13716
polyvinyl formate, far IR molecular vibrational spectroscopy by inelastic electron tunnelling 78−50546
propiolic acid, adsorbed in thin film tunnel junctions, hydrogenation and deuteration, IETS obs. 80−45547
quantum tunnelling in molecular physics 79−63894
NH-rhodanine-merocyanine films, electronic transitions, 0.5 to 2.5 eV, inelastic electron tunnelling spectra 79−41214
Schottky-barrier diodes, resonant tunnelling spectroscopy, deep centre detection 80−96968
sulphonic acids, adsorption and orientation on Al_2O_3, tunnelling spectroscopy obs. 78−34707
surface studies, rel. to inelastic electron tunnelling spectroscopy 79−4479
TCNQ compounds adsorbed on alumina, inelastic electron tunnelling spectroscopy 77−42367
thermally degenerated Schottky diodes, resonant tunnelling 80−100503
TTF-TCNQ, electronic struct. near Fermi level, tunnelling spectra 77−85126
Al-Al oxide-Pd tunnel junctions, exposed to H_2, inelastic electron tunnelling spectra 80−20327
Al-Al_2O_3-Pb, oxide-layer chemisorbed phenols, electron tunnelling spectra, 2K 77−62736
Al-Al_2O_3-Pb structure, traps in Al_2O_3 detected by tunnelling 77−8202
Al-Al_2O_3-Pb tunnel junction, depend. of conductance curves on chemisorbed ion conc. in barrier 79−15233
Al-Pb junction, intensity and line-shape measurements in inelastic electron tunneling spectroscopy 79−24104
Al_2O_3, IR spectra, comparison to inelastic electron tunnelling spectra *(French)* 78−68489
Al_2O_3, inelastic electron tunnelling spectroscopy of adsorbates, MgO comparison 80−88686
Au-Ti/SiO_2/p-Si MOS struct., interface state distrib., DC tunnelling spectra determ. 80−75611
CO chemisorbed on Fe, low energy vibr. modes studied by tunnelling spectroscopy 80−78590
$Fe(CN)_6$, adsorbed on Al_2O_3, tunnelling spectra, isotope shifts 80−29262
p-GaAs:Zn, Mn, degenerate, tunnel p-n junction and semicond.-metal struct., I-V characts. 78−72252
Ge, phonon energy variation under high press. band struct. changes, tunnel spectroscopy study *(Russian)* 80−2134
Ge:Sb(Ga), amorphous, doping effects on Fermi level, electrical meas. 79−42546
n-InAs, tunnelling spectra in mag. field, dispersion law *(Russian)* 79−60923
MgO, inelastic electron tunnelling spectroscopy of adsorbates, Al_2O_3 comparison 80−88686
Pb, single and polytextured thin films, band struct., tunnelling spectroscopy 80−80169
Pb-Si superconducting solutions, effect of hydrostatic compression on tunnelling *(Russian)* 80−65746
$Pb_{1-x}Sn_xTe$, band struct. and phonon energies, tunnelling spectroscopy 78−72070
Pt-Si thermally degenerated Schottky diodes, resonant tunnelling 80−100503
Rh, adsorption of $C^{16}O$ and $C^{18}O$, inelastic electron tunnelling spectra obs. 79−65331
Rh, adsorption of CO, inelastic electron tunnelling spectra obs. 79−46962
Rh supported catalyst particles, adsorption of CO, inelastic electron tunnelling spectra 79−3509
$(SN)_x$ single crystals, electronic structure clarification near the Fermi level *(Japanese)* 80−49954
SiO, alumina surface deposited film, SiH bond form., inelastic electron tunnelling spectra 79−69375

tunnelling spectra continued
W (100), chemisorbed Ba, inelastic tunnelling spectra 78−47664
$Zr(BH_4)_4$ catalytic reactions on Al_2O_3, inelastic electron tunnelling spectra 80−75425

tunnelling spectroscopy
AC bridge with two-freq. modulation of supply 80−13196
adhesion, inelastic electron tunnelling spectroscopy expts. 78−92440
adhesion, surface chemistry studies, anal. appls. 80−88440
anthracene, inelastic-electron tunnelling spectroscopy, exptl. test of symmetry selection rules 77−83671
applications, review 78−92588
biological applications of inelastic electron tunnelling spectroscopy 78−92770
biological applications of inelastic electron tunnelling spectroscopy 78−92771
differential tunnelling spectroscopy, bridge design 78−5309
electron inelastic tunnelling spectrometer, construction and operation 79−40646
electron-molecule interaction, in inelastic electron tunnelling spectroscopy, model 78−90257
electronic transitions obs. by inelastic tunnelling spectroscopy 79−3511
energy spectroscopy, review of principles and techniques, superconductivity 78−90253
external doping of tunnel junctions 79−3510
far IR molecular vibrational spectroscopy by inelastic electron tunnelling, polyvinyl formate appl. 78−50546
film, thick, phonon damping of virtual levels 79−4626
golden rule formalism in electron tunnelling 78−90259
inelastic electron tunnelling spectroscopy, appl. to study of lubrication 80−70302
inelastic electron tunnelling spectroscopy, conf., MO, USA (May 1977) 78−90254
inelastic electron tunnelling spectroscopy, external doping of junctions by infusion technique 78−90251
inelastic electron tunnelling spectroscopy, golden rule formalism 79−94050
inelastic electron tunnelling spectroscopy, multiple-scatt. theory of intensities 79−68285
inelastic electron tunnelling spectroscopy, past and future 78−90255
inelastic electron tunnelling spectroscopy technology 78−90261
inelastic tunnelling cross sections, calc. using self-consistent multiple scatt. 78−90260
instabilities in tunnel junctions for inelastic electron tunnelling spectroscopy 78−56235
light emission from inelastic tunnelling spectroscopy 79−3598
molecular vibrational inelastic electron tunnelling spectroscopy, effect of cooperative behaviour 78−90258
phthalocyanine films, metal-ligand and π singlet-triplet transitions, IETS obs. 78−90252
Raman spectroscopy of mol. monolayers in inelastic electron tunnelling spectroscopy junctions 80−93344
review, vibr. spectra of organic mols. 77−54632
review *(German)* 78−91776
semiconductor tunnelling, bound levels and band struct., rel. to inelastic electron tunnelling spectroscopy 79−4597
sensitivity, direct meas. using expts. on benzoic acid and p-deuterobenzoic acid 77−88605
superconductive tunnelling, appl. in inelastic electron tunnelling spectroscopy, advantages of supercond. electrodes 79−4625
superconductive tunnelling with spin polarised electrons 79−4627
surface chemistry and heterogeneous catalysis appls. of inelastic electron tunnelling spectroscopy 78−92512
theoretical interpretation of inelastic electron tunnelling spectroscopy 78−90256
trace substance detection, inelastic electron tunnelling spectroscopy appls. 78−92589
zero bias anomalies in tunnelling, review 79−4603
Al, corrosion by carbon tetrachloride, IETS obs. 80−81230
Al, tunnel junction, barrier layer structure, mol. adsorption mechanisms *(Russian)* 79−31634
Al/formvar/Al(Sn) structures, low frequency phonon spectroscopy by tunnel effect 78−23206
Al-Al_2O_3-Pb diode, external doping with organic mols. 77−72919
Al-oxidised Al-Pb tunnel junction, nature of oxide barrier for IETS 77−72922
Al_2O_3 thin film used in inelastic electron tunnelling spectroscopy, X-ray photoelectron spectrum 80−108319
CO, chemisorbed on alumina-supported transition metals, inelastic electron tunnelling spectra 77−31871
Pb/oxide/InAs structure, effective mass determ. by tunnelling spectroscopy *(Russian)* 80−44482
Pb-SiO_2-$Pb_{0.8}Sn_{0.2}Te$, prop. of insulating film for tunnelling study on zero bias anomaly 79−15608

tunnels, wind *see wind tunnels*

turbidimeters *see turbidimetry*

turbidimetry
aerosol pollutant, in situ detection using thermal anal. 77−37364
atmospheric aerosol, turbidity characts. determ. from spectral actinometric obs. 78−92986
atmospheric aerosol automatic mass conc. meas. techniques 77−64459
automatic scanning integrating spectronephelometer 77−79165
bacteria, scattering pattern analysis 78−80946
baghouse maintenace, opacity monitoring technique 79−34459
city plume aerosol size distrib. and turbidity meas. 77−37408
composition analysers, electronic self-balancing system, turbidity meter appl. 80−16754
crystallisation kinetics study of sparingly soluble salts 78−26471
digital polar nephelometer, scatt. meas. from monodisperse aerosol particles 80−9804
dioctyl phthalate, polydisperse, spectronephelometer studies 79−21797
drinking water exam., L65 turbidity meter description *(Dutch)* 77−27332
electrooptical nephelometry, characterisation of nonspherical atm. aerosol particles 80−77106
fluid electrophysical effect control by susceptibility variation *(Russian)* 79−95628
fossil-fuelled power stations, air pollution detection and control, opacity monitoring 79−100557
Freon-12(22), gas, Rayleigh vol. scatt. coeffs., spectronephelometric meas. 78−14127

turbidimetry continued
hydrographic charting by multispectral and ocean colour scanners 77−5368
immunochemical analysis, standardisation of light scatt. meas. 78−36081
laser polarimeter for active spill detection 77−21938
latex particles, size determ. by combined filtration and turbidimetry method 79−79313
LED marine beam transmittance meter 77−70870
light scattering techniques applied to water treatment 79−12150
marine hydrosol scattering meas. by submerged laser nephelometer *(Russian)* 77−60418
multichannel electrooptical turbidity meter 80−67423
nephelometer, backward hemispheric integrating, accuracy 77−45189
nephelometer, for contamination assessment in XUV spectrographs in Apollo Telescope Mount 77−60603
nephelometer, for light scatt. meas. in optical ceramics 77−10084
nephelometer, integrating, ang. truncation error in fog droplet size range 77−70861
nephelometer, integrating, atm. light scatt. meas. extension into UV 79−74955
nephelometer, meas. of Rayleigh scatt. props. of aerosols and gases 79−29865
nephelometer on Pioneer Venus Sounder and small probes 80−67511
ocean water quality instrumentation system test 77−41066
oil-fired boilers, opacimeter use possibilities *(Rumanian)* 80−87483
photoelectric nephelometer for liquids 80−101812
photoelectric turbidimeter *(Polish)* 80−31840
photometer, MEX2, construction and operation *(Dutch)* 78−21203
polyethylene, mol. wt. averages determ. by temp. drop turbidimetry 79−39207
polystyrene in cyclohexanol, polydispersities from temp.-drop turbidimetry 77−25314
polystyrene-tetrahydrofuran-water system, thermodynamic and hydrodynamic props. 79−96353
scattering media optical meas. for biomedical applications 79−83890
seawater inherent optical props. rel. to Secchi depth 79−16472
Sigrist turbidity meter, description *(Dutch)* 77−18064
spectrocolorimeter, SPEKOL, polymer characterisation by turbidimetric titrations 79−79301
spectrophotometer, controlled rapid-scan, for turbidity meas. 77−41700
sulphate turbidimetric determ., nonsegmented continuous flow method 79−70405
sunphotometer aperture effects on atmospheric turbidity meas. 79−84483
water pollution control, Rome's metropolitan water board, control system *(Italian)* 77−81953
water quality meas., continuous, in tubular columns, probes utilisation *(French)* 78−3836
zinc oxalate crystallisation kinetics determ. by turbidimetry method 78−30569
AgBrI photographic emulsion prep., double-jet nucleation turbidimetry 79−100446
SF_6, gas, Rayleigh vol. scatt. coeffs., spectronephelometric meas. 78−14127

turbidity
see also turbidimetry
aerosol size distribution by inverting spectral turbidity data 80−95796
anisodiametric particles, light scatt. functions 79−98286
aqueous polynucleotide-protein mixture, inverted turbidity versus conc. depend. 77−9165
Atlantic Ocean, anomalous bottom water south of Grand Banks due to turbidity current activity 80−4042
Atlantic Ocean, turbidity distrib. 77−56634
atmosphere, aerosol effects on diffuse and direct solar radiation at Earth's surface 77−37406
atmosphere, aerosols size distrib. and turbidity meas. over St. Louis, Project METROMEX 79−16670
atmosphere, effects on classification of remotely sensed Earth surface features 78−16204
atmosphere, ideal Rayleigh, direct solar radiation at Earth's surface calc. 78−36274
atmosphere, Monte Carlo anal. of multiply scatt. lidar returns 77−25779
atmosphere, multiple scatt. effects on refl. light pulses 77−29442
atmosphere, path length distrib. of scattered photons 77−45147
atmosphere, polarising radiometer meas., skylight at South Pole station, Antarctica 78−57320
atmosphere, pyrheliometric meas. over India 77−78424
atmosphere, radiation scatt. role of spatial inhomogeneities *(Russian)* 78−7765
atmosphere, transparency characts. calc. 78−81407
atmosphere, turbidity meas. across Los Angeles Basin 78−92982
atmosphere, turbidity meas. on Hulunbeier grassland and dust transport study *(Chinese)* 79−84485
atmosphere, turbidity meas. via polarisation of UV light of daytime sky 78−20517
atmosphere, turbidity rel. to contamination, helicopter soundings *(Spanish)* 77−9499
atmosphere, water vapour, O_3 and aerosol effects 77−78420
atmosphere at Athens Observatory, solar radiation meas. 78−7768
atmosphere boundary layer, turbidity rel. to spectral struct. of radiation attenuation *(Russian)* 78−44997
atmospheres, spherical symmetry, radiative transfer, non-conservative problem 80−36492
atmospheric, rel. to circumsolar radiation intensity 77−37405
atmospheric turbidity, solar noon at Edmonton, in Canada 79−29858
atmospheric turbidity caused by air pollutants, assessment 79−100941
atmospheric water content and turbidity in Thailand, calc. 79−5580
auroral ionosphere, radio turbidity coeff. 78−45112
Bhavnagar solar radiation, atm. turbidity and sunshine obs. 79−58072
binary critical mixture, critical turbidity, kinetics, press. jump investig. 77−47548
binary critical mixture near crit. temp., temp.-jump expts. 77−21407
biomembrane microviscosity measurement, light scatt. effects 79−39365
CBNA, nematic-isotropic transition at high press., turbidity meas. 80−92655
colloidal dispersion, spherical particle, optical turbidity and refr., particle size and relative refr. index meas. 79−92012
current head motion *(Japanese)* 79−34852
disperse system, oblate particles, reciprocal problems 79−72496

turbidity continued
disperse system, parameters determ. from turbidity spectrum, allowance for nonspherical particles 78−55302
disperse system of oblate particles, light scatt. functions 79−64180
disperse systems, turbidity spectrum, wave exponent, spherical particle size depend. 78−46514
disperse systems, turbidity-spectrum method, scatt. functions for nonspherical particle systems 78−20078
dispersed random prolate spheroids, light scatt. characts., for turbidity spectrum calcs. 78−25801
EBBA, nematic-isotropic transition at high press., turbidity meas. 80−92655
EM infinite plane wave, mutual coherence function propag. 78−1163
estuarine waters, optics, approxs. and appls. 79−66712
fine particles of dredger spoil, motion with current from dumping ground 80−17287
Funka Bay, Japan, ^{234}Th removal from seawater 80−61803
hot matter, conductive opacities and free-free Gaunt factors 80−3361
human and calf lenses, light scatt. and reversible cataracts 80−56019
hydrological instrument to meas. light absorpt. coeff. 80−82076
Kainji Lake particulate distrib. patterns, LANDSAT-1 spectral data 77−5255
Lake Kainji, W.Africa, water columns movement, LANDSAT data 79−25284
laser backscattering from turbid water-nigrosin black dye-Teflon spheres dispersion 80−1129
lens, intensity fluctuations in turbulent atmosphere, with (without) central screening 79−7080
liquid crystal, scattering centres size and conc. determ. using turbidity spectrum 79−77509
Lorenz-Mie light scatt. fine struct. 78−7242
lysozyme-salt water soln., critical mixing point, turbidity and viscosity meas. 77−86437
macromolecules, mol. wt. meas., light transmission meas. 78−17828
MBBA, nematic-isotropic transition at high press., turbidity meas. 80−92655
mesosphere, turbidity from twilight obs. 77−5318
natural waters, turbidity rel. to spectral scatt. props. 80−72560
objective sensor placement for sampling regional turbidity 79−5626
ocean, instrument to meas. light absorpt. coeff. 80−82076
ocean, light scatt. obs. in African upwelling region, suspended particle meas. 79−5483
ocean, light transmission meas. in N.Arabian Sea 77−91144
ocean, suspended sediment conc. and fluid vel. near-bottom meas., Long Island inner shelf 79−34838
ocean, turbidity current flow, computer simulation 78−15997
ocean floor abyssal regions, gigantic accumulative relief forms 77−21759
oceanic hydrosols, refr. index and turbidity effects on solar radn. flux in atm.-ocean system 77−64303
optical response of turbid media, approx. linear relationship 78−90371
phosphatidylcholine dispersion, phase transitions obs. with interference refractometer 78−44459
PMMA isotactic, syndiotactic stereocomplex formation in soln., composition, struct. 79−66292
polyethylene oxide, mol. wt. averages and polydispersity determ. by temp. drop turbidimetry 77−63959
polyethylene oxide, solns. in toluene and ethyl benzene, phase equilib., struct. and thermodynamic stability *(Russian)* 79−86871
polymer solution, determ. using SPEKOL spectrocolorimeter 79−79301
polystyrene-diethyl malonate, strongly opalescent critical isochore, scattered light intensity 80−71436
polystyrene-polydimethylsiloxane, block copolymer micelles, small angle X-ray scatt. 79−69003
potentiophotometric platelet aggregation meas. by turbidity change 80−36061
PVC, plasticised film, defect form. study, turbidity and shrinkage meas. *(Russian)* 77−62490
radiative flux, in turbid medium above reflecting surface *(Russian)* 79−72498
radiative transfer through turbid atmosphere, single-scatt. solution 79−16663
remote sensing penetration depth at green wavelengths 79−66832
reservoir, stratified layer turbidity *(Japanese)* 78−20455
rod photoreceptor disc membrane, cooperative conform. change induced by bleaching 77−81499
rubber, nitrite, heat ageing, light scatt. method study *(Russian)* 80−40407
Sargasso Sea at 3.2 km depth, organic carbon annual variation 80−41460
seawater, Mangalore coast, India, 1976-7 nearshore water conditions 80−8315
solar radiation availability rel. to atmospheric turbidity 79−58071
soot conglomerate destruction dynamics in pulsed laser radiation field 80−58617
spherical particles, fine structure of the Mie scattering, specific turbidity resonant structure of a_n and a_b 78−58913
St. Lawrence Estuary turbidity maximum, sediment, salinity, suspended matter study 80−4015
suspension, light scatt., turbidity 78−44407
turbidity over Canada 79−53515
undersea transmission characts. of laser beam in Tago Bay, Japan 77−21782
urban-rural solar radiation and atm. turbidity, meas. in Los Angeles basin 79−80024
visibility in turbid media with coloured illumination 79−72489
volume scattering function and light field characts. *(Russian)* 79−13902
water quality monitoring, modular system *(German)* 80−26186
AgBr microcrystals in dispersed photographic emulsions, dimens. determ., specific turbidity method *(Russian)* 79−26027
NO_2 optical depths rel. to atmospheric turbidity studies 77−17216
$Na_2SO_4.12H_2O$ aq. soln., dodecanol additive effect near critical micelle conc. 77−73472
SF_6, liq., near crit. point, optical props. meas. 77−72673

turbine generators *see turbogenerators*

turbines
see also compressors; gas turbines; hydraulic turbines; steam turbines; turbogenerators; wind turbines
air, for measurement of magnetic torque acting on rotating sample 80−31811

turbines continued
air lubricated sample turbine for applications in solid body multipulse spectroscopy *(German)* 80−52284
airflow through cascade of turbine blades, laser anemometry 80−59146
analogue simulation of temperature distribution *(German)* 77−68551
axial turbine blades, spatial streamline flow calcs. using pot. flux of incompressible liq. 80−59000
axial turbomachine, cascade and through-flow theories as inner and outer expansions 78−75148
blade, rotating, vibr. analysis using holographic interferometry 78−32807
blade and nozzle guide vane, transient cascade, heat transfer meas., wind tunnel 78−94768
blade arrays, turbulence characts. of stream, obs. 78−71319
blade microporosity testing using X-radiographic method 77−86276
blade natural freq. and stress meas. *(German)* 79−34260
blade profile design, flow computation including shock waves *(French)* 77−62281
blade surface temperature meas. IR pyrometer 77−17983
blade vibration analysis, time average holography 77−5901
blade vibration meas., optical methods *(French)* 78−71300
bladed disc, finite element anal. of vibr. modes 77−39250
blades, three-dimens. annular array, aerodynamic forces with nonsteady flow 80−99991
blades nondestructive testing, using scanning laser acoustic microscopes, comparison with SEM and optical microscopy results 80−58875
boundary layer charact., influence of external flow turbulence 80−87811
cascade deviation, prediction and measurement 80−24049
cascade flow, surface-oriented coords. in num. simulation 77−55018
cascades, rotating annular, test facility of DFVLR, measurement and evaluation 80−14866
disc transverse vibration initiation 79−68633
duct rotating around perpendicular axis, flow and heat transfer, finite difference method 78−94752
flow turbine casing enclosed solar electric generator *(Japanese)* 79−88001
flowmeters, turbine-type, made in Bulgaria, survey *(Bulgarian)* 80−6173
fluid, equation of state and Euler's turbine eqn. *(Rumanian)* 78−79400
freon, 10 kWe solar power plant development 79−62020
hollow symmetrical blade vibration characteristics, thin shell theory 78−59341
jet flow hydrodynamic model 80−79369
noise emission of fans, blowers, dynamic compressors, acoustic test methods *(French)* 77−19478
overlay coatings for turbine parts, physical vapour deposition techniques, economic evaluation 80−35429
ring chamber, oscillatory behaviour of confined ring vortex 80−6075
rotor shaft, US testing, sensitivity multiplication factor 80−85125
solar energy conversion, osmotic pressure utilisation 79−57418
solar energy system, based on low-temperature Rankine cycle, low-cost design, pump drive appl. 79−62021
solar power generation, survey, vapour-tubine units, using organic working fluids 79−83618
solar turbines, use of organic fluids *(French)* 79−52885
solar turbopack, using organic Rankine cycle and flat-plate collectors, thermodynamics optimisation, irrigation pump drive appl. 79−62019
subsonic gas flow, integral eqn. method *(Russian)* 79−27662
TU-20 turbine oil, 4-methyl-2,6-ditertiarybutylphenol determ., using IR spectrophotometry *(Polish)* 80−13161
turbomolecular pump in pulsed mag. field, operational effects 78−50402
turbomolecular pump with mag. bearings, fusion expt. device appl. 78−50400
wind turbines, compact shroud theory 77−72373
wind turbines, spacing in large arrays 77−73797
Co-Cr-Al-Y coated turbine airfoils, effect of electron beam deposition rate on struct. 79−23870
Ni-Cr-Co based alloy, IN-738 turbine blades, hot isostatically pressed investment castings, effect of heat treatment on grain boundary struct. 80−89270
ZrO_2 coatings for turbine components, degradation due to internal stresses 79−24671

turboalternators *see turbogenerators*

turbogenerators
1000-2000 MVA turboalternators, for LWR power station, design *(French)* 77−3153
bar insulation in stator winding of large turbogenerator, inspection using microwave defectoscope 80−35474
bearing oil film damping and stiffness coefficients determ. for dynamic behaviour stability study *(Italian)* 80−106762
compressed air energy storage plants, turbomachinery options 80−30578
concentrator/photovoltaic/Rankine cycle steam turbogenerator system efficiency 79−62002
cryogenic, stability study *(Russian)* 77−53919
cryoturbogenerator transition process simulation, cryostat damping casings electrical characteristics determination *(Russian)* 80−8996
flow turbine casing enclosed solar electric generator *(Japanese)* 79−88001
high capacity, heating reduction measures for enhanced reliability and interval between maintenance *(Russian)* 80−96175
nuclear power station outages, turbine-generator reliability assurance through large scale test facilities 77−3151
nuclear power stations, overspeed protection, reliability study, design *(French)* 77−3156
numerical computation of electrical and magnetic fields, using ELMAG program system *(German)* 77−3516
rotor and stator core thermal conductivity solution using integral representation method *(Russian)* 80−100451
short circuits, stator end windings deformation *(Japanese)* 78−11465
sound level meas. using directional microphones 79−68520
stator core losses simulation, expt. 80−88798
stator endwinding vibrations, tests *(Russian)* 77−9885
superconducting, heat transfer in rotating excitation winding using He in rotating thermosiphon loops 79−58718
tidal power stations, technical details and operating experience 80−72009
turbojet engine noise interaction of entropy fluctuations with turbine blade rows 77−80149
water-bath US coupling and piece-part testing methods *(German)* 79−74317

turbogenerators continued
water/oil cooled type TVM-300, stator winding vibration tests *(Russian)* 77−9886
wind power distribution, control and conversion, vortex augmentor concept 79−83554
wind turbine generator, control and stabilisation 80−30370
wind turbine generator dynamic stability, digital simulation 79−96415
H production from radioactive waste heat and utilisation in gas turbines 80−30326
H_2 cooled, heating-up detect. by gas stream chromatography and mass spectrography *(French)* 79−48024

turbulence
see also atmospheric turbulence; boundary layer turbulence; cavitation; laminar to turbulent transitions; plasma turbulence; shear turbulence; turbulent diffusion; vortices
1st normal stress difference meas., water rel. to polymer solns. 79−98829
ν-fluid theory, turbulence model construction for high Reynolds number 79−46295
abruptly expanding circular duct, velocity distrib. 77−65798
accretion disc, selfgravitating, model 79−25466
acoustic, heat transfer in gas 79−86425
acoustic, in gas, heat transfer, mean internal energy and oscill. absorpt. *(Russian)* 78−46962
acoustic modes, high order, turbulence-generated noise in pipes with various fittings 80−74849
acoustic noise flow-generated, acoustic power and head losses of silencers *(Japanese)* 79−23309
acoustic power distribution in a turbulent jet 78−67238
acoustic radiation from bodies in unsteady flows 80−69799
acoustic radiation pressure on sphere at high Reynolds numbers, meas. 77−79989
acoustic tones in side-branch pipe resonators, flow-induced 80−64243
acoustic wave propagation on turbulent jets using organ pipe flue 80−91946
acoustic-vortical turbulence struct. 78−83373
acoustics, scatt. and interaction of sound with sound *(Russian)* 79−18571
active ocean layer, numerical modelling *(Russian)* 78−32110
advection, scalar spectrum model 79−32474
aeroacoustic measuring techniques in or outside turbulent flows 80−53534
aeroacoustics of advanced turbopropellers, noise prediction 80−69598
aerodynamic architectural and industrial testing, Oxford University 4×2 m wind tunnel 78−22443
aerodynamic noise, acoustic interference effects and role of Helmholtz number 79−94392
aerodynamic noise from wave-turbulence interaction 80−14679
aerodynamic noise prediction, acoustic dipole model, effect of motion 77−80148
aerodynamic sound generation by unsteady subsonic flows around rigid bodies 80−69798
aerodynamically generated noise, especially jet noise *(French)* 78−14002
aerodynamics of parallel circular cylinders, finite height 80−103013
aerosol, turbulent coagulation in pipe flow 79−37385
aerosols, β-active, charging in turbulent flow 77−19642
aerothermal turbulent channel, meas. of multi-orders velocity-temp. correls. 80−79268
air conditioned buildings, two equation model of turbulent flow *(German)* 77−14994
air flow, turbulent, in infinite medium spatial speed distrib. *(Rumanian)* 80−53826
air flow and heat transfer, in horizontal pipe, thermogravit. effects 77−31305
air flow in pipe at high temp. 79−81850
air flowmeter for long-term monitoring in patient-ventilator ccts. 77−64149
air intake, at high incidence, finite element anal. 79−3999
air jet, heated, turbulent, discharged downward, temp. profiles 79−27677
air jet, vertical axisymmetric buoyant, profile meas. 78−90906
air jets, interacting two-plane parallel jets, turbulence props., hot wire meas. 80−14767
air turbulence, effect on light flux fluctuations, limiting factors in photoelectric meas. 80−13136
air-Hg flow, stratified, co-current, in rectangular channel, interfacial wave structure 80−74955
air-water surfaces, turbulence characts., mass transfer and eddies 80−14665
aircraft noise, basic aeroacoustic research, industrial appl. 80−69596
airfoil trailing edge noise, near-wake struct. and unsteady pressures at trailing edge 80−69794
airfoil trailing edge noise, pressure field at trailing edge: effect on radiated noise 80−69795
airfoils, transonic testing at high Reynolds number in shock tube 80−14852
alloy melt, inductive stirring, melt vel. 77−73250
amplitude equation anal. of two-dimens. flow fields 78−5731
analysis, recurrence rate techniques 79−50831
anemometer, cond.-type, with external mag. field, turbulence spectrum correction 78−1766
annular channels with turbulent gas flow, bilateral heating *(Russian)* 79−7375
annular channels with turbulent gas flow, unilateral heating *(Russian)* 79−10559
annular conduit, wall suction, turbulent flow *(French)* 78−18343
annular diffuses with conical walls, swirling flow and separation 80−43715
annular flow of gases with varying physical props., turbulent, heat transfer in two-sided heating 80−48702
annular gap turbulent flow calcs. 79−55417
annular spaces inner surface, heat transfer in turbulent flow 80−14686
annular turbulent flows with heat transfer 78−94718
annuli carrying turbulent flows of gases with variable physical props., heat transfer in one-sided heating 80−48701
annuli heated from both sides, critical heat flux density and turbulence 80−48694
annuli with turbulence promotors, heated, lengthwise-uniform and non-uniform heat release, boiling crisis 80−48703

turbulence continued
annulus turbulent air flow heat transfer, physical prop. variability depend., expt. 78−83482
Antarctic Circumpolar Current S of Australia, cyclonic eddy obs. from R/V Professor Zubov 79−48500
aortic stenosis, expt. model, turbulent vel. meas. 77−21550
arc, electrical characts., effects of laminar and turbulent flows 80−1870
arc column in free turbulent jet, electric field strength 80−49021
arc voltage gradient in fully-developed turbulent air flow 78−71597
arterial stenosis, turbulence press. field rel. to character of vascular murmurs 77−56398
artificial heart blood pump ventricle, mech. driven, visual study of flow field 77−56539
asbestos fibre suspension, drag reduction in turbulent flow 79−68786
asymmetrical heated tube, turbulent airflow heat transfer characts. 80−38402
asymptotic, supersonic, 2-dimens. turbulent wakes, fully developed mean flow criteria 80−14706
atmosphere, vertical heat flux determ. on basis of semiempirical turbulence theory 78−3907
atmospheric sound generated by Al plate excited by free turbulent jet *(German)* 80−102908
attached jet, anal. *(Japanese)* 79−68779
autorotating flat plate wings, moment of inertia, geometry and Reynolds number effects 79−68719
autosimilar extinction of turbulence with large Reynolds number *(French)* 79−46296
axial momentum altered transverse transport in coolant flows during oscillatory instabilities 79−17964
axial-flow fan, quadrant duct bend effect on noise emission *(German)* 77−27539
axially symmetrical turbulent free jets, in wind tunnel, higher order moments measurement *(German)* 80−33648
axisymmetric, rapid distortion 78−30271
axisymmetric confined flame, aerodynamic and heat transfer, finite difference scheme, program 78−94689
axisymmetric flow, centreline formulation in numerical computation 79−41671
axisymmetric homogeneous, direct spectral simulations compared with direct interaction approx. 77−3813
axisymmetric jet, interaction with plane obstacle, Navier-Stokes eqn. solns. *(Russian)* 80−1659
axisymmetric jets and wakes, calc. with turbulence model 78−67239
axisymmetric turbulence, return to isotropy, numerical simulation 79−32470
baroclinic finite amplitude instabilities, book contrib., review 80−19328
BBGKY equation, two-point, separation of variables 79−50707
beam wave, propag. through weak turbulence, frequency spectra 78−78911
Belousov-Zhabotinsky reaction, chem. turbulence, strange attractor representation 80−85148
Benard convection, pretransitional induced, two-dimens. numerical anal. 79−68703
benthic ocean, bottom mixed layer turbulence 80−72532
bifurcations inducing attractor in Oboukhov's turbulence system 80−1536
bispectra, one-dimens. calcs. 80−53757
bispectral analysis, turbulent rot. vel.-derivative data computations 77−920
black holes, spherical turbulent accretion rel. to gamma rays emission spectrum 78−32504
blades, three-dimens. annular array, aerodynamic forces with nonsteady flow 80−99991
blood, extracorporeal circulation connectors, turbulence obs. 80−81641
blood, normal human, reduced hydrodynamic drag 78−61210
blood, turbulent flow through natural human vitral valve 77−36975
blood flow, contrib. of semilunar leaflets 80−3666
blood flow disturbance detect. using pulsed US Doppler method 77−40724
blood flow in left ventricle 77−48834
blood plasma, human, hydrodynamic props. 77−73538
blood turbulent flow measurement with pulsed Doppler US 77−40871
blown flap, upper surface, trailing edge turbulent mixing and sound generation 77−75902
bluff body, turbulent near wake, vel. correlation struct. 78−30298
blunt body injection into supersonic flow, expt. study 79−90277
book, turbulence, second edition 78−90839
book 77−58651
bounded coaxial jets, convective heat transfer in turbulent mixing, swirling 80−64541
Boussinesq approx. for homogeneous kinematic and thermal turbulence 79−27627
Boussinesq fluids, viscosity, conductivity and power spectrum of turbulent convection 80−98543
Boussinesq turbulence, statistical theory 80−48713
branch-to-trunk area ratio, effect on transition to turbulent flow, cardiovascular system appls. 80−67108
Brownian sphere, long time fluctuations 79−85077
bubble and eddy heat diffusion in single phase flow 80−19477
bubble chamber fluid, thermal turbulence, optical distortion effect 77−3221
bubble flow, churn turbulent regime, drift flux field eqns. 78−94807
bubbly, laser meas. of local liquid velocity and void fraction *(Japanese)* 78−9693
bubbly flow, drift velocity, analytical model of distrib. mechanisms 80−99992
bubbly flows, simultaneous meas. of local liq. vel. and void fraction using gas laser *(Japanese)* 77−42947
Buleev's model of turbulent exchange, modifications and limitations 77−84231
buoyant surface jet, 2-D flow props. *(Japanese)* 80−48762
buoyant surface jets of incompressible fluid, turbulent energy balance appl. 80−38469
Burgers' equation, energy transfer 79−1161
Burgers' model, energy decay, Monte Carlo quadrature 77−909
Burgers' turbulence, similarity law and renormalisation 78−46994
Burgers' turbulence model, uniqueness and stability 79−27693
Burgers eqn. calcs., mesh Reynolds number, computational accuracy 79−3997
Burgers equations, in two dimens., finite element anal. 80−1532
Burgers turbulence, asymptotic props., Burgers eqn. shocks 79−81852
turbulence continued
burning rate in engine cylinder, swirl and turbulence effects 80−89492
burning vortex ring, turbulent, acoustic emission 78−94676
bursting events, open channel, Reynolds stress conditional probability distribs., rel. to expt. 77−39348
bursting phenomenon in bounded turbulent shear flow, streamwise vortices 80−1600
BWR, core flow fluctuations, noise source, expt. study 79−13386
BWR, global noise identification by spectral and parametric methods 79−63730
calculation methods, book contrib. 77−58655
cantilever pipes, internal flow induced instabilities 78−63496
cardiovascular flow disturbance, US detection 77−60231
cascade model of fully developed turbulence 79−46293
cascade wake pattern with trailing-edge slot or surface suction 78−90909
catchment areas, large, jet flow similitude *(French)* 79−66423
cavity, square, 2-D, recirculating flow of incompressible fluid, large Re, convergence of finite-difference schemes 80−33611
cellular flow wavelength selection, convection and turbulence 80−38380
δ Cephei, atmospheric vel. field rel. to microturbulence and macroturbulence 79−25611
channel blockage and turbulence influence on water transverse flow past cylinder *(Russian)* 80−79401
channel flow, conducting fluid in external elec. and mag. field *(Russian)* 77−3875
channel flow, convective vel. to wall press. fluctuations, numerical simulation 78−94829
channel flow, mean vel. profile 79−55359
channel flow, meas. of vorticity and turbulence prod., pattern recognition method 78−26194
channel flow, Reynolds stress and joint probability density distribs. in u-v plane 77−46996
channel flow, secondary current numerical simulation 78−94828
channel flow, velocity vector instantaneous direction meas. 79−72949
channel flow wall region, fluctuating vel. components 79−77250
channel flow with rough walls, drag 79−86512
channel flows of high temp. gases, heat transfer 78−94722
channel height effect on nearcritical flow past circular cylinder 80−14818
channel turbulent gas flow with HF press. fluctuations, heat transfer rate depend. 78−83487
channel with sudden expansion, flow model 77−89101
channels, energy aspects of turbulent flow 78−7677
channels of various cross-sections, convective heat transfer 77−11262
chaos, reinjection principle, folded and cut chaotic flows 80−12996
chaotic phenomena and statistical physics, review of the contributions made by J. Schwinger 79−63135
chaotic Taylor vortex flow, dynamic instabilities and transition 79−94630
chaotic turbulent flows, scaling behaviour, Lyapunov characteristic exponent 80−86217
charged liquid, turbulent flow, transverse charge distrib. calc. 77−84334
chemical reaction at wall, turbulent mass transfer at $Pr \gg 1$, first order 78−18357
chemical reaction in turbulent jet, light probe meas. 77−62310
chemical reactions, second-order, in turbulent fluid, model, formulation and validation 79−20349
chemical reactions, second-order, in turbulent fluid, model, appl. to atm. plumes 79−20350
chemical reactions in turbulent stream, ignition *(Russian)* 77−80229
chemical turbulence, reduced model 77−4896
chemical turbulence, steady state, theoretical anal. 77−56216
chemically reacting flows, turbulent, steady and unsteady, computation in axi-symmetrical domains 80−1697
circle theorem generalisation for const. turbulence flow *(French)* 77−39277
circular Couette flow, centrifugal instabilities in cylindrical annulus 79−18956
circular cylinder, turbulence distortion, wake and velocity fluctuations 79−68712
circular cylinder, turbulent crossflow in vortex zone 80−10252
circular cylinder with tripping wires, heat transfer, flow and wakes *(German)* 80−1589
circular jet, turbulent shear layer, shear fluctuations 79−81936
circular jet asymmetry in flowfield and surrounding acoustic field, turbulence characts. 79−77197
circular jet turbulence under suction conditions *(Bulgarian)* 78−59437
circular turbulent jet in transverse flow, inlet section 79−94690
clay-water suspension turbulent flow in tube, velocity profile and frictional losses *(Russian)* 77−31364
close binary stars, tidal friction due to envelopes turbulent viscosity 77−57013
closure models, invariance 79−68683
closure relations for the pressure-strain correlation of turbulence 80−59011
coaxial jet, Raman scattering diagnostics of turbulent flow field 78−18328
coaxial jets with and without swirl 80−48759
coaxial round jet turbulence characts., obs. 78−87372
coherent Doppler anemometer for turbulent vel. meas., potential accuracy anal. *(Russian)* 78−71406
Cole-Hopf transformation for nonlinear parabolic and hyperbolic equations, diffusion and turbulence 79−41680
collisional drift waves, nonlinear evolution, bifurcations to chaotic state 80−14666
combustion, model for molecular mixing of unmixed gases *(Russian)* 78−94849
combustion, turbulent, averaging of pulsed laser Raman signals 78−70839
combustion, turbulent, implications of probability eqns. 78−14098
combustion gas flows, concentration fluctuation measurement by Fourier analysis of Raman signals, nonintrusive technique 78−92564
combustion region of gas turbines, perturbations produced by unsteady combustion and heat addition 80−53764
combustion-driven oscillations in small tube 79−52664
cometary tails, small-scale turbulence theory 79−44411
compressible axisymmetric jet sound radiation by instability waves 80−69792
compressible fluid, spectrum and excitation of turbulence *(Russian)* 77−3837

turbulence continued
compressible gases interface, turbulent mixing 78−1683
compressible inviscid fluid, profile of isogradient vaneless diffusor with swirl flow 79−86445
compressible liquid, sound and hydrodynamic turbulence *(Russian)* 78−55633
compressible turbulent flow, kinetic theory, comparison with classical theory 77−3814
compressible turbulent tube flow, heat transfer 78−71314
computation, bispectral meas. 80−38382
computational modelling by finite elements 79−1163
condensing turbulent annular-mist flow, wall and interfacial shear stress 78−94812
conditional eddies in isotropic turbulence, higher order estimates 80−92119
conducting medium, high temp. plane flow turbulence, mag. field effect *(Russian)* 77−65811
cone formation during interaction of laminar axisymmetric jets 77−84290
conference, computation fluid dynamics, Rhode-Saint-Genese, Belgium (March 1977) 77−80134
conference, drag reduction and turbulence struct., Washington, USA (June 1976) 78−22329
conference, Moscow, USSR, (April 1972) 77−89100
conference on dynamical critical phenomena, Geneva (Apr. 1979) 80−27040
confined coaxial jets with and without swirl, vel. characts., recirculation regions 80−103055
confined turbulent coaxial jet, vel. characts. 80−64601
conical diffusers, exponential behaviour in turbulent flow 77−7374
conical tube, heat transfer with internal cooling by swirling air jet 77−55063
constant isotropic kinematic thermal turbulence, constant gravity effects *(French)* 78−30269
constricted tube, turbulent flow, haemodynamic appl. 80−53860
contracting, axisymmetric turbulent flow, rapid distortion solns., stress transport model 78−67180
convected, vortex shedding influence on noise generation 77−3830
convection, buoyant, turbulent, from source in confined region 79−59983
convection, turbulent, numerical models based on unsteady Navier-Stokes eqns. 80−38415
convection between parallel plates, result plotting method 80−24001
convection in cubic cavity heated from below 79−77092
convection in fluid layer, turbulence from Rayleigh-Bernard instability 78−42605
convection in liquid, laser beam propagation 79−98831
convection in liquid in vertical slot under turbulent flow 79−98721
convection in liquid metals in narrow cell *(French)* 78−94701
convection in vertical layer, numerical modelling *(Russian)* 78−9636
convection mode numerical modelling 79−64653
convection within rapidly rotating superadiabatic fluids with horizontal temp. gradients 78−90913
convective free and forced flow in vertical channels 80−19391
convective heat transfer, turbulent flow with polymeric additives 79−77098
convective plume in uniform isothermal atmosphere *(Russian)* 78−5738
convective wave motion in rot. layer *(Russian)* 77−58670
cosmic rays acceleration by moving magnetic mirrors, efficiency 79−44310
cosmic turbulence, Kurskov-Ozernoi transformation appl. 77−5604
cosmic turbulence, primordial, spectrum evolution 80−90589
cosmic turbulence origin rel. to galaxy form. 77−49513
cosmological turbulence theory, observational tests 80−98747
cosmology, effect of non-linear interactions on universe expansion, quantum turbulence near singularity 78−77629
Couette flow, eddy viscosity decay, phenomenological theory 79−98700
Couette flow, plane, resonance mechanism, small 3-D disturbances 80−79269
Couette flow, turbulence transition, Landau picture, stochastic attractor representation *(Russian)* 79−98692
Couette flow with adverse press. grad., zero net flow 77−72281
Couette plane turbulent flow, probability distrib. functions 77−54983
coupled Burgers equation, numerical solution for turbulent fluid motion 79−40378
coupled conduction-turbulent convection in a circular tube 78−94691
coupled transport of heat, momentum mass, numerical method *(German)* 77−11193
Craya equation for Fourier transformation of double correl. at two points, direction modelling and anal. soln. *(French)* 79−46291
creation, review *(Hungarian)* 79−23312
critical fluctuations analogy in turbulence, intermittency exponents, book contrib. 77−84214
critical heat flux in swirl flow *(Russian)* 79−10558
critical phenomena, n=−2 model *(French)* 77−3812
critical point behaviour, probability theory 79−44889
critical Reynolds number hypothesis for phenomenological turbulence model 77−39279
cross stream-jet mixing, near field influence on mass, momentum and vorticity fluxes 77−39320
cross-current-flow past circular cylinders, surface roughness influence on heat transfer *(German)* 77−35134
crossover dimensions for fully developed turbulence 79−50713
cryogenic systems, circulating cooling time for laminar and turbulent flow coolant 77−5849
curved tube bank vibration in turbulent transverse water flow *(Russian)* 80−33678
cylinder, circ., oscillating in turbulent water flow, press. fluctuations 79−59995
cylinder, vel. and temp. probability distrib. in mixing layer and wake 79−68711
cylinder heat transfer to turbulent cross-flow of water at critical Re *(Russian)* 78−34132
cylinder in low Reynolds number flow, vortex shedding mechanism 79−32525
cylinders, closely spaced row, average drag force 77−68591
cylinders in turbulent flow, heat transfer 79−1198
cylindrical straight pipe, reorganisation criteria *(French)* 77−75980
cylindrical thermocouple with plane frontal area, recovery factor in turbulent subsonic flow *(German)* 80−74882
d-dimensional homogeneous isotropic incompressible turbulence, definition 78−55634
turbulence continued
decay in inlet region of channels 79−14384
decay of grid produced turbulence, velocity correlation equations, two- and three-point 80−53741
decay processes, at large Reynolds and Peclet numbers 77−58656
decaying homogeneous turbulence, correlation term-discard closure 79−27624
decaying isotropic turbulence, passive scalar contaminant, test field model calcs. 79−94596
decaying isotropic turbulence, Wiener-Hermite expansion, renormalised time-depend. base 78−38299
decaying turbulence in neutral and stratified fluids 80−96247
density stratified turbulent liquid flows, refractive index variation elimination 79−77215
depth-mode cavity resonance in turbulent flow 79−1017
descending turbulent flow of liquid film and gas, hydrodynamics 77−7437
description and quantification using information theory *(German)* 80−106789
determinism and chaos 78−87333
developed free turbulent flow, semiempirical theory, probability density model eqn. 79−98689
developing turbulent flow, in rectangular duct, laser Doppler anemometer obs. 77−14995
DHAB, nematic, ordering change due to external DC elec. field, permittivity obs. 78−94990
diagnostics, using multiple laser-beam probe system 77−27630
diagnostics by holographic interferometry 79−60078
diffusion flow on interacting surfaces, laminar and turbulent, in Newtonian or nonNewtonian fluids *(French)* 77−27516
digital processing of unsteady periodic signals around oscillating airfoils 80−10340
direct interaction approximation, higher corrections 80−92118
discontinuous transitions into chaos after single bifurcation, hysteresis existence 80−73264
discrete model exhibiting successive bifurcations leading to onset of turbulence 78−13996
discrete model with chaotic behaviour, trajectory instability, strange attractors 78−71318
dispersion concentration valves, system for wind tunnel meas. 79−5191
dispersion in porous media, pore distrib. and flow segregation effects 80−10302
dispersive medium, photon interaction models 79−82068
dissipation in incompressible fluid 78−1647
dissipation rate for turbulent plane and circular jets 80−69889
dissipations, dynamic and thermal, ratio *(French)* 77−89099
dissociating gas in pipe flow, heat transfer crisis, flow laminarisation 79−1265
dissociating turbulent gas flow around triangular rod bundle, heat and mass transfer *(Russian)* 79−68822
dissolved gas liberation kinetics in turbulent liquid stream 77−11226
distensible tube damping effects on turbulent flow, cardiovascular system implications 80−103076
Doppler velocimetry within turbulent phase boundaries 77−11289
Doppler-difference laser anemometry, appl. to wind tunnel meas. 79−7421
double grid of cylinders with opposite grid motion, turbulence decay 80−96246
drag reducing flow, mean vel. and turbulent energy closures 78−22331
drag reducing viscoelastic fluid, heat transfer to turbulent flow 77−84249
drag reduction, dilute polymer soln., wall roughness effective slip depend., turbulence model 78−26162
drag reduction and burst cycle mechanism, dil. polymer soln. 78−26164
drag reduction by fibre injection 79−37298
drag reduction by polymer additive, mech. mixing 77−68637
drag reduction in pipe flow due to nonuniform polymer conc. 79−27672
drag reduction scale-up criteria 78−22330
drag reduction with surfactants at elevated temp. 77−68579
drag-reducing flows, calc. of velocity profiles 77−35185
drag-reducing polymers aqueous solutions, turbulent bursts rel. to wall friction 78−63454
driven mixing layer of circular jet, turbulent static pressure fluctuations spectra 79−77195
droplets in turbulent flow, heat and mass transfer 78−22410
duct, noncircular, with sharp corners, friction factors 79−81968
duct, smooth or rough, laws of turbulent motion *(French)* 78−34196
duct, triangular, fully developed flow 78−38298
duct and contraction, nearly isotropic turbulence 79−18877
duct confined turbulent flames, laminar burning vel. effect on struct. and propagation 79−90351
duct entrance region, numerical prediction of turbulent flow and heat transfer 77−80164
duct flow, heat transfer, mixing length model 78−94720
duct flow, length-scale model 77−84233
duct flow, stable turbulent flow 77−84230
duct flow, turbulent, large scale struct. 79−64770
duct flow, turbulent convective heat transfer 78−94719
duct of arbitrary cross section, parabolic procedure for three-dimens. compressible viscous flow prediction 79−94716
duct rotating around perpendicular axis, flow and heat transfer, finite difference method 78−94752
duct wall cavities, heated bottom surface, forced convection heat transfer 80−6048
Duluth-Superior Harbour, turbulent heat transport rel. to ice growth 79−2299
dynamic methods appl. 78−1640
dynamical model of intermittent fully developed turbulence 79−10552
dynamical systems, critical transition to stochasticity 80−73265
Earth core, small scale turbulent dynamo rel. to geomag. field transition periods 79−8598
eccentric rotating cylinders, flow where clearance is relatively large 78−1667
eddy dynamics, Fourier transform ambiguity 77−5300
eddy turbulent heat transfer in stabilised pipe flow, calc. 78−83474
eddy-viscosity model constructed by homogenization *(French)* 79−84407
EHD transducers, jet turbulization by EHD action *(Russian)* 77−24031
electrically conducting media with nonlinear heat release, turbulence props. 80−103024
electrolytic cells, gas sparged, mass transport anal. 80−24004

turbulence continued
electrolytic method of mass transfer meas., appl. in oscill. and pulsating tube flows 79−68828
electrostatic precipitator, particle velocity, laser Doppler anemometry study 80−59144
electrostatic precipitators, aerodynamic theory, gas turbulence, Deutsch law 80−53758
elevated-free stream turbulence, characteristics of laminar boundary layer 77−80139
EM irradiance distribution function in turbulent media, theoretical review 79−64155
EM or optical pulse arrival time statistics in turbulent media 80−48154
EM wave propagation through turbulent medium, space-time anal. 77−42472
EM wave source bandwidth and receiver response time effect on scintillation index in random media 77−42473
EM wave strong scatt. in uniform isotropic turbulence, intensity moment eqns. soln. 79−64154
emulsion, concentrated unstable, turbulent flow in pipes 80−28537
endotracheal tube as factor in meas. of respiratory mechs. 77−21549
energy spectrum, short-wave asymptote *(Russian)* 79−86409
energy transformation, models 78−1641
energy-dissipation model, flow past a rotating cylinder 77−58696
engine intake noise, high freq., ray-theory approach 80−69595
enstrophy transfer in two-dimens. turbulence, subgrid scale modelling 79−16586
entrainment interface in a stratified fluid 78−55672
entrance flow, circular pipe, kinetic energy dissipation rate two eqn. model 78−47039
entry region of pipe, temp. and vel. fluctuations 78−94717
equilibrium correlation functions, turbulent flow kinetic theory *(German)* 78−90886
equilibrium dispersed-ring water vapour flows, liq. distrib., film paramters and hydraulic resist. 80−24079
equilibrium turbulence, soliton role as liquid drops *(Russian)* 80−98804
ergodic behaviour of two-dimens. turbulence 80−28494
ethyl alcohol, free convection on turbulent horizontal layer, effect of thermocapillary forces 79−98722
Eulerian and Lagrangian renormalization in turbulence theory 78−9629
excess noise from supersonic underexpanded jets in flight 80−69815
extensional viscosity of a dilute suspension of spherical particles at intermediate microscale Reynolds numbers 80−106835
external flow, book contrib. 77−58653
external noise effect on transition to turbulent convection 80−96263
f reactor coolant interchannel interaction for prolonged flow around bunches of rods 80−73888
falling liquid film, laminar and turbulent, local mass transfer *(German)* 79−77080
fan wakes, turbulent structure 78−79322
ferrofluid devices, magnetostatic and centrifugal, nonmagnetic body motion 80−33700
ferrofluid flow in circular pipe, uniform mag. field effects 80−43782
fibre suspension, dil., mechanistic aspects of drag reduction in turbulent pipe flow 80−6102
fibre suspension, rheology, rel. to turbulent drag reduction 78−22315
fibre suspension in water, turbulent jet, analogous behaviour to polymer solns. 78−1732
field-coherence four-point function in turbulent medium 80−87319
fields with a permanence property and existing triple correlations *(German)* 77−14998
film and gas descending flow, tangential stress 77−39333
film rupture in laminar and turbulent lubrication, inertia forces effect 80−74813
filmwise condensation heat transfer coeffs. 78−63429
fine particles in axisymmetric gas stream, concentration field investigation 79−14464
fine-scale struct. of vel. field 78−51151
finite turbulence spatial scale effect, turbulence amplification by a contracting stream 80−87760
fission reactor 61-tube bundle with wire wrap 80−32329
flame, acoustic noise *(Russian)* 79−32708
flame, flow pulsation effect on chem. reaction 77−35260
flame, mass streamline, vel. and density fluctuations correlation *(Japanese)* 80−6164
flame, premixed, propag. in large-scale turbulence 79−50813
flame, premixed, theoretical predictions *(French)* 78−94853
flame, premixed, turbulent, interaction effects 77−11279
flame, premixed, variable density effects 78−5824
flame, real time study by Raman scatt. 77−72368
flame, round jet type, mass exchange between recirculation zone and outer flows, stabilisation 80−14842
flame, temp. and conc. calcs. *(Russian)* 79−32707
flame, turbulent mixed gases, thermal exchange effect on reaction rate 78−7205
flame, turbulent premixed with sequential chemistry, closure model 78−35683
flame ionisation detector, meas. fluctuating conc., in turbulent flows 80−92240
flame propagation in flowing turbulent combustible mixture *(Russian)* 77−27624
flame propagation limits, mixture turbulence effects 80−16679
flame quenching, by narrow cylindrical passage 78−15674
flame stabilisation behind bluff-body flame holder *(Japanese)* 78−67284
flame stabilisation conditions, homogeneous reactor model anal. 79−86531
flame stabilised by turbulence *(French)* 79−1952
flames, effects of finite reaction rate and molecular transport on premixed turbulent combustion 80−3348
flames, laminar and turbulent, normal vels. of propag. calc. 77−84342
flames, laser Doppler vel. meas. using spark discharge particle generator 80−59139
flames, local turbulence props., Raman spectroscopy meas. 80−64648
flames, premixed, structure investig. by light intensity distrib. meas. 80−16680
flames, turbulence rel. to noise sources 77−51127
flat duct, inlet turbulence, local heat transfer, expt. 78−83480
flat duct, inlet zone turbulence under differing boundary layers, heat transfer, expt. 78−83481
flat plate moving in homogeneous or isotropic turbulence 80−106790
turbulence continued
flat plate streaming potential investigations: hydroynamics and electrokinetic equivalency 80−106777
flat rectangular channel turbulent water flow, free stream and viscous sublayer temp. fluctuations 78−83369
flight effect of Michalke and Michel vis-a-vis Lighthill's model 80−59018
flocculation, mathematical model *(Japanese)* 80−79389
flow, turbulent mixing, velocity biasing resulting from non-uniform seeding 80−59143
flow and heat transfer in the thermogravitational generation mode 78−94684
flow at high Reynolds numbers, turbulence meas. by statistical laser Doppler velocimeter 77−3895
flow downstream of sudden expansion, vortex growth 79−32472
flow field meas., near nozzle outlet using laser Doppler anemometer 80−28582
flow fields measurement, evaluation of stereoscopic trace particle records 78−1648
flow in cylindrical chamber *(German)* 77−68572
flow in cylindrical pipe, energy equations 79−90228
flow in pipes, temp. field struct. 80−69923
flow into homogeneous porous media on inclined bedrock 79−10609
flow meas., light beam coherence effect on optical method information capacity 80−1709
flow measurement by laser Doppler anemometry, concentration and size of tracer particles, theoretical limits 78−59514
flow model based on generalised parameter optimisation method *(German)* 77−14993
flow noise in ducts, excitation of side-branch cavity 77−11182
flow noise level determination in ducts 79−86421
flow regulating system operating with Newtonian and non-Newtonian fluids *(German)* 80−1535
flow splitting tee junction, three dimens. turbulent flow field, coarse field computations 78−63494
flow structure in channel with porous walls 78−67179
flow through bends and diffusers, pressure losses, component interactions influence 78−42665
flow turbulence, influence on the inception and growth of cavitation in a liquid 78−90948
flow with drag reduction, turbulent energy dissipation model 78−79345
flow-field investigations using triple-sensor probes 80−100043
flowmeter, 360 degree bend, discharge coeffs. 79−27717
fluctuating component eqns. for turbulence anal. 79−98688
fluctuating vel. meas. by optical instrument 78−83500
fluctuation corrections by renormalisation group methods 77−42806
fluctuations, turbulent, amplitude scale characteristic 78−18273
fluctuations of intensity at two wavelengths in turbulent medium 80−87318
fluctuations of temperature and concentration *(German)* 78−59372
fluid flow and heat transfer around two circular cylinders of different diameters in cross flow 80−14687
fluid saturated porous media, 3-dimens. and multicellular steady and unsteady convection 79−94615
fluid spheres in Stokes flow, eddy motions 79−23350
fluid stream, turbulent structure determ. using thermoprobe unit *(Bulgarian)* 80−28584
fluidised beds, solids circulation and heat transfer to immersed tube banks 80−6141
Fokker-Planck dynamics, homogeneous hydromag. turbulence 78−45566
forced convection, heat and mass transfer, analogeous relationship *(Japanese)* 79−14396
forced convection in channel flows, turbulence, review 79−1195
forced convection with rheological systems, review 79−1222
forced turbulent plumes, rise times 79−100932
formation during flow around elastic membrane *(Russian)* 79−41666
formation in parallel blast mixing *(Ukrainian)* 80−6033
four wire probe for turbulent flow temp. and vel. meas. 78−67290
four-point field coherence function meas. in laser random focusing region *(Russian)* 78−58910
Fourier representation of Navier-Stokes eqns., isolating consts. of motion 77−84235
fractal approach, attractors and dispersion 78−46943
free annular jet with finite radial dimens. under entrainment conditions, initial part 79−98772
free convection heat transfer from flat vertical plate to power law fluid 78−67225
free convection heat transfer from vertical thin wire to air, laminar-turbulent transitions *(Japanese)* 80−92152
free convection in mag. field, statistical characts., vortices 80−79310
free convection loops, dissipation effects in laminar and turbulent flow 80−19372
free convective heat transfer in liq. saturated porous bed at high Rayleigh number *(German)* 80−33605
free jet development, effects *(German)* 77−84291
free shear, channel and turbulent flows, finite element anal. 79−68808
free stream turbulence, effect on flow and heat transfer in annulus inlet 77−58647
free stream turbulence effect on skin friction and heat transfer from bluff body 79−86413
free turbulent flow of incompressible liquid, self-consistency of expt. data 80−6031
free turbulent heat exchange surface, free convection liquid flow 80−64543
free turbulent jet directed against a flat surface, phenomena accompanying the impact, diversion, and distribution *(German)* 80−106827
free turbulent mixing in streamwise press. gradients, linearised k-ε anal., wakes 80−59039
free-stream, effect on aerodynamic characts. of circular cylinder *(Japanese)* 80−10229
free-stream, effect on heat transfer and skin friction 78−30276
free-stream, in air and water, control by means of honeycomb 77−35122
free-stream, influence of axisymmetric contraction ratio 77−31284
freestream turbulence statistical characts., convective heat transfer calc., boundary layer eddy viscosity 78−83366
freezing of turbulently flowing liq. in tube, steady state 78−33998
friction factor, calc. by TI-57, binary-search method 80−83788
fully developed, intermittency exponent 79−86406
fully developed, origin of intermittency 77−58658
fully developed, quasi-normal Markovian approx. 80−53756
fully developed pipe flow, turbulence struct., suction effects 79−50799

turbulence continued
fully developed steady turbulence, intermittency exponent determination, maximum principle 79−98691
fully developed turbulence, intermittency and magnetic fields 78−89059
fully developed turbulence and statistical mechanics, review 78−51150
fully turbulent free convection heat transfer, surface renewal approach 80−14697
fully-developed, renormalisation group, review 80−28495
functional smoothing method in turbulence problems 79−86407
fundamental problems in general fluid dynamics and hydromag. dynamo theory, book contrib. 77−84213
fundamental triad-interaction system in 3D homogeneous turbulence 79−27623
furnace heat transfer, 3-dimens, computer model predictions test 78−59504
galactic wake turbulence, rel. to head-tail radio sources form. 80−36703
Galaxy magnetic field, turbulent struct. from extragalactic sources Faraday rot. 78−20885
gas, heat transport meas., second order effects *(German)* 77−15030
gas, nonsteady flow through semipermeable screen to vacuum 80−100029
gas, reaction rate distortion applic. of Tsuge kinetic theory 79−7418
gas bubble dynamics in turbulent jet 79−41741
gas cooled rough rod bundles, thermofluid dynamic expts., evaluation with code SAGAPO 80−24002
gas flow in annular channels, heat transfer apparatus and technique *(Russian)* 78−34199
gas flow in tube, temp. fluctuations 78−94721
gas flow through cracks 79−98693
gas flow turbulent press. and vel. fluctuations meas. by condensation method 78−34217
gas flows, turbulent, conservation props. 79−18876
gas jet, evaporation of semidispersive drop system 77−55077
gas jet, transient section and position of turbulent zone *(Russian)* 78−47010
gas mixture turbulent concurrent double pipe heat exchanger equilib. and nonequilib. reaction 78−94856
gas pipe flow, turbulent Graetz problem, Joule-Thomson effect 78−75204
gas stream model, turbulence damping by addition of solids *(German)* 77−58774
gas transported dust, discrete particle phase effect on turbulence intensity *(Russian)* 80−79384
gas turbine combustion chamber, isothermal model, bluff body, recirculation phenomena in primary zone 79−47925
gas turbine combustion chamber flow three-dimens. calc. 80−79405
gas vibrations in tubes under action of periodically varying pressure 79−94718
gas with broadly varying entropy, turbulence statistics *(French)* 78−94646
gas-cooled annuli, turbulent heat transfer 78−94723
gas-dynamic pulsation effects on turbulent gas flow discharges *(Russian)* 79−7500
gas-liquid, turbulent co-current flow, in tube, with/without swirl 79−77257
gas-liquid ascending flow, monodispersed, funciton stress on wall, bubble size effect 80−59098
gas-liquid flow with small gas contents, liq. phase vel. profiles distrib. 77−35216
gas-liquid interaction in turbulent reacting flows, mathematical model 80−83862
gas-liquid turbulent flow, friction, velocity and gas content profiles 80−14793
gas-liquid two-phase flow, meas. by hot-film anemometry *(German)* 77−11254
gas-solid flow in cylcone, turbulent swirl velocity, particle sizes and concentrations 80−69902
gas-solid suspension, free turbulence influence on heat transfer 77−42898
gas-solid suspension, turbulent heat transfer during motion in tubes *(Russian)* 77−24020
gas-solid turbulent flow, heat transfer, model 79−1232
gas-solid turbulent suspension flow, frictional pressure drop Prandtl's mixing length anal. 79−14458
gaseous cavitation, effect on fluid transients 79−77194
generation, Lorenz eqn., horseshoe-map chaos 77−41473
geometrical aspects of statistical physics, scaling and fractals 79−58625
geophysical, buoyant flow, book contrib. 77−60459
geostrophic turbulence, book contrib., review 80−19336
glass bead-air suspension, local particle conc. in turbulent duct flow 77−11239
granular media, dynamic flow, statistical theory 78−51217
gravitational field influence on turbulent flow and heat exchange, review 79−86427
grid generated, evidence for restoration of turbulent energy for flow in distorted duct *(French)* 78−90841
grid generated, plane strain appl., Reynolds stress tensor in shear flow 79−81858
grid generated, temp. fluctuations and heat flux 78−94651
grid generated turbulence, uniform strain effect on thermal fluctuations 80−103026
grid turbulence in air and water, higher-order moments of turbulent velocity 79−94595
grid-generated, vibration of rod in annular downstream region, reactor cooling appl. 80−74836
grid-generated turbulence, temp. fluctuation decay obs. 79−32506
ground water at horizontal plane, 2-D unsteady flow *(Chinese)* 80−46205
Gulf Stream east side, cold eddy studies using satellite and ship data 79−48501
gyrotropic turbulence spectra, Wilde diagram anal. *(Russian)* 79−4000
H-shaped section cylinder in turbulent flows, aerodynamic charact. 80−106813
haemodynamic velocity profiles in prosthetic heart valves under steady flow conditions 77−56410
HDR, numerical investigation of radial mixing capabilities in strongly buoyancy-influenced vertical, turbulent channel flows 79−93751
heat and mass transfer, book contrib. 77−58693
heat and mass transfer, TURF computer schemes 79−4014
heat and mass transfer rates at high Pr, electrochemical modelling 78−83383
turbulence continued
heat emission of a rough-surfaced tube in turbulent water flow *(Russian)* 80−74837
heat exchange between jet and obstacle, turbulence effect *(Russian)* 80−1579
heat exchange in blocked annular channel in turbulent flow of air with variable props. *(Russian)* 79−94620
heat exchange in turbulent gas streams in channels during resonant vibrs. *(Russian)* 79−50723
heat exchanger, tubular bundle type, with longit. drive, forced turbulent convection *(French)* 79−86333
heat exchanger tube banks, turbulent buffeting and fluid elastic instability 79−3958
heat pipe, turbulent vapour stream gasdyanmics 79−90335
heat transfer, acoustic oscills. effect 78−59394
heat transfer, in turbulent pipe flow, fluid props., var. calcs. 77−27527
heat transfer, local, cross flow, free convection and free stream turbulence effects 77−15009
heat transfer, nonstationary, finite element calcs. 80−83795
heat transfer, turbulent non-isothermal flow, temp. pulsations 78−94712
heat transfer and heat production in turbulent gas *(German)* 78−90867
heat transfer and press. drop in tube, internal solidification effect 79−32512
heat transfer between successive cylinders in liquid crossflow, expts. *(Russian)* 78−46967
heat transfer bibliography, Japanese works 79−23317
heat transfer downstream of a fluid withdrawal branch in a tube 79−77255
heat transfer enhancement in annulus by fluid injection 79−23319
heat transfer from cylinders in crossflow at critical Reynolds no. 79−98707
heat transfer from spheres, naturally turbulent outdoor environment 77−80163
heat transfer from spheres in naturally turbulent outdoor environment 77−42701
heat transfer in a tube, mixing tee effect 79−68812
heat transfer in annular channels in turbulent flow of gases with variable props. *(Russian)* 79−90256
heat transfer in annulus, transient, heating element, reactor cooling theory 78−86569
heat transfer in channel with permeable wall 78−63426
heat transfer in circular tube during turbulent flow *(Russian)* 78−38175
heat transfer in grid-generated turbulence 78−59393
heat transfer in tube with turbulence promoter 78−94728
heat transfer in turbulent flow of dilute surfactant or polymer solns. 79−77101
heat transfer of plate, to accelerated liquid flow *(Russian)* 78−18299
heat transfer of tubes closely spaced in an in-line bank 80−59026
heat transfer turbulence models, review 79−4017
heated flows, fine scale turbulence, hot and cold wire sensitivity corrections 80−69956
heated grid, two-point turbulence meas. 77−19594
heated round turbulent jet, in coflowing stream, vel. and temp. profiles 77−27569
heated turbulent flow of He-Ar mixtures in vertical circular tubes 79−59975
heated turbulent flows, cct. for instantaneous temp. meas. 78−21137
heated turbulent jet, local isotropy and large structs. 80−6116
helical channel flow, heat transfer 80−6150
helical isotropic, Lagrangian vel. covariance 77−62240
Helmholtz equation for turbulence, with a difference approximation *(German)* 79−86411
Henon-Pomeau attractor 80−46811
n-hexane, tank flame, turbulence, holographic interferometric synchronous photography *(German)* 78−51255
high Reynolds number flow, in exponential tubes with slow variation 79−46391
high-temperature supersonic jet, noise spectrum 79−94691
higher-order nonlinear interaction among spectral components in a wake 79−72894
holographic interferometry appl. in turbulence effects on optical wavefront 78−82936
homogeneous, anisotropic, statistical coeffs. of velocity and temp. fields 78−18274
homogeneous, three-point method 78−13995
homogeneous, uniform distortion, generation of pressure fluctuations 77−27519
homogeneous 80−69772
homogeneous fluid, turbulence induced by an oscillating grid 79−3998
homogeneous fuel mixture, turbulent combustion theory 80−53883
homogeneous isotropic, energy, dimensional anal. *(German)* 77−14999
homogeneous isotropic flow-field, effect of small solid particles on the decay of turbulence intensity 79−4073
homogeneous isotropic turbulence, Heisenberg's decay eqn., stability anal. 78−30272
homogeneous isotropic turbulence, inertial convective region, scalar fluctuation spectrum *(German)* 80−92120
homogeneous isotropic turbulence, law of similarity of energy spectra *(German)* 78−55635
homogeneous isotropic turbulence energy, spectral density, wave number vector modulus anal. *(Russian)* 78−46946
homogeneous isotropic turbulence in final period of decay, triple vel. correl. *(Chinese)* 78−18277
homogeneous turbulence, chemical reactions, probability approach and particle models, comparison 80−14844
homogeneous turbulence, return to anisotropy 77−75892
homogeneous turbulence, rotation effect on double vel. correlations *(French)* 78−63435
homogeneous turbulence, theoretical progress and problems 78−94652
homogeneous turbulence decay from given state at higher Reynolds number 80−1534
homogeneous vel. and temp. fields, statistical transfer coeffs. 77−7375
horizontal elliptical conduits, turbulent film evaporation and condensation 79−1182
horizontal tube turbulent flow secondary current struct., thermogravitation effects 78−90902
hot jet, crossed beam technique for characterisation of noise sources *(French)* 77−35284
hot turbulent flow, temp. fluctuations, hot-wire anemometer *(French)* 78−42684

turbulence continued
hot wire 45° slant probe for Reynolds stresses and turbulence intensities 79−72967
hot wire anemometry method for the flow patterns in an array of heat exchanger tubes 79−90357
hot wire anemometry of turbulent compressible gas flows 79−46408
hot-wire anemometry using 'squared signals', comments and reply 80−28581
hot-wire probe, simultaneous, instantaneous, temp. and vol. component meas. in turbulent flow 78−34236
hot-wire signal analysis, flow field determ. with high/low turbulence intensity 80−1719
Howells' model for isotropic turbulence, soln. and simplification 80−48682
Hurst phenomena in grid turbulence 78−46947
Hurst phenomenon in turbulent flows 78−59377
hydrocarbons flowing through circular pipe, streaming currents developed in laminar and turbulent flows 78−87413
hydrodynamic instabilities, transition to turbulence 80−28491
hydrodynamic instabilities and turbulence, flow states, examples and meas. methods 80−92116
hydrodynamic turbulence in weak large scale mag. field, effective mag. viscosity 77−33340
hydrodynamically unsteady turbulent flow, unsteady random contact time distrib. 77−51036
hydromagnetic, appl. of Karman's energy transfer process 79−81991
hyperchaos eqn. for 79−63151
hypermixing nozzle in thrust augmentor, three dimens. turbulent mixing 78−51214
hypersonic flow, reson. Doppler velocimeter meas. and direct flow visualisation 77−35285
ice layer profile on const. temp. plate in forced convection, laminar to turbulence transition regime 80−24007
ideal fluid separated flow, turbulent wakes and vortices locations 79−98732
ignition and flame quenching in flowing gaseous mixtures 77−80230
images aberrated by turbulence, undersampling errors in moments meas. 80−1137
immiscible liquids, flow in helix, high press. boiler analogue 77−58763
inclined hot-wire response equations, for flow field having dominant tangential velocity component 78−14105
inclined open channel, stability of permanent roll waves 80−64629
incompressible conducting fluid, homogeneous turbulence, functional charact. 78−18355
incompressible flow cct. large Reynolds number, numerical simulation *(French)* 79−10550
incompressible fluid, fully developed turbulence generated by random stirring, variational approach 79−3991
incompressible fluid, isotropically turbulent stream, probability distrib. of vel. and temp. differences 80−79273
incompressible fluid flows, dissipation of turbulent energy 77−35120
incompressible homogeneous decaying turbulence, press. and vel. fluctuations calcs. 79−32475
incompressible inviscid 2D flow, exact Gaussian soln. 79−55360
incompressible liquid in planar channel, axial curvature effects 80−87762
incompressible turbulent flow problems, appl. of mixed finite element methods 79−64638
incompressible two-phase flow without mass transfer, turbulence eqns. *(French)* 79−72925
incompressible viscous fluid, homogeneous turbulence, systematic perturbation method 77−31282
incompressible viscous fluid, turbulently generated sound, pressure probability struct. 80−33581
individual realisation laser anemometry, sampling bias evaluation 77−58810
induced turbulent flow and natural convection, combined effect heat transfer rates 79−90243
infinite-dimensional turbulence, short-time and renormalised expansions 78−24670
inhomogeneous, simulation, clipping approx. 80−19331
inhomogeneous turbulence with unidirectional mean flow, Reynolds stress 79−37296
inhomogeneous turbulent flow scale characts., vortex struct. relationship 80−53754
initial flow turbulence effects on power spectrum of wall-pressure fluctuations 79−18875
instability, post-, in class of smooth functions, mathematical model 80−69649
integro-differential formulation 79−32468
interaction of external disturbance, stability 77−54977
interaction representation in turbulence theory 79−41673
interferometric measurement, turbulence spectrum reconstruction 79−2816
intermittancy in turbulence onset 80−59013
intermittency determination from passive scalar probability density function 78−42611
intermittency model in three-dimensions 78−59376
intermittent characteristics using temp. as passive scalar contaminant 77−54976
intermittent transitions to turbulence, intermittency in dissipative dynamical systems 80−106781
intermittent turbulent flows, conditioned averages 77−68574
internal flow, book contrib. 77−58654
internal flow sytems, press. losses rel. to component interactions 77−65794
internal separated flows at large Reynolds number, Poiseulle flow development in channel 80−53755
internally finned tube and annuli, turbulent flow and heat transfer 79−81979
interplanetary magnetic field, turbulence rel. to mean free path of low-rigidity cosmic rays 80−98524
interplanetary plasma turbulence spectrum, determ. from radio sources scintillation spectra 80−46361
interplentary turbulence, rel. to Earth bow shock theory 80−85816
interstellar clouds, turbulence effects on collapse, three-dimensional numerical models 80−56910
interstellar contracting clouds, influence of turbulence on solid particles growth 80−62251
interstellar dust, turbulence effect on coagulation 79−35356
turbulence continued
interstellar gas, differential rot. ahd helical turbulence rel. to galactic dynamo 78−81685
interstellar gas turbulence, effects on grain collisions 80−77470
interstellar medium, cosmic ray generated anisotropic MHD turbulence 77−45532
interstellar medium, inertial range of weak MHD turbulence 77−45528
interstellar medium, turbulence, rel. to pulsars, modified Rickett diagram 77−17609
interstellar medium turbulence rel. to scintillation, analytic soln. of second-order moment eqn. 80−26726
interstellar molecular clouds, microturbulence, systematic motions and spectral line form. 77−33586
interstellar molecular clouds, turbulent motion and radiation transport rel. to line profiles 78−93347
inviscid, two-dimens. turbulence, equilib. energy spectra 80−38383
inviscid flow on sphere, statistical mech., atm. appl. 80−90152
ion-selective membrane, flicker noise and turbulent convection in depleted layer 78−48692
ionosphere, heating by powerful radio emission with random modulation of carrier freq. 80−109310
irradiance probability distrib. in saturation regime 79−76588
isobaric turbulent reacting jet issuing into costream 78−63509
isotope cyclone separator, 3D flows and turbulence intensity *(Chinese)* 79−36418
isotropic, energy spectral density calc. 79−86410
isotropic, helicity effect at high Reynolds no. 77−58657
isotropic, in entrained air bubble channel flow, spectral struct. 78−34112
isotropic, multiple-scale cumulant expsn. 78−34111
isotropic, response to change in principal aces of strain tensor *(French)* 78−18276
isotropic, simulation, subgrid-scale models 79−50709
isotropic, theory rel. to expt. data 78−1646
isotropic and homogeneous self-similar behaviour *(French)* 80−74838
isotropic theory, second order spectral local isotropy in turbulent scalar field 77−54980
isotropic time depend. turbulence, theory 78−32682
isotropic turbulence, conditional flow struct., anal. 80−19335
isotropic turbulence spectrum determ. from optical meas. 79−3634
isotropic turbulent flowfield, smoke downstream diffusion, mass transfer characts. 80−14668
isotropic two-dimensional, energy dissipation, correl. relationships and Taylor length scale 80−19334
isotropic vorticity theory, appl. to adverse pressure gradient flow 80−59047
iterative approach to strong turbulence theory 80−92117
jet, 2Z 79−64807
jet, acoustic emission from coherent structs. *(French)* 77−65775
jet, acoustic noise due to turbulence, directivity and Mach no. depend. 79−72921
jet, air, subsonic, fully pulsed, near field vel. meas. 80−19540
jet, annular, discrete freq. noise generation props. and flow pattern 77−51092
jet, annular, outer mixing region coherent structs. 79−32613
jet, axial momentum conservation 78−67240
jet, axially symmetric, impingement on plate, heat transfer characts., inner peak in heat flux 80−28540
jet, axisymmetric, impingement region, model 77−42886
jet, axisymmetric, modelling of large eddies, harmonic forcing effect 78−90957
jet, axisymmetric, vel. distrib. and swirl effects, low speed results 79−46351
jet, axisymmetric turbulent impinging, mass transfer 77−42887
jet, buoyant, in uniform environment, near field 79−32607
jet, buoyant, integral props. 77−58752
jet, buoyant, turbulence struct. 77−58753
jet, buoyant, turbulent in cross flow, finite difference method 78−90907
jet, chem. reaction at metal surface, modelling 78−64885
jet, coaxial, initial swirl of inner and outer flows effect on aerodynamics 77−68652
jet, coaxial round, turbulent mixing, eddy Reynolds number var. 78−75179
jet, cold, subsonic, acoustically active turbulent structs., conditional sampling anal. *(French)* 79−18881
jet, convective heat transfer to flat plate 79−1226
jet, disperse phase turbulence struct. modification model, energy dissipation 77−58769
jet, drop motion 78−5789
jet, dye-dilution laser induced fluoresc. meas. 78−30397
jet, free, turbulent flow, large scale struct., discrete values meas. 78−90840
jet, heat transfer during impingement on sphere or cylinder rel. to turbulence *(Russian)* 78−38327
jet, heated, joint probability densities and quadrant contribs. 79−32597
jet, impinging on curved plate, surface press. fluctuations 78−9666
jet, incident on plate, convective diffusion 78−67242
jet, instantaneous two-dimens. conc. meas. by Mie scatt. from seeded flow 79−41670
jet, large scale struct. and vortices, linear stability theory 78−26179
jet, large-scale turbulent struct., noise prod. 79−7394
jet, mixing zone coherent struct. of hot free jet 78−94788
jet, noise, coherent struct. 77−89176
jet, noise modelling by geometrical acoustics, outside silence cone 78−34177
jet, noise radiated from convecting quadrupoles, flight effects 79−32601
jet, nonisothermal, acoustic energy 77−7431
jet, nonisothermal, turbulence fluctuation meas. by hot-wire anemometer 77−35189
jet, nonisothermal axisymmetric turbulent transfer, vel. and temp. fluctuations, correl. coeffs. 78−83445
jet, plane, development and struct. 79−37371
jet, power law, rel. to marginal instability principle 79−32458
jet, propag. in deflecting airstream, trajectories, density influence 79−86480
jet, radiative transfer 78−94578
jet, round jet/plane jet spreading rate anomaly 78−63469
jet, signal transit velocities 77−35192
jet, slowly diverging, linear instability modes 77−3856
jet, sound power output, jet into gas with different sp. ht. 78−94789
jet, sound transmission expts. 79−32600
jet, spreading rate, virtual origin 77−3855

turbulence continued
jet, submerged, US scatt. 78−50992
jet, subsonic and supersonic, laser velocimeter correlation meas. 80−106785
jet, subsonic hot free, coherent structures in mixing zone, acoustic effects 79−4052
jet, surface age meas. 78−83442
jet, three dimens., expt. 78−1702
jet, three-dimensional circular turbulent 79−98769
jet, trailing edge noise mechanism 79−41720
jet, transverse, turbulent mixing with high Mach number stream 79−32603
jet, turbulent, axisymmetric, spatial correlations 80−19539
jet, turbulent, deflected, 3-dimens. vel. field, finite-difference soln. 78−47009
jet, turbulent, free, three-dimens., k-ε model calc. using finite difference procedure 80−19468
jet, turbulent, injected into crossflowing stream, trajectory predictions 77−51094
jet, turbulent and heated, temp. and vel. meas. 78−94784
jet, turbulent mixing layer, conditional meas. 79−32598
jet, turbulent mixing layer, wave dispersion on vortex pairing 79−32612
jet, turbulent source coherence effect on noise 79−32599
jet, wavelike eddies 77−89175
jet array, propag. in bounded drift flow 77−84288
jet diffuser efficiency, fine turbulent jet injection at outlet sections 78−1707
jet engine exhaust noise, orderly struct. as a source 78−94786
jet engine exhaust noise, source coherence 78−94787
jet entrainment mechanism 79−41721
jet expansion into uniform counterflow, velocity field soln. 79−14445
jet flame, stabilisation using thick burner rim *(Japanese)* 77−68706
jet flow, moderate Reynolds no., time domain analysis 78−18329
jet flow, simulation by discrete eddy system, statistical charact. 79−98771
jet flow mixing length calc., two-equation model solution, using finite element method 78−38295
jet flow modification of uniform flow along a plane wall *(German)* 80−6120
jet flow past ellipsoid of revolution 79−81937
jet flows, correlation techniques to detect azimuthally coherent structures 80−53765
jet impinging on liq. pool, submerged biphasic region 77−31350
jet mixing layer, large-scale turbulence and vorticity 79−32611
jet mixing layers, exptl. investig. of large scale structs. *(French)* 79−41728
jet mixing noise, aircraft, in-flight simulation expt. 78−1501
jet mixing noise generation, eval. of Lighthill analogy using LV turbulence, source location and spectral noise data 80−69803
jet mixing rates with self-excited acoustic oscills. 78−47008
jet noise, aeroacoustic interaction, review 80−87765
jet noise, cross-spectral densities, extension of Ribner's theory 80−69804
jet noise, turbulent, press. depend. for choked and subsonic jets *(Chinese)* 78−67235
jet noise in flight, prediction, importance of jet temp. 80−69814
jet noise prediction, nonlinear Lilley equation 80−69805
jet noise source characterisation, conditional sampling 79−41722
jet noise source distrib., from far-field cross-correlations 77−84039
jet noise sources, meas. using shallow surface-wave simulator 77−80146
jet on cylinder wall, heat transfer and fluid mechanism study *(Japanese)* 80−83800
jet pseudoturbulent mixing efficiency in fluidised bed 77−39342
jet structure, turbulence and coherent eddies, review 80−48760
jet turbulence, interaction with pure tone sound 78−94790
jet turbulence caused by nozzle wall laminar boundary layer 77−55065
jet type turbulent flow, concentration-pulsation eqn. use 79−90300
jets, axisymmetric and flat, heat transfer in vicinity of stagnation point, turbulence effect 80−48697
jets, axisymmetric subsonic and supersonic, in parallel stream, turbulence meas. 77−31349
jets, behaviour in presence of body forces and non-self-similarity 78−1706
jets, compressible coaxial submerged and coflowing, mixing coeff. correls. 77−42883
jets, confined, flow pattern and turbulence quantities prediction *(Japanese)* 79−18923
jets, curved, investigation along curved streamline 77−51095
jets, film cooling performance 80−79272
jets, free, turbulent, acoustic effect, dual nature 78−18325
jets, influence of drag reducing polymers on cavitation inception 80−106823
jets, power spectrum of scattered acoustic signal 79−94695
jets, turbulence models for flow patterns 79−64720
jets, turbulent, heat, mass and momentum transport, into ambient air 78−51210
jets, turbulent mixing, conc. fluctuations 77−39318
jets, turbulent two-dimens., parallel, mixing 78−51209
jets, two-dimens., vel. and press. distribs. at confluence 77−24004
jets, two-dimensional water, sensitive to sound, behaviour *(Japanese)* 80−79376
jets, velocity and concentration profiles in core and transition regions *(German)* 78−34172
jets, vertical, round, effect of buoyancy on turbulence struct. 79−55403
jets, vortex-street structure 80−10280
jets and plumes, swirling, integral method model 79−60040
jets and wakes, intermittency determ. from probability density function of passive scalar 77−3827
jets of different density entering air, turbulent flow 79−72922
Jupiter convective interior, turbulent viscosity and tidal Q 77−29713
Jupiter magnetosphere, Ganymede wake turbulence rel. to field-aligned current obs. 77−25975
kinetic model *(French)* 79−14382
kinetic theory, fundamental soln. 80−27137
kinetic theory 77−75891
Kolmogoroff's −5/3 power law, statistical approach 78−1644
Kolmogoroff's theory, high Reynold's no. model, laser beam atmospheric propag. 79−7368
Kolmogoroff $r^{2/3}$ law 79−68682
Kolmogorov's −5/3 power law, statistical derivation by turbulent-viscosity approach 78−90837
Kolmogorov turbulent spectrum, direct interaction model 78−18275
turbulence continued
ladle filling, turbulent flow, math. anal. 79−46294
Lagrangian and Eulerian vel. autocorrelations 79−32469
Lagrangian history turbulence approximations, velocity and strain-based 79−59969
Lake Tahoe, California-Nevada, LF turbulence spectra in mixed layer 77−21804
large eddy simulation, numerical technique 78−9628
large eddy simulation 80−19333
large scale steady state 3-D turbulence, helicity 78−75122
laser beam degradation by two-dimens. turbulent jet 80−14375
laser beam path design for reduced thermal blooming in axial pipe flow 79−94268
laser beam propagation, thermal turbulence effects *(French)* 77−24038
laser Doppler anemometry on transparent turbulent electromagnetically driven flow 80−103090
laser Doppler velocimeter, for turbulent flow velocity meas., redesign 78−1245
laser Doppler velocity measurements, single scattering particle, data reduction 77−39379
laser instability, example from synergenetics 80−9848
laser light scatt. meas. of turbulent flow 77−35288
laser radiation thermal self-interaction in turbulent absorbing liq. medium 80−91868
laser scattered light intensity, recurrence rate correl. 78−66760
laser-Doppler anemometry and photon correlation for turbulence length scales 80−87828
light intensity in turbulent medium, two-freq. fluctuations correl. 79−98280
light propagation, turbulence spectrum reconstruction from time correlation function 77−19178
light propagation problems, probability distrib. of sum of N complex random variables 77−50617
light propogation in turbulent medium, space struct. of strong intensity fluctuations 79−98278
light scattering from turbulent flow inhomogeneities 77−54670
light scintillations in weak turbulence, source temporal coherence effects 79−50223
line vortices 79−27649
liquid, flow visualisation techniques eval. 77−58817
liquid, parametric method of integrating motion eqns. *(Russian)* 79−41672
liquid crystal, dissipative structures in turbulent movement *(Russian)* 78−55808
liquid crystals, bubble domains, generated by electrohydrodynamic turbulence *(Japanese)* 78−22413
liquid film, gas absorpt. accompanied by first order reactions 79−69327
liquid flow in heated tube at supercritical press., heat transfer 78−71316
liquid jet launched into transverse liquid flow, calc. velocity and width *(Russian)* 77−68653
liquid jets, breakup length 77−84293
liquid layer between surfaces in relative motion 79−1255
liquid metal in periodic EM field, mean MHD flow, turbulent stresses calc. *(Russian)* 78−47056
liquid metal jets, 3D fluid flow model induced in ladles or holding vessels 80−10278
liquid metal tube flow, turbulence, heat transfer, thermogravitation effect 78−71315
liquid metals, flow in tube in mag. field, turbulent transfer coeff. *(Russian)* 78−75220
liquid metals, flow velocity structure, in nonuniform const. mag. field *(Russian)* 78−75215
liquid metals, heat transfer with gas bubbled through *(Russian)* 80−38395
liquid metals, turbulent heat transfer, Nusselt no. calcs. 77−31304
liquid metals, turbulent heat transfer charact. 78−42602
liquid metals, turbulent temp. fluctuations, in heated pipe flow, theory 77−84246
liquid motion in channels with permeable walls, hydraulic resistance 78−5797
liquid pipe flow, heat exchange and resistance calc. 78−94819
liquid pipe flow, heat transfer, thermoacoustic oscills. 78−9635
liquid velocity and turbulence meas. by image sensor 79−77297
liquid-liquid dispersion, droplet size spectra in turbulent pipe flow 78−67247
liquid-liquid dispersion, in turbulent agitated motion, drop size limits 79−68787
liquid-liquid mass transfer in systems agitated by submerged jets 78−22393
liquids of different density, turbulent mixing at an accelerating interface 80−6030
LMFBR, wire wrapped assemblies, subchannel flow rates, meas. using turbulent flow split expt. 79−59140
LMFBR fuel rod, hydraulic anal. of turbulent fluid flow by Galerkin method 79−30893
LMFBR fuel subassembly temp. noise prediction, Monte Carlo approach 79−13392
LMFBR LOF accident, surface ablation in impingement region of liquid jet 79−54549
LMFBR wire wrap spaced rod bundles, laminar, transition, and turbulent parallel flow press. drop 79−26478
LMFBR wire-wrapped assemblies, turbulent mixing expt. and model 80−590
local model of turbulent medium 77−58650
localised optical heating, principle of meas. on flows *(French)* 77−31406
Loch Ness, Scotland, turbulence and mixing meas. 77−70702
log-amplitude and phase time fluctuations, turbulence spectrum parameters influence *(Czech)* 80−9774
lognormality of gradients of advected scalars 78−67181
longitudinal vel. fluctuations and zero crossings in turbulent flows, maxima universal trends 79−77076
Lorentz model, simplest limit cycle analytic form 79−86405
Lorenz attractor, origin and struct., appl. to specific model systems 78−29054
Lorenz attractor and onset of turbulence 77−11173
Lorenz attractor struct. 78−46944
Lorenz attractors, topological classification 78−77720
Lorenz equation in high Rayleigh number limit, periodic soln. using perturbation theory of nonlinear oscills. 79−68681
Lorenz model, chaos and limit cycles 78−57787

turbulence continued
Lorenz model, Feigenbaum sequence of bifurcations 80−83783
Lorenz model, intermittency, first limit cycle-second strange attractor transition 80−31674
Lorenz model, new interpretation and size of strange attractor 77−75883
Lorenz model, periodic solns. and bifurcation struct. at high R 79−81692
Lorenz model, statistical dynamics study using stochastic differential equations 79−92949
Lorenz model, transient behaviour in periodic regions 79−17346
Lorenz model, transition between turbulent and periodic states 78−71317
Lorenz model, turbulence in dissipative dynamical systems 80−90784
low and high turbulence flows, hot wire measurement based analysis 78−59511
low dimensional chaotic dynamical system for turbulent flow, time series geometry 80−103014
low frequency sound radiation due to the interaction of unsteady flows with a jet pipe 80−69787
low Mach number aerodynamic noise theory 80−69796
low quality flow boiling, turbulent forced convection and nucleate boiling heat transfer 80−14696
low Reynolds turbulent flow, vel. distribution anal. using hydrogen bubble method *(Japanese)* 80−106788
low turbulence flow, laser dual-focus flow velocimeter meas. 77−39381
low-intensity flows, turbulence meas. 79−50826
Lucke's theory of turbulence 80−99990
lunar lavas, sinuous rilles form. turbulent flows erosion 77−60654
lung, nonlinear mathematical model, parameter tracking adaptive algorithm 77−60227
lung and vascular tree structs., optimisation of diameters and bifurcation angles 78−11683
α Lyrae (Vega), microturbulence parameter from Copenicus UV spectral anal. 80−26856
Mach wave radiation of hot supersonic jets 80−69894
macroturbulence effects on stellar temp. models derived from multiplet line-centre fluxes 79−5806
magmas turbulent mixing, implications of density var. among mid-ocean ridge basalts 80−56460
magnetic dynamo α-effect, determ. for slow and fast rot. 79−40069
magnetic energy transfer in weak mag. fields 78−18350
magnetic field dynamics, turbulent dynamo theory 80−32880
magnetic field growth in helical turbulence 79−18967
magnetic gyrotropy in a medium with inhomogeneous density 79−94730
magnetostatic turbulence, cosmic rays spatial diffusion coeffs. calc. using nonlinear particle trajectories 77−45262
main eddies of recirculating zone induced by impulsively started cylinder, origin *(French)* 80−53784
main-sequence stars envelopes, hydrodynamical instabilities constraints from Li, Be and B obs. 78−93202
marine thermocline, turbulent quantities computation using Mellor-Durbin theory 80−4041
mass transfer by forced convection, at rough surfaces in annuli, rate meas. 77−27532
mass transfer cell with vibr. mixing for liq.-liq. systems 79−37425
mass transfer from rotating cylinders 78−42613
MBBA, nematic liquid crystals, wave number spectrum of dissipative structures 80−38904
mean flow near-wake characts., two-dimens. bluff models 78−42609
mean Reynolds stress turbulence models, triple vel. correlation 78−79309
measure determination problems 79−81854
measurement by laser Doppler anemometers, book contrib., review 80−19538
membrane vicinity, cation-selective type, turbulent flow meas. using scatt. laser radiation Doppler shift 79−46301
memory effects, relaxation eqn. description of Reynolds stresses *(German)* 77−11175
memory effects in turbulent flows 78−79340
metastable chaos, transition to sustained chaotic behavior in Lorentz turbulent convection model 80−4643
methane-air flame, Raman scattering diagnostics of turbulent flow field 78−18328
MHD, turbulence, development and generation *(French)* 80−79407
MHD, turbulent duct flow, turbulence suppression in liq. 78−94844
MHD channel flows, asymptotic theory 78−30368
MHD effects in turbulent medium with density gradient, appl. solar convection *(Russian)* 78−47055
MHD expt. to test turbulent flow relaxation theory 79−98814
MHD flows, residual disturbances after laminarisation, entry effects 80−6160
MHD flows and turbulence, second Bat-Sheva seminar, Beer-Sheva, Israel, (March 1978) 79−60070
MHD helical turbulence, nonlinear dynamo effect 77−3873
MHD jets, laminar and turbulent, elec. cond. fluid with transverse mag. field 79−77261
MHD shear flow, energy transfer from turbulent to mean motion 77−35252
MHD turbulence, gyrator effects 78−42670
MHD turbulence, helical, numerical simulation 78−38415
MHD turbulence, low mag. Reynolds number 78−94845
MHD turbulence, numerical simulation and closure techniques 79−90343
MHD turbulence, one dimens. model, conditions for global regularity and onset of singularities *(French)* 79−50803
MHD turbulence, statistical theory distrib. functions 79−37412
microjet noise and micropore diffuser-muffler design 78−30335
minicomputer-based scheme for turbulence measurements with pulsed Doppler ultrasound 80−26435
mist formation in turbulent convection field, critical supersaturation model 80−64611
mixed convection to air in a vertical pipe 78−90896
mixing, zero gradient points 78−94648
mixing flow, simultaneous laser measurements of instantaneous vel. and conc. 77−35287
mixing layer, turbulent, quasi-two-dimens. eddy-struct., vortex rolls 79−81896
mixing layer, vel. and temp. distribs., conditional averaging *(Russian)* 78−38296
mixing layer description from transient vortex flow results 80−1533
mixing layers, 2-dimens., statistical model of turbulence 79−68680

turbulence continued
mixing mechanism theory in turbulent flows with coherent structs. 79−7369
mixing nozzle reattachment of two-dimensional turbulent jet 79−23347
mixing process induced by the vorticity associated with the penetration of a jet into a cross flow 79−7396
mixing with react. of miscible reactant streams, simulation 80−64651
model conduction problem, MacCormacks time-splitting technique stability anal. 79−55361
modelling, large eddy simulation technique for high R turbulence flows 79−64639
modelling, subgrid, with classical closures and Burgers' eqn. 80−19332
models, integral-relation model appl. 80−43691
models, two-dimens., vortex and Fourier mode 78−46945
modified dissipativity for a non-linear evolution equation arising in turbulence 79−94594
molecular gas radiation in the thermal entrance region of a duct 80−6051
momentum transfer in curved pipes 79−68814
moving boundaries in two-phase turbulent flows 79−18932
moving surface, free liquid layer, laminar and turbulent flow, Navier-Stokes anal. 79−94589
multi-point turbulent eqns., closed set obtained with mean value theorem 78−67182
multi-scale, mixing and decay of turbulence field, use of significant dynamic length scales 79−86404
multicomponent mass transfer in turbulent flow 79−32477
multidimensional two phase flow eqn. derivation, general constitutive principle appl., turbulent stresses 80−10297
multiphase flows, various aspects *(German)* 77−15109
natural convection effect on heat transfer 78−5739
natural laminar and turbulent convection, from isothermal spheres, correlation eqn. *(German)* 80−33607
Navier-Stokes equations, averaged, closure, dynamical system approach 78−46941
Navier-Stokes equations, comparison of models 78−46939
Navier-Stokes equations, dynamical systems approach, strange attractor 78−46942
Navier-Stokes equations, finite element methods 79−1162
Navier-Stokes equations, turbulence and infinite bifurcations, five-mode truncation 80−52031
Navier-Stokes equations for turbulent and transition flows, num. soln. methods 77−54979
Navier-Stokes random forced flow ensemble mechanics 77−7363
Navy vessel fracture mechanics and flow separation, instability phenomena 80−99971
near wake of disc, annular jet, vel. characts. 78−38336
near wall vel. meas. for wall shear inference in turbulent flow 78−34234
near-critical fluids in turbulent flow through tubes, heat transfer num. prediction method 77−42832
near-wake behind step with supersonic jet 79−14448
needle shaped particles, diffusion orientation on filtration surface in turbulent flow 80−33668
Newtonian fluids, momentum transfer in curved pipes 79−68813
noise generated aerodynamically *(French)* 79−77090
noise generated by an eddy *(French)* 80−19363
noise generated by turbulence, coherent struct. model 78−94675
noise generation by laminar flames in tubes 79−86422
noise generation by transonic open rotors 80−69599
noise source mechanisms, expt. determ. in gas turbine combustors 80−69597
noise sources produced by fluid inhomogeneities 77−11181
noise spectrum, turbulent jet, approx. calc. 78−67236
nomogram for heat transfer coefficient determ., water flowing in pipes or tubes 78−9641
non Eulerian renormalized expsn. 79−64640
non isotropic homogeneous, pure rotation influence *(French)* 80−33568
non-Gaussian aspects, num. model approach 77−51037
non-isothermal flow, turbulence measurement, laser Doppler velocimetry appl. 79−41776
non-Newtonian flow, book contrib. 77−58775
non-Newtonian flow in noncircular pipes 78−18315
non-Newtonian fluid mixing, convective heat transfer theory 79−77094
non-Newtonian fluids, turbulent flow in absence of anomalous wall effects 80−69880
non-self-similar turbulent jets, flow restructuring and relaminarisation 79−98770
nonbuoyant plume, advection of scalar quantities, stochastic props. 79−32471
noncircular pipes, laminar and turbulent flow 78−18315
nonequilibrium fluctuations at onset of turbulence 78−18272
nonisothermal flow in horizontal cylindrical channel, gravitational field effects 78−83365
nonisothermal streams, turbulent velocity pulsations meas., procedure 80−19514
nonisothermal turbulent heterogeneous jet entering air filled half space 80−64599
nonisothermal turbulent jet, physiochemical processes, temp. and conc. effects 80−14849
nonisotropic, homogeneous, temp. distrib. degeneracy, statistical characts. 77−84232
nonisotropic scalar field, dynamic eqn. for concentration correl., energy spectra 77−14992
nonlinear cascade model, time depend. scaling relations 79−37300
nonlinear cascade models for fully developed turbulence 77−46995
nonlinear diffusion-reaction problems with time-dependent diffusion coefficient 79−98823
nonlinear dispersive system with small dissipation, statistical theory 78−70058
nonlinear interactions in turbulent and convective flows, barotropic and baroclinic instability 79−98706
nonlinear internal waves, turbulence, numerical anal. 80−14721
nonlinear media containing chaotic inhomogeneities, equation closure for average field 79−81601
nonlinear perturbations development in turbulent flows, predictability problem *(Russian)* 77−62238
nonlinear rheological fluids, functional description method for turbulence 79−72913
nonlinear wave in turbulent medium, with random inhomogeneities *(Russian)* 79−27134

turbulence continued
nonlinear wave modulation in strongly dispersive systems with random field 78−36840
nonsteady one-dimensional liquid flow, analytic method calcs. 80−59009
nonsteady turbulent MHD flows in plane channels and circular tubes 80−48810
W.North Atlantic Ocean, mesoscale motion space and time scales 78−49035
nozzle expansion in turbulent flow, downstream heat and mass transfer 80−1669
nozzles, quarter circle and combined, investigation *(Russian)* 78−42689
nuclear heat exchanger, shell-and-tube, flow distrib. anal., rel. to CRBRP-IHX 77−42052
nuclear reactor, two-phase flow in pin bundle, two fluid model 80−91209
nuclear reactor coolant axial flow in bare rod bundles, turbulence modeling 80−32338
nuclear reactor fuel element, turbulent flows in tubes, Nu-number determ. *(German)* 77−38432
nuclear reactor turbulent flow in fuel rod bundles 78−37400
nuclear reactor turbulent flow through wall subchannel of rod bundle 78−41802
nuclear reactor turbulent-laminar flow transitions in rod bundles, Reynolds numbers determ. 77−42036
nuclear reactor wire-wrapped core assemblies, turbulent flow split modelling and expts. 80−95370
numerical methods, conf., Swansea, Wales, July 1978 79−1155
numerical methods in statistical hydrodynamics 77−35121
numerical modelling 77−80144
numerical simulation, intermittency effects 78−59375
numerical simulation with three-dimens. vortex in cell method 80−19330
oblique flat plate, MHD flow patterns, at high Reynolds number *(Japanese)* 79−64786
oblique high-drag heat exchangers, turbulent flow and pressure losses 79−94710
observable motions, Navier-Stokes eqns. 80−10230
obstacle in potential flow, vortical and entropic distortions 79−32532
ocean, exptl. study of nonlinear baroclinic instability and mode selection in large basin 80−85669
ocean, meas., metal-film temp. and vel. sensors and self-propelled research vehicle stability evaluation 79−5672
ocean, realistically stratified, nonlinear energy and enstrophy transfers 80−101370
ocean, small-scale, statistical patterns 78−3802
ocean, Southern Hemisphere, eddy field rel. to poleward heat fluxes 79−48496
ocean, strong interaction with gravity waves *(Russian)* 77−81904
ocean, transport across diffusive interface in presence of externally imposed turbulence 77−41057
ocean, turbulence rel. to model of annual temp. var. and climatology 78−20433
ocean, turbulent spot in stably stratified fluid, dynamics *(Russian)* 78−40558
ocean, vel. fluctuations scaling in surface mixed layer 77−45009
ocean, vertical eddy viscosity effects on Rossby and Eady waves 80−51404
ocean, vertical struct. characts. 80−12426
ocean, weak turbulence of internal waves *(Russian)* 77−33089
ocean, wind forcing vars. rel. to turbulence and sea surface temp. response 79−48505
ocean, wind-induced turbulence energy distrib. rel. to mixed layer evolution *(Russian)* 80−94529
ocean current structure function for intermittent turbulence *(Russian)* 78−32109
ocean eddy fields in N.Atlantic and N.Pacific, geographic var. of intensity 77−9431
ocean horizontal turbulence, spectral struct. 78−3790
ocean inertial oscills. radiation damping, wind mixed layer turbulence 79−39730
ocean intermittent turbulence, statistical anal. *(Russian)* 77−29310
ocean internal waves and mesoscale eddies, weak interaction 77−9433
ocean reverberation spectra rel. to remote detect. of turbulence 78−38124
ocean small scale turbulence, anal. of spectra *(Russian)* 79−88360
ocean small-scale turbulence, study via towed instruments carrier 80−36423
ocean small-scale turbulence in upper layer 77−64318
ocean solitary Rossby waves over variable relief, transition to turbulent behaviour from numerical expts. 80−101372
ocean surf zone, turbulent dissipation rel. to wave height and wave celerity 77−45012
ocean synoptic eddies 79−5491
oceanic mesoscale eddies generation, numerical simulations with two and three layer quasigeostrophic models 79−57950
oceanic turbulence, generation *(Russian)* 78−16022
one-exponent scaling for very high Reynolds no. turbulence 78−42592
onset, fluctuation spectrum calc., appl. to Rayleigh Benard flow 80−23989
open cct. wind tunnel, exptl. procedures to improve characts. *(Japanese)* 80−19528
open channel thermally stratified flow, eddy diffusivity buoyancy effects, obs. 78−90904
optical beam, diffracted rays in turbulent medium 80−48153
optical beams in randomly inhomogeneous media, strong fluctuations of fields 80−99634
optical crossed beam correlation method, localised turbulence props 78−34223
optical phase fluctuations in turbulent medium 78−33668
optical plane wave intensity fluctuations in turbulent medium *(Russian)* 78−1156
optical propagation, laboratory-generated turbulence simulating atmosphere 80−9803
optical propagation in turbulent water, refr. index spectrum of temp. or salinity fluctuations 79−5487
optical resolution through turbulent medium, adaptive phase compensation 77−46692
optical source in turbulence, asymptotic parameters, scintillation scales 77−606
optical wave, log-amplitude fluctuations spectra, turbulence spectra parameters determ. 80−95797
turbulence continued
optical wave propagating through turbulence, scintillations meas. detector aperture effect *(Slovak)* 80−63921
orifice plate calibrations, extrapolation to high Reynolds no. 80−53833
oscillating jet in moving air stream, vel. meas. 78−22396
oscillators in convective biperiodic regime, velocity oscills. 80−53759
oscillatory turbulent subcooled flow, transient radial heat transport effects 77−42834
over-wing-blowing configurations, aerodynamic characts. determ. 78−5774
N.Pacific Ocean, turbulence rel. to regional depend. of low-freq. acoustic attention 77−62090
tropical Pacific Ocean, vertical eddy coeffs. rel. to thermocline displacement, simple Ekman-type model 79−48498
parametrically excited nonlinear chain, stochastic oscills. *(Russian)* 79−55363
partially coherent source in extremely strong turbulence, irradiance scintillations 79−64176
particle acceleration by MHD shock turbulence 80−87894
particle acceleration in solar flares by cyclotron damping of cascading turbulence 79−44433
particle beams, charge density vol. distrib. in turbulent stream *(Russian)* 80−74288
particle behaviour in a turbulent field, dispersive approach *(French)* 79−72882
particle diffusion in electrostatic precipitators 77−3526
particle dispersion in turbulent fluid, steady drift effects, negative vel. correlations 79−90227
particle entrainment into fluid stream, force balance model 80−43690
particle meas. concentration in turbulent jet, laser scatt. technique 77−39372
particle-fluid mixture, energy balance in turbulent flow 77−47076
particles, falling under gravity, in rot. drying drum, turbulent gas flow 78−1728
particles in turbulent fluid, statistical motion, Eulerian direct interaction 80−53841
particles suspended in turbulent fluid, dispersion 78−14073
passage central region, anal. of flow differential eqns. *(German)* 77−23939
perforated plate composite cooling in turbulent gas flow 79−98716
perforated plate generators in wind tunnels, wake, shear flow and isotropic turbulence prod. 80−69770
period doubling and turbulence onset, analytical estimate of Feigenbaum ratio 80−87761
periodic flow, wake of circular cylinder, laser Doppler correl. technique 77−35278
perturbation potential for unsteady near-sonic flows *(German)* 80−1635
perturbation theory, quasi-periodic motion, asymptotic expansion method 80−17877
phase turbulent impinging jet, struct., vortex stretching 79−32476
photochromic flow visualisation, effect of turbulence on precision of vel. and vel. fluctuation data 77−68714
photon correl. velocimetry, turbomachinery and industrial burner velocity and turbulence profiles 79−60083
photon correlation technique, appl. to sinusoidally perturbed flow characts. meas. 77−42945
physical and mathematical description *(German)* 77−14996
physical and spectral space methods *(French)* 80−28493
physical processes, math. eqns., book contrib. 77−58652
pipe, circular, developing turbulent flow, using finite element method 79−1164
pipe, energy dissipation with flow effect on heat transfer rate 77−75905
pipe, entrance region, meas. and prediction 78−42666
pipe, local heat transfer to turbulent flow, superposition principle, expt. 78−83479
pipe, turbulent velocity profiles from stability criteria 79−50717
pipe entrance region, turbulence and heat transfer meas. and prediction 77−65734
pipe flow, correlations among turbulent shear stress, kinetic energy and axial intensity 79−3996
pipe flow, enlargement, contraction effect on flow characteristics 80−6154
pipe flow, fully developed, friction factors calcs. 79−98812
pipe flow, fully developed, turbulent velocity and temp. fluctuation struct. 79−77254
pipe flow, numerical anal. by finite element method 78−18341
pipe flow, response to change in roughness 78−47040
pipe flow, rough circular pipe, vel. and heat transfer calc. 79−60065
pipe flow, smooth- and rough-walled, turbulence struct. asymptotic similarity 77−35242
pipe flow, spectrum anal. of Reynolds stress *(German)* 77−11267
pipe flow, turbulence props. in core 77−68576
pipe flow, turbulence struct., wave model 77−58649
pipe flow, turbulence with low heterogeneity and anisotropy 77−39276
pipe flow, turbulence-generated noise, book contrib. 78−59385
pipe flow, use of eddy viscosity expressions for vel. profiles in Newtonian, non-Newtonian and drag-reducing flows 80−83789
pipe flow, wall region mass transfer 78−1638
pipe flow 79−64637
pipe flow turbulence struct. drag reduction with PEO 301 dilute soln. 78−26196
pipe flow turbulent entrance region, drag reducing fluid, expt. and anal. 78−63458
pipe flow with coolant temp. depend. thermophysical props., heat transfer 78−94821
pipe flow with heat transfer and chemical reaction 79−1271
pipe flow with thermal load variation, heat transfer 78−94820
pipe-jet system in crossflow, turbulent vortex shedding modes 80−10274
pipes, smooth, turbulent velocity profile, zero centreline velocity gradient 80−74974
pipes, turbulence and heat exchange 80−24094
pipes internal flow, turbulence rel. to vibrs. and broadband sound-power radiation 77−62104
pipes with regular artificial wall roughness, laminar flow stability, turbulence 79−98803
plane channel flow, subcrit. turbulence transition 80−106787
plane channel with parallel walls, turbulent flow stability *(Russian)* 79−37295
plane horizontal turbulent buoyant jet, parameter calcs. *(Russian)* 80−79373

turbulence continued
plane jet in laminar cocurrent flow, eddy viscosity decay, phenomenological theory 79−98700
plane parallel flow, free convection in Couette and Poiseuille flows, numerical simulation 80−99995
plane symmetric sudden expansion over backward step, turbulence and separation 80−53752
plane turbulent jet, outer intermittent turbulent motion structural charcts. 79−77208
plane turbulent jet spreading rate, external disturbances 77−55062
plane turbulent wakes, intermittent bulges, spanwise struct. 78−42610
planetary atmosphere studies by occultations, wavelength depend. of turbulence effects on refr. angles 79−48697
planetary atmospheres, effect on occultations, power spectra of phase and intensity fluctuations 79−40104
planetary atmospheres, turbulence effects on atmospheric profiles derived from radio occultations 77−60696
planetary atmospheres, turbulence effects on profiles from Doppler meas. of occultations 79−2498
planetary atmospheres, turbulence effects on profiles from intensity meas. of occultations 79−2499
planetary atmospheres, turbulent, effects of inhomogeneous background on radiation propag. 78−69679
plasma jet on baffle, flow behaviour and heat exchange 79−98774
plate heat transfer rel. to external liquid flow turbulence *(Russian)* 79−81873
plate heat transfer to highly turbulent air stream, expt. *(Russian)* 79−46318
plume, axisymmetric, buoyant, turbulence meas. 78−9637
plume, buoyant, turbulent, issuing vertically into stratified or uniform ambients 77−58756
pneumatic transmission lines with and without steady flow, freq. charcts. 79−77245
polyacrylamide solution, tube flow, friction and convective heat transfer, rheological changes effect 79−1220
polyatomic gases, turbulent tube flow, heat transfer 79−14395
polydisperse system, turbulent coagulation in force field 79−57297
polydispersed flows, Doppler signal spectrum 80−103081
polyethylene oxide, drag reduction props., Congo Red additive effects 79−64717
polyethylene oxide aqueous solns., spectroscopic obs. of structural variability WRT turbulent resistance reduction 77−7356
polyethylene oxide soln., drag reduction of highest mol. wt. fractions 77−68636
polyethylenoxide additive mixing, turbulent drag reduction, schlieren obs. 78−26163
polyisobutylene in toluene solution, effect of capillary materials on drag reduction *(German)* 80−87785
polyisobutylenes, dilute solns., turbulent drag reduction, influence of mol. wt. and mol. conformation 77−80189
polymer additive effects on turbulent cloud spreading 78−22383
polymer additives effect on grid-generated turbulence 77−68638
polymer additives in pseudo-turbulent flow, nonlinear dumbbell model 78−51206
polymer solns., mass transfer and drag reduction near wall, electrochemical methods 79−77138
polymer solns., turbulent flow through smooth and rough tubes, viscoelastic flow models *(German)* 77−11224
polymer solution, channel flow, drag reduction, viscous sublayer struct. 78−22385
polymer solution, drag reduction in pipe flow, flow time scales 78−22386
polymer solution, drag reduction in turbulent flow 78−26159
polymer solution, drag reduction in turbulent flows, book contrib. 78−59432
polymer solution, molecular weight distrib. effect on drag reduction in turbulent stream 78−83437
polymer solution, pipe flow, early turbulence 78−22380
polymer solution, rheology, rel. to turbulent drag reduction 78−22315
polymer solution, turbulence structure, drag reduction 78−22381
polymer solution, turbulent jet behaviour 78−1732
polymer solution, turbulent mass transfer to pipe flow 78−1695
polymer solution pipe flow, drag reduction 78−42631
pool boiling heat transfer from horizontal plates *(Japanese)* 78−67016
power spectra for chaotic transitions in Rossler dynamical system 80−53898
power spectra in turbulent flow *(French)* 78−59373
Prandtl and Schmidt numbers from modelled transport eqns. 80−19373
premixed turbulent flame combustion, heat transfer obs. and calc. *(French)* 78−94688
premixed turbulent flame struct. 79−86515
premixed turbulent flow, spectral interpretation of the propag. vel. *(French)* 79−4090
pressure fluctuations assoc. with general eddy turbulence field 80−53750
pressure fluctuations in homogeneous turbulence associated with shear and gravity effects, correlations *(French)* 79−50708
pressure fluctuations in jets, long range effects, book contrib. 80−1663
pressure nonuniformities, compact heat transfer surface development for heat exchangers with gaseous carriers 78−30296
pressures on a slender body at high angle of attack in a very low turbulence level air stream 79−77164
pressurised turbulent flow in circular annular slot, calc. 79−90229
preturbulence in Lorenz fluid flow model 79−72883
probabilistic nature, closure of Navier-Stokes eqns. 78−1643
propane-air flame, eddy entrainment and combustion in depth process, three-region model 79−100384
propane-air flame, premixed turbulent, three region model 79−100383
propane-air flame-generated turbulence, approach stream turbulence effects 79−64793
propane-air mixture, turbulent combustion, model 79−64792
propane-air mixture, turbulent combustion zone, initial temp. fluctuations influence on reaction evolution *(French)* 79−15998
prosthetic heart valves, disc, ball and tilting disc types, fluid stresses in vitro 78−81078
proto-galactic eddies, origin 78−54040
protoplanetary cloud, turbulence rel. to ang. momentum transfer by meridional currents 77−53436
pulsatile duct flow in presence of orifice plate, discharge and press. drop coeffs. eval. 78−30306
pulsatile flow, turbulent, wall region periodicity 77−54978
pulsating turbulent pipe flow, vel. distrib. 79−32666
turbulence continued
pulse luminescence using N laser for turbulence meas. 77−24041
pulse wave propagation in turbulent media, analytical theory 79−58550
pulsed laser radiation intensity fluctuations, thermal selfinteraction in turbulent medium 80−102781
PWR, LOCA anal., turbulent flow in fuel rod bundle with partial flow blockages 79−30898
PWR power plant flow pressure fluctuations as vibration source, relationships *(Hungarian)* 80−47685
quadratic structure functions describing random tilted phase fields 80−95799
radial gas content profiles of rising swarm of bubbles in vertical pipe *(German)* 77−47062
radiation from charge moving in randomly inhomogeneous media, fluctuation effects *(Russian)* 78−71017
radiation properties of a turbulent jet excited by a sinusoidal acoustic disturbance 80−69789
radiative heat transfer between isothermal parallel plates, flow models, numerical analysis 80−14547
radiative transfer in turbulent media, theory 78−94578
Raman scattering and laser Doppler velocimetry techniques for turbulent flow field investigs. 78−34224
random advection of chemically reacting species, probability density method 78−38418
random entropy fluctuations, interaction with nonuniform mean flows, turbulence generation 79−81851
random flow statistics analysed by photon correlation anemometry 80−64522
random media, two-frequency mutual coherence function for pulse propagation 79−76589
random velocity fields, radiative transfer and line form., intensity moment transfer eqn. derivation 80−52967
random vortex methods for two dimens. large Reynolds number flow, errors 78−42614
randomly stirred fluids, long distance behaviour 79−77082
randomly transitional phenomena in the system governed by Duffing's equation 79−54055
Rayleigh-Benard convection, periodic thermal perturbation, chaotic response 78−94685
Rayleigh-Benard convection, time depend. vel., turbulence transition 77−3824
Rayleigh-Benard convection, turbulence and intermittency, expt. 80−99998
Rayleigh-Benard instability and the evolution of turbulence 79−77074
Rayleigh-Taylor instability, turbulent stage anal. 79−41669
reactant concentrations in oscillatory chem. reactions, turbulence-like behaviour 77−4895
reacting binary mixture, turbulent flow, Reynolds eqns. and heat and mass transfer *(German)* 77−11281
reacting flow, modelling, probability approach 79−72959
reacting-diffusing system, turbulent spatio-temporal dynamics 78−56880
realizability inequalities, moments of one- and multi-dimens. variables 77−55006
reattachment points, visualisation using laser-induced fluoresc. 77−35283
recirculating flow in enclosure, heat transfer rates 78−38315
recirculating flows in general orthogonal coordinates 78−38297
recirculating laminar flow between shrouded rotating disks, num. soln. 79−64667
recirculating two-dimens. turbulent flow, numerical model calcs. 80−19358
recirculatory flows, mathematical and physical modelling 79−55364
rectangular channels, turbulent forced convection, momentum and heat transfer, secondary flows *(German)* 79−77259
rectangular duct, two dimens., Reynolds number depend. of bulk flow varibles 78−94827
rectangular prisms, galloping in smooth and in turbulent flow 77−75840
red cells in dilute suspensions, turbulent flow and effect on O_2 uptake kinetics 77−60223
reservoirs, turbulent viscosity and bottom friction of wind driven currents *(Russian)* 77−70700
review, current theory and practical examples *(French)* 80−64523
review of present research 79−98687
review of progress and problems 77−39278
review of progress in last thirty years 78−89290
review of theory 80−4536
Reynolds formulation of turbulent motion eqns., flow function 77−65735
Reynolds stress expt. analysis, using laser anemometry *(Italian)* 79−4094
Reynolds stress tensor for homogeneous turbulence *(French)* 79−46292
Reynolds stress turbulence models, realisability 77−68575
Reynolds stresses calculation using improved algebraic relation 77−42805
Reynolds stresses for nonisotropic turbulence *(Russian)* 77−58648
RF propag. in turbulent atmosphere, temporal freq. spectra of multifreq. waves 77−21834
rigid shell, oscillatory flow through perforated surface, sound generation 79−18950
river bed forms and unsteady processes 77−29352
rocket engines, meas. turbulence parameters in exhaust plume, laser crossed beam correl. method 79−86541
roll waves, small amplitude, behaviour in turbulent liquid films *(German)* 78−94756
Rossby nonlinear waves, stochastic closure 77−89133
rotating and curved flow, press. gradient-vel. correls. 78−26128
rotating cylindrical pipe turbulent nonisothermal flow, temp. fluctuation and pulsatile heat flux calc. 78−83475
rotating fluid, turbulent transport coeff., rel. to stellar interiors 78−36452
rotating fluid layer, heated, turbulent convection 80−100003
rotating liquid layer heated from below, form. and interaction of three-dimens. convective cells 79−14397
rotating liquids, turbulence onset *(Russian)* 79−46327
rotating short radial blade, laminar and turbulent flow, heat transfer 78−18294
rotational Couette flow, power spectra of nonlinearly coupled waves 78−30261
rotational flow avoidance, Navier-Stokes eqns. numerical solns. *(German)* 80−59057
rotor blades in low-pressure axial flow fans, turbulent noise modelling 77−42660

turbulence continued
rough surface heat transfer, turbulent flow in annular channels, result anal. 80−24003
roughened rod in smooth channel, turbulent convective heat transfer 78−51241
roughened surface, slope and intercept of dimensionless velocity profile 80−43701
round free jet, aerodynamic noise, propagation of wavelike disturbances 80−69806
Ruelle-Takens picture, bifurcations, semiflows and Navier-Stokes eqns. 78−46940
salt-brine interface, natural convection mass transport 78−30291
saltating solid particles in turbulent flow, accel. and forces *(Russian)* 80−1675
scalar field turbulent convection, probability density functions relax. 79−27622
scalar fields, transport eqn. for probability density function, closure 80−1585
schlieren instruments threshold sensitivity to turbulent inhomogenities 78−79134
sea surface layer, dynamically passive impurity propag. by currents and turbulent pulsations 80−31063
seawater, refractive microstrcutrure from diffusive and turbulent mixing 80−8326
secondary flows determ. from Reynolds eqn. 77−35237
seminar, theoretical descriptions 78−46938
separated flows, upwind and central difference schemes 80−28539
shadow device with photoelectric recording, for turbulence meas., resolving power 79−7210
shadow instrument with photoelec. recording, signal charact. rel. to turbulence spectrum charact. 77−35267
shadow methods for studying turbulence using reflection from a mirror in the medium 80−95801
shadow optical method for turbulent flow microstruct. investig., stat. analysis problems 80−19534
shaped edge cylinders in oscillatory flow, separation and vortex shedding forces 80−53825
shield-hot turbulent jet interaction, nonstationary heat transfer 80−92136
similar solns. of mean vel., turbulent energy and length scale eqn. 77−89102
single and twophase flow over rough surfaces, heat transfer effects 78−30297
single particle drag coeff. in still air 80−33620
skewness and flatness factors, Reynolds number dependence 80−53751
slag and metal flow in ESR process, mathematic model 77−73249
slightly dissipative systems, stochastic behaviour 80−22290
slightly heated cylinder, turbulent wake, conditional sampling study, turbulence struct. 80−6063
slowly moving vapour, film condensation heat transfer 80−19376
slurries, horizontal turbulent pipe flow, deposit vel. prediction 79−90312
small particles suspended in turbulent fluid, convection, mass transfer 80−87793
small scale magnetic fields in turbulence, Saffman's approx. 80−106851
small turbulent flow vel. meas., contactless optical Doppler instrument 78−90838
small-scale, governing eqn. 78−63419
small-scale, modified DIA approach and Kolmogorov's −5/3 power law 79−14383
smoke-motion, numerical anal. by finite-element method *(Japanese)* 80−69910
solar chromosphere, turbulent motions rel. to S I 1807 Å and 1900 Å profiles 78−57517
solar convection zone, turbulent viscosity rel. to mag. fields floating-up time and 11-year cycle 80−101580
solar convective zone, outward transport of ang. momentum rel. to equatorial accel. 77−53531
solar convective zone, two-dimensional stochastic motions rel. to differential rot. problem 77−53518
solar corona, prominence turbulence causing heating and MHD wave generation 80−72907
solar corona, turbulent heating role 80−12715
solar granulation, turbulent, model rel. to spatial power spectrum 78−65581
solar nebula, turbulent flows rel. to grains as isotopic anomalies carriers 80−26757
solar photosphere, complex study of 'microturbulent' vel. and damping const., introduction *(Russian)* 80−12719
solar photosphere, improved values for microturbulent and macroturbulent filter functions 78−20796
solar photosphere, microturbulent vels. and damping const. determ. errors *(Russian)* 80−72899
solar photosphere mesoturbulence, effect on spectral line widths, Fourier anal. appl. 77−17500
solar photosphere velocity field, spatially averaged props. 79−16912
solar photospheric convection, two-dimensional spectral anal. of disc centre granulation 77−53520
solar transition region, turbulence rel. to nonthermal motions and energy balance 80−90379
solar transition zone and corona, wave refl. and wave disorder 79−12453
solar wind, small-scale inhomogeneities spectrum rel. to whistlers 78−45173
solar wind plasma, turbulence spectrum from three-satellite radio wave propag. meas. 80−101518
solid and liquid particle interaction with turbulent flow field 80−43767
solid-fluid turbulent mass transfer with instantaneous chem. react., appls. 77−3888
solidification of liquid at its freezing temp. flowing into a convectively cooled tube 78−34001
soluble fluids in laminar, turbulent flows, stretch model appls. to mixing, diffusion, react. 79−94736
sonar, synthetic-aperture sonar systems in turbulent medium 80−96080
sound absorption, acoustic energy conversion to turbulent kinetic energy 78−63420
sound generation and propagation in flows, inhomogeneous convected wave equation 80−69813
sound generation by flow-acoustic coupling 80−69793
sound generation by head-on collision of two vortex rings 80−69801
sound generation by turbulence, mean flow calcs. of large eddy struct. and flow-acoustic interaction 80−69785
sound generation by turbulent dipole, model 77−68296

turbulence continued
sound generation in flows, conf. Gottingen, Germany (Aug. 1979) 80−67937
sound radiation from a simulated jet flow, calc. of vortex configuration and sound field 80−69786
sound source location techniques 80−69802
sound spectra radiated by gas jets, influence of closely located solid surfaces 80−69800
spatially decaying, relation to mixing across density interfaces 77−7373
spectra, meas. with randomly triggered pulsed-wire anemometer 77−15141
spectral energy transfer, localness 79−77081
spectral energy transfer in high Reynolds no. turbulence 77−27513
spectral evolution of strongly interacting waves 79−77144
spectral modelling of homogeneous turbulent fields *(French)* 77−75890
spectral space, comparison between kinematic and scalar fields *(French)* 78−87334
spectral temperature measurement, line-reversal method, turbulent fluctuation effects 77−30147
spectral tensors $\Phi_{ij}(K, t)$ and $t_{ij}(K, t)$ for homogeneous turbulent field, direct modelling *(French)* 78−90813
spectral transfer of kinetic energy, EDQNM theory *(French)* 79−81849
spectral variance estimation, rel. to data anal. 79−64641
spectrally local disturbance evolution in grid generated nearly isotropic turbulence 80−48681
spectrum reconstruction from transient charact. of shadow instrument signal 79−41674
sphere drag at Mach numbers from 0.3 to 2.0 at Reynolds numbers approaching 10^7 79−81919
sphere motion in infinite conductive fluid, variable mag. dipole located within sphere case 80−19519
spherical solids melting in turbulent carrier fluid, deformation and breakup 80−92646
spherically blunted cone with massive surface blowing, laminar and turbulent flows, shocks 80−38445
spot, entrainment behaviour, flow visualisation and laser Doppler velocimetry 78−26102
stably stratified fluid, turbulence rel. to mixed layer growth 79−55358
stably stratified fluid, turbulent spot, dynamics *(Russian)* 78−40558
stagnation flow turbulence about circular cylinder, visual study 80−96248
stars, massive, convective and semiconvective mixing 80−90405
stars in main sequence, diffusion and turbulence rel. to abundance anomalies 78−89198
stationary homogeneous, Kolmogoroff's spectrum and scaling law 77−62239
stationary turbulence, path integral functional description, variation principle 79−77083
statistical analysis, non Gaussian variation models, 1-D distributions 80−6032
statistical dynamics of chaotic flows 80−106786
statistical hydrodynamics for the Burgers turbulence *(Japanese)* 80−14667
statistical irreversibility, spectral energy distrib. 78−1642
statistical properties of turbulence in the inertial subrange of the spectrum 79−98690
statistical theory, review of present trends, book contrib. 77−84234
steam, wet, drop coagulation in cross-over pipe flows 80−74982
steam jet condensation in turbulent liquid flow, heat transfer 80−33599
steam turbine nozzle cascades, local heat transfer, approach flow turbulence effects 80−38381
steam turbine turbulent flat jet condenser, nozzle hydraulic and heat transfer charact. 78−94793
steel pipe corrosion, mass transfer coeffs. under isothermal flow conditions 80−97628
stellar atmospheres, macro- and microturbulent filter functions for weak line profiles 79−53803
stellar atmospheres, review 79−30056
stellar chromospheric supersonic turbulence, Wilson-Bappu effect 77−17541
stellar convection zones dynamics, effect of rot. on turbulent viscosity and cond. 80−36612
stellar kinematics and interstellar turbulence 79−35313
stellar structure models, convection theory including turbulent kinetic energy flux 78−57543
stellar turbulence, conference, London, Ontario, Canada (1979 August 27 to 30) 80−73102
stellar turbulent convection equations, ensemble averaging 80−67698
stellar winds, turbulent mixing with interstellar gas 80−67701
stenoses model disorder distal, steady and pulsatile flow 79−57688
stenosis model, turbulence development in pulsatile flow through partially occluded tubes 78−44531
stenosis model, turbulence in water flow system 78−44530
stenosis with upstream roughness, press. and vel. fluctuations 77−56416
stenotic flow models, fluid dynamic wall interactions 77−56414
step-backward flow, with surface discontinuity, flow separation 79−77078
stirred vessel, turbulence meas. to establish scaling rules 79−23303
stochastic particle accel. by MHD turbulence 80−31203
stochastic self-oscillations and turbulence, review 80−4537
Stokes flow, attached and free eddies 80−48679
Stokes flow past a two-dimensional lens 79−77088
Stokes flows, separation 80−48680
Stokes particle, suspended in inhomogeneous turbulent incompressible viscous stream 77−75968
strain-based Lagrangian-history turbulence theory 79−37297
strange attractor type motion, simplest case 79−17345
stratified and rotating fluids, review of selected aspects 77−68660
stratified flow, turbulence, mixing 78−22400
stratified fluid, density interface, turbulent entrainment 77−35197
stratified fluid, turbulence and mixed layer deepening rate *(Russian)* 78−24292
stratified fluid with shear, instability and turbulence 79−77216
stratified gas-liq. film flow, eqns. of motion 79−37376
stratified gas/liquid flow, heat transfer, local Nusselt number prediction 80−38393
stratified medium, normal and abormal turbulent transport *(French)* 80−59095
stratified turbulent flow digital simulation using finite element method 78−90964
stratified water, turbulence and mixing, book contrib. 78−59444

turbulence continued
streaklines in a shear layer perturbed by two waves 80−59055
strong geometrical perturbation, restructing of turbulent flow, Reynolds stresses *(French)* 79−50706
structure and entrainment in turbulent spot plane of symmetry 79−10551
structures and mechanisms of turbulence, conference, Berlin, Germany (Aug. 1977) 78−94647
subgrid modelling procedures, theoretical applications 79−50710
subgrid-scale modelling, eddy diffusivity, eddy noise 77−72292
submerged turbulent isothermal jet development and min. entropy prod. principle 79−77199
subsonic, jet-mainstream interaction 80−79271
subsonic, sound propagation due to a source near the duct exit 78−83446
subsonic base pressure fluctuations on axisymmetric blunt-based body, Mach no. depend. 80−19423
subsonic gas flow in tubes, friction factor determ. method *(Russian)* 77−19635
subsonic grid turbulence, diffusion processes of small spots of electrostatically charged mols. 78−87410
subsonic jet noise, prediction method for flight effects 78−1502
subsonic turbulent jet, entry zone flow wave struct., eddies 80−14773
Sun, differential rotation for unrestricted rot. rates, 2-dimens. stochastic motions 77−56899
supercritical He I, heat transfer to turbulent flow 80−69631
supercritical water flow in tube under very high press., heat transfer charcts. *(Japanese)* 77−42840
superfluid, penetration through porous filters 79−46855
superheated steam, turbulent flow, local heat transfer during cooling *(Russian)* 79−59985
supersonic, near wake flow 78−22368
supersonic axisymmetric near wake behind bluff-base bodies 78−1665
supersonic cone flow at high angle of attack, numerical simulation, laminar and turbulent flow 79−77178
supersonic flow, meas. turbulence, using hot-film and modified hot-wire sensors 79−90356
supersonic jet, nonsteady interaction with barrier, math. model of oscillatory cycle 80−19462
supersonic jet, turbulent wake, laser velocimeter meas. 78−26173
supersonic quasihomogeneous flow, turbulence in presence of density and vel. fluctuations 80−1638
supersonic thin turbulent layer, hot-wire anemometry, error reduction 78−34235
supersonic trailing edge flow, numerical soln. of 2D laminar and turbulent flows 79−77172
supersonic turbulent flow, turbulence production 78−94767
supersonic velocity and turbulence, appl. Doppler velocimeter with Fabry-Perot interferometer 77−39377
surface active material solution, turbulent flow study by laser anemometer 77−51038
surface buoyant jet entrainment, meas. of velocity and concentration fluctuations *(Japanese)* 79−14450
surface discharging heated turbulent jet, 3D finite difference model, turbulent diffusivities 80−74845
surface noise from turbulent hot jet, temperature effects 80−69782
surface renewal in turbulent convective transport, interfacial conditions 77−913
surface renewal principle ε_m and ε_H formulation 78−42591
surfactant solns., rheological props., hydraulic loss reduction in tube flow 77−65768
suspended particle motion in homogeneous turbulence 78−22408
suspended particles, influence on turbulence struct. in tube flow 77−75969
suspended particles motion in turbulent flow in open channel 78−51225
suspension, annular flow, gas vel. profile 77−35215
suspension, combined radiative and convective heat transfer 78−9724
suspension, dil., of spherical particles in non-Newtonian liq., rheological behaviour 80−24058
suspension, heat transfer and struct. 78−9683
suspension, solid separation at wall, heat transfer 78−9685
suspension bearing flow, turbulent energy balance in pressure pipe flow 80−48777
suspension carrying stream, gravitational transport theory *(Russian)* 78−75188
suspension flow, gravitational theory, discrete model 80−48779
suspension flow in tube, turbulent energy balance *(Russian)* 77−35203
suspension in stirred tanks, complete particle suspension conditions 78−27824
suspension of asbestos fibres, heat transfer and friction coeffs. for tubular flow 78−22405
suspension of solid in gas, heat transfer rel. to turbulence 79−72928
suspension-carrying bottom layer flow, turbulent shear stress and vel. vs. height calc. *(Russian)* 77−55070
suspensions, flow in cylindrical pipe, using ultrasonic debitmetry Doppler spectra *(French)* 80−96303
suspensions, motion of particles suspended in stationary turbulent medium at large Reynolds number 80−83836
suspensions, turbulent characts. of open channel flows *(Japanese)* 77−68676
swirl, infinitely long axisymm. theoretical anal. 77−68599
swirl dynamics 79−50732
swirled flow characts. in swirl-nozzle type injector 79−86444
swirled gas flame aerodynamics, empirical results 77−58804
swirling flow, exptl. determ. of mean velocity and Reynolds stress components *(Russian)* 79−59991
swirling flow, nonisotropic turbulence model 77−55001
swirling flow 78−71337
swirling turbulent radiative arc heater flowfield, model 79−41764
symmetric free turbulence, similarity and weak closing relations 80−33569
symmetrical wake calc., two-dimens. laminar and turbulent flows 80−14707
Taylor vortex flow in long fluid columns 79−81898
Taylor-Couette flows at very high Taylor number, marginal instability 80−1599
temperature field fluctuations in raised temp. turbulent flow *(French)* 80−19371
temperature fluctuation measurement in turbulent channel, sensor wire-supports cond. influence *(French)* 79−94751
turbulence continued
temperature fluctuations, negative prod., spectral anal. *(French)* 77−19592
temperature pulsation balance in turbulent streams, differential equation 79−14385
temperature wake, axisymm. turbulent, final decay period modelling 77−3828
tensorial volume of turbulence 80−59012
theory, expectation of an exponential function of an integral 78−32686
thermal, laser beam propagation *(French)* 77−7007
thermal, temp. field meas., buoyant vortex bubbles and turbulent thermals 78−34232
thermal and velocity mixing layers, uniform distortion 78−59374
thermal blooming in laboratory expts., index of refr. turbulence effects 79−50357
thermal convection at high Rayleigh number, variation of Nusselt number 80−79300
thermal convection in presence of rot. and mag. field, stellar and planetary dynamos appl. 80−6042
thermal exchange between sensor and supports, temp. fluctuation meas. in turbulent airflow 78−21135
thermal fluctuations, effect on turbulent flow 79−77079
thermal mixing layer, intermittency 77−31283
thermal plume rising along isothermal wall, struct. and heat transfer 79−81890
thermal turbulence in plane airstream, temp. fluctuation meas., interferometric method 79−7432
thermal turbulent wake studied by 3-beam holographic interferometry *(French)* 77−62316
thermal wake of flat plate with one heated face, turbulence 78−94741
thermally developed duct flow, boundary conditions rel. to Nusselt numbers 78−91016
thin orifice plate, turbulent flow numerical modelling 78−34229
thin sheet fluid, example of kinematic waves *(German)* 77−72310
three dimensional flow in controlled atmosphere, mathematical model *(German)* 79−64636
three dimensional turbulent rectangular jets 80−14769
three-wave decay interaction, steady-state turbulence spectrum 80−96249
throttle flow characts., approx. equation 78−18362
Tollmien-Schlichting wave packet produced by turbulent spot in laminar boundary layer 79−68733
toothlike wave dispersion due to turbulent viscosity *(Russian)* 78−1676
trailing edge noise, semi-infinite rigid plate, theoretical review 79−37307
transient convective turbulent heat transfer in tubes, thermal and hydrodynamic instability 78−83485
transient decay, mathematical modelling 78−83364
transient freezing of liquids in turbulent flow inside tubes 80−6494
transient heat transfer in tube flow 77−47004
transient natural convection in rectangular enclosures, numerical anal. 79−77111
transient turbulent convective heat transfer in concentric annuli *(German)* 77−7399
transition to aperiodic behavior in turbulent systems, recursive method 80−105493
transonic flow, accuracy and space/time resolution of laser Doppler velocimetry *(French)* 77−35276
transonic flow, hot-wire anemometry and boundary layer turbulence 78−14103
transport coefficients, derivation from turbulent parameters in isotropic turbulence 78−46948
trench flow, square section, viscous liquid, laminar and turbulent conditions obs. 77−75981
triad interaction flows, isotropic and ergodic motion 79−50712
triangular array rod bundles, fully developed turbulent flow, secondary flows 80−53753
triaxial acoustic current meter for small-scale ocean turbulence resolution 77−41232
tube bundle in crossflow at low Reynolds nos., heat transfer 79−98712
tube entrance velocity and temp. distrib. with turbulent hot air flow *(Russian)* 78−14087
tube entry region, turbulent heat transfer, high Prandtl number 78−94716
tube flow, drag reducing additives and sudden enlargement of diam. 79−37397
tube flow, heat carrier with near-critical parameters 78−42600
tube flow, of water, heat transfer 79−32513
tube inlet region, high temp. gas turbulent heat transfer, temp. factor, expt. 78−83483
tube turbulent convection, effective power dependence of heat transfer coeff. 79−4006
turbine blade arrays, turbulence characts. of stream, obs. 78−71319
turbine impeller stream flow, turbulence props. in core 77−68576
turbomachine combustor, analysis and modelling of flow *(French)* 79−46401
turbulent and high frequency fluctuating flow, mean static pressure measurement 78−57889
turbulent buoyancy convection heat transfer, two-dimens., with internal heat sources 78−94540
turbulent circular jet, in presence of co-flowing free stream 78−1704
turbulent combustions, problems of bias on mean meas. *(French)* 80−53879
turbulent flame theory, probabilistic approach 77−24034
turbulent flames, statistical theory 79−70329
turbulent flames and isothermal free jets, mathematical model *(German)* 79−74387
turbulent flow in rectangular ducts with low aspect ratio having one rough wall 79−55362
turbulent free jets, subsonic and supersonic, laser velocimeter meas. 79−77307
turbulent jet noise and diffusors *(Chinese)* 79−55367
turbulent pipe flow, vertical cond. distrib. 78−1714
turbulent pipe flow with heat transfer and chem. reaction 78−51257
turbulent plane mixing layers, growth rate, structure measurements 79−50716
turbulent temporal decay, final period struct. elements 78−94653
turbulent transport, general comments 78−94650
two component reacting fluid, density fluctuations, light scatt. spectrum, Rayleigh lines 80−25397
two dimensional turbulent mixing layer, spanwise struct., vortices 80−69771

turbulence continued
two rotating discs, air flow in gap between 80−92156
two-dimens. MHD turbulence, second order closure 79−32693
two-dimensional, computational method 80−74839
two-dimensional boundary layer, Coriolis force stabilising and destabilising effects 79−81841
two-dimensional flow, evolution of point vortex energy spectrum *(Russian)* 77−39300
two-dimensional MHD turbulence, small-scale struct., singularities form. 79−46396
two-dimensional random field model for image structural analysis *(Russian)* 80−63932
two-dimensional space isothermal and nonisothermal turbulent flow *(German)* 80−28505
two-dimensional turbulence, hydrodynamic and plasma applications, dynamical eqns., diffusion, MHD, superfluidity, review 80−69769
two-dimensional turbulence in square region, inviscid Navier-Stokes eqn. calcs. 78−16656
two-dimensional turbulence transition, dynamics in mag. field *(Russian)* 77−3886
two-dimensional turbulent blunt body flows with impinging shock 80−38444
two-dimensional turbulent flow past rectangular cylinder 78−1645
two-dimensional turbulent perturbations, successive approx. appl. to nonlinear evolution 77−46997
two-dimensional turbulent wakes, influence of upstream history 78−59400
two-dimensional unsteady stream function equation, similarity transformations 78−38302
two-layer quasi-geostrophic turbulence, simple special case 78−81186
two-layered co-current flow, in open channel, turbulence *(Japanese)* 78−38393
two-phase countercurrent flow, turbulent steam condensation in a horizontal channel 80−106800
two-phase disperse-annular flow, vel. profile calc. 78−1720
two-phase flow, book contrib. 77−58775
two-phase flow in electrostatic precipitator, particle separation prediction reliability analysis *(German)* 79−4072
two-phase free-surface flow, velocity and concentration distributions *(French)* 79−98786
two-phase gas-liquid flow, turbulent characts., determ. method 80−96300
two-phase isobaric jet, turbulent mass transfer, anal. *(Russian)* 77−27586
two-phase jets 79−32636
two-phase systems, ion Karman's constant variation in turbulent motion *(Italian)* 78−14062
two-phase turbulent flows, condensed phase formation, anal. 79−81853
two-phase turbulent jet model 79−60044
two-phase turbulent round jet, turbulence dissipation 77−35208
two-point moments calcs., use of series expansions *(German)* 77−14997
unconstricted positive column of high-vel. gas flow 77−35426
underexpanded gas jet issuance into supersonic flow 80−38468
underwater turbulent jets, velocity field calcs. for expansion region *(Russian)* 77−31351
uniform fluid flow, general nondimensional relationship *(Bulgarian)* 78−12571
universal velocity profile 78−1639
universality and scaling, review 79−58548
Universe model, homogeneous, isotropic, close to cosmological singularity, long-wave disturbances 80−73078
unsteady aerofoil theory, small perturbation expns. 78−14037
unsteady convective heat transfer in fluid tube flows *(Russian)* 79−18961
unsteady flow, axisymm., Navier-Stokes eqns. in vectorial form 79−68724
unsteady high Reynolds number flow through circular aperture 79−50735
unsteady Lagally theorem for multipoles and deformable bodies 80−33560
unsteady subsonic turbulent jets, book contrib. 80−1664
variable density turbulent subsonic flow, pressure pulsation and vel. divergence correlations 80−100008
variational method 79−59968
vascular stenosis detection using flow continuity and turbulence, US Doppler method 77−40723
Vela supernova remnant, turbulent struct. from rot. meas. 80−51836
velocimeter for fluctuating temp. and vel. meas. in combustion field 80−14856
velocity correlations in randomly-stirred fluid, variational principle for path-integral functionals 78−81846
velocity sensor for three-dimensional turbulence meas. 80−46314
velocity-derivative skewness in small Reynolds number, nearly isotropic turbulence 79−32473
velocity-turbidity system, amplitude-frequency characteristic *(Russian)* 78−75195
Venus atmosphere, dynamics, winds, circulation and turbulence 77−78706
Venus atmosphere, turbulence rel. to strong horizontal winds 77−29682
vertical buoyant jet decay in uniform environment, unified scaling law 78−90905
vertical buoyant jets, decay, unified correlation and prediction in turbulence model 80−6118
vertical plane turbulent buoyant jet in confined depth channel, stability and mixing 79−90302
viscoelastic fluid, reduction of turbulent friction, rheological model 79−86408
viscosity coefficient, calc. in semiempirical formulae *(Russian)* 80−79267
viscous compressible flows at high Reynolds number, book contrib., review 80−19424
viscous flows with no-slip walls, incompressible Navier-Stokes eqn., pseudospectral method 80−69924
viscous fluid, convection energy, theory 79−86436
viscous fluid, non-equilib. props. 77−11174
viscous incompressible flow in tube, nonsteady convective heat transfer 80−19393
viscous incompressible fluid, two-dimensional turbulence in bounded region 78−30270
viscous incompressible liquid, disturbance by small particle stream *(German)* 78−94804
turbulence continued
viscous incompressible liquid, vibrational displacement, wave mechanism 80−43777
viscous laminar jet flow in slipstream calculation *(Russian)* 79−77209
viscous liquid film instability under the influence of an adjacent gas flow 80−92110
viscous toroidal eddy generation in cylinder, Stokeslet streamlines 80−19404
volume flux conservation in free turbulence 78−51152
volumetrically heated fluid layer, combined natural turbulent convection and radiation 80−74871
vortex, shed from lifting wing tip, decay, injected air jet modification 78−63434
vortex flow meas. by laser Doppler anemometer, meas. of turbulent vortex flow 80−79412
vortex interpretation of Landau's theory of turbulence generation *(Russian)* 79−77077
vortex pair, interaction with ground plane 78−1669
vortex pairing in jet noise generation 80−69807
vortex pairs, turbulent, neutral surroundings, verification of similarity soln. 78−26127
vortex region boundaries during sudden expansion of turbulent flow *(Russian)* 77−31310
vortex ring, turbulent motion 77−35148
vortex ring core, turbulence struct. 80−33615
vortex rings, turbulent motion and heat transfer *(Russian)* 77−55008
vortex zone from turbulent jet impinging on external stream plane surface 79−90301
vortices, laminar and turbulent, decay mechanism 79−50732
vortices caused by slender bodies, high angles of attack to medium of travel *(French)* 80−59041
vortices formation in mixing layer downstream of a separation in near wake of body *(French)* 80−48716
wake, behind slender propeller-driven bodies 78−38335
wake, cylinder generated, interface position 78−94742
wake, external compression effects 79−32560
wake, fluctuations in boundary 79−27646
wake, meas. with pulsed-wire and hot-wire anemometers 77−11288
wake, modelling using interaction hypothesis 78−63431
wake, of heated cylinder, turbulent temp. and thermal flux characts. using four-wire probe 80−19541
wake, thermal, behind asymmetrically heated plate 79−64664
wake, vel. and temp. distribs., conditional averaging *(Russian)* 78−38296
wake flow behind wedge, two-dimens., press. distrib. and vortex shedding freq. 77−72301
wake of axial flow turbomachinery rotor blades, numerical anal. 80−1596
wake of blunt body with chemical reaction, flow field meas. using laser Doppler anemometry 77−35262
wake of heated cylinder, interface statistical props. 77−19608
wake of heated cylinder, similarity 78−67200
wakes, turbulence memory in self-preserving wakes 79−32527
wall and shear turbulence, turbulent correlation equations 78−94673
wall flow direction probe for turbulent separating and reattaching flows 80−53903
wall turbulence of viscous incompressible fluid 77−912
water, cooling, wind-induced turbulence rel. to boundary layer thermal state *(Russian)* 78−81192
water, flow through circular pipe, pulsed NMR study 80−28566
water, turbulence vertical transport by controlled Langmuir circulations 79−23330
water, turbulent flow, effect of polymeric additives 79−1216
water channel with wall cut-out, laser Doppler anemometer flow meas. 79−46403
water droplets suspended in turbulent flow, evaporation rate rel. to $Ca(CO_3H)_2$ soln. drops 79−90771
water jets sensitive to sound, two-dimensional, velocity fluctuations behaviour *(Japanese)* 80−100020
water tank, initial turbulence determ. from results of sphere towing expt. *(Russian)* 77−68573
water tunnel turbulence measurements behind a honeycomb 79−18874
wave attenuation factor in pulsating turbulent gas flow in channel 77−42852
wave energy dissipation by turbulence *(Chinese)* 79−81908
wave propagating in turbulent medium, four-point field coherence function 79−98279
wind, crossed hot-film velocity data anal. 80−31122
wind energy conversion, wind driven turbines, review 80−7909
wind tunnel testing, modern developments 77−31405
wind-induced heat and mass transfer over large bodies of water 77−11186
wind-wave interaction, two-layer flow, numerical simulation 78−92823
wire-wrapped 61-rod bundle edge subchannel flow distrib. 79−9676
wrinkled flame speed and struct., turbulence effects 80−26015
zero-mean-shear mixed layer, turbulence meas. 80−1705
^{4}He, superfluid, electron photography *(French)* 80−54456
Al-Cu, stir cast microstructure, turbulent flow and solidification 79−20036
Ar-Ti powder two-phase jets, with Ti combustion, high temp. study 79−81934
CO_2, turbulent flow field, mol. vibr.-rot. bands, spectral absorpt. coeff., temp. depend. 80−52987
D_2-HCl electric discharge gasdynamic laser, turbulent mixing characts. 78−9366
H supersonic flames, chemical kinetics and unmixedness effects on burning 80−64649
H_2-air jet diffusion flames with finite chemical reaction rates 79−81992
H_2-CO_2, turbulent flow heat transfer, expt. and numerical anal. 78−94690
He II superfluid, turbulence during rotation, critical lengths 80−49443
He, supercritical, correlation for heat transfer in turbulent flow in small channels 78−18871
He, supercritical, heat transfer in turbulent tube flow 78−30287
He, superfluid, thermal counterflow in rot. flow, vortices and turbulence 79−86946
He, superfluid, turbulence, steady homogeneous counterflow 78−87836
^{3}He-^{4}He II, pulsed NMR investig. of ^{3}He flow vel. 77−59171
^{4}He, heat transfer and hydraulic drag in tubulent flow in circular tube 80−14821

turbulence continued
^{4}He, superfluid, fluctuations in turbulent counterflow, vortex line density fluctuation power spectra 80−84335
^{4}He, superfluid, rotating Couette flow, hydrodynamic instabilities, attenuation of second sound resonances 79−55964
^{4}He, superfluid, self-preserving structures in homogeneous turbulence 79−55962
^{4}He, superfluid, turbulence in counterflow jet 77−72732
^{4}He, superfluid, turbulence and fully turbulent state 79−65274
^{4}He, superfluid, turbulent counterflow, vortex line density by second sound burst technique 79−55963
^{4}He, superfluid, vortex-line density fluctuations 77−80666
^{4}He, superfluid turbulence, vel. and temp. depend. from thermal resist. meas. 80−20003
Hg, liq., flow transition, in mag. field, 2-dimens. to 3-dimens. turbulence *(Russian)* 77−7471
Hg, liq., turbulent channel flow, in mag. field, spatial correl. and vorticity *(Russian)* 77−3876
Hg, on stabilising thermal section, temp. fields and heat transfer 80−19366
Hg, transition and turbulent flow in curved channels under transverse mag. field 80−79396
Hg, turbulent annular flow 77−19602
N_2O_4, heat and mass transfer in turbulent stream in axisymmetric channel *(Russian)* 79−18960
N_2O_4, reactive turbulent flow, heat and mass transfer anal. *(Russian)* 77−42932
TiO_2 suspension in glycerine, Bingham plastic flow through annuli 80−64521

turbulence, atmospheric *see atmospheric turbulence*

turbulence in shear flow *see shear turbulence*

turbulent diffusion
advection-diffusion equation, weighted-mean schemes for finite-difference approx. 78−34103
aerosol coagulation and diffusion in turbulent jet 79−23355
aerosol particle diffusivity in turbulent pipe flow 78−1731
aerosol particles, gravity settling in horizontal rectangular tube with diffusion 77−84310
air, Fourier transformation of space-time transport equation 80−62595
air, turbulent diffusion of particles, analytical numerical method 78−32257
air pollutants dispersion from area sources in convective turbulence, model 78−28303
air pollution, from sources near obstacles with separated wakes, eddy diffusivity model 79−81865
air pollution, from sources near obstacles with separated wakes, conc. meas. near cylinder 79−81866
air pollution, Gaussian diffusion-deposition model for elevated point sources 77−49156
air pollution dispersion in Ekman boundary layer 77−73783
air pollution transport and turbulent dispersion over rugged mountainous terrain 79−84349
airflow over snowpack, two-dimens. turbulent diffusion model 77−78277
analytical approximations in the theory of turbulent diffusion 78−67192
atmosphere, boundary layer, dissipation effects on parallel shear instability near ground 78−69406
atmosphere, boundary layer, Gaussian plume and spectral solns. 78−24328
atmosphere, boundary layer, second-order closure modelling of diffusion 77−78300
atmosphere, buoyancy driven mixed layers modelling 77−33150
atmosphere, coeff. determ. from meteor trail photographs 78−45073
atmosphere, Lagrangian scheme of turbulent diffusion *(French)* 79−53487
atmosphere, lateral diffusion parameters vars. 79−20931
atmosphere, pollutant dispersion in horizontally-homogeneous boundary layer 78−36263
atmosphere, Rn tracer determ. of vertical mass diffusion coeff. *(Spanish)* 77−70717
atmosphere, simple exponential function as Lagrangian vel. correl. function 79−58001
atmosphere, SO_2 turbulent diffusion above and within forest 77−45055
atmosphere, spectral transfer of turbulent energy and temp. variance 78−61489
atmosphere, stability classification schemes for urban area 77−49127
atmosphere, tensor diffusivity of inert trace constituent in stratified boundary layer 77−56675
atmosphere, turbulent diffusion in surface layer 77−66950
atmosphere, turbulent viscosity rel. to turbulent thermal conductivity *(Russian)* 80−21796
atmosphere, vertical turbulent diffusion in a stably stratified fluid 79−16585
atmospheric boundary layer, mol. resistance during diffusion, universal function determ. 80−26573
atmospheric boundary layer, stratified, conc. profile, admixture-underlying surface interaction effect 80−31089
atmospheric boundary layer, turbulent diffusion of pollutants 77−41113
atmospheric boundary layer, with Rossby number similarity, turbulent diffusion 78−92896
binary gas mixtures, mass transfer analysis using model of convective diffusion for turbulent flow in tube 77−7454
boundary layer, calc. on spinning and curved surfaces 77−65737
boundary layer, drag reduction polymer molecule turbulent diffusion and degradation 80−1686
boundary layer, mixing length in wall region 77−62242
boundary layer, temp. fluctuations *(French)* 77−62248
boundary layer 78−38305
boundary layer diffusion, with surface reactions, laminar or turbulent regimes, thermal simulation method 77−75912
bubble diffusion in two-phase flow 78−18332
bubbles in turbulent flow 78−22412
buoyancy effects in entraining turbulent boundary layers: a second-order closure study 80−21815
burning vortex ring, turbulent, acoustic emission 78−94676
chemically active additive in turbulent mixing zone, stat. characts. 77−35258
chemically reacting flow, second-order closure anal. 77−39364
chemically reactive flow, probability approach to modelling 77−42928
coaxial jet, aeroacoustic characts., sound power spectral density 77−62285

turbulent diffusion continued
combustion, turbulent premixed and diffusion, engineering flow modelling computation 78−1756
concentration initial section effect on diffusion fluxes 78−59383
concentration interface in turbulent mixing layer, visual growth 80−38392
conditionally intermittent sources, calc. of diffusion characts. 79−14389
conditionally intermittent sources, conf., Haifa, Israel, (July 1977) 79−15683
contaminant cloud, passive, relative diffusion in incompressible turbulence flow 79−50774
convection, nonlinear double-diffusive, low Prandtl number, boundary layer method 80−69816
convection-diffusion problem, singular perturbation problem with nearly resonant operator 78−22352
convective heat transfer with diffusion, finite element anal. 79−4011
coolant in LMFBR fuel assembly, mixing, subchannel vels., electrolytic tracer, isokinetic sampling techniques 77−18653
cosmic ray propagation, partially averaged field approach 78−53776
cosmic rays, velocity diffusion, turbulent mag. field, Monte Carlo calc. 78−53777
diffuse electrical gas discharge, in turbulent flows 79−94834
diffusers, conical, injection for boundary layer control 78−90864
diffusers, optimum press. recovery 80−1539
diffusion flame in turbulent boundary layer on liq. propellant surface behind shock wave 80−53763
diffusion-convection equations, finite difference scheme 78−42596
direct optical meas. of vel. gradients 80−59132
discrete particle diffusion in turbulent fluid, finite difference method anal. of integro-differential eqn. 79−77089
discrete particles dispersion in turbulent fluid field 80−33580
disperse systems, coagulation, slow, turbulent 78−53259
distributed chemical reaction system, diffusion induced chaos 79−81995
double-diffusive system between infinite horizontal planes, heat and salt transfer 77−39298
drag reduction in turbulent boundary layer, diffusion of polymer soln. introduced via slit 79−68685
droplets of concentrated cloud, approx. eqn. for mass and heat flux in constrained flow 77−47073
dust entrainment in shock-induced turbulent air flow, dust entrainment 80−43763
dust laden jet, particle turbulent diffusion 78−83455
dye plumes, relative turbulent diffusion, conc. fluctuation meas. 79−94602
eddy diffusion, explicit scale-depend. coeffs., atm. and ocean appl. 78−67191
eddy diffusivity, effect on heat transfer and skin friction 78−30276
eddy diffusivity, near open channel free surface, heat transfer expt. 78−5798
eulerian-lagrangian turbulent diffusivity relation 80−103018
fast reactor, partly blocked fuel subassembly, turbulence meas. in air model 77−74965
finite-rate turbulent diffusion 78−46956
fire plume, turbulent, reaction rate, air entrainment, radiation 78−35682
flame, combustion model and calc. 78−35684
flame, free-jet diffusion type, ionis. meas. and combustion progress 80−30238
flame, interaction of flow pulsation and chem. reaction 77−58801
flame, mass entrainment, momentum flux and temp. 79−32704
flame, turbulent diffusing, analytic incorporation of probability density functions 78−75232
flame, turbulent diffusion, burning vel. *(Russian)* 77−7475
flame, turbulent diffusion, mean flow props. 78−1753
flame, turbulent diffusion, transport eqn. for probability density function, closure 80−1585
flame, visible length of vertical free flames 78−85163
flame jet, anal., pulsations of conc. and Archimedian forces *(Russian)* 77−51130
flames, high Reynolds number, rocket exhaust appl., chem. processes theory 80−45504
flames, multiple turbulent, struct., operating conditions rel. to characts. *(Russian)* 77−7476
flames, turbulent, calc. in one-dimensional approach 80−30236
fluid eddy viscosity and thermal diffusivity model *(Russian)* 78−46957
fluidised bed, binary, finely dispersed, local struct., random pseudoturbulent motion 77−75977
fluidised bed, numerical soln. to 20 unsteady diffusion eqn. for vortex flow 77−84320
fluidised bed, particle mixing, diffusion model for longitudinal particle transport 77−47087
forced plume characteristics 78−18286
free diffusion flame, length *(Russian)* 78−3334
free jet, coefficients of eddy diffusion, rel. to mean scalar quantity 77−84287
heat and salt transfer across diffusive interface, grid generated turbulence 77−7381
heat flux and temp. fluctuation prediction 80−38400
heat transfer coefficient prediction, in drag reducing turbulent pipe flow 77−51052
helical coil, effect of Schmidt number on laminar dispersion 77−80145
helical turbulence, diffusion of passive-scalar and mag. fields, computer simulation 77−11272
heterogeneous liquid stream, stress diffusion effect, molar diffusion coeff. 78−79338
highly turbulent fluids, diffusion, memory and retardation effects 80−43697
homogeneous stationary turbulence, diffusion of scalar and vector fields 78−5736
homogeneous turbulence, diffusion of passive scalar, statistical approach 80−38391
hydrocarbon turbulent diffusion flame, flame-zone model anal. 80−16684
impurity diffusion in boundary layer 77−89110
invariant props. of fluctuation distribs., contaminant cloud appl. 80−59017
ion wind enhancement of evaporation into a laminar air stream 80−53773
ionisation wave propag. in gas, turbulent diffusion effect 78−42704
jet, free, heated, turbulent, high temp., eddy diffusion, methane combustion obs. 78−30329
jet, quasi-two-dimensional description of rapid-type nucleation 77−35190

turbulent diffusion continued
jet, turbulent diffusion flames, statistical props. *(Japanese)* 79−81939
jet array, thermal diffusion downstream meas. 78−94785
jet diffusion flames, blowout and attachment mechanisms 79−72957
jet flame, effect of mol. gas radn. 77−80232
jets, axisymmetric, turbulence mixing of gases with different densities 77−58749
jets, two-phase, turbulent, particle or droplet size effect on diffusion 80−1658
jets in cross flow 79−27674
kinematic diffusion of scalar quantities in turbulent velocity fields 80−27235
Lagrangian scheme, algorithm and applications *(French)* 79−84401
Lagrangian-Eulerian relation, independence approx. 77−11180
limit theorem for turbulent diffusion 79−41679
liquid metal turbulent heat fluxes, channel flow, nucl. reactor appl. 77−42035
lognormality of gradients of advected scalars 78−67181
longitudinal diffusion in a flow through a tube 78−90974
marked fluid, approach to normality of distance-neighbour function 77−15005
mass and heat transfer between turbulent flowing fluid and solid wavy surface 80−14681
mass exchange for spherical particle in flow at high Peclet numbers and Re≤100 77−54988
mass transfer in annulus 79−14388
methane, jet, free turbulent flow, diffusion coeff. variation, mixing processs velocity 77−7480
methane tracers, single-jet mixing in turbulent tube flow, similarity and scaling law 80−14765
method of first integrals 79−37305
MHD, root mean square mag. field on turbulent diffusion 78−36449
miscible fluids, concentration fluctuations, statistical theory 77−42810
mixing at fluid interface in gravity field 77−89112
mixing meas., laser light scatt. technique 77−11285
moving liquid, numerical method for convective diffusion problem 77−89120
multiphase flow diffusion equations 78−94801
multiple time scales, appl. in turbulent transport modelling *(French)* 79−7374
non-axisymmetric, annular channel 78−75129
non-Newtonian turbulent transport in circular tube 77−39313
nonlinear double-diffusive convection 77−19607
nonlinear integrodifferential eqn., numerical soln. 78−38306
nuclear reactor, fuel element array, temp. distrib. for turbulent liq. metal flow 78−13203
nuclear reactors, connected flow passages, computer prediction using k-ε turbulence model 80−9331
nuclear reactors, connected flow passages 80−9330
ocean, admixture diffusion in vortex flow 79−2277
ocean, initial and boundary value problem *(German)* 77−86908
ocean, neighbour diffusivity in near-shore zone *(German)* 77−70668
ocean, relative diffusion meas. at small scales 78−88838
ocean refractive index microstruct. from diffusive and turbulent ocean mixing 80−56486
ocean surface layer, dye plumes diffusion, expt. 78−44871
oceanography, diffusion parameterisation of mesoscale eddy effects from numerical expt. 79−48508
one dimensional turbulence problem, equivalence to one dimens. Coulomb gas 78−5735
open channel flows, junction losses, frow anal. 80−6156
particle collectives, turbulent flow, diffusion model description, appls. *(German)* 78−59446
particle convective diffusion to rot. disc surface 78−18334
particle diffusion, two-timing theory and appl. to statistical geophysics 77−73879
particles suspended in turbulent fluid, dispersion 78−14073
particles suspension, small sphere motion in rot. vel. field 77−58771
passive scalar magnitude *(French)* 80−69778
pipe, asymmetrically heated, turbulent transport and thermal diffusivities 80−64636
pipe flow, depend. of particle deposition velocity on particle inertia 77−35219
pipe flow, drag reduction polymer molecule turbulent diffusion and degradation 80−1686
pipe fluid flow, solid particle impurity propag. 80−64630
plane-parallel flow, calc. by finite-rate diffusion equations 78−67190
plasma strong turbulence and anomalous diffusion in mag. field 80−59239
plume, buoyant, turbulent, pl./line heat sources, temp. and vel. distribs. 77−84254
plumes, vertical, round, diffusion, flow props. 80−43755
pollutant dispersion from point source with and without chem. reaction in semi-bounded waters 77−64329
pollution dispersion-convection equation, soln. for bay with currents 77−91157
polymer additives diffusion in turbulent boundary layer 77−35176
polymer soln., diffusion in boundary layer 78−87368
propagator renormalisation, combinatorial factors 77−19598
propane-air flame premixed turbulent, three region model 79−100382
pulsed extraction column, with perforated plates, efficiency 79−64809
quasi-kinematical approach, self-diffusion coeff. 77−31294
rate calculations for large Schmidt numbers 77−51049
Rayleigh-Bernard convection, forced phase diffusion 80−103019
rectangular jet distrib. in cross flow, expt. 80−19465
respiratory system, particle deposition due to turbulent diffusion 79−66478
retarded turbulent boundary layer, expt. study of turbulence energy balance components 79−86415
Reynolds analogy extension for fully rough surface 78−51159
Richardson problem, soln. in one dimension *(French)* 80−23993
rivers, turbulent open channel flow, dissipation and fine-scale structure 79−16546
second- and third-moment rate eqns. closure 78−59384
semiopen channel vel. distrib. 77−54303
shear turbulence 79−68690
single stationary object effects on rates 77−54987
smoke 78−90863
solar magnetic field, Eulerian formalism 79−16901
solid particle concentration profiles in turbulent jet, laser Doppler anemometer meas. and theoret. calcs. 79−27686
turbulent diffusion continued
soluble flat surface stability in turbulent flow 80−14676
spectral transfer model for high wave numbers of turbulent velocity and scalar fields *(French)* 77−15004
statistical approach to inhomogeneous diffusion 79−90238
stochastic model 79−18880
stratosphere, turbulence from IR astronomy data 80−12475
stress transport turbulence model, local equilib. solns. 77−54989
subgrid-scale modelling, eddy diffusivity, eddy noise 77−72292
superimposed miscible liquids, dynamic stabilization, turbulent transport through diffuse boundary layer 80−74844
supersonic flow, optical method for measuring intensity of fluctuations of conc. of inert impurity 77−80234
surface discharging heated turbulent jet, 3D finite difference model, turbulent diffusivities 80−74845
suspension, turbulent and pseudo-turbulent transport 78−14068
swirling recirculating reacting turbulent jets passing through diffusers 79−50764
thermosphere, macroturbulent scales estimation around 100 km altitude 78−61635
thermosphere, Na clouds eddy diffusion rel. to turbopause altitude vars. during night 77−78548
thermosphere, wave-induced diffusion effects on acoustic-gravity waves 78−61637
total dispersion of a scalar quantity in turbulent flow 80−28499
tracer gas axial dispersion through tube constrictions 80−64625
transonic flow, unsteady, turbulence modelling, compression waves developing into shock wave 80−74909
transport coefficients, derivation from turbulent parameters in isotropic turbulence 78−46948
tube flow, longitudinal turbulent dispersion of dye pulse, asymptotic stage, Taylor conditions 77−51050
tubes, heat transfer laws, longitudinal turbulent diffusion influence 80−33597
tubular flow reactors with first-order kinetics 79−4088
turbulent transport, general comments 78−94650
two-dimensional turbulence, hydrodynamic and plasma applications, dynamical eqns., diffusion, MHD, superfluidity, review 80−69769
type transport in inhomogeneous turbulence 78−18285
unsteady diffusion in wedge-shaped region with inhomogeneous boundary conditions, appl. of Sommerfeld-Malyuzhinets integral 77−89111
unsteady turbulent boundary layer developing in oscillatory external flow *(French)* 77−72288
urban planetary boundary layer, pollution effects on thermal struct. and dispersion 78−11986
viscoelastic flow in tube, eddy diffusion reduction for heat and momentum transfer 78−22382
viscoelastic liquid injected into Newtonian turbulent pipe flow, diffusion and drag reduction *(German)* 79−77251
vortex ring motion analysis 77−51061
water vapour, wet, boundary layer in compressible flow 80−10295
wavefronts in reaction-diffusion systems, instability and turbulence 80−106855
waves, miscible (immiscible) fluids, in closed horizontal (vertical) ducts 77−62263
CO_2 laser amplifiers, porous tube generated flow field, heat and mass diffusion 80−63969
H-air flame, premixed turbulent, three region model 79−100382
H_2-O_2 gas mixture in chem. equilib., elemental diffusional separation in nonisothermal flow 79−55429
^{4}He, superfluid, self-diffusion of turbulence through porous media 79−55961
Rn, vertical diffusion coeffs., wash-out and deposition effects 77−68726
SO_2 regional transport, three-dimensional grid model 77−37375
UO_2, condensed vapour following core disruptive accident, particle-size distribs. using first-generation model 78−13295

turbulent flow *see turbulence*

Turing machines
see also automata theory
cerebellar function, molecular information processing model 78−31759
quantum mechanical microscopic Hamiltonian model 80−101727

TV *see television*

twilight
see also night sky
aerosols from Perseid meteors, effect on twilight optical characts. *(French)* 80−46255
airglow, photographic obs. from Skylab 77−60505
airglow spectrum, new diffuse emission bands obs. 80−72662
atmospheric NO_2, tangent ray meas. technique, effects of NO_2 conc. vars. at twilight 78−32141
auroral zone, afternoon sector, obs. of pulsating aurora 78−81486
duration of twilight and darkness, var. with latit. 77−25632
intensity and polarisation, Monte Carlo simulation *(Russian)* 77−33186
ionosphere, MF absorpt. nocturnal var. and nighttime E-region 77−29563
mean twilight at zenith and scatt. coeff. height var., statistical anal. *(Russian)* 79−16666
noctilucent clouds, obs. in Poland during 1974 77−21826
noctilucent clouds, photographic obs. on 1976 June 18-19, Scotland 77−81982
Raman scattering spectrum 79−92596
sky colours, modelling 79−100944
sky polarisation during meteor showers *(French)* 77−9578
stratosphere, aerosol conc. using iterative method from twilight polarization meas. 78−20464
stratosphere aerosol meas. by solar occultation method 77−45090
Sun's meridian, single- and multiple-scattered light dependencies, on air dispersion factor *(Russian)* 79−5612
upper atmosphere emission at night and twilight horizons, Salyut 4 obs. 77−9590
visibility function of near-Sun astronomical objects 77−5321
VLF propag. during sunrise 78−93030
Li I 6708 Å twilight emission enhancement following rocket release 77−53255
N I(^{2}D) 5200 Å emission, obs. in twilight rel. to prod. in auroral zone 79−21090
NO_2, in stratosphere, spectroscopic determ. and behaviour at mid-latit. 80−17414
NO_2, stratospheric, ground based obs. 80−85697
Na I D-line profiles, interferometric studies 78−36353

twilight continued
O atom corona, of fast atoms during solar max., airglow obs. 80−101469
O I 6300 Å emission in twilight airglow, thermospheric temperature depend. 77−45215
O II 7320-7330 Å emissions meas. at twilight 78−88962
O_3 conc. meas. at high latit. during twilight 77−41128
$O^+(^2P)$ airglow, thermospheric comp. changes estimation 79−62635

twin boundaries
acoustic emission during tensile tests, H_2 assisted fracture 79−100257
n-alkenes, n even, interaction energy at twin boundary, dihedral reentrant, salient angle effect on growth morphology 78−55876
BCC crystals, atomic struct. of twin boundaries by electron microscopy 78−22735
brass (70/30), interaction of annealing twins in fcc metals and alloys 78−68712
β_1 brass containing α-precipitates, reversible shape memory effect *(Japanese)* 78−60711
coincidence grain boundary, lattice displacement, electron images 77−80516
cubic system, electron diffr. patterns of twins *(Chinese)* 79−99214
diamond, synthetic, struct. of twin seam obs. by optical microscopy 77−39596
dimethylammonium cadmium tetrachloride, far IR refractive index, extinction coeff. and dichroism obs. 80−66144
elastic energy of slightly incoherent twins 77−72616
electron microscope images 77−11568
electron microscopy, multi-beam, general extinction criteria for extended defects 77−72532
FCC metal, twin boundary, surface relaxation, lattice statics calc. 78−63925
ferroelectric substances, electron microscopy investigations, review *(Japanese)* 80−71366
gamma-ray diffractometry, phase transitions, domain structures, twinned texture studies 80−19678
Inconel 600, effects of ageing and misorientation on intergranular corrosion *(Japanese)* 79−79158
interfacial energy of planar defects, symm. variations 77−68983
martensite, habit plane 78−18572
metal, BCC, computer simulation of twin boundary and twinning dislocation struct. 78−30644
metal, BCC, stacking fault and twin boundary energies 77−76420
metal, BCC, twin boundary and stacking fault structs., computer simulation 80−59485
metal, FCC, vacancy migration near twin boundaries and stacking faults 80−39075
metal, FCC, with fibre texture, X-ray method of twin fault probability determ. 79−87817
metal, martensitic memory mechanism *(Russian)* 77−21217
metal particles, small, possible vibrations associated with twins 80−100253
metal-C system, spheroidal graphite formation, role of high angle boundaries *(Russian)* 80−81065
metals, BCC, coherent twin boundaries and interatomic pots. 78−51558
metals, FCC, dislocation barriers at coherent twin boundaries, anisotropic elasticity solns. 80−96522
metals, FCC, slip dislocation reactions at coherent twin boundaries, effect on work-hardening 79−1431
modelling of linear and surface defects 77−89450
Peierls force of boundary layer, theory 80−10552
plane coalescence, at grain boundaries 80−70221
polyethylene crystal, computer simulation of {110} twin boundary 78−30646
quartz, dissociated a-dislocation, effect on plastic deformation 79−7610
quartz, phase transformations and domain structures *(French)* 78−27509
rare earth oxide, lattice images *(French)* 78−26397
relative orientation of two crystals from analysis os spot diffr. patterns 77−47305
sapphire, shaped single crystals, porosity, microstruct. 78−2125
sodium tartrate tetrahydrate, gel-grown single crysts., charact. 77−90261
stacking fault, antiphase boundary energies, investig. methods, review, appls. to FCC metals *(French)* 79−42080
steel, austenitic, precipitation hardening, effect on fatigue strength 78−84829
steel, austenitic stainless, creep deform. effect on struct. of twin boundaries 79−8332
steel, austenitic stainless, dislocation transport and H_2 embrittlement 80−30087
steel, austenitic stainless, extrinsic grain boundary dislocations, effect on $M_{23}C_6$ precipitate nucleation 79−51118
steel, austenitic stainless, extrinsic grain boundary dislocation spreading 79−57004
steel, austenitic stainless, interaction of annealing twins in fcc metals and alloys 78−68712
steel, austenitic stainless, low-cycle fatigued at high temps., crack obs. 77−1874
steel, austenitic stainless, Ni-alloyed, Cr_2N precipitation, interface struct. and morphology 80−11644
steel, austenitic stainless, precipitation of $M_{23}C_6$ type carbide on twin boundaries 80−89226
steel, austenitic stainless, type 800, tensile creep props., coherent twin boundaries, TEM obs. 79−38885
steel, bainitic, habit plane determ., austenite orientation determ. 79−1926
steel, C, U8A, struct. after low-temp. thermomech. treatment 79−79008
steel, Cr-Mo-Ni-WV (6, 4, 3, 2 wt.%), tempering and secondary hardening, TEM obs. *(Chinese)* 80−104245
steel, Cr-Ni, bainitic habit plane determ. 79−1927
steel, CrNi, etchability of austenite *(German, English)* 80−11860
steel, Cu-Mo, tempered, cementite precipitation along twin boundaries 80−45309
steel, Hadfield, cast and crystallised, deform. resist. of grain boundaries *(Russian)* 77−21216
steel, interface model of $(3, 15, 10)_F$ martensite 78−31408
steel, low C, ferrite grain nuclei form. during polymorphic transform. *(Russian)* 80−50626
steel, Ni-C, martensitic, microstructural distrib. of cathodic H_2, autoradiography *(French)* 79−99234

twin boundaries continued
steel, stainless, aged 304, twin boundary cavitation during creep 77−86099
steel, stainless, austenitic grain growth, annealing twins role 79−57016
steel, stainless, electrohydraulic effect and struct. changes *(Russian)* 78−23783
steel, stainless, He ion bombard., in situ electron microscope examination 80−34094
steel, stainless, shock loaded, residual martensite obs. 80−104414
steel, stainless, type 304, TEM study of dislocation emission from grain boundaries 79−66121
steel, two-phase austenitic-ferritic, plastic deformation under hot working conditions 77−48466
Tishomingo Fe meteorite, taenite deform. twins obs. 79−16898
transformation twin thickness 78−95750
transition, cell-preserving, space group theory of translation, twin and translation-twin boundaries 77−19892
transition metals, stacking fault and twin energies 79−82244
Ag, annealing twins rel. to stacking fault energy 79−33006
Ag expitaxial film, twin boundaries of recrystn. type, electron microscope obs. *(Russian)* 79−4484
Ag film, twin boundary faceted struct., struct. coarsening due to dislocations *(Russian)* 79−99215
Ag particles, lattice defect influence on size effect 78−88329
Ag thin evaporated films, rel. between microstruct. and excess free energy, TEM 80−70427
Ag-Mn, annealing twins rel. to stacking fault energy 79−33006
Al bicrystal, estimation of grain boundary torque 77−7736
Al bronze, O free, annealing in photoemission electron microscope, twin density recrystallised grain size relation *(German)* 78−52850
Al, polycryst. in annealed and creep conds., dislocation interactions with grain boundaries 79−42067
Al thin foil, thin foil, electron irrad., observation of triangular loops at twin boundaries 80−34005
Al-Cu (3.93 wt.%), planar defects within theta precipitates 77−16583
Al_4Cu_9, rhombohedral γ-brass, direct imaging of struct. and structural defects 80−15115
Al_8Mn_5, rhombohedral γ-brass, direct imaging of struct. and structural defects 80−15115
Au, atomic arrangements of defects, dynamic obs. of atom movement 80−39108
Au, atomic struct. of large angle [001] twist boundary, determ. by computer modelling and X-ray diffr. study 80−70162
Au bicrystal, dislocation networks in twin boundaries, TEM obs. 78−51556
Au, coherent twin boundary, electron microscopy obs. *(Japanese)* 79−82130
Au, dislocation free bicrystal, DSC dislocation network generation in coherent twin boundary 77−62544
Au film, surface step structure imaging by dark field electron microscopy 80−15346
Au film, twin boundary struct. and migration, atomic scale electron microscopy obs. 80−107276
Au, quenched polycryst., vacancy loss at grain boundaries 80−59477
Au, thin film bicrystal, annealing twin form. by boundary dissociation 79−47729
Au/AuPd, bicrysts., in situ relax. of interphase interfaces 80−39455
Au/Pd, bicrysts., in situ relax. of interphase interfaces 80−39455
Au_4Mn, fully ordered, microstruct., high resolution electron microscopy 79−1439
Au_5Mn_2, variants in domain struct. 77−43224
β-BN, struct. of twin seam obs. by opticalmicroscopy 77−39596
Be, forest dislocation effect on single twin layer development in single crystals 78−63775
Be, twin boundaries, computer simulation 80−39109
Be_2SiO_4, phenakite, flux grown single crysts., twinning study by hydrothermal etching and X-ray diffr. 80−107271
Bi, deformed cryst., phonon scatt. by lattice defects, thermal cond. calc. 78−22802
Bi, epitaxial films, grain boundary struct., electron microscopy obs. *(Russian)* 79−46671
Bi, thermal cond. under plastic deform., phonon scatt. by dislocations and twin boundaries 77−11746
$CaCO_3$, with perfect struct., temp. depend. of rate of twinning 80−10561
Cd, twin boundaries, computer simulation 80−39109
Co base alloy, FCC, twin-slip interaction 77−51379
Co-Ni-Cr-Nb FCC alloy, electron microscope obs. of deform. twins 79−60380
Cr, twin and stacking fault energies calc. 80−2038
Cu, annealing twins, density, effect of recrystallisation temp. and electron microscope resolution *(French)* 78−31423
Cu electrocrystallisation, multiple twin form. 77−39750
Cu electrolytic form. by electrodeposition, structural defects 77−39749
Cu film, on (001) Ag, FCC and BCC metal-on-metal epitaxy, geometric factors, electron microscopy 78−22980
Cu, grain boundary character, revealed by etching and slip line continuity 79−33001
Cu, interaction of annealing twins in fcc metals and alloys 78−68712
Cu, O free, annealing in photoemission electron microscope, twin density recrystallised grain size relation *(German)* 78−52850
Cu, point and planar defects, computer simulation 80−59455
Cu, surfaces and twin faults, electronic states calc. by surface Green's functions 80−39647
Cu-Al-Ni, rubber like behaviour 77−86114
Cu-Ge (8 wt.%), anelastic effect due to deform. twins *(Japanese)* 79−20095
α-Cu-Zn-Al (18, 7 at.%), deform. and mech. props. 79−29159
Cu_2Se, VPE on mica, defect struct., temp. depend. 77−35837
α-Fe, BCC, migration of vacancies near twin boundaries 78−51535
Fe, deformation twin form. during high temp. creep *(Russian)* 79−24573
α-Fe, exam. of structural defects due to shock waves, and induced hardness 78−48427
Fe, twin and stacking fault energies calc. 80−2038
α-Fe, twin boundary struct., plane translations 79−69113
Fe-Mn-C, $\gamma \rightarrow \varepsilon \rightarrow \alpha'$ martensitic transform. 79−24523
Fe-Ni (32 wt.%), electrohydraulic effect and struct. changes *(Russian)* 78−23783
Fe-Ni martensite, twin struct. 79−77607

twin boundaries continued
Fe-Ni-C (19.5, 0.73 wt.%), banded struct. formed by deform., TEM and optical obs. 78−39869
Fe-Ni-C (21, 0.6 wt.%), stress assited and strain induced martensite morphologies 78−3187
Fe-Ni-C (24, 0.5 wt.%), struct. of burst and isothermal martensites 79−38825
Fe-Ni-C (31.9, 0.02 wt.%), metallographic study of austenite grain size effect on martensite kinetics 79−1863
Fe-Ni-Co-C, substruct. effect in mech. props. 80−30086
Fe-Si (3.25 wt.%), dislocations in twin boundaries, electron microscopic images 80−34006
$Fe_{40}Ni_{40}P_{14}B_6$ metallic glass, crystn. 80−70127
FeS_2, pyrite, high-resolution electron micrograph of twin boundary 77−65983
GaP on GaAs substrate, heteroepitaxial layers, stuct. defects *(German)* 79−23865
GaSb pulled crystal, wavy impurity patterns beside twin boundary 78−18674
GeTe, heterophase state, plasma refl. spectra, twinning domain distrib. study 79−69845
GeTe, low temp. alloys, microstruct. obs. *(Russian)* 78−19768
In crystals, twin layer broadening dynamics in temp. range 235-390K 79−65098
In, twin boundary movement by creep 80−24460
In-Tl single crystal, phase transform. X-ray topographic study *(Japanese)* 78−31405
InSb-GaSb solid solution ingots, orientation, twinning and orientation depend. reflectance 79−28001
InSb-GaSb superlattice, density of microtwins and dislocation boundaries, depend. on composition modulation 79−56930
$LaNbO_4$, single cryst., grown by Czochralski method, with (102) and (201) twinning boundaries 77−52247
Li, BCC, coherent twin boundaries and interatomic pots. 78−51558
Li, twin boundaries, computer simulation 80−39109
metal, BCC, multi-layer faults on (112) planes and interatomic pots. 78−51563
Mg, twin boundaries, computer simulation 80−39109
Mo, shock deformation twinning, shock loaded BCC and FCC metals comparison 80−104413
Mo, twin and stacking fault energies calc. 80−2038
β-$MoTe_2$, domain struct., dislocation fine struct., phase transitions 79−82332
$NH_4H_2PO_4$, defects, X-ray topographic study 78−26580
$(NH_4)H_2PO_4$, single cryst., X-ray diffr. contrast at twin boundaries, computer simulation 79−33000
$NH_4H_2PO_4$, X-ray interference fringes due to diffraction effect at grown-in twin boundary 78−38728
$4Nb_2O_5.9WO_3$, cryst. struct. determ. by 1 MV TEM 79−7581
$NdNbO_4$, single crystal grown by Czochralski method, with (102) and (201) twinning boundaries 77−52247
Ni, annealing twins, density, effect of recrystallisation temp. and electron microscope resolution *(French)* 78−31423
Ni based superalloy, interaction of annealing twins in fcc metals and alloys 78−68712
Ni, computer simulation of point defects and planar defects 78−43013
Ni, electrodeposit, linear defect obs., TEM study 79−4304
Ni, O free, annealing in photoemission electron microscope, twin density recrystallised grain size relation *(German)* 78−52850
Ni, shock-loaded, residual strengthening, effect of grain size, dislocation cell size and deform. twin spacing 79−91744
Ni single crystal foil, H_2 induced deform. during thinning, electron-optical obs. 79−57059
Ni-Cr, partial dislocation, stacking fault TEM study *(Chinese)* 80−84174
Ni-Cr-ThO_2 (20, 2 wt.%), dispersion hardened, model for high temp. deform. based on struct. obs. 78−19809
Ni-Ti (49.7 at.%) alloy, rel. to deform. behaviour and shape memory effect 77−32638
NiAl martensite, Ni-rich, precip. of Ni_3Al, mechanism 77−86033
NiTi martensite, shape memory effect, struct. characts., TEM $2^1/_2$ D imaging obs. 80−108446
NiTi, stacking faults prod. by martensite transition, lattice imaging electron microscopy obs. 79−96026
Pb, estimation of stacking fault and twin boundary energies using phonon dispersion curve 78−43031
Si, coherent twin boundaries, struct. by TEM 80−75238
Si crysts., dynamic processes associated with stacking faults and deform. twins, HVEM in-situ obs. 80−103369
Si, deformed, annealed and recrystallized, struct., implications for solar cells 80−60922
Si film, polycryst., substruct. 79−23848
Si, grain boundaries, high resolution TEM 80−103364
Si, heavily damaged ion implanted (100) and (111), development of secondary defects 79−51166
Si, ribbon, edge-defined film-fed grown, orientation depend. of defect struct. 77−1134
Si, ribbons produced through capillary action shaping, elec. and struct. characts. 78−47804
Si, semicrystalline layer, deposited on stainless steel and Pyrex glass, growth conditions and props. 79−82482
Si single crystal ingot growth from metallurgical grade Si, inhomogeneities 80−59416
Si-Fe, ferromagnetic domains and their junctions, simulation of X-ray topographs 79−78434
SiC, pyrolytic particles for high temp. reactor fuel, X-ray and SEM study *(French)* 78−22734
SiC, struct. of thin seam obs. by optical microscopy 77−39596
β-SiC whisker, failure and defects 79−96145
Ti, martensitic transformation, strain energy minimisation 77−21140
Ti, serrated $\{10\bar{1}2\}$ twin interfaces 80−84182
Ti-Al-Sn (5, 2.5 wt.%), fracture mechanism at cryogenic temps. 78−64642
TiMn, faceted parent martensite interface 80−6417
V, twin and stacking fault energies calc. 80−2038
W, incoherent twin boundary microfaceting on annealing, field ion microscope determ. 79−77608
W, twin and stacking fault energies calc. 80−2038
Zn, crack form. at grain and twin boundaries at low temp. *(Russian)* 80−66620
Zn, forest dislocation effect on single twin layer development in single crystals 78−63775
Zn, twin boundaries, computer simulation 80−39109
ZnS, sphalerite, struct. of twin seam obs. by optical microscopy 77−39596
ZnSe, single crysts., grown from melt under Ar pressure, defects form. 79−4312
Zr, martensite, furnace cooled and water quenched, strength and deform. 79−20101
Zr, serrated $\{10\bar{1}2\}$ twin interfaces 80−84182
β-Zr-Mo-(Al)(Ti)(La), metastable, deform. induced transform. 78−52805
Zr-Ru(Pd), heat treated, mech. props. and struct. 78−80571
Zr-Ti martensites, furnace cooled and water quenched, strengh and deform. 79−20101

twinning
see also twin boundaries
aggregate, polycrystalline, deform. 77−4816
n-alkanes, even, long-chain, layer interaction energies for different twin and polytypic positions 77−65985
n-alkenes, n even, interaction energy at twin boundary, dihedral reentrant, salient angle effect on growth morphology 78−55876
alloy, thermodynamic and structural changes in deform. twinning 78−2139
alloys, industrial, stacking fault energy rel. to mech. props. *(French)* 79−43339
alumina, polycryst., compressive strength, microplasticity 77−36620
amethyst quartz, α-β phase transition, interaction of Dauphine and Brazil twins 77−62641
annealing twin form., statistical anal. *(French)* 77−81281
BCC crystal, held by pair interactions, asymmetry props. 77−19970
BCC metals, plastic deform., computer simulation 80−40456
α-brass, 70:30, cold-worked, recrystallised grains nucleation on heating 80−29998
brass, 70:30, rolled, nucleation and annealing texture development 80−45320
α-brass, (211)[$\bar{1}$11] single crystal, rolling deform. 77−21174
α-brass, deformation mode during rolling *(Japanese)* 79−79001
brass, FCC rolling texture origin with rolling plane parallel to {111} 79−91674
β-brass, quenched single crystal, deform. and slip 79−79026
brass, rolling texture development and deform. struct., shear bands effect *(Japanese)* 80−84952
brass, shear band development during rolling, twinning, metallographic obs. *(Japanese)* 78−39849
brass, simulation of rolling and shear texture, using an adapted Taylor theory 78−52835
brass, two-phase α/β bicrystal, diffusion induced twins in α-phase 79−46967
brass (70:30), cold rolled, optical, X-ray and TEM exam. of deformation struct., and textures 78−88500
α-brass sheet, shear bands and recrystallisation 79−91680
brass single crystal, martensite form. and shape memory effect mech. 78−19744
caesium hydrogen tartrate, anomalous dispersion of Cs, refined struct. from modified least squares program 78−51522
calcite, sound emission on dislocation annihilation *(Russian)* 80−54246
camphor, rhombohedral, polycryst., compressive deform. and dynamic recrystn. 80−71698
carbonate minerals, deform. twinning mechanisms 80−79814
cellulose II, preparation and crystal growth, electron diffr. obs. 78−91285
ceramics, polycrystn., porosity, twinning and grain-size depend. on spontaneous cracking 80−44253
coatings, defects and their effect on props. 80−39474
composite reciprocal lattice unit cells for cubic twins, electron diffr. obs. *(Chinese)* 79−99213
composition plane as extended defect, structure-building entity, review 80−44218
computer simulations, of twins and grain boundaries, methods in X-ray topography 79−23484
corundum, bladed crystals, morphology and struct. 77−84680
crystal, asymmetrisation in the growth process, sectorial struct. and structural ordering 79−90581
crystals, re-entrant corner effect, re-investigation 79−73177
deformation, of binary alloy 77−63717
deformation, orientation changes accompanying slip and twinning 77−43273
derivative lattices, determ. of relationships 80−107012
diamond, synthesis on nondiamond substrate, electron diffr. and luminesc. exam. 77−76344
diamond, synthetic disorientation of crystallite subgrains *(German)* 77−68939
diamond, synthetic grits, crystal morphology of cyclic twins 80−2037
diffracted electron beams, equality of intensities 78−79506
diffraction by crystals with planar faults, struct. anal. using microtwins 78−91343
dimethylammonium manganese chloride, neutron diffr., 188K, cryst. struct. 77−47434
dislocation pile-up dynamics, planar 78−6058
dislocations and lattice transformations, book contrib. 80−107242
DNA salt with cetavlon, twin struct. obs. 78−71746
double martensitic transformation, distribution of austenitic orientation *(Russian)* 78−64540
elastic monatomic crystals, nonlinear, global instabilities 80−58903
electrocrystallisation, twinning nucleation, mechanism 77−62495
electron diffraction, multibeam dynamical theory appl. to twinned cryst. 77−19847
electron microscope images of twin boundaries, contrast mechanism 78−30640
electron microscope resolution improvement for crystal structure imaging and atomic movement dynamic obs. 80−70090
electron microscopy images of coincidence grain boundaries 78−30639
ethane, single cryst. X-ray struct. determ., plastic and monoclinic forms 78−63744
FCC crystal, electron diffr. anal. of twin and HCP phase *(Chinese)* 79−10763
FCC crystal, twin-twin interactions 77−47467
FCC crystal, twin-twin interactions 77−47468

twinning continued
FCC matrix, electron diff. anal. of thin twin or HCP plates 77−59020
FCC metals and alloys texture transitions, computer simulation 79−90666
FCC structure, high-order twinning, reduction to single rot. relation *(Chinese)* 79−90669
FCC to HCP transform., model and expt. evidence 77−44243
Fe, twinning under influence of plane shock wave *(Russian)* 80−92538
ζ-Fe-Zn layer formed during hot dip galvanizing, texture 79−29287
ferroelastics, incommensurate twin plane *(Japanese)* 80−29034
ferromagnetic polytwin cryst., crystallite thickness effects on mag. struct. *(Russian)* 77−80913
ferromagnetic twin crystals, Bloch mag. struct., depend. on crystallite thickness and mag. field *(Russian)* 79−42792
ferrous martensites, trace analysis of (112) transform. twins 77−86030
film defect growth and nucleation, electron microscopy and diffraction exam. *(French)* 80−59824
graphite, CTR material, the ion injection effect 78−34557
graphite, ion bombarded, light gases, structural study using TEM 80−92570
Haynes Stellite 6B, particle erosion damage, TEM obs. 78−88546
HCP metals, atom movement in twinning, {10$\bar{1}$1}, {10$\bar{1}$3} twins, {10$\bar{1}$1} {10$\bar{1}$2} double twinning, new model 80−100252
heteroepitaxial layers, dislocation structures, problems of formation 80−15100
ice, polycrystalline twinning model with cubic struct. at junctions 77−1136
Iceland spar, crystal, interaction of crack and elastic twin 77−12698
interface obs., using relative translations of adjacent crystals in TEM 78−75675
intergrowths, regular, investigation with Laves-Ernst compensator 79−96843
isotropic and anisotropic crystals, stress fields around defects of dislocation-aggregate type 77−39591
kyanite, deformed, defect struct. 77−31668
linear compressibility anisotropy under hydrostatic press. 78−51553
magnetic reversals, role of magnetostatic interaction *(Russian)* 78−39361
martensitic nucleation mechanism, FCC→BCC and other martensitic transforms. 77−36503
martensitic transform. kinetics., strain induced, FCC to HCP 77−44249
martensitic transformation, internal stress relax. effect on microstruct. and kinetic features 77−44250
mechanical, associated tensile strain 77−31675
mechanical, associated tensile strain 77−31676
mechanical result of deform. or martensitic transform. hypothesis 77−62550
merohedry detection, based on intensity statistics 80−100246
metal, BCC, appl. of results of computer simulation of screw dislocation motion 77−4102
metal, BCC, computer simulation of twin boundary and twinning dislocation struct. 78−30644
metal, BCC, struct. of twinning dislocations, computer simulation 78−2140
metal, brittle, ductility improvement by plating *(German)* 77−8954
metal, FCC, polycrystalline, quantitative anal. of cross-slip and twinning 79−90677
metal, HCP, development of Kronberg's model for {10$\bar{1}$2} twins, extension to {11$\bar{2}$2} twins 79−51119
metal particles, small, possible vibrations associated with twins 80−100253
metal particles produced by gas evaporation, form., growth and interaction 80−16220
metallic polycrystals, deform. during cooling, revealed by deposited graphite layer *(Polish)* 80−25755
metals, microstructural inhomogeneities resulting from high strain deformations 79−87705
metals, plant deform. and recrystallisation textures 78−68708
metals and alloys, FCC, model for form. of annealing twins 78−59818
metals and alloys, HCP struct., relative orientation of cryst. lattices 80−84181
modelling of linear and surface defects 77−89450
modulated struct. phenomena, survey 79−95033
multiply twinned particles, with decahedral and icosahedral pt. group symm., twin cryst. struct. 79−86801
noncubic crystals, divergent X-ray beam technique for struct., defect investigs. 77−76259
octacosane crystals, complex growth polytypism and periodic polysynthetic twins 77−47360
ordered superlattices, X-ray studies, rel. to microstructure 79−94844
β-phycoerythrin crysts., twinned by merohedry, diffr. data treatment 80−108845
plagioclase feldspar, deformed, elastic twinning, TEM obs. 77−62551
planar nine atom model 77−51392
poly-1,6-dip-toluenesulphonyloxy-2,4-hexadiyne single cryst., twinning 80−33906
polydiacetylene single crysts., twinning 78−23777
polyethylene, {110} twinning mode, X-ray obs. 77−35572
polyethylene, anisotropic surface stress 78−14562
polyethylene, high-density, semicryst., fold-surface morphology effect on deform. processes 78−34447
polyethylene film, melt-cast, deform. in equatorial region of spherulites, electron diffr. 77−25115
polymer, crystalline, in hydrostatic tension, plastic deform. of model 77−59870
polymer crystal, local plastic deform. mech., effect of lattice defect 77−28870
polymers, struct. classification, morphology and twinning *(French)* 79−51058
quartz, Brazil twins, twinning prod. by successive shears 79−19263
α- quartz, ferrobielastic hysteresis 80−19869
quartz, fundamental and second harmonic light scattering by α-β coexistence state 77−69086
quartz, light scattering polarisation props. at α-β phase transition 80−108220
α-quartz, obs. of reversible elastic Dauphine twinning 78−87684
quartz, plant deform. and recrystallisation textures 78−68708
α-quartz, secondary Dauphine twinning, visualisation method 79−51121
quartz, stressed, Dauphine twinning growth, thermodynamic theory 79−23619
twinning continued
quartz, twinned crystals, after Japan Law, investigation of regrowth 80−54162
quartz ferrobielastic twinning, electrical and acoustic emissions 79−56731
quartz ferrobielastic twinning coercive stress obs. 78−59854
α-quartz twinning and tailored domain patterns 77−40197
rare earth oxymolybdates, growth from soln., struct., props. 77−28705
rare earth-Co alloy, electron microscopy exam. 78−67722
rotation twins, matrix anal. *(Chinese)* 79−73174
ruby, structural defects due to laser irrad. *(Russian)* 80−100303
single crystals under large loads, theoretical elastic behaviour, review and appl. 80−71681
slip and twinning relns. *(Russian)* 77−65982
smectic mosaic textures, mech. twinning obs. 77−11475
sodium acetate trihydrate, whisker growth on membrane in aq. soln. 78−30854
solid state chemistry problems, appl. of electron microscopy and diffr. 79−46527
SOS films, cryst. quality improvement by Si ion channelling, annealing 80−44222
squaric acid, ferroelasticity, elastic hysteresis loop and domain struct. 79−55814
steel, α-martensite formation in crossing range of ε-martensite platelets *(German)* 78−3126
steel, Al, relax. twins in martensite, electron diffr. and electron microscopy *(Russian)* 78−47391
steel, alloy 10G2S1 welds, fracture, subjected to low-temp. fatigue 80−89350
steel, alloy structural, anomalous grain growth 80−20984
steel, austenite, carbide strain hardened, strength and plasticity, effect of Mn content *(Russian)* 80−97500
steel, austenitic, AISI 4340, effect of step quenching on microstruct. and fracture toughness 78−84834
steel, austenitic, Cr-Mn, Kh4G18F, microstruct. and mech. props. during tensile deform. *(Russian)* 79−20114
steel, austenitic stainless, plastically deformed, TEM obs. *(French)* 77−44302
steel, austenitic stainless, stacking fault effect on martensitic transform. during plastic deform. *(Russian)* 80−25696
steel, bainitic, invariant plane strain theory, determ. of habit planes and orientation relationships 80−55388
steel, C, cavitation erosion, exam. of mechanism and rates 79−5063
steel, cast, fractographic features of coarse grained intercrystalline fractures *(Czechoslovakian)* 77−36627
steel, cast, high speed, solidification, $(Fe,Mo)_6C$ form., struct. 79−24514
steel, Fe-Mn-C austenitic, deform. twinning and mech. props. 77−59868
steel, high Mn, mech. props.. strain induced martensitic transform., effect of austenite predeformation 77−16649
steel, high-C, type U12, U15, U17, cementite precipitation cryst. geometry singularities during decomposition of martensite *(Russian)* 80−7577
steel, low alloy, martensite twinning, direct anal. 80−2040
steel, low C, alloy, structural transform. during deform. and annealing *(Russian)* 79−91707
steel, low C, V(C,N) precipitation and twinning in γ→α transform. *(Polish)* 78−52807
steel, mild, impact velocity effect on fracture surface *(Japanese)* 79−96118
steel, Mn, form. of twinned struct. *(Russian)* 78−64542
steel, Mn (13.5 wt.%) hardening mechanism during friction 79−96152
steel, stainless, Cr-Mn (21, 14 wt.%), grain boundary precipitation and fracture *(Japanese)* 79−100149
steel, stainless, shock loaded, peak press. and press. pulse duration effect on crystallographic transform. 78−67769
steel, stainless, shock loading parameter effect on substruct. and mech. props. 79−52360
steel, stainless 304, deformation twins contribution to yield stress, Hall-Petch law for inter-twin spacing 79−24588
steel, stainless 304, recrystallisation, effect of dislocation structure 77−32595
steel, stainless 304, shock loading response, grain size effect 77−36601
steel, stainless type 316, in-situ HVEM studies under ion beam irradiation 80−103396
steel, thermally and thermomechanically treated, struct. and decomposition of martensite 78−19784
steel, thermomechanical treatment effect on mech. props. and microstruct. *(French, German)* 79−66090
steel, type 304, twinning and martensitic phases on hydrogen-charging, TEM 77−21222
steel, types 10G2 and 18G2F, formation of transform. microtwins in ferrite *(Russian)* 79−1866
steel, U15 and 130 Gz, upper bainite, relation between cementite and ferrite lattice orientations *(Russian)* 78−23663
steel, V, precip. and transform. kinetics, effect of N 80−97485
steel martensitic, high-C, formed from hot-worked austenite, struct. *(Russian)* 78−6950
steel plates, fatigue substructures after high cycle vibrs. 77−8945
steels, 110G13 and 40Kh10G10, hardening and structural transformations during friction *(Russian)* 77−52527
sulphide minerals, superstructure and modulated struct. 79−99146
superconductors, type II, review of mechanical behaviour and stress effects 77−86083
swinging twinning on unit cell level as cryst. struct. building operation 77−31623
texture transformations, 'brass to copper' in FCC metals 80−76246
TMMC, one-dimensional, EPR at HF and low temp. 78−80205
transition metal hydrides and deuterides, $MH_x(D_x)$, M=gp. V metal, single cryst. prep. and characterisation 79−95910
tris (3-mercapto-1, 3-diphenyl-2-propen-1-onato) Co(III), multiple twinning 80−100250
twin and stacking fault energies 79−38018
vinyl stearate multilayers, struct. determ. 79−4469
weak-beam technique, contrast from incoherent twin interfaces 79−46524
X-ray diffractometry, of superimposed twins and clusters, establishing UB matrices of single cryst. individuals 79−37586
X-ray intensity measurements of twinned or grown together cryst. 77−51275
Zircaloy-4, load relaxation and tensile tests 79−20093
Zircaloy-4-O alloys, rapidly heated and quenched, transform. charact. 79−20041

twinning continued
Ag, (211)[$\bar{1}$11] single crysts., shear band effects on rolling deformation 80−50651
Ag catalysts, multiply-twinned particles 80−15114
Ag epitaxially grown film, on Au (111), twin form., LEED detection 80−88442
Ag, filament produced by glass coated melt spinning, mech. props. 77−86125
Ag, high purity, nucleation and twinning during recrystallization, TEM study 79−29082
Ag, multiply twinned particles, internal and surface struct. by electron microscopy 80−84189
Ag, recrystallisation texture development after plane-strain deform. 77−48448
Ag, tensile deformed, dynamic recrystn. *(German)* 80−84959
Ag, thin-film bicrystals, planar lattice defects and migrating grain boundaries interaction 80−79835
Ag wire, ultrapure, cryst. forms of hillocks and voids formed by electromigration 77−31811
Ag-Cd (45 at.%) martensite, shape memory mech. and related phenomena 80−30009
Ag-Cd (47 at.%), crystal struct. and internal defects of thermoelastic martensite 77−48438
Ag-Ge (4.5 at.%), FCC, vapour-deposited, lattice imperfections, X-ray diffr. 78−72032
Ag-Ge eutectic alloys, unidirectional solidification, electron microscope study of twinning 79−61574
Al, annealing twin growth, obs. by synchrotron radiation X-ray topography 79−55753
Al, boundary dislocations gliding, on coincidence boundaries, TEM study 79−82224
Al-alloy ingots, crystallisation condition effects on fan-shaped zone struct. *(Russian)* 78−3114
Al-Fe-Si, eutectic alloy growth, by twinning plane propagation *(French)* 78−60667
Al-Ni foil, vapour deposited, multiply twinned particles, electron microscopy 77−28083
Al-Ni(Pt)(Zn), rapidly solidified, twinned dendrites 80−70572
α-Al_2O_3, sapphire lamellar crystal, growth twinning investig. 77−4113
Al_2O_3, twinning and microcrack nucleation during indentation 77−63793
Al_2O_3, unflawed polycryst., tensile failure, SEM and acoustic emission expts. 78−27598
$AlPO_4$, twinning and phase transform., X-ray diffr. obs. 77−47466
Au, electroless deposition, epitaxial initial growth with microtwinning 77−8771
Au films, condensation on alkali halides, growth, struct., stability *(French)* 78−38989
Au films, vac. condensed at oblique vapour incidence, oriented cryst. growth, electron diffr. study 80−97432
Au fine particles, adhesion, role of twinning and surface energy, TEM obs. 78−72009
Au island epitaxial films, on (111) surface of fluorite, discrimination of twin orientation 79−46983
Au, multiply twinned particles, internal and surface struct. by electron microscopy 80−84189
Au, twinned crystals, epitaxial growth on KCl crystals, electron microscopic study of microstructure 78−91566
Au wire, ultrapure, cryst. forms of hillocks and voids formed by electromigration 77−31811
Au-Cd (47.5 at.%), modified 2H and 9R martensites 78−14366
Au-Mn ordered alloy, coincidence sites in domain boundaries, high resolution TEM obs. 78−71708
AuCu II plates, growth mechanisms 77−48423
Au_8Mn_2, electron microscope exam. of ordering 78−63697
β-B, electron beam zone melting growth, crystn. and defect form. 80−15020
BC, sintered, struct. and props. 80−104181
$B_{12}C_3$, sintering and subsequent high temp. annealing, struct. and props. 80−20858
BN, artificial production of growth twins 78−30641
BN, graphite-like, twinning and shear 77−4114
BP, epitaxial, CVD on Si substrate, cryst. imperfections 78−10294
BP wafers, epitaxial growth by thermal decomp. of $B_2H_6+PH_3$, struct. imperfections 77−62774
$BaCl_2.2H_2O$, artificial production of growth twins 78−30641
$BaCl_2.2H_2O$, ferroelastic effect obs. 79−28033
$Ba_{2.09}Na_{0.72}Nb_{5.02}O_{15}$, cryst. growth, monodomenisation, detwinning, optical homogeneity, composition, dielec., spectral props. 77−44151
$BaTiO_3$, effect of phase transformation on fracture behaviour 78−48507
$BaTiO_3$, ferroelectric domain struct. and cryst. struct. changes, X-ray diffr. 77−24803
$BaTiO_3$, ferroic materials, fracture processes 80−79869
$BaTiO_3$, planar phase boundaries and domain struct. 79−69795
Be, twin and stacking fault energies 79−38018
Be, twinning dynamics of single crystal 77−4115
Be_3N_2-$BeSiN_2$ system, crystallography and phase relationships, TEM and electron diffr. study 80−92502
Be_2SiO_4, phenakite, flux grown single crysts., twinning study by hydrothermal etching and X-ray diffr. 80−107271
Bi, charge carrier interaction with twinning planes in strong transverse mag. fields *(Russian)* 80−88577
Bi epitaxial film, twinning, electron diffr. 77−35838
Bi, magnetothermal EMF, twinned layer effect 80−49784
Bi, twin shape variation under long period loads *(Russian)* 80−65007
Bi, twinning dynamics of single crystal 77−4115
Bi_3GeVO_9, dielec. props. and twin struct. 77−12350
$Bi_{12}O_{15}Cl_6$, struct. derivation from $Bi_6X_{7+n}Cl_3$ by chem. twinning 77−35520
$Bi_6O_7FCl_3$, struct. derivation from $Bi_6X_{7+n}Cl_3$ by chem. twinning 77−35520
Bi_2S_3-CuPbBiS_3 series, ordered chem. twinning 79−55717
$Bi_7Ti_4NbO_2$, mixed-layer cryst. struct., twinning, electron microscope images 77−84703
Ca-Nb-O perovskites, struct. characterisation *(French)* 78−10021
$CaBSi_2O_6$, B=Mg, Fe^{3+}, Al, pyroxenes, order-disorder interpretation 80−38987
$Ca_{0.2}Ba_{0.8}TiO_3$:Nb, conductive single cryst. growth by Verneuil method 77−85928
$CaCO_3$, calcite, form of end of free elastic twin *(Russian)* 80−6416
$CaCO_3$, Iceland spar, crack interactions with twin interlayers 77−7790

twinning continued
$CaCO_3$, with perfect struct., temp. depend. of rate of twinning 80−10561
$Ca_2NaHSi_3O_9$, pectolite, TEM obs., of microtwins and stacking faults 78−75677
CaO, single cryst. growth from molten $CaCl_2$ in wet atmosphere, habits 80−55287
$(Ca_{1-x}Sr_x)(Ca_{1/3}Nb_{2/3})O_3$ perovskites, cryst. struct., twinning phenomena obs. *(French)* 79−65044
Cd, twinning dynamics of single crystal 77−4115
Cd_3As_2, vapour phase single cryst. growth, X-ray topographic obs. of perfection 78−9976
$CdCO_3$, three-fold transformation twin in topotactic decompositon 78−44078
CdI_2, hexagonal-rhombohedral polytypic transformation, electron diffr. and X-ray diffr. obs. 80−49163
CdI_2, soln. grown, rotation twinning, arcing and polytypism 78−51557
CdS layers, epitaxial, deposited on InP substrates, vapour growth technique 77−21033
CdS-CdTe double layers on various GaAs surfaces, morphology and crystallography 80−34326
CdTe layers, on CdS substrate, cryst. perfection and defects, X-ray diffr. obs. 79−56081
CdTe, nonlinear optical effects in rotationally twinned crysts., phase matching 77−42570
Co base alloy, FCC, twin-slip interaction 77−51379
Co, Co alloy, HCP films, chem. reduced, electrodeposition on Cu, Ni FCC crysts., struct. 79−11527
Co, glide ahead of terminating {10$\bar{1}$2} twins 80−96545
Co, single crystal, cavitation erosion, role of twinning 80−107272
Co, single crysts., {11$\bar{2}$1} twins, accommodation and form. 80−96540
Co-Fe alloys, transformation induced microstructs. extended total dislocations, TEM study 79−42073
Co-Ni (33 wt.%), FCC deform. twinning kinetics, relationship to stress-strain behaviour 78−52887
Co-Ni alloy, slip charact., and fatigue, FCC twinning and FCC to HCP martensite transform. effect 80−35182
Co-Ni-Cr-Mo, mech. props., effect of twinning and FCC to HCP transform. 77−4779
Cr, BCC, electrodeposits on {100} Cu substrates, {211} twins obs. 77−47698
$CsCaCl_3$, birefringence, twinning and structural phase transitions 79−38480
CsCl, twin form. by compressive stress during phase transform. 80−49358
CsCl-type lattice, (111) superlattice screw dislocation motion, computer simulation 80−79793
$CsLiSO_4$, crystal structures of I and III phases, twins 80−70181
$CsPbCl_3$, birefringence, twinning and structural phase transitions 79−38480
$CsSrCl_3$, birefringence, twinning and structural phase transitions 79−38480
Cu, annealing twins density, photoemission microscopy 80−35208
Cu, deformation in ultramicrotomy 77−8874
Cu, electrodeposited coating, annealing effect on struct. and microhardness *(Russian)* 78−76668
Cu, electrodeposition and formation of crystallised layers on Ni(111) surface, twinning 77−24495
Cu epitaxially grown film on Au (111), twin form., LEED detection 80−88442
Cu films, vac. condensed at oblique vapour incidence, oriented cryst. growth, electron diffr. study 80−97432
Cu, mechanical twinning characts., 4.2 to 300K *(Russian)* 79−37714
Cu, mechanical twinning in (110)[$\bar{1}$12] single crystal under plane strain compression *(German)* 77−36616
Cu, single crysts., ⟨110⟩ oriented, tensile deformed, HVEM of recrystn., recrystallised state 80−89256
Cu single crysts., deformed, HVEM study of recrystn. texture 80−104179
Cu, strain hardening parameters, 4.2 to 300K *(Russian)* 79−20063
Cu, tension deformed single crystal, dynamic recrystallisation 79−47716
Cu, thick sputter deposit, microstruct., tensile props. 77−40461
Cu-Ag, solid soln., nonhomogeneity of deform. 78−84889
α-Cu-Al, mechanical twinning characts., 4.2 to 300K *(Russian)* 79−37714
Cu-Al (11 at.%) single cryst., dislocation reactions during deform. twinning 80−79795
Cu-Al (15 at.%), rolled single crysts., metallographic study of deformation struct., orientational change, shear bonds *(Japanese)* 79−24582
Cu-Al (3 wt.%), annealing twins density, photoemission microscopy 80−35208
Cu-Al (6.4 wt.%), rolled low stacking fault energy alloy, struct. and texture 78−52844
Cu-Al alloys, strain hardening parameters, conc. and temp. depend., 4.2 to 300K *(Russian)* 79−20063
Cu-Al-Ni, single variant twinned martensites, pseudoelasticity 77−28849
Cu-Al-Ni alloys, deformed, fine struct. of martensite *(Russian)* 78−6923
Cu-Al(8 at.%), single crystal, twinning deform. 77−21236
Cu-Cd, structure, electrolytic deposition on monocrystalline Cu cathodes *(Polish)* 80−44435
Cu-Cd alloy electro deposits on Cu substrate, struct. *(Polish)* 79−51437
α-Cu-Ga (3.4-15 at.%) cold-worked, lattice imperfections, X-ray obs. 77−55291
Cu-Si (6.5 at.%) alloy, easy glide deform., obs. and mechanism 77−8887
Cu-Sn, deformed, martensitic transformation *(Russian)* 79−15668
Cu-Sn (4.9 wt.%), role of mech. twinning on stress/strain behaviour 80−85004
Cu-Zn single crystal, pseudoelastic effects 79−47739
γ-Cu_9Al_4, struct. refining from diffr. meas. 78−55834
Cu_3Au, deformation twinning 77−63717
CuAu superlattice, (101) lattice twinning mode assoc. with ordering transition 77−15431
$CuFeS_2$, explosive-shock deform. 78−95108
$CuFeS_2$, natural chalcopyrite, defect struct., TEM 77−62535
Cu_2FeS_3, pseudocubic mineral, twinning obs. in point electron-diffr. photographs 77−43225
β(CuNi)Zn alloys, effect of normal stress on {112} ⟨111⟩ slip 79−47760
Cu_2Se, VPE on mica, defect struct., temp. depend. 77−35837
CuZnAl, martensitic, ordering effect on yield stress 79−100133

twinning continued
Dy, rel. to magnetoplastic deform., 70-90 kOe, 4.2K 77−8376
Dy, single crystal, plastic and magnetoplastic deform. 77−63713
Dy_2O_3, lattice conservating twin, bend contours due to upper Laue zones 80−15113
α-Fe, $(\bar{1}\bar{1}2)$ $[\bar{1}\bar{1}\bar{1}]$ anti-twinning slip system, low temp. strengthening, dislocation struct. 77−21164
Fe alloys, influence of plastic deform. on twinned martensite struct. *(Russian)* 78−88493
Fe, Armco, microstruct., effect of strain rate on change, due to tension-compression 78−80614
Fe, α-, γ-, crysts., twinning, martensitic transforms., correspondence matrices *(German)* 78−31406
Fe, cavitation erosion, exam. of mechanism and rates 79−5063
Fe, single cryst. growth by recrystn., twinning, growth length *(French)* 77−12523
Fe whisker, polycryst., FIM obs. of struct. 78−84111
Fe zone refined crystals, cryst. orientation and distrib. of stray grains 80−70509
Fe-Al, single crystal, twinning and pseudoelasticity 79−15718
Fe-Al eutectic alloy, duplex crystals, unit cell parameters, appl. of Weissenberg technique 78−67684
β-Fe-Be, pseudotwinning and pseudoelasticity 79−96056
Fe-Co-Ni-W alloy, 45KKhVN, plastic deform., electron microscope obs. *(Russian)* 78−80584
Fe-Cr (26 wt.%) effect of Ni content and austenite phase, on low temp. toughness and embrittlement 78−60754
Fe-Cr-Co alloy, spinodally decomposed, micro-twinning 80−92537
Fe-Cr-Ni-C (17.2, 7.34, 0.2 wt.%) alloy, twin related laths, fracture elongation, TEM study 79−29192
Fe-Mn, mechanical twinning of close-packed hexagonal ε-phase during plastic deform. *(Russian)* 80−60909
Fe-Mn-Cr-C, twinning and strain induced FCC to HCP transform. 77−44248
Fe-Mn-Mi, martensitic, morphology and substruct. study 77−70059
Fe-Mo quenched alloy, electron microscope exam. of planar defects 79−79000
Fe-Ni, slip and twinning, SEM and optical obs. 79−71209
Fe-Ni martensites, deform. twinning for crystals with transform. twin microstruct. 77−31677
Fe-Ni-C, HVEM study of strain induced martensite 79−20047
Fe-Ni-C, martensitic, internal friction 77−16633
Fe-Ni-C, role of strain in deform. induced martensitic transform. *(Japanese)* 78−92263
Fe-Ni-C, thin foil, high voltage TEM exam. of martensitic form. 78−92264
Fe-Ni-C (24, 0.45 wt.%), martensites, TEM observation of double twinning 78−76651
Fe-Ni-C (26.4, 0.24 wt.%) martensite, partially twinned, slip lines obs. 78−84913
Fe-Ni-C (30, 0.5 wt.%) single cryst., stress induced martensitic transform. 80−60860
Fe-Ni-C (31, 0.28 wt.%), crossings of thin plate martensites, TEM obs. 80−25756
Fe-Ni-C austenitic alloy, banded struct. formed by deform. 80−71713
Fe-Ni-Ti-C (31, 4, 0-18 wt.%), coherent precipitates in austenite, effect on martensite substruct. 77−52327
Fe-Ni-(C), substruct. of ausformed martensite 77−36548
Fe-Ni-(C), thin foil martensite, TEM obs. 77−51378
Fe-Pd (50 at.%) alloy, structural changes during ordering *(Russian)* 77−77471
Fe-Si, dynamically strained, temp. depend. of twinning charact. *(Russian)* 79−46673
Fe-Si, temp. depend. of twinning intensity, development of deform. *(Russian)* 79−51116
Fe-Si, temperature dependence of the twin growth rate *(Russian)* 79−27999
Fe-Si, twinned annealing, plastic deform., and recrystallisation *(Russian)* 77−28829
Fe-Si (3 at%), deformation and electron bombardment, influence on dislocation struct., 20-500°C *(Russian)* 80−92536
Fe-Si (3 wt.%), breaking stress grain size and grain boundary energy during onset of reversible temper brittleness *(Russian)* 77−32673
Fe-Si (3 wt.%), electron irradiated, yield strength and elongation 80−76325
Fe-Si (3 wt.%), singularities in geometry of slip, point temp. depend. *(Russian)* 79−24574
Fe-Si(3.25 wt.%), crack nucleation depend. on twins during intense slip *(Russian)* 79−100239
FeAl single crystal, compressed, dislocation arrangement 78−14354
Fe_3Al, slip geometry and pseudoelastic behaviour, effect of crystal orientation *(French)* 78−87681
$Fe_{80}B_{20}$, crystallisation of amorphous alloys, TEM and X-ray diffr. exam. of struct., growth charact. 78−79539
$Fe_3B_7O_{13}I$, twinning in orthorhombic phase, ferroelec. domain struct. with switching 78−19434
$Fe^{2+}BSi_2O_6$, B=Mg, Fe^{3+}, Al, pyroxenes, order-disorder interpretation 80−38987
FeCoC, unidirectionally transformed eutectoid, crystallography of herringbone pearlite, TEM obs. 78−31399
$Fe_2(MoO_4)_3$, cryst. struct. and twinning behaviour 80−33967
$Fe_{50}Ni_{30}B_{20}$, crystallisation of amorphous alloys, TEM and X-ray diffr. exam. of struct., growth charact. 78−79539
α-Fe_2O_3, prod. by α-FeOOH dehydration, mosaic struct. and twin form. 79−86802
Fe_2O_3, twinning dislocations, electron microscopy obs. 79−99218
α-Fe_2O_3, twinning law *(French)* 79−51038
Fe_2O_3/Fe_3O_4 transformation matrices, higher-order orientation relationships 80−100846
FeP_4, twinned cryst., synthesis and cryst. struct. 79−4278
Fe_3Pt, martensite austenite interface, twin thickness in martensite 77−32579
GaAs, defect revealing etchant, electrochem. process in $NH_4OH:H_2O$ 78−6060
GaAs:$p^+(N^+)$, struct. charact. of radiation damage produced by high energy ion implantation 79−4340
GaP crystal, structure defect formation due to annealing and stress, dendrites, slip, dislocations 80−29026
$Gd_2(MoO_4)_3$, ferroelastic, laser-induced twinning 77−76422
Ge (111) surface, 500 eV Ar^+ bombard., high temp. annealing, recovery, RHEED obs. 78−87723
twinning continued
Ge, strained crystal, annealing effect, recrystn. and struct. *(Russian)* 80−89252
Ge, twin lamellas formation due to deposition of metal contacts 78−10060
Ge-Si system alloys, growth by Czochralski method, morphology 77−15329
GeTe, effect of phase transition on mech. and elec. props. 77−51746
α-HgS, synthetic cinnabar, morphological, optical and X-ray studies *(French)* 77−43223
$HoAlO_3$, Czochralski growth and props. 77−48335
In, acoustic emission charact. of twinning, nondestructive testing evaluation 77−4873
In crystals, twin layer broadening dynamics in temp. range 235-390K 79−65098
In-Sn alloy crystals, phase changes and shape memory effect *(Japanese)* 80 108502
InBi single crystal, deform. mode under dynamic indentation 80−88163
InP, MBE, substrate temp. related degradation mechanisms 80−65385
InP single crystals, uniaxial compression deform. charact. 80−84991
InP, twin-free, prep. using liquid encapsulated Czochralski growth 80−50546
InSb, crystal growth from melt, facets and twin formation obs. *(Chinese)* 80−59409
InSb thin layers, directed crystn. on sapphire, struct. 80−35112
InSb-GaSb alloys, directionally solidified, influence of twinning on segregation, electron probe anal. 79−24513
InSb-GaSb solid solution ingots, orientation, twinning and orientation depend. reflectance 79−28001
Ir-W (0.3 wt.%), polycrystn., brittle fracture TEM study 79−61715
$K_2Cr_2O_7$, role of metastable β-phase in cryst. growth 79−32931
$K_4Fe(CN)_6.3H_2O$, nature of phase transition 79−38470
KH_2PO_4, appl. of γ-ray diffractometry to twinned crystals study 79−68987
KNO_3, orientations and twinning in the struct. transform. aragonite-type to calcite-type 77−24284
K_2SO_4, thermal phase transition 80−19738
$KTi_2Ta_5O_{17}$, chemically twinned rutile struct., X-ray study 80−107149
$LaNbO_4$, ferroelastic, cryst. struct. and twinning struct. 79−27965
$LaTiO_3$, cryst. struct. and cryst. chem., cryst. showing complex twinning 80−1984
β_{II}-Li_2CoSiO_4, disordered struct., twinning description 80−39017
Li_2GeO_3, melt-grown single crysts., polar twins, piezoelec. meas., etching behaviour 79−32999
$LiNbO_3$, twinning systems produced by plastic compression 77−1135
Li_2SiO_3, melt-grown single crysts., polar twins, piezoelec. meas., etching behaviour 79−32999
Mg, twin and stacking fault energies 79−38018
Mg-Ce, workability, aging charact. and tensile strength 80−55416
Mg-La, workability, aging charact. and tensile strength 80−55416
$MgAl_2O_4$ crystals, flux grown, artificial spinel twin form. by $BeAl_2O_4$ addition 80−96542
$MgBSi_2O_6$, B=Mg, Fe^{3+}, Al, pyroxenes, order-disorder interpretation 80−38987
MgO smoke crystals, growth twinning 79−60382
Mn-Cu (25 wt.%) alloy, critical shear stresses of glide 79−87693
Mn-Cu alloy, plastic deform. mechanism and shape-memory effect, mag. struct. obs. *(Russian)* 78−60705
Mn-Ni, single cryst. or polycryst., elastic anomalies at antiferromag. transition 78−14972
$MnCO_3$ crystals, gel. grown, Ca^{2+}, Ni^{2+} impurity influence, SEM study, cause of twinning 80−20778
$Mn_{0.75}Ga_{2.17}S_4$, twinning and cryst. struct. determ. *(French)* 78−83798
MnS-Y_2S_3, chem. twinning, electron microscopic study 79−46678
Mo, shock deformation twinning, shock press., pulse duration and grain size effects 79−5021
Mo, shock deformation twinning, shock loaded BCC and FCC metals comparison 80−104413
Mo, shock loaded, peak press. and press. pulse duration effect on crystallographic transform. 78−67769
MoO_3 topotactic transform into MoO_2, electron microscopy, X-ray anal. 80−107417
α-N_2 twinning, electron microscope and diffr. exam. 77−35574
NH_4LiSO_4, point group symm. at high press. phase 80−70150
NH_4MnCl_3, X-ray single crystal analysis, phase transitions, Mossbauer effect 79−19366
$(NH_4)_2SO_4$, mechanically twinned, orthorhombic, search for antiphase boundaries 79−37715
$(NaAl)_xSi_{2-x}O_6.H_2O$, analcite, polyhedral tilt transitions obs. at high press. 80−6515
$Na_2Al_2Si_3O_{10}.2H_2O$, natrolite, cleavage etching in acidic and neutral media 80−6407
$NaBSi_2O_6$, B=Mg, Fe^{3+}, Al, pyroxenes, order-disorder interpretation 80−38987
Na_2CoGeO_4, hydrotherm. single crysts., optical microscopy study of twinning 79−19166
$NaH_3(SeO_3)_2$, high-pressure phase transform., ^{23}Na NMR obs. 77−63380
$NaNO_2(NO_3)$, linear compressibility to 27 kbar, X-ray diffr. obs. 80−34125
$Na_2Ti_9O_{19}$, orthorhombic, unit-cell twinning of monoclinic $Na_2Ti_9O_{19}$, cryst. struct. 80−107155
Na_xWO_3, domain struct., optical microscope obs. 79−19436
$NaZr[Si_2O_6OH]$, keldyshite, X-ray structural anal. 79−14779
Nb, single crysts., plastic relaxation of internal stresses during mech. twinning at 4.2K, optical and SEM study *(Russian)* 79−66108
Nb, superconductor, deformational twinning, mag. props. *(Russian)* 79−95543
Nb-Ti, metallurgical treatment, effects on props. 79−38846
Nb-Ti(Zr), type II superconductor, mech. behaviour and stress effects 77−86083
NbO, cryst. growth and microstructure 79−95913
NbO_2, cryst. growth and microstructure 79−95913
$Nb_{12}O_{29}$, cryst. growth and microstructure 79−95913
Nb_2O_5, cryst. growth and microstructure 79−95913
Nb_xO_y structures, dislocations and related defects 77−7724
$4Nb_2O_5.9WO_3$, cryst. struct. determ. by 1 MV TEM 79−7581
$NdNbO_4$, ferroelastic, cryst. struct. and twinning struct. 79−27965
Ni, (99 wt.%), annealing twins density, photoemission microscopy 80−35208

twinning continued
Ni, cyclic flow stress and microstructural changes during multiple step testing at elevated temperatures 79−91746
Ni, deformation twins contribution to yield stress, Hall-Petch law for inter-twin spacing 79−24588
Ni, electrodeposit, change in twin faults during growth, X-ray study 79−65334
Ni electrodeposit on Cu, growth and microstruct. 77−11823
Ni, film deposit on (001)Fe substrate, misfit twin crystals 77−4273
Ni, pure, anomalous grain growth 80−20984
Ni, pure stacking fault energy eval. from twinning stress of Ni-Ge (1 to 9 at.%) *(Japanese)* 78−59820
Ni, shock loading parameter effect on substruct. and mech. props. 79−52360
Ni, textured galvanic layers, grain size determ., matrix and twinning orientations *(Russian)* 77−43461
Ni, thick sputter deposit, microstruct., tensile props. 77−40461
Ni/Ni_3Al-Ni_3Nb, directionally solidified lamellar eutectic alloy, deform. anisotropy and fracture 77−36604
Ni/Ni_3Al-Ni_3Nb eutectic, directionally solidified, plastic deformation *(Russian)* 78−39843
Ni-Ge (1 to 9 at.%), twinning stress used to eval. stacking fault energy of pure Ni *(Japanese)* 78−59820
Ni-Ni_3Al-Ni_3Nb, directionally solidified, role of twinning in cyclic stress strain behaviour 78−80605
α'_2-Ni-Zn-Cu martensite, thermoelastic, microscope obs., TEM 77−55966
$Ni_{62}Co_4Al_{34}$, fine struct. of martensite, electron microscopy obs. *(Russian)* 79−46672
Ni_2Cr ordered alloy, mech. twinning *(French)* 77−72624
NiTiCu, shape memory alloys, electron microscope and X-ray diffr. study of struct. 79−82179
Ni_3V, deform. propag., electron microscopy obs. 78−6070
α-Np, deform. modes around hardness indentations 77−20009
$PbNb_2O_6$ ferroelectric single crysts., domain struct., cryst. planes, twinning 78−64340
Pb_2OFBr, mimetic twinning, cryst. struct. determ. 79−23568
Pb_2OFCl, mimetic twinning, cryst. struct. determ. 79−23568
Pb_2OFI, mimetic twinning, cryst. struct. determ. 79−23568
$Pb_3(PO_4)_2$, ferroelastic domain struct., twinning analysis by pseudosymmetry 77−76421
PbS, film condensation on amorphous substrate, struct. and growth 78−38981
n-PbTe, cold hydroextrusion, plastic deform. rel. to thermoelec. props., struct. 77−11945
$PbTiO_3$, crysts., simple 90° twinning, X-ray study of 90° domain struct. 79−15426
$PbTiO_3$, mechanical twinning, spontaneous polarisation shielding 79−42930
$Pb(Zr,Ti)O_3$, ferroic materials, fracture processes 80−79869
$Pr_{24}O_{44}$, beta phase, high resolution cryst. struct. images 78−42991
$RbCdCl_3$, birefringence, twinning and structural phase transitions 79−38480
$RbMnCl_3$, birefringence, twinning and structural phase transitions 79−38480
$RbMnCl_3$ crystal, structural phase transition, twin struct. 80−15243
$RbMnCl_3$, twinning struct., cryst. domains, orientation mag. transition *(Russian)* 80−107275
Re film, electrodeposition on Cu, packing defects, X-ray diffr. 77−1333
Re, metallo-ceramic, deform. and cold working by cold rolling *(Russian)* 78−56655
$(SN)_x$, fibrous struct. study by electron diffr. using TEM 79−65004
$(SN)_x$, halogenated, struct. behaviour, TEM obs. 80−70126
$(SN)_x$, struct. defects, nature and origin 77−24313
Sb, twinning dynamics of single crystal 77−4115
Sc_3Co, new struct. type related to Fe_3C and Re_3B by periodic unit-cell twinning 79−4268
Si (111) surface, 500 eV Ar^+ bombard., high temp. annealing, recovery, RHEED obs. 78−87723
Si crysts., dynamic processes associated with stacking faults and deform. twins, HVEM in-situ obs. 80−103369
Si, dechannelling by twins, ^4He backscatt. spectra 78−18691
Si epitaxial film on sapphire, microtwins, TEM exam. 80−70555
Si epitaxial layer on sapphire, twin three dimens. distrib. 77−89666
Si, fivefold twinned crystals grown in Al-Si (16 wt.%) melt 80−2942
Si, implanted, dechannelling of MeV He ions by twinned regions 78−75700
Si, implanted and annealed, effect of twins on dechannelling charged particle beam 79−4315
Si, implanted annealed layers, amorphised structure formation mechanism and crystallographic nature 80−29091
Si, ion implanted, complex annealing behaviour of amorphous layers, TEM obs. of defect struct. 80−107299
Si, ion implanted, damage struct. obs. using TEM and cross section specimens 80−107298
Si layers, solid phase epitaxial growth, crystalline qualities, ^4He backscatt. and TEM exam. 78−10306
Si, on sapphire, early growth, TEM 77−24961
Si, on sapphire, early growth, models 77−24962
Si on sapphire, stacking faults and twins, TEM obs. at early stage of epitaxy 79−28233
Si, polycrystalline, grain boundary obs. by TEM, solar cell appl. 80−72057
Si, polycrystalline structure stability, stacking defects, twins grain struct. *(Russian)* 80−100248
Si, post-annealed amorphous layer, twinning struct. by transmission electron diffr. 77−76685
Si, recrystallised amorphous layer, self-ion irradiated, defect structures, TEM obs. 78−75688
Si, ribbon, edge-defined film-fed grown, orientation depend. of defect struct. 77−1134
Si ribbon parallel twinned structure development by shaped crystallisation 78−64465
Si, solid-phase-epitaxial, deposited above 380°C, defects obs. 78−63942
Si, strained crystal, annealing effect, recrystn. and struct. *(Russian)* 80−89252
Si, structural defects on (115) plane 78−87675
Si, twinned, neutron diffr. topographic obs. 78−38727
Si:Ne(Ar)(Kr), ion implantation damage, annealing, comparative study 79−10867
Si-Al-O-N system, phase analysis and TEM struct. obs. 80−108420

twinning continued
SiC, cubic, photo EMF on microtwinning lamella *(Russian)* 78−60165
n-SiC, single cryst. layers deposition on charact. substrates, morphology *(German)* 79−28943
β-SiC, twinned crystals, fracture charcts. 80−3193
B-SiC, X-ray diffr. study of anisotropic layers in twinned seams 80−107274
SnO_2:Sb, and pure cryst., microstruct., X-ray diffr., optical and electron microscope studies 78−79619
$SrAl_2Si_2O_8$, TEM obs. of feldspar aand hexacelsian polymorphs 78−83827
$SrTiO_3$, defects grown by Verneuil method 77−51390
Ta-N, domain configurations of new phase *(French)* 78−56648
Ta_2O_5, ε-modification, cryst. struct. and microstruct. 79−51083
$TaSe_2$, 1T and 2H superstruct., cryst. struct. using X-ray diffr. 80−39044
Tb, rel. to press. induced polymorphic transition mechanism 77−59113
Ti alloys, twinned hexagonal α phase crystals, electron diffr. pattern analysis 78−56647
α-Ti based alloys, deform. twinning effect on mech. props. at low temps. *(Japanese)* 78−6979
Ti, fast neutron irrad., twinning deform. at room temp. 80−65061
Ti, fracture mechanism at different temps. 77−63785
α-Ti, plastically deformed by rolling, optical and electron microscope obs. 79−91666
Ti, twinning deformation, neutron irradiation effects 80−75236
Ti-Al-Mo-V (8, 1, 1 wt.%), Widmanstatten colonies, fracture toughness 80−85031
Ti-Al-V (6,4 wt.%), strongly textured, influence of crystallographic orientation on tensile behaviour 80−7633
Ti-Al-V(Sn) alloys, plastic deformation and fracture charcts. at low temps. *(Russian)* 80−7624
Ti-Al(−V)(Mo), impact strength anisotropy, influence of texture *(Russian)* 80−20952
β-Ti-Mo, alloy, struct. changes during deformation and ageing *(Russian)* 78−39791
Ti-Mo, metastable β-phase, stress induced products formed by cold rolling *(Japanese)* 78−84843
β−Ti-Mo, thermal instability, hardness and tensile deform. *(Japanese)* 80−71703
Ti-Mo (15 wt.%) alloy, metastable β-phase, deform. charcts. 78−6975
β-Ti-Mo-Zr-Sn (10.2, 5.8, 4.7 wt.%) heat treated, tensile yield, fracture behaviour, primary deform. mode, exam. 78−60724
Ti-Mo-Zr-Sn (11.5, 6.0, 4.5 wt.%) alloy, struct. as affected by processing history 80−84972
Ti-Mo-Zr-Sn-Fe-C-Si alloy, β-III, cold deform. and annealing, effect on struct. and mech. props. *(Russian)* 79−24533
Ti-V, cyclic stress-strain response 78−60700
Ti-V, metastable β-phase, stress induced products formed by cold rolling *(Japanese)* 78−84843
Ti-V (15.5 wt.%), {332} deformation twins, optical microscopy study 79−79047
β-Ti-V metastable alloys, fatigue crack propag. 80−60964
Ti-Y(Er), dispersoid effect on deform. 79−24530
$TlBiTe_2$, epitaxial film, struct. anomalies, TEM 77−11824
$TlMnCl_3$, birefringence, twinning and structural phase transitions 79−38480
$TlMnCl_3$, weak ferromag. and mag. struct., temp. depend. 78−19219
α-U, polycrystalline, compressive deform. at low temps. 77−28856
U, two-dimensional expt. fracture map 78−95803
U-Mo-Nb-Zr-Ti (0.75, 0.75, 0.75, 0.5 wt.%), heat treatment effect on microstruct. and mech. props. 78−23729
U_3Si, reversible twinning, in-situ obs. 80−104241
V, coherent twin boundary structure *(French)* 79−60379
V, impact deform., influence of previous static loading *(Russian)* 78−6972
V, strain hardening, screw dislocations and microtwinning *(Russian)* 80−29971
V-Nb, mech. props., −196-1000°C, comp. depend. 78−39847
V-O alloys, quenched, local ordering of O, electron microscopy and diffr. 80−59453
V-Ta, mech. props. 79−61682
V-Ta (5 wt.%), strain hardening, screw dislocations and microtwinning *(Russian)* 80−29971
V_4As_3, defect struct. 77−4112
V_2MoO_8, planar defects, electron microscopy and electron diffraction meas. 77−15430
$V_{16}N_{1.5}$ solid solution, quenched, ordered structure *(Russian)* 80−88086
V_2O_5-Fe_2O_3-LiO_2 system, physical properties 78−84503
W, fan shaped twins of type II, struct. 79−90676
W twin lamellae shape of single crystal *(Russian)* 80−19812
W, twinning dislocation, math. model 77−59024
Y_2MoO_6, growth from soln., struct., props. 77−28705
Yb_2O_3, merohedral twins, many beam diffr. contrast 78−83829
Zn, deform. twin form. kinetics, Rose channel form. and interactions, twin growth rate *(Russian)* 79−60378
Zn, deformed, internal friction meas. 77−86067
Zn, dislocation mechanism of Rose channel formation under impact loading conditions *(Russian)* 79−79073
Zn II complex, hexaimidazole-zinc(II) dichloride tetrahydrate:Cr(III), D-tensor orientation, charge-compensation vacancies 80−50172
Zn, incompatible bicrystals, effect of grain boundaries on mech. props. *(Japanese)* 78−39798
Zn, low-temp. thermal fatigue, causing fracture and plastic deform. 77−28837
Zn, mechanical twins in single crystals *(German)* 79−33004
Zn monocrystal, cavitation induced multiple slip, twinning and fracture 78−39872
Zn, oriented polycrystals, tensile behaviour under hydrostatic press. *(Japanese)* 77−52417
Zn, shaped single crystal prod. from melt 78−2040
Zn, single crystal, acoustic emission during twinning 78−11468
Zn single crystals, temp. and strain rate effects on strength, slip and twinning 80−16373
Zn, twinning, influence of dislocation drag. mag. field effects 80−59472
Zn, twinning dynamics of single crystal 77−4115
ZnO-Bi_2O_3-Sb_2O_3-Co_2O_3-MnO_2-Cr_2O_3, nonohmic ceramic, microstruct. exam. 78−47292
ZnS, crystal, layered struct. microscopic observations *(Japanese)* 78−38725

twinning continued
ZnS, microregions disorientation degree anal. by birefringence, ESK and decoration methods 79−60389
ZnS, sphalerite modification, polysynthetic cryst., struct. changes due to uniaxial compression 77−15482
ZnSe, nonlinear optical effects in rotationally twinned crysts., phase matching 77−42570
ZnSe, parasitic birefringence dispersion induced by lattice plane defects 77−4617
ZnSe, recrystallisation during hot pressing 77−85952
ZnSe, twinning effect on electro-optical props. 78−68478
ZnSe, twinning on melt-growth under pressure 77−80515
ZnSe:Cr^{2+}, stress-induced alignment of Jahn-Teller centres in twinned crysts. 79−78651
ZnTe, nonlinear optical effects in rotationally twinned crysts., phase matching 77−42570
Zr alloys, acoustic emission during tensile testing 77−90433
Zr, deformation texture during rolling in sequential passes 79−11674
Zr, deformed at 77K, effect of fast-neutron irradiation on deformation twinning, TEM and optical microscopy obs. 79−37741
Zr, neutron irradiated, twinning deformation 79−14848
Zr polycrystalline, low-temp. alternating deformation and annealing, yield stress, elec. cond. variation *(Russian)* 79−74199
Zr, tensile deformation behaviour, neutron irrad. effects, dislocations, twinning inhibition 77−90393
ZrO_2, hydrous, prep. from $ZrOCl_2$ soln. and cryst. texture determ. *(Japanese)* 77−89398

twistors *see magnetic storage devices*

two-dimensional digital filters
Earth resource image processing techniques *(Italian)* 77−82063
image generation using 2-D elec. filters 77−79772
isotropic reconstruction of track-type airborne geophysical surveys, 2D filler design 79−66844
multispectral scanner imagery application 80−31152
optical fibre laser plate for optical parallel processing 79−76695
optimum linear filter, design principles, geophys. appl. *(Chinese)* 77−91281
recursive, based on system theory concept, image processing appl. 78−58934
recursive, for potential field data processing 77−2268
recursive methods for image processing, problems 78−58933
tomograph noise filtering, lung boundaries determ. using neuristic search 78−73240
US pulse echo digital processing 77−32948
wideband wavefront reconstruction in two-dimensional dispersive space 77−31191

two-phase flow
abrasive jet, parameters affecting particle velocity 77−65788
accelerating bubble flow of gas-liquid mixture, phase slip 80−53838
accelerating two-phase nozzle/diffuser flows, virtual mass effects on numerical stability 80−92204
adiabatic discharge of saturated water, from cylindrical channels, critical flow 77−84299
advanced continuous fluid Eulerian comput. scheme for flows with large density gradients 77−46236
aerated flow, longitudinal profile anal. in high velocity flow through channel *(Bulgarian)* 77−19637
aerated systems, oblong, flow and mixing, transverse circulating flow of liquid, longitudinal dispersion 80−69900
aerated water, disturbance waves 77−27581
aerocolloidal flow, radiant heating, Knudsen no. effect 77−68704
aerocolloidal suspension of solid particles, shock wave entering aerocolloid domain 78−51227
aerodynamic interaction between two spheres at Reynolds numbers around 10^4, induced forces 79−81946
aerosol, β-active, emission electrification in external field 78−83497
aerosol, charged, particle deposition in conducting tube 79−98792
aerosol, diffusion and sedimentation in Poiseuille tube flow 78−59463
aerosol, electrodiffusion precipitation of charged particles onto cylindrical channel walls 79−14463
aerosol, electrostatically charged, particle deposition in hollow cast of human larynx-tracheobronchial tree 79−43953
aerosol, interaction with surfaces past which they flow 77−80198
aerosol, laminar flow in cylindrical tube, conc. distrib. of free and attached Rn and Tn decay products 79−29412
aerosol, large particle thermophoresis theory, comparison of two methods 80−26060
aerosol, one-dimensional unsteady gas flow *(Russian)* 77−35223
aerosol, particle fallout rate under nonisothermal conditions 78−7238
aerosol, photophoretic motion of nonvolatile particles, thermal diffusion effect 78−79364
aerosol, simultaneous diffusion and sedimentation in rectang. tube 77−11266
aerosol, solid phase motion, large Reynolds no., carrying agent drag 78−79363
aerosol, spherical, binary gas mixture thermal slip along surface 78−34168
aerosol, turbulent coagulation in pipe flow 79−37385
aerosol aggregate, creeping motion of two touching spheres 77−47077
aerosol coagulation and diffusion in turbulent jet 79−23355
aerosol deposition on plate in turbulent flow 78−87380
aerosol electrostatic discharger for helicopters *(French)* 80−28863
aerosol enclosures under convective stirring conditions, quiescent boundary layer thickness 79−66364
aerosol in continuum, eqn. of motion 78−3895
aerosol in cylinder wake, local particulate vel. 77−11238
aerosol kinematic coagulation calcs. in variable-speed gas stream 80−19491
aerosol particle, in slightly rarefied gas, thermal force effects 78−1724
aerosol particle deposition in channel due to diffusion and electric charge 78−90978
aerosol particle deposition in fibrous media with dendritic pattern 77−60124
aerosol particle deposition in flow through model filters 78−1740
aerosol particle diffusivity in turbulent pipe flow 78−1731
aerosol particle response to impulse at small Knudsen no. 78−90977
aerosol particle separation efficiencies of wire grids 78−87381
aerosol particle settling in flow in parallel plate channel, diffusion effect 79−66371

two-phase flow continued
aerosol particle thermophoretic deposition, from laminar-flow gas streams 77−58766
aerosol particles, gravity settling in horizontal rectangular tube with diffusion 77−84310
aerosol particles, turbulent migration phenomenon 80−53836
aerosol particles diffusion and gravitational settling in tube 78−90976
aerosol particles in flow type chamber, coagulation, deposition 80−69908
aerosol pipe flow, heat transfer 78−9684
aerosol precipitation from laminar gas stream, free convection effect 78−83459
aerosol sampling lines, particle deposition expts. 78−81472
aerosol ultrafine particle size meas., diffusion battery anal. 79−92010
aerosol vortex jet streams, impingement zone, particle motion soln. and expt. 77−65773
aerosols, β-active, charging in turbulent flow 77−19642
aerosols, β-active, charging in variable electric field 77−11280
aerosols, asymmetric deposition motion in circ. tube, anal. by Laplace transform methods *(Chinese)* 79−37379
aerosols, diffusophoresis along curved surface 78−83432
aerosols, flowing, attachment of ^{220}Rn decay products using aerosol centrifuge 80−61167
aerosols, particle deposition from laminar flow 79−47988
aerosols, particle size distrib., effect of concentration of dispersed liquid 77−60128
aerosols, particle-droplet inertial collisions 79−47989
aggregates, solid, aerosols, dynamic shape factors meas. appls. 80−61165
agitated system, simulation model 77−11241
air bubble, in hydraulic oil, effect of diffusion on diameter change 78−90966
air bubble, rising behaviour in superposed liquid layers 77−62294
air bubble entrainment in self-aerated flow, channel or pipe flow 80−106832
air bubbles, rising in glycerine-water mixture, boundary surface velocity *(German)* 79−32631
air bubbles entrained in channel flow, isotropic turbulence spectral struct. 78−34112
air transported dust concentration, annular Venturi tube meas. *(Polish)* 79−72971
air water downflow through packed beds, apparent wall heat transfer coeff. 80−74953
air water downflow through packed beds, effective thermal conductivity 80−74952
air water two phase flow in pipe, regime map 80−69901
air-atomised water mixture, high temp. surface impact, heat transfer *(French)* 79−4015
air-bubble two dimens. plume, anal. 78−1715
air-H_2O, two phase upflow across horizontal tube bundles, void fraction and flow pattern 80−92201
air-H_2O injection into permeable bed for underground coal gasification, numerical model 80−30359
air-H_2O turbulent-turbulent stratified flow in circular tube 79−90307
air-Hg flow, stratified, co-current, in rectangular channel, interfacial wave structure 80−74955
air-liquid flow, liquid droplet disintegration mechanisms 80−74959
air-solid flow in pipe bends, circ. and elliptical, press. drops 79−32642
air-solid mixture, behaviour in pipeline of varying cross-section 78−9673
air-solid mixtures, pressure drop in pipe elbow *(German)* 78−5790
air-solids mixture in horiz. unsymmetric branches, pressure drop and solids distrib. 79−4069
air-steam mixtures, heat transfer to moving droplets 78−90997
air-stream mixture, direct contact dondensation on single droplet 77−68370
air-vapour flow in channel, laminar, with wall vapour-ice transition 79−94617
air-water, two-phase mixtures, vertical downward flow, void fraction 77−11235
air-water bubbly flow struct. through vert. venturi 79−64749
air-water bubbly mixtures, press. wave propag. *(French)* 78−22402
air-water choked flow in short pipes 77−84314
air-water film flow, transport phenomena, wary interface motion 77−35213
air-water flow, periodic instability related to continuity waves 78−1716
air-water flow, transverse intraphase vel. profiles and phase fraction distrib. influence 80−96295
air-water flow in Y-junctions 78−51218
air-water mist flows, uniform heat flux wedge, heat transfer 79−23352
air-water mixture, vertical flow, temp. influence on boundary lines between flow regimes 80−43764
air-water separated critical flow *(Japanese)* 78−42650
air-water slug flow in horizontal pipe, liquid holdup determination 79−46362
air-water stream, heat transfer, expt. meas. unit 77−42941
air-water two-phase flow, anal. of induced vibr. in horizontal piping system 77−80215
air-water two-phase flow form. in injection device 77−58765
air-water two-phase flow in a helically coiled tube 80−92206
air-water two-phase flow in concentric annulus, heat transfer 78−91002
air-water two-phase flow in vertical pipe, heat transfer *(Japanese)* 77−24011
air/water mixture mass flow meas. by drag devices and γ densitometer 80−79385
air/water vertically downward slug flow distrib., bubble vel. meas. 77−51108
airborne dusts collection by bluff bodies 79−4065
airborne dusts transport in near wakes of bluff bodies 79−4064
airdroplet flight in air, drift loss from spray cooling pond, numerical estimation 80−19471
alkali metal vapour condensation from gas flow (He,Ar,N_2) heat and mass transfer 78−75192
annular, crit. heat flux, swirl effect 80−10113
annular, entrained droplets, size distrib. and entrainment rate 80−43760
annular, multifluid modelling of adiabatic and boiling flows 79−1233
annular flow, flooding and flow reversal 78−51230
annular flow through annulus, droplet deposition 79−90311
annular flow through orifices, modelling 80−28555
annular flows, interfacial drag and wall layer height 77−39324
annular gas-liquid flow, drop sizes 77−51099
annular two-phase, two-component flow, quasi-stationary model in three-group approx. *(Bulgarian)* 80−69911
aqueous fog form. in shock tube 80−19531

two-phase flow continued
artificial membrane lung, fluid vortices and mass transfer 77−52919
asbestos fibre suspension, drag reduction in turbulent flow 79−68786
atomisation as nonequilibrium process, doplet disintegration distrib. function 78−38387
atomisation of high-viscosity liqs. by parallel flow air-liq. nozzle *(Japanese)* 78−38385
atomisation of liquid by impinging jets, expt. and theory 78−87373
axial momentum altered transverse transport in coolant flows during oscillatory instabilities 79−17964
axisymmetric annular fluid interfaces, stability at zero contact angle 79−94697
axisymmetrical sedimentation by rough plates *(Russian)* 79−79300
axisymmetrical two-phase jet, integral method for calculation *(Russian)* 78−47023
baffled shell and tube heat exchanger, two phase flow 79−77233
balance equations, computer programs for thermal-hydraulic anal. of nucl. steam supply systems 80−9332
barbotage bubble, liquid flow patterns 77−58770
bent pipe, inertial particle deposition 77−80204
binary mist flow, heat and mass transfer anal. *(Japanese)* 79−14467
blast furnace, simulated, interaction between gas and liq. flow 80−10300
blob mechanics visualisation in flow through porous media 79−4076
blowdown from horizontal pipe, unequal phase vel. and temp. theory appl. 77−39335
boiler plate restriction, hydraulic resistance calc. by energy equation 78−1734
boiler tube, serpentine geometry at high press., two phase heat transfer 78−94077
boiling, bubble growth at superheated horizontal wall, pure liq. and binary mixtures 79−41719
boiling, expt. study of outflow from accelerating two-phase nozzle 78−1721
boiling, mechanism model based on rotating vortex model with spatial heating 80−14694
boiling, nucleate, subcooled, latent heat transport contrib. 78−75046
boiling, nucleation centres interaction, obs. technique 78−14065
boiling, sustained and transient, inlet subcooling effect on flow instabilities 78−94809
boiling, two-phase boundary layer, temp. fluctuations 78−51222
boiling and bubbling heat transfer under the conditions of free and forced convection 78−90637
boiling calculations in low-pressure systems, appl. to LMFBR Na boiling 80−103068
boiling in channel, thermally induced two-phase flow instabilities, thermal nonequilib. 78−51240
boiling in two parallel horizontal tubes in solar collector receiver tubes, fluctuations *(Japanese)* 79−79377
boiling mechanism during burnout phenomena in subcooled two-phase water flows 78−94529
bottom settling of solid particles in turbulent shear flow, distribution statistical properties *(Japanese)* 80−19344
boundary layer, successive approx. method 79−32647
boundary vapour contents for critical state of heat transfer of second kind 78−1722
breakup of long slender droplets in 2-dimens. straining motion, hyperbolic flow 79−60062
bubble, of vap., with microlayer, universal growth relations 78−71266
bubble, single rising, internal mass transfer coeffs. 79−86487
bubble, spherical gas, nonlinear response to multi-freq. acoustic excitation 80−38480
bubble ageing and bursting in trace-contaminated water, rise speeds 78−26184
bubble and droplet-type contactors, wake shedding 79−4060
bubble and eddy heat diffusion in turbulent flow 80−19477
bubble cavitation in inviscid compressible liq. 80−28553
bubble chain, diffusion of dissolved substance at large Peclet nos. 79−86489
bubble coalescence and breakup in liqs. 77−62293
bubble collapse, heat transfer controlled, in isothermal tube 78−90979
bubble collapsing near free surface, cavitation 78−47026
bubble column, diam. and high gas throughput effects 79−37382
bubble columns, axial dispersion coeffs. 77−3861
bubble columns, large diameter, liq. phase duration *(German)* 79−32632
bubble containing liquids, nonsteady shock waves 79−68792
bubble detachment from wall, zero and negative gravity 77−3863
bubble diffusion in two-phase flow 78−18332
bubble distribution, eruption diam. in fluidised bed with horizontal tube bundle 80−14781
bubble dynamics, laser schlieren meas. 79−41773
bubble form in potential flow 79−86490
bubble formation during gas injection into liq. through orifice, interfacial area, press. *(German)* 79−18937
bubble formation in flowing liq. 79−64741
bubble growth and collapse, dilute polymer soln. effects in unbounded and bounded flow 79−81956
bubble growth dynamics, isothermal, gas bubble in liq. 79−14459
bubble growth in magnetic field 77−7462
bubble in liquid subject to tension pulse, model 79−55406
bubble in power-law liq., convective heat and mass exchange, Pe≤1000 78−55683
bubble layers in liquids, struct. of pressure pulses 80−38479
bubble motion and bubble-droplets in immiscible liq., photographic obs. method *(German)* 79−72931
bubble motion close to solid wall, surfactant effect 79−81954
bubble motion in an incompressible viscous liquid 78−34190
bubble motion in rotating liquid under residual gravity 78−55679
bubble motion in vertical temp. gradient, buoyancy and Marangoni forces 79−46372
bubble motion through liquid under reduced gravity 77−51100
bubble of gas rising in fluid filled tube, wall effects *(French)* 79−7399
bubble oscillations of large amplitude in fluid of infinite extent 80−96298
bubble population prediction in flow boiling, from gas bubble nucleation 78−90696
bubble profile and volume, symmetrical about vertical axis, analytical soln. 77−72346
bubble raise rate in nonuniform fluidised bed 78−67263
bubble rising in pipe, upward flowing liq. 79−32676
bubble size, rise velocity in screen-packed fluidised beds 77−31372

two-phase flow continued
bubble stagnation depth in vertically oscill. liq. column viscous effect 77−42901
bubble swarm behaviour and gas absorption in non-Newtonian fluids in sparged columns 79−4061
bubble swarm characts. in bubble column 77−42900
bubble with adsorbed film, migration in Hele-Shaw cell, rel. to materials processing in space 79−28912
bubble-flow regime, two-phase, laser Doppler anemometry 77−39366
bubbles, active nucleation site spatial distrib., bubble flow density 78−71267
bubbles, evaporating, of low-boiling liq., surface condensation of high-boiling mixture vapours 80−59021
bubbles, forced oscillation damped by acoustic radiation 80−33664
bubbles, pulsating, motion in viscous liquid half-space near boundary with inviscid liquid 80−19494
bubbles, pulsating, surface oscillations and jet production 80−33640
bubbles, single, generating apparatus and motion in water *(Korean)* 79−23387
bubbles and drops coalescence rate, ambient liq. viscoelasticity effect 78−67248
bubbles and drops driven by modulated acoustic radiation stresses, shape oscillation and static deformation 80−33274
bubbles break-up in stagnant fluids 78−75182
bubbles detection in insulating liquid flow, using spiral delay line 80−79415
bubbles diffusion in turbulent flow 78−22412
bubbles in fluidised beds, light probe detector 78−30376
bubbles in liquid column, gas holdup *(French)* 77−65781
bubbles in viscoelastic fluid, dynamics and dissolution 78−90970
bubbles with adsorbed films, motion through viscous fluid 79−18933
bubbly, droplet and particulate flows, drag coeff. and relative vel. relations 80−24072
bubbly, two-phase mixtures, numerical anal. of press. transients by explicit-implicit method 78−34185
bubbly flow, hot-wire and hot-film probes, response to passage through air-water interface 78−22438
bubbly flow, void fraction meas. by laser beam attenuation technique, theory *(Japanese)* 79−50779
bubbly flow, void fraction meas. by laser beam attenuation technique, expt. *(Japanese)* 79−50780
bubbly flow, void fraction meas. by laser beam attenuation technique, meas. accuracy determ. *(Japanese)* 79−50781
bubbly flow, void fraction meas. by light attenuation technique derivation of transmission rate reln. *(Japanese)* 80−48795
bubbly flow, wall press. fluctuations in turbulent boundary layer 77−58776
bubbly flows, simultaneous meas. of local liq. vel. and void fraction using gas laser *(Japanese)* 77−42947
bubbly flows, simultaneous meas. of local liquid vel. and void fraction by gas laser, accuracy *(Japanese)* 78−67295
bubbly liquid, choking phenomena in nozzle flows 77−62300
bubbly liquid, nozzle flow based on Wijngaarden's model 78−26182
bubbly mixtures, shock wave form. by compression wave steepening 78−38390
butane drops, nucleation in flowing water 79−1099
BWR, air clearing in H_2O-type press. suppression systems, scaling laws 79−54563
BWR, air clearing in H_2O-type press. suppression systems, scaling laws 79−54564
BWR, coolant flowrate in evaporative channel, self-oscillation parameters investigation 80−37572
BWR, core flow fluctuations, noise source, expt. study 79−13386
BWR, in-core investigation of two-phase flow using neutron-noise techniques 79−54530
BWR, momentum coupled transient thermal-hydraulic model 80−13565
BWR, Tarapur, one-loop model, dynamics anal., power transient response 78−46131
BWR Channel, two-phase flow fluctuations and continuity 80−14786
BWR channel stability, problem anal. 79−13387
BWR neutron noise local component meas., two phase flow study 78−94059
BWR pressure-suppression system, steam chugging anal., heat transfer and fluid mechanics characts. 80−95339
BWR subchannel code with drift flux and vapor diffusion transport 79−59149
CANDU-PHW, neutron flux regulation by two-phase flow absorber system 79−93799
capillary-porous submerged coating, boiling model 77−65792
carbon tetrachloride-I_2-water system, mass transfer in pulsed perforated plate column 78−71385
Casson fluid, gas bubble motion, behaviour, appl. to bubble in blood stream 79−10605
cavitation, acoustic field generated, review 80−74934
cement suspension, settling and flow props., effect of cellulose ethers and lignosulphonates 77−11242
centrifugal pumps in two-phase flow, characts. correlation 79−98790
centrifugal separators, two-phase flow distribs., nuclear power appl. *(German)* 77−6574
chamber-orifice interaction in bubble formation 77−89185
channel flow, critical flow rate 79−55410
channel flow with friction 78−59458
channel two phase flows, threshold steam qualities and cutoff heat fluxes 79−90242
channel with falling liq. film and two-phase flow, heat transfer 78−30337
channels, transient boiling flow, two-phase two-fluid approach 79−41756
channels with single- or two-phase heat transfer fluid, computer simulation of transients 78−90969
characterisation using neutron techniques, review *(Italian)* 80−19479
charged droplets evaporation and motion in electric field 78−42669
charged particle suspension, deposition in tube flow 79−37416
chemical reaction rate increase in US cavitation, diffusion model 79−96312
chemical reactor, falling-film gas-liq. type, mathematical model 79−86526
chemically active gas flow, heat exchange of small metallic bodies *(Russian)* 78−47068
chemically reactive, dynamic stability, mathematical model *(Russian)* 78−47069

two-phase flow continued
chemically reactive flow, dynamic stability, numerical anal. *(Russian)* 79−68823
chlorobenzene drops falling freely through water, breakup 80−69899
circular tube, heat transfer crisis and development for cosinusoidal thermal flux distrib. 77−35206
CIRENE LWCHW reactor, two-phase flow rods for neutron flux control, computer anal. 79−59217
clay-water suspension turbulent flow in tube, velocity profile and frictional losses *(Russian)* 77−31364
clumping instability of falling horiz. lattice 77−3866
co-current flow liquid-liquid binary mass transfer in ejectors 78−75185
coagulated colloidal suspensions, couette flow, viscosity effect 79−90317
coagulated suspensions, flow equation 78−63487
coarse angular particles in water, sedimentation fall vel. 79−74430
coaxial air stream, self-oscillatory liquid film flow regime 79−86498
cocurrent gas-liq. stratified flow, mass transfer obs. 79−18931
cocurrent two-phase downflow in tubes, flow pattern, void fraction and press. drop 79−77229
cocurrent two-phase downflow through packed beds, multiple hydrodynamic states 79−18942
cold liquid spray interaction with hot gas stream in channels 77−15108
colliding gas-slurry jets, dispersed material motion, numerical anal. *(Russian)* 79−32653
colloidal dispersions, microrheology, Brownian diffusion of doublets of spheres 77−4942
colloidal dispersions, stability in flow fields, trajectory anal. 78−5782
colloidal suspensions, coagulated, expt. props. of flow curve parameters 77−938
colloidal suspensions, coagulated, flow props., elastic floc model 77−939
colloidal suspensions, coagulated, flow props., energy dissipation in flow units 77−3862
compressed air energy storage, champagne effect modelling, improved cavern design 79−83638
compressibility effect on hydrodynamics, resistance coeff. 78−55684
compressible two-phase flow dynamics, distributed parameter model 80−24086
compression shock stability in streams of spontaneously condensing vapour 80−28563
computerised tomography meas. technique 80−59135
concentrated dispersion media, associated mass of discrete phase element *(Ukrainian)* 78−1719
condensate film flow on finned surfaces, heat transfer, heat exchanger design 78−75038
condensation heat transfer, nonequilib. temp. profiles, mass transfer engineering calc. 80−63227
condensation of laminar film on helical elliptical cylinders, governing eqns. soln. 78−9689
condensation-driven fluid motions, nuclear reactor safety 80−63228
condenser system, submerged, buble pumped augmented natural convection 78−94535
condensing flow, thermally governed transient flow surges 78−30346
condensing steam, method for calculating expansion 77−27573
condensing turbulent annular-mist flow, wall and interfacial shear stress 78−94812
conducting drop, in conducting fluid, induced motion and drop deformation in elec. field 79−7415
conducting dusty fluid, unsteady flow through rectangular channel with time depend. press. gradient 79−14486
confined burning jet, droplet vaporisation, expt. and theory 78−94855
constitutive equations for lift force and Brownian motion 77−937
constitutive laws determ. from irreversible thermodynamics 80−36861
contaminant cloud, passive, relative diffusion in incompressible turbulence flow 79−50774
contaminant lateral dispersion in open-channel flow, buoyancy effects 79−50775
continuity measurement by radioisotope method, error 79−32723
continuum two-phase theory, volume averaged balance eqns. *(German)* 80−92212
convection, forced, heat transfer in ultradeep boreholes 79−68762
convective diffusion to drop, large Peclet no., finite Reynolds no., asymptotic soln. 79−41742
cooling, by liq. boiling in capillary porous layer, statistical model 77−89196
Couette flow, asymptotic solns. 79−77223
Couette flow, of dusty gas between two infinite coaxial cylinders 78−55685
Couette flow, with uniform suction at stationary plate 79−32637
counter-current annular two-phase flow, flooding vel. 77−31363
counter-current flow, discrete polydispersed model 80−14779
counter-current flow, hold-up and particle size distrib. simulation 80−14780
counter-current two-phase flow, annuli, rod bundles, liq. film behaviour, flooding 78−59452
counter-current two-phase flow in tube, liq. film waves and flooding 78−18345
countercurrent flow, turbulent steam condensation in a horizontal channel 80−106800
countercurrent flow in tube, max. heat flux 78−90992
counterflow with freely-falling dispersed material, heat and mass transfer 78−30340
creeping flow, in cloud of round drops of arbitrary size distribution 78−9677
creeping flow mass transfer in size distrib. cloud drops, high Schmidt number 80−14783
critical flow, disperse annular flow 78−42645
critical flow in long nozzles, PWR appl. 80−13550
critical heat flux in annuli, general correlation 80−43705
critical mass flow rate, calc. *(Russian)* 80−53848
critical pressure ratio 77−84300
critical two-phase flow, bubble nuclei 80−64615
critical two-phase flow, nonequilibrium vapour production model 80−52719
critical two-phase flow models, nuclear reactor safety 80−63229
cryogenic liquids, simple, generalised charts for computation two-phase choked flow 77−47061
cyclohexane-aniline, crit. mixture with shear flow, light scatt. obs. 80−6521
cyclone, reverse flow, efficiency anal., using monodisperse methylene blue-uranine 78−34142

two-phase flow continued
cylinder in pulsating air-water spray, forced convective heat transfer *(French)* 79−7274
deagglomeration in viscous fluids, size distrib. response to shear stress 77−42903
dense suspensions, review 78−67255
density measurement by high energy photon scatt., dynamic capabilities 77−7485
density wave oscillations, linear stability anal. 80−19327
depressurised subcooled liquid, boiling boundary phase-change front transient propag. 80−43768
descending turbulent flow of liquid film and gas, hydrodynamics 77−7437
detonation development in unmixed media *(Russian)* 80−28556
detonation front compression waves, solid particle oxidation reaction *(Russian)* 78−34207
detonation sputtering, interaction between detonation waves and gas and powder flows *(Russian)* 80−16182
dibutylphthalate, supersaturated vapour, aerosol form. by mixing of flows 79−39212
dichloroethane drops falling freely through water, breakup 80−69899
diethyleneglycol-air mixture, energy dividing props. in discharge from supersonic jet *(Russian)* 77−39332
diffuse flow measurement, investigation 78−59513
diffusion coefficient determination, using Stefan cell 77−51136
digital signal processor for real-time anal. 77−80235
dilute suspension, boundary layer in presence of electric field *(Russian)* 78−63503
dilute suspension, low Reynolds number flow in slowly varying tubes 79−46389
dilute suspension of ellipsoidal particles flowing in channel, elec. field effects *(Russian)* 77−68696
disc straddling interface of two-phase flow 78−90971
discrete phase variable particle size, Euler and Lagrange methods 80−92203
disperse annular flow, crit. heat transfer, liq. distrib. 79−32209
disperse drop composition meas. in two-phase stream 78−55682
disperse ore in a gas flow, mixing stage calcs. *(Russian)* 80−106829
disperse powder interaction in high temp. gas flow *(Russian)* 80−106830
disperse system, vibr.-extrusion discharge, process optimisation 77−66772
disperse-annular flow, vel. profile calc. 78−1720
dispersed drop-vap. flow, heat transfer, wall deposition and boiling 77−75965
dispersed flow post-dryout heat transfer, review 79−1094
dispersed phase flow, heat transfer 78−90996
dispersed phase holographic analysis 80−103061
dispersed supersonic two-phase flow, shock characts., droplet size depend. at nozzle 80−106815
dispersed two-phase flow, relationship between radiation transmissivity and void fraction *(Japanese)* 80−100026
dispersed-annular isothermal flow, vel. distrib., phase conc. and droplet size distrib. in core 77−47064
dispersion, close-packed, two-dimens., gravity effect on thin film drainage 79−86486
dispersion, kinetics, doublets of rigid spheres, calc. method 77−72344
dispersion phase distribution, mass force effect in biphase liq. cylindrical vortex *(Russian)* 80−79388
dispersions, kinetics, doublets of rigid spheres, simple shear expt. 77−72345
dispersive, coeff. of internal resistance 80−19476
dissolved gas liberation kinetics in turbulent liquid stream 77−11226
drift flux field equations and vap. drift vel., theoretical bases 78−94807
drift flux formulations and calculational methods 80−103067
drop, centrally-located with thin jet in infinite viscous fluid 79−32614
drop, deformable, motion in second-order fluid 79−64754
drop, diffusional evap. in EM radiation field 78−43112
drop, evaporation in vap., slow viscous flow, heat flow asymmetry effect 77−75966
drop, impact dynamics on solid surface 79−86488
drop, mass transfer, surface-active agents effect 79−77218
drop, mass transfer accompanied by chem. reaction at surface 79−77290
drop, oscillating, immersed in 2nd fluid, induced flow field streaming 78−59454
drop deformation and orientation in shear and extensional flow fields, dynamic interfacial props. 80−107611
drop diameter, hold-up and backmixing coeffs. in liq.-liq. spray columns 78−75183
drop dynamics in shear fields, role of dynamic interfacial effects 80−107612
drop evaporation rate in forced convective flow with transverse sound fields 78−51224
drop formation hydrodynamics, macroencapsulation 80−64603
drop in ambient liq., mass transfer, combination of resistances 78−83458
drop in extensional flow, deformation and breakup 78−67250
drop in infinite viscous fluid 79−1234
drop in shear flow, deform. and burst of drop 79−32645
drop in ternary mixture, laminar condensation heat and mass transfer 79−14227
drop in uniform (shear) stream, convective heat and mass exchange, Pe≤1000 78−55683
drop in viscous fluid stream, nonstationary mass transfer *(Russian)* 79−10561
drop motion in flow with varying vel. 78−59457
drop motion in free turbulent jet 78−5789
drop motion in immiscible liquid, integral eqn. for Stokes flow 78−71389
drop motion in stream of viscous incompressible fluid 77−11252
drop of soln. moving in hot gas, solvent evaporation 77−65783
drop of soln. moving in hot gas, solvent evaporation 77−68673
drop profile and volume, symmetrical about vertical axis, analytical soln. 77−72346
drop size and dispersion in tubes and coils 77−39328
drop size in nozzle flow of moist water vapour 77−42904
drop size spectrum and phase surface calcs. from exptl. data *(Russian)* 77−31366
drop-solid surface high-speed interaction, apparatus design *(Russian)* 79−27605
droplet coalescence, film drainage 78−71387
droplet collisions, coalescence and disruption expts. 79−68768
droplet deformation in extensional flow 80−19449

two-phase flow continued
droplet deposition in turbulent annular flow 77−62299
droplet dispersion produced by rotating perforated drum 77−11244
droplet dynamic interaction, angle of collision effects 80−38475
droplet evaporation, modelled by wet porous sphere, heat-transfer meas. 78−59268
droplet evaporation in const. cross flow, with and without gas. chem. reaction 77−35214
droplet motion in inhomogeneous-in-temp. viscous liq. 77−39334
droplet size distribution in liquid phase of two-phase flow effect on characts. 80−103070
droplet vaporisation in two-phase, gas+solid particle, flow 78−55677
droplet-vapour flow, burning, conservation eqns., mass transfer 77−39363
droplet-vapour flow, normal shock waves 79−32651
droplets, vaporising, in gas stream in channel laminar entry region 78−30347
droplets in turbulent flow, heat and mass transfer 78−22410
droplets of soln. dispersed in gas flow, heat and mass transfer during evaporation 78−90998
drops, diffusion of dissolved substance at large Peclet nos. 79−86489
drops, fast-moving, interaction with liq. film surface *(Russian)* 79−64756
drops break-up in stagnant fluids 78−75182
drops driven by modulated acoustic radiation pressure, quadrupole resonance, experimental props. 80−33275
drops in immiscible liquid, intermittent elec. field heat transfer augmentation 78−94872
drops in liquid, diffusional interaction 79−81947
drops in pulsating flow, mass transfer, renewal-penetration model 77−31369
drops submerged in unbounded arbitrary vel. field, low Reynolds no. motion 78−42646
dryout charcts. of steam generator 78−90990
duct, horizontal, slugging onset 80−10296
ducts, one-dimensional models for transient gas-liquid flows 80−64614
dumbbell shaped particles in power-law liq., struct.-phenomenological theory 78−1730
dust clouds of solid fuels, ignition and flame quenching 80−28577
dust erosion by shock wave in air 78−42648
dust laden gas flow over plate, combined heat transfer, thermal fluxes 80−79289
dust laden gas in channel, combined heat transfer 78−91031
dust laden jet, particle turbulent diffusion 78−83455
dust particles and liquid in circular pipe, two-phase flow heat transfer 80−64607
dust-air cyclone separator, operation anal. 78−57362
dust-laden gas flow, heat transfer 78−14067
dust-liquid channel flow, with varying inlet temp., transient forced convection soln. 78−87375
dusty fluid, flow past wavy moving wall 80−96299
dusty fluid, laminar boundary layer flow, 2-D stagnation point near oscillating plate 80−64606
dusty fluid, motion induced by impulsive plane boundary motion and cylinder motion 78−79362
dusty fluid flow past plate, small amplitude oscillations 80−14792
dusty fluid unsteady flow through long pipe with time depend. press. gradient 79−18863
dusty fluid unsteady laminar flow through circular pipe 77−11236
dusty gas, attenuation of radiant energy 78−94579
dusty gas, flow between concentric coaxial circular cylinders 80−10299
dusty gas, hypersonic wedge flow 80−6083
dusty gas, Stokes layer stability 80−19493
dusty gas, two fluid model field eqn., time interval for soln., iteration method *(German)* 78−63489
dusty gas, unsteady flow in channel with annular sector cross section 79−77247
dusty gas, unsteady flow in cylinders, numerical soln. 78−51231
dusty gas flow in horiz. and vertical tubes, heat transfer 78−22409
dusty gas steady state flow, uniqueness criteria 77−31360
dusty gases, fully dispersed wave struct., Navier-Stokes eqns. 80−69875
dusty Maxwell flow between concentric spheres, torsional transient motion 79−90258
dusty plane viscous incompressible fluid flows, kinetic, kinematic props. 80−38482
dusty viscous conducting liquid, unsteady flow in annulus in mag. field 78−38412
dusty viscous flow between oscillating coaxial circular cylinders 79−18928
dusty viscous flow due to torsional vibrations of a circular disc 80−28548
dusty viscous flow through a cylinder of elliptic section under time-dependent pressure gradient 79−77248
dusty viscous fluid, unsteady flow through tube 78−59449
dusty viscous fluid, unsteady flow through uniform pipe 78−59450
dusty viscous fluid flow through rotating circular cylinder 77−68675
dusty viscous liquid, laminar flow through tube 79−37399
dusty viscous liquid, unsteady flow through elliptic ducts 79−50703
dusty viscous liquid flow between parallel flat plates 79−37384
dynamic two-phase layer, heat exchange and mass transfer coeffs. of flat element 77−7439
Ekman boundary layer, suspended particles effect 78−24349
elastic sphere suspension, steady flow in tube 78−67251
elastic spheres in oscill. linear flow, Frolich-Sack result, inertial effects 78−34184
electrostatic precipitator, re-entrainment, particle trajectories and gas flow 78−13642
ellipsoid freely suspended, rotation about a slow viscous flow's vorticity axis 78−38386
emulsion, concentrated unstable, turbulent flow in pipes 80−28537
emulsion, dilute, straining motion, effect of inertia on dynamic viscosity 80−87797
emulsion, films, thinning vel. and lifetime, surfactant in continuous and dispersion phases 77−84306
emulsion, relative drop-drop and drop-wall motions, slow 79−32641
emulsion films, thinning vel., surfactant in continuous and disperse phases 77−84305
emulsions, unstable water-oil type, rheological props. obs. non-Newtonian obs. 77−75866
energy separation in high vel. flows 78−9691
two-phase flow continued
entrainment from body surface under convective aerodynamic heating, numerical soln. 79−81949
entrainment of liquid from horizontal cylinder by air flow 77−15102
equation systems, characteristics, stability and short wavelength phenomena 78−38395
equilibrium dispersed-ring water vapour flows, liq. distrib., film paramters and hydraulic resist. 80−24079
erythrocyte sedimentation rate, for teaching 78−49610
ethane, flow continuity in arterial capillary systems in cryogenic heat pipes 80−64536
evaporating and condensing flows, system mean void fraction model 78−42520
external condensation problem, with suction (blowing), self-similar soln. 79−94705
falling film flow, spatially growing three dimens. wave, annular-froth flow transition 78−14071
falling particles, in rot. fluid 78−55675
fast reactor safety, thermohydrodynamics code TWOPOOL, modelling and numerical methods 79−59195
ferrofluid, convective stability of horizontal layer in mag. field *(Russian)* 77−3885
ferrofluid constitution examination by rotating test tube method 80−33693
ferrofluid droplet, interphase boundary hydrostatic charcts. in uniform mag. field 80−33692
ferrohydrodynamics, mag. relax. models 79−94706
ferroliquid, magnetoelastic oscills. 79−94639
ferromagnetic colloid, natural convection, mag. field effects *(Russian)* 77−62307
ferromagnetic suspension, heat transfer for shear flow conditions 79−46394
ferromagnetic suspension, mag. field effect on heat transfer, thermal cond. 78−59500
ferrosuspension, magnetorheologic charcts. *(Russian)* 77−65786
ferrosuspension, MHD flow, heat transfer *(Russian)* 78−26203
fibre orientation in viscous liquid flow *(Japanese)* 78−34189
fibre suspension, rheology, rel. to turbulent drag reduction 78−22315
fibre suspension flow in pipes, transition regime analysis, drag reduction 77−89186
fibre suspension in water, turbulent jet, analogous behaviour to polymer solns. 78−1732
film boiling destabilisation, liq. drop falling onto hot liq. surface 78−94588
fine particles in axisymmetric gas stream, concentration field investigation 79−14464
fine particles in gas flow, Doppler laser velocimeter meas. of motion 77−27583
finite element method, nonlinear test case 80−96293
finite element soln. technique 78−79366
fission reactor coolant depressurisation studies, transient density, press., temp. variations, during discharge 80−57833
fission reactor HCDA, debris transport in horizontal piping 79−93784
fission reactor LOCA, gravity-driven reflood hydrodynamics, EFLOD code 79−89426
fission reactor LOCA, models for estimation of critical flow in two-phase systems 79−36361
fission reactor LOCA, reflooding phenomena in single heated tool 80−27754
fission reactor pipe blowdown, expts. and nonequilib. anal. 79−30960
fission reactor pressure vessel blowdown two-phase level swell calc. using drift flux correl. 79−89428
fission reactor rod bundle blowdown heat transfer instrumentation, transient two-phase flow meas. 80−685
fission reactor safety, stability analysis and charcts. for two-phase flow eqn. systems with viscous terms 80−59103
fission reactor safety, two-phase flow, analytical simulations for safeguards design 78−46143
flame advection and propagation in fluid 80−59097
flame stabilisation mechanism in two-phase fuel-air mixture flow 79−81996
flashing adiabatic flows, calc. taking into account bubble separation freq. variation under forced flow 78−67258
flat plate, adiabatically densified fluid film, turbulent two-substance boundary layer *(German)* 78−90845
flexible cylinders, dynamics in axisymmetrically confined axial flow, two-phase flow 79−64757
flexible filament in liquid flow, dynamics using Riemann's method *(Russian)* 77−68670
flooding phenomena in inclined circular pipe flow 80−96302
flotation, noninertial, effect of particle aggregation 80−55719
flow boiling, critical heat flux, review 79−4074
flow film boiling, void fraction meas. 80−92207
flow instability in parallel multichannels 79−90221
flow regime maps for developing steady air-water two-phase flow in horizontal tubes 80−28552
flow visualization using two-phase flow 80−33714
flows with large density gradients, Eulerian finite difference technique 77−79424
fluid containing particles, laminar throughflow between corotating disks 79−77136
fluid mixture, inertia coeff. and drag coeff. 80−19475
fluid spheres, touching, motion along line of centres 79−4071
fluid spheres in Stokes flow, eddy motions 79−23350
fluid spheres in viscoelastic fluid, drag coeff., low Reynolds number *(Japanese)* 78−9694
fluid velocity meas. by radiation intensity correlation 77−75996
fluid-fluid interface, rotlet or sphere rot., torque values 79−86494
fluid-gas mixtures, tubular reactor layout *(German)* 80−1698
fluid-gas spray apparatus for conical mixing chamber *(Russian)* 79−50820
fluid-particle separation, chainlike form. of particle deposits 77−77813
fluid-solid flow, holdup, expt. 78−79361
fluid-solid flow, holdup, theory 78−79360
fluidised, determ. of flow parameters by simple model and new distributor design 78−83493
fluidised bed, gas-solid, solid circulation 78−79359
fluidised bed, jet penetration depth of multiple vertical grid jets 80−38486
fluidised bed, nonuniform, force on fixed sphere, rising gas bubble force field 78−59476

two-phase flow continued
fluidised bed, polydisperse particle entrainment in gas flow 77−65791
fluidised bed, Richardson-Zaki equation, effective gravity force calc. 77−31382
fluidised bed, two-phase model, moment method 79−37391
fluidised bed reactor, solid-circulation model, steady-state multiplicity 79−86524
fluidised bed reactors, gas flow, anal. 79−94703
fluidised beds, heat transfer to horizontal tube *(German)* 78−59387
fluidised beds, instability waves and bubble origin, two-fluid eqns. 80−92205
fluidised beds, theoretical bounding relations, for bubble void fraction 80−96296
fluidised gas-solid flow in standpipes 77−75970
foam stability relation to structure, criteria derivation w.r.t. drainage stage 80−69904
foam with high press. gradients, syneresis in Plateau-Gibbs channels, capillary press. 80−74948
forced convection in two-phase flow from jets, mass transfer near interface *(German)* 80−53782
forced convection quench data rel. to steady-state nucleate boiling data 78−90995
forced flow laminar filmwise condensation of vapour in vertical tube 80−43762
forced oscillations of nonspherical bubbles 80−33663
forced-convection boiling upflow system, instabilities in parallel channel, nonlinear model 77−57724
fouling in heat exchangers, review 79−3902
fountain effect, flow boundary conditions 79−68784
free air/water convective flow confined by 2 parallel vertical walls, variable fluid props. 79−55369
free liquid surface oscillations, gas bubble motion 80−100025
free molecule heating of micron size particles at hypersonic speeds 80−19442
free motion transition criteria for single bubbles and drops 80−64605
free moving drop in pulsating liquid, mass transfer *(French)* 77−27588
free-surface sediment conveying river bed flow, flowrate and momentum correction factors 80−36339
free-surface turbulent flow, velocity and concentration distributions *(French)* 79−98786
Freon 22, boiling in internally finned tubes, heat transfer and hydraulics 79−81694
Freon-113 vapour environment, rewetting of hot surfaces, two-phase high pressure flow simulation 80−32358
Freon-12, annular mist flow in tube, wall film mass flow rate 80−69905
frictional energy dissipation, appl. to nuclear fuel assemblies *(Japanese)* 77−55074
fuel drops, liq., blast wave initiated detonation waves 79−64691
fuel rod, time-of-flight laser anemometer meas. 77−39383
gas, finitely conducting, effect of suspended particles on hydromagnetic thermal convection instability 79−53709
gas, in contact with condensed phase, hydrodynamic eqn. and slip boundary condition 80−14791
gas and non-Newtonian liquid, stratified flow in horizontal pipes 80−48787
gas and vapour bubbles in gas/liquid solutions, growth and collapse *(Italian)* 78−22403
gas bubble, motion in rotating liquid under simulated low and zero gravity 77−55071
gas bubble, rise and cooling in viscous fluid *(Russian)* 80−74949
gas bubble boundary surfaces in turbulent liq. flow, equivalence of photographic, chem. determs. *(German)* 79−32630
gas bubble cloud motion in impulsively accelerated liquid 77−941
gas bubble collapse in viscoelastic fluid, elongational flow 78−14060
gas bubble collapse in viscoelastic fluid, elongational flow and viscosity 78−14061
gas bubble dynamics in turbulent jet 79−41741
gas bubble in acoustic field, effect of diffusion on evolution, stability 77−15105
gas bubble motion in power-law fluid, heat and mass transfer with chemical reaction 79−77227
gas bubble oscills. in viscoelastic liq. 77−80202
gas bubble plumes in stratified environments, vertical fluid transport, double plume model 78−47019
gas bubble suspensions, incompressible nonNewtonian and Newtonian fluids, dilatational props. 78−30343
gas bubble-liquid system, shock wave refl. 79−81952
gas bubble-liquid system, struct. of weak shock waves 79−86492
gas bubble-water mixture with polymer additive, shock wave propag. 78−47021
gas bubbles, flow and temp. fields, global collocation calcs. 77−47067
gas bubbles dissolving in liq. 79−90319
gas bubbles in liq., controlled vibratory movement under near-zero gravity conditions 78−14119
gas bubbles in liquid, nonlinear acoustic disturbances 80−59104
gas bubbles in low-viscosity liquids, US attenuation 80−58849
gas bubbles in vibr. liquid, selective drift in reln. to their size 79−77225
gas bubbles in vibrating liq., localisation and translational motion *(Russian)* 79−14455
gas bubbles in vibrating liq., selective bubble drift *(Russian)* 79−14456
gas dispersion turbulent flow in tubes, nonisothermicity rel. to deposit form., heat transfer 79−55409
gas emitting from liquid, model *(Russian)* 78−26187
gas flow dust content, temp. and speed meas. method 78−34216
gas flow with particles, nonsymmetric 2D nozzle, nonuniform wear 77−47075
gas injection into liquid stream, heat transfer rates 78−14075
gas injection into liquid through porous plate, squeezing out of liq. 80−64622
gas mixture, binary, condensation in boundary layer flow, numerical method 79−1236
gas mixture, binary, spherical expansion into flooded space, components separation 79−81948
gas mixtures, removal of condensing component by suction through porous walls 79−98787
gas particulate flow on flat plate, laminar boundary layer, finite difference method 80−43688
gas sparged devices for viscous liq. systems, design, bubble size 78−83454
gas stream model, turbulence damping by addition of solids *(German)* 77−58774

two-phase flow continued
gas stripping column, periodically cycled, feedback control, simulations 79−1231
gas suspension flow in long horizontal pipe, heat exchange investig. 80−19388
gas suspension vertical flow, wall-particle interaction 78−59461
gas transfer into liq. interface bombarded by liq. pulses 77−7434
gas transported dust, discrete particle phase effect on turbulence intensity *(Russian)* 80−79384
gas-conveyed solid suspension flow, press. losses 77−80197
gas-droplet flow, particle-source-in-cell model 77−84313
gas-dust mixture, wave eqns. of one-dimensional motion 79−86496
gas-evolving electrodes, mass transfer, superposition of hydrodynamic flow 78−73047
gas-foreign particle mixture, flow in Laval nozzle, direct problem soln. 77−35218
gas-hard particle mixtures, nonstationary waves, shock wave interactions *(Russian)* 77−27587
gas-liq. (liq. metal) two-phase two-component heat transfer, review 79−1239
gas-liquid, compressible, laminar, numerical investigation *(German)* 77−15111
gas-liquid, in homogeneous channel, forced oscillations anal. 77−11250
gas-liquid, response of small pitot tubes 80−92209
gas-liquid, similarity criteria and fundamental eqns. 79−98784
gas-liquid, turbulence meas. by hot-film anemometry *(German)* 77−11254
gas-liquid, turbulent characts., determ. method 80−96300
gas-liquid, turbulent co-current flow, in tube, with/without swirl 79−77257
gas-liquid agitated vessels, interfacial area meas. 79−23351
gas-liquid annular flow, wire probe meas. of liq. film thickness 79−64805
gas-liquid annular two-phase flow, wave and interfacial friction characts. 78−67249
gas-liquid ascending flow, monodispersed, funciton stress on wall, bubble size effect 80−59098
gas-liquid bed, flow props. and bubble vel. determ. method and instrument 77−72374
gas-liquid boundary layer, droplet precipitation enhancement 78−1735
gas-liquid bubble flow accelerating in nozzle, slipping of phases *(Russian)* 77−35202
gas-liquid cocurrent downflow in fixed bed in pulsed regime, mass transfer fluctuations 80−19485
gas-liquid cocurrent flow in tubes, interfacial area meas. 77−39327
gas-liquid countercurrent packed column, with intermittent voids, residence time distrib. studies 80−19483
gas-liquid dispersion, mechanically agitated, heat transfer to helical cooling coil 79−4063
gas-liquid dispersion, molar current changes in gas phase, fluid dynamical props. *(German)* 77−35200
gas-liquid film flow, stratified, eqns. of motion 79−37376
gas-liquid film interface stability behind slipping shock wave front *(Russian)* 78−55630
gas-liquid flow, bubble size and density, void fraction, sifting method meas. *(Japanese)* 78−83462
gas-liquid flow, drop size spectrum 78−34187
gas-liquid flow, holdup, expt. results 78−14063
gas-liquid flow, holdup, theoretical aspects 78−9674
gas-liquid flow, hot-film anemometer signal anal. method 79−32639
gas-liquid flow, hydraulic resistance 80−24077
gas-liquid flow, hydrodynamics and transport processes, electrodiffusion modelling method, convection and boiling 79−90309
gas-liquid flow, in vert. tube, annular flow transition at low-press. 78−94800
gas-liquid flow, mass transfer in laminar streams with circulation in wet-walled columns 79−94698
gas-liquid flow, mass transfer in upflow and downflow 79−41738
gas-liquid flow in channel, forced oscills. charact., expt. 77−11251
gas-liquid flow in channels, hydrodynamics 79−81951
gas-liquid flow in granular layer, hydrodynamic modes 78−9712
gas-liquid flow in heat exchange panel *(Russian)* 80−28550
gas-liquid flow in horizontal and inclined pipes, flow pattern transition 80−74958
gas-liquid flow in rotor pulsated apparatus, volume coeffs. of mass transfer *(Russian)* 77−84312
gas-liquid flow in triangular ducts, two-phase wall layers 78−90999
gas-liquid flow in tubes, bubble rise and liq. holdup 79−4059
gas-liquid flow in vertical tubes, Graetz problem 78−91001
gas-liquid flow through packed beds, holdup profiles, elec. cond. meas. 77−35201
gas-liquid flow with small gas contents, liq. phase vel. profiles distrib. 77−35216
gas-liquid flows with chemical reactions in hydraulic approx., mathematical modelling 79−18972
gas-liquid interaction in turbulent reacting flows, mathematical model 80−83862
gas-liquid mass transfer in packed beds, review 77−31381
gas-liquid medium, standing waves 78−9474
gas-liquid mixture, acoustic disturbance propag. 78−9473
gas-liquid mixture, bubble mode of flow in vertical pipe 80−24081
gas-liquid mixture, entrained downward flow in vert. channel 79−94704
gas-liquid mixture, flow struct. and distrib. effects in pipe 79−27682
gas-liquid mixture, outflow from large container with a slit 80−74951
gas-liquid mixture, press. perturbations propag. 78−34186
gas-liquid mixtures, flow rate meas., standard system design principles 77−76005
gas-liquid mixtures, flowing, gas conc. meas., acoustic method 78−59448
gas-liquid moving interface diffusion 78−22404
gas-liquid pipe flow, influence of return bends on velocity ratio 80−74962
gas-liquid pipe flow, stability at slugging onset 77−11237
gas-liquid reacting flow, interfacial area and liq.-side mass transfer 79−37420
gas-liquid slug flow, liq. vol. fraction correlation 78−38389
gas-liquid swirl nozzle, gas dispersion, discharge coeff. 77−89187
gas-liquid system, unsteady state determination of mass transfer coefficients 78−14106
gas-liquid system discharging from nozzle, phase slip *(Russian)* 77−55067

two-phase flow continued
gas-liquid systems, vibs. stabilisation of dynamic equilib. and mixing *(Ukrainian)* 80−10291
gas-liquid transient flow in horizontal pipes, flow pattern transitions 79−32629
gas-liquid turbulent flow, friction, velocity and gas content profiles 80−14793
gas-liquid two phase flow film thickness, tube four rectangle obstacle, expt. 78−87377
gas-liquid two phase flow film thickness, tube ring obstacle effects, expt. 78−87376
gas-liquid two-phase flow, flow pattern prediction, quantitative indication method 80−79377
gas-liquid upward flow, effect of tube size on liq. side mass transfer 78−9682
gas-liquid upward flow in granular layer, hydrodynamic conditions 78−34188
gas-particle flow, contact charging 79−81987
gas-particle flow, optical fibre sensors, appls. *(German)* 78−26215
gas-particle flow, physico-computational model 79−32650
gas-particle flow in shock tube, finite difference calc. *(Japanese)* 80−79390
gas-particle flows in shock waves, radiant interchange among suspended particles *(Japanese)* 77−15063
gas-particle mixture, downhole flow regimes 79−98791
gas-particle mixture, shock wave structs., particle specific heat effect 78−14072
gas-particle mixture flows, aerodynamic problems, French contribs. 77−42909
gas-particle mixture flows, fundamentals and applics., review 77−42913
gas-particle mixture flows, German R&D 77−42910
gas-particle mixture flows, report of European developments 77−42908
gas-particle mixture flows, research at Von Karman Inst., Belgium 77−42912
gas-particle mixture flows, UK research survey 77−42911
gas-particle mixture in tube flow 79−14460
gas-particle mixtures, effect of thermal radiation on shock wave 78−91032
gas-particle mixtures, supersonic flow past wedge, shock wave *(Japanese)* 77−47070
gas-particle plumes from finite-size combustion sources, dynamics 78−30341
gas-particulate fluidised beds, bubble formation and shock front 79−90318
gas-particulate laminar boundary layer on a flat plate 79−77068
gas-solid dispersions, heat exchange in uniform elec. field 77−11273
gas-solid flow, nonreacting, heat and mass transfer, thermodynamic approach 78−51223
gas-solid flow in cylcone, turbulent swirl velocity, particle sizes and concentrations 80−69902
gas-solid flow in pipe, conc. distrib. *(French)* 79−50769
gas-solid flow in pipe, expansion on deceleration 80−69909
gas-solid flow local heat transfer, particles distrib. 78−9686
gas-solid flowing mixtures, heat transfer 77−58773
gas-solid fluidisation, solid pot. flow around rising bubbles 79−86501
gas-solid horizontal pipe flow, vertical concentration distrib. *(French)* 80−14824
gas-solid mixture, flow in standpipes, review 79−18935
gas-solid mixture, pulsating flow, hydraulic resistance, heat transfer 78−38392
gas-solid mixture entering curved duct, particle trajectories 80−96304
gas-solid mixture hydrodynamics, use of relative velocity of gas to solids *(Croatian)* 80−14799
gas-solid mixtures, free non-Stokes particles, expt. investigation *(German)* 77−11253
gas-solid packed column, gas and solid phase axial dispersion at trickel flow 80−14807
gas-solid particle suspension, turbulent flow in curvilinear channel, local heat exchange 78−63484
gas-solid suspension, free turbulence influence on heat transfer 77−42898
gas-solid suspension, turbulent heat transfer during motion in tubes *(Russian)* 77−24020
gas-solid suspension flow, laser anemometry meas. 77−35268
gas-solid suspension flow in tube, press. drop, entry length 78−42647
gas-solid suspension flow through packed beds, convective heat transfer 79−4075
gas-solid suspensions flowing in steel and insulating coated pipes, electrification 77−77811
gas-solid turbulent flow, heat transfer, model 79−1232
gas-solid turbulent flow, press. drop, Reynolds eqn. 77−31370
gas-solid turbulent flow, press. drop, solids phase momentum eqns. 77−31371
gas-solid turbulent shear channel flow, particulate motion, numerical simulation 80−53863
gas-solid turbulent suspension flow, frictional pressure drop Prandtl's mixing length anal. 79−14458
gas-vapour droplets, nonuniform mixture, acoustic wave attenuation 78−83154
gas-water flow, heat transfer meas. *(Russian)* 80−43761
gas/liquid, hydrodynamic eqns. formulation 77−68682
gasdynamic laser, two-phase mol. vibr. relax. in gas-aerosol system 79−45807
gasdynamics of explosions, reactive systems, conf., Stockholm, Sweden (Aug. 1977) 79−64690
geopressured geothermal wells production characts. 78−81223
geothermal pressure transients, two-phase and single-phase 79−66664
geothermal reservoir simulation, numerical soln. techniques 80−12447
glass bead-air suspension, local particle conc. in turbulent duct flow 77−11239
glycerine-water drops, collision dynamics, ang. of incidence influence *(Russian)* 78−83461
grain movement on stream bed, relative protrusion effect, shear stress 77−13094
granular cohesionless material, gravity flow in chutes and channels 79−64753
granular material, double sliding free rotating model 78−38384
granular material flow in two-dimensional hoppers 79−7403
granular material pneumatic conveying, gas-to-particle heat transfer 79−18927
granular materials, flow round obstacles 80−103064
two-phase flow continued
granular materials, pneumatic conveyance, pressure drop production *(German)* 79−50782
granular materials flow, micropolar continuum theory 79−35565
granular materials minimum transport vel., in horizontal pipe 78−90965
granular materials pneumatically transported, heat transfer and lateral mixing 78−87378
granular media, dynamic flow, statistical theory 78−51217
granular media and powders model laws, especially for silo models 78−38383
granules ejected in air stream, parameters of motion under gravity 77−15103
gravitational instability in presence of suspended particles and rot. 79−64633
gravity flow of gases, liquids and bulk solids, common eqn. represent. and exptl. test 80−38477
heat and mass transfer in porous media subject to fires 79−86507
heat and mass transport eqns. derivation, closure problem 77−89188
heat conduction, unsteady, in quarter plane, appl. to bubble growth 78−75045
heat exchange between two-phase flow and nozzle wall with condensate film 79−46357
heat exchange component vibrations in liquid and two-phase cross-flow 78−90770
heat flux-flow coupling effects in the stability of vapour generators *(German)* 80−74967
heat pipe, 2-component, heat and mass transfer 80−24021
heat pipe, with header and single or two-phase artery systems 78−90981
heat transfer, between cylinder and rising two-phase flow, electrochem. method 77−55076
heat transfer between a dispersed system and a vertical heating or cooling surface 79−1069
heat transfer between flow with condensed liq. particles and wall with solid condensate layer 79−86426
heat transfer bibliography, Japanese works 79−23317
heat transfer conference, Aug. 78, Toronto, Canada 78−90624
heat transfer in convergent part of nozzle, correl. of expt. data 79−81958
heat transfer in dense layer flowing in cylindrical pipe 77−47074
heat transfer in vertical steam generating tube, at low pressures and moderate mass velocities of flow, post-dryout coeff. calc. 78−67257
heated tubes, alternate dry and rewet, flow boiling, obstruction effects 79−1181
heavy-particle impurity suspension effect on viscous shock layer gas flow 80−28554
Hele Shaw flow with horizontal temp. gradient, slow bubble motion 80−28549
Hele-Shaw cell, bubble motion, study of 2 phase flows under reduced gravity 79−14457
heterogeneous condensation, in cylindrical channel and on aerosol particles 79−57298
heterogeneous condensation 79−64488
heterogeneous flows of multi-component mixtures in porous media−review 78−59471
heterogeneous fluidised system, aerodynamic aspects of transfer processes, crit. state 80−79394
heterogeneous liquid stream, stress diffusion effect, molar diffusion coeff. 78−79338
heterogeneous porous medium, two-phase flow, multidimensional problem *(Chinese)* 80−64608
n-hexane droplets coalescence in aq. electrolyte solns. 79−64742
high loading ratio slurries, pressure flow, pressure drop calcs. in pipes 80−92202
high pressure steam/water mixture flow through cylindrical channels, obs. 80−79404
high pressure water in heated four rod bundle, flow patterns 78−89938
high speed flows, verification calcs. of fundamental eqns. *(Japanese)* 80−69907
high-temperature optical void probe, reactor safety appl. 79−93705
hindered settling in a multi-species particle system 80−14782
holdup relation verification 78−51220
hollow cone sprays, induced air flows 80−53846
horizontal coiled tube banks, two-phase flow boiling heat transfer and hydrodynamics 80−48708
horizontal gas-liquid stream, flow vel. meas. 80−96301
horizontal pipelines, two-phase flow patterns, pipe dia. and fluid prop. effects 80−48791
horizontal slug or surge flow 80−48786
horizontal stratified, 1-D two-fluid eqns. 80−91226
horizontal two-phase flow across tube banks, pressure drop predictions 80−103062
hot, temp. meas. by absolute spectral line intensity method 79−94700
hot surface quenching rate, countercurrent single- and two-phase flow effects 78−59451
hot-film anemometer for cylinder wake pattern with spray cooling 78−34238
human respiratory airways, diffusional deposition of airborne particles in curved tract 77−81519
hydraulic jump characts., air entrainment 78−79379
hydraulic lines, wave phenomena, coupled vibrations in bending and branching lines 80−14778
hydraulic resistance of channels with separation or merging of incompressible flows 77−68669
hydrodynamic crisis, in two-phase channel flow 78−14066
hydrodynamic resistance reduction by surfactant, rel. to micelle form. 77−7438
hydrodynamic suspensions, physical property variations *(Russian)* 78−47022
hydrodynamics and heat exchange in film flow 78−91000
hydrothermal flows, two-phase, in permeable media, struct. 80−85693
hypersonic bow shock interaction with ice crystal, aerodynamic shattering criterion 77−27558
hypersonic free-molecular heating of micron size particulate 79−4058
imbibition in 2-phase flow through porous medium with capillary pressure 79−20884
immersed nozzle, liq. gas discharge processes 78−83451
immiscible liquid two-phase flow in porous media, unstable displacement 80−92213
immiscible liquid-liquid system, laminar jet, vel. profiles and form 79−64752

two-phase flow continued
immiscible two-fluid system, in horizontal layer, with internal heat sources, natural convection 78−94539
inclusions in gas-liquid mixture, effect on interphase heat and mass exchange 80−103059
incompressible, through sharp-edged orifices, pressure-drop study 78−1726
incompressible Newtonian fluid, flow past wall with small particle injection *(French)* 79−46384
incompressible two-phase flow without mass transfer, turbulence eqns. *(French)* 79−72925
inert gas, in liq. metal, bubble dynamics, simplified model 77−15098
inertial coupling between components, flow regime depend. 79−27684
inertial coupling in dynamic eqns. of components 78−63483
inhomogeneous fluidised layer in reactor, 2-point boundary value problem, asymptotic anal. 80−33654
inhomogeneous media of cylindrical geometry, luminesc. 79−23377
instabilities, programme for nucl. reactor heat removal expt. at low power 78−54814
instability in parallel channels 78−94810
instrumentation calibration for mass flow rate meas. in PWR coolant two-phase flow 80−37552
instrumentation for localised meas. in PWR coolant two-phase flow conditions 80−37550
instrumentation for safety anal. of LWR LOCA 80−102259
interface of spherical particles, unsteady state mass transfer 78−47017
interface of spherical particles, unsteady state mass transfer 78−47018
interfacial stability with heat and mass transfer, appl. to Rayleigh-Taylor and Kelvin-Helmholtz cases 78−67253
intermittent flow in horiz. pipes, predictive models 79−64740
internally finned tubes, refrigerant 22, evaporative heat transfer and pressure drop 80−5919
interparticle interactions in two-phase moving media 79−14465
inviscid liquid, spherically oscillating, force acting on particle and bubble 77−35222
inviscid rotational flow through sprays 79−46328
ion Karman's constant variation in turbulent motion *(Italian)* 78−14062
isobutane-air, in packed bed, heat and mass transfer, axial mass dispersion 78−75200
isothermal expansion of a two-phase fluid in a magnetohydrodynamic generator duct 80−1695
isotope separation, using nonequilib. condensation with selective laser photoexcitation, mathematical model 79−31720
isotopic computerised tomography meas. 80−59136
jet, discrete phase penetration into constant cross flow *(Russian)* 78−47024
jet, disperse phase turbulence struct. modification model, energy dissipation 77−58769
jet, laminar, in liq.-liq. system, vel. profile, numerical analysis 80−28545
jet, liq., breakup, 3rd perturbation Cosserat soln. 79−32615
jet, liq., interaction with confined wet entraining vap.-liq. flow 79−32635
jet, liquid, turbulent, gas absorpt. *(Japanese)* 80−38473
jet, turbulence dissipation 77−35208
jet impinging on liq. pool, submerged biphasic region 77−31350
jets, turbulent 79−32636
jets, two-phase, turbulent, particle or droplet size effect on diffusion 80−1658
jets, two-phase supersonic flow around a sphere 80−6114
kerosene drops in crystallising $MgCl_2$ brine, direct contact cooling 79−1053
Lagrangian hydrodynamics meshes, discrete rezoning algorithm, hot interacting bubbles calcs. 78−42628
Lagrangian turbulence characteristics meas. using photographic techniques 77−58811
laminar aerosol flow through inclined circ. tubes, gravitational deposition of particles 77−89192
laminar boundary layer, forced convection condensation *(Japanese)* 78−34191
laminar boundary layer eqns. 80−38476
laminar channel flow, forced convection energy eqns. 77−55090
laminar dispersion, effect of tube curvature and pulsations 77−3858
laminar dispersion in rectangular conduits, side wall effects, convection 78−94636
laminar film condensation from moving vapour, with suction 78−59459
laminar flow, in circular pipe, heat transfer, inlet temp. effects 78−67265
laminar flow in channel, vel. profile 78−9675
laminar liquid film, falling, O_2 adsorpt. with zero order react. in entrance region 80−64652
laminar suspension flow, with diffusive gravit. deposition at entrance of converging and diverging channels 80−14825
laminar tube flow, gravitational deposition of growing aerosol particles 80−59099
laminar two-phase flows, particle interaction, obs. and calc. 79−72875
laminar vapour-air mixture flow, around circ. cyl. with vapour desublimation, numerical anal. *(Russian)* 79−60051
laminar zero net flow in inclined pipe 78−83457
laser velocimetry and visualisation, two-phase supersonic streams, gas-dust 79−68830
laser-Doppler technique, local size and vel. probability distrib., two-phase suspension flow 78−59517
latex suspension liquid film flow, local thickness meas. 79−4070
Laval nozzle, surface burning in two-phase flow, boundary layer interaction, Rakhmatulin model 78−83452
Laval nozzle, two-dimens. two-phase flows with nonequil. phase transition 77−51101
limiting vapour qualities in second boiling crisis 79−81970
liquefied natural gas, nonsteady-state flow calculations in horizontal pipeline systems 80−106838
liquid, spontaneously evaporating, critical discharge from channel 78−59456
liquid acceleration in channel by intermittent vaporisation, pulsed transfer of energy 79−94701
liquid containing gas bubbles, struct. of supersonic waves and cavitation development 80−33643
liquid containing small particles, eqn. of motion *(Russian)* 77−84301
liquid drop aggregate breakup in shock waves 80−24084
liquid drop coalescence, effect on disperse-phase-controlled mass transfer rates 78−26185

two-phase flow continued
liquid drop deposition in two phase dispersed flow heat transfer 79−81959
liquid drop in viscous liq., slow motions, force of resistance 77−35217
liquid drop motion in non-Newtonian media 78−75184
liquid droplets in free-mol. stream, drop size distrib. 77−35211
liquid drops, colliding in free fall 78−38396
liquid drops moving in single file in liquid continuum, heat transfer 79−46367
liquid evaporation in circulating gas, porous channel temp. determ., obs. 79−72943
liquid film, gas entrained, combined plane parallel flow, linear and nonlinear stability 80−33655
liquid film, in vertical tube with turbulent gas flow, friction coeff., press. losses 77−89189
liquid film flow, hydrodynamic and heat transfer in downward annular motion 77−89190
liquid film flowing concurrently with air in horiz. duct, flow pattern 80−43774
liquid films, vertically falling in circular tube, longitudinal flow characteristics 80−74957
liquid filtration by passing through partially saturated porous media 79−90326
liquid foams, shock wave dispersion 79−46359
liquid freon II, saturated and subcooled, two-phase critical flow 77−68678
liquid fuel droplet heating with internal circulation 78−75194
liquid hold-ups in packed column *(German)* 79−46364
liquid in centrifugal atomizer, air vortex radius 77−80201
liquid jet, burnout in nucleate boiling 78−90991
liquid layer, flowing on pipe wall, gas absorption rates 79−94696
liquid metal flow in heat pipe, low temp. region, effect of compressibility, friction and evaporation 77−47066
liquid metal gas inclusions, bubble release dynamics, mag. field effects *(Russian)* 77−3865
liquid metal MHD generator, wall-jet gas injection 80−28830
liquid metal two phase flow, gaseous phase redistrib. in strong mag. field 79−37410
liquid metal-gas two-phase MHD generator, pot. loss mechanisms, rel. to fluid dynamic processes 77−39359
liquid sprays, aerodynamic behaviour 77−35212
liquid to vapour transformations, mechanics of two phase flows 77−89532
liquid with bubbles, small perturbations propag. 78−42651
liquid with fine particles, flow instability 79−64745
liquid with gas bubbles, steady-state perturbations, wave propag. 78−5788
liquid-borne solids monitoring, optical instrument general principles 79−37424
liquid-fluidised system, axial dispersion, correlating parameters 79−46381
liquid-gas bubble mixtures, shock wave disturbances 78−22411
liquid-gas flow without mass transfer, centrifugal scaling 77−35209
liquid-gas interface, heat and mass transfer 78−30338
liquid-gas mixer, perforated disc stirring cascade type, power dissipation, mechanism and correlation 79−1238
liquid-gas system between two plates, capillary curve 80−33660
liquid-liquid agitated dispersion, droplets transitional breakage probability 79−77219
liquid-liquid dispersion, in turbulent agitated motion, drop size limits 79−68787
liquid-vapor system, shock compression, equilib. states *(Russian)* 78−9687
liquid-vapour critical flow, two-fluid model 78−90973
liquid-vapour flow, heat transfer crisis, wall shear stress 78−90986
liquid-vapour flow, wave pattern and liq. film burnout 78−90985
liquid-vapour flow in heat transfer crisis, liq. film limiting flow rate 78−90987
liquid-vapour mixture, acoustic wave propag. 78−90972
liquid-vapour system, shock wave effect on thermodynamic equilib. 79−64746
liquids with vapour bubbles, US propag. 80−33661
LMFBR, effects of Na entrainment and heat transfer with UO_2 vapour during HCDA 79−93775
LMFBR, flow behaviour of vol. heated boiling pools 80−13545
LMFBR, local boiling calculations in subchannel geometry, feasibility study using CLAYMORE code 78−25280
LMFBR, red. of two-phase thermal cond. and heat transfer by entrained inert gases 79−30897
LMFBR, transient fuel solidification and relocation from core during transition-phase conditions 79−85616
LMFBR accident anal., noncondensible void fraction effect on freezing of flowing fluids 79−31013
LMFBR core disruptive accidents, flow regime obs. in two-phase volume heated boiling pools 79−31014
LMFBR LOF-HCDA, solidification dynamics of flowing two-phase mixtures 79−49757
LMFBR postulated core meltdown, onset of foam flow regime in volume heated boiling pool 79−31015
LMFBR steam generator, few-pressure model for transient two-phase flows in networks 79−59136
LMFBR thermal hydraulics 80−27718
LOCA, blowdown phase, two-phase mass flow rate meas. using true mass flowmeters 80−778
LOCA, counter-current flow limiting phenomena with vapour condensation, model 77−61519
LOCA codes, characteristics of two-phase one component flow with slip 77−83019
local density measurements, side-scatter gamma technique 80−569
local void fraction in two phase flow, Raman effect measurement technique 79−64813
longitudinal diffusion in a flow through a tube 78−90974
loose material forced displacement processes in pipes, gas flow filtration effect 77−58783
low quality flow boiling, turbulent forced convection and nucleate boiling heat transfer 80−14696
low velocity vertical steam-water flow, void fraction in pipes 80−74964
lung airways aerosol impaction model 77−90840
LWR, analytic simulation 80−13551
LWR LOCA, anal. of LOFT drag disc turbine meter rakes 80−102260

two-phase flow continued
LWR LOCA, modelling of press. and temp. changes in two-phase, two-component flow *(Bulgarian)* 80−68904
LWR safety, critical flow of two-phase one-component mixtures *(Italian)* 79−71880
macroscopic equations 77−15095
magnetic separator, high-gradient, flow characterisation 79−41740
magnetic stabilization of the state of uniform fluidization 80−19484
magnetorheological systems, heat transfer 79−81988
mass flow instrumentation performance, during LOFT nonuclear test series 80−69952
mass flow measurement, ^{16}N tagging 79−93793
mass flow measurements of single-phase and multi-phase flows using radionuclide methods *(German)* 79−86532
mass transfer inside drops in continuous fluid, effect of pulsation *(French)* 78−55686
meas. using sharp edge orifices, correlations evaluation 78−26223
measurement, indirect, methodological error anal. and reduction 78−34241
measurement techniques, recent progress *(French)* 80−79411
measurement with orifice-couple in horizontal pipeline 79−94744
mechanics equations for porous medium saturated by a two-phase liquid 79−94699
medium containing heavy particles, convective stability 77−80203
medium with low initial water saturation, end effect in two-phase flow 80−33656
metal foams, solidification in space environment, fluid flow effects 79−47674
metallic heat carrier in loops, phase transition process, temp. field 79−55867
metallic particles, two-phase nozzle flow into vacuum, laser scatt. 77−35194
methane-H_2, in packed bed, heat and mass transfer, axial mass dispersion 78−75200
MHD coal slag particles deposition rate on channel wall, theoretical and expt. studies review *(Japanese)* 78−38413
MHD flow through cracked porous media, imbibition 78−34200
MHD pipe flow, single and two phase 80−53869
MHD pressure drop in liquid metal flow, gas-liquid slip ratio 79−23368
microconvective heat, mass transfer processes, in fluids with internal rot. 79−86435
mist flow, evaporation of droplets 77−55350
mist flow over heated cylinder, particle size and temp. difference effects 80−38409
mixed 2-D flows of supersaturated and two-phase medium with nonequilib. phase transitions 79−77224
mixing and condensation in high-speed flow, review 78−47014
mixing layer growth from turbulent and nonturbulent boundary layer 79−68686
model eqns., interfacial press. forces 78−14069
modelling, theoretical foundation, appl. to fission reactor fluid flow and heat transfer 80−103065
molten drop break up in gas flow, surface drag, capillary excitation *(Russian)* 80−100024
molten reactor core debris pool, hydrodynamic instabilities and convective mixing 78−8931
momentum and energy eqns., pressure term form 79−90315
moving boundaries in two-phase turbulent flows 79−18932
mud suspension, batch sedimentation in inclined tube 79−64743
multicomponent system interface, mass transfer relations *(German)* 80−74966
multidimensional effects in critical two-phase flow 79−14461
multidimensional two phase flow eqn. derivation, general constitutive principle appl. 80−10297
multigranular suspensions, aqueous, sedimentation in oblique plate separator under laminar flow conditions *(German)* 77−44513
multiple-jet thermal mixing in a piping tee 79−81938
natural convection in permeable medium adjacent to vertical heated surface 79−68790
Navier-Stokes eqns. 79−1235
Navier-Stokes flow with suspended particles, mathematical modelling, numerical simulation 77−72348
Newtonian fluid containing rigid particles, peristaltic pumping at low Reynolds number 79−10604
Newtonian fluids, mean velocity and vol. flow rate for steady 1-D flow 80−6132
Newtonian vapour, with liquid droplets, throughflow between corotating disks, numerical anal. 78−94802
non-Newtonian flow through porous media, fluidised beds, solid-fluid interaction *(Portuguese)* 80−38454
non-Newtonian fluid, effective diffusion of impurity in laminar flow of liquid 78−67228
non-Newtonian fluid, gas bubble form. at single submerged orifice, model 79−32640
non-Newtonian fluid, quadratic shear flow, rigid sphere and drop migration 77−84309
non-Newtonian fluid containing particles, constitutive models 79−60049
non-Newtonian liq.-air annular flow, film thickness rel. to rate 77−3860
non-Newtonian liquids, spherical gas inclusion radius change Rayleigh classical equation generalisation 80−19444
non-Newtonian liquids and gases, annular two-phase flow, press. drop and gas vol. fraction 80−10286
non-Newtonian medium, bubble motion and deformation, drag coeffs. 77−89184
nonequilibrium, phase temp. meas. 80−74950
nonequilibrium, true mass steam content meas. by diffusion indicator method 79−86538
nonequilibrium flow, spectral characts. 78−94854
nonequilibrium models, anal. using method of characteristics 80−103069
nonequilibrium subsonic/supersonic flow, acoustic vel. obs. 78−42642
nonequilibrium transient flow boiling, method of characts. soln. 80−14789
nonequilibrium two phase flow, voids fraction and vapour phase condensation 79−90310
nonequilibrium two-phase flow, relation between thermal and flow characts. 78−55694
nonequilibrium two-phase flow in Laval nozzles 79−68820
nonisothermal boundary layer, laminar flow of dilute particle suspension, self similar soln. 77−65785
nonisothermal flow in vertical channel, rel. to natural convection boiling 77−24013

two-phase flow continued
nonlinear Rayleigh-Taylor stability with mass and heat transfer 79−90224
nonspherical particle, friction coeffs. in incompressible fluid with spin 78−87350
nonstationary velocity tracking by adaptive cross-correl. algorithm 78−14074
nonstratified, adiabatic, hydraulic resistance calc. 77−7440
nozzle, convergent-divergent, choked foam flow 79−64750
nozzle, Laval, direct flow problem, numerical anal. 78−63475
nozzle, two phase, efficiency at high rates of heat and mass transfer 80−48767
nozzle design for gas-liquid flow, inverse problem formulation 78−47015
nozzle flow, max. mass flow rate determ. 78−71384
nozzle flow, specific impulse estimation 77−47065
nozzle flows from separate phase model 80−74938
nozzles, subsonic and transonic 79−81950
nuclear fuel pin model, parallel two phase flow induced vibrations 79−13388
nuclear power plant heat exchange problems 80−18372
nuclear power station, hot water leakage from first loop, 22.8 MPa initial pressure, flow characts. 78−66357
nuclear reactor, AGR, helical monotube vapour generator, density wave instability, experimental-stochastic and theoretical anal. 80−47539
nuclear reactor, interfacial mass and momentum transfer in two-phase flow 80−27725
nuclear reactor, method of characteristics anal. 78−21628
nuclear reactor, two-phase critical flow phenomena 80−27723
nuclear reactor, two-phase flow characterisation by neutron noise techniques 78−94058
nuclear reactor, two-phase flow in pin bundle, two fluid model 80−91209
nuclear reactor components, two-phase flows, high-intensity X-ray system for stochastic measurements 79−93791
nuclear reactor coolant, generalized pressure drop correlation, in two-phase flow 79−9664
nuclear reactor flow boiling anal., numerical standards 77−79448
nuclear reactor LOCA, modelling two-phase hydrodynamic phenomena, pipe blowdown with Freon-12 80−5267
nuclear reactor LOCA, reflood hydrodynamics, two-velocity two-phase flow model 79−633
nuclear reactor LOCA reflood phase, hydrodynamics, moving control vol. method 78−704
nuclear reactor LOCE blowdown flow meas., improved spool piece 80−27727
nuclear reactor pin bundle, two-phase flow, eqns. of motion 78−86570
nuclear reactor safety analysis, void fraction prediction, depressurization of diabatic systems 77−23222
nuclear reactor transient thermal hydraulic analysis, RELAP4 transform. into fully implicit iterative code 77−65257
nuclear reactor transient two-phase flow, analytical modelling 80−27722
nuclear reactor transit time estimation, improved correlation method, coolant bubbles appl. 78−94067
nuclear reactor two-phase-flow instrumentation development at Brookhaven National Laboratory 80−102261
nuclear reactors, BWR and PWR, boiling mixing studies in water loops 79−26502
nuclear reactors, two-phase flow operating conditions *(French)* 80−78348
nucleation homogeneous, gasdynamics of supersonic flow with condensation 77−62292
numerical prediction of recirculation flows with free convection encountered in gas-agitated reactors 79−10602
oil, spreading on water, rel. to surface contamination 79−43795
oil thickness variation on wavy water 80−6134
oil transport as oil-in-water emulsions 79−77192
oil-bearing layer with input parameter correction, discrete dynamic model 80−83778
oil-water emulsification, by US, large primary oil drop breakup 79−32644
oil-water interface, US emulsification drop form. by capillary wave instability 79−32643
once-though boiling flow system, density wave instability 79−22367
one component, single substance flows, probe method for phase concentration determ. 80−74954
one dimensional, critical flowrate in channel calc. 80−10292
one-dimensional, heat and mass transfer, approx. math. model 79−86495
optic cavitation and laser-produced bubbles 80−38463
optical instrumentation methods for two-phase reactor flows 80−63313
optical probe for local void fraction and interface vel. meas. 78−83505
oscillating vessel with liquid containing compressible sphere, finely disperse inclusion motion 80−74963
packed bed, temperature profile for concurrent air-water downflow, latent ht. effect 79−50789
packed bed thermal storage systems, single- and two-phase models 78−91009
packed beds, gas-liquid concurrent, wall heat transfer 79−50790
packed beds, low Peclet number particle-to-fluid heat and mass transfer 78−94799
packed beds, particle-to-fluid transfer coeffs., fluid diffusivities 77−31378
packed column, liquid distrib. and redistrib., expt. 79−18939
packed column, liquid distrib. and redistrib., theory 79−18938
packed column, trickle and two-phase flow, tracer dispersion obs. 79−86502
packed-bed particle-to-fluid heat transfer coefficient, determination from radial heat transfer measurements 78−9699
packing in flow, with longit. dispersion 79−68796
paraffin-air mixture, energy dividing props. in discharge from supersonic jet *(Russian)* 77−39332
parallel channel forced convection boiling upflow system, instabilities 80−9327
parallel channel of forced convection boiling upflow system, instabilities 77−61494
parallel corotating discs, laminar or turbulent throughflow, bulk-parameter anal. 77−39336
parallel-plate channel, convectively-cooled, liq. solidification 77−68666
paramagnetic particle stream trajectories near ferromag. fibre 79−86128
partial differential equatn. finite difference solutn. 80−18564
particle array, falling through fluid, clumping instability 77−42906
particle capture from laminar flows, review, book contrib. 77−47078

two-phase flow continued
particle cloud conc. profile in turbulent boundary layer 77−24016
particle collection, fluid inertia effects 79−18934
particle collectives, turbulent flow, diffusion model description, appls. *(German)* 78−59446
particle collisions in concurrent dispersed flows 77−15101
particle convective diffusion to rot. disc surface 78−18334
particle deposition, in laminar flow in tube, thermal effects 77−58764
particle deposition, onto rot. disc, convective diffusion, external force field 78−40081
particle deposition in channel walls, analysis *(Russian)* 79−77228
particle diffusion in electrostatic precipitators 77−3526
particle drag and induced mass, particle conc. effect 78−47016
particle EM ejection coefficient in two-phase MHD flow 79−77273
particle flow meas. by microwave Doppler-effect flowmeter 78−9732
particle free fall through oscill. liqs., eqn. of motion 77−3859
particle impacting wall diffusion layer, enhancement of mass transfer *(French)* 79−60050
particle in nonuniform flow of viscous liq. 77−89191
particle interaction, coagulation and rebound calc. 79−98789
particle meas. concentration in turbulent jet, laser scatt. technique 77−39372
particle mobility in liqs., meas. by optical and elec. transients 79−77303
particle motion in gas currents *(German)* 78−55676
particle motion in gas stream, motion parameters determ. with photographic system 78−5837
particle motion induced by liq. oscills. 77−35210
particle oscillation inducing flowfield, in container 79−50770
particle shape, in laminar flow, by optical mixing *(Russian)* 79−10619
particle sizing by capillary hydrodynamic chromatography 79−64759
particle sizing counter for in situ meas. 79−75489
particle sizing counter for in situ meas. 79−75490
particle slip, temp. depend. in gaseous medium, free mol. regime 77−11249
particle swarm moving in viscous fluid 78−26186
particle transport in laminar stream *(Russian)* 77−58768
particle transverse motion in turbulent boundary layer 78−79358
particle velocities measurement in two-phase flow using mag. markers *(German)* 77−42939
particle-fluid mixture, energy balance in turbulent flow 77−47076
particle-vapour subliming boundary-layer flow, local nonsimilar solns. 77−80206
particles, falling under gravity, in rot. drying drum, turbulent gas flow 78−1728
particles, spherical, collection efficiency of inclined tubular elutriator 79−90354
particles dispersion variation process study using theoretical kinetic methods 80−106839
particles in a fluid, convective diffusion and mass transfer, wakes, chemical reactions 80−38394
particles in laminar tube flow, thermophoretic deposition 79−46371
particles in supersonic flow, vel. lag expts. 79−7402
particles in turbulent fluid, statistical motion, Eulerian direct interaction 80−53841
particles moving in reactive, dispersive system, mass transfer interaction 79−64738
particles suspended in turbulent fluid, dispersion 78−14073
particles suspension in turbulent vortices, meas. of small sphere motion in rot. vel. field 77−58771
particulate beds, sheared, mass transport kinetics, Markov chains appl. 79−60057
particulate emission monitor calibration in gas-solid suspension 77−37454
particulate materials, cohesionless, mixing and segregation, microscopic mechanisms 79−37848
particulate materials, cohesionless, mixing and segregation, failure zone form. 79−42261
particulate sedimentation, eqn. soln. stability to small perturbations 79−77230
particulate sedimentation, stability, two-dimens. anal. 80−69768
particulate suspensions, weak wave propagation 77−80207
paste-like composite with polymer binding, rheological props., wall effect 77−47072
pattern characterisation by electrical conductance probe 80−106857
periodic capillary tube, two phase fluid flow and hysteresis 80−107615
periodic capillary tube, two phase fluid flow and hysteresis 80−107616
petroleum, two phase flow in underground reservoirs, soln. of nonlinear eqn. by random choice method 79−50773
phase distribution in two-phase steam flows, effects of probe position 80−87799
phase interfaces, balance eqns. and struct. models 78−59453
pigment dispersion rheology, kinetic model, expt. results 79−7361
pipe, annular two-phase flow, downtake turbulent film and gas flows, pressure drop 80−92218
pipe, circular, two phase flow in entrance region, effect of conc. of suspended particles 80−19481
pipe, particulate suspension flow, sticking probability and erosion, data correlations 79−41744
pipe, straight, fracture under large deflection, pipe pressures, finite difference code 77−58616
pipe flow, depend. of particle deposition velocity on particle inertia 77−35219
pipe flow, effect of mass transfer on heat transfer 78−91003
pipe fluid flow, solid particle impurity propag. 80−64630
pipe lines, on-line holdup or quality meter 80−106858
pipeline break, unsteady-state outflow 78−42658
through pipes, calc. method and simplified diagram *(German)* 77−35235
pipes, flow of liquid and gas mixture, optical representation *(German)* 80−14800
pipes, two-phase stream, stratified flow, condensation calc. 79−23349
plastic disperse systems, generalised flow theory with account of wall effect 78−87320
plate columns with dual flow, mass transfer modelling 78−51219
pneumatic transport of granular material 79−72927
polydisperse gaseous suspension, heat transfer between subsonic nozzle walls, rel. to particle motion parameters 77−24019
polydisperse materials gravitational classification in horizontal flow *(Ukrainian)* 77−68668
polydisperse particles in spouted bed, particle cycle times, size depend. 79−46365
polyethylene, melts, stratified two-phase flow, interface deform. 77−11158
polyethylene pellets, falling in air in pipe, equilib. region press. drop, friction factor 78−63479
polymer melt suspension, plastic-viscoelastic constitutive eqn. 79−60014
polymer melts, bubbles formation, non-coalescing bubbles theory appl. 78−42640
polymer melts, stratified two-phase flow, interface deform. 77−11158
polymer solution, bubble elongation dynamics, modelling with viscoelastic constitutive relations 79−37388
polymer solution one- and two-phase flow through porous media 78−42659
polymeric liquid, viscoelastic, gas bubble pulsations and assoc. dissipation effects 80−59079
polymeric liquids in pipes, non-steady two-phase stratified laminar flow 79−81832
polystyrene, melts, stratified two-phase flow, interface deform. 77−11158
polystyrene, ordered monodisperse latexes, viscoelasticity and flow props. 80−58992
polystyrene suspension, laminar flow, augmentation of heat and mass transfer, correl. of data 80−53840
porous media, diffusion-convection eqn., mixed finite element method, water flooding 80−74969
porous media, fingero-imbibition, composite expansion soln. 78−79373
porous media, two-phase flow with end effect allowance, numerical simulation 80−33659
porous media flow, finite element simulation 79−41752
porous media two-phase flow, perturbation soln. due to differential wettability 78−59470
porous medium, starting algorithm for numerical simulation 78−38388
porous particle suspension, linear shear flow 77−15094
porous particles suspension, effective viscosity, flow 79−18929
powder, triaxial test procedure and num. calc. method for flow props. 77−60028
powder flow over inclined surfaces 78−63488
powders, air fluidisation, bubbling behaviour, rel. to particle size 77−31362
power-law liquid, dil. suspensions of dipole dumbbells, rheological eqns. of state and shear flow in elec. field 79−86473
prepolymer, two-phase, US flowmeter optimisation 77−31410
pressure driven stratified laminar pipe flow 80−64609
pressure drop in bends, eval. of two-phase multiplier 80−92208
pressure drop measurement variations, analysis *(German)* 78−59445
pressure drops and hydraulic losses w.r.t. local resistances 79−77221
pressure pulse propagation in two-component slug flow 79−77235
pressurised pipe guides, nonstationary discharge of boiling liq. in thermodynamic equil. approx. 79−81711
pseudocontinuum mass transfer in media with spatially periodic boundaries 79−86500
pseudofluidised layer, hydrodynamical eqns. *(Russian)* 77−35233
pulsatile flow of dusty fluid through constricted channel 79−14468
pulsating air bubbles in water, stability using optoelectrical method *(German)* 77−27578
pulsating gas bubbles in acoustic field, thresholds for surface waves 80−33665
pulsed neutron measurement of single and two phase flow 79−50771
pulverised coal reactors, cold flow mixing rates with recirculation 79−50762
pulverised fuel gas flow distrib. in manifolds of uniformly variable section *(Russian)* 80−33666
pumps, cavitating, dynamic characts., bubbly flow model 79−32646
PWR, choice of vent flow formulation for subcompartment anal. 79−31047
PWR, small scale ECC bypass data anal. 80−18505
PWR, two phase flow modelling for LOCA *(French)* 80−78349
PWR boiler steam generators, two-phase flow problems in low press. transients *(French)* 80−78350
PWR core thermal hydraulic calculation *(Hungarian)* 78−25282
PWR LOCA, pump behaviour conveying two-phase flow *(French)* 80−78351
PWR LOCA reflooding phase, two-phase flow and heat transfer at and near quench front 80−757
PWR rod bundles, radiative heat transfer calc. method 80−33602
quinone electrochemical reduction at packed, fluidised bed electrodes, kinetic behaviour 79−57235
raindrop growth physics, for teaching 79−35502
rapid surface vaporisation with back pressure, Knudsen layer, flow Mach number 79−77168
Rayleigh-Taylor instability, two superposed cond. fluids, with suspended particles 78−87399
reacting flow, heterogeneous, balance eqns. and soln., interior ballistic phenomena modelling 79−94737
reaction near grid in fluidised beds, two-phase model 78−67280
reactive particle flow through normal shock waves 78−42676
reactor containment subcompartment flow, film entrainment determ. 79−49657
reactor coolant flow boiling crisis, tube diameter effect 79−85603
reactor cooling channels, flow anomaly diagnosis, autoregressive model appl. *(Japanese)* 80−83146
reactor core control absorber, out-reactor flow investigation 78−58389
reactor thermal-hydraulics, quality influence on the departure from nucleate boiling in cross flows through bundles 80−95340
reactor two phase flow instability, classification by density wave oscill. model 79−63731
recirculating, num. calc. procedure 77−55081
refrigerant R-113 upflow in heated tube, liq. film dryout 78−90989
resuspension of spheres from a surface using a suction-nozzle system 79−37386
RETRAN two-phase flow model, comparison with expt. 80−32330
rewetting temperature in vertical channel coolant flow 79−59117
riffle formation model 78−63482
rigid spherical particle suspension, two-phase theory, volume averaging and governing eqn. *(German)* 80−87801
ripple, annular, two phase flow, statistical characteristics 78−9672
rising flow in channels, heat and mass transfer 77−62295
rivers, sand-wave motion of sediment along nonerodible bottom in open channel flow 78−16074
rod bundle dryout, liq. film, droplet entrainment and deposition 78−13204

two-phase flow continued
rod bundle void fraction in two phase flow, fast neutron scatt. technique calibration 79−82017
rod bundle with helical spacers, air distrib. in water flow 79−30894
rods falling near vertical wall 78−9690
rotary mixer, two-phase flow over working surfaces, optimal dimensions 78−63485
rotating heat exchanger, frictionless two-phase tube flow, centrifugal accel., choked flow 80−48792
rotating spheres, heat transfer coeffs. for gas-solid two-phase flow 80−19369
rough pipe, gas-liq. flow pattern transition model 78−14084
over rough surfaces, heat transfer effects 78−30297
saltating solid particles in turbulent flow, accel. and forces *(Russian)* 80−1675
saturated steam-water mixtures, void fraction relationships for upward flow 80−14790
second-order fluid, migration of spheres in two-dimens. unidirectional shear flow 77−940
sediment hindered settling, two-phase flow anal. 77−89193
sedimentation, settling instability, horizontally homogeneous suspension 78−42652
sedimentation, three-parameter Markov model 78−34183
sedimentation Markov model for very slow settling of dilute suspension 78−22406
sedimenting suspension, conc. distrib. determ. by radioactive solids 79−32634
seeded flow, instantaneous two-dimens. conc. meas. in turbulent jet by Mie scatt. 79−41670
semi-implicit differencing method for two-phase fluid dynamics 78−42649
semi-implicit two-fluid calculational methods 80−103066
separated, air-water in LWR LOCA *(Japanese)* 79−36334
separated flow models, stratified flow, averaged formulation, high order dispersion effects 80−74960
separated incompressible boundary layer prediction, including viscous-inviscid interaction 80−1548
separated two-phase flow, pressure drop and sonic vel. 80−106840
separation by solenoid *(Russian)* 77−7466
shock boiling, liq. discharge through short nozzles, flow blocking 79−86491
shock structure in a liquid containing gas bubbles with nonsteady interphase heat transfer 78−83424
shock wave, expt. 77−68674
shock wave amplification in nonequilibrium system of liq. and solvent gas bubbles 79−18936
shock wave in dusty gas, three-dimens. shock waves 79−68788
shock wave propagation in two-phase mixture *(Russian)* 78−51196
silt suspension turbulent boundary layer, steady state model 78−28242
simple bodies in two-phase flow, aerodynamic drag 80−96294
single-component two-phase flow, one-dimens. motion 78−59455
slender particles oriented in extensional non-Newtonian flow, stress field 77−19632
slowly moving vapour, film condensation heat transfer 80−19376
slowly rotating sphere submerged in fluid with surfactant surface layer 80−48717
slug formation, horizontal and inclined pipes, gas-liq. flow model 78−14083
slug formation, wave instability effects 78−14085
slug in fluidised bed, mass transfer, wall effect 79−4079
slurries, horizontal turbulent pipe flow, deposit vel. prediction 79−90312
slurry, pressure loss reduction by addition of surfactants 77−84297
slurry flow, confined, mean vel. field skewness computation 78−63481
slurry measurement, by press. differential devices 77−35265
smoke-motion, numerical anal. by finite-element method *(Japanese)* 80−69910
smoke-particle aggregates, long-range correlations 79−46369
solar nebula, grain motion through gas rel. to role as isotopic anomalies carriers 80−26757
solid in plane-parallel vortex flow of ideal incompressible liquid 79−14414
solid particle concentration profiles in turbulent jet, laser Doppler anemometer meas. and theoret. calcs. 79−27686
solid particle pnuematic conveyance, flow characts. 79−37380
solid particles effect on homogeneous isotropic turbulence decay 79−4073
solid particles in viscous incompressible fluid, action of gravity, sedimentation *(French)* 77−75964
solid particles lateral migration in laminar flow near plane 77−35207
solid particles suspension in agitated tank 79−7400
solid spheres in oscill. fluids, mass transfer review 77−42902
solid transported by gas in pipe, heat output 78−63486
solid-gas flow, fluctuation damping 80−19478
solid-gas jet issuing into transverse stream 79−32649
solid-liquid, through vertical pipe, particle concentration distribution *(Japanese)* 78−87382
solid-liquid mass transfer in concurrent two-phase flow through packed beds 79−4066
solid-liquid mixtures, laminar flow in open channels *(German)* 77−15123
solid-liquid mixtures, rheological characts., shear stress/strain rate relationships 80−10287
solid-liquid pipe flow, cross correlation method anal. 79−32638
solid-liquid slug flow, radial heat transfer characts. 78−63495
solidifying liquid metals, flow in two-phase zone 79−81953
solids, pneumatic transport, flow, friction effects *(German)* 78−34181
solids in mass flow bins, pressure prediction using minimum strain energy 77−35221
solids-gas countercurrent vertical flow 80−10288
soluble matter initial dispersion in three-dimensional flow 79−37387
solution droplets vaporisation, in high-temp. gas flow, heat and mass transfer 78−75191
Soret driven instability, transient and steady state behaviour, analogy with laser instability 79−55413
space averaging in continuum mechanics, macrostress tensor symmetry 80−92210
space averaging in continuum mechanics, symmetry of macrostress tensor 80−96297
sphere in presence of plane fluid-fluid interface, exact soln. of Stokes' eqn. 80−79251
sphere motion in viscous fluid, boundary wall effect 79−10603
two-phase flow continued
sphere moving in viscous fluid in corner 77−15099
sphere sedimenting in viscous fluid, lateral force 79−27685
spheres, accel. in free flight, periodic discontinuities 78−79365
spheres, strongly interacting, numerical soln., Stokes flow 78−22407
spheres falling in viscoelastic fluid, interactions along line of centres 77−15106
spheres in vertical flow, transient transition boiling heat fluxes 78−90994
spherical agglomeration in conical drum 78−14064
spherical cavity gas bubble in compressible liquid, kinematics of free vibrations *(German)* 80−24074
spherical condensed phase, motion in uniform vapour gas flow, kinetic theory 78−1725
spherical contaminated bubbles in viscous fluid at arbitrary angle of attack, terminal motion 79−27687
spherical gas bubble in unsteady viscous flow, unsteady boundary layer 79−55357
spherical gas bubble in viscous fluid, initial motion 77−65780
spherical particle, lateral migration in 2-dimens. shear flow 77−15100
spherical particles, line of centre motion 79−4067
spherical solids melting in turbulent carrier fluid, deformation and breakup 80−92646
spontaneously condensing and wet steam discontinuous flows in steam turbine cascades, subsonic, transonic and supersonic, numerical investigation *(Russian)* 80−87800
spouted bed, fountain region height and struct. 79−46380
spouted beds of spherical particles, spout termination, parameters 80−64621
spray, droplet vel. meas. using laser Doppler velocimeter *(German)* 79−50818
spray, numerical computation, appl. to engines 79−37378
spray cooling, characts. and minicomputer control *(French)* 79−3889
spray drying, of highly viscous conc. solns., heat and mass transport *(Russian)* 78−83230
spray nozzle, transfer processes in droplet plume during counterdirectional atomisation in gas flow 77−24014
spray-cooled cylinder, heat transfer 79−23354
sprays, drop trajectories, aerodynamic drag effects, computing methods 77−72347
stability conditions and wave speeds 78−30344
stagnation flow at a heated curved wall, ignition condition 80−96242
stationary sphere on boundary of similar spheres, drag coeff. function extension *(French)* 78−36211
steam, 2-D two-phase flow, nucleating and wet steam, time-marching method 80−69906
steam, condensation, heat transfer 77−62297
steam, superheated, dispersion in saturated water, bubble form., heat transfer 77−47068
steam, superheated, dispersion in saturated water, bubble form., heat transfer 77−47069
steam, wet, drop coagulation in cross-over pipe flows 80−74982
steam, wet, supersonic flow, total- and static-press. probe characts. 77−84353
steam condensation in moving two-phase film, heat transfer, volumetric coefficient 80−48696
steam condensation on turbulent water surface 79−64748
steam generating channel, nonuniform heat release, heat transfer crisis location 80−64534
steam generating channels, heat exchange intensification by surface roughness in transcritical region 79−55371
steam generating tubes, burnout mechanism 78−90984
steam generator, flow distribution anal., computer code 79−49653
steam generators, steady 2-dimens. two-phase flow and heat transfer calc. 79−1237
steam mixture of bubble struct., sound velocity, damping decrement 79−55444
steam turbine cascade, mixed and discontinuous, calc. 80−79391
steam-generating channel, heat exchange in transcritical region 78−42644
steam-generating channel hydraulic characts., two phase flow instability effects 79−90333
steam-generating tube, bubble/plug flow boiling regimes, elevated press., drift vel. and void fraction determs. 78−87379
steam-generating tubes, rough (smooth), post-dryout, heat transfer 78−55678
steam-liquid, annular-dispersed flow, hydrodynamic characts. 78−94806
steam-water, flow characts. at high press. 78−94805
steam-water, high-pressure, adiabatic, hydraulic losses calc. 78−87384
steam-water annular dispersed flow, liq. distrib. between core and film 77−75971
steam-water annular flow, moisture exchange, salt method 80−24078
steam-water counterflow in porous media, model, geothermal systems appl. 79−79879
steam-water flow, mass vel. meas. by Pitot tubes 77−79411
steam-water mixture, intensive drop condensation, flow boundaries 77−35204
steam-water mixture, upward flow in tube, liq. film-core mass transfer, liq. distrib. 78−75189
steam-water systems, two-phase press. drop correlations 77−82995
steam-water two phase mixture, relative vel. of vapour phase, determ. of void fraction 78−5791
steam/air mixtures, instrument for steam fraction meas. 80−52724
Stefan flow at liquid-gas interface, with evap. or condensation 79−37381
stochastic systems, time evolution in two-phase flow, mathematical model 79−64739
Stokes flow, Faxen relations generalisation 79−32438
Stokes flow past coaxial clusters of spheres in cylinder 77−11240
Stokes particle, suspended in inhomogeneous turbulent incompressible viscous stream 77−75968
stratified cocurrent flow of gas-liquid mixtures in horizontal pipes 79−77214
stratified flow through fractures in porous media 78−5792
stratified fluids in open channel, critical flow conditions 80−74956
stratified gas/liquid flow, heat transfer, local Nusselt number prediction 80−38393
stratified horizontal flow, averaged and local instantaneous formulations, stability 80−64613
subcooled boiling flow, vapour bubble growth and recondensation 79−93692

two-phase flow continued
subcooled forced convection film boiling in forward stagnation region 80−43702
subcooled liquid boiling in duct, vapour voids size distrib. 78−5783
submerged gas injection into liquids, flow regimes 80−59101
superposed flow, interfacial instability 79−4057
supersaturated liquid, flashing incompleteness and produced phases sonic ejection 79−86493
supersaturated vapour, nucleating centre nonstationary formation rate calc. 80−34178
supersonic transverse gas stream, penetration and mixing of secondary liq. injection 77−24018
supersonic two-phase flow, nonequilib. condensation, boundary condition numerical anal. 80−64565
supersonic two-phase flow, phase separation 79−23358
suspended particle motion in homogeneous turbulence 78−22408
suspended particles, fast moving, size and vel. meas. 77−42935
suspended particles motion in turbulent flow in open channel 78−51225
suspended sediment transport theory, elliptic boundary value problem 79−14466
suspended sediments in translational flow, vertical distrib. 78−3841
suspended solids, modelling of settling 77−84298
suspension, Brownian rotational-translational particles, at finite conc., dynamics and hydrodynamics 79−7401
suspension, centrifugal sedimentation of large particles 78−59462
suspension, dielectric, convective heat transfer, rheodynamics, in horizontal coaxial cylindrical channel 78−59494
suspension, dil., of spherical particles in non-Newtonian liq., rheological behaviour 80−24058
suspension, dilute, arbitrary-shape particles, time-depend. flow, Brownian rot. effect 78−26188
suspension, dilute, single component multiphase mechanics 77−55079
suspension, finely dispersed, rheological props., steady flow 79−18930
suspension, flow through ultrafine capillaries 78−94822
suspension, hydrodynamic screening and viscous drag at finite conc. 78−35725
suspension, laminar Poiseuille flow, particle lateral migration, tubular pinch effect 79−98783
suspension, macroscopic transport coefficients, flow instability *(French)* 78−35729
suspension, memory impairment, Brownian rotation of spheroids 80−79386
suspension, memory impairment, expt. 79−41736
suspension, memory impairment, theory 79−41735
suspension, nonstationary axial-symmetric flow in viscous liq. 77−39326
suspension, nonstationary flow in viscous liq. 77−39325
suspension, nonuniform shear effects 79−96372
suspension, oscillating parallel flow in channel 77−68677
suspension, parallel flows with boundary layer characts. 77−15093
suspension, particle interactions, averaged-equation approach 78−23972
suspension, particles self-diffusion in shear flow 77−24015
suspension, Poiseuille to plug flow transition in tubes 79−90316
suspension, polar fluid microstructure, relative force 77−72343
suspension, random behaviour simulation, interval of quiescence method 78−31708
suspension, rigid ellipsoids, rheological props., specific viscosity in shear flow *(Russian)* 78−75187
suspension, settling velocity 79−46360
suspension, sheared, effective thermal conductivity 77−7436
suspension, solid separation at wall, heat transfer 78−9685
suspension, stirred, suspended particles absorpt. of solute molecules 78−30342
suspension, stress near rigid boundaries 77−80200
suspension, transversal undostatic forces prod. by border effects 77−72316
suspension, turbulent, heat transfer and struct. 78−9683
suspension, turbulent and pseudo-turbulent transport 78−14068
suspension, turbulent annular flow, gas vel. profile 77−35215
suspension, turbulent pipe flow, vertical cond. distrib. 78−1714
suspension, wave motion in flow down inclined plane *(Ukrainian)* 79−77220
suspension carrying stream, gravitational transport theory *(Russian)* 78−75188
suspension channel flow, particle-wall interactions, heat transfer 78−5787
suspension deposition in channel entrance 77−89194
suspension flow in pipe, velocity field asymmetry *(Russian)* 77−68671
suspension in nonstationary flow, rheological behaviour 80−6130
suspension in stirred tanks, complete particle suspension conditions 78−27824
suspension of asbestos fibres, heat transfer and friction coeffs. for tubular flow 78−22405
suspension of dielectric particles in plane channel, flow with perpendicular elec. field *(Russian)* 77−62305
suspension of particles during crystallisation in gaseous stream; modelling by aerothermochemistry of suspension eqns. *(French)* 80−53844
suspension of prolate spheroids in shear flow, bulk heat flux 79−46370
suspension of rigid spherical particles, impulsive motion, effect of antisymmetric stresses and particle rotation 80−106833
suspension of rods in silicone oil, interactions between rods in shear flow 77−55075
suspension of slender fibres, Poiseuille flow stability 78−71388
suspension of solid in gas, heat transfer rel. to turbulence 79−72928
suspension of solids, transfer processes, adiabatic calorimeter problem 79−23353
suspension of spheres, hydrodynamic interactions, Navier-Stokes eqn. calc. *(Russian)* 79−32652
suspension of spherical drops, mean drag and ave. velocity *(Russian)* 78−67259
suspension of spherical particles, Brownian motion effect on bulk stress 78−7246
suspension of spherical particles, sedimentation *(Russian)* 78−67254
suspension stream in horizontal pipe, local heat exchange 77−47071
suspension-carrying bottom layer flow, turbulent shear stress and vel. vs. height calc. *(Russian)* 77−55070
suspensions, creeping flow, hindered settling, particle shape effect 80−14797
suspensions, dilute, flow effects on effective thermal cond. 77−1952
suspensions, settling, accelerated by addition of buoyant particles 79−96369
two-phase flow continued
suspensions, turbulent characts. of open channel flows *(Japanese)* 77−68676
suspensions of charged particles, laminar tube flow, entrance deposition 80−59100
suspensions of spheres in viscoelastic media, alignment and aggregation effects, photographic obs. 77−80129
swirling flow in short vortex chamber 79−72924
swirling one- and two-phase liq.-gas flow in tube, heat and mass transfer 78−30339
tapered tubes, flow of closely fitting spheres and cones 80−48789
tensor formulation of the fluid-solid interaction force for multi-dimensional, two-phase flow within tube arrays 80−92211
terminal velocity of a chain of drops of bubbles in a liquid 78−9692
terrestrial atmosphere, low-density gaseous body motion, rel. to Tunguska catastrophe 79−84554
test chimney stack construction, two-phase flow model *(French)* 77−37392
thermal convection, two-phase, in porous layer, flow visualisation study 79−72930
thermal reactor containment systems, critical flow mode for air-steam-water mixtures 80−18502
thermally expandable fluid transients, finite difference method 77−79418
thermally induced flow oscillations investig. 77−42907
thermocapillary convection, unevenly heated liq. stream near gas bubble 78−59460
thermocapillary gas bubble movement, liquid screening 80−19474
thermodynamic processes, in two-component flows with phase transitions 77−27584
thermohydrodynamic equations for two-phase polydisperse medium with phase transformations and size distrib. 79−41743
thermomagnetophoresis of particles in magnetic suspensions 80−35581
thermophoreses velocity and coeff. of thermal slip of gases 77−7416
thermosiphons, two-phase heat exchange in supply zone, anal. 80−19387
thermosyphon feasibility for solar energy transport and storage 79−57491
tracer analysis in two-phase flow systems 80−24073
tracer dispersion in annular climbing film flow 79−64751
transient, drift flux approx. 79−68793
transient, drift flux approx. 79−72929
transient, interfacial heat and mass transfer, surface renewal model 79−27683
transient, theoretical interfacial constitutive models 79−86497
transient 1-D two-phase flow eqns., finite difference approx. 78−51229
transient and statistical meas. techniques, review 77−11287
transient flow boiling in duct, dynamics 78−94528
transient two-phase flow, appl. drift flux model 79−49656
transient two-phase flow reversal prediction, LOCA conditions 78−94811
transient two-phase flow system, three-dimensional numerical simulation 80−687
transonic two-phase vapour-drop flow in channel, stability singular point 77−55078
transpiration cooling system 78−22418
tube, vertical, steam generating annular flow, dry-out position prediction, computer model 78−59447
tube wall temperatures of an eccentrically located horizontal tube within a narrow annulus 79−32201
tubes, horizontal and vertical cooled, boiling crisis and critical heat flux 80−48712
tubular duct, energy balance and concentration distribution rel. to diameter *(Russian)* 77−35203
tubular duct, solid particle concentration rel. to vertical diameter *(Russian)* 77−31365
turbulence, book 78−90839
turbulence, book contrib. 77−58775
turbulence analysis, recurrence rate techniques 79−50831
turbulence flow struct., in tube, suspended particles influence 77−75969
turbulent, condensed phase formation, anal. 79−81853
turbulent, particle separation prediction reliability analysis *(German)* 79−4072
turbulent Ar-Ti powder two-phase jets, with Ti combustion, high temp. study 79−81934
turbulent boundary layer, drag reduction 78−22414
turbulent bubbly flow, laser meas. of local liquid velocity and void fraction *(Japanese)* 78−9693
turbulent film and gas descending flow, tangential stress 77−39333
turbulent flow field, solid and liquid particle interaction 80−43767
turbulent fluidised fine particles, ascending gas flow in cylindrical channel, review 78−42643
turbulent gas jet, evaporation of semidispersive drop system 77−55077
turbulent jet model 79−60044
turbulent two-phase isobaric jet, anal. *(Russian)* 77−27586
turbulent vertical gas flow, steady-state dispersed particles radial distrib. 78−55680
two immiscible liquids, mass transfer into laminar fluid stream from moving interface 78−1717
two parallel infinite plates, Couette flow of dusty gas 80−1681
two spheres rotating perpendicular to an interface 79−90313
two-component fluid, laminar boundary layer, temp. and conc. field calcs. *(German)* 78−71386
two-dimensional supersonic flow, in two-phase fluid, condensation effects calcs. *(French)* 77−84272
two-dimensional supersonic flows of mixture, vapour and drops in nozzle and submerged jet, determ. 79−23357
two-fluid model calculations, stability problems 80−19489
two-layered co-current flow, in open channel, turbulence *(Japanese)* 78−38393
two-phase flow, dryout region of forced convection evaporation, heat transfer coeff. 78−90988
two-phase nozzle flow, liq. film size at mouth, holographic meas. 79−86537
two-phase porous cooling system development 78−59477
underground porous medium, similarity anal. of fingero-imbibition 78−18338
unstable heat transfer conditions, free convection-film boiling transition 78−14006
unsteady 1-D flow, numerical soln. of eqns. *(French)* 77−68665
unsteady flow of an electrically conducting dusty viscous liquid through a channel 79−14484
unsteady processes, in high-press. subsonic channel flow 77−65784

two-phase flow continued
unsteady-state gas absorption/desorption, mass transfer product 80−79381
unstratified, in permeable tube, hydraulic resistance 77−35205
upflow, vertical cocurrent, interfacial areas determ. for mass transfer 79−86528
upflow at atmospheric press., void fraction and pressure drop 80−48781
upflow at atmospheric pressure, void fraction and press. drop 79−77222
UVUTUP two-phase separated flow models 80−48793
vapor-liquid energy transport in a porous medium 79−64762
vaporisation channels, rough and smooth, heat transfer in post dry-out region 80−96255
vaporising liquid drops in N_2 gas, drag coeff. meas. 80−19486
vapour bubble collapse with translatory motion, general and quasi-steady solns. 78−18333
vapour bubble-liquid slug heat transfer, Taylor instability mechanism for LMFBR HCDA 78−8939
vapour bubbled through liquid pool, fractional vapour content 80−106831
vapour bubbles, analysis of oscillation 80−19487
vapour bubbles, flow and temp. fields, global collocation calcs. 77−47067
vapour bubbles, oscillating, evaporation-condensation resonance frequency 80−19488
vapour flows with condensation 80−48794
vapour generator, two-phase flow dynamics 78−94808
vapour generator for K, heat transfer with drop motion in tube in super-crit. region 80−23880
vapour phase heat transfer in post critical heat flux region 79−9668
vapour-drop flow, effect of drop conc. and dispersions 80−24082
vapour-droplet mixtures, small perturbation propagation 78−95111
vapour-gas bubbles removal in arteries of low-temp. heat pipes, anal. 80−19490
vapour-liquid mixture, outflow from large container with a slit 80−74951
vapour-liquid mixture, propagation of acoustic disturbances, model 80−103058
vapour-liquid mixture in heated channel, integrated momentum model 77−31367
vapour-liquid pipe flow, data bank of expt. data *(German)* 79−41739
vapour-liquid two-phase flashing flow, isentropic streamtube model 79−55412
vapour/gas, kinetic model of cavitational oscill. in pumps 77−35186
variable cross-section channel, quasi-one-dimensional flow, numerical investigation 80−79403
vascular system, haemorheology and two-phase flow *(French)* 79−34586
velocity-turbidity system, amplitude-frequency characteristic *(Russian)* 78−75195
velocity-voidage relations for sedimentation and fluidisation 80−24076
vertical adiabatic flow in tubes, actual gas content determ. 77−11245
vertical annular laminar flow, of immiscible liqs., heat transfer 78−14082
vertical coplanar Y-junctions, two-phase steam-water flow 80−38478
vertical density surges, rel. to sound vel. *(German)* 78−42641
vertical tube, pressure loss coeff. 77−27582
virtual mass effects for interfacial transfer phenomena 80−14788
viscoelastic fluid, bubble and solid particle separation through apertures *(German)* 79−37389
viscoelastic fluid, homogeneous shear flow, rigid particle slow motion 77−84308
viscoelastic fluid, suspension of two identical spheres, interaction anal., general homogeneous flow 78−63455
viscoelastic fluids, stratified two-phase flow through rectangular duct, interfacial instability 77−31359
viscoplastic liquid film on vertical vibr. wall, with slip, shaking loose 78−59371
viscous fluid, bubbling through of air, drop entrainment 80−14787
viscous fluid, deform. of falling elastic particle 80−79149
viscous fluid drop, induced flow field in oscillating fluid 78−90980
viscous fluid with suspended particles, motion in a curved tube 80−83835
visualisation, in environmental and technical systems *(German)* 79−86540
void fraction, NMR meas. 77−15096
void fraction and phase distrib. meas. in transient flow boiling by neutron scatt. 78−94870
void fraction determ., simulation of neutron scatt. method 79−90321
void fraction determ. by slip ratio correlations 79−81955
void fraction meas. in water-steam mixtures by neutron gauge 79−80982
void fractions in the phase flow, hydrodynamic and hydraulic studies for reactors 79−55411
void traction, rotating electric field conductance gauge 77−80250
volatile highly thermally conductive spherical drop, theory of diffusio-phoresis 80−14784
vortex breakdown flowfields, spectral characts. in water 80−19408
vortex flow, calc. of discrete component motion velocity and distrib. *(Russian)* 79−90320
vortex flow, motion of near buoyant tracer particles 77−89216
vortex free downflow, in vertical drain 77−51098
vortex sheet discretised evolution with buoyancy and surface tension effects 77−27579
water, annular mist flow in tube, wall film mass flow rate 80−69905
water, saturated (subcooled), crit. discharge through differently shaped channels 78−55681
water, subcooled, choked expansion and the isentropic homogeneous equilib. model for 2-phase flow 78−91034
water and Freon-12, flow boiling crisis in horizontal tubes, fluid-to-fluid modelling 80−48785
water boiling in Laval nozzles, discharge and dynamic characteristics 80−19470
water critical flow states through pipe, modified Bernoulli theory 78−30345
water droplets in hot gas flow, transient cooling 79−1063
water droplets suspended in turbulent flow, evaporation rate rel. to $Ca(CO_3H)_2$ soln. drops 79−90771
water drops deformational breakup in wet-steam stream, differential eqns. 79−14462
water flow with air contents, partially- and super-cavitating hydrofoils in cascade, analysis method *(Japanese)* 80−14763
water in multiphase flow systems, diagnostics, laser induced Raman scatt. 77−31373
water jet impinging on hot surface, boiling heat transfer 78−90993
water pulsating flow in heat exchanger effect of pulsations on heat transfer 79−94614
water steam, boiling and nonboiling vertical two phase flow in tube, void fraction correl. 77−55073
water vapour, 2-D laminar boundary layer 80−19492
water vapour, wet, boundary layer in compressible flow 80−10295
water-air and water-steam mixtures, sound speed rel. to fluid flow 77−84029
water-air mixture, energy dividing props. in discharge from supersonic jet *(Russian)* 77−39332
water-air mixture in tube, pressure loss and thickness of liquid film 77−58767
water-air plug-train system, press. wave propag. characts. 80−59058
water-air two phase flow, oscillatory flow instabilities 80−83833
water-entrained gas flow, force on moving body 78−63480
water-fluidised bed, viscosity meas. by oscills. damping 78−59475
water-steam mixture, upflow in heated tubes, void fraction 77−62296
water-vapour velocity transient meas. by cross-correlation anal. *(German)* 77−62312
water-water vapour flow through packed bed 80−38484
water/steam, void fraction meas. by fast neutron moderation 77−34380
wavelets, initial generation by coupled shear flow instability wind wave evolution 79−94635
wedge, forced-convection film boiling, boundary layer flow 79−46366
wet steam, high speed flows, drop dimensions meas. method 80−90817
wet steam flow in nozzles, choking conditions 79−72926
wet steam tunnel expts., low press., temp. and press. differentials 80−33667
wind-wave interaction, two-layer flow, numerical simulation 78−92823
wood chip refiners, cavitation effects in two-phase flow 80−35348
Ar bubbles injected into Sn, Pb and Cu melts, under laminar flow, characts. 78−38394
CO_2-water, saturated two phase flow system, non-equilib. state transient process 80−59096
^{252}Cf neutron source for water-steam mixture void fraction meas. 79−26762
Cu spheres, electrically augmented pneumatic transport at low particle and duct Reynolds numbers 78−87409
Fe_2O_4, suspension in oil, motion in rotating mag. field *(German)* 77−75983
Ga, liq. particles-He(N_2)(CO_2)(air), nonequilib. Laval nozzle flow calib., numerical soln. 77−75967
H_2-N_2-Ar, two-phase flow film boiling, in vap. generator, heat transfer 78−75190
H_2O foams, shock wave propagation 79−64737
H_2O vapour under point corona discharge, microprocessor control for vapour generator and EHD phenomena 80−106852
He boiling tube hydraulic resistance and burnout expt. 80−24085
He, flow, of liq.-vap. mixture, frictional press. drop, adiabatic and heated conditions 78−90983
He, hydraulic resistance to forced two-phase flow in narrow channels 78−87383
He I, expt. investigation of 2-phase flow pressure drop characts. in vertical tubes 79−60052
He, liq., narrow channel flow and heat transfer characts., void fraction in steady and transient states 78−55000
He, two-phase mixture, circulation using jet pumps 80−82771
Hg-Ar, two phase flow in vertical tube, transverse mag. field, bubbles and slug flow 77−84303
N_2 bubbles coalescence in dil. aq. solns. 79−4062
N_2, evaporating in horizontal tube, local heat transfer coeff. 77−23959
N_2 gas jet injection into Hg, interaction at submerged orifice 80−59102
N_2, two-phase flow in horizontal tube, heat transfer and pressure drop over extensive pressure range 79−58747
N_2-H_2O mixtures, two-phase pressure drops in the low flowrate region 80−19480
NH_3 aqueous soln., stripping by sieve plate column without downcomers 78−22430
N_2O_4, dissociating, nonsteady flow in steam-generating channel 79−37422
N_2O_4, reactor coolant, stability in two-phase flow *(Russian)* 80−609
Na, boiling, LMFBR safety, flow rundown expts. in seven pin bundle 77−88240
Na, boiling, LMFBR safety, seven pin bundle expts., flow patterns, two-phase press. drop 77−88241
Na boiling in tubes, heat transfer and pressure drop 80−28408
Na, liq., in vert. pipe, hydraulic resistance under boiling conditions 78−90968
Na, liquid, local boiling behind local flow blockage, simulated LMFBR fuel subassembly 78−54842
NaCl gas-droplet counterflow heat exchanger, numerical model *(French)* 80−61396
O_2 bubbles, rising in water, dissolution mass transfer coeffs. 79−41737
$PbCrO_4$, paste, anomalous viscous flow 79−64617
TiO_2, aq. suspension, flocculation effect on dilatant flow 79−61916
TiO_2 suspension in glycerine, Bingham plastic flow through annuli 80−64521
U enrichment by photochemical laser, two-phase flow with condensation, mathematical model *(French)* 80−74029
U isotope separation by selective laser photoexcitation in reactive two-phase flow 79−94109

two-photon spectra
absorption, broadband detect. using intracavity dye laser spectroscopy 79−40628
absorption, semiclassical theory, finite-state model 77−58109
absorption, time varying perturbation theory *(Rumanian)* 78−46311
absorption efficiency, depend. on mode selection and mode locking of He-Ne laser 78−83023
absorption from polychromatic stationary radiation field, light coherence 78−74626
absorptivities, CNDO/S-CI calc. with second order time depend. perturbation eqns. 80−74122
absorptivity, ion cyclotron reson. photodissoc. spectra, CNDO/S-CI-perturbation theory 80−74123
alkali bromides and iodides, self-trapped exciton and F-centre form. by picosecond laser pulses 80−10546
alkali halide, two-photon absorpt. coeffs., 355 and 266 nm 78−83037
alkali halides, two-photon absorpt. 80−50292

two-photon spectra continued
alkali metal, two-photon S-S transitions, press. broadening and shift by rare gases 79−6916
alkali metal atom, two-photon transitions to Rydberg levels, dye laser reference wavelengths 78−94221
alkali metal atoms, two-photon ionisation, polarisation effects 78−1039
alkyl iodides, two-photon reson . ionis. spectra 80−28071
amines, caged, multiphoton ionisation, two-photon transition resons. 78−33558
anthracene, aromatic solvents, two-photon absorption cross section meas. by energy migration 77−58204
anthracene, mol. cryst., polariton fusion, two-photon excitation spectra 77−90139
anthracene solution, singlet-triplet-transitions influence on two photon absorpt. cross section meas. *(German)* 77−38703
antibunching in two-photon absorption 78−78980
antiferromagnetic, crysts. with spin-forbidden transitions, two-photon light absorption *(Russian)* 77−48185
aromatic hydrocarbon, centrosymmetric, two photon excited upper state fluoresc. spectra, reson. fluoresc. and vibr. mode selectivity 80−18878
atom, AC Stark effect, fluoresc., in modulated laser beams, two-photon stepwise excitation 80−42989
atom, collisionally perturbed, reson. profile and strengths, degeneracy and Doppler shift 78−55156
atom, Doppler-free two-photon absorpt. of coherent beams 78−33490
atom, effect of laser linewidth on two-photon absorption 78−46310
atom, finite laser bandwidths effects in two-photon spectroscopy 79−3424
atom, narrow reson. of super-narrow pulse 77−18876
atom, photon statistics and time depend. of two photon absorption 78−13480
atom, quantum beats in two-photon resonance fluorescence 80−91488
atom, two-photon absorpt. of two-mode laser beam with phase diffusion 79−6926
atom, two-photon absorption resonance, transit effects 79−10085
atom, two-photon ionis., time depend. model, finite bandwidth light 79−81193
atom, two-photon resonance in coherent fields 80−63606
atom or ion, two-photon absorpt. of light emitted in two-photon spontaneous decay *(Russian)* 77−61729
atom pairs in solids, cooperative two-photon absorpt. lineshape 80−84706
atomic levels, two-photon transitions 80−83333
atomic line shape in Doppler-free two-photon spectra 79−59416
atomic system, Raman scatt. and fluoresc. after two-photon excitation 79−13664
atomic two-level system, spontaneous emission in bichromatic reson. field 80−69093
atomic two-level system, two-photon transverse reson. in RF spectra 77−79594
atoms, Doppler-free two-photon excitation by multiple light pulses 77−42306
atoms, Doppler-free two-photon resonances, interference fringe form. 77−42305
atoms, Raman scatt. in presence of two-photon reson., coherence effects 79−45679
atoms, two photon excitation, time depend. emitted light spectra, perturbation theory 80−63605
atoms, two-photon photoelectron energy spectra, AC Stark splitting 78−86834
1-azo-bicyclo-2,2,2-octane, multiphoton ionis. spectra polaris. characts., two-photon symmetry assignment 78−74718
benzene, $^1B_{2u}$-$^1A_{1g}$ transition, vibronic coupling, Duschinsky effect 77−88439
benzene, cryst., vibronic spectra using 2-photon fluoresc. excitation 79−47493
benzene, crysts., Raman and two-photon reson. in three wave mixing 79−38538
benzene, liq., two-photon spectra, $^1E_{2g}$ state 79−11431
benzene, liquid, polarised light two photon thermal blooming near UV spectra 80−66216
benzene, location of $^1B_{2u}$, $^1B_{1u}$, $^1E_{2g}$ states 77−30940
benzene, mol. cryst., reson. four-wave mixing, third order susceptibilities 80−100654
benzene, mol. transilicon consignment, two-photon gas-phase spectra 77−54582
benzene, multiphoton ionis. spectra polaris. characts., two-photon symmetry assignment 78−74718
benzene, S_0-S_1 transitions, two-photon absorpt. spectra by nozzle beam-multiphoton ionisation method 80−63728
benzene, single vibronic level fluoresc. after two-photon excitation 77−6818
benzene, stimulated diffusion induced by two photon absorption *(French)* 78−90455
benzene, two-photon ionis. of mol. beam, mass spectrometer ion source 79−27118
benzene, two-photon molecular spectra using two synchronised tunable dye lasers 77−34783
benzene, UV two-photon absorpt. relative to known Raman cross section 79−81487
benzene(-d_1,d_2,d_4), two-photon $^1B_{2u}$←$^1A_{1g}$ spectrum, deuterium effect 80−32788
benzene liquid, two-photon absorption spectra and cross-section meas. 79−82993
benzene-d_0,-d_6, $^1B_{2u}$ excited states, high resolution two-photon spectra 77−506
biexciton, two-photon excitation of first vibr. state 79−7789
biphenyl, crysts., Raman and two-photon reson. in three wave mixing 79−38538
biphenyl, mol. cryst., reson. four-wave mixing, third order susceptibilities 80−100654
biphenyl crystals, electronic and vib. states, cryst. field mixing, two-photon spectra 77−59603
trans-1,3-butadiene, multiphoton ionis. spectra polaris. characts., two-photon symmetry assignment 78−74718
trans-butadiene, two-photon spectra, press. effects, transient lensing spectrosc. 78−58756
CdSe two-photon absorption, laser calorimetric obs. 80−33076
chlorobenzene, S_0-S_1 transitions, two-photon absorpt. spectra by nozzle beam-multiphoton ionisation method 80−63728
two-photon spectra continued
chloroform., liq., two-photon absorpt. meas., using nonlinear light mixing spectroscopy 77−79620
chloronaphtalene, stimulated diffusion induced by two photon absorption *(French)* 78−90455
coherent optical spectroscopy 78−1112
coherent states in degenerate four wave mixing 80−5717
coherent two-photon absorpt., near reson. media 79−14026
coherent two-photon reson. and Doppler free population inversion, perturbation anal. 77−643
colliding particle system, two-photon transition, stimulated Raman scatt. 80−9663
coumarin-6, tunable-pulse dynamic picosec. spectrosc. 79−44941
cross-section magnification and line contraction due to Dicke effect 77−6744
cyclohexane, liq., two-photon absorpt. meas., using nonlinear light-mixing spectroscopy 77−79620
cyclohexane, two-photon spectra; fluoresc. spectra, decay times, intensities obs. 77−75245
decalin, two-photon spectra; fluoresc. spectra, decay times, intensities obs. 77−75245
diatomic molecule, rot. line strengths in multiphoton transitions 80−48051
dibenzofuran, single cryst. 2-photon excitation spectrum, 4.2K 79−56807
3,4,9,10-dibenzpyrene, hexane soln., UV fluoresc. line-narrowing two-photon site selective excitation 77−88484
dichroism, circular, laser-induced, quantum electrodynamical anal. 77−75193
p-difluorobenzene, $^1B_{2u}$-^1A_g transition, two-photon spectra 78−46408
diphenylhexatriene, low-energy ^1A_g state obs., by two-photon matrix spectroscopy 78−74715
diphenylhexatriene, two-photon excitation of low-energy excited states 77−14507
diphenyloctatetraene, two photon excitation of low-energy excited states 77−14507
diphenyloctatetraene, two-photon spectra, ^1A_g state confirmation 78−17736
diphenylpolyenes, two-photon absorptivities via three wave mixing 79−68416
dipole-forbidden transitions, CNDO-CI cross sections 79−81244
Doppler free resonances, power broadening 78−5308
Doppler-free two-photon dispersion problem 80−106562
double beam two-photon absorption spectra, off-diagonal matrix elements 80−5517
dye, two-photon fluoresc. quenching, phase fluctuations and phase modulation effect 78−50570
dye solns., single and two-photon spectroscopy, using pulsed acousto-optical effect 77−68087
electric dipole susceptibility, third order, rel. to mol. spectra 79−36624
electro-optic level-crossing effect 78−37608
erythrosine dye, vibrational decay and fluoresc. in S_1 excited state 78−25605
excitonic molecule, Bose condensation, optical response 77−43512
excitonic molecules, reson. Raman scatt. and luminesc. 79−95763
excitonic molecules, secondary radiation, optical orientation effects 79−83010
F-centres, struct., quantum optics, laser spectra 77−52147
fluorene, exciton band struct., two-photon fluoresc. excitation 78−64402
fluoroacetylene, laser-microwave two-photon spectroscopy, appl. of tunable source 79−30579
fluorobenzene, S_0-S_1 transitions, two-photon absorpt. spectra by nozzle beam-multiphoton ionisation method 80−63728
fluorobenzene, two-photon contours comparison with band contours of toluene 79−41212
fluorobenzene, vap., two-photon excitation spectrum assignments 79−59519
fluoromethane-^{13}C, pulsed far IR emission 80−69370
forbidden decay modes of one- and two-electron ions, book contrib. 78−82679
generalised two photon theory, N+2 level quantum system 78−70809
generating scattering amplitude, coherent representation 78−50527
haeme protein, reson. Raman line intensity formulae applicability 77−83609
Hanle effect, saturation resonances, in presence of two-photon transitions 77−30842
harmonic-generating crysts., two-photon absorpt. coeffs., 355 and 266 nm 78−83037
1,3,5-hexatriene, two-photon spectra, failure to find low-lying excited ^1A state 77−79665
homonuclear molecules, vibrs. excitation by IR radiation 80−28068
hydrocarbons, aromatic, ultrasensitive detection by two-photon photoionisation 80−104473
hydrogenic atoms, metastable, Raman-like two-photon scatt., calc. 80−47953
7-hydroxycoumarine, one- and two-photon absorption, fluoresc. obs. 78−46407
7-hydroxycoumarine, two-photon visible absorpt. spectra, fluoresc. obs. 78−42147
II-VI semiconductor, two-photon and two-step absorption of light 80−7389
II-VI semiconductor mixed crystals, two photon absorption *(Russian)* 77−20875
II-VI semiconductors, zinc blende and wurtzite struct., two photon spectra, quantitative investigation 80−50373
III-V semiconductors, linear circular dichroism near the two-photon absorpt. edge 79−61334
indigo dye, S_1-lifetime determ. by two-photon fluoresc. 77−18966
inert gas atom, two-photon excitations, interelectron correlation 80−957
interference in two-channel two photon ionization 80−23381
iodomethane, dressed mol., ν_6 band, saturated absorption spectrosc. 79−54844
IV-VI semiconductors, two photon spectra, quantitative investigation 80−50373
laplace transform method in two-photon spectroscopy theory 79−10084
laser calorimetric meas. of two-photon absorpt., appl. to CdSe(Te) 79−44934
laser-induced line shifts and double-quantum Lamb dips 78−86825
lifetime meas., stepwise excitation by pulsed dye lasers 77−83536
lineshapes of three-level spectra in intense laser field, theory 80−69109
liquid media, vibr. two-photon reson. linewidths 77−88516
magnetic circular dichroism 79−76457

two-photon spectra continued
magnetooptic effects, theory 77−83629
many-valley semiconductor, two-photon transitions from deep neutral impurity centres, light absorpt. and drag effect 79−91478
microwave-optical double resonance, off-reson. optical radiation theory 78−25579
mixtures, two-component, two photon isotope separation, dynamics 80−102584
molecular dissociation limit, two-photon technique 77−3425
molecular gas, three-wave mixing method 78−29826
molecular IR multilevel absorpt., field broadening and pump line selection effects 77−46599
molecular transition frequencies in reson. optical field, Stark shift 77−14487
molecular two-photon spectra, theory 78−94298
molecule, forbidden Raman scatt. theory, including two-photon operators 79−54814
molecule, ordinary Raman scatt., two-photon saturation effect 78−82738
molecules, two-photon spectroscopy, dipole-forbidden transitions, double excited configurations, CNDO-CI methods 80−58332
multilayer epitaxial heterostructures, use of two-photon absorption in study 79−8185
naphthalene:anthracene, two-photon picosec. excitation, sensitised fluoresc. kinetics 79−47516
naphthalene, crysts., Raman and two-photon reson. in three wave mixing 79−38538
naphthalene, in benzene, using flashlamp-pumped dye laser spectrometer 78−16860
naphthalene, mol. cryst., polariton fusion, two-photon excitation spectra 77−90139
naphthalene, mol. cryst., reson. four-wave mixing, third order susceptibilities 80−100654
naphthalene, solns., two-photon absorpt. meas., using nonlinear light-mixing spectroscopy 77−79620
naphthalene, two-photon and mutiphoton excitation, UV fluoresc. spectra 77−88517
naphthalene, vap., Doppler free two-photon absorption spectra 78−5307
naphthalene crystal, vibronic spectra at 1.6K, two-photon fluoresc. excitation 77−59604
naphthalene molecular ion, two-photon absorpt. dissoc. 80−74210
naphthalene-h_8, gas phase two-photon spectra calcs. 78−94298
naphthalene-h_8 (-d_8), two-photon excitation spectra, vibronic coupling 77−75246
Nile blue-A-oxazone, tunable-pulse dynamic picosec. spectrosc. 79−44941
trans, trans-1,3,5,7-octatetraene, high-resolution one and two photon excitation spectra 80−78669
1,3,5,7-octatetraene, lowest excited singlet state, dipole forbidden character 79−27024
optical isolation mechanisms 77−19288
optical transients in Doppler-free two-photon excitation 78−86977
organic dye molecules, two-photon absorpt. in laser fields with arbitrary statistical characts. *(Russian)* 80−37842
organic dye solutions, vibronic struct. in two-photon absorpt. spectra *(Russian)* 79−64004
orthopositronium quenching by O_2, meas. by two-photon coincidence rate difference technique 80−74262
parametric luminescence spectra Stark effect, stimulated processes, strong field 77−10977
partially oriented molecules, uniaxial, two-photon processes, polarised spectrosc. 80−74209
n-pentadecane, two-photon spectra; fluoresc. spectra; decay times, intensities obs. 77−75245
phenanthrene, two-photon excitation spectra, exciton-phonon and intramol. vibronic coupling 80−84774
phenanthrene in glass, non-photochem. hole burning appl. to two-photon spectrosc. 79−18246
phonon assisted two-photon transitions, in mag. field, four-band model 77−36260
photon echo, two-photon transition, adiabatic vector model 77−23719
polarisation spectroscopy 80−9573
polaritons, two-photon absorption and stimulated Raman effect 77−50729
polyacenes, spectra, correlation effects 79−81199
polydiacetylene polymer crystals, one dimensional conjugated, optical props. 77−43993
polydiacetylenes, cryst., picosec. pulse, nonlinear optics appls. 79−46017
polydiacetylenes, reversible creation of defects by laser pulses 78−23480
polyenes, linear, two-photon absorptivities, SCF-PPP-CI calcs. 79−31631
polymer solution, conjugated, polymer two-photon dispersion, freq. depend., symmetry assignment and oscillator strengths 79−86094
positronium formation and quenching in Ar-O_2 mixtures, orthopositronium quenching cross section determ. 80−74261
propynal, IR-microwave double reson. and two-photon expts. 80−83396
pyrazine, two-photon spectra of gas phase 79−89724
pyrene, photoionisation in alkane liqs., laser induced fluoresc. 78−61038
pyrene in n-heptane solution, laser two-photon ionisation spectroscopy, photoionisation threshold determ. 80−78668
radiative collisions and two-photon transitions 77−46552
reson. Raman scatt. by excitons via intermediate excitonic mol., polarisation and polariton effects 78−10880
resonance Raman scatt., by excitons via intermediate excitonic mol. 77−52086
resonance two-photon absorption, theory 80−28268
resonant absorption, time and spectral resolution 77−58305
resonant absorption line profile, quadratic Doppler effect 77−34590
resonant broadening of two-photon S-S transitions *(Russian)* 79−26957
resonant processes, conserved quantity 79−45688
resonant Rayleigh-type optical mixing and relax. 78−42380
resonant three level spin system 78−30017
all-transretinal, two-photon spectrum, rel. to photophysics of vision 79−41159
rhodamine 6G-alcohol, two-photon luminesc. intensity, appl. to picosecond pulse meas. 78−71134
ruby, two-photon spectroscopy of reson. three-level spin system, reson. shift 79−82864
semiconductor, characts. of two-photon absorption under reson. conditions 77−90170
semiconductor, excitonic molecule creation by two-photon absorpt. 77−20247
two-photon spectra continued
semiconductor, impurity-level assisted two-photon interband absorption of laser radiation 78−23464
semiconductor, nonlinear light absorption, influence of transition via deep impurity centres 77−63446
semiconductor, radiative spectra from hot photocarriers 78−31249
semiconductor, shallow donor states exam. by two photon spectroscopy 79−23925
semiconductor, two-photon absorpt. spectra examination using automatic system 79−17503
semiconductor films, two-photon absorption, exciton effects *(Russian)* 80−40174
semiconductor films, two-photon interband absorpt., quantum size effects 79−43054
semiconductor wires, size-quartised, two-photon interband absorpt. 80−93256
semiconductor with superlattice, two-photon absorpt. 77−16331
semiconductors, direct-gap, two-photon absorpt. 80−50292
semiconductors, II-VI and III-VI types, competition between two-photon absorption and two-stage absorption via deep traps 80−29764
semiconductors, nonlinear effects, induced by lasers 79−94300
semiconductors, two-photon absorption in crossed elec. and mag. fields 77−85693
semiconductors, two-photon light absorption by excitons in static elec. field 80−11364
simple molecules, two-photon dissoc., spectrosc. obs. 80−32787
small molecules, spectroscopic techniques, review 77−54554
solids, two-photon transitions, selection rules 77−69240
split spectra, in Doppler-free two-photon spectroscopy 78−292
Stark effect, two photon absorption spectroscopy 80−43126
stilbene, photo excitation kinetics 77−23525
trans-stilbene, two-photon absorpt. near maximum, three wave mixing expt. 77−58106
stilbene, two-photon absorptivities via three wave mixing 79−68416
trans-stilbene, two-photon excitation, phantom photochemical singlet, assignment 77−75247
sub-Doppler line shapes, saturation and two-photon spectra, elastic collisions, review 78−82697
subnatural linewidth spectra by optical double reson. with two-photon pumping 80−74200
surface polaritons, obs. by two-photon absorpt. 77−51676
symmetric top molecules, rovibronic 2-photon transitions, rot. line strengths 78−78762
tetracene, triplet exciton diffusion and double photon absorpt., delayed fluoresc. obs. 77−36287
three level absorber, two-photon transition, self-induced transparency 79−27337
three level atom in two-photon reson. with laser field, fluoresc. spectrum 77−42273
three level molecular system interaction with two laser fields 77−54685
three-level atom, Doppler free two-photon absorption, near reson. intermediate state 77−71788
three-level atom, strong-field aspects and steady-state response 78−960
three-level atom reson., vector model, comparison, with exact two-photon soln. 77−57957
three-level optical pumping, nonabsorbing atomic coherences, excited state populations 77−3332
three-level system, 2-photon reson. fluoresc. 80−87077
three-level system, adiabatic following in two-photon transitions refr. index, line asymmetry 77−57956
three-level system, two-photon transition in two pulsed fields 79−68215
three-state atom, saturated two-photon absorpt. in perturber gas 80−106310
time-domain relaxation time measurements, by Stark switching technique 77−75248
toluene, two-photon ionisation spectrum, of $^1L_b \leftarrow S_0$ transition 80−14180
toluene vapour, two-photon excitation spectrum under low resolution 79−41212
transient resonant secondary emission spectra, theory 79−56827
triethylenediamine, multiphoton ionis. and two-photon fluoresc. excitation spectra 79−98164
triphenylene, in n-heptane cryst., 2-photon excitation spectrum 78−82760
triphenylene, in PMMA matrix, two-photon phosphoresc. spectra 77−42366
triphenylmethane dye, S_1-lifetime determ. by two-photon fluoresc. 77−18966
two level system interacting with two optical fields, generalised theory 79−36866
two-photon absorption with coherent and partially coherent driving fields 78−5191
UV transparent materials, 355 and 266 nm absolute two-photon absorption coeff. obs. 79−18493
visual chromophores, two-photon absorptivities, SCF-PPP-CI calcs. 79−31631
vitamin A, visual chromophores, two-photon spectra, lowest excited state 78−64934
yield optimisation aspects in two-photon excitation 79−6924
zinc blende structure semiconductors, two photon absorption model 79−78679
H atoms, two-photon transition matrix elements, group theory calc. 78−62776
acetaldehyde, multiphoton ionisation meas., two-photon polarisation ratio of n→3s transition 80−91610
$AgGaSe_2$, two-photon absorpt. and short pulse stimulated recombination 80−89054
AlAs-GaAs monolayer crystal, two-photon absorpt. spectrum 78−52589
$Al_2O_3:Cr_2O_3$, saturation effects by double-quantum transitions 78−80197
Ar, electron scatt. multiphoton process effects, laser-induced free-free transitions 77−79595
As_2S_3, amorphous and cryst., optically induced changes, ps. spectroscopy 80−48326
As_2S_3, cryst., vitreous or amorphous, nonlinear light absorption, temp. depend. *(Russian)* 77−48199
As_2S_3, cryst. and glassy, two-photon spectrum at room temp. 79−24334
As_2S_3, two photon light absorpt. dispersion, induced linear light absorpt. *(Russian)* 80−66231
$As_2S_{3-x}Se_x$, amorphous, picosecond relax. of optically induced absorption 80−97302
$B_3N_3H_6$, allowed character of 1900 Å band 78−74719

two-photon spectra continued
Ba, diamag. quasi-Landau spectrum near ionis. threshold, two-photon ionis. spectra obs. 78−58642
Ba, even-parity states, one- and two-photon absorpt. 77−42303
Ba ions, resonance fluorescence and optical sideband cooling of electrodynamically contained ions 79−3422
Ba, isotope shift and hyperfine splitting 78−33491
Ba, two-photon spectroscopy, highly excited even levels, J=0 spectrum anal. 79−31447
C_2, Swan transitions, relax. dynamics and two-photon excitation, in inert gas matrix 77−505
CN, matrix isolated, interstate cascading radiationless transitions 77−46594
C_2N_2, multiphoton dissociation in UV light 79−54928
CO $A^1\Pi$, Doppler free two-photon excitation 78−17641
CO, Doppler-free two-photon vac. UV absorption spectra 78−86882
CO, rot. line strengths in multiphoton transitions 80−48051
CO, two-photon excited vac. UV fluoresc. 78−5264
CO, two-photon spectroscopy with tunable ArF laser 80−37843
CO, vac. UV absorpt. spectrum, Doppler-free two-photon excitation 79−41185
CS_2, liq., two-photon absorpt. meas., using nonlinear light-mixing spectroscopy 77−79620
Ca, $4p^2\ ^1S_0-4s4p\ ^1P_1-4s^2\ ^1S_0$ cascade rate, two photon coincidence meas. technique 80−95576
Ca_2, in Kr matrix, 1- and 2-photon fluoresc. excitation 78−50567
CaCl, $D^2\Sigma$ and $X^2\Sigma$, two-photon vis. absorption, vibr. and rot. consts. 78−78764
$CaF_2:Eu^{2+}$, two-photon absorpt. spectra exam. of excited state of Eu^{2+} 77−77261
$CaF_2:Tb^{3+}(Eu^{3+})$, one- and two-photon luminesc. excitation spectra 79−83023
CdP_2, two-photon light absorpt. dispersion, allowed-forbidden transition *(Russian)* 78−15193
CdS, biexciton, low intensity nonlinear coherent mixing study 80−49619
CdS, biexciton levels, luminescence-assisted two-photon spectra 80−29795
CdS, creation of 2P excitons by two photon magneto-absorption 78−2432
CdS, excitonic region, nonlinear optical meas., 4.2K 78−68531
CdS, fine struct. of two-photon absorption, luminesc. meas. 77−24893
CdS, intrinsic exciton fine struct., two-photon absorption 77−12397
CdS, nonlinear self-action effect and absolute two-photon absorption coeff. 80−83649
CdS, reson. Raman Scatt. under two-photon excitation of excitonic mols. 78−52486
CdS, size effect of dense electron hole systems 80−7413
CdS, two photon absorpt., influence of In and Cu impurities 77−16353
CdS, two photon absorption relative to Raman cross sections 78−87098
CdS, two photon Raman scatt. at high excitation levels *(Russian)* 80−16032
CdS, two-photon absorpt., excitons *(Russian)* 78−39571
CdS, two-photon absorption coefficient rel. to inverse Raman cross section 78−6678
CdS, two-photon Raman scatt. via biexcitons, angle- and polarisation depend. 79−87446
CdS, virtually excited biexcitons polaritons dispersion, two photon Raman scatt. 80−45067
CdS:Cu(in), two-photon and two-step absorption of light 80−7389
CdS:In, two-photon absorpt. spectra exam. of effects of screening of exciton continuum 79−8166
$CdS_{0.4}Se_{0.6}$, two-photon absorpt., effect of polarisation of laser radiation 77−69856
CdSe(Te), laser calorimetric meas. of two-photon absorpt. coeffs. at 1.06 μm 79−44934
CdTe, two-photon absorption coefficient, 3-band model 79−78679
CdTe two-photon absorption, laser calorimetric obs. 80−33076
$^{113}Cd_2$, two-level system, absorpt. spectrum, subradiative struct. *(Russian)* 80−28008
Cl_2CS, excitation, singlet and triplet states, two photon absorpt., singlet-singlet energy pooling, fluoresc. obs. 80−48032
Cs, 8S hyperfine splitting, two-photon transition and fluoresc. meas. 78−37585
Cs, elec. dipole approx. and elec. quadrupole resons. allowed in multiphoton absorpt. *(French)* 78−5190
Cs, energy levels for highly excited ^2F states 78−70805
Cs, excited S- and D-states, Stark interaction by laser spectroscopy, polarisability 77−50404
Cs, fine structure splittings of $n^2D_{5/2,3/2}$ levels (18<n<23) 78−46465
Cs I, $n^2S_{1/2}$ and $n^2D_{3/2,5/2}$ states, energies 80−87066
Cs, two photon ionisation, destructive interference effect 80−74153
Cs, two-photon ionis., profiles of $6^2S_{1/2}$-$7^2P_{1/2,3/2}$ lines 80−958
Cs vapour, two-photon induced stimulated Raman scatt., optical Stark shifts 77−46756
Cs+Ar, laser two-photon ionisation, collisional line broadening, atomic forces 77−83543
Cs+Ar, two-photon ionisation spectra, satellites, absorption line shape 78−82668
Cs_2, two-photon dissoc., spectrosc. obs. 80−32787
$CsPbBr_3$, electronic and optical props. 80−25414
$CsPbCl_3$, electronic and optical props. 80−25414
Cu halides two photon spectra, quantitative investigation 80−50373
CuBr, biexciton dispersion, two-photon absorpt. 80−76045
CuBr, biexciton luminesc. 77−44056
CuBr, biexciton two-photon absorption 79−47480
CuBr, biexciton two-photon absorpt. 80−11432
CuBr, emission spectra after two-photon excitation, Raman scatt. 79−47518
CuBr, excitonic mols., two photon generation 77−43511
CuBr, multiplet struct. of P-excitons due to valence band degeneracy 78−39035
CuBr, P exciton fine struct. 80−20091
CuCl, biexciton first excited state, LO phonon assisted two-photon absorption 77−40260
CuCl, biexciton luminesc. 77−44056
CuCl, biexciton luminescence and two photon Raman emission, polarisation props. 78−80406
CuCl, biexciton resonant two-photon absorption 78−23491
CuCl, biexciton two-photon absorpt. 80−11432
CuCl, biexcitons, two-photon absorption and luminesc. 77−43513
two-photon spectra continued
CuCl, emission spectra after two-photon excitation, Raman scatt. 79−47518
CuCl, exciton mol. creation by pure and phonon-assisted two-photon transitions 78−63987
CuCl, exciton spatial dispersion determ., two-photon Raman scatt. via excitonic mol. state 80−60595
CuCl, excitonic molecules, secondary emission under two-photon reson. excitation 80−11468
CuCl, excitonic mols., two photon generation 77−43511
CuCl, giant two-photon absorption into excitonic mol., anomalous dispersion of excitonic polariton 78−27211
CuCl, luminesc. spectra, excitonic mol. reson. two phonon excitation 78−19514
CuCl, phonon interaction of excitonic molecule 80−50316
CuCl, phonon-assisted two-photon absorpt. of excitonic mol., bare-exciton approach 79−78702
CuCl, picosecond spectroscopy of secondary radiation from resonantly excited excitonic molecules 79−15461
CuCl, ps. luminesc. spectra, resonantly excited excitonic mols. 78−19555
CuCl, reson. coherent nonlinear scatt., biexciton autoionising states 79−51978
CuCl, reson. Raman scatt. and luminesc. under two-photon excitation 79−95765
CuCl, reson. two-photon Raman scatt., excitonic polariton dispersion 78−72509
CuCl, reson. two-photon excitation of excitonic mol. using circ. polarised light 78−84566
CuCl, resonantly excited excitonic molecules, time resolved spectroscopy 78−92109
CuCl, two-photon absorpt. and luminesc., biexcitons 80−11434
CuCl, two-photon reson. Raman scatt. with recoiling excitonic polariton 77−36223
CuCl, two-photon reson. Raman scatt., recoil of upper-branch excitonic polariton 78−27212
CuCl, two-photon reson. scatt. in excitonic mol., population instability 79−28826
CuCl, two-photon reson. Raman scatt. and luminesc. of excitonic mols. 79−28819
CuCl, Z_3-exciton, temp. dependent TPA linewidth 78−67946
Cu_2O, even-parity excitons assignment, from two-photon spectrum 80−6731
DCl, two photon reson.-enhanced third harmonic generation 78−87094
D_2O, pulsed opto-acoustic spectroscopy 80−62743
Eu^{2+} in aqueous solution, multiphoton excitation and emission 78−94222
FCN, IR-microwave double reson. and double photon transitions, HF Stark effect 77−14464
GaAs, epitaxial layer, 1.06 μm two-photon absorption coeff., guided wave meas. 78−46707
GaAs, nonlinear light absorpt., photoluminesc. meas. 77−66528
GaAs, nonlinear light absorption, effect of deep impurity levels 77−77259
GaAs, optical absorption near fundamental edge due to CO_2 laser pulses 78−39569
GaAs, two photon absorpt., hot electron-hole plasma, relax. time depend., picosecond spectra 79−51979
GaAs, two-photon 1.06 μm absorption coeff., absolute meas. 78−19527
GaAs, two-photon absorpt. of Nd:glass laser radiation 78−87107
GaAs, two-photon absorption coefficient, 3-band model 79−78679
GaAs, two-photon electroabsorption by excitons 79−42944
$GaAs_xP_{1-x}$ epitaxial film nonlinear light absorpt., photoluminesc. meas. 77−66528
$Ga_{1-x}In_xSe$, layered, luminescence and photocond. obs., two-photon excitation 78−76521
GaP, two photon absorption relative to Raman cross sections 78−87098
GaP, two-photon absorption coefficient rel. to inverse Raman cross section 78−6678
GaS two-photon absorpt., cond. and luminesc. meas. 77−52166
GaS, two-photon photoemission 79−28890
GaS_xSe_{1-x}, two photon absorpt. 77−69841
GaSe, two-photon absorpt., cond. and luminesc. meas. 77−52166
Ge, exciton mol. by phonon-assisted two-photon absorpt., theory 78−48197
Ge, exciton mol. creation by pure and phonon-assisted two-photon transitions 78−63987
Ge, two photon absorption of light with optical transitions between heavy- and light-hole states 79−11421
H, $3^2S_{1/2}$-$3^2D_{5/2}$ interval, two-photon lineshape theory 79−54825
H, $3^2S_{1/2}$-$3^2D_{5/2}$ interval, double quantum RF meas. 79−54826
H, $3P_{3/2}$-$3D_{3/2}$ Lamb shift, double quantum saturation spectrosc. obs. 78−94223
H Balmer-α fine struct. lines, anomalous shifts, in He-H_2 DC discharge 79−45677
H in planetary nebulae, two-photon emission contrib. to UV continuum 80−109523
H, nonresonant two-photon absorption, gauge interaction calcs. 78−37617
H, two freq. separated oscillatory field technique, multiple quantum transitions 77−71892
H, two-photon 1s-2s transition rate and absorption coeff. freq. depend., choice of gauge 78−9132
H, two-photon absorpt. of ultrashort pulses, reson. intensities 78−59077
H, two-photon bound-bound transitions, retardation effect, Coulomb Green's function 77−57907
H, two-photon radiation rel. to planetary nebulae continuous UV spectra 79−92843
H, two-photon transition, $3^2S_{1/2}$-$3^2D_{5/2}$, precision meas. 78−17642
H, two-photon transitions, parity nonconservation effects *(Russian)* 78−21892
H_2, $E,F^1\Sigma_g^+$ state, collisional and radiative props. 80−58357
H_2, metastable $c^3\Pi_u$ state, population densities and quenching times meas. 78−94296
H_2, two-photon spectroscopy with tunable ArF laser 80−37843
$H_2(E,F^1\Sigma_g^+)$, two-photon excitation, cross section, radiative lifetime, quenching rate, IR fluoresc. obs. 78−37698
H_2O, pulsed opto-acoustic spectroscopy 80−62743
He, Doppler-free two-photon optogalvanic spectroscopy 80−52960
He, Doppler-free two-photon high resolution spectroscopy 80−58197
He^+, detection of $6D_{5/2}$-$6S_{1/2}$ double quantum transition 77−61858
Hg, two photon excitation, time resolved spectroscopy 80−87075

two-photon spectra continued
Hg_2, absorpt., fluoresc. and two-photon spectroscopy 78−998
Hg_2, emission and form. kinetics, sequential two-photon absorpt. expt. 80−32767
$Hg_{1-x}Cd_xTe$, two-photon absorption coefficient, 3-band model 79−78679
$Hg_{1-x}Cd_xTe$, two-photon absorpt. spectra 80−20660
I_2, 2- and 3-photon absorpt. obs. 80−18864
I_2, energy levels near B-state dissoc. limit, two-photon spectra 78−9210
I_2, molecular dissociation limit, two-photon technique 77−3425
I_2, stepwise two-photon excitation, E-state vibr. bands, B-state vibr. rot. levels 79−26962
I_2, two-photon excitation of rovibronic levels and gerade states 77−14508
I_2, two-photon sequential absorpt. spectroscopy 77−54581
$^{129}I_2$, energy levels near B-state dissoc. limit, two-photon spectrosc. obs. 80−106367
ICl, energy levels, near first dissoc. limit, 2-photon sequential absorption obs. 78−90246
ICl, two photon UV absorpt. spectrosc. 79−89687
$^{127}I_2$, two photon excitation, rot.-vibr. structure of E-state 79−41213
In, two-photon laser spectroscopy 79−6925
InSb, two-photon absorption coefficient, 3-band model 79−78679
InSb, two-photon absorpt. spectra 80−20660
K, diamag. Zeeman shift of S,D Rydberg states, two-photon absorpt. 77−23461
K, multiphoton excitation, Rydberg transitions, ionisation detection 77−42304
K, reson. line polarisation, 2-photon excitation 77−54546
K, Rydberg states, two photon absorption, decay fluoresc. 77−71787
K, two photon excitation by opposing light beams, reson. lines polarisation studies 78−82705
KBr, self-trapped exciton and F-centre form. 79−73443
KBr, two photon absorpt., 2p excitons relax., F-centre 79−91462
KBr, UV two-photon absorpt. relative to known Raman cross section 79−81487
KCl, colour centres laser spectra, induced F' band absorpt. 80−2779
KI, UV two-photon absorpt. relative to known Raman cross section 79−81487
Kr, 6p levels, two-photon excitation, time resolved fluoresc., quenching, lifetimes and photoionisation cross section 80−78587
Li, hyperfine splitting and isotopic shift, Doppler-free two-photon spectroscopy 79−36592
Li, seeded flames, excitation, laser radiation absorpt., sound vel., opto-acoustic effects obs. 80−43345
Li, two-photon ionization spectra 80−23382
Li_2, triplet absorpt. bands, 6215-5875 Å, after two-photon excitation 79−50035
α-$LiIO_3$, energy band struct., nonlinear optical absorpt. obs. 79−64277
α-$LiIO_3$, two-photon absorption spectra, energy struct. anal. 80−99785
$LiNbO_3$, energy band struct., nonlinear optical absorpt. obs. 79−64277
$LiNbO_3$, pure, two-photon photorefractive recording 78−31220
$LiNbO_3$, two-photon absorption spectra, energy struct. anal. 80−99785
Mg, atom, forbidden Raman scatt. theory, including two-photon operators 79−54814
N_2, $a^1\Pi_g$, Doppler free two-photon excitation 78−17641
N_2, rot. line strengths in multiphoton transitions 80−48051
NH_3, Doppler free coherent two-photon transients, collision induced relax. time, meas., Stark switching 78−90249
NH_3 forbidden vibr.-rot. transitions, ν_2 band, IR-microwave two-photon spectra 77−3428
NH_3, IR-microwave two-photon spectra using CO_2 lasers 78−37664
NH_3 laser transitions, CW, two-photon pumped 80−99702
NH_3, two-photon population inversion, adiabatic rapid passage 78−78763
NH_3, two-photon transition, collisional dephasing time meas. by Stark switching 77−75248
$^{14}NH_3$, Doppler free spectroscopy, 16 micron generation applications 79−94049
$^{15}NH_3$, two-photon spectroscopy, double resonance studies with a new coincidence 78−70888
NH_4Cl, cryst., impurity overtone states, interference two-photon spectrum *(Russian)* 79−24344
NO, $^2\Pi_{1/2}$ and $^2\Pi_{3/2}$ band centre freqs., opto-acoustic detection 77−58108
NO, $A^2\Sigma^+$ state, two-photon excitation and emission spectra 77−83666
NO, $A^2\Sigma^+$ two-photon excitation, radiation lifetime, quenching 77−3426
NO, electronic quenching rates, two-photon spectrosc. meas. 79−50097
NO nonlinear laser spectroscopy, VUV harmonic generation 80−74175
NO, rot. line strengths in multiphoton transitions 80−48051
NO, simultaneous one- and two-photon spectroscopy, Λ-doubling, spin-rot. splitting 78−66560
NO, two-photon excitation to levels near and above the dissoc. limit 79−10161
NO, two-photon spectra by three-wave mixing 78−29826
NO, v=0,1 states, spectroscopic data calc. 78−86851
NO, v=2←1 absorption band two-and multiphoton spectra, Λ-doubling const. vibr. depend. 77−30942
α-NPO, two-photon fluoresc. 77−30896
$^{14}NH_3$, ν_2-band Doppler-free two-photon resons. in Stark field 77−23527
$^{15}NH_3$, and $^{14}NH_3$, laser-microwave two-photon spectroscopy, appl. of tunable source 79−30579
Na, 3^2S-4^2D two-photon transitions, isolated optical Ramsey fringes 77−83559
Na, 3S-4D and 3S-5S two-photon lines, broadening and shift by inert gases 77−75105
Na, 3s-5s transition, detuning and polarisation selection rules 78−86836
Na, (3s-4d), Doppler free spectra, 4d fine struct. splitting = 1028 ± 0.4 MHz 78−41356
Na atom perturbed by noble gas, relaxation of $4D_{3/2}$ and $4D_{5/2}$ level 78−50526
Na, atomic beam, AC Stark splitting of two-photon spectra 77−46551
Na, D-doublet in H_2-O_2-Ar flame, excitation profiles 77−88436
Na, Doppler-free two-photon linewidths, 3S-4D press. broadening coeffs. 78−25481
Na, highly excited, f-state fine struct., microwave reson. obs. 77−83535
Na, hyperfine interaction in $4D_{3/2}$ and $4D_{5/2}$ levels 78−37616
Na, hyperfine splitting, fluoresc. after two-photon excitation 79−18307
Na, mag. field quantum beats in two-photon free-induction decay 79−13692
Na, Raman transients obs. in Doppler free two-photon excitation 77−61728
Na, Rydberg states, high resolution two-photon mm spectroscopy, metrology appl. 80−43018
Na, Rydberg states, millimeter spectra, quantum defect, fine struct., polarisability, field ionis. obs. 78−82672
Na seeded flames, excitation, laser radiation absorpt., sound vel., opto-acoustic effects obs. 80−43345
Na, self-broadening of 3S-5S and 3S-4D two-photon transitions 79−26955
Na, Stark effect study, S and D excited states struct., two-photon spectra 77−54547
Na, two and three photon resonances in strong nonmonochromatic field 77−34908
Na, two-photon absorpt. processes, polarisation selection rules 80−9574
Na, two-photon absorption reson. in spatially separated fields 78−21890
Na, two-photon excitation in flame, saturation broadening, fluoresc. obs., broad-band excitation 78−74625
Na, two-photon optical free induction decay, Stark switching obs. 77−68024
Na, two-photon optical free-induction decay 78−90138
Na, two-photon polarisation rotation effect in vapour 77−68025
Na, two-photon transition, distinction of competing processes in nonlinear resonant freq. mixing 80−33080
Na, two-photon transition broadened by Ar impact 79−22681
Na vapour, two-photon reson. four-wave mixing 78−46716
Na+Ar, two-photon near-reson. light scatt. 77−30941
Na+H(Ne)(Kr) vel.-changing collisions, effect on 2 photon and stepwise absorpt. line shape 80−87221
Na+He (Ne), two-photon optical free induction decay meas. by broad-band excitation in unidirectional beams 79−76489
Na+inert gas, collisional redistrib., two-photon absorpt. with near-reson. intermediate state 80−23505
Na+Xe, nonreson. two-photon absorpt., 4s excited states and pot. energy curves, close coupled eqns. 80−48068
Na_2, Doppler free vs. Doppler broadened absorpt., near-reson. intermediate level 79−13779
Na_2, Doppler-free three-photon cross reson. obs. 77−58107
Na_2 molecule, Doppler-free two-photon transitions, $^1\Sigma_g^+$ state 77−3427
Na_2, two-photon transition, velocity tuned, polarisation depend. and Franck-Condon factors 78−90250
Na_2 vapour, near reson. two-photon absorption, polaris. depend. 77−79666
NaF, two-photon absorpt. cross sections of N_1 and F_3^+ centres 79−73991
Nd:glass, self-induced transparency on two-photon reson. line *(Russian)* 79−86221
Nd^{3+}:glass, nonlinear refractive index, two-photon resonant absorption by Nd^{3+} *(Chinese)* 80−43387
Ne, atom, isotopic shift and fine struct. for $2p^54d$ and $2p^55s$ config., Doppler-free two-photon spectroscopy 80−23387
Ne, dipole dynamic polarisabilities and two-photon photoionisation cross section calc., R-matrix approach 80−102444
Ne, Doppler-free two-photon spectra, fine struct. and hyperfine consts. of 4d′ level 77−61725
Ne, Doppler-free two-photon spectral line intensities 77−61726
Ne I, transition probabilities for 3p to 4d array 77−437
Ne+Ne(He), 7d′ states, isotope shift, press. shift, press. broadening, two-photon spectra obs. 78−55155
^{20}Ne, Doppler-free two-photon optogalvanic spectroscopy 79−89656
^{21}Ne, hyperfine interaction in 4d subconfiguration, Doppler-free two-photon spectroscopy meas. 80−18944
No, $C^2\Pi(v=0)$ state, two-photon absorpt. spectra, predissociation 77−79664
O, 2-photon excitation, cross-section calcs. 78−58641
O isoelectronic series, two photon transition probabilities 79−22680
OCS laser, two-quantum excitation, photolysis, energy transfer, for fusion expts. 78−59003
Pb stable isotopes, 2-photon spectroscopy, isotope shift of $6\text{-}^2\,^3P_0$-$7p\,^3P_0$ transition 80−87070
PbI_2, two-photon absorpt. spectrum 77−52118
PbI_2 two-photon absorpt. cond. and luminesc. meas. 77−52166
PbI_2, two-photon photoemission 79−28890
PbS, molecule, Ne matrix environment effects on vibronic emission systems 77−58070
PbTe, recombination radiation polarisation direction, two-photon selective energy valley occupation *(Russian)* 77−20924
Rb, $5^2D_{3/2,5/2}$ and $7^2S_{1/2}$ two-photon excitation stimulated and parametric emission 77−10651
Rb, 5^2S-n^2S transitions, Rydberg levels, high resolution two photon spectra obs. 80−52923
Rb Doppler-free two-photon lines, self-broadening and shift meas. 80−5506
Rb, Doppler-free two-photon absorpt. spectrum 80−42975
Rb, excited S- and D-states, Stark interaction by laser spectroscopy, polarisability 77−50404
Rb, multiphoton ionis. processes, fine struct., hybrid reson. 77−18877
Rb, n^2D states, fine struct. near ionisation limit, two-photon spectra 77−30843
Rb Rydberg levels in intense mag. field, diamag. struct. 79−26958
Rb, two-photon transitions to Rydberg levels, dye laser reference wavelengths 78−94221
Rb, vap., 1.06 micron conversion to 420 nm range 79−14040
Rb vapour, Doppler-free two-photon dispersion and optical bistability 80−95940
$^{85,87}Rb$, high Rydberg levels, press. broadening and shifts 80−52902
Rb+Rb**, freq. shift, line broadening, phase interference effects, Doppler free two photon spectra 80−58200
RbBr (I), optical absorpt. centre formation time meas. 80−40081
RbBr, two photon absorpt., 2p excitons relax., F-centre 79−91462
RbBr, UV two-photon absorpt. relative to known Raman cross section 79−81487
RbI, two photon absorpt., 2p excitons relax., F-centre 79−91462
SF_6, excitation by strong IR laser field, spectral characts. 80−32713
SF_6, excited to dissoc. threshold, IR absorption 79−81245
SF_6 molecule, resonant energy absorpt. struct. in IR laser field *(Russian)* 80−5592
SO_2, two-photon spectra by three-wave mixing 78−29826
Si, exciton mol. by phonon-assisted two-photon absorpt., theory 78−48197
SnO_2, rutile, band gap assignment by two-photon spectroscopy 79−19513

two-photon spectra continued
Sr, diamag. quasi-Landau spectrum near ionis. threshold, two-photon ionis. spectra obs. 78−58642
Sr I, Rydberg and autoionisation levels, laser ionisation spectroscopy 77−3331
SrF_2:Eu^{2+}, two-photon absorpt. spectra exam. of excited state of Eu^{2+} 77−77261
$SrTiO_3$ 78−6678
$SrTiO_3$, energy band struct., two-photon absorption spectra study 80−15453
TiO_2, two-photon absorption coefficient rel. to inverse Raman cross section 78−6678
Tl atom, two-photon laser spectroscopy and ionisation 78−55153
Tl(7^2P) states, isotopic forms, HFS, press. self-broadening, two-photon spectra 77−18879
U atomic beam, two laser irrad., two photon reson. effects., visible spectra 80−63604
Xe, doppler-free two-photon spectroscopy using degenerate four-wave mixing 79−31490
Xe, ground state, two-photon excitation spectra, fluoresc, decay 77−75115
XeBr, emission and form. kinetics, sequential two-photon absorpt. expt. 80−32767
XeO* production through collisional electronic energy transfer from two-photon excited Xe atoms 78−62775
Yb, direct two-photon excitation, hybrid resonances 79−31489
Yb highly excited levels, reson., visible two photon absorpt. spectra obs. 80−58228
Yb, highly excited states 78−70806
$Zn_{0.1}Cd_{0.9}S$:Cu, doping effect on two-photon absorpt. spectra, deep levels 77−69870
$Zn_xCd_{1-x}S$ monocrystal, optical and nonlinear optical charact. *(Russian)* 79−98442
ZnO, biexciton levels, luminescence-assisted two-photon spectra 80−29795
ZnO, excitonic molecule transitions, M-band emission 79−78742
ZnP_2, two-photon light absorpt. dispersion, allowed-forbidden transition *(Russian)* 78−15193
ZnS, two-photon absorpt. in crossed elec. and mag. fields 77−85693
ZnSe, band-edge photoluminesc., far-below band-gap excitation 80−76063
ZnSe, exciton fine struct., envelope-hole coupled exciton states, two-photon absorpt. 77−52124
ZnSe, impurity effects on two-photon absorpt. spectrum 77−59597
ZnSe, two photon absorpt. by envelope-hole coupled exciton states, polarisation depend. 77−66522
ZnSe, two photon absorption relative to Raman cross sections 78−87098
ZnSe, two-photon absorpt., effect of polarisation of laser radiation 77−69856
$(ZnSe)_{1-x}(GaP)_x$, two-photon absorpt. at ruby laser freq., clarification *(Russian)* 79−15505
ZnTe, two-photon absorpt. line shape near direct band gap and critical point 79−65898

two-photon spectroscopy
absorption measurements by time-resolved registration of difference between two laser pulses *(German)* 77−87841
amorphous semiconductor, ps. spectroscopy 80−48326
atom-strong field interactions, generalised dressed atom approach, laser theory and Bloch-Siegert shift 77−71964
atomic cascade rate absolute meas. using two photon coincidence technique, appl. to Ca 80−95576
calibration via stimulated Raman gain 78−87098
chemical analysis, uses of two-photon excited mol. fluoresc. 80−40799
chemical spectroscopy and dynamics, higher-order susceptibility effects, laser appls. 79−40625
coherent background noise elimination from saturation spectrosc. signals using freq. offset pump 80−62733
coherent two-photon NMR, standard-basis operators, coherent averaging 80−82798
computer-controlled spectrometer for organic crystals 78−58064
condensed phase fluoresc., double reson. excitation spectroscopy 80−86438
corona positive discharges, in atmospheric air, positive ions distribution determ. *(French)* 77−4015
Doppler free, high resolution spectra from actively mode-locked CW dye laser, feasibility 78−41356
Doppler free intracavity two-photon absorption 78−5307
Doppler free multiphoton spectroscopy, review 77−79707
Doppler free two photon resonances, optical Ramsey fringes 78−29167
Doppler less spectroscopy, wave front convolution in parametric nonmonochromatic wave interaction *(Russian)* 79−94280
Doppler-free, and wave-front conjugation by four-wave mixing of monochromatic waves 80−28265
Doppler-free, for mol. electronic transitions 77−79167
Doppler-free, method *(Dutch)* 79−50167
Doppler-free, occurrence of split spectra 78−292
Doppler-free, ultra-high-resolution two-photon spectroscopy 78−49909
Doppler-free laser spectroscopy seminar 78−302
Doppler-free many-photon spectroscopy 79−35845
Doppler-free multiple-pass two-photon spectroscopy 79−17499
Doppler-free two photon and saturation spectroscopy, using thermionic detector 78−46465
Doppler-free two-photon spectroscopy, appl. to mol. electronic transitions 77−74525
doppler-free two-photon spectroscopy using degenerate four-wave mixing 79−31490
dye lasers, single-mode and multimode CW, as sources for obtaining power-squared corrected two-photon spectra 80−78849
dynamic picosecond spectroscopy, tunable-pulse methods, appls. 79−44941
ELLIPSA, two-photon spectroscopy method for polarisation meas. 79−6184
elliptical polarisation state alteration technique 79−40627
experimental techniques, review 77−67510
high resolution, using counter-propagating laser beams and AC Stark effect 77−49781
high resolution spectroscopy of atoms and mols., without Doppler broadening, laser techniques 77−54631
high resolution two-photon FM laser spectroscopy of gas atoms, free of Doppler broadening 80−95748

two-photon spectroscopy continued
high-sensitivity, high-resolution spectroscopy techniques 79−40626
impurity molecules in glasses, non-photochem. hole burning appl. to two-photon spectrosc. 79−18246
intracavity dye laser spectroscopy, broadband detect. of 2-photon absorpt. 79−40628
IR Doppler free molecular spectroscopy, two photon coherence and pumping 80−48052
IR mthods 78−86900
laser, real time monitoring of atmospheric pollutants 80−7996
laser microwave double resonance spectroscopy, wide-band intracavity microwave cells 77−82580
laser nonlinear spectroscopy polaris. selective optical heterodyne detection 79−58798
laser spectroscopy, review 77−5927
laser spectroscopy, review of new techniques 78−32893
laser spectroscopy, review of progress 78−82867
laser-microwave two-photon spectroscopic tunable source 79−30579
laser-radiofrequency double quantum saturation spectroscopy 80−48105
light shifts on atomic energy levels, non-resonant irradiation effect, appls. 77−75107
light-induced frequency shifts and two-photon Lamb dips 79−36591
liquids, optical system for studying two-photon absorpt. 79−17500
luminescence-assisted two-photon spectroscopy, appl. to biexciton levels in CdS and ZnO 80−29795
molecular, two pulse technique using ultrashort pulses 80−53165
molecule, IR-microwave two-photon spectra using CO_2 lasers, appl. 78−37664
molecule, using tunable spin flip Raman laser, review 80−55762
molecules, stimulated Raman and two-photon absorpt. 80−52999
nonlinear high resolution laser spectroscopy, review of techniques 78−29171
nonlinear optical processes in atoms and mols. using inert gas halide lasers 79−59745
nozzle-beam mol. multiphoton ionisation method for determ. two-photon absorpt. spectra 80−63728
nuclear laser-induced resonant absorption of γ radiation 80−18290
optical Ramsey fringes in two-photon spectroscopy, time delayed pulsed Doppler free technique 78−82708
photoconductivity detector for measurement of picosecond light pulses from Nd-glass laser 80−77872
polarisation 80−9573
polarisation dependence, two photon absorption coeff. 78−80379
positron two-photon annihilation coincidence technique, difference mode 78−54516
quantum interference effects in two photon spectroscopy, improved techniques review 78−94224
Ramsey fringes in spectroscopy without Doppler broadening *(French)* 77−50560
resonance scattering methods in atomic spectroscopy 80−53167
resonant third-harmonic generation with ultrashort pulses, index mismatching, detuning and spectral effects 80−101844
solids, optical absorption under laser irrad. 80−34940
spectrometer, based on flashlamp-pumped dye lasers 78−16860
stratospheric gas monitoring, Doppler-free technique 77−9514
symmetric top molecule, two-photon excited fluoresc. spectroscopy, density matrix formalism 79−36716
two frequency separated oscillatory field technique for multiple quantum transitions 77−71892
using two synchronised tunable dye lasers 77−34783
two-photon fluorescence, constrast ratio decrease depend. on laser pulse intensity 80−1255
visible and far-infrared laser spectroscopy for semiconductor impurity studies 77−74524
Li, A=6,7 two-photon intracavity dye laser spectroscopy 78−82706

two-term control
cell freeze conservation control unit *(German)* 79−5410
electric furnace, muffle type, automation of temp. regime 77−61068
eye, vergence movements, heuristic feedback system model 77−21517
eye continuous movement monitoring, proportional-integral adaptive system *(German)* 79−16320
Pu fuel research facility for advanced LMFBR fuel *(Japanese)* 78−29624

TWT *see travelling-wave-tubes*

Tyndallometry *see turbidimetry*

type fonts *see character sets*

type I superconductors
see also intermediate state
Al, press. depend. of electron-phonon interaction, rel. to supercond. transition temp. 79−95106
approximate T_c formula, Eliashberg eqn. *(Chinese)* 80−107941
approximate T_c formula, Eliashberg eqn. calcs. *(Chinese)* 80−88662
critical current, in circ. mag. field 78−68124
critical current measurement, metastable current states *(Russian)* 78−43529
critical field, anal. of expt. data *(Chinese)* 80−60151
critical field for nucleation of n-domains 77−1515
current-field relation, nonlocal, differential operator method 79−69637
cylindric superconducting domain lattices in magnetic field, lattice stability determ. *(Russian)* 80−44775
cylindrical superconducting domain lattice dynamics *(Russian)* 80−93052
defects in nucleation of superconducting phase *(Russian)* 77−36025
film, crit. mag. field calc. using Ginzburg-Landau eqns. *(French)* 79−60999
film, cylindrical, domain struct. in mag. field 80−15666
flux tube nucleation, in current induced resistive state, noise 79−24109
Landau's laminar structure under inclined mag. field 78−39271
local magnetic field, penetration through large sheets 78−23211
magnetic dipoles, influence on order parameter *(French)* 77−8227
magnetic flux structures in superconductors, book 79−91199
magnetic flux-free environment creation, cryogenic appl. 80−101797
magnetisation, first stage, and metastable migration field in slab 80−15655
magnetisation in thermodynamic and metastable phases 80−93027
mixed state, Josephson condition, phase jumps *(Russian)* 80−107967
nuclear spin-lattice relaxation rate, paramagnon effect 77−32119
one-dimensional mixed state, in longitudinal mag. field 79−87213
order parameter, influence of HF fields 79−28486
order parameter, mag. dipole effect *(French)* 77−89899

type I superconductors continued
paramagnetic effects of two-dimensional mixed state *(Russian)* 79−51729
properties of selected superconductive materials 79−56366
radiation effects, conf., Argonne, Il., USA (June 77) 78−52120
rare earth iridium borides, RIr_4B_4, supercond., magnetism and metastability 80−29501
soft thin superconductors, static paramagnetic response 80−84550
spectroscopy using mag. impurity relax. of Josephson junction-Fiske modes 77−80880
superheated supercond. colloid as a total absorption detector preliminary calcs. 78−78579
superheating field for finite κ calc. 77−12060
surface impedance, anomalous skin effect, surface supercond. regime *(Russian)* 80−80459
surface resistance, theory 77−51841
thermal conductivity in intermediate state, size effect in longitudinal lamellar struct. 78−52153
thin plate surface, ponderomotive phenomena theory, magnetic forces *(Russian)* 77−12058
transition temperature, Hall const. correl. 79−47186
two dimensional mixed state *(Russian)* 78−19193
Ag film-Pb sandwich, supercond., effective renormalisation interactions 79−56397
Al, acoustomag. effect, temp. depend. *(Russian)* 77−72941
Al, bulk superconducting fluctuations in elec. resist 80−49995
Al, dielectric screening function and effective interaction strength 79−33387
Al film, crit. temp. enhancement *(Russian)* 80−93021
Al film, lattice and bulk heat capacity meas. for normal and supercond. states 80−92684
Al film, order-parameter variations meas. 80−103797
Al film, permanent resistive states created by light pulses 79−56450
Al film, quasiparticle branch mixing rates 79−78269
Al film, supercond., meas. of effective quasiparticle recombination times, density of electronic states at Fermi level 79−38264
Al, film, superconducting transition temp. and lattice dynamics 80−93028
Al film in microwave radiation field, resistive state transition *(Russian)* 80−93038
Al films, Al^{2+} irrad., increase of resist. and supercond. transition temp. 80−7027
Al films, microwave induced supercond. above crit. temp. 79−56364
Al, fluxural oscillations in longitudinal mag. field, sound attenuation, magnetoelasticity *(Russian)* 80−54844
Al granular films, self-ion implantation, supercond. transition temp. enhancement 80−103774
Al, granular inhomogeneous, supercond. 80−103795
Al, influence of effective phonon spectrum on T_c *(Chinese)* 79−51705
Al microbridges, non-equilibrium phenomena 79−56410
Al, nonequilibrium superconductivity in microwave field 79−42695
Al, nonlinear conductivity of thin films in mixed state *(Russian)* 80−80464
Al, nonlinear sound wave interactions, sound attenuation in weak superconducting state *(Russian)* 80−75310
Al, order-parameter relax. time calc. 79−4618
Al particles, Zeeman crit. field, NMR spin echo meas. 79−56453
Al, phonon absorption and pairbreaking at 35 GHz 77−32120
Al, plastic deformation meas. in normal and supercond. states, down to 0.4K *(Russian)* 79−11658
Al, point contact Josephson junction, microwave-enhanced critical currents 77−8242
Al, press. depend. of electron-phonon interaction rel. to normal state resist. 79−28063
Al, quasiparticles, nonequilib. distrib. function 78−91810
Al, remanent supercond., effect on temp. depend. of normal phase resist. 79−56362
Al, remnant superconductivity, temp. depend. elec. resistivity meas. 79−99529
Al, resistivity temp. depend., evidence for electron-electron scatt. 79−69488
Al, resistivity well above T_c, supercond. effect up to $2T_c$ 80−6810
Al small particle, NMR study, Knight shift, spin-lattice relax. time, supercond. effects 80−39710
Al, stimulation and enhancement by external micropower irradiation *(Russian)* 78−95394
Al strips, on Si substrates, microwave-enhanced crit. currents, phonon effects 79−56451
Al strips, supercond., order-parameter relaxation meas. 79−47207
Al, supercond. film, intrinsic and expt. quasiparticle recomb. times 77−15999
Al, supercond. film, quasiparticle injection, tunnel junction characts. 78−76193
Al, superconducting, quasiparticle charge distrib. due to tunnel injection 80−44771
Al, superconducting, resistive layer microstructure *(Russian)* 80−34567
Al, superconducting and normal state, anisotropic impurity scatt. and EM surface resist. 78−30970
Al, superconducting band gap anisotropy and Fermi surface anisotropy *(Spanish)* 80−84544
Al superconducting film, granular, O content and oxide barrier thickness, transition temp. meas. 79−15250
Al, superconducting film, resistive states, voltage switching effect in tunnelling systems *(Russian)* 79−7938
Al, superconducting order parameter relax. time, temp. depend. 77−77011
Al, superconducting state parameters, dielectric screening functions effect 77−4471
Al superconducting surface, layer struct. and dynamics on switching off mag. field 79−60998
Al, superconducting transition temp., electron-phonon mass enhancement, pseudopot. calcs. 78−2604
Al, superconducting transition, effect on jump-like deform. *(Russian)* 80−34538
Al, surface layer struct. arising after mag. field H>Hc is switched off 79−61000
Al, thick film, supercond., tunnelling characts., geometrical reson. in Al-Pb struct. 79−38260
Al thin films, dielectric coating effect on superconductivity 80−7026
Al, transition temp., perturbative corrections, direct and indirect ladder diagrams 80−49979

type I superconductors continued
Al tunnel junctions, superconductivity enhancement by microwaves 80−107956
Al, tunnelling characts., phonon struct. enhancement by high energy spectral weight 79−60984
Al-Formvar-Sn coupled films, Ginzburg's excitonic supercond. model 80−97039
Am, superconducting critical field, sp. ht. 80−11136
As, A1-type superconductor, critical mag. field 79−69638
Ba, superconductivity, pressure dependence, ion core 78−91805
Bi, A1-type superconductor, critical mag. field 79−69638
Bi, amorphous, superconductivity and the very strong electron-phonon interaction *(Japanese)* 79−95552
Bi crosspiece in high-resistance supercond. microbridge 80−93050
Bi, superconducting modification obtained by impact compression *(Russian)* 80−93020
Bi superconduting film, critical temp., thermal equilibrium *(Russian)* 80−80438
Bi, whiskers, hardness, elec. props. *(Russian)* 78−51874
C_8K, intercalation cpd. with graphite, supercond. props. 80−44755
Cd, electronic properties depend. on $2^1/_2$-th order phase transition under high press. *(Russian)* 80−11128
Cd, transition temp., perturbative corrections, direct and indirect ladder diagrams 80−49979
Cd whisker, crit. temp., stress depend. 77−39989
Cs, supercond., elec. resist. and phase transforms. under high press. *(German)* 80−107763
Ga film, crit. transverse mag. fields and transition temp. *(Russian)* 80−7048
Ga II, superconducting high pressure phase, sp. ht. 80−70894
B-Ga, metastable, elec. props. in normal and supercond. states *(Russian)* 80−65520
Ga, nonlinear sound wave interactions, sound attenuation in weak superconducting state *(Russian)* 80−75310
Ga, superconducting modifications in bulk samples *(Russian)* 79−65574
Ga, US anomalous penetration along electron trajectories in mag. field *(Russian)* 79−87191
Hf, valence band XPS, correl. to supercond. 79−65980
Hg films, superconducting, far-IR and electrodynamic props. meas. 80−103957
Hg, law of corresponding states, Eliashberg eqn. *(Russian)* 79−87183
Hg, supercond. transition temp. from Eliashberg eqns. 79−51709
Hg, transition temp., perturbative corrections, direct and indirect ladder diagrams 80−49979
In, crit. RF mag. field, rel. to superheating 78−2632
In, destruction in high amplitude LF varying field *(Russian)* 78−26999
In, discontinuous film, DC resist. in normal and supercond. states 79−56357
In, divided superconducting thin film, superheating and supercooling field resistive meas. *(French)* 80−44751
In, energy gap and phonon frequencies under press., tunnelling meas. 77−32112
In film, crit. current hysteresis prod. by electron overheating 79−56449
In film, current-induced resistive state, fluctuations in flux nucleation process 79−38252
In film, metastable states supercond. parameters 78−47903
In film, resistive transitions scaling behaviour 79−15248
In films, crit. temp. enhancement *(Russian)* 80−93021
In films, supercond., sp. ht. discontinuity and transition temp. meas. 79−60969
In, influence of effective phonon spectrum on T_c *(Chinese)* 79−51705
In, Lifshits transition, electron-phonon interaction 80−29502
In microbridges, non-equilibrium phenomena 79−56410
In, mixed state, two-dimensional effect study, destruction current *(Russian)* 80−93054
In, nonequilibrium superconductivity in microwave field 79−42695
In, relaxation time determ. 77−55638
In, shell model for clad particles *(Chinese)* 79−69623
In, stimulation and enhancement by external micropower irradiation *(Russian)* 78−95394
In, stress depend. of supercond. parameters 77−12045
In, supercond., expt. study of thermoelectricity 80−60138
In, supercond. and normal states, internal friction hysteresis *(Russian)* 77−36023
In, supercond. crit. temp., functional derivative with electronic density of states, Eliashberg eqns. 79−56368
In, supercond. penetration depth field depend. meas. 77−4464
In, supercond. transition temp. from Eliashberg eqns. 79−51709
In, superconducting, thermoelec. transport effect 78−39257
In, superconducting bridge, Josephson effect, flux tube nucleation 77−36028
In superconducting films, metastable states, supercooling fields 80−97031
In, superconducting transition temp., electron-phonon mass enhancement, pseudopot. calcs. 78−2604
In, surface superconducting layer in high amplitude LF EM field *(Russian)* 79−78261
In, T_c and penetration depth *(Chinese)* 79−51706
In, type I superconductor, thermoelec. power in intermediate state 78−34935
In, US attenuation in supercond. and normal state in transverse mag. field and zero field 80−54836
In ultrathin films on TbTe and Te, prep. and characterisation 77−7995
In whisker, crit. temp., stress depend. 77−39988
In-Bi, single spheres, supercond. props. 79−73617
In-Bi(Tl)(Pb), small κ supercond., phase transitions higher than second order 80−88668
In-In_2O_3-Pb, Josephson tunnel junction fabrication for MM-wave detector 80−100427
In-Sb, cryst. struct. after appl. of high press., supercond. transition temp. 80−70169
α-In-Sn, stress depend. of supercond. parameters 77−12045
Mg, superconducting transition temp., electron-phonon mass enhancement, pseudopot. calcs. 78−2604
Nb, energy gap determ. by pt. contact tunnelling 78−19185
P quench-deposited A1-type films, superconducting props. 79−15264
Pb, absolute surface reactance and penetration depth 78−68109
Pb, band structure, and electron-phonon interaction, supercond. transition temp. determ. 79−19512
Pb, crit. RF mag. field, rel. to superheating 78−2632

type I superconductors continued
Pb, crystal defect accumulation after plastic deform. in normal and supercond. state resist. meas. 77−85196
Pb, dislocation electron drag coeff. temp. depend., internal friction method, superconducting state 80−29031
Pb, dislocation inertial effects, internal-friction meas. on normal and superconducting states 79−38883
Pb, dislocation internal friction changes under the action of US vibr. 79−69630
Pb, effect of changes in $\alpha^2(\Omega)F(\Omega)$ on the zero-temp. energy gap 80−97025
Pb, effect of O ion irradiation on supercond. 78−52131
Pb, effect of supercond. transition on phonon energies and lifetimes 79−28432
Pb, energy gap and penetration depth *(Chinese)* 79−51718
Pb, fatigue testing in normal and supercond. state 78−19959
Pb film, amorphous, nucleated with Mo, supercond. and normal elec. cond. 77−24633
Pb film, current-induced flux motion, studied at 100 ns time resolution 79−47208
Pb, film, first order transition due to quasiparticle injection 78−23208
Pb film, flux nucleation in current-induced resistive state 78−23210
Pb film, monocryst., heteroepitaxial growth, struct. defects, and elec. props. *(Russian)* 80−84403
Pb film, near supercond. transition temp., Hall effect 79−42698
Pb film, supercond., flux dynamics during current-induced breakdown, magneto-optical flux detection 77−24646
Pb film, supercond., meas. of effective quasiparticle recombination times, density of electronic states at Fermi level 79−38264
Pb film, ultrathin quench-condensed, two-dimensional elec. cond., onset of supercond. 78−39233
Pb, fluxural oscillations in longitudinal mag. field, sound attenuation, magnetoelasticity *(Russian)* 80−54844
Pb foil, crit. current density, pinning force density, shadow electron microscopy obs. 80−88696
Pb, friction, wear in supercond., normal states *(Russian)* 78−39914
Pb intermediate state, Meissner effect investigation by muon technique *(Russian)* 80−107954
Pb, laser irradiated tunnel junction, nonequilibrium quasi-particle distrib. function, thermal regime *(Russian)* 79−42700
Pb, law of corresponding states, Eliashberg eqn. *(Russian)* 79−87183
Pb, mag. hysteresis meas. *(French)* 77−4463
Pb on Cu and Ag substrates, tunnel conductivity, proximity effect *(Russian)* 79−51726
Pb, Pb-Bi, anomalous thermal cond., transition induced creep *(Russian)* 77−36020
Pb, penetration field and magnetisation curve, lattice defect effects 77−28292
Pb, phonon softening, neutron scatt. at high press. 78−80091
Pb, phonon thermal conductivity of deformed cryst. below 2K *(Russian)* 78−60244
Pb, plastic deform. rate rel. to supercond. transition, temp. depend. *(Russian)* 78−31015
Pb, press. depend. of electron-phonon interaction rel. to normal state resist. 79−28063
Pb, quasi-particle recomb. time, Kapitza resistance 78−68123
Pb, quasiparticle and phonon propagation 79−42689
Pb, RF surface resist., 136 to 472 MHz and 1.5 to 4.2K 77−63029
Pb, shell model for clad particles *(Chinese)* 79−69623
Pb, single cryst., quasiparticle propag. and recomb. 77−32126
Pb single crystal, normal-superconducting transition and plastic flow 78−3166
Pb slabs, magnetisation and migration field, reversible stage 80−65737
Pb, strength loss in supercond. state, size factor effect *(Russian)* 80−88677
Pb, supercond., surface bound state, microwave surface impedance 77−12059
Pb, supercond. crit. temp., functional derivative with electronic density of states, Eliashberg eqns. 79−56368
Pb, supercond. film, intrinsic and expt. quasiparticle recomb. times 77−15999
Pb, supercond. phonon struct. in ultra-thin proximity effect tunnel junctions 78−80101
Pb, supercond. transition temp. from Eliashberg eqns. 79−51709
Pb, supercond. transition temp., theoretical calc. 79−73614
Pb, supercond. transition temp., ab initio calc. 80−25036
Pb, superconducting, phonon density of states determ. 77−20493
Pb, superconducting, press. depend. of supercond. transition temp. 78−84340
Pb superconducting amorphous film, conductivity and transition temp., ion bombardment effects *(Russian)* 80−49969
Pb, superconducting film, radiation induced critical temp. 79−87179
Pb, superconducting phase condensation in bulk sample *(German)* 79−56447
Pb, superconducting state parameters, dielectric screening functions effect 77−4471
Pb, superconducting transition temperature, resistive transition meas. 77−80861
Pb, superconducting transition temp., electron-phonon mass enhancement, pseudopot. calcs. 78−2604
Pb, superconducting transition curves, meas. during plastic deform. 79−60956
Pb, thermal conductivity, in normal and supercond. states, 0.6-7.5K *(Russian)* 80−6815
Pb, thermal conductivity in supercond. and normal states, press. effects 77−43779
Pb, thermomagnetic effect *(French)* 77−63036
Pb thin strips, supercond., optical wave illum., critical current behaviour 80−50012
Pb, transition temp., perturbative corrections, direct and indirect ladder diagrams 80−49979
Pb, transverse acoustic phonons, freq. and damping, supercond. transition temp. effects 79−42687
Pb, US oscillations and dislocation unpinning in supercond. and normal states *(Russian)* 79−11648
Pb ultrathin films on PbTe and Te, prep. and characterisation 77−7995
Pb/Cu interface, thermal conductance at low temps. in normal and supercond. states 80−49436
Pb-Al_2O_3-Al tunnel junction, Pb supercond. film behaviour in mag. field 78−14894

type I superconductors continued
Pb-Cu(Ag) double layers, intermetallic boundary effects, tunnelling 80−88692
Pb-insulator-Pb diode, US effect on tunnel current 77−16006
Pb-Pb bridge, variable thickness, DC and AC Josephson effect 78−31016
Pb-Pb bridge, variable thickness, static mag. field effects, Josephson effects 78−31017
Pb-PbO-Pb, Josephson tunnel junction fabrication for Mm-wave detector 80−100427
Pb-sapphire interface, heat transfer coeff. meas., 2-80K 80−88419
Pb-Sn bimetallic loop, thermoelec. flux effects due to penetration depth changes 77−24636
Pd, confined geometry, p-wave supercond. or itinerant ferromag. 80−11129
Pd, disordered film, supercond., occurrence and crit. temp. after He^+ irrad. 79−11261
Pd-H system, magnetisation, type I and type II supercond. behaviour, homogeneity effects 77−28291
Pd-H(D), band struct. and supercond. props., APW calc. 79−56354
Pd-H(D) system, normal state phonon resist. and supercond. tunnelling density of states 79−56402
Pd-Rh-H and Pd-Ag-H, band struct. and supercond. props., APW calc. 79−56354
PdH_x foils, supercond. props. 77−32114
PdH_x, x=0.915 to 0.996, thermoelec. power, 10 to 170K, rel. to optical phonon spectra 79−56201
PdH_x, $x \simeq 1$, type I supercond. props. 79−56448
$PdH_x(D_x)$, band struct., supercond. props., APW calcs. and neutron scatt. 78−43511
S quench-deposited A1-type films, superconducting props. 79−15264
Sb, A1-type superconductor, critical mag. field 79−69638
Sb, electronic band struct. changes due to plane straining effects *(Russian)* 80−54602
Se, A1 type, supercond. destruction by mag. field 78−91825
Sn, acoustomag. effect, temp. depend. *(Russian)* 77−72941
Sn, bulk non-equilib. quasiparticles probed by ballistic phonons 79−56391
Sn, bulk supercond., ballistic propag. of near-gap phonons 77−85384
Sn, chem. potential change on becoming superconducting 77−28301
Sn, crit. RF mag. field, rel. to superheating 78−2632
Sn, cross-like film structures, microwave irrad. stimulated superconductivity and Josephson effect 79−60988
Sn, destruction in high amplitude LF varying field *(Russian)* 78−26999
Sn, diamag. moment meas., dislocation supercond. above crit. temp. *(Russian)* 79−4619
Sn, EM detection and generation of US shear waves, theory and expt. 77−19468
Sn, effect of O ion irradiation on supercond. 78−52131
Sn film, crit. current hysteresis prod. by electron overheating 79−56449
Sn film, crit. mag. fields, temp. depend., penetration depth thickness depend. 80−70908
Sn film, crit. temp. enhancement *(Russian)* 80−93021
Sn film, energy gap reduction by quasiparticle injection 77−47941
Sn film, energy gap suppression and instability under strong quasiparticle injection 80−7042
Sn film, limitation in microwave stimulation of supercond., crit. current meas. *(Russian)* 80−88695
Sn film, phonon-injection-induced destruction of supercond. 80−6956
Sn, film, superconducting, current-voltage characts. in microwave field 79−69631
Sn, film, superconducting fluctuations, transition temp. *(Russian)* 80−65740
Sn, homogeneous supercond., phase stratification in microwave field *(Russian)* 79−82711
Sn, mag. hysteresis meas. *(French)* 77−4463
Sn microbridges, non-equilibrium phenomena 79−56410
Sn, nonequilibrium superconductivity in microwave field 79−42695
Sn, nonlinear conductivity of thin films in mixed state *(Russian)* 80−80464
Sn, paramagnetic effect fine struct. apparent mag. permeability *(Russian)* 79−95550
Sn, quasiparticle recomb. time and normal electronic density of states at Fermi surface from tunnel junction expts. 79−24108
Sn ribbon, penetration depth of nonequilibrium elec. field, temp. depend. *(Russian)* 78−23202
Sn, shell model for clad particles *(Chinese)* 79−69623
Sn, single crystal cylinder, threshold current of paramagnetic effect *(Russian)* 79−87194
Sn small particles, electron level quantisation effects, Knight shift meas. of electron spin susceptibility 78−2624
Sn, stimulation and enhancement by external micropower irradiation *(Russian)* 78−95394
Sn, stress depend. of supercond. parameters 77−12045
Sn, supercond. crit. temp., functional derivative with electronic density of states, Eliashberg eqns. 79−56368
Sn, supercond. film, electron mean free path depend. of crit. currents and pair-breaking limit 77−20504
Sn, supercond. film, intrinsic and expt. quasiparticle recomb. times 77−15999
Sn, supercond. fine particles, sp. ht., fluctuations under mag. field, crit. field and transition temp. 77−80873
Sn, supercond. transition, effect of AC EM field *(Russia)* 77−8232
Sn, supercond. tunnel junction, quasiparticle excitation by α-particles 80−103791
Sn, supercond. whiskers, HF radiation effects on current-voltage characts. 79−65619
Sn, superconducting and normal phases, damping of dislocations and supercond. attenuation 78−52155
Sn, superconducting current carrying film, resistive region boundary movement, ambient media depend. 80−44763
Sn, superconducting film, paraconductivity 80−54845
Sn, superconducting film, radiation induced critical temp. 79−87179
Sn, superconducting loops, thermally generated mag. flux 79−56452
Sn superconducting thin-film bridge, IV curves oscill. instability and quasi-particle recomb. *(Russian)* 80−44769
Sn, surface, superconductivity suppression by microwave radiation *(Russian)* 79−24098
Sn, surface superconducting layer in high amplitude LF EM field *(Russian)* 79−78261
Sn, T_c and penetration depth *(Chinese)* 79−51706

type I superconductors continued
Sn temp. depend. of energy dissipation 78−76198
Sn, thin film, supercond., acoustic wave absorpt., quasiparticle distrib. 78−10603
Sn thin strips, nonequilibrium resistive state, penetration depth meas. 79−56377
Sn whisker, crit. temp., stress depend. 77−39988
Sn whisker, supercond., current carrying 78−72304
Sn whiskers, current induced phase transition 78−10600
Sn, whiskers, current-carrying, mutual influence of votlage steps in V-I characts. 78−10601
Sn-Bi(Sb), small κ supercond., phase transitions higher than second order 80−88668
Sn-Sn bridge, variable thickness, DC and AC Josephson effect 78−31016
Sn-Sn bridge, variable thickness, static mag. field effects, Josephson effects 78−31017
Sn-SnO-Pb, supercond. tunnel struct., nonequilib. state, influence of illumination 79−15262
Ta, critical field, muon spin relaxation *(German)* 80−50015
Ta film, supercond. transition temp. rel. to struct. and deposition parameters 77−85377
Ta, flow stress at superconducting transition, temp. and strain rate depend. 78−2617
Ta:N, superconductive to normal transition anisotropy 80−25031
TaN, mag. field direction determining whether type I or II 79−15266
Te, A1 type, supercond. destruction by mag. field 78−91825
Th-Dy, dil., paramag. Dy moment relax., Mossbauer spectra study 80−65755
Th-Dy, dil., supercond. Th, paramag. relax. of Dy moments, Mossbauer study 80−39957
Zn, electrical and thermal resist. calc. 79−69489
Zn film, SAW US attenuation 79−73633
Zn film for energy selective phonon detection 80−92621
Zn, superconducting transition temp., electron-phonon mass enhancement, pseudopot. calcs. 78−2604
Zn, transition temp., perturbative corrections, direct and indirect ladder diagrams 80−49979
Zn whisker, crit. temp., stress depend. 77−39989

type II superconductors
see also mixed state
A15 binary alloys, supercond. transition temp., computer assisted estimate 79−38240
A15 compound formation by diffusion from ternary bronzes, thermodynamics 78−84740
A15 compound trends, self consistent band calcs. 78−79925
A15 compounds, coherence length and phonon softening 78−34587
A15 compounds, density of states broadening and its effect on T_c 79−65577
A15 compounds, disordered, reordering kinetics 80−96678
A15 compounds, elec. resist., phenomenological model 77−43775
A15 compounds, elec. struct., 3-D k.p model 78−2405
A15 compounds, electronic instabilities and phonon softening 79−95115
A15 compounds, electronic struct. calc. 79−37970
A15 compounds, high press.-high temp. treatment, phase props. 77−28746
A15 compounds, high supercond., T_c, attributed to linear chains or cubic symmetry 79−38221
A15 compounds, high-temp. superconductors, martensitic transform., microscopic theory based on 3-dimens. band struct. 78−19752
A15 compounds, linear muffin tin orbital band results by press. calc. 79−65356
A15 compounds, local lattice instabilities 78−19178
A15 compounds, martensitic and supercond. transition models, anisotropy of vortices and US anomaly, review *(Japanese)* 78−23216
A15 compounds, max. T_c due to electron-photon scatt. 78−91801
A15 compounds, mode softening and high supercond. crit. temp. 78−14851
A15 compounds, neutron irrad., X-ray scatt. theory 79−37740
A15 compounds, new aspect of superconductivity, Fermi level rel. to electron-phonon interaction 79−7927
A15 compounds, struct. transform., comparison of Landau theories 78−67824
A15 compounds, supercond. rel. to struct. transform. 78−14873
A15 compounds, T_c reduction due to defects, gap anisotropy mechanism 77−43773
A15 compounds, T_c related to residual resist. 79−15134
A15 films, electron beam codeposition, synthesis and props. 78−72296
A15 materials, α-particle induced defects and stoichiometry 77−32101
A15 multifilamentary high-field superconductors, status of development 79−61004
A15 ordered and disordered cpds., density of states calc. 79−87033
A15 phases, stability criterion *(Chinese)* 79−91195
A15 structure, electronic density of states and T_c changes with atomic ordering 78−91800
A15 supercond. with defects 78−76183
A15 superconductors, effects of material parameters on H_{c2} 79−61005
A15 superconductors, radiation induced Tc, gap anisotropy effects 78−52125
A15 superconductors, supercond. and phonon softening in unstable systems 79−65587
A15 type compound, props. and one-dimensionality 80−2530
A15 type compounds, A_3B type, supercond. transition temp.-solid solution range correlation 77−85373
A15 type compounds, supercond. T_c in terms of Debye temp. and effective and reduced ionisation pots. 79−28435
A15-phase superconductors, metallurgical possibilities of raising transition temp. *(German)* 77−69441
A15-type compounds, review of superconducting props. and structure 80−70909
A 15 type superconductors, acoustic phonon spectra, electronic density of state function *(French)* 80−80444
A-15, A_3B type, cryst. chemical laws 78−34914
A-15 compound, defect influence on T_c 80−20345
A-15 compound, V_3X and Nb_3X, (X=Al, Ga, Si, Ge, Sn), electronic struct., electron-phonon interactions, and low temp. anomalies 79−60701
A-15 compounds, coupling strength 79−19684
A-15 compounds, defects 77−47927

type II superconductors continued
A-15 compounds, density of states model for lattice transforms. 80−65219
A-15 compounds, disordered, resist. and supercond. transition temp. 80−107944
A-15 compounds, disordered, T_c depression, appl. to Nb_3Ge 80−7020
A-15 compounds, effect on critical temp. for supercond. of disorder, induced by α-particles 78−47897
A-15 compounds, homogeneity range 80−2172
A-15 compounds, irrad. effect on supercond. transition temp. 78−6472
A-15 compounds, models for growth kinetics, solid state diffusion 79−46847
A-15 compounds, radiation damaged, supercond. crit. temp. 78−76185
A-15 compounds, radiation induced damage, TEM and heat capacity meas. 79−56349
A-15 compounds, structured phase transition, renormalisation group theory 78−79743
A-15 compounds, supercond. props., band struct. calcs. 79−33388
A-15 compounds, superconducting props. and structural transition *(Russian)* 77−12052
A-15 compounds, superconductivity 79−60947
A-15 compounds, X-point model for mag. susceptibility 78−23014
A-15 diffusion layers, influence of additions of growth and supercond. props. *(German)* 80−11130
A-15 high-T_c supercond., apparent T^2-depend. of normal-state resist. and lattice sp. ht. 77−47921
A-15 lattice, LF maxima in phonon state density and exponential term of resist. *(Russian)* 77−80871
A-15 phase, comment on new 3-dimens. $\vec{k}.\vec{p}$ model for electronic struct. 80−10865
A-15 phase, reply to comment on new 3-dimens. $\vec{k}.\vec{p}$ model for electronic struct. 80−10866
A-15 superconductor, dHvA effect 78−75985
A-15 superconductors, transition temp., d band relative displacement *(Chinese)* 80−103770
A-15 superconductors with defects, transition temp. 78−14857
A-15 type compounds, relation between martensitic and supercond. phase transition 80−29497
AC losses for superconductor with field-dependent surface barrier 79−87216
acoustic wave velocity, temp. depend. *(Russian)* 77−4468
α-Ag-Ge, superconducting transition temp. depend. on electron per atom ratio, lattice deform. 77−8222
alkali metal ternary chalcogenides, $M_{0.33}TaS_2$ and $M_{0.5}NbS_2$, supercond. props., alkali cation and topotactic solvation influences 79−87180
alkali metal tungsten bronzes, enhanced supercond. T_c, possible explanation 78−14850
alkali metal tungsten bronzes, superconductivity at press. up to 20 kbar 79−38226
alkali tungsten bronzes, dynamic fluctuations between local struct. states in supercond. TI phase 78−26981
alkali tungsten bronzes, struct. and supercond. 79−82703
alloy, meas. and interpretation of electron distrib. 79−1572
alloy, sound absorpt. and longit. collective oscills. *(Russian)* 77−32122
alloy, transition temp., effect of transition metal impurities, role of s-d Coulomb interaction 78−88061
alloys, binary, normal state lattice thermal cond., solute at.-phonon scatt. 77−76512
alloys, Kondo effect, specific heat jump at transition temp. 78−6479
alloys, nondiagonal disorder effects on supercond. transition temp. 79−73622
alloys and intermetallic cpds., metallurgical factors influencing T_c 79−38225
alloys with ordered magnetic moment distribution, thermoelec. effect 78−91811
aluminides of non-magnetic transition metals, atomic volumes deviation from additivity 79−82178
amorphous alloys, liq.-quenched, T_c 79−38234
amorphous metals, supercond., mag. impurity interactions 80−44777
amorphous metals and alloys, review of transport props. 79−4546
anisotropic, demagnetisation effects on lower critical field 80−97043
anisotropic, lower crit. field 80−60153
anisotropic superconductors, upper critical field theory 80−75692
annular superconductor, field replication and flux shielding 77−28286
antiferromagnetic, isolated vortex line 80−70912
antiferromagnetic superconductors, new pairing state, pair destruction, theory 80−54847
applied superconductivity, conf., Pittsburgh, USA (Sept. 1978) 79−33374
Bi-Ni base alloys, heterogeneous, supercond., magnetisation meas. *(French)* 78−6477
bounded, intermediate state struct. form. near crit. field, role of surface 80−80465
Ce impurities, sp. ht. jump, unified description of demagnetisation of Ce impurities 77−69450
Chevrel phase compounds, bonding and phys. props. rel. to struct., book contrib. 80−49209
Chevrel phase materials, indirect meas. of Fermi surface parameters 79−60686
Chevrel phase supercond., resistivity meas. from 4.2 to 400K 79−56230
clean, US attenuation and thermal cond. 78−91812
clean cubic anisotropy of generalised Ginzburg-Landau parameters 79−4630
collective modes and relax. effects 77−76996
collective quantum fields for many body systems, appl. to BCS, ^{3}He and type II superconductors *(German)* 79−35917
composite wire critical current density rel. to tensile stress at 4.2K, obs. 79−33439
compound superconductors, radiation effects on critical currents 78−52175
critical current, peak effect in mag. field depend. *(Russian)* 78−47924
critical current standard 77−28322
critical field, anal. of expt. data *(Chinese)* 80−60151
critical fields, materials developments *(Czech)* 78−23213
critical state, flux jumps and oscills. *(Russian)* 80−7052
critical state stability *(Russian)* 78−56266
critical state stability anal. 77−89907
crystals of magnetic flux, review 79−99664
cubic, flux-line lattice anisotropy, boson method calc. 80−2536
cubic compounds of A15, C15 and B2 types, struct. phase transitions 77−4198

type II superconductors continued
current density distrib. in type II supercond. with normal inclusions, theory 80−80461
cylinder, magnetisation change induced by current near upper crit. field 80−70890
cylindrical tube, thick-walled, mag. field distrib. in axial region *(French)* 77−51856
dilute alloys, eqn. for crit. temp. 78−72300
dilute magnetic alloys, effects of indirect coupling upon nucl. spin-lattice relax. 77−80874
dilutely pinned, threshold criteria for pinning force 80−15668
dilutely pinned superconductors, nonlinear I-V characts. 79−56479
dirty, mixed state, vortices, transport entropy theory 78−43534
dirty superconductor, fluctuation diamagnetism *(Russian)* 79−51721
dirty superconductors, fluctuation induced elec. cond. 79−38251
disc of arbitrary shape, thermal conductivity meas. method and appl. 79−63228
dynamic instabilities in high T_c materials 78−10607
electronic component and material improvement, ion implantation techniques *(French)* 78−18667
EPR of paramagnetic impurities and conduction electrons *(Russian)* 79−1641
ferromagnetic, critical behaviour, coexistence near supercond.-ferromag. multicritical point 79−47197
ferromagnetic superconductor, supercond. Bloch wall 80−20349
film, inversion temp. in pinning of vortices by periodic struct. 78−56274
film, memory device storage of Abrikosov vortices 79−28487
film, resistive state, linear depend. on applied microwave power of second crit. current 77−32121
film, sputtered, high press. induced shifts in supercond. transition temp. 77−85374
film, stripline, propag. const., attenuation and phase vel. expressions, pulse propag. 78−43524
film, superconducting props. 79−38215
fluctuation induced diamagnetism above H_{c2} 78−80097
fluctuations in crit. region near upper crit. field 80−25048
flux distribution and hysteresis loss in round supercond. wire 80−34570
flux jump in magnetic field, at slow sweep rate, theory and expts. 79−4632
flux pinning in superconductor with current, effect on mag. field distrib. 79−65622
flux-flow noise theory 79−24115
flux-flow noise voltages, oscillations in V-I curves 80−15671
flux-line cutting 80−7055
flux-line cutting model 80−50017
flux-line lattice instability due to planar imperfections 78−23218
flux-line-cutting threshold 80−88705
fluxes, axial and azimuthal, contained in cylinder in force-free config. 79−82728
fluxon pinning, in supercond. with regularly spaced defects 78−39276
foil, DC voltage induced by superposition of AC mag. field 77−85395
gapless, localised mag. moments, EPR *(Russian)* 78−34920
giant-vortex state, temp. depend. 80−7051
Ginzburg-Landau parameters in case of non-pure supercond. 77−76997
Ginzburg-Landau theory, exact solns. for pure metals 80−49981
granular, Josephson junction array, phase transition 80−88684
granular, percolation theory, crit. props. 80−84575
granular films, percolation threshold and crit. current, theory 80−88706
granular metal, supercond. transition, increased resistance rel. to quasiparticle tunnelling 80−88689
graphite intercalation compound, $C_{8.8}K$, mag. susceptibility fluctuations near supercond. transition temp. 79−78259
graphite intercalation compounds with alkali metals and halogens, physical props. 78−31050
graphite-K intercalation compound, effect of H addition on superconducting transition temp. 80−70872
graphite-K intercalation compounds, Fermi surface, transport and supercond. props. 79−65367
group-V layer compounds, 2H-polytypes, origin of CDW, elec. susceptibility, electron-phonon interactions 77−51679
hard superconductor, flux trapping, penetration depth determ. 80−100572
hard superconductors, mag. instabilities 77−89908
heat capacity of high T_c superconds., anal. of data 79−38247
high field expts. on press. effects up to 15 kbar 79−61006
high temperature superconductors, tunnelling spectra, electron pairing anal., appl. to Nb_3Sn 79−87205
high-current superconductors, low-freq. losses, phenomenological model 78−6486
high-Tc superconductors role of quasilocal excitation 80−2508
high-temperature superconductors, clustering hypothesis 78−26984
hysteresis losses for round cross section with collective interaction 78−43513
hysteretic, flux cutting 79−73647
ideal, wire, macroscopic current in longitudinal field 78−84366
ideal vortex lattice strength *(Russian)* 77−80886
impurities with Kondo effect, Green's function calcs. 77−89894
In-Cd-Sn, supercond. transition temp. and electronic props., Brillouin zone effect 79−56345
inductive response to trapezoidal magnetic field 78−39277
inhomogeneous, impedance in Shubnikov phase *(Russian)* 78−23212
inhomogeneous superconductor, crit. fields 78−84367
inhomogeneous superconductors, nonlocal pinning, inversion temp., and crit. current 79−56475
intermetallic compounds, containing d-transition metal, hydrogenated, magnetism 80−34609
intermetallic compounds, press. depend. of martensitic and supercond. transition temp. 79−19681
intermetallic phases, technical superconductor applications *(German)* 78−27005
interstitial compounds, electronic structure and useful phys. props. 77−89683
ion implantation applications 78−52134
irreversible, flux flow in transverse mag. field 79−7949
Kondo effect in type II superconductors, upper critical field and Ginzburg-Landau parameter 78−14874
Kondo superconductor, nucl. spin-lattice relax. 78−52156
Kondo superconductor, self-consistent theory of pairbreaking 78−26989
large-scale applications, review 79−69640
layered compounds, surface supercond. *(Russian)* 78−31018
layered superconductors, Josephson coupling effects, review 80−84554

type II superconductors continued
long ferromag. supercond., metastable supercond. state 80−103771
longitudinal current, continuous vortex cutting 80−88704
longitudinal currents in a system of Abrikosov vortices, Ginzburg-Landau eqn. anal. 80−70914
low temperature depend. of elec. resist., mag. suscept., heat capacity, Hall const. *(Russian)* 78−30900
magnetic behaviour under longitudinal mag. field, irreversible force free current 80−7053
magnetic hysteresis and flux profiles, review 79−1651
magnetic properties, boson method, impurity and temp. effects 78−91826
magnetic properties, phase transition around H_{c1} at finite temp. 77−4472
magnetic superconductor, shape effects 80−103773
magnetically impure superconductors, finite relax. time at zero field transition point, exptl. obs. 78−23219
magnetisation, critical state model in nonideal supercond. 79−47212
magnetisation, rel. to anisotropy of upper crit. field 80−54832
magnetisation curves, boson method calcs. 78−39258
materials for supercond. electronics 79−28470
mechanical behaviour and stress effects, review 77−86083
metal and alloy softening at transition *(German)* 77−89898
metal hydrides, anharmonicity and superconductivity 77−15988
metallic conductors, disordered and non-crystalline, anomalous elec. cond. 78−95279
metallic glasses, electronic structure rel. to elec. cond., supercond. and mag. props. 80−65429
metallic glasses, low temperature US props., supercond. state effects 79−87192
metallic glasses, review *(German)* 79−41962
metallic glasses, structure and properties, review 78−47245
metallic glasses, transport properties, applicability of liq. metal theory 79−56179
metallic glasses props., development and appl. 80−19710
metastable alloys, review of current work 80−81002
metastable states, boundaries 80−54848
molybdenum chalcogenides, multicomponent, physical props. 80−84577
molybdenum chalcogenides, props. preparation and struct. *(French)* 79−73619
molybdenum ternary chalcogenides, structures and properties survey *(Czech)* 80−70870
molybdenum ternary sulphides, Chevrel phase, synthesis and superconductivity *(German)* 80−25038
multifilamentary composite, coupling losses in outer normal layers 79−99667
neutron effects 78−52121
neutron irrad., elec. resist., temp. depend. 79−91024
neutron irradiation effects *(Rumanian)* 78−52144
neutron scattering from imperfect flux-line lattice 79−56474
noble metal alloys, superconductivity, correlations and predictions 78−23192
nonideal, pin distrib. rel. to V-I characts. *(Japanese)* 79−33421
nonideal, with dense pinning centres, threshold criterion 80−88703
nonideal slab, AC losses in small AC mag. field of trapezoidal wave form 78−39272
nonideal type II supercond. wire, flux penetration in transverse mag. field *(Japanese)* 80−60154
order parameter, space dependence at low temps. 77−72951
order parameter change near H_{c2}, influence of transport current 80−75690
oscillations, resistive state, current density 80−44782
paramagnetic limit, Fermi surface dielectric gap *(Russian)* 80−2533
paramagnetic properties of crysts. without symm. centres, spin-orbit interaction 77−15994
$Pb_{80}In_{20}$ foil, flux-flow crit. freq. and generalised bundle size depend. on fluxoid traversal distance and length 80−7054
peak effect, static and dynamic crit. currents obs. *(Russian)* 77−85399
perturbation series for crit. behaviour near H_{c2} 77−8233
phase diagrams, exam. in terms of electronic structure 79−8278
phase diagrams, use in superconductor processing 79−11574
phonon anomalies, neutron scatt. obs., book contrib. 77−89504
phonon Raman scattering in superconductors 80−100657
pinning centres influence on voltage-current characts. 79−56470
pinning forces scaling law in nonideal supercond. 79−99663
pion condensate props. in mag. field, superconductivity, mixed state *(Russian)* 80−49974
positive muon diffusion coeff., determ. from transverse depolarisation 80−25269
power apparatus appls., research study *(Japanese)* 78−19192
precipitation-induced conductivity enhancement, analogy to precip.-hardening 77−77490
properties of selected superconductive materials 79−56366
quasi-one-dimensional superconductor, critical mag. field, transition temp. *(Russian)* 80−93058
radiation effects, conf., Argonne, Il., USA (June 77) 78−52120
radiation-induced changes in crit. props., radiation defects *(Russian)* 80−25027
randomly pinned superconductors, I-V characts. 79−56478
rare earth alloys with Cu_3Au lattice, cryst. chemistry and supercond. crit. temp. 79−86744
rare earth compound, $R_{1-x}Mo_6S_8$, magnetically ordering, supercond. props. 79−56373
rare earth compounds, phenomenological study of supercond. 78−43512
rare earth compounds, $R_xMo_6S_8$, high crit. field Chevrel phase 79−61003
rare earth compounds, $R_xMo_6S_8$ mag. susceptibility meas., 1.3-300K 78−14936
rare earth compounds, $R(Rh_{0.85}Ru_{0.15})_4B_4$, mag. ordering and supercond. 78−14861
rare earth compounds, RMo_6X_8, (X=S, Se), supercond. and long range mag. order coexistence 80−15642
rare earth compounds, RMo_6X_8, X=S,Se, coexistence of supercond. and antiferromag. order 79−65579
rare earth compounds, RRh_4B_4, coexistence of supercond. and ferromag. order 79−65579
rare earth compounds, RRh_4B_4, supercond. and long range mag. order coexistence 80−15642
rare earth compounds, ternary, superconductivity and ferromagnetism 79−69617
rare earth compounds, ternary, theory of superconductivity 79−73628

type II superconductors continued
rare earth compounds, upper crit. fields in the dirty limit, depend. on intra- and interaction exchange interactions 79−56461
rare earth cpds., $RMo_6S_8(Se_8)$ and RRh_4B_4, coexistence of supercond. and mag. ordering *(Russian)* 80−84542
rare earth cpds., RRh_4B_4 and RMo_6X_8 (X=S, Se), mag. order and supercond., neutron scatt. studies 80−44807
rare earth iron silicides, $R_2Fe_3Si_5$, superconductivity 80−49968
rare earth lead molybdenum sulphides, $R_xPb_{1\pm x}Mo_{6+y}S_8$, R=La, Nd, Pr, Gd, sputtered, supercond. props. 80−50019
rare earth metal compounds, high temp. paramagnetic-supercond. phase transitions, mag. cell symm. *(Russian)* 79−78255
rare earth metal compounds, phase stratification in superconductors *(Russian)* 79−42685
rare earth molybdenum chalcogenides, Chevrel phase correlation between struct. and supercond. transition temp. 80−7023
rare earth molybdenum selenides, supercond., mag. props., 0.7 to 295K 77−32113
rare earth molybdenum sulphides, $R_{1.2}Mo_6S_8$, low temp. magnetisation meas., and supercond. props. 79−8018
rare earth molybdenum sulphides, supercond. and magnetism coexistence *(Japanese)* 80−7025
rare earth rhodium boride system, ternary, supercond., phase diagrams at upper crit. fields 80−2531
rare earth rhodium borides, RRh_4B_4, NMR and sp. ht. in supercond. and mag. ordered phases 80−7037
rare earth rhodium tin intermetallic cpds., synthesis, supercond. and mag. props. 80−100547
rare earth systems, superconductivity, review 79−69621
rare earth ternary borides, coexistence of magnetism and superconductivity 79−73630
rare earth ternary borides, RRh_4B_4, ferromag. Curie Temp., high supercond. transition temp. 77−89893
rare earth ternary borides, RRh_4B_4, supercond., re-entrant magnetism, energy band calcs. 78−52140
rare earth ternary borides, RRh_4B_4, supercond. and ferromag., cryst. struct., X-ray diffr. 77−89423
rare earth ternary compounds, supercond. and antiferromag. coexistence 80−25030
rare-earth compounds, supercond. pairing, mag. ordering effect 80−15641
resistive domain existence, current generation *(Russian)* 80−44776
reversible, AC flux penetration on force free config. 79−56464
rotating, vortex lines *(Russian)* 77−40009
scaling relations in mag., mechanical and superconducting pinning theory 77−76403
series formula of supercond. critical temp. applications *(Chinese)* 80−54816
slab, AC losses in small mag. field of sinusoidal wave form 78−47920
small-angle scattering, of X-rays and neutrons, (fourth international conf., Gatlinburg, USA (Oct. 77)) 79−10745
solders, transition temp. determ. 77−28281
solid solution disordered alloy, conc. depend. of superconducting transition temp. *(Russian)* 79−28427
spin diffusion in inhomogeneous mag. fields 78−2618
standards for practical superconductors, development 79−33442
stress tensor of cosmic and lab. type-II superconductors 78−6485
strong coupling superconductor thin film, critical mag. field *(Chinese)* 80−54849
structure defect, effect on resistive and Hall effects *(Russian)* 79−33419
superconducting order parameter perturbation flux pinning 80−103801
surface and bulk props., determination 79−61011
surface barrier to flux entry, thermal stability 78−52163
surface resistance, theory 77−51841
synthesis from thermalised sputtering and changes in Tc and depend. of H_{c2} on temp. 79−56350
technical superconductor requirements and main properties 79−30511
thermodynamics, corrections from electron-phonon interactions 80−49387
thermodynamics near $H_{c2}(T)$ and scaling law 79−60968
thermomagnetic effects and critical state stability 80−20353
$(TMTSF)_2PF_6$, organic one-dimensional superconductor, transition temp. 80−44754
$(TMTSF)_2PF_6$, quasi-dimens. cond., diamagnetic AC susceptibility 80−103781
Tokamak requirements for supercond. materials and devices w.r.t. thermonucl. fusion *(French)* 78−13322
transition element compounds, supercond. props., lattice symm. and instability 77−8224
transition element cpds. and their dil. alloys, supercond. crit. temp., s-d Coulomb interaction 78−31012
transition metal, tunnel junctions, phonon struct., junction quality 79−11274
transition metal alloy, binary, conc., superconductivity and electron-phonon interactions, theory 78−14868
transition metal alloys, amorphous, reduced supercond. transition temps. 77−39991
transition metal alloys, deformation and solute-induced microstructural effects on superconductivity 79−7925
transition metal borides, supercond. search below 1K 80−20342
transition metal carbides, high temp. supercond., role of electronic struct. on obs. phonon anomalies 77−24363
transition metal carbides, influence of implanted ions on supercond. transition temp. 77−28276
transition metal chalcogenides, quasi-one-dimens., elec. mag., and supercond. props., review *(Russian)* 80−93022
transition metal compound refractories, electron and phonon behaviour 80−54624
transition metal compounds, phonon anomalies due to d-band effects, electron-phonon matrix elements 78−30720
transition metal compounds, phonon anomalies rel. to superconductivity 77−12055
transition metal dichalcogenides, phys. props. *(Japanese)* 77−69225
transition metal dihydrides, band struct. and electronic props., electron-phonon coupling 79−47011
transition metal glasses and amorphous films, supercond. and electronic props. 79−73612
transition metal hydrides, electron-phonon interaction const. calc. 79−65160

type II superconductors continued
transition metal hydrides, isotope effects, depend. on cryst. field energies 79−56353
transition metal hydrides, isotope effects on supercond. props. 79−65580
transition metal impurities, kinetic coeffs. *(Russian)* 77−32111
transition metal pyrites, mag. and elec. props., review *(Japanese)* 78−47941
transition metal silicides, struct. and supercond., Cu influence 80−50592
transition metal sulphides, selenides and phosphides, NaCl struct., supercond. props. 79−4613
transition metal superconductors, specific heat anharmonic components, phonon freq. temp. shift *(Russian)* 79−91183
transition metals, amorphous, superconducting transition temp. *(Chinese)* 80−54817
transition metals, and their carbides high temp. superconductivity and phonon softening 78−14848
transition metals, BCC, supercond transition temp. and press effects 77−4461
transition metals, d-band superconds., s-electron current density calc. 77−47926
transition metals, group V, low temp. sp. ht. anomalies 77−77002
transition metals, influence of implanted ions on supercond. transition temp. 77−28276
transition metals, lattice dynamics calculations, superconductivity parameters 79−7655
transition metals, resistivity and superconductivity 79−51550
transition metals, supercond., effect of s-, d-electron hybridisation *(Russian)* 78−39243
transition metals, supercond. transition temp., ab initio calc. 80−25036
transition metals, superconductivity, recent developments 79−11263
transition metals and alloys, BCC, T_c related to residual resist. 79−15134
transition metals and alloys, superconductivity, relevance of mag. interactions 80−100545
transition metals silicides, atomic volume deviations and supercond. T_c 80−75203
transport entropy of vortices, in supercond. with paramag. impurities 77−20506
upper critical field at low temps. 77−66230
virtual bound state alloys with resonant impurity scatt. centres theory 79−99654
vortex line pinning and I-V charcts. *(Russian)* 79−65623
vortex motion, and elec. cond., in weak mag. field 77−59362
vortex pinning at edge dislocations, electrostatic mechanism 80−103802
β-W type compounds, resist. charcts. in normal state 78−51963
wire, AC losses *(Japanese)* 78−84364
wires, general crit. state model in two dimens. and zero applied field, uniqueness theorem 80−93062
zero-gap dirty, cond. electron spin resonance theory 80−103888
Ag brazing alloy, type BAg-3, props. 79−1639
α-Ag-Al, superconducting transition temp. depend. on electron per atom ratio, lattice deform. 77−8222
Ag-Mn film, supercond. proximity effect and pair breaking, normal state mag. interactions 77−63035
Ag-Nb-Ga, phase relations, A15 phase diffusion layer formation 78−52764
AgH, electronic struct. and supercond., APW calc. 79−95318
$Ag_xMo_3S_4$, chevrel phase, charge transfer and valence electron conc. 78−6029
$Ag_xMo_6S_8$, Chevrel phase, lattice instabilities, X-ray diffr. meas. 78−34491
$Ag_{1-x}Sn_{1+x}Se_{2-y}$, supercond. and normal state props. 77−36008
Al, energy gap enhancment by tunnelling extraction 80−34564
Al film, granular, crit. field anisotropy and fluctuation cond. 78−26994
Al film, metastable current states 79−15265
Al film, metastable current states, mean free path variation *(Russian)* 80−2538
Al film, perforated, crit. currents associated with interaction of commensurate flux-line sublattices 78−34937
Al film, perforated with triangular lattice of 1 μm holes, critical currents 77−28332
Al film, supercond. crit. field, spin-polarized tunnelling meas., test of high-field supercond. theory 79−87220
Al film with magnetically weakened section, Josephson effect 77−28302
Al granular film, edge pinning in perpendicular mag. fields 79−4633
Al granular films, inhomogeneous supercond. transitions, microwave meas. 80−103789
Al granular films as weak link in Josephson devices 80−88685
Al, granular supercond., normal state cond. 80−88529
Al, superconducting, order parameter, spatial var. near Anderson impurity 79−60962
Al superconducting film, cylindrical, granular, crit. currents and electron mean free paths 80−7057
Al, superconducting thin film, evidence for Kosterlitz-Thouless transition 80−39721
Al:O, perforated film, RF resist. in mag. field, pinning force const. 79−56471
Al:O supercond. film, RF complex impedance meas., dynamic pinning 80−84573
Al/Ge multilayered superconducting films, crit. fields and crit. temps. 79−7945
Al-3d transition metal, dil., transport props., sp. ht. and supercond. crit. temp. calc. 77−1393
Al-Ag, torque oscillations in mag. field *(Russian)* 80−103800
Al-C(Si)(Ge) film, ion-implanted, enhancement of supercond. transition temp. 77−32103
Al-Ce, very dil., low temp. sp. ht. 79−51745
Al-Cu, dil. alloy, quench condensed thin films, supercond. and struct. from electron diffr. patterns 78−47901
Al-Cu, superconducting amorphous films of high stability 80−70889
Al-Er, dil., order parameter dynamics and collective modes, pair tunnelling meas. 79−56409
Al-Ge, film, double supercond. transition in resistance-temperature and current-voltage charcts., percolation theory 79−56365
Al-Ge thin film alloy, critical currents near metal-insulator transition 79−65626
Al-Mn, dil., superconducting and normal state, ^{27}Al spin-lattice relax. rates 79−60977
Al-Si(Ge) film, ion-implanted, percolation and superconductivity 78−26982

type II superconductors continued
- Al-V, dil., superconducting and normal state, ^{27}Al spin-lattice relax. rates 79−60977
- Al-V-Ti junction, spin-dependent electron tunnelling 79−19700
- Al_2Cu, single cryst. elastic consts., 4.2-300K 78−72803
- $Al_{10}V$, supercond. transition temp. determ., localised phonon modes 77−63016
- Au-Al-In solid soln., elastic strain energy depend. of supercond. T_c 79−38229
- Au-Ga, resist. and supercond. meas., electron-phonon interaction and Coulomb pseudopot. determ. 78−43358
- Au-Ga-In solid soln., elastic strain energy depend. of supercond. T_c 79−38229
- α-Au-Ge, superconducting transition temp. depend. on electron per atom ratio, lattice deform. 77−8222
- α-Au-Zn, superconducting transition temp. depend. on electron per atom ratio, lattice deform. 77−8222
- AuGa, and $AuGa_2$, supercond. transition temp. and crit. field 79−38232
- $AuGa_2$ film, magnetic susceptibility and Knight shift press. depend. 77−43777
- $AuGa_2$, press. depend. of thermodynamic props., theor. *(Russian)* 77−51843
- $AuGa_2$ type supercond., mag. impurity and press. effect on crit. temp. *(Russian)* 78−23189
- $(Au_{1-x}Pd_x)Ga_2$, supercond. transition temp. and crit. field 79−38232
- Ba, BCC, superconductivity under press. 78−14858
- $BaGe_2$, superconducting temperature depression due to mag. field 80−54820
- $Ba_2Mo_{15}Se_{19}$, superconducting chalcogenides containing Mo_6 and Mo_9 clusters 80−103804
- $BaPb_{1-x}Bi_xO_3$ film, RF sputtered, T_c as function of comp. and annealing conditions 79−24100
- $BaPb_{1-x}Bi_xO_3$, semiconductor-metal transition and supercond., IR absorpt. and struct. meas. 77−28278
- $BaPb_{1-x}Bi_xO_3$, supercond. T_c and crit. fields, comp. depend. 79−73623
- $BaPb_{1-x}Bi_xO_3$, superconducting thin films, RF sputtering prep. 80−76181
- $BaPb_{1-x}Bi_xO_3$, superconducting props., Hall coeff. and elec. resist. meas. 80−84531
- $Ba_{0.67}Pt_3B_2$, cryst. struct. and supercond. props. 79−38231
- $Ba_{1-x}Sr_xPb_{0.75}Bi_{0.25}O_3$, superconductivity, rel. to lattice const. 80−49966
- Be alloys, enhancement of supercond. transition temp. 80−60129
- Be-Nb-Zr alloys, glassy and partially crystalline, supercond. T_c and struct. props. 78−60239
- Be-Zr alloy, glassy, quenched from melt, supercond. props. 78−26983
- Bi, amorphous film, supercond. fluctuation effects in resist. transition 78−10609
- Bi, amorphous films, supercond. fluctuation effects in perpendicular mag. fields 79−60980
- Bi, lightly doped, superconductivity, resist. obs. 78−64160
- Bi-Pb alloy, crit. temp., effects of press. up to 30 kbar. *(Russian)* 77−20484
- Bi-Pb amorphous alloys, superconductivity and the very strong electron-phonon interaction *(Japanese)* 79−95552
- Bi-Sb film, tunnel conductivity, proximity effect *(Russian)* 79−51726
- Bi-Tl alloy, thermal cond., 1.5 to 50K, temp. depend. 78−26990
- Bi-Tl film, superconductivity and phonon spectrum *(Russian)* 79−91190
- $Bi_{1-x}Pr_x$-Al oxide-Al tunnel junction, cryst. field struct. obs. in conductance 78−84358
- $Bi_{1-x}Sb_x$, transition temp., press. depend., 30-80 kbar 77−8223
- C_8K, intercalation compound, superconductivity 78−91827
- C_8K, intercalation cpd. with graphite, supercond. props. 80−44755
- $Ca_{0.67}Pt_3B_2$, cryst. struct. and supercond. props. 79−38231
- Cd-Cr, dil., estimates of s-d interaction from supercond. transition temp. and mag. susceptibility 78−43561
- Cd-Sn alloy, superconductivity and microstructure 80−107949
- Ce, high press. superconductivity, phonon softening 78−14852
- $CeCu_2Si_2$, strong Pauli paramagnetism, superconductivity obs. 80−29499
- $Ce_{1-x}Gd_xRu_2$, superconductivity and ferromagnetism coexistence, 60 mK-4.2K, spin echo NMR 78−84349
- $Ce_{0.73}Ho_{0.27}Ru_2$, superconductors, mag. correlations and crystal-field levels 80−34547
- $Ce_{0.73}Ho_{0.27}Ru_2$:Co, spontaneous mag. order below superconducting transition temp., Mossbauer study 80−39701
- $(Ce_{1-c}Ho_c)Ru_2$, mag. props., neutron scatt. study 80−44808
- $CeRu_2$ and $Ce_{1-x}Gd_xRu_2Zr_2Co$, spin-pairing state investig. via Josephson effect 77−47942
- $CeRu_2$, change of valence of Ce ions, induced by H absorption, supercond. disappearance 79−47185
- $CeRu_2$, H absorption induced Ce valence change, mag. and supercond. props. 80−50042
- $CeRu_2$, type II supercond., ESR of Nd^{3+} meas. 79−28444
- $CeRu_2$:Nd^{3+}, supercond. state, ESR investigation 79−78514
- Co-Nb-C, obtained by liq. quenching, superconductivity 80−75699
- $Co_2Mo_6S_6O_2$, O-containing Chevrel phases, synthesis and props. 80−108368
- Cr_3Si structure, rel. between phase diagrams and superconductivity 80−88330
- $Cs_{0.33}WO_3$, supercond. and special phonons, neutron scatt. obs. 80−15643
- Cs_xWO_3, normal phase and supercond. props 80−25035
- Cu-Ga porous solid formed by shock compression 80−29905
- α- Cu-Ge, superconducting transition temp. depend. on electron per atom ratio, lattice deform. 77−8222
- Cu-Nb, supercond. wire, directional solidification of melts, supercond. ionisation temp. *(Russian)* 78−76596
- Cu-Nb (0,4 at.%), splat quenched, aged, superconductivity *(Japanese)* 77−63018
- Cu-Nb (17 wt.%) multifilamentary wires, fabrication and supercond. characts. 79−56476
- Cu-Nb alloys, origin of superconductivity 77−47918
- Cu-Nb alloys for superconducting wire, casting of dendritic structure 80−2976
- Cu-Nb filamentary composites, powder metallurgy prod., supercond. props. 79−56477
- Cu-Nb_3Sn multifilamentary tapes, in situ formed, crit. current density anisotropy 80−84576
- Cu-Nb_3Sn superconducting composite, crit. props., AC hysteretic losses 80−50014
- Cu-Nb-Sn, multifilamentary supercond. composite wires, fabrication on laboratory scale and mech. props. 80−29897

type II superconductors continued
- Cu-Nb-Sn composites, cold-powder-metallurgy processed, supercond. critical currents 79−78279
- Cu-Nb-Sn dil. alloys containing Nb_3Sn precipitates, superconductivity 78−43507
- Cu-Nb-Sn system, phase equilibria and supercond. props. *(Russian)* 80−50589
- Cu-NbTi, composite conductor, acoustic emission 80−97032
- α- Cu-Si, superconducting transition temp. depend. on electrons per atom ratio, lattice deform. 77−8222
- Cu-Sn-Nb multifilamentary alloy, high field crit. current density 78−27004
- Cu-V-Ga dil. alloys with V_3Ga particles, supercond. props. and microstruct. 78−39278
- Cu-V-Si, supercond. props. 80−107945
- Cu-V-Si, two-step supercond. transition 80−34539
- CuCl, high-temp. supercond., BCS strong-coupling limit for transition temp. 80−2511
- Cu_xLa_{1-x}, splat-cooled, phase diagram and supercond. props. 80−70881
- $Cu_{1.8}Mo_6D_8$, triclinic struct., X-ray powder diffr. anal. 80−6388
- $Cu_{1.8}Mo_6S_8$, electron tunnelling spectroscopy expts. *(German)* 80−107966
- $Cu_{1.8}Mo_6S_8$, supercond. energy gap and phonon-induced structs. in tunnelling density of states 79−51728
- $Cu_2Mo_6S_8$, normal state and superconducting property measurements 78−91660
- $Cu_2Mo_6S_8$, phonon density of states, mode softening correl. with supercond. transition temp. 79−51714
- $Cu_{2.5}Mo_6S_8$, evaporated two-phase, crit. current and scaling laws 78−91831
- $Cu_xMo_3S_4$, chevrel phase, charge transfer and valence electron conc. 78−6029
- $Cu_xMo_3S_4$, superconductivity and cryst. struct. 79−78250
- $Cu_xMo_6S_8$, $1.5 \leq x \leq 3.55$, low temp. phase diagram, 1.2-320K 77−85371
- $Cu_xMo_6S_8$, Chevrel phase, lattice instabilities, X-ray diffr. meas. 78−34491
- $Cu_xMo_6S_8$, Chevrel phase supercond. prep. and supercond. props. 79−28434
- $Cu_xMo_6S_8$, Chevrel-phase sputtered film, supercond. critical currents 77−80892
- $Cu_xMo_6S_8$, constitution diagram, 11-2000K 80−108407
- $Cu_xMo_6S_8$, evap. film prep., supercond. props., lattice parameters 78−23195
- $Cu_xMo_6S_8$, evaporated films, superconducting upper crit. fields, crit. currents 79−42714
- $Cu_xMo_6S_8$, Hall effect and magnetoresistivity 78−95400
- $Cu_xMo_6S_8$, normal-state electronic props., Fermi surface and supercond. parameter derivations 79−60850
- $Cu_xMo_6S_8$, prep. by topotactic electrode reactions, struct., supercond. 79−99158
- $Cu_xMo_6S_8$, scaling laws for pinning forces 79−47214
- $Cu_xMo_6S_8$, sintered and sputtered, supercond. upper crit. field 78−23215
- $Cu_xMo_6S_8$, sputtered, supercond. crit. currents and scaling laws 78−47923
- $Cu_xMo_6S_8$, supercond., two-phase, upper crit. field meas. 80−29509
- $Cu_xMo_6S_8$, superconducting reactively evaporated film, crit. currents 79−28492
- $Cu_xMo_6S_6I_2$, x=0 to 1.2, superconducting Chevrel-phase system, synthesis and transition temps. 79−69618
- $Cu_2Mo_6S_6O_2$, O-containing Chevrel phases, synthesis and props. 80−108368
- $Cu_xMo_6S_8(Se_8)$, prep., metallurgical and supercond. props. 77−32102
- $Cu_{0.7}Mo_3Se_4$, Chevrel-phase, low temp. struct. instability rel. to supercond. 77−47919
- $Cu_{40}Nb_{30}X_{30}$ (X=Ti, Zr, Hf), superconductors with metastable ordered structs. 80−108484
- $CuRhS_4(Se_4)$, press. depend. of supercond. transition temp. meas. 77−12050
- $Cu_{40}Zr_{60}$, amorphous alloys, supercond. transition temp., press. depend. 80−84524
- $Dy_xCe_{1-x}Ru$, supercond., mag. order 79−87189
- $Dy_xCe_{1-x}Ru_2$, supercond., mag. props. 79−11267
- $DyMo_6S_8$, long range mag. order in supercond. state 79−65653
- $DyMo_6S_8$, supercond. and antiferromag. coexistence, neutron study 78−95401
- $DyMo_6S_8$, superconductor, neutron scatt. exam. of mag. phase 79−73680
- $Dy_{1.2}Mo_6S_8$, long-range mag. order and supercond., neutron diffr. obs. 79−78320
- $Dy_{1.2}Mo_6S_8$, low temp. heat capacity anomaly rel. to antiferromag. transition in supercond. state 80−25044
- $Dy_{1.2}Mo_6S_8$, mag. ordering in supercond. state, resist. and AC susceptibility meas. 78−19194
- $DyRh_{1.1}Sn_{3.6}$, new supercond./mag. cpds., X-ray powder diffr. data 80−100215
- $Er_{1-x}Gd_xRh_4B_4$, supercond. and mag. transitions at press. up to 19 kbar 79−38236
- $Er_{1-x}Gd_xRh_4B_4$, ternary superconductor, mag. interactions 79−73613
- $(Er_{0.6}Ho_{0.4})Rh_4B_4$, reentrant supercond., magnetisation meas. near lower crit. temp. 80−25043
- $Er_{1-x}Ho_xRh_4B_4$, ferromagnet, sp. ht anomaly at lower superconducting transition temp. 79−47194
- $Er_{1-x}Ho_xRh_4B_4$, mag. and supercond. transitions, cryst. field effects 80−107950
- $Er_{1-x}Ho_xRh_4B_4$, re-entrant supercond. and mag. ordering 78−60240
- $(Er_{1-x}Ho_x)Rh_4B_4$, superconducting ferromag., Josephson effect, point contact junction meas. 80−7043
- $(Er_{1-x}Ho_x)Rh_4B_4$, superconductive and mag. interactions, hydrostatic press. effect 80−49973
- $Er_{1-x}Ho_xRh_4B_4$, ternary superconductor, mag. interactions 79−73613
- $Er_{1-x}Ho_xRh_4B_4$ type cpds., supercond., phase stratification *(Russian)* 79−42685
- $ErMo_6S_8$, long range mag. order in supercond. state 79−65653
- $Er_{1.2}Mo_6S_8$, mag. ordering in supercond. state, resist. and AC susceptibility meas. 78−19194
- $ErMo_6Se_8$, crystal field excitations, inelastic neutron scatt. obs. 79−78321
- $ErMo_6Se_8$, mag. ordering and supercond., neutron diffr. 78−68125
- $ErMo_6Se_8$, mag. supercond., neutron scatt. obs. 80−70952
- $Er_xMo_6Se_8$, long-range antiferromag. order and supercond. coexistence 78−10715
- $ErRh_4B_4$, ferromag. superconductor, vortex phase 80−80441

type II superconductors continued
$ErRh_4B_4$, film, sputter deposition and low temp. props. 80−2948
$ErRh_4B_4$, long ferromag. supercond., metastable supercond. state 80−103771
$ErRh_4B_4$, mag. supercond., NMR study of ^{11}B 80−107957
$ErRh_4B_4$, Mossbauer spectra 80−15926
$ErRh_4B_4$, reentrant supercond., mag ordering, neutron diffr. obs. 78−14879
$ErRh_4B_4$, supercond., electronic struct. and reentrant magnetism 78−10340
$ErRh_4B_4$, supercond., electronic props. of Er^{3+} using Mossbauer effect in ^{166}Sr 79−56651
$ErRh_4B_4$, supercond., thermal cond. between 0.05 and 4K 79−60967
$ErRh_4B_4$, supercond. and mag. props. 79−4631
$ErRh_4B_4$, supercond. and mag. props., influence of mag. fields 79−56374
$ErRh_4B_4$, supercond. transition temp., upper critical field, local spin fluctuations 79−38250
$ErRh_4B_4$, superconductivity destruction at onset of long-range mag. order 77−76994
$ErRh_4B_4$, superconducting and mag. transitions, alpha particle irradiation damage effects 79−60954
$ErRh_4B_4$, superconducting and normal state props. 79−73632
$ErRh_4B_4$, superconducting, magnetic dilemma 80−75680
$ErRh_4B_4$, superconducting thin films, critical mag. field 80−75693
$ErRh_4B_4$, superconductor, neutron scatt. exam. of mag. phase 79−73680
$ErRh_4B_4$, ternary superconductor, mag. interactions 79−73613
$ErRh_{1.1}Sn_{3.6}$, new supercond./mag. cpds., X-ray powder diffr. data 80−100215
$ErRh_{1.1}Sn_{3.6}$, synthesis, supercond. and mag. props. 80−100547
$Er_{1-x}Tm_xRh_4B_4$, mag. and supercond. transitions, cryst. field effects 80−107950
$Er_xY_{1-x}Rh_4B_4$, mag. and supercond. transitions 80−70874
$Er_xY_{1-x}Rh_4B_4$, supercond. phase transitions, recentering temp. to normal ferromag. state 80−7024
$(Eu,Sn)Mo_6S_8$, ternary superconductor, mag. interactions 79−73613
$EuIr_2$, superconductivity 79−78248
$EuMo_6S_8$, Chevrel phase, RE mag. isolation and supercond. 80−44470
$EuMo_6S_8$, Chevrel phase, mag. interactions, LMTO energy band studies 80−70606
$Eu_xSn_{1-x}Mo_6S_8$, Chevrel phase, cond. electron polarisation by Eu^{2+}, effect on supercond. props. 79−56650
$Eu_zSn_{1-z}Mo_6S_y$, supercond., mag. props. 77−69447
ε-Fe, low temp. supercond., transition temp. estimated 80−34540
Ga, films, distorted, crit. mag. fields *(Russian)* 78−39273
Ga-Cu, fast quenching of A15-phases *(German)* 77−36014
GaP, metallic modification, supercond. transition temp. at high temp. *(Russian)* 77−80867
$Gd_xCe_{1-x}Ru_2$, magnetic ordering by ^{155}Gd Mossbauer spectroscopy 78−27139
$Gd_xCe_{1-x}Ru_z$, coexistence of supercond. and spin glass mag. freezing 77−28283
$Gd_xEr_{1-x}Rh_4B_4$, effects of Gd ion on supercond. transition temp., mag. transition temp. and upper crit. field 79−56392
$Gd_xEr_{1-x}Rh_4B_4$, ferromag. and structural transitions, low temp. calorimetric meas. 79−55888
$Gd_xEr_{1-x}Rh_4B_4$, mag. and supercond. transitions 78−68127
$Gd_xEr_{1-x}Rh_4B_4$, mag. ordering near supercond. region 79−73696
$GdMo_6S_8$, Chevrel phase, RE mag. isolation and supercond. 80−44470
$GdMo_6S_8$, coexistence of antiferromagnetism and superconductivity, neutron diffraction study 79−99685
$GdMo_6S_8$, long range mag. order in supercond. state 79−65653
$Gd_{1.2}Mo_6S_8$, low temp. heat capacity anomaly rel. to antiferromag. transition in supercond. state 80−25044
$Gd_xMo_6S_8$, Chevrel phase, lattice instabilities, X-ray diffr. meas. 78−34491
$Gd_{0.1}Mo_6Se_8$, mag. supercond., low temp. sp. ht. meas. 79−56380
$Gd_{1.2}Mo_6Se_8$, coexistence of supercond. and long range antiferromag. order 80−84534
$Gd_xTh_{1-x}Ru_z$, coexistence of supercond. and spin glass mag. freezing 77−28283
$Gd_xY_{1-x}Rh_4B_4$, mag. and supercond. transitions 78−68127
Ge-Sn barriers, Josephson tunnelling 79−28468
$Ge_{0.6}Cu_{0.2}Au_{0.2}$ film, superconducting transition temp., resistivity meas. 77−43774
$HbSe_2$:Mn layered superconductor, crit. temp. and fields 77−51836
Hf-V, superconductivity and metallurgy of C15 materials 79−4610
Hf-V foil, rapidly quenched and heat treated, supercond. props. 80−54852
$HfC_xN_yO_z$, valence band XPS, correl. to supercond. 79−65980
$HfGe_2$ film, supercond. obs. 77−72939
HfV_2, C-15 struct., phase transitions, elec. cond., crystal lattice parameters *(Russian)* 80−54826
HfV_2, C15 Laves phase, supercond. and stoichiometry 78−39245
HfV_2, C15 supercond., dielec. transitions, temp. depend. of resist. and mag. susceptibility, 4.2-300K 79−38136
HfV_2, dielectric phase transition, elec. resist. temp. depend. 79−65525
HfV_2, elec. resist. and mag. suscept., anomalous temp. depend. 79−69491
HfV_2, supercond., dielec. phase transition *(Russian)* 78−64168
HfV_2, thermal expansion at low temp. 78−76189
HfV_2H_x and HfV_2D_x, composition depend. of supercond. crit. temp. 77−20482
$HfV_2H_x(D_x)$, superconducting transition temp. var., isotope effect 77−12047
$Hf_{1-x}Zr_xV_2$, lattice consts. at 4K and room temp., phase division at x=0.4 78−51474
$Hf_{0.5}Zr_{0.5}V_2H_x(D_x)$, enhanced supercond. transition temp. on H(D) additions 78−80083
Hg filament, crit. mag. field and supercond. transition temp. 77−16013
Hg-Xe vapour deposited films, cond. transitions, effect of disorder on supercond. 80−88659
$Hg_{2.86}AsF_6$, anisotropic supercond. caused by Hg extrusion, DTA 78−55953
$Hg_{2.86}AsF_6$, linear-chain cpd., anisotropic Meissner effect, magnetisation meas. 77−85387
$Hg_{3-\delta}AsF_6$, linear chain compound, mag. field induced residual resist., anisotropic supercond. 80−24897
$Hg_{3-x}AsF_6$, supercond., absence of surface Hg 80−20350
$Hg_{2.91}SbF_6$, anisotropic supercond. caused by Hg extrusion, DTA 78−55953

type II superconductors continued
$Ho(Ir_xRh_{1-x})_4B_4$ pseudoternary system, supercond. and mag. ordering 80−70876
$Ho_{1.15}Lu_{0.05}Mo_6S_8$, long range mag. order in supercond. state 79−65653
$HoMo_6S_8$, long range mag. order in supercond. state 79−65653
$HoMo_6S_8$, reentrant supercond., direct. obs. of long range ferromag. order 78−76190
$HoMo_6S_8$, superconductor, neutron scatt. exam. of mag. phase 79−73680
$Ho_{1.2}Mo_6S_8$, re-entrant ferromag. supercond., heat capacity and AC mag. susceptibility 79−60948
$Ho_{1.2}Mo_6S_8$, supercond. destruction by mag. ordering 77−69449
$Ho_{1.2}Mo_6S_8$, supercond. transition temp., upper critical field, local spin fluctuations 79−38250
$HoMo_6S_8(Se_8)$, mag. supercond., neutron scatt. obs. 80−70952
$Ho_{1.2}Mo_6Se_8$, crystal field excitations, inelastic neutron scatt. obs. 79−78321
In alloys, superconducting transitions temp. rel. to electronic struct. 77−80865
In film, Josephson arrays, proximity effect junctions 80−84553
In film, metastable current states, mean free path variation *(Russian)* 80−2538
In superconducting films, metastable states, supercooling fields 80−97031
In, superconductivity destruction singularities, intermediate state, hysteresis *(Russian)* 80−80460
In whiskers from Sn-In alloys, current carrying, superconductivity breakdown 80−60133
In-Bi, crit. RF mag. field, rel. to superheating 78−2632
In-Bi, mixed state, pinning centre distrib. statistics, I-V characts. *(Russian)* 80−100571
In-Bi, single spheres, supercond. props. 79−73617
In-Bi (2 at.%), supercond. film, thermal cond. in perpendicular mag. field 77−8229
In-Bi (2-33.3 at.%), phase diagram DTA, X-ray diffr. and supercond. T_c meas. 79−38795
In-Bi (22 at.%), directionally grown eutectic two phase superconductors, magnetisation behaviour 77−28293
In-Bi(Tl)(Pb), small κ supercond., phase transitions higher than second order 80−88668
In-Cr film, electronic thermal cond., 1.5 to 3K 77−47934
In-Cr(Mn) films, supercond., sp. ht. discontinuity and transition temp. meas. 79−60969
In-Mg, ordered equiatomic, lattice specific heat meas., Debye temp., superconducting transition 80−54396
In-Mn, dil., supercond. film, H_{c2} meas., mag. impurity effects, pair breaking theory 79−42708
In-Mn, discontinuity in sp. ht. at supercond. transition 79−60971
In-Pb (7 at.%) alloy cylinder, magnetisation change induced by current near upper crit. field 80−70890
α-In-Sn, stress depend. of supercond. parameters 77−12045
In-Sn alloy, Lifshits transition, electron-phonon interaction 80−29502
In-Sn alloy, phonon spectra and superconductivity, single-particle electron-tunnelling expts. 77−40005
In-Sn film, supercond. transition temp. and crit. currents *(Russian)* 77−55632
In-Sn(Pb)(Tl) alloy whisker, crit. temp., stress depend. 77−39988
In-Tl alloy, superconducting transition temp., phonon mode softening 79−1637
In-Tl alloys, supercond. transition in martensitic two phase region 77−72936
In_2Bi, magnetisation curve, interpretation using boson formulation of supercond. 78−2619
In_2Bi, press.-induced supercond. phase transform. 79−24099
In_2Bi-In, thin lamellar eutectic strips, unidirectionally solidified, morphologic and crystallographic study *(French)* 77−55264
In_2Bi-In(Bi) laminar eutectic alloy, SNS struct., Josephson behaviour *(French)* 78−26996
$In_xMo_3S_4$, chevrel phase, charge transfer and valence electron conc. 78−6029
$In_xMo_6S_8$, Chevrel phase, lattice instabilities, X-ray diffr. meas. 78−34491
$In_2Mo_{15}Se_{19}$, superconducting chalcogenides containing Mo_6 and Mo_9 clusters 80−103804
$In_{\sim 3}Mo_{15}Se_{19}$, high field supercond., crit. temp. and crit. field 79−47211
$In_xMo_{15}Se_{19}$, new ternary Mo(II) compounds, containing Mo_6Se_8 and Mo_9Se_{12} units, X-ray diffr. study 79−65056
In_3Sn, anisotropy of upper crit. field 80−20360
β-In_3Sn, crystn., decomp. and superconductivity 79−91579
In_3Sn, superconductivity, and phase diagram of In-Sb system 79−38794
In_3Sn, tetragonal supercond., lower and upper crit. field, anisotropy and temp. depend. 80−97042
$In_{0.69}Tl_{0.31}$, supercond. transition temp., specific heat, pseudopotential form factor 80−97026
In−Gd film, dil., fluctuation induced cond. above supercond. transition temp. 79−47196
Ir borides, MIr_3B_2 (M=La, Th, U), supercond. and mag. props. 80−97028
Ir, thin film, supercond. props. 79−56444
Ir-Y eutectic alloy, supercond. transition enhancement due to lattice softening 80−103775
$K_2Mo_{15}S_{19}$, superconducting chalcogenides containing Mo_6 and Mo_9 clusters 80−103804
$K_2Mo_{15}Se_{19}$, superconducting chalcogenides containing Mo_6 and Mo_9 clusters 80−103804
$K_{0.33}WO_3$, supercond. and special phonons, neutron scatt. obs. 80−15643
$(La,Ce)Al_2$ and $(La,Gd)Al_2$, magnetic impurity effect on thermal cond., normal and supercond. states 77−63027
$(La,Ce)Ru_2$, supercond. transition temp., its press. depend., and structural phase transform. 78−6473
(La, Ce)Sn_3, dil. alloys, supercond. and normal state props. 78−76184
$(La,Gd)Al_2$, normal and supercond. state, US attenuation, freq. depend. and mechanisms 80−49992
(La,Na)Sn alloys, supercond. transition temp. 79−78254
(La, Nd)Sn_3, cryst. field effects, normal and supercond. props. 79−60973
(La, Nd)Sn_3, superconducting props. 79−60958
(La,Y)Ce, dil., Kondo supercond., transition temp., susceptibility and resist. 80−65733
La, DHCP and FCC phases, phonon density of states 78−67791
La film, tunnelling investig., multiple band effects 77−8244

type II superconductors continued
La, heat capacity and supercond. props. 80−65247
La particles, supercond. props. *(Russian)* 80−7018
La, superconducting, electron-phonon coupling, hydrostatic press. depend. 78−80087
La, transition temp., press. depend., mode softening 78−14847
La-Ag alloys, amorphous, elec. resist. and supercond. 80−70885
La-Al(Ge)(Au), amorphous, alloying effect on supercond. props. 79−60951
La-Au, splat-quenched, Mossbauer effect and elec. resist., amorphous struct. 80−84676
La-Ce, Kondo system, intermediate temp. supercond. under hydrostatic press. 79−24097
La-Er, superconducting, EPR for localised Er mag. moments *(Russian)* 77−47931
La-Eu, dil., DHCP, impurity effects on T_c, electron pair breaking 77−36013
La-Eu(Gd), EPR investig. of local moment, correl. with supercond. props. 77−63282
La-Gd, dil., DHCP, impurity effects on T_c, electron pair breaking 77−36013
La-Gd(Tb,Dy,Ho,Er,Tm) alloys, FCC, supercond. transition temp. 79−4614
La-In alloys, cohesive and superconducting props. from electronic struct. calcs. 79−99113
La-pnictides, supercond. props. 77−85366
La-Pr, superconductive tunnelling, cryst. field effects 78−88085
La-Sm-Sn, dil. alloy, Kondo effect obs., supercond. transition temp. meas. 77−51837
LaAg, Tb and Pr substituted, superconductors, cryst. field transitions linewidths 80−24854
LaAg, under hydrostatic press., supercond. and phase transform, elec. resist., 1-300K 78−10595
$LaAl_2$, doped with Tb, Nd, or Pr, crystal field effects, tunnelling within mK range 80−70907
$LaAl_2$, supercond. and normal states, anomalous US attenuation and velocity change 80−80446
$LaAl_2$, Tb and Pr substituted, superconductors, cryst. field transitions linewidths 80−24854
$LaAl_2$:Gd^{3+}(Eu^{2+}), cryst. field parameters, relax. rates 78−84482
$LaAl_2$:Gd(Ce), supercond., electronic thermal cond. 77−12063
La_4As_3, superconductivity 77−20481
$La_{100-x}Au_x$, amorphous film, stability, supercond. temp. and residual resistivity 79−4636
$La_{18}Au_{22}$, amorphous, evidence for short wavelength cutoff in fluctuation spectrum 78−68113
$La_{1x}Au_x$, splat cooled amorphous alloy, sp. ht. 78−19182
$La_{78}Au_{22}$, amorphous supercond., T_c and fluctuation cond. under high press. 79−7935
La_4Bi_3, La_3Bi_2Pb and La_4BiPb_2, superconductivity 77−20481
La_2C_3, solid solution, lattice const. and superconducting transition temp. *(Russian)* 80−92496
$La_{1-n}Ce_n$, supercond. mag. alloy, effect of interconfigurational fluctuations 78−19175
$La_{1-c}Ce_cAl_2$, Kondo superconductor, self-consistent theory of pairbreaking 78−26989
$(La_{1-n}Ce_n)_3Al$, mag. impurity effects in normal and supercond. state, NMR 78−2622
$(La_{1-x}Ce_x)Al_2$, Kondo supercond., tunnelling density of states 78−14900
$(La_{1-x}Ce_x)Al_2$, Kondo supercond., tunnel junction fabrication with wax barriers, tunnelling meas. 78−19191
$La_{1-x}Ce_xAl_2$, supercond., nucl. relax. and impurity magnetism 77−20495
$La(Ce)Sn_{3-x}Pb_x$ system, mag. impurities in supercond., supercond. transition temp. and sp. ht. 78−39244
LaCeY, three normal supercond. transitions 78−26989
LaEu, mag. supercond., phase diagram, bulk susceptibility meas. 77−59353
$La_{1-x}Ga_x$ foils, amorphous, splat cooled, calorimetric and resistive meas. 79−33417
$(La_{1-n}Gd_n)_3Al$, mag. impurity effects in normal and supercond. state, NMR 78−2622
$La_{1-x}Gd_xAl_2$, supercond., nucl. relax. and impurity magnetism 77−20495
$La_{80-x}Gd_xAu_{20}$, amorphous, supercond. and spin-glass regime, magnetisation and resist. meas. 77−36011
$La_{3-x}Gd_xIn$, mag. impurity ordering and superconductivity, EPR exam. *(Russian)* 77−8400
$(La_{1-x}Gd_x)_{1.0}Mo_6Se_8$, Gd-rich, supercond. state, phase transition, lambda-type sp. ht. anomaly obs. 78−6480
$La_{1-x}Gd_xMo_6Se_8$, supercond. transition temp., upper critical field, local spin fluctuations 79−38250
$La_{1-x}Gd_xRu_2$, mag. ordered superconductor, re-entrant superconductivity 78−88059
$LaGe_2$ film, supercond. obs. 77−72939
$LaGe_x$, specific heat in range $0.07 \leq T \leq 10K$, comp. depend. 78−43517
La_3In, supercond. T_c, alloying effects 79−38227
$(La_{0.993}Lu_{0.007})_{1-x}Gd_xRu_2$, exchange enhanced supercond., compensation effect on H_{c2} 77−4474
LaM_2-Gd, M=transition metal, correl. between g-shift and stability, EPR study 80−88874
$LaMo_6S_8$ thin films, crit. currents and pinning forces 80−34575
$La_xMo_6S_8$, Chevrel phase, lattice instabilities, X-ray diffr. meas. 78−34491
$LaMo_6X_8$ (X=S, Se), supercond., sp. ht., 1 to 14K 79−51720
(LaNd)Sn_3, containing Nd impurities, supercond. and normal state props. 80−49967
$LaPb_3$, doped with Tb, Nd, or Pr, crystal field effects, tunnelling within mK range 80−70907
$LaPb_3$, Tb and Pr substituted, superconductors, cryst. field transitions linewidths 80−24854
$La_{80-x}Pr_xAu_{20}$, amorphous, mag. and supercond. props. 80−75713
$La_{1-x}Pr_xPb_3(Sn_3)$, cryst. field excitations, inelastic neutron scatt. obs. 80−15653
(LaPr)Sn_3, supercond., free energy and thermodynamical crit. field 77−32127
$La_{1-x}Pr_xSn_3$, supercond., 0.6 meV cryst. field transitions, neutron spectroscopy 78−67991
$La_{1-y}Pr_ySn_3$, neutron spectroscopy of 0.6 meV cryst. field transitions 78−30894
$LaRu_2$, H absorption induced Ce valence change, mag. and supercond. props. 80−50042
$LaRu_2$, supercond. disappearance on H absorption 79−47185
$LaRu_2$, type II supercond., ESR of Nd^{3+} meas. 79−28444
$LaS_{1.33}$-$LaS_{1.40}$, low temp. sp. ht. 80−15259
La_3S_4, high crit. mag. field supercond., elec. resist., sp. ht. and magnetisation 80−2532
$La_3S_4(Se_4)$, structural transitions, symm. anal. 80−92671
La_4Sb_3 and $La_4(Sb_{0.5}Bi_{0.5})_3$, superconductivity 77−20481
$La_{1-x}Sm_xSn_3$, Kondo scatt. from Sm ions 77−51734
$LaSn_3$, dilute alloy containing light rare earth impurities, press. depend. of supercond. transition temp. 79−47184
$LaSn_3$, doped with Tb, Nd, or Pr, crystal field effects, tunnelling within mK range 80−70907
$LaSn_3$, Tb and Pr substituted, superconductors, cryst. field transitions linewidths 80−24854
La_3Sn, cubic phase, high press. and high temp. synthesis, and characterisation 78−19687
$La_{0.98}Sn_{0.02}Mo_6Se_8$, Chevrel phase supercond., hyperfine interaction, microscopic study 79−56650
$La_{0.98}Sn_{0.02}Mo_6Se_8$, Mossbauer spectra 80−15926
$La_{1-x}Tb_xAg$, supercond., 0.6 meV cryst. field transitions, neutron spectroscopy 78−67991
$La_{1-y}Tb_yAg$, neutron spectroscopy of 0.6 meV cryst. field transitions 78−30894
$La_{1-x}Tb_xAl_2$, supercond., 0.6 meV cryst. field transitions, neutron spectroscopy 78−67991
$La_{1-y}Tb_yAl_2$, neutron spectroscopy of 0.6 meV cryst. field transitions 78−30894
$La_{1-x}Tb_xSn_3$, supercond., 0.6 meV cryst. field transitions, neutron spectroscopy 78−67991
$La_{1-y}Tb_ySn_3$, neutron spectroscopy of 0.6 meV cryst. field transitions 78−30894
$La_{0.80}Th_{0.20}Ce$, re-entrant supercond. matrix-impurity system additive pair breaking 77−69460
$(La_{1-x}Th_x)_{1-n}Ce_n$, supercond. mag. alloy, effect of interconfigurational fluctuations 78−19175
$(La_{0.80}Y_{0.20})Ce$, three superconducting crit. point behaviour 78−10625
$La_{1-y}Y_y(Ce)$ system, mag. impurities in supercond., supercond. transition temp. and sp. ht. 78−39244
$LaYSb_3$, superconductivity 77−20481
$Li_6In_2O_6$, ionic cond. rel. to cryst. struct. 79−77810
Li_7LO_7 (L=Nb, Ta), ionic cond. rel. to cryst. struct. 79−77810
Li_8MO_6 (M=Zr, Sn), ionic cond. rel. to cryst. struct. 79−77810
$LiTi_2O_4$, prep., characterisation and supercond. props. 77−40010
$LiTi_2O_4$, press. depend. of supercond. transition temp. meas. 77−12050
$LiTi_2O_4$, single-phase, prep., crystal struct. and superconducting transition characts. 80−50583
$Li_{2.6}Ti_xO_4$, upper critical field, paramag. limiting effects 77−8251
$Li_{0.33}WO_3$, supercond. and special phonons, neutron scatt. obs. 80−15643
Lu_2C_3, superconductivity 79−73621
$(Lu_{1-x}Ho_x)Rh_4B_4$, interaction between superconductivity and magnetism 79−38248
$LuMO_6X_8$ (X=S, Se), supercond., sp. ht., 1 to 14K 79−51720
$LuRh_4B_4$, superconducting and normal state props. 79−73632
Mo and Nb-Mo alloys, superconductivity and phonon softening, between electron bands and phonons 78−14859
Mo chalcogenide superconductors with $T_c > 10K$ 79−33381
Mo, electron-phonon coupling and supercond. transition temp. 79−56360
Mo, isotopic vol. effect confirmation by energy-dispersive X-ray diffr. 77−36019
Mo selenides, ternary, Chevrel phase supercond., compressibility and vol. depend. of Tc 78−31008
Mo sulphides, ternary, Chevrel phase supercond., compressibility and vol. depend. of Tc 78−31008
Mo sulphides, ternary $M_xMo_6S_8$, crit. currents in strong mag. fields *(Russian)* 77−43796
Mo superconducting film, amorphous and crystalline, transition temp. exam. by UPS 79−28433
Mo ternary chalcogenide, MMo_6X_8 (M=metal, X=chalcogen) Chevrel phase, supercond. and normal state props. 78−56267
Mo ternary chalcogenides, band struct., muffin-tin orbitals and atomic-sphere approx. 78−51871
Mo ternary chalcogenides, supercond. props. 79−38230
Mo ternary cpds., $R_ySn_xMo_6S_8$ (R=La, Ce, Pr, Eu, Gd, Ho, Lu, Y, In, U), supercond. props. 80−97023
Mo, transition temp., perturbative corrections, direct and indirect ladder diagrams 80−49979
Mo:N film, high T_c amorphous phase stabilisation by interstitial nitrogen 78−23622
Mo:N film, implantation effect on supercond. and struct. transform. 77−4462
Mo-Be solid solutions, superconducting transition, temp. changing peculiarity due to press. *(Russian)* 80−70878
Mo-chalcogenides, crit. mag. fields *(Russian)* 78−34936
Mo-Ge(Bi) amorphous films, supercond. transition temp. and residual elec. resist. *(Russian)* 79−19680
Mo-Re, σ phase alloy, critical mag. field, elec. resistance 80−54850
Mo-Re (5 at.%), enhanced lattice sp. ht. due to LF reson. modes 78−14882
Mo-Re alloys, supercond. energy gap and transition temp., tunnelling meas. 79−56405
Mo-Re film, electron beam deposited, supercond. transition temp. conc. depend. 77−28279
Mo-Ru(-Si), amorphous superconductors, prep. by electron beam evaporation and liq. quenching, crit. temp. 80−103776
Mo-Si(Ge)(Al), amorphous supercond. alloy, produced by coevaporation, struct. and supercond. 79−91179
Mo-Sn-Se system, supercond. crit. temp. and cryst. struct. *(Russian)* 80−107947
Mo-Tc system, supercond. behaviour, quick-quench production technique 78−56251
MoB_2, hexagonal, form. by plasma heating and props. 79−28996
Mo_3Ge, RF sputtered, crit. temp. 78−14853
Mo_3Ge, superconductivity, T_c related to disorder and density of states 79−15249
Mo_6NaS_8, specific heat and supercond. critical field *(Russian)* 77−77004
Mo_3Os, effect of high energy neutron irradiation on supercond. transition temp. 77−36012

type II superconductors continued
$Mo_{80}P_{10}B_{10}$, amorphous supercond. high-κ, upper and lower crit. fields 79−4629
Mo_5PbS_8 embedded in resin, composite supercond., high transition temp. 80−88660
Mo_xRe_{1-x}, (x=0.4 and 0.6), search for strong coupling superconductivity 79−28441
$(Mo_{0.6}Ru_{0.4})_{82}B_{18}$, supercond. metallic glass, neutron irrad. effects 80−29060
$(Mo_{0.6}Ru_{0.4})_{0.8}G_{0.2}$-Fe (G=P,B), amorphous supercond., upper crit. field as function of temp. 79−73646
$(Mo_{0.5}Ru_{0.5})_{80}P_{20}$, amorphous normal and mixed supercond. state, ^{31}P NMR 79−87193
$(Mo_{1-x}Ru_x)_{80}P_{20}$, amorphous alloys, superconductivity, mag. susceptibility and electronic props., liq. quenching 78−88057
$(Mo_{1-x}Ru_x)_{80}P_{20}$, amorphous, liq. quenched, mag. susceptibility, supercond. and electronic props. 79−56376
$(Mo_{1-x}Ru_x)_{80}P_{20}$, liq. quenched amorphous allot, props. 78−88057
$(Mo_xRu_{1-x})_{80}P_{20}$, amorphous supercond., high-κ, upper and lower crit. fields 79−4629
$(Mo_{0.6}Ru_{0.4})_{80}Si_{10}B_{10}$, amorphous supercond. matrix, flux pinning by MoRu precips. 80−65756
Mo_5RuTe_8, synthesis, struct., and elec. props. 80−92877
MoS_2 intercalation compounds, reaction with alkali and alkali earth metals, band struct., superconductivity 78−26541
MoS_2 molybdenite band structural props. rel. to supercond. and semicond. 80−96781
Mo_6S_8 Chevrel phases with group IIIa metals, Nb, Hg, Pb and Cu, synthesis, stability and characts. 80−71608
Mo_6S_8, relationship between electronic struct. and supercond. transition temp. 77−85368
$Mo_6S_6Br_2$, supercond., crit. temp. meas. 77−85367
$Mo_6S_6I_2$, supercond., crit. temp. meas. 77−85367
$Mo_6S_8(Se_8)$, heat capacity and mag. props., 2-30K 79−42692
$Mo_6S_8(Se_8)(Te_8)$ and halogen substituted cpds., sp. ht. capacity 80−49986
Mo_6S_xSn, triple chalcogenide, NMR spectra in supercond. state *(Russian)* 80−93194
Mo_3Se_4, low temp. struct. stability rel. to supercond. 77−47919
Mo_6Se_8, Chevrel phase, anisotropy of H_{c2} 79−56460
Mo_6Se_8, Chevrel phase, isotope effect on supercond. T_c 78−52141
Mo_6Se_8, Chevrel phase, isotope effect on supercond. transition temp., phonon modes 79−51713
Mo_6Se_8, Chevrel phase, supercond. isotope effect meas. *(German)* 80−25038
Mo_6Se_8, Chevrel phase supercond., phonon spectra, neutron scatt. meas. 79−42174
Mo_6Se_8, isotope effect, theory 78−91806
Mo_6Se_8, isotope effect on transition temp. 79−73615
Mo_6Se_8, relationship between electronic struct. and supercond. transition temp. 77−85368
$Mo_6Se_{8-x}Br_x$, supercond. obs. crit. temp. determ. 77−85367
$Mo_6Se_{8-x}I_x$, supercond. obs. crit. temp. determ. 77−85367
Mo_6Se_8Sn, triple chalcogenide, NMR spectra in supercond. state *(Russian)* 80−93194
$Mo_{70}Si_{20}B_{10}$, amorphous alloys obtained by liq. quenching, superconductivity 80−75670
$Mo_5SnGa_xS_6$ heat capacity from 2 to 25K 78−43518
Mo_5SnS_6, supercond., at 2 to 25K, lattice and electron contrib. to sp. ht. 77−77003
$Mo_{0.18}Tc_{0.82}$, search for strong coupling superconductivity 79−28441
$Mo_{0.4}Tc_{0.6}$, A15 and BCC, sp. ht., 4-20K 78−68111
$Mo_{1-x}Tc_x$, BCC, sp. ht. in normal and supercond. phases 79−87190
$Mo_6Te_{8-x}I_x$, supercond obs., crit. temp. determ. 77−85367
$Mo_{1-x}V_x$, NMR and mag. susceptibility meas. 79−56388
Mo_6X_8 (X=S, Se), phonon density of states, mode softening correl. with supercond. transition temp. 79−51714
$(NH_4)_{0.33}WO_3$, supercond. and special phonons, neutron scatt. obs. 80−15643
NaCl, high press. metallic modification, superconduction obs. *(Russian)* 79−65576
Na_xWO_3, anomalous supercond. transition temp., electron pairing by acoustic plasmon exchange 79−56358
Na_xWO_3, crit. temp., semiempirical model for lattice instabilities in non-stoichiometric materials 78−14442
Na_xWO_3, dynamic fluctuations between local struct. states in supercond. TI phase 78−26981
Na_xWO_3 enhanced T_c, interband coupling 78−91804
(Nb,Ti)N_x, metastable supercond. phase, effects of rapid quenching on transition temp. 78−2611
Nb A15 compounds, preferential order-disorder 77−84702
Nb alloy film, multisource deposition rate control using mass spectrometer as sensing element 78−72730
Nb alloys, supercond. and normal phases, electron scatt. and lattice thermal cond. 77−77001
Nb and alloys, dynamic destruction of supercond. 77−69461
Nb and Nb-Mo alloys, superconductivity and phonon softening, between electron bands and phonons 78−14859
Nb, and Nb-V alloy, T_c and H_{c2}, effect of purity and alloying with Ta, Cr, Mo or Re 77−85375
Nb, anisotropy of crit. field, magnetisation meas. 79−78260
Nb, at thermally oxidised junctions, supercond. parameters determ. 79−19699
Nb based, electron probe comp. meas. 77−12852
Nb based A-15 type, universal defect behaviour, transition temp. rel. to lattice parameter 77−69440
Nb, bulk granular supercond., thermal fluctuations compared to Josephson weak link array 78−43520
Nb cavities, RF, expectations and limitations 79−1648
Nb, clean, fluctuations and sound attenuation near T_{c2}(B) 77−15996
Nb, critical current density, deviation from critical state model 80−84578
Nb, critical field, muon spin relaxation *(German)* 80−50015
Nb, cylindrical and ellipsoidal, rotational magnetisation and torque meas. in mag. field 78−43515
Nb, effect of changes in $\alpha^2(\Omega)F(\Omega)$ on the zero-temp. energy gap 80−97025
Nb, effect of O ion irradiation on supercond. 78−52131
Nb, electron beam evaporated film, struct., supercond., purity *(German)* 77−52253
Nb, electron drag on mobile dislocations, flow stress meas. 79−91197

type II superconductors continued
Nb, electron-coupled phonon spectrum, effects of strain 79−7943
Nb, electron-phonon contrib. to phonon linewidth determ. 78−10146
Nb, electron-phonon interaction electronic contrib. 77−15524
Nb electron-phonon interaction, calc. using APW band struct. calcs. and measured phonon spectra 78−14869
Nb, electron-phonon spectral function and mass enhancement 78−26988
Nb, Eliashberg eqns., numerical solns. Fermi surface calcs. 77−1514
Nb, fabrication of supercond. weak links, electron beam lithography and ion implantation 78−47913
Nb, Fermi surface, Fermi velocity, electron-phonon interaction parameter 79−7778
Nb, field history effect of flux gradient 78−91828
Nb film, bias sputtering prep. 79−1826
Nb film, crit. temp., crit. field, and surface resist. 77−55635
Nb film, critical currents due to microwave field 80−25058
Nb, film, critical mag. fields and currents, temp. depend. *(Russian)* 80−103798
Nb film, deposited in quasi-closed vol., supercond. props. 79−91180
Nb, film, epitaxy, struct. and supercond. props., on (001) surface of fluorophlogopite *(Russian)* 80−80101
Nb film, far IR reflection and transmission spectra, room temp. 77−55792
Nb film, magnetron-sputtered, intrinsic stresses and supercond. props. 80−24772
Nb film, struct. and electrophys. props. at 4.2K 80−80436
Nb film, supercond. relax. phenomena at microwave freqs. *(Russian)* 79−47187
Nb film, superconducting tunnelling, meas. of annealing characteristics 79−7944
Nb, film, surface impedance 79−24110
Nb, film, switching, storage and erasure effects 77−8253
Nb film, transition temp. and crit. current, Gd ion implantation effects 77−39986
Nb film, transition temp. and transition width, impurity effects *(Russian)* 77−66222
Nb film, vac. deposited, deposition parameter effects on crit. temp. 80−2514
Nb, film microbridge, fabrication and I-V characts. 79−87198
Nb film sputtered onto Cu substrate, microstruct. and supercond. props. 77−85370
Nb films, ion beam sputtered, supercond., laser annealing effects 80−97024
Nb films, penetration depth measured with Nb-NbO_x-PbIn Josephson junctions 79−42691
Nb films, supercond. props. and electronic density of states *(Russian)* 79−28439
Nb, fluctuation contrib. to sound attenuation near H_{c2} 79−33397
Nb, fluxoid lattice, eqn. props., small-angle neutron diffraction measurements 80−34573
Nb, fluxoid lattice, eqn. props., magnetisation measurements 80−39725
Nb foil, cross correlation measurements on moving vortex arrays 79−24117
Nb foil, time behaviour of local flux flow noise 79−24116
Nb, for supercond. microwave cavities, secondary electron emission and AES meas. 79−56895
Nb granular films, ratio of supercond. transition temps. 80−84529
Nb granular films as weak link in Josephson devices 80−88685
Nb, granulated film, critical current temp. depend. *(Russian)* 80−103803
Nb heteroepitaxial layers on sapphire, residual mechanical stress and strain influence on superconductivity 80−15644
Nb, high crit. flux density gradient near surface 79−87221
Nb, high field de Haas van Alphen spectroscopy 79−73425
Nb, high frequency cyclotron resonance study 79−11057
Nb, hypersonic attenuation near critical field H_{c1} 77−77005
Nb, hysteresis in time depend. fields up to 3 kOe 77−24637
Nb, impurity conc. monitoring during single cryst. production, use of nuclear phys. methods 78−31337
Nb, inhomogeneity detection by penetration depth meas., proximity theory 77−28288
Nb, irradiated superconductor, fluxoid defect interactions 78−52166
Nb layer, ion bombarded, supercond. props. and struct. 80−88671
Nb, magnetoresist. and mag. breakdown in field up to 175 kOe *(Russian)* 77−20492
Nb microbridges, heating and flux flow, I-V curves and microwave mixing 79−28474
Nb, microwave cavity of muffin-tin type, for accelerator use 77−26905
Nb, momentum dependence of electron-phonon interaction 79−7665
Nb, nanobridges Josephson effect, quasiparticle diffusion time, inelastic scatt. time 80−34556
Nb, O enrichment of surface layers, penetration depth and resist. meas. 78−19180
Nb, O_2 diffusion profiles in surface layer 79−24101
Nb, optical props. and electron-phonon interactions 80−2510
Nb, peak effect due to vortex pinning in subsurface layer *(Russian)* 80−93060
Nb, phonon linewidths and electron-phonon interaction 79−73273
Nb, plastic deform., Shubnikov phase penetration, Faraday effect obs. 79−82731
Nb, plastic deform. effect on positron annihilation and supercond. transition *(Russian)* 77−39993
Nb, plastic deformation effects on superconducting specific heat transition 80−20352
Nb, plastically deformed, changing lattice dynamics 78−67793
Nb, plastically deformed, flux density gradients and pinning forces, Faraday effect obs. 79−61010
Nb point contact, 9 GHz complex impedance 77−28303
Nb point contacts, AC Josephson effect meas. at 604 GHz 77−80876
Nb, point contacts, freq. and voltage depend. in noise background 79−58796
Nb point contacts, Josephson effects in far IR, high freq. behaviour 79−1643
Nb pure single crystal, low-κ type II superconductors, determ. of low field critical parameters 79−11278
Nb pure single crystals, anisotropy in flux-line lattice symmetry of low-κ type II superconductor, neutron diffr. study 79−11279
Nb, RF superconductivity, appl. to particle acceleration, overview 79−31244
Nb, single cryst., anomalous US attenuation at low temps. 78−43076
Nb, single cryst., superconductive tunnelling meas. 79−47203

type II superconductors continued
Nb, single crysts., fluxoid pinning by small nitride precips. 80−70913
Nb slab, inductive response to trapezoidal magnetic field 78−39277
Nb spheres, residual resistivity ratio, prep. method effects *(German)* 79−8372
Nb, spin fluctuations effect on T_c, from sp. ht. and mag. suscept. 80−7030
Nb, sputter deposited film, O contamination, Auger anal. 78−52669
Nb, strong-coupling microscopic parameters, electron tunnelling obs. 78−14888
Nb, supercond., dielastic interaction of flux line lattice with internal stresses of cryst. imperfections 78−56270
Nb, supercond., influence of plastic deform. 77−85378
Nb, supercond. and normal state, thermal cond. meas., 0.05-23K 77−63025
Nb, supercond. crit. temp., functional derivative with electronic density of states, Eliashberg eqns. 79−56368
Nb, supercond. crit. temp. enhancement by radiation damage 78−2609
Nb, supercond. mixed state, US attenuation meas. near B_{c2} 78−64167
Nb, supercond. surface resistance derivative meas. for annealed and unannealed crysts. 79−33395
Nb, supercond. transition temp. from Eliashberg eqns. 79−51709
Nb, superconducting, AC losses surface effects 77−28313
Nb, superconducting, deformed, oscillation in current-voltage charact. near H_{c2} 79−28491
Nb, superconducting, state of art of tunnelling 79−69634
Nb, superconducting, thermodynamic props. 80−107955
Nb superconducting amorphous film, conductivity and transition temp., ion bombardment effects *(Russian)* 80−49969
Nb, superconducting bridges by electron beam lithography and ion implantation Josephson effect 80−20355
Nb superconducting C-band cavities for linear accelerator appl. 79−36432
Nb superconducting cavities, AES depth profile meas. on oxide layer 77−8984
Nb, superconducting critical magnetic field and crit. temp. 79−7947
Nb, superconducting film, thickness depend. of electrophys. parameter *(Russian)* 78−10590
Nb superconducting film prod. by electron beam sputtering *(Russian)* 78−15308
Nb superconducting films, crit. depairing currents, temp. and mag. field depend. 80−7058
Nb, superconducting parameters, tunnelling meas. 79−91192
Nb, superconducting phonon struct. obs. in proximity tunnelling 77−77008
Nb, superconducting point contacts, cond. mechanism 79−56440
Nb superconducting point contact, high freq. props. in far IR 80−54840
Nb, superconducting state influence on dislocation motion *(Russian)* 80−70208
Nb, superconducting transition temp., correl. with resist. anomalies and defect struct. 77−47920
Nb, superconducting transition effect on electronic work function 77−47928
Nb, superconductive transition point as reference temp. 80−107943
Nb, superconductor, deformational twinning, mag. props. *(Russian)* 79−95543
Nb, superconductor, neutron irradiation, low temp., effect on critical current 78−52180
Nb, surface effect on crit. current density 79−61014
Nb, surface effect on critical current density 79−65627
Nb, T_c control by N ion implantation 78−2606
Nb, thermal cond., 0.3-20K, temp. and impurities effects 78−14883
Nb, thermo EMF and mag. breakdown *(Russian)* 77−80884
Nb, two-band supercond., attenuation of longitudinal ultrasound 77−51847
Nb, US attenuation, hysteresis near and below H_{c1} 80−75676
Nb, upper crit. field, temp. depend. and anisotropy 80−80462
Nb wire, Cu-clad, temp. sensor below 1K using proximity effect 79−85139
Nb wire, helical propag. of flux jumps 78−14901
Nb, with Nb_2N precipitates, flux pinning, magnetization, bulk flux density gradient, and neutron scatt. meas. 79−56472
Nb:He, implant saturation and annealing, effect on struct. and supercond. props. *(Russian)* 78−43538
Nb:N, H, atomic tunnelling of interstitial pair, specific heat meas. 78−47600
Nb:N,H(D), thermal cond., 0.07 to 1.5K, influence of N interstitials 79−65601
Nb:O, type II supercond., radiation-induced flux pinning 78−80106
Nb/Cu, layered ultrathin coherent structs., supercond. props. 80−84525
Nb/Cu-Sn-Mg, effect of Mg addition to Cu-Sn matrix 80−25028
Nb/H, heat capacity and supercond. between 1.5 and 16K 80−2521
Nb/In composite superconductor, transport props. 80−88658
Nb-Al, A15 and σ-phases, supercond. and normal state electronic props. 77−43765
Nb-Al alloy, A-15 struct., influence of composition on supercond. transition temp. 77−20486
Nb-Al alloy, σ-and A15-phases, Knight shift and supercond. 77−15984
Nb-Al film, Josephson junction, tunnelling exam. 79−38257
Nb-Al proximity sandwiches, supercond. transition temp. and tunnelling meas. 80−7045
Nb-Al-Si, supercond. transition temp., Si conc. depend. 78−84339
Nb-Al-(Ge) film, superconductor, high rate sputter deposition and heat treatment 77−36399
Nb-Al(Ga,Si,Ge,Sn)-Cu, equilib. and rapidly quenched, struct. and props. 80−76235
Nb-Al(Ga)(Ge), fast quenching of A15-phases *(German)* 77−36014
Nb-B, atomic order, stability, supercond. *(French)* 80−50021
Nb-Cu-Sn, cast supercond. alloy, crit. current, degradation resistance 78−76203
Nb-epoxy, interface, Kapitza resist. in supercond. and normal states 77−66085
Nb-Ga, A15 phase, chem. deposition on Hastelloy substrate, for superconducting tape *(German)* 80−104071
Nb-Ga, phase system form. and stability of A15 phase 77−90347
Nb-Ga (16 to 28 at.%), transition temp., upper critical field and magnetisation curves 77−80866
Nb-Ga alloy, A15 type, melt produces specimens, supecond., homogeneity, transition temp. *(German)* 78−2608
Nb-Ga-Cu, fast quenching of A15-phases *(German)* 77−36014

type II superconductors continued
Nb-Ga-Cu, phase diagram, metallographic and X-ray study, annealed and as-cast supercond. crit. temp. *(Russian)* 78−56617
Nb-Ga-Fe ternary system, phase equilib. at 1000°C, supercond. transition temp. 80−35158
Nb-Ga-Ir system, phase equilib. at 1000°C and supercond., Nb-rich portion 77−36480
Nb-Ga-Sc, superconducting transition temp., X-ray, microscopic and microprobe anal. *(Ukrainian)* 80−75667
Nb-Ga-Y, X-ray and microprobe anal., isothermal section and supercond. transition temp. *(Ukrainian)* 79−38793
Nb-Ge, A15 struct. superconductor, high field transport props. TEM study 80−34574
Nb-Ge, amorphous supercond. alloy, resistivity, transition temp. 80−60126
Nb-Ge, compounds with A15 structure, films, TEM study *(French)* 80−80135
Nb-Ge, supercond. A-15 phase, supercond. transition temp. after ion implantation 80−49972
Nb-Ge, superconductor, phase diagram determ. using various methods up to temp. of 2200°C 79−8414
Nb-Ge, supersuperconducting transition temp., correl. with resist. anomalies and defect struct. 77−47920
Nb-Ge, transition metal atom stabilised superconductivity 79−7924
Nb-Ge alloys, stoichiometry and phase equilibria, X-ray diffr. study *(French)* 79−70040
Nb-Ge film, coevaporated, supercond. critical temp. and struct. 77−28275
Nb-Ge film, supercond. transition temp., rel. to prep. conditions 77−36009
Nb-Ge film, TEM expts., correl. of struct. and elec. props. 78−14628
Nb-Ge film, two-phase, tetragonal Nb_5Ge_3 phase identification by electron diffr. 77−89665
Nb-Ge superconducting film, prod. by electron beam sputtering *(Russian)* 78−15308
Nb-Ge system, phase diagram determ. 79−38796
Nb-Ge vapour deposited films with T_c of ∼20K, preps. *(Japanese)* 77−12048
Nb-Ge-Cu, phase equilib. and supercond. props. *(Russian)* 80−40332
Nb-Ge-Ni, phase composition and superconducting props., influence of Ni *(Russian)* 80−20898
Nb-Ge-Si, A15 struct. superconductor, high field transport props. TEM study 80−34574
Nb-Ge-Si, compounds with A15 structure, films, TEM study *(French)* 80−80135
Nb-Ge-Si, Si effect on raising superconducting transition temp. in pelicular specimens *(Russian)* 78−23188
Nb-Ge-Si, supercond. state transition temp., influence of Si on alloy constitution *(Russian)* 79−78244
Nb-Ge-Si film, CVD, struct., comp., stability and homogeneity 80−15421
Nb-Ge-Sn A15 cpds., CVD, superconductivity 79−38222
Nb-Ge-Sn(Pt)(Ir), A15 cpds. prod. by liq. quenching, phase stability and supercond. props. 79−95538
Nb-Ge(Si), amorphous supercond. alloy, produced by coevaporation, struct. and supercond. 79−91179
Nb-Ge(Si) and Nb-Ge-Si, A15 cpds., CVD prep. and supercond. crit. temp. 79−60949
Nb-H systems, supercond., H conc. depend. *(Russian)* 77−47932
Nb-Hf (26 at.%), mixed state, ultrasonic velocity meas. 79−60974
Nb-Hf (38 at.%) superconductor, peak effect, summation problem, mag. history flux pinning force 80−20362
Nb-I-Pb junction, double-peak structure *(Russian)* 79−82716
Nb-Ir, A 15- and σ-phases, supercond. 79−73645
Nb-Ir-O, phase struct., supercond. H-phase 78−39246
Nb-Mo system, electron-phonon coupling const. and supercond. transition temp., average T-matrix approx. 80−39707
Nb-Mo-Tc alloys, supercond., point-group symmetry 78−64163
Nb-N, superconducting layers, sputtering in high vacuum apparatus *(German)* 80−89147
Nb-N system, ion-implanted, supercond. crit. temp., effect of implantation conditions 78−19176
Nb-Nb point contact junction, supercond. weak couplings, high-freq. props. 78−68122
Nb-Nb superconducting point junctions, I-V charact. *(Russian)* 79−51727
Nb-Nb_2O_5-Pb Josephson junction formed on Nb film edge 80−107960
Nb-Nb_3(Al,Ge) multifilamentary supercond., fabrication and props. 77−20480
Nb-Nb_xO_y-Pb Josephson tunnel junction form. and ageing, adsorbed gas effect *(Russian)* 78−14899
Nb-Nb_xOy-Cu/Pb supercond. proximity junction, max. DC Josephson current, thickness depend. 79−82719
Nb-NbO_x-Pb, miniature tunnel junction, gap voltage determ. 79−7939
Nb-NbO_x-Pb tunnel junctions with high normal resists.,, crit. currents 79−56399
Nb-NbO_x-Pb tunnel junctions at 4.2K, conductance of oxide barrier 80−7046
Nb-NbO_x-PbIn tunnel junctions with ultra-thin Nb electrodes 79−56398
Nb-Nb(Nb_3Sn) supercond. point contacts, crit. currents, effect of laser radiation *(Russian)* 79−28484
Nb-Pb supercond. tunnel junction proximity effect, theory 80−65752
Nb-Pb tunnel junction, crit. Josephson current, proximity effect model 80−93047
Nb-Pt, A15 phase, comp. and order effects on supercond. props. 77−85372
Nb-Pt alloy, superconducting parameters of A15- and σ-phases 78−39242
Nb-Pt-O system, phase equilibria, diagram, unit cell parameters, supercond. 80−55352
Nb-Rh, σ-phase alloy, superconductivity and resistance behaviour 80−70882
Nb-Ru(Re)(Os), dil., impurities effect on elec. resist. at 0.4 and 77.3K *(Russian)* 79−91196
Nb-sapphire RF superconducting resonator, fabrication and props. 79−51704
Nb-Si, compounds with A15 structure, films, TEM study *(French)* 80−80135
Nb-Si compounds, CVD, struct. and supercond. props. 79−24447
Nb-Si film, superconductivity close to A15 stoichiometric phase 79−95540

type II superconductors continued
Nb-Si-Sn(Pt)(Ir), A15 cpds. prod. by liq. quenching, phase stability and supercond. props. 79−95538
Nb-Si(−V)(Zr)(Mo)(Ta)(W)(C)(B)(Ge), ductile amorphous, superconductivity 80−60131
Nb-Sn, A15 compounds, Hall coeffs. 79−33281
Nb-Sn, depend. of supercond. transition temp. on composition *(Russian)* 78−19173
Nb-Sn, diffusion couple, phase equilibria, effect on T_c and H_{c2} 79−56462
Nb-Sn, reactive diffusion *(Russian)* 77−20133
Nb-Sn, supercond. foils, phase anal. by Mossbauer spectra 78−64305
Nb-Sn alloys, stoichiometry and phase equilibria, X-ray diffr. study *(French)* 79−70040
Nb-Sn sinter material, for superconducting tubes for magnetic shielding 79−67446
Nb-Sn(Al)(Ga)(Ge)(Si)-C, phase equilib. and supercond. 80−50593
Nb-Sn(Ge), A-15 compound formation by ion implantation 78−51572
Nb-Ta (54 at.%) cylinder, superconducting mag. and resistive behaviour 77−8252
Nb-Ta bimetallic loop, thermoelec. flux effects due to penetration depth changes 77−24636
Nb-Ta fibre reinforced Cu, fatigue testing in normal and superconducting states 78−19959
Nb-Ti, annular superconductor, field replication and flux shielding 77−28286
Nb-Ti, film, composition determ. by ^{3}He elastic scatt. 78−76974
Nb-Ti, Helmholtz coils, optimisation, critical current rel. to mag. induction 79−67353
Nb-Ti, multifilament composite technical superconductors, development and manufacture 79−19707
Nb-Ti, optimised pinning struct., crit. data 1.8-4.2K 77−89913
Nb-Ti, pinning curves, high field J_c and scaling behaviour 80−93064
Nb-Ti, pinning mechanism at high mag. fields 79−95555
Nb-Ti, radiation effects on critical currents 78−52175
Nb-Ti, sheet, flux trapping, appl. to mag. shielding and levitation 80−31806
Nb-Ti, single core conductor, carrying DC transport current, alternating field losses 80−34550
Nb-Ti, superconductive materials and magnet systems developed at Intermagnetics General Corp. 79−58699
Nb-Ti, superconductivity after heavy ion irradiation at low temps. and high fluence 77−69437
Nb-Ti, thermal conductivity in low temp. range 78−39259
Nb-Ti (50%), supercond., cryostat design for magnetisation study *(Spanish)* 80−75673
Nb-Ti alloy, supercond., low-temp. plasticity 77−15992
Nb-Ti alloy, supercond. and mag. props., anisotropy *(Russian)* 77−59361
Nb-Ti alloy, supercond. and high mag. fields 79−87215
Nb-Ti alloy, supercond. Helmholtz coils, optimisation 79−2795
Nb-Ti alloy strip, crit. current anisotropy 78−10624
Nb-Ti and Nb-Ti-Zr, low temp. resist., enhancement due to short-range supercond. order 77−28157
Nb-Ti filamentary superconductor critical current density rel. to thermal treatment 79−33440
Nb-Ti films, ion beam sputtered, study by ^{4}He backscattering and nucl. reaction microanal. 79−42400
Nb-Ti multifilaments, effect of mech. and thermal treatments of supercond. props. 80−104197
Nb-Ti superconducting alloy, critical current density, heat treatment effects *(Japanese)* 78−14909
Nb-Ti superconducting cylinders, dynamically stabilised, differences in shielding versus trapping behaviour 77−47933
Nb-Ti superconducting magnet system, for short sample test on Tokamak superconductor 80−9010
Nb-Ti superconducting single layered multifilamentary coil, eddy current loss depend. on demagnetisation 80−97040
Nb-Ti superconductor, for fusion facility, cold-pressure-welded joints 78−62630
Nb-Ti/Cu composite disc, crit. state model for crit. current determ. 79−99665
Nb-Ti-Ta, pinning curves, high field J_c and scaling behaviour 80−93064
Nb-Ti-Ta alloys, metallurgical anal. and crit. current densities 79−38286
Nb-Ti-Zr, supercond. wire, anomalous increments of AC losses due to flux jumps 77−28289
Nb-Ti-Zr, superconducting, ageing effect on critical current density *(Japanese)* 79−61747
Nb-Ti-Zr, superconducting, critical current density and microstruct. correlation *(Japanese)* 79−61748
Nb-Ti-Zr, superconducting wire, coil simulation, class and instability meas. 79−71487
Nb-Ti-Zr, superconducting wire, coil simulation meas. of losses and instabilities 80−37050
Nb-Ti-Zr, wire, anomalous crit. AC 77−16014
Nb-Ti-Zr ternary alloy wires, flux jumping 79−60965
Nb-Ti-Zr ternary system, high-field supercond. 80−97045
Nb-Ti(Mo), AC loss minimum, pinning, flux distribution 80−84574
Nb-Ti(Zr), type II superconductor, mech. behaviour and stress effects 77−86083
Nb-V_3Ga mixed state, Meissner effect investigation by muon method *(Russian)* 80−107954
Nb-V(Ta) alloys, electron-phonon interaction and supercond. transition temp. *(Russian)* 79−28426
Nb-Zr, acoustic phonon anomalies and superstructure, neutron inelastic scatt. meas. 80−19892
Nb-Zr, crit. current, flow-flow resist. depend., allowance for superheating *(Russian)* 80−93061
Nb-Zr, effect of band structure on elastic constants and superconductivity 79−8313
Nb-Zr, type II supercond., radiation-induced flux pinning 78−80106
Nb-Zr sputtered film, effect of O in sputtering atm. on supercond. props. *(Japanese)* 78−52138
Nb-Zr-Al alloy, struct. determ. by optical microscopy and electron diffraction *(Russian)* 77−16628
Nb_3/Sn-Cu composites, in situ processed, supercond. props. 80−75698
Nb_3(Al,Ge) and Nb_3(Al,Si), liq. quenched, supercond. props. 80−84580
Nb_3(Al, Ge), effect of thermal treatment on superconducting props. 79−61016
type II superconductors continued
Nb_3(Al,Ge) supercond., diffused layer critical current depend. on Cu before and after annealing *(Russian)* 79−69643
Nb_3Al, $NbAl_3$, supercond. and mag. props. 77−47922
Nb_3Al, A-15 struct., converted from cold worked BCC struct., crit. currents 80−75697
Nb_3Al, BCC struct., cold working and converting to A-15 struct. 78−64553
Nb_3Al, band struct. and density of states from self-consistent pseudopotentials 79−69401
Nb_3Al base ternary solid solns., T_c meas., dopant depend. 77−1510
Nb_3Al based ternary solid solns., supercond. transition temp., paramag. susceptibility and lattice parameters meas. *(Russian)* 77−43766
Nb_3Al, bonding, electronic charge distribs. and struct. transform. from self-consistent pseudopotentials 79−69054
Nb_3Al, complex refractive index meas. 80−93264
Nb_3Al, electron energy loss spectra, AES and HEED investig. of surface 77−24635
Nb_3Al, fast neutron irrad. effects on T_c 77−55633
Nb_3Al film, electron-beam coevaporated, prep. and characts. 80−76187
Nb_3Al, liq.-quenched, crit. current density and T_c 77−72957
Nb_3Al, mechanical and supercond. props. 79−38214
Nb_3Al, metallic bonding, electronic states calcs. 78−79916
Nb_3Al multifilamentary cable fabrication and props. 79−33438
Nb_3Al, multifilamentary wires, supercond. props. 78−64175
Nb_3Al, NMR of ^{93}Nb and spin-lattice relax. time at low temp. 77−85388
Nb_3Al, neutron irrad. effects on transition temp. *(Japanese)* 79−82707
Nb_3Al, nuclear magnetic relaxation, near T_c *(Russian)* 79−42852
Nb_3Al, phonon density of states, temp. depend. 79−42183
Nb_3Al, quantum interference and Josephson effect *(Russian)* 78−56259
Nb_3Al, quasi-one-dimensional supercond., giant enhancement of nucl. relax. rate near T_c 78−56257
Nb_3Al, supercond. props. and lattice parameter, comp. and neutron irrad. effects 80−70880
Nb_3Al, superconductivity, crit. temp., paramag. susceptibility comp. depend. *(Russian)* 77−66219
Nb_3Al superconductors, sputter deposited, BCC to A15 transition, microstruct. investig. 78−27512
Nb_3Al tape, effect of thermal treatment on superconducting props. 79−61016
Nb_3Al:^{93}Nb, NQR spectra, NQR signal disappearance in supercond. state 78−19369
Nb_3Al-Nb_3Ge-Nb_3Ga system, supercond. crit. temps. 77−8218
Nb_3Al-Ni(Cr)(Fe) mag. impurities effect on supercond. props. 77−1524
Nb_3Al(Ga), NQR freq. temp. depend., supercond. transition temp. 80−93207
Nb_3Al(Ga)(Si)(Ge)(Sn), electronic struct. calcs. 79−47005
$Nb_3Al_{0.8}Ge_{0.2}$, supercond., sp. ht. meas. 77−28296
$Nb_3Al_{0.83}Ge_{0.21}$, A-15 phase, sp. ht. meas., Debye temp., energy gap and crit. field 79−19689
$Nb_3Al_{1-x}Ge_x$, RF sputtering synthesis, supercond. transition temp. variation 77−81216
Nb_3(AlSi) film, thermomodulation spectra, 1.1-2.8 eV 78−48250
Nb_3(AlSi), ternary supercond. alloy films, T_c, props. *(Russian)* 78−88055
$Nb_3Al_{0.2}Si_{0.8}$, A-15 alloy synthesis by ion implantation 78−80489
Nb_3Al(Sn), electron-phonon coupling and supercond. crit. temp. 79−33379
Nb_3As, electronic and supercond. props. 77−16011
Nb_3As, structural and supercond. props. press. effects 80−39700
Nb_3Au, A-15 struct. supercond., microhardness, bonding 78−76199
Nb_3Au, BCC, density of states, comparison with A-15 78−80095
Nb_3Au, supercond. diffusion layer prep. 79−1834
$Nb_{\sim 3}Au$, upper crit. field 79−82729
NbB_2, superconductivity below 1K 80−20342
NbC, C implanted, channelling crit. angle and min. yields 78−47458
NbC, diffuse, production and superconductive props. *(Bulgarian)* 80−80467
NbC, electronic struct. of vacancies, effect on supercond. transition temp. 80−29347
NbC, phonon anomalies, microscopic theory 78−14867
NbC, phonon anomaly rel. to Fermi surface 77−11853
NbC, supercond. critical temp., neutron irrad. effect 80−80433
NbC, supercond. transition temp. and lattice dynamics 79−56361
NbC, ultrafine powders and sintered compacts, prep. and supercond. props. 77−40015
$NbC_{0.89}$, implantation or diffusion of C rel. to supercond. transition temp. 77−69442
NbC_x, reactor irrad. effects on elec. resist. and supercond. props. *(Russian)* 78−47895
NbC_x, supercond. transition temp., light element implantation effect 80−107951
NbC(N), critical temp. enhancement, surface effect on phonon spectrum and electronic state density *(Chinese)* 80−2507
NbCN, preparation methods and supercond. properties *(French)* 79−73618
Nb(CN), supercond. critical temp., neutron irrad. effect 80−80433
NbCN superconducting films, high field critical current densities and resistive transition 79−61018
NbC_xN_{1-x}, obs. of phonon anomalies, sp. ht. meas. and supercond. transition temp., 1.5-90K 77−39985
NbC_xN_{1-x}, s.p. ht., 4.2-100K, phonon anomaly rel. to supercond. transition 78−14880
NbCn, superconducting film, high field critical current densities and resistive transition 79−73648
NbD_x, acoustic phonons conc. depend. 77−15515
$Nb_{0.75}Ga_{0.25}$, A 15 phase high transition temp., sp. ht. determ. 80−60140
Nb_3Ga, crit. temp. and struct., heat treatment and stoichiometry effects 77−43769
Nb_3Ga, critical data, under hydrostatic pressure to 15 kbar 79−47217
Nb_3Ga film, RF sputtered, supercond. and struct. props. 77−28274
Nb_3Ga, thermodynamic and expt. study of CVD 79−24441
Nb_3Ga, transition temp. increase by rapid hardening with annealing 80−76275
Nb_3Ga:^{93}Nb, NQR spectra, NQR signal disappearance in supercond. state 78−19369
Nb_3Ga-Nb_3Pt alloy, crit. temp., comp. depend. *(Russian)* 77−59347
$Nb_{78}Ga_{22-x}Mn_x$, supercond. props., influence of Mn mag. impurities 80−54825

type II superconductors continued
$Nb_{80}Ga_{20-x}Mn_x$, supercond. props., influence of Mn mag. impurities 80−54825
Nb_3(Ge,Si) A15 film, supercond. and structural props. 79−87177
Nb_3(Ge, X), X=Si, Ga, CVD tapes, supercond. props. at high mag. fields 79−38279
$NbGe_2$ single crysts., elec. resist. and superconductivity 79−38233
$NbGe_2$, superconducting transition temp. meas. of sputtered films and bulk 80−7019
$Nb_{1-x}Ge_x$, supercond., mag. field props. 80−54822
Nb_3Ge A15 cpd., bulk modulus 80−7611
Nb_3Ge, A15 superconductor, rel. between transition temp. and density of states 79−15247
Nb_3Ge, amorphous and crystalline A-15 phases 78−83896
Nb_3Ge amorphous films, X-ray diffr. analysis of microstruct. 78−72035
Nb_3Ge, amorphous nongranular thin superconducting film, thermodynamic and resistive transitions 80−34571
Nb_3Ge, and $Nb_{0.82}$, structural and supercond. props. press. effects 80−39700
Nb_3Ge, α-particle irrad., supercond. transition width 78−23193
Nb_3Ge, α-particle irrad., relationship between density of states and supercond. transition temp. 79−42684
Nb_3Ge, band struct. and density of states from self-consistent pseudopotentials 79−69401
Nb_3Ge, bonding, electronic charge distribs. and struct. transform. from self-consistent pseudopotentials 79−69054
Nb_3Ge, CVD, AC losses, temp. depend., 4-20K 77−28311
Nb_3Ge CVD supercond. tape critical current anisotropy obs. 79−33372
Nb_3Ge CVD tapes, supercond. props. at high mag. fields 79−38279
Nb_3Ge coevaporated film, high supercond. transition temp., nucleation and growth 80−76185
Nb_3Ge continuous supercond. tape, prep. by CVD 77−80893
Nb_3Ge, crit. current density temp. depend. 77−47951
Nb_3Ge, DC sputtered films, annealing and mech. deform. effects on struct. and supercond. props. 79−38217
Nb_3Ge, density of states from critical field meas. 79−42690
Nb_3Ge, effect of ^{16}O and ^{32}S ion irrad. and thermal recovery on T_c, residual resist. and slope of crit. field 79−56348
Nb_3Ge, electron energy loss spectra, AES and HEED investig. of surface 77−24635
Nb_3Ge, electron-lifetime effects on props. 80−10951
Nb_3Ge, epitaxial growth of polycryst. films with high supercond. transition temp. 77−63015
Nb_3Ge film, CVD, critical current density rel. to second phase (tetr. Nb_5Ge_3) 77−32131
Nb_3Ge film, CVD fabrication of supercond. tape for high-field magnets 78−95698
Nb_3Ge film, CVD on inside of Cu tube, AC losses 77−28312
Nb_3Ge film, crit. temp., resist., and struct., comp. depend. 78−6470
Nb_3Ge film, critical current density and flux pinning 77−20510
Nb_3Ge film, electron beam codeposition in O_2, Cl_2 or air, phase diagram 77−28728
Nb_3Ge film, electron beam co-deposited, prep. and supercond. crit. temp. 78−15310
Nb_3Ge film, far IR reflection and transmission spectra, room temp. 77−55792
Nb_3Ge film, growth by co-evaporation in O_2, critical temp. enhancement 77−28273
Nb_3Ge film, high-temp. supercond. phase stabilisation w.r.t. prep. conditions *(Russian)* 80−70871
Nb_3Ge film, in supercond. proximity sandwich, energy gap struct., appl. to electron-phonon spectra 79−56401
Nb_3Ge film, low temp. sputter deposition 78−48315
Nb_3Ge film, nucleation of high-T_c phase in presence of impurities 78−88054
Nb_3Ge film, prep. by coevaporation, supercond. props. 78−91830
Nb_3Ge film, sputtered, chemical composition versus lattice parameter a_o and supercond. transition temp. relations 77−43771
Nb_3Ge film, sputtered and evaporated, transition temp., critical field and current anisotropy 77−28328
Nb_3Ge film, supercond., intercorrelations between composition, lattice parameter a_0 and T_c 77−8217
Nb_3Ge film, supercond., epitaxial growth on Nb_3Ir and Nb_3Rh substrates 78−80473
Nb_3Ge film, superconducting, A-15 type, getter-sputtering with controlled additions of O 78−88427
Nb_3Ge film, superconductivity, relevance of mag. interactions, EPR study 80−100545
Nb_3Ge film, T_c var. with ^4He irrad. induced defects 77−8220
Nb_3Ge film, TEM obs of microstruct. foil prep. method 77−55642
Nb_3Ge film, tunnelling obs., electron and X-ray diffr. obs. 77−32123
Nb_3Ge films, α-particle induced defects and stoichiometry 77−32101
Nb_3Ge films, correl. between crit. current density and microstruct. 79−38277
Nb_3Ge films, form. of A15 phases by DC sputtering 79−38740
Nb_3Ge films, prep. by DC sputtering and solid state diffusion, supercond. props. and struct. 79−38212
Nb_3Ge, high crit. temp., prep. *(Japanese)* 79−78914
Nb_3Ge, high pressure and temp. treatment effect on supercond. props. *(Russian)* 77−1512
Nb_3Ge, high T_c, development as high field supercond. 79−61015
Nb_3Ge, high T_c film with impurity expanded lattice, form. and stabilisation 79−56099
Nb_3Ge, high T_c supercond., anal. of X-ray traces 79−56098
Nb_3Ge, hysteretic losses in parallel AC and DC mag. fields 79−87217
Nb_3Ge, low fluence alpha irradiation, behaviour of supercond. transition temp. 78−43510
Nb_3Ge, low temperature electron, neutron irrad. effects on critical temp. *(French)* 80−75669
Nb_3Ge, metallic bonding, electronic states calcs. 78−79916
Nb_3Ge, Nb_5Ge_3 and NbO content, X-ray diffr. obs. 80−2515
Nb_3Ge, neutron irradiated, A15 compound, recovery of T_c by annealing 78−52132
Nb_3Ge, ordered and disordered A15 phases, energy gaps, tunnelling 77−8235
Nb_3Ge, projected critical current, comparison with $PbMo_6S_8$ 79−69642
Nb_3Ge, RF and DC sputtered films comparison, O content effect 78−72022
Nb_3Ge, RF sputtered film, high superconducting transition temp. 77−59346
Nb_3Ge, scaling laws for pinning forces 79−47214

type II superconductors continued
Nb_3Ge, sputter-deposited, superconducting T_c and phase relationship 79−56344
Nb_3Ge, sputtered, ion scatt., AES, depth profiling 77−11806
Nb_3Ge sputtered and evaporated, struct.-depend. anisotropy of supercond. crit. currents 79−38292
Nb_3Ge sputtered film, struct. and superconducting props. 77−28337
Nb_3Ge sputtered films, Ge surface segregation exam. by AES 79−56084
Nb_3Ge, sputtered on Cu, film-substrate interface obs. by electron microscopy 80−65398
Nb_3Ge, supercond., single phase, sp. ht. meas., 4-29K 78−72307
Nb_3Ge, supercond. film, amorphous content, X-ray diffr. study, rel. to transition temp. 80−75668
Nb_3Ge, supercond. film, CVD, crit. temp., crit. current density 78−76204
Nb_3Ge supercond. film, of high transition temp., US attenuation 80−49991
Nb_3Ge, supercond. film, prep. by chem. transport reaction, critical props. 79−47635
Nb_3Ge, supercond. tape, growth technique via amorphous state 78−84708
Nb_3Ge supercond. thin films, He- and Ar-irradiated, X-ray diffr. studies 80−29503
Nb_3Ge, superconducting A-15 type compounds, transition temp., radii ratio and structure *(Chinese)* 80−44752
Nb_3Ge superconducting film preparation and props. 79−11515
Nb_3Ge superconducting films, role of O_2 in form. of struct. *(Russian)* 79−60950
Nb_3Ge superconducting film, crit. temp. correl. with resist. relations and film struct. *(Russian)* 80−15646
Nb_3Ge superconducting films, high critical temp., optimum sputtering conditions 80−15647
Nb_3Ge superconducting films, quantitative Auger anal. 80−55740
Nb_3Ge, superconducting hybridisation and bonding, XPS exam. 78−2988
Nb_3Ge superconducting long tapes, CVD prepared, high current densities at 20 T 79−33436
Nb_3Ge, superconducting thin films, energy gaps from tunnelling meas. 80−25050
Nb_3Ge, superconducting transition temp. 78−47898
Nb_3Ge tape, prep. by continuous CVD process 78−11121
Nb_3Ge tape, prepared continuously by CVD, props. 78−60257
Nb_3Ge tape conductors, strain depend. of crit. current density 79−38278
Nb_3Ge:H film, sensitivity of supercond. transition temp. to H content 78−47894
Nb_3Ge-based superconducting alloys, upper critical field temp. depend. *(Russian)* 78−10622
Nb_5Ge_3, 0.30K T_c meas. with 0.14K transition width 78−6468
Nb_3Ge(Al), anomalous resistivity, insight from band theory 78−60106
$Nb_3Ge_xAl_{1-x}$, ternary supercond. alloys, comp. variations 80−97022
$Nb_3Ge_{1-x}Ga_x$ CVD films, supercond. transition temp. depend. on lattice parameter 79−38219
$Nb_3Ge_{1-x}Ga_x(Sn_x)$ CVD films, supercond. props., 4.2 to 19K 79−42713
$Nb_3Ge_{1-x}M_x$ (M=Ga,Sn), pseudo-binary, scaling laws for supercond. crit. currents 79−24118
$Nb_3Ge_{0.8}Nb_{0.2}$, A-15 type struct. and order parameter 79−77552
Nb_3Ge(Si), amorphous films, thermally-activated internal friction peaks, structural obs. 80−80147
Nb_3Ge(Sn), electron irradiation at cryogenic temps., effect on T_c and transport props. 78−52122
Nb_3Ge(Sn), optical props. and electron-phonon interactions 80−2510
$Nb_{78}Gn_{22-x}Fe_x$, $Nb_{80}Ga_{20-x}Fe_x$, A15 phase supercond. 79−87181
NbH_x, supercond. T_c and low temp. resistivity, morphology 77−72940
Nb_3Ir, A-15 struct. supercond., microhardness, bonding 78−76199
$Nb_{80}Mo_{20}$, $Nb_{75}Mo_{25}$, phonon cond. below 1k 78−14881
$NbMo_2Be$, predicted A15 struct. and T_c=30K 78−76182
$(Nb_{0.99}Mo_{0.01})_{1-x}Ge_x$, supercond. transition temp. and crit. field 79−38220
$(Nb_{1-y}Mo_y)_3Ge$ system, composite transition metal atom supercond. 77−39984
$Nb_{1-x}Mo_xSe_2$, supercond. transition temp. and mag. susceptibility 77−12043
NbN, 2-dimens. supercond. phase transition, universal current scaling in crit. region 79−28429
NbN, critical data, under hydrostatic pressure to 15 kbar 79−47217
NbN, diffuse, production and superconductive props. *(Bulgarian)* 80−80467
NbN diffusion wires, crit. currents and supercond. crit. field under high press. 79−38287
NbN embedded in resin, composite supercond., high transition temp. 80−88660
NbN film, supercond., upper crit. field 78−64172
NbN film, ultrathin granular, zero dimensionality and Josephson coupling 78−10612
NbN, for supercond. microwave cavities, secondary electron emission and AES meas. 79−56895
NbN granular films, crit. current behaviour 80−15672
NbN granular films, supercond., crit. props. 80−88661
NbN granular films as weak link in Josephson devices 80−88685
NbN, granular thin film, phase transition between incoherent and coherent supercond. states 79−56394
NbN, granulated film, critical current temp. depend. *(Russian)* 80−103803
NbN, γ- and δ-forms, cryst. growth and supercond. transition temp. 80−107946
NbN, Nb_4N_3-NbN, Nb_2N-Nb_4N_3, Nb_2N, cryst. growth parameters and morphology of chem. vapour deposition, X-ray diffr. and SEM study 79−23861
NbN preparation, by precip. from gaseous NgF_5-N_2-H_2 mixture 80−20857
NbN, Raman spectra and superconductivity of various phases 78−68506
NbN single crystal preparation, transition temperature determination 80−60776
NbN, supercond. RF reactively sputtered films, deposition parameter effects on props. 80−80972
NbN, supercond. transition temp. and lattice dynamics 79−56361
NbN, ultrafine powders and sintered compacts, prep. and supercond. props. 77−40015
$NbN_{0.7}C_{0.3}$, cryst. growth and supercond. transition temp. 80−107946
$Nb_3Nb_{1-x}Si_x(Ge_x)$, impurity stabilised A15 supercond., transition temp., lattice consts., specific heat 80−93026

type II superconductors continued
Nb_2O_5, for supercond. microwave cavities, secondary electron emission and AES meas. 79−56895
Nb_3Pb superconducting film, prep., vac. deposition 80−89149
Nb_3Pt, neutron irrad. effects on supercond. props. 79−38224
NbS, supercond. props. at press. up to 20 kbar 79−24111
NbS_2 (2H), anisotropy of upper critical field 78−76200
NbS_2, high pressure polymorphs 78−51459
Nb_2S_4, anisotropic superconductor, critical field and specific heat meas. 80−44779
Nb_2S_4, supercond., prep. and transition temp. 78−84341
$NbS(Se)_2$, polymorphism at high press. and temps., T_c and band struct. 78−26528
$NbS_{1.6}Se_{0.4}$, layered supercond., fluctuation induced diamag. and dimensionality 77−77006
$Nb_3S_{1.7}Se_{2.3}$, supercond., prep. and transition temp. 78−84341
Nb_3Sb, NMR of ^{93}Nb and spin-lattice relax. time at low temp. 77−85388
Nb_3Sb, NQR study, ^{93}Nb nuclear relax. 78−88073
$NbSe_2$ (2H), layered, anisotropy and electron-phonon coupling effects on sp. ht. 77−51844
$NbSe_2$ (2H), pure and Fe doped, layer supercond., anisotropy and temp. depend. of H_{c2} 77−51857
$NbSe_2$ (2H), Raman scatt. from supercond. gap excitations 80−93340
$NbSe_2$ (2H), Raman scatt. by supercond. gap excitations, coupling to CDWs 80−103956
$NbSe_2$ (2H), supercond., thermodynamic props., exhibiting anisotropy and strong-coupling effect 77−12062
$NbSe_2$, high pressure polymorphs 78−51459
2H-$NbSe_2$, layer struct. supercond., H_{c2} temp. and ang. depend. 77−8248
$NbSe_2$, layered supercond., fluctuation induced diamag. and dimensionality 77−77006
$NbSe_2$ microbridges, current-voltage curves, hysteresis of crit. current *(Russian)* 77−69452
$NbSe_2$ nonstoichiometry, electrical props. *(Japanese)* 78−10593
$NbSe_2$, supercond. and normal state, thermal cond., temp. and mag. field depend. 78−26992
$NbSe_2$, upper crit. fields and reduced dimensionality 80−70910
$NbSe_2$:Mn, Kondo effect, mag. ordering and superconductivity 77−62915
$NbSe_2$-Fe, dil. alloy, magnetotransport and superconductivity 77−55516
$NbSe_3$, CDW form., supercond. and Fermi surface determ., press. study 80−70891
$NbSe_3$, chain-like compound, low temp. phase transition 78−80088
$NbSe_3$, Fermi surface, press. effects, supercond. transition at 3.5K 80−20068
$NbSe_3$, superconducting transitions and diamagnetism 80−84526
$NbSe_3$, superconductivity under press. 77−76995
$NbSe_3$, transport props. 80−20175
$NbSe_3$:Zr, dopant effect on supercond. transition temp. rel. to CDW 80−39699
$NbSe_x$, x=1.48-2.0, nonstoichiometric, elec. props., supercond. transition temps. 79−73624
$NbSe_x$, x=1.48-2.0, nonstoichiometric, press.-comp.-temp. rel. determ. by annealing 79−74139
Nb_2Se_4, supercond., prep. and transition temp. 78−84341
$NbSe_2$(2H), CDW onset temp. and supercond. crit. temp., press. effects up to 20 kbar 77−39987
$NbSe_2$(2H), I-free, anomalous resist. 77−51732
$NbSe_2$(2H) layered supercond., effect of Fe impurities on sp. ht. 79−60972
$NbSe_2$(2H), Raman spectra of soft modes at CDW transition 77−16301
$NbSe_2$(2H), specific heat and critical field, anisotropy and strong coupling effects 77−36021
$NbSi_2$, superconducting transition temp. meas. of sputtered films and bulk 80−7019
Nb_3Si, A-15 type, growth by levitation melting, transition temp. meas. *(Chinese)* 79−24424
Nb_3Si A15 phase from amorphous Nb-Si alloys, high-press. synthesis 80−93516
Nb_3Si A15 struct., high press. synthesis *(Chinese)* 80−70917
Nb_3Si, A15 struct., synthesis at high press., preferable conditions *(Chinese)* 77−48363
Nb_3Si, electronic and supercond. props. 77−16011
Nb_3Si epitaxial layers, ion implantation synthesis, supercond. transition temp. optimization 79−38218
Nb_3Si film, quasiamorphous, supercond. phase formation by heat pulse 77−63017
Nb_3Si film, supercond., obtained by vaporisation in vacuum, props. 78−14865
Nb_3Si films, form. of A15 phases by DC sputtering 79−38740
Nb_3Si, high press. phase, prod. by recrystn. of metastable sputter deposits, struct. and supercond. props. 78−60571
Nb_3Si, high T_c, supercond. props. from extrapolation of sp. ht. meas. on A-15 Nb-Si 80−25045
Nb_3Si, high T_c supercond., anal. of X-ray traces 79−56098
Nb_3Si, metastable A-15 struct. synthesis by ion implantation, supercond. transition temp. 80−55319
Nb_3Si, structural and supercond. props. press. effects 80−39700
Nb_3Si, substituted, splat cooling influence on supercond. T_c and stoichometry 80−80439
Nb_3Si, supercond., A15 film, electron beam evaporation 80−29284
Nb_3Si, supercond. phase, formation by explosive compression 79−82701
Nb_3Si, supercond. props., effect of neutron irrad. 79−38211
Nb_3Si, superconducting, high transition temp., sputtering 78−15309
Nb_3Si, superconducting A-15 type compounds, transition temp., radii ratio and structure *(Chinese)* 80−44752
Nb_3Si type with A15 struct., supercond. transition temp., depend. on stoichiometry *(German)* 77−69444
Nb_5Si_3, supercond. props. and cryst. struct. 79−78245
$Nb_{1-x}Sn_x$, sp. ht., supercond. T_c and martensitic transform. *(French)* 78−43508
Nb_2Sn, filamentary segments, flux pinning, proximity effects, percolation thresholds 78−56269
Nb_3Sn, A-15 cubic phase, band calc. using APW method 79−56120
Nb_3Sn, A-15 struct. Nb based superconductors, irrad. type influence on radiation defects 80−15093
Nb_3Sn, A-15 struct. supercond., microhardness, bonding 78−76199
Nb_3Sn, A-15 supercond. cpd., martensitic transform. 79−60499
Nb_3Sn, A-15 superconductor, dHvA effect 78−75985

type II superconductors continued
Nb_3Sn, AC losses, low field behaviour, morphology depend. 77−24655
Nb_3Sn, AC losses, surface effects 78−64171
Nb_3Sn A15 composite superconductors, hydrostatic extrusion *(French)* 80−104090
Nb_3Sn, A15 compound, exam. of deformation processing, review 78−39864
Nb_3Sn, alloying agent influence on struct. and supercond. props. *(Russian)* 80−39698
Nb_3Sn, anisotropic thermal parameters of Nb 79−99282
Nb_3Sn, annular superconductor, field replication and flux shielding 77−28286
Nb_3Sn, atomic displacements induced by radiation damage, X-ray study 80−2085
Nb_3Sn, α-particle irrad., relationship between density of states and supercond. transition temp. 79−42684
Nb_3Sn bronze process, flux pinning scaling law depend. on strain 80−75696
Nb_3Sn, cavities, quasiparticles in energy gap corresponding to weak spots 79−56386
Nb_3Sn cavities with high microwave qualities 77−26890
Nb_3Sn coatings, for RF cavities, props. 77−26891
Nb_3Sn, coherence parameter, nonlinear high temp. supercond. elements with A-15 lattice *(Russian)* 80−60127
Nb_3Sn composite, superconducting transition depend. on non-hydrostatic stress 80−107948
Nb_3Sn composite processes with Cu-Sn-Zn matrix, superconducting props. 78−84370
Nb_3Sn, composite supercond., powder metallurgical prep. 80−2981
Nb_3Sn, composite superconducting wire, critical current-bend strain relationships 80−93063
Nb_3Sn, composite wire, boundary resistance and cryogenic stability 79−69629
Nb_3Sn conductors for toroidal-field coils, forced-flow, flow characts. 79−58741
Nb_3Sn, crit. current ang. depend., prep. conditions effect 77−47949
Nb_3Sn, crit. current density, low dose fast neutron irrad. effect 78−14910
Nb_3Sn, crit. current enhancement by low temp. fast neutron irradiation 77−40014
Nb_3Sn, crit. temp. and transition width, 25 MeV O ion irrad. effects 77−69439
Nb_3Sn, critical current density 78−52176
Nb_3Sn, critical current enhancement by low temp. fast neutron induced flux pinning centres 78−52177
Nb_3Sn, critical currents, ang. depend., prep. conditions effects 77−43793
Nb_3Sn, critical data, under hydrostatic pressure to 15 kbar 79−47217
Nb_3Sn, cryostabilised conductor cooling system for Large Coil Program 78−50393
Nb_3Sn, Cu admixture in Sn bath effect on critical current and stability temp. 80−7059
Nb_3Sn, current carrying capacity increase by Hf addition 80−7056
Nb_3Sn, de Haas van Alphen meas. of Fermi surface for H≤40 T 79−73424
Nb_3Sn, de Haas-van Alphen oscills. in normal state 79−56116
Nb_3Sn, degradation mechanism of superconducting transition temp. under high energy neutron irradiation 78−52124
Nb_3Sn, delayed flux entry and surface barriers, tunnelling obs. 77−59355
Nb_3Sn, density of states from critical field meas. 79−42690
Nb_3Sn, dependence of max. trappable field on supercond. cylinder wall thickness 77−72952
Nb_3Sn diffusion layer material, characterisation 79−38213
Nb_3Sn, diffusion-processed layer, texture meas. 79−82726
Nb_3Sn disc loaded waveguide, for linear accelerator appl., fabrication and props. 77−26892
Nb_3Sn, distrib. of mag. field of transport current in type II supercond. 79−51730
Nb_3Sn, effect of changes in $\alpha^2(\Omega)F(\Omega)$ on the zero-temp. energy gap 80−97025
Nb_3Sn, effect of diffusion couple Sn content on superconductivity 79−61009
Nb_3Sn, effect of O ion irradiation on supercond. 78−52131
Nb_3Sn, effect on critical temp. for supercond. of disorder, induced by α-particles 78−47897
Nb_3Sn, electron beam deposited, microstruct., rel. to supercond. props. 79−37935
Nb_3Sn, electron energy loss spectra, AES and HEED investig. of surface 77−24635
Nb_3Sn, electron-lifetime effects on props. 80−10951
Nb_3Sn, electronic struct., APW method 78−72066
Nb_3Sn, energy gap and penetration depth *(Chinese)* 79−51718
Nb_3Sn, fast neutron irradiation, effect on critical current density 78−19197
Nb_3Sn fatigue effects in unidirectional composites, computer simulated model 80−35289
Nb_3Sn filament, crit. current stress induced degradation 77−24658
Nb_3Sn, filamentary, fatigue tests on small coils 78−64652
Nb_3Sn, filamentary, mech. props. and crit. current 77−24657
Nb_3Sn filamentary composite conductor design 79−30515
Nb_3Sn, filamentary conductors, type-II, low temp. 30 GeV proton effects on critical props. 78−52178
Nb_3Sn, filaments in Cu matrix, thermal strain effects on superconducting critical temp. 80−93032
Nb_3Sn film, electron beam evaporation, growth morphology 77−44167
Nb_3Sn film, electron beam codeposited, growth morphology and tensile props. 78−10301
Nb_3Sn film, growth by high-rate magnetron sputtering, transition temp. and crit. currents 77−28718
Nb_3Sn film, high T_c, high-rate magnetron sputtering, supercond. transition temp. meas. 77−43770
Nb_3Sn film, SQUIDs for operation above 14.5K 77−66226
Nb_3Sn film, T_c var. with ^4He irrad. induced defects 77−8220
Nb_3Sn film contacts, quantum interference at H_2 temp. *(Russian)* 77−12041
Nb_3Sn film formation, solubility, precipitating processes *(Russian)* 80−92792
Nb_3Sn film on insulating substrate, crit. mag. fields *(Russian)* 79−11277
Nb_3Sn films, α-particle induced defects and stoichiometry 77−32101

type II superconductors continued
Nb_3Sn films, deposition by quasi-closed vol. method, supercond. crit. temp. 80−15645
Nb_3Sn, flux density gradient determ. by Faraday effect 80−107969
Nb_3Sn, flux trapping and shielding capabilities in transverse fields 80−15667
Nb_3Sn, for supercond. microwave cavities, secondary electron emission and AES meas. 79−56895
Nb_3Sn forced flow superconductor design considerations for Large Coil Program 78−50394
Nb_3Sn, forced flow toroidal field coil, Westinghouse Electric conceptual design for test coil 78−50392
Nb_3Sn, gap anisotropy, electron irrad. effect on transition temp. 78−10599
Nb_3Sn, grain size in A15 reaction layers 78−14911
Nb_3Sn, high-current A-15 microcomposite material 80−44781
Nb_3Sn, high-rate sputter-deposited, effect of oxygen on microstruct. 80−20343
Nb_3Sn, high-temp. supercond., tunnelling spectra, electron pairing anal. 79−87205
Nb_3Sn, highly disordered, elec. resist. and supercond. T_c 78−52142
Nb_3Sn, influence of effective phonon spectrum on T_c *(Chinese)* 79−51705
Nb_3Sn, inhomogeneity detection by penetration depth meas., proximity theory 77−28288
Nb_3Sn, lattice dynamics at 300K 79−65155
Nb_3Sn, lattice microstrain induced metastable phase, low temp. struct. and props. 77−8482
Nb_3Sn, low fluence alpha irradiation, behaviour of supercond. transition temp. 78−43510
Nb_3Sn, low temp. irrad. with 20 MeV S ions, effect on supercond. props. 79−38223
Nb_3Sn, low temp. neutron irrad. expts., E_n=14 MeV 79−33424
Nb_3Sn, martensitic transform. coupling with supercond. transition 78−44126
Nb_3Sn, martensitic transition, lattice anharmonicity 79−8300
Nb_3Sn microfilamentary superconducting composite, critical currents, fracture props. 80−107970
Nb_3Sn monofilament wires, supercond. props., effect of Be alloying additions to bronze matrix 79−87222
Nb_3Sn monofilamentary wires, supercond. crit. current density, bending effects 80−50018
Nb_3Sn, monofilaments, radiation-enhanced diffusion growth, crit. current density 80−65758
Nb_3Sn, multifilament composite technical superconductors, development and manufacture 79−19707
Nb_3Sn, multifilament conductors, strain-crit. current meas. 78−64174
Nb_3Sn multifilament conductors, strain effect on crit. props. 78−80108
Nb_3Sn, multifilament conductors appl., production and props. *(German)* 80−3081
Nb_3Sn multifilament supercond. wire, hydrostatic extrusion processing 79−33976
Nb_3Sn, multifilament superconductors, AC losses 79−60979
Nb_3Sn, multifilament superconductor, pulsed mag. field losses and critical current densities 80−54853
Nb_3Sn, multifilamentary, optimization of high field crit. current density 79−38288
Nb_3Sn, multifilamentary composite wires, critical current strain depend. 77−20511
Nb_3Sn multifilamentary conductors, enhancement of supercond. crit. current by tensile stress 78−6490
Nb_3Sn multifilamentary conductors for large-scale magnets, crit. currents, stability, and stress effects 79−38291
Nb_3Sn, multifilamentary conductors, production using solid state diffusion technique 79−56454
Nb_3Sn multifilamentary composites, supercond. destruction by current, long N-S interfaces 79−56480
Nb_3Sn, multifilamentary conductors, stress-induced enhancement of critical currents 79−69644
Nb_3Sn multifilamentary composites, crit. currents, flux pinning, and crit. field 79−78280
Nb_3Sn multifilamentary composite supercond. wires, transverse sections prep., ion milling, TEM obs. of grain size 80−101000
Nb_3Sn multifilamentary dipole magnet, construction and performance 77−28758
Nb_3Sn multifilamentary hollow superconductor and magnet, fabrication and crit. currents 79−38289
Nb_3Sn, multifilamentary high-field superconductor, status of development 79−61004
Nb_3Sn multifilamentary supercond., Cu-stabilised, recent developments 77−28759
Nb_3Sn multifilamentary superconductors crit. current up to 18 T 77−47950
Nb_3Sn multifilamentary superconductor AC hysteresis losses 79−33437
Nb_3Sn multifilamentary supercond. composites, crystallographic texturing 80−71669
Nb_3Sn, multifilamentary superconductor preparation by 'in situ' and cold powder methods, review 80−93522
Nb_3Sn, NMR of ^{93}Nb and spin-lattice relax. time at low temp. 77−85388
Nb_3Sn, neutron irrad., elec. resist., temp. depend. 79−91024
Nb_3Sn, neutron irrad., X-ray scatt. theory 79−37740
Nb_3Sn, neutron irrad. effect on upper crit. field and crit. current 77−72954
Nb_3Sn, neutron irrad. effect on supercond. fusion magnet props. 78−52128
Nb_3Sn, neutron irrad. effects on transition temp. *(Japanese)* 79−82707
Nb_3Sn, nonstationary Josephson effect, 13-18.3K, 9-10 GHz, 20 MW *(Russian)* 78−2631
Nb_3Sn, normal state, Fermi surface, APW band calc. and de Haas-van Alphen oscills. 79−65369
Nb_3Sn, O^{4+} bombarded, Mossbauer studies 80−2672
Nb_3Sn, on $LiNbO_3$ substrate, US attenuation of SAW in applied mag. field 80−75678
Nb_3Sn patterned film, appl of refractory lift-off process using Nb-Cu bilayers 79−47626
Nb_3Sn, phonon density of states, temp. depend. 79−42183
Nb_3Sn, phonon softening and T_c, strong electron-phonon coupling 78−31009
Nb_3Sn, produced by Sn implantation, supercond. and Mossbauer effect 79−4612

type II superconductors continued
Nb_3Sn, quasi-one-dimensional supercond., giant enhancement of nucl. relax. rate near T_c 78−56257
Nb_3Sn, radiation damage effect on superconducting props. 78−52127
Nb_3Sn, stabilized multifilamentary superconductor, internal Sn diffusion process 79−61749
Nb_3Sn strip, made by diffusion method, crit. curent anisotropy, Zr alloying addition effects *(Russian)* 78−47921
Nb_3Sn, supercond., crit. fields Pauli paramag. limiting and material parameters 79−78277
Nb_3Sn, supercond., dielastic interaction of flux line lattice with internal stresses of cryst. imperfections 78−56270
Nb_3Sn, supercond., effect of trapped mag. flux on AC losses 79−33420
Nb_3Sn, supercond., fast particle irradiation effects, using anti-site defect model, electronic state influences 79−56346
Nb_3Sn, supercond., production of high current carrying strip *(Russian)* 79−33435
Nb_3Sn, supercond., thin film, US attenuation of SAWs 80−49988
Nb_3Sn, supercond. and high mag. fields 79−87215
Nb_3Sn, supercond, composite, residual stress state, crit. currents 80−80468
Nb_3Sn, supercond. crit. temp., functional derivative with electronic density of states, Eliashberg eqns. 79−56368
Nb_3Sn, supercond. props., effect of neutron irrad. 80−80463
Nb_3Sn, supercond. props. and struct., neutron irrad. dose depend. 77−15985
Nb_3Sn, supercond. props. of cold worked core wires an basis of A15 phases 77−85369
Nb_3Sn, supercond. props. and appls., state-of-the-art 79−33413
Nb_3Sn supercond. tape substrate structural changes 79−33373
Nb_3Sn, supercond. thermodynamics 79−42693
Nb_3Sn, supercond. transition temp., deform. effects 77−12051
Nb_3Sn superconducting, formed from Cu-Sn alloy, props. 79−42709
Nb_3Sn, superconducting, inelastic scattering of light 79−33390
Nb_3Sn, superconducting accelerating struct., high field exam. 79−36439
Nb_3Sn superconducting bridge junction, crit. current temp. depend. *(Russian)* 78−34938
Nb_3Sn, superconducting filament formation near edge dislocation *(Russian)* 79−4635
Nb_3Sn superconducting layers, crit. currents, struct. and prep. *(Slovak)* 78−56273
Nb_3Sn, superconducting props., effect of radiation induced atomic disorder 78−52133
Nb_3Sn, superconducting thin films, energy gaps from tunnelling meas. 80−25050
Nb_3Sn, superconducting toroidal field coils for Tokamaks 78−50388
Nb_3Sn, superconducting transition temp., crit. parameters 77−28280
Nb_3Sn superconducting wire, fabrication from Cu-Nb-Sn alloy using controlled high temp. gradient 80−25056
Nb_3Sn, superconductive materials and magnet systems developed at Intermagnetics General Corp. 79−58699
Nb_3Sn superconductors, bronze-processed, effect of Ta additions 78−95404
Nb_3Sn superconductors, mech. behaviour, diffusion *(German)* 78−39880
Nb_3Sn, T_c and penetration depth *(Chinese)* 79−51706
Nb_3Sn, TEM of radiation damage 79−65122
Nb_3Sn tapes, aPpl. of method for continuous meas. of crit. current 77−24656
Nb_3Sn tapes, transition temp. meas. using Si linear thermometer 77−57330
Nb_3Sn, ternary additions effect on upper crit. field at 4.2K 77−28316
Nb_3Sn, thick walled tube, calc. of transverse dipole mag. field distributions *(French)* 79−47209
Nb_3Sn thin film bridges, AC Josephson effect 79−42702
Nb_3Sn, thin film weak-links SQUIDs, localised region radiation damage, fabrication and properties 78−47912
Nb_3Sn tunnel junctions, tunnelling density of states and electron-phonon spectral function 79−65618
Nb_3Sn, vap. deposited supercond. film, effect of N_2 and tape heating 78−34939
Nb_3Sn, vapour deposited, supercond., surface resist. and penetration depth 79−33392
Nb_3Sn wires used in He cryostat for superconducting magnet 79−58733
Nb_3Sn, X-ray study of fission fragment induced structural damage 78−51589
Nb_3Sn, Young's modulus, 4.2-300K, behaviour near martensitic transition 80−66564
Nb_3Sn-Au, supercond. tunnel junction with microshort circuit, nonlinear phenomena 78−14898
Nb_3Sn-Cu, high-current A-15 microcomposite material 80−44781
Nb_3Sn-Cu multifilamentary wires, in situ prep., supercond. and mech. props. 79−38768
Nb_3Sn-Cu multifilamentary composite wire, Nb_3Sn filament morphology and grain size 80−100855
Nb_3Sn-Fe(Co)(Mn), mag. impurities effect on supercond. props. 77−1524
Nb_3Sn-Nb_3Sn supercond. point contacts, crit. currents, effect of laser radiation *(Russian)* 79−28484
Nb_3Sn-Pb tunnel junction, Josephson props. 79−7937
Nb_3Sn-V_3Ga concentric solenoid magnet system, 17.5 T operation 77−26353
Nb_3Sn-Zr (0.8%), supercond. tape, crit. current, two stage annealing effect *(Russian)* 77−63046
Nb_3Sn_4 film, critical currents due to microwave field 80−25058
Nb_3(Sn-Al) system, X-ray spectroscopic studies of electronic struct. of A15 cpds. 80−2900
Nb_3Sn(Al), neutron irradiated, A15 compound, recovery of T_c by annealing 78−52132
Nb_3Sn(Al)(Ga)(Ge)(Si), supercond. transition temp., rel. to A15 phase stability 78−52137
Nb_3(SnGa), wire, neutron effect on T_c, I_c and flux pinning 79−38216
$Nb_3(Sn_{1-x}Ga_x)$, bronze processed wires, critical current densities in fields up to 23.5 T 78−47922
Nb_3Sn(Ga)(Al) film, quasiamorphous supercond. phase formation by heat pulse 77−63017
Nb_3Sn(Ge), resistivity and T_c measurement after low temp. neutron irradiation 78−52123
Nb_3(SnIn) tapes, diffusion processed, high field props. 79−38266
Nb_3(SnIn) wires, prep. by ductile fabrication process and props. 79−38265
Nb_3Su-Cu supercond. composites, fabrication, magnet appl. 80−11602

type II superconductors continued
$Nb_{30}Ta_{70}$, microwave props. of 8.6 GHz supercond. cavity 77−28297
$Nb_{80}Ta_{20}$, phonon cond. below 1k 78−14881
$Nb_{0.95}Ta_{0.05}Se_3$, resist 0.5K to room temp., supercond. transition temp. and crit. field 79−82704
$Nb_{1-x}Ta_xSn_2$, supercond. transition temp. and upper crit. field 80−39723
$NbTe_2$, high pressure polymorphs 78−51459
Nb_3Te_4, supercond., prep. and transition temp. 78−84341
NbTi, acoustic emission during flux jump 80−39724
NbTi, chemical comp., supercond. films and bulk surfaces 78−76973
NbTi, composite wire, boundary resistance and cryogenic stability 79−69629
NbTi composites, cryogenic stability due to boundary resistance between filament and matrix 79−58748
NbTi, dynamic stress effects, supercond. magnet training problems 78−49870
NbTi filament reinforced Cu, superconducting composite, elastic const., temp. depend. 78−68717
NbTi, filamentary conductors, type-II, low temp. 30 GeV proton effects on critical props. 78−52178
NbTi, General Dynamics Convair conceptual design test coil 78−50389
NbTi, General Electric test coil conceptual design 78−50390
NbTi, monocore and filament conductors, crit. current densities and anisotropy factors, heat treatment effects 79−38285
NbTi monofilamentary wire in current sharing state, supercond. temp. sensor use 80−57288
NbTi multifilament supercond. wire, hydrostatic extrusion processing 79−33976
NbTi, multifilamentary composite wires, critical current strain depend. 77−20511
NbTi, neutron irrad. effect on supercond. fusion magnet props. 78−52128
NbTi, orientation effects on magnetisation 77−28287
NbTi, processing parameter optimisation for high mag. field appls. 79−38290
NbTi, RF magnetoresistance, flux flow resistivity 79−61002
NbTi, solid soln. supercond., crit. current anisotropy 79−38273
NbTi split coil superconducting magnet system, for Mossbauer spectroscopy and susceptibility meas. 79−71486
NbTi, supercond., measurement of thermal conductivity 79−58682
NbTi, supercond., thermal cond. meas 79−60970
NbTi, supercond. critical temp., appl. of cryogenic calorimetry 79−40577
NbTi, superconducting, serrated yielding meas. via dynamic stress test facility 77−77698
NbTi, superconducting multifilamentary conductors, crit. current density, bending effects *(German)* 80−39727
NbTi superconducting state, stability under localised heat pulses 79−73611
NbTi superconducting tapes, mag. field profiles 77−28326
NbTi, superconducting toroidal field coils for Tokamaks 78−50388
NbTi wire, supercond., magnetisation rel. to field orient. 78−52151
NbTi/In composite superconductor, transport props. 80−88658
NbTi-Cu, supercond. composite, use in temp. and heat transfer coeff. meas. 80−77780
$(Nb_{0.99}Ti_{0.01})_{1-x}Ge_x$, high T_c, resist. meas. 80−88531
$(Nb_{0.99}Ti_{0.01})_{1-x}Ge_x$, supercond. transition temp. and crit. field 79−38220
$(Nb_{0.99}Ti_{0.01})_{1-x}Ge_x$, supercond., mag. field props. 80−54822
$Nb_{1-y}Ti_ySe_2$, supercond. transition temp. and mag. susceptibility 77−12043
$Nb_{1-x}W_xSe_2$ x=0 to 0.15, elec. resist., mag. suscept., heat capacity, structural, supercond. transition *(Russian)* 78−31006
Nb_3X, X=Ge, Gu, Al, Sn, Pt, composition effects on T_c 77−76993
$Nb_{0.75}Zr_{0.25}$, effect of force constant, disorder on Eliashberg function 80−29504
$Nb_{0.75}Zr_{0.25}$, supercond. energy gap, proximity tunnelling method determ. 79−56404
$Nb_{1-x}Zr_x$, supercond., McMillan-Rowell tunnelling spectroscopy 79−60985
$(Nb_{1-x}Zr_x)_3$ Sn, bronze-processed tape, AC losses between 5 and 16K 79−82727
$Nb_{20}Zr_{80}$, supercond., US attenuation 80−44766
$Nb_{20}Zr_{80}$, supercond. and normal, sp. ht. meas., 2-20K 80−70893
$(Nb_{0.99}Zr_{0.01})_{1-x}Ge_x$, supercond. transition temp. and crit. field 79−38220
$(Nb_{0.99}Zr_{0.01})_{1-x}Ge_x$, supercond., mag. field props. 80−54822
$(Nb_{0.99}Zr_{0.01})_3Sn$, AC power losses in parallel AC and DC mag. fields 80−97041
$NdRh_4B_4$, possible obs. of coexistence of supercond. and long-range mag. order 79−82730
$NdRh_{1.2}Sn_{4.1}$, new supercond./mag. cpds., X-ray powder diffr. data 80−100215
Ni-Nb-C, obtained by liq. quenching, superconductivity 80−75699
Ni-Nb(-Cu)-C, NbC dispersed supercond. tapes, fabrication and charcts. 78−19773
$Ni_2Mo_6S_6O_2$, O-containing Chevrel phases, synthesis and props. 80−108368
Os borides, MOs_3B_2 (M=Lu, U), supercond. and mag. props. 80−97028
Pa, superconducting transition temp. and upper critical mag. field 80−44756
Pb alloys, meas. of small changes in calorimetric props. 77−33988
Pb creep, low-temp., thermal heating and quantum mechanisms, supercond. transition effects 80−79868
Pb, dil. alloy, dislocation inertial effects in plastic deform., internal friction meas. 77−36609
Pb film, conducting coating effect on supercond. transition temp. and normal-state cond. 77−16007
Pb, film, spatially inhomogeneous state appearance under laser pumping conditions 80−93053
Pb granular film, Josephson coupled, resistive transition 80−88683
Pb:Au(In)(Bi), type II film, penetration depth meas. 77−28285
Pb:Ni, paramag. impurity effect on work hardening at superconducting transition *(Russian)* 77−47915
Pb/Bi-I-Al tunnel injected nonequilibrium supercond. struct., diffusive quasiparticle instability, multiple gap states 80−50005
Pb-2n, work hardening in mixed state *(Russian)* 79−42707
Pb-Bi, annular superconductor, field replication and flux shielding 77−28286

type II superconductors continued
Pb-Bi, splat quenched, solubility limit, vacancy conc. and supercond. transition temp. 77−12046
Pb-Bi, supercond. tunnelling, effect of phase composition and press. 79−15261
Pb-Bi alloy, crit. mag. fields, influence of parameters 80−75691
Pb-Bi alloy, T_c evaluation, from ab initio band struct. calcs. on Pb 80−75502
Pb-Bi alloys, microwave surface resist., mag. field depend. *(French)* 77−24647
Pb-Bi alloys, phonon-electron interaction, normal and supercond. state thermal cond. and elec. resist. meas. 79−60460
Pb-Bi-Tl alloy, crit. mag. fields, influence of parameters 80−75691
Pb-Bi(Ni), creep, low-temp., thermal heating and quantum mechanisms, supercond. transition effects 80−79868
Pb-Cd, supercond. proximity effect, electron tunnelling study 78−10616
Pb-Cd lamellar eutectic composite, pair potential meas. 79−33396
Pb-Cu, (10%) T_c and penetration depth *(Chinese)* 79−51706
Pb-Cu (10%), energy gap and penetration depth *(Chinese)* 79−51718
Pb-Fe, supercond. films, modification of props. by Fe grains *(French)* 79−60957
Pb-Ga(Ge)(Si)(Mo)(Bi) amorphous films, supercond. transition temp. and residual elec. resist. *(Russian)* 79−19680
Pb-Ge thin film alloy, critical currents near metal-insulator transition 79−65626
Pb-In, containing Ag particles, flux pinning in superconducting matrix 80−2534
Pb-In, electron tunnelling under hydrostatic press. 77−51850
Pb-In, series-connected Josephson tunnel junctions, fabrication procedure diagnostics 78−47909
Pb-In, superconductive to normal transition due to external mag. fields, dynamic behaviour 80−39722
Pb-In, viscous drag on mobile dislocations, plastic deformation, critical temp. magnetic data 78−43514
Pb-In (1 to 20 at.%), upper critical field anisotropy 77−36033
Pb-In (40-60 at.%), type II superconducting Ettingshausen effect, transport entropy of vortices 78−56272
Pb-In (50 wt.%), supercond., pinning effect 80−15669
Pb-In alloys, energy gap determ. by pt. contact tunnelling 78−19185
Pb-In alloys, supercond., AC losses of EM energy, critical current densities 79−33423
Pb-In alloys, vortex pinning on grain boundaries *(Russian)* 77−89910
Pb-In film, RF sputter anodisation, Josephson junction form., ellipsometry anal. 79−29258
Pb-In film, supercond. surface sheath, dynamic pinning model of elec. dissipation 77−28320
Pb-In film, superconducting tunnel junction, pulsed quasiparticle injection 80−84565
Pb-In/Sn-In proximity sandwiches, crit. currents 79−60992
Pb-In-Ag, transport current distribution in longitudinal mag. field 80−25057
Pb-In-Au, series-connected Josephson tunnel junctions, fabrication procedure diagnostics 78−47909
Pb-In-Au alloy, Josephson junction electrode materials, strain relax. 79−38255
Pb-M, M=Bi, La, Sm, vacuum deposited supercond. films, T_c chem. comp. depend. *(Russian)* 78−19174
Pb-Mn, dil., supercond. film, H_{c2} meas., mag. impurity effects, pair breaking theory 79−42708
Pb-Na (8.4 at.%), surface flux pinning, crit. state model 80−97044
Pb-Sb, crystal struct., supercond. after subjection to high press. 78−88064
Pb-Sb, dynamic destruction of supercond. 80−2529
Pb-Si superconducting solutions, effect of hydrostatic compression on tunnelling *(Russian)* 80−65746
Pb-Sn, dil., dislocation inertial effects, internal-friction meas. on normal and superconducting states 79−38883
Pb-Sn, lamellar eutectic alloy, proximity effect, entropies, free energies and transition temps. 77−51849
Pb-Sn eutectic, directionally solidified, periodic array of supercond.-normal contacts, supercurrent and dynamic resist. 78−34928
Pb-Sn Josephson junctions, small area high current density normal resistance, RC times 80−34555
Pb-Sn lamellar eutectic alloy, supercond. normal-supercond. junction arrays 77−24641
Pb-Sn(Ag), dil. alloys, dislocation motion and electron-dislocation interactions 77−7728
Pb-Sn(Bi) alloys, dil., impurity effects on softening at T_c *(Russian)* 78−23220
Pb-Sn(Bi)(Ni), strength loss in supercond. transition, nonmag. and paramag. impurities influence *(Russian)* 80−70875
Pb-Tl, reversible surface superconducting magnetisation 78−43531
Pb-Tl (20 wt.%) rod, supercond., critical current densities in surface pinning region 79−47216
Pb-Tl alloy, crit. mag. fields, influence of parameters 80−75691
Pb-Tl-Bi-In, localised phonons studies by supercond. tunnelling 79−87210
Pb-Tl-In, localised phonons studies by supercond. tunnelling 79−87210
$Pb_{0.45}Bi_{0.55}$, influence of effective phonon spectrum on T_c *(Chinese)* 79−51705
$Pb_{0.45}Bi_{0.55}$, T_c and penetration depth *(Chinese)* 79−51706
$Pb_{0.9}Bi_{0.1}$, quasiparticle recombination time, tunnelling of junction 79−15259
$Pb_{55}Bi_{45}$ film, amorphous, supercond. energy gap and transition temp. 78−14866
PbCu film, amorphous supercond., phonon heat transport, thermal cond. meas. 78−19181
PbIn films, penetration depth measured with Nb-NbO_x-PbIn Josephson junctions 79−42691
PbIn oxidised electrodes, symm. and asymmetric supercond. tunnel junctions, subharmonic gap struct. study 79−60981
PbIn-oxide-Pb junction, two-particle tunnelling and microwave effects 78−43527
$Pb_{0.8}In_{0.2}$, flux-flow noise 79−95556
$Pb_{0.84}In_{0.16}$, barriers to flux entry and exit, magnetisation meas. 79−60963
$Pb_{80}In_{20}$, flux pinning and flux flow noise 79−56473
$PbMo_6S_8$, supercond., upper crit. field meas. up to 600 kG 80−93057
$PbMo_{5.1}S_6$, high supercond. T_c, soft mode behaviour 78−14855
$PbMo_{5.1}S_6$, supercond. wire prep. by powder technique 78−52705

type II superconductors continued
$PbMo_6S_6$, cold-worked core-wires, supercond. transition temp. and lattice instability 78−6469
$PbMo_6S_7$, fast neutron irrad. effects on T_c 77−55633
$PbMo_6S_8$ and ternary sulphides, lattice parameter rel. to supercond. T_c 78−52119
$PbMo_6S_8$, Chevrel phase supercond., phonon spectra, neutron scatt. meas. 79−42174
$PbMo_6S_8$, Chevrel-phase, electronic struct., LCAO calc. for idealised Mo_6S_8 cluster 77−43494
$PbMo_6S_8$, Chevrel-phase superconductors, lattice dynamical calcs. 79−33056
$PbMo_6S_8$, crit. current density, effect of prep. technique and press. 78−14908
$PbMo_6S_8$, electron tunnelling spectroscopy expts. *(German)* 80−107966
$PbMo_6S_8$, Hall effect and magnetoresistivity 78−95400
$PbMo_6S_8$, high crit. field Chevrel phase 79−61003
$PbMo_6S_8$, influence of Fe on superconduction transition temp., and mag. props. *(Russian)* 79−42686
$PbMo_6S_8$, normal state and superconducting property measurements 78−91660
$PbMo_6S_8$, normal-state electronic props., Fermi surface and supercond. parameter derivations 79−60850
$PbMo_6S_8$, prod. by solid state reaction, supercond. crit. temp. *(Japanese)* 79−42682
$PbMo_6S_8$, projected critical current, comparison with Nb_3Ge 79−69642
$PbMo_6S_8$, relationship between electronic struct. and supercond. transition temp. 77−85368
$PbMo_6S_8$, scaling laws for pinning forces 79−47214
$PbMo_6S_8$, sputtered film, critical current density meas. 78−84369
$PbMo_6S_8$, temp. depend. of crit. currents 80−20363
$PbMo_6S_8$ wire, powder processed, crit. current density and field 80−80466
$PbMo_6S_8$:Gd^{3+}, powder EPR spectra, cryst. field, supercond. energy gap 80−34769
$Pb_xMo_6S_8$, Chevrel phase supercond. prep. and supercond. props. 79−28434
$Pb_xMo_6S_{8-y}$, phase relns., stoichiometry, T_c 78−15378
$PbMo_6S_6O_2$, O-containing Chevrel phases, synthesis and props. 80−108368
$Pb_xMo_6S_8(Se_8)$, prep., metallurgical and supercond. props. 77−32102
$PbMo_6S_8(Se_8)(Te_8)$, Chevrel phase correlation between struct. and supercond. transition temp. 80−7023
$PbMo_6Se_8$, relationship between electronic struct. and supercond. transition temp. 77−85368
$Pb_{1.125}Mo_6Se_{7.5}$, Chevrel phase supercond., NMR study 80−49989
$Pb_{1.2}Mo_6Se_8$, Chevrel phase supercond., phonon spectra, neutron scatt. meas. 79−42174
$PbMo_6Se_8(S_8)$, anisotropy of H_{c2} 78−39274
$PbMo_6X_8$ (X=S, Se), phonon density of states, mode softening correl. with supercond. transition temp. 79−51714
PbNa, type-II superconductor, regularly ordered precipitates, peak effect, crit. current meas. *(German)* 78−19196
$Pb_{0.871}Sn_{0.129}$, supercond., hysteresis in flux flow characts., normal metal precipitates 78−80107
Pd, electron-phonon coupling and supercond. transition temp. 79−56360
Pd, electron-phonon parameters and supercond. p-state pairing 80−25041
Pd, irradiated film, supercond. 79−78249
Pd-Ag-D system, instability and superconductivity 78−39248
Pd-Cu(Ag)(Au) alloys-H solid solutions, superconducting transition temp. behaviour *(Russian)* 80−70879
Pd-H, elec. resist., temp. depend., H conc. var. *(Russian)* 77−39819
Pd-H, supercond. and phonon softening in unstable systems 79−65587
Pd-H alloys, press. depend. of supercond. transition temp. 77−63026
Pd-H like compounds, T_c increase by optical phonons 77−1509
Pd-H system, anharmonicity effects on superconducting transition temp. 79−33380
Pd-H system, instability and superconductivity 78−39248
Pd-H system, magnetisation, type I and type II supercond. behaviour, homogeneity effects 77−28291
Pd-H-Fe, Mossbauer effect, hyperfine field, effect of changing spin susceptibility 77−20494
Pd-H(D), band struct. and supercond. props., APW calc. 79−56354
Pd-H(D), isotope effect, theory 78−91806
Pd-H(D), isotope effects in supercond. properties 78−6471
Pd-H(D), superconducting transition temp., conc. depend. and inverse isotope effects 77−80864
Pd-H(D), superconductivity and electron-phonon interaction 80−49975
Pd-H(D) system, normal state phonon resist. and supercond. tunnelling density of states 79−56402
Pd-H(D) system, superconductivity and phonon softening 79−73626
Pd-Ni-H, hydride formation in high press. range 80−65235
Pd-Ni-H alloys, hydrogenation under high press., crit. temp. 78−88058
Pd-Ni-H alloys hydrogenised under high press., crit. temp. 77−51834
Pd-Pb-Bi supercond. alloy, X-ray, microscopic, thermographic anal. *(Russian)* 77−32106
Pd-Rh-H and Pd-Ag-H, band struct. and supercond. props., APW calc. 79−56354
Pd-Si-H(D) alloys, solid solution and amorphous phase regions, isotope effect 79−56347
$(PdAg_{0.2})H_2$, molar heat capacity, 2-6K, absence of supercond. transition 77−1516
$Pd_{1-x}Ag_xH_c$, superconducting transition temp. conc. var. 77−8221
$Pd_{1-y}Ag_yH_x$, electronic struct. and supercond., APW calc. 79−95318
$Pd_{1-y}Ag_yH_x$, superconducting transition temp., APW band struct. calcs. 78−95393
$Pd_{0.91}Ag_{0.045}Rh_{0.045}H_x$, supercond. transition temp. rel. to optical phonon spectrum 79−56355
$PdAl_x$ hydrides, supercond. transition temp. 79−47188
$PdAl_xH_y$ films, ion implantation prop., supercond. crit. temp. 79−87182
PdB_xH_c, superconducting transition temp. conc. var. 77−8221
$Pd_{1-x}Cu_xH_c$, superconducting transition temp. conc. var. 77−8221
PdD, electron-phonon mass enhancement factor and supercond. crit. temp. 79−87184
PdD, isotope effect on transition temp. 79−73615
PdD_x, molar sp. ht., γ-coeff. and Debye temp., 2 to 12K 77−1517
PdD_x, optical phonon spectra, supercond. tunnelling meas. 79−19701
PdH, electron-phonon mass enhancement factor and supercond. crit. temp. 79−87184
PdH, electronic struct. and supercond., APW calc. 79−95318

type II superconductors continued
PdH, isotope effect in supercond. *(Russian)* 77−89892
PdH, role of optic phonons in superconductivity 78−39251
PdH, supercond., book contrib. 80−25037
PdH, supercond., simple scaling theory of isotope effect 78−14878
PdH, superconducting transition critical temperature, BCS theory, phonon spectra *(Spanish)* 80−84535
$PdH_{0.97}$:Fe(Cr), supercond. transition temp. depression, coexistent mag. behaviour 80−49976
PdH_x, electronic props., H alloying effects, book contrib. 79−82522
PdH_x foils, supercond. props. 77−32114
PdH_x, local, soft modes, superconductivity thermal neutron inelastic scatt. *(Chinese)* 80−70331
PdH_x, optical phonon spectra by supercond. tunnelling meas. 79−19701
PdH_x, supercond. below 1.5K *(Russian)* 79−91178
PdH_x, superconducting transition temp., inverse isotope effect, Einstein model 80−65734
PdH_x, upper crit. field determ. 78−47919
PdH_x, x=0.915 to 0.996, thermoelec. power, 10 to 170K, rel. to optical phonon spectra 79−56201
PdH(D), isotopic vol. effect 77−1511
PdH(D), stoichiometric, ^1H and ^2D NMR, rel. to supercond. T_c 78 72430
PdH(D), superconducting, electronic spin density, isotope effects 78−39262
PdH(D), superconducting props., effect of hybridisation, band struct. determ. 79−69628
$PdH_x(D_x)$ films, electron-phonon coupling, elec. cond. obs. 80−50011
$PdH_x(D_x)$, superconducting transition temp., 0.2K to 4K 79−99651
$PdIn_xH_y$ films, ion implantation prop., supercond. crit. temp. 79−87182
$Pd(M_nCo)$, giant moments, Mossbauer study of ^{57}Fe 80−44969
$Pd_{1-y}Rh_yH_x$, electronic struct. and supercond., APW calc. 79−95318
$(Pd_{95}Rh_5)_1H_x$, elec. resistivity studies 80−59957
PdZr, amorphous, supercond., US props. 80−44765
$Pd_{30}Zr_{70}$, amorphous alloys, supercond. transition temp., press. depend. 80−84524
$Rb_{0.33}WO_3$, supercond. and special phonons, neutron scatt. obs. 80−15643
Rb_xWO_3, anisotropy in H_{c2} 80−6879
Rb_xWO_3, anomalous supercond. transition temp., electron pairing by acoustic plasmon exchange 79−56358
Re, plastic deform. rel. to low temp. sp. ht., supercond. *(Russian)* 78−31005
Re-based HCP-BCC binary systems, electronic struct. and supercond. *(Russian)* 79−33375
Re_5Fe_3, RF sputtered, crit. temp. 78−14853
Rh borides, RRh_3B_2 (R=rare earth), supercond. and mag. props. 80−97028
RhH, electronic struct. and supercond., APW calc. 79−95318
Ru borides, RRu_3B_2 (R=rare earth, Y, Th, or U), supercond. and mag. props. 80−97028
Ru-Fe, dil., localised spin fluctuation system, supercond. transition temp., conc. depend. 78−56253
$(SN)_x$, brominated, struct. and elec. props. 80−24914
$(SN)_x$, discontinuous film, DC resist. in normal and supercond. states 79−56357
$(SN)_x$, mag. props. in supercond. state 77−51842
$(SN)_x$, magnetization meas. in supercond. regime 79−56375
$(SN)_x$, Meissner effect, mag. susceptibility meas. 80−20351
$(SN)_x$, preparation and properties 78−27389
$(SN)_x$, supercond., fluctuation cond., crit. mag. fields 80−39712
$(SN)_x$, supercond. at high press. 78−23194
$(SN)_x$, supercond. energy gap, tunnelling meas. 79−56403
$(SN)_x$, supercond. props., press. and field depend. 78−14903
$(SN)_x$, supercond. props., press. depend., up to 9.5 kbar 78−68106
$(SN)_x$, supercond. props. rel. to fibrous morphology 80−84570
$(SN)_x$, superconducting fluctuation induced magnetoconductivity in anisotropic bulk and fibrous samples 79−95545
$(SN)_x$, thermoelec. power, 0.1 to 4.2K, phonon drag contrib. and supercond. transition 79−56356
$(SNBr_{0.4})_x$, magnetization meas. in supercond. regime 79−56375
$(SNBr_{0.4})_x$, supercond. props. rel. to $(SN)_x$ 79−65581
$(SNBr_{0.4})_x$, supercond. props., dimensionality 80−20344
Sb-Te, A1-type, superconductivity 80−29496
Sc, superconducting high-pressure phase 79−33378
Sc_4C_3, superconducting phase synthesis at high press. and temp., critical field *(Russian)* 80−65732
$ScMo_6X_8$ (X=S, Se), supercond., sp. ht., 1 to 14K 79−51720
$ScRu_4B_4$, superconducting and crystallographic data 80−33968
ScS, supercond. props. at press. up to 20 kbar 79−24111
$SmRh_4B_4$, coexistence of supercond. and antiferromag. order 80−11140
$SmRh_4B_4$, mag. ordered, persistence of supercond. 80−54834
Sn film, metastable current states, mean free path variation *(Russian)* 80−2538
Sn film, metastable supercond. alloys, produced by low temp. ion implantation 80−88670
Sn film, phonon-injection-induced destruction of supercond. 80−6956
Sn, film, superconducting transition curve stepped struct. due to microwave radiation *(Russian)* 78−2610
Sn-Au, amorphous film, elec. resist., temp. depend., supercond. transition temp. 79−91159
Sn-Bi, crystal struct. and superconductivity after appl. of high press. and quenching 80−10531
Sn-Bi(Sb), small κ supercond., phase transitions higher than second order 80−88668
Sn-Cu film, metastable supercond. alloys produced by low temp. ion implantation 80−88670
Sn-In, crit. RF mag. field, rel. to superheating 78−2632
Sn-In, dil., amplitude depend. US attenuation in normal and supercond. state 77−28299
Sn-In, dil., supercond., current-induced resistive state 79−51712
Sn-In, nonlinear conductivity of thin films in mixed state *(Russian)* 80−80464
Sn-In(Cd)(Sb)(Bi) alloy whisker, crit. temp., stress depend. 77−39988
Sn-Sb, A1-type, superconductivity 80−29496
Sn-Sn_xO_y-Sn long Josephson tunnel junction, flux flow, crit. conditions 80−80452
Sn-SnO_2-Sn, supercond. tunnel junctions, energy gap suppression by quasiparticle self-injection 78−80102
$Sn_{0.5}Eu_{0.5}Mo_6S_8$, supercond., spin polarisation, NMR, Mossbauer effect and bulk magnetisation meas. 77−43782

type II superconductors continued
$Sn_{0.75}Eu_{0.25}Mo_6S_8$, Chevrel phase supercond., spin-depairing interaction, Mossbauer obs. 80−25258
$Sn_{1-x}Eu_xMo_6S_8$, supercond., Mossbauer effect, struct. phase transition 77−12290
$Sn_{1.2(1-x)}Eu_xMo_{6.3}S_8$, supercond. transition temp., upper critical field, local spin fluctuations 79−38250
$Sn_{1-x}Ga_xMo_5S_6$, heat capacity meas., singularities at low temp. 80−49985
$SnMo_5S_6$, high supercond. T_c, soft mode behaviour 78−14855
$SnMo_5S_8$, fast neutron irrad. effects on T_c 77−55633
$SnMo_6S_8$, Chevrel phase supercond., phonon spectra, neutron scatt. meas. 79−42174
$SnMo_6S_8$, Chevrel phase, RE mag. isolation and supercond. 80−44470
$SnMo_6S_8$, Chevrel phase, mag. interactions, LMTO energy band studies 80−70606
$SnMo_6S_8$, crit. current density, effect of prep. technique and press. 78−14908
$SnMo_6S_8$, cryst. struct., superconducting characts. changes 79−86773
$SnMo_6S_8$, lattice softening, vibr. anisotropy 78−14428
$SnMo_6S_8$, phonon density of states, mode softening correl. with supercond. transition temp. 79−51714
$SnMo_6S_8$:Gd^{3+}, powder EPR spectra, cryst. field, supercond. energy gap 80−34769
$Sn_xMo_3S_4$, chevrel phase, charge transfer and valence electron conc. 78−6029
$Sn_xMo_5S_6$, supercond. props., effect of W and Re alloying additions, Mossbauer and X-ray diffr. meas. *(Russian)* 79−15245
$Sn_xMo_6S_8$ and $(Sn\text{-}Al)_xMo_6S_8$, Chevrel phase supercond. prep. and supercond. props. 79−28434
$Sn_xMo_6S_8$, Chevrel phase, lattice instabilities, X-ray diffr. meas. 78−34491
$Sn_xMo_6S_8$, struct. anal. supercond. props. 80−97023
$SnMo_6S_8(Se_8)$ Chevrel phase supercond., hyperfine interaction, microscopic study 79−56650
$SnMo_6S_8(Se_8)$, Mossbauer spectra 80−15926
$Sn_xMo_6S_8(Se_8)$, prep., metallurgical and supercond. props. 77−32102
$SnMo_6S_8(Se_8)(Te_8)$, Chevrel phase correlation between struct. and supercond. transition temp. 80−7023
$SnMo_6Se_8$, anisotropy of H_{c2} 78−39274
$SnMo_6Se_8$, Chevrel phase, RE mag. isolation and supercond. 80−44470
$SnMo_6Se_8$, high crit. field Chevrel phase 79−61003
$Sr_{0.67}Pt_3B_2$, cryst. struct. and supercond. props. 79−38231
$SrSi_2$, superconducting temperature depression due to mag. field 80−54820
Ta, effect of changes in $\alpha^2(\Omega)F(\Omega)$ on the zero-temp. energy gap 80−97025
Ta, electron-phonon interaction, calc. using APW band struct. calcs. and measured phonon spectra 78−14869
Ta film sputtered onto Cu substrate, microstruct. and supercond. props. 77−85370
Ta, plastic deform. effect on positron annihilation and supercond. transition *(Russian)* 77−39993
Ta point contact, 9 GHz complex impedance 77−28303
Ta, supercond. crit. temp., functional derivative with electronic density of states, Eliashberg eqns. 79−56368
Ta, superconductive transition point as reference temp. 80−107943
Ta, thermal cond., 0.3-20K, temp. and impurities effects 78−14883
Ta wire, emission current effect on superconductor critical parameters 79−91185
Ta wires, supercond. destruction by current, long N-S interfaces 79−56480
Ta:N, H_{c2}-anisotropy obs. 78−80105
Ta:N, superconductive to normal transition anisotropy 80−25031
Ta-N, supercond. props. 77−20507
Ta-Nb-V, solid solutions, superconductivity and charge transfer 79−7926
Ta-Nb-V BCC solid solutions, supercond. and normal state, sp. ht. meas. 78−84347
Ta-Rh, σ-phase alloy, superconductivity and resistance behaviour 80−70882
TaC, phonon anomaly rel. to Fermi surface 77−11853
TaC_xN_y, supercond. and normal props. under hydrostatic press. 77−12049
$TaGe_2$, superconducting transition temp. meas. of sputtered films and bulk 80−7019
Ta_3Ge, superconducting transition temp. 78−47898
TaN film, prep., comp. anal., and supercond. T_c 79−15605
TaN, mag. field direction determining whether type I or II 79−15266
$Ta_{70}Nb_{30}$, Abrikosov vortex formation kinetics *(Russian)* 80−93055
TaS_2 (2H) single crystal, specific heat meas. in mag. field, 0.3 to 3K, AC calorimetry technique 78−43516
TaS_2 ($4H_b$), press. effects on CDW transitions 77−51680
TaS_2 $(aniline)_{3/4}$, low-field magnetisation meas. on small cryst. in supercond. phase 79−87188
TaS_2, alkali metal and alkali metal hydroxide intercalates, lattice parameters, supercond. transition temps. 80−25029
TaS_2 intercalated with methylamine, supercond. layer cpd., crit. field enhancement and reduced dimensionality 80−60152
TaS_2, intercalated with organic cpds., upper crit. fields and reduced dimensionality 80−70910
TaS_2 intercalates with alkali metals, prep., X-ray anal. and supercond. transition temp. 78−31007
TaS_2 intercalation complexes, superconductivity 78−91803
TaS_2-copper tetra-4-dimethylaminophthalocyanine, dye intercalated layered cpd., struct. and superconductivity 78−84342
TaS_2-Fe, dil. alloy, magnetotransport and superconductivity 77−55516
$TaS_{1.6}Se_{0.4}$, pure and intercalated with organic cpds., upper crit. fields and reduced dimensionality 80−70910
$TaS_{2-x}Se_x$ layer compound, Hall coeff., 4-200K, rel. to supercond. transition temp. 78−95305
TaS_2(2H), supercond. transition temp., upper crit. field, and interlayer coupling strength 79−56406
TaS_2($4H_b$), electrical cond. and CDW transitions under press., rel. to supercond. 77−43574
$TaSe_2$-Fe, dil. alloy, magnetotransport and superconductivity 77−55516
$TaSe_3$, chain-like compound, low temp. phase transition 78−80088
$TaSe_3$, effect of press. on supercond. transition temp. 79−91182
$TaSe_3$, one-dimens. monoclinic, supercond. below 2.1K, mag. field effect *(Japanese)* 77−43767
$TaSe_3$, phase transitions and elec. props. 80−20178
type II superconductors continued
$TaSe_3$, superconducting crit. field rel. to anisotropic cryst. struct. 78−80104
$TaSe_3$, superconducting transition *(Japanese)* 78−30880
$TaSe_3$, superconducting transitions and diamagnetism 80−84526
$TaSe_3$, transport props. 80−20175
$TaSi_2$, superconducting transition temp. meas. of sputtered films and bulk 80−7019
Ta_3Si, superconducting, shock synthesis *(Russian)* 77−85957
Ta_5Si_3, transition temp. *(Russian)* 77−20485
$TaS_2(pyridine)_{1/2}$ intercalation complex, supercond. transition temp., upper crit. field, and interlayer coupling strength 79−56406
$TaS_2(pyridine)_{1/2}$, superconducting intercalation complex, proton spin lattice relaxation time 78−80096
$TaS_2(pyridine)_{1/2}$, upper and lower critical fields, supercond. props. from Ginzburg-Landau theory 79−56456
TbAl-NdAl, existence of high-temperature superconducting phase *(Russian)* 79−42685
$TbMo_6S_8$, long range mag. order in supercond. state 79−65653
$TbMo_6S_8$, superconductor, neutron scatt. exam. of mag. phase 79−73680
$Tb_{1.2}Mo_6S_8$, long-range mag. order and supercond., neutron diffr. obs. 79−78320
$Tb_{1.2}Mo_6S_8$, low temp. heat capacity anomaly rel. to antiferromag. transition in supercond. state 80−25044
$Tb_{1.2}Mo_6S_8$, mag. ordering in supercond. state, resist. and AC susceptibility meas. 78−19194
$Tb_{1.2}Mo_6Se_8$, crystal field excitations, inelastic neutron scatt. obs. 79−78321
Tc film, electrodeposited, supercond. transition, AC susceptibility meas. 79−95539
Tc film, supercond. transition, complex susceptibility 80−29495
Tc, superconducting transition temperature, resistive transition meas. 77−80861
Tc, superconductivity and Fermi surface calcs. 80−70873
Tc-Fe, dil., effect of Fe impurities on superconductivity 79−61007
Tc-Fe dilute alloys, supercond. and mag. props. 80−29494
Te-Au film, metastable supercond. alloys, produced by low temp. ion implantation 80−88670
Te-Au film, supercond. by ion irrad. 80−34544
Te-I, A1-type, superconductivity 80−29496
Th-H system, supercond., book contrib. 80−25037
Th-La(Y)(Ce)(Zr)(Bi)-H, hydride form. and supercond. 77−36007
Th-Y-Ce, supercond., magnetisation of Ce impurities, sp. ht. meas. 78−47904
Th-Zr, supercond. transition temp. depend. on constitution 78−88056
Th-Zr alloys, BCC phase, supercond. props. 79−87178
$Th_7Co_3(Fe_3)$, spin-pairing state investig. via Josephson current between weakly-coupled superconductors 77−47942
Th_7Fe_3, H induced change from supercond. to mag. ordered state 79−28525
Th_4H_{15}, H vibr. modes, neutron scatt. study, phonon density of states 79−42195
Th_4H_{15}, superconductivity and electron-phonon interaction 80−49975
Th_4H_{15}, ThH_2, phonon densities of states rel. to supercond. props. 77−27960
$Th_4H_{15}(D_{15})$, normal and supercond., low-temp. sp. ht.; Debye temp. and supercond. props. 77−4466
$ThMg_2$, cubic Laves compound, sp. ht. rel. to supercond. 79−82356
$ThRu_2$, type II supercond., ESR of Nd^{3+} meas. 79−28444
$ThRu_2$:Nd^{3+}, supercond. state, ESR investigation 79−78514
$Th_{65}Sc_{35}Ce$, supercond., magnetisation of Ce impurities, sp. ht. meas. 78−47904
Ti and Ti-Nb, plastic deform. and thermal cond., 2.5 to 10K, dislocation pinning 77−35629
Ti, for supercond. microwave cavities, secondary electron emission and AES meas. 79−56895
Ti, transition temp., perturbative corrections, direct and indirect ladder diagrams 80−49979
Ti-based HCP-BCC binary systems, electronic struct. and supercond. *(Russian)* 79−33375
Ti-Mo (3 to 35 wt.%), high pressure influence on transition temp. to supercond. 80−107952
Ti-Mo (5 at.%) based alloy, supercond. transition temp. enhancement by varying struct. state 77−20483
Ti-NB-V-Zr alloy, struct. determ. by optical microscopy and electron diffraction *(Russian)* 77−16628
Ti-Nb superconducting alloys and cmpds. with A15 struct., H_2 effect on supercond. props 79−28438
Ti-Nb-Si, amorphous alloy, supercond. props. and crystn. behaviour, TEM and DTA study *(Japanese)* 80−84536
Ti-Nb-Zr-Fe, supercond. and paramag. props., effect of Fe additions *(Russian)* 80−65730
Ti-Nb-Zr-Ta, superconducting props. comp. depend., stress effects and precipitation behaviour, X-ray scatt. 80−93059
Ti-U(Cr)(Mo)(W), dilute, superconducting transition temp. and mag. suscept. 78−47899
Ti-V (19 at.%), aged ω-phase precipitation, incomplete proximity effect 78−60252
Ti-V-Cr, electron-lifetime effects on props. 80−10951
Ti-V(Nb)(Ta), influence of different factors on supercond. transition width *(Russian)* 79−1636
$TiBe_2$, weak itinerant magnetism as inhibited superconductivity 79−51715
$Ti_{1-x}Co_x$, electronic struct. and anomalies of elec. and mag. props. 80−6710
TiN films, reactively RF sputtered, struct. and elec. props., substrate bias effects 80−96763
TiN, for supercond. microwave cavities, secondary electron emission and AES meas. 79−56895
TiN, high dispersed superconductivity 78−43505
TiN, low-energy ion-stimulated deposited, supercond. props. 80−88664
TiN, phonon dispersion curves, soft-mode behaviour, inelastic neutron diffr. 78−43083
TiN single crysts., supercond. T_c at high press. 79−38228
TiN, supercond. critical temp., neutron irrad. effect 80−80433
TiN, superconductivity 78−2605
TiN, VPE, and superconductivity *(German)* 77−24964
$Ti_{55}Nb_{45}$, supercond., anomalous phonon thermal resist. 77−69451
$Ti_{1-x}Ni_x$, electronic struct. and anomalies of elec. and mag. props. 80−6710
Tl-Pb-Bi, critical field and specific heat 79−73631

type II superconductors continued
Tl-Pb-Bi alloys, supercond., electronic density of states from heat capacity meas. 79−56383
$Tl_2Mo_{15}Se_{19}$, superconducting chalcogenides containing Mo_6 and Mo_9 clusters 80−103804
$Tl_2Mo_6Se_6$, one dimensional supercond. crystal struct., resist. and upper crit. field 80−50016
$Tl_{0.33}WO_3$ bronze, elec. resist. meas., anisotropy, supercond. 80−75569
$Tl_{0.33}WO_3$, supercond. and special phonons, neutron scatt. obs. 80−15643
TmO_6S_8, low temp. Mossbauer study and mag. susceptibility 80−80656
$TmRh_4B_4$, mag. and supercond. props., mag. susceptibility and sp. ht. meas. 79−78344
U, supercond., phonon-softening 78−10592
α-U-Mo, dil., electronic properties depend. on $2^1/_2$-th order phase transition under high press. *(Russian)* 80−11128
U_6Fe, spin-pairing state investig. via Josephson current between weakly-coupled superconductors 77−47942
$U_6Fe_{0.98}$ supercond. transition temp. reduction by neutron irradiation 77−63020
$U_xPb_{1\pm x}Mo_{6+y}S_8$, sputtered supercond. props. 80−50019
US, phonon anomalies 79−7663
$(V,Fe)_3M$, M=Si, Ge, Ga, solid soln. form. and supercond. T_c *(Russian)* 78−80512
$(V,Nb)_3Ga$, $(V,Nb)_3Ge$ and $(V,Nb)_3Si$ solid solns., supercond. T_c, absolute thermal EMF, microhardness 77−36006
$(V,Nb)_3Si$ type with A15 struct., supercond. transition temp., depend. on stoichiometry *(German)* 77−69444
$V_3Ga_{1-x}Sn_x$, lattice props. supercond., ^{119}Sn Mossbauer shift meas., 5-300K 77−1627
V, amorphous film, supercond. props., gaseous impurities effect *(Russian)* 78−72301
V, and V-Nb alloy, T_c and H_{c2}, effect of purity and alloying with Ta, Cr, Mo or Re 77−85375
V columnar films, crit. field anisotropy, depend. on prep. conditions *(Russian)* 80−93056
V, creep effect in periodically swept minor hysteresis loops 79−60964
V, effect of O ion irradiation on supercond. 78−52131
V, electron-phonon coupling constant calc. *(Russian)* 80−70624
V, electron-phonon interaction, calc. using APW band struct. calcs. and measured phonon spectra 78−14869
V, electronic density of states, effective mass, electron-phonon interaction, Coulomb pseudopot. *(Russian)* 78−26804
V, Fermi surface area, effective heat, optical masses, surface anisotropy critical temp. depend. *(Russian)* 79−90943
V film, inhomogeneous, crit. field anisotropy 79−56459
V film, resist. supercond. transition 80−25033
V film, resistive transitions scaling behaviour 79−15248
V film, resistive transitions *(Russian)* 79−95546
V film, scaling behaviour of resistive supercond. transitions 79−56363
V, fluctuation contrib. to US attenuation in mag. field near H_{c2} 77−47936
V, fluctuation contrib. to sound attenuation near H_{c2} 79−33397
V, fluxural oscillations in longitudinal mag. field, sound attenuation, magnetoelasticity *(Russian)* 80−54844
V foil, time behaviour of local flux flow noise 79−24116
V heat switches, effect of surface prep. 79−60966
V, lattice dynamics, microscopic theory 79−7664
V, low-temperature thermal and elec. cond. 79−60792
V, plastic deform. effect on positron annihilation and supercond. transition *(Russian)* 77−39993
V Si, supercond. alloy, electron distrib. vel. to Cr_3Si 77−68944
V, small particles, crystal structure, magnetic and superconducting props. 80−97121
V, soft modes, d-electron localisation 78−14872
V, spin fluctuations effect on T_c, from sp. ht. and mag. suscept. 80−7030
V, supercond., influence of plastic deform. 77−85378
V, superconducting, fluxoid pinning by VC_x precipitates 78−52169
V, superconducting, microwave biased RF-SQUID system, appl. to magnetic aftereffect 79−26089
V, superconductor, neutron irradiation, low temp., effect on critical current 78−52180
V, thermal conductivity in ultrapure normal, mixed and supercond. states *(Russian)* 79−4617
V, thin film, determ. of energy gap, tunnel effect method 79−42704
V wire, helical propag. of flux jumps 78−14901
V/H, heat capacity and supercond. between 1.5 and 16K 80−2521
V-Al junction, spin-dependent electron tunnelling 79−19700
V-Al/Cu-Ge composite superconductors, transition temp. and upper crit. field, heat treatment effects 79−38268
V-Al(Ga,Si,Ge,Sn)-Cu, equilib. and rapidly quenched, struct. and props. 80−76235
V-based A15 compounds, nuclear spin-lattice relax. time, electronic density of states 77−59354
V-Ga(Ge)(Si), fast quenching of A15-phases *(German)* 77−36014
V-Hf-Nb(Zr), multifilamentary, superconducting props. improvement 79−38267
V-M, M=Ti, Nb, Sm, vacuum deposited supercond. films, T_c chem. comp. depend. *(Russian)* 78−19174
V-Nb-Ta, elec. resist. and electron-phonon interaction parameters, comp. depend. 78−14862
V-Re system, discovery of supercond. A-15 phase 78−88060
V-Si-C film, struct., crit. temp., resist. 78−72299
V-Sn(Al)(Ga)(Ge)(Si)-C, phase equilib. and supercond. 80−50593
V-Ta, superconducting transition temp., nondiagonal disorder effects 79−73622
V-Ta alloys, electron-phonon interaction and supercond. transition temp. *(Russian)* 79−28426
V-Ti alloys, supercond., thermal cond. 77−89900
V-Ti superconducting film, electron spin effects 79−28488
V-Ti(Cr) amorphous films, supercond. transition temp. 79−60953
V-Zr-Nb alloy, rel. between density of states and martensitic and superconducting phase transition temps. 78−10594
V_1 single cryst., supercond., Ginzburg-Landau parameters, magnetisation meas. 78−2620
V_3Ga, high T_c supercond., electron-phonon coupling, effect of electronic density of states sharp struct. 78−14877
V_3Ge, superconducting filament formation near edge dislocation *(Russian)* 79−4635
V(-Ti), rotating discs, hysteresis losses and mag. phenomena 80−75695

type II superconductors continued
V_3Al film, quasiamorphous, supercond. phase formation by heat pulse 77−63017
$V_3Al(Ga)(Si)(Ge)(Sn)$ electronic struct. calcs. 79−47005
VC, metastable supercond. phase, effects of rapid quenching on transition temp. 78−2611
$(V_{1-x}Cr_x)_3Si$, elastic moduli, 4.2 to 290K, softening near supercond. transition *(Russian)* 80−92582
$(V_{1-x}Cr_x)_3Si$, mag. susceptibility, 4.2 to 320K, density of states model 80−7035
$(V_{1-x}Cr_x)_3Si$, single cryst., elec. resistivity, temp. depend. 79−56193
$V_{3-x}Cr_xSi$, x=0 to 3, struct., supercond. and mag. props. 80−1962
$V_3(Fe,Ge)$, struct. and supercond. transition temp. *(Russian)* 79−7920
$V_{0.75-x}Ga_{0.25+x}$ ^{51}V, nucl. spin-lattice relax. time, annealing and neutron effects 79−82710
$V_{1-x}Ga_x$, nuclear spin-lattice relax. and supercond. 79−56387
V_2Ga, phonon density of states, temp. depend. 79−42183
V_3Ga, A15 compound, exam. of deformation processing, review 78−39864
V_3Ga, A15 cpd., hydrogenation effects on supercond. transition temp., lattice parameters 80−103772
V_3Ga, cast, effect of hydrostatic extrusion on supercond. props. *(Russian)* 77−21215
V_3Ga, crit. temp. and field, prep. from V-Al and Cu-Ga 78−43506
V_3Ga, development by diffusion processes and use in 17.5 T supercond. magnet 79−61015
V_3Ga, diffusion-processed layer, texture meas. 79−82726
V_3Ga, filamentary conductors, type-II, low temp. 30 GeV proton effects on critical props. 78−52178
V_3Ga, grain size in A-15 reaction layers 78−14911
V_3Ga, high current density multifilament wire, neutron effects on equilibrium and transport props. 78−52126
V_3Ga, high-current A-15 microcomposite material 80−44781
V_3Ga, long-range order parameter variations determ. and correls. with supercond. T_c 77−11504
V_3Ga multifilament superconductors, AC losses 79−60979
V_3Ga, multifilament superconductor, pulsed mag. field losses and critical current densities 80−54853
V_3Ga, multifilamentary high-field superconductor, status of development 79−61004
V_3Ga, multifilamentary wire, stress effect on critical currents 77−80891
V_3Ga, multifilamentary wire, crit. current props. with third element additions 79−61013
V_3Ga multifilamentary wires, critical current densities 79−69645
V_3Ga, neutron irrad. effect on upper crit. field and crit. current 77−72954
V_3Ga, neutron irrad. effects on transition temp. *(Japanese)* 79−82707
V_3Ga, neutron irradiation and annealing 78−52130
V_3Ga, nuclear magnetic relaxation, near T_c *(Russian)* 79−42852
V_3Ga, phonon densities of states and Debye temp. calcs. 79−51212
V_3Ga, pinning characteristics *(Japanese)* 78−91829
V_3Ga, single crystal prep. by iodine transport, supercond. T_c meas. 78−48294
V_3Ga, structure effects on supercond. props. and electron spectrum *(Russian)* 77−80862
V_3Ga, supercond., μ^+ probe study *(Russian)* 79−7946
V_3Ga, supercond., neutron-induced disorder revealed by isochronal annealing 77−72938
V_3Ga, supercond. A15 phase, prep. by controlled precip. 80−81000
V_3Ga, supercond. and high mag. fields 79−87215
V_3Ga, supercond. μSR meas. 79−56667
V_3Ga, supercond. transition temp., as-cast and annealed *(Russian)* 78−56618
V_3Ga superconducting tape, diffusion-processed, cryst. textures, X-ray pole figures 79−11266
V_3Ga superconducting tape, stress effect on critical current *(Japanese)* 80−50020
V_3Ga, superconducting transition temp. and electron density of states 77−32105
V_3Ga, superconducting transition temp., metallurgical processing, struct. 77−63019
V_3Ga-Cu, high-current A-15 microcomposite material 80−44781
V_3Ga-Cu composites, supercond. props. 79−95557
V_3Ga-Nb_3Sn concentric solenoid magnet system, 17.5 T operation 77−26353
V_3Ga-V_3Pt alloy, crit. temp., comp. depend. *(Russian)* 77−59347
V_3Ge, A-15 cpds., nucl. mag. relax. in normal and supercond. state 80−49993
V_3Ge, A-15 struct. supercond., microhardness, bonding 78−76199
V_3Ge, A15 cpd., hydrogenation effects on supercond. transition temp., lattice parameters 80−103772
V_3Ge, Anderson-Gruneisen parameter, from 3rd order elastic const. data 79−33059
V_3Ge, anisotropic thermal vibrations, lattice const. X-ray study 80−34164
V_3Ge film, T_c var. with ^4He irrad. induced defects 77−8220
V_3Ge films, α-particle induced defects and stoichiometry 77−32101
V_3Ge, forbidden Bragg refls., rel. to supercond. transition temp. 79−15251
V_3Ge, low temp. props., mag. suscept. and resistance 78−19213
V_3Ge, phonon densities of states and Debye temp. calcs. 79−51212
V_3Ge, phonon density of states, temp. depend. 79−42183
V_3Ge, superconducting, high transition temp., sputtering 78−15309
V_3Ge, superconducting A-15 type compounds, transition temp., radii ratio and structure *(Chinese)* 80−44752
V_3Ge, superconducting transition temp. and electron density of states 77−32105
$V_3Ge_xOs_{1-x}$, low temp. props. 79−99652
$V_3Ge(Si)$, electron-phonon coupling and supercond. crit. temp. 79−33379
$V_3Ge(Si)$, Gruneisen parameter and thermal expansion eval. at room temp. 80−70351
$V_3Ge(Si)$, supersuperconducting transition temp., correl. with resist. anomalies and defect struct. 77−47920
V_2Hf, fast neutron irrad. effects on T_c 77−55633
V_2Hf-base C15 compounds, development as high field supercond. 79−61015
$V_2Hf_{1-x}Ta_x$, C15 supercond., electronic and lattice props. 78−68110
V_2HfZr, C-15 cryst. struct. supercond. props. 78−64173
$V_2Hf_{1-x}Zr_x$, normal and supercond. state, transition temps., mag. susceptibility and specific heat determ. *(Russian)* 80−60132

type II superconductors continued
$V_{0.62}Ir_{0.38}$, supercond., Knight shift contrib. to reson. line shift meas. 77−4467
$V_{3-x}M_xGa$, M=Ti, Cr, Mn, Fe, Co, Ni, cryst. struct. and microhardness meas. 79−86740
$V_{75-x}M_xGa_{25}$, M=Ti, Cr, Mn, Fe, Co, Ni, supercond. transition temp. and electron-phonon coupling parameter 79−60952
VN, electronic struct. of vacancies, effect on supercond. transition temp. 80−29347
$VN_{0.74}$ and $VN_{0.89}$, low-temp. specific heat and superconducting critical temp. meas., density of states 80−54835
V_3P, superconducting transition temp. 78−47898
$V_{0.76}Pt_{0.24}$, supercond., Knight shift contrib. to reson. line shift meas. 77−4467
$V_{1-x}Pt_x$, A-15 struct., Knight shift in normal state, upper crit. field curves *(French)* 78−43519
V_3Pt, supercond., Knight shift contrib. to reson. line shift meas. 77−4467
$V_{1-x}Pt_x(Ga_x)(Si_x)$, A-15 cpds., nucl. mag. relax. in normal and supercond. state 80−49993
V_3Si, ^4He induced damage, channelling effect meas. 77−62570
V_3Si, A 15 compound, Raman scatt. and phonon density of states 79−28768
V_3Si, A-15 struct. supercond., microhardness, bonding 78−76199
V_3Si, A-15 supercond. cpd., martensitic transform. 79−60499
V_3Si, A15 compound, exam. of deformation processing, review 78−39864
V_3Si, A15 compound, microscopic model of supercond. and martensitic transform. 77−8226
V_3Si, A15 compounds, Hall coeffs. 79−33281
V_3Si, A15 cpd., hydrogenation effects on supercond. transition temp., lattice parameters 80−103772
V_3Si, Anderson-Gruneisen parameter, from 3rd order elastic const. data 79−33059
V_3Si, anharmonic contrib. to mode softening 79−73241
V_3Si based ternary solid soln., supercond. T_c and paramag. susceptibility *(Russian)* 77−59348
V_3Si, channelling, at displacements and electron phonon/defect interactions 77−84815
V_3Si, chemical composition effect on phase transition and transition temp. 78−14860
V_3Si, Czochralski growth, supercond. behaviour 79−74080
V_3Si, d-spacing fluctuations above Martensitic phase transition 80−7570
V_3Si, de Haas van Alphen meas. of Fermi surface for H≤40 T 79−73424
V_3Si, de Haas-van Alphen oscills. in normal state 79−56116
V_3Si, dislocations, obs. by TEM 77−59012
V_3Si, elec. resist. below 77K, phonon assisted interband scatt. 78−14703
V_3Si, electron charge distrib., martensitically transforming single cryst., X-ray diffr. meas. 78−75631
V_3Si, electron energy loss spectra, AES and HEED investig. of surface 77−24635
V_3Si, electron spectrum characts., mag. susceptibility depend. on resistivity ratio 79−95320
V_3Si, electronic struct., electron-phonon interaction and high temp. superconductivity, APW calc. 78−14871
V_3Si embedded in resin, composite supercond., high transition temp. 80−88660
V_3Si, exam. of superconductivity and props. 79−1649
V_3Si, Fermi surface topology, positron annihilation meas. 79−56117
V_3Si film, far IR reflection and transmission spectra, room temp. 77−55792
V_3Si film, optical props. *(Russian)* 80−93418
V_3Si film, quasiamorphous, supercond. phase formation by heat pulse 77−63017
V_3Si film, sputtered, high press. induced shifts in supercond. transition temp. 77−85374
V_3Si film, struct., crit. temp., resist. 78−72299
V_3Si film, superconducting props. 79−38213
V_3Si film, T_c var. with ^4He irrad. induced defects 77−8220
V_3Si films, α-particle induced defects and stoichiometry 77−32101
V_3Si, grain size in A-15 reaction layers 78−14911
V_3Si, grown-in dislocations, diffr. contrast behaviour 79−86794
V_3Si, Hall effect, 77K to superconducting transition temp. 78−43359
V_3Si, heat capacity rel. to temp. *(Russian)* 78−52152
V_3Si, high T_c supercond., electron-phonon coupling, effect of electronic density of states sharp struct. 78−14877
V_3Si, ion irradiated, influence on struct., resist., and supercond. transition temp. 80−54823
V_3Si, low fluence neutron irradiation, behaviour of supercond. transition temp. 78−43509
V_3Si, low temp. irrad. with 20 MeV S ions, effect on supercond. props. 79−38223
V_3Si, low temp. sp. heat and thermal cond. 77−15995
V_3Si, magnetic susceptibility, density of states model for lattice transformation in A-15 compounds 80−65219
V_3Si, martensitic transform. coupling with supercond. transition 78−44126
V_3Si, martensitic transform., thermal expansion meas. in normal and supercond. states 79−56381
V_3Si, Mossbauer spectra of ^{57}Fe *(Russian)* 79−24235
V_3Si, neutron irrad., grain boundary pinning, field-depend. change of crit. current density 80−65759
V_3Si, neutron irrad., neutron diffraction studies 78−88076
V_3Si, neutron irrad., sound velocity, magnetic susceptibility and upper critical field 78−88074
V_3Si, neutron irrad. effects on transition temp. *(Japanese)* 79−82707
V_3Si, neutron irradiated, A15 compound, recovery of T_c by annealing 78−52132
V_3Si, neutron irradiated single crystal, superconducting transition temp. widths, resistivity and heat capacity meas. 78−91802
V_3Si, neutron-irrad., ht. capacity and resistivity 78−88075
V_3Si, nontransforming, press.-induced phase transformation 78−80084
V_3Si, normal, mixed and supercond. state, specific heat meas., thermodynamic and superconducting props. 80−49987
V_3Si, normal state, Fermi surface, de Haas-van Alphen oscills. 79−65369
V_3Si, normal state resistivity as function of neutron irrad. 79−56194
V_3Si, nuclear magnetic relaxation, near T_c *(Russian)* 79−42852
V_3Si, optical props. and electron-phonon interactions 80−2510
V_3Si, phonon densities of states and Debye temp. calcs. 79−51212

type II superconductors continued
V_3Si, phonon density of states at 300K, mode softening 77−11648
V_3Si, phonon density of states, temp. depend. 79−42183
V_3Si, phys. props., appl. of new three-dimens. k.p model for A-15 cpds. 78−23015
V_3Si, plastic deform. effect on supercond. props. 80−29500
V_3Si plastically deformed cryst., lattice transform., Kossel technique 78−95153
V_3Si, positron annihilation lifetime meas. 79−19946
V_3Si single cryst., A-15 compound supercond., plastic deform., at high temp. 79−20104
V_3Si, single cryst., double supercond. transitions 79−28430
V_3Si, single cryst. growth by electron beam melting 78−64467
V_3Si single crystal, radiation damage and superconductivity 78−52129
V_3Si single crystals, channelling effect studies using He ions and $^{28}Si(d,p_8)$ reaction 79−4362
V_3Si, single crystals, supercond. tunnel characts. 80−7044
V_3Si, soft mode sound vel. in mag. field rel. to density of states 78−14647
V_3Si, sp. ht. anomaly at struct. transform. 78−14426
V_3Si, supercond., crit. fields Pauli paramag. limiting and material parameters 79−78277
V_3Si, supercond. and struct. transitions *(Russian)* 78−52118
V_3Si, supercond. props., effect of neutron irrad. 80−80463
V_3Si, supercond. tape, growth technique via amorphous state 78−84708
V_3Si, supercond. transition temp. and phase transform. at press. up to 45 kbar 79−56352
V_3Si superconducting bridge junctions, vortex model appl. *(Russian)* 79−60986
V_3Si, superconducting thin films, energy gaps from tunnelling meas. 80−25050
V_3Si, superconducting transition temp. press. depend., for shear-stress induced tetragonal phase 77−36010
V_3Si superconductor film, Fourier and laser spectroscopy comparison in far IR-sub. mm. range 79−93237
V_3Si, thermal expansion, 20-300°C, using differential push-rod dilatometer 80−39320
V_3Si, thermal expansion meas., 4.2 to 293K 79−56382
V_3Si, thermodynamic study, intrinsic type II superconductivity 79−47193
V_3Si thin films, Holstein processes and electron-phonon spectral function, far IR meas., 19K 79−87445
V_3Si, thin films in supercond. and normal states, far IR laser spectroscopy 79−61453
V_3Si, transforming and nontransforming, high press. effects 78−80086
V_3Si tunnel junctions, energy gap investigation 80−84569
V_3Si, US anomaly when cooled below martensitic and supercond. transition temps. 80−20354
V_3Si-Fe, mag. impurities effect on supercond. props. 77−1524
V_3Si-M, M=Hf, Nb, Ta, Mo, W, Ni, Ge, Sb, cryst. struct., supercond. T_c comp. depend. 78−51494
V_3Si-SiO_x-Mo_3Re_2, supercond. tunnel junctions 80−107961
$V_3(Si_{1-x}C_x)$, bulk, effect of C on supercond. transition temps. and microstructure 80−54824
$V_3Si(Ga)$, coherence parameter, nonlinear high temp. supercond. elements with A-15 lattice *(Russian)* 80−60127
$V_3Si_{1-x}Ge_x$, elastic props., 77 to 290K, rel. to supercond. transition temp. *(Russian)* 80−66560
$V_3Si_{1-x}Ge_x$ solid soln., longitudinal and transverse US wave propag. rate, 4.2 to 300K *(Russian)* 80−103423
$V_3Si_xOs_{1-x}$, supercond. transition temp. and paramag. susceptibility 79−28436
V_3Sn, ultrafast quenched and subsequently tempered, supercond. T_c 78−64162
V_3Sn, $V_3Sn_{0.5}Al_{0.5}$, and $V_{2.5}Ti_{0.6}Sn$, elec. resist., temp. depend., T_c to 300K 79−65426
V_3Ti, metastable supercond. phase, effects of rapid quenching on transition temp. 78−2611
$(V_{1-x}Ti_x)Ge$, pseudobinary A15 compound, supercond. transition temp. 80−49970
W-Re amorphous alloys, phase-slip and localisation diffusion lengths 80−107747
$W_{0.65}Re_{0.35}$, search for strong coupling superconductivity 79−28441
$W_{70}Si_{20}B_{10}$, amorphous alloys obtained by liq. quenching, superconductivity 80−75670
$(Y,La)B_6$, superconducting transition temps., impurity effects 80−20341
$Y_{0.7}$ $Th_{0.3}C_{1.58}$, specific heat 78−91813
$Y_{1-x}Gd_xRh_4B_4$, mag. supercond., anomalous temp. depend. of upper crit. fields 80−29510
YGe_2 film, supercond. obs. 77−72939
$Y_xLu_{1-x}Ir_4B_4$, supercond., magnetism and metastability 80−29501
YM_2-Gd, M=transition metal, correl. between g-shift and stability, EPR study 80−88874
YMo_6X_8 (X=S, Se), supercond., sp. ht., 1 to 14K 79−51720
$Y_xPb_{1\pm x}Mo_{6+y}S_8$, sputtered supercond. props. 80−50019
YRh_4B_4, supercond., anomalous cond.-electron polaris. 80−25047
YRh_4B_4, supercond., electronic struct. and reentrant magnetism 78−10340
$Y(Rh_{0.85}Ru_{0.15})_4B_4$, mag. ordering and supercond. 78−14861
YS, soft-mode behaviour in phonon dispersion, inelastic neutron scatt. meas. 78−38807
YS, supercond., phonon anomalies, inelastic neutron scatt. 78−59901
YS, supercond. transition temp. and lattice dynamics 79−56361
YS, superconductor, resonances in generalised susceptibility and phonon anomalies 79−60443
$Y_{0.7}Th_{0.3}C_{1.55}$, superconducting crit. mag. field curve, initial slope 77−28318
$YbFe_xMo_6S_8$, singularities in mag. and supercond. props. 79−51710
$YbMo_6S_8$, low temp. Mossbauer study and mag. susceptibility 80−80656
$YbMo_6S_8$, supercond., low temp. thermal and mag. props. 78−14904
Zn-Mn, dil., Kondo effect and impurity interactions in resist., transition to supercond., 0.05-14K 78−14721
Zn-Mn, thermal cond. compared with Shiba's theory 77−8228
$ZnMo_5S_6(Se_6)$, Chevrel-phase, low temp. struct. instability rel. to supercond. 77−47919
Zr, H(D) implanted, superconductivity enhancement obs. 80−70884
Zr-Nb (20%), low-j_c supercond. vortex pinning *(Russian)* 77−80885
Zr-Nb-V-Si alloy, struct. determ. by optical microscopy and electron diffraction *(Russian)* 77−16628
Zr-Pd, metallic glasses, electronic props. and supercond. 79−73486

type II superconductors continued
Zr-Rh alloys, amorphous, thermal relax. effects on electronic and supercond. props. 79−65575
Zr-Rh-H(D), superconducting transition temp., effect of H(D) conc. 80−84532
Zr-V, superconductivity and metallurgy of C15 materials 79−4610
Zr-V foil, rapidly quenched and heat treated, supercond. props. 80−54852
Zr_xBe_{1-x} noncrystalline alloy, phonon-electron scatt., superconducting temp. 80−54330
ZrC, supercond. transition temp. and lattice dynamics 79−56361
ZrC_x, x=0.99 to 0.13, elec. cond., supercond. state 78−43504
$Zr_{70}Co_{30}$, metallic glass, low temp. resist., supercond. T_c 79−38235
$Zr_3Co_{1-x}M_x$, M=Cu, Ni, Fe, Mn, Ag, and Ru, phase stability and supercond. T_c 78−80519
$Zr_{65}Cu_{35}$, metallic glass, low temp. resist., supercond. T_c 79−38235
$(Zr_{1-x}Er_x)_3Rh$, amorphous, influence of mag. ordering on supercond. props. 80−29511
ZrGe, film, supercond. obs. 77−72939
$ZrGe_2$, RF sputtered, crit. temp. 78−14853
$Zr_3Ge(P)(Sb)(Si)$, superconducting transition temp. 78−47898
$Zr_xHf_{1-x}V_2$, polycrystalline superconductor, resist. and mag. susceptibility, transition temp., temp. depend. 80−25113
ZrN, form. in RF discharge 77−86222
ZrN, plasma-formed, ESCA and supercond. transition temp. 78−19697
ZrNb, supercond. thermal cond. meas. 79−60970
Zr_2Ni, spin-pairing state investig. via Josephson current between weakly-coupled superconductors 77−47942
$Zr_{70}Ni_{30}$, metallic glass, low temp. resist., supercond. T_c 79−38235
$Zr_{0.7}Pd_{0.3}$, amorphous supercond., sp. ht. and thermal cond., 0.1-10K 78−26991
$Zr_{75}Rh_{25}$, amorphous, evidence for short wavelength cutoff in fluctuation spectrum 78−68113
$Zr_{75}Rh_{25}$, amorphous superconductor, high-κ, upper and lower crit. fields 79−4629
$Zr_{1-x}S$, short- and long-range ordering of vacancies, rel. to supercond. transition temp. 77−19945
$Zr(V,Al)_2$, struct., supercond. props., elec. resist. and mag. susceptibility, 4.2 to 300K *(Russian)* 79−15246
$ZrV_{,2}$, supercond., dielec. phase transition *(Russian)* 78−64168
ZrV_2, anomalous softening at martensitic transform. 80−93630
ZrV_2, C-15 struct., phase transitions, elec. cond., crystal lattice parameters *(Russian)* 80−54826
ZrV_2, C15 supercond., dielec. transitions, temp. depend. of resist. and mag. susceptibility, 4.2-300K 79−38136
ZrV_2, dielectric phase transition, elec. resist. temp. depend. 79−65525
ZrV_2, elec. resist. and mag. suscept., anomalous temp. depend. 79−69491
ZrV_2, Laves-phase, cubic to rhombohedral transition, lattice electron instability 78−92261
ZrV_2, supercond., Young's modulus and internal friction meas. 79−11654
ZrV_2, supercond. rel. to struct. instability *(Russian)* 78−23196
$ZrZn_2$, weak itinerant magnetism as inhibited superconductivity 79−51715

typesetting, computer-controlled *see computer controlled typesetting*

U-centres
alkali halide:$H^-(D^-)$, local modes and colour centre absorpt. bands, analogy 80−60632
alkali halide, localised mode due to U-centre 77−20036
alkali halide, U-centre pairs, localised modes 77−7813
alkali halide crystals, mixed, impurity centre local vibrs., comp. depend. of spectral parameters 80−79898
alkali halides, electronic struct., self-consistent model 79−65406
alkali halides, local and reson. modes due to hydide ions, U-centres and additive cation impurities 79−77710
alkali halides, mixed, U-centre localised modes 80−100319
alkali halides, U_2 centres, cluster-Bethe lattice calc. for electronic density of states 79−4531
alkali halides, U-centre electronic struct. cluster-Bethe lattice calc. 80−107737
chalcogenide glasses, trap controlled transient photocond. 80−44641
chlorides, I^- or Br^- doped, optical investigation of atomic hydrogen centres 78−88351
KBr(I):D, inelastic light scattering of localised vibration of interstitial H atom in alkali halides 80−88998
metal-semiconductor disordered interface, supercond. transition temp. enhancement by bipolaron interface centres 80−84528
BaClF, localised vibr. of U-centres 78−75779
BaF_2, U-centre, electronic struct. and optical transition energies, SCF MS Xα calc. 79−4532
CaF_2, localised vibrs. due to substitutional impurities 78−22803
CaF_2, U-centre, electronic struct. and optical transition energies, SCF MS Xα calc. 79−4532
CsI:H^-, force consts. using Green's functions 79−46775
KBr:H^-, U-centre absorpt. band shape, piezodichroism dispersion curve and electron-phonon interaction 77−24873
KBr:Na, U-centres, HFS and g-factor, EPR spectra 80−39869
KBr:Rb, U-centre modes, Green's function method calc. 77−24372
KBr(Cl):OH^-, cc U_2 to H_2O^- defects conversion after UV photodecomp. 80−107230
KCN:H^-, U-centre, local mode meas. 77−1199
KCl, U-centre electronic struct., expanded unit cell model 78−72109
KCl:$CaCl_2$, KOH, complex form., U-centre influence, optical absorpt. bands 77−80502
KCl:$F^-(Br^-)(I^-)$, U-centres, local defect modes, Green's functions calcs. 80−44280
KCl:H, dichroic H- and U-centres by polarised bleaching of interstitial H 80−29766
KCl:H, migration and stabilisation of H atoms, ESR and thermolum. study 79−1430
KCl:Na(Ag), UV irrad. anionic H and D atoms, ESR and optical absorpt. expts. 79−99187
KCl-KH, F- and U-centre redistrib. at end of proton tracks, microspectrophotometric anal. 80−10583
KCl-KH cryst. stimulated by X-radiation, spatial redistribution of F and U centers 79−14804
$KCl_{1-c}Br_c$, impurity centre local vibrs., comp. depend. of spectral parameters 80−79898
KCl(Br)(I), U_2 and U_1 centres, optical excitations 80−2803

U-centres continued
KI:H^-, force consts. using Green's functions 79−46775
$K_{1-c}Na_cCl$ and $K_{1-c}Rb_cCl$, impurity centre local vibrs., comp. depend. of spectral parameters 80−79898
LiF:OH crystals, X-irradiated, H centres formation and annealing 80−54226
NaBr-U-centre containing cryst., X-ray radiation induced cation vacancy generation 80−39078
NaCl:H^-, U-centre absorpt. band shape, piezodichroism dispersion curve and electron-phonon interaction 77−24873
NaCl:Li, U-centres, HFS consts., g-factor, EPR spectra 80−39869
NaCl(Br)(I), U_2 and U_1 centres, optical excitations 80−2803
NaI:H^-, force consts. using Green's functions 79−46775
RbCl containing K additive impurity, local modes due to U-centres 78−22805
RbCl, lattice localised modes due to U-centre pairs 79−77709
RbCl, U-centre local modes calcs. 77−62603
RbCl:H^-, defect pairs of F-centres and U-centres, Raman meas. 79−7599
RbCl:Na, U-centres, HFS consts., g-factors, EPR spectra 80−39869
RbI:H^-, force consts. using Green's functions 79−46775
SrClF, localised vibr. of U-centres 78−75779
SrF_2, U-centre, electronic struct. and optical transition energies, SCF MS Xα calc. 79−4532

UBV photometry *see stellar photometry*

u.h.f. amplifiers *see ultra-high-frequency amplifiers*

u.h.f. tubes *see ultra-high-frequency tubes*

ultimate tensile strength *see tensile strength*

ultra-high-frequency amplifiers
see also microwave amplifiers
GaAs FET amplifier, varactor-tuned, for UHF SQUID magnetometer 80−31814
monolithic SAW amplifier and periodic grating oscillator 79−50447

ultra-high-frequency tubes
see also microwave tubes
No entries

ultracentrifuges *see centrifuges*

ultrafiltration *see filtration*

ultrasonic absorption
400 MHz to 2.3 GHz acousto-optic deflectors 79−50416
A-phase, order parameter collective modes, effect on NMR and US attenuation 79−46866
abietic acid, transverse US wave propag., glass and liquid transition region 80−79883
acetic acid, effect of impurities on US relaxation 78−10130
acetic acid-carbon tetrachloride, US absorption, coupled dimerisation cyclisation reaction *(French)* 79−42148
acoustic characteristics, of solid materials, instrument for direct meas. 79−14179
acrylamide aqueous solution, ultrasonic investigation *(Chinese)* 80−107371
acrylic gel, US observation of critical behaviour *(French)* 79−29414
adhesive bonds, physical modelling, US attenuation effects 78−7141
adhesive bonds, transducer materials and adhesives for high temp. US generation 80−43586
air, absorption in 10-100 kHz range, NPL report 77−7239
air, HF sound absorpt. meas. 78−1475
air gap field configuration rel. to pole piece geometry and material inhomogeneity 79−30500
n-alcohols, sound vel. and absorpt. meas. at hypersonic freqs. 78−18708
algorithm for relaxation spectra in US spectroscopy 80−79038
alkali halides, aq. solns., hypersonic sound vel. and absorpt. meas. 78−30699
alkali liquid metals, US absorption due to electrons and phonons 79−28046
alkali metal-ammonia solns., metal-insulator transition, h.f. and u.s. props. 77−1369
alloys, disordered binary, crit. US attenuation 79−99272
amorphous insulators acoustic props. at low temps., ultrasonic attenuation, dielec. props. *(French)* 77−72658
amorphous mag. substance with rare earth ions, low temp. specific heat, elec. resistance and US absorpt. *(Russian)* 79−19734
aniline-cyclohexane, hypersound velocity, absorption temp. depend *(Russian)* 80−75303
animal tissues, freshly excised, attenuation and backscatt. obs. 80−51148
p-anisalaminoazobenzene, acoustic relax. in nematic phase 77−1184
anisotropic superconductor, finite freq. US attenuation 79−1640
anthracene, mol. crystal, meas. of US attenuation coeff. by optoacoustical methods *(French)* 80−70317
APAPA, nematic liq. cryst., effect of mag. field on US attenuation *(Japanese)* 79−19144
associated liq., US absorpt. and hole theory 78−10124
attenuation, of US main waves with distance 80−5859
attenuation meas., diffraction corrections for finite size of source and receiver 80−96153
attenuation meas. using quartz transducer transmitter-receiver 78−30139
attenuation/backscattering, by mammalian organ as function of time after excision 78−7412
austenite cladding layers, damping of ultrasound 80−104390
austenitic steels at large strain amplitudes 80−19192
automatic precision test installation for US waves through solids *(German)* 79−50549
benzene-hexafluorobenzene, mixtures, dielectric relax. and US absorpt. 77−12307
benzene-similar liquids, 10 to 1300 MHz 80−39229
binary liquid mixtures, containing one rotational isomeric relaxing liquid 80−70315
binary liquid mixtures, non-aqueous solns. of non-electrolytes 79−95081
binary liquid mixtures containing cyclohexanol 77−27948
binary organic liquid mixtures, 7.56 MHz 77−39630
biological cells, intracellular temp. distrib. 80−61623
biological tissue, dependence on constituent proteins 80−61621
blood, canine, US attenuation and speed, rel. to packed cell vol., 37°C 80−41106
blood, during tumour development in exptl. animals 77−25524
blood, sickle cell, effect of deoxygenation on US absorpt. coeff. 78−44477
blood, US propag., effects of red cell shape and orientation 78−24104
bone, 2 to 8 MHz US attenuation obs. 79−57701

ultrasonic absorption continued
borosilicate glass, interaction between EM and elastic waves at low temps. 77−31724
borosilicate glass US attenuation saturation by microwaves, low-temp. obs. 77−36114
borosilicate glass US attenuation temp. dependence rel. to γ irrad. 79−46755
brain, normal and abnormal, attenuation, vel. and impedance 80−45955
breast cancer connective tissue content correl. with US attenuation 80−45997
breast malignant tumour, freq. depend. US attenuation, fast Fourier transform technique 80−45996
bromochloromethane, rotational-vibrational energy transfer, US absorpt. obs. 79−98537
bulk superconductor, nonequilibrium and superlattice effects, US attenuation meas. 79−56390
t-butanol aqueous soln., sound absorpt. coeff. meas., acoustic relax. 78−83883
n-butanol-water-Ca $(SCN)_2$ system with hypercrit. point, US absorpt. 80−49306
N-n-butoxybenzylidene-n-butylaniline, US propag. near nematic-smectic A transition, mag. field effect 80−39266
cancer thermographic diagnosis enhancement by US irradiation 79−79614
carbon tetrachloride, liq. and plastic cryst. phases, thermodynamic props., light scatt., US propag. 78−2863
CBOOA, liq. cryst., mag. aligned, smectic A-nematic transition, US absorpt meas. 78−95137
CBOOA, US absorpt. and dispersion at nematic-smectic-A transition 79−82287
CBOOA, US attenuation near nematic-smectic A transition 78−87773
cellulose acetate solutions, US absorpt. coeff in 0.1-1000 MHz range 77−35638
ceramic and thin layer US pulse-echo meas. 77−28969
ceramics, fine-grained, US attenuation and velocity obs., 5 to 500 MHz 77−39634
ceramics, US attenuation 78−67772
chalcohalide glasses of Ge-As-S-I system, acousto-optical parameters 77−36199
chalcopyrite crystal acousto-optical props. 79−46054
Chesapeake Bay, abnormal US attenuation 77−29315
o-chloroaniline-iso-octane, crit. system, comp. depend. of absorpt., US obs. *(German)* 80−19879
o-chloroaniline-iso-octane critical system, US absorpt. meas. 77−51440
o-chloroaniline-n-heptane, crit. system, comp. depend. of absorpt., US obs. *(German)* 80−19879
cholesteric liquid crystal, mag. aligned, anisotropic US propag. 78−42895
cholesteric nonanoate, US attenuation near cholesteric to smectic A transition 79−28091
cinnamyldehyde, rotational isomerism study by US absorpt. and vel. meas. 77−27196
collagen effect on US propagation in tissue 78−61212
condensed systems, vibrational relaxation times calc. from low-freq. mol. spectrum 78−2205
continuous and simultaneous recording of changes in US attenuation and vel. 78−46875
critical binary liquid systems, composition depend. of US absorpt. 79−4372
critical fluid, dynamic droplet model, freq. and temp. scaling 78−26625
crotonaldehyde, rotational isomerism study by US absorpt. and vel. meas. 77−27196
cyclic carbonates, supercooled liqs., dielec., acoustic, NMR, viscoelastic relax. props. 77−1609
cyclohexanal, liq., viscoelastic and structural relax., US rel. and absorption meas. 78−26634
cyclohexane, US absorption and vel. meas. 77−51450
cyclohexanol, orientationally disordered phase, Brillouin scatt. study 80−93351
cyst liquid of human breast, US absorption obs. 79−62319
n-decane-nitrobenzene critical system, US absorpt. meas. 78−6126
decibel meter, for US pulse echo attenuation meas. 78−1520
defect-containing crysts., US absorpt. near displacive phase transitions, anomalous temp. depend. 80−92612
di-n-decyl azoxy methyl cinnamate, smectic-A liq. cryst., anisotropic US propag. 79−55829
dialkyl carbonates, liq., US, microwave dielect. relaxation 79−56717
dibenzyl, diphenyl, near melting point 78−6127
dibromomethane, rotational-vibrational energy transfer, US absorpt. obs. 79−98537
dicalcium strontium propionate, anomalous US attenuation near ferroelec. phase transition 79−91383
dichlorodifluoromethane, US vels. and absorption coeffs., determ. of relaxation times 78−63530
dichloromethane-cyclohexane, liq. mixture, intermol. vibrational energy transfer, US study 80−70313
dichloromethane-d_0(-d_2), rotational-vibrational energy transfer, US absorpt. obs. 79−98537
dielectric medium at low temp., influence of nonequilib. phonon gas *(Russian)* 78−71795
dielectric plate, dimensional effects in ultrasonic wave absorpt. coeff. *(Russian)* 80−70321
diethylamine melanin, sound wave anomalous absorption and dispersion 79−77688
p-dioxane-H_2O at 11 and 25°C, US absorption 80−65171
dioxane-water solvent, mixed, with addition of 1-1-valent electrolyte 80−87632
dislocation internal friction in high dislocation density crystals *(Russian)* 80−34146
dispersion and attenuation, general relationships 78−83135
doped displacive ferroelectrics, sound attenuation constant, Green's function technique 79−11397
EBBA, nematic liq. cryst., effect of mag. field on US attenuation *(Japanese)* 79−19144
edge reflection SAW absorber, FM discriminator appls. 78−1517
electrolytic solution, ionic drift from 50 Hz supply, pulse echo technique 80−70314
electron ferromagnet, longit. US attenuation due to spin fluctuations 79−56588
electron-hole drops, mobility and US absorption, effect of fluctuation pairing 78−2434

ultrasonic absorption continued
Epon 828-Z, acoustical determ. of shear relax. functions 78−76686
epoxy material, filled, US props. for sonar transducers 78−59867
erythrocyte membranes in 12 to 68 MHz range 80−89727
ethanol, US studies of mol. relax. 78−22790
ethanol aqueous soln., sound absorpt. coeff. meas., acoustic relax. 78−83883
ethyl alcohol, US attenuated temp. depend. in association liq. 77−51441
ethyl alcohol, US attenuation, for vol. viscosity, 0-60°C 78−63871
ethyl formate, liquid, temp. depend. of US absorpt. and volume viscosity 78−38776
ethyl formate, second relax. interval 77−1183
ethyl lactate, sound vel. and absorpt. meas. at hypersonic freqs. 78−18708
ethylene-N_2, gas, vibr. relax. time by US meas. 79−98852
excised breast tumour US attenuation meas., 6 to 10 MHz 79−48311
exciton ferromagnet, spin-lattice relax., light and US absorption *(Russian)* 79−7960
exciton insulator, coherence factors and transport props. 79−28291
excitonic phase, collective excitation modes under strong mag. field *(Japanese)* 77−43502
excitonic phase in strong mag. field, sound absorption 77−20243
ferroelectric, uniaxial, crit. behaviour, electrostrictive coupling role 80−71329
ferroelectric crysts., meas. using optical heterodyning and Raman diffr. by US waves 79−18640
ferroelectrics, structural phase transitions, ultrasonic velocity and attenuation meas. 80−75977
ferrofluid, US attenuation anomaly in mag. field 78−68345
ferrofluid US attenuation anomalies 79−55830
ferromagnet, planar, US attenuation, spin-phonon coupling, magnons and magnetostriction contrib., calc. 80−34611
ferromagnet, pure and random uniaxial with dipolar interaction, US attenuation 80−11239
ferromagnetic single cryst., US attenuation anomalies *(German)* 77−8381
ferromagnets, uniaxial, US attenuation and kinetic coeffs. near crit. point, renormalisation group theory 79−4715
filled polymers, cumulative internal damage, US assessment 79−57180
first order displacive transformations, localized soft modes and US effects 79−73281
fluoroform, vib. relax., 183-295K, US absorpt. meas. 77−34722
Freon-12, US absorption meas. 77−24049
freons of methane series, US attenuation rel. to vibr. relaxation 77−39397
furan, liq., US relax., light scatt. meas. 77−77231
furan-cyclohexane, liq. mixture, intermol. vibrational energy transfer, US study 80−70313
furfuraldehyde, liquid, US absorpt. meas. rel. to relaxation 77−20016
gas, molecular, kinetic coeffs. calc. from ultrasonic data 78−42703
gases, resonant tube for sound absorption meas. at low freq./press. ratios 80−96156
n-Ge US attenuation due to donors and acceptors 77−28223
glass, time depend. sp. ht. rel. to US props., at low temps. 78−59957
glass, US propagation at ultralow temperatures 77−39635
glass filled solids, ultrasonic absorpt., scatt., velocity and attenuation 80−44262
glass melt, unified theory of chem. relaxation using light scattering or US absorption 79−16028
glasses, acoustic and dielec. props. at low temps., review 78−6128
glasses, US properties and short-time sp. ht. relationship 79−60440
graphite fibre reinforced epoxy, US attenuation as an indicator of fatigue life 80−85118
Gruneisen parameter for nonconducting cubic crystals 78−87744
haemolysis kinetics, US differential absorption meas. 77−77877
hepatic tissue in vitro acoustic attenuation slope spatial correlation obs. 79−57702
n-heptane-nitrobenzene, US study of crit. mixing 78−75732
heptanoic acid, soln., US relax. *(German)* 78−22792
heterocyclic liquids, 10 to 1300 MHz 80−39229
n-hexane-n-pentadecane mixtures, solns., mech. of US absorption and viscosity *(Russian)* 79−90732
n-hexane-perfluoro-n-hexane mixtures, US vel. and absorpt. mixtures 80−88281
HOBA, isotropic phase, Brillouin scatt. spectra, hypersound data determ. 79−91453
human tissue, transmission of US beams, focusing and attenuation studies 80−45948
ice, plastic deformation, ultrasonic wave attenuation by dislocations *(French)* 80−59564
inhomogeneous absorbing solid, self-focusing of intense hypersonic and US beams 77−84038
insulator, strong US wave absorption due to phonon interactions 77−89503
insulators, high-intensity US wave vel., phonon-phonon interaction effects 80−70323
insulators, nonlocal hydrodynamic of phonon gas, thermal cond. and second attenuation coeff. 79−65158
interferometer method for US props. of solids 77−23836
interferometry, US attenuation or velocity meas. 80−58874
isobutyric acid-water, crit. mixture, conc. fluctuation mean relax. time, US absorpt. and vel. meas 80−29163
isopropanol, US studies of mol. relax. 78−22790
isopropanol aqueous soln., sound absorpt. coeff. meas., acoustic relax. 78−83883
isopropanol-n-propanol aq. mixtures, US relax., US absorpt. and vel. meas. *(French)* 80−103426
itinerant ferromagnet with helical spin struct., US attenuation 79−78497
itinerant-electron ferromagnet, US propag. and struct. instabilities, screening effects 77−69653
Jahn-Teller cooperative system, US attenuation, appl. to TmZn 79−78053
Jahn-Teller cooperative systems, low-freq. dynamics 79−82565
Kneser liquids, vibrational energy exchange probabilities 78−38780
Kondo superconductor, transport props. 79−65600
leaky wave attenuation by near-surface defects 77−32757
LF absorpt. in liquids at 500 kHz, determination using reverberation technique 80−38197
liquid, UHF interferometer appl. 78−22234
liquid, weakly assoc., US wave reson. absorpt. 80−34141

ultrasonic absorption continued
liquid containing gas bubbles, investigation using acoustic streaming 80−5863
liquid crystal, smectic A and isotropic phases, Brillouin scatt., hypersound vel. and attenuation determ. 77−8591
liquid crystal, US attenuation, elec. field effects 77−15304
liquid metal, mol. motions from NQR, viscosity and sound damping 77−1615
liquid systems, 10 to 30 MHz, 25 to 60°C, undergraduate expt. using 2-transducer RF pulse method 80−69608
liquids, high resolution Bragg reflection technique 79−23160
liquids, shock excitation for diffuse-field reverberation studies 80−88267
liver pathology characterisation, clinical appl. of a US attenuation coeff. estimation technique 80−76813
liver tissue, attenuation coefficient slope statistical estimation from refl. US signals 80−46000
low-viscosity liquids containing electrolytically-generated gas bubbles 80−58849
magnetic fluids, US attenuation, MHD approach 80−60389
magnetic superconductors, spin fluctuation and US attenuation 80−80445
mammalian testes, freq. depend. of US absorpt. coeff. 78−61213
mammalian tissues, US vel. and atten. 78−57044
MBBA, hypersonic props., Mandel'shtam-Brillouin spectra obs. 79−4813
MBBA, isotropic phase, Brillouin scatt. spectra, hypersound data determ. 79−91453
MBBA, nematic, US attenuation anisotropy, temp. depend. 78−43071
MBBA, nematic liq. cryst., anisotropy of US attenuation 78−43070
MBBA, pure and mixed with bezene (chlorobenzene), nematic-isotropic transition, US absorpt., visual hysteresis 80−54355
MBBA film, nematic liq. cryst., visible interaction of low-intensity US waves 78−10126
MBBA/EBBA binary liquid crystal mixture, US absorpt. and vel. dispersion, phase transition and alignment effects *(Korean)* 80−29121
measurement, pulse echo method, minicomputer program control *(Japanese)* 80−53587
measurement using atuomatic pulse echo tracking apparatus 77−22571
medium with hysteresis type damping, signal propag. *(Russian)* 79−53986
metal, anisotropy effects on US cyclotron resonance 79−73816
metal, apparent screening breakdown mechanism in US attenuation 77−27946
metal, FCC, dislocation behaviour at high strain rates, US detection method, data analysis basis 80−85136
metal, Fermi surface local geometry ultrasonic absorpt. ang. depend., Pippard oscill. spectrum *(Russian)* 79−19507
metal, nonlinear EM absorption of short-wave sound *(Russian)* 78−43446
metal, quantum oscills. with dislocations under press. *(Russian)* 80−88273
metal fatigue monitoring by US velocity and attenuation meas. 78−60970
metallic films, ultrasound attenuation, size magnetoacoustic effect *(Russian)* 80−107869
metallic glasses, mats. props. review 77−4043
metallic systems with rare earth impurities, US attenuation in mag. field, absorpt. mechanisms 79−15336
metallic thin film surface wave attenuation due to electron-phonon interaction 79−55848
metals, sound absorpt. and dispersion, Fermi surface flattening 78−91596
metals and alloys, absorption of high intensity US 79−86845
methane, liquid, Brillouin scatt. obs., US vel. and absorpt. 80−45085
methane-d_4, solid, US attenuation, phase transitions 79−51204
methane-N_2, gas, vibr. relax. time by US meas. 79−98852
methanol, US studies of mol. relax. 78−22790
methanol-nitrobenzene-iso-octane, US vel. and absorpt., along line of plait points in ternary liq. 78−79669
methyl alcohol, US attenuation, for vol. viscosity, 0-60°C 78−63871
methyl alcohol, US attenuation temp. dpeend. in associated liq. 77−51441
methyl formate, liquid, temp. depend. of US absorpt. and volume viscosity 78−38776
β-methyl-butyl-methoxybenzylidene amino cinnamate, smectic-B liq. cryst., US attenuation anisotropy 79−55828
methylene chloride-cyclohexanol system, sound vel. and acoustic loss coeff. 77−51450
3-methylpentane-nitroethane crit. mixture, dynamical scaling for sound propag. 80−49305
3-methylpentane-nitroethane critical binary liquid mixture, US absorpt. 80−107376
methylpyridines, propag. vel. and attenuation coeff. as functions of temp. 79−14886
micellar solutions, US absorpt. 80−45571
microemulsion, sound velocity and absorption 80−81374
microwave phonon attenuation in quartz at low temperatures 79−19324
minicomputer controlled instrument for US vel. and attenuation meas. 79−86312
molecular resonance in solids, expressions for US absorption 77−24359
monochlorodifluoromethane, US vels. and absorption coeffs., determ. of relaxation times 78−63530
Mossbauer spectra obtained at US excitations of source and absorber *(Russian)* 79−47364
myocardial injury, correlation of US and enzymatic indices 77−21581
myocardial tissue, relationship between collagen and US attenuation 79−43973
myocardial tissue, US attenuation depend. on time after excision and temp. 78−11711
myocardium, acoustic microscopic anal. 80−45995
myocardium, normal and ischaemic, US attenuation 80−45954
naphthalene, mol. crystal, meas. of US attenuation coeff. by optoacoustical methods *(French)* 80−70317
nematic liquid crystal, acoustic attenuation anomaly above clearing point 78−75816
nematic liquid crystal, critical US absorption 79−65174
nematic liquid crystal, isotropic phase, light scatt., ultrasonic vel. and absorpt. meas. 78−48189
nematic liquid crystals, absorption of longitudinal and transverse waves *(French)* 77−51321
nematic liquid crystals, acoustic props., rotating mag. field study 80−88034

ultrasonic absorption continued
nitrobenzene-n-heptane, crit. mixture, conc. fluctuation mean relax. time, US absorpt. and vel. meas 80−29163
nitrobenzene-n-hexane critical mixture, ultrasound absorpt. 77−1178
nitrobenzol-n-hexane, hypersound velocity, absorption temp. depend *(Russian)* 80−75303
nitroethane-isoctane, crit. mixture, conc. fluctuation mean relax. time, US absorpt. and vel. meas 80−29163
noble metals, interaction of thermal and acoustic phonons thermoelastic relaxation, calcs. for US longitudinal waves 80−65165
nomogram for determ. of damping coeff. of transverse waves 78−56867
non-linear ultrasound absorption in an electromagnetic wave field under quantum size effect conditions 78−87745
nonanoic acid, soln., US relax. *(German)* 78−22792
ocean, attenuation of surface generated noise received deep in the ocean 78−90573
ocean microbubbles, in situ acoustic meas. 77−37207
oil-polymer mixture, acoustic attenuation CW meas., tissue simulation appl. 80−35961
oil-water microemulsions, US attenuation and structural transitions 79−61917
one-dimensional antiferromagnet, interchain coupling, effect on US attenuation 80−19880
ophthalmic tissue signature characterisation by US frequency-domain analysis 77−40857
organic crystal, US absorption, rel to lattice vibrs. 77−24358
organic liquids, US resonance absorption 78−95110
orthoferrites near spin-flip temp., magnetoelastic waves 78−19301
PAA, isotropic phase, Brillouin scatt. spectra, hypersound data determ. 79−91453
PAA, nematic liq. cryst., effect of magnetic field on US vel. and absorpt. 78−18707
PAA, nematic-isotropic phase transition, US meas. 79−90761
phase velocity and absorpt. coeff. meas. incorporating exact diffr. corrections 78−26010
phenol-chloromethane, US absorpt., phenol cyclic assoc. 77−15501
β-picoline-water solution, light scatt. spectra, ultra- and hypersonic absorpt. *(Russian)* 80−93353
piezoelectric nondegenerate semicond., magnetoacoustic effects of nonparabolic band struct. 80−96948
piezoelectric semiconductor, polarisation of Maxwell-Wagner relaxation oscillators 80−44670
piezoelectric substrate, small SAW attenuations and vel. variations 79−86281
PMMA, acoustical determ. of shear relax. functions 78−76686
PMMA, low-energy excitations and hypersonic props., Brillouin scatt. meas., 1.7 to 15K 77−90160
poly(4-methyl pentene-1), US props., glass transition, Gruneisen parameters 80−54316
poly-l-glutamic acid, soln., linear Ising chain kinetics 77−4980
polyacrylamide aqueous solution, ultrasonic investigation *(Chinese)* 80−107371
polyalkanimide, US vel. and absorpt. at liquid He temps. 78−51619
polycrystalline materials, freq. and grain size dependency of US attenuation 80−50783
polydimethyl siloxane solns., attenuation meas. 80−107372
polydimethylsiloxane networks, high freq. US absorpt. rel. to crosslink density, α-relaxation 79−95091
polyethylene, glass filled solids, ultrasonic absorpt., scatt., velocity and attenuation 80−44262
polyethylene, high press. phase, US, DTA, and X-ray diffr. study 80−75188
polymer solution, US absorpt., internal viscosity-normal mode description 79−10899
polymer solutions, dil., dynamics, model 79−73086
polymers, filled, cumulative internal damage, US assessment 80−97653
polypeptides, in aq. poly(L-glutamic acid) soln., helix-coil transition, US relax. times 80−45849
polypropylene, drawn fibres, SEM and US study 78−47249
polystyrene, US propag. at low temp. 79−55834
polystyrene solution, differential meas. of ultrasonic velocity *(French)* 80−75302
polyvinylidene fluoride, US transducers, dielec. and acoustic losses 80−48541
polyvinylidene fluoride films, HF meas., 300 to 1500 MHz 80−74667
polyvinylidene fluoride piezoelectric thin films, US atten. at high freqs. 79−65798
porous rocks, US absorpt. from wave attenuation and scattering on random inhomogeneities *(Hungarian)* 77−86791
l-proline, aqueous soln. US absorpt. 78−87743
n-propanol, US studies of mol. relax. 78−22790
n-propanol aqueous soln., sound absorpt. coeff. meas., acoustic relax. 78−83883
propyl formate, second relax. interval 77−1183
propylene, liquid, effect of libration transitions on sound absorpt. 78−2203
pulse echo waveform rel. to acoustic characteristics of continuous medium 80−67145
pulse-echo methods, effects of nonparallelism 78−55537
PVA, aq. solns., US absorpt., acetate groups effects *(Russian)* 80−65162
PVAC dispersions, US method of determining plasticiser content *(German)* 80−21257
quartz, fast neutron irradiated, saturation of 9.4 GHz hypersonic attenuation 79−23682
quartz, US absorption, influence of plastic deform. and electrostatic field *(Russian)* 80−39226
quartz, x-cut, triplepass Brillouin scatt. by induced phonons 77−28588
quartz shear wave attenuation, 9.4 GHz, AC-,BC-cut, 15-35K 78−26627
rare earth alloys and intermetallic cpds., US attenuation, temp. and mag. field depend. 80−15195
rare earth metals, electronic sound attenuation anomalies at transition to helical phase, Fermi surface topology *(Russian)* 80−92807
rare-earth metals, US attenuation, exchange striction, and spin-phonon interaction 79−33518
rare-earth metals, US attenuation in applied fields 77−51933
resonance absorption of ultrasound by moving dislocation 80−54318
Rochelle salt, polarisation relaxation, US vel. and attenuation meas. 77−28512
sand, fluid-saturated, viscous attenuation 80−33307

ultrasonic absorption continued
SAW, velocity, attenuation and reflection meas., interf. acoustical method 79−18638
SAW attenuation coeffs. and wave speeds 79−46903
SAW attenuation due to thin film finite conductivity and air loading 77−31154
SAW propagation in admittance sheet deposited on piezoelectric substrate 77−80689
scanning signal, influence of resonance filter on wave form *(Russian)* 79−55265
Schaaffs' molecular-kinetic theory of propag. in liquids, temp. and pressure changes of 'collision factor' 80−19143
semiconductor, absorption of EM and sound waves in strong coupling case, effect of acoustic superlattice 78−26630
semiconductor, electron-hole droplet 77−89814
semiconductor, ultrasound absorption, intermediate frequency, nonlinear effects 79−28380
semiconductor, US absorption of moderate freq., electron distrib. function perturbation 77−55587
semiconductor, US attenuation by impurities 77−69047
semiconductor, zincblende struct., phonon attenuation in presence of internal strains and mag. field 78−76118
semiconductor film, US propagation in quantised elec. field *(Russian)* 80−60050
semiconductors, narrow band gap, superlattices, acoustic wave absorpt. and amplification 80−29445
L-serine, in aqueous solns., US spectra using automatic recording spectrometer 78−75735
p-Si US attenuation due to donors and acceptors 77−28223
silicate glasses, low-energy excitations and hypersonic props., Brillouin spectra meas., 1.7 to 15K 77−90160
small peptide antibiotic and protein solns. 79−48286
soft tissue temp. increases due to US Doppler blood flowmeters, thermographic meas. 79−62294
soft tissue US attenuation coefficient slope estimation 77−21582
soil, physical properties study by US wave attenuation meas. *(Polish)* 77−9566
sol-gel transition, US attenuation meas. 80−101043
solids, acoustic wave emission, absorpt. and propag. in THz range 80−65164
solids meas., by acoustooptical method, losses in boundary layer evaluation *(Polish)* 78−30701
steel, medium, C, US attenuation, mag. field effect 80−89428
steel, plain C, type 304 and type 316 stainless, fatigue damage indicators, non-desructive 80−25932
steel, type AC/HT-2, grain diameters, US attenuation 80−89429
steel, US attenuation, defect effects in US inspection *(Italian)* 78−48609
styrene-butadiene-styrene triblock copolymer, US relax. 77−89502
superconducting and normal metal, non-linear acoustic props. of cond. electrons 79−60975
superconducting and superfluid substances, role of physical acoustics in investigations, review 80−96090
superconducting intermediate state, obliquely incident sound absorption *(Russian)* 78−39263
superconductor, creation of normal domains by acoustic methods 78−60248
superconductor, dirty, attenuation in mixed state 77−8231
superconductor, nonequilib., with wideband source of quasiparticles, kinetic theory 80−80442
superconductor, nonlinear acoustic attenuation effects, energy gap widening *(Russian)* 77−43780
superconductor, phonon mechanism for sound-affected energy gap *(Russian)* 77−43781
superconductor, strong coupling, finite-freq. US attenuation 77−51846
superconductor, theory of tunnel injection *(Russian)* 79−47198
superconductor, US attenuation and Fermi surface topology *(Russian)* 78−23203
superconductor, with overlapping bands, tunnelling density of states, ultrasound attenuation 79−7934
superconductor film, in nonequilib. state, US attenuation 77−47925
superconductor intermediate state, geometric resonance *(Russian)* 79−95551
superconductor with struct. transform., kinetic props. *(Russian)* 79−95544
superconductors, charged, collective excitations and longitudinal US spectrum 79−56389
superconductors, nonequilibrium states, narrow nonequilibrium sources *(Russian)* 80−88687
suppression of finite-amplitude primary wave attenuation, parametric acoustic arrays, use of bubbles 80−74563
suspensions and emulsions, highly-concentrated, sound absorption 79−41475
TBBA, US absorpt. and dispersion at nematic-smectic-A transition 79−82287
terephthal-bis-p-p'-butylaniline, pretransitional anomaly, US obs. 78−75818
tetrafluoromethane, US absorpt. for vibr. self-relax., 139-183K 78−63529
tetramethylammonium tetrachlorozincate, incommensurate phase transition, US propag. meas. 79−91382
TGS, admixed with nitroanilines or L-alanine, US vel. and absorpt., ferroelec. transition 77−32333
TGS, pure and nitroaniline-admixtured, longit. US wave propag., domain struct. effects 77−55322
TGS, US vel. and absorpt. in ferroelec. transition region 77−66461
TGS type ferroelectric, US absorpt. anomalies near T_c 77−16264
TGSe, US vel. and absorpt. in ferroelec. transition region 77−66461
TGSe, US velocity and absorpt., 10 MHz, crit. anomalies 77−15504
Thermo-Acoustic Sensing Technique for noninvasive tissue analysis 77−64117
thin film elastic constants and SAW velocity and attenuation meas. 79−56101
thin metal films, SAW attenuation and phase vel. meas. 79−46136
thiophene, meas. of absorpt. coeff. in 10-60 MHz range, existence of vibrational relaxation 80−33377
tissue, freshly excited, from rat, freq. depend. 77−86573
tissue, mammalian, survey of US vel. and attenuation data 80−46744
tissue, mammalian, US attenuation and speed determ. as function of temp. 80−41108
tissue, possible mechanisms 80−45951
ultrasonic absorption continued
tissue, soft, attenuation 80−45952
tissue, soft, attenuation vs. frequency 80−45956
tissue, temp. and freq. dependence 80−45949
tissue analysis, two-beam thermo-acoustic sensing technique 77−40716
tissue bioacoustic property determ. by US pulse echo anal. *(German)* 78−85349
tissue characterisation by attenuation, absorption, and velocity 77−64106
tissue characterisation by US frequency-dependent attenuation and scatt. 77−66832
tissue characterization in vivo by differential attenuation measurements 80−45999
tissue pulse-echo US absorption estimation model 79−48304
tissue refractive index spatial distrib. meas. by US computer assisted tomography 78−69161
tissue US absorption thermoelectric meas., beamwidth and thermocouple size effects 79−48306
tissue US attenuation and velocity meas. by direct and phase-contrast imaging 77−64114
tissue US attenuation and velocity meas. by reflection techniques 77−64115
tissue US attenuation and velocity meas. by time delay spectrometry 77−64111
tissue US backscatter and attenuation distrib. mapping, digital reconstruction 80−51188
tissue US parameters, quantitative cross-sectional imaging 79−53277
tissues, fixed and unfixed, US propagation, backscattering coeffs. and speech determ. 80−41109
tissues, mammalian, US absorpt. and attenuation determ. by thermoelectric method 80−41110
toluene-xylene liquid mixtures, appl. of Bauer-Sette theory 79−77682
torsional vibrations in metals 80−58856
transition metal dichalcogenides, US characts. rel. to Fermi surface geometry *(Russian)* 78−34749
transverse hypersonic waves at 9.4 GHz appl. to APR and attenuation meas. 78−33970
triethylamine-H_2O, crit. phenomena, US vel. and absorpt. 78−91382
triethylamine-water critical mixtures, US absorpt. 79−28045
trifluoroacetic acid, US absorpt. 77−15505
trifluoroacetic acid-acetic acid, equimolar mixture, US absorpt. 77−15505
trifluoromethane, US absorpt. for vibr. self-relax., 163-299K 78−63529
tris-sarcosine calcium chloride, ferroelec., US attenuation and vel., elastic consts., and permitt. near Curie temp. 79−37761
tube method for absorpt. meas., 4-100 kHz 77−84092
two-dimensional US attenuation coefficients, computerised tomographic reconstruction 79−57733
type II superconductor, clean, US attenuation and thermal cond. 78−91812
uniaxial ferroelectric, acoustic attenuation near transition point 80−11350
uniaxial ferroelectrics, static and dynamic crit. behaviour, elastic and electrostrictive consts., US attenuation 78−35103
US relaxation of aqueous mixtures of methanol and ethanol *(French)* 80−6468
vibrational relaxation of molecules in condensed media, survey, book contrib. 77−36295
vinyl chloride, time-dependent spectra at 1 MHz for various polymerisation conditions 80−33299
vinyl chloride suspension polymerisation monitoring by US attenuation and velocity 79−70328
vinyl-series polymer solutions, longitudinal US waves absorption 80−15192
viscous liquids, shear absorption, effect of pulse width 78−83878
water, hypersound phase vel. and damping by high resolution Brillouin spectroscopy 77−69845
water, in Bragg cell, influence on Bragg diffr. imaging 77−31188
water, supercooled, US vel. and attenuation *(French)* 79−90730
water and heavy water, US attenuation temp. depend. in associated liq. 77−51441
water-alcohol mixtures, attenuation meas., method of streaming 80−88272
Wigner crystal, long-wavelength excitations in strong mag. fields 79−82533
Ag film, damping and vel. of longit. elastic waves at 9.4 GHz 80−10596
Ag^+ superionic conductors, US attenuation due to hopping of Ag^+ ions 78−22890
Ag_3AsS_3, US absorpt. and vel., 4.2-100K 77−24361
β-AgI, piezoelectric ionic cryst., US investigation 79−77689
$AgNO_3$, molten, Brillouin scatt., hypersonic absorption and vel. meas. 77−8592
Ag_3SbS_3, pyrargyrite, US absorption, influence of illumination 79−42153
$Ag_3SbS_3(AsS_3)$, electroacoustic echo, ultrasonic wave attenuation *(Russian)* 80−88280
Al alloy sheets, type 7075-T6 used in aircraft, early detection of fatigue cracks 80−66730
Al alloys AK4-1 and D16, US structure monitoring 78−53082
Al, damping of US vibrations under high hydrostatic press. 77−55324
Al, dislocation and point defect interactions, US study under quasistatic stress *(French)* 80−2061
Al, supercond., phonon absorption and pair breaking at 35 GHz 77−32120
Al, superconducting band gap anisotropy and Fermi surface anisotropy *(Spanish)* 80−84544
Al superconducting film, 2 GHz SAW attenuation meas. of mean free path 77−39999
Al-Cu-Mg-Si-Mn (2.5, 0.7, 0.7, 0.5 wt.%), alloy AK6, US inspection of heat treatment quality 78−76681
Al-Mg, elastic and anelastic props. in relation to Guinier-Preston zones, US investigation *(French)* 79−38833
Al_2O_3-epoxy mixture, acoustic wave velocity and attenuation meas. 79−42151
β-Al_2O_3-Na_2O, non-stoichiometric, amorphous, US attenuation and velocity 80−39228
β-Al_2O_3-Na_2O 79−19396
Ar, liquid, compressional viscosity and vibrational relaxation 80−70311
Ar, US vels. and absorption coeffs., determ. of relaxation times 78−63530
Ar-monochlorodifluoromethane mixture, US vels. and absorption coeffs., determ. of relaxation times 78−63530

ultrasonic absorption continued
As, amorphous, US attenuation and sound vel. meas., 4.2 to 300K; 80−49308
As-Ge-Se and As-Ge-Se-Sb glasses, US absorpt. and acousto-optic props. 77−27327
As_2S_3, amorphous, acousto-induced struct. change, Brillouin scatt. meas. 79−27928
As_2S_3, amorphous, shear wave attenuation 80−11027
As_2S_3, amorphous, US attenuation obs. 79−46756
As_2S_3, glass, US attenuation, enhanced after elec. field removal 79−65145
As_2S_3:Ag, amorphous US props. 78−51616
As_2Se_3:Ag, amorphous, US props. 78−51616
Au film, damping and vel. of longit. elastic waves at 9.4 GHz 80−10596
$BaTiO_3$, logarithmic velocity variations for longitudinal US waves near ferroelec. transition 78−72472
Bi, damping of US vibrations under high hydrostatic press. 77−55324
Bi film, amorphous, temp. dependence of SAW attenuation 80−75679
Bi, giant quantum attenuation of sound, anomalous temp. depend. 77−76728
Bi, giant quantum attenuation anomalies of sound waves at high mag. field, temp. and freq. depend. 80−70587
Bi, giant quantum attenuation anomalies of sound waves at high mag. field, extra attenuation peaks 80−70588
Bi, US attenuation, annealed sample, 0.6 kbar, 25-120°C 78−47474
Bi, US attenuation in strong mag. fields, electron-hole correlation effects 80−11049
Bi-Sb-O-I glasses, US attenuation and acousto-optic props. 77−31121
$Bi_{12}SiO_{20}$ surface and pseudosurface wave props. 79−46908
C fibres, US attenuation factors 77−39631
C, heat-treatment and neutron irrad. effects on US atten. and Young's modulus 79−11644
$CHCl_3$ and C_2H_5OH and mixtures, velocity and damping of ultrasound 80−29120
CO, liquid, Brillouin scatt. obs., US vel. and absorpt. 80−45085
Ca, attenuation due to phonon-phonon interaction and thermoelastic phenomenon 79−77686
Cd US attenuation due to conduction electrons 79−46754
Cd, US attenuation of conduction electrons calc. 78−91588
Cd, US attenuation of conduction electrons, shear waves calc. 78−91589
$CdCl_2$, aq. solns., sound absorpt. and relax. phenomena 80−49311
CdS crystals, orientational depend. of photoacoustic effect *(Russian)* 80−65167
CdS, lattice attenuation meas. by US injection method 78−76480
CdS, photoconductive, obs. of high intensity sound self-defocusing 80−24972
CdS, semicond. piezoelec. crysts., US investigation of acoustoelectric charcts. 77−1456
CdS thin-film Lamb wave delay line characteristics and strain effects 77−31185
CdS:Cu, US absorpt. in heavily doped piezoelec. semicond. 79−11189
CeB_6, magnetostriction, US absorpt. and thermal expansion 80−66004
Cr, anomalous US damping under hydrostatic press. 79−14890
Cr, antiferromagnetic, US attenuation and phase diagram 80−103831
Cr film, damping and vel. of longit. elastic waves at 9.4 GHz 80−10596
Cr, mag. phase diagram, near, spin-flip temp., US attenuation 80−60267
Cr, US velocity and damping in Neel temp. range, thermocyclic treatment effect *(Russian)* 79−91282
Cs-NH_3, Cs-ND_3, solns., US absorption, metal-nonmetal transition 79−69194
$CsNO_3$, molten, Brillouin spectra, 420-520°C, hypersonic vel. and sound absorption freq. depend. 77−28589
$CsNiCl_3$, one-dimens. antiferromag., US attenuation, crit. behaviour 77−66308
$CsNiCl_3$, one-dimens. antiferromag., US attenuation 78−88156
$CsNiF_3$, planar ferromagnet, US attenuation, spin-phonon coupling, magnons and magnetostriction contrib., calc. 80−34611
Cu film, damping and vel. of longit. elastic waves at 9.4 GHz 80−10596
Cu, HF ultrasound, viscous and relax. components of dislocation attenuation 80−15196
Cu, US attenuation, nonlinearity parameter temp. depend. 79−42152
Cu, US attenuation by open-orbit electrons, role of deformation potential 79−73428
$Cu(ClO_4)_2$ in ethylene glycol solns., US absorpt., relaxation rel. to temp. 77−31727
$Cu(NO_3)_2$, in ethylene glycol solns., US absorpt., relaxation rel. to temp. 77−31727
$CuPbSbS_3$, piezoelectric semiconductor, electron-phonon interaction, temp. depend. 77−51464
D_2O, US attenuation, for vol. viscosity, 0-60°C 78−63871
D_2O, US excess absorption and compressional viscosity, temp. depend., hole theory 77−4157
Dy, antiferromagnetic, thermal expansion, US attenuation anomalies 79−47319
Dy, US attenuation in mag. field 77−40104
Dy, US attenuation maxima in mag. field 77−16140
Er, US attenuation, longitudinal, in mag. ordered region and at phase transitions 77−28422
Er, US attenuation in mag. field, temp. and field depend. 79−91279
Er US attenuation near magnetic transitions at 53.9 and 83.8K 79−55837
Fe and Fe alloys, US attenuation at large strain amplitudes 77−1182
Fe, cast, with uniaxial loading, changes in ultrasonic waves vel. and attenuation 79−15756
Fe, damping of US vibrations under high hydrostatic press. 77−55324
Fe-Ni (29.58 wt.%), acoustic absorpt. and emission associated with martensitic transform. 79−34035
$Fe^{2+}Fe_{0.2}{}^{3+}Cr_{1.8}{}^{3+}O_4$, acoustic props. rel. to cooperative Jahn Teller effect and structural phase transform 80−24538
Ga, anomalous US penetration at low temp., effect of trajectorial electron transfer *(Russian)* 77−43670
Ga, spiral cyclstron waves excited by US in open Fermi surface metals *(Russian)* 79−99771
Ga, US anomalous penetration along electron trajectories in mag. field *(Russian)* 79−87191
Ga, ultrasonic absorpt., intermediate state 77−72942
GaAs:Cr^{2+}, dynamic Jahn-Teller effect, relaxation time for reorientation 80−6798
GaAs:Cr^{2+}, US attenuation meas. of Jahn-Teller distorted Cr^{2+} centres 79−28048

ultrasonic absorption continued
Gd-Y (40 wt.%) alloy, magnetic phase transitions, elastic consts. meas. 78−14957
$GdVO_4$, antiferromag., US attenuation at 9 GHz 77−24728
Ge, Akhieser region, nonlinearity parameter and US attenuation coeffs., temp. depend. 79−37762
Ge crystals, orientational depend. of photoacoustic effect *(Russian)* 80−65167
Ge, electron-hole drop drag by ultrasound *(Russian)* 80−100437
Ge, electron-hole droplets, capillary-wave reson. investig. by US attenuation 77−8027
Ge, electron-hole drops, US absorpt. and recomb. radiation, 1.8 to 3.5K 77−31954
Ge, electron-hole-liquid, de Haas-van Alphen-like oscills. in ultrasound absorpt. 79−60720
Ge, photoacoustic effect, free flexural vibrs. damping 77−89813
Ge, pure and n-type, US velocity and attenuation, second and third order elastic moduli 80−70325
Ge single crysts., dislocation absorption *(Russian)* 77−62589
Ge, spectral diffusion in acceptor-hole system at low temp., ultrasonic hole-burning expt. 80−92610
Ge, US absorption, depend. on orientation 79−69197
Ge, US attenuation, temp. variation, 273K to 500K at 4 MHz *(Rumanian)* 79−77691
Ge, US attenuation and nonlinearity const., temp. depend. 78−43075
n-Ge, US attenuation by impurities 77−69047
p-H_2, rotational 0-2 transaction cross-sections *(Russian)* 80−32812
HCl in DMSO-H_2O soln., ion assoc., US absorpt. obs. 79−23513
H_2O, US attenuation, for vol. viscosity, 0-60°C 78−63871
^{3}He, superfluid, A and B phases, US props. 79−65278
^{3}He, superfluid A-phase, effect of order-parameter collective modes on NMR and US attenuation 79−51344
^{3}He, US dispersion and attenuation near liq.-gas crit. point 78−38897
^{3}He-^{4}He mixture, US propagation near tricritical point 77−59169
^{4}He, HCP, dislocation damping, MHz sound freq. depend. attenuation 77−72739
^{4}He, HCP, longitudinal sound velocity, temp. and freq. depend. 77−72742
^{4}He HCP crystals, US attenuation, dislocation damping 80−24711
^{4}He, liq., λ point, US absorption, dynamic scaling 80−44380
^{4}He, liq., US attenuation and dynamical scaling near T_λ 77−24460
^{4}He, solid BCC, plastic deform., stress-strain relations and US attenuation 78−38909
^{4}He, solid HCP, US attenuation 78−47634
$HgSb_4S_8$, photosensitive semicond., US attenuation, phase transition obs. 79−65518
$Ho(NO_3)_3$ solns., f-f transitions, intensity anal., correl. with cond. and US absorpt. 80−97292
In film, damping and vel. of longit. elastic waves at 9.4 GHz 80−10596
In, intermediate state, doping effect on US attenuation 80−2522
In, superconducting relaxation time determ. 77−55638
In, US absorption and dispersion, lineshape studies of quantum oscills., anomalous behaviour 78−63966
In, US attenuation in supercond. and normal state in transverse mag. field and zero field 80−54836
In, ultrasonic absorpt., intermediate state 77−72942
In-Sn, dil., intermediate state, doping effect on US attenuation 80−2522
In_2Bi, pre-melting absorption of sound 80−88277
InSb, US attenuation and Akhieser loss, temp. depend. 79−86842
n-InSb, ultrasound modulation in mag. field 79−69196
n-InSb, Wigner cryst., long-wavelength excitations in strong mag. fields 79−82533
K, ultrasonic attenuation at low temp., spherical Fermi surface model 80−84255
$K_2Ba(NO_2)_2$, elastic props. 80−96588
KCl, US attenuation in strained single crystals 77−1181
KCl:Cu^+ US attenuation meas., 80-300K 77−43285
$K(H_{1-x}D_x)_2PO_4$, polarisation relaxation time and Landau kinetic coeff. rel. to degree of deuteration 80−84251
KH_2PO_4, central peak susceptibility and US propag. near T_c 78−15125
$KMgF_3$:Fe^{2+}, US relax. absorpt., acoustic wave-impurity coupling, spin-orbit splitting 79−4375
$KMnF_3$, critical dynamics of sound 80−103424
$KMnF_3$, dynamic scaling and US attenuation at structural phase transition 80−44260
$KNiF_3$, isotropic antiferromag., phase diagrams, US meas. 78−68350
K_2O-B_2O_3-SiO_2 system glasses, hypersound propag., 77 to 300K, Brillouin scatt. obs. 77−84850
$K_2Pt(CN)_4Br_{0.3}.3H_2O$, lattice softening, temp. depend. of elastic consts., US meas. 78−14432
$K_2Pt(CN)_4Br_{0.3}.3H_2O$, spin-lattice model for elastic anomalies 80−15179
$KTa_xNb_{1-x}O_3$, ferroelectric transition, US attenuation, elastic consts., soft modes 78−23411
Kr, liq., US attenuation and bulk viscosity 80−49304
$(La,Gd)Al_2$, normal and supercond. state, US attenuation, freq. depend. and mechanisms 80−49992
$LaAl_2$, supercond. and normal states, anomalous US attenuation and velocity change 80−80446
Li single cryst., attenuation measurement in vicinity of martensitic phase transformation 80−75358
Li-NH_3 solution, metal-nonmetal transition, US absorption coeff. 77−51443
LiCl in H_2O, complexity investigation using US method 80−33326
LiF, cryst., ultrasonic attenuation along (111) and (110) directions 78−63813
LiF, US attenuation, 4.2 to 300K 77−47513
Li_2GeO_3, acoustic props., intrinsic piezoeffect, US absorpt. coeffs. *(Russian)* 80−29692
$LiIO_3$ crystal elastic, piezoelec., dielectric and acoustic props. 79−46740
$LiNbO_3$, acoustic characts. meas. of Z-cut single crysts. by acousto-optical method 79−3867
$LiNbO_3$, damping of elastic waves at 36.5 GHz 77−39632
$LiNbO_3$, hypersonic wave attenuation, temp. depend. long wavelength phonons 78−18710
$LiNbO_3$, y-z, x-z and 41$^1/_2$-x cuts, SAW SHG, laser probing 77−31153
Mg US attenuation due to conduction electrons 79−46754
Mg, US attenuation of conduction electrons calc. 78−91588
Mg, US attenuation of conduction electrons, shear waves calc. 78−91589
$MgAl_2O_4$, damping of elastic waves at 36.5 GHz 77−39632
$MgAl_2O_4$:Dy, US attenuation 77−89500

ultrasonic absorption continued
$MgO:Fe^{2+}$, intrinsic spin-lattice relaxation rates, nonresonant US meas. 78−80203
MnP, US vel. and crit. attenuation, longit. waves, external mag. field 78−27035
$MnSO_4$ aqueous soln. conc. depend. of third US relaxation freq. and activation energy 78−63814
$MnSO_4+H_2O$ solutions, relaxation freq. and activation energy depend. on conc. 78−55913
MnSi, mag. phase diagram, crit. US attenuation 77−12122
MnSi, mag. phase diagram, US attenuation meas. 77−63188
Mo, anomalous US damping under hydrostatic press. 79−14890
Mo, longwave dopplerons, nonlocal Hall effect, surface impedance, size effect *(Russian)* 80−80253
Mo, US attenuation meas. of mean free path temp. dependence 77−39825
N_2, liquid, Brillouin scatt. obs., US vel. and absorpt. 80−45085
N_2, liquid, US absorpt., bulk viscosity and relaxation 77−35639
ND_4Cl, ultrasonic exam. near order-disorder transition, elastic consts. 79−46799
$(NH_4)_2BeF_4$, elastic compliance, US attenuation and piezo-coeffis., 170 and 190K 79−51918
NH_4Br, order-disorder phenomena, high press. US investigation 79−37835
$NH_4Br(Cl)$, dynamic crit. phenomena 79−77690
NH_4Cl, acoustic absorption by soft modes of defects 80−59584
$NH_4Cl_{1-x}Br_x$, US exam. of order-disorder phase transform. 78−38841
Na-NH_3, solns., US absorpt. and vel. near crit. point 79−28047
NaCl, cryst., ultrasonic attenuation along (111) and (110) directions 78−63813
NaF, cryst., ultrasonic attenuation along (111) and (110) directions 78−63813
$NaNO_2$, elastic constants and US attenuation coeffs., anisotropic charact. 78−63809
$NaNO_2$, incommensurate-and-antiferroelectric phase transition, amplitude mode, ultrasonic study 80−39227
Nb, mixed state, hysteresis of US attenuation 80−84549
Nb, single cryst., anomalous US attenuation at low temps. 78−43076
Nb, supercond. mixed state, US attenuation meas. near B_{c2} 78−64167
Nb, superconducting, fluctuation contrib. to sound attenuation near H_{c2} 79−33397
Nb, superconducting, hypersonic attenuation near critical field H_{c1} 77−77005
Nb, two-band supercond., attenuation of longitudinal ultrasound 77−51847
Nb, US attenuation, hysteresis near and below H_{c1} 80−75676
Nb-Hf(26 at.%), mixed state, magnetoacoustic attenuation 77−4473
Nb_3Sn, on $LiNbO_3$ substrate, US attenuation of SAW in applied mag. field 80−75678
Nb_3Sn, supercond., thin film, US attenuation of SAWs 80−49988
$Nb_{20}Zr_{80}$, supercond., US attenuation 80−44766
Ni cryst., attenuation, phonon viscosity and dislocation drag coeffs. 80 and 298K 77−76491
Ni film, 618 MHz SAW attenuation rel. to mag. field 77−40110
Ni film, damping and vel. of longit. elastic waves at 9.4 GHz 80−10596
Ni, film, mag. susceptibility correlation with SAW attenuation 79−47310
Ni, single cryst., magnetisation and US attenuation, mag. field depend. *(Russian)* 78−6559
Ni, US attenuation, mag. field and temp. depend. 77−90008
Ni-Fe films, US generation by ferromag. reson. 78−88155
Ni-P, amorphous metallic, sound attenuation and rel. meas. 77−31722
$NiCr_2O_4$, acoustic props. rel. to cooperative Jahn Teller effect and structural phase transform 80−24538
$Ni^{2+}Fe_{0.75}{}^{3+}V_{1.25}{}^{3+}O_4$, acoustic props. rel. to cooperative Jahn Teller effect and structural phase transform 80−24538
$Ni_{78}P_{22}$, amorphous metallic alloy, US attenuation 78−75789
O_2, liquid, Brillouin scatt. obs., US vel. and absorpt. 80−45085
O_2 liquid, US absorpt., bulk viscosity and relaxation 77−35639
P, amorphous, US attenuation and sound vel. meas., 4.2 to 300K; 80−49308
Pb, dislocation internal friction changes under the action of US vibr. 79−69630
Pb film, superconducting, hypersonic attenuation investig. of crit. field, intermediate state 77−8246
Pb, superconducting and normal, electronic damping of dislocation, US meas. 79−27997
Pb, US oscillations and dislocation unpinning in supercond. and normal states *(Russian)* 79−11648
Pb/Cu(Ag) proximity effect semiconductor, US surface wave attenuation 79−60994
$(Pb_{1-x}Ba_x)_5Ge_3O_{11}$, ferroelec. transition blurring, US relax., dielec. and opt. props. 78−95559
$Pb_5Ge_3O_{11}$, ferroelec. transition, US and elasto-optic props. 80−60527
$Pb_5(GeO_4)(VO_4)_2$, $Pb_5(SiO_4)(VO_4)_2$, and Pb_5GeO_{11}, elastic nonlinearity and acoustic losses 80−59554
PdSiCu, amorphous, US attenuation and vel. studies 80−19881
PdSiCu, amorphous, US attenuation and vel. studies at low temps. 80−88278
$Pd_{0.775}Si_{0.165}Cu_{0.06}$, metallic glass, intensity-depend. US attenuation at low temps. 78−79671
$Pd_{0.775}Si_{0.165}Cu_{0.06}$, metallic glass, 0.01-10K, relax of tunnelling systems by conduction electrons, US expts. 79−14889
$Pd_{0.78}Si_{0.16}Cu_{0.06}$, phonon propagation below 1K 78−71824
$RbAg_4I_5$, superionic cond., US absorpt., ionic cond., relaxing sp. ht. 78−14505
$RbAg_4I_5$, US attenuation near 208K phase transition 79−33085
RbH_2PO_4, ferroelectric, US propag. near ferroelectric phase transition temp. 78−23417
RbH_2PO_4 powder, phase transition in paraelectric (upper) phase by measuring damping const. and amplitude of phonon echoes 79−19855
$RbHSO_4$, anisotropy of US anomaly near ferroelec. phase transition 78−72473
$RbHSO_4$, ferroelec. phase transition, US attenuation and velocity 78−39511
$RbH_3(SeO_3)_2$, US vel. and absorpt. near ferroelec. Curie temp. 80−97206
$RbMnF_3$, isotropic antiferromag., phase diagrams, US meas. 78−68350
$RbMnF_3$, isotropic antiferromag., crossover behaviour of mag. phase boundary, US meas. 78−80145

ultrasonic absorption continued
Rb_2ZnCl_4, US vel. and attenuation at normal-incommensurate phase transition pt. 79−55833
Rb_2ZnCl_4, US velocity and attenuation, around normal-incommensurate phase transition 80−40072
SO_2, liq., vibr. relax., US absorpt. and vel. meas. 80−34147
SO_2-tetrachloromethane, solns., near critical point, ultrasound absorpt. obs. 80−65160
SR, attenuation due to phonon-phonon interaction and thermoelastic phenomenon 79−77686
Sb, dislocation internal friction changes due to high-amplitude US oscills. *(Russian)* 80−10556
Sb_2S_3, dielec. and acoustic nonlinearity 78−15107
$Sc_2(SO_4)_3+Al_2(SO_4)_3$ aq. solns., complex form. reacts., kinetics, US relax. investig. 79−1942
Se, acoustic props. near first-order phase transition 77−20014
Se, amorphous, sound propag. at low temps. 77−72657
Se, amorphous, US attenuation at low temp., internal friction peak 80−65152
Se, amorphous, US wave attenuation and vel., near glass transition 77−89501
a-Se, hole form. energy, heating time and cooling rate depend. 79−41958
Se, liquid, US absorpt. meas. 78−2202
Si, amorphous sputtered thin film, US anomalies, 0.5-300K 80−34145
Si, photoacoustic effect, free flexural vibrs. damping 77−89813
Si, pure and n-type, US vel. and attenuation, evaluation using elastic moduli 80−70325
p-Si, US attenuation by impurities 77−69047
P-Si:B, US spectroscopy, energy splitting of acceptor ground state 79−33260
SiC, acoustic props. study at 9.43 GHz 80−65169
SiC, sound absorption 78−88000
SiO_2, amorphous, low temp. acoustic absorpt., 9 to 20K and 15 to 65 MHz, Anderson model interpret. 78−26633
SiO_2, and $SiO_{0.7}$, amorphous sputtered thin film, US anomalies, 0.5-300K 80−34145
SiO_2, vitreous, Suprasil-I, spectral diffusion at 0.5K, acoustic hole burning expts. 79−60439
SiO_2, vitreous Brillouin scatt., 35 GHz phonon vel. and absorpt. below 1K 80−100664
SiO_2-Al_2O_3, vitreous US vel. and absorption 80−107380
SiO_2-B_2O_3 glasses, Brillouin scattering meas. of attenuation and vel. of hypersounds 80−100309
SiO_2-TiO_2, vitreous, US vel. and absorption 80−107380
Sn intermediate state, US attenuation 79−42694
Sn, superconducting and normal phases, damping of dislocations and supercond. attenuation 78−52155
Sn, US attenuation and dislocation damping 79−95086
Sn, white, cyclotron effective masses, US attenuation meas. 77−15753
Sn-In, dil., amplitude depend. US attenuation in normal and supercond. state 77−28299
Sn-In, dil., intermediate state, US attenuation 79−42694
Ta, shear elastic constant, anomalous temp. behaviour, US study 80−79855
Tb-Ho, US attenuation and elastic consts. in 3 mag. phases, 4.2 to 300K 77−72645
Tb-Ho (50%), antiferromagnetic, thermal expansion, US attenuation anomalies 79−47319
$Tb_{0.3}Dy_{0.7}Fe_2$, US velocity and attenuation obs. 77−28423
$Tb_2(MoO_4)_3$, elastic wave attenuation and velocity near ferroelec. transition 79−73257
Ti-Ni, internal friction and US props. *(Russian)* 80−84247
$TmFeO_3$, acoustic vel. and attenuation shifts at spin reorientation phase transition 80−65986
V, attenuation due to electron-phonon interaction 79−77687
V, mixed state, US attenuation purity depend., crit. temp. and energy gap 77−47935
V, superconducting, fluctuation contrib. to US attenuation in mag. field near H_{c2} 77−47936
V, superconducting, fluctuation contrib. to sound attenuation near H_{c2} 79−33397
V-Ti (42 at.%), mixed state, US attenuation meas. at 4.14K 80−15657
VO_2, phase transition, temp. variation of US attenuation and phase vel. 77−31723
V_2O_3 phase transition, temp. variations of US attenuations and phase vel. 77−31723
V_3Si, supercond. mixed state, low temp. tetragonal-domain-reorientation phenomena, US expts. and thermal props. 80−60141
V_3Si, US anomaly when cooled below martensitic and supercond. transition temps. 80−20354
W, absorpt. of ultrasonics, temp. depend. *(Russian)* 79−51203
W, attenuation due to electron-phonon interaction 79−77687
W, longwave dopplerons, nonlocal Hall effect, surface impedance, size effect *(Russian)* 80−80253
W, US attenuation meas. of mean free path temp. dependence 77−39825
YAG:Dy(Er)(Tm)(Tb)(Yb), US attenuation 77−89500
YAG:rare earth, phonon impurity scatt., lattice thermal cond. and US attenuation meas. 78−87748
YAG:rare earth metal, US absorpt. meas., relax. model 80−24539
YB_{68}, melt grown, props. meas. 77−11518
YIG, thermal attenuation of US waves, 500-1000 MHz 77−84854
ZN, anomalous US damping under hydrostatic press. 79−14890
Zn, damping of US vibrations under high hydrostatic press. 77−55324
Zn film, supercond., SAW US attenuation 79−73633
Zn US attenuation due to conduction electrons 79−46754
Zn, US attenuation of conduction electrons calc. 78−91588
Zn, US attenuation of conduction electrons, shear waves calc. 78−91589
Zn, US attenuation under high hydrostatic press., dislocation mechanism 77−43284
$ZnCl_2$ in H_2O, complexity investigation using US method 80−33326
$ZnCl_2$-LiCl(NaCl)(KCl)(CsCl), molten, US absorption coeffs. and bulk viscosity coeffs. *(Japanese)* 80−88271
$ZnCl_2$-$PbCl_2$, molten, US velocity and absorpt., thermodynamic quantities and bulk viscosity *(Japanese)* 80−84249
ZnO monocrystal and RF sputtered heteroepitaxial film, SAW attenuation comparison 79−56063

ultrasonic applications
see also biomedical ultrasonics; ultrasonic materials testing; ultrasonic welding
acoustic detection of high energy particle showers in water 79−85862
acoustic holography system, Sonoscan using microprocessor 80−38184
acoustic imaging, electric coupling effects in transducer array 80−43587
acoustic imaging, phase sampler, improved image quality *(French)* 80−79088
acoustic imaging with nematic liquid crystals *(French)* 80−69617
aerosol droplet size rel. to liquid viscosity 79−47998
air jets, free and constrained, acoustic emission, gas leak detection conditions 80−5895
alloy melt, US treatment *(Russian)* 77−44259
assisted radiant heat transfer into water and air 79−46169
biochemical research using sonicator processor 79−18639
biological surgery, severing corpus callosum in rats 80−26306
bituminous coal emulsification 79−47997
blood flow detection in human heart, US pulsed Doppler flowmeter system, microcomputer based 80−104690
blood flowmeters, design considerations 80−23853
blood vessel localisation appl. 77−77956
bonding displacement meas. by He-Ne laser interferometer 77−37972
bubble detect. and meas. in liquids, blood appls. *(Japanese)* 80−1712
cast stoneware, quality control, use of US methods 78−11490
cavitation detection PW reactor coolant water pumps, *(German)* 77−74906
ceramic, US treatment, without abrasion suspensions 77−44375
cervical dilation during labour, continuous meas. with US device 77−86574
characteristics and appl. patient diagnosis appl. *(German)* 78−1527
chelation study of aspartic acid with Zn(II), Cd(II) and Hg(II) 77−44464
cinefilm cleaning system using focused ultrasonic energy source 80−31916
cleaners and disintegrators, review, latest instruments 79−37101
cleaning by chlorine solvents, US cavitation intensity measurement *(Polish)* 80−38464
cleaning of microscopic optics, using solvents in US field *(Czech)* 79−40608
cleaning of optical fibres, deleterious effect 78−33821
cleaning of optical materials, deleterious effects 77−42631
cleaning using Freon 113, ethylene tetrachloride, methylene chloride anisotropic mixtures *(Polish)* 79−15839
coal slurry diagnostics by US transmission 78−87216
colloid submicron particle size measurement, ultrasonically induced birefringence technique 80−30290
computer tomography, radionuclide imaging and ultrasonography in hepatic mass lesions 79−88211
conference, Brighton (1977) 78−59223
conference, New Orleans, LA, USA 80−73101
correlation of return signals with bipolar digital representation of broadcast waveform 80−99897
cubic crystal orientation determ. from meas. sound vels. 79−55691
cubic single crystals, rapid crystallographic orientation determ. method using US vel. anisotropy 78−6027
data collection aperture, based on long-wavelength imaging system 80−99905
density meas., impedance and velocity meas. methods comparison *(Russian)* 77−37846
density meas., online system 78−718
device development and application trends 79−23155
dispersion of Na salt crystals in aqueous slurries, particle size distrib. determ. 79−61918
Doppler flowmeter employing continuous wave modulation *(Japanese)* 79−37429
Doppler US flowmeters, operating principle 79−50817
drying of pulverised coal in vacuum filtration 77−32539
Duraluminium, erosion at surface due to US activation *(German)* 79−57122
elastic modulus of Tb, meas. using CdS transducer 77−11151
electrolytes, US determ. of hydration numbers 78−20027
ferrous material fractured surface exam., oxide scale removal 78−95886
fields radiated into liquid by normal modes of plate driven by pulsed US beam 78−50995
film cleaning by ultrasonic liquid cavitation and acceptable solvents 80−62769
fish finder, with colour TV display 78−38159
fission reactor US testing to ensure safety, trends *(German)* 77−26847
flotation of hydrophobic minerals, US activation of non-polar collectors 78−63250
flow meas., with US meas. of float position *(Russian)* 77−42943
flowmeter, computer interface development 78−38426
flowmeter, correlation and spectral props. of flow modulated US signals 77−42948
flowmeter, for pure and high polluted fluids *(German)* 79−77319
flowmeter, open channel acoustic flowmeter, error sources and calibration 78−30389
flowmeter, ultrasonic cross correl. flowmeter 78−30393
flowmeter DUS 20 for liquids, operation *(French)* 79−50819
flowmeter for natural gas industry 78−30392
flowmetering 79−50832
fluid flow meas. by contactless techniques *(Italian)* 80−53891
glass workpiece, US drilling, structural alterations 78−48555
graphite impregnation by low melting point metals using ultrasound *(Russian)* 78−46876
heat transfer systems 80−74723
heating process parameter meas. and registration system *(Polish)* 79−12798
HF probing method for investigation of hydrodynamic cavitation in viscous liquid 80−87676
historical review 77−27404
hollow drop production by injection of gas bubbles into liquid jet and US excitation 78−1710
holograms, recording via suspension method 77−14857
holographic visualisation *(Slovak)* 79−41527
hot-pressing chamber, with US activation facility 77−59709
ice detection using surface acoustic waves 78−18129
imaging, visualization and characterization, conf., Houston, TX, USA (Dec. 1979) 80−106672
imaging and holography using US, devices, medical uses *(French)* 77−827

ultrasonic applications continued
imaging system using random phase mask and stationary-point receiver 77−80035
imaging techniques *(Japanese)* 80−19190
imaging using Bragg diffraction *(French)* 79−81664
information transmission, nondestructive testing, review *(German)* 79−50550
insulants, thermophysical meas. by US method 77−45830
interface erosion rate meas. using pulse-echo US method 78−182
internal friction meas. instrument for use at high temps. 78−13977
invisible information imaging techniques 77−5819
lapping of conical surfaces 78−44235
laser, double heterostruct. junction type, US wave freq. modulation anal. 78−83009
laser beam spatial coherence control by progressive US wave 80−78885
level detection appl. 80−27268
liquid atomisation, using US piezoelectric resonators *(German)* 79−66359
liquid atomisation developments 79−66360
liquid cavitation technique for cleaning cinefilm 80−31918
liquid crystal film, imaging of US in air 80−38166
liquid filtration US enhancement 78−59526
liquid ultrasonic meter for the intensity of pulsed beams of charged particles 79−68110
LMFBR safety application of US thermometry 79−45400
LMFBR vessel, austenitic steel welds testing 77−1903
manometer for low press. based on US interferometer 77−67455
marine sediments, correl. between geotechnical and acoustic props. bottom refl. coeff. meas. near sea floor 79−96756
marine sediments, reflected and scatt. US waves, granulometric mode determ. *(French)* 78−92815
mechanical engineering, excitation and stabilisation of reson. modes in US rod systems 77−14839
metal powder, atomised, refining by ultrasound 77−44187
metallic glass surface oxide film removal *(Russian)* 78−72935
microbiology, status and problems of methods used 80−21592
microelectronic appls., use of broadband vibratory systems 80−74613
microscopy, principles and appls. 78−18133
microscopy at optical wavelengths 78−71251
mobility aid for blind people 80−56290
monitoring of local phase transitions during vinyl chloride polymerisation 80−33299
mulitary appls., multilayered tape for perimeter warning device for combat troops 80−19200
nebuliser, for inductively coupled plasma-atomic emission spectrometry, detect. limits efficiency 77−68361
nebuliser, US, in plasma jet emission spectroscopy, parameter, Mn determ. appl. 78−68960
neutrino detection, using thermoacoustic effect in water, particle-induced EM cascade 79−29960
ocean small-scale turbulence study *(Russian)* 77−78201
ocean-dumped sewage sludge tracking, using 200 kHz echo sounder 77−2182
oceanographic sensors, US abatement of fouling on glass *(German)* 77−5342
optical coherence modulation by US waves, partial coherence depend. on US parameters 80−58453
particle coagulation using acoustic radiation pressure 79−32152
PET fibre, molecular orientation determ. by US propag. velocity 77−58961
petroleum prospecting, digital recording of ultrasonic signals [petroleum prospecting] 78−73552
photodetector metrological certification, using acoustooptical modulators 80−23727
pickling of atomised Fe powders, particle size effect on degree of purification 79−28985
pipe/boiler wall thickness meas., test equipment *(German)* 78−18136
plastic extrusion cylinder and feed channel wall temp. and pressure control and meas. 77−27448
Polaroid Sonar One-Step camera, US automatic focusing 78−78011
polymer processing, US effects casting appl. *(German)* 77−48388
polymers in soln., mean mol. wt. determ. from attenuation and velocity meas. *(German)* 77−54641
powder purification by US cleaning and pickling, effectiveness of working liq. comp. 77−63587
pressure vessels, acoustic emission inspection, during water-pressure testing, NDT 77−1901
pressure vessels, C-fibre reinforced plastics, acoustic emission detection, immersion technique 77−1902
probes in AP-10KI series 78−53116
pseudorandom signal-correlation system 80−43547
random signal analysis, conf., London (April 1977) 77−44822
refractory metal dichalcogenides and Ga alloys, mixing powders using US treatment 79−24454
rock sample compressional and shear wave vel. meas. by profiling 78−44786
rocks characteristics examination *(German)* 77−91314
scanning electron microscopy, US imaging technique 80−95192
signal processing in ultrasonics, conf., London, England, Jan. 1980 80−33351
small surface crack size estim. using SAW 78−76793
soldering, industrial applications 77−58499
sonar, US imaging system, design and construction 79−3831
specimen preparation for TEM, ultrasonic separation method 79−52561
spectrographic anal., atomisation of solns., US method, aerosol dispersion, sensitivity, reproducibility *(Russian)* 77−1964
spectroscopy appl. in NDT 80−79090
spring strip production, flattening mill employing US and electroplastic effect 78−84941
steel, casting, US study 79−66252
steel, stainless, atomized 0Kh18N9 powder, activated sintering, US treatment 77−90291
steel, surface hardening by US treatment *(Russian)* 77−73364
steel, US cleaning incorporation in continuous annealing plants 77−1884
strengthening of cryst. mats., instrument for US attack at low temp. 77−49732
surface, mech. and corrosion props. improvement using US energy *(Rumanian)* 79−15821
surface cleaning, electrolytic method for quality control 79−34233
surface hardening and finishing by US peening *(German)* 78−85020
surface waves height meas., new acoustical methods 79−1276

ultrasonic applications continued
switch, two-board design, alarm and data transmission systems appl. 78−46870
technological processes monitoring using US devices with elastic strip waveguides 77−839
telemetry for monitoring heart/respiration rate and body/skin temp. of scuba divers 77−90929
temperature meas. using US resonance method 78−16792
testing techniques review 77−74899
thermal diffusivity and sp. ht. meas., ultrasonic method 77−89015
thermometer using sound velocity in air, cct. and operation *(French)* 79−35739
thickness gauge, echo-pulsed digital 77−74359
thickness meas., precision, echo technique appl. *(French)* 78−29089
thin layer thickness measurement, US waves, phase vel. and damping *(Russian)* 78−36969
thin tube wall thickness meas. using US echo-pulse thickness gauge *(Russian)* 78−49797
through-water diver communication system Wet-Phone, voice or switch operated, 31.5 KHz carrier, 1350 m range 80−38187
time-coordinate convertor for distance meas., design aspects *(Russian)* 78−77857
transmission tomography 80−94301
tube expansion force reduction expts. 78−59186
underground remains detection, acoustic meas. with computer data processing 79−76921
underwater imaging system using multifreq. US holography 79−98556
underwater imaging using US image convertor tube 77−19499
underwater sound props. determ. using US temp.-depth profile meas. system *(Japanese)* 77−70864
UNIPAN 545 thickness gauge, with digital readout 80−47019
US leak detection for piping systems in reactor environment 77−61528
vibration systems, appl. in power ultrasonics *(Chinese)* 80−43568
washing and drying of multiwire chambers 80−105624
water pollution detect. by US sonar *(Italian)* 77−91335
welding of Ag metal oxide contact materials 78−29095
wideband Fresnel focusing array response, echography appls. 80−74640
wire drawing, anal. of radial-mode US tool with statically loaded inner surface 78−183
ZrO_2 powders, stabilised, for plasma spray-coatings 80−20869
Al, erosion at surface due to US activation *(German)* 79−57122
Al surface cleaning process 78−11417
Al_2O_3, ^{27}Al NMR, strain effects, US modulation technique 79−28636
Al_2O_3, residual stress reduction by ultrasonics 79−24575
Au conductor bonding performance and failure mechanisms 79−71436
LaB_6, US comminution of refractory compound powders 78−23656
Nd:glass laser with US modulated emission 80−48309
Ni-Al-Cr-Ti-W-Mo, US vibration applied during solidification, improved strength, corrosion resistance *(Russian)* 78−15382
Ni-Cr (33.3 at.%) alloy, ordering after US deform., microhardness and elec. resist. meas. *(Russian)* 79−20113
Si wafers, preparation of preselected areas for TEM 78−24887
SiC, US comminution of refractory compound powders 78−23656
$SrO.HfO_2(ZrO_2)$, US comminution of refractory compound powders 78−23656
Ti alloy VT9, fatigue strength estimation after US hardening 77−12746
TiB_2-TiC(20 wt.%), sintered, US machining 77−21325
W strip production, flattening mill employing US and electroplastic effect 78−84941
Y_2O_3, US comminution of refractory compound powders 78−23656
ZrC, US comminution of refractory compound powders 78−23656

ultrasonic delay lines
1.2 GHz temperature stable SAW oscillator 78−59226
300 MHz oscillators using SAW resonators and delay lines 78−59255
acousto-optic real-time radar and sonar signal processing 79−72515
broadband SAW delay lines using weakly piezoelectric substrates 78−22230
buffer memory, SAW/CCD device 79−46137
capillary and clad acoustic fibre delay line storage 78−9504
capillary tubing delay lines for operation at 20 MHz 80−74654
chirp transform processors using US strip dispersive delay lines, implementation 80−53577
clad-rod delay line with sinusoidally perturbed core-cladding interface, torsional modes coupling 77−79999
composite strip piezoceramic US receiving array 78−42511
convolution by membrane waves, using transversal piezoelectric effect of PVF_2 film 79−3859
disc delay line beamguide 'optical' transfer function 77−31183
electronically variable delay using a SAW tapped delay line and digital shift register 78−63241
flexible capillary US delay line characts. 77−7269
fused silica clad delay lines 77−46859
gap-coupled SAW devices, transverse modes 79−46138
GHz bandwidth bulk acoustic delay line using mosaic transducers and stagger tuning 80−74657
high-speed correlometer, based on US delay line 77−75757
Lamb wave excitation in yz-cut plates *(Russian)* 78−55483
low-distortion FM demodulator using SAW delay device 78−51014
metal film-coated, measurements of SAW attenuation 80−74619
parallel-channel SAW filter bank transfer function synthesis 77−23828
phased array US imaging delay line bandwidth reduction 79−50552
piezoactive waveguide, anisotropic dispersion relations for normal waves 77−88975
piezoelectric transducer, resonant, construction and delay line contract, US thickness meter 78−53100
piezoelectric vibrators, elec. steered line array, US probe characts. 80−35486
radar pulse Doppler processing with low-loss SAW delay line 77−31184
Rayleigh wave line with continuously variable optically controlled delay 77−68360
SAE, for real-time spectral anal. of D_2O far IR laser pulses 79−45983
sapphire torsional wave delay line, dispersion rel. to information storage 77−84053
SAW, combined triple-transit and bulkwave suppression 80−53565
SAW, physical props. and communication signals processing applications and devices 80−38162
SAW, triplet-transit suppression technique 79−64453
SAW, TV receiver ghost image cancelling circuit appl. *(Japanese)* 77−27429
SAW and optical signal processing techniques compared 80−48173

ultrasonic delay lines continued
SAW CdS delay lines, electronic control for optical image scanning 78−26006
SAW components review for signal processing equipment *(French)* 78−51013
SAW delay line and resonator oscillators for phase locking 78−59254
SAW delay line complex transfer coeff. calc., Shockley-Ramo induced current theorem 79−7264
SAW delay line filters, wideband, low insertion loss, VHF band 80−28398
SAW delay line signal processors using acousto-optic interactions, real time system 80−28384
SAW delay lines, true quadrature taps 78−87222
SAW devices, appls. of amorphous magnetic-layers 80−28389
SAW dispersive delay lines, new cut of quartz for temperature stability 80−19185
SAW in-line chirp filter applications 78−59207
SAW oscillator for UHF radio receiver 79−7272
SAW tapped delay line suppressing reflection from interdigital transducers *(Japanese)* 78−63247
SAW tapped delay-line for US imaging 80−74636
SAW transduction on Si substrates with polyvinylidene fluoride films 80−74618
SAW transmitting hydrophone development and performance 79−53586
SAW transversal equaliser using SAW tapped delay line and PIN diode control ccts., characts. 79−68532
SAW X-ray topographical representation 79−47870
SAW/CCD high-speed analogue programmable tapped delay line 77−39167
shallow bulk acoustic wave delay line filters, narrowband and wideband implementations 80−28400
shallow bulk acoustic wave excitation by interdigital transducers 78−59251
shallow bulk acoustic wave generation by interdigital transducers 79−51411
spiral SH_0 waveguide, Al film evaporated on $Pb(Zr,Ti)O_3$ disc, characts. 77−72123
surface elastic wave devices, RF leakage *(Slovak)* 78−55522
surface wave delay lines, fabricated using simple mask printers 78−59229
surface wave recirculation loops, for signal processing 78−22228
thin stretched foils, membrane wave excit. 78−90578
transverse surface waves, on cylindrical surfaces of anisotropic solid 78−10270
trimming using stroboscopic method of signal-to-time conversion 80−19191
two-phase PSK modulator employing SAW delay line, fundamental performance 80−33398
U-path HF periodic grating oscillator 77−23847
UHF single-phase line acoustic wave transducers 78−79180
unidirectional transducer for Lamb-wave delay lines 77−68354
VHF piezoelectric transducer-delay line systems 77−7277
wideband chirp and Barker code correlations with storage convolver 77−23832
wrap-around delay lines, Gulyaev-Bleustein and Rayleigh wave reflection 77−80028
Al strip 1.8 MHz dispersive delay line for US NDT system using pulse compression 77−32730
AlN/Al_2O_3, for fabrication 2.148 GHz SAW oscillator 80−74680
BeO ceramic, appl. for short time delay lines 77−51447
CdS bulk wave-$LiNbO_3$ SAW piezoelectric coupling 77−23845
CdS thin-film Lamb wave delay line characteristics and strain effects 77−31185
$LiNbO_2$ SAW-CdS bulk wave piezoelectric coupling 77−23845
$LiNbO_3$ acousto-optic convolver with large time-bandwidth product 77−27432
$LiNbO_3$ delay line, bulk wave generation due to nonlinear interaction of SAW 79−42359
$LiNbO_3$, SAW, delay line for acoustoelectric integrating correlator 77−88990
$LiNbO_3$, tapped SAW delay line, coupling with CdS bulk wave 77−1289
$LiTaO_3$ SAW delay line with −70 dB spurious responses 77−31182
Ni, film, mag. susceptibility correlation with SAW attenuation 79−47310
Ni film, RF sputtered on $LiNbO_3$, SAW delay variation obs. 79−56102
PVF_2 Lamb wave delay line, highly temp. dependent 80−106687
Pd-Si, amorphous alloys, elastic props. and temp. coeff. of delay time, appl. to US delay lines *(Japanese)* 79−96069
Si array/$LiNbO_3$ gap-coupled imaging devices 79−46057
Si SAW delay line design, inclusion of cond., equivalent cct. 77−88989
Si-SiO_2, influence on frequency-temp. coeff. of SAW devices 80−79066
Si-SiO_2 structure, SAW device, appl. to integrated oscillators 78−83186
SiC, acoustic props. study at 9.43 GHz 80−65169
ZnO film, elastic-surface-wave device with zero first-order temp. coeff. 77−88987
ZnO-on-Si SAW convolver development 77−27430

ultrasonic devices
see also ultrasonic delay lines; ultrasonic transducers
2-D separated media semiconductor convolver for acoustic Fourier transforms of optical images 80−74308
acoustic strip surface waveguide, diffr. and guidance anal. 78−13828
acousto-optic tunable filter, programmable 80−74511
aerial ultrasonic generators using metal resonators *(French)* 80−79074
apparatus for simultaneous velocity meas., of longitudinal and transverse waves at high temp. 78−59213
atomiser of solns., spectrochem. anal. appl. *(Russian)* 77−1964
broadband vibratory systems for microelectronic appls. 80−74613
cervical dilation during labour, continuous meas. 77−86574
characteristics and appl. *(German)* 78−1527
concentrator, calculation of arbitrary configurations 79−94430
concentrators, spheriform and cylindriform 77−50816
concentrators for US tools, wave propag. in curved rods of var. cross section 78−9484
convergent sound sources, using flexurally vibrating circular diaphragms 77−50845
crystal cleaner, use of US 79−49216
cylindrical interferometer, optical alignment of end face, theoretical criterion 77−14861

ultrasonic devices continued
cylindrical shell, coupled vibrations giving high intensity US radiators 78−59236
development and application trends 79−23155
differential US velocimeter, for meas. of dilute suspensions 77−78065
disc-rod US tool, gain enhancement technique 77−35010
disc-rod US tool 77−39134
distance measuring device with decremental acquisition of the measuring results *(German)* 80−19199
Doppler alarm systems, piezoelectric transducers appl. *(Italian)* 78−42508
driven equilibrium Fourier transform sensor operating at 100 MHz 80−74612
echocardiophone, CW swept freq. US echo location system 77−70514
elastic sphere radiometer, appl. to US intensity determ. 77−68342
electrically steerable US detector 78−51026
EM generation of US guided waves in ferromag. metal polycrysts., model 78−22236
engineering US rod systems, excitation and stabilisation of reson. modes 77−14839
etched arrays for medical imaging 79−25057
exponential solid horn, finite element analysis 78−94496
flow meter for liquids *(Spanish)* 80−6181
flowmeter, multichannel 80−103089
flowmeter, non-intrusive, theoretical and expt. uncertainty determ. 78−30391
flowmeter, PLL cct. *(Japanese)* 80−79414
flowmeter, time differential clamp on ultrasonic flowmeter, performance and appls. 78−30390
flowmeter *(French)* 79−1274
flowmeter for measuring rapidly changing gas flows, freq. range, excitation and signal processing *(German)* 78−83502
flowmeter for small time-interval meas., methods *(Russian)* 77−65824
flowmeter output characteristic linearity 78−42685
flowmeter performance anal. 79−14500
fluid flow measurement 80−1710
focusing probe selection criteria, NDT appl. *(German)* 78−7147
high-temperature US apparatus for elasticity charcts. and thermal cond. meas. of materials 78−5705
image Fourier transform correlator using US light modulator *(Russian)* 77−58264
image processing device status and prospects 80−48446
imaging and holography using US, devices, medical uses *(French)* 77−827
imaging systems, including Sokoloff tube 79−98575
integrated optic spectrum analyser, design of Bragg cell 80−74515
laser communication system, using US light modulator, for teachers 79−40321
leak detection systems, piezoelectric transducers appl. *(Italian)* 78−42508
lenses, three compartment variable focus US lenses 78−94499
light modulators, multichannel optical processing and spectral anal. of radio signals 77−23763
liquid-crystal film for US visualisation 80−5893
mechanical waveguide using circular cylindrical rod for HF intense US production *(Japanese)* 78−33983
memory correlator based on photoinduced surface storage of SAW patterns in $LiNbO_3$ 80−74309
mobility aid for blind people 80−56290
multistrip coupler for coupling of surface skimming bulk waves 80−74630
nebuliser, for inductively coupled plasma-atomic emission spectrometry, detect. limits, efficiency 77−68361
nuclear materials safeguards, ultrasonically identified security seals for CANDU safeguard systems 80−63297
ocean digital survey fathometer, providing chart display and digital output 79−5665
optical matched filtering with multichannel US modulators *(Russian)* 77−58426
parametric radiator, influence of dispersive medium on charcts. 78−94470
parametric US radiator, saturation-limited operation 78−94467
phase-locked loop device, for fine freq. anal. of bats biosonar signals 77−56392
piezoelec. face plate response anal., for imaging systems 79−14169
planar reflector in interior/on surface of test objects, charcts. *(German)* 80−43569
prism couplers for Rayleigh and Lamb waves, anal. 80−69619
probe, rocking-beam, radiation pattern, NDT appl. 77−90572
probes, multielement, for immersion inspection of contact butt welds 77−90569
pulse-phase interferometer, appl. to $LiIO_3$ cryst. as wide-band transducer 77−14868
Q-switch, ultrasonic, for Nd:glass laser 80−64034
quartz resonators, electron irradiated, optical and anelastic absorptions and resonator freq. 78−64385
quartz temperature-stable shallow bulk acoustic wave devices 79−55293
radial US vibration generation by circular plate 79−18663
reflective dot array for high-performance signal processing, development 80−74623
remote controlled US pre-service and in-service inspections of reactor pressure vessels 78−89955
resonant US thermometer for nuclear reactor appls. 78−57948
resonator cell, new design for millilitre liquid samples 78−87213
rod concentrators, equiv. circuit anal. 78−50997
scanning high resolution microscope 78−1529
scrubber for air pollution abatement 77−33180
shear wave probes, beam shape theory 79−24714
short column vibrator, apparent elasticity analysis and applications 78−59242
signal processors using multichannel SAW correlation and convolution 80−74611
Splav-VM, automated US device for inspecting hollow extruded profiles 80−7747
standing wave US Bragg cell, appl. to laser communication system, theory 78−25958
standing wave US Bragg cell, appl. to laser communication system, expt. results 78−25959
strengthening of cryst. mats., instrument for US attack at low temp. 77−49732
switch, two-board design, alarm and data transmission systems appl. 78−46870
technological processes monitoring using US devices with elastic strip waveguides 77−839
thermometer, high temp., based on sound velocity temp. depend. 80−52202
thermometers, nuclear fuel temp. profile meas., TRESON expts. 78−57955
thickness gauge, resonant immersion-type, dynamic range of magnetic modulator 79−11756
transmission scanning acoustic microscope, single lens 80−87669
transmission/reception system with single crystal, principle, biomedical appl. *(Japanese)* 77−84093
trapped-energy ceramic resonator with improved response charcts. *(Japanese)* 78−9522
tuning fork for HF operation, second-mode, finite element anal. and expts. 80−102980
underwater US image convertor optimal working frequency estimation *(Russian)* 78−30111
US-optical correlator for spatial freq. meas. 80−95995
UT-31MTs pulsed ultrasonic thickness gauge 78−24761
wideband annular US imaging array response 79−55306
$LiTaO_3$ temperature-stable shallow bulk acoustic wave devices 79−55293
PVF_2 polymer probe for mapping pressure field from arrays 80−74669
$PbMoO_4$, polychromatic acousto-optical deflector *(Russian)* 77−58429
ZnO piezoelec. film, fabrication and appl. *(Japanese)* 78−23616

ultrasonic diffraction
anisotropic medium, US diffr. expt., cryst. elastic anisotropy theory verification 77−84846
beams in single crystals, diffr. and propag. 78−94468
Bragg diffraction scanner for ultrasonic tissue characterisation in vivo 77−77949
caustics in non destructive evaluation, diffraction at crack like defects 80−43680
diffraction corrections for finite size of source and receiver in US vel. and attenuation meas. 80−96153
ellipsoidal inclusions, plane elastic wave diffraction 77−84020
interaction of two diffracting sound beams and directional US radiators 78−38121
large aperture bowl transducers, diffr. pattern 80−58833
light modulation, temporal, by ultrasound, synthesis of formulae 79−76907
nondestructive evaluation transducer figure of merit 77−27457
nonperiodic wave diffr. anal. *(French)* 80−48486
penny-shaped cracks in metals, theory and expt. 80−33267
periodic surface characterisation by US diffraction spectroscopy 78−60974
phase velocity and absorpt. coeff. meas. incorporating exact diffr. corrections 78−26010
pulse production mechanism, in crack sizing 79−83429
radiator for narrow, slightly diverging beam form. 79−90105
scanner for in vivo tissue characterisation 78−61226
SH wave diffraction in half-space with crack 79−53981
stress pulse propagation, in water, effect of diffr. 78−90568
surface wave diffraction, expt. and anal. 80−5898
swept-frequency diffraction by cylinders and arrays for tissue characterisation 78−53461
tissue characterisation 77−21585
transducer, US sound field diffr. losses, numerical calc. *(German)* 77−3705
transducers, curved, coaxial pair system, diffr. losses 77−31195
two-dimensional monolithic mosaic transducer array 79−46156
US flaw detection, diffraction of normal modes by a compliant disk 80−87603
wave fronts image profiles in schlieren obs. 77−11093
welded joint, US reflection from irregularities 80−104389
$Bi_{12}SiO_{20}$ surface and pseudosurface wave props. 79−46908
$LiNbO_3$, y-z, x-z and $41^1/_2$-x cuts, SAW SHG, laser probing 77−31153
$LiTaO_3$ SAW delay line with −70 dB spurious responses 77−31182

ultrasonic dispersion
amorphous materials, dielec. and US dispersion at low temps. freq. and temp. depend. 79−95092
attenuation and dispersion, general relationships 78−83135
binary alloys, acoustic modes in random and correlated alloys, order-disorder transform. 80−65189
bone, cortical, US velocity dispersion obs., 1 to 10 MHz 77−21583
CBOOA, US absorpt. and dispersion at nematic-smectic-A transition 79−82287
chlorobenzene, liq., vibr. relax., Brillouin scatt. and US vel. meas. 79−77692
coherent THz acoustic wave launching by far IR photon-phonon conversion 77−39135
composite materials, scatt. coeff. and uel. dispersion 79−86844
curved rods of variable cross section, wave dispersion and amplitude conc. 78−9484
diethylamine melanin, sound wave anomalous absorption and dispersion 79−77688
ethanol, US studies of mol. relax. 78−22790
ethylene glycol liquid, hypersonic dispersion and attenuation depend. on sound freq. and viscosity 79−37609
ethylene-N_2, gas, vibr. relax. time by US meas. 79−98852
isobutyric acid-water critical mixtures, US hypersonic study 80−88268
isopropanol, US studies of mol. relax. 78−22790
liquid, weakly assoc., US wave reson. absorpt. 80−34141
machine-made paper orthotropic US plate wave theory and expt. 79−68460
magnetically polarised nonferromag. metals, US excitation and detection 78−56856
measurement by phase comparison of continuous harmonic waves 79−1035
metallic ore processing, effects of ultrasonics and their appls. 78−92214
metals, sound absorpt. and dispersion, Fermi surface flattening 78−91596
methane-N_2, gas, vibr. relax. time by US meas. 79−98852
methanol, US studies of mol. relax. 78−22790
methanol-nitrobenzene-iso-octane, US vel. and absorpt., along line of plait points in ternary liq. 78−79669
β-methyl-butyl-methoxybenzylidene amino cinnamate, smectic-B liq. cryst., US attenuation anisotropy 79−55828

ultrasonic dispersion continued
nitrobenzene-i-octane, soln., with critical point, US dispersion 77−1179
PMMA, oriented, hypersound propag., elastic props. 78−75737
polyethylene glycol liquid, hypersonic dispersion and attenuation; depend. on sound freq. and viscosity 79−37609
n-propanol, US studies of mol. relax. 78−22790
Rayleigh wave propagation in strongly magnetostrictive materials 77−40111
sapphire torsional wave delay line, dispersion rel. to information storage 77−84053
SAW, phase velocities on solid-liquid boundary 78−83151
SAW EM transducer range resolution improved by pulse compression 77−19509
SAW multistrip coupler mode analysis 77−27419
steel, cold worked layer of used railroad rail, Rayleigh wave dispersion 79−1014
TBBA, US absorpt. and dispersion at nematic-smectic-A transition 79−82287
tissue, freshly excited, from rat, freq. depend. 77−86573
tissue bioacoustic property determ. by US pulse echo anal. *(German)* 78−85349
transition metal dichalcogenides, US characts. rel. to Fermi surface geometry *(Russian)* 78−34749
triethylamine, Rayleigh line and acoustic spectra, fine struct. 77−39629
water, supercooled, sound vel. dispersion, struct. relax. effect, Brillouin scatt. obs. 80−107375
Ag_5SbS_4, electron absorption and dispersion of ultrasound velocity 80−15197
$BF_3+BF_3(D_2)$ (inert gas), US dispersion meas. 78−17758
$BeSO_4$ soln. in H_2O, methanol-H_2O, US dispersion, 3-60 MHz *(German)* 78−59862
CdS, US dispersion of high intensity waves, nonlinear electron absorpt. *(Russian)* 78−26916
$CoSO_4$ soln. in H_2O, methanol-H_2O, US dispersion, 3-60 MHz *(German)* 78−59862
^3He, US dispersion and attenuation near liq.-gas crit. point 78−38897
$Ho_{0.58}Tb_{0.2}Dy_{0.22}Fe_2$ magnetoelastic surface wave dispersion obs. 79−47321
$LiNbO_3$-Si acoustically-matched surface elastic wave transducer 78−90623
$MgO:Fe^{2+}$, intrinsic spin-lattice relaxation rates, nonresonant US meas. 78−80203
$NiSO_4$ soln. in H_2O, methanol-H_2O, US dispersion, 3-60 MHz *(German)* 78−59862
SF_6 gas acoustic dispersion obs. by double-crystal US interferometry *(Japanese)* 79−4100
Si, amorphous sputtered thin film, US anomalies, 0.5-300K 80−34145
SiO_2, and $SiO_{0.7}$, amorphous sputtered thin film, US anomalies, 0.5-300K 80−34145
UF_6 gas acoustic dispersion obs. by double-crystal US interferometry *(Japanese)* 79−4100
W-Cu composite materials, vel. dispersion and scatt. of transverse US waves 78−91383
WF_6 gas acoustic dispersion obs. by double-crystal US interferometry *(Japanese)* 79−4100

ultrasonic effects
air flow through capillary under action of ultrasound 80−6149
alcohols, US effects on shear viscosity 78−59184
alkali metal salt solution, Ar saturated, sonoluminesc. as acoustic cavitation probe 79−60437
alloy, hard, powder mixtures, porosity and hardness during pressing, u.s. vibration effects 77−1821
alloy melt, US treatment *(Russian)* 77−44259
amino acid formation in ultrasound in water masses of primordial Earth 77−37409
bean roots, non-thermal inhibition of growth and detect. of acoustic emissions, 1 MHz US 80−104643
binary liquid mixtures, excess internal press. and intermolecular interaction 78−35640
bioeffects of pulsed US 80−51155
birefringence induced in nematic liquid crystals, image detector appls. 79−41537
bone, piezoelectric effect on exposure to US, effect of sample rot. 78−80913
bone regeneration, morphology, effect of US 80−41111
bruising modification in quinea-pig pinna 79−16248
bubbel nucleation in oscill. press. field 79−32216
bubble layers in liquids, struct. of pressure pulses 80−38479
C Fe Armco, cumulative fatigue damage at US freqs., thermal activation 77−70181
carnauba wax, orientation prod., by mech. press. or US waves 78−64314
cavitation, bubble number kinetics in US field 77−15085
cavitation, production of pressure and light impulses *(French)* 80−33297
cavitation at a fluid-solid boundary, cleaning and erosion 80−65158
cavitation bubbles in water, elec. pulses production 79−47407
cavitation emission from insonated plant tissues 78−59185
cavitation in liquid crysts. 80−87633
cavitation in liquids due to effects of simultaneous action of US vibrations of different freqs. 79−94396
cavitation in water, effect of transducer radiating surface coatings *(German)* 77−42653
cavitation intensity in liquids, organic comparisons 80−106820
cavitation-induced capillary waves in US atomization 80−33328
cavitation-produced stress in solid 77−24354
cells of Chinese hamster, US treatment at high intensities and long exposures 77−5026
chemical reaction rate increase in US cavitation, diffusion model 79−96312
Chinese hamster ovary cell colony size and giant cell form. after 1 MHz US irrad. 78−28000
Chinese hamster V-79 cells, US lethality obs. 80−85443
chromosome aberrations in vivo effect of US alone and in combination with X-rays 78−20210
coagulation of Re hydrosols 80−58853
cochlear, struct. and functional changes following US irrad. 80−89791
collagen synthesis stimulation, human fibroblasts, role of US-induced cavitation 80−85442
conducting media, ultrasound excitation, varying EM fields 80−87635

ultrasonic effects continued
corn seed treatment with ultrasound, changes in production, yield, chemical composition 79−79597
crystallising bar, oscillations, EM excitation 80−84845
4-cyano-4′-octylbiphenyl, smectic A phase, defect patterns induced by ultrasounds 79−86695
cylindrical light beam diffr. on wideband US signal 78−50698
dextran, activation of acid hydrolysis by ultrasound, mech. stress effect on reactivity 79−74375
dielectric, regulated, thermal capacity, strong US waves effects *(Russian)* 80−65240
diffraction of laser light, nonlinear liquids 80−64270
drawing, of continuous round ultrasonically perturbed profiles, stressed states at centre of deformation *(Russian)* 80−59557
Drosophila eggs, killing on exposure to traveling and standing US wave fields 80−101223
E. coli, effect of US at 1.5 MHz 80−72212
E. coli B, combined US and gamma irrad. 78−20211
Elodea, cell death thresholds for 0.45-10 MHz US 80−67149
EM field induction in vacuum by US wave in magnetostrictive conductive half space, anal. 77−73415
epoxy resin compositions, highly filled, influence of combined action of mechanical vibr. and ultrasound 79−56952
erosion testing based on Al foil damage using light scatt. 77−36695
erythrocytes, avian, US effects on transport 79−96613
erythrocytes, haemolysing action of u.s. 77−2019
fluorocarbon liquid, effect of US irrad. on breakdown characts. 79−91361
free convective heat transfer, from inclined plate in water, effect of US vibr. 77−51055
freezing effect, creation of const. volumetric periodic struct. *(Russian)* 78−63843
gamma resonance spectroscopy under HF excitation, review 77−48113
gamma-quantum coherent scatt. in field of US waves, kinematic theory 80−80649
gamma-ray resonant interaction with matter, control, suppression using acoustic excitations *(Russian)* 79−4748
gas cavitation nuclei, radii determ. by filtering gelatin 79−81612
gas cavitation nuclei stabilization using skins of varying permeability 79−81611
graphite, wetting by molten Al, effects of US 79−15629
holographic interferometry used in US field investigations, theoretical analysis of light intensity distrib. 80−32903
hydrocarbon liquid, effect of US irrad. on breakdown characts. 79−91361
hydrodynamic siren, acoustic excitation of cavitation 78−94776
hydrodynamic wave excitation at tangential discontinuity by high-intensity US beams 80−58851
hyperthermia, deep local, induction by US and EM fields, problems and choices 80−94283
hyperthermia in tissue-like substances, EM and US induction 80−98012
II-VI semiconductors, high intensity US effects on synthesis and growth 77−819
incinerator smog reduction by US vibration induced water mist 77−32845
Josephson current, acoustic perturbation 79−42706
laser beam modulation by Fresnel acousto-optic conversion 77−27371
laser speckle reduction in image plane by US modulation of spatial coherence 80−106459
leucocytes, human, sister chromatid exchange anal. 79−96612
light diffraction, adjacent US beams 80−87629
light diffraction by acoustic wave from transducer array 79−18527
light diffraction by two adjacent parallel US waves, soln. of boundary value problems 78−90358
light passage, in homogeneous isotropic dielec. 77−599
light temporal modulation, in thick-screen diffr. by ultrasound beam plus amplitude grating 77−50755
light wave diffr. by complex spectral composition US 80−95939
lipid bilayer, 1 MHz US effects on cond. and capacitance 78−77082
liquid crystal, orienting action of US related to theorem of min. entropy prod. 79−77498
liquid crystals, instabilities generated by US field, review 78−91235
liquid dielectric breakdown characts. *(Korean)* 77−90101
liquid dielectric breakdown influence of US excitation 80−15964
liquid flow through porous media, 20 kHz US stimulation 77−31385
liquid He, subharmonic responses 80−33327
liquid light diffraction, Fresnel approx. 80−48135
liquid surface relief prod. by US field, holographic interferometry meas. 78−1519
liquid vibration 80−43559
liquids, US induced birefringence, temp. depend. study by optical farfield method 78−16826
lymphocyte cell DNA damage by US diagnosis 80−67148
lymphocytes, human, 1.5 MHz irradiation 79−96609
macromolecules in solution, US degradation simulation program 79−14148
magnon kinetic eqns. in parametric ultrasonically excited frromagnets 80−44820
mammalian cells, in vitro US irrad. at hyperthermic temps. 80−94282
mammalian cells and chromosomes in vitro, 65 kHz 78−40240
MBBA, liq. crystal, hydrodynamic instabilities and elastic deformation created by US 77−19873
MBBA, nematic liq. cryst., acoustohydrodynamic instability 77−4036
MBBA film, homeotropic nematic cell, subjected to ultrasound, impedance variations 79−41948
medical US and its biological effects 79−96614
metal, fracture under influence of high power US waves *(Russian)* 79−5034
metal, hydroextrusion, effect of longitudinal US vibrs. 79−96046
metal, US heating *(Russian)* 77−44258
metal plastic deformation, influence of mech. vibrations 78−60722
metal rod, US heating to onset of plastic deform., temp. field calc. 77−69049
metallic ore processing, effects of ultrasonics and their appls. 78−92214
metals, erosion accompanying simultaneous action of laser emission and ultrasound *(Russian)* 80−7442
metals, hydroextrusion, effect of longitudinal US oscills. *(Russian)* 79−34071
Mossbauer absorption spectra variations induced by LF excitations 80−102904
Mossbauer effect, ultrasonic excitation, phase effects 80−55004

ultrasonic effects continued
Mossbauer emission and absorption spectra, effect of anharmonic US vibrations excited in cryst. 78−72443
mouse, effect on adult mortality and litter size 78−69135
mouse uterine smooth muscle, US induced contractions 79−25028
natural flow and US cavitation erosion comparison 78−59435
nematic liquid crystal, effect of ultrasound on orientation *(French)* 77−59067
nematic liquid crystals, acoustohydrodynamic instability 79−94397
nematic oriented film, birefringent stripe pattern generation by ultrasonic waves 77−76301
nucleic acid components, low-intensity US effects 77−32874
oedema experimentally induced in rats by $AgNO_3$, effect of US on response 80−104642
oil, slurries, ultrasound assisted filtration 78−94504
oil-water emulsification, by US, large primary oil drop breakup 79−32644
oil-water interface, US emulsification drop form. by capillary wave instability 79−32643
optical diffraction by US wave rel. to molecular parameter calc. 77−48144
optoacoustic interactions obs. method 78−94498
organic molecules in solution 78−31260
particle coagulation using acoustic radiation pressure 79−32152
pearlitic transformation, effect of ultrasound *(Russian)* 78−67823
perturbation obs. at cellular level 78−61214
phosphatidylcholine monolayer vesicles, US irradiation formation, quasielastic laser light scatt., dynamics 77−48764
piezoelectric probe, radiation and reception field investigations, pulsed mode, Kirchhoff approx. 80−87636
piezoelectric semiconductors, US ionisation of shallow impurities 77−43538
Pisum sativum roots, 2 MHz US effects on growth and mitotic index 78−7385
plant root growth, cavitation as mechanism for effects 80−21489
platelet aggregation induced by US under specialised conditions in vitro 80−45963
platelet morphology and function modification by US exposure 77−77929
PMMA, ultrasonically modulated tensile stress produced fracture surface 79−91815
polycaproamide, US degradation in H_2SO_4 soln. 80−15191
polyethylene, sonic frequency vibration effect on stress relaxation 77−86072
polyethylene terephthalate fibres, high freq. US effects on physical and chem. structs. *(Polish)* 78−51446
polymer soln. US atomisation efficiency and particle size distrib. rel. to supply volume rate 79−68468
polymethylstyrene, mech. scission by US irradiation *(Japanese)* 78−59190
polystyrene solutions, US degradation obs. 78−95989
postpartum survival of mice exposed 'in utero' 79−96610
pregnant mice, acute US exposure at different stages of gestation 80−94284
pregnant mice and embryos in utero 78−35880
protein synthesis in human fibroblasts in vitro, US stimulation, role of cavitation 80−8100
PTFE fibres, US effects on structure *(Polish)* 78−68702
pupa, Drosophila melanogaster survival after 1 MHz US exposure 79−88114
PVC, mechanochemical degradation in primary struct., mech. vibration effects, IR spectra *(German)* 78−19769
rabbit liver, kidney and testicle, thresholds for lesion prod. 77−81527
rat cardiac muscle, mech. props., effect of 1 MHz ultrasound 78−96062
resonance driving of ellipsoidal oscillations of liquid drops 77−31164
resonance suppression of anomalous X-ray transmission *(Russian)* 77−89347
resonant bubbles, stable arrays in standing wave acoustic field 77−79988
root growth, Zea mays, combined effect of US and cytotoxics 77−5025
root meristem cells, 2 MHz US effects on DNA, RNA and protein synthesis 77−9218
root meristem cells, Vicia faba, micronuclei induction, X-ray rel. to US exposure 79−96633
root meristem cells of Pisum sativum, increased G_2 duration after sonication obs. 80−56117
sonochemical reactions, cavitation induced, rate dependence on US intensity 77−36732
static flow stress, decrease, by superimposition of ultrasonics 79−7652
steel, austenitic, pearlite transform. kinetics, effect of US deform. *(Russian)* 77−21136
steel, austenitic 30KhGSN2A, bainite transform., US strain effects *(Russian)* 77−73269
steel, C, siliciding in US field 79−39043
steel, Cr, influence of ultrasound on tempering processes *(Russian)* 78−52827
steel, Mn, influence of ultrasound on tempering processes *(Russian)* 78−52827
steel, stainless, atomised powder, effect of ultasonic refining on processing preps. 79−33972
steel, stainless, fixing pins for fractured bones, strength, ultrasound effect 80−71710
steel, stainless, Mossbauer radiation modulation by coherent US excitation 79−61277
steel, type 30KhGSN2A, influence of US on γ-α transformation kinetics *(Russian)* 79−74148
steel SS-41, plastic working with vibr., US hardness tester 78−53044
strengthening of cryst. mats., instrument for US attack at low temp. 77−49732
superconductor tunnelling, sum rules *(Russian)* 79−87195
surface and absorption heating in US field in liquid medium *(Japanese)* 77−72110
surfactant vesicles, low-ang. light scatt. and photon correlation spectroscopy 79−79484
suspensions, changes in physical props. 80−23825
suspensions, particle concs. rel. to interference maxima, appl. to US holograms recording 77−14857
thermocytes, rat, US-induced changes in rates of influx and efflux of K^+ in vitro 80−89793
thyroid substances levels in blood serum of rats exposed to 0.2, 0.6 and 1 W/cm^2 of US energy 78−69134
ultrasonic effects continued
transkull transmission of an intense focused US beam, lesion production at 500 kHz 80−89792
tumour irradiation with intense US, hamster 80−8099
tumours, spontaneous, in dogs and cats, treatment by ultrasound-induced hyperthermia 79−62290
ultrasound generation, at metal-electrolyte interfaces, preliminary meas. 78−91526
US hardening kinetics rel. to dislocations 80−50644
vapour bubble, nonsteady behaviour in US field 77−15107
vapour bubble growth in US field 77−34989
vapour bubble growth in US field 80−87608
wear resistant material, US welding effect on struct. *(Slovak)* 79−74185
Al alloy, AK4-1, dispersion-hardening, US effects on ductility and thermal resist. *(Russian)* 77−32582
Al alloy AL22, influence of ultrasonics application on creep during multistage ageing *(Russian)* 79−91708
Al, mechanical deformation with superimposed insonation, volume effects 78−60723
Al, strength changes on US treatment in programmed loading *(Russian)* 77−32583
Al, struct. changes in single cryst. under influence of static and dynamic stresses *(Russian)* 78−92300
Al, US fatigue crack propagation obs. 77−40451
Al, US hardening kinetics rel. to dislocations 80−50644
Al-Cu(Mg), age-hardenable, US cavitation erosion mechanisms, effects of comp. and heat treatment 78−53002
Al-Li (2.8 wt.%), ageing in US field, precip. hardening *(Russian)* 80−29968
Al-Mg alloy AMg6, US vibr. during superplastic deform. effect on struct. 79−38911
Al-Mg alloy A99, intercrystalline fracture during US treatment 79−15795
Al-Si-Mg (1, 0.6 wt.%), plasticity due to superimposed macrosonic and static strains 78−60719
$BaTiO_3$, vacuum condensates on US irrad. substrates, props. 77−66466
$BaTiO_3$-based nonpiezoelectric ceramic, acoustic convolution in paraelectric phase 80−6467
$Bi_{95.6}Mn_{4.4}$, magnetisation of ferromag. precipitates, effect of ultrasonic pulses 80−2121
$CaF_2:Gd^{3+}$, cubic, strain effects on EPR by UMER method 77−1592
Cu electrodeposit, US agitation effect on hardness, porosity and grain size, work-hardening 77−60075
Cu, soft crystal, US irrad. induced dislocation distrib. 77−32584
Cu, struct. changes in single cryst. under influence of static and dynamic stresses *(Russian)* 78−92300
Cu, US fatigue crack propagation obs. 77−40451
Cu, US hardening kinetics rel. to dislocations 80−50644
Cu, wire, polycryst., internal friction, ultrasonic vibrations effect *(Russian)* 78−76685
Cu-Be alloys, ageing kinetics, ultrasonic effects *(Russian)* 79−78997
Cu-Ti (3.5 wt.%), aged by US strain, struct. and props. *(Russian)* 80−21003
Cu-Ti (3.5%), coherent precipitates, US irrad. effect on struct. and hardness *(Russian)* 77−48446
emerald:Cr^{3+}, spin-lattice coupling consts. 79−99761
Fe, Armco, crack and slip band form. during US fatigue 78−56723
Fe, Armco, fatigue cracking under 23 kHz loading at 23°, 60° and 100°C 78−60763
Fe, C and Cr diffusion *(Russian)* 77−59144
Fe powder, supersonic vibration effect on pressing *(German)* 78−64500
Fe, US oscillatory stress superimposition effects on deformation 80−35287
Fe, under US vibrs., initial struct. effect on C diffusion *(Russian)* 78−38876
Fe-Si (3 wt.%), deform., effect of superimposed US oscillatory stress *(Japanese)* 78−31461
Fe-Si (3 wt.%), US oscillatory stress superimposition effects on deformation 80−35287
$FeCO_3$, siderite, powder, Mossbauer spectra, acoustic-excitation-induced asymmetry of quadrupole splitting 78−27145
Ga, spiral cyclstron waves excited by US in open Fermi surface metals *(Russian)* 79−99771
Ge, single cryst., ultrasound effects on dislocation struct. and impurity atoms diffusion 77−69119
H_3PO_4, wet process, influence of high-intensity US 79−15993
He I, stable microscopic bubbles and evaporation-condensation resonance 78−91381
^4He, superfluid, US generated quantised vorticity 78−38893
n-InSb, HF EM and acoustic oscill. generation in LF electric field 78−64068
InSb:Te, cryst. growth from melt, pulling method, US effects on facet growth 80−76169
KCl, US plastic deform., dislocation struct. 80−19809
$LiNbO_3$, Mossbauer radiation modulation by coherent US excitation 79−61277
Mg, dislocation struct. after US deform. *(Russian)* 80−29027
Mg, US hardening kinetics rel. to dislocations 80−50644
$MgSO_4$, soln., electrolytic cond. dispersion, 1-6 MHz, caused by US propag. 80−44343
Mo single crystal, effect of prior ultrasonic working on hardness, crystal orientation and creep resistance *(Russian)* 79−34056
Mo, US working effect on single cryst. during deform., strengthening effect, plasticity resource *(Russian)* 79−34107
NaCl, US deformation, stress anal. by polarised light method *(Russian)* 77−11641
$Na_2[Fe(CN)_5(NO)]$ powder, Mossbauer spectroscopic study of ultrasonic anharmonicity 78−52411
$Na_2[Fe(CN)_5NO].2H_2O$, powder, Mossbauer spectra, acoustic-excitation-induced asymmetry of quadrupole splitting 78−27145
Ni, acoustic hardening, influence of US treatment temps. and material purity *(Russian)* 80−11656
Ni, electrical resistance in DC mag. field after ultrasonic deform. *(Russian)* 80−54671
Ni electroless plating, effect of ultrasonic irrad. 79−33953
Ni, US deform., electron microscope exam. *(Russian)* 78−35447
Ni, US deformation at low temps. *(Russian)* 79−11656
Ni, volume-strained sintered porous, physicomech. props., u.s. vibration propag. velocity 77−1823

ultrasonic effects continued
Ni-base alloys, US vibration during crystallisation, effect on mech. props. *(Russian)* 78−19827
Ni-Cr (Mo), solid soln., US deform., electron microscope exam. *(Russian)* 78−35447
Ni-Cr (33 at.%), US deform. effect on short range order form. *(Russian)* 78−39839
Ni-Cr-Ti(Al), effect of ultrasound on crystallisation, dendritic structure, and plasticity *(Russian)* 80−11637
Ni-Cr(Mo), solid soln., US effect on mech. props. *(Russian)* 78−23819
$Pb_3Ge_2O_7$, vacuum condensates on US irrad. substrates, props. 77−66466
Sb, dislocation internal friction depend. on high ampliutde US vibrations *(Russian)* 79−90727
Se, crystallisation kinetics correlation with molecular structure 78−94998
Si, perfect cryst., X-ray acoustic reson. 79−27873
Si, X-ray acoustic reson., Borrmann effect reson. suppression by transverse US vibrs. 79−32852
Si:B, ion-implanted, influence of US waves on charged particle channelling 79−23668
SiO_2, fused, US cleaning effect on laser damage threshold 77−62024
$SrTiO_3$, vacuum condensates on US irrad. substrates, props. 77−66466
Ti alloy VT9, fatigue strength estimation after US hardening 77−12746
Ti, mechanical deformation with superimposed insonation, volume effects 78−60723
TiB_2 thick film on low C steel substrate, CVD in US field, crystallite size 80−84854
TiN, CVD growth in US field, effect on adherence and hardness 77−59696
W, plastic working of wires, combined action of US and high-density current 79−57002
W, US working effect on single cryst. during deform., strengthening effect, plasticity resource *(Russian)* 79−34107
Zn, US hardening kinetics rel. to dislocations 80−50644

ultrasonic equipment
acoustic imaging with electronic ccts., book 80−99899
acoustic lense-design with elliptic surfaces 80−48530
amplifier for directly driving solid-dielectric capacitance speakers 80−19186
array system, computer-controlled, acoustic beam steering and focusing, with variable frequency array transducers 80−38191
atomizer, construction, fatigue strength, elec. charact. 78−81959
austenitic steel, US test equipment and practice *(German)* 79−74316
B-scan imaging with automated water-delay system 80−98041
beam detector, two-dimensional 78−94495
beamformer with programmable time delay and sum 80−53592
biomedical, Aberdeen phased array, real-time US scanner with dynamic focus 80−72276
biomedical imaging system, CCD devices appl. in electronic focusing 80−56148
biomedical real-time scanner with pulsed Doppler and T-M facilities, obstetrical appls. 80−67172
blood flow measurement by US Doppler method, computer-aided determ. of angles *(German)* 78−80931
blood pressure analysis system for treadmill stress testing 80−81674
blood velocity noninvasive meas. in large vessels, broadband pulsed Doppler US system 78−61224
boxcar integrator/US recording unit using sample-and-hold circ., for student lab. 80−27083
Brillouin scattering cell for liquids 80−106694
bubble quantification system, appl. to decompression of animals and man 80−76869
calorimeter for beam power meas. 77−39181
cardiotocograph for foetal heart-rate monitoring *(German)* 77−86566
cleaners and disintegrators, review, latest instruments 79−37101
combination probe for US flaw detect. 80−35492
computed tomography of breast, progress 80−51196
concentrators, optimum geometry 80−102952
contact B-scanners, calibration method 79−23161
cross correlation flowmeter, HWR appl. 78−25283
decontamination system for reactor fuel transfer pool, remotely operated 80−68916
defectoscope, electromechanical attachment, model EMP-3 78−72975
defectoscope echo-pulse, testing of annular welds 78−53090
delay lines, transducer bonding material investigations *(Japanese)* 80−79097
design of instruments with elec. controlled directivity patterns 77−838
diagnostic equipment, US power and intensities produced 78−69162
Diasonograph incorporating pulsed Doppler system 77−77955
digitiser/processor for extraction of clinical parameters from Doppler-shift waveforms 80−36042
direct and angled text fixtures *(German)* 78−44298
disperser for powder, suspension and emulsion production 78−23636
Doppler US equipment design and biological applications *(Spanish)* 78−7409
Doppler US flowmeters, operating principle 79−50817
Doppler US flowmeters, optimum vel. resolution 77−957
dual-mode transducer and liq. acoustic line, testing of bulky irregular objects 78−56855
dynamic imaging, high resolution 80−17042
dynamically focused electronic sector scanner based on CCDs 80−98042
echo distribution evaluation, for biomedical appls. *(German)* 78−80934
echo probes, flexible, and prospects for use in oncology 80−56147
echo pulse thickness gauge, portable, range 0.1 to 300 mm, with digital readout 78−70108
echo sounding equipment *(Italian)* 78−55530
echo-oculometer, accurate meas. of eye length 77−37030
echoencephaloscope, two-probe three-mode design 78−44567
Echosimulator, function generator for meas. of US diagnostic equipment charact. *(German)* 80−104685
fission reactor materials safeguarding, fuel assembly identification using US signatures, statistical aspects 80−69620
fission reactor materials safeguarding, US signatures for remote-controlled identification of fuel assemblies 80−63296
fission reactor primary coolant flowmeter 80−73912
flaw detector for welded seams, with automatic registration of flaw parameters 77−90570
flow-meters, compensation-type, development of structs. *(Russian)* 80−83866

ultrasonic equipment continued
flowmeter, for Na cooled FBR coolant flow meas. *(Japanese)* 78−78455
flowmeter, propagation time of acoustic signal 80−6175
flowmeter, wide beam 80−106856
flowmeter DUS 20 for liquids, operation *(French)* 79−50819
flowmeters, recalc. of charact. and calibration 80−103086
focusing probes for flaw detection 80−104383
foetal breathing monitor for humans in utero, US pulsed Doppler instrument 78−69164
gas analyser for lung closing vol. meas. 78−61223
gas jet evacuation system in vacuum UV source chamber 77−13763
gating device, beam width, position and direction control 80−38192
goniometer, for measurement of surface stress in steel 79−15947
heart-lung machine blood flow line gas bubble US detector 77−77954
holography, US-field display device with transducer and LED linear arrays 80−23843
image reconstruction in parallel processing analog electronic systems, secondary images 79−81638
imaging system, 3rd generation development, high resolution, 3-D 77−86575
imaging system, Bragg-diffraction, with partially coherent light illumination 79−14175
immersion apparatus for determination of HF storage and loss moduli for polymers and polymeric composites 80−74668
improvements in ultrasonic testing, narrow-band transmitter pulses of continuously variable wavelength 80−93706
impulse-F instrument for solid-state material studies 79−94433
Indian status in 1979, industry and medicine appl. 80−81668
intraoesophageal imaging, heart dynamics 80−94303
lens, symmetrical doublet with F 1 aperture 77−14869
LMFBR Na flow meas. using US flowmeter 80−32412
lung tissue characterisation by US, instrumentation, model and results, book 78−44575
mean frequency Doppler modulator performance, blood flow meas. appl. 80−45991
medical instrumentation standardisation, physician's need 78−69168
medical probes, main parameters and characterisation 79−25056
microcirculation semiquantitative demonstration using US noninvasive meas. method *(German)* 78−85348
microscope techniques, book 79−49283
microsphere probe for pressure field meas. up to 10 MHz 80−96159
multiple section tomogram simultaneous display equipment 78−61227
multiple use US receiver *(French)* 79−64457
nebuliser system, for radioaerosol delivery 77−2050
neonatal peripheral circulation, human, characterisation by US pulsed Doppler technique 80−76815
oscillating US heavy plate body testing equipment, computer controlled, working experience *(German)* 80−93720
pseudo-continuous-wave monitor for measuring acoustic props. of substances 79−68525
pulse apparatus UD-22UM for monitoring materials with high US atten. coeff. 79−3868
pulse spectroscopy method, investigation apparatus 80−35483
pulse-echo equipment, US tissue equiv. test objects for routine performance checks 78−73182
pulsed thickness meter with digital readout 77−45823
pulsed-echo thickness meters calibration using liquid-thickness model 79−37102
radial-mode tool with statically loaded inner surface, anal. 78−183
radiation-force balance, portable, for use with diagnostic US equipment 78−69163
radiator for narrow, slightly diverging beam form. 79−90105
real-time US spectroscopy in suspensions, pulse transmission system 77−19495
receiver, based on suppressed total reflection of light *(German)* 77−75760
receiver response, optimised by fast-attack detector 77−80034
remote control circuit using US transducer 80−10097
safety standards, review of BRH, FCC, CPSC, FDA and OSHA regulations 77−57311
scanner for imaging appls. in medicine 80−72388
scanners, ceiling suspension 80−30815
scanning laser acoustic microscope for US vel. meas. of mammalian collagen threads 79−43972
schlieren quantitative visualization, using closed circuit TV system 78−46867
sector scanner, real time servo controlled, for high resolution image prod. 78−94501
shadow flaw detectors, metrological peculiarities when inspecting thick rolled steel sheet 80−81263
signal shape anal., ultrasonic pulsed measuring instrums. 80−87678
sloped probe for angular type reflector, US inspection appl. 80−104391
sonicator processor, for biochemical research 79−18639
sonoprobe for Si crystal microcracks detection 80−76462
spectrometer, double-pulse comparison technique for meas. US vel. changes 78−1526
Splav-VM, automated US device for inspecting hollow extruded profiles 80−7747
storage oscilloscope system for US grey scale display 78−3569
student laboratory, US pulse generation for vel. meas. in liqs. by optical diffraction 79−62963
test unit for abrasive granular materials, failure charact. in US field 80−85112
testing applications, review 77−74899
tissue analysis, comprehensive system 80−51189
tissue characterisation by computer-aided US method *(German)* 78−80932
transceiver for US inspection units 80−89458
transducer manipulator outside link of coupling fluid in US expts. 80−106693
transmission microscope optimisation 78−51022
underwater, for biological object vel. measurement, design principles 80−19195
underwater imaging system using multifreq. US holography 79−98556
UNIPAN 545 thickness gauge, with digital readout 80−47019
US diagnostic instrument performance evaluation, work of USA AAPM and AIUM 78−69170
US grey scale scanner dynamic range testing 78−69169
US temp. profiling system for critical heat flux meas. of nuclear reactor fuel assembly 80−37032

ultrasonic equipment continued
US velocity and damping coeff. meas. of polymers *(French)* 80−7723
viewing system for reactor fuel assemblies under liquid Na 80−57875
water-bath US coupling and piece-part testing methods *(German)* 79−74317
waterfilled US testing tanks, appl. of filled rubber material system to echo absorpt. 80−96059
Al-Mg-Si alloy, dispersion hardened, concentrators, US waveguides appl. *(Polish)* 80−89237

ultrasonic materials testing
1 kV SCR pulse generator for US pulse echo excitation 79−70290
200 to 500 MHz A-scan defect characterisation 79−47873
acoustic, stress determ. improvement of accuracy 78−15631
acoustic channel, correction of freq. response by electronic circuits 78−85111
acoustic characteristics, of solid materials, instrument for direct meas. 79−14179
acoustic defectoscopes, low freq., elec. simulation of compound piezoelec. transducers 80−102956
acoustic emission, digital memory storage and source isolation 78−27712
acoustic emission, phenomenological model, calc. of intensity 78−85110
acoustic emission, principles of technique and measuring instrums. 80−28375
acoustic emission, structural calibration technique for quantitative appl. 78−9509
acoustic emission, time-domain deconvolution technique for signal identification 79−20306
acoustic emission, transducer for inspecting weld quality 79−94444
acoustic emission anal., signal recovery technique for martensitic transformation study 78−60965
acoustic emission appl. 80−11854
acoustic emission detection for small components production testing, review 80−16632
acoustic emission detection system sensitivity, direct comparison method 78−56848
acoustic emission detection technique, industrial NDT appl. *(Japanese)* 78−27721
acoustic emission detection using Michelson interferometer and laser 77−90510
acoustic emission leak detection, attenuation of elastic waves in pipelines 78−27711
acoustic emission measurement transducers, comparison of piezoelec. and optical sensors 79−14192
acoustic emission monitoring difficulties overcome by optical detectors 78−60968
acoustic emission NDT of aircraft struct. 78−53177
acoustic emission parameter and interpretation 77−40508
acoustic emission pulse signature anal., optimal design and eval. criteria 77−48596
acoustic emission pulses evaluation, freq. anal. appl. 78−18126
acoustic emission signal, amplitude distrib., information context 80−108666
acoustic emission signal sorting by computerised pattern recognition 77−40516
acoustic emission signals interpretation during tensile testing 77−9030
acoustic emission source identification using signal anal. 77−44415
acoustic emission sources, localisation 78−87220
acoustic emission systems, method for evaluation efficiency 79−39079
acoustic emission techniques, improvement in noise immunity 80−21213
acoustic emission test apparatus 80−61041
acoustic emission transducer construction principles evaluated 78−59239
acoustic flaw detection, contactless electrogasdynamics 78−53120
acoustic flaw detector with sound indicator 78−53140
acoustic holographic techniques 79−86300
acoustic holography for flaw image form. *(German)* 77−56196
acoustic holography in tandem arrangement for interpretation of US indications *(German)* 77−16763
acoustic microscopes, nondestructive material testing appls. 80−48537
acoustic microscopy appl., scanning 80−16612
acoustic microscopy appl. to materials charact. 79−74335
acoustic microscopy using scanning laser beam as remote sensing microphone 77−81382
acoustic ranger for tube and pipe inspection 78−85092
acoustic signalling unit for US echo type flaw detector 78−53117
acoustic spectral flaw detector 79−39089
acoustic spectral flaw detector 79−34248
acoustic spectral inspection unit piezoreceiver, operation conditions 79−64465
acoustic surface waves, studies via broadband probe 78−23904
acoustic testing methods, for materials exam. review 78−72987
acoustic wave probing techniques 80−71855
acoustical spectral nondestructive-testing method 79−34234
acoustically active material, fatigue strength testing installation, electric and magnetic field effects 78−39995
acousto-elastic effect, appl. to rail stress meas. 79−91870
acousto-optical imaging, resolution 78−53165
acrylate adhesive coating on glass substrate, mech. props. determ. using transfer functions of US oscillations *(Russian)* 79−87644
adhesive bond eval., computer controlled 79−96253
adhesive bond strength prediction, Fisher linear discriminant function 79−61808
adhesive bond testing, US trapped modes in layered media 77−32761
adhesive bonded joints, testing using US probe 79−57182
adhesive bonds, physical modelling, US attenuation effects 78−7141
adhesive disband detection, US impulse induced resonance utilizing damping 78−44287
advanced fibre composite, C-scan technique for fibre misorientations, delaminations, bond failures 78−95882
AE, spectral anal. 79−43496
AE locator, receiving channels, selection of number 80−108676
AE monitoring, indust. appl. 78−68850
AE monitoring of multipass submerged arc welding 77−73394
aerospace acoustic emission instrumentation and applications 77−33322
amplifier for US flaw detector, special frequency response 79−70276
AMUR-6 instrument to detect defects and indicate their location 80−104402
angle probes, influence of membrane dimensions on sound field 79−23168
annular array search units, potential appl. in conventional US testing systems 80−35446

ultrasonic materials testing continued
annular welds, echo-pulse defectoscope 78−53090
aperiodic piezoelectric transducers, ceramic, structure and operating principles 78−85109
applications in medicine, seismology and communications 80−21198
artillery projectile inspection by noncontact EM transducers 79−47872
attenuation, of US main waves with distance 80−5859
attenuation charact., expt. determ. using Roney generalised theory 78−88596
austenite cladding layers, damping of ultrasound 80−104390
austenitic stainless steel weld metal, US propag. 80−45452
austenitic stainless steel weld metal defect detection, shear-wave polarisation effect 78−44337
austenitic steel, US test equipment and practice *(German)* 79−74316
automated rail flaw detection, US wheel probe variation problems 79−47862
automated ultrasonic testing system for piping in nuclear power plant *(Japanese)* 80−71839
automated US units for inspecting thin walled tubing 78−88606
automatic, tank test systems for crystal defects location *(German)* 79−83406
automatic, US in-service inspection for reactor pressure vessels *(German)* 77−90538
automatic acoustic emission analysis system with programmed control *(Russian)* 78−46866
automatic inspection, thin walled large diameter pipes flaw size classification 78−60949
automatic inspection of tubing 78−56865
automatic inspection system, computer aided *(German)* 77−4877
automatic installations for weld testing on tubes and tanks *(German)* 77−1894
automatic monitoring of tube butt welds, sensitivity and reliability 79−79205
automatic system for US inspection of pipes 78−76813
automatic US equipment for monitoring drill and casing tubes 78−53085
automatic US inspection of heated objects by SGK-2Ts system 78−95894
axial resolution, of US testing by signal processing *(German)* 80−7736
B fibre reinforced Al, real-time NDT during fatigue loading 77−86264
b-scan Fourier transform holography 79−83421
babbitting tester, semiautomatic, for US inspection 79−66245
beam control, defect classification and reconstruct. by phased arrays *(German)* 80−35448
beam detector, two-dimensional 78−94495
bidimensional array design for B- and C-scan US imaging system 79−47877
bimetal, explosively welded, dissipation of US oscillations at boundary layers 78−53124
bimetal, explosively welded, US oscillation dissipation at boundary layer 78−53157
bolt preload 78−53174
bond evaluation, anal. of problem 80−71847
bond US inspection, aspects of model anal. and pattern recognition 78−31611
bone, human, acoustic emission in restressing 80−3704
bone, tibia, human, physical stress effect on state, US meas. 78−24088
bone, US propag. 78−24105
bone, US surface waves for studying props. of human tibia 77−25619
book 77−90577
Bragg-diffraction imaging 79−64463
brass wire, US inspection, immersion method 80−66757
brittle lacquer for acoustic testing 78−53045
brittle material, surface energy determ. from AE, automatic system 79−91899
brittle porous materials, US fractography appl., expts. on glass 77−44336
bulk wave electromagnetoacoustic excitation 79−57195
bulky irregular objects, using dual-mode transducer and liq. acoustic line 78−56855
BUS-2 scan control unit for automatic interference reduction 79−5126
butt welded joint defects inspection 80−81244
C-scan grey scale recorder, calibration method 78−95878
calculation and experimental determination of corrections for diffraction in the pulse mode 79−52568
capacitative excitation of elastic oscillations 80−71862
case hardening depth meas. using ultrasonic goniometer, corner reflection method, book contrib. 79−100325
caustics in non destructive evaluation, diffraction at crack like defects 80−43680
cavitation mechanical strength, US assessment of materials in various media 77−16772
ceramic, automatic US defect detection for tile grading and packing processes 78−23885
ceramic, piezoelectric, US instrument for determ. charact. 80−66752
ceramic, thermal stability determ. by US monitoring 77−44441
ceramic and thin layer pulse-echo meas. 77−28969
ceramic inclusions meas. and characterisation, Si_3N_4 80−76474
ceramic surface flaw detection by SAW scatt. 79−47866
ceramics, fine-grained, US attenuation and velocity obs., 5 to 500 MHz 77−39634
ceramics, high temp. props., conf., Baden-Baden (Feb. 1978) *(German)* 79−70135
ceramics, thermal shock resistance meas. by AE *(German)* 79−70233
ceramics, US investigation, porosity, mech. and dielectric strength *(Polish)* 79−52565
circuit board materials, high voltage 78−88597
circuit for electrochemical recording of defect records in US inspection 79−66246
circular transducer array for ultrasonic inspection of plates and sheets 79−29293
coarse grain anisotropic structure materials 77−16767
coarse-structure materials, inspection of part quality using LF US methods, review 80−81264
cold rolling rolls, US monitoring of hardened thickness with low hardness gradient 78−60955
combination probe for US flaw detect. 80−35492
composite aircraft materials 80−81274
composite grip design for extraneous noise elimination during AE testing 79−15915

ultrasonic materials testing continued
composite material delamination visualisation, US pulsed schlieren method 79−70289
composite materials, fracture, elastic mismatch and interfacial bonding influence 80−40506
composite piezotransducer for LF acoustic inspection using electrical models 80−104393
composite strip piezoceramic US receiving array 78−42511
computer-assisted, review 79−43536
computer-controlled system for measuring two-dimensional acoustic velocity fields in solid samples 80−76468
computerised image processing of US and radiographic images 79−79195
computerized US signal processing for crack detect. under installed fasteners 77−19490
concrete, acoustic emission at prior loading meas. method 78−27703
concrete, compressive strength *(German)* 78−68847
concrete, deep foundations 78−88585
concrete, porosity determ. from combined US and gamma absorption meas., mech. props. 79−29295
concrete, US assessment, of strength at early ages 77−25225
concrete, US testing of strength under load and of reinforced concrete structs. 77−36707
concrete analyser, pulse velocity method 80−45472
concrete column, strength estimation by US pulse velocity method, aggregate variation effects 77−63867
concrete quality assessment, US pulse vel. meas. practical use 80−100991
conducting media, ultrasound excitation, varying EM fields 80−87635
contact fluid 79−52586
contact layer thickness optimization for resonance method inspection 79−34236
contact media for US thickness meas. and defect inspection over wide temp. range 80−104395
contact tip of transducer, method of joining 78−53086
contactless electromagnetic acoustic method, high powder radiofrequency pulse generator for US vibration excitation 79−5110
contactless electrostatic-acoustic transducer equivalent cct. analysis 77−19507
counterflow crystal. process from melt, US method of monitoring 77−56175
crack and flaw detection, basic instrument 79−5108
crack depth measurement, ultrasonic techniques, review 78−95903
crack depth measurement by US techniques 80−71859
crack detection, automatic recording and heat treatment monitoring system 77−90542
crack detection, conference, England, (Dec. 1974) 77−32754
crack dimensions, US determ. studies survey 79−11744
crack fracture parameter estimation by long wavelength scatt. 79−24709
crack growth and coordinate determ. by acoustic emission 79−5119
crack growth measurement, instrum., expt. 77−73421
crack propagation, acoustic emission transients meas., appl. to low alloy steel 79−8407
crack propagation, and prepack damage study with US attenuation 80−40656
crack size and acoustic emission pulses correlation, theory and exp. 77−90568
crack sizing, diffraction techniques 79−83429
crack-like flaw identification and crack parameter determ. in US testing *(German)* 80−50794
cracks, action as elastic wave radiation, rel. to AE signal charact. 78−60952
critical evaluation of test results, representation, processing *(German)* 78−7145
CrMoV, surface coating to prevent oxidation during high temp. AE 80−16539
curved surfaces calibration 78−39977
cylindrical articles, acoustic channel in echo-defectoscope eqn. for angled beams 77−77705
damping coeff. meas. 77−90575
data acquisition system for processing and recording of acoustic emission signals, on-line 80−57266
defect classification, automatic, by US spectral method 79−66240
defect coordinate determ. by calibration of AE method 80−35473
defect coordinate determ. in struct. with arbitrary surface, AE method 79−66239
defect coordinates, in anisotropic cylindrical shell with aid of stress waves emission 80−3282
defect coordinates in anisotropic shells, plates, determination using acoustic emission 78−80707
defect position location technique *(German)* 77−86275
defect reconstruction, from US methods, mathematical model *(German)* 78−44295
defect scanning method for metal *(German)* 78−15620
defect sizing 79−29291
defect sizing 79−83402
defect visualisation, instantaneous imaging in transparent medium 79−87811
defectometry reliability for welds in 22K steel 78−56858
defectoscope, electromechanical attachment, model EMP-3 78−72975
defectoscopy, development of and problems in theory of normal waves, review 80−81265
defects in opaque solids, visualisation of US wavefronts using pulsed LED 78−85091
defects reconstruction by signal locus curves *(German)* 78−92435
delaminations in thin sheets, elongated, interaction with Lamb waves, book contrib. 79−98574
deposited metal, US echo inspection procedure 80−89425
detection limit, comparison with eddy current methods 78−60957
differential probe head for impedance type defectoscopes, transducer design 77−73409
differential probe head for impedance type defectoscopes 77−73408
diffraction model for US frequency analysis and flaw characterisation 77−21337
digital recording system, for automatic US flaw detection system 78−76815
dimensional tube testing techniques 77−32738
direct and angled text fixtures *(German)* 78−44298
dispersive delay line for US NDT system using pulse compression 77−32730
dissimilarly oriented defects detection 78−53079

ultrasonic materials testing continued
Doppler effect, nonstationary, freq.-phase methods of investig., control of production processes 80−45464
drill pipe, exam. of propag. of US surface waves 79−5102
drill pipe, exam. of propag. of US surface waves 79−15934
drill pipe 79−34243
drill pipe with welded end couplings, US inspection 79−5124
dual-gate depletion-mode FET/piezoelectric film transducer 79−50563
echo method of inspection for complicated shapes 78−44317
echo method with immersion, attenuation coeff. meas. 78−60962
echo pattern and amplitude, construction of AVG diagrams *(German)* 80−108657
echo pulse flaw detectors, use of auxiliary sensitivity regulation 78−60951
echo signal amplitude of US flaw detector, automatic measuring instrument 79−79212
echo signal amplitude relationship to value of angle type reflector 78−53160
echo type flaw detector, frontal resolution investigation 78−53109
echo-mirror method with transform. of elastic waves 80−108663
efficient transducer arrays for NDT 79−57194
elastic anisotropy, analysis, by acoustic ellipsometry 79−47864
elastic media, flaw characts. from ultrasonic scatt. data 79−79188
elastic moduli meas. by travelling normal wave method for thin wire 78−53110
elastic stress monitoring 78−53176
elastic wave applications 77−19470
elastic wave scatt. from localised defects in solids, long-wavelengths 79−87794
elastic wave scatt. theory for anal. and design of flaw characterisation expts., long-wavelength limit 79−83408
electrodynamic transducers, US wave generation, material testing *(German)* 78−44294
electron beam closure weld on press. vessel 77−40480
electron beam welds, NDT by AE to detect lack of fusion *(German)* 77−56193
electroslag welds, using tandem probe techniques 78−27692
ellipsoidal inclusions, plane elastic wave diffraction 77−84020
ellipsometer design and performance 79−57196
EM transducer dynamic range optimisation 77−19506
EM ultrasonic flaw detection *(Chinese)* 78−11452
emission technique principle and prospects 77−12767
end cap welds in thin walled fuel elements 77−32740
energy measurement and significance in acoustic emission testing 78−31594
energy processing techniques for stress wave emission signals 79−86297
epoxy adhesion, curing time investigation 79−83430
epoxy resin curing, elastic moduli changes, US wave propagation monitoring technique 79−20305
equipment for production line inspection 79−29320
error sources, reference bodies and nonlinearity in echo display equipment *(German)* 79−34222
extruded billets, residual stress determ. from acoustoelastic meas. 80−76467
failed steam accumulator anal., role of metallography and NDT 78−95877
failure prediction by US scatt. 77−21349
fatigue crack depth meas. in threaded part of drill pipe by US inspection 79−1930
fatigue crack growth, AE monitoring 78−27706
fatigue crack growth in aircraft wing test, AE detection 78−60925
fatigue crack growth investigation, testing equipment 80−81247
fatigue crack propag., constructive and destructive interference in acoustic emission 79−86313
fatigue cracked sample stress meas. by US phase shift detection 77−28971
fatigue cracks, US visualization, advantages over pulse-echo methods 80−66738
fatigue cracks as standards for ultrasonic flaw evaluations, book contrib. 79−100327
fatigue cracks in metals, US device for determining growth rate 78−60917
fatigue cycling, radius optimisation of specimen with circ. gauge profile 79−79190
fatigue damage, procedure for early detect. and remaining life prediction 80−71848
fatigue damage detection, book contrib. 79−100326
fatigue damage early prediction by acoustic and exoelectron emission 78−53170
fatigue monitoring, new technique 77−28938
fatigue testing, use of standard equipment and background noise effects elimination, expt. 77−73423
fatigue testing of different materials with equivalent vibration charact. 80−11847
fatigue tests, determination of magnification and resonance length of samples 79−15948
fault detection, MatEval computerised test system *(French)* 79−52564
fault location, foreshortened projected distance concept *(German)* 80−16625
ferrite, US testing 78−53084
ferrites, void, conc. and dimensions determ. by acoustic charact. 80−35472
ferritic steel, size meas. and characterisation of non-planar defects 79−87812
ferrous metal rolled repetitive sections 79−87770
fibre reinforced composite, fatigue damage, early detection by NDT 77−28951
fibre reinforced composite, fibre/matrix adhesion, AF testing *(Japanese)* 77−70254
fibre reinforced composite failure analysis, by AE 78−80691
fibre reinforced composite laminate, fracture mode determ. by AE 79−57187
fibre reinforced composites, acoustic imaging 79−15918
fibre reinforced composites, AE monitoring review 79−11735
fibre reinforced composites, US diagnosis of elastic characts. and struct. parameters 80−40663
fibre reinforced composites, US method for evaluating strength props. 78−76796
fibre reinforced plastic, curing time investigation 79−83430
fibre reinforced plastic laminates, US evaluation of hygrothermal effects 80−7730

ultrasonic materials testing continued
fibre reinforced polymer, US spectroscopy location of delaminations 77−81352
fibre reinforced porous composite anal. by US wave velocity meas. of fibre vol. and matrix porosity 78−95902
fibreglass rings, ultimate load determ. by AE method 78−48604
fibres, elastic moduli determ., automatic laboratory display unit 79−55349
filled polymers, cumulative internal damage, US assessment 79−57180
filled polymers, US study of internal damage, nonlinear elastic effects, theory 80−49307
filtering and correlation by SAW devices 78−60969
fission reactor component reliability, non-destructive testing and flaw evaluation *(French)* 79−24711
fission reactor materials, intrareactor facility for physicomechanical props. investig. by pulsed US spectroscopic method 78−70591
fission reactor pressure vessel walls, ultrasonic inspection reliability 79−24713
flaw detect., tolerance on operating freq., sensitivity standardisation 78−53089
flaw detection, Born approx. theory for elastic-wave scatt., expt. aspects 79−100307
flaw detection, diffraction of normal modes by a compliant disk 80−87603
flaw detection, FD-410S US detector by Mitsubishi, Japan 79−5098
flaw detection, focusing probes 80−104383
flaw detection, high temp. long duration US transducer tests 80−43586
flaw detection, informative shape index for nature of flaws 77−73407
flaw detection, progress in theory and principles 80−81262
flaw detection, structural products and structures, restricting portion of signal analysis 78−44318
flaw detection, US reference reflection parameter determ. from amplitude and time of travel meas. *(German)* 79−91877
flaw detection, using equivalent defect sizes, sliderule construction 77−90576
flaw detection, using pulsed thermoelastic generation of 20 MHz wave at constrained surface 77−35007
flaw detection equipment, acoustic section bandwidth increasing techniques 77−73410
flaw detection in thin-sheet objects, based on variational method used in dynamics of irregular solid waveguides 80−5857
flaw detection sensitivity enhancement by focusing system, theory 78−53112
flaw detection sensitivity enhancement by focusing system 78−53113
flaw detector, automatic, for butt welds *(Japanese)* 80−25976
flaw detector, portable, supply voltage stabilisation 77−90573
flaw detector, pulse-to-analogue convertor 79−39102
flaw detector, UD-22UM, materials with large US attenuation appl. 79−52585
flaw detector for welded seams, with automatic registration of flaw parameters 77−90570
flaw detector UDM-3, measurement errors 79−8409
flaw indication evaluation by US pulse amplitude and phase spectroscopy *(German)* 77−32743
flaw parameters determ., plastic strain and growing cracks identification 80−81252
flaw size determ. accuracy by US focusing probes and holography 79−29296
flaw sizing of real defects, review 78−53041
flaw width investigation by inclined scanner with regulated directivity diagram 80−89452
flaws, elastic wave scattering, Born approx. 77−79984
flaws, size and shape meas. by US spectrum method 80−7745
flaws, size and shape meas. method of ultrasonic spectrum pt.II 80−7746
flaws in elastic materials, US scatt. theory 77−79983
flow detection, mirror shadow method sensitivity expression and analysis 78−53088
flow detectors, tuning methods for time depend. sensitivity control unit 80−108667
fluid bi-inclusion in elastic solid, geometry and mech. props. from US pulse scatt. 77−21348
fluoropolymer components, pulsed US quality control of heat treatment 78−60953
focused sound field appl. to NDT 78−7105
focusing improvement, dynamic, using analogue-switch phase shifters 77−52856
forgings, untreated surface, US monitoring, sensitivity comparison 80−66751
fracture mechanics evaluation, role of NDT 78−68862
fracture surface by replicas, determ. of reflector size by scanning 78−27689
fracture toughness testing, acoustic emission, inspection technique 78−68860
fracture toughness testing by US, crack extension monitoring 77−16758
frequency analysis, Fourier model 77−40504
fretting fatigue development, sonic monitoring 77−12770
friction material, US inspection 78−60931
fusion reactor vacuum vessel welds, ultrasonic scanner 80−99288
future development, review 79−79196
gas turbine sand casting 78−88594
GFRP laminate, damage assessment by stress wave emission and dynamic mech. meas. 78−11461
glass fibre reinforced plastic, filament wound tube, US defect detection 80−7734
glass fibre reinforced plastic, NDT of strength after immersion in hot water 77−90530
glass fibre reinforced plastic pipe, on-line US inspection 77−86263
glass fibre reinforced plastics, dry-entry ultrasound transmission, through polyurethane 77−90563
glass wool reinforced polymer, relationship between Young's modulus and dissipation of energy *(German)* 79−96064
glasses, US props., review 77−69048
glued members, low frequency acoustic flaw detector inspection 78−60954
goniometer, surface wave appl., corner reflection method 79−100324
grain size meas. of austenitic thin gauge plates by US backscattering *(German)* 79−91878
granular materials, abrasive, failure and strength characts. in US field, test unit 80−85112
graphite, inspection apparatus for complex profiles 79−5109
graphite, reactor material, ultrasonic nondestructive testing *(Japanese)* 79−43520
graphite composite aircraft structures, flaw detection by US methods 78−44288
graphite fibre reinforced epoxy, correlation of tensile strength with US stress wave factor 79−87798
graphite fibre reinforced epoxy, impact damaged, acoustic emission 79−91875
graphite fibre reinforced epoxy, US attenuation as an indicator of fatigue life 80−85118
graphite fibre reinforced epoxy laminate, containing interlaminar paper inclusions, AE monitoring 79−34229
graphite fibre reinforced polyimide, correl. of US attenuation and shear strength 78−19968
graphite fibre reinforced polyimide acoustic emission spectral anal. 79−47850
graphite reinforced epoxy, NDT 79−96254
graphite reinforced epoxy laminates, imminent fracture detection using acoustic emission 79−20302
graphite-epoxy aircraft rudders (DC-10), description of US methods for inservice inspection 78−76798
grating acoustic scanner for material defects 79−47878
grating acoustic scanner for underwater imaging and NDT 79−57198
gray tone display processor for CRT display, cct. 78−44284
head type acoustic wave use 79−5114
heat exchanger tubes, US inspection by rotating search units method 79−9667
heterogeneous duplex grain structure in 304 austenitic stainless steel, US spectroscopy 80−30204
hexagonal honeycomb core shear wave progagation 79−47879
high-speed stress detection and imaging, 100-element acoustic phased array 79−47876
high-temperature contactless testing by EM acoustics 78−85095
hodographs, for analysing methods of adjusting impedance inspection units 80−7744
hologram numerical reconstruction in NDT *(German)* 80−97667
holography for defect size meas. at inservice inspections of nuclear components 79−45372
homogeneity improvement of inspection trace of line focused US probe *(German)* 79−94428
human tibia, US surface wave velocity, mech. props. relation 77−32937
hydraulic liquids, cavitation-erosion props. assessment using ultrasonic dispergator 80−71832
imaging, new technique, sonoscan 79−83403
imaging applications of US and acoustic methods *(Dutch)* 78−27719
imaging cell for direct visualisation of defects in solids 79−20324
imaging system, digitally controlled electronically scanned and focused 80−74659
imaging system, high resolution 78−53169
imaging techniques for NDT 77−81381
imaging using electronic scanning 79−66230
immersion inspection of contact butt welds, using multielement US probes 77−90569
immersion testing, effects of curved entry surfaces on calibration, steel sample expts. 80−71849
immersion type, dead-zone minimization and data-bearing parameters of ultrasonic echo signals 80−66753
immersion unit for inspecting thin wire and fibres 80−66757
impact excitation of vibrations in the acoustic spectral inspection method 79−70273
impedance flaw detector, acoustic, feasibility of standardless check 78−53158
impedance method, variations, methods of treating information and adjusting apparatus 80−7743
impedance method charact. and inspection transducer 79−96270
improvements in ultrasonic testing, narrow-band transmitter pulses of continuously variable wavelength 80−93706
impulse thickness gauges, inspecting wall thickness of tapered profiles 78−72988
inclined probes employing test pulses 78−53087
inclusion cleanliness assessment *(French)* 80−104411
Inconel, cracks under pressure vessel cladding, detection, causes, danger 80−52760
industrial, Indian 1979 status 80−81668
ingots, struct. effect on flaw detection 80−66722
inspection of cast explosive billets for air voids 78−3287
inspection of large diameter pipe and stock 78−48593
inspection of metallic atomic power station equip., portable unit 80−104394
inspection of rails for flakes, mechanised US unit 78−44330
inspection of seamless drill casting and linepipe, review 78−95879
inspection result reproducibility on welded joints of tubes in boiler surfaces 78−60948
inspection slanted probes, prism material choice 78−92428
inspection unit, UDM-1M, modernisation 79−39106
inspection with given reliability, optimal conditions 78−95895
instrument for crack detection by AE 79−52582
instrument limitation, flaw detection instruments, programmed automatic corrections 78−7103
insulators, acoustic emission detection prior to elec. breakdown 80−88924
interface waves between bonded solids, optical meas. of US waves 80−71825
isotropic materials, third-order elastic moduli meas. using Rayleigh waves *(Russian)* 80−50786
joints, visualisation using transmission-type scanning acoustic microscope 77−90511
Lamb wave equivalent US mode propagation in thin-walled tubing 79−68459
laminate, bonding inspection, by acoustic amplitude method 78−48591
large aperture bowl transducers, diffr. pattern 80−58833
laser induced shock waves in microwelds 79−43498
layered composite materials NDT, US spectrum anal. 77−81357
layered structure, vibroacoustic quality control 79−70274
leak detection, threshold sensitivity eval. criteria 80−104401
leak detector 79−39090
leaky wave attenuation by near-surface defects 77−32757
leaky waves, interaction with subsurface flaws 77−63868
light optical imaging, of focused US field *(German)* 80−3275

ultrasonic materials testing continued
liquid-filled crack, Rayleigh wave reflection and transmission calc. 77−32762
Listokhod-1 US flaw detector system 79−52583
LMFBR, liquid Na-limestone concrete interaction following HCDA, US meas. 80−78412
loose material moisture content determ. by UHF Brewster method 77−40488
low-frequency acoustic nondestructive test methods, survey 79−79204
low-pass spatial filtering 79−47869
LWR, heavy water moderated, prototype, pressure tube monitoring with US devices 77−88268
LWR pressure vessels, inspection of spherically shaped perforated areas 78−17339
magnetic sound determ. of H_2 absorpt. in metals *(Russian)* 77−60009
magnetically polarised nonferromag. metals, US excitation and detection 78−56856
magnetized samples, defects, magnetostrictive conversion of US waves into EM fields 80−66008
magnetostrictive SAW generation efficiency meas. of residual stress 77−28972
material deformation parameters measurement, ultrasonic fatigue systems, new technique 80−97676
mechanised US testing, technological advances 79−79193
metal, acoustic emission technique appl. *(Russian)* 77−44439
metal, acoustic signal shape produced by high density electron fluxes 80−108674
metal, crack propagation meas. via stress wave emission, propag. model 77−63837
metal, fatigue testing at US frequency, hardness change 77−44440
metal, FCC, dislocation behaviour at high strain rates, US detection method, data analysis basis 80−85136
metal, high frequency fatigue crack initiation and propagation, US meas. 78−60978
metal, internal friction determ. using sound emission during vibration 77−77715
metal, Rayleigh waves detect. via electrostatic transducer 77−19498
metal, US propag. factor rel. to fracture toughness props. 78−80698
metal, US quality control standardisation 78−53142
metal adhesive bond quality meas., digital US signal analysis 79−47863
metal defect meas. using cepstral processing 78−73010
metal ellipsoidal flaw characterisation by US scatt. 79−47865
metal fatigue crack detection using nondestructive evaluation (NDE) methods 80−71826
metal fatigue monitoring by US velocity and attenuation meas. 78−60970
metal film on polymer base, adhesion determ. using cavitation 79−91865
metal flat plate, electromagnetic-acoustic conversion 78−44320
metal pipe wall thickness, variable, analysis of method.errors in inspecting 78−72983
metal plastic flow through ultrasonic vibrated die, mechanism *(Rumanian)* 77−70242
metal powder density meas. by US velocity 77−32760
metal specimen, ultrasonic technique for stress anal. 78−64790
metall, thin section fusion weld, US inspection 79−15916
metallic materials, deformation process, stage-by-stage nature investigation using acoustic emission *(Russian)* 80−40434
metallurgical noise reduction in austenitic welds testing 80−76466
metals, coarse grained structure, US inspection, structural reverberation interference 80−45456
metals, contactless transducer, for thickness meas. and flaw detection 78−44312
metals, echo-mirror method with transform. of elastic waves 80−108663
metals, mechanical props., testing and modelling 80−25811
metals, strain, US characts., meas. apparatus 78−60898
metals, thermal props. at high temps. meas., acoustic method 79−14222
methylundecanhydride hardened phenol formaldehyde resin, hardening kinetics and mech. losses 80−66520
metrological defectoscopy, US materials testing refinements *(German)* 78−15638
metrological provisions for means of NDT 78−73001
microprocessor utilization in ultrasonic nondestructive inspection systems 80−71845
microscopic defects in stressed materials, rel. between acoustic emission and defect development 80−85127
microscopy, with microwave freq., determ. of mech. props. of materials 80−48535
mineral filled plastics, US meas. 77−40482
monitoring heated components, probes and contact fluids 78−44316
monolithic cascade CCD ultrasonic lens applications 78−22231
multichannel shadow flaw detectors, accuracy and reliability of inspection 78−44306
multichannel US inspection unit, indicator of working order of electronic-acoustic circuits 78−92425
multifrequency US flaw detectors, parameters 79−5118
multilayered constructions, US time method using normal waves 78−72959
multiparameter system for investigating high-power US effects on metals 80−7742
multiple scattering structural noise, expt. method of isolation 79−52571
nanosecond acoustic pulses, optical excitation and detection 78−53159
NDT probe array using 4 transducers 80−35499
near-surface defects, US detection and analysis *(German)* 80−93728
noise suppression circuit for automatic flaw indicator 79−5111
nomogram for determ. of damping coeff. of transverse waves 78−56867
non-contact 77−70238
noncontact EM transducer design improvement 79−46151
noncontact thickness testing by US and electromagnetic waves 78−48603
noncontact transducers compared 79−46149
nondestructive evaluation transducer figure of merit 77−27457
nondestructive testing review including ultrasonic methods *(German)* 77−77724
nonlinear layer in linear medium, US transmission 79−47867
nonmetallic materials including glass, ceramics 78−80690
notch like defects, echo signal depend. on sound field and frequency *(German)* 77−90537
nuclear materials safeguards, use of US identified seals 79−85677
nuclear power plant system, optimisation with regard to design, materials and testing *(German)* 80−42739

ultrasonic materials testing continued
nuclear power station, US metalwork flaw detection system *(Russian)* 78−25302
nuclear power station fuel rods, weld checks 79−5116
nuclear reactor materials, US test results, data evaluation problems 79−9770
nuclear reactor pressure vessels, remote controlled US pre-service and in-service inspections 78−89955
nuclear reactor pressure vessels, thick steel sections, inspection by US nondestructive examination 80−102258
nuclear reactor pressure vessels, US pulses propag. by means of acoustic emission *(German)* 80−3274
nuclear reactor vessel, recording instrument for US inspection results 79−5104
oblique entry inspection, random error of defect coord. meas., anal. 78−40006
oblique entry probes for examining pipe welds, determination of optimal inclination angles for piezoelectric plates 78−76808
oblique entry US inspection of welds, defect coord. meas., error anal. 78−40008
offshore structures 78−27691
online inspection, steel plate manufacture appl. 78−80702
oscillating US heavy plate body testing equipment, computer controlled, working experience *(German)* 80−93720
oxide coating, thermal sprayed, AE study of porosity 80−25927
part inspection with surface temp. up to 500°C, transducer 79−98584
particle size analysis, irregular shape particles, from acoustic emissions 79−61825
parts hard-faced by electric-arc welding, expt. 77−73411
periodic magnet noncontact transducer theory and application 79−46150
phase contrast imaging with electronic scanning 77−31190
phase technique for stress region meas. 77−25219
phase-insensitive receiver theory and CdS acoustoelectric convertor 79−47871
piezoelectric probe, conversion ratios 80−69624
piezoelectric probe in defectoscope, electroacoustic channel in echo type defectoscope 78−53156
piezoelectric probes, US defectoscope, theory of operation, fundamental equations of electroacoustic channel 78−53123
piezoelectric radiators, heat-treatment method for improved resoln. 80−104196
piezoelectric transducer, aperiodic, for US radiation, design for testing applic. 78−36996
piezoelectric transducer, contactive, spectrum of natural freqs. 80−69623
piezoelectric transducer, resonant, construction and delay line contract, US thickness meter 78−53100
piezoelectric transducer, sensitivity meas. 78−49821
piezoelectric transducer, surface excited, US field 80−64331
piezoelectric transducer, thick, operating as radiator or receiver, performance characts. 80−35484
piezoelectric transducer matching with shock excited oscillator for US flaw detectors 77−73422
piezoelectric transducer with oblique bottom immersion chamber inspection of plane parallel objects 78−53111
piezoelectric transducers, broadband, production 80−61044
piezoelectric transducers, energy and spectral evaluations of broadband excitation 80−35485
piezoelectric transducers, for AE signal investigation 78−42507
piezoelectric transducers, prep. method problems for UF-90PTs instrument, for US testing of concrete 78−90622
piezoelectric transducers, surface-driven, input impedance calc. 80−35493
piezoelectric transducers for contactless US product inspection 79−34238
piezoelectric vibrators, elec. steered line array, US probe characts. 80−35486
pipe, review 79−100316
pipe, thick walled, increasing efficiency of automated ultrasonic inspection of segregate defects 79−11755
pipe-wall thinning in coal gasifiers 77−52593
pipeline inspection, welding flaw detect. 78−19984
pipes, large-diameter, US testing of welds 78−3267
pipes, soldered, device for automatic scrapping 79−29308
pitch-catch technique 79−91874
plastic elasticity, hardness, creep, and relaxation meas. with Vickers indenter by electroacoustic method *(German)* 78−48584
plastic pipe inspection by rotational ultrasonics 79−20323
plastic tubing, pulse echo US thickness gauging 77−73392
plate, flaw reconstruction by automatic US testing *(German)* 80−61059
PMMA, crack velocity meas. using US fractography 79−15772
polycrystalline materials, freq. and grain size dependency of US attenuation 80−50783
polycrystalline structure testing by US backscatter meas. 77−21347
polycyclic aromatic hydrocarbons sorbed on fly ash, recovery for quantitative determ. 80−61177
polyethylenepolyamine hardened epoxy resin, hardening kinetics and mech. losses 80−66520
polymer, acoustic props. appl. in US flaw detection 79−47857
polymer, oriented, dynamic shear modulus determ. by acoustic method 78−23911
polymer materials, NDT, rigidity and hardness from acoustic, thermal, optical and dielectric props. *(Russian)* 77−48601
polymeric materials, inelasticity degrees estimation, hysteresis friction model appl. rel. to US testing 80−3136
polymers, filled, cumulative internal damage, US assessment 80−97653
polymers, mech. props. testing 79−70249
polymers, US velocities and damping coeff. meas. *(French)* 80−7723
polymers, using fast longitudinal and shear wave techniques 80−50793
polymers, velocity-of-propagation meter 78−19976
porous ceramics, with non-spherical holes, US wave vel. and elastic moduli evaluation 77−60031
porous layer, angle dependence of impedance of polyurethane foam 80−81243
portable digital US thickness gauge 78−92427
postweld eval., by AE 79−96252
precision tubes, US inspection system *(German)* 77−90539
pressure and interference fields *(German)* 80−89436
pressure vessel of PWR reactor, in-service inspection *(Czech)* 78−29658
pressure vessels hydrotest, acoustic emission monitoring 77−46206
pressure vessels weld quality assessment, NDT methods and equipment 78−56871
probe evaluation, using photoelastic visualisation method 78−80688

ultrasonic materials testing continued
probe specification and assessment 79−24686
probes, assessment and specification rel. to standards 79−23175
probes and flaw detectors for inspection of plastics and rubber materials 79−52558
probes in AP-10KI series 78−53116
production inspection of parts, automatic noise-blanking, pulse-timing discriminator 80−76472
protective coating on steel, US testing 78−23908
pseudorandom binary noise US correlation system for nondestructive evaluation 79−52612
PTFE and filled PTFE, nonlinear creep, compression bulk modulus 80−66593
pulse apparatus UD-22UM for monitoring materials with high US atten. coeff. 79−3868
pulse delay time calculation for testing of industrially produced substances *(German)* 80−3280
pulse echo meas. at 200 MHz, appl. to film thickness determ. 77−23834
pulse echo method, CRT displays *(German)* 78−7153
pulse echo techniques for locating flaws in metal components *(French)* 80−55613
pulse operation of piezoelectric vibrator against solid half-space load, anal. 77−77709
pulse propag. meas. and appl. 78−53167
pulse spectroscopy method, investigation apparatus 80−35483
pulse-echo instrument linearity meas. 77−66725
pulse-echo systems, improved sensitivity using pseudo-random binary-code phase-modulated signals 80−38182
pulsed thickness gauge, inspection of tapered profiles, error anal. 78−40007
PVF_2 bulk wave transducers for nondestructive evaluation 79−57199
Pyrex, stress intensity factors of surface cracks and fracture stress, acoustic meas. 79−47845
quality control, US transducer, exam. of design configuration 78−73003
quality estimation *(German)* 79−91903
quantitative ultrasonics, defect characterization using US scatt. 79−79194
radial-bolt-hole cracks in mechanically fastened aircraft structs., measurement of size using Doppler shift 80−55597
rail joint, thermit-welded, US flaw detection probe 78−56852
rail quality monitoring, by mirror-shadow method, using EM acoustic convertors 77−90551
railway track rail testing using defectoscope car, acoustic contact stability 77−77710
railway track rail-inspection transducers lateral position automatic control 79−57200
raw kaolin, acoustical investigations of the effect of additives on elastic props. 80−66559
Rayleigh and Lamb waves pickup with wedge type transducers, efficiency anal. 77−77708
reactor pressure vessel, automatic compound scanning US inspection system 77−1892
real-time imaging with shear, Rayleigh, and Lamb waves 77−32759
receiver-transmitter for ultrasonic inspection units 80−89458
rectangular probe under impulse conditions, directivity of emission curves 79−96276
reference blocks and transducers, survey 78−68858
reflecting echo method and single-stage monitoring 78−23890
reflection pattern interpretation, error analysis *(German)* 80−45470
reflector geometry for acoustic microscopy and NDT 79−47874
reflector shape and size determ. by US spectroscopy, use of radiation field theory 77−25227
refraction angle of sound waves produced by angle probe, temp. depend. 80−55618
refractories, elastic moduli meas, US method for up to 2000K *(French)* 80−104373
refractories, elastic props., test unit for up to 1500°C 79−57167
reinforced plastics, low frequency acoustic flaw detector inspection 78−60954
reproducible adjustment of test equipment, procedure utilising computer controlled electronics *(German)* 78−60927
research and development, book 79−100321
residual stress drawing 80−97674
resonance method, appl. in inspection of symmetrical products 80−89449
resonance method for accurate thickness meas. 78−48590
resonance splitting in ultrasonic spectroscopy 78−87214
review 80−104360
review of methods 79−43504
review ultrasonic testing devices, creativity aspects *(German)* 77−73426
rig for testing effect of stress on cavitation erosion 78−15545
rock mechanics, appl. of AE *(Japanese)* 78−56845
rocking-beam probe, radiation pattern 77−90572
rolled sheet, artificial surface cracks, reflection of normal shear waves 80−89448
rotor forgings, crack detection, US holography method 77−66730
rubber gasket inspection system, gas pipe appl. 80−30178
sandstone, fracture toughness and acoustic emission charcts. *(Japanese)* 79−34810
SARD-1 automatic system with digital recording 77−77712
SAW, velocity, attenuation and reflection meas., interf. acoustical method 79−18638
SAW EM transducer harmonic operation 79−46152
SAW EM transducer model and flexible design for NDT 77−23844
SAW EM transducer range resolution improved by pulse compression 77−19509
SAW inverse filter for NDT 77−28970
SAW transducer array for surface defect imaging in metals 80−74660
SAW X-ray topographical representation 79−47870
scan control unit, BUS-1 78−53143
scanner heads, with variable incidence angle of US beam, exam. of design 79−15942
scanning, digital, with adjustable step 77−90574
scanning laser acoustic microscope, biomedical research and materials science appls. 78−46878
scanning laser acoustic microscope 79−7263
scanning laser acoustic microscope applications *(German)* 80−3271
schlieren quantitative visualization, using closed circuit TV system 78−46867
sealed radioactive sources, US leak and surface contamination tests *(Czech)* 80−27846
selection of focusing US probe *(German)* 78−7147
self-exciting reflection oscillator US spectrometer 77−32758
semiautomatic ultrasonic flaw detector for studs 79−66247
semiconductor surface eval. using SAW convolver 80−97677
sensitivity adjustment by use of new measuring scales 79−52567
sensitivity adjustment for focusing probes, testing of planar and curves surfaces *(German)* 78−7152
sensitivity selection based on probabilistic techniques 79−91871
separable combination scanner, macrostruct. inspection of rolled bars 80−45457
service life of equipment in creep, AE appl. to technical diagnostics 79−96271
shadow flaw detector, acoustic section anal. 77−77706
shadow flaw detectors, metrological peculiarities when inspecting thick rolled steel sheet 80−81263
shadow immersion exam. of defects, dimension determ., error anal. 78−44305
shadow immersion flaw detection in rough surfaced objects, registration threshold selection 77−73413
shadow immersion flaw detector, pulsed, operating characts. for multiple shadow mode 78−44304
shafts of power plant machinery, metal fatigue crack detect. 77−77716
shaping process for acoustic field of head type wave in test medium 79−96269
shear wave probes, beam shape theory 79−24714
shear wave scatt. by flat-bottomed hole in Al, intensity distribution mapping using EMAT 77−19503
sheet material, Lamb wave inspection, pulsed and impact excitation of transducer 79−34244
sheet materials, using correlation method 77−75759
signal shape anal., ultrasonic pulsed measuring instrums. 80−87678
signal to noise ratio improvement for material exhibiting coherent noise *(German)* 79−83416
sintered material, relation between density and sound velocity 78−53173
sloped probe for angular type reflector 80−104391
small bore appl. 78−80697
Snezhinka-5 ultrasonic transducer kit 79−39098
soil, physical properties study by US wave attenuation meas. *(Polish)* 77−9566
solder melting point, US exam., equipment design 79−15937
soldering fusion instant recording by US method 78−44319
solid solution breakup, anal. by meas. US wave vel. 78−23887
solids, visualisation using Schlieren photoelastic apparatus *(Italian)* 80−88274
sonograms, sound pattern and capability of US test heads *(German)* 79−79199
sonoprobe for Si crystal microcracks detection 80−76462
sound field corrected US indications display *(German)* 78−27714
sound field data evaluation with distance-law for sound press. *(German)* 77−32742
source location on spherical or plane surface 78−92421
specimen with varying thickness for US inspection 78−53137
spectral anal. of flaws, theoretical study 78−95897
spectral density of echo signals, attenuation effect 79−5117
spectral method for determ. of nature of defects 79−5115
spectrometry, physical basis *(German)* 79−7265
spectroscopic NDT 78−76805
spectroscopy, impulse response eval. of US echoes *(German)* 78−26012
spherical material parts, defect coordinates, location via acoustic emission method 78−35626
spherical tanks for liquified natural gas, weldments 79−29290
spherical voids, elastic wave scatt. at long wavelengths 80−48480
Splav-VM, automated US device for inspecting hollow extruded profiles 80−7747
spot welding process, acoustic emission signals, anal. *(German)* 78−44296
sputter target cracking, acoustic emission testing 80−81248
stainless steel, intercrystalline corrosion test by nondestructive methods *(Russian)* 78−56827
stainless steel, pipe, small-diameter ribbed-bore, Lamb-wave ultrasonic inspection for defect detection 79−15944
static flow stress, decrease, by superimposition of ultrasonics 79−7652
status and prospects 77−21346
steam generator tube, EMAT probe develop. 80−76464
steel, acoustic emission, quantitative evaluation from plastic zone growth, book contrib. 79−100328
steel, acoustic emission associated with phase conversions 79−70275
steel, acoustic emission sources and dislocation patterns 80−61040
steel, acoustic hardness testing 79−39088
steel, alloy, mechanical props. meas. by acoustic methods, chem. composition influence 80−104384
steel, austenite, pipe, ultrasonic testing of grain size 78−44313
steel, austenitic, optimum freq. for US testing *(German)* 80−30195
steel, austenitic, tubing, heavy walled, US inspection 79−39107
steel, austenitic, weld, with natural flaws, US test techniques *(German)* 78−27713
steel, austenitic stainless, microstructural effects on US attenuation 78−11455
steel, austenitic stainless, pipe welds, US inspection pattern recognition reflector classification feasibility study 80−16615
steel, austenitic stainless, type 07Kh25N12G2T, US monitoring of fatigue crack growth 78−60917
steel, austenitic stainless, US fatigue meas. 80−40489
steel, austenitic stainless, welds, false indications, cause and influence 78−31599
steel, austenitic stainless weld, US inspection, focusing probe significance *(German)* 77−73397
steel, austenitic weld, review *(German)* 78−53068
steel, austenitic welds, US longitudinal wave examination 80−50784
steel, austentic stainless, butt welds, US exam. 80−93710
steel, ball bearing rods, inspection installation 80−81268
steel, C, EM excitation of US 80−33412
steel, C, ferromagnetic rods, direct and inverse electromagnetic conversion 79−52569
steel, C, hot rolled, ultrasonic echo inspection method 79−87772
steel, casting, C-scan method of US inspection, developments 79−29294
steel, castings for use at high temp., correlation between US and radiographic inspection *(German)* 78−88599
steel, Co-Cr-Mo, type HY 180 correl. between advanced NDT evaluation methods and fracture mech. parameters 80−97675

ultrasonic materials testing continued
steel, coarse grained Kh18N9T, US amplitude inspection, efficiency estimation 78−48592
steel, Cr-Ni-Mn, AISI 4340, correl. between advanced NDT evaluation methods and fracture mech. parameters 80−97675
steel, crack detection, single probe US technique 77−66732
steel, fatigue crack depth meas. by US technique 77−9006
steel, ferritic, clad with austenitic steel 309, US detection of undercladding microcracks *(Italian)* 80−108683
steel, ferritic weldment, US testing of defects, charact. and size 78−7104
steel, flocculation detectability factor in US inspection in quality control 78−3268
steel, fracture ductility, determ. in bending tests and US emission 78−23899
steel, fracture initiation moment, I-integrals critical value determ., ultrasonic method 80−61049
steel, grain size determ. 78−40015
steel, H embrittlement detection by US velocity 79−52613
steel, high strength, alloy, initiation of cracks at delayed fracture, AE study 78−72868
steel, high-strength castings, AE study of intercrystalline crack form. 80−104403
steel, hot 78−88586
steel, hot blooms, US inspection to detect internal pipe 80−97655
steel, HSLA and Low C, weldment, AE monitoring 79−87800
steel, inclusion cleanliness, US meas. 80−25978
steel, inclusion content, ultrasonic method of determination *(French)* 79−52555
steel, medium, C, US attenuation, mag. field effect 80−89428
steel, mild, bolt thread strain meas. by US reflection 78−60972
steel, mild, residual stress meas., acoustoelastic, in a patch-welded disc 79−27604
steel, mild, rolled, critical angle US reflectometry of stressed bar, book contrib. 79−100324
steel, mild, US detect. of H embrittlement 80−71822
steel, nitride coated, brittleness eval. by AE *(Chinese)* 78−11453
steel, nuclear reactor pressure vessel materials, AE assessment 79−83422
steel, pearlitic, austenitic weld, US testing, frequency and beam angle choice 78−60950
steel, pearlitic/ferritic, pearlite interlamellar spacing and grain size effect on US attenuation 79−34230
steel, phase conversion kinetics, exam. using ultrasonic method, apparatus design 80−21203
steel, plain C, type 304 and type 316 stainless, fatigue damage indicators, non-desructive 80−25932
steel, plastic deform. effect on third-order elastic moduli, dislocation anharmonism *(Russian)* 80−50786
steel, possibilities and limitations 78−19979
steel, pressure vessel, acoustic emission during loading by pulsating internal press. *(German)* 78−19973
steel, rail, AE use for mech. tests 80−35467
steel, round bar inspection, EM-acoustic techniques 78−60973
steel, round bar used for seamless tube manufacture, US testing 77−40479
steel, sheet, cold-rolled, US inspection for mech. prop. anisotropy 78−23750
steel, Si-Mn-Ni-Cr-Mo, acoustic emission during stress corrosion cracking appl. to materials testing 78−53042
steel, SS-41, plastic working with vibr., US hardness tester 78−53044
steel, stainless, cracks under pressure vessel cladding, detection, causes, danger 80−52760
steel, stainless, LWR appl., US and AE testing of welds 79−36330
steel, stainless, type 12Kh18N10T, US inspection for intergranular corrosion 78−60912
steel, stainless, ultrathin walled tubing, equipment for US structural inspection 78−72990
steel, stainless, US methods for intergranular corrosion inspection 78−95898
steel, stainless austenitic welds, time domain approach to crack location and sizing 80−50781
steel, stainless austenitic welds, US inspection 80−71821
steel, statistical methods in anal. of real defects 78−72976
steel, strength, acoustic monitoring 80−35479
steel, strip, US inspection by differential method using binary comparative probes 79−70285
steel, strip components, automatic US macrostruct. monitoring 79−79203
steel, surface stress measurement using US goniometer 79−15947
steel, susceptibility to lamellar tearing assessment 77−25231
steel, temp. depend. of elastic, moduli US obs. *(Japanese)* 80−25750
steel, thick-rolled sheet with unfinished surface, defect assessment expt. 77−77720
steel, tubes, helical welded, computerised US quality control 78−35601
steel, type AC/HT-2, grain diameters, US attenuation 80−89429
steel, US attenuation, defect effects in US inspection *(Italian)* 78−48609
steel, US attenuation sorting of normally and partially annealed sheet *(German)* 77−77692
steel, US charact., change with stress appl., exam. 78−48579
steel, US critical angle reflectivity, near-surface metallic prop. gradient effect 80−70516
steel, US inspection to 1000°C, hot-metal defectoscopy 80−66750
steel, US internal flaw detection system 77−66717
steel, US testing, sensitivity adjustment for focusing probes, testing of planar and curves surfaces *(German)* 78−7152
steel, US testing of strength 79−39104
steel, weld, flaw-size meas. by US frequency anal. 77−44429
steel, welded specimen AE testing by external static loading of cold cracking susceptibility 78−40013
steel 20, deformation process, stage-by-stage nature investigation using acoustic emission *(Russian)* 80−40434
steel bar reinforced concrete member, effect of steel bars on US testing 78−60923
steel Cr-Mo (2.25, 1 wt.%), duplex LMFBR steam generator tubing, US equipment for NDT 78−11469
steel Eh1415, US attenuation, heat treatment effects 78−44315
steel forgings, variable attenuation coeff. effect on flaw detect. 77−77707
steel high-temperature ultrasonic testing *(Italian)* 79−96242
steel microstructure study 80−76469
steel mild, high temp., by EM-acoustic surface wave test head 78−95901
ultrasonic materials testing continued
steel pipe, flaw detection by US pulse-echo method 80−66756
steel plates, dynamic evaluation of flaw size 79−15949
steel pressure level flaw size meas. *(French)* 77−68347
steel pressure vessel plates, PISC trials result 80−52746
steel pressure vessel plates, US examination, PISC project 80−57861
steel pressure vessel US examination, PISC trials result anal. scheme 80−57863
steel products, hot thick, US inspection system 80−40661
steel stainless, intergranular corrosion, effect on acoustic props. for US inspection 79−11745
steel tape, inspection method exam. 79−15943
steel to plastic joints, correl. between peel strength and amplitude of interf. waves 78−72960
steel wire, US inspection, immersion method 80−66757
steels, eutectoid 79−15889
stell, austenitic stainless, deformation process, stage-by-stage nature investigation using acoustic emission *(Russian)* 80−40434
stratified medium reflection coeffs. estimation by signal processing techniques *(French)* 80−81242
stress corrosion crack growth over extended period, US pulse high difference method of recording 79−70235
stress field effect on US energy reflected from discontinuity in solid 78−53168
stress meas. acoustoelasticity appl. 79−34259
stress measurement, calibration expt. results *(German)* 80−53725
stress wave emission techniques for monitoring laser welds 79−100329
strobe impulse former in inspection zone of part with variable thickness 79−39100
structural ceramic components eval. 80−76473
structural material defect characterisation by US signal processing 79−52614
superconductors, high field, large internally cooled, development, production and testing 79−54144
surface crack penetration, by US surface wave method 77−16768
surface defects in metals estimation, Rayleigh wave scattering technique *(French)* 80−55612
surface wave scatt. from elliptical cracks for failure prediction 80−55608
symmetrical Lamb wave scatt. at pair of thin slots 79−47868
synthetic focus digital acoustic imaging for nondestructive evaluation 79−52611
T-joint welds, acoustic system charcts., optimisation 77−73412
tandem method for testing zone determ. *(German)* 77−56194
techniques for engineers, interpretation of reflection patterns in tube thickness meas. *(German)* 80−35451
Temp-1 system for the ultrasonic inspection of bulky aluminium alloy plates 80−66755
temperature investigation of AE 78−44336
test piece defects, quantitative meas. *(German)* 80−85122
testing in casting quality control *(German)* 77−4876
thermally sprayed nonfused coating, adhesive bond strength NDT 79−83433
thermoelastic expansion flexible acoustic probe 80−16618
thick specimen visualisation and joint characterisation by scanning acoustic microscope 79−47875
thickness gauge, improved readout device 78−95896
thickness gauge, Kvarts-6, design of automatic control block 78−73005
thickness gauge, model ST-211, improved version, exam. 79−15941
thickness gauge, pulse-echo, transistorised, with reduced dead zone 77−12766
thickness gauge, resonant immersion-type, dynamic range of magnetic modulator 79−11756
thickness gauge for continuous exam., instrument description 78−72981
thickness meas., destructive and nondestructive methods compared *(French)* 78−15611
thickness meas. of deep treated and corroded surface layers 79−34237
thickness meas. US inspection, variability of meas. 79−24704
thickness meter, digital *(Czech)* 78−49795
threaded pieces, stress calc. from US meas. 78−56859
three layered medium, dispersion relation for interference waves 78−72980
time-interval meter for digital display pulse echo thickness gauges 78−48594
tone-burst spectroscopy, influence of phase cancellation and pulse shape artifacts 80−81276
transducer, low frequency US flaw detector appl. 79−98580
transducer characterization methods at the NBS 79−27481
transducer evaluation for inspection and diagnostic appls. 79−27480
transducer head construction *(German)* 78−76804
transducer performance, theoretical anal. 80−30176
transducer size choice in monitoring austenitic welded joints 78−60961
transducer testing freq. definition techniques 79−23172
transducer-head and test piece coupling problems *(German)* 78−60930
transducers, effect of component preparation and assembly, on transducer parameters 78−73004
transducers operating in pulse mode, directivity determ. 78−71258
transient piezoelectric wave scatt. from crack 79−52615
transmission line of probe for hot metal inspection, spurious signals 80−66754
transmitter pulse of variable frequency and distrib. of frequency *(German)* 79−20313
transparent materials, appl. of ultrasound visualisation technique 77−14863
tube flaw detection by annular US transducers 78−60971
tube testing, relationship between ultrasonic field and testing zone *(German)* 77−1893
turbine rotor shaft, US testing, sensitivity multiplication factor 80−85125
UD-24 instrument, piezoelec. US transducers 80−108664
ultrasensitive US system for NDT, medical diagnosis and nonlinear US 78−59224
ultrasonic and eddy current testing of welded titanium tubes *(Japanese)* 80−108651
ultrasonic imaging systems, including Sokoloff tube 79−98575
ultrasonic pulse echo technique for location of discrete flaws in metal components 80−74548
underwater continuous testing techniques for metallic specimens *(German)* 78−92420
underwater testing of materials by ultrasonics *(German)* 80−97670
underwater testing parallel, cylindrical, conical pieces, echo sounder appl. *(German)* 78−88604

ultrasonic materials testing continued
unipolar transducers for nondestructive eval. 80−76471
US aperiodic piezoelectric sensor, fabrication and design problems 77−77713
US excitation and detection in mag. polarised nonferromag. metals, elastic displacements 78−53091
US flaw detector, microprocessor controlled, for flaw classification in welded plates 80−100992
US spectroscopy appl. in NDT 80−79090
US wave interaction with adhesive bonds, modelling concepts 77−21335
US wave visualisation, use as teaching aid 77−57136
vibration-acoustic diagnostics, random signal patterns recognition, with aid of computer *(Slovak)* 79−18612
vibrations, propag. time meas., accuracy increase with UK-10P instrument 79−96277
vinyl chloride suspension polymerisation monitoring by US attenuation and velocity 79−70328
visualisation of US propag. in solids, for NDT 80−22424
visualization of acoustic vibrations of material surfaces 79−39105
water-bath US coupling and piece-part testing methods *(German)* 79−74317
water/Al/adhesive/Al/water five layer struct., time domain anal. of US propag. 79−20319
wave damping in solid material, instruments for determ., review 78−92429
wave reflection location techniques *(German)* 79−15921
wave refraction/reflection phenomena appl., transducers *(German)* 78−35615
weld flaw study using ultrasonic holography *(Dutch)* 78−68855
weld inspection, AE analysis *(German)* 77−36698
weld inspection 77−86254
weld inspection system for Space Shuttle external fuel tank, automatic, interim report 80−76463
weld inspections with freq. scanned SH waves 80−76465
weld interrogation distance amplitude curve, attenuation effects 77−40505
weld joint, fatigue crack progress, acoustic emission frequency determ. *(German)* 78−19971
weld joint, inspection probe 78−92426
weld joints, austenitic, practical appl. of US testing 80−40655
weld monitoring, in-process, with acoustic emission 80−16620
weld quality, in spiral-welded gas pipes 77−90550
welded corner pipes flow detection, method 77−77711
welded joint, reflection of ultrasound from irregularities 79−39086
welded joint, ultrasound reflection from breaks of reinforcing rollers 79−79213
welded joint, US reflection from irregularities 80−104389
welded joint inspection using special US scanning system 79−34235
welded joints, in USSR, survey 79−87768
welded joints, US inspection of defects, recording nominal length and height 79−52577
welded joints in sugar extraction diffusion apparatus 80−93703
welded joints of tube headers, US inspection feasibility study 79−11746
welded lengthwise seam, US inspection of cylindrical testpieces 79−39087
welded structure reliability estimation, acoustic emission signal appls. 80−93702
welded T-joint, US inspection possibility by normal entry probe on far side of main member 79−52570
welded tee joint, by no reference standard method, echo-signal amplitude characteristics calc. 77−90549
welding defects, dependence of echo-signal amplitude on distance from defect 79−11743
welding seams, automatic US inspection system 79−29310
welds, contact electric, quality monitoring 78−56854
welds examination, book 78−48608
wideband spherically concave transducers, for wideband probes, exam. of basic characts. 78−72979
Wiener filtering appl. to nondestructive evaluation 79−11732
wire fatigue properties, fast testing method using 23 kHz US frequency 80−89460
wood, standing trees, US pulse echo method for flaw detection 80−66731
wrap-soldered tubing, inspection using UDT-6Sm us apparatus 78−3276
Ag, granular thin film, adhesion measurement 80−50807
Ag solder strip continuity, US inspection 79−52605
Al, A999, US inspection of purity and dislocation struct. 79−70286
Al alloy, 2124-T851, fracture toughness via acoustic emission 78−7109
Al alloy, acoustic stress wave emission during plastic deform., dislocation motion explanation 77−36697
Al alloy, fracture toughness testing, acoustic emission, inspection technique 78−68860
Al alloy, strain response to acoustic excitation, statistical props., comparison with C fibre reinforced plastic 79−43502
Al alloy, US characts., with stress appl., exam. 78−48579
Al alloy, US inspection of overheating in parts 79−52607
Al alloy, US testing of cold worked surface, quality evaluation 78−48602
Al alloy 7075, comparative US response of machined slots and fatigue cracks 77−40506
Al alloy D16T, acoustic emission temp. depend. 78−53136
Al alloy sheets, type 7075-T6 used in aircraft, early detection of fatigue cracks 80−66730
Al alloy V95T1, endurance determ. method over wide range of load asymmetry 78−56836
Al alloys, fatigue, microcrack development, acoustic SHG study 80−35440
Al alloys AK4-1 and D16, US structure monitoring 78−53082
Al and Al alloy, rolled sheet, transverse US wave attenuation, thickness meas. 79−52573
Al, cast, testing of moulds and die-casting machines 78−53097
Al, dislocation line movement at low temp., obs. by US meas. *(French)* 79−95025
Al, porosity determ. in ingot, US signal integration technique 77−44430
Al, surface wave scatt. from elliptical cracks for failure prediction 80−55608
Al-Al adhesive bond system, US determ. of bond strength due to surface prep. variations 77−21336
Al-Cu, US wave propag. velocity, exam. 78−72982
Al-Mg weldment, US testing, defect acceptance criteria, electron strength 77−70239

ultrasonic materials testing continued
Al-Si-Mg (1, 0.6 wt.%), plasticity due to superimposed macrosonic and static strains 78−60719
Al_2O_3, crack detection caused by thermal shock, AE technique *(Japanese)* 80−21248
Al_2O_3, elastic moduli meas., US method for up to 2000K *(French)* 80−104373
Al_2O_3, film on stainless steel in water, Gaussian ultrasonic beam refl., appl. to testing material under coated surface 78−67896
Al_2O_3, fracture toughness testing by AE *(German)* 79−70234
As_2S_3, determination of stoichiometric discontinuity, using US velocity 79−5242
B fibre, US inspection, immersion method 80−66757
B fibre reinforced epoxy resin, real-time NDT during fatigue loading 77−86264
B fibre reinforced W double coaxial composition rod, waveguide, normal mode US propag. 79−100317
Be, welded acoustic emission 78−39976
C brick, nondestructive acceptance testing by ultrasound *(German)* 77−4878
C fibre reinforced plastic, cross plied, US determ. of lay-up order 77−60007
C fibre reinforced plastic aircraft structural appl., non destructive testing 78−35599
C fibre reinforced plastic, strain response to acoustic excitation, statistical props., comparison with Al alloy of strain response to acoustic excitation, statistical props. 79−43502
C fibre reinforced plastic, fatigue failure mechanism identification, AE detection using piezoelectric strain gauge 79−96239
C fibre reinforced plastic, deform. and failure using AE method *(Russian)* 80−40630
C fibres, durability, elastic props. and struct., heat treatment temp. effect, US meas. methods 80−40446
$CaAl_2O_4$ hydration, US wave propag. study 79−39114
$CaAl_2O_4$, phase transform. accompanying hydration, US and X-ray obs. 79−39115
Cd thermal neutron filter, in-cell US inspection 80−68791
M-1Cu, deformation process, stage-by-stage nature investigation using acoustic emission *(Russian)* 80−40434
Fe, cast, US flaw detection by boxcar integration 80−89437
Fe, cast, US study of sections undergoing deform. or thermal cycling 80−104285
Fe, cast, u.s. detection of spongeosis in pipes *(German)* 77−4879
Fe nodular parts, comparison of sonic-resonance and US velocity techniques for quality control 80−97654
Fe, pig, liquid gas bubble form. at nozzles, acoustic exam. 78−52723
Fe, porous, volume strained, correlation between strength and acoustic props. 77−16770
Fe-Ni, sintered, porosity determ. by US attenuation and sound vel. meas. *(German)* 80−76437
Fe-Ni-C, martensitic transform., new investigation method *(French)* 79−91881
$Fe_{80}B_{20}$, Metglas 2605, Young's modulus meas. using piezoelectric US composite oscillator technique 80−108656
GaAs, during deformation, acoustic emission rel. to cracks, dislocations 80−35441
He gas jet use in AE anal. 78−80701
MgF_2, polycrystalline, elastic moduli, press. and temp. depend. US meas. 77−21202
MgO and MgO-dolomite, crack detection caused by thermal shock, AE technique *(Japanese)* 80−21248
Mo film, constrained, 20 MHz thermoelastic wave generation 79−47880
Mo wire, US inspection, immersion method 80−66757
Na_2O-Al_2O_3-SiO_2, porous glass, crack shape, US fractography obs. 77−44336
Nb ingot, US flaw detection sensitivity enhancement by focusing system 78−53113
Nb-H system, temp.-stimulated acoustic emission, hydride precip. 80−3044
Ni alloy ZhS6U, US method of porosity detection 80−71828
Ni, electrical resistance in DC mag. field after ultrasonic deform. *(Russian)* 80−54671
Ni, ferromagnetic rods, direct and inverse electromagnetic conversion 79−52569
Ni-Cr-Ti-Al/Au-Ni brazed joint, high temp., AE under elev. temp. and loading *(German)* 78−31597
Ni-Cu-Al(Si), spinodal decomposition, morphology of microstructure, elastic strain energy anisotropy effect 78−15354
Ni-Si melt, ultra acoustic study *(Russian)* 78−15613
PVF_2 thin film SAW tranducers for 8 MHz delay line 80−58876
Si crystal microcrack detection by ultrasonoprobe 80−66733
Si, power devices, high frequency US testing 79−47851
Si wafers eval. using SAW 80−76470
Si_3N_4, bending strength, deformability, elastic moduli and brittleness 80−81191
Si_3N_4, hot pressed, surface wave scatt. from elliptical cracks for failure prediction 80−55608
$SrGa_2Si_2O_8$-$SrGa_2Ge_2O_8$, solid solution, exam. of elastic and electrical props. 79−96057
Ti alloy, tubing, heavy walled, US inspection 79−39107
Ti alloy tensile strength, correlation with ductility and fracture detection 78−31601
Ti alloys, US wave propag. velocity, exam. 78−72982
Ti, US interactions with thin gap discontinuities, resonance effects on energy flux coeff. 77−12761
Ti, US wave scatt. from ellipsoidal cavities, Born approx. theory comparison 79−100307
Ti-Al-V (6, 4 wt.%), high temp. cyclic oxidation, AE monitoring 79−83413
UO_2, in-reactor meas. of modulus of elasticity, US spectroscopic method 77−23210
W alloys, sintered relation between density and sound velocity 78−53173
W wire, US inspection, immersion method 80−66757
Zn, single crystal, acoustic emission during twinning 78−11468
Zr, acoustic emission during deformation, expt. 77−73425

ultrasonic measurement
see also ultrasonic velocity measurement
absolute calibration of piezoelectric transducers 80−79099
absorption in solids, by acoustooptical method, losses in boundary layer evaluation *(Polish)* 78−30701

ultrasonic measurement continued
acoustic surface waves, broadband probe for materials testing 78−23904
air bubble growth meas. by rectified diffusion at 22.1 kHz 80−96155
angle measurement by device using US impulses *(German)* 79−80572
anisotropic media, determination of second-order adiabatic elastic coeffs. 79−73256
aortic haemodynamics meas. in humans using US pulsed Doppler transoesophageal method 80−30808
arc-welding seam defectoscope *(Russian)* 80−43564
attenuation measurement of soft tissues, signal processing of broadband pulsed US 78−77094
automatic meas. method of US transducer constants *(Japanese)* 78−33972
bats, biosonar signals, fine freq. anal. via phase-locked loop device 77−56392
beam power meas. calorimeter bridge for 1 to 15 MHz 77−27446
beam power meas. using US calorimeter 77−39181
beam scanner, automatic US beam meas. system *(Dutch)* 79−27473
biological object vel. measurement, underwater, design principles of instrums. 80−19195
biomedical crown rump length meas., comparison of methods 80−45992
blood flow, quantitative meas. by pulsed Doppler technique 80−45990
blood flow echography using Doppler techniques *(French)* 80−26303
blood flow velocity profiles, US MTI meas. 80−36033
blood US correlation technique for blood flow meas. 77−36968
broadband US spectroscopy, appl. to layered media study 79−14177
calibration, and medical device output meas. 77−39183
calorimetric cell for US flow meas. 77−42674
composite torsional quartz transducer for shear US measurements of aqueous liquids 80−53599
conference, meas. for safe use of radiation, Gaithersburg, USA (Mar. 1976) 77−40794
cross-correlation flow meas. error estimation and reduction 79−3194
cylindrical horns, US power monitoring 77−19500
damping coefficient 77−90575
decibel meter, for US pulse echo attenuation meas. 78−1520
defects equivalent dimensions sliderule construction 77−90576
densitometer development for two-phase flow density meas. in pressurised water reactor 80−77759
differential optical interferometry 77−72120
digital trigger delay unit for automatic variable-path-length US meas. 77−11095
distance measuring device with decremental acquisition of the measuring results *(German)* 80−19199
echography for medical diagnosis *(French)* 80−26305
elastic const. changes in Va and $Nb_{53}Ta_{47}$ caused by addition of H, effects of hydrostatic pressure 80−75287
electrostatic US transducer, broadband, props. appl. 79−18642
field intensity meas. using wideband piezoelectric convertors *(Russian)* 80−38209
field meas. by optical holography 80−14532
flaw detection in metal components by pulse echo techniques *(French)* 80−55613
flow measurement, microcomputer-controlled 80−24111
flow of two-phase prepolymer, US flowmeter optimisation 77−31410
flowmeter, 240 Clampitron, applicability study 80−24108
flowmeter, Danfoss, using electronic unit and piezoelectric transducers 80−6172
gas, molecular, kinetic coeffs. calc. from ultrasonic data 78−42703
gases, resonant tube for sound absorption meas. at low freq./press. ratios 80−96156
glass, US detector applications 78−33974
imaging system using random phase mask and stationary-point receiver 77−80035
inertialess sensing with US measurement systems 80−64315
intensity, dilatometric method 79−3865
intensity, primary determ. method using elastic sphere radiometer 77−68342
interferometer method for US props. of solids 77−23836
interferometric holography, linearised subfringe, for US travelling wave visualisation 79−1036
larynx height and vocal fold vibratory pattern 80−98184
level detection 80−27268
light scattering technique, Doppler-shifted, 3D meas. of US waves in transport solids 78−90613
liquid, chemically active, device for meas. props. via US vibrations 77−72122
liquid level measurements using longitudinal, shear extensional and torsional waves 80−77757
LMFBR Na flow meas. using US flowmeter 80−32412
low-temperature CW US expts., appl. of rotatable sample holder with voltage readout 78−13873
marine sediments, correl. between geotechnical and acoustic props. bottom refl. coeff. meas. near sea floor 79−96756
medical probe power, use of semiconductor strain gauges 80−87679
microsphere probe for pressure field meas. up to 10 MHz 80−96159
nuclear appls. of US thermometry 80−73365
nuclear reactor steam generator duplex tubing 80−32379
optical holographic equipment for US field visualisation in optically transparent media 79−18643
optical interferometric meas. and appls. to medicine 77−39184
optical-acoustic probing of heterogeneous condensed media 80−38211
particle motion 3D sensing via multibeam laser system 80−83722
phase velocity and absorpt. coeff. meas. incorporating exact. diffr. corrections 78−26010
piezoelectric transducer, US refl. from transducer with coupling layer *(German)* 79−10440
piezotransducers, surface-excited, calc. and meas. of US fields 80−102957
PMMA Doppler scatt. optical determ. of US radiation patterns 79−76930
polydimethyl siloxane solns., attenuation meas. 80−107372
power meas. via acoustio-optic method 77−832
power measurement using const.-flow calorimeter, 1.5 to 3 MHz 77−50843
pressure field visualisation using microphone matrix *(German)* 79−32151
progressive US wave visualisation by acoustic stroboscopy *(French)* 79−18635
pulse echo meas. at 200 MHz, appl. to film thickness determ. 77−23834
pulse excitation method for solids 78−5624
ultrasonic measurement continued
pulse selector, linear, for US investigs. 78−5623
pulse-echo diagnostic equipment performance meas. methods 77−77957
pulsed US grating obs. in optical farfield 79−41534
quartz crystal US vibrations, SEM obs. 79−56733
radiation balance for US power meas. 79−83863
radiation-force balance, portable, for diagnostic US transducer output power meas. 78−69163
reference block calibration procedures 77−62126
resonance splitting in ultrasonic spectroscopy 78−87214
rough surface scattering and characterisation of parameters, 2 to 25 MHz *(French)* 79−41538
SAW, particle motion fields anal. 80−79042
SAW amplitude measurement, optical probe 79−28185
SAW standing waves, heterodyne optical probing of partial standing waves 78−13870
shear waves, EM detection and generation in supercond. Sn 77−19468
single transducer swept frequency ultrasonic reflection measurements 80−14534
soldered materials, US method for compatibility evaluation 77−40486
solids, measuring equipment for determ. of propag. vel. and attenuation of US waves *(German)* 79−37104
sound field, in air, quantitative visualisation *(French)* 78−87212
spectrum anal. using frequency-tracked gated RF pulses 80−79079
standard probe transducers, calibration 77−840
standing and travelling waves in water-filled wedge, obs. by frequency-shift holography 80−79089
Steatit ceramic strength determination by measuring US dynamic elastic modulus *(German)* 79−43301
Stonely waves, direct meas. at Ni-Pyrex rel. to crustal seismic waves 78−10268
stress analysis by US pulse spectroscopy 77−42788
stroboscopic visualisation, surface wave travelling on a glossy plane *(French)* 78−79175
surface acoustic impedance, meas. technique for oblique incidence angles of 10-160 kHz 77−54848
surface characterisation meas. of randomly rough surfaces by US backscatter at normal incidence *(French)* 80−52165
surface defects in metals estimation, Rayleigh wave scattering technique *(French)* 80−55612
tethered float radiometer for US therapy equipment output power meas. 80−104691
thickness, precision, echo technique appl. *(French)* 78−29089
thickness gauge, pulse-echo, transistorised, with reduced dead zone 77−12766
thin layer US reflection coefficient meas., substitution method 77−31189
tissue acoustic parameter characterisation by induced transient thermal gradient 77−64116
tissue characterisation, US propag. parameter meas. 80−45953
transcutaneous blood flow measurements using pseudorandom noise Doppler system 80−36035
transducer characterisation using cholesteric liquid crystals 78−42512
transducer directivity, semi-automatic meas. 77−84102
transducer power meas. at MHz freq., calorimetric method 79−23180
transducers, variable-angle, qualitative evaluation by photoelastic visualisation method 78−18143
transverse hypersonic waves at 9.4 GHz appl. to APR and attenuation meas. 78−33970
tube method for absorpt. meas., 4-100 kHz 77−84092
ultrasound visualisation, use of LED as short duration stroboscope 77−14863
underwater acoustic transducers, reciprocity calibration by FM signal correl. methods 77−68298
US Doppler spectragrams refreshed display and haemodynamic parameter meas. 80−41152
US fields investigation, appl. of holographic interferometry 78−1519
US magnetostriction vibrator efficiency meas. *(Japanese)* 78−9523
VHF wave production and detection above 1 GHz 77−50852
vibration visualization in piezoelectric ceramics using IR telethermography 78−33966
visualization using small Al flakes *(Japanese)* 78−33973
vortices in wind tunnel expts. meas. using US pulses 80−10334
wavefront visualisation and meas. methods 79−64459
Al-SiC cermet elasticity, porosity meas. by US means 80−81101
LiCl aqueous solns., dynamical props. by ultrasonic propag. meas. 80−76517
$LiNbO_3$, electrostatic probe for absolute measurement of SAW amplitude 79−50543
UF_6, vibr. relax., US meas. 77−83696
UF_6 vibrational relaxation, ultrasonic meas. in UF_6-Ar-N_2 mixtures 80−1050

ultrasonic paramagnetic resonance *see acoustic paramagnetic resonance*

ultrasonic propagation
see also ultrasonic diffraction; ultrasonic dispersion; ultrasonic reflection; ultrasonic refraction; ultrasonic relaxation; ultrasonic scattering; ultrasonic transmission
acrylamide aqueous solution, ultrasonic investigation *(Chinese)* 80−107371
alkanes, fourth order nonlinearity acoustic parameter 78−51612
anisotropic crystal surface $\Delta V/V$ waveguide SAW propagation and mode excitation 77−31161
anisotropic crysts., 3-D representations of bulk acoustic wave props. 80−75311
anisotropic media, determination of second-order adiabatic elastic coeffs. 79−73256
antiferromagnet, first order orientational transition, sound propag. anomalies 77−1580
attenuation and dispersion, general relationships 78−83135
beams in single crystals, diffr. and propag. 78−94468
benzene, hypersound propagation temp. depend., Mandelshtam-Brillouin spectra meas. 78−31210
benzene, nonlinear acoustic coeff. determ. *(French)* 77−1175
biological tissue, phase and amplitude fluctuations 80−8097
borosilicate glass, interaction between EM and elastic waves at low temps. 77−31724
breast tissue, US ref. index and attenuation images 80−17036
bubbly liquids, theory 79−90067
N-n-butoxybenzylidene-n-butylaniline, US propag. near nematic-smectic A transition, mag. field effect 80−39266

ultrasonic propagation continued
caster oil, calculation of nonlinearity parameters thermodynamic method 80−79880
ceramic piezoelectric transducer, anomalous radiation pattern due to parasitic Lamb wave generation 80−96170
cholesteric liquid crystal, mag. aligned, anisotropic US propag. 78−42895
cloud of isotropic scatterers, air bubbles in water appl. *(French)* 80−53507
collinear h.f. sound beams, nonlinear interaction in weakly dispersive media 77−807
composites, random particulate, US wave propagation, velocity as function of frequency and volume fraction of inclusions 80−59583
concrete, ultrasonic wave velocities and density, calc. and meas. 79−52545
condensed matter, conf., Zilina, Czechoslovakia (Sept. 1978) 80−82563
conducting media, ultrasound excitation, varying EM fields 80−87635
crystals under quasihydrostatic compression, elastic characts. 77−51445
curved rods of variable cross section, wave propag. 78−9484
defectoscopy, development of and problems in theory of normal waves, review 80−81265
dielectric medium at low temp., influence of nonequilib. phonon gas *(Russian)* 78−71795
dielectrics, nonlinear phonon-photon interactions, physical basis 77−61998
diethylamine melanin, sound wave anomalous absorption and dispersion 79−77688
dispersive media, pulse propagation in human soft tissues 80−81644
Doppler effect, nonstationary, freq.-phase methods of investig., control of production processes 80−45464
Doppler-shifted cyclotron resonance, anomalous propag. of US waves 79−73429
drill pipe, exam. of propag. of US surface waves 79−5102
drill pipe, exam. of propag. of US surface waves 79−15934
elastic half spaces, parametric model of loose bonding 77−11061
excitonic insulators, study of coherence factors using US attenuation 78−76338
ferrofluid, US response time, mag. field depend. 79−1702
ferromagnet, domain walls, hypersound effect *(Russian)* 79−51810
ferromagnetic fluid, resonance excitation of ultrasound 78−95112
ferromagnetic metal, EM generation of US guided waves, model 78−22236
ferromagnetic metal, itinerant electron model, for US propagation and structural instabilities 78−95508
ferromagnetic metals, itinerant electron, theory of crit. US propag. 77−69655
fibrous networks in viscous media, appls. of theory of acoustic motion 77−86733
gas, molecular, kinetic coeffs. calc. from ultrasonic data 78−42703
glass, US propagation at ultralow temperatures 77−39635
glass fibre reinforced plastics, ageing by boiling in water, effect on physicomech. props. 80−60892
glass prisms, vel. meas. by pulse technique and propag. theory 79−18636
p-p′-heptyloxyazoxybenzene, smectic-C phase, mag. aligned, anisotropic US propag. 77−84630
hexagonal honeycomb core shear wave progagation 79−47879
human tissue, transmission of US beams, focusing and attenuation studies 80−45948
hypersonic waves, theory of self action 78−75010
interaction of two diffracting sound beams and directional US radiators 78−38121
Invar, antiferromagnetic Cr-Fe-Mn alloy, Elinvar charact., US wave propag. charact. 77−11640
Josephson junctions, collective excitations in superconductors below T_c, tunnel current fluctuations 79−33403
Lamb wave equivalent US mode propagation in thin-walled tubing 79−68459
light beam diffraction, phase geometry variation analysis 80−106441
light diffraction by US waves, in optically active crystals 77−43965
liquid, cavitation effects of simultaneous action of US vibrations of different freqs. 79−94396
liquid crystal US expts. and phase transitions 79−46571
liquid crysts., mesophases and phase transitions 78−79667
liquid mixtures, US propag. parameters, effective Debye temp. 80−79882
liquid-solid interface, US leaky-waves, interaction with subsurface flaws 77−63868
liquids with vapour bubbles 80−33661
liquids with very low US propag. velocities for use in biomedical optical computer 80−28392
longitudinal US wave propag. near surface of a solid 78−95217
machine-made paper orthotropic US plate wave theory and expt. 79−68460
magnetic metals, crit. transverse US attenuation, spin fluctuations 78−48022
mammalian tissues, compilation of empirical US props. 78−88727
mammalian tissues, compilation of literature on empirical US props. 80−98007
marine sediments, penetration as function of physico-mech. characts. *(French)* 80−33324
MBBA, hypersonic props., Mandel'shtam-Brillouin spectra obs. 79−4813
MBBA film, nematic liq. cryst., visible interaction of low-intensity US waves 78−10126
medium with hysteresis type damping, signal propag. *(Russian)* 79−53986
metal, EM generated ultrasound, position dependent amplitude 79−37763
metal, nonferromagnetic polycryst., EM-acoustic oscills. during EM field emission by inductive convertor *(Russian)* 77−11638
metal, superconducting and normal, attenuation, EM generation and detection of US shear waves 78−39261
metals, anomalous sound propag. by cond. electrons 80−11048
metals, spurious ringing in pulse NMR 79−93187
metals, ultrasonic wave propagation by open-orbit electrons at reson. condition 78−51877
mixtures and suspensions, flow rate meas., ultrasound propagation and scatt. approach 80−43806
molecular acoustics, time correlation functions 77−51451
Mossbauer spectrum, ultrasonic sideband intensity depend. on acoustic field statistics 80−75905
multiple nomogram for US propag. calcs. 80−28371
ultrasonic propagation continued
nematic liquid crystals, review 78−63668
nonlinear effects in cavitating liquids, optical visualisation 80−106651
nonlinear US fields in air, numerical representation, microphone signal example *(French)* 80−53521
nonlinearity in free progressive waves at 20 kHz 80−33394
nonlinearity parameter for solids, relationship with Gruneisen parameter 80−74561
nonreciprocal effect, during light passage through US beam 80−106443
organ-puncture needles, needle surface and tissue propag. 80−96052
organic liquids, propag. of longit. and shear hypersonic waves, light scatt. meas. 77−51442
paper fibre suspension, meas. and modelling 77−27447
periodically corrugated piezoelec. cryst., Bleustein-Gulyaev waves behaviour 80−96115
permafrost soil, compressional and shear wave vels. using US pulse technique 77−17081
phase velocity and absorpt. coeff. meas. incorporating exact diffr. corrections 78−26010
phonon echoes and amplification of ultrasonic waves in a microwave electric field 79−19635
β-picoline-water solution, light scatt. spectra, ultra- and hypersonic absorpt. *(Russian)* 80−93353
piezoactive waveguide, anisotropic, normal waves propagation 77−88975
piezoelectric plate, thickness waves, dispersion characts. near cutoff freqs. 79−19841
piezoelectric semiconductors, attenuation, carrier conc. depend. 78−72206
piezoelectric substrate coated with admittance films, attenuation and vel. of surface waves 79−98540
polyacrylamide aqueous solution, ultrasonic investigation *(Chinese)* 80−107371
polycrystal of orthorhombic symmetry, US scatt. and vel. determ. 77−84848
polydimethyl siloxane solns., attenuation meas. 80−107372
polymethylsiloxane-2, liq., thermodynamic props. at high press., US propag. meas. *(Russian)* 80−65157
polyvinylidene fluoride films, SH and Lamb waves propag. 80−75948
pulse propagation in elastic waveguides *(Russian)* 79−18576
pulsed US field display by laser *(Chinese)* 79−32158
quartz, shear elastic waves, conical refr. and collinear interaction 77−62588
quartz crystal, γ-irradiated, US shear wave propag., beat obs. 77−43283
quartz plate, X-cut, phase shift freq. depend. rel. to US vel. meas. 77−14866
radiation force variation with differing propagating media gas content 79−32128
rays, curvature limitations for computerised tomography 80−94301
rotation of US plane of polarisation under ESR saturation conditions 80−29123
rough walled waveguide 78−90549
SAW propagation along X axis on Y-cut plate of Se 80−75313
Schaaffs' molecular-kinetic theory of propag. in liquids, temp. and pressure changes of 'collision factor' 80−19143
sedimentary rocks fluid saturation effects on dynamic elastic properties 77−17082
self focusing of acoustic waves during cavitation 79−3821
semiconductor, absorpt. and amplification of US at moderate freq. 78−19102
shear velocity of muscle tissues, mech. props. determ. 80−108930
skeletal muscle fibre orientation, US attenuation meas. 80−30763
smectic liquid crystal, shear wave attenuation 78−9944
Solenhofen limestone, US propag. at high press. 79−29756
solid layer-liquid system 80−31522
solids, acoustic wave emission, absorpt. and propag. in THz range 80−65164
solids, measuring equipment for determ. of propag. vel. and attenuation of US waves *(German)* 79−37104
solids, visualisation using Schlieren photoelastic apparatus *(Italian)* 80−88274
sound pulses interfering in continuous stratified medium, reciprocal action *(German)* 77−68285
spherically curved transducers, anal. of focusing action 80−64332
square-well liquids, equation of state, acoustic properties 79−99270
stationary thermal self-focusing of US and hypersonic waves in nonlinear media 77−813
steel, alloy, mechanical props. meas. by acoustic methods, chem. composition influence 80−104384
steel, austenitic welds, US longitudinal wave examination 80−50784
steel, stainless austenitic welds, time domain approach to crack location and sizing 80−50781
Stonely waves, direct meas. at Ni-Pyrex rel. to crustal seismic waves 78−10268
stratified media, US investigation method theory, acoustic impediography *(French)* 79−11990
stress pulse propagation, in water, effect of diffr. 78−90568
superconductor, nonequilib., hypersound enhancement *(Russian)* 80−34552
superconductors, US studies of cond. 79−60976
suspensions, effects of particle shape and orientation 78−59171
TGS, domain wall thickness determ. from longit. US wave propagation meas. 77−66463
TGS, ferroelec. single crystal, low freq. nonlinear effects 80−84490
TGS, US propag. and vel. rel. to growth defects 79−28049
TGS and deuterated cpd., ferroelec. US relax. time constant 80−84257
thermoelastic generation of 20 MHz wave, pulsed excitation of constrained surface 77−35007
thermoelastic material, deformed isotropic, thermal effect on acoustoelasticity 80−33276
thermooptical US generation due to moving laser source in liquid 80−102903
thin-plate waves, Schlieren study 77−80001
three dimensional US wave model for refractional diffracted waves *(Chinese)* 77−62080
tibial bones, of highly trained athletes phys. stress effect type as measured by US techniques 80−16992
tissue, freshly excited, from rat, freq. depend. 77−86573
tissue, human, model of backscatt. 77−40715
tissue, mammalian, survey of US vel. and attenuation data 80−46744
tissue characterisation, US propag. parameter meas. 80−45953
tissue characterisation, US propag. props. 80−45950

ultrasonic propagation continued
tissue characterisation by attenuation, absorption, and velocity 77−64106
toluene, nonlinear acoustic coeff. determ. *(French)* 77−1175
torsional modes, couplers, in clad-rod with sinudoidally perturbed core-cladding interface 77−79999
underwater, 2 MHz, expts. on intensity modulation of laser beam crossing field 79−76906
US nonstationary self-focusing in nonlinear media 77−27412
visualisation of US propag. in solids, for NDT 80−22424
visualisation of US travelling waves, by linearised subfringe interferometric holography 79−1036
water layer between solid plates, elastic wave propag. 77−4158
wave attenuation and scattering in medium with randomly distributed inhomogeneities, theory *(Hungarian)* 77−86791
wavevector reversed ultrasound studies of phase transitions 80−75306
AgCl, US wave propagation, direct obs. 78−59864
$AgNO_3$, electrolytic solution, sono-conductance rel. to temp. 77−15496
Al cylindrical rod, stress wave propag. from electrical discharge 78−59866
Al disk, US wave excitation by electron beam 79−14888
Al, US scatt. and vel. determ. 77−84848
Al_2O_3-Epon 828-Z, mixture, acoustic wave prop. characts., using differential-path US technique 79−42151
As_2S_3, amorphous, low temp. US meas., two-level systems role 78−30703
B fibre reinforced W double coaxial composition rod, waveguide, normal mode US propag. 79−100317
BaO, NaCl struct., elastic props., US meas. 78−18697
$BaTiO_3$, ferroelectric polydomain crysts., piezoresonance effects, appl. as transducer 79−4779
Bi, US propagation anomalies, under hydrostatic press. *(Russian)* 78−83884
Bi:Te(Sn,Sb,Pn), US attenuation meas. 80−92614
C fibre, supersonic wave propag. and damping as function of thermal treatment temp. 77−89499
C fibres, durability, elastic props. and struct., heat treatment temp. effect, US meas. methods 80−40446
CaO, NaCl struct., elastic props., US meas. 78−18697
$Cd_3P_{2-x}As_x$ solid soln., US wave prop. velocity, composition depend. 77−20013
CdS, cylindrically rounded cryst., Gulyaev-Bluestein wave propag. 77−84852
CdS, semicond. piezoelec. crysts., US investigation of acoustoelectric characts. 77−1456
$Cd_{3-x}Zn_xAs_2$ solid soln., US wave prop. velocity, composition depend. 77−20013
Co-P, metallic glass, phonon propagation at low temp. 78−87756
Fe-Cr melts, ultrasonic propag. and isothermal compressibility using pulse-phase method *(Russian)* 79−51202
Ge, pure and n-type, US velocity and attenuation, second and third order elastic moduli 80−70325
^4He, solid and liq., US finite amplitude wave propag. 80−80024
Ho-Tb (50 wt.%) alloy, mag. phase diag. from anomalous US propag. 78−6526
In, US wave polarisation plane and ellipticity rot. in mag. field, doppleron interactions *(Russian)* 79−15335
n-InSb, ultrasound modulation in mag. field 79−69196
$KMgF_3$, elastic moduli, press. and temp. depend., US technique 80−6453
K_2O-B_2O_3-SiO_2 system glasses, hypersound propag., 77 to 300K, Brillouin scatt. obs. 77−84850
LiF, elastic moduli meas. by US pulse superposition, high-temp. behaviour 77−11621
$LiNbO_3$, acousto-optic interaction, phase grating production 79−41454
$LiNbO_3$, crysts., elec. field influence on hypersonic wave propag. 80−44668
$LiNbO_3$, damping of elastic waves at 36.5 GHz 77−39632
$LiNbO_3$ $\Delta V/V$ waveguide SAW propagation obs. and modal analysis 78−38128
$LiTaO_3$, crysts., elec. field influence on hypersonic wave propag. 80−44668
$MgAl_2O_4$, damping of elastic waves at 36.5 GHz 77−39632
MnO, antiferromag., temp. depend. of elastic consts., US study 80−79854
MnSi, crit. transverse US attenuation, spin fluctuations 78−48022
ND_4Cl, order-disorder transformation, elasticity and heat capacity temp. depend., US obs. 78−71851
$(NH_4)_2BeF_4$, Mandelstam-Brillouin and US exam. of phase transitions 77−12347
NaCN, elastic const. temp. depend., Brillouin and US exam. 77−80572
NaCl:Mn^{2+}, elastic wave damping, 300-1800 MHz, acousto-optical obs. 79−69198
NaF, elastic moduli meas. by US pulse superposition, high-temp. behaviour 77−11621
NbO_2, low temp. elastic consts. and Debye temp. 78−47463
Pd-Si, amorphous metallic, sound propag. at low temps. 77−72656
Pd-Si, metallic glass, phonon propagation at low temp. 78−87756
PdZr, amorphous, supercond., US props. 80−44765
Rb_2CoF_4, critical fluctuations near Neel temp., US attenuation study 80−108013
RbH_2PO_4, longit. US wave propag. near ferroelectric phase transition temp. 78−84536
SbSI, nonlinear sound propagation in case of polarisation switching 79−27458
Si, perfect crystal, dispersion surface of X-ray radiation, X-ray acoustic resonance method 79−41908
Si, pure and n-type, US vel. and attenuation, evaluation using elastic moduli 80−70325
SiO_2, fused, US study by harmonic generation, elastic consts., Gruneisen parameters 78−83735
SiO_2, vitreous, fast neutron irrad., low temp. US meas., two-level systems role 78−30703
SrO, NaCl struct., elastic props., US meas. 78−18697
Ti-Ni, internal friction and US props. *(Russian)* 80−84247
$V_3Si_{1-x}Ge_x$ solid soln., longitudinal and transverse US wave propag. rate, 4.2 to 300K *(Russian)* 80−103423
W, rot. of polarisation plane and ellipticity of US waves near doppleron-phonon reson. *(Russian)* 79−19325
Xe sound propag., near crit. point, theoretical anal. 77−69046
ZnO/substrate higher order mode SAW propagation obs. 79−46909

ultrasonic radiation *see ultrasonic waves*

ultrasonic reflection
angular type defect, methods of calc. 80−104391
arterial walls, simulated, US refl. amplitude 77−25534
austenitic stainless steel weld metal defect detection, shear-wave polarisation effect 78−44337
bat echolocation system, optimum phase modulation for insensitivity to acceleration 79−53163
beam displacement of US transverse wave, reflection at free boundary surface *(German)* 80−87580
brass/water interface leaky Rayleigh wave reflectivity loss meas. 78−59187
case hardening depth meas. using ultrasonic goniometer, corner reflection method, book contrib. 79−100325
dead-zone minimization and data-bearing parameters of ultrasonic echo signals 80−66753
echo distribution evaluation, for biomedical appls. *(German)* 78−80934
echo pulse shape improvement in low impedance materials 78−1489
elastic rod on viscoelastic half-space, forced longit. vibr., appl. to muscle study 78−44538
exact fractions US interferometer algorithm and circuitry 77−39182
foam, US characts. of open-cell polyurethane foam layers for airborne appls. 80−96597
focusing reflectors in kidney stone destruction by shock waves 77−32946
and friction 77−27494
glass, two pulse echo, low temp. 78−18709
grooved reflective array SAW compressor and resonator performance 77−23820
grooved SAW reflective grating, field theory 77−31162
hepatic tissue characterisation by US reflection, estimator variance reduction 79−48307
impedance image reconstruction, reflection and transmission techniques 79−53202
inhomogeneous elastic slab impedance soln. 79−44745
intensity profiles of reflected beams near Rayleigh angle, numerical integration method 80−64242
layered composite materials, US reflection spectrum rel. to NDT 77−81357
layered media, US transmission and refl. coeffs. 78−13827
liquid-filled crack, Rayleigh wave reflection and transmission calc. 77−32762
liquid-solid interface, nonspecular refl. near longit. crit. angle 80−48483
liquid-solid interface, superimposed grating, backward displacement of waves 77−1288
liquid-solid interface, US wave interaction at Rayleigh angle 77−39132
liver, estimating acoustic attenuation coeff. slope from reflected US signals 80−5876
liver sector scans, echoes across diaphragm 78−69165
longitudinal wave, conversion into transverse wave by reflection from boundary of half space 80−5860
lung, US tissue characterisation 77−40717
marine sediments, correl. between geotechnical and acoustic props. bottom refl. coeff. meas. near sea floor 79−96756
NDT, US wave refl. visualisation appl. as teaching-aid 77−57136
nonspecular reflection effects for liquid-solid-liquid layered media 80−102882
nonspecular reflection from isotropic solid plate in a liquid 77−23788
ocean sediment classification by seismic reflectivity meas. 77−5370
ophthalmic tissue signature characterisation by US frequency-domain analysis 77−40857
piezoelectric transducer, US refl. from transducer with coupling layer *(German)* 79−10440
planar reflector in interior/on surface of test objects, characts. *(German)* 80−43569
plane wave reflectivity from water-metal interface, stress effect 79−81586
polyurethane foam layers, open-cell, refl. characts. for ultrasound in air 78−83139
porous layer, angle dependence of impedance of polyurethane foam 80−81243
powder material US pulse echoes and suppression 77−28520
pulse-echo determination of thermal injury in deep dermal burns 77−70511
pulse-echo scanning, echo struct. 77−52857
pulse-echo systems, improved sensitivity using pseudo-random binary-code phase-modulated signals 80−38182
pulses from surfaces, appl. to location of discrete flaws in metal components 80−74548
receiver, based on suppressed total reflection of light *(German)* 77−75760
reflective dot array SAW filter 77−23825
reflective strip swept-frequency imaging 77−31192
reflector geometry for acoustic microscopy and NDT 79−47874
SAW, velocity, attenuation and reflection meas., interf. acoustical method 79−18638
SAW filter triple transit suppression by mech. and regeneration reflection cancellation 77−23829
SAW grating resonators, reflection-dependent coupling 77−23822
SAW reflection from quartz powder on piezoelec. substrate 80−74565
SAW reflector performance rel. to fabrication tolerances 77−27452
SAW resonator reflector and transducer characteristic effects 77−39168
sea surface, diffuse reflection, mathematical treatment *(French)* 77−45016
self-exciting reflection oscillator US spectrometer 77−32758
single transducer swept frequency ultrasonic reflection measurements 80−14534
solid plates and half-spaces, non-specular reflection 78−1464
sound propagation conf., France (May 76) *(French)* 77−42638
spatial echo distrib. processing for interface props. determ. 78−1490
special total reflection on anisotropic crystals 79−56054
spectral information display in colour ultrasonogram 77−21584
steel, mild, bolt thread strain meas. 78−60972
steel, mild, rolled, critical angle US reflectometry of stressed bar, book contrib. 79−100324
steel, US critical angle reflectivity, near-surface metallic prop. gradient effect 80−70516
stratified medium reflection coeffs. estimation by signal processing techniques *(French)* 80−81242
thin layer US reflection coefficient meas., substitution method 77−31189

ultrasonic reflection continued
tissue analysis using pulse echo US and freq. domain deconvolution 77−40720
tissue US attenuation and velocity meas. by reflection techniques 77−64115
tissues, inhomogeneous media model 80−108981
water-sediment interface US reflection with bidirectional displacement 78−60017
water/Al/adhesive/Al/water five layer struct., time domain anal. of US propag. 79−20319
weighted SAW transducers, electrostatic neighbour and end effects 77−31200
welded joint, US reflection from irregularities 80−104389
Al_2O_3 film on stainless steel in water, Gaussian ultrasonic beam refl. 78−67896
Al_2O_3 layer on stainless steel in water, leaky wave generation 80−75419
$Bi_{12}GeO_{20}$, reflection of Gulyaeb-Bluestein waves from end of acoustic channel 77−84852
Cu, elastic constants, up to 2500 bar, −196-25°C, US pulse echo obs. 79−87680
Hg, liq., sound vel. near metal-nonmetal transition, up to 1600°C and 2000 kg/cm^2 80−39222
n-InSb, ultrasound modulation in mag. field 79−69196
$LiNbO_3$:Fe, polarization echo signals amplification *(Russian)* 78−43780
Nb, elastic constants up to melting point, US meas. 77−86081

ultrasonic refraction
angle probe produced waves, temp. depend. 80−55618
attenuation, of US main waves with distance 80−5859
breast tissue, US ref. index and attenuation images 80−17036
breast tissue characterisation in vivo by US TOF computed tomography 80−51186
isotropic nondispersive solid, meas. method for vel. of sound 80−69616
lens transmission variations and interfacial effects 78−59176
tissue refractive index and attenuation distrib. reconstruction from time-of-flight and amplitude profile 77−64113
tissue refractive index spatial distrib. meas. by US computer assisted tomography 78−69161
tomography, refractive index field reconstruction for strongly refractive asymmetric fields 80−4760

ultrasonic relaxation
acetic acid, effect of impurities on US relaxation 78−10130
acetic acid, liq., sp. ht. of 2nd relax. step *(German)* 79−37766
acetic acid-carbon tetrachloride, US absorption, coupled dimerisation cyclisation reaction *(French)* 79−42148
acoustic wave absorption processes in atmosphere 80−53531
air, HF sound absorpt. meas. 78−1475
algorithm for relaxation spectra in US spectroscopy 80−79038
n-alkanes, liq., hypersonic attenuation, temp. depend. of Brillouin spectra 79−11426
amorphous solids, structure and low temp. props. 79−37631
associated liq., US absorpt. and hole theory 78−10124
associated liquids, correl. between dielec. and acoustic relax. times 78−9925
benzene, mean free path meas., US relax. 80−59585
benzene-similar liquids, 10 to 1300 MHz 80−39229
binary liquid mixtures, containing one rotational isomeric relaxing liquid 80−70315
t-butyl alcohol, aq. solns., US relax. freqs., clathrate-hydrate model 78−30704
CBOOA, US attenuation near nematic-smectic A transition 78−87773
cellulose acetate solutions, US absorpt. coeff in 0.1-1000 MHz range 77−35638
cellulose solutions, acoustic relax. mechanisms *(Russian)* 79−90733
chlorobenzene, liq., vibr. relax., Brillouin scatt. and US vel. meas. 79−77692
chlorocyclohexane 80−24540
condensed matter, conf., Zilina, Czechoslovakia (Sept. 1978) 80−82563
condensed systems, vibrational relaxation times calc. from low-freq. mol. spectrum 78−2205
cyclohexanal, liq., viscoelastic and structural relax., US rel. and absorption meas. 78−26634
cyclohexane, US absorption and vel. meas. 77−51450
cyclohexanol, US relaxation at 0.5 to 45 MHz 78−59868
deep ocean LF attenuation data, review 80−33318
2,4-di-p-bromophenyl pentane, polystyrene model mol., US relax., mol. dynamics 79−73258
dibromomethane, 60-700 MHz, high resolution Bragg refl. method 77−84853
dichlorodifluoromethane, US vels. and absorption coeffs., determ. of relaxation times 78−63530
dichloromethane, 60-700 MHz, high resolution Bragg refl. method 77−84853
dichloromethane, mean free path meas., US relax. 80−59585
p-dioxane-H_2O at 11 and 25°C, US absorption 80−65171
2,4-diphenyl pentane, polystyrene model molecule, US relax. 77−6965
elastic moduli in ferroelectric transition region 78−6646
electrolyte solutions, fluctuations rel. to acoustic relaxation and light scatt. 77−15497
ethanol, aq. soln., conc. fluctuations, shear and longit. relax., Brillouin scatt. and pulse techniques 78−71792
ethanol, US studies of mol. relax. 78−22790
ethyl alcohol, US attenuation, for vol. viscosity, 0-60°C 78−63871
ethylene-N_2, gas, vibr. relax. time by US meas. 79−98852
experimental data of relaxation times, bounded error anal. of expt. distribs. 79−88924
explosion waves, vibrational relaxation effects on atmos. attenuation and rise times 79−7244
fluid, correlation functions in mol. acoustics 77−51451
fluorobenzene, liq., vibr. relax., Brillouin scatt. obs. 79−51206
fluoropropylmethylsiloxane fluids, viscoelastic behaviour 79−14361
freons of methane series, pulsed US investigation of vibr. relaxtion 77−39397
furan, liq., US phase vel. decay in space and time 80−99891
furan, mean free path meas., US relax. 80−59585
furfuraldehyde liquid, US relaxation meas. 77−20016
n-Ge US attenuation due to donors and acceptors 77−28223
glass, backward-wave phonon echoes 77−76513
glass, linewidth and anomalous dispersion of ultrasound 77−39636
glass, spectral diffusion, phonon echoes and US saturation recovery 78−10149

ultrasonic relaxation continued
glass filled solids, ultrasonic absorpt., scatt., velocity and attenuation 80−44262
glass-plastic, Young's modulus, expt. study 77−52389
glasses, US props., review 77−69048
graphite-epoxy composite, hydrothermal ageing 77−21189
gylcerol, influence of electrolytes on acoustic props. 78−75728
heptanoic acid, soln., US relax. *(German)* 78−22792
heterocyclic liquids, 10 to 1300 MHz 80−39229
n-hexane-perfluoro-n-hexane mixtures, US vel. and absorpt. mixtures 80−88281
hexantriol-1,2,6, influence of electrolytes on acoustic props. 78−75728
isobutyric acid-water critical mixtures, US and hypersonic study 80−88268
isopropanol, US studies of mol. relax. 78−22790
isopropanol-n-propanol aq. mixtures, US relax., US absorpt. and vel. meas. *(French)* 80−103426
Kneser liquids, vibrational energy exchange probabilities 78−38780
liquid, weakly assoc., US wave reson. absorpt. 80−34141
liquid metal, mol. motions from NQR, viscosity and sound damping 77−1615
MBBA, hypersonic props., Mandel'shtam-Brillouin spectra obs. 79−4813
MBBA/EBBA binary liquid crystal mixture, US absorpt. and vel. dispersion, phase transition and alignment effects *(Korean)* 80−29121
metal, anisotropy effects on US cyclotron resonance 79−73816
metallic glasses, low temperature US props., supercond. state effects 79−87192
methane-Ar liquid mixture, viscoelastic props., acoustic relax. *(Russian)* 78−75736
methanol, ethanol, aqueous mixtures *(French)* 80−6468
methanol, US studies of mol. relax. 78−22790
methyl alcohol, US attenuation, for vol. viscosity, 0-60°C 78−63871
methylene chloride-cyclohexanol system, US props. and relaxation mechanisms 77−51450
micellar solutions, US absorpt. 80−45571
molten salt, hydrodynamic correlation functions 77−31577
monochlorodifluoromethane, US vels. and absorption coeffs., determ. of relaxation times 78−63530
nematic liquid crystals, US relaxation time, temp. depend. 78−18712
nitrobenzene and n-heptane critical mixture, US and hypersonic acoustical props. 80−65170
noble metals, interaction of thermal and acoustic phonons thermoelastic relaxation, calcs. for US longitudinal waves 80−65165
nonanoic acid, soln., US relax. *(German)* 78−22792
oligobutenes, anomalous behaviour of viscoelastic props. 77−63704
optical glasses, Brillouin scattering meas., sound vels., Pockels coeffs., phonon damping 79−95792
PAA, nematic liq. cryst., effect of magnetic field on US vel. and absorpt. 78−18707
phospholipid bilayers, US relax. spectra in transition zone 79−92169
poly(alkyl methocrylates), US determ. of relax. 77−51449
poly-2,6-dimethyl-p-phenylene oxide solns., US and viscoelastic relax., conformational changes 77−31033
polyalkanimide, US vel. and absorpt. at liquid He temps. 78−51619
polydimethyl siloxane, Brillouin scatt. and hypersonic relax. 77−55795
polydimethylsiloxane networks, high freq. US absorpt. rel. to crosslink density, α-relaxation 79−95091
polydimethylsiloxane oligomers, Brillouin scatt. obs. of hypersonic sound speed and loss, mol. wt. depend. 79−91457
polyethylene, crystallised from oriented melt, mech. and thermomech. props., framework struct. 77−63756
polyethylene, glass filled solids, ultrasonic absorpt., scatt., velocity and attenuation 80−44262
polyisobutylene, Brillouin scatt. and hypersonic relax. 77−55795
polymers, amorphous, Brillouin scatt., hypersonic relax. 79−4811
polypropylene, atactic, Brillouin scatt. and hypersonic relax. 77−55795
polystyrene, atactic, chain length depend. of hypersonic relax., Brillouin spectra 77−55797
polystyrene, monosubstituted, US relaxation, dynamics of mol. chains 80−29124
polystyrene, soln., macromol. dynamics, us relax. 80−19882
polyvinyl acetate, Brillouin scatt. and hypersonic relax. 77−55795
n-propanol, US studies of mol. relax. 78−22790
propylene, liquid, effect of libration transitions on sound absorpt. 78−2203
pyridine, liquid, vibrational double relaxation 79−42154
pyridine, mean free path meas., US relax. 80−59585
quartz, smoky, HF US relax. 78−71796
sea water, sound absorpt., chemical relaxation involving Mg and carbonic acid 79−68466
semiconductor, US absorption of moderate freq., electron distrib. function perturbation 77−55587
L-serine, in aqueous solns., US spectra using automatic recording spectrometer 78−75735
p-Si US attenuation due to donors and acceptors 77−28223
smectic liquid crystal, shear wave attenuation 78−9944
solvents, acoustic relax. mechanisms *(Russian)* 79−90733
steel, US critical angle reflectivity, near-surface metallic prop. gradient effect 80−70516
styrene-butadiene-styrene triblock copolymer, US relax. 77−89502
2,4,6,8-tetraphenylnonane soln., macromol. dynamics, us relax. 80−19882
TGS, US vel. and attenuation just above T_c 77−35637
TGS and deuterated cpd., ferroelec. US relax. time constant 80−84257
thiophene, mean free path meas., US relax. 80−59585
thiophene, US and hypersonic investigations of vibrational relaxation 80−33377
1,1,2-trichlorethane, soln. in acetone, US relax., solvent effects 79−99275
triethanolamine, intermol. H bonds redistrib. 77−69050
triethylamine, Rayleigh line and acoustic spectra, fine struct. 77−39629
UHF range, high resolution Bragg reflection technique 79−23160
underwater sound, acoustic absorpt. by $MgCO_3^0$ ion-pair relaxation 79−74914
vinyl-series polymer solutions, longitudinal US waves absorption 80−15192
water, US vel. meas. by Brillouin scatt., supercooled to boiling range 77−15495
Al, cold worked, effect of bias stress on US attenuation induced by geometrical kinks mobility *(French)* 77−31728

ultrasonic relaxation continued
Al, cold-worked, dislocation-pinning defects, US attenuation obs. 77−31673
Al, lattice resistance stress, Bordoni relax., microdeform. and US attenuation results 80−25747
Al_2O_3-MgO spinel, 9.4 GHz US wave damping, defect and phonon scatt. 77−39637
β-Al_2O_3-Na_2O, Young's modulus and internal friction obs. 77−35624
β-Al_2O_3-Na_2O 79−19396
Ar, US vels. and absorption coeffs., determ. of relaxation times 78−63530
Ar-Kr liquid mixtures, volume and shear viscosities *(Russian)* 77−84961
Ar-monochlorodifluoromethane mixture, US vels. and absorption coeffs., determ. of relaxation times 78−63530
$BeSO_4$ soln. in H_2O, methanol-H_2O, US dispersion, 3-60 MHz *(German)* 78−59862
Bi:Te(Sn,Sb,Pn), US attenuation meas. 80−92614
$CdCl_2$, aq. solns., sound absorpt. and relax. phenomena 80−49311
Co, US damping temp. and mag. field depend. *(Russian)* 78−23313
$CoSO_4$ soln. in H_2O, methanol-H_2O, US dispersion, 3-60 MHz *(German)* 78−59862
$CsNO_3$, molten, Brillouin spectra, 420-520°C, hypersonic vel. and sound absorption freq. depend. 77−28589
$Cu(ClO_4)_2$ in ethylene glycol solns., US absorpt., relaxation rel. to temp. 77−31727
$Cu(NO_3)_2$, in ethylene glycol solns., US absorpt., relaxation rel. to temp. 77−31727
D_2O, US attenuation, for vol. viscosity, 0-60°C 78−63871
Fe tourmaline, microwave acoustic relax. absorpt. 78−22791
Ga, elastic moduli, temp. depend., anharmonic effects *(Russian)* 77−31708
GaAs:Cr^{2+}, dynamic Jahn-Teller effect, relaxation time for reorientation 80−6798
Ge, single cryst., US absorption by dislocations *(Russian)* 77−62589
Ge, US attenuation and nonlinearity const., temp. depend. 78−43075
H_2O, US attenuation, for vol. viscosity, 0-60°C 78−63871
^3He, liquid, fluctuation contrib. to sound vel. and damping above superfluid transition temp. 80−15324
$K(H_{1-x}D_x)_2PO_4$, polarisation relaxation time and Landau kinetic coeff. rel. to degree of deuteration 80−84251
KH_2PO_4, central peak susceptibility and US propag. near T_c 78−15125
$KMgF_3$:Fe^{2+}, US relax. absorpt., acoustic wave-impurity coupling, spin-orbit splitting 79−4375
$KMgF_3$:Cr^{2+}, dynamic Jahn-Teller effect 77−66416
LiCl in H_2O, complexity investigation using US method 80−33326
$LiNO_3$ in N,N-dimethylacetamide, Raman, IR and US relaxation studies 80−50315
LiSCN in N,N-dimethylacetamide, Raman, IR and US relaxation studies 80−50315
$MgAl_2O_4$, transverse elastic wave damping at 36.5 GHz 77−80583
Mn-Cu alloys, mechanical damping at 40 kHz 78−23755
MnP, US vel. and crit. attenuation, longit. waves, external mag. field 78−27035
$MnSO_4$ aqueous soln. conc. depend. of third US relaxation freq. and activation energy 78−63814
$MnSO_4+H_2O$ solutions, relaxation freq. and activation energy depend. on conc. 78−55913
N_2, liquid, US absorpt., bulk viscosity and relaxation 77−35639
N_2, moist, relaxation freq., sound tube meas. 78−1058
N_2-ethylene, gas, vibr. relax. time by US meas. 79−98852
N_2-methane, gas, vibr. relax. time by US meas. 79−98852
NH_4Cl, λ-type phase transition, hypersonic study using Brillouin scatt. 80−34165
$NH_4H_2PO_4$, phase transition, phonon echo method *(French)* 78−6640
NaF, γ-irradiated cryst., relaxational damping of elastic waves and activation energy of motion of defects 79−14891
$NaNO_3$ in N,N-dimethylacetamide, Raman, IR and US relaxation studies 80−50315
NaSCN in N,N-dimethylacetamide, Raman, IR and US relaxation studies 80−50315
Nb, plastically deformed, hydrostatic pressure effect on dislocation relaxation, US exam. 78−76696
Ni cryst., US wave attenuation, phonon viscosity and dislocation drag coeffs. 80 and 298K 77−76491
$NiSO_4$ soln. in H_2O, methanol-H_2O, US dispersion, 3-60 MHz *(German)* 78−59862
O_2 liquid, US absorpt., bulk viscosity and relaxation 77−35639
O_2-CO_2 mixture, temp. difference of molecular vibr. relaxation freq. from 300 to 675K 80−74238
O_2-H_2 mixture, temp. difference of molecular vibr. relaxation freq. from 300 to 675K 80−74238
O_2-He mixture, temp. difference of molecular vibr. relaxation freq. from 300 to 675K 80−74238
$(Pb_{1-x}Ba_x)_5Ge_3O_{11}$, ferroelec. transition blurring, US relax., dielec. and opt. props. 78−95559
$Pb_5Ge_2O_{11}$ acoustic relax. assoc. with phase transition at hypersonic freq. 78−88267
$Pb_5Ge_3O_{11}$ acoustic relaxation near ferroelectric transition 78−2814
$Pb_5(GeO_4)(VO_4)_2$, $Pb_5(SiO_4)(VO_4)_2$, and Pb_5GeO_{11}, elastic nonlinearity and acoustic losses 80−59554
$RbAg_4I_5$, superionic cond., US absorpt., ionic cond., relaxing sp. ht. 78−14505
SF_6 gas acoustic dispersion obs. by double-crystal US interferometry *(Japanese)* 79−4100
$Sc_2(SO_4)_3+Al_2(SO_4)_3$ aq. solns., complex form. reacts., kinetics, US relax. investig. 79−1942
Se, amorphous, relax of sound velocity, struct. determ. 78−38786
Se, amorphous, retardation of deform. near T_g point 80−84256
Se, liquid, US absorpt. meas. 78−2202
P-Si:B, US spectroscopy, energy splitting of acceptor ground state 79−33260
UF_6 gas acoustic dispersion obs. by double-crystal US interferometry *(Japanese)* 79−4100
WF_6 gas acoustic dispersion obs. by double-crystal US interferometry *(Japanese)* 79−4100
YAG:rare earth metal, US absorpt. meas., relax. model 80−24539
YIG, thermal attenuation of US waves, 500-1000 MHz 77−84854
Zn single crystal, US flow detection in dislocation relaxation investigations 80−29122
$ZnCl_2$ in H_2O, complexity investigation using US method 80−33326

ultrasonic scattering
A-mode echo computer spectral anal. 80−51193
animal tissues, freshly excised, attenuation and backscatt. obs. 80−51148
arrival times of scattered signals from solid inclusion in elastic material 79−72735
backscatter analysis, from human tissue, imaging 77−86576
backscatter of short US pulses by solid elastic cylinders at large ka 80−43502
backscattered wave minima for solid metal cylinder immersed in water *(French)* 80−53510
backscattering by mammalian organ as function of time after excision 78−7412
backscattering in water due to elastic cylinder, short pulse backscatter *(French)* 80−53511
backscattering measurements in laboratory waveguide 80−64259
blood, angular dependance 77−81542
blood, US backscattering, haematocrit and erythrocyte aggregation depend. 80−45961
blood, US propag., effects of red cell shape and orientation 78−24104
blood, US scattering, theoretical study 80−51147
blood flow measurement by Doppler method, effects of geometrical spectrum broadening 77−40725
bone, cancellous, US attenuation and dispersion 80−51149
cardiac pressure noninvasive US measurement, scatt. from encapsulated bubbles 80−36048
caustics in non destructive evaluation, diffraction at crack like defects 80−43680
ceramic surface flaw detection by SAW scatt. 79−47866
cerebral tissue, freq.-dependent US backscatter obs. and correl. 79−79620
circular crack, quasistatic approx. of US scatt. 78−67080
cloud of isotropic scatterers, air bubbles in water appl. *(French)* 80−53507
composite materials, scatt. coeff. and uel. dispersion 79−86844
compressional impulse interaction with slot normal to surface of elastic half space 79−50626
Doppler spectra, transit time and geometrical broadening 78−44576
erythrocyte aggregation detect. by US scatt. 77−40721
erythrocyte US scatt. frequency dependence obs. 77−64119
eye and eye socket, short US pulse scatt. 77−37008
failure prediction 77−21349
flaw detection, Born approx. theory for elastic-wave scatt., expt. aspects 79−100307
flaws in elastic materials 77−79983
fluid, near liq.-gas crit. pt., local order effects on dynamic props., US and light scatt. 78−67806
fluid bi-inclusion in elastic solid, geometry and mech. props. from US pulse scatt. 77−21348
forward sound scatt. by small nylon cylinders in water 80−96054
glass filled solids, ultrasonic absorpt., scatt., velocity and attenuation 80−44262
heart and liver, quantitative meas. 80−45959
human tissues, theoretical models 78−7411
Indian Ocean, fluctuation spectrum of US field scattered by inhomogeneities 79−88367
inertial transducer, rotational perturbation detection appl. 78−9524
leaky wave attenuation by near-surface defects 77−32757
liver, human, theoretical modelling 80−89785
liver, US backscatter from human tissue, depend. of freq. and protein/lipid content 80−45960
long elastic wave scatt., inverse problem 79−55819
lung surface US tissue signature 80−45957
lung tissue characterisation by US, instrumentation, model and results, book 78−44575
metal ellipsoidal flaw characterisation 79−47865
mixtures and suspensions, flow rate meas., ultrasound propagation and scatt. approach 80−43806
myocardial and hepatic tissue US backscatter comparison 79−48310
ocean turbulence, small-scale, study by acoustic scatt. method 80−26540
ophthalmic tissue signature characterisation by US frequency-domain analysis 77−40857
piezoelectric crystals, class $C_{6v}(C_{4v})$, shear wave scatt. by low resist. cylinder and cylindrical void 78−95113
plane axial-shear wave, scatt. by circular semiconducting piezoelectric cylinder 78−2806
polycrystal, US scatt. by grains 80−2122
polycrystalline materials, freq. and grain size dependency of US attenuation 80−50783
polycrystalline structure testing by US backscatter meas. 77−21347
polyethylene, glass filled solids, ultrasonic absorpt., scatt., velocity and attenuation 80−44262
polymer, liq., Brillouin scatt. and segmental motion, appl. to polypropylene glycol 78−91217
pulse-echo scanning, echo struct. 77−52857
randomly rough surface backscatter anal., autocorrelation theory *(French)* 80−53508
Rayleigh wave scattering by surface breaking crack, ray analysis 80−69575
Rayleigh waves scatt. by thin surface strip 77−11773
real-time imaging with shear, Rayleigh, and Lamb waves 77−32759
rough surface scattering and characterisation of parameters, 2 to 25 MHz *(French)* 79−41538
rough surfaces, scatt. by different roughness amplitudes and profiles 77−809
SAW propag. along boundary with periodic inhomogeneities 80−102905
SAW scattering by surface breaking cracks 79−56058
SAW scattering from surface cracks, angular and frequency dependence obs. 79−57197
SAW scattering in piezoelectric material, by metallic electrodes anal. 78−83157
scanning laser probe for acoustic wave phenomena observation at liquid-solid interfaces 80−100386
Schlieren observations of short US pulses scattered from elastic cylinders *(French)* 80−53500
shear wave scatt. by flat-bottomed hole in Al, intensity distribution mapping 77−19503
soft tissue characterisation by US backscatter analysis 77−21586
spectral struct. from random sea surface 78−63225
spherical cavity in metallic solid, longitudinal acoustic wave scatt. 78−38108
spherical voids, elastic wave scatt. at long wavelengths 80−48480

ultrasonic scattering continued
structural material defect characterisation by US signal processing 79−52614
submerged turbulent jet in liquid 78−50992
surface characterisation meas. of randomly rough surfaces by US backscatter at normal incidence *(French)* 80−52165
suspensions and emulsions, highly-concentrated, sound absorption 79−41475
suspensions of spheroidally-shaped particles 79−98539
symmetrical Lamb wave scatt. at pair of thin slots 79−47868
theory, scatt. by single objects 80−99892
tissue, human, model of backscatt. 77−40715
tissue bioacoustic property determ. by US pulse echo anal. *(German)* 78−85349
tissue characterisation by angle scan and freq.-swept scatt. technique 80−45958
tissue characterisation by backscattered field space-time processing 79−48305
tissue characterisation by scattering 77−64107
tissue characterisation by US backscattering 79−70595
tissue characterisation by US frequency-dependent attenuation and scatt. 77−66832
tissue characterisation by US scatt. frequency and angular dependence 77−64118
tissue macrostructure determ. by swept-frequency US scatt. 77−64120
tissue US backscatter and attenuation distrib. mapping, digital reconstruction 80−51188
tissues, fixed and unfixed, US propagation, backscattering coeffs. and speech determ. 80−41109
transient piezoelectric wave scatt. from crack 79−52615
transmission image reconstruction, inverse scatt. and tomography 78−61231
turbulence in water, interaction with 1 MHz waves 80−87619
underwater sound, volume scattering strengths and zooplankton distributions at acoustic frequencies between 0.5 and 3 MHz 80−33317
volume scattering at 25 kHz in presence of temp. discontinuity layer 80−38157
W-Cu composite materials, vel. dispersion and scatt. of transverse US waves 78−91383

ultrasonic transducers
A-scanners, performance assessment using system transfer functions 79−23169
absolute calibration by impulse techniques 79−23179
absolute calibration of piezoelectric transducers 80−79099
acoustic emission transducer for inspecting weld quality 79−94444
acoustic vibrating systems, use of nonlinear phenomena for IC microwelding appls. 80−74656
acoustooptic Bragg deflector, wide-band guided wave, using tilted-finger chirp transducer 80−14440
acoustooptic effect calc., integrated 80−91944
adaptive control system realisation algorithm *(Russian)* 77−54853
air-coupled, for non-contact transduction of kinetocardiogram 77−86568
angle probes, influence of membrane dimensions on sound field 79−23168
annular, for focusing field upon transmission 78−44574
annular array search units, potential appl. in conventional US testing systems 80−35446
annular array with dynamic focusing 77−32947
aperiodic piezoelectric sensor, fabrication and design problems 77−77713
aperiodic piezoelectric transducers, ceramic, structure and operating principles 78−85109
applications, conference, Brighton (1977) 78−59223
arbitrarily electroded piezoelec. plate acoustic spatial response determ. 80−99910
arc array with automatic sector scan echo signals presentation system *(Italian)* 79−96637
array, transducer elements tuning 80−87684
array review 79−59898
array technology, 2-D, state of art review 77−844
arrays, broadband directional reception 80−96126
arrays, electric coupling effects in acoustic imaging 80−43587
artillery projectile inspection by noncontact EM transducers 79−47872
aspiration-biopsy transducer development 78−61233
asymmetric three-transducer configuration analysis 77−39165
automatic meas. method of US transducer constants *(Japanese)* 78−33972
axisymmetric transducers, under various conditions of baffle, nearfield radiation patterns determ. 80−99909
baffled planar, calc. of acousto-optic (Raman-Nath) parameter for entire sound field 80−74689
bandpass filters with quarter wave reflections, design 80−19183
beam scanner, automatic US beam meas. system *(Dutch)* 79−27473
beam scanning by SAW transducer arrays 79−55266
bidimensional array design for B- and C-scan US imaging system 79−47877
biodynamic research, US/EMG transducer, speech appl. 78−77164
biomedical low-loss wideband for noninvasive appls., charcts. 78−48846
blind children's CW FM sonar 79−70708
blood velocimeters, US transesophageal meas. of human haemodynamic parameters 80−41146
bolt clamped Langevin longitudinal transducer *(Japanese)* 79−27483
bolt-clamped Langevin type transducer, effect of surface conditions on performance *(Japanese)* 80−48543
bonding material investigations, US delay lines *(Japanese)* 80−79097
broad band clinical transducers, pulse echo beam profiles through attenuating and non attenuating media 80−45945
broadband chirp transducers for integrated optics spectrum analyzers 80−74514
broadband constant beamwidth, theoretical new approach 78−90616
broadband constant directivity transducer, array shading function 79−14188
broadband fluid loaded US transducers, design 80−19202
broadband matching of piezo-transducers for acousto-optical devices *(Russian)* 80−64329
bulk wave electromagnetoacoustic excitation 79−57195
calibration by He gas jet 77−835
calibration by measuring total nearfield force, theoretical results 80−33400
calibration method using laser interferometry 79−23177

ultrasonic transducers continued
capacitative appl. to elimination of transducer bond correction in US wave vel. meas. 77−46873
capacitative excitation of elastic oscillations 80−71862
cellophane film condenser transducer, operation in air, 0-100 kHz 78−42509
ceramic piezoelectric transducer, anomalous radiation pattern due to parasitic Lamb wave generation 80−96170
ceramic transducer, spatially-bounded US wave response 80−48542
characterisation using cholesteric liquid crystals 78−42512
characteristics deviation 79−98581
characterization methods at the NBS 79−27481
characterization standards, tissue equivalent testing for hospital use 79−29651
charge distribution for non-periodic transducers using cct. model 80−74691
circular and rectangular transceivers, effect of range on US echo 79−94434
circular piston, Gaussian-Laguerre description of US fields 80−64239
circular transducer array for ultrasonic inspection of plates and sheets 79−29293
cleaners and disintegrators, review, latest instruments 79−37101
coaxial circular spherical array for US imaging 78−9513
composite piezoelectric US transducer, finite element simulation 79−41541
composite piezoelectric US transducer, finite element simulation *(Japanese)* 79−68537
composite strip piezoceramic US receiving array 78−42511
composite torsional quartz transducer for shear US measurements of aqueous liquids 80−53599
computer-controlled system for measuring two-dimensional acoustic velocity fields in solid samples 80−76468
concave, confocal pair, appl. of polyvinylidene fluoride piezoelec. film 78−22241
conical solid horn with flange, FEM analysis of free vibrations *(Japanese)* 80−79045
contactless electrostatic-acoustic transducer equivalent cct. analysis 77−19507
contactless EMA excitation of US bulk waves *(German)* 78−59234
contactless transducer, for thickness meas. and metal flaw detection 78−44312
curved, coaxial pair system, diffr. losses 77−31195
cylindrical horns, US power monitoring 77−19500
cylindrical transducer scatter scanner for medical ultrasonographic imaging 80−96154
cylindrical tubes, high-intensity US radiators *(Japanese)* 80−33404
damping by multilayer front face 79−55301
design rel. to vibration geometrical effects 79−83871
dielectric acoustoelectric transducer, freq. charcts. 78−38167
differential probe heads of impedance-type defectoscopes, design 77−73409
diffraction corrections for US vel. and attenuation meas. 80−96153
diffraction corrections under impulse conditions 79−32175
digital gauge, for ventricular dimension meas. 78−20238
directivity determ. in pulse mode operation 78−71258
disc impedance meas. and US transducer CAD program 79−46157
Doppler, single-transducer system, circuit construction 79−81680
Doppler blood flowmeter, directional, transducer design 77−25535
Doppler blood flowmeter, geometrical spectrum broadening anal. 77−86567
Doppler flowmeter average frequency processor 79−83873
Doppler flowmeter employing continuous wave modulation *(Japanese)* 79−37429
Doppler proximity detector alarm system 79−64477
Doppler sonographic flow meas. over small cross-sections in vitro and in vivo *(German)* 78−88729
Doppler US flow transducer for human milk flow meas. 79−53200
dual-gate depletion-mode FET/piezoelectric film transducer 79−50563
dynamic focusing transducer design for diagnostic image quality improvement 80−41155
echo sounder transducer field plotter 78−59238
efficient transducer arrays for NDT 79−57194
electret US transducer performances and prospects 78−59244
electrodynamic transducers, US wave generation, material testing *(German)* 78−44294
electromechanical filter torsional mode transducer analysis 77−27436
electronic scan US tomography, array transducer, shading function design *(Japanese)* 77−84100
electronically scanned US diagnostic systems, electromechanical coupling coeff. for plank-shaped transducers 80−33383
electronically-addressed bulk acoustic wave Fourier transform device 80−74637
electrostatic, broadband, for US meas. in liquids, props. 79−18642
electrostrictive material for transducers, proposal of method for evaluation 80−38208
electrostrictive US transducer electroacoustic efficiency and load matching 79−68541
ellipsometer design and performance 79−57196
EM, calc. of acoustic field produced in nonmag. metal 77−11101
EM periodic SAW transducers 78−13880
EM transducer dynamic range optimisation 77−19506
energy criterion for performance in pulse mode 78−87227
epoxy material, filled, US props. for sonar transducers 78−59867
evaluation and calibration conf., London 1977, May 79−23167
evaluation by cross-sectional mapping in near field using point reflector 79−94440
evaluation for inspection and diagnostic appls. 79−27480
evaluation in exptl. and theoretical domains 79−46153
excitation at odd subharmonics 79−98583
extensional trapped energy mode transducer bandwidth, influence of tuning inductor 79−55303
eye movement non-contacting recording appl. 78−7414
fabrication, effect of component preparation and assembly, on transducer parameters 78−73004
face centred array, for acoustic emission source location 79−24708
farfield angular radiation pattern generated from arrayed piezoelectric transducers using finite element anal. 80−33401
fibre-optic pressure sensor 80−58878
field homogeneity enhancement 77−68358
field intensity distribution measurement, liquid-surface relief method, transient behaviour for pulsed transducers 80−95073

ultrasonic transducers continued
field intensity meas. using wideband piezoelectric convertors *(Russian)* 80−38209
film cleaning by ultrasonic liquid cavitation and acceptable solvents 80−62769
finite SAW transducer, surface charge density and elec. field distrib., moment method 80−23857
flaw detector, automatic, for butt welds *(Japanese)* 80−25976
flowmeter, 240 Clampitron, applicability study 80−24108
flowmeter, Danfoss, using electronic unit and piezoelectric transducers 80−6172
flowmeter, multichannel time-freq. type, operating principle 77−72387
flowmeter appl., computer interface development 78−38426
flowmeter cell unconventional designs 78−59528
flowmeters, petroleum and similar fluids 80−43804
focused, for acoustical imaging of objects buried in seafloor sediment 80−79036
focusing, field pattern criteria 79−14196
focusing device with IDT on thin piezoelectric plate 80−1398
focusing improvement, dynamic, using analogue-switch phase shifters 77−52856
focusing piezoelectric type, pulsed operation 79−68539
focusing transducers 80−33410
Greens function method for quasi-static anal. of interdigital transducers 80−69621
HF, lumped bandpass filter equiv. ccts., quarter-wave matching charact. 80−1397
HF Lorentz force hydrophone theory and practice 78−42510
HF strain transducer for acoustic wave signal processing 77−88991
high power applications in gases 79−23165
high resolution, with toroidal acoustic lens, biomedical appl. 77−65656
high-efficiency narrowband transducers and arrays, development 80−58880
high-power US transducer performance rel. to ceramic location 79−50561
highly electrostrictive ceramic capacitor 79−47390
hydrophone, cylindrical, theoretical shape of directional pattern 79−81609
hypersonic generation and detection using Josephson junction *(Polish)* 77−14870
imaging, single-transducer technology, state of art review 77−843
imaging biomedical piezoelectric micro-array technology for improved image quality *(German)* 80−98052
impedance flaw detector, resonant transducer 79−52572
impedance flaw detectors, unified procedure for transducer calc. 79−90109
impedance method charact. and inspection transducer 79−96270
implantable, accuracy of CW Doppler flow meas. 77−25537
incoherent image two-dimensional Fourier transform by optoacoustic transducer 79−50243
inertial, based on dynamic scattering, rotational perturbation detection appl. 78−9524
inspection apparatus for warp-soldered tubing 78−3276
integrated optical effect produced by US fields, study using light diffraction technique 80−23848
interacting SAW transducer equivalent circuits 77−27456
interdigital, equiv. cct. parameters from surface waves dispersion relations 77−39187
interdigital, generation and detection of surface and bulk acoustic waves 77−39186
interdigital, scatt. parameters 77−39188
interdigital SAW transducers, freq. charact. improvement *(Japanese)* 79−23164
interdigital transducer, book contrib. 80−1400
interdigital transducer, electroelastic surface wave excitation, detect. and scatt. 77−812
interdigital transducer and 1.1 GHz SAW oscillator, photolithographic contact printing *(Japanese)* 78−33981
interdigital transducer design, redefined element factor 79−7266
interdigital transducer design and component specification tradeoffs 77−27455
interdigital transducer design with spectral weighting frequency response 77−27454
interdigital transducer models for accurate design implementation of SAW transversal filters 80−28396
interdigital transducer transverse electrostatic end effects 77−27453
interdigital transducers, fabricated using simple mask printers 78−59229
interdigital transducers for one-port SAW resonators, narrow band filters appl. *(Japanese)* 79−27478
internally lossless transducer conjugate matching, power transfer and backing impedance 79−46158
Lamb wave excitation in yz-cut plates *(Russian)* 78−55483
Lamb-wave device with three operation modes 79−14183
large aperture bowl transducers, diffr. pattern 80−58833
level detection appl. 80−27268
level sensor, for tank and pipe water level meas. and control 77−37845
LF sandwich transducers for underwater acoustics analogy between fluid and solid horns 80−38213
$LiNbO_3$ wedge waveguide apodised interdigital transducer evaluation 77−27451
liq. cryst. cell for US visualisation *(German)* 78−79179
loading, monitoring by impedance bridge technique, effect of US field geometry 80−102950
longitudinal wave, for US inspection of hot thick steel products 80−40661
low frequency US flaw detector appl. 79−98580
low-loss wide-band US transducer design for noninvasive medical appls. 79−44021
lumped wideband equaliser design optimisation 79−46159
magnetically tunable ultrasonic transducers for shear waves 80−74682
magnetostrictive, matching with cavitating water 78−94503
magnetostrictive US probes using extensional, torsional and flexural waves 79−50562
magnetostrictively coupled meander-coil EM transducers, horizontally polarised shear wave generation in ferromagnets 79−46144
manipulator outside tank of coupling fluid in US expts. 80−106693
matching systems calc. 79−94445
materials and adhesives, high temp. long duration tests 80−43586
for materials quality control, exam. of design configuration 78−73003
materials testing appl., wave refraction/reflection phenomena *(German)* 78−35615
ultrasonic transducers continued
materials testing reference blocks and transducers, survey 78−68858
measurement systems, inertialess sensing 80−64315
medical, design 79−100685
medical diagnosis, routine eval. of US transducers 79−23173
medical imaging, ceramic and PVF_2 transducers compared 79−57734
medical imaging, modelling *(French)* 80−26302
medical Pulse-echo transducer standardization 78−73181
medical transducer evaluation by optical interferometry 77−39184
medical ultrasonics, transmitters and receivers from piezoelectric materials 80−76819
medical US imaging technology status 78−24174
metal defect scanning method for metal *(German)* 78−15620
metal flat plate, electromagnetic-acoustic conversion 78−44320
metal-dielectric contact, surface barrier Rayleigh wave transducer 79−98578
microprocessor-controlled digital compound scan system 79−57735
microwave ultrasound in liquid generation, piezoelectric film transducer of $\lambda/4$ operation, effective attenuation analysis *(Japanese)* 78−30145
mixed matrix representation of interdigital transducers 80−19184
mulitary appls., multilayered tape for perimeter warning device for combat troops 80−19200
multicomponent ring transducers, mechanical loss resistance calc. technique 78−38166
multilayer electroacoustic transducer containing active layers 79−64482
multilayer electroacoustic transducer containing active layers electrically connected in parallel 80−5902
multiphase interdigital transducers and the crossed-field model 80−92006
multitrack nonperiodic multistrip couplers, cct. model 78−75026
NDT probe array using 4 transducers 80−35499
near-field transient acoustic beamforming with short pulse arrays 79−57738
noncontact EM transducer design improvement 79−46151
noncontact transducers compared 79−46149
nondestructive evaluation transducer figure of merit 77−27457
nonlinear parametric radiation study using Fourier anal. *(French)* 79−41485
nonpiezoelectric materials, technique for excitation of surface and shear acoustic waves 78−66997
oceanographic data acquisition system using high sensitivity US current meter 77−41211
ophthalmological, with controlled weight, eye axial length meas. appl. 78−20239
optical determ. of low US powers of circular piston transducers 80−64319
optical multimode fibre acoustic sensor, using mode-mode interf. 79−50553
optically controlled piezoelectric transducers for ultrasonic volume waves 79−18662
optically-controlled acoustic transducers, piezoelect. and electrostrictive 80−74638
opto-acoustic, for biomedical diagnostic imaging, equiv. cct. and simulation 77−60283
opto-acoustic transducer structs., recent investigations 80−74688
opto-acoustic transducers, improved equivalent cct. 80−74658
opto-acoustic transducers for sensitive US imaging 78−5625
optoacoustic transducer characteristics for US imaging 79−50560
parametric, for high-resolution sonar 80−14539
part inspection with surface temp. up to 500°C 79−98584
performance, theoretical anal., material testing appl. 80−30176
periodic interdigital transducer for SAW 79−7269
periodic interdigital transducers with arbitrary voltages, generalized model 79−68534
periodic magnet noncontact transducer theory and application 79−46150
phase insensitive acoustoelectric transducer, operation and optimisation procedures 78−90617
piezoceramic aperiodic transducer, mech. load study 80−87700
piezoceramic transducers, transient charact. 80−106704
piezoelectric, calc. of amplitude-frequency and phase-frequency curves 79−68531
piezoelectric, design US imaging equipment appl. 78−9525
piezoelectric, included scanner for corner reflector acoustic channel 80−106705
piezoelectric, pre-energised nonuniform, delay rod loaded, subject to body force, mechanical response 77−27449
piezoelectric, US energy meas. for echography 80−36044
piezoelectric ceramic plates, expt. data for design of line arrays, medical diagnostics appl. 77−84099
piezoelectric discs, radial vibrs. 80−96166
piezoelectric radiator of longitudinal acoustic waves with an inhomogeneous elec. field 80−87693
piezoelectric rectangular plate vibrating mode, US array appl. 77−80046
piezoelectric shear-mode acoustic wave receiving, transfer charact. 80−87696
piezoelectric strip transducers with nondirectional sound radiation *(German)* 79−98576
piezoelectric surface excited, thick, transient, pulse and amplitude-frequency charact. 80−102958
piezoelectric thickness vibrator, digital computer simulation 77−88998
piezoelectric transducer, aperiodic, for US radiation, design for testing applic. 78−36996
piezoelectric transducer, resonant, construction and delay line contract, US thickness meter 78−53100
piezoelectric transducer, thick, operating as radiator or receiver, performance charact. 80−35484
piezoelectric transducer, US refl. from transducer with coupling layer *(German)* 79−10440
piezoelectric transducer parameters testing equipment 79−50555
piezoelectric transducers, energy and spectral evaluations of broadband excitation 80−35485
piezoelectric transducers, integrated acousto-optical effect prod. by pulsed sound fields 77−31193
piezoelectric transducers, surface-driven, input impedance calc. 80−35493
piezoelectric transducers for contactless US product inspection 79−34238
piezoelectric transducers of tall, narrow elements of acoustic imaging array 80−74690
plot system developed for nondestructive materials testing exam. 78−53067
polymer, acoustic props. appl. in US flaw detection 79−47857

ultrasonic transducers continued
polyvinylidene fluoride, US transducers, dielec. and acoustic losses 80−48541
polyvinylidene fluoride film appl., poled, short duration unipolar stress pulse detection, generation 80−106695
polyvinylidene fluoride film polymer transducer, with US appl., durable lead attachment techniques 80−79094
polyvinylidene fluoride piezoelectric film, acoustic wave reson. meas. 77−81058
polyvinylidene fluoride SAW transducers, evaluation of performance 80−74617
power meas. at MHz freq., calorimetric method 79−23180
power measurement using const.-flow calorimeter, 1.5 to 3 MHz 77−50843
power output meas. using modulated radiation pressure 78−59230
pressure gauge, using single-transducer sing-around system 77−13742
probe calibration procedure, practical appls. *(German)* 79−81677
probe for measuring US energy density in liquids *(Polish)* 78−5617
probes, assessment and specification rel. to standards 79−23175
pulse excitation method for solids 78−5624
pulse excited, reference spectrum 79−23171
pulse frequency-response curves for a contact piezoelectric transducer 79−68538
pulse-echo transducers, tone burst testing 79−27479
pulsed, sound field description, evolution equations 80−87682
pulsed acoustic radiation of plane damped transducers 77−84101
pulsed fields radiated by thick piezoelectric discs immersed in petrol, expt. study *(French)* 80−53512
pulsed transducer, semi-automatic meas. of effective directivity 77−84102
PVF_2 bulk wave transducers for nondestructive evaluation 79−57199
PVF_2 film composite resonator for concave focusing US transducer 79−46155
PZT transducer manufacture and testing 79−23174
quality control, appl. of ultrasound visualisation technique 77−14863
quartz, ST plate, efficient bulk wave excitation 77−15502
quartz acoustic bulk wave resonators using AT-cut crystals, tolerance effects 80−53601
quartz crystal, influence of tabs thickness and resonating props. 78−18140
quartz X-cut crystal transducer, laser intensity distrib. meas. using US diffr. 80−64092
radiation patterns of acoustical arrays with quantized time delays 80−74566
random signal US, transducer limitations 77−25536
rare earth-Co permanent magnet EM acoustic transducer design 77−19508
receiver response, optimised by fast-attack detector 77−80034
receiving array having power response 80−74653
reciprocity calibration of acoustic emission transducers 80−28401
reciprocity calibration of arbitrarily terminated transducers 80−53574
reciprocity technique for estimating the diffuse-field sensitivity of piezoelectric transducers 80−48538
remote control circuit using US transducer 80−10097
response dependence on fluid layer coupling *(French)* 80−43580
rolling transducer, for automatic inspection systems 79−3881
rolling ultrasonic low-frequency probe 79−98582
rotatable sample holder with voltage readout, angle sensing mechanism 78−13873
sandwich, transcendental equation adaptation for simplified calc. 79−18661
sandwich and disc transducer characteristics for gaseous media 78−59241
sapphire rod, ZnO coated, for pulse echo meas. at 200 MHz 77−23834
SAW, apodized, radiation conductance 80−96174
SAW, micro-fabrication technique for Al electrode 77−80042
SAW, on Si substrate with nonzero conductivity, calcs. of fractional velocity 78−1533
SAW, parameter calc. with power scattering coeffs. *(Russian)* 80−64317
SAW, surface to bulk wave conversion at local surface defects 78−38165
SAW, tunable, appl. of nonlinear interaction of SAW with Josephson junction 77−85392
SAW, wedge transducers, efficient broadband design using coupled-mode theory 78−63253
SAW asymmetrically truncated transducers with finite impulse response 78−87225
SAW delay line triplet-transit suppression technique using symmetric and antisymmetric transducers 79−64453
SAW delay lines, true quadrature taps 78−87222
SAW digital FM compression system *(Russian)* 78−55541
SAW edge bonded transducer design and application 79−55304
SAW EM transducer harmonic operation 79−46152
SAW EM transducer model and flexible design for NDT 77−23844
SAW EM transducer range resolution improved by pulse compression 77−19509
SAW filter interdigital transducers, manufacturing inaccuracies influence on transmission characts. 79−10434
SAW filter triple transit suppression by mech. and regeneration reflection cancellation 77−23829
SAW filter with low insertion loss using group-type unidirectional interdigital transducer *(Japanese)* 78−33980
SAW filters, low insertion loss, using multiphased unidirectional transducers 80−28397
SAW IDT, Al evaporation conditions 80−92007
SAW IDT, bulk wave radiation suppression, theoretical investigation of crystalline orientation 80−58886
SAW IDT, electrode charge distrib. as element factor, anal. 80−1396
SAW interdigital transducer, electromechanical coupling coeff. 79−23163
SAW interdigital transducer transfer function rel. to fabrication tolerances 77−27452
SAW interdigital transducers, equivalent network model 79−46145
SAW interdigital transducers, excitation profiles 79−41544
SAW interdigital transducers, finger withdrawal admittance eval. by normal mode anal. 78−33978
SAW Lamb wave transducer with three operation modes, communication system appls. 80−43583
SAW resonator, as stress sensor, freq./stress sensitivty 77−2645
SAW resonator cavities with unidirectional transducers 77−23849
ultrasonic transducers continued
SAW resonator reflector and transducer characteristic effects 77−39168
SAW scattering by interdigital transducer, model and appl. to SAW track changer 79−59899
SAW transducer, new model 78−59232
SAW transducer array for surface defect imaging in metals 80−74660
SAW transducer with capacitive electrode weighting, band-pass filters 80−48544
SAW transducers, equivalent circuit model 77−46870
SAW transducers on Si substrates with polyvinylidene fluoride films 80−74618
SAW two dimensionally periodic transducer *(Japanese)* 78−33984
SAW two-port resonator using long interdigital transducers *(Japanese)* 78−33982
SAW unidirectional transducer with 3 electrode groups for Lamb wave devices 78−51034
scanner, real-time rotating transducer, for heat and abdomen exams. 79−20603
scanners, phased-array, angular response of piezoelectric elements 79−64471
seismoscopes, pulse output generator 77−9537
semiconductor-metal contact, depletion depth, acoustic determ. 79−99621
sensitivity measurement 78−49821
shallow bulk acoustic wave excitation by interdigital transducers 78−59251
shallow bulk acoustic wave generation by interdigital transducers 79−51411
shear-wave transducers for laboratory sediments 78−51033
shear-wave vel. meas., bone elastic moduli determ. 78−83201
short pulse, field phenomena 79−23170
short pulse transducers, comments 79−23166
short pulse transducers, design and characterisation using PZT5A 78−87228
single-transducer coupler for diagnostic pulsed Doppler or pulse-echo US instrumentation 78−61236
size choice in monitoring austenitic welded joints 78−60961
slotted transducer arrays with matched backings for underwater imaging 80−38214
sonar transducer arrays, image prod., signal processing methods comparison 78−18122
sonic transducer, Langevin type, made from $Pb(Zr,Ti)O_3$ type 1 ceramic, performance characts. 80−79095
sonograms, sound pattern and capability of US test heads *(German)* 79−79199
sound field, numerical calc. of diffraction losses *(German)* 77−3705
speckle reduction in US B-mode images of human tissue, using transducer and signal processor 80−74634
spherical arrays, reconstruction of three dimens. US reflectivity images 80−38203
spherically curved transducers, anal. of focusing action 80−64332
standard probe transducers, calibration 77−840
static and dynamic calibration using optical interferometric techniques 79−23178
steel high-temperature ultrasonic testing *(Italian)* 79−96242
stepped-array, acousto-optic deflector with 200 MHz bandwidth 77−58467
stereoscopic imaging synthesis allowing for real positioning of operator's head *(Russian)* 79−64391
stress determ. for bolt preload 78−53174
submicron SAW interdigital transducer fabrication by contact printing 79−46147
superconducting transducers for 50-1000 GHz range 77−50851
surface charge on unapodized periodic IDI 80−91947
surface excitation 79−76935
surface excited thick piezoelectric transducer, output current form 80−87701
surface skimming bulk wave transducers, specific appls. 79−81678
surface skimming bulk waves, excitation and detection on rotated Y-cut quartz 80−43492
Swzawa wave broadband thin-film interdigital transducers 80−74681
testing aspects, transducer head construction *(German)* 78−76804
testing freq. definition techniques 79−23172
thermographic-photographic technique for US intensity pattern characterisation 80−106689
thickness gauge, pulse-echo, transistorised, with reduced dead zone 77−12766
thickness gauges calibration, thickness standards 79−35669
thickness gauging on hot surface, combination double transceiver probe 79−3882
thickness mode design, computer simulation using Thevenin equivalent ccts. 78−30143
thickness mode piezoelec. US probe design factors 79−68540
thickness mode piezoelectric, method for stress const. determ. 79−14187
thickness-extensional trapped energy mode transducer array, increased bandwidths and mode shapes 80−74633
thin film interdigital transducers for SAW devices at GHz freqs. form. by electron beam lithography 80−4702
tilted-finger chirp transducer for design of wideband guided-wave acousto-optic Bragg deflector 80−74510
Tonpilz piezoelec. transducer design using nonlinear goal programming 80−106696
tracking focusing annular array transducer *(French)* 80−26301
transformless broadband equaliser, design algorithm 79−94436
transmit/receive 2D ceramic piezoelectric arrays, construction and performance, medical, NDT appls. 78−87223
transmitter calibration, acoustic pressure meas. 77−65657
transparent-solid US transducer field visualisation 79−55285
tube flaw detection by annular US transducers 78−60971
tumour irradiation, closed-loop energy and temp. control 79−83874
two-dimensional photoacoustic image processing with longitudinal waves 79−50244
UHF single-phase line acoustic wave transducers 78−79180
ultrasonic pulser requires no step-up transformer 78−79182
undersea acoustic holographic transducer array development 78−59209
underwater, parabolic reflector as nearfield calibration device 80−48528
underwater acoustical compliance element, elastic problem of flattened cylinder type 80−33309
underwater acoustical compliance tube for sound projectors, stress and deformation analysis 80−33310
underwater data communication US standing-wave radiator 79−46104

ultrasonic transducers continued
underwater transducers, reciprocity calibration by FM signal correl. methods 77−68298
underwater US magnetostriction vibrator efficiency meas. *(Japanese)* 78−9523
unidirectional SAW transducers with ZnO film on glass substrate 77−68355
unidirectional transducer for Lamb-wave delay lines 77−68354
unipolar transducers for nondestructive eval. 80−76471
US Doppler flowmeter spectra for asymm. transducers 78−31880
US implantable CW Doppler blood flowmeter, optimal system design 78−53460
US inclined probe, construction improvements 80−33411
US phase flowmeter, pulsating flow rate meas. error evaluation 77−72388
US velocity meas., fixed-path interferometer, phase error elimination 78−83197
variable-angle, qualitative evaluation by photoelastic visualisation method 78−18143
variable-focus US membrane transducer, medical imaging appls. 77−39185
velocity-of-propagation meter, based on interferometer 80−79084
VHF wave production and detection above 1 GHz 77−50852
vibration amplitude distrib. meas. by holographic technique *(Japanese)* 77−88999
vibration amplitude distribution meas. by holographic technique 77−42678
vibrations of very small amplitude, measurement using laser probe 80−73443
water-loaded, air-backed discs, impulse response 79−27482
wedge type for NDT, Rayleigh and Lamb waves pickup efficiency anal. 77−77708
wedge-type backing for US transducers 79−41546
wedged, with improved signal-to-scattered-noise ratio 79−3880
weighted SAW transducers, electrostatic neighbour and end effects 77−31200
wide-band, transmission, and reception of short US pulses 80−10099
wideband, tissue characterisation, 1 to 10 MHz 79−16262
wideband spherically concave transducers, for wideband probes, exam. of basic characts. 78−72979
ZnO, microwave acousto-optical device applic., 0.2 to 18 GHz 77−58465
Al alloy D16T, acoustic emission temp. depend. 78−53136
$BaTiO_3$-metal contact, surface barrier Rayleigh wave transducer 79−98578
CdS film SAW two-dimensional image processor 77−39164
CdS piezoelectric thin film transducers, testing via light diffr. by acoustic waves 77−23840
CdS, ultrasonic transducer, multilayer systems, amplitude-freqn. characts. *(Russian)* 77−23843
CdS, use in meas. elastic modulus of Tb 77−11151
Fe-Al (12 wt.%) alloy 23 kHz US transducer piezomagnetic props. 78−59240
$FeBO_3$, magnetically tunable ultrasonic transducers for shear waves 80−74682
$KTaO_3$-metal contact, surface barrier Rayleigh wave transducer 79−98578
$LiIO_3$, Z-cut cryst., appl. as wide band transducer in US pulse-phase interferometer 77−14868
$LiNbO_3$ acousto-optic convolver with large time-bandwidth product 77−27432
Y-Z $LiNbO_3$, radiation patterns of bulk acoustic modes from finite interdigital transducer 80−43491
$LiNbO_3$ UHF SAW filters using group-type unidirectional interdigital transducers 78−59252
$LiNbO_3$-Si acoustically-matched surface elastic wave transducer 78−90623
N_2O_4 liquid *(Russian)* 79−59863
Na_2O; SiO_2, use as US transducer bond 79−83437
PVF_2 film transducers, review *(Japanese)* 79−98579
PVF_2 Lamb wave delay line, highly temp. dependent 80−106687
PVF_2 thin film SAW tranducers for 8 MHz delay line 80−58876
$Pb(Z,Ti,Mg,W)O_3$, low-Q ceramics, props. and transducer appl. 80−75944
Si monolithic US transducer array 79−3877
$SrTiO_3$-metal contact, surface barrier Rayleigh wave transducer 79−98578
TeO_2 crystal multichannel acousto-optic modulator 77−39100
YIG, magnetoelastic SAW transducers, approximate theory 79−68533
ZnO, CVD of epitaxial films on sapphire, SAW interdigital transducer fabrication 80−66430
ZnO film concave transducer, for focusing microwave ultrasound 77−7276
ZnO film concave transducers for scanning acoustic microscopes 80−74663
ZnO integrated optical transducer arrays 79−50444
ZnO piezoelectric film US transducers obtained by DC diode sputtering, dielec. breakdown props. 80−40066
ZnO thin-film transducer, bulk wave generation due to nonlinear interaction of SAW 79−42359
$ZnO-SiO_2$-Si SAW device, interface transduction 80−102949

ultrasonic transmission
alabaster, US waves in crack preparation region rel. to seismic waves 77−9405
attenuating materials, transmission time meter with digital readout 77−40485
erythrocyte-rouleaux formation, US detect. by spectral anal. 78−40280
ethylene glycol liquid, hypersonic dispersion and attenuation depend. on sound freq. and viscosity 79−37609
foam, US characts. of open-cell polyurethane foam layers for airborne appls. 80−96597
impedance image reconstruction, reflection and transmission techniques 79−53202
layered composite materials, US transmission spectrum rel. to NDT 77−81357
layered media, US transmission and refl. coeffs. 78−13827
lens transmission variations and interfacial effects 78−59176
liquid-filled crack, Rayleigh wave reflection and transmission calc. 77−32762
liquid-metal interface, surface wave generation by US wave *(French)* 78−18885

ultrasonic transmission continued
liquid-solid-liquid layered media 80−102882
nonlinear layer in linear medium 79−47867
plates immersed in fluid, acoustic transmission theories verified 78−59183
polyethylene glycol liquid, hypersonic dispersion and attenuation; depend. on sound freq. and viscosity 79−37609
resonance splitting in ultrasonic spectroscopy 78−87214
smectic B_A, B_C and E_A liquid cryst., transmission of US shear waves *(French)* 77−51309
tissue, time post-mortem effects 78−28025
tissue characteristics, swept freq. meas. of US attenuation and vel. 78−40278
transkull transmission of axisymm. focused US beams, 0.5 to 1 MHz 80−51184
transmission line of probe for hot metal inspection, spurious signals 80−66754
velocity and damping of ultrasound, in $CHCl_3$ and C_2H_5OH and mixtures of these 80−29120
n-GaP:S, elastic moduli and mode gammas 79−73242
Hg, liq., sound vel. near metal-nonmetal transition, up to 1600°C and 2000 kg/cm^2 80−39222
LiAl(In)(Zn), elastic moduli and Debye temp., US meas. 79−91724
$LiIO_3$, US wave tunnelling across piezoelectric gap 78−87857
NaIn(Tl), elastic moduli and Debye temp., US meas. 79−91724
Ni-Fe films, US generation by ferromag. reson. 78−88155

ultrasonic velocity
see also ultrasonic dispersion
abietic acid, transverse US wave propag., glass and liquid transition region 80−79883
acetic acid, liq., sp. ht. of 2nd relax. step *(German)* 79−37766
acetic acid, vapour, chem. reaction effect on speed of sound 80−103100
acetic acid-acetone mixture, physical parameters 80−2716
acetone-methanol, acetone-CCl_4, methanol-CCl_4 and acetone-methanol-CCl_4 mixtures, acoustic and physicochem. obs. 79−96347
acetonitrile-carbon tetrachloride-n-butanol, mixtures, compressibility, free length, molar and available vol., US meas. 78−2200
acetonitrile-methanol, excess vol. and isentropic compressibility, from density and US vel. meas. 78−79776
acetonitrile-toluene-n-butanol, mixtures, compressibility, free length, molar and available vol., US meas. 78−2200
acrylic gel, US observation of critical behaviour *(French)* 79−29414
adamantane, elastic props., press. depend. rel. to intermol. forces 80−54297
n-alcohols, sound vel. and absorpt. meas. at hypersonic freqs. 78−18708
alkali halides, aq. solns., hypersonic sound vel. and absorpt. meas. 78−30699
alkali metal-ammonia solns., metal-insulator transition, h.f. and u.s. props. 77−1369
aluminates with perovskite struct., elasticity meas. to 6 kbar 77−51428
amine solutions, US analysis method 78−7277
amorphous materials, dielec. and US dispersion at low temps. freq. and temp. depend. 79−95092
amorphous polymers, localised low-energy excitations 79−73322
aniline, under press., determ. of thermodynamic props. *(Japanese)* 77−59068
aniline hydrobromide, ferroelastic, acoustic softening near transition temp. 80−96617
aniline-cyclohexane, hypersound velocity, absorption temp. depend *(Russian)* 80−75303
aniline-phenol, liq., US vel., adiabatic compressibility, H-bonded complex form. 77−35635
p-anisalaminoazobenzene, acoustic relax. in nematic phase 77−1184
aortic wall, canine, speed of 10 MHz sound, effects of temp., storage, formalin soaking 80−56112
aqueous non-electrolytes, solution structure, adiabatic compressibility studies 78−87605
aqueous solutions of acetamide, dimethyl urea, β-alanine interferometric obs. 80−19878
associated liquids, US vel. and absorpt. rel. to hole theory 78−10124
benzene, high press. Brillouin scatt., hypersonic speed 77−48182
benzene, liq., sound velocity between 283 and 463K, up to 62 MPa 79−55827
benzene binary liquid mixtures, US vels. and mol. interaction 77−15494
benzene-acetone-chloroform ternary liq. mixture, US vels. rel. to interactions 77−69044
benzene-ethanol, excess vol. and isentropic compressibility, from density and US vel. meas. 78−79776
benzene-n-heptane, excess vol. and isentropic compressibility, from density and US vel. meas. 78−79776
benzene-tetrahydrofuran, soln., excess thermodynamic props. and interactions, US vel. and density meas. 80−39288
benzene-toluene and benzene-o-xylene mixtures, US vels., compressibility, expsn. coeff. 79−33038
benzyl alcohol-n-butanol, excess vol. and isentropic compressibility, from density and US vel. meas. 78−79776
binary electrolyte solns. thermodynamics using US props. 78−73946
binary liquid mixture, energy of vaporisation evaluation 80−65209
binary liquid mixtures, US props., molecular interaction between components 78−63657
biological tissue, dependence on constituent proteins 80−61621
blood, canine, US attenuation and speed, rel. to packed cell vol., 37°C 80−41106
blood, during tumour development in exptl. animals 77−25524
blood, US propag., effects of red cell shape and orientation 78−24104
bone, cancellous, US attenuation and dispersion 80−51149
bone, human cortical, US properties and microtexture 80−51144
bone, surface wave propag. 78−44578
bovine blood vessel walls 78−85333
brain, normal and abnormal, attenuation, vel. and impedance 80−45955
brass, elastic constants, third order, from US velocity meas. 78−76687
brass, meas. method for isotropic nondispersive solids 80−69616
bromobenzene + m-xylene, US vel. and adiabatic compressibility 78−51614
butanol-methylethyl ketone, soln., excess thermodynamic props. and interactions, US vel. and density meas. 80−39288
t-butyl alcohol, aq. soln. 80−88237
n-butyl alcohol, dil. aq. soln., US vel., 4.04 MHz 78−67770
carbon tetrachloride, liq. and plastic cryst. phases, thermodynamic props., light scatt., US propag. 78−2863

ultrasonic velocity continued
carbon tetrachloride, US vel., 265-435K 80−6464
chalcohalide glasses of Ge-As-S-I system, acousto-optical parameters 77−36199
o-chloroaniline-iso-octane critical system, US absorpt. and vel. meas. 77−51440
chlorobenzene, liq., vibr. relax., Brillouin scatt. and US vel. meas. 79−77692
cholesteric liquid crystal, mag. aligned, anisotropic US propag. 78−42895
cholesteric liquid crystal, temp. depend. 77−11637
cinnamyldehyde, rotational isomerism study by US absorpt. and vel. meas. 77−27196
collagen effect on US propagation in tissue 78−61212
composite materials, scatt. coeff. and uel. dispersion 79−86844
composites, random particulate, US wave propagation, velocity as function of frequency and volume fraction of inclusions 80−59583
compressible liquid flow with heat transfer 79−14131
computerised tomography, var. of acoustic speed with temp. in excised human tissues 80−51150
concrete, ultrasonic wave velocities and density, calc. and meas. 79−52545
concrete, US wave propag. and microcracking *(French)* 80−39225
crotonaldehyde, rotational isomerism study by US absorpt. and vel. meas. 77−27196
cryogenic binary mixture, ultrasonic velocity, compressibility, heat capacity, at 298.15K 79−10898
cubic crystal orientation determ. from meas. sound vels. 79−55691
cubic crystals, US vels. rel. to third-order elastic consts. meas. 77−80566
cubic single crystal misorientation angle determ. by US speed meas. 80−54315
cubic single crystals, rapid crystallographic orientation determ. method using US vel. anisotropy 78−6027
cyclic carbonates, supercooled liqs., dielec., acoustic, NMR, viscoelastic relax. props. 77−1609
cyclohexanal, liq., viscoelastic and structural relax., US rel. and absorption meas. 78−26634
cyclohexane, under press., determ. of thermodynamic props. *(Japanese)* 77−59068
cyclohexane, US absorption and vel. meas. 77−51450
cyclohexane-acetone-butanol ternary liq. mixture, US vels. rel. to interactions 77−69044
cyclohexane-acetone-ethanol ternary liq. mixture, US vels. rel. to interactions 77−69044
cyclohexane-benzene-carbon tetrachloride ternary liq. mixture, US vels. rel. to interactions 77−69044
cyclohexanol, orientationally disordered phase, Brillouin scatt. study 80−93351
DC Bi:Te, elastic consts., electronic contrib. 77−84826
di-n-decyl azoxy methyl cinnamate, smectic-A liq. cryst., anisotropic US propag. 79−55829
dibenzyl, diphenyl, near melting point 78−6127
dicalcium strontium propionate, elastic stiffness consts., determ. in US freq. region 79−37752
dichlorodifluoromethane, US vels. and absorption coeffs., determ. of relaxation times 78−63530
dichloromethane-cyclohexane, liq. mixture, intermol. vibrational energy transfer, US study 80−70313
dioxan(-oxalic acid)(-benzoic acid), solns., compressibility, internal press., US vol., H-bonding 79−82272
dioxan-acetone, dioxan-chloroform mixtures, US props., molecular interaction between components 78−63657
dioxan-cyclohexane-chloroform, mixtures, compressibility, free length, molar and available vol., US meas. 78−2200
dioxan-methanol system, US vel., compressibility, complex form. 79−82283
p-dioxane, aq. soln., excess molar heat capacities, 298.15K, US vel. obs. 80−6523
dioxane-alcohol mixtures, US vel. behaviour with dioxane conc. 79−73254
elastic constant determ. for low trigonal symmetry cryst. 78−2187
elastic waves in crystals, invariance relations 80−84250
electrolyte, aq. soln., US vel., ionic drift depend. 79−19327
electrolytic aqueous solution, US study of apparent molar compressibility 78−10125
electrolytic solution, ionic drift from 50 Hz supply, pulse echo technique 80−70314
Epon 828-Z, acoustical determ. of shear relax. functions 78−76686
epoxy material, filled, US props. for sonar transducers 78−59867
ethanol-H_2O mixture, liq. and solid, US vel., −80 to 20°C, 1-5 MHz 78−59933
ethyl alcohol, dil. aq. soln., US vel., 4.04 MHz 78−67770
ethyl lactate, sound vel. and absorpt. meas. at hypersonic freqs. 78−18708
exam. of glass forming region, properties and crystallisation 78−88454
ferroelectrics, structural phase transitions, ultrasonic velocity and attenuation meas. 80−75977
ferrofluid, US vel. anisotropy in mag. field 78−68344
ferromagnet, itinerant electron, magnetoelastic contribs. to US vel., elastic consts., and susceptibility 80−75829
fibre reinforced composite, containing voids, elastic consts. and US velocity, theory 77−89498
fibre reinforced composite, ultrasonic vibrs. propagation velocity, dependence on composites elastic props. 80−5975
filled polymers, cumulative internal damage, US assessment 79−57180
first order displacive transformations, localized soft modes and US effects 79−73281
fluorobenzene, liq., vibr. relax., Brillouin scatt. obs. 79−51206
freons of methane series, US vel. rel. to vibr. relaxation 77−39397
furan, liq., US phase vel. decay in space and time 80−99891
furan, liq., US relax., light scatt. meas. 77−77231
furan-cyclohexane, liq. mixture, intermol. vibrational energy transfer, US study 80−70313
glass filled solids, ultrasonic absorpt., scatt., velocity and attenuation 80−44262
glass prisms, vel. meas. by pulse technique and propag. theory 79−18636
glass with frozen structure, viscous flow, valence configuration flow theory 80−39335
glass-ceramic, machinable, elastic const. temp. depend. 80−79852
glasses, acoustic and dielec. props. at low temps., review 78−6128
glasses, US props., review 77−69048

ultrasonic velocity continued
graphite fibre reinforced epoxy, US attenuation as an indicator of fatigue life 80−85118
heavy lanthanide perchlorator, aq. solns., US vel. and solvation numbers meas. 79−19319
n-heptane-nitrobenzene, US study of crit. mixing 78−75732
n-hexadecane-β,β'-dichlordiethyl ether exfoliating mixture, light scatt. and hypersound vel. 77−28586
n-hexane, superheated liq., US wave vel., adiabatic compressibility, heat capacity 78−2198
n-hexane-perfluoro-n-hexane mixtures, US vel. and absorpt. mixtures 80−88281
HOBA, isotropic phase, Brillouin scatt. spectra, hypersound data determ. 79−91453
inert gases, speed of ultrasound at 298-15K *(French)* 79−82027
insulators, high-intensity US wave vel., phonon-phonon interaction effects 80−70323
invariance relations for acoustic waves in cryst. deformed by hydrostatic press. 79−95087
isobutyric acid-water, crit. mixture, conc. fluctuation mean relax. time, US absorpt. and vel. meas 80−29163
isopropanol-n-propanol aq. mixtures, US relax., US absorpt. and vel. meas. *(French)* 80−103426
kaersutite, sound vels. and anisotropy, rel. to upper mantle seismic struct. 80−26501
kerosene-base mag. fluid, sound vel. meas. 77−63969
Kneser liquids, vibrational energy exchange probabilities 78−38780
liquid, Rao's acoustical constant, temp. depend., from C_1-parameter 80−6462
liquid, US vel. determ. using optical diffr. by short acoustic pulses, for teaching 79−62963
liquid binary mixtures of organic chemicals, excess internal pressure and Van der Waals' constant, Flory's theory 80−70310
liquid crystal, smectic A and isotropic phases, Brillouin scatt., hypersound vel. and attenuation determ. 77−8591
liquid metals, Debye temp. determ. from US vels. and thermodynamic data 79−99289
liquid mixtures, binary, hydrogen bond interactions 80−79881
liquid n-H_2, n-D_2, Ne mixtures, deviation from Rao-Wada rule 78−75729
liquids, hole theory rel. to US propag. 78−38775
liquids, repulsive exponent, Rao's and Kuczera's relations 80−79878
magnetic crystal, sound velocity temp. depend. anomaly 77−72891
magnetoelastic SAW velocity on magnetised ferrite substrate, non-reciprocity 80−80587
mammalian tissues, US vel. and atten. 78−57044
MBBA, isotropic phase, Brillouin scatt. spectra, hypersound data determ. 79−91453
MBBA, US propag., nonlinear effects 77−59069
MBBA/EBBA binary liquid crystal mixture, US absorpt. and vel. dispersion, phase transition and alignment effects *(Korean)* 80−29121
metal, degree of deform. effect on thermophys. props. at high temps. 78−26694
metal, FCC, dislocation behaviour at high strain rates, US detection method, data analysis basis 80−85136
metal, US velocity, effects of deform. and high temps. 78−26626
metal nitrates, molten mixtures, US vel., thermodynamic interpretation *(French)* 78−79670
metal specimen, ultrasonic technique for stress anal. 78−64790
metallic glass, phonon transport below 100K 78−14422
metals, strain, US characts., meas. apparatus 78−60898
methane, liquid, Brillouin scatt. obs., US vel. and absorpt. 80−45085
methane(-d_4), liq., Brillouin scatt. and refr. index measurements 80−76035
methane-d_4, solid, sound velocity meas., 4-77K 78−75734
methanol-nitrobenzene-iso-octane, US vel. and absorpt., along line of plait points in ternary liq. 78−79669
methyl alcohol, dil. aq. soln., US vel., 4.04 MHz 78−67770
β-methyl-butyl-methoxybenzylidene amino cinnamate, smectic-B liq. cryst., US attenuation anisotropy 79−55828
methylene chloride-cyclohexanol system, sound vel. and acoustic loss coeff. 77−51450
methylethyl ketone-butanol, soln., excess thermodynamic props. and interactions, US vel. and density meas. 80−39288
3-methylpentane-nitroethane critical binary liquid mixture, US absorpt. 80−107376
2-methylpyridine+D_2O, p-T-X miscibility dome critical point, US vel. meas. 77−27979
methylpyridines, propag. vel. and attenuation coeff. as functions of temp. 79−14886
microemulsion, sound velocity and absorption 80−81374
microwave phonon attenuation in quartz at low temperatures 79−19324
mixtures and suspensions, flow rate meas., ultrasound propagation and scatt. approach 80−43806
molten salt mixtures, binary, excess thermodynamic props. and US vel. *(French)* 77−27943
monochlorodifluoromethane, US vels. and absorption coeffs., determ. of relaxation times 78−63530
myocardium, acoustic microscopic anal. 80−45995
β-Na_2O-Al_2O_3 low temp. ultrasonic vel. meas., temp. depend. 80−79885
nematic liquid crystal, acoustic attenuation anomaly above clearing point 78−75816
nematic liquid crystal, isotropic phase, light scatt., ultrasonic vel. and absorpt. meas. 78−48189
nitrobenzene-aniline, US vel., sp. ht. and compressibility 79−33037
nitrobenzene-n-heptane, crit. mixture, conc. fluctuation mean relax. time, US absorpt. and vel. meas 80−29163
nitrobenzol-n-hexane, hypersound velocity, absorption temp. depend *(Russian)* 80−75303
nitroethane-isoctane, crit. mixture, conc. fluctuation mean relax. time, US absorpt. and vel. meas 80−29163
nylon 6, stress depend. of US velocity *(Japanese)* 78−26629
optical glasses, Brillouin scattering meas., sound vels., Pockels coeffs., phonon damping 79−95792
organic binary liquid mixtures, US vel. rel. to non-ideal behaviour 78−95109
organic liquid mixtures, excess free vol. US vel. meas. 77−51294
organic polar liquids, US sound vel. meas. 78−87742
organic ternary liquid systems, intermolecular interaction, US vel. meas. 80−79879

ultrasonic velocity continued
organosilicon ladder polymer, vel. meas. of longitudinal and shear US waves 78−95114
orthoferrites near spin-flip temp., magnetoelastic waves 78−19301
PAA, isotropic phase, Brillouin scatt. spectra, hypersound data determ. 79−91453
PAA, nematic liq. cryst., effect of magnetic field on US vel. and absorpt. 78−18707
PAA, nematic-isotropic phase transition, US meas. 79−90761
permafrost, US vels. and elec. props. 77−78157
PET fibre, molecular orientation determ. by US propag. velocity 77−58961
phase transition with valency change, sound vel. renormalisation *(Russian)* 78−79963
phenol-aniline (quinoline) (pyridine), liq., US vel., adiabatic compressibility, H-bonded complex form. 77−35635
piezoelectric nondegenerate semicond., magnetoacoustic effects of nonparabolic band struct. 80−96948
piezoelectric SAW velocity rel. to uniaxial biasing stresses 77−27416
piezoelectric substrate, small SAW attenuations and vel. variations 79−86281
piezoelectric substrate coated with admittance films, attenuation and vel. of surface waves 79−98540
plane wave reflectivity from water-metal interface, stress effect 79−81586
PMMA, acoustical determ. of shear relax. functions 78−76686
PMMA, low-energy excitations and hypersonic props., Brillouin scatt. meas., 1.7 to 15K 77−90160
PMMA, oriented, hypersound propag., elastic props. 78−75737
poly(4-methyl pentene-1), US props., glass transition, Gruneisen parameters 80−54316
poly(4-methyl-1-pentene), semicrystalline, bulk and film, hypersonic vel., temp. depend. 79−42982
poly(alkyl methocrylates), US determ. of relax. 77−51449
poly-4-methylpentene-1, elastic parameters, US velocity meas. at 2.1-240K 80−40415
polyalkanimide, US vel. and absorpt. at liquid He temps. 78−51619
polyamide fibre, chain-segment orientation, US vel. meas., humidity effects *(German)* 78−75590
polycarbonate, amorphous US vels. from Brillouin scatt., room temp. to 250°C 79−91454
polycarbonate films, amorphous and crystalline, temp. depend. of US vel. 78−91575
polycrystal of orthorhombic symmetry, US scatt. and vel. determ. 77−84848
polydimethylsiloxane networks, high freq. US absorpt. rel. to crosslink density, α-relaxation 79−95091
polydimethylsiloxane oligomers, Brillouin scatt. obs. of hypersonic sound speed and loss, mol. wt. depend. 79−91457
polyesterimides, solns., ultrasonic vel. and Rao formulism 80−103422
polyethylene, glass filled solids, ultrasonic absorpt., scatt., velocity and attenuation 80−44262
polyethylene, high press. phase, US, DTA, and X-ray diffr. study 80−75188
polyethylene glycol solns., US studies 77−72655
polymer films, Brillouin scatt. at transitions 80−70312
polymers, filled, cumulative internal damage, US assessment 80−97653
polymers in soln., mean mol. wt. determ. from attenuation and velocity meas. *(German)* 77−54641
polypropylene, drawn fibres, SEM and US study 78−47249
polystyrene, US propag. at low temp. 79−55834
polystyrene solution, differential meas. of ultrasonic velocity *(French)* 80−75302
polyurethane, foaming parameters determ. from US wave vel. 80−71885
polyvalent electrolyte apparent molal adiabatic compressibility and US vel. obs. 78−61028
porous ceramics, longitudinal US wave velocity 77−55323
porous medium, US bulk compressional wave obs. 80−64235
propagation in austenitic stainless steel weld metal, effect of anisotropy 80−45452
n-propanol mixtures, US vel. depend. on association compounds 79−60436
n-propyl alcohol, dil. aq. soln., US vel., 4.04 MHz 78−67770
propylene, liquid, sound vel. and absorpt. rel. to libration transitions 78−2203
quartz, crystal growth in fluoride environment, growth features and props. 80−6373
quartz, fused, second press. derivatives of elastic moduli, US vel. meas. 79−23670
quartz, synthetic piezoelectric, US vel. meas. rel. to elastic characts. 78−6638
quartz plate, X-cut, US vel. meas. via phase shift freq. depend. 77−14866
quartz SAW velocity/temperature dependence calc. 79−56062
rare earth Co Laves phase cmpds., elastic props. rel. to temp., mag. field 79−51834
rare earth metals, elastic props., connection with electron struct. *(Russian)* 80−19895
rare earth metals, thermodynamic props. determ. form US vel. meas. 78−55912
rare earth-Fe alloys, magnetostrictive, elastic props. 78−84469
rare earth-iron alloys, elastic vs. magnetoelastic anisotropy 78−68347
raw kaolin, acoustical investigations of the effect of additives on elastic props. 80−66559
Rochelle salt, polarisation relaxation, US vel. and attenuation meas. 77−28512
rocks, US pulse transit times, simultaneous stress and strain monitoring 77−91046
rubber, US vel. in 25-150 kHz range 77−31726
sample chamber for ultrasonic vels. and elastic consts. meas. *(German)* 78−46868
in sandstone, stress and size-depend. sonic vel. 77−9417
sandstone elastic wave velocity, function of moisture content 80−56459
tris-sarcosine calcium chloride, elastic props., US damping 80−84229
SAW, phase velocities on solid-liquid boundary 78−83151
SAW propagation in admittance sheet deposited on piezoelectric substrate 77−80689
Schaaffs' molecular-kinetic theory of propag. in liquids, temp. and pressure changes of 'collision factor' 80−19143
sea ice, US vel. meas. 77−33094
ultrasonic velocity continued
silicate glasses, low-energy excitations and hypersonic props., Brillouin spectra meas., 1.7 to 15K 77−90160
simple fluid near crit. point, homogeneous phase sp. ht. at const. vol. 78−71832
sintered materials, relationship between vel. and density 78−53173
smectic liquid crystals, acoustic props., US velocity and anisotropy in mag. fields *(Russian)* 79−90547
Solenhofen limestone, US propag. at high press. 79−29756
squaric acid, struct. transition, US vel. meas. 78−79770
squaric acid, structural phase transition, US vel. meas. as function of temp. below and above T_c 79−14927
stannates with perovskite struct., elasticity meas. to 6 kbar 77−51428
steel, austenitic stainless, Mn alloy, sound vel. anomalies near spin glass transition 79−82795
steel, C, stress depend. of US velocity *(Japanese)* 78−26629
steel, C, US exam. of yield and breaking strength 79−15755
steel, cold worked layer of used railroad rail, Rayleigh wave dispersion 79−1014
steel, meas. method for isotropic nondispersive solids 80−69616
steel, sheet, cold-rolled, US inspection for mech. prop. anisotropy 78−23750
steel, stainless austenitic welds, time domain approach to crack location and sizing 80−50781
steel, stainless type 304, elastic const. variability, US vel. meas. 80−55446
steel, tool, US vel. meas., 20-900°C 80−70318
steel, US critical angle reflectivity, near-surface metallic prop. gradient effect 80−70516
steel cone, phase velocity of longit. impact wave *(Japanese)* 78−9600
steel railway line, acoustoelastic and third-order elastic constants meas. 77−4798
stishovite, polycrystalline, US vels. and elasticity 77−5189
stressed anisotropic solid, Rayleigh wave vel., third-order elastic constants 77−11772
styrene-butadiene-styrene triblock copolymer, US relax. 77−89502
terephthal-bis-p-p'-butylaniline, pretransitional anomaly, US obs. 78−75818
ternary liquid mixtures, molecular interaction and thermodynamic props. 78−59861
ternary liquid mixtures, nonlinear effects with high amplitude US prop. 78−51613
ternary liquid mixtures, physical props., determ. by density and US vol. meas. 79−37751
tetracosane melt, Brillouin spectroscopy obs. of struct., 65-250°C 79−55642
tetrahydrofuran-benzene, soln., excess thermodynamic props. and interactions, US vel. and density meas. 80−39288
tetramethylammonium tetrachlorozincate, incommensurate phase transition, US propag. meas. 79−91382
TGS, admixed with nitroanilines or L-alanine, US vel. and absorpt., ferroelec. transition 77−32333
TGS, paraelec. phase, elastic and thermoelastic consts. 77−47503
TGS, perfect and imperfect, sp. ht. and sound vel., crit. anomalies 80−71331
TGS, pure and nitroaniline-admixtured, longit. US wave propag., domain struct. effects 77−55322
TGS, sound group vel. vector direction, temp. depend. 78−67774
TGS, US propag. and vel. rel. to growth defects 79−28049
TGS, US relax., just above T_c, velocity and attenuation coeffs. 77−35637
TGS, US vel. and absorpt. in ferroelec. transition region 77−66461
TGSe, acoustic and thermal anomaly correlation near ferroelec. transition 79−4775
TGSe, cryst., US vel., crit anomaly and electromech. effects 79−55832
TGSe, US vel. and absorpt. in ferroelec. transition region 77−66461
TGSe, US velocity and absorpt., 10 MHz, crit. anomalies 77−15504
thermoelastic material, deformed isotropic, thermal effect on propag. vels. 80−33276
thermometer using sound velocity in air, cct. and operation *(French)* 79−35739
1,2,5-thiadiazole, liq., light scatt. from orientational and density fluctuations, hypersonic vel. 77−81110
tissue, freshly excited, from rat, freq. depend. 77−86573
tissue, mammalian, survey of US vel. and attenuation data 80−46744
tissue, mammalian, US attenuation and speed determ. as function of temp. 80−41108
tissue, soft, temp. depend., rel. to temp. distrib. monitoring 80−45994
tissue analysis, two-beam thermo-acoustic sensing technique 77−40716
tissue characterisation by attenuation, absorption, and velocity 77−64106
tissue characteristics, swept freq. meas. of US attenuation and vel. 78−40278
tissue US parameters, quantitative cross-sectional imaging 79−53277
tissues, fixed and unfixed, US propagation, backscattering coeffs. and speech determ. 80−41109
titanates with perovskite struct., elasticity meas. to 6 kbar 77−51428
tourmaline, elastic consts. by US phase-comparison method 80−2108
triethylamine-H_2O, crit. phenomena, US vel. and absorpt. 78−91382
tris-sarcosine calcium chloride, ferroelec., US attenuation and vel., elastic consts., and permitt. near Curie temp. 79−37761
TTF-TCNQ, sound vel. in a a dand b directions, 0-300K 77−84851
US velocity in crit. region water 80−59582
US velocity rel. to mineral content 80−45962
vinyl chloride suspension polymerisation monitoring by US attenuation and velocity 79−70328
water, calc. based on Brownian motion theory and counteracting molecular forces, 25 to 80°C 80−88265
water, hypersound phase vel. and damping by high resolution Brillouin spectroscopy 77−69845
water, mag. treatment affecting props., proposed mechanism 78−84827
water, metastable liquid, US vel. under atmospheric press. 79−10897
water, Rayleigh-Brillouin scattering and compressibility 79−91455
water, speed determ. over wide range of pressure and temp. 80−23821
water, supercooled, Brillouin scatt. 78−43884
water, supercooled, sound vel. dispersion, struct. relax. effect, Brillouin scatt. obs. 80−107375
water, supercooled, US vel. and attenuation *(French)* 79−90730
water, supercooled to −33°C, sound vel. determ. by acoustic levitation method 80−88269
water, superheated, ordinary, heavy, US velocities, thermodynamic props. 80−65156

ultrasonic velocity continued
water, thermodynamic props. at high pressures from US vel. 79−94474
water, US vel. meas. by Brillouin scatt., supercooled to boiling range 77−15495
water and saturated monatomic alcohol mixtures, effects of chlorides on struct. 79−86840
water supercooled, hypersonic sound vel., thermodynamic interpretation 78−59860
water-2-propanol, density, US vel. meas. 78−18529
water-dioxane mixtures, compressibility, density, US vel. rel. to temp., conc., struct. *(German)* 77−43263
water-ethanol(methanol) mixtures, nonlinear acoustic coeff. meas., 0-50°C *(French)* 80−34142
water-urea-valeric acid systems, sound vel. and liquid structure *(Japanese)* 77−1177
Wigner crystal, long-wavelength excitations in strong mag. fields 79−82533
Zerodur, glass-ceramic, thermoelastic props. 78−27550
Ag film, damping and vel. of longit. elastic waves at 9.4 GHz 80−10596
Ag_3AsS_3, US absorpt. and vel., 4.2-100K 77−24361
AgBr-AgCl mixed crystal, elastic consts., temp. and press. derivatives 77−11620
Ag_2HgI_4, order-disorder transform. at 51°C, sound vels. and dielec. losses 78−10129
$AgNO_3$, molten, Brillouin scatt., hypersonic absorption and vel. meas. 77−8592
Ag_3SbS_4, dielec. and acoustic props. *(German)* 78−64335
Ag_3SbS_4, electron absorption and dispersion of ultrasound velocity 80−15197
Al alloy A3B2, stress depend. of US velocity *(Japanese)* 78−26629
Al film on α-quartz, SAW velocity/temp. dependence 77−31861
Al, high-temp. US vels. rel. to validity of Nernst-Lindemann eqn. 77−72695
Al, meas. method for isotropic nondispersive solids 80−69616
Al, US scatt. and vel. determ. 77−84848
Al, US velocity, anomalous response to applied stress 78−63811
Al, US velocity, depend. of applied stress and third order elastic const. *(Japanese)* 79−29124
Al, US velocity, temp. depend., stress effects 80−75307
Al-Mg, elastic and anelastic props. in relation to Guinier-Preston zones, US investigation *(French)* 79−38833
Al-Mg, single crystal elastic consts., ultrasonic meas. during ageing 78−11263
Al-Mg solid solns., decomposition studied by ultrasonic meas. of elastic props. 80−35184
Al_2Cu crystal, Young's modulus, Poisson ratio, elastic consts. determ. by extensometry and US meas., anisotropy discussion *(French)* 79−50683
Al_2O_3-epoxy mixture, acoustic wave velocity and attenuation meas. 79−42151
β-Al_2O_3-Na_2O, non-stoichiometric, amorphous, US attenuation and velocity 80−39228
$Al(PO_3)_3$-LiF system glasses, microhardness and US vel. 79−99274
$Al(PO_3)_3$-NaF system glasses, microhardness and US vel. 79−99274
$AlPO_4$, berlinite, piezoelectric coupling for SAW applications 79−56055
α-$AlPO_4$, berlinite, SAW velocity and piezoelec. coupling obs. 79−56056
$Al_2(SO_4)_3$ soln., adiabatic and apparent molal compressibility determ. from US vel. meas. 78−63797
AlSb, molten, temp. depend. of vel. of sound and adiabatic compressibility 77−27944
Ar, US vels. and absorption coeffs., determ. of relaxation times 78−63530
Ar-monochlorodifluoromethane mixture, US vels. and absorption coeffs., determ. of relaxation times 78−63530
As, amorphous, US attenuation and sound vel. meas., 4.2 to 300K; 80−49308
a-As, second and third order elastic consts., ultrasonic velocity meas. 80−103408
As-Ge-Se and As-Ge-Se-Sb glasses, US vels. and acousto-optic props. 77−27327
As_2Ge_2SeTe, semiconducting glass, elastic props., US vel. meas. 78−26628
$As_2Ge_3T_{15}$, semiconducting glass, elastic props., US vel. meas. 78−26628
AsGeTe, semiconducting glass, elastic props., US vel. meas. 78−26628
As_2S_3, amorphous, acousto-induced struct. change, Brillouin scatt. meas. 79−27928
As_2S_3, amorphous, low temp. US meas., two-level systems role 78−30703
As_2S_3, amorphous, ultrasonic velocity, 1.5 to 296K 79−37764
As_2S_3, determination of stoichiometric discontinuity, using US velocity 79−5242
As_2S_3, semiconducting glass, elastic props., US vel. meas. 78−26628
As_2S_3:Ag, amorphous US props. 78−51616
$As_2S_3(Se_3)$ glasses, elastic moduli, hydrostatic press. effect, US wave vel. meas. 80−34115
As_2Se_3, amorphous, ultrasonic velocity, 1.5 to 296K 79−37764
As_2Se_3 glass, mech. props. var. due to high press. phase change 77−76481
As_2Se_3, semiconducting glass, elastic props., US vel. meas. 78−26628
As_2Se_3:Ag, amorphous, US props. 78−51616
Au film, damping and vel. of longit. elastic waves at 9.4 GHz 80−10596
Au film on α-quartz, SAW velocity/temp. dependence 77−31861
Au-Cd (47.5 at.%), single cryst., temp. and press. derivatives of elastic consts. near transform., US meas. 77−63667
Au-Co alloys, molten, compressibility and partial struct. factors determ. 77−69045
Au-Co melts, struct., compressibility, X-ray and neutron diffr. 77−11614
B fibre reinforced Al, orthotropic elastic stiffness consts., US vel. meas. 80−49289
B_2O_3, amorphous, acoustic props. at 20 GHz, Brillouin scatt., 3-300K 80−24536
Ba, elastic properties, Debye temp., 20°C, 20 to 70 kbar, US wave velocity meas. 78−87735
Ba I-Ba II phase boundary, Ba I fusion curve peak at high press. *(Russian)* 80−2165
$Ba_{0.92}Ca_{0.08}TiO_3$ ceramic, uniaxial stress effects, US dilatometric and dielec. meas. 78−52454
BaF_2, fluorite-struct. compound, high-temp. elasticity, US pulse meas. 77−81878
$BaMnF_4$, phase transitions review 79−78378
$BaMnF_4$, spectroscopy near ferroelec. transition, dielec. anomalies near mag. ordering temp. 80−75965
ultrasonic velocity continued
$Ba(NO_3)_2$, press. derivatives of elastic-moduli, ultrasonic velocity meas. 78−95102
BaO-La_2O_3-GeO_2, exam. of glass forming region, properties and crystallisation 78−88454
BaO-P_2O_5, glass, US velocity rel. to elastic props. 80−103425
$BaTiO_3$, isotropic dielectric, US vel. and longit. elec. field *(Russian)* 78−38785
$BaTiO_3$, logarithmic velocity variations for longitudinal US waves near ferroelec. transition 78−72472
$BaVS_3$, polycrystalline, elastic behaviour, 40 to 350K 79−60498
BeO ceramic, US vels. rel. to appl. as material for delay lines 77−51447
Bi, liq., US vel. and thermophysical props. meas., 500-1000K 78−38778
Bi, US velocity, renormalisation in mag. field 77−59246
Bi:Sn(Pb)(Sb)(Te) polycrystal elastic constants for US velocity obs. 79−69180
$Bi_{12}GeO_{20}$, third-order elastic moduli determ., US vel. meas. 80−65121
$Bi_{12}SiO_{20}$, third-order elastic moduli determ., US vel. meas. 80−65121
C, vitreous, low temp. sp. ht., thermal cond. and US vel. meas. 78−47533
$CHCl_3$ and C_2H_5OH and mixtures, velocity and damping of ultrasound 80−29120
CO, liquid, Brillouin scatt. obs., US vel. and absorpt. 80−45085
CaF_2, fluorite-struct. compound, high-temp. elasticity, US pulse meas. 77−81878
$CaGeO_3$ perovskite, elasticity meas. to 6 kbar 77−51428
CaO, elastic moduli, pressure and temp. derivs. 77−62577
CaO-P_2O_5, glass, US velocity rel. to elastic props. 80−103425
Cd, Fermi surface, strain depend., from US vel. oscills. 78−84133
Cd, liq., US vel. and thermophysical props. meas., 500-1000K 78−38778
Cd-Bi, liq., US vel. and thermophysical props. meas., 500-1000K 78−38778
Cd-$CdCl_2(Br_2)(I_2)$ molten solution, US velocity and compressibility 77−84844
$CdCl_2$-NaCl, KCl molten salt mixtures, US velocity and adiabatic compressibility obs. 78−75730
CdF_2, ionic conducting fluoride fluorite, US velocity meas. 80−107381
$Cd_6Ge_3As_4$, semiconducting glass, elastic props., US vel. meas. 78−26628
$Cd_xHg_{1-x}Se$, phase transition and elastic consts., US vel. study 80−75354
$Cd_3P_{2-x}As_x$ solid soln., US wave prop. velocity, composition depend. 77−20013
$Cd_{3-x}Zn_xAs_2$ solid soln., US wave prop. velocity, composition depend. 77−20013
Ce, elastic properties up to 84 kbar, US vel. meas. *(Russian)* 79−60434
$CeH_{1.98}$, $CeH_{2.98}$, elastic props. at high press. 77−84825
$Ce_2(SO_4)_3$ soln., adiabatic and apparent molal compressibility determ. from US vel. meas. 78−63797
CoF_2, elastic constant determ. by US pulse echo overlap 79−14874
Cr, antiferromagnetic, polarisation domain effects on US velocity 78−52329
Cr film, damping and vel. of longit. elastic waves at 9.4 GHz 80−10596
Cr, US velocity and damping in Neel temp. range, thermocyclic treatment effect *(Russian)* 79−91282
Cr_2O_3, elastic consts., distance depend. of mag. interactions, US vel. meas. 77−4539
$CsCdF_3$, nonlinear elastic behaviour, US velocity, 1 bar-3 kbar 78−59851
CsH_2AsO_4, elastic props., photoelasticity near ferroelectric phase transition 80−29107
CsH_2AsO_4, Mandelstam-Brillouin spectra and US vel. meas. near ferroelec. Curie point 79−38553
$CsMnCl_3.2H_2O$, diagonal elastic const., thermal expansion coeffs., ultrasonic velocity meas. 80−79853
$CsNO_3$, molten, Brillouin spectra, 420-520°C, hypersonic vel. and sound absorption freq. depend. 77−28589
$CsPbBr_3$, US vel. around successive phase transition points 77−80581
$CsPbCl_3$, O_h^1-D^5_{4h} transition, US and thermodynamic props. 78−67826
Cu film, damping and vel. of longit. elastic waves at 9.4 GHz 80−10596
Cu, HF ultrasound, viscous and relax. components of dislocation attenuation 80−15196
Cu, stress depend. of US velocity *(Japanese)* 78−26629
Cu, US velocity, depend. of applied stress and third order elastic const. *(Japanese)* 79−29124
Cu, US velocity, temp. depend., stress effects 80−75307
Cu, ultrasonic velocity meas., mag. field depend. 78−19104
Cu, ultrasonic velocity response to stepwise change of stress *(Japanese)* 79−38905
Cu-Mn, spin glass, US meas. of crit. exponent α′ 79−78384
Cu-Mn alloy, spin-glass, US exam. 78−68351
β-Cu-Zn-Al, US elastic const. meas. near martensitic transform. temp. 78−39827
Cu-Zn-Al martensite, β-phase, single cryst., elastic waves behaviour as function of temp. 79−55807
n-D_2, fluid, eqn. of state from P-V-T and US vel. meas. up to 20 kbar 78−63837
D_2, liq., 22-35K *(Russian)* 78−75731
D_2O-H_2O mixtures, US vel. at 298.15K, adiabatic compressibility 78−10127
$DyFe_2$, amorphous, mag. struct., US meas. 79−99683
$DyFe_2$, amorphous, ultrasonic exam. below T_c 79−73793
$ErFeO_3$, sound velocity meas. at high press., spin-reorientation transition 78−76254
Fe, cast, with uniaxial loading, changes in ultrasonic waves vel. and attenuation 79−15756
Fe, elastic consts. and mech. losses at elevated temps., α-γ transition anomaly 78−75830
Fe-Ni, sintered, porosity determ. by US attenuation and sound vel. meas. *(German)* 80−76437
Fe-rare earth alloys, amorphous, magnetoelasticity and moment rot., US vel. calc. and neutron scatt. meas. 80−65992
Fe-Si, 6.3-25 at.% Si, single crysts., adiabatic elastic consts., room temp. US pulse echo meas. 77−48467
$Fe^{2+}Fe_{0.2}{}^{3+}Cr_{1.8}{}^{3+}O_4$, acoustic props. rel. to cooperative Jahn Teller effect and structural phase transform 80−24538
$(Fe_{1-x}Mn_x)Si$, rel. to mag. struct. and phase transforms *(Russian)* 77−47976
$Fe_{80}P_{13}C_7$, amorphous ferromag. ribbons, US rel. meas. 77−80582
$Fe_{75}Si_{15}B_{10}$, amorphous ferromag. ribbons, US rel. meas. 77−80582
Fe_2TiO_5, anisotropic spin glass behaviour 79−99707

ultrasonic velocity continued
Fe_2TiO_5, anisotropic spin glass type behaviour 80−60296
Ga, liq., Brillouin scatt. obs., vel. of sound determ. 77−24858
Ga-Sn alloys, compressibility, US velocity meas. *(Russian)* 77−59060
Ga-Te alloys, liq., compressibility and US velocity meas. 77−51426
GaSb, molten, temp. depend. of vel. of sound and adiabatic compressibility 77−27944
Ge film, amorphous, LF vel. of sound for Young's modulus mode 77−35636
Ge, pure and n-type, US velocity and attenuation, second and third order elastic moduli 80−70325
Ge-Al (1.15 wt.%), US wave vel. meas. for anal. of solid soln. breakup 78−23887
Ge-As-Se glasses, elastic moduli, US vel. and reson. freq. meas. 78−23756
Ge-Ga (1.13 wt.%), US wave vel. meas. for anal. of solid soln. breakup 78−23887
Ge-Se glass, elastic props. under press., US interferometry 78−79658
GeS_2 glass, temp. and press. depend. of elastic props. 77−15476
H_2, liq., 18.25-32.38K *(Russian)* 78−75731
H_2, liquid, US vel. and intermol. interactions *(Russian)* 79−65144
$HClO_4$, aq. soln., anomalous u.s. props. 77−1176
He-Ar(Xe) mixtures, US vel. meas., phase separation 79−27738
^{3}He, liquid, fluctuation contrib. to sound vel. and damping above superfluid transition temp. 80−15324
^{3}He-^{4}He mixture, US propagation near tricritical point 77−59169
^{4}He, HCP, longitudinal sound velocity, temp. and freq. depend. 77−72742
^{4}He HCP crystals, US vel., temp. and freq. depend. 79−56016
^{4}He, liq., low-momentum phonon dispersion relation, press. depend., US velocity meas. 77−47635
^{4}He, solid-fluid, eqn. of state, melting props. under press. 80−96721
^{4}He, superfluid, phonon dispersion 80−10722
Hg, liq., Brillouin scatt. obs., vel. of sound determ. 77−24858
Hg, liquid, velocity depend. on density 78−43073
$HoFe_2$, amorphous, ultrasonic exam. below T_c 79−73793
$Ho_xTb_{1-x}Co_2$ lave phase compounds, elastic props., temp. and magnetic field dependence 80−60393
In, elastic consts., from room temp. to MP, US pulse echo meas. 77−24342
In film, damping and vel. of longit. elastic waves at 9.4 GHz 80−10596
In, US velocity dispersion in external mag. field 80−20446
In-Cd alloys, elastic-phase transition, US study 78−6919
In-Pb alloys, elastic consts. of three phases, acoustic mode softening from US vel. meas. 80−30006
In-Tl, BCC alloys, stability and elastic consts., US vel. 79−42133
InSb, molten, temp. depend. of vel. of sound and adiabatic compressibility 77−27944
InSb, third-order elastic consts. meas. at 300, 80K 77−31711
n-InSb, Wigner cryst., long-wavelength excitations in strong mag. fields 79−82533
$K_2Ba(NO_2)_2$, elastic props. 80−96588
$KBrO_3$, trigonal, elastic, thermoelastic and dynamic piezoelec. props., US vel. meas. 77−32328
KCN, elastic functions meas. by US pulse-echo method and Brillouin scatt. 77−84829
$K(CN)_{1-x}Cl_x$, elastic functions meas. by US pulse-echo method and Brillouin scatt. 77−84829
KCl, liq., Brillouin scatt. determination of hypersonic vel. 79−82288
KCl molten salt, thermodynamic function, Brillouin spectroscopy, hypersonic vel. *(French)* 78−35161
K_2CuF_4, Brillouin scatt. and US meas. of phonons, elastic moduli and Debye temp. calc. 79−87454
$KD_3(SeO_3)_2$, acoustic phonon softening and spontaneous strains 78−26652
$KH_3(SeO_3)_2$, acoustic phonon softening, US vel. meas. 78−14429
$KH_3(SeO_3)_2$ and $KD_3(SeO_3)_2$, ferroelastic phase transition, mech. stress effect 80−70394
$KH_3(SeO_3)_2$, phase transition, acoustic phonon softening 77−27997
$K_2Mn_2(SO_4)_3$, elastic props. using piezoelec. reson. and US vel. meas. 80−15180
K_2NiF_4, 2D antiferromag., volume depend. of superexchange, US velocity meas. of T_N 78−19237
K_2O-B_2O_3-SiO_2 system glasses, hypersound propag., 77 to 300K, Brillouin scatt. obs. 77−84850
K_2O-SrO-SiO_2, glass, elastic constants 77−16630
$K_2PbCu(NO_2)_6$, US vel. near cooperative Jahn-Teller phase transitions 79−23680
$K_2Pt(CN)_4Br_{0.3}.3H_2O$, lattice softening, temp. depend. of elastic consts., US meas. 78−14432
K_2SeO_4, Brillouin scatt. at paraelectric-incommensurate phase transition, hypersonic waves 79−78690
K_2SeO_4, elastic props. at commensurate-incommensurate transition, Brillouin scatt. and US study 80−93248
K_2SeO_4, ultrasonic study in temp. range of incommensurate phase transform. 80−88276
K_2SnCl_6, elastic consts., inelastic neutron scatt. and US meas. 80−59553
$LaAl_2$, supercond. and normal states, anomalous US attenuation and velocity change 80−80446
LaB_6, elastic consts. at room temp., US vel. meas. 77−43268
$LaH_{2.96}$, elastic props. at high press. 77−84825
$LiIO_3$ crystal elastic, piezoelec., dielectric and acoustic props. 79−46740
$LiNO_3$-$NaNO_3$-$AgNO_3$, molten salt mixture, excess thermodynamic props. and US vel. *(French)* 77−31720
$LiNbO_3$, light induced ultrasonic wave velocity change, refractive index 80−97236
$LiNbO_3$, polydomain, nonstoichiometric crysts., elastic, piezoelec., dielec. constants. 77−8513
Li_2O-Al_2O_3-SiO_2, glass, study of elastic props. 80−104205
Li_2SO_4, liq. and plastic crystalline phases, Brillouin scatt. 79−99897
Li_2SO_4, molten, Brillouin spectra, refr. index meas., hypersonic vel. 78−68523
^{6}Li, and natural Li, elastic consts., temp. and press. depend. 78−30692
$Mg(Al,Cr,Fe)_2O_4$, spinel, elastic moduli calc. 78−6960
MgF_2, elastic constant determ. by US pulse echo overlap 79−14874
MgO-P_2O_5, glass, US velocity rel. to elastic props. 80−103425
γ-Mn-Ni-C, elastic anomalies, martensitic transformation in Mn rich alloys 78−84807
MnF_2, elastic constant determ. by US pulse echo overlap 79−14874
MnP, US vel. and crit. attenuation, longit. waves, external mag. field 78−27035

ultrasonic velocity continued
$MnSO_4$ aqueous soln. conc. depend. of third US relaxation freq. and activation energy 78−63814
MnSi, US velocity anomalies near mag. transition 78−19302
Mn_5Si_3, elastic moduli, phase transitions, ultrasonic velocity 80−92589
Mo, elastic moduli meas. *(Russian)* 78−75704
Mo, Fermi surface ang. shear deform., US vel. quantum oscill. meas. 79−77985
N_2, liquid, Brillouin scatt. obs., US vel. and absorpt. 80−45085
N_2-methane mixture, US propag. vel. up to 40 kbar, additivity deviation 77−42959
ND_4Cl, ultrasonic exam. near order-disorder transition, elastic consts. 79−46799
$(NH_4)_2BeF_4$, elastic props., US damping 80−84229
NH_4Br, λ-type phase transition, Brillouin scattering 78−79725
$NH_4Br_xCl_{1-x}$, cryst., order-disorder phase transitions, US investig. 80−6378
$(NH_4)_{2(1-x)}Rb_{2x}SO_4$, mixed crystal, dielectric and US meas. of ferroelec. phase transition *(Japanese)* 80−7305
Na-NH_3, solns., US absorpt. and vel. near crit. point 79−28047
NaCN, cubic, KCN-type anomalous thermoelastic behaviour 77−84823
NaCl dilute solution, US vel. meas. by differential velocimeter 77−78065
NaCl, elastic props. at press. up to 9 GPa, ultrasonic wave velocities 79−95073
NaCl, liq., Brillouin scatt. determination of hypersonic vel. 79−82288
NaCl, molten salt, thermodynamic function, Brillouin spectroscopy, hypersonic vel. *(French)* 78−35161
NaCl, Poisson's ratio and shear modulus meas., 9 GPa 77−4140
$NaClO_3$, lattice vibrations and sp. ht., neutron spectroscopic study 80−107388
Na_2CoGeO_4, single cryst. growth and study of their piezoelec. and elastic props. 79−4906
NaF, US vel., Poisson's ratio and shear modulus meas., 9 GPa 77−4140
$NaNO_2$, incommensurate-and-antiferroelectric phase transition, amplitude mode, ultrasonic study 80−39227
Na_2O-SiO_2 glass, acoustic and thermal Gruneisen parameters 80−59608
Nb third-order elastic consts. using nonlinearity parameter 78−75733
Nb-H(D)(T) system, BCC, US vel. changes caused by H isotope dissolution 80−65117
Nb-Hf (26 at.%), mixed state, ultrasonic velocity meas. 79−60974
Nb-Mo, BCC, press. derivatives of elastic moduli, Fermi surface topological changes, band struct. 79−61639
$NbSe_2$, layered dichalcogenide, US vel. rel. to CDW 77−76490
Nb_3Sn, acoustic soft modes in high mag. fields, soft sound vel. meas. 77−43482
NbTi/Cu, room temp. elastic consts., US determ. 77−59839
Ne, liquid, US velocity at 5 MHz *(Russian)* 78−83879
Ni film, damping and vel. of longit. elastic waves at 9.4 GHz 80−10596
Ni-P, amorphous metallic, sound attenuation and rel. meas. 77−31722
Ni-P, amorphous metallic, logarithmic temp. depend. of sound vel. 77−31725
$NiCr_2O_4$, acoustic props. rel. to cooperative Jahn Teller effect and structural phase transform 80−24538
$Ni^{2+}Fe_{0.75}^{3+}V_{1.25}^{3+}O_4$, acoustic props. rel. to cooperative Jahn Teller effect and structural phase transform 80−24538
$NiTe_2$, acoustic phonon dispersion, inelastic neutron scatt. meas., elastic consts. and sound vels. 79−95098
O_2, liquid, Brillouin scatt. obs., US vel. and absorpt. 80−45085
P, amorphous, US attenuation and sound vel. meas., 4.2 to 300K; 80−49308
Pb, elastic consts., from room temp. to MP, US pulse echo meas. 77−24342
Pb, liquid, US wave velocity *(Japanese)* 79−60438
Pb-Bi, elastic moduli, internal friction from US velocity meas. 79−15717
$(Pb_{1-x}Ba_x)_5Ge_3O_{11}$, ferroclec. transition blurring, US relax., dielec. and opt. props. 78−95559
PbF_2, US vel. near press. induced cubic-to-orthorhombic transform. 80−103476
$Pb_5Ge_3O_{11}$, ferroelec. transition, US and elasto-optic props. 80−60527
$Pb_5(GeO_4)(VO_4)_2$, $Pb_5(SiO_4)(VO_4)_2$, and Pb_5GeO_{11}, elastic nonlinearity and acoustic losses 80−59554
$Pb_{1-x}Ge_xTe$, TO phonon interaction with acoustic phonons near phase transition temp. 79−90776
PbI_2, cubic, elastic consts., hydrostatic press. effect, US vel. meas. 80−49292
$Pb_2KNb_5O_{15}$ piezoelectric coupling for SAW applications 79−56055
$Pb(NO_3)_2$, press. derivatives of elastic-moduli, ultrasonic velocity meas. 78−95102
PbO-SiO_2 glass, acoustic and thermal Gruneisen parameters 80−59608
PbS-As_2S_3 glass, elastic props. temp. depend. 78−71780
Pb(Zr,Ti)O_3:Nb ceramic, stress effects on ferroelec. hysteresis, macroscopic strain, US vel. 79−4778
Pd-Si, amorphous, US velocity, freq. and temp. depend. 78−63812
Pd-Si, amorphous metallic, sound propag. at low temps. 77−72656
PdSiCu, amorphous, US attenuation and vel. studies 80−19881
PdSiCu, amorphous, US attenuation and vel. studies at low temps. 80−88278
$Pd_{0.775}Si_{0.165}Cu_{0.06}$, metallic glass, 0.01-10K, relax of tunnelling systems by conduction electrons, US expts. 79−14889
Pu-Ga (1 wt.%) alloy, single cryst. elastic consts. 77−20005
$RbAg_4I_5$, third order elastic consts. at room temp. using 110 cut 78−59848
$RbCaF_3$, nonlinear elastic behaviour, US velocity, 1 bar-3 kbar 78−59851
$RbCdF_3$, nonlinear elastic behaviour, US velocity, 1 bar-3 kbar 78−59851
RbH_2PO_4, electrostrictive effects, US rel. 80−75941
RbH_2PO_4, ferroelectric, US propag. near ferroelectric phase transition temp. 78−23417
$RbHSO_4$, acoustic and dielectric props. near phase transition 80−55053
$RbHSO_4$, ferroelec. phase transition, US attenuation and velocity 78−39511
$RbH_3(SeO_3)_2$, US vel. and absorpt. near ferroelec. Curie temp. 80−97206
Rb_2ZnCl_4, US vel. and attenuation at normal-incommensurate phase transition pt. 79−55833
Rb_2ZnCl_4, US velocity and attenuation, around normal-incommensurate phase transition 80−40072
Re, Fermi surface, strain depend., from US vel. oscills. 78−84133
SO_2, liq., vibr. relax., US absorpt. and vel. meas. 80−34147

ultrasonic velocity continued
SO_2-tetrachloromethane, solns., near critical point, ultrasound absorpt. obs. 80−65160
$SbGe_xSe_y$ glasses with const. Sb content, heat capacity, thermal expansion, US vel. and elastic moduli 77−76574
Se, acoustic props. near first-order phase transition 77−20014
Se, amorphous, relax of sound velocity, struct. determ. 78−38786
Se, amorphous, sound propag. at low temps. 77−72657
Se, amorphous, US wave attenuation and vel., near glass transition 77−89501
Se, elastic and piezoelec. consts., US phase vel. meas. 79−86834
Se, liq., US rel. temp. depend., melting effects 78−38782
Se, vitreous, elastic coeffs. about glass transition temp. US study *(French)* 80−19865
Se, vitreous, temp. depend. of sound vel. 77−84855
Se-As 36.4 at % amorphous alloy, heat treatment effect on acoustic props. 79−86843
Si film, amorphous, LF vel. of sound for Young's modulus mode 77−35636
Si, pure and n-type, US vel. and attenuation, evaluation using elastic moduli 80−70325
SiC delay line at 9.43 GHz, acoustic props. study 80−65169
SiO_2, glass, acoustic and thermal Gruneisen parameters 80−59608
SiO_2, glass, HF phonon phase vel. meas., below 1K, tunnelling model 77−7818
SiO_2, vitreous, fast neutron irrad., low temp. US meas., two-level systems role 78−30703
SiO_2, vitreous, hypersound velocity meas. from Brillouin scatt. freq. 80−27349
SiO_2, vitreous, neutron irrad. effects on heat capacity, thermal cond., US velocity temp. depend. 78−83851
SiO_2, vitreous, US velocity, freq. and temp. depend. 78−63812
SiO_2, vitreous Brillouin scatt., 35 GHz phonon vel. and absorpt. below 1K 80−100664
SiO_2-Al_2O_3, vitreous US vel. and absorption 80−107380
SiO_2-B_2O_3 glasses, Brillouin scattering meas. of attenuation and vel. of hypersounds 80−100309
SiO_2-TiO_2, vitreous, US vel. and absorption 80−107380
$SmCo_5$, single-cryst. and liq. phase sintered, elastic stiffness consts., US velocity obs. 77−73066
Sn, liq., US vel. and thermophysical props. meas., 500-1000K 78−38778
Sn, liquid, US wave velocity *(Japanese)* 79−60438
Sn-Bi, liq. US vel. and thermophysical props. meas., 500-1000K 78−38778
SrF_2, fluorite-struct. compound, high-temp. elasticity, US pulse meas. 77−81878
$Sr(NO_3)_2$, press. derivatives of elastic-moduli, ultrasonic velocity meas. 78−95102
SrO-P_2O_5, glass, US velocity rel. to elastic props. 80−103425
$SrTiO_3$ based solid solns., ferroelec., US study 79−38476
$SrTiO_3$, semicond., structural phase transitions, US velocity meas. 79−28692
TGSe, anomalous sound velocity near ferroelec. phase transition at high pressure 78−52456
Ta-W BCC, press. derivatives of elastic moduli, Fermi surface topological changes, band struct. 79−61639
TaS_2, layered dichalcogenide, US vel. rel. to CDW 77−76490
Tb, magnetic phase diagram, US meas. of elastic const. 80−15721
$Tb_{0.3}Dy_{0.7}Fe_2$, elastic vs. magnetoelastic anisotropy 78−68347
$Tb_{0.3}Dy_{0.7}Fe_2$, magnetoelastic coupling meas. by US method 77−69652
$Tb_{0.3}Dy_{0.7}Fe_2$, sound velocity mag. field and temp. depend. elastic moduli calcs. 80−39839
$Tb_{0.3}Dy_{0.7}Fe_2$, US velocity and attenuation obs. 77−28423
$TbFe_2$, amorphous, mag. struct., US meas. 79−99683
$Tb_2(MoO_4)_3$, elastic wave attenuation and velocity near ferroelec. transition 79−73257
Te, elastic and piezoelec. consts., US phase vel. meas. 79−86834
Te, liq., US rel. temp. depend., melting effects 78−38782
Ti-V-Cr, BCC, press. derivatives of elastic moduli, Fermi surface topological changes, band struct. 79−61639
Ti-V-H system, BCC, hydrogen effects on anisotropic elastic props. 79−24565
Ti_2O_3, press. depend. of elastic consts. at 296K. 79−42134
$(Ti_{1-x}V_x)_2O_3$, US velocities in high mag. field 78−84262
$TlAsS_4$, struct. and soft mode behaviour 78−91327
Tl_3AsS_4, crystal growth by Bridgman-Stockbarger method, exam. of props. 79−11506
$TlCdF_3$, nonlinear elastic behaviour, US velocity, 1 bar-3 kbar 78−59851
Tl_3VS_4 single-crystal substrate SAW filter performance 77−31186
$TmFeO_3$, acoustic vel. and attenuation shifts at spin reorientation phase transition 80−65986
TmSb, cryst. field effects on elasticity, rot. and higher order interactions 77−63251
UAl_2, elastic consts., temp. and mag. field depend. 80−55450
UN, sound velocity temp. depend. anomaly 77−72891
UN, sound velocity temp. depend. anomaly in elastic consts. determ. 77−72892
UO_2, elastic props. at high press., US meas. 77−4141
V, shear elastic constant, anomalous temp. behaviour, US study 79−28031
V, ultrasonic velocity meas., mag. field depend. 78−19104
V-Cr, elastic moduli, US pulse echo meas. 78−84881
V-H(D)(T) system, BCC, US vel. changes caused by H isotope dissolution 80−65117
V-Ti (42 at.%), ultrasonic vel. in mixed state 80−75689
VO_2, phase transition, temp. variation of US attenuation and phase vel. 77−31723
V_2O_3, high temp. mag. phase transition studied by US vel. meas. *(Russian)* 79−33520
V_2O_3 phase transition, temp. variations of US attenuations and phase vel. 77−31723
V_2O_3, US vel. and elastic const. meas., 150-273K 77−15478
V_2O_3:Cr, pure and doped, sound vels. and elastic consts. from phonon dispersion curves 79−55844
V_3Si, soft mode sound vel. in mag. field rel. to density of states 78−14647
$V_3Si_{1-x}Ge_x$ solid soln., longitudinal and transverse US wave propag. rate, 4.2 to 300K *(Russian)* 80−103423
W, conduction electron g-factor, US vel. quantum oscills. 77−28100
ultrasonic velocity continued
W, Fermi surface, uniaxial strain depend., quantum oscills. in magnetostriction, US vel., with torque 77−28094
Zn, liquid, US wave velocity *(Japanese)* 79−60438
$ZnCl_2$-LiCl(NaCl)(KCl)(CsCl), molten, US velocity, thermodynamic quantities and struct. *(Japanese)* 80−88270
$ZnCl_2$-$PbCl_2$, molten, US velocity and absorpt., thermodynamic quantities and bulk viscosity *(Japanese)* 80−84249
ZnF_2, elastic constant determ. by US pulse echo overlap 79−14874
ZnF_2, elastic props., 4.2-300K, incipient ferroelec. transition 78−30691
ZnSe, resonant Brillouin scatt. by injected acoustic waves 77−12394
ZrV_2, Laves-phase, cubic to rhombohedral transition, lattice electron instability 78−92261

ultrasonic velocity measurement
acoustic characteristics, of solid materials, instrument for direct meas. 79−14179
acoustooptically active solids, laser beam probing of standing wave 78−33965
automatic precision test installation for US waves through solids *(German)* 79−50549
binary liquid mixtures of aromatic amines with carbon tetrachloride, theoretical evaluation 80−39224
biological material dilute suspensions, meas. via differential US velocimeter 77−78065
blood, US Doppler velocimetry, experimental appls. *(French)* 79−34610
bone, longitudinal and shear wave velocity meas. for elastic moduli 77−25623
bone, temp. range of room temp. to 90°C 80−76787
Brillouin scattering frequency high-precision meas., rel. to hypersound velocity meas. 80−27349
Brillouin spectroscopy, high-resolution, for hypersound phase vel. meas. 77−69845
cell for meas. under hydrostatic press. 78−55534
ceramic, piezoelectric, US instrument for determ. charcts. 80−66752
ceramics, fine-grained, US attenuation and velocity obs., 5 to 500 MHz 77−39634
collagen threads, mammalian, US meas. using scanning laser acoustic microscope 79−43972
concrete, ultrasonic wave velocities and density, calc. and meas. 79−52545
continuous and simultaneous recording of changes in US attenuation and vel. 78−46875
continuous meas. of changes in US velocity 80−87675
coral skeleton US velocity and Young's modulus anisotropy obs. 79−57837
correlation method using quartz transducer transmitter-receiver 78−30139
crystals, precision meas. via phase shift freq. depend. 77−14866
cyclohexane+n-heptyl alcohol 80−38200
diffraction corrections for finite size of source and receiver 80−96153
digital electronic instrument using pulse-echo overlap method 79−37097
digital US vel. meter using freq. counter 80−38202
Doppler ultrasonic flowmeter 79−68889
elastic wave transit time meas., 100 kbar apparatus 78−79176
ethyl methyl ketone+cyclohexane, measurements for determination of excess props. 80−37910
ethyl methyl ketone+n-butanol, measurements for determination of excess props. 80−37910
exact fractions US interferometer algorithm and circuitry 77−39182
femur, human, pulse-echo technique for US vel. meas. in vivo 80−89812
fibre reinforced porous composite anal. by US wave velocity meas. of fibre vol. and matrix porosity 78−95902
filled polymer materials, simple approx. method, acoustic impedance 80−64314
fixed-path interferometer, phase error elimination 78−83197
flowmeter, distorted profile effects 79−68860
flowmeter, non-intrusive, theoretical and expt. uncertainty determ. 78−30391
flowmeter, open channel acoustic flowmeter, error sources and calibration 78−30389
flowmeter, time differential clamp on ultrasonic flowmeter, performance and appls. 78−30390
flowmeter, using frequency difference method 79−68851
flowmeters, applications and development 79−68893
interferometer method for US props. of solids 77−23836
interferometry, US attenuation or velocity meas. 80−58874
isotropic nondispersive solid, meas. method for vel. of sound 80−69616
laser light diffraction, appl. to meas. of acoustic and acousto-optic props. of crystals *(Polish)* 78−76425
liquid, pulsed exptl. arrangement, press. to 2000 atm. *(Russian)* 79−94427
liquid, UHF interferometer appl. 78−22234
liquid density determination as function of pressure, based on acoustic method 79−12771
liquid metals, pulse-echo overlap technique 80−99906
liquid systems, 10 to 30 MHz, 25 to 60°C, undergraduate expt. using 2-transducer RF pulse method 80−69608
liquids, high resolution Bragg reflection technique 79−23160
liquids, high-accuracy differential meas. in different liquids 80−5889
in liquids, meas. technique for freq. range 20 to 1000 kHz 77−14867
liquids, pulse technique, monostable multivibrator and oscilloscope technique 80−64313
liquids, US vel. meas. method for elastic const. determ. w.r.t. temp. and pressure 80−15177
liquids and small biological tissue specimens, phase meas. 80−76786
liquids with very low US propag. velocities for use in biomedical optical computer 80−28392
longitudinal and transverse waves, experimental apparatus for simultaneous velocity meas., at high temp. 78−59213
longitudinal US vibrations meas., based on interferometer 80−79084
metal, US surface wave vel. meas. on plane and cylindrical samples, optical methods 77−46875
metal fatigue monitoring by US velocity and attenuation meas. 78−60970
metal powder density meas. by US velocity 77−32760
metals, SAW attenuation coeffs. and wave speeds 79−46903
metastable liquids, optical schlieren method 78−55535
meter, UF-91 Shch 78−59221
methane, solid, thermodynamic props. from US velocity obs. 79−46753
mid-radius flow, US meas. 79−68852

ultrasonic velocity measurement continued
minicomputer controlled instrument for US vel. and attenuation meas. 79−86312
oil, US flow measurement in laminar-turbulent transition region 79−68850
optical heterodyning method for ferroelec. crysts., with Raman diffr. by US waves 79−18640
optical probe for meas. local elastic props. in transparent media 79−14174
paper fibre suspension, modelling 77−27447
phase and group vel. meas. by phase comparison of continuous harmonic waves 79−1035
picrite, calculation of Gruneisen parameter and specific heat from measurements 80−41436
polycarbonate film, oriented, US speed −180 to 160°C, orientation influence 79−19326
polymers, US velocities and damping coeff. meas. *(French)* 80−7723
pulse echo method, minicomputer program control *(Japanese)* 80−53587
pulse propag. meas. and appl. 78−53167
pulse superposition technique, apparatus assembled from discrete instruments 80−74650
pulse velocity meas. by time selector and frequency counter *(German)* 78−13876
pulse-echo methods, effects of nonparallelism 78−55537
quartz transducer, multimodality influence on US vel. and attenuation meas. 77−11100
review 77−84094
SAW, velocity, attenuation and reflection meas., interf. acoustical method 79−18638
SAW velocity meas. by phase-sensitive laser probe 79−46911
scanning signal, influence of resonance filter on wave form *(Russian)* 79−55265
sheet materials testing, using correlation method 77−75759
signal shape anal., ultrasonic pulsed measuring instrums. 80−87678
sing-around meter, IC 80−38198
sing-around system, high-speed, automated 79−90101
solid solution breakup, anal. by meas. US wave vel. 78−23887
solid state pulse interferometer to measure ultrasonic velocities in crystals 79−23154
solids, measuring equipment for determ. of propag. vel. and attenuation of US waves *(German)* 79−37104
solids, with allowance for statistical charact. of bonding layers 80−5894
solutions in alcohols, ultrasonic vel. and density meas. used to calc. compressibility, intermol. free length and salvation no. 80−96150
sonic interface detection for multiproduct liquid transportation by pipeline, developments 80−33382
spectrometer, double-pulse comparison technique for meas. US vel. changes 78−1526
steel, austenitic, type 304, 304L, 316L, US wave vel. meas. rel. to cold working 80−99908
steel, low alloy, 38NiCrMo$_4$, US wave vel. meas. rel. to cold working 80−99908
superheated water, Brillouin scatt., sound velocity meas. 80−95631
surface wave velocimeter, phase sensitive 80−102947
surface wave velocity measurement using reflections from laser scribed grooves 78−90614
ternary organic liquid mixtures 80−38201
tetrachloromethane+n-heptyl alcohol 80−38200
thin film elastic constants and SAW velocity and attenuation meas. 79−56101
three-dimens. fluid vel. vector and temp. fields from acoustic transmission meas. 78−30394
time of flight tomography, reconstruction of US vel. distribs. in soft tissue 77−48850
tissue, meas. device 80−45993
tissue, temp. depend., appl. to noninvasive temp. monitoring 78−40281
tissue characterisation by backscattered field space-time processing 79−48305
tissue US attenuation and velocity meas. by direct and phase-contrast imaging 77−64114
tissue US attenuation and velocity meas. by reflection techniques 77−64115
tissue US attenuation and velocity meas. by time delay spectrometry 77−64111
transducer, shear-wave vel. meas., bone elastic moduli determ. 78−83201
transducer bond corrections, elimination by use of capacitative transducers 77−46873
transmission time meter, with digital readout 77−40485
TTF-TCNQ, sound vel. measurements using capacitive transducers 79−72775
vibration propag. vel. meas. in solids using broadband amplifier 78−1521
Al-Cu, US wave propag. velocity, exam. 78−72982
α-AlPO$_4$, berlinite, X-axis boule cut SAW props. 79−56061
Cr_2O_3, US wave vel. near mag. transition 78−84263
Cu-Sn (15 at.%), temp. depend. of elastic consts. above martensitic transition temp., US exam. 78−76695
Cu-Zn-Al (19.3, 13.0 wt.%), effect of hydrostatic or uniaxial stress on elastic consts., near martensitic transformation point 78−76697
Fe nodular parts, comparison of sonic-resonance and US velocity techniques for quality control 80−97654
Hg, liq., sound vel. near metal-nonmetal transition, up to 1600°C and 2000 kg/cm^2 80−39222
Li single cryst., measurement in vicinity of martensitic phase transformation 80−75358
LiCl in H_2O, complexity investigation using US method 80−33326
$LiNbO_3$, acoustic charact. meas. of Z-cut single crysts. by acousto-optical method 79−3867
$LiNbO_3$, SAW propag. velocity meas. 80−92003
Li_2O-Al_2O_3-SiO_2, glass ceramic, elastic props. at high press., US meas. 78−83863
NH_4Cl, λ-type phase transition, hypersonic study using Brillouin scatt. 80−34165
$Pb_{0.97}La_{0.02}(Zr_{0.92}Ti_{0.08})O_3$, ferroelec. ceramic, stress effects 80−2119
$Pb_{0.99}Nb_{0.02}(Zr_{0.95}Ti_{0.05})_{0.98}O_3$, ferroelec. ceramic, stress effects 80−2119
Ti alloys, US wave propag. velocity, exam. 78−72982
V, determination of effect of H on elastic moduli 80−75288
Zn-Cd alloys, liq. and solid, ultrasound speed and compressibility meas. 80−102941
$ZnCl_2$ in H_2O, complexity investigation using US method 80−33326

ultrasonic wave propagation *see ultrasonic propagation*

ultrasonic waves
see also surface acoustic waves; ultrasonic propagation
Bragg anisotropic diffraction of light *(Russian)* 77−10833
cavitation shock pressures in venturi, 10 kHz-1 MHz 77−24002
diamond, sound excitation orientational effect due to channelled electrons 80−84254
distortion of ultrasound beams in tissue and tissue-equivalent media 80−45945
elastic wave transit time meas., 100 kbar apparatus 78−79176
generation by focused modulated electron beam, appl. to US imaging in scanning electron microscopy 80−95192
generation in insulators, detection prior to breakdown 80−88924
hypersonic waves, theory of self action 78−75010
hypersound resonant excitation by 2-dimens. plasmons *(Russian)* 79−78032
integrated optical effect produced by US fields, study using light diffraction technique 80−23848
Lamb waves, leaky, in solid plate with water loading on one side *(Japanese)* 77−3690
liquids, photoelastic visualisation 80−28374
metals, generalised Gruneisen tensor from solid nonlinearity parameters 80−84275
molecular crystal, optical rotation induced by ultrasonic wave *(Russian)* 80−93270
Mossbauer spectrum, ultrasonic sideband intensity depend. on acoustic field statistics 80−75905
multidomain structure, RF excited spectrum 78−68056
multilayer metal films, EM excitation of sound, Mossbauer study *(Russian)* 79−99795
paramagnetic metals, EM excitation of sound, Mossbauer study *(Russian)* 79−99794
piezoelectric transducer, surface excited, US field 80−64331
plane wave reflectivity from water-metal interface, stress effect 79−81586
pressure field visualisation using microphone matrix *(German)* 79−32151
propagation in austenitic stainless steel weld metal, effect of anisotropy 80−45452
pulsed fields radiated by thick piezoelectric discs immersed in petrol, expt. study *(French)* 80−53512
SAW, nonlinear interaction in 2-6 MHz range *(French)* 80−33296
SH wave magnetostrictive generation model for ferromag. materials 79−55836
shock waves emitted by cavitation at rotating perforated plate, wear, thickness effects 77−27565
standing and travelling in water-filled wedge, obs. by frequency-shift holography 80−79089
standing wave acoustic field, stable arrays of reson. bubbles 77−79988
standing waves in liquid, directional independence of freezing-in-effect *(German)* 77−50786
Stoneley US waves on boundaries, surface bonding effects 79−56059
transmission through rough surface *(Russian)* 80−100387
US excitation and detection in mag. polarised nonferromag. metals, elastic displacements 78−53091
visualization using schlieren technique 78−30118
Fe-Ni, mechanisms of EM generation and detection of US Lamb waves 78−39382
GaS(Te)(Se), elastic characteristics, Debye temp., ultrasonic study *(Russian)* 80−79872
Ge, electron-hole drop drag by ultrasound *(Russian)* 80−100437
$PbMoO_4$, elastic wave excitation and amplification by laser radiation 80−103419
SmS, film, laser generation of US using metal-insulator transition 79−90734
Sn, u.s. surface generation, below 20K 78−2353

ultrasonic welding
IC microwelding using nonlinear phenomena of acoustic vibratory systems 80−74656
microcontacting in thin metallic layers *(German)* 80−55624
UV radiation effects on welded joints and substrate surface 80−37008
Ag metal oxide contact materials 78−29095
$Ni_{40}Fe_{40}P_{14}B_6$ metallic glass alloy, US spot welding to Cu 79−21730

ultrasonics
see also acousto-optical effects; ultrasonic applications; ultrasonic devices; ultrasonic equipment; ultrasonic waves
conference, New Orleans, LA, USA 80−73101
n-hexane, superheated, thermodynamic props. from ultrasound speed 80−92036
historical aspects 79−46105
interferometry, pseudo-stationary US fields in fluids 79−81610
internal losses in metals subjected to high intensity US flexural vibrations 80−6460
minerals, ultrasonic damping due to internal friction, freq. depend. *(German)* 80−90078
physical and technical acoustics and ultrasonics, conf., USSR (Apr. 75) 77−800
symposium, Annapolis (1976) 77−19469
symposium, Cherry Hill (1978) 79−50472
symposium, Phoenix, AZ, USA (Oct. 1977) 79−46096
trends in research work *(Japanese)* 78−33946
$MgSO_4$, aq. soln., electrolytic conduct. affected by US waves 79−23997

ultraviolet astronomical observations
0 and B stars, UV obs. of mass loss effects 77−17551
0B-type stars, O VI obs. in stellar winds 80−8630
108-76°1, new halo planetary nebula, chemical abundances 77−45510
0254−334/2, high-redshift QSO without Lyman α emission or absorpt., spectroscopic obs. 79−92886
0406+121, optical spectra 4950-7950 Å, of possible BL Lacertae object 80−51895
1309−216, probable BL Lacertae object with absorpt. red shift 1.49, optical spectrum 80−67856
1978 RA, fast-moving asteroidal object UBV photometry 78−85887
1978 SB, positions and UBV photometry 78−96422
A0035, large southern ring galaxy, obs. 77−45559
2A 0042+323 (3U 0042+32) optical candidate, photometry and spectrum 78−54088
2A 0311−227 optical counterpart, identification as AM Herculis type star 79−30149

ultraviolet astronomical observations continued
2A 0311−227 optical counterpart, simultaneous photometric and spectroscopic obs. 80−90572
2A 2251−179, X-ray quasar, UBV photometry 80−82349
A- and B-type stars, B abundance from B II reson. line obs. 79−21276
A- and F-type stars, absolute energy distribs. 77−17554
A-type central stars of three planetary nebulae 79−17064
A-type stars, predicted and observed spectral energy distribs. 78−4208
A-type supergiant stars, reson. line profiles from IUE and Copernicus spectra 80−90424
Abell 426 and 1367, surface brightness and colour distribs. of elliptical galaxies 78−81681
Abell 46, planetary nebula, eclipsing binary nucleus, hot component UV continuum obs. by IUE 80−98693
absorption at 2175 Å, correl. with interstellar features 77−45401
active galaxies, implications of UV obs. 80−105390
active nuclei of galaxies and quasars, role of UV obs. *(Italian)* 78−32577
AGK2+81°266, hot subdwarf, spectral type 78−45323
Am stars, τ Ursae Majoris and 15 Vulpeculae, energy distrib. from spectral obs. 80−85949
Am-stars, ANS UV photometry of 26 objects 78−61869
o Andromedae, Be star, radial vels. obs. 79−58355
o Andromedae, Be star, spectrographic obs. from (1967 to 1976) 77−71116
o Andromedae, binary star, UV spectrum 77−45485
RT Andromedae, eclipsing binary, three-colour photoelectric obs. and improved ephemeris 80−22043
RT Andromedae, light curve anal. of short period eclipsing binary 80−46603
α Andromedae, Mn star, UV spectrophotometry from TD 1-A/S 59 77−29848
λ Andromedae, spectroscopic binary, UV and optical obs. of chromospheric lines 79−30087
Z Andromedae, symbiotic star, IUE obs. of UV spectrum 80−109450
Z Andromedae, UV spectra, 1979 Feb. 17, quiescent phase 79−40202
α Andromedae, UV spectrum of Mn star 78−69802
ET Andromedae (HR 8861), Ap star, light vars. and period 80−46571
Ap Si stars, UV spectral vars. 79−8927
Ap stars, CN lines identification 77−91551
Ap stars, heavy element abundances from Copernicus UV data, reference stars α Lyrae and α Canis Majoris A 78−28688
Ap stars, photoelec. obs. of light vars. *(German)* 78−20841
Ap stars, summary of physical and chemical props. from UV obs. *(Italian)* 78−32479
Ap stars in open clusters, rot. vels. and mag. braking 77−33500
Ap-stars, ANS UV photometry of 79 hot and cool objects 78−61869
Ap-stars, UV spectra in 1350-2550 Å range, TD1 satellite obs. 78−36581
Ap-type stars, mag. fields and atmospheres struct. *(Russian)* 77−17594
α and β Aquari, G-type supergiants, evidence for hybrid atmospheres and winds from UV spectra 80−72948
AE Aquarii, cataclysmic variable, IUE satellite UV obs. 80−72985
AE Aquarii, cataclysmic variable, rapid light oscills. rel. to white dwarf oblique rotator model 80−36634
α Aquarii, chromospheric event detect. from UV spectrum obs. 80−31299
U Aquarii, R Coronae Borealis star, extraordinary comp. rel. to unusual s-processing event 80−17588
R Aquarii, symbiotic long-period variable, spectrum of assoc. nebulosity 80−90450
R Aquarii, UV obs. of hot component 80−56854
σ Aquarii (A0 IVs), hot metallic-line star, spectrum and abundance anal. 80−90415
R Aquarii (M7+pec), late type variable star, IUE obs. of circumstellar emission 80−82370
Aquila X-1, UBV photometry during 1978 X-ray outburst *(Russian)* 79−101224
Aquila X-1 (4U 1908+00), optical outburst, obs. 78−69911
η Aquilae, classical Cepheid, companion star detect. and distance determ. 80−90443
α Aquilae, Copernicus UV spectral obs. 77−33480
KO Aquilae, eclipsing binary system, UBV photoelectric study 80−62198
θ Aquilae (B9.5 III), spectrum and abundance anal. 80−90415
V603 Aquilae (Nova 1918), periodic light vars. detect. 80−82391
V1301 Aquilae (Nova 1975), VBLUW photometry, absolute magnitude, distance and reddening 79−58342
387 Aquitania, slow spinning asteroid with rot. period of nearly one day, photometric evidence 80−17529
Arakelian galaxies, emission line spectra 77−74138
Arakelyan 120, Seyfert galaxy, spectrophotometry 79−62913
β Arietis, Am star, spectroscopic obs. and curve of growth anal. 77−22237
UX Arietis, Copernicus UV obs. of Lyman α and Mg II emission 78−81651
κ Arietis, double-lined Am star, spectroscopic obs. and curve of growth anal. 77−22237
SX Arietis, He spectrum variable, UV photometry with ANS 78−36585
56 Arietis, spectrophotometry of Ap star, continuum features vars. 80−36638
asteroid families, obs. evidence for common origins 77−91468
59 Aurigae, δ Scuti star, light curves periodogram anal. 80−62141
SX Aurigae, early-type semidetached binary, UBV photometric anal. 79−44521
ε Aurigae, eclipsing binary, International UV Explorer obs. 79−17027
ζ Aurigae, eclipsing binary, UV obs. of supergiant atmos. 80−94836
IU Aurigae, massive triple system, obs. 77−64798
ε Aurigae, spectrum outside eclipse 77−71129
ε Aurigae, UV spectrum using IUE 79−71071
α Aurigae (Capella), Mg II lines obs. rel. to chromosphere model 78−40931
T Aurigae (Nova 1891), old nova, photometric and spectroscopic obs. 80−90446
AA Aurigae field, UBV photoelectric magnitude sequence 77−74073
B2 1652+39, BL Lacertae-type object, photoelectric intraday photometric obs. 78−36681
B, A and F stars, spectrophotometry, effective temps. 78−57546
B, A and F stars in selected areas, intrinsic uvby β indices, distances and colour excesses 78−89171
B-, A- and F-type stars, photoelec. K-line indices 79−16953
B- and A-stars, spectral class. from S2/S68 UV expt. 77−29839
B-type stars, He weak, UV flux distrib. 78−96477
B-type stars, search for weak interstellar lines in spectra 77−74124
B-type stars, UV obs. of six rapidly rotating objects 77−56938
B-type stars, uvby indices, empirical effective temps. and bolometric corrections 77−45429
B-type stars, XUV obs. and constraints 78−93232
B-type stars absolute UV spectrophotometry, continua and absorpt. features 77−22217
Balloon-borne UV Stellar Spectrograph, first obs. results 79−70955
Balloon-borne UV Stellar Spectrograph, instrumentation and obs. 79−70954
Barnard Loop Nebula, far UV imagery 77−29911
Basle catalogue of 1906 blue objects at high galactic latitudes 78−32360
BD+10°2179, BD−9°4395, extreme He stars, UV spectra 79−16976
BD+10°2179, C rich H deficient star, UBV photometric obs. 80−90437
BD+33°2642, galactic halo blue star, mass loss determ. from IUE obs. 80−72947
BD+39°3226, BD+34°1543, hot subdwarfs, spectral types 78−45323
Be 94, UBV photometric obs. of young distant open cluster in Cepheus 78−61892
Be and shell stars, mass loss from Copernicus UV data 77−56986
Be and shell stars, UV spectra, circumstellar absorpt. lines 79−62832
Be and shell stars, UV spectrophotometry with TD-1 satellite 80−90438
Be stars, evidence for mass loss in mid-UV spectra 78−8010
Be stars, photometric behaviour, UV excess, emission indices, galactic distrib. 80−36637
Be stars, UV radiation intensity obs. *(French)* 78−81635
Be-stars, UV fluxes 78−61870
Be-stars, UV Si IV/C IV ratio, Skylab obs. 77−56987
Be-stars 77−56985
Be-stars showing poles, far UV spectra 77−56990
776 Berbericia, slow spinning asteroid with rot. period of nearly one day, photometric evidence 80−17529
Berkeley 11, compact open cluster, UBV obs. 80−94840
Bochum 15 stellar aggregate, photoelectric and spectroscopic obs. 77−87490
44=i Bootis, eclipsing binary, variable light curve obs. and implications 78−61887
α Bootis, search for Ti II 3080 Å multiplet emission 80−51769
α Bootis, spectrophotometric profile, 3200-3600 Å 80−62118
α Bootis (Arcturus), Ca II K-line rel. to variable mass loss and giant convective elements 77−22213
α Bootis (Arcturus), far UV spectrum, coronal temp. determ. 78−16407
α Bootis (Arcturus), line identifications in UV spectrum 79−25598
α Bootis (Arcturus), UV obs. of chromospheric emission line profiles 78−81620
ξ Bootis A, active dwarf star, chromospheric emission lines obs. 80−12762
BPM 25114, southern mag. white dwarf, spectrophotometric obs. 79−92765
bright galaxies, optical redshifts 78−89252
bright quasars discovery program, preliminary results 77−17715
bright southern stars, Stromgren photometry rel. to spectral classification 79−88645
Byurakan 2, open cluster, UBV photometry 77−2345
3C 120, Seyfert galaxy, spectrophotometric obs. of assoc. nebulosity 80−67890
3C 273, far UV spectrophotometry of quasar using Faint Object Telescope 79−25481
3 C 273, H I spectral line intensities *(Russian)* 79−88763
3C 273, IUE obs. of quasar spectrum 79−71149
3C 273, quasar, detailed UV obs. with IUE 80−94886
3C 273, quasar, UV emission line spectrum 77−87567
3C 273, quasar, UV spectrophotometry 78−12401
3C 273, UBV obs., (1975 to 1979) 80−62309
3C 273, UV spectrum, 1200-1700 Å, cosmological implications 78−45425
3C 33, 98, 184.1 and 218, rotation axes 80−26997
3C 371, BL Lacertae-type object, photoelectric intraday photometric obs. 78−36681
3C 390.3, obs. of radio galaxy with International UV Explorer 79−67101
3C 66 A, BL Lacertae-type object, photoelectric intraday photometric obs. 78−36681
3C 98, 3C 178, 3C 192, 3C 327, narrow-line radio galaxies, optical spectra 77−33664
Ca II K line emission widths in solar and stellar spectra 77−41373
Z Camelopardalis, dwarf nova, spectrophotometry at standstill and in eruption 80−82366
AX Camelopardalis (53 Camelopardalis), Ap star, UBV photoelectric photometry and period of var. *(Italian)* 80−90448
α Camelopardalis (O9.5 Ia), stellar wind terminal vel. short time changes from UV spectrum 80−36625
38 Cancri, δ Scuti star, UBV photometric obs. of variability 80−22021
AH Cancri, contact binary in M67, spectrum and photometry 79−40222
49 Cancri, spectrophotometry of Ap star, continuum features vars. 80−36638
R Canis Majoris, eclipsing binary, multiband photoelectric photometry 77−53633
CW Canis Majoris, eclipsing binary, UBV photometry 77−37615
UW Canis Majoris, eclipsing binary, UV photometry and primary component shape and atmospheric struct. 78−40992
α Canis Majoris, EUV obs., Sirius B model atm. 77−33489
α Canis Majoris, Lα obs., interstellar H and D determ. 79−21275
UW Canis Majoris, O7f supergiant, UV lines P Cygni profiles rel. to mass loss rate 80−67736
27 Canis Majoris, spectroscopic obs. in 0.14-4.7 μ range 78−85957
α Canis Majoris (Sirius), B abundance 77−53585
α Canis Majoris (Sirius), search for surrounding nebulosity 78−93242
α Canis Majoris (Sirius B), EUV obs., evidence against photospheric origin of 0.25 keV flux 78−49481
α Canis Majoris (Sirius B), spectral energy distrib. 80−8629
α Canis Majoris B (Sirius B), search for far UV emission 79−5821
β Canis Majoris stars, ANS UV photometry 80−26871
β Canis Majoris stars, UV flux obs., basic data obtained with TD-1A satellite 80−51783
β Canis Majoris stars, UV obs. by TD-1A satellite 78−20839
β Canis Majoris stars in southern hemisphere, photometric search 78−12243

ultraviolet astronomical observations continued
α Canis Minoris, Copernicus UV spectral obs. 77−33480
α Canis Minoris, Utrecht UV spectrophotometer obs. 78−69793
α Canis Minoris (Procyon), CH and CN bands obs. rel. to CNO abundances 78−93222
VZ Canum Venaticorum, eclipsing binary star, photometric elements and intrinsic variability 77−45487
TX Canum Venaticorum, evolution from cataclysmic to stationary P Cygni stage 79−12479
RS Canum Venaticorum, out of eclipse light var. and comparison with similar stars 80−109489
α^2 Canum Venaticorum, UV flux distrib. 79−80313
ζ Capricorni, Ba star, white dwarf+giant, UV spectra obs. 80−105284
ν Capricorni (B9.5 V), spectrum and abundance anal. 80−90415
χ Carinae, β Canis Majoris type variability discovery from UBV photometry 79−80326
η Carinae, IUE spectral obs. 79−71051
AG Carinae, luminous star in symmetric nebulae, IUE low-dispersion spectrum 80−46560
η Carinae, optical and UV line emission of ionised Fe 77−13364
η Carinae, reddening of optical radiation 77−41385
β Carinae, UV spectra, comparison of synthetic and observed spectra 77−29820
η Carinae, UV spectrum and expansion vel., IUE obs. 79−30071
QZ Carinae (HD 93206), massive multiple system in great Carina Nebula, spectral types and orbits 79−97027
QZ Carinae (HD 93206), O-type quadruple eclipsing system, spectroscopic and radial vel. study 80−105275
VY Carinae field stars, spectra and photometry rel. to cepheid absolute magnitude 77−64764
Cassiopeia A supernova remnant, abundance inhomogeneities 80−12797
TV Cassiopeiae, Algol variable, UBV photometric obs. 79−35306
γ Cassiopeiae, Be star, new UV C IV and Si IV shell lines 79−84802
γ Cassiopeiae, Be star, polarisation rapid vars. 80−22022
γ Cassiopeiae, Be star, spectrophotometric variability from UV and Hα obs. 79−5829
SU Cassiopeiae, Cepheid variable, spectrophotometric determ. of effective temp. 80−90435
VX Cassiopeiae, early-type irregular variable, photometric variability *(Russian)* 80−72973
RZ Cassiopeiae, eclipsing binary, spectroscopic orbit 80−22040
DO Cassiopeiae, eclipsing binary, three-colour photoelectric investigation 78−16462
AB Cassiopeiae, eclipsing binary with δ Scuti primary, light vars. preliminary anal. 80−94831
κ Cassiopeiae, effective temp. radius, mass loss and luminosity 80−51748
γ Cassiopeiae, N I interstellar absorption in γ Cassiopeiae direction, UV obs. 80−51823
γ Cassiopeiae, UV and optical spectral var. rel. to coronal emission 78−93251
SU Cassiopeiae region, field stars photometry rel. to Cepheid distance and pulsation mode 78−89204
cataclysmic variables, visual continuum flux distribs. 80−36636
cD galaxies in poor clusters, photometry, spectra and redshifts 79−48907
cD galaxy in Abell 2029, envelope spectra rel. to dynamics and struct. 79−92850
CD-31°622, spectroscopic obs. of DC white dwarf candidate 77−67090
186 Celuta, slowly spinning asteroid, photometry rel. to rot. period and comp. type 78−61782
proxima=V645 Centauri, dMe flare star, quiescent corona, transition region, and chromosphere obs. 80−56850
BV Centauri, dwarf nova, identification as spectroscopic binary 80−51775
V436 Centauri, dwarf nova, photometry during superoutburst (May 1978) 80−46570
SZ Centauri, eclipsing binary, four-colour photometry, photometric elements, dimensions and He content 77−41391
V346 Centauri, eclipsing binary, spectroscopic orbit 79−58378
μ Centauri, far UV spectra analysis of pole-on Be-star 79−48805
β Centauri, occultation by Earth, satellite obs., atm. O_3 density meas. 77−53259
β Centauri, occultation by Earth's atmosphere rel. to O_3 and Cl meas., OAO 3 obs. 77−9580
ω Centauri, SEC Vidicon photometry of main sequence 80−90491
ζ Centauri, shell star, Copernicus UV obs. 77−56989
μ Centauri (B2 IVe), new circumstellar shell development, spectroscopic obs. (1980 June 10 to 12) 80−94808
V748 Centauri (Centaurus X-4?), high-latit. eclipsing system, VBLUW photometry 79−44529
V810 Centauri (HD 101947), yellow variable supergiant near Cepheid instability strip, VBLUW photometry 80−98672
α Centauri A, Be abundance and constraints on Be form. 77−41379
α Centauri A, Utrecht UV spectrophotometer obs. 78−69793
α Centauri A and B, IUE spectra and transition region models 80−46543
α Centauri C (Proxima Centauri), EUV flare obs. rel. to flare star scaling theory 77−45453
central stars of planetary nebulae, UV spectral obs. from TD-1 satellite 80−31300
EI Cephei, Am eclipsing binary, light curve anal. 77−33560
9 Cephei, B2-type supergiant, circumstellar CO lines discovery 79−84793
β Cephei, Copernicus UV obs. 77−33502
U Cephei, eclipsing binary, gas stream effects in UV spectrum, IUE obs. 80−26898
U Cephei, eclipsing binary, hot/cool spots obs. in UV light curves 78−57577
T Cephei, long-period variable, radial-vel. obs. 79−88684
NY Cephei, massive eclipsing binary star, progress report from UBV photometry 80−67789
T Cephei, Me variable, Tc discovery 78−32483
U Cephei, photoelectric obs. of recent eclipses 79−67061
VV Cephei, supergiant eclipsing binary UV spectrum 80−82415
VV Cephei, UB photoelec. obs. 77−17633
EM Cephei, UBV, photometry rel. to constancy or variability of period 80−105286
VV Cephei, UBV photometry during ingress phase of 1976-78 eclipse 78−20862
U Cephei, UV excess, mass transfer in eclipsing binary system 77−33555
ultraviolet astronomical observations continued
VV Cephei, UV spectrum in 1978, flux distrib. 79−88698
VV Cephei, UV spectrum obs. during chromospheric eclipse phase 80−109498
λ Cephei, variable outflow in Of star, spectroscopic obs. 79−35263
9 Cephei (B2 Ib), circumstellar CO obs. 80−94795
β Cephei stars, search south of declination −20°, B-type giants and subgiants 78−61863
VV Cephei system, distant, in Puppis, spectral classification, UBV photometry and polarimetry 80−51810
Cepheid variables, VBLUW photometry rel. to intrinsic colours and physical props. 78−28696
Cepheids, in Magellanic Clouds, UBV photometry, evidence for interstellar reddening 77−2435
Cepheids, short period, in N.hemisphere, UBV photometry rel. to search for double mode Cepheids 80−94814
UV Ceti, continuum and Hβ emission vars. during large flare 77−45456
TV Ceti, F-type eclipsing binary, four-colour photometric obs. 79−40217
κ Ceti, IUE obs. of far UV spectra of G-type dwarf 80−56831
TX Ceti, UBV obs., photometric elements of eclipsing binary star 79−8950
o Ceti (Mira), H I emission line profiles *(Russian)* 79−16990
o Ceti (Mira), long-period variable, radial-vel. obs. 79−88684
o Ceti (Mira), rapid light vars. of companion star during 1977 light min. 78−96492
o Ceti AB, IUE obs. of UV spectrum 80−22027
RS Chamaeleontis, eclipsing binary, four-colour photometry rel. to photmetric elements, absolute dimensions and He abundance 80−67783
Chu's object in Perseus, UBV photometry and spectrum rel. to identification as galactic star 80−62132
classical Cepheids colour excesses 77−22242
CoD−38°10980, white dwarf, photometry and spectroscopy rel. to gravit. redshift 78−24511
CoD −35° 10525, bright YY Orionis star, spectrum and UBV photometry 78−36566
Collinder 132a, b, UBVβ photometry of two sparse open clusters 78−32540
μ Colombae line of sight, Copernicus UV obs. 77−33591
Coma cluster, new stellar standard sequence 78−93436
14 Comae, A-type shell star, spectroscopic obs. 78−7992
17 Comae A, magnetically variable Ap star, spectroscopic obs. 77−17595
Comet Arend-Roland (1957 III), visible and UV spectra anal. *(Chinese)* 80−12709
Comet Bennett (1970 II), CN (0-0) band brightness profile obs. rel. to CN prod. 80−82303
Comet Bradfield (1979l), UV spectrum, UE obs. 80−90371
Comet Kobayashi-Berger-Milon (1975 IX), Lyman-α obs. 80−4301
Comet Kohoutek (1973 XII), C and O prod. rates 77−49331
Comet Kohoutek (1973 XII), Mariner 10 UV obs. of Lyman-α line 79−96970
Comet Seargent (1978m), UV spectral obs. by IUE 78−96436
Comet Seargent (1978m), UV spectrum 79−44413
Comet Tago-Sato-Kosaka (1969 IX), H and OH prod. rates 78−28580
Comet West (1975n), Lyman α obs. 77−82163
Comet West (1975n), photography and narrow-band photometry 77−17429
Comet West (1976 VI), CN (0-0) band brightness profile obs. rel. to CN prod. 80−82303
comet West (1976 VI), emission bands and continuum flux heliocentric depend. 80−36575
Comet West (1976 VI), Lyman α isophotes 80−46485
Comet West (1976 VI), spectrophotometry after perihelion passage, emission features vars. 78−57503
comets, recent, periodic, photometry rel. to gas and dust props. 79−70997
comets recent UV and IR obs. and prospects for Spacelab 77−33425
compact galaxies, spectroscopic and photometric obs. 78−77603
compact nebulae, very-low-excitation, in Magellanic Clouds, spectra 78−32556
cool giant stars, chromosphere mass loss determ. from Mg II UV line obs. 80−85935
cool stars, local interstellar H and D Lyman α towards four objects 79−5886
cool stars, Mg II flux profiles and chromospheric radiative loss rates 80−36611
cool stars, outer atms. struct., solar-type and non-solar-type stars 79−48791
cool stars, UV spectra obs. by International Ultraviolet Explorer (IUE) 78−96475
S Coronae Austrinae, a bright southern YY Orionis star, spectroscopic obs. 77−29818
S Coronae Austrinae, identification of absorpt. lines, irradiated amethyst 79−25601
S Coronae Austrinae, YY Orionis star, satellite UV spectrum 79−67016
α Coronae Borealis, binary star, UV spectrum 77−45485
R Coronae Borealis, search for graphite feature at 2200 Å 77−87419
R Coronae Borealis type variables and related objects, UBV photometric obs. 80−90437
coronal forbidden lines in 975-3000 Å range, Skylab obs. 77−60734
coronal hole, radio and EUV obs. 77−78753
coronal hole structrue from UV and radio obs. 77−53513
coronal holes, locations, sizes and evolution during June 1973 to January 1974, EUV obs. 77−56893
cosmic background radiation at 1440 Å 79−71159
CPD−26°389, central star of NGC 1360, radial vel. obs. 80−4350
CPD-26°389, central star of NGC 1360, spectroscopic binary within planetary nebula 77−45494
3CR, radio galaxies, spectrophotometry spectral energy distrib. 79−21413
Crab Nebula outskirts, remarkable spectra and element abundances 78−36662
BI Crucis, new symbiotic star, spectrum 80−109442
31 and 32 Cygni, ζ Aurigae stars, UV spectroscopic obs. 80−109499
P Cygni, Copernicus obs. 79−30066
SS Cygni, dwarf nova, spectrophotometry rel. to accretion disc models in erruption and at min. light 80−36635
CG Cygni, eclipsing binary, changing light curve obs. 79−48857
V367 Cygni, eclipsing binary, spectroscopic study 78−53984
GO Cygni, eclipsing binary, UBV photometry rel. to period changes 80−72999

ultraviolet astronomical observations continued
P Cygni, effective temp. radius, mass loss and luminosity 80−51748
P Cygni, extreme B-type supergiant, UV spectroscopy 80−22004
ν Cygni, far UV spectra analysis of pole-on Be-star 79−48805
P Cygni, high resolution UV spectrum obs. 80−26873
32 Cygni, IUE obs. and effects of B-type star within late-type supergiant upper chromosphere 80−22036
V382 Cygni, IUE spectra of massive close binary 80−8659
χ Cygni, long-period variable, radial-vel. obs. 79−88684
α Cygni, mass loss from mid UV spectrum obs. 78−93217
V832=59 Cygni, mass-losing Be star, changes in UV spectrum 80−46561
V389 Cygni, peculiar (Ap-type) binary, spectroscopic obs. 78−85975
V1500 Cygni, post-nova light curve development, UBV and Hβ obs. 77−71115
57 Cygni, spectroscopic binary, search for systematic radial vel. anomalies 80−17617
α Cygni, supergiant, near UV spectrum 78−7991
CH Cygni, symbiotic star, IUE obs. during active phase 79−62846
CH Cygni, symbiotic star, rapid and slow light vars. 80−51792
V1500 Cygni, UV photometry 77−64766
59=V832 Cygni, variable mass flux from spectroscopic obs. 80−41840
V1341 Cygni (Cygnus X-2), UBV photometry and light vars. 79−5833
V1341 Cygni (Cygnus X-2), UBV photometry and possible 82-minute quasi-periodic bursts obs. *(Russian)* 79−17140
α Cygni (Deneb), Copernicus obs. of UV spectrum 78−45330
V1500 Cygni (Nova 1975), flux distribs. rel. to shell electron temps. and densities 79−30068
V1500 Cygni (Nova 1975), line spectrum evolution 78−32493
V1500 Cygni (Nova 1975), linear polarization obs. 78−36601
V1500 Cygni (Nova 1975), photometric and spectroscopic obs. 78−36604
V1500 Cygni (Nova 1975), polarimetric and photometric obs. 78−36612
V1500 Cygni (Nova 1975), small amplitude light var. 78−36608
V1500 Cygni (Nova 1975), spectral energy distrib. 78−36605
V1500 Cygni (Nova 1975), spectrographic obs. *(Chinese)* 79−16982
V1500 Cygni (Nova 1975), UBV photometry, short period variability 78−61862
V1500 Cygni (Nova 1975), UBVR Hα photometry and polarimetry 78−36611
V1500 Cygni (Nova 1975), UBVRI photometry and polarimetry 78−36614
V1500 Cygni (Nova 1975), UV photometry after visual max. 77−82260
V1500 Cygni (Nova 1975), visible and near UV photoelec. photometry 78−36610
V1500 Cygni (Nova 1975), visible and near UV spectrophotometric obs. 78−32492
V1500 Cygni (Nova 1975), visible and near UV spectrophotometry 78−32494
V1500 Cygni (Nova 1975), visible and UV spectra and light curve 80−12771
V1500 Cygni (Nova 1975), visible-band linear polarimetry 78−36621
V1500 Cygni (Nova 1975) photometric obs. at Skalnate Pleso Observatory 78−36617
V1668Cygni (Nova 1978), linear polarisation obs. 80−26875
V1668 Cygni (Nova 1978), multifilter photometry and polarimetry 80−90454
V1668 Cygni (Nova 1978), spectroscopic and photometric obs., (1978 to 1979) *(Russian)* 80−109444
V1668 Cygni (Nova 1978), UBV light curve 80−46565
V1668 Cygni (Nova 1978), UV spectrum, emission lines 79−62837
V1500 Cygni (Nova Cygni 1975), low resolution spectrophotometry 77−49403
V1500 Cygni (Nova Cygni 1975), spectrophotometric obs. 77−49402
P Cygni in far UV *(Russian)* 79−8919
CI Cygni symbiotic star, UV and optical spectrum changes during eclipse 80−105258
Cygnus Loop, far UV emission line spectrum, C depletion in interstellar medium 79−21398
Cygnus Loop, SNR, abundances and filament shock vel., UV obs. 80−94848
Cygnus Loop, supernova remnant, UV spectral obs. of bright filament 78−45387
Cygnus Loop, Voyager 2 UV spectrometer obs. 79−92816
Cygnus OB2 number 12, spectral classification and membership of association 80−51760
Cygnus X-1, discovery of synchronous binary polarization 78−41087
Cygnus X-1, evidence for 39 day period 78−8165
Cygnus X-1, new period in X-ray binary system *(German)* 78−81712
Cygnus X-1, UV shot noise upper limit 80−4458
Cygnus X-1 (HDE 226868), search for 78.4 day period in U-band polarisation 79−75297
Cygnus X-1 (HDE 226868) system, search for third star 77−45606
Cygnus X-1 (V1357 Cygni), optical light curve vars. rel. to X-ray vars. 80−109560
Cygnus X-1 (V1357 Cygni), optical photometry (1980 May 25 to July 7) 80−90578
Cygnus X-2, rapid UV flux vars., IUE obs. 80−12833
D and cD galaxies in poor clusters, struct. and photometry 78−32580
DA 240, radio galaxy, high-vel. gas in jet 78−28773
degenerate star candidates, photoelectric and spectroscopic obs. 80−12763
degenerate stars, UV spectrophotometry, IUE obs. 79−53810
Deimos, spectral evidence for carbonaceous chondrite surface comp. 80−41754
HR Delphini, UV spectrum, stellar wind 80−26880
HR Delphini (Nova 1967), short period light vars. from UBV photometry 80−67744
δ Delphini stars in Michigan Spectral Catalogue, uvbyβ photometry rel. to spectral types 80−4377
diffuse cosmic far UV background, rocket obs. 80−46708
diffuse cosmic UV background, spectrum 80−17696
diffuse galactic light, S2/68 sky-survey telescope UV obs. 79−12519
diffuse interstellar bands at far UV wavelengths, obs. 78−32554
diffuse sky background, D2B satellite ELZ photometer survey 80−105404
distant cluster of galaxies, photometry and red shift 78−12377
DO white dwarfs, spectrophotometry rel. to effective temps. and He abundances 79−35249
S Doradus, LMC Hubble-Sandage variable, IUE and ground based spectroscopic obs. 80−101595

ultraviolet astronomical observations continued
β Doradus, Mg II h- and k-lines in UV spectra of Cepheid 79−40196
β Doradus, UV photometry of Cepheid by ANS 79−35272
S Doradus (HD 35343), luminous LMC supergiant, long time baseline VBLUW photometry 80−22007
S Doradus (HD 35343), luminous LMC supergiant, long time baseline VBLUW photometry 80−36630
30 Doradus central object (HD 38268), interstellar and nebular lines obs. 80−51839
30 Doradus complex, in LMC, UV reddening law 78−96516
30 Doradus nebular complex, chemical comp. and struct. obs. 80−62226
30 Doradus region, far UV extinction anomaly 78−45386
30 Doradus region, in LMC, interstellar extinction and stellar population 78−96517
30 Doradus region, uvbyR surface photometry 78−81670
double spiral galaxies, UBV photometry, magnitudes and colour indices 79−62914
ζ Draconis, line identifications in UV spectra 77−87384
ϕ Draconis, Si Ap-star, UV vars. rel. to patchy stellar surface model 77−49389
CR Draconis, UV Ceti variable, flares colour behaviour 80−22020
BV Draconis (ADS 9537A), W Ursae Majoris type star, photoelectric photometric obs. 79−35296
BW Draconis (ADS 9537B), W Ursae Majoris type star, photoelectric photometric obs. 79−35296
BY Draconis-type stars, spectroscopic binary incidence 77−87401
dwarf novae, eruption types and superhumps, obs. 79−75212
dwarf novae, EUV obs. from Apollo-Soyuz Test Project 78−93252
dwarf novae, satellite UV obs., temp. calc. 77−57033
dwarf novae, spectra *(Russian)* 80−8638
dwarf novae, spectrophotometry, 1250-7500 Å region 80−46577
E3 (ESO-037-SC 01) dying globular cluster, photometry and stellar content rel. to tidal truncation 80−105291
E/S0 radio galaxies, ionized gas obs. 79−17105
early A-type stars, UV spectral classification 78−69794
early Be stars, macroscopic radial atmospheric motions 78−8009
early O-type star in SMC, discovery 79−5820
early type stars, 206-287 nm UV spectra of Ap, Bp, Be, Bn and shell stars 80−51776
early type stars, 'normal', with anomalous mid UV spectra 80−26857
early type stars, intermediate-band photometry 77−49385
early type stars, Mg II lines near 2800 Å 78−12229
early type stars, mid UV spectra obs. 80−21995
early type stars, normal, near UV line blocking depend. on spectral type and luminosity 80−36619
early type stars, rotation effects, TD-1A obs. 79−44476
early-type star Lyman α and β profiles 77−87391
early-type stars, catalogue of 0.2 Å far UV spectra meas. by Copernicus 77−56843
early-type stars, Copernicus UV obs., of He I lines 80−41825
early-type stars, interstellar C IV and Si IV column densities 80−73018
early-type stars, interstellar gaseous Fe depletion from Fe II resonance 79−44584
early-type stars, near UV obs. of line blocking factors 78−45329
early-type stars, radial vel. meas. and standard wavelengths 77−17547
early-type stars, Skylab UV obs., MK spectral types 78−40933
early-type stars, spectral classification from TD1 satellite low dispersion UV spectra 78−16421
early-type stars, UV spectrophotometry 77−29836
early-type stars, vacuum UV spectrophotometry and effective temps. 79−30060
early-type stars and cool stars, UV spectroscopy of outer layers 80−72922
faint early-type stars in neighbourhood of H II region RCW 38, UBV photometry 80−4352
early-type stars in Perseus, UV spectrophotometry, energy distrib. 79−88653
early-type stars in southern hemisphere, four colour photometry and spectral types 78−40945
early-type stars with Balmer emission, near UV (2000-3000 Å) spectra 80−94811
early-type stars with six degrees of galactic anticentre direction, radial vels. 78−7990
early-type supergiants, spectrum variability, UV obs. *(Italian)* 78−32458
SW eclipsing binary, period study, photometry and spectra obs. 80−82424
eclipsing binary runaway, orbital data, UV obs. 80−85952
emission line stars, Mg II obs. near 2800 Å, absolute flux calibration 77−13350
emission regions, C III spectral line obs. by IUE 79−71089
emission-line variable (No.86) in core of M 15, UBV photometry, probably W Virginis star 80−77458
equatorial and southern bright stars, UVBYβ photometry 77−22205
γ Equulei, peculiar A-type star, line identification study, 3086 to 3807 Å 79−88659
ε Eridani, UV line spectrum of active chromosphere star, models 80−77394
eruptive blue variables at high galactic latit., spectrophotometry 78−32482
ESO 012-G21, Seyfert 1 galaxy, spectrum, redshift, UBV photometry and X-ray identification 80−8695
ESO 113-IG45, galaxy and/or quasar, spectrum, photometry and struct. 78−28782
ESO 113-IG 45 (=Fairall 9), Seyfert galaxy, spectroscopic and multiaperture photometric obs. 80−31362
ESO 140-G43 (Fairall-51), new southern Seyfert 1 galaxy, discovery and red shift 78−54044
247 Eukrate, UBV photometry, light curve and rot. period 80−21942
Europa, UV emissions and possibility of O and H clouds 79−5775
EUV source detect. in Pavo region at 500 Å 78−28675
EUV spectroscopic method for electron density determ. in stellar atms. 79−16836
EUV/soft X-ray background, Apollo-Soyuz sky survey results 79−71160
exciting stars of Orion triple emission nebula, UBV photometry 77−13430
extragalactic emission line objects, third list from Curtis Schmidt thin prism survey 78−28538
extragalactic emission-line objects, second list from Curtis Schmidt thin prism survey 78−28537

ultraviolet astronomical observations continued
extragalactic objects UV spectra, International Ultraviolet Explorer (IUE) obs. 78−96540
extragalactic optically variable objects, calibration of photoelec. comparison sequences 77−87537
extreme galactic B and A supergiants, light vars. 77−56927
F, G, K-type stars, electron concs. in photospheres, Fe line obs. *(Russian)* 77−49376
F- and G-type stars, C and N abundances 77−91530
F- and G-type stars, props. determ. by spectral quantification 77−29791
faint blue stars, southern, UBV photometry 80−82349
faint blue stars near galactic anticentre, spectral types 79−71021
faint blue stars near galactic anticentre, UBV photometry 78−40932
faint blue stars UVBY photometry, second list of southern stars 77−45424
faint quasars, spectroscopy and props. of CTIO 4 metre survey 78−32592
faint red stars at intermediate galactic latit., UBVR photometric obs. 78−32457
Fairall 160, 182, UBV photometry 80−82349
Feige 24, EUV obs. of hot white dwarf, temp. determ., interstellar H I density calc. 78−16422
Feige 24, hot white dwarf, EUV obs. and stellar charact. 77−9746
Feige 24, hot white dwarf, OAO-2 UV photometry 77−9747
Feige 4, hot white dwarf, identified with bright EUV source 78−89200
Feige 7, mag. white dwarf, spectroscopic studies 79−25603
Feige 86, UV high-resolution spectrum 80−41834
Feige 86, UV spectrum of peculiar hot halo stars 79−48811
flare stars, photoelectric monitoring (1974 to 1976) 79−44509
flare stars discovery in Ophiuchus-Scorpius region *(Chinese)* 78−69804
flare stars in Orion Nebula region, new objects and repeated outbursts 80−56852
flare stars in Pleiades, photometric obs. *(Russian)* 77−91536
flare stars in Pleiades, UV and photographic obs. of flares *(Russian)* 77−13367
G200-39, hot hybrid white dwarf, spectroscopic obs. 80−26852
G292.0+1.8, abundance anomalies, radial vels., possible Crab-like SNR 80−46628
G292.0+1.8, supernova remnant, optical identification and spectrum 79−84839
G292.0+1.8, young supernova remnant, high vel. material obs. 80−22064
G35-26, high-velocity mag. degenerate, obs. 78−73709
G-type dwarf stars, far UV Si emission line analysis 80−56829
galactic bright nuclei, survey of 448 galaxies 78−32569
galactic clusters observed in three colours, catalogue and distances 79−40089
galactic distrib. of interstellar absorpt. from Celescope catalogue, UBV and Hβ obs. 77−60810
galactic G-type supergiants, UBV photometry 80−41824
galactic globular clusters colour excess ratio, rel. to interstellar absorpt. law 78−28797
galactic halo, evidence for hot gaseous component from IUE UV obs. of (3C 273) 80−94886
galactic high-latitude regions, balloon-borne UV survey 80−41891
galactic light, rocket-borne photometry 79−35372
galactic poles, Apollo 17 far UV obs. of cosmic background 78−93401
galactic structure around l=140°, b=0°results from stellar UBV photometry 78−24555
galactic UV background, TD-1 satellite obs. 77−13504
galaxies, early-type, rot. curves meas. 78−54034
galaxies, elliptical and S0 colour-absolute magnitude relation 78−8108
galaxies, energy distribs. from OAO UV photometry 79−35360
galaxies, interacting, with compact components, UBV photometry 78−20888
galaxies, irregulars and blue compacts, chemical comp. and evolution from spectrophotometry 80−36711
galaxies, southern, UBV photometry of 262 objects 79−35364
galaxies, southern, with broad emission lines 78−20891
galaxies, UBV photoelectric photometry and photometric parameters 80−67855
galaxies, with UV continuum, tenth list *(Russian)* 77−91445
galaxies from ESO/Uppsala list, first catalogue of spectroscopic obs. 77−22113
galaxies nuclei, vel. dispersions meas. 77−57083
galaxies with UV continuum, ninth list *(Russian)* 77−49464
galaxies with UV continuum, photoelectric UBVR photometry *(Russian)* 80−36721
galaxies with UV continuum, twelfth list 80−67585
galaxies with UV excess, second list 80−67584
galaxies with UV excess and double and multiple nuclei, spectral study 80−67848
Galaxy nuclear bulge, stellar UBV photometry 78−53926
Ganymede, stellar occultation obs. by Voyager 1 rel. to exospheric atmosphere 80−26792
GCl 0422−213, distant globular cluster in Eridanus, preliminary photometry and spectroscopy 80−17624
GD 229, mag. white dwarf, spectroscopic studies 79−25603
Gd 428, variable star, photometry and spectrum rel. to nature of dwarf Cepheids 78−73720
GD 90, magnetic white dwarf, circular polarisation obs. 78−16409
ε Geminorum, occultation by Mars, evidence for atm. tides 77−37550
β Geminorum (Pollux), Mg II lines obs. rel. to chromosphere model 78−40931
giants, emission lines in UV spectra of α Bootis and α Tauri 79−71028
globular cluster giant stars, blanketing differences meas. 80−4345
globular clusters, ANS far UV photometry of blue horizontal branches 79−71080
globular clusters, ANS UV obs. in 1550-3300 Å range 77−91598
globular clusters, evidence for H II in cores 78−8065
globular clusters, radial UBV colour distribs. 79−25648
globular clusters, southern, surface-brightness profiles rel. to struct. and stellar content 79−71078
globular clusters, UBV photometry 78−16468
globular clusters, UBVR photometric obs., dust patches 78−81662
globular clusters, UV energy distribs. from Orbiting Astronomical Observatory photometry 80−73009
globular clusters, UV spectroscopic meas., central surface brightness distribs. 79−67067
globular clusters (M3, M5, M13, M15), equidensity curve meas. *(Russian)* 79−97041
ultraviolet astronomical observations continued
globular clusters evolved stars, CN strengths and UV excesses from DDO photometry 77−64753
β Gruis (M2 II), S I emission obs. in EUV spectrum 80−82359
GX 17+2 (3U 1813−14), photometry of optical candidate 78−28849
H 2155−304, optical counterpart position and spectrum 78−93478
H 2252−035, optical counterpart photometry and spectrum 80−101651
h 4866 B, vars. in spectral type and radial vel. 78−32518
H Lyman α and β lines, OSO 8 disc centre obs. compared with theoretical profiles 79−8888
Haro 15, spectrophotometry and morphology of galaxy with UV excess *(Russian)* 78−93387
HBV 475 (V1329 Cygni), high-excitation emission lines obs. 78−40955
HD 101065 light variations, comparison stars UBV photometry 78−69812
HD 102567, optical counterpart to 4U 1145−61, atm. model from UV obs. 80−105396
HD 105056, ON supergiant, radial vel. study 80−90427
HD 105902 (ADS 8448), Ba star in visual binary, spectra and photometry 77−78805
HD 116458, Ap-star, photometry, spectrum and orbit 77−64767
HD 116890, Ap star, 5200 Å depression index and light variability 77−64767
HD 116994, uvby photometry, var. period determ. 77−13358
HD 118216=HR 5110, radio outburst and UV spectra of RS Canum Venaticorum-type binary 79−62844
HD 118246, new Be star at high galactic latit., photometry and spectrum 78−73721
HD 137613, C rich H deficient star, UBV photometric obs. 80−90437
HD 149499 B, IUE obs. of hottest white dwarf 80−41828
HD 152667, =OAO 1653−40, photometry, spectrum and physical parameters 79−17021
HD 153919, Of supergiant, X-ray binary 3U 1700−37 optical counterpart, light curve anal. 78−32470
HD 153919 (3U 1700−37), binary X-ray source, radial vel. data in blue spectral region 78−61888
HD 153919 (3U 1700−37), X-ray binary, UV photometric obs. 77−45490
HD 153919 (3U 1700−37), X-ray eclipsing binary, VBLUW photometric obs. 79−17135
HD 153919 (3U 1700-37), binary X-ray source, radial vels. in blue spectral region 78−49556
HD 153919 (4U 1700−37), optical oscills. obs. 78−96572
HD 15570, Of/WN7 spectral classification problem 80−51786
HD 156385, WC7 star, anomalous 2200 Å absorpt. band 77−64769
HD 159378 (Tr 27-102), yellow variable supergiant near Cepheid instability strip, VBLUW photometry 80−98672
HD 161698, Hg-Mn star, chemical elements identification in spectrum 79−58354
HD 17576, UV subdwarf companion discovery from uvbyβ photometry 78−96479
HD 190073, a0ep star, Ca II lines struct., nightly vars. and line profiles interpretation 77−17578
HD 190603, effective temp. radius, mass loss and luminosity 80−51748
HD 192163, 191765, Wolf-Rayet stars, optical interstellar spectra obs. 80−17640
HD 192273, EUV flux upper limit, Voyager 1 obs. 80−77406
HD 193793, Wolf-Rayet star, photometric evidence for C-rich dust cloud 80−26861
HD 199892, spectrographic binary, spectrograms and orbital elements 79−21359
HD 200120, Be star, UV spectra vars. 77−5534
HD 200775, Be star, optical and UV extinction by dust in (NGC 7023) 80−109515
HD 206860, G0 V star, IUE obs. of active region 79−92766
HD 215038, Ap star, line identification list 78−32484
HD 221568, Ap star, light var. period 80−56856
HD 26676, unusual radio star, not close binary 78−73707
HD 26676 (HR 1307), UV spectrum, possible radio star 79−101150
HD 28497, distant unreddened star, Copernicus UV obs. 77−33591
HD 30466, double wave photometric variable Si star 77−87410
HD 33579, 35343, HDE 286757, 269006, most luminous LMC supergiants, long time baseline VBLUW photometry 80−22007
HD 33579, HD 35343 (S Doradus), HDE 268757, HDE 269006, most luminous LMC supergiants, long time baseline VBLUW photometry 80−36630
HD 34452, Si Ap star, spectroscopic study 78−65634
HD 3473, A2p star, spectrograms, Si and rare earth elements overabundance 77−74071
HD 3580, 187473, 212432, Si stars, uvby photometry and periods 78−96487
HD 3980, late Ap star, photometric and mag. variability obs. 80−56845
HD 39937, 101379, 155555, 174429, southern RS Canum Venaticorum stars candidates, radial vel. study 80−98686
HD 4174 (=EG Andromedae), peculiar M giant, spectra obs. 80−94798
HD 45677 or 50138, hot Bep stars with circumstellar dust IR excesses, UV obs. 78−93250
HD 49798, H-deficient subdwarf O-type binary, non-LTE spectral anal. 79−16978
HD 50169, Ap star, uvby photometric obs. 77−22236
HD 50896, distant unreddened star, Copernicus obs. of interstellar lines 77−26036
HD 50896, Wolf-Rayet star, detect. of polarisation struct. across emission lines 79−97008
HD 50896, Wolf-Rayet star, linear polarisation periodic vars. rel. to binary star nature 80−72972
HD 50896, Wolf-Rayet star, UV spectral energy distrib. 77−22211
HD 51480, shell star, spectroscopic obs., atmospheric struct. and distance 80−31305
HD 64740, He rich star, UV spectral vars. 80−22016
HD 77581 (3U 0900-40), X-ray binary, spectroscopic orbit and masses of components 78−16461
HD 77581 (Vela X-1), four colour photometric obs. and light curve anal. 77−17621
HD 87892, central star of NGC 3132, obs. of visual companion 78−20859
HD 88661, Be star, photometry and light vars. *(French)* 78−57562
HD 90657, Wolf-Rayet spectroscopic binary, spectroscopic obs. 77−13357

ultraviolet astronomical observations continued
HD 91805, spectrum anal. rel. to nature of Bidelman-MacConnell weak G-band stars 78−49432
HD 92664, Ap star, photometric variability and period from uvby photometry 79−40199
HD 93131, probably single WN7 star, spectroscopy and photoelectric photometry 79−8924
HD 94033 ultra short period cepheid, obs. 80−22024
HDE 226868 (Cygnus X-1), variable UV polarisation 77−37622
HDE 226868 (Cygnus X-1), X-ray and UV spectra from HEAO 2 and IUE 80−82543
HDE 245770, possible counterpart of variable X-ray source A 0535+26, line and continuum vars. 80−17600
HDE 245770 (A0535+26), UBV photometry during X-ray outburst 79−67024
HDE 245770 (Ariel 0535+26), photoelectric UBV photometry 78−36592
HDE 283048, hot subluminous star, spectrum 78−20823
HDE 313846, most extreme Of star, spectroscopic obs. and mass outflow 79−88682
He-3 1863, unusual high latit. Be star, spectral obs. 77−87418
HEAO-1 spacecraft pointing and scanning obs. 78−45185
Henize 715 (4U 1145−61), Be-type star, colour and luminosity vars. (1976-1980) 80−72979
Henize 787 (SAO 251905), five-colour photometry 77−29846
Henize 788 (Wray 977), counterpart of 3U 1223-62, five colour photometry 77−29846
Herbig-Haro object, far UV spectrum obs. rel. to nature of object 80−67714
Hercules X-1 (HZ Herculis), Bowen fluorescence mechanism evidence 78−53985
ι Herculis, B3 IV type star, Copernicus UV spectral atlas 80−67583
α^2 Herculis, circumstellar absorpt. lines rel. to absolute mass loss scale for red giants 78−7997
DY Herculis, dwarf Cepheid, radial vel. and radius 79−58358
DY Herculis, dwarf Cepheid, uvbyβ photometry and evolutionary status 79−58357
DI Herculis, eclipsing binary, photometric obs. anal. rel. to relativistic motion of periastron 80−94830
ϕ Herculis, Hg-Mn star, corona search, UV obs. 80−72986
AM Herculis, high speed photometric obs., 186 min. var., dwarf nova model 77−64806
AM Herculis, IUE UV obs. 79−67051
τ Herculis, line identifications in UV spectra 77−87384
AM Herculis, low-mass X-ray binary, radial vels. and line intensities 77−78826
α Herculis, M-type supergiant, Mg II h and k emission obs. 78−53945
AM Herculis, multicolour photometry, slow optical pulsar 78−28693
AC Herculis, RV Tauri star, UBV obs. 80−56857
BL Herculis, short-period Population II variable, chem. comp. determ. 79−8923
AM Herculis, spectrophotometric obs. at min. light min. light 80−98692
u Herculis, synthetic light curve soln. of OAO-2 UV light curves 80−4399
AM Herculis, X-ray eclipsing binary, UV and visible spectra anal. 80−109563
AM Herculis (3U 1809+50), simultaneous three-channel photometry rel. to optical flickering mechanism 80−82411
AM Herculis (3U 1809+50), UV spectrum obs. 80−67782
HZ Herculis (Hercules X-1), IUE obs. spectrum and light var. 80−73069
HZ Herculis (Hercules X-1), optical and UV obs. 80−109487
high velocity clouds, absorption line obs. by Copernicus, review 77−37640
high-velocity stars, southern, radial vels. 80−21988
high-velocity stars, southern, UBV colours 80−21989
horizontal-branch A-type stars, astrophysical parameters determ. 79−62829
hot stars, UV spectra obs. by International Ultraviolet Explorer (IUE) 78−96474
hot stars in LMC, far UV spectral evidence for hot gaseous galactic corona 79−67097
hot subdwarfs in Carnochan and Wilson catalogue, UV spectra 80−82354
hot white dwarfs, EUV flux interstellar absorpt., local clumpiness factor determ. 80−36627
hot white dwarfs, luminosity function, spectral type anal. 80−90418
HR 1099, Copernicus obs. of UV interstellar absorption lines 78−93358
HR 1099, RS Canum Venaticorum binary, optical spectrophotometry during major flare outburst 79−21342
HR 1099 (V711 Tauri), Copernicus UV obs. of Lyman α and Mg II emission 78−81651
HR 1170, δ Scuti-type star, light and colour curves 77−74058
HR 1300 spectroscopic binary Am star, orbital elements 77−49438
HR 2142 and 7084, mass loss from UV spectra obs. 80−109485
HR 2172, double-lined binary, radial vels. and equivalent widths *(French)* 77−17625
HR 3089, He-rich star, anal. of UV spectrum 77−9751
HR 3413, Ap star, photometric vars. and period *(French)* 78−32471
HR 4665, spectroscopy of bright long-period RS Canum Venaticorum system 80−36665
HR 5999, variable shell star, VBLUW photometry 78−28701
HR 6127, chemically peculiar star, spectral lines and equivalent width lists, visible obs. 80−82387
HR 6392, double star with very high luminosities, photometry, and spectra 77−45493
HR 8752, superluminous star, hot companion discovery by IUE 79−16947
HR 9049, (HD 224113), eclipsing spectroscopic binary star, period determ. 80−46609
Hyades stars, Be abundances 77−53584
Hydra I cluster, photometric obs. of brightest galaxies 77−33659
χ^2 Hydrae, eclipsing binary, four-colour photometry, orbital elements, dimensions and He abundance 78−65653
AI Hydrae, light curves and photometric elements of eclipsing binary 78−65652
TT Hydrae, UBV photometry, improved light elements 78−69837
RW Hydrae, UV obs. of hot component 80−56854
β Hydri, nearby subgiant star, XUV radiation upper limit 79−12471
HZ 43, EUV obs. of hot white dwarf. temp. determ., interstellar H I density calc. 78−16422

ultraviolet astronomical observations continued
IC 2149, planetary nebula, two-photon emission of H in UV spectrum 77−22301
IC 2944, stellar aggregate surrounding HD 101205, spectrographic and photometric obs. 77−17636
IC 3568, planetary nebula, struct. and internal extinction 80−31338
IC 361, open cluster, preliminary photometry 78−89228
IC 418, planetary nebula, UV spectra and C abundance 80−67832
IC 418, planetary nebula C abundance from visible and IUE obs. 80−82451
IC 4756, open cluster, uvby β photometry, distance modulus 78−53997
ϵ Indi, late type dwarf star, spectrum rel. to model atmosphere and comp. 80−90425
intermediate brightness stars, for UV photometry from ASTP 79−71027
International Ultraviolet Explorer, orbiting telescope, 1978 observations *(French)* 80−8540
International Ultraviolet Explorer (IUE), in-flight performance 78−96383
International Ultraviolet Explorer (IUE), obs., new era in UV astronomy 79−48671
International UV Explorer satellite, obs. of sample targets 78−32315
interplanetary H, Lyman α radiation meas. with absorpt. cell spectrophotometer 78−28519
interplanetary Lyman α emissions, Mariner 10 obs., rel. to solar wind latit. struct. 79−35085
interstellar 2200 Å feature, anomalous strength in Cassiopeia-Taurus association stars 80−77469
interstellar absorpt. in five stars, Copernicus obs. 77−33598
interstellar absorption lines in ζ Puppis spectrum 78−65665
interstellar abundance and depletion models for B, V, Cr, and Co 80−46630
interstellar C I lines, obs. in ζ Puppis and ζ Ophiuchi 79−35332
interstellar Cl and P abundances towards 10 stars, Copernicus obs. 78−36646
interstellar cloud surfaces, O VI absorption 79−97049
interstellar CO absorption in spectrum of ζ Ophiuchi, Copernicus obs. and cloud density 78−36656
interstellar D/H ratio in lines of sight to ζ Puppis and γ Cassiopeiae 77−37633
interstellar diffuse bands, 2175 Å band correl. with other features 77−60813
interstellar diffuse EUV radiation field obs. 79−30099
interstellar extinction, satellite obs. 79−67083
interstellar extinction feature at 220 nm and diffuse 443 nm band, ANS obs. 80−62244
interstellar gas, UV absorption line obs. of vel. distrib. 78−89235
interstellar gas in diffuse regions, Copernicus UV obs. *(Italian)* 78−32552
interstellar gas near 30 Doradus, UV absorpt. in stellar spectra 80−85978
interstellar grains, interaction of light with small-particle system 77−74111
interstellar H_2 column densities, Copernicus UV obs. 78−8070
interstellar H I Lyman α and β obs. by Voyager UV spectrometer 78−81673
interstellar HD, rotationally excited, towards ζ Ophiuchi, column density 79−25674
interstellar He, 584 Å obs. rel. to local density, correction 79−92834
interstellar He I, obs. with gas absorpt. cell, implications for local interstellar medium struct. 80−62234
interstellar high velocity cloud near ζ Orionis, density, temp. and comp. 77−22291
interstellar high-velocity gas clouds, abundance vars. 77−26039
interstellar lines in 67 stars, S 59 obs. rel. to Fe, Mn and Mg depletion 79−2563
interstellar lines towards 15(=S) Monocerotis 80−90494
interstellar lines towards Cepheus OB2 association, anal. 80−22052
interstellar local He I density from EUV obs. 78−4331
interstellar low mass dust clouds in solar vicinity, photometric survey results 80−36512
interstellar matter in front of χ Ophiuchi, optical obs. 79−25673
interstellar matter towards Orion OB1 assoc. stars ϵ Orionis and π^5 Orionis, Copernicus obs. 80−22050
interstellar medium, International Ultraviolet Explorer (IUE) spectroscopic obs. 78−96524
interstellar medium, UV obs. by Voyager in 500-1700 Å range 79−53878
interstellar medium Lyman α emission, line profile, temp. and polarisation from geocoronal absorpt. 77−67120
interstellar Mg column density towards nearby stars from Mg II obs. 78−41023
interstellar N_2 in diffuse clouds, Copernicus search, upper limits 79−25661
interstellar N abundance from XUV absorption line obs. 79−5741
interstellar Na I and/or Ca II lines, obs. towards 47 stars 79−25676
interstellar O I lines, O abundance determ. 78−16498
interstellar O VI, spectroscopic tracer for hot interstellar gas, Copernicus obs. 78−16505
interstellar OH and H_2O searches in diffuse clouds, Copernicus UV obs. 79−40233
interstellar radiation field, galactic latit. depend. of 1530 Å radiation 77−33704
interstellar reddening in high-latit. field around ω Bootis 79−101185
interstellar semitorrid gas obs. in direction of γ^2 Velorum and Gum Nebula 79−48890
interstellar Ti II 3384 Å in 68 stars, photoelectric scans and Ti abundances 78−57611
interstellar UV absorption lines assoc. with Vela SNR 77−33604
interstellar UV extinction obs. in galactic plane from TD1 satellite 78−93382
interstellar UV radiation field, obs. from S2/68 sky-survey telescope 80−77523
interstellar UV radiation field from ionization equilib. of C, S, Fe and Ca 77−87508
interstellar wind, Mariner 10 meas. of Lyman α and He I 584 Å interplanetary emissions 78−65474
interstellar wind, Mariner 10 UV obs. and solar radiation models 79−48736
interstellar wind properties from Lyman α and He I 584 Å interplanetary emissions 78−65475
Io, evidence of SO_2 from UV obs. 80−36561

ultraviolet astronomical observations continued
Io, global SO_2 abundance upper limit 80−77332
Io plasma torus, Voyager 1 EUV spectrum obs. 80−26792
irradiation flux determ. in 150-210 nm range 77−17509
IUE, first year of obs., conference, London, England (1979 April 4 to 6) 80−51960
IUE satellite, observing experience 80−36476
JL 76, spectroscopic obs. of DC white dwarf candidate 77−67090
Jupiter, atmospheric absorption in blue and UV 79−40125
Jupiter, auroral hot spots obs. 78−16333
Jupiter, far UV (1200-1900 Å) spectrum, rocket-borne multichannel spectrometer obs. 77−25974
Jupiter, H I Lyman α and Io torus, Voyager 2 EUV obs. 80−77338
Jupiter, Lyman α albedo, Copernicus UV obs. 80−94747
Jupiter, Lyman α emission var. with solar cycle 80−41759
Jupiter, O^+ forbidden emission detect. in inner magnetosphere 80−51687
Jupiter, polar regions limb darkening obs. and atmospheric props. 79−62790
Jupiter, upper atmosphere temperature, Voyager 1 meas. 80−17536
Jupiter, Voyager 1 EUV obs. 80−26792
Jupiter atmosphere map at 2400 Å from Voyager 2 obs. 80−77336
Jupiter spectrum, obs. from 1500 to 2000 Å with IUE 80−56752
K648, halo planetary nebula, spectrophotometry and element abundances 78−41011
Kron 3, SMC globular cluster, identification with X-ray source (4U 0026−73) 79−5919
KUV09313+4052, variable UV excess object, discovery, position and photometry 80−62159
Lacerta OB1 association stars, spectral classification and distances 77−37626
AR Lacertae, eclipsing binary, photometric obs., intrinsic variation 77−22271
EV Lacertae, flare star, photometry and spectrum rel. to starspots and rot. period 80−98665
EV Lacertae, high-speed five-colour photometry of flare star 77−56956
BL Lacertae, optical monitoring by three-colour photographic photometry 78−16525
BL Lacertae, photoelectric intraday photometric obs. 78−36681
EV Lacertae, UV Ceti variable, flares colour behaviour 80−22020
BL Lacertae type objects, linear optical polarisation study *(Russian)* 78−57640
Landolt celestial equatorial UBV standard stars, spectral classifications 79−75199
late B-type stars, rot. and incidence of HgMn stars 78−89199
late B-type stars, spectral class. from TD1 UV obs. 77−91529
late-type field stars in S.hemisphere, radial vel. study rel. to possible duplicity 80−98686
late-type stars, Copernicus survey of Mg II emission 79−80301
late-type stars, search for C IV reson. doublet, TD1 satellite UV obs. 77−5526
late-type stars, search for Ti II 3080 Å multiplet emission 80−51769
late-type stars intermediate-band photometry, calibration of indices 78−49424
LB 3459, short period eclipsing binary system containing two O-type subdwarfs, uvby photometry 78−53987
ρ Leonis, effective temp. radius, mass loss and luminosity 80−51748
ρ Leonis, expanding envelope OAO-3 spectra *(Russian)* 78−4224
η Leonis, mass loss from mid UV spectrum obs. 78−93217
20 Leonis, triple system with a δ Scuti variable, spectroscopic obs. 77−49440
AD Leonis, UV Ceti variable, flares colour behaviour 80−22020
48 Librae, Be star, shell spectrum line profiles 80−62146
AP Librae, BL Lacertae object, emission line obs. in (1976) 77−29932
48 Librae (FX Librae), shell star, spectroscopic study 78−96486
limb darkening in 3033-7297 A range 77−53507
LMC, Apollo 17 far UV spectra 77−13461
LMC, catalogue of UV obs. in 30 Doradus region 77−64844
LMC, integrated photometric props. 78−54054
LMC, interstellar extinction meas., UV sky-survey telescope obs. 79−35384
LMC, IUE obs. and 2200 Å feature detection towards reddened supergiants 79−16959
LMC, stellar photoelectric UBV photometry *(German)* 80−21932
LMC, UV surface brightness meas., TD-1 sky survey 79−71125
LMC, yellow stars UBV photometry and LMC members number 78−93417
LMC disc, underlying stellar component photometry rel. to population struct. 77−33633
LMC H II regions, ANS UV obs. of exciting stars 79−71017
LMC interstellar extinction, visible and UV obs. 80−51877
LMC OB and supergiant stars, deep objective prism survey catalogue 79−40090
LMC OB associations, Apollo 16 for UV spectra 77−33634
LMC X-2 optical candidate, UBV photometry and variability 79−17136
LMC X-4 optical candidate, binary nature 77−64879
local interstellar H and D densities, Copernicus obs. 78−16487
local interstellar medium, He component anal., UV obs. 79−30100
local interstellar medium, intermediate-vel. gas obs. 78−36655
long-period variable stars, radial vel. obs. 79−88684
long-period variable stars in S.hemisphere, narrowband polarimetry 80−98666
loose stellar clusterings in southern Milky Way, continued photometric studies 80−36679
loose stellar clusters in southern Milky Way, spectral type and UBV obs. 80−94839
low galactic latitude stars, proper motions, UBV photometry and mean secular parallax 78−57542
LP182-44, faint high-vel. degenerate star with probable C features, photometry and spectrum 79−67007
LP 145-141, C_2 white dwarf, spectrum, strong UV absorpt. obs. by IUE 80−67715
LP 790-29, southern mag. white dwarf, spectrophotometric obs. 79−92765
LS I+61°303, radio, optical, X-ray, gamma-ray Be star, optical and radio obs. 79−88755
LS I +61°303, radio variable Be star, UV spectrum, stellar models 80−26879
LS II+33°5, new H deficient B-type star, spectrum 78−93265
LSI+61°303, possibly optical counterpart of GT 0236+610, absence of variability 78−49438

ultraviolet astronomical observations continued
LSS 1916, 3371, new VV Cephei stars, spectra and colours 79−35299
luminous stars in M31 80−36622
luminous stars in symmetric nebulae, IUE low-dispersion spectra 80−46560
lunar total eclipse, 1975, May 24-25, UBV photometry 77−22126
RU Lupi, far UV spectrum of T Tauri type star 79−44494
α Lupi, UV light curve of β Cephei-type star 78−36570
Lyman α sky background, Copernicus high-resolution obs. 77−29963
Lyman alpha scattering meas. by Venera 9 in interplanetary space, interstellar medium parameters determ. 79−80180
RR Lyncis, Am eclipsing binary, photometry and spectroscopy, abundances 77−33558
Lynga 6, open cluster, photometry rel. to reality and membership of Cepheid TW Normae 77−87491
β Lyrae, eclipsing binary, random vars. in UV spectrum 77−22273
β Lyrae, photoelectric photometry rel. to orbital period variability 80−72997
RR Lyrae, UV photometry from Orbiting Astronomical Observatory, light curve interpretation 77−45435
α Lyrae, UV spectrum, line identifications 77−17552
β Lyrae, UV spectrum 78−8048
α Lyrae (Vega), B abundance 77−53585
α Lyrae (Vega), Copernicus UV obs. of C II and Si II lines 80−8627
α Lyrae (Vega), spectral anal. from Copernicus 80−26856
RR Lyrae stars, atlas of light and colour curves 77−82228
RR Lyrae stars, VBLUW photometry rel. to reddening and blanketing 79−48806
RR Lyrae stars in ω Centauri, UBV photometry rel. to comps. 78−73719
RR Lyrae stars in galactic bulge, spectra and comp. 77−26012
RR Lyrae stars in M4, UBV photometry 77−78802
RR Lyrae type variable discovery near M4 *(Chinese)* 78−69804
RR Lyrae variables in globular cluster NGC 6121 (M4), UBV photometry 80−22018
M101, spectra of H II regions, comp. gradient across spiral galaxy 78−65683
M104 (Sombrero galaxy), mass spectrum of star form. 77−17675
M15-K1082, two-hour variable UV-bright star in NGC 7078 (M15), spectra 79−88681
M25, young open cluster, UBV obs., photoelec. calibration, distance, reddening 79−8956
M25 (IC 4725), open cluster, stars four colour and Hβ photometry 78−8067
M31, globular clusters colour indices, rel. to interstellar absorpt. law 78−28796
M31, rocket far UV imagery 79−5897
M31, UV image 80−98716
M31 and M32, IUE spectra of nuclei 79−71117
M31 and M81 nuclei, UV continua, spectrophotometry obs. from ANS satellite 80−77478
M32-1, planetary nebula in M32, spectrophotometry and filter photometry 79−25664
M33, supergiants distrib. rel. to spiral struct. and star form. 79−21437
M33, UV integrated magnitudes of spiral galaxy 80−31368
M34, open cluster, UBV photoelectric photometry 78−12307
M67, open cluster, stellar proper motions rel. to membership 77−22281
M83, H II regions spectral characts. and chemical abundances 80−56927
M87, dynamical evidence for central mass concentration 78−49529
M87, interstellar gas vel. dispersion rel. to presence of large central mass 80−94873
M87, UV spectrum, IUE obs. 80−82502
M87 jet knots, polarisation and spectroscopic props. 80−12817
M92, globular cluster, giant star C and N abundances 77−87496
M-type variable stars, obs. in DDO photoelec. system, spectral classification 78−32463
Magellanic Cloud supernova remnants, forbidden O II spectra rel. to optical emission from shocks 79−92831
Magellanic Clouds, gaseous corona, evidence from stellar spectra 80−82490
Magellanic Clouds, spectrophotometry of nebulae suitable as standards 78−12350
Magellanic Clouds, UV brightness maps and UV spectra 80−85994
main sequence stars, F- and G-type, Be abundances 77−13332
main-sequence reddened stars, ANS photometry, UV colours 80−77400
Mariner 10 UV spectrometry of inner solar system 77−45337
Markarian 185, 186, UBV surface photometry *(Russian)* 77−91614
Markarian 205, electronographic and spectroscopic obs. rel. to distance 79−97058
Markarian 231, Seyfert galaxy, substructure with UV excess, UV and visible obs. 80−82512
Markarian 298 (=IC 1182-4), multicolour photometry *(Russian)* 78−57641
Markarian 325, irregular galaxy, emission clumps observational props. 80−67869
Markarian 335, Seyfert galaxy, spectroscopic investigation *(Russian)* 79−101204
Markarian 501, UV and X-ray obs. of BL Lacertae-type object 80−36717
Markarian 509, brightness variability meas. *(Russian)* 77−17671
Markarian 59 , supergiant H II region in SBm galaxy NGC 4861 spectrum and struct. 80−98705
Markarian galaxies, emission line intensities depend. on colour index *(Russian)* 77−17672
Markarian galaxies, nature from photometry and classification 78−28781
Markarian galaxies frequency on objective prism photographs at Tautenburg Observatory 77−67128
Markovian 297, IUE UV spectra of clumpy irregular galaxy 80−26981
Mars, atm. O_3 vertical distrib., Mariner 9 UV spectral obs. 79−66952
Mars, dust complex refractive index, wavelength depend. and comp. 77−29695
Mars, H I Lyman α emission meas. at solar minimum 79−12417
Mars, UV spectra and photometry by TD1A and OAO-2 satellites 77−91459
Mars atmosphere, O_3 layer and two aerosol layers detect. by Mars 5 spacecraft UV obs. 78−49357
Mars upper atmosphere, H Lyman α radiation meas. with absorpt. cell spectrophotometer 78−28519

ultraviolet astronomical observations continued
MCG 8-11-11, X-ray Seyfert galaxy, recent optical activity in nucleus 79−25701
Melotte 66, oldest open cluster, colour-magnitude diagram rel. to age 80−17621
Mercury, atm. comp. from Mariner 10 data 77−9684
Mercury, EUV albedo 77−33378
Merope nebula, uvby photometry and dust grains phase function in UV 78−32553
Merope reflection nebula, near UV photometry of surface brightness 77−29896
metallic line stars, spectral energy distrib. *(Russian)* 80−72975
meteor, fast sporadic spectrum 78−93170
meteor bright line spectra, study via astronomical TV system 78−61817
meteors OH emission, UV photometric obs. 78−7943
9 Metis, UBV photometry, light curve and rot. period 80−21942
Monoceros R2 association, stellar UBV photometry and spectra 77−13409
19 Monocerotis, β Canis Majoris variable, photometric obs. 80−4379
15=S Monocerotis, interstellar lines 80−90494
V616 Monocerotis (A 0620−00), UBV photometry 80−56846
Moon, EUV albedo 77−33378
Moon, far UV albedo meas. by Apollo 17 77−37513
α Muscae, β Canis Majoris type variability discovery from UBV photometry 79−80326
θ Muscae, Wolf-Rayet binary, spectrum and photometry 77−22235
MXB 1735−44, optical bursts obs. 78−61937
MXB 1735−44, X-ray burst sources, 3 s delay in optical burst 79−58442
MXB 1837+05 (Serpens X-1), detect. of optical burst coincident with X-ray burst 80−27013
N132 D, SNR in LMC, rapidly moving material, visible and UV solns. 80−82449
N70, giant filamentary shell in LMC, emission lines profiles rel. to dynamics 80−90511
NAB 0137−01, quasar, UBV photometry and brightness vars. 80−56967
NAB 0137−01, spectrophotometry of possible X-ray quasar 77−13490
nearby stars, Mg II interstellar resonance doublet absorption 78−45391
Neptune, UV albedo meas. 80−82295
NGC 1068, Seyfert galaxy, UBV photometry 77−67132
NGC 1068, type 2 Seyfert, recombination spectrum and reddening 80−90519
NGC 1084, NGC 7331, spiral galaxies, surface photometry and mass distrib. 79−40265
NGC 1261, globular cluster, colour-magnitude diagram 80−17623
NGC 1275, Seyfert galaxy, nucleus, emission line intensities rel. to gas and radio source structs. *(Russian)* 79−48936
NGC 1275, Seyfert galaxy, vars. of emission line spectrum and conditions in nucleus envelope 77−17688
NGC 1275, spectroscopic and photometric obs. 77−33630
NGC 128, S0 galaxy, rot. curve 77−33631
NGC 157, spiral galaxy, surface photometry and mass distrib. 79−40264
NGC 1851, 6624, globular cluster, abundance gradients spectroscopic investigation 80−82437
NGC 1904 (M79), UBV photometry, colour-magnitude diagram of halo globular clusters 78−32528
NGC 205, UV image 80−98716
NGC 2110, Seyfert 2 X-ray galaxy, optical studies 80−22071
NGC 2243, old open cluster, UBV photometry 77−78835
NGC 2264, open cluster, reddening, blanketing and metallicity from spectroscopic obs. 80−26916
NGC 2420, old disc cluster, photometry and spectra rel. to stars chemical comp. 80−46620
NGC 2439 association, photometric and spectroscopic study 78−16470
NGC 2527, galactic cluster, UBV photometry 78−16479
NGC 2571, open clusters, UBV anal. 79−58386
NGC 300, NGC 1365, southern galaxies, H II regions comp. 80−4441
NGC 3105, young open cluster, photoelectric UBV obs. 77−64811
NGC 3115, s0 galaxy, photometric obs. 77−29917
NGC 3227, Seyfert galaxy, photoelectric and spectroscopic study and comparison with galaxy chain (VV 150) 80−98724
NGC 3242, 7009, 6210, high excitation planetary nebulae, high dispersion EUV obs. 80−77466
NGC 3242, UV emission lines, Copernicus obs. of planetary nebula 79−12501
NGC 3247, RGU photometry of open cluster, catalogue of 129 stars *(German)* 77−82290
NGC 3324, very young open cluster in Carina spiral feature UBV β photometry 77−22282
NGC 3379, elliptical galaxy, spectroscopic obs. rel. to rot. and vel. dispersion 78−49529
NGC 3516, SBO type Seyfert galaxy, extended nebulosity, UV and visible obs. 80−82487
NGC 3516 Seyfert galaxy, optical spectrum 77−26052
NGC 3532, southern galactic cluster, stellar photoelectric sequences 77−45502
NGC 3532, southern open cluster, UBV photometric study 80−46621
NGC 3603, luminous young cluster, UBV photometry 78−36643
NGC 4151, Seyfert galaxy, for UV line profiles 80−22083
NGC 4151, Seyfert galaxy, nuclear region far UV spectrum 78−32573
NGC 4151, Seyfert galaxy, optical polarimetry, circumnuclear dust envelope 78−61916
NGC 4151, Seyfert galaxy, UV spectrum 77−13468
NGC 4151, UV photometry and extended spectrum of Seyfert galaxy 78−89249
NGC 4235, Seyfert galaxy, spectrum and radial. vel. 78−49536
NGC 4314, barred spiral galaxy, UBV surface photometry of central region 80−77482
NGC 4321, IUE UV and visible obs. of supernova (1979 April) 79−53834
NGC 4321, UV and visible obs. (1979 April-May) of supernova 79−58363
NGC 4378, anaemic Sa galaxy, extended rot. curve 79−8990
NGC 5053, haloglobular cluster, photometric study 77−74103
NGC 5102, lenticular galaxy, dust and young stars obs. 79−44609
NGC 5102, peculiar SO galaxy, UBV photometry 77−13452
NGC 5128, southern radio galaxy, OAO UV photometry, energy distrib. 79−40255
NGC 5128, struct. and evolution from multicolour photography 79−53913

ultraviolet astronomical observations continued
NGC 5128 (Centaurus A) optical struct., picture processing anal. 79−53907
NGC 5195, companion of M51, rot. and relative mass 77−22306
NGC 520, Irr II galaxy, new photographic and spectroscopic obs. 80−41889
NGC 5236, spiral galaxy peculiar nucleus continuum and reddening 80−73031
NGC 604, 5471, giant extragalactic H II regions, IUE UV spectra 80−77467
NGC 6087, galactic cluster, four-colour and Hβ photometry 80−62208
NGC 6144, globular cluster, and neighbouring region, photometric obs. 80−51816
NGC 6231, young open cluster, main sequence stars photometry and spectra 79−88709
NGC 6240 (=VV 617+MCG 0-43-4), interacting Seyfert with reddening *(Russian)* 79−58426
NGC 6266, globular cluster, colour magnitude diagram, distance and metallicity 78−61894
NGC 6302, emission nebula, direct evidence for energetic stellar wind 80−67835
NGC 6383, photometry and spectral classifications, age and distance of open cluster 78−93342
NGC 6383, young open cluster, central core stars obs. 78−41003
NGC 6528, metal-rich globular cluster, colour-magnitude diagram from UBV photometry 80−4406
NGC 6530, open cluster, broadband photometry 77−45504
NGC 6530, UBV photometry of variable stars in open cluster 77−74106
NGC 6530, young open cluster, UBV photometry, magnitudes, reddening, distance, age 78−93341
NGC 6541, globular cluster, UBV photometry, metallicity and distance 79−35316
NGC 6543, planetary nebula, electronographic data rel. to struct. 78−20869
NGC 6546, open cluster, assoc. with Cepheid AV Sagittarii disproved 79−58387
NGC 654, young open cluster, UBV photometric study 80−109502
NGC 6720 (Ring Nebula), strong forbidden N II emission and element abundances 77−26035
NGC 6752, globular cluster, blue horizontal-branch stars photometry 78−49488
NGC 6752, globular cluster, main sequence from UBV photometry 79−71079
NGC 6822, new compact H II regions discovery 80−51854
NGC 6822, UBV photometry of dwarf irregular galaxy 79−62903
NGC 6888, around Wolf-Rayet star HD 192163, IUE obs. of absorpt. by hot gas 79−53896
NGC 6914b, surface brightness and UBV colorimetry *(Russian)* 77−13446
NGC 7000 (North America Nebula), rocket UV imagery 80−82440
NGC 7023, refl. nebula, surface brightness study 80−56903
NGC 7027, interstellar extinction 164-2170 nm obs. of planetary nebula 79−67082
NGC 7027, planetary nebula, continuum obs. and electron temp. 77−2462
NGC 7027, planetary nebula, UV emission line spectrum rel. to interstellar reddening, IUE obs. 78−96524
NGC 7027, planetary nebula, UV spectrum rel. to physical conditions and CNO elements abundances 80−82459
NGC 752, DDO astrophysical study 79−48864
NGC 7582, narrow emission line X-ray emitting nucleus, UV spectra 80−101640
NGC 7654 (M52), open cluster, stars four colour and Hβ photometry 78−8067
NGC 7662, Ne IV forbidden $^2D \rightarrow {}^4S$ lines obs. in UV spectrum of planetary nebula 79−48896
NGC 7662, planetary nebula, rocket UV spectrum and models 78−28746
NGC 7789, open cluster, DDO and UBV photometry 77−53648
NGC 931, interacting Seyfert galaxy, struct. and spectra 79−25716
NGC 935-IC 1801, close pair of spiral galaxies, rot. curves and mass distribs. 77−45556
NHC 4594 (Sombrero Galaxy), H II regions and ionised interarm gas detect. 78−36685
Norma dark cloud region, stellar photometry rel. to cloud struct. 78−16494
northern early-type stars at intermediate galactic latits., UBV photometry and MK spectral classification 77−82221
Nova Centauri 1979, UBV photometry and spectrum, identification with X-ray transient 79−62842
Nova Cygni 1975, Copernicus near UV spectral obs. 77−29844
Nova Cygni 1975, spectrum obtained with small image-intensifier spectrograph 78−73647
Nova Cygni 1978, spectroscopic obs. 78−89213
Nova Cygni 1978, UBV photometry and short-period vars. 79−5835
Nova LMC 1977b, VBLUW photometry, absolute magnitude, distance and reddening 79−58342
Nova Sagittarii 1977, early spectrum 78−32496
Nova Serpentis 1978, VBLUW photometry, absolute magnitude, distance and reddening 79−58342
Nova V3888 Sagittarii (1974), UBV and uvby photometry during decline stage 78−20836
Nova Vulpeculae 1979, spectroscopic and photometric obs., possible exceptionally slow nova 79−48820
novalike object in Vulpecula, photoelectric UVB obs. (1979 June 9 to 15) 79−80323
novalike object in Vulpecula, photometry, June 1980, and spectral classification 80−94807
novalike object in Vulpecula, UBV photometry (1979 August 6 to September 20) 80−8644
novalike object in Vulpecula, UV decline and expanding cooling photosphere 80−67741
O3 to O5.5-type stars, spectra 77−33481
O-B stars, spectrophotometric and UBV colorimetric parameters *(Russian)* 77−17569
O-type stars, effective temps., far UV photometric obs. 79−88656
O-type stars, in LMC, uvby photometry 77−60756
O-type stars, mass loss rate from UV spectra 80−82346
O-type stars, O VI P Cygni profiles hourly vars. 77−37596
O-type stars, radial vels. and K-term 77−56922

ultraviolet astronomical observations continued
O-type stars in open cluster IC 1805, C IV UV reson. line P Cygni profiles 80−31296
OAO 1653-40, 38 s X-ray pulsar, optical counterpart, spectroscopic search 80−73072
OB stars, Copernicus UV spectral data of rotation 79−84795
OB stars, in LMC, spectroscopic obs., galaxy distance determ. 79−71111
OB stars, stellar wind mass loss determ. spectral obs. 80−94789
OB stars, UV P Cygni profiles long-term changes 78−12234
OB-type stars in SA 98, UBV photoelectric meas. 80−46535
OB-type stars in vicinity of long period Cepheid VZ Puppis, UBV β photometry 78−45339
OBN, OBC stars, radial vels. and short period binaries frequency 78−53951
UZ Octantis, W Ursae Majoris system, UBV light curves 80−22042
Of-type stars, search for 2200 Å absorpt. band anomalies 77−64769
ζ Ophiuchi, identification of interstellar lines in UV spectrum 78−93212
ζ Ophiuchi, interstellar C I UV lines obs. 79−35332
U Ophiuchi, massive eclipsing binary star, spectrophotometry 80−26900
RS Ophiuchi, recurrent nova, spectrum obs. 79−62848
ζ Ophiuchi, search for interstellar Sc II 80−82445
ω Ophiuchi, UBV photometry of Ap star, periodicity in luminosity vars. *(French)* 78−57559
ζ Ophiuchi cloud, Copernicus UV obs. of interstellar C_2 78−41022
ζ Ophiuchi clouds, interstellar abundances 79−48875
OQ 172, quasar, H_2 lines in absorpt. spectrum 80−36734
Orion, far-UV rocket survey 77−64762
Orion Nebula, C abundance from visible and IUE obs. 80−82451
Orion nebula, C and Mg abundances from UV spectrum 80−41882
Orion Nebula, far UV imagery 78−4326
Orion Nebula, IUE obs. of UV continuous spectrum 80−90499
Orion Nebula (NGC 1976), long-slit spectroscopy in rocket UV 80−105297
Orion Nebula peripheral regions, spectrum obs. rel. to element depletion and ionisation 80−36686
Orion OB1 assoc., expanding gas shell, UV obs. 79−71086
Orion OB 1 association, photometric study 77−82128
Orion reflection nebulosity, UV photometry from OAO-2 78−65668
β Orionis, B8 Ia star, UV spectrum 77−22221
42 Orionis, Copernicus UV spectra and IR photometry 77−49437
κ Orionis, expanding envelope OAO-3 spectra *(Russian)* 78−4224
ι Orionis, high-vel. interstellar H I absorpt. features obs. and implications 79−48891
δ, ε and ι Orionis, interstellar D/H ratio from D absorption features 79−53865
ζ Orionis, interstellar MgI line structure, balloon UV obs. 79−35251
β Orionis, line blocking, reddening empirical effective temp. determ. 77−87389
β Orionis, mass loss and shell, IUE and balloon UV obs. 80−51765
β Orionis, mass loss from mid UV spectrum obs. 78−93217
22 Orionis, nonradial m-mode changes in 53 Persei variable 80−72939
λ Orionis, obs. of UV radiation scattered by interstellar dust 80−56918
α Orionis (Betelgeuse), UV flux meas. 77−22231
θ^2 Orionis A, 4U 0531−05 optical candindate, Copernicus obs. 79−67050
η Orionis A, binary star, UV spectrum 77−45485
λ Orionis A, far UV flux, emission line obs. of surrounding H II region 78−93303
δ Orionis A, UV spectrophotometry and optical polarimetry, stellar wind variability 79−21277
λ Orionis association, photometric props. of young cluster 78−16478
θ^2 Orionis B, long-slit spectroscopy in rocket UV 80−105297
θ^1 Orionis C and θ^2 Orionis A, UV spectra 80−90499
σ Orionis E, period and luminosity stability from uvby β photometry 78−8017
Palomar 5, remote globular cluster in galactic halo, chem. comp. 77−87482
Parsamyan 22, surface brightness and UBV colorimetry *(Russian)* 77−13446
γ Pavonis, C and N abundances 77−91531
MW Pavonis, eclipsing binary, UBV light var. and orbital elements 77−49429
peculiar central stars of planetary nebulae, spectroscopic characts. 77−87405
peculiar extragalactic sources, multiaperture UBV photometry 78−28772
EQ Pegasi, active dwarf binary star, chromospheric emission lines obs. 80−12762
AU Pegasi, binary Type II cepheid, photometric and spectroscopic study 80−26866
o Pegasi, hot Am star, spectroscopic obs. and curve of growth anal. 77−22237
β Pegasi, M-type giant star, Mg II h and k emission obs. 78−53945
AG Pegasi, OAO 2 UV obs. of symbiotic binary 79−53814
AG Pegasi, symbiotic binary system, UV and optical spectrum rel. to nature of components 80−109449
γ Pegasi, UV spectrum of early B-type star, Copernicus obs. 78−81621
Periodic Comet Ashbrook-Jackson (1977g), spectroscopic obs. 78−96437
Periodic Comet Giclas (1978k), spectroscopic obs. 78−96437
Periodic Comet Schwassmann-Wachmann 1, CO^+ obs. near minimum brightness 80−82305
ϕ Persei, Be star, Fe III metastable states and mass loss 79−5832
KT Persei, dwarf nova, brightness oscills. during two outbursts 77−2438
B Persei, eclipsing binary, Mg II 280 nm line profile, calcs. and UV obs. 80−82421
RY Persei, eclipsing binary, spectroscopy and physical parameters of atmospheres 80−101618
β Persei, eclipsing binary, study of light curve at 3428 Å 77−53634
β Persei, eclipsing binary, UV obs. from TD-1A satellite 80−77447
AG Persei, massive eclipsing binary star, spectrophotometry 80−26900
IW Persei, metallic-line close binary star, photometric and spectroscopic obs. 80−62186
ζ Persei, obs. of weak interstellar lines below 3400 Å 77−45509
21 Persei, spectrophotometry of Ap star, continuum features vars. 80−36638
20 Persei, visual binary, radial vel. obs. 78−73736
β Persei (Algol), gas stream producing absorpt. features in red wings of Mg II reson. lines 78−24524
β Persei (Algol), UV photometry and spectrum rel. to primary component rot. 80−72996
V400 Persei (Nova Persei 1974), photoelectric obs. 78−4252

ultraviolet astronomical observations continued
α Persei cluster, OAO 2 photometry 78−93331
α Persei cluster, stellar spectral types 79−58385
α Persei star cluster, polarisation wavelength depend. 79−48865
Perseus II complex, ζ Persei direction, Copernicus obs. 78−4301
PG 0026+129, Lα/Hβ/Pα ratio following IUE UV obs. of quasar 79−12537
PHL 1092, narrow line quasar, discovery of extreme Fe II emission 80−77508
PHL 957, Lyman α emission halo upper limit 77−33678
PHL 957, quasar, H_2 and CO absorpt. lines obs. *(Russian)* 79−101216
Phobos, composition, evidence for carbonaceous chondrite surface from spectral anal. 78−49365
SX Phoenicis, dwarf cepheid, spectrum 77−49405
SX Phoenicis, short period dwarf Cepheid, UBV photometric obs. 78−57561
SX Phoenicis light curve, colour effect obs. 78−93248
δ Pictoris, β Lyrae-type eclipsing binary, satellite UV obs. 77−57033
Pismis 6 and 8, open clusters, photometry and spectra rel. to proximity to (Wat 6) 79−88712
PK 60−7°1, nebula around FG Sagittae, spectrophotometric study 79−40240
PKS 0237−23, absorpt. spectrum obs., absorpt. lines origin 78−41074
PKS 0528−250, abundances in absorbing material towards QSO 79−40288
PKS 1157+014, spectral obs., of QSO with no Lα emission 80−31384
PKS 2155, BL Lacertae object, UV flux meas. by IUE 80−12833
PKS 2155−304, BL Lacertae object, spectral slope from far UV obs. 80−82509
PKS 2322-12, narrow-line radio galaxy, optical spectrum 77−33664
planetary nebula IC 418, search for absorpt. in CO fourth positive system 80−46647
planetary nebula in irregular galaxy NGC 6822, spectrophotometry and He, N, O and Ne abundances 80−41867
planetary nebula obs. in red globular cluster NGC 1852 in LMC 77−17668
planetary nebulae, C IV 1550 Å lines fluxes meas. and C abundances 79−17051
planetary nebulae, EUV spectra of young objects 79−35336
planetary nebulae, IUE satellite obs. of high excitation objects 80−94860
planetary nebulae, low excitation, of small ang. size, spectral studies 80−17646
planetary nebulae, moderately bright, spectroscopic study 79−84835
planetary nebulae, O/H ratios meas. rel. to Galaxy O enrichment 80−105328
planetary nebulae, review of UV obs. 80−109523
planetary nebulae, spectrophotometry, emission line intensities, physical conditions 78−36651
planetary nebulae, UV spectra 79−92843
planetary nebulae central stars, Cassegrain image-tube scanner obs. 77−22214
planetary nebulae central stars, UV radiation meas. 78−28679
planetary nebulae central stars, variability from UV obs. 78−36668
planetary nebulae photometric obs., interstellar extinction determ. 77−17660
Pleiades stars, wavelength depend. of polarisation 77−45500
Pleione (28 Tauri), envelope behaviour in 1976, spectroscopic obs. 80−8636
Pleione (28 Tauri), metallic-line shell spectrum anal., (1973-1976) 80−8637
PN 108-76°1, halo planetary nebula, spectrophotometry and element abundances 78−41011
PN 49+88°1, halo planetary nebula, spectrophotometry and element abundances 78−41011
pulsars, search for thermal EUV radiation 77−22259
VV Puppis, AM Herculis type binary, accretion column absorpt. spectrum obs. 79−101176
VV Puppis, AM Herculis type binary spectrophotometric obs. 79−5860
VV Puppis, dwarf nova, spectroscopic obs. during active phase 79−80322
V Puppis, eclipsing binary, circumstellar matter obs. 77−13385
ζ Puppis, interstellar C I UV lines obs. 79−35332
ζ Puppis, of supergiant, mass flow var., visible and UV obs. 80−90431
ζ Puppis, Of-star, UV spectrum, line identifications 77−45441
RX Puppis, peculiar emission-line object, spectrum and UBV photometry 79−44497
ζ Puppis, spectral line profiles, mass ejection 77−33507
VV Puppis, spectroscopic obs., broad absorpt. features discovery 79−44502
ζ Puppis, UV spectral energy distrib. 77−22211
ζ Puppis, visible and UV spectroscopy of stellar wind var. 79−16949
R Puppis (HD 62058), G-type supergiant, UBV photometry and variability confirmation 80−41824
T Pyxidis, recurrent nova, photoelectric obs. 78−4252
Q0353−383, QSO abundance anomalies, UV and visible spectral obs. 80−82532
Q 0932+501, bright quasar with broad absorption features 80−46697
Q 0957+561 A,B, UV spectra and gravit. lens interpretation 80−82537
Q 1246−057, absorpt. line spectrum, presence of outflowing material 78−93453
Q 2204−408, IUE UV spectrum of high redshift radio-quiet quasar 79−35424
Q 2240.9-3702, Q 2238.9-4115, optically selected QSOs with broad-lined absorpt. systems spectra 80−4456
QSO candidates, spectroscopic obs., indentifications 80−31385
QSOs, Fe II UV lines, spectrophotometry obs. 80−73063
QSOs, high-redshift, Image Dissector Scanner (IDS) spectrometry and redshifts 80−22111
QSOs, Lyman α/Hβ intensity ratio 77−45600
QSOs of small and intermediate emission redshift, absorpt. lines homogeneous survey results 80−31218
quasar, strong emission line, with redshift z=0.189, spectrum and photometry 80−8710
quasar emission lines 80−27009
quasar near companion galaxy NGC 5296, photometry and redshift 77−13489
quasars, absorpt. line spectra and redshift systems 77−13488
quasars, absorpt. lines statistics and line-locking 78−57681
quasars, emission-line, survey, new discoveries and faint quasars number limits 79−92884

ultraviolet astronomical observations continued
quasars, gas and high energy particle interactions, B line search 78−4388
quasars, high-redshift, emission-line spectra rel. to radio or optical selection 77−53696
quasars, implications of UV obs. 80−105390
quasars, low-red shift, photoelectric UBV photometry *(French)* 80−51904
quasars, Mg II 2798 Å and Hβ emission, line profiles 80−12807
quasars, O VI 1035 A emission and Lyman β 77−2483
quasars, optically selected, with 3.0<z<3.5, spectrophotometry rel. to absorpt. line problem 79−25746
quasars in CTIO 4 m survey, visible and UV spectrophotometry 80−86009
quasars in region of NGC 1629 companion galaxy, spectra and redshifts 80−56965
quasars M87 and 3C 273, imaging polarimetry 78−41076
quasars near peculiar pair of galaxies NGC 7714−7715, spectra and redshifts 78−28835
quasars of Michigan-Tololo survey, spectrophotometry 80−22105
quasars relative luminosities determ. from emission line strengths 78−61931
quasars with high redshift, discovery and spectroscopic obs. 77−45594
quasi-stellar objects, luminosity indicators in emission-line spectra 77−57103
quasi-stellar objects, variable, photometry and completeness of faint blue objects in Sandage-Luyten field 78−54069
quasi-stellar radio sources from 4C and Parkes catalogues, spectra and photometry 78−65714
radiation background, far UV at high galactic latits., D2B−Aura satellite obs. 79−17143
radio galaxies, broad-line Mg II 2798 Å and Hβ emission, line profiles 80−12807
radio galaxies, narrow-lined, spectrophotometry 78−93391
radio galaxies, optical emission-line spectra 78−57643
radio sources in south polar cap, optical identifications 79−75284
radio sources south of declination −75°, optical identification 77−64863
RCW 107 (NGC 6164/5), ionisation struct. of southern H II region 77−45526
red giant stars in globular clusters M92 and NGC 6397, C abundances 79−48785
red giants in globular cluster NGC 6752, DDO photometry and spectra 79−71079
rotating early-type stars, V and i from Copernicus UV obs. 77−33492
Rubin-152, possible massive O-type star on galactic fringe, spectroscopic obs. 80−98656
S147, supernova remnant, assoc. interstellar CO detect. 80−67836
2S 1254−690 optical counterpart, identification, photometry and spectrum 79−12545
2S 1702−363 optical counterpart, UBV photometry 80−82349
SA 133 field near galactic centre, three-colour stellar photometry *(German)* 80−36618
HM Sagitaae, emission-line star, UBV photometry and spectral obs. in (1978) *(Russian)* 80−36648
HM Sagittae, emission-line star, polarimetry, (1977 to 1978) *(Russian)* 80−36649
HM Sagittae, emission-line star, spectrum vars. (1978 to 1979) 79−58347
HM Sagittae, photometric and spectroscopic obs. rel. to proto-planetary nebula mass ejection 78−85947
U Sagittae, photometric study of eclipsing binary 77−22270
WZ Sagittae, recurrent nova, eclipsing binary, outburst of December 1978, UV obs. 80−72982
WZ Sagittae, recurrent nova, IUE obs. in outburst 80−109448
WZ Sagittae, recurrent nova, spectroscopic obs. and model for superhump phenomena 80−82368
WZ Sagittae, recurrent nova, spectroscopic obs. during 1978 outburst 80−26862
WZ Sagittae, recurrent nova, spectroscopic study during 1978 outburst 80−56849
WZ Sagittae, spectroscopic obs. (1978 December 1 and 2) 79−16983
FG Sagittae, spectrum of assoc. nebula 78−49498
HM Sagittae, UBV photometry and spectral obs. (1977) *(Russian)* 79−16991
XZ Sagittarii, Algol system, UBV photometric investigation 80−22041
μ Sagittarii, binary star, B8 star eclipse obs. during (June 1979) 80−4401
AV Sagittarii, Cepheid, assoc. with open cluster NGC 6546 disproved 79−58387
V1647 Sagittarii, light curves, photometric elements and apsidal motion 77−60795
V356 Sagittarii, massive eclipsing binary star, spectrophotometry 80−26900
MV Sagittarii, R Coronae Borealis variable, brightness decline obs. and UBV photometry 80−8641
υ Sagittarii, UV spectrum 79−35300
Saturn, Lyman α emission from disc and ring system 78−12150
Saturn, rings, four colour phase curves, analysis 80−4295
Saturn, satellite associated clouds, Pioneer UV photometry obs. 80−82288
Saturn, UBV photoelectric pinhole scans of disk 79−40135
Saturn, UV spectra and photometry by TD1A and OAO-2 satellites 77−91459
Saturn A and B rings, surface brightness obs. *(Russian)* 80−72872
Saturn atmosphere, acetylene detect. using IUE satellite 79−48731
Saturn far UV spectrum, rocket obs. 78−53867
Saturn globe and rings, optical reflectance polarimetry and interpretations for B-ring 80−31248
α Scorpii, circumstellar absorption lines in UV spectrum 80−51804
τ Scorpii, Copernicus UV spectral atlas 78−12220
μ′ Scorpii, eclipsing binary, UV obs. 80−77447
τ Scorpii, expanding envelope, mass loss rate 78−65613
ζ¹ Scorpii, extreme B1 supergiant, IUE obs. of line spectrum and continuum energy distrib. 80−17583
ζ¹ Scorpii, extreme B1 supergiant, UV reson. lines obs. 80−4349
ζ¹ Scorpii, extreme B-type supergiant, UV spectroscopy 80−22004
V861 Scorpii, X-ray emission and UV spectra rel. to unseen companion 78−89226
V861 Scorpii =OAO 1653−40, photometry, spectrum and physical parameters 79−17021
α Scorpii (Antares) nebula, spectrum 78−41014
ultraviolet astronomical observations continued
ζ¹ Scorpii (HD 152236), UV spectroscopic and photometric vars. 80−101594
V861 Scorpii (OAO 1653-40?), simultaneous UV and X-ray obs. 80−17616
Scorpius region, UBV surface brightness photometry of Milky Way from Helios 1 78−57634
Scorpius X−1, interstellar extinction and UV flux distrib. 79−25754
AI, WZ and XX Sculptoris, southern δ Scuti stars, photoelectric study 80−90452
RY Scuti, eclipsing binary, ephemeris and UBV obs. 80−94832
V373 Scuti (Nova 1975), VBLUW photometry, absolute magnitude, distance and reddening 79−58342
Seyfert 2 galaxies, spectrophotometry 78−93391
Seyfert and emission-line galaxies, UBV obs., light vars. 79−30134
Seyfert galaxies, exploratory obs. of gas near nuclei 79−48906
Seyfert galaxies, Mg II 2798 Å and Hβ emission, line profiles 80−12807
Seyfert galaxies, optical emission-line spectra 78−57643
Seyfert galaxies nuclei, optical variability from U, B, V and Hα photometry 78−96543
Seyfert galaxies with large z, electronographic survey 77−91624
Shahbazian 1 group of galaxies, dynamics from spectroscopic, obs. 80−67878
Sk 160, optical counterpart of SMC X-1, VBLUW photometry 77−82277
sky surveys, review 78−93111
SMC, surface brightness meas. with UV Sky Survey Telescope 78−93414
SMC, UBV photoelectric photometry *(German)* 78−77594
SMC Cepheids, five-colour obs. and comparison with galactic Cepheids 77−29923
SMC probable members and foreground stars, spectral types and UBV, photometry 79−40091
SMC Shapley wing, UV obs. from S2/68 sky-survey telescope 79−25717
SMC star clusters catalogues, identifications and coordinates 78−89086
SMC X-1, VBLUW photometry, evidence for accretion disc 78−12409
SN 1006 optical remnant, peculiar spectrum obs. 79−21371
SN 1973f in NGC 4944, photometric obs. 79−21318
solar active region loops, evidence for opposed currents 77−2403
solar active regions, OSO-8 obs. of UV brightenings 78−28630
solar active regions, Salyut-4 UV spectra 77−82211
solar active regions and quiet Sun, EUV fluxes, OSO-4 spectroheliograms 77−49358
solar active regions and X-ray bright points, birthplaces 80−12739
solar atmosphere, C III 1909 Å and Si III 1892 Å emission lines, echelle obs. 80−31277
solar B abundance, photoelectric meas. 77−29753
solar background corona, Skylab study near solar minimum 78−28616
solar C I multiplets at 1560 and 1657 Å, overlapping emission peaks obs. and theory 78−93178
solar chromosphere, C II reson. lines obs. by OSO 8 rel. to temp. struct. 78−53896
solar chromosphere, EUV network in quiet regions 77−2386
solar chromosphere, limb spectra from Skylab, 2000-3000 Å region 77−45376
solar chromosphere, motions, EUV obs. by OSO-8 *(Italian)* 78−81602
solar chromosphere, quiet and active, Lα spectra and models based on partial redistrib. diagnostics 79−75169
solar chromosphere, vels. from Si II 1816 Å line, OSO-8 obs. 77−13301
solar chromosphere and transition region, OSO-8 obs. of wave propag. 78−93183
solar chromosphere and transition region, persistent vel. fields, OSO-8 obs. 77−9730
solar chromosphere flares, Lyman emission obs. rel. to soft X-ray heating effects 79−40170
solar chromosphere limb flare, 1959 July 25, spectrum rel. to physical conditions 80−105227
solar chromosphere-corona transition region, mass motions in impulsive flarelike brightenings, OSO-8 obs. 79−35217
solar chromosphere-corona transition region, optically thin lines, OSO-8 obs. 77−9729
solar chromosphere-corona transition zone, dynamics over sunspot, OSO-8 obs. 77−9728
solar chromosphere-corona transition zone instabilities, spectroscopic far UV obs. 77−17479
solar chromospheric oscillations obs. in C II 1336 Å line by OSO-8 78−28625
solar chromospheric oscillations obs. with OSO-8, average phase spectra for Si II 79−62801
solar chromospheric oscillations obs. with OSO-8, average power spectra for Si II 79−62800
solar chromospheric oscillations obs. with OSO-8, basic meas. and analytical methods 79−62799
solar chromospheric plages, Mg II obs. rel. to physical props. models 78−89153
solar CO emission lines in UV spectra of sunspots and flare 79−53795
solar cool corona pressure and energy balance over sunspots 77−13291
solar corona, dynamical props. from line intensities and widths of EUV forbidden lines 79−35213
solar corona, EUV anal. of polar plumes 78−4178
solar corona, mag. loops and downflows obs., rel. to convection 78−93175
solar corona, N I isoelectronic sequence line ratios and electron densities 79−16906
solar corona, temps. and temp. gradients from OSO-7 spectroheliograms 77−17506
solar coronal holes, radio and EUV meas. of temp. distrib. and electron density *(Russian)* 78−16378
solar coronal lines, 1175 to 1965 Å, identifications, wavelengths and intensities 79−25559
solar coronal mass ejection event, 1973 December 19, kinematics 78−28640
solar coronal obs. with Skylab 77−56891
solar coronal temp. and nonthermal motions in coronal hole, quiet and active regions 77−33449
solar equatorial K-corona, temporal evolution 78−28618
solar eruptive prominence of June 8, 1974 Ca II K-line spectra 77−22182
solar EUV flux changes, AEROS spacecraft obs. and resulting ionospheric vars. calcs. 79−44293

ultraviolet astronomical observations continued
solar EUV flux variation at end of solar cycle 20, AE-C satellite obs. 77−71075
solar EUV impulsive bursts, characts. 78−77539
solar EUV line emission obscuration near limb 79−48762
solar EUV spectrum, H_2 emission lines obs. 79−16908
solar filament-corona transition region, OSO-VI EUV obs. 78−28620
solar flare, 1973, June 15, UV spectral lines list from 1000 to 1940 Å 78−89139
solar flare, 1973 August 9, decay phase, X-ray and UV obs. 79−53780
solar flare, 1973 June 15, Skylab XUV spectra, allowed transitions 77−78730
solar flare, 1973 June 15, Skylab XUV spectra, intersystem and forbidden transitions 78−4159
solar flare, 1974 January 21, single loop obs. in Fe XV emission lines 79−66991
solar flare, C line profiles and continua obs. and upper chromosphere semiempirical model 79−40148
solar flare, EUV and X-ray obs. of thermal phase 79−8886
solar flare 80−26829
solar flare EUV continuum emission, Skylab obs. 79−30046
solar flare impulsive heating using EUV obs. *(Russian)* 77−91502
solar flare kink instability obs. in XUV by Skylab 77−45370
solar flares, ATM evidence for low nonthermal proton/electron energy flux ratio 79−8887
solar flares, electron densities from Ca XVII line ratios 77−87358
solar flares, EUV (1420-1960 Å) continua, Skylab obs. 79−30028
solar flares, EUV and hard X-ray bursts interrelationship 78−61845
solar flares, EUV and hard X-ray sources relationship 80−46512
solar flares, EUV continuum obs. rel. to temp. min. region struct. and flare heating mechanisms 79−12458
solar flares, Fe XXI 1354 Å obs. from Skylab rel. to ionisation equilib. calcs. 80−21956
solar flares, forbidden Fe XIX, Fe XX and Fe XXI lines obs. 78−57519
solar flares, H spectral lines obs. rel. to mechanism investigation *(Russian)* 79−16925
solar flares, impulsive EUV and hard X-ray emission 78−65578
solar flares, Lyman continuum obs., energy transfer, chromospheric evaporation 79−21266
solar flares, O I 1355.6 Å and C I 1355.8 Å lines obs. 80−90381
solar flares, obs. of lines between 171 and 630 Å 78−49406
solar flares, XUV electron density diagnostics 79−88633
solar flux distribution, comparison with stellar flux distribs. and solar B−V and U−B colours determ. 79−66970
solar full-disc fluxes, 250-1940 Å rocket obs. 77−87360
solar H_2 emission in UV spectra of sunspots and flare 79−53794
solar H Balmer emission lines, Skylab obs. of active regions 77−33441
solar H Balmer emission lines, Skylab obs. of quiet Sun and polar coronal hole 77−33440
solar He II Balmer α line components 77−33436
solar ionising radiation, meas. during 1973 June 30 eclipse 79−8901
solar limb active regions, 1175 to 1940 Å emission-line spectra 78−96446
solar limb darkening meas., 1945-3245 Å, Skylab data 79−12439
solar limb spectrum, newly identified Fe II lines 77−33442
solar limb spectrum, Si I series identifications from 3000 to 1200 Å 77−56882
solar loop prominence system, flare assoc., high temp. corona 79−53782
solar Lyman α line, wavelength and profile meas. 79−8896
solar Mg II core absorption, wavelengths meas. and evidence for atmospheric downflow 79−12451
solar Mg II h and k lines, Skylab high-resolution obs. 78−36544
solar Mg II h and k lines in active regions and network, wing profiles and photospheric models 78−57518
solar Mg II lines obs. above limb from Skylab 77−33450
solar Mg II resonance-line wings, faint emission features obs. 78−32429
solar photosphere, UV continuum high resolution photographic obs. 80−17565
solar prominence, EUV limb spectra, Skylab obs. 80−12717
solar prominence, EUV spectrum rel. to horizontal temp. gradient meas. and prominence condensation 80−26832
solar prominence spectra taken at Ondrejov Observatory, inclined spectral features obs. 80−62098
solar prominence-corona interface compared with chromosphere-corona transition region 77−29786
solar quiescent prominences, Ca II K spectra and vertical struct. of line of sight and vel. field 77−53522
solar quiescent prominences, EUV obs. from Skylab 79−66987
solar quiescent prominences, middle Balmer decrement meas. 80−12737
solar quiet limb, optically thin UV lines obs. 77−17454
solar S I 1807 Å and 1900 Å lines, anal. of profiles 78−57517
solar Si II and Si III EUV emission line profiles, centre-to-limb vars. 78−28627
solar Sn abundance from Sn I line intensity profiles 78−20772
solar spectra, far UV, Salyut-4 orbiting solar telescope obs. 78−53783
solar spectra, He II Balmer 9 and 11 lines obs. 79−66981
solar spectrum in vicinity of Si IV 1122 and 1128 Å 78−4170
solar surge, EUV limb spectra obs. from Skylab 80−17560
solar system objects, International Ultraviolet Explorer (IUE) obs. 78−93133
solar transition zone, area var. of supergranule network features with temp. 78−89152
solar transition zone, energy balance and press. for network and active region features 80−21957
solar transition zone, search for turbulent free region 78−4174
solar transition zone, Si IV line profile vars., rel. to MHD disturbances 78−28626
solar transition zone lines, quiet Sun, limb broadening, OSO-8 obs. 79−48752
solar UV continuum, absolute intensities, centre to limb vars. and Laplace inversion between 1400 and 2100 Å 79−62803
solar UV emission spectrum, beam-foil spectroscopy appls. 77−41314
solar UV light, polarisation at solar limb 78−45302
solar UV line intensities brightness fluctuations during shock wave passage 79−66990
solar UV spectra, preliminary results from OSO-8 LPSP instrument 78−49317
solar vacuum UV centre-to-limb variation obs. *(Japanese)* 78−28604
solar wind flux depletion at high ecliptic latits., Mariner 10 UV obs. 78−96371
solar wind latitudinal vars., Mariner 10 H I Lyman α obs. 79−48635

ultraviolet astronomical observations continued
solar XUV He I and He II emission lines, intensities and gross centre-to-limb behaviour 78−40888
solar-type stars, in open clusters, spectroscopic differences from Sun 78−36560
solar-type stars, photoelec. scanner obs., search for solar spectral analogues 78−40938
southern dark clouds, survey for Herbig-Haro objects and Hα emission stars 78−28536
southern peculiar A-type stars, spectra and atmospheric anals. 78−24517
southern peculiar emission-line stars, observational data rel. to mass ejection 80−41843
southern quasars and quasar candidates, UBV photometry 78−32595
spectral classification of UV sources 78−65602
spectral energy distribution for 50 stars, 3200-7550 Å region *(Russian)* 78−65620
spiral and irregular galaxies, brightest superassociations as distance indicators 80−62260
spiral galaxies, early-type, multiaperture UBV photometric props. 80−98706
spiral galaxies, UBVR surface photometry and mass distrib. 79−71123
spiral galaxies nuclei, spectra and stellar population 80−56926
SS 433, UV spectral search and 8 GHz linear polarization 79−71048
standard stars, IUE photometric calibration, UV spectra 80−77383
standard stars for uvby photoelectric photometry south of declination +10°, obs. 77−2347
starfield in direction to Scutum Cloud, RGU photometry 79−35242
starlight scattering by interstellar dust, Apollo 17 far UV obs. 78−65726
stars, atlas of UV spectra from OAO 2 spectrometer flux data 79−48691
stars, balloon-borne UV spectroscopy using echelle and SEC-vidicon system 79−25482
stars, catalogue of photometric parameters meas. in Geneva Observatory system 77−73974
stars, early-type, in northern Milky Way fields, UBVβ photometry 77−2424
stars, new UBV photoelectric sequences in Puppis (l=250°, b=0°) 77−45426
stars, photometry in Geneva seven colour system, second catalogue 77−13252
stars, spectra, second OAO atlas 80−72786
stars, UBV photometry, influence of Balmer discontinuity on reductions 77−74046
stars, UV chromospheric and transition-layer emission 80−56823
stars, UV fluxes, S2/68 obs. of 31215 objects 79−8852
stars, UV lines in O, B and A-type spectra 77−78787
stars, UV photometry from Cosmos 215 satellite *(Russian)* 77−64750
stars, Walraven VBLUW photometry 77−17377
stars, young, in galactic anticentre direction, photometry and spectra rel. to outer Galaxy struct. 80−22079
stars hotter than B 1, Copernicus obs. of C IV doublet 79−44463
stars in 3U 1538-52 field, photometric search for optical candidates 78−12412
stars in Magellanic Clouds and Milky Way, five-channel photometric obs. 78−16398
stars of B6 to A0 spectral types, UV line blocking factors 77−22216
stars of Carina-Crux-Centaurus region, UBV photometry rel. to interstellar extinction 79−40242
stars of upper Scorpius region, spectrophotometry 79−88647
stars with peculiar interstellar polarisations, interstellar lines and grains props. 77−53659
stellar coronae, evidence for existence from X-ray and UV obs. 80−12756
stellar coronae, IUE search 80−4233
stellar flux distributions, comparison with solar flux distrib. and solar B−V and U−B colours determ. 79−66970
stellar flux measurements, comparison of S2/68 and OAO-2 calibrations 77−87372
stellar low-dispersion objective prism spectra from UK 1.2 m Schmidt telescope 77−45311
stellar occultation by Earth, upper atm. H_2 and O_2 densities by Copernicus satellite 77−9579
stellar photoelectric photometry at Hvar Observatory, colour systems and extinction meas. 77−78643
stellar photoelectric photometry at Wise Observatory, performance assessment 78−73657
stellar photoelectric UBV sequences, in fields of eight low-red shift quasars *(French)* 80−51904
stellar photometry, UBVR sequences around globular clusters (NGC 5946, 6440 and 6624) 79−88702
stellar spectra, atlas, line features use in spectral classification 78−12215
stellar spectra, balloon-borne echelle spectrograph obs. 78−49318
stellar spectra, interstellar Mg lines obs. rel. to existence of circumstellar clouds 80−94782
stellar spectra, Texas Univ. UV catalogue 77−78662
stellar spectral classification from UV line features, Am and Ap stars appl. 79−21272
stellar spectral classification using Copernicus UV data 78−12216
stellar spectral classification using Fe III UV lines 78−16404
stellar spectral classification using satellite UV photometric data 78−16402
stellar spectral classification using Skylab UV objective-prism spectra 78−16403
stellar spectral energy distribution in 3500 to 7500 Å region, absolute calibration 80−67710
stellar spectral energy distributions, results from Fourier transform spectrometry 77−82215
stellar spectrophotometric standards, obs. rel. to extinction monochromatic coeffs. on Terskol Peak *(Russian)* 79−44246
stellar UV photometry from S2/68 obs. on TD1 satellite 77−78775
stellar UV spectra, IUE preliminary results, workshop, Udine, Italy (1978 October 12) *(Italian)* 80−86033
subgiant stars, F-, G- and K-type, Be abundance rel. to post-main sequence evolution 77−13333
Sun, 1973 August 14 loop prominence, XUV emission and density 80−56807
Sun, absolute intensities in 1750-2100 Å range, vars. with solar activity 77−2405
Sun, active region coronal loops, gyroresonance absorption evidence 80−56792
Sun, active region McMath 12628, EUV and X-ray obs. 80−67692

ultraviolet astronomical observations continued
Sun, aeronomical reference spectrum for solar UV below 2000 Å 79−25379
Sun, atomic line profiles of active limb filament, OSO-8 UV obs. 79−44446
Sun, C III line intensity ratios, Skylab obs. 79−53786
Sun, C IV 1548 Å profile in quiet region, interpretation 79−96980
Sun, C IV profiles at 1548 Å, OSO 8 time series rel. to chromospheric oscills. 79−53785
Sun, chromosphere line profiles from OSO-8 satellite 80−67690
Sun, chromosphere-corona transition region, OSO 8 UV obs. of optically thick region 80−56788
Sun, chromospheric spicules, He ζ/H8 relative intensities in spectrum 78−40904
Sun, CO fluoresc. obs. in EUV spectrum 78−93184
Sun, coronal and transition zone plasma evolution during 1973 August 9 compact flare 79−5792
Sun, coronal EUV holes, rot. charact. from Fe XV 284 Å spectroheliograms 77−53547
Sun, coronal holes, EUV and radio spectrum 80−56802
Sun, coronal holes and arches, brightness temps. at 169 and 408 MHz rel. to UV obs. 79−8893
Sun, coronal holes and assoc. solar wind, sunspot cycle 20 survey 78−40911
Sun, coronal holes rel. to magnetic fields and model of formation in solar cycle 78−40909
Sun, coronal loop structures, temporal var., time-lapse sequence obs. 80−72909
Sun, coronal loops in an active region, physical props. XUV obs. 80−90376
Sun, cycle 21 development rel. to EUV spectrum and atmospheric absorption 79−75174
Sun, electron density at 10^5K from O IV intersystem line obs. in EUV 78−53903
Sun, EUV composite spectra of representative features 78−96447
Sun, EUV emission line nonthermal broadening near quiet limb 79−48748
Sun, EUV emission line profiles meas. near solar limb 79−16909
Sun, EUV emission line spectra of flare, analysis of Skylab obs. 78−40913
Sun, EUV Fe, Si and S line intensities, OSO-7 obs. of limb brightening 78−69759
Sun, EUV spectra from Skylab Apollo Telescope Mount spectrograph expt. 77−60598
Sun, EUV spectroheliograms from Apollo Telescope Mount expt. S082A 77−60597
Sun, EUV structure of small flare, Skylab obs. 78−40912
Sun, H_2 lines detect. in EUV spectra 78−12184
Sun, H I Lyman α flux near solar minimum 80−90393
Sun, H I Lyman-α and Lyman-β calibrated full disc profiles 78−93185
Sun, He I 584 Å reson. line profile and intensity meas. 79−40153
sun, He I 58.4 nm line profile, monitoring using resonance absorption spectrometer 80−62019
Sun, He I and He II XUV emission lines intensity ratios and distrib. functions 78−57516
Sun, high-resolution Lyman α filtergrams 80−82323
Sun, impulsive EUV bursts, C IV 1548 Å line profiles, OSO-8 obs. 80−90401
Sun, mass motions in active transition zone from EUV spectra 78−85922
Sun, Mg I, Mg II reson. lines obs. in active region 79−40163
Sun, Mg I λ2852 supergranular line profile var. 79−40164
Sun, Mg II UV doublet obs. *(Japanese)* 78−61831
Sun, plage Ca IV K-line, peak separation due to microturbulence 80−109407
Sun, relative chemical abundances in different solar regions 80−46518
Sun, reversal wavelengths of H I, Mg II and Ca II lines, temporal var. 78−93186
Sun, Si II lines 1808-1817 Å, observed and theoretical profiles 78−49412
Sun, Si V 1393 Å line in coronal hole and quiet Sun, OSO-8 obs. 77−91511
Sun, spectral line polarisation in VUV, technique and data reduction 80−67691
Sun, structure of lower corona and transition zone from Skylab NRL spectrograms 79−48744
Sun, supergranular vels. from UV obs., height var. 79−30025
Sun, supergranulation structure in coronal holes 80−51729
Sun, transition-zone plasmas, electron densities and mass motions in flares 80−56804
Sun, UV radiation, ferrioxalate actinometer meas. 80−41731
Sun, XUV spectra obs. by grazing incidence spectrograph on Skylab 77−60601
Sun EUV image, obs. by Skylab Apollo Telescope Mount TV monitor 77−60600
Sun extreme limb spectra, spatial struct. obs. in lines in 3398 to 3526 Å region 79−12449
Sun instantaneous XUV images, obs. and recording on ATM television monitors 77−60605
Sun polar coronal hole, EUV lines obs. anal. 79−5797
sunspot, UV emission line spectrum obs. 77−13296
sunspot transition region, emission meas. in far UV 77−78750
sunspot umbrae, Ca II H and K lines shapes and centre to limb. bar. 77−22178
supergiant stars, B2 to G0, small amplitude light vars. 78−32469
supergiant stars in LMC, spectral types and magnitudes, catalogue of 1882 objects 78−32361
supergiant stars with stellar winds in LMC luminosity and extinction values, UV obs. 80−77477
supergiants, C IV resonance lines in B- and early A-type objects 80−46550
supergiants, emission lines in UV spectra of α Orionis and α Scorpii 79−71028
supergiants assoc. with groups of luminous OB stars, photometry and spectra 77−17555
supergiants in LMC, IUE obs. of UV spectra and flux distribs. 80−101593
supernova in anonymous galaxy in Cygnus, UBV photometry and spectrum 79−5846
supernova in NGC 4321, UBV photometry, light curve and type 79−67045

ultraviolet astronomical observations continued
supernova in NGC 4321, UBV photometry 79−53835
supernova in NGC 4321, UBVR photometry 80−77428
supernova remnants, UV spectra interpretation using radiating shock wave models 80−90498
supernovae in NGC 488 and NGC 977, UBV photometry 79−62857
supernovae stellar remnants, spectroscopic search 80−26890
87 Sylvia, UBV photometry, light curve and rot. period 80−21942
ζ Tauri, apparent wavelength depend. of v sin i 78−12240
CD Tauri, eclipsing binary star, intermediate-band photometric anal. 77−13389
λ Tauri, eclipsing binary star, mass loss from UV spectra obs. 80−109485
T Tauri, flare obs. in U-band *(Russian)* 77−22228
ζ Tauri, high-resolution rocket spectra of λ1920 and λ1720 features 78−4236
DR Tauri, highly variable young star, spectrometric and photometric obs. 78−20829
T Tauri, integral brightness and Hα emission vars., 1971-77 period *(Russian)* 78−61852
λ Tauri, massive eclipsing binary star, spectrophotometry 80−26900
ζ Tauri, near UV spectrum, TD-1A satellite obs. 77−56988
ζ Tauri, near UV spectrum of shell star 78−81653
α Tauri, search for Ti II 3080 Å multiplet emission 80−51769
DR Tauri, T Tauri star, Balmer line profile changes and inverse P Cygni profiles 80−101591
V471 Tauri, U photometry of eclipses and flares 79−71072
β Tauri, UV spectrum of Mn star 78−69802
V471 Tauri, white dwarf eclipsing binary, IUE UV spectra 80−26912
α Tauri (Aldebaran), Mg II lines obs. rel. to chromosphere model 78−40931
V711 Tauri (HR 1099), Lyman α H I and D I interstellar absorption 80−8658
α Tauri (K5 III), S I emission obs. in EUV spectrum 80−82359
BU Tauri (Pleione), UV photometry during shell phase 77−64768
28=BU Tauri (Pleione) Be shell star, 3167 to 4924 Å spectrum atlas 80−98673
RV Tauri and yellow semiregular variables, photometric investigations 80−26865
T Tauri like stars, far UV photometry 78−20827
T Tauri stars, seven-colour TV photometry, obs. methods *(Russian)* 77−64756
T Tauri stars, seven-colour TV photometry, variability *(Russian)* 77−64757
Tautenburg objective prism survey objects, high-resolution spectra and redshifts 80−4436
BL Telescopii A, yellow variable supergiant near Cepheid instability strip, VBLUW photometry 80−98672
17 Thetis, opposition effect and surface material, UBV photometry *(Russian)* 79−58294
Tololo emission-line galaxies, nature from photometric and spectroscopic obs. 78−49531
Ton 1542, Seyfert galaxy, electronographic photometry *(French)* 77−45547
Ton 1542, Seyfert galaxy nucleus, optical polarisation *(French)* 77−26053
Tr 27-102 (HD 159378), possible long-period Cepheid, light vars. obs. 78−45336
Triton, diameter and reflectance, spectral and radiometric obs. 80−17546
Trumpler 1, open cluster, UBV photometry 77−74105
Trumpler 27, heavily-reddened young open cluster, spectra and photometry 77−78836
47 Tucanae, globular cluster, photometry and spectra rel. to stars chemical comp. 80−46620
47 Tucanae, metal-rich globular cluster, UBV photometric study 77−57065
4U 1543−62, optical candidate obs. 78−77625
4U 1626−67, X-ray pulsar, optical candidate photometry 78−12418
4U 1636−53 (MXB 1636−53), X-ray burster, optical candidate photometry 78−12418
4U 1735−44 (MXB 1735−44), optical identification and similarity to (Scorpius X-1) 78−93468
4U 1735−44 (MXB 1735−44), X-ray burster, optical candidate photometry 78−12418
4U 1755−33, optical candidate obs. 78−77625
4U 1837+04, UBR plates of Davidson optical counterpart 78−81714
3U 1956+11 optical counterpart, photometry and spectrum 78−49554
4 U 2129+47 optical counterpart, spectrum and photometry rel. to 80−17693
UBVRGI photometric measurements of 1297 stars, catalogue on mag. tape 78−40839
Uranus, disc profiles, narrow waveband, 6000-8500 Å region 79−66960
Uranus, UV albedo meas. 80−82295
CQ Ursae Majoris, Ap star, UBV photometry, light vars., period determ. 79−88667
ε Ursae Majoris, Ap star, UV spectral scans, line identifications 77−45440
XY Ursae Majoris, eclipsing binary, observational evidence for large-scale spot activity on primary component 80−109491
AW Ursae Majoris, light curve anal. of contact binary 80−56875
AN Ursae Majoris, nova-like variable, extremely high circular polarisation obs. 78−8018
W Ursae Majoris, OAO-2 UV photometry 77−13393
α Ursae Minoris region, field stars uvbyβ photometry rel. to reddening of Polaris 79−58356
UV5, in globular cluster NGC 1851, He abundance determ. 78−49441
UV 1758+36, He deficient hot subdwarf B star, atm. parameters, radial vel. 78−53944
variable compact object discovery in Perseus, bright blue N-galaxy, photometry and spectrum 79−12524
variable stars, UBV photometry at geographic latit. 69°22′ north 79−44376
variable UV excess object, discovery 79−40280
variable UV excess object in Bootes, UGR photometry, position 79−48942
Vela SNR, IUE UV spectrum 80−101635
Vela X-1 (HD 77581), binary source, spectral obs. 80−94892
AI Velorum, dwarf Cepheid, nature from uvbyβ photometry 77−78801
γ Velorum, interstellar absorption lines in UV spectrum 79−35324

ultraviolet astronomical observations continued
λ Velorum, K-type supergiant, UV spectrum rel. to chromosphere and wind struct. 80−72948
CV Velorum, light curves, photometric elements and absolute dimensions 77−60796
δ Velorum, UV spectra, comparison of synthetic and observed spectra 77−29820
γ_2 Velorum, Wolf-Rayet binary, orbital element determ. from spectral obs. 80−85950
γ_2 Velorum, Wolf-Rayet binary star, UV obs. from TD-1A satellite 80−77447
Venus, cloud images from Pioneer orbiter 80−46432
Venus, cloud structure, high-contrast UV detail 80−51682
Venus, exosphere, nonthermal H population, Venera Lyman α obs. 78−93136
Venus, H I and D I Lyman α radiation scattering, Venera obs. 77−78703
Venus, H Lyman α emission rel. to exosphere temp. day-to-night var. 79−35164
Venus, Mariner 10 photometric obs. 77−29685
Venus, Pioneer nephelometer expts. results 80−46430
Venus, regional polarization, 1950-77 obs. 80−8570
Venus, rotation of upper atmosphere *(French)* 80−36534
Venus, SO_2 detect. in UV spectrum 79−62781
Venus, spectral detection of SO_2 and CS_2 *(French)* 79−62776
Venus, ultraviolet photometry and cloud struct., Venera obs. 80−56738
Venus, upper atm., rot., photographs 1927-1975 in UV *(French)* 79−2504
Venus, UV and IR simultaneous images, correl. of features 79−53744
Venus, UV markings, Venera 9 cloud top data analysis 80−17521
Venus, UV markings contrast spectral depend. 79−62783
Venus, UV nightglow, IUE obs. 79−62782
Venus, vortex circulation, Mariner 10 polar stereographic UV images 79−35167
Venus atmosphere, circulation development and vars., Mariner 10 TV pictures 78−57479
Venus atmosphere, scattering layer over absorbing clouds, Venera 9 and 10 UV photometry 77−78700
Venus atmosphere, SO_2 detect. by IUE 79−101101
Venus cloud cover, obs. by Venera 9 orbiter 80−51680
Venus clouds, UV absorbers, Pioneer data 80−46433
Venus cloudy layer, TV observation of UV and violet region from Venera station orbiter *(Russian)* 79−53747
Venus dayglow spectrum, 1250 to 1430 Å, Pioneer Venus obs. 80−77311
Venus polarisation, wavelength depend. obs. rel. to UV cloud model 80−82250
Venus UV spectroscopy, initial results from Pioneer Venus orbiter 79−48711
Vesta, UBV photometry and lightcurve 80−36546
BF Virginis, β Lyrae-type eclipsing binary, light curves 77−13395
32 Virginis, Am star, spectroscopic obs. and curve of growth anal. 77−22237
α Virginis, binary star, UV spectrum 77−45485
α Virginis, Copernicus UV obs. 77−33502
CU Virginis, He spectrum variable, UV photometry with ANS 78−36585
α Virginis, UV interstellar lines in 935-2960 Å range 79−35323
visual binaries containing GK giants, CN strengths, mixing and supermetallicity 77−56930
visual double stars, spectral classification and UBV photometry 77−74084
Vulpecula OB2 stars, photometry and spectra rel. to membership of 67 day Cepheid S Vulpeculae 80−41831
BW Vulpeculae, UV light curve of β Cephei-type star 78−36570
NQ Vulpeculae (Nova 1976), UV and visual spectra analysis *(Chinese)* 80−12770
NQ Vulpeculae (Nova Vulpeculae 1976), photoelectric obs. 78−4252
VV 150, galaxy chain, photoelectric and spectroscopic study 80−98724
VV 493 (UGC 07910), unusual extragalactic object, morphology and spectrum rel. to probable nature 80−98718
Wat 6, open cluster, photometry and spectra rel. to proximity to (Pismis 6 and 8) 79−88712
white dwarfs, hot, effective temps. 79−25602
white dwarfs, southern, Stromgren photometry 78−32456
white dwarfs in globular cluster NGC 6752, UB photometry 78−93233
white dwarfs in open clusters, obs. rel. to progenitor stars upper mass limit 80−51738
Wolf-Rayer stars, UV obs. 78−40965
Wolf-Rayet stars, ANS obs. of UV variability 78−65632
Wolf-Rayet stars, ANS UV spectrophotometric obs. 80−22023
Wolf-Rayet stars, atlas of Copernicus UV spectra 78−57557
Wolf-Rayet stars, faint, photometry and spectrography 79−40200
Wolf-Rayet stars, in M33, spectral obs. 77−64779
Wolf-Rayet stars, interstellar N V lines, IUE obs. 80−101634
Wolf-Rayet stars, Si IV and C IV, absorpt. lines, IUE obs. 80−67748
WRA 977, high-speed UV photometry of periodic modulation 78−16442
X-ray sources, UV spectra obs. by International Ultraviolet Explorer (IUE) 78−96569
yellow semiregular and RV Tauri variables, photometric investigations 80−26865
young emission-line stars in S Hemisphere, image tube spectrograms 78−8016
young open clusters, UVBYβ photometry rel. to bimodal star form. 77−49374
zodiacal light, search at 1550 Å 79−16882
zodiacal light, spectrum in middle UV 77−29720
zodiacal light, UV obs. from D2B-Aura satellite 79−58299
zodiacal light, UV spectroscopy at 20° elongation 78−20728
zodiacal light UV observations by Astro 7 rocket expt., reddening 78−96427
VII Zw 466, ring galaxy, UBVR photometry 79−8991
I Zw 92, III Zw 77, compact galaxies with broad emission lines, spectra 78−73760
B II 1362 Å, interstellar line detect. in front of κ Orionis 80−51841
H deficient and He weak stars, uvby photometry, variability 80−46579
H I survey from Lyman α absorption meas. towards 100 stars 78−93357
H II condensation in NGC 2175, obs. of involved stars 78−20883
H II regions in Perseus arm, spectrophotometry and reassessment of galactic abundance gradients 80−22055

ultraviolet astronomical observations continued
H II regions near nucleus of spiral galaxy NGC 3310, exploratory investigation 80−62235
H I+molecular/H II shells from 1 to 1200 pc dia. in LMC, obs. and origin 79−25678
Hα emission stars in southern dark clouds, UBVR photometry 78−81633
Hα emission stars in young cluster NGC 2264, UBVRI obs., pre-main sequence stars 79−35267
He I, II in interplanetary space, EUV photometer obs. of 58.4, 30.4 nm lines 77−45309
HgMn stars, spectrophotometry 80−26867
HgMn stars, UV spectra rel. to thin Hg layers and diffusion model 80−105243
Mg I 2852A line obs. towards moderately reddened stars 78−20874
N deficient supergiants in loose assoc., LTE and non LTE abundance anals. 79−44478
O VI interstellar survey, UV spectra of OB stars 78−36679
Ti II 3384 Å line obs. towards ζ Persei, interstellar Ti vel. distrib. 79−53877
U stars and related objects, spectroscopic study 78−49465

ultraviolet astronomy
see also ultraviolet sources (astronomical)
aeronomical reference spectrum for solar UV below 2000 Å 79−25379
Apollo Telescope Mount and solar instruments of Skylab, overview 77−60593
Apollo Telescope Mount television monitors, obs. and recording of instantaneous images 77−60605
aspheric grating for EUV astronomy 78−57451
automated spectrum scanner, 3000-11000 Å region 79−53724
background radiation in far-UV as probe of dense hot intergalactic medium 79−92897
Balloon-borne UV Stellar Spectrograph, first obs. results 79−70955
Balloon-borne UV Stellar Spectrograph, instrumentation and obs. 79−70954
BUSS, echelle and SEC-vidicon for balloon-borne UV spectroscopy 79−25482
coma-free two-mirror systems, astronomical appls. *(Russian)* 77−64641
conference, Erice, Sicily, 1975, May *(Italian)* 78−32436
cosmic background radiation at 1440 Å 79−71159
deep photographic survey from Spacelab 79−25474
detector, self-scanned anode array, for Mariner Jupiter/Saturn spectrometer 77−78632
detectors, UV response of InGaAsP photocathodes 77−57387
diffraction grating, transmission efficiencies on EUV and soft X-rays 77−60621
diffraction mountings, conical and classical, for XUV gratings 79−3780
diffuse cosmic UV background, spectrum 80−17696
diffuse sky background, D2B satellite ELZ photometer survey 80−105404
dust, UV opacity effects on stellar spectra 80−90505
echelle spectrograph, high-resolution, for far UV and visible astronomy, design and performance 80−26744
electrographic image detectors, development, and applications in UV astronomy and scientific research 80−43465
electrographic instrumentation for ultraviolet imaging and spectrography 80−46399
EUV instruments, computer aided calibration technique 80−85839
EUV solar image TV monitor on Skylab Apollo Telescope Mount 77−60600
EUV solar line emission weakening short of 912 Å wavelength 80−21962
EUV spectra and solar atmosphere plasma diagnostics 79−30050
EUV spectrograph, Skylab Apollo Telescope Mount expt. S082B 77−60598
EUV spectrograph with single toroidal grating, stigmatic performance 80−36498
EUV spectroheliographic, in Apollo Telescope Mount experiment S082A 77−60597
EUV spectroheliometer for photometry of dynamic phenomena 78−53825
EUV spectroheliometer on Apollo Telescope Mount 77−60594
EUV spectroheliometer on Skylab Apollo Telescope Mount, photometric calibration 77−60595
EUV spectrum of hot, optically-thin interstellar plasma 78−81665
EUV telescope, high performance, design 79−58245
EUV/soft X-ray background, Apollo-Soyuz sky survey results 79−71160
extragalactic work with IUE 80−105357
Fabry-Perot scanning interferometer with piezoelec. spacers, appl. to solar UV spectrum 80−12678
Faint Object Camera calibration 79−25479
Faint Object Camera on Space Telescope 79−25478
Faint Object Spectrograph for Space Telescope 79−25483
Faint Object Telescope for far UV spectrophotometry of galaxies and quasars 79−25481
far UV spectrograph with microchannel plate detector,for rocket-borne astronomy 77−22086
FAUST, far UV camera on Spacelab 79−25476
FAUST instruments, high focal ratio telescope for UV imagery 80−41724
Feige 4, hot white dwarf, identified with bright EUV source 78−89200
galactic neutrinos and decay to UV photons 80−109566
gratings for UV space instrumentation, comprehensive analysis 79−8839
grazing incidence telescopes, design, fabrication and performance, for EUV obs. 78−49329
Grazing-Incidence Solar Telescope facility 79−70956
Gurzadyan UV stellar group in Auriga, UBV and uvby photometry 78−45373
He II 304 Å line redshifted to 1450 Å in far UV background 80−41893
high resolution UV solar spectroscopy, review 78−45313
high-resolution optical telescope design 80−90335
holographic grating, calc., for very wide field camera *(French)* 78−81547
IKA-65 UV stellar photometric equipment on Cosmos 215 satellite *(Russian)* 77−64642
image convertor-intensifier detector for interference spectroscopy in balloon UV 80−56707
instrumentation for EUV astronomy 79−25484
International Ultraviolet Explorer, geosynchronous satellite 78−89060
International Ultraviolet Explorer, results after one year 79−96915

ultraviolet astronomy continued
International Ultraviolet Explorer, spacecraft, instrumentation and program *(Italian)* 78−32320
International Ultraviolet Explorer (IUE), in-flight performance 78−96383
International Ultraviolet Explorer (IUE), new era in UV astronomy 79−48671
International Ultraviolet Explorer (IUE), spacecraft and instrumentation 78−96382
International Ultraviolet Explorer (IUE) second European conference (Tubingen, Germany, 1980 March 26 to 28) 80−82584
International UV Explorer satellite, obs. of sample targets 78−32315
interstellar clouds, diffuse UV radiation penetration 80−56901
interstellar grains and molecules, UV obs. from Spacelab 80−41871
interstellar H_2 vibrational excitation in intense UV fluxes 78−36647
interstellar medium, role of H I Lyman-α 1216 Å flux 77−2459
interstellar UV grain albedos rel. to C I 79−92818
IUE, search for stellar coronae 80−4233
IUE preliminary results, workshop, Udine, Italy (1978 October 12) *(Italian)* 80−86033
IUE satellite, observing experience 80−36476
IUE ultraviolet telescope, initial results *(French)* 79−84639
Jupiter, Lyman α albedo rel. to solar activity 80−98601
Lyman α camera, for high resolution solar Lyman α filtergrams 80−82323
Lyman alpha coronagraph 79−25486
Mariner 10, UV spectrometer airglow expt. 77−64611
Mariner 10 UV spectrometer, Mercury occultation expt. 77−67023
measurement of UV radiation, accurate techniques 80−47103
metal mirrors, Al, Ni and Au surfaces, EUV reflection efficiencies 79−14073
middle UV low light level imaging devices 77−41319
mirrors with highly reflective coatings, for satellite instrumentation *(French)* 77−67022
monochromators of concave grating mounting for space telescopes, VUV region 78−73629
multi-anode microchannel arrays for detector systems 79−25480
Multipurpose Utility Pointing and Stabilisation System *(Italian)* 77−82114
nebulae, UV radiative pumping of N^+ fine structure levels 79−53871
nonejecting novae as EUV sources 78−12238
numerical image manipulation and display, Skylab EUV solar obs. appl. 77−60618
objective-prism spectrograph, for UV stellar spectral obs. from Skylab 77−60609
OSO-8 Univ. of Colorado UV spectrometer expt., optical design 78−49326
OSO-8 UV spectrometers, computer-controlled mission operations 80−41723
Penning source, continuous discharge, with 50 Å to 300 Å emission lines 79−50363
photographic photometer, three-channel, for stellar obs. from Skylab 77−60608
Pioneer Venus Orbiter cloud photopolarimeter 78−57429
Pioneer Venus Orbiter UV spectrometer, design and operation 80−67503
planetary nebulae, advances in UV obs. 80−109524
polychromator, Astro 7, UV, for zodiacal light obs., absolute radiometric calibration 78−49336
primaeval galaxies, model emission spectra 80−46655
QSOs, dust opacity and photoionization in far UV 80−46696
QSOs UV emission lines, photoionization model analysis 79−71148
review of vac. UV astronomy 79−2488
Salyut 6 200-260 nm UV receiver 80−67566
satellite-borne instrument development problems and solns. 77−82111
satellites, Earth-orbiting, study of hot components and extended coronas 80−109379
silicates, optical props. in far UV 78−53875
sky survey project EXUV 10-1000 Å waveband, proposed mission 80−82165
sky surveys, review 78−93111
Skylab, experience, with Schumann-type XUV film 77−60599
Solar Maximum Mission UV polarimeter design, operation and calibration 79−80225
solar stratospheric station, automatic, construction, selection of variant *(Russian)* 79−96913
solar ultraviolet Doppler camera 79−25485
solar UV flux, cyclic vars. 80−101577
solar UV spectrum, 140 to 350 nm, NASA meas. using SURF storage ring calibrations 80−94721
solar UV vars. rel. to climatic changes 80−26607
solar XUV, grazing incidence spectrograph on Skylab 77−60601
space astronomy, new instrumentation, conference (Tel Aviv, 7-18 June 1977) 79−25473
space instrumentation, techniques 79−25519
Space lab integrated UV and X-ray astronomical payload proposal *(Italian)* 77−82112
Space Telescope, prospects for spectroscopic and direct work 78−57444
Space Telescope 79−25477
space-borne opportunities 78−61704
spectral classification of UV sources 78−65602
spectrograph balloon-borne UV, for stellar obs. 78−49318
spectrometer, microchannel plate life tests 77−61117
spectrophotometry absolute calibration, 1750-3350 Å region 79−70963
spectrophotometry of faint astronomical objects, rocket instrument description 80−62014
spectroscopy, fabrication of transmission gratings 80−14490
spectroscopy with Copernicus satellite 78−16310
stars, atlas of UV spectra from OAO 2 spectrometer flux data 79−48691
stellar spectra, second OAO atlas 80−72786
stellar spectrograph BUSS, optical system, appls. *(Dutch)* 78−7880
stellar spectroscopy, spaceborne instrumentation 79−25518
Sun, N III and O IV intersystem multiplets as density indicators for solar plasmas 80−31264
Sun and stars, high resolution UV spectrography appl. 79−25520
T Tauri stars, for UV radiation *(Russian, English)* 79−75217
transition radiation from relativistic intergalactic dust grains 79−75272
transmission grating, facet-type, aberrations for cosmic X-ray and XUV spectroscopy 78−85851
Ultraviolet Spectrometer and Polarimeter on Solar Maximum Mission 80−51661

ultraviolet astronomy continued
UTEX, integrated UV and X-ray astronomy facility on Spacelab 79−25475
vacuum UV monochro-collimator *(Japanese)* 77−73957
wide field UV cameras, Marseille Obs. *(Italian)* 78−32346
Wolter-Schwarzschild optics for Berkeley stellar spectrometer and EUV Explorer 80−82197
XUV astronomy, review *(German)* 80−109372
XUV solar flare kernels, electron density meas. 79−16913
XUV spectroheliometer on SMM 79−25487
D_2 gas discharge lamp as UV continuum source, space appls. 80−36505
N III lines for solar diagnostics 79−30031
O I isoelectronic sequence, excited level populations, line intensity ratios, solar corona appl. 80−32637

ultraviolet communication *see optical communication*

ultraviolet detectors
arc quasistationary plasma, scatt. diagnostics using periodically pulsed UV lasers 78−67481
biological application, UV meas. 80−35963
C-CD, thinned back-illuminated, for extreme UV direct detect. 80−77852
C-CD Si detectors for space astronomical appl., UV sensitization 79−84668
calibration of radiation detectors in VUV, using wall-stabilised Ar cascade arc 79−80679
calorimeter, pulse gas, for vacuum UV rad. meas. 80−251
ceramic channel electron multiplier, detect. efficiency in vacuum UV 78−12759
coordinate gas counters for vacuum UV and ultrasoft X-ray spectra 79−89014
discrete wavelength detector at 214 nm, for high performance liquid chromatography 79−75595
dosimeter, direct-response TLD using MgO 77−13010
dosimeter, for natural radiation meas. in study of photodermatoses and drug photosensitivity 78−40339
dosimeter for UV radiation meas. *(Russian)* 77−90902
dosimeter response correction, spectral distrib. of natural radiation under clear day conditions 77−41171
double-junction Si photodiode, high UV responsivity 77−74504
echelle and SEC-vidicon for balloon-borne UV spectroscopy 79−25482
electrographic instrumentation for ultraviolet imaging and spectrography 80−46399
electronic imaging techniques in EUV spectral region 79−30564
ferrioxalate actinometer for solar UV radiation meas. 80−41731
gas filled phototube, photoionisation of excited atoms 77−87823
gas filled phototubes as sensitive UV detectors, excited atom photoionisation mechanism 77−61122
gas-filled photoelec. sensors, flame detector appl. 77−168
high-speed photographic camera for UV spectrum range *(Russian)* 77−34051
HPLC, high sensitivity UV detector 78−45709
HPLC, UV absorption detector 78−45707
HPLC, UV detection 78−45706
HPLC, UV variable wavelength monitor 78−45708
inert gas photoelectron counter, XUV intensity meas. 78−32842
light-flux generated by single-lens illuminator, spectral composition for UV region 80−87450
liquid chromatograph detector for high concentration and flows 80−71960
liquid chromatograph for homogeneous mixture analysis 80−16757
measurement of UV radiation, accurate techniques 80−47103
measurement techniques, industrial, medical appl. 78−37954
measurement techniques, solar radiation, industrial, medical UV radiation appl. 78−37057
metal photocathodes, for absolute intensity meas. in soft X-ray and vac. UV region 77−71412
microchannel detector arrays, multi-anode, development 79−25480
microchannel plate detector for far UV spectrograph, rocket-borne astronomy appl. 77−22086
microchannel plate life tests 77−61117
microchannel plate multiplier for self-scanned anode array UV detector 77−78632
microcomputer controlled UV ozone calibrator 80−13149
monochromator, photon counting, solar radiation UV limit meas. at Earth surface 78−49134
multiwire gas counter for VUV region coordinated meas. 79−67384
optical communication, atmospheric UV propagation 77−79770
photocell, 0.22-0.36 μm 77−71376
photochemotherapy, absolute radiation dosimetry 79−12008
photoconducting device for psoriasis photochemotherapy source output monitoring 78−53473
photodiodes, windowless XUV, with Al_2O_3, W photocathodes, photoefficiency 20 to 250 eV 78−65963
photon counting, vacuum UV region, 120-200 nm, detection limit of apparatus *(German)* 78−45691
plasma broadband radiation, detect. in Tokamak using photoelectric effect and photodiode array 79−90464
plasma spectroscopy, broadband stable detector 78−87495
radiation standards and meas. for health and safety 78−74056
radiation standards for source spectral emission and detector spectral sensitivity 77−39007
radiometric standards at NBS 77−38011
recorders, latest trends 79−54117
secondary electron conduction vidicon digital TV camera 78−54457
selective receivers for 0.2 to 0.3 μ spectral region 79−30560
semiconducting dosimeter, 200-400 nm range 78−74059
semiconductor ratemeter of UV radiation 78−285
seminar, optical radiation meas., San Diego, CA, USA (Aug. 1979) 80−86036
semitransparent multialkali photocathodes, UV response, efficiency 77−167
sodium salicylate, vac. UV scintillators, characteristic props. at 253.7 nm 79−71525
solar UV meas. and physics 80−41784
solid-state imaging devices, conference, San Diego (1977) 78−66944
spatial imaging detector system for pulsed plasma extreme ultraviolet diagnostics 80−33821
spectral radiance calibrations, 165-300 nm, interlab. comparison 77−74478

ultraviolet detectors continued
spectral sensitivity of radiation detectors using Ar-cascade arc, report *(German)* 78−82037
spectrofluorimeter design with vacuum, luminescence meas. from thin films 79−71538
Spectroline DM series, UV appl. 80−77854
standards, at Australian Nat. Meas. Lab. 80−31704
temperature units, USSR special standards 77−30148
p-terphenyl, vac. UV scintillators, characteristic props. at 253.7 nm 79−71525
UV radiation meas. in agricultural production, instrument *(Russian)* 78−65969
UVB spectral irradiance monitoring at 9°, 39° and 71°N 79−58070
VUV detector, using photodetector sensitised by alkali halide coating 79−85180
VUV detectors absolute efficiency, meas. using VEPP-2M storage ring synchrotron radiation 80−82824
VUV Eagle spectrometer, 2 m, design, construction, operation *(German)* 78−45732
water vapour instrum. for stratospheric aircraft using UV fluorescence 80−82100
Zn_3P_2, UV photoconductive detectors 80−4766
Ag-Al_2O_3-Al structure, photoinduced currents, UV detection characts., 325 nm 77−53979
Al_2O_3:Si,Ti photostimulated thermolum., and appl. to UV dosimetry 78−53511
Au-Si surface-barrier detectors with increased UV sensitivity 78−4696
CaF_2:Dy (TLD-200), practical UV dosimeter 77−60258
CaF_2:Dy sensitivity to UV and ionising radiations, temp. treatment effect 79−26763
$CaSO_4$:Dy phosphor powder, effect of grinding on thermoluminescent sensitivity 79−33852
$CaSO_4$:Dy thermoluminescence sensitivity and glow curves, 700° to 1300°C 79−85815
$CaSO_4$:Tm intrinsic thermoluminescence stability for UV dosimetry 80−12262
$GaAs_{1-x}P_x$-Au, surface-barrier struct., photodetectors of visible and UV radiation 77−20437
InGaAsP photocathodes for astronomical detectors, UV response 77−57387
LiF, photostimulated thermolum. as UV radiation dosimeter 77−16984
Mg, SiO_4:Th TLD phosphor, γ-ray induced sensitisation and phototransfer 79−33851
MgO, thermoluminescence of single crystal 77−16986
Mg_2SiO_4:Tb, TLD material, UV induced thermolum. and phosphoresc. 78−92707
Si detectors, vac. UV performance, 500-2000 Å 77−26397
Si, n-type, thermally oxidised, natural inversion layer, UV photodiode construction 79−30559
Si, photodiode, violet and near UV sensitive, prep. and expt. study *(Chinese)* 79−49285
Si UV detectors coated with thin film scintillators 80−86412
Zn-In-S ultraviolet detector *(Russian)* 80−18014
$Zn_xCd_{1-x}S$ film, prep. and use as heterojunction optical energy converters 79−95488

ultraviolet lamps *see lamps*

ultraviolet radiometry *see photometry*

ultraviolet sources *see light sources*

ultraviolet sources (astronomical)
accreting magnetic degenerate dwarfs, X-ray and UV emission 80−41826
accreting nonmagnetic degenerate dwarfs, X-ray and UV radiation 79−40184
3C 273, quasar, detailed UV obs. with IUE 80−94886
cosmic background radiation at 1440 Å 79−71159
Cygnus X-2, rapid UV flux vars., IUE obs. 80−12833
diffuse cosmic far UV background, rocket obs. 80−46708
EUV point sources, contrib. to diffuse EUV background 80−62324
EUV/soft X-ray background, Apollo-Soyuz sky survey results 79−71160
Feige 86, UV high-resolution spectrum 80−41834
galactic UV radiation, role in interstellar gas heating 80−67839
HD 192273, EUV flux upper limit, Voyager 1 obs. 80−77406
HD 192273, high latitude EUV source, low-mass binary 80−4353
HD 192273, optical spectral obs. of proposed EUV source 79−35256
HD 219150, F0 V star with remarkable UV excess, optical and UV photometry and spectrum 80−90429
hot subdwarfs in Carnochan and Wilson catalogue, UV spectra 80−82354
interstellar UV radiation field, obs. from S2/68 sky-survey telescope 80−77523
KUV09313+4052, variable UV excess object, discovery, position and photometry 80−62159
RU Lupi, T Tauri star, for UV radiation rel. to chromosphere, corona and X-ray emission *(Russian)* 80−51770
nearby main sequence and subgiant stars, XUV radiation upper limits 79−12471
NGC 4151, Seyfert galaxy, for UV line profiles 80−22083
NGC 7023, refl. nebula, far UV brightness rel. to HD 200775 reddening and dust albedo and scatt. 80−51832
observations by Earth-orbiting satellites of hot components and extended coronas 80−109379
observations with International Ultraviolet Explorer (IUE), new era in UV astronomy 79−48671
PKS 2155, BL Lacertae object, UV flux meas. by IUE 80−12833
planetary nebulae, advances in UV obs. 80−109524
planetary nebulae, review of UV obs. 80−109523
Seyfert galaxies, nonthermal UV sources vars. rel. to dust thermal emission vars. 80−67865
Seyfert galaxies, type 1, nuclei props., UV emission, colour index *(French)* 79−48923
stars in high-latitude regions, balloon-borne UV survey 80−41891
supernova, nearby, UV and gamma radiation effects on terrestrial atmosphere 80−94584
T Tauri, Lyman continuum energy spectrum rel. to nebula ionisation and emission line spectrum 80−67820
variable UV excess object, discovery 79−40280
H I+molecular/H II shells from 1 to 2000 pc dia., wind-driven or supernova remnants 79−25678

ultraviolet spectra of inorganic solids *see visible and ultraviolet spectra of inorganic solids*

Umklapp process
actinide metals and compounds, nearly magnetic, thermoelec. power 78−84197
actinide systems, nearly magnetic, thermoelectric power determ. 78−56133
alkali metal, crossing of dispersion curves in (ζ00) direction 78−38795
alkali metal, electron-phonon drag effects in elec. cond. and thermoelec. power 77−15824
alkali metals, electron distrib. function enhanced, phonon-limited electrical resistivity 78−6346
commensurate and incommensurate structural phase transitions in Jahn-Teller system 80−70403
dielectric material, phonon thermal conductivity, Umklapp process, comparison with LiF data 80−39367
electric field depinning of charge density waves 79−73454
electron gas, 1-D, 2-D Coulomb gas, and 2-D epitaxial monolayer problems, family of mappings 80−34346
electron-electron scatt. and elec. resistivity of metals 79−95396
Fermi one dimensional gas with long range potential, renormalisation group, exchange, Umklapp interactions 80−2351
incommensurate systems, transitions, solitons 79−77714
metal, closed Fermi surface, galvanomagnetic phenomena, in intermediate magnetic fields *(Russian)* 78−34822
metal, dirty, resist. temp. depend., causes of Matthiessen's rule deviations *(Russian)* 77−69291
metal, low-freq. longit. sound attenuation, viscous and induction mechanisms 77−8152
metal, quasi-one-dimensional, elec. resist. due to electron-electron scatt. 79−4549
metal, rel. to thermal resist. calc. 77−62894
metals, normal hexagonal, temp. depend. anisotropy of phonon scatt. resist. 78−51967
multivalley semiconductor, rel. to donor binding energies, variational calc. 78−23041
normal metals, low temp. resistivity, correl. with electron-phonon scatt. anisotropy 79−56190
one-dimensional electron system, with short-range attraction, case of one electron per atom 77−4281
one-dimensional Hubbard model, correl. functions *(Russian)* 77−31929
one-dimensional metal, cond., electron-electron scatt. 80−10957
Peierls transition, inhomogeneous state 78−67943
Peierls transition in quantizing mag. field, possibility 80−103441
Peierls-Frohlich state, effect of Umklapp processes on dynamics *(Russian)* 77−47752
phonon drag by sound 79−28062
quasi one-dimensional system, Peierls-Frohlich state, cond., Umklapp processes *(Russian)* 79−38059
semimetal, two-stage drag of electrons by phonons 77−15843
solid, three phonon processes, separation of normal and Umklapp processes 79−55857
superconductivity, high-temp. electron-hole 80−2512
superlattice, plasma oscillations 77−72878
thermal phonon drag by coherent acoustic waves, Umklapp processes 78−14417
three-photon Umklapp processes, variational techniques 79−37785
TTF-TCNQ, commensurate ordering 77−7829
two-dimensional Wigner-crystal-liquid-surface system, eigenmodes and instability of charged liq. surface 80−10896
Al, magnetoresist., linear growth in strong. mag. fields *(Russian)* 78−51972
Al, Nernst-Ettingshausen coeff., electron-phonon Umklapp scatt. 78−26848
Al, positron annihilation, ang. correl. meas., electronic momentum density calcs. 77−4284
Al, positron annihilation, angular distrib., Umklapp effects *(French)* 80−50454
Al, positron annihilation studies using high-density proportional chambers 80−25478
As, electrical and thermal props. 78−14747
BN thermal diffusivity meas. using ruby laser beam *(Spanish)* 79−90835
C_8Cs, intercalation cpd., theory of order-disorder phase transitions 80−19908
Cs, elec. and thermal resist. calc. using modified noncentral force model 79−91016
Cu, conduction band, high momentum components determ. from annihilation radn. ang. correlation 79−19508
Cu, elec. resist., electron-electron scatt., Fermi surface calc. 78−64023
Cu, electrical resistivity, at low temp., temp. depend. 78−23071
Cu, point-geometry ang. correl. curves, enhancement in positron annihilation 79−95873
Cu, positron annihilation studies using high-density proportional chambers 80−25478
Cu surface, (001) and (111), angular resolved photoelectron spectroscopy 78−95652
Cu, umklapp annihilation of positrons, rot.-specimen method 78−2410
β_1Cu-Zn, structural Umklapp processes at low and high temp. lattice kinetics of phase transformation isotherms *(German)* 78−30707
β_1-Cu-Zn mixed crystal, metastable structural Umklapp process, isothermal phase transform. *(German)* 78−22798
α-$Cu_{0.7}$ $Zn_{0.3}$, point-geometry ang. correl. curves, enhancement in positron annihilation 79−95873
$FeCl_2$, antiferromag., magnon-phonon interactions in thermal cond. 80−65315
GaAs, boundary scattering and phonon conductivity, 2-10K 78−63888
GaAs, lattice thermal cond. from three phonon scatt. relax. rate 78−51755
GaAs-$Ga_{1-x}Al_xAs$, superlattice umklapp processes in resonant Raman scattering 78−64362
GaAs-$Ga_{1-x}Al_xAs$ superlattices, resonance enhanced Umklapp Raman process 78−39547
GaP, multiband and multivalley effective mass theory for impurities 79−65409
Ge, lattice thermal conductivity three phonon processes 78−34662
H_2, solid, thermal cond. at varying o-H_2 conc. 78−51786
He, liq., Wigner 2-dimens. lattice, on surface, reson. linewidths 79−86949

Umklapp process continued
InSb, lattice thermal cond. from three phonon scatt. relax. rate 78−51755
Ir, (111) surface states, surface Umklapp effects, photoelectron spectra 80−93457
K, thermomagnetic and thermoelectric properties, phonon scatt. processes 80−29390
K, ultrasonic attenuation at low temp., spherical Fermi surface model 80−84255
$K_2Pt(CN)_4$, quasi-one-dimens. Peierls system, phonon dispersion and neutron scatt., calc. 80−24550
Li, elec. and thermal resist. calc. using modified noncentral force model 79−91016
Li MIM struct., electron-phonon interaction function investigation by microcontact spectroscopy 79−95108
Li, phonon limited resistivity struct. depend., Umklapp scatt., elastic consts. 80−88532
Mg_2Ge, three-phonon relaxation rate and phonon conductivity 78−14416
Na MIM struct., electron-phonon interaction function investigation by microcontact spectroscopy 79−95108
Na, phonon limited resistivity struct. depend., Umklapp scatt., elastic consts. 80−88532
Ne, solid, rel. to thermal cond., 0.5-10K 77−43396
PbI_2, thermal cond., 2 to 30K, Umklapp processes and phonon boundary scatt. *(Russian)* 79−10991
Si, Auger recombination 78−26883
Si, doped, basis functions for studying intervalley effects 79−69442
Si, impact ionisation, threshold energies calcs. for electons and holes 77−62933
Si, multiband and multivalley effective mass theory for impurities 79−65409
Si, screening of donor ions by delocalised electrons 79−69466
Si:Al, valley-orbit splitting of bound exciton states 79−28290
$TaSe_2$ (2H), optical absorpt., band struct., plasmons, and CDW 80−45104
$TaSe_2$(2H), plasmon behaviour at charge density wave onset 80−10900
TiO-MeO (Me=Ni, Co, Mn), solid soln., lattice thermal cond. 79−23791
β-Zr, phonon dispersion, modified Sharma-Joshi model 80−100311

uncertainty principle *see indeterminancy*

underground cables
see also cable laying
convectively cooled cable, temp. distribs., heat transfer correlations 78−71262
convectively cooled cable, vel. distribs., press. drop correlations 78 71330
EM shielding of sources within metal-cased borehole 77−40979
fibre optical cable, buried, transmission characts. meas. *(German)* 78−33865
oil-cooled, laminar friction factor and heat transfer 80−10247
optical cable transmission meas. 78−50942
optical fibre 1.8 km cable, operational, installation *(German)* 79−3783
optical waveguide air refractive index thermal fluctuation obs. 78−9452
optical waveguide beam distortion by air convection 77−62063
telephone cables laying, seismology appl., rocks location verification 80−72456

underground distribution systems
see also distribution networks
convectively cooled cable, temp. distribs., heat transfer correlations 78−71262
convectively cooled cable, vel. distribs., press. drop correlations 78−71330

underwater acoustics *see underwater sound*

underwater cables *see submarine cables*

underwater sound
see also hydrophones; oceanography; sonar
3-layer waveguide, wave numbers and phase difference between components of sound field 80−38144
absorption, chemical relaxation studies using resonator method 80−96073
absorption in sea water, theory 78−1481
absorption in viscoelastic medium containing short cylindrical cavities 77−84049
absorption of sound by sound 78−59180
acoustic, backscattering, from thin air-filled spherical shells in water 78−13838
acoustic absorption by $MgCO_3^0$ ion-pair relaxation 79−74914
acoustic array, noise immunity in presence of weak external disturbances 79−64386
acoustic array design, environmental influences 80−83721
acoustic array gain, rel. to correl. coeffs. and patch size 77−31158
acoustic arrays, focused nonuniformly spaced, 2-dimensional minimax optimization 79−59897
acoustic channel stability meas. 79−41495
acoustic CW phase fluctuation spectra, estimation and interpretation 77−46850
acoustic field in shallow water, transition ranges, bottom-reflection loss *(Chinese)* 77−58500
acoustic hologram correction for nonuniform relative motion 79−46119
acoustic holographic image reconstruction for moving objects 78−75019
acoustic imaging, real-time signal processing techniques 79−90089
acoustic line array operation in water layer 80−5866
acoustic measurements, appl. of FM signal modulated by smoothed random telegraph signal 78−18130
acoustic motional source transfer function characts., ocean profile anal. appl. 78−66982
acoustic phase, modulation by internal wave vertical vel. 77−46852
acoustic phase modulation by first-mode directional internal wave, simulation 77−62089
acoustic propagation in deep underwater channels, sonar appl. *(French)* 79−72745
acoustic pulse reflected from water surface, spectrum 80−87627
acoustic radiation and scatt. anal., use of linear system theory 77−75729
acoustic reflection, from absorbing and nonabsorbing cylinders 78−1479
acoustic scatterers, classification, experimental appls. involving fish 79−41502
acoustic signal processing, influence of time- and space-varying random filters 78−5615
acoustic signals, classification using environmentally adaptive approach 79−46114

underwater sound continued
acoustic transducers, reciprocity calibration by FM signal, correl. methods 77−68298
acoustic transmission in isospeed channel, effect of random ocean current 78−13840
acoustic transponder navigation, for ships 79−32167
acoustic underwater antenna arrays, adaptive 79−64467
acoustical compliance element, elastic problem of flattened cylinder type 80−33309
acoustical compliance tube for sound projectors, stress and deformation analysis 80−33310
acoustical energy conservation-dissipation theorem 78−90561
acoustical imaging, US visualization and characterization, conf., vol.8, Key Biscayne, FL, USA (May-June 1978) 80−83720
Acoustical Soc. Amer. 96th meeting, Hawaii, 1978 Nov. 78−90545
acoustics, speech and signal processing, conf., Tulsa, USA, 1978, April 78−63242
acoustics, speech and signal processing, IEEE international conf., Washington, DC, USA, 1979 Apr. 79−55275
acoustics, time delay estimation in presence of source or receiver motion 77−88977
active sonar detection range, Adriatic Sea refract. effect *(Croatian)* 79−57945
adaptive array processing, time and frequency domains 79−59874
adaptive cross-sensor beam forming with planar arrays 78−18121
adaptive linear prediction filtering for airborne underwater acoustic signal processors 79−64388
adiabatic mode theory in range dependent environment 78−55497
aerospace systems and electronics, IEEE conference, Washington D.C., USA, 26-29 Sept (1976) 77−5420
ambient noise, statistical anal. 77−79996
ambient noise depth-dependence models and their relation to low-frequency attenuation 80−43514
ambient noise in low-loss, shallow water channel, theoretical model 80−64265
ambient noise levels meas., Cochin backwaters 79−25256
ambient sea noise directionality, meas. and processing techniques 78−16025
amplitude fluctuation spectra, of tone-burst signals refl. from ocean surface 77−3695
amplitude fluctuations due to temp. microstructure 80−19140
AMTE/OUEL underwater jet noise rig, working report for 1977/78 80−79286
AMTE/OUEL underwater jet noise rig, working report for 1978/79 80−79287
angle-depth diagram uses 77−11067
apex approximation for mean-square phase and phase-rate fluctuations 79−41498
approximate ray angle diagram, construction from sound vel. profile 77−46843
arbitrary continuously stratified environments, propagated, reflected and transmitted acoustic waves 78−13829
array processing using freq.-wavenumber approach 78−66974
array processors for noise and interference suppression and signal-to-noise resolution enhancement, error corrections 78−30132
arrays, line and planar, effects of random shading, phasing errors and element failures on beampatterns 79−64468
arrival angle estimation by multiple cross-correlation meas. 78−66978
NE Atlantic, volume scatt. strength obs. at 2 kHz 77−11073
Atlantic bottlenose dolphin, echolocation signal propag. 78−88721
Atlantic shallow water off Argentinian coast, bottom reverberation-derived scattering strengths 78−65321
attenuation of surface generated noise received deep in the ocean 78−90573
axisymmetric turbulent boundary-layer flow, noise generation 77−47001
background ambient noise, estimation from spectral anal. of time series 77−84046
backscattering cross-sections of live fish, probability density functions and aspect 80−64260
backscattering from discrete targets at 87.5 kHz 78−87181
backscattering from elastic cylinders of finite length 77−50811
backscattering from very rough water surfaces 79−41499
backscattering of sound by the sea surface under shadowing conditions 78−94473
backscattering spectra of zooplankton 77−79994
basic principles and problems 80−53536
bathymetry, high resolution for seabed flatness analysis, use of resobath system 77−21921
beam displacement, cycle distances, and attenuations for rays and normal modes 80−74580
beam output noise due to shipping, statistical meas. 79−3836
beam pattern side lobes, significance in fluid flow measurement 80−19136
beamforming a towed line array of unknown shape 78−63230
bearing estimation bias resulting from source motion 78−29084
bedload transport oscillations, circuit for acoustic detect. 77−45168
Benthic Untethered Multipurpose Platform for underwater acoustic TV 80−46319
Bermuda Eleuthera Acoustic Range environmental meas. buoy 77−41229
biological object vel. measurement, design principles of instrums. 80−19195
bistatic surface scatt. strength at short wavelengths 78−55499
Black Sea, first expts. with Pisces submersible vehicles 79−44267
bottom layering influence on reflected FM signal characts. 78−50991
bottom reflection loss for a class of marine sediments, effects of density gradients 78−55498
bottom reverberation for narrow band signal and horizontal receiver array, space correlation *(Russian)* 77−46858
bottom-reflected sound field, defocusing in inhomogeneous antichannel 78−1484
bounded deep ocean channel, multipath acoustic propagation with moving source 77−23795
broadband detection system, anal. 79−3827
broadband echo ranging system for freq. charact. meas. of fish schools 79−64390
broadband target classification using bionic sonar 78−18123
broadside vertical array in shallow water, comments on array gain 80−19138
broadside vertical array in shallow water, reply to comments on array gain 80−19139

underwater sound continued
broadside vertical line array gain in shallow water 79−41497
bubble oscillations, modification by nearby objects, comment 79−90064
bubble oscillations of large amplitude 80−96298
bubble swarm acoustics, insertion loss of a layer on a plate 80−96072
bubbly liquid, acoustical determs. of bubble-size spectra 78−9735
C-mode US imaging by electronically scanned coaxial circular spherical receiving array 78−59222
calibration of acoustic transducers using complex exponential signal representation 78−79183
caustic field, regular and cusped, mathematical analysis *(French)* 77−42650
cavitating water, matching optimisation for magnetostrictive transducers 78−94503
cavitation threshold meas. for polyalkylene glycol and castor oil 80−107374
cavitation tunnel hydroacoustic transfer function, meas. and anal. *(Croatian)* 80−92002
cavitation zone, shock wave theory rel. to acoustic and hydrodynamic cavitation 77−27567
channel with range-depend. parabolic vel. profile, mode coupling 79−7245
Chesapeake Bay, abnormal US attenuation 77−29315
clustered sensor array, turbulent boundary layer induced noise suppression 80−96121
coherence estimates based on amplitudes of signals reradiated by rough sea surface, unreliability 80−58847
coherence estimates for signals propagated through acoustic channels with multiple paths 79−50479
coherent interference, rejection by amplitude shading of sonar transducer arrays 77−62094
coherent ray propagation through Gulf Stream ring 78−11906
communications, undersea acoustic channels, modelling of sea surface scattering channels 79−1022
compact planar array, mutual interaction of nearest neighbours 78−50979
complex structures, in-fluid response rel. to orthotropic spheres 77−23797
composite compliant baffle anal., comments 80−48482
composite piezoelectric US transducer, finite element simulation *(Japanese)* 79−68537
composites of wood, steel and rubber, underwater acoustic reflection 79−94394
compound random process for underwater ambient acoustic noise 80−83699
compressional wave attenuation in deep ocean sediments 80−79033
computer model for generating World ocean sound velocity profile 80−87624
conference on acoustic propag., Marseille, France, 1978, May *(French)* 79−41484
Confidence bounds for magnitude-squared coherence estimates 78−66979
conformal array beam patterns and directivity indices 78−55523
conical acoustic lens, fabrication and test results 78−51019
conical acoustic lens, opto-acoustic feasibility design 78−51020
correlation of pseudonoise signals in reflection from layered ocean bottom 80−87626
correlation sonar for ship's velocity meas. 79−27474
correlator compensation requirements for passive time-delay estimation with moving source or receivers 80−58843
cosmic-ray air showers, acoustic detect. 79−66901
coupled power equations for cylindrically spreading waves 77−23796
creeping waves on curved body, rel. to normal modes of vibr. 77−50817
crossing rate statistics for finite bandwidth or modulated multipath signals 80−64262
curved face parametric projector for marine sediment penetration 78−51032
CW coherence meas. at low freq. for long underwater paths 80−106654
CW line spectra, determination of struct. using integration time and acoustic multipaths 79−59860
CW source motion effects on total acoustic field, isospeed channel appl. 77−7242
CW tones received at long ranges, acoustic sidebands obs. 77−7244
cylindrical elastic shell, fluid-filled, excitation and propagation of normal modes 79−64385
cylindrical shell executing harmonic vibrations, determination of pressure of fluid on cylinder 79−64384
cylindrical steel shells in water, thick-walled, distrib. of normal surface vel. and acoustic radiation *(German)* 80−102899
data communication US standing-wave radiator 79−46104
deep ocean, l.f. coherence transverse to propag. direction 77−818
deep ocean acoustic propagation, effect of currents and tidally varying sound speed 77−79995
deep ocean LF attenuation data review 80−33318
deep ocean seamount detection using reconnaissance sonar 78−69551
deep ocean sound transmission, anal. of source-motion effects 77−62088
deep sound channel, mesoscale variations and effects on LF propag. 79−98529
deep towed seismic profiling system, multichannel hydrophone array, sub-bottom oceanic structure study appl. 80−26550
deep water, study of propag. loss into shadow and convergence zones *(French)* 79−41504
deep-water acoustical analysis of stationary and moving broadband sound sources 78−63226
detection, fibre-optic technique 78−13871
detonation wave, reflection from water surface 80−87628
differential Doppler shift estimation 80−19162
diffusion loss in refractive sound channels, bottom loss effects 78−9482
diffusion loss in stratified sound channel 77−11072
digital beamforming 78−50989
direction finding device for bearing determ. of whale sounds, real-time device 80−96079
directional spectral spreading in randomly inhomogeneous media 80−19133
directivity pattern of particle vel. detectors near a baffle 77−50813
distant shipping noise statistics, Edgeworth series 78−55496
Doppler effects, for randomly moving scatterers and platforms 77−62093
Doppler sonar, digital processing of signals 77−46856
Doppler sonar fish counting system, feasibility study 78−50980
Doppler sonar for ship's velocity meas. in deep water 79−27475
Doppler tracking using optimization techniques 78−55526

underwater sound continued
duct problems, variational anal. techniques 78−90574
duct with liquid layer lying over half-space (Pekeris branch cut) 79−68464
East Australian Current eddy, sound propag. 78−65322
echo location, determ. of depths of underwater objects in presence of refr. 77−34986
echo sounder transducer field plotter 78−59238
echo sounders, magnetostriction effects appl. *(German)* 78−23311
Eckart's formulation, surface correlation effect on average scattered pressure 80−96070
education, acoustical propag. in ocean, appl. of parabolic approx. 79−25794
elastic cylinder submerged in water, scattered form function determ. 78−30105
element failure and random errors effect on sidelobe level for linear array 80−106670
end-fire line arrays, nearfield beam patterns 77−46857
envelope spectra for signals and noise in vertically directional beams 79−86283
environmental-acoustic model for deep moving ocean, stochastic 80−64267
excess sound propag. loss in stochastic environment 78−9478
explosion generation of sound wave pulse, nonlinear region 80−56493
explosion of detonating gas with high initial bulk energy density 80−5867
explosion produced toroidal cavity, pulsation anal. using acoustic approx. 78−83423
explosion shock waves, comment on weak shock soln. 79−90068
explosions, source depth determ. from spectra obs. at long range 77−7243
explosions as acoustic sources, distrib. of measured bubble pulse periods 79−5495
explosions in shallow water, determination of acoustic source levels 80−19131
explosions scaling law for shock waves 77−14838
explosive accoustic waves, empirical and theoretical laws comparison *(Russian)* 80−109150
explosive shock waves, formulation of weak shock soln. 80−10070
explosive shock waves, weak-shock soln. 78−26003
explosive signals in shallow water, computer simulation 78−79160
explosive sources, model evaluation and data interpretation 77−11068
explosive wave profile transformation, time constant derivation 80−48485
Fermat paths, phase and amplitude 78−79159
field amplitude, in rays refl. from curvilinear boundary 77−33874
finite amplitude wave refl. in parametric array 77−84036
fish, target strength at any aspect 78−30115
fish backscattering cross section, swimbladder effect in gadoid and mackerel 80−89787
fish stock count by acoustic target strength meas. of individual fish, comparative anal. 80−19129
fish target strength functions, model for averaging 80−43512
fishing-boat noise, freqs. affecting albacore catch 79−90063
flexural wave transmission across line inhomogeneity on plate in liquid, radiation of sound 80−38159
flow noise effect on pressure and pressure gradient hydrophones 79−81605
fluctuating ocean, computations of strength and diffraction parameters 80−33320
fluctuating stratified ocean, sound propagation, comments 77−11075
fluctuations, theory using parabolic vel. profile 77−31159
fluid-loading influence coeffs. for finite cylindrical shell 77−23799
focusing by spherical compliant-tube Luneburg lens, theory 77−46842
forward reflection from rough sea surface statistical anal. 78−50983
forward scatt. and freq. depend. on medium 79−50496
frequency and time coherence in random multipath channels 77−84047
frequency modulation model for surface reflection of CW tone 78−83161
frequency spread of backscattered sound, facet model for rough sea surface 78−87184
fundamental and second harmonic pressures meas. in field of circular piston source 80−33322
gain limitations of passive vertical line array in shallow water 80−96117
gas bubbles forced radial oscills., thermal effects and damping mechanisms 77−31375
GATE acoustic echo sounder, preliminary results 77−33080
Gaussian acoustic signal detection using array processors, performance eval. 80−83696
generalised wave theory applied to propagation of sound in deep water *(French)* 80−53505
generation of sound in water heated in cell by laser pulses 77−50812
geometric construction of multipaths 80−74575
geophone and hydrophone recordings in Californian offshore sediment 80−46192
glacier obs. by side-scan sonar 77−5270
grating acoustic scanner for underwater imaging and NDT 79−57198
Green's function field soln. in plane multilayered medium, theoretical and numerical 80−33314
Greenland Sea, LF sound propag. in marginal ice zone 78−85567
guided acoustic waves in the ocean, review 79−39753
Gulf Stream north wall, sound speed structure across anticyclonic eddy 79−2257
Helmholtz and parabolic equations for sound propag., relation between solns. 77−84048
Helmholtz eqn., test of Born and Rytov approx. using Epstein problem 78−63212
Helmholtz resonator as high-power deep-submergence LF source 80−74576
HF acoustic scatt., from submerged cylindrical shells coated with viscoelastic absorbing layers 78−1478
high resolution cross sensor beamforming for uniform line array 78−50988
high-resolution ocean subbottom survey data analysis model 80−46211
holographic transducer array development 78−59209
holographic viewing experimental system 79−46121
horizontal acoustic refraction through ocean mesoscale eddies and fronts 80−96085
horizontal directionality estimation considering array tilt and noise field vertical arrival structure 80−64302

underwater sound continued
hydrophone array response calc. errors due to two dimensional beam pattern assumption 78−66972
hydrophone performance, geometric factors 77−50846
hydrophone shadowing by seamounts 80−33308
hydrophone signal phase stability, meas. using moving source 80−87623
imaging, techniques and characts. 79−64462
imaging of objects buried in seafloor sediment using focused US transducer 80−79036
imaging systems characts. and appls. 78−33945
impedance calculations for refracting layer 79−90065
Indian Ocean, fluctuation spectrum of US field scattered by inhomogeneities 79−88367
infrasonic field structure in shallow sea, machine expt. 80−14512
infrasonic flow noise, meas. by H-58 omnidirectional hydrophone 77−47119
infrasonic noise at Mid Atlantic Ridge near 37°N 77−25691
infrasonic sea noise, meas. and experimental problems 78−11902
infrasound and sound prod. by nonlinearly interacting ocean waves 77−11069
intensity fluctuations and fourth-order coherence function in random media 80−78774
intensity fluctuations spectrum in internal wave freq. range 80−64268
Inverted Echo Sounder for ocean thermal structural variations and currents 80−46312
inverted echo sounders, for meas. thermocline depth vars., MODE results 77−87108
J-9 sound projector, freq. response in typical experimental tank 79−50556
lake surface reverberation, statistical props. 79−1020
laser produced cavitation in water, behavioural study by holocinematography *(German)* 78−87371
l.f. attenuation and seawater bulk viscosity, Be and B influence 77−3696
LF backscattering by wind-generated air bubbles undersea with large-scale roughness 79−86285
LF coherent wave transmission range meas. system, portable 77−88976
LF multipath fluctuations in the ocean, statistical anal. 78−90571
LF propag. off Mission Beach, California 80−79035
LF sandwich transducers, analogy between fluid and solid horns 80−38213
LF sound waves propag. in Arctic channel with irregular ice boundary 77−11079
LF volume attenuation meas. in sea, influence of range-dependent environments 77−46845
LF wide-band high-power sound source using flextensional transducer 79−3883
liquid surface relief prod. by US field, holographic interferometry meas. 78−1519
liquid surface waves, generation by sound *(Russian)* 77−46841
local spectrum of underwater ambient noise field 79−37078
Loch Ness, bubble clouds in freshwater lake, detect. by acoustic refl. 79−66722
long range propag. in oceans, signal speed variations 78−50984
long-range sound propagation, Doppler effects 78−30116
Lorentz force hydrophone for low MHz frequencies 78−59243
low-freq. absorption in seawater, borate-complex relaxation 80−36304
low-frequency absorption contour chart for Atlantic, Indian and Pacific Oceans 80−36303
low-frequency acoustic fluctuations, rel. to internal gravity waves in ocean 77−50809
low-frequency parametric radiator, using nonlinearity of water 77−39128
low-frequency sound absorpt. in the ocean, pH depend. 77−84052
magnetostrictive sonar transducer, hollow spherical scatterer effects on radiation resistance at air-water surface 77−39125
magnetostrictive transducer at air-water surface, effect of spherical scatterer on radiation reactance 80−48531
magnetostrictive underwater sound transducers, use of rare earth alloys 80−19204
marine biological choruses observed in tropical waters near Australia 79−2085
marine meas. technology appl. *(Japanese)* 80−87625
marine organisms, acoustic target strengths 79−46103
marine particulate plume density and distrib., acoustic assessment 80−45843
marine sediments, correl. between geotechnical and acoustic props. bottom refl. coeff. meas. near sea floor 79−96756
marine sediments, in situ acoustic impedance meas. method 78−9519
marine sediments, saturated, nonlinear parameter 80−19132
marine sediments, sound velocity gradients 79−68465
marine sediments, water-saturated, finite-amplitude wave propag. 78−1476
marine sediments and rocks, ratio of compressional wave vel. to shear wave vel. and Poisson's ratios 80−12404
marine sediments and rocks, sound vel.-density relations 78−50982
maximum-likelihood estimation of source parameters from time-sampled outputs of linear array 77−75751
measurement of acoustic noise effects on behaviour of marine organisms 80−106657
measurements, FM signal correl. methods 77−62086
microwave ultrasound generation, use of piezoelectric film transducer of $\lambda/4$ operation, effective attenuation analysis *(Japanese)* 78−30145
midocean environment, fluctuations in reciprocal acoustic transmission 80−10069
miniature transmitters for fresh water, operating freq. choice 77−54826
mode conversion rates, due to scatt. from ocean bottom roughness 78−63228
mode coupling effect on multipath time stretching 79−98536
mode interactions in isovelocity ocean of uniformly varying depth 80−33321
mode theory of propag. in bilinear medium, WKB approx. 77−7229
modulation of monochromatic waves *(French)* 79−41503
monochromatic US signal interaction with AF noise 79−14147
monolithic cascade CCD ultrasonic lens applications 78−22231
moored acoustic buoy system (MABS) 77−49187
multibeam sonar systems, data flow requirements 77−3697
multielement array underwater acoustic instrumentation 80−43571
multilayered media, layer-indexed acoustic reflection model 80−43517
multipath anal. of explosive source signals in ocean 80−79034
multipath channels, comments on coherence estimates 80−58832
multipath interference nulls in long-range, low-frequency acoustic propagation by normal modes 80−33315

underwater sound continued
multipath propagation, impact of ocean acoustic transfer function on coherence of propagations 79−59861
multipath scintillation spectra, phase and fluctuation 77−11076
multipath separation and passive localisation using horizontal wavenumber spectrum 80−91952
multipath signal, individual pulse resolution, maximum likelihood signal processing 78−83176
multiple refl. from rough surface, correl. characts. 77−68288
multiple rough surface scattering, coupled mode analysis 79−98527
multiple scatt. between a rigid steel cylinder and plane 77−23793
narrow band signals, FFT and Prony algorithms for bearing estimation in ocean environment 77−46855
narrow-band signals and noise amplitude fluctuations in sea 78−9479
nearfield array for use in acoustic backscattering cross section meas. 77−14862
nearfield axial levels of exponentially shaded end-fire arrays 77−39127
nearfield measurement system for computing farfield radiation characts. of transducers 80−10101
negative bottom loss, critical-angle shift and interpretation of bottom refl. coeff. 77−46853
New England shelf-slope water mass interfaces, acoustic imaging 78−3784
noise correlation functions for arbitrary receiver orientation and steering direction in vertically anisotropic, azimuthally isotropic noise fields 80−58864
noise fields in randomly inhomogeneous moving media, probabilistic characts. 79−64383
noise level rel. to wind vel. *(Russian)* 79−34834
noise measurement of rotating sources *(Croatian)* 78−46869
noise radiated by incompressible boundary-layer transition 80−33319
noise spectra produced by fishing boats affecting albacore catch, comment 80−58844
nonacoustic noise interference in measurements of infrasonic ambient noise 80−19135
nondirectional sound sources in layer of fresh-water reservoir, determination of strength 80−58845
nonhomogeneous, contiguous and discontinuous domains, numerical approx. of hyperbolic evolution problem and appl. to underwater propag. *(French)* 79−41489
nonlinear reflection of short impulsive waves at water surface 80−33298
normal mode amplitudes in random ocean, statistical theory 78−50981
normal mode sound field in shallow water, positive sound vel. gradient, random fluctuation surface *(Chinese)* 77−34982
normal modes in bottom, effect on ocean acoustic field 80−106653
normal modes in ocean sound channel with range depend. parabolic sound speed profile 78−33941
North Pacific, variation of vertical directionality of noise with depth 80−19130
ocean, acoustic bottom loss measurement using multipath resolution 79−5652
ocean, acoustically relevant statistics for stochastic internal-wave model 77−46854
ocean, amplitude and phase fluctuation periods for long-range propag. 77−50808
ocean, development of research programmes in USSR 79−64382
ocean, fluctuating, long-range sound transmission, book 79−86286
ocean, internal waves influence on sound propag. 77−14837
ocean, long-range acoustic transmission variability of NW.Atlantic 80−90091
ocean, pH depend. of low-freq. sound absorpt. 77−49072
ocean, point source transmission through sinusoidal surface 79−14142
ocean, powerful acoustic signals propag., approx. eqns. *(Russian)* 79−98526
ocean, radiated noise meas. from data buoys and cycloidal propellers 78−33960
ocean, scattering of sound by internal waves 79−14141
ocean, sound propagation in an ocean shelf zone of arbitrary profile 78−90576
ocean, turbulent, nature of sound fluctuation 79−7250
ocean, turbulent, nature of sound fluctuation 79−7249
ocean, two-point coherence function models with inhomogeneous background and anisotropy 80−81922
ocean, US temperature-depth profile measuring system, expt. *(Japanese)* 77−70864
ocean acoustic background noise, detection of sinusoids 80−33347
ocean acoustic methods *(Russian)* 77−25798
ocean acoustic model inputs/sensitivity 79−5492
ocean acoustic multipaths, stability and identification 80−83697
ocean acoustic propag., long range, statistical anal. of signal intensity 78−90569
ocean acoustic tomography, for large scale monitoring 80−4119
ocean acoustic transfer function impact on coherence of undersea propag. 80−58842
ocean acoustic transmission rel. to finestructure meas. 77−64311
ocean acoustics, book 79−57970
ocean ambient noise levels, freq-freq. correls. 77−64302
ocean bed carbonate sediments, acoustic stratigraphy 80−21709
ocean bottom, influence of range dependence on adiabatic approximation 80−10066
ocean bottom, ray theory model of acoustic interaction 79−98532
ocean bottom, sloping, effects of tidally varying sound speed on propag. 80−10062
ocean bottom and surface reflections, correlation measurement of coeff. 80−58848
ocean bottom input impedance meas., particle vel. hydrophone appls. 78−94475
ocean bottom interaction, plane wave reflection loss model based on numerical integration 79−10425
ocean bottom loss and mode attenuation per cycle 79−90061
ocean bottom plane-wave reflection loss model including sediment rigidity 80−33311
ocean bottom reflected signals, isotopicity of correlation characts. 79−86284
ocean bottom reflection data processing by digital deconvolution 77−33223
ocean bottom reflections, nonparametric estimation of plane wave refl. coeff. 79−7252
ocean bottom reflectivity at low freqs. 78−40559
ocean bottom reverberation meas. at low grazing angles 79−14143
ocean bottom roughness effects on LF propag. 79−41501

underwater sound continued
ocean bottom-reflected pseudonoise signals, correlation with transmitted signal 80−58846
ocean channel, deep, analysis of acoustical effects of receiver and source motions at short ranges 80−10063
ocean channel with linear sound speed, effects of class of random currents 80−87621
ocean current parameters meas. from drifting ship 77−49189
ocean cyclonic eddies, influence on short-range acoustic transmission 80−33316
ocean density profile remote sensing by acoustic pulses, numerical algorithm 77−70893
ocean density profile remote sensing pulses, numerical algorithm 78−20429
ocean ducts, range dependent, acoustic flux formulae 80−96075
ocean eddies, calcs. of acoustic transmission 80−64264
ocean eddy effects on sound transmission 78−11905
ocean environment, range dependent, examination of multipath processes within context of adiabatic mode theory 80−19134
ocean floor, refl. and attenuation obs. at 4 kHz 77−2140
ocean internal waves, acoustic reverberation data 80−41562
ocean internal waves, induced acoustic phase fluctuations 77−7240
ocean LF sound absorpt. rel. to temp., pH, B conc. and pressure 78−40560
ocean microbubbles, in situ acoustic meas. 77−37207
ocean mooring monitoring, acoustic phase tracking technique 78−30138
ocean multipath propagation effects on sonar design and performance 78−5602
ocean receivers for acoustic signals from moving radiating sources, computer-aided analysis 79−59859
ocean sediments, experimental studies of attenuation 80−10067
ocean sound channels, ray calcs. using pocket programmable calculator and Incomplete Beta Function 79−68467
ocean sound velocity field fine struct. meas. method 77−64479
ocean subbottom data analysis through simulation, theoretical vertical and lateral model 80−74571
ocean surface, forward scatter freq. spreading, physical models 79−14145
ocean surface backscattering, diffr., refl., and interf. at near grazing and near normal incidence 78−90570
ocean surface characteristics affecting acoustic scatt. 80−46194
ocean surface ducts with rough boundaries 78−55493
ocean surface layers, explosive pulse propag. 79−94395
ocean surface probing for measurement of directional-frequency spectrum 80−79032
ocean surface reverberation model 77−34984
ocean surface scattering problem, connection between small-waveheight solns. 78−13839
ocean temperature microstruct. effects on LF propag. in S.Tasman Sea 77−86910
ocean velocity profile, horizontal range, and travel time series expansions 78−5604
ocean-dumped sewage sludge tracking, using 200 kHz echo sounder 77−2182
ocean-surface directional-frequency spectra, inverse scattering problem 80−79031
oceanic background in high-gain acoustic array, nonstationary and nonuniform 80−64263
oceanic finestructure effects on acoustic transmission, numerical simulation 80−43511
oceanic guided waves, acoustic flux methods 80−96077
oceanic internal struct. exploration using sonar methods *(French)* 79−44274
oceanic layered finestructure in Arctic, acoustic variability, 10 to 60 kHz 79−90060
oceanic microstructure scattering, detection with large aperture array 79−98530
oceanic sound transmission, calc. of strength and diffraction parameters 80−74572
oceanic waveguide, normal mode theory of acoustic Doppler effects 79−50497
oceanic wind speed and stress estimation from ambient noise meas. 79−74963
oceanographic fronts identification by long range acoustic propagation meas. 79−66705
oceans, randomly fluctuating, modelling of propag. using radiation transport eqn. 79−90062
oceans, three dimensional sound ray paths in basins, troughs and near seamounts using ray invariants 78−30113
Oceans 1976 conference, Washington (Sept 1976) 77−5241
Oceans '77, conf., Los Angeles, USA (Oct. 77) 78−36193
optical generation of sound in liquid half-space bounded by solid layer 80−38158
optimum range and bearing estimation with randomly perturbed arrays 80−96119
oscillating gas bubbles damping, meas. by appl. of subharmonic threshold 77−31374
NE.Pacific, depth depend. of ambient noise 78−88840
E Pacific, volume scatt. layers in tropical regions 77−2181
N.Pacific mesoscale phenomena, oceanographic model and acoustic survey comparison 80−46195
S.Pacific Ocean, acoustic cross-section (Project Kiwi One) 80−36330
Pacific Ocean, geographic variation of LF sound absorption 79−44189
N Pacific Ocean, regional depend. of low-freq. attenuation 77−62090
N.Pacific Ocean, west, depth, var. of temp., salinity and sound vel. meridional gradients 80−51429
parabolic approx., correction based on second range derivative 79−14146
parabolic approximation, path-integral approach 79−98533
parabolic reflector as nearfield calibration device for transducers 80−48528
parabolic wave theories and applications 80−51436
parabolic-equation technique, accuracy improvement via sound-speed profile modification 78−1480
parametric acoustic arrays, historical background and theory 78−5621
parametric acoustic arrays formed by diverging sound beams 77−27418
parametric acoustic arrays with intermediate directivity in water, expt. study 80−74569
parametric acoustic receiving array vibration sensitivity anal. 78−66971
parametric acoustic source, numerical method for nearfield calc. 78−63221
parametric acoustic source beamwidth control 78−75011
underwater sound continued
parametric hydrophone, compact, using nonlinear interaction within cylindrical rubber waveguide 79−98535
parametric receiving array with large aperture, expt. 79−64469
parametric source, specialized drive waveforms 78−33985
parametric source aperture factors 77−841
parametric source for underwater acoustic communications 77−7247
partially random sonobuoy array directivity index analysis 80−43518
passive coherence processing sonars, near-field performance 80−33346
passive detection, adaptive approach 78−5607
passive detection and spatial coherence testing 79−46113
passive listening, influence of spatial coherence of background noise 79−64387
passive localisation of moving source 79−3826
passive ranging of acoustic source 78−71241
passive tracking acoustic array evaluation, nonlinear filtering lower bound algorithms 80−96088
Pekeris model, reflection loss and mode attenuation 79−98534
Pekeris model, uniform asymptotic evaluation of continuous spectrum contrib. 80−87622
penetration into a sand sediment of difference-frequency sound generated by a parametric array 78−63227
penetration of marine sediments as function of physico-mech. characts. *(French)* 80−33324
phase-coherence detector and estimator, formed via overlapped FFT 79−59870
phased arrays use in very shallow water 78−1482
piezoceramic cylindrical transducer, increase of bandwidth via two transition layers 77−14871
piezoelectric transducer, response equalization using low-pass filter 78−30144
piston source, circular, meas. of fundamental and second harmonic pressures in acoustic field 79−46101
plane wave propag. in ocean, fluctuations of arrival angle at line array 80−43515
plane wave reflection, existence of Stoneley waves as loss mechanism 79−50498
plane-wave refl. coeff. of ocean bottom, meas. technique 80−96081
plane-wave reflection coeff. for inhomogeneous plane waves 79−90059
plates immersed in fluid, acoustic transmission theories verified 78−59183
Poisson reverberation envelope, statistical props. 78−66984
polymer additive effects on sound propag. in water containing bubbles 77−50810
polyvinylidene fluoride transducers, underwater acoustic meas. 79−14184
porous media, fluid-filled, propag. and decay 79−7248
portable acoustic tracking system, for underwater construction teams tracking 79−3874
pressure field in presence of gravitational and rotational forces, derivation of acoustic wave eqn. 79−98528
pressure unit, 0.01 to 1 Hz, USSR state standard 78−38160
projector, improvement of fidelity using technique involving modern control theory 79−98549
propagation equation solution, theory of modes, deep and shallow water appl. *(French)* 77−42651
propagation in an inversion and reflection at the ground relevance of underwater acoustics 77−14835
propagation in fluctuating media 77−53073
propagation in frozen random media 77−50814
propagation in presence of randomly perturbed parabolic profile 78−94477
propagation in shallow water expts. for long range communication systems 80−33323
propagation in spatially variable medium, analysis *(French)* 77−42649
propagation paths to Midway Is., using shallow explosion sources 79−41496
propagation prediction measuring system at sea, WPA prototype 78−69552
propagation stability of a doubly spread underwater channel 77−31156
propagation vel. depend. on elec. cond., temp. and hydrostatic press. *(Russian)* 78−65332
Proteus, advanced signal processor system 77−65648
prototype fast reactor, transmission of sound through subassembly wrapper immersed in water 79−81608
psychophysical struct. 77−77908
pulsation noise damping from small air bubbles in water 80−64253
pulse compression system, signal processing methods 80−56630
quadratic sound channel, first order scatt. resulting for temp. fluctuations 78−83136
radial spatial coherence from near ocean surface source 78−30117
random acoustic field model 79−50495
random ocean, normal mode amplitudes, comparison with Monte Carlo simulation 78−87179
randomly perturbed one dimens. wave eqn., multiple-scales space-time anal. 78−8247
range dependence of underwater echoes from randomly rough surfaces 78−63229
ray paths plotting in potential layer from bathythermograms 77−41037
ray theory for sound speed profiles with two dim. variation 78−50987
ray tracing technique, modified phase integral approx. 77−7241
ray-phase perturbations due to ocean-environmental variations, simplified calculation 80−64266
receiver-source motion at intermediate ranges in deep ocean, anal. of acoustical effects 80−96082
reciprocal transmission in midocean environment, current monitoring appl. 78−11907
refl. from bottom with sound vel. and density gradients 80−102901
reflected and lateral waves for Sommerfeld model 77−11074
reflection coefficient, for transverse waves in absorbing solid 78−9470
reflection coefficient for layered bottom, freq. and ang. response 77−11078
reflection from a variable-index half space 78−94472
reflection from layered elastic absorptive cylinders, matrix methods 77−46826
reflection from sea bottom with linearly increasing sound speed 80−33312
reflections from Al cylindrical shells immersed in water 79−7251
resonance theory of acoustic waves interacting with an elastic plate 80−33268
resonant acoustic scattering by swimbladder-bearing fish 78−87183

underwater sound continued
reverberant and distortional channels, homomorphic deconvolution 78−90606
reverberation from surface of sea, simulation *(French)* 77−14836
reverberation of 4 κHz and 20 kHz tone bursts in water filled tank 80−83695
reverberation spectra rel. to remote detect. of turbulence 78−38124
rough interface between two fluids, coherent acoustic scatter 80−96074
rough sea surface reflected signal and sea wave spectrum 78−94474
sand, water-saturated, broadband meas. of acoustic attenuation 80−83719
SAW hydrophone system using resonator-controlled oscillators 80−74631
scattering, from planar grating of compliant cylindrical shells, sonar appls. 77−31157
scattering at rough boundary, interaction models 79−7247
scattering by coated hollow cylinder, sonar cross section 77−46844
scattering by finite elastic cylinder in water 80−96062
scattering by large sea surface inhomogeneities, phase function shape in shadowing conditions *(Russian)* 80−94530
scattering by layered elastic and viscoelastic obstacles in water 80−96061
scattering by marine organisms, review 80−64269
scattering by rows of cylindrical obstacles 78−87182
scattering by waveguide inhomogeneities, single-scatter theory 77−7245
scattering channels, signal correl. function after several reflections 77−7246
scattering from fluid sphere, appls. to marine organisms 77−46846
scattering from fluid-filled elastic spherical shells, isolation of resonant component 79−46106
scattering from moving rough surface 79−7246
scattering function for multiple-bounce underwater acoustic channels 78−83162
scattering in anisotropic random medium, numerical calc. 79−81587
scattering layer composition, acoustic estimation 77−86909
scattering of boundary wave generated by grazing incidence at slightly rough rigid surface 80−10064
scattering of sound by sound, relation to the parametric receiving array 78−90563
scattering of spherical pulses by slightly rough surfaces 80−10065
sea bed mapping, signal processing technique *(Dutch)* 77−64478
sea explosion waves, comparison of empirical and theoretical laws of parameter variation 80−36325
sea floor analysis with deep tow techniques 78−33942
sea ice, US vel. meas. 77−33094
sea noise, LF ambient levels in S.Fiji Basin 79−72744
sea surface scattering, mechanism 80−106656
sea surface scattering channel and undersea communications, modelling 79−1022
sea water, absorption, chemical relaxation involving Mg and carbonic acid 79−68466
sea-floor reflectivity obs. 80−98302
seawater and distilled water nonlinearity parameter meas. 78−75727
seawater sound speed eqns. for varying salinity and temp. 78−81193
sediment classification by ocean subbottom acoustic Q meas. 80−46168
sediment refraction of sound, for sonar studies 80−81902
sediment rigidity effect on ocean bottom reflection loss in typical deep sea sediment 80−96083
sediment shear wave effects on ocean bottom refl. loss, ray path anal. 80−96084
sediments, penetration of highly directional acoustic beams 80−14511
seismic signal processing using inverse diffraction technique 80−74608
selected mode excitation in shallow-water sound propagation 78−59182
semiinfinite plate, immersed in a fluid, flexural modes 77−50819
sensor arrays, optimization technique 79−64405
shadow zones in horizontal plane 79−41494
shallow ocean water propagation, Naval Research 79−25258
shallow sea, influence of bottom on formation of acoustic field 80−102900
shallow water, acoustic normal modes, attenuation coeffs. 77−86932
shallow water, measurement of freq. dependence of normal modes 79−7262
shallow water, mode conversion, scatt. from rough ocean floor 77−84050
shallow water, pseudoresonances and virtual modes 79−14144
shallow water, spatial filtering of modes 78−59181
shallow water horizontal spatial coherence meas. 78−5605
shallow water propag., beam forming and freq. dependence of mode identification 80−28373
shallow water propag., soln. of wave eqn. based on eigenfunctions of Schrodinger eqn. *(French)* 79−41505
shallow water propag. overlying consolidated bottom 77−816
shallow water propagation under downward refr. conditions 77−34983
shallow water wave propagation, Pekeris operator resolvant 78−90575
shallow water with negative vel. gradient, average sound intensity *(Chinese)* 78−1477
shallow water with rough boundaries, attenuation of sound coherent component 77−62091
shallow-water propag. over low-velocity bottom 80−74579
shallow-water propagation, investigation using reduced scale model *(French)* 79−3825
shallow-water sound propagation 79−5493
shear layer scatt. of acoustic wave, linearised theory with causality 77−42643
shell of revolution immersed in liquid, freq. distribution function 80−69587
ship hull, acoustic radiation from point excited rib-reinforced plate 77−80003
ship noise, source level model for propeller blade rate radiation 80−43513
ship propeller induced underwater acoustic disturbance obs. 79−68463
ships, acoustical determination of course speed and lateral drift 80−5892
ships, prediction of post-detection data load for passive sonars 80−96125
sidebands from CW sources towed in deep ocean 78−50985
signal coherence limits in random ocean environment 80−46193
signal response, in two-path medium, average array 80−87657
signal timing, determ. of freq. shift arrival time 79−3875
single-mode transmission and backscatter measurements in laboratory waveguide 80−64259
slotted transducer arrays with matched backings for underwater imaging 80−38214
slow waveguide, in water, Helmholtz eqn. soln. 78−30114
small submersible, acoustic communications system design 79−5666

underwater sound continued
SOFAR channels, strongly range-dependent, paraxial and nonparaxial ray speeds 79−7253
sonar, directional charact. of cylindrical receiving arrays with nonuniform hydrophone response 77−88979
sonar, directivity of underwater horns 78−18138
sonar, evaluation procedure for refl.-reduction coating 78−9468
sonar, side looking, picture improvement 79−84516
sonar appl., passive, use of directional transducer arrays *(Spanish)* 80−69586
sonar communication systems 79−18574
sonar performance, incoherent and coherent processing against echo fading in shallow water 80−19142
sonar range prediction, inherent errors 78−66977
sonar target recognition experiment 79−86298
sonar transducer arrays, image prod., signal processing methods comparison 78−18122
sonomagnetic pseudoradiation from submerged acoustic sources 78−18093
sonomagnetic pulses from underwater explosions and implosions 80−43510
sound propagation conf., France (May 76) *(French)* 77−42638
source extraction problem, general formulation 77−84043
source location and motion estimation, joint reduction of bias and variance 80−96087
source location in random dispersive media using generalised reducion methods 80−43509
source micromotion effects on acoustic signal in freq., time, and space domains 80−74574
source motion effects on acoustic signal in freq., time, and space domains 80−74573
source power spectrum measurement in shallow water 80−19141
space scales of reflected signal fluctuations from ocean bottom 79−90066
sparse line array, cross-sensor beam forming 77−39126
spatial coherence loss, cylindrically symm. formulation 77−34985
spatial coherence of white noise, determ. using model *(French)* 79−41487
spatial filtering of modes of propagation, Pekeris theory, mathematical treatment *(French)* 77−42652
spatial noise spectrum meas. in ocean for small observation baseline 80−102902
speed in aq. salt solns. as function of conc., temp., and press. 78−79668
speed of sound in seawater at high press., meas. 78−13837
spherical targets, dynamics of acoustic resonance scattering appl. to gas bubbles in fluids 80−10068
static pressure influence on operation of hydrodynamic radiating system 80−102954
statistical model for backscattering from a randomly fluctuating surface 79−27459
steerable US beam due to leaky Lamb waves in plate with water loading *(Japanese)* 77−3690
steered planar nearfield transducer calibration array 78−59214
steered vertical line arrays, response to anisotropic noise 79−90103
stochastic ray theory relations, exptl. agreement 77−84051
stochastic ray tracing in ocean waveguide 77−3694
Stoneley wave effects on plane wave reflection coeffs., bottom reflection charact. 78−87180
stratified ocean as slowly varying waveguide 78−4490
stress pulse propagation, in water, effect of diffr. 78−90568
sub-bottom absorption profiles, acoustical effects 79−41500
submerged elastic bodies, resonance excitation by sound scatt., linear approx. theory 78−55495
submerged elastic shell, acoustic radiation 78−90572
submerged plate with finite number of reinforcing ribs, acoustic backscattering 80−74586
submerged plate with one reinforcing rib, acoustic backscattering 80−74585
supertanker radiated noise spectra in deep ocean, origin 78−33959
surface duct propag., influence of submerged duct 80−5865
surface duct propagation model based on radiation transport eqn. 80−46196
surface ducts, attenuation 78−63231
surface generated noise in stratified ocean, spatial correlation 80−87620
surface ripples generation, parametric subharmonic reson. theory 77−46849
surface-duct propag., evaluation of models of effects of surface roughness 80−64261
surface-generated noise received deep in ocean, attenuation 78−9481
swept carrier acoustic underwater communications 79−3835
swimbladder resonance in fish, experimental investigation 79−98531
symmetric line array, source passive location, variance bounds 78−9480
synthetic aperture imaging using acoustical holography 79−3863
synthetic aperture radar underwater mapping, array processing 78−69549
synthetic aperture sonar system prototype 77−46867
S.Tasman Sea, LF acoustic propag. meas., Project TASMAN TWO 78−11904
telephone equipment for underwater sonar communications type 2008 system 78−94478
temperature variation of acoustical props. of laboratory sediments 80−96069
testing of materials by ultrasonics *(German)* 80−97670
thermal excitation of acoustic waves by periodic sequence of nanosecond laser pulses 79−95084
thermal self-action of sound waves, beam defocusing 77−3692
thermocline, depth determ. by sonar in Caspian Sea *(Russian)* 77−13132
thin elastic cylindrical shell submerged in water, backscatter calc. from Kirchhoff approx. 78−30104
thin plate, effect of line-discontinuity admittance on sound scattered by plate vibration 78−55494
thin stiffened Al plate, underwater acoustic backscattering and echo struct. charact. 78−55492
three level coincidence-correlator detectors, underwater sound appls. 78−63245
through-water diver communication system Wet-Phone, voice or switch operated, 31.5 KHz carrier, 1350 m range 80−38187
time delay estimation, cross-correl. and smoothed coherence transform methods compared 80−96086

underwater sound continued
time delay estimation, quantitative study of optimum and sub-optimum filters in generalized correlator 79−59866
time-frequency-space generalised coherence and scatt. functions 78−5603
time-spread channel bandlimited impulse response display 78−66983
time-varying shallow water channel weighting function meas. 78−5606
towed arrays, hydroacoustic sources of locally generated sound, hose material 80−23822
towed arrays, hydrodynamics 80−23823
towed hydrophone systems tests by high speed research vessel Athena 77−41213
towed-line array, iterative technique for ambient-noise horizontal-directionality est. 78−55525
tracking system for divers, PATS 80−91949
transducer, ceramic, spatially-bounded US wave response 80−48542
transducer, constant beamwidth, theoretical new approach 78−90616
transducer array directional response anal., model 78−66973
transducer array for acoustic holography *(Japanese)* 77−80029
transfer function of the ocean for motional source 79−14140
transient pulses generation in water by ceramic transducer 78−1483
transmission from air into rough ocean, expt. 77−11071
transmission paths in dispersive systems, determ. of importance 77−72106
triangulation ranging using beta density angular errors 79−72758
triaxial acoustic current meter for small-scale ocean turbulence resolution 77−41232
turbulent boundary-layer press. fluctuations cancellation 77−88978
ultrasonic testing parallel, cylindrical, conical pieces using echo sounder, nondestructive testing appl. *(German)* 78−88604
ultrasound speed determ. over wide range of pressure and temp. 80−23821
undersea acoustic signal coherence fluctuations 80−46191
undersea acoustics, review of history (to 1950) 77−45667
undersea platform location by acoustic signature processing 80−43519
unified wave propagation theory, tenuous random medium 78−4491
unipolar acoustic pulses, quantitative schlieren visualization 78−38125
upper ocean, spatial variability 80−51435
US appl. to studies of small-scale turbulence *(Russian)* 77−78201
US applications, conference, Brighton (1977) 78−59223
US backscattered wave minima for solid metal cylinder immersed in water *(French)* 80−53510
US backscattering by elastic cylinders in water *(French)* 80−53511
US cavitation in water, effect of transducer radiating surface coatings *(German)* 77−42653
US continuous testing techniques for metallic specimens *(German)* 78−92420
US fish finder, with colour TV display 78−38159
US focusing device with IDT on thin piezoelectric plate 80−1398
US image convertor optimal working frequency estimation *(Russian)* 78−30111
US imaging system using multifreq. US holography 79−98556
US magnetostriction vibrator efficiency meas. *(Japanese)* 78−9523
US propag. in water with air bubbles *(French)* 80−53507
US pulse propag. and reflection by small targets 78−50986
US pulse transmission and reception by wide-band transducers 80−10099
US receiver, multiple use *(French)* 79−64457
US scatt. by submerged turbulent jet in liquid 78−50992
US scatt. spectral struct. from random sea surface 78−63225
US scattering by turbulence 80−87619
US video system *(German)* 78−94471
US waves in liquids, photoelastic visualisation 80−28374
velocity inversion in a stratified medium with separated source and receiver 80−96071
velocity meas. sonar system, transfer function model 77−7275
vibrating sphere near rigid or compliant wall, near field and impedance 78−94476
Virtual modes and mode amplitudes near cutoff 79−81607
virtual modes and surface boundary condition 77−31160
viscous attenuation in suspensions and high-porosity marine sediments 80−74577
VLF attenuation from deep-water ambient noise field meas. 77−11070
VLF wind-generated noise produced by turbulent pressure fluctuations in atmosphere near ocean surface 80−19137
vol. reverberation from scatt. layers and biological meas. 78−81194
volume scatt. and biological content from sea bottom echo fluctuations 78−50990
volume scattering at 25 kHz in presence of temp. discontinuity layer 80−38157
volume scattering strengths and zooplankton distributions at acoustic frequencies between 0.5 and 3 MHz 80−33317
water-sediment interface US reflection with bidirectional displacement 78−60017
wave direction-finding by full-aperture beam forming delay line 80−48527
wave eqn. derivation for inhomogeneous ocean 80−33313
wave equation, comparison of two normal-mode solns. based on different branch cuts 77−84044
wave propagation and underwater acoustics, book 78−90577
wave-theory peaks in range-averaged channels of uniform sound velocity 80−96076
weak acoustic shocks and solitons, short-wave asymptotics 77−37763
wedge-shaped ocean with penetrable bottom 80−74578
wide-angle acoustic field in ocean with range-depend. vel. profiles, computation technique 77−79993
wideband acoustic characterisation method for fish schools and long-range propag. channels 80−43551
Wilson's sound speed meas. reevaluation for pure water 77−23794
wind-generated noise produced by impact of spray with ocean surface, low freq. 80−106655
D_2O, sound speed rel. to normal water as a function of temp. and press. 78−2201

undulator radiation
angular-spectral distribution and polarization of synchrotron radiation from a 'short' magnet 79−94137
BESSY, a 800 MeV storage ring dedicated to synchrotron radiation, review 79−68021
BNL National Synchrotron Light Source, 100 to 700 MeV booster synchrotron 79−67973

undulator radiation continued
BNL National Synchrotron Light Source, 2.5 GeV X-ray ring, design status 79−68023
BNL National Synchrotron Light Source, 700 MeV VUV storage ring 79−68031
book, synchrotron and undulator radiation 77−75402
bunches in waveguide *(Russian)* 79−76561
coherence, directional pattern, wavelength spread, polaris. 79−55043
coherence, extension to short wavelengths 79−55042
coherent radiation from electrons in transverse periodic fields 80−78748
coherent X-ray emission from relativistic electron beam 80−91739
electron beam self-bunching in resonantly absorbing medium, radiation amplification feasibility 80−102605
electron bunch coherent radiation, electron distrib. effects 78−66734
electron laser, stimulated undulator radiation from relativistic electrons, physical processes 79−45921
electron motion in magnetic undulator *(Russian)* 79−7064
electron relativistic beam in synchrotron, ang. spread of vel. using undulator radiation electron 80−14021
electron storage ring, horizontal wiggler, modelling of effect on beam parameters 79−68029
electron undulator radiation, spectrum and ang. distrib. meas. 79−41313
electrons in medium in field on intense wave, induced and spontaneous radiation *(Russian)* 77−31056
emission from 'Pakhra' synchrotron *(Russian)* 78−5409
free electron devices for light prod., history, book contrib. 79−27147
free-electron lasers and masers with quasicircular undulators 79−55102
hard, in dispersive medium, in dipole approx. 80−23608
IR emission from modulated electron beam in EM field *(Italian)* 77−3525
irregularity effects 80−99614
microwave to X-ray up-conversion, by undulated electron beams 77−62006
oscillator at flight in homogeneous medium over plane boundary with periodically-inhomogeneous dielectric *(Russian)* 78−1138
polarisation, circular or linear generation by relativistic helically moving particle 77−75401
polarised electron bremsstrahlung γ-quanta from ultrarelativistic electrons in mag. field *(Russian)* 78−46502
polarization characteristics 80−69305
protons in synchrotron, beam parameter diagnostics via IR undulator emission *(Russian)* 78−836
quasi-monochromatic synchrotron radiation from undulators 78−63000
reflection and catching of charged particles by plane EM wave in undulator 78−58894
relativistic charged particles, in irregular undulator, radiation spectra *(Russian)* 80−63900
relativistic electron beam in resonant structure with waveguides and apertures 77−19152
relativistic electron emission characts. from Sirius electron synchrotron 80−63904
relativistic electron radiation in variable undulator *(Russian)* 77−75397
relativistic electrons, change in form of polarisation in undulator radiation *(Russian)* 78−50683
relativistic electrons, motion and radiation in mag. undulator *(Russian)* 78−62997
relativistic electrons in mag. undulator *(Russian)* 79−86121
relativistic particles in dispersive media *(Russian)* 79−59624
relativistic particles in mag. undulator *(Russian)* 78−66729
review 80−9794
shortwave coherent undulator radiation, classical theory 80−23195
SIRIUS synchrotron, experimental study of the spectral, angular and polarization properties of undulator radiation 80−91338
SPEAR storage ring, initial operation of mag. wiggler 79−68025
spectrum and polaris. characts. effect of beam parameters 77−75400
spin effects during electron movement in undulation *(Russian)* 78−13652
Stanford Synchrotron Radiation Laboratory, operation and development, review 79−68020
storage rings, free electron laser amplifier operation 79−68399
SURF II, 250 MeV storage ring for UV synchrotron radiation, progress report 79−68032
synchrotron radiation source, Daresbury 2 GeV storage ring with 600 MeV booster synchrotron, review 79−68022
visible spectrum undulator radiation, ang. variation, polarisation 79−41314
waveguide, rectangular, with finite length undulator, charge oscills. 78−71021
X-ray and VUV source, specified spectrum 79−10251
X-ray synchrotron source, design status 79−68024

unified field theories
see also supergravity; Weinberg model
(1+1) dimensional model field, fermion-boson correspondence, Klein transformation 80−42379
5-dimensional generation structure, possible signature for SU(5) semi-simple grand unification 80−82930
γ-W^0 mixing as an alternative to unified weak-electromagnetic gauge theories 79−2966
Abelian and non-Abelian gauge theories, mass generation, renormalisation, chiral and unified theories 80−4871
affine gauge theory of gravity and strong interactions, GL(4,R) spinor fields 79−93331
affine manifolds, 3-D, existence of metric 80−82695
anisotropic Bianchi II cosmological models with matter and electromagnetic fields 79−48976
astronomical bodies, mag. field, cosmological interpretation 80−46714
asymptotic catastrophe, temporary freedom in lepton and quark interactions 79−85253
asymptotic freedom constraints, review 80−62914
asymptotically free E_6 model of particle interactions 78−24922
asymptotically free SU(2)×SU(2)×SU(4) model of unified interactions 78−16968
asymptotically free SU(5) grand unification, proton stability, renormalisation group 80−82929
atomic parity conservation, left-right symm. unified theoreies 78−70306
atoms, handedness and parity non-conservation 78−29757
attempts at unification, general review 80−13250
axial chromodynamics, signatures 79−40729
axial gauge for unified gauge models, renormalisation constants 79−12930

unified field theories continued
axial superfield and the supergravity group *(Russian)* 79−17319
axial vector anomalies, weak-EM interactions nonrenormalisability 80−62859
axion avoidance without massless quarks, chiral symmetry dynamical spontaneous breakdown 79−63403
axion production, astrophys. implications of new light Higgs boson 79−22007
axion production search in low energy electron bremsstrahlung 79−63401
axions, astrophys. constraints on axion mass and number of quark flavours 79−36009
axions, very low mass, astrophysical bounds and stellar-energy loss 80−109353
B-L as fourth colour in an $SU(2)_L \times U(1)_R \times U(1)$ model 79−97589
B-L conservation and B nonconservation in unified models of quarks and leptons 80−95229
baryon decay effective lagrangian flavour struct. and renormalisation, grand unification 80−27447
baryon nonconservation in grand unified theories, rel. to Universe isotropy and homogeneity 80−22125
baryon number generation in grand unified theories 79−26279
baryon number nonconservation limits, grand unified theory nucleon decay modes 80−411
baryon production through primordial black holes in grand unified theories 80−101970
baryon- and lepton-nonconserving processes in grand unified theories 80−13253
baryon/photon ratio bounds due to human existence, grand unification 80−62345
beta decay, unification of EM and weak interaction *(French)* 79−89270
Bhabha-Gupta field coupled to external EM and gravitational fields, causality 78−4767
bi-scale theory of gravitational and strong interactions 79−12696
Bianchi type II exact cosmological model with matter and EM field 80−105560
Big Bang primordial fluctuations and Universe smoothness in grand unified theories 80−56987
bimetric gravitation theory, fields due to finite-size charged body 79−88862
bimetric gravitation theory, fields due to point charge 79−88861
black-hole evaporation, unified gravit. and electromag. field theory 78−53979
Bonnor electrovac counterparts of Tomimatsu-Sato solns. of Einstein eqn. 78−57835
Bonnor transform. extension 80−31643
Borel multipliers for the Bondi-Metzner-Sachs group 80−18088
boson field operator constructed from even number of fermion field operators 80−27416
bounds on number and masses of quarks and leptons 78−58151
Brans-Dicke Maxwell fields, static Weyl solutions 79−85033
Brans-Dicke static axially symmetric Maxwell fields 79−97278
Brans-Dicke theory, generalised static EM fields 80−12972
broken colour gauge theories, effective weak vertex, colour contrib. 79−40750
Cabibbo angle, CP violation quark masses 78−33016
Cabibbo angle and discrete symm. 78−29288
canonical neutral-current predictions from the weak-electromagnetic gauge group $SU(3) \times U(1)$ 80−95242
causal theory, removal of Einstein's objections to quantum theory, unification 80−31572
causality and relativity 78−81901
charge quantisation in curved spacetime, Kaluza-Klein background, Mandelstram field 79−2695
charged fluid sphere, general relativity soln., Einstein-Maxwell eqns. 80−68088
charm, elementary particle theories, properties *(Spanish)* 80−73681
charm particles, implication for unified theory of elementary particles *(French)* 79−67522
chiral symmetry spontaneous breaking, using vacuum stability condition 79−35986
classical geometrodynamics, for gravit. and electromagnetism, complex bivector formalism 78−77786
classical non-Abelian gauge theories in the space of reference frames 80−31977
classical quark confinement from general relativity 78−45842
classical quark confinement from general relativity 78−58162
classical Yang-Mills fields in a Robertson-Walker universe 79−2692
Clifford algebra based unified theory for quarks and leptons 80−47228
collective phenomena of fermion-antifermion pairs 79−12687
colour embeddings, charge assignments and proton stability 79−6309
colour-flavour symm., renormalisation effects in guage theories 78−33018
compact gauge groups for unified weak and EM interactions, representations and classifications 79−22008
compact rotating gravitational instanton from Einstein eqn. solns. 79−9161
complementary aspects of gravitation and electromagnetism 77−37795
conceptual foundations of the unified theory of weak and electromagnetic interactions, review 80−95237
conference, quarks and leptons as fundamental particles, Schlamding, Austria, (Feb.-Mar. 1978) 80−17709
conformal and superconformal gravity and non-linear representations 79−17308
conformal electrodynamics in Einstein spacetime 80−31644
conformal relativity, 6-dimens., unified gravit. and electromag. theory 77−2594
conformal relativity, based on $SO_{4,2}$ 78−8311
conformal relativity, classification of metric bosons 78−93803
conformal relativity, Klein-Kaluza scheme 77−74297
conformal relativity, particle species classification, symms., space time origin of isospin 78−93815
conformal supergravity, superconformal group, nonlinear representation 79−12695
conformally flat Einstein-Maxwell spaces, Newman-Penrose formalism 80−62559
conservation of energy in the unified field theory 79−71676
continuity equations, for transverse multipole amplitudes, EM and gravitational fields 79−58609
cosmological baryon asymmetry origin, unification mass 80−31398
unified field theories continued
cosmological baryon number domain structure, from symmetry breaking in grand unified field theories 79−84876
cosmological baryon production, kinematical constraints for heavy boson decay 80−51932
cosmological constant, broken gauge theories and 3K black-body radiation 78−28870
cosmology and elementary particle review 79−101061
coupled Einstein SO(3) gauge field eqn. solns. 79−274
coupled EM and scalar fields, in cylindrically symm. space-time 79−85035
coupling constant renormalisation anal. in unified theories, generalised gauge hierarchies 79−97556
covariant gravitational theory using Yang-Mills fields *(German)* 79−21615
CP violation and off-diagonal neutral currents 79−13008
current status in elementary particle physics 79−40651
current trends in the theory of fields, conf., Tallahassee, Florida, 6-7 April 1978 79−12923
currents in Su(5) and E_7 unified gauge theories 78−54600
curved space-time, neutrino fields with geodesic and shear-free rays, zero rest-mass fields 77−17890
cylindrically symmetric electrovac universes satisfying vacuum field eqns. 79−17303
D-type nondiverging and nontwisting electrovac soln. with λ 80−115
de Sitter gauge invariance based unified field theory 80−22255
development and expansion 80−95239
differential eqns., strength concept review, appl. to Einstein-Maxwell eqns. 78−16706
Dirac equation as basis for unified treatment of electromagnetic and gravitational theory 78−8314
Dirac particle creation in Einstein-Cartan-Sciama-Kibble theory 80−4622
direct interaction between particles, strings and membranes 78−86433
direct interactions between membranes, gauge invariant theory 78−4551
direct lepton generation in strong interactions, unified model, colour quark state *(Russian)* 80−82933
discrete finite nilpotent Lie analogs: new models for unified gauge field theory 78−66025
discrete symmetries, Cabibbo universality, flavour mixing angles, in gauge model with six quarks 78−62346
dual electromagnetism and neutral-current interactions 79−71678
dynamically broken gauge models, natural mass hierarchy, unification 80−68409
E6 unified gauge model, breaking patterns, quark-lepton symmetry and mass scales 78−86434
E_6 model of unified interactions, asymptotically free, mass relations and interactions 80−73642
E_6 unifying gauge symmetry, strong, weak and EM model embedding 79−9325
E_7 exceptional group, calc. of 6_j symbols 78−57800
E_7 gauge theories with proton stability *(Russian)* 79−17659
E_7 grand unification, neutral currents problem in $SU(2) \otimes [U(1)]^3$ gauge theory *(Russian)* 80−62913
E_7 grand unification using $SU(3) \times (U(1))^3$ gauge group, neutral currents 80−27444
E_7 group generators, calc. of 3jm factors and matrix elements 79−93330
E_8 group, branching rules, Kronecker, products 80−27438
E(6) grand unified theories, one loop renormalisation effects, stepwise symmetry breaking 80−32058
early big bang, asymptotic freedom, rel. to cosmic microwave background isotropy 80−46712
effective field theories, functional integration, renormalisations 80−86648
effective hamiltonian for $\Delta C = 1$ nonleptonic interactions in the Kobayashi-Maskawa model 80−86667
effective potential for spontaneously broken gauge theories and gauge hierarchies 80−18080
eight-dimensional unified theory of weak, EM and gravit. interactions 77−37797
eight-lepton and eight-quark unification based on Grassmann algebra 80−105824
Einstein, EM induction, field equation soln. 79−2696
Einstein's, structure of charged particles 77−30073
Einstein's 1925 unified field theory, equivalence with relativistic theory of the nonsymmetric field 79−58484
Einstein's impact on theoretical physics 80−77677
Einstein's non-symmetric unified field theory, universal symmetry and Klotz metric 80−62555
Einstein's nonsymmetric theory, field eqns. 77−2588
Einstein's nonsymmetric unified field theory extension, geom. props. 79−44833
Einstein's strong field eqns. variational derivation 78−4544
Einstein's theories extended, book 80−22164
Einstein's theory, nonsymmetric connection eqns. 77−49657
Einstein's unified field eqns., strength 80−52103
Einstein's unified field theory, axially symm. approx. solns. 77−67365
Einstein's unified field theory, field equations soln. for H-atom space-time struct. 79−21634
Einstein's unified field theory eqn. soln. 77−82429
Einstein and the quantum theory, review 80−22237
Einstein field equations, covariant splitting, spherical symmetry models *(German)* 79−21616
Einstein Maxwell generalised field eqns., characteristic surfaces and initial data 79−97279
Einstein Maxwell static field eqns. 79−58594
Einstein nonsymmetric unified theory, nonsingular particle solns. 80−57163
Einstein symposium, Berlin, Germany (Mar. 1979) 80−90596
Einstein theory, Faraday's EM inductron prop. 80−117
Einstein unified field theory, wave solns. *(Italian)* 79−49147
Einstein unitary field theory with tele-parallelism, Dirac's classical theory of electrons 79−12685
Einstein Universe, with source-free EM field 79−85036
Einstein vacuum and Einstein-Maxwell space-times, infinitesimal holonomy group structure and geometrization 80−73252
Einstein-Cartan theory, rel. especially to elementary particle weak interactions 78−37171
Einstein-Cartan theory in the spin coefficient formalism 80−101742
Einstein-Kaufman generalised theory, EM tensor 77−79017
Einstein-Maxwell, field theory with teleparallelism and Dirac electron *(German)* 79−9168

unified field theories continued
Einstein-Maxwell, homogeneous fields admitting transitive group of motions 79−40437
Einstein-Maxwell, Reissner-Nordstrom black holes, instability of the Cauchy horizon 79−67201
Einstein-Maxwell eqn., static electrovac soln. 80−31642
Einstein-Maxwell eqns., algebraically special space-times with nontwisting rays 80−42114
Einstein-Maxwell eqns., exterior stationary axisymmetric solns. 79−21622
Einstein-Maxwell eqns., generation of Lewis solns. from Weyl solns. 79−93019
Einstein-Maxwell eqns., Robinson, Schild and Strauss soln. 80−46901
Einstein-Maxwell eqns., solns. for cylindrically symmetric space-time 79−12657
Einstein-Maxwell eqns., some exceptional electrovac type D metrics with cosmological constant 79−75419
Einstein-Maxwell eqns., static stationary solns. 80−4617
static Einstein-Maxwell eqns., three parameter soln. 79−58593
Einstein-Maxwell eqns. with axial symmetry, exact solns. 80−118
Einstein-Maxwell equations: gauge formulation and solutions for radiating bodies *(German)* 80−27194
Einstein-Maxwell equations, charged solution, type-G 80−46904
Einstein-Maxwell equations, EM and gravitational wave spacetimes, similarity solutions 80−57154
Einstein-Maxwell equations, inhomogeneous stationary cosmological solns. 80−62556
Einstein-Maxwell equations, static electrovac solns., complexification technique 80−68114
Einstein-Maxwell field, symplectic structure 78−29028
Einstein-Maxwell field eqns., new solns. from electrovac space times with isometries 78−62128
Einstein-Maxwell field equations, charging transforms 80−95017
Einstein-Maxwell field equations, connection approach 79−88860
Einstein-Maxwell field equations in vacuo, consideration of axially symm. metric 79−85034
Einstein-Maxwell field theory, generalised mull EM fields 79−58606
Einstein-Maxwell fields, stationary solns. by combining Demianski algorithm with Kinnersley method 80−90758
Einstein-Maxwell fields for massless charge 79−44804
Einstein-Maxwell fields in asymptotically null-spherical coords., news functions 78−12631
Einstein-Maxwell generalised field theory, pp-wave soln. 79−6034
Einstein-Maxwell instantons charge quantization 79−80489
Einstein-Maxwell non-static field eqn. solns. 80−42128
Einstein-Maxwell nonstatic-source free symmetric coupled zero-mass and EM fields 79−63111
Einstein-Maxwell null field metric, exact cosmological solns. 79−67122
Einstein-Maxwell scalar eqns., axial symmetric field singularities 79−71327
Einstein-Maxwell space-times, infinitesimal holonomy group structure, Lie algebra 80−12976
Einstein-Maxwell stationary eqns., symmetries 80−31627
Einstein-Maxwell stationary field eqns. 80−31626
Einstein-Maxwell stationary field eqns. 80−98840
Einstein-Maxwell system, covariant quantum field theory 80−68119
Einstein-Maxwell theory, cosmological model with gravitational, electromagnetic, and scalar waves 80−86188
Einstein-Straus unified field theory, cosmological appl. 79−67123
Einstein-Strauss and Einstein Kaufman unified field theories relationship 78−73912
Einstein-Yang-Mills system in six dimensions, static solution 80−8883
Einstein-Yukawa theory, unified 78−29240
Einsteins unified field theory, electric cylindrically symmetric solns. 80−22254
electro-gravitational induction, relativistic theory 79−85040
electrodynamics and gravitation, closed theory 80−52445
electromagnetic and gravitational Hertz potentials 79−2680
electron anapole moment, static parity violating coupling to EM field, unified gauge theory 80−68390
electron-muon mass ratio, $SU(2)\times U(1)\times D_4$ symmetry model 79−89090
electroweak and strong interactions without the t quark 80−73640
electroweak force, grand unification and superunification 79−93333
electroweak gauge models with heavy W bosons, $SU_2\times U_1\times U_1'$ scheme *(Russian)* 80−86652
electroweak gauge models with sequential W and Z bosons 80−101971
electroweak interaction model based on $U_L(2)\otimes U_R(2)$ left-right symmetric gauge group 80−57544
electroweak interactions, dynamically broken gauge theories, CP nonconservation without elementary scalar fields 80−86613
electroweak mixing angle, renormalisation 80−86651
electroweak symmetry group, B-L U(1) generator and quark-lepton symmetry 80−57549
elementary particle classification and quark model, symmetry breaking gauge theories, unified theories 79−346
elementary particle forces identical at 10^{-29} cm 80−105827
elementary particle interactions, advances towards a unified theory 80−91039
elementary particle interactions, review of unification schemes 78−74197
elementary particle interactions, unified theories from non-Abelian gauge theories 80−62903
elementary particle physics, information from astronomical observations 80−51935
elementary particle theory, mathematical method, conf., Liblice, Czechoslovakia (June 1978) 79−21891
EM, weak and strong interactions, massless fermions coupling to vector mesons 80−73637
EM and gravitational field unification, development attempts *(Norwegian)* 80−4615
EM and weak interaction unification, bearing of Weinberg model and gauge invariance *(German)* 80−32054
EM and weak interactions, generalised unified theory, local gauge invariance and P invariance 80−82928
EM approach to fundamental states of matter, book 80−73103
EM field in space with torsion, semi-minimal coupling principle 80−77675
EM field inside the nucleus, Salam-Strathdee phase transitions, vanishing Cabibbo angle 78−37296
EM fine struct., Fermi weak coupling, Newtonian grav. constants, unified relation 80−101974
unified field theories continued
EM phenomena induced by weak grav. fields, possible gravitational wave detector 80−82692
EM soliton in weak and EM unified field theory 79−9323
energy momentum tensor for vector-tensor theory of gravity and electromagnetism 78−12633
Eotvos expts. and weak interactions, anal. 78−78129
equivalence of vacuum Yang-Mills gravitation and vacuum Einstein gravitation 79−25924
etergy-momentum tensors, characterization in gravitational field eqns. 79−88846
Euclidean gravity, asymptotically flat self-dual solns. 78−45834
exact classical solutions of the massless α-model with gauge fields in Minkowski space 79−17619
exceptional gauge groups and quantum theory 79−35983
exceptional groups, patterns of symmetry breaking 80−42356
explosive cascade-decays of leptons. quarks, virtual photons, weak vector bosons and Higgs scalars 80−86641
extended phase space, unified meson fields 80−86551
extended phase space, unified spin 1/2 fields 80−86552
extended supergravity, higher order invariants in Riemann curvature tensor 79−35614
extended technicolour scalarless theories 80−78001
Extended Technicolour scaleless models 80−73636
fermion generations in grand unified theories, SU(8) model 80−78012
fermion mass, unified gauge model based on E6 80−32053
fermion masses and hierarchy of symmetry breaking, u and d quarks 80−86618
fermions, light, mass hierarchy, grand unification, SU(N) theory 80−62911
fermions and bosons, interacting models 79−21629
fermions and bosons in a unified framework, physical foundations of local (algebraic) approach 79−21628
fermions and bosons in unified framework, math. structures and phys. questions 79−21630
fibre bundles, gauge theory of strong and EM interactions 78−54574
field equations for field ϕ with homotopic charge 79−13006
fine structure constant, estimate in unified theories with unstable proton 80−9133
finite-struct. and gravit. const. in unified theories 77−41802
Finzi's nonsymmetric theory, plane wave solns. 80−8885
Finzi unified field eqns., wave solutions 78−70036
five-dimensional theory of interacting scalar, electromagnetic, and gravitational fields 80−105833
flavour mixing in ambidextrous $SU(2)_L\times SU(2)_R\times U(1)$ gauge theory 78−12805
flavour unification in SU(11) 80−62912
fractionally charged quarks, binding in unified gauge theory with Abelian massless gluons 78−29296
Free vector field in a homogeneous space with torsion 80−90759
fundamental constituents of matter and unification of weak and electromagnetic interactions 80−62940
fundamental length hypothesis, concept in gauge vector field theory 78−93836
gauge field masses and degenerate pots., Yang-Mills and Higgs field unification 79−17647
gauge field theories and coupling constant trajectories 77−22675
gauge field theory, geometrical consideration 78−12809
gauge field theory as unification of elementary forces of nature 77−65067
gauge field theory for weak and EM interactions with $SU(3)\times U(1)$ symmetry 78−58153
gauge field theory with torsion, symmetries 78−89386
gauge fields and supersymmetry 78−58150
gauge group theory of combined gravitational and e.m. interaction 77−80
gauge hierarchies, book contrib. 80−42384
gauge hierarchies beyond the tree approximation 79−67470
gauge hierarchy in presence of discrete symmetry, $U(1)_L\times U(1)_R$ and $SU(2)_L\times SU(2)_R\times U(1)$ 80−9094
gauge hierarchy problem, proposal for elimination in unified theories 79−75707
gauge invariance, minimal coupling, and torsion 78−78084
gauge model, weak interactions of leptons and quarks 80−22556
gauge models of weak and EM interactions, quantisation and renormalisation of gauge theories, book contrib. 79−30669
gauge scheme of weak and electromagnetic interactions, review *(Russian)* 79−26278
gauge SU(3)×U(1) model of weak and EM interactions 79−22003
gauge supersymmetry, spontaneous breaking, supergravity gauge invariance 79−9277
gauge symmetry, generalised local, Ward identities 77−10171
gauge symmetry, spontaneous breakdown, grand unification of QCD and SU(2)×U(1) 79−49380
gauge theories, facts and prospects, conf., Schladming, Austria (Feb.-Mar. 1978) 79−26203
gauge theories 80−73652
gauge theories of weak, EM, and strong interactions, book contrib. 79−30694
gauge theory, suppression of flavour changing effects from neutral spinless meson exchange 79−40716
gauge theory and neutrino physics, book 79−30726
gauge theory of gravit., e.m., mag. monopole fields 77−57263
gauge theory of gravity and supergravity on a group manifold 79−21635
gauge theory unification, appl. to origin of baryons in Universe 79−62938
gauge unification of fundamental forces, review 80−95238
general relativistic unification of gravitation and EM 77−45777
general relativity, quantum field theory, vierbein formalism 80−22263
general relativity, SL(2,C)Yang-Mills field theory description, in curved twistor space 79−21602
general relativity, unified treatment of null and spatial infinity 78−65848
general relativity, vacuum field equations, fifth dimension, ratio of EM to gravitational force 80−77679
general relativity conference, Trieste, Italy, 1975, July 78−8285
general relativity singularity-free extended particle model 78−54255
generalised field theory of general relativity, field eqns. 77−79013
generalised gravitation theory, with electromagnetism, derivation of conservation laws 79−49146

unified field theories continued
generalized Einstein-Maxwell field theory, asymptotic behaviour 80−86184
geodesic in gauge supersymm. 78−12634
geometric unification of classical gravitational and EM interactions 80−57165
geometrical gauge theory of gravit., strong interactions, EM interactions 78−70041
geometrical unification of gauge and Higgs fields 80−99077
geometrisation of physics or physicalisation of geometry 80−90760
global equivalence of Euclidean gauge and Higgs fields 78−8527
Goldberger-Treiman relation, corrections, unified gauge-field model 78−16969
grand unification, neutron oscillations and massive neutral Majorana leptons, baryon number 80−91033
grand unification from neutral currents in gauge models 80−78009
grand unification gauge groups, const. 79−71338
grand unification mass scale, cosmological origin 79−88773
grand unification of strong, weak and EM interactions 78−54598
grand unification with exceptional group E_6, symmetry breaking, SU(5) relations, quark masses 80−68407
grand unification with the exceptional group E_8 80−105828
grand unified field theories, mass relations and renormalisation effects 79−49436
grand unified gauge theories, running coupling constants and unifying mass scale 80−91029
grand unified model, Yukawa coupling radiative corrections, lepton and quark masses 79−97555
grand unified model with a stable proton and no axion problem 80−95234
grand unified O(10) model, quark mass formulae and number of flavours 79−75730
grand unified theories, baryon asymmetry of the Universe, SO(10) model 80−4619
grand unified theories, compatibility with big bang cosmology, superheavy monopoles 80−86647
grand unified theories, mag. monopoles and cosmological implications 80−86643
grand unified theory from broken SO(8) extended supergravity, SU(5) theory 80−99081
grand unified wave function for quarks and leptons 80−91034
gravitation, gauge covariant theory, cosmological constant 79−88865
gravitation, gauge field actions and their principle bundle formation *(Chinese)* 79−71331
gravitation, gauge formulations, relationship to Riemannian holonomy struct. 80−42131
gravitation, gauge theory, special relativistic limit 80−22256
gravitation, particle masses, instantons, unified theory 78−37168
gravitation and electromagnetism field equations, metric-affine gravit. framework 78−45547
gravitation-electromagnetism unification, Planck length, five dimensional principal U_1 bundle theory *(Chinese)* 80−86181
gravitational, electromagnetic, and nuclear theory 79−71677
gravitational and EM field in flat space time, relationship, hierarchy hypothesis 77−5732
gravitational and EM fields, purely geometric *(German)* 77−57264
gravitational and fine struct. consts., grand unification and proton quasistability *(Russian)* 80−77680
gravitational and strong interactions, unified gauge theory 80−95016
gravitational charge of uniton-quark 79−63400
gravitational field, nonlocalisation, connection with geometrical theory of gauge fields 80−82696
gravitational field and arbitrary gauge field, equations of motion, Heisenberg and classical, force term, spin-curvature coupling 80−57158
gravitational field interaction with fermion and boson fields 78−86208
gravitational field theory, ten-dimensional manifold of local inertial reference frames 80−46903
gravitational indistinguishability of neutrino field and stokesian fluids 79−30159
gravitational instanton contribution to spin 3/2 axial anomaly 79−17321
gravitational instanton symmetries, classification 79−63110
gravitational multi-instantons 79−2693
gravitational pseudoparticles in higher rank gauge theories 77−45960
gravitational theory of matter 79−21627
gravitational trace anomaly renormalisation in QED 80−57532
gravitational-inertial field of Universe, generalised metric tensor theory 78−89275
gravity, broken symmetric theory, unified gauge field breaking 79−30343
hadron spectroscopy, quark models and SU(5) grand unification scheme 80−4958
hadron strong interactions, theory from general relativity 79−49143
heavy Higgs scalars, in $SU(2)_L \times SU(2)_R \times U(1)$ gauge theory, no decoupling at low energy 79−13018
heavy lepton decay, selection rule, $SU_2 \times U_1$ gauge model 79−49500
heavy Majorana particles, cosmological and astrophysical implications 80−90331
hidden gauge symmetry, appl. to elementary particle fundamental interactions 79−30658
hierarchical fermion masses from grand unification 80−105832
Higgs boson mass, 10 GeV? 79−63406
Higgs boson mass, perturbation constraint 79−67493
Higgs bosons, masses, gauge hierarchies, SU_5 model 80−47236
Higgs bosons in $SU(2) \times SU(2) \times U(1)$ left-right gauge field, coupling strength 79−13017
Higgs mechanism and the inverse Einstein-Infeld-Hoffman problem 79−63100
Higgs meson prod., possible signals in high energy collisions, gauge groups 78−89649
Higgs scalars, decay into vector mesons and photons 79−49442
Higgs-Boson mass, weak interactions at very high energies 78−8540
Higgs-Kibble mechanism and electron-muon mass ratio 78−66065
High energy behaviour of weak interactions and renormalisable theories, book contrib. 78−78164
historical contributions *(Hungarian)* 80−46900
history of gravitational and unified theories, book contrib. 80−22259
history of quantum field theory, search for unity 78−28904
horizontal symmetries dynamical symmetry breaking and neutrino masses 80−105830
horizontal-quantum-flavor-dynamics approach to the fermion mass spectrum in $[SU(2) \times U(1)]_{WS} \times U'(1)$ gauge 80−52474

unified field theories continued
infrared attractive fixed points, gauge symmetries, QED and anti-grandunification 80−95213
instanton effects on axion mass 78−58127
integer spin zero-rest-mass field, irreducible representation of Lorentz group 80−68110
integer-charged quarks in the SU(5) grand unified theory 80−68410
isotopic spin sources, motion, gauge theories 80−12977
Jordan's five dimensional theory, stationary axially symmetric solns. 79−88863
Jordan Thiry theory in five dimensional Riemannian manifolds 79−44832
Jordans 5-D unified theory of gravitation, Ehlers-Harrison type transform 80−8882
K3 gravitational instanton, physical interpretation 79−17320
Kaluza-Klein bundle, unified theory 80−37153
Kerr black hole, gravitational perturbations 79−44819
Kerr-Newman metric, perturb. equations, EM test fields 80−62557
Killing fields, evolution for dust matter space time *(French)* 79−21617
L-A pair of coupled eqns. for gravitational and EM fields *(Russian)* 79−88859
Lagrangian formalisms in scalar pregeometry, quantum mechanical equivalence 79−54024
Lagrangian formulation for gauge theory of strong+EM interactions defined on Cartan bundle 78−16964
large Numbers, explanation via classical unified theory 80−57166
left-right symm. gauge model, neutral gauge boson 78−29289
left-right symmetric gauge models, parameter constraints from neutral current data 80−86588
left-right symmetric model from general horizontal symmetry, Cabibbo angle, CP violation 80−101972
left-right symmetric SU(N) gauge models, parity violation in atoms 79−21966
left-right-symm. unified theory of quarks and leptons 78−41466
left-right-symmetric theory of weak interactions in unified gauge theory, constraints on phenomenology 78−21369
LEP, design, tests of unified field theories and quark properties, search for new quarks and leptons 80−74048
lepton structure model 80−91063
lepton-quark and space-time symmetry 78−16967
lepton-quark mass relation in unified theory 79−97560
lepton-quark model, supermultiplet of weak bosons and Higgs scalar 78−62345
leptons, SU(3) electroweak theory 80−86638
leptons and quarks, unification within conformal relativity 79−93343
lh theory of leptons and hadrons, unification in $GA_{4,R}$ gauge 80−86639
linearisation stability of Yang-Mills and Einstein-Yang-Mills eqns. 79−49142
linearised gravity, eqns. of motion, uniform acceleration, Robinson-Trautman fields 79−71308
linearised gravity eqns. of motion, run away sources 79−71309
local B-L symmetry of electroweak interactions, Majorana neutrinos, and neutron oscillations 80−73643
local conserved currents in unified field theory 79−17307
local symmetry groups and fermion families 79−13030
magnetic monopoles, existence in unified field theories 79−25957
Majorana-Weyl fields, development of unified models 78−33015
mass scales, alternatives to SU(5) 80−27441
massless boson, unified nonlinear theory 80−376
massless fermion representations in grand unified gauge theories 79−97553
massless scalar and EM field equations interacting with gravit. field, particle-like solns. 79−54290
massless spin 3/2 field, covariant canonical quantisation in general covariant gauges 79−40440
massless spin 3/2 field, irreducibility 79−35620
massless spin two field, covariant quantisation in general covariant gauge 78−66027
mathematical origins of general relativity and of unified field theories 80−95009
Maxwell, Dirac and Yang-Mills eqns., octave algebra 79−2967
Maxwell equations in Riemann-Cartan space, spin-torsion coupling const. 80−82697
ME-EM field model of free electron state 78−49988
mesons and numbers of quarks and leptons, unified model 78−21370
metric existence in 2-D affine manifolds 79−85039
metric-affine gravit. theory, vol. preserving and canonical transform. 79−44826
metric-affine unification of gravity and gauge theories 79−63109
milliweak gauge models of CP violation 80−73633
minimal O(10) grand unification, ν mass 80−57546
MIT bag model, static electroweak props., PCAC 80−73645
mixing angle and proton lifetime, two-loop corrections 80−13249
mixing matrix and CP violation for n quark generations 80−101986
mixing of leptons with different quantum numbers in gauge theories of weak and EM interactions *(Russian)* 78−54601
monopole solutions for strong gravity coupled to SO(3) gauge fields 80−4621
multidimensional theory, 11-dimens. space, 7 compacted dimens., 0(8) symmetry 79−26275
multidimensional unified theory of gravit., EM and weak interactions 78−41462
N=1 supergravity, chiral invariance in four dimensions 79−40441
N=2 extended supersymmetry, Noether current multiplets, extended supergravity 79−40438
N=8 supergravity theory, lagrangian 79−17311
Nambu-Jona-Lasinio type model for gravity, effective Lagrangian 77−74628
Nambu-Jona-Lasinio type unified model for gravitational and EM forces 78−65850
net baryon number and CP nonconservation with unified fields 80−62349
neutral current phenomena, gauge model of parity nonconservation 79−17656
neutral current struct. in unified gauge theory 79−2975
neutral currents, strength limit at PETRA energies 80−105839
neutral currents in generalised $SU(2) \times U(1)$ gauge models 78−45832
neutral currents in left-right symmetric unified gauge models 79−45044
neutral-current weak interaction without electroweak unification 80−105835

unified field theories continued
neutrino, Maxwell, and scalar fields in the cylindrical magnetic or plasm universe 80−120
neutrino, oscillations, mass and mixing scales 80−105823
neutrino number and isotropy of Universe 80−85852
neutrino oscillations, Majorana and Dirac mass mixing 80−101969
neutrino oscillations of weak interactions 80−105825
neutrino-generated static space-times 80−52107
neutrinos, gauge theories, EM props., forbidden processes and currents with anomalous Lorentz struct. 78−54599
non Abelian gauge theories, relation between fields and pot. 80−22529
non conventional monopoles in field theory, book contrib. 79−58919
non-Abelian gauge potential, decomposibility in Cartan geometry with zero torsion *(Chinese)* 79−17624
non-integral gauge theories 79−12675
non-symmetric, plane wave-like solns. 78−29031
nonexistence theorem for a unified field theory in plane symmetry 79−25956
nonlinear EM effects induced in vacuum by gravitational interaction 79−44827
nonlinear gauge fields and the structure of gravity and supergravity theories 78−77791
nonlinear Heisenberg-Klein-Gordon equation, localised solns. in flat Schwarzschild space-time 80−4620
nonlinear realisation, unified interaction, spontaneous symmetry breaking 79−13010
nonlinear realizations of compact and noncompact gauge groups, grand unification 80−47183
nonlinear wave propagation in relativistic continuum mechanics 80−22203
nonlocal neutrino gravitational interaction and field self interaction 80−91037
nonlocal spinor field theory of matter 79−49141
nonlocalization concept 78−21324
nonminimally coupled gravitational and EM fields, Lagrangian 79−71328
nonrelativistic quark model with one gluon exchange pot., baryon spectroscopy in SU(6)⊗O(3) 78−78147
nonsingular gravitational collapse, Yang-Mills cosmos 79−21621
nonsymmetric unified field and covariant extensions 77−9936
nonsymmetric unified field theory, conservation laws, Bianchi type identities 78−73910
nonsymmetric unified field theory, metric and local invariance group 80−90754
nonsymmetric unified field theory, metric hypothesis, spinor analysis 80−68404
nonsymmetric unified field theory, physical interpretation and light propag. 79−21618
nonsymmetric unified field theory implied cosmology metric 79−53943
nonsymmetric unified field theory of Einstein, cosmological implications, Universe expansion 78−73911
nonsymmetric unified field theory of Einstein, metric tensor determ. 78−73909
nuclear decays as test of elementary particle theory, review 78−21361
nucleon decay, T violation possibility and consequences in superunified theories 80−82917
nucleon decay operator anal., superunified theories selection rules 80−13302
O(10), SU(4) colour subgroup, fractional charged gauge boson, proton half-life 80−73644
O(10) theory of strong, weak and EM interactions, masses and mixing 80−13248
O(4)⊗U(1) gauge model for weak and EM interactions 79−71681
observability differences between classical EM and gravitational gauge fields 80−36925
octonionic quark confinement 79−17669
octonions and exceptional groups in field theory, unified interaction model *(Russian)* 79−67491
P violation, neutral currents, $SU(2)_L \times SU(2)_R \times U(1) \times U(1)$ 79−6308
parity violation in He and Cs atomic electrons and e-e interaction effects 79−54788
parity-violating nucleon-pion amplitude in unified gauge-invariant models 77−6070
partial unification of strong, weak and EM interactions, B-meson decay 80−18106
particles and fields in simple model of physical system, unified view 79−25951
Pati-Salam model, higher order parton transition effects in deep inelastic scatt. 80−78008
Pati-Salam neutral vector gluons, possible expt. search in e^+e^- collisions 80−37202
Pati-Salam $SU(2)_L \times SU(2)_R \times SU(4)$, gauge-c 78−12851
Peres space-time, generalised, algebraic props. and solns. 80−106
perturbative QCD and exptl. signatures of weak bosons 78−93916
Petrov type II twist free metrics, solns. to Einstein Maxwell eqns. 79−49115
phenomenological ideas toward a field theory of matter, unification of EM and gravity fields 80−378
phi meson as light scalar boson in unified weak and EM interactions 79−17706
photino and goldstino, scatt. cross sections on matter 79−97558
physico-geometrical remarks on unified gauge field and supersymm. concepts 78−37167
Pontecorvo neutrino oscillations for Dirac and Majorana masses, CP nonconservation 80−105829
pre-quarks and fractional charges 80−91048
precocious chiral grand unification based on $SU(8)_L \times SU(8)_R$ semi-simple gauge group *(Russian)* 80−42382
pregeometry, gravity with composite metric 79−35619
preon model for hadron and lepton struct. 78−78124
primal cosmic energy field, Birkhoff hypothesis consistent with relativity 77−30072
primordial baryons, generation by black holes 80−98750
primordial magnetic monopoles in unified gauge theories 80−91035
proton and neutron disintegration, concepts of leptons and quarks *(French)* 80−91038
proton decay, confirmation of unification of forces, book contrib. 80−42383
proton half life, Dirac approach to large number coincidences 80−27501
pseudoinvariant gauge Lagrangians for Einstein gravity and supergravity 79−12680

unified field theories continued
pure gauge fields on coset space 79−40673
QCD contributions to vacuum polarization 80−105834
QCD theories of interactions, CP conservation, in presence of pseudoparticles 78−16923
quantum field theory, lattice-limit definition of functional integrals 80−27396
quantum gravity, choral of symmetries in general relativity 80−105565
quark and lepton mass determ., unified weak and EM theory without scalar fields 79−75709
quark confinement, unified theory of gravity and strong interactions 77−22681
quark flavour, unified theory with SU(5) subgroup 79−89102
quark mass, electroweak contrib. 80−101990
quark models and unified field theories, review 79−80805
quark structure model 80−91063
quark-lepton unification in SU(N>5) 80−73646
quarks, mass differences of up and down quarks, grand unification 80−62978
quarks and leptons, EM and weak interactions, flavour $SU_3 \times U_1$ gauge model 79−97554
quarks and leptons, high energy and nuclear physics interface 80−41974
quartz resonator, large mag. field effect on rate of time 80−27195
quaternion limitations on higher dimension spacetimes for unified field theories 78−45545
radional field theory, corpuscular theory, origin of natural forces 78−77785
Reggeization of elementary fermions in arbitrary renormalizable gauge theories 80−68367
Reggeization of gauge vector mesons and unified theories 79−97562
Reissner-Nordstrom black hole, perturbation treatment using Newman-Penrose formalism 79−44820
Reissner-Nordstrom perturbations, coupled Einstein-Maxwell eqns. 80−68108
relativistic discrete unified field theories, computer field interaction simulation system 80−68412
relativity, seven-dimensional, 4-D gravity coupled to Yang-Mills fields 80−82699
relic monopoles from big bang, cosmological problem for standard unified theories 80−77532
Riemann gravitational theory, cosmic time asymmetry *(German)* 79−35610
riemannian-Maxwellian invertible structures in general relativity 80−4618
right translation invariant metrics and variational principles on principal bundle, gauge theories *(Chinese)* 80−101743
Robinson-Trautman fields, motion of sources 79−71329
S_3-symmetrical model, use of permutation symmetry 79−26280
scalar field solutions to Yang-Mills and Vierbein field theories 79−12682
scalar free unified theory, order-R vacuum functional, with spontaneous scale breaking 80−78003
scale invariance in superspace 79−17313
self duality in 4-dimens. Riemannian geometry, Yang-Mills eqns. 78−78073
semisimple unified gauge theories 78−70282
$\sin^2\theta_w$, grand unified gauge theories and proton decay 80−73634
six-quark model of quantum flavourdynamics, Cabibbo angle and quark masses 78−33017
six-quark theory, calc. of t-quark mass and flavour mixing angles based on $SU(2) \times SU(2)_R \times U(1)$ 79−80811
sixth quark mass in $SU(2)_L \times SU(2)_R \times U(1)$ gauge group 79−26291
SL(2n,C)⊗SL(2,C), invariant gravitational model, spontaneous symmetry breakdown 77−46009
SO_{10}, soft CP violation and complex Majorana mass relations 80−78010
SO_{10} hierarchical breaking and neutrino masses 80−22550
SO_{11} group for interaction unification, charge and coupling constants 79−2965
SO(10), p decay modes 80−13301
SO(10) grand unified theories, one loop renormalisation effects, stepwise symmetry breaking 80−32058
SO(10) grand unified theory, breaking scheme and neutrino mass 80−47230
SO(10) unification, composite structs., quark and lepton composite models 80−57547
SO(10) unified model, phenomenological group, symmetry breaking chain low energy effects 80−86645
SO(1,3)-gauge theory of gravity 79−129
SO(2N) grand unification in an SU(N) basis 80−62906
SO(3,2) gauge theory, geom. of Einsten-Cartan theory 79−75425
SO(4,1) de Sitter gauge theory, general relativity as gauge theory limit 79−58598
SO(4,2) dynamical symmetry, unified description of bradyons and tachyons, book contrib. 79−44834
$SO(4) \times U(1)$ model of weak and electromagnetic interactions 79−13009
SO(8) extended supergravity 78−16970
SO(N) grand unified gauge theories, eigenvalue conditions and asymptotic freedom 79−22010
soft CP violation, renormalisable gauge model for strong, weak and EM interactions 78−74196
some electrovac models of homogeneous gravitational force fields in general relativity 80−95014
source-free Yang-Mills theories 79−12956
$Sp(4) \times U(1)$ theory of weak and EM interactions, little groups and discrete symmetry 79−26283
space-times admitting a three-parameter isometry group with two-dimensional null orbits 79−85019
spin, supersymmetry, and square roots of constraints 79−12676
spin 1/2 classical particle, supersymmetric actions 79−2952
spin 3/2 field, axial and trace anomalies 79−2690
spin 3/2 field interacting with EM field, quantisation 80−82698
spin 3/2 particles with minimal EM interaction, inconsistencies of Glass's eqn. 79−67207
spin (10) grand unified theory, monopole mass 80−99080
spin-2 gluon-graviton model with baryon-number nonconservation 80−57565
spin-2-gravity coupling, consistency problems 80−77681
spin-couplings 3/2, consistency 79−44824
spinor-type fields with linear, affine and general coordinate transformations 79−25949

unified field theories continued
spontaneous CP nonconservation in theories with more than four quarks 80−47212
spontaneous origin of Newtons const., modified Einstein eqns., matter interactions in weak gravit. fields 78−12853
spontaneous symmetry breaking in interaction of scalar field with external vector field 78−8545
spontaneously broken chiral $U(1)_4$, weak-interaction singlet and strong CP invariance 79−80781
stable hadrons containing massive stable quarks, cosmological constraints 79−54308
stable heavy neutrinos, dynamical interactions and astrophys. effects 79−5743
stable tangent bundle in differential geometry and unified field theory, generating method 79−5974
standard electroweak gauge model with light W and Z bosons 80−95236
standard weak-EM gauge model, six-quark phenomenology and Grand Unification 80−37204
static coupled zero-mass and source-free EM fields, generalised Laplace eqn. 80−52102
static electric spherically symmetric field, particle soln. in Bonner unified field theory 79−67205
stationary charged C-metric 80−17849
stationary Einstein-Maxwell equations, gravitational and EM potentials 80−86185
stochastic-field multieikonal theory, high-energy hadron dynamics 78−8634
strangeness changing neutral currents, avoidance in gauge theories of weak and EM interactions 79−22005
stratifying strong, weak, EM and gravit. interactions in five dimens., geometrical model 78−37166
strengths of Proca and Brans-Dicke space times eqns. 77−37794
strong+EM+weak interactions, unified gauge theory, improved Pati-Salam model 79−318
strong and gravitational interaction unified theory, hierarchy of universes, large numbers explanation 79−17654
strong and gravitational interactions 79−17662
strong gravity, field equations, strong interactions, de Sitter microsphere idea of hadrons 80−68111
strong gravity and Dirac numbers 78−21372
strong gravity contrib. to nucleonic axial-vector form factor in SU(3) 80−4902
strong gravity with torsion and the Cabibbo angle 80−4913
strongly interacting Higgs bosons, gauged nonlinear σ-model, $SU(2)_L\times U(1)$ extension 80−86656
$(SU_2\times U_1)\times S_n$ flavour dynamics, flavour number bound, n quark and n lepton generations unification 80−4907
$SU_3\times U(1)$ gauge models and neutral current reacts. 78−89648
$SU_4\times U_1$ and the origin of the Cabibbo angle, charged gauge boson mixing 80−73639
SU_4 gauge model of weak and EM interactions, u- and d-quark masses 80−13254
SU_5 theory, superheavy particles, decoupling at low momenta 80−52431
SU_7 grand unification model, two (V−A) and one (V+A) generations of quarks and leptons 80−57538
$SU_L(24)\times SU_R(24)$ model for the unification of interactions *(Chinese)* 79−54291
$SU_L(2)\times SU_R(2)\times U(1)\times[SU(3)\times SU(3)]_c$ gauge model, chiral colour symmetry breaking 80−47234
$SU_L(4)\times SU_R(4)\times U(1)$ gauge model, u- and d-quark mass generation 79−63419
SU_N gauge group uniqueness in grand unified model, U_1 color, proton stability 79−316
$SU(10)_{flavour}\times SU(10)_{colour}$ unified hadron lepton theory 79−67509
SU(2,1), graded Lie algebra, irreducible representations 80−82913
SU(2,1) generation of electrovacs from Minkowski space 79−75427
SU(2|1) electroweak interactions, implications for 6 extra time dimensions 80−77998
$SU(2)_L\times(T_3)_R\times U_V(1)$ gauge group, grand unification, symmetry breaking and Z bosons 80−73641
$SU(2)_L\times(T_3)_R\times U_V(1)$ gauge unified model, neutral current interactions, ed and ν scatt. 80−18107
$SU(2)_L\times SU(2)_R\times U(1)$, CP invariance, global chiral U(1) symmetry, axion-quark coupling 79−22009
$SU(2)_L\times SU(2)_R\times U(1)$ gauge model, possibility of b-quark weak interactions 79−26285
$SU(2)_L\times SU(2)_R\times U(1)$ gauge model for weak/EM interactions, u-d quarks mass difference 78−12850
$SU(2)_L\times SU(2)_R\times U(1)$ gauge models, neutral currents, P-violation 79−54293
$SU(2)_L\times SU(2)_R\times U(1)$ gauge theory, left-right symm., neutral current struct. 78−41420
$SU(2)_L\times SU(2)_R\times U(1)$ gauge with permutation symmetry, quark mass and Cabibbo angles 80−47232
$SU(2)_L\times SU(2)_R\times U(1)$ Higgs scalars, vacuum expectation values, quark mass ratios 79−49404
$SU(2)_L\times SU(2)_R\times U(1)$ model, weak and EM interactions, Higgs scalars, vac. instability 79−317
$SU(2)_L\times U(1)$, natural flavour conservation of Higgs couplings and Cabibbo mixing conflict 80−37200
$SU(2)_L\times U(1)$, nonlinear realisation of Weinberg-Salem model for chiral $SU(4)\times SU(4)$ meson theory *(Russian)* 79−30693
$SU(2)_L\times U(1)$, strong CP-violating phase, one-loop corrections, Higgs particles 80−62910
$SU(2)_L\times U(1)$ gauge theory, four flavours, Cabibbo angle natural relations and bounds 80−57550
$SU(2)_L\times U(1)$ primitive particle model 79−40708
$SU(2)_L\otimes SU(2)_R\otimes U(1)$ calculability, fermion mass matrix and CP invariance violation 80−13252
$SU(2)_L\otimes SU(2)_R\otimes U(1)$ gauge models confronting neutral current data 79−22013
$SU(2)_L\otimes SU(2)_R\otimes U(1)$ weak model, ν mass and spontaneous P nonconservation 80−62884
$SU(2)_L\otimes U(1)$ theory, CP violation and Cabibbo angle 80−52447
SU(2), unification of isospin and hypercharge, electroweak interactions of leptons 80−27439
$SU(2)\times SU(1)\times SU(3)$ unifying mass scales without intermediate schiral colour symmetry 80−22555
$SU(2)\times SU(2)\times U(1)$ supersymmetric gauge model, atomic parity violation and neutral current predictions *(Russian)* 79−54294
$SU(2)\times U1$ unified theory, symmetry and renormalisation 80−22551
unified field theories continued
$SU(2)\times U(1)$, gauge invariance and fermion mass dimensions 80−62907
$SU(2)\times U(1)$, gauge theory of weak interactions 78−21328
$SU(2)\times U(1)$, $K^0\leftrightarrows\bar{K}^0$ transition amplitude in MIT bag model 79−63450
$SU(2)\times U(1)\times G$ expanded gauge models of neutral currents, propagator momentum transfer 80−47237
$SU(2)\times U(1)\times SU_F(2)$ gauge symmetry, CP violation, neutron elec. dipole moment, muon number changing process 79−89091
$SU(2)\times U(1)\times U(1)$ gauge theory of weak and EM interactions in unified SU(6) scheme 78−41465
$SU(2)\times U(1)\times U(1)$ model, Cabibbo angle and Higgs coupling strangeness conservation 80−47233
$SU(2)\times U(1)\times U(1)$ model, neutral current, quark mass reactors, spontaneous broken Lagrangian 79−97563
$SU(2)\times U(1)$ gauge model, chiral $SU(2)\times SU(2)$ symmetry and electron mass 80−57542
$SU(2)\times U(1)$ gauge model, muon anomalous mag. moment, charged Higgs boson contrib. 80−78011
$SU(2)\times U(1)$ gauge models, CP violation origin, Yukawa interaction 79−40712
$SU(2)\times U(1)$ gauge theories, successes and current issues 80−18064
$SU(2)\times U(1)$ gauge theories of weak and EM interactions, neutral current contraints 78−70272
$SU(2)\times U(1)$ gauge theory, μ-e mass ratio and CP violation as quantum effect 79−30691
$SU(2)\times U(1)$ gauge theory of weak, EM and dual EM interactions 80−52448
$SU(2)\times U(1)$ model, fermion and Higgs multiplet structure, universality 80−62909
$SU(2)\times U(1)$ scheme, CP violation parametrization, quark n-doublet weak interaction *(Russian)* 80−13231
$SU(2)\times U(1)$ symmetry group, μe universality breaking in neutral current weak interactions *(Russian)* 79−58918
$SU(2)\times U(1)$ theories, weak isospin breaking, higher order corrections 80−95235
$SU(2)\times U(1)$ unified gauge field, Euclidean space and O_4 invariance 80−91031
$SU(2)\times U(1)$ unified gauge theory threshold effects 78−82098
$SU(2)\times U(1)$ unified model, universal Yukawa coupling 80−91032
$SU(2)\times U(1)$ vectorlike model: new leptons, quarks, and the axion question 79−40711
$SU(2)\times U(1)$ Weinberg-Salam model, weak mixing angle, grand unified gauge theories 79−89093
$SU(2)\otimes U(1)$ gauge model of EM and weak interactions, fermion mass restriction *(Russian)* 78−89650
$SU(2)\otimes U(1)$ gauge models of weak and electromagnetic interactions and the μe universality *(Russian)* 80−13257
$SU(2)\otimes U(1)$ standard and SU(5) grand unification models, neutral current data implications 80−78000
SU(2) gauge theory, polarised eN scatt. anal. 78−58193
SU(2) symmetry, classical quark confining solns. incorporating colour 79−339
$SU(3)_c$ gauge symmetry, unification of fundamental forces in nature, elementary particle constituents, review 80−27448
$SU(3)\times U(1)$ electroweak model, strong extension, flavour and colour gauge exchange symmetries *(Chinese)* 80−101975
$SU(3)\times U(1)$ gauge theory, electro-weak interaction, helicity mixed representation 80−78013
$SU(3)\times U(1)$ low-energy symmetry within the unifying $SU(4)_F\times SU(4)_C$ gauge group 79−67489
$SU(3)\times U(1)$ theory of weak-electromagnetic interaction with charged-boson mixing 79−35988
$Su(3)\times U(1)$ unified gauge theory without μ-e universality 79−26274
SU(3) gauge model of weak and EM interactions, Weinberg angle, Han-Nambu quarks 80−52452
$SU(3)\times U(1)$ gauge theory with different muon and electron neutral currents 78−58152
$SU(4)_F\times SU(4)_C$ synthesis of strong, weak, and electromagnetic interactions 80−13255
$SU(4)^4$, determ. of unifying mass scale 78−45830
$SU(4)\times U(1)$ gauge theory, Cabibbo mixing, new approach, CP nonconservation calc. 79−71657
$SU(4)\times U(1)$ unified gauge theory, CP nonconservation 79−71656
$SU(4)\times U(1)$ unified gauge theory, muon number conservation 79−71655
SU(4) and SO(4) supergravity relations, anomalies and field transformations 79−9170
SU(5|1) superunified model in 6-dimens. 79−97557
SU(5), gauge invariance and fermion mass dimensions 80−62907
SU(5), Higgs scalars number and m_b/m_τ ratio 80−105826
SU(5), p decay modes 80−13301
SU(5), unification of weak, EM and strong interactions, review 80−105814
$SU(5)\times SU(2)$ unification, horizontal symmetry due to quantised motion along internal axes 80−62905
$SU(5)\times U(1)$ unified theory, neutral current anal. 80−73647
SU(5) and O(10) grand unified theories, fermion and Higgs boson mass bounds 80−9134
SU(5) and SO(10) grand unification, flavour mixing and proton instability *(Russian)* 80−68413
SU(5) electroweak-strong interaction model, broken colour symmetry and gluon mass 80−73650
SU(5) electroweak-strong interaction model, mass relations and mixing angles 80−73649
SU(5) gauge model, masses, mixing angles, CP violation and b-quark decay 80−78006
SU(5) grand unification, cosmological baryon asymmetry 80−86640
SU(5) grand unification, fermion mass and Higgs representations 80−27446
SU(5) grand unification, flavour number estimate 79−85264
SU(5) grand unification, heavy coloured Higgs scalars, b-quark mass 80−57543
SU(5) grand unification, nucleon lifetime, bag model calc. 80−52450
SU(5) grand unification, p lifetime and branching ratio, bag model wavefunctions 80−78004
SU(5) grand unification, spin from isospin, half integer spin charge monopoles 80−68406
SU(5) grand unification, strong CP violation, quark-lepton mass ratio 80−32057

unified field theories continued
SU(5) grand unification, superheavy fermions and proton lifetime *(Russian)* 80−91036
SU(5) grand unification embedding in SU(N), SU(9) theory, flavour unification 80−32059
SU(5) grand unified model, inherent mixing and proton lifetime 79−49441
SU(5) grand unified theories, proton decay, flavour mixing effects 80−377
SU(5) grand unified theory, flavour number limit from fermion mass higher order corrections 80−4904
SU(5) grand unified theory, proton lifetime estimate accuracy 80−101967
SU(5) grand unified theory, t-quark mass 79−97559
SU(5) grand unified theory weak vector boson masses 80−68411
SU(5) invariant theory, B-L nonconservation and neutron oscillation 80−78005
SU(5) model, dyons and monopoles 80−82931
SU(5) model, gauge hierarchy for grand unified theory prototype 79−75711
SU(5) monopoles, magnetic symmetry and confinement 80−99078
SU(5) theories with both proton stability and cosmological baryon-number generation 80−86642
SU(5) unification, Higgs potential, coupling constants, and gauge hierarchy 80−86637
SU(5) unified gauge theory, non-Abelian electric and mag. flux 80−57545
SU(5) unified model of strong, weak and EM interactions, matter instability 79−35985
SU(5) without symmetry constraints, unified model of quarks and leptons, conservation laws 80−101968
SU(5/1) supergroup based strong-electroweak unified model with supersymmetry 80−101977
SU(6) based renormalisable unified gauge model with calculable masses 78−89647
SU(6) gauge theory, hierarchy of gauge symm. and CP nonconservation 78−41464
SU(6) grand unification model, hierarchy of symmetry breakings and neutral currents 80−52446
SU(6) grand unified theories, one loop renormalisation effects, stepwise symmetry breaking 80−32058
SU(6) unified gauge field theory of weak, EM and strong interactions 79−17658
SU(6) unified gauge model, based on SU(3)×U(1) and colour SU(3) subgroups 78−12847
SU(7) grand unified theory with heavy colour 80−42380
SU(8) grand unification, natural embedding of SU(3) horizontal symmetry 80−86646
SU(9) grand unification of flavor with three generations 80−13251
SU(N>5) chiral grand unification 80−91028
SU(N) conformal supergravity, gauge theories for extension 78−8577
SU(N) grand unification with several quark-lepton generations 80−27443
SU(N) unification of extra strong interactions, no-go theorem 80−32056
SU(S) based grand unified theory, monopoles and vector bosons, symmetry breaking 80−99079
SU(s) grand unification, neutrino mass and oscillations, B-L nonconservation 80−52449
subquark model of leptons and quarks, unification, currents and exotic states 80−86683
super-dense matter, phase transitions in gauge theories and cosmology, review 79−44654
superconducting early Universe, cosmological baryon prod., CP invariance grand unification 80−90592
superconductivity and elementary particles theory, review 80−4911
superconductivity unified model of weak, EM and strong interactions 77−49888
superconformal invariance of superspace with nonminimal auxiliary fields 79−17317
superconformal unified field theory 78−12848
superfield formulation of supergravity 79−17312
superfields in higher-dimensional spacetime 79−17316
superfluid as a source of all interactions 79−21620
supergrand exceptional unification and quark-lepton constituents 80−91030
supergrand unification in E_8, quark-lepton assignments, symmetry breaking scheme 80−68408
supergravity, and superconformal gravity linearisation 79−12679
supergravity, auxiliary fields 79−17315
supergravity, constraint-free superfield formalism 79−17309
supergravity, critique of superfield theories 79−54028
supergravity, elimination of redundancy in superspace eqns. 79−12678
supergravity, exact plane wave soln. to coupled field equations 79−30337
supergravity, failure of minimal coupling, superfield covariant derivative 79−6035
supergravity, fundamental supergeometrodynamic theory of hadron 79−40725
supergravity, introduction 79−49149
extended supergravity, N=2, auxiliary fields in 5, 6 space-time dimens. 79−30339
supergravity, O(2) extended, exact plane wave solns. 79−25955
supergravity, prepotentials in superspace formulation, superconnections 79−12683
supergravity, relation between vector and scalar multiplets and gauge invariance 79−12684
supergravity, rigid simple and extended 79−30336
supergravity, SO(3) and SO(4), finiteness and renormalisability of scalar multiplet coupling 78−4821
supergravity, superspace formulation, component formalism transform props. 79−12688
supergravity, superspace-time local symmetry, Ferru torsion preservation, renormalisability 79−12689
supergravity, supersymmetric generalisation of differential geometry tensors 78−45546
supergravity, symmetry breaking by instantons 79−21625
supergravity, Weyl and Einstein, unified approach to matter coupling 78−54275
supergravity and unification of laws of physics *(Polish)* 80−36926
supergravity as limiting case of gauge supersymmetry 77−2593
supergravity group structure 79−21619

unified field theories continued
supergravity groups, struct., complex conjugated superspace general covariance groups 79−6036
supergravity in superspace, algebraic approach 79−17314
supergravity spin 5/2 with SO_9 inernal symmetry 79−21624
supergravity with general scalar interactions, super Higgs effect, gravitinos, spontaneously broken supersymmetry 79−6037
supergravity without cosmological constant, spontaneous symmetry breaking and Higgs effect 79−17310
superheavy magnetic monopoles, cosmological prod. in grand unified models 80−8884
superspace, generally covariant theories of gauge fields 78−54568
superspace as a fibre space 79−17637
supersymmetric gauge models of weak and EM interactions 78−58106
supersymmetric gauge theories and their possible applications to the weak and electromagnetic interactions 79−49419
supersymmetric models of weak and electromagnetic interactions 79−26276
supersymmetry, physico-geometrical comments, unified field theories and supergravity, gauge transformations 80−364
supersymmetry as means to unified field theory 80−91040
superunified field theories, geometrical transformation laws 79−63117
superunified theories, $\Delta B \neq 0$ processes 80−73635
superunified theories, geometry of gauge invariance 78−24723
superunified theories in superspace 80−8886
symmetric versus antisymmetric mass matrices in grand unified theories 80−99082
symmetry violation natural suppression, muon and electron lepton number nonconservation 78−8574
t-quark mass in O(10) unified field theory 79−75708
taming of the dipole ghost in relativistic quantum field theory 78−66035
tensor gauge theory, Kerr type exact soln. 79−21631
Titius Bode Rule for solar planets and planetary satellites, c.f. Bohr atomic orbitals 79−101057
topless model for grand unification 80−73653
twister space, complex fibration, fibration structure deformation, Einstein vacuum eqns., Maxwell's eqns. 78−12854
twistor theory in Weinberg-Salam and Georgi-Glashow SU(5) model 80−73651
U_3(W) gauge models, neutral currents 79−49443
$U_L(1)\times U_R(1)\times R_R$ group, mass ratio and symmetries of electron and muon, model 79−58917
$U(1)\times SU_L(2)\times SU(3)$ theory, integer charge quarks, lepton hadronic processes *(Russian)* 80−86653
U(1)×SU(2) unified gauge field theories, field function O(4) invariance 80−37201
U(1) colour symm., Higgs coupling, proton stability 78−29290
unification hypothesis invalidation by non-asymptotically free known interactions 79−89092
unification mass and gauge hierachies for O(10), E_6 and $[SU(4)]^4$ models 79−80782
unification of gravitation and matter, crossing terms in Einstein's eqns., singularity 78−21039
unified actions for gauge fields and gravitation *(Chinese)* 79−17305
unified description of quarks and leptons using colour and flavour degrees of freedom 80−27445
unified gauge field underlying supersymmetry space, physico-geometrical remarks 79−13007
unified gauge theories and the baryon number of the universe 78−85842
unified Lagrangian formulation for massive and massless tensor fields 79−12686
unified model for atomic parity violation and neutral currents in gauge theories 80−4912
unified theories with spontaneously broken colour symmetry, QCD scalar parton effects 79−80783
unified thoery of matter, derivation of fundamental physical law 78−20982
unified Yang-Mills-Einstein-Higgs gauge theory, hadron struct., quark confinement 79−9275
unitary field theory, preliminaries and recent developments, review 79−35613
unitary spin, colour and unified theory, consideration of many-dimensional space-time 78−8570
universal supersymmetry and its need for grand unification theories 80−13230
Universe, closed or open, Fornax system density profile, strong gravitational interactions 80−90587
Universe and microcosm, gravitational-inertial field theory 80−8721
Universe baryon asymmetry, left-right symmetric grand unified models 80−82559
universe ultimate fate, effect of finite proton lifetime 80−82560
$V_2\times V_2$ space-time wave solns. to new unified theory 77−67363
vacuum symmetries of gauge supersymmetry, quantum effects 79−17634
vertical-horizontal symmetric minimal grand-unification 80−47229
very early Universe, nonequilib., grand unified particle interactions, baryon number violating bosons 80−36752
very early Universe, phase transitions and mag. monopole prod., grand unification 80−51934
vortices topology of unified intrinsic field quantities for elementary particle systems 79−40653
VV+AA gauge model 78−29246
weak and EM interaction unification with strong interactions following τ and Υ, book contrib. 80−47235
weak and EM interactions, book contrib. 78−81908
weak and EM interactions, semi simple SU(3l) gauge groups for hadrons 78−74195
weak and EM interactions at high energy [conf. Les Houches, France (July 1976)] 79−80785
weak currents of hadrons, unified gauge theories 79−80786
weak gauge boson doubling in standard SU(2)⊗U(1) model, W, Z bosons 80−62916
weak hypercharge embedding in strong gauge groups 79−30692
weak interaction models explaining null parity violation in Bi, tests on other weak interactions 79−2974
weak interactions of ultra heavy fermions 78−93838
Weinberg angle, renormalisation effects 78−62344
Weinberg-Salam theory, quantisation 78−89646
Weyl's geometry appl. 78−65843
Weyl and Papapetrou axisymmetric space-time as geodesics of hyperbolic complex plane 79−49126

unified field theories continued
Weyl-Dirac theory with torsion, complex Dirac field, conservation equations 80−68112
Weyl-Dirac theory with torsion 80−52106
Yang's gravitation theory, homogeneous cosmological models 79−17304
Yang-Mills, unified spatial and isotopic symmetry 79−21952
Yang-Mills equations in Riemann spaces, spherically symmetric solns. *(Russian)* 79−30666
Yang-Mills instanton in Taub-NUT space 79−2691
Yukawa spherical diffuse massless sources in relativity 77−87931
Z-boson and two-boson models, neutral current phenomena, μ-e universality 80−18109
$e^+e^-\rightarrow$ jets, transversely polarised annihilation, charged gluon jets, Pati-Salam model 80−86739
e^+e^- collisions, weak neutral current effects, unified theories of dimension *(Hungarian)* 79−9326
$e^+e^-\rightarrow F\bar{F}$, with polarised particles, weak asymmetries, unified gauge theory anal. 78−8636
$e^+e^-\rightarrow\gamma X$, angular asymmetries, weak contribs. 80−101976
$e^+e^-\rightarrow$Higgs boson$+\gamma$ in standard SU(2)×U(1) model, resonance enhancement 79−54331
$e^+e^-\rightarrow l^+l^-$ via many-vector boson exchange, cross sections from unified models 80−22597
$e^+e^-\rightarrow\mu^+\mu^-(\tau^+\tau^-)$, cross sections, charge asymmetry, polarisation in SU(2)×SU(2)×U(1) models 79−97616
eN deep inelastic scattering asymmetries, gauge theory predictions 79−22104
$en\rightarrow en\pi$, pol. e, P-odd asymmetry and cross sections, SU(2)xU(1), SU(3)xU(1) calcs. *(Russian)* 80−62998
eN interactions, parity nonconservation, $SU(2)_L\times SU(2)_R\times U(1)$ gauge model anal., Z boson decay widths 80−47302
eN scatt., polarised e, testing unified gauge theories prediction 79−17732
$e^-N\rightarrow e^-\Delta(3/2, 3/2)$, P-odd asymmetry, P nonconserving neutral current interaction 80−57611
$e^-N\rightarrow e^-X$, parity violating asymmetry, constraint on right-handed electron weak charge 79−17734
$e^+p\rightarrow e^\pm\gamma+X$, deep-inelastic bremsstrahlung, quark charges, colour gluon mass 78−74216
μ anomalous mag. moment, weak correction in gauge models 78−16965
$\mu\rightarrow e\gamma$, and other rare decays, in SU_6 superunified gauge theory 78−21408
$\mu\rightarrow e\gamma$, SU(2)×U(1) unified guage theory 78−8643
μe universality breakdown of neutral weak currents in $SU_2\times U_1$ gauge *(Russian)* 79−75712
$n\rightarrow\bar{n}$ oscillations in nuclei, detectable annihilation rate, grand unification 80−101966
ν decay in gauge theory of weak and EM processes *(Russian)* 79−22087
ν mass, second-order effect in Higgs coupling 79−75716
ν_μ mass limit in absence of muon-lepton-number conservation, unified gauge theories 78−21368
P decay, baryon number-lepton number conservation or violation, grand unification implications 80−27425
p decay, flavour gonimetry 80−99100
p decay lifetime in SU(5) grand unified theory 79−71749
$p+N\rightarrow\mu^-\mu^+X$, 400 GeV, charged gluon effects, broken colour gauge model study 79−49473
t-quark mass in SU(2)×U(1) 79−40710
t-quark mass in super unified O(10) model 79−49439
θ vector particles, calibration interaction macroscopic confinement radius *(Russian)* 80−47257
Υ, quixotic interpretation as $Q\bar{Q}$ bound state 80−13280
$Z\rightarrow H\gamma$, decay rate determ. in SU(2)×U(1) gauge theory 79−40717
Z-mass prediction as test of standard model 80−47239
^{209}Bi, P violating eN pot., determ. of effects by optical rotation meas. 79−26277
H, parity mixing of atomic states, spin-depend. weak interaction coupling const. 78−8572
H parity violations, fundamental struct. of weak current, unified gauge theories 78−12849

unijunction transistors
negative resistance as phase transition, critical exponents *(French)* 80−49746
transition critical exponents, negative resistance phenomena 80−44713

unimolecular layers *see monolayers*

uninterruptible power supply *see emergency power supply*

units (measurement)
see also constants; dimensions; measurement; nomenclature and symbols
acoustics, change to SI problems *(German)* 77−27403
American Society of Photogrammetry, use of International System of Units 79−21692
ampere, absolute meas. using NMR 80−98941
ampere, kilogram and fundamental constants, suggestion of systematic effect in weighing measurements 79−85127
ampere, realization expts. at NBS 80−98938
ampere as standard electric current unit *(German)* 77−22574
ampere determ. and proton gyromagnetic ratio, review of last 15 years' results 78−57887
ampere determination from levitation of supercond. mass 77−30178
ampere realization and gyromag. ratio of proton meas. at NPL 80−98940
ampere realization by means of current balance at NPL 80−105678
angular, ambiguity of status 80−8951
astronomical unit, determ. from radar obs. of Venus 79−88570
astronomy and SI units 77−78672
CGS to SI conversion for electromagnetism 78−16592
coherent-radiation spectral power density unit reproduction, USSR standard 78−37957
COMECON standard ST SEV 1052-78 for establishing units of physical quantities 80−42189
conference on metrology and fundamental constants, Varenna, Italy (July 1976) 80−105603
constant angular acceleration unit, USSR standard, metrological charcts. 79−30430
continuous laser radiation relative power-density distribution unit reproduction, USSR 78−37956
conversion to SI, US units of length, area, volume based on international, US survey foot 78−77836
decibel, definition, meter calibration and hi-fi equipment *(Spanish)* 79−54092
definitions, of units, standards and measurement methods *(French)* 80−27264
depth profiling using ion sputtering, ion dose unit, Wehner 77−8753
derived SI radiation dosimetrical, phys. quantities used in radiation safety monitoring 80−99344
dose equivalent unit 79−79658
education, SI units, classification 78−36962
electrical, realisation progress *(German)* 78−160
electrical and mechanical, two new variants for SI systems *(Polish)* 77−53851
electrical quantities, units, symbols and definitions *(German)* 80−86248
electrical unit reproduction at German ASMW, developments 80−98944
electricity/fuel substitution coefficients, energy units and balance sheets *(French, English)* 79−92053
electromagnetic phenomena, relativistic aspects *(Rumanian)* 79−17382
electromagnetism, dimensions and symmetry considerations, duality transformations 80−28139
electron and energy fluxes meas., 5 to 50 MeV, Soviet primary standard 77−75031
flow, gas, measurement techniques, rel. to significance and treatment of phys. quantities *(German)* 78−1775
Gauss system, conversion to SI *(Polish)* 79−88904
geomagnetism, SI units *(German)* 78−65391
gross surgical specimen photography, centimetre rule/elevator rod technique 78−61287
health physics quantities and units 80−8193
heliotechnics, basic values, symbols, units and definitions *(Rumanian)* 80−57243
HF current intensity unit, USSR state standard 78−36979
historical review and current systems in use *(German)* 80−68166
International Bureau of Weights and Measures, 1978 activities and news 80−188
introduction of SI system in Poland *(Polish)* 78−29082
ion motion in electrolyte solns. due to elec. field, teaching appl. 77−14
IR radiation brightness unit reproduction error anal., USSR standard 78−45699
kilogram as standard mass unit *(German)* 77−22532
light measurement, units and terminology for photometry and displays 79−21691
linear thermal expansion coeff. unit, 4.2 to 90K, USSR state standard 78−37001
magnetic meas., terms and concepts 79−97334
magnetism, SI units 79−2743
magnetism teaching w.r.t. chemistry, guide to units 80−12871
mass, force and weight, relationship 80−27273
medical measurements, SI units *(Croatian)* 80−104797
metallurgy, international system of units *(German)* 77−22519
metre, Canadian standard 79−12768
metre as standard length unit *(German)* 77−22528
metric and imperial systems of measurement, comparison of apparent accuracy 79−12755
mole, amount of substance 77−87723
mole, importance in school chem. courses 77−87589
mole, introduction in teaching of ideal and real gases 77−87611
noise units and traceability *(Japanese)* 78−18104
optical radiations, effects on men, directives and unit derivation *(Hungarian)* 78−57040
particle fluence concept 78−77837
photometric, SI system 78−93644
photometric radiation equivalent and meas. units *(German)* 79−54166
photometry and radiometry, new candela and lumen definitions 79−6162
photometry and radiometry 77−61108
photometry radiation energy units reproduction, error anal. 78−45670
physical meaning of units and counting units in different processes 79−97338
physical quantities, terminology and definition 79−75485
physical quantities, unit unification trends 78−41267
physicochemical quantities and units, symbols and terminology 79−63187
Polish conversion to SI system of units, technical aspects *(Polish)* 77−74346
power and energy units reproduction for optical, elec. and mech. quantities 77−71287
pressure measurement, definitions of units 80−77745
pressure unit, optimum metric, for thermodynamic standard state 80−8950
pulmonary function, SI unit system 77−21541
pulsed coherent radiation intensity unit reproduction, USSR standard 78−37955
quantity-of-heat, standard for organometallic compounds calorimetry 79−17421
radiation dosimetry, new SI units *(Spanish)* 79−62365
radiation effects meas., units selection 80−98870
radiation protection, SI units and ICRP recommendations 78−5054
radiation therapy level dosimeters, choice of meas. quantity 79−92379
radiation units in SI system, conversion problems 80−57244
radioactivity, definitions and interrelations 80−17914
radiology, SI units 77−12980
radiometric exploration meas. standardisation advantages and methods 78−28325
reactor technology, sources, phys. units and biological factors *(German)* 78−46180
review, the measures of man 77−9981
second as standard time unit *(German)* 77−22534
SI, definitions, table *(Polish)* 77−53852
SI, development and implementation in Portugal *(Portuguese)* 77−37839
SI, development and world-wide adoption *(Rumanian)* 78−49791
SI, for physical quantities, in Germany *(German)* 77−41564
SI, fundamentals *(French)* 80−95059
SI, guidelines for use, US National Bureau of Standards 80−68167
SI, of physical quantities, draft state standard, experience 77−87722
SI base units, rel. to fundamental physical constants 77−87724
SI metric units, in college phys. texts 80−101697
SI system, need for periodic recalibration of laboratory equipment 80−31705
SI system *(Japanese)* 78−4583
SI system implementation, in USA 77−5799

units continued
SI system introduction into Poland *(Polish)* 77−67407
SI units, conventions and practices, physics teacher's viewpoint 80−36968
SI units, for dosimetry of ionising radiation *(Hungarian)* 77−3167
SI units, group props., dimensionality 80−17746
SI units, group props. 80−17745
SI units, introduction in Hungary, ionising radiation aspects *(Hungarian)* 78−8379
SI units, introduction in Hungary, practical aspects *(Hungarian)* 78−8380
SI units, introduction in Hungary *(Hungarian)* 79−49189
SI units, rationalisation and need for approximation to SI 80−36969
SI units applied to chemistry, consequences *(German)* 79−97339
SI units in Journal of Physics E: Scientific Instruments 77−13733
sI units in permanent magnet calculations 79−30406
SI units in radiochem. and radiology 78−81939
SI units in radiological protection 78−86235
SI units status in Hungary *(Hungarian)* 79−44897
solar energy, units and symbols 79−12756
sound level, decibel unit, definition and eqns. *(Italian)* 79−9201
specific physical quantity interpretation 78−8381
spectral luminous efficacy maximum, definition *(German)* 78−54333
standard for unification within COMECON framework 80−42187
surface science, change to SI, proposals 78−62175
tesla (T) unit acceptance in SI system for magnetic induction, history *(Slovenian)* 79−40526
thermodynamics, SI units *(Croatian)* 80−189
time, rel. to angle meas., history 78−20931
transition to SI system, NBS guidelines 78−77835
underwater sound pressure unit, 0.01 to 1 Hz, USSR state standard 78−38160
units in measurement *(German)* 79−6076
vacuum measurement *(French)* 77−53925
volt, method and equipment for realization based on fundamental physical consts. and superconductivity phenomenon 80−98943
volt, realization of standard by means of Josephson effect *(German)* 79−71401
volt dissemination method and standard cell enclosure design 80−98876
watt determination by elect. and calorimetric methods, wattmeter accuracy 79−167

universe *see cosmology*

universe models *see cosmology*

untuned power amplifiers *see power amplifiers*

unwinding *see winding (process)*

upper atmosphere
see also exosphere; ionosphere; magnetosphere; mesosphere; radiation belts; thermosphere
ablation model for large meteorite entry, theory and obs. 79−66967
acoustic gravity waves, atmospheric, harmonic generation 78−88956
acoustic-gravity waves, diffr. around spherical Earth 78−4016
acoustic-gravity waves, relaxational dissipation 78−4018
acoustogravity waves generation mechanism 79−66776
aeronomical models, diurnal averaging 78−49186
aerospace environment, upper atmosphere and solar-terrestrial relations, book 80−8466
air density at 300 km altitude from China 2 rocket orbit anal. 77−91341
air density variations, from January 1972 to April 1975 near 200 km 78−57377
air density variations at 435 km altitude from Skylab 1 orbital elements 79−5694
air radiation in photographic meteor spectra 77−29733
airglow emissions, semi-annual vars. 78−28360
albedo obs., middle UV, by TAIYO satellite *(Japanese)* 79−44281
albedo particles ionization losses calc. with allowance for geomag. field 79−53621
ambipolar diffusion coefficient estimates from radio meteor method 78−45064
Arecibo coord. tidal obs. 79−2410
artificial aurora, optical emission excited by electron ejection from rocket 80−51592
artificial satellite laser ranging for upper atmosphere wind determ. 77−64485
astronomical hard X-ray telescope, balloon borne, background noise calc. 77−5427
Astronomical Netherlands Satellite, orbit prediction 79−21139
atmospheric-ionospheric disturbances, seasonal vars. 77−53289
atom and ion radiative recombination, rate coeffs. 78−40758
atomic processes, book contrib. 77−37482
atoms and radicals in situ reson. fluoresc. meas. in upper atmosphere 79−53600
Auger electrons form. during ionisation by X-ray pulse 78−53767
Auger processes and photoelectron spectra formation 79−2403
aurora, dayside morphology from large scale obs. at 6300 Å, 5577 Å and 3914 Å 80−85786
aurora, time-depend. model, particle precip. effects on atm. props. 78−4021
auroral emissions during 1974, March 16 magnetic storm 77−49209
auroral kilometric radiation, ISIS 1 obs. at source 79−84558
auroral $O(^1S)$ production and loss processes, artificial auroral expt. Precede meas. 79−66855
auroral particle instantaneous energy deposition, determ. from optical emissions 78−81491
auroral protons energy and pitch angle spectra vars. in upper atm. 79−75032
auroral secondary electrons spectrum at low altitudes, collisionless effects 79−40008
auroral X-rays, balloon obs. in Canada rel. to X-ray illuminating regions determ. 80−31156
auroral zone, joule and particle heating 77−45218
auroral zone electric currents, ground-based obs. using two-dimensional magnetometer array 80−90245
Ba vapour releases, induction of pulsating aurora 77−49211
blow-off mechanism rel. to Van Allen belt populations 77−29524
bremsstrahlung produced by precipitating electrons, theoretical characts. 79−66862
Central Aerological Observatory, USSR, historical review 77−70798
circulation flow patterns, laboratory simulation of abrupt changes, catastrophe theory appl. 78−40721

upper atmosphere continued
composition measurement, comparison of satellite self-contamination expts. and scatt. return flux calcs. 78−40722
conference, New Delhi, India (Jan. 1979) 80−94912
constituents, absolute high-resolution far IR meas. 77−41249
constituents detection, submillimetre wave heterodyne radiometry 78−49183
Cooperative Tidal Observations Program 79−2409
cosmic antiproton-proton flux ratio at top of atmosphere 78−40783
cosmic ray ion-pair production rate above 18 km altitude, parametrisation 78−65469
cosmic ray pion spectrum, at top of atmosphere 78−53780
cosmic ray secondary protons, fluxes above 500 MeV at 200-300 km 77−64497
cosmic rays, short-term fluctuations obs. 80−67483
coupling between neutral and ionized atmosphere, NATO conf. proceedings (Spatind, Norway, 1977 April 12-22) 80−27036
dayglow spectrum, far UV N and N_2 emissions 78−28361
daytime neutral winds, Li release tracking by photometer 79−39871
density, accuracy of nonspherical model from satellite drag obs. 77−29520
density derivation from near-circular satellite orbits, effect of temp. diurnal var. 80−21867
density distribution, from Cactus accelerometer flight results in Castor satellite 80−77251
density models rel. to drag on artificial satellites 80−17428
density semiannual variations form. mechanism 77−25807
density variations and meteor rates correl. with solar activity 77−53485
diffusion coefficient and height relation from radar meteor echoes 78−49187
diffusion equations, coupled time-dependent, numerical method using self-diffusion coeff. 80−109285
discrete auroras near midnight, occurrence and lifetimes 80−67447
disturbances, seasonal vars. in latit. struct. 78−32264
diurnal tide meas., 80-100 km altitude, Arecibo radar obs. 77−2290
drag perturbations on artificial satellite orbits 80−67522
dynamical properties 79−75005
E-region neutral wind, simultaneous obs. by different techniques at low and mid-latits. 77−53303
eddy current torques, air torques, and spin decay of orbiting cylindrical rocket bodies 78−93074
electric fields and currents, origin and structure *(German)* 78−32196
electrical coupling to lower atmos., quasi-static model 80−61865
electrojet induced press. and vel. fluctuations 80−82118
electron beam injection into neutral gas, laboratory study 80−54004
electron beam scattering in atoms, sounding rocket expt. (POLAR-5) 80−77212
electron capture processes, cross sections calc. 79−5693
electron energy degradation in N_2, spatial yield spectra, microplume model 79−98235
electron impact cross-sections of atmospheric gases 78−28398
electron impact on atmospheric gases, yield spectra 78−28401
electron precipitation daily vars., rocket meas. 78−69575
electrostatic V-shocks in auroral plasma, approximate equipotentials 80−21870
energy balance, importance of IR radiation 79−8729
energy fluxes propagated by diurnal oscills. 77−37473
equatorial aeronomy, conference, Townsville, Australia, (25-31 August, 1976) 78−36339
equatorial gravity waves, generation and props. 78−36232
escape of ions to space, ion chem. and low altitude accel. effects 80−85798
Excede 2 test, artificial auroral expt., ground-based optical meas. 78−89038
far IR atmospheric emission and absorption spectrum calc. program 79−35020
gamma ray angle and energy distrib., 2-25 MeV 78−12033
gamma rays, medium energy, spectrum meas. 79−9030
gamma-quanta flux, short-period pulsations rel. to Sun surface oscills. *(Russian)* 77−9638
gas clouds released at satellite orbital velocity, dynamics expts. 80−14748
gas releases, collisionless-diffusive flow transition 80−12577
Geminid meteor shower, radar obs. statistical modelling 78−61816
geocorona, collisional model for spectral line profiles 78−77508
geocorona, Lyman β and Balmer α emissions meas. during Apollo 16 mission 77−37476
geocorona, rocket borne resonant absorption spectrometer and photometer for He obs. 80−4155
gravity wave critical level flow, viscous stabilization 77−45074
gravity wave emission from moving sources 77−60504
gravity wave propagation, 'potential' well treatment 80−67396
gravity waves, obs. during tornado outbreak (1974, April 3) 78−85753
gravity waves, obs. during tornado outbreak (1974 April 3) 78−85753
gravity waves, possible effect on Loran-C 100 kHz signals 80−109304
gravity waves, ray tracing, tornadic storms and hurricanes warning system 78−73448
gravity waves, rel. to equatorial ionosphere total electron content fluctuations 78−36360
gravity waves, rel. to ionosphere radio waves phase path changes 79−35043
gravity waves at E-region heights, obs. of Es 80−72657
gravity waves in ionosphere, radar obs. of electron density 80−77182
gravity waves in nighttime F-region, TID distrib. and occurrence 80−77206
gravity waves interaction with $O_2(^1\Sigma)$ airglow 79−29918
gravity waves propag. through critical layer 80−51591
H chemistry, role of H-implanted interplanetary dust grains 78−65445
handbook, of upper atmosphere, ionosphere and magnetosphere 78−73557
heating, by solar wind energy 77−37471
HF radio meteor echoes duration rel. to dense trains deionisation 79−5697
high latitude expts., conf. (Ajaccio, Corsica, 24-29 April 1978) 79−35019
high-latitude ionosphere-atmosphere interactions 77−22000
hydrodynamical accelerator, numerical modelling *(Russian)* 78−16225
hypersonic free-molecular heating of micron size particulate 79−4058
incoherent scatter results for co-ordinated special intervals at St. Santin (France) 79−2416
infrasound, refr. by winds 77−33229

upper atmosphere continued
internal gravity waves, generation and relation to ionospheric valley electron density inhomogeneities 77−91348
internal gravity waves, interpretation of experimental data *(Russian)* 78−16224
internal gravity waves and assoc. travelling ionospheric disturbances, electron density power spectra obs. 78−28394
internal gravity waves meas. in meteor zone 77−25806
internal gravity waves nature obs. from OH emission 77−41246
International Magnetospheric Study (IMS) and Antarctic and Southern Hemisphere Aeronomy Year (ASHAY) 77−87210
ion chemistry, ion+mol., rate consts., in situ ion comp. meas. 80−31154
ion-molecule reactions, exothermic, review 78−33563
ion-neutral collision frequencies and mean temps., 80-100 km altitude, Arecibo radar meas. 78−88957
ionization inhomogeneities advected neutral gas motions, geomag. field effects 80−26677
IR brightness obs. 80−94629
IR emission, obs. with Meteor satellite 79−62632
IR emission at high latitudes from Meteor satellite, radiometer obs. 80−72655
IR emissions in auroral regions, origin 77−33247
IR radiation, model 78−12035
IR radiation flux in upper atmosphere, meas. in 4 to 6 μm spectral range 80−61929
IR radiation from mol. vibr.-rot. transitions 79−5695
irregular motions, radiometric meas. and origin *(Russian)* 78−96333
LF signals attenuation due to meteor trains 78−40726
lunar tide influencing equatorial electrojet 80−61937
M_2-lunar tide, determ. from lunar daily geomag. vars. at Tucson 78−96136
mean flow, rate of energy transfer from internal waves *(Russian)* 77−13101
mean zonal circulation in meteor zone above France and Sweden 79−75003
mesopause, energy characts. of internal gravity waves obs. by OH emission *(Russian)* 79−12324
mesopause region, ion-clustering during winter anomaly, temp. and NO density vars. effect 79−21087
meteor bright line spectra, study via astronomical TV system 78−61817
meteor head echoes, heights anal. 78−36537
meteor heights, results from decay rates of 18000 meteor echoes 77−82175
meteor ionisation trails, characts. 77−71069
meteor particles, ion prod. function in E-region 79−12336
meteor radar rates correl. with geomag. activity and solar wind sector struct. 78−65553
meteor region, travelling quasi 2-day wave 78−81480
meteor region, winter motions meas. in S. hemisphere 80−109287
meteor trail, maximum ionization height detect. method 80−8487
meteor trail diffusion, radio refl. determination 80−46329
meteor trails, causes of fluctuations in effective linear electron density 78−73687
meteor trails, effect of thermal on measured drift speed 77−21955
meteor trails, influence of recomb. on under-dense radio-meteor data 79−80279
meteor trails, ionised, initial radius, height and time depend. investigation 79−58301
meteor trails, scattered radio waves trapping by ionospheric ducts 80−4172
meteor trails initial expansion 77−2373
meteor wakes, red afterglow origin 78−36536
meteor wind data for global comparisons 79−2413
meteor wind observations from Sheffield, during January 1976 winter anomaly 78−45070
meteor wind profile comparison with electron density obs. 77−9587
meteor wind study at Kyoto University 79−48595
meteor winds over Sheffield, radar obs. 79−2415
meteor zone, seasonal variations of solar and lunar tides 77−87134
meteoric ionisation column, radiowave scatt. 77−87337
meteoric material influx rate from photographic obs. of bright meteors 79−21233
meteoritic material, meas. from spacecraft 77−53486
meteoroids, odd N prod. 79−2404
meteors, ionization curve length and vaporization altitude var. with speed 79−21232
meteors, luminous efficiency coeff. from photographic obs. 78−96440
meteors ionisation columns, initial radii meas. 80−94762
meteors overdense trails, determ. of diffusion coeff. and initial radius 77−13140
meteors television spectra, prod. and study 77−67076
MeV gamma radiation, theoretical zenith angle distrib. at high balloon altitudes 77−45208
MHD waves, absorpt. rel. to neutral upper atmosphere heating 79−53588
midlatitude electric fields at ionospheric heights, magnetospheric effect 79−2433
mountain ridge, causing upper atm. perturbations *(Russian)* 80−105018
neutral atm., density, temp. and winds, review 79−75006
neutral atm. disturbances, reaction of midlatit. ionosphere 77−25805
neutral atmosphere, dynamics rel. to ionosphere primary ion-electron prod. rates change 80−72675
neutral atmosphere, semi-empirical models based on turbopause height and exospheric temp. vars. 79−21085
neutral atmosphere dynamics, rel. to magnetospheric convection 77−29525
neutral atmospheric motions effects on two-stream irregularities in equatorial electrojet 79−16742
neutral composition, magnetic storm circulation significance 77−49206
neutral composition, vars. rel. to negative ionospheric storms numerical simulation 79−25393
neutral composition variations at F-region heights, meas. from incoherent scatt. and nightglow obs. *(Portuguese)* 80−41584
neutral gas composition during winter anomaly, cryo mass spectrometer meas. 78−45192
neutral gas diffusion in nonuniform chemically reactive atmosphere, three-dimensional time depend. modelling 79−66846
neutral gas expansion numerical simulation 79−12325
neutral temperature at 100-120 km altitude, compared to T_e 80−77211
neutral waves determ. from AE satellite meas. 79−58139
neutral wind, seasonal var. of semi-diurnal components 77−70895
upper atmosphere continued
neutral wind and composition, rel. to F_2-layer hemispherical differences 78−69603
neutral wind gradients, meteor radar obs. 80−41575
neutral wind in upper atmosphere, rel. to magnetospheric disturbances in aurora borealis zone *(Norwegian)* 78−24399
neutral wind profiles between 115 and 175 km altitude in dayside auroral oval 80−98494
neutral winds, rocket determs. compared with partial refl. drifts 77−87019
neutral winds and nighttime F-region maintenance 77−29555
nightglow, 557.7 nm line and Herzberg bands excitation 79−75008
nightglow, OH, Na D-line and O I 5577 Å emissions correl. 79−80067
nightglow, rocket meas. of O_2 atmospheric system and OH Meinel bands *(Japanese)* 80−94631
nightglow O I 5577 Å line, intensity var., related to solar tides *(Russian)* 80−12585
nightside auroral oval, instantaneous, from electron precip. equatorward boundary obs. 78−32289
nighttime ionization by energetic particles, 120-200 km altitude 79−62666
noctilucent clouds over W.Europe (during 1979) 80−109289
O I nocturnal 6300 Å luminesc., profiles from incoherent scatt. radar and photometry *(Portuguese)* 80−41591
outgas flow from spherical spacecraft, Bhatnagar-Gross-Krook model 79−94676
perturbations caused by mag. storms, review of obs. 80−98495
photoelectron energy spectra 78−49190
photoelectron spectra allowing for Auger effect 78−69557
photographic observations from Skylab 77−60505
physics of atmospheres, book 79−62568
pitot pressure measurements for density determ. between 50 and 120 km, W.Europe Winter Anomaly Campaign 78−45193
polar atmosphere, penetration by monoenergetic and unidirectional proton beams 77−29528
polar wind morphology in mag. quiet conditions 80−72713
positron annihilation line at 511 keV, balloon obs. 80−41582
Precede, artificial auroral expt., summarised results 78−89037
prevailing wind altitude-latit. struct., 80-100 km altitude 79−29829
processes in neutral and ionized atmosphere in 60-150 km altitude range, problems 77−21961
protonosphere, Gliddon's model of heat cond. 78−32294
protonosphere, stationary isothermal plasma flows 77−60502
protonospheric-ionospheric modelling of magnetospheric VLF ducts 78−28446
quadrupole mass spectrometer applics., book contrib. 77−25911
radar for observing middle and upper atmosphere, Yaggi antenna array design 80−90255
radar meas. 80−72661
radar meteors rate depend. on geomag. activity and coronal activity 80−67662
radiating molecules, in upper atm., rot. relax., IR emission and vibr.-rot. transitions calcs. 77−65462
radiation transfer eqn. approx. soln. *(Russian)* 77−13122
radiative transfer, inverse problems method in transport and filter theory 79−29920
radiative transfer, non-LTE, in CO_2 15 μm band *(Russian)* 78−36341
radiative transfer in CO_2 4.3 μm band with non-LTE *(Russian)* 78−88914
radio aurora in dayside auroral oval, rel. to field-aligned currents and energetic particles 78−88966
radio meteor rates observed with meteor wind radar during non-shower period 79−84753
radio meteor wind data, anal. using finite element approximation 78−81475
radiometeors, forward scatter, amplitude distrib. index, D-region absorpt. effect 78−65552
radiometeors characts. assessment, statistical analysis of time-dependent series *(Russian)* 80−56777
radiowave scattering theory appl. to radio meteor obs. 79−5696
radiowaves in magnetised plasma, modulation instability saturation *(Russian)* 77−47203
rare earth rich submicron grains, solar vs. terrestrial origin 78−12180
relativistic electron beam localisation, stabilising effects *(Russian)* 80−21868
Rossby neutral mode, secular stability 80−81983
rotation rate and density, obs. of satellite orbit 80−85785
rotation rate from Proton 4 satellite orbit determ. 77−64632
rotational rate and winds, determ. from China 2 rocket (1971-18B) orbit 80−4231
rotational vel. from Interkosmos 10 inclination var. analysis 80−41693
secondary cosmic ray electrons, fluxes at equator from Kosmos-428 data 78−45168
solar activity effects, mid-latit. ionospheric disturbance of corpuscular origin 78−28374
solar eclipse, 1973, June 30, atmospheric waves obs. 77−53302
solar EUV output rel. to aeronomy, present knowledge and future meas. techniques 78−57535
solar flare X-rays, atmosphere reflected fluxes rel. to flare spectrum beyond 200 keV 80−51710
solar radiation extinction, theory 77−78546
solar terminator, gravity waves generation rel. to E_s-layers form. 79−12337
solar UV irradiation flux meas. between 120 and 400 nm, current position and future needs 78−57536
solar-terrestrial energy orders of magnitude *(German)* 77−70940
sounding rocket expts., during 1979 February 26 total solar eclipse 79−58145
Space Shuttle, orbital environment 78−36430
space shuttle reentry, unsteady nonequilib. chemically reactive flow, parallel computation 78−47065
spacecraft re-entry and meteorite supersonic movements, ablation problems 79−32780
spectra, Galatry profile convolved with Fabry-Perot instrument function 77−78642
spectrally integrated transmittance in O_2 Schumann-Runge bands and O_2 column density, 76-102 km altitude 79−70902
splash and re-entrant albedo electrons, energy spectra 78−69630
Standard Atmosphere, 1976, rel. to previous standards 78−11975
structure, composition, temperature and motion, general review 79−39997

upper atmosphere continued
structure and composition, daily vars. at midlatits., reference system 77−29521
subsatellites launched from Spacelab, for atm., magnetospheric and plasma physics research 77−21944
sunrise effect on elec. pot. near ground, origin in upper atmos. 80−61866
super-rotation, effect of momentum of meteoroids 77−56877
telemetry, automation of information input and processing 77−78429
temperature, comparison of measured and inferred values from AEROS-B 77−21958
temperature, measured using new aperture for interferometry of airglow 80−82075
temperature, turbulence and N_2 composition, 95-150 km altitude, 1967-75 obs. 80−51588
temperature and humidity anomalous profiles remote determ., errors *(Russian)* 77−17266
temperature and ion chemistry at nighttime, 400-450 km altitude, Ogo 6 data 80−90267
temperature and wind distrib. between 100 and 120 km altitude *(Russian)* 77−29527
thermosphere, lower, electric current and atmospheric motion, symposium, Seattle, Washington, 1977 August to September 80−62371
tidal interaction effects on geomagnetic and ionospheric variations 77−87137
tidal observations at Millstone Hill for the August 1974 and October 1975 special periods 79−2414
tidal wind variations, upper mesopause region, ionospheric reflection height *(German)* 77−87139
tide (solar semidiurnal), zonal motion and meridional temp. gradient effects 80−98399
tides, electromagnetic force effect 77−87136
tides, theoretical work since 1970, review 80−94589
tides and planetary waves *(French)* 77−21962
tides and winds meas. from meteor radar obs. 79−66851
tides at meteor altitudes, CTOP radar obs. 80−77181
tides in equatorial thermosphere, semidiurnal and terdiurnal 80−82119
trace gas concentration determ. by Spacelab passive sounding expt. 77−21950
tropical UV airglow, mag. storm effects 77−45214
turbopause, altitude vars. during night 77−78548
turbulent diffusion coeff. determ. from meteor trail photographs 78−45073
twilight sky polarisation during meteor showers *(French)* 77−9578
Urbana Meteor Radar observations during GRMWSP/CTOP periods 79−2412
UV extinction meas. of O_2 density 79−2406
UV fluoresc. excited by electron beam, POLAR-5 rocket expt. at 391.4 nm 80−77214
UV radiation sources, modelling 80−1288
UV solar radiation effects on upper atmosphere, review of Saha's work 79−53599
UV spectrophotometric obs. from Spacelab 77−21964
vertical winds effects on medium scale internal gravity waves propag. 79−75004
Vertical-6 rocket flight results 80−90268
viscosity spatial inhomogeneity and dynamic effects 79−53590
viscosity tensor of neutral component 79−62633
visual observations from space 80−21825
VUV solar scatt. radiance, aurora and nightglow, satellite obs. 80−90272
wave structures in meteor zone, obs. by Illinois University radar 77−41205
waves, relaxational dissipation, basic formulation 78−4017
wind, meas. with airglow Fabry-Perot spectrometer 80−77156
wind, obs. by radio meteor drift, 80-100 km altitude over Adelaide 80−46328
wind and temperature measurement, laboratory discharge lamp source appl. 80−4148
wind as cause of ionospheric disturbance dynamo 80−82134
wind determination by meteor track movement *(French)* 80−51589
wind field disturbances, 90-100 km altitude, rel. to stratospheric warmings *(German)* 77−70894
wind in lower ionosphere, obs. by Kyoto meteor radar 80−67444
wind in neutral atmos. at F-region height, servo model of ionosphere 80−101486
wind in upper mesopause, diurnal variation of zonal and meridional components 80−109284
wind meas. errors from meteor trails 77−49202
wind observed at solar eclipse, 80-100 km altitude 80−46327
wind shear, rel. to E_s-layer form. at middle latits. 77−13157
wind velocity fluctuations in 95-100 km altitude region rel. to lower atm. wave processes *(Russian)* 77−29523
winds, effects on propag. of auroral infrasonic wave emission 77−29534
winds and aerodynamic lift effects on S3-1 satellite orbit inclination 77−53262
winds from Cosmos 408 rocket orbit 78−73559
winds from radio meteor meas. over Atlanta 79−2411
winds from satellite 1973-101A orbit 78−73560
winds in meteor region, periodic fluctuations of recurrent nature 80−90266
winds of 95 km altitude, meteor obs. at 45°N 80−46330
X-ray aurorae prod. by energetic electrons precip., imaging from Spacelab 78−61608
zonal wind speeds determ. from satellite 1966-51C orbit anal. 77−56786
zonal winds, determ. from satellite orbit anal. 77−13143
zonal winds, var. with height and local time, satellite orbit anal. 77−56785
zonal winds at 95 km altitude, correl. with radar meteor echo rates 80−56775
γ-ray flux above 40 MeV 77−53257
Al hydration, in vap. phase, rel. to upper atmosphere chemiluminesc. 79−29362
Ba^+ clouds, early time striation struct. due to presence of BaO flow 77−25833
CH^+, obs. following trimethylaluminium high altitude release 79−48591
H chemistry, role of H-implanted interplanetary dust grains 78−65445
H distribution and daily density vars. 77−29522
H, energetic, from radiation belts, rel. to interplanetary H origin 77−9645

upper atmosphere continued
H escape flux, charge exchange induced, diurnal and solar cycle vars. 78−93022
H Lyman α reson. emission, obs. during 1973 June 30 solar eclipse 79−8901
H thermal dissipation near baropause 78−45062
H^+ loss during solar cycle, charge exchange processes 78−93021
H^+, O^+, conc. meas., Aureole 2 satellite mass spectrometer obs. 78−53766
H_2 and O_2 densities near 100 km altitude, from UV stellar occultation obs. 77−9579
He distrib., dynamical model 77−70896
He dynamical model, use of Jacchia (1977) empirical model for background gas press. 78−77381
He I 584 Å dayglow obs. by rocket-borne reson. absorpt. cell 77−64503
Li releases, daytime, obs. via high resolution photometer rel. to winter anomaly 78−45023
Mg, Mg^+, photochemistry 77−21954
N and O radiative recomb., source of NO γ and δ bands auroral emission 77−91343
N content temporal vars. 77−60501
N production, photochem. model, far UV dayglow 80−90271
N_2, band emission as source of 1027 Å aurora 79−80064
N_2 bands in proton-induced poalr cap aurora, intensities 78−77389
N_2 dissociation by electron impact and EUV photoabsorpt., rel. to aurora and airglow 78−58847
N_2 gas, electron energy degradation, Monte Carlo study 80−69969
N_2 in aurorae, vibrational distrib. 79−80068
N_2, N_2^+ auroral bands, airborne spectroscopic studies 77−29533
N_2 photochem. rel. to solar cycle phase, 285-375 km altitude 80−85783
N_2 vibrational energy distribution, effects of soft electron precip. 77−33261
N_2 vibrational level distrib. in upper atmos., theory 80−41576
N_2^+ 1 NG emissions from proton aurora, anomalous vibr. distrib. 80−67448
$N(^2D)+O_2$, chemiexcited NO form., 90-180K IR obs. 78−90163
NO, 2150 Å auroral emission, excitation 77−9594
NO abundance meas. in equatorial region 77−78547
NO airglow, 2150 Å (1,0) γ-band intensity meas. with polarising NO photometer 78−45076
NO, concs. in aurora 77−2291
NO density, high-altitude rocket meas. 78−45068
NO, density profile from airglow obs., 72-120 km altitude 80−105094
NO, gamma band emission rate factor, rel. to upper atm. comp. determ. 77−54572
NO, Salyut 4 IR spectral obs. in upper atmosphere mid-latitudes 78−16223
NO, time-depend. profile rel. to temporal vars. in HF ionospheric absorpt. 77−53305
NO^+ cluster ion formation in D-region, temp. control by ion obs. 80−61931
$NO^+ + N_2$, vibrational radiation quenching in upper atmosphere 79−3543
$NO_2^+ + O \rightarrow NO^+ + O_2$, rate constant rel. to atm. ion chem. 77−41245
$NO^+.H_2O + O \rightarrow NO_2^+ + H_2O$, rate constant rel. to atm. ion chem. 77−41245
$NO^+(\nu=1,2) + N_2$, vibr. transfer, vibr. absorption coeff. 79−6994
$N(^2P)$ in auroral arc, excitation and collisional deactivation processes 80−72658
Na daytime abundance, absorpt. studies 77−87140
Na enhancement at 95 km altitude, airglow and lidar obs. 80−101466
Na I twilight and nightglow; interferometric studies of D-line profiles 78−36353
Na layer, laser sounding and interp. in terms of global atmospheric parameters 78−20570
Na layer, lidar obs. of wave-like struct. 78−88955
Na winter nightglow, correl. with radio absorpt. 77−33239
$Na + O_3 \rightarrow NaO^* + O_2$, in upper atm., rel. to Na I nightglow intensity vars. 79−70905
NaI night airglow, D-line excitation mechanism 79−84562
O, 557.7 nm spectral emission mechanism at 100 km altitude 80−61933
O, airglow intensity of green line rel. to atom density *(Chinese)* 80−90269
O and N density determ. by optical reson. absorpt.-reson. fluoresc. techniques 77−21951
O and N density meas. by Apollo-Soyuz UV spectroscopy 77−33228
O and N_2 densities, OSO-7 meas. 77−21960
O atoms in exposure, polar corona atom distrib. 80−82120
O I, $3s'\ ^3D^0$ and $3d\ ^3D^0$ levels excitation and radiative decay 79−80064
O I 1304 Å, nadir intensity/column prod. rate ratio rel. to airglow studies 77−45213
O I 5577 Å green line, nighttime var. of 2-15 min fluctuations 78−49193
O I 5577 Å nightglow, meas. via two-channel rocket photometer 78−45078
O I 5577 Å nightglow intensity latit. var., Chapman's mechanism 77−37474
O I 557.7 nm nightglow in central polar cap 77−33238
O I 6300 Å airglow rel. to O atoms creation and destruction 79−8735
O I 6300 Å emission, nighttime vertical distrib. models 79−53602
O I 6300 Å red emission, first obs. in Guinea 79−58146
O I and N I forbidden lines emission in nightglow, historical review 79−5699
O II 7319-7330 Å dayglow, meas. and theory 77−37475
O, low-energy electrons integral scatt. cross section 78−69556
O, UV photoionisation cross-section calc., 304 and 584 Å 80−43015
$O^+ + N_2$, charge exchange collision, rate coeff. and ionosphere implications 80−87224
$O^+ + O_2$, charge exchange collision, rate coeff. and ionosphere implications 80−87224
O_2, (0-1) spectral emission band in upper atmos. 80−61933
O_2 and O semi-annual and annual vars. 79−53589
O_2 density at D-region attitude, obs. of Lyman-α extinction 80−77180
O_2 photoabsorption cross section near Lα line, temp. depend. 77−64499
O_2 UV absorpt. cross section and column density at 70-120 km altitude 77−53263
$O_2^+ + N \rightarrow NO^+ + O$, rate constant rel. to atm. ion chem. 77−41245
O_3, 9.6 μm band radiance calc., excitation processes 78−36350
O_3, Cl abundances, OAO 3 stellar occultation meas. 77−9580
O_3 content of atmos. rel. to solar activity 80−41488

upper atmosphere continued
O_3, nighttime equatorial density determ. from UV stellar occultation obs. 77−53259
$O(^1D)$ production by O_2^+ dissociative recomb. 77−41251
$O^+(^2D)+N_2$ charge exchange, rate coeff. temp. depend. 80−77179
$O_2(^1\Delta_g)$ airglow, emission height profile meas. during winter anomaly event 78−45077
OH airglow layer (90 km), atmosphere warming during 1976-77 winter *(Russian)* 79−88518
OH emission, waves and winds, 80-100 km altitude 78−93025
OH emission layer waves, comparison with F_2-layer waves 78−45065
OH, NO, NO^+, inverted populations due to moving bodies and ejected gas 78−32265
OH nightglow emission, intensity meas. during 1969 NASA airborne auroral expedition 77−29529
OH nightglow IR photographs, evidence for wave systems 77−45212
OH, submicron airglow bands correl. studies during Spacelab simulation 79−25381
$O(^1S)$ formation, comparison of Chapman's and Barth's mechanisms 79−62636

uranium
see also nuclei with .....
see also fission of uranium
^{235}U enrichment, steady state cascade performance, cost anal. 79−59264
α phase, lattice dynamics 79−95101
γ-irrad., EPR and luminesc. studies of U^{5+} and U^{6+} centres 79−51854
abundance determ. for rocks using NaI detectors 79−80043
abundance in Archaean granites from NE.Minnesota 78−61356
abundance in Indian kimberlites 77−60376
abundance in Precambrian basement, W.Canada, petrologic and tectonic controls 80−17257
accumulation mechanism in Black Sea sediments 77−91105
adsorption of water and O_2, XPS study 80−7473
adsorption on C, scanning-transmission electron microscope obs. 77−51597
advanced high U-density reduced-enrichment plate-type fuel development for test and research reactors 80−23101
AES and loss spectra, changes on oxidation 77−20965
S.African and South West African deposits 79−84268
alkali-alumino-phosphate:U, rontgenoluminesc. and fluoresc., radiative transitions obs. 80−103977
in alkaline earth tungstates, incorporation during growth, effective distrib. ratios, luminesc. characts. 79−42094
analysis in geological samples, delayed neutrons method *(Rumanian)* 79−88507
analysis in phosphate fertilisers and other materials using liq. scintillation spectrometry 78−53280
assay, experimental comparison of the active well coincidence counter with the random driver 80−78503
assay in phosphate-containing materials by solvent extraction-liquid scintillation method 79−22447
assay of natural samples, meas. of gamma- or neutron activity of short-lived fission products 80−61179
atom, 4 eV odd levels, hyperfine struct., double reson. spectrosc. 79−81171
atom, ab initio effective core pots., relativistic corrections 78−50483
atom, absolute pair prod. cross sections 79−63973
atom, excited state radiative lifetime, sputtering technique 78−17602
atom, gf-values, level mean lifetimes, electronic excitation and delayed coincidence meas. 78−21878
atom, high-lying levels in vapour near ionisation limit 78−21842
atom, highly selective multistep ionisation by laser radiation 79−59408
atom, ion induced K-shell ionisation cross-sections determ. by comparison with nuclear Coulomb excitation 79−76500
atom, isotope shift and configuration interaction 79−31468
atom, isotope shifts rel. to $|\psi(0)|^2$ 78−17580
atom, L-shell Auger and Coster-Kronig intensities from relativistic theory 79−93962
atom, L-shell photoionis., transition radn. ang. distrib. 78−33486
atom, L-shell X-ray photoelectric cross sections, fluorescence spectra 78−58636
atom, L-subshell ionisation cross-section ratio by ion beam impact, projectile charge and vel. depend. 77−6920
atom, laser fluoresc. spectroscopy using pulse hollow cathode lamp 80−27973
atom, lifetime meas. of electron excited states, rel. to laser isotope separation 77−34591
atom, M-shell X-ray emission obs. by photoelectron spectrosc. 77−54529
atom, matrix isolation studies with Fourier transform IR 78−45740
atom, oscillator strengths, 2289.8-2860.3K, 355.2-359.4 nm 79−10069
atom, photoionisation, by Ar ion laser radiation, appl. to U laser isotope separation 78−42233
atom, radiative lifetime, appl. to laser isotope separation 79−50152
atom, relativistic Dirac-Slater calcs. *(Japanese)* 77−42252
atom, reson. absorption meas. using Zeeman tuned arc lamp 78−17593
atom, sputtered, absorpt. spectra in hollow cathode glow discharge 80−32643
atom, X-ray L shell emission spectra *(Spanish)* 79−98016
atom+^{3}He(^{4}He)(Ne), collisional relax. of highly excited states, laser-induced fluoresc. obs. 80−58205
atom+molecule, collisional relax. of highly excited states, laser-induced fluoresc. obs. 80−58205
atom and ions, shell energy struct., SCF calc. by Dirac-Fock-Slater method 80−52877
atomic beam, two laser irrad., two photon reson. effects., visible spectra 80−63604
atomic model 79−41095
atomic motion on thin C substrate, low-temp. obs., biomolecule marking appl. 79−25176
atomic structure, valence energy levels, SCF relativistic Xalpha calc. 79−85912
atomic X-ray spectra, parity violation, from electron-nucleus weak currents *(Russian)* 79−22642
atoms, form. in chem. reaction, conc. determ. by laser fluoresc. excitation *(Russian)* 77−9156
atoms, Rydberg levels, time-resolved stepwise laser photoionisation obs. 77−27038
Australia, genesis of Proterozoic U deposits 79−84270
Australian reserves, development program 78−4983
Australian resources, review 79−87941

uranium continued
autoionic images of dislocation struct., computer interpretation 77−62453
automated analyser, delayed neutron counting, geological sample analysis appl. 78−3769
basalts from DSDP Leg 37 cores, U and Pb abundances 77−91123
binding, by brown coal, from seawater, IR spectroscopic obs. 78−82855
blood, U conc. meas. 80−21532
borehole assay using Ge gamma spectrometers 79−53571
borehole logging by prompt fission neutron technique, log interpretation 79−53567
borehole logging system, delayed neutron activation anal. method using ^{252}Cf source 79−53569
boreholes, in situ assay using prompt fission neutron technique 77−37441
breeder reactors, current status in Europe 80−27796
bronchogenic carcinoma among former U mine workers at Port Radium, Canada 80−89802
Canada, U occurrences and mode of origin, N.Saskatchewan 79−84272
in Canadian deposits, reconnaissance programme *(French)* 78−88827
CANDU fuel radioactive decay props., natural uranium fuel cycle 77−71655
charge density wave, first order transition 80−10664
chemical and isotopic anal. of U, Pu, and Th in nuclear fuel materials 79−81046
chest survey, in vivo, confirmation by autopsy specimen anal. 77−66859
chondritic meteorites, U isotopic comp. 78−4157
commercial, γ- and β-hardened, recrystallisation, effect of impurity distrib. 78−70602
compressive deform. at low temps. 77−28856
conference, natural fission reactors, Paris, France, 1977 80−17716
Conference, nuclear materials, safeguards and accountability meas., Williamsburg, USA (May 1978) 79−81045
content anomaly of sediment under Galapagos hydrothermal mounds 80−56434
content in natural samples, γ spectrometric determ. *(Russian)* 78−92562
content in some Indian coal and flyash samples 80−104547
continental crust evolution, granitic rock formation and destruction rel. to U deposits 79−84201
core and valence band spectra, XPS obs. 80−50530
core fuel elements, of A-1 reactor, volume growth *(Czech)* 80−27745
denatured fuel cycles for international safeguards 79−41011
dental porcelains, determ. of U content and dose to oral mucosa 80−89830
deposit distribution patterns and formation investigation *(Russian)* 79−30926
deposits, distribution and mode of occurrence 79−84266
determ. in coastal sediments and seawater, activity ratios, disequilib. 78−27851
determination, automated spectrophotometric method for sub-milligram amounts 79−11870
determination, in environmental samples, neutron activation, neutron assay and fluorometric methods 78−61087
determination, in fuel rods, by passive gamma-ray spectrometry 78−92576
determination, in natural waters, spectrophotometric method *(German)* 78−70952
determination, in porcelain dentures, rapid anal. by delayed fission neutron method 78−15907
determination, in water, by AAS after ion exchange preconcentration 78−85231
determination, using automated fluorometer 79−11871
determination by computer-controlled titration system, evaluation 79−16113
determination in environmental waters by epithermal neutron activation 79−53010
determination in fossil bones 79−52846
determination in natural water by ion exchange separation, delayed neutron counting 77−36847
determination in obsidian from northern New Zealand, archaeological sourcing method appl. 79−2239
determination in sea water by preconc. on Chelex 100 and neutron activation 79−53009
determination in soln. using automatic controlled-potential coulometer 77−25335
determination in whole rock samples by fission track method 77−73880
determination of ^{238}U, ^{234}U, ^{230}Th, ^{226}Ra and ^{210}Pb in U ores, dusts and mill tailings 78−15736
development possibilities of energy resources, review *(German)* 80−21355
diffusion enrichment plant by Eurodif and Coredif, France 77−358
diffusion in Ta and W, determ. by neutron fission tracks meas. 77−89587
diffusion of U III and IV in alkali chloride eutectic melts 77−80637
distribution of speculative uranium resources 80−78369
Earth mantle, U conc. rel. to Earth thermal evolution 80−89988
EBR-II delayed neutron monitor, response to tramp uranium and fission prod. test source 79−67919
educational module, nature and exploration in US sandstone deposits 80−36799
Edwards carbonate aquifer, Texas, U isotopes fractionation rel. to aquifer oxidation/reduction 80−98362
electron stopping power, continuous slowing down approx., range difference for 0.2 to 10 MeV electrons 80−39187
electronic band struct. and props. 80−10861
emission spectrum, visible region, wavenumber meas. by Fourier transform spectroscopy *(French)* 77−57407
enriched U, lower costs 80−106111
enriching gas centrifuge cascade, computer program for performance anal. 79−85805
enriching gas centrifuge cascade, reflux effect, enrichment enhancement control 77−54346
enrichment, asymmetric separation process, value function, separative power 77−75001
enrichment, centrifuge, URENCO facilities at UK and Netherlands *(German)* 78−86666
enrichment, centrifuge process, LWR fuel *(German)* 80−68905
enrichment, commercial centrifuge plants in UK and Netherlands, prospects 78−5000
enrichment, critical status report 77−34419

uranium continued
enrichment, demonstration centrifuge plants at Capenhurst and Almelo, progress report 78−29626
enrichment, HAGA radial separating nozzle centrifuge process, cost 78−46155
enrichment, Italian activities 79−31126
enrichment, jet membrane process 79−26683
enrichment, laser R&D 77−54364
enrichment, layout of gas centrifuge cascades 79−26587
enrichment, market survey *(German)* 78−4999
enrichment, project using gas centrifuge at Centar, USA 77−357
enrichment, separation nozzle process 79−31124
enrichment, using advanced gas centrifuge technology, for commercial use 77−356
enrichment by electrostatic filtration *(French)* 77−18707
enrichment by gas centrifuge, Japan 79−31123
enrichment by gaseous diffusion, Japan, research and development, economic evaluation 79−31121
enrichment by gaseous diffusion process *(French)* 79−31120
enrichment by isotope separation, HAGA radial-separating-nozzle centrifuge process 79−67954
enrichment by laser isotope separation *(Japanese)* 80−68960
enrichment by photochemical laser, two-phase flow with condensation, mathematical model *(French)* 80−74029
enrichment by plasma centrifuge, partial pressure distrib. obs. 78−74501
enrichment by plasma centrifuge, rotational velocity meas. 78−74502
enrichment by two step photoionisation laser isotope separation *(Japanese)* 79−49865
enrichment changes, impact on utility fuel management, 1978-1985 period 79−63796
enrichment facility, based on separation nozzle process, materials management w.r.t. safety 79−85747
enrichment for power reactors, laser isotope separation 77−6953
enrichment in volcanic rocks of E.Avoca-Ballard mineralised belt 78−69346
enrichment induction in test and research reactors, US program 80−22949
enrichment methods, efficiencies and costs *(Dutch)* 80−37634
enrichment plant criticality analysis *(Japanese)* 78−46156
enrichment plants, 1979 status *(French)* 80−807
enrichment plants, general world situation, survey 77−355
enrichment plants in France 77−14257
enrichment processes in France *(French)* 79−31127
enrichment prospects for 1980's 77−46368
enrichment services availability 79−26695
environmental distribution and movement, agricultural product distrib., Japan 77−90921
environmental impact of phosphate and related industries, need for radiation controls 77−56483
in environmental samples, determ. by gamma spectroscopy of 1.0015 MeV radiation in ^{234}U 77−1954
exploration, ^{222}Rn gas detection using Track Etch system 80−98488
exploration, airborne phoswich detector system 79−53576
exploration, delayed fission neutron and prompt fission neutron logging, comparison of predicted signals 79−39879
exploration, photomultiplier tube, solid-state, for improved gamma counting techniques 79−54748
exploration, pulsed neutron logging, minimisation of neutron absorber effects 77−37446
exploration, radiation transport anal. for borehole logging probes 79−53565
exploration and assay, nuclear methods 77−41228
exploration and evaluation techniques for ore bodies 79−26536
exploration and international cooperation 78−86628
exploration and production increase, 1977 survey *(Czech)* 77−83035
exploration and prospecting methods 80−85768
exploration in Australia, Alligator Rivers Uranium Province 79−30922
exploration in Australia 79−48471
exploration in developing countries, facts and trends 80−16764
exploration of the Oklo natural fission reactors, review *(French)* 80−21753
exploration with computer-processed LANDSAT data 78−7777
exploration with electronic alpha cups 78−7781
explosively clad uranium targets 80−18737
exposure standards for U mining 80−46055
extraction, by underground leaching of ore-enclosing rock 77−61626
extraction by transfer between liq. phases, laser radiation effect 80−66795
extraction from friable ore-bearing rocks, underground leaching 77−70664
extraction from natural water *(Russian)* 79−31112
extraction from sea water, around British coastal power stations 78−21788
extraction from sea water in Japan 79−31113
extraction from sea water using polyacrylamide gel containing metal hydroxides 78−54861
extraction from sea-water by interfacial electrolysis *(Japanese)* 77−1931
extraction from seawater, by sorption techniques 79−29902
extraction from seawater, feasibility 80−37564
extraction from seawater, tests of adsorbents 78−36198
extraction from seawater *(Japanese)* 78−36199
extraction from seawater by polymer-bound macrocyclic hexaketone 79−92052
extraction from seawater using composite absorbents, Ti(IV)-Fe(II) oxide 80−24730
extraction from seawater using magnetic adsorbents 80−37563
extraction from seawater using Ti based composite hydrous oxides *(Japanese)* 80−804
extraction process for systems, with 2 extractable macrocomponents, graphical calc. 79−31098
FBR fuel, U-Pu extraction by equilibrium water systems with 0.15 to 1 M HNO_3 acidity 79−71940
Fermi surface and effective masses of α-phase, de Haas-van Alphen meas. 80−65426
field-emission microscopy, emissive props. 78−88409
film, condensed on cold substrate, electronic props. *(Russian)* 79−7912
film for bombardment targets, prod. techniques 77−389
fissile material accountancy using controlled potential coulometry 80−63298

uranium continued
fissile material assay, cyclic method of neutron activation and delayed-neutron counting 77−34395
fission reactor fuel, resources and future demand 77−10468
fission reactor fuel, U enrichment, optimal blending 78−13309
fission reactor fuel demand and reprocessing requirements estimate, 1976 to 2000 77−14232
fission reactor fuel enrichment, US 1978 policy and future recommendations 79−36393
fission reactor fuel waste, burning in three phase pellet for inertial confinement fusion systems 77−61600
fission reactors, integral experiments for testing Th and ^{233}U data 80−27707
fission track dating using U glasses, error analysis 80−95503
foil and powder, oxidation kinetics in CO_2, 375 to 602°C 77−50240
fossil fuels, determ. of trace amounts by neutron activation anal. 79−83531
fuel, enrichment by gaseous diffusion process *(French)* 78−70622
fuel, future requirements, planning amidst uncertainty 79−63792
fuel, isotope separation processes development *(French)* 78−66361
fuel, low-enriched, appl. of Raschig Ring Standard 79−26528
fuel, system-wide feed and enrichment requirements of expanding nuclear economy with advanced reactors 77−61624
fuel cycle, supply, enrichment and irradiated fuel reprocessing developments *(French)* 80−18565
fuel elements recycling and thermal re-irradiation, technical, economic and safety problems *(German)* 80−99269
fuel enrichment, asymmetric process, separative power, resoln. of inconsistencies 78−29622
fuel enrichment, flow profile meas. of gas in rotating cylinder 77−46382
fuel enrichment, nondestructive determination by Ge(Li) spectrometer *(Czech)* 77−46371
fuel fabrication in 1980s changes in process equipment and facilities 79−63797
fuel for HWR, radiation stability *(Russian)* 79−13424
fuel reserves, technological status 77−34398
fuel resources and supply outlook for 1985 79−63795
fuel supplies security up to year 2000 *(French)* 80−3480
gamma ray analysis of K, U and Th for dose-rate estimation in thermoluminescent dating 79−79333
gas centrifuge with differential rot., U enrichment 77−54363
gas-discharge fission reactor, fuel element component conc., plasma temp. profile instabilities 80−63253
gaseous, U fueled reactor, use as power supply for nuclear pumped laser system 80−63247
gaseous core reactor U plasma radiative temp. calc. 79−9807
genesis and exploration, USA 79−84267
geochemical cycle 79−84275
geochemical prospecting methods 80−72635
geological exploration, LANDSAT data merged with geol. and geophysics data 80−56651
geological exploration by Rn mapping, exclusion of ^{220}Rn signal 80−61916
geological samples, f/α particle track anal. for U, Th and isotropic disequilibria 78−7799
geological samples, rapid determ. using X-ray fluorescence anal. methods 79−88479
geophysical exploration, via Rn long-distance migration in Earth, subterrestrial fluid convection hypothesis 77−37246
geophysical prospecting, ^{222}Rn mapping using mat to avoid hole drilling 80−82087
geophysical prospecting, use of alpha sensitive plastic films 79−39980
geophysical prospecting by γ-ray logging of borehole, factors affecting resolution 80−98463
gravimetric titration, automated, determ. of U in safeguard materials 80−622
half-life determ., sample preparation 79−9936
heat capacity, from 80 to 1000K of high purity metallic sample 80−34201
heat of solution in aq. HCl acid 79−83495
heavy ion beam source, high charge and intensity beam prod. 79−12884
hollow cathode discharge, opto-galvanic spectroscopy-electron temp., isotope ratio analysis 79−77437
hollow cathode tube, inert gas buffered U, time resolved optogalvanic effect 79−37564
HTGR, economies in U reserve use 77−42175
HTGR fuel, French, fabrication, irrad. performance *(French)* 79−30934
HTGR fuel, recovery by graphite fuel element and C fluidised bed combustion 78−13314
HTR fuel cycle program in the Federal Republic of Germany 80−644
HTR fuel of low/medium enrichment 80−645
Hugoniot data, ultrahigh press. (TPa) shockwave from underground nuclear explosion 80−59580
hybrid fusion reactor, Tokamak type, with fissioning matter, blanket parameters 77−34446
hydrochemical prospecting, APDC coprecipitation and X-ray spectrometry for trace element determ. 77−37445
hypercompression by profiled explosion method 78−50296
in situ leach mining, environmental considerations rel. to water quality 80−3543
in-resonator spectroscopy via isotope filtration of dye laser radiation *(Russian)* 77−54752
induced magnetisation density 78−47952
interband, collective and atomic (p,d) excitations, Z-160 eV, fast EELS 80−93443
international resources assessment 80−99215
ion, electron cyclotron resonance source *(French)* 78−29680
ion beam prod. at 50 keV by charge exchange in gas and metal vapour targets 78−70675
ion impact on C foil, energy loss 78−55902
ion source using surface ionisation process 80−68999
ionisation potentials, 2nd-6th, thermochemical calcs. 79−98248
ions, electronic props., Dirac-Fock studies 78−60094
irradiation growth during fission fragment and proton bombard. 80−92568
isotope enrichment, laser methods for nuclear fuel reprocessing 77−38378
isotope enrichment for fission reactors 77−67851
isotope enrichment in CVD system 77−23301
isotope separation, ^{237}U from ^{241}Pu 79−71980
isotope separation, chemical and ion exchange unit 77−34474

uranium continued
isotope separation, chemical treatment of irrad. targets *(French)* 77−26883
isotope separation, gas centrifuge 79−3227
isotope separation, new processes 79−31128
isotope separation, porous barrier fabrication, powder metallurgy problems *(Italian)* 78−88439
isotope separation, separative performance transients in a gas centrifuge 79−67957
isotope separation, throughput limit in mass spectrographs 79−21850
isotope separation and ratios, neutron irrad. of natural U in Japan Material Testing Reactor *(Japanese)* 80−52730
isotope separation appl. to nucl. fuel cycle, teaching module 80−36805
isotope separation by Redox chromatography 80−37565
isotope separation by selective laser photoexcitation in reactive two-phase flow 79−94109
isotope separation in centrifuge, pressure recovery at high Mach number rotation 79−22480
isotope separation in countercurrent vortex tube, energy consumption *(German)* 79−27099
isotope separation in Fe^{3+}(III) water-glycerine solution-U(IV) cationic resin 79−41025
isotope separation processes, w.r.t. economics, reliability and safety *(French)* 80−806
isotope separation using gas centrifuge 79−49815
isotope separation using ion exchange chromatography, U(IV)-U(VI) exchange isotope effects 79−36376
isotope separation with rot. plasma 79−13842
isotopes, in soil, determination using alpha-spectrometry 80−45601
isotopic analysis by resin-bead mass spectrometry for materials safeguards 80−78392
isotopic composition, determ. using precise absolute gamma spectroscopic meas. 80−66916
isotopic composition, determ. using thermal ionisation spectrometry with automatic data eval. 80−66913
isotopic compostion, determ. using thermal ionisation mass spectrometry 80−66914
isotopic depletion curves at Oklo natural fission reactor *(French)* 80−21759
isotopic evidence for U exchange during low-temp. alteration of oceanic basalt 79−29744
labile component, on marine sediment particle surfaces, surface layer thickness meas. 78−40592
laser enrichment, implications for nucl. weapons proliferation 77−67849
laser enrichment plant, optimum operating conditions 79−54578
laser induced fluoresc. spectroscopy, using induction heated oven 78−21230
laser isotope separation, atomic spectroscopy requirements 78−33638
laser isotope separation 77−38418
laser isotope separation techniques and efficiency 79−31721
laser using U in organic soln., nuclear pumping 78−5470
leaching, design criteria for criticality safety of dissolution vessel 80−13772
liquid, electronic density of states, shock vaporization technique 80−29300
liquid, enthalpy and heat capacity meas. using neutron heating 77−20078
liquid, hard-sphere model, phys. prop. meas. interpret., adjacent solid phase implications 77−19866
logging by prompt fission neutrons, effect of neutron-absorbing rock anal. 77−64477
losses, at eluting agent interface in anion exchange chromatography, prevention 78−48706
lunar drill sample, neutron activation and radiochemical anal. *(German)* 80−51673
lung-stored U, meas. using NaI and solid-state detectors 78−28090
LWR fuel, partial partitioning of U and Pu by coprocessing solvent extraction 79−36382
LWR fuel appl., properties 78−8911
LWR fuel utilisation improvement 79−59160
LWR fuel-cladding gap, Cs-U-Zr-H-I-O system, chemical thermodynamics 78−82440
M shell prod cross section of Au, Pb and U for 75 to 150 keV p and e excitation 79−47552
management information system, at BWR fuel fabrication plant 79−85750
in marine basalts, conc. and distrib. rel. to oceanic U sink 77−81886
marine rocks, content distrib. and meas. by neutron induced fission track method 79−79809
martensitic behaviour at low temp., variations, α-phase 78−41818
martensitic behaviour of α-phase 79−29058
martensitic behaviour of α-phase 79−29059
mass analysis for accountability in nucl. fuel processing 79−16112
mechanical properties of α-phase crysts., very high strain rates, double-notch shear test use 80−85131
melting crucible, use of Y_2O_3 coated graphite 77−32712
metal oxide:U^{6+}, luminesc. sensitivity to vibrational fine structure 78−6772
metal oxides, mixed, luminesc., of U^{6+} 79−33765
metamorphism, higher grade, behaviour of U 79−84274
microdistribution in stony meteorites 79−75162
migration, and trapping of D in U and UO_2 during D^+ implantation 80−34243
mill radiological effluent and environmental monitoring guidelines 78−94153
mill tailings, attenuation of Rn flux by consolidation 79−66563
mill tailings, meas. of surface Rn flux, effect of moisture content 78−5056
mill tailings pile, health effect estimations 77−40800
milling waste management in USA 79−31077
mineral analysis using alpha particle absorption by cellulose nitrate *(Spanish)* 77−70358
mineral deposit, Saima alkaline massif, NE China 79−16470
mineral deposits, Canadian Uranium Reconnaissance Program 77−37439
mineral deposits, in situ assay logging system using delayed fission neutrons 77−37440
mineral deposits, organization in Mouana, Gabon district *(French)* 80−21741
mineralisation rel. granite magmatism, British Isles 79−84273
mineralization of Witwatersrand and Dominion Reef systems 77−86890
minerals, fissile nuclide concentration ratios *(Spanish)* 77−33067

uranium continued
minerals, isotopic composition due to terrestrial neutron flux *(Spanish)* 77−5195
minerals, quantitative microprobe anal. 78−61126
minerals, radiogenic Pb migration in hydrothermal metamorphism 77−56627
minerals, redistribution and mobility during metamorphism of volcanogenic formations 77−64283
miners, chromosome aberrations as biological dose-response indicator 80−17019
miners, lung cancer rel. to radiation exposure time distrib. 79−79605
miners Rn daughter inhalation and pulmonary cancer incidence 78−96080
mining, CEA and Cogema activities *(French)* 80−626
mining, manufacture and purification processes, safety and waste disposal *(Spanish)* 79−63785
mining, processing and transportation, in Western US, impact 80−45621
mining, radioactive mining waste disposal *(Dutch)* 80−21418
mining, surface, assoc. radiation exposures 77−64140
mining and milling, effects on ground water in Grants Mineral Belt, New Mexico 77−56657
mining and milling radioactive waste management N.Australia 79−31076
mining in Canada, health hazards associated with Rn daughter inhalation 79−88140
minor isotope concentration meas. for safeguarding U enrichment cascade 80−63283
mode softening and lattice instability under press. 77−51833
modern prospecting techniques evaluation, Athabaska sandstone deposits 79−26537
molybdates, alkaline earth, U activated, scheelite struct. luminesc. props. vibr. modes and quenching temp. 80−60651
monitoring in gaseous CO_2 coolant by gamma spectrometry 79−89374
National Uranium Resource Evaluation (NURE) programme, aerial radiometric survey data interpretation via principal components anal. 80−101438
natural, absorbed dose rate rel. to depth in tissue 79−88194
natural, induced to spontaneous fission ratio, B and Li effects 79−45305
natural fission reactors, parametric study of criticality conditions *(French)* 80−21768
natural fission reactors, requirements for formation, search for new examples 80−21772
natural resource survey, NURAB system for processing neutron activated samples 79−11847
natural resources, aerial radiometric data anal. using line-intensity estimation code MAZAS 79−62627
natural U fuel with improved performance, CANDU experience 79−71894
neutron activation anal. for U ore assay in situ 79−34989
neutron activation delayed analysis, U content in Hueco and Guadalupe Mountain Indian ceramics 80−85230
neutron criticality, solid angle computations using computer code 80−13726
neutron spectra in fast neutron systems using ^{6}Li sandwich counter 80−27884
neutron yield calcs., electron beam incidence 78−95622
nondestructive assay of leached Zr-hulls in reprocessing plant 79−81070
nondestructive assay of mixed samples using neutron activation anal. 80−18423
nondestructive assay reference materials 79−49702
nondestructive assay using continuous fast-neutron source 79−52849
nondestructive element and isotope assay 80−71870
nondestructive measurement of U and Th conc. and quantities using XFA and gamma spectrometry 80−71877
nuclear fuel, burn-up, chemical separation, ion exchange 80−42746
nuclear fuel, impact of fusion-fission hybrid reactors on world demand 80−95404
nuclear fuel, power distrib. comparison of U and Pu in KWO PWR core 77−14224
nuclear fuel, thermal near-breeder reactor, effect on future U utilization 78−17322
nuclear fuel, world resources, technological status 77−67911
nuclear fuel conversion plant, nondestructive assay 80−66761
nuclear fuel cycle, demand and supply estimates, U supply 79−26694
nuclear fuel decontamination, sorption and distillation methods, review *(Czech)* 78−82496
nuclear fuel particle prep. by ion exchange resin loading *(German)* 78−82499
nuclear fuel reprocessing, displacement re-extraction, math. simulation 77−61586
nuclear fuel reprocessing, re-extraction with weak acid, math. simulation 77−61587
nuclear fuel standard materials, analytic chemistry of trace impurities, and standard sample preparation 79−26521
nuclear fuels, elemental and isotopic conc. anal. using nondestructive assay 79−49691
nuclear reactors, initial fissile U requirements for fuel cycle, computer simulation 78−17320
nuclear reactors in use in West, important types, effects on reserves *(German)* 78−74463
oceanic crust abundance, heat flow implications, basalt fission track anal. 80−8287
oceanic lithosphere, distribution and evolution 79−84226
oceanic rocks of DSDP Leg 37, U concs. 77−91075
Oklo fossil nuclear reactors, ion analysis exam. of U grains and gangue *(French)* 80−21758
Oklo natural fission reactor, computer calc. of neutron balance and flux distrib. *(French)* 80−21767
Oklo natural fission reactor, dating from U-Pb isotopic data 80−21763
Oklo natural fission reactor, eval. of neutron temp. from ^{176}Lu/^{175}Lu and ^{156}Gd/^{155}Gd isotopic ratios *(French)* 80−21766
Oklo natural fission reactor, isotopic anal. of rare earth metals *(French)* 80−21761
Oklo natural fission reactor, radioactive dating from Pb and Th meas. *(French)* 80−21762
Oklo natural fission reactor, Ru isotopic anal. *(French)* 80−21765
Oklo natural fission reactors, formation, propagation and control, review *(French)* 80−21774
Oklo natural fission reactors, geology, review *(French)* 80−21770
Oklo natural fission reactors, geophysical eval. of U distrib., topography, sedimentology and structure *(French)* 80−21755

uranium continued
Oklo natural fission reactors, migration in core sample, appl. to dating of reactions *(French)* 80−21760
Oklo natural fission reactors, migration paths for radioactive products 80−21773
Oklo natural fission reactors, review of French geological research *(French)* 80−21744
Oklo natural fission reactors, U radiometric meas. and isotopic anal. *(French)* 80−21754
Oklo natural fission reactors geological environment, tectonic anal., petrography, geochemistry *(French)* 80−21742
Oklo natural reactors, control and propag. of nuclear reactions, thermal effects *(French)* 80−21769
Oklo natural reactors, data on stability and remobilisation, summary *(French)* 80−21771
Oklo natural reactors, mining, geology and tectonics *(French)* 80−21743
Oklo natural reactors, review of mineralogical and petrographic studies at Strasbourg *(French)* 80−21745
optical absorption meas. 0.15 to 2.0 eV, polycryst. α-U 80−108223
ore, in situ mining, Wyoming State regulations and environmental monitoring 79−88510
ore, radioisotopic X-ray anal. by K-shell fluorescence 79−79353
ore, Ru isotopic anal. 80−21764
ore, solution mining, appl. of solution flow prediction computer models 79−88013
ore, solution mining, environmental impact, groundwater restoration 79−88012
ore, solution mining, in situ leach method 79−87983
ore, solution mining facilities, operational and environmental aspects 79−87984
ore, U content determ., radioisotopic X-ray technique using Compton scatt. 77−70357
ore, Witwatersrand Basin, fluid inclusion study 77−86891
ore assaying by delayed fission neutron process 79−53536
ore at Oklo, appl. of Ep-pH diagrams to problems of retention and migration of fissiogenic elements 80−21757
ore bodies ground level radiometric surveys, overburden effects correction techniques 79−88485
ore body rel. to excess ^{4}He in Teggau Lake, NW.Ontario 78−65353
ore dating from meas. of ^{238}U and Ru conc. 80−21863
ore deposit, H_2 as reducing agent 78−36169
ore deposits, fossil nuclear reactors, review 77−60377
ore deposits, review of methods of prospecting *(German, English)* 77−21925
ore deposits, sulphide-free, unusual mineral assocs. in oxidation zone 77−25682
ore deposits in collapse calderas, structural-geological features 77−25681
ore detection, Rn gas concentration meas. using alpha sensitive plastic detectors 80−94617
ore detection using integrated meas. of long-distance transport of ^{220}Rn 80−98476
ore exploration, Rn gas conc. meas. using alpha sensitive plastic films 80−94618
ore grade direct determ. by photoneutron assay method 79−53570
ore processing by filtration-free sorption method 79−26664
ore processing using nonfiltration sorption method *(Russian)* 79−31110
ore systems, morphogenetic grouping 78−81158
ore treatment plants and techniques *(French)* 79−26699
ore zone logging, corrections for prompt fission neutron data 79−88353
ores, $^{13}C/^{12}C$ isotope fractionation of assoc. organic matter induced by alpha irradiation 79−57932
ores, effective γ-ray attenuation coeffs. 77−25680
ores, estimation of ratio of induced to spontaneous fission 78−53234
ores, lower grade, cost saving techniques 77−34418
ores treatment, in France and African countries *(French)* 80−805
oxidation in air and CO_2, Al content effect 77−50236
oxide:U^{6+}, struct. sensitivity of luminesc. 77−90187
particle etch track technique determ. of U trace content in normal human blood 80−89910
particulate biogeochemistry of coastal zone 79−29787
personnel monitoring, 16 yrs. experience 79−76149
phosphate fertilizer, specific activity of U and Th rel. to particle size 80−106244
phosphates, U content, α-ray autoradiography, fluorimetry, estimation 78−20414
phosphorite nodules on sea floor off Peru and Chile, U isotopes 78−7612
photoelectric cross-section at K-edge measurements 78−2983
photoelectric interaction around the K edge 78−5183
photoelectron spectra study, core and valence levels 80−66394
photoionisation, isotope separation and enrichment by Ar ion laser *(Japanese)* 79−81192
photoneutron yields released by incident electrons, improved calc. 80−27630
PIXE elemental anal. at $\mu g\ g^{-1}$ levels in ore samples 80−55758
plasma, fission fragment effect on electron energy distrib., radiative transport 77−24062
plasma, high temp., opacity calcs. 78−79414
plasma, opacity and radiative energy current calc., 5000-8000K 78−83535
plasma, present research status with appl. to gaseous core reactors 78−33244
plasma, Saha's ionisation eqn. soln., input for opacity calcs. 77−39412
plate-type research and test reactors, near-term reduced enrichment conversions 80−22951
poor ore radiometric enrichment, plant flow scheme *(Russian)* 79−26700
powder, hydriding kinetics, 13.3 and 26.6 kPa, 50-250°C 80−16725
power reactor enrichment calcs. and fuel requirements, basic information 77−74959
power reactor fuel cycles, Pu, Th and U evaluation 79−26706
power station ashes, Th, U, and K conc. meas., dose rates in Poland 79−100754
production by U_xS_y irrad. in reactor, chem. separation, yield 77−63986
production from low grade Swedish shale 79−31111
production in New Mexico, constraints 80−42843
prospecting, ^{222}Rn and ^{210}Pb meas. 79−53573
prospecting, airborne radiometric meas., ground conc. estimation 79−53575
prospecting, appl. of barrier technique for Rn isotope separation 78−21770
uranium continued
prospecting, influence of disequilib. and ^{222}Rn emanation factor variability 79−62498
prospecting, intrinsic Ge detector for use in borehole sonde 77−9547
prospecting, pattern recognition appl. 77−66999
prospecting, quantitative determs. from gamma-rays logs, digital time series analysis 79−48580
prospecting, use of Ge(Li) and intrinsic Ge detectors in borehole sondes 77−37442
prospecting at exploratory borehole, spatial depend. of delayed-neutron signals 78−7817
prospecting by active neutron logging, evaluation models 80−98480
prospecting for U deposits, use of ^{222}Rn content of air *(Spanish)* 77−78303
prospecting method, using Ra accumulation in animal thyroid glands, anal. 78−27853
prospecting of sandstone-type ores, charged particle track analysis 80−91405
pulsed-neutron U logging, probing distance determ. 77−64476
Purex kinetics, U extraction with tributylphosphate *(German)* 80−57937
Purex process, concs. of U, Pu, HNO_3, fission products, in LMOM2 extractor, expt., graphical determ. 78−41843
Purex solvent extraction process for fuel recovery and recycling 79−36387
PWR, physics of U-Pu fuel cycle 77−50278
PWR, U-Pu, mixed oxide fuel, physical props. 77−67814
radioactivation analysis, of biological and geological materials, separation methods *(French)* 77−90700
radioactive dating, open system model appl. 79−29874
radioactive waste reprocessing for U extraction, methods and risks *(German)* 77−42157
radioactivity of thermal and mineral springs in Slovenia 80−7963
radiometric determ. of U contents, using liquid scintillation spectrometers *(Czech)* 78−69487
rare metal ores, quantitative relns. between Ta, U, Th and Zr 77−56629
reactivity enhancement in transportation and storage arrays from density reductions 77−57756
reactivity with Y_2O_3, exam. by thermal anal. 78−85154
reactor fuel, correlation of U and Pu isotope compositions with burn-up 79−63746
reactor fuel, determination of microamounts of Pu for burnup estimation *(Czech)* 77−6521
reactor fuel, selected enrichments for minimisation of blending losses, optimal set 78−17402
reactor fuel enrichment, random-walk model of holdup time of gas mols. in separation process 79−22481
reactor fuel enrichment by chemical exchange process *(Japanese)* 79−26661
reactor fuel processing plant development in Spain review *(Spanish)* 79−59231
reactor fuel supply, exploration and production capacities, review 79−22388
recovery from manufacture of phosphatic fertilisers 78−17398
recovery in slags containing calcium and magnesium *(Spanish)* 78−8955
redox titrimetry for accurate determ. of 5 to 25 mg 79−87932
removal from P_2O_5 in Spain, pilot plants *(Spanish)* 79−30927
reprocessing and supplies in 1980s, trends 78−720
resource conservation using pebble bed prebreeder reactor 79−49697
resource exploration and assessment technology survey 79−53564
resource potential, geochemical surveys of large areas in USA and Alaska 79−30924
resource research using Pennsylvania State Univ. reactor 79−12159
resource utilisation and antiproliferation reactor concept 79−9735
resources, consumption and 30 year fuel commitments for Canada and the world, 1975-2025 78−82456
resources, optimisation of LWR and FBR power prod. strategy 80−99253
resources and accessibility, reliability of nuclear fuel supply 80−99216
resources and prospecting techniques and equipment development in India 79−30923
rivers, evidence for higher natural U content 79−44208
rock samples, meas. by track registration in plastic detectors 78−73533
rocks, isotope disequilibrium, due to α-recoil and soln. effects 80−98314
rocks, U-bearing, radioactive disequilib. determ., isotopes relative abundance meas. 78−57330
rolling texture formation, computer simulation in HCP and orthorhombic metals 80−3095
safeguarding, 5 to 20 mg determ. by constant current coulometric titration 80−78381
safeguarding, determ. of trace amounts by pulsed laser fluorometry 80−78382
safeguarding, determ. of U and Pu content of fuels using isotope correl. tech. 80−68834
safeguarding using resin bead mass spectroscopy 80−73984
safeguards, computerised nondestructive assay for materials management 80−78388
safeguards accountability, NDA of crated waste by gamma-ray and neutron coincidence counting 80−83166
sand grains containing high ^{238}U and ^{232}Th concentrations, enhanced natural radiation exposure *(German)* 80−51018
N.Scotland, regional geochemistry rel. to U deposit formation 79−84269
seawater, conc. and $^{234}U/^{238}U$ activity ratios in open ocean 78−36197
seawater, U in sea foams and adhered to sea sands *(Japanese)* 79−29785
second Hugoniot relationship 77−35659
sedimentary distrib. rel. to O_2 in Precambrian atmosphere 77−5272
sedimentary rocks, Th and U abundances rel. to crustal evolution and sedimentary recycling 80−85654
separation, by column extraction chromatography 78−44421
separation from spent Th nuclear fuel elements, avoidance of third phase *(German)* 79−6756
separation from urine, meas. by fluorometry 79−57788
SIMS quantitative analysis 77−73498
soil, U and Ac series nuclides radioactive disequilibrium 80−4014
solar nebula, Th, U, Pu and Cm condensation and fractionation 79−35154
solenoid, partially disintegrated superhigh field, for fusion reactor *(Russian)* 77−7584
solubility in the Oklo reactor 80−21756

uranium continued
solubility of O_2, and composition of lower phase boundary of UO_2 at 1950K 80−49366
solubility of Y at 1700K 77−89545
solutions, conc. changes, proton induced X-ray emission obs. 77−25325
solvent extraction kinetics 79−26685
spall, one dimensional 77−80579
specific heat, Debye temp. for α-U 80−15258
specific heat anomalies at low temp., polycryst. α-phase sample 77−35708
spectrochemical analysis, U concentration in fuel reprocessing streams, determ using acid-compensated dual-wavelength tech. 80−78430
spent reactor fuel, burnup determ., isotopic comp. and conc. determ. by mass-spectrometric isotope dilution 79−89373
spent reactor fuel burnup determ. using anal. chem. [conf. Piestany, Czechoslovakia (Sept. 1978)] 79−89371
sphere, enriched, water-reflected, critical measurements 79−26569
spraypainting of deposits for nuclear measurements 80−18736
sputtered atom angular distrib., mass effects in Mg plasma 79−87538
sputtered atoms, laser fluorescence spectroscopy 80−66359
sputtering yield meas. by fission track technique 78−39646
sputtering yield meas. by obs. of fission tracks in mica 77−88340
St. Severin chondrite, U and Pu distrib. 80−72889
stain artefacts in electron microscopy, technique for minimizing occurrence 79−84040
superconductivity, phonon-softening 78−10592
superstructure of α-phase, neutron scatt. obs. near 43K 79−95116
supplies, United States industry and restrictive measures 78−686
supply, Canada's role 78−86627
supply and demand for reactor fuel, industrial and commercial considerations 79−26535
supply situation in the Federal Republic of Germany 79−30916
supply study in Western world *(German)* 78−8960
surface, mol. beam bombardment, aggregate form. *(French)* 79−74047
surface structure, $He^+(Ne^+)(Ar^+)$ impact, appl. of double pass cylindrical mirror analyser 78−72658
N.Sweden, evolution of U province 79−84271
symbiotic energy system, U fuelled, economic anal. using SYMECON code 80−106172
symbiotic system, managing fusion burn, economic analysis 80−106173
tailings management, economic impact on nuclear fuel cycle 80−18494
target, microwave laser irrad., plasma form., inhibited electron thermal cond., laser intensity threshold Z-depend. 80−48928
thermal expansion coeff. and cones of zero expansion in α-phase single crystal 78−34635
thermal properties, anomalous behaviour at low temp. 77−28018
thermionic spacecraft reactors with ^{233}U as fuel, reflector drums as control mechanism 80−47686
trace determination of U impurity in Si, by fission track method 79−79354
tungstates, alkaline earth, U activated, scheelite struct. luminesc. props. vibr. modes and quenching temp. 80−60651
tungstates, U-doped, perovskite struct., luminesc. quenching, QMSCC calcs. 80−71470
urine analysis by delayed neutrons 80−26331
vacancy formation and phase transformations by positron annihilation 80−49215
valence and 5f states, XPS and bremsstrahlung isochromat spectroscopy 80−66393
vapour prod. by sputtering, Ne, Ar, Kr, carrier agents, density meas. *(French)* 78−86967
vapour production using pulsed hollow cathode lamp *(French)* 79−82107
Venus surface rock, radioactive element concs., Venera 9 and 10 meas. 77−78691
Vitro Mill Tailings at Salt Lake City, Utah, remedial action 77−46315
VVER reactors, relative accumulation of ^{232}U and ^{233}U during ^{232}Th irrad. 79−71923
in water samples, conc. determ. by fission track registration technique 80−12565
well logging, gamma-ray spectra calc. using discrete ordinates transport code 79−53572
world resources, effect on development of nuclear power 80−55826
X-ray fluorescence isotopic anal., apparatus construction and testing *(Czech)* 77−50244
α-particle detectors, two layer proportional counter for measuring U content in solid-waste mats. *(Russian)* 80−27904
$\mu^-{}^{238}U$ atom, shape isomeric γ-decay 77−34245
$Al_2TeO_6:U^{6+}$, luminesc. spectrum 79−56845
Au-U conglomerates, Witwatersrand type, significance of diagenesis for origin 79−84265
α disintegration, liquid scintillation counting 80−27873
BaF_2:U, absorption band spectra following neutron irrad. 80−29763
BaF_2:U, neutron irrad., absorpt. band attributed to F_2- centres 80−7380
$BaF_2:U^{3+}$, single crystal, superhyperfine interaction of tetragonal centres 79−42834
CaF_2:U, charge conversion of U^{3+}, ESR spectra 80−7150
CaF_2:U, electron irrad. defect aggregates, ordering, impurity effects 80−75216
CaF_2:U, electron microscopy study of lattice deformation due to electron irrad. 79−65077
CaF_2:U, U^{5+} centres, nonoctahedral symmetry 80−11266
CaF_2:U single crystal, Czochralski-Kyropoulos grown, U ion localization 79−91580
$CaF_2:U^{3+}$, anomalous magnetooptic props., optical detection of ESR and cross-relax. resonances 80−93287
$CaF_2:U^{3+}$, cryst. field splittings, ab initio MO calcs. 77−20520
$CaF_2:U^{3+}$, cubic site substituent, EPR spectra obs. 78−72392
$CaF_2:U^{3+}$, Na^+, EPR, orthorhombic U^{3+} centre 77−77100
$CaF_2:U^{4+}$, EPR hyperfine struct. 80−15781
$CaF_2:U^{5+}$, charge compensation, struct. 79−15124
$CaF_2:U^{5+}$, rhombic centre EPR spectrum, heat treatment effects 78−72407
$CaF_2:U^{5+}$, single cryst., EPR 78−19325
$CaF_2:U^{5+}$, trigonal centres, hyperfine parameters, EPR 78−43643
$CaF_2:U^{5+}$, trigonal EPR spectrum 78−15021
^{252}Cf neutron assay system for nondestructive assay of enriched U 79−81067
$CsCl-BaCl_2:U^{3+}$, melt, diffusion coeffs. and mechanisms 79−73330
H isotope removal from flowing Ar, U and Ce as hydriding materials 78−17438

uranium continued
$H^+ + U(Ni)(Au)(Sn)$, 4.88 GeV, K-vacancy production cross sections 77−19036
$HfSiO_4:U^{4+}(U^{5+})$, opt. spectra 78−88334
KF:U, X- and γ-irrad., EPR of U^{5+} centre charge compensation mechanism 77−90030
$KF:U^{5+}$ EPR of U^{5+} centre meas. 77−20684
$KPO_3.Al(PO_3)_3$:U, vibronic excitation, absorption and emission spectra 78−52524
LMFBR, U-Pu-Zr fuelled breeding potential assessment 79−9685
LMRBF, ^{233}U-Th fuelled pin diameter optimisation 79−9687
$LaBr_3:U^{3+}$, luminesc., fluoresc. lifetimes 79−33768
$LaCl_2:U^{3+}(5f^3)$, polarised absorption spectra and energy levels 80−16063
$LaCl_3:U^{3+}$, cryst., spectrum anal., cryst. field parameters 80−76057
LiF:U, Mn, EPR of Mn^{4+} centre, g-values and hyperfine struct. 77−12192
LiF:U, X- and γ-irrad., EPR of U^{5+} centre, charge compensation mechanism 77−90030
LiF:U, X-ray and γ-ray irrad., EPR of U^{5+} centres 79−91295
$LiF:U_3O_8$, X- and γ-irrad., U^{5+} luminesc. molecular centres, optical and ESR expts. 77−48224
$LiF:U^{5+}$, absorption and laser-excited fluoresc. 79−99927
$LiPO_3.Al(PO_3)_3$:U, vibronic excitation, absorption and emission spectra 78−52524
$Li_3WO_4:U^{6+}$, luminescence meas. 77−32432
$Li_4WO_5:U^{6+}$, vib. fine struct. in luminesc. spectra 77−8620
NaF:U, luminesc. spectra, Vibr. struct. 80−80840
NaF:U, single crystals, luminescence and electrical conductivity 78−72588
NaF:U, X- and γ-irrad., EPR of U^{5+} centre, charge compensation mechanism 77−90030
$NaF:U^{5+}$, U isotope abundance determ. by EPR hyperfine struct. 79−91296
$NaF:U^{6+}$ luminesc. spectrum, obtained using chronospectroscopic method and phase spectra 79−54199
$NaPO_3.Al(PO_3)_3$:U, vibronic excitation, absorption and emission spectra 78−52524
natural, isotope separation from ^{234}Th by extraction column chromatography using TnOA and filter paper 79−43659
Pb/U in two-billion-year granulites in Late Precambrian metamorphic basement along S.Peruvian coast 78−28204
in $PbWO_4$, incorporation during growth, effective distrib. ratios, luminesc. characts. 79−42094
Se:U, cryst. and amorphous, impurity conc. and distrib., solid state nuclear track detection 79−46694
Th, absorption coefficients, near O_{IV} O_V thresholds, 5d cross sections calc. 78−90134
Th-^{233}U fuel cycle, in molten-salt reactor, efficient fuel utilization without Pu separation 79−26499
$ThBr_4:U^{4+}$, absorpt. spectrum, zero phonon line *(French)* 80−11443
$ThBr_4:U^{4+}$, IR luminesc., zero phonon lines 79−33769
$ThBr_4:U^{4+}$, single cryst., absorpt. and emission spectra 77−90174
$ThO_2:U^{4+}$, paramag. acoustic reson. absorpt. in cubic field 77−20680
$ThO_2:U^{4+}$, spin-lattice relax. time calc., nearest neighbour point charge model 77−16146
ThO_2-^{233}U exponential expts. anal., cross section library sets, resonance integral correls. 77−23215
$ThSiO_4:U^{4+}(U^{5+})$, opt. spectra 78−88334
U (VI) extraction from sea water, by adsorption on gel particles containing $Ti(OH)_4$ *(Japanese)* 77−54347
U blanket management, effects of power and irradiation behaviour 78−86595
α-U, CDW at 43K 80−80198
U exploration in Egypt, exploration under arid conditions 79−26538
U fuel, burnup determ., using ^{148}Nd 78−82459
U fuel, reprocessing of highly active fast reactor fuel 79−26666
U I, 5027 Å line, ^{235}U odd-even staggering coeff. 77−30828
U I, electronic configs., HF relativistic calc., spin-orbit const.-Slater integral relation 77−18793
U I, hyperfine struct. meas. of high-lying levels 79−54796
U I, isotope and relative isotope shifts for ^{234}U, ^{236}U and ^{238}U 77−30823
U I, laser spectroscopy, using stepwise excitation and fluoresc. detect. 79−54802
U I, relative branching ratios for excited level decay 77−57922
U I, relative isotope shifts, specific mass shifts 78−90122
U I, visible spectrum, ^{238}U-^{235}U isotope shift 79−788
U II, oscillator strengths for calibration 77−42280
U III, IV, line identification on relative intensity basis 80−95561
U III, in hexamethyl phosphoric triamide soln., absorption spectrum, intensities, oscill. strengths 78−74599
U ion, range calc., number of primary atoms created in diatomic target *(French)* 79−1473
α-U, mech. behaviour, strain rate influence, 300 to 550°C 79−38907
U, Mo and V, complex recovery from sedimentary ores 79−26701
U ore detection, using trace detection sensitive to ^{222}Rn α-particles *(Hungarian)* 78−77339
α-U, orthorhombic, computer simulation of rolling texture formation 80−3095
α-U, pseudo-single cryst. and polycryst., low temp. sp. ht. 78−83972
U requirements for advanced fuel cycles in nuclear power systems 79−18027
U series nuclide conc. in soil particles rel. to their size 77−33073
U, specific α radioactivity meas. rel. to size using aerosol centrifuge 79−76255
α-U, spin density determ. by polarised slow neutron scatt. 77−28375
α-U, strain rate effect on flow and fracture 80−100887
α-U, strain rate effect on tensile flow and fracture 80−84992
U, two-dimensional expt. fracture map 78−95803
U^+, 70 GeV beam, propag. through fusion target chamber, stability 78−26303
U^+, atomic model 79−41095
U^{3+}, screening factors *(French)* 78−72119
U^{4+}, cryst. field effects and screening factors *(French)* 78−72119
U^{4+} electron configuration from nuclear information 80−58146
^{92}U, self-consistent relativistic density-functional theory 80−91441
U^{n+} (n=0 to 6), electronic struct., multiconfig. Dirac-Fock calcs. 79−45646
U/(Zr-Cu-Mo alloy) welded joints, mech. characts. determ. 20 to 750°C 79−29113

uranium continued
U/Pu separation, use of carboxylic acids 77−38377
U/Te thin film junctions, combined electron, proton and X-ray beam obs. 77−85041
U/Ti welded joints, mech. charact. determ. 20 to 750°C 79−29113
U-^{238}Pu-^{237}Np GCRF fuel cycle to produce isotopically denatured Pu for LWR 80−78427
U-graphite subcritical assembly, resonance escape probability meas. 77−71632
U-He plasma, radiation-induced, electron energy distrib. 77−24054
U-light water slab, meas. of space depend. ang. thermal neutron spectra 77−14208
U-Pu, isotope separation in HNO_3 by exchange resins 78−74782
U-Pu radial redistrib., effect of fuel rod parameters and fuel porosity *(German)* 79−49799
U-SbO_3 catalyst, dynamic measurements of electrical conductivity during adsorption and catalysis 80−13096
U-UH_3 powder, appl. in Lyman alpha radiation source 78−13775
U-ZrH system, neutron spectrum in critical pile 79−45322
U+F surface reactions, UF_6^- form. 77−73465
U+H_2, surface reaction, temp. depend. 79−91996
U+H^+, L X-ray production cross sections, 0.3-1.8 MeV, expt. rel. to PWBA prediction 80−53115
U+H^+, L-shell ionis., 0.5-3.5 MeV, X-ray emission obs. 77−54528
U+H^+, relativistic K-shell ionisation cross-section meas. 78−33593
U+$H^+(D^+)$, L-subshell vacancy production, Coulomb deflection effects 80−9711
U+$H^+(He^+)$, 2-18 MeV, L-subshell ionis. cross section, projectile energy depend. 77−19031
U+Kr, momentum transfer cross-section, 0.1 eV 79−45783
U+Kr^{n+}, K-L level matching, X-ray obs. 79−63948
U+NO_2, UN reaction product identification in Ar matrix, vibr. energy distrib. 77−9066
U+O_2, assoc. ionisation, electron energy distrib. 78−35656
U+O_2, chemi-ionisation reaction involving laser excited atoms *(Japanese)* 79−13830
U+O_2, laser excited atoms, chemical reactions 77−90594
U+O_3, assoc. ionis. cross sections, in crossed beams, mass spectra obs. 78−94317
U+Pb, K-vacancy form., rot. coupling effect in quasimol. L-shell 78−25692
U+U, K-shell ionis., classical relativistic trajectory method appl., 1, 10 GeV/n 80−43129
U+U, superheavy quasimolecule, direct Coulomb formation of 1sσ vacancies 77−3450
U+X^+, X=O, N, N_2, CO_2, charge transfer cross-section, 1-500 eV 78−82835
U^++$N_2(D_2)(CD_4)$, endothermic reactions, heat of formation 77−73444
U^++$O_2(CO)(CO_2)(COS)(CS_2)(D_2O)$, reaction cross-sections, ion beam apparatus study 80−97691
U^++U, symmetric charge exchange, below 1 keV, cross sections calcs. 77−532
U^++U^+, critical two-centre distance, HFS relativistic calc. 79−22801
U^++$U(U^+)(U^{2+})$, elastic scatt. in plasma, interaction pots. and momentum transfer 80−38534
U^{36+}+N(Ne)(Ar)(Kr), radiative charge exchange, 16, 64, 256 MeV/amu 78−55234
U^{40+}+Ne, highly charged very slow Ne recoil ions, K X-ray transition 80−91649
UI, absorption line shape change, pulsed hollow cathode source *(French)* 80−47927
UI plasma, absolute emission coeff. 80−64693
UI, precision isotope shifts meas. in visible, near IR 80−63587
U(IV) photochem. prod. for use as reductant for Pu(IV) 79−36383
UV, energy levels and UV spectral anal. 80−106290
U(VI) extraction from sea water using hydrous metallic oxide binded with hydrophilic polymers *(Japanese)* 79−48102
U(VI) removal from rat body by DTPA, DTPP, EDDIP, decontamination efficiency 78−44617
UX_1, separation from U, using silica gel ion exchanger 78−86961
^{A}U, A=235, 238 cumulative fission yield meas. by neutron dosimetry techniques 79−41041
^{A}U, A=235,238, muonic atom lifetimes from muon induced fission 80−69269
^{230}U, production, tracer appls., α-spectra 77−61644
^{233}U and Pu fuels, relative occupational hazards 78−94101
^{233}U droplets burning in air, aerosol generation investig. rel. to inhalation hazards 79−67959
^{233}U, enhanced fuel prod. using Th-Li hybrid reactor blanket with UO_2 multipliers 80−13810
^{233}U, fissile fuel preparation by spallation of ^{232}Th *(Russian)* 79−22441
^{233}U, production by ^{232}Th cycle, review 79−45388
^{233}U, role and importance in extension of nuclear fuel resources 79−45325
^{233}U safeguards, expt. nondestructive assay using a random driver 80−83164
^{233}U, transuranic trace analysis using resonance ionisation spectroscopy of inert gases 80−93833
^{233}U-^{232}Th fuel cycle alternatives to LMFBR 79−9741
^{233}U-^{232}Th reactor as burner of actinide wastes 77−23235
^{233}U-^{235}U fuel, nondestructive isotopic meas. using fission neutron counting 80−32385
^{234}U excess, ageing effect in confined waters, comment 77−9449
^{234}U excess in groundwater, ageing effect in confined waters, comment 77−5252
^{234}U/^{235}U/^{238}U ratios in sediment from W. coast of India 77−41020
^{234}U/^{238}U ratio disequilibrium in natural samples, mechanisms involving recoiling alpha-emitting nuclei 79−16466
^{234}U/^{238}U/^{226}Ra ratios in fracture zone water of N.Kirgizia 77−33108
^{234}U→^{230}Th→^{226}Ra, superposition soln. of transport of decay chain through sorbing medium 80−37500
^{234}U→^{230}Th→^{226}Ra decay chain, hydrogeological migration anal. 80−37501
^{235}U, anal. by cyclic activation of delayed neutrons 78−53296
^{235}U burn-up determ. by mass spectrochemical anal. 80−71989
^{235}U, conc. in $UO_2(NO_3)_2$ aq. soln., pulsed NMR determination 80−2658
^{235}U content determination, from 0.186 MeV ^{235}U γ-ray intensity meas. 79−5240
^{235}U content in enriched samples, fission track registration technique, solid state detectors 77−56291

uranium continued
^{235}U, depleted fuel, reactivity worths of fixed neutron absorbers 78−21654
^{235}U, determ. of amount in urine by delayed-neutron counting 79−25118
^{235}U enrichment, separation nozzle process 79−31106
^{235}U enrichment, using double deflection separation nozzle *(German)* 77−46383
^{235}U enrichment, using laser based two-phase photoionisation and photodissociation methods *(Czech)* 77−61583
^{235}U enrichment analyzer based on interference spectroscopy, fabrication and performance *(Japanese)* 78−29625
^{235}U enrichment by laser isotope separation 77−19113
^{235}U enrichment by laser isotope separation process, cost anal. 77−42160
^{235}U enrichment by pulse gas diffusion 79−36380
^{235}U enrichment by separation nozzle systems with dynamic flow deflection 79−49825
^{235}U enrichment staggering of initial fuel charge of 770 MWe BWR *(German)* 77−61582
^{235}U fission product γ radiation for short irrad. times, energy distrib. 80−73929
^{235}U foil, sputtered, energy spectrum, fission track technique 78−68593
^{235}U, ground and 1st excited states, hfs, laser fluoresc. and laser-RF double reson. spectroscopy 80−58170
^{235}U, ground-state hyperfine structure high-precision meas. by laser-RF double reson. 79−26942
^{235}U, high precision meas. of hyperfine struct. of 620 cm^{-1} atomic level 79−45660
^{235}U, hyperfine struct. and isotope shift meas., laser separation by two-step photoionisation 78−78822
^{235}U, in aq. soln., assay by pulsed neutron interrogation 78−68966
^{235}U isotope separation, efficiency improvement by nuclear excitation by electron transition 78−55039
^{235}U isotope separation, laser photochemistry appl., LASL developments 79−31719
^{235}U isotope separation enhancement with RF hyperfine transitions 79−41249
^{235}U isotopic content determ. of nuclear materials using gamma spectrometry 79−85756
^{235}U, large scale enrichment using separation nozzle 79−94654
^{235}U, nondestructive active assay in $(U,Pu)O_2$ fuels 80−71873
^{235}U, nondestructive assay, appl. to decommissioning of fuel reprocessing facility 80−81269
^{235}U, nondestructive assay techniques for control and accountability 80−81270
^{235}U, nondestructive determ. of content in fuel elements using passive gamma ray spectrometry 80−18418
^{235}U, recovery from enrichment plant tailings by laser isotope separation 80−83212
^{235}U, resonance energy neutron radiography using dynamitron accelerator 79−52480
^{235}U, separation nozzle process for enrichment 78−21739
^{235}U to ^{238}U enrichment, ultracentrifuge, gas diffusion and nozzle separation techniques comparison, w.r.t economics 77−18680
^{235}U var. and natural abundance in ore bodies 77−41014
^{235}U/^{238}U isotope ratio determ. in UF_6 samples using gas quadrupole mass spectroscopy 80−78376
^{235}U/^{238}U ratio, non-destructive field meas. for geophysical prospecting 80−21862
^{235}U-^{239}Pu, initial conversion, fast fission, and relative fission product activity ratios 78−58347
^{235}U-fission track micromapping, exam. of U mobilisation processes in Precambrian sediments 80−98477
^{235}U-mica, solid state nuclear track detector, neutron response 80−27876
^{236}U in LWR spent fuel, recycling in enriching plant 77−18684
^{238}U, ^{235}U, decay consts. for use in geochronology and cosmochronology 78−28189
^{238}U ($^5L_6^0$) from hollow cathode lamp, laser absorpt. spectroscopy *(French)* 79−59402
^{238}U, conc. in Florida phosphate materials 80−30615
^{238}U concentration in ore, absolute determ. by gamma-ray spectroscopy 77−13133
^{238}U content determination, from 0.0925 MeV ^{234}Th doublet γ-ray intensity meas. 79−5240
^{238}U, determ. of time since arrival in matrix existing at time of discovery in Pakistan 79−34822
^{238}U enrichment by linear accelerator for LWR 79−13497
^{238}U enrichment by proton accelerator 79−13498
^{238}U I, lifetime, branching ratio and absolute transition probability of 6395.42 Å transition 79−3402
^{238}U I, transition probabilities meas. by time resolved optical pumping 77−46545
^{238}U in UO_2, Doppler effect in GCFR critical assemblies, 300-1100K 78−29574
^{238}U, isotope shifts and inherent quadrupole moments *(French)* 79−7032
^{238}U, neutron spectra for fusion + hybrid reactor materials 80−23142
^{238}U, radioactivity in Straits of Malacca marine environment 79−12135
^{238}U, single charged, numerical anal. of longitudinal motion of 9.5 GeV 79−54737
^{238}U, terrestrial beta radiation field in natural environment, numerical evaluation 78−81161
^{238}U vapour, hollow-cathode generator, energetic yield 80−47724
^{238}U/^{226}Ra dating of quaternary corals by γ-spectrometry 79−88221
^{238}U/^{232}Th comparative breeding potential in LMFBR blankets 80−22948
^{238}U/^{235}U in Allende meteorite rel. to early Solar System ^{247}Cm 80−90347
^{238}U/^{235}U in chondritic meteorites, search for isotopic anomalies 80−85903
$^{238}U^{n+}$+Z, Z=6 to 92, 3.6 to 5.9 MeV/amu K-vacancy prod. 79−31672
^{238}U+^{238}U (^{136}Xe), nuclear Coulomb excitation, inner shell ionisation and internal conversion, quasimol. formation 78−94026
$U(f^3ds^2)$+molecule, collisional relax. of $^5K_5^0$ and $^5L_7^0$ states, laser-induced fluoresc. obs. 80−52925
U(g)+nC(graphite)→UC_n(g) (n=1 to 6), enthalpy changes 80−7842
U(n,X), Japan Material Testing Reactor, U and Pu isolation and isotopic ratios *(Japanese)* 80−52730
ZrO_2:U, thermoluminescence, traps and emission centres 79−24373

uranium continued
$ZrSiO_4$, zircon, U content estimation using plastic track detector *(French)* 77−64445
$ZrSiO_4$:U^{4+}(U^{5+}), opt. spectra 78−88334

uranium alloys
crystal structure rel. to anomalous props. of γ-phase alloys 77−19910
shell, explosive expansion, deform. and rupture modes and mechanisms 80−85064
shell, explosive expansion, rupture behaviour 80−85063
strengthening rules, high temp. 77−21157
ternary alloy, Al_4Ba-$ThCu_2Si_2$-type structure, geometrical charact. 77−58977
thermal creep and swelling, characterisation 79−74226
Al-Sn-U alloy, phase equilib. exam. by metallographic and X-ray anal. 77−21102
Hg-U system, thermodynamic props., vap. press. and EMF expts. 79−91625
$(Np_{1-x}U_x)Fe$, Mossbauer spectra, magnetism and hyperfine interactions 80−20529
RhU, mol. vapour above Th-U-Rh-graphite, dissoc. energy, mass spectra 78−78832
Th-Pu-U-Zr (20, 4, 8 wt.%) metal fuels, compatibility with cladding alloys for FBR appls. 80−102242
Th-U, Kondo alloys, spin and phonon resistivity independ. 78−47777
Th-U (20 wt.%) metal fuels, compatibility with cladding alloys for FBR appls. 80−102242
Th-U alloy fast reactor fuel element, design basis considerations 79−54503
Th-U alloy fuel behaviour in organic-cooled reactor 78−86605
Th-U metal alloys, LMFBR appl. 77−83040
Th-U Na-bonded metal fuel, transient heating test 78−86607
Th-U-Pu metal alloys, LMFBR appl. 77−83040
Th-U-Pu-C-O-N, kernel migration for HTGR fuel 77−38335
Ti-U, dilute, superconducting transition temp. and mag. susceptibility 78−47899
(U, Me)C, Me=Hf, Ti, Zr, Nb or Ta, effects of alloying and interaction with C 79−45350
U-Al, storage of unirradiated fuel in borated concrete, criticality safety anal. 80−13608
U-Al, transform. and struct. changes, cooling, cooling rate effect *(Korean)* 77−63660
U-Al (0.78 at.%), behaviour of metastable phases under neutron irrad., application of model 78−48408
U-Al alloy components, process control analysis of ^{235}U during fuel element manuf., neutron absorpt. method 79−85720
U-Al fuel elements in light water, neutron multiplier, criticality studies for ^{252}Cf source 78−25367
U-Ce-C system, phase equilibrium exam. *(German)* 78−23670
U-Co(Ce)(Fe)(Mn)(Ni)(V) metallic glasses, glass form. and thermal stability 80−75183
U-Cr, absolute thermoelec. power values 77−20303
U-Cr-Al (0.2, 0.1 at.%) fuel elements with high swelling resistance for KS-150 reactor 78−78471
U-Fe(Ni)(Co)-B, isothermal section of phase diagram, X-ray obs. 79−52157
U-Ga system cpds., elec. resist., paramag. susceptibility magnetis., temp. depend., mag. struct. 77−20559
U-Hg system, phase relations determ. 79−91624
U-Mo, absolute thermoelec. power values 77−20303
α-U-Mo, dil., electronic properties depend. on $2^1/_2$-th order phase transition under high press. *(Russian)* 80−11128
U-Mo (10 wt.%), commercial alloys, influence of metallurgical factors on fracture processes *(French)* 78−60751
U-Mo (10 wt.%), gaseous O_2 and hydrogen embrittlement, exam. 78−60811
U-Mo (1.5 wt.%), superplastic behaviour 450 to 720°C *(French)* 79−74203
U-Mo (1.5 wt.%) metallurgical study of forging *(French)* 78−21737
U-Mo (2 wt.%), depleted, effect of microstruct. on mech. props. 80−108497
U-Mo and U-Mo-Zr, shear martensitic transform. during quenching, plastic deform. and annealing 77−28815
U-Mo-Nb-Zr-Ti (0.75, 0.75, 0.75, 0.5 wt.%), heat treatment effect on microstruct. and mech. props. 78−23729
U-Mo-(Zr), ductile-brittle transition *(French)* 77−66693
U-Mo(Nb)-(Zr), gamma stabilised, internal H_2 embrittlement 77−28883
U-Mo(Re), high temp. phase diagram, thermodynamic props. of refractory metal solutes in liquid U 77−25022
U-Mo(Ti)(Q^4)(Q^5), Q^4-quad, Q^5-quint, stress corrosion cracking in moist air, salt water, salted moist air 78−35562
U-Mo(2 wt.%), mech. props., effect of ageing 77−8914
U-Nb, absolute thermoelec. power values 77−20303
U-Nb (14 at.%), exam. of shape memory effects 78−76694
U-Nb (14 at.%), martensitic and polymorphic transformations 80−60861
U-Nb (4.5 wt.%), correlation between oxidation and stress corrosion cracking 79−20253
U-Nb and U-Nb-Zr, shear martensitic transform. during quenching, plastic deform. and annealing 77−28815
U-Nb-C system, phase equilibrium exam. *(German)* 78−23670
U-Nb-Zr, BCC alloys, solubility of H_2 and D_2 gas 79−96302
U-Nb-Zr (16.6, 5.6 wt.%), stability of BCC phase 79−66039
U-Nb-Zr (7.5, 2.5 wt.%), elastically bent, ageing induced shape instability 77−16622
U-Nb-Zr (7.5, 2.5 wt.%), texture development role in shape memory effect 79−87661
U-Nb(2-3, 4.5, 6.0 and 8.0 wt.%), SCC in air 77−73363
U-Ni dilute alloy fission product source design and use at EBR-II 79−9932
U-Pt, paramag. suscept. 79−61047
U-Pu carbides, advanced LMFBR fuels, equilib. thermodynamics 79−67862
U-Pu-Zr metal fuel remote alloying and casting 79−89477
U-Pu-Zr(-Th) LMFBR metal fuel elements; development and performance 80−57856
U-Re system, γ-solid solns., thermo-EMF, temp. depend. *(Russian)* 79−73496
U-Re-C, crystalline struct. of a compound 77−25023
U-Si-Al fuel rods, Zr-Nb cladding, irradiation behaviour with peripheral voidage 78−54835

uranium alloys continued
U-Ti (0.75 wt.%), quench rate sensitivity, effect on microstruct., mech. props., ageing 77−70077
U-Ti system, γ-solid solns., thermo-EMF, temp. depend. *(Russian)* 79−73496
U-Ti(0.75 wt.%), mech. props., effect of ageing 77−8914
U-UNi_2-UCo_2, system, phase equilibria, lattice constants *(German)* 80−50598
U-V (0.2 wt.%), mech. and struct. props., effect of internal H *(French)* 77−21253
U-Zr, absolute thermoelec. power values 77−20303
U-ZrH low enrichment fuel for TRIGA and plate-type reactors 80−22950
UAL_2, band magnetism due to f-electrons, T_{sf} 77−73039
UAl_2, dynamical susceptibility, diffuse neutron scatt. study 79−24138
UAl_2, elastic consts., temp. and mag. field depend. 80−55450
UAl_2, high field, high press. mag. props. 80−11172
UAl_2, inelastic neutron scatt. 80−11165
UAl_2, low temp. mag. susceptibility 79−38301
UAl_2, low temp. sp. ht., spin fluctuation phenomena 77−28405
UAl_2, spin fluctuations, mag. field effect, electronic sp. ht. and elec. resist. 80−108026
UAl_2, transport props., susceptibility and sp. ht. 80−11174
UAl_2-UNi_2, phase relationships, thermal, microscopic and X-ray exam. *(German)* 78−88447
$UAl_2+2Al \rightarrow UAl_4$, effect on Young's modulus and rupture strength in dispersion reactor fuel *(German)* 78−62596
UAl_3, thermoelectric power, 5-300K 79−65444
UAl_4, clusters, band struct., variational Xα calc. 79−4508
UAl_4, clusters, X_α calculations *(Japanese)* 79−82519
UAl_x dispersion nuclear fuels, development and irrad. performance 80−78368
UAl_x plate-type reactor fuel element fabrication 79−49822
UAl_x-Al dispersion fuel for thermal high flux reactors, irradiation 77−18660
$UAl_2(Co_2)$, surface comp. and electronic struct., photoemission study 80−66382
UAs, localised cryst. field states, neutron inelastic scatt. obs. 78−14697
U_3As_4, high-field magnetisation, field-induced phase transition near hard (100) directions 77−28413
UAs(Sb), anisotropic mag. ordering and mag. structural transitions 79−78324
UB_2, thermochemistry and stability 80−97723
UBe_{13}:Gd, Van Vleck paramagnet, exchange parameters, ESR determ. 77−4557
UCo_2, cubic Laves phase, prep. and stoichiometry 79−24459
UCo_2, elec. resist. and mag. susceptibility meas., non-stoichiometry influence 77−63088
UCo_2 Laves phase, alloy systematics, rel. to the long periodic table 79−37649
UCo_2, mag. props., ferromag. transition *(Russian)* 78−68148
$UCo_{5.3}$, mag. props., cryst. and domain struct. *(Russian)* 77−4529
$UCo_{5.3}$, mag. props. and cryst. struct. *(Russian)* 77−51925
$U(Co_{1-x}Fe_x)_2$, ferromag. onset, susceptibility and resist. meas. 80−70967
$U(Co_xNi_{1-x})_2$, cryst. struct. and mag. props. at 4.2K 80−54175
$U_{10}Co_{51}Si_{33}$, crystal struct., dimensions, space group and coord. *(Russian)* 80−88085
$U_2Co_3Si_5$, cryst. struct. 78−47285
$U_6Co_{30}Si_{19}$, X-ray cryst. struct. determ. 80−107111
UCu_5, core and valence band spectra, XPS obs. 80−50530
UCu_5, mag. props. and NMR 77−20734
UFe_2, giant magnetoelastic deform. of cryst. struct. mag. props. *(Russian)* 80−93159
UFe_2, mag. anisotropy of single crysts. 79−56527
UFe_2, magnetisation, neutron diffr. and Mossbauer expts. 77−63137
UFe_2, magnetisation meas. 79−51756
UFe_2, Mossbauer diffr., combination type maxima, hyperfine interactions on nuclei 80−25263
UFe_2, nonstoichiometry effects on Curie temp., susceptibility obs. 80−25131
UFe_2, thermodynamic props., agreement with Campbell correlation of laves phase compounds 78−15370
U_6Fe, spin-pairing state investig. via Josephson current between weakly-coupled superconductors 77−47942
$U_6Fe_{0.98}$ supercond. transition temp. reduction by neutron irradiation 77−63020
UGa_2, cryst. struct., mag. and magnetoelastic props. *(Russian)* 79−38364
UGa_2, mag. and magnetoelastic props. 80−15775
UGa_3, thermoelectric power, 5-300K 79−65444
UGe_3, compensated metal, topological props. of Fermi surface, magnetoresist. meas. 78−6350
UGe_3, de Haas-van Alphen effect, band struct. calc. 78−72068
UGe_3, spin fluctuation phenomena, band struct. calcs. and de Haas-van Alphen meas. 77−20225
UGe_3, thermoelectric power, 5-300K 79−65444
UGeS, mag. props., 4.2-300K 78−10667
UGeSe, mag. props., 4.2-300K 78−10667
UGeTe, mag. props., 4.2-300K 78−10667
UHg prep. from uranyl ion using two-compartment electrolyser 80−802
$U_{11}Hg_{45}$, cryst. struct. determ. 79−77555
UIn_3, thermoelectric power, 5-300K 79−65444
UIr_3, (100) surface reconstruction, LEED, AES, electron energy loss spectra study 78−75918
UIr_3, de Haas-van Alphen effect, Fermi surface obs. 77−28099
UIr_3, uncompensated metal, topological props. of Fermi surface, magnetoresist. meas. 78−6350
$UIr:X_2$ (X=Si,Ge), cryst. struct. 80−1964
UMn_2, mag. props., ferromag. transition *(Russian)* 78−68148
UMn_2, structural transition from cubic to monoclinic, neutron and X-ray obs. 78−75833
UMn_2, transport props., influence of lattice distortion 80−100452
UMn_2-UCo_2, mag. props., ferromag. transition *(Russian)* 78−68148
UMn_2-UFe_2, mag. props., ferromag. transition *(Russian)* 78−68148
UNi_2, mag. phase transition, elec. resist. meas. 80−97094
UNi_5, core and valence band spectra, XPS obs. 80−50530
$UNi_{0.5}Cu_{4.5}$, core and valence band spectra, XPS obs. 80−50530
$UNi_{5-5x}Cu_{5x}$, NMR and press. effects 80−25230
$UNi_{5-x}Cu_x$, thermoelectric power, 5-300K 79−65444
$U_3Ni_3Sb_4$, and related compounds, X-ray diffr. cryst. struct. determ. 79−42009

uranium alloys continued
$U_3Ni_4Si_4$, X-ray cryst. struct. determ. 80−33931
UPb_3, crystal field energy levels, magnetisation and susceptibility, neutron spectra obs. 80−50064
UPd_3, anomalous behaviour in low temp. props. 79−28108
UPd_3, crystalline elec. field studies using neutron inelastic scatt. at NRCN 80−10931
UPd_3, crystalline electric field levels of U, neutron scatt. exam. 78−60267
UPd_3, U^{4+} mag. form factor meas. by inelastic neutron scatt. 78−52221
UPd_4, localised cryst. field states, neutron inelastic scatt. obs. 78−14697
UPd_2Si_2, magnetic phase transition, neutron diffr. meas. 79−47284
UPt, valence bands, XPS spectra 80−50520
UPt, weak ferromag., magnon heat capacity, magnetisation and mag. entropy 77−24685
URe, mag. susceptibility 78−68182
$U_4(Re_{0.17}Si_{0.83})_{13}$, X-ray diffraction anal. of crystal struct. *(Ukrainian)* 78−83773
$U_4Re_7Si_6$, X-ray diffraction anal. of crystal struct. *(Ukrainian)* 78−83773
URh_3, de Haas-van Alphen effect, Fermi surface obs. 77−28099
URh_3, magnetisation density 78−52203
URu_3, sublimation thermodynamics 80−97722
USb, antiferromag., neutron diffr. exam. of ordered state 77−20557
USb, crit. neutron scatt. 77−24674
USb, localised versus itinerant 5f electrons exam., reflectivity meas. 79−19905
USi_3, thermoelectric power, 5-300K 79−65444
U_3Si, crystalline elec. field studies using neutron inelastic scatt. at NRCN 80−10931
U_3Si, heat capacity and thermodynamic props., 1 to 1203K 77−72697
U_3Si, reversible twinning, in-situ obs. 80−104241
U_3Si, tensile ductility from 25 to 320°C 79−74225
U_3Si, X-ray diffr. exam. 78−75629
USn_3, crystalline elec. field studies using neutron inelastic scatt. at NRCN 80−10931
USn_3, inelastic neutron scatt. 80−11165
USn_3, thermoelectric power, 5-300K 79−65444
$U_{1-x}Th_xAl_2$, ferromag. spin fluctuation system, sp. ht. and elec. props. 77−20604
$U_{1-x}Th_xAl_2$, mag. susceptibility, low temp. depend. 80−11173
δ-UZr_2, computed X-ray powder diffr. patterns and densities 77−43172
^{235}U-Al castings in water, pulsed reactivity meas., Monte Carlo anal. 79−26522
^{235}U-Al castings in water moderated lattices, pulsed reactivity meas. 79−26529
$V_{0.97}U_{0.03}$, phonon spectrum, quasi-local vibrs., inelastic incoherent neutron scatt. 77−15519
Y-Mo, BCC alloys, solubility of H_2 and D_2 gas 79−96302
Y-Nb, BCC alloys, solubility of H_2 and D_2 gas 79−96302

uranium compounds
see also uranium alloys
bis-2-AC-benzofuranato uranyl complex, IR spectra 78−980
bis-3-acetyl-4-hydroxy coumarinate, uranyl complex, IR spectra 78−980
alkali metal uranyl nitrates, IR spectra, force constants, bond orders 77−30873
alkaline earth fluoride solid solns., MF_2-UF_4-CeF_3, surface degradation, complex admittance anal. 78−55980
alkaline earth-uranium mixed oxides, EPR spectra 78−27090
and UO_2-Gd_2O_3 solid soln., high temp. thermal expansion, 298-1700K 78−83979
BWR island-design Pu recycle fuel assemblies, nuclear fuel performance meas. 79−30907
carbides, solvent for NaCl type monocarbide and sesquicarbide fission products, solubility rules 78−59953
ceramic fission reactor fuels, high temperature chemistry, nonstoichiometry, review 77−14238
chalcogenides, electronic struct., relativistic single-site scatt. model 79−87040
chalcogenides, mag. anisotropy 79−42754
complexes, equatorial bonds, MO calcs. 78−82621
dipnictides, elec. and mag. props. 78−84399
fill-gas comp. and eccentric gap geometry effects 78−13284
mono-furfural 4-(2-pyridyl thio semicarbazonato) uranyl complex, IR spectra 78−980
in fused salts, redox and chem. props. 77−29038
GCFR core-catcher crucible, material compatibility for UO_2-316 stainless steel BN system 79−59171
graphite-UF_6 intercalation compounds, NMR exam. 78−39416
guanidinium uranyl sulphate trihydrate, new ferroelec., dielec. props. 78−43824
guanidinium uranyl sulphate trihydrate, X-ray diffr., crystal struct. 78−14331
high temp. (2300-2500°C) treatment, metallographic cross sections, microradiographic anal. *(German)* 78−29586
HTGR fuel recycle technology 79−59246
HTR oxide fuel, retention of solid fission products 79−54507
K X-ray fluoresc. anal. 77−81449
bis-3-methyl-4-(p-methyl phenylazo)-5-pyrazolonato uranyl complex, IR spectra 78−980
mill tailings, radiation pathways and potential health impacts 79−85826
mill tailings generated between 1975 and 2030, environmental impact 79−85825
milling operations, radiological assessment methodology 79−85827
mineral deposits, criticality study using ore model *(Spanish)* 77−70655
mineral identification in Black Sea sediments *(German)* 78−65257
minerals, luminescence spectra, chemical bond effect 78−72597
minerals from Shinkolobwe, Zaire *(French)* 77−86873
minerals in Witwatersrand Triad, geochronology 77−86892
minerals of U, Pu content, ore model calcs. comparison with expt. *(Spanish)* 77−70654
mixed U-Pu oxide O_2 potential and O/M ratio determ. by solid-state galvanic cells 79−96324
mixed-oxide fuel fabrication in 1980s changes in process equipment and facilities 79−63797
monazite mineral, high-energy alpha emitters, E≥10.6 MeV 79−48467
nitrides, matrix isolation studies with Fourier transform IR 78−45740
nitrides, solvent for NaCl type mononitride fission products, solubility rules 78−59953

uranium compounds continued
ore, solution mining, effect of Environmental Protection Agency requirement for underground injection 79−92101
ores, ^{210}Pb determ., radiochem. method 77−56266
oxide fuels, irrad. behaviour, chemical process, densification, corrosion *(Japanese)* 77−83033
oxides, matrix isolation studies with Fourier transform IR 78−45740
phosphate glass: UO_2^+, Sm^{3+}, energy transfer from UO_2^+ to Sm^{3+} 79−78732
pnictides, electronic struct., relativistic single-site scatt. model 79−87040
pnictides, mag. anisotropy 79−42754
sintering uranium oxide resistance furnace appl. and characteristics *(Italian)* 77−81239
sodium uranyl acetate, fluoresc., circ. dichroism 79−38598
stainless, type 1.4970, density, thermal expansion 79−65223
swelling in mixed-oxide fuel pins 79−22393
tailings piles, potential population dose from ^{222}Rn 79−85824
tetragonal compounds, mag. props. 80−15704
thermal reactor fuel cycles, actinide wastes toxicity limitations *(German)* 80−99220
(U, Pu)O_2 fuel, remote fabrication experience in FRG 80−13753
UC_xO_y, fissile fuel, SiC-fission product reaction kinetics in thermal gradient 80−47570
UNO_3, gravimetric standards, best fit calibration curve parameters, error estimates 79−87931
uranates, luminesc. 79−33765
uranyl acetates, cubic crysts., optical spectra fine struct. 77−1693
uranyl complexes, fluoresc. state, rel. to electronic struct. *(Russian)* 78−5274
uranyl complexes, IR spectra, complexation effects on force consts. and bond lengths 78−980
uranyl complexes, IR spectra and bond distances 80−74167
uranyl complexes, MCD spectra, electronic struct. of lowest excited states *(Japanese)* 79−27014
uranyl pentafluoride complexes, normal coordinate anal. 79−22596
uranyl propionates, cubic crysts., optical spectra fine struct. 77−1693
uranyl salts, cryst., multiphonon relax. 80−15208
uranyl solns. in perchloric acid, radioluminesc. due to self-alpha-radiation of U^{238} *(Russian)* 77−55831
US, large magnetic anisotropy exam. 77−20585
X-ray absorption spectra, meas. of energy shifts of K absorption edge and K X-rays 78−11020
$AgUO_2(NO_3)_3$, fluoresc. decay rates, temp. depend. 80−25429
AmO_2-UO_2, target possibilities for waste incineration, simulation study 80−32419
$(AsO_4)_2H_2(UO_2)_2.8H_2O$, point group symmetry for ferroelec., antiferroelec. and paraelect. phases 78−42983
BaO-B_2O_3: UO_2^{2+}, Eu^{3+} glass, nonradiative energy transfer 77−59602
BaO-B_2O_3:UO_2^{2+}, Nd^{3+} glass, radiative and nonradiative energy transfer 78−60508
BaO-B_2O_3:UO_2^{2+}→Er^{3+} glass, energy transfer 78−2895
$Ba_{1-x-y}U_xCe_yF_{2+2x+y}$, solid soln., ionic cond. 79−99356
Be_2C-graphite-UC_2 fuel development for pulsed reactors 79−67856
BeO-UO_2 fuel testing, annular core pulse reactor 78−86593
CC UF_6 conversion to UO_2, reactor fuels, review 80−23099
$(CH_3)_4NUO_2(NO_3)_4$, fluoresc. decay rates, temp. depend. 80−25429
CO-UF_6 nuclear pumped laser, expansion cooled, vibr. excitation distrib. 80−63997
$Ca_2Cu(UO_2)(CO_3)_4.6H_2O$, voglite, cryst. and powder diffr. data 80−24421
$Ca_{1-x-y}U_xCe_yF_{2+2x+y}$, solid soln., ionic cond. 79−99356
$CaUNb_2O_8$, monoclinic-quadratic phase transform. *(French)* 77−27998
$Co(UO_2AsO_4)_2.8H_2O$, prep. cryst. struct. characterisation 78−30589
CoU_2S_5, mag. struct. and props. 80−11166
$CrUSe_3$, mag. struct. and delocalized moments, powder neutron diffr. obs. 77−69496
Cs_2SnCl_6:$UO_2Cl_4^{2-}$, luminesc., vibronic anal. 79−33767
$Cs_2UO_2Br_4$, force consts., IR spectra 78−5216
$Cs_2UO_2Cl_4$, low-lying excited electronic levels, fluoresc. decay meas. 79−47491
$CsUO_2(NO_3)_3$, ^{15}N isotope shifts in electronic spectrum, internal mode identification 80−55098
$CsUO_2(NO_3)_3$, fluoresc. decay rates, temp. depend. 80−25429
$Cs_4(UO_2)_4O_2Cl_8(H_2O)_4$, cryst. data 77−76367
$CsUO_2(PO_3)_3$, synthesis and struct. 79−86767
Cs_2ZrCl_6:$UO_2Cl_4^{2-}$, luminesc., vibronic anal. 79−33767
Cu-U-O system, equilib. relationships *(German)* 80−35163
$Cu_2U_6S_{13}(Se_{13})$, cryst. struct. and magnetic props. *(French)* 80−96496
F_2+UO_2, reaction kinetics, molecular beam study 78−46157
Gd_2O_3-UO_2, behaviour as control rod in commercial reactor 78−8918
$HUO_2AsO_4.4H_2O$ and $HUO_2PO_4.4H_2O$ layered cpds., struct. investigs. below antiferroelec. transition temps., H bond ordered structs. 80−107416
$HUO_2AsO_4.4H_2O$ and $HUO_2PO_4.4H_2O$ layered cpds., single and polycryst., proton cond. behaviour w.r.t. antiferroelec. transition temps. 80−107481
$H_{5n-2}UO_2(IO_6)_n.4H_2O$, n=0.5 to 2.0, high proton cond. 80−107562
$H(UO_2P(As)O_4)4H_2O$, H motion, PMR obs. 78−80239
$HUO_2PO_4.4H_2O$, H^+ ion cond., struct. mechanism, X-ray diffr. obs. 78−34651
$HUO_2PO_4.4H_2O$, H^+ ion solid electrolyte, cryst. struct. 79−14759
$HUO_2PO_4.4H_2O$, high proton cond. 79−77809
$HUO_2PO_4.4H_2O$, film fabrication and appl. as solid electrolyte in electrochromic displays 80−70462
$HUO_2PO_4.4H_2O$ solid proton conductor, appl. as electrochromic cell 80−89497
He-UF_6 gas mixture, velocity slip in free jet expansions 78−90951
$HuO_2P(As)O_4.4H_2O$, water deficiency, enthalpy of dehydration, thermogravimetric anal. 80−65251
K_2UF_6, X-ray photoelectron spectra 77−32491
KUO_3, EPR and mag. susceptibility, temp. depend. 79−33451
$K_2UO_2Br_4$, force consts., IR spectra 78−5216
$K_5(UO_2)F_9$, optical spectra, vibr. freqs. calcs. *(Russian)* 78−31205
$KUO_2(NO_3)_3$, fluoresc. decay rates, temp. depend. 80−25429
$K_2UO_2(NO_3)_4$, fluoresc. decay rates, temp. depend. 80−25429
$K_2(UO_2)_4O_2(OH)_2Br_4(H_2O)_6$, cryst. data 77−76366
$K_2(UO_2)_4O_2(OH)_2Cl_4(H_2O)_6$, cryst. data 77−76366
$K_2[(UO_2)_3F_8$-$H_2O].3H_2O$, cryst. struct. *(French)* 80−49193
LiF:U_3O_8, X- and γ-irrad., U^{5+} luminesc. molecular centres, optical and ESR expts. 77−48224
LiF+UO_2^+, optical absorpt. spectra 77−81129

uranium compounds continued
$LiUO_3$, EPR and mag. susceptibility, temp. depend. 79−33451
$Li_xUO_2F_2$, $0 \leq x \leq 2$, use in electrochemical batteries 80−50858
$Mg_yU_{1-y}O_{2+x}$, thermodynamics from EMF meas., high Mg conc. 78−43143
$Mg_yU_{1-y}O_{2+x}$, thermodynamic props., EMF meas. 80−29187
$(NH_4)_2Cd_2(SO_4)_3:Mn^{2+}$, UO_2^{2+}, luminesc., vibr. modes 79−38629
$NH_4UO_2(NO_3)_3$, fluoresc. decay rates, temp. depend. 80−25429
$NH_4UO_2(NO_3)_3$, IR spectra, force consts., bond orders 77−30873
$(NH_4)_2(UO_2)_4O_2(OH)_2Cl_4(H_2O)_6$, cryst. data 77−76366
Na_2UBr_6, phase transformations, elec. cond. and entropy meas., synthesis *(French)* 78−79763
$NaUO_3$, anomaly in mag. susceptibility-temp. curves 77−32152
$NaUO_3$, EPR and mag. susceptibility, temp. depend. 79−33451
$Na_3UO_2F_5$, IR and Raman spectra, struct. *(French)* 79−11409
NdP-UP solid soln., cryst. field parameters 80−10927
$Nd_{1-x}U_xCo_5$, mag. props. and spin-reorientation phase transitions *(Russian)* 78−60284
$Ni(UO_2AsO_4)_2.8H_2O$, prep. cryst. struct. characterisation 78−30589
$Ni[UO_2(SO_4)_2].4H_2O$, revision of crystallographic data 78−22699
$(Pu,U)O_2$, <5 wt.% PuO_2, criticality data generated by SU-HAMMER 79−3198
$(Pu,U)O_2$ assemblies, fission and explosive energy releases 77−65295
$(Pu,U)O_2$, core materials development for water cooled reactor systems 77−46296
$(Pu,U)O_2$, criticality data generation using SU-HAMMER code 78−29581
$(Pu,U)O_2$, low-enriched fuel assemblies, profiles of activity ratios of ^{134}Cs, ^{137}Cs and ^{106}Ru fission products 77−57713
Pu+U mixed oxide aqueous solns., limiting critical concs., multiplication factor 77−26859
PuO_2-UO_2 mixed oxide fuel, plutonia particle behavior during sintering in Ar-H_2 (8%) atmosphere 79−8258
PuO_2-UO_2-Na aerosol, from LMFBR HCDA conditions, characterisation 78−94104
$RbUO_3$, EPR and mag. susceptibility, temp. depend. 79−33451
$RbUO_2(NO_3)_3$, fluoresc. decay rates, temp. depend. 80−25429
$Rb_4(UO_2)_4O_2Cl_8(H_2O)_4$, cryst. data 77−76367
$Rb_2(UO_2)_4O_2(OH)_2Br_4(H_2O)_6$, cryst. data 77−76366
$Rb_2(UO_2)_4O_2(OH)_2Cl_4(H_2O)_6$, cryst. data 77−76366
$Sr_{1-x-y}U_xCe_yF_{2+2x+y}$, solid soln., ionic cond. 79−99356
$(Th,U)_2$, chemical form of solid fission product simulating high burnup 80−616
(Th,U)C advanced FBR fuels, radiological assessment of reprocessing 80−73983
$(Th,U)O_2$, burnup simulated, high O_2 pot., chem. state 80−91220
$(Th,U)O_2$, D_2O cooled, relative conversion ratio 78−29582
$(Th,U)O_2$ fuel conversion to $(Th,U)C_2$ for reprocessing 79−54579
$(Th,U)O_2$ fuel kernel prep. by external gelation of Th 79−93802
$(Th,U)O_2$ fuel kernels, simplified preparation 78−86668
$(Th,U)O_2$ low burnup fuels, densification-related pellet diameter shrinkage 79−54510
$(Th,U)O_2$ microspheres, fabrication 80−801
$(Th,U)O_2$ reactor fuel, dissolution in HNO_3-HF mixtures, fuel reprocessing study 78−59951
$(Th,U)O_2$ recycled fuel elements, composition calc. 79−13504
$(Th,U)O_2$, thermal conductivity model for temps. to melting 79−93732
Th-U non-oxide compounds, use as refractory breeder fuels 78−86612
Th-U(Pu) fast breeder fuels, chemical, thermodynamic and selected transport props. 79−54505
Th-U(20 wt.%) alloy fuel, compatibility performance of candidate cladding alloys 79−54509
Th_3As_4-U_3As_4, cryst. growth by chem. vap. transport 78−23588
Th_3As_4-U_3As_4 solid soln., electronic props. 80−34469
ThO_2-UO_2 (0.1 wt.%), ^{133}Xe release after low dose irradiation 77−74919
ThO_2-UO_2 fuel performance after irradiation 78−86621
ThO_2-UO_2 in PWR fuel rod, LIFE-THERMAL computer code anal. 78−86623
ThO_2-UO_2 solid solns., props. of importance for use as nuclear fuels 79−54506
$Th_{0.81}U_{0.19}O_2$, irradiated fuel particles, meas. and interpretation of CO and Kr-Xe content 78−25287
$Tl_2U_yF_{x+4y}$, cryst. growth from flux, crystallographic charact. *(French)* 77−77364
(U,Ce), U self-diffusion 80−92711
$(U,Gd)O_2$ sintered pellets, homogeneity determ. by ceramographical method *(German)* 79−49804
(U,La)C, U self-diffusion 80−92711
$(U,Pn)O_2$, LMFBR fuel pin lattices, calcs. of k_{eff} valves 80−13569
$(U,Po)O_2$, liq., v.p. meas. at 5000K 77−20077
(U, Pu) C, nuclear fuel, irradiation induced creep meas. 80−93605
(U,Pu) O_2, pore struct., characterisation for gas exchange anal. *(German)* 79−49687
(U,Pu)-oxide nuclear fuel, near and non-stoichiometric, O_2 potential, thermogravimetric and galvanic cell meas. comparison 79−63744
$(U,Pu)_{2+x}$, elec. cond., pure state and Mo addition influence, 350 to 750°C 77−20320
(U,Pu)(C,N) and (U,Pu)N, high burn-up simulated, Pu self diffusion 80−92712
(U,Pu)C FBR fuel pins, irrad. behaviour w.r.t. fission gas release, fuel/clad compatibility, Pu migration 80−57847
(U,Pu)C fuel, interaction with molten stainless-steel shroud 78−86592
(U, Pu)C, LMFBR carbide fuel cladding damage anal. at TREAT 80−13602
(U,Pu)C LMFBR fuel elements, transient overpower test results 77−46334
(U,Pu)C LMFBR fuel, Na-bonded, consequences of rapid Na loss on fuel behaviour 80−102238
(U,Pu)C, pellet and sphere-pac nuclear fuels, comparative irrad. tests 80−78367
(U,Pu)C, porosity in MX-type fuel and its stability 78−86629
(U,Pu)C possibility for GCFR fuel 77−18667
(U,Pu)C, self-diffusion meas. 80−6544
$(U,Pu)C_{1\pm x}$, evap. behaviour, 1500-2458°C 77−27994
(U,Pu)CN, porosity in MX-type fuel and its stability 78−86629
$(U,Pu)C_{0.8}N_{0.2}$, self diffusion processes 78−50259
$(U,Pu)C_{1-x}N_x$ LMFBR MX-type fuels, fission gas release and microscopic swelling 80−73921
(U,Pu)CNO irradiated fuel, electron microprobe anal. 78−70601
(U,Pu)N, porosity in MX-type fuel and its stability 78−86629
uranium compounds continued
(U,Pu)N, self-consistent normal fluid eqn. of state, press., density, and enthalpy of vaporisation calc. 78−8909
(U,Pu)N, self-diffusion meas. 80−6544
$(U,Pu)O_2$ 80−63252
$(U,Pu)O_2$ 316 stainless steel clad rods for GCFR high temp. fast flux irrad. tests 77−18666
$(U,Pu)O_2$ (30 wt.%), oxidation behaviour 79−66210
$(U,Pu)O_2$, anal. of densification in BWR 79−49685
$(U,Pu)O_2$, autoradiographic anal. of PU distrib. 79−49811
$(U,Pu)O_2$, build-up and decay of actinide nuclei in fuel cycle of BWR, PWR, HWR, HTGR and LMFBR 78−17314
$(U,Pu)O_2$, ceramographic exam. of Dounreay PFR fuels, data bank storage 79−49811
$(U,Pu)O_2$, close coupled O-to-metal ratio anal., rapid thermogravimetric method 79−11878
$(U,Pu)O_2$ FBR fuel cycle, review 80−47682
$(U,Pu)O_2$, FBR fuel pellets, gel-supported precipitation conversion and prep. 80−813
$(U,Pu)O_2$, FBR fuel pellet fabrication, control of O_2-to-metal ratio 80−13760
$(U,Pu)O_2$ FBR fuel pin thermal design, effect of fuel stoichiometry 80−18570
$(U,Pu)O_2$, fission gas release and retention in irrad. nuclear fuels 80−57841
$(U,Pu)O_2$ fuel, criticality control, critical mass meas., fission rate distrib. by solid state dosimetry 80−13723
$(U,Pu)O_2$ fuel performance, effect of O_2-metal ratio 80−13762
$(U,Pu)O_2$ fuel pin behaviour during FFTF 3c/s reactivity insertion event, TREAT expt. anal. 80−102240
$(U,Pu)O_2$ fuel-cladding chemical interaction, effect of O_2-metal ratio 80−13763
$(U,Pu)O_2$ fuels, eqn. of state up to 5000K, high-temp. laser technique 77−27971
$(U,Pu)O_2$ fuels, O distrib. during irradiation, calc. using CODIF program 78−70604
$(U,Pu)O_2$ GCFR fuel behaviour, effect of O_2-metal ratio 80−18569
$(U,Pu)O_2$, hyperstoichiometric, oxygen potentials determ., 1500-1850K 77−20095
(U, Pu)O_2, hypostoichiometric fuels for FBR, effect of O_2 pot. on fuel props. *(German)* 79−49800
$(U,Pu)O_2$, in pile creep 77−42060
$(U,Pu)O_2$, irradiated fuel, O_2 pot. meas. using galvanic cell 79−49689
$(U,Pu)O_2$ LWR high burnup fuels, remote fabrication and performances 80−13755
$(U,Pu)O_2$, lattice defects and irrad. damage, review 77−27873
$(U,Pu)O_2$, liq., v.p. up to 5000K 77−1239
$(U,Pu)O_2$, microsphere fabrication, hydrolysis process 77−23204
$(U,Pu)O_2$, mixed oxide fuel elements, lenticular pore movement 78−78460
$(U,Pu)O_2$, mixed oxide fuel elements, Pu redistribution 78−78463
$(U,Pu)O_2$, neutron activation determ. of O_2 coeff. 80−37457
$(U,Pu)O_2$, oxidation rates 80−37557
$(U,Pu)O_2$ powder, FBR fuel prep. by Au/PuC coprecipitation process 80−814
$(U,Pu)O_2$, power reactor fuel manufacture, technological aspects 79−640
$(U,Pu)O_2$ rare earth, Y impurities separation, at. emission anal. 77−52723
$(U,Pu)O_2$, substoichiometric, unified model for defects, thermodynamic functions 77−20094
$(U,Pu)O_2$, thermal creep in 40 to 100 N/mm^2 stress range 77−28881
$(U,Pu)O_2$, vapour press. eqn. of state, VENUS-II code studies 78−8908
$(U,Pu)O_{2-x}$, chemical diffusion of O *(French)* 79−42300
$(U,Pu)O_{2-x}$, fuel, particle cavitation during reduction by H_2 78−8958
$(U,Pu)O_{2-x}$, mixed oxide fuel, final stage densification 79−49681
$(U,Pu)O_{2-x}$, O_2 thermomigration described by cluster model 78−22888
$(U,Pu)O_{2\pm x}$, cluster model approach to thermodynamic props. 77−20093
(U, Pu)$O_{2\pm x}$, O chemical diffusion coeff. 79−10977
$(U,Pu)O_{2\pm x}$, solid state transport as mechanism of O thermomigration 79−19395
$(U,Pu)O_3$, prod., recycling for use in LWR *(Spanish)* 79−63786
$(U,Th)O_2$ fuel pellet fabrication using gel microspheres 80−42844
$(U,Th)O_2$ fuel rods, analytical stressing in hot cell 80−18566
$(U,Th)O_2$, γ-active pellet fuels fabrication, conceptual design of remotely operated plant 80−32340
$(U,Th)O_2$ reactor fuel, annealing test up to 2500°C *(German)* 79−3228
(U,Y)C, U self-diffusion 80−92711
(U,Zr)C, U self-diffusion 80−92711
U complex, $[UO_2(CO_3)_3]^{4-}$, vibr. and low-temp. optical spectra, rel. to U recovery from oceans 79−73939
U complex, bis-hexafluorocetylacetonate uranyl tetrahydrofuran, laser-induced dissoc. 80−53071
U complex, cyclopentadienyl-U-halides, paramag., U IV ligand interaction, mag. susceptibilities, 1-300K *(German)* 79−15279
U complex, tetrakis(dipivaloylmethanato)uranium IV, in CS_2 soln., ^1H NMR, intromol. rearrangement 79−19784
U complex, tetramethylethyl-cyclopentadienyl uranium trichloride, prep., NMR and IR spectra 79−76428
U complex, UCl_4.3DMBA(.3MAA), mag. exchange interaction 79−78303
U complex, $U(acac)_4$, cryst. fields, mag. susceptibility, chem. shift *(French)* 78−84179
U complexes, tetranuclear halogenocomplexes, preparation, vibr. spectra *(French)* 77−83596
U complexes, UT_5 and $UTCl_4$, (T=tropolone), synthesis, cryst. struct. parameters 80−33945
U loaded cation exchange resin, fabrication for HTGR fuel kernels, processing variables effect 78−8951
U solution systems, high-enriched benchmark critical expts. 79−63748
U^{3+}, U^{4+}, shielding factors, cryst. field effects 80−10926
U-Ba-C FBR nuclear fuels, phase anal., 1400°C 80−66487
U-C system p-T diagram, 1000-2600°C, 0-10^{-16} atm. 77−73265
U-C-N system, high temp. X-ray diffr. exam. of structure *(French)* 78−72765
U-H system, phase diagram and thermodynamic parameters 77−21124
U-O system, infrared spectroscopy 77−8573
U-O system, phase equilibrium, thermal, X-ray and cond. meas. 78−35371
U-Pr-C FBR nuclear fuels, phase anal., 1400°C 80−66486
U-Pu aqueous solutions of oxides and nitrates, criticality, effect of Gd, Gd-B neutron absorbers 77−34393

uranium compounds continued
U-Pu mixed oxides, impurities, emission spectrometric anal., single carrier method 78−68944
U-Pu-C system, segregation and v.p. obs. 77−28793
U-Pu-C-N system, phase relationships and equil., effects of oxygen, review 77−21126
U-Pu-O system, substoichiometric phase range obs., high temp. thermodynamic parameters 77−21125
U-Re-C and U-Tc-C systems, phase relationships 77−21127
U-Sr-C FBR nuclear fuels, phase anal., 1400°C 80−66487
U-UH_3 powder, appl. in Lyman alpha radiation source 78−13775
U-Y-C FBR nuclear fuels, phase anal., 1400°C 80−66485
U-ZrH fission reactor fuel options for TRIGA Mk.III 80−5235
(U-Pu)C, new CRBRP reload core design 79−59155
(U-Pu)O_2, fuel and fuel elements for fast and power reactors 79−616
(U-Pu)O_2 interaction with stainless steel cladding, corrosion products, electron microprobe anal. 79−26524
(U-Th) oxide, carbide, nitride and metal fueled LMFBR breeding performance 79−59175
(U-Th)C fueled reactor system, large plant, performance parameters 79−26500
UAs, anisotropic susceptibility 79−42754
UAs, anisotropic susceptibility 80−7087
UAs, mag. props. 78−43554
UAs, magnetic struct. in high mag. fields, neutron diffr. study 80−34597
UAs, magnetisation, ferrimag. spin struct. 80−7088
UAs, magnetisation, in fields up to 40 T 79−33505
UAs, NaCl struct., band struct. 80−6714
UAs, search for lattice distortions at low temps. 80−79759
UAs, sp. ht. meas., 5-300K, mag. transition obs. 80−50101
UAs, U 4f ESCA spectra 80−16148
UAs, U_3As_5, cryst. growth by chem. vap. transport 78−23588
UAs_2, and U_3As_4, positron annihilation, mean ionic radius calc. 79−15550
UAs_2, heat capacities, antiferromag.-paramag. transitions 78−76253
UAs_2, positron annihilation ang. distrib., valence electrons and Fermi surface 77−28093
U_3As 13a 3-5→5-3_4, heat capacity, 5-300K, ferromag. transition obs. 80−88769
U_3As_4 (110), (211) single crystal, Bitter figure obs. 79−65693
U_3As_4, elec. resist. in vicinity of Curie point, influence of mag. field 77−69314
U_3As_4, ferromag., mag. field induced phase transitions 80−65887
U_3As_4, ferromagnetic transitions and heat capacities from 5 to 950K 78−14955
U_3As_4, high-field suscept. at He temp. 77−89935
U_3As_4, mag. anisotropy, magnetisation meas. 80−50085
U_3As_4, mag. phase transitions, symmetry changes 77−20597
U_3As_4, mag. struct., mag. refls. in paramag. state 77−20559
U_3As_4, magnetisation in strong fields, 4.2 to 200K anisotropy and exchange forces 80−54886
U_3As_4, mol. field approx. study of mag. ordering, Curie temp., paramag. susceptibility 79−78410
U_3As_4, rhombohedral distortion of low temp. 77−7828
UAsS(Se)(Te), positron annihilation ang. distrib., valence electrons and Fermi surface 77−28093
UAsS(Se)(Te), positron annihilation, mean ionic radius calc. 79−15550
UAsSb, prep. and struct. 77−68951
UAsSe, strongly anisotropic ferromag., negative magnetoresist. meas., 77-135K 77−89774
UAs_xSe_{1-x}, lattice distortion below Curie temp. 77−63252
UAsTe, crit. behaviour, Ising-like props. 78−43605
UB_{12}, exam. of electronic structure, using X-ray emission spectra *(Russian)* 79−33865
UBC, crystallographic relationship with with CrB, α-MoB, ThBC 79−42025
$U(BH_{4-x})_y^+$, identified in vap. above $U(BH_4)_4$, IR spectra 79−36639
$U(BH_4)_4$, and d-16, IR specra, gas, matrix, isolated and film 79−36639
$U(BH_4)_4$, IR and UV spectra of gas phase 78−62798
$U(BH_4)_4$, in $Hf(BH_4)_4$, excited state assignments and E-symmetry ground state, near IR MCD obs. 80−66153
UBi, mag. props. 78−43554
UBi, NaCl struct., band struct. 80−6714
UBi_4, mag. phase transitions, symmetry changes 77−20597
UBi_4, mol. field approx. study of mag. ordering, Curie temp., paramag. susceptibility 79−78410
UBr_3, cryst. field levels, neutron scatt. determ. 80−65509
UBr_4, paramag., U IV ligand interaction, mag. susceptibilities, 1-300K *(German)* 79−15279
UBr_5, cryst. struct. investig., powder neutron diffr. 78−91321
UBr_4O_2 ions, force field calc., vibr. amplitude and rot. distortion consts. 79−98245
U(C,N), N vapour pressures and thermodyanmic props. 80−84918
UC 80−15046
UC, chemical compatibility with Cr-Fe-Ni cladding alloys, thermodynamic model 80−63263
UC, compatibility with transitions metals used in stainless steel 77−46293
UC, creep, irradiation induced, transient state, kinetic eqn. treatment 80−88251
UC, effect of porosity on fission-gas-induced swelling 78−8959
UC, electronic struct., comparison with photoemission spectra 80−91450
UC FBR fuel fabrication by reaction sintering of UO_2 and UC_2 80−812
UC, fission dose depend. of lattice parameter changes 77−24333
UC, high-temperature carbide targets for fast on-line mass separation of alkali and noble gas elements 79−22515
UC, low temp. reactor irradiation 80−39168
UC, MX-type LMFBR fuels, TEM exam. of microscopic swelling 78−70596
UC, miscibility with rare earth nitrides *(German)* 80−96654
UC, nuclear fuels, irrad. induced kinetics, diffusion and fission gas resoln. 80−59523
UC, nuclear reactor fuel element performance anal. with UNCLE-I 77−42086
UC, partially filled f bands, configurational and relativistic effect sensitivity 79−78002
UC, phonon dispersion, three-body-force shell model 77−1191
UC, polycrystalline, creep mechanism interpretation 78−8898
UC, power reactor fuel manufacture, technological aspects 79−640
uranium compounds continued
UC, quasi-self-consistent energy band structures using relativistic KKR calcs. chemical bonding 79−51484
UC, quenched-in defects, formation, migration and resistivity 80−64990
UC response to transient heating 77−46333
UC, sintering, role of Ni as sintering additive 80−84892
UC, temp. depend. of Gruneisen parameter and lattice vibr. freq., between 298 to 2500K 80−29142
UC Tokamak fusion-fission breeder, blanket fuel selection 79−22468
UC, transient capillary wave generation on laser irradiated surface 78−21653
UC, UC_2, U_2C_3, and $UC+UC_2$, elec. resist., 4 to 1900K 80−59953
UC, vapour, thermal conductivity, theoretical prediction 77−72402
UC, weak and resin derived fuel microspheres 77−79454
UC:O, sample prep. method importance in O determ. *(Japanese)* 80−23100
UC/PuC, grain boundary energy to surface energy ratio, as determ. from pore geometry 80−34291
UC-(PuC), ceramic fission reactor fuels, fabrication and performance, review 78−58392
UC-NbC, UC-ZrC and UC-ZrC-NbC, solid soln. strengthening rules, physicomech. prop. changes 77−28826
UC-PuC, carbothermal synthesis *(German)* 77−18661
UC-UC_2, alloyed, electron bombarded, enhancement of U_2C_3 deposition 77−27911
UC-UN, in equilibrium with UC_2 and/or C, relationship between N_2 pressure and composition, phase relationships 79−43223
$UC+UC_2$, neutron irradiation, U_2C_3 deposition 78−33253
UC_{1-x}, influence of parameters on sintering behaviour and properties 79−100100
$UC_{1\pm x}$, C diffusion 80−49428
$UC_{1.5}$, creep behaviour and phase change under compression stress 78−35432
UC_2 and (8Th, 1U)O_2 fuel kernel, experimental containing CVD ZrC coatings, irradiation behaviour 77−3103
UC_2, fissile fuel, SiC-fission product reaction kinetics in thermal gradient 80−47570
UC_2, fission fuel, HTGR TRISO, SiC-fission product reaction under isothermal conditions 80−42744
UC_2, HTR fuel elements, chem. prod. processes *(German, English)* 77−14256
UC_2, high temp. thermal diffusivity, thermal conductivity, spectral emissivity 77−28052
UC_n (n=1 to 6), formation and atomization energies by high temp. mass spectrometry 80−7842
UC_n-PuCn, refabricated fuel for breeder reactor, C determ. 79−11877
UC_x, computer simulation of C activity and transport 78−86618
UC_x, partial molar thermodynamic quantities, semi-invariant cumulants method 80−65250
UC_x, self-diffusion and nonstoichiometry, modified Monte Carlo method 77−69114
UC_x, x=1 to 2, high temp. thermodynamic props. 79−60524
U_2C_3+UC, MX-type LMFBR fuels, TEM exam. of microscopic swelling 78−70596
UCN, quenched-in defects, formation, migration and resistivity 80−64990
$UC_{0.60}N_{0.40}$ optical phonon splitting 78−71810
$UC_{1-x}N_x$, low temp. elec. resist., temp. depend., 3 to 90K 77−20321
$UC_{1-x}N_x$, NMR of ^{13}C and ^{15}N, 5f electrons nature, mag. susceptibility, spin fluctuations 77−20736
$UC_{1-x}N_x$, nonstoichiometric, atomic short-range order obs. by diffuse neutron scatt. 77−24315
UC_xN_{1-x}, self diffusion processes 78−50259
U(CO), influence of parameters on sintering behaviour and properties 79−100100
UC_xO_y fission fuel, HTGR TRISO, SiC-fission product reaction under isothermal conditions 80−42744
U(CON), influence of parameters on sintering behaviour and properties 79−100100
UCl_3-CsCl melts, density, surface tension and viscosity 78−67764
UCl_3-RbCl melts, density, surface tension and viscosity 78−67764
UCl_4, cryst. field transitions obs. by neutron spectroscopy 77−47780
UCl_4, equatorial bonds, MO calcs. 78−82621
UCl_4, heat of solution in aq. HCl acid 79−83495
UCl_4 molten mixtures with alkali metal chlorides, physicochemical props. 78−38915
UCl_4, paramag., U IV ligand interaction, mag. susceptibilities, 1-300K *(German)* 79−15279
UCl_4, UCl_6^{2-}, UCl_6^-, UCl_8^{3-}, reduced partition function ratio calc. 77−12819
UCl_4, vaporisation thermodynamics 78−44394
UCl_5, ESR, g-factor 77−43864
UCl_5, IR absorpt., ground config. splitting, spin-orbit coupling 77−55778
UCl_5, mag. susceptibility, ESR and g-value, crystal field model anal. 79−91292
UCl_5, single crystal, thermal broadening of IR energy levels 78−35121
UCl_6, electronic struct., photoelectron spectra and SW Xα calcs. 79−72355
UCl_6, equatorial bonds, MO calcs. 78−82621
UCl_4O_2 ions, force field calc., vibr. amplitude and rot. distortion consts. 79−98245
UCo_5Si_3, X-ray cryst. struct. anal. 79−60342
UCr_2O_6, hydrothermal cryst. growth, 40 kbar, 873K, cryst. struct. *(French)* 78−35342
UD_3, crystalline elec. field studies using neutron inelastic scatt. at NRCN 80−10931
UD_3, dissoc., isotope effect 80−26174
β-UD_3, electronic props., metallic character 80−6693
UF_3, $4f_{7/2}$ electron XPS obs., in condensates and ion-bombarded UF_4 79−45763
UF_4, 5f element fluoride bond length-strength anal. 80−54166
UF_4, AES and loss spectra 77−20965
UF_4, absorption spectrum indicating presence of resonantly localised continuum state 80−58173
UF_4, condensate and ion-bombarded powder, $4f_{7/2}$ electron XPS obs., spectra of UF_3 79−45763
UF_4, crystalline elec. field studies using neutron inelastic scatt. at NRCN 80−10931
UF_4, equatorial bonds, MO calcs. 78−82621
UF_4, inner conversion electron spectra, electron orbit hybridisation *(Russian)* 80−87227

uranium compounds continued
UF_4, interband, collective and atomic (p,d) excitations, Z-160 eV, fast EELS 80−93443
UF_4, matrix isolated. IR spectra, interactions with frozen gas 78−9148
UF_4 matrix with ^{235m}U isomer, conversion process electron role in valence band *(Russian)* 80−13416
UF_4 optical interference layers, electron-beam decomposition 78−34541
UF_4, paramag., U IV ligand interaction, mag. susceptibilities, 1-300K *(German)* 79−15279
UF_4, photoacoustic spectra determ. of amorphous deposits from plasma 78−53303
UF_4, solid, photoacoustic spectra 78−58044
UF_4, vaporisation behaviour 80−84283
UF_4, X-ray photoelectron spectra 77−32491
UF_4-CF_4 mixture, gas core fission reactor, fission based plasma engine 80−63366
UF_4-LiF(KF) molten binary mixtures, viscosity meas. 80−65270
UF_4-MF (M=Na or K), ion-molecule equilibria, heat of form. and dissoc. and electron affinities determ. 80−104480
$UF_4+F_2 \rightarrow UF_5$, UF_6, IR matrix isolation spectra 77−12787
UF_5, electronic struct., Hartree-Fock-Slater and Dirac-Slater calcs. 79−31370
UF_5, electronic struct. calc. 80−6716
UF_5, electronic struct. and geometry, ab initio calcs. using relativistic ECP 80−32606
UF_5, monomer struct. and pot. consts., IR and Raman spectra in inert gas matrices 78−5215
β-UF_5, single cryst. struct., coordination of U^V 77−11512
UF_5, thermochem., heat of formation, dissoc. energy, ionis. pot. 77−70326
UF_5, transient mol., IR absorption spectrum, 580-630 cm^{-1}, assignments, mol. struct. 79−68227
UF_5, transient species formed in UF_6 laser flash photolysis, 17 micron IR spectrum 79−45715
$UF_5 \rightarrow UF_5AU_2F_{10}$, dimerisation equilib. of gas phase, 600-870K 79−87838
UF_6, ^{235}U enriched, moderation control 77−65315
UF_6, 360 to 420 nm absorpt., intraresonator laser spectroscopy technique 77−50448
UF_6, $3\nu_2$ vibr. spectra 78−55183
UF_6 ($^{235,238}U$), vibrational overtone spectra calc. 78−66534
UF_6 admixture effect on N_2 and Ar excited state lifetimes 79−10281
UF_6 anal. with in-line gas chromatograph 77−63982
UF_6 arc emission discharges, compared to UI plasma emission coeff. 80−64693
UF_6, CW CO_2 laser spectroscopy 80−83367
UF_6 centrifuge cascade, power supply loss accidents anal. 79−13502
UF_6, collisionless multiple photon absorpt. photodissociation using IR lasers 79−22772
UF_6, convection-diffusion eqn. soln. for centrifuge axisymm. vel. field, rel. to isotope separation 78−17434
UF_6 conversion for nuclear fuel appls. 80−99266
UF_6 conversion to UO_2 by fluid bed 79−97879
UF_6, critical parameters determ. using thermodynamic and mol. similarities 77−43310
UF_6, cryst., overall vibr. band struct., excitons 77−90136
UF_6 crysts., density of exciton states, two-particle and mixed cryst. spectra 78−2829
UF_6, electron affinity, MS Xα calc. 77−30778
UF_6, electronic struct., non-relativistic Hartree-Fock-Slater method 78−50469
UF_6, electronic struct., relativistic MS Xα calc. 79−85911
UF_6, electronic struct. and transitions, SCF-Xα-SW calcs. 78−78627
UF_6, electronically excited, laser-induced time-resolved emission, self-quenching 78−42114
UF_6, electronically excited, emission quenching by organic mols. 78−42115
UF_6, electronically excited, emission quenching by inorganic mols. 78−42116
UF_6, emission and absorpt. spectra at 80 to 600 nm, decomp. products 77−23212
UF_6, energy levels and bonding, relativistic SCF Dirac-Slater calcs. 77−6691
UF_6, equatorial bonds, MO calcs. 78−82621
UF_6, excitation spectra after electron impact, 30-75 eV impact energy 79−45854
UF_6, fission fragment excitation of optical radiation 77−23665
UF_6, fluoresc. lifetime, temp. depend. 77−58065
UF_6, gas, laser-induced fluoresc., A-X band 78−94275
UF_6 gas acoustic dispersion obs. by double-crystal US interferometry *(Japanese)* 79−4100
UF_6 gas fueled reactor development, for space and earth-bound appl., NASA-sponsored program 79−49829
UF_6, gas phase thermal decomp., dissoc. energy of U-F bond *(German)* 79−29353
UF_6, gaseous fuel reactor research 78−21736
UF_6, gaseous fuel reactor applications 80−63367
UF_6, high temp. fissioning plasma core reactors, fluid mechanical confinement 80−63248
UF_6, IR multiphoton dissociation using 16 μm CF_4 laser 79−22773
UF_6 in Ar matrices, fluoresc. and Raman spectra, vibr. anal. 78−66585
UF_6 in gas centrifuge, fluid flow anal., computer calcs. 77−75924
UF_6 in sealed container, detection and meas. by passive neutron technique 77−67954
UF_6, isotope enrichment, ^{19}F NMR in gas, liq. and solid 78−23364
UF_6, isotope separation by mol. laser *(German)* 77−6954
UF_6, isotope separation by NH_3 laser far IR radiation 77−38867
UF_6, isotope separation cascade, random walk model 77−58190
UF_6, laser chemistry 80−69198
UF_6, laser flash photolysis, transient UF_5 IR spectrum 79−45715
UF_6 laser isotope separation for fuel enrichment 77−54618
UF_6, laser isotope separation, characts. of optically pumped 12.08 μm high power NH_3 laser 78−74923
UF_6, matrix isolated, laser fluoresc. spectrosc. at 12K 79−68253
UF_6, matrix isolated, vibronic fine struct. in fluoresc. spectrum 80−83406
UF_6, matrix isolation spectra and photolysis 79−50043
UF_6, mining, manufacture and purification processes, safety and waste disposal *(Spanish)* 79−63785
UF_6, mol. vibrs. and reaction pathways, min. energy coords. and compliance consts. 77−57966
uranium compounds continued
UF_6 molecular dissociation by DF_4 laser radiation 80−91619
UF_6 molecule dissociation in two-frequency IR laser field 80−66855
UF_6, multiphoton irradiation, spectra and modeling of laser induced emission 80−69160
UF_6, multiple photon absorpt. of 16 μm radiation at 300K 79−76475
UF_6, near UV fluoresc., quantum efficiency, decay time 77−61776
UF_6, neat and mixed cryst. emission spectra, lowest charge transfer state, Jahn-Teller effect 78−67992
UF_6, negative surface ionisation investigation using sensitive detector and pressure gauge 80−31781
UF_6, non-equilibr. condensation calcs. for laser isotope separation 80−10132
UF_6, nucl. lasing, population inversion mechanism 80−63980
UF_6 nuclear pumped lasers, electron impact cross section meas. 80−63985
UF_6, ν_3 manifold 3-quantum transition probabilities, spectral assignment 78−58648
UF_6 on C-coated Pt(Pt-W), mol. negative surface ionisation 78−56913
UF_6, orthorhombic crysts., Raman spectra, int./external mode separation and factor group anal. 77−90135
UF_6, photodissoc. through light scatt. of UF_5 particles, influence of N_2 as collisional partner 80−95698
UF_6, photodissociation dynamics at 266 nm, recoil flight time 78−73062
UF_6, photophysical props., laser study 80−28040
UF_6, plasma expts. related to plasma core reactors 78−8977
UF_6, present technology status for gas core reactors 78−33254
UF_6, quenching action in N_2-He ion nuclear pumped lasers 80−64001
UF_6, Raman scatt. cross section and density meas. 77−75160
UF_6, reactions inducing plasmas, neutron irrad. UV and visible spectra obs. 80−64784
UF_6, relativistic scattered wave calculations 80−63538
UF_6, room temp., IR absorpt. obs., isotope shift of fund. band and combination bands, freq. depend. 80−23421
UF_6, safeguarding of enriched UF_6 bulk transfers 80−68814
UF_6, standard enthalpy of formation of gas and solid 79−96349
UF_6, strong UV-visible emission and weak ionisation induced by focused KrF laser 79−64034
UF_6, supercooled, IR absorpt. spectrum 77−23574
UF_6, temp. and density profiles in freely expanding gas for laser enrichment 78−74458
UF_6, thermodynamic functions and elec. cond. at 1000 to 11000K and 0.1 to 100 atm. 77−42964
UF_6, U isotope separation by velocity slip process, calcs. 79−94100
UF_6, UF_4, reduced partition function ratio calc. 77−12819
UF_6, UF_6-H_2 gas dissociation in pulsed IR and UV laser fields 80−91620
UF_6, UF_6^+, and UF_6^-, electronic struct., ab initio calcs. using relativistic core pots. 79−97987
UF_6, UV photophysics, energy balance through quantum efficiency meas. 80−9634
UF_6, UV spectra, electronic and vibronic states in gas and solid phases 77−14445
UF_6, universal eqns. of state and thermodynamic similarity 77−35290
UF_6, valence electron spectra, vibr. band struct. 77−23520
UF_6, valence energy levels, SCF relativistic Xalpha calc. 79−85912
UF_6, vap., high-resolution spectroscopy by density modulation and UV spectrum 77−31023
UF_6 vapor release in postulated accident 79−22442
UF_6, vapour press., phase transform. enthalpy *(German)* 78−51654
UF_6, vibr. excitation kinetics, IR-UV reson. methods 79−45739
UF_6, vibr. relax., US meas. 77−83696
UF_6, vibr. strength, IR intensities calcs. 77−34608
UF_6 vibrational relaxation, ultrasonic meas. in UF_6-Ar-N_2 mixtures 80−1050
UF_6, visible fluoresc. obs., 374 and 270 nm excitation 79−3490
$^{235}UF_6$ isotope separation by CO_2 laser beam four-photon mixing IR source 77−54760
UF_6-graphite intercalation cpds., prep. and props. 80−40686
UF_6-H_2, near UV and visible excitation, quantum yield from photodissociation 80−35549
UF_6-H_2/HF nuclear pumped laser, characts. 80−78847
UF_6-He circulating gas critical expts. 79−13488
UF_6-He fission pumped nucl. laser, power deposition 78−58987
UF_6-He mixture, ballistic piston fissioning plasma 78−5038
UF_6-$MF_5(MF_6)$, dil. solns., (M=Te, Mo, W, V, Sb, Ta), liq.-vapour equilib. 77−62632
UF_6+alkali atom(dimer), ionis. reactions, electron affinity 77−81398
UF_6+Cs, collisional ionisation, crossed beam obs. 79−68299
UF_6+Cs, ion pair form. and atom abstraction reactions 79−1946
UF_6+e (K)(Na)(Cs), positive and negative ion formation, electron affinity, bond dissoc. energy 77−75314
UF_6+H_2, laser induced dielectric breakdown obs. 77−28992
UF_6+$K_2(CS_2)$, ionisation reactions, absolute cross sections 80−99565
UF_6+K(Cs), crossed beam reaction cross sections 77−77740
UF_6+K(Cs), ionisation reactions, absolute cross sections 80−99565
UF_6+SiH_4, IR laser single photon absorption reaction chemistry, solid state 79−66308
UF_6+SiH_4, photoinduced reaction in low temp. SiH_4 matrix 80−30256
UF_6 +Ar, UF_6 internal excitation 80−106386
$UF_4(Cl_4)$, electronic struct., MS-SCF-Xα calcs. and VUV photoelectron spectra 80−63710
$UFe_3B_2(B_4)$, Mossbauer effect of ^{57}Fe nuclei, mag. props. 80−103907
$U(Fe_{1-x}Mn_x)_2$, Curie temp. and saturation moment at 4.2K 80−70966
UFe_2O_6, hydrothermal cryst. growth, 40 kbar, 873K, cryst. struct. *(French)* 78−35342
UGe_3, induced magnetisation density and f-d bonding, polarised neutron diffr. study 80−50063
UGe_3, magnetisation density, neutron scatt. meas. 80−50038
UGeY, (Y=S, Se, Te), mag. ordering, neutron diffr. obs. 78−72329
UH_3 critical mass calc. by Monte Carlo methods as function of ^{238}U enrichment 79−36320
UH_3, dissoc., isotope effect 80−26174
UH_3, hyperfine splitting of proton determ. by inelastic neutron scatt. 77−43814
UH_3, magnetic props., book contrib. 79−82754
UH_4, thermochem., heat of formation, dissoc. energy, ionis. pot. 77−70326
UH_6, Dirac-Fock one-centre calcs. 79−6837
UH_6, Dirac-Fock one-centre expsn. calc. 80−5485
$U(H_2P_2O_5)_2$, prep., identification, thermal stability 79−15970

uranium compounds continued
$U(HPO_3)_2.2H_2O$, prep., identification, thermal stability 79−15970
$U(H_2PO_4)_4.2H_2O$, prep., identification, thermal stability 79−15970
UI_3 sublattice magnetisation, mechanism 77−55671
UI_4, paramag., U IV ligand interaction, mag. susceptibilities, 1-300K *(German)* 79−15279
UI_6-alkali metal halide system, prep. 80−50568
UIr_3B_2, supercond. and mag. props. 80−97028
$UMnNiO_6$, hydrothermal cryst. growth, 40 kbar, 873K, cryst. struct. *(French)* 78−35342
UMn_2O_6, hydrothermal cryst. growth, 40 kbar, 873K, cryst. struct. *(French)* 78−35342
$U_2Mn_3Si_5$, cryst. struct. 78−26550
UN, antiferromag., mag. susceptibility, elec. resist. and elastic consts. meas. 77−69510
UN, band struct., SAPW calcs. 78−26810
UN, band struct. and density and states, PES meas. 79−42454
UN ceramic fuel, fission enhanced creep, in-pile meas. 77−67807
UN, compatibility with transitions metals used in stainless steel 77−46293
UN, cubic antiferromag., anisotropic critical neutron scatt. behaviour 79−61112
UN, density of states calc. 80−6715
UN, electronic struct., relativistic energy band struct. calc. 80−34354
UN, electronic struct., comparison with photoemission spectra 80−91450
UN, fission enhanced creep and swelling, in-pile meas. 77−42061
UN form. by reaction of C in NH_3 and H_2-N_2 mixture 78−21738
UN form. by UO_2 reaction with C in NH_3 and N_2-H_2 mixture 79−47914
UN formation, mechanism and kinetics, reaction of UO_2 with C and N_2 78−48649
UN, HTR fuel, X-ray phase anal. of thermodynamic stability 79−59165
UN, identification in AR matrix, IR spectra, vibr. freqs. 77−9066
UN, lattice parameters determ. by X-ray diff. 79−19212
UN, low temp. elec. resist., temp. depend., 3 to 90K 77−20321
UN, mag. inelastic scatt. 80−7079
UN, mag. props. 78−43554
UN, mag. susceptibility under press. 80−7086
UN, magnetisation, in fields up to 40 T 79−33505
UN microspheres, prep., effect of process variables 78−8956
UN, N vapour pressures and thermodynamic props. 80−84918
UN, NaCl struct., band struct. 80−6714
UN, nuclear reactor fuel element performance anal. with UNCLE-I 77−42086
UN, phonon dispersion relation near Neel temp., neutron coherent inelastic scatt. 78−59900
UN, photoelectron spectra study, core and valence levels, antiferromag. transition effects 80−66394
UN, power reactor fuel manufacture, technological aspects 79−640
UN, relativistic energy bands, LMTO calcs. 80−65442
UN, search for lattice distortions at low temps. 80−79759
UN, single crystal, electronic props. 77−77061
UN, single crystal, mag. props. 77−77042
UN, sound velocity temp. depend. anomaly 77−72891
UN, sound velocity temp. depend. anomaly in elastic consts. determ. 77−72892
UN, synthesis from UO_2 through carbide 80−73980
UN, system with two singlet levels, fluctuations, excitations and induced moments 79−61022
UN, temp. depend. of Gruneisen parameter and lattice vibr. freq., between 298 to 2500K 80−29142
UN, U 4f ESCA spectra 80−16148
UN, vapour, thermal conductivity, theoretical prediction 77−72401
UN-(PuN), ceramic fission reactor fuels, fabrication and performance, review 78−58392
UN-YN, solid soln., decomp. press.-temp. relations 78−52780
UN-ZrN, Young's modulus antiferromagnetic anomaly 80−92583
$(UN_6)^{15-}$, electronic struct., variational Xalpha cluster calc. 80−39499
$U_2N_2As(P)(S)(Se)$, mag. susceptibility, 4.2 to 1000K, cryst. field and exchange interactions 77−20569
$U_2N_2Bi(Sb)(Te)$, mag. props. 78−72333
$U(NO_3)_6^{2-}$, reduced partition function ratio calc. 77−12819
U_2N_2Te, and related cpds., crit. behaviour 78−43605
U_2N_2Te, mag. struct. 77−63119
U_2N_2Te, powdered, high field magnetisation 78−35008
$U_{1-x}Nd_xS$, mag. phase diagram 80−71027
$UNi_{1.4}Si_{3.6}$, X-ray determ. of crystal struct. *(Russian)* 77−76361
UNi_2Si_3, X-ray determ. of crystal struct. *(Russian)* 77−76361
UNi_xSi_3, X-ray crystal struct. determ. 77−7701
UO, fission reactor fuel, suitability of spent fuel shipping casks 80−27757
UO, nuclear oxide fuel anal., coulometry, emission anal., chromatography, X-ray anal. 80−18420
UO, spectroscopic data rel. to thermodynamic functions 80−34208
$UO^+ + Ar$, collision-induced dissoc. cross section and threshold 80−95706
$UO^+ + O_2(CO)(CO_2)(COS)(CS_2)(D_2O)$, reaction cross-sections, ion beam apparatus study 80−97691
UO_2 80−63252
$UO_{2\ and\ 2.11}$, temperature factor determ. by powder elastic neutron diffraction 78−10152
UO_2, ^{236}U activity meas. *(Spanish)* 78−44822
UO_2, 5d X-ray spectra 78−88382
UO_2, 5f-magnetic semiconductor, spectroscopic data, review 80−97299
$UO_2(NO_3)_2$, establishing traceability to standard reference material 79−81052
$UO_2(NO_3)_2$, preparation of uranium nitrate standards for X-ray fluoresc. anal. 79−81053
UO_2, (110), (100), and (111) surfaces, struct. study using He^+ ion scatt. spectroscopy 80−40206
UO_2 (111), $He^+(Ne^+)(Ar^+)$ impact, appl. of double pass cylindrical mirror analyser 78−72658
UO_2, (111) and (553) surface struct., He^+ ion scatt. spectra 78−75917
UO_2 (~100), vicinal surfaces, LEED and AES expts. 79−4464
UO_2, (uraninite), crysts., vibr. spectra, approx. calc. method *(Russian)* 78−35148
UO_2, alpha radiation damage, point defect ingrowth and annealing behaviour 77−27926
UO_2 and (U, Pu)O_2 nuclear oxide fuels, vapour pressure meas. for fast reactor safety anal. by laser techniques to 5000K 80−13591

uranium compounds continued
UO_2 and (U,Pu)O_2, determ. of H_2O, Hz content by hot extraction methods *(German)* 79−49808
UO_2, and U_3O_8, AES and loss spectra 77−20965
UO_2 and U_4O_9 single crysts., optical props. rel. to chem. bonding 77−28598
UO_2 and UC, creep props. under irradiation 77−42059
UO_2 and UC drops, fragmentation on entering Na pool in LMFBR 79−3225
UO_2 and UO_2-Ni, surface, grain boundary and interfacial energies 78−21649
UO_2, antiferromag., new type of mag. domains *(Russian)* 77−59430
UO_2 BWR fuel rod design to remedy fuel-cladding interactions 80−42766
UO_2 blanket in rodded GCFR lattice, axial meas. 79−81037
UO_2, boundary heat transfer from volumetrically boiling pools following LMFBR HCDA 80−47654
UO_2, build-up and decay of actinide nuclei in fuel cycle of BWR, PWR, HWR, HTGR and LMFBR 78−17314
UO_2, burnup determ. in PWR and BWR using NDA of neutron emission rates 80−83148
UO_2 ceramic fuel fabrication, simulation of thermal processes by emanation thermal anal. 80−811
UO_2, closed boiling system, effect of condensation on dispersion following LMFBR HCDA 78−8936
UO_2, cluster-type fuel for ATR, lattice parameter meas. and neutron behaviour 77−46282
UO_2, clustering phenomena effect, anal. based on shock wave model 78−21652
UO_2 coated particle fuel, amoeba endurance parameters 77−79439
UO_2, commercial fuel pin, irradiation induced volume changes, comparison with model 78−78465
UO_2, comp. of lower phase boundary at 1950K 80−49366
UO_2 compact, density distrib. determ. using autoradioagraphy 77−25234
UO_2 compact, first power emergence, pressure excursion in fuel elements 78−82477
UO_2 complexes, cubic crysts., low temp. optical spectra *(Russian)* 78−92083
UO_2, compressed, dislocation substructure obs. *(French)* 78−78461
UO_2, computer model of Young's modulus 78−31450
UO_2, condensate solidification onto steel struct. in above-core region of LMFBR after HCDA 78−17364
UO_2, condensed vapour following core disruptive accident, particle-size distribs. using first-generation model 78−13295
UO_2, config. and climb rate of dislocation links, contrib. to anelastic creep 77−52431
UO_2, contact conductivity between core and cladding, statistical processing of experimental data 80−5238
UO_2, controlled porosity reactor fuel 77−23205
UO_2 cracked fuel pellets, wetting by molten stainless steel, in LMFBR transient undercooling accident 78−4993
UO_2, creep, irradiation induced, transient state, kinetic eqn. treatment 80−88251
UO_2 critical clusters in D_2O perturbation anal. of buckling 78−29573
UO_2, cross over, discontinuous to continuous phase transition in external mag. field 78−43592
UO_2, cryst. growth by chem. transport 80−16166
UO_2, crystalline elec. field studies using neutron inelastic scatt. at NRCN 80−10931
UO_2 crystallite growth from oxide plasmas, growth morphology 80−59417
UO_2, crystn., specific heat anomaly 80−84299
UO_2, cumulative diffusional release of fission product gases from an equivalent sphere, generalised anal. 80−47569
UO_2 cylindrical fuel rods, thermal neutron flux depression meas. 79−81010
UO_2, D migration and trapping during D^+ implantation 80−34243
UO_2 defective fuel pin fission product release and detection 77−83061
UO_2 dense microsphere production by sol-gel technique *(Czech)* 80−68906
UO_2, dense solid reactor fuel particle preparation by sol-gel technique 79−31136
UO_2, desintering of unrestructured UO_2 fuel during film boiling testing, grain boundary separation 80−22997
UO_2, differential thermal anal. of irradiated material 79−62484
UO_2, diffusion mobility of gas bubbles 80−39357
UO_2, diffusion of Kr and Xe fission gas atoms 79−6746
UO_2, dislocation creep, creep deform. predictions 78−19815
UO_2 dynamic vaporisation, rate effects rel. to fast reactor safety anal. 79−31034
UO_2 effect of Be impurity on Pu breeding control 78−21740
UO_2, effect of H_2O vapour during sintering by sol-gel process *(Czech)* 79−31092
UO_2, effect of pellet density and axial restraint on failure threshold 78−17367
UO_2, effect of point defects on nonequilibrium bubble behaviour 79−93722
UO_2 effective eqn.-of-state meas. to determ. vapour pressure, rel. to LMFBR safety 79−31036
UO_2, elastic props. at high press., US meas. 77−4141
UO_2, electronic contribution to thermodynamics, sp. ht. 79−7699
UO_2, electronic distributions by X-ray spectroscopy 80−97407
UO_2, electronic struct. and bonding, molecular cluster approx. 77−51657
UO_2, electronic struct. contribs. to excess enthalpy at 3000K and in liq. phase 80−15265
UO_2, electronic struct. and Coulomb correl. energy, XPS and bremsstrahlung spectra 80−55272
UO_2, electronic transitions, crystal field effects and phonons, phase transition 80−97303
UO_2, energy depend. Doppler factor meas. using lead slowing-down time spectrometer 78−17310
UO_2 epitaxial films, epitaxial, channelling studies 79−49683
UO_2, equatorial bonds, MO calcs. 78−82621
UO_2 equiaxed grain growth modelling 80−13589
UO_2, equilib. conc. of fission products, ^{235}U induced fission and ^{238}U spontaneous fission *(Spanish)* 78−44823
UO_2, equilib. conc. of fission products, calc. comparison with expt. values *(Spanish)* 78−44824
UO_2 film, vacuum evaporated, He^+ ion energy loss parameter 78−50253
UO_2, fine grained, low-stress creep study, metallographic obs. 79−43312
UO_2, first to second order transition crossover 78−10709

uranium compounds continued
UO_2 fission fragment, range calc., number of primary atoms created in diatomic target *(French)* 79−1473
UO_2, fission gas bubble distrib. from high temp. irradiated SGHWR fuel pins 77−46284
UO_2, fission gas release during irradiation 79−17978
UO_2, fission gas release and retention in irrad. nuclear fuels 80−57841
UO_2 fission reactor fuel fragmentation gas thermodynamics 79−13458
UO_2 fission reactor fuel, response to simulated thermal transients 79−22391
UO_2 fission vapourised fuel, aerosol close in sampling, accident safety 79−49779
UO_2 fluorides, $M_2^I[M^{II}(H_2O)_6][(UO_2)_2F_8]$, M^I=K, Rb, or Cs and M^{II}=Mn, Co, Ni, Cu, Zn or Cd, struct. and IR spectra 77−35525
UO_2 fracture strength meas. of sintered specimens by diametral compression testing, effect of temp. and deformation rate 79−79074
UO_2 fragmentation by capacitor discharge 77−88227
UO_2 fuel, density, thermal conductivity, specific heat, thermal diffusivity, flash method 77−55362
UO_2 fuel, dynamic intragranular fission gas behaviour model, DIGRAS computer code 80−32345
UO_2 fuel, fission product gas emission measurement 79−17980
UO_2, fuel, Zircaloy-2 cladding bonding mechanisms determ. by SEM and EPMA 78−17317
UO_2 fuel crust, submerged, mechanical stability 77−46323
UO_2 fuel element/sheath, heat transfer meas. 78−29580
UO_2 fuel elements, gas evolution kinetics 77−46291
UO_2 fuel fabrication by AUC powder process 79−59240
UO_2 fuel fabrication by the AUC powder process 80−13744
UO_2 fuel melting and Zircaloy cladding thermal failure during LWR PCM transient 80−42834
UO_2 fuel modelling *(Japanese)* 77−71648
UO_2 fuel pellet, bending strength, fabrication and microstruct. effect 80−2986
UO_2 fuel pellet fabrication using gel microspheres 80−42844
UO_2 fuel pin specifications 79−97812
UO_2 fuel rod, fine struct. meas. of fission density distrib. using solid state track detector 77−57715
UO_2 fuel rod, Zircaloy clad, chemical activity determ. of fission product 79−49682
UO_2 fuel vapour, condensation on vertical steel substrate 77−46330
UO_2 fuel-coolant interaction, film boiling and vapor explosion phenomena 80−95363
UC_2 fuels, in-pile meas. of fission gas release 79−93697
UO_2, gas bubble mobility 80−91222
UO_2, grain boundary diffusion, sintering and creep correlation, reinterpretation of creep mechanism 79−66111
UO_2, grain growth, in-reactor and lab. testing 79−74184
UO_2 grain growth studies, grain size and activation energy meas., rel. to nuclear fuel evaluation 79−93808
UO_2, green pellet with zinc stearate as additive, effect on sintering 80−68908
UO_2, growth by chem. vapour transport, using $TeCl_4$+Ar 78−35284
UO_2, Gruneisen coeff., lattice vibrational frequencies in range 298-2300K 78−79712
UO_2, γ attenuation coeffs. meas. for burn-up determ. correction *(Russian)* 78−82597
UO_2 heat-generating, molten, interaction with MgO brick 79−13468
UO_2, high burnup nuclear fuels, relation between fission product release and fuel microstruct. 80−57845
UO_2, high density, fuel kernel, burn-up swelling *(German)* 77−46283
UO_2, high temp. irradiation, effect on microstruct. and unstable fission products 78−33250
UO_2, hyperstoichiometric, O_2 chemical diffusion coefficient 79−85608
UO_2, in reactor densification 78−21648
UO_2 in UO_2-PuO_2, fast reactor fuel pins, Cs interaction 79−6743
UO_2, in-reactor meas. of modulus of elasticity, US spectroscopic method 77−23210
UO_2, infinite medium, containing liq. Na sphere, heat transfer, temp. profile 77−75783
UO_2 inhaled particle distrib. and clearance on first bifurcation and trachea of rats 78−73267
UO_2, interaction with Na, dropping experiments and subassembly test 78−82460
UO_2 interaction with water, in-pile meas. 77−42097
UO_2, interconnected grain edge porosity 79−17979
UO_2 ion in Na_2O-CaO-SiO_2 glass, fluorescence and absorption spectra of UO_2 ions 77−66531
UO_2, ionic model partial struct. factors, radial distribs. 77−84617
UO_2, ionisation potential, cohesive, electronic and redox props. 79−47916
UO_2, irradiated, fission gas release and swelling study, model 77−6488
UO_2 irradiated, grain edge porosity growth 79−19285
UO_2, irradiated, intergranular fission gas bubbles 78−21651
UO_2, irradiated, spacing of intergranular fission gas bubbles 78−66340
UO_2, irradiated, T loss during oxidative processing in air 79−97831
UO_2 irradiated fuel, densification algorithm 79−78913
UO_2 irradiated fuel, unstable fission product release 80−617
UO_2, irradiated sample, 1000 to 2100K, swelling and fission gas obs. 78−78462
UO_2, irradiation induced lattice defects 78−33251
UO_2, irradiation induced vol. change 78−67740
UO_2, isolated rod, exptl. and calculated resonance integrals 80−22986
UO_2, isothermal crack healing and strength recovery, thermal shock effects 77−36625
UO_2, LMBR fuel, burnup rate determ. using Nd isotope separation, anal. 77−44553
UO_2, LMFBR, boiling pools with internal heat generation, void distrib. 78−21626
UO_2, LMFBR fuel, mechanical response to transient heating, HCDA conditions 77−14237
UO_2, LWR fuel, microstruct. and chemical props. of powder and pellet 80−629
UO_2, LWR fuel, prep. and advantages of CARAMEL, a sheeted fuel of UO_2 pellets 80−630
UO_2, lattice defects and irrad. effects, review 77−27873
UO_2, lattice shear distortions 79−99221
UO_2, lenticular void migration rate in thermal gradient 78−21642
UO_2, liq., sp. ht. eqn. for high temp. 77−51510
UO_2, liq., splashed on Na, no evidence of entrapment 79−41000
UO_2, liquid, eqn. of state 79−14910

uranium compounds continued
UO_2, liquid, pressure generated by encapsulated Na *(Italian)* 78−82454
UO_2, liquid, reactor safety research, laser experiments *(German)* 80−42787
UO_2, liquid, struct. differences between ionic and molecular fluid models 78−26423
UO_2, liquid, surface tension 79−7733
UO_2, localised versus itinerant 5f electrons exam., reflectivity meas. 79−19905
UO_2, low enriched coated fuel particles for HTGR, anal. of O_2 partition equilibrium 80−68769
UO_2 low temp. fluorination in 3-inch diam. fluoridised beds *(Japanese)* 79−81056
UO_2 low-enriched HTR fuel, performance data review 80−42780
UO_2, mag. ordering lattice internal rearrangement transition, theory 80−20402
UO_2, mag. phase transitions, symmetry changes 77−20597
UO_2, mag. struct. 77−59389
UO_2, matrix swelling rate 78−8900
UO_2, Mg Kα and He(II) photoelectron spectra, origin from multiconfigurational Dirac-Fock calcs. 80−66387
UO_2 micropore sintering, irradiated below 1100°C, in Winfrith SGHWR 80−5255
UO_2 microspheres, prep. from UO_3 $(NH_3)_2$, exam. of mech. and physical preps. 79−6758
UO_2, microstructure in rods operated above critical heat flux 77−42098
UO_2, microwave heating in nuclear fuel preparation 80−37556
UO_2 minimum particle size to survive thermal stress fragmentation by fuel-coolant interaction 79−67886
UO_2, mobility of intergranular gas bubbles 80−15310
UO_2, mobility of intragranular bubbles during irradiation 77−6520
UO_2, modified Ashby's computer method for constructing sintering diagrams 79−43165
UO_2, molecular geometry determ. from IR spectra vibr. assignments 77−50437
UO_2, molten, effect of radiative heat transfer on thermal fluid behaviour 79−93783
UO_2, molten, fragmentation in flowing Na under TOP accident conditions 79−30978
UO_2 molten, interactions with steel and graphite 79−49700
UO_2, molten, interaction with stainless steel claddings during LMFBR TOP accident 79−54515
UO_2 molten fuel debris, 1-D penetration into concrete following FBR HCDA 80−47640
UO_2, molten fuel freezing in shield plug following LMFBR HCDA 78−8941
UO_2 molten fuel radial motion during a LWR high temp. transient 80−42833
UO_2, molten LMFBR fuel, characterization of fragmented fuel from a thermal fuel-sodium interaction 80−68774
UO_2, molten pool, heat transfer to concrete slab following LMFBR HCDA 78−8930
UO_2 molten pool prod. by internal heating, heat transfer meas. 77−88214
UO_2, monocrystalline, fission gas release charact. during irradiation 78−4985
UO_2, natural, reactor fuel, lattice cell meas. in ZED-2 hot loop facilities 78−58347
UO_2, neutron and electron irradiated, imperfect dislocation loops *(French)* 79−7606
UO_2, neutron diffr. extinction, wavelength depend. 78−38588
UO_2, neutron irrad., ^{99}Mo separation by vacuum sublimation 77−90893
UO_2, neutron irrad., sublimation separation of ^{99}Mo 77−9257
UO_2, neutron irradiated, diffusion of fission product T 78−67866
UO_2, neutron irradiated, thermal recovery of defects 79−45348
UO_2 neutron transmission temp. depend. 79−82265
UO_2, non-stoichiometric, oxidation reactions and dopants 79−42087
UO_2, nonstoichiometric, surface and interfacial props. 77−69161
UO_2, nucl. Doppler effect in fast and intermediate spectra measured by direct flux depression in neutron beam expt. 77−50232
UO_2 nuclear fuel, eqn. of state and thermodynamic props. 80−13592
UO_2 nuclear fuel, exam. of neutron yield on O(α,n) reaction 80−86912
UO_2 nuclear fuel element, lenticular pore movement 78−21644
UO_2 nuclear fuel preparation, emanation thermal anal. for characterisation of uranyl gel microspheres 80−95391
UO_2 nuclear fuels, fission gas release at high burn-ups 80−57852
UO_2 nuclear fuels, irrad. induced kinetics, diffusion and fission gas resoln. 80−59523
UO_2, O diffusion during UO_2-Zircaloy interaction 79−10986
UO_2, O diffusion mechanism 78−33249
UO_2, optical props. and electronic struct. 78−68527
UO_2, oxidation effects in CANDU spent fuel storage canister 77−6539
UO_2, oxidation rates 80−37557
UO_2 particle preparation by deposition on a fluidised bed 79−26707
UO_2 pellet, interaction between cladding in water reactor fuel pins 78−25286
UO_2 pellet fuel, radiation induced densification 77−6519
UO_2 pellet reactor fuel rods, fission gas release in high burnup range 80−635
UO_2 pellet storage facility, large dry, criticality eval. 79−26668
UO_2 pellet surfaces, β-$UO_{2.33}$ formation in air at 229 to 275°C, X-ray diffr. study 80−35362
UO_2 pellets, irrad., ^{129}I, ^{3}H distrib., radiochem. anal. *(German)* 77−16880
UO_2, pellets, pore size distrib. for optimisation of dimens. behaviour *(German)* 79−49801
UO_2 pellets, quantitative characterisation of structural parameters *(German)* 79−49803
UO_2 pellets, retention and release of water 79−67923
UO_2 pellets, sinterability, particle size effect 80−104098
UO_2 pellets, thermal densification *(Korean)* 78−44065
UO_2 pellets-graphite-Zircaloy cladding, evaluation of graphite lubrication 80−32342
UO_2, performance in organic-cooled reactor 78−25292
UO_2 phase, thermodynamic props. 80−13594
UO_2, phase transition crossover from first- to second-order in symmetry-breaking field 79−82805
UO_2, photoelectron spectra study, core and valence levels 80−66394
UO_2 pin meltdown simulation by direct electrical heating 77−88215
UO_2 pins, electrical resistance meas. at high temp. 77−15848

uranium compounds continued
UO_2, pitchblende and sooty uraninite, U extraction by underground leaching with H_2SO_4 77−61626
UO_2, point defects and electronic props., theoretical survey 77−31657
UO_2, polycrystalline, 400-600°C, Ar solubility and diffusion 77−20130
UO_2, polycrystalline, oxidation in air at room temp. 77−23206
UO_2 porous HTGR kernels, restoration of CO_2 equilibrium 77−79438
UO_2 powder, characterisation and quality control 79−49806
UO_2 powder, effect of impurities on sinterability 79−49806
UO_2 powder, precompaction effect on compressibility 78−41846
UO_2 powder, sintering charact. 78−35341
UO_2, powder, sintering effect of compaction 80−20874
UO_2 powder, temp. depend. of atomic thermal displacements, Rietveld profile-refinement procedure 80−49190
UO_2, powder and pellets, determ. of f and metal impurities *(German)* 79−49807
UO_2 powder and pellets, fabrication by integrated dry route process 79−59239
UO_2 powder compaction, force transmission and friction 80−71620
UO_2 powder prep., effect of ammonium uranate props. 78−66363
UO_2 powders, cond. between sintering and agglomeration phenomena 79−9830
UO_2 powders, sintering characterisation 79−43189
UO_2, power reactor fuel manufacture, technological aspects 79−640
UO_2 preparation, thermal treatment of U^6 xerogels during calcination 79−49813
UO_2, preparation by sol-gel technique, intermediate products characterisation *(Czech)* 79−67921
UO_2 pyrocarbon-coated HTR fuel particles, fast neutron influence on fission product transport 80−42777
UO_2, quantitative spectrographic anal. of rare earth and other impurities 79−59232
UO_2, quenched and neutron irrad., recovery processes, vacancy migration 77−28048
UO_2, radioactive gas release during irradiation 77−74922
UO_2 rate-dependent heat capacity, rel. to fast reactor safety 79−31035
UO_2 reactor fuel, high burnup performance in LWR 80−634
UO_2 reactor fuel, in linear accelerator driven and regenerative reactors 79−81064
UO_2 reactor fuel, removal of T and ^{85}Kr in O_2 medium 77−67850
UO_2, reanal. of neutron diffr. data 80−15084
UO_2 reduction by H_2, modulated mol. beam mass spectra 77−25305
UO_2, refractory, chemical reduction by atomic hydrogen 79−93830
UO_2, relative growth rates of fission-gas bubbles on grain faces 79−6739
UO_2, resolution of fission gas from grain edge bubbles, porosity effect 79−85607
UO_2, review of diffusion coeff. of fission product rare gases 78−33248
UO_2 rods, 2.35 wt.% ^{235}U enriched, in water with fixed neutron poisons, benchmark calcs. for subcritical clusters 79−26674
UO_2 rods, 2.35 wt.% ^{235}U enriched, in water with fixed neutron poisons, critical separation between subcritical clusters 79−26673
UO_2 rods, 4.75 wt.% ^{235}U enriched, in lattices in water, critical expts. 79−63790
UO_2, SiC coated, small surface area determ. by Kr adsorption 80−44429
UO_2, single crysts., nucl. neutron diffr. intensity meas. analysis, extinction 79−27957
UO_2, single-cryst. neutron diffr. data, reanal. using third cumulants 80−100130
UO_2, sintered, fuel manufacturing technology *(Czech)* 78−50290
UO_2, sintered, production by gel calcination and drying, thermal anal. *(Czech)* 80−45260
UO_2 sintered dense spheres from sol-gel technique intermediate products, characterisation *(Czech)* 79−22443
UO_2, sintered pellet, isothermal grain growth kinetics 77−18663
UO_2, sintered pellets, relationship between intercept length and grain diameter 78−52743
UO_2 sintering, effect of impurity 79−33962
UO_2 sintering, thermal anal., hexavalent uranium xerogel drying, thermal treatment modelling *(Czech)* 79−36378
UO_2, sintering, use of NH_3, grain size changes 77−55920
UO_2 sol-gel particles, low temp. sintering and props. 79−100101
UO_2, solid state diffusion of Pu 79−7711
UO_2 spectral emissivity meas. up to 3800K 80−24625
UO_2, spectroscopic data rel. to thermodynamic functions 80−34208
UO_2, spin wave spectrum, mag. susceptibility, sp. ht. *(Russian)* 79−33470
UO_2, stoichiometric, sintering diagram *(Rumanian)* 79−87602
UO_2, strain rate and temp. depend. of yield stress 77−46281
UO_2, strength recovery and crack healing 77−8918
UO_2, superplastic creep 79−15730
UO_2, surface energy, determ. by Hertzian indentation 80−93641
UO_2, surface energy *(German)* 79−7742
UO_2, surface props. of low index faces, calc. 80−6604
UO_2, swelling and gas release at low and intermediate temps. 77−50241
UO_2, temp. depend. of 5f to $6de_g$ absorption edge and intra-5f transitions 79−24314
UO_2, thermal and in-reactor densification 78−66364
UO_2, thermal and transport props., electronic contrib. 80−15432
UO_2, thermal cond. by comparative longit. ht. flux, use of generalised Bessel functions 78−26741
UO_2, thermal cond. meas. under simulated in-reactor conditions 78−94079
UO_2, thermal creep in 40 to 100 N/mm^2 stress range 77−28881
UO_2, thermodyn. props., calc. for liq. and solid phases 77−43348
UO_2, thermodynamics, defect props. 77−67810
UO_2, threshold stress in particle inhibited diffusive creep 79−38922
UO_2, transfer of fission gas between grain faces and edges 78−79815
UO_2 two-phase fuel expansion in LMFBR HCDA 79−93775
UO_3, U_2O_5, U_3O_8, and UO_3, bonding and valence obs. by ESCA and EPR 77−28696
UO_3, U_3O_8, U_2O_5, shake-up satellites and band struct. 77−55861
UO_2, unrestructured fuel, intergranular fracture during film boiling 80−3169
UO_2, uranyl cpds., X-ray photoemission spectra obs. of electronic struct. 77−28695
UO_2, valence electronic configuration determ. by photoelectron spectroscopy 78−15284
UO_2 vapour, saturated, thermodynamic state and gas kinetic relaxation to 5000K 80−13593
UO_2 vapour, thermal conductivity prediction 77−68733

uranium compounds continued
UO_2 vapour condensation from rising bubble, effects of internal circulation velocity and noncondensable gas 78−50258
UO_2, vapour press. meas. up to 500K, critical point data prediction, present state of art 79−45347
UO_2, vapour press. meas. up to 5000K, appl. of laser pulse heating 80−52230
UO_2 volatization pot. of metallic inclusions in irrad. nuclear fuel during LOF overheating transients 80−57895
UO_2 volume boiling pools, meas. and calc. of average void fraction for LMFBR HCDA anal. 80−47653
UO_2 waste material, dry recovery 79−63787
UO_2, weak acid resin derived fuel microspheres 77−79454
UO_2, Y_2O_3 stabilised, O self diffusion 79−28135
UO_2, Zircaloy sheathed, CEA expt. on transient behaviour *(French)* 80−18417
UO_2^{+}, $^{2+}$ valence energy levels, SCF relativistic Xalpha calc. 79−85912
UO_2^{2+}, precipitation reaction in KSCN 80−26040
UO_2^{2+}, aq. soln., ionic mobility meas., conductivity method 77−31791
UO_2^{2+}, electronic struct., secondary ligands effects, Dirac-Slater model 77−411
UO_2^{2+}, electronic struct. theory, applied to solid phase $Cs_2UO_2Cl_4$ and $CsUO_2(NO_3)_3$ 79−73476
UO_2^{2+}, excited, in liq. and glassy media, luminesc. decay processes, temp. activation 79−91978
UO_2^{2+} γ-irrad. frozen solns. in dimethyl sulphoxide, radiothermolum. and temp. deactivation *(Russian)* 79−33854
UO_2^{2+} in aq. solns., luminescence quenching by metal ions 78−39588
UO_2^{2+} in aq. solns., luminescence quenching by H_2O mols. 78−39589
UO_2^{2+} in aqueous solution, time resolved luminesc. for lifetime, $U_2O_4H^{4+}$ exciplex 79−61417
UO_2^{2+}, in $HClO_4$ soln., photoluminesc. intensity, conc. depends. of uranyl and H^+ 77−68069
UO_2^{2+} luminesc., excited states anal. 79−33766
UO_2^{2+}, n-propanol soln., ionic mobility and assoc. consts. 77−31792
UO_2^{2+}, relativistic X_α scatt. wave calcs. 78−46268
UO_2^{2+}, $UO_2F_5^{3-}$, $UO_2Cl_4^{2-}$, $UO_2Br_4^{2-}$, $UO_2(NO_3)_3^{-}$, reduced partition function ratio calc. 77−12819
$^{235}UO_2$ single crystals, electrochemical prep. 78−37478
$^{235}UO_2$, visualisation of fissionable radionuclides in rat lung using neutron-induced autoradiography 78−28055
UO_2:Cr_2O_3, fission gas release and swelling 80−47567
UO_2:Nb_2O_5, additions on elec. cond. 80−49712
UO_2/Gd_2O_3, grain boundary energy to surface energy ratio, pore geometry 80−34291
UO_2/Na, fuel/coolant thermal interaction in FBR, out of pile preliminary tests *(Italian)* 78−54828
UO_2/PuO_2, grain boundary energy to surface energy ratio, pore geometry 80−34291
UO_2/Zircaloy pellet/cladding interaction, eval. of lubrication of graphite 79−67857
UO_2-20CeO_2 mixed powder, X-ray and microprobe exam. of homogenisation 80−25609
UO_2-(Ni), surface, grain boundary and interfacial energies 78−71905
UO_2-(PuO_2)(BeO), ceramic fission reactor fuels, fabrication and performance, review 78−58392
UO_2-(Zr Nb) system, high-temp. reaction 78−66344
UO_2-Gd_2O_3, determ. of H_2O, Hz content by hot extraction methods *(German)* 79−49808
UO_2-Gd_2O_3, interfacial energy meas. 77−59763
UO_2-graphite interaction in operating reactor fuel elements 77−18669
UO_2-graphite interactions, effect of stainless steel, temperature on reaction rate 79−59172
UO_2-Mg reactor fuel, U potentiometric and mass spectrometric determ. 79−97811
UO_2-Na contact interface temp., effect of internal radiation 79−13477
UO_2-Na interaction, thermophysical behaviour of type 304 stainless steel impacted by jet of molten core debris 77−46319
UO_2-P-uO_2 rods, isotopic anal., gamma-ray spectrometric meas. calibration appl. 77−81440
UO_2-PuO_2, actinide redistribution in the outer regions of mixed-oxide fuel 79−36321
UO_2-PuO_2, effects of stoichiometry on cladding attack 79−26523
UO_2-PuO_2, irradiated fuel pins with various initial stoichiometries, radial O_2 distrib. *(German)* 77−46285
UO_2-PuO_2, mixed oxide fast reactor-fuel pin, fission gas bubble distrib. 78−78459
UO_2-PuO_2, possible Pu particle detection by neutron radiography, simulated fuel expts. 77−71637
UO_2-PuO_2, reaction with Zircaloy-2 79−17982
UO_2-PuO_2 fuel, O_2 diffusion at low temps. 78−8899
UO_2-PuO_2 fuel pin, hyperstoichiometric, post irradiation examination 80−63258
UO_2-PuO_2 fuelled lattice, reactivity predictions using multigroup transport theory 78−89957
UO_2-PuO_2 powder compacts, homogenization kinetics study by X-ray diffr. technique 79−37883
UO_2-SiO_2, 1000-1400°C, Ar solubility and diffusion 77−20130
UO_2-ThO_2, LWR and HWR fuel anal. of exponential expts. with WIMS-D code and data 79−81000
UO_2-Triso (propene), high temp. (2300-2500°C) treatment, metallographic cross sections, microradiographic anal. *(German)* 78−29586
UO_2-U_3O_8 thin films, sputtering under influence of fission fragments at low irrad. doses 77−48282
UO_2-U_4O_9, thermal cond., effect of microstruct. and microcracking 79−97810
UO_2-UC microspheres, coated, coating permeability meas. 80−95343
UO_2-UC_2 HTGR fuel, pyrocarbon coating permeability effect on U redistrib. 77−40460
UO_2-UC_2-C, HTGR fuel microspheres, carbothermic conversion process 80−42845
UO_2-UC_2-C microspheres, carbothermic prep., rate-controlling preps. 80−45257
UO_2-water tightly-packed lattices, ENDF/B-IV data evaluation 79−9805
UO_2-Zircaloy fuel element behaviour in PWR power plants 80−631
UO_2-zircaloy-4, reaction kinetics at high temps., O_2 diffusion 80−16667
UO_2-Zr fuel performance evaluation in power ramp tests 79−26544
UO_2-Zr fuel pins, high burnup pellet and Vipac type, overpower performance analysis 77−46230
UO_2-Zr fuel pins, ramp testing 78−86591

uranium compounds continued
UO_2-Zr high burnup nuclear fuel rods, Xe, Kr, He release 80−57846
UO_2+Na, fuel-coolant interaction, UO_2 fragmentation by thermal stress and pressurisation 77−88226
UO_2+ZrC, high temp. reactions 80−3320
UO_2^++Ar, collision-induced dissoc. cross section and threshold 80−95706
$UO_{2+\alpha}$, ternary sintering diagram, grain boundary diffusion 79−59234
UO_{2+x}, C coated particles, variation of O/U ratio and $CO+CO_2$ press. 77−61504
UO_{2+x}, configurational entropy of defect complexes, Mayer cluster theory calcs. 79−77591
UO_{2+x}, corrosion of austenitic steel effect on tensile props. *(German)* 77−70216
UO_{2+x}, defect complexes model, rel. to lattice gas virial coeffs. 79−97308
UO_{2+x} dissolution in MgO, shell model calcs. of enthalpy, computer program for formation energies 79−42251
UO_{2+x}, elect. cond. and thermoelectric power 78−52020
UO_{2+x}, possible anionic clusters and mixed valence effects 78−43333
UO_{2+x}, sintering mechanism 77−21071
UO_{2+x}-ThO_2-MgO system, in air, phase rel., X-ray diffr., electron probe and metallography anal. 79−74137
$UO_{2\pm x}$, model of response of fission gas bubbles to dynamic behaviour of point defects 79−37735
$UO_{2\pm x}$, O self and chem. diff. coeff. 78−71879
$UO_2^{2+}{}_{(aq)}+UO_2NO_3^+{}_{(aq)}$, ground and excited state interaction, struct., thermodynamic functions, photochemistry obs. 80−32779
$UO_{2.12}$ hyper-stoichiometric, defect struct., anal. of neutron diffr. data 78−26562
UO_3, 5d X-ray spectra 78−88382
γ-UO_3, inner conversion electron spectra, electron orbit hybridisation *(Russian)* 80−87227
UO_3, microwave heating in nuclear fuel preparation 80−37556
γ-UO_3, neutron powder profile obs. 77−15337
UO_3, spectroscopic data rel. to thermodynamic functions 80−34208
γ-UO_3, standard enthalpy of formation 78−88654
UO_6^{6-}, electronic struct., discrete variation and scatt. wave X_α methods 80−917
UO_6^{6-} group, in perovskite type hosts, luminesc. var. with chem. environment 77−16374
UO_6^{6-} in oxides, excitation and emission transitions involved in green luminesc. obs. 77−16372
UO_6^{6-}, octahedral uranate group, charge transfer transition and luminesc. 80−97324
$(UO_8)^{12-}$, $(UO_6)^{10-}$, electronic struct., variational Xalpha cluster calc. 80−39499
UO_n^{6-2n} ion in cryst. matrices, luminesc. 78−84640
U_3O_8, radioiodine release in O_2 and inert gas atm., chem. identities 77−57712
U_3O_8, ^{235}U enriched aerosol, characterisation by solid state track recorders 78−17538
U_3O_8 aggregates, solid, aerosols, dynamic shape factors meas. 80−61165
α-U_3O_8, cryst. struct. 78−6039
U_3O_8 demand projections using a diaggregated market penetration model 80−99214
U_3O_8, differential thermal anal. of irradiated material 79−62484
U_3O_8 enrichment standards, gamma-ray spectra 80−78378
U_3O_8, λ-type heat capacity anomalies 77−20080
U_3O_8, microwave heating in nuclear fuel preparation 80−37556
U_3O_8, oxidation rates 80−37557
U_3O_8 preparation from ammonium diuranate, thermal anal. 79−81009
U_3O_8, recovery from phosphoric acid *(Spanish)* 78−37428
U_3O_8 recovery from seawater, R and D program 80−99217
U_3O_8, supported fission foils for laser excitation, preparation method 77−68218
U_3O_8 two near-term alternatives for improved nuclear fuel utilization in PWR 80−95347
U_3O_8-Al cermet fuel for research reactors 79−9835
U_3O_8-$Y_2O_3(Sc_2O_3)$, solid soln. electrode, high temp. electrochem. appl. 80−6828
U_3O_{8-x}, phase transition to U_8O_{21+x}, study by elec. cond. meas. 80−100489
U_3O_{8-z}, therm. cond. from 200 to 750K using scanning temp. method 79−37886
U_3O_{8-z}, thermal expansion, phase transforms. rel. to temp. 77−35721
U_4O_{9-y}, doped, phase transitions, heat capacity meas. 77−18664
U_4O_{9-y}, thermal conductivity and diffusivity, 250 to 415K 77−50234
UO_2Br, X-ray struct. determ., heavy-atom method *(French)* 77−80454
UO_2Br_2, and hydrates, standard enthalpies of formation and solution 79−24811
UO_2Br_2, high temp. enthalpy increments and thermodynamic functions 80−29189
UO_2Cl_2, high temp. enthalpy increments and thermodynamic functions 80−29189
$(UO_2)_2Cl_3$, prep. and cryst. struct. 78−38674
$(UO_2Cl_4)^{2-}$, equatorial bonds, MO calcs. 78−82621
$U_2O_2Cl_5$, prep. and cryst. struct. *(French)* 80−84150
$UO_2(DMSO)_5^{2+}$ in DMSO soln. kinetics of DMSO exchange by NMR method 79−81214
α-UOF_4, neutron diffraction study 78−14327
UO_2F_2, ^{18}O isotope effects on electronic spectrum, temperature effect 79−31541
UO_2F_2, high temp. enthalpy increments and thermodynamic functions 80−29189
UO_2F_2, in soln., UV-visible spectra, ^{18}O isotope effects 77−52116
UO_2F_2, methanol soln., O isotope photochem. enrichment 79−36786
UO_2F_2 powder, F elimination kinetics 77−50235
UO_2F_2, standard enthalpy of form., from enthalpy of soln. in HF 77−48677
$UOF_4.nSbF_5$ (n=1, 2 or 3), preparation and cryst. struct. *(French)* 79−51062
$U_2O_4H^{4+}$ exciplex, in UO_2 aq. soln., time resolved luminesc. spectra 79−61417
$U(OH)_2SO_4$, antiprismatic crystal field, paramag. susceptibility, 4.2 to 300K 79−1655
$U(OH)_2SO_4$, cooperative Jahn-Teller effect, mag. susceptibility meas. 78−72121
$U(OH)_2SO_4$, mag. susceptibility, heat capacity anomalies at 21K 80−11151

uranium compounds continued
UO_2I_2, and hydrates, standard enthalpies of formation and solution 79−24811
UO_2(II), selective separation from rare earth elements on chelate ion exchangers 78−58861
UO_2(Li) pellets, release of tritium on heating after neutron irradiation 78−40071
$UO_2(NH_2O)_2(H_2O)_2.H_2O$, cryst., Raman and IR spectra 77−63409
$UO_2(NH_2O)_2.2(NH_3O).2H_2O$, neutron diffr. cryst. struct. determ. 79−19206
$UO_2(NH_2O)_2.3H_2O$, low temp. neutron anal X-ray diffr. exam. 78−2068
α-$UO_2(NH_2O)_2.4H_2O$, low temp. neutron diffr. exam. 78−26518
$UO_2(NO_3)_2$, aq. soln., pulsed NMR relax. time, ^{235}U enrichment depend. 80−2658
$UO_2(NO_3)_2$ complexes, IR spectra, normal coordinate anal., vibr. assignments, force consts. and ligation effects 80−9608
$UO_2(NO_3)_2$ highly enriched solns., benchmark critical expt. calc. study, KENO-IV code 79−18026
$UO_2(NO_3)_2$ highly enriched soln. with $Cd(NO_3)_4.4H_2O$ neutron poison, criticality expts. 80−13724
$UO_2(NO_3)_2$, mechanoluminesc., cryst. size depend. 79−38685
$UO_2(NO_3)_2$, particle fuel prep., wet chem. process for LWR, FBR and HTR *(German, English)* 77−65314
$UO_2(NO_3)_2$ solutions, cryoscopy and activity coeffs. 78−11544
$UO_2(NO_3)_4$, secondary criticality control, use of chlorinated PVC piping 80−13607
$(UO_2NO_3^+)_{aq}+UO_2^{2+}{}_{(aq)}$ ground and excited state interaction, struct., thermodynamic functions, photochemistry obs. 80−32779
$UO_2(NO_3)_2.2H_2O$, in n-butanol, ionic mobility determ. 78−34642
$UO_2(NO_3)_2.6H_2O$, 420 nm absorpt. band, electronic-vibr. struct. calc. 79−10119
$UO_2(NO_3)_2.6H_2O$, in n-propanol, ionic mobility determ. 78−34642
$U_6O_4(OH)_4(SO_4)_6$, antiprismatic crystal field, paramag. susceptibility, 4.2 to 300K 79−1655
α-UO_2SO_4, enthalpies of soln., form. determ. 78−27813
β-UO_2SO_4, X-ray and neutron powder diffr. cryst. struct. anal. 79−14760
$UO_2S_2O_3.H_2O$, IR and Raman spectra, possibility of nonexistence of cpd. of given formula *(French)* 77−24279
$UO_2SO_4.2CO(NH_2)_2$, and $U_2OSO_4.3CO(NH_2)$, lattice parameters, space groups, X-ray crystallography 78−59798
UO_2SeO_3, cryst. struct. 78−51490
UO_2SeO_3, enthalpies of soln., form. determ. 78−27813
UO_2SeO_4, α- and β-phases, X-ray and neutron powder diffr. cryst. struct. anal. 79−14760
β-UO_2SeO_4, enthalpies of soln., form. determ. 78−27813
UO_2TeO_3, cryst. struct. 78−51490
$(UO)_2V_2O_7$, V-O-V bridge stretching freq. correl. with bond angle 78−74636
UOX_2 (X=Cl, Br, I) crystal struct., IR spectra, and mag. meas. *(French)* 79−60331
$UO_2(-Nb_2O_3)$, kinetics of initial state of sintering stoichiometric and nonstoichiometric oxide 79−91609
$(UO_2)_2[SiO_4](H_2O)_3$, synthetic soddyite cryst. stuct., powder photographs 80−39050
$UO_2.HCONH_2.0.5H_2O$, prep., cryst. struct. and charact 80−29010
$UO_2.(NO_3)_2$, highly enriched solution systems, benchmark critical expts. 79−18025
UO_2(acac)DMSO, in DMSO soln. kinetics of DMSO exchange by NMR method 79−81214
UOs_3B_2, supercond. and mag. props. 80−97028
UP, anisotropic susceptibility 80−7087
UP, low temp. elec. resist., temp. depend., 3 to 90K 77−20321
UP, mag. props. 78−43554
UP, magnetisation, in fields up to 40 T 79−33505
UP, NaCl struct., band struct. 80−6714
UP, U 4f ESCA spectra 80−16148
UP, vol. changes at mag. transitions 80−7107
UP-PrP (NdP) systems, mag. phase diagrams 78−84424
UP_2, positron annihilation ang. distrib., valence electrons and Fermi surface 77−28093
UP_2, positron annihilation, mean ionic radius calc. 79−15550
U_3P_4, Knight shift, paramag. susceptibility 77−66430
U_3P_4, mag. phase transitions, symmetry changes 77−20597
U_3P_4, magnetocryst. anisotropy, torque meas. at 0.34, 0.65 and 0.91 T, 118K 78−47969
U_3P_4, mol. field approx. study of mag. ordering, Curie temp., paramag. susceptibility 79−78410
U_3P_4, press. effects on elec. resist. and Curie temp. 80−75559
U_3P_4, rhombohedral distortion of low temp. 77−7828
U_3P_4, single cryst., Barkhausen effect 77−28410
$(U_{1-y}P_y)O_{2-x}$, thermodynamics 78−70594
$UP_{1-x}S_x$, sp.ht. and electronic struct. 79−91240
UPTe, crit. behaviour, Ising-like props. 78−43605
$U_xPb_{1\pm x}Mo_{6+y}S_8$, sputtered supercond. props. 80−50019
$U_{1-x}Pr_xS$, mag. phase diagram 80−71027
$(U_{0.8}Pu_{0.2})C$, enthalpy, 1039 to 2421K 77−74920
$U_{0.8}Pu_{0.2}C_xN_{1-x}(0\leq x\leq 1)$, MX-type LMFBR fuels, TEM exam. of microscopic swelling 78−70596
$U_{0.8}Pu_{0.2}N$, self diffusion of ^{238}Pu 78−78457
$(U_{0.8}Pu_{0.2})N$, self diffusion of ^{238}Pu 78−82461
$(UPu)O_{2-x}$, thermal expansion as a function of deviation from stoichiometry *(French)* 78−21645
$U_{0.75}Pu_{0.25}O_{2-x}$, variation in O_2 potential with simulated burnup 78−70597
$U_{0.77}Pu_{0.23}O_{2\pm x}$, oxygen potential in temp. range 1523 to 1822K 80−106113
$(U_1Pu)O_2+x$, O_2 chem. diffusion *(French)* 80−49427
$(U_{1-y}Pu_y)O_{2-x}$, thermodynamics 78−70593
$U_xPu_{1-x}O_2$, theoretical study of electronic thermodynamic and valence props. 79−37655
US, band struct., SAPW calcs. 78−26810
US, band struct. and density and states, PES meas. 79−42454
US, density of states calc. 80−6715
US, elastic consts. temp. depend. in para- and ferromag. regions 79−77666
US, electron spin polarisation 79−65978
US, electronic struct. and exchange band splitting, optical refl. meas. 80−66226
US, ferromag., AC mag. susceptibility at high press. 80−7085

uranium compounds continued
US, ferromagnet, electronic structure, reflectivity *(German)* 80−49567
US, low field mag. props. 77−73047
US, magnetisation, temp., mag. field and orientation depend. 77−63232
US, magnetisation temp. and field depend. 77−20565
US, NaCl struct., band struct. 80−6714
US, optical props. and electronic struct. 80−25410
US, optical reflectivity and electronic density of states 80−16053
US, photoelectron energy distrib. and spin polarisation, electronic and mag. props. 80−16146
US, relativistic energy bands, LMTO calcs. 80−65442
US, spin polarisation and magnetism, photoelectron study 80−40219
US, U 4f ESCA spectra 80−16148
US-UC_2, solution studies 77−21120
US-UC-UC_2 system, potential nuclear fuels, phase solid soln. studies, prep. and props. exam. 79−40996
$(US_6)^{10-}$, electronic struct., variational Xalpha cluster calc. 80−39499
U_2S_3, mag. props. temp. depend. 77−8287
U_2S_3, sp. ht. at low temps., mag. behaviour 80−60353
U_xS_y, reactor irrad., U, Pu, Am, Cm production, chem. separation, isotope fractional conc. determ. 77−63986
$US_xN_yO_z$, neutron diffraction exam. of structure 78−79777
$U(SO)_2.4H_2O$, antiprismatic crystal field, paramag. susceptibility, 4.2 to 300K 79−1655
USb, anisotropic susceptibility 80−7087
USb, collective elementary magnetic excitation, neutron inelastic scatt. obs. 79−24141
USb, mag. props. 78−43554
USb, magnetisation, in fields up to 40 T 79−33505
USb, NaCl struct., band struct. 80−6714
USb, neutron inelastic scatt. from collective excitation 80−7080
USb, neutron inelastic scatt. meas., phonon spectra, mag. response, anisotropy 80−50065
USb, reflectivity spectrum, band struct. 80−7368
USb, relativistic energy bands, LMTO calcs. 80−65442
USb, search for lattice distortions at low temps. 80−79759
USb, short-range spin correlations, neutron study 78−39293
USb, UPS and XPS, surface oxidation 80−7465
USb, USb_2, U_3Sb_4, cryst. growth by chem. vap. transport 78−23588
USb_2, heat capacities, antiferromag.-paramag. transitions 78−76253
USb_2, positron annihilation ang. distrib., valence electrons and Fermi surface 77−28093
USb_2, positron annihilation, mean ionic radius calc. 79−15550
USb_2, single crystal growth, structural perfection 80−15024
U_3Sb_4, ferromagnetic transitions and heat capacities from 5 to 950K 78−14955
U_3Sb_4, mag. phase transitions, symmetry changes 77−20597
U_3Sb_4, mol. field approx. study of mag. ordering, Curie temp., paramag. susceptibility 79−78410
$USb_{0.8}Te_{0.2}$, magnetisation and polarised neutron studies 79−56515
$USb_{0.8}Te_{0.2}$, magnetisation and neutron meas., mag. moments 80−15703
$USb_{0.9}Te_{0.1}$, multiaxial mag. ordering, magnetisation and neutron scatt. meas. 79−51750
$USb_{0.9}Te_{0.1}$, multiaxial mag. structure 80−15696
$USb_{1-x}Te_x$, mag. struct. and mag. phase diagram, neutron diffr. study 80−50059
$UScS_3$, cryst. struct. determ. *(French)* 78−79576
USe, anisotropic mag. moments 79−42754
USe, electronic struct. and exchange band splitting, optical refl. meas. 80−66226
USe, ferromag., spin polarisation of photoelectrons 79−78831
USe, optical reflectivity and electronic density of states 80−16053
USe, photoelectron energy distrib. and spin polarisation, electronic and mag. props. 80−16146
USe, spin polarisation and magnetism, photoelectron study 80−40219
U_2Se_3, mag. props. temp. depend. 77−8287
U_3Se_4, mag. phase transitions, symmetry changes 77−20597
U_3Si, crystalline elec. field studies using neutron inelastic scatt. at NRCN 80−10931
U_3Si, interaction with ZI_4, 700 to 800°C, exam. using metallographic and local X-ray spectral anal. 79−90831
U_3Si production, for heavy-water-cooled ractor, arc melting and hydrogenation methods comparison *(Chinese)* 79−85721
$USiO_4$, cryst. field parameters, paramag. susceptibility, 2-500K 77−55658
$U_xSn_xMo_6S_8$, supercond. props. 80−97023
UT_3, ^{3}He distrib. 78−30661
UT_3, ^{3}He distribution from triton decay, NMR meas. 78−19360
UTe, crit. exponents, neutron and magnetisation meas. 80−88823
UTe, critical mag. fluctuations near T_c 80−7122
UTe, electronic and spin struct. negative spin polarisation of photoelectrons 79−19514
UTe, electronic struct. and exchange band splitting, optical refl. meas. 80−66226
UTe, ferromag., negative electron spin polarisation in photoemission 79−19967
UTe, magnetisation and neutron meas., mag. moments 80−15703
UTe, magnetisation and polarised neutron studies 79−56515
UTe, photoelectron energy distrib. and spin polarisation, electronic and mag. props. 80−16146
UTe, photoemission energy distrib. curve and electron spin polarisation 79−52074
UTe, relativistic energy bands, LMTO calcs. 80−65442
UTe, spin polarisation and magnetism, photoelectron study 80−40219
U_3Te_4, mag. phase transitions, symmetry changes 77−20597
U_xTe_y, mag. props. temp. depend. 77−8287
UTe_xSb_{1-x}, photoemission energy distrib. curve and density of states 79−52074
UTe_xSb_{1-x}, photoemission, densities of states 80−16147
$U_xTh_{1-x}As$ (Sb), electronic struct., relativistic KKR-averaged T-matrix approx. method 80−107702
$U_xTh_{1-x}As$, mag. phase diagram, magnetisation meas. 80−60271
$U_{1-x}Th_xO_2$, solid solution, single crystal growth by chemical transport reactions 78−72708
$(U_xTh_{1-x})S$, mag. props. rel. to elec. struct., 1.5-300K 77−1557
$(U_xTh_{1-x})S$, metallic, 5f virtual bound states, elec. resist. and mag. susceptibility meas. 77−28363
$(U_xTh_{1-x})Sb$, magnetisation, U valence change 80−7089
$U_xTh_{1-x}Sb$, valence change of U accompanied by singlet-ground-state ferromag. 80−70965
uranium compounds continued
$(U_xTh_{1-x})Se$, metallic, 5f virtual bound states, elec. resist. and mag. susceptibility meas. 77−28363
$(U_xTh_{1-x})S(Te)$ solid solns., electronic struct., mag. susceptibility and elec. resist. obs. 77−20551
U(VI) gel, prep. by internal gelation, determ. of region of existence 77−9136
U(VI) peroxo complex ion precipitation with Co(III) complex cation 78−80728
U(VI) sulphito complex ion precipitation with hexammine Co(III) chloride cation 78−92495
$(U_{0.3}Y_{0.7})O_{2-x}$, ionic cond. 80−6828
UZr_6FO_{14}, X-ray cryst. struct. determ. and refinement *(French)* 80−107122
$U_xZr_{1-x}Fe_2$, Curie temp. and saturation moment at 4.2K 80−70966
UZrH low enrichment fuels, test programs and analysis 80−9398
$^AUO_2(NO_3)_2$, a=233, 235, slab tanks for criticality control, neutron multiplication calc. 80−13606
^{233}U fuels for HTGR, remote fabrication 80−13752
$(^{233}U, Th)O_2$ fuels for HTGR, remote fabrication 80−13752
$(^{233}U, Th)O_2$ pellet-type fuels for CANDU reactors, remote fabrication plant design 80−13751
$^{233}UO_2$, reactor fuel, neutron multiplication factors, temp. depend. 78−29557
$^{233}UO_2/ThO_2$ water-moderated lattice analysis with ENDF/B-IV data 79−9800
$^{235}UF_6$ enrichment equipment, running-belt and rotary-disc concentrators, transient Knudsen diffusion 80−32421
^{238}U complex, α-induced defects, vibronic luminesc. band fine struct. 79−87489
$^{238}UO_2$ grains distrib. in graphite matrix, effect on resonance integral 80−68768
UF_6, mass spectrometric determ. of ^{235}U content 80−68961
$^{233}Uo_2$-ThO_2 fuelled core, spent fuel rod assay, reactivity perturbation method 77−18654
$VO[UO_2(SO_4)_2].6H_2O$, synthesis and crystallographic data 78−26532
VUS_3, mag. struct. and delocalised moments, powder neutron diffr. obs. 77−69496
Xe-MF_6, M=W, Mo, U, Re, Ir, charge transfer interactions, VUV and IR obs. 78−50664
$Zn(UO_2AsO_4)_2.8H_2O$, prep. cryst. struct. characterisation 78−30589
ZrO_2-UF_4, orthorhombic struct., X-ray and electron diffr. study *(French)* 78−67689

Uranus
ε ring, precession 80−26804
albedo and brightness temp., 5 μm IR obs. 80−82300
albedo and spectral features from IR obs. 80−82299
astrolabe obs. during 1977 at Santiago, Chile 79−58298
astrometry, obs. with Danjon Astrolabe of Santiago during 1975 and (1976) 78−12151
astrometry, positions determ. with Odessa meridian circle, (1974 to 1975) *(Russian)* 79−44394
atmosphere, ammonia and water vapour contents 80−90366
atmosphere, appl. of methane band-model parameters to visible and near IR spectrum 80−98609
atmosphere, D/H ratio from visible spectra obs. 80−82296
atmosphere, IR radiation, review 80−8568
atmosphere, limb and polar brightening at 7300 Å 77−56873
atmosphere, methane absorpt. band in spectrum 78−45275
atmosphere, Raman scatt. 78−28571
atmosphere, review 77−5470
atmosphere, saturation model 77−60723
atmosphere, thermal struct. 79−84735
atmosphere, whole-disc optical polarization meas. 77−45356
atmosphere model, methane cloud 77−37567
basic props. 77−45357
brightness temperature at sub-mm wavelengths 79−53743
clouds, particle comp. 80−31253
contaminant terrestrial microorganisms, limitations to growth 77−41355
decimetric radio obs., brightness temp. 80−46474
disc profiles, narrow waveband, 6000-8500 Å region 79−66960
disk structure in 7300 Å methane band 80−17544
ethane, long path photoelec. absorpt. spectra 4200-10600 Å, appl. to Uranus 77−83592
ethane emission, unsuccessful search 78−16344
far IR obs., temp. determ. 79−12431
figure, hydrostatic equilib. eqn. numerical soln. 79−62773
formation of planet and satellites *(Chinese)* 78−69712
geometric oblateness from digitized photographs, Stratoscope II balloon obs. 80−67649
geometrical and dynamical flattening 79−48734
insolation, latitudinal, seasonal and atmospheric effects 77−60704
ionosphere, model, ionization by galactic cosmic rays and solar EUV radiation 78−4142
IR spectrum from 0.8 to 2.5 microns, obs. 80−21946
limb brightening, visible spectrum 78−61797
limb brightening within methane 7300 Å band 78−85902
Love numbers 78−16338
lunar occultation obs., 1977 February 10, radius, limb darkening and polar brightening at 6900 Å 80−17545
magnetic field, hydromagnetic dynamo in core 80−90365
magnetic field origin 80−36564
magnetosphere, plasma dynamics in mag. field laboratory simulation 79−16757
magnetosphere, review 78−12145
methane(-H_2), long path photoelec. absorpt. spectra 4200-10600 Å, appl. to Uranus 77−83592
methane 6819 Å line interpretation rel. to inhomogeneous scattering models 78−53871
methane 6825 Å band, obs. 77−78715
methane band limb-brightening, obs. 79−84742
microwave brightness temperature, evidence for increase 78−93150
microwave radiometry and interferometry 80−56766
Miranda, influence on struct. of Uranian ring system 78−4148
Miranda (Uranus V), appulse to BD−14°3996 on 1977, March 10, predictions 77−2369
Neptune-Uranus general planetary theory, short-periodic term elimination 79−75153
Oberon, near IR spectra and JHK photometry, mass and dia. measurement 80−56761

Uranus continued
observing in 1977, prospects 77−56874
occultation of faint blue star on 1977, Aug. 26 77−53470
occultation of SAO 158687, 1977, Mar. 77−33407
occultation of SAO 158687, 1977 March 10, obs. at Tokyo Astron. Obs. 78−61716
occultation of SAO 158687, 1977 March 10, rings discovery 78−69743
occultation of SAO 158687, 1977 March 10 77−87322
occultation of SAO 158687, estimation of true external errors of Tokyo meridian circle obs. 78−28487
occultation of SAO 158687, evidence for satellite belt 77−29718
occultation of SAO 158687 by ring system, obs. at Perth and Mauritius 77−67068
occultation of SAO 158687 by Uranus (1977 Mar. 10) 77−22044
occultation of SAO 158687 on 1977, March 10, predictions 77−29717
occultations by eclipsed Moon, 1850-2050 period 77−49319
orbit second-order perturbations, semi-major axis secular vars. *(French)* 79−2474
orbital perturbations by Pluto, representation *(French)* 80−26724
photometric observations for solar luminosity monitoring 77−53500
photometric var. in 1953-76 period 78−85901
polar moment of inertia determ. 80−94694
positions, reduction of 19th century obs., method comparison 80−94691
proposed sixth satellite, mass estimate 79−35190
radio emission in H_2O 1.35 cm line 78−20664
radius and ellipticity from SAO 158687 occultation obs. 80−67648
regular satellite system, form. model rel. to masses 78−69714
ring, form. and stability 80−82302
ring occultation possibilities for two faint 11-12 mag. stars 77−56875
ring system, origin and location of narrow rings 80−56764
ring system, quantitative anal. of Dermott-Gold theory 78−4147
ring system, radii rel. to break-up and accretion limits and origin 79−84737
ring system, review of physical studies 80−72874
ring system, statistical mechanics of Keplerian orbits 78−20625
ring system, struct. from photoelec. obs. of 5AO 158687 occultation 80−77348
ring system, summary of recent research 80−72875
ring system, theory, orbital reson. with Ariel, Titania and Oberon 77−64698
rings, as volatile material in satellite orbits, model 80−26807
rings, BD−15°3969 occultation obs. 78−89118
rings, geometric albedo upper limit 78−36510
rings, ice sputtering by radiation belt protons 78−89116
rings, nature and origin, orbital resonance 79−96967
rings, new discovery 78−45274
rings, occultation obs. *(French)* 80−82281
rings, occultation of SAO 158687, 1977 March 10, photoelec. obs. and anal. *(Chinese)* 78−69657
rings, occultation of SAO 158687, 1977 March 10, photoelec. obs. 79−30007
rings, occultations of stars, existence of rings confirmation and radii calc. 78−53872
rings, occultations of stars during 1977-1980, predictions 78−16343
rings, optical search 77−67067
rings, possible obs. by William Herschel 79−48733
rings, prediction in 1972 based on Alfven critical vel. effect 79−2518
rings, radii and widths from 1978 April 10 occultation of SAO 158687 79−8878
rings, radii from SAO 158687 occultation 78−89117
rings, reson. orbit theory and prediction of undiscovered satellite 78−81585
rings, S/N ratios for stellar occultations, 1977-80 period 78−32392
rings, size, shape and periods of rotation *(French)* 79−48735
rings, stellar occultation predictions for December 77−82161
rings, theory 79−21226
rings and regular satellite system formation 80−41746
rings discovery *(Danish)* 78−69742
rings origin, orbital reson. effects 78−53874
rotation, equatorial flow theory 80−67653
rotation period, effects of seeing on reflected spectrum 80−46479
rotation period, spectroscopic determ. 80−51691
rotation period meas. 78−7920
rotation periods rel. to methane band strength var. 78−49376
rotation velocity determ. 78−36508
rotational period, modified spectroscopic technique 78−16345
rotational period from spectral line tilts 78−20726
SAO158687 occultation, obs. possibilities in methane bands 77−29719
SAO 158687 occultation by rings, identifications and sizes 77−45358
satellite ε-ring, variable width and ellipticity, orbital considerations 78−40870
satellite belt, numbers and positions from SAO 158687 occultation 77−33408
satellite occultation of SAO 158687, Kavalur obs. 77−53473
satellite ring system, new features from Kavalur photoelectric record of SAO 158687 occultation 78−12152
satellite rings, KAO obs. of SAO 158687 occultation 77−53471
satellite rings, occultation of SAO 158687 77−37568
satellite rings, Perth Observatory obs. of SAO 158687 occultation 77−53472
satellite rings occultation of SAO 158687, discovery accounts 77−74009
satellite system, orbit-orbit resons. 78−4093
satellites, astrometric obs. 80−67654
satellites, narrow band spectrophotometry of Ariel, Umbriel, Titania and Oberon 79−16879
satellites masses and Laplace relation 77−5492
satellites position meas. 78−81573
secular brightness increase, 1972-76 period 78−16346
spectrum in 5-20 micron range, obs. 78−32393
stellar occultation, 1980 August 15 to 16, reality of additional occultations questioned 80−109396
stellar occultation by Uranus and rings, 1980 August 15 to 16, obs. 80−98610
stellar occultations by ring system, 1977-1980, colours and magnitudes of stars 78−16277
structure and evolution in three-layer interior model 80−72877
structure and magnetic field, theory using two-layer model 80−4298
synchrotron radiation upper limit at 34.3 MHz 77−60724
thermal evolution, comparison with Neptune 78−85903
thermal structure from IR meas. 78−36509

Uranus continued
Titania, near IR spectra and JHK photometry, mass and dia. measurement 80−56761
Titania and Oberon, IR photometry rel. to membership of new class of satellites 78−12146
Umbriel, near IR spectra and JHK photometry, mass and dia. reassessment 80−56761
upper atmosphere, mean temp. and temp. vars. 80−46477
upper atmosphere, struct. from SAO 158687 occultation obs. 80−17547
upper atmosphere, temp. struct. 79−62791
Uranus satellite rings, identifications and sizes from SAO 158687 occultation by 77−45358
UV albedo, meas. 80−82295
Voyager low energy charged particle experiment 78−20618
Voyager magnetic field experiment 78−24431
Voyager mission objectives 78−24426
Voyager UV spectrometer experiment 78−24429
D/H ratio in atmosphere, meas. from HD line 78−57497
H_2 quadrupole lines detect. in spectrum 78−93149
H_2 rotational quadrupole lines, theoretical brightness temps. 78−7917
HD detect. at 6063.88 Å, D/H abundance ratio calc. 78−57495
NH_3 in atmosphere, evidence for depletion 78−53870

urban planning *see town and country planning*

utility programs
bWR servicing and refueling improvement program 80−9390
rectangular and triangular diagram printer-plotting FORTRAN routines 77−5325

u.v. astronomy *see ultraviolet astronomy*

u.v. detectors *see ultraviolet detectors*

V-centres
see also H-centres
alkali halide: monovalent cation, recomb. luminesc. $(V_K+e)_A$-type emission 77−28615
alkali halide:Sn^{2+}, V_c^--centres, vacancy induced splitting of excited states, Sn^{2+} structure 78−51931
alkali halide, activated, luminesc. and stored light sum 78−6738
alkali halide, dynamics of nonrelaxed and self-trapped holes *(Russian)* 80−80607
alkali halide, hole capture kinetics, influence of autolocalised and zone holes *(Russian)* 80−54714
alkali halide, impurity-vacancy dipole interaction with relaxed and nonrelaxed holes *(Russian)* 78−75661
alkali halide, V_k-centre, electrostatic energy 79−27978
alkali halide crystal, defect formation in thermal equilibrium state of self-localised exciton 80−44205
alkali halide crystal, irrad., chemiluminesc. process during dissolution *(Russian)* 78−92133
alkali halide crystals, radiation damage products, impurities and colour centres *(German)* 78−10086
alkali halide crysts., thermal motion theory for V_k-centres *(Russian)* 77−47451
alkali halides, gamma and additively coloured, dissolving in pure water, lyoluminesc. mechanism 80−100693
alkali halides, luminesc. induced by ion impact, −160 to 200°C 77−8654
alkali halides, self trapped exciton, optical detection of spin relax. processes 78−60358
alkali halides, self-trapped holes, ESR *(Japanese)* 79−73811
alkali halides, V_k-centres, vibr. modes, calc. 80−84269
alkali metal halides, F_2^- mag. reson. absorpt. spectrum 77−73079
alkali metal halides, F-colouring role of impurities 80−64995
alkali metal halides, hole self-localization and capture, temp. depend. 80−92526
alkali metal halides, hyperfine struct. of V_K and $(XY)^-$ centres, valence band wave functions 77−11873
alkaline earth fluorides, radiation damage and photochromism in doped and undoped crysts. 79−51148
halogen molecule negative ion, pot. curve calc. 77−10596
ionic crystal, exciton mechanism model for defect form. 80−80187
KBr, γ-irradiated and additively coloured, chemiluminescence origin *(Russian)* 77−32453
molecular model for V_k centre 77−85567
nonmetals, V_K-centre dynamic model, fluctuation production of barriers, diffusion *(Russian)* 78−47372
phosphate glass, electron-irradiated, charge accumulation, comp. depend. 78−2159
semiconductors, recombination processes, review 79−38088
trialkylammonium, iodides, absorpt. and luminesc. spectra of self-localized excitons 80−97340
trihalide ions, V_k-centre motion in alkali and alkaline earth halides 77−26984
Zeeman interaction, relativistic corrections and very small g-shifts, contrib. to EPR 78−72393
$AgBr_{1-x}Cl_x$, self-trapped holes, ESR meas. 77−36131
Al_2O_3, γ-irrad., hole centres, luminesc. and EPR obs. 77−32256
Al_2O_3, UV dosimetry grade, thermolum. glow curves and emission spectra, 90-500K 78−72615
a-As_2Se_3 chalcogenide glass, influence of thermally induced defects on transport props. 80−49766
a-As_2Se_3 film, metallic impurity effect on transport props. 80−49963
BaF_2, mag. hyperfine const. and lattice distortion of V_k-centre 77−62864
BaF_2:RF_3, cryst., absorpt. spectra, γ-ray effects 77−12409
BaO, electronic struct. of V^- and related centres 80−2355
BeO, ceramic and single cryst., EPR-ENDOR study of [Li]° centre 77−85569
CSI:Na cryst., V_K-Na^0 centre pairs, tunnelling recomb. 78−91952
CaF_2, doped, colour centre form. by UV irrad., afterglow, thermolum. and EPR obs. 78−10047
CaF_2, mag. hyperfine const. and lattice distortion of V_k-centre 77−62864
CaF_2:Dy(Ho)(Pr)(Tb), V_k-centre recomb. kinetics, phosphoresc. 77−55817
CaF_2:M, M=Mn, Fe, Co, Ni, X-irrad., impurity effects on defect prod. 80−92525
CaF_2:Ni, X-irradiated, optical and EPR meas. 80−108235
CaF_2:Tm temperature dependence of V_k-centre generation efficiency *(Russian)* 78−48203
$CaMoO_4$, scheelite struct., intrinsic hole centres, EPR study 78−64274
CaO, electronic struct. of V^- and related centres 80−2355

V-centres continued
CaO, undoped and Cl-, F- or Al-doped, X-ray and UV luminesc., electron-hole recombination processes *(Russian)* 78−76528
$Ca(OH)_2$, V-centres, EPR obs. 77−48051
$CaWO_4$, scheelite struct., intrinsic hole centres, EPR study 78−64274
Cl_2^-, in ion pairs with metals, ESR, in AR matrix, V-centre theory 77−16172
CsBr, self trapped hole, hopping motion equilib. lattice config., electronic excitation energy, activation energy calc. 78−10046
CsBr:Tl^+, ESR of [X_2^-] centres 79−33533
CsCl, self trapped hole, hopping motion equilib. lattice config., electronic excitation energy, activation energy calc. 78−10046
CsCl:Tl^+, ESR of [X_2^-] centres 79−33533
CsI, correl. between UV emission band at 300 nm and self-trapped excitons, 4.2K 78−75998
CsI, self trapped hole, hopping motion equilib. lattice config., electronic excitation energy, activation energy calc. 78−10046
CsI:Na, self-trapped exciton emission polarisation 80−49607
CsI:Na, tunnelling recomb. of electron-hole pair, optical detection of ESR and circ. dichroism 79−47360
CsI:Na, X-ray irradiated, optical and ESR studies in IR absorption band 80−80828
CsI(Br)(Cl):Tl, [X_2^-] centre dynamic props. 79−65730
GaAs:Ge, vap. grown, diatomic complex donor and acceptor model 78−80003
β-Ga_2O_3, doped, photolum., emission centres struct. 78−52557
GaP:Fe(Cr), photo-ESR of annealed crysts. 80−15795
GeO_2:Sc^{3+}(Y^{3+})(In^{3+}), trapped-hole centres, ESR meas. 79−77597
KBr and KBr:Sr X-irradiated, optical investig. of Br_3^- centres 77−16348
KBr, cation defects creation mechanism 80−75224
KBr, defect accumulation under electron irrad. at 4K 80−107233
KBr, efficiency of V_k- and Ag^0-centres generation *(Russian)* 80−39080
KBr, electron irrad. at 4K, role of V_K centres in equilib. among centres 78−67712
KBr, kinetic eqns. of formation of F-centres and V_4-centres 78−67713
KBr, pulse radiolysis of metastable interstitial centre of high temp. 80−20658
KBr, pure and Sr^{2+} doped, X-irrad., hole Br_3^- centre creation and destruction 77−15411
KBr, thermolum. and reactions of freed interstitial and trapped hole centres 78−23538
KBr, V- and X-centres accumulation *(Russian)* 80−54228
KBr whisker, X-irrad., defect form., thermolum. and ionic cond. obs. *(Russian)* 78−84666
KBr, with Frenkel cation defects, EPR and thermolum. of V_F, V_2-centres 78−10769
KBr, X-irrad. crysts., halogen aggregation, absorpt. spectra obs. *(Russian)* 80−66234
KBr, X-irradiated, at 80K, interstitial K ions associated with interstitial Br ions *(Russian)* 78−75655
KBr:Ag, formation of electron centres and self-localised holes, ESR exam. 78−91947
KBr:H^+(H_2^+), absorption bands, V_4- and M-centres 77−48204
KBr:Li^P(Na^+), electronic struct. of $(V_K e)_A$ 78−95269
KBr:NO_2, Na effect of Na^+ impurity on self-trapped hole *(Japanese)* 78−67982
KBr:NO_2, X-irrad., paramag. and nonparamag. hole centres 77−16176
KBr:Na, X-irrad., luminesc. from self-trapped excitons 77−28614
KBr:Tl excitation in fund. absorpt. region, luminesc. and thermolum. 80−50433
KBr(Cl), X-ray irrad., tunnelling recomb. luminesc. 80−2873
KBr(Cl)(I):Tl^+, recomb. luminesc. kinetics 77−16366
KBr(I), photostimulated recomb., electron spin polarisation 80−60673
KCl (Br) crystals, thermally stimulated luminescence accompanying recombination of V_F and F centres 80−55201
KCl and KCl:NO_2, X-irrad. crysts., Cl_3^- centres photodissoc., optical anisotropy and creation mechanisms *(Russian)* 80−66235
KCl, cryst., colour centres, ionic cond., X-ray effects, thermoluminesc. *(Russian)* 78−6056
KCl, electron-irrad., positron-capture centres, thermal annealing kinetics 79−95875
KCl, gamma-irradiated crystal, interrelation between V_2 and V_3 centres *(Russian)* 79−69862
KCl, irrad., V_3-band in absorpt. spectra, model *(Russian)* 79−56821
KCl, irradiated, determ. of molar extinction coeff. and oscillator strength of V_2-centre *(Russian)* 78−80384
KCl, irradiated crystal, determ. of oscillator strength of V_3-centre *(Russian)* 78−92095
KCl, luminescence induced by tunnelling recombination between neutral Ag atoms and V_k centres 79−61442
KCl, Raman spectra and vibrational modes of V_K centre meas. 78−80338
KCl, thermal annealing of F, V_2-, V_3-centres *(Russian)* 80−54229
KCl, V- and X-centres accumulation *(Russian)* 80−54228
KCl, with Frenkel cation defects, EPR and thermolum. of V_F, V_2-centres 78−10769
KCl:Ag(In)(Tl), excitation in fund. absorpt. region, luminesc. and thermolum. 80−50433
KCl:Ag(Tl), formation of electron centres and self-localised holes, ESR exam. 78−91947
KCl:Cu,Tl, plastic deform., charge exchange of hole centres *(Russian)* 77−11876
KCl:Eu, additively coloured, ESR obs. of $^{2+}$ complex 77−16170
KCl:I crystals, V-band development using X-rays 78−88337
KCl:$SnCl_2$, photostimulated hole recombination luminesc. *(Russian)* 80−80833
KCl:$SnCl_2$, Sn^+ centres, polarised luminesc. and EPR 79−65076
KCl:Sr^{2+}, X-irrad., thermolum., impurity aggregation, trapping centre form. 78−88367
KCl:Sr(Ca), thermoluminescence and colour centre thermal stability in irradiated sample 78−43941
KCl:Tl, ESR of trapped electron and hole centres 79−78516
KCl:Tl, hole capture kinetics, influence of autolocalised and zone holes *(Russian)* 80−54714
KCl:Tl, thermal glow of trapped electron and hole centres 79−78762
KCl:Tl^+, optical absorpt. spectra following X-irrad., F- and V-centres 79−99912
KH_2PO_4:KH_2AsO_4, X-irrad., EPR 77−32257
KI crystals, containing excess of halogen, optical and thermal properties *(Japanese)* 77−59596

V-centres continued
KI, intrinsic luminesc. quenching, by X-ray induced coloration 78−19539
KI, optical bleaching of V_2 and V_3 bands 79−33739
KI, surface, 420 nm band laser-stimulated emission, V_2 centres 78−84633
KI, V-centres, optical and thermal bleaching of V_2 and V_3 bands 77−85751
KI, X-irrad., V-centres, Raman spectra 79−91429
KI:Eu^{2+}(Sr^{2+})(Mn^{2+}), elec. field effect on mech. of recomb. 78−80397
KI:Tl, electron-hole and V_k-Tl recomb., TSC and thermolum. study *(French)* 80−34461
KI:Tl, excitation in fund. absorpt. region, luminesc. and thermolum. 80−50433
LaF_3, gamma-ray induced coloration, role of impurities 77−35586
LiCl, neutron irradiated, EPR exam. 78−76309
LiF, Raman spectra and vibrational modes of V_K centre meas. 78−80338
LiF, thermoluminescence mechanism, extension of Mayhugh-Christy model 78−80425
LiF, V_k and F centres, efficiency of formation, temp. depend. 79−7600
LiF, V_k-centre generation, temp. depend. 78−18644
LiF, V_t centre (F_3^{2-}) identification, ESR spectrum anal. 80−7164
LiF:Mg(Ag), electron spin-lattice relax. of V_k-centre 78−95518
$MgAl_2O_4$, γ-irradiated crystal, TSC, thermoelec. power, thermolum. and afterglow 80−75583
MgF_2, gamma- or neutron irradiated, ESR meas. on hole centres 77−12201
MgO, ^{25}Mg superhyperfine struct. of V-type defects, ENDOR 77−66439
MgO, cryst. short-wave luminesc. V-centre electron recomb., impurity effects *(Russian)* 77−20921
MgO crystals, dipolar defects, thermally stimulated depolarisation 80−66101
MgO, defect centres, thermolum. examination 78−15235
MgO, electron irrad., V^--centres, stress-induced optical dichroism, absorpt. spectra 79−61406
MgO, radiation induced O interstitials, EPR meas. 78−55866
MgO, single crystal, thermolum. meas. *(Japanese)* 78−19577
MgO, single crystal, thermal and optical stimulation processes of V-centres *(Japanese)* 80−11485
MgO, V^- centres, electronic struct., rel. to optical absorption 77−28140
MgO, with paramag. surface defects, elec. cond., 20-250°C, H_2 atm. effects 77−20313
MgO:Al(Li)(F)(Sn), hole processes in photostimulated luminesc., electron emission, X-ray irrad., ESR relaxation 79−69889
MgO:Li, $[Li]^0$ defect, high temp. and ionisation induced effects 78−34509
MgO:Li, $[Li]^0$ defect, stress induced optical dichroism 78−35179
MnF_2, radiation damage, optical absorpt. and luminesc. expts. 78−2161
NaCl crystals, electronic and hole centres and surface, quantum-chemical calcs. 80−65489
NaCl, emission of Cl atoms during V_k centre decomposition 80−10578
NaCl, irradiated, determ. of molar extinction coeff. and oscillator strength of V_2-centre *(Russian)* 78−80384
NaCl, luminescence induced by tunnelling recombination between neutral Ag atoms and V_k centres 79−61442
NaCl, V- and X-centres accumulation *(Russian)* 80−54228
NaCl:Ag, excitation in fund. absorpt. region, luminesc. and thermolum. 80−50433
NaCl:Ag, formation of electron centres and self-localised holes, ESR exam. 78−91947
NaCl:Ca^{2+}, X-ray induced luminescence 78−23516
NaCl:Mn^{2+}, radiation-induced colouring, room temp. kinetics 79−55736
NaCl:Mn^{2+}, thermolum. spectra, mechanisms 80−80873
NaCl:Pb, γ-irrad., centres in thermoluminescent emission 77−85816
NaCl(Br), X-ray or UV irradiated, cation defects creation mechanism 80−75224
NaF:U, luminesc. spectra, Vibr. struct. 80−80840
NaI:Cu^+, luminesc. of iolated V_K-centres 78−84641
NaI:Tl, scintillation excitation mechanism 80−2857
$NaMgF_3$, defects induced by X- and vacuum UV irrad., optical and elec. study 80−107319
RbBr (I), optical absorpt. centre formation time meas. 80−40081
RbBr, suprapure, thermolum. glow and emission studies at room temp. 80−7423
$RbCaF_3$, V_K centres, lattice distortion in tetragonal phase, EPR meas. 77−20699
RbCl, Raman spectra and vibrational modes of V_K centre meas. 78−80338
RbCl(Br), cation defects creation mechanism 80−75224
RbI, intrinsic luminesc. quenching, by X-ray induced coloration 78−19539
RbI, luminesc. spectra induced by pulsed Ne^+ and electron beams and X-rays 80−80851
RbI, photostimulated recomb., electron spin polarisation 80−60673
RbI:AgI, thermal reorientation kinetics of I_2^-, decay of optical anisotropy 77−52138
$RbMgF_3$:Mn, low-temp. radiation damage, optical absorption meas. 78−22761
$RbMnF_3$, radiation damage, optical absorpt. and luminesc. expts. 78−2161
Si:Ar(Ne)(O)(N), ion-implanted, defect reverse annealing, 550-650°C 80−88875
SiO_2, fused, γ-irrad., O-associated trapped-hole centres, optical absorpt. and ESR spectra obs. 79−65729
$SrCl_2$:K^+(Na^+)(Rb^+) X-irradiated, recomb. luminesc. between trapped electron and self trapped holes 77−73162
SrF_2, mag. hyperfine const. and lattice distortion of V_k-centre 77−62864
SrF_2:Dy(Ho)(Pr)(Tb), V_k-centre recomb. kinetics, phosphoresc. 77−55817
SrF_2:Tb, and pure, UV induced processes 77−32452
SrO, electronic struct. of V^- and related centres 80−2355
SrO, hydrogenated, EPR and ENDOR meas. of γ-irradiated cryst. 77−8403
SrO, trapped hole defects, ENDOR and EPR spectra of V-centres 77−32255
SrO:D, γ-irrad., V_{OD} defects, EPR and ENDOR 78−27116
$SrTiO_3$, EPR of Fe^{3+}-V_O centre, above T_c 80−39870
SrO, x-irradiated, intrinsic V^- and V^0 centres, ESR exam. 77−40126
TiO_2:Ga^{3+}, EPR spectra 78−80214

V-centres continued
Y_2O_3, formation and changes in point defects, EPR, optical transitions and thermolum. spectra 78−2118
ZnS:Cl, single cryst., deep centre study by impurity electroabsorpt., photocond. meas. 77−12411
ZnSe, ODMR expts., A and V^--centres, origin of emission bands 78−80255
ZnSe, optically detected mag. reson. of V^- centre and donors 78−10805
V_H-centres *see H-centres*
V-VI semiconductors *see semiconductor materials*
vacancies (crystal)
see also Frenkel defects; impurity-vacancy interactions; Schottky defects; vacancy condensation loops; vacancy-dislocation interactions
A15 compounds, disordered, reordering kinetics 80−96678
A15 ordered and disordered cpds., density of states calc. 79−87033
activation energy of self diffusion, temperature dependence 78−91470
adamantane, cryst., vacancy formation energy, positron annihilation study 80−60706
adsorption on internal boundaries, rel. to recrystalln. and precip. 78−10084
alkali halide:Eu^{2+} cation vacancy complexes, binding energies 80−96513
alkali halide:Me^{2+}, nearest-neighbour theory of dipole polarisation and depolarisation, cation vacancies 77−16243
alkali halide, chalcogen^{2-} vacancy centres, absorpt. and fluoresc. spectra 78−48204
alkali halide, crystal, irradiation-induced defects 80−107316
alkali halide, dipolons, graphical method for binding energy determ. 78−59805
alkali halide, energy of movement of vacancies, zeroth order calc. 77−89571
alkali halide, migration enthalpy of cation vacancy correl. with MP 77−76606
alkali halide crystals, defect fermion properties, ionic cond. calcs. 80−59457
alkali halide crystals, inhomogeneous transport at low temp. 77−43382
alkali halide F-centres, cation vacancy model, rot. mechanism 77−76393
alkali halides, binding energies of vacancy pairs 78−51533
alkali halides, defect formation, kinetics 78−67713
alkali halides, free energy of formation of vacancy determ. 77−76597
alkali halides, intrinsic point defects, generalised Mott-Littleton approach 77−51698
alkali halides, mass transport, contrib. of vacancy defects 79−46831
alkali halides, NaCl and CsCl type structs., comparison of migration entropy for cation and anion vacancy motion 77−62519
alkali halides, polarization, photoinduced, rel. to exchange between vacancy and impurity 80−59914
alkali halides, shell model calc. of defect energies, crystal-independent interionic potential parameters 79−28141
alkali halides, XPS, trapped electrons at F-centres and anion defects, photoionis. cross sections 77−90249
alkali metals, vacancy formation energies calc. 79−82197
alkali metals, vacancy formation energy calcs., electron density functional method 80−19801
alkali perchlorates, elec. transport during struct. transforms. 78−59971
alkaline earth fluoride based solid solns., ion transport 80−107545
alkaline earth fluoride crysts., ion transport, defect energies calc. 77−55382
n-alkane binary mixtures, melting and solid-state transition 77−72685
alloy, binary, conc., with short and long range order, computer simulation of diffusion 78−30778
alloy, binary, kinetic behaviour of vacancies and atoms 79−28129
alloy, binary substitutional, short-range ordering kinetics, vacancy behaviour 78−55867
alloy, dispersion hardened, work hardening due to Orowan loops, temp. depend. *(Japanese)* 80−66534
alloy, solid substitutional soln., diffusive creep *(Russian)* 79−55816
alloy, vacancy formation energy, new method for determining 78−47345
alloy random, binary, diffusion correlation factors calc., comparison of matrix inversion, Monte Carlo and diffusion of probability techniques 78−30779
alloys, conc., radiation induced, segregation of preferential defect migration, theory 79−77633
alloys, concentrated, vacancy formation energies determ. 78−63756
alloys, effects of temp. an order-depend. elec. resist. 77−31992
alloys, irradiated, segregation, inverse Kirkendall effect, effect of constitution on void swelling 78−91472
amorphous solids, vacancies and vacancy clusters, stability under relaxation 80−15005
anthracene crysts., mol. orientational disorder calc. vacancies, dislocations, photodimerisation 77−4915
antiferromagnetic alloy, stoichiometric depend. of elec. resist. 77−69312
atom flux inequality with vacancy counter flux 78−95178
atomic diffusion mechanisms *(Hungarian)* 78−38868
atomistic computer experiments of point and extended defects 78−30610
austenitic steel, solid solution decomposition at defects, TEM meas. 77−12656
BCC metal, heavy ion implanted, vacancy annealing stage, Mossbauer meas. 78−39463
BCC metals, stressed, computer simulation of vacancy and divacancy migration 78−47573
BCC structures, simulation of vacancy-thermotransport 78−47570
bicrystals, diffusion growth of pores under creep conditions 77−15404
bimetal system, diffusion kinetics taking into account nondiagonal coeff. of Onsager matrix *(Russian)* 78−38871
binary alloy, phenomenological theory of interdiffusion, role of nonequilib. vacancies *(Russian)* 78−59966
binary alloys, FCC lattice, mean distrib. of vacancies, computer program 77−62444
binary alloys, ordered, self-diffusion kinetics 80−10698
binary alloys, quenched, vacancy concs. 80−107212
binary metallic solid solns., thermodynamic quantities rel. to vacancy and diffusion characts. 79−95204
binary substitutional solid solution, diffusion, correl. effects and jump freq. ratios 79−99350
brass, α and $\alpha+\beta$ type, positron annihilation, short-range order, clustering and lattice defects influence 79−29107
α-brass, electron irradiated, vacancy migration props., effect on enhanced atomic mobility 79−46829
β-brass, vacancy form., ordering effect, positron annihilation obs. 80−93427
vacancies continued
brass, vacancy form. enthalpy, determ. from threshold temp. for positron trapping in vacancies 78−80433
brass, vacancy formation energies in mixed $\alpha+\beta'$ phase 80−59456
brass, vacancy formation enthalpy, composition depend., position annihilation obs. in Cu rich phase 79−95872
γ-brass type alloys, faulted defects, nature determ. by image matching technique 78−63777
brass-like alloys, constitutional vacancies 80−84168
α-brasses, cold worked, atomic diffusion kinetics to stacking faults, Laplace transformation method 80−19977
cavity growth anal. during superplasticity 80−60923
cavity nucleation at second phase particles in grain boundaries 78−59819
chemical potentials of structural elements of compounds and face or dislocation specificity, thermodynamic parameters 80−96514
classical solid solutions, beyond-mean-field approx. 77−20039
clustering of S in Au 77−4100
clustering of vacancies, effect of impurity atom 77−84789
concentration of vacancies in crystal in temp. gradient, kinetic anal. 80−49217
condensed media, low-temp. particle transport theory, impurity electron transfer 80−19974
continuum model for diffusion in region with multiple diffusivity 79−77801
corundum, packing errors in structure, X-ray diffr. obs., charact. features 79−46655
covalent semiconductor, single vacancy, relax. energy and form. vol. calcs. 78−38691
covalent semiconductors, vacancy screening, dielec. const., exchange correl. pot., Thomas-Fermi description 80−44528
creep, irrad. induced in transient irrad. environments 80−92598
creep, swelling and growth, radiation induced, bias factors estimated from self-consistent model 80−88249
creep and growth, irradiation induced, solute effects on defect precip. rate 80−88252
creep and growth, radiation induced, fundamental mechanisms 80−92596
creep crack growth, model based on vacancy diffusion along grain boundaries 78−75716
crowdion elastic interaction with extended at. defects in isotropic media 77−76454
cryst. with defects 78−60478
crystal field splitting, parametrisation of temperature dependence 78−91652
crystallites with two and three vacancies, models, topological approach 80−44202
crystals, with diamond struct., vacancy formation energy rel. to plastic state transition temp. *(Russian)* 80−19795
cubic crystal, close packed clusters of 5 substitutional point defects, configs. 78−59802
cubic crystal, non-Arrhenius diffusional behaviour and high-field nuclear spin relax. 77−47611
cubic crystals, random motion, of vacancies, correl. factor and NMR diffusion parameters determ. 78−2284
cubic crystals, randomly migrating vacancies, computer simulation of correlated self-diffusion 78−2283
cubic lattice, self-diffusion via vacancy mechanism, correl. effect 80−59693
defect diffusion coeffs., site blocking, correlated defect motion 80−84315
defective crystals, diffusion processes and multistate diffusion 79−19389
depth distribution of vacancies produced by ion implantation 80−65024
diamond, defect electronic struct. and lattice config., MO approaches 80−65495
diamond, GR 2-3 absorpt. line, uniaxial stress effects 78−72563
diamond, GR defect, high resolution optical spectra after electron irrad. 78−56515
diamond, high temp. ion implantation EPR meas. 79−23623
diamond, irradiated, MCD spectrum of GR1 line, neutral vacancy model 77−69850
diamond, Jahn-Teller coupling at ND1 and GR1 centres 78−56103
diamond, natural, subthreshold defect formation due to electron irrad., cathodoluminescence study *(Russian)* 80−45152
diamond, natural semicond., isothermal annealing of electron radiation damage 77−7764
diamond, neutral vacancy, generalised val. bond calc. 77−55493
diamond, radiation-induced optical absorption spectrum, 0.4-2.0 MeV electrons 77−84798
diamond, thermal conductivity, high temp., electron irrad. effects 80−65318
diamond, vacancy, mol. orbital theory of transitions 77−85757
diamond, visible absorpt. spectrum, vacancy charge states 77−90177
diamond-type crystals, vacancy formation and stability due to noncentral force 80−70192
dielectric, dipolar point defects, studied by ITC 80−6405
diffusion, activation enthalpy and entropy and defect form., basic thermodynamic relation, validity limit 78−47557
diffusion coeff. and correlation factors, exact analysis 78−59968
diffusion correlation factors, Monte Carlo computer simulation 77−15615
diffusion data obtained by NMR and Mossbauer expts., interpretation, mol. dynamics study 78−47567
diffusion processes in ohmic sintering, temp. distrib. influence 80−92704
diffusion tensor for atomic migration in crystals 79−7705
dilation induced by vacancy, effect on form. energy and vol. 77−15406
dilute alloy in dissociative equilibrium, solute and solvent diffusion 77−76593
dislocation bias and point defect relaxation volumes 79−99248
disordered distributions of vacancies or altervalent ions, electrostatic energy 78−9995
disperse systems, solubility increase, phase composition, size effect calcs. 80−70418
displacement spike annealing, Mont Carlo method computer expteriments 78−30672
Earth mantle materials, radioactivity rel. to vacancies creation and creep rate 79−92520
edge dislocation screening in metals and superconductors, metal softening *(Russian)* 80−64997
n-eicosane, triclinic phase, self-diffusion, 295 to 309K 80−88359
elastic continuum point defect model, inhomogeneity correction 77−27878

vacancies continued
elastic-diffusion interaction of closely situated pores *(Russian)* 77−76592
electromigration, electron wind, vacancy vol. relax. and shape 79−69277
electron micrographs, possible source of error in determ. of small lattice defect type 77−65941
electron solid, two-dimens., defects and implications for melting 80−39076
entropy, excess, effect of surface boundary conditions and localised vibr. modes 77−11542
entropy of formation due to anharmonic effects 77−62521
entropy of solubility of substitutional impurities 77−4202
externally stimulated interstitial release followed by vacancy-interstitial annihilation, kinetics 78−34535
F-centre formation efficiency, dependence on lattice vacancy concentration 79−82203
fast volume diffusion during cryst. growth 79−99352
FCC crystal, field-ion images, computer simulation of contrast of dislocation loops 77−11561
FCC crystals, close packed vacancy clusters, enumeration of migration, growth and contraction mechanisms 78−47352
FCC lattice, computer simulation of low energy displacement cascade 78−47367
FCC lattice, elastic interaction between point defects, nonlocal theory 78−38689
FCC metals, dislocation loops and voids, growth kinetics, role of divacancies 79−99196
fermi crystal, mag. props. of vacancies *(Russian)* 79−46881
ferrite film, plasma sputtering, influence of heating support on struct. and props. *(Russian)* 79−78445
ferromagnetic metal, magnetisation density in vacancies, μ^+ probe, theory 77−28504
Fick's equations solutions for impurity diffusion, dislocations, interstitials, vacancies 80−70469
field ion microscopy, developments, lattice imperfections 79−67445
film, microporosity described in terms of vacancies and voids 80−24769
fission oxide fuels, intergranular densification model due to the diffusion of pt. defects and pore destruction 79−73345
fission reactor materials, point defect nucleation and growth, rate theory model for simultaneous clustering 80−13604
fluorite ceramics, doped, short range order anal. by electron diffr. 78−83672
fluorite structured crystals, high temp. disorder and elastic consts. 78−30689
fluorochloroapatite, synthetic, defect struct. and colour centres obs. *(Russian)* 78−30612
fluorphlogopite, valence transition of Ti impurity, ESR and optical absorption data 77−16155
formation energy, correl. with compressibility 78−2112
formation energy, nonspherical contribution 78−83810
formation energy and vibr. freq. of atom in dislocation core region 80−103322
formation enthalpy measurements, via positron experiments 78−47337
formation parameters from specific heat data 80−75221
formation volume in solids, stress-assisted diffusion theories 79−95201
formation volume of vacancies calc. 79−19244
formation volume per vacancy, anal. of diffusion expts. under press. 78−55971
free energy, 2-dimensional triangular lattice classical high-temp. limit 77−65974
fusion of metals, vacancy theory 80−44299
fusion reactor first wall material, mobile He inclusion in void swelling rate theory model 80−34069
fusion reactor materials, atom displacement and He prod. using fusion reactor first wall neutron spectrum 78−46168
fusion reactor metals, irradiated, defect cluster nucleation, He injection effect 80−34091
gas behaviour in closed porosity body, exam. 80−24642
grain boundaries, molecular dynamics studies, use of coincidence lattice theoretical model 78−30645
grain boundary cavities, star-shaped unstable growth 79−46679
grain boundary Gibbs thermodynamics anal., interaction with vacancies *(Russian)* 80−2034
grain boundary migration vacancy generation, and drag force 80−15090
graphite, electronic props., self consistent LCAO calc., point vacancy in 2-dimens. cryst. 78−51932
graphite, fast neutron irrad. damage, chem. rate theory applic. effect of annealing and thermal equilib. defect concs. 77−67804
graphite, fast neutron irrad. damage theory and modifications 77−67805
graphite, irrad., lattice expansion, vacancies and interstitials contrib., bond order role 80−65042
graphite, neutron induced changes, exam. of lattice consts., elastic modulus, elec. cond 79−95053
graphite, neutron irradiation, electron transport, annealing study 80−39165
graphite, new force const. model 77−72643
graphite, point defects and self diffusion 78−63758
graphite, surface morphology changes after irrad. with energetic He ions 78−21767
graphite vacancy and substitutional impurities, moderately-large-embedded-cluster approach 80−49663
growth of point defect aggregates during irradiation, model 77−89468
halides, vacancy-interstitial pair prod. by electron-hole recomb. 79−4530
hardening during creep, effect of interstitial and vacancy dislocation loops *(Russian)* 77−81271
harmonic crystals, Helmholtz free energy, vacancy defects interactions calc. by cell cluster method 80−107443
harmonic crystals, thermodynamic props., effects of vacancy defects determ. by cell cluster method 80−79959
harmonic solids, free energy, vacancy defect effects calcs. 77−1198
heat of transport in cryst. solids, vacancy diffusion 77−55383
heat of transport in solids, computer simulation of a vacancy in FCC cryst. 79−14955
Heusler alloys, ternary, order-disorder transitions, Bragg-Williams approx. 79−90756
homogeneity and struct. vacancies 77−84937
hopping, appl. of dynamic quadrupole spin relax. 77−8436
hydrocarbon crystal, calc. of internal friction resulting from molecular defects 78−31448
hyperfine interaction detected by γ-ray PAD 77−43913
ice, vacancy conc. calc. from self-diffusion const. 77−35553
ice surface layer, viscosity, from thermal contraction meas., 0 to −50°C 80−49469
ice surface viscosity, activation energy, vacancy migration 80−107458
III-V compounds, deep centres exam., review 79−11086
III-V oxide interface state and Schottky barrier form., unified mechanism 80−44724
III-V semiconductor, localised defects, one-electron pseudopot. 77−24533
illite, vacancy ordering, transition state cluster model, electron diffr. 77−47547
Inconel 600, mechanisms of dynamic strain ageing and jerky flow 79−79024
inert gas crystals, Monte Carlo calc. of conc. of lattice vacancies, method of overlapping distribs. 80−39077
inert gases, solid, long-range many-body interaction and monovacancy heat of form. 80−38996
infinite linear array of atoms, vacancy migration, Morse pairwise pot. calcs. 77−76331
interaction, with vacancies and vacancy clusters Monte Carlo simulation 78−71754
intermetallic phases, B2 struct., substitutional and triple defects, enthalpies of formation 80−96520
interstitial cluster nucleation at the onset of irradiation 78−79635
ion implantation, net recoil density 80−88175
ion polarisation and point defect resistivity in metals 80−103672
ionic compounds, hopon mechanism for ion transport 79−14957
ionic crystal distortion, energy of vacancy form. 77−89429
ionic crystal pair, AB-AC, mutual diffusion, vacancy supersaturation 77−59153
ionic crystal with vacancies, coherent neutron scatt., calc. 80−59346
ionic crystals, coupling of interface charge transfer to bulk transport props. 78−95183
ionic crystals, imperfect, positron stabilisation 80−40182
ionic crystals, migration volumes calc. 80−103324
ionic crystals, thermodynamics and kinetics of lattice defects 77−84738
ionic crysts., thermodynamic ion-vacancy complexes *(Spanish)* 80−75222
ionic electret behaviour, ionic thermoconductivity technique 80−7274
ionic impurity, drift mobility in electric field, computer simulation 79−82388
ionic-covalent crystal transition to plastic state 79−90717
irradiated materials, cascade damage and self-ion injection effects on swelling 78−34549
irradiation creep, temp. depend. 77−43252
irradiation creep due to dislocation and glide 77−69009
irradiation effects, low dose, void incubation, rate theory approach 79−77635
irradiation enhanced diffusional mass transport 79−14844
irradiation growth, contrib. of grain shape to anisotropy 80−92556
irradiation induced creep, point defect absorption at dislocations 78−19842
irradiation produced point defects; rel. to stress induced mass transport, anal. soln. 79−60401
irradiation-induced, recombination rate with interstitials 80−96516
jellium residual resistivity of vacancies 78−6348
KCl, pure and Ba-doped, γ-irrad., point defect form. and interaction, X-ray and optical studies 79−65078
kinks, solitons, and nonlinear transport in solids 80−65421
lattice atom displacements near end of implanted μ^+ tracks 78−55890
layered transition metal dichalcogenide, diffuse intensity contours in electron diffr. patterns, struct. interpretation 80−38878
linear lattice of atoms, Lennard-Jones pot. basis, for teachers 78−61997
liquid alloys, positron annihilation due to vacancy trapping, simplified model *(Russian)* 80−71511
long-lived point defect formation from unstable vacancy-interstitial pairs 77−59008
low dislocation density crystal, vacancy loss during quenching 78−75656
melting, vacancy mechanism 78−38814
melting, vacancy mechanism 78−38815
melting, vacancy model 79−28080
metal, Arrhenius plot of diffusion, curvature, disappearance under press. with single-vacancy model 79−10975
metal, atomic defect config. from X-ray and neutron scattering studies 78−47322
metal, atomic defect configuration from high resolution TEM 78−47324
metal, atomic defect props., conf., Argonne, IL, USA, (Oct. 1976) 78−47318
metal, BCC, effective valence, from phonon data, rel. to vacancy formation energies 80−79781
metal, BCC, high temp. positron annihilation 78−47421
metal, correlation of annealing temp. for radiation damage fields to melting point in DPAD expts. 78−43737
metal, dynamic study of defect mobility using HVEM 78−47327
metal, electron scatt., effect of surface on lattice defects, surface Landau level reson. 79−65534
metal, equilibrium vacancy conc. 78−38694
metal, FCC, props. of vacancies and divacancies 80−10545
metal, FCC, small vacancy clusters, structures and energies, computer simulation 80−39073
metal, FCC, vacancy migration near twin boundaries and stacking faults 80−39075
metal, FCC and BCC, self-diffusion along edge dislocations by vacancy mech. *(Russian)* 78−87810
metal, FCC and BCC, vacancy diffusion along single edge dislocations, computer modelling *(Russian)* 77−47612
metal, formation entropy per vacancy, anal. of exptl. data 78−75657
metal, H and He impurities, electronic struct. 78−10402
metal, HCP, atomic struct. of defects 78−30611
metal, HCP, self-migration energies, elastic calc. 79−95205
metal, He ion implanted, statistical model of low temp. blister formation 78−67754
metal, He migration and defect interactions, role in radiation damage processes 77−28041
metal, ion beam damage, distinguishing between models of radiation damage using TEM *(German)* 78−30680
metal, irrad., containing self-interstitials and vacancies, electronic transport props. 78−60105
metal, irradiation creep and swelling, cascade damage effect 77−19991
metal, NDT using positron annihilation technique 78−3294
metal, nonlinear electron density distribution around point defects, formulation 79−19548

vacancies continued
metal, nonlinear electron density distribution around point defects, applications 79−19549
metal, nucleation of vacancy precipitation during quenching 77−72612
metal, oxidation of high temp. material, lattice vacancy effect 77−70203
metal, plastic flow, role of osmotic forces in low cycle fatigue, vacancy generation *(Russian)* 79−60430
metal, point defects, μSR studies 79−56703
metal, point defects, lattice theory 78−47321
metal, positron trapping at defects, positron-phonon scatt. effect 77−89736
metal, positron-phonon scatt. effect on positron trapping at monovacancies 78−26829
metal, positron-vacancy interactions, equilib. temp. depend. of positron annihilation 78−76547
metal, pure, vacancy injection during oxidation, reexamination of evidence 78−60864
metal, radiation stimulated diffusional flow, neutron irrad. *(Russian)* 79−29132
metal, resistomatic studies of lattice defects review *(Japanese)* 78−59799
metal, self-diffusion, atomic jump processes 78−47562
metal, self-diffusion, vacancy migration energy 78−51723
metal, self-diffusion 78−47561
metal, self-diffusion acceleration by dissolved H_2 *(Russian)* 78−34647
metal, simple, vacancies and vacancy clusters, electronic struct. 79−11077
metal, simple, vacancy and divacancy form. energies and divacancy binding energy 77−35554
metal, thermal cond. changes at melting point, vacancy model 79−33279
metal, thermal expansion coeff. of defect-entropy volume 78−26707
metal, unstable vacancy-interstitial atom pair, scatt. of electrons 79−15129
metal, vacancies, energy charact. *(Russian)* 77−24314
metal, vacancies and change of surface free energy at melting point 79−42219
metal, vacancies and interstitials, electronic struct. 78−47320
metal, vacancy concentration 78−47319
metal, vacancy defect mobilities and binding energies obtained from annealing studies 78−47325
metal, vacancy diffusion during plastic deform., possibility of stimulated electron emission obs. *(Russian)* 79−5007
metal, vacancy form. energy, validity of lattice statics at all temps. 77−27877
metal, vacancy formation energies and volumes, exam. of models 78−47349
metal, vacancy formation parameters and Gruneisen constant 78−22709
metal, vacancy formation volume, self consistent electron theory 77−89426
metal, vacancy properties, semilinear approach 77−89425
metal, vacancy-solute interaction 78−47409
metal BCC, divacancy binding energy, appl. stress effect, computer simulation 77−15408
metal couple, porous homogeneous vacancy migration and void form. 77−55401
metal crystallite, BCC, mechanisms of growth of vacancy complexes 78−14338
metal halide intercalated graphite, acceptor sites 80−49218
metal halides, fluorite structure, retarded ionic motion 80−88361
metal oxides, boundary conditions of formation of primary nonstoichiometry 77−21115
metal swelling, max. point on temp. scale rel. to point defect generation *(Russian)* 78−38751
metal vacancy conc. studies using positron annihilation spectroscopy 77−11544
metal-insulator transition, chemical mechanism, thermodynamics, vacancies 80−103626
metallic surface, surface traps and vacancy trapping, slow positron obs. 79−87522
metals, atomic binding energy and surface energy rel. to prediction of physical props. 80−59434
metals, cubic, relationship between defect resist. and bulk resist. at melting temp. 78−6344
metals, defect chemistry, He desorption spectrometry *(Dutch)* 80−96737
metals, dynamical props. of point defects, book contrib. 80−103317
metals, effect of vacancy migration upon annihilation of trapped positrons 77−48271
metals, electrons around vacancies, electron density calc. 78−64003
metals, FCC, pair potentials calc., appl. to point defect props. 80−19798
metals, HCP, vacancy and interstitial config. 79−65071
metals, He vacancies, random coalescence 79−51168
metals, heat capacity near melting point, vacancy mechanism of melting 80−10641
metals, interstitial loop growth, pulsed irrad. effects 80−88210
metals, irradiated, solute segregation and annealing kinetics at sinks 79−23640
metals, irradiated, void growth, appl. of Langevin method 79−77632
metals, irradiation induced swelling, bias factor 80−2062
metals, lattice defects, positron annihilation study, book contrib. 79−99977
metals, melting temp., press. depend., vacancy mechanism 80−103460
metals, noble, dilute alloys, solute vacancy binding energy, Dingle temp. 80−49177
metals, nontransition, jellium approach to vacancy energetics 78−47347
metals, point defect and microstruct. behaviour during irrad., appl. to fusion reactors 79−23638
metals, point defect diffusion controlled reaction theory, book contrib. 80−103318
metals, point defect dynamic props. and diffusion controlled reactions, book 80−101674
metals, point defect relaxation volumes, dipole tensors and Kanzaki forces 80−54222
metals, quenched, vacancy cluster form. process 80−92706
metals, radiation damage production in stage II, temp. and impurity effects 77−68997
metals, resistance fluctuation spectroscopy, power spectrum of density fluctuations 79−65428
metals, scoring resistance under dry friction *(Russian)* 79−99267
metals, simple, model for vacancies, including ionic pot. in self-consistent density calc. 77−51369
vacancies continued
metals, submicroscopic defects, influence on HVEM in-situ expts. 80−103392
metals, two and one interstitial model explanation of elec. cond. variations 80−88143
metals, vacancies, corrected spherical model 78−34802
metals, vacancy form. vol. from positron annihilation meas. 78−47339
metals, vacancy porosity kinetics at high irradiation doses of fast neutrons 79−28018
metals, void growth and time-lag, statistical theory 80−88208
metals, void lattice form, spinodal decomp. of vacancies 78−92234
metals 77−27879
metals and alloys, radiation damage prediction and measurement 78−75693
metals and alloys, relaxation, rel. to defect struct. *(Russian)* 78−19801
metals and alloys, stress relaxation, in-reactor study at low temps. 80−93588
metals and alloys, vacancies and lattice elec. cond. determ. method at high temp. 79−37695
metals and intermetallic cmpd., monovacancy form. enthalpy 79−90649
microcrystallites, LCAO-MO calcs, in HMO approx., influence of lattice distortion adsorption, absorpt. of gases *(German)* 78−30584
migration and formation energies rel. to Debye temp. and melting point 78−22710
migration energy in pure metals and dil. alloys 78−47572
migration induced by subthreshold collisions, computer simulation exam. 78−47365
molecular crystal, impurity and vacancy, struct. disturbance and lattice relax. calc. 79−51099
molybdates, nonstoichiometric, IR spectra rel. to vacancy struct. *(French)* 78−43867
Mossbauer line broadening, effect of diffusion by vacancy mechanism 77−40161
Mossbauer line broadening due to Mossbauer atom diffusion via vacancies 79−73868
NaCl, dislocation charge photostimulated variation kinetics *(Russian)* 80−79806
neutron irradiated, 573 to 923K, damage struct. 79−99247
neutron irradiated, positron annihilation at temps. 350 to 1000°C 78−55894
nickel calcine, reactivity, contact I-V meas. 77−85975
Nimonic, ageing, role of quenched-in vacancies 77−52363
Nimonic alloy PE-16, irradiated, numerical simulation of void nucleation, dislocation densities, pt. defect. conc. 79−73208
NMR spin relaxation, motion-induced, in low. temp. HF limit 80−60443
NMR spin-lattice relax., effect of correlated atomic diffusion 80−107495
noble metal, van der Waals forces and their contrib. to vacancy form. energy and phonon dispersion 78−91635
noble metals, divacancy contrib. to impurity diffusion 78−79812
noble metals, electron statistical vacancy model 77−76390
nonlinear diffusion 80−39338
nonmetallic crystals, collapse of tracks formed by fission fragments 80−24510
nonstoichiometric compounds, physicochem. props. depend. on short-range order struct. 80−100227
nonuniformly stressed crystal, statics and kinetics of vacancies *(Russian)* 78−55863
norbornylene and norbornane, HCP plastic cryst. phases, radiotracer self-diffusion obs., monovacancy mechanism 79−33111
nuclear fuel, gas release and swelling, operational model, grain boundary gas 80−95346
nuclear fuels, creep, irradiation induced, transient state, kinetic eqn. treatment 80−88251
nucleation, heterogeneous theory, appl. to precipitate nucleation at Guinier-Preston zones 77−36509
n-octane, relax. about porphyrin defects and vacancies, Monte Carlo calcs. 79−46577
ordered binary crystals, charcts. of equilib. distrib. of vacancies 80−59458
ordered vacancy compounds, lattice dynamics 78−75770
oxide, defect struct., nonstoichiometry and elec. cond., pentavalent oxide dopant effect 80−24442
oxide ceramic, ferroelectric, with perovskite struct., cond. and polarisation, vacancy mechanism 77−12325
oxide films, diffusing pt. defects recomb. 79−19475
oxide fuels, in-pile densification by vacancy boil-off and vacancy knockout, model 79−8259
oxides, nonstoichiometry influence on plasticity *(German)* 79−24592
perovskite oxides, point defects, elec. cond., and electron energy spectra 80−70706
perovskite-related oxides, oxygen-deficient, oxygen ion conductivity 77−20119
perovskites, $A_2^{2+}B^{3+}U_{5/6}^{6+}\nu_{1/6}O_6$, struct., cation vacancies, X-ray diffr. study *(German)* 80−107147
perovskites, nonstoichiometric, ordering of oxygen vacancies, model *(French)* 77−68963
phase stability under irradiation, chem. vacancy effect 79−77634
plastically deformed metal, positron annihilation examination of recrystallisation *(German)* 77−70252
plastically deforming solid, creep cavitation by vacancy diffusion 78−48471
point defect distrib. in bounded media under irradiation 77−7712
point defect model for materials failure 77−16669
point defect production in irradiation, swelling, cascade diffusion theory 80−34044
point defect trapping, reaction consts. sink conc. depend., random walk theory model 79−65072
point defect trapping and migration, calcs., in presence of rare gases and dislocations 79−77834
point-defect clustering during irradiation 80−92521
polycomponent metallic solid soln., creep and diffusion of vacancies *(Czech)* 79−43340
polycrystalline materials, diffusion controlled stress rupture 77−32681
polycrystalline materials, diffusion-controlled stress rupture 80−3186
polyethylene, cryst., transverse deform. and transverse movement of defects 80−38958
polyethylene, crystalline, steric struct. modelling of end defects 80−6371
polymer crystal, local plastic deform. mech., effect of lattice defect 77−28870
pore nucleation in radiation damaged solid solns. 79−99237

vacancies continued
pore shrinkage, diffusional mechanisms 79−28131
pores in system with excess vacancies extraneous inclusion role in nucleation *(Russian)* 79−73164
porous solid sintering, role of gas in healing of isolated pore by volume vacancy diffusion 78−15330
porphyrin in n-octane Shpolskii matrix, defect props., Monte Carlo obs. 80−63533
positron annihilation in cryst. materials, determ. of vacancy conc. *(French)* 79−69901
positron lifetime meas. of defects 79−28857
positron trapping, temp. depend., vacancy form. energy 77−90215
positron trapping rate into vacancy clusters in metals 80−2890
precipitate free zones, X-ray microanal. 80−108768
precipitate hardened material, intergranular cavity growth inhibition 80−50677
precipitate re-solution in low dose irradiations 80−93559
n-propanol, glassy and crystalline forms, trapped electrons, conc. of mol. vacancies determ. 77−65948
quantum crystal, delocalisation of vacancy local phase stratification and impurity free region creation *(Russian)* 78−47637
quantum crystal, ground-state lattice vacancies and Bose-Einstein condensation 77−7943
quantum crystals of spinless fermions, collective modes, vacancy motion-lattice vibr. coupling 79−86960
α-quartz, CNDO/2 calcs., electronic props. of perfect cluster, EPR parameters of O^- vacancy 80−107701
quartz, electron-hole centres, energy characts. assoc. with point radiation defects 79−32991
quartz, thermoluminesc., sensitivity, heat treatment effects 77−59622
quartz, vacancy attenuation of elastic waves at high temp. 79−86846
quartz glass, effect of O vacancies and hydroxyl-group concs. on crystn. 77−16533
quartz glasses of various grades, natural luminescence and lattice vacancies *(Russian)* 77−28625
quasielastic neutron scattering and correlated self-diffusion in cryst. 77−84967
quenched in vacancies, clustering, stochastic theory, continuum model 79−77593
quenched-in vacancies, clustering, stochastic theory, solvable model 79−65074
quenched-in vacancies, stochastic theory for clustering, general mathematical props. 79−65073
quenched-in vacancy defects behaviour, electron microscopy study 77−1120
radiation blistering, interpreatation based on radiation stimulated vacancy migration 80−49265
rel. to radiation cascades in void generation 79−73210
radiation damage cascades, stochastic theory of particle transport 80−54291
radiation defect production, exact solns. of models for continuous and pulsed irrad., implications for stability and fluctuations 80−65041
radiation enhanced diffusion, approx. solns. of chem. rate eqns. and appl. to expts. 79−73344
radiation induced solute segregation, kinetic model, GEAR package of subroutines 78−30673
radiotracer diffusion rates in ionic solid, influence of transmutation products 77−89568
rare earth metals, heat capacity near melting pt., vacancy mechanism of melting 80−15221
rare earth oxide film, short-range order to long-range order transition 78−10288
rare earth zirconate, $R_2Zr_2O_7$, Raman spectra, anion disorder characterization 80−25358
rare gas, crystal, quasi-atomic and quasi-molelcular exciton states *(Russian)* 80−103628
recombination of vacancies and interstitial atoms in primary cluster of radiation defects *(Russian)* 79−1429
resistance fluctuations, anal. independ. of thermal voltage noise 80−84495
sapphire, vacuum UV spectra, Cr^{3+} impurity and anion vacancy conc. 78−84605
self-diffusion, flux of vacancies and atoms, computer simulation 79−73332
semiconductor, atomic displacements and enthalpy of vacancy formation 78−38690
semiconductor, bulk evaporation, injection of nonequilibrium vacancies 80−39273
semiconductor, deep levels, review 80−103640
semiconductor, elastic stresses effect on diffusion processes 78−10226
semiconductor, entropy of fusion allowing for dissociation at melting point 77−55348
semiconductor, ion implantation, radiation defect form. in presence of force fields 79−51126
semiconductor, radiation defects, formation kinetics, successive capture of vacancies by impurities 79−10873
semiconductor, with defects or impurities, local density of electron states 80−92857
semiconductor defects, electronic structure and lattice distortion, Green's function methods *(French)* 80−59917
semiconductor defects, entropy of ionisation and temp. variation of ionisation levels 77−11871
semiconductor displacement energy threshold 77−89430
semiconductor with inhomogeneous impurity distrib., irrad. effects, annealing effects 79−10875
semiconductors, amorphisation by high-energy ion irrad. 79−51172
semiconductors, annihilation processes of radiation-produced vacancies and interstitials 77−89432
semiconductors, cryst. defects induced by radiation, review 79−55776
semiconductors, dangling-bond states theory 80−24840
semiconductors, radiation damage studies on implanted Te, Sb and Sn by Mossbauer spectroscopy 78−2176
semiconductors, ternary and quaternary solid solutions with nearly perfect sublattices, stoichiometry invariants 79−51270
semiconductors, Watkins-type radiation defects, low temp. form. mechanism 80−15153
semiconductors, Z 80−19799
silicates, nonstoichiometry influence on plasticity *(German)* 79−24592
simple cubic lattice, vacancy, diffusion harmonic theory, heat of transport 77−84962
vacancies continued
simple metal, single vacancy, relax. energy and form. vol. calcs. 78−38691
simple metals, monovacancy formation parameters, temp. depend. 78−75658
small particles, cause of reduction in lattice spacing *(Russian)* 80−38967
solid electrolyte dielectric permeability, phase transition to superionic state *(Russian)* 80−49403
solid electrolyte with structural disorder, current flow mechanism 80−19982
solid solns., determ. of degree of imperfection 77−80624
solid solution, binary, radiation-induced instability, contrib. of dissipative processes 80−65039
solids, vacancy migration vol. 80−10701
solute-induced jump correlations during diffusive processes 79−51297
spatial pore lattice, parameter of vacancy pores, temp. depend. 79−27976
specific heat, const. press., press. variation of vacancy contrib. 79−1510
specific heats, macroscopic calc. 79−32989
spinodal decomposition, void lattice formation 79−10845
steel, austenitic, Cr-Mn-N, plastic deformation influence on internal friction, relaxation processes *(Russian)* 80−100870
steel, austenitic stainless, creep, rel. to radiation swelling and stacking fault energy *(Russian)* 78−27562
steel, austenitic stainless, effect of Soviet BR-5 reactor operating conditions on vacancy porosity 79−32990
steel, austenitic stainless, HVEM irrad., point defect trapping influence on void swelling 79−23652
steel, C, diffusion of H_2, effect of quenching and tempering 77−7908
steel, Cr-Mo (2.25, 1 wt.%), interrelationship between creep deform. and creep rupture 79−61664
steel, neutron irradiated, liberation of He in uniform heating 77−50248
steel, stainless, atom displacement and He prod. using fusion reactor first wall neutron spectrum 78−46168
steel, stainless, electron irradiated, dislocation assisted vacancy diffusion 78−55891
steel, stainless, irradiated, vacancy loop effect on swelling 79−14852
steel, stainless, irradiation creep and swelling, microstructural modelling 77−52407
steel, stainless, type 316, irradiated, numerical simulation of void nucleation, dislocation densities, point defect conc. 79−73208
steel, stainless, void swelling, Si point defect trapping, interstitial loop growth rate temp. depend. obs. 80−49270
steel, stainless type 316, effect of damage rate on void growth, point defect conc., microstruct. development 79−73209
steel 0Kh16N15M3B, neutron irradiated, kinetics of nucleation and growth of vacancy pores and dislocation loops *(Russian)* 77−51408
strain ageing, and serrated yielding, mechanism 80−88245
stress field-point defect elastic interaction energy 79−77631
succinonitrile, defects in plastic phase, positron annihilation obs. 80−11504
superionic crystal, domain formation, thermodynamic theory 77−84963
superionic fluorites, disordered anions exam. 79−42299
superionic fluorites, structure and transport 80−84318
surface, ion bombardment, equilib. at. struct. 79−56051
surface and interface defects, electronic struct., scatt. theory 80−84498
surface vacancies in close packed crystals 79−77871
swelling during self-ion bombardment, effect of implanted interstitials 78−10099
tetrahedral semiconductor, interstitial type dislocation loop form. by vacancy precipitation 78−67715
tetrahedrally coordinated covalent semiconductor point defects, multiple scatt. Xα model 80−54636
tetrahedrally coordinated semiconductors, electronic nature of vacancies 77−62863
thermal expansion, temp. depend., vacancy effects 80−79962
thermodynamic properties, phase transitions 78−47518
TiO, single cryst., short range ordering of vacancies, X-ray anal. 79−73163
titanomaghemite, synthetic, cation distrib. 78−55856
topological approach to vacancy modelling 80−10543
tracer diffusion, effect of vacancy conc. on correlation factors 79−4425
transition metal alloys, disordered, formation energy of vacancies 77−27876
transition metal ferrocyanide selective sorbents for alkali metals, sorptive props. w.r.t. struct. 80−101051
transition metal ferrocyanides, crystal structures and ion-exchange props. 77−15362
transition metal hydrides, proton diffusion mechanisms, NMR determ. 77−90060
transition metal oxides, corrosion, defect. struct. and cation transport 79−100277
transition metal oxides, XPS, trapped electrons at F-centres and anion defects, photoionis. cross sections 77−90249
transition metal-V_O pair centers, microscopic struct. 79−60354
transition metalloids, t-matrix theory of thermal and nonstoichiometric softening 79−86788
trapping process of vacancies by foreign atoms 79−90696
triangular lattice, thermodynamic props., effect of vacancy defects determ. by cell cluster method 80−79959
triangular lattice, two-dimens., vacancy pair free energy 79−14799
vacancy and divacancy diffusion 79−82377
vacancy distribution along mag. sublattices in β-brass type ferro and antiferromagnetic alloys *(Russian)* 80−79783
vacancy formation energy calc. within density functional and second order perturbation formalisms 78−67975
vapour growth, element incorporation 78−30556
VC-EVAC graft copolymer, mech. props., effect of heat treatment *(German)* 77−63702
VIII-IIIA, transition metal alloys, B2 struct., vacancy conc. and thermodynamic props. calc. 78−59801
void growth and incubation, stress effect 79−51147
rel. to void nucleation, steady state, spatial correl. effects 78−67705
void sink strength depend. on mutual recombination, point defect loss to fixed sinks 80−33995
void swelling, role of divacancies 79−99236
void swelling simulation, effect of self ion injection 78−22772
voids, coated, capture efficiency 80−96515
zero-gap semiconductors, reson. states, review 79−82558

vacancies continued
zinc blende type ionic semiconductors, vacancies, bound state energy level calcs., tight binding approx. 80−44694
zinc blende-type semiconductors, interstitial PDs, electronegativity diff. and effective ionic charges 77−76766
Zircaloy, in-pile temp. depend of yield strength and growth, under neutron irrad. 79−73219
Zircaloy, post irradiation recovery of growth 79−46711
Zircaloy-2, interstitial/vacancy nature of neutron induced dislocation loops, TEM study 79−42110
Zircaloy-2, irradiation growth, reaction rate theory calcs. 80−88212
Zircaloy-2, irradiation growth, shape and volume changes 80−92562
Ag (100) and (111) surfaces, positronium form. due to slow positron trapping 80−107748
Ag, Ag-Cd(In) dil. alloys, electron irrad., stage I_E recovery 77−39616
Ag, diffusion of ^{110}Ag in temp. gradient, local vacancy conc. determ. 78−87812
Ag, electron irradiated, exam. of vacancy migration energies, and annealing kinetics 78−47571
Ag film, defect density, thickness depend., elec. resist. obs. 80−70568
Ag film, void growth, TEM obs. 80−59833
Ag halide, photographic image form., defect and impurity states, LCAO calc. 78−16876
Ag, injection of vacancies by electrochem. etching at high temp. *(German)* 80−49219
Ag, positron annihilation spectra, Doppler-broadened, temp. depend., 9 to 1098K 80−71510
Ag, positron trapping by vacancies using ^{19}Ne source 78−47341
Ag, vacancy and divacancy diffusion 79−82377
Ag, vacancy formation energy, thermal expansion meas. 79−14798
Ag-Fe, dil., ion implanted, phase comp., Mossbauer study 80−7244
α-Ag-Zn, electron irrad., atomic mobility enhancement by defects, dynamic characts. 79−37871
Ag-Zn, vacancy prod. rate by displacement cascades, anelastic meas. during neutron irrad. 80−19794
Ag-Zn (30 at.%), electron irrad., mobilities of self-interstitials and vacancies 77−84795
AgBr, Ag^+ migration vol. for vacancy and interstitial motion, influence of anharmonicity 79−14965
AgBr and AgBr:$PbBr_2$, emulsion grains, dielec. loss, ionic cond. and surface space charge 77−28038
AgBr, diffusion of Fe^{3+}, vacancy migration evidence 78−47603
AgBr, self-diffusion of ^{82}Br by both single vacancies and vacancy pairs 78−55978
AgBr:Cl, impurity diffusion, vacancy pair and single vacancy contribs. 79−77830
AgBr:Ni^{2+}, low-temp. EPR 77−77091
AgBr(Cl):$Ru^{3+,2+}$, dopant vacancy config., EPR 79−91288
AgCl, irradiated, surface defect center, XPS study 79−28894
AgCl:$CdCl_2$, point defect model, free energy and radial distrib. functions 80−44201
AgCl:Ni^{2+}, low-temp. EPR 77−77091
AgCl:Pd^{2+}, EPR, role of vacancies in impurity based trapping 77−28439
AgCl(Br), point defect form. energies, atomistic calc. and surface pot. meas. 80−107221
α-AgI electrolyte, degree of disorder of anion lattice 78−59975
AgI:Cd, polycrystalline, thermoelectric power meas. 80−59698
Al, Al-Ag(Mg) dil. alloys, electron irrad., stage I_E recovery, interstitial trapping 77−15405
Al alloy, precipitation hardening, creep deform. effect 77−16601
Al and Al-Cu (1.5 at.%), vacancy charact. study by electrical resistance derivative method, rel. to temp. 78−47361
Al and Al-Mg alloys, thermal generation of vacancies involving dislocation climb 77−59808
Al bimetal film with Cu, Ti(V,Ni) and alloy MLT(RS-3710), struct. and macroscopic defects *(Russian)* 79−1555
Al, CC vacancy, electron and positron densities and temp. depend. of positron lifetime 78−19001
Al, creep, rel. to radiation swelling and stacking fault energy *(Russian)* 78−27562
Al, deformed, efficiency of dislocation as sink for vacancies, resist. obs. 77−36570
Al, dislocation loops, interstitial, size distrib. for metal irradiated in high voltage electron microscope *(Russian)* 80−103335
Al, effect of microvoid size on positron annihilation and residual resist. 77−48272
Al, electron and neutron irrad., Doppler broadened positron annihilation meas. *(German)* 77−62563
Al, electron density distrib. around vacancy, Thomas-Fermi eqns. 77−15791
Al, electron-irrad., NQR, EFG around vacancies and interstitials 78−88220
Al, empirical pot. methods, use of Wedepohl pot., vacancy form energy 80−39230
Al, foil, influence of O_2-pressure on oxidation rate, TEM study 80−104355
Al, high purity, neutron irradiated, void annealing kinetics 80−44234
Al, mechanical multipole moments determ. 78−55868
Al, monovacancy thermodynamic parameter calcs., temp. dependence 78−2114
Al, neutron irrad., μ^+ mobility and trapping by vacancies, muon spin rot. meas. 79−4757
Al, plastic flow, role of osmotic forces in low angle fatigue, vacancy generation *(Russian)* 79−60430
Al, positron annihilation, effects of quenching, annealing and neutron irrad. 80−20732
Al, positron annihilation ang. correl., trapping by mono- and multivacancies 77−32466
Al, positron annihilation and vacancy formation, Doppler broadening study 80−60708
Al, positron annihilation rel. to thermocyclic treatment 79−52040
Al, positron annihilation with high-momentum core electrons, vacancies study 80−25481
Al, positrons around vacancies 77−40297
Al, pressure effect on diffusion, theoretical study 78−47566
Al, quenched, diffusion solution for point defects in stress field, steady state and transient 78−30780
Al, quenched, irradiated, anisotropic electron scatt. on defects 79−95397
Al, quenched, irradiated, and quenched plus irradiated, grain boundary hardening 80−3162
vacancies continued
Al, quenched, $muon^+$ trapping at vacancies, compared with positron annihilation 80−15937
Al, quenched, positron annihilation study, vacancy clustering 78−27348
Al, quenched, vacancy agglomeration, elec. resist., splat-cooling effects 77−51365
Al, quenched, vacancy annihilation at surface and dislocation loops 79−60351
Al, quenched, vacancy-Fe interactions 78−47412
Al, quenched-in lattice defects, Mossbauer anal. of associated ^{57}Co 78−39820
Al, radiation damage with radioactive probes, TDPAC meas. 77−24336
Al, rigidity modulus, neutron irrad. and quenched, point defects 78−27546
Al, single vacancy formation energy, determ. using energy bands and wave functions, from LCAO calc. 78−47348
Al, single vacancy formation energy calc., SCF-LCGO modified solid state scatt. theory 80−54637
Al, splat cooled, vacancy transformations, resist. meas. 77−59770
Al, vacancy and divacancy diffusion 79−82377
Al, vacancy distribution, interbonding atoms, heat peaks in scattered cascades *(Russian)* 80−39169
Al, vacancy double jumps and atomic diffusion 78−6175
Al, vacancy double jumps at high temp. 78−47569
Al, vacancy electron density, local electronic struct. theory 79−1580
Al, vacancy electronic struct. LCGO calcs., solid state scattering theory 79−78044
Al, vacancy form. energy from positron annihilation meas. 78−47340
Al, vacancy form. enthalpy, simultaneous positron lifetime and momentum meas. 78−47335
Al, vacancy formation energy and entropy, migration, quenched-in resist. meas. 77−11540
Al, vacancy formation energy, thermal expansion meas. 79−14798
Al, vacancy formation enthalpy, positron annihilation spectroscopy 78−67707
Al, vacancy formation volume, temp. depend. 78−47350
Al, vacancy loop formation, quenched-in vacancy clustering, continuum model 79−77594
Al, vacancy migration energy at high temp. 78−43010
Al, vacancy-solute interaction 78−47413
Al:H, impurity energies and geometrics, self-consistent jellium calc. 79−99507
Al-^{57}Co, implanted, Mossbauer effect obs. of annealing 80−39126
Al-Ag (0.10 at.%), channelling meas. of trapping efficiencies of solute atoms for self-interstitials 79−86829
Al-Ag (1.03 at.%) alloy elec. resist. meas. above room temp., Ag atom configuration correlation 78−35534
Al-Al_2O_3 alloys, dilatometric method for studying relaxation of conc. of defects 77−55288
Al-Co, defect structs. introduced by electron irrad., Mossbauer study 80−7239
Al-Co alloy, dil., fast neutron radiation damage, interstitial trapping, Mossbauer spectra and elec. resist. meas. 77−27914
Al-Cu-Mg(:Fe,Si) alloys, double-ageing, resist., hardness meas. 77−28822
Al-Cu-Ni, vacancy ordering, electron microscope and electron diffr. obs. 79−27954
Al-Cu-Sn, ageing process, effect of Sn atoms, ^{119}Sn Mossbauer spectra obs. 80−7598
Al-Er, dil., lattice location of ^{169}Er ions after implantation, Mossbauer effect of ^{169}Tm 78−39460
Al-Fe (0.02 at.%), rapidly quenched, ^{57}Fe Mossbauer spectrum associated with vacancy 78−23378
Al-Fe (0.02 wt.%), Mossbauer spectrum of ^{57}Fe associated with vacancies 77−85636
Al-Fe alloys, dil., quenched, secondary defects, Mossbauer spectroscopy 77−28491
Al-In, dil., vacancy trapping and detrapping at ^{111}In, PAC spectra 78−39461
Al-Li alloy, annealing of vacancies and ageing, resist. and TEM obs. 77−21172
Al-Li alloy, dil., quenched and irrad., recovery, resist. and internal friction obs. 78−52848
Al-Mg, dilute, dislocation loops, interstitial, size distrib. for metal irradiated in high voltage electron microscope *(Russian)* 80−103335
Al-Mg, foil, oxidation in O_2 atm., TEM study 80−104356
Al-Mg, Si alloy, void form. under different precip. conditions, after Al ion irrad. 80−59529
Al-Mg (1 wt.%), mechanisms of dynamic strain ageing and jerky flow 79−79024
Al-Mg (5.7 wt.%) alloy, pre-precipitation, elec. resist. investig. 77−32601
Al-Mg_2Si (1 wt.%), precipitation reactions, vacancy formation 80−11652
Al-Ni, positive muon trapping at vacancies 79−56704
Al-Sc, dil., thermomigration of Sc 79−69280
Al-Si, internal friction and Si precipitate nucleation 78−60690
Al-Si (1.2 wt.%), dispersion hardened, work hardening due to Orowan loops, temp. depend. *(Japanese)* 80−66534
Al-Sn alloys, heat treatment effect on ^{119}Sn Mossbauer spectrum 80−7228
Al-Zn, dil., grain boundary diffusion 78−91475
Al-Zn, X-ray diffr. after omnidirectional compression *(Russian)* 80−88262
Al-Zn (10 wt.%), ageing at low temp., effects of fluctuation of solute conc. 80−76287
Al-Zn (10 wt.%), ageing at low temp., effects of fluctuation of solute conc. 80−76288
Al-Zn (10 wt.%), solid soln., decomposition meas. by resistivity meas. under isothermal conditions *(French)* 79−20025
Al-Zn (12.5 wt.%) alloy, rel. to retardation of precip. reaction by DC stress 77−55969
Al-Zn (22 at.%), rel. to segregation, X-ray scatt. expts. *(French)* 79−96032
Al-Zn-Mg, decomposition calorimetric study *(German)* 79−74165
Al-Zn-Mg alloys, decomposition kinetics, resistivity meas., extended jump model 78−84766
Al-Zn-Mg superplastic alloy, cavity growth under creep conditions 80−60940
$Al_xGa_{1-x}As$ DH lasers, deep-level luminesc. 79−65913
$Al_xGa_{1-x}As$, defect state identification associated with Ga vacancy 77−69269

vacancies continued
$Al_xGa_{1-x}As$:Cu, variable-gap semicond., impurity props., carrier recomb. 80−96907
$Al_xGa_{1-x}As$:N, ion implantation, in situ annealing photoluminesc. obs. 80−10567
$(Al_xIn_{1-x})_2S_3$, x=0-0.33, cryst. struct., X-ray diffr. 79−55710
$Al_4(Ni, Co)_3$ ternary phase in Al-Ni-Co system, cryst. struct., vacancy controlled phase *(Chinese)* 80−70164
α-Al_2O_3, crystal defects from X-ray irradiation, F-centres, X-ray luminesc. obs. 80−55176
Al_2O_3, defect microstructure due to ion bombardment, TEM study 80−34100
Al_2O_3, polycrystalline, conditions for formation of anion vacancies 79−10844
α-Al_2O_3:Er(Cr), crystal defects from X-ray irradiation, F-centres, X-ray luminesc. obs. 80−55176
β″-Al_2O_3-Na_2O, nonstoichiometric, correl. effects in diffusion, Haven ratio, point defect interactions 80−107505
AlO_xN_y spinel, crystal struct. model 78−91333
Ar crystal, Monte Carlo calc. of conc. of lattice vacancies, method of overlapping distribs. 80−39077
Ar, solid, vacancy conc., X-ray study at const. vol. 80−64991
Ar, vacancy, electronic structure, Green's function theory 80−39525
As-Se(S), glassy and crystalline, point defect exam. by positron annihilation 78−72637
Au (111) film, sputtered, surface struct., HV electron microscopy and theoretical model 78−22981
Au, conduction electron scatt. from vacancies 77−76735
Au, deformed, annealing kinetics of vacancies, elec. cond. meas. and computer simulation 78−47353
Au, deformed, annealing kinetics of vacancies *(Japanese)* 80−88139
Au, elec. resist. and vol. change due to lattice vacancy 79−51101
Au, electron and neutron irrad., quenched, Doppler broadened positron annihilation meas. *(German)* 77−62563
Au, electron irradiated, exam. of vacancy migration energies, annealing kinetics 78−47571
Au, electron irradiated, interstitials and their clusters, diffuse X-ray scatt. study 80−33997
Au film, excess vacancy diffusion to free surfaces and voids, resist, decay 79−65237
Au film, rel. to void growth in early stages of ageing and electromigration 78−38991
Au films, (111), sputtering in high voltage electron microscope 80−35027
Au, heavy ion irrad., cascade energy density effect on defect cluster type 80−107340
Au, magnetoresist of quenched and annealed metal, defect scatt. 79−4981
Au, monovacancy and divacancy parameters, positron annihilation meas. 77−35550
Au, pure metal and Au-Sn dil. alloy, vacancy clusters, quenching and ageing 78−76671
Au, quenched and annealed, cond. electron scatt., de Haas-van Alphen Dingle temp. meas. 77−89688
Au, quenched and annealed, conduction electron scattering 78−47774
Au, quenched polycryst., vacancy loss at grain boundaries 80−59477
Au quenched single crysts., vacancies, diffuse scatt. and resist. obs. 80−33994
Au, stacking fault tetrahedra, critical nucleation temp. 78−26581
Au, stacking fault tetrahedra formation, quenched-in vacancy clustering, continuum model 79−77594
Au, thin foil, growth of stacking fault tetrahedra 80−19815
Au, vacancy and divacancy diffusion 79−82377
Au, vacancy props. 78−47326
Au, vacancy size effect, surface energy in small particles and bulk specimens 80−75223
Au/Ag couple, diffusion induced stresses and plastic deform. 78−26736
Au/Pb thin film couple, room temp. interdiffusion study 79−28154
Au-Ag, radiation damage and diffusion 80−24645
Au-Ag alloy, vacuum-deposited monocryst., rel. to internal friction, 200-3000 Hz, 20-850°C *(Russian)* 77−21197
Au-Cd system, cryst. struct. of $AuCd_3$ and existence of $AuCd_{\sim 5}$ phase *(German)* 77−25020
Au-Cu, dil., electron irradiated, interstitials and their clusters, diffuse X-ray scatt. study 80−33997
Au-Fe, dil., ion implanted, phase comp., Mossbauer study 80−7244
Au-Pd (1(50) wt.%), quenched, vacancy annihilation and short-range order formation, elec. resist. 80−108487
$(Ba,La)TiO_3$, defect chemistry and elec. cond., thermogravimetric meas. 77−39580
Ba ferrite powder, effect of lattice defects on coercivity *(German)* 79−24194
BaF_2, NMR relax., ionic cond. and self-diffusion 78−23362
$Ba_5Nb_4O_{15}$, 5H polytype, perovskite related phase, electron microscope obs. 77−51391
$Ba_xSr_{1-x}Nb_2O_6$, reduced, elec. cond., effect of oxygen vacancies 77−35939
$BaTiO_3$, acceptor-doped defect equilibria, elec. cond. 77−39579
$BaTiO_3$, defect chem., elec. cond. obs. 77−4097
$BaTiO_3$, defect chemistry and elec. cond. improved positive temp. coeff. model 77−39859
$BaTiO_3$, doped, defect chemistry and elec. cond. kinetics of equilib. restoration 77−39700
$BaTiO_3$, oxygen vacancies and partial pressures 77−84938
$BaTiO_3$, reduction inhibition by impurity ions 80−101018
$BaTiO_3$, single cryst., elec. cond., 800-1200°C, nonstoichiometric disorder 78−51989
$BaTiO_3$:C, solubility of C at low O_2 potentials, 800°C 80−100334
$BaTiO_3$:Gd, positron lifetime spectra meas. 78−43956
$BaTiO_3$:La and undoped, defect chemistry elec. cond. at high temp. meas. 77−39858
$BaTiO_3$:X(X=Cr, Mn, Fe, Co, Ni, Zn, Ga), annealed in H_2 and O_2, valence change in phase stability 80−20600
$BaTiO_3$-$Ba_{1/2}NbO_3$, defective solid solns., reduction 77−81395
$BaTiO_3$-$BaNbO_3$ system, solid solns., thermal ionic relaxation, vacancy form. 77−8499
$Be_4^{I}Te^{0}[O_7\square]^{c}$, singularities of atomic arrays as compared with $Al_2^{0}Mg^{}[O_4]^{c}$ spinel struct. type 79−19242
Bi, equilib. vacancy conc., thermal expansion meas. 77−59007
Bi, neutral point defect electronic struct., self consistent method 78−91641
vacancies continued
Bi_2O_3, elec. props. of α, β, γ and δ phases 79−23771
Bi_2O_3-CdO system, solid-state reaction, kinetics and mechanism 77−90303
$Bi_{1-x}Sr_xO_{1.5-x/2}$ vacancy-type solid soln., anionic cond. *(French)* 80−49407
α-brass, serrated yielding, tensile tests and TEM obs. 79−34110
C, vacancy, tight-binding calc. 80−24844
Ca fluorapatites, carbonated, B-type, EPR of F^+-centre after X-irrad. *(French)* 80−108065
CaF:Eu(Gd)(Dy)(Tb), dimer reorientation activation volume 80−107285
CaF_2, anion-void superlattices *(Danish)* 79−14796
CaF_2, cation jump freq., isotope effect, lattice dynamical calc. 80−88357
CaF_2, phonon resonances associated with vacancy 80−19893
CaF_2:alkali metal cation, thermal depolarisation study 80−108147
CaF_2:Li(Na)(K)(Rb), dielec. relax., activation energy, rel. to vacancy pair reorientation 80−88917
CaF_2:Na, vacancy motion activation vol., complex dielec. const. meas. 80−39356
CaF_2:O_2^-, OH^-, ion incorporation by reaction with surrounding atm. 80−55143
$CaF_2.3Ca(PO_4)_2$, apatite, fission damage detection, absorpt. spectra 78−84617
$CaMoO_4$, exam. of electrical conductivity, absorption spectrum 79−51301
$Ca_2Nb_2O_7$-$CaTiO_3$ system, mode of formation and stability of $A_nB_nO_{3n+2}$ phases *(French)* 78−3110
CaO, single cryst., tribolum. obs. 79−52031
$Ca_{10}(PO_4)_6Cl_2$, nonstoichiometry effect on X-irrad. induced electron-excess centres 77−62525
CaS, polycryst., point defects, EPR obs. 79−61214
$CaTi_{0.7}Al_{0.3}O_{2.85}\square_{0.15}$, ionic conductivity 77−20119
$CaWO_4$, solid-phase synthesis, disordering and vacancy defect form. 77−8774
$CaWO_4$:Gd, site occupation 79−28608
$Ca_2XFe_xTi_{3-x}O_8$, X=Ca, Sr, Ba, Y, La, Gd, struct. and O vacancy ordering *(French)* 77−11520
Cd, lattice defects studied by gamma ray angular correlation 79−51895
Cd-Ag, polycryst. quenched foil, the influence of Ag on the recovery spectrum 78−76661
$CdCr_2S_{4-x}Se_x(O_x)$ X=0, 4, and solid solns., imperfect struct. model from cryst.-chem. investigs. 79−42053
$CdCr_2Se_4$, temp. depend. of resist. and magnetoresist., influence of Se vacancies 78−60130
$CdCr_2Se_4$:Ag, ferromag. reson. field and linewidth anisotropy, Se vacancy effects 78−60338
$CdCr_2Se_4$:In, influence of Se-deficiency on props. 78−30921
CdF_2, polarisation phenomena due to vacancy migration 78−76377
CdF_2:NaF thin films, electroluminescence obs. at 77K *(French)* 80−80866
$CdGa_2Se_4$ ordered vacancy compound, Raman scatt. 79−99870
$Cd_xHg_{1-x}Te$, diffusion and struct. of defects 77−84775
$Cd_xHg_{1-x}Te$, long term stability at 300K, rel. to device appl. 80−59978
$Cd_xHg_{1-x}Te$, solid soln., pure and Ag(In) doped, defect struct. model, Hg self-diffusion coeff. 79−95213
$Cd_xHg_{1-x}Te$, vacancy electron states, acceptor behaviour, electron mobility 80−70193
CdS, 200 keV electron induced defects, low temp. annealing 77−80796
CdS, deep level IR luminescence, origin 80−20704
CdS, electron and hole trapped centres, EPR, photoluminescence, photoconductivity study 80−108071
CdS, epitaxial film, conductivity control by S vacancy form., light modulation appls. 77−4455
CdS, neutron irradiated, intrinsic defects 78−51599
CdS, photocond. peaks due to exciton transition and S vacancies 77−8131
CdS, polycrystalline evaporated layers, donor and trap densities 80−20213
CdS:Cu, diffusion doping, photolum. 79−91493
CdS:Cu, IR photolum. at 10K, Cd^{2+} vacancy model 79−28824
CdS:Li film, photocond., effects of annealing, S vacancies, and O_2 adsorption 78−34854
CdSe, comp. and evap. kinetics on vacuum heating, effects on deposited film characts. 77−85940
CdSe crystals, photocurrent and electrorefl. spectra, stoichiometry defects revealed by annealing *(Russian)* 77−52134
CdSe, defect struct. in Se vapour 78−64043
CdSe film, vac. deposited, elec. resist. and surface changes by laser annealing 80−2491
$CdSnAs_2$, electron induced defects, p- to n-type cond. inversion, Hall meas. 77−24557
CdTe, growth on Te substrate by solid-state reaction 79−95287
CdTe, high-resistivity, irradiation effects on carrier transport and trapping process 78−2164
CdTe, Li diffusion, 300°C 77−43383
CdTe, Yb^{3+} implantation, nonstoichiometry effect 77−15440
CdTe:Cl, LPE from $CdCl_2$ soln., elec. props., defects 80−39689
CdTe:Cu, doping effects on evaporation kinetics and electronic props. during high-temp. annealing in vacuum 78−22743
CdTe:Cu films, impurity behaviour, Hall mobility and hole density meas. 80−80420
CdTe:P, annealing induced lattice defects, TEM obs. 80−2010
Ce, vacancy formation enthalpy in γ phase, positron annihilation meas. 79−99182
CeO_2, nonstoichiometric, defect struct. and elec. props. 79−60827
CeO_2:$CaO(Y_2O_3)$, oxygen ion cond. and defect struct. 80−107553
CeO_2:S, acceptor properties of S, free electron concentrations 80−34395
CeO_2-rare earth oxides, complexes of the 'two impurity ions-vacancy' type 79−95004
CeO_{2-x}, 1.5<O/Ce<2, physicochemical equilibria, statistical thermodynamics model *(French)* 78−38688
CeO_{2-x}, small polaron mobility, elec. cond. and nonstoichiometry meas. 78−47785
Co, FCC, self-diffusion and isotope effect, influence of mag. order-disorder transition 80−29205
Co, phase transformations and vacancy form. by positron annihilation 80−2155
Co, positron trapping, monovacancy form energy 79−74016
Co-Al, positron lifetime and angular correl. curves 79−47538
Co-Al, X-ray K-absorption spectrum 80−97378

vacancies continued
Co-Ga β' quenched single crystals, annealing-out of point defects 80−55426
Co-Ga system, exam. of thermodynamics of α and β' phases 78−71870
$CoFe_2O_4$, cation self-diffusion, 1231 to 1390°C, vacancy migration mechanism 77−1260
$Co_{1-y}Fe_{2+y}O_4$, role of vacant and chemisorbed O and charge transfer effect 78−79868
β-CoGa, Cu addition effects on defect struct. *(German)* 77−11546
CoGa, ordered electronic cpd., self-diffusion of ^{60}Co and ^{72}Ga 79−65238
CoGe, vacancy conc. in B2 phase exhibiting triple defects 79−42058
CoM_2O_{4+x} (M=Rh,Mn), anomalous $^{57}Fe^m$ charge states, Mossbauer study 80−40017
$Co_{1-x}Mg_xO$ ceramics as O_2 sensors, phase stability, elec. cond. and thermoelec. power meas. 78−3420
CoO, electrotransport 80−2196
CoO, isotope effects in CoO diffusion rel. to vacancies 80−84319
CoO, Mossbauer lines, quadrupole splitting due to defects 80−2670
CoO, total conc. of point defects and deviation from stoichiometry 77−15407
$Co_{1-x}O$ single crystal of controlled stoichiometry, ^{60}Co self-diffusion 77−43369
γ-CoSe, d-electron deficit model, electrochem. meas. of free enthalpy *(French)* 78−30605
Cr condensates, lattice const., internal stresses *(Russian)* 80−107141
Cr, thermal vacancies, energy of form. and conc. 80−29014
CsCl, impurity and defect sites, elec. field gradient calc. 79−78034
CsCl:Fe, defect struct., Mossbauer spectra and X-ray diffr. obs. 80−7237
CsCl-type crystal, cation vacancies migration energies 80−2192
CsI, isotope diffusion 78−75875
Cu, ^{110}Ag diffusion, activation energy, form. enthalpy of vacancies 78−51736
Cu (111) surface, positronium form. due to slow positron trapping 80−107748
Cu, annealed, positron lifetime changes during cyclic fatigue, vacancy generation and condensation 79−43060
Cu, Ar^+ ion irradiated, defects study by electron microscopy *(German)* 80−2087
Cu, Ar^+ ion irradiated, small defect clusters, electron microscopy contrast *(German)* 79−99253
Cu crystal, cohesion and vacancy form., electron statistical model 80−54169
Cu, defect annealing around stage III, $\gamma\gamma$ ang. correlation expt. 79−14846
Cu, defects at thermal equilib. and melting, positron annihilation meas. 77−76391
Cu, dlectron irrad. at 130K, positron lifetime investig. of stage III recovery mechanism 77−47484
Cu, electrical resistivity changes at high temp. due to vacancies 78−26565
Cu, electron and neutron irrad., Doppler broadened positron annihilation meas. *(German)* 77−62563
Cu, electron irrad., positron lifetime exam. of annealing recovery 78−47354
Cu, electron irrad., rel. to stage III recovery kinetics 78−63792
Cu, electron irradiated, evidence for vacancy migration in stage III 78−38693
Cu, electron irradiated, exam. of vacancy migration energies, and annealing kinetics 78−47571
Cu, electron irradiated, small-angle X-ray scatt. investig. of stage III recovery 77−7763
Cu, electron irradiation, vacancy clustering study by small angle X-ray scatt. 79−14845
Cu, electron-irradiated, monovacancy migration during stage III annealing, NQR study 80−107576
Cu, entropy factors for vacancy formation and migration 78−75866
Cu film, electron transport props., struct. defects role 77−40117
Cu film, heavily oxidised, hole form. on vac. annealing due to vacancy clustering 77−12738
Cu, formation entropy, diffusion const. by determinant and Green's function methods 79−77595
Cu, He-vacancy clusters, computer simulation 77−39583
Cu, interatomic pot., vacancy form., migration energy from phonon dispersion curves 78−42950
Cu, ion bombard. by 5 keV Ar^+, sub-surface damage 80−103399
Cu, mechanical multipole moments determ. 78−55868
Cu, monovacancy and divacancy parameters, positron annihilation meas. 77−35550
Cu, monovacancy formation enthalpy 79−65217
Cu, nucleation and growth of oxidation zones during diffusional creep *(Russian)* 79−52431
Cu, oxidation kinetics, influence of intermediate annealing treatment 80−89412
Cu, point and planar defects, computer simulation 80−59455
Cu, positron annihilation ang. correl., trapping by mono- and multivacancies 77−32466
Cu, positron annihilation with high-momentum core electrons, vacancies study 80−25481
Cu, positron trapping by vacancies using ^{19}Ne source 78−47341
Cu, positron-lifetime study of 4.5-25 MeV proton irrad. effects 79−33021
Cu, prevacancy temperature depend. of positron annihilation, Doppler broadening lineshape parameters 80−60709
Cu, pure and Ge doped, vacancy formation energy 79−51464
Cu, quenched, Hall coefficient, relaxation times, Fermi surface 80−84460
Cu, radiation damage, vacancy migration induced by subthreshold focused collisions 77−19982
Cu, radiation damage and diffusion 80−24645
Cu, radiation damage with radioactive probes, TDPAC meas. 77−24336
Cu, radiation damaged, temp. depend. of elec. field gradient, DPAC expt. 78−43727
Cu, screening charge density round $\Delta Z=-1$ impurities, vacancies, NQR study 80−103897
Cu, self interstitial struct. determ., and vacancy clustering, X-ray exam. 78−47351
Cu, self-diffusion of ^{64}Cu, 737-1079°C, monovacancy and divacancy contribs. 79−19394
Cu, vacancies-gas impurity interactions in vacuum condensates *(Russian)* 79−15036

vacancies continued
Cu, vacancy, lattice vibrs., reson. and localised modes 80−39236
Cu, vacancy and divacancy diffusion 79−82377
Cu, vacancy annealing exam. by positron annihilation 79−14801
Cu, vacancy form. enthalpy, positron annihilation meas. 80−97371
Cu, vacancy migration energy in FCC lattice by computer simulation 77−11722
Cu, volume change due to point defects and He bubbles, isotropic elasticity theory 78−47445
Cu:H, interaction of H and vacancies, positron annihilation, Doppler broadening 78−80434
α-Cu-Al, binary substitutional, short-range ordering kinetics, vacancy behaviour 78−55867
α-Cu-Al, kinetic behaviour of vacancies and atoms 79−28129
Cu-Al, positive muon trapping at vacancies 79−56704
Cu-Al (14.8 at.%), vacancy formation energy determ. 78−63756
Cu-Al (15 at.%), vacancy migration, and short range ordering, comparison of exp. results with theory 78−47356
α-Cu-Al (15 at.%) alloys, low temp. neutron irrad. induced point defects behaviour 77−43251
Cu-Al alloy, vacancy formation energy, determ., using new method, elect. cond. meas. 78−47345
Cu-Al-Ni, positron annihilation study of vacancies before and after martensitic transform. 79−99971
Cu-Al-Ti, formation of modulated structure rel. to barrier nucleation of new phase *(Russian)* 77−32580
Cu-Au, vacancies and divacancies, quenching effects and elec. resist. meas. 80−39072
Cu-Au alloys, vacancy and divacancy migration activation energies, elec. cond. meas. 80−88140
Cu-Be (0.25 at.%), channelling meas. of trapping efficiencies of solute atoms for self-interstitials 79−86829
Cu-Co (1.5 and 4 wt.%) alloy, coherent Co-rich separations obs. by positron annihilation *(Russian)* 80−89082
Cu-Fe, dil., ion implanted, phase comp., Mossbauer study 80−7244
Cu-Ge, dil., point defect props., density functional approach 80−29013
Cu-Ge alloys, equilib. defects *(German)* 79−86789
Cu-In, dil., point defect trapping after ion implantation, DPAC meas. 78−43728
Cu-Mn, positrons as probe of phase transforms. 78−31401
Cu-Ni, annealing effect on oxidation kinetics, reduction in vacancy level 80−50760
Cu-Ni, nucleation and growth of oxidation zones during diffusional creep *(Russian)* 79−52431
Cu-Ni-Nb (30, 0.9 at.%), precipitate free zones, X-ray microanal. 80−108768
Cu-Zn alloy, molecular dynamic exam. of perfect and imperfect cryst. 77−39647
Cu-Zn(30 at.%), electron irrad., positron annihilation, defect recovery 79−74018
$CuAl_2$, constitutional defect struct., from X-ray and density meas. proposed substitutional-vacancy model 79−37696
Cu_3Au, 5-100 keV Cu^+ ion bombardment, displacement cascades, TEM investig. 77−11601
Cu_3Au, heavy-ion or neutron bombardment, disordered zone form., TEM diffr. contrast 77−11600
Cu_3Au, vacancy migration during fast and thermal neutron irradiation 79−42114
CuCl, defect and impurity bands, lattice consts. 80−54638
Cu_5FeS_4, bornite, superstructuring, vacancy clustering, high-resolution electron microscopy 78−42981
Cu_5FeS_4, mag. ordering and vacancy clustering, mag. susceptibility and Mossbauer spectra meas. 77−85625
CuH dilute alloy, Hall coefficient, relaxation times, Fermi surface 80−84460
CuI and CuI:CdI_2, ionic cond., vacancy and interstitial mobilities, phase transitions 77−20116
CuI, pure and CdI_2 doped, ionic cond. obs. 77−15626
$Cu_{0.5}In_{2.5}Se_4$, transition state and domain struct. by electron microscopy and diffr. studies 80−15095
Cu_xNbS_2, $0.8<x<1$, order-disorder transitions and incommensurate superstruct. 77−15587
Cu_2O, defect levels, TSC 77−66138
Cu_2O, residual conductivity, role of vacancies, photoluminesc. and photocond. 77−15901
CuPt equiatomic alloy, effects of quenching temp. on monovacancy, divacancy and thermal equilibrium vacancy ordering *(Japanese)* 79−43285
Cu_2S, defect models of different allotropic varieties, thermal reactions of Hall coeff. *(French)* 77−47448
$Cu_{2-\delta}S$, Cu chem. diffusion, and nonstoichiometry, 400°C, electrochem. determ. 79−28132
$Cu_{2-\delta}S$, $Cu_{2-\delta}Se$ and $Cu_{2-\delta}(S,Se)$, ionic and electronic cond., thermopower and Hall coeff. 77−20117
Cu_9S_5, digenite, superstructuring, vacancy clustering, high-resolution electron microscopy 78−42981
$Cu_{2-x}Se$, electrical activity of Cu vacancies 80−39606
$Cu_{2-x}Se(Te)$ crystals, struct. 79−90608
$Cu_{2-x}Te$, electrical activity of Cu vacancies 80−39606
$Cu_{2-x}Te$, x=0 to 0.3, elec. cond., Hall const., carrier mobility, conc., thermoelec., density, lattice parameter 77−11915
D NaCl:Fe, defect struct., Mossbauer spectra and X-ray diffr. obs. 80−7237
DX, X=Cl, Br, I, thermodynamic properties, phase transitions 78−47518
$DyCoO_3$, anomalous $^{57}Fe^m$ charge states, Mossbauer study 80−40017
ErO_x, nonstoichiometric film, short-range order characts. and its effect on elec. behaviour 79−99435
Er_2O_3, pure and HfO_2-doped polycryst., Er self-diffusion 80−29207
Er_2O_3:CaO, elec. cond. and nonstoichiometry 79−11112
$EuCoO_3$, anomalous $^{57}Fe^m$ charge states, Mossbauer study 80−40017
EuO, Eu rich, insulator-metal transition, model Hamiltonian 78−2422
EuO, nonstoichiometric film with excess EU, O vacancy formation 79−8204
EuO nonstoichiometric film, ESR spectra and exchange interaction 80−93176
EuO, reflectivity spectra near absorpt. edge 79−47471
EuSe, annealed, AC conductivity and dielectric anomaly 80−34445
EuSe, polarisability of shallow donors, permittivity meas. 80−24833
α-Fe, BCC, migration of vacancies near twin boundaries 78−51535
Fe, BCC, void nucleation following electron irrad. 80−29054

vacancies continued
α-Fe, BCC metals, stressed, computer simulation of vacancy and divacancy migration 78−47573
Fe crystallites, vacancy diffusion and vacancy lattices semi-empirical mol. orbital calcs. 77−1121
Fe, defect trapping of ion implanted D, depth profile, diffusion eqn. calcs. 80−2047
α-Fe, deformation induced intergranular creep cavitation 78−31473
Fe, Doppler broadened positron annihilation lineshapes, prevacancy lattice expansion 78−27349
α-Fe, electron irradiated, vacancy annealing 79−55785
Fe, electron-irradiated, positron lifetime meas. 80−93431
α-Fe, formation entropy and diffusion const. by determinant and Green's function methods 79−77595
α-Fe, heavy ion irradiated, TEM exam. 79−7638
α-Fe, interaction of foreign interstitial atoms with vacancies 78−6052
α-Fe, irradiation induced void swelling, Cr additions effect 80−55408
α-Fe, neutron irradiated, mobile C atom trapping, anelastic and magnetic relaxations 80−100306
Fe, oxidation at elev. temp., scale/metal interface charact. 79−74286
Fe, phase transformations and vacancy form. by positron annihilation 80−2155
Fe, point defect estimation from specific heat and volume in plastically deformed pure metals *(Russian)* 80−54223
Fe, positron annihilation, temp. depend. 78−56540
Fe, pure and doped, electron irrad., mag. aftereffect 80−88838
α-Fe, stress induced interaction of point defect pairs, in BCC solutions 78−79608
α-Fe, vacancy, lattice vibrs., reson. and localised modes 80−39236
Fe vacancy form. by positron annihilation in thermal equilibrium 78−10041
Fe, vacancy formation energy by positron annihilation 78−51531
α-Fe, vacancy migration, annealing expt. study, irradiation induced defects 78−6956
Fe, vacancy mobility determ., HVEM expts. 80−33993
Fe, vacancy recovery stage, radiation doping, elec. resistivity meas. 79−51102
Fe, volume changes and defect healing due to plastic deform. *(Russian)* 80−81139
Fe:^{133}Xe, heavy ion implantation, recovery, Mossbauer effect meas. 78−52393
α-Fe:C, electron irrad., vacancy-C interaction, positron lifetime meas. 80−75264
Fe:I, ^{131}I NMR, vacancy associated impurity sites 78−91964
Fe:Y, ion implanted, deep D traps due to Y-vacancy complex 80−103372
Fe-Al, positron lifetime and angular correl. curves 79−47538
β-Fe-Al, struct. defect obs. 78−14337
Fe-Al, vacancy formation energy 78−18638
Fe-Al (40 at.%), ordered, plastically deformed, neutron irrad. damage and recovery, resist. meas. 77−19993
Fe-Al (50.5 at.%), ordered, neutron irrad. enhanced defect diffusion, resist. meas. 77−11598
Fe-Al (51 at.%), crystal vacancies, dilatometric and field ion microscopy exam. 78−47346
Fe-C, electron-irradiated, positron lifetime meas. 80−93431
Fe-Co(-V) alloys, neutron irradiated, influence of dislocation doping on recovery 79−46715
Fe-Cr, irradiation induced void swelling, Cr additions effect 80−55408
Fe-Cu (0.34 wt.%), neutron irradiated, field-ion microscope detection of ultra-fine defects 79−42116
Fe-Ni (50 to 94 wt.%), FCC, form. and migration energy of vacancies, induced magnetic anisotropy *(French)* 78−2110
Fe-Si (3 wt.%), grain oriented, MnS-AlN-inhibited, precipitate morphology 77−12648
FeAl intermetallic, constitutional vacancies, lattice parameter and thermal vacancy conc. obs. 79−23599
Fe_3Al, vacancy conc. and ordering conc. 78−18639
$FeAl_{2-x}Cr_xO_4$, spinel, elec. cond. behaviour during oxidation 79−19593
γ-$(Fe_{1/3}Al_{2/3-y}Cr_y)_2O_3$, lacunar spinels, elec. cond. behaviour during oxidation 79−19593
FeCo, isothermal annealing effect on lattice const. *(Japanese)* 79−20076
FeCo, ordered and disordered alloy, annealing of point defects created by neutron irrad. at 20K *(French)* 79−1467
$Fe_{50}Co_{50}$, neutron irradiation, close pair recombination *(French)* 80−39162
$FeCo_2V$, ordered and disordered alloys, annealing of point defects created by neutron irrad. at 20K *(French)* 79−1467
$Fe_{49}Co_{49}V_2$, neutron irradiation, close pair recombination *(French)* 80−39162
$(Fe^{2+}Fe_{2-x}{}^{3+}M_x{}^{3+})O_4{}^{2-}$ ($M^{3+}=Al^{3+}$, Cr^{3+}), oxidation to γ lacunar spinels, rate law vs. O_2 press. 80−50849
$Fe_{1.67}Ge$, Mossbauer and X-ray expts. 79−1734
$Fe_{1-x}O$, wustite, defect struct. 80−107216
$Fe_{1-x}O$, wustite, vacancy and interstitial ion order, equilib. conditions, neutron diffr. obs. *(French)* 78−14336
$Fe_{1-x}O$, wustite, struct. at high temp., neutron diffr. obs. *(French)* 79−86754
$Fe_{1-z}O$, wustite, struct. at high temp., neutron diffr. *(French)* 80−1982
Fe_2O_3 based γ defective spinels, elec. cond. behaviour during transform. to α rhombohedral phases *(French)* 80−49354
γ-Fe_2O_3, small particles, vacancy sintering 77−65975
γ-Fe_2O_3, struct. vacancy distrib., effect on $\gamma\rightarrow\alpha$ transform. heat 78−6051
α-Fe_2O_{3-x}, nonstoichiometry effect 77−47583
$Fe_{3-x}O_4$, vacancy diffusion from relax. of deviations from stoichiometry 79−23769
Fe_3O_4, magnetite, cation diffusion, correlation and isotope effects 80−96686
Fe_3O_4, magnetite, defect content, gas-phase comp. effects 77−43336
Fe_3O_4, substituted magnetite, correl. between IR spectra, X-ray diffr., and struct. vacancy distrib. 80−84753
$Fe_{0.9}S$, ferrimag. transition, mag., thermodynamic props., kinetics 79−47280
$Fe_{1-\delta}S$ chemical diffusivity and nonstoichiometric props. 78−10217
$Fe_{1-x}S$, NC-type, wave distrib. of vacancies 79−99178
Fe_9S_{10}, antiferro- to ferrimag. transition, Mossbauer and mag. exam., diffusion of Fe during transition 79−73716
Fe_9S_{10}, polytypism, Fe diffusion near antiferromag. to ferrimag. transition 80−44830
vacancies continued
$FeSb_xO_{4-y}$, defect struct. and mag. transition, elec. transport and Mossbauer expts. 78−59803
Fe_7Se_8, test of Okazaki's 3c and 4c superstruct. model, Mossbauer expt. 77−66445
α-$Fe_{1-x}Si_2$, vacancy ordering, cryst. stabilisation energy aspects 80−103325
Fe_2SiO_4, nonstoichiometry influence on plasticity *(German)* 79−24592
Fe_xTaS_2, vacancy ordering, transition state cluster model, electron diffr. 77−47547
$Fe_{(1+x)}Ti_{2(1+x)}S_4$ non-stoichiometric cpds., vacancy-cation distrib., Mossbauer spectra 80−15900
Fe_xVS_2 ($0.20<x<1.00$), phase diagram and order-disorder transition of vacancies 80−81039
Ga, vacancy equilib. config., pseudopot. estimation 77−39582
GaAlAs, native defects, stoichiometry, doping effect 77−11541
GaAlAs, surface vacancies, bound state energy levels calc. 80−80340
GaAs (111), Ga-As-H-Cl CVD system, adsorption of Cl, GaCl, As, As_4, Ga, AsGaCl, 973 to 1223K, equilib. adsorption layers 79−23858
GaAs, annealing rel. to stoichiometry deviation, Hall effect, electron microscope meas. 77−24410
GaAs, anodic native oxide, vacancy transport mechanism for O 79−61767
GaAs, defect state identification associated with Ga vacancy 77−69269
GaAs, electron and neutron irrad., defect clusters 80−2077
GaAs, electron-irrad., deep-level defect anal. using 2γ positron annihilation and IR absorption spectra 80−16120
GaAs, electronic states of neutral vacancies 77−11875
GaAs, fast neutron irrad., effect on cryst. lattice period, X-ray diffr. meas. 79−37743
n-GaAs, heat treated, origin of 1.41 eV emission band, photolum. expt. 78−72579
GaAs, ideal vacancy, electronic struct., tight-binding calc. 79−4529
GaAs, ion bombarded, defect distrib., photolum. meas. 77−20920
n-GaAs, low energy photolum., 77K, deep centre obs. 77−69877
GaAs, native vacancies study using positron lifetime technique 79−83052
GaAs, semi-insulating substrate, characterisation and modification 77−81215
GaAs, surface, vacancies, bound state energy level calcs., tight binding approx. 80−44694
GaAs VPE layers, role of diffused Ga vacancy in degradation 78−95050
GaAs, Xalpha cluster model, electronic dangling bond effect elimination 79−99504
GaAs:Cd, lattice defects caused by quenching, elec. cond. 79−56160
n-GaAs:Cu, contaminated single cryst., deep level photoluminesc. model 78−68554
GaAs:Ge, ion-implanted, photoluminesc., deep emission centres 80−34965
GaAs:Ge, solubility and point defect-dopant interactions 79−90689
GaAs:Ge, vap. grown, diatomic complex donor and acceptor model 78−80003
GaAs:Se, Ga, dual species ion implantation, elec. characts. 80−103377
n-GaAs:Si, ion implanted and/or annealed, As vacancy form., photolum. line 77−27875
GaAs:Sn, implantation, annealing, impurity-defect struct., Mossbauer study 80−54269
GaAs:Sn, nature and conc. of point defects over conc. range 10^{17} to 6.10^{18} cm^{-3} 79−14802
GaAs:Sn, solubility and point defect-dopant interactions 79−90688
GaAs:Sn^+, impurity-defect complex from ^{119}In implantation, Mossbauer study 80−59486
n-GaAs:Te, electron-irrad., absorpt. spectra *(Russian)* 78−15200
GaAs:Te, preferential precipitation on dislocation loops 79−7612
GaAs:Te, solubility and point defect-dopant interactions 79−90687
GaAs-Cu:Tl, cathode luminescence spectra, Hall effect, cryst. defects 80−76087
$GaAs_{0.6}P_{0.4}$:Zn, rel. to control of Zn diffusivity by multiple implantation 78−38877
$GaAs_{1-x}P_x$, $0\leq x\leq 1$, evidence for common nature of certain deep-level radiative centres 78−6767
GaN:Zn(Fe)(Ni)(Cr), influence of N vacancies on lattice parameters 79−73153
β-Ga_2O_3, doped, photolum., emission centres struct. 78−52557
Ga_2O_3:Mg(Zr) single crystals, quenched, ionic and elec. props. 78−30922
GaP, electronic states of neutral vacancies 77−11875
GaP, electronic structure of neutral phosphorus vacancy, empirical pseudopotential 79−78042
GaP, internal friction due to reorientation of Ga divacancies, calc. 80−2116
GaP, localised states in presence of P vacancy, pseudopot. calc. 78−18992
GaP:Fe, double Fe-thermal acceptor centre, energy states 80−96823
GaP:Fe, heat treated, EPR spectra, struct. defects 80−7158
GaP:Fe(Cr), photo-ESR of annealed crysts. 80−15795
GaP:Zn, isolated Ga vacancy due to electron irrad., EPR study 78−95519
$GaS_xSe_{(1-x)}$ solid solns., electrical props. meas. 78−84216
GaSb and alloys, struct. defect, photoluminesc. 80−25459
GaSb, defect concentration determ. model, Hall effect 80−103385
GaSb, sputtered films, on GaAs, growth, Hall effect, impurity levels 80−20334
GdO film, new reduced variant due to annealing 77−89660
$Gd_xZr_{1-x}O_{2-x/2}$, elec. cond. of ceramic solid solutions 80−107554
Ge, amorphous, 1 MeV electron irrad. influence on kinetics of crystallisation 77−89476
Ge amorphous film, effects of ion implantation on structure 78−55881
Ge, entropy and enthalpy of vacancy form., comparison of theory with quenching expts. 77−11872
Ge film, amorphous, ^{74}Ge ion implanted, defect struct. obs. 78−51848
Ge, form. of divacancies anchored to self-interstitials under electron bombard. 77−80501
n-Ge, group V doped, point defect form. due to γ-ray irrad., carrier density, mobility meas. 78−71759
Ge, ideal vacancy, electronic struct., tight-binding calc. 79−4529
Ge, irradiation at about 6K, low temp. annealing of defect 78−2162
Ge, localised vacancy state 79−82543
Ge, migration energy of intrinsic point defects in different charge states 77−89582

vacancies continued
Ge, n- and p-type, solubility and diffusion of Na, vacancy mechanism 77−89592
Ge, polarisation of implanted ^{12}B 78−43653
Ge, positron annihilation, effect of vacancies 79−24385
Ge, quenched n- and p-type, intrinsic defects migrating near 100°C 77−62670
Ge, self-diffusion, activation energy and entropy factors 80−88353
Ge, self-interstitials, vacancies and their clusters 77−80500
Ge, shallow acceptors produced by quenching 79−51523
Ge, single cryst., proton irradiated, defect study using X-ray diffuse scattering 79−95048
Ge, unrelaxed vacancy states appl. of local formalism 77−4313
Ge, vacancy, tight-binding calc. 80−24844
Ge, vacancy formation and stability due to noncentral force 80−70192
Ge, vacancy paradox 78−59804
n-Ge:O, impurity-saturated, dislocation-free, anomalously high magnetoresist., vacancy effects 77−43629
Ge:Sb, neutron irradiated, hopping cond. between shallow defect levels 77−4347
Ge:Sb, thermal defects, influence on radiation defect formation and annealing 77−55281
Ge-Si, electron irradiation and annealing 77−55305
GeO_2, gamma-ray generation of O vacancies and O diffusion 79−99358
GeO_2, hexagonal and glassy, X and γ-irrad., thermolum. and paramag. centres 77−63472
GeTe, stoichiometry deviations influence on mech. props., 25-500°C 80−103410
H, metallic, defect form. energy, Einstein-Kanzaki model 78−34676
He, solid, activation energy of vacancies 77−28064
He, solid, impurities and vacancies 79−65289
He, solid, theory and thermodynamic props., book contrib. 77−47646
He, solid, vacancies and dislocations *(Japanese)* 78−91507
He, solid, vacancy tunnelling freq. calc. 77−80678
He, vacancy activation energy, from high temp. sp. ht. data 77−15657
^{3}He, BCC, vacancy bandwidth determ. by sp. ht. 78−79854
^{3}He, entropy of vacancy formation 79−33156
^{3}He, FCC, vacancy induced spin polarons 80−59756
^{3}He, HCP, vacancy-induced transitions 80−88395
^{3}He on graphite, two dimensional quantum crystal *(Russian)* 78−60001
^{3}He, solid, as mag. semicond., analogy to Mott insulator 80−96720
^{3}He, solid, mag. phases *(Russian)* 77−72743
^{3}He, solid, magnetic polarisation around vacancies, on two-dimens. lattice 79−51368
^{3}He, solid, rotating, structure of vacancies *(Russian)* 79−90843
^{3}He, solid, spin diffusion coeff. *(Russian)* 77−80679
^{3}He, solid, struct. of vacancy induced spin polarons 79−95244
^{3}He, solid, vacancy mobility *(Russian)* 77−85015
^{3}He, submonolayer on Grafoil, vacancy induced ferromag. 78−14536
^{3}He, vacancy relaxational phenomena *(Russian)* 78−95203
^{3}He, vacancy struct., neighbouring ferromag. domains *(Russian)* 77−20161
^{3}He-^{4}He, solid soln., struct. of vacancies 80−2242
^{4}He, plastic deform., athermal processes 79−56017
^{4}He, quantum cryst., ground-state lattice vacancies and Bose-Einstein condensation 77−7943
^{4}He, small liq. drop model for vacancy 78−51784
^{4}He, solid, impuriton vacancy mols. 78−79853
^{4}He, solid BCC, plastic deform., stress-strain relations and US attenuation 78−38909
^{4}He, solid BCC, vacancy tunnelling at finite temp. 78−38907
HfO_2:Er_2O_3(Y_2O_3)(Eu_2O_3), elastic props., sonic reson. meas. 80−7612
HfO_2-Y_2O_3, solid soln., diffuse X-ray scatt. by vacancies 78−71728
Hg-S binary system, phase relations, bulk resist. meas. 79−66040
HgCdTe, electron irradiated, high temp. defects 79−78122
$Hg_{1-x}Cd_xTe$, long-term Hall-type conversion by vacancy diffusion at room temp. 79−65498
$Hg_3In_2Te_6$, complex ordered-vacancy cpd., struct. and lattice dynamics 78−34496
HgSe, point defect model rel. to elec. props. and phase diagram 77−4339
HgTe, vacancy doping, effect on elec. characts. 79−82595
HgTe, vacancy doping by off-stoichiometry, influence on transport props. 78−55862
HgTe, vacancy electron states, acceptor behaviour, electron mobility 80−70193
HgTe, vacancy mech. of resorption of Hg droplets 80−39070
HgTe-CdTe(ZnTe) solid solns. form., equil. vacancy conc. changes 77−43208
In, positron annihilation, vacancy form. vol. 78−15245
In, positron annihilation lineshape meas., 74 to 430K, positron trapping by vacancies 77−36308
In, positron annihilation line Doppler broadening, self-trapping and vacancy form. 77−40298
In, vacancy formation and activation volume, macroscopic model 80−54221
In, vacancy size effect, surface energy in small particles and bulk specimens 80−75223
InAs, intrinsic point defects, nature and influence on electrophys. props. 78−79609
InAs, obtained by liquid-seal method, deviation from stoichiometry 77−40345
In_2O_3, defect chemistry and struct. stability, impurity incorporation 77−35552
In_2O_3, lattice defects, optimum prep. conditions w.r.t. stoichiometry 79−27974
InP, electronic structure of neutral phosphorus vacancy, empirical pseudopotential 79−78042
InP, low temp. diffusion of radioactive Ag 78−75884
InP, surface vacancies, bound state energy levels calc. 80−80340
InSb, thin film, carrier scatt. by vacancies and interstitials 79−65568
In_2Te_3-type semiconductor, mechanism of electrically inactive impurities 80−24834
Ir (111), $(\sqrt{3}\times\sqrt{3})30°$ S overlayer struct., LEED obs. 80−15365
Ir_5Sn_7, cryst. struct. determ. *(German)* 79−27952
K, defect calcs., vacancy form. and migration energy 79−19185
K, vacancies and elec. resist. 79−82575
K, vacancy superlattice 77−7713
KBr, electrolytically coloured single cryst., F-centre diffusion rel. anion vacancy density 77−62937
KBr, point defect concs., effect of plastic deform. 77−1124

vacancies continued
KBr, proton irrad., divacancies, positron capture, ionic cond. and TSC study 80−54289
KBr, X-irradiated, at 80K, interstitial K ions associated with interstitial Br ions *(Russian)* 78−75655
KBr:Cl^-, diffusion traps for divalent ions, dielectric loss and ionic thermocurrent techniques 80−6566
KCl, and KCl:Ca^{2+}(Sr^{2+})(SO_4^{2-}), conductivity, self-diffusion coeffs., lattice defect props. 77−4216
KCl crystals, Eu^{2+} concentration effect on lattice parameter and density of crystals 80−88169
KCl, electrolytically coloured single cryst., F-centre diffusion rel. anion vacancy density 77−62937
KCl, electron-irrad., positron-capture centres, thermal annealing kinetics 79−95875
KCl, fine structure of X-ray absorption spectra 80−71514
KCl, γ-irrad. and doped, lattice relax., cold neutron scatt. obs. 77−7715
KCl, thermal annealing of F, V_2-, V_3-centres *(Russian)* 80−54229
KCl, vacancy comaplex formation and binding energies in zeroth approx. 80−24441
KCl, with divalent impurity, reorientation of impurity-vacancy complexes, thermally stimulated depolarisation 77−65977
KCl, X-ray irradiated, vacancy conc. determ., thermal expansion meas. 80−79782
KCl:Eu_3 flow stress 77−36577
KCl:Eu^{2+}, X-ray irrad., cation vacancies, conversion to anion vacancies, F centre formation 79−55778
KCl:H^-, diffusion traps for divalent ions, dielectric loss and ionic thermocurrent techniques 80−6566
KCl:Pb_3 light induced ionic polarisation 80−7264
KCl:Pb^{2+}, highly doped, state of dispersion of Pb^{2+} 77−1144
KCl:Pb^{2+}, low temp. sp. ht. 80−2178
KCl:Sn^{2+}, EPR exam. of struct. and prod. of $Sn^-(5p^3,4S)$ defects 79−61215
KCl:$SnCl_2$, action of ionising radiation on Sn aggregation processes 78−34543
KCl:Sr, positron annihilation and trapping in A-centres 80−84802
KCl:$SrCl_2$, H_{Na} annealing, X-ray irrad., H centre capture by IV dipoles 78−10927
KCl:Tl, F-centre formation efficiency 79−82203
KCl-KBr mixed crystals, microhardness studies, nonlinear depend. on composition 78−83872
KCl(Br)(I) with alkali and halogen impurities, colour centre deformation induced nonradiative decay 80−7387
KCl(I), electron range-energy relation, thermally created lattice vacancies effect 80−92574
$KClO_4$, ClO_3^- detection by EPR of ClO_3 radicals created by X-irrad. 78−76311
$KHSO_4$:Fe^{3+}, DC cond. meas., mechanism 80−65285
KI, electrolytically coloured single cryst., F-centre diffusion rel. anion vacancy density 77−62937
KI:S^{2-}, photoinduced polarisation and depolarisation 79−33738
$K_2Mg_4Mo_4O_{16}(OH)_2(H_2O)_2$ study of non-stoichiometry *(French)* 78−30604
$K_2Mg_4Mo_4O_{16}.(OH)_2(H_2O)_2$, dehydration processes rel. to stoichiometry *(French)* 79−24734
$KNbO_3$, elec. and thermoelec. props., influence of O defects 80−29401
$KTaO_3$, defect struct. and elec. props. 78−91695
$K_xWO_{(3+y)}$, direct imaging of ordering 77−11511
Kr, solid, vacancy conc., X-ray study at const. vol. 80−64991
$(La,Gd)Al_2$, normal and supercond. state, US attenuation, freq. depend. and mechanisms 80−49992
La-Co-O system, stability of ternary phases, nonstoichiometry 80−24434
$LaAl_{0.85}Mg_{0.15}O_{2.925}\square_{0.075}$, $LaAl_{0.8}Mg_{0.2}O_{2.9}\square_{0.1}$, $LaNb_{2.6}Zr_{0.4}O_{8.8}\square_{0.2}$, ionic conductivity 77−20119
$(La_{0.8}Ca_{0.2})MnO_{3+y}$, non-stoichiometry and lattice consts. 80−100212
$LaCoO_3$:Ca(Sr), anomalous $^{57}Fe^m$ charge states, Mossbauer study 80−40017
LaF_3, ionic transport, NMR and cond. studies 80−107555
$La_2Fe_{1.76}S_5$, cryst. struct. *(French)* 78−51499
$La_2Fe_2S_5$, $La_2Fe_{1.87}S_5$, struct. *(French)* 77−55277
$La_{1-x}Na_xFeO_{3-x}$, defect perovskite system, Mossbauer effect 77−36159
$La_2Ti_2O_7$-$CaTiO_3$ system, mode of formation and stability of $A_nB_nO_{3n+2}$ phases *(French)* 78−3110
Li, defect calcs., vacancy form. and migration energy 79−19185
Li:Mg(Eu)(Co), dissociated state with cation vacancy, elec. cond. 79−7709
β-Li-Al, lattice parameters, density, defect struct. 80−24440
LiCl:Fe_2 defect struct., Mossbauer spectra and X-ray diffr. obs. 80−7237
LiCl:Ni^{2+}, first order induced Raman scatt. from Ni^{2+} and cation vacancies 77−48169
LiF, γ-irrad. induced defects, positron capture and annealing obs. 80−60707
LiF single crystal, void disappearance 78−55864
LiF:Mg, X-ray irrad., trapping processes, Z-centres and dipoles, two models 80−49222
LiF:OH:Mg, γ-irrad. induced oxyhydryl complexes 80−92555
$LiGd(MoO_4)_2$, defect struct. and phase transitions 79−28697
LiH, cluster cryst., extended HMO calc. of defects 79−51521
LiH, ionic cond., thermocurrent and photocond., defect and electronic props. 77−15621
LiH, self-diffusion of Li and H ions 78−59974
LiIn, electrical resist. and thermal expansion temp. depend., 30 to 400°C, vacancy form. 77−24547
$LiInS_2$, blue-band emission 80−76062
Li_3N, ionic conductor, single cryst. defect struct. anal. data reduction and struct. refinements, 153-678K 79−32988
Li_3N, ionic transport mechanism and defect props. 80−107528
$LiNbO_3$, γ-irradiated and annealed, elastic and piezoelectric props. 78−2807
$LiNbO_3$, XPS and UPS from surface defects 80−76136
$LiNbO_3$:Fe, ferroelectric, treated in Li_2CO_3, formation of Fe^{2+} state, Mossbauer effect 78−92003
$LiNbO_3$:Fe, origin of photoelectrons and conc. of point defects 77−43645
$LiNd(MoO_4)_2$, defect struct. and phase transitions 79−28697
$Li_2O.nAl_2O_3(7.3\text{-}n)SiO_2$, metastable solid soln., Al^{3+} vacancy incorporation 77−12593
$LiTaO_3$:M, optical damage of transition-metal-doped ferroelectric 78−95571
Mg alloy, quenched-in defect behaviour, effect on flow stress 79−61625

vacancies continued
Mg, HCP, vacancy and interstitial config. 79−65071
Mg, HCP, vacancy clusters and interstitials, computer simulation study 80−64992
Mg, lattice distortion around vacancy 79−42192
Mg, single crystal, Green's function method of lattice statics, monovacancy 78−55865
Mg:H, impurity energies and geometrics, self-consistent jellium calc. 79−99507
Mg-Ag, dil., ion irradiated, interaction between Ag and defects, channelling meas. 78−38766
Mg-Ag (0.18 at.%), channelling meas. of trapping efficiencies of solute atoms for self-interstitials 79−86829
Mg-Al(-Zn), solute-vacancy binding energies from hardness meas. 78−39789
Mg-H^+ $2p_{3/2}$ vacancy alignment electron capture role 80−83465
$Mg_xFe_{1-x}O$, diffusion of ^{59}Fe and elec. cond. 80−59700
MgO, defect surface, chemisorption of mol. H_2, quantum mechanical approach 77−62761
MgO, single cryst., tribolum. obs. 79−52031
MgO:Al^{3+}, positron capture by cation vacancies, positron annihilation meas. 77−8681
MgO:Al^{3+}(Fe^{3+}), defect struct., shell model calcs. 79−99180
MgO:Fe, Fe^{2+} oxidation and Fe^{3+} reduction kinetics, EPR obs. 79−70399
Mg_2SiO_4, directional depend. of transport for Mg interstitials and vacancies 79−69285
Mn film, heat treated, lattice distortion energy, resist. meas. 79−19492
Mn-MgF_2 cermet, heat treated, lattice distortion, resist. meas. 79−19492
Mn-Pt alloys, diffusion of ^{54}Mn, radioactive tracer study *(French)* 79−86915
α-MnS, defect energetics and range of homogeneity 78−47317
MnZn ferrite, thermal cond. of single crystals 77−36079
MnZn ferrite, Ti substituted, vacancy contents and phase equilibria 80−29012
$Mn_{0.53}Zn_{0.35}Fe_{2.12}O_4$, and Ti substituted, acoustic losses 79−24207
Mo, BCC, void nucleation following electron irrad. 80−29054
Mo cryst., radiation induced vacancies and D_2^+ implantation 80−65076
Mo, desorption of He, during stage III annealing, vacancy model 77−1123
Mo, diffusion anomalies, vacancy model *(French)* 77−43366
Mo, diffusion of Li, Cs, vacancy and divacancy mechanisms *(Russian)* 80−70472
Mo, effect of microvoid size on positron annihilation and residual resistivity 77−48272
Mo, electron irrad., positron trapping in vacancies and vacancy clusters 79−52039
Mo, electron radiation damage and props. of point defects 77−11590
Mo, He ion irradiated, TEM 77−19994
Mo, interatomic pot. from phonon spectra 77−76355
Mo, neutron dose depend. of elec. resist., vacancy-interstitial recomb. *(Russian)* 77−80546
Mo, neutron-irradiated, positron lifetime study 79−23654
Mo, point defect migration, stage III annealing 77−80548
Mo, positron annihilation and vacancy formation 80−16119
Mo, vacancy diffusivity from width of grain boundary void denuded zone 77−47615
Mo, vacancy mutation to divacancies by He trapping, percolation onset 78−51601
Mo, vacancy recovery stage, radiation doping, elec. resistivity meas. 79−51102
Mo, void lattice and depend. of vacancy porosity on irradiation dose *(Russian)* 79−27972
Mo wire, laser shock induced microstructural changes, rel. to explosive shock induced phenomena 78−67768
Mo:N single cryst., interaction of N with vacancies 79−82261
Mo:Xe, BCC, heavy ion implanted, vacancy recovery, Mossbauer spectroscopy 79−82896
MoO_3, reduction at low temp., role of defects, electron microscope obs. 77−77755
NH_4Cl, acoustic absorption by soft modes of defects 80−59584
NH_4Cl:$[MoOCl_5]^{2-}$, single cryst., struct. investigations 77−66524
$(NH_4)H_2PO_4$:Cr^{3+}, EPR exam. above and below T_c 78−68363
Na, at. migration 79−69279
Na, defect calcs., vacancy form. and migration energy 79−19185
Na, diffusion data under press., anal. 78−55975
Na, electron density distrib. around vacancy, Thomas-Fermi eqns. 77−15791
Na, monovacancy thermodynamic parameter calcs., temp. dependence 78−2114
Na, self-diffusion, quasielastic neutron scatt. obs. 79−90818
Na, single vacancy relax. energy 77−84741
Na, vacancy double jumps and atomic diffusion 78−6175
Na vacancy formation energy value from phonon data 79−77592
Na, vacancy formation volume, temp. depend. 78−47350
Na, vacancy superlattice 77−7713
Na, vacancy thermal expansion coeff., lattice statics calc. 79−37698
$NaAl_{11}O_{17}$, β-alumina, local electroneutrality 79−65054
Na_2CO_3, rel. to elec. cond., 270-830°C 78−10216
NaCl, calc. of migration volume of vacancies 78−75872
NaCl cleaved surface structure, electron microscope 79−7735
NaCl, electronic structure calculation, CNDO semi-empirical methods *(Russian)* 80−10909
NaCl, filamentary crystal, vacancy-enriched surface layers 78−51536
NaCl, γ-irrad. and doped, lattice relax., cold neutron scatt. obs. 77−7715
NaCl, monocrystalline, defect struct. and intrinsic ionic cond. relationship 79−95211
NaCl, pure, undoped, luminesc. obs., ion-vacancy interactions 77−32412
NaCl, thermal expansion meas. after X-ray irrad., F-centre bleaching 80−44338
NaCl type compounds, vacancy ordering, atomistic approach 79−94947
NaCl, vacancy comaplex formation and binding energies in zeroth approx. 80−24441
NaCl, X-ray irrad., vacancy conc., thermal expansion meas. 80−6431
NaCl:Ca^{2+}, spin-lattice relax. meas., 160 to 360°C, vacancy contrib. 77−28477
NaCl:Mn^{2+}, CN^-, EPR spectrum rel. to Mn^{2+}-vacancy-CN^- complex 80−54942
NaCl:Pb^{2+}, activation energy for clustering of Pb^{2+} vacancy pairs 77−72610
vacancies continued
NaCl:Sr, dimer and trimer aggregate formation by NMR, ionic cond. and dielectric losses 80−15094
NaCl:Sr, positron annihilation and trapping in A-centres 80−84802
NaCl:V^{2+}(Ca^{2+})(Mn^{2+}), X-irrad. effects on divalent metal aggregates, EPR and ionic cond. meas. 79−82263
NaCl-NaBr mixed crysts., ionic cond., 42-450°C, cation vacancy migration 78−59970
NaF:Ca_i migration enthalpy and entropy, TSC obs. 80−54716
NaF:Fe^+_{2+}, ENDOR associated with Na^+ vacancy 79−61264
NaI:Ca^{2+}, pure and doped, ionic thermocurrents meas. 80−80677
NaI:Ca^{2+}, pure and doped, lattice defects, entropy and enthalpy of formation and migration 80−96687
$Na_xIn_xSn_{1-x}S_2$, intercalation-substitution compounds, NMR study 80−44952
$NaNO_3$, dielec. loss anal., Debye type loss peaks 80−50260
$NaNbO_3$, elec. and thermoelec. props., influence of O defects 80−29401
$NaNbO_3$-based ferroelec. solid solns., morphotropic transitions and elec. props., enhanced vacancy conc. 80−55048
Na_2O-K_2O-SiO_2, Na diffusion 78−26724
Na_2O-SiO_2:Ce photochromic glass absorption centres 79−27352
$Na_2O.5Al_2O_3$, diffusion of Na, vacancy availability, computer simulation 77−24431
$NaPO_3$ glass, Na diffusion 78−63875
$Na_2Sn:Mn^{2+}$ single crystal, EPR expts. and interpretation 79−1708
Nb, BCC, void nucleation following electron irrad. 80−29054
Nb, channelling study of irradiation damage by $^4He^+$, effect of dissolved O_2 79−82270
Nb, defect annealing in 7 MeV-irrad. samples, positron annihilation obs. 80−24497
Nb, diffusion anomalies, vacancy model *(French)* 77−43366
Nb, elec. resist. changes with plastic deform. 77−89749
Nb, Fe diffusion mechanism, self diffusion enhancement 77−84992
Nb, ion bombard. by 5 keV Ar^+, sub-surface damage 80−103399
Nb, neutron induced defect structs., TEM exam. 77−84802
Nb, positron annihilation and vacancy formation 80−16119
Nb, positron trapping and annihilation at vacancies 80−29823
Nb, rel. to self diffusion, 1353-2693K 78−47576
Nb, stress induced interaction of point defect pairs, in BCC solutions 78−79608
NbC, electronic struct. of vacancies, effect on supercond. transition temp. 80−29347
NbC, nonstoichiometric, simple shell model for phonon dispersion 77−24370
NbC, nonstoichiometric, simple model for phonon dispersion, rel. to C vacancies 78−30718
NbC, valence band XPS meas., comparison with X-ray emission spectra and band struct. spectral calcs. 80−50535
NbC_x, supercond. transition temp., light element implantation effect 80−107951
NbC_x, thermophysical props. at high temp., thermal vacancies form. 78−43141
NbC_x, x=0.868, 0.834, 0.766, self-diffusion of ^{14}C 80−29206
Nb_xC powders, plastic deform. characts. on vibratory milling 78−11183
NbO, single cryst. with 25% vacancies, neutron damage 77−15459
$Nb_{12}O_{29}$-Nb_2O_5, oxide defect structures of stable and metastable phases, 800 to 1100°C 79−46651
$Nb_{28}O_{70-x}$, O diffusion, rel. to Nb_2O_5 nonstoichiometry *(French)* 78−47583
Nb_3Sn, A-15 struct. Nb based superconductors, irrad. type influence on radiation defects 80−15093
Nb_3Sn, supercond. props., effect of neutron irrad. 80−80463
$Nd_{1-x}S$, grown-in defect exam. 78−43014
$Nd_2Ti_2O_7$-$CaTiO_3$ system, mode of formation and stability of $A_nB_nO_{3n+2}$ phases *(French)* 78−3110
$Nd_xZr_{1-x}O_{2-x/2}$, elec. cond. of ceramic solid solutions 80−107554
Ne, vacancy, electronic structure, Green's function theory 80−39525
Ni 200, C interstitial effect of yield point develop. during static strain ageing, model 78−88498
Ni 200, static strain ageing, 373 to 473K 77−36558
Ni and alloys, heavy ion irrad., defect cluster obs. 80−107341
Ni binary alloys, constituent segregation during irradiation 79−55791
Ni, cold rolled, influence of impurities on recovery and recrystallisation, positron annihilation meas. 79−15696
Ni, cold-worked, impurity-induced vacancy clustering 79−99972
Ni, computer simulation of point defects and planar defects 78−43013
Ni, creep, rel. to radiation swelling and stacking fault energy *(Russian)* 78−27562
Ni crystallites, vacancy diffusion and vacancy lattices, semi-empirical mol. orbital calcs. 77−1121
Ni, defects at thermal equilib., positron annihilation meas. 77−76391
Ni, Doppler broadened positron annihilation lineshapes, prevacancy lattice expansion 78−27349
Ni, electroplated, fuchsin additive effect on low-temp. annealing characts., resist. meas. 77−32725
Ni, electroplated layer, field ion microscope study 79−28246
Ni Ga, defect struct. 78−30608
Ni, H diffusion, trapping and mobility near vacancies, dislocations and cracks 80−49426
Ni, hardness after-effect studied by anelastic relaxation 80−66570
Ni, in situ rare gas ion irrad., cluster creation obs. by electron microscopy 80−107343
Ni, irradiated, numerical simulation of void nucleation, dislocation densities, pt. defect conc. 79−73208
Ni, mass transfer parameters, lattice defect effects under laser pulse action *(Ukrainian)* 80−6537
Ni, oxidation kinetics, influence of intermediate annealing treatment 80−89412
Ni, phase transformations and vacancy form. by positron annihilation 80−2155
Ni, plastically deformed, recovery stages III and IV investig. by positron annihilation 77−31715
Ni, point defect estimation from specific heat and volume in plastically deformed pure metals *(Russian)* 80−54223
Ni, positron annihilation ang. correl., trapping by mono- and multivacancies 77−32466
Ni, positron capture by dislocations, vacancies, rel. to temp. *(German)* 78−30606
Ni, positron lifetime meas., 4.2 to 1700K, monovacancy form. enthalpy 80−97370
Ni, positron trapping, temp. depend., vacancy form. energy 77−90215

vacancies continued
Ni, positron trapping by vacancies using ^{19}Ne source 78−47341
Ni, push-pull fatigued polycrystals, point defects, elec. excess resist. meas. 80−100910
Ni quadrupole interaction of vacancy associated with Te impurity, β-γ TDPAC meas. 78−43730
Ni, quenched vacancies, effect of oxidation *(French)* 78−27686
Ni, rel. to self-diffusion, 813-1193K 77−15618
Ni, vacancy and divacancy diffusion 79−82377
Ni, vacancy diffusivity from width of grain boundary void denuded zone 77−47615
Ni, volume changes and defect healing due to plastic deform. *(Russian)* 80−81139
Ni:Mn, radiation-enhanced diffusion, effect of point defect fluxes 77−89588
Ni-Al, B2 type, vacant sites on Ni sublattice and p-d stabilization energy 79−60357
β_2-Ni-Al, elastic consts., supersaturated thermal vacancy effects 80−54298
Ni-Al (51 to 55 at.%), vacancy defective, TEM exam. of structure 78−76677
Ni-Co-Cr-Al-Ti-Mo superalloy IN738, casking porosity removal using hydrostatic press. sintering 80−55322
Ni-Cr (33 at.%), US deform. effect on short range order form. *(Russian)* 78−39839
Ni-Fe (20at.%), vacancy-C interaction, Lomer's model insufficiency *(French)* 77−76456
Ni-Ge , defect-solute interactions and radiation-induced segregation 80−25705
Ni-Ge (2 at.%), vacancy cluster form. during deform. positron lifetime meas. 79−56882
Ni-In, dil., symmetry of lattice defect, DPAC meas. 78−43729
Ni-In, dil., uncorrelated radiation damage, TDPAC meas. 78−43343
Ni-NiAl solid soln., high temp. transforms *(Russian)* 79−56973
Ni-S, defect control by heat-treatment in S atmos. 79−43293
Ni-Si, defect-solute interactions and radiation-induced segregation 80−25705
Ni-Zn ferrites, comp., lattice imperfections, sintering 78−3080
β'-NiAl, dislocation climb, hot stage TEM 77−24318
β'-NiAl, ordered, hardness after-effect studied by anelastic relaxation 80−66570
NiAl, thermal defects, dilatometric study *(Japanese)* 80−15092
$Ni_{1-x}Al$ solid solution, vacancy ordering exam. by electron diffr. after annealing 78−3123
$Ni_3Al(Ga)$, off-stoichiometric alloy, inverse mag. susceptibility rel. to defect conc. 80−60216
$Ni_{0.5-x}Co_xZn_{0.5}Fe_2O_4$ ferrospinal solid solutions, cryst. lattice defects and props. 80−19796
$Ni_{1-3x}^{2+}Fe_{2+2x}^{3+}Vac_xO_4^{2-}$ (Vac=cation vacancy), solid solns., cryst. lattice imperfections 80−39069
NiGa, vacancy conc. in B2 phase exhibiting triple defects 79−42058
Ni_3Mn, vacancy migration during fast and thermal neutron irradiation 79−42114
$Ni_{65}Mo_2Fe$, O_2 effect on secondary recrystallisation and mag. props. 80−35201
Ni_xNbS_2 vacancy ordering, transition state cluster model, electron diffr. 77−47547
NiO (001) surface, chemisorption of H, surface and second-layer defect effects 80−65369
NiO, diffusion of ^{35}S 77−15629
NiO, diffusion of ^{35}S by two different modes 80−59720
NiO, diffusion of Ni in bulk and along dislocations 79−82381
NiO, dipole orientation from bound polaron hopping 80−84437
NiO, elec. cond. and chem. diffusion coeff. at high temps. 79−23962
NiO, elec. cond. meas. at 1000°C 78−10451
NiO, H chemisorption, perfect surfaces, cation vacancies, self-consistent HF-VB calcs. 79−69351
NiO, stress appl. high temp. creep and point defects, creep rate obs. 80−49297
NiO, thermodynamic study of point defects, anal. of elec. cond. results 79−23963
NiO_2, elect. cond. under low O_2 press., kinetics interpretation 79−82587
$Ni_{1-x}O$, electronic cond. at high temp., vacancies and interstitials effect *(French)* 78−79990
β-Ni_3S_2, formed during sulphidation of Ni, defect struct. and chemical diffusion 78−2115
NiSb, dilute alloy, impurity-induced vacancy clustering 79−99972
β-NiSe, d-electron deficit model, electrochem. meas. of free enthalpy *(French)* 78−30605
$Ni_{1-x}Te_2$, mixing energies of Ni atoms and vacancies 79−27975
NpC_{1-x}, nonstoichiometric, atomic short-range order obs. by diffuse neutron scatt. 77−24315
PLZT composition, effect on its switching characts. 79−42917
PLZT, diffuse phase transitions, Curie temp., dielectric props. 80−75979
$(Pb,Ba)(Zr,Ti)O_3$, diffuse phase transitions, Curie temp., dielectric props. 80−75979
Pb, electron irradiation at 4.7K and below 3K, annealing expts. 77−11595
Pb, energy of form. of monovacancies, positron annihilation obs. *(German)* 78−71721
Pb, liq., generation and motion from coordination statistics 77−1063
Pb, perturbed γ-ray angular distrib. of ^{210}Po, temp. depend., radiation damage effects 78−43736
Pb, positron annihilation, Doppler broadening, 4.2 to 600K 79−47540
Pb, positron trapping by vacancies, high resolution lifetime meas. 77−1759
Pb, vacancy and divacancy props., exam. via quenching and annealing 78−47343
Pb-As (~0.01 wt.%), enhanced precip. phenomena, invest. of mechanism by elec. resist. meas. 80−104162
Pb-Au, interstitial and substitutional distrib. 80−84204
Pb-Bi, splat quenched, solubility limit, vacancy conc. and supercond. transition temp. 77−12046
Pb-Sb-As (1.1-1.8, ~0.01 wt.%), enhanced precip. phenomena, invest. of mechanism by elec. resist. meas. 80−104162
Pb-Tl, vacancies, positron capture, function of Tl concentration *(German)* 80−49213
Pb-Tl alloys, positron trapping in vacancies, varying concentration effects *(German)* 80−25477
PbF_2 based solid solns., ion transport 80−107545
vacancies continued
PbF_2, cubic and orthorhombic, press. and temp. depends. of ionic cond. 79−95207
β-PbF_2, solid electrolyte, mobile species mobility and conc., temp. depend. 77−20113
PbS:Tl, self-compensation of acceptors by vacancies, Hall coeff. meas. 80−92913
PbS_xSe_{1-x}, chalcogen interdiffusion, electron microprobe obs. 79−28145
PbSe:Tl, self-compensation of acceptors by vacancies, Hall coeff. meas. 80−92913
$PbSe_xS_{1-x}$, comp. depend. of density, effect of defects 77−11538
$Pb_{1-y}Sn_ySe$, electron irrad., change in elec. and recomb. props. due to form. of Se vacancies 79−56227
PbSnTe, electron irradiated, high temp. defects 79−78122
p-$Pb_{0.82}Sn_{1.8}Te$, Hall coeff. sign-inversion temp. 78−52010
$Pb_{1-x}Sn_xTe$, electron irrad., elec. and recomb. props., changes due to form. of Te vacancies 79−56227
$Pb_{1-x}Sn_xTe$ solid solutions, EPR at Te vacancies *(Russian)* 77−48050
$Pb_{1-x}Sn_xTe$:Cd, distrib. of Cd atoms in cryst. lattice after compensation metal vacancy sites 79−69292
PbTe epitaxial layers, submillimetre spectroscopy 79−83048
PbTe, TO phonon softening, free carriers and defects effects 78−79720
PbTe, undoped, nature of defects, X-ray diffr. and optical absorption meas. 77−43211
PbTe:Cd, distrib. of Cd atoms after compensation of metal vacancy sites 79−69292
$Pb(Ti,Zr)O_3$, kinetics of initial stage of sintering 77−85973
$PbTiO_3$-$La_2O_3.3TiO_2$, struct. and dielec. props. 80−54200
$Pb(Ti_{0.47}Zr_{0.53})O_3$, elec. cond. rel. to O_2 partial press. 77−51742
$Pb(Ti_{0.47}ZrO_{.53})O_3$, small polaron cond. mechanism, elec. cond. and thermopower meas. point defects 78−43380
$Pb(Zr,Ti)O_3$ pyroelectric ceramics 79−47649
Pd, localised vacancies produced by thermal neutron capture recoil 78−26598
$Pd_3P_{0.8}$, pure and deuterated, cryst. struct., neutron diffr. study 80−84152
$Pr_{40}O_{72}$, ε-phase, defect cryst. struct. 79−90645
Pr_9O_{16}, ζ-phase, defect cryst. struct. 79−90645
Pt foil, quenched, 1.2 MeV electron irrad., subthreshold irrad. effects 78−51585
Pt, interstitial thermal conversion study by elec. cond. meas. 80−15096
Pt, quenched, coprecipitation of vacancies and C atoms 79−78978
Pt, quenched, deviations from Matthiessen's rule 77−69289
Pt, radiation damage with radioactive probes, TDPAC meas. 77−24336
Pt, recovery spectrum after thermal neutron irrad., resist. obs., Au addition effect and defect conc. depend. 80−65057
Pt, thermal and fission neutron produced defect configurations 78−47432
Pt wire, single vacancy form., activation energy meas. 80−49212
Pt-Au (4.0 at.%), ion irradiated, direct obs. of vacancy struct. of (220) platelet 78−51534
Pt-In, dil., damage induced quadrupole interactions, DPAC exam. 78−39465
PuO_2, substoichiometric, unified model for defects, thermodynamic functions 77−20094
$R_{1-x}Co_x$, rare earth amorphous alloys, thermal stability, elec. cond. enthalpy 80−100172
Rb, defect calcs., vacancy form. and migration energy 79−19185
RbCl, with divalent impurity, reorientation of impurity-vacancy complexes, thermally stimulated depolarisation 77−65977
$RbCl:Co^{2+}$, dielectric loss, impurity sites 79−91348
$RbMgF_3$:Mn, low-temp. radiation damage, optical absorption meas. 78−22761
Sc_2O_3:MgO, defect struct., X-ray diffr. and pyrometric density 78−34524
Sc_2O_4, polycryst., form. conditions of anion vacancies, phase comp. 80−54220
a-Se, hole form. energy, heating time and cooling rate depend. 79−41958
Se, undeformed rhombohedral, dislocations, electron microscope obs. *(French)* 78−51548
n-Si, 300 keV proton irrad., temp. depend. of defect prod. 78−6113
Si (110) surface, chemisorption of H, UPS spectra meas. and LEED 77−20186
Si (111), adsorption of Cl, H, Si, SiCl, $SiCl_2$, equilib. adsorption layers 79−23858
Si (111) 1×1, surface, chemisorption of Cl in vacancies 79−77910
Si (111) surface reconstruction, milk-stool model, quantum chem. ab initio calc. 80−49477
Si, amorphisation by $^{31}P^+$ ion irrad. 79−51172
Si, amorphisation by ion implantation, homogeneous or heterogeneous nucleation 77−11578
Si, amorphous, large vacancy cluster annealing by ion bombard, EPR investig. 77−68965
Si, amorphous layer prod. by ion implantation, diffusion broadening, ESR study 80−92552
Si, annealing of vacancy clusters produced by ion bombardment 77−89485
Si, CW laser annealed, defect luminesc. 80−50388
Si, charge disturbance around neutral defect, simple new method, appl. to ideal vacancy 79−82554
Si, crucible grown, virgin and implanted, laser irradiation effects on surface structure 80−92768
Si, Czochralski grown, dislocation free, swirl defect form., doping effect 80−92519
Si, deep level defects, struct. bonding, amphoteric centres 80−88506
Si, deep-level point defects, effective-mass nature 80−59922
Si, defect formation kinetics during charged particle irrad. 80−29096
Si, defects, divacancy and split 100 interstitial, electronic structure calc. 80−65494
Si, diffusion mechanism of P, migration channels along vacancies and interstices 80−79996
Si, diffusion of P, excess vacancy generation by E-centre dissociation 77−72720
Si, dislocation free, C and O impurity clouds, heat treatment influence on light scatt. 80−6427
Si, divacancies due to proton irrad., IR absorpt., annealing effects 80−20673
Si, divacancies orientation induced by IR light, EPR spectra 80−25209
Si, divacancy, hyperfine interactions from ENDOR meas. 79−42868
Si, divacancy, positive, EHT calcs. 79−99184

vacancies continued
Si, divacancy charge states, photoconductivity spectra 77−15899
p-Si divacancy charge transfer during annealing after fast neutron bombard., piezo-spectroscopic study *(Russian)* 77−28607
Si, EPR of radiation damage due to complete stopping of 30 MeV protons 77−65994
n-Si, efficiency of radiation defect generation by electron bombardment, influence of Fermi energy 77−11596
Si, electron irrad., limiting position of Fermi level, elec. cond. and optical absorpt. meas. 79−65484
Si, electron irrad., multivacancy-O complexes, EPR expt., correl. with IR absorpt. data 77−28443
Si, electron irrad., two-vacancy defect EPR 80−29619
p-Si, electron irrad. induced defects, thermally stimulated capacitance 77 11933
Si, electron irradiated, EPR of C-O divacancy complex 77−69691
n-Si, electron-irrad., surface defect distrib., deep-level transient spectroscopy 79−1459
Si, electron-irradiated crystals, positron trapping, temp. depend. 80−104009
Si, electronic states of vacancies, covalent states 79−23926
Si, electronic vacancy states by chemical pseudopot. method 79−23929
Si, entropy and enthalpy of vacancy form., comparison of theory with quenching expts. 77−11872
Si, extended Huckel theory calculations for positive divacancy 78−87938
Si films, polycryst., annealing of paramag. vacancy-type defects, EPR obs. 79−10848
n-Si, gamma ray irrad., impurity composition influence on recombination centre formation 80−6872
p-Si, heat-treated, mechanism of vacancy generation 79−69531
Si, hyperfine interaction of divacancies, ENDOR meas. 77−4579
Si, ideal vacancy, electronic struct., tight-binding calc. 79−4529
Si, ideal vacancy, self consistent Green's function calc. 78−91640
Si implanted layers, interaction of defects and impurities stimulated by induced ionisation, ESR 80−11270
n-Si, influence of deform. on capture of electrons by divacancies 77−1449
Si, interstitials and lattice vacancies 78−10038
Si, ion implanted, voids, electron microscopy 78−67757
Si, ion irradiation prod. of stable vacancy-interstitial pairs 77−27925
Si, ion-implanted, secondary defects development, three-stage model 78−87725
Si, irrad. with Cr^+, form. and annihilation, of defects, ESR investigation 79−90707
Si, isolated vacancy, electronic struct., SCF method 80−80208
Si, Jahn-Teller distorted vacancy, electronic struct. 80−10869
Si, lifetime of free vacancies 79−10851
n-Si, lightly doped, electron irrad. induced divacancies as electron traps 77−4126
Si, localised defect, self consistent Green's function calc. 80−10919
Si, migration energy of intrinsic point defects in different charge states 77−89582
Si, nearly perfect crysts., point defect aggregates, high resolution diffuse X-ray scattering study 80−49211
Si, neutral undistorted vacancy 78−91638
Si, neutral vacancy, generalised val. bond calc. 77−55493
Si, neutral vacancy electronic struct. 77−62865
n-Si neutron and electron irrad., isochronous annealing influence on edge absorpt. 80−11449
Si, neutron irrad., small angle neutron scatt. meas. 80−29073
Si, neutron irradiated, charact. of defect form. 78−14382
Si, neutron irradiated, direct band gap transition, IR absorpt. 79−73980
Si, neutron irradiated, influence of defects and temp. on positron annihilation 77−4699
Si, neutron transmutation doping, at. displacement effects 80−19852
Si, oxidation induced stacking fault growth, role of point defects 78−10061
Si, oxidation-induced stacking faults, control by Cl implantation 79−46682
Si, paramagnetic defects produced by electron irrad., EPR 79−19779
p-Si, photoabsorpt. associated with divacancies 79−15502
n-Si, photoionisation of doubly charged divacancies 79−51526
Si, plastically deformed, EPR spectra of point defects., temp. depend. 77−90033
Si plate, internal friction temp. depend. 77−15491
Si, point defect clusters identification by TEM 77−43210
Si, point defects, multiple scatt. Xα model 80−54636
Si, point defects, negative-U props. 80−49660
Si, positively charged divacancy photoionisation cross section by photocapacitance meas. 80−6901
Si, proton irrad., efficiency of form. and nature of defects, Hall meas. 80−6444
n-Si, quenched, fast electron irradiated, annealing of defects 80−89259
Si, radiation defect clusters, form. kinetics and parameters 77−11545
p-Si radiation defects due to 30 MeV proton irrad., rel. to solar energy convertors 78−71776
Si, radiation-stimulated vacancy diffusion, mechanisms 77−55396
Si, reconstructed surface physics, review 80−10766
Si, rel. to anomalous passage of positrons, expt. 79−95052
Si, rel. to oxidation effects on diffusion of P 79−51309
Si, Schottky barrier structs., proton bombarded, defect states 80−29356
Si, self-consistent pseudopotential cal. of electronic states associated with reconstructed vacancy 79−73465
Si, self-diffusion, activation energy and entropy factors 80−88353
Si, self-interstitials, vacancies and their clusters 77−80500
Si, semivacancy and pair of semivacancies calc. by CNDO/2 method 78−51537
Si, single crystal, kinetics of annealing of vacancy complexes 78−87666
Si, solubility of Au, gettering by P 78−83961
Si, status of defect studies 77−84742
Si, thermal oxidation, mechanism of appearance of surface roughness and surface defects 77−7956
Si, thermal oxidation kinetics, steady-state transport anal. 80−71773
Si, thermal oxidation kinetics, theoretical perspective 80−76387
Si, vacancies and interstitials 80−29015
p-Si, vacancy, charge states, Jahn-Teller stabilisation energy 80−80209
Si vacancy, defect electronic energy levels calc., optimisation 79−28315
Si vacancy, electron states, Anderson negative-U system 80−96820
Si, vacancy, local energy levels in Wannier approx. 77−20264
Si, vacancy, possible Anderson negative-U system 80−2358
Si, vacancy, self consistent Green's function method 80−24843
vacancies continued
Si, vacancy, self-consistent electronic states 80−29354
Si, vacancy, tight-binding calc. 80−24844
Si, vacancy cluster props., effect of natural anisotropy *(Russian)* 77−62522
Si, vacancy electronic struct., self-consistent approach 79−78043
Si, vacancy electronic struct., self-consistent Koster-Slater method 80−10920
Si, vacancy formation and stability due to noncentral force 80−70192
Si, vacancy paradox 78−59804
Si, vacancy screening, dielec. const., exchange correl. pot., Thomas-Fermi description 80−44528
Si, wafers, HCl etched, surface morphology, etch pit origin 79−96166
Si:Al, electron irrad. induced defects, transient capacitance study 80−59516
Si:As, displacement effect beam energy depend., vacancy trapping 80−33996
p-Si:B, defect energy levels with 1 MeV electron irrad. and annealing, transient capacitance spectra 77−62860
Si:B, implanted, effectiveness of charged vacancies in diffusion 80−34239
Si:B, ion implanted, radiation defect accumulation and annealing, X-ray diffr. obs. 79−37726
Si:B, irrad. with fast neutrons true profiles of impurity photocond. bands from piezodichroisms 79−91103
Si:B (0.2 wt.%) ion implanted, B atom displacement due to low temp. irrad. 80−88234
p-Si:B(Al), radiation defect form. and annealing study using Hall effect, cond. and carrier diffusion length 80−84214
Si:B(P), proton enhanced diffusion, vacancies diffusion length 80−29226
n-Si:Cs, ion implanted, minority carrier lifetime and defect struct., annealing effect 78−6395
Si:Cu, interaction between vacancy emitting absorbing precipitates and dislocations, TEM obs. 78−71755
Si:Gd, radiation defect form., effect of Gd impurities, elec. and optical meas. 78−71764
Si:H, defects in monovacancy Si cluster, semi-empirical calc. 78−43329
a-Si:H, spin defect and recombination influence on electronic transport 80−50409
Si:In, electron irrad., Hall effect meas. 80−2401
Si:O, heat treated, excess carrier recomb. rate, defect levels 80−75579
Si:O,C, electron irradiated, indirect vacancy-interstitial recomb., IR absorpt. meas. 77−43209
Si:P, diffusion eqn. numerical soln. 79−51311
Si:P, diffusion of P, 900-1100°C, distrib. of excess vacancies 77−72631
Si:P, excess vacancy generation by P diffusion *(Japanese)* 77−89460
Si:P, optically induced divacancy reorientation, EPR spectra 78−80216
Si:P, P diffusion, vacancy mechanism 77−7906
Si:P(As)(B)-SiO_2 interface oxidation kinetics, high doping levels, experiment 80−11828
Si:P(B), high temp. impurity diffusion via vacancies and self-interstitials 80−24667
Si:P(B)(As), proton enhanced diffusion and vacancy migration 78−67747
Si:Sb, electron irrad. damage, Sb-vacancy pair trapping centre 77−39798
Si:Sn, Mossbauer study of defects due to ^{119}In implantation 80−80641
Si-As(Sb) temp. depend. of irradiation-induced displacement of impurities, backscattering meas. 78−26605
Si-SiO_2 interface oxidation kinetics, high doping levels, theory 80−11827
SiC, B diffusion, polytype struct. effect 78−59983
β-SiC, cubic, electronic props. of vacancies and divacancies 77−76767
SiC, influence of plastic deform. on struct. of photoluminesc. spectra 77−55824
SiC, synthesis by ion implantation of diamond, role of struct. imperfections 78−34529
n-SiC, thermal defects, ESR study 80−88876
SiH_1-like centres, in cryst. Si, vacancies and chem. trapping obs. 79−99916
SiO_2, amorphous and crystalline, with O vacancy, cathodolum. meas. 77−24901
SiO_2 clusters, CNDO/2 calc., appl. of cyclic boundary conditions 78−72110
SiO_2, disperse, EPR, O_2 vacancy relax. rel. to substrate struct., gas adsorpt. *(German)* 79−95645
SiO_2 film, form. by reactive sputtering, effect of defects in Si wafer 77−89676
SiO_2, g-tensor and ^{29}Si hyperfine tensors of E_1'-centre for model of O^- vacancy 79−19777
SiO_2, surface defect studies, AES, theoretical model, and expt. 79−7738
SiO_2, vitreous, luminescence centres at 396 and 280 nm 80−103996
SiO_2, vitreous, semi-empirical mol. orbital model, appl. to radiation compaction 79−73433
SiO_2-Si interface, interaction of point defects, electron microscope exam. 77−7979
SiO_{2-x}, vitreous, $\rightarrow\beta$-cristobalite, polymorphic transformation with stoichiometry changes 77−43325
SiO_x, oxidation, film defect equilibria and growth reactions 78−11377
SmO film, new reduced variant due to annealing 77−89660
SmS, cryst. struct. in homogeneity region 78−91334
Sm_3S_4, sp. ht. anomaly 77−89550
α-Sn, ion implanted, defect struct., Mossbauer spectra 80−80214
Sn, single cryst., equilib. vacancy conc., length and lattice parameter change meas. 79−60352
Sn, thermally induced vacancies, positron trapping 80−89083
Sn, vacancy formation and activation volume, macroscopic model 80−54221
Sn-Bi, eutectic, superplastic anisotropy *(German)* 80−25808
SnO_2 CVD coating on glass, elec. resist. rel. to cryst. microstruct. 80−84520
SnO_2, nonstoichiometric crystal, free electron density anal. 79−99108
SnO_2, rare earth ion doped, luminesc. and charge compensation 78−76532
SnO_2 thin films, O_2 vacancy diffusion 80−107467
SnSe, electronic props., region of existence *(French)* 77−35885
SnTe-PbTe solid solns., defects from susceptibility meas. 77−84737
$SrCl_2$, ionic cond., self-diffusion, rel. to defect motion, mol. dynamics study 80−65282
$SrCl_2$, point defect parameters, ionic cond. study 80−107490
$SrCoO_{3-\delta}$, crystal struct. and mag. props., O vacancy effect 79−95587

vacancies continued
$Sr_3NbO_{5.5}\square_{0.5}$, $Sr_2CaTaO_{5.5}\square_{0.5}$, $Sr_2CaNbO_{5.5}\square_{0.5}$, $SrZr_{0.8}Yb_{0.2}O_{2.9}\square_{0.1}$, $SrZr_{0.8}Mg_{0.2}O_{2.8}\square_{0.2}$, ionic conductivity 77−20119
SrO, proton, neutron irradiated, fluorescence from anion vacancies, F^+ centre model 78−48221
SrO, single cryst., tribolum. obs. 79−52031
SrO-Fe_2O_3, EMF meas. with solid state cell, Mossbauer effect and magnetic props. *(Korean)* 77−28493
$SrTiO_3$ ferroelectric modes, Raman spectra, neutron scatt. meas. 80−80727
$SrTiO_3$, pure and Nb doped, heat treated, Hall effect, electrical cond., optical absorpt., defect states 78−47812
$SrTiO_3$, semicond., structural phase transitions, US velocity meas. 79−28692
$SrTiO_3$, semiconductor, soft modes, zone boundary mode 80−71357
$SrTiO_3$-Ni, electrochromism, optical and elec. meas. 79−95732
$SrTiO_{3-x}$, anion deficiency and anion vacancy ordering 78−51532
$SrTiO_{3-x}$, X-ray and electron diffr. obs. of anion deficiency 78−22708
Ta, diffusion anomalies, vacancy model *(French)* 77−43366
Ta, positron annihilation and vacancy formation 80−16119
Ta, positron trapping and annihilation at vacancies 80−29823
Ta, stress induced interaction of point defect pairs, in BCC solutions 78−79608
Ta, vacancy formation and migration energies, positron annihilation meas. 77−84739
Ta:Xe, BCC, heavy ion implanted, vacancy recovery, Mossbauer spectroscopy 79−82896
Ta_2O_5, anodic film, thermally stimulated exo-electron emission 80−11546
Te, anelastic relax. in $Pb_{0.84}Sn_{0.16}Te$ single cryst. *(Russian)* 77−51437
Te, electron irradiated, dose-depend. and recovery behaviour of transport props. 78−71761
ThC_{1-x}, nonstoichiometric, atomic short-range order obs. by diffuse neutron scatt. 77−24315
ThO_2-CaO, and ThO_2-$YO_{1.5}$, solid solns., defective oxides, ionic cond. 80−107548
ThO_2-CaO electrolyte, cond. rel. to dissociated vacancies and vacancy-impurity complexes 77−8156
Ti, deform. and H_2 inclusion effect on annihilation γ-ray ang. correl. curve shape 78−31273
Ti, heat capacity near polymorphic transition, temp. depend., vacancy mechanism 79−86884
Ti, neutron irradiated, characterization of dislocation loops 80−88155
Ti, point defect estimation from specific heat and volume in plastically deformed pure metals *(Russian)* 80−54223
Ti, volume changes and defect healing due to plastic deform. *(Russian)* 80−81139
β-Ti-Mn, exam. of reloading yield points 78−72822
TiC, nonstoichiometric, simple model for phonon dispersion, rel. to C vacancies 78−30718
TiC_{1-x}, substoichiometric, electronic density of states 80−2319
TiC_x (x=0.97, 0.90, 0.80), Raman scatt. induced by C vacancies 78−52500
TiC_x, effect of structural vacancies on neutron radiation damage 77−35591
TiC_xN_y, neutron diffr. investig. 77−51355
TiC_xO_y, lattice completeness and period 78−22706
Ti(Fe, Co), off-stoichiometric alloy, inverse mag. susceptibility rel. to defect conc. 80−60216
TiN, powder defect struct., thermal and elec. props. 77−59286
TiO, ordered phase, vacancy-strain coupling 78−79549
TiO_2 (rutile), (001) and (110) faces, UPS and LEED obs. 80−45206
TiO_2, nonstoichiometry study, thermal emission of electrons 80−108317
TiO_2 treated with quinoline, electron transfer between O ion vacancy in TiO_2 and surface state 79−66352
TiO_2:Nb and TiO_2, reduced, thermoelec. power meas. at high temp., point defect model 77−32030
TiO_2:Nb_2O_5(Ta_2O_5), conduct. rel. to defect structure, obs. 77−76392
TiO_2:S, acceptor properties of S, free electron concentrations 80−34395
TiO_2:V(Cr)(Mn)(Fe), impurity levels, photocurrent and ESR meas. 80−29346
TiO_{2-x}, and $TiO_{2-x}F_x$, rel. to differences in photoelec. behaviour 79−28371
TiO_{2-x}, reduced, cond. between elec. props. in equil. at 1100°C and after quenching, defects role *(French)* 80−44582
TiO_x, (x=0.88, 1.27), effect of heating at high press. on struct. 78−10190
TiO_x, heat of form. of structural vacancies 79−14797
TiO_x, quenched and high temp. specimens, vacancy-vacancy and vacancy-electron interactions 78−79607
TiO_x, struct. vacancies in unit cell 80−107213
TiO_x, vacancy ordering, transition state cluster model, electron diffr. 77−47547
$Ti_{1+x}S_2$, vacancy ordering, transition state cluster model, electron diffr. 77−47547
$Ti_xV_{1-x}Cy$ solid solutions, mag. susceptibility and band struct. 79−51739
TmSe, nonstoichiometry, high temp. chem. and valence instability *(German)* 79−23743
$(U,Pu)_{2+x}$, pure state and Mo addition, stoichiometry depend. of elec. cond. 77−20320
$(U,Pu)O_2$, substoichiometric, unified model for defects, thermodynamic functions 77−20094
$(U,Pu)O_2$, substoichiometric high temp. thermodynamic parameters 77−21125
$(U,Pu)O_{2-x}$, O_2 thermomigration described by cluster model 78−22888
$(U,Pu)O_{2\pm x}$, cluster model approach to thermodynamic props. 77−20093
U, irradiation growth during fission fragment and proton bombard. 80−92568
U, vacancy formation and phase transformation by positron annihilation 80−49215
UC, fission dose depend. of lattice parameter changes 77−24333
UC, quenched-in defects, formation, migration and resistivity 80−64990
UCN, quenched-in defects, formation, migration and resistivity 80−64990
$UC_{1-x}N_x$,nonstoichiometric, atomic short-range order obs. by diffuse neutron scatt. 77−24315
UO_2, irradiation induced vol. change 78−67740
UO_2, O diffusion mechanism 78−33249
UO_2, quenched and neutron irrad., recovery processes, vacancy migration 77−28048

vacancies continued
UO_2, thermodynamics, defect props. 77−67810
$UO_{2\pm x}$, model of response of fission gas bubbles to dynamic behaviour of point defects 79−37735
$UO_{2.12}$ hyper-stoichiometric, defect struct., anal. of neutron diffr. data 78−26562
$(U_{1-y}Pu_y)O_{2-x}$, thermodynamics 78−70593
V, Doppler broadened positron annihilation lineshapes, prevacancy lattice expansion 78−27349
V, electron-irradiated, positron annihilation study 80−70259
V, polycryst., rel. to creep behaviour, 790-880°C 79−24578
V, positron annihilation, temp. depend. 78−56540
V, positron annihilation and vacancy formation 80−16119
V, stress induced interaction of point defect pairs, in BCC solutions 78−79608
V-O alloy, temp., dose and conc. depend. of void form. following V^+ ion beam irradiation 78−10105
V-S system, order-disorder transition of metal vacancies, statistical thermodynamics 78−43012
V-S system, quenched, order-disorder transition of metal vacancies, DTA and X-ray analysis 78−30576
V-Se system, quenched, order-disorder transition of metal vacancies, DTA and X-ray analysis 78−30576
V-Ti, exam. of intrinsic diffusion and vacancy flow effects 79−4430
VC_x, VN_x, vacancy ordering, transition state cluster model, electron diffr. 77−47547
VC_xO_y, conc. depend., of unit cell filling degree 80−54199
VN, electronic struct. of vacancies, effect on supercond. transition temp. 80−29347
VN_{1-x}, vacancy ordered structure in cubic mononitride phase, transition entropy determ. 78−43011
$VO_{1.30}$, ordered phase, X-ray anal. of defect struct. 79−99177
VO_2 film, ion bombard. effect on metal-dielec. phase transition, optical props. meas. 79−90963
VO_x, defect ordering, electron diffr. obs. 79−23595
VO_x, defect struct., local ionic arrangements in disordered phase 80−10532
VO_x, struct., model based on O vacancy superlattice 77−84707
V_2O_5 and lower oxides, defect structures and related props., review 80−59454
V_2O_5 EPR of O vacancy 78−72406
V_3Si, phase transition and transition temp., chemical comp. effects, defect struct. exam. 78−18651
V_3Si, supercond. props., effect of neutron irrad. 80−80463
W, diffusion anomalies, vacancy model *(French)* 77−43366
W, diffusion of Li, Cs, vacancy and divacancy mechanisms *(Russian)* 80−70472
W, electrical resistivity -temperature scale and vacancy parameters 78−71727
W, electron irrad., or ion irrad., stage II, point defect struct., FIM 77−80542
W, implantation effects of ^{133}Xe, annealing behaviour, Mossbauer study 80−40011
W, ion irradiated, defect clusters obs. 80−2089
W, neutron irrad., at thermal energies, annealing exam. of recovery 78−47355
W, positron annihilation and vacancy formation 80−16119
W, positron trapping and annihilation at vacancies 80−29823
W, surface energies and vacancy-surface interactions calc. 79−19448
W, vacancies, quenching and recovery invest., resist. and TEM study 80−39074
W, vacancy recovery stage, radiation doping, elec. resistivity meas. 79−51102
W, vacancy struct. of depleted zones after ion irrad. 79−73224
W, vacancy structure in near surface depleted zone following ion bombard. 80−70267
W, vacancy-defect clustering, due to annealing and quenching, TEM and elec. cond. exam. 78−47344
W wire, laser shock induced microstructural changes, rel. to explosive shock induced phenomena 78−67768
W:Kr, He trapping at substitutional Kr, vacancy creation 77−43258
W:Xe, BCC, heavy ion implanted, vacancy recovery, Mossbauer spectroscopy 79−82896
$YCoO_3$, anomalous $^{57}Fe^m$ charge states, Mossbauer study 80−40017
$YFe_{5-x}Al_xO_{12}$, impurity redistrib. kinetics, temp. depend., vacancy effects 80−75263
$YFe_{5-x}Ga_xO_{12}$, impurity redistrib. kinetics, temp. depend., vacancy effects 80−75263
YIG, nonstoichiometry and electronic defects, thermogravimetric expts. and anal. of elec. data 78−6050
YIG:B,Pb, IR spectrum, localised modes, rel. to impurities and O vacancies 80−50377
YIG:Ca, O diffusion depend. on defect conc. 78−67857
YIG:Ca, oxidising effects of high temp. annealing in reducing atmosphere 80−66696
Y_2O_3, nonstoichiometry study, thermal emission of electrons 80−108317
zircalloy-2, annealed, neutron irradiated, 573 to 923K, damage struct. 79−99247
Zn, 6.1 MeV α-particle irrad., stage III and IV recovery kinetics, defect diffusion 77−76474
Zn, defect recovery after low temp. electron irrad. 78−10090
Zn, growth from melt, conditions influencing dislocation struct. *(Russian)* 80−97424
Zn, thermal recovery and stress-strain relations 78−11266
Zn, vacancy conc., lattice parameters meas. 78−10040
Zn, vacancy concentration meas., lattice parameter and length changes, form. parameters 79−37697
$ZnAl_2S_4$-$ZnCr_2S_4$, nonstoichiometric spinel solid solns., synthesis and cryst. chemistry 77−35526
$ZnGeP_2$, P vacancies, lattice parameters, optical props. depend. on thermal treatment *(Russian)* 78−71729
$Zn_xHg_{1-x}Te$, vacancy electron states, acceptor behaviour, electron mobility 80−70193
ZnO, electron irrad., vacancies and interstitials, EPR meas. 79−14803
ZnO, F^+-centre exam., ground and first excited energy level 77−39800
ZnO, irradiation in high voltage electron microscope dislocation loops study 80−88157
ZnO, vaporization from spinel solid solns. 77−76541
ZnS, high-resist., optical transmission thermal processing effects 77−63431
ZnS, ion implantation effects on luminesc., thermo-EMF 80−88178

vacancies continued
ZnS, ODMR of Zn vacancy obs. 80−108121
ZnS:Ag, TSC and induced impurity photoconductivity, existence of two electron trapping centres 80−44655
ZnS:Mn, phosphor, surface changes following interaction with H *(Russian)* 78−72602
ZnS:Mn-H atom systems, surface physiochem. changes, radical recombination luminesc. investig. 79−56863
ZnS_xSe_{1-x}, electron trap associated with anion vacancy, DLTS study 80−80210
ZnSe, electron trap associated with anion vacancy, DLTS study 80−80210
ZnSe, electronic struct. of charged Zn vacancy, cluster model 77−47764
ZnSe, heat-treated in controlled partial press. of Zn or Se, TSC 80−59910
ZnSe, pure and Cu doped, elec. props. after heat treatment in Zn or Se vapour 79−99505
ZnSe, single crysts., opt. band gap and Mn^{2+} EPR, effects of prep. conditions 77−47730
ZnTe, nonlinear absorpt., temp. depend. *(Russian)* 77−20899
ZnTe:Al,Cl, photolum., complex acceptor, ionization energy 80−20693
ZnTe:In(Al), pure and doped, Zn vacancy energy levels, elec. and optical props. 79−4827
Zr alloys, creep and growth, irradiation induced, rate theory approach 80−89294
Zr alloys, creep and growth, irradiation induced, microstruct. depend. 80−93602
Zr and Zircaloy, polarisation in high temp. water 77−52540
Zr, irradiation growth, reaction rate theory calcs. 80−88212
Zr, neutron irradiated, dislocation loop nature 77−47489
Zr neutron irradiated, faulted loops 78−10094
α-Zr, vacancy recovery following 1.5 MeV electron irrad., positron annihilation meas. 77−47485
Zr-Au (0.3 and 0.2 wt.%), irradiated, backscattering meas. of Zr self-interstitial atom trapping by Au 77−69014
Zr-base alloy as reactor core material, microstruct., deform. and fracture 78−4988
Zr-base alloys, annealed specimens, irradiation growth 80−49276
Zr-Nb alloy, direct imaging of point defects using TEM 77−35453
ZrC, sintering shrinkage, effect of struct. vacancies in interstitial phases 78−60630
ZrC_x, thermophysical props. at high temp., thermal vacancies form. 78−43141
$ZrH_{1.9}$, neutron irrad. induced defects, nature and thermal stability 77−50246
ZrN, thermodynamic props. of vacancies 77−11539
ZrN_x:Cs, thermionic emission, metallic sublattice vacancy effects 78−68597
ZrO_2 $1.6H_2O$, anion defect formation and annealing during thermal decomp. in vacuum 77−51366
ZrO_2, cubic, anion vacancy form. during electrolysis, density change 77−80648
ZrO_2, cubic, nitride stabilised 78−92223
ZrO_2:Y_2O_3, low-temp. specific heat, oxygen vacancy effects 80−49376
ZrO_2-CaO, and ZrO_2-$YO_{1.5}$, solid solns., defective oxides, ionic cond. 80−107548
ZrO_2-CaO system, fluorite related ordered compd. prep., struct. 77−68958
ZrO_2-Gd_2O_3, solid solution with fluorite and pyrochlore structure; exam. of elec. conductivity *(German)* 79−23766
ZrO_2-Y_2O_3, solid solns., density meas. rel. to O vacancy model 78−2113
ZrO_2-Y_2O_3, solid soln., diffuse X-ray scatt. by vacancies 78−71728
ZrO_2-Y_2O_3, stabilised, struct. of single crysts. 77−35527
ZrO_2-Y_2O_3, ZrO_2-CaO system, fluorite related ordered compd, prep., struct. 77−68958
ZrO_2-$YO_{1.5}$-$TaO_{2.5}$, cubic fluorite phase, elec. cond. 80−107551
$Zr_{1-x}S$, short- and long-range ordering of vacancies, rel. to supercond. transition temp. 77−19945
$ZrSiO_4$, isomorphous replacement of Zr^{4+} by Tb^{3+}, charge compensation 77−47424

vacancy condensation loops
see also prismatic dislocations
capture efficiency of dislocation loops, effect of nonlinear elasticity 80−59461
dislocation loop growth during intrinsic point defect-impurity atom mobile complex formation *(Russian)* 79−90653
faulted dislocation loops induced by elastic interaction, climbing motion 80−75227
fusion reactor metals and alloys, microvoid form., gaseous impurity atom effects, positron annihilation study 80−49275
irradiated materials, cascade damage and self-ion injection effects on swelling 78−34549
irradiation induced creep rate, vacancy dislocation loop contribution 79−42141
metal, nucleation of vacancy precipitation during quenching 77−72612
metal, point defect clusters, TEM obs., review 78−26564
metals, FCC, small vacancy clusters, structures and energies, computer simulation 80−39073
metals, irrad., mechanism of formation of vacancy dislocation loops *(Russian)* 80−65053
metals, irradiation creep strain, produced by vacancy loops, calc. of magnitude 78−72815
metals, irradiation-induced creep, transient stage, vacancy loop contrib. *(Russian)* 80−29115
metals, point defect simultaneous clustering during irrad. 79−95000
radiation effects, distrib. functions of point defects and moving gas filled holes 77−55302
steel, ST M316, heavy ion irrad., numerical evaluation of combined self-ion injection and vacancy loop prod. 79−7635
steel, stainless, type 316, point defect simultaneous clustering during irrad. 79−95000
vacancy dislocation loop microstruct. formed during heavy particle bombardment 79−99250
void swelling rate, vacancy dislocation loop effect 80−2084
Al, creep behaviour, at high temp., influence of oxidation 80−97538
Al, neutron damage, positron annihilation 80−65056
Al, vacancy loop formation, quenched-in vacancy clustering, continuum model 79−77594
Al-Ce (0.06 at.%) alloy, rapidly quenched from melt, vacancy loops and precipitates, TEM 77−59769

vacancy condensation loops continued
Al-Cu-Mg (1.3, 1.3 at.%) alloy, natural ageing, meas. of quenching vacancy dislocation loops 79−15704
Al-Li, ageing mechanism, metastable δ′ phase and stable δ phase precip. *(Russian)* 77−8858
Al-Mg (0.1 at.%), neutron damage, positron annihilation 80−65056
Al-Ni (2 at.%) alloy, rapidly quenched from melt, vacancy loops and precipitates, TEM 77−59769
Au foil, radiation damage, in situ study by HV electron microscopy 78−6101
Cu, dlectron irrad. at 130K, positron lifetime investig. of stage III recovery mechanism 77−47484
$Cu_{83}Pd_{17}$, Cu^+ (Au^+) ion-bombarded, displacement cascades and disordered zones, TEM studies 80−15167
Fe:Yb(Au), radiation-damage evolution, influence on lattice-location meas. 80−6426
Fe-Cr-Ni, α-particle induced precip. and phase instability 79−1470
Fe_3Al, Cu^+ (Au^+) ion-bombarded 80−15167
GaAs:Li diffused, lattice imperfections, TEM 77−80521
GaAs:Si, faulted and prismatic loops, TEM obs. 77−51386
GaAs-GaAlAs bicrystal struct., dislocation half-loops, nucleation and generation 79−95009
KCl:Ba^{2+}, localised stress relaxation in excess vacancy system, prismatic loops *(Russian)* 80−88160
Mg, vacancy loop behaviour on high-temp. oxidation, X-ray topography 77−76414
MgO, a⟨100⟩ dislocation loops, TEM obs. 78−38710
Mo, ion irrad., defect anal., electron microscopy, appl. of theory of non-edge loop image contrast 80−70200
Mo, self-ion damage, influence of material purity and irradiation temp., electron microscope exam. 77−35562
Nb single crystals, growth by pulling from a melt on a pedestal, charact. arrangement of dislocations 79−4911
Ni and alloys, heavy ion irrad., defect cluster obs. 80−107341
Ni, in situ rare gas ion irrad., cluster creation obs. by electron microscopy 80−107343
Pt, ion irrad. damage, temp. depend., electron microscopy obs. of defect kinetics 80−107339
Pt, neutron damage, positron annihilation 80−65056
Pt:^{181}Hf, interaction of implanted impurity with radiation induced lattice defects, TDPAC meas. 80−24494
Si, swirl defect characterisation in floating-zone cryst., comment 77−4098
Si:B, ion implanted, laser annealed, thermal annealing effect 79−73191
Ti, neutron irradiated, characterization of dislocation loops 80−88155
Zr and alloys, neutron irrad. at 573 to 923K, damage struct. 80−107334
Zr neutron irradiated, faulted loops 78−10094

vacancy-dislocation interactions
BCC metal, discrete-continuum hybrid method for dislocation-point defects interaction 77−89467
BCC metals, vacancy-edge dislocation interactions, computer simulation 78−83845
diffusion growth of dislocation loops in saturated soln. of point defects 77−68974
edge dislocation climb, numerical anal. 78−71736
edge superdislocations, resist. to motion, temp. depend. expressions *(Russian)* 80−79789
FCC anisotropic crystals, extended screw dislocation, ⟨110⟩ misfit defect elastic interactions 80−100232
FCC crystal, elastic interaction of 60° and screw dislocations with point defects 78−63786
graphite, fast neutron irrad. damage, chem. rate theory applic. effect of annealing and thermal equilib. defect concs. 77−67804
graphite, fast neutron irrad. damage theory and modifications 77−67805
HCP crystals, dislocation-point defect interactions in slip systems 78−47417
ice, edge dislocation dipole form. by heat treatment, X-ray diffr. topography 79−99203
ionic crystal, solid soln. hardening by aliovalent cations 77−44265
ionic crystal. interaction energies between point defects and dislocations, shell-model calc. 78−22759
mass flux, irradiation enhanced, dislocation interactions 80−88206
metal, BCC, ⟨111⟩ screw dislocation−vacancy interaction energies 77−15415
metal, FCC and BCC, self-diffusion along edge dislocations by vacancy mech. *(Russian)* 78−87810
metal, FCC and BCC, vacancy diffusion along single edge dislocations, computer modelling *(Russian)* 77−47612
metal, vacancy-dislocation interaction, tight-binding calc. 80−92554
metals, point defect simultaneous clustering during irrad. 79−95000
metals and alloys, vacancies and lattice elec. cond. determ. method at high temp. 79−37695
Nimonic PE16, He injected, bubble-void transitions in Ni ion bombard. 80−34095
random sink models, vacancy loss during quenching 78−60698
stress field-point defect elastic interaction energy 79−77631
stressed crystal, point defect interaction with dislocation 77−80537
AgBr:Cd^{2+} (Sr^{2+}), single cryst., stress-induced migration and aggregation of solute ions, internal friction 79−51200
Al and Al-Mg alloys, thermal generation of vacancies involving dislocation climb 77−59808
Al, quenched, vacancy annihilation to non-uniformly distributed dislocations 78−6096
Al, zone refined, vacancy annihilation to dislocations, annealing profiles 77−80536
Al-Cu (96.5, 3.5 wt.%), charact. of disappearance of excess vacancies on dislocations 80−33991
Au, deformed, annealing kinetics of vacancies *(Japanese)* 80−88139
Au, polycrystn., deformed, computer simulation of vacancy annihilation to dislocations *(Japanese)* 80−88205
Co-Ni, deformed and isochronally annealed, positron lifetimes, annihilation at dislocation trapped monovacancy 80−55221
Cu-Ni alloys, chemical interdiffusion under uniaxial stress 80−65307
α-Fe, internal friction peaks from dislocation relax. in plastically deformed and/or neutron irrad. sample 78−48438
α-Fe:He, impurity clustering in vacancies bound to edge dislocations 78−91358
Fe-Ni alloy, N27T2 and N28, internal friction peaks after reverse martensitic transform. *(Russian)* 78−92287

vacancy-dislocation interactions continued
$GaAs_{0.6}P_{0.4}$ LED, luminesc. investig. of degradation, deep-level form. at dislocations 77−40287
Ge, defect form. under radiation-accelerated diffusion conditions 80−19854
Ge, edge dislocation struct., lattice distortion and surrounding vacancy distrib. 77−19954
GeTe, stoichiometry deviations influence on mech. props., 25-500°C 80−103410
He, solid, vacancies and dislocations *(Japanese)* 78−91507
KCl, thermal hysteresis in ionic cond., dielec. loss meas. 78−34652
MgO, interaction energies between vacancies and edge dislocations, shell-model calc. 78−22759
MgO, interaction energies, atomistic model calcs. 80−59513
NaCl, moving dislocations, interaction with defects, elec. effects meas. in plastic deformation *(Hungarian)* 80−10572
Ni 200, C interstitial effect of yield point develop. during static strain ageing, model 78−88498
Ni 200, static strain ageing, 373 to 473K 77−36558
Se, radiation damage expts. review, defect interaction 77−84800
Si, defect form. under radiation-accelerated diffusion conditions 80−19854
Si, edge dislocation struct., lattice distortion and surrounding vacancy distrib. 77−19954
Si, radiation defects, influence of dislocations on accumulation, elec. props. 80−92558
Te, electron irrad., mobility increase due to defect prod. 80−24501
Te, radiation damage expts. review, defect interactions 77−84800
ZrN, microhardness and resist. to brittle fracture 79−87715

vacuum apparatus
includes apparatus for producing, maintaining and handling vacuum per se
see also vacuum gauges; vacuum pumps; vacuum techniques
acoustic delay line efficiency in synchrotron radiation storage ring system protection 79−88965
adhesion strength meas. of organic coatings 80−105663
AES, depth profile analysis, influence of impurity gases in UHV systems 78−76958
AES-LEED, satellite vac. system with sample transfer capability 77−7639
ALA, high luminosity e^+e^- storage ring, 1.2 GeV, design study 79−72066
Alcator Tokamak, vacuum system, surface props. 78−71549
all-metal autoionisation microscope construction and equipment 79−67433
asymmetric diode system design for RF sputtering device, vac. system *(German)* 77−12527
atom probe time-of-flight field-ion microscope, computer-controlled, for metal defects study 77−82645
atomic beam spectrometer using a LiF analyzer crystal, for surface studies in UHV 78−71651
Auger electron microscopy, instrumental capabilities 78−70227
backing pressure automatic regulation device 79−49241
bakable Al vacuum chamber and bellows with flange and seal for ultrahigh vacuum 79−30486
bakeable vacuum feedthrough 79−40582
BEBC, bell jars for research into strong interactions at SPS energies *(Dutch)* 77−46463
BNC-JJ coaxial floating shield bakable and coolable vacuum feedthrough useful from dc to 4 GHz 78−54381
Boersch's electron optical bench, modifications 80−87286
break-seal shattering, novel method 78−41322
Calcutta variable energy cyclotron vacuum system design, testing and commissioning 78−86707
camera, vacuum-cold, appl. to astronomical near IR photography 80−90341
capacitive displacement system for UHV operation 80−31737
cavity of rotating He cryostat, centrifugal field rel. to residual press. 80−42232
cell for saturating specimens with liq., true and apparent density determ. of ceramics 80−62636
cell for surface studies using IR transmission spectroscopy 78−41361
ceramic vac. chamber, bunched beam EM field penetration 77−83368
chamber-bell jar with built-in cooling body 80−90860
channelling experiment apparatus, test results on LiF crystal at 4 torr H_2O 79−2779
cold trap, improved design 78−81990
cold-bore system design for proton storage rings POPAE 77−83226
compensating work holder for coating two sides of substrate uniformly 80−22372
condensate removal system, for vac. metallisation chamber 79−58752
conference, vacuum science, Jerusalem, Israel (April 1978) 79−67322
constant calibrated gas feed system for vacuum use 79−67321
coupler, for connection of H-flanges *(Japanese)* 80−13083
couplings, small bore British system, complementary to ISO recommendations 78−21148
cryogenic extreme high vac. chamber 77−67449
cryogenic sorption trap for high-vacuum system protection 79−88963
cryogenic vacuum feedthrough, with isolated shield, DC to 6.5 GHz 79−67324
Dependex fittings, modification for sealing with Cu 77−65040
deposition equipment cleaning, practical procedures 80−57318
Dewars, vacuum space saving via simple valve seal 77−5851
differential Burnett apparatus, virial coeff. meas. at various temps. 80−22373
differential pumped bellows, for ISX-B Tokamak devices 78−55025
differentially pumped six-inch metal sealed gate valve 78−70137
double-beam spectrophotometer, VM-3, principle and assembly 79−75624
eccentric inlet for rotational or reciprocating motion 77−13762
education, positron annihilation in solids, high temp. vacuum chamber for source protection, crystal defect obs. 79−9068
electric breakdown initiation, implications for JHV technology 78−30509
electric furnaces for quenching developed in USSR 78−84872
electrical feedthrough for probe meas. in vacuo 78−71543
electrical leadthrough, heavy duty, for vapour deposition resistively heated box sources 79−40584
electron microscope, high resolution, obs. at liq. He temps. 80−86517
electron microscope specimen preparation, VUP-2K vacuum station improvement 77−38058

vacuum apparatus continued
electron optical demountable system for studying image tube designs 79−81575
electronograph cryogenic trap construction 80−31766
electrophysical properties measurement apparatus for films 78−4654
energy analyser for charged particle energy and angle meas. in ultrahigh vacuum 78−86750
envelope for high press. mass spectrometer 78−61077
epoxy resin, outgassing and its reduction 77−71333
evacuated chamber with specimen cooling via a mechanical switch [for optical measurements] 79−35765
extraction system for vacuum stoving and sample melting 78−21146
fast gas valve for gas injection into vacuum 78−74011
fast gas valve for injection into vacuum system 78−57970
fast H gas injection system for plasma physics expts. 78−71550
feedthrough, bakeable, with 22 pins, for monitor system of proton synchrotron 78−21798
feedthrough, coaxial, multipin and combined multipin *(Japanese)* 79−6132
feedthrough, multipin, compact design 78−70139
feedthrough employing coax. cable for high vac. and low temp. 77−79101
feedthroughs, coaxial and multipin, cryogenic performance 80−8995
Fermilab antiproton cooling ring, injection, magnet and vacuum systems 79−72139
ferrite, 350 NNI, for use in superhigh vacuum systems 80−108478
field emission micro SEM, for UHV surface anal. 80−86519
field emission scanning electron microscope 80−86520
field in microscope specimen exchange device for ultra-high vacuum use 79−67437
flanged joints, appls. in cryogenic and vacuum technology *(German)* 80−101801
flanges and couplings, small bore British system, complementary to ISO recommendations 77−26316
flowmeter for gas throughput meas. 77−67451
FMIT accelerator vacuum system 79−71993
furnace, inexpensive design 77−2657
furnace for laboratory appls. 79−71454
furnace system for heat treatment, ultrahigh vacuum conditions 80−52222
fusion reactor, Demonstration Power Tokamak Reactor, vacuum outer containment and metal seals feasibility study 80−95458
fusion reactor, Doublet III, vacuum vessel neutral beam armour 80−95462
fusion reactor, ETA-BETA II RFP, vacuum system design and operation 80−95450
fusion reactor, neutral beam injection reionisation power losses in duct, model 80−99385
fusion reactor, PLT, neutral beam duct reionisation losses, obs. and power loss model 80−99383
fusion reactor, TFTR, large noncircular ports, development of bakeable seals 80−95454
fusion reactor, TFTR, neutral beam-torus connecting duct 80−99302
fusion reactor, TFTR, vacuum vessel bellows, strength and fatigue anal. 80−95455
fusion reactor, TMX, config., liq. N_2 supply and operation of vacuum system 80−95448
fusion reactor blanket, NOEL (No External Leak), thermal anal. and tests 80−95459
fusion reactor neutral beam injector vacuum system transient simulation anal. 80−95453
fusion reactor vacuum system (Princeton TFTR), description, operation, safety 78−74497
fusion reactor vacuum system transient simulator, appl. to Princeton TFTR 78−74496
fusion reactor vacuum vessel, large, ultra high vacuum, design and manufacturing problems 80−99276
fusion reactor vacuum vessel, performance of silver-coated metal seals, 20 to 450C *(German)* 78−81996
fusion reactors, TMX, installation and operation of cryoliners in vacuum system 80−95449
fusion reactors Doublet III neutral beam injector system, outgassing rate meas. and residual gas anal., coating props. 80−95457
GANIL separated sector cyclotron, vacuum chamber description 79−54640
gap breakdown initiation by microparticle impact 80−96413
gas circulating pump, closed system, without moving parts 78−180
gasket, large diameter elastic metal gasket for ultra-high vacuum flange connections 80−95106
gate valve, bakeable, for UHV microwave tube expt. 77−5854
glazed high alumina cement vacuum chamber 79−40585
grazing incidence concave grating spectrometer for ultra soft X-ray emission spectra 78−62273
grazing incidence monochromator, ultra high vac., SSRL, design considerations and operating experience 78−62269
grazing incidence monochromator FLIPPER, ultra high vac., for synchrotron radiation 78−62237
greases, desorption characts. 78−21147
heated vacuum monochromator for 40-280 nm spectroscopy 80−33176
hermetically sealed box, dynamic testing system, vacuum or controlled environment *(French)* 80−61060
high speed vacuum seal 79−93151
high vacuum chamber for thermokinetic studies of solid surface thermal shock 80−73373
high vacuum two crystal monochromator for soft X-ray synchrotron radiation 78−62272
high voltage, compact feedthrough 77−26315
high-speed rotational vacuum tap for discharge gas sampling 78−57969
high-vacuum, for degassing studies 80−100814
high-vacuum system control and diagnosis by monitoring total press. and per cent N content 80−95105
high-voltage vacuum feedthrough, fully screened 78−24814
history and development 80−31775
hospital supply, central source, pipelines to outlets 77−90942
hot press, continuous, for transparent ceramics prod. 78−23643
integrated approach to vacuum systems engineering 78−70134
interlock, for production sputtering systems 79−66006
ion microprobe mass analyser, adaptation for liq. metals ion bombardment 77−49805
ion source, magnetic-discharge pump for pulsed H injection 77−23318
IR window mounting for ultrahigh vac. appl. 80−82778

vacuum apparatus continued
ISABELLE storage rings vacuum system, design charcts. 77−83224
KEK proton synchrotron vacuum system design and construct. 77−83225
Kelvin method contact PD meas. manipulator 78−57979
knife-edge flange, sealing after high temp. vacuum firing 80−77793
leak detection in large vacuum vessels 78−74012
leak detector, sparking, using semiconductor switching diodes 80−31774
leaks to amosphere, N_2 press. meas. technique by mass spectrometry 78−70133
low energy ion scattering spectroscopy, UHV apparatus *(Japanese)* 80−20746
magnetic discharge cells with nonuniform periodic magnetic field 80−101799
magnetic liquid vacuum seals 79−63244
magnetic safety valve 80−8966
manipulator attachment for azimuthal sample rotation with elec. readout 79−210
manometric tube wih vacuum valve 80−47066
mass exchange in closed high-vacuum systems 77−11222
mass selective outgassing rate meas., direct mol. beam method 79−85146
mass spectrometer high-speed vacuum lock 79−67421
mechanical boosters incorporating self-limiting power transmission 78−70138
melting furnaces and casting techniques 78−84727
metal secondary electron emission coefficient recorder 78−58094
metal-seal valve for high radiation use in high vacuum 80−233
metal-sealed all-metal gate valve, design developments 79−63243
metallic superhigh-vacuum apparatus for 10 eV photoelec. meas. 78−21145
Michelson interferometer, for deform. meas. in UH vacuum system at high temps. 77−2650
microstructure observation apparatus, observation during heating, stressing, under vacuum, photography facility 77−73403
MKh 1303 mass spectrometer, small-scale device for moving solid specimens in vacuum chamber 78−315
molecular density directional detector 79−80626
molecular flow measurement, precision, and control for single and multigas systems 78−70135
monochromator, integration with 1000 W H discharge lamp 77−42582
monochromator low-temp. attachment construction and optics 80−31764
multipurpose vacuum installation 78−86279
multistage sluice-gate loading devices 78−60576
neutral beam injection system vacuum chamber, for Tokamak fusion test reactor 78−55021
neutral beam injection vac. components, for fusion reactor 78−74493
NUMATRON project test accumulation ring, vacuum system *(Japanese)* 80−18724
O-ring, for ultrahigh vacuum, heat cycle test of stainless hollow *(Japanese)* 80−13084
O-ring type gaskets in metal vacuum systems, replacement for Au gaskets 80−57316
optical coating production, vacuum system development, review 77−58493
optics test chamber for cryogenic meas. at high vacuum, upgrading design 79−23098
parodontosis treatment portable vacuum apparatus 79−39593
PDX vacuum vessel, glow discharge conditioning 80−79607
PEP vacuum chamber, parasitic mode losses in cylindrical cavities with beam ports 77−83271
permeation cell for studying H desorption from Fe into ultrahigh vac. system 80−86326
PETRA vacuum system, RF parasitic mode losses, fabrication cost, new techniques 77−83217
photoacoustic cell resonances from standard ultrahigh vacuum components 79−12862
piezoelectric quartz cryst. microbalance for sorption studies under dynamic conditions 80−73323
porous vacuum gas accumulator preparation and conductance 79−67319
pressure balance estimation in high vacuum systems 77−67453
pressure due to adsorbed mols., upper bound 77−67446
pressure response in elementary system 78−37027
proton storage ring, NAP-M, mag. and vacuum system 77−65362
PTFE seal for superfluid He 78−4625
pyrometer for ultrahigh vac. systems, using Si photovoltaic cell 77−5908
radiative and mol. heat transfer in high vacuum systems 78−94574
recrystallisation annealing, induction apparatus for brass tubes 79−57021
remotely operable large vacuum seals for fusion reactors 78−50405
rotary manipulator, ultrahigh vacuum, with direct cooling 77−26317
rotatable support, for B deposition in ultra high vacuum 79−40586
rubber rings wrapped in In for vacuum packings *(German)* 77−74411
sample holder with magnetic rotational drive 77−41628
sample manipulation and rotation using ultra high vacuum angle resolving photoemission chamber 80−57317
sample manipulator and heater for ultrahigh vac. for electron spectroscopy 79−44988
sample positioning, two axes rot. mechanism 77−61076
sample transfer mechanism 80−77765
sample transfer system for transferring samples between chambers in UHV 79−12809
sample transfer system for ultrahigh vacuums using conventional manipulators 79−88964
scattering chamber, rotatable lid, vacuum sealed, with semicond. detector arrays, INS cyclotron accessory 77−6599
scattering chamber, ultra high vacuum, for metal-semicond. and metal-metal thin film studies 79−2780
seal, demountable, for low temp. conditions 77−45857
seal, for rotary motion 80−31772
seal between stainless steel and Al_2O_3 ceramic, bakeable and moveable 79−35767
seal design, construction and application 80−82780
seals, Cu-ceramic, metallisation process 80−37046
SEM vacuum system specification and design 80−82779
semiconductor film X-ray and electrical characteristics meas. chamber 78−86396
separated sector cyclotron, design of vacuum chamber for magnets 79−54639
Serpukhov proton synchrotron ion-getter pumps, operation evaluation 77−83347
vacuum apparatus continued
shiva and Argus target diagnostics vacuum systems 79−81079
space chamber, tracer slug leak detection 79−80627
Spacelab pallet, meas. of mol. streaming fields 80−82173
specimen manipulator, for analytical vacuum instrumentation 79−63245
spectrograph, 6.600 m grazing incidence, construction, adjustment and performance 79−26146
spherical chamber, molecule-surface collision rate 78−76570
sputter coating unit conversion for SEM sample preparation 77−34058
steel, stainless, vacuum components, pre-vacuum surface finish influence on electron stimulated desorption in ultrahigh vacuum 80−57320
stop cock consisting of glass, O ring and metal *(Japanese)* 79−54146
storage ring, ISABELLE, beam tube material and vacuum chamber design 79−76199
stored beam energy loss to vacuum components, particle bunch simulation meas. at PETRA 77−83258
system construction material selection and degassing 80−82783
Tandem Mirror Experiment, vacuum system 78−55023
target transfer device, intercontinental test 78−70132
technology, medium, high and ultrahigh vacuum, conf., Oxford, England (Apr. 1978) 79−63242
teflon rope, vacuum sealing material 80−98925
thermocouple reference junction box, used for vacuum chamber 80−90844
thermoelectric coolers, fast transient response of novel Peltier junctions 78−21141
thermovacuum chamber, criteria for choice of elastomer seals 79−71466
thermovacuum system, thermal system design for temp. range 173-373K 79−35764
toroidal vacuum chamber, large, elastomer seal 80−27315
toroidal vacuum vessel, for Joint European Torus 78−55024
transfer system, 15 cm diameter ultrahigh vac. type, for remote plasma-wall interaction expts. 80−86327
transparent chambers for CERN ISR interaction areas 79−76211
UH vacuum sample chamber for combined ion implantation and ion beam anal. 77−4970
UHV bakeable vacuum chamber, use of Al alloy *(Japanese)* 80−52248
UHV beam line at SSRL for spectral range 4-4000 eV, monochromatised radiation 78−62673
UHV gate valves for systems used in plasma discharge studies 79−54147
UHV microbalance, with ion gun, absolute meas. of sputtering yield *(Japanese)* 80−17951
UHV system and He discharge lamp connection using unbacked Al windows 79−97397
ultra high vacuum, HT facility for heavy ion simulation of neutron radiation damage 77−57786
ultra high vacuum device, for annealing of Nb single crysts. *(German)* 80−89169
ultra-high vac. harmonic drive as rotary motion feedthrough 77−2661
ultra-high vacuum evaporation apparatus for deposition of metallic thin films 80−100791
ultra-high vacuum system for thin film and surface preparation and anal. 79−69986
ultra-high vacuum systems for surface anal. 79−67323
ultrahigh vacuum adsorption, Haul-Gottwald empirical isotherm origin 78−21149
ultrahigh vacuum and cryogenic feedthrough, with 48 pins 79−97399
ultrahigh vacuum chamber for quantitative surface anal. by medium energy ion scatt. 77−8704
ultrahigh vacuum chamber for Raman studies of gases adsorbed on metals 78−81991
ultrahigh vacuum equipment for Kelvin meas. of surface charge of alkali halide crystals 78−12708
ultrahigh vacuum sample transfer system 79−80628
ultrahigh vacuum setup for photo- and thermostimulated electron emission and luminesc. obs. *(Russian)* 80−66383
ultrahigh vacuum system design for gauge calibration 78−21157
ultrahigh vacuum system for ISABELLE full cell 80−77798
ultrahigh vacuum system for ultramicrogravimetric study of samples loaded in controlled environment 79−80580
ultrahigh vacuum systems, modelling using polystyrene 79−44912
ultramicrobalance, for surface studies 79−71465
universal ultrahigh-vacuum system 80−105664
UPS ultrahigh vacuum apparatus, appl. to clean and gas covered Si(III) surfaces *(Japanese)* 80−37125
vacuum chamber, for arc investigations *(Polish)* 79−82120
vacuum seal for 5000 r.p.m. rotation 77−53923
vacuum-arc plasma extracted ion precipitation unit 80−35106
valve, baffle and trap design and construction 80−82781
valve, compact small aperture straight through, design and operation 78−74014
valve, fast closing, for Berkeley 88″ cyclotron 77−10501
valve for gas chromatograph/mass spectrometer system 79−39245
valves, and valve traps, for production appl. 78−70140
valves, for high and ultrahigh vacuum 79−63246
variable aperture, externally operable, for ultrahigh vac. appl., design 80−77799
virtual leak, influence on pressure in high and ultrahigh vacuum systems 79−97398
volume ratio determ. by successive expansion method 79−172
water-cooled equipment, emergency switch design 78−81962
Wisconsin Synchrotron Radiation Center, UHV Seya-Namioka and adjustable slit 'Grasshopper' monochromators 78−62234
Al vacuum chamber and bellows, proton synchrotron appl. 79−68056
Al wire gaskets for demountable, bakeable ultrahigh vac. seals *(Japanese)* 79−93154
BaF, CaF windows, process for vacuum tight joints prod. 77−26312
Cu vacuum gaskets, basic problems 80−47064
He desorption spectrometer, clustering of Kr in W (100) obs. 80−77908
LaB_6 cathodes, residual gas poisoning in vac. system, thermionic emission decay 78−27364
TiN film as protective coating for vacuum deposition chamber, Auger electron spectroscopy study 80−25922
WC vacuum sintering furnace systems 78−84737

vacuum control
backing pressure automatic regulation device 79−49241
compressor, air, reciprocating, capacity control system 80−90859
cyclotron, vacuum chamber pumping system automatic control *(Japanese)* 79−85842

vacuum control continued
electron storage ring, bakeable weldable vacuum gauge 79−40589
electron storage ring, vacuum control system for synchrotron radiation beam lines 79−68027
triode and diode ion sputtering pumps, power supply, press. control *(Spanish)* 77−37902
vapour pressure temperature estimation method in ultra high vacuum range *(Chinese)* 80−232

vacuum deposited coatings
AgBr, thin layers, struct. and photographic charact. 78−49919
amorphous, vac. evaporated, doping, transport and optical props. 80−49715
anthracene, electroabsorption in disordered solids 78−95590
anthracene, evaporated films, fluoresc. 77−85777
anthracene, film substruct., vacuum deposited, low temp. luminesc. *(Russian)* 78−15226
anthracene, thin film vacuum deposited, exciton reflection spectra *(Russian)* 78−15194
anthracene, ultrathin films on fused quartz and sapphire 80−59812
anthracene thin films, struct. rel. to substrate temp., thickness, condensation rate 78−30845
anthracene-tetracene amorphous films, host-guest energy transfer 78−60505
antireflection coatings, thickness monitoring during deposition 80−19114
astronomical mirror reflection coefficient checking against control samples 79−75106
beam splitter phase coatings, for producing phase quadrature interferometer outputs 78−77974
benzene, vacuum UV absorpt. spectrum, 1100-2500 Å, effect of deposition temp. 78−23542
brass, prep. 77−59693
broadband dielectric mirror interference coatings, scatter losses 79−50365
butane RF plasma, etching, prior to deposition of C 79−66224
chalcogenide glass semiconductor film kinoform production *(Russian)* 77−14670
chalcogenide semiconductor amorphous film comp. monitoring by EPR 77−51940
conducting, appl. to brittle fracture growth dynamics obs. 78−83347
conference, vacuum science, Jerusalem, Israel (April 1978) 79−67322
constant-thickness film formation on axially symmetrical substrate 79−27453
copper phthalocyanin, thermal behaviour *(Japanese)* 80−24753
deposition on glass surface heated between room temp. and 300°C 77−90277
deposition profile with shadow effect, theoretical model 79−82473
diamond-like C film, plasma stream condensation with RF pot., props. 79−15612
dielectric coatings, optical charact., effect of electric field during film condensation 80−69539
dielectric film, electron beam produced pore form. mechanism, statistical model *(Russian)* 80−6667
dielectric film, formation during ion implantation, electric field effects 78−2801
dielectric interference coatings, optical props. variation with time 79−99963
dielectric thin film stack, control by stationary ratio method, refractive index dispersion influence *(French)* 80−60693
N,N-dimethyl-p-nitrosoaniline, coherent anti-Stokes Raman spectra, negative peak intensities 77−72805
diphenyl anion salts, sublimed layer, electronic and IR absorpt. spectra 80−66189
electron beam deposited alloy coating for gas turbine superalloy, defects 77−40473
ferromagnetic thin film edge domain structures, Bitter pattern. obs. 77−73063
film on Si substrate, eutectic point displacement on annealing *(Russian)* 80−100850
film sandwich structures Auger anal. 78−72030
films, elec. and galvanomag. props., microstruct. 80−70859
films, metal-semicond. and metal metal studies in ultra high vacuum scatt. chamber 79−2780
fluoride, contamination by 1 MeV proton bombardment, backscatt. obs. 77−11811
glass films, struct. mech. and optical props. *(Czech)* 78−80469
graded-thickness, filters for solar corona obs. appl. 80−76164
graphite on Cu, interf. films deposited on diffr. gratings, for solar selective absorbers 79−14103
growth and composition on NaCl substrate 77−89677
heteroepitaxial vacuum deposited films, doping *(German)* 77−84779
n-hexatriacontane film, vacuum deposited on alkali halide crystals, structure and heat treatment 80−103600
high rate film growth, book contrib. 78−11117
interference coatings perpared by electron beam evaporation, UV optical strength 79−59779
intrinsic stress determ. by cantilevered plate method, substrate bending 80−54571
ion beam milling, amomalous sputter yield behaviour 80−108624
ion deposition techniques, AES exam. of surface cleaning methods 79−15878
large-area uniform thickness evaporated thin films 78−76605
laser deposition with periodically pulsed CO_2 laser, film charact. 79−28926
margaric acid, evaporated film, X-ray diffr. anal. and mass-spectrography 77−15718
mass change, optical transmittance, and reflectance, simultaneous meas. apparatus 79−75501
mechanical properties, stress generation mechanisms 78−75968
metal, deposition condition relationship with struct. and props. 78−11369
metal, grain struct., influence of impurities and alloying elements *(Russian)* 78−56048
metal, on supercond. film, effect on T_c and residual resist. 78−47900
metal, thickness, X-ray fluoresc. meas. method, appls. *(Russian)* 78−56582
metal film, elec. field effect on residual struct. 78−51836
metal film, evaporated, resistivity change on oxidation *(Japanese)* 79−11723
metal film, thickness meas., using nondestructive radioisotopic technique 80−68179
metal film, vac. deposited, internal friction *(Japanese)* 78−47685

vacuum deposited coatings continued
metal film, vacuum deposited, sputtering rates by O^+ bombardment 78−88390
metal mirrors, diamond turned, evaporated and sputtered, surface and optical studies 78−79098
metal-semiconductor contact junction formation by ion evaporation 77−90285
metallic, for aperture stops of electron microscopes 79−85202
metallic, two-phase, ductility maximum, weakening and strengthening 79−11681
metallic films, vapour deposited on polymer, ageing, adhesion, elec. cond., electrochem. pot. *(Russian)* 79−33362
metallic mirror coatings, protected and unprotected specular reflectance 79−76792
microporosity and absorptivity in vacuo meas. apparatus 80−9053
millimetric and IR discontinuous-metal-film detector 78−289
monochromatic Maximeter control system for thin multidielectric films, stopping criterion *(French)* 80−60694
multidielectric film, optical control by method of static ratios *(French)* 77−69993
multidielectric film production monochromatic modulator controlled thickness *(French)* 78−75008
multidielectric stack control using chromatic maximeter, Fourier series anal. of signal *(French)* 78−83111
multilayer superlattice stacks, very thin nonideal, wavelength variation of transmissivity, refl. 80−100701
naphthalene derivatives, struct., electron microscope and diffr. obs. 79−11029
opaque metal coatings on plastic scintillator 78−3049
optical, improved film quality, progress in vacuum generation and deposition technology 80−35101
optical, struct. and mechanical properties 79−76772
optical film, Rayleigh scatt., 441.6 nm, scatt. losses correl. with deposition parameters 79−78782
optical multilayer coating production with continuous thickness reoptimisation 79−76890
optical reflectivity and transmissivity, DC resistivity, in situ meas. in ultrahigh vac. at low temp., Au appl. *(French)* 78−39617
orientation axis tilt rel. to vapour angle of incidence 80−88456
oxidation protective coating for Ni base TaC eutectics 77−40475
oxide, molecularly-deposited on cathode, elec. cond. 78−11062
oxide, vacuum deposited layer adhesion to glow-discharge treated-surfaces *(Russian)* 77−44372
palmitic acid, evaporated film, X-ray diffr. anal. and mass-spectrography 77−15718
particle flux ang. distrib. anal. *(Ukrainian)* 77−69189
parylene, electronics appl. 80−108607
pentacene, evaporated on quartz, optical absorption, substrate temp. depend. 78−2932
Permalloy, obliquely deposited, mag. anisotropy, annealing and deposition parameter effects *(Russian)* 77−80971
Permalloy, oxidised film, magnetic noise, low temp. depression *(Russian)* 79−99734
Permalloy film, multi- and single-layer, reson. curves subjected to tangential mag. reversals *(Russian)* 80−50195
Permalloy film corrosion characterisation by crystal oscillator microbalance and resistance meas. 78−7101
Permalloy films, domain propelling tunnel, domain struct. displacement *(Russian)* 79−99736
Permalloy films, domain struct., nonuniform rotation of magnetisation *(Russian)* 79−47313
polyethylene, adhesion on Al and Cu 79−61793
polyferrocene, in MIM sandwich, I-V and I-d charact. 78−80064
polyferrocene film, plasma polymerised, dielec. props., 40 kHz to 50 MHz, 30-400°C 78−52439
polypropylene, electron trap depth, TSC meas. for MIM struct. 79−95535
polystyrene film formed by RF electrodeless excitation, dielec. props. 77−24795
porosity rel. to deposition conditions 78−56057
porphyrin films, methine bridge substituted, surface photovolt. depend. on fabrication method 80−60119
prep. by evap. and ion plating, AES determ. of comp. profiles 77−89675
p-quaterphenyl oriented layers, charge carrier transport, hopping model 80−2506
rare earth element sulphides, condensates, struct. and optical transmittance 80−20727
rare earth oxides, electron beam evap., optical and mech. props. 77−79907
rare earth-iron alloy amorphous film, crystn., TEM obs. 79−87019
rare earth-transition metal, amorphous, microstruct. and magnetism 78−64230
rare earth-transition metal alloys amorphous thin films, anisotropic mag. and microstruct. props. 78−95487
rare earth-transition metal film, amorphous, microstruct., TEM obs. 78−72018
reference fission foils preparation by fluoride deposition, characterisation 80−23218
refractory coatings, deposited by electron evaporation, struct. and props. 79−23871
refractory metal films, evaporated, optical props., rel. to struct. 80−55211
resistive foils, manufacture and props. of multicomponent alloys *(Polish)* 80−35131
self-supporting films, method for coating substrate with parting agent 78−11112
semiconductor, or semimetal, on supercond. film, effect on T_c and residual resist. 78−47900
semiconductor films for solar collectors, absorbing surfaces at collectors 78−5580
a-Si:H highly homogeneous, for low-cost solar cell fabrication 80−72053
silicone, film deposition, glow discharge polymerisation, elec. and thermal charact. 78−6467
space environment effect on coatings 78−85827
spectrally selective surfaces for photothermal conversion of solar energy 80−101125
squarylium dye films, surface photovolt. 80−75594
stable structure formation use of borosilicate glass intermediate layer 80−80979
stearic acid, film, for low-loss capacitors 80−71317
stearic acid films, evaporated, vac. effects 80−97435

vacuum deposited coatings continued
strain gauge constantan alloy-film/ceramic steel system, electromech. behaviour 78−6634
stress measurement method using real-time holographic interferometry 78−84099
structure and properties, basic relationship 78−6236
substrate prep. for film deposition using glow discharge techniques 79−24438
surface strengthening of Al single crysts. on coating with evaporated films 77−8972
surface temperature measurement, on thin films 80−57297
p-terphenyl, hopping cond. among localised states 80−70861
tetrabenzo[a, cd, j, lm]perylene evaporated film, crystn., time depend. as function of purity 80−88449
tetracene, disordered, vapour deposited on glass substrate, fluoresc. and energy transfer 80−84761
tetracene, hopping cond. among localised states 80−70861
thermal evaporation industrial techniques for obtaining uniform thickness *(Polish)* 78−84710
thickness meas., low temp., quartz thickness monitor 77−79052
thickness meas., low temp., quartz thickness monitor 78−41275
thickness measurement, quartz, thickness monitor nonlinearity 78−29091
thickness measurements, digital frequency meter and quartz crystal oscillator system 78−89436
thickness monitoring techniques *(Japanese)* 80−60783
transition metal film, amorphous, temp. stability 78−63948
transition metal-boron alloy amorphous film, crystn., TEM obs. 79−87019
transition metals, BCC, films, vac. evaporated, optical cond. 80−76100
TTT film, hopping cond. AC and DC meas. and EPR 80−11111
two-layer, thermal strength, recrystn. influence 79−87748
ultra-high vacuum system for thin film and surface preparation and anal. 79−69986
ultra-microhardness tester, for expts. on vacuum deposited films 78−53161
vacuum deposited film, as first wall material, sputtering yield mea. *(Japanese)* 80−25513
vacuum UV special application coatings, reflectance, transmission, technology 79−59788
ALF_3, evaporated layers DC props. and α-particle scatt. 78−14845
Ag, defect density, thickness depend., elec. resist. obs. 80−70568
Ag, defect density and activation energy depend. on deposition rate 80−29294
Ag, deposited from hot hollow-cathode source, adhesion rel. to ion precleaning 77−8754
Ag, evaporated film, density, adhesion, intrinsic stress, substrate temp. effects 77−15709
Ag film, adsorbed CO, enhanced Raman scatt. mechanism in ultrahigh vacuum 80−107645
Ag film, Ge coated, electrical resistance and ageing *(Russian)* 80−103759
Ag film, in situ struct. determ. by internal stress meas. 80−54569
Ag film, substrate surface structure effects on absorptance 78−19585
Ag film, surface roughness determ. from light scatt. meas. 78−5541
Ag film, surface roughness, light scatt. meas. 80−107624
Ag film, twin boundary faceted struct., struct. coarsening due to dislocations *(Russian)* 79−99215
Ag film deposition, thermal effects, influence on internal stress meas. 80−96767
Ag, film growth on C, conductance meas. 79−82495
Ag film growth on Pd substrate, interface cpd. form., AES study *(French)* 80−80131
Ag film vacuum deposition and ion plating, effects on surface topography 79−82427
Ag films, electrodeposited and vac. deposited, AES depth profiling anal. 77−59232
Ag, growth on C replica stripped from pure and doped NaCl single crysts., elec. memory expts. 77−76691
Ag, high temp. stabilisation using SiO_2 78−1319
Ag, initial stages of growth on Si (111) 7×7, LEED, AES and UPS expts. 78−38988
Ag, internal friction vibr. reed technique 78−43276
Ag, internal stress and its depend. on gas adsorption 80−6683
Ag, island film on Ni foil substrate, elec. props. 77−43745
Ag, on Cu, ion-induced intermixing 80−15420
Ag, on evaporated AgBr layers, growth mechanism 80−35095
Ag, on MgF_2 and SiO substrates, internal stresses correl. with struct. 79−87026
Ag, on Si (111), interface struct., AES 78−14589
Ag on V{100}, layer-growth, total current spectroscopy 77−36329
Ag overlayer on Cu laser mirror, microstruct. and 10.6 μm reflectivity 77−42543
Ag particles on graphite, particle motion rel. to heating in gaseous environments 78−34695
Ag, polycryst. boundary layer on seed cryst., role in hydrothermal growth mechanism of sodalite 78−30571
Ag, quartz crystal, crystal damping during deposition 78−11116
Ag, specimen charging control for SIMS and AES 80−101875
Ag, thickness meas. using X-ray fluoresc. technique 79−90911
Ag, thin film, elec. resist., effect of annealing In electrodes 80−80416
Ag, ultra-microhardness testing for vacuum deposited film and bulk specimen 78−79910
Ag ultra-thin film, deposited on MgF_2 and SiO substrates, struct. and internal stress 78−91572
Ag, vac. deposited films, surface pot. and work function rel. to thickness 79−42672
Ag, vac. deposition of oriented coating on doped alkali halide substrate 80−2303
Ag, vacuum condensate, effect of Ge coatings on ageing kinetics *(Russian)* 77−59340
Ag vacuum condensates, on Cu substrate, struct. and substruct *(Russian)* 79−73412
Ag vacuum deposited coating on glass, strength 80−55505
Ag, vacuum deposited film, surface struct., HEED meas. 78−6234
Ag, vacuum-condensed film, structural changes under glow discharge *(Russian)* 79−15852
Ag/stearic acid layer periodic struct. prep. and optical props. 77−69199
Ag-LiF, alternating plasma-dielec. five layer system, ATR angular spectra 79−19943
Ag-Ni supersaturated metastable solid solns. formed by ion beam mixing 80−107425

vacuum deposited coatings continued
Ag-SiO_2, coevaporated films, neutral density filters for near IR radiation 79−72673
AgBr thin films, influence of bromine vapour on spectral props. 77−71393
AgBr vacuum evaporated thin films, sensitometric obs. 78−78010
AgBr(Cl) vapour-deposited epitaxial film, surface structure 80−59814
AgI-RbI films, vacuum deposited, cond. determ. 77−39689
$Ag_2S.HgI_2$ and $Ag_2Se.HgI_2$ thin films, transmission spectra and photochromism 79−52032
Ag_2Se thin film, switching and Ag movement, point contact technique 80−60107
Al alloy-Cu alloy evaporated couples interdiffusion *(Russian)* 77−43389
Al, condensed film, phase and struct. nonuniformity *(Russian)* 80−54536
Al, electron beam evaporation, on Kapton laminates, and characterisation 78−11373
Al evaporated on quartz substrate, surface irregularities 79−90920
Al film, condensed and fused, on Ge, press. and residual gas comp. influence on struct. 77−16497
Al film, H incorporation effect on stress and electromigration 80−80139
Al film, MBE and field emission deposition on III-V semiconductors, comparative study 79−87016
Al film, nucleation and growth on C layers, adsorption energy and surface diffusion 79−99451
Al film, vacuum deposited, rate and press. depend. of contamination 78−72732
Al film, vacuum deposited, structural changes during annealing at temp. near melting point 78−84096
Al film, vacuum deposited, O_2 contamination effect on form. 79−82487
Al film, vacuum evaporation growth, impurity presence, effects *(Hungarian)* 80−7495
Al film deposition on Kapton laminates by electron beam evaporation 78−76603
Al, film growth on C, conductance meas. 79−82495
Al films on Cr-Mo aircraft steels 79−70231
Al foils, high strength, vapour deposited on curved surfaces, quantitative characterisation 80−80144
Al, lattice dimens., difference between vacuum condensates and massive specimens *(Russian)* 77−31912
Al, low vacuum condensates, struct., IR refl. obs. *(Russian)* 78−30850
Al, morphology and purity determ. of 7 to 65 μ films 77−76699
Al, on CdS, bonding and interdiffusion, XPS obs. 80−80000
Al, on single cryst. Si slices, long-term tests 79−33346
Al, solar radiation props., grey-reflector appl. 77−20098
Al, sputtered and electron gun evaporated films, grain size and orientation obs. 78−10308
Al, step coverage optimisation by computer simulation and SEM 78−51838
Al, structural singularities and porosity *(Russian)* 78−75950
Al, thin film, elec. resist., effect of annealing In electrodes 80−80416
Al thin films, influence of film thickness on internal stresses magnitude *(Russian)* 79−37938
Al underlayer, effect of deposition parameters on mag. props. of Ni-Fe-Co film 77−77078
Al, vacuum condensate, struct. and mech. props. depend. on deposition conditons 80−15417
Al vacuum deposited coating on glass, strength 80−55505
Al vacuum deposition on GaAs (001), perfect and facetting growth 79−47632
Al, vacuum-condensed film, structural changes under glow discharge *(Russian)* 79−15852
Al/Al_xO_y vacuum deposited laminates, struct. and mech. props. 79−28219
Al-Ag, struct. of two-layer film 79−23851
Al-Cu, epitaxial film on NaCl(001), orientation obs. *(French)* 79−95294
Al-Cu alloy, vacuum deposited thin film, abnormal grain growth before melting transition and subsequent struct. change 79−60663
Al-Cu alloys, condensed films, metastable states 79−15046
Al-Cu film bilayers, growth kinetics of θ phase, He^+ backscatt. and X-ray exam. 78−84105
Al-Cu films, deposition rate, mol. beam incidence angle influence on struct., film props. *(Russian)* 79−60646
Al-Cu thin films, microstruct. rel. to electromigration 80−44355
Al-Pd(Si) film, preferred sputtering on surface, mass and bonding difference effects, AES obs. 79−87552
AlF_3, disordered film, optical transitions as function of prep. conditions 78−27340
AlF_3 film, dielec. characts. 77−85650
Al_2O_3, thick vacuum condensates, electron microscopy struct. investig. *(Russian)* 78−95242
Al_2O_3, vacuum condensate, struct. and mech. props., second phase effect *(Russian)* 80−71705
$Al_2O_3(Al_2O_3$-MgO)-Ag(Au)(Cr)(Cu) cermet selective surfaces for evacuated solar collectors 79−43785
As-Ge-Se system, synthesis and phys. props. of amorphous layers 77−52252
As-S semiconducting glass film holographic recording media *(Russian)* 77−10864
As-Se(Te)-Ge, fabrication of amorphous semicond. thin films with graded band struct. *(Japanese)* 77−55623
As_2S_3 amorphous film waveguide and grating coupler 80−53448
As_2S_3 chalcogenide film surface relief hologram selective etching *(Russian)* 79−94181
As_2S_3, electron beam deposited film, photoinduced birefringence and dichroism *(Russian)* 78−2934
As_2S_3 film, effect of light exposure and heat cycling 78−94417
As_2S_3 film, optical recording, light scatt. enhancement due to coherence 80−97362
As_2S_3 film, selective etching characts. obs. *(Russian)* 80−3207
As_2S_3, single-layer vac. antirefl. coatings for near IR spectral region 80−33099
As_2S_3, spt. spectra of vac. deposited coatings *(Russian)* 77−48264
As_2S_3 thin films, vacuum deposited on Ge and PbS, sealing props. and TEM 80−35097
As_2S_3, vapour-deposited, pure and doped, hole mobility 80−49728
As_2Se_3, amorphous, hole emission defect states 80−49759
As_2Se_3 chalcogenide film surface relief hologram selective etching *(Russian)* 79−94181

vacuum deposited coatings continued
As_2Se_3, film, influence of electric field on crystallisation kinetics 78−42914
As_3Se_2 chalcogenide film surface relief hologram selective etching *(Russian)* 79−94181
$AsTeS_x(Se_x)(Sb_x)(Bi_x)$, chalcogenide glass, thin film crystallisation 79−7758
Au, adhesion on oxide or glass with interposed fluoride film 78−19667
Au, biological specimen prep. for SEM 79−5421
Au, discontinuous, evaporated on C and SiO, struct. and elec. cond. 80−39686
Au, discontinuous, morphology and size distribs. of islands, electron microscope obs. 77−62766
Au, discontinuous, substrate radiation damage effect on resist. and strain gauge stability 79−95520
Au, discontinuous films, glass substrate 78−6246
Au, evap., temp. change and gas adsorpt. effect on opt. consts., ellipsometric obs. *(German)* 80−89081
Au film, adsorbed CO, enhanced Raman scatt. mechanism in ultrahigh vacuum 80−107645
Au film, epitaxial growth, whisker form. 77−76713
Au film, MBE and field emission deposition on III-V semiconductors, comparative study 79−87016
Au, film continuity, observations by Auger spectroscopy 78−64433
Au film deposition, thermal effects, influence on internal stress meas. 80−96767
Au film sandwiches, recovery kinetics and early stages of diffusion, DC resist. expts. 79−77971
Au fine particles, morphological features using TEM weak-beam dark-field technique 80−15410
Au, growth on C replica stripped from pure and doped NaCl single crysts., elec. memory expts. 77−76691
Au, growth on clean and contaminated GaAs (001) surfaces 78−26785
Au, internal stress and its depend. on gas adsorption 80−6683
Au island film, on NaCl cleaved surface, growth, effect of perp. elec. field *(German)* 77−76697
Au island film, on SiO_x, growth and struct., effect of perp. elec. field *(German)* 77−76696
Au, microporosity induced by nucleation and growth processes, TEM expts. 78−10303
Au, on Al, Ni, EUV reflection efficiencies 79−14073
Au, on CdS, bonding and interdiffusion, XPS obs. 80−80000
Au, on Cu, ion-induced intermixing 80−15420
Au, on Cu, sputtering yield by substrate Auger meas. 79−95889
Au, on MgF_2 and SiO substrates, internal stresses correl. with struct. 79−87026
Au, on Si or CaF_2, oriented crystn., formation of coincidence orientations on interphase boundary 79−90922
Au on V{100}, layer growth, total current spectroscopy 77−36329
Au, thin film, elec. resist., effect of annealing In electrodes 80−80416
Au, ultra-microhardness testing for vacuum deposited film and bulk specimen 78−79910
Au, vac. deposited films, surface pot. and work function rel. to thickness 79−42672
Au vacuum deposited coating on glass, strength 80−55505
Au, vacuum deposited film, surface struct., HEED meas. 78−6234
Au vacuum deposited layer on KI, nucleation and growth 79−61516
Au vacuum deposition on dielectric substrates, ellipsometric and electron microscopic meas. 79−74011
Au, void growth in early stages of ageing and electromigration 78−38991
Au/Sn, microstructure and texture, TEM obs. 80−39481
Au/Sn thin film couples, evaporated, TEM study 80−59832
Au-Cu-Cr, deposited on glass or Si substrate, X-ray microanalysis *(French)* 80−50902
Au-GaAs, film-substrate interface alloying behaviour, electron microscopic study 79−60652
Au-GaAs Schottky barrier diode, X-band applications 77−8192
Au-Ge (27 at.%), metastable phase struct. determ. by electron diffr. 78−83780
Au-Pd, biological specimen prep. for SEM 79−5421
Au-Sn evaporated films, comp. and annealing behaviour, 20-400°C 77−76695
Au_8 particles, vacuum-deposited, degree of faceting during sintering 80−84411
AuAl formation by thin film interactions, identification by X-ray diffraction 79−99442
AuMn alloy, ordered, vacuum deposited epitaxial films, orientation control by external stress 80−100426
Au_3Mn thin films, electron diffr. study 80−92793
$Au_{35}Si_{65}$, amorphous vacuum-deposited and liquid-quenched films, diffusion and crystn. 80−84094
Au_xSi_{1-x} amorphous films, phys. studies 80−75476
B, evaporated, electronic struct., XPS, SXS and isochromat investig. 80−76143
B films, amorphous, prep., struct., props., review, book contrib. 78−48321
B-transition metal, amorphous thin film, crystallisation, TEM obs. 79−19483
Ba film, deposited on W (100), struct. determ. using LEED 79−90902
Ba film, work function and struct. 78−80040
Ba getter film, initial reaction probability with O_2, water, CO and CO_2, AES obs. 80−61153
Ba, oxidation, SXAPS 77−73189
Ba, structure effects on work function, electron micrographs and photoemission meas. 79−83107
$BaCl_2$, non-cryst., very-low-freq. inelastic light scatt. 80−25367
BaFCl, non-cryst., very-low-freq. inelastic light scatt. 80−25367
BaO, on W cathode, struct. transforms., LEED obs. 78−11061
$BaTiO_3$, nonstoichiometry of vac. condensates, effect on dielectric props. 77−16260
$BaTiO_3$, vacuum condensates on US irrad. substrates, props. 77−66466
Be film, opt. filter in He discharge lamp for photoelectron spectroscopy 78−79115
BeO film, amorphous or polycryst., dielec. function, refl., from electron energy loss meas. 78−43947
BeO specimen supporting films for high resolution electron microscopy of single Au particles 77−27793
Bi, automatic fabrication and simultaneous computer-controlled measurement equipment 79−69984
Bi, evaporated film, internal friction 77−7998
vacuum deposited coatings continued
Bi film, evaporated, lattice distortion spectrum, elec. resistance temp. variation 80−54806
Bi film, vap. deposited, effect on deposition parameters and substrate condition on crystallinity 78−10290
Bi, high-mobility, quantum size effects, struct. and kinetic charact. improvement 79−91174
Bi, on LiF single cryst., surface failure induced by laser impulse *(Russian)* 77−35585
Bi-Sb alloy, amorphous nature, AC and DC cond. and Hall coeff. obs. 80−11114
BiF_3 thin films, optical props. 79−32005
$Bi_{12}GeO_{20}$ vacuum-deposited film elec. and photoelec. props. *(Russian)* 78−60237
Bi_2O_3 films, dielec. props., 90 to 298K, freq. range 0.1 to 10 kHz, ageing effect 80−55036
Bi_2O_3, thermally grown, I-V charact., current controlled neg. resist. 80−15637
$Bi_{2-x}Sb_xTe_3$, solid soln. film on mica substrate, effect of stresses on elec. cond. 78−51859
C, amorphous, density meas., microcrystalline model of struct. 80−2313
C, amorphous, diamond-like 3-fold coord. 80−50323
C, amorphous, struct. and semicond. props. and heterojunction form. with single cryst. Si 80−25002
C amorphous thin films prepared by vac. evaporation, density meas. 77−80714
C, arc evap. film, optical props., 0.6-3.8 eV 77−81166
C, deposition processes, coating struct., for prosthetic devices 77−40374
C, diamond-like, ion deposited, hardness and mech. stability 80−2314
C, diamond-like, ion-plated, electron energy loss spectra characterisation 80−2308
C, effects of Ni substrate surface on deposition 77−28721
C, film, work function, heat treatment 78−64563
C, for prosthetic coatings, wear behaviour 79−43440
C, graphitisation, electron microscopy 80−40265
C on Pt for radiative heat transfer gauges, prod. technique *(Chinese)* 79−38742
C, SRO from radial-distrib. curve analysis 77−89662
Ca, film struct., mass-thickness depend. 78−80040
Ca films, thin and ultrathin, struct. and photoemission meas. 80−11538
Ca, oxidation, SXAPS 77−73189
Ca, photoionisation coeff. from photoemission meas. 79−91569
Ca, structure effects on work function, electron micrographs and photoemission meas. 79−83107
CaF_2 thin films, initial ionic thermocurrent meas. 80−97018
$CaF_2:Gd^{3+}$ evaporated film, struct. of impurity centres, substrate temp. effects 79−99943
Cd films, microstruct. exam., X-ray diffr. profile anal. 79−46973
Cd, freshly deposited, 77K, refl., annealing effect, thickness depend. 77−16413
Cd, HCP, crystal struct. changes on ion bombard. 77−69018
Cd, HCP, microstruct., X-ray obs. 80−10827
Cd, thin film, vac.-deposited, X-ray diffr. struct. obs., props. 79−37937
Cd-Sb alloy condensate film, phase transform. kinetics 77−15721
Cd_3As_2 film on NaCl substrate, vacuum deposition, growth morphology, microstructure 80−75479
Cd_3As_2 films, nucleation processes, on NaCl substrates 80−59813
n-Cd_3As_2, Shubnikov-de Haas effect 79−99644
$CdCr_2Se_4$, spinel film, struct. SEM study, props. 78−79905
$CdGa_2S_4(Se_4)$, optical absorpt., and energy gaps 78−11012
$Cd_xHg_{1-x}Te$, vac evap. film struct. rel. to carrier scatt. 77−85116
$CdIn_2S_4$ films, vac. deposited, struct. and photoelec. props. 79−87006
$CdIn_2S_4$, growth, struct., optical and photoelectronic props. 80−10831
CdS evaporated films, growth rate and resist. determ., in situ meas. technique 79−77940
a-CdS film, DC cond. Seebeck data 77−24626
CdS film, heterojunction with copper sulphide, ordinary glass with silver layers as substrate 78−2525
CdS film, prep. by hot wall technique, morphology and semicond. props. 79−95292
CdS film, strain-induced modulation of photoconductivity 79−24009
CdS films, vac. evaporation from $CdS.Cr_2O_3$ system, photoelec. props. 78−80074
CdS, for solar cells, struct. and elec. props., thickness depend. 78−72289
CdS, polycryst., optical spectra, 0.5-6.5 eV 80−55212
CdS polycrystalline layers, electron trapping depend. on preparation conditions 79−78232
CdS, pure and Al doped, vacuum deposited film, photoelectric props., optical absorption 78−60162
CdS vacuum evaporated film photoconductivity and In doping effects *(Japanese)* 79−87174
CdS:Ag, recrystn. by H_2S heat treatment 80−34328
CdS:Cu, Cl films, photocond. growth and decay time 80−60041
CdS:Cu, dynamic quenching of photocapacitance, deep levels obs. 77−85175
CdS:Cu(Cl), thin layer, electron pulse induced cond. relax. 80−2501
CdS:In, flash evaporated, prep. and elec. props. 80−20792
CdS:In, high cond., high transmittance, growth by evaporation method, and characterisation 77−77386
CdS:In films, growth, elec. and optical props. 79−51460
CdS:M, M=Zn, Te, doping and solid soln. prep. during VPE 77−85353
CdS:Mn, vacuum deposited film, Mn migration, EPR and X-ray study 80−65411
n-CdS/p-$ZnIn_2Se_4$ thin film solar cell, photovoltaic props. 80−89628
CdS-CuI film heterojunction photocells, prep , photoelec. props. 78−80044
CdS_xSe_{1-x}, flash evaporated, prep. and elec. props. 80−20792
CdS_xSe_{1-x} photosensitive films, prep., props., and use for photodetectors 80−55298
CdS(Se)(Te), growth and struct., HEED obs. 80−29292
CdSe, electrical resist. and surface changes by laser annealing 80−2491
CdSe evaporated films, struct. and epitaxy, TEM, RHEED, and X-ray diffr. obs. 79−77939
CdSe evaporated films, photoconductivity and effect of deposition conditions 79−95442
CdSe film, electrophys. props. rel. to evap. rates and comp. of initial cryst. 77−85940
CdSe, film, specific resist., deposition conditions, depend. 77−85363
CdSe film, stimulated recrystn. influence on photocond. 77−43754
CdSe film photoanodes for electrochem. photovoltaic cells, fabrication and evaluation 80−76641

vacuum deposited coatings continued
CdSe film polycryst., thermal diffusion of Cr, 240-400°C 80−80001
CdSe, stabilisation by heat treatment in vac. *(French)* 79−95532
CdSe, structure, resist. and Hall mobility 77−76974
CdSe-Si n-p heterojunction, vacuum deposition, photovoltaic effects *(Korean)* 77−28243
CdSe-ZnO thin film n-n heterojunctions, prep. elec. and optical props. *(Korean)* 77−28244
CdTe, electron mean free path, 350-1450 eV 80−103707
CdTe, formation on glass substrates, influence of sublayers of recrystn. stimulators 77−43455
CdTe-Te film, prep. by combined hot-wall-flash evaporation method, and characterisation 80−55296
$CdTe_{1-x}Se_x$ solid solution films, prep., struct., and photocond. 80−54541
$Cd_xZn_{1-x}S$ film, vacuum evaporated, struct. 78−38985
CeO_2 coatings on Gd-Fe amorphous films, Kerr magneto-optical effect enhancement 79−19866
CeO_2-$SiO_2(MgF_2)$, multilayer refractory oxide interf. coatings 79−7192
Co film, columnar struct. depend. on degree of texture 80−54567
Co film, texture and adsorption of CO *(German)* 77−24485
Co film, texture and columnar struct. 80−54566
Co, HCP, crystal struct. changes on ion bombard. 77−69018
Co vacuum condensates, Cr alloying addition effect on texture charact. *(Russian)* 80−108471
Co vacuum deposited coatings on metal substrates, cryst. struct. and stability 80−75481
Co-CoO films, evaporated, exchange anisotropy 80−88841
Co-Cr films, mag. props. in range of transition from thin-film to hypercritical state *(Russian)* 79−51824
Co-Cr(-Al-Y) coatings, hot corrosion resist., ductile-brittle transition 79−24674
Co-Gd amorphous film, struct., mag. anisotropy consts., saturation magnetisation *(Russian)* 79−99735
Co-O thin films, exam. of oxide phase reduction, by electron photographic analysis *(Russian)* 79−34359
Co-Si film system, diffusion marker expts. 78−79824
Co-Si film system, interaction kinetics 78−79823
CoP amorphous alloy, heat treatments influence on opt. props., struct. and DC resist. obs. 80−80892
Co_3Pd film, ordered, stacking fault obs. by TEM and interpret. using many-beam theory 80−107680
^{57}Co, on Ni (111), Mossbauer effect emission 79−80735
Cr, columnar struct. rel. to deposition conditions 78−52675
Cr containing Cr_2O_3, film struct., oxide percentage determ. and temp. coeff. of resist. 80−103607
Cr, die cast Zn as substrate 78−6238
Cr, evap. film, refl. and struct. 78−72021
Cr film, evaporated, concurrent ion bombard. effects 80−80142
Cr film, residual stress meas. by X-ray diffr. using $\sin^2\psi$ method 79−15059
Cr, film, vac. deposition onto low temp. substrate, cryostat *(Japanese)* 78−27403
Cr film, vacuum evaporated, particularities in growth on alkali halides with Pb colloids and F-centres 79−82496
Cr film on glass substrate with ZnS or MgF_2 underlayer, thermal strength, recrystn. influence 79−87748
Cr, films, vac. deposited, defects *(Russian)* 79−33203
Cr, lattice dimens., difference between vacuum condensates and massive specimens *(Russian)* 77−31912
Cr, on die-cast Zn, microstruct. and intrinsic stresses, substrate temp. effects 78−10304
Cr, on polycryst. CdS, thermal diffusion, 240-400°C 80−80001
Cr, quantitative mass anal. by colorimetry, angle of incidence depend. 77−69998
Cr, stratification phenomenon, interf. metrology *(French)* 77−59225
Cr vacuum deposited coating on glass, strength 80−55505
Cr, with A-15 struct., prep. and characterisation 77−62768
Cr-Si, for resistor manufacture, residual gas atmosphere analysis *(German)* 80−6681
Cs, on MgO secondary emitter, increasing of emission efficiency 78−2960
Cs_3Sb vacuum deposited photoemitter, XPS study 80−89122
Cu, adsorption and desorption of water vapour, relative humidity effects 80−49505
Cu alloy film, multicomponent secondary ion emission meas. of composition var. laws *(Russian)* 77−80704
Cu alloy vacuum condensed films, alloying addition influence on electrophysical props., elec. cond. *(Russian)* 80−34529
Cu alloy-Al alloy evaporated couples, interdiffusion *(Russian)* 77−43389
Cu, breakdown stress, thickness depend. *(Russian)* 77−59238
Cu, condensates of different thicknesses, polycrystalline, mech. props. 79−65350
Cu evaporated layer on Ge, RHEED Kikuchi bands, anomalous contrast 78−87597
Cu, film, deposited in UHV by thermal evaporation, surface struct. 79−69381
Cu film, in situ struct. determ. by internal stress meas. 80−54569
Cu film, on Au substrate, oxidation and interfacial behaviour, ion scatt. spectroscopy study 80−66691
Cu film, on W substrate, cementation, vac. deposition, and electroplating, growth charact. 79−95291
Cu film, oxidised in ^{18}O, ion scatt. anal. 77−40463
Cu film, pure and CO covered, optical consts., ellipsometry meas. 79−78645
Cu film, struct., oxidation, and exoelectron emission rel. to bulk samples *(Russian)* 79−37927
Cu, film continuity, observations by Auger spectroscopy 78−64433
Cu film deposition, thermal effects, influence on internal stress meas. 80−96767
Cu film growth on amorphous C, energy charact., in situ electron microscope determ. 79−11027
Cu film on Ni, AES comparison of ion plated and vacuum evaporated films 79−28250
Cu, ion bombardment induced preferential orientation 80−100290
Cu, lattice dimens., difference between vacuum condensates and massive specimens *(Russian)* 77−31912
Cu on Fe (001) substrate, orientation relationship 80−65415
Cu, separation from leucosapphire substrate during annealing *(Russian)* 77−7997
Cu, thickness meas. using X-ray fluoresc. technique 79−90911
vacuum deposited coatings continued
Cu, thin film, elec. resist., effect of annealing In electrodes 80−80416
Cu, ultra-microhardness testing for vacuum deposited film and bulk specimen 78−79910
Cu, vacancies-gas impurity interactions in vacuum condensates *(Russian)* 79−15036
Cu vacuum coating on steel substrate, influence of precipitation conditions on porosity *(Russian)* 80−54578
Cu, vacuum condensate, struct. and mech. props. depend. on deposition conditons 80−15417
Cu, vacuum deposited film, surface struct., HEED meas. 78−6234
Cu, vacuum-condensed film, structural changes under glow discharge *(Russian)* 79−15852
Cu vapour deposited mirror on SiC substrate, pulsed laser damage characts. 80−48314
Cu-Ag, thickness meas. using X-ray fluoresc. technique 79−90911
Cu-Al, vacuum condensate, struct. and mech. props. depend. on deposition conditons 80−15417
Cu-Al alloy film comp. struct. resistivity 78−6852
Cu-Al films, elec. cond. of vacuum condensates depend. on composition, annealing *(Russian)* 80−65709
Cu-Al thin film multistructure, Xe^+ ion beam cratering 80−66708
Cu-Al_2O_3, dispersion-strengthened, vapour-deposited, tensile creep 78−11115
Cu-Al_2O_3 thin film ceramets, TEM study of composition and struct. 79−99437
Cu-based alloys, deposition condition relationship with struct. and props. 78−11369
Cu-Ge codeposited film, elec. resist. and thermoelec. power, rel. to struct. 79−87168
Cu-Mn alloys, vacuum deposited, electrophys. props. 77−63006
Cu-Ni film, coevaporated, AES anal. and ion sputtering effects 79−15044
Cu-Ni thin films, ferromag., Hall effect meas. 80−80428
Cu-Ni/Au-Ni multilayer films, ohmic behaviour, use as strain gauge 80−65713
Cu-Ni/Au-Ni multilayers obtained by co-evaporation in UHV, ohmic stability and TCR 79−78226
Cu-S, thin film, phase formation conditions *(Russian)* 79−56078
Cu-Sb-S-I amorphous film formation and stimulated crystallisation, electrophysial props. *(Russian)* 78−30838
Cu-Sn(Al)(Ga) reflecting surface absorpt. coeffs. at 10.6 μm 80−95984
Cu-Zn multilayer condensate, diffusion process, brass formation 78−43186
CuAu alloy, ordered, vacuum deposited epitaxial films, orientation control by external stress 80−100426
CuBr(I), reflectance and thermoreflectance spectra, electronic struct. 80−71444
CuFe film, metastable polycrystalline optical props. 79−83044
CuGaTe, flash evaporated, growth and optical props. 79−95296
$CuInS_2(Se_2)$, absorpt. coeff. 78−72621
$CuInSe_2$ amorphous thin film, flash evaporation, struct., stoichiometry 80−89150
$CuInSe_2$, evaporation source temp. effect, on comp. 80−39478
p-$CuInSe_2$ film, prep. from vac. evaporation of $CuInSe_2$, optical and elec. props. 79−82697
$Cu_{2-x}S$ films, vacuum deposited, electrical conduction and phase transitions 78−84332
$Cu_{2-x}S$, ordering process, electron diffr. study 80−39477
$Cu_{2-x}S$-CdS heterojunction V-I characteristic and max. photovoltage, long-term changes *(Russian)* 78−43468
Cu_xS evaporated layer growth in vacuum, compositional and optical characterisation, solar cell appls. 80−97437
Cu_xS evaporated thin films, composition, prep. and charact. 80−25569
CuSe film, phase transforms. and decomp., electron diffr. obs. 79−42418
Dy_2O_3, phase transforms. on annealing 79−95285
Er, elec. resist., thickness depend. 77−76956
Er, film, evap., CO effect on work function 78−39188
Er, film, reaction with H_2O vapour, spectroscopic and X-ray diffr. obs. 77−40575
Er-H_2 system, work function changes correlated with phase changes, elec. resist. meas. 77−11828
ErD_2, thin film, reaction with H_2O vapour, spectroscopic and X-ray diffr. obs. 77−40575
ErO, vac. deposited films, struct. changes due to annealing 79−77741
Eu chelate, fluoresc. lifetime, depend. on optical environment 80−9630
Eu complex, benzoyltrifluoro-acetone-chelate, refr. index determ. of fluoresc. films 80−40175
EuS film, influence of prep. on mag. props. 79−24201
EuS films, mag. and elec. props. rel. to stoichiometry and defects 80−97122
EuS_x film, vacuum deposited, composition depend. on substrate temp. and deposition rate 78−84107
Fe based dispersion strengthened thick condensates, struct., mech. props. 77−90361
Fe, columnar struct. rel. to deposition conditions 78−52675
Fe, epitaxial film on Sb, ultrahigh vac. deposition 78−56572
Fe, epitaxial growth on Au platelets, dislocations 80−96760
Fe, evaporated, adsorbed acetylacetone, XPS study 80−76133
Fe, evaporated at oblique incidence, optical and mag. anisotropies 80−7134
Fe film, coated, interface magnetism by Mossbauer spectroscopy 80−75890
Fe film, stopping power meas. of 0.3 to 2.6 MeV ^4He ions 79−3329
Fe films, vacuum evaporated, exam. of texture for various vapour beam incidence angles *(Japanese)* 78−48318
Fe granular deposits, plasma reson., rel. to interstellar dust extinction curve 79−21387
Fe, granular film, microstructure using X-ray, electron diffr. and TEM 79−65344
Fe, Hall resist., effect of N impurity codeposition 78−64146
Fe, lattice dimens., difference vacuum condensates and massive specimens *(Russian)* 77−31912
Fe, on Au (111), interaction layer formation mechanism 80−54559
Fe, polycryst., heat of adsorpt. of H_2 and D_2 78−91530
Fe, thermally evaporated, contamination effects obs. 80−49545
Fe vacuum deposits on Ni(Cu)(Ag) (111) FCC substrates, orientation relationships 80−59836
Fe-Al, dil., NMR spin echo, rel. to struct. inhomogeneities *(Russian)* 80−29644
Fe-Au (111) interface, nature of interaction layer 79−99433

vacuum deposited coatings continued
Fe-B, amorphous to cryst. transition 80−88048
Fe-Co, dil., NMR spin echo, rel. to struct. inhomogeneities *(Russian)* 80−29644
Fe-Cr based coatings, hot corrosion resist. 79−24674
Fe-Cr-Al, Kanthal films, vac. deposited, evaporation charact., comp., struct. and elec. props. 80−88646
Fe-Gd, amorphous, mag. props., mean field analysis 78−64236
Fe-Gd, amorphous, O_2 contamination effects on mag. props. 78−64231
Fe-Gd amorphous film, struct. and mag. props. 80−20439
Fe-Ni, depth profiles, sputter etching obs. 79−83079
Fe-Ni, internal stresses, thickness and comp. effects *(Russian)* 77−80713
Fe-Ni, mag. and struct. props., effect of O_2 partial press. during deposition 79−90903
Fe-Ni films, lattice constants rel. to mag. moments *(Russian)* 77−32218
Fe-Pd, depth profiles, sputter etching obs. 79−83079
Fe-rare earth, amorphous thin film, crystallisation, TEM obs. 79−19483
Fe-refractory compound, dispersion strengthened, thick vacuum condensate, control of struct. and mech. props. 80−16324
Fe-refractory compound condensate, struct. and mech. props., disperse particle content depend. *(Russian)* 78−19772
Fe-Si amorphous film, struct. and crystallisation, Mossbauer study 80−11300
$(Fe\text{-}Ni)_{1-x}(SiO)_x$, cermet film, internal strsses *(Russian)* 78−75951
FeF_3, thin film, optical absorpt. meas. 79−15546
FeF_3 thin film prep. and charact. *(French)* 78−64470
α-Fe_2O_3, photochem. props. of sintered and doped samples for solar photoelectrochem. cell appls. 80−89651
Fe_xO_y films, electron microscopy and energy-loss spectroscopy 80−80137
Fe_xO_y, thermally evaporated, contamination effects obs. 80−49545
FePd, epitaxial, for thermomag. recording, mag. and magneto-optical props. *(Russian)* 78−60319
$Fe_{1-x}Pd_x$ film, air-exposed, comp. profiles by AES, ESCA and ion sputtering 78−95245
$Fe_{1-x}Pd_x$ films, vacuum deposited, mag. and corrosion props. 79−56574
$Fe_{1-x}Pd_x$, oxidation and corrosion, AES, XPS and STEM obs. 79−100286
FePt, epitaxial, for thermomag. recording, mag. and magneto-optical props. *(Russian)* 78−60319
FeSb solid solution, supersaturated, mag. hyperfine field, Mossbauer study 80−44961
$FeSi_2$ films, structural and Anderson transitions, cond. and IR reflectance meas. 79−15200
Fe_xSn_{1-x} amorphous alloy films, magnetisation meas. and Mossbauer spectra 78−95489
Ga, freshly deposited, 77K, refl., annealing effect, thickness depend. 77−16413
Ga, monoclinic, elec. cond., classical size effect 77−89881
Ga, on GaAs or Si, anodic oxidation, Ga_2O_3 film prep. 77−81338
Ga, supercond. T_c and residual resist., variation with coating thickness 78−47900
Ga, vacuum deposited film characterisation *(French)* 79−51447
GaAs amorphous film, effective medium theory and freq. depend of conductivity 79−24090
n-GaP, Au-coated semicond. electrode, photoelectrochem. behaviour in water 77−21399
GaP, vac. deposited film, structural, elec. and photoelectric props. 79−82698
GaSb film, gamma-irradiated, struct., TEM and SEM obs. 79−15033
GaSb films, amorphous and cryst., vac. evaporated, Elec. cond. thermoelec. power and optical absorpt. 80−2504
Ga_2Se_3, vapour phase deposited films, struct. 78−2383
GaTe, hexagonal, vacuum deposited, physical parameters and substruct. 78−2393
Ga_2Te_3, vapour phase deposited films, struct. 78−2383
Gd, deposition parameters effects on struct. 79−90912
Gd-Ag, vap. quenched alloys, struct. and mag. props. 78−84461
Gd-Co, amorphous, for bubble device appl., prep. and perpendicular anisotropy 77−69641
Gd-Co, amorphous, phase separation as source of perpendicular anisotropy 78−64244
Gd-Co, amorphous ferrimagnet, mag. anisotropy, effect of ion bombard. during prep. 79−1692
Gd-Co, evap. amorphous film, mag. props. 77−24720
Gd-Co, evap. amorphous films, anisotropy, magnetisation and FMR meas. 77−66392
Gd-Co, evaporated amorphous film, perpendicular anisotropy by controlled O_2 contamination 77−89990
Gd-Co, thermally evap. amorphous film, mag. anisotropy 77−16122
Gd-Co film, evaporated and sputtered, struct. and mag. anistoropy 79−56578
Gd-Tb (10 wt.%) film, nuclear echo signals, crystal anisotropy consts. *(Russian)* 79−99790
GdCo film structure, dependent on substrate type *(Russian)* 80−24747
GdFe film structure, dependent on substrate type *(Russian)* 80−24747
$GdFe_2$ films, electron beam deposited, amorphous and cryst., mag. and struct. props. 79−4710
Ge, amorphous, density meas., microcrystalline model of struct. 80−2313
Ge, amorphous, non-destructive density meas. 80−6680
Ge amorphous film, effective medium theory and freq. depend of conductivity 79−24090
Ge amorphous film, O depth profiling by SIMS 80−39480
Ge amorphous film, ultra high vac. prep., DC elec. cond. 80−49721
Ge, amorphous layer, on single cryst. Si, heteroepitaxy by laser annealing 79−77952
Ge amorphous thin films prepared by vac. evaporation, density meas. 77−80714
Ge epitaxial film, vac. deposited on GaAs, doping effect of annealed GaAs surface 80−65718
Ge, evaporated film, lattice parameters and phase transition temp., surface influence of glass substrates 78−94996
Ge, film, vac. deposition onto low temp. substrate, cryostat *(Japanese)* 78−27403
p-Ge, fragmented struct., elec. cond., Hall coeff. and magnetoresist. meas. 77−15979
Ge, on Si(111), solid phase heteroepitaxy 80−6670
Ge thin films on glass substrates, annealing by Ar ion bombardment 80−80136

vacuum deposited coatings continued
Ge-Ga amorphous alloy, co-evaporated elec. and optical props. 80−70860
Ge-metal film, polycryst., struct. props. determ. 79−4494
Ge-metal films codeposited, amorphous and polycryst., struct. and elec. props. 80−24766
Ge-Si, UHV-produced epitaxial structs., electrophys. props. 78−3060
a-Ge-Si crystal interface, low resist. elec. behaviour 77−89843
$Ge_{15}As_4Te_8$, film, influence of electric field on crystallisation kinetics 78−42914
GeO, optical props., rel. to possible appl. in holography 80−29816
GeP, thin films, vacuum-deposited, struct. characterisation 77−47691
GeS film, between Al(Zn)(Sn) electrodes, Schottky and Poole-Frenkel cond. mechanisms 80−54799
$GeSe_2$ chalcogenide film, struct. changes due to laser induced transmittance oscill., SEM obs. 78−6240
Ge_2Se_3, vitreous, evaporation kinetics and amorphous film deposition 80−97434
Ge_4Se_5Te amorphous layers, prep. and elec. props. 80−97436
GeTe, electro-reflectance meas. 80−11496
GeTe films, elec. props. and struct., influence of annealing and condensation conditions 80−15388
H_2-D_2 solid films, struct. study transmission electron diffr. obs. *(Russian)* 79−11035
HfO_2, for multilayer reflector in near UV 77−34924
HfO_2, vac. deposited, near UV multilayer reflector 77−39014
Hg-Xe vapour deposited films, cond. transitions, effect of disorder on supercond. 80−88659
HgTe, electrical props., 78-420K 80−11119
Ho-Co film, evaporated, struct. and mag. anistoropy 79−56578
In electrode, annealing, effect on elec. resist. of metallic thin film 80−80416
In film, $\sqrt{3}$ and $\sqrt{31}$ submonolayer superstructures on Si (111) isothermal desorption, RHEED meas. 79−86992
In film, vacuum evaporation growth, impurity presence, effects *(Hungarian)* 80−7495
In, film growth on C, conductance meas. 79−82495
In films, growth conditions effect on elec., optical, and structural props. 79−78215
In, freshly deposited, 77K, refl., annealing effect, thickness depend. 77−16413
In on Au, ultrathin quantum size effect *(French)* 77−20466
In particles, grown in ultra-high vac. on KCl substrates, struct. and orientation 80−10814
In, recrystallisation of films prep. by vacuum evap. 79−4488
In-PbTe contacts, fabrication and props. 80−60078
In-S system, vac. deposited films, form., reacts. 78−43259
InAs, thin film prep. and elec. props. 79−1633
In_2O_3 films, reactively evaporated, elec. props. 80−84521
In_2O_3, In_2O_3-SnO_2, transparent thin films for satellite temp. control 79−80187
In_2O_3, thermally evaporated film, struct. and elec. props. 80−104066
In_2O_3, transparent electrode deposition on PLZT ceramic, elec. and opt. props. 78−74848
InP-Al interface struct., low temp. interaction, AES study 80−107661
InSb amorphous film, effective medium theory and freq. depend of conductivity 79−24090
InSb film, gamma-irradiated, struct., TEM and SEM obs. 79−15033
InSb films on $LiNbO_3$, prep. and props. 80−35093
InSb, synthesis by 2-source mol. beam technique and AES characterisation 78−72729
InSb thin films for acoustoelectronics 80−103765
InTe thin films, flash evaporation, electrical props. 80−65722
Ir, CO adsorption, IR refl.-absorpt. spectroscopy 80−34925
Ir, electron beam deposition and ion plating 77−44166
KI microcrystals, UV spectra by diffuse reflectance technique, surface electronic transitions obs. 80−75614
Kb_2S_3, condensates, struct. and optical transmittance 80−20727
Kr, HCP, vap. phase grown thin films 78−18917
Kr:N_2O, cryodeposited film, exciton-enhanced KrO excimer luminescence 77−36288
LaB_6, prep. by electron beam evaporation, and optical and elec. props. 80−20793
LaF_3 films, electron beam evaporated, dielec. props. 79−91375
$LaSi_2$, thin film, exam. of phase transitions during vacuum annealing 79−95281
La_5Si_3 thin film, exam. of phase transitions during vacuum annealing 79−95281
Li aggregated deposits, optical props., 1-6 eV 77−66549
Li, on MgO secondary emitter, increasing of emission efficiency 78−2960
LiF film, intrinsic stress meas. 80−71696
LiF film, refractive index as function of time, ATR meas. 79−65940
LiF, polycrystalline and single-cryst., comparative study of phonons by electron spectroscopy 80−25505
LiF, ultra-microhardness testing for vacuum deposited film and bulk specimen 78−79910
LiF(Cl)(Br) film, electron emission under metastable He and Ne atom impact 80−20747
Li_xWO_3, electrochromic characteristics 78−6653
Mg and Mg-Fe films, defect energy distrib., elec. resist. meas. during annealing 80−54808
Mg film, Fuchs Sondheimer theory, size effect, elec. cond., Fermi surfaces 79−99637
MgF_2, bounded by Ag films, ATR ang. spectra, assoc. reson. EM oscills. 79−15541
MgF_2, destruction props. obs., suitability for integrated optics assessment *(Slovak)* 80−33224
MgF_2, disordered film, optical transitions as function of prep. conditions 78−27340
MgF_2, origin of mech. stress 79−90925
MgF_2, tensile stress, meas. and calc. 79−87027
MgF_2, ultra-microhardness testing for vacuum deposited film and bulk specimen 78−79910
MgF_2-Na_3AlF_6 thin film deposits, quenched ageing by chopping 80−97364
MgO film, vacuum deposited on NaCl-type alkali halides, struct. characterisation 79−82490
MgO, IR spectroscopy and RHEED analysis 77−89664
MgO, with ordered structure, slow electrons escape depth 77−20971

vacuum deposited coatings continued
Mn coated BN powder particles, X-ray investig. of thermal stresses generated in vac. deposition 77−40455
Mn, contact to p-Si, barrier height 80−34510
Mn, deposited in elec. field, resist., struct. 80−103761
Mn film, elec. resist., deposition rate effect 80−97010
Mn film, H(D) uptake kinetics and energetics 80−88430
Mn film, resistivity-temperature variation 79−24085
α-Mn, low temp. resist., rel. to deposition conditions 79−78223
Mn-Al alloy, vacuum codeposited, disorder of $MnAl_6$ phase in recovery process 78−51854
Mn-MgF_2 cermet film, resistivity-temperature variation 79−24085
Mn-SiO, annealed cermet films, elec. resist., composition depend. 80−97007
Mn-SiO cermet films, DC and AC resist. 80−54804
Mn-SiO cermet films, elec. resist., annealing behaviour 80−54803
MnBi films, prep. by ionised-cluster beam deposition technique, magnetooptical props. 80−100790
MnBi, magnetic reversal mechanism, hysteresis loops for polycryst. and single cryst. specimens *(Russian)* 78−60318
MnTe film, elec. props. 78−43498
Mo, carbonyl coating, deposition and props. 77−28725
Mo, epitaxially grown on W tips, field evaporation, struct. obs. 77−28723
Mo, evap. film, refl. and struct. 78−72021
Mo, evaporated, annealing behaviour, SEM obs. 80−65397
Mo film, evaporated, grain size and resist. 80−88650
Mo film, silicide formation during growth by electron beam evaporation *(German)* 78−84717
Mo, film, vacuum deposited, elec. cond., internal stresses, surface corrosion, MOS gate appl. *(Japanese)* 78−80073
Mo film, vacuum deposited onto SiO_2-Si substrates, elec. resist. 78−76166
Mo, supercond. T_c and residual resist., variation with coating thickness 78−47900
Mo, with Nb, Ni or Al_2O_3 impurity, prod. by simultaneous condensation from 2 sources, growth direction *(Russian)* 77−21026
Mo-Ni thin film junction, phys. vap. deposition parameters effect on thermoelec. power 77−39922
Mo-Si(Ge)(Al), amorphous supercond. alloy, produced by coevaporation, struct. and supercond. 79−91179
MoC coatings, produced by plasma flux deposition in vacuum, exam. *(Russian)* 80−11567
MoO_3 film, evaporated, electrochromism *(Japanese)* 79−38686
MoO_3, optical absorpt. after ion irrad., appl. to ion beam profile monitoring 79−26181
Na, for expendable filter in VUV, use and preparation technique 80−33193
Na-NH_3, quench-condensed, anomalous elec. cond. obs. 77−32057
Na_3AlF_6, effect of temp. var. on light transmission 78−79136
Na_3AlF_6, electron bombard. effect on secondary electron emission, Auger peak shifts 80−2903
Na_3AlFe_6, opt. spectra of vac. deposited coatings *(Russian)* 77−48264
NaF(Cl) film, electron emission under metastable He and Ne atom impact 80−20747
$NaSbSe_2$ films, struct., photoelec. and opt. props. 78−51834
Nb, deposited in quasi-closed vol., supercond. props. 79−91180
Nb, electron beam evaporated film, struct., supercond., purity *(German)* 77−52253
Nb films, supercond. props. and electronic density of states *(Russian)* 79−28439
Nb on Mo, Ti, evaporation, carburisation and diffusion behaviour 77−44410
Nb, superconducting, deposition parameter effects on crit. temp. 80−2514
Nb, superconducting film, thickness depend. of electrophys. parameter *(Russian)* 78−10590
Nb, superconducting thin film, devitrified glass or ruby substrate, elec. props. 77−55635
Nb, thin-film SQUID working at 4.2K, fabricationa and characterisation 80−100570
Nb/Cu, layered ultrathin coherent structs., supercond. props. 80−84525
Nb-Fe, formed on laser irradiation of Nb-Fe interface, Mossbauer spectra *(Russian)* 79−60560
Nb-Ge(Si), amorphous supercond. alloy, produced by coevaporation, struct. and supercond. 79−91179
NbC, vacuum condensate, struct. and mech. props., second phase effect *(Russian)* 80−71705
Nb_3Ge, electron beam co-deposited, prep. and supercond. crit. temp. 78−15310
Nb_3Ge sputtered and evaporated, struct.-depend. anisotropy of supercond. crit. currents 79−38292
Nb_3Ge, supercond., electron beam evaporation technique 78−6470
Nb_3Pb superconducting film, prep., vac. deposition 80−89149
Nb_3Si film, supercond., obtained by vaporisation in vacuum, props. 78−14865
Nb_3Sn, electron beam deposited, microstruct., rel. to supercond. props. 79−37935
Nb_3Sn, electron beam evaporation, growth morphology 77−44167
Nb_3Sn film, electron beam codeposited, growth morphology and tensile props. 78−10301
Nb_3Sn-Al_2O_3 composite, electron beam deposited, microstruct., rel. to supercond. props. 79−37935
$NdAlO_3$ films, preparation, electrophys. props. in MIM structs. 77−24956
$Nd_{0.35}Co_{0.65}$, vacuum evaporated, magnetisation ripple struct., TEM and defocused Lorentz microscopy 80−7136
Ni 78−7099
Ni based Rene 80 superalloy, initial stages of pack aluminisation 80−76188
Ni deposited on liquid-He-cooled sapphire, galvanomag. props. 79−95519
Ni, electron beam evaporated, ductility and struct. 78−11439
Ni, epitaxial film on NaCl, struct. and purity 78−72047
Ni, ethylene adsorption and reactivity with adsorbed H, surface pot. meas. 79−86995
Ni, evaporated, adsorbed acetylacetone, XPS study 80−76133
Ni, evaporated at oblique incidence, residual stress, mag. anisotropy meas. 78−22992
Ni, few atomic layers thick, transition from Pauli paramag. to band ferromag. 80−44885

vacuum deposited coatings continued
Ni film, evaporated, elec. resist. and galvanomagnetic props. 80−80411
Ni film, layer mode growth on Fe (001) surface, AES study 80−49540
Ni film, multi- and single-layer, reson. curves subjected to tangential mag. reversals *(Russian)* 80−50195
Ni film, stopping power meas. of 0.3 to 2.6 MeV ^4He ions 79−3329
Ni film, struct., oxidation, and exoelectron emission rel. to bulk samples *(Russian)* 79−37927
Ni film, vac. deposited, hexagonal phase *(French)* 78−63944
Ni films, adhesion on graphite 80−80141
Ni films on Pyrex, AES, purity 77−8755
Ni, lattice dimens., difference between vacuum condensates and massive specimens *(Russian)* 77−31912
Ni on Fe (001) substrate, orientation relationship 80−65415
Ni, ultrathin film, field effect meas., influence of CO adsorption 80−11108
Ni, vacuum-condensed film, structural changes under glow discharge *(Russian)* 79−15852
Ni/Au film on silicon vacuum deposited, electron impact mass spectrometric exam. of surface contaminants 78−75957
Ni-(Co)-Cr, aluminide coating, microstruct. and chem. 80−76189
Ni-Al, co-evaporated, comp.-depend. struct. and morphological changes 79−87020
Ni-Al, high-temp. condensed, electron diffr. and elec. resist. *(Russian)* 79−4485
Ni-Al films, evaporated, grain size and microstruct. 80−15423
Ni-Al_2O_3 alloy, electron beam evaporated, struct. and mech. props. 78−11114
Ni-Al_2O_3(ZrO_2), dispersion strengthened, thick vacuum condensate, control of struct. and mech. props. 80−16324
Ni-Co films, electron-beam evaporated, magnetoresist. anisotropy, deposition temp. effect 80−34528
Ni-Co-Cr-Al-Y, electron beam deposited, for Ni-base superalloy, fatigue crack initiation and propag. 78−11438
Ni-Cr, comp. and temp. coeff. of resist., AES obs. 79−91161
Ni-Cr, struct. transforms. induced during annealing, resist. obs. 79−77965
Ni-Cr, vac. deposition, elec. props. and comp. struct. 79−77966
Ni-Cr based coatings, hot corrosion resist. 79−24674
Ni-Cr film, resistance stabilisation by surface oxide formation 79−78214
Ni-Fe, differential susceptibility, struct. const. and losses 79−91271
Ni-Fe (20 wt.%), thin film ferromagnetic band, magnetisation under domain creep conditions *(Russian)* 79−91262
Ni-Fe (20%) film, condensed, struct. from electron diffr. 77−59222
Ni-Fe-Co (17,3 wt.%), thin film ferromagnetic band, magnetisation under domain creep conditions *(Russian)* 79−91262
Ni-Ge-Au evaporated contacts on GaAs, TEM obs. 80−75449
Ni-SiO composite film, acoustic damping capacity and struct. *(Russian)* 77−59070
Ni-SiO_2 composite film, influence of hardening phase on yield stress *(Russian)* 79−5001
Ni-ZrO_2, electron-beam-evaporated condensate, cold deform. and annealing effects on microstruct. 80−16331
NiF_2 film preparation and characterisation 80−59815
$Ni_{0.625}Ge_{0.375}$, amorphous film, crystn. mechanism *(Russian)* 77−51623
NiP amorphous alloy, heat treatments influence on opt. props., struct. and DC resist. obs. 80−80892
NiSe, phase transformation, electron microscope studies 80−2302
O_2 solid film, optical and structural props. 78−56052
Pb film, conducting coating effect on supercond. transition temp. and normal-state cond. 77−16007
Pb film, vacuum deposited, reflectance spectra, structural rearrangement effects 77−24905
Pb, polycrystalline film, electron diffr. evidence by off coincidence grain boundaries 77−47469
Pb, splat-cooled and vapour-deposited, metastable structs. 79−87018
Pb, supercond., T_c and residual resist., variation with coating thickness 78−47900
Pb, thermal strain depend. on thickness and grain size 79−90926
Pb, vapour deposited FCC, normal and oblique incidences, microstructure, X-ray diffr. study 80−20048
Pb-Ar films, atomic arrangements, high energy electron energy diffractogram study, Ar conc. depend. 79−99444
Pb-M, M=Bi, La, Sm, vacuum deposited supercond. films, T_c chem. comp. depend. *(Russian)* 78−19174
PbF_2, antireflection coating deposition technique, 2.87 μm laser damage threshold 80−33264
β-PbF_2 film between metal electrodes, vac. evaporated, AC study of elec. props. 80−2207
PbF_2, opt. spectra of vac. deposited coatings *(Russian)* 77−48264
β-PbF_2, thin films, cond. mechanisms, struct. 77−84970
$Pb_3Ge_2O_7$, vacuum condensates on US irrad. substrates, props. 77−66466
PbI_2:KI alloys, fundamental abs. edge, potential as solar convertor 80−101128
PbO, reactively evaporated, photocond., H_2O induced phase transform. 80−60122
PbS, film condensation on amorphous substrate, struct. and growth 78−38981
PbS islands, vacuum deposited, electron microscope obs. 80−103601
PbS, optical and phys. props. 80−2315
PbS, polycryst. and epitaxial, small-angle X-ray scatt. and electron density inhomogeneities 80−96758
PbS, vap. deposited film, island growth obs. by optical diffr. from electron micrograph 78−10291
PbS-Al coatings, absorptivity, emissivity, as function of PbS thickness 78−46731
PbS-PbO vacuum evaporated films, elec. cond. and photocond. 80−75656
$PbSnF_4$, anionic conductor, thin films and ceramics 80−107556
$Pb_{1-x}Sn_xSe$, film struct. and elec. props. 77−80708
$Pb_{1-x}Sn_xTe$ film, deposition, elec. and piezoresist. props. 78−6465
$Pb_{1-x}Sn_xTe$ heterojunction lasers, instantaneous vacuum evaporation grown, threshold current density 80−5759
PbTe film, residual conductivity 78−2595
PbTe films, thermal cond. and elec. props., 4.2 to 300K 79−28162
PbTe(Se) vacuum deposited thin films, struct. and growth 79−19482
$Pb(Zr,Ti)O_3$, thin film evaporated on stainless steel, photovoltaic effect 79−4580
$Pb(Zr,Ti)O_3$ thin layers, tan δ temp. dependence obs. *(Bulgarian)* 78−88259

vacuum deposited coatings continued
Pd, electron beam deposition and ion plating 77−44166
Pd, ethylene adsorption and reactivity with adsorbed H, surface pot. meas. 79−86995
Pd on Al_2O_3 substrate, controlled vapour growth of small particles 78−75958
Pd, on Si, ion-induced intermixing 80−15420
Pd particle arrays on C film, UPS, Pd valence band width 78−88403
Pd particles formed by evaporation on alkali halide crystals, orientation and struct. 78−84108
Pd, resistivity and thermoelec. power, annealing effects 80−39684
Pd-Ag, deposited on glass or Si substrate, X-ray microanalysis *(French)* 80−50902
Pd-Fe (1 wt.%), alloy component surface conc. changes kinetics under vac. sputtering and volatilisation *(Russian)* 79−60608
Pd-Se, thin layers, phase identification and struct., electron diffr. 77−51615
Pd-Si structure, epitaxial silicide growth, LEED and AES study 80−103590
PdGe, Pd_2Ge, growth kinetics and structure on Ge substrate 79−11514
$PdH_{0.65}$ film, thermoreflectance spectra 78−56463
PrB_6, prep. by electron beam evaporation, and optical and elec. props. 80−20793
Pt, electron beam deposition and ion plating 77−44166
Pt, ethylene adsorption and reactivity with adsorbed H, surface pot. meas. 79−86995
Pt evaporated film, optical props. meas. in VUV, 220 to 150 Å 80−45159
Pt film, growth on amorphous Si:H, AES and LEED study 80−88447
Pt, on Au, crit. thickness of pseudomorphic film growth, substrate size depend. *(Russian)* 80−29286
Pt, on Si, ion-induced intermixing 80−15420
Pt-Ni vacuum condensates on Si and SiO_2, thermally treated, X-ray anal. *(Russian)* 80−70559
PtSi film, on (001) Si, crystallography 78−75955
Re, phase comp. depend. on thickness, deposition rate and substrate temp. 77−31915
Re, supercond. T_c and residual resist., variation with coating thickness 78−47900
Sb, amorphous film on glass substrate, effect of substrate temp. on crystallisation 80−39468
Sb, evaporated, crystallite struct., texturisation 77−7991
Sb evaporated film crystallisation rel. to substrate temp., −50° to 170°C 78−47680
Sb film, elec. cond., and struct., thickness depend. 78−26974
Sb, film, microrelief, electron microscope obs., grain size and condensation rate 77−55469
Sb, film growth mechanism, action of residual gases rel. to deposition conditions 79−23850
Sb, splat-cooled and vapour-deposited, metastable structs. 79−87018
Sb-Au amorphous film, quench condensed, struct. and stability 79−99459
Sb-Au amorphous films quench-condensed, resistivity and Hall effect meas. 79−99638
Sb_2S_3, amorphous and crystalline thin films, optical consts. 79−91518
Sb_2S_3, amorphous layer, scattering of visible light, rel. to substrate temp. during deposition 79−65950
Sb_2S_3, vacuum deposited films, struct. and photoelec. props. 77−85092
Sb_2Se_3 film, struct. and photoelec. props 77−85257
Sb_2Te_3-Sb_2Se_3 thin layers, struct., phase comp., and elec. cond. 80−15389
Sc thin films, obtained in vac. of 10^{-5}-10^{-6} Torr, struct. and elec. resist. 80−107931
Se, amorphous, block formation during crystn., electron microscope obs. 79−11030
Se, amorphous, density meas., microcrystalline model of struct. 80−2313
Se, amorphous, localised states in band gap 80−59928
Se, amorphous, struct. and crystn., far IR transmission spectrum and DSC obs. 77−85106
Se, amorphous, vac. deposition on polymer substrates, use of temp. gradient vac. coating device 80−35099
Se, amorphous, vac. deposited on polymeric substrates, with dynamic coating device 80−100792
Se, amorphous electrophotographic layers, resolution parameters 80−31926
Se, amorphous evaporated layers, struct. inhomogeneities due to prep. technology fluctuations 77−76710
Se, amorphous film, crystn., thermal and photo-effects 77−47692
Se, amorphous film, highly disordered, UPS study 80−76148
Se amorphous films, structural relax., viscosity, creep, heat capacitors, and IR spectra meas. 79−42424
Se amorphous layer structure, influence of vacuum deposition conditions *(German)* 78−63957
Se, film, effect of thermal history and substrates or crystn. by vac. condensation 77−15713
Se film, vacuum deposited, struct. asymmetry, reflectivity elec. cond. 79−23855
Se film on brass, ESCA interface study 78−43269
Se, noncryst., controlled vapour deposition, crystn., and optical props. 78−39696
Se, thin film selective absorber coatings, prod. using an oblique vacuum deposition technique 80−81488
Se, vacuum evaporated film, photoinduced amorphous-crystalline transition obs. *(German)* 79−82156
Se-Bi-I, amorphous, high sensitivity visible-near IR photoconductor development and characterisation 78−39153
Se-Ni-Mylar multilayered struct., interfacial bonding effect on adhesion, ESCA obs. 79−95274
Si, amorphous, epitaxial regrowth, structure and impurities effect 80−84401
Si, amorphous evaporated, picosecond optoelectronic detect., sampling and correlation meas. 80−100478
Si amorphous film, annealing behaviour of void network 78−18551
Si, amorphous film, electron beam evaporated, freq.-depend. dielec. behaviour 79−99549
Si, amorphous film, in Ti-Si-Ti struct., elec. cond. processes and threshold switching 79−78207
Si, amorphous film, oxidised, vacuum deposited, cond. change due to electron irrad. 78−10089
Si amorphous film, vacuum deposited, microscopic voids, gas absorpt., crystn. study 80−49534

vacuum deposited coatings continued
Si, amorphous ultrahigh vacuum evaporated films, ESR obs., deposition effects 79−33534
Si, amorphous vacuum deposited p/undoped photodiode and diode-voltage variable resistor combination 80−61380
Si and Si:H amorphous films, porosity and oxidation of evap., sputtered and plasma-deposited films 80−10838
Si, covered with Al layer, solid-phase crystn. obs. 77−85100
Si, electron-beam-evaporated amorphous thin films, noise meas. 79−24091
Si epitaxial layers, vacuum deposited, conditions for impurity migration from B, P, Sb doped sources *(Russian)* 80−107570
Si film, amorphous, glow discharge deposited, for low cost solar cells 80−61355
Si film, polycryst., for photovoltaic appl., grain size effects 78−72034
Si films, elec. and struct. props. 79−1632
Si films, electron beam evaporated, for MIS solar cells 80−93490
Si films, electron-beam-deposited on W substrates, growth and struct., AES and SEM obs. 79−46972
Si homoepitaxy in high vac., stacking fault nucleation, crit. temp. for SiC growth 78−14620
Si on Al, interf. films deposited on diffr. gratings, for solar selective absorbers 79−14103
Si photoconducting films, amorphous, undoped, I-V characts. of vacuum deposited films 80−60049
Si, semicrystalline layer, deposited on stainless steel and Pyrex glass, growth conditions and props. 79−82482
Si solar cells, realisation by laser induced diffusion of deposited Sb 80−93998
Si, thin film, evaporated amorphous, hydrogenation by plasma treatment 78−91555
Si, ultra high vacuum epitaxy on Si substrates *(German)* 77−47702
Si vacuum deposited polycryst. films, p-n junctions investigation 77−28249
Si vacuum sublimated thin film structure impurity distrib. 78−95354
a-Si, vapour species rel. to amorphous film deposition 78−14641
Si:Ga(Al), MBE, growth, struct. and elec. props. 77−89458
Si:H, evaporated amorphous film, prep. elec. cond. and photocond. 79−38201
Si:H amorphous films for solar cells, optical and elec. props. of RF glow discharge deposited films 80−54576
Si:Li(Na)(K)(F)(Cl), amorphous, implantation effects on elec. props. 80−49716
Si:Sb vacuum deposited coating, p-n junction, pulsed electron beam annealing doping, diffusion 80−75480
Si-Pd film, preferred sputtering on surface, mass and bonding difference effects, AES obs. 79−87552
Si-Pd-Ti, silicide form. in evaporated films 80−80006
SiC, on Si and metal silicides, formation characteristics and mechanism, by ion backscattering techniques 79−60653
SiGe, ultra high vacuum epitaxy on Si substrates *(German)* 77−47702
$Si_{0.92}Ge_{0.08}$ film on Si, elastic strain, misfit dislocation density 77−85119
SiO, amorphous, density meas., microcrystalline model of struct. 80−2313
SiO amorphous thin films prepared by vac. evaporation, density meas. 77−80714
SiO, antireflection coatings for InP/CdS solar cells 78−50871
SiO, binding energies, XPS meas. 77−7989
SiO condensate distrib. from extended aspherising source 79−52118
SiO double deposition, homogeneous surface alignment of nematic liq. cryst., appl. to displays 79−4239
SiO evaporated film, dielec. function 8 to 33 μm, spectrophotometric and refl. meas. 80−80883
SiO, film, thickness influence on nematic MBBA orientation 80−59384
SiO film, vacuum evaporation on NaCl single cryst., IR absorption spectra 80−35098
SiO, obliquely evaporated, topography, effect on liq. cryst. orientation 78−38987
SiO, single-layer vac. antirefl. coatings for near IR spectral region 80−33099
SiO_2 as high temp. stabiliser for Ag films 78−1319
SiO_2, IR spectra and elec. props., influence of prep. conditions 79−87176
SiO_2, stoichiometric condensate form. during electron beam evaporation of quartz, electrophysical props. 77−16496
SiO_2, surface charge, effect of doping with P+B, differing vacuum deposition conditions *(French)* 77−85286
SiO_2 thin films, comparison of RI and IR spectra 80−11497
SiO_2, vacuum deposited, 7-10 μ, microhardness and structure 78−19669
SiO_x, in MIM sandwich, elec. props. 77−72933
SiO_x, phase comp., electron spectroscopy obs. 78−60042
SiO_x, powder and vac. deposited, amorphous struct., X-ray diffr. meas. 80−1931
SiO_x protected Al mirror, far UV refl., UV irrad. effect 79−7191
SiO_x-GaAs, vacuum evaporated system, acoustoelec. signal, interface props. 80−75646
SmB_6, prep. by electron beam evaporation, and optical and elec. props. 80−20793
$SmCo_5$, vacuum-deposited, eutectoid decomp. *(Russian)* 77−66621
SmS, metallic, transmission, refl. and absorpt. spectra 78−19587
Sm_2S_3 films, refl. and transmission spectra at 300K 80−80889
Sn film, effect of rate of deposition on supercond. props. and struct. 80−2954
Sn film, substrate and substrate temp. effects on struct. 80−107677
Sn film, vacuum deposited, reflectance spectra, structural rearrangement effects 77−24905
Sn film epitaxially grown on KCl substrate 79−99441
Sn, globular film, interf. and diffr., solar selective props. 79−4860
Sn globular film, solar selective props., effect of dielec. layer addition 79−4861
Sn on Au, ultrathin, quantum size effect *(French)* 77−20466
$Sn_{1-x}Ge_xTe$, evaporated thin films, characts. 79−60944
SnO_2, optical and elec. props., rel. to stoichiometric deviation and struct. 77−47701
SnO_2, transparent electrode deposition on PLZT ceramic, elec. and opt. props. 78−74848
SnO_2:Eu, RF cosputtering, cryst. site of Eu, cathodolum. obs. 77−7987
SnO_2:Sb film on glass substrates, elec. props. 80−88652
SnO_2-copper phthalocyanine-Ag systems, elec. and electroluminescent behaviour 80−80864

vacuum deposited coatings continued
SnO_2-Si solar cells, electron-beam deposited, struct., photovolt. props. 80−50956
SnTe, electro-reflectance meas. 80−11496
$(SnTe)_{1-x}(PbSe)_x$ films on glass-ceramics, struct. and elec. props. 77−52251
Sr, film struct., mass-thickness depend. 78−80040
Sr, oxidation, SXAPS 77−73189
Sr, structure effects on work function, electron micrographs and photoemission meas. 79−83107
Sr-Te-O system, amorphous thin film, vacuum deposited, elec. cond., current cut-off *(Japanese)* 77−24625
$SrCl_2$, non-cryst., very-low-freq. inelastic light scatt. 80−25367
$SrTeO_3$, ferroelec. vacuum condensates 77−40180
$SrTiO_3$, vacuum condensates on US irrad. substrates, props. 77−66466
T-metal, thin film contact, time evolution of photovoltaic effect 80−65687
Ta film, amorphous, UHV deposited, elec. and struct. props. obs. 78−6233
Ta film, vacuum-deposited, gas adsorpt. effects on photoelec. props. 78−15298
Ta films, H^+ and D^+ sputtering in energy range 0.6 to 15 keV 79−78808
Ta, optical const. var. with struct., ellipsometric meas. 77−63478
Ta, superconducting transition temp. rel. to struct. and deposition parameters 77−85377
Ta thin film, elec. cond., strain gauge factor, ion bombardment effects 80−80417
Ta-Co(Ni)(N)(Ar), amorphous metal films, struct. and elec. characterisation 79−87017
Ta-Ni alloy film, amorphous, UHV deposited, elec. and struct. props. obs. 78−6233
Tb, nucl. echo signals, cryst. anisotropy *(Russian)* 79−99790
Tb-Fe, undoped and O-doped, amorphous, microstruct. and mag. props. 79−91273
TbF_3 thin films, AC conduction obs. 80−70868
Te, amorphous, phonon-assisted hopping cond. 80−2392
Te coating of PbTe surfaces, struct. and junction characts. 80−50743
Te, crystallinity and electronic props., annealing effect 77−85107
Te, effects of electron irradiation on surface coverage *(Japanese)* 79−82477
Te evaporated film nucleation on Au oriented islands, grain growth 78−2388
Te film, surface morphology depend. on vacuum deposition angle 80−103553
Te, growth and morphology of crysts. 80−96766
Te, hexagonal film vac.-evaporated at normal incidence, X-ray Fourier line shape anal. 79−99454
Te, on NaCl, crystallite growth and morphology, electron microscopy 80−65401
Te, thermally evaporated, elec. cond., Hall voltage and thermoelec. power. 77−47913
Te, thin evaporated films, 130 Å, temp. depend. of elec. props. 79−95529
Te, thin film selective absorber coatings, prod. using an oblique vacuum deposition technique 80−81488
Ti alloy, VT3-1, vacuum-chromized, fretting-corrosion in couple with unprotected BT3-1 and steel 40KhNMA *(Russian)* 78−56804
Ti coated BN powder particles, X-ray investig. of thermal stresses generated in vac. deposition 77−40455
Ti, deposition on Si wafers, backscattering anal., of layer structure, silicide formation 79−69377
Ti diffusion coated cast Fe, wear resistance 79−52459
Ti, electrochem. oxidation, AES, XPS and electrochem. characterisation 78−7086
Ti, film, elec. resist. Hall effect and absolute differential thermoEMF *(Russian)* 79−24083
Ti, film, evap., CO effect on work function 78−39188
Ti, in $LiNbO_3$ substrate, planar optical waveguides construction *(Czech)* 79−41452
Ti, overlaid thin films, D pumping speed 78−33286
Ti, vacuum deposited, cryst. struct. and elec. props. 78−79908
Ti-Al alloy film, evaporated, anodisation characts. obs. *(Polish)* 80−55574
Ti-N_2, condensate formed by plasma flow precipitation in vacuum, cryst. and surface props. *(Russian)* 80−100788
TiB_2, TiB_2-ZrB_2, refractory compounds, direct evaporation deposition, struct. and props. 77−44392
TiB_2, TiC, vacuum condensate, struct. and mech. props., second phase effect *(Russian)* 80−71705
TiH_x film, kinetics of H_2 interaction 80−6620
TiN, low-energy ion-stimulated deposited, supercond. props. 80−88664
TiN, synthesis using enhanced reactive evaporation 80−2953
TiO_2, amorphous, struct. and crystn., TEM obs. 80−2291
TiO_2, destruction props. obs., suitability for integrated optics assessment *(Slovak)* 80−33224
TiO_2 layers, activated reactive evaporation and absorpt. indices 80−97363
TiO_2-SiO_2 multilayer vacuum coatings, optical props. 80−97361
TiO_2-SiO_2 reactive evaporation technique for multilayer coatings 77−10994
TiO_x deposition on Ti by reactive evaporation in O_2, optical consts. and heat resist. 79−65951
Tl film, Fuchs Sondheimer theory, size effect, elec. cond., Fermi surfaces 79−99637
TlI-PbF_2 graded-index film coating technique and results 80−33265
Tm_2O_3, electron beam deposition, elec. props., and struct. 79−87580
UO_2 film, vacuum evaporated, He^+ ion energy loss parameter 78−50253
V film, vac. evaporated, elec. props. 80−80414
V, superconducting vacuum-deposited film, electrophys. props. *(Russian)* 77−59345
V-M, M=Ti, Nb, Sm, vacuum deposited supercond. films, T_c chem. comp. depend. *(Russian)* 78−19174
V_2O_5 amorphous film, photochromism and thermochromism 80−93254
V_3Si-SiO_x-Mo_3Re_2, supercond. tunnel junctions 80−107961
W film, silicide formation during growth by electron beam evaporation *(German)* 78−84717
W, on Mo, strengthening effect *(Russian)* 77−66714
W, produced by carbonyl method, struct. *(Russian)* 77−43441
W-Cu(N) amorphous metal films, struct. and elec. characterisation 79−87017

vacuum deposited coatings continued
WO_3, amorphous, density meas., microcrystalline model of struct. 80−2313
WO_3, amorphous, struct. and crystn., TEM obs. 80−2291
WO_3 electrodes, electrochromic processes, digital simulation model 80−76518
WO_3 film, amorphous, struct. and crystn., TEM obs. 80−103606
WO_3 film, evaporated, electrochromism *(Japanese)* 79−38686
WO_3 film, evaporated, mech. of elec. cond. 80−44747
WO_3 films, electron struct. changes during electrocoloration, XPS obs. 80−40217
WO_3, optical absorpt. after ion irrad., appl. to ion beam profile monitoring 79−26181
WO_3 thin film, Li diffusion, appl. of AC techniques 80−70468
WO_3-MoO_3, film, evaporated, electrochromism *(Japanese)* 79−38686
W_2O_{5-x} current noise due to adsorption of water 78−6421
WS_2 films, exciton peaks in absorpt. spectra, press. and temp. depend. 79−51496
Xe, HCP, vap. phase grown thin films 78−18917
Y, prepared in ultrahigh vac., optical meas. 6 to 14 eV 79−78767
Y_2O5d3 films, preparation, electrophys. props. in metal-oxide-metal structs. 77−24956
Yb_2O_3 film, amorphous, electron beam deposited, dielec. props. 79−91339
Yb_2O_3 thin film on Cr substrate, refr. index depend. on thin film thickness 80−108290
Zn film, hexagonal struct., vacuum deposited, X-ray peak shift anal. 79−65335
Zn film, vac. deposited, X-ray diffr. study of microstruct. 78−26796
Zn, film, vac. deposited, X-ray diffr. study of microstruct. 78−75966
Zn, film growth on C, conductance meas. 79−82495
$Zn_xCd_{1-x}S/Cu_2S$ heterojunction solar cells, fabrication and performance 79−79397
$Zn_xCd_{1-x}S/Cu_2S$ heterojunction solar cells, junction anal. 79−92080
ZnF_2:Mn, thin films, electroluminescence, brightness voltage characts. hysteresis 80−20709
$ZnIn_2S_4$ (I), one-packed polytype, resist., photocond. and luminesc. 79−1608
ZnS, destruction props. obs., suitability for integrated optics assessment *(Slovak)* 80−33224
ZnS, effect of temp. var. on light transmission 78−79136
ZnS evaporated film, refl. loss on UV irrad., ZnO form. 80−99813
ZnS evaporated film optical props. 160 to 2000 A 79−15544
ZnS film, defect form. and development 80−96759
ZnS, film, vac. deposition onto NaCl cryst. in H_2S environment 78−63945
ZnS films prepared by thermal evaporation in vac., nature of defects 80−10835
ZnS, origin of mech. stress 79−90925
ZnS, ultra-microhardness testing for vacuum deposited film and bulk specimen 78−79910
ZnS, vacuum-evaporated conducting films, prep. and props. 79−66007
ZnS, ZnS-CeF_3, single-layer vac. antirefl. coatings for near IR spectral region 80−33099
ZnS:Ag, IR quenching of photocapacitance, deep levels obs. 78−56180
ZnS:Cu_3 Cl, Mn film, AC electrolum. 80−60680
ZnS:Tb^{3+}, NdF_3 film, electrolum. energy transfer 80−2861
ZnS-Ag, broad band visible heat reflecting mirror 77−39017
ZnS-MgF_2 alloy films, struct. and optical props. 79−90910
ZnS-MgF_2 mixtures, triple-layer broad band antireflection coatings 79−32011
ZnS-MgF_2/MgF_2, homogeneous mixed dielecs. as antirefl. coatings effective at two visible wavelengths 79−76770
ZnS-MgF_2/MgF_2 double-layer antireflection coatings, transmittance meas. 79−36967
ZnSe, high conductivity films appl. to p.n. heterojunctions 78−68100
ZnSe, IR laser window coating absorption rel. to deposition conditions 79−14061
$ZnSiP_2$-Au(Ni) Schottky contact, production and props. 79−7901
ZnTe film preparation and props. using single-source method *(Japanese)* 80−6664
ZnTe films, grown on glass using atomic layer evaporation 80−44453
Zr-N_2, condensate formed by plasma flow precipitation in vacuum, cryst. and surface props. *(Russian)* 80−100788
ZrB_2, refractory compounds, direct evaporation deposition, struct. and props. 77−44392
ZrC, ZrC-ZrB_2, refractory compounds, direct evaporation deposition, struct. and props. 77−44392
ZrO_2 film, electron beam deposition, refr. index and microporosity 78−90467
ZrO_2 thin film, optical props. rel. to cryst. struct. 80−97357
ZrO_2, ZrB_2, vacuum condensate, struct. and mech. props., second phase effect *(Russian)* 80−71705
ZrO_2-SiO_2, protective antirefl. coatings, electron beam evaporation on glass 77−31143

vacuum deposited thin films *see vacuum deposited coatings*

vacuum deposition
used for EVAPORATED layer production in vacuum
see also electron beam deposition
actinide target prep. for synthesis of transactinide elements 80−23206
alloy, vacuum coating deposition by vaporisation *(Russian)* 79−74093
alloy deposition processes, rate controlling and composition analysis by electron impact emission spectroscopy 77−44165
alloy film, monitoring and controlling techniques, review 78−11113
alloy film, rate controlled deposition using electron impact emission spectroscopy based instrument *(German)* 80−89152
American Vacuum Society National Symposium, Boston, USA (Nov 1977) 78−72718
amorphous film formation by vacuum deposition review *(Japanese)* 77−66590
annular wedge-shaped layer coatings, apparatus for prod. 77−14817
aspherising layer prod., monitoring by interf. fringes in periscopic microscope 77−14820
automatic high vacuum coater, automatic, using minicomputer or microprocessor, IC semiconductor industry appl. 78−48317
automation and programming of production plants *(Hungarian)* 77−4736
binary alloys, kinetic nucleation model 77−85118
borosilicate glass intermediate layer, stable structure formation 80−80979

vacuum deposition continued
brass, vacuum coating deposition by vaporisation *(Russian)* 79−74093
brass coating 77−59693
chalcogenide glass, prep. by laser evaporation, and characterisation 77−12533
closed field sputtering equipment 80−50556
coevaporation technique for basic and applied research 78−72735
cold light mirror multilayer coating deposition 80−87464
cold light production by high vacuum deposition of multilayer interference coatings *(German)* 80−53486
compact system, design, construction and operation 77−90275
condensate removal system, for vac. metallisation chamber 79−58752
condensation of nuclei, stabilisation of sizes 79−8248
conference, New York, USA (Oct. 79) 80−73093
constant-thickness film formation on axially symmetrical substrate 79−27453
cryogenic thin film ultrahigh-vaccum evaporation/sputtering apparatus 80−20790
cryopumping panel, liquid He cooled, appl. in vacuum deposition system 78−56581
crystal resonator electrode deposition from nozzle beam type metal vapour source 77−40376
cyclohexane, monolayers and thin crystals grown on Pt (111), LEED obs. 77−59230
DC glow discharge techniques for surface treatment and coating 78−11374
deposition on glass surface heated between room temp. and 300°C 77−90277
device for cleaving rocksalt for clean surface prep. 77−13738
device for simultaneous condensation on many substrates, temp. depends. determ. *(Russian)* 77−32524
di-butyl-sebacate, HV evaporation, mass transfer in evaporating space *(Japanese)* 80−50558
discrete-pulse evaporation, films of substances with complicated composition production 80−50557
double-layer antireflection coatings for plastic lenses, evaporation coating process 80−14491
electric arc deposition of coatings using extracted ion precipitation unit 80−35106
electric-arc metal vaporizer with cathode spot magnetic confinement 77−77383
electron beam gun with multi-crucible for evaporation in ultra high vac. 78−27404
epitaxial growth process at UHV, electron microscope study 78−55790
epitaxy, fine struct. formation *(French)* 78−43275
equipment cleaning, practical procedures 80−57318
euglenoid flagellates, sputter and vacuum evap. coating, comparative effects on delicate features 78−24205
evaporation, ion enhanced film bonding 79−95931
evaporation rate monitor with quartz sensor 79−28921
evaporation source, molecular emission pattern meas. *(French)* 77−70000
evaporation source, molecular spatial and vel. distrib. *(French)* 77−69999
evaporator, large-capacity, with filtering element, for SiO film prod. 77−14819
field emission deposition sources 79−83127
film, thickness uniformity on rot. spherical substrate on planar wave holder 79−65351
film formation by ionised-cluster beam deposition 79−33934
film thickness monitor, quartz crystal, based on SAW oscillator 78−3036
film thickness monitor 77−36401
films, deposition profile with shadow effect, theoretical model 79−82473
films and coatings using conc. energy sources *(Russian)* 79−74090
fissured biological object prep. for SEM, vacuum deposition and cathode sputtering comparison 80−72390
fluoride layer, nematic liquid crystal tilt control by vacuum deposition alignment 79−10797
Fluorolon-3, utilisation factor determ. during electron beam sputtering *(Russian)* 79−66008
freeze etching and related techniques, resist. monitor for automatic film thickness regulation 78−49810
frozen hydrated tissue section prep. for X-ray microanalysis using satellite vacuum coating and transfer system 78−24200
gas exchange in closed volume during vapour condensation, residual gss density change 77−59692
graded-thickness film, optical filter appl. 80−76164
high rate film growth, book contrib. 78−11117
high temp. materials conf., Reutte, Austria, (May 1977) 79−57124
high vacuum evaporation system with low-temperature substrate for superconducting meas. 78−84716
HV, mass transfer in evaporating space *(Japanese)* 80−50558
II-VI semiconductor film technology 78−23621
inorganic thin layers, two-stage formation 79−27450
interference coating deposition by Balzers BA-710 vac. system, photometric monitoring 78−46850
interference coating production, new ideas 79−32098
interference coatings on projector reflectors, vac. deposition 77−75725
ion assisted deposition, review *(Japanese)* 77−73227
ion beam sputtering 77−55887
ion beam utilisation for etching and film deposition, review 77−32522
ion plating industrialisation, appl. of induction heating 77−8764
ion-enhanced film bonding 79−83126
IR multilayer interference filter manufacture, supposed longwave limit 80−9989
isotope target preparation by laser beam evaporation techniques 80−18735
Josephson microbridges, submicron, fabrication using optical projection lithography and liftoff techniques 79−28458
laser deposition of metal, semicond. and oxide films, using periodically pulsed CO_2 laser 79−28926
laser evaporation of chem. element films with Nd:glass laser 79−47633
laser fusion targets, vapour deposited coatings, surface finish obs. 78−60863
using low pressure plasmas 77−40361
margaric acid, evaporated film, X-ray diffr. anal. and mass-spectrography 77−15718
masks, using rib-supported structures, solving stencil problem 78−23615
mass spectroscopic measurements, validity for pressures exceeding 10^{-4} mbar 79−85198

vacuum deposition continued
materials for evaporation, review 77−24957
metal, heating of polymer substrate surface during deposition 78−48319
metal, surface properties improvements, using vacuum thermal process techniques 79−100283
metal coating of optical fibres, for strengthening and surface protection 78−30103
metal dispersion in vac., thickness, X-ray fluoresc. meas. method, appls. *(Russian)* 78−56582
metal on Schottky barrier solar cell, optimum thickness indicator 78−21120
metal-GaAs junctions, thermal stability improvement, using transition and near noble metals 79−7143
metallic substrate, temp. meas. during evap. 77−69997
metallic substrates, enhanced vacuum deposition by pretreatment with plasmatron discharge 78−76604
metallic thin film, early stage obs. using microbalance technique and electron microscopy *(Japanese)* 80−54554
metallic thin films, pressure operated shutter for thickness control and monitoring 79−15607
metallic thin films, vacuum deposition, ultra-high vac. technique 80−100791
metallurgical coatings, vapour deposition processes in vac. 80−35430
microelectronics and thin film components frontiers 80−73123
multicomponent alloy films, struct. form. laws and elec. prop. changes obs. during vacuum condensation 78−6850
multidielectric film, optical control by method of static ratios *(French)* 77−69993
multilayer cotaings, reactive evaporation technique for TiO_2 and SiO_2 films 77−10994
multistage sluice-gate loading devices 78−60576
nucleation rate in vacuum condensation in presence of inhomogeneously distributed adsorbed atoms 77−15722
ohmic contacts, sputter-etch plus evaporated film technique for contacts to Si devices 78−23165
opaque metal coatings on plastic scintillator 78−3049
optical coatings, improved film quality, progress in vacuum generation and deposition technology 80−35101
optical component rotation in vac. system, using linear asynchronous motor drive system 80−102874
optical film deposition, thickness monitoring with optical time-domain reflectometer 79−55254
optical films, dissoc. and recomb., packing density 77−752
optical filter fabrication, reducing variation in transmission band location 77−14816
optical multilayer interference filter production for CO_2 ν_2 band 77−10998
optical thin film coating manufacture, automated deposition control system, design principles 80−64220
organic thin film prep. methods in ultrahigh vacuum *(Japanese)* 80−84851
palmitic acid, evaporated film, X-ray diffr. anal. and mass-spectrography 77−15718
n-paraffins, monolayers and thin crystals grown on Pt (111), LEED obs. 77−59230
phase transition dynamics, investigating device 78−22967
plasma flow condensation with ionic bombardment *(Russian)* 79−61517
polyethylene stretched, film, effects of vapour phase application of compounds 77−90276
polyimide thin film vacuum deposition 78−39695
polymer thin film deposition device 77−77384
polypropylene, low mol. wt., vapour phase epitaxial growth 78−67924
quartz crystal thickness sensor isotope target preparation 80−17923
quartz film thickness monitors, effect of accumulated film layers on accuracy 78−72734
rare earth films, prep., struct., and props., general review 80−54556
rare earth metal oxide dielectrics using electron beam, capacitor, characts. and design considerations *(Russian)* 77−1638
rare earth metal refining *(Russian)* 77−59687
Re-sputtering and implanting sputtered atoms during deposition 80−16137
refractory metal expitaxial layers *(Russian)* 77−59227
relative supersaturation, formula valid for different technological conditions *(Russian)* 78−84081
resistively heated box sources, heavy duty vacuum leadthrough 79−40584
saturation density of nuclei, substrate temp. depend. 78−18932
SEM specimen preparation thin film coating techniques 80−68308
semiconductor thin film deposition *(Polish)* 79−47630
semiconductor thin films, methods *(Polish)* 79−56932
shell, deposited in vacuum, elastic characts. meas. by short time static extension *(Russian)* 78−39961
shutter for multiple-position planetary workholder 77−81221
solar cells manufacture, Si or Si/Cu_xS, w.r.t. optimum yield, Baude process appl. *(French)* 79−96448
solar furnace application for thin film production 80−89148
specific thickness profiles 78−95697
strip source, onto arbitrarily oriented rotating cylinder 78−95696
substrate and film surface temp. meas. 80−57297
substrate bending during thin film evaporation due to temp. difference between substrate faces 80−54571
substrate heating by special lamp 78−59164
substrate heating in vac., heating method rel. to spectral characts. 77−7223
substrate temp. meas. by laser beam 80−20794
surface vaporisation under conc. energy sources, thermal model development *(Russian)* 79−74091
targets manufacture, Al_2O_3, by powder metallurgy *(German)* 80−11586
technology, conf., Uppsala, Sweden (Aug-Sept. 1976) 77−90270
Teflon-4, utilisation factor determ. during electron beam sputtering *(Russian)* 79−66008
thickness monitor using freq. demodulation technique 79−67249
thin film composition gradient production 80−55295
thin film prep. for solar energy utilisation 80−84847
thin film thickness monitor shutter 78−56583
thin films, deposition techniques, review 80−80964
thin films thermal evaporation industrial techniques for obtaining uniform thickness *(Polish)* 78−84710
tube source for deposition of extremely uniform thin films 77−90278
tubular-type evaporator, radiation-heated, ZnS film deposition 80−76191
ultra high vacuum technology developments *(Japanese)* 78−49845

vacuum deposition continued
ultra-high vacuum system for thin film and surface preparation and anal. 79−69986
ultrapure materials preparation, in orbiting ultrahigh vac. facility 78−7855
ultrathin metal film, evaporation cryostat for elec. and optical meas. under ultrahigh vac. 77−87769
V-VI-VII ferroelectric semiconductor film growth, effect of artificial nucleation centres 79−11032
vacuum deposited film, as first wall material, sputtering yield mea. *(Japanese)* 80−25513
vapour sources for thin film evaporation technique *(Polish)* 78−56580
waveguides construction, optical, diffusion of Ti in $LiNbO_3$ substrate *(Czech)* 79−41452
Ag, condensation on glass, temp. depends. *(Russian)* 77−32524
Ag, condensation on glass, temp. depend. *(Russian)* 77−32525
Ag, film, condensate obtained in electric field, anisotropy of elec. props. 80−44743
Ag film, vacuum deposited onto SiO, C and mica, quantitative study of nucleation 79−77959
Ag film, vacuum deposition on Pb (111), substrate diffusion effects, RHEED, LEED, AES 80−65410
Ag film growth on Si (111), nucleation and growth modes, SEM study 80−100423
Ag film vacuum deposition and ion plating, effects on surface topography 79−82427
Ag, fine particles prep. by vacuum evap. onto running oil substrate 79−28925
Ag, on AgBr evaporated layers, vacuum deposition at room temp. 79−20409
Ag, on evaporated AgBr layers, growth mechanism 80−35095
Ag, vac. deposited films, surface pot. and work function rel. to thickness 79−42672
Ag, vacuum deposited on Al substrate, recrystallisation 78−60044
Ag-Au, nucleation and growth on substrates 79−77956
Ag_2S film, oriented growth by vacuum evaporation 77−21028
Ag_2S film, vacuum deposition and struct. 77−73233
Ag_3SbS_3 film prep. 77−52250
Al alloys, optical contrast enhancement by vacuum deposited ZnTe layers 78−44301
Al and other metals, improved evaporation filament/strip source 77−85941
Al, condensate, effect of growth conditions on critical thickness 79−69985
Al, film, condensate obtained in electric field, anisotropy of elec. props. 80−44743
Al film, condensed and fused, on Ge, press. and residual gas comp. influence on struct. 77−16497
Al film, deposition on grooves of grating-polariser for IR spectral region, optimisation 79−55221
Al filters, for use on Apollo Telescope Mount XUV spectrograph fabrication 77−60602
Al, on Si, effect of vacuum ambience on Al-Si contacts 77−43718
Al thin films, vacuum deposited, crystal growth in presence of O_2 and Ni 80−15409
Al, vacuum evaporation appl. of TiB_2-TiC and TiB_2-BN for crucibles 79−74094
Al/GaAlAs, film, epitaxial growth on (100) GaAs by hot vac. deposition and characterisation 79−56085
Al-Cu, evaporation, successive dilution method for reproducible control 77−69994
Al-Zn thin film, prep. using Sn-Zn evaporant source 80−100789
Al_2O_3 film growth on MBE GaAs 78−39706
As-Ge-Se system, synthesis and phys. props. of amorphous layers 77−52252
As_2S_3 thin films, vacuum deposited on Ge and PbS, sealing props. and TEM 80−35097
As_2Se_3, vacuum evaporation, composition of condensates 78−44012
Au clusters, coalescence on NaCl substrates at room temp. 78−18935
Au, condensation kinetics on KCl substrate, evolution of size distrib. function 79−28243
Au, condensation on Si (111), AES obs. of very first stages 78−14633
Au, crystallite, surface decoration, depletion zone anal. along KCl slip step 79−90868
Au film, deposition on polymer substrates, effects of glow discharge on nucleation characts. 79−77963
Au film, early growth stages on amorphous C, cluster migration obs. 79−77964
Au film, integrated condensation coeff. on NaCl cleavage faces, Rutherford ion backscatt. obs. 80−59827
Au film growth on Mo (110) surface, AES, LEED, thermal desorption study 80−80130
Au films, vac. condensed at oblique vapour incidence, oriented cryst. growth, electron diffr. study 80−97432
Au island film, on NaCl cleaved surface, growth, effect of perp. elec. field *(German)* 77−76697
Au island film, on SiO_x, growth and struct., effect of perp. elec. field *(German)* 77−76696
Au, nucleation on NaCl from new vapour source, temporal and electron micrograph obs. 79−77954
Au, nuclei on KCl, collective behaviour, monatomic step influence 77−15719
Au, on mica, saturation density of nuclei 78−18932
Au, vac. deposited films, surface pot. and work function rel. to thickness 79−42672
Au, vac. deposited thin film, Auger spectroscopy 80−2952
Au vacuum condensation on KCl, spatial distribution of nuclei 78−18931
Au, vacuum deposition, on (100) surfaces of KBr, KCl and NaCl substrates with colloidal centres *(Rumanian)* 78−60579
Au, vacuum evaporated particle coalescence behaviour on doped alkali halides 79−77961
Au-Ag, deposition on alkali halide, kinetic nucleation model 77−85118
Au-$Cd_xHg_{1-x}Te$(CdTe) contacts, photo-effect in the 77-300K range, barrier height estimation 80−107850
Au-GaAs, film-substrate interface alloying behaviour, electron microscopic study 79−60652
B, electron beam deposition, rotatable support for ulta high vacuum system 79−40586
B films, amorphous, prep., struct., props., review, book contrib. 78−48321
vacuum deposition continued
B, prep. by vacuum decomposition of purified BI_3, purity 79−91589
^{10}B self supporting target preparation up to 500 $\mu g/cm^2$ 80−18745
^{11}B self supporting target preparation up to 500 $\mu g/cm^2$ 80−18745
Ba film, supercond. A1-type quench-condensed, prep. and crit. temp. 77−69443
$BaTiO_3$, film deposition by HF cathode sputtering 77−36398
Be, ultra-thin fabrication 79−33933
Bi, amorphous, microbridge prep. and transition from superconducting to normal state 78−34933
Bi film deposition by vacuum evaporation on $NaNO_3$ single cryst. cleavage 80−35091
BiOCl, crystalline, growth 77−40364
$Bi_2TE_{3-x}Se_x$, solid solution films, prep. and props. 78−44013
C, effects of Ni substrate surface on deposition 77−28721
C thin layers, thickness determ. by objective colorimetry 78−77844
Ca, nuclear target preparation 80−23224
Cd films, nucleation and growth, props. 80−29878
Cd, thin film, vac.-deposited, X-ray diffr. struct. obs., props. 79−37937
Cd-Sb thin film prep. by vacuum deposition, elec. props. 78−92194
$CdCr_2Se_4$ film, ferromag. semicond., prep. by vacuum condensation 77−28724
$Cd_xHg_{1-x}Te$ film, vacuum deposited, struct. and elec. props. 77−59344
CdS film, double-layered polycrystalline on $LiNbO_3$ substrate, fabrication and props., rel. to SAW appl. 78−64480
CdS film, high cond., high transmittance, growth by evaporation method, and characterisation 77−77386
CdS, thin films, deposition onto hot substances, vapour phase method 78−95694
CdS, vacuum epitaxial growth on $CuInSe_2$ 78−92193
CdS-PbTe and CdS-Te heterojunctions, electron irrad. effect on electrophys. props., prep. conditions depend. 79−28421
CdS(Se), electron irrad. effect on electrophys. props., prep. conditions depend. 79−28421
CdS_xSe_{1-x} photosensitive films, prep., props., and use for photodetectors 80−55298
CdS(Se)(Te), evap. onto electron bombarded NaCl substrates, epitaxial growth and characts. 79−28948
CdSe film, resistivity rel. to vapour deposition parameters 77−12033
CdSe, film, vacuum condensation thermodynamics, starting powder comp. effects 77−81220
$CdSe_xTe_{1-x}$ film, polycrystalline, deposition and physical props. 77−4741
CdTe film formation on glass substrates, influence of sublayers of recrystn. stimulators 77−43455
n-CdTe layers, growth and characterisation, heterojunctions and Schottky barriers fabrication *(German)* 80−89151
CdTe-Te film, prep. by combined hot-wall-flash evaporation method, and characterisation 80−55296
Ce film, supercond. A1-type quench-condensed, prep. and crit. temp. 77−69443
Co ferrite film prep. by vac. evaporation and annealing 77−85939
Co, ultrafine particles prepared by vacuum evap. on running oil substrate, mag. behaviour 79−28565
CoO, evaporation curve struct. from AC arc electrodes *(Russian)* 78−3051
Cr, film, vac. deposition onto low temp. substrate, cryostat *(Japanese)* 78−27403
Cr film, with A-15 struct., prep. and characterisation 77−62768
Cr film vacuum deposition on glass display panels 78−39694
Cr films, props. prep. and appls., expt. *(Hungarian)* 77−4737
Cr, films, vac. deposited, defects *(Russian)* 79−33203
Cr source material, particle press. anal. 78−72731
Cr-Si coatings, for resistor manufacture, residual gas atmosphere analysis *(German)* 80−6681
Cr-SiO cermet film, silicide form. during deposition 77−12535
$CrSi_2$ formation on Pd_2Si and PtSi, radioactive Si tracer obs. 78−60578
Cs film, supercond. A1-type quench-condensed, prep. and crit. temp. 77−69443
Cu film, vacuum deposition on Pb (111), substrate diffusion effects, RHEED, LEED, AES 80−65410
Cu, film growth on graphite and amorphous C, electronic struct. by photoemission and Auger obs. 79−77947
Cu films, vac. condensed at oblique vapour incidence, oriented cryst. growth, electron diffr. study 80−97432
Cu, vac. deposited thin film, Auger spectroscopy 80−2952
Cu vacuum condensate on PET film 77−77385
Cu, vacuum deposited on Al substrate, recrystallisation 78−60044
Cu-Be, condensation *(Russian)* 78−44014
Cu-Mn-Ni, thin film, vacuum deposited, struct., elec. cond. *(Russian)* 78−19668
Cu-Zr, vapour quenching prod. (thermal evaporation and r.f. sputtering), amorphous film for electron microscopy 78−6851
Cu+Fe+Cd, nuclear target preparation by evaporation and rolling 80−23224
Cu+Fe+Sn, nuclear target preparation by evaporation and rolling 80−23224
p-$CuInSe_2$ film, prep. from vac. evaporation of $CuInSe_2$, optical and elec. props. 79−82697
$CuInTe_2$, vac. deposited film, growth, struct. and elec. characts. 77−69995
$Cu_{1.8}S$ film, vacuum evaporated, props. rel. to elec. cond. 77−36001
Cu_2S films, prpe. methods, appl. to Cu_2S-CdS solar cells 80−80980
Cu_2S-CdS solar cell, fabrication using solid state reaction 77−16498
Cu_2S-CdS solar cells, fabrication by evaporation technique with solid state reaction 79−74515
$Cu_{2-x}S$ on CdS, low temp. growth, AES obs. 79−28924
Cu_xS evaporated thin films, composition, prep. and characts. 80−25569
Cu_xS/CdS, sequential evaporation, for solar cell applic. 80−93902
Cu_xS-CdS solar cell improvement by Cu treatment and front contacting 79−61987
Dy, appl. of deposition system using liq. He cooled cryopumping panel 78−56581
$ErD_{2-x}T_x$ films, on Cr underlays on Cu substrates, vacuum deposition conditions for optimum hydriding 79−78891
Fe, ultrafine particles prepared by vacuum evap. on running oil substrate, mag. behaviour 79−28565
FeF_3 thin film prep. and charact. *(French)* 78−64470
FeO-Fe_2O_3, evaporation curve struct. from AC arc electrodes *(Russian)* 78−3051

vacuum deposition continued
FeSb alloy films, vapour-deposited, formation of metastable phase 80−44437
Gd, appl. of deposition system using liq. He cooled cryopumping panel 78−56581
Gd-Co film, amorphous, for bubble device appl., prep. and perpendicular anisotropy 77−69641
Ge amorphous evaporated film, to metal contact resist. diffusion and microstruct. 77−89880
Ge, epitaxial growth of very thin electron microscopy specimens 80−100793
Ge film, amorphous, vac. deposited, XPS and elec. props., evidence for polycryst. phase 77−28691
Ge, film, vac. deposition onto low temp. substrate, cryostat *(Japanese)* 78−27403
Ge, thin single crystal, (110) orientation, preparation technique 79−95930
Ge-As-Se, amorphous film, condensation formation and struct. props. *(Russian)* 78−38629
Ge_2Se_3, vitreous, evaporation kinetics and amorphous film deposition 80−97434
GeTe, high temp. mass spectrometric obs. of vaporis. 77−76542
$Ge_{15}Te_{81}X_4$ amorphous semicond. switches, fabrication technology *(German)* 80−7493
HgTe thin film Hall sensor fabrication 80−2951
In, epitaxial growth and desorption on W tips, high field microscopy obs. 79−69380
In, film, vac. deposited, influence of ion bombardment during condensation 79−82483
In-$Cd_xHg_{1-x}Te$(CdTe) contacts, photo-effect in the 77-300K range, barrier height estimation 80−107850
In-S system, vac. deposited films, form., reacts. 78−43259
InAs, thin film prep. and elec. props. 79−1633
In_2O_3 transparent conductive coating production 80−35092
InSb, evaporation kinetics, rel. to film growth 78−3050
InSb film, prep. by rotary type flash method *(Japanese)* 77−40372
InSb film, synthesis by 2-source mol. beam technique and AES characterisation 78−72729
InSb-SiO-Al MIS structure, prep. and characts. *(Italian)* 78−84715
La film, supercond. A1-type quench-condensed, prep. and crit. temp. 77−69443
Li, nuclear target preparation 80−23224
Li_3N thin film, vacuum evaporation on WO_3, retarded deposition 80−108351
MgF_2-ZnS multilayers, high vacuum deposition for cold light mirror prod. *(German)* 80−53486
Mn film, variation of elec. resist. with deposition conditions 77−43746
Mn film, variation of resist. with deposition rate 77−43747
Mn-Bi film, amorphous, form. and crystn. 79−28923
Mn-MgF, cermet film, evaporated, variation of elec. resist. with prep. conditions 77−43746
Mn-SiO cermet film, silicide form. during deposition 77−12535
$Mn_{2-x}Cr_xSb$ film, prep. and mag. props. 78−48009
Mo, arc, steady, vac., plasma ion mass and energy diagnostics 78−51385
Mo, arc, vac., stabilised, plasma props. 78−51384
Mo film, epitaxial growth on cooled W tips at 78K, struct. obs. 77−28723
Mo, in-situ coating, vacuum deposition on, Hastelloy-X substrate 79−3237
Mo, on sapphire, epitaxial layer production by electron beam deposition in vacuum *(Russian)* 77−59228
Nb Josephson junctions, submicron, fabrication by evaporation 79−28920
Nb-Ge film, coevaporated, supercond. critical temp. and struct. 77−28275
Nb-Ge film, supercond. transition temp., rel. to prep. conditions 77−36009
Nb-Nb Josephson junctions, submicron, thermally recyclable, fabrication and characts. 80−100566
Nb_3Ge film, sputtered and evaporated, transition temp., critical field and current anisotropy 77−28328
Ni, film growth on graphite and amorphous C, electronic struct. by photoemission and Auger obs. 79−77947
Ni films, props. prep. and appls., expt. *(Hungarian)* 77−4737
Ni, fine particles, prep. by vacuum evaporation, crystal habits 78−88437
Ni foil, crystal struct. as function of substrate temp. during deposition 80−18742
Ni, ultrafine particles prepared by vacuum evap. on running oil substrate, mag. behaviour 79−28565
Ni-Cr film, vac. deposition, elec. props. and comp. struct. 79−77966
Ni-Cr thin-film resistors, props. prep. and appls., expt. *(Hungarian)* 77−4737
NiCr thin film resistor, 'clean vacuum' deposition equipment suitability obs. *(Polish)* 79−15611
NiO, evaporation curve struct. from AC arc electrodes *(Russian)* 78−3051
P, nuclear thin red target preparation 78−46196
Pb, atomic beam impinging on mica and SiO in vac. deposition, thermal accommodation 79−77960
Pb film, vacuum deposited onto SiO, C and mica, quantitative study of nucleation 79−77959
PbO thin films, elec. props. *(Korean)* 79−60943
PbSe films, synthesis characts. 80−35094
PbSe, vacuum evaporation, composition of condensates 78−44012
$Pb_{0.8}Sn_{0.2}Te$ film, growth in quasi-closed space, single and polycryst. 79−33930
$Pb_{1-x}Sn_xTe$, epitaxial growth on $LiNbO_3$, electron diffr. and microscopy exam. 77−1331
$Pb_{1-x}Sn_xTe$, large single crystal growth, on quartz surface, non-seeded 78−48293
PbTe films grown from vapour, optimum conditions and elec. characts. 79−52117
PbTe, thick epitaxial film, laser deposition technique 78−68629
PbTe-ZrO_2 (SiO_2), epitaxial MIS struct., fabrication and elec. props. 80−2472
Pd, film growth on graphite and amorphous C, electronic struct. by photoemission and Auger obs. 79−77947
Pd-Ag (Cu) alloys, epitaxial growth and surface characterisation 78−14638
Pd_2Ge, PdGe, growth kinetics on single cryst. and evaporated Ge 78−22985
vacuum deposition continued
Pt foil, crystal struct. as function of substrate temp. during deposition 80−18742
Re epitaxial film growth on sapphire *(Russian)* 78−35311
Rh film, evaporation onto single crystal Ag films and mica cleavages 77−40375
Se, amorphous, vac. deposition on polymer substrates, use of temp. gradient vac. coating device 80−35099
Se, evaporation kinetics from temp. programmed large area source 77−69996
Se film, noncryst., controlled vapour deposition, crystn., and optical props. 78−39696
Se layer in metal crucible, radiation emissive power theory 78−22874
Se-As alloy film, thickness, substrate temp. effects 79−15610
Se-Bi-I, amorphous, high sensitivity visible-near IR photoconductor development and characterisation 78−39153
SeS gas, thermodynamic props., quadrupole mass filter study 80−16716
Si, combined with Sb ion implantation *(Japanese)* 78−88428
Si, combined with Sb ion implantation technique *(Japanese)* 79−28005
Si epitaxial layers, grown by sublimation in vacuum, TEM study of surface 79−46982
Si, solid-state epitaxial growth of amorphous layer 80−10803
Si, source, with two independent filaments 80−76190
Si thin-film polycrystalline vacuum-deposited solar cells, TiB_2 bottom electrode, 10% efficiency 80−93489
Si vacuum deposition combined with Sb ion implantation, neutron activation anal. 79−47631
Si, vacuum deposition of polycrystalline film on metal substrate 79−91588
Si:Ga(Al), MBE, growth, struct. and elec. props. 77−89458
Si/Al-Si system, rate controlling and composition anal. by electron impact emission spectroscopy 79−91591
SiC, epitaxial layers on diamond, electron diffr. patterns 77−15720
SiC, on Si and metal silicides, formation characteristics and mechanism, by ion backscattering techniques 79−60653
SiO condensate distrib. from extended aspherising source 79−52118
SiO, evaporation geometry for film deposition 78−48320
SiO film, vacuum evaporation on NaCl single cryst., IR absorption spectra 80−35098
SiO_2 films, vac. thermal evaporation, parameter stabilisation 80−87571
SiO_2, prop. of insulating film for tunnelling study on zero bias anomaly in Pb-SiO_2-$Pb_{0.8}Sn_{0.2}Te$ 79−15608
Sn, film, vac. deposited, influence of ion bombardment during condensation 79−82483
SnO_2 thin film gas sensor, prep. 80−39691
SnO_2, transparent electrode deposition on PLZT ceramic 78−74848
SnS_2, cryst. growth, photoconductivity 77−85912
SnSb film, defect density variation with deposition rate, annealing, elec. resist. meas. 77−21027
SnTe, expitaxial film, early stages of growth, replication and TEM obs. 79−65348
SnTe-InTe system, solid soln. films prep. under quasi-equilibrial conditions 79−33931
SnTe-PbSe, semicond. film, growth, phase composition, condensation temp. rel. to cond. type 77−28266
$SrTeO_3$, ferroelec. vacuum condensates 77−40180
Ta, deposition parameters, struct., and elec. props. 77−81222
Te film, evaporated, predeposited Ag, Sn, Bi, Al and Se nucleation centres effect on grain growth 77−4739
Te film, growth on (111) KBr films deposited on mica, TEM and electron diffr. obs. *(Japanese)* 78−64473
Te textured thin films, prep., high solar absorptivity by multiples refl. 80−11568
Te-Se-Cd, sandwich structure, fabrication and characteristics 80−60089
Ti, deposition on Si wafers, backscattering anal., of layer structure, silicide formation 79−69377
Ti line fabrication, shadow deposition method using optical lithography for 0.15-0.3 μm widths 79−43148
Ti, vacuum deposited, cryst. struct. and elec. props. 78−79908
Ti-Al-V (6,4 wt.%) alloy foil, substrate temp. effect on struct. 80−7497
TiO_2 layers, activated reactive evaporation and absorpt. indices 80−97363
TiO_2, reactive evap. of Ti-O phases, refr. index 77−19372
V, film, vac. deposited, influence of ion bombardment during condensation 79−82483
W film production 77−21029
W, notched wire flashing method 78−35309
Zn film growth, HEED and projection microscope obs., surface orientation depend. on deposition parameters 77−32523
ZnS, epitaxial growth, appl. to electronic devices, review *(Japanese)* 80−55281
ZnS film, epitaxial growth on Si in ultrahigh vacuum, source nonstoichiometry effects 77−77387
ZnS films prepared by thermal evaporation in vac., nature of defects 80−10835
ZnS-MgF_2/MgF_2, homogeneous mixed dielecs. as antirefl. coatings effective at two visible wavelengths 79−76770
ZnS(Se)(Te), relative supersaturation, formula valid for different technological conditions *(Russian)* 78−84081
ZnSe, amorphous thin film, prep. and electronic props. 77−85350
ZnSe, electron irrad. effect on electrophys. props., prep. conditions depend. 79−28421
ZnSe, evap. onto electron bombarded NaCl substrates, epitaxial growth and characts. 79−28948
ZnSe multispectral aircraft window materials, production processes 77−73237
ZnSe-ZnTe heterojunction, prep. and props. 79−95483
ZnTe film preparation and props. using single-source method *(Japanese)* 80−6664
Zr source for ultrahigh vacuum surface expts. 79−12810

vacuum gauges
see also barometers; ionisation gauges; manometers; vacuum measurement
absolute pressure vacuum gauges, testing and calibration automation 80−22378
Bayard-Alpert gauge, modulated, reverse X-ray currents *(Japanese)* 80−13087
bimetallic, temperature difference type *(Japanese)* 80−13089
Brownian motion press. gauge, diamag. levitation technique 78−24807
calibration, 10^{-4} to 10 Pa, by orifice flow method 78−82000

vacuum gauges continued
calibration, attenuation meas. on buffer gas scatt. of mol. beam *(French)* 79−58669
calibration, by expansion-reduction method 80−77807
calibration, by static method 80−52258
calibration, compact bakeable ultrahigh vacuum system design 78−21157
calibration, rate of rise method extension 77−57342
calibration, review 77−22563
calibration apparatus, flowmeter designs for gas throughput meas., review 77−26319
calibration of vac. gauge, techniques review *(German)* 77−87778
calibration using simple volume ratio method 80−31780
capacitance manometer with stainless steel bellows-sealed membrane 78−54383
chemisorption gauge, using depend. of elec. cond. of β-carotene on O_2 pressure *(Czech)* 77−139
control of pumping process, 'Pirani', 'Penning' and ionisation gauges *(Czech)* 80−52256
electron storage ring, SRS, press. meas. 79−63264
electrostatic electron oscillator design optimisation, ion source and vacuum gauge 78−74107
electrostatic-ion pumps in a vacuum calibration system 78−57971
extremely high vacuum meas. by modulated B-A gauge *(Japanese)* 79−71473
field electron emission gauge, to indicate surface gas coverage 79−71476
field emission microscope for determ. of hydrocarbon contamination in vacuum systems 77−18002
Granville-Phillips, series 275, convectron, sensitivity to various gases 79−93156
Granville-Phillips, series 275, Convectron, sensitivity to various gases 80−77804
Granville-Phillips' Convectron design comparison, Rational Needs Analysis technique appl. 78−77926
interfacing device for use with supervisory computer 78−8409
ionisation vacuometers, cold or hot cathode, with automatic control *(Czech)* 80−73376
Knudsen manometer, modified, for meas. of low gas press. and thermal accommodation coeffs. 77−26320
leak detector, mass spectrometer, meas. range extension 80−73375
manometer, capacitance diaphragm, electrostatic calibration between 10^{-4} and 10^{-1} Torr 77−2663
McLeod gauge, capillary depression phenomena, Hg vapour drag effect 80−98923
nuclear technolgoy, vacuum gauge design 78−17546
orbitron device, electronic injection, ionisation phenomena and space charge influence 79−40587
organic solid surface-conductivity vacuum meter *(German)* 77−57340
oscillating vane gauge, for determ. gas composition of binary gas mixtures 79−97401
partial pressure measurement and gauges for ultrahigh vacuum meas. 80−57323
Pirani, appl. to integrating radiation dosimeter, 10^4 to 10^8 rad. 79−747
Pirani, bakeable, weldable, for electron storage ring 79−40589
Pirani gauge, constant resistance thermistor 78−45642
Pirani gauges, performance reproducibility 80−77806
Pirani type, dimension- and gas-dependence of characteristics *(Japanese)* 80−13086
Pirani type, with TaN thin films *(Japanese)* 80−52257
pressure ranges, error sources and calibration *(French)* 78−49846
resistance vacuum gauge for 10^{-3} torr *(Polish)* 79−71472
resistance vacuum meter, range extrusion method *(Polish)* 79−54148
spinning rotor gas friction gauge, calibration against fund. vac. press. standard 80−82787
standardisation, international 77−87774
testing and calibration for low absolute pressure 77−57341
thermal compensation for accuracy improvement 79−67332
thermocouple, gas analyser appl. 80−61183
thermocouple type gauge, appl. to molar flow rates determ. in dilution refrigerators 77−10032
three grid modulated Bayard-Alpert gauge *(Japanese)* 80−13088
types, principles and ranges, review 79−71477
types and charact., reviews 79−26064
ultrahigh vacuum system for ISABELLE full cell 80−77798
US interferometric manometers for low and medium vacua 77−67455
vapour pressure meas. gauge of ^3He for use up to 0.3K 80−68207
vibrating vane gauge for 10^{-3}-10^{-1} torr range 78−49793
TaN film, press. depend. of elec. props. appl. to press. meas. 79−78241
TaN film, simple vacuum gauge, 10^5 to 10^{-3} Pa press. range 78−70148

vacuum measurement
see also vacuum gauges
automatic pressure recording method, 5 to 10^{-2} torr 79−85148
automatic range-changing amplifier, ionisation current pH and vacuum measurement appls. *(French)* 79−63262
beam experiment press. meas. system, 0.5-10^{-2} Pa 79−88971
binary gas mixture, determ. gas composition, oscillating vane gauge 79−97401
cold traps, influence on low-vacuum pressure meas. 78−37026
control of pumping process and vacuum apparatus *(Czech)* 80−52256
corrosive atm. pressure or vacuum meas. isolation chamber 77−30174
cryogenic environment, H_2 and He press. meas. 78−77925
differential membrane manometer 80−31777
dynamic expansion method for press. scale realisation in 10^{-3} to 10^{-8} torr range, uncertainty analysis *(German)* 78−37025
dynamic torsion-effusion pendulum, video obs. 77−61077
electron storage ring, SRS, press. meas. 79−63264
field electron emission gauge, to indicate surface gas coverage 79−71476
gas flow method *(Croatian)* 79−17434
gas-operated free-piston pressure-gauge, effect of rot. on meas. 77−41631
hot filament ionisation gauges, press. meas. limit up to 10 mm Hg *(German)* 79−17431
impedance probe calibration, for vacuum meas. in single component two-phase mixture *(Italian)* 80−62677
industrial vacuum system, cryopump design and performance 77−87777
interferometric oil micromanometer 79−63263
interferometric oil micromanometer as primary vacuum standard 79−88970
ion source, press. determ. from discharge charact. 77−57423

vacuum measurement continued
ionisation vacuometers, cold or hot cathode, with automatic control *(Czech)* 80−73376
JG ionisation gauge, effect of electrode voltages on elec. field distrib. 77−49737
magnetic discharge manometric convertor 80−31779
mass spectrometer, design and operation 79−63322
mass spectrometer materials, set up for meas. released gas 80−105746
mean sojourn time of molecules on surfaces, meas. in practical vacuum system *(Japanese)* 80−57315
method using silicate glass defect liquidation 77−41627
nuclear technolgoy, vacuum gauge design 78−17546
partial pressure measurement and gauges for ultrahigh vacuum meas. 80−57323
partial pressure measurement method in extremely high vacuum range *(Japanese)* 79−71475
partial pressure measurements in extremely high vacuum *(Japanese)* 79−71474
piezoceramic transducer for 760 to 10^{-5} torr 78−86283
Pirani type vacuum gauge, with TaN thin films *(Japanese)* 80−52257
positive-displacement vacuum pump speed meas. 78−81993
pulsed pressure meas., using piezoelectric pick-up 80−31778
rapid and accurate meas. apparatus for press. and vol. 79−88972
standardisation, international 77−87774
standards intercomparison, 8×10^{-5}-8×10^{-2} Pa 80−86333
supersonic molecular beam source, simple calibration method 80−82845
technology, medium, high and ultrahigh vacuum, conf., Oxford, England (Apr. 1978) 79−63242
transition metal carbides, coated emitters, thermionic emission props., appl. in vacuum meas. *(Japanese)* 77−40322
trends and problems *(French)* 77−53925
ultra high vacuum generation and meas. *(Japanese)* 78−45640
ultra-high vacuum, total pressure meas. 80−31782
units, gauges, error sources and standards *(French)* 78−49846
units and measurement in vacuum technology *(German)* 77−79100
in vacuum tubes, techniques *(Japanese)* 79−26065
vapour pressure temperature estimation method in ultra high vacuum range *(Chinese)* 80−232
Hg use and abuse for vacuum production and meas. 78−81998

vacuum polarisation *see quantum electrodynamics*

vacuum pumps
see also cryopumping; diffusion pumps; ion pumps
absorption, magneto-optical cryostat, optical meas. at 0.4K 80−73369
applications of perfluoropolyethers *(Japanese)* 78−229
AVEhD 40/800 arc-sorption pumping system 78−227
categories, review 79−75541
condensation pump with preevacuation 77−74414
cryogenic pump for US gas jet evacuation in vacuum UV source chamber 77−13763
cryopump and extremely high vacuum *(Japanese)* 79−71468
crystal units, vacuum system for cleaning and cold welding *(Polish)* 80−31776
CVD, problems with creating vacuum *(French)* 80−101803
dental suction system, at Guy's Hospital, London 79−8556
differential pumping, of gas discharge columns, ionisation enhancement 79−67330
Diffstaks with integral cold traps 78−70144
diffusion and getter pumps, operation and specifications *(Hungarian)* 77−71334
diffusion pump, CMOS monitor cct. 77−5855
electron microscope backing pump system, high-performance oil-free design 80−99011
electrostatic-ion pumps in a vacuum calibration system 78−57971
ELMO-G quiet running vacuum pumps and compressors for plant noise reduction 80−5872
fast pumping for UPS for study of transients and unstable species 77−83764
fluids, types and props. 79−75540
freeze-drying corrosive materials 77−41580
fusion plasma experiments, vacuum developments 79−63260
fusion reactor, pumping and vacuum requirements 77−57744
fusion reactor, TFTR, vacuum pumping system 80−95447
fusion reactor, TFTR Flexibility Modification, in-torus surface pumping, Ti and Zr/Al gettering 80−95451
fusion reactor, vacuum system design 77−57747
fusion reactor vacuum system (Princeton TFTR), description, operation, safety 78−74497
gas cooled rotating piston pumps *(French)* 78−21153
gas mixtures, pumping in high vacuum region 80−95107
gas-cooled roots, WGK-C, chemical series 78−70146
gasdynamic tubes, performance estimation 79−12811
getter pumping for economical sputtering with Xe 77−40371
HV AC Penning discharge, vacuum pumping charact. 78−93713
Indian rotary vacuum pumps, defects and performance 78−81997
liquid ring pumps, capabilities and limitations 79−40588
mechanical, design and manuf. aspects 77−57339
mechanical boosters incorporating self-limiting power transmission 78−70138
mechanical pumps, operation and charact. *(Hungarian)* 77−74413
miniaturised turbo-molecular pump, for space appl. *(French)* 80−42234
National Synchrotron Light Source, vac. system 79−81106
oil, rotational, function, construction and operation *(Slovak)* 80−68206
oil backstreaming in turbomolecular and oil diffusion pumps 79−80636
oil-vapor vacuum pump made of glass *(Japanese)* 77−82539
oil-vapour vacuum pump, glass, construction *(Japanese)* 77−18000
operating principles and applications *(German)* 77−79100
optical coating production, vacuum system development, review 77−58493
orbitron ion-getter, small non-cooled and low power consumption 80−52352
orbitron pump, modified, pumping speeds of He, Ar and Xe, 288 to 418K 77−57338
perfluoro polyethers, props. and use in vacuum appls. 78−70136
perfluoropolyethers as vac. pump fluids 78−32828
PETRA electron-positron storage ring, vacuum system techniques and problems 78−17452
plasma etching, problems with creating vacuum *(French)* 80−101803
positive-displacement vacuum pump speed meas. 78−81993
pressure range extension by getter pumps 79−67327
primer for low to ultra high vacuum 77−26106

vacuum pumps continued
production sputtering systems, design, use of high rate magnetron source 79−66006
pumpdown time eqn. and system selection 80−82785
pumping down curve, P(t), rel. to adsorption isotherm *(Japanese)* 80−52249
roots pump and oil-sealed mechanical pump combination for low back-streaming 80−57322
Roots pumps, mechanical booster pump, clean vacuum, reduction of oil backstreaming *(French)* 80−17954
rotary, back-migration 79−12812
rotary, vacuum use of perfluoro polyether as pump fluid 80−52251
rotary and sublimation pump system, pumping charact. 77−22562
semiconductor production problems and safety precautions *(German)* 80−86330
sliding-vane rotary, with selected accessories, appl. in vacuum processing 78−70145
solid membrane superpermeability rel. to gas evacuation 79−74422
sorption pump, design of cheap pump 79−63255
sorption pump, high vacuum, pumping speed and condensation coeffs. determ. 78−21156
sorption pumped system for high vacuum 79−71470
Space Shuttle, methods of improving vacuum for expts. 78−32825
sputtering application, cryogenic versus turbomolecular pumping 79−80629
standardisation, international 77−87774
steam jet ejectors, capabilities and limitations 79−40588
summary of new laboratory pumps 80−22375
TEM modifications allowing continuous failsafe pumping 77−22626
TFTR, vacuum system design, performance curves 78−70625
TFTR vacuum system transient simulator 78−74496
thermal desorption spectra, effect of vacuum system time consts. 78−22960
and thin film technology, conf., Uppsala, Sweden (Aug-Sept. 1976) 77−90270
Toepler pump improved design 77−22561
turbo molecular pump, performance for H_2 *(Japanese)* 80−13085
turbomolecular pump, development and use 79−63251
turbomolecular pump, miniaturized for space appl. 80−52254
turbomolecular pump development 77−41630
turbomolecular pump evaluation 78−77924
turbomolecular pump in pulsed mag. field, operational effects 78−50402
turbomolecular pump vacuum system for the Princeton Large Torus 78−71521
turbomolecular pump with mag. bearings, fusion expt. device appl. 78−50400
turbomolecular pumps, advances, review 80−62676
turbomolecular pumps, development trends 79−67328
turbomolecular pumps, operation and fields of operation *(Hungarian)* 77−74412
turbomolecular pumps for high gas flow applications 79−80632
turbomolecular pumps in mag. fields, problems 78−70143
turbomolecular pumps with corrosion resistant oil 77−87776
turbomolecular vaccum pump, grease lubrication of bearings 79−80630
vapour pumping groups, single struct. 79−67329
vapour-handling, new series 78−70147
very high vacuum appl. of field electron emission gauge 79−71476
water content meas. and display with AF3 80−22376
Al wire gaskets for demountable, bakeable ultrahigh vac. seals *(Japanese)* 79−93154
H_2 evacuation, magnetic discharge pump durability improvement 79−67326
H_2 evacuation, permeation through Pd membrane under different gas and membrane boundary conditions 79−71469
He condensation forevacuum pump 78−86282
N_2 forevacuum trap 78−86281
Pd alloy membrane pump, for thermonuclear fusion devices 78−89980
Ti sorption pump for molecular beam detector 78−21150
Ti sublimation pump, behaviour in 10^{-11} Torr range 77−57336
Ti sublimation pump, deuteriding inhibition by surface contamination 77−57335
Ti sublimation pump, methane outgassing 80−77796
Ti sublimation pump, pre-cleaned, atomically clean surface environment, confirmation using field electron emission 80−52250
Ti sublimation pump *(Japanese)* 78−24806
Zr-Al getter pumping in beam driven Tokamaks 78−50401

vacuum sintering *see sintering*

vacuum techniques
includes techniques for producing, maintaining and handling vacuum per se
see also cryopumping; getters
28 GeV proton synchrotron and intersectig storage rings 78−86706
adsorption vacuum measurements, standard devices 79−71464
air density direct determination in balance through artifacts characterised in evacuated weighing chamber 79−88916
American Vacuum Society National Symposium, Boston, USA (Nov 1977) 78−72718
analysis, design and operation of small mass spectrometers 79−63322
analytical, specimen manipulator 79−63245
Araldite, high vacuum sealant at liq. N_2 temp. 80−57319
artificial satellite molecular wake shields of various shapes for vacuum expts. 79−88966
ATJ graphite, ultrahigh vac. compatibility, outgassing charact. 79−81080
atomically clean surface environment, confirmation using field electron emission 80−52250
bakeable seals development for large noncircular ports on Tokamak fusion test reactor 80−82777
biological specimen replication at −150°C with improved freeze-fracture apparatus 80−85560
calibration of vac. gauge, techniques review *(German)* 77−87778
catalysis reaction studies on single cryst. surface in XHV system limitations 77−9126
ceramic-metal seal technology, history and trends 78−81992
CERN ISR, cold bore expt. 79−76212
CERN-ISR, vac. techniques 77−83250
chopper system, UHV compatible, for meas. of energy spectrum of neutral D atoms 80−79587
cleaning procedures for vacuum equipment 79−71467
contribution to powder metallurgy 78−84736
crossed fields nitriding in air atm. 80−84867
cryogenic pressure-vacuum valve 78−37020
cryogenic-vacuum chamber, shaft seal method for rotation transmission 77−26314
cryostats, twin-chamber flexible vacuum connection 80−73368
degassing metals for extreme low pressures 80−98924
deposition equipment cleaning, practical procedures 80−57318
differential Burnett apparatus, virial coeff. meas. at various temps. 80−22373
differential evacuation system for electron beam emission into atmosphere 79−35890
diffusion-pumped vacuum system, contamination minimization 79−44913
discharge, cathode spot, models analysis 80−19636
discharge, cathode spot parameters, existence diagram method applic. 80−24276
education, undergraduate and post-experience courses 79−62954
eductation, advanced undergraduate expts. in vacuum physics and mass spectrometry 80−73153
elastometer materials, selection for vacuum seals 80−77797
electron microscopy of epitaxial growth process at UHV 78−55790
electron spectroscopy of solid surfaces in ultrahigh vacuum, measurement using versatile spectrometer 79−58849
electron storage ring, vacuum system for synchrotron radiation source 79−63830
epoxy, reinforced, outgassing rate in vacuum, control by pretreatment 79−40583
etching, prior to deposition of C, in RF butane plasma 79−66224
etching, vac. colour, for investigating hot plastic deform. of C steel 80−61036
evacuated tubular solar collector integration with LiBr absorption cooling systems 80−3493
evaporation cryostat for vac. meas. on ultrathin metal film 77−87769
extraction device with mass spectrum analyser for determ. of gas-forming admixtures in metals 80−22371
far IR spectroscopy, variable path length solution cell, for use in vacuum 78−45736
fast pulsed gas valve for injecting gas pulses 80−62675
freeze drying of pharmaceuticals 77−70010
furnace, vacuum, regulated particle-delivery system 78−21139
fusion plasma experiments, vacuum developments 79−63260
fusion power plant, vacuum outer containment, safety, T control and monitoring 78−74498
fusion reactor, Heliotron E, vacuum chamber construction using electron beam welding 80−106180
fusion reactor, STARFIRE project, T handling and vacuum requirements 80−106187
fusion reactor, vacuum engineering *(Japanese)* 78−58401
fusion reactor vacuum vessel welds, ultrasonic scanner 80−99288
fusion reactors development wall contamination avoidance *(German)* 78−21769
Gaede, Wolfgang, memories on 100th anniversary of birth 79−67133
gas exchange in closed volume during vapour condensation, residual gss density change 77−59692
gas leak detection principles and practice 78−81995
gases in metals, detection by vacuum spark technique, appl. to Al wire 78−61094
glass ceramics, machinable, vac. compatibility 79−93152
glow discharge treatment of vac. tube, sputtering and reactive effects 78−70141
halogen leak test *(Japanese)* 79−93153
heat treatment, efficiency 80−81089
helium mass spectrometer leak detector, design and appl. to industrial leak detection 79−63247
high efficiency solar collector development 79−62051
high pressure preparation lock for surface analysis in ultrahigh vacuum chamber *(German)* 80−52261
high vacuum, for large capacity system *(Japanese)* 77−82538
high-vacuum system control and diagnosis by monitoring total press. and per cent N content 80−95105
hot pressing, continuous, of transparent ceramics, press design criteria 78−23643
inert gas atoms, desorbing from solid surface, ultrahigh vacuum apparatus for detection 78−32915
intense pulsed neutron source, vacuum system 79−63261
ion accelerator, atomic collision processes rel. to vacuum system, review 80−54290
joint, welded, through defects, study using vacuum bubble method of airtightness inspection 79−52599
K-ramic®, ultrahigh vac. compatibility, outgassing charact. 79−81080
leak detection, trapless, use of reversed diffusion pump 77−2662
leak detection, ultrasensitive 80−47065
leak detection using liquid spray 80−234
leak telescope for mol. flow direction detect. in large vacuum chamber 77−49735
leak testing with search gases, He leak detectors with mass spectrometer anal. *(German)* 80−101802
LEP, electron positron storage ring, vac. chamber, glow discharge surface cleaning 80−58010
liquid jet vacuum seal, inflow, rel. to electron beam emergence into atmosphere 80−78469
low energy ion scattering spectroscopy, UHV apparatus *(Japanese)* 80−20746
low pressure manometer calibration method using vacuum technique 78−74015
low pressure plasma system, design and operating characteristics 79−64880
low-cycle testing unit for use in vacuum and at high temp. 79−52503
lubricant vapour pressure and evap. rate in vacuum, determ. using ambient press. meas. 78−29123
manometer calibration method in high- and ultrahigh-vacuum regions 78−16807
mass selective outgassing rate meas., direct mol. beam method 79−85146
mass spectroscopic measurements, validity for pressures exceeding 10^{-4} mbar 79−85198
MBE, vacuum interlock system 78−48330
mean sojourn time of molecules on surfaces, meas. in practical vacuum system *(Japanese)* 80−57315
Meissner coils in high-vacuum applications, anomalous behaviour 78−32826

vacuum techniques continued
melting furnaces and casting techniques 78−84727
metal filings and wires, thermal processing encapsulated under vac. in metal tubulations 77−59810
metal hollow O-ring seal, for UHV and cryogenic use *(Japanese)* 80−22374
metal melting in suspended state, large vol. and mass samples *(Russian)* 78−44036
metal refining in superhigh vacuum, condensation from vap. and zone recrystallization *(Russian)* 79−15604
metallurgical industries, vacuum furnace developments, heat treatment, high speed steels *(German)* 79−100174
metallurgical industries, vacuum hardening of high speed steels *(German)* 79−100175
metallurgy, vacuum, using electron beam techniques, technical problems *(German)* 80−84850
metals and alloys, fatigue behaviour, vacuum effect, review 80−35309
microbalance, Cahn RG-2000, improvement in sensibility 80−77794
microbalance system, detection of minimum weight difference *(Japanese)* 79−26032
microweighing techniques and use of beam microbalance, book 80−62401
molecular sieves, adsorpt. of atmospheric gases, comparison of 13X and 4A at low temp., press. *(German)* 80−88423
monochromator for investigating scattering objects in vacuum UV 77−74523
Monte Carlo analysis of backscattering and sputtering in vacuum systems 80−235
mounting method for thermocouple gauge tubes 80−77795
multilayer insulation materials, ambient temp. outgassing rate 80−84370
Nb, pure, production by carbothermic reduction-electron beam melting combination method 80−89177
orbiting ultrahigh vacuum facilities, appls. and characts. 78−7855
outgassing, effect of ambient and other pretreatment 80−17953
outgassing material selection and treatment 78−81994
outgassing meas. of noncryst. materials, diffusion theory *(Chinese)* 80−57313
outgassing rate in dynamic vacuum system during particle bombard. of walls 79−44911
permanent joining techniques 80−82782
PETRA electron-positron storage ring, vacuum system techniques and problems 78−17452
PETRA vacuum system, RF parasitic mode losses, fabrication cost, new techniques 77−83217
Pioneer Venus large probe neutral mass spectrometer for measurement of composition and abundance of atmospheric gases 79−88563
plasma confinement, mirror, multichambered neutral beam line, self-consistent background gas density calc. 78−34352
PLT Tokamak vacuum vessel, residual gas and surface comp. changes with H_2 discharge cleaning 79−80631
polyimide thin film gasket seal fabrication for ultrahigh vac. 77−57334
polymer thin film, tensile testing multiposition unit, for testing in vacuo and gaseous media 78−11478
pressure vessel, effects of method of return to atm. press. *(French)* 80−42233
production, field electron emission gauge, to indicate surface gas coverage 79−71476
production sputtering systems, design, use of high rate magnetron source 79−66006
programmable quadrupole mass spectrometer *(Japanese)* 77−86415
protection of internal components from contaminants of large systems 80−105666
protective coating plasma polymerisation in vacuum chamber 79−70183
proton storage ring, NAP-M, vacuum chamber evaporation techniques 77−65362
pulse type H_2 diffusion leak 77−87751
pulsed high voltage measurement using 2 MV resistive voltage divider 80−31803
pumpdown, nomogram for required time or pumping capacity 77−10035
pumpdown time eqn. and system selection 80−82785
pumping down curve, P(t), rel. to adsorption isotherm *(Japanese)* 80−52249
quenching of die steel 79−38861
reactor defective fuel detection using vac. slipping technique 80−9389
refractory metals, internal friction meas. from 20 to 2000°C in superhigh vac. 77−86249
refractory metals and alloys, processing by powder and vacuum melting techniques 79−33966
retort for vac. thermogravimetric apparatus used in evaporation kinetics determ. 77−37865
review of vacuum physics progress *(Chinese)* 79−35768
RF sputtering, bias voltage control using vacuum press. controller 77−28720
rotary pump, back-migration 79−12812
rotary/push-pull vacuum feedthrough 78−32827
sample heater, high vacuum, using Zener diode 78−12690
seal, demountable, operating at low temps. 77−67445
seal with thermomechanical drive of Ti-Ni 80−31773
sealing LiF window to thin-walled Au or Cu cylinder using PbF_2 77−54820
seals, high-speed cryogenic mag. fluid for high-vacuum chambers 80−57314
seals for $MgFl_2$ windows 78−94457
SEM, secondary electron emission dependence on electron beam density dose, surface interactions from AES and ELS 80−61209
SEM and Auger electron spectroscopy, vacuum improvement technique 80−27381
SEM vacuum techniques, and contamination management 79−17575
sensitivity limitations on force and weight meas. in vac. 78−65908
solar flate plate evacuated collector design 79−62099
Space Shuttle, wake shield expt., true and net outgassing rates 79−48645
Spacelab pallet, meas. of mol. streaming fields 80−82173
steel, stainless type 304, radiation induced outgassing 80−624
surface analysis, system, modular combined ESCA, UPS, AES, and SIMS 78−73107
surface and thin film phenomena 78−86280
surface potential meas. in high vac., vibrating capacitor method modification 77−71343
system engineering, integrated approach 79−67320
technical standardisation *(Czech)* 78−65940
vacuum techniques continued
technology, medium, high and ultrahigh vacuum, conf., Oxford, England (Apr. 1978) 79−63242
thermal fatigue testing, in ultra high vac. environments *(Japanese)* 80−93716
thermal system design, for thermovacuum chamber, temp. range 173 to 373K 79−35764
thermovacuum aquameter for moisture meas. 77−82537
thin window gas absorption apparatus suitable for storage ring synchrotron radiation sources 78−62955
Tokamak, Petula, vac. vessel and RF coils for compressional transit time mag. pumping heating 78−70634
Tokamak reactors impacts of plasma perform. parameters on vacuum and T system design 79−76131
transfer device for Tokamak in situ surface anal. 79−2778
transition metals processing technology and appl. *(Hungarian)* 80−55318
trapless leak detection, counter-flow mass spectrometer leak detector 79−63248
tunnelling expts., thermal drive apparatus 77−8175
UHV fatigue drive, design and performance 80−86328
UHV photoelectron spectroscopy, VUV He reson. line radiation source 78−89602
uHV technique for intervacuum sample transfer 79−85147
ultra high and high vacuum appl. *(Japanese)* 78−45641
ultra high vacuum generation and meas. *(Japanese)* 78−45640
ultra high vacuum technology developments *(Japanese)* 78−49845
ultrahigh vacuum and cryogenic feedthrough, with 48 pins 79−97399
ultrahigh vacuum system, for channelling backscattering experiments *(Japanese)* 79−26061
ultrahigh vacuum system for ISABELLE full cell 80−77798
ultrahigh vacuum technology for electron and proton storage rings 77−83213
ultramicrobalance, for surface studies 79−71465
universal ultrahigh vacuum manipulator for LEED camera 77−43121
UPS ultrahigh vacuum apparatus, appl. to clean and gas covered Si(III) surfaces *(Japanese)* 80−37125
vacuum chamber, for arc investigations *(Polish)* 79−82120
Vacuum Society conf., San Francisco, USA (Nov. 1978) 79−77862
vacuum tightness monitoring in components with unclosed cavities, automatic mass spectrometer 79−52592
virtual leak, influence on pressure in high and ultrahigh vacuum systems 79−97398
visible-IR window assembly for ultrahigh vacuum systems using polycrystalline ZnSe 78−54380
Al storage ring vacuum chambers, glow discharge processing versus bakeout 78−70658
CO, chemisorpt. on Pd particles supported on mica, ultra high vacuum technique 78−71960
Cu (100) surface, electronically-activated N_2 chemisorption 79−66348
Cu, commercial pure, creep-rupture props., vacuum, *(Japanese)* 78−72843
Cu-Ge solders for electric vacuum instruments, Mn and Ag additives effect on evaporation 79−42231
H evacuation at 25 m^3/sec by electric arc unit 78−21144
$H_2(D_2)$ pumping by Ti film, pumping speed comparison 78−51819
He desorption spectrometer, clustering of Kr in W (100) obs. 80−77908
Hf-Ta alloy prep. by carbide-oxide reaction 77−12554
In seal fabrication by prepressing 80−101800
Mg, purification by vacuum distillation 79−52138
N_2 supply, liquid, to vacuum installations 80−31762
Nb single crystals, for tunnel meas., annealing in ultra high vac. device *(German)* 80−89169
Ni superalloy, transient liq. phase diffusion bonding and mechanism *(Japanese)* 78−2279
PLZT porosity and transparency affected by vacuum hot pressing 77−12556
Sm, vacuum sublimation method of prod. *(Russian)* 79−70012

vacuum tubes
see also diodes; pentodes; tetrodes; triodes
1/f fluctuations *(Japanese)* 78−43448
Brillouin electron beam critical current rel. to vacuum level 79−7068
emission detector sensitivity to γ-rays 77−54462
erosion phenomena on contaminated cathodes due to electrical discharges 79−41889
field emission electron tube, pump for compact IR semiconductor laser 79−59725
HV vacuum accelerator tube, microparticle obs. 80−864
orbitron, radial electronic charge distrib. 77−57827
triggered vacuum gap, semicond. coated dielec., firing characts. 77−47286

valence bands
adsorbates, valence photoemission book contrib. 78−95672
adsorbed atom on solid surface, photoemission from valence band, surface plasmon emission, model Hamiltonian calcs. 80−50525
alkali graphite intercalation compound, evidence for alkalilike cond. bands 80−45201
alkali graphite intercalation compounds, evidence for alkali-like conduction band, UPS study 80−45208
alkali graphite intercalation cpds., selection rules and restricted valence band self-convolution for KVV Auger transition 80−29832
alkali halides, piezo-optical properties, temperature dependence 78−92050
alkaline earth fluorides, orbital binding energy and ionicity relations, XPS meas. 80−97399
aluminosilicate minerals, X-ray spectral study, emission bands, quantum yield, tetrahedra valence band 77−28660
amorphous semiconductor, local order as determined by electronic and vibrational spectroscopy 79−37627
amorphous semiconductor, tetrahedrally bonded, effects of quantitative disorder on electronic struct. 79−47003
anthracene, cryst., cyclotron reson. and carrier scatt. 77−76746
anthracene, solid, electronic struct., comparative ESCA study of polyacenes 78−52631
benzene, solid, electronic struct., comparative ESCA study of polyacenes 78−52631
borides, MB_{12}, exam. of electronic structure, using X-ray emission spectra *(Russian)* 79−33865
Cain model, two-band, dispersion and iso-energy surfaces of valence and conduction bands *(Russian)* 80−24783

valence bands continued
β-carotene, electronic struct., classical and double beam photoemission obs. 78−9285
β-carotene, XPS obs. 78−24030
chalcogenide lone-pair semicond. charged impurities, effect on carrier concs., Street-Mott model 78−67984
core and valence electron enhancement factors from positron annihilation-correlation curves 80−25479
covalent semiconductor, valence band calc. using many-electron theory 80−15434
degenerate semiconductors, heavy hole-phonon bound states for valence band with degeneracy point *(Russian)* 80−15461
degenerate valence band semiconductors, polariton effect 79−15102
diacetylene polymers, photoelectron valence band spectra 78−43979
diamond, natural, free exciton luminesc. line shape 80−40165
diamond, photoionisation cross-sections of valence s- and p-electrons *(Ukrainian)* 77−73211
diamond, semiconducting, electron-hole liquid formation conditions and parameters 79−78013
diamond, state density and X-ray photoelectron spectra of valence bands calc. 77−28679
diamond, valence band calc. using many-electron theory 80−15434
diamond, valence electrons, energy-depend. photoionisation probability calc. 77−16462
diamond structure, energy levels of direct exciton formed by split-off valence band 78−91624
difluorides, rutile type, tight-binding calc. for upper valence band 77−55480
dimethyl zinc, valence band and Zn 3d levels, electric field gradients 77−88495
electron mean free path, stopping and straggling 78−91367
$(ethylene)_x$, mol. crystals, quantum theory, mol. tight binding method calcs. 80−49572
exchange interactions in semiconductors and insulators, mean free path and energy gap effects 80−88522
excitons, Wannier and Frenkel, simple model for unified treatment 79−69422
extrinsic semiconductors, carrier concs. and Fermi levels 77−66112
ferromagnetic semiconductors, dielectric function depend. on magnetisation, light absorpt. coeff. *(Russian)* 80−15467
finite-energy f-sum rules for valence electrons 78−88276
fluoride perovskite- and tysonite-type, upper valence bands, tight binding calc. 77−80730
fluorite-type crystals, universal valence bands 77−35864
$(formamide)_x$, mol. crystals, quantum theory, mol. tight binding method calcs. 80−49572
gapless semiconductor valence band in mag. field 80−49600
graphite, Compton profiles, momentum densities, comparison with glassy C 80−2895
graphite, diamagnetism with quasilinear dispersion law, orbital susceptibility, valence bands *(Russian)* 80−80475
graphite, high energy cond. and valence band states, XPS 78−39664
graphite, X-ray emission and absorption, XPS, electronic struct. 77−16431
graphite, XPS and Auger KVV valence band spectra 78−11028
graphite intercalation compound, interaction between one or two s orbitals *(French)* 80−65440
graphite monofluoride, self-consistent semi-empirical LCAO calcs. of electronic band struct. 77−85142
ice, UPS, valence band struct. 79−33890
II-IV-V_2 semiconductors, heat of formation from spin-orbit splitting in valence bands 77−31985
II-VI and III-V compounds, Compton line shapes of atoms 77−44080
intrinsic semiconductors, indirect exchange interaction, finite temp., valence bands and energy gaps effect 80−59943
ionic crystals, surface electron states in continuous spectrum 78−26931
laser diode, spontaneous emission linewidth, calcs. 77−10927
metal, valence band Auger spectra, effect of edge anomaly 79−69908
metal electron response to local fields, X-ray processes 78−23584
metallic compounds, cohesive props., augmented-spherical-wave calcs. 79−94952
metatungstate mixed valence anions, XPS spectra, oxidation states 78−6824
mixed valence system, far IR intervalence tunnelling transition, vibronic coupling model 78−58646
molecular crystal, band structure, excitonic processes, trap distrib. 80−6720
molecules, valence and core photoionisation, spectral lines, many body effects 80−47853
MOS structure, p-channel, effect of isotropic stress on Si valence band struct., press. transducer appl. 80−25011
$Na_2[Fe(CN)_5NO]$, valence levels, X-ray photoelectron and X-ray spectra 77−88500
naphthalene, solid, electronic struct., comparative ESCA study of polyacenes 78−52631
noble metal, XPS of valence bands, ang. depend. 77−44122
one-dimensional semiconductor, delocalisation and superalternation effects in nonlinear susceptibilities 77−11840
optical joint density of states, oscillator strength effects 77−11838
OPW method, instability rel. to error in core eigenvalues 78−63963
organic molecular crystals, photoemission, book contrib. 80−16158
p-n heterojunctions, forward-biased, charge accumulation 80−107902
passive layer, on Fe electrode, semiconductor model, appl. to electrochem. reactions, review 80−26022
photoelectron spectroscopy, review 78−39668
photoelectron spectroscopy of solids, review 80−55263
photoemission in solids, book 80−12860
phthalocyanine compounds, valence band studies, UPS meas. 77−52221
phthalocyanines, UV photoemission, valence band struct. 77−85884
poly(2-vinyl pyridine), electronic struct., molecular-ion states and dielectric props. 79−37969
polyacetylene:I, electronic structure, XPS and UPS meas. 80−66385
polyacetylene, band struct. valence Hamiltonian minimal STO-3G basis calc., nonempirical model pot. 80−54596
polydiacetylene-bis(toluenesulphonate), XPS valence band obs., binding energies 77−77339
polyethylene, band struct. valence Hamiltonian minimal STO-3G basis calc., nonempirical model pot. 80−54596
polyethylene film, soln.-cast, low energy electron scatt. obs. of band struct. 80−16131
polypeptide chains, struct. of conduction and valence band 80−76700
polypeptides, electronic struct., side-chain disorder effect 80−76706
pyrene, band structure, excitonic processes, trap distrib. 80−6720
α-quartz, CNDO/2 calcs., electronic props. of perfect cluster, EPR parameters of O^- vacancy 80−107701
α-quartz, electronic energy band struct. calc. 79−23894
α-quartz, valence electron states and X-ray emission spectra, pseudopot. and OPW calcs. 77−35866
α-quartz, valence electron states calc. by pseudopotential method 77−20239
rare earth aluminate, scandate and zironate film coatings, electrophys. props. w.r.t. prep. technology 80−60781
rare earth metals, heats of vaporisation and valence band energies, theory 78−91431
rare earth metals, X-ray 5p emission bands, valence energy band 80−104016
rare earth sulphides L-X-ray absorpt. spectroscopy, conc. of ions with various numbers of f electrons 77−28646
rare earth tellurides, electron density distrib. from Mossbauer spectra 78−23374
rare earths, and their alloys and cpds., photoemission, rel. to electronic struct., book contrib. 80−16157
$retinal_1$, all-trans, XPS obs. 78−24030
semiconductor, carrier number and effective bandwidths *(Spanish)* 78−18954
semiconductor, covalent, molecular cluster model 78−43283
semiconductor, direct band gap, electronic Raman scatt. of polarised light on donor levels 80−93309
semiconductor, intrinsic, indirect exchange interaction, finite temp. effects 80−71003
semiconductor, narrow band gap, ferromagnetism of electrons in filled band *(Russian)* 79−78300
semiconductor, nearly cubic, acceptor ground state calc., appl. to GaAs 77−28113
semiconductor, p-type, Faraday effect due to free holes 80−97247
semiconductor, p-type, infrared absorption and plasma reflection 80−97284
semiconductor, p-type, intervalence-band transitions, saturation, theory 80−75997
semiconductor, relaxation of nuclear spins interacting with holes 78−48073
semiconductor, tetrahedral, bond orbital model on CNDO basis 77−47720
semiconductor, Wannier excitons, fine structure, lineshape and dispersion, review 80−44520
semiconductor, zinc-blende struct., shallow acceptor contribution to near-resonance spin-flip Raman scatt. 79−95754
semiconductor, zincblende-type, valence band effective mass strain depend. 78−51880
semiconductor thin films, degenerate one-valley and many-valley, photogalvanic effect calcs. 80−34487
semiconductors, photoelectron spectra and band struct., book contrib. 80−16155
semiconductors with degenerate valence band, diamg. excitons, and oscillatory magnetoabsorpt. of GaSb 77−76754
silicate minerals, X-ray spectral study, emission bands, quantum yield, tetrahedra valence bands 77−28660
simple metals, photoemission theory, book contrib. 80−16159
single crysts. and thin films, absorpt. edge temp. depend., gap energy changes 79−42991
SOS MOS devices, hole mobility under residual stress, Hall meas., valence band struct. 78−88039
surface electron state characterisation by X-ray techniques 77−55868
surface electron states, valence band spectroscopy in ultrasoft X-ray region 77−55852
TCNQ, electron- and phonon-polaron effects in valence and cond. bands 77−76757
TCNQ, infinite stacks, all valence electron band struct. 78−39001
ternary chalcopyrite semiconductors, energy band struct. 78−34767
ternary semiconductor, struct. effects on energy band struct. 78−39021
tetracene, solid, electronic struct., comparative ESCA study of polyacenes 78−52631
tetrahedral semiconductors, valence band degeneracy, polar electron-phonon interaction effect, exciton binding energy 79−56140
tetraselenotetracene, electronic structure, conductivity studied by ESCA 79−4889
tetrathionaphthalene, electronic structure, conductivity studied by ESCA 79−4889
tetrathiotetracene, electronic structure, conductivity studied by ESCA 79−4889
tight binding calc., overlap and next-nearest-neighbour interaction effects 78−72059
transition metal, 3d, energy parameter, Auger spectra, quasi-atomic behaviour 77−20966
transition metal alloys, band filling 77−4288
transition metal carbides, APW bands rel. to covalent binding 77−59245
transition metal clusters, particle size rel. to bulk metallic props. 80−44490
transition metal compounds, valence band struct., X-ray spectroscopic study 80−29319
transition metal monosulphides of first-row, XPES and UV PES 80−20760
transition metal nitrides, APW bands rel. to covalent binding 77−59245
transition metal oxides, APW bands rel. to covalent binding 77−59245
transition metal phosphides, valence electron energy spectrum, deduced from X-ray spectra and XPS 79−99984
transition metal surface (adsorbate), intermediate UPS/XPS synchrotron radiation study 78−52633
transition metals, 3d, XPS of valence bands 78−35249
transition metals, alloys, and cpds., XPS asymmetry of core electrons and electronic struct. parameters 80−93460
transition metals, and their alloys and cpds., photoelectron energy distrib. curves, rel. to band struct., book contrib. 80−16156
transition-metal perovskitelike compounds, covalency effects, partial densities of p- and d-states photoelectron spectra 79−38718
TTF, infinite stacks, all valence electron band struct. 78−39001
tunnelling MIS structures photovoltaic energy conversion, band struct. 80−92995
V_2VI_3 compounds, electronic struct., X-ray emission, XPS, UPS obs. 78−52638
W-dichalcogenide, valence band nature, elec. and mag. props 78−39014

valence bands continued
wurtzite-type semiconductor, exciton binding energy, effect of electron-hole exchange and valence bands 79−51494
X-ray photoelectron spectral characterisation of solids *(French)* 77−36367
zinc-blende semiconductors, quantum resonances in valence bands under uniaxial stress 79−99480
zincblend structure, energy levels of direct exciton formed by split-off valence band 78−91624
zincblende structured ternary alloy semiconductor valence bands, LCBO coherent potential approximation *(Japanese)* 78−47699
Ag, 4d spectrum, high resolution X-ray photoelectron spectra, comparison with APW calc. 77−1784
Ag (110) surface, photoelectron spectroscopy and surface order, UPS and XPS obs. 78−56568
Ag, AES, valence band spectra, solid-state and atomic features 78−72646
Ag, atomic cross-section effects in soft X-ray photoemission from valence bands 77−1783
Ag, Auger spectra obs. 78−76563
Ag halides, tetrahedrally coordinated, semiempirical band struct. model 77−51655
Ag halides, valence and cond. states, UPS, temp. depend. 77−20997
Ag-Cd, behaviour of Cd d-bands, comparison with Hg and Au alloys 79−37972
Ag-Mn, dil., valence and core level spectra, XPS study 80−84838
Ag-Ru(Rh)(Pd) film, valence band spectra, XPS meas. 78−52618
Ag-Sn alloys, UV photoelectron spectroscopy of valence bands 77−24924
$AgAsS_2$, cryst. and amorphous, band struct., photoemission and refl. spectra obs. 77−66581
AgCl, photoconductivity and photoluminesc., 6.8 to 80K, exciton and valence band states 77−43644
AgCl(Br), thermal shifts in energy level separations, ESCA 77−8723
$AgGaSe_2$, and Ag_9GaSe_6, XPS, Auger and direct electron spectra 78−52620
AgI, superionic conductor, density of valence states, photoelectron spectra meas. 80−25523
β-AgI:Cu, pure and doped, photoconductivity, band struct., trap nature 79−95449
Ag(111), valence band struct. along Λ, angle resolved photoemission spectra 79−95316
Al, angle-resolved XPS from valence levels, Brillouin zone averaging 78−48285
Al, single cryst., surface reson. and oxidation 78−72225
Al, valence band Auger spectra, surface effect 80−80915
Al-Mn(Ni)(Cu), dil., core and valence band spectra, XPS study 80−84837
$Al_xGa_{1-x}As$, valence and core level photoemission spectra 79−19973
Al_2O_3, corundum, band struct. calc. using semiempirical Mulliken-Rudenberg method 80−80177
Al_2O_3, electronic struct., XPS meas. 77−73217
Al_2O_3, valence band density of states from self-deconvolution of $L_{23}VV$ Auger spectrum 79−47561
Ar, solid gaseous, valence and inner shell excitonic band struct. 80−6735
Ar, vacancy, electronic structure, Green's function theory 80−39525
Ar, valence electron distrib., pseudopotential calcs. 80−2335
As, interband, magnetorefl. for circularly polarised radiation 78−2840
As-Se amorphous film, density of upper valence band states, annealing effects, UPS obs. 80−29845
As-Se chalcogenide glass, optical const. photoinduced changes mechanism 80−7321
As_2S_3, amorphous, density of valence states, XPS and UPS obs. 77−48308
As_2S_3, crystalline and amorphous, surface charging effects on valence band spectra in XPS 77−8725
$As_xS_{100-x}(Se_{100-x})$, localised states density near valence band edge *(Russian)* 80−103638
$As_2(Se,Te)_3$ glasses, X-ray absorption and photoelectron spectroscopy study 80−7463
Au, AES, valence band spectra, solid-state and atomic features 78−72646
Au, angle resolved XPS, temp. independence 79−19975
Au, angle-resolved XPS from valence levels, Brillouin zone averaging 78−48285
Au, Auger spectra obs. 78−76563
Au clusters on alkali halide surface, size depend. of valence bands, XPS study 80−65647
Au film, photoelectron emission, intershell interaction influence on 3d and 5d branching ratio 80−104038
Au, photoemission, polarisation and ang. dependencies 77−12495
Au subshell photoelectron branching ratio meas. using synchrotron radiation 80−66397
Au, valence bands, angle-resolved photoemission meas. using synchrotron radiation 77−24930
Au, XPS, achromatic X-ray source, spectrum iterative deconvolution, doublet and valence band 78−72689
Au-Cd, behaviour of Cd d-bands, comparison with Hg and Ag alloys 79−37972
Au-Cd(Ga)(In) alloy, UPS exam. of valence bands 79−19511
Au-Cs(Mg)(Rb)(Zn), charge transfer, Mossbauer effect ^{197}Au isomer shifts, XPS valence-band spectra 80−2676
Au-Fe(Co)(Ni), dil., valence and core level spectra, XPS study 80−84838
Au-M (M=Cd, In, Sn, Sb, Te), charge-transfer and valence-band behaviour using ^{197}Au Mossbauer and X-ray photoemission spectra 79−60695
Au-Si interface, valence band and core levels, Si diffusion, alloy form., photoelectron spectra obs. 80−45205
Au(111), Λ-line valence bands, angle-resolved photoemission determ. 80−108323
B, evaporated, electronic struct., XPS, SXS and isochromat investig. 80−76143
BN, cubic, energy band and piezoelec. calcs. 78−72071
BP-BAs solid solns., electronic struct. of valence bands and nature of interatomic interaction 78−34764
BP_xAs_{1-x} system, electron struct. and interatomic interactions, X-ray spectroscopy 80−20736
$BaCl_2$ film, UPS exam. 79−38716
BaF_2 film, UPS exam. 79−38716
BaF_2, width of upper valence band, tight-binding calc. 78−26814
BaO, XPS valence bandstruct. 80−89117
valence bands continued
$BaTiO_3$, band struct. calc., interpretation of XPS and UPS spectra 80−70597
$BaTiO_3$, electronic struct., XPS and band struct. calc. 79−38708
$BaTiO_3$, photoelectron and optical spectra derived from self-consistent charge MO and band calcs. 80−96785
$BaTiO_3$, undoped and Cu doped, Γ_{15} phonon freezing, electronic instability, LCAO calc. 80−25318
$BaTiO_3$, valence band UPS and partial p and d density of states 80−71560
$BaTiO_3$, XPS, band struct., density of states, photoionisation cross sections 78−52629
Be, HCP metals, K-emission valence bands, structure and bonding 80−7438
Be, polarised K-emission valence bands 77−16429
Be, XPS investigation of density of states 78−6829
Bi electron properties, carrier spectrum, review 78−84137
Bi, film, oxidation, UPS, valence band, cond. band and 5d core states 77−20995
Bi film, oxidation kinetics and interfacial bonding using final states 77−56127
Bi, solid and liq., valence band structure, XPS meas. 77−32504
BiI_3, layered semicond., valence bands UPS and XPS obs. 78−11078
BiI_3, octahedrally coordinated, layer cpd., electronic struct. using synchrotron-radiation photoemission spectroscopy 79−74058
$(Bi_{1-x}Sb_x)_2Te_3$, highest valence band struct., Shubnikov-de Haas effect 78−14661
Bi_2X_3, (X=O,S,Se,Te), X-ray photoelectron spectra and electronic struct. 77−32493
C, amorphous, inelastic electron scatt., valence electron contrib. 80−55240
C, glassy, Compton profiles, momentum densities, comparison with graphite 80−2895
C:Ni, X-ray photoemission studies 80−76138
CaF_2, width of upper valence band, tight-binding calc. 78−26814
CaO, XPS valence bandstruct. 80−89117
$CaSi_2$, X-ray spectra, valence band struct. *(Russian)* 79−1798
Cd-P compounds, X-ray emission bands intensity distrib., influence of chem. bonds 77−28658
Cd_3As_2, valence band struct., optical absorpt. meas. 80−50293
$CdCr_2Se_4$, optical absorption due to transitions between bands and local levels 79−38537
CdF_2, struct. determ. by photoemission meas. 79−47591
$CdGa_2S_4(Se_4)$, band struct., pseudopot. method 80−92816
$CdGa_2Se_4$, struct. of valence band, photocond. and reflection spectra meas. 80−6719
CdI_2, valence-band XPS meas. 77−12487
$CdI_2(Br_2)(Cl_2)$, dielec. function and band struct., EELS meas. 80−40195
$CdIn_2S_4$, electronic states, sensitivity to cryst. struct., UPS study 80−45209
$CdIn_2S_4$ single crystals, recombination process and localised levels 80−93383
$CdIn_2S_4$, valence band densities of states, XPS meas. 79−28892
α-$CdIn_2Se_4$, defect zincblende struct., electronic props. 77−15767
$CdIn_2Se_4$, defect zincblende semicond., valence band, cryst. struct. effects 78−48278
CdP_2, role of metal d states in valence band formation 79−65380
CdP_4, role of metal d states in valence band formation 79−65380
Cd_2P_3, role of metal d states in valence band formation 79−65380
Cd_3P_2, role of metal d states in valence band formation 79−65380
CdS, band structure calcs. by modified orthogonalised plane wave (MOPW) method 80−54609
CdS:F(Cl), shallow donors electronic Raman scatt., reson. enhancement 80−45068
CdSe-Si n-p heterojunction, vacuum deposition, photovoltaic effects *(Korean)* 77−28243
$CdSiP_2$, electronic struct., X-ray spectroscopic investigation 80−108300
$CdSiP_2$, pseudodirect bandgap semiconductor, natural birefringence 79−65834
n-$CdSnAs_2$, optical absorption rel. to energy spectra *(Russian)* 78−75994
CdTe:Li, excitation spectrum of Li acceptor and valence band parameters 79−28795
Ce and Ce-Al alloys, XPS valence band spectra meas. 77−48306
γ-Ce, valence band exam. by XPS and UPS 79−37977
α-Ce, valence band photoemission intensity, giant enhancement 79−19972
Ce-pnictides, XPS exam. 79−38717
CeN, electronic struct., XPS exam. 78−6269
CeP_5O_{14}, photoemission spectra, 4f, 5p and 5s giant reson. enhancement 78−95660
CoAl, bonding, self-consistent energy bands 78−91610
$CoCl_2$, energy spectrum of valence electrons, X-ray emission spectra 77−16430
CoF_2, valence-electron density of states, XPS meas. 77−69963
CoO and Co_3O_4, XPS interpretation, valence band structure 77−12497
CoO, electronic struct., XPS and UPS expts. *(French)* 79−38711
CoO, valence band struct., cryst. field anal., photoelectron data 79−47007
Co_3O_4, electronic struct., XPS and UPS expts. *(French)* 79−38711
$CoS_2(Se_2)$, core-level and valence-band XPS 80−93450
CoSb, electronic struct., XPS meas. 78−2990
CoSi, plasma refl., 80 to 300K, energy overlap of valence and conduction bands 79−28366
CoSi, X-ray emission spectra obs. of valence band states *(Ukrainian)* 77−69935
CsAu, photoelectron spectroscopy and energy bands calc. 78−76581
CsBr, (110) surface, electronic struct. of valence bands calc. *(Russian)* 80−75621
CsCl, (110) surface, electronic struct. of valence bands calc. *(Russian)* 80−75621
CsI, (110) surface, electronic struct. of valence bands calc. *(Russian)* 80−75621
Cu (110), valence bands, angle-resolved photoemission spectra meas. 79−74056
Cu, AES, valence band spectra, solid-state and atomic features 78−72646
Cu, ang. depend. XPS valence-band spectra meas. 77−21006
Cu, angle resolved photoemission, thermally induced breakdown of direct-transition model 77−77346

valence bands continued
Cu, Auger spectra obs. 78−76563
Cu clusters, valence band and core binding energies, UPS meas. 79−38721
Cu, energy band dispersions and lifetimes using angle-resolved photoemission 79−77998
Cu film, photoelectron emission, intershell interaction influence on 3d and 5d branching ratio 80−104038
Cu film, valence bands, XPS excited by Zr Mζ radiation 80−40236
Cu, film growth on graphite and amorphous C, electronic struct. by photoemission and Auger obs. 79−77947
Cu halides, reflection spectra, 4.5-7.5 eV, bond struct. scheme 79−61402
Cu halides, tetrahedrally coordinated, semiempirical band struct. model 77−51655
Cu, $L_{2,3}VV$ and MVV Auger spectra 78−68583
Cu, $L_3M_{4,5}M_{4,5}$ and $M_{2,3}M_{4,5}M_{4,5}$ Auger line shapes, independent electron calc. 77−63500
Cu, MVV Auger spectra, atomic model and valence band features 78−72644
Cu molybdates, valence band X-ray induced Auger spectra and XPS 78−80813
Cu oxides, valence band X-ray induced Auger spectra and XPS 78−80813
Cu, photoemission from valence bands 77−20996
Cu, surface d-band narrowing, angle resolved XPS 78−19635
Cu, valence band splitting, X-ray K-emission spectroscopy 80−40189
Cu, valence bands, angle-resolved photoemission meas. using synchrotron radiation 77−24930
Cu, XPS, angle-resolved, valence band density of states distrib. 77−44123
Cu-Fe(Co)(Ni), dil., valence and core level spectra, XPS study 80−84838
Cu-Zr, metallic glasses, valence band struct. investigation 80−11533
$Cu_{0.7}Al_{0.3}$, chemical effect on valence electronic states, AES and SXAPS meas. 79−47558
CuBr, multiplet struct. of P-excitons due to valence band degeneracy 78−39035
CuBr, UPS, temp. depend., dynamic hybridisation 77−20998
CuCl, UPS meas., electronic struct. 80−50529
CuCl, XPS and Auger spectroscopy, elec. struct. 80−29852
$CuGaS_2$, tetragonal distortion, crystal field splitting, temp. depend. 79−47060
$CuGaSe_2$, obs. of energy transitions from lower valence band states 78−95576
$CuGaSe_2$, temp. depend. of fundamental absorpt. edge 78−92090
CuI, thermoreflectance spectrum, 4-7 eV region 79−19904
$CuInTe_2$, optical transitions from valence band states 79−87416
$(Cu_xNi_{1-x})S_2$, XPS of valence band meas. 77−85885
Cu_2O, pure and Fe doped, carrier cyclotron resonance impurity scattering effects, polar mass extrinsic origin 79−56614
Cu_2O, self-consistent energy bands 80−59869
CuP_2, Cu_3P, electronic struct. of valence bands, X-ray spectra and XPS 78−92176
$Cu_{0.75}P_{0.25}$, chemical effect on valence electronic states, AES and SXAPS meas. 79−47558
CuPd, chemical shift effects and origin of Pd 3d core level satellite 80−104039
$Cu_{0.67}S_{0.33}$, chemical effect on valence electronic states, AES and SXAPS meas. 79−47558
$Cu_{0.9}Si_{0.1}$, chemical effect on valence electronic states, AES and SXAPS meas. 79−47558
CuZr, photoemission study 80−104046
Cu(100), photoemission via Bloch states and evanescent band gap states, polarised synchrotron irradiation 79−61492
$EuCu_2Si_2$, valence fluctuation and temp. depend. of Cu nuclear quadrupole interaction 80−15818
$EuCu_2Si_2$, XPS studies, valence band, 4-f region 78−6831
Fe, photoemission and electronic spectra, exchange splitting 77−4717
Fe-B amorphous alloys, valence band spectrum, XPS study 80−50534
Fe-Ni alloys, electronic struct., XPS study 80−29842
FeAl, bonding, self-consistent energy bands 78−91610
FeB and Fe_2B, ESCA and mag. spin data, electronic struct., isomer shifts, valence bands and chemical bonding 80−75489
$Fe_{0.5}Cu_{0.5}Cr_2S_4$, ESR spectra, elec. and mag. props., Curie temp. 80−97137
FeF_2, valence-electron density of states, XPS meas. 77−69963
FeO, valence band XPS and UPS, LCAO-MO calcs. 80−45197
$Fe_{1-x}(P,B)_x$, amorphous and crystalline, photoemission and band structure 80−60754
FeS_2, core-level and valence-band XPS 80−93450
$Fe_{1-x}S$, soft X-ray emission and AES study 79−91535
$FeSb_2$, quasi-magnetic semicond., mag. susceptibility 80−39757
FeSi, $FeSi_2$, valence shell XPES 79−43105
GaAS, O_2 chemisorption on (110) surface, bonding sites 78−38938
$Ga_{1-x}Al_xAs$ electrodes, interface capacitance meas., flatband pot., conduction and valence band boundaries *(French)* 79−33339
GaAs (110), valence band Auger spectra 78−35230
GaAs (110), valence band Auger spectra, from Ga and As CCV transitions 78−92149
GaAs (110)-Al(Ga) interface, interface states, photoemission study 78−95359
GaAs, angle-resolved photoemission and valence band dispersions 80−7469
p-GaAs, electronic props. 78−68040
GaAs, electronic surface props., interaction with Au and O adsorbate layers 77−20385
GaAs, high resist., linear electroabsorpt., characts., valence band splitting 77−44018
n-GaAs, interband transition times, luminesc. depolarisation obs. *(Russian)* 79−33831
GaAs, surface states, band struct. by discontinuous potential method 80−20276
GaAs, valence band fine struct. from light mod. with nonequilib. opt. phonons 78−39568
GaAs, valence band struct. obtained by magnetophonon effect 77−76748
GaAs, valence band structure, CPA, bond orbital calcs. 78−87909
n-GaAs, valence band studies of clean and O_2 exposed surfaces 78−43298
GaAs, valence-band dispersions, electron and hole lifetimes, angle-resolved photoemission 80−80947

valence bands continued
p-GaAs:Cd, (110) cleaved surface, defect-induced surface states 80−6925
GaAs:Cr, carrier equilibrium effects, impurity states, elec. resistivity 80−65488
GaAs:Cr, local level near valence band, photocapacitance 79−11080
GaAs:Sb, resonance levels of isoelectronic impurities 80−107740
$GaAs-Ga_{1-x}Al_xAs$, superlattice umklapp processes in resonant Raman scattering 78−64362
GaAs-Ge heterojunction, band discontinuities, angle-resolved UPS obs. 79−7878
GaAs-Ge structure, electronic struct., ang.-resolved photoemission obs. 80−49881
$GaAs_{1-x}P_x$ electrodes, interface capacitance meas., flatband pot., conduction and valence band boundaries *(French)* 79−33339
GaN, electron struct., ESCA study 80−89116
GaP (110), electronic surface states, initial steps of O_2 chemisorption 80−49844
GaP, cleaved (110) surface, electron surface props. 80−11067
GaP, valence band structure, CPA, bond orbital calcs. 78−87909
GaP:Fe, electron exchange via val. band between Fe acceptor centres, Mossbauer spectra 77−55741
GaP-liq. NH_3 soln. junctions, elec. characts. *(French)* 80−2460
GaS, valence and conduction bands, synchrotron radiation photoemission spectra 77−63536
GaS, XPS and valence band density of states, tight binding approx. 78−63974
GaS_xSe_{1-x}, valence band states, composition depend., photoemission spectra study 80−100434
GaS_xSe_{1-x}, wavefunction symm. and binding energies, synchrotron radiation photoemission spectroscopy 80−50532
GaSb, degenerate valence band, diamag. excitons and oscillatory magnetoabsorpt. 77−76754
GaSb, solid solns., impact ionisation, cond. and valence band effects 80−65583
GaSb, valence band structure, CPA, bond orbital calcs. 78−87909
p-GaSb:Zn, hole transport props. from 77 to 300K 79−73530
GaSe, layer, upper valence bands using bond-orbital model 79−15078
GaSe, spatial symm. of valence band struct. by angularly resolved XPS 77−69961
GaSe, valence and conduction bands, synchrotron radiation photoemission spectra 77−63536
GaSe, valence band struct., angle-resolved photoemission spectroscopy 77−1360
GaSe, wave function symmetries of valence band states revealed by polarisation effects in angle-integrated photoemission spectroscopy 79−67395
Gd and Gd-Al alloys, XPS valence band spectra meas. 77−48306
Gd-Fe, mag. moment of Fe, multiplet splitting in photoemission 79−78846
$Gd_{0.67}La_{0.33}P_5O_{14}$, photoemission spectra, 4f, 5p and 5s giant reson. enhancement 78−95660
Ge, direct gap recombination, at high excitation level and low temp. 79−38650
Ge, dislocation energy band width, carrier lifetime anal. 77−11874
Ge, electron-hole drop freq. depend. damping 80−88482
p-Ge, hole drift vel. in high field 79−95415
Ge, ion implanted, cond. and valence bands study by X-ray bremsstrahlung and photoelectron spectra 80−2360
Ge, photoemission spectroscopy of surface states and oxidation 77−55863
Ge, photoionisation cross-sections of valence s- and p-electrons *(Ukrainian)* 77−73211
p-Ge, saturable absorption isolator for CO_2 laser systems 77−19284
Ge, transmission Faraday rot., due to intervalence band transitions 79−38521
Ge uniaxially deformed, cyclotron resonance of RF field heated hot holes, *(Russian)* 80−44925
Ge, valence band effective mass strain depend. 78−51880
Ge, valence band relaxation energies during XPS 78−39657
Ge, valence band splitting in mag. field, LCAO interpolation *(German)* 77−59251
Ge, valence band struct. obtained by magnetophonon effect 77−76748
Ge, valence electrons, XPS, LCAO and OPW calc. 77−12496
Ge:Cu, hot photoexcited holes at low temp. 78−30954
Ge/GaAs (110) heterojunction, valence band discontinuity in XPS spectra, precise determ. 80−84834
Ge-GaAs heterojunction, electrostatic dipole shifts contrib. to valence band discontinuities 79−51657
Ge-GaAs heterojunctions, electronic struct. 78−19138
Ge-rare earth alloys, nature of chemical interaction, X-ray emission, absorpt. and photoelectron study *(Russian)* 80−55261
Ge-Si cpds., effect of short-range order 77−59252
GeS, amorphous, UPS and XPS, valence band struct. 77−90247
GeS, density of valence states, tight binding calc. 79−77976
GeS(Se)(Te), XPS investig. of valence band struct. 77−48311
GeSe, amorphous, UPS and XPS, valence band struct. 77−90247
GeSe, density of valence states, tight binding calc. 79−77976
GeTE, density of valence states, tight binding calc. 79−77976
GeTe, amorphous, UPS and XPS, valence band struct. 77−90247
$(HCN)_x$, mol. crystals, quantum theory, mol. tight binding method calcs. 80−49572
H_xWO_3 bronzes, Anderson transition, XPS 80−107705
^3He, solid, valence band struct., zero-point motion effect 80−65333
Hf, valence band XPS, correl. to supercond. 79−65980
HfC-TaC alloys, microhardness rel. to valence electron conc. 77−86130
$HfC_xN_yO_z$, valence band XPS, correl. to supercond. 79−65980
Hg, valence band spectra by PES study 80−4822
Hg-Cd, behaviour of Cd d-bands, comparison with Au and Ag alloys 79−37972
HgSe, interband $\Gamma_6 \rightarrow \Gamma_8$ magnetoabsorption, temp. study 80−76032
HgTe, mag. sub-band struct. under uniaxial stress 77−11883
II-VI semiconductor-electrolyte boundaries, electrolyte boundaries, photo e.m.f. meas., semicond. energy bands 77−1481
In inorganic and organometallic cpds., photoelectron spectra, valence bands, ligand field broadening 77−63525
InAs, valence band structure, CPA, bond orbital calcs. 78−87909
$In_{1-x}Ga_xAs-GaSb_{1-y}As_y$, new heterostruct. characts. 78−72247
$In_xGa_{1-x}As_yP_{1-y}$, valence band struct., CPA calc. 79−73435
InP, III-V semicond., electronic struct. of valence and conduct. bands 77−28110

valence bands continued
InP, oscillatory interband magnetoabsorption meas. 79−73909
InP, valence band fine struct. from light mod. with nonequilib. opt. phonons 78−39568
InP, valence band structure, CPA, bond orbital calcs. 78−87909
InP-$In_{1-x}Ga_xP_{1-y}As_y$, valence band discontinuity, quantum well luminesc. 79−91483
In_2S_3, valence band densities of states, XPS meas. 79−28892
InSb, conduction and valence band effective mass parameters 79−60689
InSb, cyclotron harmonic transitions, warping and inversion asymm. effects 78−68383
InSb, intraband photocond. in mag. fields 79−47123
p-InSb, magnetophonon reson. of holes 79−95424
p-InSb, quantum resonances in valence band under uniaxial stress, far IR meas. 79−99481
p-InSb, stress induced k-linear terms in band struct. 80−49595
InSb, valence band struct. obtained by magnetophonon effect 77−76748
InSb, valence band structure, CPA, bond orbital calcs. 78−87909
InSe, angle resolved photoemission, 15-29 eV, valence band struct. 77−48319
InSe, spin orbit split off valence bands, exciton transitions, Hopfield's quasicubic model, visible absorpt. spectrum 80−50370
InSe, valence and conduction bands, synchrotron radiation photoemission spectra 77−63536
IrO_2, electronic struct., XPES obs., rel. to TiO_2, RuO_2 78−52632
K surface, clean and O_2-exposed, X-ray and UV photoelectron spectra 78−52636
KBr, electronic states at (100) surface, accounting for spin-orbit interaction *(Russian)* 78−91750
KCl, electronic states at (100) surface, accounting for spin-orbit interaction *(Russian)* 78−91750
KCl:Tl, low-temp. ionisation of activator, photoexcitation, in region of interzone transitions *(Russian)* 79−28320
KI, electronic states at (100) surface, accounting for spin-orbit interaction *(Russian)* 78−91750
$KNbO_3$, electronic struct., XPS and band struct. calc. 79−38708
$KNbO_3$, XPS, band struct., density of states, photoionisation cross sections 78−52629
$KTaO_3$, electronic struct., XPS and band struct. calc. 79−38708
$K[Fe_4S_3(NO_7)]$, valence levels, X-ray photoelectron and X-ray spectra 77−88500
La and La-Al alloys, XPS valence band spectra meas. 77−48306
LaB_6, UPS and XPS of valence band 78−84703
LaB_6, valence band dispersions, angle-resolved photoemission 80−11536
$LaCrO_3$, spin states, XPS meas. 78−68599
LaOF, features of formation of band structure 79−33232
$LaTiO_3$, spin states, XPS meas. 78−68599
Li, cryst. and electronic props., Hartree-Fock calcs. 79−60698
Li, valence band Auger spectra, surface effect 80−80915
LiC_6, intercalated, charge-transfer and non-rigid-band effects 80−44496
LiC_6, spatial distribution of valence electrons 79−37983
LiF, evaporated film, UPS, valence and cond. band struct. 77−63528
LiH, valence band struct., XPS exam. 79−69416
$LiNbO_3$, valence band UPS and partial p and d density of states 80−71560
Mg, HCP metals, K-emission valence bands, structure and bonding 80−7438
Mg, $L_{23}VV$ Auger spectrum 78−39634
Mg, XPS investigation of density of states 78−6829
Mg-Cu alloy, electronic struct., X-ray emission obs. 77−16428
Mg_2Ge, valence band, XPS meas. 77−8018
MgO, electronic struct., XPS meas. 77−73217
MgO, single crystal, thermal and optical stimulation processes of V-centres *(Japanese)* 80−11485
MgO, valence electron distrib., pseudopotential calcs. 80−2335
MgO, XPS valence bandstruct. 80−89117
Mg_2Si, valence band, XPS meas. 77−8018
Mg_2Si, valence band density of states, pseudopot. calc. 78−72067
$MgSiP_2$, electronic struct., X-ray spectroscopic investigation 80−108300
Mg_2Sn, valence band, XPS meas. 77−8018
$MnCl_2$, energy spectrum of valence electrons, X-ray emission spectra 77−16430
MnF_2, d-orbital directed photoemission using AlK_α radiation 79−95901
MnF_2, valence-electron density of states, XPS meas. 77−69963
$MnS_2(Se_2)$, core-level and valence-band XPS 80−93450
MnS(Se)(Te), core level binding energies and valence band spectra, XPS meas. 78−80455
MnSb, electronic struct., XPS meas. 78−2990
MnSi, Mn_5Si_3, valence shell XPES 79−43105
Mo X-ray electron spectra, paramag. susceptibility, depend. on plastic deform. for single crystals 77−28683
Mo-dichalcogenide, valence band nature, elec. and mag. props. 78−39014
MoS_2, UPS meas. band struct. determ. 78−35250
NH_3, solid, UPS, valence band struct. 79−33890
Na, XPS investigation of density of states 78−6829
NaCl, valence electron distrib., pseudopotential calcs. 80−2335
NaCl-type crystals, donor levels due to dislocations, calc. 80−6771
Na_xWO_3 bronze, oxidation state of W, oxidation by air exposure 77−8719
Na_xWO_3, vacuum UPS exam. 78−84700
$Na_2[Fe(NO)_2(S_2O_3)]_2$, valence levels, X-ray photoelectron and X-ray spectra 77−88500
Nb-V alloy, X-ray M- and L-emission bands obs. *(Russian)* 78−19602
Nb-Zr-C (0.1, 0.01 wt.%) plastic deform. influence on electronic state of Nb atoms 80−40463
NbC, high-temp. plastic deform. effects on elec. props. 77−44370
NbC, valence band struct. *(Russian)* 78−6268
NbC, valence band XPS meas., comparison with X-ray emission spectra and band struct. spectral calcs. 80−50535
$Nb_3Os(Ir)(Pt)(Au)$, XPS of valence electrons meas. 77−21003
NbS_3 and Nb_3S_4, electronic struct. and predicted cond. props. 80−92815
Ne, vacancy, electronic structure, Green's function theory 80−39525
Ni (001) surface, electronic struct. of ordered S overlayers 80−84835
Ni (111), band struct. and temp.-depend. mag. exchange splitting, angle resolved photoemission obs. 78−60546
Ni, chemisorptive binding of O, CNDO calc. of potential energy curves *(German)* 80−44431
Ni clusters, valence band and core binding energies, UPS meas. 79−38721
valence bands continued
Ni, film growth on graphite and amorphous C, electronic struct. by photoemission and Auger obs. 79−77947
Ni films, HCP and amorphous, RF sputtered, O_2 incorporation, ESCA obs. 80−10832
Ni, photoemission spectra, valence band and core level satellite due to excitation of d electron 80−97408
Ni, valence-band photoemission spectra, self-energy corrections effect 80−11534
Ni, XPS valence band spectra 77−21007
Ni-O system, oxidized polycryst. Ni films, H_2 reduction, AES 77−12472
NiAl, bonding, self-consistent energy bands 78−91610
β'-NiAl, density of states, XPS meas. 78−48284
NiF_2, valence-electron density of states, XPS meas. 77−69963
$NiS_2(Se_2)$, core-level and valence-band XPS 80−93450
NiSb, electronic struct., XPS meas. 78−2990
NpO_2, XPS of 5f electrons 77−73216
Pb, inorganic and organometallic cpds., photoelectron spectra, valence bands, ligand field broadening 77−63525
$PbCl_2(Br)(I_2)$, valence band electronic struct., XPS and UPS obs. 78−6826
$Pb_{1-x}Ge_xTe$, Raman scatt. from soft TO-phonon modes 79−95773
$Pb_{1-x}Ge_xTe$, solubilities, elec. and optical props. 77−35940
PbI_2 (2H), layer cpd., band parameter determ. 79−95332
PbI_2 intercalated with organic mols., energy band splitting *(Russian)* 78−76027
PbI_2, layered semicond., valence bands UPS and XPS obs. 78−11078
PbI_2, octahedrally coordinated, layer cpd., electronic struct. using synchrotron-radiation photoemission spectroscopy 79−74058
PbI_2, press. depend. of band-gap excitons, 77K, optical absorpt. spectra 79−8157
PbI_2, valence-band XPS meas. 77−12487
PbN_6, electronic transitions and energy band struct. 79−74053
p-PbS, dispersion law investigation, valence band density of state effective mass 79−95314
p-PbS, struct. of valence band, transport processes study 80−20081
PbS, temp. effects on valence bands, UPS study 80−11537
PbS, valence band struct., angle-resolved photoemission spectra obs. 77−48310
PbS(Se), valence band struct. determ. by optical absorpt., size quantization effects 80−59871
PbS(Se)(Te), XPS investig. of valence band struct. 77−48311
PbSe, spin-orbit splitting in valence bands, angle-resolved UV photoemission 78−2991
PbSe, temp. effects on valence bands, UPS study 80−11537
p-PbSe, valence band structure, IR refl. and absorpt. meas. 77−55791
PbSe, valence band structure from angular resolved photoemission spectra 78−84143
PbSe, valence band struct., Hall and transverse Nernst-Ettingshausen effects, optical absorption 79−11064
$Pb_{1-x}Sn_xSe$, valence zone struct. effect on mobility/inherent conc. ratio *(Russian)* 79−73437
$Pb_{0.82}Sn_{0.18}Te$, thermomagnetic, thermoelectric props., valence band struct. *(Russian)* 80−54724
$Pb_{1-x}Sn_xTe$, DH laser, gain-freq.-current relation, k.p band model 77−61951
$Pb_{1-x}Sn_xTe$, hole effective mass near zero bandgap, IR refl. study 80−108205
$Pb_{1-x}Sn_xTe$, narrow gap solid solns., mag. susceptibility and energy band spectrum 79−28276
$Pb_{1-x}Sn_xTe$, valence band struct., Hall effect meas. 78−39016
$Pb_{1-x}Sn_xTe$:Ge, anomalous behaviour of impurity centres under press. *(Russian)* 80−65491
PbTe, struct. of second valence band 77−89697
Pd (111), energy dispersions for valence and conduction bands 79−38719
Pd catalytic clusters, electronic structure, XPS obs. 77−77345
Pd clusters, valence band and core binding energies, UPS meas. 79−38721
Pd, film growth on graphite and amorphous C, electronic struct. by photoemission and Auger obs. 79−77947
Pd particle arrays on C film, UPS, Pd valence band width 78−88403
Pd, photoemission spectra, valence band and core level satellite due to excitation of d electron 80−97408
Pd-Si, metallic glasses, XPS and UPS studies 79−74062
Pd-Zr, metallic glasses, valence band struct. investigation 80−11533
PdZr, photoemission study 80−104046
Pt, absorption of CO on (111) surface, photoemission, 40-150 eV 77−16465
Pt, angle resolved XPS, temp. independence 79−19975
Pt band-structure determ., angle-resolved photoemission 80−66398
Pt catalytic clusters, electronic structure, XPS obs. 77−77345
Pt subshell photoelectron branching ratio meas. using synchrotron radiation 80−66397
$Pt_{0.97}S_2$, optical props. at absorption edge 78−35140
Pt(111), Λ-line valence bands, angle-resolved photoemission determ. 80−108323
Pu, oxidation, binding energies, Auger and X-ray photoelectron spectra study 80−76550
PuO_2, XPS of 5f electrons 77−73216
RbAu, photoelectron spectroscopy and energy bands calc. 78−76581
RbCl(Br)(I), thermal shifts in energy level separations, ESCA 77−8723
RuO_2, electronic struct., XPES obs., rel. to TiO_2, IrO_2 78−52632
$(SN)_x$, film, brominated, XPS, electronic struct. 78−72678
$(SN)_x$, polycryst. films, single crysts., UPS, valence band struct. 77−69967
S_4N_4, film, brominated, XPS, electronic struct. 78−72678
$(SNH)_x$, density of states, CPA calcs., effect of H impurities 79−42431
Sb inorganic and organometallic cpds., photoelectron spectra, valence bands, ligand field broadening 77−63525
SbI_3, valence band, UPS meas. with synchrotron radiation 79−56914
Sb_2S_3, amorphous, density of valence states, XPS and UPS obs. 77−48308
Sb_2S_3, fundamental absorpt. edge, optical props. 79−56817
Se, trigonal, luminesc. identification of indirect transition 80−55189
Se, trigonal, NMR chem. shift, tight-binding calc. 78−2759
Se, trigonal and amorphous, electronic struct. and nonempirical calc. of struct. props. 80−59866
Se-Te-Sb glasses, electronic transport 80−88579
Se_8, monoclinic, XPS and valence band struct., comparison with trigonal form and S_8 77−44124

valence bands continued
n-Si (001) on sapphire, galvanomag. effect for holes, valence band 79−91166
Si (111), (100) and (110) ideal surfaces, valence-band Auger lineshape theory 77−48286
Si (111) 7×7 clean surface and O chemisorbed stage valence band density of states from $L_{23}VV$ Auger spectra 80−100717
Si (111) surface, clean, ESCA obs., Ni(Au) surface impurities 78−52640
Si, AES, convolution and deconvolution 78−52601
Si, amorphous, clean and O_2 adsorbed, light sensitive electron laser meas. 79−24396
Si, amorphous, position of Fermi level, spectroscopic and transport determ. 80−6706
Si, amorphous, topological and electronic struct. 77−28102
Si, clean and gas (O_2 and H_2O) covered surface, appl. of UPS ultrahigh vacuum apparatus *(Japanese)* 80−37125
Si, core and valence electron excitations, AES, chemical shift and line shape 80−2365
Si, electronic struct., non-spherical local pseudopotential calcs. 80−39496
p-Si, high ohmic material, deep level investigation, vacuum growth *(Russian)* 80−54654
p-Si, hole drift vel. in high field 79−95415
Si, hole mobility temp. depend., valence bandstruct. 77−80771
Si, hot holes, drift and diffusion 79−78110
p-Si, interband transitions, contrib. to conductivity at submillimetre wavelengths 80−34473
p-Si, millimetric and far IR cond., evidence for interband transitions 78−52022
Si on sapphire, residual strain effect on elec. props. *(Japanese)* 80−84522
Si, photoionisation cross-sections of valence s- and p-electrons *(Ukrainian)* 77−73211
Si, state density and X-ray photoelectron spectra of valence bands calc. 77−28679
Si surface, local density of states method and bond orbital model calc. 77−8165
Si surface, valence band Auger line shape, corrected numerical results 78−52602
Si, valence band model, nonlocal exchange and correl. pot. 77−43492
Si, valence band relaxation energies during XPS 78−39657
Si, valence bands, XPS excited by Zr $M\zeta$ radiation 80−40236
Si, valence bond Wannier functions calcs. 78−60053
Si, valence electrons, energy-depend. photoionisation probability calc. 77−16462
Si:F(,H), amorphous, electronic struct., orthogonalised LCAO calc. 80−44486
Si-H, amorphous film, in situ prepared, photoemission studies 80−35060
Si-SiO_2 boundary, surface charge transport in valence band of Si 80−70789
SiAs, monoclinic, OPW calc. 77−59255
$Si_xGe_{1-x}O_2$, $0 \le x \le 1$, XPS and UPS, electronic struct. 77−48318
Si_5H_{12} cluster, Si valence band Auger spectrum, cluster approach, comparison with experimental spectrum 80−40191
Si_3N_4 amorphous film, CVD, core and valence electron excitations, low energy electron loss spectroscopy and AES 80−2365
SiO molecule, true potential energy curves, dissoc. energy, ionisation potential 77−6704
SiO_2 amorphous film, thermal, core and valence electron excitations, low energy electron loss spectroscopy and AES 80−2365
SiO_2, orthosilicates, mica, soft X-ray spectra and photoelectric yield spectra 78−72640
SiO_2, thermally grown film, optical absorption and photocond. 78−64421
SiO_2, valence band density of states from self-deconvolution of $L_{23}VV$ Auger spectrum 79−47561
SiO_x system, cluster plus effective medium tight-binding study 79−33216
SiP_2, pyrite structure, density of states 77−15733
SiS molecule, true potential energy curves for various states, dissoc. energies 77−6704
Si_3Si_5, X-ray spectra, valence band struct. *(Russian)* 79−1798
$SmCo_5$, electronic struct., X-ray photoelectron spectra 77−20992
Sm_2S_3-Sm_3S_4, valence related optical and other studies, review 78−31215
$SmS_{1-x}P_x$, valence changes, XPS and UPS study 80−97402
Sn inorganic and organometallic cpds., photoelectron spectra, valence bands, ligand field broadening 77−63525
$SnBr_2$, UPS, 40.81 eV, valence band struct. 79−33891
$SnCl_2$, UPS, 40.81 eV, valence band struct. 79−33891
$SnCl_2$, valence band electronic struct., XPS and UPS obs. 78−6826
SnF_2, valence bands, electronic struct., UPS 78−39656
$Sn_{1-x}Mn_xTe$, IR reflectivity, elec. susceptibility mag. order effects 79−47433
SnO_2, electronic struct. and densities of states, tight-binding calcs. 80−15447
SnO_2, rutile, band gap assignment by two-photon spectroscopy 79−19513
SnS, tight-binding calc. of density of valence states 78−34760
SnS_2, conduction and valence band density of states 77−62817
SnS_2, octahedrally coordinated, layer cpd., electronic struct. using synchrotron-radiation photoemission spectroscopy 79−74058
$Sn(S_xSe_{1-x})_2$, valence band states, composition depend., photoemission spectra study 80−100434
SnS(Se)(Te) XPS investig. of valence band struct. 77−48311
SnSe, tight-binding calc. of density of valence states 78−34760
$SnSe_2$ spatial symm. of valence band struct. by angularly resolved XPS 77−69961
SnTe, cubic semicond. with ellipsoidal valleys, magnetoresist. 80−80300
SnTe, Raman scatt. from soft TO-phonon modes 79−95773
SnTe, tight-binding calc. of density of valence states 78−34760
SrF_2, width of upper valence band, tight-binding calc. 78−26814
SrO, electronic struct., XPS meas. 77−73217
SrO, XPS valence bandstruct. 80−89117
$SrTiO_3$, electronic struct., XPS meas. 77−73217
$SrTiO_3$ semicond. electrode, electrochem., photoelectrochem. props. 80−3352
$SrTiO_3$, valence band UPS and partial p and d density of states 80−71560
$SrTiO_3$, XPS, band struct., density of states, photoionisation cross sections, theoretical determ. 78−52629
valence bands continued
TaS_2 (1T), angular resolved photoemission at low energy and high atomic number 77−36373
Te, hole susceptibility anisotropy, spin contrib. and total 77−85413
Te, hydrostatic press. effect 77−47724
Te, intervalence band absorption, press. and defects influence 80−55149
Te, opt. props. under high press., band struct. transform. 80−55112
Te, trigonal, NMR chem. shift, tight-binding calc. 78−2759
Te, trigonal, self-consistent ground state, X_α calcs. 80−54604
Te, trigonal and amorphous, electronic struct. and nonempirical calc. of struct. props. 80−59866
Te, uniaxially stressed, submm. cyclotron reson., deform. pots. and k.p coeffs. 80−54606
Te, valence band struct. under press., spin-orbit splitting, intraband absorpt. spectra 80−2330
Te, valence-band X-ray emission spectrum 78−84682
ThPt, valence bands, XPS spectra 80−50520
Ti (0001), valence band struct. and chemisorption, XPS and UPS study 80−35062
Ti-Zr alloy, X-ray M- and L-emission bands obs. *(Russian)* 78−19602
TiC, valence band electron distrib., photoelectron spectra obs. 77−44120
TiC, valence X-ray photoelectron spectrum, density of states 77−81197
TiC_x, single cryst., core level shifts, valence band struct., ESCA 77−32499
TiGa, $TiGa_2$, Ti_5Ga_3, X-ray K- and L-bands, electronic struct. *(Russian)* 79−1797
TiGe, $TiGe_2$, Ti_5Ge_3, X-ray K- and L-bands, electronic struct. *(Russian)* 79−1797
TiO_2, clusters, surface electron struct. and defect states, DV-Xα calc. 80−20268
TiO_2, cond. and valence band struct., gap anisotropy 77−47729
TiO_2, electronic struct., XPS obs., rel. to RuO_2, IrO_2 78−52632
TiO_2, subsidiary valence band extrema, piezospectroscopic exam. 79−19516
TiP, TiP_2, electronic struct. of valence bands, X-ray spectra and XPS 78−92176
$TiPd_3$, X-ray emission spectra *(Russian)* 77−40304
TiS_2, valence density of states 80−44465
$TiS_2(Se_2)$, valence density of states, Gilat-Raubenheimer method 80−88465
TlBr, polymorphism, XPS obs. 80−97398
TlBr, XPS of valence bands 78−76578
TlCl, polymorphism, XPS obs. 80−97398
TlCl, UPS, valence band struct., dynamic hybridisation 77−20999
TlCl, valence band electronic struct., XPS and UPS obs. 78−6826
TlCl, XPS of valence bands 78−76578
TlI, XPS of valence bands 78−76578
Tl_xTe_{1-x}, amorphous, bonding and electrical conduction 79−90951
Tm monochalcogenides, valence related optical and other studies, review 78−31215
U, core and valence band spectra, XPS obs. 80−50530
$UAl_2(Co_2)$, surface comp. and electronic struct., photoemission study 80−66382
UCu_5, core and valence band spectra, XPS obs. 80−50530
β-UD_3, electronic props., metallic character 80−6693
UNi_5, core and valence band spectra, XPS obs. 80−50530
$UNi_{0.5}Cu_{4.5}$, core and valence band spectra, XPS obs. 80−50530
UO_2, ionisation potential, cohesive, electronic and redox props. 79−47916
UO_2, U_2O_5, U_3O_8, and UO_3, bonding and valence obs. by ESCA and EPR 77−28696
UO_2, U_3O_8, U_2O_5, shake-up satellites and band struct. 77−55861
UO_2, valence electronic configuration determ. by photoelectron spectroscopy 78−15284
UPt, valence bands, XPS spectra 80−50520
V, and its cpds. with light elements, surface state, XPS investigation 78−11070
V, electronic structure, X-ray spectra and XPS meas. 77−85842
V oxides, XPS and AES study, electron correl. effects, semicond.-metal transition 80−7467
V_3Au, effect of atomic ordering on XPS of valence bands 77−52224
V_3Au, XPS of valence electrons meas. 77−21003
VC, valence band struct. *(Russian)* 78−6268
V_2O_5, energy band structure, tight-binding method 80−70602
V_3O_5, high-temp. phase transition, resistivity, valence photoelectron spectra 80−49357
W, XPS, angle-resolved, from valence bands, obs. of strong temp. depend. and direct-transition effects 80−60752
WO_x, nonstoichiometric, XPS meas. 77−48307
Xe crystal, photoelectron spectroscopy, hole-electron valence bound state 77−36369
YOF, band structure formation, valence band 79−33232
$YbAl_3$, XPS studies, valence band, 4-f region 78−6831
$YbCu_2Si_2$, valence fluctuation and temp. depend. of Cu nuclear quadrupole interaction 80−15818
Zn, Fermi surface-Brillouin zone interaction, XPS obs. 79−52078
Zn, HCP metals, K-emission valence bands, structure and bonding 80−7438
ZnF_2, valence-electron density of states, XPS meas. 77−69963
$ZnGa_2S_4$, band struct., pseudopot. method 80−92816
$ZnGeP_2$, pseudodirect bandgap semiconductor, natural birefringence 79−65834
$ZnIn_2S_4$, valence band photoemission spectroscopy 78−56569
ZnO (0001), (000$\bar{1}$) and (10$\bar{1}$0), UPS rel. to elec. struct. 78−15288
ZnP, Zn_3P_2, electronic struct. of valence bands, X-ray spectra and XPS 78−92176
ZnS, band structure calcs. by modified orthogonalised plane wave (MOPW) method 80−54609
ZnS, Compton profile, state of valence electrons 78−11018
ZnS:Ag film, photocapacitance IR quenching, hole photoionisation energy and spectral distrib. 79−87127
ZnS_2, XPS of valence band meas. 77−85885
ZnSe, cubic, valence band parameters, magnetoreflectance of Γ_6-Γ_8 exciton 78−60056
ZnSe, effective mass parameter, two-photon absorpt., envelope-hole coupled exciton states 77−52124
ZnSe, two photon absorpt. by envelope-hole coupled exciton states, polarisation depend. 77−66522
ZnSe, valence-band parameters and g-factors from free-exciton magnets reflectance 79−73905

valence bands continued
ZnSe(Te), photolum. excitation spectra of tightly bound holes, valence band contrib. 80−60658
$ZnSiAs_2$, pseudodirect bandgap semiconductor, natural birefringence 79−65834
$ZnSiP_2$, electronic struct., X-ray spectroscopic investigation 80−108300
$ZnSiP_2$, pseudodirect bandgap semiconductor, natural birefringence 79−65834
ZnTe clean and adsorbed O_2 (110) surfaces, UV photoemission spectra *(Japanese)* 80−93456
ZnTe, spin flip scatt. of laser light 77−43976
ZnTe, spin flip scatt. of laser light 77−43977
ZnTe, valence band parameters and free exciton reduced mass, free exciton magnetoreflectance 80−45046
ZnTe:As(P)(Li), electronic Raman scatt. and IR absorpt. spectra of shallow acceptors 79−73978
Zr, valence-band meas. using XPS 79−69958
Zr-Co, amorphous and crystalline, d-band struct., alloying effects 80−59862
Zr-Ni, amorphous and crystalline, d-band struct., alloying effects 80−59862
Zr-Ni, energy spectra of valence electrons *(Ukrainian)* 78−6814
Zr-Ni alloys, energy spectra, X-ray emission obs. *(Russian)* 78−19604
ZrC high-temp. plastic deform. effects on elec. props. 77−44370
ZrC, valence band struct. *(Russian)* 78−6268
$ZrH_{1.65}$, valence-band meas. using XPS 79−69958
ZrN high-temp. plastic deform. effects on elec. props. 77−44370
$ZrPd_2$, X-ray emission spectra *(Russian)* 77−40304
ZrS_2, valence density of states 80−44465
$ZrS_2(Se_2)$, valence density of states, Gilat-Raubenheimer method 80−88465

valence bond calculations *see VB calculations*

valency
actinide materials, valence transitions and intermediate valence states 79−42496
actinides, lower oxidation states in molten salts 77−29088
actinides, valence fluctuation model, physical prop. response 80−6791
β-AgI, valence state and impurity-vacancy dipole formation, Mossbauer effect meas. 78−68435
atoms and ions, valence region energies, electronegativity, Politzer-Parr partitioning, finite difference approx. 78−78612
borides, proposed classification 80−19741
brass-like alloy phases, binding and cryst. struct., valence arguments 80−88081
ceramic 22KhS, glass phase, valence state of Ti and Mn ions, ESR determ. 77−43871
concept development, reln. to chemical bonds, teaching approach *(Hungarian)* 79−756
Covalency and hyperfine interaction on the impurity ion in crystals 78−23063
epoxy resins, correlation between valence energies and low temp. flexibility 80−25815
fluctuating oxidation states in cpds. 78−60089
garnets, cation site distrib. and valence states 79−99167
inorganic complexes, chem. bonding, quantum mech. ideas development and use 80−12878
inorganic complexes, chem. bonding, quantum mech. ideas development and use 80−12879
metal, BCC, effective valence, from phonon data, rel. to vacancy formation energies 80−79781
metal, noncubic, conduction-electron elec. field gradient, probe valence effects 78−47749
metallic phase structures, dimensional analysis, bonding information from valency effects appearing as artefacts 80−96471
optical fibres, material dispersion 79−27377
polyethylene, correlation between valence energies and low temp. flexibility 80−25815
rare earth alloys, $RIn_3(Sn_3)$, ^{111}Cd quadrupole coupling consts. and valence states, PAC meas. 77−48102
rare earth and actinide halides and oxides stability study, energy difference between trivalent and tetravalent metal states 78−79553
rare earth dihalides, rel. to stability and enthalpy of formation 79−91000
rare earth elements, valence changes in cpds. 79−91000
rare earth intermetallics, valence, coordination no., polyhedral at. vols. 80−19742
rare earth materials, valence transitions and intermediate valence states 79−42496
rare earth metal, 4f levels, obs. by bremsstrahlung isochromat and XPS spectroscopy 79−24411
rare earth metals, 4f level energy position relative to Fermi energy 80−6764
rare earth metals, elastic props., connection with electron struct. *(Russian)* 80−19895
rare earth metals, lower oxidation states in molten salts 77−29088
rare earths, compounds, K X-ray line shift associated with valency change and isomorphous phase transitions 79−47553
rare earths, valency, ionicity and electronic config. 80−18775
rare-earth metals, surface valence state from surface tension props. 79−95462
semiconductors, valence bond test, for validity of structure 79−10830
spinels, MCr_2O_4 and MV_2O_4, valency and ionicity rel. to magnetism 78−52229
TCNQ, charge transfer complexes, changes in valence electronic structure 80−7477
transition elements, 3d, ESR for valency assessment, appl. to ceramics and glass industries *(German)* 80−34757
transition metal, 2nd and 3rd long period, covalence of atoms 78−47274
transition metal atoms, valency in metallic alloys 77−4288
transition metal-Yb(Ce) alloys, valence state of Yb and Ce 79−77545
Z=114, Dirac-Fock one-centre calcs., tetravlent hydride prediction 77−34551
Al alloys, dil., size effect, valency factor and point defect interactions 79−51143
Al matrix, capture radius of impurities 80−20110
β-Al_2O_3-Na_2O:Fe, coordination site, oxidation state, Mossbauer, absorpt., emission spectra, mag. susceptibility meas. 78−68431
Am cpds., prep. and stability of highest oxidation states in phosphoric acid. soln. 77−29029
Am(VI) formation in molten salts 77−29039

valency continued
As_2S_3, amorphous, time resolved spectroscopy of valence alternation pair luminesc. 80−50400
As_2Se_3-$GeSe_x$-$SnSe_x$ (x=1,2), exam. of Sn valency and physical props. 79−4753
Au, surface valence state from surface tension props. 79−95462
B_2O_3-PbO-GeO_2-Fe_2O_3 glass, Mossbauer exam. of Fe valence states 79−78597
$BaTiO_3$:X(X=Cr, Mn, Fe, Co, Ni, Zn, Ga), annealed in H_2 and O_2, valence change in phase stability 80−20600
CaF_2:Eu, oxidation and reduction of Eu, EPR and optical studies 80−25199
$Ce(Cu,Ni)_2$, pseudobinary phases, struct. and mag. props. rel. to Ce valence 78−6032
$CeNb_3O_9$, $CeNbO_4$, $CeNbO_{7.6}$, electron config. of Ce ions, mag. sucept., L_3 absorpt. edge, resist. 79−43063
Ce_3NbO_x, $CeNbO_x$ and $CeNb_3O_x$, redox processes, elec. resist., phase anal., mag. suscept., thermogravimetric meas. 78−34482
$CeNi_2$-$CePt_2$ system, structural and mag. studies on valence behaviour of Ce 80−103809
$CeRu_2$, change of valence of Ce ions, induced by H absorption, supercond. disappearance 79−47185
$CeRu_2$, H absorption induced Ce valence change, mag. and supercond. props. 80−50042
$CeSn_3$, valence instabilities 79−78546
Cf, surface valence state from surface tension props. 79−95462
CfO_x-O_2 system, for 1.50<O/Cf<1.72, temp., press. and stoichiometry depends. 77−28009
Co oxides, effective atomic charge rel. to chemical shifts in transition metal compound XAS 79−78788
Cr^{3+} impurity ions in MgO single crysts., valency conversion by UV irradiation *(German)* 78−84620
CrO_2, valence states of Cr, XPS obs. 80−40216
$Cs_2Au_2Cl_6$, electronic state of Au at high press., Mossbauer spectra 80−60467
Cu alloys, dil., size effect, valency factor and point defect interactions 79−51143
Cu in Al film on Si substrates, electromigration and diffusion, effective valency 79−77820
$CuCr_2Se_4$, mag. reson. and valence state of Cu and Cr ions 80−60413
$Cu_{1-x}Fe_{2+x}O_4$, cation distrib. and valence state 78−63732
EuB_6, valence state of Eu, X-ray line displacement meas. 80−70633
$EuPt_x$ compounds, partial valence change, ^{151}Eu Mossbauer and magnetisation obs. 80−70167
Fe oxides, effective atomic charge rel. to chemical shifts in transition metal compound XAS 79−78788
Fe^{3+} impurity ions in MgO single crysts., valency conversion by UV irradiation *(German)* 78−84620
α-Fe:B(C)(N)(O), valency effect of interstitials 80−65502
Fe^{3+}/Fe^{2+} in frozen solns., stabilisation on ^{57}Co decay, electron scavenger effects, Mossbauer obs. 77−40562
Fe-Co alloys, at. valence states *(Ukrainian)* 78−2656
Fe-Ni alloys, atomic valence states *(Ukrainian)* 78−2656
GaAs:Cr, semi-insulating, defect chemistry, EPR study 79−99754
In_2Te_3-type semiconductor, mechanism of electrically inactive impurities 80−24834
IrO_x, anodic films, electrochem. characts., electrochromic system 78−80316
KCl:Pb, impurity valence, heat treatment influence, absorpt. spectra obs. 79−38574
La-Sm-Au, amorphous, surface effects on Sm valence, XPS and X-ray absorption meas. 80−108325
$LaRu_2$, H absorption induced Ce valence change, mag. and supercond. props. 80−50042
$Li_xCr_yV_{1-y}S_2$, Mossbauer and mag. studies 79−73869
$Li_xFe_yV_{1-y}S_2$, Mossbauer and mag. studies 79−73869
$LiNbO_3$:Fe, impurity valence state charge on X-ray irrad., Mossbauer meas. 80−7235
$Li_xV_{1-y}Fe_yS_2$, intercalated battery cathode material, Mossbauer studies 80−44984
$MgO:Mn^{2+}(Fe^{2+})(Cr^{2+})$, redox behaviour of ions, ESR and X-ray diffr. 78−52341
Mn oxides, effective atomic charge rel. to chemical shifts in transition metal compound XAS 79−78788
$MnFe_2O_4$, valence states, NMR investig. *(Czech)* 78−72420
$MnFe_2O_4$, valency states, NMR 77−51987
Na_xWO_3 bronze, oxidation state of W, oxidation by air exposure 77−8719
NiO_2, $Ni(O_2)_2$, coordination of mol. O_2 with Ni, EHT calcs. 77−18795
$NpAs_2$, magnetic props., 4.2 to 77K, Mossbauer study 80−39937
Np(V)/Np(IV) catalytic redox reactions, kinetics and mechanisms 77−29006
Np(VII) formation in molten salts 77−29039
$Pd_{21}Ge_8$, cryst. struct. *(German)* 78−18586
Pu(IV) catalytic redox reactions, kinetics and mechanisms 77−29006
Pu(VII) formation in molten salts 77−29039
$RbFeS_2^+$, ^{57}Fe Mossbauer hyperfine interaction, covalency effects, point charge model 78−39484
S, concentration and valence state in pollution samples, X-ray fluoresc. anal. 79−48027
^6S state ions, overlap and covalency contrib. to zero field splitting, LCAO-MO calc. 80−24850
^{125}Sb, in HCl solns., valency states investig., radioanal. tracer preparation, stability 77−63943
Si, semiconductor charge densities with hard-core and soft-core pseudopotentials 79−33266
Si_3N_4, CVD, chem. bond nature, Compton scatt. expts. 80−49539
Sm metal, valence transition at surface of Sm 80−70652
Sm surface, valence change 79−56280
Sm, surface valence state from surface tension props. 79−95462
Sm, XPS, 50-250 eV, 4d→4f transition and surface mixed valence 79−15588
Sm, XPS, electronic struct. determ. for surface 80−20765
Sm-Au, amorphous, surface effects on Sm valence, XPS and X-ray absorption meas. 80−108325
Sm-Fe, dil., valence impurity state, inference from mag. susceptibility 78−95270
Sm_3S_4, cryst. struct. and valence state of Sm *(German)* 78−75636
Sn compounds, Sn(II) valency config., Mossbauer and X-ray electron determ. *(Russian)* 77−8483

valency continued
Sn-In dil. liq. alloy, electrodiffusion and electroconvection, effective diffusion coeff., apparent effective valence 78−87802
Sn-Sb dil. liq. alloy, electrodiffusion and electroconvection, effective diffusion coeff., apparent effective valence 78−87802
$TbCrO_4$, valence states of Cr, XPS obs. 80−40216
Ti, effect on elec. cond. of Al_2O_3-SiO_2-TiO_2-RO glass-cryst. material 79−60876
Ti^{4+}, valence transition in fluorphlogopite, ESR and optical absorption data 77−16155
TmS(Se)(Te):Gd^{3+}, EPR studies of valence states of Tm 77−77095
$U_xPu_{1-x}O_2$, theoretical study of electronic thermodynamic and valence props. 79−37655
$(U_xTh_{1-x})Sb$, magnetisation, U valence change 80−7089
V_2O_5-TeO_2 glasses, ESR spectra 78−10755
YAG:M^{3+}, ESR absorption spectra, line broadening of Fe^{3+}, Cr^{3+}, Gd^{3+} 78−91940
YIG:Ru, optical absorpt. and MCD obs. of Ru^{4+} site occupancy 80−71456
Yb intermetallic compounds, mag. susceptibility, 1.4 to 1060K, investig. of Yb valency 77−20543
$YbAl_3$, valence instabilities 79−78546
YbB_{12}, mag. props., cryst. struct., valence of Yb *(Russian)* 78−60263
YbB_{12}, valence state and mag. props. 80−50031
$YbNi_{(2)}$-$YbCu_{(2)}$ system, valency state, Yb behaviour *(French)* 80−45277
YbPd-YbAg, valency state, Yb behaviour *(French)* 80−45277
YbPt-YbAu system, valency state, Yb behaviour *(French)* 80−45277
Yb_xSy, synthesis and mag. props. 78−23242
ZnO-Cr_2O_3, crystal structure, valence of chromium ion rel. to variation of Cr/Zn ratio *(Rumanian)* 79−65057
ZnS:Cu, film effect of Cu valency on cond. 79−11246

value analysis *see value engineering*

value engineering
see also operations research; optimisation; quality control
effluent monitoring, purpose and value 78−89986
Co permanent magnet material savings *(German)* 80−103851

valve voltmeters *see voltmeters*

valves
see also diaphragms
1300 MW nuclear reactor steam isolating valve blowdown tests *(German)* 80−22967
acoustic noise measurement from pipe vibration *(French)* 77−39158
adjustable, selection for arbitrary Reynolds number *(German)* 78−22439
aortic and mitral regurgitation patient surgery and vectorcardiogram changes 79−44050
aortic and mitral valve prostheses, in vitro flow visualisation 77−86703
aortic concave-convex pivoting disc valve prosthesis, hydrodynamic evaluation 79−84027
aortic leaflet valve prosthesis, optimal design and longevity anal. 77−90958
aortic valve opening, haemodynamics 78−20208
aortic valve prosthesis, Hancock porcine xenograft, comparison of models 242 and 250 77−56532
aortic valve prosthesis, Reul-Ghista optimal tri-leaflet, in vitro performance tests 79−92432
aortic valve prosthesis, wall shear stress in Bjork-Shiley and Starr-Edwards types in vitro *(German)* 78−81067
aortic valve prosthesis water hammer pulse effect *(Japanese)* 78−3676
aortic valve replacement with subcoronary ball valve, early expts. 77−56524
artificial, mitral valves, insufficiency, press. and work losses *(German)* 78−88764
artificial heart, electronic pressure control with fast variable aperture valve *(French)* 77−40928
artificial heart valve closing element, kinematics photoelectric recorder 79−48370
artificial heart valve closing element surface pressure distrib. 79−57811
automatic inlet system with pneumatic changeover valves for isotope ratio mass spectrometer 79−49333
bellows valve, large rectangular for mirror fusion reactors 78−50404
bellows valve of all-metal construction 77−49715
Bjork-Shiley aortic prosthesis, in vitro vel. meas. using laser-Doppler anemometer 80−17196
Bjork-Shiley tilting disc heart valve 77−56525
blood pump, controlled high pressure, for heart support systems *(German)* 79−8580
blood pump, pulsatile, stabilisation of unsteady ball valve motion 78−44708
blood pump artificial heart valve *(German)* 78−81065
blood pump pressure servovalve control, moving coil system *(German)* 78−24182
BWR containment, influence of safety relief valve discharge loads 80−42793
BWR turbine valve closure, pressure transients 79−89441
BWR with fracture live steam line, isolating valve loading *(German)* 77−38340
CANDU-PHW, valve maintainability, design, application, layout, administrative factors 78−25318
cardiac assist devices, selection of prosthetic valves 78−44730
cardiac valve dynamics, fluid physics appls. *(French)* 79−34589
cardiac valve motion obs. CW FM sonar 78−61230
cavitation and aerodynamic noise level estimation 77−84076
Cocatron, servo valve for liq. He II level control, superfluidity and supercond. applic. 78−18855
compressible fluid flow in pipes and valves, acoustic noise calcs. *(French)* 77−19477
compressible gas flow through exhaust valve, analytical calc. using flux analysis method *(Japanese)* 80−69896
control valve noise prediction 79−72754
Cooley-Cutter heart valve prosthesis 77−56526
coronary perfusion pressure programmable control circuit 79−92278
cryogenic pressure regulator 78−57963
cryogenic pressure-vacuum valve 78−37020
cryogenic valve design and materials 79−71462
Dewars, simple valve seal for vacuum space saving 77−5851
dual pilot operated valve for switching the flow of a cryogenic liquid 80−98918

valves continued
electro-osmotic valve, implantable, for controlled drug administration 78−40399
electronically controlled insulin pump and valves for diabetes patients 78−53565
emergency cold valve, operating in He II 80−22367
fast gas valve for gas injection into vacuum 78−74011
fast gas valve for injection into vacuum system 78−57970
fast pulsed gas valve for injecting gas pulses into vacuum system 80−62675
fission reactor containment structures, integrity and safety, isolating valve provision and testing aspects *(Spanish)* 79−93738
flapper-valve flow characts., interferometry appl. 77−24040
friction area and nozzle area as flow parameters 77−42895
fusion reactor, T_2 valve, pulsed gas feed into Tokamak reactor 78−66412
fusion reactor control valve, low-noise, rolling closure 78−54888
gas flow rate meas. up to 2.8 m^3/sec, dynamic volumetric method 77−72380
gas injection technique, rapid response, design 78−94865
gas thermometry, constant volume valve design 80−4711
gate valves, angle valves and safety valves, for high and ultrahigh vacuum 79−63246
glass-PTFE stopcocks for use at elevated temps. and pressures 77−10000
heart artificial valve with convex closing body *(German)* 78−81066
heart valve bioprosthesis, devel. from xenograft (1965-77) 77−56528
heart valve bioprosthesis, porcine 77−56529
heart valve prostheses, fluid shear stress 77−90833
heart valve prostheses, past and future 77−52924
heart valve prostheses development 77−56523
heart valve prosthesis, mech. props. of SnO_2 coated bioceramics *(German)* 79−12028
heart valve prosthesis, theoretical limit to flow design 77−60302
heart valve prosthesis design, role of simulation studies 79−12033
heart valve prosthesis mean press. gradient meas. under in vitro pulsatile flow 77−56531
hermetically sealed valve for the safety systems of a nuclear power station *(Russian)* 78−89952
high pressure gas valves, supersonic air flow noise and flow pattern obs. 80−59067
hybrid field-effect liquid crystal light valve, sensitometry control 80−23788
hydraulic single-bellows valve use at 1K in dilution refrigerator 78−225
hydrocephalus surgical treatment, valve system design *(Japanese)* 78−31963
laryngeal prosthesis for fistula speech after laryngectomy 77−78056
liquid N_2 transfer valve 77−136
liquid-metal valves, materials selection 78−82449
LMFBR, equipment design, Na-NaK engineering handbook 79−97815
magnetic safety valve 80−8966
main steam isolating valves, back pressure light, PWR appl. 78−29602
metal-seal valve for high radiation use in high vacuum 80−233
metal-sealed all-metal gate valve, design developments 79−63243
mitral valve prosthesis in vitro tester, unique design 78−40426
mitral valve prosthesis with flexible fabric leaflets 77−78057
mitral valve velocity meas. by digital echocardiographic tracking system 77−21579
molecular flow in vacuum valve, Monte Carlo method for conductance 78−71398
noise analysis industrial process control valve systems 78−79163
noise control methods 78−50999
noise reduction in steam power, chemical, petrochemical industries 78−51002
nuclear power plant, isolation and relief valve/piping transient force anal. program 78−50287
nuclear power reactor, austenitic stainless steel, appl. 77−3102
nuclear reactor emergency core cooling system motor operated valves, failure criteria 78−70592
nuclear steam supply, emergency core cooling system motor operated valves, failure mode anal. 78−54866
nuclear steam system, globe main steam isolation valve unbalanced forces and novel actuator design 78−50288
pivoting disc heart valve prosthesis, clinical results and new all-C model 77−52923
plasma chromatograph/mass spectrometer column overload prevention valve 80−16748
pressure reducing, generated noise reduction methods 79−27463
pressure reducing, noise abatement 79−46108
pressure regulators, self-contained, selecting and sizing 80−82759
prosthetic aortic valve, Bjork-Shiley, steady flow in vitro vel. 78−44735
prosthetic aortic valve, Reul-Ghista optimal tri-leaflet Avcothane design performance 78−44736
prosthetic aortic valve stress analysis using finite element compute program 78−48930
prosthetic cardiac valve, concave-convex pivoting disc two-dimensional model 79−84028
prosthetic heart valve design flow evaluation using finite difference transforms 78−44733
prosthetic heart valve flow pattern visualisation by laser technique 78−44734
prosthetic heart valves, disc, ball and tilting disc types, fluid stresses in vitro 78−81078
prosthetic heart valves, laser Doppler anemometer for velocity meas. 79−57814
prosthetic heart valves, rigid leaflet and caged-ball types, diastolic ventricular mechs. 78−81079
prosthetic mitral valve, pressure drop and flow pattern obs. 79−92430
pulsatile blood pump, vortex diode used as outflow valve 78−44724
PWR containment isolation using butterfly valves 78−13256
PWR power plant steam dump valve stability anal. 78−50289
RF sputtering systems, discharge suppression within piezoelectric gas admission valves 80−100110
ruby valve, lambda-tight, for liq. He II transfer 77−30159
self-opening, for N_2 decanting siphon 80−57310
shock tube, fast-acting valve, construction and characts. 77−72372
shock tubes, use of fast-acting valves, shock wave formation 80−24052
small air jet and quiet valve noise obs. 78−83165
Smeloff-Cutter heart valve prosthesis 77−56527
sorption pump, design of cheap pump 79−63255
sphygmomanometer control valve, improved design 77−60266
sprung needle valve, VV-2500 type 78−22434

valves continued
switch valve, lightweight, remotely actuated, for rebreathing exercise studies 80−101278
UHV gate valve, bakeable, for microwave tube expt. 77−5854
UHV gate valves for systems used in plasma discharge studies 79−54147
vacuum, and valve traps, for production appl. 78−70140
vacuum, differentially pumped six-inch metal sealed gate valve 78−70137
vacuum, fast closing valve, for Berkeley 88″ cyclotron 77−10501
vacuum, mounted on pressure pickup 80−47066
vacuum value for gas chromatograph/mass spectrometer system 79−39245
vacuum valve, baffle and trap design and construction 80−82781
vacuum valve, compact small aperture straight through, design and operation 78−74014
vapour pump, recent developments 79−63250
wedge-gate valve of cast Fe with stainless steel trim for under water use, corrosion protection by dip-applied coating 80−93677
He distribution, low-temperature equipment development *(Czech)* 77−61069
^{4}He pumping lines, low press. safety value 78−32822
NO, combustion gas sampling system and valves for sampling during engine expansion process 78−24380

valves (electronic) *see electron tubes*

Van Allen radiation *see radiation belts*

Van Allen radiation belts *see radiation belts*

Van de Graaff accelerators
8UD Pelletron tandem accelerator, fast neutron time-of-flight spectrometer facility 79−85856
14UD Pelletron accelerator at ANU, energy calib. using $^{12}C(p,\alpha)$ 78−17449
alkali metal solid ion source for low-energy Van de Graaff accelerator 79−31292
beam optical components, anal. of misalignment effects 78−13355
bremsstrahlung thick-target, spatial distrib. of energy transfer meas. with miniature dosimeter 78−15897
British Science Research Council's new accelerator at Daresbury 78−66433
bunched beams, transport, second order aberrations 80−52801
calibration method 79−45479
CAMAC and microprocessor appl. to target room control 78−37468
CN type, Berlin, conversion to heavy ion injector 78−25346
corona stabilisation systems 78−29668
corona stabiliser, effect of insulating gas comp. 79−13559
Daresbury 30 MV tandem, ion exchange processes in vacuum accelerator tube 79−45478
Daresbury 30 MV tandem accelerator, current status 79−45473
Daresbury heavy ion Van de Graaff, gas foil stripper system 79−67988
double focusing bending magnet, meas. of optical props. with thin alpha source 78−55073
electrostatic generator computer control 78−29666
EN Tandem, corona stabilisation system 79−18061
EN-tandem, foil stripper *(German)* 79−36437
fast electrostatic chopper of low power consumption 79−31284
FN tandem, absolute excitation energy meas. using electrostatic analyser 77−30741
FN-7 tandem, matching of heavy-ion direct extraction Penning source 78−13357
FN-Tandem at Saclay, up-grading 78−33313
focusing electrode improved ion source extraction system 79−76179
foilless diodes, hollow relativistic electron beam generation 79−76170
heavy ion facility, target production 80−23213
heavy ion tandem, injection into ORIC for radioactive nuclei acceleration 77−10502
heavy ion-nucleus reactions, use of accelerators *(Norwegian)* 79−13316
Heidelberg postaccelerator for heavy ions, design criteria and experience 80−18722
Holifield 25 MV heavy ion tandem accelerator, radiation safety 79−45483
hoops, circular and oval, stress multiplicating factor 80−74043
HV vacuum accelerator tube, microparticle obs. 80−864
injection to linear accelerator, beam dynamics, computer simulation 80−13989
ion beam, precision energy meas. using generating voltmeter 78−58508
ion drift time measurement in gap 79−694
ion exchange currents (microdischarges), in vacuum accelerator tube 78−55057
JAERI 20 MV tandem accelerator *(Japanese)* 78−33308
Lamb shift polarised ion source at FN tandem Van de Graaf at Univ. of Cologne 78−55065
Lamb-shift polarized ion source for the tandem accelerator center, the University of Tsukuba 79−93853
Laval 7 MV accelerator, upgrading using triply charged beams 79−45476
LECH, beam energy stabilization analysis 78−25343
LECH, main data 78−25342
Los Alamos P-9 accelerator facility, CAMAC data acquisition system 79−45607
Middleton type negative ion sputter source for Van de Graaff terminal operation 78−17455
Mobley compression system, time resolution 77−26897
MP tandem, magnetic suppression on inclined field acceleration tubes 78−46184
MP tandem, Rochester, operating experiences since upgrading 78−25348
MP tandem Van de Graaff, large aperture accelerating tubes, use at high pots. 78−33316
MP-Tandem at Munich, diagnostic and control system 78−29667
MP-Tandem at Munich, light link coupled current monitor 78−33311
Munich heavy ion postaccelerator 79−22500
Munich MP tandem, beam optical components, anal. of misalignment effects 78−13355
neutron primary beam and shielding radiation quality and absorbed dose obs. 80−12281
Orsay, $^{14}C^-$ beam prod. from TaC and Ta_2C *(French)* 79−76243
Orsay MP tandem, review 78−13352
Orsay MP tandem, zero degree detection system 78−13353
picosecond bunching system at the Munich MP-tandem accelerator 79−85835
polarized ^{3}He ion source for a CN Van de Graaff accelerator 79−68106

Van de Graaff accelerators continued
RF superconducting resonators for booster linac 79−54623
Rossendorf tandem EGP-10-1, exptl. results 78−13358
small van de Graaff accelerator, appl. to ^{14}C detect. 79−11844
Spectrum 151, tandem accelerator at Daresbury *(Spanish)* 79−6777
stack insulators, acceleration tube elements, construction in 5 MV Van de Graaff at Atomki 78−33317
subnanosecond pulsing using passive coaxial pulse shaper 78−46186
suppressed accelerator tube installations, design, performance 78−33319
T acceleration in FN tandem using Cs beam sputter ion source 78−55070
Tandem, 3.5 MeV, Greengate and Fabreeka belt performance 78−29669
tandem, appl. to meas. of ^{10}Be distrib. in geophysical samples 80−61924
tandem, appl. to radioisotope detection in terrestrial and extraterrestrial samples 80−61923
tandem, beam quality restoration through gas prestripping of molecular ions 78−46185
tandem, data acquisition system 79−89529
tandem, in-beam γ-ray spectroscopy 78−13373
tandem, review and subsystem developments 78−13351
tandem, Saclay, principle and description *(French)* 79−689
tandem 700 keV accelerator 79−54621
tandem accelerator, appl. to ^{36}Cl anal. in environmental water samples 79−20895
tandem accelerator, design, assembly installation of insulating stack 79−67993
tandem accelerator for meas. of ^{10}Be in Mn nodules 79−74967
tandem accelerators, MV heavy ion injection 78−13356
tandem accelerators and nuclear phys. conf. 78−13349
tandem electrostatic 30 MV accelerator, nuclear struct. facility at Daresbury Lab. 78−55056
tandem electrostatic accelerators, phase space acceptance and emittance 77−31058
tandems, review of research appl. 78−13350
two component ion beam accelerator system, for interactive surface effect studies 79−49880
upgrading using RF structures, comparison of techniques 79−45477
VICKSI 6 MV Van de Graaff and split pole cyclotron, present status 79−67987
XTU tandem of Lab. Nazionali di Legnaro (Padova) 78−13354
As ion prod. in 2 MV Van de Graaff 80−14031
C, stripper foil prepared by cracking hydrocarbon vapour in glow discharge 79−31286
C stripper foils for heavy ions, preparation method 79−22516
^{14}C dating technique using cyclotrons, or Van de Graaff as mass spectrometer 80−5414
^{123}I, prod. using 6 MeV Van de Graaff accelerator 79−53243
^{127}I ions, 20 MeV, emerging from gas stripper, absolute charge state yields 78−55066
^{13}N prod. by accelerators for nitrosourea-^{13}N prep. 79−53242
Se ion prod. in 2 MV Van de Graaff 80−14031
W ions, fractionally charged, search 78−29083

Van de Graaff generators
cryopump system, for use in HV centre terminal of tandem Van de Graaff 79−63253
neutron detection and neutron reaction cross-sections, Van de Graaff generator and cyclotron facility 80−47805
neutron experiments, Braunschweig accelerator facility, data acquisition and anal. 80−47806
nuclear physics experiments, teaching appls. 77−74178
pressurised, operational characts. 77−30675
resistor chain use to improve axial and radial voltage gradient, electrolytic field mapping 77−54377
tandem, mag. spectrometer for heavy ion induced reaction study *(French)* 79−707
terminal discharges, transient radial elec. field in breakdown channel 79−22501
transient behaviour using up charge and down charge processes 79−76178
pp, elastic scatt., teaching expt. using Van de Graaff generator 77−74178
$^{19}F(p,\alpha\gamma)^{16}O$, reson. reaction, teaching expt. using Van de Graaff generator 77−74178

Van der Pol oscillators *see relaxation oscillators*

Van der Waals forces
adatom interaction with solid substrate, effect of mechanical stress on chem. pot. 80−10784
adsorption, gas on solid substrate, Van der Waals model 80−29271
alkali halide cryst., interaction energy eval. 78−71705
alkali halide crystal, Gruneisen parameter, vol. depend. anal. 80−2135
alkali halides, electronic and static dielec. consts., strain derivative theory 79−95701
alkali halides, interionic potentials, completely independent specification of Born-Mayer potentials 78−55828
alkali halides, repulsive hardness parameters, crystal-independent 80−64947
alkali halides estimation of van der Waals dipole-quadrupole interactions 77−80441
alkali metal atoms, calc. of Van der Waals energies, variation-perturbation method 77−510
alkali metal halides, crystal properties, cohesive energy, bulk modulus and press. depend., interionic force model 80−15035
alkali metals, heavy, crystal structure, effect of Van der Waals forces 79−99111
alkaline-earth fluorides, electronic and static dielec. consts., strain derivative theory 79−95701
n-alkanes, liq. mixtures, thermodynamics 80−55700
alkanes, van der Waals dimers, PCILO calcs. 79−36542
aromatic five-membered heterocyclic ring system, covalent radii determ. method 80−23332
atom between two perfectly conducting plates, retarded Van der Waals pot. 78−78122
atom interaction with pair of conducting plates 79−97990
atom-atom systems, spherically symm. van der Waals pot. theoretical model 77−34713
atom-diatom complexes, metastable level widths, energies with lifetimes 79−89727
atom-diatom van der Waals complex, Born-Oppenheimer separation of radial and ang. motion 78−29828
atomic forces, finite size effects, linear response theory 79−81252

Van der Waals forces continued
atomic nonresonant collisions in intense mag. field, van der Waals pot. 77−3440
benzene, van der Waals interaction energy calc., perturbation theory, MO LCAO method 77−42373
biexciton, change of binding type and dissoc. in strong mag. field 78−62744
bimetallic junction, van der Waals interaction 79−24048
biological surfaces, van der Waals interactions 77−44609
borosilicate glass samples, Van der Waals interaction, influence of optical absorpt. 79−95273
bounds for Van der Waals coeffs. using oscill. strength sum rules 79−41219
bounds on van der Waals coeffs., oscillator strength sum rules 80−27941
brittle crack in gas, role in crack-tip decohesion 77−90440
Brownian particles, deposition rates calc., interaction forces lumped into boundary condition 77−9131
calculation method, based on phenomenological Hamiltonian for polarised system interaction with EM field *(Russian)* 78−5316
Casimir effect in dielectrics using source theory, surface tension and latent heat 79−8109
Casimir self-stress on a perfectly conducting spherical shell 79−13859
chromatography, hydrodynamic, role of colloidal forces 78−48717
cluster, gas phase, vibr. predissoc., rel. to matrix isolated O_2 multiphonon vibr. relax. 80−18861
collision anisotropy and spectral line impact contour *(Russian)* 80−52942
complexes, PCILO calcs. 79−36542
condensed media, space correlation functions of particle numbers and energy densities *(Russian)* 78−1971
conducting media, macroscopic theory of van der Waals force 78−30876
crystal, cohesive energy, many-body theory calcs. 77−76348
crystal, equation of state, from Bogolyubov chain temp. expansion *(Russian)* 77−13705
crystalline state, P-V-T diagram, Holmholtz free energy, mean-field model, for teaching 77−33784
diatomic bonding energy, changes due to Van der Waals interactions with other atoms 78−95012
diatomic molecule, bound-states, new trigonometric pots. 79−72383
dielectric continuum theory of van der Waals interaction 77−11976
4,4′-dinitrobiphenyl complexes, intermol. interacts. and geometry of non-rigid mols., vibr. spectra 78−88294
2,4-dinitrophenol, cryst. and mol. struct. 77−15394
dipolar Van der Waals forces between molecules of ellipsoidal shape 79−89729
dispersion force calculations, use of finite atomic radius 78−51467
DNA conformation, influence of intermol. interactions 80−16900
dynamic polarisabilities and dispersion force coeffs., bounds 79−68290
electrolyte solutions, van der Waals forces, force density 78−42877
emulsion drop coalescence with liq. cryst., van der Waals pot. 77−12834
ethyl p-methoxybenzilidene aminocinnamate, dimer, mesogenic, intermol. interactions 79−46564
ethylene, van der Waals dimer, PCILO calcs. 79−36542
ethylene dimer, CO_2 laser induced photodissoc., pulsed mol. beam obs., van der Waals bond 80−9660
ethylene molecules, long range forces in multipole expsn., ab initio calcs. 78−9219
film, spherical, van der Waals' forces contrib. to thermodynamic props. 77−15724
film, van der Waals interactions, dispersion depend., semiempirical anal. from Lifshitz theory 77−15728
film adsorbed on graphite, two-dimensional phase transitions 80−107653
fluid, classical one-dimens. Lennard-Jones type, eqn. of state 80−24562
fluid, inhomogeneous, free-energy theory 80−10751
fluid, internal energy calcs. 77−28025
fluid, transport props., shear viscosity calcs. 77−35738
fluid interfaces, mol. theory 77−7949
fluids with assoc. mols., van der Waals type eqn. of state 77−967
fluoride crystals, rutile-type, interionic pots., cohesive energy, bulk modulus, calc. 80−79741
friction forces, contrib. of macroscopic van der Waals interaction *(Russian)* 77−16867
frictional force, contrib. of macroscopic Van der Waals interactions 78−55613
gas, thermodynamic props. review 80−31694
gas-liquid phase transition, Van der Waals' model 78−14445
glass, inorganic, calc. of microhardness and glass transition temp. 79−5059
glassy linear polymer, mol. model *(Russian)* 77−62610
glyoxal in supersonic jet, fluoresc. excitation, collision-induced intersystem crossing, van der Waals complex 79−81223
graphite, Van der Waals interactions, in and between layers of atoms 77−84695
ground state atoms, Van der Waals coeffs., polarisabilities and oscill. strengths calcs. 79−93913
hadrons, Yang-Mills pots., Van der Waals force and fermion motion 80−52465
halogens, van der Waals dimers, PCILO calcs. 79−36542
Hamaker functions, calc. from coagulation data, influence of Stern layers 78−48698
HCl-inert gas mixtures, van der Waals molecules, far IR spectra 80−95610
hexagonal layered structure, Van der Waals interactions, in and between layers of atoms 77−84695
I_2He, I_2He_3, and I_2He_3, photodissoc. products energy distrib. 79−100410
imperfect gas, van der Waals eqn. of state derivation 77−89221
inert gas crystal, correlation forces *(Russian)* 78−22686
inert gas crystal, dielec. const., Brillouin scatt., short-range at. interaction effect 78−43881
inert gas dimers, electron impact ionis. 80−58400
inert gases, viscosity, expt. and derived from statistical models *(French)* 77−35302
interface forces and interactions, roughness and ductility depend. 77−24476
intermolecular energies calculation from delocalised pictures, artifacts and elimination 80−18899
interpolation formula for interaction of 2 parallel cylinders 79−92122
ionic crystals, evaluation of photoelastic consts. 80−50297
ionic crystals, van der Waals potentials 78−83767
Kapton H, aromatic, polyimide, conformational investig., X-ray method, pot. energy calcs. 77−3498

Van der Waals forces continued
laser-induced atom-atom collision line shape 80−9691
layer compound, expansivities and thermal degradation 77−89554
Lifshitz constant for calc. of van der Waals force between two solids *(French)* 80−107658
linear molecules, spherical harmonics expsn. 78−5312
lipid bilayer membrane interaction forces in zone of contact 78−53345
liquid crystal, isotropic-nematic phase transition, van der Waals theory 77−31757
liquid crystal, lyotropic, phase diagrams and NMR, solubilised mols. effect on struct. 77−84628
liquid crystals with large dielec. anisotropy 77−15317
liquid film, free, stabilised with ionic surfactants, EHD 78−87403
liquid or gas, many-particle correl. attenuation *(Russian)* 77−27798
liquid thin films, calcs. using Lifshitz theory 77−72755
liquid-liquid interfaces in isolation, and in interaction, review 77−47651
liquid-vapour interface, surface tension-compressibility relation 80−44397
long range forces in quantum theory, book contrib. 78−82811
long-chain interactions, quadrupole effects, many-body anal. 77−83675
between loose macromolecular struct. 78−95996
macroscopic theory of Van der Waals forces between dielectrics 78−15139
many-body attraction between two equal spheres, easily calculable approx. 77−9134
many-body Van der Waals attraction between two spheres 79−24837
membrane bilayers, quasitwo dimens., theoretical models 80−76713
mesomorphic monolayers, quasitwo dimens., theoretical models 80−76713
metal, interacting metal half spaces, effect of retarded-surface-plasmon dispersion and Van der Waals interaction 79−69452
metal, pair potential between two ions in electron gas 78−47723
metal, van der Waals energy estimation 78−91634
metal surface, normal mode anal. of image pot. 79−33325
metal surface, van der Waals, interaction with mol., effect of spatial dispersion 78−10534
metal surface-void van der waals interaction energy 78−10036
metal surfaces, Van der Waals forces computation 79−15204
metallic surface, coupling to fluctuating atomic dipole, screening of point charge by surface plasmons 77−59217
metals, surface effects in hydrodynamic model review 79−78148
metastability, spinodal fixed point, renormalisation group anal. 79−40509
methane-propane(pentane)(n-heptane)(n-decane)(H_2S) mixtures, densities calc., van der Waals model 78−79740
methyl iodide, van der Waals mol., electron self-scavenging 80−95727
mica and quartz plates, calcs. from complete dielectric data 77−32340
mica surfaces, van der Waals interactions 78−30973
mixtures, phase equilibrium, augmented Van der Waals theory 78−79737
molecular interactions, two-body van der Waals coeff., combination rules 80−78677
molecule, matrix isolation spectrosc. 79−80688
molecules, higher-order vibr. eigenvalues calcs. 79−36722
molecules, long range interaction energy, ab initio calc. 78−62868
molecules, photo-induced vibr. predissoc. 79−41209
molecules, pot. functions, level spacings and thermodynamic props. 80−14185
molecules, review, book contrib. 77−38709
moment between anisotropic bodies, calc. 79−94547
monolayer, physically adsorbed, many-body interactions 78−84068
multipole long-range interaction coeffs., two- and three-body van der Waals interactions 80−37847
nematic fluid, anchoring at interface, effects of long range van der Waals forces 77−7662
nematic liquid crystal, generalised van der Waals theory 77−72547
nematic liquid crystal, self-consistency requirements 78−18541
nematic liquid crystal, surface tension, mol. theory 77−1075
nematic liquid crystals, surface and anchoring energies, van der Waals contrib. 80−92455
nematic liquid crystals, surface and interfacial free energy, Van der Waals dispersion force contrib. 79−99399
nematogenic solutions, binary, Van der Waals theory 79−27916
nematogenic solutions, Van der Waals theory 79−27915
net repulsive van der Waals forces between different particles, macromolecular, or biological cells in liqs., appls. 80−34274
neutral atom collisions, hyperfine component broadening and shift of spectral lines 80−74136
neutral atom scattering, long range, from solid cylinders, quantum theory 80−71549
neutral particles interaction pot. with surfaces *(Russian)* 80−6937
noble metal, van der Waals forces and their contrib. to vacancy form. energy and phonon dispersion 78−91635
noble metals, effect of forces on crystal structure 78−2062
nonelectrolyte solutions, liq. theory, review, book contrib. 77−39523
nonlocality effects influence on interaction between two macroscopic bodies *(Russian)* 77−81077
nonuniform fluid state, Van der Waals theory, thermodynamics, struct. and phase stability 79−77475
nucleotide base stacking interactions in vacuum, field mass spectrometry 80−81526
one-dimens. model of van der Waals forces 77−61824
oscillator strength sums, dynamic polarisabilities, one-term approximations 79−22782
oxide crystals, rutile-type, interionic pots., cohesive energy, bulk modulus, calc. 80−79741
palmitic acid-choleic acid complex, cryst. struct. and van der Waals energy 80−64983
paraffin oil, aq. emulsion, polyelectrolyte stabilised, mech. props. 79−39223
particle transport to rotating disc surface under external force field 78−15718
phospholipid bilayers, van der Waals interactions, total potential curves 78−77006
poly-n-phenyleneterephthalamide, conformational and structural props. *(Russian)* 77−61889
polyatomic molecule, crit. consts. evaluation from intermol. force consts. 80−37844
polyatomic molecules, struct. and dynamics calcs. 79−41097
polyatomic molecules, vibr. predissoc., rel. to van der Waals triatomic mol. theory 78−55208

Van der Waals forces continued
polyatomic molecules, vibr. predissoc. rel. to van der Waals mol. theory, anharmonicity effects 78−55209
polyethylene, oriented, stress-strain curve, analogy with van der Waals isotherm 77−59869
polyethylene glycol solns., US vels. to Van der Waals forces 77−72655
polypeptide lyotropic liq. crystals, van der Waals-Lifshitz forces 77−84624
polystyrene, glass-like, intermol. interactions temp. depend., IR spectra *(Russian)* 79−51967
pure fluids, augmented van der Waals theory 78−18518
pure gas, enthalpy, Carlson-Thodos van der Waals eqn. calcs. 80−83878
QCD colour singlets, long range forces 78−86441
quantum chemical intermolecular integrals, calc. using truncated Gaussian expansions of atomic orbitals 77−88520
quantum mechanical system dynamic polarisability, van der Waals constants 80−46867
quartz, Van der Waals interaction between two crystalline samples, influence of optical absorpt. 79−95273
reaction rates, diffusion controlled, effect of van der Waals force, Smoluchowski's formula 79−100335
real gas thermodynamics, Van der Waals model approach 80−38515
Riemann-Hugoniot catastrophe and P, ρ, T surfaces of real gases 79−6066
semiconductor, donor van der Waals interactions, spectral lineshapes 80−11450
semiconductor surface plasma, van der Waals interaction with neutral atom, mag. field effects 77−59316
soap film, light scatt., van der Waals forces determ. 77−85028
soft-sphere mixture viscosity, nonequilib. mol. dynamics 80−19680
solids in air, direct meas. 78−43461
solvent structure, in particle interactions, short range forces 78−83709
solvent structure in particle interactions, asymptotic regime 78−83708
solvent-rod mixture, two phase, interfacial free energies, quartic van der Waals theory 80−59377
spatial dispersion effects on van der Waals interaction between molecules 77−35817
spatial dispersion effects on van der Waals interaction between molecules 77−79672
spectral line broadening, growth curves 80−102548
sphere and half-space, van der Waals attraction energy 80−16735
sphere-wall attraction, many-body formula, approximation 78−21000
statistical theory of viscoelastic relax. van der Waals liq. 77−68907
styrene-methacrylic acid copolymer, glass-like, intermol. interactions temp. depend., IR spectra *(Russian)* 79−51967
sum-rule functions, parametrized, C_6 consts. 77−27000
surface plasmons around cavity in semiinfinite metal *(French)* 78−56196
tetracene-Kr(Xe), intramol. intersystem crossing in supersonic beam, external heavy atom effect 80−14167
tetrazine-Ar, van der Waals bond, nonstatistical vibr. energy distrib., photochemical reaction effects 80−30255
time-dependent Hartree theory, elec. quadrupole effects 77−6882
transport properties of a Van der Waals fluid near the critical point 79−46537
triatomic, molecules, vibr. predissoc., rel. to polyatomic complexes, theory 78−55208
triatomic molecule, vibr. predissoc. model 77−71838
tris(ethylenediamine)metal(III), H bonding *(French)* 80−87241
tris-butadienyl metal D_3 complex pairwise chiral discriminations, stereochem. basis, extended transition monopole model 78−74725
TTF dimer, nonbonding intermolecular forces 80−83443
TTF-TCNQ, organic metal, Van der Waals donor stacking 80−15037
Van der Waals constant, liquid, binary mixtures of organic chemicals, US velocity and excess internal pressure, Flory's theory 80−70310
Van der Waals equation, statistical anal. of RT_c/P_cV_c *(Spanish)* 80−74213
van der Waals molecules, vibr.-rot. spectrum 79−13698
voids and particles, Van der Waals energy between them, from asymptotic to close contact 80−80351
water, Van der Waals interaction, Kramers-Kronig eqn. with full spectral data vs. oscillator model approx. 78−5998
pp scatt., low energy, strong van der Waals interaction 78−41563
Ag (110), CN^- chemisorbed, Raman scatt. 80−45075
Ag film, on amorphous C and Si substrates, dispersion force contrib. to adhesion *(French)* 80−59842
Ag halides, cryst., van der Waals coeffs. calcs. 80−96459
Ag halides, van der Waals energy, cohesive energy calc. 77−51343
AgCl(Br)(I), van der Waal dipole-dipole and dipole-quadrupole energies, Born and Slater-Kirkwood models 79−27947
Al film, on amorphous C and Si substrates, dispersion force contrib. to adhesion *(French)* 80−59842
Al I line broadening and shifts by van der Waals interaction with Ar and He atoms 79−6912
Ar line broadening by at. collisions, meas. of oscillator strength of ArI lines reson. *(French)* 78−5172
Ar-acetylene van der Waals molecule, radiofreq. spectroscopy and Stark effect meas., equilib. struct. and props. 80−91543
Ar-HBr, intermol. pot. energy surfaces calcs. 80−91625
Ar-HCl, van der Waals mol., far IR spectra 77−79611
Ar-HCl, Van der Waals mol., far IR spectrum, anisotropic intermol. force effects 78−62869
Ar-O_3 Van der Waals complex, struct. and props., RF and microwave obs. 80−32704
Ar_2, accurate ab initio calc. of intermol. energy 80−18899
Ar_2, photoionisation 77−54578
ArHX, (X=F,Cl,Br,I) van der Waals mols. vibr. and thermodynamic props., WKB calcs. 77−71740
Au deposited on alkali metal substrates, calc. binding energy of Au atoms to substrates 79−33208
Au film, on amorphous C and Si substrates, dispersion force contrib. to adhesion *(French)* 80−59842
Au film, van der Waals energy of interaction with heavy alkali atoms 77−11829
CO+Ar(He)(Ne)(Kr)(Xe), intermol. pot. energy surfaces from electron gas model, ang., distance, and vibr. depend. 79−3520
Ca_2, in Kr matrix, 1- and 2-photon fluoresc. excitation 78−50567
Ca_2, matrix isolated, vis. and near IR spectra 78−5214
Ca_2, van der Waals mol., in Kr matrix, absorpt. and emission spectra 77−83611

Van der Waals forces continued
^{114}Cd λ326.1 nm reson. line, self-broadened, temp. depend. of parameters 79−63964
CdI_2-$CdBr_2$ mixed layer cpds., rigid layer modes and van der Waals interactions, Raman spectra obs. 79−33700
Cr-covered objects, dispersion forces at 132-670 nm distances 79−42681
Cs, crystal struct., van der Waals and repulsive interaction 80−84137
Cs+Ar(Kr)(Xe), spectral line breadth and shift, Van der Waals pot. calc. 78−90126
CsBr, evaluation of van der Waals dipole-dipole pot. 78−22692
CsCl, evaluation of van der Waals dipole-dipole pot. 78−22692
CsCl-structure compounds, lattice energy and elastic consts. for 3-body Van der Waals interaction 77−72580
CsI, evaluation of van der Waals dipole-dipole pot. 78−22692
Cu film, on amorphous C and Si substrates, dispersion force contrib. to adhesion *(French)* 80−59842
Cu halides, van der Waals energy, cohesive energy calc. 77−51343
CuCl(Br)(I), van der Waal dipole-dipole and dipole-quadrupole energies, Born and Slater-Kirkwood models 79−27947
D+HCl(HBr), elastic scatt., van der Waals pot. meas. 77−58120
GaAs, donor van der Waals interactions, spectral lineshapes 80−11450
H bonded solids, neutron diffr. data, rel. to van der Waals criterion 78−91292
H+H, multipole-multipole dispersion interaction, Pade approximants 79−31638
H+HCl(HBr)(HI), elastic scatt., <50 meV, Van der Waals pot. 79−54937
H+He, H Balmer-α fine struct. lines, anomalous shifts, in He-H_2 DC discharge 79−45677
H+He, H Balmer-α fine-struct. line shift and broadening 80−37783
H+He(Ne)(Ar)(Kr)(Xe), low energy elastic scatt. cross section MCSCF calc., van der Waals forces 78−70897
H+Ne(Ar)(Kr)(Xe), orbiting resons., van der Waals pots., beam scatt. obs. 79−89739
H_2 in organic solvents, proton chem. shift, Van der Waals solvent effect contrib. 77−68062
H_2, triplet state, pot. curve van der Waals region, MS-MA calcs. 77−79551
H_2, Van der Waals constants, upper and lower limits, analytic eqns. 78−29831
H_2-H_2, intermol. pot. surface, ang. depend., nonorthogonal CI calc. 77−46613
H_2-H_2 intermol. pair pot., ab initio SCF-CI surface 80−91457
H_2-like molecules, change of binding type and dissoc. in strong mag. field 78−62744
H_2+Ar(Kr)(Xe), orbiting resons., van der Waals pots., beam scatt. obs. 79−89739
H_2+H_2, van der Waals pot., electron tunnelling, charge transfer 77−54588
$(H_2)_2$, $(D_2)_2$, $(HD)_2$ and H_2-D_2, Van der Waals complexes, mol. symmetry 80−42963
$(H_2)_2$, ab initio calcs., perturbation dispersion energy versus CI treatment 77−26976
H_2Ar, van der Waals complexes, lifetimes calcs. 78−13564
HBr, fundamental IR band, solvent effect *(Russian)* 78−13501
HCl(-acetone)(-acetonitrile), soln., IR absorption, H-bonding, solvent effect 78−29778
H_2O, Van der Waals dispersion coeffs., 2 well separated mols., sum rule moment calc. 78−5156
He, 2(^{1,3}S) excited states and ground state, dynamic polarisabilities, van der Waals force consts. 77−34773
He, films, inhomogeneities 77−76641
He-Ar, van der Waals pot. determ. 79−10167
He-He, exchange dispersion energy, multiple expansion, rate of convergence 77−46614
He+Ar, van der Waals pot., from crossed at.-mol. thermal beams scatt. 79−27053
He+H_2, pot. energy surface, ab initio calcs., van der Waals const. determ. 80−106372
He+H_2, Van der Waals pot., ab inito SCF model 78−74728
He+methane $(NH_3)(H_2O)(SF_6)$, differential scatt. cross-section, intermol. pot. 79−36728
He+$N_2(O_2)(CO)(NO)$, anisotropic intermol. pots., crossed beam expts. 79−31639
HeI_2, van der Waals mol., vibr. predissoc. lifetimes 79−68278
HeI_2, Van der Waals mol. vibr. predissoc. anharmonicity effects 80−52971
$HeNO_2$, vibr. predissoc., rel. to van der Waals triatomic mol. theory 78−55208
$HeNO_2$, vibr. predissoc. rel. to van der Waals mol. theory, anharmonicity effects 78−55209
^{3}He, liq., reinforcement of low temp. surface ferromag. instability due to ^{3}He-wall attraction 79−51373
^{3}He, liquid, surface ferromagnetic instability, attraction to solid substrate 79−46863
^{3}He-^{4}He mixture, adsorbed film, systematic exptl. study 80−107603
^{3}He-^{4}He mixtures, liq., coherence length effects on nucleation of superfluid transitions 77−66069
^{3}He-^{4}He solution film, thermodynamic theory including effect of Van der Waals potentials 77−4238
^{4}He, liq., reflection coeff. for ^{3}He atoms at free surface meas. 77−15644
^{4}He superfluid film, neutron scatt., surface effects 78−10251
^{4}He, superfluid film, solitons at low temps., Korteweg-de Vries eqn. 80−96717
He($2s^1$S,2^3S)+Ne(Ar)(Kr)(Xe), Van der Waals forces, one-electron model pot. calcs. 80−14094
HfS_2, layer compound, expansivities and thermal degradation 77−89554
Hg 6 ^{1}S$_0$-Hg 6 ^{1}P$_1$, Van der Waals term in interaction, blue satellite line *(French)* 80−37848
I_2He, Van der Waals mol., photodissoc. lifetime, I_2 vibr. depend. 79−6977
$I_2Ne_aHe_b$ van der Waals complexes photodissoc. 80−50864
I_2*He, vibrational predissociation, van der Waals molecules, vibration-translation scaling theory 80−43135
K, crystal struct., van der Waals and repulsive interaction 80−84137
Kr-HCl, intermol. pot. energy surfaces calcs. 80−91625
Kr_2, photoionisation 77−54578
KrAr, photoionisation spectra of ground and excited states 78−5297
KrHCl, van der Waals complexes, struct., RF and microwave spectra, isotope effects 80−37806

Van der Waals forces continued
Li, dipole oscill. strength sums, dipole-dipole and dipole-quadrupole van der Waals consts. 78−9127
Li^+, 2(^{1,3}S) excited states and ground state, dynamic polarisabilities, van der Waals force consts. 77−34773
Li+H(He) 78−9127
LiF+inert gas atom, interaction anisotropy, Van der Waals forces 79−6985
Mg, spectral line broadening, by inert gas collisions 77−79580
Mg_2 matrix isolated, vis. and near IR spectra 78−5214
Mg_2, $X^1\Sigma_g^+$ state, pot. curve, coupled pair many electron theory calc. 79−89621
$(N_2)_2$, Van der Waals molecule, struct. and internal rot. barriers determ., interaction pot. from ab initio calcs. 80−91626
NH_3, gas phase proton solvation energetics, mol. beam-photoionis. obs. 79−29345
N_2O, pure and in mixtures, electron attachment near 1 atm., microeave cond. meas. 80−1063
$(N_2O)_2$, photo-induced vibr. predissoc. of van der Waals mol. 78−90242
Na-Hg high-press. discharge, Na reson. radiation, self-reversed maxima shifts 80−92411
Na+Ar→NaAr, quasimol. form., laser spectroscopic obs. 77−57920
NaAr, ground and excited state pot. curves, dispersed fluoresc. spectrum 79−98140
NaNe, laser spectroscopy, interat. pot. curves 78−86871
NaNe, van der Waals mol., form., laser spectroscopy 78−29797
NaO_2, physical mechanisms of phase transitions 80−6381
Ne+H_2, Van der Waals pot., ab inito SCF model 78−74728
Ne_2, van der Waals mol., vibr.-rot. spectrum 79−13698
Ne_2, van der Waals mols., interatomic energy, SCF supermol. ab initio calcs. 77−42370
Ni (001) surface, chemisorbed O_2, electronic struct. and overlayer struct. theory 79−28391
O_2+inert gas atom, absolute total elastic cross sections 78−9220
$O(^3P)$+inert gas atom, absolute total cross sections, 0.6-2.0 km sec^{-1}, model pots. 77−19010
P, black allotrope, orthorhombic bonding, up to 26.6 kbar, neutron diffr. obs. 79−99106
Rb, crystal struct., van der Waals and repulsive interaction 80−84137
Rb+Ar(Kr)(Xe), spectral line breadth and shift, Van der Waals pot. calc. 78−90126
$^{87}Rb+^{129}Xe$, spin-exchange cross-section meas. 80−78686
S atom, van der Waals radius, mean statistical value 77−83515
Se, vitreous, elastic coeffs. about glass transition temp. US study *(French)* 80−19865
Si, van der Waals electron correlation energy 78−95013
Si-borosilicate, Van der Waals interaction, influence of optical absorpt. 79−95273
Si-Si system, Van der Waals interaction, influence of optical absorpt. 79−95273
SiO_2, fused, van der Waals forces between flat plate and spherical surface 79−37924
$SnS_2(Se_2)(SSe)$, layer compound, expansivities and thermal degradation 77−89554
Sr_2, matrix isolated, vis. and near IR spectra 78−5214
Sr_2, Van der Waals dimer, inert gas matrix-isolated, laser excited emission spectra 78−78744
TiS_2, layer compound, expansivities and thermal degradation 77−89554
Tl halides, cryst., van der Waals coeffs. calcs. 80−96459
Tl halides, van der Waals energy, cohesive energy calc. 77−51343
TlCl(Br)(I), van der Waal dipole-dipole and dipole-quadrupole energies, Born and Slater-Kirkwood models 79−27947
TlI, atomic fluorescence, D_2 pressure effect on width and shift 80−99475
Xe+Cl_2 classical trajectory calcs., energy threshold for collision induced dissoc. determ., 80−95709
Xe_2, photoelectron spectra, $X^1\Sigma^+_{(1/2)g}$ ground state pot. 78−5280
Xe_2, van der Waals mol., photoionisation 77−18991
XeAr(XeKr) photoionisation spectra of ground and excited states 78−5297
ZrS_2, layer compound, expansivities and thermal degradation 77−89554

Van der Waals molecules *see quasimolecules*

vanadium
see also nuclei with .....
abundance in early A-type stars 79−21314
adsorption on W, effect on work function 77−51607
AES, extended fine struct. above L-shell appearance pot. thresholds 78−92148
air pollution, transport from urban to remote marine areas 77−37355
alkali bromide (chloride):V^{2+}, electron spin transfer 78−87949
alkali chloride: V^{2+}, phonon induced zero field splitting 78−39073
alloying addition to low-alloy steel, role in austenitic grain growth 77−44255
amorphous film, supercond. props., gaseous impurities effect *(Russian)* 78−72301
annealing after irradiation with 210 keV He at 625°C at high fluences 78−67751
anodisation, oxide struct., electronic current, and const. current efficiency 78−15575
anodisation, source of O in oxide films 79−100389
anodisation, use of nucl. reaction to trace source of O 79−52683
anodised layer, structure and stoichiometry, thickness effects 77−77634
anomalous slip under compressive deform. 77−63737
APS thresholds, extended fine struct., effect of central atom pot. 80−66329
atom, fine struct. levels fitting, config. interaction effect, spin-orbit and electrostatic interaction parameters 80−69248
atom, hyperfine struct., laser-RF double-reson. obs. 79−41141
atom, ionisation potential, term value, correlation energy by vertical anal. 78−41964
atom, $K\alpha^h$ hypersatellite spectra and K-shell double photoionisation cross-section 78−21874
atom, $K\beta/K\alpha$ ratio anomalies, K-capture rel. to bremsstrahlung excitation 77−18825
atom, K-shell ionisation cross sections, proton induced 77−23556
atom, model pots., STO calcs. 77−408
atom, $O^{2+,3+,4+,5+}$ induced K-shell X-ray production cross section, 7 to 24 MeV 77−61850
atom, X-ray fluorescence, $K\alpha$ hypersatellites 77−18830
atom, X-ray production by protons by 0.5 to 2.0 MeV energy 78−66646

vanadium continued
atomic energy levels in all stages of ionisation, data anal. 78−94207
atomic transition probabilities, oscill. strengths 78−74601
atomisation, for graphite furnace AAS, using graphite platform 78−32877
Auger electron appearance potential spectroscopy 78−72647
band effective mass, Animalu TMMP theory 80−29312
band electron momentum distributions calc. 78−18950
band structure, X-ray emission bands, self-consistent calc. 77−28104
band structure and X-ray emission spectra calcs. 77−28105
BCC, stress-induced interaction and ordering 79−42057
blister form. and stress build-up, under He bombardment, surface prep. effects 78−95094
blister form. by He and H ion bombardment, target struct. effect 78−95087
blistering after Ar^+ ion bombard., irrad. mode effect 80−39176
catalysis, Fe-based oxides containing V for NO_x reduction 79−12285
CdS:Cu, V, photoluminescence spectra 79−83027
channelling studies on the trapping of deuterium in vanadium by O-interstitials 79−4316
charged particle prod. cross sections for 14 MeV neutrons, Ti, V, Cr, Mn 80−42648
chemisorption, competitive, on metallic films, IR spectra, oil matrix technique 77−9118
coherent twin boundary structure *(French)* 79−60379
columnar films, crit. field anisotropy, depend. on prep. conditions *(Russian)* 80−93056
Compton profiles, anisotropic 80−97368
Compton profiles, comparison with band struct. calcs. 78−84675
concentration in snow of Mt. Blanc rel. to air pollution 78−81258
creep, substruct. changes *(Russian)* 78−23782
creep behaviour of polycryst., V, 790-880°C 79−24578
creep rate in vacuum, grain size effect 80−108514
crystal field potential calc. 77−59366
Debye-Waller exponent, 4.2 to 296K, incoherent elastic neutron scatt. 79−4382
deformation behaviour, stress relax. and slip plane patterns of zone refined single crystals 79−29163
dehydrogenation by annealing with Zr foils 80−96736
density, rel. to elastic const. calc. from US meas. 77−86079
deoxidation of Fe by V, phase equilibrium with V_2O_3 *(Russian)* 80−16275
depth profiling of ^{3}He ion implantation 78−59830
determ. by atomic absorption, using low temp. flames 80−30307
determination, in Mg alloy, emission spectrographic DC arc-powder technique 78−48713
determination in sea and surface waters, preconc. on charcoal, neutron activation anal. 77−44549
determination of microconcs. by polarography 79−16072
diamagnetic lattice, EPR parameters of V^{4+}, cryst. field effects 78−64263
dielectric screening and phonon frequencies using isotropic noninteracting s-d-band model 79−19343
diffusion and solubility in Be 77−35757
diffusion and trapping of O_2 79−77816
diffusion characteristics in Ag, 1051 to 1220K 80−15308
diffusion in Cu 77−62674
diffusion in Mn steel, electron probe microanalysis *(Czech)* 77−59149
diffusion in Mn steel with varying Mn content *(Czechoslovakian)* 77−35743
diffusion in molten Fe *(Japanese)* 77−51531
diffusion of H_2, in single crystal, Debye-Waller factor, neutron spectroscopy 79−37881
diffusion of H_2, isotope effects, crystal field stabilisation 80−59728
diffusion of $H_2(D_2)$, quantum rate theory for symmetric double well pot. 78−55970
diffusion of H_2 *(Japanese)* 78−10221
diffusion of H, book contrib. 79−82390
diffusion of H, neutron radiography meas. 77−39696
diffusion of H and D, effect of impurities on coeff. 78−47604
diffusion of H and trapping 80−70447
diffusion of O and N, least squares computer technique 78−38881
diffusion of O and N, statistical calcs. on Arrhenius lines 80−59722
diffusion of positive muons 78−47601
diffusion of Ta, 1100 to 1800°C 77−24443
dimer, formation, spectra, electronic struct. 77−54642
dynamic deformation, influence of previous static loading *(Russian)* 78−6972
elastic constants, pure metal and with O_2 additions, 4.2 to 300K, hardening 79−90712
elastic constants in pure and hydrogenated crystals, effect of pressure 80−7614
elastic consts., changes caused by addition of H and effects of hydrostatic pressure 80−75287
elastic moduli, determination of effect of H based on US vel. meas. 80−75288
elastic properties, at high temp. 80−30007
elastically deformed, quadrupole effects, NMR line intensity *(Russian)* 78−56400
electrical resistivity, 200-2100K 79−33277
electrical resistivity due to interstitial H (D) 80−96848
electrnic sp. ht. and heat conduction, temp. depend. 78−71865
electro- and thermotransport of O and N 77−28040
electromigration measured by resistance method, for H and D impurities 79−23783
electron distribution, HF calc. 78−75979
electron energy losses due to H, obs. by scanning TEM 80−79850
electron-irradiated, positron annihilation study 80−70259
electron-phonon coupling constant calc. *(Russian)* 80−70624
electron-phonon interaction, calc. using APW band struct. calcs. and measured phonon spectra 78−14869
electronic density of states, effective mass, electron-phonon interaction, Coulomb pseudopot. *(Russian)* 78−26804
electronic structure, APW calcs., self-consistency and exchange effects 77−66109
electronic structure, model potential calcs. *(Russian)* 80−100431
electronic structure, thermoreflectance studies 80−76047
electropolishing for TEM obs. 78−31605
electrotransport in Th, 1370-1665°C 78−59979
electrotransport of H(D) at high H concs. 80−34246
emissivity, integral normal, in 1300-2000K range 77−35728

vanadium continued
emittance at 400 to 850K and normal spectral reflectance at room temp. 77−20813
energy bands, calcs. using LCGO method 78−91608
energy bands, Compton profile, optical cond., SCF LCAO calcs. Gaussian orbitals 78−47698
energy gap determ. by optical methods *(Russian)* 78−30867
enthalpy and heat capacity determ., 1345-2173K 78−71866
epitaxial films on sapphire by electron beam evaporation *(Russian)* 77−76701
erosion coeff. temp. depend., electron beam melting 78−17418
Fermi surface and magnetic breakdown, magnetoresistance and thermopower behaviour 79−33222
Fermi surface area, effective heat, optical masses, surface anisotropy critical temp. depend. *(Russian)* 79−90943
Fermi surface topology, associated plane wave calcs. 78−14660
film, BCC, optical props. 79−78781
film, electron beam evaporator for in situ deposition studies in UHV electron microscope 80−40264
film, evaporated, optical props., rel. to struct. 80−55211
film, resist. supercond. transition 80−25033
film, scaling behaviour of resistive supercond. transitions 79−56363
film, supercond. crit. temp., crit. field, resist. and struct. *(Russian)* 77−4475
film, superconducting tunnelling, meas. of annealing characteristics 79−7944
film, vac. deposited, influence of ion bombardment during condensation 79−82483
film, vac. evaporated, elec. props. 80−80414
film on sapphire substrate, orientational growth, epitaxial textures, nucleation textures *(Russian)* 80−75454
film on Si, ion implanted, inert-gas-bubble form., TEM and Rutherford backscatt. anal. 79−90682
film vapour-deposited on Be substrate, diffusion anal. by ion backscatt. 77−35752
films, vac. evaporated, optical cond. 80−76100
fine particles, appearance of mag. moment 78−68152
fine particles formed by gas-evap. technique, cryst. struct. and habit 79−27935
flow stress temp. depend., effect of interstitial atom clustering and embrittlement *(Russian)* 78−34538
fluxural oscillations in longitudinal mag. field, sound attenuation, magnetoelasticity *(Russian)* 80−54844
foil, air-oxidised, reversible switching, mechanism determ. 79−28387
foil, electron energy loss spectra 80−7452
foil, rolling procedures 80−23225
foils, coated with thin H-permeable Pd film, AES and SIMS 79−52467
fusion reactor first wall material, cyclic deform. tests 80−30074
fusion reactor first wall material, irrad. with 40 keV ^{4}He ions, blistering 78−55897
fusion reactor material, ^{4}He irrad., depth profiles, migration, release, surface effects, blistering 77−35606
fusion reactor material, blister behaviour during 200, 2000 keV He irrad., temp. depend. 77−35607
guanidinium aluminium sulphate hexahydrate, ESR of V^{3+}, 21.5 GHz, 4.2K 78−91942
hydrogenated, grain size depend. of tensile strength 77−36657
hyperfine particles, appearance of mag. moments, mag. susceptibility meas. 77−36097
hyperfine particles, surface magnetisation, explanation of expt. work 78−23303
implanted Li atoms, depth profiles and sputtering anal. by optical spectra 77−35579
impurity defect interaction influence on radiation hardening and embrittlement 80−35199
impurity in Al nuclear reactor fuel tubes, proton activation determ. 80−27741
impurity in II-VI semiconductors, absorption and luminesc. spectra 78−15203
interatomic pair potential, phonon spectra 80−33927
internal friction, low temp., H_2 effects 80−40419
internal friction α-peak origin 78−95773
internal friction and elastic constants, reson. vibrs. of metal spheres 78−15443
internally oxidised, neutron irradiated, annealing effect on mech. props., elec. cond. and electron microscope obs. *(Japanese)* 79−15701
interstellar abundance and depletion models 80−46630
interstitial impurity and substitutional solute interaction, internal friction meas. 78−10082
ion implanted, energy dependent channelling and backscatt. anal., $^4He^+$ ions, 1 to 2.8 MeV 79−4360
ion implanted with 2 MeV He under pulsed conditions, microstructure obs. 80−29088
irradiation with 2 MeV He ions, low cycle at elev. temp. 78−95086
ISSEC selection for fusion reactor 80−57950
Kohn anomalies and phonon dispersion, model including exchange-correl. corrections 78−59886
lattice atom displacements near end of implanted μ^+ tracks 78−55890
lattice defects, relax. studies, computer simulation 78−79604
lattice distortion, due to O and N di-interstitial clusters 78−71726
lattice distortion and migration energy of H impurities 78−30796
lattice distortion in migration energy of O impurities 78−30796
lattice dynamics, local frequency spectrum, mean thermal displacement of H 80−59604
lattice dynamics, microscopic theory 79−7664
lattice dynamics, modified Sharma-Joshi model 79−51221
lattice dynamics, phonon dispersion and atomic force constants, phenomenological model 78−26640
lattice dynamics, seven parameter model 79−90739
lattice dynamics, vibr. spectrum and sp. ht., CGW model 78−22793
lattice dynamics and cryst. equilib. 78−75753
liquid, elec. resist., melting pt. to boiling pt., temp. depend. 80−96839
liquid, multiple scatt. calcs. of resist. 78−76039
liquid, sp. ht. eqn. for high temp. 77−51510
liquid, spectral emissivity and brightness-temp. meas. at MP 77−43356
liquid, thermal volume expansion, MP to BP 79−90802
liquid, viscosity at melting point, free energy *(Russian)* 80−92699
low temperature depend. of elec. resist., mag. suscept., heat capacity, Hall const. *(Russian)* 78−30900
low-temperature thermal and elec. cond. 79−60792
lower critical field anisotropy 78−76201
vanadium continued
luminescence characteristics of pure surfaces acted on by flux of field emission electrons 80−100695
magnetic form factors, neutron diffr. study 79−47234
magnetic moment near surface, one-electron band model 79−82747
magnetic susceptibility, model pot. theory 80−75710
magnetic susceptibility, orbital, calc. 80−7075
mechanical properties, O, N_2 and C addition effects 79−52356
microstrain at room temp., with different grain sizes *(German)* 77−36614
mixed state, US attenuation purity depend., crit. temp. and energy gap 77−47935
Mossbauer fraction, press. depend. 77−59493
Mossbauer fraction for ^{57}Fe, press. depend. 77−16226
muon$^+$ spin resonance, diffusion, temp. depend. 78−39490
muon diffusion, μ^+SR meas. 78−39487
muon diffusion, LAMPF results 80−71285
muon diffusion and trapping 79−56686
muon localisation and lattice dilation, μSR 79−56694
muon trapping, Knight shift, rel. to H interstitials 80−50247
neutron activation analysis for determ. of V in crude oil 78−20109
neutron diffraction determ. of O, N, C, interstitial sites 77−19944
neutron diffraction measurements, search for antiferromagnetism *(Russian)* 78−6516
neutron irrad., yield stress and activation vol. 77−90418
neutron irradiated, void swelling, O_2 effect 78−6106
neutron irradiation effect, comparison of high purity V with V-O 77−84805
neutron low energy interaction cross sections, gravitational spectrometer meas. 80−24521
neutron multiple scatt. calcs., expt. verification using polarisation anal. technique 78−42865
nuclear acoustic resonance absorption and dispersion via coupling to mag. dipole moment 77−48065
O_2 getters for LMFBR fuel pins 78−74437
optical absorption spectrum, 0.25-14 μm *(Russian)* 77−81118
optical properties and electronic props. 79−42439
oxidation during energetic particle irrad., influence of reactive gases on sputtering and secondary ion emission 78−72656
oxidation to form VO_2, ionic cond. 79−51299
oxidised in air during laser irradiation, switching effect *(Russian)* 80−24977
oxidized, electron stimulated desorption of O^+ ions 79−99428
partial densities of states, electron-phonon interaction 78−51869
phonon dispersion curves, extended du Launay model 77−4162
phonon dispersion using non-central force model 78−91392
phonon frequencies calc. 79−19329
phosphate glasses:V^{4+}, EPR, optical spectra 78−72399
photoelectric cross sections at 52.4, 60, 72.2 and 84.4 keV 80−69187
photoelectric cross sections of low energy photons 78−46309
plastic deformation, struct. changes *(Russian)* 78−48447
plastic deformation effect on positron annihilation and supercond. transition *(Russian)* 77−39993
plasticity and strength change in temp. range 20 to 1000°C, impurity effects 80−35235
pollution, low level meas. 77−41239
polycrystalline, 20 keV protons penetration depth, ultrasonic meas. technique 78−30677
polycrystalline plate, struct. facators, time of flight neutron diffr. 78−47212
positron annihilation, Doppler broadened lineshapes, prevacancy lattice expansion 78−27349
positron annihilation, temp. depend. 78−56540
positron annihilation and vacancy formation 80−16119
powder, crystal structure, magnetic and superconducting props. 80−97121
pressure equation derived, Hartree-Fock approx. 78−72103
proton bombardment induced blistering 77−7770
purification and plastic props. 80−25810
quantitative anal., for D, by ion microanalysis 78−56945
radiance temperature at melting point, surface roughness depend. 80−59683
radiation hardening and plastic instability *(Russian)* 78−39842
resistivity variations caused by H and D interstitials, isotope effects 77−89750
rolling textures, microstructure, micro orientation *(Russian)* 79−91663
ruby:V^{3+}, cross-relax. 80−71163
Saguenay fjord sediments, distrib. and partition of Co, Ni, Cr and V 77−33100
secondary electron emission, on proton and deuteron irrad., 0.5-2.5 MeV 77−63512
secondary ion emission, energy spectra, 0-55 eV, contamination levels 79−15573
secondary ion emission, normalised energy spectra from Hg^+ impact, anomalous behaviour 80−45193
self diffusion, 1170 to 1893°C *(German)* 79−86917
self diffusion meas. 77−89570
self-powered flux detectors, response characts. in CANDU reactors 78−82594
self-powered neutron flux detector response in mockup Bruce reactor core 78−58391
self-transport, electro- and thermo-, 1480-1822°C 79−42297
shear elastic constant, anomalous temp. behaviour, US study 79−28031
single cryst., surface investigation by positron annihilation 79−15552
skeletal system V incorporation mechanism 79−82341
slip, anomalous, suppression by O interstitials 77−28875
slip geometry and dislocation struct., rel. to degree and temp. of deform. *(Russian)* 78−38717
solubility in α-Ti, 400-700°C 78−83959
sorption investigation of (100) surface, using total current spectroscopy of slow electrons 77−8694
spallogenic isotopes in Fe meteorites, radial distrib. 80−67488
sputter-erosion and impurity emission under low energy ion bombardment 78−95628
sputtered film, compressive stress transition 78−10310
sputtered particles from D bombardment, ion fraction and energy anal. 77−36345
sputtering by fusion neutrons meas. 77−36321
sputtering under 14.1 MeV neutron impact 77−48281
steel-V interface, diffusion above 500°C *(German)* 79−28156
stopping power for 28 MeV α-particles, re-evaluation 78−79651

vanadium continued
stopping powers for 28.8 MeV α-particles 77−80556
strain hardening, screw dislocations and microtwinning *(Russian)* 80−29971
strength, ductility, 4.2 to 400K, O_2 effect 77−36529
stress induced interaction of point defect pairs, in BCC solutions 78−79608
stress relaxation test, appl. to discerning frictional and internal stresses 77−63712
structural changes in single crystal under single electric impulse discharge *(Russian)* 79−65086
superconducting, creep effect in periodically swept minor hysteresis loops 79−60964
superconducting, fluctuation contrib. to sound attenuation near H_{c2} 79−33397
superconducting, fluctuation contrib. to US attenuation in mag. field near H_{c2} 77−47936
superconducting, fluxoid pinning by VC_x precipitates 78−52169
superconducting, Ginzburg-Landau parameters, magnetisation meas. 78−2620
superconducting, microwave biased RF-SQUID system, appl. to magnetic aftereffect 79−26089
superconducting, rotating discs, hysteresis losses and mag. phenomena 80−75695
superconducting, spin fluctuations effect on T_c, from sp. ht. and mag. suscept. 80−7030
superconducting film, inhomogeneous, crit. field anisotropy 79−56459
superconducting film, resistive transitions *(Russian)* 79−95546
superconducting film, resistive transitions scaling behaviour 79−15248
superconducting foil, flux flow noise cross-correl. functions 77−36034
superconducting foil, time behaviour of local flux flow noise 79−24116
superconducting heat switches, effect of surface prep. 79−60966
superconducting props., effect of voids 78−52168
superconducting rotating disc, flux expulsion and trapping 78−6488
superconducting T_c and H_{c2} effect of purity and alloying with Ta, Cr, Mo or Re 77−85375
superconducting thin film, determ. of energy gap, tunnel effect method 79−42704
superconducting transition temperature, ab initio calc. 80−25036
superconducting vacuum-deposited film, electrophys. props. *(Russian)* 77−59345
superconducting wire, helical propag. of flux jumps 78−14901
superconductivity, anisotropy of generalised Ginzburg-Landau parameters 79−4630
superconductivity, influence of plastic deform. 77−85378
superconductor, neutron irradiation, low temp., effect on critical current 78−52180
superconductor, soft modes, d-electron localisation 78−14872
surface, adsorbed C^+ layer removal, by 20-30 keV Ar^+ bombardment, in plasma 77−76103
surface, chemisorption of Br_2, struct., Na adsorption effects 80−101039
surface, clean, nearest neighbour spacings from extended appearance pot. fine struct. 79−69329
surface, H^+ ion bombardment, surface blistering, influence of temp. and crystallographic orientation *(Russian)* 78−95083
surface, He ion bombard., blister diameter and skin thickness, SEM obs. 79−28019
surface, particle valence by neutrons 80−25493
surface, secondary ion emission mechanism, under Hg^+ ion bombardment 79−100013
surface, spin fluctuations, finite temp. mag. props. study 80−107994
surface blistering, SEM and TEM obs., ion energy, dose and target temp. depends., review 77−43261
surface interaction with O_2, H_2, H_2+O_2, and H_2O, SIMS, EID and flash filament signals 77−62753
surface state, XPS investigation 78−11070
synergic extraction and photometric determ. in presence of phenols, using N-hydroxy-N-p-tolyl-N'-(3-chloro-4-methylphenyl)-p-toluamidine as reagent 79−79345
target bombard. with medium-energy protons, ^{43}K recovery, separation, medical appls. 77−81572
thermal conductivity, 1200-1900K range 78−95282
thermal conductivity, elec. resist. and Seebeck coeff. meas., 6-300K 77−39818
thermal conductivity in ultrapure normal, mixed and supercond. states *(Russian)* 79−4617
thermal shock resistance, original struct. effects 77−63803
thermodynamic props., calc. for liq. and solid phases 77−43348
thermophysical props. at temps. up to 7000K 80−103497
Tokamak reactor ISSEC 78−41860
transport of H, study by neutron radiography, review of results 78−59961
twin and stacking fault energies calc. 80−2038
ultrafine particles, sp. ht., 1.3-10K, supercond. transition 77−12061
ultrasonic velocity meas., mag. field depend. 78−19104
US attenuation due to electron-phonon interaction 79−77687
US waves interaction with cond. electrons, double-pulse comparison spectrometer appl. 78−1526
V-V_xO_y-Pb tunnel junctions, IV characts. of SQUID 79−19704
vapour laser, operation by dissoc. of metal complex 77−54702
void formation from 200 to 700°C following heavy-ion irradiation 78−10104
volt ampere characteristics during electron melting process *(Russian)* 80−75336
VPE on sapphire, highly oriented film prod. 77−66097
wire, deformed in torsion, internal friction, H effect 80−76300
X-ray (110) scattering factor, absolute meas. 78−71706
X-ray band spectra calcs. 79−33860
X-ray Compton line shape, effect of valence state 77−8682
X-ray emission spectra, low energy plasmon satellites 79−65957
X-ray $K_{\beta 5}$ emission band, reinterpretation *(Russian)* 77−59645
X-ray resonant Raman scatt. and fluoresc. near K-absorpt. edge 79−52042
XPS, valence bands 78−35249
XPS and AES study, electron correl. effects 80−7467
XPS escape depths and relative photoionisation cross section for 3p subshell 77−73212
ZnS:V^{2+}, impurity states by Green's function method 80−92855
μ^+ meson spin relax. in cryst. lattices *(Russian)* 79−28664
Al determination, Fe and Al alloys, in presence of V *(Polish)* 80−35605

vanadium continued
α-Al_2O_3:(V^{3+}), optical absorption spectra, DC and AC field effects 78−10925
α-Al_2O_3:Cr(Ti)(V), impurities effect on thermoluminesc. 80−40170
Al_2O_3:V, gamma-irrad., low temp., induced absorpt. spectra 79−56820
Al_2O_3:V, V^{3+} pairs studied by phonon freq.-crossing spectroscopy 78−39068
Al_2O_3:V, valency changes of V ions, γ irradiation, thermal cond. optical absorption and EPR meas. 77−80541
Al_2O_3:V^{3+}, frequency crossing signals of V^{3+} ions, conc. depend. study using thermal phonons 78−95115
Al_2O_3:V^{3+}, $g_\perp/g_\parallel$ determ. by freq. crossing spectroscopy using thermal phonons 78−23055
α-Al_2O_3:V^{3+}, ground state spin Hamiltonian parameters and electric field effect 77−15801
Al_2O_3:V^{3+}, hyperfine splitting and magnetoelastic consts., freq. crossing spectroscopy 80−107392
Al_2O_3:V^{3+}, Jahn-Teller effects, ground state 80−75528
α-Al_2O_3:V^{3+}, local deform. due to uniaxial stress 80−34140
Al_2O_3:V^{3+}, magnetocaloric effect in high magnetic fields 80−25140
α-Al_2O_3:V^{3+}, near IR spectra, line lifetime, 2, 10, 77K 78−10972
Al_2O_3:V^{3+}, phonon scattering, comparison between theory and experiment 78−95116
Al_2O_3:V^{3+}, phonon spectroscopy study of V^{3+} ion pairs 79−87068
Al_2O_3:V^{3+}, spin-phonon coupling, rot. mode role 80−70329
α-Al_2O_3:V^{3+}, stress-induced linear dichroism in $^3A_2(^3T_1)\rightarrow{}^3T_2$ transition, Jahn-Teller effect 80−34884
α-Al_2O_3:V^{3+}(V^{4+}), optically and thermally stimulated reactions, absorpt. spectra 80−80825
Al_2O_3:V^{4+}, dil. solution, stimulated phonon emission 78−63817
α-Al_2O_3:V^{4+}, emission spectrum, Jahn-Teller effect in $^2T_{2g}$ and ^2E_g states 79−83007
Be-Li-V, phase diagram, metallurgical aspects for fusion blanket use 80−32467
CaO:V^{3+} orbital triplet, intermediate Jahn-Teller effect, APR 80−34758
CdI_2:V^{2+}, EPR 78−68362
CdTe:V, optical props. meas. 79−73969
CrN-VN, rhombic distortion of cryst. lattice at low temp. 78−2253
evaporated layers, ion bombardment effect on superconducting transition temp. 78−52136
Fe:V surface, laser doping with V *(Russian)* 78−95065
Fe-Ni-V, cryogenic toughness, strength, rel. to reactive metal addition 78−39885
GaAs:V, ion implanted, luminesc., level splitting 80−97338
GaP:V, ESR exam. 79−11344
GeO_2:V^{4+}, crystal field splitting from ESR and optical absorpt. results 79−47063
GeO_2:V^{4+}, direct mechanism in supertransferred hyperfine interaction 79−23936
H solubility, and diffusivity around room temp. 80−29225
H_2 permeability, surface impurity layer effect 77−24440
He preinjected, void swelling on neutron irradiation 77−7765
KBr:V, covalency effects EPR meas. 77−85557
KCl:V^{2+}, EPR spectrum temp. depend., crystal field theory 77−16163
KCl:V^{2+}, EPR spectra above 300K 80−34765
KCl:V^{2+}, spin-lattice relaxation 78−91941
$KMgF_3$:V^{2+}, ^{51}V ENDOR meas., spin Hamiltonian parameters 79−28638
$KMgF_3$:V^{2+}, 3d→4d absorpt. band exam. 77−63435
$KMgF_3$:V^{2+}, combined spin-orbit and Jahn-Teller coupling, method of soln. 79−60773
$KMgF_3$:V^{2+}, dynamical Jahn-Teller effect on spin orbit multiplets, intensity quenching 79−95374
$KMgF_3$:V^{2+}, first and second order Jahn-Teller coupling const. calc. 79−65906
$KMgF_3$:V^{2+}, MCD and linear dichroism, 3d→4s transitions 79−56768
$KMgF_3$:V^{2+}, zero-phonon line splitting in T×ε_g Jahn-Teller problem 78−19006
$KZnF_3$:V^{2+}, ^{51}V ENDOR meas., spin Hamiltonian parameters 79−28638
$KZnF_3$:V^{2+}, calc. of t_{2g} antibonding mol. orbital in $|VF_6|^4$, rel. to ESR 80−50174
LiCl:V, electron transfer absorption bands 79−95810
Li_2O-Al_2O_3-P_2-O_5:V^{4+}, glass exam. of ESR spectrum of V^{4+}, optical spectra, and structure 78−88180
Mg:V^{2+}, coupling of T_{1u} and T_{2u} vibr. to $^2E_g\rightarrow{}^4A_{2g}$ transition 77−63453
MgF_2:V^{2+}, MCD and linear dichroism, 3d→4s transitions 79−56768
MgO:V^{2+}, $^4A_{2g}\rightarrow{}^4T_{2g}$ spectra, new expt. results 80−11441
MgO:V^{2+}, first and second order Jahn-Teller coupling const. calc. 79−65906
MgO:V^{2+}, Jahn-Teller system, zero-phonon line broadening due to non-radiative transitions 80−108258
MgO:V^{2+}, mag. circular dichroism in split zero-phonon line 78−56460
MgO:V^{2+}, zero-phonon line splitting in T×ε_g Jahn-Teller problem 78−19006
MgO:V^{3+}, HF phonon spectroscopy using supercond. tunnel junctions 80−65178
MnO_2:V, Zn^{2+} ion specific adsorpt. kinetics, ^{65}Zn γ-ray scintillation investig. 80−70529
MoO_2:V, current carrier sign, Fermi surface cross section variations *(Russian)* 80−84420
MoO_2:V, growth by VO_2 transfer reacts. 79−43116
$MoTe_2$:V, single cryst. growth and vapour phase transport 79−28903
MvO:V^{2+}, octahedral clusters, quadratic Jahn-Teller effect and tunnelling splitting 77−72840
$(NH_4)_2SO_4$:VO^{2+}, ferrielectric phase transition, two-sublattice model, EPR of polar VO^{2+} probes 78−48127
NaBr:V, covalency effects, EPR and optical spectra 77−85557
NaCl:V^{2+}, EPR and optical absorpt. spectrum temp. depend., crystal field theory 77−16163
NaCl:V^{2+}, EPR spectra above 300K 80−34765
NaCl:V^{2+}, elec. field effect on Z-like centres spectrum 80−2802
NaCl:V^{2+}, spin-lattice relaxation 78−91941
NaCl:V^{2+}, X-irrad. and unirrad., EPR of isolated V^{2+} ions 79−15347
NaCl:V^{2+}, X-irrad. effects on divalent metal aggregates, EPR meas. 79−82263
Nb, effect of O ion irradiation on supercond. 78−52131
Ni-V system, interdiffusion, kinetics of phase growth *(Russian)* 80−29230
PbI_2:V^{2+}, EPR 78−68362
PbO-SiO_2:V^{4+} glass, EPR 78−39392

vanadium continued
RbBr:V, covalency effects, EPR meas. 77−85557
RbCl:V^{2+}, EPR spectrum temp. depend., crystal field theory 77−16163
RbCl+V^{2+}, spin-lattice relaxation 78−91941
n-Si:P,V, degeneracy ratios and impurity levels of V, resist. and Hall effect meas. 77−20260
Si:V p-n junctions, thermal emission rates and capture cross sections of majority carriers at V centres 80−96980
SnO_2:V^{4+}, direct mechanism in supertransferred hyperfine interaction 79−23936
$SrTiO_3$:V, Jahn-Teller impurity, V^{4+} EPR 80−29608
TiO_2:V, impurity levels, photocurrent and ESR meas. 80−29346
TiO_2:V, localisation and migration of V^+ ions, ESR and ESCA study *(French)* 79−33529
Ti_3O_5-V; semicond.-metal transition, resist., enthalpy and mag. susceptibility changes obs. 77−62965
$TiSe_2$:V, transport props. and phase transition 78−72149
U, Mo and V, complex recovery from sedimentary ores 79−26701
(V,Ti)C+Ni cermet, binder grain size 80−44401
V cathodic deposition, from crude V, V_2C and VC, hardness meas. *(Japanese)* 79−78908
V, electron irradiated, positron study 78−76555
V, electronic structure, X-ray spectra and XPS meas. 77−85842
V I, IR emission spectrum meas. 78−62746
V I, photographic emission spectrum remeas. 78−62750
V I in solar photosphere, oscillator strength computation 78−40905
V II, spectrum, $3d^3$5s and $3d^3$4d config. *(Spanish)* 79−22636
V III, absolute oscill. strengths determ. 78−82691
V III, semiempirical calc. of energy spectra 77−46499
V IV, $3d^2$-3d4f tranistions obs. 190 to 650 Å 78−62758
V, neutron irradiated, saturable trap anal., of solute segregation applied to O_2 trapping 79−77645
V thin film-amorphous Si interface, V silicide formation, backscattering diffraction meas. 80−2285
V V, spectrum, 100-8500 Å, ionisation energy 77−65432
V VI, autoionising transitions ns^2np^6−nsnp^{6}mp 77−88419
V VII, VIII, IX, X, 3s-3p and 3p-3d transitions, oscillator strength and energy levels calcs. 80−83251
V XII, level struct. and predicted intercombination lines 80−14098
V XIII, wavelengths and energy levels, spectra obs. 77−428
V XX, Be I like spectra from laser-produced plasma, classification 78−67410
V XXII, He-like ion resonance line satellites 79−10064
V XXII, X-ray spectra from laser plasma 78−17596
V^{2+}, configuration interaction method for hyperfine contact interaction 77−3274
V^{2+}, doped ion in divalent metal cpds., correl. between Szigeti charge and hyperfine coupling consts. 80−96832
V^{3+} in crystal field, intercombination transition intensities, symmetry reduction method 78−84175
V^{4+}, cryst. field effect on ESR parameters 77−36116
V^{4+}, doped in single crysts. bonding character and g-factor interpretation 77−55704
V^{4+} in glasses, numerical optimisation of ESR spectra 79−38370
V^{4+} ion complexes in diamagnetic crystals, ground state wavefunctions, hyperfine interaction parameters, EPR meas. 78−19311
V^{4+} ions in garnets, effects of covalency on mag. props. V^{4+} ion, effect of covalency 78−64010
V^{4+} on tetragonally distorted tetrahedral sites, Jahn-Teller effect and hyperfine parameters 77−69276
V^{5+}, in $(VO_4)^{3-}$ ions, metal X-ray K absorption spectra, low energy maxima interpretation 79−74019
V:N, ion bombard., void form. 80−34097
V:N, non-pure supercond., Ginzburg-Landau parameter 77−76997
V:O, lattice location study, of 0, 1 MeV deuteron channelling 79−10846
V:O, neutron irrad., void form., 673-1073K 80−29066
V:transition metal, linear expsn. temp. coeff., polymorphic transition temp. shift 78−6164
V/Al_2O_3 composite film, optical props., rel. to solar collector appls. 78−72622
V/Al-Al_xO_y-Pb tunnel junction, superconducting transition, critical currents, Josephson effect *(Russian)* 80−29507
V/MgO composite film, optical props., rel. to solar collector appls. 78−72622
V/SiO_2 composite film, optical props., rel. to solar collector appls. 78−72622
V-Al junction, spin-dependent electron tunnelling 79−19700
V-Al_2O_3 heterophase film, elec. props. rel. to Al_2O_3 content 77−15969
V-C film layer structure, obs. of supercond. transition temp. and crit. mag. field oscills. 77−69438
V-C sandwiches, energy gap fluctuations *(Russian)* 78−34930
V-CdS-In Josephson structures, light-sensitive 79−99660
V-CdS-In preparation and behaviour obs. Josephson junctions 80−100559
V-H, BCC, tetrahedral interstitial site H band modes, neutron scatt. obs. 79−55852
V-H, H effect on tensile props. at moderate temps. *(Japanese)* 78−19831
V-H, H on polycrystalline V, H detection by SIMS, flash-desorption obs. 79−24405
V-H, incoherent spinodals, meas. by Gorsky effect 78−19712
V-H single crysts., critical current and flux pinning *(Russian)* 77−47946
α-V-N solid solns., quenched ordered structures *(Ukrainian)* 77−69088
V-N system, TEM of V-$V_{16}N$ precipitates 77−16590
V-Ni(Fe) interface, diffusion above 500°C *(German)* 79−28156
V-O alloy, temp., dose and conc. depend. of void form. following V^+ ion beam irradiation 78−10105
V-SiO_2 interface reaction, identification of diffusion species 78−75890
V-V_xO_y-Pb tunnel junctions, Josephson characteristics *(Russian)* 77−47938
V-VO_x-Pb Josephson tunnel junction, crit. currents exam. 78−23209
V+F^{q+}, (q=6, 8, 9), target and projectile cross-sections, X-ray prod. yields 79−81269
V+H^+, K X-ray production, 0.2-0.5 MeV, ionis. cross-section 79−31459
V+H^+ ion collisions, K_α satellite intensity meas. 77−23550
V+$O_2(NO_2)$, oxidation, VO chemiluminesc. 77−9077
$V^{2+}F^-$, $V^{2+}F^-V^{2+}$ π-electron systems, transferred hyperfine interaction, HF calc. 80−24859

vanadium continued
VH_x, Knight shift and spin-lattice relax. of proton NMR, local electronic environment of protons 77−16194
VH_x, proton Knight shift and mag-suscept., high resolution meas. 77−55716
$VH_x(D_x)$, H conc. detect. by neutron interferometry, precipitation effects 78−67735
V(V), biamperometric iodometric determ. using Pt-graphite electrode system 77−70359
^{50}V, nucl. quadrupole moments from laser-RF double reson. spectroscopy 80−57682
^{50}V quadrupole moment and atomic ground state hyperfine intervals, laser spectroscopic determ. 79−89234
^{51}V, K_β/K_α intensity ratios, chem. effects 79−63949
V{100}$_1$ Au(Au) layer growth, total current spectroscopy 77−36329
Va+N^+, X-ray production cross section, $K\beta/K\alpha$ ratio, 0.5-2.5 MeV/amu 77−54526
YIG:V, mag. anisotropy and magnetostriction, effect of V 78−27029
$ZnCs_2(SO_4)_2.6H_2O$:VO^{2+}, single cryst., X-band EPR meas. 77−90024
$ZnSiF_6.6H_2O$:V^{2+}, paramagnetic impurity ion spin multiplet initial splitting parameter, immediate environments distortion influence on sign 79−65720
$ZnSiF_6.6H_2O$:V^{2+}, spin-lattice relax. at normal and high press. 80−2632
Zr_2-SiC-C-V, refractory cermet hot pressing and oxidation resist. 80−3231
ZrF_4-ThF_4-BaF_2:V^{3+} glass, absorpt. spectra *(French)* 79−99918
$(ZrO_2)_{0.9}(Y_2O_3)_{0.1}$:$VO^{2+}$, ESR of V^{4+} at room temp., spin Hamiltonian parameter determ. 77−16167

vanadium alloys
see also vanadium compounds
A15 compounds, mode softening and high supercond. crit. temp. 78−14851
A15 compounds, self-consistent LMTO band calcs. 79−37954
A-15 superconductor, dHvA effect 78−75985
BCC ternary, solid soln. hardening model, compared with expt. results 77−44262
binary alloys with group IIIB and IVB elements, coord. polyhedra 78−9997
Cr-Mo-V steel turbine rotor, fatigue tests 78−39912
environmental fatigue crack propag., texture influence 79−91802
fusion reactor first wall, thermal stress and creep fatigue limitations 79−76132
fusion reactor first wall and blanket material, props. for struct. appl. 80−30071
fusion reactor first wall/blanket system, thermal-hydraulics and fatigue life modelling 78−58453
fusion reactor first-wall and blanket material, mech. props. 80−34074
fusion reactor materials, He and simultaneous damage production simulation 80−32480
fusion reactor materials, performance and economics 80−32433
low-alloy, strength and ductility at high temp. and different strain rates 80−16401
magnetic susceptibility and Knight shift meas., d-metal alloys 80−66055
neutron irrad., elec. resist., temp. depend. 79−91024
Permendur 49, ordered and disordered, clean mild wear 80−16508
polycrystalline alloy, thermal cond., 1200-1900K range 78−95282
steel, 30N9K4, effects of Mo, V, and N on grain growth, tempering, hardenability, strength and toughness 78−44202
steel, Al-Ti-(Mo), Al-Ti-V-(Mo), Al-Ti-Nb-(Mo) and Al-V-(Mo) low-alloy, toughness improvement through Ti additions 80−66525
steel, alloy, Cr-Mo-V, fatigue, failure probability based on residual strength 78−68797
steel, alloy, Cr-Mo-V-P, quenched, temper brittleness in relation to V and P concs. 78−52986
steel, alloy, cyclic strength after strain hardening and tempering, precip. hardened 40FT 78−52988
steel, alloy, Fe-Cr-Mo-Si-V, various steels, short rod stress intensity factor tests up to 700K, exam. 78−60815
steel, alloy, Fe-Ni-Cr-Mo-V-C, H_2S stress corrosion cracking, effects of overload, exam. 78−60886
steel, alloy, Fe-Ni-Cr-Mo-V-C, HY130, effect of H_2 and impurities on brittle fracture, review 78−60765
steel, alloy, V-W-Mo-Cr, exam. of carbide transformation 80−16299
steel, alloy, W-Mo-Cr-V, blanks welded to steel 45, optimal high temp. tempering 80−16351
steel, austenitic, Mn-V-C, discontinuous precipitation, grain boundary struct. effect 79−29068
steel, austenitic stainless, biphase, ferritic, ageing and thermomech. treatment effects on struct. and props. 80−35226
steel, austenitic stainless, V alloyed, creep mechanism 77−36591
steel, Cr, carbide form. depend. on Mn, Cr, V additions, cementite stabilisation, microstruct. *(Russian)* 80−55399
steel, Cr-Mo and Cr-Ni-Mo, V effects on recrystallisation *(Russian)* 77−66654
steel, Cr-Mo-V, 1% Cr, chem. comp. and struct. effect on deform. props. *(German)* 79−1888
steel, Cr-Mo-V, austenite to bainite transformation under cooling conditions, effect on creep 80−3033
steel, Cr-Mo-V, biaxial cyclic deformation behaviour 80−16431
steel, Cr-Mo-V, brittle failure resistance obs. influence of cold plastic deform. 78−72858
steel, Cr-Mo-V, cast, strain intensity approach of high temperature fatigue crack growth and failure 79−20175
steel, Cr-Mo-V, combined Cr-Mn addition effects on hardenability 78−7046
steel, Cr-Mo-V, creep, effect of microstruct., heat treatment, transform. temp. 78−11248
steel, Cr-Mo-V, creep crack growth temp. depend., 525 to 600°C 78−64634
steel, Cr-Mo-V, creep deform. under const. and cyclic temp. 79−38914
steel, Cr-Mo-V, creep fatigue interaction 78−60841
steel, Cr-Mo-V, creep fatigue interactions obs., strain controlled and load controlled tests 78−44214
steel, Cr-Mo-V, creep fracture, microstruct. effects 78−64668
steel, Cr-Mo-V, creep/fatigue interaction 78−64632
steel, Cr-Mo-V, cyclic oxidation and crack growth during high strain fatigue 78−31586
steel, Cr-Mo-V, ductility and heat resistant prop. prediction rel. to fine struct. and solid soln. state 79−15751

vanadium alloys continued
steel, Cr-Mo-V, environmental crack growth during isothermal high strain fatigue and temp. cycling 79−5082
steel, Cr-Mo-V, fatigue crack growth rate and threshold under oxidising conditions 79−20272
steel, Cr-Mo-V, high temp. main steam pipe, residual stresses in butt welds 80−21059
steel, Cr-Mo-V, high temp. steam pipe weld, defect distrib. and growth 80−25979
steel, Cr-Mo-V, high-temp. cumulative damage for stage I crack growth 78−19883
steel, Cr-Mo-V, low alloy, creep fatigue interaction 78−64673
steel, Cr-Mo-V, low alloy, V effect on creep *(Czech)* 77−86088
steel, Cr-Mo-V, medium strength, correlation between crack initiation, propag. and microstruct. 78−60787
steel, Cr-Mo-V, press. vessel, fracture, effect of tempering 78−60799
steel, Cr-Mo-V, rupture ductility rel. to cavitation, density and SEM obs. 79−34142
steel, Cr-Mo-V, strength and ductility in creep, purity influence 80−66598
steel, Cr-Mo-V, stress relief cracking mechanism 78−64669
steel, Cr-Mo-V, stress rupture strength at high temps. *(German)* 80−40474
steel, Cr-Mo-V, thermal fatigue and rupture strength 78−72857
steel, Cr-Mo-V (0.5, 0.5, 0.25 wt.%), comparison of methods of correlating creep crack growth 78−60826
steel, Cr-Mo-V (0.5, 0.5, 0.25 wt.%), creep crack growth, temp. effect 78−64667
steel, Cr-Mo-V (0.5, 0.5, 0.25 wt.%), heat treated, microstructure effect on threshold region fatigue 78−56757
steel, Cr-Mo-V (1, 0.5, 0.25 wt.%), long-time stress relaxation props. 77−12666
steel, Cr-Mo-V (1 wt.%) oxidation assisted crack growth during high cycle fatigue at 550°C 77−16742
steel, Cr-Mo-V alloy, crack growth during strain fatigue at 825K 78−39890
steel, Cr-Mo-V austenitic, creep resist., high-temp. props. residuals effect 80−66600
steel, Cr-Mo-V creep crack growth, relation between engineering and metallurgical factors 78−11321
steel, Cr-Mo-V low-alloy, high-temp. ductility and crack growth, impurities effect 80−66652
steel, Cr-Mo-V low-alloy, mech. props. and stress relief cracking, effects of impurities and deoxidation practice 80−66599
steel, Cr-Mo-V low-alloy, prior austenite grain boundary embrittlement by B 80−66657
steel, Cr-Mo-V low-alloy, stress relief cracking, impurity and alloy content effects 80−66654
steel, Cr-Mo-V low-alloy with high residual element content, cavitation control 80−66663
steel, Cr-Mo-V press. vessel, crack growth under creep 78−60827
steel, Cr-Mo-V-W, crack-growth and thermal-mech. fatigue 80−21072
steel, Cr-Mo-W-V, long term creep rupture props., turbine blade *(Japanese)* 77−59909
steel, Cr-Mo-W-V, long time stress relaxation props. *(Japanese)* 77−59841
steel, Cr-Ni-Mo-V, magnetic induction, struct. dependence *(Czech)* 80−50141
steel, Cr-Ni-Mo-V, Mossbauer austenitometry and mag. props. 80−40003
steel, Cr-Ni-Mo-V-Nb (12,8,1,1.5,0.4 wt.%) Ce addition effects on strength and hardness *(Russian)* 78−15454
steel, Cr-V (1.5, 0.5 wt.%), ferritic, effect of temp. and microstruct. on creep damage 79−5023
steel, Cr-W-V-Mo (3.9 to 4.5, 1.5 to 2, 0.9 to 1.2, 3.9 to 4.4 wt.%), heat resistant, type 8Kh4M4V2F1-Sh, mech. props. 80−16464
steel, CrMoV, compact tension specimen, thickness effect 78−68764
steel, CrMoV, creep and creep strength under alternate tension/compression *(Czech)* 77−63728
steel, CrMoV, failure in post yield regime using single edge notched tension specimens 78−68765
steel, CrMoV, low alloy, dispersed phase of VC, hardening mechanism *(Czech)* 78−60676
steel, CrMoV (1 wt.%), high temp. creep and fracture 77−36598
steel, fine grained C-Mn-V-Al-N, relationship between ferrite and austenite grain size 80−3001
steel, high speed, W-Mo-Cr-V, production by powder metallurgy 77−12574
steel, high V-W-Mo, high speed, phase composition and struct. of atomized powders 77−90323
steel, HSLA, V effect on mech. props. *(Korean)* 80−29987
steel, ledeburite, fracture during hot plastic deformation exam. 78−56755
steel, low C, Al-killed, effect of V on mag. props. 79−83339
steel, low C Mn-V, VC effects on strength and brittleness 77−70055
steel, low-alloy, V effect on mech. props. 80−35312
steel, medium C, microalloying with V and Ti, effect on hardness and structure 80−11750
steel, microalloy V-Nb, V, Nb effects on strength and formability of cold rolled sheets 77−55979
steel, Mn-Cr-V, crack propag. resist. at hardness indentation, and fracture toughness *(German)* 79−29220
steel, Mn-Cr-V, structural changes during solution annealing *(Czech)* 78−84864
steel, Mn-V reinforcing type, strain ageing characts. rel. to mech. props. 80−84969
steel, Mo-V, creep rupture strength, heat treatment effects *(German)* 78−72834
steel, Mo-V, creep rupture strength, rel. to microstruct. *(German)* 78−35467
steel, Nb,(V),(Al), hot-rolling, laboratory simulation, recrystn. of austenite 80−97512
steel, Nb-V, cold rolled, HSLA, prod. by precipitation hardening, annealing 78−88471
steel, Nb-Va microalloyed, mech. props. *(French)* 80−35252
steel, Ni-Cr-Mo-V, stress corrosion cracking 77−52542
steel, Ni-Cr-Mo-V, turbine rotor shaft, fracture toughness, validity criterion for K_{IC} 78−72861
steel, Ni-Cr-Mo-V low-alloy, additive remedy for temper brittleness 80−66659
steel, NiCrMoV, stress corrosion cracking, cold work effects 78−11383
vanadium alloys continued
steel, pearlitic, Cr-MoV and Mo-V, heat resist., Mo content rel. to mech. props. 79−20134
steel, Si-Cr-Mo-W-V (2,4,1,3,2 wt.%), heat treatment and props. 80−16349
steel, stainless, ferritic, Ni-free, effect of V, Ti addition on ductility 79−79048
steel, Ti-V, Ti and V effects on precipitation, hardness and annealing *(German)* 77−55968
steel, V, carbide eutectic presence, solidification and struct. 80−50624
steel, V, precip. and transform. kinetics, effect of N 80−97485
steel, V, tempering, initial stages of carbide form., electron diffr. *(Russian)* 78−19760
steel, V-Nb, supercooled austenite isothermal decomp., struct., strength and fracture characts. 80−60966
steel, VN precipitation after heat treatment 79−29067
steel, W-Mo-Cr-V tool, laser surface melted, struct., heat treatment effect 80−76424
steel, WC reinforced surface layer, serviceability improvement by Ni, Cu-Ni, V alloying additions 77−21290
steel Cr-V (1.5, 0.5 wt.%), cavitation effect of temp. and C content 78−64638
steel electrode, erosion resist., influence of C and carbide-forming elements *(Russian)* 78−11389
steel precipitation, low C, precipitation of Nb and V, critical temperature identification, by meas. electric resistance *(Slovak)* 77−4781
steel W-Mo-V-TiC, powder, TiC effect on milling, pressing and sintering 78−60607
strengthening in internal oxidation *(Japanese)* 78−11493
thermal conductivity at slow temps., temp. depend. *(Russian)* 79−91019
U-V metallic glasses, glass form. and thermal stability 80−75183
V-Fe (29-35 at%), ferromag., mag. props. near crit. conc. for ferromagnetism 78−19225
V-Ru, electronic states calculation 78−95255
Vicalloy 1, dilatometric anomalies and α to γ transform., effect of heating rates *(Russian)* 78−39762
vicalloy-2, high heating rate effect on mag. props. *(Russian)* 77−81328
VT22, hot deform., microstruct. form. and mech. props. *(Russian)* 77−28830
Al alloy 7075, $CrAl_7$ form., effect of V and Zr 78−44132
Al-V, dil., electron irradiated, interaction of self interstitials with undersized solute atoms 78−63789
Al-V, dil., screening charge around 3d impurities, NQR meas. 77−32287
Al-V, dil., supercond., nucl. spin relax. and quasiparticle excitations 80−88680
Al-V, dil., superconducting and normal state, ^{27}Al spin-lattice relax. rates 79−60977
Al-V alloys, anomalous sp. ht. and nuclear spin-lattice relax. 79−46814
Al-V-Ti, SiC coated B fibre reinforced, tensile and compressive strength, prior thermal treatment effect 78−11264
Al-V-Ti junction, spin-dependent electron tunnelling 79−19700
$Al_{10.4}Ga_{0.08}V$, low temp. thermal expansion 78−95167
$Al_{10}V$, low temp. thermal expansion 78−95167
$Al_{10}V$, supercond. transition temp. determ., localised phonon modes 77−63016
$Al_{10}V$, well defined local modes 78−26648
$Al_{10}V$-Ga, dil., well defined local modes 78−26648
Au-V, dil., ^{51}V CW NMR line width anal., RKKY broadening 78−15033
Au-V, dil., Kondo alloy, spin dynamics, nuclear spin relax obs. 78−68155
Au-V, UPS study, localised states 80−93449
Au-V Kondo alloys, mag. susceptibility and NMR Knight shift in conc. independent region 77−77027
Au_4V, effect of structural changes on phys. props. 78−31400
Au_4V, partially disordered, magnetisation distrib., polarised neutron diffr. study 79−47244
Au_4V single crystal, ordered, mag, props., domain models 80−39770
B_4C-V, contact reaction with liq. Ni 80−55707
C-Mn-V power station component, fracture toughness and fatigue characts. 79−20192
Co-^{48}V, nucl. orientation of ^{48}V, γ-ray anisotropy obs. 80−97169
Co-Fe-V-Ni, mag. and mech. props., heat treatment and stress effects 80−60363
Co-V, Co rich, ferromag. behaviour, mag. moments, Curie temp., and NMR spectrum 80−70964
Co-V, ferromag. struct. in nucl. spin echoes 80−60453
Co-V, solid and liq., mag. susceptibility and electronic struct. 80−39738
Co-V (10 to 23 wt.%) system, phase constitution, X-ray and elec. resist. meas. 80−3007
Co-V (12.4-18.7 at.%), ferromag. behaviour 79−24163
Co-V (20.7 wt.%), cryst. struct., electron and X-ray diffr. study 80−44172
Co-V alloy system, Co rich, low temp. phase, electron microscopy 77−84766
Co-VC (12 wt.%), directionally solidified eutectic, oxidation 80−11821
Co-VC((Ti,V)C), eutectic alloy, unidirectional solidification, oxidation and tensile tests 78−52790
Co(GaTiV) alloys, ferromag. onset, electron conc. depend. 80−60203
$Co_2Ga_{2-x}V_x$, elec. resist. anomalies 79−38044
$Co_2Ga_{2-x}V_x$, ferromag., local configuration studies, neutron scatt. and spin echo NMR 77−63114
$Co_2Ga_{2-x}V_x$, ferromag., site selectivity and moment distrib. 77−77031
$Co_2Ga_{2-x}V_x$, mag. props. and order 77−12093
CoV, dil., low temp. specific heat and magnetisation 80−65925
CoV, phase dependent MNR spectra 80−108114
Co_2VAl, hyperfine fields of Fe impurities, Mossbauer spectra 80−71255
$Co_2VAl(Ga)$, ferromag., hyperfine fields meas. by NMR 77−63315
Co_2VGa, ferromag. Heusler alloy, spin echo NMR meas. 77−63319
Cr-Co-V alloys, dil., elec. resist. min. 80−54680
Cr-Fe-V, calc. of phase equilibria using thermodynamic values from different models 78−60646
Cr-Fe-V, dil., V effect on para- to incommensurate and commensurate transitions 78−68260
Cr-Fe-V, effects of V on mag. transition, elec. and mag. props. 77−69554
Cr-Fe(Co)-V, dil., antiferromag., elec. resist. min., press. and impurity effects 80−59970
Cr-La-V-Nb-Ta, La, V, Nb Ta effect on hardness and strength *(Russian)* 79−34050

vanadium alloys continued
Cr-Mo-V, steamline bends, restorative heat treatment effects 78−68716
Cr-Mo-V steel, creep rupture tests on notched cylindrical specimens at 600°C 77−32670
Cr-Mo-V-Nb, supercooled austenite isothermal decomp., struct., strength and fracture characts. 80−60966
Cr-Si-V, (2, 0.1 at.%), paramag. to commensurate spin density wave transition 80−65875
Cr-Si-V, dil., V effect on para- to incommensurate and commensurate transitions 78−68260
Cr-V, binary continuous solid solution, elec. resist. and thermoelec. power behaviour 79−69492
Cr-V, cast, B additions effect on struct. and props. *(Russian)* 78−19891
Cr-V, dil., mag. susceptibility, 77 to 400K *(Russian)* 80−50066
Cr-V, disordered, extension of Taylor's theory of lattice vibr. 79−4387
Cr-V, Invar alloys, thermal expansion, plasticity *(Russian)* 79−55907
Cr-V, itinerant electron antiferromag., spin fluctuations, low temp. specific heat 80−107439
Cr-V, strain wave and spin density wave intensities, neutron diffr. 78−60266
Cr-V-B-Y system, fatigue strength and fatigue fracture at 20 and 1100°C, SEM study 80−3194
Cr-V-Fe, mag. moment of Fe, mag. suscept. meas. 79−61079
Cr-V-Fe alloy, resistivity minimum, press. effect 79−38043
$Cr_{1-x}V_x$, nucl. spin relax., spin fluctuation effect 80−34811
$Cr_{1-x}V_xCo$, localised mag. moment of Co impurity 78−27014
$Cr_{1-x}V_xCo$, mag. state of Co impurity, NMR exam. 78−27100
$Cr_{1-x}V_xCo$, $x \leq 0.05$, antiferromag., nucl. mag. relax. 78−6590
$Cr_{2.8}V_{0.7}Fe_{3.4}C_3$, stacking fault study, morphology, comp. and struct. 80−84190
Cu-V, dil., local mag. moments and Kondo effect, theoretical model 79−69651
Cu-V, dilute, Knight shift of ^{51}V reson., and host satellite resonances 77−85594
Cu-V alloy, phase equilib. diagram exam. *(French)* 77−21100
Cu-V-Ga dil. alloys with V_3Ga particles, supercond. props. and microstruct. 78−39278
Cu-V-Si, supercond. props. 80−107945
Cu-V-Si, two-step supercond. transition 80−34539
$(Fe, Co, Ni)_3V$, control of ordered struct. and ductility 80−21029
$(Fe,Ni,Co)_3V$, long-range ordered alloy for fusion reactor appl. 80−32481
Fe-^{48}V, nucl. orientation of ^{48}V, γ-ray anisotropy obs. and NMR meas. 80−97169
Fe-C-V-Cr, white cast, effect of abrasion on carbide microstructure *(German)* 78−88540
Fe-Co alloy, V addition effect on atomic order parameters, dislocation struct., mechanical props. 79−91762
Fe-Co-V, anelastic phenomena, related to atomic order, exam. of magnetostriction *(French)* 78−80579
Fe-Co-V, neutron irradiated, influence of dislocation doping on recovery 79−46715
Fe-Co-V, neutron irradiated, damage rates 79−77646
Fe-Co-V, ordered and disordered, dynamic ageing *(French)* 80−16355
Fe-Co-V, plastic flow, order-disorder transform. effect on creep, traction and relaxation *(French)* 80−35180
Fe-Co-V, Vicalloy, $\alpha \rightarrow \gamma$ transform. under plastic deform., morphological singularities *(Russian)* 77−32576
Fe-Co-V, Vicalloy, magnetisation reversal by stretching and twisting 80−34733
Fe-Co-V, Vicalloy 1, γ-phase morphology and structural inheritance depend. on heating rate *(Russian)* 79−70059
Fe-Co-V (2 wt.%), gamma phase 77−36514
Fe-Co-V (2%), annealing of point defects produced by plastic deform. *(French)* 78−72829
Fe-Co-V (33, 33 at.%), BCC β phase, high temp. creep, existence of master curve 80−55473
Fe-Co-V alloy, Remendur, heat treatment effects on mech. and struct. props. 77−8846
Fe-Co-V alloys, effect of V on struct., electron diffr. and Mossbauer meas. *(Russian)* 77−77507
Fe-Co-V wire for high-speed matrix printers, wear resistivity obs. *(Japanese)* 80−55540
Fe-Co-V-Cr alloys, struct. transform., appl. of mag., thermomag. methods *(French)* 79−20318
Fe-Co-V(-Ni), annealing effect on microstruct. rel. to mag. and mech. props. 80−89267
Fe-Co-V(2%) alloy, correl. of resistivity with microstructure 78−72896
Fe-Co-2 V, (49, 2 wt.%), solid soln., rheological study of crystallographic order on creep *(French)* 80−97548
Fe-Cr-Co ductile magnet alloys, phase diagram and mag. props., V or V+Ti addition effects 77−8959
Fe-Cr-Co-V alloy, microstruct. and mag. props. 78−68221
Fe-Cr-Co-V-(Ti) hard magnets, V and V-Ti effects on mag. and mech. props. 79−91810
Fe-Cr-Co-V(-Ti), phase equilib., X-ray diffr. meas. *(Russian)* 79−47658
Fe-Cr-Ni-Mo-V, Mo and V effects on segregation *(German)* 77−55942
Fe-Cr-V-C, X-ray microanal. of carbide phases rel. to V conc. *(Russian)* 78−88467
Fe-F, thermophysical props. and elec. cond., temp. depend. 80−96842
Fe-Hl (Si) (Ti) (V), molten, gaseous O_2 absorption 80−11836
Fe-Mn-Nb-V, high Mn, dispersion strengthening 77−16602
Fe-Mn-Ni-V-C (0.5, 3.0, 1.0, 0.2 wt.%), austenite decomp., isothermal transform. characts. 80−97477
Fe-Mn-V-C (0.5, 1.0, 0.2 wt.%), austenite decomp., isothermal transform. characts. 80−97477
Fe-Mn-V-C austenitic steel, discontinuous precipitation, morphological changes 80−3078
Fe-Nb-V-C-N, equilibrium comp. and solubility in steels, model of ideal solns. *(Russian)* 80−60832
Fe-Ni-Co-V, effects on fusion reactor neutronics performance 80−47705
Fe-Ni-V, austenite, martensite elec. cond. depend. on heating *(Russian)* 79−70177
Fe-Ni-V, concentration ferromag. antiferromag. phase transition and mag. state diagram. *(Russian)* 80−20401
Fe-Ni-V, effect of low temp. ageing on props. during high temp. ageing *(Russian)* 78−39811
Fe-Ni-V, nitrided austenitic alloys, modulated substitutional interstitial solute atom clustering 79−74160
Fe-Ni-V alloy, ageing of martensite *(Russian)* 78−39808

vanadium alloys continued
Fe-Ni-V-C alloy, reverse α to γ transformation, previous deformation influence on struct. and props. *(Russian)* 79−100139
Fe-Ni-V-Co, Co influence on age hardening *(Russian)* 78−68703
Fe-Ni-V-(CO) alloy, lattice parameter variation during ageing *(Russian)* 78−39812
Fe-Ni-V-(Cu) (12, 2, 2 wt.%), Cu addition strengthening at 77K, mech. props. 80−60875
Fe-O-V melts, phase equilib. *(Russian)* 80−16273
Fe-Sb-V, dil., interactions and precip., Mossbauer study 80−39997
Fe-Sb-V, interactions and segregations, Mossbauer and X-ray diffr. study 80−70415
Fe-Si-V, eutectic alloy, exam. of eutectic temp., composition, and oxidation resistance 78−52767
Fe-Ti-V-C-N, equilibrium comp. and solubility in steels, model of ideal solns. *(Russian)* 80−60832
Fe-V, ^{59}Fe self-diffusion *(Czech)* 80−88352
Fe-V, BCC, ferromag., high-field susceptibility 80−7083
Fe-V, conc. depend. of mag. moment distrib., polarised neutron diffr. meas. 78−19218
Fe-V, Curie temp. determ. using deviation from Mattheisen's rule 79−15306
Fe-V, dil., high freq. induction melting and centrifugal casting, working curve sample prep. photoemission anal. *(Japanese)* 78−53050
Fe-V, dil., local mag. moments, polarised neutron elastic diffuse scatt. 80−50088
Fe-V, dilute, irradiation softening effect on yield stress 80−76319
α-Fe-V, dilute alloy, Mossbauer diffusion line broadening, exponential fitting evaluation 78−52379
Fe-V, dislocation mobility and internal friction, effect of alloying in α-Fe *(Russian)* 77−31671
Fe-V, elec. resist. between 78 and 1200K 77−8065
Fe-V, ferromag. struct. in nucl. spin echoes 80−60453
Fe-V, H permeability, 300-700°C *(Russian)* 77−15627
Fe-V, hardness after nitriding, metallographic, electron microscopic and microprobe anal. 78−51608
Fe-V, local environment effect on atomic moments, itinerant model 78−68188
Fe-V, local environment effect on magnetic states 79−56491
Fe-V, nitrided, struct. and props. 78−19950
Fe-V, nitrided by const. activity ageing, X-ray studies 77−32720
Fe-V, order-disorder transition and σ-phase form. 80−7555
Fe-V, polarised neutron diffr., appl. of multiband CPA theory 77−77033
Fe-V, split bands evidence from sp. ht. and elec. transport data 77−24515
Fe-V, unlimited component solubility, intercrystallite internal adsorption *(Russian)* 80−39294
Fe-V, with atomic short range order, local environment effects on electronic struct. 78−67936
Fe-V, X-ray exam. of dynamic characts. *(Russian)* 77−62608
Fe-V (1 wt.%), nitrided and annealed, struct. 77−8998
Fe-V (10 to 50 at.%), solid soln., tempered, exam. of long and short range order, using Mossbauer effect *(Russian)* 79−29105
Fe-V (1.06, 5.23, and 15.55 wt.%), nitriding 78−3253
Fe-V alloys, hyperfine fields at solute and solvent sites rel. to mag. moments 77−8461
Fe-V alloys, Mossbauer study, hyperfine field effect on formation of local moments 78−27134
Fe-V solid solution, diffusion of V 79−90817
Fe-V-C, austenite to ferrite+precipitate reaction, TEM/STEM study 80−3075
Fe-V-C (0.3, 0.05 wt.%), interphase precipitation obs. in assoc. with Widmanstatten ferrite lateral growth 80−40365
Fe-V-C melts, electron struct., mag. susceptibility meas. *(Russian)* 78−47729
Fe-V-S-(C), sulphide nature exam. by X-ray spectral anal., solidification effects *(Russian)* 79−52191
Fe-VC alloys, struct. and mech. props. 79−52171
Fe-VC-WC(TiC), sintering, densification 80−25615
Fe-VN-C-Mn-Si, dispersion hardening effect on mech. props. 78−3137
Fe-VN-(C), dispersion hardening effect on mech. props. 78−3137
$FeCo_2V$, ordered and disordered alloys, annealing of point defects created by neutron irrad. at 20K *(French)* 79−1467
$Fe_{49}Co_{49}V_2$, neutron irradiation, close pair recombination *(French)* 80−39162
$Fe_{65.4}Cr_{20.5}Al_{10.7}V_{3.4}$, effect of Al and V on form. of $L2_1$ superstructure and stratification 77−77474
FeSi-Ca-V complex alloy oxidation of steel, nonmetallic additions *(Russian)* 80−93685
Fe_3Si-V, dil., cond. electron polarisation and moment perturbations 78−68224
FeV (2 at.%), NMR spin echoes, domain wall effects 80−75883
$Fe_{0.85}V_{0.15}$ film, ^{51}V NMR, spin echo expts., 77 and 300K 77−69728
$(Fe_{1-x}V_x)_3Ge$, magnetic and X-ray studies 80−1966
$(Fe_{100-x}V_x)_{79}P_{13}B_8$ amorphous alloys, splat cooled, mag. and transport props. 80−84593
Fe_2VSi, Heusler type material, mag. props. 77−40042
$Fe_{3-x}V_xSi$, Fe hyperfine fields 79−78055
$Fe_{3-x}V_xSi$, limits of solubility, mag. props. and electron conc. 78−10670
$Fe_{3-x}V_xSi$, selective site substitution and spin polarisation 79−78583
$Fe_{3-x}V_xSi$, struct., magnetisation, and spin echo expts., rel. to local environment model 77−20518
Gd-V amorphous films, spontaneous Hall effect and elec. resist. 80−80251
$(Hf,Zr)V_2$, phase transition, sp. ht. anomalies meas., 70-150K 77−35691
Hf-V, superconductivity and metallurgy of C15 materials 79−4610
Hf-V foil, rapidly quenched and heat treated, supercond. props. 80−54852
HfV_2, C-15 struct., phase transitions, elec. cond., crystal lattice parameters *(Russian)* 80−54826
HfV_2, C15 Laves phase, supercond. and stoichiometry 78−39245
HfV_2, C15 supercond., dielec. transitions, temp. depend. of resist. and mag. susceptibility, 4.2-300K 79−38136
HfV_2, dielectric phase transition, elec. resist. temp. depend. 79−65525
HfV_2, elec. resist. and mag. suscept., anomalous temp. depend. 79−69491
HfV_2, latent heat of structural transform. 80−24589
HfV_2, supercond., dielec. phase transition *(Russian)* 78−64168
HfV_2, supercond. compound, thermal expansion at low temp. 78−76189
$HfV_2H_{2.1}$, proton NMR relax. time and Knight shifts, diffusional activation energies meas., sorption props. 80−75871

vanadium alloys continued
HfV_2H_x and HfV_2D_x, composition depend. of supercond. crit. temp. 77−20482
$HfV_2H_x(D_x)$, superconducting transition temp. var., isotope effect 77−12047
$Hf_{1-x}Zr_xV_2$, lattice consts. at 4K and room temp., phase division at x=0.4 78−51474
$(Hf_{1-x}Zr_x)V_2$, supercond., Young's modulus and internal friction meas. 79−11654
$Hf_{0.5}Zr_{0.5}V_2H_x(D_x)$, enhanced supercond. transition temp. on H(D) additions 78−80083
α-IrV, internally deformed struct. as source of homogeneous linear struct. 78−26497
Mn-Ni-V, non-ferromagnetic Elivar type 77−48473
Mn-V, spin fluctuations effect on sp. ht. 79−82788
Mn-V-Al, magnetic props., heat treatment effects 79−29233
Mn-V-Al, phase stability 77−48397
Mn-V-Mo-C master alloys, development for low alloyed PM steel 80−50576
$Mn_{1-x}V_xAs$, mag. props., phase diags. 77−66300
$Mn_{2-x}V_xSb$, $0.08 \leq x \leq 0.25$, mag. props. modification by V 77−36071
Mo-(Zr+V+C) (1.1 wt.%) alloy, phase composition, carbide phase microhardness *(Russian)* 80−60834
Mo-Cr-V-P, load curves, structure states boundaries and strain hardening *(Russian)* 80−89241
Mo-Ru-V alloys, phase equilib. and corrosion resist. *(Russian)* 79−52165
Mo-V, binary continuous solid solution, elec. resist. and thermoelec. power behaviour 79−69492
Mo-V, elec. resist. and thermo-EMF, conc. depend., 4.2 to 1500K *(Russian)* 80−80247
Mo-V-C, hot-worked, substructural hardening and high-temp. strength *(Russian)* 80−25731
$Mo_{1-x}V_x$, supercond., NMR and mag. susceptibility meas. 79−56388
Nb-V, binary continuous solid solution, elec. resist. and thermoelec. power behaviour 79−69492
Nb-V, negative muon Coulomb capture ratio and Lyman series intensities 80−14255
Nb-V, resistivity due to H incorporation 80−70666
Nb-V, valence bands, X-ray M- and L-emission bands obs. *(Russian)* 78−19602
Nb-V (20 at.%), optical props., 0.1-25 eV, band models 78−10892
Nb-V alloys, electron-phonon interaction and supercond. transition temp. *(Russian)* 79−28426
Nb-V oxidation in air, rate determining process *(Russian)* 80−21170
Nb-V system, H_2 absorpt. 80−59808
Nb-V system, short-range order exam. by diffuse X-ray scatt. *(Russian)* 77−31644
$Nb\text{-}V_3Ga$ mixed state, Meissner effect investigation by muon method *(Russian)* 80−107954
Nb-V-O solid soln., thermodynamics of O_2 78−68673
Nb-V-Si, ductile amorphous, superconductivity 80−60131
Nb-V(-Cr), oxidation resist., Cr and V effects *(Russian)* 80−40585
Nb_3Ga, comp. and LRO effects on supercond. T_c 77−39992
$NbV\text{-}VO_x\text{-}Pb$ Josephson tunnel junction, VO_x effect on props. 79−87203
$Nb_{1-x-y}V_xH_x$, interaction between interstitial H and V, NMR meas. 77−59471
Ni-Cr-Mo-V steel disc, rolling contact fatigue and residual stress on contact surface 77−32671
Ni-Mo-Al-V, high-resist., struct. transforms., TEM *(Russian)* 78−19762
Ni-Mo-V, struct. changes on annealing *(Russian)* 77−21145
Ni-V, del. alloy, anisotropy consts., K_3 and K_1, determ. 77−4512
Ni-V, dil., mag. props. at elevated temps. 77−63089
Ni-V, dil., optical absorpt., electronic struct. 80−108227
Ni-V, dil., oxidation behaviour at 1200°C 77−77636
Ni-V, elementary excitations, exchange stiffness const., inelastic neutron scatt. study 79−47294
Ni-V, ferromag. reson. meas., anisotropy consts. determ. 78−39410
Ni-V, interdiffusion coeffs. in phase transform. range, 810-1175°C *(Russian)* 78−91490
Ni-V, low temp. sp. ht. near ferro-paramag. transition 77−63218
Ni-V, magnetocryst. temp. and conc. depends., rel. to resistivity 77−40052
Ni-V, solid and liq., mag. susceptibility and electronic struct. 80−39738
Ni-V, solid soln., diffusion and thermodynamic props. 80−65278
Ni-V, spin wave stiffness consts., RPA CPA band model 79−61088
Ni-V, weak ferromag., stiffness const., low-temp. meas., rel. to RPA-CPA theories 78−31063
Ni-V system, conc. depend. of interdiffusion coeff., 810-1175°C, rel. to phase diagram *(Russian)* 79−4429
Ni-V system, interdiffusion, kinetics of phase growth *(Russian)* 80−29230
NiAl-V join, phase relations and eutectic directional solidification 78−31396
$Ni_2Mn_xV_{1-x}Sn$, Heusler alloy, mag. moment exam. 77−24682
$Ni_2Mn_xV_{1-x}Sn$, mag. hyperfine fields, ^{119}Sn Mossbauer spectra study 80−55003
Ni_3V, dissociation of $^1/_2\langle 112\rangle$ perfect dislocations and nature of slip dislocations 78−43022
Ni_3V, ordered, domain size effect on mech. props. 79−79027
Ni_3V, stacking faults, twinning deform., electron microscopy obs. 78−6070
Pd-Ru-V, elec. resist. and thermal cond. *(Russian)* 78−19017
Pd-V, alloy and bilayer, silicide form. solid phase reaction with Si 80−6568
$Pd_2Mn_xV_{1-x}Sn$, Heusler alloy, structural disorder, Mossbauer study 80−80650
$Pd_{82-x}V_xSi_{18}$, amorphous, effect of structural relax. on elec. resist. 79−56186
$Pd_{82-x}V_xSi_{18}$, metallic glasses, effect of press. on elec. resist. 80−6805
Pt-V, Matthiessen's rule breakdown 77−15823
Pt-V dil. alloy, 0.5 at.%, ^{195}Pt NMR for local mag. susceptibility 78−84484
PtV, dil. alloys, NMR obs. of ^{51}V 80−71203
Re-Zr-V, constitutional diagram *(Russian)* 79−56956
$Sm_2(Co, Cu, Fe, V)_{17}$, permanent magnet, improved props. 77−89978
Ta-Nb-V, solid solutions, superconductivity and charge transfer 79−7926
Ta-Nb-V BCC solid solutions, supercond. and normal state, sp. ht. meas. 78−84347
vanadium alloys continued
Ta-V system, short-range order exam. by diffuse X-ray scatt. *(Russian)* 77−31644
Ta(C,N)-Ni-VC, sintering behaviour, VC effect 80−93520
(Ti,V)C carbides, prep. and mech. props. 78−64518
Ti-6Al-4V, oxidation kinetics, water vapour, comparison with pure Ti 77−21321
Ti-6Al-4V, stress distrib. for steady axisymmetric extrusion 80−3103
Ti-A-V (6, 4 wt.%), castings, fatigue crack initiation 79−29186
Ti-Al-Cr-Mo-U, alloy VT22, phase composition and fatigue strength 78−3219
Ti-Al-Cr-Mo-V, alloy VT22M, exam. of ageing and phase transitions *(Russian)* 79−11641
Ti-Al-Cr-Mo-V, effect of structure and heat treatment on tensile strength, ductility, fatigue limit and notch sensitivity 78−56711
Ti-Al-Cr-Mo-V alloy VT-22, effect of heating rate on phase recrystallisation *(Russian)* 79−34077
Ti-Al-Mo-V, crack resistance in chloride soln., electrochem. protection, polarization effect 80−55589
Ti-Al-Mo-V (8, 1, 1 wt. %), stress corrosion cracking and slow strain rate H_2 embrittlement 78−48569
Ti-Al-Mo-V (8, 1, 1 wt.%), environmental fatigue crack propag., texture influence 79−91802
Ti-Al-Mo-V (8, 1, 1 wt.%), Widmanstatten colonies, fracture toughness 80−85031
Ti-Al-O, V effect on thermal stability and mech. props. 77−21171
Ti-Al-U (6,4 wt.%), low and high cycle fatigue rupture at same load 78−3217
Ti-Al-V, (6,4 wt %), fracture mode, tearing topography surface fracture 80−7670
Ti-Al-V, (6,4 wt.%), history dependent steady state creep rate 78−39866
Ti-Al-V, (6,4 wt.%), single and dual ion irrad., microstruct. studies 80−29077
Ti-Al-V, (6.7, 4.3 wt.%), fatigue crack growth and fracture resistance enhancement, due to annealing 78−35510
Ti-Al-V, alloy 685, fatigue life, creep and dynamic strain ageing effect, 25 to 400°C *(French)* 80−45384
β-Ti-Al-V, annealed, differing interstitial O content, fatigue crack propag. resist. 79−11696
Ti-Al-V, containing 0-6000 ppm ^3He, sensitivity of tensile props. 80−39197
Ti-Al-V, environmental effects in alloy fretting, effect on fatigue props. 78−56787
Ti-Al-V, erosion resistant boride coating 79−20290
Ti-Al-V, friction coeff. reduction on injection with TiC particles 80−85086
Ti-Al-V, fusion reactor blanket structures, radiation resistance 80−63379
Ti-Al-V, impact strength anisotropy, influence of texture *(Russian)* 80−20952
Ti-Al-V, irrad. induced creep 80−39163
Ti-Al-V, long-term corrosion stability rel. to use in joint endoprostheses 78−36059
Ti-Al-V, oxidation by water vapour *(French)* 78−76787
Ti-Al-V, plane strain toughness and resistance to crack propagation *(French)* 78−23813
Ti-Al-V, rolled, elastic stiffness and Bauschinger effect accompanying anisotropic hardening *(Russian)* 80−40435
Ti-Al-V, VT6 alloy, butt welded joints, electron beam welding conditions effecting interstitial impurities distribution 80−39136
Ti-Al-V (4.7, 2 wt.%) pseudo alpha alloy, laminar struct. singularities, β to α transformation *(Russian)* 80−7552
Ti-Al-V (6, 4, wt.%), delayed retardation phenomena of fatigue crack growth, exam. 78−56745
Ti-Al-V (6, 4, wt.%), texture influence on fracture toughness and deformation 79−91801
Ti-Al-V (6, 4 wt.%), annealed and rolled plate, elevated temp. plastic anisotropy 79−61663
Ti-Al-V (6, 4 wt.%), α-β anneal, recrystn. anneal, β-anneal, room temp. creep 79−61662
Ti-Al-V (6, 4 wt.%), cavitation induced erosion, under mill annealed, soln. treated and aged, and beta annealed conditions 79−8371
Ti-Al-V (6, 4 wt.%), compliance calibration results 78−19798
Ti-Al-V (6, 4 wt.%), corrosion resist. in marine environments *(French)* 80−50767
Ti-Al-V (6, 4 wt.%), deform. charact. under isothermal forging conditions 77−36600
Ti-Al-V (6, 4 wt.%), dynamic crit. stress intensity vs. crack vel. 80−2115
Ti-Al-V (6, 4 wt.%), fatigue crack growth data 77−73332
Ti-Al-V (6, 4 wt.%), fatigue crack propag. under dwell time conditions 78−80639
Ti-Al-V (6, 4 wt.%), fretting corrosion of orthopaedic implant materials by bone cement 80−104813
Ti-Al-V (6, 4 wt.%), friction characts. improvement by O_2 dissolution and controlled surface hardening *(French)* 80−45401
Ti-Al-V (6, 4 wt.%), gust spectrum fatigue crack propag. 80−21105
Ti-Al-V (6, 4 wt.%), high temp. cyclic oxidation, AE monitoring 79−83413
Ti-Al-V (6, 4 wt.%), hot isostatically pressed casting, fatigue crack initiation 79−79078
Ti-Al-V (6, 4 wt.%), improvement of props. by ion implantation 80−16601
Ti-Al-V (6, 4 wt.%), repassivation and pitting corrosion 80−30143
Ti-Al-V (6, 4 wt.%), ring test, evaluation for strain rate sensitive materials 78−39991
Ti-Al-V (6, 4 wt.%), solution treatment temp. effect on fracture morphology 79−61620
Ti-Al-V (6, 4 wt.%), stress corrosion cracking, composition, microstruct. and texture effects 79−11725
Ti-Al-V (6, 4 wt.%), superplastic, mech. behaviour and hardening characts. 79−83269
Ti-Al-V (6, 4 wt.%), targets, metallographic features after ballistic tests 79−79046
Ti-Al-V (6, 4 wt.%), temp. distrib. for steady axisymmetric extrusion 80−11670
Ti-Al-V (6, 4 wt.%), temp. distrib. for steady axisymmetric extrusion numerical results 80−11671
Ti-Al-V (6, 4 wt.%), texture effect on fatigue crack path 78−27633
Ti-Al-V (6, 4 wt.%), textured, anisotropy of fracture toughness over various specimen orientations 79−8353

vanadium alloys continued
Ti-Al-V (6, 4 wt.%), texture depend. stress corrosion cracking 80−104334
Ti-Al-V (6, 4 wt.%), type IMI 318, internal friction study of martensitic transformations 80−7573
Ti-Al-V (6, 4 wt.%), type IMI 318, stability of martensitic phases 80−7574
Ti-Al-V (6, 4 wt.%), void formation and growth, tensile fracture, exam. 78−80637
Ti-Al-V (6, 4 wt.%), Widmanstatten, microstructurally sensitive fatigue crack growth obs. 78−27627
Ti-Al-V (6, 4 wt.%) effect of high temp. oxidation on eddy current conductivity 78−76770
Ti-Al-V (6, 4 wt.%) slow crack growth in air and fracture toughness, H content effect *(French)* 80−45385
Ti-Al-V (6,4 wt %), superplasticity, effect of temp. 80−7639
Ti-Al-V (6,4 wt%), cyclic temp. creep, transition effect 80−97539
Ti-Al-V (6,4 wt.%), age hardened, deform. charact. 77−36608
Ti-Al-V (6,4 wt.%), alloy plate, fatigue crack propag. under in-plane loading, expts. 79−52337
Ti-Al-V (6,4 wt.%), alloy plate, fatigue crack propag. under in-plane loading, anal. 79−52338
Ti-Al-V (6,4 wt.%), α/β interface phase formation charact. 79−52272
Ti-Al-V (6,4 wt.%), α/β interface phase influence on tensile props. 80−30034
Ti-Al-V (6,4 wt.%), β-annealed, subsurface fatigue crack initiation 80−108553
Ti-Al-V (6,4 wt.%), corrosion fatigue behaviour, surgical implant material 79−39027
Ti-Al-V (6,4 wt.%), cyclic stress-strain response 77−21170
Ti-Al-V (6,4 wt.%), D profiles after D_3^+ implantation 80−37581
Ti-Al-V (6,4 wt.%), D trapping in fusion reactor materials, temp. dependence 80−37577
Ti-Al-V (6,4 wt.%), effect of air exposure on fracture charact. 80−100890
Ti-Al-V (6,4 wt.%), fatigue crack growth, influence of dwell-time 79−43380
Ti-Al-V (6,4 wt.%), fretting fatigue resistant coating, for steel/Ti-Al-V mating surfaces 78−64721
Ti-Al-V (6,4 wt.%), fretting fatigue behaviour of temps. up to 600°C 80−21104
Ti-Al-V (6,4 wt.%), H related fatigue fracture 80−76344
Ti-Al-V (6,4 wt.%), heat treated and rolled, texture instability 77−63689
Ti-Al-V (6,4 wt.%), heavy ion irrad. effect on microstructure 79−10884
Ti-Al-V (6,4 wt.%), high temp. fretting fatigue, fatigue and fretting wear 80−3197
Ti-Al-V (6,4 wt.%), hot salt stress corrosion susceptibility, microstruct. effects 77−36688
Ti-Al-V (6,4 wt.%), improved toughness from prior β-grains 78−15522
Ti-Al-V (6,4 wt.%), ion irradiated, microstruct. study using TEM 80−96572
Ti-Al-V (6,4 wt.%), laser surface melted, topographical charact. 79−70200
Ti-Al-V (6,4 wt.%), microstruct. improvement by cyclic heating *(Japanese)* 79−100185
Ti-Al-V (6,4 wt.%), microstruct. effect of base metals on diffusion welding *(Japanese)* 80−89296
Ti-Al-V (6,4 wt.%), phase transformation after hydrogenation 80−7560
Ti-Al-V (6,4 wt.%), plastic flow instability and multiple necking during superplastic flow 77−8896
Ti-Al-V (6,4 wt.%), porous compacts, determ. of effective stress in hot pressing 80−100807
Ti-Al-V (6,4 wt.%), quenched, struct. and age hardening rel. to treatment temp. 80−11657
Ti-Al-V (6,4 wt.%), strongly textured, influence of cryst. orientation on fracture toughness 78−84951
Ti-Al-V (6,4 wt.%), strongly textured, influence of crystallographic orientation on tensile behaviour 80−7633
Ti-Al-V (6,4 wt.%), superplasticity microstructural influences 79−52323
Ti-Al-V (6,4 wt.%), surface cracking under unidirectional loading 78−56753
Ti-Al-V (6,4 wt.%), surface and grain boundary free energy, zero-creep determ. 79−4313
Ti-Al-V (6,4 wt.%), surface residual stresses, surface topography, fatigue behaviour 79−52366
Ti-Al-V (6,4 wt.%), surgical implant ion beam textured, stress/strain relations, fatigue charact. 78−73297
Ti-Al-V (6,4 wt.%), sustained loading charact. and H_2 effects 78−48515
Ti-Al-V (6,4 wt.%), to H effect on fracture props. and microstruct. 80−40512
Ti-Al-V (6,4 wt.%) alloy, fatigue crack closure eval. with electric potential method 79−50678
Ti-Al-V (6,4 wt.%) alloy foil, substrate temp. effect on struct. 80−7497
Ti-Al-V (6,4 wt.%) for TiC reactively sputtered coatings, adherence, XPES and wear study 80−25565
Ti-Al-V (6,4 wt.%) superplastic deform. 78−31471
Ti-Al-V (6,4 wt.%) superplastic alloy, maximum attainable ductility 80−60919
Ti-Al-V (6,4wt.%), galvanic couple with Al alloys, velocity effect on corrosion 78−35566
Ti-Al-V (6.4 wt.%), electron beam melting for scrap recycling 77−66604
Ti-Al-V (6.4 wt.%) cast alloy, with improved microstruct., mech. props. *(Japanese)* 80−71701
Ti-Al-V alloy, thermophysical meas. above 1450K, using subsecond transient technique 78−95161
Ti-Al-V alloys, 17.5 MeV Cu ion irradiation, resistance to void damage 79−55795
Ti-Al-V-Be-B, melt-extracted polycryst., mech. props. 80−76360
Ti-Al-V-Cr-Mo-Zr (3,8,6,4,4 wt.%), beta-C, microstruct. effect on mech. props. 78−27577
Ti-Al-V-Cr-Zr-Mo (3, 8, 6, 4, wt.%), phase transforms. 79−100113
Ti-Al-V-Cr-Zr-Mo-Fe (3.4, 8.3, 5.8, 3.9, 4.2, 0.06 wt.%), shock loaded, residual strength 77−36589
Ti-Al-V-Fe-Cu, melt-extracted polycryst., mech. props. 80−76360
Ti-Al-V-Fe-Si, alloy VT6, phase transform. kinetics and Young's modulus *(Russian)* 77−81258
Ti-Al-V-Sn (5.5, 5.3, 2.3 wt.%) fatigue crack growth and fracture resistance enhancement, due to annealing 78−35510
Ti-Al-V-Sn (5.5, 5.5, 2 wt%), crack growth, slow, H-induced 80−104272

vanadium alloys continued
Ti-Al-V-Sn (6, 6, 2 wt.%) weldments, heat treated, transangular fracture 80−40524
Ti-Al-V-Sn (6, 6, 2 wt.%), fatigue crack growth, cyclic freq. and microstruct. influence 80−55515
Ti-Al-V-Sn (6,6,2 wt.%), H_2 induced crack growth, in-situ scanning Auger anal. 79−8355
Ti-Al-V-Sn (6,6,2 wt.%), α-β type 662, fusion zone fracture behaviour in weldments 80−30093
Ti-Al-V-Sn (6,6,2 wt.%), depend. of K_{ISCC} on loading rate and crack orientation 80−45427
Ti-Al-V-Sn (6,6,2 wt.%) solid metal embrittlement by Cd, Ag and Au 80−16551
Ti-Al-V-Sn (6,6,2 wt.%) fusion weldment, substruct. charact. 80−84183
Ti-Al-V-Sn-Zr alloy TS5, annealing effect on ductility and strength *(Russian)* 78−35427
Ti-Al-V-Sn(Mo-Fe), heavy section extrusion, fabrication and mech. props. 78−6985
Ti-Al-V-(Cr)(Mo), electrochemical behaviour under tensile stress in boiling H_2SO_4 and acidic chloride solns. 78−95851
Ti-Al-V-(Mo), Widmanstatten, quantitative anal. of microstruct. effect on fatigue crack growth 79−79071
Ti-Al-V-(Sn), SCC, subcritical flow growth, comparison of aircraft alloys in NaCl soln. 78−53028
Ti-Al-V-(Sn), surface finishing effect on internal stresses, X-ray study *(German)* 79−34210
Ti-Al-V(Sn) alloys, plastic deformation and fracture charact. at low temps. *(Russian)* 80−7624
Ti-Al-V(6,4 wt.%), electrical potential method, unusual potential drop 77−16761
Ti-Al-V(6,4 wt.%), environmental fatigue crack propag. 77−36632
Ti-Al-V(6,4 wt.%), partially ordered, i.r. absorptance, 0-600°C 77−4632
Ti-M-V-Cr-Mo, RMI 38644, shock loaded, age hardening 79−29112
Ti-Mo-V (8 wt.%, 8 wt.%), FCC phase, decay of β-solid soln., electron microdiffr. 79−15670
Ti-Mo-V-Al-Cr-Fe (4.8, 4.7, 5.2, 1.1, 1.0 wt.%), structural changes during heating up to 1000°C, DTA study *(Russian)* 80−93552
β-Ti-Mo-V-Fe-Al (8, 8, 2, 3, wt.%), exam. of stress induced H_2 migration 78−87823
Ti-Mo-V-Fe-Al (8,8,2,3, wt.%), exam. of stress controlled fatigue response 79−61734
β-Ti-Mo-V-Fe-Al (8,8,2,3 wt.%), metastable, high cycle fatigue crack initation, grain size effect 77−86145
β-Ti-Mo-V-Fe-Al (8,8,2,3 wt.%), metastable alloy, microstruct. and mech. props. ageing time and temp. effect 78−64569
β-Ti-Mo-V-Fe-Al(8,8,2,3 wt.%), metastable factors affecting stress corrosion cracking 77−28928
Ti-Nb, IR absorption peculiarities 79−65876
Ti-Nb alloys, Fe, Mo, V, Ta alloying additions on microstruct. after combined treatment *(Russian)* 77−59826
Ti-Nb-V-Zr, superconductor, struct. determ. by optical microscopy and electron diffraction *(Russian)* 77−16628
Ti-Nb-V(25 wt.%, 15 wt.%), precipitation of β and ω phases during ageing at 350°C 77−8838
Ti-Nb-Zr-Fe-Mo-V, cold worked, struct. and phase transform. during ageing 78−3153
Ti-V, anomalous elec. resistivity, mag. susceptibility, soft-phonon induced structural inhomogeneities 78−60104
Ti-V, cyclic stress-strain response 78−60700
Ti-V, elastic moduli, comparison with paramagnetic Cr, V-Cr, rel. to bandstructure 80−7615
Ti-V, elastic moduli, electron conc., pulse echo overlap meas. 80−59550
Ti-V, IR absorption peculiarities 79−65876
Ti-V, influence of different factors on supercond. transition width *(Russian)* 79−1636
Ti-V, metastable β-phase, stress induced products formed by cold rolling *(Japanese)* 78−84843
Ti-V, metastable diffusionless equilibria, high press. conditions 80−71627
α-Ti-V, Mossbauer spectra, metastable θ- and ω-phases 80−20556
Ti-V (10 at.%), $\alpha \rightarrow \omega$ transformation, electron diffr. evidence of intermediate BCC phase 80−81051
Ti-V (15.5 wt.%), {332} deformation twins, optical microscopy study 79−79047
Ti-V (19 at.%), aged ω-phase precipitation, incomplete proximity effect 78−60252
Ti-V (27 and 30 wt.%), fatigue crack propag., in single and poly. crystals 79−5048
β-Ti-V (40 at.%), BCC, flow stress asymmetry and cyclic stress-strain response 77−36583
Ti-V (40 at.%), BCC, single crystal, fatigue and slip 78−19854
Ti-V (40 at.%), microcracks intersecting fatigue crack, exam of origin 78−80638
Ti-V (40 wt.%), effects of H on anisotropic elastic props. 79−74192
β-Ti-V metastable alloys, fatigue crack propag. 80−60964
Ti-V-Cr, BCC, press. derivatives of elastic moduli, Fermi surface topological changes, band struct. 79−61639
Ti-V-Cr, electron-lifetime effects on props. 80−10951
Ti-V-Cr, type Ti-15-333, irrad. induced creep 80−39163
Ti-V-Cr-Al (13, 11, 3 wt.%) alloy spring wire, torsional fatigue props. 77−77649
Ti-V-Cr-Al (13, 11, 3 wt.%), stress corrosion cracking in methanolic solutions 80−50752
Ti-V-Cr-Mo, fracture resistance at low temps. 80−104284
Ti-V-Fe-Al (10, 2, 3 wt.%), fracture toughness and stress corrosion resistance 80−100904
Ti-V-H system, BCC, hydrogen effects on anisotropic elastic props. 79−24565
Ti-V-Mo alloy system, phase equilibria and interstitial effects, TEM and X-ray diffr. study 79−43204
Ti-V-Mo-Cr system, β-phase stability 80−55353
Ti-V-Ru system, metastable phases form. *(Russian)* 77−21098
Ti-V-Si, equlibrium silicide, X-ray and electron diffr. obs. 78−27483
Ti-V-Si, Si effects on precipitation and strengthening 77−55970
Ti-V-Si (30, 1 at%), quenched and aged, hardness, tensile behaviour and phase transform. 79−11646
βTi-V-Si (40, 1 at.%), Si effect of precipitation and age hardening 77−63676
Ti-Zr-Mo-V, alloy VT20, exam. of plasticity in temp. range 20 to 1000°C 78−56712

vanadium alloys continued
TiN-VN alloys, synthesis in low-temp. plasma, phys.-chem. props. *(Russian)* 79−38761
Ti(V,Ni)/Al bimetal film structure, macroscopic defects *(Russian)* 79−1555
Ti_xV_{1-x}-H_2 system, reaction and press.-composition isotherms meas. 80−108391
U-Q^5, Q^5=quint, stress corrosion cracking in moist air, salted moist air and salt water 78−35562
U-V (0.2 wt.%), mech. and struct. props., effect of internal H *(French)* 77−21253
$(V,Fe)_3M$, M=Si, Ge, Ga, solid soln. form. and supercond. T_c *(Russian)* 78−80512
$(V,Nb)_3Ga$, $(V,Nb)_3Ge$ and $(V,Nb)_3Si$ solid solns., supercond. T_c, absolute thermal EMF, microhardness 77−36006
$(V,Nb)_3Si$ type with A15 struct., supercond. transition temp., depend. on stoichiometry *(German)* 77−69444
(V,Ti)C+(Ni,Mo) cermet systems, effect or V/Ti ratio or Mo partitioning 79−79099
$V_3Ga_{1-x}Sn_x$, lattice props. supercond., ^{119}Sn Mossbauer shift meas., 5-300K 77−1627
V cathodic deposition, from crude V, V_2C and VC, hardness meas. *(Japanese)* 79−78908
V Si, supercond. alloy, electron distrib. vel. to Cr_3Si 77−68944
V/Cu-Ga, composite superconductor, V_3Ga phase form., TEM obs. *(Russian)* 80−84933
V/H, heat capacity and supercond. between 1.5 and 16K 80−2521
V-Al, band struct. and density of states, KKR method and X-ray meas. 80−10863
V-Al, conduction band states, X-ray spectra obs. *(Russian)* 80−29317
V-Al thin film system, phase growth kinetics, electrochemical anode etching 77−72805
V-Al/Cu-Ge composite superconductors, transition temp. and upper crit. field, heat treatment effects 79−38268
V-Al/Cu-Ge composite tape, transition temp., upper crit. field 78−68126
V-Al-C, ternary system, phase relationships 80−76230
V-Al(Ga, Si, Ge, Su)-Cu, rapidly quenched, comp. and phase equilib. 80−76235
V-based ternary solutions, containing H, thermodynamics 80−19961
V-C alloys, low carbides struct. rel. to ht. treatment 77−48458
V-C system, ordering and phase equilibrium processes 79−99311
V-CO(Ni) sigma phase alloys, NMR and electric-field gradients 80−108109
V-C(N) system, mutual phase orientation, X-ray diffr. exam. *(Russian)* 77−62498
V-Cr, elastic moduli, comparison with paramag. Cr, Ti-V, rel. to band-structure 80−7615
V-Cr, elastic moduli, US pulse echo meas. 78−84881
V-Cr, electronic density of states, temp. depend. of elec. resist. and mag. susceptibility 77−11891
V-Cr (15 wt.%), fusion reactor struct. alloys, dual-ion irrad. effects 79−45403
V-Cr (15 wt.%), radiation-induced solute segregation 80−29086
V-Cr (wt.%), 3.5 MeV $^{51}V^+$ irrad. induced void swelling and solute segregation 79−7637
V-Cr alloys, absorption of H_2, thermodynamic parameters 78−87862
V-Cr effect of alloying additive on thermoelectric props. 77−35927
V-Cr-H system, electronic sp. ht. 80−49378
V-Cr-Ti, fusion reactor first wall structural materials, prediction of life limiting props. 78−62605
V-Cr(Fe)(Nb)(Ti), diffusion of H_2 *(Japanese)* 78−10221
V-Cr(Mo)(Nb), thermopower composition depend. 79−65445
V-D, prod. using Pd layer coating technique 79−47816
V-D alloys, low frequency internal friction study 78−48444
V-D alloys, positron annihilation radn. angular correlation, electronic struct. study 79−43058
V-D system, phase equilibria study *(Japanese)* 79−78936
$V-D_{0.01}$, enrichment of D during the ion bombardment 80−54288
V-Fe, ^{57}Co Mossbauer spectra, diffusion mechanism of Fe 80−15292
V-Fe, ferromagnetism to mictomagnetism at low Fe conc. 78−91878
V-Fe, force constant change with pressure, relative Mossbauer fraction 80−34163
V-Fe, mag. ordering temp. depend. on atomic short-range order from susceptibility meas. 79−61159
V-Fe (5.0 at.%), stress relaxation test, appl. to discerning frictional and internal stresses 77−63712
V-Fe (5.0 at.%), work softening at elevated temps. *(Japanese)* 77−52347
V-Ga-Cu, fast quenching of A15-phases *(German)* 77−36014
V-Ga-Cu, phase diagram *(Russian)* 77−25014
V-Ga-Sc, phase diagram, metallographic and X-ray meas., solubility boundaries *(Russian)* 78−56618
V-Ga(Ge)(Si), fast quenching of A15-phases *(German)* 77−36014
V-H, BCC, quasimolecular Jahn-Teller reson. states 80−44550
V-H, BCC, tetrahedral interstitial site H band modes, neutron scatt. obs. 79−55852
V-H, effect of neutron irrad. on electrical resistance, magnetic susceptibility 80−29063
V-H, electron work function, 300 to 600 degrees C, contact potential difference meas. 80−29462
V-H, fusion reactor first wall material, cyclic deform. tests 80−30074
V-H, H effect on fatigue crack propag. 78−48516
V-H, incoherent spinodals, meas. by Gorsky effect 78−19712
V-H, NMR of anomalous diffusion of H and phase transition 77−16571
V-H, phase diagram, resistometric contribution 78−15372
V-H, thermokinetics of H_2 generation from transition metal-H compounds 79−74421
V-H rods, twisting effect, anelastic deviations on thermal cycling 80−21043
V-H single crysts., elastic consts., temp. depend., H effects 80−66563
V-H system, crystallography of βVH precipitation 77−52326
V-H system, DTA, phase diagrams, low temp. phase 78−6903
V-H system, phase equilibria studies *(Japanese)* 79−78935
V-H(D), metallographic and thermal differential anal., potential for H energy storage appls. 80−45281
V-H(D) system single cryst. prep. and characterisation 79−95910
V-H(D)(T) system, BCC, US vel. changes caused by H isotope dissolution 80−65117
V-Hf-Nb(Zr), multifilamentary, superconducting props. improvement 79−38267
V-HfV_2-$HfCr_2$-Cr, phase diagram *(Russian)* 77−52288

vanadium alloys continued
V-Mn, equiatomic, ordering kinetics and antiphase domain coarsening 80−7559
V-Mn-Cr, disordered BCC state, mag. phase diagram, mag. and elec. props. 77−63185
V-Mo, corrosion in high purity liquid Na containing ≈1 ppm O, at 700°C for 500 h 79−8383
V-Mo, effect of ion plated Mo on corrosion in liquid Na, mech. props. 78−53020
V-Mo, effects of heat treatment on mech. props. 77−21176
V-Mo, mechanical properties, O, N_2 and C addition effects 79−52356
V-Mo, X-ray K-emission spectra *(Russian)* 77−55851
V-Mo (25 wt.%), corrosion behaviour in high temp. impure He gas 80−76402
V-Mo effect of alloying additive on thermoelectric props. 77−35927
V-N, BCC solid soln., superperiodicity of lattice in quenched ordered struct. *(Russian)* 78−56662
V-N α-solid solution, struct. transform. during annealing and quenching *(Russian)* 77−81257
α-V-N solid solns., quenched ordered structures *(Ukrainian)* 77−69088
V-N system, ordering and phase equilibrium processes 79−99311
V-N system, phase formation *(Russian)* 78−39739
V-N(O)(C) system, specimen prep. for metallography *(German, English)* 80−89439
V-Nb, effects of heat treatment on mech. props. 77−21176
V-Nb, mech. props., −196-1000°C, comp. depend. 78−39847
V-Nb, supercond. T_c and H_{c2}, effect of purity and alloying with Ta, Cr, Mo or Re 77−85375
V-Nb, vacuum deposited supercond. films, T_c chem. comp. depend. *(Russian)* 78−19174
V-Nb, X-ray K-emission spectra *(Russian)* 77−55851
V-Nb-Mo(Cr), corrosion in liquid Na, O_2 effects 77−8987
V-Nb-Ta, supercond., elec. resist. and electron-phonon interaction parameters 78−14862
V-Nb-Ti-N alloy, dispersion hardened, fracture charact. 79−15794
V-Nb-Ti-N alloy, with dispersed second phase, ductile-brittle transition 80−93653
V-Nb(Ti)(Zr)(Cr)(Mo)(Fe)(Cu), H solubility and diffusivity around room temp. 80−29225
V-Ni, ion bombard., void form. 80−34097
V-Ni alloy, onset of ferromag. 79−56533
V-Ni-Al, phase equilib., elect. cond., hardness *(Russian)* 77−66627
V-Ni-Mo, structure in alloy crystallisation region, peritectic equilibria *(Russian)* 80−50622
V-Ni-Mo alloy, annealed at 1150°C, isothermal section *(Russian)* 79−52154
V-O, neutron irradiated effects, comparison with high purity V 77−84805
V-O (1 to 4 at.%), solid soln., void swelling, V ion beam irradiation, 550 to 905°C 78−63795
V-O alloy, temp., dose and conc. depend. of void form. following V^+ ion beam irradiation 78−10105
V-O alloys, quenched, local ordering of O, electron microscopy and diffr. 80−59453
V-O solid soln., BCC, modelling of interstitial solute behaviour 79−77748
V-Os system, equilib. phase fields, X-ray diffr., elec. resist., DTA, and EPMA meas. 79−47661
V-Pd, dil. alloys, surface segreg. 78−18883
V-Pd, H mobility and solubility, appearance pot. spectra obs. 80−55231
V-Pt, dilute, inelastic neutron scatt. and quasilocal vibrs. *(Russian)* 77−80595
V-Pt, sp. ht. and mag. meas. in ordered and disordered phases 80−70422
V-Re, X-ray K-emission spectra *(Russian)* 77−55851
V-Re alloy, thermo-EMF and resistivity at 0 to 1500°C 77−43571
V-Re system, discovery of supercond. A-15 phase 78−88060
V-Rh, constitution diagram 77−44216
V-Rh alloys, short range atomic order exam. *(Russian)* 78−63696
V-Si, A15 compounds, Hall coeffs. 79−33281
V-Si, strengthening by internal oxidation 80−55424
V-Si-C film, superconductivity 78−72299
V-Si-Cu, struct. and supercond., Cu influence 80−50592
V-Si(Ti)(Sn-Ti), corrosion resistance and some physicomechanical props. 77−70229
V-Sm, vacuum deposited supercond. films, T_c chem. comp. depend. *(Russian)* 78−19174
V-Sn(Al)(Ga)(Ge)(Si)-C, phase equilib. and supercond. 80−50593
V-Ta, mech. props. 79−61682
V-Ta, superconducting transition temp., nondiagonal disorder effects 79−73622
V-Ta, X-ray emission spectra *(Russian)* 77−55851
V-Ta (5 wt.%), strain hardening, screw dislocations and microtwinning *(Russian)* 80−29971
V-Ta alloys, electron-phonon interaction and supercond. transition temp. *(Russian)* 79−28426
V-Ti, and V-Ti-Be(Zr), 4 MeV Ni^{++} irrad., He gas bubble form. 80−29085
V-Ti, exam. of intrinsic diffusion and vacancy flow effects 79−4430
V-Ti, supercond., rotating discs, hysteresis losses and mag. phenomena 80−75695
V-Ti, vacuum deposited supercond. films, T_c chem. comp. depend. *(Russian)* 78−19174
V-Ti (20wt.%), corrosion in liquid Na, O_2 effects 77−8987
V-Ti (42 at.%), mixed state, US attenuation meas. at 4.14K 80−15657
V-Ti (42 at.%), ultrasonic vel. in mixed state 80−75689
V-Ti alloys, supercond., thermal cond. 77−89900
V-Ti superconducting film, electron spin effects 79−28488
V-Ti-C, elemental anal. by EELS 80−101069
V-Ti-C, elemental anal. of second phase carbides using electron loss spectroscopy 79−20500
V-Ti-C, high temp. carbide form., electron microscopy study 80−89228
V-Ti-O single crystal alloy, mech. props. 77−25112
V-Ti(Cr) amorphous films, supercond. transition temp. 79−60953
V-W, effect of alloying additive on thermoelectric props. 77−35927
V-W, X-ray K-emission spectra *(Russian)* 77−55851
V-Zr, strengthening by internal oxidation 80−55424
V-Zr (2 wt.%), internally oxidised, neutron irradiated, annealing effect on mech. props., elec. cond. and electron microscope obs. *(Japanese)* 79−15701

vanadium alloys continued
V-Zr-C, erosion coeff., temp. depend. reactor wall swelling due to He ion bombardment 78−17418
V-Zr-C, radiation hardening and plastic instability *(Russian)* 78−39842
V-Zr-C-Y alloy weld metal, hardening phase precipitates examination, TEM appl. 80−7576
V-Zr-N quasi-binary section, long term hardness to compare heat resistance 78−3223
V-Zr-Nb alloy, rel. between density of states and martensitic and superconducting phase transition temps. 78−10594
V-ZrO_2(HfO_2), eutectic system, metallographic investigation *(Russian)* 77−66629
V_3Ga, high T_c supercond., electron-phonon coupling, effect of electronic density of states sharp struct. 78−14877
V_3Ge, superconducting filament formation near edge dislocation *(Russian)* 79−4635
VAl, X-ray spectra, electronic structure 79−78793
V_3Al film, quasiamorphous, supercond. phase formation by heat pulse 77−63017
γ-V_5Al_8, γ-brass, cryst. struct. redeterm. 77−47377
$V_3Al(Ga)(Si)(Ge)(Sn)$ electronic struct. calcs. 79−47005
$V_3Al(Ga)(Si)(Ge)(Sn)$, electronic struct., electron-phonon interactions, and low temp. anomalies 79−60701
V_4As_3, defect struct. 77−4112
V_3Au, effect of atomic ordering on XPS of valence bands 77−52224
V_3Au, supercond., electronic density of states and T_c changes with atomic ordering 78−91800
V_3Au, XPS of valence electrons meas. 77−21003
VBe_{12}, coated limiters, first wall protection 80−32483
VBe_{12} coating, erosion rates under H^+ ion bombard., fusion reactor appls. 80−39179
VBe_{12}, fusion reactor material, low energy ion erosion expts., Kaufman source appl. 80−68942
VC base alloys, ordering processes *(Russian)* 77−36462
V_3Co, nuclear spin-lattice relax. time, electronic density of states 77−59354
$(V_{1-x}Cr_x)_3Si$, elastic moduli, 4.2 to 290K, softening near supercond. transition *(Russian)* 80−92582
$(V_{1-x}Cr_x)_3Si$. mag. susceptibility, 4.2 to 320K, density of states model 80−7035
$(V_{1-x}Cr_x)_3Si$, single cryst., elec. resistivity, temp. depend. 79−56193
$V_{3-x}Cr_xSi$, x=0 to 3, struct., supercond. and mag. props. 80−1962
$VD_{0.77}$, Compton profile, electronic struct. *(German)* 78−92140
V_2D, BCC α-phase, metal atom-induced diffuse X-ray scatt. from short range order 79−60358
V_2D, short-range interstitial order above crit. temp., diffuse X-ray scatt. obs. 79−95159
V_4D_3, multistage ordering process, neutron diffr. obs. 77−59114
$V_3(Fe,Ge)$, struct. and supercond. transition temp. *(Russian)* 79−7920
$V_{1-x}Fe_x$, low temp. sp. ht. and mag. props. 80−2548
$V_{75-x}Fe_xGa_{25}$, Mossbauer exam. 77−90078
$V_{1-x}Fe_xH_n$, low temp. sp. ht. and mag. props. 80−2548
V_3G_3Ga multifilamentary wires, effect of low temp. neutron irrad. 77−32132
$V_{0.75-x}Ga_{0.25+x}$ ^{51}V, nucl. spin-lattice relax. time, annealing and neutron effects 79−82710
$V_{1-x}Ga_x$, A-15 cpds., nucl. mag. relax. in normal and supercond. state 80−49993
$V_{1-x}Ga_x$, nuclear spin-lattice relax. and supercond. 79−56387
V_2Ga, phonon density of states, temp. depend. 79−42183
V_3Ga, A15 compound, exam. of deformation processing, review 78−39864
V_3Ga, A15 cpd., hydrogenation effects on supercond. transition temp., lattice parameters 80−103772
V_3Ga, band theory, semiself-consistent band calcs. 78−2406
V_3Ga, cast, effect of hydrostatic extrusion on supercond. props. *(Russian)* 77−21215
V_3Ga, composite-processed, with improved current carrying capacities in high mag. fields 79−38272
V_3Ga, development by diffusion processes and use in 17.5 T supercond. magnet 79−61015
V_3Ga, diffusion-processed layer, texture meas. 79−82726
V_3Ga, filamentary conductors, type-II, low temp. 30 GeV proton effects on critical props. 78−52178
V_3Ga, grain size in A-15 reaction layers 78−14911
V_3Ga, high current density multifilament wire, neutron effects on equilibrium and transport props. 78−52126
V_3Ga, high-current A-15 microcomposite material 80−44781
V_3Ga layer on bronze, diffusion of Ga *(Russian)* 80−65297
V_3Ga, long-range order parameter variations determ. and correls. with supercond. T_c 77−11504
V_3Ga multifilament superconductors, AC losses 79−60979
V_3Ga, multifilament superconductor, pulsed mag. field losses and critical current densities 80−54853
V_3Ga multifilament wire, crit. current props. above 4.2K 77−32135
V_3Ga, multifilamentary high-field superconductor, status of development 79−61004
V_3Ga multifilamentary stranded compd. supercond., design, processing, mech., supercond. props. 77−76999
V_3Ga, multifilamentary supercond., prod. by ECN powder metallurgy method, and props. 77−28762
V_3Ga multifilamentary supercond. wire, fabrication and props., crit. review 79−38271
V_3Ga, multifilamentary wire, stress effect on critical currents 77−80891
V_3Ga, multifilamentary wire, crit. current props. with third element additions 79−61013
V_3Ga, NMR and mag. suscept. *(Russian)* 78−39420
V_3Ga, neutron irrad. effect on upper crit. field and crit. current 77−72954
V_3Ga, neutron irrad. effects on transition temp. *(Japanese)* 79−82707
V_3Ga, neutron irradiation and annealing 78−52130
V_3Ga, nuclear magnetic relaxation, near T_c *(Russian)* 79−42852
V_3Ga, phonon densities of states and Debye temp. calcs. 79−51212
V_3Ga, self-consistent APW band struct. calc. 78−47697
V_3Ga, single crystal prep. by iodine transport, supercond. T_c meas. 78−48294
V_3Ga, structure effects on supercond. props. and electron spectrum *(Russian)* 77−80862
V_3Ga, supercond., μ^+ probe study *(Russian)* 79−7946
V_3Ga, supercond., neutron-induced disorder revealed by isochronal annealing 77−72938

vanadium alloys continued
V_3Ga, supercond., pinning characteristics *(Japanese)* 78−91829
V_3Ga, supercond., prep. from V-Al and Cu-Ga, crit. temp. and field 78−43506
V_3Ga, supercond., projected upper limits to crit. current density 77−36037
V_3Ga, supercond. A15 phase, prep. by controlled precip. 80−81000
V_3Ga, supercond. and high mag. fields 79−87215
V_3Ga, supercond. μSR meas. 79−56667
V_3Ga superconducting composite, bronze process, metallurgy 80−3004
V_3Ga superconducting mutlifilamentary wires, critical current densities 79−69645
V_3Ga superconducting tape, diffusion-processed, cryst. textures, X-ray pole figures 79−11266
V_3Ga superconducting tape, stress effect on critical current *(Japanese)* 80−50020
V_3Ga, superconducting transition temp. and electron density of states 77−32105
V_3Ga, superconducting transition temp., metallurgical processing, struct. 77−63019
V_3Ga, superconductive fixed points for temperatures above 0.5K 79−63221
V_3Ga-Cu, high-current A-15 microcomposite material 80−44781
V_3Ga-Cu, supercond. in situ composites, stress effects on crit. props. 80−65757
V_3Ga-Cu composites, supercond. props. 79−95557
V_3Ga-Nb_3Sn concentric solenoid magnet system, 17.5 T operation 77−26353
V_3Ga-NbN point-contact Josephson junction, fabrication and charact. 78−19189
V_3Ga-V_3Pt, supercond. crit. temp., comp. depend. *(Russian)* 77−59347
V_3Ge, A-15 cpds., nucl. mag. relax. in normal and supercond. state 80−49993
V_3Ge, A-15 struct. supercond., microhardness, bonding 78−76199
V_3Ge, A15 cpd., hydrogenation effects on supercond. transition temp., lattice parameters 80−103772
V_3Ge, Anderson-Gruneisen parameter, from 3rd order elastic const. data 79−33059
V_3Ge, anisotropic thermal vibrations, lattice const. X-ray study 80−34164
V_3Ge, band theory, semiself-consistent band calcs. 78−2406
V_3Ge, bronze-processed, stress-induced enhancement of supercond. T_c 78−64159
V_3Ge film, T_c var. with ^4He irrad. induced defects 77−8220
V_3Ge, forbidden Bragg refls., rel. to supercond. transition temp. 79−15251
V_3Ge, Gruneisen parameter and thermal expansion eval. at room temp. 80−70351
V_3Ge, low temp. props., mag. suscept. and resistance 78−19213
V_3Ge multifilamentary superconductor, formation by composite diffusion process, and crit. temp. determ. 77−85959
V_3Ge, phonon densities of states and Debye temp. calcs. 79−51212
V_3Ge, phonon density of states, temp. depend. 79−42183
V_3Ge, resist. characts. in normal state 78−51963
V_3Ge, superconducting, high transition temp., sputtering 78−15309
V_3Ge, superconducting A-15 type compounds, transition temp., radii ratio and structure *(Chinese)* 80−44752
V_3Ge superconducting film, α-particle induced defects and stoichiometry 77−32101
V_3Ge, superconducting transition temp. and electron density of states 77−32105
V_3Ge, superconducting transition temp., correl. with resist. anomalies and defect struct. 77−47920
V_3Ge, third order elastic consts. 78−88490
$V_3Ge_xOs_{1-x}$, low temp. props. 79−99652
$V_3Ge(Si)$, electron-phonon coupling and supercond. crit. temp. 79−33379
$VH_{0.71}$, Compton profile, electronic struct. *(German)* 78−92140
VH_x, Knight shift and spin-lattice relax. of proton NMR, local electronic environment of protons 77−16194
VH_x, proton Knight shift and mag-suscept., high resolution meas. 77−55716
V_2H, long-range order and β to β' transition, X-ray scatt. obs. 79−95160
$V_2(Hf,Zr)$, Laves phase compounds, electrical resistivity, temperature dependence 78−76047
$V_2(Hf,Zr)$, NMR and mag. susceptibility, density of states determ. *(Russian)* 80−66053
V_2Hf base Laves phase compound tapes, supercond. props., prep. 77−40011
V_2Hf, NMR meas., mag. susceptibility, Knight shift and elec. field gradient determ. *(Russian)* 78−23359
V_2Hf, supercond., fast neutron irrad. effects on T_c 77−55633
$V_2Hf_{1-x}Ta_x$, C15 supercond., electronic and lattice props. 78−68110
V_2HfZr, C-15 cryst. struct. supercond. props. 78−64173
$V_2Hf_{1-x}Zr_x$, normal and supercond. state, transition temps., mag. susceptibility and specific heat determ. *(Russian)* 80−60132
V_3In, hypothetical, electronic struct., lattice parameters and possible supercond. transition temp. 79−23891
$V_{0.62}Ir_{0.38}$, supercond., Knight shift contrib. to reson. line shift meas. 77−4467
V_xIr_{1-x}, nuclear spin-lattice relax. time, electronic density of states 77−59354
$V(Ir_{1-x}Pt_x)_3$, mag. props., ferromagnetism, comp. depend. 77−77039
$V(Ir_{1-x}Pt_x)_3$, NMR study of ferromag. 79−65760
V_3M, M = Si, Sn, Ge, Ga, Al, electronic struct., electron-phonon interactions and X-ray spectra 78−91613
$V_{3-x}M_xGa$, M=Ti, Cr, Mn, Fe, Co, Ni, cryst. struct. and microhardness meas. 79−86740
$V_{75-x}M_xGa_{25}$, M=Ti, Cr, Mn, Fe, Co, Ni, supercond. transition temp. and electron-phonon coupling parameter 79−60952
δ-VMn, ordering and disordering behaviours 77−48428
V_xMo_{1-x} solid soln., mag. susceptibility 79−91208
$V_{16}N_{1.5}$ solid solution, quenched, ordered structure *(Russian)* 80−88086
VNb-NbO_x-Pb Josephson tunnel junction, compared with VNb-VO_x-Pb 79−87203
$V_{2-x}Nb_3Hf$, NMR of ^{51}V and mag. susceptibility, 20-300K *(Russian)* 80−93192
$V_{77}Ni_{23}$, nuclear spin-lattice relax. time, electronic density of states 77−59354
α-$V_{0.97}O_{0.03}$ solid soln., impurity vibrs., inelastic neutron scatt. study 80−92635

vanadium alloys continued
$V_{50}O_{50}$, nuclear spin-lattice relax. time, electronic density of states 77−59354
V_3Pd, nuclear spin-lattice relax. time, electronic density of states 77−59354
$V_{0.76}Pt_{0.24}$, supercond., Knight shift contrib. to reson. line shift meas. 77−4467
$V_{1-x}Pt_x$, A-15 cpds., nucl. mag. relax. in normal and supercond. state 80−49993
$V_{1-x}Pt_x$, A-15 struct., Knight shift in normal state, upper crit. field curves *(French)* 78−43519
V_3Pt, supercond., Knight shift contrib. to reson. line shift meas. 77−4467
V_xPt_{1-x}, nuclear spin-lattice relax. time, electronic density of states 77−59354
V_3Rh, nuclear spin-lattice relax. time, electronic density of states 77−59354
VRu, soft X-ray emission, photoelectron spectra and electron structure 79−37978
VSi_2 thin film growth rel. to annealing environment and interposed layers 78−2395
VSi_2-Si interfaces, chemical state, AES expts. 78−91767
VSi_3, cubic-tetragonal phase transition two-band (s-d) model 79−56193
$V_{1-x}Si_x$, A-15 cpds., nucl. mag. relax. in normal and supercond. state 80−49993
V_3Si, ^4He induced damage, channelling effect meas. 77−62570
V_3Si, A 15 compound, Raman scatt. and phonon density of states 79−28768
V_3Si, A-15 struct. supercond., microhardness, bonding 78−76199
V_3Si, A-15 supercond. cpd., martensitic transform. 79−60499
V_3Si, A15 compound, exam. of deformation processing, review 78−39864
V_3Si, A15 compound, microscopic model of supercond. and martensitic transform. 77−8226
V_3Si, A15 cpd., hydrogenation effects on supercond. transition temp., lattice parameters 80−103772
V_3Si, Anderson-Gruneisen parameter, from 3rd order elastic const. data 79−33059
V_3Si, anharmonic contrib. to mode softening 79−73241
V_3Si, band theory, semiself-consistent band calcs. 78−2406
V_3Si based ternary solid soln., supercond. T_c and paramag. susceptibility *(Russian)* 77−59348
V_3Si bridge contacts, nonstationary props. 80−103793
V_3Si, CDW instability and anharmonicity 78−79734
V_3Si, channelling, at displacements and electron phonon/defect interactions 77−84815
V_3Si, chemical composition effect on phase transition and transition temp. 78−14860
V_3Si, complex refr. index and reflectivity of thin film, microscopic charcts. and superconductivity 78−31267
V_3Si, Czochralski growth, supercond. behaviour 79−74080
V_3Si, d-spacing fluctuations above Martensitic phase transition 80−7570
V_3Si, de Haas van Alphen meas. of Fermi surface for H≤40 T 79−73424
V_3Si, de Haas-van Alphen oscills. in normal state 79−56116
V_3Si, dislocations, obs. by TEM 77−59012
V_3Si, E_g optical phonon, Raman scatt. meas. 79−24316
V_3Si, EFG and band struct. 77−35861
V_3Si, elec. resist. below 77K, phonon assisted interband scatt. 78−14703
V_3Si, electrical resistivity, saturating contrib. from electron-phonon interactions 80−2376
V_3Si, electron charge distrib., martensitically transforming single cryst., X-ray diffr. meas. 78−75631
V_3Si, electron energy loss spectra, AES and HEED investig. of surface 77−24635
V_3Si, electron spectrum charcts., mag. susceptibility depend. on resistivity ratio 79−95320
V_3Si, electronic props. calc. 79−7780
V_3Si, electronic struct., electron-phonon interaction and high temp. superconductivity, APW calc. 78−14871
V_3Si, electronic struct., charge distrib. and X-ray emission spectra 79−51481
V_3Si electronic struct. from three-dimens. k.p model 78−84139
V_3Si embedded in resin, composite supercond., high transition temp. 80−88660
V_3Si, exam. of superconductivity and props. 79−1649
V_3Si, far IR transmission spectrum 77−38041
V_3Si, Fermi surface, positron annihilation study 79−4869
V_3Si, Fermi surface, positron annihilation meas. 79−87039
V_3Si, Fermi surface determ. by positron annihilation 80−2326
V_3Si, Fermi surface studies by the positron annihilation technique 79−82515
V_3Si, Fermi surface topology, positron annihilation meas. 79−56117
V_3Si film, far IR reflection and transmission spectra, room temp. 77−55792
V_3Si film, optical props. *(Russian)* 80−93418
V_3Si film, quasiamorphous, supercond. phase formation by heat pulse 77−63017
V_3Si film, sputtered, high press. induced shifts in supercond. transition temp. 77−85374
V_3Si film, superconductivity 78−72299
V_3Si film, superconducting props. 79−38215
V_3Si film, T_c var. with ^4He irrad. induced defects 77−8220
V_3Si formation by bronze process 77−86032
V_3Si, grain size in A-15 reaction layers 78−14911
V_3Si, grown-in dislocations, diffr. contrast behaviour 79−86794
V_3Si, Gruneisen parameter and thermal expansion eval. at room temp. 80−70351
V_3Si, H_{c2} anisotropy in high field, grain boundary flux pinning 78−43532
V_3Si, Hall effect, 77K to superconducting transition temp. 78−43359
V_3Si, He irrad., computer simulation of channelling 79−55800
V_3Si, heat capacity rel. to temp. *(Russian)* 78−52152
V_3Si, high T_c supercond., electron-phonon coupling, effect of electronic density of states sharp struct. 78−14877
V_3Si, intra-atomic Coulomb interaction effect on band type of Jahn-Teller effect 79−78057
V_3Si, ion irradiated, influence on struct., resist., and supercond. transition temp. 80−54823
V_3Si, lattice defect, high voltage electron microscopy *(French)* 79−27993

vanadium alloys continued
V_3Si, lattice dynamics, inelastic coherent neutron scatt. 78−26645
V_3Si, low fluence neutron irradiation, behaviour of supercond. transition temp. 78−43509
V_3Si, low temp. irrad. with 20 MeV S ions, effect on supercond. props. 79−38223
V_3Si, low temp. sp. heat and thermal cond. 77−15995
V_3Si, martensitic transform. coupling with supercond. transition 78−44126
V_3Si, martensitic transform., thermal expansion meas. in normal and supercond. states 79−56381
V_3Si, mixed state, ultrasonic anomaly 77−55644
V_3Si, mixed state A15 struct., Gibbs free energy and lower crit. field temp. depend. 77−55643
V_3Si, Mossbauer spectra of ^{57}Fe *(Russian)* 79−24235
V_3Si, NMR meas. near struct. transform. *(Russian)* 80−44942
V_3Si, NMR of ^{51}V above and below 21K struct. transition *(Russian)* 80−34796
V_3Si, neutron irrad., grain boundary pinning, field-depend. change of crit. current density 80−65759
V_3Si, neutron irrad., neutron diffraction studies 78−88076
V_3Si, neutron irrad., sound velocity, magnetic susceptibility and upper critical field 78−88074
V_3Si, neutron irrad., volume pinning force, summation and saturation behaviour 79−95554
V_3Si, neutron irrad. effects on transition temp. *(Japanese)* 79−82707
V_3Si, neutron irradiated, A15 compound, recovery of T_c by annealing 78−52132
V_3Si, neutron irradiated single crystal, superconducting transition temp. widths, resistivity and heat capacity meas. 78−91802
V_3Si, neutron-irrad., ht. capacity and resistivity 78−88075
V_3Si, nontransforming, press.-induced phase transformation 78−80084
V_3Si, normal, mixed and supercond. state, specific heat meas., thermodynamic and superconducting props. 80−49987
V_3Si, normal state, Fermi surface, de Haas-van Alphen oscills. 79−65369
V_3Si, normal state resistivity as function of neutron irrad. 79−56194
V_3Si, nuclear magnetic relaxation, near T_c *(Russian)* 79−42852
V_3Si, phase transition and transition temp., chemical comp. effects, defect struct. exam. 78−18651
V_3Si, phonon densities of states and Debye temp. calcs. 79−51212
V_3Si, phonon density of states at 300K, mode softening 77−11648
V_3Si, phonon density of states, temp. depend. 79−42183
V_3Si, phys. props., appl. of new three-dimens. k.p model for A-15 cpds. 78−23015
V_3Si, plastic deform. effect on supercond. props. 80−29500
V_3Si, positron annihilation lifetime meas. 79−19946
V_3Si, powdered, Debye-Waller factors and lattice consts., 25-1000K, X-ray diffr. obs. *(German)* 79−33060
V_3Si, press. depend. of positron lifetimes 78−11015
V_3Si single cryst., A-15 compound supercond., plastic deform., at high temp. 79−20104
V_3Si, single cryst., anharmonicity determ. from X-ray refl. intensities 79−73284
V_3Si, single cryst., computer simulation of channelling meas. 79−51180
V_3Si single cryst., creep deform. 80−71695
V_3Si, single cryst., double supercond. transitions 79−28430
V_3Si, single cryst. growth by electron beam melting 78−64467
V_3Si single crystal, radiation damage and superconductivity 78−52129
V_3Si single crystals, channelling effect studies using He ions and $^{28}Si(d,p_8)$ reaction 79−4362
V_3Si, single crystals, supercond. tunnel charcts. 80−7044
V_3Si single crysts., elec. resist. and Hall coeff., temp. depend., 17-300K *(Russian)* 77−69292
V_3Si, soft mode sound vel. in mag. field rel. to density of states 78−14647
V_3Si, sp. ht. anomaly at struct. transform. 78−14426
V_3Si, static compressibility, up to 20 kbar 77−43281
V_3Si, supercond., crit. fields Pauli paramag. limiting and material parameters 79−78277
V_3Si, supercond., sp. ht. meas., internal heating effect obs. in mixed state 77−12067
V_3Si, supercond. and struct. transitions *(Russian)* 78−52118
V_3Si, supercond. film, electron beam codeposition, synthesis and props. 78−72296
V_3Si, supercond. mixed state, low temp. tetragonal-domain-reorientation phenomena, US expts. and thermal props. 80−60141
V_3Si, supercond. props., effect of neutron irrad. 80−80463
V_3Si, supercond. structure and properties *(German)* 80−93631
V_3Si, supercond. tape, growth technique via amorphous state 78−84708
V_3Si, supercond. transition temp. and phase transform. at press. up to 45 kbar 79−56352
V_3Si, superconducting, optical props. and electron-phonon interactions 80−2510
V_3Si superconducting bridge junctions, vortex model appl. *(Russian)* 79−60986
V_3Si, superconducting diffusion wires, high field expts. on press. effects up to 15 kbar 79−61006
V_3Si superconducting film, α-particle induced defects and stoichiometry 77−32101
V_3Si superconducting props. and structural transition *(Russian)* 77−12052
V_3Si, superconducting thin films, energy gaps from tunnelling meas. 80−25050
V_3Si, superconducting transition temp. press. depend., for shear-stress induced tetragonal phase 77−36010
V_3Si, superconducting transition temp., correl. with resist. anomalies and defect struct. 77−47920
V_3Si superconductor film, Fourier and laser spectroscopy comparison in far IR-sub. mm. range 79−93237
V_3Si, temp. depend. of mag. susceptibility *(Russian)* 77−36053
V_3Si, thermal expansion, 20-300°C, using differential push-rod dilatometer 80−39320
V_3Si, thermal expansion meas., 4.2 to 293K 79−56382
V_3Si, thermodynamic props. determ. using ternary phase equilibria 78−91449
V_3Si, thermodynamic study, intrinsic type II superconductivity 79−47193
V_3Si thin film far IR laser thermal spectroscopy 80−60144
V_3Si thin films, Holstein processes and electron-phonon spectral function, far IR meas., 19K 79−87445

vanadium alloys continued
V_3Si, thin films in supercond. and normal states, far IR laser spectroscopy 79−61453
V_3Si, third order elastic consts. 78−88490
V_3Si, transforming and nontransforming, high press. effects 78−80086
V_3Si tunnel junctions, energy gap investigation 80−84569
V_3Si, US anomaly when cooled below martensitic and supercond. transition temps. 80−20354
V_3Si, V_3Sn, V_3Ge, V_3Ga, V_3Al, electronic struct., electron-phonon interacs., X-ray spectra 78−91613
V_3Si volume changes during phase changes, meas. low temp. differential scanning dilatometer *(Russian)* 79−34224
V_3Si, X-ray emission spectra, electron struct. 77−48278
V_3Si, XPS and APS of valence band 77−20994
V_3Si-Fe, mag. impurities effect on supercond. props. 77−1524
V_3Si-M, M=Hf, Nb, Ta, Mo, W, Ni, Ge, Sb, cryst. struct., supercond. T_c comp. depend. 78−51494
V_3Si-SiO_x-Mo_3Re_2, supercond. tunnel junctions 80−107961
V_5Si_3, thermodynamic props. determ. using ternary phase equilibria 78−91449
$V_3(Si_{1-x}C_x)$, bulk, effect of C on supercond. transition temps. and microstructure 80−54824
$V_3Si(Ga)$, coherence parameter, nonlinear high temp. supercond. elements with A-15 lattice *(Russian)* 80−60127
$V_3Si(Ge)$, A-15 compounds, interlattice displacements, elastic consts. 78−55906
$V_3Si(Ge)$, plasma energies, tight-binding energy-band model 78−84159
$V_3Si_{1-x}Ge_x$, elastic props., 77 to 290K, rel. to supercond. transition temp. *(Russian)* 80−66560
$V_3Si_{1-x}Ge_x$ solid soln., longitudinal and transverse US wave propag. rate, 4.2 to 300K *(Russian)* 80−103423
$V_3Si_xOs_{1-x}$, supercond. transition temp. and paramag. susceptibility 79−28436
V_3Sn, A-15 cpd., normal-state elec. resist. 80−75542
V_3Sn, elec. resist., temp. depend., T_c to 300K 79−65426
V_3Sn, ultrafast quenched and subsequently tempered, supercond. T_c 78−64162
$V_3Sn_{0.5}Al_{0.5}$, elec. resist., temp. depend., T_c to 300K 79−65426
VTi alloys, blister behaviour during 200, 2000 keV He irrad. temp. depend. 77−35607
V_3Ti, metastable supercond. phase, effects of rapid quenching on transition temp. 78−2611
$V_{2.4}Ti_{0.6}Sn$, elec. resist., temp. depend., T_c to 300K 79−65426
$V_{0.97}U_{0.03}$, phonon spectrum, quasi-local vibrs., inelastic incoherent neutron scatt. 77−15519
V_2Zr, NMR meas. mag. susceptibility, Knight shift and elec. field gradient determ. *(Russian)* 78−23359
$V_2Zr(Hf)$, struct. transform. at low temp., X-ray diffr. anal. *(Russian)* 80−45298
Ve-Fe-Ga system, phase obs. at 800 and 820°C *(Russian)* 78−23662
Zr-Al-V, H sorption props. for H storage, influence of Al 80−45794
Zr-Mo-Nb-V-Sn (1,2,2,2 wt.%), heat treatment, transform. reactions and mech. props. 79−24545
Zr-Nb-V-Al (Fe) alloys, decomp. of β solid soln., metastable and equilib. phases 79−11632
Zr-Nb-V-Fe (12 wt.%, 6 wt.%, 4 wt.%), struct. changer during decay of BCC β solid soln. 79−15669
Zr-Nb-V-Si superconductor, struct. determ. by optical microscopy and electron diffraction *(Russian)* 77−16628
Zr-V, superconductivity and metallurgy of C15 materials 79−4610
Zr-V foil, rapidly quenched and heat treated, supercond. props. 80−54852
Zr-V-H, synthesis at high H pressure exam. of props. 80−29924
$Zr(Co_xV_{1-x})_2$, H absorption and desorption props. 77−55448
$Zr(Fe_xV_{1-x})_2$, H absorption and desorption props. 77−55448
$Zr_xHf_{1-x}V_2$, polycrystalline superconductor, resist. and mag. susceptibility, transition temp., temp. depend. 80−25113
$Zr(V,Al)_2$, struct., supercond. props., elec. resist. and mag. susceptibility, 4.2 to 300K *(Russian)* 79−15246
$ZrV_{2.2}$, supercond., dielec. phase transition *(Russian)* 78−64168
ZrV_2, anomalous softening at martensitic transform. 80−93630
ZrV_2, C-15 struct., phase transitions, elec. cond., crystal lattice parameters *(Russian)* 80−54826
ZrV_2, C15 supercond., dielec. transitions, temp. depend. of resist. and mag. susceptibility, 4.2-300K 79−38136
ZrV_2, dielectric phase transition, elec. resist. temp. depend. 79−65525
ZrV_2, elec. resist. and mag. suscept., anomalous temp. depend. 79−69491
ZrV_2, Knight shift vs. susceptibility plot 80−75712
ZrV_2, latent heat of structural transform. 80−24589
ZrV_2, Laves-phase, cubic to rhombohedral transition, lattice electron instability 78−92261
ZrV_2, supercond. rel. to struct. instability *(Russian)* 78−23196
$Zr(V_{1-x}Co_x)_2$, relation between electronic struct. and H_2 storing props. 80−76662
$Zr(V_xCo_{1-x})_2$, Laves phase, phenomenological model for H_2 absorption capacity 77−84935
$ZrV_2D_{4.5}$, deuterated cubic Laves phase, D atom distrib., neutron diffr. anal. 80−29006
$ZrV_2D_x(H_x)$, site occupation modes and cryst. struct., neutron diffr. study 80−59440
$Zr(V_xM_{1-x})_2$ (M=Fe, Co), H_2 absorpt. capacity 80−88433

vanadium compounds
see also vanadium alloys
alkali bromide-VBr_2 systems, cryst. struct., DTA investig. *(German)* 78−72766
alkali halide:VO^{2+}, impurity behaviour, elec. cond. and IR absorpt. obs. 77−8607
alkali metal complex vanadates, $M^+{}_3M^{3+}(VO_4)_2$, $M^+{}_2M^{4+}(VO_4)_2$, M^{3+}=Sc, La, B, Al, Ga, In, M^{4+}=Ti, Zr, Sn, phosphors 77−48217
alkali metal vanadium fluoride bronzes, cryst. struct. examination by electron diffr. using TEM 79−23583
alkali metal-V_2O_5 bronzes, single cryst., elec. cond., 300 to 900K 77−20369
anodised layer, structure and stoichiometry, thickness effects 77−77634
deuteride, Compton profiles 79−8206
guanidinium vanadium sulphate hexahydrate, mag. behaviour in applied fields below 1K 77−66376
guanidinium vanadium sulphate hexahydrate, singlet ground state system, low temp. mag. props. 80−44843
guanidinium vanadium sulphate hexahydrate, susceptibility meas. spin-lattice relax. effects 77−66279
hexa-urea aluminium complex: VO^{2+}, cryst., one-dimens. interactions, EPR 77−73074
hexacarbonyl, EPR in frozen glasses, optical spectra in soln., solid, assoc., bonding 77−6807
hexaurea aluminium perchlorate:VO^{2+}, single cryst. ESR 77−16158
hydride, temperature limits for stable existence, ionic state *(Russian)* 77−7690
oxide, phase transformation interference reversible light reflector material, visualisation of CW EM radiation 79−71531
oxides, change in phonon damping due to metal-insulator transition 80−103625
oxides, FTIROS, polarisation of recorded image spectrum 77−75439
oxides, FTIROS thermochromic materials, colour and visual contrast 80−33100
oxides, XPS and AES study, electron correl. effects, semicond.-metal transition 80−7467
oxides, XPS study, electron binding energies, spin orbit splittings, exchange splittings 79−78839
oxides mixture, thermochromic material, appl. to laser beam indicator/visualiser 80−9976
oxovanadium carboxylates, near one-dimensional antiferromagnetism, thermal and mag. props. calc. 77−20602
oxygen bronzes of type $M_xV_{12}O_{30}$, synthesis and thermal props. of single crysts. 77−84717
phthalocyanide, thermal stability obs., by DTA *(German)* 80−11945
potassium oxalate, VO^{2+} EPR spectra 80−39858
potassium oxalate monohydrate:VO^{2+}, cryst., IR absorpt. 80−55134
rare earth vanadites, X-ray fluoresc., IR and UV spectra 77−77206
refractory carbides, borides and nitrides, wetting by and interactions with liq. metals 80−54473
resin:VO^{2+}, interaction with ligands, EPR meas. 78−10756
slag enrichment by oxide reduction during plasma melting *(Russian)* 78−52716
TGS:VO^{2+}, polarisation reversal, static hysteresis loops, switching, EPR 78−43633
transition metal vanadates, elec. and mag. props., stoichiometry 78−51991
tris sarcosine calcium chloride:VO^{2+}, EPR and absorpt. spectra 78−60330
V_2O, semicond.-metal transition, hysteresis effects, appl. in optical information storage 78−88006
V-V_xO_y-Pb tunnel junctions, IV characts. of SQUID 79−19704
vanadyl alkanoates, ^{51}V NMR, quadrupole splitting in nematic phases 79−28637
vanadyl bisacetylacetonate, frozen soln., proton ENDOR, ligand hyperfine tensors 79−99792
vanadyl bisacetylacetonate, polarised X-ray absorption and double refraction 80−50459
vanadyl carboxylates, EPR and mag. susceptibility, near one-dimens. antiferromagn. 77−63265
vanadyl octaethylporphyrin, radical cation EPR linewidth inversion, relax. theory 77−10693
vanadyl phthalocyanine, exciton electroabsorpt., optical density spectra 77−85746
vanadyl phthalocyanine, sublimed layer, IR absorption, vibr. assignments 78−55174
vanadyl porphyrins, anion radicals and dianions, reson. Raman spectra 77−471
VI_2, mag. structs. and props. 79−61063
XPS, p-shell, multiplet struct. 78−76580
$24BaO.V_2O_5.25P_2O_5$, ESR and absorpt. spectra, V(IV) ions conc. 78−64266
$24CaO.V_2O_5.25P_2O_5$, ESR and absorpt. spectra, V(IV) ions conc. 78−64266
$Ag_xV_2O_5$, diffusion of Ag 77−20120
$Ag_xV_2O_5$, thermodynamic, elec. and electrochem. props. 78−84265
Al_2O_3-V_2O_3-VO_2 system, phase equil. at 1273K *(French)* 77−35668
$(Al_xV_{1-x})_2O_3$, heat capacity anomalies, metal-insulator transition, phase diagram 77−11701
AuV, gas, bond dissoc. energy, from high-temp. mass spectra of V-Nb-Mo-Au 79−45860
B_2O_3-V_2O_5, thermal cond. of melt in region 900 to 1100°C, effect of convection 78−2309
B_2O_3-V_2O_5-P_2O_5, glass, mech. and elec. props 80−84228
$BaBr_2.2H_2O:VO^{2+}$, EPR meas. 77−16145
$BaCl_2.2H_2O:VO^{2+}$, EPR meas. 77−16145
BaO-Al_2O_3-B_2O_3-V_2O_5 glass, spectra, oxidation-reduction behaviour, DC cond. 77−76814
BaO-B_2O_3-V_2O_5 glasses, polaron hopping cond., optical absorpt. and ESR spectra 79−23966
BaO-B_2O_3-V_2O_5(Fe_2O_3)(Cu_2O), glass, resist. and activation energy, reduced valency 77−51749
BaO-K_2O-VO_2-SiO_2, glass, elec. cond. rel. to ion polarisability, polarons 80−49729
BaO-$La_{0.6}O$-VO_2-SiO_2, glass, elec. cond. rel. to ion polarisability, polarons 80−49729
BaO-V_2O_5-CuO, P_2O_5-V_2O_5-CaO-CuO glasses, EPR, Cu impurity effect on elec. props. 79−51849
BaO-V_2O_5-CuO semiconducting glasses, impurity effects, elec. resist. and EPR study 80−103692
$BaVS_3$, polycrystalline, elastic behaviour, 40 to 350K 79−60498
$BaVS_3$:Fe, Mossbauer and mag. studies, electronic state of Fe 80−108130
$BaVSe_3$, one-dimensional, struct. and mag. props. 80−28993
$Ba(V_{1-x}Ti_x)S_3$, synthesis and struct. phase transitions 80−107415
BeO-Al_2O_3 V_2O_5, mixture kinetics and mechanism of formation of cryosoberyl 79−11535
Bi_2O_3-V_2O_5, sintered, high oxide ion cond. meas. 78−14503
β'-$Cu_xV_2O_5$, mag. and spectroscopic study, semiconductor to metal transition 80−2628
$C(NH_2)_3V(SO_4)_2.6H_2O$, low temp. mag. props., mag. sp. ht. *(Japanese)* 78−19268
CO_2, metallic, one-electron dispersion relations 77−62794
$Ca_{2x}Bi_{3-2x}Fe_{5-x-y}V_xIn_yO_{12}$, ferromagnetic relax. meas., 4.2-300K 80−44923
$Ca_3Fe_{3.5}V_{1.5}O_{12}$, ferrogarnet, crystallisation field in CaO-V_2O_5-Fe_2O_3-PbO 77−16548

vanadium compounds continued
- $CaO-B_2O_3-Al_2O_3-V_2O_5$ glass, cond. mechanism, current carriers, V_2O_5 conc. effects 77−62668
- $CaO-V_2O_5-Fe_2O_3-PbO$, crystallisation field of Ca-V ferrogarnet 77−16548
- $CaO-V_2O_5-SiO_2$ system, compatibility triangles 80−81037
- $CaO.V_2O_5$, reduction by Al powder for V production 78−44049
- $Ca_3Ti_{2x}V_{1.5-x}Fe_{3.5-x}O_{12}$, garnet, mag. and neutron diffraction investigation 77−16044
- CaV ferrite garnet, large grained, mag. props. 78−64222
- CaVG, polycryst. IR transmission spectra rel. to Faraday rotator and modulator appl. 78−10900
- $(CdSO_4)_3.8H_2O:VO^{2+}$, polycryst., struct., EPR 78−15014
- Co salts:VO^{2+}, EPR, spin-lattice relax. time meas., 180-380K 78−64268
- $CoK_2(SO_4)_2.6H_2O:VO^{2+}$, ESR, ion orientations 78−48029
- $Cr_2O_3-V_2O_3-VO_2$ system, phase equil. at 1273K *(French)* 77−35668
- $Cr_{1-x}V_xN$, solid soln., mag. struct. *(French)* 78−6519
- $Cr_{1-x}V_xN$ solid solution, X-ray diffr. structure exam. at low temp., deformation study *(French)* 78−2069
- $(Cr_{1-x}V_x)_5S_6$, mag. props. 77−69548
- CsV primary clock performance of NRC 77−74370
- $CsVCl_3$, antiferromag. coupling in linear chains, molecular orbital approach 78−52239
- $CsVI_3$, Mossbauer spectra, struct., electronic and mag. props. 79−91320
- $CsVI_3$, Mossbauer spectra, struct., electronic and mag. props. 80−15908
- $CuO-V_2O_5-P_2O_5$ glass, elec. cond. and switching *(Japanese)* 80−34492
- α-$Cu_xV_2O_5$, EPR and mag. susceptibility meas. 80−2627
- $Cu_xV_2O_5$, nonmetallic bronze, low field sp. ht. and mag. suscept. 78−72357
- CuV_2S_4, preparation, cryst. struct. and physical props. *(French)* 79−55714
- $Cu_{0.75}VS_2$, cryst. struct. and phys. props. *(French)* 78−14328
- Cu_3VS_4, out of equil. mixed cond., off-centre positions and order-disorder transition, ultrafast nucl. relax. obs. 80−108103
- Cu_3VS_4, out of equil. mixed cond., chem. origin of mobile ions, spin-lattice relax. and NQR obs. 80−108104
- Cu_3VS_4, Raman active modes 80−11414
- $Eu_3VTa_2O_9$, prep., characterisation and mag. props. 78−26535
- (Fe, Mn)-V spinels, complex, oxidation, effect of Cr_2O_3, TiO_2, MgO additions 79−43453
- $FeCs_2(SO_4)_2.6H_2O:VO^{2+}$, EPR, spin Hamiltonian parameters 79−19771
- $Fe_xNb_xV_{2-2x}O_4$ complex solid solns., synthesis and phase diagram, semicond.-metal transition temp. 79−43214
- $Fe_xNb_xV_{2-2x}O_4$, NMR analysis of semiconductor transitions 78−52367
- $Fe_2O_3-PbO-V_2O_5$ fluxed melt system, solubility and relative supersaturation meas. 80−64934
- $Fe_2O_3-V_2O_5$ system, elec. transport 79−51576
- $Fe_xTa_xV_{2-2x}O_4$ complex solid solns., synthesis and phase diagram, semicond.-metal transition temp. 79−43214
- $Fe_{1+x}V_{2-x}O_4$ spinels, prep. and negative resist. charact. *(Korean)* 78−39119
- $Fe_xV_{1-x}O_2$, X-ray diffr. obs. 77−27858
- $Fe_xV_{2-x}O_4$ solid solutions, specific heat near semiconductor-metal transition 80−24612
- θ-$Fe_xV_2O_5$, spin glass and paramag. props., susceptibility, EPR and Mossbauer studies 80−75782
- $(Fe_xV_{1-x})V_2S_4$, and $(Fe_xV_{1-x})V_4S_8$, mag. props. 78−27034
- $Ga_xV_{1-x}O_2$, resistivity, EPR, enthalpy and entropy meas., rel. to semicond.-metal transition 78−88004
- HfV_2D_4, disordered solid solution, order-disorder transition 80−88321
- KCl-NaCl-NaF-K_2NaVF_6 system, phase diagram 79−66049
- $KH_2PO_4:VO^{2+}$, EPR spectra, Hamiltonian parameters, ferroelec. transition 78−39387
- $KH_3(SeO_3)_2:VO^{2+}$, electron spin reson. obs. 78−80196
- $K_2O-V_2O_3-Al_2O_3$ melt, soln. of Al_2O_3 single crystal 80−20910
- $K_2SO_4:VO^{2+}$, polycryst., struct., EPR 78−15014
- $Li_{0.5}Fe_{2.5}O_4-Bi_2O_3(V_2O_5)$ systems, phase diagrams, sintering conditions 78−35366
- $LiH_3(SeO_3)_2:VO^{2+}$, ferroelectric, 298K, EPR 79−51846
- $Li_xM_yV_{1-y}S_2$ (M=Fe, Cr) physical props., effect of metal substitution of Li intercalation 79−100395
- $Li_2O-V_2O_5-Al_2O_3$ melt, soln. of Al_2O_3 single crystal 80−20910
- $Li_xV_{1-y}Fe_yS_2$, intercalated battery cathode material, Mossbauer studies 80−44984
- $Li_xV_2O_5$ ($0.1<x<1.0$), phase relationship in ambient temperature system 80−20912
- β-$Li_xV_2O_{5-y}$ bronzes, thermodynamic props. by coulometric titration 80−34209
- $LiVS_2$, intercalation cpd., NMR 77−90048
- $Li_2VS_2(Se_2)$ based topochemical cells, low voltage behaviour 79−92069
- Li_xVSe_2, intercalation cpds., electron chem., ionicity 80−89501
- $Mg(NH_4)_2(SO_4)_2.6H_2O:VO(H_2O)_5^{2+}$, proton ENDOR meas. used to determine hyperfine coupling tensors 80−66075
- $Mg(NH_4)_2(SO_4)_2.6H_2O:VO^{2+}$, polycryst., struct., EPR 78−15014
- $MgO-V_2O_5$ system, heat treated, EPR meas. *(Russian)* 77−90025
- $NH_4H_2PO_4:VO^{2+}$, EPR of VO^{2+} ions in antiferroelec. cryst. 79−47329
- $NH_4HSO_4:VO^{2+}$, ferroelastic, inernal strains, ferroelec. transitions, EPR 79−47400
- $(NH_4)_2SO_4:VO^{2+}$, EPR spectrum, temp depend. 110-300K 80−11249
- $(NH_4)_2SO_4:VO^{2+}$, ferrielectric phase transition, two-sublattice model, EPR of polar VO^{2+} probes 78−48127
- $(NH_4)_2SeO_4:VO^{2+}$, EPR spectrum 79−61207
- Na-V-O system, low O_2 potential 77−50238
- $NaH_3(SeO_3)_2:VO^{2+}$, ESR spectra 79−4718
- $Na_2O-SiO_2:VO^{2+}$ glass, optical absorption spectra *(Japanese)* 78−42918
- $Na_2O-V_2O_5-Al_2O_3$ melt, soln. of Al_2O_3 single crystal 80−20910
- $Na_2O-V_2O_5-(VO_2)_2-V_2O_3$, phase comp. and equilib. 80−35172
- $NaVO_3-BaV_2O_6-SrV_2O_6$, phase diagrams, simple eutectic system 78−48379
- $Na_{0.33}V_2O_5$, quasi-one-dimensional conductor, anisotropic cond. meas., 18-400K 77−85204
- $Na_xV_2O_5$ β-phase single cryst., phase transitions EPR meas. 78−95514
- $Na_xV_2O_5$, nonmetallic bronze, low field sp. ht. and mag. suscept. 78−72357
- $Na_3V_2(PO_4)_3$, synthesis and cryst. struct. *(French)* 79−32964
- $NaVS_2$, intercalation cpd., NMR 77−90048
- Na_xVS_2, intercalation cpd., mag. phase transitions 77−69558
- Na_xVS_2, mag. and elec. props. rel. to struct. transitions 78−91848
- Na_xVS_2, Na_xVSe_2, charge density waves, electron localisation 79−47038
- $Na_xVS_2(Se_2)$, intercalation compounds, phys. props. 80−44179

vanadium compounds continued
- Na_xVSe_2, intercalation cpd., mag. and structural phase transitions 77−69558
- Na_xVSe_2, mag. and elec. props. rel. to struct. transitions 78−91848
- $Na_2V_2Ti_6O_{16}$, characterisation and mag. props., 90-800K, $Na_xTi_4O_8$ bronze isotypes *(French)* 80−39735
- $Na_2Zn(SO_4)_2.4H_2O:VO^{2+}$, EPR spectra at X-band, spin-Hamiltonian parameters 79−56606
- $Na_3[V(NCS)_6].12H_2O$, single crysts., X-ray diffr. cryst. struct. anal. 78−95021
- $Nb_2O_5-V_2O_5-P_2O_5$, glasses and glass ceramics, elec. cond., struct. 80−84466
- NbV-VO_x-Pb Josephson tunnel junction, VO_x effect on props. 79−87203
- $Nb_{1-x}V_xSe_2$, elec. and mag. anomalies at CDW transition 80−107722
- $Nb_{0.87}V_{0.13}Se_2$(4Hb), stacking layer study, appl. of convergent beam electron diffr. 80−39116
- α-$PVW_{17}O_{40}^{5-}$, α_2-$P_2VW_{17}O_{12}^{8-}$, aq. soln., hydrodynamic radii from ESR line width 79−78504
- $RbH_3(SeO_3)_2:VO^{2+}$, EPR spectra, spin Hamiltonian parameters 80−100609
- Si-V_2O_5 p-n heterostructure, photocond. *(Russian)* 79−42622
- Si-V_2O_5-Al, current-voltage characts., oxide film effects 80−70841
- SnCaV garnet polycrystal, ferrimag. resonance loss rel. to grain size 77−85581
- SnO_2-VO_x-PdO ceramic, switching and oscill. phenomena 78−6417
- $Sr_3VTa_2O_9$, prep., characterisation and mag. props. 78−26535
- TeO-V_2O_5 glass system, X-ray diffr. study 79−10805
- $TeO_2-MoO_3-V_2C_5$, phase comp. determ. using X-ray diffr., electron microscopy and DTA *(German)* 80−88046
- $TeO_2-V_2O_5$ glass threshold devices, reversible monopolar switching 80−2434
- $TeO_2-V_2O_5-Fe_2O_3$ system, phase equilib. and analysis, primary crystn. fields 77−66628
- $TeO_2-V_2O_5-Li_2O(Na_2O)(K_2O)(Cs_2O)(Ag_2O)$, glass, IR spectra of crystalline phases 79−38536
- (Ti,V)C, activated reactive evaporation deposited films, annealing study, microstructure 80−24762
- (Ti,V)C carbides, prep. and mech. props. 78−64518
- $(Ti,V)_2O_3$, magnetisation, field and temp. depend., down to 1.6K 77−8284
- Ti-V-C-N, solid solns., quasibinary cross sections 78−23676
- $(Ti_{1-x}V_x)_2O_3$ spin glass, mag. props., metallic antiferromagnetism 79−82791
- TiC-VC, mag. susceptibility, elec. cond. and thermoelec. props. 80−50033
- TiC-VC, prod. and props. 77−28772
- TiC-VC carbide alloys, thermophys. props., temp. depend., specific elec. resist. 79−86908
- TiN-VN refractory powder composite, resistors, produced in low temp. 78−11182
- TiO-VO, solid soln. formation 77−89541
- $Ti_2O_3:V_2O_3$, XPS, band states 77−20986
- $(Ti_2O_3)_{1-x}(V_2O_3)_x$, lattice polarisability, electronic contribs. IR refl. obs. 78−59904
- TiVC, on steel, sputter deposited, adhesive quality 77−12531
- $Ti_xV_{1-x}C$, electronic struct. and X-ray emission spectra, cluster MO calc. 80−65444
- $Ti_xV_{1-x}Cy$ solid solutions, mag. susceptibility and band struct. 79−51739
- $Ti_{1-y}V_yH_x$, electronic props., H alloying effects, book contrib. 79−82522
- $(Ti_{0.9}V_{0.1})_2O_3$, spin glass, dynamic mag. susceptibility meas. 80−39792
- $(Ti_{0.98}V_{0.02})_2O_3$, lattice parameters, temp. depend. 77−11855
- $(Ti_{0.99}V_{0.01})_2O_3$ spin glass, sp. ht. anomaly and entropy change 79−56546
- $(Ti_{0.9975}V_{0.0025})_4O_7$, metal-insulator transition, struct. aspects 79−86752
- $(Ti_{1-c}V_c)_4O_7$ order-disorder and metal-insulator transition theory 80−24802
- $(Ti_{1-x}V_x)_2O_3$, crystal struct. determ., metal-metal distance, effect on electronic struct. 77−47431
- $(Ti_{1-x}V_x)_2O_3$, nonlinear magnetisation at spin glass phase transition temp. 79−78403
- $(Ti_{1-x}V_x)_2O_3$, $O<x<0.1$, magnetisation and mag. moments 80−65772
- $(Ti_{1-x}V_x)_2O_3$, single crystal, anisotropic susceptibility 79−87228
- $(Ti_{1-x}V_x)_2O_3$ solid soln., struct. changes comp. depend. 77−55275
- $(Ti_{1-x}V_x)_2O_3$, spin glass, nonlinear susceptibility and sp. ht. 80−60304
- $(Ti_{1-x}V_x)_2O_3$, spin glass props. and anisotropy, comp. depend. 77−66368
- $(Ti_{1-x}V_x)_2O_3$, spin glass to antiferromag. regime 78−52276
- $(Ti_{1-x}V_x)_2O_3$, spin glass and metallic antiferromagnetism 78−68268
- $(Ti_{1-x}V_x)_2O_3$, spin-glass props., 0.05-300K 80−25149
- $(Ti_{1-x}V_x)_2O_3$, susceptibility and ^{51}V NMR expts., spin glass behaviour 77−66369
- $(Ti_{1-x}V_x)_2O_3$, US velocities in high mag. field 78−84262
- $(Ti_{1-x}V_x)_4O_7$, elec. cond. and phase diagram near metal-insulator transition 80−11054
- $(Ti_{1-x}V_x)_4O_7$, mag. susceptibility calcs. 78−91850
- $(Ti_{1-x}V_x)_4O_7$, metal-insulator transition investig. by resist., sp. ht. and X-ray diffr. 77−43497
- $(Ti_{1-x}V_x)_4O_7$, metal-insulator transition and mag. behaviour 78−51895
- $(Ti_{1-x}V_x)_4O_7$, metal-insulator transitions, EPR, elec. and mag. props. 80−2336
- $(Ti_{1-x}V_x)_4O_7$, order-disorder and metal-insulator transitions 80−39504
- $Ti_{1-x}V_xS_2$, resistivity, Hall effect and mag. suscept. 78−79991
- $Ti_{0.99}V_{0.01}Se_2$, negative mgnetoresist. and nonlinear cond. 79−87105
- $Ti_{0.99}V_{0.01}Se_2$, negative magnetoresist. and nonlinear cond. 80−44617
- $Ti_{1-x}V_xSe_2$, mag. susceptibility, 4.2-300K 80−60188
- $(Ti_{1-x}V_x)_2O_3$, metallic antiferromag. struct., neutron studies 80−65797
- Tl-V-S system, crystallographic data and phys. props of some phases *(French)* 79−99163
- TlBr-VBr_2 system, cryst. struct., DTA investig. *(German)* 78−72766
- TlV_5S_8, prep., props. and cryst. struct., metallic behaviour 77−27864
- Tl_3VS_4, cryst. struct., X-ray diffr. obs. *(French)* 79−14763
- Tl_3VS_4, for SAW devices, temp. compensated cuts with zero power flow 77−12313
- $Tl_xV_6S_8$, prep., struct., props. 77−19935
- UF_6-VF_5, dil. sol., liq.-vap. equilib. 77−62632
- UO_3, semiconductor-metal transitions, photoelectron spectra meas. 78−84144
- V (III) complex, alcoholic VCl_3 soln., fluoresc. and photoreduction 78−85177
- V complex, $[C(NH_2)_3]V(SO_4)_2.6H_2O$, mag. sp. ht., low-temp. crit. behaviour *(Japanese)* 78−56340

vanadium compounds continued
V complex, α-α′-dipyridil iminodiacetato oxovanadium (IV), cryst. struct. 79−69086
V complex, BaVO(EDTA).6H_2O, cryst. and mol. struct., X-ray diffr. obs. *(Russian)* 78−30601
V complex, VOCL $[Co(cyclopentadienyl)_2]_{0.16}$, synthesis and struct. 80−44176
V complex, vanadyl ion-pyridyliminonitroxide radical mag. interactions, ESR 77−83623
V complex with carboxylate, channel model in exchange theory 78−14950
V complex. triaminomethyl vanadium sulphate hexahydrate, S=1 ground state, mag. props. in external field 80−11157
V complexes, ^{51}V quadrupole coupling tensors form EPR meas. 80−88866
V III, fluoro complexes anomalous magnetic properties, theoretical basis using magnetic field approximation 79−41093
V-C-O, phase relations 79−96012
V-D, exam. of phase diagram, using DTA and calorimetry, isotope effect 78−80527
V-Ge, thermophysical props., at elevated temp. 80−103493
V-H, effect of neutron irrad. on electrical resistance, magnetic susceptibility 80−29063
V-H, electron work function, 300 to 600 degrees C, contact potential difference meas. 80−29462
V-H, exam. of electron structure 80−29306
V-H system, DTA, phase diagrams, low temp. phase 78−6903
V-H(D), anelasticity due to long-range diffusion 80−60904
V-H(D), hydrogen ordering, review 80−60850
V-H(D), phase diagrams, struct. studies 80−66491
V-H(D) system single cryst. prep. and characterisation 79−95910
V-Mn-O system, phase comp. during oxide prep. 78−27447
V-N system, X-ray determ. of phase equilibria *(Russian)* 77−55952
V-O, dislocation pinning, impurity interactions, strengthening *(Russian)* 80−92532
V-O coordination complexes, CNDO calcs. of stability and bonding *(German)* 79−31404
V-O solid solutions, solubility and thermodynamic props. 77−7866
V-O system, chemical transport of non-stoichiometric phase 79−69972
V-O system, structure of γ-phase *(Ukrainian)* 79−51063
V-O system β phase BCT, X-ray diffr. study of additional scatt. effect *(Russian)* 80−10537
V-S system, order-disorder transition of metal vacancies, statistical thermodynamics 78−43012
V-S system, quenched, order-disorder transition of metal vacancies, DTA and X-ray analysis 78−30576
V-Se system, quenched, order-disorder transition of metal vacancies, DTA and X-ray analysis 78−30576
V-Ti-C precipitation, high temp. coarsening, of dispersions in ferrite 78−84874
V-VO_x-Pb Josephson tunnel junction, crit. currents exam. 78−23209
V-W-O system, phase diagram and thermodynamic props. at high temps., in region W-WO_2-VO_2-V_2O_3 80−104133
$V_{0.985}Al_{0.015}O_2$, insulating T-phase cation disproportionation and V-V pairing 77−62825
$V_{0.985}Al_{0.015}O_2$, struct. aspects of metal insulator transitions 78−18965
$V_{1-x}Al_xO_2$, phase diag. 77−52308
$V_{1-x}Al_xO_{2\pm y}$, mag. and struct. props. meas. 78−2658
VB, nuclear quadrupole parameters 80−103896
VB_2, energy shift and struct. of K-absorpt. edge of V 79−38694
VBe_{12}, plasma-sprayed coatings on Cu and stainless steel, fusion reactor appl. 80−18619
VBr_2 growth on V due to Br_2 chemisorption 80−101039
VBr_4, mol. struct., vibronic interactions, dynamic Jahn Teller effect, gas phase electron diffr. 79−31711
V(C,N), precipitation in γ→α transform. in low C steel *(Polish)* 78−52807
VC, bond energy and ionization efficiencies from SIMS 79−24400
VC, damage sustained during neutron irradiation 77−1841
VC electronic structures calc. and obs., by APW method and X-ray photoelectron spectroscopy *(Japanese)* 79−15074
VC, energy band struct., chem. bonding 78−18958
VC, energy schemes 77−39778
VC, energy shift and struct. of K-absorpt. edge of V 79−38694
VC, exam. of brittle fracture props., using Hertzian indentation 79−11686
VC, final-state effects in C Auger spectra 78−6818
VC, high-temperature carbide targets for fast on-line mass separation of alkali and noble gas elements 79−22515
VC, metastable supercond. phase, effects of rapid quenching on transition temp. 78−2611
VC, micropowder, abrasive props. 77−63821
VC, precipitation, high temp. coarsening, of dispersions in ferrite 78−84874
VC, precipitation in ferrite and pearlite, during C steel transformation, TEM exam. 78−52812
VC single cryst., Vickers microhardness, slip mechanism 80−71732
VC, soft X-ray emission, excitation pot. spectra, excited level binding energy 80−35009
VC, TiC and TiN, charge distrib. and bond ionicity 78−63961
VC, valence band struct. *(Russian)* 78−6268
VC, X-ray emission band exam. and electronic struct. 77−8689
VC, X-ray emission spectra, interpretation in terms of relativistic elec. dipole transition probabilities 79−3459
VC-NbC, phase diag. calc. 77−90329
VC-Ni, fracture mode determination, using Auger electron spectroscopy 80−7680
VC-TaC, phase diag. calc. 77−90329
VC-TiC, deposited by activated reactive evaporation, TEM and hardness 79−23872
VC-TiC coating, high rate deposition by activated reactive evaporation, and characterisation 78−11372
VC_x coating, C steel vanadisation by CVD 80−44454
VC_x, complex phases with NaCl struct., microhardness rel. to electronic structure 77−90438
VC_x electron band struct. and X-ray spectra *(Ukrainian)* 79−51482
VC_x precipitates, fluxoid pinning in supercond. 78−52169
VC_x, static distortions and Debye temp. determ., neutron diffr. exam. *(Russian)* 77−80482
VC_x, surface state, XPS investigation 78−11070
vanadium compounds continued
VC_x, vacancy ordering transition state cluster model, electron diffr. 77−47547
V_2C crystal struct., X-ray determ. of rhombic modification *(Ukrainian)* 79−77564
V_4C_3, determ. in cementite by annealing in moist H_2 *(German)* 79−39231
VC_xN_y, superstructure induced by ageing, neutron diffr. obs. *(Russian)* 80−49195
$V(CN)_5NO^{3-}$, struct., FSGO calcs. 78−70736
$V(CN)_6NO^{4-}$, struct., FSGO calcs. 78−70736
$V(CO)_6$, cryst. and mol. struct., Jahn-Teller distortion, mol. vib. and librational correction 79−32949
$V(CO)_6$, paramag. matrix isolated species, MCD spectrosc. appls. 78−46378
VC_xO_y, conc. depend., of unit cell filling degree 80−54199
V_2Cg, struct. and orientation of rhombic modification *(Russian)* 77−55270
VCl_3, electronic struct. and struct. phase transition 80−59644
VCl_4, intensity changes between He(I) and He(III) photoelectron spectra 78−21969
VCl_4, liq., struct. factor, mol. dynamics calc. 80−38898
VCl_4, liq. struct. by neutron diffr. 79−73088
VCl_4, photoelectron and UV spectra, SINDO theory 77−50360
VCl_4, Raman spectra and selection rules, Jahn-Teller splitting 78−988
$VCl_4(Br_4)$, vibronic systems, degenerate ground states, statistical sums, thermodynamic func. calcs. 80−27997
$V_{1-x}Cr_xO_2$, VPE and elec. and optical characterisation 78−3053
$(V_{1-x}Cr_x)_2O_3$, Raman scatt. and phase transitions 80−71420
$(V_{1-x}Cr_x)_2O_3$, thermal props., rel. to phase transition 77−35709
$(V_{1-x}Cr_x)_2O_3$, vapour phase transport, single cryst. growth *(French)* 77−24940
$(V_{1-x}Cr_x)_2O_{3+y}$, elec. props. and struct. 80−84494
$V_xCr_{3-x}S_4$, elec. and mag. props. 79−28523
VD, structs. phase diagrams, morphologies, prep. methods, book contrib. 80−25675
$VD_{0.68}$, anisotropic Compton profiles 80−97368
α-$VD_{0.7}$, interstitial vibr., coherent neutron scatt. study 79−42196
α-$VD_{0.7}$, vibrations of interstitial D, coherent neutron scatt. 80−96612
$VD_{0.77}$, Compton profile, electronic struct. *(German)* 78−92140
$VD_{0.77}$, Compton profiles, comparison with band struct. calcs. 78−84675
$VD_{0.8}$, antiphase domains during ordering, neutron diffr. 77−90348
V_2D, elec. resistivity studies of order-disorder phenomena 79−78961
V_2D, ordered, distortion-induced superstruct. modulation, from X-ray scatt. 80−49186
V_2D, single crystal, superstructure modulation and long range order, X-ray obs. 78−71712
V_4D_3, multistage ordering process, neutron diffr. obs. 77−59114
VF_2, nearly one-dimensional, paramag. susceptibility 79−15278
VF_2, prep., struct., heat capacity 5-300K, mag. ordering 79−86746
VF_3, energy shift and struct. of K-absorpt. edge of V 79−38694
VF_5, normal coord. anal., generalised valence force field calcs. 77−58195
$V_{1-x-z}Fe_xMo_zO_2$, Mossbauer effect exam., Fe conc. and precise struct. characteristics 78−31141
$V_{0.986}Fe_{0.014}O_2$, metal-insulator phase transition, effect of hydrostatic press. 80−6725
$V_{1-x}Fe_xO_{2-y}$, Mossbauer effect exam., Fe conc. and precise struct. characteristics 78−31141
$V_{1-x}Fe_xO_{2-x}F_x$, $0<x<0.2$, phase diagrams, ^{57}Fe-Mossbauer spectra, X-ray diffr. studies *(German)* 80−29663
$V_{1-x}Fe_xO_{2-x}F_x$, $0<x<0.20$, magnetic susceptibility and electron cond. *(German)* 80−39754
$V_{1-x}Fe_xO_{2-x}F_x$, mag. susceptibility *(German)* 79−78305
V_3Ga composite prep. and testing for high-field supercond. magnet 79−30513
$V_{1-x}Ga_xO_2$, M1→T phase transition, X-ray and mag. meas. 77−11692
$V_{1-x}Ga_xO_2$, phase transitions, semicond. metal transition, antiferromag. props. 77−11969
VH, electronic struct. and X-ray emission spectra 77−52201
β-VH, precipitation crystallography, TEM obs. 77−77480
VH, structs. phase diagrams, morphologies, prep. methods, book contrib. 80−25675
$VH_{0.07}$, diffusion of H, neutron scatt. study 79−60550
$VH_{0.51}$, optic modes study by neutron spectroscopy 80−19891
$VH_{0.55}$, ultra-high vacuum cleavage, H_2 desorption 80−54514
$VH_{0.71}$, Compton profile, electronic struct. *(German)* 78−92140
$VH_{0.71}$, Compton profiles, comparison with band struct. calcs. 78−84675
VH_4, electronic structure, ab initio calcs. 79−89601
VH_x, diffusion of H atoms, quasielastic neutron scatt. obs., book contrib. 79−82383
VH_x, electronic props., H alloying effects, book contrib. 79−82522
VH_x, NMR, phase transition obs., activation energy for H diffusion meas. *(Russian)* 78−27506
VH_x, positron annihil. lineshape Doppler broadening, H conc. and temp. depend., 20-500K 79−61463
VH_x, reluctance, Hall effect 79−38102
V_2H, elec. resistivity studies of order-disorder phenomena 79−78961
$VH(SO_4)_2.4H_2O$, cryst. parameters and X-ray powder diffr. data *(French)* 79−14765
V_2Hf-base C15 compounds, development as high field supercond. 79−61015
VI_2, antiferromag., zone-boundary phonon Raman scattering, modulation of exchange interaction 80−11386
VI_2, antiferromagnet, phonon Raman scatt. from spin superstructures 80−16030
VI_2, lattice dynamics and ionic charge 80−10615
VI_2, MCD spectra, interpretation rel. to mag. struct. 80−66222
VI_2, mag. 'Bragg' scatt. obs. through Raman scatt. 80−66179
VI_2, mag. struct., long- and short-range order and Mossbauer spectroscopy 80−65803
VI_2, mag. superlattice, neutron oscill. and Weissenberg photography 80−65802
VI_2, Mossbauer spectrum, electronic and mag. props. 77−32302
VI_2, noncollinear magnetic order and spin wave spectrum in presence of competing exchange interactions 80−65834
VI_2, single crysts., growth from vapour phase 80−66410
VI_2, spin-dependent Raman scatt. from phonons 80−97274
$V_{1-2x}M_x^{2+}N_x^{6+}O_2$, (M=Ni,Cu,Mn, N=W,Mo,Te) cryst. struct., transitions and thermal effects 77−68950
$V_{1-2x}M_x^{3+}Nb_xO_2$, (M=Fe,Cr) cryst. struct., transitions and thermal effects 77−68950

vanadium compounds continued
- V_2MoO_8, planar defects, electron microscopy and electron diffraction meas. 77−15430
- δ-VN, cryst. growth by floating zone and zone annealing techniques 77−69983
- VN, electronic struct. of vacancies, effect on supercond. transition temp. 80−29347
- VN, energy shift and struct. of K-absorpt. edge of V 79−38694
- VN, interatomic interactions from XPS 80−49171
- VN, lattice phonons, dispersion and density-of-states 79−99283
- VN, opt. consts. and physicochem. spectra 77−85677
- VN, optical props. and charact. electron energy loss spectra 79−52056
- VN powder, defect struct., thermal and elec. props. 77−59286
- VN, soft X-ray emission, excitation pot. spectra, excited level binding energy 80−35009
- VN, V(CN), VC, particle coarsening reactions in low alloy steels, effect of cold deform. 80−71664
- VN-CrN solid solutions, thermal cond., Lorentz number 80−15317
- VN-CrN system solid solns., electrophys. and galvanomag. props., 77 to 1300K 77−24567
- VN-CrN systems, solid solns., mag. props. 77−12086
- VN-Mn, solid solns., electrophys. props. 77−35914
- $VN_{0.74}$ and $VN_{0.89}$, low-temp. specific heat and superconducting critical temp. meas., density of states 80−54835
- VN_{1-x}, vacancy ordered structure in cubic mononitride phase, transition entropy determ. 78−43011
- VN_x, surface state, XPS investigation 78−11070
- VN_x, vacancy ordering, transition state cluster model, electron diffr. 77−47547
- β-V_2N, neutron powder profile-refinement cryst. struct. determ. 80−15060
- $(V_{1-x}Nb_x)_2$ C, C ordering formation of varieties 80−38968
- $(V_{1-x}Nb_x)_2C$, modulated structs., periodic antiphase domains 79−94969
- $V_{11-z}Nb_zGe_8$, cryst. struct. *(French)* 78−38675
- $V_{1/3}NbS_2$, Hall coefficient and resistivity 80−39610
- $V_{1/3}NbS_2$, magnetic susceptibility, function of temp. 80−39756
- $V_{0.5}NbSe_2$, cryst. struct., metallic cond., mag. and phys. props. *(French)* 80−33956
- $V_{1-x}Nb_xSe_2$, CDW anomalies, Nb substitution effects, mag. susceptibility, 16-300K 79−38005
- VO, $^4\Pi$ states, spin-spin coupling consts., ab initio calc. 79−97981
- VO, (001) surface, spectral density of states 78−39187
- VO, energy band spectrum, APW and Green's function method calcs. 79−7783
- VO, energy band struct. and density of states *(Russian)* 80−44493
- VO, from V oxidation, bandhead anal. 77−9077
- VO, investigation of Fermi surface from electron energy spectrum *(Russian)* 80−75496
- VO, octahedral clusters, electronic struct., Xα discrete variation and SW methods 78−63976
- VO, surface states in unreconstructed (001) surface 77−32060
- VO^{2+}, behaviour as spectroscopic probe for characterisation of glasses 79−78510
- VO^{2+}, EPR and optical absorption in strontium formate dihydrate 77−40112
- VO^{2+} EPR in solids, review 80−11254
- VO^{2+}, fluoresc. quenching of organic excited singlet states, rate meas., mechanism 77−38685
- VO^{2+} ion, in calcium tartrate tetrahydrate, optical absorption spectrum 78−6713
- VO^{2+} ion impurities, in hydrated crysts., EPR obs. 80−97130
- VO^{2+} spin probes, slowly tumbling, in nematic liq. crysts., EPR 79−50985
- VO^{2+}+alkyl dinitriles, reaction, CN stretching freqs., bonding effects 77−16820
- $VO_{1.23}$, electron diffr. study of diffuse scattering due to atomic displacements 79−99327
- $VO_{1.25}$, ^{51}V NMR studies, microscopic mag. props. 80−108086
- $VO_{1.30}$, ordered phase, X-ray anal. of defect struct. 79−99177
- VO_2, absorbing film parameters determ. by ellipsometry 80−254
- VO_2, amorphous thin films, phase transition, resistivity and opt. transmission discontinuities 77−47871
- VO_2, CVD behaviour *(German)* 78−23625
- VO_2, change in optical props. at semicond.-metal transitions 77−28597
- VO_2, chemical transport, mass spectrometric study 79−24860
- VO_2 clusters in metallic and semiconductor phases, electronic struct., Xα calcs. 78−63977
- VO_2, cylindrical specimen, thermal switching 80−44679
- VO_2, diffuse X-ray scatt. due to lattice instability near metal-semiconductor transition 78−56074
- VO_2, discontinuous metal insulator and spin dimerisation transition, Hubbard model 78−51893
- VO_2, doped, morphology, structure and props. *(German)* 78−59823
- VO_2, elec. cond. and dielec. props. 79−11379
- VO_2, electronic struct., quadrupole coupling, Mulligen-Wolfsberg-Helmholtz calcs. 78−87948
- VO_2, ferroelastic metal-insulator transition, electronically triggered crystallographic phase transition 80−70614
- VO_2, film, absorption spectra, semicond.-semimetal transition 78−19512
- VO_2 film, dynamic hologram recording *(Russian)* 77−10873
- VO_2 film, dynamic holography, coherent props. of Cu vapour laser 79−13929
- VO_2, film, IR induced metal-semicond. phase transition *(Russian)* 77−15769
- VO_2 film, ion bombard. effect on metal-dielec. phase transition, optical props. meas. 79−90963
- VO_2 film, metal-dielec. transition, refl. after 40 keV ion bombardment 79−23899
- VO_2, film, metastable metallic phase due to laser and electron beam irrad., refl. spectra 79−19944
- VO_2 film, negative resist. region, applic. as oscillator element and transducer *(Russian)* 77−85359
- VO_2 film, optical and elec. props., 0.8 to 4.2 mm, near metal-semicond. transition 77−32473
- VO_2 film, optical charact. of phase transition, ion bombardment effects 79−28281
- VO_2, film, optical consts. and electrical props. near phase transition *(Russian)* 77−59631
- VO_2 film, optical props. meas. near semicond.-metal transition 77−1742
- VO_2, film, semicond.-metal transition, carrier density, mobility and Hall meas. 77−43751

vanadium compounds continued
- VO_2 film, semicond.-metal transition, light absorption by metallic drops *(Russian)* 77−59579
- VO_2, film, semiconductor-metal phase transition, fast laser kinetic studies 79−69419
- VO_2 film, sensitivity to heat perturbation and current noise, effect of temp. 77−66215
- VO_2, film, visualisation of microwave and IR radiation 80−5839
- VO_2 film as holographic recording medium, diffr. efficiency 80−28180
- VO_2 film based recording medium, holographic characteristics calc. *(Russian)* 79−7092
- VO_2, film prep. under equil. conditions, struct. and elec. props. 80−108352
- VO_2 film sub-mm wave modulators and switchable polarisers 77−75664
- VO_2 films, chemically deposited, chemical transition layers at interface with substrate, AES and SEM obs. 79−95533
- VO_2 films, elec. cond. near metal-semicond. phase transition 77−1503
- VO_2, first principles calc. of intra-atomic correlation energy 79−23920
- VO_2, from oxidation of metallic V, ionic cond. 79−51299
- VO_2 in air oxidised V foil reversible switching 79−28387
- VO_2 interference films, colour valencies as function of thickness and phase change *(German)* 78−56533
- VO_2, laser induced metal-insulator transition, thermal switching dynamics 77−76885
- VO_2, lattice instability and metal-insulator transition 78−63834
- VO_2, light scatt. near semicond.-metal phase transition 78−60414
- VO_2, magnetic susceptibility in insulating and metallic phases, electron-electron and electron-lattice interactions 80−96788
- VO_2, metal-insulator transition meas. by microcalorimetry *(French)* 77−47733
- VO_2, metal-insulator transition, resist. meas. 78−14770
- VO_2 metal-insulator transition, technical appls. possibilities *(German)* 79−99587
- VO_2, metal-insulator transitions, effect of isotopic substitution 80−2337
- VO_2, metal-insulator transition, electron correls. and spin dimerization, thermodynamical study 80−70615
- VO_2, metal-insulator transition and electronic struct., ion bombard. effects 80−92948
- VO_2, metal-semiconductor transition, i.r. detection model 77−1442
- VO_2, metal-semiconductor transition, effect of deviations from cryst. lattice periodicity 79−23898
- VO_2, metallic, electronic struct., lattice instability 78−14664
- VO_2, metallic, magnetisation distribution and band structure 78−76223
- VO_2, metallic phase, electronic props., plasma freq., Hall coeff. 78−84195
- VO_2 needles, switching, voltage oscills. 79−15199
- VO_2, nonlinear wave generation in system with metal-semicond. transition, wave propagation velocity *(Russian)* 79−73549
- VO_2, nonstoichiometry influence on electron struct. and metal-insulator phase transition 80−44507
- VO_2, phase transition, temp. variation of US attenuation and phase vel. 77−31723
- VO_2, photoacoustic effect at first order phase transitions at increasing and decreasing temp. 80−70320
- VO_2 pyrolytic film, phase transition and electrical cond. 77−89890
- VO_2, quasi-one-dimens. system, appl. of qualitative theory for phase transitions 78−31086
- VO_2, reduced, microstruct., crystallographic shear planes, electron microscope obs. 79−1443
- VO_2, semicond. phase, optical spectrum, CNDO CI calc. 78−27258
- VO_2, semicond.-metal phase transition, fast laser excitation, kinetics obs. 79−47018
- VO_2, semiconductor-metal transition LCAO cacl., cryst. distortions 77−4294
- VO_2, semiconductor-metal transition, effect of ^{18}O substitution 78−84268
- VO_2 single cryst., noise in presence of current filament 80−92952
- VO_2 single cryst., switching, visual obs. of metallic and semicond. domains 78−52041
- VO_2 single cryst. film, ion-irrad., 'splitting' of semicond.-metal transition 80−11053
- VO_2 single crystal, elec. switching 80−92946
- VO_2, single crystal, fluctuations of current and switching time 79−38137
- VO_2 single crystal, positron annihilation, metal-insulator transition obs. 77−85830
- VO_2, single crystal and polycrystalline, synthesis and resist. near metal-semicond. phase-transition 80−44680
- VO_2, sputtered, switching effects in four-electrode structures 78−2596
- VO_2, switching effect, temp. depend. 80−20259
- VO_2, thermal cond. meas., metal-dielectric phase transition, phonon scatt. mechanism 78−87831
- VO_2, thermal mechanism of switching effect 77−15919
- VO_2, thermochromic film, visualisation of microwave radiation using metal-semiconductor phase transition 79−65845
- VO_2 thin film semiconductor-metal transition applications 80−49835
- VO_2, thin films, doping by ions of Ar, B, P 77−84781
- VO_2 thin films, light modulation appls., optical props. at metal-insulator transition 80−87547
- VO_2 thin films, resist.-temp. characts. and structure at phase transition temp. *(German)* 77−28265
- VO_2, $V_{1-x}Nb_xO_2$, crysts. and polycryst. films, metal-semicond. transition, polarised Raman scatt. 77−90151
- VO_2, V_2O_3, V_3O_5, isotope effect on metal-dielectric phase transitions temp. *(Russian)* 78−34771
- VO_2, VPE and elec. and optical characterisation 78−3053
- VO_2 variable-reflectance mirror for CO_2-N_2-He 10.6 μm scan laser 80−38026
- VO_2, X-ray determ. of lattice constants and thermal expansion coeffs. near transition temp. 79−86747
- VO_2, X-ray Lα emission spectra of V 78−2947
- VO_2:Al, photoacoustic effect study of phase transitions 80−69615
- VO_2:Al(W), thin layer prep. by reactive DC sputtering doping effectiveness *(German)* 78−6847
- VO_2:Ga, Mo, conductivity transitions 78−76121
- VO_2:Ga(Al)(Fe), phase transforms., influence of nonstoichiometry 77−85274
- VO_2:M^{3+}, M=Al,Ga,Fe, anisotropy of thermoelec. power, hole conductivity 77−11946
- VO_2-α-Fe_2O_3-Si, transverse elec. field effect on switching V-I characts. *(Russian)* 77−55591
- VO_2-$CrNbO_4$, solid solns., synthesis and phase diagram 80−35171

vanadium compounds continued
VO_2-$VO_{2.5}$-H_2O system, hydrothermal exam. *(French)* 77−52244
$VO_2+Er_2O_3$, high-pressure reaction, cryst. struct. and mag. props. of $ErVO_3$ 80−19773
VO_4^{3-}, charge transfer transition, bond length effects calcs. 77−83721
VO_4^{3-}, electronic struct. determ. from X-ray spectra 78−86885
VO_4^{3-}, triplet levels obs. by luminesc. meas. 79−69874
$VO_{(0.67\ to\ 0.44)}C_{(0.20\ to\ 0.70)}$, production by carbothermic reduction of VO_3, evaluation as ladle addition to molten steels 78−40049
$VO_{(2n-1)/n}$, metal-semicond. transition temps. 80−59876
VO_x, anodic film, optical anisotropy 77−20942
VO_x, defect ordering, electron diffr. obs. 79−23595
VO_x, defect struct., local ionic arrangements in disordered phase 80−10532
VO_x, diffuse scatt., relation to curvature of free energy surface 79−99025
VO_x, mag. susceptibility temp. depend. 79−47229
VO_x, minimum conductivity and electron localisation near metal-insulator transition 78−30960
VO_x, struct., model based on O vacancy superlattice 77−84707
VO_x, surface state, XPS investigation 78−11070
$V_{0.97}O_{0.03}$, lattice dynamics exam., neutron scatt. 79−23689
$V_{13}O_{24}$ long-period Magneli phase as product of V_6O_{11}-V_7O_{13} periodic microsyntactic intergrowth 80−50618
V_2O, γ-phase, struct., O at. position 79−10834
V_2O_{2n-1}, V_6O_{13}, V_2O_5, Magneli phases, chem. transport using $TeCl_4$ *(German)* 78−31343
V_2O_3, 500 to 530K, magnetic susceptibility meas., high temp. transition, interacting Hubbard bands 78−39325
V_2O_3, alloying into Ti_2O_3, semicond. to semimetal electrical transition, lattice parameter changes 79−60714
V_2O_3, crystallographic structure changes due to phase transition, electron microscope study *(French)* 79−7688
V_2O_3, effect of metal-insulator transition on V K-absorption spectrum 79−19950
V_2O_3, electron structures calc. using models, ESCA and X-ray spectral data 77−35863
V_2O_3, electron-density studies, deform. density at 295K, metal-metal bonds 80−107118
V_2O_3, film, absorption spectra, semicond.-semimetal transition 78−19512
V_2O_3 film, reactively sputtered on sapphire, electron microscopy exam. 78−84106
V_2O_3, film prep. under equil. conditions, struct. and elec. props. 80−108352
V_2O_3, high temp. mag. phase transition studied by US vel. meas. *(Russian)* 79−33520
V_2O_3, high-temp. transition domain, small angle diffuse neutron-scatt., 400-600K 77−69231
V_2O_3, hydrostatic compression, X-ray diffr. meas. 79−99269
V_2O_3, impurity doping effects, elec. props. obs. 80−75609
V_2O_3, insulating phase, mag. struct. 79−38305
V_2O_3 insulating phase, realistic Hartree-Fock calc. 79−38306
V_2O_3, lattice parameter anomalies at high temp. 78−47522
V_2O_3, lattice parameters and anomalous high temp. behaviour 78−87790
V_2O_3, low temp. antiferromag. phase, mag. struct. 78−52213
V_2O_3, low temp. crystallographic struct. domains 78−83765
V_2O_3, metal-insulator transitions, effect of isotopic substitution 80−2337
V_2O_3, metallic differential refl. spectra and band struct. 77−1699
V_2O_3, phase equilibrium with Fe deoxidized by V *(Russian)* 80−16275
V_2O_3 phase transition, temp. variations of US attenuations and phase vel. 77−31723
V_2O_3, phase transitions, Raman scatt. expts., 20-300K 78−39538
V_2O_3, polarised Raman scatt. in metallic and semicond. phases 77−90152
V_2O_3, pure and Cr doped, metal-insulator transition 79−37989
V_2O_3, Raman scatt. and phase transitions 80−71420
V_2O_3, semiconductor-metal transitions, photoelectron spectra meas. 78−84144
V_2O_3, semiconductor-metal transition, effect of ^{18}O substitution 78−84268
V_2O_3, thermal cond. meas., metal-dielectric phase transition, phonon scatt. mechanism 78−87831
V_2O_3, thermal expansion tensor, phase transitions, X-ray diffr. obs. *(French)* 79−1515
V_2O_3, US vel. and elastic const. meas., 150-273K 77−15478
V_2O_3, vapour phase transport, single cryst. growth *(French)* 77−24940
V_2O_3:Al, struct., props., rel. to V_2O_3:Cr, X-ray diffr. and elec. resist. obs. 78−2531
V_2O_3:Cr, anomalies in X-ray diffuse scatt. at high temp. metal-insulator transition 79−87042
V_2O_3:Cr, metal-insulator transitions, XPS and UPS 79−33236
V_2O_3:Cr, pure and doped, sound vels. and elastic consts. from phonon dispersion curves 79−55844
V_2O_3:Cr, struct., props., rel. to V_2O_3:Al, X-ray diffr. and elec. resist. obs. 78−2531
V_2O_3-Al_2O_3 solid soln., interactions between V atoms, comp. and temp. depend. of mag. susceptibility 77−8056
V_2O_3-H_2, interaction with surface, quantum chemical study 80−45549
V_2O_3-M_2O_3, M=Ti, Cr, struct. and mag. props. 78−27041
V_2O_3-Ti_2O_3-TiO_2, phase equilib. at 1473K 77−16562
V_2O_3-VO_2-GeO_2, phase equilibria as function of O_2 pressure at 1173K *(French)* 79−42216
V_2O_3-VO_2-M_2O_3, (M=Ga, In or Y), phase equilibria as function of O_2 pressure at 1273K *(French)* 79−42216
$V_2O_3+{}^1/_2O_2+Fe=FeV_2O_4$ react., free energies of form., 1400-1750K, electrochem. method determ. 79−43613
$V_{2O_{3+x}}$, $0\leq x\leq 0.08$, mag. and elec. props. 80−49833
V_2O_{3+x}, nonstoichiometric compositions, mag. transition exam. by Mossbauer effect 77−28385
V_2O_{3+x}, nonstoichiometric, microscopic mag. props., NMR and inelastic-spin-flip neutron scatt. 79−38323
$^{57}CoV_2O_4$, after effects of orbital electron capture 79−73870
V_2O_4 films, characterisation using XPS, metal-semiconductor transition 79−28900
V_2O_4, struct. from electron microscopy of Tyep F-2 fibre 78−2087
V_2O_5, (001) surface modification, during catalytic oxidation of propene *(French)* 80−45557
V_2O_5, amorphous, electronic cond., effect of random glass struct. 79−23972
V_2O_5, amorphous, hydration and fibrous texture, EPR study *(French)* 79−24826
vanadium compounds continued
V_2O_5 amorphous film, photochromism and thermochromism 80−93254
V_2O_5 amorphous films, CVD prep., structural characts. 80−49114
V_2O_5 amorphous layers, gel deposited, semicond. props. 80−92887
V_2O_5, amorphous semicond., solubility and fibrous texture 80−75162
V_2O_5 and lower oxides, defect structures and related props., review 80−59454
V_2O_5 cathode, used in Li-V_2O_5 reserve cells, microstruct. optical reflectance, elec. cond. meas., chem. anal., SEM obs. 79−43752
V_2O_5 containing melts, activation energy of electron mobility and electronegativity 77−35971
V_2O_5, core levels, cryst.-field splitting, X-ray emission study 80−66328
V_2O_5 crystal, photoinduced threshold switching in VO_2 channel 80−29450
V_2O_5, dielec. polarisation, permittivity meas., 50-200K *(Russian)* 78−39498
V_2O_5 EPR of O vacancy 78−72406
V_2O_5, effect on magnetic props. of Li-Zn ferrite *(Japanese)* 77−28415
V_2O_5, elec. cond. in strong fields, tunnelling mechanism 78−91699
V_2O_5 electrochromism obs. and mechanism, thin film growth *(Russian)* 77−77249
V_2O_5 electrode, anodic dissolution in aq. acid soln. *(German)* 79−91826
V_2O_5, electron beam induced decomposition, appearance pot. spectroscopy 80−85203
V_2O_5, electronic, optical, structural and surface props., review 80−88120
V_2O_5, electronic and band struct. and spectra, CNDO CI cluster method 79−11091
V_2O_5 energy band struct. rel. to expt. studies 80−70603
V_2O_5, energy band structure, tight-binding method 80−70602
V_2O_5, etching characts. by plasma reactive sputter etching 78−27661
V_2O_5, fast ion transport and electrochem. storage, Li reactions 80−61324
V_2O_5, ferroelec. semicond., dielec. and elec. meas. 80−60516
V_2O_5 film, amorphous, CVD prep. method 80−55299
V_2O_5 film, amorphous, thickness, density and refr. index determ. from reflectance interference spectra 80−55206
V_2O_5 film, electrochromism, X-ray electron spectra 78−48146
V_2O_5 film, optical absorption in 1.0 to 5.5 eV range 78−19586
V_2O_5, hydrated amorphous, EPR, struct. and electron mobility *(French)* 77−15319
V_2O_5, interaction with adsorbed propene, IR emission spectra obs. 79−90881
V_2O_5, laser induced damage *(Russian)* 79−43069
V_2O_5 layer, amorphous, photocond. investig. using V_2O_5-n-Si system 77−76875
V_2O_5, $Li_xV_2O_5$, and $Na_xV_2O_5$, catalytic behaviour in decomp. of isopropanol, 186-300°C 78−11553
V_2O_5, low dislocation density cryst. growth, opt. props. 77−63551
V_2O_5, low-melting additive to $Li_{0.5}Fe_{2.5}O_4$ 77−85494
V_2O_5, optical characts., far IR transmission spectra 78−72525
V_2O_5, quadrupole broadening in ^{51}V NMR spectrum 80−20469
V_2O_5, reduction in butyllithium, ESR study 80−100611
V_2O_5 single crystals, contact-limited conduction 79−95493
V_2O_5 single cryt. microhardness and anisotropy of mech. props. *(French)* 80−50713
V_2O_5, splat-cooled, crystallisation, high-press. effects 78−9956
V_2O_5, switching mech. 78−60175
V_2O_5, thermal expansion tensor, phase transitions, X-ray diffr. obs. *(French)* 79−1515
V_2O_5, thermally stimulated exoelectron emission *(German)* 80−66404
V_2O_5, thermoelec. props., 500-1500K 80−29423
V_2O_5 type liquid semiconductor, elec. props. control, by O_2 partial press. *(Russian)* 78−72142
V_2O_5, VO_2, thermal switching, resist.-temp. charact. 78−64071
V_2O_5, water in noncryst. solid, quenching of molten V_2O_5 *(French)* 78−42912
V_2O_5, wedge shaped cryst., electron lattice image interpret. 80−103319
V_2O_5, X-ray Lα emission spectra, excited states calcs. 79−59488
V_2O_5:Fe^{3+}, EPR, 5-300K 77−81002
α-V_2O_5:Li(Na)(Cu), far IR absorption spectra meas. 77−73158
V_2O_5:Na(Li), pure and doped, elec. cond. and thermoelec. power meas. 80−10987
V_2O_5-$AlNbO_4(GaNbO_4)(TiNb_2O_7)$ systems, interfacial reactions, efficient boundary conditions and solid state reactivity 80−76542
V_2O_5-As_2O_3-RO, R=Ba, Ca, Pb, semicond. glass, electronic props. 80−88557
V_2O_5-B_2O_3-ZnO semiconductivity glasses, optical and modulated absorpt. spectra in band gap region 77−48189
V_2O_5-BaO-K_2O-ZnO glasses, elect. props. and struct. 80−15547
V_2O_5-based glasses, amorphous and crystallized electronic cond. and related props. 79−99547
V_2O_5-Cr_2O_3, phase diagram 77−70040
V_2O_5-CsV_2O_5 system, phase comp. and phase diagram for conditions of inert atmosphere 77−25030
V_2O_5-CuO-BaO glass, unpaired electron localisation, ESR study 80−66026
V_2O_5-Fe_2O_3 solid solution, Mossbauer investig. of cryst. props. *(French)* 77−4592
V_2O_5-Fe_2O_3-Li_2O ternary system, charge compensation of Fe ions, Mossbauer obs. 78−52410
V_2O_5-Fe_2O_3-LiO_2 system, physical properties 78−84503
V_2O_5-Ge, elec. props., molecular deposition method 80−34525
V_2O_5-GeO_2 glass, effect of thermal processing on elec. and thermal props. *(Russian)* 77−63814
V_2O_5-GeO_2-PbO glasses, memory and threshold switching 78−23142
V_2O_5-$In(Tl)_2O_3$, ceramic, elec. resist., dielec. props., porosity 77−8093
V_2O_5-MoO_3, solid soln. thermogravimetric anal., ion formation on crystallisation 77−20076
V_2O_5-MoO_3 solid soln., number of V^{4+} ions, magnetic and thermogravimetric exam. 78−52199
V_2O_5-MoO_3 solid solns., small polaron cond., elec. resist. and thermoelec. power meas. 80−34447
V_2O_5-MoO_3 system, X-ray diffr., IR absorption spectra, NMR and thermal analysis 77−24379
V_2O_5-MoO_3-P_2O_5 glass, semicond., DC cond., dielec. props 79−91044
V_2O_5-n-Si system, carrier transport mechanisms 77−62999
V_2O_5-$NaPO_3$-P_2O_5 threshold switches, elec. props. 77−35974
V_2O_5-P_2O_5, glass, DC cond. meas. high temp. range 78−6376
V_2O_5-P_2O_5 (70-30), electrical cond. and thermoelectric meas., Au-glass-Au sandwich 80−29403

vanadium compounds continued
V_2O_5-P_2O_5 based glasses, specific heat effect of fast neutron irradiation 77−69096
V_2O_5-P_2O_5 glass, density and O molar volume 78−59759
V_2O_5-P_2O_5 glass, dielec. relax. mechanism, SDRC investigation, Schottky barrier formation in metal-glass-metal systems 78−60388
V_2O_5-P_2O_5 glass, EPR investig., samples with varying V^{4+} content and cond. 77−8389
V_2O_5-P_2O_5 glass, electrical 1/f noise and DC cond. 79−91109
V_2O_5-P_2O_5 glass, in metal-semicond.-metal struct., TSC of dielec. relax. *(Russian)* 77−35998
V_2O_5-P_2O_5 glass, in SnO_2/V_2O_5-P_2O_5/Si heterojunction, static optoelectronic charact. 79−87146
V_2O_5-P_2O_5 glass, switching and memory behaviour, Pt point contact effects 77−11970
V_2O_5-P_2O_5 glass, thermoelec. power meas. 78−84242
V_2O_5-P_2O_5 glasses, anomalous cond. mechanism 77−76832
V_2O_5-P_2O_5 glasses, Raman spectra 79−78667
V_2O_5-P_2O_5 glasses, secondary electron emission 79−87534
V_2O_5-P_2O_5 glasses, threshold and memory switching 77−76887
V_2O_5-P_2O_5 glasses containing metallic particles, elec. props. 79−42547
V_2O_5-P_2O_5-CaO glass with metal electrodes, elec. charact., thermal conditions effect *(Russian)* 78−47884
V_2O_5-P_2O_5-Cs_2O(Na_2O) glasses, enhanced secondary electron emission yield 80−93441
V_2O_5-P_2O_5-H_2O, formation of $VOPO_4.2H_2O$ 77−44228
V_2O_5-P_2O_5-Nb_2O_5 glasses, switching 80−88604
V_2O_5-PbO, acoustooptic props. from comp. and density 80−76000
V_2O_5-Si, sandwich system, photocond. in range 380-1000 nm 77−32034
V_2O_5-TeO_2 glasses, ESR spectra 78−10755
V_2O_5-TeO_2 system, vitreous, struct. obs. using neutron scatt. 78−22667
V_2O_5-TiO_2 interface, role of struct. props. in interfacial reactions 78−31688
V_2O_5-V_2O_4-$BaZnO_2$ glass, V ion states, mag. and elec. props. 80−88556
V_2O_5-WO_5, solid soln. thermogravimetric anal., ion formation on crystallisation 77−20076
V_2O_5-water, EPR of VO_{aq}^{2+} formed by solar light photoreduction, electrolysis appl. 78−11540
V_2O_5-ZnO-B_2O_3 glass, sputtered, optical absorpt., band gap and Urbach tail 77−8597
V_2O_{5-x}, O_2 equilib. press. at 600°C 77−81421
V_2O_{5-x}, O_2 equilib. press. above oxide system, thermodynamic props. 79−16029
V_2O_{5-x}, O_2 equilib. press. as measure of O_2 binding energy in oxide system 79−16030
$V_2O_{5(3)}$-aluminophosphate melt, resistivity, 800-1200°C 77−39903
V_3O_5, cond. transition at 154°C, effect on props. *(German)* 79−42594
V_3O_5, dielec.-metal transition obs. and interpretation *(Russian)* 78−23023
V_3O_5, electrical, thermodynamic and mag. props. at metal-semicond. transition, homogeneity range 77−4413
V_3O_5, film prep. under equil. conditions, struct. and elec. props. 80−108352
V_3O_5, high-temp. phase transition, resistivity, valence photoelectron spectra 80−49357
V_3O_5, increase of X-ray refl. intensities and profile widths at phase transition temp. 79−69052
V_3O_5, insulator-metal phase trnasition at 450K, properties 78−39023
V_3O_5, low-temp. modification, cryst. struct. and valency distrib., importance of very weak reflections 80−92493
V_3O_5, mag. anisotropy 77−85441
V_3O_5, metal-insulator transition, effect of doping *(German)* 78−30869
V_3O_5, metal-insulator transitions, effect of isotopic substitution 80−2337
V_3O_5, metal-semicond. transition, pressure-temp. phase diagrams anal. 79−87132
V_3O_5, Mo,Ti, and Ga doping effects on conductivity transition 77−11971
V_3O_5, phase transform., heat capacity anomaly near 425K 77−47576
V_3O_5, phase transition, X-ray diffr. and DTA meas. 77−28001
V_3O_5, phase transition temp., hydrostatic press. depend. 77−62827
V_3O_5, resistivity switching due to phase transition, 154°C 79−19642
V_3O_5, semiconductor metal transition, IR spectra obs. *(German)* 78−23456
V_3O_5, semiconductor-metal transition, effect of ^{18}O substitution 78−84268
V_3O_5 single crysts., prep. by chem. transport reacts. props. 79−43115
V_3O_5, spin order, one-dimensional, Neel transition 80−39799
V_3O_5, steady-state elec. switching charact., simple thermistor model 77−8159
V_3O_5, struct. and electronic aspects of cond. transition 78−15078
V_3O_5, thermal cond. meas., metal-dielectric phase transition, phonon scatt. mechanism 78−87831
V_3O_5-Ti_3O_5, DTA, mag. susceptibility and X-ray diffr. study 80−70970
V_3O_7, ESR spectra of V^{4+} ions 77−28437
V_3O_7, hyperfine interactions, inelastic spin flip neutron scatt. 77−28372
V_3O_7, microscopic mag. props., NMR 80−7177
V_4O_7, cryst. atomic struct., 120K and 298K 78−34486
V_4O_7, metal-insulator phase transition temp. depend. on hydrostatic press., DTA meas. 79−73438
V_4O_7, sublattice magnetisation temp. depend., ^{51}V NMR 79−91301
V_4O_9, defect structures and related props. of V_2O_5 and lower oxides 80−59454
V_4O_9, electronic, optical, struct. and surface props., review 80−88120
V_5O_9, metal-insulator phase transition temp. depend. on press. 80−29327
V_6O_{11}, metal-insulator phase transition temp. depend. on press. 80−29327
V_6O_{11}, metallic Magneli phase, electron state 79−94946
V_6O_{11}, microsyntactic intergrowth 79−99149
V_6O_{11} single crystals, heat capacity anomaly at 172K 78−10197
V_6O_{11}, sp. ht., 0.4-50K 78−72358
V_6O_{13}, cathode materials for secondary Li cells 79−92073
V_6O_{13}, defect structures and related props. of V_2O_5 and lower oxides 80−59454
V_6O_{13}, electronic, optical, struct. and surface props., review 80−88120
V_6O_{13}, low temp. phase, cryst. struct. 78−42979
V_6O_{13}, optical props. in metallic and semicond. phase 80−40135
V_6O_{13}, semicond., IR vibration spectra 80−88997
V_7O_{13}, metallic Magneli phase, electron state 79−94946
V_7O_{13}, microsyntactic intergrowth 79−99149
V_nO_{2n-1} ($3 \leq 3 \leq 9$), Magneli phases, mag. susceptibilities at low temp. 80−20389

vanadium compounds continued
V_nO_{2n-1}, cryst. growth and characterisation 78−31311
V_nO_{2n-1}, insulating Magneli phases, mag. susceptibility and sp. ht. meas. 80−34604
V_nO_{2n-1} Magneli phases, elec. and mag. props. 79−37990
V_nO_{2n-1}, Magneli phases, sp. hts. 0.4 to 50K 79−42774
V_nO_{2n-1}, microsyntactic intergrowth 79−1402
V_nO_{2n-1}, X-ray Lα emission spectra of V 78−2947
V_nO_{2n+1}, X-ray Lα emission spectra of V 78−2947
V_xO-M_yO, (M=Ni, Co, Mn), solid solutions, exam. of thermal conductivity 78−79827
V_xO_y, energy shift and struct. of K-absorpt. edge of V 79−38694
V_xO_y film, prep. by thermal decomp. of vanadium naphthenate, and elec. props. *(Japanese)* 78−88425
V_xO_y, film, preparation by calcining vanadium naphthenate, formation process exam. *(Japanese)* 78−30849
V_xO_y, metal-insulator transition, external mag. field effects 80−92819
VO_2(:Al,W), layers, liq. phase prep., resist.-temp. behaviour *(German)* 77−77435
VOCl, and $Li_{0.8}VOCl$ intercalation cmpd., magnetic, optical and electrical props. 79−95402
$VOCl_3$, liq. struct. by neutron diffr. 79−73088
$V_2O_{3-x}F_x$ ($0 \leq x < 0.3$), preparation and physical props. 78−76619
$(V_2O_5)_{0.93}(MoO_3)_{0.07}$ solid soln., struct. transform. in oxidizing and reducing gas atm. 79−23740
2-$VOPO_4$, IR absorpt. spectra, bond freqs. 80−108192
$VOPO_4$, prep. of cryst. from H_3PO_4 and V_2O_5 80−35068
$(VO)_2P_2O_7$, cryst. struct. determ. 80−15081
$(VO)_2P_2O_7$, IR absorpt. spectra, bond freqs. 80−108192
$VOSO_45H_2O$, single cryst. X-ray cryst. struct. determ., H_2 bonding *(French)* 79−73138
β-$VOSO_4.5H_2O$, X-ray cryst. struct. determ. and refinement *(French)* 80−107121
$VOSO_4.6H_2O$, single-cryst. X-ray diffr. struct. determ. *(French)* 80−39021
$VOSb_2O_4$, synthesis and struct., stereochem. influence of lone pair *(French)* 77−15367
$VOWO_4.3H_2O$, chemical behaviour and paramag. centre suitability 77−48670
$VO[UO_2(SO_4)_2].6H_2O$, synthesis and crystallographic data 78−26532
$mV_2O_5.(100-m)P_2O_5$, (m=100-2), V(IV) complexes conc., absorpt. and ESR spectra 78−64266
V_4O(β-phase), X-ray study of precipitated phase *(Ukrainian)* 78−6928
$V_{0.4}Os_{0.6}B_2$, V_2OsB_2, cryst. chem. and struct. 78−42995
VO(tartrate)$_2$ complex, EPR study of VO^{2+} ions in Rochelle salt crystal 80−34762
VP, cryst. struct., X-ray obs. 77−72594
V_3P, superconducting transition temp. 78−47898
$V(PO_3)_3$, cryst. struct., bond lengths, angles 77−80477
VPO_4, IR absorpt. spectra, bond freqs. 80−108192
VPO_5, cryst., vibr. spectra 77−52064
$V_{1+x}P_{1-x}O_{5-c/2}$, density and struct. from X-ray scatt. meas. 77−89380
$V_{1+x}P_{1-x}O_{5-c/2}$ glasses, structure, adiabatic hopping conduction model 77−43588
$V_4(P_2O_7)_3$, IR absorpt. spectra, bond freqs. 80−108192
$V_x(PO_4)_y$, neutron activation determ. of macrocompounds *(Russian)* 77−32859
$V_{1-x}Re_xO_2$ ($0 \leq x \leq 0.15$), insulator-metal transition, DTA, X-ray, mag. and elec. meas. 78−10353
VS through V_3S_4, nonstoichiometric, phase relations and thermodynamics 80−29188
VS_2 (1T), electronic struct. using nonspherical cryst. pot. 80−44498
VS_2, non-stoichiometric phase, physico-chemical props. 80−29532
VS_3, energy shift and struct. of K-absorpt. edge of V 79−38694
$V_{1+x}S_2$, local moment formation, X-ray, mag. susceptibility and NMR meas. 77−69511
V_2S_3, enthalpy and specific heat, temp. depend. 80−54406
V_2S_5, amorphous, electrochemistry in Li cells 80−76626
V_3S-type structures, α- and β-forms, atomic coord. and bonding 79−60330
V_3S_4, antiferromag. order, ^{51}V NMR spectrum 79−56625
V_3S_4, itinerant antiferromag. spin fluctuations, NMR studies 80−93198
V_3S_4-V_5S_8 system, exam. of thermodynamic props. at temp. from 650 to 800°C 78−52784
V_5S_8, antiferromag., NMR meas. 77−36140
V_5S_8, itinerant antiferromag. spin fluctuations, NMR studies 80−93198
V_5S_8, metallic evidence of spin flopping by magnetoresist. meas. 78−6352
V_5S_8, non-stoichiometric phase, physico-chemical props. 80−29532
V_5S_8, paramag. cryst., struct. factors using polarised neutron diffr. 80−15691
V_5S_8, single cryst., mag. props. 78−88098
V_5S_8:Fe, Mossbauer and mag. studies, electronic state of Fe 80−108130
$VS_2(Se_2)$, and alkali metal intercalates, phys. props. 80−44179
VSb_2, free-energy, heat and entropy of formation, 430-600°C *(Ukrainian)* 80−7837
V_3Sb_2, struct. study, space groups *(French)* 77−68949
$VSbO_4$, catalyst particles, converger beam electron diffr. 78−83685
$V_{2-x}Sb_xO_4$, defect struct. exam. 78−18635
VSe_2, 1T, band struct. calc. 79−95324
VSe_2, 1T, quasi-octahedral layer compound, band struct. and Fermi surface 77−76747
VSe_2, 1T polytype, layer cpd., thermal props. at CDW transition 77−47750
VSe_2 (1T), deform. modulated superstruct., electron diffr. expts. 78−51515
VSe_2 (1T), electronic struct. using nonspherical cryst. pot. 80−44498
VSe_2 (1T), Fermi surface calcs. 77−51640
VSe_2 (1T), incommensurate periodic lattice distortion, X-ray diffraction study 80−107414
VSe_2, angle-resolved UPS, Fermi surface determ. 80−55257
VSe_2, CDW and accompanying periodic structural distortions 78−72094
VSe_2, CDW states, correl. mag. and transport props. 79−73494
VSe_2, CDW states, intrinsic mag. props., mag. susceptibility and NMR obs. 78−68397
VSe_2, electrochemical charact. in Li cells 79−1959
VSe_2, fast ion transport and electrochem. storage, Li reactions 80−61324
VSe_2, k-dependent photohole scatt. in photoemission 79−56912
VSe_2, layer dichalcogenides, reflectivity 6 to 40 eV, electronic deep level excitation 77−55801

vanadium compounds continued
VSe_2, metallic behaviour obs., anomalous elec. and mag. props., temp. effects 77−15819
VSe_2 phase, stability and Se equilib. vapour press., homogeneity range 78−43133
VSe_2, press. depend. of CDW transitions, role of Coulomb correlations, elec. props. 78−87927
V_3Se_4, antiferromag. order, ^{51}V NMR spectrum 79−56625
V_3Se_4, itinerant antiferromag., spin fluctuations, NMR study 80−75874
V_5Se_8, itinerant antiferromag., spin fluctuations, NMR study 80−75874
V_xSe_2 (x=1.04,1.13,1.15), crystallographic parameters correlation to heats of formation and reduced length 79−27963
$VSe_{2-x}S_x$ ($0<x<2$) solid solutions, characterisation 80−88730
VSi_2, energy shift and struct. of K-absorpt. edge of V 79−38694
VSi_2, form. from solid phase reaction between Si and Pd-V 80−6568
VSi_2, thermodynamic props. determ. using ternary phase equilibria 78−91449
V_3Si, mixed state, hysteresis in elastic characteristics *(Russian)* 80−103799
V_3Si plastically deformed cryst., lattice transform., Kossel technique 78−95153
V_3Si, quasi-one-dimens. band struct. 78−19596
$(V_{1-x}Ta_x)_2$ C, C ordering formation of varieties 80−38968
$V_{1/3}TaS_2$, Hall coefficient and resistivity 80−39610
$V_{1/3}TaS_2$, magnetic susceptibility, function of temp. 80−39756
VTe, mag. and elec. transport props. 80−92897
$(V_{1-x}Ti_x)Ge$, pseudobinary A15 compound, supercond. transition temp. 80−49970
$V_{1-x}Ti_xO_{1.75}$, synthesis and mag. susceptibility obs. 78−23243
$V_{1-x}Ti_xO_2$, metal-insulator transition, resist. meas. 78−14770
$(V_{1-x}Ti_x)_2O_3$, solid solution, phase transition exam. 77−15590
$(V_{1-x}Ti_x)_2O_3$:Fe, metallic antiferromagnetism, Mossbauer spectra 80−15881
$V_xTi_{1-x}S_2$, elec. and mag. props. 79−65504
$V_xTi_{1-x}Se_2$, cryst. struct. and elec. props. 79−47133
VUS_3, mag. struct. and delocalised moments, powder neutron diffr. obs. 77−69496
$VW_5O_{19}^{4-}$, aq. soln., hydrodynamic radii from ESR line width 79−78504
V_2WO_6, magnetic structure, stability of mag. modes, neutron diffraction study *(French)* 80−39744
$V_xW_{1-x}O_2$, phase relations, vacuum seal study and DTA obs. 79−100122
V0, electronic polarisability of ions 77−40175
Va_2D, neutron diffr. meas. of disorder-order phase transitions 80−29947
$VaH_x(D_x)$, cryst. struct., phase diagrams, order-disorder transition 78−55836
Vo_2, crystal growth by I_2 vap. transport 79−43116
Vo_2, reactively sputtered film, influence of manufacturing parameters on film struct. and props. *(French)* 77−81218
WV_2O_6, magnetic susceptibility, behaviour in terms of quasi-isolated binuclear units 80−97073
α-$W_xV_2O_5$, paramag. defect study by ESR 80−103881
YAG:V_2O_5, CaO, V^{4+} ion impurity spectral anal. 79−78719
$ZnCs_2(SO_4)_2.6H_2O:VO^{2+}$, optical absorpt. spectra obs. 80−40146
$ZnSO_4.7H_2O:VO^{2+}$, single cryst., struct., EPR 78−15014
$ZrV_2D_{4.5}$, deuterated cubic Laves phase, D atom distrib., neutron diffr. anal. 80−29006

vanadium phosphate semiconductor glasses *see amorphous semiconductors*

vaporisation
see also boiling; evaporation; heat of vaporisation; sublimation
ablating material surface, hydrodynamic boundary conditions 79−10939
actinide oxide/rare earth oxide system, high temp. vaporization, valence effects 79−99309
aerosol particles, volatile, diffusion-phoretic motion 77−56259
alkali halides, sputtering, thermal effects, review 80−35033
alloy, complex melt, processes taking place during vaporisation *(Russian)* 79−73298
alloys, binary, vaporisation kinetics from one source with feed maintenance *(Russian)* 79−37824
arc roots, high current, vaporisation effect 78−30496
binary liquid mixture, US evaluation of excess energy of vaporisation 80−65209
binary mixtures, hydrostatic and external field effect, anal. 80−19929
bubble growth, noncondensing gas-vap. injected into liquid 78−55553
ceramic fission reactor fuels, high temperature chemistry, nonstoichiometry, review 77−14238
ceramic substrate, surface spark discharge, channel spreading and substrate vaporisation 77−89336
comet nuclei, vaporisation effects on light curves and life times 80−56772
compound conductors, impulse heating, Cu vapour conc. determ. 80−75346
confined burning jet, droplet vaporisation, expt. and theory 78−94855
correlation range behaviour in gravitational field *(Russian)* 77−62633
cylinder, in vaporisable liq., temp. distrib. calcs. *(French)* 77−14874
diffusion pump jet assembly and vaporiser design optimisation 78−81999
droplet, vaporising, internal temp. field 78−51042
droplet convection vaporization with unsteady heat transfer in circulating liq. phase 80−53771
droplet interactions, vaporisation effects 80−24106
droplet vaporisation in moderately-high temp. stationary media, Chang model 78−34609
droplet vaporisation in two-phase, gas+solid particle, flow 78−55677
droplets, atomized, polydisperse system, nonisothermal vaporisation, algorithm for calc. vaporisation parameters 80−48782
droplets, vaporising, in gas stream in channel laminar entry region 78−30347
electric-arc metal vaporizer with cathode spot magnetic confinement 77−77383
electron beam heating, scattering of beam by target vapour *(Russian)* 77−59825
entropy of vaporisation, var. with temp. up to critical conditions 77−31760
entropy/surface tension relation near melting point *(Japanese)* 79−99397
falling film vaporising surfaces, heat transfer coeff. 78−9542
fluid, combustion, vaporisation and heat transfer under elec. field 80−7798

vaporisation continued
fluid, electric field induced promotion of combustion, vaporisation, and heat transfer 79−20370
fluoride-opacified glass melt, time depend. of volatilisation losses 80−70381
fracture of material through the action of an internal heat source 78−67025
free energy change, classroom example for teaching thermodynamics 80−42010
Freon-113, correlation properties near phase-separation boundary, gravitational field effect 80−107410
fuel-coolant interactions in a shock tube geometry 80−13660
glass melt, high-temp. transpiration apparatus 80−52231
heat flux channel close-up time *(Russian)* 77−55994
high melting particle heating, melting and vaporisation in hot gas 80−6201
high temperature vapours, phase transitions, equations of state, appl. of laser pulse heating 80−52230
high-temperature materials, vaporisation meas. using laser heating system 77−77699
Holbrook chondritic meteorite, experimental vaporisation and mass spectrometry 78−65568
humid atmosphere, water droplet vaporis. model with natural convection 78−33999
hydrodynamic effects, in thermal model of condensed media under action of intense EM radiation *(Russian)* 79−69922
hypervelocity particle impact, heating and vaporisation, temp. estimation 78−59290
internal boiling and superheating in vaporizing multicomponent droplets 79−3906
ionic solid volatilisation, surface charge effects 78−14457
kinetic theory, physical-mathematical problems *(Italian)* 79−40505
kinetics of crystalline surfaces *(Russian)* 77−43424
Kolmogorov statistical model, monolayer, for cryst. vaporisation kinetics, pt.I 79−95151
Kolmogorov statistical model, monolayer, for cryst. vaporisation kinetics pt.II 79−95152
laminar boundary layer flow along vaporising liq. layer *(German)* 78−83403
Langmuir method of vaporisation meas., compact collector device 78−6150
laser heating and burnthrough of opaque solid 77−69940
laser vaporisation of metals for prod. of low energy metal neutral beams 80−77910
laser vaporised surface, free jet expsn. of vapour 78−1703
Leidenfrost phenomena, spheroidal state min. wall temp., total vaporisation times 80−38246
liquid acceleration in channel by intermittent vaporisation, pulsed transfer of energy 79−94701
liquid fuel droplet heating with internal circulation 78−75194
liquid metal, vaporisation in arc heated gas stream, model 79−46795
liquid mixtures, superheat limits, homogeneous vapour nucleation 80−38247
liquid organometallic compounds vaporizer 77−77388
liquid scintillation wastings, vaporisation apparatus *(Japanese)* 80−63502
liquid vaporisation, radiation induced, spinodal singularity manifestation 80−2152
mass and heat exchange in high temp. gas, Sherman eqn. calcs. *(Russian)* 80−39270
metal, partial pressure meas. *(Japanese)* 80−34179
metal cone, vaporisation, solution by wave front method 78−5640
metal film, vaporisation kinetics on absorbing laser radiation *(Russian)* 77−43423
metal film vaporisation by laser, vaporisation front relativistic velocities *(Russian)* 80−66337
metal surface crater form., by laser pulse, frontal method, approx. soln. 77−77327
metal vaporisation, optical spectral methods of vapour press. meas., review 79−66381
metal vaporisation by laser irrad., effect of plasma 79−1800
metal vaporization rate improvement in electron-beam vaporizers with water-cooled crucibles 78−21266
metallic mirrors, laser damage, temp. depend. of absorptance, vaporisation and vap. heating 79−81471
metallic particle, surface tension depend. on size, vaporisation time *(Russian)* 80−34290
metals, erosion accompanying simultaneous action of laser emission and ultrasound *(Russian)* 80−7442
metals, expansion, isentropic, vaporisation and condensation kinetics anal. 77−66623
metals vaporisation by laser beams, effect of delivery pressure time dependent behaviour *(Russian)* 79−55877
methyl salicylate, vapour phase, absorption and fluorescence spectra 79−81232
molecular spatial and vel. distrib. from evaporation source *(French)* 77−69999
molecular spatial and vel. distrib. meas. from evaporation source *(French)* 77−70000
molecule cluster fluid, phase changes, theory 77−15534
multi-droplet system in vapour flow, time-evolution, mathematical formulation 79−41733
multidroplet system, condensation-evaporation by kinetic theory 80−7873
nonisotropic systems near liquid-vapour critical point, similarity hypothesis, gravitational effects 80−17913
nonstoichiometric cpd., excess component conc. meas. 78−43113
opaque solid slab, laser heating and burnthrough, anal. 77−48284
oxides, sputtering, thermal effects, review 80−35033
packed bed, temperature profile for concurrent air-water downflow, latent ht. effect 79−50789
partial wave propag., influence of rapid particle fluxes *(Russian)* 79−38696
particles, vaporisation calc. taking account of rarefaction of medium *(Russian)* 80−24575
particles in nonisothermal plasma jet, trajectory and temp. calcs. *(Russian)* 80−7514
pentane-benzene solution, vapour-liquid equilibrium study, vaporisation critical state *(Russian)* 80−79931
plasma arc contamination by electrode vapour 77−65924
porous moist body, contact heating moulding, temp. distrib. heat/mass transfer 77−75784

vaporisation continued
powder, polydisperse, heating and vaporisation in plasma stream *(Russian)* 77−59707
pulsed laser light stimulated desorption and local vaporization 77−16432
radiating gas flow over blunt body with intense vaporisation 77−35255
radioiodine volatilisation problem, soln. using plexiglas iodination box 77−56484
rapid surface vaporisation with back pressure, Knudsen layer, flow Mach number 79−77168
rare earth compound vaporisation by cathode ray and HF ion-plasma methods 77−77380
rare earth halides, prep. and props., book contrib. 80−54211
rare earth metal-B systems, phase equilibria, phase diagrams, book contrib. 78−48389
rare earth nitrides, Knudsen cell vaporization, vaporization enthalpies 79−10936
refractory materials, vaporisation by electron bombardment in UVN-71R-3 installation 77−28722
refractory metal-Al_2O_3 systems, vaporis. at elevated temp., mass spectrometric obs. 79−29388
refractory oxide, high temp. props. conf., Odeillo, France (June/July 1977) 79−100125
rock vaporising to elements, meteorite impact study 80−36583
rotating radial pipe with liq. film, Coriolis effect, film width and vaporisation 79−18955
selective volatilisation, in DC arc, direct-reading spectrometer obs. 77−73480
simple fluid, continuity of isochore slopes and divergence of curvature of vaporisation curve 77−39670
solution, binary, and pure material, isomorphism of crit. vapour form phenomena *(Russian)* 77−13723
solution droplets vaporisation, in high-temp. gas flow, heat and mass transfer 78−75191
spherical drop combustion, asymptotic, drop shrinkage and flame movement, heat and mass transfer 77−81405
spray cooling, characts. and minicomputer control *(French)* 79−3889
superheated liquid discharge from nozzle, pressure calc. 80−92199
superheated liquids, vapour generation in steady flashing flow, appl. to fission reactor LOCA anal. 80−23004
surface vaporisation under conc. energy sources, thermal model development *(Russian)* 79−74091
thermal pulse shape effects on vaporisation of plate *(Russian)* 77−54858
thermoelectric materials vaporisation suppression, p-type $(Cu,Ag)_2Se$, using inert and reactive coatings 79−48149
TTF-TCNQ, mass spectroscopy 77−1224
two-phase flow dynamics in vap. generator 78−94808
two-phase nonequilibrium flow, spectral characts. 78−94854
vaporisation kinetics in vacuum *(Russian)* 77−72683
vaporisation sites, number variation with fluid layer height 78−59273
vapour deposited coatings, two-component from two sources, geometrical aspects of prod. *(Russian)* 79−38743
vapour pressure measurement, effusion method, review 80−51995
volatile highly thermally conductive spherical drop, theory of diffusiophoresis 80−14784
volatile liquid, boundary viscosity, meas. by blowoff method 79−11006
water, vaporisation and thermoelastic press. due to CO_2 laser pulse 80−84227
water droplet, explosive vaporisation on 10.6 μm radiation exposure, inhomogeneous internal heat evolution 80−29162
water films vaporisation in rot. pipes 79−14228
Ag, vaporization, thermodynamic props. determ. by mass spectroscopy 78−22841
Al fracture speed during phase explosion due to electron beam irrad. *(Russian)* 80−76336
Al, laser pulse damage at 10.6 μm, single cryst. target in vac. 77−50706
Al, neutron activation analysis, trace element removal technique 79−57309
Al oxidative vaporisation, thermochemical analysis 78−11447
Al, rhodamine 6G laser radiation interaction 80−97387
Al_2O_3, high temp. gas phase equilib. formation enthalpy, dissoc., mass spectra 78−23925
Al_2O_3, vaporisation process, mass spectrometric exam. 77−1220
$3.5Al_2O_3.2SiO_2$, mullite, decomposition by SiO_2 volatisation 80−61082
^{241}Am high-purity solid, reln. to electronic structure and mag. props. 77−28011
As, (111) surface, freshly cleaved, vaporisation, surface morphology changes obs. 77−80612
As_2S_3, amorphous film, light enhanced vaporisation, photolithographic process, photographic appls. 77−5949
As_2S_3 films, kinetics of light-enhanced vaporisation rel. to photocond. 77−84919
As_2S_3, mass spectrometric analysis 78−22843
Au-Cl system, high temp. vaporisation chemistry incl. form. of vapour complex species 79−47963
B_2O_3, volatility, effect of batch composition of liquating glass 77−27995
Bi, vapour, optical activity, Faraday effect, parity nonconservation, mag. transitions *(Russian)* 80−55070
C, into nonequilib. stagnation point boundary layer, Jupiter probe heat shield 79−1264
CO, vaporisation temp. and press., state eqn. *(French)* 77−43323
$CaSO_3$, thermal decomp., enthalpy of form. 77−73460
CdS single cryst., vaporization and form. of negative whiskers 80−92659
CdS(Se), uncoated and liq. layer coated, vaporisation mechanism, surface morphology 77−35683
Cr oxidative vaporisation, thermochemical analysis 78−11447
Cr, volt ampere characteristics during electron melting process *(Russian)* 80−75336
Cs, vaporisation by laser impact for production of atomic beam pulses 80−37123
Cs_2CO_3 and Cs_2SO_4, ionic equil., mass spectra obs., heats of reaction and form. of ions 79−87867
Cu fracture speed during phase explosion due to electron beam irrad. *(Russian)* 80−76336
Cu, vaporization, thermodynamic props. determ. by mass spectroscopy 78−22841
Cu, vapour production method, hollow cathode arc., Ar buffer gas 78−86981
$EuBr_2$, vaporisation thermodynamics, enthalpy sublimation 78−22837
Eu_2O_3+$EuPO_4$ in Mo crucible, $EuMoO_4$ and $EuMoO_3$ atomisation energy 78−40073
vaporisation continued
$EuPO_4$ in Mo crucible, $EuMoO_4$ and $EuMoO_3$ atomisation energy 78−40073
EuS, vaporisation thermodynamics, Knudsen cell mass spectra 77−47569
Fe-Cr (25 wt.%), vaporisation kinetics in vacuum *(Russian)* 77−72683
$FeBr_2$, UV-visible absorpt. spectrum, vaporisation thermodynamics 78−13512
$Fe_{1-x}O$, wustite, vaporisation, mass spectrometric analysis of gaseous phase 78−48652
Fe_3O_4, magnetite, vaporisation, mass spectrometric analysis of gaseous phase 78−48652
GaAs vaporisation during laser annealing 80−25495
Ga_2S_3, partial vapour press. of Ga_2S, anomalous temp. depend. 77−62634
GdS, vaporisation thermodynamics and dissoc. energy obs. 78−67822
GeTe, high temp. mass spectrometric obs. 77−76542
Hg, in NAA from samples and standards *(Russian)* 80−41128
$Hg_{1-x}Cd_xTe$, vaporisation under Knudsen effusion conditions 80−2154
Ir oxidation and vaporisation of the volatile oxides, gravimetric exam. comparision with losses due to vacuum annealing *(Russian)* 79−57136
K_2CO_3 and K_2SO_4, ionic equil., mass spectra obs., heats of reaction and form. of ions 79−87867
KD_2PO_4, transparent dielec., thermal analysis of laser-induced damage 80−66336
$K_2Mo_3O_{10}$ melt volatility, solubility of $YAl_3(BO_3)_4$ 80−65211
K_xO_y, thermodynamic props. 80−29184
K_2SO_4, effusion studies of vaporisation/decomposition 79−95153
K_2SO_4, mass spectrum obs. of vaporisation, vapour comp. and press., transition and form. heats 80−19933
K_2SO_4, vaporisation thermodynamics, MHD generation appls. 77−9112
La-B, phase and thermodynamic props., vaporisation 78−51660
LaB_x, phase relationships, chemical activity and work function obs., thermionic appls. 77−90234
$LaCrO_3$, vaporization in oxidizing atmos. 80−24579
Li-LiH two-phase equil. system, vaporis. diagram at high temps. 80−19926
Li_2O, mass-spectrometric study of vaporization of solid and thermochemistry of gas 79−10940
LuS_n, high-temp. vaporisation and thermodynamics 79−73325
Lu_3S_4, high-temp. vaporisation and thermodynamics 79−73325
Mg, heating by shock compression, of porous material, vap. form. *(Russian)* 78−2195
Mg, vaporisation from inductively stirred melt, meas. and prediction 78−51659
Mg, vaporised, evidence for gas-surface exchange 78−91532
$MgAl_2O_4$-Cr_2O_4, vaporization 79−99308
MgO, vaporization in O_2-H_2O atmos. *(Japanese)* 79−74279
MgO-$(Cr_2O_3)(AP_2O_3)(Fe_2O_3)(SiO_2)$, vaporization 79−99308
MgO-Al_2O_3-Cr_2O_3, vacuum vaporisation, Langmuir method 78−95149
MgO-Cr_2O_3, vaporisation rate, O_2 partial press. effect *(Japanese)* 78−63848
Mg_2SiO_4, vaporization 79−99308
MnSe, vaporization, thermodynamic study by Knudsen-cell mass spectrometry 79−10937
Mo, vaporisation, influence of inert gases on losses *(Russian)* 79−55878
Mo, volt ampere characteristics during electron melting process *(Russian)* 80−75336
Na, vaporisation from capillary-porous structs. (heat tubes, vap. chambers) crit. heat flux 78−90631
NaCl, interpolational eqn. of state with allowance for melting, vaporis., dissoc. and ionis. processes 80−24566
NaCl, thermodynamic equilib. vapourisation, transpiration mass spectrometry 80−52356
Na_2O-B_2O_3-GeO_2 glass-forming melts, thermodynamic props. and vaporisation processes, mass spectrometric study 80−79926
Na_2O-SiO_2 glass, influence of $p(O_2)$ on Na vaporisation at 1345°C 80−6502
Na_2SO_4, thermodynamic equilib. vapourisation, transpiration mass spectrometry 80−52356
Nb, vaporisation, influence of inert gases on losses *(Russian)* 79−55878
Nb, volt ampere characteristics during electron melting process *(Russian)* 80−75336
Ni-Cr-Co-W (47.5, 25, 12, 8.75 wt.%), vaporization of IN-643, high-temp. mass spectrometry 79−7685
Ni-Si melt refining by electric fields, ionic conduction of Ni, Si *(Russian)* 80−65273
Ni-V, solid soln., diffusion and thermodynamic props. 80−65278
Ni_3S_2, exam. of vaporisation kinetics, using a levitation technique 78−51658
O_2, vaporisation temp. and press., state eqn. *(French)* 77−43323
P_4S_{10}, gas, vaporisation and thermal dissoc. obs. *(French)* 78−47511
P_4S_3, gas, vaporisation and thermal dissoc. obs. *(French)* 78−47511
P_4S_7, gas, vaporisation and thermal dissoc. obs. *(French)* 78−47511
PbO-Re_2O_7 system, gas phase components obs. using mass spectrometry *(Russian)* 79−96354
Pd-Fe (1 wt.%), alloy component surface conc. changes kinetics under vac. sputtering and volatilisation *(Russian)* 79−60608
Pt oxidative vaporisation, thermochemical analysis 78−11447
Pt-Ba cathode, vaporisation expts., heat of adsorpt. and migration of Ba on Pt 78−10272
Pt-Rh alloys, surface behaviour on heating in air, XPS and SIMS *(French)* 77−40327
$(SN)_x$, mass spectroscopy 77−1224
Sb_2Se_3 solid, vaporization, thermodynamic props. of molecules formed 80−11943
ScP, thermodynamics and high temp. vaporisation 80−88310
$ScPO_4$, $Sc(PO_3)_3$, mass spectra 77−47567
Sc_xS, high temp. vaporisation, enthalpy, atomisation, dissoc. energies 77−1223
Si oxidative vaporisation, thermochemical analysis 78−11447
SiO_2 based glass melt, Na vaporisation, H_2O vapour effects 77−55353
SiO_2, vaporisation in steam atmosphere 80−44306
SmF, sublimation, Knudsen effusion method 80−6508
SrO, heated on W, vaporisation behaviour, mass spectrometric thermal anal. 77−56277
Ta, vaporisation, influence of inert gases on losses *(Russian)* 79−55878
ThO_{2-x} phase, high temp. vaporisation behaviour 79−54508
ThO_x:Y_2O_3 solid electrolyte high-temp. vaporisation obs. 78−14456
Ti-Pt link on Si_3N_4-SiO_2-Si substrate, laser vaporisation, interference effects 77−69941

vaporisation continued
TiO, high temp. thermodynamics, vaporisation, and pressures over 80−10685
TiO, high temp. vaporisation and thermodynamics, stoichiometry, mass spectra 77−59109
TiO, high temp. vaporisation and thermodynamics, vapour press. temp. coeff. 77−59110
TiS, vaporisation chemistry and thermodynamics, computer-automated simultaneous Knudsen-torsion effusion 80−48837
UCl_4, vaporisation thermodynamics 78−44394
UO_2 dynamic vaporisation, rate effects rel. to fast reactor safety anal. 79−31034
UO_2 phase, thermodynamic props. 80−13594
UO_2 volatization pot. of metallic inclusions in irrad. nuclear fuel during LOF overheating transients 80−57895
V, volt ampere characteristics during electron melting process *(Russian)* 80−75336
W, heat resistant particles in low temp. Ar plasma, heating, melting, vaporisation *(Russian)* 80−40384
W high-current multicavity thermionic cathode, erosion mechanisms, sputtering 79−55570
W, vaporisation, influence of inert gases on losses *(Russian)* 79−55878
W, volt ampere characteristics during electron melting process *(Russian)* 80−75336
ZnO, from defective spinel powders, in vac. 80−16675
ZnO, vaporization from spinel solid solns. 77−76541
ZnS, negative whisker form. by solid-liq.-vapour mechanism 77−35684
ZnS, uncoated and liq. layer coated, vaporisation mechanism, surface morphology 77−35683
ZrI_4, thermodynamics of vaporisation and high temp. enthalpy 78−91432
ZrI_4, thermodynamics of vaporisation from substoichiometric solid Zr iodides 80−3393
ZrO_2, substoichiometric, thermodynamic props. at lower phase boundary 80−29185
ZrO_2-Y_2O_3-Nd_2O_3, high-temp. thermophys. props. 78−26663

vaporising *see vaporisation*

vapour density *see density of gases*

vapour deposited coatings
see also CVD coatings; plasma deposited coatings; sputtered coatings; vacuum deposited coatings
adhesion measurement methods 80−50822
alumina deposition by activated reactive evaporation, struct. obs. 77−44176
automated vapour deposition apparatus based on programmable calculator 78−44022
backscattering yield of 2 MeV ^4He, target texture influence 79−4875
carbide coating, oxidation protection 77−32704
ceramics, glazing with gaseous P_2O_5 80−108609
chloroaluminium phthalocyanine, sublimed layer, IR absorption, vibr. assignments 78−55174
cobalt, phthalocyanine, sublimed film, absorption spectra and association 78−48174
columnar microstructure, shadowing mechanism 78−22987
condensed alloy film vaporisation method 77−85942
condensed two-dimensional phases on foreign substrate, structural aspects 77−20209
copper phthalocyanine, sublimed film, absorption spectra and association 78−48174
Cr on Kh25N20S2 steel, structural transformations, oxidation effect 79−57154
diamond-based, fabrication and wear resist. 80−40576
dichloride 2.4′-bis (trimethylammonium-acetamide)-benzal-fluorene, thin layers, behaviour in electric field *(Rumanian)* 80−35108
dielectric films, refractive index and structure, deposition temp. depend. 79−4857
dielectric layers on semiconducting substrate, ellipsometric monitoring 79−49272
dimethyl stilbene chloride, organic semiconductor thin film on glass, voltampere charact. *(Rumanian)* 79−38196
3,4-dimethyl-1,2,5-thiadiazol plasma polymerised film for holographic recording 80−106490
diphenyl anion salts, sublimed layer, electronic and IR absorpt. spectra 80−66189
film, evaporated at oblique incidence, columnar grains inclination angle 80−75468
fluoride films, refractive index and structure, deposition temp. depend. 79−4857
glass 7059, film acousto-optical props. for integrated optical Bragg cell 79−55251
growth morphology, effect of absorbed gas 78−11370
In_2O_3-SnO_2, thin films deposited on cold substrates, life stability 79−23867
industrial appl. 78−72042
ion implantation simultaneous with deposition, gas impurity distrib. 79−69146
ion plated filament, improved strength *(Japanese)* 77−90282
ion plating, surface treatment comparison *(French)* 79−57132
ion plating, techniques and applications 77−70005
ion-beam-activated vacuum deposition, struct. and props. of deposits 80−15422
laser beam metal-coated apodising apertures 77−19439
laser deposited dielectric thin films, optical and struct. props. 80−7506
low energy stopping powers of ^3He and ^2H, new meas. method 79−4351
magnetic anisotropy rel. to columnar microstruct., calc. 80−39822
manganin thin film microtransducers for elastohydrodynamic lubrication studies 80−37048
mech. props. 78−6247
metal, chemisorpt. of O_2 active sites, chemiluminesc. and vacuum microbalance obs. 78−22950
metal coatings, obtained by vacuum evaporation and sputtering, mech. props. rel. to prep. conditions 77−59239
metal film, evaporated, surface area rel. to temp., gas adsorpt., nature of substrate 78−79909
metal films, evaporated, interaction with BCl_3, HCl, adsorpt. 78−75945
metal oxide, highly dispersed, transparent coatings, electrically conductive 79−24637
metal vapour condensate, anisotropy in electric field 80−15624
metallic layer, vapour deposited, struct., resist. component manufacture appl. *(German)* 77−55467

vapour deposited coatings continued
metallurgical coatings, conf., San Diego, USA (23-27 Apr., 1979) 80−12848
metastable phases, convergent beam electron microscopy obs. 80−108689
microporosity described in terms of vacancies and voids 80−24769
morphological features, struct. defects, laser evaporated thin films 78−67926
naphthacene film, electron escape depth, energy depend. 79−38709
naphthalene, microcryst. and evaporated film, excimer emission 80−2823
nuclear targets, thin, techniques used in preparation 79−85201
optical, thickness monitoring using quartz cryst. monitor 78−5592
optical fibre preform diagnostics, nondestructive noncontacting method 79−27376
optical film, thickness monitoring 78−5591
optical films, optical, struct. and mechanical properties 79−76772
oxide, pore size distrib. and permeability 79−24641
oxide films, refr. index and struct., deposition temp. depend. 79−4857
pentacene, disordered solid layer, absorpt. spectra 80−93417
pentacene, evaporated film elec. cond. meas. for various temps., SCL 78−10584
perylene film, electron escape depth, energy depend. 79−38709
polypropylene coating, glow-discharge-polymerised, adhesion and hydrophilicity 79−15829
prism-film coupler, for investigation of thin films condensed onto cold substrate 78−24873
pyrocarbon, agglomerate model 77−79458
pyrocarbon, coating process and model 77−79459
rare earth oxide films, optical absorpt., refractive index, band gap and zone struct. *(Russian)* 78−76544
rare earth oxides, reactively evaporated, struct. and polymorphic transforms. 79−51441
rare earth-transition metal alloy magnetic thin films, influence of gaseous phase on mag. props. *(Polish)* 80−39820
rare earth-transition metal amorphous film, microstruct. 77−51619
refractory compound hard coating, electron beam evaporation in reactive atm. 77−44396
refractory films, stability, high temp. and electron irrad. effects 77−39747
screen printing, in solar cell metallisation 80−85291
SEM, non-conductive specimens, determ. of thickness and grain size of deposited films by TEM 78−77170
silicide coating, oxidation protection 77−32704
temperature meas., precise, using combination of Pt resistor and Au-Pt thermocouple 79−49227
tetracene, disordered solid layer, absorpt. spectra 80−93417
texture formation in films obtained by oblique mol. beams, texture formation *(Russian)* 77−66592
thin film growth, mean thickness at which films reach continuity 79−51459
thin film growth, surface self-diffusion coeff., adhesion energy of evap. material 78−84080
two-component from two sources, geometrical aspects of prod. *(Russian)* 79−38743
vanadyl phthalocyanine, sublimed layer, IR absorption, vibr. assignments 78−55174
Ag, evaporated, chemisorption effects on reflectance and elec. resist. 80−11495
Ag film, ion plated, on AT-cut quartz crystal, crystallographic structure obs. 80−2280
Ag film, lattice defects, convolution relations for X-ray line breadth calcs. 78−51394
Ag, ion beam plating using mass analysed ions, SIMS and AES expts. 78−19673
Ag, on Cu, defects and their effect on props. 80−39474
Ag, on mica, microstruct. changes 78−72013
Ag, on W, scanning Auger microscopy, effect of backscatt. electrons on resolution 79−2898
Ag ultrafine particles evaporated on glass, optical transmittance meas. 79−78772
Ag-Ge (4.5 at.%), FCC, lattice imperfections, X-ray diffr. 78−72032
Ag-Pd, composition modulated foils, layer struct. and mech. props. 79−95300
AgBr, evaporated layers, use as registrating system *(Bulgarian)* 80−52344
Al cathodes for He-Ne lasers, performance improvement by Cu addition 80−5748
Al, corrosion in distilled water, ellipsometric obs. 77−48590
Al, film and polished bulk specimens, initial stages of oxidation obs. using SIMS 80−81239
Al, ion plated through mask hole, thickness nonuniformity *(Japanese)* 79−19999
Al on Kh25N20S2 steel, structural transformations, oxidation effect 79−57154
Al, on NaCl, defects and their effect on props. 80−39474
Al thin films evaporated on rough quartz substrates, surface irregularity, light scattering measurements *(Polish)* 80−88450
Al/Cu laminates, vapour deposited, strength enhancement 79−24576
Al-Al_2O_3-GaAs MOS struct., mol. beam reaction growth of Al_2O_3 film, C-V charact. 80−11095
Al-Be, two-layer foils, mech. props. *(Russian)* 78−51858
Al-Cu (0.5 wt.%), evaporated layers, electromigration, linewidth depend. 80−65277
Al-Cu (1 to 10 wt.%), vapour deposited films, ion scattering spectrometry characterisation 80−15386
Al-Cu film, galvanostatic formation anodic oxide, Rutherford backscattering and depth profiling 78−92395
Al-Ge film, random percolation, elec. resist. meas. 79−28418
Al-Ni with multiple layer plasma coating, exam. of cohesion strength *(Russian)* 80−7714
Al-SiO_x-Al evaporated film anomalous dielectric dispersion under high DC field 80−15620
AlN, nonlinear optical susceptibility, SHG expts. 78−30012
Al_2O_3, layer, obtained by reactive evap., surface struct. and morphology *(Polish)* 79−28242
Al_2O_3-Cu composite, dispersion-strengthened, hardness, tensile strength and struct. 77−70063
As, film A1-type supercond. vapour-quenched transition temp., A7-type phase transition 78−52145
As_2S_3, amorphous, elec. cond. mech. obs. *(Japanese)* 80−11028
As_3S_3 and As_4S_4, valence states, thermal and photo-induced changes UPS study 80−93459

vapour deposited coatings continued
Au, as deposited film, voids 77−69194
Au bicrystalline film, lattice imaging of low angle tilt boundaries by TEM 78−79620
Au black solar absorber, struct. comp. and optical props. 78−27339
Au film, on Si, coincidence site phase boundaries 78−67927
Au films, condensation on alkali halides, growth, struct., stability *(French)* 78−38989
Au, ion beam plating using mass analysed ions, SIMS and AES expts. 78−19673
Au, ion plated, defect growth structs., SEM obs. 80−24768
Au, mean thickness at which films reach continuity 79−51459
Au, nuclei interaction on KCl (100) surface 77−89670
Au, on alkali metal substrates, calc. binding energy of Au atoms to substrate 79−33208
Au particles, small vapour deposited multiply twinned, struct. anal. using TEM 79−82488
Au, surface struct. and lattice const., TEM obs. 77−1326
Au-Co, co-evaporated, struct. and ohmic behaviour 79−87021
Au-Ge evaporated film, effect of substrate on conductivity 79−78213
Au-Ni, composition modulated foils, layer struct. and mech. props. 79−95300
Au-Sn layer system, on glass, thin film interdiffusion 77−20134
AuFe alloy films, mag. susceptibility, Fe concentration and annealing depend. 79−61119
B, amorphous film, Raman scatt. exam. 78−39545
B film growth by phys. vapour deposition 80−16200
B-transition metal thin films, amorphous to cryst. transformation 80−7563
BaO on Ir, thermionic props., Auger, LEED, and emission microscopy 79−43089
Be film, vapour quneched, mech. stresses and elec. cond. 79−73414
Bi, film A1-type supercond. vapour-quenched transition temp., A7-type phase transition 78−52145
Bi, superconducting ultrathin film, metastable, supercond. props. *(Russian)* 79−7917
Bi, vapour deposited on NaCl cleavages, crystallinity depend. on deposition parameters 78−63955
$Bi_{1-x}Sb_x$ film, evaporated, cross-sectional struct., electron microscopy and replica technique study *(German)* 78−22977
C fibre, Al-coated, stress rupture 78−80628
C films with high conductivity, prep. and props. 80−80983
C, ion-plated, on metal, deposition method, graphitic struct., and tribological props. 78−11440
C, transparent and hard insulating layer, struct. and props. 80−10830
CaF_2, Na-resistant glass cell, coating apparatus 80−90874
$CdCr_2S_4$, ferromagnetic semiconductor films, prep. and props. *(Japanese)* 79−47308
CdI_2, sublimed films, preparation, struct. 77−24491
CdS film, surface stoichiometry rel. to CdS-Cu_2S cell performance 78−2956
CdS film preferred orientation, internal stress, and interface characteristics 78−26795
CdSe thin film transistor on Cr substrate, cryst. struct., substrate defect effects 80−70563
CdTe, film grown in quasi-closed volume, struct. *(Russian)* 78−75952
$Cd_{1-x}Zn_xS$ 10 μm film optical and electrical characterisation *(French)* 78−64153
Co, evaporated, uniaxial mag. anisotropy 77−51929
Co, ferromag. film, ion plating prep., coercive force and magnetoresist. 77−12546
Co, on Ni-Cr type alloys, surface pretreatment to attain pore-free aluminised coatings 80−40612
Co-Ni, ferromag. film, ion plating prep., coercive force and magnetoresist. 77−12546
Cr film, vapour deposited on low temp. KCl substrates, struct. obs. 80−10826
Cr, on mild steel, hardness and protective props., rel. to grain size 78−11436
Cr, physically vapour deposited, struct., mech. props. 77−36400
Cr ultrafine particle selective absorption of solar energy 79−62035
Cr ultrafine particles, selective solar energy absorption 78−18027
Cr-$NdAlO_3$, dielectric films, phase composition and structure 80−39464
Cr-SiO cermet film, silicide form. during deposition 77−12535
CrN, deposition by hollow cathode discharge process, and hardness 79−24452
CsI, secondary emission yield, primary electron ang. of incidence effects 78−2961
Cu alloy solid solution condensed films, influence of alloying components on phase composition and lattice spacing *(Russian)* 80−20047
Cu, ion plated, defect growth structs., SEM obs. 80−24768
Cu, ion plating onto ABS plastics, expt. study *(Japanese)* 78−6858
Cu ion-plated coating, grain structure 79−28249
Cu, on ceramic substrate, RF bias ion plating process and microstruct. 78−11132
Cu on Mo and steel, substrate limiting temp. during vaporisation and condensation coating in vacuum *(Russian)* 80−100787
Cu, on polystyrene, surface complex, XPS obs. 78−72026
Cu, on polystyrene, unusual core level spectra, XPS obs. 79−24415
Cu-Cr, vapour deposited, electron irrad., resistance behaviour *(German)* 78−47779
Cu-Fe, vapour deposited, electron irrad., resistance behaviour *(German)* 78−47779
Cu-Ni evaporated thin film couple interdiffusion obs. 78−43187
Cu-Ni(Pd), composition modulated foils, layer struct. and mech. props. 79−95300
CuBr, evaporated film, magneto-optical effects on exciton bands 78−72624
CuCl, evaporated film, magneto-optical effects on exciton bands 78−72624
$CuInS_2$ single phase thin film prep. by flash evaporation 80−100796
$Cu_xMo_6S_8$, superconducting reactively evaporated film, crit. currents 79−28492
Er-diphthalocyanine complex, electrochromism *(Japanese)* 80−20611
Fe evaporated at oblique incidence, columnar grain struct. using anisotropy field meas. 77−59231
Fe film, evaporated at oblique incidence, columnar and textural struct. *(Japanese)* 77−62776
Fe on Al_2O_3 substrate, controlled vapour growth of small particles 78−75958
Fe-Co (46%), evaporated, uniaxial mag. anisotropy 77−51929

vapour deposited coatings continued
Fe-Cr-Mo and Fe-Cr-Mo-Si alloys, amorphous films, corrosion resist. and ion plating use 80−89423
Fe-Cu alloy, struct. and thermal stability 78−43265
Fe-Fe_2O_3 composite films, structural props., microhardness, 250 to 700K 78−84095
Fe-Ni-Cr, vapour-deposited film, effect of condensation temp. on form. of metastable phases and mag. props. 79−65700
Fe-Ni-Cr vapour deposited film metastable phase formation *(German)* 78−38984
FeF_3 thin film prep. and charact. *(French)* 78−64470
$Fe_{32}Ni_{36}Cr_{14}P_{12}B_6$, Metglas amorphous films, corrosion resist. and ion plating use 80−89423
Ga, film, polymorphism, electron diffr. obs. *(French)* 78−18922
$Ga_xAl_{1-x}N$ film, growth and props. 78−39702
GaAs film, vapour-grown, effect of gas-phase stoichiometry on deep levels 78−10393
GaAs layers, from gas phase, impurity influence on growth micromechanism 80−45237
GaAs, vacuum deposited Shottky barrier metallisation 79−78153
Ga_2O_3 thin films, reactively evaporated, props. *(Japanese)* 79−99648
Gd-Ag (0-16 at.%), vapour-quenched, struct. and mag. props. 78−38980
Gd-Co, vapour quenched amorphous, struct., electron diffr. meas. 77−28086
GdFe homogeneous amorphous films, compensation point switching, magneto-optical Kerr signal anal. 80−15726
Ge alloy, amorphous film, formation and stability criteria 79−10799
Ge film, amorphous, prepared by evap. or sputtering, AC loss meas. 80−65560
Ge-Al(Cu), alloying effects on elec. transport props. of amorphous and crystalline Ge films 79−51689
H_xWO_3 films, proton diffusion coeffs. 80−6548
HfN on stainless steel, activated reactive evaporated coatings, high rate deposition, microhardness 80−25580
HfO_2, obtained by vapo-condensation, exam. of structure and phase props. *(French)* 79−19489
Hg lamps, RF-excited, dark film anal. 80−92789
Ho-Co, vapour quenched, amorphous, struct., electron diffr. meas. 77−28086
In-Ge film, random percolation, elec. resist. meas. 79−28418
In-In_2O_3-Pb, Josephson tunnel junction fabrication for MM-wave detector 80−100427
$In_{1-x}Ga_xSb$ films, elec. props., preparation 80−100473
In_2O_3, films, activated reactive evaporation technique of prep. 80−80989
In_2O_3, reactive ion plating onto insulating substrates, and elec. and optical props. 79−87588
In_2O_3, transparent heat mirror formation by ion plating on ambient temp. substrates and props. 80−25578
In_2O_3:Sn, films, activated reactive evaporation technique of prep. 80−80989
n-InP film, polycryst., deposited on Mo sheets, elec. props. obs., w.r.t. varying deposition conditions 79−4608
Ir, electron beam deposition and ion plating 77−44166
LiF, secondary emission yield, primary electron ang. of incidence effects 78−2961
$LiNbO_3$ SAW filter bulk wave suppression by triangular metal film overlay 77−23830
Mn-MgF, cermet film, evaporated, variation of elec. resist. with prep. conditions 77−43746
Mn-MgF, cermet film, variation of resist. with deposition rate 77−43747
Mn-SiO cermet film, silicide form. during deposition 77−12535
MnBi film, electrical props., in situ annealing effect 80−65708
Mn_3Ge_2, $Mn_{11}Ge_8$, amorphous thin films, quasieutectic model, electron diffr. investigation of short range order 79−69013
Mo, condensed layers, restricted growth texture formation singularities *(Russian)* 77−7982
Mo film on Si surface, $MoSi_2$ form. conditions *(French)* 78−43270
Mo heater-substrate system design, model of radiant heat exchange appl. *(Russian)* 78−95701
Mo, on ceramic substrate, RF bias ion plating process and microstruct. 78−11132
Na-NH_3 film, vapour deposited, elec. resistivity, metal-nonmetal transition 78−84317
Nb, film, evaporated, adsorpt. of SO_2, corrosion 78−79897
Nb films electron beam evaporated, struct. defects *(German)* 77−76684
Nb layer, ion bombarded, supercond. props. and struct. 80−88671
Nb-Ni, amorphous thin film, vapour quenched, elec. resistivity and thermoelectric power 79−33275
Nb_3Sn patterned film, appl. to refractory lift-off process using Nb-Cu bilayers 79−47626
Nb_3Sn, supercond., surface resist. and penetration depth 79−33392
Nb_3Sn, vap. deposited supercond. film, effect of N_2 and tape heating 78−34939
$NdAlO_3$, dielectric films, phase composition and structure 80−39464
Ni, evaporated, uniaxial mag. anisotropy 77−51929
Ni, ferromag. film, ion plating prep., coercive force and magnetoresist. 77−12546
Ni film, evaporated, chemisorpt. of CO, ellipsometric investig. *(German)* 80−61156
Ni film on leucosapphire, island growth as annealing in Ag vapour *(Russian)* 78−51830
Ni, on graphite, formation and decomposition of Ni_3C 79−15055
Ni, precise temp. meas. using combination of Pt resistor and Au-Pt thermocouple 79−49227
Ni-Co-Cr-Al-Y, electron beam evap., low press. gas scatt. 77−40474
Ni-Cr film, long range order 79−60657
Ni-Fe (15%), evaporated, uniaxial mag. anisotropy 77−51929
Ni-ZrO_2, thin layers, vapour deposited, dispersion strengthened, exam. of struct., mech. props. 78−80554
Ni_3C film, thermal decomposition, AES meas. 78−56056
$NiSi_2$, layer, on Si, ion implantation damage, channelling obs. 78−30676
$PaCl_2$, thin films, reduction to Pd by Ne^+ ion irrad., 2 MeV He^+ ion backscatt. anal. 79−4493
Pb film tunnel junction, thermal cycling stability enhancement using substrate with large thermal expansion 79−87200
Pb-PbO-Pb, Josephson tunnel junction fabrication for Mm-wave detector 80−100427
PbF_2 film, ionic conduction, effect of hydrostatic press. *(French)* 79−28259
PbIn films strengthening, by preventing formation of misfit dislocations 80−84858

vapour deposited coatings continued
PbO layer vapour deposition, structure, and props. 80−65408
PbO layers, crystal platelets orientation and thickness, X-ray diffr. obs. 78−87890
PbO, on vitreous SiO_2, interdiffusion reactions, UV spectroscopy obs. 78−51750
PbO, polycrystalline layers, influence of prep. conditions on phase comp., texture and struct. 79−4495
PbO, reactively evaporated photoconductive film, phase transform. induced by water vapour 79−78233
PbSe films, synthesis and growth 80−45236
$Pb_{0.8}Sn_{0.2}Te$:La, evaporated thin films, low carrier conc. 80−65414
PbTe 80−45236
Pd, electron beam deposition and ion plating 77−44166
Pd-Si, amorphous thin films, laser irrad., metastable phases 80−96622
Pd_2Si layer, on Si, ion implantation damage, channelling obs. 78−30676
Po-Ge film, random percolation, elec. resist. meas. 79−28418
Pt, electron beam deposition and ion plating 77−44166
Pt ion plating on $\alpha+\beta$ Ti alloy Ti-6242, creep property improvement 80−16408
Pt, on Ir and W, defects and their effect on props. 80−39474
Pt-Si, amorphous thin films, laser irrad., metastable phases 80−96622
$RbAg_4I_5$ film, thermopower meas. temp. depend., correl. effects role 80−107539
Ru layer, 2-3 μm thick, ion plating and characterisation 78−11131
$(SN)_n$* radicals polymerisation to $(SN)_x$ in thin films, optical spectra 80−16656
Sb film A1-type supercond. vapour-quenched transition temp., A7-type phase transition 78−52145
$SbNbO_4$, ferroelec. film charact. 77−48127
Sb_2O_3-SnO_2 film vapour deposition in conveyor furnaces *(French)* 78−15311
Sb_2S_3, thin film, dielectric props. 79−15392
Se, amorphous, evap. layers, electrophotographic props. depend. on thermal treatment of initial material 77−76978
Se, amorphous films, evaporated, ageing and crystn., DTA 80−65413
Se electrophotographic film current density/voltage characteristic rel. to substrate temp. *(German)* 77−55629
Se, gas-evaporated, selective absorpt. charact. and emissivity 80−50998
Se, thin film selective absorber coatings, prod. using an oblique vacuum deposition technique 80−81488
Si large grain films on metallurgical Si substrates, chem., struct., elect. and photovoltaic props. 80−61357
n-Si-Ag(Au) evaporated contact photoelectric props. *(Russian)* 78−43473
Si-H(-D), film, IR and Raman spectra, H bonding effects 78−72515
Si-In_2O_3:Sn heterojunctions for solar cells 78−64107
SiC, film, synthesized by RF reactive ion plating, struct. 77−40391
β-SiC, fluidised bed deposited coatings for nucl. fuel granules, microstructural obs. by SEM 77−14233
SiC, oxidation protective coating on C fibres *(Polish)* 79−52408
Si_3N_4 film acousto-optical props. for integrated optical Bragg cell 79−55251
Si_3N_4 protective coatings on Mo, RF reactive ion plating 78−3250
SiO amorphous thin film capacitor, EPR, elec. cond. 78−68358
SiO_2 film, bombardment by B^+ ions, waveguide layer form. 79−27454
SiO_2, on Si, internal stresses 77−24499
Sn-Au(Cu), amorphous film, optical props. 79−69895
SnO_2, reactive ion plating onto insulating substrates, and elec. and optical props. 79−87588
Ta, film, evaporated, adsorpt. of SO_2, corrosion 78−79897
Ta_2O_5 film acousto-optical props. for integrated optical Bragg cell 79−55251
Tb-Fe, amorphous ferrimag. film, thermomag. writing using He-Ne laser 77−12163
Tb-Fe, undoped and O-doped, amorphous, microstruct. and mag. props. 79−91273
Te, gas-evaporated, selective absorpt. charact. and emissivity 80−50998
Te, thin film selective absorber coatings, prod. using an oblique vacuum deposition technique 80−81488
(Ti,V)C, activated reactive evaporation deposited films, annealing study, microstructure 80−24762
Ti, film, evaporated, adsorpt. of SO_2, corrosion 78−79897
Ti, on ceramic substrate, RF bias ion plating process and microstruct. 78−11132
Ti-Pt-Au, nonalloyed ohmic contacts to n-GaAs by pulse-electron beam annealed Se implants 80−2466
TiC, activated reactive evaporation and sputter deposition, friction and wear charact. 77−44394
TiC, activated reactive evaporation and sputter deposition, ancilliary props. 77−44395
TiC, activated reactive evaporation deposited films, annealing study, microstructure 80−24762
TiC, CVD and activated reactive evaporation on WC-TiC-Ta(Nb)C-Co, substrate-layer interactions, AES obs. 79−24679
TiC coated high speed steel, machining of steel 4340, tool life 78−11435
TiC, deposited by activated reactive evaporation, TEM and hardness 79−23872
TiC, on WC-NbC-Co, ion plating, and cutting tests 79−24678
TiC, wear resistant film, activated reactive evaporation form. 77−44411
TiC-Au film, prep. by activated reactive evaporation, struct. and mech. props. *(Japanese)* 78−3252
TiC_x film, formation by hollow cathode discharge reactive deposition process, on mild steel sheet 79−24451
TiN film as protective coating for vacuum deposition chamber, Auger electron spectroscopy study 80−25922
TiN layers formation, on steel substrate, microchardness and structure obs. *(Hungarian)* 80−2965
TiN, on WC-NbC-Co, ion plating, and cutting tests 79−24678
TiN, reactive ion plating with auxiliary discharge deposition conditions influence on film props. 80−20801
TiN, wear resistant film, activated reactive evaporation form. 77−44411
TiN-Ti_2N, activated reactive evaporation formed deposits, microstructure, transformation depend. on depositing conditions 80−24761
TiN_x, deposition by hollow cathode discharge process, and hardness 79−24452
TiN_x, synthesis by enhanced activated reactive evaporation 78−39705
TiO_x film, growth and struct. determ. 78−48328
VC-TiC, deposited by activated reactive evaporation, TEM and hardness 79−23872
vapour deposited coatings continued
VC-TiC, high rate deposition by activated reactive evaporation, and characterisation 78−11372
V_2O_5 film, amorphous, thickness, density and refr. index determ. from reflectance interference spectra 80−55206
W-Al_2O_3 cermet films, oxide evaporation deposited on Mo, Ti, Al_2O_3 substrates, struct., props. 80−25581
WO_3 evaporated film composition and chem. structure rel. to electrocoloration 77−77175
Y_2O_3, in MIM struct., electroforming props. 80−65705
$Zn_xCd_{1-x}S$, thin solid soln. films, vapour deposited, elec. and optical charcts. 80−60110
ZnO film, prep. by reactive ionized cluster beam deposition, and characterisation 80−10829
ZnO film acousto-optical props. for integrated optical Bragg cell 79−55251
ZnO, rate of deposition and morphology 78−84719
ZrO_2, obtained by vapo-condensation, exam. of structure and phase props. *(French)* 79−19489

vapour deposited thin films *see vapour deposited coatings*

vapour deposition
see also chemical vapour deposition; crystal growth from vapour; electron beam deposition; ion plating; plasma deposition; sputtering; vacuum deposition
alkali-halide crystals, two-dimens. nucleation and hole nucleation, mol. beam method *(German)* 80−93499
amorphous ferromagnetic alloys, form. and stability 77−16515
automatic deposition of optically active layers, single and multicoated on industrial scale *(Hungarian)* 77−75718
borosilicate glass film, vapour-deposited, structural model, IR spectra meas. 77−1084
carbon tetrachloride, prep. of glassy state, DTA 77−24388
ceramic, coating, vapour deposition by plasma activated process 79−57125
ceramics coating by physical vapour deposition processes *(Japanese)* 80−55306
coating techniques, for SEM and X-ray microanalysis 79−12783
composite material, B-Ti, for loudspeaker's diaphragm *(Japanese)* 80−58883
crystal nucleation on substrate, two-barrier thermodynamic pot., nuclei size distrib. 78−10300
diamond, polycrystalline film growth from gas phase 78−48332
dichloride 2.4′-bis (trimethylammonium-acetamide)-benzal-fluorene, thin layers, behaviour in electric field *(Rumanian)* 80−35108
diffusion barrier layer evaporation, improved Cr-Zr source 80−76163
directory of crystal growth and solid state materials production and research 79−65988
electron bombardment in thin film formation, model *(Russian)* 77−55894
film, adatom diffusion and capture by clusters, random-walk problem 78−2385
film deposition and characterisation, book contrib. 79−1563
film growth, island growth and coalesc. stage, computer model 79−11034
film growth kinetics, mol. beam deposition *(Japanese)* 78−91563
film growth kinetics under high adatom conc., surface diffusion parameters 77−28088
films, thermionic deposition 77−48349
GaAs solar cells, thin film growth tech. and characterisation 80−89631
glass optical fibre, vapour phase materials and processes, review 80−58825
high-rate vapour quenching techniques and use in amorphous phase prep. 80−80977
interference coating, optical charcts. topography var. 77−72102
ion assisted deposition, review *(Japanese)* 77−73227
ion evaporation techniques based on the electron beam evaporation source only 80−16203
ion implantation simultaneous with deposition, gas impurity distrib. 79−69146
ionised-cluster beam deposition and epitaxy, for electronic device fabrication 78−11133
ionized-cluster beam and reactive ionized-cluster beam deposition, new developments 80−16202
ionized-cluster beam deposition and epitaxy 79−83137
laser beam heating, complex film deposition *(Russian)* 77−48353
layer thickness-distance function modification, at high-rate evaporation *(Hungarian)* 79−87568
metal film, laser photodeposition 79−100061
metal film, positive particle beam deposition 77−85948
metal nuclei evaporated on to C, SiO_2 films, atm. contamination, AES meas. 77−4264
metal-semiconductor junction, deposition and post-deposition treatment effects on electrical props. 77−89853
metallic film, island surface coverage, determ. by optical interference 77−1810
metallic thin films, deposition by organometallic cpd. decomp. 80−71599
metallurgical coatings, conf., San Diego, USA (23-27 Apr., 1979) 80−12848
metallurgical coatings, conf., San Francisco (Apr. 1976) 77−40363
molecular beam deposition apparatus, design and construction *(Japanese)* 78−23632
molecular beam deposition apparatus *(Japanese)* 78−23631
molecule desorption and surface diffusion from critical deposition rate 80−92786
optical fibre, low-loss high-numerical-aperture, fabrication by vapour-phase axial deposition 80−1315
optical fibre cable made by vapour phase axial deposition, charcts. *(Japanese)* 80−58691
optical fibre fabrication, OH-free 80−99887
optical fibre preparation methods and performance factors 80−69557
optical fibre with ultra wide bandwidth, fabrication by vapour axial deposition method 80−69508
optical fibres, 30.4 km graded index vapour-phase axial deposited fibre, props. 80−64149
optical fibres, single-mode, fabrication by VAD 80−83687
optical fibres, ultimately low OH content achievement, by optimised dehydration 80−99845
optical fibres, vapour-phase axial-deposition, OH-ion reduction 79−94376

vapour deposition continued
optical fibres manufactured by MCVD and VAD for transmission system *(Japanese)* 80−58692
optical film, monitoring of props. during deposition, wide band monitoring system 79−81582
optical film polariser, design, prep. and optical characterisation 79−76866
optical thin-film waveguides fabrication, review *(Polish)* 79−3775
organic films, electronics and communications engineering appls. *(German)* 78−44011
oriented film deposition *(French)* 77−21030
overlay coatings for turbine parts, physical vapour deposition techniques, economic evaluation 80−35429
oxide film prod. by pulsed evap., capacitor prod. and characts. *(Russian)* 78−60584
phosphosilicate glass, deposition on contaminated Si wafer, Au redistrib. during growth 77−4121
phosphosilicate glass film, vapour-deposited, structural model, IR spectra meas. 77−1084
piezoelectric crystal surface, periodic film form. due to SAW 78−72038
polyhexamethyldisiloxane thin film form. in glow-discharge flow system 78−68631
rare earth metal refining *(Russian)* 77−59687
review of basic technique, chemistry, materials and applications *(Italian)* 80−89153
ring gap discharges for high rate vac. coating 77−69991
saturation cluster density in vapour deposited thin films, general formula 80−15408
semiconductors, plasmatron appl. *(Russian)* 79−77428
source configurations in thermal evaporation technique, deposition distrib. eqns. *(Polish)* 78−31339
surface coating technology, conference, London (1978) 79−83358
surface treatment, ionic deposition and electron bombardment industrial equipment, pollution control *(French)* 80−7699
thermal evaporation on rotary cylinder with locked mask *(French)* 78−80471
thin film Congress Loughborough, England, (Sept. 1978) 79−77949
thin film deposition technique, review *(Japanese)* 80−35107
thin film growth, computer modelling, condensation coeff. influence evaluation *(Czech)* 79−77935
thin film growth, surface self-diffusion coeff., adhesion energy of evap. material 78−84080
transition metal complexes, dimethylglyoxymate films, prep. and physical props. 79−90923
V-VI-VII complex ferroelec. semiconductor monocrystalline film production 79−78905
VAD optical fibre cables, characts. 80−43461
VAD optical fibres for transmission system field trial 80−43462
vapour deposition of wear resistant coatings 77−21307
wear resistant coatings 77−21307
wear resistant coatings on steel 79−56935
Ag, film, ion deposition *(Japanese)* 77−36407
Ag, vapour-deposited on rotating substrate at oblique angle, X-ray struct. anal. 77−62775
Al, coating prod. by thermal decomp. of Al alkyls 80−104076
Al film, internal stress, effect of residual gas press. 77−66100
Al film, using pulsed ruby laser *(Czech)* 79−52126
Al, vapour deposition on substrates, splash-free, using modified W helix 78−52689
Al-Cu alloy, deposition from RF induction source, onto laminated polyimide substrates and characterisation 80−16535
Al-Ni foil, vapour deposited, multiply twinned particles, electron microscopy 77−28083
AlN, cpd. form. reaction in reactive evaporation, quadrupole mass analysis *(Japanese)* 78−23628
γ-Al_2O_3, film, enhanced activated reactive evaporation process, ion effect 79−66013
Al_2O_3, high temp. amorphous film, transport props., prep. conditions effect 77−12040
As_xS_y, bulk and vapour deposited films, comparison of struct., X-ray diffr. meas. 77−69195
Au, growth, optical and elec. prop. meas. during depositon *(French)* 77−70007
Au island condensate, on LiF or NaCl, nucleation kinetics, influence of ionised atoms 77−11816
Au, on ceramics with Cr interlayer 77−20202
Au, sputter etching to improve adhesion, line definition and contact resist. 79−43145
Au_xSi_{1-x} amorphous alloy, crystallisation, elec. cond. study 80−103246
B and B-rich borides, protective coatings, in situ prep. for controlled nuclear fusion devices 79−3238
B_2O_3-SiO_2, optical waveguide glass, sintering kinetics 80−84898
Bi, evaporated film, nuclei size distrib. 77−11802
C, films, hard and transparent, prep. by condensation of ionised organic species 79−83132
CaF_2 on glass, Na-resistant cell, coating apparatus 80−90874
Cd, influence of source material and shape on sublimation props. 78−80474
CdS photoanode, for photovoltaic cells, prep. and characts. 78−14818
CdS thin films, growth and evaluation for fabrication of high performance photovoltaic solar cells 80−93501
CdSe film, stimulated recrystallisation 77−4272
CdSe film, struct. props., influence of O_2 partial press. and substrate temp. during vapour deposition 77−39751
CdSe, influence of source material and shape on sublimation props. 78−80474
CdSe thin-film transistors, sputter etching to improve adhesion, line definition and semicond. props. 79−43145
CdTe film, low-resist., prep. by multi-source evaporation method, and characterisation 80−25582
CdTe, laser window material, vap. deposition, mech. props. 77−46776
CdTe layer deposition by ionised cluster beam technique 77−48351
CdZnS thin films, growth and evaluation for fabrication of high performance photovoltaic solar cells 80−93501
Co, particle formation by evap., electron microscopy obs. of interaction processes 80−104053
CoO deposition on glass using laser beam 79−83364
Cr, film, defects and mechanical stability, different deposition methods *(Bulgarian)* 80−44438
Cr, on O treated polystyrene, microscopic interactions 80−3407

vapour deposition continued
Cr-Au layers RC circuits, sputter etching to improve adhesion, line definition and contact resist. 79−43145
$CrSi_2$, kinetics of growth 77−43454
Cs condensation on fused quartz meas. by torsion microbalance *(German)* 77−35839
Cu alloy, precipitation strengthened compositions with oxide particles, condensed, struct. criteria and thin layer possibilities *(Russian)* 80−89236
Cu-Ag film preparation with const. comp., by diffusion-limited evaporation from liquid 77−21038
$CuInS_2$ single phase thin film prep. by flash evaporation 80−100796
$CuInS_2$ thin films, growth, struct., and elec. props. 79−38729
$Cu_xMo_6S_8$, evap. film prep., supercond. props., lattice parameters 78−23195
Cu_2S-CdS solar cells, prep. and stoichiometric control of Cu_2S film 78−2560
Cu_xS-CdS solar cells, cu_xS growth kinetics and composition analysis by absorbance transient and galvanic electrochemical measurements 80−92797
Es film, preparation and characterisation 80−15405
EuS, film, anisotropic growth on amorphous substrate 77−12547
Fe, Fe-Ni, deposition of layers from carbonyl vapour 77−4727
Fe, particle formation by evap., electron microscopy obs. of interaction processes 80−104053
Fe-Ni-Cr, vapour-deposited film, effect of condensation temp. on form. of metastable phases and mag. props. 79−65700
FeF_3 thin film prep. and charact. *(French)* 78−64470
α-Fe_2O_3 film, prep. by reactive condensation and mag. props. 78−64241
Fe_3O_4 film, prep. by reactive condensation and mag. props. 78−64241
GaAs, prep. of thin films by ionised-cluster beam deposition *(Japanese)* 80−25576
Ge film, evaporated amorphous, angle of deposition effects, electron microscopy 77−43451
HfN on stainless steel, activated reactive evaporated coatings, high rate deposition, microhardness 80−25580
n-$(In,Sn)O_x$-p-InP solar cell, growth, efficiency 77−72910
In submonolayer growth on Si(111)7 surface, superstruct. 79−77930
In_2O_3, pure and Sn-doped, prep. by activated reactive evaporation, and characterisation 80−80989
InP solar cells, thin film growth tech. and characterisation 80−89631
InSb, prep. of thin films by ionised-cluster beam deposition *(Japanese)* 80−25576
InSb, thin film prep. with remelting, elec. props. 77−52255
InSe luminescent film, production and characterisation *(Russian)* 78−39581
KCl, two-dimens. nucleation rate on the (100) surfaces, mol. beam method, 289-343°C *(German)* 80−93500
MnBi, ionized-cluster beam and reactive ionized-cluster beam deposition 80−16202
MnTe, film, vapour deposition 78−47677
Mo_3Sn, thin films with A-15 struct., prep. 78−80478
Na vapour deposition rates and gas flow patterns in LMFBR 80−68732
NaCl, mol. beam condensation on Ir and Pt substrates, adsorbed C effects 77−66593
Nb, onto hot strip, mathematical model *(Russian)* 78−80476
Nb thick layer vapour deposition by photoresist stripping 79−83135
Nb-Al, prep. from gaseous phase *(Russian)* 78−27451
NbC, deposition with vapour-gas phase circulation in closed circuit 77−55927
Nb_3Ge film, growth by co-evaporation in O_2, critical temp. enhancement 77−28273
Nb_3In, thin films with A-15 struct., prep. 78−80478
Nb_3Sn, crit. current ang. depend., prep. conditions effect 77−47949
Ni alloy, precipitation strengthened compositions with oxide particles, condensed, struct. criteria and thin layer possibilities *(Russian)* 80−89236
Ni, deposition of layers from carbonyl vapour 77−4727
Ni, on O-treated polystyrene, microscopic interactions 80−3407
Ni, particle formation by evap., electron microscopy obs. of interaction processes 80−104053
Ni, thin film, growth on Au (001) substrates *(French)* 80−44446
Pb, on Au (100), initial stages of condensation 78−91569
PbSe, complex-composition film production method *(Russian)* 78−95702
PbSe films, synthesis and growth 80−45236
PbTe 80−45236
PbTe, complex-composition film production method *(Russian)* 78−95702
PbTe, high mobility polycrystalline layer, mol. beam deposition 79−83138
$(SN)_x$ film, evaporated on low temp. substrate, elec. cond. 77−63003
Sb film on NaCl, effect of ion irradiation on form., struct. and props. 77−36408
$Se_{5,6}$, influence of source material and shape on sublimation props. 78−80474
Si, post-annealed amorphous layer, twinning struct. by transmission electron diffr. 77−76685
Si, whisker, amorphous, growth method for field desorption mass spectrometry 79−28262
SiC, coating, vapour deposition by plasma activated process 79−57125
SiO, on liq. cryst. for surface alignment treatment 77−19871
SiO_2 film deposition on high-resistance Ge substrate by pyrolysis of tetraethoxysilane 77−1818
SiO_2, high temp. amorphous film, transport props., prep. conditions effect 77−12040
SiO_2, low temp. vapour phase growth 79−95936
SiO_2 wideband dielectric mirror production, spectral transmission 79−76897
SiO_2-GeO_2 optical fibre fabrication, 21.2 km graded-index VAD fibre with low loss and wide bandwidth 80−53414
SiO_2-P_2O_5 cladding vapour-phase axial deposition fibres at 1.3 μm and 1.6 μm 80−9996
SiO_x film, reactively evaporated, substrate temp. depend. of optical props. 77−70006
Sn film, vapour-deposited on NaCl single cryst., nucleation, growth, microstruct. 78−91561
SnO_2, transparent, on glass plates, in tunnel furnace *(Hungarian)* 78−35303
SnTe, complex-composition film production method *(Russian)* 78−95702
TiC, CVD and activated reactive evaporation on WC-TiC-Ta(Nb)C-Co, substrate-layer interactions, AES obs. 79−24679

vapour deposition continued
TiC, cpd. form. reaction in reactive evaporation, quadrupole mass analysis *(Japanese)* 78−23628
TiC single crystal, vapour deposited on Mo and W wires, electron microscope study 77−1795
TiN film as protective coating for vacuum deposition chamber, Auger electron spectroscopy study 80−25922
TiN, reactive ion plating with auxiliary discharge deposition conditions influence on film props. 80−20801
TiO_2 wideband dielectric mirror production, spectral transmission 79−76897
U film, for bombardment targets, prod. techniques 77−389
W-Al_2O_3 cermet films, oxide evaporation deposited on Mo, Ti, Al_2O_3 substrates, struct., props. 80−25581
Zn film, on Cu_2O, effect of ion irradiation on form., struct. and props. 77−36408
ZnO film, prep. by reactive ionized cluster beam deposition, and characterisation 80−10829
ZnS film, ion beam deposition 77−70008
ZnS, film, laser evaporation synthesis, surface struct. 79−28954
ZnS, laser evaporated film, microstruct. TEM obs. 79−82479
ZnS(Se)(Te) film, on semicond. substrates, early stages of growth, electron microscope obs. *(Russian)* 78−38976
ZrC coating on refractory metal fibre, diffusion barrier, deposition 77−4759
ZrC, deposition with vapor-gas phase circulation in closed circuit 77−55927

vapour-liquid transformations *see liquid-vapour transformations*

vapour phase epitaxial growth
see also molecular beam epitaxial growth
adsorption of oriented overgrowths, pairwise interaction approach 77−62759
anthracene, selective epitaxial growth on soln. grown anthracene substrate 77−63558
benzoic acid, ENSH method of oriented thin film growth 79−99443
C GaP on GaAs substrate, heteroepitaxial layers, stuct. defects *(German)* 79−23865
chemoepitaxial nucleation during reaction diffusion, thermodynamic anal. *(Russian)* 80−15394
chemoepitaxy and chemoendotaxy on metals 77−11827
compound semiconductor, heteroepitaxial growth and characterisation, book contrib. 79−83133
condensed two-dimensional phases on foreign substrate, structural aspects 77−20209
conf., Nagoya, Japan, (July 1978) 79−24431
copper phthalocyanine, on graphite, epitaxial growth of new polymorph 77−80712
covalently bonded materials, surface reconstruction effects, review 77−89669
CVD reactors, transport phenomena meas. 78−39701
cyclohexane, monolayers and thin crystals grown on Pt (111), LEED obs. 77−59230
deep level studies, growth by time difference method at controlled vapour pressure 80−39522
diamond, deposition on powder form methane 77−11805
diamond, epitaxial synthesis by C-ion deposition at low energy, and struct. 79−1559
diamond-graphite epitaxial film deposition on diamond substrate 77−4271
dielectric films, low temp. epitaxy in laser sputtering 80−34335
dopant incorporation during growth, theory and expt. 79−99229
doping, retrodiffusion cell design and applic. 77−84773
durene, ENSH method of oriented thin film growth 79−99443
electron microscopy of epitaxial growth process at UHV 78−55790
epitaxial film, dopant incorporation model 79−99228
epitaxial films, condensed from vapour or molecular ion beams, impurity distrib. 80−65032
epitaxial growth on Bi substrate 78−95246
film formation by ionised-cluster beam deposition 79−33934
film growth kinetics, mol. beam deposition *(Japanese)* 78−91563
fine structure formation *(French)* 78−43275
growth mode characterisation, physical methods 78−87885
growth processes, in-situ obs. *(Japanese)* 80−35104
heteroepitaxial surface morphologies and misalignments *(Japanese)* 80−15411
heterostructures for integrated optics 77−39112
n-hexatriacontane film, vacuum deposited on alkali halide crystals, structure and heat treatment 80−103600
horizontal CVD reactor, anal. of gas flow dynamics, book contrib. 79−82498
horizontal epitaxial reactor having multiple elongated-inclined susceptors 78−80475
hot wall epitaxy, review 78−52678
ice crystals, epitaxial, influence of environmental saturation and elec. field on growth and evaporation 79−42408
II-VI semiconductor, hot wall epitaxy, review 78−52678
II-VI semiconductors, heteroepitaxial, for SAW and electro-optic device appl., prep. and props., book contrib. 79−83134
II-VI semiconductors, thin epitaxial layer, direct synthesis *(German)* 80−104070
III-V semiconductor, flow graph model of VPE growth of $A^{III}B^{V}$ compounds 79−56088
III-V semiconductor, superlattices and related structures *(Slovak)* 80−88620
III-V semiconductor, vapour transport reactions and kinetics 79−28931
III-V semiconductor ternary alloys, VPE growth lattice mismatch effects 79−28220
III-V semiconductor ternary layers, on-time comp. determ. 78−67915
III-V semiconductors, CVD 78−92195
III-V semiconductors, heteroepitaxial, for SAW and electro-optic device appl., prep. and props., book contrib. 79−83134
III-V semiconductors, heteroepitaxy *(Japanese)* 77−24968
III-V semiconductors, p-n heterostructures, epitaxial growth techniques, appl. to optoelectronics, review 80−54770
III-V semiconductors, recent advances, book contrib. 79−66011
III-V semiconductors, VPE by metalorganic CVD *(Japanese)* 80−50562
III-V semiconductors prep. *(Czech)* 80−89131
III-V semiconductors using organometallics and hydrides *(French)* 79−33936
impurity profile computer-aided control 80−2962

vapour phase epitaxial growth continued
$In_{1-x}Ga_xAs_yP_{1-y}$ quaternaries, 0.75 to 1.35 eV band gap range 79−69987
InAs, gas-phase epitaxy, prep. thermodynamics, use of partial pressure diagrams 79−79279
ionised-cluster beam deposition, epitaxy *(Japanese)* 78−48329
ionised-cluster beam deposition and epitaxy, for electronic device fabrication 78−11133
ionized-cluster beam and reactive ionized-cluster beam deposition, new developments 80−16202
ionized-cluster beam deposition and epitaxy 79−83137
IV-VI narrow gap semiconductors, fabrication, IR laser and detector appls. 77−77415
IV-VI semiconductor, hot wall epitaxy, review 78−52678
kinetic model of oriented growth of nucleating curves during vacuum condensation *(Russian)* 79−74092
mass diffusion in two-dimens., perturbation method 79−2737
menthol, nucleation and growth on C, glass and fused quartz 77−7992
metal, nucleation, oriented island growth on point defects 78−87889
metal, on muscovite and fluophlogopite substrates, orientation rels. *(Russian)* 77−31910
metal-InP contacts, metal beam epitaxy, struct. and elec. props. of films on ion bombarded InP 79−28922
metallic epitaxial film growth with ionised beams and surface imperfections 77−32529
microscopic mechanism of film growth from non-condensed phases, kinetic anal. 80−54565
minerals, vapour growth and epitaxy, comparison of growth methods 79−23856
monocrystalline film, from gaseous phase, gasdynamic and heat transfer processes *(Russian)* 80−55301
multicomponent epitaxial structure synthesis device 77−77414
naphthalene, ENSH method of oriented thin film growth 79−99443
naphthalene crystal nucleation on anthracene microcrystals suspended in vapour-gas stream 80−76165
narrow-band semiconductor, growth of epitaxial layers, activation by UV and IR radiation 80−71598
NMP-TCNQ film, oriented, preparation and properties obs. 79−15040
nonmetallic materials, epitaxial film growth by sputtering, review 77−32521
oriented film deposition *(French)* 77−21030
n-paraffins, monolayers and thin crystals grown on Pt (111), LEED obs. 77−59230
periodic structures, props., prep., use 78−51982
phthalocyanine monolayers and vapour-grown films, surface struct., LEED 77−35830
polycyclic aromatic quinone, epitaxy on alkali halides, adsorbed water effect 79−28239
polypropylene, low mol. wt., vapour phase epitaxial growth 78−67924
potentially superior method of preparing semicond. devices *(Czech)* 78−44027
rare earth garnets, prep. and props. book contrib. 80−44193
reactive closed-space vapour transport, simplified theory 80−15396
refractory metal, electron-microscope exam. of film prod. *(Russian)* 77−59227
reproductive epitaxy, exam. 80−55303
review of growth and appl. 78−22966
selective epitaxial growth and morphology control 77−77378
semiconductor, CVD, book contrib. 77−12544
semiconductor, mol. flow in vac., free carriers effect on doping impurity distrib. 78−47682
semiconductor compound films, formation and structure *(Japanese)* 78−22979
semiconductor device fabrication by ionised-cluster beam deposition and epitaxial techniques 77−81227
semiconductor epitaxial film growth with ionised beams and surface imperfections 77−32529
semiconductor epitaxial groove and tunnel growth mechanism 80−10804
semiconductor film growth, multilayer systems, spectroscopic ellipsometry, review 80−103603
semiconductor layer CVD, appl. to Si, II-VI and III-V semiconductor growth 77−32530
semiconductors, heteroepitaxial, for electronic devices, prep. and props., book 79−83116
semiconductors, VPE growth, book contrib. 79−69997
Si epitaxy, vapour phase deposition technology 80−75472
stepped substrate-adsorbed layer interaction, selective effect on epitaxy 78−14616
synthetic crystals, vapour growth and epitaxy, comparison of growth methods 79−23856
tetracyanoethylene, oriented adsorption on KCl, LEED-AES study 77−62737
ultra high vacuum technology developments *(Japanese)* 78−49845
vapour growth, element incorporation 78−30556
Volmer-Weber mode of epitaxy, post-nucleation phenomena 79−77955
VPE on sapphire, highly oriented film prod. 77−66097
Ag epitaxial growth, cluster mobilities, in-situ electron microscopes obs. 80−15407
Ag, epitaxial growth and reaction with SnTe substrates 78−14640
Ag, epitaxial growth on InP (001) by at. beam deposition in ultrahigh vac. 77−59691
Ag film, elongated epitaxial (111) island growth on Cu(001), interface misfit, dislocations 79−82493
Ag film, epitaxial growth, characterisation of [001] tilt boundaries 78−84097
Ag film, epitaxial growth, effect of electron bombard. of NaCl substrate, TEM and AES obs. 79−90916
Ag film, epitaxial growth on O_2 conditioned (001)MgO film, TEM obs. 79−82489
Ag film, epitaxial growth on isolated Au patches covered with amorphous C layer 80−40270
Ag film, ion plated on AT-cut quartz crystal, crystallographic structure obs. 80−2280
Ag film, on Pd, AES and LEED obs. of growth modes and substrate influences *(French)* 80−84408
Ag film, vacuum deposited on NaCl, microstructure and orientation, surface condition influence 79−82486
Ag, form. simultaneously on (111) and (100) NaCl 77−11826
Ag, growth on electron bombard. NaCl(111) surfaces, RHEED and AES 80−15419

vapour phase epitaxial growth continued
Ag, on W (110), alignment of (111)FCC-(110)BCC epitaxial metal pairs 79−19488
Ag, oriented crystallisation on active amorphous C centres 79−7762
Ag, vac. deposition of oriented coating on doped alkali halide substrate 80−2303
Ag/Si (111), metastable 2D condensations, epitaxy, growth modes, exp. techniques, book contrib. 80−49558
AgCl on TGS, model system for orientation mechanism determ. 79−11022
Al on Pd, alloying effects 77−62785
Al/GaAlAs, film, epitaxial growth on (100) GaAs by hot vac. deposition and characterisation 79−56085
n-AlAs, VPE on GaAs, for heterojunction devices 77−1814
n-AlAs/p-GaAs, VPE growth for solar cells 77−77391
AlAs-GaAs film heterojunction, VPE growth and charact. 78−6439
Al_xCy, on diamond 77−72758
(AlGa)As laser system, VPE growth and degradation mechanism 80−99748
$Al_{0.3}Ga_{0.7}As$-GaAs DH mesa stripe laser, metalorganic VPE growth and characterisation 79−98391
$Al_xGa_{1-x}As$ grown by organometallic VPE, luminesc. efficiency 79−78892
$Al_xGa_{1-x}As$, monolithic optical integration for new devices 77−75714
$Al_xGa_{1-x}As$, organometallic VPE growth, and characterisation 79−78899
$Al_xGa_{1-x}As$, recent advances, book contrib. 79−66011
$Al_xGa_{1-x}As$, VPE and LPE growth, electron mobility 79−91165
$Al_xGa_{1-x}As$, VPE growth and characterisation 78−35315
p-$Al_xGa_{1-x}As$:Be layer, MBE growth, Be doping and diffusion 77−51397
$Al_xGa_{1-x}As/Al_yGa_{1-y}As$ DH lasers grown by metalorganic CVD, CW operation in wavelength range 760-780 nm 80−64053
$Al_xGa_{1-x}As$-GaAs, CW 300k quantum-well heterojunction laser, optical and injection pumping operation 80−5735
$Al_xGa_{1-x}As$-GaAs, heterojunction, interface width, AES obs. 80−20290
$Al_xGa_{1-x}As$-GaAs DH lasers, metalorganic CVD growth and performance charact. 80−53312
$Al_xGa_{1-x}As$-GaAs heterostruct. lasers, metallorganic CVD 80−23692
$Al_xGa_{1-x}As$-GaAs multiple-quantum-well injection lasers grown by metal-organic CVD, room temp. continuous operation 80−1218
$Al_xGa_{1-x}N$ epitaxial layers, growth and props. 79−11522
AlN, epitaxial growth, by ammonolysis of $AlCl_3$, thermodynamics 77−8758
AlN film, epitaxial growth by reactive evaporation *(Japanese)* 78−23629
AlN, impurity-doped film, cathodoluminescence spectra 79−83038
AlN, VPE by closed space vapour process, and optical absorpt. edge 78−88371
Au, effect of intermittent deposition on nucleus formation and growth on alkali halide substrates 79−23853
Au epitaxial growth, cluster mobilities, in-situ electron microscopes obs. 80−15407
Au, epitaxial growth in NaCl with continuous C-intermediate film, electron microscope obs. 78−84102
Au film, epitaxial growth, whisker form. 77−76713
Au film, epitaxial growth, characterisation of [001] tilt boundaries 78−84097
Au film, epitaxial growth, effect of electron bombard. of NaCl substrate, TEM and AES obs. 79−90916
Au film, epitaxial growth on Ag(111) surface, LEED meas. 78−14632
Au, film, on C/Ag system, epitaxial growth in ultra high vacuum 77−1336
Au, film, on sapphire substrate, nucleation, growth and postdeposition thermally induced epitaxy 79−77946
Au, growth and nucleation on NaCl during ion bombardment 79−11024
Au, growth on clean and contaminated GaAs (001) surfaces 78−26785
Au, mobility of small crystallites on KBr cleavage planes 79−23857
Au, nucleation on NaCl, role of surface steps 78−79902
Au on Pd alloying effects 77−62785
Au, on W (110), alignment of (111)FCC-(110)BCC epitaxial metal pairs 79−19488
Au on W (110), LEED and AES 77−69198
Au, vacuum evaporated particle coalescence behaviour on doped alkali halides 79−77961
Au vapour deposited particles, with pentagonal profiles struct. by TEM imaging techniques 79−77566
Au, vapour deposited particles, with hexagonal profile, struct. determ. using TEM imaging 79−77567
Au-Pd alloy, on rock salt, epitaxial growth and struct. 77−20211
AuMn alloy, ordered, vacuum deposited epitaxial films, orientation control by external stress 80−100426
$AuPb_2$, epitaxial layer, formation during Pb absorpt. on Au, LEED, AES study of Au/$AuPb_2$ interface 78−71988
BP, CVD on Si substrate, cryst. imperfections 78−10294
BP, diffused layers formed in Si substrates, device appls. 78−56585
BP, epitaxial growth on Si substrate, Si impurity profile, ion microanal. 78−87886
BP, epitaxial growth using B_2H_6-PH_3-H_2 system 79−28937
BP wafers, epitaxial growth by thermal decomp. of $B_2H_6+PH_3$, struct. imperfections 77−62774
$Ba_xSr_{1-x}TiO_3$, ferroelec. film, heteroepitaxial growth in cathode sputtering 80−93486
$BaTiO_3$, vacuum condensates, epitaxial growth on $SrTiO_3$ crysts., electron diffr. and TEM anal. 79−15051
Bi, decoration of Sb surface 79−28227
Bi film, elec. cond., obs. of epitaxial growth mechanism *(French)* 78−84329
Bi film deposition by vacuum evaporation on $NaNO_3$ single cryst. cleavage 80−35091
Bi, orientation on mica, effect of deposition parameters 77−28085
Bi, vapour deposited on NaCl cleavages, crystallinity depend. on deposition parameters 78−63955
Bi-Sb-Te system, epitaxial film prep. in closed-crucible 77−52230
$Bi_{12}TiO_{20}$, RF sputtered epitaxial film on $Bi_{12}GeO_{20}$, for optical waveguiding 78−9462
CaO, epitaxial layer growth by chem. transport reaction 77−52254
CaO, epitaxial layers by CVD *(Russian)* 79−56934
(Cd,Hg)Te epitaxial structures, comp. profile depend. on deposition parameters 80−100795
Cd chalcogenides, thin films, VPE, needle-like cryst. growth 80−80148

vapour phase epitaxial growth continued
Cd, epitaxial monolayer, nucleation and growth on Ge (111) 77−7986
$Cd_xHg_{1-x}Te$, isothermal growth of epitaxial layers 78−60577
$Cd_xHg_{1-x}Te$ solid solns., epitaxial growth under isothermal conditions 77−16504
$Cd_xHg_{1-x}Te$, VPE on CdTe *(Russian)* 78−11129
CdS, epitaxial growth and nucleation, on monocrystn. ZnS, substrate real struct. influence 80−88455
CdS, epitaxial layers on (111) Ce, growth and defect struct. 78−18920
CdS, grown by vac. evaporation on Si 80−25567
CdS heterojunction solar cells by CVD method 80−45685
CdS layers, epitaxial, deposited on InP substrates, vapour growth technique 77−21033
CdS, vacuum epitaxial growth on $CuInSe_2$ 78−92193
CdS:M, M=Zn, Te, doping and solid soln. prep. during VPE 77−85353
CdS/InP epitaxial thin films on NaCl, HEED and TEM study 80−88446
CdS-CdTe double layers on various GaAs surfaces, morphology and crystallography 80−34326
CdS-CdTe solar cell, prep. by VPE, junction struct. and photovoltaic props. 77−73235
CdS-CdTe solar cells fabrication *(Japanese)* 79−87992
CdS-InP(CdTe)(GaAs)(Ge), solar cell heterojunctions, CVD fabrication, photovoltaic response 80−93878
CdS-Si n-p heterojunction photodetector, fabrication and charact. 78−52068
CdS(Se)(Te), condensation from gas phase of controlled comp., and props. 80−54562
CdS(Se)(Te), evap. onto electron bombarded NaCl substrates, epitaxial growth and charact. 79−28948
CdSe, epitaxial growth by transport reactions in closed system 77−52232
CdSe on ZnTe (111), monocrystalline layers 78−14631
CdSe:In, epitaxial layers, synthesis and elec. props. 77−47909
CdSe-Ge (111) heterojunctions, epitaxial, azimuthal rotation 78−84085
CdSe(Te) films, oriented, epitaxial growth by epitaxial nucleation in submicroscopic holes method 80−59834
$CdSe_xTe_{1-x}$, solid solns., epitaxial layer prod. 78−23619
CdTe epitaxial films, on CdS substrate, closed-tube vapour growth 80−55302
CdTe epitaxial films, surface morphology, layer and spiral growth 80−10823
CdTe, film grown by hot wall epitaxy, elec. props. 79−82696
CdTe, film grown in quasi-closed volume, struct. *(Russian)* 78−75952
CdTe, films grown by hot wall epitaxy, elec. props. 79−28420
CdTe, growth by photostimulated VPE, electrophys. props. 77−40390
CdTe homojunctions from VPE growth, solar cell appl. *(French)* 77−43453
CdTe on GaAs, cryst. struct. and phys. props. 79−33202
CdTe thin films, oriented, VPE growth, infrared transmission, photovoltaic cells 80−59825
CdTe-CdS heterojunctions, growth by closed-tube chem. transport, elec. props. 80−60070
CdTe-PbTe(InSb) superlattices, laser deposition of multilayer heteroepitaxial structs. 80−44450
CdTe-Si heterojunctions, epitaxy and electrical props. *(Japanese)* 77−32074
$Cd_{1-x}Zn_xS$, epitaxial growth of single crystal layers on (111) GaAs substrate, close-space geometry 78−92198
$Cd_{1-x}Zn_xS$-p-GaAs heterojunctions, elec. and photovolt. props. rel. to growth technique 80−29466
$Cd_{1-x}Zn_xSe$, epitaxial layer growth with Zn content from doping to solid soln. formation 77−85094
Cr film, on sapphire, epitaxial relations 79−60649
$CrCl_2$, epitaxial relationships studied by RHEED and Auger emission spectra *(French)* 78−22990
CrO_2, epitaxial growth on rutile, possible appl. as bit oriented mag. material 77−16127
CrO_2, epitaxial growth on sapphire in air 78−27414
CrO_2, ferromag. films, epitaxial growth in air, electron diffr. and SEM obs. 79−42410
CrPt film, on sapphire, epitaxial relations 79−60649
Cs, VPE on W emitter, FEM obs. 80−70552
Cu film, on W substrate, cementation, vac. deposition, and electroplating, growth charact. 79−95291
Cu films on Ru (0001), growth, struct. and electronic props. 79−77958
Cu on Au, alloying effects 77−62785
Cu, on W (110), alignment of (111)FCC-(110)BCC epitaxial metal pairs 79−19488
Cu/Ag (111), metastable 2D condensations, epitaxy, growth modes, exp. techniques, book contrib. 80−49558
CuAu alloy, ordered, vacuum deposited epitaxial films, orientation control by external stress 80−100426
$CuGaTe_2$ films deposited on GaAs substrates by flash evaporation, struct. and elec. cond. 80−24755
CuI films, reactively sputtered, epitaxial growth on rocksalt substrates 79−4918
$CuIn_{0.7}Ga_{0.3}Se_2$ epitaxial layers, on GaAs substrates, struct. and elec. props. 80−107670
$CuInS_2$, epitaxial thin film on GaAs, exam. of growth, electrical props. 80−24754
$CuInSe_2$, heteroepitaxy on {111} oriented Ge by flash evaporation, struct. 80−108333
$CuInTe_2$ epitaxial layers, on GaAs, growth and props. 80−108359
Cu_2S, epitaxial overgrowths on Cu films, charact., TEM and RHEED obs. 78−84101
Cu_2Se, VPE on mica, defect struct., temp. depend. 77−35837
$Er_3Fe_5O_{12}$, low temp. CVD epitaxial film growth and mag. props. 79−42406
$(Eu,Y)_3Fe_5O_{12}$, low temp. CVD epitaxial film growth and mag. props. 79−42406
$(Eu,Yb)_3Fe_5O_{12}$, low temp. CVD epitaxial film growth and mag. props. 79−42406
EuSe, VPE by hot-wall technique 80−80958
Fe deposited W tip, FIM obs., epitaxial growth 78−79904
Fe, epitaxial film on Sb, ultrahigh vac. deposition 78−56572
Fe epitaxial growth on Au single crystals, substrate temp. effect on morphology 78−26798
Fe, epitaxial growth on Au platelets, dislocations 80−96760
γ-Fe, FCC film, epitaxial growth on CuAu (111) surfaces, strong ferromagnetism 80−70557

vapour phase epitaxial growth continued
Fe, on Au, growth processes, ultra high vac. in situ electron microscopy 78−30842
Fe, on W tip, depositing direction depend. 80−10812
Fe/Cu (100), metastable 2D condensations, epitaxy, growth modes, exp. techniques, book contrib. 80−49558
Fe-Au interface, two types of dislocation dependent on deposit thickness *(French)* 77−85109
$FeCl_2$, epitaxial relationships studied by RHEED and Auger emission spectra *(French)* 78−22990
(Ga,In)As, growth of epitaxial layers 77−12542
GaAlAs on GaAs thin film stacked multiple-bandgap solar cell structs., prep. using CVD techniques 80−94083
GaAlAs/GaAs heterostructures, ellipsometric assessment of epitaxial layer during growth in organometallic VPE system 79−37933
GaAlAs-GaAs lasers, channelled substrate, prepared by combination of organometallic pyrolysis and LPE 80−99745
$Ga_{1-x}Al_xAs$ based layer structures, optimum growth conditions, comp. and struct. perfection 80−104069
$Ga_{1-x}Al_xAs$, solar cells appl., technology advancements 79−43776
$Ga_{1-x}Al_xAs$ VPE layers, X-ray diffr. 80−29296
$Ga_{1-x}Al_xAs$-$Ga_{1-y}Al_yAs$ DH laser, grown by organometallic CVD, room temp. operation 78−29950
$Ga_{1-x}Al_xAs$-GaAs, CVD laser diodes, operation and growth processes 78−46598
$Ga_{1-x}Al_xAs$-GaAs, room temp. DH laser, CVD growth 78−37912
$Ga_{1-x}Al_xAs$-GaAs DH injection lasers grown by metalorganic CVD, props. 80−99751
$Ga_{1-x}Al_xAs$-GaAs heterostructure lasers grown by metalorganic CVD, prep. and props. 79−36918
$Ga_{1-x}Al_xAs$-GaAs laser, DH, grown by metalorganic CVD, room temp. operation 78−13702
$Ga_{1-x}Al_xN$, VPE growth on sapphire, RHEED obs.of orientation rels. 77−20208
$Ga_xAl_{1-x}Sb$, closed tube transport technique 79−28935
GaAs (100), VPE, role of Cl, LEED, RHEED, and AES obs. 77−1327
GaAs antireflecting MOS solar cells, epitaxial and polycryst. using OM-CVD techniques 80−94072
GaAs, bulk purification by chemical vapour transport 79−24437
GaAs, by CVD, vapour-solid interface, expt. anal. *(French)* 79−33940
GaAs, by pyrolysis, producing power GaAs MESFETs 78−23623
GaAs, CVD in Ga-$AsCl_3$-H_2 system with different input supersaturations *(Russian)* 78−68098
GaAs, CVD mechanism, product catalysed reaction of Me_3Ga with AsH_3 77−48345
GaAs, CVD using Ga-As-H-Cl system, theoretical anal. of equilib. adsorption layers 79−23858
GaAs, chem. transport by water vapour, thermodynamic calcs. 77−12539
GaAs compensated VPE thin film, electron Hall mobilities 80−107932
GaAs, device quality, epitaxial growth on Ge/Mo substrates 79−69988
GaAs, epitaxial, polycryst., monocryst. layers and whiskers growth by CVD, SEM obs. electron diffr. study *(French)* 79−43150
GaAs, epitaxial, Si and Ge doping 80−24470
GaAs, epitaxial deposition from organometallic cpds. 77−47689
GaAs, epitaxial deposition, growth kinetics *(French)* 80−2961
GaAs epitaxial growth, in GaAs-$AsCl_3$-H_2 system, elec. field effect 80−2306
GaAs epitaxial growth, CVD-organometallics method, reactional efficiency in solar cell elaboration 80−93498
GaAs, epitaxial growth and etching rate meas. method 77−35829
GaAs, epitaxial growth for microwave devices *(French)* 77−48360
GaAs, epitaxial growth in $Ga(CH_3)_3$-AsH_3-H_2 system 78−35312
GaAs, epitaxial growth under different intake supersaturations in GaAs-$AsCl_3$ gas transport system *(Russian)* 78−26776
GaAs, epitaxial layer, micron and submicron vap. phase growth, for FET 80−11577
GaAs, epitaxial layer growth by chloride process, μ and subμ thickness 78−23624
GaAs epitaxial layer high power Gunn diode developement and fabrication 80−16199
GaAs epitaxial layers, growth below 700°C electrophysical props. 79−1827
GaAs, epitaxial layers, electron irrad. deep level trap energy depend. 80−80205
GaAs, epitaxial multilayer, electron irrad. defect study by transient capacitance 79−99241
GaAs, epitaxy by metallorganic and chloride depositions, defect characterisation at growth interface 80−59817
GaAs, epitaxy on semiinsulating GaAs, elec. props. of transitional layers rel. to growth conditions 77−15977
GaAs, epitaxy using TMG and AsH_3, chloride etching effect 78−76606
GaAs film, epitaxial deposition from gas phase, transient processes, elec. cond. 77−16501
GaAs film on recrystallised Ge film, solar cell appl. 78−19671
GaAs films for solar cells appl., deposition and characterisation 80−84853
GaAs, gas-phase composition during growth by chloride method 77−12537
GaAs, gas-phase epitaxy, mass exchange during 79−78901
GaAs, gas-phase epitaxy, step stopping centre form. kinetics 80−65407
GaAs, growth method at low H_2 press. 79−28936
GaAs, growth method using low press. organometallics 79−100054
GaAs, growth rate anal. 78−52680
GaAs, heterogeneous reactions in chemical transport by water vapour, growth kinetics of epitaxial layers 77−16500
GaAs homoepitaxy, vicinal surfaces of substrates, characterisation 77−20207
GaAs, homoepitaxy and epitaxy, surface anal. during growth using RHEED and Auger spectroscopy 80−66433
GaAs, hydride VPE growth for FETs, and characterisation 78−27407
GaAs, in Ga-$AsCl_3$-He_2 system, expt.-statistical analysis *(Bulgarian)* 78−60580
GaAs, influence of growth parameters, $AsCl_3$ transport method 80−29881
n-GaAs layer, VPE, influence of growth conditions on incorporation of deep levels 77−4310
GaAs layers, high resistivity, growth for microwave device appl. 79−100056
GaAs, MBE with ionised dopant 77−40338
GaAs MESFET layers, low-temp. halide epitaxial growth 77−77403
GaAs MESFET layers, low temp. VPE growth by halide process 77−90279
GaAs, multi-wafer growth technique using $AsCl_3$-Ga-N_2 system with horizontal reactor 79−28934
GaAs, multilayer epitaxial growth with Sn doping 77−47690
GaAs, ohmic contact formation with thin film 77−8756
GaAs on GaAs and Ge, epitaxy, mechanism, effect of substrate surface struct. 77−51614
GaAs on Ge thin film stacked multiple-bandgap solar cell structs., prep. using CVD techniques 80−94083
GaAs, optical integrated circuits appl. 77−65644
GaAs optical waveguides, oxide confined, formed by lateral epitaxial growth 80−58815
GaAs, partial press. diagrams use for thermodynamic represent. 79−33201
GaAs, produced by VPE using trimethylgallium and arsine, controlled doping 78−6855
GaAs, residual donor impurities 77−76679
GaAs, review of growth techniques *(French)* 79−33935
GaAs ribbons from Ga-$AsCl_3$-H_2 epitaxy 80−7498
GaAs, selective in situ vapour etch of substrate and growth 80−2958
GaAs, sequential multiple layer epitaxy, method 77−12545
GaAs, substrate prep. effect on surface morphology 78−26780
GaAs substrates, out-diffusion of Cr 80−10708
GaAs surface, during vapour phase epitaxial growth, characterisation techniques and meas. *(French)* 77−1817
GaAs, thermodynamic analysis of Si contamination 79−28932
GaAs, thermodynamic factor influencing growth rate and layer purity in Ga-$AsCl_3$-H_2 system 79−28933
GaAs type FET with buffer, bias effects due to deep centres in struct. *(French)* 80−107917
GaAs, ultrathin film growth by cracking of organometallic compounds at 40 to 100 torr *(French)* 78−44023
GaAs using organometallic method, deep trap levels 80−10923
GaAs, VPE, electron Hall mobility meas., attempted correlation with growth parameters 78−43417
GaAs, VPE, fast growth at low temp. and high partial pressure 79−51446
GaAs, VPE, growth parameters effect 77−28726
GaAs, VPE, incorporation of deep levels, effects of growth conditions 80−20111
GaAs, VPE, surface defects rel. to technological parameters 78−44015
GaAs, VPE by Ga-$AsCl_3$-H_2 process, role of Si 77−40380
GaAs, VPE by single flat temp. zone method, elec. props. 79−95526
GaAs VPE film growth, in Ga-$AsCl_3$-H_2 system, O_2 injection effect 79−100057
GaAs VPE growth, in situ surface anal. 79−95937
GaAs, VPE growth, surface morphology study by optical microscopy 79−60651
p-GaAs, VPE growth and characterisation, doping levels 80−10841
GaAs, VPE growth by single flat temp. zone method, residual doping level 77−48352
GaAs, VPE growth on {110} cryst. plane 80−10840
GaAs, VPE growth rate variation with distance along substrate within const. temp. zone 78−2384
GaAs, VPE in CVD systems, anisotropic phenomena 80−54563
GaAs, VPE in Ga-$AsCl_3$-H_2 system at reduced temp. 79−11519
GaAs, VPE in inert gas-H_2 mixed carrier system, thermodynamic analysis 78−11120
GaAs, VPE layer growth with abrupt doping profile 80−24746
GaAs, VPE layer props. control using boundary layer characts. 80−50561
GaAs VPE layers, elec. props., semi-insulating substrates effect 80−11123
GaAs, VPE layers, growth conditions effect on deep levels 79−95360
GaAs VPE layers, role of diffused Ga vacancy in degradation 78−95050
GaAs VPE layers for FET devices, impurity characterisation 80−29491
GaAs, VPE on Ge substrate, and characterisation 78−72736
GaAs, VPE thin layers, thickness uniformity, main factor anal. 80−76197
GaAs, VPE UV stimulated 78−35313
GaAs, vapour phase epitaxy using computer control 79−38744
GaAs, vapour phase epitaxial appl. to hyperabrupt varactor fabrication 80−29288
n-GaAs vapour phase epitaxial film electrophysical props. rel. to growth temp. *(Russian)* 80−49961
GaAs, vapour-phase epitaxial growth, transfer mechanism of Si 77−51616
p-GaAs:Be layer, MBE growth, Be doping and diffusion 77−51397
GaAs:Cr, VPE grown, exam. of doping GaAs using $Cr(CO)_6$ 78−72737
GaAs:Cr, VPE growth, carrier conc. profiles 79−74099
GaAs:Fe, for FET, VPE and characterisation 78−19672
GaAs:Ge, VPE, doping, electrophysical characts. meas. 78−43493
GaAs:Ge, vap. grown, diatomic complex donor and acceptor model 78−80003
GaAs:S epitaxial layers, dopant conc. control method 77−1807
GaAs:Si(Te)(S), vapour phase epitaxial grown layers, photoluminesc. and emission spectra 80−29774
n-GaAs:Sn, VPE growth, reactor design 80−2956
GaAs:Zn films, VPE growth and photoluminesc. props. 79−38642
GaAs-(Ga, Al)As heterostructure transmission photocathode, characts. *(French, English)* 78−52616
GaAs-AlAs, alternate monolayer single cryst., optical waveguides 77−72065
GaAs-GaAlAs DH laser with low threshold current, metalorganic CVD 79−50293
GaAs-GaAlAs heterostructure, growth by metal-alkyl-hydride process 78−15313
GaAs-GaAlAs superlattices, metalorganic VPE growth, in sites ellipsometry monitoring 80−70547
GaAs-$In_yGa_{1-y}P$, CW room temp. DH lasers prep. by VPE 77−10942
GaAs-S VPE layers, thickness and carrier conc. variations 79−100060
GaAsP epitaxial film, composition self modulation, defect struct. 80−34331
GaAsP, VPE, lattice forbidden band composition depend. *(Hungarian)* 80−6669
$GaAs_{0.6}P_{0.4}$, CVD growth for LEDs 79−19998
$GaAs_{1-x}P_x$ epitaxial layer prep. for electroluminescent diodes *(Czech)* 77−21032

vapour phase epitaxial growth continued
$GaAs_{1-x}P_x$ epitaxial layers prep., photoluminesc. and electroluminesc. props. *(Czech)* 78−48233
$GaAs_{1-x}P_x$, solid soln. comp. control during gas-phase heteroepitaxy 77−85091
$GaAs_{1-x}P_x$, VPE on Ge substrate, and LED characts. 78−72736
$GaAs_{1-y}Sb_y$ organometallic VPE, use of trimethyl As and trimethyl Sb 80−45238
$GaAs_{1-y}Sb_y$, organometallic VPE growth using trimethylantimony 80−60788
GaInAs, efficient photodiode for near IR detection 78−16848
$Ga_{1-x}In_xAs$ epitaxial layer growth by organometallic pyrolysis, homojunction LED prep. 80−76194
$Ga_{1-x}In_xAs$ organometallic VPE, use of trimethyl As and trimethyl Sb 80−45238
$Ga_{1-x}In_xAs$, organometallic VPE growth using trimethylarsenic 80−60788
$Ga_{1-x}In_xAs$-GaAs low-misfit epitaxial interface, electron microscope contrast 79−73416
$Ga_xIn_{1-x}As$, VPE growth, thermodynamic anal. 80−2933
$Ga_xIn_{1-x}As$-InP heterostructure, growth by MBE 79−8251
GaInAsP, VPE growth and props. 80−16194
$Ga_{1-x}In_xAs_{1-x}P_x$, VPE growth and characterisation 78−22970
$Ga_xIn_{1-x}As_yP_{1-y}$/Inp DH laser emitting at 1.15 micron grown by low-pressure CVD 80−64052
$Ga_xIn_{1-x}P$, recent advances, book contrib. 79−66011
$Ga_{1-x}In_xSb$, epitaxial, vapour-phase growth using open-tube flow system 79−33943
$Ga_{1-x}In_xSb$, vapour phase epitaxial growth by open tube method 78−84109
GaN CVD layer props. rel. to Ga-GaCl conversion efficiency and HN_3 decompositon 77−77404
GaN, epitaxial growth kinetics in Ga-HCl-NH_3 77−80710
GaN, epitaxial growth on sapphire substrates, elec. props., X-ray diffr. anal., photoluminescence spectra 79−4919
GaN, epitaxial layer prep. and elec. props. 77−85097
GaN epitaxy, sapphire substrate prep. 78−39929
GaN film, heteroepitaxial deposition, growth kinetics and catalytic effects 79−4487
GaN film, preparation by pyrolysis of $Ga(CH_3)_3$ in NH_3, cathodoluminesc. 77−4691
GaN, growth rate influence on elec. and luminesc. props. 80−100702
GaN, high-press. VPE and elec. characts. 78−14627
GaN, initial growth, on Al_2O_3 and spinel *(German)* 80−107664
GaN, on sapphire, crystallographic aspects 78−2387
GaN on Si, form. with GaCl-NH_3-H_2(He), ESCA and RHEED meas. 79−90909
GaN, requirements and structural etching of Al_2O_3 substrates *(Polish)* 77−43440
GaN VPE for blue LEDs *(French)* 79−28928
GaN:Al, VPE grown, luminesc. and elec. props. depend. on doping conc., bound excitons 80−20688
GaN:Mg, and undoped, epitaxial growth from vapour, orientation, elec. props. 77−4740
GaN:Zn, low voltage LED, epitaxial layer, growth and electrolum. *(Russian)* 77−77297
GaN:Zn, VPE growth, photoluminesc. rel. to doping conditions 80−55159
GaN-AlN, solid solution, epitaxial growth and electrical props. 77−73236
Ga_2O_3 on spinel and sapphire, VPE and orientation *(Japanese)* 77−51611
GaP, CVD mechanism, product catalysed reaction of Me_3Ga with PH_3 77−48345
GaP crystal, electroluminesc. 77−28631
GaP, epitaxial growth by $GaPO_4$-C system 79−99448
GaP, epitaxial layer prep. and elec. props. 77−85096
GaP for yellow-LEDs, prep. and props. *(Czech)* 78−48234
GaP, heteroepitaxial CVD on Si, dual process, film characts. 77−16503
GaP, heteroepitaxial growth on Si, substrate misorientation effects 78−3055
GaP, layer structures for LED's, SEM, and TEM obs. of dislocation density reduction expt. 80−100425
GaP layers grown in Ga-PCl_3-H_2 system, surface defects 77−7993
GaP, two-stage vapour/liq. epitaxial growth on Si 78−3054
GaP, VPE Ni contaminant detection, IR photoluminescence of Ni 78−15212
GaP:N, epitaxial layers, N concentration determination by two independent methods 80−39142
GaP-Si, heteroepitaxial growth, electronic and optical props. 80−104075
GaP_xAs_{1-x} solid soln., specularly smooth epitaxial layers, superlattice struct. 77−24959
GaP_xAs_{1-x}, surface defects and comp. inhomogeneity during gas-phase heteroepitaxy 77−85090
GaSb, CVD using organometallics, epitaxial growth 80−29879
GaSb high-purity and doped layers grown by LPE and VPE methods 78−6863
Gd film, deposition parameters effects on struct. 79−90912
Ge, epitaxial and amorphous film growth, low energy ion beam deposition 77−28729
Ge epitaxial film, vac. deposited on GaAs, doping effect of annealed GaAs surface 80−65718
Ge, epitaxial film growth by hydride-iodide method 77−48343
Ge epitaxial films, structural perfection rel. to deposition conditions 78−43258
Ge, epitaxial growth from monogermane at 685°C 78−51833
Ge, epitaxial growth of very thin electron microscopy specimens 80−100793
Ge, epitaxial layer deposition by vacuum pyrolysis 78−52676
Ge, film, epitaxial growth on Si, interdiffusion, plasmon energy loss anal. 77−31916
Ge film, prep. by low press. reactive deposition process 79−24449
Ge, ion sputtering, growth mechanism, struct., props. 77−31917
Ge, on n-GaAs, with Ni overlayer, smooth and continuous ohmic contact form. by solid-state diffusion 78−68086
Ge, polycrystalline epitaxial film, exam. of growth kinetics and props. 80−55304
Ge:B, epitaxial film, exam. of doping during chemical deposition from gas phase 79−1446
Ge:P, doping of epitaxial layers, in chloride and hydride processes 78−43036

vapour phase epitaxial growth continued
Ge-Si alloy, epitaxial growth by getter sputtering, characts. 79−28915
$Hg_{1-x}Cd_xTe$, epitaxial layer, vapour phase growth 79−1829
$HgCr_2Se_4$-$CdIn_2S_4$ heterojunction, prep. and photovoltaic prop. *(Japanese)* 78−34889
$HgCr_2Se_4$-$CdIn_2S_4$ heterojunctions, prep. and photovoltaic prop. 78−34892
HgS, RF sputtering on NaCl, growth and struct., electron diffr. and TEM obs. 77−90271
HgSe, epitaxial growth on CdSe, struct. and electrophysical props. 77−12540
HgSe/CdSe lattice-matched heterostructs. as Schottky barriers, CVD epitaxial growth and elec. props. 80−49877
HgTe, conditions for oriented crystn. 79−52124
HgTe, heteroepitaxial growth by close-spaced technique of confined type *(Japanese)* 77−24967
HgTe, VPE growth control by EM irrad. *(Russian)* 80−34338
HgTe-CdTe, epitaxy by evap. and interdiffusion under isothermal conditions book contrib. 77−12549
In epitaxial growth, cluster mobilities, in-situ electron microscopes obs. 80−15407
In, growth and desorption on W tips, high field microscopy 79−69380
In ultrathin films on TbTe and Te, prep. and characterisation 77−7995
InAs epitaxial layers, on GaAs substrate, electron diffr. and SEM exam., electronic props. 79−1552
InAs, heteroepitaxial film, orientation and struct. investigation 79−82480
InAs heteroepitaxial layers, VPE grown, effect of $AsCl_3$ mole fraction on elec. props. 79−11255
InAs, organometallic VPE growth on InAs and GaSb 80−16193
InAs, possibility of local epitaxy in depressions on unmasked substrates 79−42415
$InAs_{1-x}Sb_x$, organometallic VPE growth on InAs 80−45233
InGaAs, lattice-matched VPE on (100) InP, photodiode appl. 80−35102
InGaAs on (100) InP substrate, VPE 80−40267
InGaAs-InGaP vapour-grown ternary heterojunction laser struct., reliability 79−98385
InGaAs-InP punch-through type photodetector fabricated by VPE 80−68253
n-$In_xGa_{1-x}As$ film, epitaxial growth on GaAs, using CVD system 77−1812
$In_xGa_{1-x}As$, planar photodiodes made by VPE 79−49286
$In_xGa_{1-x}As$, VPE on (100), (111)A, and (111)B InP substrates 80−15382
$In_xGa_{1-x}As$-$InAs_xP_{1-x}$ mixed crystal composition rel. to vapour pressure *(Japanese)* 77−55893
InGaAsP, expitaxial growth by chloride CVD process, thermodynamic anal. 80−64936
(InGa)(AsP) laser system, VPE growth using metal organic sources or halide transports 80−99748
InGaAsP/InP DH, vapour phase growth by dual-growth-chamber method 80−50559
InGaAsP-InP CW lasers, 1.5-1.7 μm, VPE 80−78861
InGaAsP-InP vapour-grown quaternary heterojunction laser struct., reliability 79−98385
InGaP/InGaAs struct. for transferred electron photocathodes, VPE growth and characterisation 80−76193
$In_{1-x}Ga_xP$ LEDs and electron-beam-pumped lasers 80−2281
$In_xGa_{1-x}P$, solid solns., gas phase epitaxy from Ga-In-HCl-PH_3-H_2 systems 78−34722
$In_{1-x}Ga_xP_{1-z}As_z$ LEDs and electron-beam-pumped lasers 80−2281
InN, epitaxial layer prep. using $InCl_3$-NH_3 system 78−3056
InN, epitaxial layer prep. and X-ray analysis 79−38747
InP, CVD 79−28927
InP, epitaxial, kinetics of VPE 80−60790
InP, epitaxial growth, thermodynamic conditions 77−89661
InP film, prep. by low press. reactive deposition process 79−24449
InP films, organometallic VPE grown, props. 80−96753
InP, heteroepitaxial, deposition on GaAs substrate, using close-spaced method, X-ray analysis *(Czech)* 77−15710
InP, heteroepitaxy on CdS substrates using InI_3 as transport agent 79−56083
InP, high-purity VPE, by PCl_3/In/H_2 technique, progress in control 78−6857
InP, homoepitaxial film by MO-CVD process, for heterojunc. solar cell fabrication 79−8250
InP, organometallic growth by cracking of $In(C_2H_5)_3$ and PH_3 80−11575
InP, planar reactive deposition on CdS, heterostruct. formation and elec. evaluation 78−72738
p-InP, prep. of single and bi-crysts., epitaxial layer and polycryst. films 77−81211
InP, pure and S doped, VPE, exam. of molar fraction controlled impurity in In-PCl_3-H_2 78−56587
InP VPE, growth kinetics and controlled doping 79−87569
InP VPE, In-H_2-PCl_3 chemistry 80−11549
InP, VPE, thermodynamics of transfer by water vapour 78−43260
InP, VPE growth for MESFET's 80−103602
InP, VPE layer props. control using boundary layer characts. 80−50561
InP VPE with new metallorganic compound 80−55278
InP, vapour phase epitaxial growth in presence of O_2, elec. props. 79−46971
InP:Si(Mg), ion implantation and PH_3 ambient annealing under VPE conditions 79−42085
InP:Sn film, mol. beam epitaxial growth 77−16505
p-InP:Zn, vapour grown, prep. and props. 80−54268
InSb, heteroepitaxial film, orientation and struct. investigation 79−82480
InSb thin films prepared by ion beam epitaxy system *(Japanese)* 78−22976
InSb-GaSb, compositionally modulated sputtered superlattice, growth and interlayer diffusion 79−56930
InSb-PbTe(CdTe) superlattices, laser deposition of multilayer heteroepitaxial structs. 80−44450
Ir, epitaxial growth on (001)W and (001)Mo 79−99450
$K_xLi_{1-x}NbO_3$, epitaxial growth of single-cryst. films on $K_2BiNb_5O_{15}$ substrate by RF sputtering 79−15041
$LiNbO_3$, heteroepitaxial growth on MgO by RF sputtering, SHG 79−27323
$Mg_{1-x}Ca_xO$, epitaxial layers by CVD *(Russian)* 79−56934
MgO, epitaxial layers by CVD *(Russian)* 79−56934
MgO epitaxy on alkali halides with NaCl-type struct., RHEED meas. 78−67920

vapour phase epitaxial growth continued
MnBi, ionized-cluster beam and reactive ionized-cluster beam deposition 80−16202
MnTe, film, vapour deposition 78−47677
Mo film, epitaxial growth on cooled W tips at 78K, struct. obs. 77−28723
Mo, film on sapphire substrate, orientational growth, epitaxial textures, nucleation textures *(Russian)* 80−75454
Mo, on sapphire, epitaxial layer production by electron beam deposition in vacuum *(Russian)* 77−59228
Mo, vacuum deposition on fluorophlogopite at 650 to 1050°C, orientation rels. *(Russian)* 77−48342
NaCl (001) substrate, preferential epitaxy of evaporated films induced by electron bombard. or elec. field 80−10824
Nb, film, epitaxy, struct. and supercond. props., on (001) surface of fluorophlogopite *(Russian)* 80−80101
Nb, film on sapphire substrate, orientational growth, epitaxial textures, nucleation textures *(Russian)* 80−75454
Nb on sapphire, highly oriented film prod. 77−66097
Nb_3Al film, electron-beam coevaporated, prep. and characts. 80−76187
Nb_3Ge, epitaxial growth of polycryst. films with high supercond. transition temp. 77−63015
Nb_3Ge film, supercond., epitaxial growth on Nb_3Ir and Nb_3Rh substrates 78−80473
Ni, epitaxial growth, on NiO(100), by low pressure hydrogen reduction *(French)* 80−11578
Ni, on diamond 77−72758
Ni, on W (110), alignment of (111)FCC-(110)BCC epitaxial metal pairs 79−19488
$Ni_3B_7O_{13}Cl$, boracite, on Cr-Cl boracite, gas phase synthesis of epitaxial layers 79−60650
$NiFe_2O_4$, on NdGG, structural and ferromagnetic reson. meas. 77−1574
NiO, formation on Ni (110), initial stage kinetics, RHEED and X-ray emission 78−15588
PLZT ferroelectric thin films, epitaxial growth and optical props. 80−70543
PLZT film, epitaxial growth by RF sputtering, and characterisation 77−85937
Pb film, monocryst., heteroepitaxial growth, struct. defects, and elec. props. *(Russian)* 80−84403
Pb, on Ag (111) and Cu (111) LEED, RHEED, AES study 78−84090
Pb ultrathin films on PbTe and Te, prep. and characterisation 77−7995
$Pb_{1-x}Cd_xS$ metastable epitaxial films, growth and physical props. 78−27417
PbS, epitaxial layer, structural nonuniformities and dislocation struct. 79−23852
n-PbS, $PbS_{1-x}Se_x$ layers prepared by hot-wall epitaxy 77−16481
PbS-PbSe-PbS DH laser, fabrication, CW operation up to 120K 77−23692
PbS_xSe_{1-x} film, prep. by co-evaporation method *(Japanese)* 78−64477
PbS_xSe_{1-x}, film prep. by co-evap., elec. props. *(Japanese)* 78−80470
PbSe, epitaxial growth, cluster mobilities, in-situ electron microscopes obs. 80−15407
PbSe, monocrystalline film prod. by laser pulse *(Russian)* 78−3059
PbSe(Te), low-temp. epitaxial film form., on KCl(Br), laser spraying *(Russian)* 77−73238
$PbSe_xTe_{1-x}$ epitaxial layers, growth, struct., elastic strain and Hall mobility 77−15717
PbSnTe film epitaxial growth on BaF_2 substrates 78−11134
$Pb_{0.8}Sn_{0.2}Te$:La, evaporated thin films, low carrier conc. 80−65414
$Pb_{0.82}Sn_{0.18}Te$ films, VPE, hot wall technique, struct., elec. props. 79−37926
$Pb_{1-x}Sn_xTe$, on $LiNbO_3$, electron diffr. and microscopy exam. 77−1331
$Pb_{1-x}Sn_xTe$ optically pumped lasers, power output and wavelength, 4 to 30K 78−79035
$Pb_{1-x}Sn_xTe$, x=0.2, monocrystal, photoelectric props. of p-n structures *(Russian)* 80−70808
$Pb_{1-x}Sn_xTe$:In epitaxial layers, growth, elec. props., and luminesc. 80−54542
$(Pb_{1-x}Sn_x)_{1+y}Te_{1-y}$ system, VPE parameters influence on epitaxial film props. 79−28229
PbTe, and $Pb_{1-x}Sn_xTe$, VPE growth control by EM irrad. *(Russian)* 80−34338
PbTe, continuous epitaxial film, grain size, growth cond. depend. 78−26786
PbTe, epitaxial film on fluorphlogopite, effects of annealing in Te vapour 77−80709
n-PbTe, epitaxial layers, elec. characts. rel. to explosive evap. in closed vol. 77−89885
PbTe IR diode, epitaxially grown and ion implanted, minority carrier lifetimes, efficiency 77−20411
PbTe, nonstoichiometric, evap. and growth of epitaxial layers 80−104072
PbTe, thick epitaxial film, laser deposition technique 78−68629
PbTe, VPE film growth under near equilib. conditions 77−32526
PbTe:Bi-PbSmTe-PbTe, epitaxial laser struct., growth, p-n junction position and lasing region 79−89908
PbTe-CdTe(InSb) superlattices, laser deposition of multilayer heteroepitaxial structs. 80−44450
PbTe-$Pb_{1-x}Sn_xTe$ n-p^+ heterojunction photodetector, hot wall evaporation technique 80−65673
PbTe-$Pb_{1-x}Sn_xTe$-PbTe DH, LPE and VPE, stimulated emission 77−75526
$PbTe_{1-x}Se_x$, epitaxial layers synthesis, cryst. struct. perfection and elec. characts. 79−87587
Pd, epitaxial growth, cluster mobilities, in-situ electron microscopes obs. 80−15407
Pd, epitaxial growth on (001)W and (001)Mo 79−99450
Pd, epitaxial growth on MoS_2, epitaxial orientation variation *(French)* 78−43256
Pd film, VPE growth on Au(111), interface struct. 79−95297
Pd growth on MoS_2, reorientation of small particles 78−84103
Pd particles formed by evaporation on alkali halide crystals, orientation and struct. 78−84108
Pd/W (110), metastable 2D condensations, epitaxy, growth modes, exp. techniques, book contrib. 80−49558
Pd-Ag (Cu) alloys, epitaxial growth and surface characterisation 78−14638
Pt, epitaxial growth on (001)W and (001)Mo 79−99450
Pt film, on sapphire epitaxial relations 79−60649
Pt-Rh alloy, on rock salt, epitaxial growth and struct. 77−20211

vapour phase epitaxial growth continued
Re *(Russian)* 77−43443
Re epitaxial film growth on sapphire *(Russian)* 78−35311
Rh, epitaxial growth on (001)W and (001)Mo 79−99450
S on Cu∼(111), selective effect of substrate steps rel. to adsorbed layer interaction 78−14616
$(SN)_x$, epitaxial crystallisation on alkali halide substrates, theory 77−24496
S_2N_2, epitaxial crystallisation on alkali halide substrates, theory 77−24496
Se film, epitaxially grown on Te substrates, crystallinity, RHEED and SEM meas. 77−40373
Si (111) face, cryst. film growth, transfer of impurity during condensation of mol. beams 78−10299
Si, autoepitaxy, displacement of microrelief 80−2307
Si beam epitaxy for epitaxial film growth and p-n junction formation in high vacuum 80−16187
Si, CVD growth, inelastic light scatt. as in situ probe of chem. reaction 77−40383
Si, CVD mechanism, epitaxial growth, IR obs. 79−23859
Si, CVD on SiO_2 and Si_3N_4, SEM study *(Dutch)* 80−2960
Si, CVD using Si-H-Cl system, theoretical anal. of equilib. adsorption layers 79−23858
Si crystal, obtained by local epitaxial accretion, facing and shape meas. 77−4270
Si, deposition chambers cleaning, improved method using KOH solution 78−64478
Si, deposition on rotating disc, one-dimens. model 80−75461
Si, dopant inclusion model *(German)* 79−42088
Si, effect of deposition parameters, migration props. *(French)* 77−59236
Si, epitaxial and amorphous film growth, low energy ion beam deposition 77−28729
Si epitaxial detector fabrication, crystal growth and preferential etching 78−37505
Si epitaxial film, high electron mobility, grown on sapphire at high growth rate 77−81225
Si, epitaxial film growth by hydride-iodide method 77−48343
Si epitaxial film growth on sapphire in SiH_4-H_2 system, optimum deposition 77−77397
Si, epitaxial film growth on Si(111) and sapphire ($1\bar{1}02$), simultaneous RHEED/AES study 80−10833
Si epitaxial films on Czochralski sapphire, optimisation of deposition conditions in SiH_4-H_2 system 80−75464
Si, epitaxial growth, adsorbed layer model for autodoping mech. 80−7505
Si epitaxial growth, in $SiCl_4$-HCl-H_2 system, model based on flow graph 79−42405
Si, epitaxial growth, novel reactor for high volume, low cost prod. 79−24442
Si, epitaxial growth by partially ionized vapour deposition, low temp. 77−40389
Si, epitaxial growth kinetics in damp H_2 77−44171
Si, epitaxial growth kinetics, experimental verification of theoretical model 79−95278
Si, epitaxial growth on ion-implanted Si:As 78−6243
Si, epitaxial growth on sapphire by partially ionised vapour deposition, RHEED-AES obs. 80−80985
Si epitaxial interface migration, theory and expt. test 80−29290
Si, epitaxial layer deposition by ion beam methods 80−100417
Si epitaxial layer growth in vacuum, Ar, Xe ion bombardment effect 80−39463
Si epitaxial layers, temp. dependence of P dopant inclusion in gas phase deposition *(German)* 79−52127
Si, epitaxial layers on ribbon substrates, solar cell prod. and characterisation 77−77354
Si epitaxial reactor, doping system, transient steady state response, transfer function approach 79−42086
Si epitaxy and oxidation, first-order process models 78−72049
Si, epitaxy lateral autodoping kinetics 78−6087
Si film, epitaxial growth on Si, impurities, plasmon energy loss anal. 77−31916
Si film deposition, small-scale system design and operation 79−43151
Si, from $SiCl_4+H_2$, in vertical cylinder reactor, transport processes analysis 77−48344
Si, gas-flow dynamics in horizontal CVD reactor, book contrib. 79−82498
Si, growth mechanisms 79−28929
Si, growth processes, in-situ obs. *(Japanese)* 80−35104
Si, heteroepitaxial, prep. and props., book contrib. 79−83128
Si, heteroepitaxial early growth island morphology rel. to deposition conditions 78−6245
Si heteroepitaxial films on sapphire, vac. deposited, struct. and elec. props. 80−15390
Si heteroepitaxial growth using SiH_4 in He-H_2 atm. 77−77396
Si, heteroepitaxial growth using SiH_4 in H_2-He atm. 80−20049
Si homo-epitaxial deposition, deposition techniques 80−7501
Si, homoepitaxy, local selective, at reduced temp. using Si-I transport system 79−24444
Si homoepitaxy in high vac., stacking fault nucleation, crit. temp. for SiC growth 78−14620
Si horizontal epitaxial reactor transport expt. and model 77−77399
Si, impurities incorporation kinetics *(French)* 78−22749
Si layer growth by CVD on Sn-coated background *(Dutch)* 80−7502
Si, low press. epitaxial reactor for multi-wafer growth 79−43153
Si, mechanism of cryst. growth during chemical reactions in Si-H-Cl system 78−2392
p-Si, monocryst., diffusion of As, Henry const., temp. depend., 1448 to 1523K 79−42399
Si, nucleation, analytical model 77−62770
Si, of submicrometer thickness 79−95932
Si, on sapphire, early growth, TEM 77−24961
Si, on sapphire, early growth, models 77−24962
Si on sapphire, stacking faults and twins, TEM obs. at early stage of epitaxy 79−28233
Si $p^+\pi p n \nu n^+$ structure form. for IMPATT diode 77−76906
Si, pattern shift comparison in vertical, horizontal, and cylindrical reactor geometries 78−27408
Si, photocell, ionized cluster beam deposition and epitaxy, cell characts. 77−77416
Si, power transistor and solar cell epitaxy from SiH_2Cl_2 source 77−77402

vapour phase epitaxial growth continued
Si, reduced pressure, advances 80−40242
Si, selectivity of deposition from $SiCl_4$ 77−24958
Si, state of art 79−33937
Si, tangential growth, thickness meas. 77−35836
Si technology, phys. and thermodynamic props. data for $SiCl_4$ 79−65218
Si, thickness meas. during deposition using diffraction *(German)* 79−97355
Si thin autoepitaxial layers low temp. growth mechanism in $SiCl_4$-H_2 system 80−20795
Si, using SiH_2Cl_2/H_2 as source for epitaxial films on insulators 78−48327
Si, VPE, stationary model, appl. to $SiCl_4$-H_2 system 78−52679
Si, VPE at reduced pressure, autodoping 77−77389
Si, VPE growth, in process monitoring and control of doping gas conc. 79−24443
Si, VPE layer props. control using boundary layer characts. 80−50561
Si, VPE via SiH_2Cl_2 in barrel reactor 78−52685
Si, vapour epitaxy, optimum growth conditions 78−76608
Si:AS, lateral autodoping kinetics 78−39699
Si:B, autodoping during epitaxial growth from SiH_4 77−47476
Si:Ga(Sb), epitaxial film, doping efficiency *(Japanese)* 79−73201
Si:P, doping element incorporation, temp. depend. in CVD epitaxy 80−45234
Si:P, epitaxial layer, vapour phase grown, temp. dependence of dopant inclusion, differential molar solution enthalpy *(German)* 79−52128
Si-epitaxial film, ionised-cluster-beam deposited, cryst. and elec. characts. 80−70553
Si-Ge heteroepitaxial layers, Ge/Si ratio transfer curve from gas phase to solid phase obtained by epitaxial growth 77−73234
SiC (6H), blue-emitting diodes by CVD 80−97439
SiC (6H) epitaxial layers, growth by CVD, morphology 79−24446
SiC, appl. for solid state devices *(Japanese)* 80−11579
SiC, CVD film growth, morphological, chem. and cryst. struct. investig. 77−40385
SiC, crystal growth from gas phase role of Si in mass transfer 79−8233
α-SiC crystals, broad-band semiconductors, growth in Acheson furnace 80−84841
SiC, epitaxial film, effect of impurities on polymorphism during growth 80−15414
SiC, epitaxial growth by sublimation sandwich method, effect of impurities 80−25568
SiC, epitaxial growth by direct synthesis in vacuum 80−40262
SiC epitaxial layer, vapour phase growth, investigations of kinetic and thermal conds. 79−42407
SiC epitaxial layer growth from sublimation in vac., kinetics 80−20791
SiC, epitaxial layer polytypism 77−62781
SiC, epitaxial layer polytypism 77−62782
SiC epitaxial layers, energy distrib. in photolum. spectra, influence of synthesis conditions 79−52009
SiC epitaxial layers, growth techniques 80−108360
SiC film, growth on Si ribbon surface, TEM anal. 78−84094
SiC, H_2 effects on epitaxial growth rates 78−22968
β-SiC, heteroepitaxial growth on Si substrate using $SiCl_4$-C_3H_8-H_2 system 79−24445
SiC, monocryst., and epitaxial layer growing, temp. distrib. study in high temp. furnaces 79−65989
SiC p-n junction, epitaxial, grown by sublimation, elec. and struct. props. *(Chinese)* 80−60067
SiC, VPE kinetics study in SiC-C system 79−37934
SiC, VPE layers, growth kinetics, polytypism 77−11809
SiC, vacuum deposition on diamond, electron diffr. patterns 77−15720
SiC:Al epitaxial layers, growth, Al distrib. and solubility 80−15391
SiC:N, conversion factor at high doping levels 78−22744
SiC-N_2 system, high temp.-processes, thermodynamics 77−85105
SiO_2, growth kinetics on Si by low-temp. oxidation of monosilane 77−8763
Sn film epitaxially grown on KCl substrate 79−99441
$Sn_{1-x}Pb_xTe$, epitaxial layers synthesis, cryst. struct. perfection and elec. characts. 79−87587
SnTe, expitaxial film, early stages of growth, replication and TEM obs. 79−65348
$Sr_{1-x}Ca_xO$, epitaxial layers by CVD *(Russian)* 79−56934
SrO, epitaxial layers by CVD *(Russian)* 79−56934
Ta epitaxial layers, formation conditions influence on struct. *(Russian)* 80−20045
Ta, film on sapphire substrate, orientational growth, epitaxial textures, nucleation textures *(Russian)* 80−75454
Te, ENSH method of oriented thin film growth 79−99443
Te, evaporated film epitaxial and amorphous-crystalline phase transition growth and struct. 79−51449
Te film, on electron irrad. KBr, epitaxial growth and surface coverage 80−10825
Te film growth on KBr (111) on mica *(Japanese)* 78−79903
Ti, oxide film form. during thermal treatment, morphological and struct. study *(French)* 80−50766
TiC, and $TiC_{1-x}N_x$, using $TiCl_4$-CCl_4-H_2 and $TiCl_4$-CCl_4-N_2-H_2 systems *(German)* 77−24964
TiN, and $TiC_{1-x}N_x$, using $TiCl_4$-N_2-H_2 and $TiCl_4$-CCl_4-N_2-H_2 systems *(German)* 77−24964
TiN-TiC_x double layer coating, deposition on C steel, X-ray diffr. study 79−65338
TiO_x evaporated films, epitaxial growth on NaCl, electron microscopy obs. 80−10822
TiO_x film, growth and struct. determ. 78−48328
Tl, on Ag (111) and Cu (111) LEED, RHEED, AES study 78−84090
TlI films, polymorphic, double epitaxy and growth on KCl, X-ray and optical obs. 79−77944
V epitaxial films on sapphire by electron beam evaporation *(Russian)* 77−76701
V, film on sapphire substrate, orientational growth, epitaxial textures, nucleation textures *(Russian)* 80−75454
VBr_2 growth on V due to Br_2 chemisorption 80−101039
$V_{1-x}Cr_xO_2$, VPE, and elec. and optical characterisation 78−3053
VO_2, VPE, and elec. and optical characterisation 78−3053
W, CVD growth, inelastic light scatt. as in situ probe of chem. reaction 77−40383
W, film on sapphire substrate, orientational growth, epitaxial textures, nucleation textures *(Russian)* 80−75454
W-Os system films, condensation temp., conc., and phase comp. effect on struct. and props. *(Russian)* 80−24749

vapour phase epitaxial growth continued
W-Re, electron beam deposition, conditions for epitaxial growth on (100) Mo *(Russian)* 77−24490
YIG, CVD defect free epitaxial growth, conditions depend. 77−16502
YIG, monocrystal film growth by chem. transport in closed system 77−77392
Zn chalcogenides, thin films, VPE, needle-like cryst. growth 80−80148
Zn film growth, HEED and projection microscope obs., surface orientation depend. on deposition parameters 77−32523
$Zn_xCd_{1-x}S$ layers on ZnS substrate, VPE growth 77−77420
$Zn_{0.7}Ni_{0.3}Fe_2O_4$ film, epitaxial deposition, comp. and mag. prop. obs. using Mossbauer effect 79−38748
ZnO, CVD of epitaxial films on sapphire, SAW interdigital transducer fabrication 80−66430
ZnO epitaxial film with smooth surface from CVD onto a sputtered ZnO film on sapphire, waveguide appl. 78−56588
ZnO, epitaxial layers, influence of deposition conditions on luminescence, electrical props. 79−99924
ZnO epitaxial layers, rel. between elec. and photoluminesc. props. and their deposition conditions 79−95530
ZnO film, growth rate and defectiveness, rel. to deposition conditions and substrate orientation 78−3057
ZnO film, optical waveguide fabrication, CVD on sputtered ZnO film on sapphire 79−86269
ZnO film, prep. by reactive ionized cluster beam deposition, and characterisation 80−10829
ZnO, high rate epitaxy on sapphire by planar magnetron RF sputtering 79−28916
ZnO on Zn (0001), oxide film growth, at. and electronic struct. 78−15587
ZnS, epitaxial film, CVD growth, photolum. spectra *(French)* 77−36403
ZnS, epitaxial growth, appl. to electronic devices, review *(Japanese)* 80−55281
ZnS epitaxial growth, in H_2, mass transport processes and effects of bypass flow 79−23860
ZnS, epitaxial growth by Zn-S-H_2 CVD method 78−27413
ZnS, epitaxial layers on Ge and GaAs substrates, exam. of growth 79−1828
ZnS, epitaxy in quasiclosed volume 77−85093
ZnS film, on Si in ultrahigh vacuum, source nonstoichiometry effects 77−77387
ZnS, heteroepitaxial growth on GaP by closed space technique 79−28939
ZnS, horizontal epitaxial growth systems, transport kinetics 79−4920
ZnS, on GaP in open tube system 79−28938
ZnS(Se), growth kinetics on CaF_2 by vapour phase transport *(French)* 80−54572
ZnS_xSe_{1-x}, epitaxial film, CVD growth and characterisation *(French)* 77−36403
ZnS_xSe_{1-x}, VPE on CaF_2 substrate, in flowing H_2, growth and characterisation *(French)* 80−107678
ZnSe, epitaxial growth, orienting semiconductive substrate effects 77−47688
ZnSe, epitaxial growth by vapour flow method 78−64482
ZnSe, epitaxial layers, close-spaced technique, preparation and optical props. 79−47637
ZnSe epitaxial layers, organometallic CVD prop., growth kinetics and luminescent props. 79−51458
ZnSe epitaxial layers, prep. by chem. transport reactions 80−16192
ZnSe, evap. onto electron bombarded NaCl substrates, epitaxial growth and characts. 79−28948
ZnSe on GaAS, role of interaction between gas and solids *(French)* 77−62769
ZnSe, organometallic CVD, on GaAs, and photolum. 79−8249
ZnSe-Ge(GaAs)(mica) epitaxial heterostructs., growth struct. 78−43257
ZnTe, epitaxial film growth initial stages 77−80707
ZnTe, epitaxial growth on GaAs by closed-tube chemical vapour transport method, elec. props. 79−99449
ZnTe film preparation and props., by single-source vacuum deposition method *(Japanese)* 80−6664
ZnTe-CdS(Se)(S_xSe_{1-x}) heterojunctions, prep. and electrolum. characts. 77−24610
ZnTe-CdSe single cryst. film heterojunctions, prep. and props. 79−19652

vapour pressure
see also humidity; vaporisation
adsorbed film, adsorbent effects on props., empirical relns. 78−6217
adsorbed layers, clustering, bulk vapour pressure behaviour 79−4473
alcohols, self-association in binary mixtures, 2-const. model, vap. press. meas. *(German)* 78−18532
alkali metal hexachloroniobates and hexachlorotantalates, thermodynamic props. from VP meas. 79−34345
n-alkanes, vap. press. eqn. appls. 77−69091
amines, self-association in binary mixtures, 2-const. model, vap. press. meas. *(German)* 78−18532
α-amino acids, mass spectrometers study of evaporation 77−86402
ammonium sulphates, nucleation of new particles in atmosphere 79−81708
anormal fluids, saturated liq. densities, four-parameter corresponding state theory 79−33066
anthracene, optical determ. of vapour conc., vap. press. and heat of sublimation 78−22840
arc, DC, AC, for spectrochem. anal., correlation between anal. signals, plasma parameter changes 79−52828
associated one-component unsaturated vapour, press., composition changes, eqns. *(Russian)* 80−55696
atmospheric water content and turbidity in Thailand, calc. 79−5580
azobenzene, vapour press. meas, using torsion-weighing effusion apparatus 77−89530
benzene, benzene-d_6, vibrational anharmonicity, condensation effect, vap. press. isotope effect 78−58657
benzene, tables of thermodynamic props. 77−24419
benzene, vapour press., 5-80°C, isotope effects 78−59939
benzene-cyclohexane system, vap. press., excess free energies, isotope effects 78−59939
benzene-cyclohexane system, vap. press., isotope effects, theory 78−59940
benzophenone, vapour press. meas, using torsion-weighing effusion apparatus 77−89530

vapour pressure continued
binary mixture, inert solvent and self-associating component, Wilson consts. 79−82351
1,4-bis[2-(5-phenyloxazolyl)]benzene, saturated vap. press., absorpt. and fluoresc. spectra 79−76442
carbon tetrachloride-n-octanol-water miscible liq. systems, isopiestic vapour press. meas., activity coeffs. determ. 77−48679
carbowax in benzene, evaporation, vapour press. determ. from gaseous diffusion coeff. 80−10654
chloroform-methanol mixtures, thermodynamic props. 79−87865
colligative properties of simple solns. 77−21466
constrained fitting of limited data 78−34615
critical exponent optimal determ. 79−51271
curves for pure substances in terms of conic sections 80−44304
cyclohexane, vap. press. from 451K to crit. temp. and press. 78−47512
cyclohexane, vapour press., 5-80°C, isotope effects 78−59939
dibutyl phthalate, vapour press. determ. by submicron droplet evaporation 79−88993
dibutyl sebacate, from submicron aerosol droplet evap. obs. 79−43639
dibutyl sebacate, vapour press. determ. by submicron droplet evaporation 79−88993
dielectric gases and gas mixtures, maximum electric strength and vapour pressure relationships 80−92249
dimethylsulphoxide, density up to 257°C, vap. press. up to 189°C, crit. density 79−90768
dioctyl phthalate, vapour press., determ. by submicron droplet evaporation 79−88993
3,5-diphenyl-1,2,4-oxadiazole, saturated vap. press., absorpt. and fluoresc. spectra 79−76442
dodecan-1-ol+n-hexane, vap. press. and thermodynamic props., 298.230 to 342.824K 78−47528
droplet evaporation, diff. coeffs., vap. press. and Lennard-Jones pot. function determ. 77−80262
electrolyte solution, hydration number determ. by vapour press. meas. 79−87868
equation coefficient, procedure for estimation and extrapolation 79−10958
equation of state, modified Redlich-Kwong-Soave, liq. state representation 77−27968
equation of state, nonanalytic, modification for low density limit, appl. to ethylene 79−46779
equations, comparison, correlation and estimation 79−10957
ethanol, Benedict-Webb-Rubin parameters 77−39660
ethanol, evap. rate var. with vap. press. 78−18758
ethylene deuterates, VP isotope effect in liq. and solid, chromatographic purification 77−43337
exfoliated graphite, adsorbed Ne, vapour press. meas., 15-30K 79−69350
fluoroform., ^{13}C vap. press. isotope effect 78−59938
fumaric acid, vapour press. meas, using torsion-weighing effusion apparatus 77−89530
graphite intercalation compounds, coherency strains and staging 80−44167
halomethanes, vap. press. and boiling point data tables 79−77736
heat of evaporation and liq.-vapour equilib., appl. to real substances 79−4409
heat pipe, centrifugal, cylindrical, heat transfer, heat flux density and vap. press. effects 78−79188
n-heptane/3-pentanone mixture, vap. press. meas., thermodynamic functions calcs. 80−75345
heterogeneous system, thermodynamic theory of nucleation on charged particles 79−39216
hexan-1-ol+n-hexane, vap. press. and thermodynamic props. 298.230 to 342.824K 78−43129
n-hexane, viscosity meas. at 353 to 436K, and corresponding vapour press. 77−69107
n-hexane/3-pentanone(acetone) mixtures, vap. press. meas., thermodynamic functions calcs. 80−75345
hydrocarbons, heavy liq., vapour press. and enthalpies of vaporisation by group-contrib. method 80−40726
hydrocarbons, reduced vap. press. eqn. 79−37823
hydrocarbons, thermodynamic props. correls., third parameters 79−95184
hydrogen, and isotopic forms, cryogenic data relevant to mag. fusion energy 80−8746
ice, $H_2{}^{16}O$ and $H_2{}^{18}O$ samples, vap. press. isotope effects, −50 to 0°C 78−18757
ice vapour pressure formulation using thermodynamic calcs. 78−43117
internal pressure of liquid effect, statistical mech. relationship 79−33094
isotherm data processing, error anal. in Barker's method *(German)* 79−77764
isotope effects, bibliography 80−77558
Kelvin equation, effect of surface tension on vapour pressure, derivation 80−2248
liquid, var. of vapour press. with temp. up to critical conditions 77−31760
liquid alloys, vapour pressure, pseudopot. and Gibbs-Bogoliubov calcs. 78−83935
liquid metals, vapour pressure, pseudopot. and Gibbs-Bogoliubov calcs. 78−83935
liquid systems, pure component Gibbs energy using structural group contribution method 79−90797
liquid vaporisation, radiation induced, spinodal singularity manifestation 80−2152
liquid-liquid-ideal vap., isothermal condition, 3-phase equilib. line special point *(Russian)* 80−54345
liquid-vapour equilibrium, azeotropic props. meas., differential tensimetrical titration appl. *(Russian)* 80−54363
liquid-vapour equilibrium, systems with components of very different volatility, total press. static method meas. 79−14922
liquids, medium cluster model, vapour press. isotope effects, mol. orientation effect 77−72542
liquids, medium cluster model, vapour press. isotope effects 77−65943
magnetic solids, surface rate processes and vapour press. 80−34182
methane, liq., medium cluster model, vapour press. isotope effects 77−65943
methane, liq., medium cluster model, vapour press. isotope effects, mol. orientation effect 77−72542
methanol, viscosity meas. at 353 to 463K and corresponding vapour press. 77−69107
mixtures, perturbed hard chain theory, thermodynamic props., appls. in chem. technology 79−34343
vapour pressure continued
monolayer on graphite, sp. ht. and u.p., size and steric effects 77−85073
naphthalene, vapour press. meas, using torsion-weighing effusion apparatus 77−89530
nonpolar substances, generalised vapor press. eqns. 78−63861
octafluorocyclobutane+n-butane mixtures, 233K, surface tension meas., vapour press. 79−19371
octamethylcyclotetrasiloxane-cyclohexane liq. mixtures, u.p. and excess Gibbs free energy determ. 77−30225
polar and H-bonding compounds, vap. press. behaviour, generalised treatment 78−2227
polar compounds, liq. props. representation, by modified Redlich-Kwong eqn. of state 78−34590
polyatomic substances, thermal eqns. of states *(French)* 78−91413
polyphenyl ether in benzene, evaporation, vapour press. determ. from gaseous diffusion coeff. 80−10654
polypropylene-chloroform (chloromethane), χ-parameters, heat of mixing, vap. press. and microcalorimetric meas. 78−34626
polyurethanes, vapour press. of solvent above swollen crosslinked networks rel. to rubber elasticity theory 80−45536
porous solid with below-freezing pt. adsorbate, isothermal adsorption and dimensional changes obs. 78−75925
prediction, using equation of state 80−103443
predictive equation, behaviour between triple and crit. pts. 78−30744
pure substances, equations for determining vap. press. *(German)* 79−77763
pure substances, vapour-press. curves, conic section representation 80−92658
rare earth metals, preparation methods and properties, review 79−69969
rare earth nitrides, Knudsen cell vaporization, vaporization enthalpies 79−10936
refractory compounds, metallic, equilib. pressure of gaseous components, determ. by Knudsen method 79−52529
salicylic acid, vapour press. meas, using torsion-weighing effusion apparatus 77−89530
salinity gradient power utilising vapour pressure differences in water 80−76652
saturation vapour pressure computation, polynomial approx. 77−64462
solutions, dilute, colligative props., kinetic derivation from elastic collision processes 78−91048
stoichiometry deviation exam. by tensimetric meas. 79−69258
submillimetric pulsed laser with optical pumping, charact. rel. to vapour pressure *(Russian)* 79−94215
TCNQ, enthalpy of sublimation and vapour press. meas. 80−92661
temperature dependence, two-parameter eqn. based on kinetic theory of fluids 77−89520
temperature estimation method in ultra high vacuum range *(Chinese)* 80−232
ternary dil. soln., free energy of transfer determ. by vapour press. method 78−64871
ternary system isothermal Gibbs-Duhem eqn., direct numerical soln. 79−1511
p-terphenyl, saturated vap. press., absorpt. and fluoresc. spectra 79−76442
tetrachloroisophthalonitrile, vapour press. by effusion method, solid phase eqn. of state 80−49350
tetrafluoromethane, vap. press., triple pt. to 173K 80−6522
3,3,4,4-tetrahydrothiophene-1,1-dioxide, vap. press. by effusion method 78−26680
toluene, tables of thermodynamic props. 77−24419
toluene, viscosity meas. at 353 to 463K and corresponding vapour press. 77−69107
TTF, enthalpy of sublimation and vapour press. meas.. 80−92661
TTF-TCNQ, enthalpy of sublimation and vapour press. meas. 80−92661
vacuum system construction material selection and degassing 80−82783
vapour-liquid equilibrium, data reduction, extension of Barker's method 78−79735
vibrational anharmonicity, condensation effect, vap. press. isotope effect 78−58657
water, evap. rate var. with vap. press. 78−18758
water, $H_2{}^{16}O$ and $H_2{}^{18}O$ samples, vap. press. isotope effects, 0-170°C 78−18757
(Ag, Tl, Ca)NO_3, aqueous solutions, meas. 80−6504
(Ag,Tl,Cd)NO_3, mixed aq. solns., vapour press., 98.5°C, Brunauer-Emmett-Teller isotherms 78−51655
Ag, heat pipe meas. of corrosion and vapour press. 80−23878
Ag, vaporization, thermodynamic props. determ. by mass spectroscopy 78−22841
Ag, vapour press. above different crystallographic planes *(Russian)* 78−18762
Ag-Te-O, partial pressure diagrams 77−36681
$AgNO_3$-$TlNO_3$-$Cd(NO_3)_2$-H_2O mixtures, Henry's law, excess free energy 78−68908
$Ag_2S(Se)(Te)$, solid and liquid, mass spectrometric obs. of VP, heats of form., comp. 79−42266
Al-Mg alloys, vapour press. temp. depend., 1104 to 1637K 80−24576
Al-Zn, liq. solutions, thermodynamic properties *(Polish)* 80−49380
Al_4C_3, vaporis. thermodynamics, 1321-1607K 80−66859
AlI_3, UV absorbance, dimer-monomer dissoc. equilib., vap. press. of solid 78−13511
Am, vap. press., 1200-1600K, heats of vap. and La mixing 80−15232
^{241}Am high-purity solid, reln. to electronic structure and mag. props. 77−28011
Ar, effect of high mag. fields on vapour pressure 78−38825
Ar, phase transition, anharmonic cryst.-gas transition 80−6510
Ar, solid, enthalpy of sublimation, internal energy, determ. from vapour pressure 78−91435
Ar, solid, high-temp. thermal expansion charact. 80−59680
Ar, vapour press., entropy and enthalpy, thermodynamic consistency, two-parameter eqn. 77−80613
Ar-O_2, vapour press. meas., free energy difference between FCC and HCP solid Ar 77−11700
As_2O_3, vapour phase equilibria over GaAs 79−66181
As_4S_4, VP and thermodynamic functions calc. 77−36470
Au, determ. above 3000K, by pulsed-electron-beam meas. 77−15567
Au, heat pipe meas. of corrosion and vapour press. 80−23878
AuV, gas, bond dissoc. energy, from high-temp. mass spectra of V-Nb-Mo-Au 79−45860
Ba-H_2 system, equilib. H_2 press. and enthalpy of forml of BaH_2 79−86893

vapour pressure continued
BaB_6 powder, surface struct. effects on thermionic emission characts. and vapour pressure *(Japanese)* 80−50506
$BeSO_4.2H_2O$, composition of saturated solutions from 360 to 570K 78−22857
Bi, vapour pressure calc. from transpiration expts. on Mg-Bi and Pb-Bi alloys 77−76571
BiSeI, sublimation, vapour pressure 77−11686
Br_2, liq., entropy, computer simulation, Widom method 79−77486
C_5 hydrocarbons, in binary mixtures, phase equilibria *(German)* 79−37822
COS, vapour pressure and critical properties 79−95149
CS_2, ^{13}C and $^{33,34}S$ isotope effects 78−18756
CS_2, liq., vap. press., isotope effects, mass spectrometric determ. 77−24412
Ca_2, new ground state, photolum. obs. vibr. consts., dissoc. energy 80−5576
$CaCl_2$-NaCl-H_2O, conc. solns., vap. press. meas. 79−23713
Cd-Zn-Hg alloys, liq., comp. and temp. depend. of Hg VP, activity, free energy and enthalpy *(Russian)* 77−20087
$CdCr_2S_4$, $CdCr_2Se_4$, variation of elec. props. with chalcogen content of gas phase, 500-700°C 77−20310
$CdGeP_2$, CdP_2, Cd_3P_2 77−90634
CdS-CdSe system, overall vapour pressure determ. by Knudsen effusion method 77−28010
CdSe, meas. of partial press., by optical absorption method *(Japanese)* 78−51661
CdSe, partial press. meas. by optical absorption 80−15234
CdTe, meas. of partial press., by optical absorption method *(Japanese)* 78−51661
CdTe, partial press. meas. by optical absorption 80−15234
^{247}Cf, vapour pressure, thermodynamic functions 80−6509
Cl_2, 206 to 270K and 334 to 417K 80−19931
Cl_2, liq., entropy, computer simulation, Widom method 79−77486
$CoCl_2$, vapour pressure meas. 77−89534
Cr, vapour press. above different crystallographic planes *(Russian)* 78−18762
Cs, 860 to 1060K, 340 to 2010 mm Hg 77−26313
Cs, liq., vapour press., thermodynamic functions determ., Knudsen-effusion radiotracer method 78−26678
Cs-SiO_2-Al_2O_3 system interactions, getter development for radiocaesium 80−83208
Cs_2CrO_4, mol. beam obs. of evap., saturated vapour press., 656.8 to 1151K 80−107411
Cu, heat pipe meas. of corrosion and vapour press. 80−23878
Cu, vaporization, thermodynamic props. determ. by mass spectroscopy 78−22841
Cu, vapour press. above different crystallographic planes *(Russian)* 78−18762
Cu-Ge solders for electric vacuum instruments, Mn and Ag additives effect on evaporation 79−42231
$CuCl_2$-water solution, Nd-glass laser radiation induced vaporisation, press. history 80−2153
CuF_2, thermochemical props. 78−31674
$CuSO_4.5H_2O$ dehydration kinetics depend. on water vapour press. 79−15986
DI, thermodynamic properties 78−47517
$DyCl_3$, vapour press. and sublimation thermodynamics, mass loss effusion meas. 80−88313
EuS, evaporation, thermodynamic data 78−2248
Fe, vapour press. above different crystallographic planes *(Russian)* 78−18762
Fe-Ni-Cr system, absolute partial pressures and chem. activities of component metals 80−50600
Fe-Zn, homogeneous phases, Gibbs free energies of form., Knudsen effusion method 80−66481
$Fe_{1-x}O$, wustite, vaporisation, mass spectrometric analysis of gaseous phase 78−48652
Fe_3O_4, magnetite, vaporisation, mass spectrometric analysis of gaseous phase 78−48652
G_2-B_2O_3 melt, thermodynamic props. from mass spectroscopy 80−39318
Ga, heat pipe meas. of corrosion and vapour press. 80−23878
GaAs, elec. cond., effect of As vapour press. at 200-1000°C 77−15846
GaAs in Sn, vap. press. of P and As 77−51485
GaN, thermodynamic anal. of prep. methods 80−55328
GaP in Sn, vap. press. of P and As 77−51485
Ga_2S, partial vapour press., above Ga_2S_3, anomalous temp. depend. 77−62634
Ga_2Se_3, evaporation, thermodynamic props. 80−54365
$GdCl_3$, vapour press. and sublimation thermodynamics, mass loss effusion meas. 80−88313
GdP, vapour comp. and dissoc. pressure 77−84916
Ge, heat pipe meas. of corrosion and vapour press. 80−23878
H_2, 4 to 30K, isotope effects 77−72674
H_2, thermometric fixed points determ. 77−82511
n-H_2, vap. press. eqn. between triple and critical pts. 77−55351
HBr, triple-point temp. and pressure, vapour pressure of liquid to 205K 79−7683
HBr-HCl, thermodynamics of binary liquid mixtures 78−64876
HBr-Xe, thermodynamics of binary liquid mixtures 78−64876
HI, thermodynamic properties 78−47517
H_2O, at triple point, technique and results 77−43338
H_2O, vapour press. formulation in range 0 to 100°C 77−69078
H_2SO_4, tropospheric or stratospheric gas-particle conversion 80−94560
He, liquid, controlled by manostat to 4 torr 79−35757
He, Stirling cryocooler, milliwatt refrigeration at temps. 3 to 4K 79−67307
^3He, significant structure theory, thermodynamic props. 78−51774
^3He-^4He mixture, transport props. near superfluid transition and tricritical point 80−29242
^4He film growth on graphite, MgO, and Mylar substrates, vap. press. meas. 80−70499
^4He films, adsorbed on graphite substrate, layering and thermal cond., heat capacity and vapour press. meas. 79−51386
^4He films adsorbed on graphite, transition temp., entropies, internal energies and heats of desorption, vapour press. meas. 80−2238
^4He layered films on ZYX graphite, thermal resist. below 2K 80−70500
^4He, nonsuperfluid liq., neutron scatt. dynamic struct. factor, saturated vap. press. 78−42878
Hg, liq., vapour press. and crit. points determ. from elec. cond. meas. 77−59273
vapour pressure continued
Hg use and abuse for vacuum production and meas. 78−81998
Hg-Cd, liq. amalgam, vapour press. and crit. points determ. from elec. cond. meas. 77−59273
Hg-U system, thermodynamic props., vap. press. and EMF expts. 79−91625
HgS, melting point and vapour pressure 77−15549
IF_5, vapour press., phase transform. enthalpy *(German)* 78−51654
IF_7, vapour press., phase transform. enthalpy *(German)* 78−51654
In, heat pipe meas. of corrosion and vapour press. 80−23878
In, In+In_2O vapour press. over In+$MgIn_2O_4$+MgO mixture, 1095-1350K 78−91433
In-P system, liquid-vapour equil., VP functional depend., 1023 to 1123K 79−42228
In-Zn, liq., Zn activity meas. by Knudsen torsion-effusion method, Zn vap. press. meas. 79−10950
InAs, soln. in liq. Sn, vapour phase partial press. meas., rel. to LPE 78−34610
$In_xGa_{1-x}As$-$InAs_xP_{1-x}$ VPE mixed crystal composition rel. to vapour pressure *(Japanese)* 77−55893
InP, soln. in liq. Sn, vapour phase partial press. meas., rel. to LPE 78−34610
In_2Se_3, vapour press. temp. depend., heat of evap. and form. 80−59642
K-Cs solution, activity and saturated vapour press. of Cs, reson. line absorpt. obs. 77−51509
KCl-$AlCl_3$, molten mixture, vap. pres. meas. 78−87779
$KO_{0.5}$-$AlO_{1.5}$-SiO_2 system, activities calc. from vapour press. meas. and known data 79−91985
K_2O-Al_2O_3 system, high temp. thermodynamics and phase equilibria 78−80521
K_2O-SiO_2, vap. press., thermodynamic props. and phase diagram at high temps. 78−83932
K_2SO_4, mass spectrum obs. of vaporisation, vapour comp. and press., transition and form. heats 80−19933
Kr, solid, enthalpy of sublimation, internal energy, determ. from vapour pressure 78−91435
Kr, solid, high-temp. thermal expansion characts. 80−59680
Kr, vapour press., entropy and enthalpy, thermodynamic consistency, two-parameter eqn. 77−80613
Kr-NO, thermodynamics, monomer-dimer assoc. of NO, vap. press. meas. 79−90798
Kr+ethene, liquid mixture thermodynamic excess functions 78−48690
La_2S, unsaturated and saturated vapour press., 673-1173K, thermal dissoc. pattern 80−104457
La_2S_3-LaS_2, p-T-x phase diagram of La-S system 77−21112
Li-ND_3, near liq.-liq. crit. point, conc. fluctuations, neutron diffr. long wavelength thermodynamic limit 79−10948
Li-Pb, thermodynamic study using Knudsen effusion mass spectrometry 80−24578
LiCl-$AlCl_3$, molten mixture, vap. pres. meas. 78−87779
Li_2O, mass-spectrometric study of vaporization of solid and thermochemistry of gas 79−10940
Mg-Bi, thermodynamic study vapour pressure measurement by transpiration 78−44395
$MgCl_2$-NaCl-H_2O, conc. solns., vap. press. meas. 79−23713
Mn-(Fe)-Si-C, activity determ. by vapour press. meas. *(Japanese)* 77−63631
Mn-C(Si), activity determ. by vapour press. meas. *(Japanese)* 77−63631
Mn-Si liquid alloy, vapour-pressure meas. using torsion effusion method 79−42215
Mn-Si-O, phase equilibrium *(Russian)* 77−66630
MnSe, vaporization, thermodynamic study by Knudsen-cell mass spectrometry, vap. press. meas. 79−10937
Mo, vapour press. above different crystallographic planes *(Russian)* 78−18762
MoF_5, prep., melting temp., vapour density, press., enthalpy of fusion, meas., assoc. 78−38813
MoF_6, vapour press., phase transform. enthalpy *(German)* 78−51654
Mo_3Sb_7, Sb decomp. press. and enthalpy of form., Knudsen effusion meas. 79−87840
N_2, effect of high mag. fields on vapour pressure 78−38825
N_2, solid low-press. diffusion of vapour 78−22842
NH_3, isotope effect, relevance to isotope exchange reaction calcs. 80−39272
NH_3-ethylene (propylene) mixtures, crit. curves at high-press. 79−23715
NH_3-metal, soln., thermophysical props., review 79−77758
Na thermodynamic props. for reactor safety analysis 79−13478
Na-Cs solution, saturated vapour pressure of Cs over solution 78−26688
$2NaBO_2$-B_2O_3 melt, thermodynamic props., mass spectra 80−65252
NaCl-$AlCl_3$, molten mixture, vap. pres. meas. 78−87779
NaCl-$CaCl_2$, electrolyte mixture, evaporation from multi-component droplets, in stream of air 77−56255
Na_2O-B_2O_3-GeO_2 system glass-forming melts, mass spectrometry obs. of thermodynamic props. 80−97468
Na_2O-B_2O_3-GeO_2 vitreous melts, thermodynamic props. from mass spectra 80−65253
NbO_x, phase comp. on heating 2000-4000K 80−21267
$NbSe_2$, thermal dissociation 78−44370
Ne, vapour press. and triple point, influence of impurities 78−79756
Ne-H_2 liq. mixtures, phase equilib. effects, thermodynamic perturb. theory *(Russian)* 80−92663
Ni, vapour press. above different crystallographic planes *(Russian)* 78−18762
O_2, effect of high mag. fields on vapour pressure 78−38825
O_2, vapour pressure meas., 90 to 154.6K, eqn. 77−27993
Pb, vapour press., meas. using transpiration method, thermodynamic props. determ. 78−3365
Pb-Bi alloy, vapour press., meas. using transpiration method, thermodynamic props. determ. 78−3365
$PbIn_2S_4$, computer-automated meas. by simultaneous Knudsen torsion-effusion method 80−73334
PbTe, epitaxial film on fluorphlogopite, effects of annealing in Te vapour 77−80709
Pb(Zr,Ti)O_3, thermodynamic properties and formation data 80−29939
$PrCl_3$, sublimation press. and thermodynamics, mass loss effusion meas. 79−99307
PrP-I, heterogeneous equilib. 77−36777
Pu, pure, vap. press. at high temp. 79−55880
Pu vapour pressure determ. 1724 to 2219K by Knudsen effusion technique 80−654

vapour pressure continued
PuO_2 nuclear fuel, eqn. of state and thermodynamic props. 80−13592
S_2, vapour press. rel. to sulphide form. on Ge surface 79−43152
Sb, vaporisation behaviour, transpiration and boiling temp. studies 80−29161
Sb-S, saturated vap. press. 78−43116
SbI_3, vapour pressure 79−60496
SbSeI, sublimation, vapour pressure 77−11686
ScI_3, mass spectra and vapour press., and thermochemistry for dimerisation 78−27809
$ScPO_4$, $Sc(PO_3)_3$, mass spectra 77−47567
Si-Te system, phase diagrams 80−89209
SiC:Be, gas-phase equilib. comp., thermodynamic analysis rel. to cryst. growth and doping 77−85909
$SiCl_4$ physical and thermodynamic properties, rel. to Si technology 79−65218
SmF, vaporisation, sublimation, Knudsen effusion method 80−6508
Sn, heat pipe meas. of corrosion and vapour press. 80−23878
Sn-S system, use of boiling points to investigate vapour pressure 80−54361
$SnSe_2$, sublimation, temp. depend. of equilib. constants 80−88312
Sr, vapour pressure below 660K, heat of vaporisation 79−37825
SrF_2, vaporisation and sublimation thermodynamics *(German)* 80−81355
Ta_3As, arsenic decomp. pressures and enthalpy of form. 77−70329
$TbCl_3$, vapour press. and sublimation thermodynamics, mass loss effusion meas. 80−88313
$ThCl_4$, thermodynamics of vaporisation and melting 79−60492
Ti-Ir alloys, Ti-rich, thermodynamic study at high temp. using Knudsen cell mass spectrometry 80−45539
Ti-Ir system, high temp. thermodynamic investig. of Ir-rich portion by Knudsen cell mass spectrometry 77−12595
Ti-S, pressure-temp.-comp. phase diagram, TiS_2 growth by chem. vapour transport 77−59764
TiO, high temp. thermodynamics, vaporisation, and pressures over 80−10685
TiO, high temp. vaporisation and thermodynamics, vapour press. temp. coeff. 77−59110
TiS, vaporisation chemistry and thermodynamics, computer-automated simultaneous Knudsen-torsion effusion 80−48837
Tl-Cd-Sb, liq., Cd vapour pressure and thermodynamic functions *(Russian)* 79−51247
$TlCl(Cl_2)$, vap. press. and thermodynamics 80−6503
$(U,Pu)C_{1\pm x}$, evap. behaviour, 1500-2458°C 77−27994
(U,Pu)N, self-consistent normal fluid eqn. of state, press., density, and enthalpy of vaporisation calc. 78−8909
$(U,Pu)O_2$ fuels, eqn. of state up to 5000K, high-temp. laser technique 77−27971
$(U,Pu)O_2$, liq., meas. to 5000K 77−20077
$(U,Pu)O_2$, liq., v.p. up to 5000K 77−1239
$(U,Pu)O_2$, vapour press. eqn. of state, VENUS-II code studies 78−8908
U-Hg system, phase relations determ. 79−91624
U-Pu-C system, segregation and v.p. obs. 77−28793
U(C,N), N vapour pressures and thermodyanmic props. 80−84918
UCl_4, vaporisation thermodynamics 78−44394
UF_4, vaporisation behaviour 80−84283
UF_6, vapour press., phase transform. enthalpy *(German)* 78−51654
UN, N vapour pressures and thermodynamic props. 80−84918
UO_2 effective eqn.-of-state meas. to determ. vapour pressure, rel. to LMFBR safety 79−31036
UO_2 nuclear fuel, eqn. of state and thermodynamic props. 80−13592
UO_2, vapour press. meas. up to 5000K, appl. of laser pulse heating 80−52230
V-S system, order-disorder transition of metal vacancies, statistical thermodynamics 78−43012
V_2O_{5-x}, O_2 equilib. press. at 600°C 77−81421
V_2O_{5-x}, O_2 equilib. press. above oxide system, thermodynamic props. 79−16029
V_2O_{5-x}, O_2 equilib. press. as measure of O_2 binding energy in oxide system 79−16030
VSe_2 phase, stability and Se equilib. vapour press., homogeneity range 78−43133
W, vapour press. above different crystallographic planes *(Russian)* 78−18762
WF_6, vapour press., phase transform. enthalpy *(German)* 78−51654
Xe, solid, enthalpy of sublimation, internal energy, determ. from vapour pressure 78−91435
Xe, vapour press., entropy and enthalpy, thermodynamic consistency, two-parameter eqn. 77−80613
Zn-Cu-Se system, condensed phase equilibria, 800-1000°C, vapour pressures of Zn, Se_2 77−16553
Zn-Te-O, partial pressure diagrams 77−36681
$ZnGeP_2$ dissoc. press., vapour comp. and press., thermodynamic characts. 77−24934
$ZnSO_4.7H_2O$, meas. of water physically adsorbed rel. to water of crystallisation *(Japanese)* 80−6622
$ZrCl_4$-CsCl melt, equilib. phase diagram and vapour press., equilib. reaction 77−66764
ZrO_2-HfO_2(Y_2O_3) solid soln. complex refractories, sublimation *(Russian)* 78−47513

vapour pressure measurement
atomic vapour pressure, optical absorpt. method 79−22865
computer-automated meas. by simultaneous Knudsen torsion-effusion method 80−73334
controller, liq. ^{4}He applic. 78−16900
effusion method, review 80−51995
electron-beam heating method, above 3000K, appl. to Au 77−15567
gas flow method *(Croatian)* 79−17434
heat pipe, gas controlled, for meas. thermophysical props. 80−23878
high temperature vapours, phase transitions, equations of state, appl. of laser pulse heating 80−52230
high-temperature materials, vapour press. meas. using laser heating system 77−77699
Knudsen torsion-effusion pendulum method, computer-automated acquisition system 79−49214
liquid mixtures, apparatus 77−30225
lubricant vapour pressure and evap. rate in vacuum, determ. using ambient press. meas. 78−29123
metal vaporisation, optical spectral methods of vapour press. meas., review 79−66381

vapour pressure measurement continued
metallic vapour, partial pressure meas. *(Japanese)* 80−34179
metals and alloys, room temp. to critical and supercritical temps., high accuracy 77−26313
metals and alloys, sulphidation, high-temp., thermobalance for studying kinetics 78−23876
molecular weight determ. by vapour pressure osmometry 77−46658
multicomponent solid and liquid solution, thermodynamic activity meas., Knudsen method appl. 78−79783
partial atomic vapour pressure, meas. by forward light scatt., transverse mag. field 79−16087
partial vapour pressure, determ. for volatile component by static method 80−37150
pure liquid vapour pressure determination apparatus 78−41274
pyridine N-oxide, in benzene, dipolar assoc. investig. 80−107035
pyrometric-laser heating technique for up to 5000K 77−1239
rapid and accurate meas. apparatus for press. and vol. 79−88972
reference materials, vapour pressure tables 77−71289
static method, evaluation 77−74378
temperature estimation method in ultra high vacuum range *(Chinese)* 80−232
thermo-balance method for expts. under controlled vapour press. 80−47021
thermometric barometer for remote locations and data buoys 80−46300
torsion-effusion method, automatic data acquisition 80−52188
torsion-weighing effusion vapour pressure measurements, appl. to organic compounds 77−89530
trifluoromethanesulphonic acid monohydrate, electrochemical props. and use as fuel cell 79−61969
ultralow, determ. by submicron droplet evaporation 79−88993
unsaturated two-component associated vapour, press., comp., thermodynamic calcs. *(Russian)* 80−64671
water vapour sensor of P_2O_5 type 80−98907
Cs vapour, electric-discharge pressure gauge for 0.1 to 10 torr range 79−17432
Fe-Ni-Cr system, absolute partial pressures and chem. activities of component metals 80−50600
H_2, 2 to 4.5K, influence of thermal radiation 77−5848
H_2O, at triple point, technique and results 77−43338
H_2SO_4, partial press. meas. with tunable diode laser *(German)* 80−43361
He vapour pressure scale determ. using paramag. salt thermometer and NPL-75 gas thermometer scale 80−95060
^{3}He, high precision, capacitive gauge for use up to 0.3K 80−68207
In amalgam lamp, Hg vapour partial pressure meas. 78−67488
Sn, SVP measurement by line absorpt. method in atomic absorpt. spectroscopy of SnI 80−55747
UO_2, and (U, Pu)O_2 nuclear oxide fuels, vapour pressure meas. for fast reactor safety anal. by laser techniques to 5000K 80−13591
UO_2, liquid, reactor safety research, laser experiments *(German)* 80−42787
UO_2, vapour press. meas. up to 500K, critical point data prediction, present state of art 79−45347

vapour-solid transformations *see solid-vapour transformations*

varactors
bounds on nonlinearity of varactor diode capacitor 79−54090
crystal parabolic frequency/temp. characteristic compensation 79−55294
GaAs FET amplifier, varactor-tuned, for UHF SQUID magnetometer 80−31814
hyperabrupt, fabrication from vapour phase epitaxial GaAs 80−29288
hyperabrupt junction, C-V index, junction parameters depend. 80−49876
multilayer p-n junction varactor diode, computer simulation, characts. 79−42625
step-index fibre transmission system variable equaliser 79−55243
strip-coupled varactor SAW convolvers, parametric cct. anal. 78−71245
thermometer appl., sensor, differential meter and stabiliser *(Czech)* 78−29115
H maser cavity, tuning using variable capacitance diode 79−72545
HgCdTe photodiode, heterodyne detection for CO_2 isotope laser freq. calibration 77−19230

variable-frequency oscillators
see also swept-frequency oscillators
audio oscillator, modified transistor radio, for teachers 78−81772
digital controlled acoustic beam steering and focusing 80−38191
electronic music synthesis, using an almost locked oscillator circuit 77−68340
far IR Josephson junction voltage-tunable differential heterodyne spectroscopy 79−30578
frequency measurement, using beat frequency display with LED 79−63191
high speed, appl. to Fermilab booster low level RF system 79−68049
laser Doppler velocimeter calibration burst generator 79−77321
magnetic field intensity changes detected by an oscillator employing a saturable-core reactor 78−12729
resistance thermometer, novel circuit *(German)* 77−74394
resonance-tracking circuit for acoustic levitation expts. 78−46874
SAW in-line chirp filter applications 78−59207
tunable variable bandwidth/frequency SAW resonator 78−59247
VLF oscillator providing variable freq. between 0.1 and 10 Hz, teaching appl. 79−62977
voltage-controlled SAW resonator oscillators 77−27450

variable speed gear
optomechanical device frictional elements, solid lubricant tests 79−52388
rigid-vane artificial heart development 79−84025

variable stars
see also eclipsing binary stars
10-day Cepheids, theoretical models 78−49449
HR 1099, RS Canum Venaticorum type binary, light and colour curve meas. 80−73004
χ Cygni, Hα emission line profile obs. of long-period variable 79−25618
2A 0042+323 (3U 0042+32) optical candidate, variable emission-line star obs. 78−54088
2A 0311−227 optical counterpart, binary star, light curve Fourier anal. 80−82549
2A 0311−227 optical counterpart, high speed photometry 80−82547
2A 0311−227 optical counterpart, identification as AM Herculis type star 79−30149
2A 0311−227 optical counterpart, possibly AM Herculis type white dwarf 79−35434

variable stars continued
2A 0311−227 optical counterpart, simultaneous photometric and spectroscopic obs. 80−90572
2A 0526−328 optical candidate, high speed optical photometry 80−51917
2A 0526−328 optical counterpart, spectroscopic obs. 80−77515
2A 0526−328 optical counterpart, X-ray emitting cataclysmic variable, spectrum and photometry 79−97103
ZA 0536−328, AM Herculis-like star identification confirmed 79−40296
A 0538−66, X-ray burster position and optical candidate in LMC 80−73076
2 A 1052+606, X-ray and optical variability of RS CVn star 80−31331
A-type stars, rot., mixing and variability 77−87397
activity of solar type, observational aspects 77−56918
adiabatic non-radial oscillations with moderate or large l, theory 80−56819
AE 1, He-rich variable, spectroscopy and photometry 80−41836
Am stars, time scale 77−29849
Am-stars, scanner obs. 79−5827
o Andromedae, Be star, radial vels. obs. 79−58355
o Andromedae, Be star, spectrographic obs. from (1967 to 1976) 77−71116
o Andromedae, Be star, spectroscopic evidence for new shell episode 80−90444
FF Andromedae, BY Draconis variable, spectroscopic binary, orbit and active region model 77−33527
λ Andromedae, high-press. transition region in model chromosphere 80−26847
AC Andromedae, mass determ. of triple-mode Cepheid 78−93261
AC Andromedae, multiperiodic RR Lyrae star, pulsation theory and models 77−87431
GP Andromedae, photoelectric photometry of RRs variable *(German)* 79−71044
AC Andromedae, pulsating variable, mass, luminosity and evolution 77−29845
SW Andromedae, RR Lyrae variable, uvbyβ photometry 78−12249
o Andromedae, shell star, UBV photometry 77−82227
CG Andromedae, Si binary star, spectrum variable, short period radial vel. variability determ. 80−72968
W Andromedae, SiO maser emission obs. 78−4225
σ Andromedae, spectrographic obs. of suspected δ Scuti star 78−61867
BM Andromedae, spectroscopic and photometric obs. of T Tauri-type star 80−62130
ζ Andromedae, spectroscopic binary, photometric and spectroscopic obs. *(Russian)* 78−57588
Z Andromedae, symbiotic star, IUE obs. of UV spectrum 80−109450
AC Andromedae, triple mode variable, oscillating c-type RR Lyrae star 78−57560
o Andromedae, UBV photoelectric obs. of shell star 79−71046
AC Andromedae, UBV photometry of triple mode variable star 78−93260
Z Andromedae, UV spectra, 1979 Feb. 17, quiescent phase 79−40202
λ Andromedae, UV spectrum obs. by International Ultraviolet Explorer 78−96475
λ Andromedae, V photometric obs. during 1976-77 period 78−40994
EG Andromedae (HD 4174), symbiotic star, spectroscopic obs. 80−85945
ET Andromedae (HR 8861), Ap star, light vars. and period 80−46571
ET Andromedae (HR 8861), spectrum variable, period from photometric measures *(French)* 77−17579
anomalous Cepheids in Draco dwarf galaxy, masses 77−2434
Ap stars, spectrum vars. rel. to mag. latit. of metals 79−58341
Ap stars 56 Arietis and HD 9996, spectrum vars. rel. to mag. fields and precession 77−2432
S Apodis, photographic B mag. and visual estimate (1977, March) 77−53609
S Apodis, R Coronae Borealis variable, visual magnitude estimates 77−53611
R Aquarii, 43 and 86 GHz obs. of SiO maser 79−71036
AE Aquarii, cataclysmic variable, IUE satellite UV obs. 80−72985
AE Aquarii, cataclysmic variable, rapid light oscills. rel. to white dwarf oblique rotator model 80−36634
R Aquarii, Mira variable, 14.9 GHz obs. 79−75210
U Aquarii, R Coronae Borealis star, extraordinary comp. rel. to unusual s-processing event 80−17588
CY Aquarii, RRs type star, BV photometric obs. *(Italian)* 80−90449
R Aquarii, symbiotic long-period variable, spectrum of assoc. nebulosity 80−90450
R Aquarii, symbiotic star, radio mol. maser line obs. 80−72960
R Aquarii, UBVRI polarimetric obs., orbital motion effect *(Russian)* 80−36646
R Aquarii, UV, visible and 85 GHz continuum obs. 80−85946
R Aquarii, UV obs. of hot component 80−56854
U Aquarii, visual magnitude estimates 1976, Oct. 77−2429
R Aquarii (M7+pec), late type variable star, IUE obs. of circumstellar emission 80−82370
Aquila X-1, UBV photometry during 1978 X-ray outburst *(Russian)* 79−101224
Aquila X-1 (4U 1908+00), optical outburst, obs. 78−69911
Aquila X-1 (4U 1908+00), optical outburst obs. 80−67909
V794 Aquilae, AM Herculis-like brightness vars. 79−92804
η Aquilae, Cepheid variable, absolute energy distrib. in radiation spectrum *(Russian)* 80−72974
U Aquilae, Cepheid variable, detect. as long-period binary by radial vel. spectrometer 80−51667
η Aquilae, classical Cepheid, companion star detect. and distance determ. 80−90443
R Aquilae, IR star, very long baseline interferometric obs. of assoc. OH maser source 77−53699
V923 Aquilae, motion in shell and atmosphere 77−60776
TW V586 and V1079 Aquilae, photometry, photographic obs. *(Russian)* 78−20842
T Aquilae (Nova 1891), spectrophotometry of shell 80−72955
V603 Aquilae (Nova 1918), IUE obs. of periodic light vars. 80−105251
V603 Aquilae (Nova 1918), old nova, eclipses obs. 80−90476
V603 Aquilae (Nova 1918), periodic light vars. detect. 80−82391
V1301 Aquilae (Nova Aquilae 1975), dust grain IR emission model 80−105254
V1301 Aquilae (Nova Aquilae 1975), IR development 77−17570
R Aquilae Mira variable, 14.9 GHz obs. 79−75210

variable stars continued
UX Arietis, binary star, radio obs. 77−64793
UX Arietis, co-ordinated UV, optical and radio obs. of RS Canum Venaticorum binary 79−16963
SX Arietis, He spectrum variable, UV photometry with ANS 78−36585
TT Arietis, nova-like cataclysmic variable, photoelectric photometry 80−82382
UX Arietis, RS Canum Venaticorum binary, two-freq. radio polarimetry 79−21335
β Arietis, suspected var. of highly eccentric spectroscopic binary 79−17026
UX Arietis, V photometric obs. during 1976-77 period 78−40994
UX Arietis (H0324+28), RS Canum Venaticorum system as coronal X-ray source 79−16979
Astrographic (Carte du ciel) Catalogues, variable star positions 77−49393
59 Aurigae, δ Scuti star, light curves periodogram anal. 80−62141
KR Aurigae, brightness history from 1890 AD 80−105245
ε Aurigae, dual aspect of wavelength depend. fluctuations 80−62190
AR Aurigae, eclipsing binary Hg star, peculiar spectral var. during eclipse 80−98679
RW Aurigae, IR spectroscopy with contact-type image tube 79−92768
KR Aurigae, irregular variable as black hole candidate 79−58362
KR Aurigae, optical spectrum, variability *(Russian)* 78−36597
KR Aurigae, peculiar variable star, possible black hole *(Russian)* 77−87420
AA Aurigae, photoelectric magnitude sequence 77−74073
RW Aurigae, T Tauri star, far UV spectra, emission measure obs. 80−94788
KR Aurigae, X-ray source nearby, X-ray, IR and visible obs. 80−67742
KW Aurigae (14 Aurigae A), ellipsoidal variable and δ Scuti pulsating star, tidal l=1 p_5-modes 79−97028
T Aurigae (Nova 1891), old nova, photometric and spectroscopic obs. 80−90446
SS Aurigae star fields, comparison star sequences, photometry obs. 80−82433
B 1 Ia-0 supergiants, mass loss meas. 79−16948
B-type stars, nonradial pulsations, line profile variations 78−4228
B-type variable star in LMC, possible identification with LMC X-3, spectral type 79−5923
BAV results for 1973-5 period *(German)* 77−71118
BD+30°448 and BD+27°4642, age of BT Draconis-type stars *(Russian)* 77−64774
BD+61° 1211 (2A 1052+606), RS Canum Venaticorum binary star, spectroscopic obs. 80−36663
BDS 1269 A, metal-poor δ Scuti star, pulsation periods from b-band photometry 80−105247
Be stars, review 79−84809
Be stars, search for rapid Hα and Hβ line variability 77−26014
Be stars, variability search, 1971-8 photometric obs. 80−36650
Be stress, bright, Hα emission variability 79−67027
beat Cepheids, Fourier anal. 78−69811
beat Cepheids, model constraints 79−5831
blue star-like objects in field of M31, photometric obs. 77−9744
UZ Bootis, cataclysmic variable similar to WZ Sagittae, outburst charcts. 80−17596
γ Bootis, classical evolved δ Scuti star 79−75219
BPM 30551, ZZ Ceti star, high freq. oscills. 77−2445
BPM 30551, ZZ Ceti-type variable, light curves and power spectra 77−56948
BPM 31594, new southern hemisphere variable white dwarf 77−5531
bright IR star monitoring at 2.7 μm 78−16433
bump Cepheids, mass anomaly as opacity effect 79−16964
X Caeli, temp. and radius vars. 77−49395
53 Camelopardalis, Ap star, Ca II K and Hδ lines rapid vars. *(Russian)* 80−90458
Z Camelopardalis, dwarf nova, photometric obs. and light curve (1973-77) 80−56853
Z Camelopardalis, dwarf nova, spectrophotometry at standstill and in eruption 80−82366
SV Camelopardalis, eclipsing binary containing BY Draconis variable, motion round third component 79−67055
RU Camelopardalis, photometric behaviour, (1966 to 1977) 78−89206
53 Camelopardalis, photometric vars. 80−4367
XX Camelopardalis, R Coronae Borealis star, photometry in optical and IR ranges 80−101601
SS Camelopardalis, UBV photometry and light curve soln. for eclipsing RS Canum Venaticorum binary 80−41854
AX Camelopardalis (53 Camelopardalis), Ap star, UBV photoelectric photometry and period of var. *(Italian)* 80−90448
38 Cancri, δ Scuti star, UBV photometric obs. of variability 80−22021
RS Cancri, late-type variable star, spectral energy distrib. and spectral types *(Russian)* 78−40958
RS Cancri, OH emission obs. 78−8026
V Cancri, Zr isotope abundances 78−53957
BT Cancri (38 Cancri), δ Scuti star, multiple periods rel. to radial and nonradial pulsation periods 80−85948
38 Cancri in Praesepe cluster, δ Scuti variable, pulsation anal. from light curves 80−77419
VY Canis Majons, late supergiants to maser star, radial vel. determ. 80−77410
β Canis Majoris, β Cephei star, Fourier anal. of radial vel. changes 80−105246
VY Canis Majoris, apparent orbit, rotating holey dust cloud hypothesis 79−40191
VY Canis Majoris, circular polarisation of stellar radiation scattered in circumstellar cloud, theory 78−96428
VY Canis Majoris, circumstellar shell heterodyne interferometry 78−8000
VY Canis Majoris, diameter upper limits 79−16974
VY Canis Majoris, expanding circumstellar cloud, SiO 8 μm band obs. 79−62840
YZ Canis Majoris, flare star, coordinated X-ray, optical and radio obs. 78−8012
VY Canis Majoris, H_2O source, linear polarisation of 22 GHz line emission 78−77612
VY Canis Majoris, IR obs. with new photometer 77−26017
VY Canis Majoris, irregular supergiant, OH maser source, UHF spectra obs. 80−90550
W Canis Majoris, luminous C star in Canis Major OB1 78−12312

variable stars continued
VY Canis Majoris, OH and H_2O microwave maser emission obs. 78−53949
VY Canis Majoris, OH masers very long baseline interferometric obs. 78−36712
VY Canis Majoris, OH/IR star, 1612 MHz OH maser multibaseline VLBI obs. 80−12766
VY Canis Majoris, relation to mol. cloud complex rel. to luminosity and evolutionary state 78−24536
VY Canis Majoris, supergiant OH maser source, optical radial vel. 77−49378
VY Canis Majoris IR star. very long baseline interferometric obs. of assoc. OH maser source 77−53699
W Canis Majoris rel. to assocs. Canis Major OB1 and R1 and NGC 2353 cluster, uvbyβ obs. 78−85985
β Canis Majoris stars, ANS UV photometry 80−26871
β Canis Majoris stars, observational aspects of multiperiodicity 77−87424
β Canis Majoris stars, UV flux obs., basic data obtained with TD-1A satellite 80−51783
β Canis Majoris stars, UV obs. by TD-1A satellite 78−20839
β Canis Majoris stars in southern hemisphere, photometric search 78−12243
β Canis Majoris variables, β photometry of early B-type stars 78−77562
β Canis Majoris variables, luminosity calibration and evolution 78−96488
YZ Canis Minoris, negative flares and dips of UV Ceti-type star 79−80317
YZ Canis Minoris, red dwarf star, weak radio flares interferometric obs. 78−65633
YZ Canis Minoris, spectroscopic flare obs. 79−92780
YZ Canis Minoris, UV Ceti-type flare star, simultaneous 1420 MHz and optical obs. of flares 78−49464
4 Canum Venaticorum, δ Scuti variable, photoelectric photometry 77−53601
4 Canum Venaticorum, BV photometry of δ Scuti star 79−35268
Y Canum Venaticorum, C_3 and IR spectrophotometry of C star 78−65619
Y Canum Venaticorum, C star, IR spectrum between 1.2 and 30 microns 80−46544
TX Canum Venaticorum, cataclysmic variable, P Cygni type, visible spectral obs. 80−105249
TX Canum Venaticorum, evolution from cataclysmic to stationary P Cygni stage 79−12479
AM Canum Venaticorum, orbital period increase 80−12765
RS Canum Venaticorum, out of eclipse light var. and comparison with similar stars 80−109489
V Canum Venaticorum, semiregular variable, polarization across TiO bands 79−97005
RS Canum Venaticorum binaries, observational selection and evolution 78−89208
RS Canum Venaticorum binary stars, introduction to series of papers 79−21329
RS Canum Venaticorum binary stars, radio luminosities and spectra 79−21333
RS Canum Venaticorum stars, Hα line variability, visible spectra obs. 80−105277
RS Canum Venaticorum stars, intrinsic light vars. due to starspots, model 79−35295
RS Canum Venaticorum systems, candidate list for southern HD stars 80−4395
RS Canum Venaticorum systems, X-ray obs. and coronal model development 80−56873
RS Canum Venaticorum type binaries, evolutionary status 79−67029
χ Carinae, β Canis Majoris type variability discovery from UBV photometry 79−80326
VY Carinae, Cepheid, luminosity and membership of assoc., visible obs. 80−94797
VY Carinae, cepheid variable, absolute magnitude 77−64764
l Carinae, Cepheid variable, Fourier anal. of light var. 80−90442
η Carinae, circumstellar shells and rel. to Carina nebula 77−87520
η Carinae, distance from interstellar colour excess 77−64744
η Carinae, earliest spectroscopic obs. and interaction of star with Carina Nebula 77−45433
η Carinae, high angular resolution obs. (35-175 μ) 79−8925
η Carinae, high-resolution IR radiation maps of homunculus, spectral and spatial distrib. 80−12767
R Carinae, intrinsic linear polarisation narrow-band struct. 77−49397
η Carinae, IR ang. diameter 78−93271
η Carinae, IR Fe II lines and interpretation of IR excesses 78−32478
η Carinae, IUE spectral obs. 79−71051
η Carinae, location in H II region (NGC 3372) 80−4383
AG Carinae, luminous star in symmetric nebulae, IUE low-dispersion spectrum 80−46560
η Carinae, new Fe II identification, IR spectrum 77−45463
η Carinae, optical and UV line emission of ionised Fe 77−13364
η Carinae, optical linear polarization map and outburst 79−67030
AG Carinae, P Cygni supergiant, spectrum of ring nebula 77−67100
η Carinae, possible assoc. with X-ray source 77−2492
η Carinae, reddening of optical radiation 77−41385
l Carinae, search for comparison stars, uvbyβ photometry, colour excess 80−62136
η Carinae, silicate grains size distrib. in Homunculus Nebula 80−4382
η Carinae, soft X-ray results from OSO-8 Wisconsin Expt. 78−36722
η Carinae, spectral obs. at 4 microns 78−4237
η Carinae, spherical circumstellar dust shell model, radiative transfer 78−36577
DY Carinae, UBV photometry of suspected double-mode Cepheid 79−48825
η Carinae, UV spectrum obs. by International Ultraviolet Explorer (IUE) 78−96474
ν Carinae, X-ray emission obs. from star and surrounding nebula 80−26876
η Carinae and Carina Nebula, polarimetric study 79−67043
η Carinae nebulosity, proper motion meas. in complex outer shell 78−28687
R Cassiopeia, airborne IR spectrophotometry, H_2O and CO absorpt. bands 78−32465
TV Cassiopeiae, Algol variable, UBV photometric obs. and deviations from mean light curve 79−35306
γ Cassiopeiae, Be star, new UV C IV and Si IV shell lines 79−84802
variable stars continued
γ Cassiopeiae, Be star, polarisation rapid vars. 80−22022
γ Cassiopeiae, Be star, possible identification with MX0053+60 transient X-ray source 77−49401
γ Cassiopeiae, Be star, rapid linear polarisation variability *(Russian)* 80−77417
γ Cassiopeiae, Be star, spectrophotometric variability from UV and Hα obs. 79−5829
γ Cassiopeiae, Be star, spectroscopic variations rel. to assoc. with X-ray source MX0053+60 77−22250
SU Cassiopeiae, Cepheid, distance and pulsation mode 78−89204
SU Cassiopeiae, Cepheid variable, spectrophotometric determ. of effective temp. 80−90435
TU Cassiopeiae, double-mode Cepheid, periods and amplitudes 79−48804
VX Cassiopeiae, early-type irregular variable, photometric variability *(Russian)* 80−72973
AB Cassiopeiae, eclipsing binary with δ Scuti primary, light vars. preliminary anal. 80−94831
VX Cassiopeiae, fast irregular variable, H_α and H_β lines obs. *(Russian)* 77−87400
TU Cassiopeiae, Fourier anal. of beat Cepheid 78−69811
γ Cassiopeiae, Hα and Hβ emission lines equivalent widths, scanner obs. 77−2430
γ Cassiopeiae, IUE obs. of Be-star 80−82383
R Cassiopeiae, late-type giant, possible H_2O thermal emission identification 78−81628
TU Cassiopeïae, mass determ. of triple-mode Cepheid 78−93261
R Cassiopeiae, Mira variable, vel. struct. in SiO maser spectrum 78−12248
V Cassiopeiae, Mira variable rel. to new H2309+59 X-ray source 78−28859
TU Cassiopeiae, periods and amplitudes from radial vels. 79−101159
UV Cassiopeiae, R Coronae Borealis star, photometry in optical and IR ranges 80−101601
WZ Cassiopeiae, semiregular variable star, variable CaCl absorpt. bands 79−88683
SU and TU Cassiopeiae, short-period Cepheids, photometry and spectra rel. to radius anomalies 80−26864
PZ Cassiopeiae, supergiant OH maser source, optical radial vel. 77−49378
TU Cassiopeiae, third period in beat Cepheid 78−16424
TU Cassiopeiae, UBV photoelectric obs. of double-mode Cepheid 78−77556
R Cassiopeiae, VLBI obs. of SiO maser in Mira variable 79−92779
o Cassiopeiae (HD 4180), Be star, IR and optical vars. 79−58353
V509 Cassiopeiae (HR 8752), emission-line spectrum rapid changes 80−36645
V509 Cassiopeiae (HR 8752), no emission at Hβ (1979 July 31) 79−92782
V509 Cassiopeiae (HR 8752), spectrum variable supergiant, Hα emission obs. 79−88672
V509 Cassioperae (HR 8752), light vars. during period of spectrum vars. 79−101161
cataclysmic, accretion disc models H line blocking of UBV colours 79−101155
cataclysmic binaries, circumstellar material geometrical and photometric parameters 80−109492
cataclysmic binaries, evolution and origin 80−56885
cataclysmic binaries, role of white dwarf component 80−82356
cataclysmic binary formation through common envelope evolution 80−8651
cataclysmic binary stars (CBS), critique of polarimetric evidence on physical parameters and orbital inclination 80−109486
cataclysmic variable stars, multiple periodicities 77−87434
cataclysmic variables, apsidal motion and evolution 79−62834
cataclysmic variables, emission lines from accretion discs 80−51774
cataclysmic variables, period change due to mass transfer 80−82425
cataclysmic variables, pulse timing meas., accretion disc models 79−62831
cataclysmic variables, review of structure 77−26018
cataclysmic variables, role of accretion disks *(Polish)* 80−26739
cataclysmic variables, short-period light oscills. rel. to non-radial oscills. of rot. stars 78−32477
cataclysmic variables, stability of non-synchronous stars in close binary systems 79−40223
cataclysmic variables, theoretical UBV colours of accretion discs 78−61865
cataclysmic variables, visual continuum flux distribs. 80−36636
cataclysmic variables, XUV emission *(German)* 80−109372
cataclysmic variables and nova explosions 77−82242
cataclysmic variables in globular clusters, preliminary report 80−109505
cause of variability, 18th. century studies by Goodricke and Pigott 79−44690
CD−42° 14462, binary nature of nova-like variable 77−87435
CD −33°12119, 3U 1727−33 candidate, UBV photometry 78−12251
V553 Centauri, C rich Cepheid, C and N abundances 80−4378
V553 Centauri, CH-type Cepheid, chemical comp. and luminosity 79−62849
Proxima=V645 Centauri, coordinated X-ray, optical and microwave study 79−5830
proxima=V645 Centauri, dMe flare star, quiescent corona, transition region, and chromosphere obs. 80−56850
BV Centauri, dwarf nova, identification as spectroscopic binary 80−51775
V436 Centauri, dwarf nova, no periodic modulation in quiescent state light curve 79−88677
V436 Centauri, dwarf nova, photometry during superoutburst (May 1978) 80−46570
ω Centauri, JHK photometry of globular cluster, giant branch spread 78−16476
ν Centauri, single-lined spectroscopic binary, β Cephei-type star 79−48821
UW Centauri, visual magnitude estimates, UBV photometry 78−40962
μ Centauri (B2 IVe), new circumstellar shell development, spectroscopic obs. (1980 June 10 to 12) 80−94808
V810 Centauri (HD 101947), yellow variable supergiant near Cepheid instability strip, VBLUW photometry 80−98672
V743 Centauri (HD 116994), light variability 79−97006
α Centauri C (Proxima Centauri), EUV flare obs. rel. to flare star scaling theory 77−45453

variable stars continued
V645=Proxima Centauri optical flares during 1977 May, S.African obs. 78−32480
δ Cephei, atmospheric vel. field 79−25611
ε Cephei, B photometry of δ Scuti-type star 79−44500
β Cephei, Copernicus UV obs. 77−33502
δ Cephei, Hα radial vel. behaviour 80−51788
δ Cephei, interstellar reddening 77−22243
μ Cephei, late-type supergiant, possible H_2O thermal emission identification 78−81628
λ Cephei, linear polarization variability in emission line O star 78−36571
T Cephei, long-period variable, radial-vel. obs. 79−88684
T Cephei, Me variable, Tc discovery 78−32483
β Cephei, non-radial pulsations detect. attempt 79−40198
RZ Cephei, RRc-type star, period var. *(Italian)* 77−91546
μ Cephei, semi-regular, supergiant, narrow-band polarimetry 79−25617
T Cephei, SiO maser emission obs. 78−4225
DI Cephei, spectrum vars. in T Tauri star 80−8628
EM Cephei, UBV, photometry rel. to constancy or variability of period 80−105286
IV Cephei (Nova 1971), ejecta He abundance 79−40203
β Cephei instability strip, effects of stellar mass loss 80−90436
β Cephei star search, northern photometric and spectroscopic obs. 77−74057
β Cephei stars, effective temps., ang. diameters, distances and linear radii 80−17584
β Cephei stars, line profile variables, pulsational modes 80−85951
β Cephei stars, line profiles and oscill. modes 77−33521
β Cephei stars, magnetic fields in nine variables 78−65631
β Cephei stars, mid UV spectra obs. 80−21995
β Cephei stars, models, He^+ ionization driving 79−8922
β Cephei stars, models nonradial stability 77−49390
β Cephei stars, non-radial oscillators, single period variables 79−25613
β Cephei stars, nonradial oscills., linear nonadiabatic analysis 80−56836
δ Cephei stars, parallaxes and distance scale, max. likelihood technique 80−51746
β Cephei stars, photometric search of southern B-type stars 79−71040
β Cephei stars, possible polarization effects 79−84807
β Cephei stars, pulsation effect on period-luminosity relation 80−72970
β Cephei stars, pulsation excitation mechanisms 77−87425
β Cephei stars, pulsations and evolutionary status 80−85959
β Cephei stars, radial and non-radial models 77−82235
β Cephei stars, radiation pressure and pulsational instability 79−84806
β Cephei stars, search in open cluster NGC 4755, evolutionary stage determ. 79−8921
β Cephei stars, search south of declination −20°, B-type giants and subgiants 78−61863
β Cephei stars, theoretical models with new radiative opacities 77−13347
β Cephei stars, vel./light curves for six objects 79−75214
β Cephei type variables, atm. radial shock effects, models 79−53807
Cepheid, hot ultrashort period, in M15 globular cluster *(Chinese)* 77−71121
Cepheid binary detection from U-V curve obs. 80−98667
Cepheid bump mass anomaly, resonance effects 78−4238
Cepheid distance scale, depend. on Hyades Cluster distance 78−8121
Cepheid instability strip, lower part, search for photometric variability in evolved Am stars 80−62145
Cepheid instability strip 80−56833
Cepheid masses from observations and pulsation theory 79−48802
Cepheid model, transitory R-type ionisation front 79−75209
Cepheid pulsation period variability and convective efficiency 80−26885
Cepheid variable distance determ., geometric method 77−74066
Cepheid variable stars, simulated, for introductory astronomy course 79−44664
Cepheid variables, amplitudes in instability strip 79−44491
Cepheid variables, cosmic distance measurement 79−84920
Cepheid variables, effects of atmospheres finite extent on colour indices and radii determ. 78−32450
Cepheid variables, incidence of duplicity 80−90453
Cepheid variables, intrinsic colours 79−84797
Cepheid variables, long-period, absence from Galaxy rel. to obs. of yellow variable supergiants 80−98672
Cepheid variables, mag. fields effects on pulsational behaviour 80−31302
Cepheid variables determ. of colour term in period-luminosity colour relation 80−94812
Cepheid variables kinematics, appl. to galactic spiral structure parameters derviation 80−17665
Cepheid variables masses, implication of mass and ang. momentum losing stars evolution 79−25591
Cepheid-type stars, stability against nonradial oscills. 77−91552
Cepheids, anomalous, in Draco dwarf spheroidal galaxy, instability strip 78−28695
Cepheids, anomalous, in dwarf spheroidal galaxies, binary system model 77−45451
Cepheids, binary star frequency from UBV photometry 77−45465
Cepheids, BVI photometric determ. of reddening 78−65630
Cepheids, classical, radii and temps. 78−49446
Cepheids, convective energy flux in atm. with gravit. field changes *(Russian)* 78−49422
Cepheids, distance determ. method 77−45467
Cepheids, double mode, in N.hemisphere, search using new UBV photometry 80−94814
cepheids, double mode, in northern hemisphere, search using existing obs. 80−8634
Cepheids, double mode pulsation, iterative treatment 80−82369
Cepheids, double-mode, freq. anal. 80−31308
Cepheids, double-mode, masses 79−35278
Cepheids, double-mode, period ratios from linear and nonlinear theory 78−40953
Cepheids, double-mode, photoelectric radial vels. and BVRI photometry 79−88675
Cepheids, double-mode, surface He enhancement, linear theory period ratios 79−67021
Cepheids, double-mode, Wesselink radii 80−31311
Cepheids, double-mode and bump, revised masses 77−56949
Cepheids, double-mode and bump, rot. and convection effects on period ratios 78−93249
Cepheids, enhanced He abundance effects on visible spectra 80−12759
Cepheids, freq.-period distribs. in Local Group galaxies 78−28694
Cepheids, galactic distrib. between l∼294° and (331°) 79−48910
Cepheids, Hα emission in southern beating objects 79−21301
Cepheids, H profile, previous mixing and loops in H-R diagram during core He burning 77−29792
Cepheids, He enrichment effects in atm., models 80−26884
Cepheids, hot ultrashort period type, general props. *(Chinese)* 78−69805
Cepheids, in different galaxies, progression in period-amplitude diagrams characts. 78−53956
Cepheids, in galaxy NGC 2403, distance 77−2471
Cepheids, in LMC, BV photometric obs., galaxy tilt determ. 79−53912
Cepheids, in LMC, BVI obs., period-luminosity-colour relation 79−71055
Cepheids, in Magellanic Clouds, evidence for interstellar reddening 77−2435
Cepheids, in southern hemisphere, VBI photometry 77−53612
Cepheids, intrinsic colours and physical props. from Walraven VBLUW photometry 78−28696
Cepheids, kinematics rel. to Galaxy local struct. determ. *(Russian)* 78−77608
Cepheids, long period, colour excess scale and intrinsic colour props. 77−29858
Cepheids, mass calc. methods, anomalies 78−49466
Cepheids, membership in open clusters from star and cluster age determ. *(Italian)* 80−90489
Cepheids, method for constructing envelopes and the period-amplitude relation 78−20840
Cepheids, multimode, two-zone models, resonances 80−36641
classical Cepheids, nonvariable supergiants and bright giants, spectrophotometric comparison 80−56837
Cepheids, observational and theoretical review 77−87428
dwarf Cepheids, period changes 80−62142
Cepheids, period-age relation 79−21317
Cepheids, period-luminosity-colour relation, numerical simulations 80−82393
Cepheids, Popularion I, kinematical trend of vel. residuals 79−48863
Cepheids, pulsation theory and multiperiodic variables 77−87429
Cepheids, radii determ. via method of max. likelihood 77−45459
Cepheids, reddenings from mean UBV colours 79−71056
Cepheids, relation between UV excess and superficial gravity 77−53604
Cepheids, short-period, radial vels., BVRI photometry, radii 80−31309
Cepheids, southern, BVI photometry 77−60772
Cepheids, stellar pulsation problem, time dependent convection local theories 80−72964
multimode Cepheids, two zone rel. to classical models 80−72967
Cepheids, ultrashort period, classification from photometric and astrometric data 80−62135
Cepheids in Crux-Centaurus region, new objects 79−12477
Cepheids in Dunsink LMC II region, BV photographic photometry 78−45340
sinusoidal Cepheids in LMC, first overtone pulsations, photometry obs. 80−77422
Cepheids in LMC and SMC, UBVRI obs. 77−71113
Cepheids in M31, use in determ. of S4 spiral arm struct. *(Russian)* 80−82515
Cepheids in M31 (Andromeda galaxy), assoc. with interstellar gas and star complexes *(Russian)* 80−90455
Cepheids in Magellanic Clouds, colour luminosity-amplitude relations 77−91554
Cepheids in Magellanic Clouds, extrinsic model of anomalies 80−4361
Cepheids in Magellanic Clouds, Wesenheit function, reddening correction 77−91553
Cepheids masses, effects of He deficient stellar winds 78−57556
Cepheids with He enriched inhomogeneous outer layers, three mode reson. 80−101600
δ Ceti, β Canis Majoris variable, period meas. and detect. of period decrease 80−105257
δ Ceti, β Cephei variable, spectroscopic binary, radial vels. and period var. 80−82376
UV Ceti, anomalous flare activity obs. 78−89202
WX Ceti, cataclysmic variable similar to WZ Sagittae, outburst characts. 80−17596
UV Ceti, IR obs. of flares *(Russian)* 78−93278
δ Ceti, period changes of β Cephei type star 78−32487
T Ceti, semiregular variable, Tc I absorpt. line obs. 78−28689
o Ceti, SiO maser variability at 86 GHz 80−41839
UV Ceti, variations of Hβ emission line during large flare 77−45456
o Ceti, vars. in spatial distrib. of 11 micron radiation 79−5828
o Ceti (Mira), diameter apparent var. at 10.2 μm 78−93267
o Ceti (Mira), enhanced activity of B-type component at 1976 light minimum 78−81636
o Ceti (Mira), H I emission line profiles *(Russian)* 79−16990
o Ceti (Mira), long-period variable, radial-vel. obs. 79−88684
o Ceti (Mira), mass loss rate determ. 79−48831
o Ceti (Mira), observing campaign around 1979 October 18 light max. 79−92786
o Ceti (Mira), polarized Balmer emission lines, spectropolarimetry 79−21302
o Ceti (Mira), rapid light vars. of companion star during 1977 light min. 78−96492
o Ceti (Mira), spectrum of companion star 78−4253
o Ceti (Mira), strong TiO-related dia. vars. 78−16429
o Ceti (Mira), variable 2.6 mm CO emission obs. 78−12241
o Ceti (Mira) at 1978 max., visible spectropolarimetry 80−94799
o Ceti (Mira)-type stars, colour curves for Me and Se types 77−29857
o Ceti AB, IUE obs. of UV spectrum 80−22027
UV Ceti flare stars, review *(Russian)* 78−28685
UV Ceti stars, ^{7}Li nucleosynthesis in flares 79−30073
ZZ Ceti stars, constraints on possible long-term variability 80−90428
UV Ceti stars, photometric features near flare initial phase 80−105252
ω Ceti stars, Sio J=1→0 ν=1 and 2 masers relative intensity and vel. 80−4339
ZZ Ceti stars, southern hemisphere survey 77−56948
ZZ Ceti stars and pulsations, physical props. 79−48781
ZZ Ceti stars search, photometric obs. of apparently quiescent stars 80−22005
UV Ceti type stars, weak Ca II triplet absorpt. lines *(Russian)* 79−88691
ZZ Ceti white dwarfs, implications of seismological theory for non-radial oscills. periods 80−17577

variable stars continued
ZZ Ceti white dwarfs, non-radial oscills. theory 80−82356
UV Ceti-type flare stars, simultaneous 1420 MHz and optical obs. of flares 78−49464
RS Chamaeleontis, δ Scuti variable and eclipsing binary, four-colour photometry 80−67783
Z Chamaeleontis, eruptive binary, model from photoelectric data anal. 80−72961
Z Chamaeleontis, gravitational waves from eclipsing cataclysmic binary 80−90439
Circinus X-1, changes in optical, IR and radio emission 80−67910
Circinus X-1, radio flare phenomena Dec. 1979 and Jan. 1980 obs. 80−36731
Circinus X-1 (3U 1516−56), vars. of optical and radio counterpart 78−12414
circumstellar shell model for H_2O maser emission 77−60765
classical Cepheids, distance determ. via ang. dia. method, check on phase shifts 78−16439
classical Cepheids, light and radial vel. curves phase matching 77−17574
classical Cepheids, light curves, optimal curve fitting procedure appl. 77−78795
classical Cepheids, mass-luminosity relationship 79−35278
classical Cepheids, surface brightness and radii *(Polish)* 79−58359
classical Cepheids colour excesses 77−22242
close binary systems, reflection effects evaluation, generalised approach 79−25631
CoD −35° 10525, bright YY Orionis star, spectrum and UBV photometry 78−36566
α Columbae, rapid spectral vars., cross correlation analysis 79−48808
17 Comae A, Ap star, mag. field meas. and rot. period *(Russian)* 80−90457
FK Comae Berenicis, age of BY Draconis-type star *(Russian)* 77−64774
comparison star sequences, BV photoelectric photometry and reliability 79−97039
comparison stars near OJ287 and ON325, variability, period determ. 80−26882
composite object 0246+18, bright galaxy with superposed variable star, UBV colours 79−71130
cool C stars, nearby, distances 78−49434
cool Mira variables, shock waves accel. in photosphere 77−13352
S Coronae Austrinae, a bright southern YY Orionis star, spectroscopic obs. 77−29818
S Coronae Austrinae, identification of absorpt. lines, irradiated amethyst 79−25601
S Coronae Austrinae, line profiles in YY Orionis star 79−84808
S Coronae Austrinae, spectroscopic and photometric vars. of YY Orionis star 79−48812
S Coronae Austrinae, T Tauri star, red-displaced absorpt. features obs. 78−4221
R, S, T Coronae Austrinae, T Tauri stars, long period vars. 80−82350
S Coronae Austrinae, YY Orionis star, satellite UV spectrum 79−67016
R Coronae Borealis, 1977, February 17-26 magnitude fading 77−29854
β Coronae Borealis, Ap star, Ca II K and Hδ lines rapid vars. *(Russian)* 80−90458
β Coronae Borealis, Ap star, mag. deform rel. to secular mag. var. 77−45454
R Coronae Borealis, decline 1977, Mar., visual magnitude esimates 77−37606
R Coronae Borealis, He I λ10830 line obs. at 1978 pre-maximum phase 79−16975
R Coronae Borealis, light curve, Poisson statistics 77−56942
R Coronae Borealis, origin of 1100 day periodicity in IR excess 77−45462
R Coronae Borealis, search for graphite feature at 2200 Å 77−87419
R Coronae Borealis, UBVRIHKLMN photometry, interpretation 80−67756
R Coronae Borealis, visual magnitude estimates (1977, March-May) 77−53609
R Coronae Borealis and He stars, post-giant evolution 77−56947
R Coronae Borealis in quiet state, spectral energy distrib. *(Russian)* 80−51781
R Coronae Borealis stars, long-term IR behaviour 78−96490
R Coronae Borealis stars rel. to Type I supernovae, appl. to Crab Nebula 79−5845
R Coronae Borealis type variables and related objects, UBV photometric obs. 80−90437
CPD −62° 1837 (HDE 308122), long-period variable member of triple 80−105260
CRL 3099, highly evolved C star, IR photometry and spectrum 78−49436
cross correl. detection of rapid stellar var. using two telescopes 77−82127
β Crucis, β Canis Majoris star, photometric obs. 80−17595
BI Crucis, new symbiotic star, spectrum 80−109442
CSV 6110 in Taurus, *o* Ceti type variable, visible obs. 80−67745
CSVS 6997 as counterpart for OP 313 radiosource 77−33515
CH Cygni, 1977 April surge before September outburst 77−87412
CH Cygni, 5700-8700 A spectrograms 77−87415
29 Cygni, λ Bootis type star, photometric variability 77−64765
V1500 Cygni, (Nova 1975), emission line profiles during early nebular stage 79−53826
V1500 Cygni, (Nova 1975), photoelec. obs., period decrease, visual magnitude estimates 77−22252
SS Cygni, ANS detection of both soft and hard X-ray emission 78−36579
V389 Cygni, BV photometry of peculiar variable 79−44534
V Cygni, C star, 1-4 mm continuum emission obs. 79−88670
V492 Cygni, Cepheid, not a member of open cluster (Byurakan 2) 77−2345
X Cygni, Cepheid, radial vels. 78−73723
V1057 Cygni, CH radio emission obs. 77−87512
V1057 Cygni, circular polarisation of stellar radiation scattered in circumstellar cloud, theory 78−96428
SU Cygni, classical Cepheid and spectroscopic binary, UBVRI photometry 79−62852
SS Cygni, colour variations during dwarf nova outbursts 80−46576
V1057 Cygni, composite, spectra rel. to three models of FU Orionis type star 78−65617
V460 Cygni, cool C star, atmospheric $^{12}C/^{13}C$ ratio 78−93223
P Cygni, Copernicus UV obs. 79−30066

variable stars continued
χ Cygni, diameter of Mira-type star from speckle interferometry 80−67728
XX Cygni, dwarf Cepheid, composition and motion, visible photometric and spectrographic obs. 80−77424
SS Cygni, dwarf nova, identification as hard X-ray source by HEAO 1 scanning modulation collimator 79−2548
SS Cygni, dwarf nova, rapid optical oscills. phase variability 80−85947
SS Cygni, dwarf nova, soft X-ray pulsation obs. 80−46563
SS Cygni, dwarf nova, spectrophotometry rel. to accretion disc models in erruption and at min. light 80−36635
SS Cygni, dwarf nova, UV spectrum obs. by International Ultraviolet Explorer (IUE) 78−96474
SS Cygni, dwarf nova, X-ray polarisations discovery 78−65628
P Cygni, effective temp. radius, mass loss and luminosity 80−51748
P Cygni, electron scattering in expanding atmosphere 79−21311
P Cygni, extreme B-type supergiant, UV spectroscopy 80−22004
V1016 Cygni, forbidden Fe VI emission rel. to electron density 79−8970
V1057 Cygni, FU Orionis star, IR spectroscopy with contact-type image tube 80−17587
V1057 Cygni, FU Orionis type, UBVR photometry 78−12230
V1057 Cygni, FU Orionis-type star, flare up in 1720 MHz OH line 79−62843
P Cygni, Hα and Hβ emission lines equivalent widths, scanner obs. 77−2430
P Cygni, H Balmer line profiles, accel.-decel. envelope, mass loss 79−40205
P Cygni, H Paschen α obs. 80−62156
P Cygni, high resolution UV spectrum obs. 80−26873
V1057 Cygni, hydromag. model of peculiar activity *(Russian)* 78−49442
V1016 Cygni, image-tube spectrograms 80−8639
59=V832 Cygni, IR emission increase, spectrum scanner obs. 80−94809
V1016 Cygni, IR spectrum 78−93266
CH Cygni, linear polarisation vars. rel. to circumstellar dust grains form. 78−69808
χ Cygni, long-period variable, radial-vel. obs. 79−88684
V832=59 Cygni, mass-losing Be star, changes in UV spectrum 80−46561
V1057 Cygni, mean B-band magnitude (1978 July 30 ± 2^d). 79−84792
χ Cygni, Mira variable star, variable 2.6 mm CO emission obs. 78−12241
V1016 Cygni, near-IR spectrographic obs. 80−94810
CH Cygni, new active period, model, double system with accretion disc *(Russian)* 78−69813
V1016 Cygni, new spectroscopic obs., simultaneous presence of increasing excitation and cool features 80−26874
V1057 Cygni, OH obs. 80−36629
NML=V1489 Cygni, OH/IR star, 1612 MHz OH maser multibaseline VLBI obs. 80−12766
CH Cygni, outburst and spectral changes, 1977 August 31 obs. 77−82231
χ Cygni, P Cygni profiles obs. in Na I and K I reson. lines 77−13362
V389 Cygni, peculiar (Ap-type) binary, spectroscopic obs. 78−85975
V1016 Cygni, peculiar emission object, M star model 77−53598
V1016 Cygni, photometric and spectroscopic obs. rel. to proto-planetary nebula mass ejection 78−85947
V1500 Cygni, post-nova light curve development, UBV and Hβ obs. 77−71115
R Cygni, pure S star, new molecules identification 78−28700
SS Cygni, radial vel. of dwarf nova 79−62833
V1331 Cygni, radial vels. of spectra lines in unusual T Tauri star 79−71045
CH Cygni, red giant, mag. field interpretation for outburst 78−4250
R Cygni, S-type star, Keenan band identification problem, IR obs. 80−72946
SS Cygni, spectroscopic binary variable, X-ray source, orbital element determ. 80−105288
CI Cygni, spectroscopic obs. using multichannel analogue detector system 78−36461
CH Cygni, symbiotic star, 1977 outburst, radial vel. and atm. struct. determ. 80−72969
CH Cygni, symbiotic star, binary model 80−62158
V1016 Cygni, symbiotic star, IR variability obs. from VJHKL photometry *(Russian)* 80−105263
CH Cygni, symbiotic star, IUE obs. during active phase 79−62846
CH Cygni, symbiotic star, rapid and slow light vars. 80−51792
CH Cygni, symbiotic star, spectroscopic obs. during 1977 to 1978 outburst 79−75211
CH Cygni, symbiotic variable, flickering obs. during outburst, binary model 79−8929
V1500 Cygni, UV photometry 77−64766
V832=59 Cygni, variable mass flux from spectroscopic obs. 80−41840
CH Cygni, visible and near IR spectra 77−82232
V1500 Cygni, visual magnitude estimate (1977, February 10) 77−29853
R Cygni, Zr isotope abundances 78−53957
V645 Cygni (AFGL 2789), Ae star, perplexing spectrum 80−73066
V645 Cygni (CRL 2789), bipolar nebula, O-type exciting star 78−4392
V1357 Cygni (Cygnus X-1), brightness var. rel. to disk accretion subphotospheric layers *(Russian)* 79−25764
V1357 Cygni (Cygnus X-1), critique of polarimetric evidence on physical parameters and orbital inclination 80−109486
V1357 Cygni (Cygnus X-1), no long-term light vars. (1928-77) 80−41861
V1357 Cygni (Cygnus X-1), optical light curve vars. rel. to X-ray vars. 80−109560
V1357 Cygni (Cygnus X-1), optical photometry (1980 May 25 to July 7) 80−90578
V1357 Cygni (Cygnus X-1), UBVR obs. and accreting disk radiation *(Russian)* 79−25645
V1341 Cygni (Cygnus X-2), halo population binary 79−97099
V1341 Cygni (Cygnus X-2), IUE obs. of rapid UV flux vars. 80−12833
V1341 Cygni (Cygnus X-2), possible 82-minute quasi-periodic bursts obs. *(Russian)* 79−17140
V1341 Cygni (Cygnus X-2), shortest optical variability *(Russian)* 80−17695
V1341 Cygni (Cygnus X-2), UBV photometry and light vars. 79−5833
V645 Cygni (GL 2798), IR and EHF spectroscopy 80−72956
V1329 Cygni (HBV 475), symbiotic variable, photometric and spectroscopic history 80−62148

variable stars continued
V1500 Cygni (Nova 1975), 3.35 hour 1978 light curve, rel. to possible double period 79−67039
V1500Cygni (Nova 1975), 3 hour photometric period stabilisation 79−92776
V1500 Cygni (Nova 1975), 3 hour var. 79−16966
V1500 Cygni (Nova 1975), Balmer line emission profiles evolution in early decline phase 80−82371
V1500 Cygni (Nova 1975), binary nature, spectral meas. 77−87446
V1500 Cygni (Nova 1975), brightness meas., (1917 to 1976) 78−36618
V1500 Cygni (Nova 1975), BV photometric obs. 78−36613
V1500 Cygni (Nova 1975), BV photometry 78−36619
V1500 Cygni (Nova 1975), continuous energy distrib., IR obs., thermal bremsstrahlung 79−80315
V1500 Cygni (Nova 1975), emission line vars. rel. to struct. of central object 80−82367
V1500 Cygni (Nova 1975), fine-struct. lines rel. to 10 micron excess 78−93269
V1500 Cygni (Nova 1975), Hα and Hβ emission line vars. 80−4389
V1500 Cygni (Nova 1975), H I emission line profiles vars., envelope ejection vels. determ. 79−35281
V1500 Cygni (Nova 1975), He abundance of ejecta 78−28691
V1500 Cygni (Nova 1975), heavy element abundances 79−21295
V1500 Cygni (Nova 1975), high-energy gamma-ray flux upper limit 78−36603
V1500 Cygni (Nova 1975), light curve for 1975 Aug.-1977 July period 80−4372
V1500 Cygni (Nova 1975), light fluctuation period var. 79−97012
V1500 Cygni (Nova 1975), line spectrum evolution 78−32493
V1500 Cygni (Nova 1975), linear polarization obs. 78−36601
V1500 Cygni (Nova 1975), luminosity and distance, light curve obs. 80−72981
V1500 Cygni (Nova 1975), meas. and nova outburst model 77−87448
V1500 Cygni (Nova 1975), mechanism of quasieclipses after outburst *(Russian)* 78−93280
V1500 Cygni (Nova 1975), model for spectrographic obs. 77−87444
V1500 Cygni (Nova 1975), multiband photometry 77−87445
V1500 Cygni (Nova 1975), near IR spectroscopy 78−36599
V1500 Cygni (Nova 1975), near IR spectrum 78−36606
V1500 Cygni (Nova 1975), obs. of magnitude and spectrum changes *(French)* 77−82258
V1500 Cygni (Nova 1975), optical polarisation obs. 78−36622
V1500 Cygni (Nova 1975), photoelectric obs. 78−36620
V1500 Cygni (Nova 1975), photometric and spectroscopic obs. 78−36604
V1500 Cygni (Nova 1975), photometric obs. 78−36616
V1500 Cygni (Nova 1975), photometry, light curves, magnitude estimates 78−85960
V1500 Cygni (Nova 1975), photometry rel. to 3.3 hour var. and flickering 78−36591
V1500 Cygni (Nova 1975), polarimetric and photometric obs. 78−36612
V1500 Cygni (Nova 1975), polarisation obs. *(Chinese)* 77−67097
V1500 Cygni (Nova 1975), pre-maximum spectra 77−87449
V1500 Cygni (Nova 1975), radio emission from expanding shell 80−26868
V1500 Cygni (Nova 1975), radio obs. and analysis 80−67726
V1500 Cygni (Nova 1975), review of development *(French)* 80−17598
V1500 Cygni (Nova 1975), shell electron temps., densities and other props. 79−30068
V1500 Cygni (Nova 1975), short-term light vars. 78−36609
V1500 Cygni (Nova 1975), small amplitude light var. 78−36608
V1500 Cygni (Nova 1975), spatial and kinematic envelope model 78−36600
V1500 Cygni (Nova 1975), spectral energy distrib. 78−36605
V1500 Cygni (Nova 1975), spectral evolution 77−87447
V1500 Cygni (Nova 1975), spectrographic obs. *(Chinese)* 79−16982
V1500 Cygni (Nova 1975), spectrophotometric study *(French)* 77−82259
V1500 Cygni (Nova 1975), spectroscopic data 79−16988
V1500 Cygni (nova 1975), spectroscopic obs., three hour periodicity, nebular model 78−12235
V1500 Cygni (Nova 1975), spectroscopic studies, models for 3 hour profile vars. 79−8920
V1500 Cygni (Nova 1975), spectroscopic studies, nebular and central binary system 79−62830
V1500 Cygni (Nova 1975), spectrum variations 78−36607
V1500 Cygni (Nova 1975), thirteen-colour photometry and anal. of short period variability 79−92788
V1500 Cygni (Nova 1975), three hour light var. 79−80314
V1500 Cygni (Nova 1975), TV photometry 78−36602
V1500 Cygni (Nova 1975), UBV photometry, short period variability 78−61862
V1500 Cygni (Nova 1975), UBVR Hα photometry and polarimetry 78−36611
V1500 Cygni (Nova 1975), UBVRI photometry and polarimetry 78−36614
V1500 Cygni (Nova 1975), UV photometry after visual max. 77−82260
V1500 Cygni (Nova 1975), visible and near UV photoelec. photometry 78−36610
V1500 Cygni (Nova 1975), visible and near UV spectrophotometric obs. 78−32492
V1500 Cygni (Nova 1975), visible and near UV spectrophotometry 78−32494
V1500 Cygni (Nova 1975), visible and UV spectra and light curve 80−12771
V1500 Cygni (Nova 1975), visible spectroscopy 78−36598
V1500 Cygni (Nova 1975), visible-band linear polarimetry 78−36621
V1500 Cygni (Nova 1975), visual magnitude estimates (1977 Aug.-1978 Jan.) 78−32474
V1500 Cygni (Nova 1975), visual magnitude estimates (1977 May-Aug.) 77−82230
V1500 Cygni (Nova 1975), wide-band IR photometry 78−36615
V1500 Cygni (Nova 1975) as thermonuclear runaway event 77−82261
V1500 Cygni (Nova 1975) photometric obs. at Skalnate Pleso Observatory 78−36617
V1668 Cygni (Nova 1978), BV photometry 79−67035
V1668Cygni (Nova 1978), linear polarisation obs. 80−26875
V1668 Cygni (Nova 1978), multifilter photometry and polarimetry 80−90454
V1668 Cygni (Nova 1978), optical light curve, uvby photometry 80−62154
variable stars continued
V1668 Cygni (Nova 1978), photoelec. photometry, rapid flickering 80−36640
V 1668 Cygni (Nova 1978), spectral development 80−51789
V1668 Cygni (Nova 1978), spectrographic obs. around max. brightness *(French)* 79−58343
V1668 Cygni (Nova 1978), spectroscopic and photometric obs., (1978 to 1979) *(Russian)* 80−109444
V1668 Cygni (Nova 1978), UBV light curve 80−46565
V1668 Cygni (Nova 1978), UV spectrum, emission lines 79−62837
V1668 Cygni (Nova 1978), visual mag. estimate (1979 April 25) 79−53824
V1668 Cygni (Nova 1978), visual magnitude estimates, 1978 Nov.-1979 Apr. 79−48819
V1668 Cygni (Nova 1978), visual magnitude estimates, 1979 June 79−80324
V1500 Cygni (Nova Cygni 1975), interstellar reddening and distance 78−4230
V1500 Cygni (Nova Cygni 1975), low resolution spectrophotometry 77−49403
V1500 Cygni (Nova Cygni 1975), minute time scale flickering and 6.6 hour light period 77−17582
V1500 Cygni (Nova Cygni 1975), shell phase obs. 77−49392
V1500 Cygni (Nova Cygni 1975), spectral features during early decline phase 77−22245
V1500 Cygni (Nova Cygni 1975), spectrophotometric obs. 77−49402
V1500 Cygni (Nova Cygni 1975), spectrum around max. light 77−87411
V1500 Cygni (Nova Cygni 1975), visual magnitude estimates (1977, April-May) 77−53610
V1668 Cygni (Nova Cygni 1978), post-max. short period oscills., photoelectric photometry 80−82380
P Cygni in far UV *(Russian)* 79−8919
P Cygni mass loss, equivalent two-level-atom approach 78−93255
CI Cygni symbiotic star, UV and optical spectrum changes during eclipse 80−105258
P Cygni type, line radiation transfer in collapsing molecular clouds 78−73626
Cygnus OB2 number 12, spectral classification and membership of association 80−51760
Cygnus X-1 (HDE 226868), optical photometry, (1972-1976) 78−32609
Cygnus X-1 (HDE 226868), search for 78.4 day period in U-band polarisation 79−75297
Cygnus X-1 X-ray binary, SHF obs. 80−73071
Cygnus X-2 optical counterpart, TV photometric obs. *(Russian)* 78−57697
DA white dwarfs, kinematics rel. to nonvariable DA stars 78−53947
degenerate dwarfs nonradial oscills., theoretical review 77−87398
HR Delphini, UV spectrum, stellar wind 80−26880
HR Delphini (Nova 1967), cataclysmic binary spectrum 80−4359
HR Delphini (Nova 1967), circumstellar envelope props. *(Russian)* 78−77564
HR Delphini (Nova 1967), emission line spectrum peculiarities 79−35280
HR Delphini (Nova 1967), emission lines at nebular stage *(Russian)* 80−17597
HR Delphini (Nova 1967), envelope, photoionization models in nebula stage, 1969 June-July 79−62835
HR Delphini (Nova 1967), He I radial vel. var. 77−82249
HR Delphini (Nova 1967), models of envelope ionization 77−87439
HR Delphini (Nova 1967), photoionisation models, binary system evolution 80−17590
HR Delphini (Nova 1967), photoionisation models of envelope in nebular stage, obs. data 78−61864
HR Delphini (Nova 1967), physical conditions of different regions of envelope 80−4369
HR Delphini (Nova 1967), premax. and principal absorpt. line systems in spectrum 79−35279
HR Delphini (Nova 1967), premaximum mass loss rate, H line anal. 80−82378
HR Delphini (Nova 1967), radio emission from expanding shell 80−26868
HR Delphini (Nova 1967), short period light vars. from UBV photometry 80−67744
HR Delphini (Nova 1967), short period photometric vars. obs. 79−44503
HR Delphini (Nova 1967), simultaneous X-ray, UV and optical obs. 80−109440
HR Delphini (Nova 1967), spectra, line identification, radial vels. 80−17594
HR Delphini (Nova 1967), spectral evolution during decline 77−87440
HR Delphini (Nova 1967), spectroscopic orbit 79−44510
δ Delphini stars, abundance anal., metallicism and pulsation 77−33506
δ Delphini stars in Michigan Spectral Catalogue, uvbyβ photometry rel. to spectral types 80−4377
discoveries by John Goodricke, history 79−49005
Dopplers, Hα line freq. depend. general relativistic formula, appl. to (SS 433) 79−97010
β Doradus, Cepheid, reddening determ. from nearby star UBV obs. 80−101598
S Doradus, LMC Hubble-Sandage variable, IUE and ground based spectroscopic obs. 80−101595
β Doradus, Mg II h- and k-lines in UV spectra of Cepheid 79−40196
β Doradus, UV photometry of Cepheid by ANS 79−35272
S Doradus (HD 35343), luminous LMC supergiant, long time baseline VBLUW photometry 80−22007
S Doradus (HD 35343), luminous LMC supergiant, long time baseline VBLUW photometry 80−36630
double mode Cepheids, masses and radii 77−82236
double mode pulsation as resonance phenomenon 79−67015
double periodicity in light vars. 77−87423
double star photometry and variability 79−44554
double-mode Cepheids, UBV photometry of four suspected stars 79−48825
BY Draconis, area and temp. of surface spots *(Russian)* 77−64775
K Draconis, Be star, search for short time scale vars. in Hα emission 80−109441
CX Draconis, binary Be star, UBV obs. 80−82388
73 Draconis, CH lines in spectrum of Ap star *(Russian)* 77−56958
BC Draconis, double-mode Cepheid, mass, luminosity and evolution 77−29845

variable stars continued
BY Draconis, dwarf binary, flare star, rotational hypothesis for quasi-sinusoidal light variations 78−4234
BY Draconis, flare star, Ca II emission variability 77−33528
AD Draconis, flare star, coronal soft X-ray emission obs. by (HEAO 1) 79−101140
BY Draconis, late-type flare star, metal abundances 77−78779
BY Draconis, magnitudes, colours and photometric period changes *(Russian)* 77−64771
BY Draconis, prototype spotted flare star, pre-main-sequence nature 80−36633
BC Draconis, radial pulsation period indicating Population II Cepheid 78−32491
ϕ Draconis, Si Ap-star, UV vars. rel. to patchy stellar surface model 77−49389
BY Draconis, spectroscopic binary flare star, BVRI obs. 77−53595
73 Draconis, spectroscopic study and model atm. anal. of Ap star 77−33531
CR Draconis, UV Ceti variable, flares colour behaviour 80−22020
AB Draconis star fields, comparison star sequences, photometry obs. 80−82433
BY Draconis stars, angular momentum initial distrib. and evolution 80−85954
BY Draconis stars, luminosity vars. and light curve period changes 79−71039
BY Draconis stars, out of eclipse light var. and comparison with RS Canum Venaticorum stars 80−109489
BY Draconis stars, photometric radii compared with luminosity class V stars *(Russian)* 78−57564
BY Draconis stars, rot. vels. rel. to pre-main sequence evolutionary stage 80−51767
BY Draconis syndrome among dMe stars, photometric survey 78−16428
BY Draconis type variables, flare activity and quiescent variability 78−45338
BY Draconis type variables, photometry, amplitudes and phases 79−67038
BY Draconis-type stars, Hα emission line profiles, rapidly rot. gaseous envelopes *(Russian)* 78−65625
BY Draconis-type stars, spectroscopic binary incidence 77−87401
BY Draconis-type stars of 1 M$\odot$, photoelectric obs. *(Russian)* 77−64772
dwarf Cepheids, double-mode, theoretical periods and masses 79−44488
dwarf Cepheids, linear survey of models, pulsation 79−35259
dwarf Cepheids evolutionary stage, anal. and conclusions 80−46562
dwarf Me-type stars, cyclical photometric vars. interpretation 77−74059
dwarf novae, cataclysmic variables, review of spectroscopic and photometric obs. 77−56959
dwarf novae, eruption types and superhumps, obs. 79−75212
dwarf novae, HEAO-A2 soft X-ray survey during optical outburst 80−46574
dwarf novae, quasi-periodic oscills. and nonradial pulsations of accretion disks 80−46568
dwarf novae, rapid brightness oscills. obs. 78−40968
dwarf novae, search for light oscills. during outbursts 78−40966
dwarf novae, spectra *(Russian)* 80−8638
early-type stars, suspected variability and line emission, Hα obs. 79−67036
early-type stars with gas-dust envelopes, IR spectral energy distrib. 80−67732
early-type ultra-short-period variable stars, new class identification and photometry 79−88662
eclipsing variable stars, Fourier analysis of light curves, error anal. in freq. domain 80−31214
eclipsing variable stars with extended atmospheres, Fourier anal. of light curves 80−46604
eclipsing variables, Fourier anal. of light curves, geometric elements soln. 79−25634
eclipsing variables, Fourier anal. of light curves, photometric perturbs. for partial eclipses 79−25635
eclipsing variables, Fourier anal. of light curves 79−25633
eclipsing variables, Fourier anal. of light curves 79−25632
eclipsing variables, Fourier anal. of light curves 79−30088
eclipsing variables, Fourier analysis of light curves 79−8946
eclipsing variables, Fourier analysis of light curves 79−8945
education, variable star, digitally synthesized, diagram 79−9067
ellipsoidal binaries with single optical component, light vars. 79−92806
emission line stars, spectrographic obs., 5650 to 11000 Å *(French)* 79−48815
emission variable in Sagitta, magnitudes 77−17599
emission variable in Sagitta, photographic magnitudes from Harvard patrol plates 77−2431
emission-line object candidate for 4U 1630-47, photometric and spectroscopic obs. 77−82324
emission-line star in core of M15, spectrum, photometry and position 79−5840
emission-line stars in galactic cluster NGC 663, emission line variability 80−4363
emission-line variable (No.86) in core of M 15, UBV photometry, probably W Virginis star 80−77458
equatorial and southern bright stars, UVBYβ photometry 77−22205
ν Eridani, β Cephei star, Fourier anal. of radial vel. changes 80−105246
ν Eridani, β Cephei variable atm. parameters from H and He spectral obs. 80−67739
CC Eridani, BY Draconis variable, Hα variations 77−87406
Z Eridani, circular polarisation of stellar radiation scattered in circumstellar cloud, theory 78−96428
RX Eridani, RR Lyrae variable, radius 77−2436
40 Eridani C, flare star, possible X-ray emission 79−97035
40 Eridani C, X-ray image of dM4e flare star 80−105282
eruptive blue variables at high galactic latit., spectrophotometry 78−32482
eruptive variable in Andromeda, posn. and mags. (1979 Sept.) 79−101163
eruptive variable stars, IR spectra rel. to grains props. 80−26943
eruptive variables, magnetic field effects 79−62845
evolved stars, thermal and nuclear modes coupling 79−84785
extragalactic distance indicators 78−93396
extratidal variables and dynamics of Sculptor dwarf galaxy 79−67088
extreme galactic B and A supergiants, light vars. 77−56927
extremely metal-poor stars, theoretical evolution and radial mode pulsational stability 78−28677

variable stars continued
extremely red stars on Palomar prints, optical variability search 78−57563
F and G-type supergiants, search for light vars. 79−88657
fast irregular variables, UBV and JHKL photometry *(Russian)* 78−28684
flare star, near Orion Nebula, UBV obs. *(Russian)* 77−82223
flare star 2329−03, spectra, chromospheric emission 77−74070
flare star discovery obs. *(French)* 77−87409
flare star search in Cassiopeia region near W3 77−37603
flare stars, anomalous Balmer decrement, stimulated transitions between highly excited atomic levels 78−5176
flare stars, catalogue of 68 objects in solar neighbourhood 77−53431
flare stars, chromosphere theory, fast electrons hypothesis 78−24514
flare stars, combined optical and radio obs., long-duration events 79−53827
flare stars, dM stars as source of interstellar ^{3}He 79−48810
flare stars, dynamical parallax, absolute magnitudes and masses *(Russian)* 79−88690
flare stars, energy storage and release, model constraints 78−65491
flare stars, fast electron hypothesis 77−78796
flare stars, flare data reduction and interpretation, interactive method *(Italian)* 80−8552
flare stars, flare emission spectrum rel. to fast electron hypothesis 80−67731
flare stars, identification with transient soft X-ray sources questioned 78−96485
flare stars, large-scale winds driven by mass loss, effects on interstellar matter 78−32464
flare stars, mean colours of flare continuum 77−13349
flare stars, model chromospheres, Balmer-line profiles 80−46558
flare stars, multichannel spectrophotometry 80−105256
flare stars, nature of flares optical continuum *(Russian)* 80−109445
flare stars, nature of nearby radiosources 78−12388
flare stars, nonmonotonic optical light curve model 77−29842
flare stars, opaque envelope clearing 79−35238
flare stars, photoelectric monitoring (1974 to 1976) 79−44509
flare stars, photographic photometry, discovery of five new stars 77−56943
flare stars, photographic photometry of four new objects 78−89207
flare stars, physical characts. 78−12242
flare stars, possible galactic cosmic ray sources 78−49240
flare stars, source of galactic cosmic rays, hypothesis 80−46559
flare stars, theory of flare mechanism *(Russian)* 78−49444
flare stars, vars. 79−16954
flare stars, X-rays influence on optical light curve 77−29843
flare stars as candidates for new class of transient soft X-ray sources 78−45337
flare stars discovery in Ophiuchus-Scorpius region *(Chinese)* 78−69804
flare stars in Orion Nebula region, new objects and repeated outbursts 80−56852
flare stars in Pleiades, new discoveries *(Russian)* 77−13366
flare stars in Pleiades, photometric obs. *(Russian)* 77−91536
flare stars in Pleiades, possible cyclic recurrence of flare activity *(Russian)* 78−49443
flare stars in Pleiades, spatial distrib. using recovery method *(Russian)* 80−94722
flare stars in Pleiades, UV and photographic obs. of flares *(Russian)* 77−13367
flare stars in Praesepe field, plate records and cluster membership 77−53652
flare stars in Scorpius-Ophiuchus region, discoveries *(Chinese)* 80−77418
flare stars in solar neighbourhood, physical parameters 80−51777
flare stars in Taurus Cloud, comparison with ρ Ophiuchi flare stars, visible obs. *(Chinese)* 80−85957
flare stars physical characts. 77−41383
flares, data acquisition and processing at Italian observatories *(Italian)* 79−62751
flares, IR obs. *(Russian, English)* 79−75216
flares in stellar aggregates, freq. function *(Russian)* 79−8918
G 208-44/45, possible double flare star, spectral obs. 80−67727
galactic G-type supergiants, UBV photometry 80−41824
GC 17353, Ap star with large photometric var., period *(French)* 79−2545
GD 154, new pulsating white dwarf, obs. 78−40928
GD 428, extreme dwarf Cepheid 77−78798
GD 428, photometry and spectrum rel. to nature of dwarf Cepheids 78−73720
U Geminorum, 1978 February magnitude estimates 78−36589
U Geminorum, dwarf nova, visual magnitude estimates, (1979, March 23 to 24) 79−44501
U Geminorum, dwarf nova, visual magnitudes during outburst, (1980 May 6 to 9) 80−72978
U Geminorum, visual magnitude estimates during outburst (1980 Oct.) 80−109439
General Catalogue and international cooperation 77−78663
Gliese 815, dMe spectroscopic-visual triple 79−12493
Gliese 82, dM4e star, flare activity discovery 77−91539
Gliese 867, flares obs. on both components of visual binary 79−48861
globular cluster metal-rich horizontal branch stars, evolution 77−45466
in globular clusters, problems 78−81641
RS Gruis, dwarf Cepheid in binary system 78−77559
RS Gruis, RRs variable, photoelectric radial vels. 77−5533
H 2252−035, cataclysmic variable, photometry and spectrum rel. to orbital and rot. periods 80−101651
H 2252−035, spectrophotometry, no periodic linear polarization (1980 Sept.) 80−105401
H 2252−035, X-ray flux modulation, compact star rotation 80−101652
h 4866 B, vars. in spectral type and radial vel. 78−32518
Harvard Photographic Collection, recent novae and variable star research 78−32486
HBV 475 (V1329 Cygni), high-excitation emission lines obs. 78−40955
HD 101065, Przybylski's star, light variability freq. anal. 80−62152
HD 101065, search for light vars. 78−69812
HD 101065 (Przybylski's star), Ap-star model rel. to light vars. and temp. 79−101151
HD 101947, yellow supergiant star, Cepheid with 125 day period 79−88671
HD 102567 (4U 1145−61), IUE obs. of Be-star 80−82383
HD 10783, Ap star, spectrophotometric obs. 80−98663

variable stars continued
HD 108102 (T111), possible RS Canum Venaticorum system in Coma star cluster 79−67020
HD 111133, Ap star, 5200 Å flux depression variability *(German)* 79−44496
HD 116458, Ap star, search for light variability 77−64767
HD 116890, Ap star, photometry and var. period 77−64767
HD 116994, uvby photometry, var. period determ. 77−13358
HD 118216=HR 5110, radio outburst and UV spectra of RS Canum Venaticorum-type binary 79−62844
HD 118246, new Be star at high galactic latit., photometry and spectrum 78−73721
HD 124224, He Si variable, spectroscopic obs., starspots, oblique rotator model 78−12239
HD 128220, peculiar spectroscopic binary, photometric separation of components *(French)* 77−57014
HD 129041, new δ Scuti star, period and amplitude 79−2547
HD 129494, new pulsating δ Delphini star, photometric obs. and luminosity 80−67750
HD 129708, new bright short-period Cepheid variable with unusual spectrum, photometric obs. 80−67751
HD 13970, photometry of probable close binary component 79−8948
HD 15165, σ Scuti type star in BDS 1269 visual binary system 80−4397
HD 153747, freq. anal. of early-type δ Scuti star 79−71053
HD 153919 (3U 1700−37), X-ray eclipsing binary, VBLUW photometric obs. 79−17135
HD 159378 (Tr 27-102), yellow variable supergiant near Cepheid instability strip, VBLUW photometry 80−98672
HD 184279, B-type subgiant, variability 79−84804
HD 184927, He variable star, spectroscopic props. 80−51790
HD 184927, He variable star, spectrum obs. 77−22249
HD 185332, new δ Scuti star, photometric and spectroscopic obs. 80−90451
HD 191639, B-type main sequence star, variability 79−84804
HD 193793, Wolf-Rayet star, circumstellar dust form. episode 80−31301
HD 193793, Wolf-Rayet star, photometric evidence for C-rich dust cloud 80−26861
HD 193793(=BD+43°3571), near IR magnitude increase 77−87413
HD 196517, new δ Scuti type variable star 78−49462
HD 200925 radial vels. of new short period δ Scuti star *(French)* 80−90441
HD 206860, G0 V star, UBV and IUE obs. of active region 79−92766
HD 21479, brightness microvariability and non-radial pulsations *(Russian)* 80−67754
HD 221568, Ap star, light var. period 80−56856
HD 224085, K2e star, long-term variability 79−48849
HD 224085, spot-covered red dwarf, light curves 77−74093
HD 30466, double wave photometric variable Si star 77−87410
HD 30849, periodic variability photometric obs. *(French)* 79−101157
HD 31908, freq. analysis of δ Delphini star 80−46581
HD 33579, HD 35343 (S Doradus), HDE 268757, HDE 269006, most luminous LMC supergiants, long time baseline VBLUW photometry 80−36630
HD 34452, Si Ap star, spectroscopic study 78−65634
HD 3580, 187473, 212432, Si stars, uvby photometry and periods 78−96487
HD 3980, late Ap star, photometric and mag. variability obs. 80−56845
HD 4174 (=EG Andromedae), peculiar M giant, UV spectra obs. 80−94798
HD 45088, BY Draconis binary, surface activity from high rot. vel., visible obs. 80−77425
HD 45677, peculiar Be-star, 0.12-12.6 μm obs. 80−72957
HD 47732, young close ellipsoidal variable in NGC 2264, photometry and struct. 78−57575
HD 50169, Ap star, uvby photometric obs. 77−22236
HD 52788, freq. anal. of δ Delphini star 79−35276
HD 64740, He rich star, UV spectral vars. 80−22016
HD 64740, He variable star, X-ray source 4U 0750−49 optical candidate 78−36584
HD 65750, photometric vars. of red giant, obs. of surrounding refl. nebula IC 2220 78−36567
HD 77581 (Vela X-1), discovery of optical pulsations 77−82327
HD 77581 (Vela X-1), optical pulsations discovery 78−20911
HD 80383, UBV photometry of β Cephei type star 80−36644
HD 8781, freq. anal. of low-amplitude δ Scuti star 80−46575
HD 88661, Be star, photometry and light vars. *(French)* 78−57562
HD 91619, 96919, B-supergiants, peculiar H_α profile variations 77−17577
HD 92664, Ap star, photometric variability and period 79−40199
HD 94033 ultra short period cepheid, obs. 80−22024
HDE 226868 (Cygnus X-1), anomalous light curve during X-ray increase of 1975 April-May 78−28850
HDE 226868 (Cygnus X-1), black hole candidate, optical and X-ray vars. 78−16577
HDE 226868 (Cygnus X-1), long-term circular polarisation variability 79−9031
HDE 226868 (Cygnus X-1), temporal and spectral var., X-ray rocket obs. 78−8163
HDE 245770, possible counterpart of variable X-ray source A 0535+26, line and continuum vars. 80−17600
HDE 245770 (A0535+26), UBV photometry during X-ray outburst 79−67024
HDE 245770 (Ariel 0535+26), photoelectric UBV photometry 78−36592
HDE 245770 (Ariel 0535+26), UBV photometry during X-ray flare-up 78−28705
HDE 326333, new β Canis Majoris star, photometric obs. 80−17595
He2-442, UVRK photometry and spectroscopic obs. *(Russian)* 80−94817
He 2-467, yellow symbiotic star, emission lines and continuum 80−62155
Henize 2-38, symbiotic star, steam and CO absorpt. obs. 78−40970
Henize 715 (4U 1145−61), Be-type star, colour and luminosity vars. (1976-1980) 80−72979
Henize 788 (Wray 977), counterpart of 3U 1223-62, five colour photometry 77−29846
AC Herculis, curve-of-growth analysis of RV Tauri variable 80−22026
DY Herculis, dwarf Cepheid, radial vel. and radius 79−58358
variable stars continued
DY Herculis, dwarf Cepheid, uvbyβ photometry and evolutionary status 79−58357
AH Herculis, dwarf nova, changes in rapid oscills. during outburst 79−88686
AH Herculis, dwarf nova outburst, rapid oscills. evolution 80−94805
OP Herculis, irregular variable, Tc I absorpt. lines obs. 78−28689
OP Herculis, late-type variable star, spectral energy distrib. and spectral types *(Russian)* 78−40958
88 Herculis, light and colour vars. of shell star 79−53817
AM Herculis, polar, IR photometric obs. 80−98687
AM Herculis, possible cataclysmic variable of Z Camelopardalis type 77−33497
AC Herculis, RV Tauri star, UBV obs. 80−56857
BL Herculis, short-period Population II variable, chem. comp. determ. 79−8923
BL Herculis, Stromgren uvbyβ photometry 78−85954
YY Herculis, symbiotic star, radio continuum detect. 79−25615
YY Herculis, symbiotic star, radio emission report refuted 79−35274
AM Herculis (3U 1809+50), simultaneous three-channel photometry rel. to optical flickering mechanism 80−82411
AM Herculis (4U 1813+50), rapid light variability obs. *(Russian)* 80−8662
HZ Herculis (Hercules X-1), optical behaviour, 1976 Aug.-1977 Nov. 79−53855
HZ Herculis (Hercules X-1), optical pulsations rel. to accretion disc/mag field interaction *(Russian)* 80−51799
DQ Herculis (Nova 1934), high time resolution spectrophotometry 80−22017
DQ Herculis (Nova 1934), light curve and double maxima 77−82255
DQ Herculis (Nova 1934), masses of interactive binary 79−97029
DQ Herculis (Nova 1934), short-period oscills. modulation and pulsed emission lines asymmetry interpretation 80−22044
DQ Herculis (Nova 1934), white dwarf rot. period rel. to nova remnant shape 80−105244
V446 Herculis (Nova 1960), ejecta He abundance 79−92775
V533 Herculis (Nova 1963), 63 sec. oscill., UBV photometry 80−17592
V533 Herculis (Nova 1963), periodic light oscills. obs. 78−93285
α Herculis A, M-type supergiant, Li abundance in atmosphere *(Russian)* 80−72950
AH Herculis star fields, comparison star sequences, photometry obs. 80−82433
high-latitude blue variables, slit spectra 79−21312
TU Horologii, ellipsoidal variable, UBV photometry 78−4292
HR 1099, 10 GHz radio emission from RS Canum Venaticorum binary 80−82427
HR 1099, binary stars, radio obs. 77−64793
HR 1099, co-ordinated UV, optical and radio obs. of RS Canum Venaticorum binary 79−16963
HR 1099, flare activity observed at 2.8 cm wavelength 78−36590
HR 1099, flare emission at 2.8 cm (1978 February) 78−32476
HR 1099, new bright RS Canum Venaticorum variable, spectrum 77−9754
HR 1099, noneclipsing RS Canum Venaticorum binary, radio flare obs. 77−17632
HR 1099, optical linear polarisation meas. 78−53958
HR 1099, radio emitting variable star, photoelectric photometry 77−53602
HR 1099, radio flux vars. obs. and optical ephemeris 78−36641
HR 1099, RS Canum Venaticorum star, 4U 0336+01 optical counterpart 78−32475
HR 1099, RS Canum Venaticorum type binary, radio emission detect. 77−9772
HR 1099, UV spectrum obs. by International Ultraviolet Explorer 78−96475
HR 1099, V photometric obs. during 1976-77 period 78−40994
HR 1099 (V711 Tauri), RS Canum Venaticorum star, Hα line variability, visible spectra obs. 80−105277
HR 1170, δ Scuti-type star, light and colour curves 77−74058
HR 1170, HR 7331, nonradial δ Scuti pulsators, photometry multiperiod anal. 79−88663
HR 1217, Ap star, spectrum and light vars. relationship 80−26878
HR 1225, δ Scuti star, photoelectric study and periodogram anal. 80−109436
HR 2557, light vars., luminous δ Scuti-type star 78−32490
HR 3517, new δ Scuti star, discovery and photometry 78−12243
HR 432, 515 and 8006, δ Scuti stars, spectrographic obs. 80−36639
HR 4594, freq. anal. of low-amplitude δ Scuti star 79−35275
HR 4594, pulsating marginal metallic line (Am) star, obs. 78−49448
HR 5153, Ap star, rot. vel. and light vars. period 77−17593
HR 5597, irregularly variable magnetic star 77−74061
HR 5999, circumstellar dust around variable shell star, photometry 79−8926
HR 5999, lightcurves for irregular variable shell star 78−77557
HR 5999, variable shell star, VBLUW photometry 78−28701
HR 5999 (V856 Scopii), multicolour photometry, circumstellar dust shell 79−48828
HR 6684, β Cephei-type star, radial vel. vars. from microphotometer scans 78−77581
HR 6684, β Cephei-type variable, radial vel. var. 78−45344
HR 7331, δ Scuti star, relation between radial vel. and light vars. 77−9752
HR 8102, uvby anal. of δ Scuti type star 78−53965
HR 8210, freq. anal. of low-amplitude δ Scuti star 79−35275
HR 8210, pulsating marginal metallic line (Am) star, obs. 78−49448
HR 8752 (HD 217476), superluminous superiant, line spectrum changes rel. to expanding shell 79−80308
HR 9070, Be star, spectral vars. obs. 80−12773
Hubble-Sandage type, discovery in M33, light curve, magnitude 78−73717
Hubble-Sandage variables, mass accretion model 80−26877
VX Hydrae, dwarf Cepheid, uvbyβ photometry 77−29856
EX Hydrae, dwarf nova, IR and optical light curves 80−67747
EX Hydrae, dwarf nova lightcurve, periodic and secular vars. 80−77413
W Hydrae, long-period variable, suspected Zeeman splitting in OH masers 80−36632
W Hydrae, long-period variable star, cyanodiacetylene detect. 77−82238
W Hydrae, OH/IR star, new SiO transition detect. 78−53954
EX Hydrae, spectra of dwarf nova 80−98670
EX Hydrae, U Geminorum type star, possible counterpart of (4U 1249-28) 78−36729

variable stars continued
RW Hydrae, UV obs. of hot component 80−56854
VW Hydri, cataclysmic variable, light curve superhumps model 80−4381
VW Hydri, colour variations during dwarf nova outbursts 80−46576
VW Hydri, dwarf nova, IR light curves 80−67747
WX Hydri, dwarf nova, obs. of superhumps during supermaximum 79−88677
IC 4997, compact planetary nebula, central star, UV radiation changes rel. to rapid emission-line vars. 79−92838
instability, broadened definitions for stars in thermal imbalance 78−16397
interferometry of star cluster with prominent variable 79−84680
IR source in 2S 1702−363 field, IR brightening, probably Mira variable 78−81705
IR stars, H_2O maser source in circumstellar envelope 78−73724
IR stars, line radiation transfer in collapsing molecular clouds 78−73626
IR stars, search for 18 cm OH emission 78−8026
IR stars, search for OH 18 cm emission 78−40949
IR stars, USAF satellite obs. 77−49406
IRC+10216, C star, IR obs. 80−90568
IRC+10216, C star, near IR obs. of new mol. feature 79−92762
IRC+10216, spatial spectra from 2.2 to 20 microns, deviations from spherical symmetry 80−41911
IRC+30219, variable C star, optical emission-line phase obs. 80−90569
Jacobi's virial eqn. soln. for celestial bodies 79−8832
K1082, in globular cluster M15, suspected ultrashort period variable star 80−26883
Kuiper 41, orbit and flare activity of visual red dwarf pair 79−97032
Kustner 1082 in globular cluster M15, hot ultrashort period Cepheid *(Chinese)* 77−67096
KUV09313+4052, variable UV excess object, discovery, position and photometry 80−62159
Kuwano's novalike object in Vulpecula, IR photometric obs. 80−62147
L19-2, low-amplitude ZZ Ceti type variable, UBV colours, period determ. 78−4242
L19-2, ZZ Ceti-type variable, light curves and power spectra 77−56948
12 and 16 Lacertae, β Cephei stars, light var. anal. and photoelec. photometry 80−77412
AR Lacertae, eclipsing binary, photometric obs., intrinsic variation 77−22271
EW Lacertae, Fe II emission line spectra 77−56978
EV Lacertae, flare star, hot-plasma model of strongest flares 78−20838
EV Lacertae, flare star, photometry and spectrum rel. to starspots and rot. period 80−98665
EV Lacertae, flare star, polarimetric and photometric obs. *(Russian)* 77−13368
EV Lacertae, high-speed five-colour photometry of flare star 77−56956
EV Lacertae, IR obs. of flares *(Russian)* 78−93278
EW Lacertae, motion in shell and atmosphere 77−60776
12 Lacertae, nonradial oscills. of β Cephei type star 80−4366
DD=12 Lacertae, obs. study of secular var. and pulsational stability 80−41833
12=DD Lacertae, radial vel. and line profile var. 77−78797
EW Lacertae, shell spectrum change, 1978 Dec. radial vels. 79−21306
EV Lacertae, UV Ceti variable, flares colour behaviour 80−22020
12=DD Lacertae, vel. curves and period charge, spectrograms 77−26016
12 Lacertae (DD Lac), spectral variations 77−71114
CP Lacertae (Nova 1936), ejecta He abundance 79−92775
large-amplitude red variables, luminosities and space motions 77−22244
late-type giant variables, ang. dias. by lunar occultation technique 77−74048
late-type stars, O-rich, 16 to 39 micron spectroscopy 80−22002
LDS 678B (EG 131), white dwarf, spectrum vars. 78−40946
Leo I dwarf galaxy, 23 new variables discovered 78−53953
R Leonis, airborne IR spectrophotometry, H_2O and CO absorpt. bands 78−32465
R Leonis, circumstellar shell heterodyne interferometry 78−8000
ρ Leonis, expanding envelope OAO-3 spectra *(Russian)* 78−4224
AD Leonis, flare conditions from photometry and spectra 79−92773
AS Leonis, flare star, chromospheric emission lines in nonflare red spectrum 79−21294
AD Leonis, flare star, Hα emission short-period variability limits 79−48807
R Leonis, IR atomic line spectrum of Mira variable 80−46557
R Leonis, IR spectroscopy of Mira variable, H_2O vibr. rot. bands 79−35258
AQ Leonis, light var. anal. of RR Lyrae star 77−56941
R Leonis, Mira variable, CO and OH IR vibr.-rot. overtone bands 78−36574
AD Leonis, nature of radiosource near flare star 78−12388
AQ Leonis, Population II double-mode RR Lyrae star, theoretical period ratio 80−62134
R Leonis, SiO maser variability at 86 GHz of Mira variable 80−41839
R Leonis, strong TiO-related dia. vars. 78−16429
20 Leonis, triple system with a δ Scuti variable, spectroscopic obs. 77−49440
AD Leonis, UV Ceti variable, flares colour behaviour 80−22020
AD Leonis, UV Ceti-type flare star, simultaneous 1420 MHz and optical obs. of flares 78−49464
AD Leonis, X-ray emission from flares, HEAO 1 obs. 80−41837
CW Leonis (IRC+10216), Mira variable and IR C star, intrinsic polarisation origin 80−67730
48 Librae, Be star, shell spectrum line profiles 80−62146
EH Librae, BV photoelectric photometry of dwarf Cepheid 79−44498
EH Librae, dwarf Cepheid, BV photometry 77−82226
48 Librae (FX Librae), Be star, search for short time scale vars. in Hα emission 80−109441
48 Librae (FX Librae), shell star, spectroscopic study 78−96486
line profile variable B-type 79−5823
Lk Hα 120, T Tauri star, spectrum 77−74052
LMC 186, luminous C-type Mira variable in LMC, obs. 78−28670
LMC X-2 optical candidate, UBV photometry and variability 79−17136
long period, OH radial vel. pattern rel. to period 79−35427
long period, system constitution *(Russian)* 80−36651
long period Cepheids, UBVRI photometry and classification 77−71112
long period variable in globular cluster NGC 6541, UBV photometry 79−35316
long period variable maser stars, radial vel. determ. 80−77410
long period variable stars, emission lines rel. to periodic shock waves and mass loss 79−44487

variable stars continued
long period variables, nonlinear coupling between pulsation and convection 77−13356
long period variables in globular clusters, high sensitivity search for main-line OH emission 80−62207
long period variables in the Galaxy *(Russian)* 77−45470
long period with OH, H_2O or SiO maser emission, catalogue 79−70965
long-period, radial and expansion vels. from SiO line 78−40956
long-period, vel. structure of photospheres, theory 79−53815
long-period, weak maser emission pedestal assoc. with SiO maser in circumstellar shells 78−93256
long-period Cepheids between l=294° and 331°, UBV and 21 cm obs. 79−12478
long-period variable stars, maser activity rel. to Hδ emission, obs. 79−88685
long-period variable stars, OH maser lines struct. and saturation 78−93264
long-period variable stars, radial vel. obs. 79−88684
long-period variable stars in S.hemisphere, narrowband polarimetry 80−98666
long-period variables, CO and SiO millimetre line emission obs. rel. to circumstellar shell props. 78−49423
long-period variables, discovery of new 1665/1667 MHz OH/IR sources 77−64763
long-period variables, H emission line form., models 78−28709
long-period variables, mass loss and circumnebular shells form. 78−8014
long-period variables, pulsation from near IR photometry 78−4248
long-period variables, SiO in 4 μ spectrum 77−13360
long-period variables, SiO maser pump mechanism and luminosity 79−92772
low amplitude variables in Cepheid instability strip, photoelectric photometry 77−17580
LS55° −8, high-speed photometric obs. of new nova-like variable 78−57565
LS I+61°303, radio, optical, X-ray, gamma-ray Be star, optical and radio obs. 79−88755
LS I +61°303, radio variable Be star, UV spectrum, stellar models 80−26879
luminous blue variable stars in M31 and M33, IR detect. 78−49437
luminous variable stars in M31 and M33, spectra and photometry 78−28686
α,τ Lupi, β Canis Majoris stars, photometric obs. 80−17595
RU Lupi, far UV spectrum of T Tauri type star 79−44494
RU Lupi, T Tauri star, chromosphere and corona parameters and expected X-ray fluxes *(Russian)* 80−51770
α Lupi, UV light curve of β Cephei-type star 78−36570
RU Lupi T Tauri star, far UV spectra, emission measure obs. 80−94788
SZ Lyncis, BV photoelectric photometry of dwarf Cepheid 79−44498
2 Lyncis, spectrographic obs. of suspected δ Scuti star 78−61867
ι Lyrae, Be star, Hα emission disappearance 79−5834
MV Lyrae, cyclotron lines in spectrum of nova-like star *(Russian)* 80−67753
XY Lyrae, late-type variable star, spectral energy distrib. and spectral types *(Russian)* 78−40958
δ^2 Lyrae, M-type supergiant, Li abundance in atmosphere *(Russian)* 80−72950
MV Lyrae, polarisation and spectrum obs., polar class candidate *(Russian)* 78−93322
MV Lyrae, soft X-ray emission from nova-like object 79−92787
RR Lyrae, UV photometry from Orbiting Astronomical Observatory, light curve interpretation 77−45435
α Lyrae (Vega), evidence for light and vel. vars. 79−75208
RR Lyrae blue variables in M22, photometry 78−85945
RRab Lyrae field stars, metallicity rel. to luminosity 78−77561
RR Lyrae pulsators as He indicators in globular clusters 80−51778
RR Lyrae star, in metal-rich globular cluster NGC 6366, photometry 77−5462
RR Lyrae star distrib. according to metal abundance, galactic evolution active phases *(Russian)* 77−74144
RR Lyrae star in globular cluster NGC 6717, photometric investigation 80−46624
RR Lyrae star system ellipticities in globular clusters 77−60805
RR Lyrae stars, absolute proper motions for 64 stars *(Chinese)* 79−80319
RR Lyrae stars, atlas of light and colour curves 77−82228
RR Lyrae stars, bibliographical catalogue at Strasbourg Stellar Data Center 78−16431
RR Lyrae stars, Ca and Fe decoupling 79−30069
RR Lyrae stars, convection depend. on pulsation phase, theoretical red edge of instability strip 77−17572
RR Lyrae stars, convective steady-state models, theoretical red edge of instability strip 78−4229
RR Lyrae stars, cycle area in two colour diagram 79−21297
RR Lyrae stars, effective temp. and colour, metallicity effects 80−56841
RR Lyrae stars, hydromagnetic processes as cause of period changes 80−105261
RR Lyrae stars, in 47 Tucanae, membership and metallicity 80−62206
RR Lyrae stars, in Baade's window region, metal abundances 77−9749
RR Lyrae stars, in globular cluster NGC 3201, BV photometry 77−2458
RR Lyrae stars, in southern hemisphere, VBI photometry 77−53612
RR Lyrae stars, inconsistency in local mixing-length convection theory 80−26841
RR Lyrae stars, instability strip red edge depend. on luminosity and comp. 77−53600
RR Lyrae stars, kinematics rel. to Galaxy initial contraction 80−62204
RR Lyrae stars, multiperiodic, observational review 77−87430
RR Lyrae stars, multiperiodic, pulsation theory 77−87431
RR Lyrae stars, parallaxes and distance scale, max. likelihood technique 80−51746
RR Lyrae stars, period-luminosity-colour relations, metallicity effects 80−56842
RR Lyrae stars, photoelectric UBV obs., second list 78−81639
RR Lyrae stars, pulsation theory and multiperiodic variables 77−87429
RR Lyrae stars, reddening and blanketing meas. 79−48806
RR Lyrae stars, semiconvection and period changes 79−30072
RR Lyrae stars, theoretical period ratios 80−62134
RR Lyrae stars, theoretical red edge of instability gap, overtone pulsation 77−78794
RR Lyrae stars, van Hoof's variation appl. to radii determ. by Baade's method 77−53613

variable stars continued
RR Lyrae stars, vel. ellipsoid 78−77563
RR Lyrae stars in ω Centauri, UBV photometry rel. to comps. 78−73719
RR Lyrae stars in galactic bulge, spectra and comp. 77−26012
RR Lyrae stars in globular clsuters, period-amplitude relation and ω Centauri anomalous horizontal branch 79−67019
RR Lyrae stars in globular cluster M4, metal abundances 79−58351
RR Lyrae stars in globular cluster NGC 1216, photometry rel. to cluster distance 80−17623
RR Lyrae stars in globular cluster NGC 5986, periods and light curves 79−5868
RR Lyrae stars in globular cluster NGC 6266, photometry and distance 78−61894
RR Lyrae stars in globular clusters, physical mechanism for Oosterhoff dichotomy 77−78837
RR Lyrae stars in globular clusters, transitional period-luminosity depend. 77−53614
RR Lyrae stars in IC 4499 globular cluster, periods and light curves 79−44490
RR Lyrae stars in LMC, list of 76 objects 77−91549
RR Lyrae stars in M22 and ω Centauri globular clusters 79−16962
RR Lyrae stars in M4, UBV photometry 77−78802
RR Lyrae stars in M 15 globular cluster, period behaviour 77−45444
RR Lyrae stars in Microscopium, VBLUW photometry and proposed intergalactic dust cloud 80−56851
RR Lyrae stars in NGC 6235 globular cluster 78−4305
RR Lyrae stars in Palomar-Groningen fields, luminosities, distances and kinematics 78−93276
RR Lyrae stars models, radial pulsations 80−26863
RR Lyrae type variable discovery near M4 *(Chinese)* 78−69804
RR Lyrae variables, three-dimensional motion 80−12754
RR Lyrae variables in ω Centauri cluster, spectroscopic obs. 79−5824
RR Lyrae variables in globular cluster NGC 6121 (M4), UBV photometry 80−22018
RR Lyrae variables in N.Galactic pole fields, metal abundances 79−88660
RR Lyrae variables in NGC 1851, periods and light curves 78−73714
in M13, globular cluster, proper motions and membership probabilities from astrometry 79−75252
M13, globular cluster, two colour photographic photometry of variable stars 77−87492
M15-K1082, two-hour variable UV-bright star in NGC 7078 (M15), spectra 79−88681
M22, globular cluster, light curves of red variables 77−64808
M22, photometry of giant branch variable stars 78−32537
M31 field, van den Bergh variables 77−74056
in M3, globular cluster, proper motions and membership status 80−8665
in M4, discoveries *(Chinese)* 80−77418
M5, globular cluster, bright variable star obs. 77−91590
M-type, obs. in DDO photoelec. system, spectral classification 78−32463
M-type giant stars, spectral energy distribs. and effective temp. scale 78−28678
M-type Miras, IR photometry 80−41823
Magellanic Clouds, ratio of total-to-selective absorpt. from Cepheid obs. 77−29927
magnetic star phenomena *(German)* 77−67103
magnetic stars measurement with improved Abbe comparator 77−67043
magnetic variable Ap stars, review 77−87426
magnetic variables, intrinsic rot. vels. 78−40967
main sequence, chromospheric var. from Ca II line obs. 77−56936
main-sequence stars, F to M-type, comparison of activity cycles to old and young stars 80−105235
marginal metallic line (Am) stars, metallicism and pulsation 78−49448
maser stars, search for water vapour absorpt. lines 77−78804
mass accretion, luminosity vars. rel. to particles orbital motion, accretion and ejection 79−44338
materials motion around a source whose luminosity changes 79−12394
Me-type dwarf stars, long-term variability 78−93254
Medium-Amplitude Red Variables, UBVRI photometry 77−45438
ZZ Microscopii, radius of dwarf Cepheid from BV photometry 78−77560
AT Microscopii, X-ray emission from flares, HEAO 1 obs. 80−41837
Mira (*o* Ceti) stars, kinematics rel. to Galaxy local struct. determ. *(Russian)* 78−77608
Mira and semiregular variables, microwave and IR obs. of H_2O vapour maser emission 79−67037
Mira envelopes, OH maser luminosity and expansion vel. gradient 79−71043
Mira objects, SiO maser sources, 43 GHz obs. 79−16942
Mira phenomena, AlO IR bands 78−69801
Mira stars, OH main lines, IR pumping 80−46632
Mira type, mass outflow vel. rel. to luminosity 78−93270
Mira type stars, luminosity props. from spectra and light curve elements 80−105253
Mira type variables, Me and Se types, UBV photometry 80−82375
Mira type variables atm., OH maser, IR line overlap pumping mechanism 80−72764
Mira variables, airborne IR spectrophotometry, H_2O and CO absorpt. bands 78−32465
Mira variables, angular diameters from lunar occultations of three objects 79−44475
Mira variables, discovery of 123 new stars in Palomar 10 globular cluster region 78−40837
Mira variables, discovery of 7 new SiO maser sources 78−32467
Mira variables, effective temps; ang. dias. and reddening determ. from 1 to 5 μm flux curves 79−44458
Mira variables, envelope pulsational instability rel. to planetary nebula form. 80−26928
Mira variables, H_2O emission characts. 77−45447
Mira variables, identified with Type II OH/IR sources, 1612 MHz obs. at low galactic latits. 77−17704
Mira variables, intrinsic amplitude and TiO absorption 78−36580
Mira variables, intrinsic props. from observational data 78−45333
Mira variables, IR Photometry and OH maser pumping efficiency 80−82379
Mira variables, light and colour variations 77−64770
Mira variables, mass loss and OH maser emission 79−16969
Mira variables, mass loss and red giant stars evolution 77−17571
Mira variables, observations in wavelength range 370 to 550 nm, energy distribution 79−84798
variable stars continued
Mira variables, OH emission high-sensitivity search 78−89203
Mira variables, OH maser sources, accurate position meas. 80−46646
Mira variables, polarisation variation detect. in absorption features 77−33496
Mira variables, pulsation and mass loss 79−25608
Mira variables, radial vel. meas. 77−56951
Mira variables, S-type, absolute magnitudes, galactic distrib. and population-type characts. 79−88651
Mira variables, SiO 86.2 GHz masers polarisation props. 80−4449
Mira variables, SiO maser luminosity and spectral type correl. 77−33512
Mira variables, statistical anal. of galactic concentration *(German)* 80−4390
Mira variables, supersonic mass ejection 77−53605
Mira variables, supersonic mass flow theory 79−35270
Mira variables around globular clusters, freq. distrib., cluster membership 80−36676
Mira variables in globular cluster NGC 6356, photometric obs. 78−32530
Mira variables in IRC catalogue 79−62841
Mira variables kinematics towards galactic centre 80−46578
Mira-type, Tc in late-type stars, spectral analysis 80−8623
Miras, angular dia. in near IR, 2-5 μm speckle interferometry 80−27010
molecular spectra of pure S stars 78−77554
V493 Monoceros, C star, discovery in two-micron objects survey 80−8555
19 Monocerotis, β Canis Majoris variable, photometric obs. 80−4379
1 Monocerotis, δ Scuti star, oscillation modes from photoelectric radial vels. and BVRI photometry 80−51787
1 Monocerotis, δ Scuti star, photometry and anal. 78−32495
21 Monocerotis, δ Scuti type star, freq. anal. 77−49398
R Monocerotis, bipolar nebula, optical and IR polarimetry 78−36658
CV Monocerotis, Cepheid variable in anon. open cluster 79−58349
R Monocerotis, Fe II forbidden line intensity changes *(Russian)* 79−8907
15=S Monocerotis, interstellar lines, UV obs. 80−90494
AU Monocerotis, mathematical anal. of photometric peculiarities 80−77448
R Monocerotis, model for assoc. cometary nebula NGC 2261 79−21372
R Monocerotis, T Tauri star, long period vars. 80−82350
V616 Monocerotis (A 0620−00), UBV photometry 80−56846
V616 Monocerotis (Ariel 0620-00), distance from interstellar colour excess 77−64744
R Monocerotis (NGC 2261 cometary nebula), spectrophotometry *(Russian)* 77−49446
V616 Monocerotis (Nova 1975=A0620−00), 8-day modulation 77−87442
V616 Monocerotis (Nova 1975=A0620−00), spectral characts. 77−87443
V616 Monocerotis (Nova 1975=A0620−00), spectroscopic obs. 77−82257
V616 Monocerotis (Nova 1975=A0620−00), X-ray and visible light curves 77−82331
V616 Monocerotis (Nova 1975=A 0620−00), UBV photometry *(Russian)* 79−58360
V616 Monocerotis (Nova 1975), photographic photometric obs. 78−36587
multimode Cepheid variables, masses and radii from period ratio diagrams 78−28698
multiple periodic variable stars, IAU Colloquium, Budapest, Hungary (1-5 Sep., 1975) 77−87422
α Muscae, β Canis Majoris type variability discovery from UBV photometry 79−80326
TZ Muscae, UBV photometry of suspected double-mode Cepheid 79−48825
θ Muscae, Wolf-Rayet binary, spectrum and photometry 77−22235
MWC 349, Be star, spectral EHF obs. 80−105262
MX 1608−52, transient X-ray source, faint variable optical candidate 78−28860
neutron stars, luminosity enhancement following X-ray bursts 78−32502
NGC 1261, globular cluster, Oosterhoff type I system, variable star obs. 77−53651
NGC 2287, open cluster, spectral classification of brightest stars 80−26919
in NGC 2298, globular cluster, variable stars photometry 77−13353
NGC 2419, globular cluster, variable star obs. 77−60804
NGC 4833, southern globular cluster, BV photometry of variable stars 78−4304
NGC 5286, B photometry of variable stars, globular cluster membership 78−32534
in NGC 5986, globular cluster, periods and light curves 79−5868
NGC 6121 (M4), near IR photometry of metal-poor globular clusters 77−41398
NGC 6530, UBV photometry of variable stars in open cluster 77−74106
NGC 6535, photometric study of variable stars in globular cluster 78−32529
in NGC 6584, globular cluster, new objects 80−62137
NGC 6638, globular cluster, Mira and RR Lyrae variable obs. *(French)* 78−16475
NGC 6913 galactic cluster, photoelec. photometry of brighter stars, variability obs. 80−46625
in NGC 6934, globular cluster, variable stars photometry 80−56891
nonradial oscillation mode splitting, effects of differential rotation 78−4211
nonradial pulsation hypothesis with simulated line profile vars. 80−8618
nonradial stellar oscillations, avoided crossing of modes 77−60748
GU Normae, Cepheid, assoc. with galactic cluster (NGC 6067) 77−45464
S Normae, Cepheid, luminosity and membership of NGC 6087 visible obs. 80−94797
TW Normae, Cepheid, membership open cluster (Lynga 6) 77−87491
S Normae, Cepheid in NGC 6087, distance and luminosity from cluster four-colour and Hβ photometry 80−62208
TW Normae, long period Cepheid rel. to open cluster Lynga 6 77−17639
TW Normae rel. to Lyngå 6 and age of galactic open cluster *(Italian)* 77−91591
Nova Centauri 1979, optical novalike object discovery and identification with X-ray transient 79−62842
Nova Centauri 1979, radio detect. of novalike object 79−67026

variable stars continued
Nova Cygni 1978, discovery report 78−85962
Nova Cygni 1978, spectrum, distance and absolute magnitude 78−89212
Nova Cygni 1978, spectrum, polarisation and visual magnitude estimates 78−89213
Nova Cygni 1978, spectrum, precise position and photometry 78−89211
Nova Cygni 1978, spectrum and visual magnitude estimates 78−89210
Nova Cygni 1978, UBV photometry and short-period vars. 79−5835
Nova Cygni 1978, visual magnitude estimates (1978 September 10 to 12) 78−85963
nova in Magellanic Clouds (LMC), premaximum spectrum 79−62853
probable nova in Sagittarius (1978), magnitudes (1978 June 30 to October 3) 79−101164
nova light curves, as manifestation of nonuniform stellar wind 80−62160
Nova Sagittae 1977, visual magnitude estimates (1977 November 6 to 1978 January 7) 78−36593
Nova Sagittarii 1977, photometry, spectrum, absolute magnitude and distance 78−53955
Nova Serpentis 1978, evolution of dust shell 80−90430
Nova Serpentis 1978, IR magnitudes and BVR photometry 78−65629
Nova Serpentis 1978, IR photometry 80−4365
nova shell ionisation, time-depend. model 79−53816
Nova Vulpeculae 1979, photometric history (1898 to 1978) 79−53819
Nova Vulpeculae 1979, prediscovery obs. and visual magnitude estimates 79−48817
Nova Vulpeculae 1979, slow nova, pre-maximum light curve 80−4364
Nova Vulpeculae 1979, spectroscopic and photometric obs., (1958 and 1968) 79−58344
Nova Vulpeculae 1979, visual magnitude estimate, (1979, May 2) 79−58348
nova-like variables, photometric obs. 77−82245
novae, dust formation and ionisation in envelopes 80−98678
novae, effect of binary companion on outburst 80−82394
novae, effects of white dwarf rot. on remnants shapes 80−105244
novae flare-ups theory, exact analytic self-similar solns. 79−35269
novalike object in NGC 5272, photometry and identification as W Virginis variable 79−75224
novalike object in Vulpecula, 1980 May-June spectra and magnitudes 80−82392
novalike object in Vulpecula, light curve, photometric and spectroscopic obs. 80−67758
novalike object in Vulpecula, photoelectric UVB obs. (1979 June 9 to 15) 79−80323
novalike object in Vulpecula, photometry, June 1980, and spectral classification 80−94807
novalike object in Vulpecula, UBV photometry (1979 August 6 to September 20) 80−8644
novalike object in Vulpecula, visual and red photographic magnitudes 79−92784
novalike object in Vulpecula, visual magnitude estimates 79−88673
novalike object is Vulpecula, visual magnitude estimates (1980 February 2 to May 9) 80−72980
novalike variable in Virgo, discovery, approximate positions and magnitudes, (1980 July and August) 80−98674
NQ Vulpeculae (Nova 1976) spectroscopic obs. 79−21316
UV Octantis, VBRI obs. of RRab star, radius determ. 79−8928
Of stars, search for rapid Hα and Hβ line variability 77−26014
OH/IR sources, microwave spectra, galactic distrib., radial velocity 78−16432
old novae, search for rapid photometric oscills. 78−4251
Y Ophiuchi, anomalous Cepheid, evidence for duplicity 78−53990
χ and 66 Ophiuchi, Be stars, search for short time scale vars. in Hα emission 80−109441
XX Ophiuchi, emission-line star, near IR spectrum 77−49404
RS Ophiuchi, recurrent nova, spectrum obs. 79−62848
ω Ophiuchi, UBV photometry of Ap star, periodicity in luminosity vars. *(French)* 78−57559
V843 Ophiuchi (Kepler supernova 1604) remnant, soft X-ray emission detect. 79−40244
Ophiuchus-Scorpius region, ZB flare stars and nebular variables *(Chinese)* 78−28702
Orion population stars, light curve characts. and emission line intensities 80−67721
α Orionis, 14.9 GHz obs. 79−75210
V380 Orionis, B8-A2e star, assoc. interstellar CH emission obs. 80−51856
α Orionis, CO and SiO millimetre line emission search rel. to circumstellar shell props. 78−49423
FU Orionis, composite spectra rel. to three models 78−65617
NU Orionis, exciting star of M43, radio and IR obs. 78−54012
κ Orionis, expanding envelope OAO-3 spectra *(Russian)* 78−4224
UX Orionis, fast irregular variable, H_α and H_β lines obs. *(Russian)* 77−87400
U Orionis, H I emission lines rapid variability *(Russian)* 79−16989
FU Orionis, IR spectroscopy with contact-type image tube 80−17587
U Orionis, Mira variable, relation between 1612 MHz flare and light curve 80−56844
V380 Orionis, near IR spectrum line identifications, equiv. widths *(Russian)* 78−61861
22 Orionis, nonradial m-mode changes in 53 Persei variable 80−72939
U Orionis, outbursts in main line OH emission 79−101158
YY Orionis, spectroscopic and photometric obs. 78−93225
U Orionis, stellar OH maser VLBI obs. rel. to mag. field 79−25742
α Orionis, supergiant, mass loss, visible spectra obs. 80−67755
LL Orionis, surrounding shocklike struct., distorted interstellar bubble theory 79−71088
V380 Orionis, T Tauri star, struct. of assoc. refl. nebula (NGC 1999) 80−94856
σ Orionis E, He star, radial vels. 77−45443
σ Orionis E, He-rich B star, period and luminosity stability 78−8017
σ Orionis E, mag. field discovery 78−93268
θ^1 Orionis E, suspected variable, photographic photometric obs. 79−58380
FU Orionis mechanism 80−51763
U Orionis OH maser flare detect. 79−40197
YY Orionis stars, UBV photometry 79−44499
YY Orionis stars in Chamaeleon T-assoc. 79−30064
YY Orionis stars in Orion population, UBV photometry of young emission-line objects 80−46552
YY Orionis stars line profiles, spectral line form. in axisymmetric moving envelopes 80−41813

variable stars continued
FU Orionis type stars, eruptive phenomena in early stellar evolution 78−12233
γ Pegasi, β Cephei star, dynamics of photosphere and shells 78−49447
EQ Pegasi, active dwarf binary star, chromospheric emission lines obs. 80−12762
AU Pegasi, binary Type II cepheid, photometric and spectroscopic study 80−26866
DY Pegasi, dwarf Cepheid, revised ephemeris, period decrease 79−67040
57 Pegasi, long-period pulsating variable, spectrographic and photometric obs. 79−21305
AG Pegasi, OAO 2 UV obs. of symbiotic binary 79−53814
RU Pegasi, radial vel. of dwarf nova 79−62833
θ Pegasi, spectrographic obs. of suspected δ Scuti star 78−61867
AG Pegasi, symbiotic binary system, UV and optical spectrum rel. to nature of components 80−109449
AG Pegasi, symbiotic nova, radio emission obs. 77−22232
EQ Pegasi (BD+19°5116), flare active binary system 78−61868
II Pegasi (HD 224085), surface-active binary star, spectroscopic obs. 80−90480
RU Pegasi star fields, comparison star sequence, photometry obs. 80−82433
period determination, maximum entropy method accuracy 80−56712
period determination method *(French)* 78−36465
period-finding technique, Fortran IV computer program 79−21195
X Persei, 13.9 minute periodicity, 3U 0352+30 optical counterpart 77−22247
AX Persei, 1978 Jan.-Feb. outburst of Z Andromedae-type object 78−36588
X Persei, 580 day and other periodicities 78−16435
AW Persei, binary cepheid variable, radial vel. meas. 77−74072
X Persei, BV magnitudes 77−91542
UY Persei, Cepheid, membership of h and χ Persei association 77−74069
UV Persei, dwarf nova, characts. of outbursts 79−71052
RT Persei, eclipsing binary, V light curve 77−53636
X Persei, energy distrib., light vars. 1972-76 period 78−16437
X Persei, IUE obs. of Be-star 80−82383
21 Persei, magnetic variable, Fe, H_γ and H_δ obs. *(Russian)* 77−49388
IW Persei, metallic line ellipsoidal variable, photometric and spectroscopic obs. 80−62186
53 Persei, nonradial mode identification 80−8632
53 Persei, nonradical pulsator, light var. rel. to line profile changes 80−4362
S Persei, periodic nature of semiregular variable 77−67099
X Persei, photometric behaviour, 1964 to 1979, and binary star model 79−53820
1 Persei, photometric variability, possible eclipsing binary 78−32489
S Persei, supergiant 22 GHz H_2O maser emission temporal var. 78−49461
S Persei, supergiant OH maser source, optical radial vel. 77−49378
S Persei, supergiant OH star, conditions for circumstellar OH emission 77−22218
b Persei, UBV photometry and spectroscopic study of ellipsoidal variable 80−36666
53 Persei, undulations of B-type star 78−89201
X Persei, V-band polarization variability 78−49455
GK Persei, visual magnitude estimates (1978 July) 78−69809
GK Persei, X-ray outburst detect. from old nova 79−67033
X Persei (2U 0352+30), photoelec. obs., light vars. 78−40999
X Persei (3U 0352+30), evidence for 581 day modulation in X-ray pulse period 77−53708
X Persei (3U 0352+30), photometry, search for optical 13.9 minute period 78−16426
X Persei (3U 0352+30), reality of massive companion questioned 77−13495
X Persei (4U 0352+30), balloon obs. of hard X-ray flux variability 79−48803
X Persei (4U 0352+30), Be star, evidence for 6-year photometric periodicity 80−109446
X Persei (4U 0352+30), light vars., tidal distortion by massive unseen companion 78−36640
X Persei (A 0535+26), Prognoz-6 obs. of X-ray fluxes and energy spectra *(Russian)* 80−109562
GK Persei (Nova 1901), nearby new X-ray source (Ariel 0327+43) discovery 78−69910
GK Persei (Nova 1901), visual magnitude estimate for 1978 July 78−69807
GK Persei (Nova 1901), visual magnitude estimates for 1978 Jul. 78−73718
V400 Persei (Nova 1974), spectral evolution 78−73715
V400 Persei (Nova Persei 1974), photoelectric obs. 78−4252
TZ and UV Persei star fields, comparison star sequences, photometry obs. 80−82433
PG 2337+12, high latitude blue variable, possible old nova 77−22241
SX Phoenicis, dwarf Cepheid, light and radial vel. vars. 79−25612
SX Phoenicis, dwarf cepheid, spectrum 77−49405
SX Phoenicis, evolutionary stage of RRs star 80−46583
SX Phoenicis, period changes 79−48822
ξ Phoenicis, periodic variability, photometric obs. *(French)* 79−101157
SX Phoenicis, short period dwarf Cepheid, UBV photometric obs. 78−57561
SX Phoenicis, simultaneous photometric and polarimetric obs. 78−49451
ρ Phoenicis, temp. vars. of δ Scuti type star 78−53960
SX Phoenicis light curve, colour effect obs. 78−93248
photoelectric obs. at Mt. Kobau (1970-3) 77−56955
photoelectric photometry, reduction of obs. to standard system *(Russian)* 77−64657
physical and eclipsing variable stars, review of surveys and obs. 80−12772
19 Piscium, C star, violet spectrum line identification and radial vel. 80−82361
53 Piscium, confirmed β Canis Majoris type variable 79−44492
TX Piscium, disc brightness distrib. and envelope obs. from lunar occultation meas. 80−67725
SS Piscium, RRc variable uvbyβ photometry 77−33526
UV Piscium, RS Canum Venaticorum star, identification with X-ray source H0118+067, X-ray obs. 80−101654
SZ Piscium, RS Canum Venaticorum star, photometric obs. rel to starspot model 80−109490
RZ Piscium, UBV photometry, light minima *(Russian)* 78−93323

variable stars continued
planetary nebulae central stars, rapid variability theory 77−45439
planetary nebulae central stars, variability from UV obs. 78−36668
Pleiades region stars, radio and optical obs. of flares *(Russian)* 78−93245
polytropic gas bodies, stability problem *(Chinese)* 79−16937
Population II Cepheids and RR Lyrae stars in globular cluster M19, photographic obs. 78−41002
pulsating star, atm. expansion due to periodic shock waves *(Russian)* 78−93244
pulsating stars, hydromagnetic flow near oscillating porous limiting surface 78−12200
pulsating stars, mixing length theory of convection 77−49367
pulsating stars, modal selection theory rel. to double-mode Cepheids 80−82372
pulsating stars asymptotic theory, boundary layer method 80−82389
pulsation, local stellar stability theory 77−5521
pulsation modes, simple props. 79−35260
pulsation periods of stars with convection zones 77−33499
pulsation rel. to He abundance 78−28690
pulsation theory, recent developments 79−84786
pulsational stabilities of star in thermal imbalance, comparison between methods 78−45316
pulsations, nonlinear coupling 80−62115
pulsations, statistical theory of turbulent convection *(Chinese)* 78−28703
RX Puppis, 2 μm spectroscopy, H_2O and CO absorpt., symbiotic binary model 79−67032
VV Puppis, AM Herculis type binary spectrophotometric obs. 79−5860
BX Puppis, cataclysmic variable, possible member of Hyades-like cluster (NGC 2482) 80−31289
ρ Puppis, chromospheric activity and atm. dynamics of δ Scuti star 77−17581
VV Puppis, dwarf nova, spectroscopic obs. during active phase 79−80322
ρ Puppis, line profile variable, pulsational mode-typing 80−90432
VZ Puppis, long period Cepheid, photometry of nearby OB stars 78−45339
VV Puppis, obs. in faint state 79−25643
RX Puppis, peculiar emission-line object, physical model 78−61871
RX Puppis, peculiar emission-line object, spectrum and UBV photometry 79−44497
VV Puppis, polar, IR photometric obs. 80−98687
L_2 Puppis, semiregular variable, Ca I uneven distrib. from narrowband polarimetry 80−98666
VV Puppis, spectroscopic obs., broad absorpt. features discovery 79−44502
ρ Puppis, temp. and radius vars. 77−49395
R Puppis (HD 62058), G-type supergiant, UBV photometry and variability confirmation 80−41824
CP Puppis (Nova 1942), soft X-ray emission detect. 79−80325
T Pyxidis, recurrent nova, photoelectric obs. 78−4252
PZT suspected variables photoelec. UBV photometry obs. 80−77392
R548, pulsating white dwarf, photometric obs., light curve anal. 78−32488
R548, pulsating white dwarf, photometric props. 77−9742
R 136, central star in 30 Doradus, nebula, variability *(German)* 77−45448
radial and nonradial stellar oscills. effect on light, colour and vel. vars. 80−31310
radio emission survey of variable and peculiar stars 77−22248
radius determ. by Wesselink method, appl. to nonradially oscill. star 79−48824
red dwarfs, double-peaked flare events and solar 'sympathetic' flares 77−56963
red dwarfs, X-ray flares rel. to galactic X-ray background 77−9755
red giant variable stars, multiple periodic vars. 77−87427
red giant variables, in metal-rich globular clusters, near IR photometry 77−45503
red variable star, possible optical candidate of 2S 1702−363, spectroscopic obs. 78−77566
red variable stars, amplitude extension and amplitudes limit 79−62836
red variable stars, narrow-band polarisation effects 78−16427
red variable stars in M13, photometric investigation 77−74104
red variable stars in SMC globular cluster NGC 419, C star content 78−53962
red variable stars in SMC OB association NGC 371, periods 78−53961
red variables, medium-amplitude, UBVRI obs. 77−82224
rotating, variable stars, period-radius-rot. vel. relation 79−2546
RRs and δ Scuti variables, theoretical aspects 77−87433
RRs type variable stars, periods rel. to evolutionary status 77−87432
2S 1702−363 optical counterpart, BV photometry and spectrum 78−54082
S-type stars, list of brightest stars in IR 77−41382
HM Sagitaae, emission-line star, UBV photometry and spectral obs. in (1978) *(Russian)* 80−36648
Sagitta emission variable, photographic magnitudes from Harvard patrol plates 77−2431
FG Sagittae, 1975-8 spectral obs. of peculiar variable 80−72959
WZ Sagittae, 1978-9 outburst of dwarf nova, spectra 80−94801
FG Sagittae, anomalous planetary nebula, spectrophotometry and UBV photometry (1968 to 1977) 79−88687
WZ Sagittae, B mags. and total visual magnitude estimates 79−21308
WZ Sagittae, cataclysmic variable, light curve superhumps model 80−4381
HM Sagittae, continuum spectrum, model, dense nebular around hot star *(Russian)* 78−69814
HM Sagittae, emission line variable, near IR spectrum *(Russian)* 78−81637
HM Sagittae, emission variable, optical spectrograms and IR magnitudes 77−67098
HM Sagittae, emission variable as embryonic planetary nebulae 77−56950
HM Sagittae, emission-line star, polarimetry, (1977 to 1978) *(Russian)* 80−36649
HM Sagittae, emission-line star, spectrum vars. (1978 to 1979) 79−58347
HM Sagittae, emission-line variable star, radio emission detect. 78−28706
WZ Sagittae, eruptive binary, model from hot spot eclipses anal. 80−72962
variable stars continued
HM Sagittae, eruptive BQ forbidden line star, obs. 78−20835
Hm Sagittae, eruptive variable, IR variability 79−25614
FG Sagittae, Fe-peak and s-process elements abundance *(Russian)* 78−12253
WZ Sagittae, image-tube spectroscopic obs. of 1978 Dec. outburst 80−72958
HM Sagittae, IR spectrum 78−93266
V Sagittae, light curve coherent oscills. 78−8022
HM Sagittae, near emission-line object, optical and IR obs. 78−36575
HM Sagittae, new spectroscopic obs., simultaneous presence of increasing excitation and cool features 80−26874
FG Sagittae, nonstable star, spectrophotometric obs. 78−28683
HM Sagittae, photometric and spectroscopic obs. rel. to proto-planetary nebula mass ejection 78−85947
FG Sagittae, photometric radius and pulsation mass 78−36576
FG Sagittae, planetary nebula central star, radial vel. meas. rel. to binary star model 80−98664
HM Sagittae, radio emission flux density 77−60770
WZ Sagittae, recurrent nova, IUE obs. in outburst 80−109448
WZ Sagittae, recurrent nova, spectroscopic obs. and model for superhump phenomena 80−82368
WZ Sagittae, recurrent nova, spectroscopic obs. during 1978 outburst 80−26862
WZ Sagittae, recurrent nova, spectroscopic study during 1978 outburst 80−56849
FG Sagittae, spectral type and element abundances *(Russian)* 78−93281
FG Sagittae, spectrophotometric study of surrounding nebula (PK 60−7°1) 79−40240
WZ Sagittae, spectroscopic obs. (1978 December 1 and 2) 79−16983
WZ Sagittae, spectroscopic obs. and photoelectric V-magnitudes 79−16984
FG Sagittae, spectrum of assoc. nebula 78−49498
HM Sagittae, symbiotic star, IR variability obs. from VJHKL photometry *(Russian)* 80−105263
HM Sagittae, UBV changes and planetary nebula emission lines 77−71120
HM Sagittae, UBV photometry and spectral obs. (1977) *(Russian)* 79−16991
HM Sagittae, variable emission object, spectrophotometry 80−17599
WZ Sagittae, visual magnitude 1979 April 8 79−44508
WZ Sagittae, visual magnitude estimate 1979 June 20 for recurrent nova 79−84800
WZ Sagittae, visual magnitude estimates, 1978 Nov., 1979 Jan.-Feb. 79−30075
WZ Sagittae, visual magnitude estimates, (1978, November 28 to December 11) 79−12481
HM Sagittae, visual magnitude estimates 77−87416
HM Sagittae, young planetary nebula, 2.8 cm flux density secular increase 79−67025
HS Sagittae (Nova 1977), visual magnitude estimates, (1978, August 5 to September 3) 78−89209
HS Sagittae (Nova 1977), visual magnitude estimates 78−61872
HS Sagittae (Nova 1977), visual magnitude estimates 1978 June 78−85961
HM Sagittae as young planetary nebula 79−48801
AQ Sagittarii, C star, ang. dia. from lunar occultation meas. 80−22008
AV Sagittarii, Cepheid, assoc. with open cluster NGC 6546 disproved 79−58387
RY Sagittarii, decline and magnitudes (1977 September-August) 77−87414
V3955 Sagittarii, field RV Tauri/SRd variable 79−88665
MV Sagittarii, H deficient variable, nature of circumstellar envelope 77−9756
V3876 Sagittarii, identified with Nova Sagittarii 1978=IRC−20494 78−49459
VX Sagittarii, IR star, very long baseline interferometric obs. of assoc. OH maser source 77−53699
RY Sagittarii, light-curve at minimum 78−61874
W Sagittarii, magnetic field from Zeeman meas. 78−4240
RY Sagittarii, magnitude estimates for R Coronae Borealis-type star 77−78800
VX Sagittarii, OH/IR star, new SiO transition detect. 78−53954
V1437 Sagittarii, Population II Cepheid, identification and dist. 80−82396
RY Sagittarii, pulsating R Coronae Borealis star, IR variability 77−45462
MV Sagittarii, R Coronae Borealis variable, brightness decline obs. and UBV photometry 80−8641
RY Sagittarii, spectra near min. light 80−36642
VX Sagittarii, supergiant OH maser source, optical radial vel. 77−49378
RY Sagittarii, visual magnitude estimates, 1977, Sept. 77−91541
RY Sagittarii, visual magnitude estimates (1977 Oct.) 77−91543
RY Sagittarii, visual obs. of 1977 Sept.-Oct. minimum 78−49463
VX Sagittarii, VLBI obs. of SiO maser in supergiant 79−92779
V3888 Sagittarii (Nova 1974), line identifications and radial vels. 77−22246
V4021 Sagittarii (Nova 1977), visual magnitude estimates for 1978 May and July 78−69806
σ Scorpii, β Cephei star, Fourier anal. of radial vel. changes 80−105246
3 Scorpii, He weak star, mag. field obs. and rot. period 79−88676
V866 Scorpii, linear polarization obs., wavelength depend., circumstellar dust envelopes 79−53809
KQ Scorpii, long-period Cepheid evidence for membership of OB association 79−88666
V879 Scorpii, M-type long period variable, visible obs. *(Chinese)* 80−85956
U Scorpii, recurrent nova, spectroscopic obs. during outburst 79−75225
V703 Scorpii, RRs variable, photoelectric radial vels. 77−5533
AH Scorpii, supergiant OH star, conditions for circumstellar OH emission 77−22218
V818 Scorpii (Scorpius X-1), Prognoz-6 obs. of X-ray fluxes and energy spectra *(Russian)* 80−109562
V818 Scorpii (Scorpius X-1), rapid variability simultaneous X-ray and optical obs. 80−62322
V818 Scorpii (Scorpius X-1), UV, visible, IR and X-ray obs. 80−82541
Scorpius-Ophiuchus region, discoveries *(Chinese)* 80−77418
Sculptor dwarf spheroidal galaxy, catalogue of 602 variable stars 79−58431
VY Sculptoris, novalike variable, precise position 80−101597

variable stars continued
VY Sculptoris, novalike variable, spectrum during faint state 80−98675
AI, WZ and XX Sculptoris, southern δ Scuti stars, photoelectric study 80−90452
V367 Scuti, double-mode Cepheid, pulsation mass calc. 77−67102
V367 Scuti, double-mode Cepheid in NGC 6649, anomalous open cluster 79−5866
δ Scuti, line profile variable, pulsational mode-typing 80−90432
δ Scuti, temp. and radius vars. 77−49395
V373 Scuti (Nova 1975), spectral evolution 78−73715
δ Scuti and related stars, review 79−62847
δ Scuti and RRs stars, observational view of multiperiodicity 77−87432
δ Scuti and RRs type variables, theoretical aspects 77−87433
V367 Scuti in open cluster NGC 6649, double-mode Cepheid nature 78−49460
δ Scuti stars, absolute energy distribs. 77−17554
δ Scuti stars, empirical period-luminosity-colour relations 79−25610
S Scuti stars, linear survey of models, pulsation 79−35259
δ Scuti stars, oscill. theory and mode coupling 77−5536
δ Scuti stars, period changes in dwarf Cepheids 80−62142
δ Scuti stars, period computation from complex signals *(French)* 78−85949
δ Scuti subgiants, possible model 79−48809
δ Scuti type pulsation, theory for metallic-line stars 79−97004
δ Scuti type stars, dynamical parallax, absolute magnitudes and masses *(Russian)* 79−88690
δ Scuti variables, photometric search of Hyades cluster 80−36677
δ Scuti variables, photometric survey of α Persei cluster 78−93246
δ Scuti variables, southern survey 78−96489
δ Scuti variables, spectrographic obs. of σ Andromedae, θ Pegasi and 2 Lyncis 78−61867
δ Scuti-type stars, chromospheric activity and atom. dynamics 77−17581
semi-detached eclipsing binary systems, revised photometric elements 78−20858
semi-regular variables, SiO 86.2 GHz masers polarisation props. 80−4449
semi-regular variables in stellar groups, absolute magnitudes 77−5537
semiregular, M-type, atmospheric anal., chem. comp. *(Russian)* 78−65623
RT Serpentis, symbiotic star/nova, possible H_2O maser obs. 79−8932
RT Serpentis (Nova 1909), spectrum in 1964, 1975 and (1978) 80−46566
FH Serpentis (Nova 1970), outburst model test 77−82253
FH Serpentis (Nova 1970), radio emission from expanding shell 80−26868
FH Serpentis (Nova 1970), thick inhomogeneous shell model for radio emission 78−12236
FH Serpentis (Nova Serpentis 1970), dust grain IR emission model 80−105254
short-period Cepheid blue variable in M22, photometry 78−85945
short-period variables, max. entropy spectral anal. appl. 78−16436
simulator 77−22357
slow novae and symbiotic stars, late-type components spectral classifications 80−94813
SMC, atlas of variable stars, clusters, emission regions and supergiant stars, book 79−44619
SMC Cepheids, five-colour obs. and comparison with galactic Cepheids 77−29923
solar luminosity variation, Ca H and K behaviour at solar minimum and cycle 21 onset 79−16907
southern hemisphere, variable stars discovery *(Spanish)* 77−64782
spectrum variables, He weak and He strong stars 78−4243
spotted stars, spot sizes 80−41812
SS 433, 10 GHz variability and thermal radio emission hypothesis 80−31307
SS 433, 164^d period as precessional motion, massive black hole and pulsar models 80−62138
SS 433, 180 mm interferometric obs. of triple structure 80−105259
SS 433, 1979 May-June radio flare, 3.24 GHz obs. 80−46567
SS 433, 6.55 day periodicity in emission line wavelengths 80−51784
SS 433, accreting black hole model 80−85958
SS 433, accretion disc viscosity determ. using slaved disc model 80−62110
SS 433, associated filamentary optical nebulosity detect. 79−88723
SS 433, B V photometry and short-term light vars. (1979 July 23 to September 17) 79−101165
SS 433, beam acceleration, radiation and precession theory 80−72971
SS 433, beam models, energetics anal., possible triple system 80−90433
SS 433, binary star model including mag. white dwarf 80−4385
SS 433, change in radio struct., 1980 January to June, from VLBI obs. 80−109557
SS 433, deviations from standard model 80−98669
SS 433, discrepancy between optical and radio positions 80−31303
SS 433, disk-driven precession 80−94803
SS 433, dissipative infall model 80−67749
SS 433, early-type binary model 80−56843
SS 433, emission line radical vels. and no periodic signals 79−80327
SS 433, emission regions and black hole accretion disk 80−67746
SS 433, enormous periodic Doppler shifts obs. 80−17593
SS 433, general spectral features 80−77421
SS 433, Hα blue component wavelength obs. and weak lines interpretations 79−67023
SS 433, Hα emission object, 21.6 and 43 GHz obs. 79−92783
SS 433, Hα radial vel. obs. (1979 July) 79−88674
SS 433, H I absorption obs. and distance 80−56848
SS 433, IR and visible obs., IR excess and emission processes 80−4387
SS 433, IR energy distrib. obs. 80−31312
SS 433, IR light curves from BVIJHK photometry, period and ephemeris 80−8642
SS 433, IR photometry, and search for short period variability 79−58346
SS 433, IR spectral obs., reddening and emission 80−4388
SS 433, IR variability obs. 80−98676
SS 433, kinematic model for line wavelengths vars. 79−75226
SS 433, light curves, double peak and binary-like period, photometry 80−94804
SS 433, light minimum epoch and period 80−26886
SS 433, line posn. vars. interpretation 79−75218
SS 433, magnetic X-ray binary model 80−109447
SS 433, mass accel. and collimation mechanisms 80−4368
variable stars continued
SS 433, mass loss rates and lifetime from W50 optical filaments 80−12804
SS 433, models of supercritical accretion discs around black holes 80−105272
SS 433, nature and evolutionary state *(Russian)* 80−36647
SS 433, near IR (600 to 1100 nm) spectra, 1979 June and September 79−97009
SS 433, near IR spectrum obs. 79−84803
SS 433, nearby faint, highly-contorted nebular filament discovery 80−94855
SS 433, no 6-day periodicity in 1978 June-1980 Feb. obs. period 80−62150
SS 433, Of star orbited by neutron star, model 80−22025
SS 433, photometric and astrometric obs. 79−84801
SS 433, photometry, 1979 July to October, and 6.5 day period identification 80−8643
SS 433, precessing ring model, test by spectral line obs. 79−101152
SS 433, radial vel. curve low amplitude section, visible spectra anal. 80−67737
SS 433, radio and optical obs. 79−88661
SS 433, radio jet discovery 80−31381
SS 433, reality of 6-day periodicity in spectral lines wavelengths var. 80−67743
SS 433, review of obs. and theories 80−72987
SS 433, search for radio spectral lines in UHF 80−109556
SS 433, short term Hα central intensity increases 80−4375
SS 433, spectral features interpreted a precessing neutron star with jets, possible binary 80−90447
SS 433, spectroscopic obs. and probable binary nature 80−51780
SS 433, UV spectral search and 8 GHz linear polarization 79−71048
SS 433, V band photometry and broad min. prediction (1980 April-May) 80−82390
SS 433, visible and IR photometric and polarisation obs. 79−80321
SS 433, visible and JHKL photometry and light vars. periodicity 79−53821
SS 433, VLBI detect. and ang. struct. 80−31304
SS 433 (H 1908+050), X-ray obs. 79−71153
SS 433 (W50), assoc. optical supernova remnant discovery 80−56916
SS 433 as veiled pulsar 80−41842
SS 433 inside SNR, unique spectrum 80−82381
SS 433 model, precessing jets in ultra-close binary system 80−4384
star associated with variable cometary nebula, spectrum and brightening 78−4333
stars in thermal imbalance, vibrational stability 78−40916
stellar and solar flares, review 78−7973
Stepanyan's star, obs. of G8 V absorpt. spectrum and emission spectrum 80−67788
Stepanyan's star, possible cataclysmic variable, eclipses obs. and orbital period refinement 80−62195
Stepanyan's star found to be eclipsing binary, possibly cataclysmic 80−51806
Stephenson-Sanduleak 433, 1.2-2.5 μm spectroscopy, photometry and polarimetry 80−41838
Stephenson-Sanduleak 433, model, precessing ring around massive black hole 79−88678
Stephenson-Sanduleak 433, moving emission features, dynamical models 79−67034
Stephenson-Sanduleak 433, nature, special relativistic effects, binary model 79−88679
Stephenson-Sanduleak 433, possible double jet struct. 79−48827
Stephenson-Sanduleak 433, spectral variability 79−62839
Stephenson-Sanduleak 433, Thomson scatt. lines in spectrum, relativistic gas motions 80−22019
Sun, implications of photosphere struct. and dynamics *(French)* 79−2540
supergiant stars, B2 to G0, small amplitude light vars. 78−32469
supergiant stars, in LMC, long-term light vars. 78−45326
supergiant stars, late-type, in Magellanic Clouds, IR photometry 79−35254
supergiants, semi-period of variation for B2 to G0 type stars 78−61854
supergiants, semi-period-luminosity-colour relation 78−61853
symbiotic star candidates in LMC, optical spectroscopy and IR photometry 80−62139
symbiotic stars, 2 cm emission obs. 78−93274
symbiotic stars, binary model with super-critical accretion 77−45458
symbiotic stars, evolutionary considerations 80−62144
symbiotic stars, magnetic field generation by close binary interaction 80−26903
symbiotic stars, models, spectral characts. *(Polish)* 79−88689
symbiotic stars, obs. of unidentified bands at 6830 and 7088 Å 80−46573
symbiotic stars, survey at 1612 MHz 80−12774
symbiotic stars and slow novae, late-type components spectral classifications 80−94813
symbiotic stars variations, rel. to stability of white dwarfs undergoing spherically symmetric steady-state accretion 80−77402
TASV 030645, possible new variable star in Perseus 78−69810
NML Tauri, airborne IR spectrophotometry, H_2O and CO absorpt. bands 78−32465
41 Tauri, Ap star, Ca II K and Hδ lines rapid vars. *(Russian)* 80−90458
ζ Tauri, Be star, rapid linear polarisation variability *(Russian)* 80−77417
SU Tauri, brightness increase, visual magnitude estimates 77−29852
V711 Tauri, change in nature of light curve, and flare, 1979 October to December 80−26906
SU Tauri, emission lines at min. and BV photoelectric photometry 80−8640
T Tauri, flare obs. in U-band *(Russian)* 77−22228
T Tauri, H_α line profile, fast variations obs. *(French)* 78−61859
T Tauri, Hα line profile vars. 78−40944
DL Tauri, Hα profile in T Tauri type star *(French)* 78−8003
DR Tauri, highly variable young star, spectrometric and photometric obs. 78−20829
T Tauri, integral brightness and Hα emission vars., 1971-77 period *(Russian)* 78−61852
T Tauri, ionisation source of emission nebula *(Russian)* 77−49375
SU Tauri, light curve, Poisson statistics 77−56942
RV Tauri, linear polarization obs., wavelength depend., circumstellar dust envelopes 79−53809

variable stars continued
T Tauri, Lyman continuum energy spectrum rel. to nebula ionisation and emission line spectrum 80−67820
44 Tauri, periodogram analysis of light curves of δ Scuti star 79−84799
DR Tauri, pre-main-sequence star, brightening, 1970 to 1979, and historical light curve 80−31297
SU Tauri, R Coronae Borealis star, photometry in optical and IR ranges 80−101601
SU Tauri, R Coronae Borealis variable, brightening after long minimum, 1980 August to September 80−109438
SU Tauri, R Coronae Borealis variable, fading, visual magnitude obs. 79−92785
V711 Tauri, radio flare on 1978 Nov. 6 at 15.5 GHz 79−5836
T Tauri, rapid Hα vars. nonconfirmation 78−73706
RR Tauri, rapid periodicity, photometric investigations 80−26853
DR Tauri, T Tauri star, Balmer line profile changes and inverse P Cygni profiles 80−101591
DF Tauri, T Tauri star, He I triplet-to-singlet ratio 78−28680
DR Tauri, T Tauri star, mass flow var. in envelope, visible spectra 80−85939
SU Tauri, visible and IR photometry and polarimetry *(Russian)* 78−61860
SU Tauri, visual magnitude esimates 77−37606
SU Tauri, visual magnitude estimates (1977, January-April) 77−53609
44 Tauri δ Scuti star, periods, least-squares determ. 79−62850
V711 Tauri (HR 1099), 1977-1978 photometry before radio outburst 79−21337
V711 Tauri (HR 1099), 1978 photometry during radio outburst 79−21338
V711 Tauri (HR 1099), Ca II and H and K emission enhancement during February 1978 radio flare 79−21341
V711 Tauri (HR 1099), Hα region spectrophotometry during February 1978 radio flare 79−21344
V711 Tauri (HR 1099), H and Ca II emission during February 1978 radio outburst 79−21340
V711 Tauri (HR 1099), Lyman α H I and D I interstellar absorption 80−8658
V711 Tauri (HR 1099), nonthermal flare emission during February 1978 outburst 79−21332
V711 Tauri (HR 1099), optical spectrophotometry during major flare outburst 79−21342
V711 Tauri (HR 1099), rapidly variable polarisation obs. at radio freqs. 79−21336
V711 Tauri (HR 1099), RS Canum Venaticorum binary, Hα profile obs. 79−21343
V711 Tauri (HR 1099), RS Canum Venaticorum binary, radio obs. at 8.0 GHz 79−21331
V711 Tauri (HR 1099), RS Canum Venaticorum binary, strong radio flaring discovery 79−21330
V711 Tauri (HR 1099), RS Canum Venaticorum star, BV light curve during (1978-79) 80−105279
V711 Tauri (HR 1099), RS Canum Venaticorum type binary, strong radio flaring obs. 79−84821
V711 Tauri (HR 1099), two-freq. radio polarimetry 79−21335
V711 Tauri (HR 1099), VLA radio obs. during 1977 international campaign 79−21334
V711 Tauri (HR 1099) and related Ca II emission binaries, Hα emission survey 79−21339
20 Tauri (Maia) and related stars, photometric constancy 79−58338
V471 Tauri (Nova 396 AD), identification of possible outburst *(Russian)* 79−101162
BU Tauri (Pleione), envelope behaviour in 1976, spectroscopic obs. 80−8636
BU=28 Tauri (Pleione), envelope during shell phase, 1972-75 period 78−28707
BU Tauri (Pleione), in Pleiades, Hα and O I photometry 79−35315
BU Tauri (Pleione), metallic-line shell spectrum anal., (1973-1976) 80−8637
BU=28Tauri (Pleione), spectral var. during 1969-1975 period 77−33532
BU=28 Tauri (Pleione), spectrum vars., 1938-75 period 78−36578
BU = 28 Tauri (Pleione), UBV obs. and light curve 77−56979
BU Tauri (Pleione), UV photometry during shell phase 77−64768
BU Tauri (Pleione), wavelength depend. of polarisation 77−45500
28=BU Tauri (Pleione) Be shell star, 3167 to 4924 Å spectrum atlas 80−98673
RV Tauri and yellow semiregular variables, photometric investigations 80−26865
T Tauri like stars, far UV photometry 78−20827
T Tauri star, extremely young, and assoc. nebula, fading 78−93236
T Tauri star formation, regulatory force in dark mol. cloud evolution 80−85980
T Tauri star groups enveloped by small dense molecular clouds 79−58400
T Tauri stars, effects of D burning on early evolution and outbursts 80−51736
T Tauri stars, for UV radiation *(Russian, English)* 79−75217
T Tauri stars, gas flow from line profiles 79−67004
T Tauri stars, H_2 emission obs. 78−93230
T Tauri stars, Hα emission line core formation in chromosphere 80−94792
T Tauri stars, infall model 77−13329
T Tauri stars, location in (J-H), (H-K) diagram 77−78790
T Tauri stars, OH and NH_3 emission line obs. 79−25662
T Tauri stars, optical luminosity mechanism and FU Orionis type flares *(Russian)* 77−22229
T Tauri stars, outflowing envelopes models 78−96482
T Tauri stars, photometric and spectral props. 79−21282
T Tauri stars, photometric vars. 77−9741
T Tauri stars, radial vels. and spectral types 77−56921
T Tauri stars, role of accretion disks *(Polish)* 80−26739
T Tauri stars, seven-colour TV photometry, obs. methods *(Russian)* 77−64756
T Tauri stars, seven-colour TV photometry, variability *(Russian)* 77−64757
T Tauri stars, subgroups on two colour diagram 79−71041
T Tauri stars ρ Ophiuchi dark cloud, photometry obs. 80−72942
T Tauri stars among new Hα stars in NGC 2264 and NGC 7000/IC 5070 regions 80−62120
T Tauri stars and Herbig Ae-Be stars, broad-band IR photometry 78−4217
T Tauri stars and related objects, IR meas. 78−8002
variable stars continued
T Tauri stars and related objects, UBV photometry 79−44499
T Tauri stars assoc. with Taurus-Auriga dark clouds, proper motions 80−41821
T Tauri stars atmospheres, sphere and low chromosphere model 80−36623
T Tauri stars in dust cloud Lynds 134, mass loss causing cloud turbulence 80−94845
T Tauri stars in mol. cloud in NGC 2264, nearby OH and NH_3 obs. 80−94847
T Tauri stars in Orion Nebula (M42), possible coronal X-ray emission obs. 78−28852
T Tauri stars in Orion population UBV photometry of young emission-line objects 80−46552
T Tauri stars near Herbig-Haro objects, obs. during search for exciting stars 80−67720
T Tauri type stars, hydromag. model of peculiar activity *(Russian)* 78−49442
T Tauri-like stars in Taurus dark cloud complex, IR study 79−8963
RR Telescopic, spectra, rel. to term anal. of Fe IV 78−82677
RR Telescopii, C III spectral lines, IUE obs. 79−71089
BL Telescopii, eclipsing binary, unusual variability of bright supergiant companion 77−64797
RR Telescopii, slow nova and symbiotic stars 77−82256
RR Telescopii, symbiotic star, steam and CO absorpt. obs. 78−40970
BL Telescopii A, yellow variable supergiant near Cepheid instability strip, VBLUW photometry 80−98672
Tr 27-102 (HD 159378), possible long-period Cepheid 78−45336
R Trianguli, Mira variable, narrow-band polarimetry 79−25617
U Trianguli Australis, beat Cepheid, mode interaction 78−4235
U Trianguli Australis, double-mode Cepheid, mass, luminosity and evolution 77−29845
U Trianguli Australis, Fourier anal. of beat Cepheid 78−69811
EK Trianguli Australis, SU Ursae Majoris dwarf nova, superhumps, light curve UBV obs. 80−105255
U Trianguli Australis, UBVRI obs. of beat Cepheid, pulsation energy changes 80−4360
U Trianguli Australis, UBVRI obs. of beat Cepheid 79−53833
4U 1626-67 optical candidate, optical pulsations discovery 78−65720
4 U 2129+47 optical counterpart, spectrum and photometry rel. to 80−17693
UBV photometry, at geographic latat. 69°22′ north 79−44376
UBV photometry for N.Norway during auroral activity, technique and results 79−40084
unpublished observations, IAU archives and 1978-79 data 79−88688
CQ Ursae Majoris, Ap star, UBV photometry, light curves, colour indices 78−49454
UX Ursae Majoris, eclipsing nova-like variable, time-series photometry 80−77446
AN Ursae Majoris, nova-like variable, extremely high circular polarisation obs. 78−8018
AN Ursae Majoris, polar, IR photometric obs. 80−98687
SU Ursae Majoris, probable 1980 March super outburst 80−51785
SU Ursae Majoris, soft X-ray halo around dwarf nova 80−98677
AN Ursae Majoris, steady low luminosity state 79−40219
SU Ursae Majoris stars, important sub-group of dwarf novae, photometric props. 80−101596
γ Ursae Minoris, high dispersion spectroscopy 80−41853
α Ursae Minoris (Polaris), interstellar reddening from field stars uvbyβ photometry 79−58356
α Ursae Minoris A (Polaris A), interstellar reddening determ. 78−8005
V1341 Cygni (Cygnus X-2), X-ray polarisation obs. from OSO 8 80−90571
V1357 Cygni (Cygnus X-1), X-ray polarisation obs. from OSO 8 80−90571
V80 in dwarf spheroidal galaxy in Ursa Minor, eclipsing binary star with RRc primary 80−109505
AH Velorum, Cepheid, radial vel. study, possible binary, coude spectrograms 77−49394
AH Velorum, classical cepheid, binary detect., UBV obs. 80−109443
AI Velorum, dwarf Cepheid, nature from uvbyβ photometry 77−78801
SW Velorum, long-period Cepheid evidence for membership of OB association 79−88666
AI Velorum, nature from BVRI photometry and photoelectric radial vels. 80−94815
AI Velorum, oscills., pulsation models 79−48813
AH Velorum, radius, delta luminosity and pulsation mode of δ Cepheid 80−46572
AI Velorum, RRs variable, photoelectric radial vels. 77−5533
γ^2 Velorum, WR binary, photometry and polarimetry 77−29847
vibrating white dwarfs, ultra-short var. 79−21287
vibrational stability of stars in thermal imbalance, energy methods 77−13320
α Virginis, β Cephei type pulsation characts. 80−56835
32 Virginis, A-type main-sequence and Am-type star components 79−30091
α Virginis, Copernicus UV obs. 77−33502
α Virginis, decline of β Canis Majoris pulsation 79−12482
EQ Virginis, dK5e star, new absorpt. line obs., possible infalling gas 77−37602
EQ Virginis, dMe flare star, chromosphere model and activity 79−48773
EQ Virginis, dwarf binary, flare star, rotational hypothesis for quasi-sinusoidal light variations 78−4234
XX Virginis, field Population II Cepheid, absolute mag. 80−41832
CU Virginis, He I 4026 Å line var., photoelectric meas. 78−77555
CU Virginis, He spectrum variable, UV photometry with ANS 78−36585
EQ Virginis, late type dwarf flare star, temp. minima, chromosphere model 80−67717
EQ Virginis, late-type flare star, metal abundances 77−78779
AR Virginis, RR Lyrae variable, photographic photometry and mean light curve *(Russian)* 80−12769
XX Virginis, Stromgren uvbyβ photometry of field BL Herculis star 78−85954
CU Virginis (HD 124224), Ap star, spectrophotometric obs. 80−98663
W Virginis stars, in southern hemisphere, VBI photometry 77−53612
virial energetic pulsations rel. to brightness vars. 79−48665
visual binaries with variable components, orbital elements, visible obs. *(Russian)* 80−77455
S Vulpeculae, 67 day Cepheid, case for membership in (Vulpecula OB2) 80−41831

variable stars continued
SV Vulpeculae, Cepheid, period change meas. rel. to evolution 79 92777
WW Vulpeculae, fast irregular variable, H_α and H_β lines obs. *(Russian)* 77−87400
21 Vulpeculae, new luminous long period δ Scuti star, photometry 80−31306
BW Vulpeculae, UV light curve of β Cephei-type star 78−36570
BW Vulpeculae, V photometry, light curve, quadratic ephemeris 80−26881
NQ Vulpeculae, visual magnitude estimates (1977, January-February) 77−29853
LV Vulpeculae (Nova 1968 No.1), spectroscopy 77−87438
NQ Vulpeculae (Nova 1976), CO emission and η Carinae stage 79−25609
NQ Vulpeculae (Nova 1976), Hα emission line profiles in 1976 November to December *(Russian)* 78−40971
NQ Vulpeculae (Nova 1976), Hα var. 79−58352
NQ Vulpeculae (Nova 1976), IR photometry, dust form. in exploded shell 79−48832
NQ Vulpeculae (Nova 1976), isothermal dust condensation phase, broad-band photometry 78−36586
NQ Vulpeculae (Nova 1976), spectral evolution 78−89205
NQ Vulpeculae (Nova 1976), UV and visual spectra analysis *(Chinese)* 80−12770
NQ Vulpeculae (Nova 1976), visual magnitude estimates 77−22254
NQ Vulpeculae (Nova 1976), visual magnitude estimates (1977 June 20-July 27) 77−74064
NQ Vulpeculae (Nova 1976), visual magnitude estimates for 1978 Aug.-Oct. 79−5839
NQ Vulpeculae (Nova 1976), visual magnitudes, 1977 Nov.-1978 Jun. 78−65626
NQ Vulpeculae (Nova 1976), visual magnitudes (1978 June 29 to July 13) 78−85959
NQ Vulpeculae (Nova 1976), X-ray emission upper limits, Ariel V data 77−64781
NQ Vulpeculae (Nova Vulpeculae 1976), photometric obs., visual magnitudes 77−60767
NQ Vulpeculae (Nova Vulpeculae 1976), spectroscopic obs. of slow nova 78−85955
NQ Vulpeculae (Nova Vulpeculae 1976), visual magnitude estimates (1977, April-May) 77−53610
NQ Vulpeculae (Nova Vulpreculae 1976), visual magnitudes (1977 Aug.-Nov.) 78−16434
white dwarf variable stars, multiple periodicities 77−87434
white dwarfs, nonradial nonadiabatic oscillations 77−56925
white dwarfs, pulsating, thermal stability of H burning shells 78−40929
white dwarfs, pulsational props. of high-luminosity He burning degenerate stars 77−5519
Wolf 424, UV Ceti-type flare star, simultaneous 1420 MHz and optical obs. of flares 78−49464
Wolf 630, visual multiple system including dwarf or degenerate stars 79−17019
Wolf-Rayet stars, ANS obs. of UV variability 78−65632
Wolf-Rayet stars, search for rapid Hα and Hβ line variability 77−26014
Wolf-Rayet stars in SMC, spectral classification 78−73716
WRA 977, high-speed UV photometry of periodic modulation 78−16442
Wray 977, optical counterpart to X-ray binary pulsar, 4U 1223−62, optical spectra 80−72984
X-ray sources, light and X-ray vars. rel. to masses 78−12430
X-ray sources optical counterparts, appl. of simultaneous fast double head UBV photometer 80−72775
yellow semiregular and RV Tauri variables, photometric investigations 80−26865
young emission line objects in S Hemisphere, image tube spectrograms 78−8016
young stars, absorpt. and emission features, IR spectrophotometry obs. 80−72954
young stars, circumstellar mols. 80−22013
young stars, nonspherical thermal instability 79−48779
ZB 33, RR Lyrae type star, light curve study *(Chinese)* 80−8633
Be-stars, TV obs. of Hα and Hβ line profile rapid vars. *(Russian)* 79−16992
C star, variable, in open cluster, Stock 8, spectroscopic and photometric obs. 79−84791
C stars, $^{12}C/^{13}C$ ratios 79−35257
C stars, 3.9 micron absorpt. band identification 78−93231
C stars, enhanced C abundances in long-period variables 77−33501
C stars, form. of carbyne and cyanoacetylene in stellar atm. 80−67708
C stars, IJHKL photometry obs. 80−98657
C stars, N-type, luminosity and C enhancement 78−93247
SS Cygni, soft X-ray emission detect. during optical outburst 80−46574
U Geminorum, soft X-ray emission detect. during optical outburst 80−46574
H deficient and He weak stars, uvby photometry, variability 80−46579
H_2O masers, detect. of new sources 78−32466
H_2O masers assoc. with late-type stars, structure 79−71037
Hα emission line star near Gum nebula, UBVRI photometry and variability 78−32449
Hα emission stars in and near NGC 7000, search for variability 77−13363
Hα emission stars in southern dark clouds, UBVR photometry 78−81633
Hα-emission stars in Perseus OB1 assoc. region 80−56855
He rich stars, intermediate and extreme, spectral atlas in 3700 to 4600 Å range 80−94806
He variable stars, IR excesses obs. 80−67733
He weak and He strong stars, spectrum variability 79−40201
RR Lyrae stars in Sonneberg fields near north galactic pole, distances, density distrib. 77−82229
OH 26.5+0.6, late-type variable star, spectrophotometry from 2 to 40 microns 78−24568
OH large-scale sky survey at 1612 MHz 78−32358
OH Mira variables, light curve shapes rel. to mass loss 77−56944
OH/IR unidentified Type II stars, galactic distrib. and kinematics from 1612 MHz survey 78−49450
OH-IR stars, time var., correl. with visual magnitude 77−60764
Si stars, UVBY photometry, variability obs. 77−22233
SiO maser emission obs. in eight long-period variables 78−4225
Tc stars, search for TcO spectral bands 78−40935

variable structure systems
see also multivariable systems
hybrid simulation 77−41470

variational calculus *see variational techniques*

variational techniques
(2+1) dimensional compact QED, combined WKB-variational method, vacuum tunnelling 80−101960
$\lambda\phi^4$, spontaneous symmetry breakdown, approx. ground state, variational approach 77−79229
AB_2, bent molecule, ab initio force fields, appl. of Simons-Parr-Finlan expansions 79−41218
ablation of elastic solid, variational principle 78−90698
acetylene, mean polarisability derivatives, variational calc. procedure 79−27108
acoustic deformation pot. polarons, linear energy-momentum relations 80−80196
acoustic resonator variational soln. using field-source reaction concept 79−55302
acoustic wave propagation, in nonuniform ducts, wave-envelope technique 78−9464
adsorption system surface properties variational calcs., binding energy, Lang model 80−29279
aerodynamic ablation of melting bodies, effect of temp.-depend. heat capacity 79−37431
air pollution diffusion transport, variational imbedding calc. method 77−73785
airborne clock synchronisation by minimum variance methods 77−37853
alkali metal atom, valence electron ground states, model potentials 78−50476
alkali metal atoms, calc. of Van der Waals energies, variation-perturbation method 77−510
alkali metal hydride, variational time-dependent H-F calcs. in pseudopot. framework 77−10588
alkali metal ion, with filled shell, dipole polarisability 80−9501
alkaline earth positive ions, valence electron ground states, model potentials 78−50476
alloys, dilute mag., local moment formation, nonequivalent orbitals model 80−11164
amorphous Heisenberg ferromagnet, variational cluster method 80−39728
analogy between dynamics and statics, related by variational techniques 78−28934
analytic radial orbitals, optimisation on variational parameters 80−42941
Anderson model, ground state, var. trial function approach 80−59913
Anderson model, ground-state energy 79−99511
Anderson model, impurity pair interactions, local moment form., var. method 80−92854
anharmonic oscillator, classical, variational method test, sp. ht., elec. susceptibility and oscillation freq. *(Portuguese)* 80−77611
anharmonic oscillator, computation of energy eigenvalues of Hamiltonian 80−12925
anharmonic oscillator, trial Hamiltonians for quantum statistical treatment 80−77652
anisotropic and laminated plates, dynamic response, variational method, general functional 77−3770
anisotropic antiferromagnet, phase transition, with external mag. field 79−11316
anisotropic reinforced plate, stress distrib. near recesses, variational anal. *(Russian)* 79−27521
anisotropic thermoelastic shells dynamical coupled problem, variational theorem *(Russian)* 79−14255
apodizing filters for optimum Sparrow resolution in coherent systems with annular aperture 80−53435
approximately relativistic Lagrangians for classical interacting point particles 78−54179
astrodynamics, perturbed boundary-value problems, variational formulae 79−21161
atmospheric diffusion transport models, variational imbedding soln. 77−37381
atom, bound state quantum fluctuations and variational method, relativistic HF calc. with radiative effects 80−42918
atom, dynamic multipole polarisability, hydrodynamic model, variational approximations 80−23340
atom, symmetric deorthogonalisation 78−37540
atom, two-electron, dynamic polarisability calc. 77−14599
atom+atom, resonance energies, complex, diverging wave functions, least squares bivariational method 78−17741
atom+diatom collinear collisions, exponentiating trajectories and statistical behaviour, variational eqns. 78−27742
atom+ion scattering, Schwinger variational principle 79−45780
atom electron scattering length calc. with imprecise target wave function, variation principle 79−72375
atom-ion collision, polarisation and energy loss by time-depend. method 79−59536
atomic and molecular computations, containing nonlinear parameters, nonexistence of maxima 79−6816
atomic and molecular structure, metric-constrained method 79−22579
atomic correlation energies calc., Wilson's scaling parameter evaluation 80−5486
atomic dynamic polarisability, variational calc. 78−22047
atomic dynamic polarisability, variational calcs. with mode pot. *(Russian)* 78−902
atomic electron scatt., modified variational method 78−1081
atomic electron scatt. length, target ground-state wave function imprecisely known, variational principle 77−58164
atomic electron scattering, resonant scattering, complex-coordinate method 79−86070
atomic electron scattering, Schwinger variational principle 79−45780
atomic excited state structure, electron correl., var. collapse theory 79−6890
atomic independent particle pots. comparison 80−52846
atomic resonance theory, appl. to two-level at. S autoionising states 80−23329
atomic Rydberg states, Coulomb and Yukawa pot., wave functions and quantum defects, Schwinger's var. principle 80−63549
atomic scattering, variational methods appls., review 78−86951
atomic state, single-term, $2<Z<55$, props. by variationally optimised local central pot. calcs. 79−41123
atomic structure, variational technique,73 variational technique, for two-electron atom, for teachers 79−21505

variational techniques continued
atomic three-body systems, channel coupling array theory 77−19005
atoms, approximate and exact state wavefunctions, ionisation potentials, energy difference calcs. 79−97967
atoms, perturbation var. calc. with contact interaction, effect of approx. zero order wavefunctions 80−58107
atoms, two-body correls., variational approach 80−91455
atoms, variation-iteration procedure, by numerical integration scheme 78−17551
atoms and molecules, second-order properties, coupled perturbed Hartree-Fock method improvement 80−58148
atoms of Group IIb, dipole polarisabilities from compact variational trial functions 80−63568
attenuation of solns. to eqns *(Russian)* 78−65753
Auger decay theory at. orbital non-orthogonality, Wentzel Ansatz 77−18871
avoided crossings, for exact states, model calcs., theory 79−10156
avoided-crossings, spurious, variationally calc., perturbation theory approach 78−5295
axisymmetric heat exchange, variational method *(Ukrainian)* 78−1547
Bach-Lanczos identity derivation from modified Hilbert variational principle 78−32737
band structure, generalised APW method using variational expression 80−6695
baryonium four body problem, Schrodinger eqn. soln. by stochastic variational method 79−36008
basis states generation by variational methods 78−78295
beam, initially stressed hyperelastic, incremental motion from variational principle 79−68638
beam, unilaterally constrained, Euler critical and buckling load, variational theory 79−37203
beam in transverse vibr., optimisation of higher order eigenfrequencies 77−78971
beam torsional vibration frequency optimisation 78−83288
beams, thin walls, stress-strain state determ., method of segments 80−28424
Beck's rod, nonconservative flutter system, variational principle 79−1132
bending, of plate, powerful finite element method for computing 78−1583
bending, plates, bilinear and biquadratic quadrilaterals, variational principles, numerical convergence 80−48576
bending of plates, finite difference variational method 80−92045
bending of thin plates, finite element anal., variational principle, simplified modified potential energy technique 80−52029
benzene, ab initio model calc., variational 77−46492
benzene, dynamic polarisabilities, calcs., superposition method of excited config., nonstationary perturbation theory eqns. 80−69257
benzene, electronic struct., mag. susceptibilities, ab initio calcs. 78−74571
biexcitons, symmetric trial function 77−68142
bifurcation from rotationally invariant states 78−77671
bimetal rolling, calc. of strains by variational method *(Polish)* 80−45323
binary boson system, ground state props., appl. to dil. ^{3}He-superfluid ^{4}He mixtures 79−73372
Biot's variational principle, consequence of invariance in thermal cond. 78−33988
bistability and anomalies in absorption and resonance scattering of intense light 79−95803
Bloch unified nuclear reaction theory, variational principle 77−14083
bond and site percolation, renormalisation group results 79−149
book, variational methods and appl. 78−81809
Bose gas, hard-disc, low density, two-dimens. many-body problem 78−95195
Bose system, Jastrow wavefunction, hypernetted chain method 80−17866
boson matter, Euler-Lagrange equations and hypernetted chain calcs. 79−40871
boson mixtures, binary, ground state configs. 80−105570
boson scattering, variational method 79−255
Boson system, hard spheres, condensed phase, Jastrow wave function 78−84018
boson system, many particle, radial distribution function, functional derivative 78−137
bound excitons, ground state energies for all mass ratios 79−60729
bound polaron, non-perturbative variational method 80−88485
bound states in quantum mechs. and AFT, eqns. of motion, variational principles, WKB approx. 78−54540
boundary layer, Gyarmati principle appl. 79−3993
boundary problems in static elasticity, distortion trivector pot., variational principle *(Russian)* 80−79146
boundary value problems, stability evidence 77−84167
boundary value problems with constraints, solution by direct method 77−22386
boundary-value problems, variational principles and hypercircle 78−57749
boundary-value problems for cracks and seepage 78−83331
boundedness, definiteness of functional eqn. for nonconforming trial functions, finite element method, variational principle 79−2608
bounds to excited states from generalised Brillouin-Wigner eqn. 78−45507
buckling, stability anal. of rectangular plates, complementary energy method 80−48611
buckling, unilateral, of thin plate, variational techniques *(French)* 80−74780
CANDU, optimum burnup distribution in a continuously fueled reactor 79−36305
cantilever minimum weight design with plural torsional frequency constraints 79−68629
cantilever plate flexure, variational method *(Russian)* 79−7310
capillary surface problems with prescribed contact angle, max. and min. principles 79−37907
carbonyl compounds, metastable triplet states, var. and perturbational calcs. 77−61680
catastrophes and bifurcations in variational problems 80−8789
causality and relativity 78−81901
celestial mechanics, ELP soln. of Moon main problem *(French)* 80−62044
cellular model for mol. and cryst. elec. struct. 78−29726
charge transfer, variationally consistent approximation scheme 79−22825
chemical equilibria, variational principle 77−36780
variational techniques continued
chemical equilibrium, optimal physical cluster definition *(Russian)* 79−61895
chemical kinetics, eigenvalue and eigenfunction anal. of Kramer's theory 79−29330
chemical reactions, decomposition theory, transition matrices, var. calcs. 78−20005
chemical reactivity, multiple site, interaction field modified Hamiltonian method 78−11498
CIDN(E)P, infinite elements, in variational soln. of stochastic-Liouville eqn. 79−94014
circular plates of variable thickness, variational approach to static and dynamic behaviour 77−75841
clamped-free rod subjected to tangential follower forces 79−50594
classical mechanics, new variational approach 77−71206
classical mechanics, numerical methods, Newtonian, Lagrangian and Hamiltonian mechanics, book 79−63024
classical systems, particle distrib. function, theoretical method 80−64856
classical systems with non-integrable constraints, quantisation 80−36901
climate models stability estimate *(Russian)* 78−69437
closed-shell atoms, Jastrow wave functions, var. calcs. 80−83249
cluster expansion formalism, independ. pair correlations 78−73922
cluster variational calcs. for extended nuclear systems 77−6279
collapsing bubble attached to solid wall 79−68791
collective inertiae, in variational frameworks, canonical approach for auxiliary Hamiltonian *(French)* 77−87657
collective open chemical systems, variational-Lagrangian thermodynamics of evolution 78−41255
collocation variational method for solving Fredholm integral eqns., convergence condition 78−57764
complementary variational principles, review 78−41135
complementary variational principles for Maxwell's equations 80−32876
complementary variational principles for Maxwell's equations 80−99603
complex eigenfrequencies 80−28631
complex meas. system error correlation matrix *(Russian)* 77−9979
complex nuclei scatt., variational method in RGM based on GCM kernel 78−564
composite particle scattering, generator coord. method, Kohn-Hulthen variational principle 77−2957
compressible finitely conducting rotating fluid in mag. field, Rayleigh-Taylor instability 80−10228
compressible flow, variational principle and finite element method 79−46336
compressible heavy fluid, variational principle 78−83426
computational methods, book 78−81820
conductivity of inhomogeneous media with macroscopic inclusions 80−49685
configuration interaction, iterative variational method calcs. 78−55127
conformal invariance of multiple integral var. problem 77−71222
conservation equation, numerical soln. by variational approach, mass transfer problem appl. *(French)* 80−19317
constant mean curvature and canonical time, concept generalisation 78−98
contact problems with slip and cohesion 78−63398
container subjected to forced pitching oscillation, liquid motion, nonlinear anal. 80−96270
continuous medium and grav. field, eqns. of state from variational method 80−42122
continuous quantum systems, variational principle for pressure, entropy, free energy, convexity consequences 79−40453
continuous renormalisation transformation, variational calcs., rel. to Potts model 78−93618
convection, natural, laminar, in open vertical channel, numerical soln. method 78−5799
convex analysis and variational inequalities *(Japanese)* 80−77606
correlated electronic wavefunctions, Schrodinger eqn. variational form, generalised k-particle Brillouin conditions 79−81146
cosmological principle appl. to variation methods for Friedmann universes *(French)* 80−77529
cosmology, Lagrangian or Hamiltonian formulations, shift vector field restrictions, symmetry group 80−67923
cosmology, maximum information universe 79−30157
cosmology, Newtonian, generalised Clebsch representation for velocity field of fluid, variational formulation 80−51930
coupled channel variational method for microscopic study of reactions between complex nuclei 79−13263
coupled channel variational method for multi-step direct nuclear reactions. I. Formalism and numerical test 78−66258
coupled fluid-structure systems, vibrations, substructure element variational anal. 79−55333
coupled-evolutional system, variational calc. of vibr., appl. to ARIANE launcher *(French)* 77−72234
covalent semiconductor, valence band calc. using many-electron theory 80−15434
covalent semiconductors, electronic struct. of localised defects, review 80−44535
covariant inverse problem of calculus of variations, corrigendum 78−77773
covariant reverse problems of variational calculus 77−74278
creep, generalised variational principles, Lagrange multiplier method applied to flow theory *(Chinese)* 80−79171
creeping flow in closed cylindrical cavity, numerical calculation 80−16976
critical exponents in three dimensions, derivation from ϕ^4 field theory with Gaussian propagator 80−4686
critical principal connections and gauge-invariance 79−6287
crystal band struct., variational cellular method, electronic struct. calcs. 80−54591
crystal with many particle interactions, variational quasiharmonic approx. *(Russian)* 77−11642
crystals, Schrodinger eqn. calcs. variational cellular method, general formulation 78−94192
cubic semiconductor, Zeeman split acceptor levels, calc. method 79−28322
cylindrical shell, buckling, combined action of axial compression and internal pressure 80−28447
cylindrical shell with elliptic cross section, subject to torsion, creep buckling 78−34040
D^--centre electronic struct. in strong mag. field 78−51928
dam seepage, variational inequality appl. to flow through porous media 80−100028

variational techniques continued
DC plasmatron with axially-blown arc, optimisation *(Russian)* 77−39476
deformable solids, variational theorems for thermodiffusion *(Russian)* 78−62169
deformation energy of nuclei, one particle spectrum, self consistent calcs., Hartree Fock variational method 78−12957
deformation potential polaron, perturbation theory breakdown 80−84440
degenerate semiconductors, ionised impurity scattering cross-section, variational calc. 80−20180
degenerate semiconductors, longitudinal thermo-EMF in quantising mag. field, scatt. mechanism *(Russian)* 80−24960
dense Fermi systems, energy expectation values, numerical study of Fermi hypernetted chain method 79−40874
density functionals in unrestricted Hartree-Fock theory 79−89583
density matrix equation, macroscopic cell representation and optimal choice of projectors by variational principle 77−74321
density operators, time depend., var. principle, rel. to linear decoupling procedures for propagators 80−63514
diamond and sphalerite type crystals, with spin-orbit interaction, indirect exciton energy levels 80−24804
diamond semiconductors, electronic structure, self consistent local description 80−20067
diamond-type crystals, energy levels of Mott excitons 78−6282
diatomic molecule, electron scatt., low energy, multichannel variational calcs., static exchange approx. 80−83483
diatomic molecule, vibr. energies and functions, cubic splines method calcs. 80−78594
diatomic transition operators, L^2 basis expansions 80−63519
diatonic molecules, Stark effect variational and perturbational calcs. 80−1022
dielectric particles, variational principle for light scatt. 79−18348
dielectrics, hyperelastic, with saturated polarisation, variational and invariance principles 80−74730
diffused optical waveguide mode analysis 77−88956
diffusion, nonlinear, stability 78−8366
diffusion approximated model neuron firing interval moments 78−96041
diffusion coefficient measurement in solid materials, geometry factor from variational principles 79−42290
diffusion eqns., finite element anal. *(French)* 77−78965
diffusion equation, soln. by mixed finite elements *(French)* 77−71283
diffusion-controlled defect recombination, quasi-steady radius, tunnelling and elastic interaction *(Russian)* 80−10908
direct method appl. to mixed boundary-value problems 77−67252
Dirichlet forms, construction of stochastic processes 80−8921
discrete variational Xα cluster calculations, applic. to metal clusters 78−90332
disordered system, diamag. susceptibility, variational calcs. 77−8265
disordered systems, density of states, variational melthod 80−49565
dissector one-electron current pulse timing, delayed self-coincidence method 79−26846
dissipative materials, deform. stresses, shape, using variational principle *(Japanese)* 77−23896
Djukic-Vujanovic method, reln. to classical variational methods 77−13578
drift wave eigenvalues, variational calc. 79−68920
dual extremum principles for heat transfer problems with variable thermal props. 78−66999
dual variational principles 78−77676
dynamic variation principle taking into account geometric nonlinearity 79−23227
dynamical systems, Clebsch potentials and variational principles 78−24657
Dyson eqn., exact soln. for mean value of Green's function 78−4559
Earth crust radiogenic heat production, depth depend. modelling by variational approach 80−72464
Earth EM induction, model refinement for one-dimensional problem 79−44096
eddy current calc. in thin conducting plates 78−90341
eddy current losses in thin conducting sheets 79−41296
edge resonance in semi-infinite plate, variational anal. 77−78987
education, classical mechanics, Hamilton's principle, variational formulation approx. solns., simple pendulum 77−33774
education, soap film on wire frame in zero gravity, variation problem branching 79−9057
effective action, quantum mechanical definition using time depend. variational principle 80−57457
eigenvalue problems with a parameter 79−77338
eigenvalues characterisation, orthonormality-constrained variation method 78−45457
eigenvalues lower bounds for quantum Hamiltonians, classical limit of quantum theories 78−41200
eikonal eqn., underlying geom. struct. 77−60957
Einstein-Cartan generalised theory, field eqns. and contracted Bianchi identities 79−12681
Einstein-Cartan theory of gravitation, generalized 78−73895
elastic beams hung at both ends, lateral buckling, variational anal. methods 79−86361
elastic design problems, optimality, iterative solutions, finite element analysis and variational method 80−23887
elastic flexible body dynamics, finite element anal., Hamilton's principle 78−24667
elastic incompressible body, contact problems involving forces and moments, rigid punch problems 80−53719
elastic medium, extremum problem for distributed parameter, and determ. of optimum props. 79−88811
elastic plate stability conditions, variational formulations 80−69701
elastic plates, annular, clamped edges, asymmetric bending, Ritz method 80−58907
elastic scattering, reson. width, stabilisation method 77−19011
elastic sheel, cylindrical, closed, laminated, longitudinal crack, elastic eqn., energy approach *(Russian)* 80−87740
elastic stability, cantilevers, flutter load, discontinuity, variational technique 80−58944
elastic stress analysis of constrained cylinders by special finite element method 80−106718
elastic wave propagation in fibre reinforced composite rectangular rods *(French)* 80−83749
elastic-plastic body, min. principles and strain uniqueness, stress fields 77−3734
elastic-plastic body, strain and stress fields, min. principles 77−3735
variational techniques continued
elastic-plastic solid, operator method for variational principles *(Polish)* 77−54898
elastic-plastic torsion, variational inequality concept, finite element anal. 80−23907
elastic-viscoplastic boundary value problem, stress anal. variational method 77−35051
elasticity, beam bending on Pasternak foundation, reciprocal variational inequalities 80−92091
elasticity, local effects and energy methods *(Chinese)* 80−42060
elasticity, one-dimens. problems, diagonal mass matrices and finite element eqns. 78−73857
elasticity, variational formulation of integral eqns. *(French)* 77−72181
elasticity theory, finite element formulation 78−69985
elastodynamics, time harmonic, pointwise variational principle for mixed boundary value problems 80−31510
elastokinetics and elastostability, equation structure from D'Alemberts principle *(German)* 79−63046
elastoplastic shell bifurcation loads *(German)* 77−42755
elastoplasticity, finite strain, rate problems, energy theorems, Lagrangians 80−74766
elastoplasticity, variational method using mixed finite elements *(French)* 79−72819
elastoplasticity, velocity discontinuities, variational formulation of boundary-value problems *(French)* 79−32284
elastoplasticity algorithm, finite difference and variational methods in flow theory models 77−871
elastostatics, variational and minimal theorems 79−88807
electric conductance and resistance, anisotropic body of arbitrary geometry 80−32865
electroacoustic wave variational expression derivation 78−1488
electrodynamics and electrostatic problems, solns. 80−1105
electrolyte, solutions, 1-1 and 1-2, extended mean spherical approxs. 79−4216
electromagnetic fields, static and stationary, determ. using variation calculus *(Hungarian)* 80−87259
electron+ion scattering, Schwinger's variational principle, Rydberg states 80−78713
electron affinity, variation-perturbation approach 77−54513
electron correlation, variational description, loop driven graphical unitary group approach, $SO_2(2^1A')$ appl. 80−47903
electron correlation problems, lattice statistical aspects, Gutzwiller approx. 78−84160
electron gas, two-dimensional, variational approach to ground state, CDW instability 80−39517
electron liquids, inhomogeneous, variational approach, appl. to metallic H_2 79−38013
electron scattering theory 77−42408
electron-atom (molecule) scatt., minimum-variance method 77−83734
electron-electron scatt. and elec. resistivity of metals 79−95396
electron-hole pair condensation and liquefaction in strong mag. field, RPA and variational calcs. 78−63984
electrons in surface phonon field 80−107885
electrostatic problems in presence of linear and isotropic quadrupole matter *(German)* 80−37924
electrostatics, two-dimensional problems *(Hungarian)* 78−58879
elliptic problems, representations of first variations, appl. to optimisation and sensitivity anal. 78−77674
EM field problem, variational expression derivation, unified approach 77−6970
EM field theory, derivation of variational expressions using unified approach 78−9295
EM field theory, Shwinger's variational principle 79−76549
EM fields, static and stationary, solving methods 79−36815
EM fields analysis, stationary, by Trefftz's method, using quasiharmonic polynomials *(German)* 79−27128
EM induction, irregularity shaped plates, slow ramped field, eddy current heating, anal. 80−91722
EM resonator eigen-oscillations, variational treatment *(Russian)* 77−79730
EM scattering from random rough surfaces, variational principle 78−55285
EM wave scattering from random rough-surface model, comparison of variational, perturbational and exact solns. 78−66724
EM waves propagation, ray surface equation and Fermat's principle, in moving anisotropic media 80−106425
EM/acoustic waves, systematic derivation 78−93536
emissivities for halfspace geometry, variational procedure 78−87245
end-temperature in semi-infinite rod, distributed parameter optimal control problem 78−13886
energy eigenvalues lower bounds for quantum Hamiltonians in lattice field theories 78−45575
energy momentum tensor for vector-tensor theory of gravity and electromagnetism 78−12633
EPR spectral simulation via finite elements, variational method and stochastic-Liouville eqn. 79−85157
estimation aided by instrumental variables, regression model *(German)* 78−29080
ethane, barrier and one electron charge transfer states in strong orthogonal group function theory 78−13421
ethane, mean polarisability derivatives, variational calc. procedure 79−27108
ethylene mean polarisability derivatives, variational calc. procedure 79−27108
Euler-Lagrange differential in fibred manifolds 78−45469
exciton-neutral donor complex, binding energy 79−60715
exciton-phonon coupling, variational solns. 80−10601
excitonic molecules, binding energy, variational calc. 80−10891
excitons, Wannier-Mott, interaction with screw dislocations *(Russian)* 79−4513
excitons in electron-hole plasma, dynamical screening and self-energy 79−15093
exercise ECG processing principles and multivariate analysis results 78−7511
exterior linear elliptic problem, numerical method, appl. to 2-dimens. wave resistance 80−28485
fast reactor system, eval. of variational method for estim. of neutron detection efficiency 79−80992
FBR, multiplication factor evaluation of bare and reflected small fast assemblies using variational method 79−85583
Fermi hypernetted chain equations, optimal correl. function 79−40870

variational techniques continued
Fermi system, hard-sphere, energy and momentum distrib., Jastrow variational wave functions 80−73261
Fermi system, Jastrow wavefunction, hypernetted chain method 80−17866
fermion matter with spin depend. correlations, variational theory 79−63614
fermions, constrained variation in Jastrow method at high density, neutron system, liquid ^{3}He appls. 77−5753
ferromagnet, spin wave stiffness coefficient, spin density functional theory 78−76230
few-body quantum system stochastic variational method for all conventional N-N pots. 77−53799
Feynman's variational method applied to the randomly forced Duffing equation 80−73201
Feynman's variational principle for real path integrals, generalisation 78−89365
fibre bundles in field theory, variational principles on rth order jets 78−86168
field problem structure, equilibrium, eigenvalue and propagation problems *(Rumanian)* 78−45520
field theory, Lie-Backlund operators props. from variational derivatives 80−37159
filtering, nonlinear, conditional laws, smoothness, stochastic calculus of variations *(French)* 80−68128
finite elastic cylinders, Ritz solns. for axisymm. temp. and stress fields 78−38190
finite elements in fluids, book 79−32441
finite medium freezing (melting), variational anal., radiation and convection effects 80−38244
finite sample, mag. rearrangements near surface 80−11240
finned-pipe solar energy collector, optimal material distribution 79−83631
finned-pipe solar energy collector optimal profile 79−62065
fission reactor blanket neutronic performance, influence of design variations, variational interpolation techniques 77−34437
flat galaxies dynamics, integral eqn. for normal modes in matrix form 77−33637
flexible strings mechanism, variational principle in Euler representation *(Russian)* 78−54172
flow past an arbitrary body, extended variational principle, local pot. method 77−89089
fluid, randomly-stirred, vel. correlations, variational principle for path-integral functionals 78−81846
fluid, with anisotropic spatially inhomogeneous viscosity, frictional force and torque 79−37367
fluid bidimensional flow past symmetric profile 77−60942
fluid channel desing using global variational method 78−38408
fluid channels indirect design using global variational method with trial functions 77−27595
fluid computations using infinitesimal functionals, variational approach 79−14365
fluid dynamics, book contrib. 79−32456
fluid dynamics, complementary variational principles for steady and unsteady Poiseuille flow in porous pipe 80−92225
fluid mechanics, Hamilton's principle 77−68559
fluidised bed at high Archimedes numbers, variational formulation of hydrodynamics 77−11257
Fokker-Planck equation, variational method for soln. 77−33928
force-free magnetic fields, variational approach and appl. to solar active regions mag. field 80−62011
forced convection heat transfer near forward stagnation pt. of cylinder, variational method 79−98726
forced van der Pol oscillator, variational eqn. bifurcations 78−77681
foreign gas broadening, translational heat-bath model, variational methods 78−9124
fracture, brittle, energy release rate, equivalent to Rice integral *(French)* 80−64457
fracture mechanics, variational bounds, qualitative method 78−67134
fracture mechanics, variational bounds and qualitative methods 78−79283
fracture mechanics anal. by displacement hybrid finite element model 77−3792
frame nonlinear postbuckling behaviour, finite element analysis 77−62183
free convection boundary layer flow and heat transfer, variational technique 80−106796
free energy derivatives, bounds, upper and lower, renormalisation group methods 80−68162
free molecular channel flow, complementary variational principles 79−64708
free surface problems, resolution methods, review 77−54954
free-surface flows, stream functions variational principle, finite element anal. appl. 79−64675
Frisch-Lloyd random system, low-lying electronic tail spectrum by path integral method and coherent state representation variational method 80−105580
functional integral method appl. to classical and quantum spin models 80−15676
fusion reactor neutronics, higher-order variational functional derivation 79−9880
fusion reactor neutronics analysis using generalised variational principles 80−57947
g- and p-modes of non-adiabatic self-gravitating fluid, perturbational-variational expansion 78−32337
gas dynamic variational problems, nonlinear programming methods *(Russian)* 77−51074
gasdynamic three dimensional flow, variational principle for *(Russian)* 77−35157
Gaussian laser beam, nonlinear self-focusing in plasma 79−27786
Gel'fand-Levitan equations with comparison measures and comparison potentials 80−12931
Gelfand-Levitan eqn. and Korteweg-de Vries eqn. 78−32708
general relativistic phenomenological theory 80−2518
general relativity, combined Dirac-Einstein-Maxwell field eqns., tetrad field variation 78−4536
general relativity, Einstein eqns. derivation from Lagrangian with internal symm. 77−64976
general relativity, perfect and imperfect fluids, variational principle 80−90733
variational techniques continued
general relativity with torsion and non-metricity, variational principle 77−67347
generalised polarisabilities, new variational bounds 78−45502
generating forms of K-generalised Lagrangian and Hamiltonian systems 78−4475
geodesy, Helmert type variance-covariance-component estimator props. 80−101318
geodetic boundary-value problem, variational formulation 78−92772
geometric formulation of Hamilton's Principle, spin particles 78−45482
geometrical nonlinear shell theory, dual extremum and complementary stationary principles 80−4526
global element method, appl. in discontinuous nuclear pot. calc. 79−3089
gravitation, appl. of Palatini-type variational principle to SL(2,C) gauge invariant Lagrangian density 78−78059
gravitational eqns. of Bianchi identity type vac. 80−4599
gravitational field equations of fourth order and supersymmetry 79−12674
gravitational gauge theories, difficulties assoc. with variational principles 77−17884
gravitational superpotentials, affine connection, Riemann tensor, field eqns. 78−107
gravity waves on stratified liquid, linear initial-boundary value problems 77−39301
Green function complex pole calc. by variational technique 80−98822
Gurtin's principle, 1-D theories of motion for beams 78−18179
Gurtin's variational principles in linear dynamic theory of viscoelasticity 77−46934
hadrons, string state, WKB-like wave functional and path-dependent phase factor, colour flux 80−52481
half-space with crack, local loss of stability *(Russian)* 79−18821
halogen ion, with filled shell, dipole polarisability 80−9501
Hamel-Boltzmann eqns. of motion, variational principle involving conditional extremum 77−17801
Hamilton type variational principles, for nonlinear thermoelasticity 78−54190
Hamilton-Jacobi eqn., generating function soln. for shocks in fields *(French)* 77−9890
Hamilton-Jacobi generalised theories 79−2681
Hamilton-Jacobi method generalised, for nonholonomic systems, appl. to classical mechanics 77−71207
Hamilton-Jacobi problem and canonical transform., first order system from variational principle 79−17193
Hamiltonian, complex-rotated, reson. props. 79−31427
Hamiltonian action of lagrangian, second variation extension *(French)* 77−82381
Hamiltonian formalism, Lagrangian function, variational technique constraints *(German)* 79−88799
Hamiltonian formalism for self gravitating relativistic perfect fluid, Lagrangian variational principle 78−16289
Hamiltons principle appl. to large deformation and flow problems 80−48600
hard core fluid with two-Yukawa tail, appl. to Ar 80−59618
hard sphere Fermi gas, variational energy, Jastrow correlations 79−40451
hard sphere system, high densities, Kirkwood eqn., variational principles 77−65942
Hartree Fock problem, using variational principle 79−93537
Hashin Shtrikman bounds, effective elastic moduli, hexagonal, trigonal and tetragonal polycrysts. 80−75282
Hashin-Shtrikman bounds, effective elastic moduli, monoclinic polycrysts. 80−70291
heat and mass transfer, non-stationary, coupled, with convective motion and relaxation, variational principle 80−106797
heat conduction, Biot variational eqn. generalisation 80−43591
heat conduction, combination of Lagrange and Euler methods 79−76941
heat conduction, interior algorithm for optimisation of forms *(French)* 77−72130
heat conduction, third boundary-value problem, variational soln. 77−7282
heat conduction equation, hyperbolic, integral variational principle *(Russian)* 78−83213
heat conduction problems, Langrangian formulation and its complementary form 79−55309
heat conductivity, nonlinear problems, variational formulation *(Russian)* 80−74700
heat convection in channel flow, temp. distrib., variational soln. 79−72886
heat equation, domain perturbation and Green kernels, variational formula 79−97321
heat transfer, nonlinear, iterative-variational method 78−94511
heat transfer calc., circular fins with heat generation optimisation 77−65658
heat transfer in boundary layers, variational description 77−68581
heavy ion+atom collisions, mol. M-X-rays, self-consistent relativistic HF-Slater many electron correl. diagrams 77−14567
heavy ion collision, K-shell vacancy sharing, variation-perturbation mol. model 79−31665
heavy ion reactions, coupled channel approx., treatment of resonances 79−9621
heavy ion reactions, time-dependent variational approach 78−50193
Heisenberg ferromagnet, spin waves at low temp., method of variational derivatives 79−24152
Heisenberg ferromagnet, structurally disordered. variational method for cluster model 78−91839
Heisenberg matrix mechanics and variational principles in quantum theory 79−63085
Hellinger-Reissner mixed variational principle, stiffness matrix determ. for nonlinear anal. of deep arches 78−18161
Hemlholtz-Cartan theorem for simple integral of higher order *(French)* 79−71238
hepatic tissue characterisation by US reflection, estimator variance reduction 79−48307
hermitian operators, upper and lower bounds to eigenvalues, variational calcs. 78−36882
heterogeneous mixture, variational hydrodynamic model in Eulerian and Euler-Lagrangian formulations *(Russian)* 79−90211
heterogeneous mixtures, variational hydrodynamic model in Euler- and Euler-Lagrange formulations 80−92100

variational techniques continued
high-density fluid-perturbation theory, based on inverse 12th power hard-sphere reference 79−99042
holes, in degenerate bands, variational principle for Landau levels, const. mag. field 79−33219
hot atom chemistry, general variational principles 80−11941
Hubbard model, partly filled narrow band, electron correlation and mag. props. 78−67968
Hubbard model, single band, magnetic phase diagram, cluster variational calc. 80−60340
Hubbard model, strong coupling limit, asymptotically exact variational approach 77−11836
hybrid deformation elements for elastic media 80−92049
hydrocarbons, mol. Raman intensities calcs. 80−52993
hydrodynamic lubrication, free boundary problem, variational inequalities 80−62475
hydrodynamics, variational principle generalisation in Euler represent. *(Ukrainian)* 77−30011
hydrodynamics models, nonstationary gas flow, two dimens., variational approach to finite difference scheme 78−51147
hypersonic flow, body form for minimum heat transmission *(Russian)* 79−37131
hypertensive left ventricular hypertrophy, orthogonal ECG multivariate analysis 79−39579
hypervirial theorems and symmetry, optimal variational wave function 80−17841
ideal gas, self-trapping of electrons, variational model 79−2662
immiscible mixtures, variational theory 79−27885
impact vibration, steady, body with impact hysteresis charact., stability anal. 78−51099
impurity scattering of current carriers in quantizing mag. field 78−51954
incompatible basis functions in boundary value problems, limitations of simplified variational principles 80−48587
incompletely optimized variational parameters, corrections, perturbation theory anal. 78−41180
incompressible flow fields, finite element dual variational anal. 79−40375
incompressible fluid, fully developed turbulence generated by random stirring, variational approach 79−3991
industrial odorous pollution rel. to perceived sensory discomfort 77−37391
inert gas atom, two-photon excitations, interelectron correlation 80−957
ingot, hollow cylindrical, temp. field and crystallisation front calc. *(Russian)* 78−63690
inhomogeneous medium, effective cond., iteration series and variational estimates, Herring method 80−70663
initial and boundary value problems, unconstrained variational statements 78−93518
initial value problems, finite element, unconstrained variational approach 77−67256
initial value problems for nonlinear systems, variational formulation 77−13579
initial value problems soln., finite element unconstrained variational formulation 77−87637
initially-stressed solids, variational-Lagrangian irreversible thermodynamics 78−29074
inner-shell excitation in heavy ion collisions, variational method 79−31428
instantons, variational anal. 78−24934
insulators, improved effective mass for impurity levels 78−87941
integral equations for three-dimensional fields, isoparametric finite element, variational solution 77−87635
integrated load increment method for finite elasto-plastic stress analysis 80−92072
intermediate valence, three-site, six-electron model, variational calc. 80−20126
intermediate valence system, local polaron model 80−107717
intermolecular forces, ab initio calcs. applicability and accuracy 80−18898
internal nonlinear waves in stratified fluid in closed basin 78−75159
interpolation of linear functionals of inhomogeneous eqns. 78−49638
intramolecular energy transfer, crit. energy calcs. 77−9046
invariant tori and cantori, variational principles 80−37666
invariant tori of fixed freq., Langrangian variational principle 79−25833
ion+atom, slow collision, K-shell ionisation, variational calcs. 78−42162
ion+atom collisions, asymmetric, polarisation and binding of inner-shell electrons, recoil in close encounters 80−18915
ion+electron scatt., static exchange approx. Schwinger variational principle, photoionisation cross section 80−43192
ion recombination in low-density ambient gas, variational principle, equiv. to quasiequilib. condition 79−37443
ion-atom electron excit., variational method 77−23547
ion-dipole capture in noncentral field, variational and trajectory investigation 80−63739
ionic crystal, simple, high temp. dynamics, var. approach 80−29130
ionic solution theory, variational approach 77−7645
irreducible cluster expansion for the logarithm of the s-particle density matrix of a many-boson system 79−21657
irreversible process thermodynamics, exergy representation 78−65892
irreversible thermodynamics of heat and mass transfer in porous solids 79−4081
irreversible transport processes, noncoupled, nonstationary, classical variational principles 78−4567
irrotational symmetric steady flow in channel, soln. by variational method *(French)* 79−18954
Ising, 2- and 3-dimens. antiferromag. lattices, appl. of Kadanoff's variational approx. 80−2583
Ising chain, in transverse field, variational treatment, static props. at zero temp. 79−4642
Ising model, antiferromag. case, modified Kadanoff variational renormalisation method 80−88710
Ising model, appl. of square lattice variational approxs. 79−56555
Ising model, free energy, variational calc. for 3 dimens. system 80−42167
Ising model, transverse, quantum crossover 78−43596
Ising model, two-dimens., in external field, variational approach 79−80538
Ising model, two-dimens., in transverse mag. field, renormalisation group studies 80−71042
variational techniques continued
Ising model, variational approx. for renormalization group transforms. 79−61139
Ising model on square and triangular lattice, variational renormalisation group method 78−16740
Ising systems, coupled, variational renormalization group approach 77−2616
isoelectronic series, var. energy functionals involving 1-electron operators 77−83484
isovector meson interaction, static source, use of coherent states 78−16921
iterative finite element meth. using Kantorovich technique, MHD appl. 77−74205
Jahn-Teller cooperative phase transition, helical ordering 79−46778
Jahn-Teller E-e system, low lying vibronic energy levels, variational calcs. 77−76780
Jahn-Teller effect, linear, variational approach 77−71759
Jastrow correlations and nuclear photoeffect 78−4927
jellium metal, surfaces props., statistical calc. 80−24987
jellium metal surface densities, electronic density, variational calc. 79−15205
Jourdains variational principle, use in nonlinear mechanics and transport phenomena 79−9093
Kadanoff's variational approximation applied to the 2-D antiferromagnetic Ising lattice 79−73659
kernels and ranges in the variational formalism 79−21529
ket vector variation, orthonormality-constrained variation method 78−45457
kinetic theory, ideal monatomic gas, thermal cond. coeff. 77−968
kinetic theory, projection and variational methods 80−6189
Klein Gordon equation, equivalent variational integral, numerical soln. by finite element method 78−78064
Klein-Gordan equations with logarithmic nonlinearities, classical theory 79−5996
KLL Auger transition energies, relativistic multiconfig. calcs. 77−18873
Kohn-Hulthen var. method for bound-state problems 78−62109
Lagrange formalism, direct and inverse variational characterisation of linear non conservative systems 78−93527
Lagrange formalism, in heat conduction theory 77−50858
Lagrange variational problem, use of Schwartz distribs. 79−2596
Lagrangian formulation for continuous media 77−57192
Lagrangian-Hamiltonian systems, partial quantisation *(Portuguese)* 80−77653
laminar boundary layer, optimal control, group theoretic approach 79−32452
laminated composite shells, mixed isoparametric finite element models 77−78979
laminated viscoelastic composite, wave propag., dispersion relations, mode shapes, variational methods 78−18215
Langevin eqns., generalised action principle 79−40444
Langmuir soliton solns. with high nonlinearities, energy principle 80−24156
lattice, gas, entropy and phase transitions in partially ordered sets 78−77808
lattice Hamiltonian for arbitrary couplings 78−16746
lattice instability theory of fracture 80−84244
Lennard-Jones gas, second virial coeff. calc. using equilib. Wigner distrib. function variational principle 80−4685
LF EM rad. scatt. by dielec. body, variational principles 79−89837
light propagation in lens-like media 77−27347
linear accelerator cavity code, based on finite element method 78−33307
linear elastic continua, variational principles, finite element techniques *(German)* 79−9113
linear elastic half space, frictional unloading problem 80−33542
linear elastic half-space, frictional unloading problem, variational soln. for stress analysis 78−59350
linear filter matrix, variational principle, functional max. value 80−27243
linear hydrodynamics exterior problems, variational formulation 79−32434
linear molecules, dispersion forces calcs. 80−9675
linear operator equations, convergence rates of variational solns. 77−33
linear shell theory, dual complementary variational principles generated from dual functionals *(German)* 79−97196
linear structures, complex, eigenvalues numerical bracketing *(French)* 80−42053
linear transport relaxation equations, matrices, variational principle 80−17785
linearised inverse problems, variational approach 79−71259
linearized theory of elastic wave propagation in initially stressed bodies *(Russian)* 78−83318
Liouville-Green approximation, general connection formulae in complex plane 79−9083
liquid ^{4}He, trimer binding in two dimensions 79−69306
liquid metal flow in curved channels, transversely applied mag. field 80−14829
liquid surface tension, statistical mechanical theory 79−82414
liquid surface waves, natural oscillation solns. *(Russian)* 77−80176
liquid-filled crack, Rayleigh wave reflection and transmission calc. 77−32762
local approach, molecular correlation energies, intraatomic correlations 78−41967
localised site cluster expansion, interacting paramagnetic sites, spin symmetry projection 79−7951
localised site cluster expansion, wave function ansatze, many body theory 79−6827
localised site cluster expansion, wave function higher ansatze, linear Heisenberg model 79−7959
lossy anisotropic inhomogeneous media, variational formulation of EM problems 79−13866
lossy anisotropic inhomogeneous media, variational solns. of EM problems 78−77735
Love waves in infinite strip with surface step, transmission, reflection and diffraction 79−88260
Lowdin canonical orthonormalisation, variation approach 79−12574
lowest order constrained method for binding energy of nuclear matter 77−18463
lubrication, hydrodynamic, free boundary problem including surface tension 80−19542
macroscopic cell representation by density matrix eqn. 79−63130
magnetic impurities in metals, appl. of variational method 80−103814

variational techniques continued
magnetic impurity interactions, nondegenerate Wolff model, variational method extension to include orbital degeneracy 79−38302
magnetic thin films, charged domain walls, variational method calc. 80−11235
magnetisation curve analytic functions, numerical parameter calc., variational methods appl. *(Russian)* 80−14267
magnetisation of easy plane amorphous wire, variational calc. 80−71098
magnetofluid dynamics, relativistic, eqns. of motion for charged particle and charged fluid 80−87821
magnetostatic field, rotational-symmetrical, modelling, variational method, difference equations *(Polish)* 79−81319
magnetotelluric analysis, soln. of electrometry inverse problem via variational method *(Russian)* 77−44915
many body systems, low lying excited states, extension of ground state variational methods 79−36177
many component plasmas with self consistent field, variational principles and canonical theory 80−87856
many-electron atoms, self-consistent theory of induction and dispersion forces, HF approx. 79−36725
many-electron molecule, self-consistent theory of induction and dispersion forces, HF approx. 79−36725
many-electron system, Wigner cryst., electron chain and CDW in strong mag. fields 78−60067
many-particle systems, stochastic var. method 77−41891
many-valley semiconductor, electronic structure of D^- ion 79−95369
many-valley semiconductor, energy states calc. of negative donor ion, high stress and stress free cases 78−2444
many-valley semiconductor, Mott transition, critical carrier conc. 77−47747
Mars probe, optimal atmospheric entry trajectories with two-dimensional control 77−91400
Mathieu eqn., var. method 78−57743
Matrix variational Pade approximants and multi-step square-well potentials 79−71283
maximal entropy distrib. determ., using variational technique with Lagrange multipliers 78−24754
maximal variational principle for transport theory 78−62166
maximum entropy spectral estimation of frequency and arrival angle 80−96129
measurable selection theorem *(French)* 80−42045
mechanics, mountain massif, pre-face zone, stressed state, finite difference method *(Ukrainian)* 80−74735
melting elastic solid, variational principle 77−84894
membranes, excitable, statistical theory, nonlinear force-flux reln. and fluctuation 77−9179
meniscus joining vertical rod to liquid bath, stability 77−4247
metal, perfectly imaging, physical adsorption of atomic H, variational cals. 79−33188
metal, thermal resistivity, var. calc. 77−43562
metal, Ziman's variational expression for resistivity, use 80−15494
metal solidification, variational formulation of stationary free boundary problem *(French)* 80−96626
metal surface, ground state, variational self-consistent-method 78−56204
metal surface props., Rayleigh-Ritz variational calcs. 79−69570
metal surfaces, adhesion theory, electron distribution tail effective length *(Russian)* 79−99430
metal with magnetic impurities, variational method, Wolff model 78−80110
metal-insulator transition region, narrow energy bands, electron correlation, Gutzwiller variational method 80−84426
metallic film, electron density and potential, variational calc. 79−78218
metals, acoustic attenuation in collision regime, variational principle 79−82648
metals separated by dielectric, electronic component of metal-metal interaction force, calc. 78−52056
meteorological fields variational adjustment 79−39837
methane, mean polarisability derivatives, variational calc. procedure 79−27108
methane, mol. multipole polarisabilities, extended variational method calcs. 79−36558
methane+methane (He)(Ne)(Ar), dispersion forces 78−13565
methylene, triplet ground state, var. and perturbational calcs. 77−61680
metric fields, generally invariant Lagrangians 79−44708
metric-affine variational principle for Einstein's field eqns. 77−87678
MHD, variational principle using Lagrangian approach for infinitely conducting fluid 79−32683
MHD channel, frame type, optimal selection of frame and transverse cross section form 78−91164
MHD charged gas flow, multicomponent eqns. *(Russian)* 79−14488
MHD generator, Faraday type, current profile optimisation, electrode cond. profile 78−94939
microwave breakdown in gases, Schwinger variational princple 79−41788
Migdal-Kadanoff renormalisation scheme, surprising effectiveness 79−35652
Milne's integral eqn., general variational method 79−8828
minimum principles, stress field derivation in elastic-perfectly plastic solid 77−878
minimum principles in elastic-plastic solid, stress and strain fields 77−879
MIS, and MISIM structs., electron energy and potential evaluation 77−51819
miscible fluid mixtures, mechanics and thermodynamics, variational approach 79−93084
mixed boundary value problem in three dimens. 77−71184
mixed spatial elasticity problems, variational soln. *(Russian)* 79−9110
mixture of two elastic solids, variational theorem in linear theory for quasi-static case 78−9561
modulated perturbation theory, mol. interactions, STO expansions nonlinear parameter minimisation 77−57871
molar molecule heat and mass transfer phenomena, generalised variational principle 80−79104
molecular and atomic structure, variations preserving orthonormality 79−76326
molecular collisions, diatomic transition operator, separable approx., variational approach 78−42150
molecular correlation energy, var. calcs. 77−30791
molecular electron scattering, continuum wave functions, discrete basis set method 79−22829
molecular electronic multipole polarisabilities, variational calcs. 79−7035

variational techniques continued
molecular energy levels, conditional probability amplitudes, variational principle 77−79530
molecular ionisation energies, self-consistent-charge Hartree-Fock-Slater calcs. 77−6687
molecular magnetic properties optimal gauge parameters, var. calcs. 77−71760
molecular multipole polarisabilities, extended variational method calcs. 79−36558
molecular orbitals, variationally deorthogonalised localised molecular orbitals 79−97968
molecular polarisabilities calcs., superposition method of excited config., nonstationary perturbation theory eqn. 80−69257
molecular polarisability, CNDO calcs. including polarisation functions in the basis set 79−6891
molecular vibrational wave functions, semiclassical Gaussian basis set method 80−9583
molecules, approximate and exact state wavefunctions, ionisation potentials, energy difference calcs. 79−97967
molecules, direct CI calcs. with multiconfigurational reference state 80−63506
molecules, Schrodinger eqn. calcs., variational cellular method, general formulation 78−94192
molecules, symmetric deorthogonalisation 78−37540
molecules, two criteria for labelling approx. treatments as fully quantal ones 80−23289
Mooney-Rivlin rubber-like materials, finite element anal. 78−46894
multi-step amplitudes, variational approach, exact T-matrix and DWBA amplitude differences 79−3167
multicomponent continual system, dynamic processes, variational principle *(Russian)* 79−12595
multiconfigurational HF calculations, quadratically convergent reference state optimisation procedure 79−97966
multivalley semiconductor, donor binding energies calc. 78−23041
multivariate and conventional ECG analysis programs compared 78−7492
N-body problem, variation eqns. and eleventh integral *(French)* 77−25921
Navier-Stokes equation soln. method, finite element anal., 2D unsteady viscous flow 77−89088
Navier-Stokes equations, stream function-vorticity formulation incorporating no-slip conditions, variational principle 78−38267
negative ion, singly-charged Thomas-Fermi-Amaldi eqn., approx. variational soln. 80−52870
nematic liquid crystal, cluster variational const.-coupling theory, thermodynamic props., nematic-isotropic transition 77−24265
nematic liquid crystal, simplified variational model for bidimensional coupled evolution eqns. 79−73092
nematic liquid crystals, tridimensional variational approximated model, existence, uniqueness and regularity of solns. 80−59379
nerve membrane, steady-state finite cable model, complementary variational principles 79−34545
neutral bound excitons, accurate binding energies, variational method calc. 80−107715
neutron density in slab geometry, transport soln. props., piecewise polynomial variational approx. 77−54269
neutron detector efficiency estimation 78−62601
neutron diffusion and transport theory, discontinuous variational approx. 78−46129
neutron diffusion theory in rectangular and cylindrical coordinates 79−17949
neutron matter mag. susceptibility, lowest-order constrained variationsl calc. 79−75884
neutron resonance escape in slab lattices, variational method 79−85572
neutron second order transport eqn., variational formulation and projectional methods 80−164
neutron spectra unfolding from activation data 79−13375
neutron stochastics, variational method 79−13373
neutron streaming along fusion reactor ducts, perturbation and variational corrections 80−23143
neutron transport, contribution Monte Carlo technique, variational derivation 80−5194
neutron transport, variational coarse-mesh method based on constrained ang. trial functions 77−65245
neutron transport discrete-ordinate transport eqn., variational difference schemes 77−65250
neutron transport equation, perturbation method to estimate functionals 80−27698
neutron transport theory, buckling approximation inclusion in finite element calcs. 78−17276
Newtonian mechanics, inverse problem, Lagrangian computation method 78−89329
noble metals, electron statistical vacancy model 77−76390
non-associated plasticity and elastoplasticity, rate boundary value problems, variational principles 80−87726
non-classical variational problems and evolution eqns., numerical methods 77−67258
non-integrable N-body Hamiltonian systems, variational solns. 78−93524
non-Lagrangian field equations, variational principles 79−21565
non-Newtonian creeping flow around rotating spheroidal spindle, torque calcs. 77−15073
non-Newtonian fluid, creeping flow, variational principles, entropy prod. 77−75946
non-Newtonian fluid, incompressible, variational principle for flow 78−51207
non-self-adjoint problems and essential boundary conditions 79−44732
nonconservative circulatory systems, variational formulation 80−48584
nonconservative mechanical systems, variational principles, finite element approach 79−49027
nonconservative systems which are conservative in a higher sense, Hamiltons variational principle extension 79−44742
nonequilibrium nonlinear statistical thermodynamics, variational principle *(Russian)* 79−85058
nonequilibrium states, variational approach to Fokker-Planck eqn. 77−87717
nonisothermal finite strain mechanics of porous solids, thermomolecular diffusion, variational Lagrangian thermodynamics 77−65668
nonisothermal heat transfer equations, hyperbolic, derivation from variational principle *(Russian)* 79−68543
nonlinear anisotropic simultaneous transport processes, variational principle *(Russian)* 79−88893

variational techniques continued
nonlinear boundary-value problem, incremental var. formulation, rel. to elasticity *(German)* 77−33866
nonlinear differential equations, similar to Schrodinger eqn., variational principle application 79−63065
nonlinear elasticity, relaxed continuity requirements, generalised variational principles 79−92942
nonlinear heat transfer, soln. by variational imbedding 77−65669
nonlinear interdependent heat and mass transfer, variational solution *(Russian)* 79−88894
nonlinear mass and energy transfer, variational soln. 79−12740
nonlinear physical media, boundary valve problem soln. by finite element anal. 79−17214
nonlinear problems of thin shells appl. 78−5673
nonlinear shell analysis via mixed isoparametric elements 78−1566
nonlinear shell problems, hybrid stress finite element model 79−14251
nonlinear simultaneous transport processes, complimentary form of variational principle *(Russian)* 79−54076
nonlinear simultaneous transport processes, variational principle *(Russian)* 79−58653
nonlinear stability problem, direct variational method 77−57174
nonlinear stochastic differential equations, approx. soln. by statistical linearization method, variational procedure 77−17789
nonlinear unsteady heat conduction, Laplace transform, small parameter, R-function and variational methods joint appl. 79−94451
nonlinear unsteady heat conduction, variational principle 77−42698
nonlinear variation eqns., convergence of finite element solns. 78−86127
nonlinear viscoelasticity, variational principles for isothermal problems *(Russian)* 78−28950
nonlinear viscoelasticity problem with geometric nonlinearity, variation principle 77−62176
nonlinear viscoelasticity variational formulations of boundary problems *(Russian)* 79−18749
nonlinear wave propagation and unsteady transonic flow, variational formulations 78−55660
nonrelativistic particle scatt. in presence of strong EM wave, Schwinger variational principles 79−93329
nonstationary heat transfer phenomena, variational description 78−89416
nonstationary multicomponent continuous systems, variational priciple, eqns. of motion *(Russian)* 79−27512
nonstationary temperature field determination, in a crystal on a substrate *(Russian)* 78−18158
nonuniform helical delay system anal. *(Russian)* 79−18336
normal mode initialisation technique, variational nonlinear, atm. gravity waves appl. 79−5584
normal modes of laterally homogeneous Earth, one dimens. example 78−88797
normal modes of self-gravitating fluids in perturbed configurations, perturbational-variation procedure 78−32336
nuclear and chemical reactions, variational techniques 77−60966
nuclear and neutron matter N-N potentials, variational calcs. 78−37292
nuclear breakup amplitudes, 2→3 cluster, variational principles 77−10375
nuclear free energy, variational description 79−45199
nuclear many-body problem, variational calculations in harmonic oscillator basis 77−6263
nuclear matter, finite temperature props., variational theory, effective mass 80−5084
nuclear matter, noncommuting pair correl. functions 78−58244
nuclear matter, review of variational theory 79−89262
nuclear matter, static density waves, cluster-variational investigation 79−40868
nuclear matter, variational and Brueckner-Bethe calcs., review 78−93959
nuclear matter, variational theory 79−40867
nuclear matter, wave functions, correlation operators, review 80−22748
nuclear matter binding energy variational calcs. in two- and three-body cluster approx. 77−26603
nuclear matter model calc. with fermion lowest order constrained variational method 77−14053
nuclear matter model energy calcs. in Jastrow variational approach 78−74322
nuclear matter theory, review, comparison of perturbative to variational techniques 78−33136
nuclear matter theory, technical aspects, review of theoretical techniques, nuclear interaction investigation 78−62497
nuclear matter variational calc. using new integral eqn. meas. 78−82301
nuclear reactor optimal control using Walsh function variational synthesis technique 77−38347
nuclear reactor theory, source-driven systems, second-order generalised perturbation theory 79−36304
nuclear reactors, fission gas behaviour, calc. fo diffusive flow to spherical boundary 80−47574
nuclear struct., pairing motion, large amplitude, time-dependent Hartree-Fock method 78−4908
nuclear structure, ^{16}O ground-state energy, nonunitary model operator approach 80−83030
nuclear structure, charge independent pairing Hamiltonian, variational approach 78−86488
nucleon fluid, constrained variational calc. of symmetry coeff. 78−46022
nucleon fluid, excitation to N*(1234) state, lowest order constrained variational calcs. 79−40864
ocean topographically bound vortices, variational theory 79−57956
one component plasma fluid, derivation of eqn. of state in strong coupling 80−33741
one-dimensional backward-scattering model with generalised coupling const., variational soln. 78−66036
one-dimensional systems, variational soln. of sine-Gordon theory and Luther-Emery backward scatt. model for one-dimens. systems 79−40447
one-electron polynuclear systems, Dirac eqn., variational soln. 80−83242
open shell restricted HF eqns., role of coupling operators 79−758
optic fibre light propagation, review of analytic methods of study *(French)* 79−90001
optical absorption spectrum of D^- centre in strong magnetic field 80−20670
optical correlation instrument field-of-view, intensity distrib. selection 79−72688
optical directional couplers with graded index profile, variational analysis 80−96037
optical fibres, radially inhomogeneous, vectorial wave anal. using finite elements method 78−37999

variational techniques continued
optical fibres, truncated parabolic-index, with minimum mode dispersion, anal. 78−38000
optical waveguide, strip-loaded diffused, modal analysis by variational method 78−46776
optimal design problems with singularities, soln. 77−72151
optimal elastic design for prescribed maximum deflection 79−75343
optimal rod and shell shape determ. using variational principle 80−5929
orbit-orbit interaction, new tensor expansion, matrix and graphical forms 80−14064
orbitals, max. and min. overlap, localised, and hybrid, orthonormality-constrained variation method 79−6830
orthonormally constrained variation method, basis vector sets, pair orthogonality 77−75050
otolith membrane, finite element model, computer soln. of differential eqns. 77−40636
pairing Hamiltonian, general, approximate solns., by variational method 78−36931
Palatini variational principle, in scalar-tensor gravitational theories 77−2592
parameter dependent renormalisation group transformations 78−87768
partially coherent beam intensity fluctuation calc. in turbulent atmosphere 80−78775
partially random sonobuoy array directivity index analysis 80−43518
particle motion in classical gauge field, variational derivation and uniqueness of equations of motion 79−40658
partition function, modified Lippmann-Schwinger variational principle 80−86233
patched variational principles, appl. to elliptic and mixed elliptic-hyperbolic problems 77−89144
path integrals and lower bounds for density matrices 80−138
path-integral methods in nonequilibrium thermodynamics and statistics 79−26018
pendulums, massive cord, oscill. freq. calcs. 78−54121
periodically structured elastic ring, free modes 77−35075
perturbation analysis 77−82404
perturbation theory, Hyleraas type base *(Russian)* 77−37775
perturbation theory, variable basis sets, numerical finite perturbation vs. analytic approach 79−59330
perturbation theory, variational methods, evaluation of second-order matrix elements 80−12936
perturbed eigenvalues, perturbation expansions and variational constraints 78−16670
phaseshift variational calc., s-wave scattering, non-zero energy 79−88822
physical systems instabilities, variational principles for complex eigenvalues 79−21527
physical-chemical solids with finite deformation, variational irreversible thermodynamics 79−6067
piezoceramic bar transducers, inhomogeneous, analysis using Reissner mixed variational principle 79−64479
piezoelectric devices, variational principle for soln. of nonlinear acoustoelectronic problems 78−90621
piezoelectric plate HF vibrations, two-dimensional eqns. 77−39143
piezoelectric problem parameters 79−81594
plane symmetric rolling mill, vector field system soln. *(German)* 78−63333
plane thermal boundary layer, temp. distrib. determ. by var. formulation 77−23947
plane wave reflection from nonlinear absorbing medium 79−81478
plasma, axisymmetric ring, method of complementary variational principles appl. to equilib condition *(French)* 77−7579
plasma, current-driven drift-wave eigenmodes, stability criteria 79−32769
plasma, electrical conductivity, complementary variational principles 79−46427
plasma, EM wave response 77−80310
plasma, laser-irradiated, Langmuir soliton generation at crit. density 80−6267
plasma, stratified, partially ionised, hydromagnetic stability 78−26276
plasma, transport coeffs., relativistic Boltzmann theory, variational method 78−47096
plasma drift waves in sheared mag. field, variational method calcs. 80−106910
plasma in uniform mag. field, complementary variational principles on elec. conductivieies 79−46430
plasma MHD, numerical simulation, variational approach 80−28625
plasma nonlinear problem variational soln. *(French)* 78−63539
plastic flow, isotropic body, finite element method for volume integration 80−74770
plastic incompressible material with non-associated flow law 78−67050
plasticity, inhomogeneous problems *(Russian)* 77−23892
plasticity, three-dimensional problem soln. *(Russian)* 78−75079
plasticity of compressible media, variational method 78−94602
plasticity theory, variational inequalities and multilevel optimisation techniques 78−79224
plate bending, transient problem, variational and reciprocity principles 77−50898
plate buckling, variational formulation for hybrid finite element method 78−18205
plate problems, biharmonic oscill., finite element discretisation, preconditioned conjugate grad. method 79−72795
plate with steady state thermal boundary layer flow, appl. of governing principle of dissipative processes 79−50722
plates, isoparametric finite elements, variational formulation of plate equilib. problem *(French)* 80−43608
plates, large deformation anal., variational formulations 80−92067
plates and shells, elastic-plastic, cyclic loading anal. variational method 79−37198
plates design, circular, rigid-plastic, w.r.t. minimum-cost 77−68440
plates on elastic foundations, variational approach 80−79160
Poiseuille flow, complementary variational principles 80−96310
Poisson's equation for impurity ion in medium with spatially variable dielec. const., variational principle 78−60084
polar molecule-electron systems, variational method for bound state calc. 78−46261
polar orthotropic circular plate, var. calc. of axisymm. vibr. 77−31237
polar semiconductor, exciton dispersion, influence of optical phonons, effective exciton mass, variational calc. 79−15091
polarisability, at. and mol., dynamic, below 1st excitation freq. 77−50552

variational techniques continued
polarisable and magnetisable medium, internal momentum, MHD and state eqns. *(Russian)* 77−65804
polaron, bound, variational calc. of ground state energy 78−84152
polaron effects on excitons 80−24811
polaron energy, bound to Coulomb potential 80−88487
polarons, Frohlich, mean field theory, phase transitions 80−34371
polarons, strong coupling theory, variational approach 80−54621
polyatomic molecules, triplet states, var. and perturbational calcs. 77−61680
position space LCAO wave function, momentum space variation approx., many centre integrals 80−27926
position-space renormalization approach 79−30404
positive column with two-step ionisation 80−70056
positive-definite-matrix-conjugate vector, construction and constrained variation 78−8267
positron+H(He), second-order nonadiabatic polaris. pot. for elastic scatt. 79−22836
post-buckling behaviour of structures using a finite element-nonlinear eigenvalue technique 80−92078
potential operators and the inverse problem of classical mechanics, differential eqns. 79−2618
potential scatt., variational methods calcs., comparison of convergence 80−52043
potential scattering, matrix Pade approximants, variational bounds 77−65120
potential scattering, refined Born approx. 80−77
Potts model, discrete, three spin thermodynamic behaviour, Kikuchi cluster variational method anal. 79−35640
power flow equation, variational soln. rel. to random bends in graded index optical fibre 79−18549
power-law fluid, two-stream mixing along flat plate, variational solns. 80−53817
prestressed cablenets, 3-D, finite element anal. 78−5650
primitive wave function in theory of intermolecular interactions 80−95703
principle of least action, minimal interpretation, variational calcs. 80−68039
projector variation method, general outline 79−97244
PWR core, variational estimate of eigenvalue of neutron diffusion eqn. 78−58322
PWR manoeuvring strategy optimisation 79−629
QED bound states 79−21992
QED on lattice, Hamiltonian variational approach to physics of weak-coupling region 79−35979
quantal nonrelativistic N particle systems, appl. of variational techniques to bound states 79−35579
quantum energy levels, statistical mechanics method, perturbative variational approach 80−62513
quantum expectation values variational calc., second order error 77−33894
quantum lattice spin theory, Jastrow wave functions 79−25999
quantum liquids and crystals, computer modelling 80−54472
quantum mech. Gaussian path integrals and semiclassical propagator 77−22432
quantum mech. phase-space formulation, variational principle, harmonic oscill. ground state 77−2558
quantum mechanical perturbation theory, convergence props., energy series 78−80
quantum scatt. theory, gauge transform. for variational method 77−65
quantum scatt. theory, variational principles and virial theorem 78−54231
quantum statistical variational principles 79−75452
quantum systems with discrete energy levels, variational method 78−31074
quark bag model, variational principle description *(Russian)* 79−40757
quark-quark interaction, phenomenological, from s-wave baryon spectrum 80−101984
quasi-local algebras over lattice, variational princple 79−71371
quasi-one dimensional metals, variation function in theory 79−23887
quasibound states, variational principle 77−3251
R-matrix theory, atomic continuum processes 77−83478
radiative ablation of melting solids, Biot's variational method 77−31203
radiative transfer, variational and discrete ordinate calc. methods 77−53188
radiative transfer albedo problem in inhomogeneous isotropically scatt. atmospheres 80−36398
radioactive tracer kinetics, compartmental system identification by optimum sampling 77−86615
radius perturbation theory, appl. to NN system and pionic atoms 78−21007
random heterogeneous materials, statistical theory of effective elec. thermal and mag. props. 77−48118
random Ising model, press., variational principle 78−8352
random Ising model, variational principle for distrib. function in the Bethe approx. 80−15674
random two-phase material, thermal cond., var. calcs. of upper and lower bounds 78−9550
rare earth compounds electron-phonon interaction influence on electronic phase transitions *(Russian)* 78−47743
rare earth pnictides, phase diagram for cubic model in Kikuchi cluster variational method 79−35639
reactor, fuel element nonlinear transient heat conduction, variational calc. 79−93685
reactor boundary changes, generalised perturbation theory 78−4980
reactor materials burnup anal., depletion pertubation theory for coupled neutron-nuclide field 79−45339
real-space renormalisation group transformation based on cumulant expansion 79−12730
rectangular parallelepiped compression, small elastoplastic deformation, variation anal. *(Russian)* 79−32294
red blood cell elastic deforms. 77−56400
Reissner's variational principle linear theory of elastic plates and shells *(Russian)* 77−17819
relativistic field theories 77−82417
relativistic multicomponent systems, transport coeffs., variational calcs. 77−15151
relativistic theories involving torsion, variational principles 77−60990
reload core design optimisation 79−604
renormalisation group approx. 79−63169
variational techniques continued
renormalisation group transformations, Kadanoff's variational approx. 77−37822
renormalisation group transforms, optimal variational approx. 77−87699
renormalisation theory, variational principles 78−73951
resonance positions, complex-rotation technique for direct calcs. 78−33549
resonance width and energy, variational calc. 78−33445
resonances, energies and widths, variational calc. 77−83506
resonances, width and energy calc. method 77−30798
resonances, width and energy calc. method 77−61690
resonator vibration analysis, combined plate eqn. and finite element method 79−55296
Riemann curvature tensor, expressed as third-order potential tensor with symmetry props. *(Italian)* 79−49129
right translation invariant metrics and variational principles on principal bundle, gauge theories *(Chinese)* 80−101743
rigid punch problems, forces and moments by reciprocal variational techniques 80−23967
ring, multilayer elastic, forced vibration, variational principle effectiveness in Ritz method *(Russian)* 79−68616
Ritz-Givens-Householder method, anharmonicity type λx^{2m}, Schrodinger operator energy levels 78−28970
rocket propulsion using nuclear reactor, optimisation problem, calculus of variation 80−27694
rod, naturally twisted curvilinear, asymptotic variational method anal. *(Russian)* 80−38251
rotated hamiltonians, complex-coordinate rotation and least-squares variational method 80−68075
rotating stars, normal modes, general variational principle 80−12750
rotating stars, perturbs. and stability, eigenvectors and variational principle 80−46537
rotating stratified fluid, hydromagnetic stability 78−55692
rotational viscometric flow around rotating sphere *(German)* 77−80187
rotationally inelastic scatt., coupled eqns. for single initial state, variation-iteration method 79−68301
RS perturbation theory, E_3 variational principles 78−58570
rubber bonded cylinder, Lagrange anal. of dynamic props. 79−14304
S-matrix, variational principle for calculating poles 78−74165
S-wave phaseshifts bounds, least norm variational principle tests, appl. to $H+e^-(e^+)$ 80−5619
Saint Venant-von Mises materials, two-field variational methods *(French)* 77−17816
sandwich system, near transition temp., proximity effect and Josephson current 80−7039
scalar electrodynamic pot., convolutional functional *(Polish)* 79−50205
scalar field, exterior case, identification of variational principles *(French)* 80−73220
scalar field, modified stationary action principle, field eqns. for perfect fluid *(French)* 80−52076
scalar partial differential eqns., variational principles 79−30255
scalar-gluon field theory, variational approach to bound states 77−6025
scale-covariant gravitation and electromagnetism, variational principle 79−85027
scattering, multichannel, optimised anomaly-free and restricted anomaly-free variational methods 79−3515
scattering, multichannel, optimised Kohn method 79−49108
scattering, single-channel, optimised Kohn method 79−49107
scattering amplitude, phase, uniqueness, variational calc. 80−86156
scattering calculations, variational, error estimation 79−111
scattering from rough surfaces, principles 77−79724
scattering in generator coord. method, appl. of variational principle with natural boundary conditon 77−54196
scattering lengths, variational calcs. 77−57218
scattering phase, variational principle 80−68084
scene principal vector analysis by multiple spatial filtering 80−48179
Schrodinger's variational quantisation method in stochastic framework 80−105532
Schrodinger eqn., approximated solns. 77−30029
Schrodinger eqn., mixed local-global variational approach and its application to a discontinuous potential 79−58564
Schrodinger eqn. with discontinuous pots., global trial functions 77 30035
Schrodinger equation, nonseparable, series solns. and variational principle, appl. to H_2^+ and He 79−36504
Schrodinger equation, strongly nonlinear, variational approach 79−58583
Schrodinger equations, three-body problem, bound state eigenvalues lower bounds, upper bounds by Rayleigh-Ritz method 80−68068
Schrodinger operator, interaction of type $\lambda x^2/(1+gx^2)$ 79−91
Schrodinger operator eigenvalue calc., linear error minimisation *(German)* 77−33880
Schwinger and Kohn variational phase shift calculations, comparison 80−78672
Schwinger principle, method for numerical appl. 77−78959
Schwinger variational principle, appl. to electron-mol. ion scatt. 80−48086
Schwinger variational principle *(Russian)* 78−89361
Schwinger variational principle for bound states and scatt. problems 78−16932
Schwinger variational principle for dynamic susceptibilities 80−4639
Schwinger variational principle in nonstationary theory *(Russian)* 79−30668
screened Coulomb pot., Schrodinger eqn. with Hulthen pot., variational soln. 77−23427
seepage flow variational inequalities by finite element method 77−68688
seismic dispersion curves, methods of computing partial derivatives 77−37149
seismology, variational approach to elastic wave propag. in anomalous layers 79−44260
self-adjoint operator, eigenvalue bounds, variational approach *(German)* 79−25886
semiclassical two electron atom, appl. of semiclassical equivalent of Hylleraas var. method 80−58111
semiconductor, deep impurity centres, two-electron model 79−65411
semiconductor, donor-acceptor pair in elec. field, anomalous Stark shift of ground state energy 79−19564
n-semiconductor, electron-phonon drag in longit. quantising mag. field 77−76805
semiconductor, impurity ion pot., nonlinear Poisson eqn. soln., variational principles 78−67976

variational techniques continued
semiconductor, impurity ion pot., nonlinear Poisson eqn. soln., var. principles 80−29350
semiconductor, impurity ion pot., nonlinear Poisson eqns. 77−20265
semiconductor, three-impurity clusters, ionisation energies and electron affinities 80−65496
semiconductor, with spatially varying dielec. const., impurity ion pot., variational calc. 79−7800
semiconductor longitudinal magnetoresist. in quantising mag. field, var. calc. 77−43630
semiconductors, excitonic polarons, Pollmann-Buttner variational method, donor and exciton binding energies 79−42469
semiconductors, multiply charged impurity centers, energy spectrum 79−69469
separable optical potential theory, Schwinger variational principle *(Russian)* 79−3122
shallow shell bending, mixed variational eqn. 80−77618
shell, circular cylindrical with varying wall thickness, creep buckling, variational methods 80−14595
shell, conical, stress distrib. near hole, orthotropy effect 80−43630
shell, cylindrical, with spiral groove, Kirchhoff's boundary conditions deduced from energy principle 80−74741
shell, ribbed conical, subjected to harmonic load, forced vibrations 80−43658
shell, shallow, limit analysis and optimal design *(Russian)* 77−42752
shell, spherical, subjected to external pressure, matching conditions 80−1447
shell equations via extended variational principle *(German)* 77−72166
shells, cylindrical, large elastic deflections, numerical anal. 79−98613
shells, flexible, self checking stepping calc. process 80−68044
shells, Kirchhoff-Love, structural stability, mixed variational principles and non holonomeous constraints *(French)* 80−74779
shells, large elastic deflections of axially compressed cylindrical and conical structs. *(Polish)* 78−13937
Signorini's problems, reciprocal variational inequalities soln. 79−41585
simple elastic materials, variational principle 77−71213
Singer polymal tempering methods 80−52845
singular stress field at crack front edge in elastic body, crack propagation 79−50656
Slater determinants, energy functional, extremum problem, Hartree-Fock equations, gradient method 80−62573
slip flow in porous medium, effective diffusion coeff., variational method 79−90325
small-aperture diffraction polarisability coefficients rel. to wall thickness 79−68355
solar evolving force-free magnetic fields, variational formulation 78−93182
solid, self-consistent numerical-basis-set LCAO model, local density formalism 77−76725
solid theory, hard sphere melting law 77−47359
solidifying metal ingots, phase interface motion and variational Biot method 79−83189
solitary Rossby waves, atmospheric, variational principle 80−56539
solitary solutions collision in nonlinear field theory, variational anal., ϕ^4 appl. 79−35922
soliton equations, perturbed, variational approach 78−89366
soliton perturbations, variational calcs. 80−46825
spatial curved bars, kinematic elements of mechanisms, movement equations 80−46809
spatial reactor control methods 77−83056
spatially periodic convective flow, stability and fluctuations 80−19394
spectral filter, optimisation for arbitrary criterion by method of basic extremals 80−96011
spectral shifts, variational study, relativistic aspects *(French)* 80−21909
sphere, method of variation of consts. appl. to excitation by elec. and mag. currents 78−86989
spherical cavity, variational anal. of stability *(Russian)* 77−50885
spin and isospin stability of dense neutron and nuclear matter with hard core interaction 79−26386
spin glass, quantum effects 80−2581
spin glass binary mixture at T=0, energy and variational props. 80−39794
spin-density gradient expansion for kinetic energy of electron gas, variational calc. 79−93917
spinning particle, Lagrangian function using variational formalism 79−40356
spurious avoided crossings, noncrossing rule calcs. 77−6661
square lattice Ising type models statistical mechanics, variational approx. 79−44873
stability of spinning liquid-filled solid bodies 80−43609
stagnation point steady and non-steady laminar viscous flow, variational solns. 77−27510
stamp problem, elastic layer or half space, variational formalism, numerical soln. 79−1106
standard sample homogeneity evaluation, optimal obs. planning 80−93721
star clusters, isotropic relativistic, multi-term trial function stability anal. 78−73742
Stark effect, perturbation and variation treatments, appl. to H(1s) reson. 80−14105
stationary phase principle, generalisation 79−30199
stationary turbulence, path integral functional description, variation principle 79−77083
statistical models, thermodynamic properties, variational calc. 77−85405
steady homenergic compressible flow with finite shocks, variational principle 80−69874
steel plate collapse, anal. by live energy minimisation 78−52910
Stefan problem simulation and control, associated variational inequality 78−67009
stellar magnetic configurations linear oscills., unrestricted second-order tensor virial eqns. 79−44461
stochastic control, regularity of weak solns. of variational irregularities *(French)* 79−54053
Stoke's problem in velocity pressure formulation, mixed finite element approx. *(French)* 78−86164
stress anal., direct and variational principles rel. to approx. techniques 80−28420
stress field in composite laminates, theory based on Reissner's variational principle 78−67038
stress intensity factors, anal. determ. by variational method for eccentric cracks 78−67115
variational techniques continued
strong coupling method reformulation on the basis of the Schwinger variational principle *(Russian)* 78−89836
strong coupling QCD, variational approach, Schrodinger eqn. and effective Hamiltonian 80−95245
structural dynamics, finite element reduction scheme, variational theorem 77−890
structural dynamics, polynomials and variational methods 77−68393
structural element design calc. under creep conditions 80−48598
structural systems, time-varying stresses calc. by variational principle 77−3732
subsonic compressible flow, past symmetric profile, num. soln. method *(French)* 77−58720
subspace quantum mechanics and the variational principle 78−70002
superconducting vortices, interaction energy using constrained var. calc. 79−78256
superconductivity, general relativistic phenomenological theory 80−2518
superconductor tunnelling system, approx. Hamiltonian *(Chinese)* 80−44768
superfluid wave propagation, variational and reciprocity principles 77−72727
supergravity, self-duality in superspace, functional anal. 80−46902
surface-fluid-shell system, finite element anal. of dynamically coupled motion 77−19536
symmetrical Lamb wave scatt. at pair of thin slots 79−47868
symmetry-adapted Wannier functions, variational procedure 80−2323
symmetry-adapted-cluster expansion, variational determ., open-shell orbital theory applic. 78−54213
systems containing noninteracting mols., variational CI calcs. 77−67988
tank with fluid, variational anal. of dynamic reaction *(Ukrainian)* 79−32234
TDHF Hamiltonian, variational derivation 79−93536
TDHF time depend. phases, TDHF variational principle 79−93535
TDMF phase, unique implication of variational principle 80−27583
thermal conduction, generalised *(Russian)* 78−59265
thermal conductivity, nonlinear, variational formulation, counter functional, exactness of soln. *(Russian)* 80−90800
thermal conductivity in homogeneous isotropic solid body, variational principles *(Hungarian)* 78−22247
thermal reistance minimisation, solid with heat-exchanging surfaces, variational method 78−94512
thermal stress anal., finite element variational method 77−7310
thermal stress variational anal. 77−7311
thermal stresses in rectangular plates, variational and finite element solns. 78−51082
thermodynamic partition function, analytic props. of Lippman-Schwinger variational approx. *(German)* 78−36953
thermodynamic properties of permanent dipoles on lattice 78−88246
thermodynamics, finite time processes, step-Carnot cycle 77−67400
thermodynamics, irreversible, internal variable theory, Lagrangian formulation 80−73291
thermodynamics of irreversible processes, variational principles *(German)* 78−81936
thermodynamics of viscous compressible heat conducting fluids 77−50868
thermoelasticity, uniqueness theorem and variational principle 80−92056
thermoelasticity with finite wave speeds 78−65772
thermoplasticity, time evolution under quasistatic conditions, existence theorems 80−74764
thermorigid dielectrics, nonlinear thermodynamic theory 80−10149
thermoviscoelasticity, bound dynamical problems, approx. calc. methods for crit. thermal states *(Russian)* 78−28949
thermoviscoelasticity, variational techniques *(Russian)* 78−13922
thin circular cylinders, vibration characteristics for different end conditions 79−86376
thin elastic shells, general theory 79−25857
thin elastic shells, stability, variational method *(Russian)* 79−32321
Thirring model, iterative variational anal., fermion field theory on lattice 78−41426
Thomas-Fermi screened Coulomb systems, thermodynamic props. calcs. 77−67399
three-body problem, eigenvalue calc., appl. to He atom *(German)* 77−33881
three-body systems, number of bound states and Efimov's effect 80−31536
three-dimensional gasdynamic flows, variational principle in Euler description, vortex conservation 80−48731
three-layer elastic-viscoelastic beam damping characteristics *(Japanese)* 78−9575
three-photon Umklapp processes, variational techniques 79−37785
tides, oceanic and shallow water, spectral method of computation *(French)* 78−28321
tides, spectral modelling, finite element method, appl. to M_2 tide in English Channel 78−61579
time-dependent variational principle and effective action 79−63359
time-dependent variational principles, Schrodinger eqn. 77−26208
Tokamak, asymmetrical collisional tearing mode growth rate, variational treatment 79−32803
Tokamak, plasma MHD equilib., var. method *(Russian)* 80−106960
topology, propagation of surfaces of weak discontinuity, broken extremals in classical field theory 78−93541
toroidal plasmas, equilib. energy principle with global invariants 80−92366
torsion of elastic bars, 2-D optimisation problem *(Russian)* 77−23877
transient temp. field in nuclear fuel rod, calc. by variational procedure 79−9772
transition metal complexes, discrete variational Xα cluster calcs. 80−15444
transition state theory, absolute rate theory and variational formulations, Porter Karplus pot. surface 80−16642
transition state theory generalisations 80−26002
transition state theory generalisations 80−26003
transmission probability of free molecular flow through a tube 79−94662
transonic aerodynamics, finite element method, book contrib. 79−32556
transonic aerodynamics, variational formulation and finite element anal., book contrib. 79−32555
transonic airfoil problem, variational principles 78−42626
transport problems, variational techniques appl. 78−89415
transport process optimal control adaptive criterion study 77−17931
transport theory, two-group integral transport equation, variational method 80−68156

variational techniques continued
transport-relaxation equations, time-depend. variational principle and reciprocity theorem 78−12655
transversally nonhomogeneous waveguide EM wave propagation, using variational methods *(Czech)* 80−33155
trapped particle instability in Tokamaks, book 78−83562
triangular Ising lattice, anal. of Kadanoff lower-bound renormalisation-group, approx. 80−8930
triangular plate elements, numerical investigation using variation principles with relaxed continuity conditions *(German)* 79−10465
triangular renormalisation group transformation, var. approximation 78−49776
truncated exponential density sequence, estimator asymptotic variance comparison 78−12539
turbomachine airfoil cascades, variational and dual extremum principles for aerodynamic problems *(Chinese)* 80−43729
turbulence theory, variational method 79−59968
turbulent channel flow transport, inequalities, variational principles 79−60063
two body scatt., non-relativistic, variational matrix Pade approximants *(German)* 78−54247
two-bar frame, eccentrically loaded, nonlinear stability anal. 78−63343
two-centre scattering amplitudes, var. determ. 77−78998
two-dimens. U(1)-Goldstone model, QFT on lattice 78−74158
two-dimensional multiply connected regions of arbitrary shape and boundary conditions, temp. field calc. 79−86317
two-dimensional quantum systems at zero temp., liquid to gas phase transitions 78−77798
two-electron system, natural orbitals, pseudo-eigenvalue eqn. and long-range behaviour 79−85886
two-electron systems, ground-state energy, var. calcs. 77−61679
two-particle interactions, new variation-perturbation principle 79−10006
two-phase Stefan problem, numerical anal. by variational inequalities 79−82315
two-stream mixing, variational soln. 78−38266
unbounded contact between elastic and elastic-rigid media, variational calcs. 79−98670
unconstrained variational statements for initial and boundary value problems, comment and reply 79−75327
unconstrained variational statements for initial and boundary-value problems 79−92927
underwater acoustic propagation, duct problems, variational anal. techniques 78−90574
underwater acoustic source location and motion estimation, joint reduction of bias and variance 80−96087
unidirectional fibrous composite, mixture theory for longitudinal wave propagation, computational procedure 79−50632
unidirectional wave motions, book 78−77730
unified field theory, five-dimensional theory of interacting scalar, electromagnetic, and gravitational fields 80−105833
unified theory of atoms and atomic aggregates, self consistent theory 80−102418
unitary variational method for atoms and mols. 77−71743
universal variational functionals of electron densities, first-order density matrices, and natural spin-orbitals and solution of the v-representability problem 80−95516
variation-iteraction soln. of Hartree Fock eqns., Green's integral operator, SCF formalism 79−6842
variational equations solved one as function of other, wave propagation appl. *(French)* 77−41493
variational inequality related to elasticity operator, soln., dual problem 79−9109
variational Lagrangian irreversible thermodynamics of nonlinear thermorheology 77−27467
variational [1/1] matrix Pade approx. in pot. scatt., exact solns. 77−22447
vectorcardiogram diagnostic algorithm improvement by outlier elimination 79−39572
vibrations of multilayer orthotropic shells *(Russian)* 78−13968
vibronically coupled systems, cluster model 79−19540
viscoelastic fibre-reinforced composites, wave propag. 79−76992
viscoelastic fluid, stability of steady shearing flows, energy method and parabolic maximum principle 80−74926
viscoelastic plate, buckling and stability, convolution var. principle 77−35052
viscoelastic solid, linear quasi-static theory, variational and minimum principles 80−10157
viscoelasticity, geometrically nonlinear 77−880
viscoelasticity, linear theory *(Japanese)* 80−48599
viscoelasticity, linearised theory, variational principles *(Russian)* 78−87279
viscoplasticity with hardening, quasi-variational problems *(French)* 77−14913
viscosity stratified fluid layer, heated from below, thermal instability 77−58762
viscous fluid, variable thermal conductivity, variational calc. of vel. profile and temp. in laminar boundary layer *(French)* 78−55625
viscous fluid mixture with thermomolecular diffusion, new variational-Lagrangian thermodynamics 79−49185
viscous gas eqn., movable net difference scheme *(Russian)* 79−50838
viscous incompressible Stokes flow, primitive eqns. solns., variational models 79−18857
voids, sink strength of random array, steady-state diffusion problem, variational technique 80−49266
Warren-Averbach method verification, distortion model calc. *(German)* 77−58921
water, deep, direct variational anal. of oscillatory irrotational waves *(Italian)* 78−83415
wave equation for simultaneous heat and mass transfer in moving media 79−44747
wave functions, stability, continuity, symmetry 77−23409
wave functions, variation-iteration principle, bound and scatt. states 78−54227
wave propagation in viscous heat cond. gas, Gurtin type props. 77−27645
waves in stratified heavy incompressible fluid, variational principle 78−59495
waves reflection and transmission at interface between elastic waveguides 77−84027
wavevector-dependent spin susceptibility, variational principle 78−91586
wear of body rotating in viscous abrasive medium *(Russian)* 79−79114

variational techniques continued
Weyl-Dirac theory with torsion, complex Dirac field, conservation equations 80−68112
whole-Earth dynamics, variational method 77−60340
X-ray dose mean value of specific energy, variational meas. 80−12276
X-Y model, spin 1/2, ground state energy, long-range order determ. by variational method 78−72322
Yukawa Bose fluids, Jastrow wave function, Monte Carlo computation 79−73375
Yukawa potential-ground state boson interaction, Monte Carlo study 78−51768
Z_+^N action on compact space 77−53825
Z(2) lattice gauge theory, variational approach, two phase struct., phase transition 80−68361
zero energy scattering quantities, bounds 78−49686
zero-component field theories, high order behaviour without $n \rightarrow 0$ limit 79−75438
zero-gap semiconductor, variational approach to resonances 79−82559
zinc blende semiconductors, small-gap, electron scatt. and transport props. 78−95294
zinc blende semiconductors, small-gap, electron scatt. and transport props. 78−95295
β-stable nuclear matter, electrically neutral, constrained variational calc. 78−58243
Δ mass, three quarks bound state, variational method calcs. 78−21396
NN dynamics, variational matrix Pade approximants 78−62427
Ag, electronic contribution to thermal cond. at low temps. 79−95384
Ar, liq., variational eqn. of state and entropy 79−28070
Ar, nonempirical calc. of X-ray K-absorpt. spectra 77−88465
BH, elec. polarisabilities and dipole moments, var. perturbation obs. 80−63527
BH^{5+}, spurious avoided-crossings, variationally calc., perturbation theory approach 78−5295
$B_3N_3H_6$, electronic struct., mag. susceptibilities, ab initio calcs. 78−74571
Be, polarisability and London coeff., ab initio variation perturbation calc. 79−13635
^{8}Be, cluster formation, multicentre variational model *(Chinese)* 78−25128
(Br,Zr) system, 1 s σ orbital, variational calc. 78−37707
C, ground and excited states, atomic polarisability calc. 77−83756
C-C σ bonds, mag. suscept., refined variational calc. 77−68136
C-H bonds, mag. suscept., vector pot. variational calc. 77−68137
C_3, Renner effect, vibronic levels and wavefunctions, ab initio variational method 80−14127
CO, electronic struct., binding energy and interatomic distance, SCF variational cellular calc. 80−9498
CO, photoabsorption, photoionisation cross-section, separated channel static exchange Stieltjes-tchebycheff calc. 79−3502
^{12}C, α-particle model 77−82839
^{12}C, three α model calcs. and O_2^+ state 79−75856
Ca_2, mol., vibr. quantum numbers of rotating vibrator 79−85949
^{42}Ca, collective states, quasi-degenerate intrinsic Hamiltonian, variational methods 80−68505
$Cd_xHg_{1-x}Se$ mixed cryst., electron mobility and electron scatt. 78−95296
Cs halides, F_x-centres, variational calc. of energy levels 79−82204
Cs halides, F-centre energy levels, ion-size effects, calc. 80−96519
CsX,(X=F,Cl,Br,I), ionis. energy, relativistic Dirac-Slater and nonrelativistic HF-Slater calcs. 77−26983
Cu (001) monolayers, electronic struct. 78−72233
Cu, electronic contribution to thermal cond. at low temps. 79−95384
CuCl, energy bands and effective mass 80−10859
D_2, c, I and i states, pot. energy curves and vibr. levels, Born-Oppenheimer approx. 78−931
Fe atoms and condensed matter in strong mag. fields, var. calc. ground-state energy 77−75046
GaAs, exciton ground state and oscillatory absorption spectra in mag. fields, variational calc. 79−11071
GaAs, excitons, diamond like semiconductor, variational calculation of binding energies 78−79938
GaAs, excitons in arbitrary mag. fields 80−96798
GaAs, impurity scattering of current carriers in quantizing mag. field 78−51954
GaAs, self-consistent localised electronic struct. 79−42445
GaP, donor states theory, camel's back struct. influence 80−59921
GaP, scatt. mech., mobility tensor 80−6826
Ge, acceptor ground state, stress effects 80−34385
P- Ge, acceptor wavefunctions in spherical approx. and piezoresist. 80−29405
Ge, donor polarizability, multivalley effective mass calc. 80−96817
Ge, far IR magnetoabsorption of free and bound excitons 78−52474
Ge, self-consistent localised electronic struct. 79−42445
n-Ge:Au, electron capture by negatively charged traps, effect on hot electron enrgy energy distrib. 78−43398
(H,H) system, 1 s σ orbital, variational calc. 78−37707
H atom spectra, homogeneous mag. field, variational approach 79−22629
H bound states in strong mag. field 80−99438
H, condensed, spin-aligned, props. from variational calcs. 80−4637
H, electron elastic scatt., local pot. method, bound states 77−75296
H, electron impact excitation of resons. below n=3 levels, algebraic variational calc. 78−9254
H, electron impact excitation of n=2 to n=3 transition, algebraic variational method close coupling calcs. 80−91678
H, electron scatt., equivalent exchange pots., algebraic variational method, 2p-2p and 2s-2p transitions 80−18931
H, freq. depend. multipole polarisability and dispersion energy between interacting pairs 79−18306
H, He atmosphere, hyperfine press. shift, MCSCF-variational procedure 77−6735
H, quasibound states, Stark effect, variational 77−3251
H, Rydberg Stark ionis. threshold scaling laws 77−6721
H, spin-polarised atom, binding to free surface of liq. ^{4}He 80−34277
H, Wannier functions, variational calc. 77−15740
H^-, bound states in mag. field, binding anal., variational calcs. 80−42940
H^-, energies and widths of $^1P^0(1)$ and $^1S(2)$ resonant states 79−18130
H^-, photodetachment cross section, perturbation-variation method 79−6921

variational techniques continued
H-He, H hyperfine struct. shift, commutator computational method 78−78608
H-like ion+H, two-body dispersion interaction, freq. depend. multipole polarisability, variational calc. 80−37758
H-like systems in arbitrary mag. field, excited states, variational approach 79−77973
H-quark interaction, var. method calcs. 78−37771
H_2, D_2, photoionisation, body-frame Hund's case b description 78−94295
H_2, dynamic polarisabilities, variation-perturbation calcs. 80−87243
H_2, electron scatt., iterative approach to Schwinger variational principle 80−99580
H_2, electron scatt., Schwinger variational principle, static-exchange approx. 80−63820
H_2, HD, c, I and i states, pot. energy curves and vibr. levels, Born-Oppenheimer approx. 78−931
H_2, mag. susceptibility vector pot. variational method, gradient transform. function selection 80−69258
H_2, metallic, ground-state energies of liq. and solid phases, variational and Monte Carlo methods 80−70502
H_2, metallic, liq., ground state energy at zero temp. 79−38006
H_2, triplet state, pot. curve van der Waals region, MS-MA calcs. 77−79551
H_2, Xα theory appls. approximations 80−9510
H_2^-, variational calcs. of resonant states 79−3571
H_2^+ bound states in strong mag. field 80−99438
H_2^+, dynamic dipole polarisability, variational perturbation theory 78−94330
H_2^+, electron elastic scatt., two-centre variational calc. of s-wave phase-shift 79−3570
H_2^+ energy spectrum, variational cellular method calcs. 78−94192
H_2^+, high (10^9 G) mag. fields, dissoc. energy, electron binding energy and equilib. separation 80−52910
H_2^+, hyperfine struct., refined var. calcs. 77−75067
H_2^+, ionisation energy, internucl. separation in intense mag. fields, var. calcs. 77−57898
H_2^+, ionisation energy in strong mag. field, variational calcs., equilib. internucl. separation 77−46654
H_2^+, modulated perturbation theory variational calc., ground state second order energy 77−57872
H_2^+, nonadiabatic vibrational energies, ab initio calcs. 78−90142
H_2^+, spurious avoided-crossings, variationally calc., perturbation theory approach 78−5295
H_2+H, diatomic operator, separable approx., variational approach 78−42150
H_2+H_2, dispersion forces calcs. 80−9675
H_3^+, ab initio calcs. of vibr. spectrum 77−6753
H_3^+, dipole polarisabilities, variational perturbation theory calcs. 78−70765
H_3^+, struct. props., in mag. fields, var. calcs. 78−21843
HCl, nonempirical calc. of X-ray K-absorpt. spectra 77−88465
HD, ground state props., nonadiabatic var. calcs. 78−58576
HD, perturbation var. calc. with contact interaction, effect of approx. zero order wavefunctions 80−58107
HD, spin-spin coupling constant convergence, comparative study 80−63536
HD^+, nonadiabatic vibrational energies, ab initio calcs. 78−90142
HF, nonempirical calc. of X-ray K-absorpt. spectra 77−88465
HF, vib.-rot. props. of $X^1\Sigma^+$ and $B^1\Sigma^+$ states, variational calcs. 77−50422
$H_2O+D_2O \rightleftharpoons 2HDO$, vibr. anharmonicity effect on equilib. 79−74410
^3H Sussex interaction, g-matrix and variational calcs. 79−3091
$^3H_\Lambda$, and contrib. of spin forces to Λ-N interaction *(Russian)* 77−79319
^4H, nuclear cluster model, energy levels by interaction set anal. 78−25136
He, ^1S ground state, variational perturbation calc., teaching 78−41129
He, appl. of semiclassical equivalent of Hylleraas var. method appls. 80−58111
He, bound states in mag. field, binding anal., variational calcs. 80−42940
He, diamag. suscept., form factor, variational method 77−18813
He, double photoionisation calcs., variational method 80−37734
He, dynamic polarisability, 2^3S_1 and 2^1S_0 states var. perturbation calcs. 77−54507
He, electron impact, ^3P_g and $^{1,3}D_u$ states excitation, electron correlation influence, Rudge-type approx. 78−74771
He, freq. depend. multipole polarisability and dispersion energy between interacting pairs 79−18306
He, generalised oscill. strength, variational determ., extremum principle appls. 78−94213
He, Hartree eqn. variational method 79−49941
He, isoelectronic sequence, 2^1S states, analytic wave function 80−9525
He, isoelectronic series, ground state specific mass shift, HF variation perturbation calc. 80−47889
He, isoelectronic series, var. energy functionals involving 1-electron operators 77−83484
He isoelectronic series 79−85894
He, muonic three-particle system with Coulomb interaction, correl. wavefunctions calcs. 77−68144
He, Pade type variational functions, appln. to ground state 80−87025
He, scattering, differential cross sections, variational calc. electron elastic scattering, differential cross sections, variational calc. 79−89785
He, variational energies for highly excited states 78−62737
He^-, isoelectronic sequence, triply excited bound state, variational calc. 80−9526
He^+, isoelectronic series, Lamb shift, Bethe mean excitation energy 78−9092
He-like ions, H^- through Mg^{10+} 1^1S state variational wave functions 77−34545
He-like ions, He through Mg^{10+}, 2^1S, 2^3S, 2^1P and 2^3P states variational wave functions 77−34546
He+He(Li), intermol. forces, ab initio VB calc. using nonorthogonal basis set 80−23490
$^4He_2$, bound state at small and large separations, variational calcs. 78−50609
HeH^{2+}, pot. energy curves for 2pπ and 3dδ excited states 78−29756
$He_2(He_2^+)$, variational electronic struct. calcs. using Hylleraas type wavefunctions 77−88375
$HeLi^{4+}$, pot. energy curves for 2pπ and 3dδ excited states 78−29756
^{3}He, Jastrow-type variational calc. methods 79−77854

variational techniques continued
^{3}He, liq., binding energy, variational calcs. by Pandharipande's method 80−101752
^{3}He, liq., binding energy and effective interactions, interactions, variational calcs. 80−107596
^{3}He, liq., surface tension, density profile, variational calcs. 78−67882
^{3}He liquid, binding energy calcs., Pandharipande method 79−65269
^{3}He, liquid, ground-state props., variational method using Fermi hypernetted-chain approach 77−35781
^{3}He, liquid, shear viscosity and thermal cond., s- and p-wave approx. 79−1535
^{3}He, liquid, surface tension and density profile at 0K 79−55997
^{3}He, normal, acoustic impedance, variational theory 79−42334
^{3}He, solid, variational calcs. using antisymmetric trial functions 79−65290
^{3}He, solid BCC, physical origin of large four spin exchange 79−56031
^{3}He, superfluid A-phase, current-driven textural transition 79−55993
$^3He_2$, variational calc. of binding energy 77−54503
^{3}He-^{4}He few atom mixed mols., binding energy, size, particle distrib. 80−32864
^{4}He ground state binding energy, near threshold behaviour in 2 and 3 dimens. 80−91716
^{4}He, liq., atomic scattering at free surface 78−56003
^{4}He, liq., binding energy, variational calcs. by Pandharipande's method 80−101752
^{4}He, liq., excited states, variational calcs. 80−80017
^{4}He, liq., ground state, self consistent description of long- and short-range correlations 80−107592
^{4}He, liq., hydrodynamic theory, variational methods 79−42331
^{4}He liquid, binding energy calcs., Pandharipande method 79−65269
^{4}He, liquid, surface structure 78−87837
^{4}He, liquid, three body correlation 78−87834
^{4}He superlattices on graphite, ground-state energy, variational calc. 80−24710
^{4}He, threshold condition for forming atomic trimer 80−63741
^{4}He trimer and tetramer, ATMS appl., bounding and ground state energies 79−86026
$^4He(\alpha,\alpha)$, size change of α effect on phase shift, generator coordinate and variational methods *(Chinese)* 80−68683
$^4He(d,d)_2$, distortion effects, orthogonality condition model 80−63190
$^4He(t,n)^6Li$, cross section using var. calcs. in generator coordinate method 78−13122
$^4He(t,t)^4He$, cross section using var. calcs. in generator coordinate method 78−13122
$(^{3,4}He)_3$ molecular bound state, variational and exact studies 77−27214
HgTe, resonance states in scatt., variational methods 79−60754
HgTe, zero gap semiconductors, Coulombic resonance states 79−38020
HgTe, zero-gap-semiconductor, variational approach to resonances 79−82559
K (001) surface, electronic struct. by density matrix method 79−60900
KH_2PO_4, variational treatment of proton-photon system 78−88261
Li halides, F-band energies press. effect 78−60086
Li, lowest $^2P^0$ and $^4P^0$ states, variational Hylleraas-type wavefunction 79−10023
Li, multipole polarisabilities, shielding factors calc., hydrodynamic analogy to quantum mechs. 77−68134
LiF, ground and excited state props., local density formalism 78−10349
LiH, mol., vibr. quantum numbers of rotating vibrator 79−85949
LiH, mol. elec. polarisabilities and dipole moments calcs. 78−41976
LiH_3 variational Hylleraas-type wavefunction, correl. 78−9082
LiH^{3+}, pot. energy curves for 2pπ and 3dδ excited states 78−29756
^{6}Li, cluster formation, multicentre variational model *(Chinese)* 78−25128
$^6Li(\alpha,\alpha)^6Li$, cross section using var. calcs. in generator coordinate method 78−13122
Mg, polarisability and London coeff., ab initio variation perturbation calc. 79−13635
Mg_2, mol. consts. calcs., inverted perturbation approach 77−57969
MoO_6^{6-}, electronic struct., discrete variation and scatt. wave X_α methods 80−917
N, ground and excited states, atomic polarisability calc. 77−83756
N_2, electronic struct., binding energy and interatomic distance, SCF variational cellular calc. 80−9498
N_2, Xα theory appls. approximations 80−9510
N_2+N_2, dispersion forces calcs. 80−9675
Na, variational cellular method, electronic struct. calcs. 80−54591
NbO, electronic struct. from photoelec.- and X-ray emission spectra and X_α calcs. of NbO_6^{-10} cluster 79−23892
Ne, atomic struct. calc., symmetry adapted pair functions, Rayleigh Schrodinger HF variational perturbation theory 80−42944
Ne, CI-Hylleraas variational calc. of ground state 77−18798
Ne, ground state, configuration interaction, iterative variational method calcs. 78−55127
Ne, nonempirical calc. of X-ray K-absorpt. spectra 77−88465
Ne, second-order correl. energy calcs. 78−33436
Ne, temp. perturbed Thomas Fermi eqn., variational principle 80−69074
Ni, chemisorption of H, Xα cluster calcs. *(Japanese)* 78−72002
Ni, effective Coulomb interaction momentum depend. band model 79−78298
Ni, FCC, H-Ni_n self-consistent electronic screening charge density 79−33255
Ni, Xα theory appls. approximations 80−9510
β′-NiAl, self consistent embedded cluster model for Fe, Co, Ni mag. impurities 80−2549
$NpAl_4$ clusters, band struct., variational Xα calc. 79−4508
$NpAl_4$, clusters, X_α calculations *(Japanese)* 79−82519
O, ground and excited states, atomic polarisability calc. 77−83756
O_2, singlet state radiative lifetime, perturbation-variation calc. 77−14496
O_3, line and band strengths in IR spectra, variational calcs. 80−87112
O_3 vibr. and rot. variational calc., isotope shifts 77−57967
O_4 molecule, equilib. struct., vibr. freqs., SCF closed shell calcs. 80−74101
^{16}O, binding energy, wave function of ground state, orthogonal schema model 79−63582
$^{16}O(d,p)^{17}O$, coupled channel variational method for multi-step direct nuclear reactions. II. Test on a (d,p) reaction 78−66259
Poisson's equations for impurity ion in medium with spatially variable dielec. const., variational principle 78−60085
$PuAl_4$ clusters, band struct., variational Xα calc. 79−4508
$PuAl_4$, clusters, X_α calculations *(Japanese)* 79−82519
S, static multipole polarisability, frozen core approx. 79−36791

variational techniques continued
Si, ab initio self consistent calcs., charge density and band struct., Wannier function scheme 79−69409
Si, donor polarizability, multivalley effective mass calc. 80−96817
Si, shallow donor states, substitutional donors 79−65403
Si-SiO_2, n-type inversion layer, theory of impurity-shifted intersubband transitions 80−20324
SmS intermediate valence, low lying states 80−96826
SmS, nonorthogonal orbitals in intermediate valence 78−43323
p-Te, transverse and longit. Nernst-Ettingshausen effect, theory and expt. 78−76095
$ThAl_4$ clusters, X_α calculations *(Japanese)* 79−82519
TiO_2, clusters, surface electron struct. and defect states, DV-Xα calc. 80−20268
UAl_4, clusters, band struct., variational Xα calc. 79−4508
UAl_4, clusters, X_α calculations *(Japanese)* 79−82519
UO_6^{6-}, electronic struct., discrete variation and scatt. wave X_α methods 80−917
$(UO_8)^{12-}$, electronic struct., variational Xalpha cluster calc. 80−39499
$(UX_6)^{n-}$, X=N,O,S, electronic struct., variational Xalpha cluster calc. 80−39499
VO_4^{3-}, charge transfer transition, bond length effects calcs. 77−83721
WO_6^{6-}, electronic struct., discrete variation and scatt. wave X_α methods 80−917
Zn^{2+}, electron pair correlation energies 79−93927
ZnSe, self-consistent localised electronic struct. 79−42445

varistors
instability effect of varistor frequency transducers on radiometer sensitivity, anal. *(Russian)* 77−22598
Si, bicrystals, grain boundary states and varistor characts. 80−24829
ZnO based, analysis of highly nonlinear current-voltage characts. 77−11983
ZnO based varistors, evolution and role of chem. constituents rel. to prep. method, influence on elec. props. *(French)* 78−31367
ZnO based varistors, nonlinear cond. theory 79−78192
ZnO, ceramic varistor, physical props. of elec. barriers by AES and electron microscopy 77−20326
ZnO ceramic varistors, I-V characts., single grain junction meas. 79−15225
ZnO ceramic varistors, trapping by localized states, effect on dielec. and elec. props. *(Russian)* 79−28671
ZnO ceramic varistors, thermal breakdown 80−88928
ZnO, low temp. AC props. 79−38434
ZnO, sintered grains, cond. model 78−14736
ZnO, statistics and grain size effects on breakdown characts. 80−34010
ZnO, varistor action, homojunction breakdown mechanism 78−60193
ZnO varistor ceramics, current-voltage characts., inhomogeneities and single barriers 80−80273
ZnO varistors, barrier voltage determ. 79−56306
ZnO:Ba, Co, rare earth metal varistors, microstructure-prop. relations 80−100249
ZnO-based, grain-boundary segregation, thin film X-ray spectroscopy obs. 80−35185
ZnO-based ceramic varistors, current-voltage characts., leakage and breakdown regions, 100 to 1300°C 79−56231
ZnO-grainboundary-ZnO junction in ceramic varistor, capacitance-voltage characts. 80−65689
Zn0 based, analysis of highly nonlinear current-voltage characteristics 77−39917

varnish
brittle, strain sensitive, for stress, strain testing of surfaces of loaded structs. 79−29311
ester-imide, electroinsulating, thermal resist. *(Polish)* 78−84014
glaze-porcelain system, intermediate layer investig. by electron probe microanalysis 77−8965
polyester, electroinsulating, thermal resist. *(Polish)* 78−84014
resin based on diacid prepared from 4,4′-oxydibenzoic aldehyde and dihydroxymethyl propionic acid *(Polish)* 77−28776
shellac, electrical cond. mechanisms, Schottky and Poole-Frenkel processes and work function 80−29402
stress anal. during drying 79−34183
wood panel coatings, electron-beam curing 77−70200

Vavilov-Cherenkov radiation *see Cherenkov radiation*

VB calculations
π-bonding, increased valence theory calcs. 77−46500
ab initio effective core pots., reduction of all electron to valence electron calcs. 77−14361
acetylene, and $C_2H_2^+$, ionis. pots., photoelectron spectra, ab initio VB calcs. 77−88396
actinide compounds, BOA valence bonding with f-character 80−6790
alkali metal+HX (X=F,Cl,Br,I), reaction, semiempirical pot. surfaces calcs. 79−74362
alkali metal hydrides, VB calcs., equilib. internuclear separation, dissoc. energies 77−71756
alkali trimers, London pot. energy surfaces 79−6893
allene, vertical valence ionis. pots., ab initio UB calcs. 79−85917
allyl radical, ionisation potential, ab initio valence bond calcs. 79−31407
atom, one-centre integrals of exact effective valence shell Hamiltonian 80−74128
benzene, charge and current densities 77−3261
benzene, ground, singlet and triplet states, ab initio VB STO, GTO calcs. 77−75060
benzene, noncrossing and degeneracy in Hubbard models 80−14096
benzene, VB calc. with CI, basis sets orthogonality problem 77−23435
bioorthogonal VB method, approx. natural orbitals 77−50368
trans-1,3-butadiene, valence electronic excited states, SCF ab initio GVB and CI calcs. 79−31423
butadienes, cis- and trans-, ionisation potential, ab initio valence bond calcs. 79−31407
butatriene, vertical valence ionis. pots., ab initio UB calcs. 79−85917
charge and current densities, approx. wavefunctions, valence bond, molecular orbital methods 77−3261
cyanamide, ab initio VB wave functions, π-electrons 78−70748
cyclobutadiene, noncrossing and degeneracy in Hubbard models 80−14096
dialkalis, VB calcs., equilib. internuclear separation, dissoc. energies 77−71756
discontinjous approx. mol. electronic wave functions, ab initio LCAO and VB ZDO appls. 77−50340
electron transfer, intramol., electron propagator method 77−34560

VB calculations continued
electronic states and initial steps in oxidation 78−91534
electrostatic isopotential maps for large biomolecules, STO transferable bond calc. 80−3571
ethylene, ionisation potential, ab initio valence bond calcs. 79−31407
expansion of MO wave functions into VB work functions 78−74580
extended correlated electronic systems, charge transfer transitions 80−29362
extended lattice VB theory, long range order spin pairing 80−52136
formaldehyde, Rydberg states, excitation energies, oscillator strengths ab initio GVB-CI calcs. 77−54518
geminal product approx., optimisation of molecular wavefunction 80−37733
halogen molecule negative ion, Cl_2^-, Br_2^-, I_2^-, $ClBr^-$, ClI^-, pot. curve calc. 77−10596
Heisenberg linear chains, dimerisation, variational localised-site cluster expansions 79−60670
trans,trans-1,3,5-hexatriene, valence electronic excited states, SCF ab initio GVB and CI calcs. 79−31423
honeycomb extended lattice VB theory, long range order spin pairing 80−52136
hydrocarbons, Compton profiles, deviations from bond additivity, rel. to strain energy 79−81240
inert gas monohalides, hyperfine interactions, struct., valence bond calcs. 78−66473
intermetallic diatomic compounds, with multiple bonds, bond energy, VB calcs. 79−31440
intramolecular electron transfer amplitude, basis function overlap effect 78−9080
ionis. pot. calc. from VB and MO wavefunctions 78−82616
Koopmans atomic valence electron ionisation energy, 1/Z expansion method, reorganisation corrections 78−78623
localised mol. orbital struct., octet rule violations, fractionality 78−25445
many-body VB theory, variational localised-site cluster expansions 79−60669
methane, valence bond calc. convergence 78−9081
methane, VB calc. using minimal Slater basis set, $^1A_1$ ground state 78−62729
mixed donor-acceptor stacks, mag. gap and partial charge transfer, VB calc. 78−76008
molecular electron correlation, valence bond perturbation theory 79−18120
narrow band conductors, valence bond theory 80−24777
organic charge transfer salts, valence bond theory 79−73473
organic charge-transfer salts, neutral-ionic interface, energy states and mag. props., VB anal. 79−4537
pairwise correlated generalised valence bond model, electron correl. model 78−41959
pairwise correlated GVB model, multiconfig. overlap approx. calcs. 79−31408
pi systems representation, efficient computer manipulation 79−81148
polyacetylene, band struct. valence Hamiltonian minimal STO-3G basis calc., nonempirical model pot. 80−54596
polyethylene, band struct. valence Hamiltonian minimal STO-3G basis calc., nonempirical model pot. 80−54596
potential energy surface, generalised diatomics-in-mols. in VB framework 79−97970
potential energy surfaces, of mols., VB diatomics-in-mols. method 79−85919
pyridine, π-electronic structs., ab initio VB calcs. 78−70749
pyrrole, 6-electron 5-centre bonding units, increased valence theory calcs. 77−46500
quantum mechanics, molecular, book 77−79538
self consistent electron pair theory, perfect pairing valence bond generalisation 80−63532
small molecules, HMO-CI, HMO-AO-CI methods, quantum chemistry model studies *(German)* 78−29753
subtilisin charge-relay system, electrostatic pot. map, STO transferable bond calc. 80−3571
surfaces and interfaces, quantum chemical calc. methods 80−49849
trihalide anions, VB pseudopot. calcs. on electronic states 77−26984
two-electron ats. and ions, low lying S states, pairwise correlated generalised VB method 77−65427
two-electron bond, energy expectation values from density matrix partitionings 77−75059
XY_8 molecules of D_{2d} symmetry, G, F and Σ matrices *(French)* 80−970
Ag_2, AgAu, AgCu, AgH, AgLi, wave functions, interatomic distance and dissoc. energy values 77−57883
α-Al_2O_3, IR intensities, valence-band dynamic and electrooptic models 80−34906
ArH, excited states, theoretical pot. curves 80−95548
Au_2, AgAu, AuCu, AuH, AuLi, wave functions, interatomic distance and dissoc. energy values 77−57883
BeH, $^2\Sigma^+$ states, spin-coupled valence bond theory of molecular electronic struct. 80−83285
BeH_2, pot. energy curve, minimal basis ab initio VB calcs. 78−50477
C, one-centre integrals of semiempirical theories of valence, ab initio calcs. 80−102441
CH, one-centre integrals of semiempirical theories of valence, ab initio calcs. 80−102441
$CH_3(CH_3^+)(CH_3^-)$, HF, GVB and CI calcs. 77−75063
Cu_2, AgCu, AuCu, CuH, CuLi, wave functions, interatomic distance and dissoc. energy values 77−57883
$F+H_2 \rightarrow HF+H$ energy profile, minimal basis ab initio VB calcs. 78−50477
FH_2, pot. energy surface, valence states, VB diatomics-in-mols. method 79−85920
FNO, four electron three centre bonding units, ab initio valence bond calcs. four electron three centre bonding units, ab initio valence bond calcs. 80−27949
Fe halides, electronic charge and spin distrib. from interpretation of hyperfine interactions 79−60776
GaAs (110), electronic states and initial steps in oxidation 78−91534
GaAs (110), reconstruction and oxidation initial stages, ab initio calc. 80−49473
$H+Br_2 \rightarrow HBr+Br$, pot. energy surface, ab initio generalised valence bond calc. 78−73026
H^++Cs, elastic and charge exchange collisions, projected valence bond method 78−78804

VB calculations continued
$H^+ + Kr$, mol. orbit approach, spin-orbit interaction, adiabatic pot. and projected valence band treatments 77−533
H_2 biorthogonal VB method, approx. natural orbitals 77−50368
H_2, chemisorption on metals, quantum chem. model, valence bond calcs. *(German)* 77−31909
H_2, electron momentum distributions from valence-bond wave functions 79−6868
H_2, electronic struct., valence bond model, pairwise correlation 80−78543
H_2, electronic struct., valence bond orbital method appl. 80−106268
H_2, mag. susceptibility calc. by distinguishable electron method 78−897
H_2, pairwise correlated GVB model, multiconfig. overlap approx. calcs. 79−31408
H_2^{2+}, two-electron bond, energy expectation values from density matrix partitionings 77−75059
$H_2^+ + H_2$, pot. energy surface and nonadiabatic regions, charge exchange and reaction, VB calc. 78−40027
H_3, biorthogonal VB method, approx. natural orbitals 77−50368
H_3, interrelationships between effective hamiltonians 77−30767
H_3^+, two-electron bond, energy expectation values from density matrix partitionings 77−75059
H_4, excited potential energy hypersurfaces, trapezoidal geometry, rel. to photochem. 2s+2s processes 77−30797
H_4, excited potential energy hypersurfaces, 'triply right' (C_{2v}) tetrahedral geometries 77−83501
H_4, pot. energy surfaces, valence bond calcs. 80−74129
HF, ab initio valence band calcs. 79−6869
HF, low lying states, GVB and CI calcs. 77−14362
HF, pot. energy curve, minimal basis ab initio VB calcs. 78−50477
HF_2^-, four electron three centre bonding units, ab initio valence bond calcs. 80−27949
HNO, four electron three centre bonding units, ab initio valence bond calcs. 80−27949
H_2O, ab initio VB and localised HF MO hybridisation 77−57852
H_2O, minimal Slater basis set VB calcs. 78−46272
H_2O, perfect pairing valence bond model, ab initio SCF calcs. 77−6689
H_2O, sum rule props., SCF optimizations of MO and VB calcs. 78−5156
H_2O, VB minimal Slater basis set calcs., comparison with H_2S, MO calcs. 79−36536
H_2S, gas-phase, states in valence photoelectron spectrum 78−94284
H_2S, VB minimal Slater basis set calcs., comparison with H_2O, MO calcs. 79−36536
$Hbr + Cl_2(BrCl)$, four-centre reaction, quasiclassical trajectory study 79−57213
$He + H_2$, collision-induced dipole, ab initio VB calc. 78−94202
He+He(Li), intermol. forces, ab initio VB calc. using nonorthogonal basis set 80−23490
He_2H^+, ground state pot. energy surface for form. by collinear collision, DIM calcs. 79−97996
Kr_2F, semi-empirical VB calcs. of hyperfine interactions and struct. 79−85902
Li, core charge polarisation, HF calcs. 79−45627
Li_3 and Li_3^+, ΔE SCF ionis. and excitation energies, transition functional method 77−88404
LiH, electronic struct., valence bond orbital method appl. 80−106268
LiH, pairwise correlated GVB model, multiconfig. overlap approx. calcs. 79−31408
LiNO, four electron three centre bonding units, ab initio valence bond calcs. 80−27949
LiON, four electron three centre bonding units, ab initio valence bond calcs. 80−27949
$Mo_2Cl_8^{4-}$, low lying states, weak electronic coupling, Xα valence band theory 79−72237
N_2, (e,2e) spectra, valence momentum distribs. and config. interaction 77−19101
NH_3 low lying states, generalised VB and CI calcs., vertical excitation energies 77−30789
NO_2^-, ab initio VB wave functions, π-electrons 78−70748
$NeHe_2^+$, electronic structure calcs., extended valence bond diatomic calcs., applications to method of diatomics-in-molecules 79−45635
Ni_2 and Ni_2^+, lowest electronic states, GVB and POL-CI calcs. 79−31409
NiH, pot. energy curves, Hartree-Fock and valence bond methods 78−41958
NiH_2, pot. energy curves, Hartree-Fock and valence bond methods 78−41958
NiO, electronic states, VB and CI calcs. 78−62728
NiO, H chemisorption, perfect surfaces, cation vacancies, self-consistent HF-VB calcs. 79−69351
O_3, ab initio VB wave functions, π-electrons 78−70748
O_3, cyclic, stability, ab initio GVB-POL-CI calcs. 78−915
$P_2O_4(OH)_4^{2-}$ group, electronic struct. calcs. 78−67971
SF_2, generalised VB calcs. of electronic struct. 77−57881
SF_4, generalised VB calcs. of electronic struct. 77−57881
SF_6 and SF_6^+, excited states investig. 77−57882
SF_6, generalised VB calcs. of electronic struct. 77−57881
$S_2N_{2,4}$, π-bonding, increased valence theory calcs. 77−46500
$S_4N_3^+$, π-bonding, increased valence theory calcs. 77−46500
S_4N_4, 6-electron 5-centre bonding units, increased valence theory calcs. 77−46500
SO, pot. energy curves, pseudopot. multi-struct. valence bond calcs. 78−9094
Si_2, electronic struct. and bonding, atomic effective pot. appl. 80−95745
$Si_2O_6(OH)_2^{6-}$ group, electronic struct. calcs. 78−67971
Xe_2F_3, 6-electron 5-centre bonding units, increased valence theory calcs. 77−46500
XeH^+, pot. energy curves, VB calcs. 77−61688

vector diagrams *see vectors*

vector meson dominance model
σ SU(3) model, quark-loop contrib., low-energy meson dynamics 78−12869
additive quark model in quasi-two-body hadronic reactions, Δ and vector meson prods. relation 78−41494
charged pseudoscalar meson photoprod. from H and D with 16 GeV linearly polarised photons 80−13318
charm particle nonleptonic weak decays, pole dominance model 79−63475
contact EM terms and nuclear shadowing of high energy photons, absorpt. by nucleons and nuclei 77−49980
core valence quark model, vector meson dominance total photoproduction cross section 79−49497
deep inelastic processes, charm prod., mass scales, parton model, generalised VDM 77−13930
diffractive neutrino prod. of charged vector mesons, VMD model 77−61277
EM form factors, gauge independ. two body amplitudes 77−74645
EM mass splittings, Born-term contribs. 78−78181
generalised, electroprod. and photoprod. of vector mesons 78−41519
generalised VMD off-diagonal terms and asymptotic SU(4) 77−30349
generalized vector dominance, photon-hadron interaction anal., review, book contrib. 80−47265
hadron EM interactions, review 80−412
hadron photoproduction, diffractive high energy processes, review, book contrib. 80−47309
hadron photoproduction total cross-section, VDM and Lipkin's 'third component' 77−82745
hadronic gauge couplings in meson decays 80−102037
hadronic props. of photons, book contrib 78−82217
heavy vector meson photoprod., vector meson dominance model anal., Regge trajectories 78−78195
meson radiative decay, consistency with vector dominance, quark models 77−79265
meson radiative decay, SU(3) octet-broken VMD anal. 77−71517
meson resonances, strong and EM decays, particle mixing and meson pole dominance 80−18127
nuclear shadowing, hadron photoproduction on nuclear targets H-U, 1.0 to 10.5 GeV 77−82748
nuclear shadowing of electromagnetic processes, vector dominance model anal., review, book contrib. 80−47266
nucleon EM structure, ψ(3.1) in VDM of nucleon form factors 78−50034
photon shadowing in nuclei, vector meson dominance model 79−89162
photon-nucleus scattering, photon shadowing, two component model, GVMD model 77−46159
photons, effect of large intermediate masses in hadron-mediated photon-nucleus interaction 80−27625
photoprod. of heavy hadrons, peripheral and VMD models 78−33074
pomeron-photon analogy, vector-meson photoproduction 77−87984
pseudoscalar Dalitz decays, form factor slopes, VDM with subtracted dispersion relation 78−58181
QCD tests in γ-γ collisions and high p_T photon production 79−89129
radial excitations and q^2 depend. in VDM, appl. to ψ radiation decay 78−452
radially excited states, photon and hadron interactions 78−82170
radiative decay rates for V→Pγ, P→PPγ, P→γγ and V→PPP, symmetry, angle mixing 77−49969
radiative decays, SU(4) and OZI violations 77−74688
radiative decays of vector mesons, single parameter scheme 80−86720
radiative transitions of low-lying positive-parity mesons, VMD and single-quark selection rules 77−18279
reggeon and photon coupling relns. 79−13063
relativistic confining potential model, current spectral functions, meson dominance calc. 79−71734
relativistic many-body bound systems, electromagnetic props. 77−74765
rising hadronic cross section effects on EM processes, generalised vector dominance formulation 78−93868
scaling in bound state models 77−38181
shadowing in nuclear photoabsorpt. 77−2976
SU(3)-breaking models, meson radiative decays, VDM 77−18282
sum rules for vector meson-nucleon scatt. 78−45810
supersymmetric vector-like model of lepton interaction 78−412
T′ (10040) as an I=1 vector meson resonance 80−47241
tensor meson dominance, internal symmetries, and meson mixing for the new particles 80−102036
tensor meson production in photon-photon collisions 79−93414
thermal states, KMS states, of vector meson model in two dimens. space time 77−5987
V→Pγ, effect of SU(3) admixture in VMD model 77−49970
vector and pseudoscalar two-body decays in broken SU(4) 77−67648
vector meson photoprod., Carlitz-Green-Zee mechanism and vector meson dominance model 79−13137
vector meson radiative decay, off-shell factors in vector dominance model 79−22084
vector meson radiative decays, vector dominance model in broken SU(3) 80−73711
virtual photon-nucleus scatt., VMD model alternative space-time view 77−54090
weak decays, calc. of coupling constant occurring in effective Hamiltonian density 77−54102
weak nucleon formfactors in modified vector dominance model *(Russian)* 80−68437
Zweig suppressed decay of heavy 1^{--} vector mesons, two gluon exchange 78−54616
$A_2 \rightarrow \pi\gamma$, suppression factors for VMD couplings calc., duality constraints anal. 77−13960
β-decay, strong meson dominance model and second class currents 80−63132
cc̄ meson radiative decays, generalised VMD mechanism 78−8606
χ particles, radiative decay widths calc., broken SU(4) model 78−62395
χ/εc(3.41) tensor meson dominance for cc̄ states, $\psi' \rightarrow \varepsilon c\gamma$ and $\varepsilon c \rightarrow \psi\gamma$ 79−3019
D meson decay, SU_4 20-plet dominance model, inclusive branching ratios 80−13299
D meson parity violating nonleptonic decays, vector meson dominance model 80−78058
D^+-D^0 mass difference, form factors, SU(4) coupling, vector meson dominance model 79−391
$D\bar{D}^*$ production and decay, VDM, dual amplitude anal., e^+e^- annihilation 77−49992
Δ(1236) isomer production, by charged and neutral currents 79−17711
δ(980)→ωγ, radiative decay width using a vector dominance model 78−82205
δ(980)→πγγ, radiative decay width using a vector dominance model 78−82205
δ(980)→ργ, radiative decay width using a vector dominance model 78−82205

vector meson dominance model continued
e^+e^- annihilation and deep inelastic scatt., VDM approach, vector meson+photon coupling 77−46068
$e^+e^-\rightarrow$baryon-antibaryon pairs, vector meson dominance model 78−21442
e^+e^- EM annihilation into quarkonium states with even charge conjugation, vector dominance 79−93438
$e^+e^-\rightarrow\eta'(X^0)\gamma$, generalised VMD theory 77−10268
$e^+e^-\rightarrow$hadrons, scaling and quark binding anal., generalised vector dominance 77−249
$e^+e^-\rightarrow\pi^0\gamma$ or $\eta\gamma$, reaction rate, weak neutral current corrections, 3γ background 77−46069
$e^+e^-\rightarrow\pi^+\pi^-$, vector meson dominance anal. for π form factor 78−70370
eN, pion production, vector-like theories *(Russian)* 78−37221
ep, polarised deep inelastic scatt., vector meson dominance anal. 78−33073
ep elastic scattering, VDM, p EM form factor *(Russian)* 78−17026
$ep\rightarrow ep\phi$, Q^2 depend. of diffractive slope, decay ang. distrib., vector dominance model 79−89169
$ep\rightarrow ep\rho^0$ or eX, polarised beam and target, cross section asymm. 77−6135
η decays of ψ's, VMD and colour model coupling const. calcs. 77−26516
$\eta\rightarrow\gamma\gamma$, radiative widths, δ and S* background, SU(3) and VDM anal. 80−419
$\eta\rightarrow\gamma\mu^+\mu^-$, vector dominance model *(Russian)* 79−58954
$\eta\rightarrow\rho\gamma(\gamma\gamma)$, C-even meson radiative decay, SU(3), and VDM anals. *(Russian)* 80−68460
$\eta'\rightarrow\rho\gamma$, radiative widths, δ and S* background, SU(3) and VDM anal. 80−419
F parity violating nonleptonic decays, vector meson dominance model 80−78058
F^+ decay, SU_4 20-plet dominance model, inclusive branching ratios 80−13299
$f_c(3.55)$ absolute γ-decay rates from tensor meson dominance and QCD pots. 79−9377
γ-N reactions, book contrib. 78−82335
γN, cross sections, contrib. of $q\bar{q}$ and $c\bar{c}$ vector mesons 78−58192
$\gamma n\rightarrow\rho^0(p\pi^-)$, 7.5 GeV, cross channel isospin amplitude meas. and anal. 77−18299
γp, heavy quark particle photoprod., QCD model, vector dominance implications 80−86730
Γp, total cross sections, contact EM terms in inclusive photo- and electroprod., generalised VMD 78−70348
γp cross-section observed increase, jets as source, QCD and vector-meson dominance model 80−22620
$\gamma p\rightarrow pe^+e^-$, 900 to 1500 MeV, 1100 MeV struct. confirmation, $\rho'(1250)$ leptonic decay obs. 79−30738
γp total cross sections, 18 to 185 GeV, VDM calc. 78−54635
J/ψ decay, via ω, ϕ, ρ^0 poles and cascade decays, vector meson pole dominance 79−85295
K charge radius, coloured quark field theory 80−62945
K form factor and struct. funct. in extended VDM 78−25046
$K_L{}^0\rightarrow\mu^+\mu^-$, VDM calc. of decay probabilities *(Russian)* 78−41539
$K_L{}^0\rightarrow\mu^+\mu^-\gamma$, VDM calc. of decay probabilities *(Russian)* 78−41539
$K^*\rightarrow K\pi\pi$ decay rate, vector meson couplings 77−30373
$\nu(\bar{\nu})$N high energy scatt., scaling violation and generalised vector meson dominance 77−67644
$\nu p\rightarrow\nu$+vector meson + X, neutral currents, generalised VDM, Regge pole anal. 78−41532
$\omega\rightarrow\pi\gamma$, suppression factors for VMD couplings calc., duality constraint anal. 77−13960
$\omega'(1.78)$ vector meson props., quark model, VDM 77−54103
p deep inelastic structure function, large-x depend. in GVMD 77−30350
pγ, one-gluon exchange, quark loop contrib. to photon total cross sections 80−4999
$pp\rightarrow(K_s{}^0, \Lambda$, or $\bar{\Lambda})\pi^\pm$+X, 405 GeV/c cross section determ., vector meson dominance 79−89207
pp inelastic collisions, ρ-dominance in collision model 78−37238
ϕ photoproduction, quark multiple scatt. model anal. under vector meson dominance 79−54350
$\phi\rightarrow\pi\gamma$, suppression factors for VMD couplings calc., duality constraints anal. 77−13960
π charge radius, coloured quark field theory 80−62945
πN, strength of parity violation in vector meson dominance 79−71653
$\bar{\pi}$p inelastic interactions at 205 GeV/c, three-fireball model, computer simulation 78−474
$\psi(3.1)$ photoproduction, vector dominance model 77−18302
ψ and related particle decay, data anal. using quark model and VMD 77−54101
ψ dipionic decays, extended vector dominance model 78−58184
$\psi\rightarrow\eta'\gamma$, radiative decays, vector dominance model 79−26330
$\psi\rightarrow\eta\gamma$, radiative decays, vector dominance model 79−26330
ψ family, VDM anal. of contrib. to total photon cross sections 79−22083
ψ particles, off-mass-shell coupling consts. and radiative decays in VDM 78−70371
ρ chiral SU(3)×SU(3) representation, spontaneous symm. breaking, VDM, PCAC 77−57512
$\tau\rightarrow\nu\pi\pi\omega$, decay width and form factor calc. using vector dominance hypothesis *(Russian)* 80−47271
$\tau^-\nu_\tau\pi^-\gamma$, π form factors, axial-vector and structure dependent, vector meson dominance model 80−62989
$\Upsilon'\rightarrow\gamma 2^{++}(\bar{b}b)$, photonic decay widths in tensor meson dominance 79−75754
$\bar{b}b2^{++}\rightarrow\gamma\Upsilon$, photonic decay widths in tensor meson dominance 79−75754
Fe+$\mu\rightarrow$multimuons+X, 150 GeV/c, charmed particle prod. 77−38177
$\gamma N\rightarrow\eta X$, 9.7 GeV, inclusive η photoprod. on H- and ^{2}H-targets, ρ^0-dominance model anal. 79−63486

vector mesons *see meson resonances*

vectors
AC vector diagram, demonstration using CRO 77−37685
analytic iterability of formal power series vectors *(German)* 77−53736
arbitrary moving magnetic dipole, EM field calc. *(Russian)* 80−9772
atoms, general adiabatic-diabatic transformation matrix, electronic non-adiabatic transitions 80−93751
bifurcation into invariant tori at points of reson., use of Poincare maps 79−44707
bundles with connection theory and gauge field theory, identity of theories 77−18184

vectors continued
chemical kinetics, vector representations 77−21361
co-ordinatization of the kinematical vectors 79−35543
constant of motion with discontinuities, Runge-Lenz vector 79−92932
coupled vector systems of nonlinear parabolic partial differential eqns., soln., geophys. appl. 77−41468
crystal physics, multivector analysis, comparison with vector anal. 80−100196
crystallography, best proper rotation to relate two sets of vectors 78−91184
deformation function, construction for anisotropic medium 79−98633
ECG vector and isopotential maps, convertibility and comparison 79−39554
education, nabla^2 derivation in cylindrical and spherical polar coords. 77−78927
education, rotation matrix for rot. around arbitrary axis, Euler vector representation 78−62011
education, vector calculus and algebra geometrical meaning of curl operation 77−45639
elliptic polarisation, Stokes parameters, vector trihedron, optical element evaluation 80−53209
Feynman diagrams, dimensionally regularised, symbolic evaluation, quantum gravity application 80−13259
field determ., using theory of distributions *(Rumanian)* 79−80415
first integrals and symmetries, geometrical obtention 80−22535
general relativity, killing vectors and maximal slicing 80−77667
generalised representation, of physical situation, appl. to hydrodynamics *(Russian)* 80−69760
geometrical vector flux and some new nonimaging concentrators 79−72650
geometrical vector flux field, ideal flux concentrators 79−72651
Helmholtz theorem, decomposition of solenoidal vectors 77−2556
hologram interferometry, sensitivity vector determ., two known object rots. 80−95840
interatomic vectors construction, of crystal without calculating Fourier series 79−94840
interference theorems of scattering theory in vector problems of low-frequency diffraction 79−86115
ket vector variation, orthonormality-constrained variation method 78−45457
Laplace (Runge-Lenz) vector, origins 77−13565
Lie derivative of a differential form, invariance conditions and phys. laws 78−65748
Lorentz transformation, vector formulation, as student introduction to special relativity *(Italian)* 78−12447
magnetostatics, integral equations 79−72453
molecular vibration, Wilson-Decius s-vectors with out-of-plane wag, derivation 78−74628
motion in spherically symmetric force fields, vector consts. 78−85833
multispectral images, vectoral representations, arithmetic processing *(Japanese)* 79−35532
Newtonian nature of any smooth 2n-dimens. vector fields 78−32648
normal coordinates, rel. to natural coords., theory 77−22343
optical system of three plane mirrors, transform. of vectors 77−75654
orientational average, of $\exp[2\pi i(\mathbf{h}.\mathbf{x}+\mathbf{k}.\mathbf{y}+\mathbf{l}.\mathbf{z})]$ 79−7519
orthogonal decomposition of 2-D periodic discrete vector fields 77−67196
palaeomagnetism, Zijderfeld vector diagrams use in multicomponent magnetisation studies 80−17420
physics teaching, vector concept *(German)* 80−82623
plane to spherical wave conversion by volume holograms, vector effects 80−106496
polarized waveform dectors, matrix and Stokes vector representations, teleseismic waves appl. 78−12008
positive-definite-matrix-conjugate vector, construction and constrained variation 78−8267
precession theory, vector-matrix notation 80−51642
quaternion physical quantities 77−45671
relativistic vector formulation, of electric and mag. fields *(Italian)* 78−12448
Riemannian manifold with quasi-concurrent vector field 77−26142
rigid body, vector anal. of finite rotations, literature review 78−36819
rotated image correlation by gradient vector sum histograms 79−75647
rotations, nonlinear vector products calc. methods 77−71201
spherocardiogram applicability of vectorcardiographic and polarcardiographic infarct criteria 79−39582
spiral vibration of rotating shaft rubbing against interference element *(German)* 78−87252
square roots of measures 77−17765
stable limit cycles of vector fields, new negative criteria 78−57756
stellar magnetic fields, vector-operator algebra technique for stationary states determ. 78−73698
teaching, curl operator when A.curl A$\neq$0 78−62020
teaching acceleration and velocity, racetrack game 80−31458
teaching undergraduates EM theory 77−71167
thermodynamics, irreversible, vector forces and fluxes 78−24753
thick ellipsoidal coil and ferromagnetic ellipsoid system, vector potential 79−41269
Tomita-Takesaki theory for von Neumann algebras with separating and cyclic vector 77−17755
topological theorem for bounded vector field, nematic liq. cryst. appl. 79−67171
Umov vector, electrodynamic and electrotechnical importance in EM field calc. *(Russian)* 77−50591
vector symmetry, in crystallography, basic theorems 79−23556
vector-matrix differential eqn., convergence of assoc. eigenfunction expansions 78−69965
vectorcardiogram diagnostic algorithm improvement by outlier elimination 79−39572

vehicles
see also electric vehicles; locomotives; road vehicles; space vehicles
air pollution analysis, automated X-ray fluorescence technique *(French)* 77−41234
air pollution survey vehicle *(Dutch)* 78−81365
cab noise control 78−55511
coherent optical processor for vehicle tracking and identification using laser diode light sources 80−37957
dumper, modifications to reduce noise levels 77−68325
dynamic interaction with structures, simulation using Lagrange multipliers 80−64357

vehicles continued
emission control, nitrogen oxides reduction on industrial furnace 79—52995
flywheels, performance of retainerless bearings for vehicular energy storage appls. 80—30567
H-fuelled passenger bus, design 80—40924
mobile incubator transport for premature and newborn babies *(German)* 79—16336
railway vehicle internal design and wayside noise abatement 78—55514
roadway aerosol filter samples, proton-induced X-ray emission analysis 77—41233
Stirling engine powered total energy system for recreational vehicle appls. 80—30538
vibrations of moving vehicle, ground induced response 79—32346
wheelchairs, electric, PWM control DC motors drive system *(German)* 77—56491
H cryogenic storage and refuelling for automobiles 80—30604
H fuel, survey of liquid hydrogen container technology for highway vehicle fuel system applications 80—30607
H storage by metal hydrides for automotive propulsion 80—40922
H_2 fuelled vehicles, design and engine modifications with Fe-Ti hydride storage 80—40925
H_2-powered, high temp. hydrides for H storage 80—45793

velocity
see also acoustic wave velocity; ion mobility; light velocity
δ Cephei, atmospheric vel. field 79—25611
double use in hydrodynamics *(French)* 79—75349
education, speed, Galilean and Einsteinian concepts, vel., rapidity and celerity 80—73130
galaxies, bright, nearby, vel. field and Local Group peculiar motion rel. to Virgo cluster 80—36699
Hamels spiral flow, temp. and vel. distribs. *(German)* 80—87779
interplanetary shock waves during second STIP interval (1976, March 15-May 15), vels. 78—81514
interstellar shocks, post-shock gas temp., density and vel. profiles, analytical results 80—56911
laser velocimeter, appl. to aerodynamics, operating principle *(Spanish)* 80—53902
MHD generators, Window-Frame, with nonuniform velocity and conductivity in transverse plane, electric effects, anal. 79—68960
monkey/hunter problem and possible solutions 79—75306
NGC 5383, barred spiral galaxy, vel. field 78—24549
photosphere velocity research, effects of apparent yearly precession of Sun 78—20809
planetesimal population, equilib. vels. 80—31219
position operators, systems exhibiting special relativistic relation between momentum and vel. 78—89335
quasars, transverse motions determ. from relativistic Doppler formula for redshift *(Chinese)* 80—105379
radio galaxies components, fly away velocities upper limits *(Russian)* 80—62306
radio sources, extragalactic, with speeds exceeding speed of light, kinematic models *(Danish)* 78—36715
solar granulation, mean vertical vel. 80—62094
solar photosphere, vel. gradients retrieval from line asymmetries, linearised approach 80—62093
solar photosphere velocity field, spatially averaged props. 79—16912
solar wind, α-particle/proton streaming vels. in three-fluid model 78—57418
solar wind, particle vel. distribs. rel. to plasmadynamical processes *(German)* 80—109323
spiral galaxies bulges, vel. dispersions meas. 80—26965
superluminal velocities in compact radio sources, role of spontaneous form. of knots in relativistic flows 80—105369
teaching acceleration and velocity, racetrack game 80—31458
wind velocity gust factors, analytical expression and wind tunnel simulation 80—31107
Cr_2O_3, elastic consts., distance depend. of mag. interactions, US vel. meas. 77—4539

velocity analyzers *see particle separators*

velocity control
Anglo-Australian 3.9 m telescope, computer-controlled slewing, setting and tracking 77—17371
autotransfusion, variable-speed pump head control 78—57121
hardness meas. device, speed control of indentor 77—1907
heavy ion separation velocity selector 77—88324
Mossbauer spectrometer, absolute vel. control via laser interferometer 77—71715
pump head speed control for autotransfusion 77—52918
radiation therapy, computer control 79—25099
rotating mirror deflector motor and control system selection 77—58484
rotation speed control attachment for rotary viscometer with weight-driven rotor 79—50822
solar collectors, design and data rate requirements of computer-based sun following system 79—83573
spacecraft final descent vel. control in Mars atmosphere, autonomous navigation algorithm 77—29620
spacecraft relative motion around orbiting station, guidance method 78—16263
speed-optimal control synthesis in near spherical symmetry problems *(Russian)* 79—9095
starship, single-stage constant-power, optimal exhaust vel. programming 78—20613
stroboscopic monitoring method *(Russian)* 79—97365
vehicle, electric, using Pb-acid battery, response to chopper-controlled discharge 79—48120
wind turbines, vertical axis, tilting using overspeed control 80—97757

velocity measurement
see also acoustic wave velocity measurement; anemometers; angular velocity measurement; flow measurement; flowmeters; laser velocimeters; light velocity measurement; stroboscopes
accelerometer/velocimeter, range of 10^{-5} g to 10^{10} g and time resolution of few nanoseconds 77—45826
acoustic, procedure *(German)* 79—93106
air, using hot-wire anemometer, calibration at low vels. 79—27724
air, using triple hot-wire probe, response and transformations eqns. 79—27718
air bubbles, rising in glycerine-water mixture, boundary surface velocity *(German)* 79—32631
air flow, by triple hot-wire probe 77—62315

velocity measurement continued
air stream, subsonic, using laser Doppler interferometer system, errors analysis *(Russian)* 80—27336
air track direct vel. readout, conservation of momentum demonstration 77—82346
aircraft velocity and altitude measurements using a tunable diode laser 80—13042
airflow using wind-speed measuring instrums., calibration using low-vel. facility 80—1718
analogue electrical methods review *(German)* 79—178
anemograph, digital, for wind direction and average speed meas. *(Czech)* 80—77174
anemometer, pneumatic type, operational description and calibration *(Russian)* 77—37420
annular flow, vel. distrib., expt. determ. 80—38510
astronomy, Doppler broadening parameters and Doppler shifts meas. without spectrograph 78—20646
atmospheric attenuation and turbulence simulation in pulsed laser Doppler velocimeter system 78—73513
axial flow compressor stator blade wake guidevane, method 80—95085
biological objects underwater, design principles of US instrums. 80—19195
Bjork-Shiley aortic prosthesis, in vitro vel. meas. using laser-Doppler anemometer 80—17196
blood, instantaneous values, ultrasonic Doppler system appl. *(Dutch)* 78—31832
blood, pulse-wave vel. meas. in humans *(German)* 80—81751
blood flow echography using Doppler techniques *(French)* 80—26303
blood intravascular mean vel. meas. using crosscorrel. technique 80—81763
blood velocimeters, US transesophageal meas. of human haemodynamic parameters 80—41146
bubbles, measurements using RF probe 80—6177
bubbly flows, simultaneous meas. of local liquid vel. and void fraction by gas laser, accuracy *(Japanese)* 78—67295
cable length, vel. and tension meas, using DBS-2 remote counting block 79—12314
capillary blood flow, dual beam laser velocimeter anal. 80—75015
cavitation bubble dynamics recording using laser holocinematography 79—86147
channel, 2-dimens. rectangular, vel. profiles and fluctuations, laser Doppler anemometry 80—53864
conductive fluids local induced voltage velometry *(German)* 79—86517
contactless, of running strips of bands, transit time determ. by pick-up *(German)* 80—14862
contactless devices survey, industrial appl. *(French)* 79—93105
contactless using laser light speckles *(German)* 77—9991
convergent cylindrical shock wave parameters meas. in metals by elec. methods 79—46407
correlation sonar for ship's velocity meas. 79—27474
correlator, for velocity meas. 79—40544
correlator, Malvern, based on photon correlation and laser scattering spectroscopy, development and appl. 80—5741
cross-wind velocity meas., interference fringe visibility and spacing, atmospheric turbulence effects 80—51572
deep ocean navigation, acoustic beacon-aided 79—32166
dielectric flows, EM method for flowrate and velocity meas. 80—53893
diffuse object real-time velocity meas. using laser speckle zero-crossings 80—77760
diffuse object vel. meas. by speckle intensity fluctuations 79—97366
digital, error calc. *(Russian)* 80—86266
digital monitor for rotational-speed instability 79—97363
discreteness periods, selection 79—30433
dispersions, particle size and velocity distribution, in flowing media, meas. methods *(German)* 78—34213
Doppler sonar for ship's velocity meas. in deep water 79—27475
drag sphere velocity probe, miniature, development and testing 78—55705
dust particles, charged, vel. meas. using laser Doppler velocimeter 80—95083
dust trajectory photography for compressible flow velocity meas. 79—82008
early-type stars photospheric expansion, meas. via. Fourier anal. technique 78—93224
eddy-current speed meter operating characteristic analysis 79—40543
education, homodyne microwave Doppler velocimetry, accel. meas. 77—78920
electrical discharge in optically transparent media, apparatus using photomultipliers 79—19086
electrodiffusion method for convective heat transfer characts. in various liquids 79—94746
electrodiffusion velocity sensor, freq. characts. calcs. 80—96675
electronic speed sensing facility 79—30427
EM velocimeters, for flow rate meas. of conductive liquids 79—68859
EM velocity meter, with cylindrical magnet, output voltage, vel. profile effects *(Russian)* 78—45600
error estimation in photographic techniques *(German)* 78—304
Fabry-Perot spherical mirror interferometer for wind velocity meas. *(Chinese)* 79—77308
fast ion beam vel. distrib. meas. with probe 79—13890
filament velocity measurement, during spinning, streak photography 78—41367
fission reactor control rod drop damping and velocity meas. instrumentation *(German)* 80—5248
flames, laminar, rise velocity meas., spectroscopic method 78—74064
flow fields, multidimensional, of any turbulence intensity, analysis 79—27720
flow fields, using hot-wire probe, effects of cooling law and probe adjustment 79—27721
flow in pipe, slanting hot-wire anemometer appl. 77—62313
flow mean velocity very close to a wall, hot-wire anemometer meas. errors 80—79413
flowpath velocity meas., semiconductor hot element anemometer 80—48823
fluid film lubrication, velocity profile meas., using ZnS phosphorescent tracer method 78—94866
flux gradient accelerometer, working model tests 77—26274
formaldehyde, mol. beam, vel. meas. by Doppler effect on RF spectrum splitting *(French)* 78—13627
freely sinking probe horizontal velocity meas. interpretation 80—46321
gait abnormality detection by tachographic data anal. 77—48938

velocity measurement continued
gas cooled reactors, velocity flow field near moving cascade, meas. using hot wire technique 77−50195
gas-gun projectile vel., direct display 78−177
gas-gun projectile vel. meas., magnetoflyer method 78−49805
graphite, shock wave, prod. by explosion, vel. meas. 80−59074
Gulf of Alaska SeaSat Experiment 14.6 GHz scatterometer surface wind obs. 80−46200
heavy water, US velocity experimental determ. using freq. pulse method 78−21734
hemisphere-cylinder, using laser velocimeter, concept 77−74375
high surface vels. using K-band microwave interferometry 80−77761
highly separated transonic flow, first vel. and RMS vel. fluctuation meas. 79−77166
holographic double exposure method for quadratic motion analysis 77−61927
holographic interferometry, for displacement or flow velocity distrib. meas., fringe analysis 78−25820
holographic method for hypervelocity particle meas. 78−36978
horizontal gas-liquid stream, flow vel. meas. 80−96301
hot-film probe, calibration in liquids 79−27723
hot-film velocity sensors, cylindrical, low Reynolds number calibration 79−64815
human motion three-dimensional monitoring by optoelectronic means, calibration 77−86658
impact, internal meas. of shear and compression waves, gauge lead effects 80−74817
impact ejecta parameters depend. on primary vel. 78−59291
instantaneous linear velocity meas. by scanistor 79−67261
interference effects by pair of two-freq. laser beams, for extremely low velocity meas. 77−79071
internal combustion engine, measurement of pulsating temp. and vel. using US flowmeter 80−1704
internal contraction engine, highly loaded, exhaust gases temp. and velocity meas. using two thermometer method *(German)* 80−31754
ion beam, fast, meas. using Doppler shift method 80−9083
laboratory's absolute velocity meas. 80−95081
laminar fluid flow measurements employing white light fringe image velocimeter 79−64816
laser anemointerferometer, for simultaneous velocity and density meas. 79−18976
laser Doppler anemometer measurements, bias correction 80−24114
laser Doppler anemometer-computer system, for flow rate meas. 79−68881
laser Doppler blood velocimetry *(Japanese)* 80−94310
laser Doppler velocimeter, accuracy, turbulence effects 79−55433
laser Doppler velocimeter, for turbulent flow velocity meas., redesign 78−1245
laser Doppler velocimeter for meas. of specified velocity vector 80−47040
laser Doppler velocimeter for surface velocity measurement 79−63193
laser Doppler velocimeter instantaneous, using fast wavelength tracking Michelson interferometer 79−7430
laser Doppler velocimeter with direct spectral anal., for instantaneous vel. meas. 80−99782
laser Doppler velocimeter with variable frequency shift for combustion flow meas. *(Japanese)* 78−67294
laser interferometer system, for velocity-time history recording 78−45602
laser interferometry measurement system 79−6171
laser speckle, time-differentiated, first order statistics, vel. meas. 80−82750
laser speckle photography for fluid flow vel. meas. 78−14112
laser surface speed measurement by correlation, industrial paper machine test *(French)* 80−95082
laser technique for simultaneous particle size and velocity meas. 78−70096
laser velocimeter, differential Doppler system, transverse vel. meas. at remote point 77−65816
laser velocimeter optical scanning system 77−58481
laser velocimeter with Doppler frequency discriminator 78−81954
lasers in metrology and testing, review 77−5817
layer velocity meter, freq. biased, for meas. on vibrating surface 79−98675
light curtain for measuring speed trajectory, of object *(German)* 78−12738
light scattering techniques, digital correlation appl. 78−57916
light velocity, interference methods, accuracy 78−17997
lip and jaw motion during speech, video-scanning system 77−56388
liquid, vel. meas. by coherent diffusion using triggered ruby laser *(French)* 77−68711
liquid film flow down inclined plane, polarographic velocity meas. method *(French)* 78−34214
liquid metals, flow vel. meas., using EM system, vel. profile effects on output voltage *(Russian)* 78−45600
liquid metals, MHD rot., vel. meas. by vane type sensor *(Russian)* 77−47123
liquid velocity and turbulence meas. by image sensor 79−77297
liquid velocity measurement and flow trajectory, using image sensor, appl. to stirred vessel 80−69950
low-reactive meas. of motion, trnasducer effects on body under investigation *(German)* 80−105621
low-speed motion irregularity meas. equipment, portable 78−54346
lung model, human, velocity distrib. and pressure drop. expt. 79−96602
magnetic tape linear velocity meas. scanistor 79−71425
Maxwell vel. distrib. determ., Cenco kinetic theory appl. 77−78916
metal-film temp. and vel. sensors and self-propelled research vehicle stability evaluation for ocean turbulence meas. 79−5672
meteorites, radar technique *(Spanish)* 79−5759
meter, appl. of photodiodes, for internal combustion engine 77−57303
microhardness meas. by ball dropping/recoil velocity ratio 77−81363
microscale sensing array for ocean meas. 78−85720
microwaves non-conventional appl. survey *(Italian)* 80−13093
mitral valve velocity meas. by digital echocardiographic tracking system 77−21579
motile spermatozoa, speed distrib. by light scattering obs. 77−37061
motion parameter measurement by comparison with motion of standard 79−30434
mucociliary tracheal clearance vel., radiological method for determ. 80−104727
natural convection air flows, vel. meas. using laser velocimeter 79−82016
velocity measurement continued
natural convection flows, hot wire measurements, fluid temp. and mixed convection effects 79−64817
non-contact velocimeter for moving objects using statistical method 80−105622
non-isothermal flow, turbulence measurement, laser Doppler velocimetry appl. 79−41776
noncontact velocity meter using sensing arrays 79−58677
ocean current meas. by Lagrangian drifting buoys 78−45049
ocean current meas. near surface, general problems, review 78−45048
ocean current meters, for continental shelf deployment, development and testing 79−5674
ocean current parameters meas. from drifting ship 77−49189
ocean currents velocity profiler based on geomag. induction principles 78−61569
ocean sediment free-fall penetrometer with Doppler telemetry 80−46320
ocean surface wind speed, SeaSat-A scatterometer 77−29626
ocean velocity microscale studies, stable platform development 79−5669
oceanic wind speed meas. using HF skywave radar sea scatter 77−29481
on-axis velocity component measurement with laser velocimeters 80−19526
optical Doppler microscope 80−68251
optical sensor, for liquid flow *(Russian)* 78−1759
N.Pacific Ocean current, vel. field diagnostic calc. comparison with obs. *(Russian)* 78−61428
pack ice, drift observed using radar buoys *(Japanese)* 78−96224
particle in fluids, meas. via small pressure-gradient hydrophone *(German)* 77−72118
particle velocity distrib. meas. by holography 80−5705
particle velocity measurement in Fraunhofer plane using double exposure holograms 79−44904
particulate, using microwave Doppler effect 77−27628
photocardiogram contact microphone 77−21634
photochromic flow visualisation, effect of turbulence on precision of vel. and vel. fluctuation data 77−68714
plasma wave group velocity measurement by FM technique 79−73047
plastic plate velocity measurement, as continuum, by streak camera technique 78−37095
polymer soln. highly elastic, vel. meas. in die entry region of capillary rheometer 80−99988
pulsed Doppler blood velocity meter readout 78−69158
relative motion, problem of boat crossing flowing rivers 77−60883
relativistic electron beam, technique for amplitude and phase vel. meas. of slow space charge wave 78−54508
rivers/open channels flow, remote sensing, cross correlation techniques 78−57328
rotating annular jets, velocity distrib. and profile meas. 79−50829
rotating body surface velocity, meas. via high-resolution spectroscopy 78−96403
rotating sphere in still fluid, hot-wire anemometer appl. *(Japanese)* 77−35112
rotational speed, digital measurement method, suitable for automatic testing of electric machines *(Czech)* 79−71419
rotational speed of sandpaper disc meas. by scanning laser velocimeter 77−791
saline containing dissolved O, velocity magnitude transducer 79−21733
SeaSat scanning multichannel microwave radiometer 80−46248
SEASAT-A satellite microwave scatterometer for wind sensing 77−5417
seismic Rayleigh waves, inversion of global average group vels. and attenuation coeffs. 79−12090
seismic Rayleigh waves attenuation and group vel., regionalisation and pure path models 79−12091
seismic surface waves, group vel. meas., error estimation 77−86805
seismic waves, vel. components determ. in media with elliptical vel. depend. 79−5454
ship speed determ., new acoustical method 79−14178
ships, acoustical determination of course speed and lateral drift 80−5892
shock wave physics, interferometric laser technique for accurate vel. meas. 77−50972
shock wave vel. determ. by laser schlieren method 77−39370
shock wave vel. meas. in liquid H_2 77−75999
shocked specimens diffuse back surfaces, meas. via Michelson field-widened interferometer 77−61050
simple linearised hot wire anemometer, performance characts. 80−53904
solar atmosphere downflow, evidence from Mg II core absorpt. wavelengths 79−12451
solar photosphere, total vel. field determ. using weak absorpt. lines *(Russian)* 78−40894
solar surface radial velocity, meas. via reson.-scatt. spectrometer 78−96393
solar velocity fields meas. using magneto-optical filter 79−25507
solid body motion parameters, determination reliability improvement using redundancy methods 79−30431
sonar, rel. resolution with linear-period-modulated pulse 77−54825
speckle, dynamic props., zero-crossing study 80−63923
speckle pattern time-space cross-correlation for in-plane vel. meas. 80−105623
speckle photography, vel. contour generation 77−2638
speckle photography and interferometry, for fluid velocity meas. 78−26221
speech production process, articulatory characteristics of tongue and jaw point movements in connected sounds of Japanese 80−26243
spherical particle velocity and size meas., crossed-beam light scatt. interferometry 80−47011
sports activities, velocity meas., stroboscopic photography, teaching appl. 79−44679
sputtered particles, vel. meas. by Doppler-shift laser spectrometer 80−62638
standing sound waves, particle vel. detect. via hot wire anemometer 77−62124
stellar atmospheres, vel. gradients determ. from spectral lines differential Doppler shifts 78−57538
stellar barycentric radial velocities, computation with classical perturbation theories 77−45291
stroboscopic monitoring method *(Russian)* 79−97365
submicron particles, holographic interferometry 77−19203
surface velocity meas. using laser beams 78−49806
suspended particles, fast moving, size and vel. meas. 77−42935
tachygraph, appls. to flow velocity and positional meas. 79−72977
telescope light source displacement *(Russian)* 77−41306

velocity measurement continued
three-dimensional flow field, novel arrangement for vel. vector meas. 77−72378
time-of-flight velocity measurement circuit 79−58485
turbine-vane passage, laser Doppler velocimeter appl. 80−95086
turbulent bubbly flow, laser meas. of local liquid velocity and void fraction *(Japanese)* 78−9693
turbulent free jets, subsonic and supersonic, laser velocimeter meas. 79−77307
two-dimensional, for rotating liquids, using automatic analysis of trace particle motion 79−64810
ultracentrifuge with magnetic suspension contactless meas. 77−16776
US Doppler signal analyser, real-time, multichannel, blood vel. meas. appl. 77−73551
US transducers for medical imaging *(French)* 80−26302
vehicle, contactless method using spatial filter *(Japanese)* 79−75504
velocimeter, non-contact, using laser produced speckle patterns *(Japanese)* 78−178
velocimeter for fluctuating temp. and vel. meas. in combustion field 80−14856
velocity gradients and laminar and turbulent diffusion, direct optical meas. 80−59132
velocity sensing interferometer (VISAR) modification 79−17481
vibrating string, wave velocity propag. meas., mass tension ratio *(Spanish)* 80−74592
vibrational, using analogue photoelectric velocities, systematic errors determ. 80−79246
viscogravitational flow in vertical channel, vel. meas. 79−32671
walking speed meas. methods and characteristics, humans *(Croatian)* 78−44624
water, oscillatory boundary layer beneath waves, meas. using laser Doppler anemometry 79−27719
wind, anemometer design using transistors 79−71420
wind, sea surface, multichannel scanning microwave radiometer, for Nimbus-G and SeaSat-A 77−29625
wind meas., new microwave radar 77−33195
wind meas. system, computerised 77−56742
wind meter, digital 80−207
wind obs. in clear air using FM-CW Doppler radar 78−57271
wind profile determ. X-band solid-state radar system 78−12028
wind speed intensity distrib. anal. using pulse height analyser 78−88937
wind velocity, remote meas. using video equipment for pollution monitoring *(French)* 80−7990
wind velocity meas. near wind power plant in Sweden 80−61883
xerographic cascade flow, carrier bead velocity distribution meas. probe 80−47136
H ions, velocity measurement by Doppler shift of H atoms line spectra after traversing thin C foil 78−16778
Mn nodule mining and processing with nuclear meas. 77−4975

velocity meters *see velocity measurement*

velocity microphones *see microphones*

velocity-modulation tubes
No entries

velocity spectrometers *see mass spectrometers*

Veneziano model
ψ meson, hadronic decay, generalised Veneziano model 78−58182
extended PCAC+Veneziano type model, Goldberger Treiman relations, $\eta\rightarrow\gamma\gamma$or $\pi^+\pi^-\gamma$ 78−21354
generalised Veneziano model, dynamical suppression 77−34136
hadrons, extended, stochastic description 78−431
impact parameter amplitude *(Russian)* 78−37187
interference terms, phases, 1/N expansion, Lee-Veneziano model 77−18247
multi-jet structure of hadronic final states and trajectory slope 78−93843
multi-Regge limit 78−29274
multi-Regge limit of Veneziano model, exchange of new trajectories 78−33043
multi-Regge limit of Veneziano model, unconventional trajectories props. 78−33044
Nahn partition function of the dual spectrum 77−87952
P-f identity hypothesis, resolution problems 79−75747
pseudoscalar meson decay constants, Goldberger Treiman relations in charm sector, three point function Veneziano model 79−293
quark-parton model from dual topological unitarization 79−93361
Regge behaviour of 6-point function and new trajectories 78−16998
Regge spectra of charmed baryons in dual resonance amplitudes 79−13088
Regge trajectory renormalisation in dual models 79−30721
sister trajectories *(Russian)* 78−41513
space-time anomalous dimension in Venziano and Neveu-Schwarz models *(Russian)* 80−68434
three particle decay, two body resonance approx., Veneziano amplitude expansion 78−82174
triple-Pomeron couplings in dual models 79−358
Veneziano model anal., $K\bar{K}\pi$ Dalitz-plot density calc. 79−26331
Yang Mills string theories 77−79216
K electromag. form factor Veneziano-type scatt. amplitudes *(Japanese)* 78−17019
$\bar{p}n\rightarrow\pi^+\pi^-\pi^-$, 1.09 to 1.43 GeV, spin-parity function, Veneziano model anal. 79−13148
pp scatt. at 90°, Veneziano like model with 2q2$\bar{q}$ meson trajectory 79−13087
πNN Veneziano-type form factor, test by fitting to np→pn and $\bar{p}p\rightarrow\bar{n}n$ $d\sigma/dt$ data 79−17725
$\pi^-p\rightarrow\psi n$, generalised Veneziano models 80−22638
$\pi\pi$ scatt., ρ-meson N/D calc. in Veneziano model 77−67627
$\pi\pi$ scattering amplitudes, Veneziano model representation 79−26313
$\psi\rightarrow 3\pi$, generalised Veneziano model, 3π Dalitz plot 79−381
$\rho'(1600)$, quantitative anal., two pion decay mode suppression 77−46031

ventilating *see ventilation*

ventilation
see also air conditioning
artificial lung, mechanical properties monitoring, parameter estimation 77−21642
building with porous walls for air ventilation, heat transmission 79−4016
BWR, heating, ventilation and air conditioning systems *(Japanese)* 80−91212
diesel-driven chiller system simulation, with multi-tank thermal storage system, for large commercial buildings 79−48187
electrophotographic copier photoconductor drum cooling methods 78−62245
fan systems and energy 80−6145
fans types survey, characteristics and appl. 78−63238
high efficiency particulate air filters, efficiency testing at large pressure transients rel. to nuclear facility safety 79−81020
louvres, sound transmission loss for various louvre geometries 80−45839
mechanical ventilation systems noise control, design approach 78−42489
modified window air conditioner, laboratory temperature control 80−68192
noise abatement for induction motors in air/air heat-exchangers for ventilation *(Hungarian)* 80−102923
noise and vibr. control of large plant 77−54834
noise survey at Liverpool University 77−7251
nuclear fuel reprocessing plant ventilation control 80−5318
nuclear power project, 480 V and 125/250 V auxiliary elec. unit design 77−3143
particle accelerators, radiation exposure 80−5350
patient, automatic control, pulmonary model 77−21556
PWR nuclear power station, heating, ventilating and air conditioning systems *(Japanese)* 80−91213
radioactive tracer appls. to ventilation and air pollution studies, review 78−28306
solar energy collection and storage, space heating *(French)* 80−61299
sound attenuators, attenuation characts. 78−30123
sound attenuators, ideal characts. 77−54836
sound emission prediction 77−7252
turbulent flow in air conditioned buildings, two equation model *(German)* 77−14994

ventilators *see ventilation*

Venus
1151 year period discovery, Babylonian or Persian? *(German)* 79−35166
airglow, Mariner 10 UV spectrometer expt. 77−64611
airglow, O_2 emission from atom recomb. 79−31576
asteroid 1685 Toro, orbital resonances with Earth and Venus 79−2513
astrometric radar meas. in 1977, results 80−17522
atmosphere, 0 to 200 km, physical parameters from Pioneer Venus mission *(French)* 80−46421
atmosphere, aerosol distrib. changes, 1972-75 period 77−64681
atmosphere, aerosol model 80−101545
atmosphere, anal. by automatic interplanetary stations (Venera-4, 5, 6 and 8) 78−28520
atmosphere, C and N species prod. by thunderstorms 80−98587
atmosphere, chemical comp., Venera 12 gas chromatography *(Russian)* 79−66948
atmosphere, chemical composition deduced from twilight glow obs. 80−56739
atmosphere, circulation development and vars., Mariner 10 TV pictures 78−57479
atmosphere, $Cl+SO_2$ reaction significance 79−84353
atmosphere, cloud and temp. struct., from 12-20 μm spectrum 79−66946
atmosphere, cloud microphysics anal. 79−16853
atmosphere, cloud patterns, waves and convection 77−5473
atmosphere, CO_2 IR absorption, extrapolation from liquid to gas 77−493
atmosphere, CO_2 IR spectrum, laboratory expt. 77−3362
atmosphere, CO_2 lines equivalent widths, multiple scatt. calcs. 78−4095
atmosphere, composition and structure, Pioneer results 80−46230
atmosphere, composition and structure 77−73992
atmosphere, cyclic and diurnal vars. in thermosphere and exosphere 80−51683
atmosphere, daytime, density, press. and temp., Venera radio probing results 79−80253
atmosphere, diffr. effects in radio transmission 77−64682
atmosphere, dynamical processes, three-dimens. model 78−32376
atmosphere, dynamics from power spectrum anal. of Mariner 10 images 79−53746
atmosphere, electron cooling by electron impact excitation of CO_2 78−57481
atmosphere, electron energy deposition in CO_2, excitation, ionization and heating 79−45857
atmosphere, Fresnel refl. of Sun estimates 77−87305
atmosphere, greenhouse effect 80−101544
atmosphere, H_2O content from narrow band photometry data 79−62779
atmosphere, H_2SO_4 aerosols characts. from isophotes, spacecraft obs. 78−81575
atmosphere, H distrib. and escape, charge exchange effects 77−29674
atmosphere, height depend. of temp., 52-90 km altitude, model 79−8866
atmosphere, impact ejecta trajectories, drag and gravity effects, analytic solns. 78−40854
atmosphere, information from equivalent widths in spectropolarimetry 79−70976
atmosphere, internal gravity waves 79−5770
atmosphere, IR extinction meas. from Pioneer Venus IR radiometer expt. 79−48719
atmosphere, IR radiation absorpt. induced by press., mol. collision between CO_2, N_2, O_2 *(Russian)* 80−56600
atmosphere, kinetic energy of circulation 77−13261
atmosphere, light polarization and scattering 79−96814
atmosphere, lighting conditions in 0.5-1.1 μ range, Venera 9 and 10 meas. 77−78696
atmosphere, microwave absorption in 21-117 GHz range 77−71040
atmosphere, model from radio, radar and occultation obs. 80−46420
atmosphere, multidimensional radiative transfer 77−64638
atmosphere, net radiation meas. by Pioneer small probe 80−46435
atmosphere, neutral gas comp., diurnal vars. 80−46427
atmosphere, nighttime, radioscopy by Venera 9 and 10 probes 79−62777
atmosphere, nighttime, radiowave fluctuation and turbulence, Venera radioscopy data 79−80254
atmosphere, noble gases *(German)* 79−58289
atmosphere, O_2, $^1\Delta g\rightarrow{}^3\Sigma g^-$ band prod. mechanisms 80−82251
atmosphere, O_2, Ar, CO abundances, error of Pioneer Venus chromatography obs. 80−105189
atmosphere, O spectral line shape following mol. dissociative excitation 80−105097
atmosphere, orographically scattered gravity waves 77−67057
atmosphere, photoelectrons caused by solar photons of less than 80 Å 80−56744

Venus continued
atmosphere, photoelectrons energy deposition 77−9687
atmosphere, Pioneer Orbiter cloud photopolarimeter meas. 78−57429
atmosphere, Pioneer Venus nephelometer expt. preliminary results 79−48716
atmosphere, probe flight characts., scale model expts. 78−7854
atmosphere, radiance meas. using Pioneer Venus Solar Flux Radiometer 80−82198
atmosphere, radiation-induced cooling 78−85885
atmosphere, radiative transfer, far IR opt. consts. of H_2SO_4 droplets 77−8574
atmosphere, radiative transfer, line form. level 80−17487
atmosphere, radiative transfer in 2.86-4.16 μm window 79−8863
atmosphere, radiative transfer of solar radiation, model based on Venera 10 data *(Russian)* 80−12698
atmosphere, radio occultation obs. by Venera-9 and Venera-10 satellites 79−48698
atmosphere, reality of strong winds 77−29682
atmosphere, remote sensor, high resolution Fourier transform spectropolarimetry 78−57469
atmosphere, response to heat sources and perturbations *(Chinese)* 80−85748
atmosphere, retrograde rot., Fabry-Perot meas. 78−65525
atmosphere, review of Venera data 80−72804
atmosphere, role of gaseous S_2, S_3, S_4 and H_2S_n 80−17518
atmosphere, scatt. solar radiation in cloud layer, multiple scatt. theory inversion 79−8865
atmosphere, scattered solar radiation, day sky spectrum, Venera meas. 80−56573
atmosphere, scattered solar radiation fluxes spectral and altitude distrib. 80−62059
atmosphere, scattering coeff. from Venera 9 and 10 photometry 80−8572
atmosphere, solar radiation spectral comp. rel. to Venera 9 and 10 illumination meas. 79−88612
atmosphere, spectral detection of SO_2 and CS_2 *(French)* 79−62776
atmosphere, spectral line profiles and phase curves for Rayleigh scatt. 77−29684
atmosphere, struct., and light, heat and wind regimes from space vehicles 80−62062
atmosphere, struct. and comp. from refl. sunlight polarisation calc. and obs. 80−36533
atmosphere, sunlight absorption 80−46434
atmosphere, surface layer turbulence from Venera 9 and 10 data 79−62780
atmosphere, temp., cloud structure and dynamics from IR remote sensing 80−46429
atmosphere, thermal contrast from Pioneer probe data 80−46229
atmosphere, thermal radiative transfer, numerical modelling 80−8574
atmosphere, thermal regime exploration methods *(Czech)* 78−32374
atmosphere, turbulent mixing coeff. and homopause height 78−49354
atmosphere, upper, barotropic instability, model 78−89091
atmosphere, upper, temp. and dynamics from Pioneer Orbiter IR radiometer meas. 80−26766
atmosphere, UV markings space-time relationships 77−5472
atmosphere, Venera 9 and 10 radio transmissions near limb 77−78694
atmosphere, Venera-8 optical meas. interpretation 79−8864
atmosphere and climate, early evolutionary stages 79−8696
atmosphere and review of studies of planet *(Russian)* 77−25966
atmosphere dynamics, winds, circulation and turbulence 77−78706
atmosphere press. and density for different chem. comps. *(French)* 79−21214
atmosphere profile from Mariner 10 radio occultation, statistical and computational uncertainties 79−96938
atmosphere radio transirradiation by Venera 9 and 10 satellites 77−82140
atmosphere structure instruments on Pioneer entry probes 80−67562
atmosphere structure up to 110 km, Pioneer Venus entry probes preliminary results 79−48715
atmosphere thermal balance, review 77−73994
atmosphere turbulence from Pioneer multiprobe radio scintillations 80−46437
atmospheric, review 78−32377
atmospheric banding, hydrodynamic mechanism 79−44386
atmospheric buoyant station, placed by inflated balloon entry 78−4058
atmospheric composition, Venera 11 and 12 mass spectrometer meas. *(Russian)* 79−66947
atmospheric conditions and clouds theory *(German)* 77−25968
atmospheric constitution, struct. and dynamics 80−105186
atmospheric precipitation, props. and possibilities of detect. 80−56741
atmospheric scatt., effect of varying scale height of scatt. particles 77−29679
atmospheric temp. and press. from high resolution IR spectra 77−60701
basalts, redox state 78−77217
bow shock, attachment to ionosphere 77−37541
bow shock, comments 77−71042
bow shock, depend. on solar wind strength 80−41748
bow shock, Pioneer magnetometer obs. 80−36535
bow shock location compared with Mercury, Mars and Earth 78−28560
bow shock observations, 4th Dec. 1978 80−41747
brightness temperature at sub-mm wavelengths 79−53743
capture into resonance rotation, tidal friction 77−78620
chemistry of lower atm. prior to Pioneer Venus mission 79−16857
climatic change on terrestrial planets, review 79−53742
cloud cover, obs. by Venera 9 orbiter 80−51680
cloud cover obs. and recording 78−49355
cloud layer, optical model from spectral photometric data from entry probes and orbiters 78−4130
cloud layer, struct. according to Venera 9 televised pictures 80−67604
cloud layer, Venera 9 and 10 narrow-band photometric probing 77−78697
cloud layer model, Venera-10 optical meas. interpretation *(Russian)* 79−21215
cloud layer moisture, Venera 4 ionization densimeter meas. 77−33379
cloud microstructure, optical props., H_2SO_4 atmosphere-aerosol study 80−72808
cloud microstructure 80−46431
cloud model using radiative transfer theory 77−82138
cloud optical properties and atmos. layered struct. 80−51681
cloud particles, Venera 9 and 10 nephelometric meas. 77−78695
cloud particles phase function, Mariner 10 data 79−40105

Venus continued
cloud properties from airborne obs. of near-IR reflectivity spectrum 78−53850
cloud structure, high-contrast UV detail 80−51682
clouds, aerosol size distrib., coagulation sedimentation and turbulent mixing effects 77−71041
clouds, anisotropic scattering model 78−53852
clouds, coagulation effects on droplet size distrib. 77−67056
clouds, H_2SO_4 aerosol medium IR optical props. and spectrum 78−65526
clouds, IR absorption and scattering, particle size dispersion effect 80−109384
clouds, IR radiation, Venera 9 and 10 radiometer meas. 77−78699
clouds, particle size distrib. meas. 79−48717
clouds, review 77−73993
clouds, UV absorbers, Pioneer data 80−46433
clouds, UV absorbers identification 78−20665
clouds spectropolarimetry, lines equivalent widths information content 80−31215
cloudy layer observation in UV, violet regions, Venera station orbiter TV system appl. *(Russian)* 79−53747
colour photographs from space probe *(German)* 77−53445
core, formation, history and energetics 79−84694
crustal evolution in silicate planets, review 78−61774
dark face, atmospheric constitution, pictures from NASA Venus Pioneer space vehicle *(French)* 80−94735
day sky spectrum, Venera 11 and 12 spectrophotometric obs. *(Russian)* 79−66949
dayglow spectrum, 1250 to 1430 Å, Pioneer Venus obs. 80−77311
dayside ion densities 80−46444
daytime ionosphere, two-freq. radioscopy results from Venera 9 and (Venera 10) 78−4129
daytime ionosphere, Veneras 9 to 10 dual-freq. radio occultation expts. studies 79−96939
daytime magnetosphere 79−96937
density and composition, comparison with Earth 77−29680
development and structure, Earth and Moon comparison *(German)* 77−67055
diameter meas. by occultation obs., teaching expt. 78−12457
disc brightness distrib. from photometry rel. to models 79−40107
disk, linear polarization, wavelength dependence 79−66942
distance from Earth determ. using radar, appl. to space craft navigation 80−109386
dust ring, evidence from Venera 9, 10 obs. 79−75131
dust ring possibility from Venera 9 and 10 spectroscopy 80−8573
dynamical flattening from meas. of trajectories of Venera-9 and -10 79−35168
Earth-synchronous rotation, theory 79−25531
electrical discharges in atmosphere *(Russian)* 79−66950
electron obs. and ion flows, Pioneer orbiter plasma analyzer expt. 80−46448
equatorial and polar limb-darkening 79−88613
equatorial IR brightness diurnal vars., obs. during 1975 apparition 79−16858
equatorial zone surface topography, radar obs. from USSR 77−87303
exosphere, hot hydrogen origin 80−36536
exosphere, hydrogen Lyman α emission 80−105188
exosphere, nonthermal H population, Venera Lyman α obs. 78−93136
exosphere non-thermal H, ionospheric source and H budget 79−12416
exosphere temperature, consequences of day-to-night var. 79−35164
exospheric density and escape fluxes of atomic isotopes 79−5771
exploration by space craft, review 78−12076
far IR obs., temp. determ. 79−12431
far IR photometry, atm. thermal models 79−75151
far IR spectrum, 45-115 μm obs. 77−29681
gas comp. meas., implications for origin of planetary atmospheres 80−51678
geologic evolution of terrestrial planets 77−53442
geomorphological obs. from Venera 9 and Venera 10 78−7895
global thermal emission and radiometric albedo *(Russian)* 78−4132
gravitational spectrum, determ. from Pioneer Venus orbiter tracking 80−41744
gravity anomalies and tectonics, review 80−98593
gravity field, by line of sight tracking of orbiting craft 80−77312
gravity field from Pioneer tracking 80−46439
hothouse theory of recent cosmological catastrophe 80−41749
impact cratering and tectonic activity, evidence from radar obs. 80−46426
induced magnetosphere 79−84699
inert gases in atmosphere, accretion from protoplanetary nebula 80−109385
infrared spectra near superior conjunction, CO_2 bands 80−56740
interior, solid-state convection, obs. evidence 79−84692
internal structure, computation from terrestrial seismic data 77−87298
internal structure evolution, calc. 77−82137
interplanetary dust concentration toward Venus orbital plane, zodiacal light obs. 79−21228
ionopause, shocked solar wind viscous flow behaviour 79−75068
ionopause altitude variability model 79−75128
ionosphere, characts. and interaction with solar wind 77−73995
ionosphere, CO_2 and CO electron vibr. cooling rates 80−41750
ionosphere, comprehensive model 78−57480
ionosphere, day and nighttime radio sounding meas. from Venera 9, 10 spacecraft 79−8867
ionosphere, dayside ion comp. dynamic effects, Pioneer obs. 79−48703
ionosphere, dayside ion composition, Pioneer meas 79−48702
ionosphere, daytime, two-freq. radio transillumination data using Venera-9, 10 probes 80−21936
ionosphere, daytime topside, plasma transport 78−4131
ionosphere, distrib. of elec. currents induced by solar wind interaction 77−64683
ionosphere, diurnal ion comp. vars., Pioneer orbiter meas. 80−46440
ionosphere, electron temps. and densities, Pioneer Orbiter meas. 79−48705
ionosphere, ion comp., photochemical and thermal diffusion control 80−46445
ionosphere, ionic reactions in lab. and planetary atmospheres, probe data 80−59168
ionosphere, mag. flux ropes nature *(Russian)* 80−77313
ionosphere, magnetic flux rope obs. by Pioneer Orbiter 79−70980

Venus continued
ionosphere, nighttime, two freq. radioscopy by Venera 9 and 10 probes 79−62778
ionosphere, photoelectrons and electron temps. 78−77511
ionosphere, Pioneer Venus magnetic field meas. on dayside 79−48700
ionosphere, plasma diagnostics meas. by Venus Orbiter *(German)* 79−96941
ionosphere, thermal diffusion calcs. 80−72806
ionosphere, thermal structure and energy influx 80−46443
ionosphere, thermal structure and major ion comp., Venus Orbiter retarding potential analyzer obs. 79−48704
ionosphere, whistler mode wave absorption 80−46446
ionosphere and airglow, calcs., Pioneer Venus prospects 78−89092
ionosphere composition, meas. by ion mass spectrometers on Pioneer Venus Bus and Orbiter 80−67499
ionosphere energetics, model based on Pioneer obs. 79−75127
IR brightness temp., daytime minima 80−77309
IR emission spectrum, 17-38 μm, aqueous H_2SO_4 droplets in CO_2 atm. 78−40855
IR image obtained at time of Pioneer Venus probe encounter 79−48714
IR polarization interpretation 79−53745
IR radiometer on Pioneer Venus orbiter 80−36469
IR spectrometer obs. on Venera 9 and 10 spacecraft 77−78698
IR spectrum, high spectral resolution ground-based obs. in 450 to 1250 cm^{-1} region 77−91456
isotope abundances in atmosphere 79−58284
lightning, Pioneer Orbiter obs. 79−70979
lightning discharges in atmosphere, frequency of occurrence 80−56743
lightning in atmosphere, chemical impact 79−96940
line profiles and curves of growth for isotropic scatt. 77−37538
liquid content of lower clouds, Mariner 10 radio occultation data 79−40106
lithosphere global TRM in presence of central dipole field, theory 80−31223
lower atmosphere composition, anal. by gas chromatography 79−48721
lower atmosphere composition, preliminary results from Pioneer Venus 79−48720
lower atmsopheric layer struct., appl. of penetrative convection model *(Russian)* 78−24335
luminous flux from Sun on surface and in atmos., Venera-9 and Venera-10 meas. 77−37544
magneti field, nightside Pioneer magnetometer obs. 80−46447
magnetic field, dimensional anal., simple model 79−58286
magnetic field, spacecraft meas. 79−2503
magnetic field and magnetosphere 80−56737
magnetic tail, unipolar induction effects 80−62060
magnetic tail formed by solar wind interaction 80−51679
magnetosphere, evidence for boundary layer and magnetotail from Mariner 10 obs. 77−9686
magnetosphere press. balance, outside dayside ionopause 80−90353
Mariner 10 expedition stages *(Norwegian)* 78−49291
Mariner 10 images, digital processing 77−78647
Mariner 10 photometric obs. 77−29685
Mariner 10 radio occultation obs., pressure-temp. profiles 78−28563
Mariner 10 UV images normalisation 77−56850
Mariner 10 UV spectrometry results 77−45337
Mayan architectural orientations rel. to Venus rising and setting positions *(German)* 77−2352
Mayan astronomy, Venus studies 79−88782
mesosphere and thermosphere temp. struct., day-night variations 77−33381
meteoric material distrib. near terrestrial planets, methematical modelling 79−96976
microrelief irregularites mean height, determination from radio transillumination data 80−72807
middle atmosphere, IR remote sounding from Pioneer orbiter 79−48712
millimetre radiation, short wave, obs. with wide-band radiometer based on superconducting point contact 79−96916
mm wavelength spectral lines detectability 79−5769
moment of inertia and non-hydrostatic equilib. state *(Russian)* 77−45339
motion, numerical theory using radar, optical and Venera satellite obs. data 78−16325
mountain heights and creep props. of rock 79−84700
natural satellites, theory of escape 78−16323
natural satellites escape rel. to planet's slow rot. 79−25529
neutral atmosphere, radio sounding meas., Venera-9, 10 spacecraft 79−8868
night airglow excitation, O_2 Herzberg II bands 77−41340
nightglow spectrum, $O_2(C^3\Delta_u$ to a $^1\Delta_g)$ bands identification 79−16856
nightside ionopause config. 79−80256
nightside ionosphere, electron currents meas. in optical shadow by Venera satellites 78−4133
nightside ionosphere, electron temp. and density models 80−46442
nightside ionosphere, formation process, ionization, mixing ratios 80−41751
nightside ionosphere, origin and maintenance 77−2359
nightside ionosphere, Pioneer orbiter radio occultations 80−46441
nighttime ionosphere, electron interaction in optical umbra 79−80259
nighttime ionosphere, two-freq. radioscopy results from Venera 9 and (Venera 10) 77−91454
nighttime ionosphere, two-freq. sounding by Venera-9 and Venera-10 probes 77−37543
nighttime luminescence, CO molecule identification 77−78702
nighttime luminescence, Venera 9 and 10 spectroscopic obs. 77−78701
nonresonance rotation 79−66944
occultation by Moon 5 October 1980, positions 80−67605
orbit and radius determ. from radar obs. in 1962-1977 period 79−88570
oxidation state of Venus atmosphere and crust, Pioneer Venus results 80−98586
phase effect at 3.4 mm wavelength *(Japanese)* 78−89095
photographic position meas. *(Russian)* 78−93121
photographic position meas. *(Russian)* 78−93135
photographic posns. Fk4 corrections 79−8851
physical properties, brief review 79−75132
Pioneer and Venera spacecraft 79−62721
Pioneer gas chromatograph analyses, laboratory simulation 80−46362
Pioneer Orbiter, radar imagar surface scan, preparation of atlas *(German)* 79−96961
Pioneer Orbiter spacecraft, magnetometer expt. system 77−87229
Pioneer radar data, planet's topography *(German)* 80−105190
Venus continued
Pioneer rephelometer expts. results 80−46430
Pioneer Venus, initial results 79−48699
Pioneer Venus, Unified Abstract Data Library and Quick Look Data Delivery System 80−67494
Pioneer Venus 1978, prospects 78−36436
Pioneer Venus a first report 79−84701
Pioneer Venus Bus neutral gas mass spectrometer 80−67513
Pioneer Venus Differential Long Baseline Interferometry expt. 80−67578
Pioneer Venus large probe neutral mass spectrometer for measurement of composition and abundance of atmospheric gases 79−88563
Pioneer Venus mission, expts. descriptions 77−73928
Pioneer Venus mission, first results 79−66945
Pioneer Venus mission photographs 79−84698
Pioneer Venus mission to study planetary atmosphere 79−44331
Pioneer Venus Multiprobe entry phase, telemetry recovery 80−67493
Pioneer Venus Multiprobe mission 79−84632
Pioneer Venus occultation experiment, radio science data generation 80−67492
Pioneer Venus Orbiter, electron temp. probe 80−67500
Pioneer Venus Orbiter, neutral gas mass spectrometer expt. 80−67502
Pioneer Venus Orbiter, planar retarding potential analyser plasma expt. 80−67501
Pioneer Venus Orbiter, plasma analyser expt. 80−67498
Pioneer Venus Orbiter, plasma wave investigation 80−67497
Pioneer Venus Orbiter, radar mapper design and operation 80−67495
Pioneer Venus Orbiter fluxgate magnetometer design and operation 80−67496
Pioneer Venus Orbiter radiometer (VORTEX) 80−67504
Pioneer Venus Orbiter UV spectrometer, design and operation 80−67503
Pioneer Venus program, 1978 mission 77−73926
Pioneer Venus program, spacecraft, objectives and payloads 77−73927
Pioneer Venus results, surface and atmosphere 80−17523
Pioneer Venus small probes net flux radiometer experiment 80−67512
Pioneer Venus Sounder and small probes nephelometer instrument 80−67511
Pioneer Venus Sounder Probe gas chromatograph 80−67507
Pioneer Venus Sounder Probe IR radiometer 80−67509
Pioneer Venus Sounder Probe neutral gas mass spectrometer 80−67506
Pioneer Venus Sounder Probe Particle Size Spectrometer 80−67510
Pioneer Venus Sounder Probe Solar Flux Radiometer 80−67508
Pioneer Venus spacecraft, design and operation 80−67491
Pioneer Venus spacecraft programme 78−61707
Pioneer-Venus, Venera 11 and 12 research results on atmosphere and surface topography *(German)* 79−80260
plasma meas. by Venera 9 and 10 wide-angle analysers 78−96418
plasma meas. from Mariner 5, reexamination 79−80258
plasma wake, viscous flow 77−87302
plasma waves, solar wind interaction, Pioneer electric field meas. 79−48701
polar clearing in clouds, Pioneer Orbiter 1 obs. at 11.5 μm 79−70978
polar heating and shape of planet, 6 cm. wavelength obs. 79−70981
polar ionosphere, Pioneer orbiter radio occultations, electron density 79−48706
polarisation, wavelength depend. obs. rel. to UV cloud model 80−82250
polarisation variation over disc, comment 77−2358
positional observations at Ukrainian Main Astronomical Observatory, (1972) *(Russian)* 79−44390
positions, photographic obs. (1967-72) from Nikolaev *(Russian)* 79−92689
program for exploration 77−73990
radar brightness and altitude images from 12.6 cm obs. 79−35163
radar image, 46 to 75° latit., 290 to 10° longit. 77−5474
radar observation of surface relief, soil and atmos. 80−36537
radar observations, delay time and Doppler freq. correction 78−7897
radar studies of Venusian surface using refraction attenuation 80−4280
radiative fluxes and equilib. temp. profile *(Russian)* 77−91455
radio emission in H_2O 1.35 cm line 78−20664
radiowave propag. for atmosphere composition anal. 79−21204
radiowaves attenuation in atmosphere of Venus by bistatic radar method 80−62061
regional polarization, 1950-77 obs. 80−8570
resonance rotation 80−109387
retrograde winds, possible periodic vars. 79−25530
review of current knowledge 77−73991
rock density, method, equipment and results of Venera 10 meas. 78−28564
rotation, possible dynamical evolution since formation 80−56742
rotation and atmospheric tides 78−85877
rotation axis, free wobble damping time 80−17516
rotation period and atmospheric circulation, problems 79−70977
rotation pole 79−66943
S-band radar imagery and surface lava flow features 77−64685
scattering layer over absorbing clouds, Venera 9 and 10 UV photometry 77−78700
scattering layers above visible clouds vertical structure 79−62775
SO_2 detect. in UV spectrum 79−62781
solar wind 79−80181
solar wind circulation behind planet, model 80−98531
solar wind interaction, plasma meas. using wide-angle instruments on (Venera 9 and 10) 77−91396
solar wind interaction, review of present understanding 79−58288
solar wind interaction 80−41687
solar wind interaction region, struct. from meas. of ion-flux characts. by (Venera 9 and 10) 78−4051
solar wind interaction with ionosphere, electrodynamic model 79−84624
solar wind plasma expt. results from Pioneer 79−48637
solar wind wake, Mariner 10 magnetic field obs. 78−96417
Soviet lunar and planetary exploration, handbook 80−62398
spacecraft orbital transfer from Earth, minimal flight time calc. 78−4090
spectral line shifts due to blending 78−62851
spectrum, interpretation of weak absorpt. lines 78−24481
spin and atmospheric tides 77−87301
spin evolution 80−46423
spin vector determ. by radar obs. 80−105185
stratosphere, large-scale turbulence, model 80−12699
stratosphere, retrograde rotation meas. with Fabry-Perot radial vel. spectrometer 79−44389
subcloud atmosphere, thermal radiation fluxes altitude distrib. 77−29676

Venus continued
subcloud lower atmosphere, IR radiation absorption calc. method 77−53446
sulphur chemical cycles, involving S, sulphite, sulphide and sulphate 80−50837
surface, atmosphere and ionosphere, spacecraft meas. 79−92690
surface, bistatic radiolocation by Venera-9 and Venera-10 satellites 79−48698
surface, evidence of diverse landforms from radar obs. 77−78705
surface, geologic interpretation of new radar obs. 78−20666
surface, preliminary analysis of images from Venera-9 and -10 77−17395
surface, structure, atmosphere, magnetic field, development *(Hungarian)* 77−73987
surface, Venera 9 and 10 landers, visible radiation 80−46425
surface and interior 77−73996
surface bistatic radar survey, using Venera 9 and 10 satellites 77−87304
surface characteristics, radioaltimeter meas. in Venera 8 descent vehicle landing area 77−29677
surface degradations, Venera 9 and 10 data anal. 77−78704
surface dust detected by Venera 9 and 10, radiant flux obs. 80−72803
surface features, Pioneer orbiter topographic and surface imaging 80−46438
surface panorama and atmospheric boundary layer structure, Venera 9 and 10 obs. 77−78688
surface panoramas, photometric analysis of Venera 9 and 10 obs. 77−78686
surface panoramas at Venera landing sites, contrasts and relief 80−8571
surface reflections of Pioneer Venus descent vehicles radio emission, atm. data 80−105187
surface reflectivity in equatorial region, radar obs. 77−17394
surface relief, Venera 9 and 10 bistatic radar obs. results 77−78689
surface relief, Venera 9 and 10 contrast evaluation 77−78687
surface relief meas. using bistatic radar on Venera 10 satellite 77−64684
surface rock, radioactive element concs., Venera 9 and 10 meas. 77−78691
surface rock density meas. by Venera 10 lander 77−78690
surface rocks, mineral composition prediction 80−17519
surface structure forecast, based on thermal conditions 78−77502
surface TV expts. of Venera 9 and 10 probes 77−78599
surface wind vel., Venera 9 and 10 anemometer meas. 77−78692
tectonics, comparison with Earth and Mars 80−26767
tectonics and composition, theory 80−72805
thermal anomalies, atmospheric, persistence and size 78−85876
thermal asymmetry, Venera 9 and 10 IR meas. 77−53447
thermal evolution, calc. 79−2501
thermal history 78−73665
thermal IR temperature maps, anal. 78−89094
thermal radiance maps, anomalous features 79−101102
thermal radiometry by Venera 9 and 10 of cloud tops 80−46424
thermosphere, acoustic-gravity waves 80−17520
thermosphere, comp. meas., temp. profile and homopause altitude 79−48707
thermosphere, depend. of struct. on solar activity 77−64686
thermosphere, H global circulation and distrib. 78−89093
thermosphere, heat sources prod. by solar UV radiation absorpt. 77−25965
thermosphere and exosphere, Pioneer Venus 1 drag meas. 79−48709
thermosphere during daytime, nitrogen chemistry 80−17517
thermosphere eddy coeffs. and lower atmosphere He content 79−80255
tidal theory and torque balance 80−46422
troposphere, chem. model, vertical zoning, comp., diurnal vars. 78−45251
troposphere, circulation calc. using 20-layer model *(Russian)* 77−33380
ultraviolet photometry and cloud struct., Venera obs. 80−56738
undercloud atmosphere, spectral struct. and thermal radiation spatial distrib. *(Russian)* 77−29678
upper atmosphere, aerosol layer obs. from polarimetry 80−90352
upper atmosphere, diffusion model 79−2505
upper atmosphere, N detect. 80−77310
upper atmosphere, rot., photographs 1927-1975 in UV *(French)* 79−2504
upper atmosphere, rotation *(French)* 80−36534
upper atmosphere density from Pioneer orbiter drag meas. 79−48710
upper atmosphere mean circulation, diagnostic model using remote temp. soundings 79−58287
upper atmosphere neutral composition, Pioneer quadrupole mass spectrometer obs. 79−48708
upper atmosphere structure and dynamics, review 77−33382
UV and IR simultaneous images, correl. of features 79−53744
UV cloud images from Pioneer orbiter 80−46432
UV markings, Venera 9 cloud top data analysis 80−17521
UV markings contrast, spectral depend. 79−62783
UV nightglow, IUE obs. 79−62782
UV nightglow and thermospheric circulation 80−46428
UV spectroscopy from Pioneer Venus orbiter, initial results 79−48711
Venera 11 and 12 first results *(Russian)* 79−35165
Venera 9 and 10, aerodynamics and dynamics during motion in Venus atmosphere 77−91399
Venera 9 and 10, descent vehicles and atmospheric parameters meas. 77−78597
Venera 9 and 10, preliminary results 77−78596
Venera 9 and 10 construction, instrumentation and preliminary results 77−41339
Venera 9 and 10 obs. 77−45338
Venera 9 and 10 panoramas and surface features *(Russian)* 77−25967
Venera 9 and 10 satellites, Venus atmosphere and surface radiosounding 80−101543
Venus Orbital Imaging Radar (VOIR), stereo side-looking radar accuracy anal. 80−56646
vortex circulation, Mariner 10 polar stereographic UV images 79−35167
wake, plasma, electron obs. 78−77510
wake region, ionosheath plasma diffusion model 79−80257
wind speed meas. by anemometers on Venera-9 and Venera-10 probes 77−37542
wind vel. and turbulence, Venera 9 and 10 Doppler meas. 77−78693
wind velocities, anal. of Venera spacecraft data 77−29683
wind velocities, vector determ. by radio interferometry 79−48722
windblown dust, threshold speeds and particle sizes 77−45083
winds, retrograde zonal movement below clouds 80−46436
winds, spectroscopic obs., techniques and data reduction 79−75130
Venus continued
zonal winds, vertical extent 78−85875
Ar isotope abundances in Venus thermosphere, upper limits 80−4281
^{36}Ar excess in Venus atmosphere, implications for Venus accretion 80−12700
CO_2 7883 Å band, high-dispersion spectroscopic obs. near superior conjunction 78−53851
CO_2 8689 Å band high-dispersion spectroscopy near superior conjunction 79−75129
CO_2 band spectroscopic obs. at 7820 Å 77−37540
CO_2 equivalent widths, phase variation obs. 77−37539
CO_2, IR absorpt. bands, 3900-10000 cm^{-1}, assignment 78−7896
CO_2 line profiles, phase variation 77−82139
CO_2 photoionisation and photoelectron energy distrib. in thermosphere 79−2506
CS_2 as candidate for 3150 Å band 79−40108
H I and D I Lyman α radiation scattering, Venera obs. 77−78703
H_2SO_4 aerosol cloud model implications 78−3312
NO production by lightning in clouds, odd N chem. reactions 80−26768
$O_2(^1\Delta)$ airglow and nightglow emission 80−17515
S chemistry and thermodynamics 79−44391
SO_2 IR absorption spectra *(Russian)* 79−25328
SO_2 in atmosphere, distrib. and implications 79−101100
SO_2 in atmosphere, IUE detect. 79−101101
Verdet constant *see Faraday effect*
Verneuil process *see crystal growth from melt*
vertex functions
see also elementary particle interactions; elementary particle theory; quantum field theory of interactions
$(\phi^3)_6$ field theory, deep inelastic lepton-headron scatt., cut vertex theory and reciprocity relation 80−57466
ϕ^4 theory, Euclidean, local existence of Borel transform of Schwinger functions 80−77932
alkali metal, electron-electron scatt. in terms of dielec. and vertex functions 79−95351
chronological exponential, renormalised system of equations 79−30661
conformal spin-1/2 systems 77−38085
electron gas, two-dimens. longit. and transverse dielec. function including exchange correls 77−66133
gauge invariance in non-Abelian gauge theories, triple-gluon vertex 80−42326
Gell-Mann and Low renormalisation group and ψ^6 theory 77−71439
Ising model, convergence of Feynman diag. expansions 78−16750
magnetic impurity in metal, Ward relation between vertex function and one-electron Green's function 79−61052
many-body problem, vertex function and crossing symmetry 80−62515
massless fermion coupled to single axial vector field in U(1) model, AAA triangle diagram 79−35965
multipolar development for two final particles *(French)* 77−49615
multipolar development in arbitrary reference frame *(French)* 77−49614
nλZ vertex in Weinberg-Salam model *(Russian)* 77−2821
parton model interpretation of cut vertex formalism 80−86566
QED tests of electron propagator, vacuum polarisation 80−77994
quantum field theory, n-point functions, renormalised G-convolution, convergence in Euclidean case 80−77930
quarkonia states, heavy, strong decay into other heavy flavours, and triple-gluon vertex 80−47279
reactions involving higher spin particles, gauge invariance 77−41844
Reggeon vertices and finite mass sum rule, bootstrap eqn., dual resonance model 80−13292
renormalised Feynman amplitude, high energy behaviour 80−86555
s-channel helicity conservation at $\gamma V,\gamma\gamma$ and NN vertices, vanishing of spin-zero covariant coupling 79−40691
superconducting Fermi-liquid, electromagnetic response, formal solutions 80−100548
three-photon vertex, weak interaction contributions 77−2787
vertex function, spectral representation, ghostless electron propagator, infra-red and ultraviolet behaviour considerations 79−58911
Wess-Zumino model, massive, dimensional regularisation, supersymmetry 80−27398
D$\rightarrow$K$\pi l\nu$, charm-changing weak hadronic current, models 80−57585
dnp vertex form factor, ed elastic scatt. at high momentum transfer 80−82977
Δ_{33} energy region, electroproduction, simple-pole model, $\gamma N\Delta_{33}$ vertex 80−22625
γNN vertex form factor, ed elastic scatt. at high momentum transfer 80−82977
NNρ couplings, parity-violating, QCD and MIT bag model, $1/2^-$ resonance contribs., $SU(6)_w$ symmetry 80−57540
pp$\rightarrow$pp+N clusters, multiperipheral process, interference terms in transition, amplitudes, correlation expansions 80−62953
πNN form factor, $\Delta(1236)$ contrib., calc. 80−22609
πNN vertex, EM nucleon form factor sidewise dispersion relations, inelastic effects 78−82212
πNN vertex function, dispersion theory calc. 77−57509
πNN vertex function and off-mass-shell πN scatt. 80−73739
$Q\bar{Q}$ systems, two gluon decay widths, short range quark gluon effective vertex 80−86669
vibrating bodies
see also elastic waves; pendulums; piezoelectric oscillations; vibrations
2D finite amplitude acoustic waves radiating from flat plate in arbitrary periodic vibrations 80−33283
absorbing structures, vibr. energy propag. 78−9596
acoustic baffles, effectiveness against flexural wave noise 79−90069
acoustic emissions during flexion *(French)* 80−48625
acoustic field anal. of oscill. body of revolution 78−90583
acoustic generation by vibrating bodies in homentropic potential flow at low Mach number 80−23826
acoustic half-space, transient response to rotating point load 79−3844
acoustic radiator, rheological behaviour of liquid on surface 79−94573
acoustical properties of porous plates vibrating in fluid *(Japanese)* 79−81590
acoustomechanical characts. of laminated first-order transducers 80−14537
aerial camera stabilised mounts, calc. of parameters 80−9059
aerofoil cascade with sinusoidal vibration, induced velocity in wake *(Japanese)* 77−15031
aerofoil stall flutter with acoustic flow control 80−23991
air cushion system, plenum, duct effects on heave stability 79−17202

vibrating bodies continued
aircraft, fuselage, light, interior noise, laboratory studies 78−90596
aircraft, general aviation types, interior noise, acoustic field studies 78−90595
aircraft engine inlet guide vanes, acoustic fatigue due to intake flow distortions 80−53542
aircraft structures, ang. vibr. prediction 77−39253
amplitude modulation of a forced system by parameter variation 79−64578
AC Andromedae, triple mode variable, oscillating c-type RR Lyrae star 78−57560
anisotropic media oscillations *(Russian)* 78−87293
anisotropic plates, dynamic response variational method, general functional 77−3770
annular membrane, harmonic props. 79−94425
annular narrow plates, flexural vibrs., rectangular plate equiv. 77−68487
annular plate, free vibr. freq. spectrum 78−63348
annular plates, uniform in-plane compressive forces, free flexural vibrations 80−106741
annular plates elastically restrained against rotation along edges, transverse vibrs. 80−38312
annular plates under periodic radial loads, dynamic stability 79−1129
annular plates under pulsating loads, parametric resonance 79−14325
annular radial-mode concentrators, calc. 80−5869
annular sector plates, semi-analytic solution for force vibration 79−81761
antisymmetric laminated plates, finite element analysis 80−53683
arbitrarily shaped membrane with point supports 80−23937
arbitrarily-shaped membrane, fund. freq. 80−106743
arbitrary elastic structure in infinite inviscid fluid, acoustic radiation and scatt. 79−7318
arches with flexibly supported ends, freqs. and critical loads 78−30218
attenuation of resilient mounts and dampers under actively vibrating machines 80−14514
automobile whip antenna, first overtone vibrational mode obs. 80−17747
autonomous third order systems stability, comments and reply 79−94539
autoparametrically coupled systems, stochastic stability of stationary response 78−20961
baffled thin rectangular plates, radiation efficiencies 77−27405
bar, curved, in-plane vibrs., shear deform. and rotatory inertia effects 80−43646
bar, curved, out-of-plane vibrs. analysis 79−94522
bar, elastic, resonant longitudinal vibrs. *(German)* 79−90178
bar, radially rotating, of variable cross-section, deflection and lateral vibr. *(Japanese)* 80−94954
bar, thin curvilinear elastic; natural freq. of vibr. optimisation *(Russian)* 80−19266
bar with two natural freqs., minimum mass design 79−46246
bar with various bends, dynamic stress conc. due to flexural wave propag. 77−23904
bar-shaped resonators excited electromechanically in flexural vibration, equiv. electric circuit 77−42677
bars, transversely vibrating, equivalent electrical networks and appls. 79−68469
base excited cantilever beam, whirling motion, comments 80−48488
base excited system with Coulomb and viscous friction, response determ. 80−19269
beam, 2-span, transverse vibr. under moving conc. load *(Russian)* 78−34063
beam, annular, torsional oscillations *(German)* 80−106752
beam, buckled, eqns. for nonplanar, nonlinear motions 78−83316
beam, composite anisotropic, torsional vibration, torsional wave dispersion *(French)* 77−14934
beam, coupled flexural-torsional vibrations 78−90751
beam, deflection under equally spaced moving loads, analytical approx. *(German)* 77−75835
beam, doubly tapered, transverse vibrs. 77−68511
beam, dynamic influence coeff. in forced vibr., fast-Fourier transform 77−72233
beam, dynamically loaded circular, on elastic foundation, natural freqs. 80−79209
beam, elasticity inverse problem soln. using amplitude and natural freq. data 77−2119
beam, forcing with time-varying frequency, solid viscosity and rotatory inertia effects 79−68619
beam, hinged, large amplitude vibration 79−46258
beam, homogeneous, initial boundary value problem of transverse vibr. 79−40367
beam, homogeneous, initial boundary value problem of transverse vibr. 79−41601
beam, infinite, periodic support system, reduction on response 78−83314
beam, multiplicity of solns. of inverse problem 80−28462
beam, nonlinear elastic foundation, comment on fundamental freq. of vib. 78−90756
beam, nonuniform cross section, influence of shearing deformation and rotatory inertia on lateral vibr., pt.II *(Japanese)* 77−68518
beam, nonuniform cross section, influence of shearing deformation and rotatory inertia on lateral vibr., pt.III *(Japanese)* 77−68519
beam, optimum distrib. of additive damping 80−38310
beam, periodically varying length, instability of motion 80−69716
beam, pretwisted, slender, coupled torsional and longitudinal vibr. 79−18770
beam, random vibration against stops 80−74796
beam, rigid plastic cantilever, in damping medium, motion under transverse impact 77−39243
beam, rotating slender, bending vibrs., Galekin method anal. 80−1465
beam, subjected to elastic constraints, free vibrs. 78−83309
beam, Timoshenko, curved, with internal damping, steady state in-plane response 80−64429
beam, Timoshenko's shear coeff. variation with frequency 79−32367
beam, with attached concentrated mass, nonlinear vibrs. 77−19557
beam and attached mass vibration and stability under axial and tangential compressive loads 79−68622
beam and circular plate with compliant boundaries, vibr. response 78−13952
beam boundary conditions vibratory identification 77−27480
beam dynamic deflection under external force of time-dependent frequency 78−83289
beam in transverse vibr., optimisation of higher order eigenfrequencies 77−78971
beam min. wt. design 77−80059
vibrating bodies continued
beam of finite length joined to infinite plate, mechanical admittance 77−11080
beam of linearly varying channel cross-section in centrifugal force field, coupled vibr. 78−18217
beam on inertial elastic foundation, response to moving load 78−5680
beam on nonlinear spring support, random vibr. 78−55585
beam on nonlinear spring support, random vibr. 80−33515
beam or spring connected structures, simple buckling and vibration anal. 79−72843
beam reinforced plate, acoustic radiation 79−18580
beam self-induced vibrations by thermal stress 78−75084
beam structure, continuous, natural freq. evaluation 78−83301
beam structures, thermally induced vibrations and heat conduction problem, numerical method 80−64427
beam subjected to gravity loading, Timoshenko shear coeff. 80−79159
beam subjected to time dependent force, dynamic behaviour 79−23248
beam torsional vibration frequency optimisation 78−83288
beam with heavy tip mass, freq. eqn. 80−43657
beam with moving load, numerical anal. of vibration 80−23943
beam with nonlinear elastic constraints, transverse vibr. 80−38309
beam with one end spring-hinged and translational restraint at other end 77−14944
beam with variable axial restraint, nonlinear vibr. 78−94605
beam with varying thickness, fundamental freqs. determ. 77−31238
beam-reinforced infinite plate excitation by transverse force 77−31253
beam-reinforced plate, flexural wave excit. 78−94612
beam-type disordered periodic systems. flexural wave motion 79−50636
beams, bending torsion vibrations under lateral parametric excitation 78−90749
beams, calc. of higher freqs. by simultaneous iteration technique 79−23258
beams, constraints on optimal design *(Russian)* 77−72158
beams, continuous mass distrib., effect of damping on vibration-stability reln. 77−19558
beams, crack effects on bending frequency *(Japanese)* 77−27487
beams, curved, viscoelastic, anal. of the clamped forced vibratory response 78−90760
beams, effect of support flexibility on fundamental frequency 80−69591
beams, elastoplasticity, flexural motion, finite element anal. 79−46223
beams, eqn. of motion of large amplitude vibration of beams *(Japanese)* 80−33511
beams, free vibr., shear effect *(Polish)* 78−13966
beams, fundamental natural freqs., upper and lower bounds 78−13957
beams, inelastic response under sinusoidal and random loads 79−94530
beams, isotropic, Timoshenko's correction for shear 77−72226
beams, large amplitude vibration damping by viscoelastic layers 78−63363
beams, linearly tapered, transverse vibr. 80−48627
beams, non-linear vibrations, stability analysis method 80−53686
beams, optimal design, iterative procedure 80−1457
beams, plates with varying thickness, fundamental freqs. 79−32324
beams, radiation efficiencies, flexural vibration 80−53541
beams, stationary random oscillations, covariant anal. *(German)* 80−106753
beams, tapered clamped, large amplitude vibr. 78−83311
beams, tapered hinged, large-amplitude free vibrs. 78−38226
beams, thin walled open section, free torsional oscills., secondary effects influence 79−32363
beams, thin-walled with complex profiles, LF normal modes 79−23268
beams, transient response prediction by Laplace transform techniques 78−1596
beams, uniform non-homogeneous undergoing transverse vibrs., optimal design 79−14315
beams and plates, longit. or inplane deform. and inertia effect on large amplitude flexural vibrs. 77−31251
beams and plates with elastic restraints, dynamic stability conditions 79−68612
beams. elastic, under tension, nonlinear transverse vibrs. 80−74803
beams of fibre-reinforced material, vibration analysis 77−68482
beams of variable thickness layers, free transverse vibrations 80−23940
beams with elastically restrained ends, large-amplitude vibrations 78−90747
bearings, rolling, varying compliance vibrations 78−90582
Beck's column, harmonic nonlinear response to lateral excitation 79−10517
Beck's column, influence of tip mass offset on stability 79−72842
Beck's column, subjected to planar harmonic excitation, flexural-flexural oscillations 79−18781
Beck's column on elastic foundation, stability 78−13964
Bernoulli-Euler beams, maximum stiffness, bending, transverse vibrs., singularities in design 79−81802
biaxial slip of mass on foundation subjected to earthquake motions 77−54915
biharmonic action on oscillator *(Russian)* 78−12556
bladed disc, finite element anal. of vibr. modes 77−39250
bladed discs, finite element dynamic anal. 79−37230
blast loaded prestressed flat plates, dynamic response 79−50637
bluff structures, aerodynamic mechanism of torsional flutter 80−53689
bone, vibr. propag. through human femur 77−25494
bone resonance, effects of geometrical parameters, shear and rot. inertia, finite element model 77−29165
bound formula for determining the fundamental frequency 79−81790
bowed string, self sustained oscillations, Hammerstein eqn. 79−98567
bowed string dynamics, general class of models 79−98566
bowed violin strings, investigation of oscillations *(German)* 80−64312
branched torsional systems with multiple junctions, analysis 77−31248
bridges, buffeting due to wind action 79−14321
bridges, flutter due to wind action 79−14320
buckled beams and plates, nonlinear vibration studies, magnetoelastic strange attractor 80−87735
building structure, estimation of structural system parameters from ambient vibrations 80−28456
building-ground interaction by SH-waves *(German)* 77−72204
buildings, damping by natural rubber mounts 80−87643
buildings, traffic-induced vibration 80−96098
built-up structures, math. modelling of resonances using meas. data 80−69718
BWR-4 neutron noise anal. of incore instrum. tube vibr. and impacting 79−36353
cable in sag-span plane *(Polish)* 77−54919

vibrating bodies continued
cables, transverse vibration technique for meas. tension 79−37269
cambered helicoidal fan blades vibr. anal. by shell finite element theory 79−3946
cantilever, lower bound for fundamental torsional frequencies 77−19565
cantilever, type-2 problem, optimum shape under specified fundamental freqs. 77−72208
cantilever beam, base-excited, whirling response 79−68472
cantilever beam, lateral stability under non-conservative load 79−94531
cantilever beam, pre-twisted, torsional vibr. 77−58583
cantilever beam, rot., bending freq. calc. 79−68637
cantilever beam, stability on viscoelastic foundation with shear layer subjected to circulatory force 79−86374
cantilever beam, with unequal breadth/depth tapers, transverse vibrations 78−63373
cantilever beam axial vibration, min. mass structures determ. 78−63278
cantilever beam chattering against a stop, Bernoulli-Euler beam theory treatment, photographic meas. of deflections 80−83752
cantilever beam of periodically varying length, parametric instability investigation 79−81758
cantilever circular cylindrical shells, linear formula for critical freqs. 78−38240
cantilever column, influence of elastic end support 77−11144
cantilever column under transient follower forces 78−1590
cantilever follower force problem, non-conservative load, boundary conditions and stability 77−46956
cantilever minimum weight design with plural torsional frequency constraints 79−68629
cantilever of cantilever-electro-piano, harmonization of vibration *(Japanese)* 79−18634
cantilever plate immersed in water, mode shapes and natural freqs. 79−81782
cantilever plates, extended transfer matrix-finite element method 80−102984
cantilever plates, free vibr. anal. by method of superposition 77−39249
cantilever plates, with biaxial subtangential loading 78−90762
cantilever plates connected by rods, natural vibration form and frequency calc. 77−62203
cantilever sandwich beams, natural freqs. of vibr. 78−18212
cantilever strips with inserts, damping characts. 80−38315
cantilever subjected to follower force, coupling effects 79−50638
cantilever with asymmetrically attached tip mass. natural freqs. 78−63350
cantilevered column with stretching follower force 79−37233
cantilevered cylindrical shells, ovalling oscillations induced by cross-flow 79−86375
cantilevers, joined by a rigid connector nat. freq. determ. 78−83298
cantilevers, neutrally buoyant inflatable, free vibration in ocean environment 79−14333
characteristic eqns. for homogeneous elements of mechanical structures 79−30265
circular annular plates of parabolically varying thickness, buckling and vibrs. 80−69698
circular arches, lateral-torsional instability with motion-dependent loading 77−89049
circular arches with flexibly supported ends, spatial symmetrical vibrations and stability 79−3953
circular bar in elastic half-space, longitudinal harmonic excitation 79−10518
circular cantilevered rod in nominally axial flow, effect of trailing end geometry 80−28455
circular cross-section cantilever pipes, approx. expression for natural freqs. 78−63365
circular crystal plates, accel. effects on resonance freqs. 78−59189
circular cylinder with variable thickness free flexural vibrations 79−68620
circular cylinders in confined fluid, hydrodynamic mass anal. 77−80099
circular cylindrical shells, free vibration 77−58587
circular cylindrical shells, integral calc. involving characteristic beam functions 78−63359
circular cylindrical shells, large amplitude vibrations 79−3959
circular cylindrical shells, ring corrugation reinforced, natural frequencies 79−55336
circular cylindrical shells with cutouts reson. freqs. 77−84178
circular diaphragm, flexurally vibrating, in sound sources generating convergent ultrasounds 77−50845
circular double-plate systems, vibr. characts. 78−79162
circular elastic ring free vibrations, accurate nonlinear eqns. and perturbation soln. 79−64576
circular membrane, transient response to eccentric annular impact load 78−34056
circular pipes, mode-selective energy transfer to walls from internal sound propag. 80−87586
circular plate, edge-clamped, sound radiation study using optical holography 77−836
circular plate, elastic moduli meas., appl. of contactless vibr. excitation and detection method *(Polish)* 79−94571
circular plate, finite amplitude vibr. 78−30214
circular plate, freq. depend. of acoustic radiation *(Japanese)* 79−90070
circular plate, full and annular composite orthotropic, flexural vibrations 79−94528
circular plate, influence of Poisson's ratio on lower natural freqs. of transverse vibration 79−23256
circular plate, min. weight *(Russian)* 77−50951
circular plate driven by noncentral force, clamped 80−64274
circular plate of arbitrary dimension, fundamental vibrational mode frequency calc. 79−98658
circular plate of variable thickness, antisymmetric modes of vibration 78−38239
circular plate on floating central collar, moving load stability theory 77−46863
circular plate systems, free vibrations with restrained edges and initial tension 77−23907
circular plates, arbitrary thickness, free vibration 80−102990
circular plates, asymmetric responses at nonlinear resonances 79−3951
circular plates, elastically restrained, of variable thickness, static and dynamic behaviour 77−75841
circular plates, temp. effects on large amplitude vibrations 78−13951
circular plates, transverse vibrations, non-uniform edge constraints 80−96210

vibrating bodies continued
circular plates, variable thickness, study of buckling and flexural vibrs., Frobenius' method 78−90758
circular plates of arbitrary thickness, free vibration 79−3842
circular plates of variable thickness, buckling and vibrations 79−81774
circular plates subjected to transient loads, nonlinear dynamic response 78−16648
circular plates with conc. mass, large amplitude vibrations 77−50958
circular plates with varying thickness, large amplitude vibrations 77−50960
circular ring segment, damped, test vs. theory for forced vibr. 80−38326
circular rings, inextensional vibrations 78−13949
circular rings, stability obs. *(Russian)* 79−76990
circular rings on radial supports, free vibration 80−23946
circular rod, controlled impact on isotropic, elastic half-space 79−90167
circular rod, elastic, on elastic half space or stratum, forced torsional vibrations 79−41508
circular sandwich plates, free asymmetric vibr. 80−1459
circular segment shaped plates vibration anal. 80−58957
circular tubes subjected to liquid cross flow, dynamic responses 80−53693
circular wire, nonlinear mode coupling of elastic waves 77−79990
circular-plates, effect of initial thermal stresses on large amplitude vibrs. 79−3949
circumferentially travelling radial loads on rings and cylinders 78−1564
clamped beam with branched elastic arm carrying concentrated mass, steady-state free and forced vibrations *(Japanese)* 80−83745
clamped beams with two symmetric steps, nonlinear free vibrs. *(Japanese)* 79−14334
clamped circular membranes dynamic anal. *(Japanese)* 79−35541
clamped circular plate of variable thickness, Rayleigh-Ritz method 77−58582
clamped cylindrical shells, bounds to natural freqs. 77−14938
clamped rectangular orthotropic plates, natural freqs. of vibr. upper and lower bounds 78−83284
clamped rectangular orthotropic plates, natural freqs. using asymptotic solns. from a modified Bolotin method 79−3962
clamped rhombical plates, upper and lower bounds for vibration freqs., method not using boundary conditions 80−79200
clamped skewed plates, elastic deformations by dynamic relaxation 78−34049
clamped square plates, Rayleigh-Ritz vibration analysis with modified Bolotin flexural freq. estimates 78−42563
clamped square plates, vibration anal. using modified Bolotin method, comments 79−72849
clamped square plates, vibration analysis by Rayleigh-Ritz method, modified Bolotin method 80−69720
clamped-free rod subjected to tangential follower forces, variational principle 79−50594
close-coupled systems, vibratory response 79−81767
closed circular cylindrical shells freq. formula for variety of boundary conditions 80−102989
clustered arbitrary discrete vibr. isolators under actively vibr. body, vibr.-isolation efficiency 77−68303
clusters of cylinders in liquid-filled channels, free vibrations 78−38238
clusters of flexible cylinders in axial flow, dynamics 80−28460
coaxial circular cylinders of two elastic phase materials, pulse propagation 79−72747
coherence functions and input/output quantities, statistical errors in meas. 79−3965
column, free flying, asymptotic solns. to problem of lateral stability 79−14242
columns and plates, lower bounds to fund. freq. and buckling loads 79−10469
complex mechanical structures, sound radiation determ. using reciprocity principle 79−23124
complex mechanical structures with random parameters, error of calc. of vibrations 79−23267
complex plates, anal. non-stationary random vibrations 80−102991
complex structures, in-fluid response rel. to orthotropic spheres 77−23797
complex structures, modal confidence factor in vibration testing 79−27607
complex vibrators, mean-value method of predicting dynamic response 80−64273
complex Young's modulus determ. by resonant rod vibrs. *(German)* 78−18259
component mode analysis of nonlinear and nonconservative systems 80−79211
composite beams, effects of fibre orientations 80−87734
composite beams, vibration and buckling anal. 79−1123
composite circular membrane fastened at circumference, symmetrical vibr. 79−37216
composite cylindrical shell, torsional vibr. in mag. field 80−48624
composite materials elastic characts. by vibr. tests and discrete conservative model calcs. *(French)* 80−45337
composite panel under fluid loading, reflection and free wave props. 80−14603
composite plates, thick fluid loaded, acoustic reflection and radiation 79−94381
composite plates with cut-outs, clamped, dynamic response 78−30222
composite plates with cut-outs, simply-supported, dynamic response 78−30221
composite rectangular membrane consisting of strips, free vibr. anal. 77−39252
composite rods, strongly anisotropic, dispersion longit. waves *(French)* 78−12573
composite-material plate, optimal design for max. fundamental freq. 77−50956
concentrical shell system coupled by viscous fluid, dynamics 77−84176
concrete plates, sound transmission at junctions 80−87652
cone with spherical caps twisted by periodic terminal couples, forced torsional vibr. 77−27485
conical sandwich shells, axisymmetric free vibrs. 79−37215
conical shell of compressible nonlinear elastic material, axisymm. proper vibr. 78−30211
conical shells, membrane vibrations 79−23244
conical shells, non-linear free vibrations 79−81795
conical shells, thin, calculation of lowest natural freqs. 79−81770
conical solid horn with flange, FEM analysis of free vibrations *(Japanese)* 80−79045

vibrating bodies continued
connected plates, vibr. power flow, cross-spectral density appl. 78−13947
conservative discrete-continuous system, free vibration *(Russian)* 80−23950
constained plates, Rayleigh-Ritz method using Lagrange multipliers 77−68502
continuous beams with concrete slabs under load, vibration problems of method proposed for crack prevention in slab *(Japanese)* 80−83760
continuous curved beams, natural freqs. of out-of-plane vibrations 80−74588
continuous shallow spherical shells, axisymmetric vibration 79−55335
continuous systems, displacement excitation 77−39254
continuous systems with damping, forced vibration anal., comments 79−23257
continuous Timoshenko beam vibrations on Winkler Pasternak foundations 79−3955
contrast of time-averaged speckle patterns produced by small vibrations of diffuse objects 79−94169
convex polygonal membrane, two dimensional Helmholtz eqn. soln. 80−19271
cooling towers with column supports, free vibration analysis 78−83292
correlation technique appls. to noise and vibration anal. 79−81617
Coulomb-damped flexible mounting, transmissibility curves 79−81768
coupled dynamic systems, loss and coupling loss factors 78−38230
coupled fluid-structure systems, vibrations, substructure element variational anal. 79−55333
coupled mechanical structures, vibration anal. 79−23266
coupled plates, in situ determ. coupling loss, power injection method 80−102983
coupled resonators, normal mode anal. 79−14327
coupled strings, responses for random forcing functions 78−63235
coupled thermoviscoelastic structures, sustained periodic vibrs., finite element anal. 79−7315
coupled vibratory sources, low freq. discrimination 78−18096
coupled-evolutional system, variational calc. of vibr., appl. to ARIANE launcher *(French)* 77−72234
coupling loss factor across a rib, influence of fluid loading and compliant coating 79−23243
creep deformation rate of vibrating structs. 77−11136
crystal plates, higher-order effects of initial deform. on vibrs. 77−46862
curved bars, in-plane vibrations of connecting system 80−43647
curved bars, out-of-plane vibrations of connecting system 80−43648
curved beam elements, free vibr. freq. spectrum 78−63348
curved beams, eigenfrequencies, animated film eigensolns. *(German)* 79−90174
curved box girders, coupled free vibrations 78−30217
curved elastic arcs, perturbation analysis for calculating inextensional natural freqs. 79−23242
curved elements, asymptotic solutions to nonlinear vibrs. 78−90757
curved rods of variable cross section, wave propag. 78−9484
curvilinear elastic rods, vibrations 80−57095
cylinder, acoustic surface intensity measurements for determination of machine noise 80−43577
cylinder, composite isotropic circular, longitudinal vibrations 78−67087
cylinder, elastic, of finite length, free oscill. calc. 77−35078
cylinder, longitudinal vibrs., gravity effects 78−34061
cylinder, of arbitrary dimension, fundamental vibrational mode frequency calc. 79−98658
cylinder, propag. of nonlinear acoustic waves, 2-dimens. case 79−23120
cylinder, propag. of nonlinear acoustic waves, 3-dimens. case 79−23121
cylinder dynamic behaviour in the vicinity of the fundamental radial-mode frequency *(Ukrainian)* 80−69709
cylinder in near-critical flow, influence of acoustic surface vibrs. on drag 78−5729
cylinders, mass transfer 77−62100
cylinders, resonantly vibrating, vortex-excited lift and reaction forces 78−13961
cylinders, solid or hollow, approx. separation of variables appl. to vibr. problems 78−1605
cylinders, stiffened with cutouts, free vibration characts. determ. 77−72221
cylinders, thick-walled, in air and water, calc. of natural freqs. *(German)* 79−50619
cylinders and plates, dynamic deform. at high frequencies *(Russian)* 78−18223
cylinders coupled by fluid gap, generalised hydrodynamic mass for beam mode vibr. 77−68515
cylindrical panel, motion stabilisation *(Russian)* 77−68498
cylindrical pipes, modal density and damping 78−13948
cylindrical shell, arbitrary cross section, transient motion in acoustic medium 78−38244
cylindrical shell, coupled vibrations giving high intensity US radiators 78−59236
cylindrical shell, dynamic stress response to conc. periodic force 77−84172
cylindrical shell, liquid filled under nonlinear resonance conditions, vibration stability 80−99954
cylindrical shell, nonlinear natural vibr. *(Russian)* 78−34062
cylindrical shell, reinforced laminer, intrinsic oscill. 80−99957
cylindrical shell, submerged 79−18715
cylindrical shell, vibration characts. *(Japanese)* 79−64565
cylindrical shell, viscoelastic, forced axisymmetric oscillations 77−50933
cylindrical shell driven by line force, sound radiation 78−94480
cylindrical shell in fluid executing harmonic vibrations, determination of pressure of fluid on cylinder 79−64384
cylindrical shell in rigid baffle, model efficiencies of sound radiation and additional mass coeffs. 78−38129
cylindrical shell in supersonic flow, response to shock load 77−42771
cylindrical shell of variable thickness, natural frequencies *(Russian)* 77−50967
cylindrical shell with cutout, dynamic behaviour 77−75735
cylindrical shell with stiffened spherical end caps, free vibrations 77−3758
cylindrical shells, dynamic instability 78−59334
cylindrical shells, eqn. for natural freqs. 79−23264
cylindrical shells, finite, of various wall thicknesses, axially symmetric vibrs. 77−72205
cylindrical shells, fluid-filled, vibr. and buckling under torsion 78−79253
cylindrical shells, influence of loading behaviour on stability 79−72846
cylindrical shells, natural transverse vibr. *(Russian)* 77−58593
vibrating bodies continued
cylindrical shells, orthotropic, noncircular, problem solubility *(Ukrainian)* 79−32255
cylindrical shells, vibr. anal. by finite element formulation 78−34048
cylindrical shells and panels, natural frquencies in vac. and in fluid 78−83295
cylindrical shells and panels in vacuum and fluid, natural freqs., comments 79−23252
cylindrical shells of varying thickness, natural freqs. and buckling loads 78−1597
cylindrical shells of varying thickness in incompressible fluid, non-linear vibrations 79−81796
cylindrical shells with finite regions of structural discontinuity, wave propag. 78−13841
cylindrical shells within initial imperfections, resonance phenomena in nonlinear vibrations 80−99958
cylindrical sleeves, non-linear forced vibrs. *(German)* 80−53698
cylindrical surfaces with nonuniform vel. distribs., radiated power and radiation loading 78−50969
cylindrical tube, free vibration in viscous incompressible liquid *(Russian)* 78−55636
damped, sandwich beam subjected to moving forces, forced vibr. 78−13953
damped 3-layer plates, finite element analysis of harmonic response 80−53691
damped acoustic systems, finite element anal., reactive mufflers performance evaluation 77−14844
damped continuous systems, forced vibrations, Galerkin and Hamilton-Ritz methods 80−53684
damped plates, vibratory modes 80−69715
deformable shell containing compressible fluid and gas, spectral anal., vibr. modes *(French)* 77−72209
dielectric, polarised, small longitudinal vibr. 79−18772
diesel engine, freq. content of surface vib. rel. to noise reduction 77−80011
diesel engine pistons, simulation of slap at TDC 77−72222
diesel engines, piston slap, assessment of contribution to overall noise and vibration 80−79055
disc, axisymmetric nonuniform quickness distrib., influence of shearing deformation and rotatory inertia on lateral vibr., pt.II *(Japanese)* 77−68518
disc, axisymmetric nonuniform thickness distrib., influence of shearing deformation and rotatory inertia on lateral vibr., pt.III *(Japanese)* 77−68519
disc, centrally clamped rotating, nonlinear vibration 79−59938
disc, circular HF axisymmetric vibrs. analysis *(Russian)* 77−41491
disc with or without baffle, acoustic field study *(French)* 79−98541
disc with Poisson ratio 1/3, freq. spectra calc. for axially symmetric extensional vibr. 78−90745
discrete models in eigenvalue vibration problems of continuous systems 77−89057
discrete spectra for elastic plates without deflection, mixed boundary conditions *(German)* 79−27579
discrete systems, conservative dynamic, K-Quotient for determ. of upper bound 79−18777
discrete-continuous system, vibrations 80−23951
discs, varying radial thickness, finite element dynamic anal. 79−37229
discs with linearly varying thickness, membrane effects on transverse vibration 79−55334
disk, flexible spinning, deflections under stationary transverse load 79−32361
dissipative circulatory structural systems, dynamic behaviour 78−63364
distorted cylindrical shell response to internal acoustic excitation below cut-off freq. 77−80005
distributed mechanical system with nonstationary boundaries, parametric pulse excitation 77−89021
double-cantilever beam, forced vibration technique for meas. of material damping 78−19964
doubly connected membranes governed by Helmholtz eqn., eigenvalue determ. 79−23253
drives, rotational, damping of torsional vibrations, experimental determ. *(Russian)* 80−74816
Duffing asymmetric model, mech. struct. dynamic prop. 77−19556
dynamic balancing, electrical measuring methods *(German)* 78−86261
dynamic coefficient of an elastically supported, pre-stressed beam 79−14306
dynamic response of a pressurized plane strain cylinder under impulsive distributed loading using finite elements 79−18788
dynamic response of elastic shell of revolution in acoustic medium 77−19566
dynamic response of structural panel by Bolotins method 79−90164
dynamic vibration absorber, consisting of three permanent magnets 78−9614
Earth core vibrs., electromechanical effects of short-period geomag. field vars. 79−57847
eccentrically stiffened plates, large amplitude flexural vibration 80−58959
education, Hooke's law oscillator, ideal, anharmonic vibrs. 78−36743
education, normal modes of vibr. between coupled bodies using stroboscope 77−87607
education, student expt., vibrating plate reson. chracts., quality factor and nonlinearity 80−73133
education, vibrating string, tuning guitar by television 80−73134
elastic bars in circulatory systems, influence of end supports on stability 78−30224
elastic beam, flexural vibrs., method of asymptotic expansions *(French)* 78−51112
elastic beam, short rectangular, bidimensional anal. of longitudinal vibration *(French)* 77−7328
elastic body, framework model, oscillations, crack detect. appl. 79−41607
elastic curved body, relation between creeping waves and normal modes of vibr. 77−50817
elastic cylinder of finite length, axisymmetric vibrations 79−86383
elastic cylinders, finite length, longit. modes 77−68306
elastic discs, axisymmetric planar vibr. HF spectrum *(Ukrainian)* 78−83283
elastic discs, high frequency vibr. spectra, second order approx. theory potentiality *(Russian)* 79−10515
elastic half-space, steady state vibr. elastic contact problem, dual integral eqns. appl. 78−18219

vibrating bodies continued
elastic plate, fluid-loaded, response to free and forced waves 79−81769
elastic plate, stability via Lyapunov's Second Method 77−54914
elastic plates, reflectivity and transmittivity, comparison of exact and approx. methods 79−3964
elastic plates, vibration and sound transmission due to a spherical sound wave *(Japanese)* 80−33330
elastic plates, viscoelastic material coated, transverse vibrations *(French)* 80−79215
elastic plates and shells, method of edge-functions 77−72231
elastic properties measurement, apparatus for elevated temps. *(Polish)* 79−96279
elastic rod on viscoelastic half-space, forced longit. vibr., appl. to muscle study 78−44538
elastic rods, wave propag. 77−60939
elastic shell, appl. FEM to coupled structural-acoustic radiation system 80−83691
elastic shells, excitation and stress field in compressible fluid 78−51183
elastic shells, fluid-coupled spherical, transient response to incident pressure pulse 79−68454
elastic shells, reciprocity theorem for sound field determ. 79−32129
elastic solid, effect of gravitational waves, oscills. *(German)* 78−81904
elastic solid, scattering of elastic waves by pores 79−86372
elastic spherical shells, fluid-filled, isolation of resonant component 79−46106
elastic strips, flexural vibrations, active suppression 79−32354
elastic systems, static response rel. to fundamental freq. 77−68484
elastic thin circular plate and particle of mass free vibr. analogy 78−1600
elastic thin plates, nonlinear dynamic stability 77−3759
elastic-plastic oscillators under random excitation 80−28458
elastic-viscoelastic-elastic beams, compressional damping in vibratory response 79−32323
elastically constrained structures, forced vibration response 79−81786
elastically supported circular plate, sound radiation 79−41507
elastically supported membrane eigenfunctions 79−14341
elastically-restrained prestressed annular plates, flexible core links, resonance freq. and mode shapes 80−69714
elasticity with thermodiffusion, vibr. boundary value problems 78−41164
electro-dynamic vibration exciters used in resonance testing of structures, force distortion 79−81779
electrodes on vibrating sphere, mass transfer 80−61106
electromechanical vibration-mounting, for machine vibration active suppression 78−18102
elliptic arc bar, vibrs. perpendicular to plane 78−26076
elliptic ring membrane, fundamental frequencies 77−50978
elliptic thin cylindrical shells, hydrostability 77−75830
elliptical plates, nonlinear vibration, use of von Karman and Galerkin methods 80−102992
epoxy resin compositions, highly filled, influence of combined action of mechanical vibr. and ultrasound 79−56952
external disturbance transformation into boundary layer waves 80−28523
fabricated unit structures, forced modes of vibration 77−65708
fan blade, vibration frequency of a curved beam with tip mass 79−37223
ferrite disc, isotropic, topographs of resonant vibrations 79−64394
ferroelectric cylinders, radially polarised, normal modes and electoacoustic sensitivity 77−62131
ferroelectric cylindrical shells, appl. of one-dimensional finite elements to normal mode anal. 77−31163
fibre composites, orthogonally reinforced, wave propagations 78−41168
finite beam subjected to travelling loads with accel. dynamic behaviour 78−34055
finite elastic struct. immersed in acoustic medium, finite element anal. of vibr. 79−7254
finite Euler-Bernoulli beam, analytical soln. for free and forced vibr. 79−27578
finite periodic beams, response to convected loading 78−38234
finite plate, concidence freq. *(Japanese)* 77−68490
finite plates and beams, energy eqns. 79−23265
fixed free rod with mass at free end, vibr. characts. *(Japanese)* 77−62101
fixed-free generally orthotropic beam vibration finite-element models 79−68621
flat rectangular anisotropy plates, supersonic flutter 77−62196
flat skin-stringer structures, finite strip analysis 78−30220
flexible cylinder, structural-acoustic response of mech. excitation, finite element anal. 79−3839
flexible guideway, vibro-excitation under influence of crossing long train *(German)* 77−54870
flexible membrane, acoustic wave scatt. near reson., panel deflection and vel. pot. field 77−42657
flexible rods, stability under follower forces 80−19273
flexible shafts on oil-film bearings, external damping 77−62199
flexible structures, dynamic simulation by substructure synthesis 80−87733
flexible thread in transverse flow with varying vel. *(Russian)* 80−74789
flexural mode resonators, mechanical susceptance slope parameter 77−80000
flexural mode vibration reduction using impedance systems 78−18225
flexural vibr. of elastic plate, energy flux vector *(Russian)* 77−42773
flexural vibration mode shape change by defects 79−7335
flexural-mode concentrators with varying cross-section 79−90072
flexurally vibrating bars supported by steel wires, broken line approx. matrix method *(Japanese)* 77−68489
flexurally vibrating beam-reinforced plate, compensation of radiation 77−68302
floating gyroscope with vibrating base, perturbing moments *(Russian)* 80−40
floating rod with loaded end, damping during transverse vibr. 80−79205
flow stability mechanical model using Orr-Sommerfeld eqn. 79−81856
fluid and flat plate with harmonic excitation, nonlinear interaction 79−23250
fluid carrying pipes, elasticity of supports and critical velocity calc. *(German)* 80−58914
fluid filled cylindrical shell, response to moving load 78−38236
fluid loaded elastic plate, intersection of dispersion curves 79−77003
fluid loaded structures, vibration response to low speed flow noise 77−84056
vibrating bodies continued
fluid loaded vibration of elastic plate carrying concentrated mass 77−84057
fluid-coupled coaxial cylindrical shells 77−19582
fluid-filled thin cylindrical elastic shell, normal modes with point force excitation 79−94550
fluid-immersed body, design considerations rel. to fluid/struct. coupling 77−84190
fluid-loaded panels, line transfer and line drive admittance approx. 80−64432
fluid-loaded plate, real roots of eqn. defining free wavenumber 79−94398
fluid-loaded thick plates, bending waves 79−72748
fluid-loading influence coeffs. for finite cylindrical shell 77−23799
flywheel, buckling and vibr. of rotating spoke, anal. 78−71288
force transmissibility of resilient mounts supporting a vibration damped object 77−34992
forced vibration of a damped linear system 79−18789
forced vibration prevention by damped dynamic absorber 78−63355
forced vibrations of continuous systems with damping Rayleigh-Ritz-Galerkin approx. 78−59332
forced vibrs. shell, viscoelastically damped, filled with pressurised liq., forced vibrs. 78−9584
free circular plate, vibration under non-conservative edge loading 80−23948
free discs, axisymmetric flexural vibrations 78−51114
free vibrational analysis of frame structures 79−32329
free-free beam, with end-loads, discrete model stability 79−3950
free-free beam with axial thrust and directional control, comments 77−14945
free-free beam with end loads, vibration and stability 79−37222
frequency and time domain responses of system modified by attached subsystem 77−31250
fundamental frequency of vibration of a rectangular plate on a nonlinear elastic foundation 80−69712
Galerkin's method, non-uniform convergence 78−83304
gear systems, analysis of vibratory excitation, tooth error representations 80−33506
gear systems, vibratory excitation 78−63233
gear wheel, free vibration anal. 80−102993
general beam systems, optimal dynamic vibration absorbers 79−23255
glaciers, floating, vibrating mechanism for iceberg calving 78−81197
glass fibre reinforced composite plate, under vibr. load, strength testing, device 79−29318
gravimeter, LaCoste and Romberg, vibr. characts. *(Japanese)* 78−65400
grid in viscous medium, damping, basis for electrostatic viscometer 80−38308
guitar, vibr. modes at Helmholtz and first top-plate resonances 77−35003
guitar body, depend. of natural vibrs. on number and distrib. of ribs. on reson. board *(French)* 77−80030
guitar resonance board, effect of radial ribs on nodal lines, holographic study *(French)* 77−80031
gyroscope, with shock absorber, errors due to spatial vibr. *(Russian)* 78−13892
gyroscope drift, elastic deform. effect on rot. gimbals with base vibr. *(Russian)* 77−14894
gyrotron, freq. characts. determ. *(Russian)* 79−14241
hand-arm system, vibrational responses of hand 78−7380
hard spring, nonlinear systems, modified single mode approach 79−86371
harmonic oscillations of annular wing in steady ideal fluid flow 79−94552
head, spheroidal model, effect of bending on axisymm. vibrs. 77−29168
heat exchange component vibrations in liquid and two-phase cross-flow 78−90770
heat exchanger radial tube bank vibration in transverse liquid flow *(Russian)* 79−81973
heat exchanger tube, vibratory contact with support plate, forces produced 77−88211
heat exchanger tube banks, cross-flow induced vibrations 79−3957
heat exchanger tube banks, flow-induced vibrs. 78−46929
heat exchanger tube banks, turbulent buffeting and fluid elastic instability 79−3958
heated plates with two opposite edges simply supported 80−38314
helical spring of small pitch, free waves propag. 78−9598
helicopter multibladed rotor flutter, effect of phase angle 77−7333
helicopter pilot's seat structure, vibrational response 77−31246
hemispherical shells partially filled with liquid, expts. on vibration 79−81792
highly prestressed anisotropic plates, numerical perturbation technique 78−18214
hinged-hinged beam, material damping in terms of mode of vibration *(Japanese)* 80−91954
hollow cylinder containing small oscillator, motion on inclined plane 77−19516
hollow symmetrical blade vibration characteristics, thin shell theory 78−59341
horizontal beam carrying concentrated mass under gravity, parametric response 79−32362
horizontal piping system, anal. of vibr. induced by two-phase flow 77−80215
human skull, experimental analysis of vibrational characts. 79−81780
hybrid many body systems, elastic part guided motion, vibr. behaviour *(German)* 79−90175
hybrid oscillation systems with elastically coupled rigid bodies, eigenvalue problems *(German)* 79−90176
hysteretic structural system, response to white random load 79−41509
I-beams, normal modes 78−9597
ideal string, extremal solutions of inverse eigenvalue problems with finite spectral data 80−101712
idealized straight beam, free and harmonically forced vibration with dynamic friction 80−96220
impact response, two degrees of freedom system, effect of damping 80−74587
impact vibration, steady, body with impact hysteresis characts., stability anal. 78−51099
impulsively forced nonlinear systems with 2 degrees of freedom, internal resonance effects 79−76998
in-plane vibrational analysis, time-averaged moire method 79−68665

vibrating bodies continued
inelastic critical strength prediction by vibration testing 78−35611
inextensible beams, clamped-free and free-free, non-linear free vibrations 79−81791
infinite elastic bar, induced oscills., normal and associated wave propagation 80−5980
infinite flat plate with fluid loading, input admittance behaviour 79−14322
infinite flexurally vibrating plate, radiation compensation at subcritical freqs. 77−50820
infinite periodic array of vibr. strips in plane acoustically compliant baffle, radiation calc. 77−68305
infinite periodic structures, response to harmonic loads 80−83751
infinite plate driven by moving load, sound radiation 79−64396
infinite plate reinforced by finite beam set and driven by point force, sound radiation anal. 78−1496
infinite plate wave properties, influence of reinforcing beam 77−50821
infinite plate with losses, flexural vibrs. in fluid 78−83319
infinite rod, velocity calc. of zero symmetrical modes for vibrations 79−50641
infinite thin elastic plate under fluid loading, point admittance 78−13959
infinite thin elastic plate under fluid loading, point admittance, comments 79−32348
infinite thin plate driven by longitudinal force, acoustic radiation 78−50998
inhomogeneous elastic structures, active compensation of vibrs. 78−18103
insonified thick elastic plate, displacement field examination 80−102987
integrally stiffened skew plates on irregularly spaced elastic supports, free vibration and transient forced response 80−14604
internal resonance in forced vibration nonlinear two-degree-of-freedom system 77−62192
inverse problems under loading 80−99955
irregular plates, non-linear analysis of vibrations 77−50954
irregularly shaped clamped plates, free vibration 79−37231
isolation of vibration, survey of use and characterization 80−19144
isotropic elastic body, asymptotic distrib. of natural freqs. *(Japanese)* 78−30121
isotropic elastic circular plate, flexural vibrs., Mindlin's theory 80−43650
isotropic elastic strip, vibration excitation by surface and volume forces 79−32355
isotropic isoceles right-angled triangular plate on elastic foundation, thermal-shock induced vibr. 77−35070
isotropic layered circular plates, axisymmetric nonlinear oscillations 79−94538
isotropic random surfaces, profile spectra and spectral densities 78−9593
kinked rods, resonant freqs. using vibration eqn. *(German)* 79−98649
Kirchhoff shells, static and dynamic anal. based on mixed finite element formulation 79−32328
Lagrange gyroscope type body, periodic solns. to eqns. of motion *(Russian)* 78−86142
laminated composite elliptic plates, free vibration analysis, computerised symbolic manipulation 79−32327
laminated composite panels, flutter instability, shear deformation and damping effects 79−72841
laminated plate, reinforced by beams of different mech. impedances 78−90584
laminated plates, dynamic response variational method, general functional 77−3770
laminated plates flutter and buckling anal. 77−65698
laminated rectangular antisymmetric angle ply plates, shear deform. effects on vibr. 78−63356
laminated rectangular plates, nonlinear flexural vibrs., general mode approach 79−32359
laminated structures, of viscoelastic and elastic layers, damping mechanism analysis *(Japanese)* 80−5968
laminates, fibre-reinforced, optimum design under natural frequency restraints 80−53688
laser fusion reactor, cylindrical shell, thermal vibrs., general soln. 80−95433
laser speckle patterns of vibrating panels, interpretation for mode shape information 77−51004
layered circular plates, free vibrations 79−23254
layered cylindrical shells, normal modes 79−94548
layered cylindrical shells vibrating in axially symmetric modes, damping props. 77−14943
layered shells of revolution, torsional vibrations 78−34053
libration in systems of many degrees of freedom *(Russian)* 78−86141
lightly damped tubular arrays, damping props, flow induced vibr. tests 80−68760
limacon-shaped membrane, approx. expression for fundamental frequency 80−53695
line-stiffened plate with fluid loading, flexural vibration analysis 77−31247
linear displacement meas. accuracy meas. accuracy improvement under vibration 80−90815
linear dynamic systems, response to product random processes 78−34054
linear mechanical systems, dynamic vibration absorbers for impulsive excitations 79−23271
linear one degree of freedom system with random excitation 78−34057
linear oscillatory systems, stability with proportional damping *(German)* 80−106751
linear random vibrs., covariance anal., appl. to multi axle vehicles *(German)* 79−90181
linear stable structure maximax response estimates compared 79−68626
linear structure, lightly damped, white noise generated non-stationary random vibrs. 78−90742
linear structures' greatest maximum response analysis 78−38241
linear systems with periodic coeffs., stability determ., numerical method 77−2535
linear vibratory system, multivariate joint probability density function 78−59329
linearly tapered annular plates, axisymmetric vibrations under in-plane force 79−94537
lipid bilayer thermal excitations detect. by light beating spectroscopy 77−48762
liquid filled distorted circular cylindrical shell, acoustic and structural mode coupling 79−3840
liquid-filled shell, nonlinear parametric oscills. 77−58598
local response of structures to random pressure fields, cross-modal terms 78−63234
loudspeaker, cone, vibration analysis using finite element method *(Japanese)* 79−18660
loudspeaker surrounds, stiffness at fund. reson. freq. *(Japanese)* 80−92009
lumped parameter beam models, transient response 80−19270
lumped-parameter systems, synthesis of stiffness of elastic elements 79−37218
machine fault diagnosis, vibr. anal., bispectrum method 79−8404
machine noise, solid and air borne sound and vibration, causes and remedies *(German)* 79−3847
machinery, resilient mounting on platelike and modified platelike substructs. 77−50818
machines, anal. of structural-vibr. related noise 77−84077
made shapes, selective optimal orthogonalisation of measured modes 79−92938
magneto-elastic plates under mixed boundary conditions 79−7328
magneto-elasto dynamics, mixed initial and boundary value problems, vibr. circular plate in mag. field 78−67034
magnetoelastic strange attractor, chaotic type non-periodic motions 80−23945
mass eccentrically fixed to elastic rod, periodic vibrations *(German)* 77−46965
mechanical networks and applications *(Japanese)* 80−10072
mechanical networks and appls. 79−81615
mechanical oscillator, effect of spin on non-linear reson. motions 77−75839
mechanical structures, noise and vibration conf. Repino, Leningrad, 1977 Oct. 79−18579
mechanical structures, realistic fatigue modelling 78−31517
mechanical vibrators miniaturisation 78−18229
mechanics of vibr., introduction, book 79−80439
membrane, composite rectangular, consisting of strips, forced vibration analysis 79−81784
membrane, infinite, acoustic radiation due to fluid loading discontinuity 78−90579
membrane, nonhomogeneous, isoperimetric inequality connecting fundamental frequency with equilib. energy of Poisson problem *(French)* 77−7327
membrane and plate, functionals method for lateral vibr. freqs. determ. *(Japanese)* 80−12918
membrane elements freq. charcts. *(Russian)* 79−27563
membrane shell, forced axisymmetric vibrs., including inner friction effects *(Russian)* 79−32368
membrane speckle pattern analysis 80−106769
membrane with circular outer boundary and eccentric circular inner boundary 77−58586
membrane with rigid centre, free axisymmetric oscillations *(Russian)* 80−38302
membranes, fixed, on the first eigenfunction 77−50980
membranes, wedge-like, isoperimetric norm bounds for first eigenfunction 77−14950
metal plate, effectiveness of stiff two-layer vibr. absorbing coating 77−824
metal rods and metal plates, US transducers, piezoelectric discs, radial vibrs. 80−96166
metallic bar, 30 MeV proton excitation of reson. oscills. 80−64431
micropolar elastic cylinder, free vibrs., wave propag., asymptotic anal. 78−51111
micropolar elastic layer, asymptotic anal. of vibr. 77−89061
Mindlin annular plate of varying thickness, steady state response 80−48626
Mindlin plates, elastically connected, subjected to moving load 79−81788
Mindlin plates, finite strip models for vibration 79−3966
Mindlin plates, Rayleigh-Ritz vibration anal. 80−96218
Mindlin-Goodman method of solving problems with time-dependent boundary conditions, comments 80−53694
mitral valve vibration anal. to detect first heart sound freq. 78−40233
modal analysis, general introduction for managers 80−91955
mode finding, experimentally, when several contribute to a reson. 78−83310
modelling by freq. response data curve fitting 77−54922
modulated backscatter from reed switch loaded dipole 77−75386
mono-coupled periodic systems with single disorder, general method for free wave propag. 79−37225
mono-coupled periodic systems with single disorder, response to convected loadings 79−37226
motion of a gyroscope with a cavity filled with a viscous liquid *(Russian)* 79−18696
motor car horn diaphragms, free vibr. anal. 80−74687
moving coil and supporting piece in dynamic cone speaker, vibr. charcts. *(Japanese)* 77−62101
moving strip, transverse vibrations 80−28459
moving vehicle, ground induced response 79−32346
multi-degree-of-freedom systems, discrete, maximax response 79−81712
multielectrode piezoelectric bar, flexurally vibr., derivation of equiv. electric circuit 78−94481
multilayer orthotropic shells *(Russian)* 78−13968
multiple input systems, effect of input cross spectra on freq. response estimation 79−55261
multiple resonance in vibrating mechanical system anal. using electrical transmission line analogy 78−59188
multiple responses, interdependence of spectral densities 80−96221
multiply connected thick plates, oscillations, elastic medium model anal. *(Ukrainian)* 79−94525
multivariate random systems, synthesis, autoregressive-moving average model 77−84060
musical acoustics wave motion experiment, phase vel. meas. using spring 80−8762
N coupled resonant oscillators, statistical energy anal. 78−59191
noise radiation from vibrating machine systems, prediction by analytical method 80−43521
non-circular cylindrical panels, arbitrary boundary conditions 80−96222
non-circular plates, fundamental freq. estimation, comments 80−23942
non-circular plates with free circular cutouts, fundamental freq. 78−59325
non-uniform beam, direct analytical soln. 78−63361

vibrating bodies continued
non-uniform beams, ref. freqs. for validation of numerical solns. of transverse vibrations 79−32344
non-uniform rectangular plate on elastic foundation, free transverse vibrations 79−32347
nonconservative system resonance, modal analysis 78−42557
nonhomogeneous cylinders and cylindrical shells, torsional oscillations anal. 79−18768
nonlinear, note on weighted mean square linearisation method 78−83303
nonlinear beam carrying concentrated mass, random vibrations 78−33948
nonlinear interaction of fields with plates under harmonic excitations 79−23246
nonlinear oscill. of beam system *(Russian)* 78−13969
nonlinear oscillator, randomly excited, energy envelope approx. 79−14319
nonlinear oscillator problems, weighted mean square linearization method, comments 79−37220
nonlinear oscills. of round plate, difference eqn. approx., Lyapunov methods *(Russian)* 77−39259
nonlinear panel flutter, finite element anal. 79−7316
nonlinear plates, response to random loads 78−94604
nonlinear spatial vibr. of rigid body with active vibr. suppression system *(Russian)* 77−50969
nonlinear structural eigenvalue calcs., mode finding 78−51102
nonlinear systems, forced vibrs., appl. to Duffing eqn. 77−60925
nonlinear systems, modified single mode approach 79−86371
nonlinear systems, multi-degree-of-freedom, harmonic excitation, instability 80−73162
nonlinear systems, third order, forced periodic response stability 78−90763
nonlinear third order systems, pulse response 78−83313
nonlinear two-degrees-of-freedom system, internal resonance, forced vibrations 78−12551
nonlinear vibrating system, combination reson. response amplitude calcs. *(German)* 79−10527
numeric displays, effect of vibration on reading 80−104582
oblique panels, large-amplitude vibrations 78−55505
one-dimensional linear oscillator impacting under harmonic excitation, steady-state response 80−53690
one-mass vibroshock system, forced random oscills., treatment by Markov process methods 79−14335
orthogonally stiffened structures, anal. by combined finite element-transfer matrix method 77−62201
orthotropic circular plates elastically restrained against rotation, large amplitude axisymmetric vibrations 80−83750
orthotropic composite circular plates, axisymmetric vibrations 79−37228
orthotropic continuous plate, natural freqs., approx. formula 78−90766
orthotropic continuous plates, reduction method 77−23906
orthotropic cylinders under initial stress, natural vibrations 79−14318
orthotropic cylindrical shells, resonant response 77−84182
orthotropic elliptical plate, natural frequencies 77−87650
orthotropic plate on elastic foundation, force vibration 80−53682
orthotropic plate vibrating problems, reduction method generalised procedure 78−8246
orthotropic plates, clamped or supported, random vibrs. 78−51104
orthotropic plates, nonlinear vibration anal. by finite element method 77−7237
orthotropic polygonal plates, determ. fund. freq. 80−106739
orthotropic sandwich plates, simply supported, forced vibrs. 77−46861
orthotropic shallow spherical shells under concentrated central load, nonlinear flexural oscillations 79−37234
orthotropic shells of revolution, free oscillations *(Russian)* 79−18796
orthotropic shells of revolution, maxi-element anal. for free vibrs. 78−13955
orthotropic skew plate, shear effects on vibrations 79−14328
orthotropic spherical shells, axially symmetric free vibrs. *(Italian)* 79−27559
oscillating spheroids, acoustomechanical characts. 77−34991
oscillation rods in viscous fluids, added mass and damping, finite element anal. 80−58967
oscillations of firmly clamped, end-stiffened, right circular cylindrical shells *(German)* 80−106750
oscillator with dry friction, forced vibrs., response random process treatment *(Russian)* 80−36841
oscillator with non-linear spring, numerical soln. for free vibr. 80−68034
oscillators, transient behaviour for two harmonic signals *(Russian)* 77−14895
overhead lines, effect of added mass on galloping oscillations 79−81777
overload cables, wave solns. of dynamics 77−35028
panel, circular cylindrical, comments on free vibrs. 78−83315
panels, influence of in-plane loading on flutter and divergence 78−1599
panels, support location influence on flutter, Galerkin method 78−1598
parallel elastically-coupled flat plates, supersonic flutter analysis 77−75838
parametric dynamic systems, combination reson. determ., generalised harmonic balance method 78−90753
parametric excitation of linear systems having many degrees of freedom 77−84177
parametric excitation system instability region determ. 79−23201
partition and glass windows, influence of vibration damping on acoustic transmission *(French)* 77−31176
passive acoustic antivibrators for vibration absorpt. 79−23269
periodic line-supported plate, approx. theory for sound radiation 79−37080
periodic structure response, modal anal. 78−63360
periodically structured elastic ring, free modes 77−35075
periodically-supported fluid-conveying pipe parametric instabilities 79−68627
phase relationships for damped and undamped systems *(German)* 80−106746
physical analysis in factor analysis *(German)* 79−49024
piano string, longitudinal vibrations and inharmonic sound box tone *(Japanese)* 78−13865
piano strings, coupled motion 79−64452
piezoactive complex vibratory systems, matrices of parameters for six-pole equivalent circuits 77−68304
piezoceramic bar transducers, inhomogeneous, analysis using Reissner mixed variational principle 79−64479
piezoceramic cylinders, finite axially polarised, vibr. anal. 77−11081

vibrating bodies continued
piezoelectric bar transducer under influence of body force, response 77−72125
piezoelectric crystals, vibrations, waves, flexure, fracture, fundamental equations 80−60505
piezoelectric infinite plate, critical reflection of antisymm. SH waves 77−34990
piezoelectric plate, loaded, thickness normal modes, generalised orthogonality conditions 78−90585
piezoelectric plate, thickness vibrations, natural freq. spectrum 80−15979
piezoelectric plate transducer, electrical response under influence of body force 77−58520
piezoelectric polymer transducer, effect of acoustic radiation on equivalent circuit 79−94380
piezoelectric resonator with vibrating wall, impacting oscills. simulation *(Japanese)* 78−9483
piezoelectric unbounded plate with circular electrodes, resonances 77−84175
pipe carrying flowing fluid, response to random excitations 77−68488
pipe conveying fluid, wave propag. and vibration response 78−9592
pipe walls, randomly vibrating, broadband sound-power radiation efficiency estimation 77−62104
pipes and beams, structure-borne power flow, cross spectral density methods 80−106742
pipes carrying fluid flow, oscillation stability *(German)* 78−87298
piston engines, elastically suspended, nonlinear vibr. under kinematic stochastic excitations *(Polish)* 78−18221
plane frames and trusses with inclined members 78−59328
plate, annular, axisymmetric flexural vibrations under uniform internal compression 78−83302
plate, annular, variable thickness, free vibration, spline technique method 80−79195
plate, beam-reinforced, edge support influence on admittance 78−1497
plate, bending vibrations and acoustic pressure *(Russian)* 80−23949
plate, circular, elastically supported, elastically restrained edge, initial radial tension, random vibrs. 78−90755
plate, circular, elastically supported, free axisymm. vibr. 77−14942
plate, circular, parabolical tapered, buckling and vibrs. 79−64540
plate, circular, thermally induced vibr. analysis 79−94524
plate, circular, with annular circle constraints, vibrs. and buckling 79−98652
plate, clamped, arbitrary shaped, with in-plane stress, vibr. fundamental freq. 77−14939
plate, clamped, with multi-holes, free vibr. freq. and modes *(Japanese)* 80−53697
plate, completely free, rectangular, free vibr. analysis by method of superposition 78−83300
plate, elastic, under aerodynamic tension, flutter, bending stiffness effect 78−30208
plate, elastic rectangular randomly inhomogeneous, free vibrs. 77−84180
plate, elastically supported, free vibr. 79−72836
plate, flexural motion, effect of accelerometer mass 78−90741
plate, in flowing water, loss factor rel. to fluid vel. *(German)* 77−820
plate, increase of first natural freq. and buckling load by optimal fields of initial stresses 78−13945
plate, inelastic thick, dynamic response, rectangular finite element development 79−94520
plate, isotropic circular, with parabolically varying density, transverse vibrs. 77−42767
plate, linearly elastic, free harmonic vibration fundamental frequency, approx. solution 79−46256
plate, orthotropic, irregular, on elastic foundation, vibrs. under in-plane forces 78−79251
plate, orthotropic multilayered, acoustic transmission loss 78−83143
plate, orthotropic multilayered, vibr. modes, acoustic transmission 78−83142
plate, orthotropic rectangular, nonlinear fluxural vibrs. 77−84179
plate, orthotropic rectangular, with varying thickness, natural freq. 77−7248
plate, plane rectangular hydrostatically acted, clamped and supported edges, exact calc. 77−39256
plate, polygonal, clamped, free vibrs. analysis 79−94523
plate, rectangular, deflections, bending moments, nodal line anal. 79−32366
plate, rectangular, dynamic stability, periodic compressive forces 77−23910
plate, rectangular, forced vibrs., magneto-elastic boundary-value problem 79−49046
plate, rectangular, Krylov-Bogolyubov method, dissipative props. effect *(Russian)* 77−58580
plate, rectangular, of arbitrary thickness, free vibr. 78−13954
plate, rectangular, variable thickness, stability and vibr. anal., finite element method 77−54918
plate, rectangular, with clamped/simply supported edge conditions, free-vibr. anal. 78−59340
plate, rib stiffened, studies on vibrations 78−83297
plate, round thick, natural frequencies of vibrs. symm. in thickness *(Ukrainian)* 77−68476
plate, thick, vibration anal. using Mindlin plate elements 80−38305
plate, thin, nonlinear oscillations *(Russian)* 79−10525
plate, thin circular elastic material, Poisson's ratio effect on natural freqs. 77−84181
plate, thin flat, transverse vibrs., eqns. of motion, kinematic elements *(French)* 80−5977
plate, thin harmonically vibrating, improved extended field method numerical results 80−36833
plate, thin isotropic rectangular, with edge beams, vibrs. 80−79193
plate, two-layered, with imperfect bonding, resting on fluid half-space, vibrations 80−74792
plate, vertical, free convection boundary layers and heat transfer 80−59002
plate, vibration mode, damping of Brownian motion by cold load 78−13967
plate clamped along contour, vibr. problem, exact soln. 78−18228
plate having circular inside edge and cornered outside edge consisting of arcs 80−33507
plate in turbulent pressure-fluctuation field, vibrations and sound radiation 78−38130
plate infinite, oscill. in strong rarefied gas under constant force 79−10623

vibrating bodies continued
plate on elastic foundation, lowest natural frequency of large amplitude free vibrs. 77−7330
plate rectangular, with eccentric circular inner boundary, transverse vibration 80−106737
plate structures with intermediate frames, free vibrations 79−32345
plate thin harmonically vibrating, extended field method free vibration solns. 80−38311
plate under impact of elastic sphere, radiation of transient sound 80−38168
plate vibrating in water, stress meas. by interferometric holography 79−3653
plate with eccentric inner boundary, transverse vibr. 77−68514
plate with intermediate continuous elastic supports subjected to initial membrane forces 80−106744
plate with random inhomogeneities, random flexural vibrations 78−94613
plate with straight line boundaries, method for solving vibration problems, Fourier expansion 80−64433
plate with varying thickness, fundamental freqs. determ. 77−31238
plate with water loading on one side, leaky Lamb waves *(Japanese)* 77−3690
plate-spring struct., dynamic characteristic determ. by rigid finite element method *(Polish)* 78−18220
plates, 3-layered damped sandwich composites 79−81794
plates, active vibration suppression 79−23125
plates, asymptotic theory, stationary plane wave freq. 79−23238
plates, circular, free transverse vibration, axisymmetric, Hamiltons energy principle 80−53679
plates, circular and annular, with ring mass *(Japanese)* 79−18783
plates, clamped orthotropic rectangular, with varying thickness, natural frequencies 79−46253
plates, composite, natural vibr. anal. using finite elements 77−68495
plates, continuous mass distrib., effect of damping on vibration-stability reln. 77−19558
plates, dynamic instability anal. by finite element method 77−3769
plates, isotropic rectangular, with two opposite edges simply supported, finite difference anal. 79−18782
plates, large amplitude vibrations, freq. analysis 77−62197
plates, long narrow, vibrations, asymptotic theory 79−27573
plates, long narrow, vibrations, asymptotic theory 79−27574
plates, mechanical vibr. damping based on continuous system anal. 77−72214
plates, mixed method in elastodynamics appl. to plate theory 77−65709
plates, orthotropic, reduction method for vibr. problems 77−14940
plates, orthotropic, shear and rotatory inertia effects 78−63351
plates, orthotropic rectangular, nonlinear vibrations by displacement formulation 79−64579
plates, periodically varying length, instability of motion 80−69717
plates, pre-stressed, 3-D problems, basis systems of homogeneous solns. *(Ukrainian)* 80−10177
plates, prestressed, numerical-perturbation technique for transverse vibrs. 77−27486
plates, rectangular, with internal rigid support, bending vibration 80−102981
plates, rectangular elastically supported, vibration and sound radiation 77−72112
plates, rectangular isotropic and orthortropic buckling and freq. of flexural vibrs., Rayleigh's method 79−32313
plates, rectangular thin, effect of different edge flexibility coeffs. on transverse vibrs. 78−83294
plates, rectangular with parabolically varying thickness, nonlinear vibrs. 80−19267
plates, reposing on springs, numerical solutions and eigenvalues *(French)* 78−79245
plates, sandwich, rectangular, singly curved, with clamped boundaries, iterative calc., using Kantorovich method *(Japanese)* 80−5970
plates, thick orthotropic on elastic foundations, freq. anal. using triangular plate bending element 79−46273
plates, thin, converged stress solns. by extended field method 80−38306
plates, thin elastic with initial irregularity, free nonlinear vibrs. eqns. *(Bulgarian)* 77−23912
plates, thin rectangular, fundamental vibration freq. 78−38231
plates, thin rectangular, initially imperfect, free flexural vibr. with large elastic amplitudes 77−896
plates, unconstrained layer damping treated, response to random acoustic excitation 80−74798
plates, unconstrained layer damping treated, response to random acoustic radiation 80−74799
plates, uniform circular, holographic interferometry study of flexural vibrs. 77−68504
plates, varying thickness, natural freq., numerical integration *(German)* 80−106747
plates, vibrating elastic, transcendental equation solns. 79−53980
plates, vibration response using general Dirac delta function method to loads along arbitrarily closed lines 80−23938
plates and beams supporting elastically mounted masses, dynamic behaviour 77−62187
plates and membranes, large amplitude vibrations 77−50959
plates and shells, internal damping, influence of geometry 78−50996
plates joined at right angles with fluid contact, diffraction problem 78−18224
plates of arbitrary shape, new analytical approach 80−53692
plates on elastic foundation subjected to shock waves, dynamic response 77−72217
plates on elastic foundations, nonlinear dynamic behaviour 78−13956
plates on Pasternak-type elastic foundation, large amplitude free vibrs. 79−64556
plates stiffened, large amplitude flexural vibrs. 78−83307
plates with initial stresses, large amplitude vibrations 79−23251
plates with integral rib-stiffening, vibration studies 77−46958
plates with irregular shock response, sound power level and noise reduction parameters *(German)* 79−81616
point loaded beam, vibrs. with coupling between different wave types *(German)* 80−102979
point-driven elastic plate, influence of shear, rotary inertia and longitudinal vibrs. on acoustic emission 80−5871
polar orthotropic annular discs, vibration anal. 80−23941
polar orthotropic circular plate, var. calc. of axisymm. vibr. 77−31237
polar-orthotropic sector plates, free vibrations 80−53687
polygonal plates, analysis of doubly connected problem 80−33508

vibrating bodies continued
poroelastic hollow cylinders, torsional vibrs. 79−64557
poroelastic semi-infinite cylinder, torsional vibr. 79−32334
poroelastic semi-infinite solid, torsional loading 79−32335
porous elastic fluid filled spherical shell, radial vibr. 79−18771
porous material surface sound radiation *(Japanese)* 79−68474
porous materials, acoustic radiations anal. 80−87640
porous plates in fluids, sound absorpt. props. of plates near rigid walls 80−87730
power press, relationship between force waveform and sound radiation 80−74596
pre-twisted beam, elements based on approximation of displacements in fixed directions 77−75843
pressure vessel, skirt supported, free vibrs., engineering appl. of Timoshenko beam theory. 78−83299
prestressed beam, dynamic response and natural freqs. 77−39230
prestressed non-uniform cantilever cylindrical shells, axisymmetric vibration 80−14605
prestressed plate on compressible fluid half-space with moving load 77−14937
prismatic plate assemblies, buckling and vibr. anal. with compact computer program 78−90737
prismatic plate structs. submerged in liquid, natural freq. and vibr. modes 78−79256
proportionate Coulomb and viscously damped isolation system 78−42561
pump-induced acoustic pressure distribution in an annular cavity bounded by rigid walls [pressurised water reactor] 79−72848
PWR internals, vibration mode shape computation and expts. 79−13444
PWR pressure vessel vibration excitation, noise correlation and modelling 79−13442
quantum elasticity theory, natural vibrations of rectangular parallelepiped and plate 77−27483
quartz crystal flexure bars and tuning forks, frequency-temp. characts. 80−5971
quartz plate, bevelled AT-cut, thickness-shear vibrations 79−90166
α-quartz plates vibrating in thickness, doubly rotated, zero polarizing effect 80−55038
radial impeller blades, unsteady aerodynamic forces and moments, singularity method obs. 80−58952
radial rotating beams, natural freqs. 78−59326
radial vibrations of a gravitating sphere with a material boundary 79−41609
radial-mode disc concentrators, reson. dimens. and gain 77−68301
radiation impedance of circular plates subject to various edge conditions 80−102913
radiation of plane circular source, nonlinear solutions *(French)* 80−33280
random excitation of system with autoparametric interaction 80−73165
random parametric vibr. of hollow cylindrical shells *(Russian)* 79−27572
reaction of continuous dynamic systems with complex form under time-space random fields 78−65767
reactor absorber, two-group theory of noise 79−26468
reactor struct. seismic response, modal response method 77−83059
record player tone arm resonant frequencies and their avoidance *(Japanese)* 80−33329
rectangular and circular plates supporting masses, fundamental vibration freq. 78−30209
rectangular anisotropic plates, elastically restrained against rotation, transverse vibrations 79−94536
rectangular bars and plates, thick, HF flexural vibr. 79−18779
rectangular beams with thin walls, vibration wave propag. 79−23262
rectangular cylinders in heaving mode, aeroelastic instability 79−3954
rectangular panel in infinite baffle, acoustic impedance 79−94399
rectangular parallelepiped, free vibrs. *(Russian)* 77−50964
rectangular parallelepiped cryst. free vibr. rel. to orthorhombic crysts. elastic consts. determ. 77−84849
rectangular plate, initially stressed, forced motion, elasticity solution 78−38235
rectangular plate, response to nonstationary random load 79−68471
rectangular plate, supported at arbitrary number of points 80−23947
rectangular plate, supported on sides and some segments, free vibration 78−12550
rectangular plate, thin elastic, resting on nonlinear elastic foundation, vibration and stability for large deformation 80−53696
rectangular plate, transverse vibration, analytical treatment 79−86373
rectangular plate complex mode vibration and sound radiation 78−83163
rectangular plate of variable thickness, approximate strain energy expression 80−38317
rectangular plate of variable thickness elastically restrained on three edges, free vibrations 79−72844
rectangular plate subjected to elastic constraints, free vibrations 79−81775
rectangular plate vibration, time-dependent boundary conditions 79−68625
rectangular plate with in-plane forces, vibration anal. by finite strip method 80−14607
rectangular plate with non-uniform thickness, forced vibrations 77−84185
rectangular plate with nonuniform thickness, forced vibrations 80−14606
rectangular plate with oblique supports, free vibrations 79−14326
rectangular plate with thermal gradient vibration anal. 79−27567
rectangular plates, averaging technique for nonlinear vibrations 78−63362
rectangular plates, edges having different degrees of rotational restraint, free vibrations 80−69713
rectangular plates, elastically restrained against rotn. along three edges and free on the fourth, transverse vibr. 79−3963
rectangular plates, elastically supported orthotropic, natural freqs. 77−31243
rectangular plates, flexural vibr., simply supported functions in Rayleigh's method 79−3947
rectangular plates, free vibration, generalized orthogonality relations for modes of vibration 80−102988
rectangular plates, in-plane loaded buckling and vibr. by unified Ritz approach 79−3945
rectangular plates, inelastic lateral support on diagonals, free vibr. anal. 79−1128
rectangular plates, non-linear vibration, theoretical anal. 78−90750
rectangular plates, nonlinear vibrations, comments 79−37221
rectangular plates, nonuniform, anal. of large amplitude vibrs. 78−90761

vibrating bodies continued
rectangular plates, orthotropic, effects of large amplitude, shear and rotatory inertia 79−81764
rectangular plates, semi-analytic solution for free vibr. 79−18778
rectangular plates elastically restrained against rotation and translation, free vibrations 78−59330
rectangular plates of linearly varying thickness, analysis of lower modes of vibration 80−33502
rectangular plates of variable thickness 77−50961
rectangular plates subject to in-plane normal and shear forces, transverse vibrs. 79−14314
rectangular plates subjected to transient loads, non-linear dynamic response 79−81766
rectangular plates with elastically restrained edges, transverse vibrations 78−13960
rectangular plates with linearly varying thickness, approximate formulas for natural freqs. 77−50952
rectangular strip-plates, free vibration and stability 79−32340
rectangular vibrating plates separated by liquid filled gaps, viscosity friction calc. *(German)* 80−105504
reflection characts. of torsional waves in semi-infinite cylindrical rod connected to elastic half space 80−96095
regular polygonal and circular plates, stepped thickness over a concentric circular subdomain, fundamental freq. of vibration 80−87732
regular polygonal clamped plates carrying concentrated masses, free transverse vibration 78−42559
reinforced annular circular plates, axisymmetric vibrations with impulsive loads 80−23939
resonance demonstration, shattering glass with sound 77−57129
resonance phenomena with incidence of acoustic waves on a sphere *(Russian)* 80−58965
resonance phenomena with incidence of waves on a cylinder *(Russian)* 80−58964
resonance testing of complex structs., first-order formulation 80−28457
resonance theory of acoustic waves interacting with an elastic plate 80−33268
resonantly vibrating surface, nearfield determ. of complex radiation efficiency and intensity distrib. 79−55262
response analysis of a vibrational system of multi degrees of freedom subjected to an arbitrary force 80−12912
RF vibr. crystals, inverse problem of Mossbauer spectroscopy 79−37081
rib-reinforced plate, point excited, acoustic radiation 77−80003
ribbed cylindrical shell immersed in liquid, dispersion curves and coeffs. of distribution function 80−87736
ribbed cylindrical shell with solid body, free oscill. 80−99956
ribbed panel, transmission of free waves across rib 77−39248
rigid body systematic deflection by suspension vibration in mag. field *(Russian)* 79−9223
rigid disc on elastic half-space, surface response due to harmonic vibration 78−59333
rigid mass connected to elastic half-space by elastic rod or spring, forced vibrations 77−58585
rigid sphere in elastic medium, effect of random compressional waves 80−53681
rigid sphere vibrating parallel to plane wall, acoustic near field and impedance 80−102910
Rijke tube, contrib. to asymptotic theory *(French)* 78−1491
ring, oscillatory behaviour, influence of Coriolis forces on power transmission belts *(German)* 78−87255
ring subjected to distributed impulsive load, dynamic response 78−13946
ring vibr., approx. theories cf. with complete bending theory 77−19563
rings on periodic radial supports, free vibration 78−9591
rings with circular cross section, vibrations 79−90172
road vehicles, response to profile-imposed excitation 77−72219
rocket engine oscills. due to burning instability *(Russian)* 77−14893
rod, cantilever, constrained end, transverse vibrs., energy dissipation 80−19278
rod, elastic unrestrained, mathematical anal. by Fourier anal. 77−39258
rod, method for estimating forcing point 79−68473
rod, type-2 problem, optimum shape under specified fundamental freqs. 77−72208
rod system in liquid 79−94551
rod with varying elasticity clamped at one end, forced vibr. 80−43653
rods, heterogeneous anisotropic, nonlinear dynamic theory 77−42730
rods, ideally elastic, nonlinear bending, discrete anal. 77−46953
rods, natural twist, influence on oscillations *(Russian)* 79−76996
rods, numerical method for analysing elastic wave propag. due to impact 79−32352
rods and clad rods, elastic waves anal., tutorial review 78−94608
rods axisymmetric motions, experimental assessment of Mindlin-McNiven rod theory 78−1595
rods with nonlinear elasticity relation and nonlinear internal friction, parametrically excited oscills. 80−99947
rotary structural joints, energy dissipation 78−30245
rotating bars, extensional vibrations 78−30213
rotating beam with tip mass, vibration 80−58960
rotating cantilever with offset root, natural freqs. 80−28454
rotating deformable elastic disc, vibr. stress anal. *(Russian)* 80−19265
rotating flexible rod, effect of small tip mass on vibr. 79−41608
rotating flexible rods at transitional parameter values, vibr. and buckling, off-clampings 80−1464
rotating machinery diagnostics, signal extraction and filtering 80−23840
rotating non-uniform disc, spline interpolation technique for calculation of free vibration 80−43656
rotating shaft, with nonlinear spring characteristics, vibrs. 77−75836
rotating shafts, torsional vibration meas., laser Doppler system 79−50685
rotating viscoelastic tapered cantilever, circulatory force at free end, influence of angle of attack on stability 80−69686
rotationally periodic large space structures, finite element transfer matrix dynamic analysis, 100 m parabolic dish 80−74731
rotationally periodic structures, vibr. behaviour, forced response to rot. force 80−69730
rotor, elastic, parameter excited vibrs. *(German)* 79−90179
rotor blades, dynamic characts. 77−39251
rotor systems, characteristic behaviour *(German)* 80−106748
rotor with many degrees of freedom, natural vibr. *(Russian)* 77−57178
rotors, unbalanced flexible, bending vibration behaviour and accel. through critical speeds 79−81783
rubber bonded cylinder, Lagrange anal. of dynamic props. 79−14304
sandwich beam shear-damping reduction effects 78−42560

vibrating bodies continued
sandwich beam with central mass, free vibr., freq. relations 77−31252
sandwich beams, tapered symmetric, frequency and loss factors 78−38247
sandwich circular cylindrical shell, natural vibrations 77−89062
sandwich plates with conc. mass, spring and dashpot, transverse vibrs. 77−68486
sapphire rod, numerical description of torsional vibrs. 77−51435
sapphire rod, torsional waves at low freqs. 77−84053
sapphire rod, wave propag. 77−51434
saws, control of vibrations through thermal tensioning 80−48516
sectorial plates, large amplitude vibration 77−72223
segmental cylindrical shells vibrations, Fourier series component mode anal. 80−58958
segmented beams, Fourier series component mode method 78−38237
semi-infinite plate, variational anal. of edge reson. 77−78987
semilunar valvular motion vibr. model during early diastole, rel. to second heart sound 78−44533
semilunar valvular vibration in early diastole, rel. to second heart sound 78−44544
shaft transverse vibrations resulting from longit. and transverse quasiharmonic forces *(Russian)* 77−58591
shaft-disk systems, lower bound for fundamental torsional frequencies 77−19565
shaft-supported plates, finite element formulation for vibrations 77−68485
shafts with restraints and attached masses, torsional vibration freq. bounds 79−32342
shallow cylindrical panel, on nonlinear elastic foundation, nonlinear vibrations 80−53680
shallow spherical shells, small amplitude vibr., dynamic anal. 79−32365
shear beam, transient response to correlated random boundary excitation 78−38245
shell, axially loaded isotropic cylindrical, asymmetric imperfections effect on vibrs., buckling 77−31241
shell, circular cylindrical, infinite, dynamic stresses under conc. impulsive loads 77−42765
shell, cylindrical, dynamic instability due to attached mass *(Ukrainian)* 80−38297
shell, cylindrical, dynamic response to conc. periodical force, displacement response 77−58579
shell, cylindrical, free vibrs., asymptotic integration solns. *(Russian)* 80−1463
shell, cylindrical, thin, tentative equation for vibrational analysis 80−5969
shell, cylindrical, viscoelastic core, parametric vibrations 77−27489
shell, cylindrical in supersonic flow, vibration, finite element anal. 80−5973
shell, elastic, containing ideal fluid, anharmonic vibr. 80−5978
shell, elastic, containing ideal fluid, nonaxisymm. vibrs. 77−35077
shell, elastic cylindrical, ribbed, with weight on springs, free vibr. freqs. 80−69725
shell, filled with compressible liq., internal press. effect on free oscill. freq. *(Russian)* 80−23934
shell, multilayer spherical, membrane analogy for vibr. problem *(Russian)* 77−35074
shell, orthotropic, axisymmetric vibrs. in mag. field, asymptotic solns. 80−2620
shell, shallow, approx. methods for linear and nonlinear anal. 78−51101
shell, thin cylindrical, dynamic behaviour under high-speed rotation 77−75834
shell, viscoelastic orthotropic, vibrations in various media 77−27488
shell, with negative curvature, free vibr. calc. *(Russian)* 80−23936
shell segments and non-axisymmetric shells, free vibration analysis using isoparametric finite elements 80−23944
shells, axisymmetric multilayer, finite element technique for thermal and press. loading, vibr. modes *(French)* 77−50973
shells, circular cylindrical, dynamic stability under periodic compressive forces 78−90754
shells, circular cylindrical, with longitudinal interior partitions, free vibrs. 79−18776
shells, cylindrical, containing swirling fluid flow, dynamic stability 77−68510
shells, cylindrical, finite element anal., solid of rev., thin shell and interphase elements 80−74744
shells, cylindricals, composite, buckling and vibrational response to axial compression 80−64423
shells, finite cylindrical, of various wall thicknesses, flexural vibrs. 78−1588
shells, laminated, high-precision ring element 79−81789
shells, laminated cylindrical, a high precision ring element 78−90752
shells, orthotropic, cylindrical, axial pressure wave effects 80−10183
shells, prolate spheroidal, const. thickness, natural freq. 78−83306
shells, random vibrations, cross-correlations 77−50957
shells, shallow, viscoelastic, transverse vibrs. 78−83293
shells, stiffened cylindrical under external load, vibration and buckling correlation 79−50629
shells, thick hyperelastic, spherical, large amplitude free and forced oscillations 80−74794
shells, thin, effect of median surface curvature on large amplitude flexural vibrs. 79−18780
shells, thin, free vibr. anal. with approx. methods *(Russian)* 78−42564
shells, thin, shallow and orthotropic, density of natural frequencies *(Russian)* 77−80097
shells, thin stiffened reinforced, stability and vibrs. 80−14610
shells, truncated conical, natural vibr. freqs. and modes, rib effects 80−69726
shells, two layer, natural vibrs. *(Russian)* 77−68479
shells and plates loaded by dynamic moments 77−7249
shells of revolution, expansion of vector functions *(Russian)* 77−54921
shells with internally attached structures, transient response 79−3941
shock spectrum of two degree of freedom nonlinear vibratory system 77−27421
short column vibrator, apparent elasticity analysis and applications 78−59242
short sandwich beams, vibrs. 77−75842
simple frame with circulatory load, elastic stability 79−94532
simply supported beam, Poisson sum formula evaluation of infinite sums 79−86377
simply supported circular, cylindrical panel, vibration with initial bending 79−32343

vibrating bodies continued
simply supported circular plates, accurate natural freqs. determ. 80−102986
simply supported circular plates, partial elastic boundary constraints 80−106740
simply supported plates carrying concentrated masses subjected to hydrostatic in-plane stresses 78−30223
simply supported regular polygonal plates, second natural freq. determ. 78−30120
simultaneous continuous and discrete stochastic processes, compact eqn. *(German)* 79−55337
singly modified damped elastic surface systems, forced vibration 77−7250
singular optimal control problems in vibrating struct. design 77−89058
sinusoidally oscillating cylinder in Newtonian fluid, mass transfer *(French)* 77−57287
skeletal elastic structures, forced, damped vibr. anal. procedures 79−32330
skew plate free vibration, B-spline coordinate functions 79−68623
skew plates, anisotropic, nonlinear flexural vibrations 79−81778
skew plates, large amplitude vibrs., including shear and rotatory inertia effects 78−90743
skew plates, shear and rotatory inertia effects on large amplitude vibr. 77−75734
skew plates of variable thickness, fundamental freq. of vibration 79−81781
skirt-supported pressure vessel free vibrations, finite element analysis 79−68632
skull-brain system, human, prolate spheroidal viscoelastic shell containing viscoelastic fluid, axisymm. vibrs. 78−80901
slender beams and thin plates, deformation effects, comments and reply 78−38229
slightly bent slender beams, lateral vibration, axial end displacement 80−74797
small free vibrations of shell of revolutions in an ideal liquid *(Russian)* 80−73168
smooth circular cylinders mounted in tandem, in-line flutter 78−13958
solid cylinders, axially symmetric natural vibrations 78−38131
solid systems, errors associated with resonance curves 79−7255
sound field attenuation of diverse sources in plate by means of surface corrugations 80−14515
sound field calculation *(Japanese)* 80−48493
sound radiation by plane structures with diffuse flexural-wave field 80−102912
sound wave diffraction by hollow elastic cylinder in partial annular layer of finite thickness 80−14506
spacecraft, flexible, in gravitational field, stability 77−25906
sphere near rigid or compliant wall, near field and impedance 78−94476
spheres, mass transfer, horizontal transverse vibr. effects 80−57220
spheres, moving on circular path, mass transfer rates 77−3890
spherical 3-layer shell, eqns. of motion for free vibr. *(Russian)* 79−23241
spherical floating gyroscope, perturbing viscous friction moment in suspension due to vibr. *(Russian)* 78−13893
spherical shell, constrained fluid-loaded, vibrations and noise associated with response to turbulent boundary layer excitation 79−90239
spherical shell accelerating in fluid medium, generation of waves 78−13843
spherical shell moving in acoustic medium, transient response 77−35067
spherical shells, nonclassical treatment of vibr., power series method *(Russian)* 77−50966
spherical shells, transient response of thin elastic spherical shells 80−96217
spinning annular plates reinforced with edge beams, vibration and stability 78−38225
spinning cable with tip mass, free vibr. anal. 78−94609
spinning elastic disc with transverse load system, stability anal. 77−19562
spinning polar orthotropic annular plates, edge beam reinforced, vibration and stability 79−94534
spring-loaded mass system vibration analysis *(German)* 80−96224
spring-mass system, optimum design of untuned viscous dynamic vibration absorber 79−86370
spring-mass system, single degree-of-freedom, rms accel. response to band-limited white noise 79−81787
springs, cylindrical helical, dynamic coupling of torsional and flexural strains 77−62202
springs, helical, cylindrical, natural frequencies of transverse vibrations 80−77630
spruce wood beam of square cross section, wind excited vibrations 78−59331
square cantilever plate immersed in water, finite element method 79−37224
square laminated panels, forced transverse vibr. expt. *(Japanese)* 78−22298
square plate with parabolic thickness variation 79−68628
stars, pulsation freqs., linked poloidal-toroidal magnetic fields 78−96470
stars, search for oscills. 78−93203
stars of about 1 $M_\odot$, semiconvection and vibr. stability 77−22204
stayed columns, concise buckling, vibration and static anal. 79−18755
steady impact vibration of body with quadrilateral hysteresis loop for restitution force 77−23905
steady-state response of internally damped circular plates 80−106658
steel bar, effectiveness of rigid vibration-absorbing coating 78−18226
steel SS-41, plastic working with vibr., US hardness tester 78−53044
stepped beams, nonlinear vibrations, transfer matrix method *(Japanese)* 79−64566
stepped strings and beams, freq. eqn. 77−31249
stepped thickness plates, fundamental freq. determ. method 77−46960
stiff string with piezoelec. polymer film, vibration mode meas. 80−99959
stiffened panels, acoustic noise transmission 80−102922
stiffening ring, longitudinal-mode and flexural-mode impedances 78−83320
storage ring, feedback-stabilised, resonator wall instability caused by ponderomotive forces 80−5418
stranded wire helical spring, general axial response 80−33453
stretched circular membrane, vibrational props. *(Japanese)* 77−42655
stretched strings, intrinsic nonlinear effects 80−82607
stretched strings, superharmonic vibrations of order 3 79−3843
string, acceleration discontinuity propagation due to solid friction *(French)* 80−22196
vibrating bodies continued
string, density determ. from spectral data 77−9856
string, harmonic waves, introduced through Fourier synthesis, for teaching 80−27080
string, harmonically forced finite amplitude vibration 77−68383
string, nonlinear stretched, randomly excited, anal. 78−83312
string, partial elastic or anelastic impact against wall *(Italian)* 77−68380
string, partially elastic or anelastic impact against wall *(Italian)* 77−72143
string, stochastic vibr., mean displacement determ. by successive approx. 79−27523
string, stretched, appl. of optimisation methods to vibr. control 78−83305
string, vibrating, motion above a concave obstacle, second order hyperbolic problem with unilateral constraints 80−57101
string, vibrational motion under frictional force *(French)* 79−32326
string instruments, body modes calc. 77−7267
string instrums., secondary waves arising from self-excitation *(German)* 79−76918
string linear displacement transducer design *(German)* 77−79085
string vibr. against point shaped obstacle, energy theorem 78−81824
string vibr. through moving ring 78−81823
string vibrating against rigid wall, partially elastic or anelastic impact, energy calcs. 78−67028
string with time-varying length 79−50620
strings, stiffened, dynamic behaviour 77−75837
strings, stretched, vibr. control by an external distributed force 78−83308
strip and plate, end resonance for materials of varying Poisson ratio 77−51438
strip radiator, power output considerations 80−69577
struck string, discrete model 79−3838
structural elements having 1- and 2-section; freedom, vibr. characts., optimum design 77−72207
structural foundations, excitation by seismic surface wave 80−10182
structural models with closely spaced modes of vibration, design method 79−32349
structural vibration anal. using subspace iteration 78−38233
structural vibration modes, inverse perturbation calcs., minimal change theory 79−18691
structural vibrations under random excitation, energy anal. 79−27568
structure borne sound insulation on pipelines, insulation 79−50501
structure frequency analysis by integrated force method 79−18692
structure radiation of simple emitters, radiated sound power *(French)* 77−19471
structure seismic design, probable simultaneous response by response spectrum method 77−83060
structure with coulomb friction, dynamic characts. 79−94535
submerged cylinders, forced oscills. test in water 78−5728
submerged spherical shell, axisymmetric free vibration 80−74546
submerged spherical shells, free vibrations 78−63358
submerged tube surrounded by rigid tubes, hydrodynamic inertia coeffs. 77−7335
Sun, diameter pulsations phase coherence 79−92747
Sun, first twenty modes of radial oscill. of 1968 non-standard solar model 77−41371
Sun, oscillations, review 78−69777
Sun, pulsation period rel. to rot. and sunspot cycle periods 77−53519
superconducting five coil partial torus, buckling and vibrs. 77−79128
supersonic flutter of heated circular cylindrical shells with temperature-dependent material properties 78−71289
surface plastic deformation, damping effect, vibration theory anal. 79−94511
surfaces, procedure for measuring sound intensity near vibrating surface 80−53580
symmetric system nonlinear forced vibrs., group representation theory 77−2536
symmetrical free vibrations of a thin elastic plate with initial condition as a generalized function 79−59939
systems with discontinuities, exact and direct analytical solns. 78−13962
systems with mixed boundary conditions, nonorthogonal eigenfunctions 77−14941
tapered beam finite elements for vibration anal., mass and stiffness matrices 79−81759
tapered beams and beams carrying mass, vibrations, finite element formulation, comments and reply 78−13950
tapered cantilevers, nonlinear vibrations 78−34052
tapered circular plates elastically restrained against rotation at edges, nonlinear vibs. 79−18791
tapered orthotropic plates having thermal gradient, natural freqs. 80−53685
tapered unconstrained beams, vibration damping 78−51106
tensioned bar with initial curvature, parametric excitation 80−43654
tensioned sheet, with central opening, buckling behaviour and parametric reson. investigation 78−90759
tensioned sheet with rectangular opening, static and dynamic behaviour 77−27482
thick circular plates, sector finite element for dynamic anal. 79−72845
thick circular rings, in-plane vibrations 77−50955
thick flexible ring rotating at high speed, vibration anal. 79−37227
thick multiply connected plates with nonsymmetric stress tensor, oscillations *(Ukrainian)* 79−41602
thick plates driven by uniform line moment, input and transfer admittances 79−23249
thin annular plate having parabolic thickness variation, flexural vibrations 80−69719
thin beam-reinforced plates and shells, wideband sound radiation 79−18581
thin circular cylinders, vibration characteristics for different end conditions using variational techniques 79−86376
thin circular membrane, forced symmetric vibrs. 80−10181
thin crystal, surface stress effect on natural freq. 77−7325
thin cylindrical shell, compression dynamics, nonlinear evolution of Rayleigh-Taylor instability 78−79243
thin elastic plate, acoustic wave scatt. near reson., panel deflection and vel. pot. field 77−42657
thin elastic plate of const. width, vibr. energy propag. 78−9599
thin elastic plate with arbitrary shape, method for solving problems 80−87641
thin elastic plates, nonlinear vibr. 78−1593

vibrating bodies continued
thin elastic shells, variational eqns., comments 77−14946
thin electroelastic sheets, fluttering, thermodynamic effects *(German)* 80−106749
thin I-shaped plates, exptl. determ. of transverse vibration modes 80−28474
thin infinite cylindrical shells, active vibration suppression 79−18797
thin infinite panel, sound insulation dependence on effective loss coeff. 80−87737
thin orthotropic plates, bending stability and free vibration 79−3961
thin panels, magnetoaeroelastic stability *(French)* 77−65702
thin plate, effect of line-discontinuity admittance on sound scattered by plate vibration 78−55494
thin plate, Young's modulus meas. by composite vibrator method *(Japanese)* 79−50599
thin plate dynamics, elastic asymptotic anal. of boundary and initial conditions 80−43640
thin plate flexural modes, synthesis of vibr. suppression system 78−9494
thin plates with complex form, vibr. statistics 79−3937
thin rectangular plates, influence of thermal grad. on natural freq. 79−32353
thin rectangular plates, stability and vibration anal. by simplified mixed finite elements 78−34058
thin shells, infinite, response to initial stress 77−31236
thin shells of revolution, large amplitude asymmetric vibrations 77−80006
thin stretched foils, membrane wave excit. 78−90578
thin strip, dispersion of flexural normal modes 78−1604
thin tubes conveying fluid, collapse and flutter, comments and reply 78−34060
thin walled tank containing compressible liq., vibr. anal. *(Russian)* 80−1462
thin-walled beams, forced vibration anal. 79−23263
thin-walled nonuniform elastic tubes containing incompressible inviscid fluid, wave propag. 77−79981
third order nonlinear differential eqns., stability criterion, comments and reply 79−94540
third-order systems, stability 77−14947
three arm plate tuning fork, anal., mechanical filter appl. 78−22300
three dimensional acoustic radiation, problems, boundary integral solns. 79−3818
three-layer beams with viscoelastic cores, nonlinear vibrations, expt. 79−32341
three-layer structure, axisymmetrically driven, acoustic radiation 78−1507
three-layer structures, calc. of antisymmetric modes 77−50975
thrust foundations, resulting vibrs. in viscoelastic bodies *(German)* 79−90177
Timoshenko beam, coupled bending and twisting vibration 77−58584
Timoshenko beam, elastically supported, moving harmonic load 78−42566
Timoshenko beam, transverse vibr. without transverse deflection 77−50976
Timoshenko beam of varying cross-section, determination of steady-state response using spline interpolation technique 79−81772
Timoshenko beam with axial force, vibration characts. 79−3956
Timoshenko beams, approx. dynamic analysis and application to tapered beams 79−98656
Timoshenko beams, effect of rotary inertia and shear deform. on freq. eqns. 78−83296
Timoshenko beams, finite element eigenvalue anal. 78−59327
Timoshenko beams, finite element for vibr. anal. 79−18774
Timoshenko beams, second freq. spectrum 77−62200
Timoshenko beams on Pasternak foundations, natural freqs. 77−60938
Timoshenko beams resting on elastic foundation, dynamic stability using finite element model 79−18775
Timoshenkos beam theory, natural frequency of continuous beam 78−83322
tip heavy beam, vibration anal. by Dunkerley's method 80−102994
toroidal shell, calculation of lowest eigenfrequencies and vibrational modes 77−19561
torsional mass in gravimeter, vibration damping *(Russian)* 78−4015
torsional vibrators, design by computer optimisation *(Japanese)* 80−33405
transducer, performance calc. 80−77771
transmission line aeolian vibrations, effect of 4R dampers 79−23259
transmission lines with dampers, higher modes of vibration 79−81773
transtropic thick plates, multiply-connected, forced oscills. *(Russian)* 77−39241
transversally vibrating string, Stieltjes functions and approximate solutions of an inverse problem 79−49094
transverse, circular plates of linearly varying thicknesses, soln. by polynomial coord. functions 80−64425
transverse vibrations of circular plates having nonuniform edge constraints 79−86366
triangular plates on Vlasov elastic half-space 78−13963
triangular slab on elastic foundations, thermally induced vibrations 79−3960
tube, cylindrical, elastic, shearing oscills. *(Chinese)* 79−64555
tube, viscoelastic, containing flowing fluid, bending vibrs. 79−94521
tube arrays in cross-flow, flow induced vibrs. 78−46984
tube banks in air crossflow, hydrodynamic vibration models *(Russian)* 78−46981
tube bundle in turbulent water crossflow, bent tube vibrations 80−92124
tube rows and arrays, fluid elastic whirling 78−46928
tube/fluid vibrations, effects of fluid viscosity 79−3967
tubes and flexible hoses carrying moving liquid excited in transverse vibrations, nonconservative boundary-value conditions 79−63056
tubes containing fluids, vibr. freqs. and flow parameters 78−1492
tubes with inclined terminal nozzle, stability boundaries for flow induced vibrations 80−19512
tuned equipment-structure systems, response spectra design methods 79−3952
tuning fork, generalised, vibration mode anal. 80−96097
tuning fork, longit. vibr. mode 80−38
tuning fork for clock, vibr. anal. using speckle method 79−21737
tuning fork for HF operation, second-mode, finite element anal. and expts. 80−102980
tuning forks, electrically driven, Melde's experiment apparatus 80−42022
tuning forks, forced parametric vibrs. *(Russian)* 77−68299

vibrating bodies continued
tuning forks, quartz crystal, finite element analysis of displacement at base portion 79−68470
turbine disc transverse vibration initiation 79−68633
turbomachine cascade wing profile oscills., aerodynamic damping, ang. of attack influence 79−37344
turbomolecular pump, development and use 79−63251
turntables, vibration estimation method using holographic interferometry *(Japanese)* 79−90071
two coupled conductors, stab. anal. 80−96219
two dimensional distributed resonator, math. model 80−64275
two-dimens. structs., finite dynamic element for free vibr. anal. 78−83287
two-layer plate in a liquid, free flexural vibrations 79−23261
two-section beam with time dependent boundary conditions, transient response 78−63366
two-way continuous rectangular plate free vibration theory 79−68631
U-type vibrator, resonant freq. and vibration mode *(Japanese)* 77−42656
unconstrained discrete systems, determ. lowest freq., extended bound formula method 80−102985
underwater beam with circular section, vibr. anal. 79−3948
unhomogeneous bars, normal mode response, stress anal. by boundary operator method 80−19239
US rod systems, excitation and stabilisation of reson. modes 77−14839
vacuum gauge, vibr. vane, sensitivity 78−49793
vapour diffusion pump, vacuum behaviour of perfluoro polyether 79−63254
vapour pump, recent developments 79−63250
variable thickness discs subjected to centrifugal and thermal stresses 77−84184
variable-thickness elastic orthotropic annular plate nonlinear oscillations 79−68630
variably constricted beams, transversal oscillations and critical loads *(Italian)* 78−51113
vertical tube with liq. flow, free and forced oscills. 77−7457
vibrating rotor gyroscope, sensitivity increase *(Russian)* 79−27503
vibration insulation, natural rubber in transport engineering 80−96099
vibration of thin plates using the Ritz method 80−64426
vibration problems, element spaces and separation for determining bounds to eigenvalues 79−14317
vibration regulation laws *(Japanese)* 77−80007
vibrator, flexural piezoelectric, split-electrode, suppression of spurious responses *(Japanese)* 78−83204
vibrohydrodynamic instability in liquid crystals, threshold calcs. and mol. reorientation determ. 78−91249
viscoelastic bar, vibrs., correlation between random parameters 79−32325
viscoelastic beam, constrained, flexural vibrating, response to random excitation of white noise and turbulent boundary layer type 80−53671
viscoelastic beam, continuous, dynamic response 78−9569
viscoelastic beam, with viscoelastic end supports, parametric response 79−81765
viscoelastic bodies with small loss tangent, vibr. anal. 77−65706
viscoelastic body, forced, geometrically nonlinear vibrations 77−3762
viscoelastic circular rod, in-plane vibr. effects of shearing deform. and rotary inertia 77−84174
viscoelastic cylinder, transverse vibrs. 77−19544
viscoelastic cylindrical shells with moving loads, steady state forced response 79−27566
viscoelastic hinge supported rod, parametric oscills. *(Russian)* 79−50624
viscoelastic materials, design evaluation of damping treatments 79−18799
viscoelastic orthotropic layered cylindrical shell in acoustic medium, numerical anal. 77−54828
viscoelastic orthotropic rectangular plates, free vibrations 79−41597
viscoelastic plate with circular outer boundary and eccentric circular inner boundary 79−81760
viscoelastic plate with eccentric circular constraint 79−90165
viscoelastic plates, cross-supported, vibrs. 77−62095
viscoelastic rod driven by sinusoidal displacement, thermomechanical response 77−89056
viscoelastic rod with small nonlinearities, vibr. anal. 79−98657
viscoelastic shells, axisymm., transient vibrations 80−10179
viscoelastic spring rod, vibration heating, amplitude depend. *(Ukrainian)* 80−38301
viscoelastic vibrating reed under gravity 79−90169
viscoelastic Voigt column, influence of elastic end support on stability 79−37238
viscoelastically damped beams, shock response 78−38232
viscoelastically damped cantilever beam, effect of boundary conditions 79−23245
vortex noise emission in flow past vibrating rigid bodies 79−23310
VVER anal. of relative motion between pressure vessel and its internals 79−67882
wedge, free oscillations in a tight cavity *(Russian)* 80−58953
white dwarf stars, ultra-short var. 79−21287
wide-band plane wave scattering and transmission by fluid loaded plates 80−106646
wind turbine blade, non-linear dynamic response 79−81771
wind-induced bending torsional galloping vibration of rigid body, minimal wind velocity determ. 80−48623
wire, self-induced vibrations by thermal stress 78−75084
yawed circular cylinders, vortex excited oscills. 78−46982
Al plate, improved freq. resolution from impulse tests with short record lengths 79−81797
Al plate excited by free turbulent jet, generation of vibrs. and atmospheric sound *(German)* 80−102908
Al rod, measurement of small amplitude vibrations using multiple-beam interferometer 80−4759
MnZn ferrite disc, excitation of radial mode vibration due to AC 79−69708

vibration control
see also damping
acoustic materials for noise and vibration control 77−11089
active suppression systems, effectiveness of criteria for placement of compensating sources 78−18099
active vibration-mounting techniques 78−18102
active vibration-suppression systems, automation 78−18098

vibration control continued
active vibration-suppression techniques for mechanical systems with many degrees of freedom 78−18101
aeroautoelasticity, active control and suppression of flutter in aircraft *(Russian)* 78−67079
aeroplane, deformable control systems, numerical anal. of lateral dynamic stability 78−51057
backward-wave-mode thickness vibration energy trapping by piezoelectric reaction control 79−56728
beam-reinforced plate, vibr. energy propag. in absorbing structs. 78−9596
bearings, rolling, varying compliance vibrations 78−90582
buildings, use of natural rubber mounts 80−87643
cantilevered bench, vibration isolation for balances 80−68183
compound metal sheet, means *(German)* 77−19481
computerised rotating laser light beam appl. *(Russian)* 78−71299
contact resonance of vibration pick-up and its control *(Japanese)* 78−33949
damping, polymeric coatings 80−10178
double-pendulum vibration oscillator or seismograph 78−16200
dynamic balancing, influence coefficient method, balancing of rigid rotors 80−53724
dynamic damping effect in small force measurement *(Russian)* 78−12687
dynamic vibration absorber, consisting of three permanent magnets 78−9614
electrodynamic vibration test beds, feedback signals for correcting characteristics 80−53543
epoxy resin use in noise and vibration control 77−50829
flexible shafts on oil-film bearings, external damping 77−62199
flexural mode vibration damping by reinforcing beams 78−18097
force controlled vibration isolation system 78−18100
gyrosystem, optical methods *(Russian)* 80−8983
harmonic gear transmission drives, method 79−88949
inhomogeneous elastic structures, active compensation of vibrs. 78−18103
IR detector balanced common module coolers 80−95142
isolation of industrial machinery 79−72868
lathe off-balance during metal removing, systems reviews *(Russian)* 78−70118
legal remedies for noise and vibration problems 80−10084
linear mechanical systems, dynamic vibration absorbers for impulsive excitations 79−23271
machine, power flow through isolation systems 80−64436
machine, wave propagation and power flow, beam-stiffened foundation plates 80−64435
machinery, resilient mounting on platelike and modified platelike substructs. 77−50818
machinery, special treatments for reduction of plant noise 77−54833
machines and power transmission mechanisms, approximate analyses of beam and plate foundations 80−64434
materials for noise and vibr. control, review 78−13854
metal plate, effectiveness of stiff two-layer vibr. absorbing coating 77−824
metal plate, optimality of constrained vibration-absorbing coatings 77−823
metal ribbed strip filled with acoustically absorbent material, vibr. damping *(Russian)* 77−46864
modal anal., digital simulation *(French)* 80−42216
natural rubber in transport engineering 80−96099
noise and vibration control systems, review 77−11090
noise and vibration control systems, review 78−30127
optical equipment, precision, insulation against vibration using springs and viscoelastic substances *(German)* 80−17986
optical structures, vibr. electronic damping using piezoelec. transducers 79−50372
optimum vibration isolation forces for system with random excitations 77−39240
physical and technical acoustics, conference, Zvenigorodskii, USSR (Sep. 1977) 78−18081
plate vibr. suppression by rate optimal response, numerical study 78−30229
polymeric materials, engineering structures, design and meas. 78−87185
resonance bar damping meas., reson. freq. control 77−2649
rotor, CO_2 laser appl. *(Russian)* 78−70115
rotor in small angular oscillation, feedback control system appl. *(Russian)* 78−70116
rotors, flexible asymmetric, convergence factor for residual unbalances 79−81785
sound and vibration fields coupling in compensation of radiation from plate at subcritical freqs. 78−18110
sound and vibration fields suppression, synthesis of systems 78−9494
string, stretched, appl. of optimisation methods to vibr. control 78−83305
strings, stretched, vibr. control by an external distributed force 78−83308
structure-borne sound source data, prediction of vibration isolation efficiency 80−102909
survey of use and characterization of vibration isolation 80−19144
vacuum and gas pumping lines, vibration reduction 78−74010
ventilation plant, noise and vibr. control 77−54834
vertical pumps, solving the vibration problem 78−87186
vibration damping materials, testing and development 77−84059
viscoelastic materials, design evaluation of damping treatments 79−18799
viscously damped dynamic absorbers of conventional and novel design 77−62096
CO_2 laser method in stabilisation of ionisation-thermal instability 77−19302
He-Ne laser interferometry appl. *(Russian)* 78−70117

vibration measurement
see also seismometers
Γ-shaped crack elastic energy evolution rate in laminate determ. by pliability vibr. meas. 78−83348
acceleration sensor device for recording vibrations of tall structures 80−95084
accelerometers, gravimetric calibration 79−71444
acoustic noise meas. methods and instrum. *(German)* 77−42670
acoustic problems modal anal. techniques 79−18651

vibration measurement continued
acousto-optical fibre interferometer for reflective surface motion meas. 80−13127
aerospace instrumentation, conference, Las Vegas, Nev., USA, (May 1977) 78−12075
amplitude and phase determ. by double exposure holography 77−58292
AT-cut quartz plate vibration anal. using light modulated oscillator 78−71255
automated dynamic balancing, rotating laser light beam appl. *(Russian)* 78−71299
automated rotor balancing system using CO_2 laser *(Russian)* 78−70115
automatic balancing of rotors subject to small angular oscill. *(Russian)* 78−70116
automatic rotor off-balance meas. using laser interferometry *(Russian)* 78−70117
automatic system for measuring, recording, analysing 77−53895
automatic system for simulating and analyzing wide-band random vibrations 80−53730
automatic testing of vibration installations, certification results processing 80−22336
axial flow compressor stator blade wake guidevane, method 80−95085
beam oscill. in balance scales using laser interferometer, construction *(German)* 77−79090
blade, rotating, vibr. analysis using holographic interferometry 78−32807
blast vibrations measurement, recording system 77−88984
BWR in-core instrument tube vibration obs. by reactor noise techniques 78−94064
calibration of devices, ring comparison meas. of equipment *(German)* 80−52189
capacitive transducer with superconducting resonator for mechanical vibration meas. 78−21127
cardiac sound and vibration recording, electro-optical sensor 77−21648
circular plate, elastic moduli meas., appl. of contactless vibr. excitation and detection method *(Polish)* 79−94571
computerised vibrational spectroscopy, using piezoelectric polymer transducers 78−29105
contact resonance of vibration pick-up and its control *(Japanese)* 78−33949
contactless meas. by fibre-optic and capacitive transducers 78−8400
contactless photoelectric fibre-optic vibration transducers 77−57319
data logging system requirements for vibr. monitoring 77−68351
decrement recording as function of amplitude with fully automatic system 78−15630
digital instruments, Bruel & Kjaer products review 78−94493
digital voltmeter for noise and vibration meas. 78−55538
double exposure holography, many-component motion anal. 79−7329
drives, rotational, damping of torsional vibrations, experimental determ. *(Russian)* 80−74816
dynamic balancing, influence coefficient method, balancing of rigid rotors 80−53724
dynamic laser speckle interferometry, appl. to transient flexure 78−32861
ear, using light scatt. heterodyne interferometer 77−2073
ear drum, human, vibr. meas. using electronic speckle pattern interferometry 79−53205
eardrum vibration meas. using electronic speckle pattern interferometry 80−67209
elastic element characteristic vibrational-frequency meas. errors 77−74391
elastic properties measurement, apparatus for elevated temps. *(Polish)* 79−96279
electrical meas. devices, method *(Russian)* 79−97378
electro-capillary element appl. *(Russian)* 77−41594
electrodynamic vibration test beds, feedback signals for correcting characteristics 80−53543
electroglottograph application experience 77−78062
electron microscope laboratory floor vibration detection by record-player cartridge 79−54233
electronic equipment components, vibration charact. determ. by holographic interferography 78−29916
electronic speckle pattern interferometry, small vibr. detection and meas. 77−72253
electronic speckle pattern interferometry, small vibrations meas. 78−32865
electronic speckle pattern interferometry, vibr. phase mapping 77−5897
electronic speckle pattern interferometry, vibrating object meas., use of chopped laser light 79−85165
electrostatic instrums., types, appl. *(German)* 77−41584
EM transducers for recording translations and vibrs. 77−67421
errors evaluation, due to pulse signals 80−23972
explosions, quarrying, use of electronic transient recorders for meas. explosion noise and vibration 80−67023
fibre optic heterodyne interferometer for vibr. meas. in biological systems 78−77101
fibre optic laser-Doppler probe, mechanical vibr. meas. 78−30248
flat surface, holographic and fringe projection methods appl. *(Polish)* 79−183
floors in maisonettes, effect of woodwool shuttering on sound transmission 78−94487
flux gradient accelerometer, working model tests 77−26274
Fourier analyser signal processing system 77−68335
free damped mech. vibration logarithmic decrement, optoelectronic meas. 80−92095
frequency meter, for vibr. etching of rolled wire technical parameters meas. 79−14356
frequency translated holography, S/N, smallest detectable vibr. 77−7022
gas turbine rotor, contactless system *(Russian)* 80−8982
gelatinous light modulating media, dynamic deform obs. by laser interferometry 79−32072
ground, problem aspects including transducer attachment 79−18578
gyroscope rotor, scanning laser based detector *(Russian)* 80−22351
gyrosystem, optical methods *(Russian)* 80−8983
harmonic gear transmission drives, method 79−88949
hearing mechanism, vibr. charact. obs. by holographic interferometry with optical fibres 80−76879
heterodyning two laser beams, meas. small mech. displacements 80−73309
high frequency vibr. meas., phase interpolation and modulation principle *(Chinese)* 79−37262
high-temperature US apparatus for elasticity charact. and thermal cond. meas. of materials 78−5705

vibration measurement continued
hologram interferometry, time-averaged, for vibr. anal. 80−63953
holograms, time-averaged, for 3D vibr. analysis 79−18840
holographic interferometry, accurate interpretation of fringes 77−2651
holographic interferometry, general shift reference 80−1150
holographic interferometry, linearised subfringe, modulation errors effect 80−78803
holographic interferometry, model interferogram construction 77−82592
holographic interferometry, phase mapping using bright fringes 77−65582
holographic interferometry, stroboscopic, for mech. vibrs. anal. in industrial environment 79−32422
holographic interferometry, stroboscopic, vibr. anal. with space-variant phase 77−58296
holographic interferometry, stroboscopic analysis of asymmetric membrane vibrs. 78−66786
holographic interferometry, time average, real time obs. of vibrating structs. 78−25813
holographic interferometry, transient wave motion obs. from single doubly-exposed hologram 78−25825
by holographic interferometry *(German)* 80−91759
holographic interferometry appl., real-time, using finite fringe field of background *(Czech)* 80−58989
holographic interferometry appl. to displacement, deformation and vibration meas. *(Italian)* 78−54337
holographic interferometry for vibrations investigation, beam modulation methods *(Polish)* 79−3649
holographic interferometry with swirl type shutter, stroboscopic and time-average methods *(Japanese)* 80−69748
holographic method, short exposure and biasing, for vibr. superposed on random motion 77−58288
holographic technique for vibrational modes in compressor blades 79−41355
holographic vibration analysis, computer-aided, for vectorial displacements of bladed discs 78−71056
holographic vibration measurement, review *(German)* 78−33709
holography, pulsed sandwich, exam. of electric drill vibrs. 78−33701
holography, shifted reference, advantage of freq. translation error 78−42304
horizontal contact resonances of vibration pickup with rectangular bases on soil surfaces 80−96160
hydrodynamic instabilities in heated channel, identification using appl. of vibration signals 80−28500
in-plane, real time speckle interferometry meas. with aid of liq. cryst. light valve 80−53734
in-plane mechanical vibrs. meas. by speckle imaging, sub Å range 78−30247
inductive magnetic transducer for ferromag./nonferromag. object displacement meas. 79−6154
industrial centrifuges, vibration monitoring, safety and economic aspects 79−49218
industrial noise, instrumentation, evaluation method, calibration *(German)* 77−80039
insects, sound radiating cuticular motion, measurement by irradiance modulation technique 79−84057
instrumentation for dynamic meas. in sound and vibration 77−72124
interference fringe method, TV detect. and electronic image processing 80−103004
interferometry, two-wavelength investigation of deform. and vibration of objects 77−46976
internal friction meas. servo system 77−39265
introduction, as diagnostic and monitoring technique 80−37025
J_0 ratio method for measuring small vibration amplitudes 79−81827
laboratory equipment for resonance meas. in solids *(Spanish)* 80−86285
laser beam appl. Selcom System 1000 *(Swedish)* 78−63402
laser beam meas. of small mechanical oscillations or vibrations 79−77032
laser Doppler vibr. meas. system using bispectral anal. 80−38357
laser Doppler vibrometer, reflecting surfaces appl. 79−6117
laser interferometer, acoustic vibration meas. 78−71253
laser interferometer appl. 79−6094
laser interferometer for meas. linear vibration report 78−86243
laser interferometric method, using LF phase modulation, for small vertical vibrations 77−37970
laser interferometry, vibratory processes investigation appls. 77−118
laser speckle, appl. to vibrational charact. 79−94569
laser speckle in diffr. field from vibr. object, dynamic statistical props. 79−22895
laser speckle interferometry, vibration anal. of plate and shell 77−10008
laser speckle interferometry of periodic nonsinusoidal vibrs. 77−41673
laser speckle patterns of vibrating panels, interpretation for mode shape information 77−51004
laser vibration meter, high sensitivity, using fibre-optic probe 79−7351
laser vibration probes, for remote surface 77−87756
laser-Doppler meter, 100 Å to 10 cm *(French)* 78−30250
lasers in metrology and testing, review 77−5817
lathe off-balance during metal removing, systems reviews *(Russian)* 78−70118
layer velocity meter, freq. biased, for meas. on vibrating surface 79−98675
LMFBR PHENIX vibration-induced neutron noise obs. 79−13453
logarithmic instruments, error estimation *(Russian)* 77−2648
long tow-wire complex vibration obs. and empirical drag law 80−46309
loudspeaker cabinet panels, source identification 77−54827
low-speed motion irregularity meas. equipment, portable 78−54346
machine testing and dynamic balancing 80−23971
manufacturing machines, spectral analysis of vibration data, failure prediction 80−79048
measurement of fan vibration using double pulse holography 79−30462
mechanical, in precision units, testing by real-time holography *(German)* 80−38366
mechanical, laser interferometry appl. *(French)* 78−67156
mechanical oscillations, elec. and optical sensing techniques, review *(French)* 77−2646
mechanical vibration, amplitude-frequency charact. recording, resonating systems 77−45829
mechanical vibration meas. optical heterodyne systems 77−13746
membrane speckle pattern analysis 80−106769
metal-electrolyte interface, vibratory process meas. apparatus 77−39732
methods survey, dynamics, sensitivity and accuracy aspects *(Dutch)* 78−36999

vibration measurement continued
microtremor, laser interferometer, He-Ne laser *(Japanese)* 80−9025
modal anal., digital simulation *(French)* 80−42216
modal anal. of vibrating structures using transient excitation 77−62220
modal analysis techniques, prediction of point mobility plots 80−106659
modal confidence factor in vibration testing 79−27607
moire fringes holography vibration anal., facilitation of fringes counting 80−64504
motion, combined and general forms, laser speckle interferometric obs. 78−74054
motion picture apparatus vibration meas. by holographic interferometry *(Russian)* 80−37112
multiple shaker testers, production and military applications 80−64276
multiplied moire fringes holography, vibration anal., expansion of meas. limitation 80−64505
noncontact optoelectronic position transducers 79−50406
nuclear power plant, PWR, constructional elements, vibrations due to cooling medium flow *(Hungarian)* 80−63304
nuclear power plant equipment vibrations caused by flow, indirect meas. methods *(Hungarian)* 80−18453
nuclear power plant machinery surveillance and diagnostics automation 79−641
off balance interferometric bridge, using heterodyne detection for recording vibratory phenomena 78−70119
online Reactor Noise, Vibration and Loose Parts Monitor 79−3212
optical fibre as flexible coherent probe of vibr. 78−25975
optical vibration analyser, meas. principle 79−6119
optoelectronic method, non-contact and non-reactive, at 60 kHz *(German)* 78−32805
optoelectronic vibration transducer based on coordinate photodetector 79−75495
oscillation period, digital method 78−93676
pallaesthesiometer automatic signalling and signal fixation unit, vibr. sensibility threshold meas. 79−57784
parametric resonance in complex objects, multichannel installation for stabilising vibration 80−58990
particle size and density determ., bispectral anal. of laser Doppler vibr. meas. 80−98880
phasemeter for small mech. vibrs. meas. 78−54359
piezoceramic accelerometers, construction and appls. 79−50686
piezoceramic accelerometers and associated instrumentation for vibration meas. 80−10073
piezoelectric accelerometer, magnetic fastening using new magnetic material $SmCo_5$ 79−77035
piezoelectric transducer, HF vibration measurement using time-average electronic speckle pattern interferometry system 80−37966
piezoelectric transducer systems, noise suppression and prevention for shock and vibration meas. 80−22353
planoconvex AT-cut quartz resonator vibration displacement meas. by laser interferometry 77−37976
plastic material specimens, free oscillation attenuation constant meas. *(Czech)* 79−41634
plate vibration analysis by time-averaged projection-moire method 80−79241
polymer glass-transition point meas. apparatus using vibration meas. of immersed plate *(Russian)* 78−71842
portable laser Doppler velocimeter for vibrating surfaces 79−68666
power generation, vibration monitor for rotating machines, ave. frequency technique 78−13299
power spectrum estimation using maximum entropy method, data analysis appl. 80−37006
production testing, multiple shaker considerations 80−79047
PWR components, using correlation techniques *(German)* 80−79247
PWR internal vibrations, neutron noise monitoring 79−13445
PWR power plant, vibr. and press. signals, information for online vibr. monitoring system 77−18674
quartz resonator tangential vibrations, using SEM 80−71323
random vibration simulator, practical realisation 80−53732
re-entry vehicle acoustic/vibration environment expt. 78−20620
reflective object displacement and vibration meas. *(Russian)* 79−21695
relative phase meas. by wavefront modulated holography 79−3652
resonance amplitude in dynamic elastic moduli meas., use of capacitance sensor 77−23923
resonance-bar damping, automated meas. system 77−2649
rotating machines, vibr. monitoring 77−68352
rotating machines, vibration monitor using average freq. technique 79−97748
rotating object, vibration anal., image detector in hologram interferometry and speckle photography 78−59351
rotating shafts, torsional vibration meas., laser Doppler system 79−50685
rotating system balancing in uninterrupted operation 78−90746
rough surface small vibrs., light scatt. meas. 80−1494
rough surface vibr. meas. by gaussian beam illumination 79−97356
sediment analysis using vibration-frequency method 79−49202
seismic microvibration frequency analysis by 50 m interferometer 80−109276
shadow-Moire time-averaged method for vibr. amplitude determ. 77−71364
shaft on two supports with cantilever-mounted pinion, method 79−88950
shock absorber, elastic damping props. determ. unit 78−5703
simulating system optimisation, rel. to efficiency and cost 80−53728
simulating system optimisation 80−53729
simulator design, optimisation 80−53731
sinewave generator, simultaneous supply of fifty strain transducers, ship vibration testing 80−62652
sinusoidal phase modulated stroboscopic holography, for vibration anal. 78−29919
skull and auditory ossicle vibr. anal., human preps., using holographic interferometry 80−67210
small amplitude, using multiple-beam interferometer 80−4759
small amplitude vibration meas., J_0 ratio method *(Chinese)* 79−1140
soil surfaces using vibration pickup, horizontal resonant freqs. 80−10102
sound and vibration monitoring, signal processing developments 78−83181
speckle, photographic recording, Chladni method 77−604
speckle applications *(French)* 77−67494
speckle interferometry, real-time meas. of vibrations and displacements *(Italian)* 78−54336
speckle method for meas. mechanical translations (10^{-11} to 10^{-3} m) *(German)* 80−17924

vibration measurement continued
speckle pattern, time-averaged, contrast for vibrating object 78−50703
speckle pattern TV interferometer, principle and appl. 78−58014
speckle produced in diffr. field of vibr. object, appl. to vibr. analysis 79−76595
spinning disc, vibration anal., using image derotated holographic interferometry 79−81822
steam turbine blades, using radio linked telemetry 77−68538
steel, low C, Young's modulus and internal friction meas. *(Polish)* 79−96279
strobe-hologram method, interference effect, linear approx. 78−1192
stroboholograhic method of investigations 77−54681
structural dynamics, modal anal. 78−39993
structural dynamics analyser development, microcomputer-based 80−53733
structural failure detection by vibration detector 78−15641
structural freq. response testing, impulse technique 78−39992
structure-borne sound, procedure for meas. sensitivity of building structures to stationary excitation *(German)* 80−64287
superconducting resonators, coaxial type, characts., appl. 77−74383
surface displacement and vibration meas. using laser speckle *(French)* 78−4686
surface oscillations meas. by 1.06 μm laser heterodyne method 79−50339
testing by simulated vibrations, expt. problems 80−58855
thin I-shaped plates, exptl. determ. of transverse vibration modes 80−28474
time averaged holographic interferometry 77−79837
time-average hologram fringe pattern interpretation 77−38838
time-average reflection-moire method for vibration analysis of plates 79−72863
time-averaged holography theory, for three dimens. vibrs. at single freq. 78−90397
torsional, on rotating machinery, system with photoelectric rotary shaft encoder 79−23287
torsional vibration meas. concepts, transducers 78−57937
torsional vibration meas. with laser Doppler system 78−45612
train induced ground vibration, measurement and analysis 80−48494
transducer, gel electrocapillary transducer type, appl. *(Polish)* 78−26094
transducer design for nuclear reactor environment 78−823
transducer dynamics *(Russian)* 80−105638
transducers, meas. errors due to surface compliance of vibrating body *(Japanese)* 80−79046
transversal micro-vibration meas. on diffusing objects, real time, random moire principle 79−85123
tuning fork for clock, vibr. anal. using speckle method 79−21737
turbine blade vibration meas., optical methods *(French)* 78−71300
turbine blades, time average holography 77−5901
turbines, gas and steam, blading overspeed, optical methods 77−74387
two-dimensional structure in-plane vibr., stress analysis by laser speckle method 80−103006
tympanic membrane, human, phase sensitive holographic technique *(German)* 78−3513
tympanic membrane investigations in living man using holographic interferometry 80−67207
tympanic membrane vibr. studies in living man using holographic interferometry 80−67208
US transducer, amplitude distribution by holographic technique 77−42678
US transducer vibration amplitude distrib. meas. by holographic technique *(Japanese)* 77−88999
US transducers, measurement of vibrations of very small amplitude using US probe 80−73443
US travelling wave visualisation, by linearised subfringe interferometric holography 79−1036
vibration signatures, computation method 77−80004
vibration-acoustic diagnostics, random signal patterns recognition *(Slovak)* 79−18612
vibrometers, photoelectric, analogue, systematic errors determ. 80−79246
vortex-excited vibration mechanism of cylindrical struct., photographic evidence 79−46406
waveform measurement using temporally modulated holography, in biomedical appl. 80−67212
$Bi_{12}SiO_{20}$, photorefractive, vibr. struct. mode pattern visualisation, phase conjugation and dynamic holography 80−95938
Fe heterogeneous plate, holographic interferometry method, up to 21.5 kHz *(German)* 77−74388
MnZn ferrite disc, excitation of radial mode vibration due to AC 79−69708
$Pb(Zc,Ti)O_3$ crystal, appl. to identification of resonant frequencies of rotating beams 79−81824
Se photocell optical vibration transducer 80−77768

vibrational states in disordered systems
acetone, liq., C-C stretching mode relax., Fermi reson. influence 80−25352
acetone, vibr. dephasing theories, test using selective coherent ps. Stokes scatt. 80−59609
acetonitrile, in dilute CCl_4 soln., far IR spectra and mol. dynamics models 79−99876
acetonitrile, in liq. phase, Ramon band profiles, calc. using IR intensities 80−2741
actinides, lattice vibrs. role in transport props. determ. 77−28158
adamantane, deuterated single plastic cryst., normal modes and librations, group-theoretical anal. *(French)* 79−14905
adamantane, lattice dynamics in disordered phase 78−55923
alkali aluminometaphosphate glass, $MPO_3.Al(PO_3)_3$:U (M=Li,Na,K), vibronic excitation, absorption and emission spectra 78−52524
alkali borates, vitreous and cryst., vibr. spectra and struct. comparison 78−23470
alkali halides, molten, mode coupling theory of charge fluctuation spectrum 80−92451
alkali metal halide melts, phonon lifetime 77−51527
alkali metal tetrafluoroborates, intramol. force fields and mean vibr. amplitudes 80−2743
alkali metaphosphate glasses, low frequency Raman scattering and glass transitions 79−95745
alkali-alkaline earth ceramic solid solutions, with tetragonal tungsten bronze struct., low freq. optical modes 78−76477
allene, liq., orientational dynamics, Raman obs. *(French)* 79−28746

vibrational states in disordered systems continued
alloys, force-and-mass disordered, average local-information transfer approx. 80−88290
alloys, substitutional, self consistent cluster theory for off diagonal disordered systems 80−84272
alloys, Taylor's theory extension 79−4387
alloys with diagonal and geometrically-scaled off-diagonal disorder, coherent locator approach to lattice vibr. 79−73279
aluminophosphate glass, multicomponent, 3.2 micron broad absorption band computer anal., residual H_2O vibr. 78−52478
amorphous, s-p superconductor, Eliashberg function, phonon spectrum 78−88066
amorphous alloy, vibr. props., appl. to Si_xGe_{1-x} 77−4176
amorphous dielectric solids, low energy atomic motions and anomalies at low temps. 78−30724
amorphous film, surface phonon assisted tunnelling at low temp. 77−4421
amorphous linear chain, distrib. of vibr. modes, truncated T-matrix approx. 77−51466
amorphous materials for IR and microwave absoprtion, temp. and freq. depends. 78−39539
amorphous metal, elec. resist., anharmonicity effects 78−14700
amorphous metals, elec. resist. temp. depend., phonon characterisation 79−60782
amorphous metals, electron-phonon coupling const. and Eliashberg function 80−39567
amorphous metals, rel. to elec. resistivity temp. depend. calc. 78−6342
amorphous phonon echo *(Russian)* 77−80596
amorphous pyramidally bonded solid, electronic and phonon densities of states 77−8001
amorphous semicond., optical props. and densities of states *(French)* 77−72809
amorphous semiconductor, local order as determined by electronic and vibrational spectroscopy 79−37627
amorphous semiconductor superconductivity feasibility model *(Russian)* 78−80092
amorphous semiconductors, vibr. props., effects of topology versus disorder 77−69063
amorphous solid, calc. using analogy with spin waves in amorphous ferromag. 79−7979
amorphous solid, frozen liquid phonons disorder parameter, Anderson localisation 78−75784
amorphous solid, glass transition temp. rel. to low temp. phonon mean free path 79−51226
amorphous solid, phonon scatt. by density fluctuations and thermal cond. 80−10626
amorphous solid, surface phonons, tunnelling states and propagation characts., low temps. 79−69337
amorphous solid, very far IR props. 78−80344
amorphous solids, low-energy excitations of phonons, magnons, electrons rel. to struct. factor 80−44488
amorphous solids, structure and low temp. props. 79−37631
amorphous solids, vibr. sp. ht. enhancement from force-const. variations 80−88333
amorphous tetrahedrally coord. solids, bond charge model 80−49108
anharmonic system, generalisation of CPA 78−75783
As-S-Br glasses, IR spectra 79−95780
binary alloys, three mode, long wavelength optical vibr., appl. to Ge_xSi_{1-x} 78−6135
binary disordered system, effective-medium and augmented space method, pseudofermion approach 79−60668
biological system, cooperative behaviour, Bose condensation, Frohlich model 78−35797
biphenyl in Ne or Ar matrix, biphenyl ring torsion by vibronically resolved spectra 79−81228
biphonon spectra, CPA calc. 80−70341
biphonon spectra, light absorpt. coeff. and density of states, CPA calc. 80−84271
borate glass:Cr, Raman spectra of Cr^{VI} 77−52076
p-bromochlorobenzene, vibr. relax., Raman active phonons temp. depend. 80−29139
t-butyl bromide, vibr. relax. in pure liq. and soln., Raman spectra 80−66167
t-butyl chloride, vibr. relax. in pure liq. and soln., Raman spectra 80−66167
C, diffusely scatt., X-ray diffr. investig. of coherence strain, thermal vibr., preferred orientation 77−31595
cancerous cell culture, phonons, long-range coherence, microwave effects 78−35816
carbon tetrachloride, solid, phase transition, Raman study 78−80345
CBOOA, isotropic, nematic, smectic-A phases, Brillouin scatt. 80−11421
cellular system with strong short range order, effect of off-diagonal randomness 77−47531
chloroform, liq. vibr.-translational energy exchange, temp. depend., Brillouin scatt. obs. 79−73959
coarse-grained quantities and short-range order 78−75787
condensed H-containing media, cold neutron total section data interpretation 80−33857
conference on lattice dynamics, Paris, France (Sept. 1977) 78−59869
configurational properties of liquids near glass transition 78−26662
4-cyanobiphenyl and 4′-alkyl- or 4′-alkoxy-substituted liq. cryst. derivatives, soln., absorpt. and fluoresc. spectra 80−87164
1,1-cyclobutane dicarboxylic acids and K salts, IR and Raman vibr. spectra *(French)* 80−2758
cyclohexane, liq. and soln., Raman scatt. for vibr. and rot. relax. 79−82969
Debye solid, amorphous and disordered harmonic, struct. factors 78−9954
defect-clusters in linear chain, effect of second neighbour interaction on freq. 78−63826
diacetylene polymers, high freq. vibr. mode modelling 79−19346
p-dichlorobenzene, vibr. relax., Raman active phonons temp. depend. 80−29139
dichloromethane, liq. state dynamics, models 79−73087
dichloromethane-decalin glass, mol. dynamics, from dielec. loss meas., 107-148K, 293K 78−76379
diffusion of particle in disordered system 78−22885
dimethyl aniline, IR spectra, 250-4000 cm^{-1}, vibr. anal. 78−62797
2,2-dinitropropane-d_0(-d_6), phase polymorphism, vibrational assignments, IR and Raman study 80−16031
disordered chains with short-range order, freq. spectra 78−10148

vibrational states in disordered systems continued
disordered semiconductors, resonance Raman scatt. 79−11419
disordered systems, mode softened unified theory 79−55637
dispersion relation of phonon-like excitations 78−18727
elasticity of bulk and film from multipass Brillouin spectra 78−76485
electrolyte solutions, strong, at high concs., collective vibrational modes 77−81105
epoxy resin, low temp. thermal props., phonon states and crosslinked struct. *(German)* 78−75846
epoxy-resins, sp. ht. and thermal cond., 0.1 to 80K, phonon scatt. 79−65215
equations of motion technique 78−51634
ethane, liq., correl. function modelling, third order memory function method 80−7339
ethyl-p-azoxybenzoate, far IR and Raman spectra, smectic polymorphism 80−76022
ferroelectric liquid crystal, soft modes 79−55653
ferromagnetic, amorphous, magnetic and phonon rotons 79−61087
flass, phonon avalanches, exptl. conditions for obs. 78−71822
fluorite type crystal, effects of anharmonicity and disorder on Raman scatt. at high temp. 78−80349
force constants for disordered system with cryst. topology 77−27966
glass, acoustic phonons lifetime at low temps. 78−26650
glass, alkali-alkaline earth nitrates, Raman spectra, vibr. perturbations effect 79−8132
glass, anomalous sp. ht. at low temp. 77−80631
glass, elementary defect creation during glassmaking, model 78−22668
glass, far IR anomalous excitation obs. 77−40245
glass, ion motion and mixed alkali effect analysis 78−30793
glass, IR total internal refl. spectrum, surface polaritons *(Russian)* 77−20861
glass, localised acoustic phonons, effects on thermal cond. and Raman spectra 77−81092
glass, low-freq. Raman scatt., 6-700K, excess scatt. 78−23473
glass, phonon echoes and self-induced transparency 78−79710
glass, porous Vycor, surface phonons, Raman and IR reflectivity spectra meas. 78−38931
glass, Schott BG20 and FG18, forced Rayleigh scatt. anomalies 79−82988
glass, spectral diffusion, phonon echoes and US saturation recovery 78−10149
glass, spectral diffusion 78−59914
glass, thermal conductivity effect of strain at 0.1K 77−89602
glass, tunnelling systems, intrinsic elec. dipole moment, coherent elec. echo obs. 80−29705
glass, US propagation at ultralow temperatures 77−39635
glass, vibrational modes, conjecture effect of small anharmonicity 79−95112
glass density fluctuations from elastic dipoles at low temps. 78−79709
glass-forming polymer, paramag. spin-lattice interactions 80−7149
glasses, acoustic and dielec. props. at low temps., review 78−6128
glasses, thermal, acoustic, and dielec. props. at low temps. 79−65164
glasses, thermal cond. rel. to diffusion process due to phonon-defect interaction 80−34259
glasses, time-dependent sp. ht. at low temps. 79−60520
glasses, US properties and short-time sp. ht. relationship 79−60440
glycerol, supercooled liq., dynamical struct. factor, Mossbauer spectroscopy 78−27126
glycerol($-d_3$), single cryst., glassy, and supercooled, polarised Raman spectra, anharmonic multiphonon interactions 79−91419
Goldstone system with off-diagonal disorder, freq., spectrum of lattice vibrations, pseudofermion approx. 79−60466
graft copolymers, normal vibrs., calc. method *(Russian)* 78−29871
harmonic approx. for vibr. spectra of disordered solids 78−51635
harmonic systems, disordered, spectrum of dynamical matrix 78−30705
heavy water, collective excitations in 10^8 cm^{-1} momentum range 78−43087
hexafluorobenzene-benzene, liq., mol. interactions, IR and Raman lineshape obs. 80−28907
hydrates, vibrational spectra, H^+ and OH^n aq. soln. 79−73916
ice, amorphous, 2500-4000 cm^{-1} Raman and IR spectra, vibr. anal. 77−59562
ice, disordered phase TO-LO splitting 79−91420
ice, IV, 4000-400 cm^{-1} IR spectra, H-bonding and assignments, orientational disorder 80−16022
ice and amorphous solid water, D_2O-H_2O, intramolecular stretching spectrum, role of Fermi resonance 79−93973
ice I, assignment of O-H stretching bands in disordered state 78−19454
IR continua, phonon theory 80−29729
isotopically disordered vibr. crystal quantum transport eqn., electron-phonon coupling 78−39081
Lennard-Jones, glass, Raman spectrum calc. 78−48165
light scattering from configurational fluctuations in disordered solids 79−11428
linear chain of oscillators, disordered, physical props., Monte Carlo approach 77−4177
linear system with a short-range order, self-consistent continued-fraction method 77−69062
liquid, Debye temp., short-range order, theory 78−2264
liquid, ionic, binary mode coupling theory of charge fluctuation spectrum 80−92451
liquid, mol. vibr. dephasing, hydrodynamic model 79−64968
liquid, thermal response to weak external field, molecular dynamics 78−71660
liquid, vibr. modes, direct and indirect dephasing 78−48162
liquid metal, mol. motions from NQR, viscosity and sound damping 77−1615
liquids, picosecond laser techniques for obs. of vibr. modes 80−5800
liquids, vibr. energy relax., nonMarkovian effects 80−74230
liquids, vibrational relaxation studied by picosecond or Raman spectros. 80−80797
local modes in disordered crysts., two-time Green's functions 80−6480
local structural excitations model for lattice dynamics of disordered or unstable lattices 78−75790
long time correlations reln. to replica correlations 79−75437
mass-disordered harmonic Hamiltonians, LF density of states 78−47488
MBBA, Raman spectra in cryst., frozen glassy, and liq. cryst. states 80−60601
melting, dislocation model, appl. to FCC cryst. 78−26658
melting, dislocation model 78−26657
metal, amorphous, electronic and vibr. props. 78−10151

vibrational states in disordered systems continued
metal oxide metaphosphate glasses, vibr. study of metal cation reduction at surface 78−56797
metallic glass, phonon transport below 100K 78−14422
metallic glasses, temp. depend. of elec. resist. 78−14702
methanol, vibr. dephasing theories, test using selective coherent ps. Stokes scatt. 80−59609
α,ω-methoxy-poly(ethylene oxide) effect of swelling on longitudinal acoustic mode 80−29739
methyl anilines, IR spectra, 250-4000 cm^{-1}, vibr. anal. 78−62797
mixed alkali glasses, Raman and far IR spectra, vib. at cation site, struct. 78−60435
molecular crystal, orientationally disordered, translation-rot. dynamics, soft modes 78−83906
molecular glass, density of states for IR active internal modes of tetrahedral mols. 78−75788
molecular liquid, depolarised Rayleigh-Brillouin spectra, theory 79−69850
molecular liquid, vibr. correl. function, dephasing and depopulation 79−99048
molecular pair, fluoresc. depolarisation, using stochastic Liouville eqn. with radiative terms 80−16074
naphthalene, melting of rotational degrees of freedom near cryst.-liq. transition 80−54352
nematic liquid crystal, vibrational IR and Raman spectra 79−73913
nitrate salts, Raman spectra, thermally disordered energy states 78−35122
p-nitroaniline, Raman spectra, mol. struct. in molten state 79−91435
nylon, H-bridge interactions, far IR spectra study 80−11374
one dimensional mixed crystal short range order, frequency spectrum 79−95093
one-dimensional amorphous solid, short-range order effect on spectral density of excitations 77−76514
one-dimensional disordered lattice, classical diffusion of localised excitations 78−72114
one-dimensional system, phase fluctuations, disorder, nonlinearity 80−54331
optical energy transfer, phonon-assisted 78−92105
optical fibres, single-mode, Brillouin spectrum 79−46032
optical glasses, Brillouin scattering meas., sound vels., Pockels coeffs., phonon damping 79−95792
optical spectra, rel. between simple analytic models 78−76473
ordered vacancy compounds, lattice dynamics 78−75770
n-paraffin, longitudinal acoustic mode, perturbing forces 80−70348
n-paraffins, Raman spectra obs. of longitudinal acoustic modes intensities 78−84584
n-paraffins, solid and liq., Raman spectra, longitudinal acoustic vibr. mode 78−31183
partially disordered crystal, lattice dynamic model 78−83897
pentachloronitrobenzene, single cryst., far IR absorption 79−73940
phonon assisted energy transfer 79−38610
phonon lifetimes, struct. disorders effects 78−34584
phonon modes, lattice Green function expansion method 80−79900
phonon-like excitations, dispersion and damping 80−49331
phosphate glasses, cation-site interactions, IR and Raman spectroscopy 80−2744
PMMA, amorphous, LF Raman modes, strain and temp. effects 77−36219
PMMA, C-H stretching and bending vibrs. in Raman spectra 80−93300
PMMA, low-energy excitations and hypersonic props., Brillouin scatt. meas., 1.7 to 15K 77−90160
PMMA, oriented, hypersound propag., elastic props. 78−75737
poly-1,6-di-p-toluenesulphonyloxy-2,4-hexadiyne, thermal polymerisation, Raman spectra 80−35531
polyacetylene, doped and neutral, resonance Raman scatt. 80−55107
polyacetylene, vibr. excitations of charged solitons 80−108201
polyalkenamers, longitudinal accordion mode, low frequency Raman spectroscopy 80−25369
polybut-1-ene, cryst. forms I and II, far IR spectra 79−33708
polyethyl ethylene and deuterated derivatives, modification I, vibrational spectra and normal coordinate anal. 79−87434
polyethylene, CH_2 Raman scissor modes *(French)* 79−69825
polyethylene, drawing-out effect on vibrational normal modes *(French)* 77−15527
polyethylene, H bonding effects on skeletal optical and longitudinal acoustical modes 80−34914
polyethylene, linear, bulk-crystallised, morphology study 79−32918
polyethylene, linear, far IR absorpt. spectrum, temp. depend., 14K to melting pt. 79−1758
polyethylene, low temp. thermal cond. 79−73351
polyethylene, oriented, Raman active modes 78−23457
polyethylene, perdeuterated, skeletal vibr. spectrum 78−23445
polyethylene, phase characterisation, Raman spectra study *(French)* 80−93303
polyethylene, phase orientation by stretching, Raman study *(French)* 80−93304
polyethylene, Raman spectra, drawing effect on longit. acoustic mode *(French)* 77−24828
polyethylene, Raman spectra obs. of longitudinal acoustic modes intensities 78−84584
polyethylene, solid, IR spectra, interference distortion of 73 cm^{-1} absorpt. line 80−11375
polyethylene, straight chain segment length distrib., from Raman LAM-1 band 79−41981
polyethylene, uniaxial, deuterated, interchain forces effects on acoustic phonon branches, neutron scatt. study 79−51228
polyethylene oxide, cryst., lowest laser Raman active accordion oscillations, elastic moduli effect 80−29734
polyethylene oxide, Raman scatt. from longitudinal acoustic modes of crysts. swollen by oligomers 78−27226
polyethylene terephthalate, simultaneous mech. loading, UV rad. effects on overstrained chem. bonds 79−52706
polymer, amorphous, high temp. thermal transport, phonon modes 77−62691
polymer, amorphous, translational motion and lattice vibr. obs. by Raman scatt., T_g phenomena 78−23469
polymer, defect solid, local and resonance vibrations, appl. to deuterated polyethylene 79−99287
polymer, general composite perturbed elastic rod soln., longitudinal acoustic mode 78−18726
polymer, longitudinal acoustic mode, perturbing forces 80−70348

vibrational states in disordered systems continued
polymer, neutron scatt. obs., book contrib. 77−89505
polymer, vibrational spectra of chain, Green's function anal. 78−18724
polymer, vibrational spectra of chain, Green's function anal., Fourier method for perfect infinite chain 78−18725
polymer chain, longit. acoustic mode, composite elastic rod model 77−7816
polymer glass, sp.ht. discontinuity at glass transition 80−19954
polymers, accordion-type laser-Raman oscills., elastic moduli 79−55854
polymers, longitudinal acoustic mode, appl. of general theory to planar zigzag of general theory to planar zigzag methylene chains 78−14421
polymers, longitudinal acoustic mode in 79−73277
polymers, melting theory, phonon anharmonicity effects 78−67659
polymers, Raman active longitudinal-acoustical mode spectra interpretation 80−103950
polymers, structure and molecular dynamics, neutron scatt. meas. 79−51009
polymethineimine, all-trans, ab initio cryst. orbital calcs. 79−77530
polymethylene crystals, lattice vibrations 80−59607
polyoxymethylene, melt-crystallised, longit. acoustic mode obs. 77−59572
polyphenyls, inelastic neutron scatt. study of structural phase transitions 79−51255
polypropyl ethylene and deuterated derivatives, modification I, vibrational spectra and normal coord. anal. 79−87435
polypropylene, isotactic, melt-crystallised, longit. acoustic mode obs. 77−59572
polypropylenes, iso- and syndio-tactic, Raman tacticity bands, vibr. spectrum 80−66193
polystyrene, amorphous, LF Raman modes, strain and temp. effects 77−36219
polystyrene, isotactic, normal vibrational anal. 78−43869
polystyrene, methacrylic acid/(PSMA) ionomers, far IR studies of ion clustering 79−87436
polystyrene, solid, low freq. Raman scatt., vibr. density of states, 29-300K 78−72516
polystyrene, uniaxially oriented atactic, laser Raman scattering 79−73920
polystyrene and model cpds., conformational struct. influence on normal modes of benzene ring, Raman study 80−14144
polysulphur nitride, Kohn anomalies in phonon dispersion 80−24555
polytetrafluoroethylene copolymers and oligomers, melt and solid, Raman active longit. acoustic modes 78−19484
polytetrahydrofuran, H bonding effects on skeletal optical and longitudinal acoustical modes 80−34914
polyvinyl alcohol, doubly orientated, polarized Raman spectra 79−65872
polyvinylidene fluoride, heat capacity, 5 to 200K 79−86900
polyyne, linear infinite chain, ground-state props., ab initio studies 79−95306
PTFE, vibrational assignment problem, far infrared spectrum 77−52087
PVC, structural studies by Raman spectroscopy 79−7044
PVTE, heat capacity, 5 to 200K 79−86900
quartz, amorphous and crystalline, surface polaritons and splitting of optical frequencies 78−72090
quartz, fused, hyper-Raman scatt. and longit.-transverse splitting of vibrs. 79−73953
quartz, fused, IR total internal refl. spectrum, surface polaritons *(Russian)* 77−20861
quartz, fused phonon lifetimes at 2.4K 77−62605
quartz glass, spectral absorpt., 3000-4000K 80−25401
quinzarin in alcohol glasses, electron-phonon coupling, photochemical hole burning 80−97265
Raman scattering cross section for LF spectrum study 80−25363
random anharmonic system, self-consistent approx. 77−62798
random chain of oscillators, CCPA calcs. of spectral density 79−37792
random chain of oscillators, exact spectral density 77−39651
randomly disordered chain, classical anal. of reson. modes 77−89514
rare earth sulphides-1.8 Ga_2S_3 glasses, vibr. spectra, electronic transitions, short range order 77−69820
rare earth-gallium sulphide glass, R_2S_3-1.8Ga_2S_3, vibr. and electronic spectra, short-range order 78−27228
relaxation mechanism in mol. solids 77−7817
rigid molecules, dil. soln. in decalin, mean librational freqs. 80−6479
semiclassical model of vibr. energy relax. in simple liqs. and compressed fluids 80−33865
semiconductors, amorphous, short-range order, theory and probes 80−79698
semiconductors, disordered, phonon-assisted interband optical absorption 80−34947
semiconductors, elemental amorphous, vibr. props., review 77−84873
shell models, CPA calc. 80−70347
short-range order and off-diagonal randomness 78−75782
silane molecules, substituted, chemical effects on freq. of Si-H vibrations 79−51227
silicate glass:Cr, Raman spectra of Cr^{VI} 77−52076
silicate glasses, low-energy excitations and hypersonic props., Brillouin spectra meas., 1.7 to 15K 77−90160
silicate glasses, phonon echoes at low temps., deformation pot., two level system coupling 79−65163
smectic liquid crystal, vibrational IR and Raman spectra 79−73913
solid with thermal or static disorder, one electron props. 79−37957
solution, of polar mols., local order and vibr. coupling, Raman bands, dielec. const. 79−99868
spectra, IR and Raman, of disordered solids, analytical models 80−7336
spontaneous echoes in disordered systems, spectral diffusion decay 80−84270
statistical copolymers, normal vibrs., calc. method *(Russian)* 78−29871
superionics, with fluorite structure, Brillouin scattering and lattice defect energetics 78−80369
TBAA, smectic B phase, deform. vibrs. of alkyl chains, Raman spectra obs. 77−39531
TBBA, phonon dispersion curves in cryst. and smectic phases 79−86863
Teflon, bond charge model for vib. props. *(German)* 78−75781
tellurite glasses: Ho^{3+}, nonradiative relax. 77−24881
tetraalkylammonium bromide, solid and liq., Raman spectra, longitudinal acoustic vibr. mode, mol. dimensions of ions 78−31183
tetrabromomethane, in disordered phases, IR active mode Raman line shape, dipole-dipole interaction 80−9603
tetrafluoromethane, in disordered phases, IR active mode Raman line shape, dipole-dipole interaction 80−9603
tetrahedral glass AX_2, band limits and vibrational spectra 79−73935

vibrational states in disordered systems continued
tetramethylsilane, liq., electron drift vel. saturation, skeletal vibr. 80−34451
thermal conductivity, Callaway eqn., phonon scatt. in highly disordered systems 80−20000
thermotropic liquid crystal, formation, dynamic approach 78−47239
time dependent spectral transfer, Monte Carlo calc. 80−11464
toluene sulphonate diacetylene polymer, vibr. modes, strain depend. using Raman spectra 80−20626
trans-polyacetylene, intrinsic, electron-phonon coupling 80−79901
trichloroethane, CH_3-stretching modes, Raman spectra reson. energy transfer obs. 78−48162
trichlorotrimethyl benzene, disordered solid, vibr. state, itinerant oscill. model 79−73278
two dimensional random lattice, struct. and vibr. props. 77−7820
vibrational dephasing in liquids and solids 79−38552
vibrational dynamics of liquids and solids, Raman scatt. of picosecond light pulses 78−94414
vibrational relaxation times calc. from low-freq. mol. spectrum 78−2205
water, collective excitations in 10^8 cm^{-1} momentum range 78−43087
water, low-density amorphous solid, IR spectrum, OH stretching region 79−11411
water, low-density amorphous solid, OH stretching spectrum 79−11413
water, low-density amorphous solid, Raman spectra, OH stretching region 79−11410
water-carbon tetrachloride soln., fundamental H_2O IR spectrum, liq. struct. 80−23419
zero photon high freq. conductivity 78−91718
Ag-As-S system glass, struct., props. and vibr. spectra 79−65901
AgI, lattice dynamics of binary superionic conductors 80−107393
α-AgI, superionic conductor, Raman scattering evidence for sublattice melting 78−80350
AgI, superionic conductor, Raman study 78−80353
AgI, superionic conductor, lattice dynamics 79−95111
$(AgI)_x(Ag_2O\ B_2O_3)_{1-x}$, amorphous superionic compound, ^{11}B lineshape and relaxation 80−108107
$(AgI)_x(Ag_2O.B_2O_3)_{1-x}$ glass, ionic cond. and disorder modes 80−39344
Al, liq., density fluctuations, neutron scatt. anal. 80−70349
Al, liquid, dynamical struct. factor 78−71667
Al-Ag, force-and-mass disordered alloys, vibrs., average local-information transfer approx. 80−88290
AlF_3-M_2F glasses, M=alkaline earth, density-of-states and structural forms, Raman spectra study 80−97255
$3Al_2S_3.La_2S_3$:Ho^{3+}, radiative and multiphonon relax. 79−33794
As, amorphous, bonding coordination defects, Raman scatt. and IR absorption meas. 78−60498
As, amorphous, electron and phonon density of states calcs., comp. to XPS 78−56066
As, amorphous, optical, vibr., transport and defect-related props., review 79−51935
As, amorphous, phonon freq. distrib. 78−30723
As, amorphous, phonon states 79−60464
As, amorphous, vibr. excitations at defect sites, IR and Raman spectra calc. 80−49329
As, amorphous, vibrational excitations of defect sites 80−49332
As, amorphous and cryst., NQR for tunnelling modes and local struct. order 79−61261
As, amorphous and cryst., phonon density of states calc., comp. to IR absorpt. and neutron scatt. data 78−55924
As, bulk amorphous, sp ht. meas., 1.8-20K 78−22866
As, bulk and sputter-deposited amorphous, vibr. props., Raman spectra meas. 77−63411
As-S, glass, IR vibr. spectra, optical charact. calc. 80−40119
As-S glasses, resonance Raman scatt. 80−50325
As-S-I system, glasses, Raman spectra, struct. 79−65857
As-Se-Ge(-S), photostructural change in Urbach tail 80−76021
As_2O_3, amorphous, network dynamics, vibr. band splittings 79−42199
As_2O_3, vitreous, local struct. and vibrational spectra 80−55091
As_2O_3, vitreous, Raman and IR spectra 79−73933
$As_{2-x}S_{3+x}$, hydrogenated chalcogenide glasses, prep. by plasma decomposition 80−49735
As_2S_3, amorphous, acousto-optical effects *(Japanese)* 79−82946
As_2S_3, amorphous, low temp. US meas., two-level systems role 78−30703
As_2S_3, two-phonon vibrational spectra, crystalline and amorphous forms, Raman and IR spectra 78−39537
As_2S_x glass, Raman and IR spectra, struct. model 78−80330
$(As_2S_3)_{1-x}(As_2Se_3)_x$ and $(As_2Se_3)_{1-x}(As_2Te_3)_x$ pseudobinary glasses, comp. depend. of opt. props. 77−90157
$As_2S_3Ge_x$ glasses, vibr. props. and struct., IR refl. and Raman scatt. 79−78682
$(As_2S_3)_{1-x}(GeS_2)_x$ and $As_2S_3Ge_x$ glasses, struct. and vibr. spectra 79−91440
$As_2S_3(Se_3)$, amorphous, network dynamics, vibr. band splittings 79−42199
$As_{2-x}Se_{3+x}$, hydrogenated chalcogenide glasses, prep. by plasma decomposition 80−49735
As_2Se_3, amorphous chalcogenides, optically broadened lattice vibration spectra 79−77712
As_2Se_3 glass, mol. struct. model 80−100179
As_2Se_3, glassy, Cu, Ag and O impurities influence on electronic energy spectrum and mol. vibr. spectrum 77−90181
As_2Se_3-$GeSe_2$ glass, bulk and impurity IR absorpt. 80−71455
$As_4Se_5Ge_1$, amorphous chalcogenides, optically broadened lattice vibration spectra 79−77712
B, amorphous film, Raman scatt. exam. 78−39545
B_2O_3 glass, struct. and phonon spectra 80−50324
B_2O_3-Na_2O-BaO glass, rare earth doped, nonradiative decay and multiphonon relax. 77−85802
B_2O_3-SiO_2 glass film, CVD, differential IR studies 80−55213
$BaCl_2$, non-crystalline film, disorder-induced Raman scatt. 80−11387
BaFCl, non-crystalline film, disorder-induced Raman scatt. 80−11387
$BaTiO_3$, electron energy loss spectra, 0.02-2 eV 78−39642
$BaTiO_3$, phonon spectroscopy, amorphous versus crystalline material 78−83898
BeF_2, vitreous, band limits and vibrational spectra 79−73935
BeF_2, vitreous, IR and reduced Raman spectra, weak Raman bands 78−68498
Br_2-Ar liquid mixture, vibr. relax., 1-D mol. dynamics study 79−73079
C, amorphous, diamond-like 3-fold coord. 80−50323

vibrational states in disordered systems continued
CS_2, coherent Brillouin spectrum, Raman induced Kerr effect, acoustic phonon excitation study 79−59754
CS_2, in carbon tetrachloride soln., Raman scatt. 79−65850
CS_2, liq., props. from allowed light scatt. spectra 80−25364
CS_2, vibrational dephasing meas. with CW mode-locked dye lasers 79−65846
$CaO-Al_2O_3-SiO_2$ glasses, density-of-states and structural forms, Raman spectra study 80−97255
$Ca_3(PO_4)_2$, amorphous, reduced intensity functions, thermal vibr. coupling 78−42910
$CdS_{1-x}Se_x$ mixed crystals, free excitons, disorder effects 80−34365
$CdS_{1-x}Se_x$, zone edge phonons 78−76475
Cs-Graphite, interaction ordered and disordered cpd., Raman spectra 80−11393
Cu halides, lattice dynamics of binary superionic conductors 80−107393
CuI, superionic conductor, Raman study 78−80353
CuI, superionic conductor, lattice dynamics 79−95111
$Cu_{46}Zr_{54}$, metallic glass, dynamical struct. factor and freq. distrib. meas. 80−54136
D_2O, isolated in glassy H_2O, IR spectrum, deuteron tunnelling 78−27207
Eu^{3+} fluoresc. lineshape in glass, temp., time and conc. depend., two-phonon Raman scatt. 78−64406
α-Fe, vibrational states, phonon dispersion, phonon softening 80−88289
$(Fe_2O_3)_x$-$(3B_2O_3.PbO)_{1-x}$ glass, thermal cond. and diffusivity obs. 79−60561
Ga, liq.-solid transition, collective mode dynamics, quantum corrections 77−15554
$Ga_{1-x}Al_xSb$, small wave vector modes 78−75785
$GaAs_{1-x}H_x$, amorphous, vib. props., Raman and IR meas. 80−50322
GaAsP, composition dependence of phonon frequencies 78−75764
GaInP, composition dependence of phonon frequencies 78−75764
$Ga_{1-x}In_xP$, zone edge phonons 78−76475
$3Ga_2S_3.La_2S_3:Ho^{3+}$, radiative and multiphonon relax. 79−33794
Ge, amorphous, electronic struct., far infrared absorption 80−45051
Ge, amorphous, IR absorpt., first-order effective charges due to at. displacements 77−48164
Ge, amorphous, pure and hydrogenated, Raman spectra 79−61358
Ge, amorphous, tunnelling states simulation and sp. ht. 79−37791
Ge, amorphous, vibrational spectra, struct. model calcs. 78−22806
Ge amorphous film, disorder induced phonon absorpt. meas. using double beam Fourier spectrometer 80−105725
Ge amorphous film, high freq. phonon scatt. 80−49328
Ge, hydrogenated amorphous and cryst., IR spectra 79−61359
Ge, nearest-neighbour atom mean-square relative displacements, EXAFS spectra 79−91532
Ge-Se glass, Raman and IR spectra obs. *(Japanese)* 77−43989
GeO_2, amorphous, phonon freq. distrib. 78−30723
GeO_2, glassy high freq. vibr. bands, central force model 80−49330
GeO_2, tetrahedral glass, Raman studies 78−71823
GeO_2, vitreous, band limits and vibrational spectra 79−73935
GeO_2, vitreous, LO vibrational modes, Raman and IR spectra 77−7819
GeO_2-Na_2O-BaO glass, rare earth doped, nonradiative decay and multiphonon relax. 77−85802
GeS_2, cryst. and glass, Raman spectra, struct. *(Russian)* 79−51966
GeS_2 glass, molecular to band-like modes 77−66012
GeS_2, glassy, high freq. vibr. bands, central force model 80−49330
$GeSe_2$, cryst. and glass, Raman spectra, struct. *(Russian)* 79−51966
Ge_xSe_{1-x} glasses, vibr. props. 78−2219
$(GeSe_2)_x(As_2Se_3)_{1-x}$, vibr. excitations of large atomic clusters, Raman and depolarisation spectra 77−20856
Ge_xSi_{1-x}, long wavelengths optical vibr. 78−6135
H-bond, symmetric $AHA^{(\pm)}$, A-H stretching vibr., liq. IR band shape, strong coupling phonon model 78−64358
H_2, vibr. population relax. in gas and fluid 80−29775
HCl, liq., IR spectral intensity and Raman cross-section meas. 80−2742
$HClO_4$-H_2O, aq. soln., IR and Raman spectra, conc. depend. *(Russian)* 80−53002
HF, H-bonded chains, vibr. modes in liq. and solids 78−59873
HNO_3, aqueous soln., reflectance and complex refractive index, IR spectra, vibr. modes 80−66168
HNO_3-H_2O, liq. and glass, mol. assoc., ion pairs, Raman obs. 79−28749
He, liquid, charged surface vibrations in metal approx. *(Russian)* 80−10718
Hg_2Br_2, powder, Raman spectra, press. effects 78−2837
Hg_2Cl_2, powder, Raman spectra, press. effects 78−2837
K_3AsO_4-$KAsO_3$, glass and cryst., Raman and IR spectra 79−99862
KBr, liquid inelastic neutron scatt. obs. from short wavelength charge fluctuations 78−47487
KBr, molten, charge fluctuations, neutron diffr. anal. 79−42198
KBr(I), oscillatory and diffusive regime, above and below melting point, IR thermal emission spectra 78−83985
KCN, disordered ordinary and metastable phases, light scatt., press. depend. 78−95151
$KCl_{1-x}Br_x$, phonon densities of states, dispersion relations 78−75761
$K_3Cu(CN)_4$, isotopic mixed crystal with ^{12}C and ^{13}C, Raman scattering 78−76476
KOH, amorphous and aqueous soln., depolarised Rayleigh scatt., phonon-like excitations 77−81109
K_cRb_{1-c}-alloys, lattice dynamics of substitutional alloys, force constant disorder 78−75786
$K_{1-x}Rb_xBr$, lattice dynamics on pseudo-crystal model 78−75762
$K_xRb_{1-x}Cl_yBr_{1-y}$, IR reflection spectra 78−76474
La-B, amorphous, B-rich, low freq. modes, Raman scatt. obs. 80−108202
LiCl, and LiBr, glassy aq. solns., Raman spectra, rel. to amorphous ice and liq. water 79−47423
$Mg_{70}Zn_{30}$ metallic glass, struct. and dynamics 79−37632
N_2:CO_2(N_2O)(methane-d_4), liq., vibr. relax., Raman scatt. obs. 78−92061
N_2-Ar mixture, picosecond dephasing of coherently excited vibrations 78−22172
N_2+$H_2(D_2)$, vibr. relax. in liquid phase 79−847
NH, ND, vib. relax. in amorphous solid inert gas systems 77−7817
NH_4Br and NH_4I, Raman scatt., 1 bar-7 kbar, 86-295 K 80−34909
NH_4Br, λ-type phase transition, Brillouin scattering 78−79725
NH_4Br, partially disordered, librational modes below disorder-order phase transition temp. 78−79680
$NH_4Cl_{1-x}Br_x$, phonon dispersion 78−75760

vibrational states in disordered systems continued
NO_3^-, in aq. nitrate solns., vibr. dephasing process, Raman obs. 79−51936
NO_3^- in aqueous electrolyte solution, vibr. relax. theory 79−94862
N_2O_2, IR spectra of solid, Raman spectra of solid and liq., vibr. anal. 77−81093
Na, liquid, entropy calc. using phonon theory of liquids 80−39310
Na_2S-GeS_2 system, glass formation, struct. and ionic conduction 80−54138
NaCN, Brillouin scatt., acoustic phonon mode freqs. 77−48181
NaCl, molten, dynamical struct. factors 78−47228
NaCl(Br), oscillatory and diffusive regime, above and below melting point, IR thermal emission spectra 78−83985
$Na_2O-B_2O_3$ glass, negative thermal expansion, LF Guneisen parameter, numerical analysis 77−11707
Na_2O-SiO_2 glass, acoustic and thermal Gruneisen parameters 80−59608
NaOD solution in D_2O, collective excitations in liquid and amorphous state, 77 to 300K 80−92636
NiO, bulklike powder, sp. ht., 14-280K 79−69260
$Ni_{78}P_{22}$, amorphous metallic alloy, US attenuation 78−75789
$Ni_{1-x}Pt_x$, disordered, phonon dispersion relations using neutron inelastic scatt. 79−69212
$Ni_{1-x}Pt_x$, phonon dispersion relations using pseudo unit cell model 79−28066
O_2, liq., stimulated Raman scatt., vibr.-translational relax. rate, schlieren technique meas. 80−9955
P, amorphous, red, far IR absorpt. spectra 80−34923
P, amorphous, vibrational excitations of defect sites 80−49332
P, amorphous red, Raman scattering 80−11416
P, bulk red amorphous, Raman scatt. and IR absorption 79−24323
PD_3, liq. and plastic cryst. states, vibr. dephasing and correl. functions 79−69036
PH_3, liq. and solid, Raman spectra., vibr. correl. functions, rot. motions 80−55087
PHD_2, vibr. dephasing in liq. and solid PD_3, calcs. 80−19884
P_2O_5, glassy, high freq. vibr. bands, central force model 80−49330
P_2O_5, pure vitreous, Raman spectra and struct. 79−69838
P_2O_5-Na_2O-BaO glass, rare earth doped, nonradiative decay and multiphonon relax. 77−85802
Pb-As-S semiconductor glasses, far IR transmission and Raman scattering 77−63419
Pb-Ge-S semiconducting glasses, far IR transmission and struct. 79−65855
$PbO-B_2O_3$, glass exam. of Raman spectra *(Japanese)* 79−19894
$PbO-GeO_2$, glass, exam. of Raman spectra *(Japanese)* 79−19894
$PbO-SiO_2$, glass IR and Raman spectra, heat treatment conditions effect 79−66088
$PbO-SiO_2$ glass, acoustic and thermal Gruneisen parameters 80−59608
$PbO-SiO_2$ glass, IR and Raman spectra interpreted in terms of struct. 78−27213
$PbO-SiO_2$ glasses, density-of-states and structural forms, Raman spectra study 80−97255
$(PbO)_x(SiO_2)_y$ glass, vibrational spectroscpic exam. 79−11417
Pd-Si amorphous alloy, heat treated, low temp. lattice sp. ht. 80−75368
Pd-Si glass, rel. to thermal cond., 0.1-30K 77−20286
Pd-Si-Fe amorphous alloy, Mossbauer spectra, struct. and bonding 80−7224
$Pd_{70}Ag_{30}$, force-const. disorder system, obs. of reson.-like phonon mode 79−90745
$Pd_{80}Si_{20}$ metallic glass, vibrational spectrum, inelastic neutron scatt. meas. 79−60465
$Pd_{0.78}Si_{0.16}Cu_{0.06}$, phonon propagation below 1K 78−71824
PdZr, amorphous, supercond., US props. 80−44765
Rb, liq., dynamic struct. factor, two-relax. time model 77−1068
Rb, liq., phonons, collective modes calcs. 78−2218
RbBr, liq., dynamic density fluctuations, diagonalized relax. theory 78−47230
RbO_2-Na_2O-P_2O_5 glasses, Raman and far IR spectra, vib. at cation site, struct. 78−60435
Rb_2O-Li_2O-P_2O_5 glasses, Raman and far IR spectra, vib. at cation site, struct. 78−60435
SF_6, dissolved in O_2 and Kr, cryogenic liqs., mol. motions, IR and Raman spectra 79−69823
$(SN)_x$, phonon evolution during polymerisation of SN units 78−79711
SO_2 liquid, short range orientation effects, vibr. Raman spectra 80−2759
Sb, amorphous, vibrational excitations of defect sites 80−49332
Sb, amorphous sputter-deposited film, vibr. props., Raman spectra meas. 77−63411
$SbCl_3/AlCl_3$ molten mixtures, Raman spectra 80−93305
SbSBr glass, IR reflectivity spectra 80−71403
Se, amorphous and liq. states, Raman scatt. meas. 80−50328
Se, glass, sp. ht. excess rel. to far IR absorption 77−84874
Se, trigonal, vitreous and red amorphous, phonon density of states comparison 80−54329
Se, trigonal and vitreous, sp. ht. and thermal cond., 3 to 300K 80−59676
Se-Ge glass, lattice vibr. spectra, photostruct. change, far IR absorpt. 78−72494
$Se_{0.84}Ge_{0.16}$ glass, sp. ht. excess rel. to far IR absorption 77−84874
Si, amorphous, chemical effects on freq. of Si-H vibrations 79−51227
Si, amorphous, electronic struct., far infrared absorption 80−45051
Si, amorphous, IR absorpt., first-order effective charges due to at. displacements 77−48164
Si, amorphous, pure and hydrogenated, Raman spectra 79−61358
Si, amorphous, Raman spectra, vibrational properties 79−99881
Si, amorphous, reduced intensity functions, thermal vibr. coupling 78−42910
Si, amorphous, tunnelling states simulation and sp. ht. 79−37791
Si, phonon spectroscopy, amorphous versus crystalline material 78−83898
Si:F, amorphous, pure and doped, vibr. excitations at defect sites, IR and Raman spectra calc. 80−49329
Si:F, amorphous alloys, RF sputtering prep. in SiF_4-Ar gas mixture, spectra 80−80772
Si:H, amorphous, Brillouin scattering from acoustic bulk and surface waves 80−11425
Si:H, amorphous films, plasma-deposited, defect states, IR, ESR, and refractive index meas. 79−65944
a-Si:H, structural interpretation of vibr. spectra 79−69864
Si:H alloy, amorphous, dihydride model of vibrational spectra 80−80827
Si:H amorphous films, IR spectrum and struct. 80−97277

vibrational states in disordered systems continued
Si:H film, amorphous, H-associated disorder modes, PMR spin-lattice relax. time meas. 80−93202
Si_xGe_{1-x}, amorphous, vibr. props. 79−23693
Si_xGe_{1-x}, vibr. props. 77−4176
$Si_{1-x}H_x$ amorphous sputtered films, IR vibr. spectra 79−43051
Si_3N_4 films, amorphous, CVD, IR spectra 77−21031
SiO amorphous film, high freq. phonon scatt. 80−49328
SiO thin films at 60 mK, high-freq. phonon propagation 79−19347
SiO_2, amorphous, chemical effects on freq. of Si-H vibrations 79−51227
SiO_2, amorphous, effect of second nearest neighbour forces on vibr. 78−59915
SiO_2, amorphous, fast-time heat capacity, heat pulse propagation 78−51700
SiO_2, amorphous, intrinsic surface phonons, Raman scatt. and IR refl. 80−24728
SiO_2, amorphous, low temp. acoustic absorpt., 9 to 20K and 15 to 65 MHz, Anderson model interpret. 78−26633
SiO_2, amorphous, phonons, cluster-Bethe lattice approach 78−10150
SiO_2, amorphous, surface phonon theory 78−84044
SiO_2, amorphous and crystalline, surface polaritons and splitting of optical frequencies 78−72090
SiO_2 and SiO_2-B_2O_3 glasses, struct. and phonon spectra 80−50324
SiO_2, electron energy loss spectra, 0.02-2 eV 78−39642
SiO_2 fibres, LF optical phonons, Raman spectra 80−80789
SiO_2, glass, acoustic and thermal Gruneisen parameters 80−59608
SiO_2, glass, HF phonon phase vel. meas., below 1K, tunnelling model 77−7818
SiO_2 glass, IR spectral emissivity and absorpt. coeff. at 600 to 1700K 80−16018
SiO_2 glass, molecular to band-like modes 77−66012
SiO_2 glass, phonon scatt., $>10^2$ GHz, by supercond. junction spectrosc. 80−10625
SiO_2 glass, relax. times of mol. OH^- ions at very low temps., elec. dipolar echoes 79−78616
SiO_2, hydroxylated amorphous, small-particle dynamics, neutron scatt. 80−79899
SiO_2, phonon spectroscopy, amorphous versus crystalline material 78−83898
SiO_2, tetrahedral glass, Raman studies 78−71823
SiO_2, vitreous, band limits and vibrational spectra 79−73935
SiO_2, vitreous, fast neutron irrad., low temp. US meas., two-level systems role 78−30703
SiO_2, vitreous, LO vibrational modes, Raman and IR spectra 77−7819
SiO_2, vitreous, multiphonon IR absorpt. 80−25381
SiO_2, vitreous, valence-attenuation pair defect, states, IR and Raman spectra 79−91442
SiO_2, vitreous Brillouin scatt., 35 GHz phonon vel. and absorpt. below 1K 80−100664
SiO_2:OH^-, vitreous, elec. dipolar echoes 78−52430
SiO_2-Na_2O-BaO glass, rare earth doped, nonradiative decay and multiphonon relax. 77−85802
SiO_2-TiO_2 glass phonons, IR and Raman spectra meas. 79−91447
$SnCl_2$-$AlkAlCl_4$ melts (Alk=Li, Na or Cs) 79−99874
$Sr_{1-x}Cd_xF_2$, IR and Raman meas. 78−75763
$SrCl_2$, non-crystalline film, disorder-induced Raman scatt. 80−11387
Te, amorphous, Rayleigh scatt. of Mossbauer radn., lattice dynamics 80−15845
Te-Si glassy alloys, IR transmission and sp. ht. changes in glass interval, vibr. modes, struct. models 78−23474
TeO_2, glass, phonon density of states, Raman spectra *(French)* 77−20841
TeO_2-Al_2O_3-WO_3 glass, rare earth doped, nonradiative decay and multiphonon relax. 77−85802
TiO_2 devitrified glass, Raman spectra 79−78677
TiO_2, electron energy loss spectra, 0.02-2 eV 78−39642
TiO_2, phonon spectroscopy, amorphous versus crystalline material 78−83898
TiO_2-SiO_2 glass system, Raman and hyper-Raman light scatt. spectra 80−66187
$TlAsS_2$, IR spectra *(Russian)* 77−66512
$Tl_{1-x}Se_x$, amorhpous, IR spectra, structure 77−77194
V phosphate glasses, vibr. spectra 77−52064
V_2O_5-P_2O_5 glasses, Raman spectra 79−78667
Y-B_x amorphous, B-rich, low freq. modes, Raman scatt. obs. 80−108202
Yb^{3+}:phosphate glass, relation between absorption and equilib. luminesc. spectra 77−85754

vibrations
see also lattice dynamics; molecular vibration; vibrating bodies
3-D cable networks, finite element study of free vibration 79−23197
acoustic noise propagation models, railway lines 80−48500
acoustically induced, human response to house vibr. caused by sonic booms or air blasts 78−90589
acoustically induced vibration of circular cylindrical rods 77−62098
acousto-structural vibrations, approx. numerical soln. 79−3841
acoustoelasticity, theory, natural modes and forced response to sinusoidal excitations 77−84058
active damping of vibrations in elastic systems with distributed parameters, active stabilisation *(Russian)* 79−27577
aeroelastic system, flutter eigenvalue problem, rigid-body degrees of freedom elimination 79−98651
aeroelastic vibr. elimination, appl. of Pontriagin max. principle 78−55584
aeroelastic vibr. elimination, optimal control method 80−33514
aeroelasticity in separation streamline flow 80−5979
aerospace guidance computer 78−21313
AF, buildings, transmission by columns 80−74602
air column resonance spectra, meas. using basic lab. apparatus 80−41998
aircraft, deformable, dynamic model for natural vibration anal. by finite elements 78−46909
aircraft, noise and vibration ride comfort criteria 79−41512
aircraft angular vibration power spectral density prediction model 78−83323
ambient vibrations of building struct., estimation of structural system parameters using exploratory-confirmatory analysis 80−28456
annular plate, radially stiffened, free vibr. studied by Ritz method 80−69707
anti-vibration systems, Fick boundary value problem soln. *(Russian)* 79−35540
vibrations continued
arterial stenosis, in vivo and model expts., flow-induced wall vibrs. 78−3535
asymmetric elastic medium, electrically conducting, magneto-thermo-elastic waves anal. 80−15772
autonomous excitation by electrodynamic vibrator *(Russian)* 77−50970
axisymmetric free vibration of submerged spherical shell 80−74546
band (tape), endless, torsional vibrs. during const. axial vel., damping effects *(German)* 78−34065
bar, impact excitation, longitudinal vibr. 78−94606
bar, impact vibr., motion and dynamic stability analysis 78−26081
bar, localised damage region effect on parametric excitation 78−30215
bar, nonuniform elastic, longit. vibr. dynamics of impact excitation 78−75086
bar carrying concentrated masses, vibr. motion under longitudinal impact *(Russian)* 79−50627
bar undergoing bending oscillations, shape optimisation *(Russian)* 79−37210
basilar membrane model using digital filter for voice features extraction 78−77069
basilar membrane nonlinearity 77−25461
beam, buckled, forced oscillations, global bifurcations and chaos 79−27580
beam, clamped, hinged, sudden change of boundary conditions, support failure vibrs. *(German)* 80−1456
beam, elastic, on elastic half-space support, forced flexural vibr. 78−63353
beam, initially stressed hyperelastic, incremental motion from variational principle 79−68638
beam, nonuniform, sectionalization and averaging method for calc. natural freq. and normal modes *(Chinese)* 80−43643
beam, nonuniform, static and dynamic instability analysis 78−13942
beam, out-of-plane vibr. including nonlinear inertia and nonlinear curvature effects 79−64558
beam, rigid plastic, stepped, impulsively loaded, optimal design for asymmetric mode motions 78−90723
beam, two-span, with curved initial path contour, transverse vibrs. 80−38324
beam column, axially creeping viscoelastic under initial axial compression, free lateral vibration 79−50639
beam containing fluid flow, on elastic base, flexural vibration stability 79−46248
beam vibration frequencies by Schelkunoff iteration with HP-65 calculator 78−1592
beam-like lattice trusses, numerical analysis, shear deformation 80−14566
beamlike dynamic vibration absorbers, anal. 80−53539
beams, buckling loads and fundamental freqs. improved lower bounds 80−64416
beams, fixed-free with support asymmetry, nonlinear, nonplanar, resonant oscillations 79−37212
beams, inextensional, nonlinear flexural-flexural-torsional dynamics, equations of motion 79−64494
beams, inextensional, nonlinear flexural-flexural-torsional dynamics, forced motions 79−64495
beams, nonlinear oscillation computation using space and time finite elements *(German)* 79−37213
beams, rectangular, of arbitrary depth, free vibr. 79−98647
beams, rigid plastic, quasimodel form solns. for dynamic response 79−90170
Beck's column subjected to vertical+follower forces, vibr., stability 78−9583
Beck's rod, nonconservative flutter system, variational principle 79−1132
bending waves in fluid-loaded thick plates 79−72748
bifurcations in dynamical systems with internal resonance 79−46255
biophysical effects, continuous manual control 78−61169
biophysical effects, visual acuity 78−61168
book, physics of vibrations and waves 77−41494
bound formula for determining the fundamental frequency 79−81790
bowed string, vibr. demonstrations 77−13532
brain, pulsations of third ventricle, mathematical description 77−64081
branched systems, single-junction, analysis using Rayleigh-Kohn and Newton Raphson methods 80−52035
bridge, appl. of finite difference method to numerical study of dynamic effects *(French)* 78−36826
building structs., eigenvalue routines 78−26078
bulk solids, strength and flow props., vibrations effect 79−37237
cantilever bars under axial load, parametric reson. by combined freqs. method 79−1131
cantilever beam, minimum mass struct., axial vibrs., numerical determ. 79−10519
cantilever beams, free transverse bending vibrs., secondary effect influence *(French)* 79−18785
cantilever of cantilever-electro-piano, harmonization of vibration *(Japanese)* 79−18634
cardiac response sensitivity to time relationship between vibr. and cardiac cycles 77−56407
cavitating orifice under reattached flow conditions, noise and vibration characteristics 80−83829
cavitation bubbles, forced oscills. rel. to noise subharmonic component 77−14851
cavity-backed panel anal. for sound transmission in air *(French)* 80−38164
circular disk resonators in vicinity of thickness resonance, vibration mode anal. 80−48634
circular plates resting on viscoelastic half space, dynamic response 79−18801
classical string problem, constants of motion 80−27113
classical string problem, evolution eqn. 80−27114
colliding elastic bodies, nonlinear surface waves *(Ukrainian)* 79−32331
column buckling criteria determ. using vibr. data 78−34098
complex elastic systems, unsteady vibrs. method of dynamic compliances generalisation *(Russian)* 79−81755
complex moduli derived from vibrations of Timoshenko beam 80−38163
complex submerged structures, vibr. anal. by discrete element techniques 77−68520
composite materials, fibre reinforced, rectangular rods, elastic wave propagation *(French)* 80−83749
composite materials, rational bonding of structures, fracture resistance 80−5990

vibrations continued
compound elastic systems, natural frequency spectra *(Russian)* 79−17230
computer tomography detector vibr. sensitivity 78−35955
concrete, fresh, behaviour under a vibr. action, large particle segregation *(Japanese)* 80−88329
construction element, optimal design in case of impulsive loading 79−86382
continuous system simulation by periodic structs. harmonic load response 79−18705
continuous viscoelastic structural members, transient dynamic response 80−64442
couple stress effects on elastic waves and vibr. 79−14307
coupled bending-torsion flutter in cascades, aeroelastic stability boundaries 80−64424
coupled dynamic problems of thermoviscoelasticity quasilinearisation method 77−72188
coupled flexural and longitudinal vibrations of finite structures, energy absorpt. estimation 78−1495
coupled fluid-structure systems, vibr. anal. by displacement method 79−7323
crane bridge, damping calc. 80−101711
critical damping of simple-harmonic motion, for teachers 79−17
crossply glassfibre, cantilever beams, nonlinear damping for nonsinusoidal strain 79−47762
crystal resonators with increased immunity to acceleration fields in any shock/vibration environment 80−91953
curved beam with viscous damping forced vibrations 79−50622
curved beams, nonlinear dynamic anal., finite element method 80−96213
curved tube bank vibration in turbulent transverse water flow *(Russian)* 80−33678
cylinder, elastic thin walled, vibrations under axial stress 79−59937
cylinder, hollow, linear viscoelastic, dynamical loading by internal press. 79−18793
cylinder, torsional vibr. superposed on finitely deformed state 80−19263
cylindrical elastic tube torsional oscillations under large internal and external press. 78−79249
cylindrical rod, periodic structure, torsional vibrations, interfacial elastic parameters 80−96215
cylindrical shell, dynamic response to concentrated impact load, radial displacement, stresses 78−67072
cylindrical shell with elastic filler, eigenfrequency spectra, dynamic instability regions, nonaxisymmetrical vibrations 78−63367
cylindrical shell with liquid, resonance frequencies determ. 80−43661
cylindrical shells, correlation between vibration and buckling 80−28463
cylindrical shells of viscoelastic material, natural transverse vibrations 80−43660
damped, differential eqn. soln., teaching appl. 79−62950
damped axisymmetric vibrations of double layered cylindrical shells, refined theory 79−75338
damped linear systems, free and forced vibrations, stability 79−64568
damped linear systems, free vibrs., principal modes 77−68512
damped linear systems, freely vibrating, eigenvalue lower bounds 79−27569
damped linear systems, vibr. 79−18790
damped string, vibr. freq. depend. on kinematical nonlinearities 79−14296
damped system, resonant peak amplitudes estimation 77−53771
damping, internal, in 2 and 3 dimens. continua 78−13970
damping on one degree of freedom system *(German)* 79−32369
decrement determ. of nonlinear hysteresis type system from resonance peak width 77−84191
deformable media, equivalence of force systems *(Russian)* 77−50886
Dicke-type Hamiltonians with hidden variables 78−74874
diffuse vibration field propag. in structs. with periodic inhomogeneities 80−86093
discomfort assessment of dual-axis whole-body vibration 78−13842
discrete dynamic system with series structure, non-linearity of vibration 78−28935
doubly rotated α-quartz plate vibration, polarising effect 79−14186
droplets, forced vibr., Raman scatt. obs. 80−34929
Duffing's eqn. forced by periodic impulses, harmonic solns. 78−89325
Duffing eqn., large nonlinearity, subharmonic solns. 79−65
duration effects on human comfort and task proficiency 80−26247
dynamic linear dipolar elasticity eqns. soln., convergence to classical elastodynamic solns. 77−888
dynamic shear loading at boundary between elastic space and cylindrical rigid enclosure *(German)* 80−58896
dynamic stabilization of multiphase media subjected to vibrations under low gravitation conditions 80−7511
Earth, torsional vibrations, damping effect 79−44121
earthquake response of nonlinear plates 80−13955
earthquake waves made visible by stroboscopic effect 77−25660
EBR-II subassemblies, 61-pin wire-spaced, exptl. confirmation of design to minimize vibr. and wear 79−67825
effect of noise and vibration on human beings, summary of symposium, Southampton Univ. (Dec. 1978) 80−35958
effectiveness rating of vibration-absorbing coatings 80−5870
EHV power transmission lines, reduction by damper, description 77−5660
elastic, numerical characts. determ. *(Russian)* 80−38181
elastic body, justification of two scale method for class of integro-differential eqns *(French)* 78−28947
elastic constants determ. by resonant vibr. in thin disk, apparatus 77−56182
elastic cylinder, end resonance under axisymmetric vibr. *(Ukrainian)* 80−23932
elastic cylindrical resonator in liquid filled cavity *(Russian)* 80−38303
elastic half-bounded medium, unidimensional deformation under vibr. loading *(Ukrainian)* 80−5933
elastic half-space, epicentre solns. for pt. multipole sources 79−81798
elastic half-space with rigid circular disc inclusion 77−72170
elastic hydrostatic sliding bearing, forced vibrs. of vertical rotor 79−18798
elastic mechanical systems, vibr. damping by dampers with filled voids *(Russian)* 80−58954
elastic ring, nonlinear flexural vibr. 79−18805
elastic shell revolution, transient motion in acoustic medium 79−7333
elastic stability of linear system, simplified algorithm 77−62180
elastic stability theory, nonlinear partial differential eqns. *(Russian)* 79−9128

vibrations continued
elastic system, rotation effects on natural vibr. frequency *(Russian)* 79−7319
elastic tube, cylindrically symmetric vibr. *(German)* 79−7330
elastic-viscoplastic frames, dynamic responses, strain hardening effects 80−79178
elastically viscous systems, crit. flutter loading, approx. determ. *(Russian)* 78−30212
elasticity, contact problem, vibration of partially adhering stamp 80−69656
elasticity, St. Venant planar theory, nonhomogeneous problem, logarithmic decrement *(French)* 78−49664
elasticity, variational formulation of integral eqns. *(French)* 77−72181
elastokinetics and elastostability, equation structure from D'Alemberts principle *(German)* 79−63046
elastomechanical systems, theoretical models correction method *(German)* 78−38
electrically conducting elastic plate, vibrs. in transverse mag. field, shear deformation *(Russian)* 79−81756
electron microscope, HV 3 MV type, mech. vibr. sources and effects *(French)* 80−82848
electrorheological suspension flow, vibr. effect *(Russian)* 80−53877
ellipsoids of revolution, stationary movements, stability of orientations *(Russian)* 77−87646
engine structure vibrations, transmission path and dynamic behavior, background and static tests 80−43520
engine structure vibrations, transmission path and dynamic behavior, motoring tests 80−48487
epicentre motion of elastic halfspace due to suddenly applied buried point source 79−72840
extrusion, benefit of vibrations 78−51135
ferrite disc, isotropic, topographs of resonant vibrations 79−64394
fibre reinforced composite waveguides, axisymm. elastic vibrs. 80−102995
fibreguide transmission, vibr. induced intensity modulation 77−23743
filled system, vibrational thinning, visoelasticity and strength 77−8795
finite orthotropic cylinder with penny-shaped crack, transient response under torsion 80−48640
finite-amplitude oscillations of a spherical cavity in a nearly-incompressible elastic material 79−64553
fission reactors, flow-induced structural vibrations anal. 80−42795
flames in tubes, dynamical props. 77−31388
flexible bar, min. vol. design by dynamic programming *(Polish)* 78−13965
flexible thread in a stream, natural freq. *(Russian)* 79−90163
flexural, accel. meas., effect of strain sensitivity of piezoelectric accelerometers 80−58991
flexural, HF, of thick rectangular bars and plates 79−18779
flexural, large amplitude, of thin shells, effect of median surface curvature 79−18780
flexural, radiation efficiencies of beams 80−53541
flexural vibrations in beams and plates, active suppression 77−27422
flexural vibrations of full and annular composite orthotropic plates 79−94528
flexural-flexural, non-linearly coupled, of Beck's column subjected to planar harmonic excitation 79−18781
floor, acceptability scales for occupant-induced vibrations 80−91956
floor, footfall-induced, effect on sensitive instruments 80−64277
floor, nature and effect on precision, machinery, isolation methods 80−43522
floor, pneumatic isolators with two-chamber damping systems, isolation of very sensitive meas. apparatus *(German)* 80−69590
flow around obstacles, in reactor cooling system, Strouhal criterium appl., vibr. excitation *(Czech)* 78−66331
flow induced vibrations design considerations rel. to fluid/struct. coupling 77−84190
flow-induced, fluid excitation forces 77−42776
flow-induced oscillations, bifurcation to divergence and flutter, infinite dimensional anal. 78−89336
flow-induced vibration anal. of nuclear reactor components 79−22380
flowmeter, float-area-type, jumping instabilities of float 80−14855
fluid, ideal, in elastic shell, nonaxisymm. vibrs. 77−35077
fluid and structural dynamics, transient 3-D potential flow problems, SING-S 80−48668
fluid coupled concentric cylindrical vessels, normal mode solution 79−37157
fluid impregnated solids, elastic and dynamic response regimes 78−90713
fluid saturated porous elastic cylinders, vibrations 79−10521
fluid-elastically coupled coaxial cylindrical shells, response to external flow 77−89063
fluidised bed, vibrofluidised, shallow, vibr. grid gas flow influence on hydrodynamics 79−86509
flutter eqn., continuation and direct soln. 78−34047
Fokker-Planck eqn. eigenfunction expansion soln. extension, first order system 80−31668
forced, lower bound on forcing amplitude for stability, third order nonliner system 80−52013
forced, orthotropic plate on elastic foundation 80−53682
forced periodic response stability in third order non-linear systems, comments 79−81763
forced periodic response stability in third order nonlinear systems, comments 79−81762
forced torsional vibration of elastic circular rod on elastic half space or stratum 79−41508
forced vibrations of freely supported continuous beam *(Rumanian)* 78−75085
forced vibrations of systems with retardation and damping 78−83290
forced vibrs. of nonlinear systems, Duffing eqn. 77−33842
fractal resonators, mode distribution 80−8782
frame, plane, impulsively loaded, large deflections, mode approx. technique extension 80−83757
free, non-linear oscillator, numerical soln. 80−68034
free body mass matrices condensation using flexibility coeffs. 78−63349
free contour plate with point fixing, frequencies and oscillation modes 77−80098
frequencies synthesis, appls. of extension of Southwell-Dunkerley methods 77−39217
frequencies synthesis, principles of extension of Southwell-Dunkerley methods 77−39216
frequency anal. of unsupported structures 79−32333

vibrations continued
frontal solution algorithm for finite element frequency analysis 79−3942
fuel rod vibration induced by coolant water and air/water flow *(Japanese)* 78−74429
g- and p-modes of non-adiabatic self-gravitating fluid, perturbational-variational expansion 78−32337
gas bubbles oscillating in liquid, modification by nearby objects, comment 79−90064
gas flow in duct, self-excited oscillations 78−55670
gas lasers, vibration immunity for interference work 78−5489
general physics and heat, book 79−25814
general representations of soln. of steady-state elastic vibr. eqns. 77−894
generation techniques using induction motors 77−42790
glaciers, floating, vibrating mechanism for iceberg calving 78−81197
glass panels, sound transmission loss and vibr. in nonreverberative conditions 77−7258
glottal sound source, self-oscillating model *(Japanese)* 78−92654
Green function expansion into eigenfunction set 80−22205
ground vibration by traffic, effects on LaCoste and Romberg gravimeter meas. *(Japanese)* 78−65400
ground vibrations for seismic detonation of buried source 77−73667
ground vibrations from cut-and-cover tunnel construction 79−3845
gyro-stabilisation platform, nonlinear loss of stability and trembling *(Chinese)* 80−62457
gyroscope, forced vibrations, shock absorber selection parameters 80−43659
gyrotachometer, error autocompensation at angle vibr. of base *(Russian)* 78−16782
hair cells of organ of Corti, thermal noise 78−15845
Hamiltonian system, two-dimensional, stability of equilib. position in case of equal frequencies *(Russian)* 78−36814
Hamiltonian systems satisfying the Rosenberg conditions for normal modes 80−64444
hand-arm vibration, analytical model of hand vibr. response characts. 77−64074
hand-arm vibration, subjective response characts. to hand-induced vibr. 77−64062
hand-arm vibration, vibr. transmission characts. including meas. techn-qiue 77−64075
harmonic oscillations of single degree of freedom systems 80−33516
harp, false gut string displacement meas. 78−75020
heart, quantitative characterisation by multipolar acoustic heart model, minicomputer method 78−85429
heat exchanger true vibrations numerical soln. 78−75094
heat exchanger tube arrays fluidelastic vibration 78−94615
heat exchanger tube banks, crossflow induced vibr. 78−50245
heterogeneous *(French)* 79−7317
holographic system path length difference controller *(Russian)* 79−22916
homogeneous elastic sphere, spheroidal mode props., displacement radial depend. special reference 79−14312
HTGR, acoustic environment determ. 79−89352
HTGR core, 2-D vibr. test and simulation anal. for vertical slice model *(Japanese)* 78−58328
human biodynamics, statistical anal. 78−92672
human response to whole-body vibr. duration effect on comfort 77−17011
human whole-body vibrations, statistical anal. 78−92672
humans, discomfort caused by rot. vibr. of seated subjects, effect of position of axis of rot. 78−85461
humans, subjective equivalence of sinusoidal and random whole-body vibrs. 77−13050
hybrid element method, calc. of vibr. freq. 77−26173
hydroelastic systems, spectrum and normal modes 77−68494
hyperelastic spherical cavity, finite amplitude oscillations 79−32332
hysteresis damping, continuum description 78−67078
hysteretic structural vibrs. under white random load 79−41509
hysteretic systems under random excitation, equivalent linearisation 80−79210
impact vibrations, steady, of body having hysteresis collision characteristics 80−14602
incremental deformations of initially stressed media with couple stresses 78−62077
induction motors due to homopolar alternating fluxes, anal. 77−78981
inhomogeneous solid weakened by circular slit 79−86381
inhomogeneous viscoelastic Voigt-Kelvin rod, stress propag. and harmonic vibrs. 79−94543
instability regions determ. in system with parametric excitation 80−90662
interferometer, data handling in high vibration environment 80−95132
interferometer design for high vibration environment 80−95131
internal losses in metals subjected to high intensity US flexural vibrations 80−6460
isoenergetic stability 77−49587
isolation, fluid-saturated porous solids 80−53726
isolation, machines and power transmission mechanisms, approximate analyses of beam and plate foundations 80−64434
isolation of vibration in presence of Coulomb friction 79−81768
isotropic elastic body, asymptotic distrib. of natural freqs. *(Japanese)* 78−30121
iterative methods, accelerated automatic root search algorithm 78−59321
Koite's modified energy functional, appl. to cantilever circular cylinder shell freqs. 79−1130
laminate, anisotropic cylindrical shell, optimal problems of vibrations 78−1602
laminate, piecewise-homogeneous elastic medium with plane parallel boundaries of separation, vibrations 77−84188
laminated half space under influence of vibrations *(Russian)* 78−63370
large deflections of a plate sealing a liquid 79−27508
layered rod on sagging elastic supports, aeroelastic stability, vibr. modes 78−51115
layered spherical shell, torsional oscills. overtones, eigenfreq. pattern 79−14311
LF oscillograph system for demonstrating mechanical vibrs. 77−64908
linear damped system, of finite degrees of freedom, numerical solution 78−24656
linear elastic discrete system, effect of damping on vibration-stability reln. 77−19558
linear lumped-parameter systems, synthesis with prescribed mode shape 80−23881
vibrations continued
linear models of frequency-independent internal friction *(Russian)* 79−18834
linear system, rigid moment relation for random parametric vibr. excitation *(German)* 79−90180
linear systems, damped free motion 79−64569
linear viscoelastic material vibrations, integro-differential eqn., two-scales method soln. 79−72839
liquid, in vessel, vibr. amplitude determ., structural damping and surface tension applied to stress anal. 80−19417
liquid metal-vibrating solid surface, equipment for investigating interaction at US freqs. 77−51589
liquid-filled vibr. beaker, spatial reson., energy transfer mechanism 77−39255
liquid-to-gas surface, dynamic behaviour in near weightlessness *(Russian)* 77−68611
LMFBR steam generators, flow induced vibr., review 77−23240
loudspeaker cones, effect of voice-coil and surround on vibration and sound pressure level 80−96172
machine, power flow through isolation systems 80−64436
machine, wave propagation and power flow, beam-stiffened foundation plates 80−64435
machine tool, stability assessment method 78−87316
machine vibrations anal. and obs. block deformability influence *(Italian)* 78−51108
machinery, association with acoustic noise 77−34999
magnetic repelling force system, with cylindrical rare-earth magnets *(Japanese)* 80−4744
magnetovibration analyser for magnetite suspension 78−4668
manual control operator performance, gain and vibration effects interaction 78−44756
material anelastic behaviour, anal. using 3-lumped vibr. model *(Japanese)* 78−47473
mathieu stability analysis of non-linear third-order weakly forced systems 79−30261
matrix methods, appl. to elastic string and spring-mass systems *(Dutch)* 77−41451
mechanical, two dimensional, numerical analysis acoustic phenomena, thin plates *(French)* 78−59337
mechanical dished supports, oscillation and stability conditions based on mixed finite elements *(German)* 78−87299
mechanical system, anal. by combined holographic interferometry and finite element anal. *(German)* 78−90806
mechanical system, random parametric excitation, internal and combination resonances 77−72230
mechnical coupled-transmission lines 78−52
membrane, fundamental free eigenvalue, lower bounds 80−38319
membrane, infinite, acoustic radiation due to fluid loading discontinuity 78−90579
membrane, prestressed rectangular, forced vibration, near resonance response 79−68611
membrane with both curved and straight line boundaries, dynamic response 80−64440
metal, fatigue and inelasticity testing apparatus in symmetrical bending mode, 36 to 330 Hz 78−27722
metal, ferromagnetic, mechanically stressed, magnetic-inductive method of discontinuous vibration detection, theory *(German)* 79−20315
metal cutting, with slowly varying system parameters, self vibrs. *(Ukrainian)* 77−68477
metal particles, small, possible vibrations associated with twins 80−100253
metals, elastic consts., resonance method for determ. within 80-300K temp. range 78−46918
micropolar elastic bars with rectangular cross section, wave motion and vibrs. 79−77000
micropolar elastic half space, steady state response to moving loads 77−58577
micropolar thermoelasticity, axial symmetric problems, stationary vibrations 79−68572
micropolar thermoelasticity, Green formula for infinite domain with cavity 79−30241
micropolar thermoelasticity, half-space problem 79−30237
micropolar thermoelasticity, radiation conditions, uniqueness theorems 79−12606
micropolar thermoelasticity, three dimens. theory, pot. method 77−68414
Mindlin plate elements, free vibration anal. 79−46244
Mindlin-Goodman method of solving problems with time-dependent boundary conditions, comments 80−53694
minimal normal modes, existence and bifurcation 79−72837
mixture burning in Soundhaus' tube, radial self excited vibr. regimes *(Ukrainian)* 78−68892
modal damping bounds by component modes method using Lagrange multipliers, natural freqs. 80−79213
modal test methods and applications 78−79252
modes, closely spaced, in structural models, design method 79−32349
moving load in initially stressed thick plates attached together by a flexible core 79−81752
multi-degree of freedom mechanical systems, antiresonances *(Chinese)* 80−42049
multi-degree of freedom system, Holzer's method 78−34059
multilayer plates, viscoelastic, equations of forced vibrs. 78−67084
multimass undamped system, decoupling from large structure 78−57774
multiparametric discrete-continual elastic systems, characteristic series coeff. *(Ukrainian)* 79−40368
multiparametric elastic system, lower frequencies and crit. loadings *(Russian)* 79−44739
multiphase media, dynamic behaviour of bubbles under vibr. in weak gravitational field *(Russian)* 79−77226
multiple parameter system vibrations and stability, book 78−93532
musical string vibrations, teaching 77−49536
natural, orthotropic cylindrical panel with glued circular ribs 78−22299
non-homogeneous elastic shells transient displacement and stress 77−65684
non-Newtonian fluid, Poiseuille flow, influence of vibrs. 79−7391
non-Newtonian fluid exit flow through capillaries, effect of vibrations 80−79358
noncollinear three-phonon interaction in an isotropic plate 78−66970
nonconservative elastic systems, induced oscillations, transition through resonance *(Ukrainian)* 79−98654
nonhamiltonian systems with one degree of freedom, forced periodic motion *(Russian)* 78−20959

vibrations continued
nonlinear dispersive and dissipative wave propagation 77−74231
nonlinear dissipative systems, oscillatory resistance forces *(Russian)* 77−80061
nonlinear elastic cylinder, parametric biharmonic vibrs., reson. modes *(French)* 79−10522
nonlinear elastic systems, linear damping coefficients, experimental determ. 79−50680
nonlinear higher harmonic generation in complex systems *(Russian)* 77−50950
nonlinear mechanical systems, periodic vibr. 78−55583
nonlinear mechanical systems, periodic vibr. 80−33513
nonlinear mechanical systems with time optional condition 80−31492
nonlinear multidegree-of-freedom system, superdivision harmonic oscillations due to fourth order nonlinearity 77−57175
nonlinear oscillations with slowly varying system parameters 79−37219
nonlinear oscillator, stroboscopic phase portrait and strange attractors 78−54177
nonlinear oscillator and reflectors, periodic vibr. and impact characteristics 80−92089
nonlinear oscillators, normal modes, uncoupling and stability 80−27115
nonlinear oscillators, random excitation, response envelope statistics 79−6052
nonlinear plate problems, unconditional stability of finite element scheme, nonlinear vibrs. *(Japanese)* 79−77004
nonlinear plates, response to random loads 78−94604
nonlinear resonant, gyro with damping system on vibrating base *(Russian)* 77−71312
nonlinear system, one degree of freedom, parametric vibration 77−53770
nonlinear system random vibr., Gaussian closure technique, bilinear hysteretic system 79−18802
nonlinear system under combined forcing and parametric excitation 77−68517
nonlinear system with stops, viscous-Coulomb damping influence 80−36842
nonlinear systems, vibrations under space-time stochastic loads 80−33524
nonlinear systems in resonance, governed by hyperbolic differential eqns. 77−39242
nonlinear two-degree-of-freedom system, internally resonanced, forced vibrs. 80−36838
nonlinear vibr. eqns., modified stroboscopic method for approx. determination of periodic solns. 80−38313
nonlinear vibr. systems, secondary resonances generated by harmonic forces *(Polish)* 79−64563
nonlinear vibrating systems, fourth order parametric resonance, influence of frictions 77−58620
nonlinear vibration decoupling using canonical transformation *(German)* 80−28451
nonlinear vibratory system, ultra-subharmonic oscillations analysis 77−50944
nonstationary nonlinear vibratory system feedback oeration effects 79−14316
nonstationary random vibrations of multiple-mass systems 80−69728
nonsymmetric vibrations of piezoelectric ceramic rings polarized along the thickness 80−7299
normal modes of coupled nonlinear oscillators, stability 78−89330
normal modes of self-gravitating fluids in perturbed configurations, perturbational-variation procedure 78−32336
nuclear containment vessel with attached masses, seismic anal. 77−3181
nuclear fuel pin model, parallel two phase flow induced vibrations 79−13388
nuclear heat exchanger and boiler designs 78−66333
nuclear power plant piping systems under seismic motion, method of residues 77−3182
nuclear power plant seismic floor response spectra 78−819
nuclear reactor, reactivity and neutron density noise excited by random rod vibr. 77−50203
nuclear reactor component vibration investigation using fast Fourier transform analysers 80−63315
nuclear reactor core, VVEH type, neutron noise, diagnostic method of mech. vibrs. *(Czech)* 77−3120
nuclear vibrations, review 79−89219
nucleation of crystallization centres, low frequency vibration effects on rate *(Russian)* 78−15383
ocean free surface vibrations caused by internal waves, experimental investigation *(Russian)* 79−16478
one-dimensional inhomogeneous structure of finite length, vibrational energy propag. 79−32356
open tubes, resonant oscillations of gas 77−68628
optimal design of freely vibr. elastic bodies *(German)* 78−65775
optimum vibration isolation forces for system with random excitations 77−39240
ore-mill foundation, prevention of vibration by damping and stiffness addition 80−69588
orthotropic elliptical plate with similar hole, free vibration 80−43649
oscillator, linear, excitation by stationary random force *(Russian)* 80−27116
oscillator, linear parametrically excited, random vibration and stability 79−64491
oscillators, with nonlinear damping, first passage failure time anal. 79−6053
oscillatory damped linear systems, eigenvalue bounds and subcritical damping 79−77005
oscillatory flow induced vibration, linearisation eqns. 80−64449
out-of-plane, natural freqs. of continuous curved beams 80−74588
oval cylindrical shells, free vibrs. modal method calcs. 79−7332
panels, induced edge crack growth rates, excited by convected random pressure fields 80−69737
parametric vibrations of elastoviscous rod 77−3763
parametrically excited systems, stability 79−80425
particle vibrational movement under impulse perturbation of an inclined plane *(Russian)* 80−17791
passive vibr. isolation, shock absorber selection 78−55556
pendulum accelerometers, error anal. *(Russian)* 78−77874
percussion instrument acoustics, multidimens. vibrs., review for teaching 77−57128
periodic heterogeneous ring, harmonic vibrs. *(French)* 79−50621
piecewise continuous elastic systems, eigenvalue lower bounds, stability and vibrations 79−50604
piezoceramic disc resonators, dispersion of thickness vibrs. 78−22237

vibrations continued
piezoelectric cylindrical shell, longitudinal wave propagation 78−92026
piezoelectric solid, perturbation theory for linear electroelastic eqns. 79−1739
pipe mode characteristics determination, pipe flow conditions effects *(French)* 78−79246
pipework, use in control valve acoustic noise measurement *(French)* 77−39158
piping conveying swirling liquid, free harmonic wave propagation 77−84187
piping systems, gas, time domain identification of standing wave parameters 79−18558
piping systems under seismic excitation, modal anal. 80−33512
plane elastic standing waves of finite amplitude 78−18218
plate, annular, elastically supported, with central rigid mass, free vibrations *(Japanese)* 80−96226
plate, circular, elastically supported, with conc. mass at centre, large amplitude vibrs. *(Japanese)* 80−96227
plate, circular arc aerofoil shaped, vibrational characts. 79−10516
plate, circular elastic, transient response to applied fluid pressure 79−64572
plate, circular thin nonhomogeneous, with circular hole, extensional vibr. 79−94546
plate, deform. vibrs., acoustic thermal relax. method for thermophys. props. determ. of group V metals at high temp. 79−85143
plate, elastic with rib, vibr. freq., Weierstrass condition *(Russian)* 79−81757
plate, heated, vibr. anal., thermal buckling 78−26073
plate, high freq. long wave vibrs., two-dimens. eqns. 78−83321
plate, thick free circular, axisymmetric flexural vibrations 79−64575
plate, thin, thermally stressed, vibrations 80−48628
plate, thin elastic, Chladni patterns in random vibration 79−81714
plate, variable thickness, on elastic foundation, bending, closed form soln. 80−79179
plate, viscoelastic, free and forced vibrs., transient response 79−32360
plate excitation, difference of structure-borne-sound levels in point excitation and large area excitation *(German)* 80−53538
plate on eccentric annular elastic support, transverse vibr. 80−14601
plate stability, numerical anal. *(Russian)* 79−3935
plate with hole, rigidly clamped, natural vibrs. 80−33520
plates, anisotropic skew, large amplitude vibrs., transverse shear, rot. inertia, theory 80−79207
plates, anisotropic skew, large amplitude vibrs., transverse shear and rot. inertia, numerical results 80−79208
plates, annular, of variable thickness, natural vibr. eigenfreq. Mindlin eqn. integration 80−38318
plates, clamped elliptical with concentrated mass, nonlinear vibration amplitude-freq. characts. 79−64561
plates, continuous, with arbitrary number of equal spans, eigenfreqs. 80−64438
plates, laminated anisotropic composite, penalty plate bending element 80−96200
plates, nonlinear vibrs., reson. phenomena under Duffing's eqn. 79−14305
plates, polar orthotropic laminated annular, asymmetric vibrations 79−76993
plates, rectangular, stability and vibrations *(Chinese)* 80−43644
plates, rectangular stepped thickness, with edges elastically restrained against rotation 78−90740
plates, sandwich, large amplitude vibration amplitude-frequency characteristics 79−64580
plates, thick, higher order theory 78−26074
plates, thick circular, axially symmetric vibration, elastodynamic deformation 79−37214
plates, thin circular, modal anal. of transient asymmetric response 80−23931
plates, thin elastic, large amplitude vibrs. by conformal transformation method 80−19262
plates, thin rectangular, with arbitrarily oriented stiffeners, free vibrs. 78−1591
plates, transversely isotropic rectangular, nonlinear vibrations 79−64559
plates, uniform circular, with free edge, natural modes and freqs. 80−48638
plates at elevated temp., vibr. and buckling, fundamental freq. 80−23935
PMMA, cracking kinetics, effect of small vibrs. 79−57108
Poiseuille flow in non-Newtonian fluid, influence of vibr. 79−81930
polarisable dielectric crystals, mean internal stress pot. *(Italian)* 79−65797
polybutadiene, complex modulus meas. using forced vibrations at ultralow frequency 77−70258
polyethylene, sonic frequency vibration effect on stress relaxation 77−86072
polymer, stress-relaxation apparatus, stress and vibration relaxation in sound frequency range 77−1905
polymer, vibrational thinning, viscoelasticity and strength 77−8795
polymer, viscoelastic prop. determ. with VR-72 vibrorheometer 77−70259
polymer, viscoelastic prop. meas. method in fluid and highly elastic states using forced vibrations 77−70258
polymer, viscofluid, extensional vibrorheometer 77−70257
polymer melt flows, propag. of large amplitude low frequency vibration 77−65770
poroelastic cone, inhomogeneous, forced torsional vibrs. 79−32338
poroelastic cylinders, torsional vibrs., wavelength, phase and group vel. 80−79214
powder, moist, granulation on vibrated chute *(Japanese)* 78−95710
powder behaviour in vibrating field from cond. obs. *(Japanese)* 78−95711
powder fluid bed forming in vacuum under vibratory action model 78−11147
power ultrasonic applications of vibration systems *(Chinese)* 80−43568
primary circuit of CHINON 3 reactor, noise sources, amplification 77−6545
propane, vibr. combustion, modulation in injection-vibr. apparatus *(Russian)* 77−9083
pulsar magnetosphere, vibrations generation by klystron mechanism 78−53971
pulsed excitation of flexural modes in infinite plates 80−38167
pulsed holography for interferometric anal. of superposition of three sinusoidal vibrs., theory 77−71955

vibrations continued
PVC, mechanochemical degradation in primary struct., mech. vibration effects, IR spectra *(German)* 78−19769
PWR, internal vibration calc. rel to operational safety condition *(Czech)* 78−8915
PWR core barrels with and without holes, various edge conditions, hydrodynamic vibrations 80−78406
PWR internals, flow induced random vibr. anal. 77−83016
PWR neutron noise interpretation by vibration analysis 78−94073
PWR power plant flow pressure fluctuations as vibration source, relationships *(Hungarian)* 80−47685
PWR reactor core barrel, influence of boundary conditions and co-vibrating liquid obs., using model 79−36302
quadrature representation of viscoelastic correspondence principle in frequency domain 79−46233
quartz plates, rotated-Y-cuts, high frequency vibrations 80−96216
radiotelescope, behaviour anal. using dynamic equivalent models *(German)* 77−2342
railway ground noise, underground systems 80−48490
railway tunnels, structure-borne sound levels and spectra 80−48499
random, statistical data digital processing method *(Japanese)* 80−64430
random compressional waves, effect on rigid sphere in elastic medium 80−53681
random vibration analysis, correlation function *(Chinese)* 80−43645
randomly loaded elastic body dynamics, probability characts., of solns. to boundary-value problems *(Russian)* 77−41490
reactor components, quality control systems by acoustic emission 79−93758
reactor multiple-support excitation piping problems, automated anal. 79−9773
rectangular laminated plate, free vibrs., freq. and shape determ., complex boundary conditions 80−79203
rectangular parallelepiped, natural vibrs. from 3D elasticity and plate theory *(Russian)* 80−79199
rectangular plates, moderately thick, free flexural vibr., effect of geometric nonlinearity 79−3940
rectangular plates, vibrations and buckling anal. *(Japanese)* 77−80084
rectangular plates subject to in-plane normal and shear forces, transverse vibrs. 79−14314
rectangular regions, plane stress problem using functions related to beam flexure 78−59297
reduced model theory, hydrodynamical approach for vel. autocorrelation functions 80−27135
reinforced plastic cylindrical shells, optimal design under dynamic constraints 80−102996
relay systems, bifurcation and stability from third order differential equation *(Russian)* 79−46247
resonance phenomena in multi-degree of freedom systems, effects of geometrical nonlinearities 79−98648
resonant nonlinear vibrations, continuous system, undamped case 80−28450
resonant nonlinear vibrations, continuous systems, damped and transient behaviour 80−33504
response analysis of a vibrational system of multi degrees of freedom subjected to an arbitrary force 80−12912
ribbed cylindrical shell carrying a fixed absolutely rigid body, free oscillations 79−10523
rigid body impact on elastic half-space, Fourier synthesis of steady state vibr. 77−80101
rigid sphere embedded in elastic medium, response to incident stochastic waves 80−64451
ring, multilayer elastic, forced vibration, variational principle effectiveness in Ritz method *(Russian)* 79−68616
road traffic noise, effect of structure-borne tunnel vibrations on buildings 80−48492
road vehicles, digital modal analysis system 80−38173
rod, cantilever, constrained end, transverse vibrs., energy dissipation 80−19278
rod, short elastic, in viscous liquid axial flow, stability and transverse oscillations 80−33521
rod shaped continua, stability of free vibrs. 77−68493
rod with nonlinear curvature, dynamic stability theory, lateral bending problem under torsion *(German)* 78−54
rods, elastic, high-freq. long wave vibrs. 80−96211
rolling, vibratory, contact strains *(Russian)* 77−65722
rotating asymmetric shaft, unequal pedestal stiffness influence on unstable vibrs. 79−18803
rotating flexible rods, unstable vibration and buckling 78−79242
rotating flexible structures, modal anal. 77−31235
rotating machinery subharmonic vibration diagnosis 79−3971
rotor, flexible, on flexible bearing, viscous-damping, vibr. and balancing 78−63352
rotor, passing through crit. speed, with gyroscopic effect, asymptotic calc. 78−63354
seismic response of flexible cylindrical liquid storage tanks 79−31241
self-excited vibrations in lubricated friction 80−58984
semiconductors, elastic consts., resonance method for determ. within 80-300K temp. range 78−46918
shaft, symmetrical, nonlinear elastic and internal damping props., flexural vibrations 78−71290
shell, cylindrical, dynamic stability under periodic axial load 79−14302
shell, cylindrical, fibre reinforced, fluid conveying, vibr. characts., flow effects 80−14600
shell, cylindrical, fibre-reinforced, axisymmetric damped vibrations calc. 79−14297
shell, cylindrical, optimal natural freq. vibrs., rib eccentricity influence 80−38325
shell, cylindrical, under external press., vibr. and buckling 80−102975
shell, cylindrical elastic, dynamic response in potential fluid 80−64446
shell, elliptical cylindrical, nonlinear vibrs., freq.-amplitude characts. *(Russian)* 79−81753
shell, multilayer composite, optimisation, buckling under stability and vibr. conditions *(Russian)* 80−53667
shell, nonlinear elastic cylindrical biharmonic excitation, parametric vibrations *(French)* 78−87294
shell, ribbed conical, subjected to harmonic load, forced vibrations 80−43658
shell, spherical, with rigidly clamped edges, Poisson ratio influence on natural vibrs. 80−33523
shell, thin cylindrical, stiffened with viscoelastic rings, vibr. damping characts. 80−28452
vibrations continued
shell, thin elastic, containing liquid, free vibrs. *(Russian)* 80−33505
shell and surface rigidity, pseudobending, vibrs. and stability loss *(Russian)* 80−33470
shell of revolution, resonant oscillation obs. by holographic interferometry *(Russian)* 78−22297
shell of rotation exposed to vibrs., optimum shape and reinforcing struct. 79−18792
shells, applicability limits for approx. theories *(Ukrainian)* 80−23933
shells, circular cylindrical, wide band random axisymmetric vibrs. 80−48637
shells, conical, axisymmetric torsional vibrs. from tangential inertial force 80−64443
shells, cylindrical, nonlinear parametric vibrations calcs., deflection *(Russian)* 79−46191
shells, flexible shallow elastic-plastic, natural vibrs. and buckling 80−33519
shells, spherical, investig. of ultralow frequency vibrations *(Russian)* 78−55580
shells, thick cylindrical hyperelastic, large amplitude oscillations 79−64560
shells, thin elastic, recent advances in linear theory 79−59921
shells, thin stiffened reinforced, stability and vibrs. 80−14610
ship propeller shaft dynamics, forces between shaft and bearings, root bearing rigidity depend. 79−81801
Shiva mechanical systems 78−63135
silicone oils, props. determ. by harmonical shear vibr. *(German)* 78−67164
single mass vibroimpact system, response to white noise random excitation 80−64454
single-degree-of-freedom system under sinusoidal forces, anal. using double-end cantilever absorber 77−74217
slab sector of variable thickness, free vibration calc. 79−64571
slender damped structures, vortex excited aeroelastic oscills., mathematical model *(German)* 78−94616
small damped vibrations, Krylov method for freq. determ. 78−67088
small free vibrations of shell of revolutions in an ideal liquid *(Russian)* 80−73168
solar pulsations at periods from 7 to 70 minutes, observational search 78−93180
solid friction damping, math. model approach 77−42764
solid systems, errors associated with resonance curves 79−7255
solid systems, non-linear vibration properties *(French)* 77−54937
solid-liquid system, connectedness of liquid and solid movements *(Ukrainian)* 79−50623
solutions using high precision finite elements, comments and reply 77−72224
sound radiation, critical freq. of flat plates in dense fluids *(German)* 80−38165
spherical pendulum in fluid flow, transverse vibrations *(Russian)* 77−87644
spherical shell of variable Young's modulus, radial vibr. 78−94607
spiral vibration of rotating shaft rubbing against interference element *(German)* 78−87252
stability of interaction between oscillator and tie in relative motion *(Polish)* 77−53789
star shaped membranes, new bounds of Poincare const. *(French)* 79−25860
stars, distorted, Clairaut coordinates and vibr. stability 80−90408
stationary random processes, spectral density structure estimation *(Russian)* 78−24736
stationary vibrations in 2-dimensional micropolar thermoelasticity 80−74793
statistical models of coupled dynamical systems and the transition from weak to strong coupling 79−50500
statistical prediction of vibr. distrib. and random noise in higher level region *(Japanese)* 79−1023
statistical treatment of vibration level distrib. in digital form *(Japanese)* 77−23805
steady state stochastic nonlinear vibrs., covariance anal. *(German)* 79−88880
steam, film condensation in tube, heat transfer, vibr. effect 78−51044
steel, austenitic, rod, coupled flexural and torsional vibrs., energy dissipation 80−89281
steel, ferromag., rod, coupled flexural and torsional vibrs., energy dissipation 80−89281
steel, fully annealed tool, cantilever beams, nonlinear damping for nonsinusoidal strain 79−47762
steel, high strength, surface work hardening effect on life 77−70234
steel, low C, absolute dimensions effect on logarithmic decrement of torsional vibrs. 80−3150
steel rod, transverse vibrations, energy dissipation, static longitudinal load effect 80−81099
steel VNS-2, damping capacity, magnetomechanical, phase transform. effects 78−31445
stretched strings, occurrence of subharmonic resonances of order 1/3 78−90580
stretched wire, vibr. freq., stiffness corrections for undergraduate expts. 78−12473
string, stretched, appl. of optimisation methods to vibr. control 78−83305
string, vibr. of segments of string anal. 77−9
string, wave velocity propag. meas., mass tension ratio *(Spanish)* 80−74592
string vibrations, linear and nonlinear, physical discretisation 78−45480
string with time-variable length, free and forced vibrs. 79−92953
string with time-varying length 79−25870
structural analysis, dynamic condensation method 79−3943
structural dynamics, system identification by pseudoinverse 77−72232
structural dynamics, vibrs., eigenrelations 78−1589
structural dynamics problem soln., generalised Euler method 79−46245
structural noise and vibration problem solution by statistical methods 79−23126
structural panel, rectangular, with elastic edge constraints, dynamic response, Bolotin's asymptotic method 78−75091
structural systems with internal gaps, dynamic and under axial impact loading 77−3092
structural vibration, aircraft noise induced, noise meas. 78−87187
structural vibration damping by rot. slip in joints 77−89059
structure vibrations, reduction by increase in damping factor *(French)* 77−19472

vibrations continued
structure-fluid interaction between vibrating wall and channel flow 77−38325
student laboratory exercise, simple harmonic motion, to waves 77−60880
Sturm-Liouville system with discontinuous coeffs., direct soln. for vibr. and heat conduction 80−23930
subharmonic and superharmonic synchronisation in weakly nonlinear systems 77−2534
superconducting coil, buckling, vibr., lateral constraint and damping effects 78−63344
Superphenix internal shells, vibr. anal. *(French)* 78−50247
supersonic potential flow, panel flutter, finite element calc. 78−26152
tactile receptor response to stepped and sinusoidal vibrs. of hair, crayfish 77−70481
taut string, Chladni patterns in random vibration 79−81714
teaching, Newtonian motion anal. using micro-computer simulations *(Japanese)* 80−31462
test rig for wear meas. of granules 78−56840
testing materials and structures 78−3298
thermal accommodation coefficients by high speed vibr. of solid sample, alkanes on Al(Fe) 78−92506
thermal stresses in conducting materials due to high current pulse 79−7287
thermoacoustic vibration generation, in heated channel laminar flow 78−14029
thermoacoustic vibrations of subcritical press., vibrs. onset mechanism 77−47026
thermoelastodynamics mixed boundary value problem, algorithm *(French)* 77−50979
thermoviscoelastic material, sensitivity of thermomechanical response to thermal boundary conditions and material constants 79−77001
thick circular rings, T or I cross section, in-plane vibrs. 80−48639
thin walled sphere in contact with elastic or acoustic media, interior dynamics 80−5981
third order nonlinear differential eqns. anal., multiple time scaling 77−82369
three-support bearing shaft system, flexural amplitude determ. and reduction method 78−46890
timing periodic events, half-column method for student expt. 78−12516
Timoshenko arcs with variable cross section, in-plane vibr. 80−28453
Timoshenko beams, eigensolns. for coupled thermoelastic vibrations 79−64577
torsional, isotropic circular cylinder, periodic shearing stress 78−75087
torsional, iterative methods of finding natural freqs., change of stiffness method 80−74589
torsional, natural freq. sensitivity anal. 77−74218
torsional vibrations, optimal damping *(Russian)* 77−57179
torsional vibrs. of spherical shell, numerical results 78−59322
torsional wave propag. in infinite piezoelec. cylinder (622) cryst. class 80−87642
train generated ground vibrations, propagation and wayside effects 80−48489
train induced ground vibration, propagation pathway prediction 80−48491
transformer cores, calc. method 77−74219
transient response of continuous elastic structures with viscous damping 79−46254
transient vibration problems, solution bounds 77−67226
transmission line vibrations, effects of Stockbridge type dampers 79−14323
transport vibration prevention approaches 78−55506
transportation, ride quality criteria 79−90076
transverse vibr. of systems with account of inadequate material elasticity *(Ukrainian)* 77−68475
tube, cylindrical, thick-walled, finite twist and external press., stability, vibrs. 78−83286
tube bank, in-line, acoustic reson. generation mech. 78−46958
tube bundle in water, freq. response 77−83028
tuning fork oscillator internal random disturbances *(Russian)* 80−62459
turbine blade natural freq. and stress meas. *(German)* 79−34260
turbogenerator endwinding, type TVV-800-2, tests *(Russian)* 77−9885
turbogenerator stator winding, tests *(Russian)* 77−9886
turbomachinery for central power stations, review of vibration and noise 80−23835
twisted strip, in centrifugal and unsteady aerodynamic force field 79−1127
two channel drive dynamics with differential wave mechanism *(Russian)* 80−28449
two-mass system, free vibrs., damping factor optimisation *(Russian)* 80−42
two-phase AC servomotor rotor, reduction method *(Japanese)* 77−45704
uniform cantilever with a point rot. constraint, vibr. freqs. 79−18804
unstaggered tube bank vibration induced by viscous liquid flow *(Russian)* 80−33677
unsteady aerodynamic modelling for arbitrary motions 80−19433
upper bounds for amplitudes of harmonic components of excitation 80−64445
US exponential solid horn, finite element analysis 78−94496
US strengthening of cryst. mats., instrument for US attack at low temp. 77−49732
US torsional vibrations in metals, measurement of absorpt. 80−58856
US vel. propag. meter for NDT of polymers 78−19976
variable systems subjected to arbitrary source functions and boundary conditions 77−7234
vibration induced polarisation modulation 79−27385
vibration problems, element spaces and separation for determining bounds to eigenvalues 79−14317
vibrations and waves in physics, undergraduate text book 78−54203
vibratory tools, hand-arm energy dissipation and accel. levels 78−96116
vibroisolation parameter selection method and stability for two machines on elastic beam 80−87738
vibroisolation with harmonic forcing, optimal choice of noninertial system *(Polish)* 79−64564
violin G-string, resonant response and excitation of wolf-note 80−53540
viscoelastic body eigenfrequency determ., finite element method *(German)* 79−23270
viscoelastic cylinder with elastic shell, vibration when subjected to random forces 79−59941
viscoelastic cylindrical shell, short, resonance vibrations 80−58962
vibrations continued
viscoelastic rod, fundamental solutions of wave equations with delay time 79−27576
viscoplastic liquid film on vertical vibr. wall, with slip, shaking loose 78−59371
viscous incompressible liquid, vibrational displacement, wave mechanism 80−43777
vocal cord vibration, computer simulation of pathological conditions 77−16940
volumetrically controlled hydraulic drive, calc. 79−35571
vortex shedding induced on two cylinders, one in wake of other 77−58589
vortex-excited vibrations, energy constraints 79−37327
water boiling, vibr. effect on heat transfer crisis 80−33423
water drop vibration analysis in near-zero gravity 77−7426
wave diffraction theory appl. to free floating and moored rigid structs. 79−7321
wedge, plane composite, singular eigenfunctions for plane harmonic problems 80−79206
wedge region with mixed boundary conditions, elasticity theory, dynamic problems soln. 80−43641
wedge-shaped straight elastic bars, new method for longitudinal and torsional vibration freq. calc. 78−59338
weightlessness vibr. effects and prospects for space technology 77−58597
whole-body low-frequency vibrations, subjective freq. doubling expts. 77−64063
Zienkiewicz four-time-level scheme for numerical integration 78−1594
AL, laminate, free-free plates, predicted and expt. natural modes 79−10520
Al alloy disc, quality factor of vibr. rel. to gravit. radiation detector 78−75093
Al, cantilever beams, nonlinear damping for nonsinusoidal strain 79−47762
Al-Cu-Mg-Mn-Si-Fe, torsional vibrations decrement, deformed vol. effect 80−76326
Al-Mg(Cu)(Si), (5.0(4.5)(11.8) wt.%), ingots, vibr. effect during solidification on porosity formation 80−108426
Cu, annealed polycryst., torsional vibrations decrement, deformed vol. effect 80−76326
Cu, electrical grade, fatigue damage eval. from freq. change of natural vibrs. 79−52498
Fe, cast, wear, effect of vibrations 79−52389
Mn-Cu (25 wt.%) rod, transverse vibrations, energy dissipation, static longitudinal load effect 80−81099
Mn-Cu (75, 25 wt.%), rod, coupled flexural and torsional vibrs., energy dissipation 80−89281
p-Si:B, reduction of vibration noise, suitable orientation of element, rel. to crystallographic axes 79−11123
vibrations, crystal lattice *see lattice dynamics*
vibrations, molecular *see molecular vibration*
vibrations of crystal lattices *see lattice dynamics*
vibrometers *see vibration measurement*
vibronic states of molecules *see molecular vibronic states*
video recording
airborne passenger entertainment, dual language Super 8 mm sound system 80−4785
aphasia treatment session recording, momentary and interval sampling 79−96704
biomedical US data recording method using videotape *(German)* 80−81666
C-CD camera, implantable, for continuous recording of sheep ovary images during reproductive cycle 78−40442
cardiac radiographic image sequence analysis and recording 78−57069
cassette recorder for analogue data, biomedical appls. 79−44009
cassette videotape recording of computer images, video-sync mixer, biomedical appl. 79−29604
chalcogenide films, laser-beam recordings by thermal creation of holes 80−35010
cinematographic film recording of information transferred from video magnetic tape 79−21835
cinematography, development and introduction of TV facilities *(Russian)* 80−22465
colour NTSC signals, 16 mm colour print film by laser beam 77−74537
comet debris (meteors) spectra studies video techniques appl. 79−80241
computerised tomography, picture documentation and filing 79−66554
digital holographic storage of TV signals 80−87353
digital information optical recording in pictorial format 79−31831
disc information retrieval by optical readout 80−43284
disc master recording, high density, replication by contact printing 80−62761
discs, apparent size of reflecting polygonal obstacles, diffr. theory 79−89844
disk pit geometry, control, optical techniques 80−5775
echocardiograph signals, M-mode, analogue storage using video tape 80−94298
educational aids, general report *(German)* 78−69954
educational applications 79−35491
EEG physiological data teletransmission system 77−86687
electronic editing system *(Russian)* 79−89029
equipment and services, 1979 video yearbook 79−14197
film projection, sound track synchronisation, new system *(German)* 79−67402
FIM, video recorder registration of unstationary images 78−24897
gamma camera pulse quantitative reproduction from video tape recordings 78−53496
gradient-index imaging, theory 80−69331
holographic, general principles 77−34844
holographic colour video memories, recording and playback technique 80−9833
holographic interferogram anal. with TV picture system 80−106489
holographic recording of digital colour TV signals on photographic film *(German)* 78−22101
image quality transfer 80−68279
Image Transform tape to film transfer 78−45742
in-lab video studio of modest cost and mobile 77−67165
interferometric investig. of electrolytic conc. polarisation at electrodes 78−68896
intraoperative use of X-ray TV chain with video recorder 79−92334
laser engineering and appls., conf., Washington, USA (May-June 1979) 80−1216

video recording continued
laser scanning system, He-Ne, for information identification *(German)* 80−106557
LEED intensity meas. using video camera and video tape recorder 79−73074
lens, gradient-index spherical, design for optical pickup systems 80−69483
light scatt. from three-dimensional obstacles with complex refractive index 77−75415
lip and jaw motion during speech, video-scanning system 77−56388
magnetic powder appl., Fe-Co-Ni alloy *(Russian)* 77−55910
magnetic tapes properties, ferromagnetic dispersions structural and magnetic characteristics *(Russian)* 78−16886
mass spectra, automatic recording microphotometer modification 77−12845
materials for optical recording *(Japanese)* 80−105730
medical laser video recorder 80−36065
microscopy, applications 80−98972
minicomputer-controlled high-speed transient recording system *(Russian)* 77−9992
movie camera, laser based, operation and applications 80−57405
multicoloured photothermoplasticity process, coding and decoding indices *(Russian)* 77−67523
multitrack video tape recorder, exercise ECG examination and cardiological telemetry appl. 77−70561
optical video disc, acoustooptic travelling wave transcription signal recording 79−36986
optical video discs, laser read-out system diffraction theory, focus error alteration influences 79−50338
Philips video long play system, bi-aspherical objective lens 79−46026
physics, videotape instruction, low-cost systems 79−29
processor for computer calc. of press.-vol. indices from left ventriculograms 78−53495
radiometrically calibrated imagery for thermography 77−40893
radionuclide computer-assisted cardiology, off-line viewing using videotape 78−65119
reconnaissance sensor data, real time recorder and display 79−32081
schools and colleges, Tasmania, TV programme storage systems 79−80404
SEM, dynamic, with video tape recording 78−32952
SEM, real-time stereo, techniques used in microdissection of biological tissues 79−80724
SIT vidicon detector system, for Palomar 1.5 metre telescope 79−92674
solar XUV instantaneous images, obs. and recording on ATM television monitors 77−60605
stroboscopic interferometry, active mirror testing appl. 79−58782
surface-relief phase gratings 77−19429
TEM image recording and processing TV system 79−58851
time control system, Q-Lock, for editing, dubbing, VTR appl. 80−68278
tutored videotape instruction advantages for science and engineering courses 78−8194
TV signals on cine film, electron beam recording *(Russian)* 78−21251
uncontrolled thermographic mosaic compilation and videotape processing 77−29502
US B-scan recording on video tape-recorder 78−77095
vapour pressure measurement, torsion-effusion method, automatic data acquisition 80−52188
videodensitometric camera and video disc system 77−40761
VLBI, Japanese domestic system, recording signal generator *(Japanese)* 80−21924
wideband recording facility, stress-wave emission signals recording appl. 77−37873
X-ray TV, high-resolution system for medical work 78−24120
AlGaAs high-power constricted DH diode laser, for optical recording 80−43351
Te film, hole machining using (Ga,Al)As DH laser, high-density optical recording 79−89954
Te film and trilayer antireflection structure for optical recording 79−94329
Te trilayer for high-performance optical recording 79−50382

video signals
acousto-optic modulator temporal response, physical optics model in low scatt. efficiency limit 78−66897
analogue video transmission feasibility using laser diode, over 30 km at 1.3 μm 80−58737
analytical video stereoscopy, extended images, real-time photogrammetry 78−88926
automatic TV complex for chromaticity analysis of cinematographic, photographic images *(Russian)* 79−89026
bandwidth compression effect on military target observers' detection and recognition performance 80−106484
biofeedback for alpha monitoring of brain activity 78−20299
coherent image processing photodiode array 79−55076
coherent light valve optical processor for GHz bandwidth signals 78−78937
colour image scanner, using one-colour laser and modified γ-Ruticon image buffer 79−27373
edge detection, numerical, optical and hybrid methods compared 80−102662
electronic imager observer performance rel. to display S/N ratio 77−40679
electronic speckle pattern interferometry, fringe contrast analysis 79−72506
equipment and services, 1979 video yearbook 79−14197
fibre optic video link, review of NASA tasks 78−42441
fibre optical PFM transmission, noise performance, cable attenuation 77−65634
fibre-optic transmission by laser diode analogue baseband modulation 80−58738
full duplex transmission link over single strand optical fibre 78−1341
hospital integral picture processing and communication system 78−57104
hybrid image processing system, space and time picture oscillation, by active incoherent feedback 78−58924
image analysis in radiology *(Japanese)* 79−29599
image feedback processor, ghost image elimination from TV display 78−46519
interferogram analysis by TV camera-microprocessor system 80−73440
IR calibrator, continuous-temp., for temp. measurement using IR scanner 79−75530
LED analogue transmission, LED linearisation by predistortion 78−37993
lightwave communications, Bell system evaluation in Chicago 78−46821
nuclear medicine, composite output signal from GAMMA-11 computing system 79−29610
optical video discs, laser read-out system diffraction theory, focus error alteration influences 79−50338
propagation over real terrain, computer-aided field strength anal. 79−25373
raster display control apparatus *(German)* 79−67265
remote sensing, image transformation and coding in conventional colours via electron system 80−4117
seawater transmission props. for underwater laser communication 80−33069
SEM information representation by equal signal lines 80−95196
semiconductor-dielectric structure, photoresponse on electron beam scanning, video signal enhancement *(Russian)* 77−47863
strain meas. speckle photography with hybrid optical/electronic image processing 80−106768
thermal viewing system, image integral scanning effectiveness 79−50402
three dimensional video images formed by parallax panoramagrams, real-time transmission 79−31807
transient astronomical phenomena, video detection and analysis techniques 79−80239
TV holographic system signal frequency spectrum 77−7036
USSR and E.German time scale comparison by transportable atomic clocks and TV signals 77−79067
videodensitometry and image analysis, minimum computer system 79−34664
X-ray image convertor with video signal output 80−36125
PtSi Schottky-barrier monolithic IRCCD focal plane 80−86427

videophones *see videotelephony*
videotelephones *see videotelephony*
videotelephony
switched audiovisual communications system, Picturephone, hospital appl. 79−74786
X-ray picture transmission over voice grade telephone channels 78−44607
videotext *see viewdata*
vidicons *see television camera tubes*
viewdata
Prestel viewdata system, introduction 80−42013
viewing screens *see screens (display)*
virial coefficients *see equations of state*
virtual storage
nuclear cross section tabular file generation, utilisation techniques 77−23397
virtuons (virtual phonons) *see phonons*
viscoelasticity
see also creep; internal friction; stress relaxation
ABA poly(styrene-b-butadiene) copolymer, physical props., casting solvent effects 77−55935
acetic acid, Rayleigh-Brillouin scatt., 20-115°C, viscoelastic theory anal. 79−28774
acoustic scattering, HF from submerged cylindrical shells with viscoelastic coatings 78−1478
acrylonitrile-styrene copolymer melts, rheological behaviour *(German)* 77−51012
activation energy, apparent, of viscoelastic deform., creep T-jump expt. 79−37264
Adam-Gibbs theory, for conc. polymer soln. 78−83353
adhesion of solids, review of physical mechanisms *(French)* 78−6231
adsorbed polymer layers, hydrodynamic thickness, Navier-Stokes eqn. calcs. 77−65726
aging viscoelastic contact 80−64486
aliphatic-aromatic block copolyamides, synthesis, struct. and dynamic viscoelasticity, DTA and X-ray anal. *(Japanese)* 78−31377
alkali borate and phosphate glasses, mech. and dielec. relaxs. and interpet. 78−27159
amorphous solids, time-temperature-pressure superposition phenomena, free volume theory 78−26059
amylopectin, glycerin impregnated, dynamic viscoelasticity *(Japanese)* 80−104203
amylose, glycerin impregnated, dynamic viscoelasticity *(Japanese)* 80−104203
anisotropic layer, nonstationary torsional waves problem *(Russian)* 80−53678
anisotropic reinforced resin laminate, cyclically reversing load, strain behaviour determ., approx. method *(German)* 79−5096
anisotropic solids with magnetic symm., unified dynamic theory 78−77713
anisotropic viscoelastic ageing materials, linear irreversible thermodynamics and phenomenological consts. 77−14922
ankle joint, human, compliance 78−57034
aorta, human, morphological and functional aspects of study of mech. props. 77−25499
aorta model, two chambered, viscoelastic, press. estimation in ascending and descending aorta 78−77076
apolar viscoelastic dielectrics, thermodynamic theory, linear effects 78−67059
approximate method of solving problems 77−80082
aqueous liquids, shear US meas. with composite torsional quartz transducer 80−53599
aquifer, viscoelastic model appl. to subsidence due to pumping 77−91175
arterial segments, canine, nonlinear anisotropic viscoelastic props. 78−20205
arterial wall empirical linear response models 77−90831
articular cartilage, normal, quasi-linear viscoelastic props. 80−108937
articular cartilage, viscoelastic properties *(Japanese)* 80−101215
articular cartilage matrix, flow-independent viscoelastic props. 79−43952
articular cartilage of normal rabbit, viscoelastic shear behaviour 77−36973
asphalt, glass transition temp. and viscosity 79−77045
asthenosphere, readjustment during earthquake cycle rel. to surface deform. 78−85490
automatic system for short-time stress relaxation 77−63710
azoxy compound, liquid cryst. mixture, nematic, elec., optical and viscoelastic props. 79−55803

viscoelasticity continued
balance rheometer, inertia effects in rheometrical flow systems 77−68722
bar, elastic and viscoelastic, impact loading model 77−23911
bar, vibrs., correlation between random parameters 79−32325
bars with nonlinear characteristics, stability 80−10174
beam, conical viscoelastic, torsion, accumulated injury influence *(Russian)* 79−94512
beam, constrained, flexural vibrating, response to random excitation of white noise and turbulent boundary layer type 80−53671
beam, forcing with time-varying frequency, solid viscosity and rotatory inertia effects 79−68619
beam, nonlinear viscoelastic, torsion creep 79−18745
beam column, axially creeping viscoelastic under initial axial compression, free lateral vibration 79−50639
bending of orthotropic rectangular plates, conformal orthotropy concept 78−38204
benzene-polystyrene, semidilute solns., viscosity and reptation time 79−99345
bimolecular lecithin membranes, artificial, rheological and viscoelasic props. 80−26252
biological soft tissue nonlinear viscoelastic behaviour 78−69128
biological tube dynamic rheology 79−62274
biomaterial growth phenomena and behaviour, math. theory 77−81458
biosystems under stress, prerupture behaviour 79−39437
birefringence of viscoelastic dielectrics under combined stresses 78−68470
bitumens, oil sand, rheological props. 80−64506
BKZ fluid tubular membrane, simultaneous elongation and inflation 79−90294
BKZ viscoelastic fluids, acceleration waves of arbitrary form 77−62224
blood, haematocrit dependence and interdonor difference compensation 79−62277
blood, rheological behaviour, viscoelastic model *(French)* 80−76779
blood, rheological parameters for viscosity, viscoelasticity and thixotropy 80−16963
blood, viscoelastic properties, transient flow obs. 80−97980
blood plasma, normal and haemophilic, coagulation kinetics study 80−67107
blood rheology, clinical changes in peripheral vascular disease and smokers 80−16965
blood rheology, erythrocyte rigidity effects on viscoelastic dilatancy 80−61610
body eigenfrequency determ., finite element method *(German)* 79−23270
bone, cortical, US velocity dispersion obs., 1 to 10 MHz 77−21583
bone dynamic mechanical props., postmortem transition 77−21554
bone from Cu deficient chicks, viscoelastic props. 79−79578
bone viscoelastic behaviour, anal. on basis of microstruct. 80−85429
bony tissue, compact, from human tibia, creep under tension 77−25487
brain injury, pulse loading effect 78−57029
brain tissue, human, nonlinear constitutive relations 78−80910
bronchial elasticity and air flow, mathematical anal. 80−45942
Brownian particles, rotating, angular velocity autocorrelation function rel. to viscoelastic effects 77−27932
bubble translational motion in a viscoelastic liquid, retarded motion approx. 80−83777
bubbles and drops coalescence rate, ambient liq. viscoelasticity effect 78−67248
buckling and stability of viscoelastic plate, convolution var. principle 77−35052
buckling of viscoelastic plates 78−13932
buried impulsive load, effect on viscoelastic layer on elastic half-space 80−28428
butadiene-styrene block copolymer, containing free polybutadiene mols., viscoelastic behaviour 77−56015
butadiene-styrene block copolymer, viscoelastic props. 79−8336
butadiene-styrene gum elastomers, compounds, viscoelastic props., stress relaxation meas. 77−7321
butanediol-1,3, viscoelastic props., digital correlation Brillouin scatt. 78−2865
butodiene-styrene copolymer, viscoelastic props., crosslinkage in presence of active silica *(Polish)* 78−79231
cantilever beam, stability on viscoelastic foundation with shear layer subjected to circulatory force 79−86374
capillary jets of elasticoviscous fluid, stability 79−90303
cardiac muscle, passive, viscoelastic theory and obs. 80−94273
Cauchy and periodic unilateral problems for ageing linear viscoelastic materials 78−30191
cell suspensions, stability to small disturbances in circular Couette flow 80−56099
cell wall, Acetabularia, deform. rel. to genetic and geometric factors 77−56348
cell wall deform. and morphogenesis, local control of viscoelastic deform., Acetabularia 77−56349
celluloid, nonlinear viscoelastic deform. under superimposed hydrostatic pressure 79−34116
cellulose acetate-dimethylphthalate gel, mech. props., substitution effect *(Russian)* 79−23291
cellulose esters, plasticiser effects on mech. and dielec. relax. 80−40047
cellulose nitrate, nonlinear viscoelastic deform., hydrostatic press. and third invariant of deviatoric stress tensor 80−93587
circular plates, thermoviscoelastic anal. of a thermorheologically simple material 80−10161
circular plates resting on viscoelastic half space, dynamic response 79−18801
circular rod, in-plane vibr. effects of shearing deform. and rotary inertia 77−84174
circular viscoelastic porous shell, dispersion of longitudinal waves *(Russian)* 78−42556
coating, free, of vert. surface, by viscoelastic (viscoplastic) fluid 78−42576
colloids, nonlinear rheological behaviour and shear dependent struct. 79−7358
column, eccentrical axial load and top-deflection, analytical relationship *(Italian)* 79−14273
complex dynamic moduli and loss angles 77−68451
complex moduli, error anal. using coated beam method 79−27565
complex moduli derived from vibrations of Timoshenko beam 80−38163
composite material, mechanical behaviour, book 80−94935
composite material, structural anisotropy in viscoelasticity 77−86073
viscoelasticity continued
composite material viscoelastic properties modelling 78−75082
composite materials, self-consistent estimates for viscoelastic creep 78−13921
composite media, macroscopic behaviour with dissipation *(French)* 79−21564
composite polymers, viscoelasticity theory, appl. 80−64397
composite semi-infinite rod, wave propagation 80−10180
composites, spatially reinforced, viscoelastic props. determ. using averaging methods 80−102973
compression struts, of nonlinear viscoelastic materal time dependent load bearing capability *(German)* 78−48474
concavity techniques, point mass impact on elastic, viscoelastic or nonlienar elastic rod 79−37172
cone and plate rheometer, press. distrib. in gap for viscoelastic fluid with high shear rate *(German)* 77−51143
conference, computational methods in nonlinear problems in mechanics and engineering, Austin, Texas, USA (March 1979) 80−51945
conformational entropy effects in viscoelastic flow, continuum description 78−1621
consolidating semi-space, axisymmetric punch problem with mixed boundary, permeability conditions 78−51087
consolidation theory, viscoelastic media, internal mobility effects, dual mechanics correlation 79−14280
constitutive equation derived from Lodges network theory 79−90207
constitutive equation for viscoelastic interface 78−84028
constrained viscoelastic damping composites, noise and vibration insulation 80−83743
contact between viscoelastic bodies 77−46944
continuous viscoelastic beam, dynamic response 78−9569
continuous viscoelastic structural members, transient dynamic response 80−64442
continuum model, allowing non-affine deform. 77−42793
contractile polymeric structures, deformative props., artificial muscles 77−25595
converging pipe flow, vel. vectors and radial stresses, rheological model and laser anemometry 79−60028
cortical bone, wet, non-linear constitutive eqn. of viscoelastic props. 80−30754
cortical bone, wet, torsional and biaxial viscoelastic props. obs. 80−30752
cortical bone, wet, viscoelastic props., relax. mechs. 80−30753
Cosserat continuum, thermomechanical behaviour 77−19539
Cosserat viscoelastic inversion problems, models *(German)* 77−84166
coupled dynamic problems of thermoviscoelasticity quasilinearisation method 77−72188
coupled thermoviscoelastic structures, sustained periodic vibrs., finite element anal. 79−7315
crack growth in viscoelastic medium *(Russian)* 78−18252
crack growth kinetics under cyclic loads in viscoelastic bodies *(Russian)* 80−87739
crack growth law derivation, linear viscoelastic solids, fracture process zone concept 80−92088
crack growth law using energy and COD fracture criteria 79−32378
crack growth prediction in nonhomogeneous viscoelastic media 78−75098
crack growth relations, for orthotropic, prestrained media 78−90772
crack propagation, adhesion *(French)* 77−89065
crack propagation in linear viscoelastic medium 80−53700
crack tip viscoelastic losses, detachment of glass sphere from viscoelastic mass *(French)* 78−42536
cracked linear bodies, stress and strain under tension and compression 77−7342
cracked linear viscoelastic solid, dynamic anal. by finite element method 80−53706
cracks in viscoelastic body, durability calcs. 80−79227
creep and relaxation phenomena for linear on non-linear bodies 77−876
creep generalisation for viscoelastic bodies with non-stationary loading 77−877
creep meas. of rotating disks 80−38360
creeping flow of viscoelastic fluid through tapered contraction 77−55050
cross-supported plates, vibrs. 77−62095
cyclic carbonates, supercooled liqs., dielec., acoustic, NMR, viscoelastic relax. props. 77−1609
cyclohexanal, liq., viscoelastic and structural relax., US rel. and absorption meas. 78−26634
cylinder, hollow, elastic coating, thermomech. responses 78−79230
cylinder, hollow, nonlinear viscoelastic material, dynamic pressure loading 80−38289
cylinder, optimal management of diffusion treatment rel. to conc. depend stresses 79−94510
cylinder, short, visioelastic, expt. and theoretical investigation of heat evolution in cyclic compression 78−13929
cylinder, viscoelastic, transverse vibrs. 77−19544
cylinder contact with visocelastic lubricant, friction 78−7056
cylinder oscillating in viscoelastic fluid, secondary flow 79−60037
cylindrical impact waves in inhomogeneous viscoelastic media 79−14295
cylindrical rod, dynamic torsion 77−3739
cylindrical shear wave propag., inhomogeneous viscoelastic solids 78−75090
cylindrical shell, arbitrary cross section, transient motion in acoustic medium 78−38244
cylindrical shell, viscoelastic, forced axisymmetric oscillations 77−50933
cylindrical shells, forced axisymmetric motions 77−89038
cylindrical shells of viscoelastic material, natural transverse vibrations 80−43660
cylindrical shells with moving loads, steady state forced response 79−27566
cylindrical viscoelastic waves, diffraction by circular obstacle, calc. *(Russian)* 77−54895
cylindrical wound shell with viscoelastic core in axial compression, optimisation 77−4821
damped cantilever beam, effect of boundary conditions 79−23245
deformation, numerical simulation of dynamic processes 79−46220
deformation and convected derivatives, quasilinear models 79−60013
deformation kinetics, Gibbs eqn. and nonequilibrium thermodynamic models *(Ukrainian)* 78−90720
deformation taking into account influence of accumulated defects 80−19252
deformation theory with account of thermodiffusion *(Ukrainian)* 78−67052

viscoelasticity continued
deformation wave processes, corrected nonlinear eqns., stresses and strains 80−102998
deformed sphere motion in viscoelastic fluid 79−81831
p-p′-dibutyl-azoxybenzene, DIBAB, light scatt. studies *(Dutch)* 80−33885
die swell problems, viscoelastic fluid flow, collocation and Galerkin finite element anal. 80−14751
N,N-diethylacrylamide, cross-linked copolymer, improved mech. props. 80−61091
differential eqn. method approximation, for solving dynamic viscoelastic problems 80−14585
diffusion in viscoelastic layer, mathematical analysis *(Russian)* 77 51539
dipolar dumbbells in a viscoelastic Oldroyd liquid, dilute soln., electric field effect on rheological behaviour 80−6009
direct solution method using Laplace transforms 79−17228
discontinuity propagation, non-homogeneous thermoviscoelastic media 80−102972
discontinuity surface, nonequilib. thermodynamics, appl. to n-component viscoelastic mixture 78−93638
dislocation-creep, minimisation of free energy due to viscoelastic strain and dislocations 77−24348
displacement vector growth estimates 79−27552
dissipation measures in viscoelastic media 78−42540
dissipative rubberlike material rod, nonisothermal nonlinear waves 79−86380
disturbances in viscoelastic medium due to impulsive forces on spherical cavity 78−67076
disturbances under transient tangential force and mag. field 80−92070
DNA, Tetrahymena, viscoelastic meas. 79−100570
dolomite, strain rate depend. meas. rel. to viscoelastic response 77−44977
double-T of nonlinear viscoelastic material, stability *(Russian)* 79−32290
drag on sphere accelerating rectilinearly in elastico-viscous fluid, Fourier transform technique 78−51145
drag reducing viscoelastic fluid, heat transfer to turbulent flow 77−84249
drag reduction of an oscillating flat plate with an interface film 80−10268
drop, deformable, motion in second-order fluid 79−64754
droplet break-up, in nonuniform shear flow 80−64588
duralumin, shock-compressed, compression and rarefaction waves obs., 150-250 kbar 77−77535
dynamic behaviour of a visco-elastic body with stripwise loading *(German)* 78−87281
dynamic response of a slab of elastic-viscoplastic material that exhibits induced plastic anisotropy 80−83737
dynamic response of viscoelastic halfspace, complex moduli concept 80−23902
dynamic shear response of viscoelastic fluid, Maxwell model 77−35106
dynamic simple shear expt., deviation by velocity gradient profile from gap loading and surface loading 77−72257
dynamic torsion and nonstationary wave propagation in viscoelastic cylinders *(Russian)* 79−50634
dynamic torsion of two-layer viscoelastic beam 77−7318
dynamical problems, approx. soln. of integral eqns. 80−10164
dynamics, linear, soln. by equiv. correspondence method 77−35058
Earth, free oscillations attenuation theory 80−21652
Earth, kinematic viscoelastic model of 1906 San Francisco earthquake 77−73671
Earth, viscoelastic model appl. to Earth tides theoretical study 80−67333
Earth crust, viscoelastic deform. by finite quasi-static sources 79−39686
Earth interior, pulse propag. in viscoelastic medium with freq. depend. Q 80−72438
Earth mantle, upper layer, heat convection rel. to viscoelasticity instability 77−41010
ebonite, viscoelastic, linearity conservation 80−108492
elastic adhesion problems, rel. to linear fracture mechanics *(French)* 80−14617
elastic circular plate with clamped edge on viscoelastic foundation with centre load 78−18176
elastic fluid, homogeneous and inhomogeneous stretching 79−86392
elastic plate, right angled isosceles triangle, on Pasternak-type viscoelastic foundation, deflection 78−75075
elastic waves in viscoplastic-elastic media under complex strain *(French)* 79−27570
elastic-viscoelastic correspondence principle for harmonic oscills., alternative representation 77−65710
elastic-viscoelastic-elastic beams, compressional damping in vibratory response 79−32323
elastic-viscoplastic structures, accommodation to periodic loading, stress and strain fields *(French)* 77−46928
elastic/viscoelastic bar interface, impact wave behaviour 78−26075
elastic/viscoplastic media, constitutive eqn. covering wide range of strain rates *(Japanese)* 80−79862
elastic/viscoplastic plate, combined longitudinal/torsional stress wave propag. *(Japanese)* 78−38227
elasticity parameters of viscoelastic materials, true moduli determ. using superposition method 79−18744
elastico-viscous liquid, atomisation, drop size rel. to elasticity 77−35220
elastico-viscous liquid flow in axisymmetric pipe of slowly varying cross-section 80−83774
elastodynamic stress states rel. to photoviscoelastic model *(Russian)* 78−75080
elastohydrodynamic lubrication, non-Newtonian effects of volume relaxation 80−103009
elastohydrodynamic lubrication at high press., non-Newtonian behaviour 79−46350
elastohydrodynamic traction, non-Newtonian thermo-viscoelastic, from combined slip and spin 80−103043
elastomer, relaxation time spectra calc. from stress relax. data *(Russian)* 77−44288
elastomeric network, finite linear viscoelastic theory, time-depend. deform. behaviour 80−38292
elastomers, viscous flow, strength characteristics, activation energy, fracture behaviour *(German)* 79−57105
electrolyte solutions, fluctuations rel. to viscoelastic props. spatial dispersion 77−15497
viscoelasticity continued
electrolyte solutions in glycerol, investigation by US shear strains 80−88266
emulsion, dilute, straining motion, effect of inertia on dynamic viscosity 80−87797
emulsions, concentrated, rheological props. 80−99981
entangled monodisperse polymers kinetic network model for nonlinear viscoelastic flow props. 80−28538
entangled polymers, viscoelastic props., transient network model 78−13918
epichlorohydrin/bisphenol A epoxy polymer concrete, viscoelastic props. 80−45340
epithelium of small intestine, mech. props. of intercellular contacts 78−53351
epoxy, curing composition, viscoelasticity in critical region 77−62228
epoxy resin, Cl-containing, relation between static and dynamic deform. characts. 80−3137
epoxy resin, heat generated by fatigue *(Spanish)* 80−11736
epoxy resin, meas. of glass transition temp., linear viscoelasticity 80−29157
epoxy resin, time-temp. superposition of creep data, linear viscoelastic props. 80−30045
epoxy resin composites, cooldown residual thermal stresses, viscoelastic response 80−60941
epoxy resin hardened with maleic anhydride and PMMA, viscoelastic props. 77−25089
epoxy resin parabolic shells, exam. of viscoelastic creep 79−43307
equation of state for class of viscoelastic deforms. 78−26060
equations, stability of numerical soln. 78−16647
erythrocyte membrane viscoelastic props., area and vol. of cells entering micropipette 77−29114
ethanol, aq. soln., conc. fluctuations, shear and longit. relax., Brillouin scatt. and pulse techniques 78−71792
ethyl acrylate ionomers, stress relax. 80−104200
ethylene-propylene copolymers, mech., photoelastic props. rel. to chain microstruct. 77−48468
extended plane fluid sheet, swelling finite element anal. 79−37277
extruded polymer soln. through capillary, flow instability and electrostatic effects 79−60035
failure and instability in tension 80−87720
fatty acid monolayers, capillary waves, photon correlation spectroscopy, viscoelastic props. 79−75608
fibre reinforced composite, fibre geometry and filler vol. influence on fracture stresses 80−45397
fibre reinforced composites, viscoelastic thermal shrinkage stresses 80−38287
fibre reinforced ionomer composites, fatigue strength, dynamic viscoelastic props. and fracture surface exam. *(Japanese)* 78−92339
fibre reinforced materials, therm. stresses in unit cell 80−10160
fibre reinforced plastics, creep damage *(Japanese)* 77−32702
fibre reinforced silicone rubber composites, interfacial slip and damping 79−5010
fibre-reinforced composites, wave propag. 79−76992
fibrous composite, residual stress form. during hardening 78−1575
filled polymer mechanical properties, particle shape effect, review 80−100864
filled system, vibrational thinning, visoelasticity and strength 77−8795
first normal stress difference prediction and dynamic moduli from steady flow viscosity 77−75868
flexible string under transverse impact, dynamic deform. and possible unwinding from drum *(Russian)* 78−22279
flexible string under transverse impact loading, eqns. of motion *(Russian)* 78−22280
flexible viscoelastic cylindrical shell, dynamic stability 78−5678
floating ice plate, time depend. deflections, linear viscoelasticity theory 77−17107
flow, cooperative phenomenon, theory 80−69878
flow, of 2nd order fluid down inclined plane, finite amplitude long wave stability 79−37365
flow, pulsatile, of viscoelastic liq. in elliptic cross-section channel 79−7392
flow, steady, of viscoelastic liq. about rot. disc 79−32586
flow along conical rotor, of viscoelastic fluid film 78−1697
flow between rotating disc and stationary porous disc 77−54964
flow past an oscillating plate in a viscoelastic fluid 79−27670
flowing viscoelastic fluid, bubble and solid particle separation through apertures *(German)* 79−37389
fluid, free surface problems, domain perturbations of rest state 77−68549
fluid, laminar flow, combined generalised measure approach, pseudoplasticity 80−64586
fluid, motion of rigid particles 80−103044
fluid, oscillatory flow past infinite porous plate with variable suction 78−38373
fluid, reduction of turbulent friction, rheological model 79−86408
fluid, stability of steady shearing flows, energy method and parabolic maximum principle 80−74926
fluid, steady shear viscosity meas. using falling ball viscometer 79−94565
fluid, work estimate, convergence to equilib. 79−64718
fluid filled viscoelastic tube, nonlinear waves, mathematical anal. 79−55395
fluid flow, eqns. of state and motion, direct numerical soln. 79−60021
fluid flow, mixed finite element anal. 77−39315
fluid flow between rotating coaxial disks, numerical anal. 79−77041
fluid flow in fixed geometry, collocation and Galerkin finite element methods 80−14750
fluid flow past sphere, anomalous separation, wake formation 77−51091
fluid flow past sphere, creeping and boundary layer flows, drag coeff. 77−51090
fluid layer, thermal instability, lift and thermocapillary forces effect 79−86434
fluid lubrication, viscoelastic, slider-bearing config., non-Newtonian normal stresses 80−69753
fluid systems, local equilib., discontinuity surface 79−84960
fluid theories based on left Cauchy-Green tensor history 80−4534
fluid theory, entropy effects 77−14971
fluid unsteady flow through tubes 80−14753
fluid-like viscoelastic liquid, coupling of orientational and translational motions, LF depolarised (VH) scatt. 77−7642
fluid-saturated cracked solids, viscoelastic props. 78−36154

viscoelasticity continued
fluids, axial compliance reduction, in a R-17 Weissenberg rheogoniometer 80−106859
fluids, die-swell theory, analytical results 77−58624
fluids, heat transfer at low Deborah numbers, rheological effects 80−19445
fluids, Lodge-Meissner step-shear relation 78−90809
fluids, shear-thinning, elastic, Carreau viscosity eqn., creeping motion of spheres 80−87753
fluids, third grade, viscometric flows 80−69883
fluoropropylmethylsiloxane fluids, viscoelastic relaxation 79−14361
forced, geometrically nonlinear vibrations of viscoelastic body 77−3762
forced vibrs. shell, viscoelastically damped, filled with pressurised liq., forced vibrs. 78−9584
foundation dynamic interaction with viscoelastic half-space *(German)* 78−79228
fractional calculus for formulation of models, appl. 79−98627
fracture mechanics 78−67145
free vibrations of viscoelastic orthotropic rectangular plates 79−41597
gas bubble oscills. in viscoelastic liq. 77−80202
gel, appl. to study of viscoelastic props. at small constant shear stresses 79−54123
gel, cylindrical, in silicone oil, method for viscoelastic consts. meas., longit. vibrs. 77−73619
gelatin gels, in water and glycerol/water mixtures, dynamic viscoelastic props. 80−64508
generalised thermorheologically simple porous materials, thermomechanical theory of viscoelasticity 80−33479
geometrically nonlinear, variational formulation 77−880
glass, internal friction in region of transition to viscous-flow state 79−66101
glass, relax. of props. during isothermal swell period, method of calc. 78−67654
glass, tempering, stress and structural relaxation 78−64574
glass, viscous deformation during heating and cooling 80−89314
glass and glass-forming liq., viscoelastic properties, comparison with Lennard-Jones model 80−84983
glass ball adherence to viscoelastic $^{1}/_{2}$-space, coming-on expts. *(French)* 79−1113
glass beads in polystyrene soln., suspension, time depend. viscoelastic behaviour 80−99982
glass fibre reinforced polycaproamide, viscoelastic, linearity conservation 80−108492
glass punch impact on viscoelastic solid *(French)* 78−42535
glass-transition temp., thermodynamic criterion 77−59783
glasses, commercial, viscosity and stress relax. in glass transition region 80−93589
glycerol, liq. and glass, thermal diffusivity meas. 79−82394
gravitational wave effect on EM radiation, viscoelastic media 78−54267
Green-Rivlin representation, accuracy 79−18750
half-space, analytic solns. to boundary-value problems 77−75816
half-space, dynamic indentation and impact by axisymmetric rigid body, iterative method anal. 80−14626
hard sphere fluid, elastic modulus and viscosity coeff. 77−30086
head injury model with viscoelastic brain tissue, mech. response 78−69117
head viscoelastic model, impact response 78−40234
heart muscle preparations, isolated, viscoelastic props., math. model *(German)* 79−53167
heat instability in thermoviscoelastic coupled dynamic problems *(Russian)* 79−10489
hereditary operators, methods of extending class 78−81841
heterogeneous or anisotropic bodies, error estimation in viscoelastic problem soln., using method of approx. 80−19253
high mol. wt. polymer melts, viscoelastic props., relaxation and retardation spectra 80−19310
hollow viscoelastic cylinder, plane nonaxisymmetric deform., dynamic behaviour 79−98635
homogeneous isotropic viscoelastic medium, wave propagation eqns. with time lag 79−35573
homogeneous viscoelastic mixtures, speed of sound 80−33272
HTGR, annular fuel rod, contact viscoelastic stress anal. *(Japanese)* 78−54817
hydrodynamic stability of structurally viscous medium, effect of elastic factor 80−19303
hydrodynamics, generalised, extension to molecular dimensions 79−25864
2-hydroxyethyl methacrylate-methacrylonitrile or acrylonitrile copolymer network, mech. response 79−57031
hysteretic friction in small velocity approx., linear viscoelasticity eqns. 79−37252
ice, floating sheet, viscoelastic response under prolonged loading 78−51093
ice, static loading expt., viscoelastic behaviour *(Japanese)* 77−81914
Il'yushin kernels, analytical representation 78−67055
impact absorber with linear spring and quadratic law damper 77−7332
impulsive response to constraints and finite one-dimens. viscoelastic deform. *(French)* 78−51092
incompressible liquid oscills. in variable cross section viscoelastic tube due to pulsating press. 80−31519
incompressible simple fluid with fading memory, stability 80−43741
incompressible two dimensional slow flow, finite deform of viscous ellipsoidal inhomogeneity 77−51013
incompressible viscoelastic fluid, accel. influence on shear initiation 77−54943
incremental formulation in nonlinear mechanics, large strain elasto-plasticity 78−77692
inelastic rate problems, improved soln. methods 79−18733
inelastic solids, anelastic relaxation anal., extended to creep at high temp., appl. to internal friction *(French)* 78−63806
inertial effects in rheometrical flow systems, orthogonal rheometer theory 77−51016
infinite power law viscoelastic body, crack propag. by rigid wedge, stress intensity 80−64476
infinite viscoelastic liquid, unsteady slow flow due to rot. sphere 78−75112
information theory approach, stress predictions from available strain history 77−57191
inhomogeneous anisotropic linear thermoviscoelastic medium, asymptotic stability proof 79−21554
inhomogeneous bodies, deformation under quasistatic loading 80−14587

viscoelasticity continued
inhomogeneous flows of non-Newtonian fluids: generation of spatial concentration gradients, stress and diffusion effects 79−60032
inhomogeneous viscoelastic body, effective props. 80−19256
inhomogeneous viscoelastic Voigt-Kelvin rod, stress propag. and harmonic vibrs. 79−94543
inhomogeneous viscoelastoplastic media, wave propagation *(Russian)* 79−32337
instantaneous moduli, determ. from long-term static test results 80−38286
integro-differential eqns. with small parameter, solns. *(Russian)* 78−62078
integro-differential viscoelasticity dynamics 80−14586
integrodifferential eqn., abstract, existence and asymptotic stability of solns. 79−12608
integrodifferential eqn. system, Cauchy problem soln. 77−50931
interfacial stresses in viscoelastic adhesive-layers due to moisture sorption 79−90145
ionene polymers, counterions and absorbed water influence on mech. relax. 77−40430
ionene polymers, ion conc. effect on mech. relax. 77−44284
isotropic linear material characteristics, finite element method *(German)* 78−32681
isotropic linear viscoelastic material, connection between shape and volume change *(German)* 79−27531
isotropic solid, viscoelastic characterisation using harmonic dispersion of longit. reson. 79−10538
IUPACA polyethylene melt, elongational behaviour, strain rate, stress depend. 79−32429
knee semilunar cartilage, viscoelastic props. 79−70568
laminar flows of viscoelastic fluids in concentric annuli with axially moving boundaries 78−79295
laminar shells, with viscoelastic binder, stability 80−10165
laminar viscoelastic boundary layers, role of fluid relaxation time 79−81829
laminate, residual stress form. during hardening 78−1575
laminated viscoelastic composite, wave propag., dispersion relations, mode shapes, variational methods 78−18215
large nonisothermic elastoplastic and elastic-viscoplastic deformations 77−75817
layered composites, wave propag., dispersion and dissipation effects 80−102982
layered medium, transient wave propagation normal to layering 80−53676
LDPE melt, nonlinear shear creep and constrained elastic recovery 78−87318
ligament, canine anterior cruciate constitutive nonlinear viscoelastic behaviour eqn. 79−96592
linear, Boltzmann and Maxwell theories, review 77−71216
linear, exterior problem 78−71283
linear, finite element method variant 80−69692
linear, improved estimates for least work 79−64535
linear, isotropic integro-differential models *(French)* 79−80443
linear, scalar and vector-valued optimisation 78−5665
linear, theory 79−68602
linear Cauchy and Piola-Kirchhoff constitutive theories for stress in solids 79−37173
linear dynamic theory, use of modified Gurtin's variational principles 77−46934
linear dynamic viscoelast., stability conditions for solns. 79−30240
linear one-dimensional viscoelastic solid, flow and relaxation distribution 78−36833
linear solid, crack propag. 79−23225
linear solids, stress/strain tensor eqns. *(French)* 80−53656
linear theory solns. by model γ-irradiation, polarisation-optical method 80−33485
linear tube, axially symmetric wave motion of viscous liquid, haemodynamics model 77−73537
linear viscoelastic behaviour simulation using simple electrical device 79−57179
linear viscoelastic bodies, approx. anal. using Legendre polynomials, finite element soln. *(Japanese)* 78−83266
linear viscoelastic body, opening and closing of growing crack under alternating tensile and compressive loads 79−23282
linear viscoelastic fluids, Stokes' problems 78−51142
linear viscoelastic material, crack propagation due to increasing applied stress 78−18246
linear viscoelastic material vibrations, integro-differential eqn., two-scales method soln. 79−72839
linear viscoelastic materials of the integro-differential type 79−81741
linear viscoelastic media, dynamic problems, approx. soln. 80−69679
linear viscoelastic media, generalised Maxwell and Voigt models *(Russian)* 79−94513
linear viscoelastic media with concealed parameters, free energy concept *(French)* 77−42754
linear viscoelastic systems, constant strain rate and stress relax. obs. 78−90727
linear viscoelastic waves, theory of diffraction *(Russian)* 78−65787
linear viscoelasticity, positivity constraints and approx. methods 79−92944
linearised theory, variational principles *(Russian)* 78−87279
linearised thermoviscoelasticity with high temperature variations and related periodic problems 78−89343
liquid, flow through porous channel, free and forced convection effects 80−53861
liquid, heat transfer in rot. flow, suction and injection effects 80−33596
liquid, horizontal layer, thermal instability 77−68545
liquid, second normal stresses meas. using rot. sphere viscometer 78−79391
liquid, viscoelastic, boundary-layer flow past symmetric wedge or right circular cone 80−64513
liquid continuous flow squeeze film, load-bearing capacity 78−87306
liquid film flow in rot. mixer 79−90291
liquid flow in viscoelastic tube, wave propag. 78−9714
liquid in corner, flow under pressure *(German)* 78−94772
liquid injected into Newtonian turbulent pipe flow, diffusion and drag reduction *(German)* 79−77251
liquid layer, electrohydrodynamic instability 80−14832
liquid props. review, viscoelasticity and lubrication 79−7356
liquids, prop. determ. method between 4 and 160 kHz *(Dutch)* 79−77040

viscoelasticity continued
liquids, relation between viscoelasticity and shear-thinning behaviour 80−19307
liquids, structural relax., fast and slow relax. limits 79−47465
liquids, viscoelastic props. meas. using torsion resonator, 20-1200 KHz *(Russian)* 80−52196
low-frequency fluctuation, dissipation and relaxation properties 80−39661
LPDE melt, tensile stress overshoot in uniaxial extension, single integral constitutive eqn. 80−1507
lubricants in human joints 79−57699
magneto-viscoelastic wave propag. in Voigt type material 78−31100
magnetostrictive viscoelastic cylinder, nonhomogeneous, torsional deformation 79−37169
magnetothermoviscoelastic waves reflection at semi-infinite solid boundary 80−48633
magnetoviscoelastic initially-stressed conducting medium, plane Lamb's problem 79−37183
magnetoviscoelastic solids under initial stress, surface waves 79−84140
maltrose syrup, separation of elastic and shear thinning effects in capillary rheometer 78−42691
mammalian DNA, rat obs. 80−8078
materials with memory, intrinsic physical limits, viscoelasticity, viscoplasticity, hydromorphic materials 79−64523
materials with memory, nonlinear integral representations 77−42732
matrix operators for viscoelasticity with ageing *(French)* 79−18729
matter, cosmological evolution, causal thermodynamics *(Russian)* 79−101232
Maxwell fluids, immiscible, hydrodynamic flow through non-conducting rectangular channel 80−100038
MBBA, shear modulus and viscosity relax. near isotropic-nematic phase transition *(Russian)* 77−39543
measurement, mech. drive tester *(Japanese)* 79−34232
mechanics of growing materials 79−18736
media in plane stress and strain, local memory system qualitative props. 77−11142
medial collateral ligament substitute specification and design 78−36060
membrane, circular, nonlinear viscoelastic material 80−64380
membranes, nonlinear viscoelastic, axisymm. deform. 78−90808
metals, continuum props. of constitutive relationships 77−35053
metals in nuclear reactors, thermo-elasto-visco-plasticity and neutron irradiation 77−3111
methylstyrene rubber, relaxation time spectra calc. from stress relax. data *(Russian)* 77−44288
micropolar fluid, second order, fund. and constitutive eqns., thermodynamics and flow 78−20970
micropolar viscoelastic fluid motions, universal stability 77−11165
micropolar viscoelastic materials with stretch, memory-dependent, linear theory 78−73855
mineral oils, viscoelastic behaviour at high press., relax. spectrum 77−65727
mixed protein phospholipid films, viscoelastic behaviour and Marangoni effect 80−3602
monolayer, viscoelastic, of apoprotein, dynamic surface potentials 80−3603
moving rigid punch on unlubricated viscoelastic half plane 79−64598
multilayer plates, viscoelastic, equations of forced vibrs. 78−67084
multiple filament yarn, finite extension, slender curved rods theory 78−75076
multiple surface waves on viscoelastic half-space 78−79254
muscle, elastic and viscous props. of resting frog skeletal muscle 77−44700
muscle, skeletal, deriving viscoelastic modulus from transient pulse propag. 78−77077
muscle, skeletal, dynamic behaviour modelled as unidimens. viscoelastic medium 77−25484
muscle, three-element model with viscoelastic passive elements 77−32930
muscle viscoelastic props. determ., appl. of forced longit.-vibr. of elastic rod on viscoelastic half-space 78−44538
NBS polystyrene, memory-function determ., relax. tests 78−1619
nematic liquid crystal, viscoelastic properties, spectral noise intensity of scattered laser light obs. 79−23522
nematic liquid crystals, Rayleigh scatt. 77−39538
non-ageing materials, quasi-constant operators in viscoelasticity theory *(Russian)* 80−53650
non-homogeneous, Lagrange equations and Galerkin method, boundary value problems 80−53654
non-linear model, constitutive equation testing with free. vol. relax. spectrum 80−6011
non-linear viscoelastic behaviour, numerical anal. 78−59318
non-Newtonian fluid, viscoelastic boundary-layer flow past a parabola and a paraboloid 80−83817
non-Newtonian liquid, convective stability, energy method 80−38455
non-Newtonian liquids, resist. to tensile stress 80−1505
noncrystalline solids, thermally stimulated creep method for mol. motions investig. 78−22787
nonhomogeneous viscoelastic media, propag. of initially plane waves 77−11145
nonisothermal elastic-plastic and elastic-viscoplastic deforms., stress/strain relations 78−22276
nonlinear, estimate for work 78−55572
nonlinear, one-dimens. model 77−67290
nonlinear, stress relaxation, Volterra integral equation, numerical analysis 80−53646
nonlinear, variational formulations of boundary problems *(Russian)* 79−18749
nonlinear, variational principles for isothermal problems *(Russian)* 78−28950
nonlinear behaviour in 1- and 2-dimens., elastoplastic hysteresis, flow and relaxation *(French)* 79−46229
nonlinear deform. wave propagation in dissipative medium, interaction and reverse problems 78−53
nonlinear elastic laminated composite, wave propag., geometrical acoustics anal. 77−42774
nonlinear functional relations and superposition principles 80−42065
nonlinear strain waves in viscoelastic rod *(Russian)* 80−1460
nonlinear thermoviscoelasticity theory for generalised thermorheologically simple material *(Russian)* 78−57785
nonlinear viscoelastic fluid, kinematical flow anal. *(Polish)* 77−55049
nonlinear viscoelastic fluid, steady shearing flow instability 79−32461
nonlinear viscoelastic materials, creep and relax., book 77−11141

viscoelasticity continued
nonlinear viscoelastic materials, stress formulation relations *(German)* 79−76987
nonlinear viscoelastic materials, thermodynamics and fracture, integral expansions 77−3736
nonlinear viscoelastic media, 1-dimens. deformation waves 79−50645
nonlinear viscoelastic media constitutive eqn. 78−81839
nonlinear viscoelastic rods, shock wave front definition *(Russian)* 79−50635
nonlinear viscoelastic spherical membrane, quasistatic inflation, bifurcation of response 78−46897
nonlinear viscoelastic wave of very small amplitude *(French)* 80−8803
nonlinear viscoelastic wave propag., effect of time dependent compressibility 77−39244
nonlinear viscoelasticity, a method of successive approxs., based on nonlinear correspondence principal 80−5953
nonlinear viscoelasticity, bifurcation and uniqueness, Hadamard stability 80−43621
nonlinear viscoelasticity, convergence of successive approx. method with integral transforms 80−19255
nonlinear viscoelasticity, uniqueness theorem 77−82392
nonlinear viscoelasticity problem with geometric nonlinearity, variation principle 77−62176
nonlinearly viscoelastic bodies one dimensional dynamic stability 79−32282
nonviscometric flow, drop suspension model, deformation and vorticity 79−60022
novel Weissenberg effects in liqs. set in motion by rot. rod 77−62225
numerical solution of viscoelasticity eqns., methods 77−89042
nylon 6 fibres, dynamic mech. props., interpretive nonlinear viscoelasticity 79−4994
nylon 6-Li halide mixtures, viscoelastic behaviour, stress relaxation 80−58995
nylon-6, viscoelastic props., meas. with modified torsion pendulum *(Spanish)* 77−31264
octyloxycyanobiphenyl, smectic-A phase, dislocation effects on viscoelastic props. 77−84633
oligobutenes, anomalous behaviour of viscoelastic props. 77−63704
one-dimensional linear viscoelastic solids, Burger and generalised models in K'_+ algebra 79−81740
optimal strain paths in linear viscoelasticity 80−5956
orientable polymer fluid, Ericksen's anisotropic fluids theory extension 80−79359
orthogonal fibre reinforced viscoelastic composites 78−42558
oscillating cup expt., shear elasticity in liqs. digital computer simulation 77−72190
oscillating pipe, effect on flow rate 79−60031
oscillatory tube flows of viscoelastic fluids 79−77252
parametric vibrations of elastoviscous rod 77−3763
pathological synovial fluids, viscoelastic props. at different shear rates 79−32430
pathological synovial fluids, viscoelastic studies *(German)* 79−79585
penny-shaped crack in infinite medium, stress field anal. 77−31254
perfluorinated polymer, Krytox 143-AB, viscous, viscoelastic and dielectric properties 80−70440
periodically layered medium, wave propag. normal to layering, viscoelastic analogy 80−48636
perturbation of front of flat plastic wave 79−5980
PET fibre, aminolyzed, dynamic viscoelasticity and thermal behaviour *(Japanese)* 79−38880
photoviscoelastic data, two procedures for recording and analysing on a μs time scale 79−37188
pitch and coke-pitch disperse system 80−1500
plane circular shearing, incompressible fluids and solids 77−75822
plane interface between two viscoelastic superposed cond. fluids, instability in mag. field 80−1694
plane punch on viscoelastic half-plane, hysteretic friction 77−68450
plane shear waves in viscoelastic fluids as motions with proportional stretch history 79−64613
plane squeeze-film flows, in convected coords. 78−90940
plane transient wave propag. in viscoelastic layer, interaction of deformation fields with temp. *(Ukrainian)* 79−30259
plane waves in electrically conducting and magnetizable viscoelastic isotropic solids subjected to a uniform magnetic field 79−28580
plant cell walls, viscoelastic props., hysteresis loop in the stress-strain curve 79−25009
plant cell walls, viscoelastic props., mathematical formulation for stress relax. 79−25008
plant cell walls, viscoelastic props., pre-extension rate effect on stress relax 79−29542
plant cell walls, viscoelastic props. 80−67106
plastic, static relaxation behaviour, test rig design *(German)* 79−39081
plastics, fatigue fracture props. correl. with viscoelastic damping 78−52993
plastics, nonlinear viscoelastic anisotropic, creep 80−35249
plastics, viscoelastic, fatigue testing, using hollow cylindrical specimens *(German)* 78−44292
plastics reinforcement theory, functional model *(German)* 77−58564
plate, guided harmonic waves 80−79194
plate, rectangular, variable thickness, stability and vibr. anal., finite element method 77−54918
plate, round, viscoelastic, deformation and creep *(Russian)* 79−32291
plate, star shaped, soln. of temp. problem by photo-thermo-viscoelastic method *(Russian)* 79−86343
plate, viscoelastic, free and forced vibrs., transient response 79−32360
plate, viscoelastic, heated, bending, Kelvin Voigt model 80−106731
plate, viscoelastic, prestressed, on nonlinear dissipative foundation, travelling load soln. 78−63331
plate of arbitrary shape, crack growth kinetics *(Ukrainian)* 77−68523
plates and shells, dynamic plastic anal. using stress resultant finite element formulation 79−37191
plates and shells, viscoelastic, flexible, thermomech. behaviour during cyclic loading 80−33478
plates at elevated temp., vibr. and buckling, fundamental freq. 80−23935
PMMA, biaxially oriented, shrinking kinetics in transform. range 78−27588
PMMA, craze zones at crack tips, validity of Dugdale model 80−108534
PMMA, laser damage mechanism rel. to viscoelastic props. 80−55233
PMMA, nonlinear viscoelastic behaviour in torsion 79−61640

viscoelasticity continued
PMMA, partial draining of low-molecular weight polymers with flexible chains 80−23592
PMMA, strain rate effects on viscoelastic crack bifurcation 78−35473
PMMA, viscoelastic props. in plastic zone, cooling rate effect 80−40418
PMMA, visoelastic props., γ-irrad. influence *(Russian)* 78−88492
PMMA and PPMA, glassy state, cyclic loading effects on internal damping, shear modulus, heat capacity and density 77−43275
PMMA fracture toughness, flame-retardant additive effect obs. 80−16470
Poiseuille flow of viscoelastic fluid between eccentric cylinders 80−1652
poly(ethylene oxide), partial draining of low-molecular weight polymers with flexible chains 80−23592
poly(spiro[2,4]hepta-4,6-diene) molecular characterisation, glassy state props. 80−64928
poly-2,6-dimethyl-p-phenylene oxide solns., US and viscoelastic relax., conformational changes 77−31033
poly-α-methyl styrene, viscoelastic relaxation and methyl group tunnelling 79−57038
poly-γ-benzyl-L-glutamate, lyotropic liq. cryst., trifluoroacetic acid effect on viscoelasticity, susceptibility 77−84644
poly-n-benzamide, mols. in soln., dynamic birefringence and rigidity *(Russian)* 77−32349
polyacrylamide, aq. soln. viscoelastic effect in flow through porous media 79−94684
polyacrylamide, very dil. drag reducing soln., nonlinear viscoelastic props. 79−7355
polyacrylamide gel, audiofrequency very slow propagating mode 79−74429
polyacrylamide gel structure inhomogeneity from permeability and viscoelasticity 77−89384
polyacrylamide solns., anomalous effect in first normal stress difference meas. 77−80130
polyacrylamide-maltose syrup soln., meas. of viscoelastic flow props. 78−1622
polyacrylonitrile-dimethylformamide soln., viscoelasticity and shear modulus meas. *(German)* 80−38374
polyalkaneimide, mech. and thermophys. props. at liq. He temps. 80−3117
polyamide, viscoelastic, linearity conservation 80−108492
polyamide, viscoelastic behaviour determ. from reln. between creep and relaxation *(German)* 77−62174
polyamide 6, alkaline, viscoelastic meas. *(German)* 77−84204
polyamide-polyoxirane copolymers, mechanical properties evaluated 80−11700
polyamide-polyurethane copolymer dispersions, structurisation and relax. props., coating from props. 80−76559
1,2-polybutadiene, crosslinked in states of strain, entanglement networks, swelling anisotropy obs. 80−79666
1,2-polybutadiene, dynamic viscoelastic props. in curing process 80−76298
cis-1,4polybutadiene, lightly crosslinked, isothermal and nonisothermal creep 77−25106
polybutadiene, linear and star branched, rheology 80−23977
cis-1,4-polybutadiene, vulcanised composite system, viscoelasticity 77−75823
polybutadiene blend, viscoelasticity using Rheovibron, Massa correction for loss tangent meas. 78−83349
polycarbonate, glassy state, rel. between thermal pre-treatment and viscoelastic behaviour 79−79038
polycarbonate, secondary flow and stress birefringence patterns in pressure hole 80−64590
polycarbonate, viscoelastic ductile, delayed yielding of plane stress viscoelastic Dugdale model 78−27569
polycarbonate, viscoelastic props. in plastic zone, cooling rate effect 80−40418
polycrystalline materials, effect of grain boundary sliding on anelasticity 80−96592
polycrystalline materials, high temp. creep, role of grain boundary sliding 80−34128
polydecamethylene-oxide, dynamic mechanical measurements using a dynamic viscoelastometer *(Spanish)* 79−61636
polydimethylsiloxane chains, end-linked, swollen model networks, stress/strain isotherms and elastic modulus 80−79668
polydimethylsiloxne, end-linked chains, viscoelastic losses 78−46898
polydisperse polymers, viscoelasticity of melts 78−67160
polyester, unsat., copolymers, crosslinking effect on viscoelastic props., free torsion oscill. study *(Russian)* 79−34093
polyester model material, strain rate effect 79−83245
polyester-polyurethane semi-interpenetrating networks, mech. props., morphology 80−45362
polyesters, linear aliphatic, chem. struct. rel. to viscoelastic props. 79−41977
polyether ester-PVC blends, annealed, dynamic mechanical and sonic velocity behaviour 80−25740
polyethylene, effect of morphology on viscoelastic props. *(Polish)* 79−51008
polyethylene, expanded, dynamic model rel. to drop impact 78−7160
polyethylene, fatigue, fractographic study 80−30101
polyethylene, fatigue crack growth charact. 80−30100
polyethylene, high density, inorganic filled, calendered sheet, crystallisation in capillary viscometer *(Japanese)* 77−70112
polyethylene, high mol. wt., inorganic filler, calendered sheet, melt, flow props. *(Japanese)* 77−70111
polyethylene, linear, cold-deformed, texture and molecular chain mobility 78−19805
polyethylene, low density, linear viscoelasticity, relaxation func. determ. 79−7359
polyethylene, low density, melt elongation, stress and recovery maxima 79−90209
polyethylene, low density, nonlinear viscoelastic model, creep and recoil rates 77−42794
polyethylene, low density, rheology and molecular struct. effect on viscoelasticity 77−62227
polyethylene, melt, low density, filler effect on viscosity and viscoelasticity 77−68546
polyethylene, melts, stratified two-phase flow, interface deform. 77−11158
polyethylene, partial draining of low-molecular weight polymers with flexible chains 80−23592
viscoelasticity continued
polyethylene, phosphonate derivatives, dynamic mech. behaviour 79−15713
polyethylene melt, low density, filler effect on viscosity and viscoelasticity 78−46919
polyethylene melt, nonlinear shear behaviour, strain-dependent memory function 78−67161
polyethylene melt, rheology and molecular struct., relaxation spectra, charact. relaxation time 77−72255
polyethylene melt, viscoelastic property measurement using improved design rheometer 79−37276
polyethylene melts, low-density, viscosity and viscoelasticity, filler effect 80−10222
polyethylene oxide, aq. soln., mech. props. in parallel superposed flows, geometric effects 80−19448
polyethylene oxide, aq. soln., nonlinear dynamic viscoelasticity 79−94576
polyethylene oxide, dil. aqueous solns., dynamical shear characts. *(Russian)* 79−86393
polyethylene oxide aqueous solns., spectroscopic obs. of structural variability WRT turbulent resistance reduction 77−7356
polyethylene oxide melts, viscoelasticity meas. 78−87324
polyethylene terephthalate, preoriented sheet, plastic deform., anisotropic behaviour 79−8335
polyethylene terephthalate, thermally stimulated creep method for mol. motions investig. 78−22787
polyethylenes, molten, Weissenberg effect 78−9616
polyhydroxyethyl methacrylate swollen network filled with polyhydroxyethyl methacrylate, viscoelastic and ultimate behaviour in rubbery region 79−83247
polyisobutylene, Aerosil-filled, solution, periodic and unidirectional deform. effects 77−42791
polyisobutylene, memory-function determ., relax. tests 78−1619
polyisobutylene, relax. of birefringence and stress, extension ratio depend. 77−43962
polyisobutylene, RQP method of inferring a mechanical relaxation spectrum 79−37195
polyisobutylene melt, thermodynamic constitutive eqns., adiabatic deform. expts. 78−1620
polyisobutylene soln., start-up tests, relaxation meas. of shear and normal stress *(German)* 78−67166
polyisobutylene solns. in thermodynamically different solvents, conc. dependence of viscoelastic props. *(German)* 77−46980
polyisobutylene solution in cetane, hyperelasticity, filler effect 80−10223
polyisoprene, blend, viscoelasticity using Rheovibron, Massa correction for loss tangent meas. 78−83349
polymer, amorphous, molecular origin of relaxations 78−26058
polymer, breakup of anisometric drops on mixing 77−40578
polymer, chain dynamics, hydrodynamic boundary conditions 77−11155
polymer, dynamic mech. anal. 78−60697
polymer, fatigue, fractographic study 80−30101
polymer, fatigue crack growth charact. 80−30100
polymer, filled, rheology, steady state shear flow and periodic deform., relaxation time, spectra, viscosity 79−96066
polymer, glass transition due to plastic deform., high-molecular linear polymer of narrow molecular mass distrib. 79−96065
polymer, glassy, tensile stress/strain curve description 78−67158
polymer, high-modulus, behaviour in solid state, nonlinear irreversible thermodynamics approach 80−44154
polymer, linear viscoelastic model and dynamic behaviour, elec. transmission line representation *(Spanish)* 77−72185
polymer, linear viscoleastic creep under arbitrary temp. variations 79−95075
polymer, long-term durability prediction methods 79−20320
polymer, melt and solution, molecular weight distribution correlations 77−84207
polymer, microrelax. model for moment effects interpret. 79−20098
polymer, relaxation properties investigation method and instrument 78−39967
polymer, relaxation time spectra calc. from stress relax. data *(Russian)* 77−44288
polymer, relaxation times and dynamical modulus, viscoelasticity theory *(Russian)* 79−52293
polymer, thermomechanics in transition and rubber regions 78−59354
polymer, vibrational thinning, viscoelasticity and strength 77−8795
polymer, viscoelastic ductile, delayed yielding of plane stress viscoelastic Dugdale model 78−27569
polymer, viscoelastic prop. determ. with VR-72 vibrorheometer 77−70259
polymer, viscoelastic prop. meas. method in fluid and highly elastic states using forced vibrations 77−70258
polymer, viscoelastic-plastic, birefr. relation 77−31266
polymer blends, viscoelastic props. *(Russian)* 78−72808
polymer chain, elasticity for different vibr. modes, algorithm 78−66696
polymer chain, viscoelastic, local relax. props. anisotropy, internal friction influence *(Russian)* 78−37780
polymer chain consisting of interacting chain units, mol. dynamics, relax. times *(Russian)* 79−31753
polymer chains with rigid bonds, local relax. times, mol. dynamics study *(Russian)* 80−59373
polymer creep, energy considerations *(German)* 77−80081
polymer diffusion equation with hydrodynamic interaction, equiv. normal coord. 80−79966
polymer film, adsorbed monolayer, rheological behaviour 79−95245
polymer film, in adhesive joint contact layer, intermol. interaction with substrate and filler *(German)* 79−8421
polymer film, swollen, diffusion-relax. cojpling, two-stage sorption correl. 79−94864
polymer film, viscoelastic props., capacitance change meas. *(Japanese)* 78−23752
polymer flow, birefringence meas. of normal and tangential stresses 77−58625
polymer fluids, complex modulus, freq. depend. var. during extensional flow 79−55351
polymer glass transition, dynamic props., mol. model *(Russian)* 78−87777
polymer liquid, entangled, phenomenological consequences of Doi-Edwards viscoelasticity theory 80−79250
polymer liquids, elastic and Newtonian, vel. distrib. determ. in channel terminals 79−77046
polymer melt, flow birefringence, in shear flow, rel. to time depend. rheological props. 77−36198

viscoelasticity continued
polymer melt, particulate mixing, fluid dynamics, rheological and energetic considerations 80−43686
polymer melt, viscoelastic, 2-dimens. nonisothermal processing between calender rolls, mathematical model 79−68670
polymer melt, viscoelasticity, rheological props., prep., transport and processing effects, tensile and shear flow *(German)* 78−13982
polymer melt, viscosity, normal stress coeffs. determ. method *(German)* 79−7360
polymer melt and soln., nonlinear network model 79−3985
polymer melt network models, loss of junctions due to stretching of material planes 79−77043
polymer melt spinning, mechanics of nonisothermal process 77−51010
polymer melt spinning mechanics, relaxation time spectrum 77−31267
polymer melts, elongational properties, microscopic stretch history 80−23981
polymer melts, flowing, irreversibility assumption of network disentanglement, effects on elastic recoil predictions 80−6006
polymer melts, isothermal and non-isothermal stress relaxation following steady state shear flow *(German)* 79−77044
polymer melts, meas. of elongation props. with universal extensional rheometer 80−6004
polymer melts, normal stresa and Barus effect 80−64589
polymer melts, quasistatic bulk strength meas., specially built apparatus 80−7737
polymer melts, stratified two-phase flow, interface deform. 77−11158
polymer melts, viscoelastic model of uniaxial and biaxial stretching 77−68547
polymer melts and solutions, rheological equations, review 79−86391
polymer mixture, particle size in dispersed phase, effect of component viscoelasticity 77−44514
polymer network, crosslinks and trapped entanglements, two-network model 80−38962
polymer network, Riemann's metric degeneration to graph metric demonstration, chain entanglement problems 80−38963
polymer network formation, relaxational props. variation 80−38961
polymer network in solution, free energy of deform. 80−38900
polymer rod, fluid-permeable, longit. stability during creep 79−57066
polymer rod, longit. oscills., continuous viscoelastic spectra *(Russian)* 77−19546
polymer soft lossy, viscoelastic props. determ. from torsional vibr. of laminated bar 77−62218
polymer solids, viscoelasticity and relaxation phenomena of polymer solids 77−68439
polymer soln., viscoelasticity, rheological props., prep., transport and processing effects, tensile and shear flow *(German)* 78−13982
polymer solns., entangled, relax. dynamics, viscoelastic response functions 77−31578
polymer solns., parameter affecting the onset of drag reduction 79−77189
polymer solns., shear and normal stress behaviour, flow hardening *(German)* 78−67165
polymer solns., vap. bubble growth from gas nuclei, viscoelasticity effect 77−89172
polymer solution, bubble elongation dynamics, modelling with viscoelastic constitutive relations 79−37388
polymer solution, conc., appl. to study of viscoelastic props. at small constant shear stresses 79−54123
polymer solution, constitutive eqn. derived from network theory 77−75947
polymer solution, drag reduction, laminar to turbulent transition, rot. disc expt. 78−75173
polymer solution, drag-reducing, turbulent wall motion 77−55047
polymer solution, elastic, load bearing capaicty of squeeze film flow 80−103051
polymer solution, flow visualization near rot. disc 79−72914
polymer solution, individual bead contribution to intrinsic viscosity 77−84206
polymer solution, jet thrust technique for normal stresses 78−9669
polymer solution, laminar wake behind cylindrical body 79−37355
polymer solution, viscoelastic, in annular die entry, upstream flow characts., instability onset 79−60036
polymer solution, viscoelastic properties, direct meas. method using channel flow 79−37265
polymer solution rheology based on a finitely extensible bead-spring chain model 80−83775
polymer solutions, dilute, normal stress difference and shear rate 80−83776
polymer solutions, dilute, production, pulsation and damping of air bubbles 80−69879
polymer solutions, dilute, viscoelastic props. 78−94626
polymer solutions, mol. dynamics, review, book contrib. 77−39268
polymer solutions, normal stress meas. using flight velocity 79−77039
polymer solutions, single-relaxation-time constitutive model 77−11156
polymer solutions, surface wave calcs. 79−32593
polymer solutions, viscoelastic, tubular entry flow, vortex characts. in stable flow 79−32428
polymer spherulite, cryst. lattice strains, mech. behaviour, X-ray diffr. detect. 80−59558
polymer spherulites, deformation mechanism, linear isothermal viscoelasticity theory 80−58924
polymer viscoelasticity and strength characterisation, advanced light scatt. techniques 80−11857
polymer with macrodefects, fracture mechanism *(Russian)* 78−35500
polymer-based composite solid propellants, viscoelastic fracture mech. 79−43431
polymer-elastomer mixtures, temp.-time analogy 79−19317
polymeric fluids, entropy effects in viscoelasticity 78−9618
polymeric liquid, gas bubble pulsations and assoc. dissipation effects 80−59079
polymeric liquids, nonlinear viscoelasticity, stress-temp. equiv. eqns. 77−80128
polymeric liquids, rheology, fluid mechanics, book 77−65772
polymeric material, temperature shear function and temp.-time analogy in linear thermoviscoelasticity region 79−18747
polymeric materials, inelasticity degrees estimation, hysteresis friction model appl. rel. to US testing 80−3136
polymeric systems, fluid, rheology, characterised by mol. int. distrib., review 80−1504
polymeric systems, rheology, review 78−87317

viscoelasticity continued
polymeric systems, supported on inert substrates, dynamic thermomech. study 80−55623
polymers, amorphous, segmental distrib., crystallisation and viscoelastic relax. meas. 78−51443
polymers, and their solns., dynamic storage and loss compliances determ. from creep data 80−5948
polymers, conversion of dielectric to viscoelastic data 78−48109
polymers, creep under plane stress, nonlinear viscoelasticity models appl. 80−89308
polymers, electrification by metals, contact time effect obs. 80−70829
polymers, entangled, ternary blends of monodisperse homopolymers, viscoelastic props. 80−19301
polymers, entangled, viscoelastic props., binary blends of monodisperse homopolymers 79−96062
polymers, entangled, viscoelastic props., interchain-intrachain entanglement model 78−42575
polymers, fluid, harmonic distortions, under nonlinear periodic deform. 80−28482
polymers, fraction exponential function use for viscoelastic behaviour *(Russian)* 80−53652
polymers, glassy, viscoelastic relaxation processes role in macrodeformation 79−72825
polymers, linear, unimolecular approx. 79−50613
polymers, linear, viscoelastic props. under flow conditions, transition to highly elastic state *(Russian)* 79−50690
polymers, multicomponent, props. and struct., review 78−44076
polymers, temp. depend. under dynamic conditions, linear theory of thermoviscoelasticity 79−61642
polymers, thermosetting, linear hereditary theory appl. *(Bulgarian)* 79−86357
polymers, viscoelastic, deform., depth of polymerisation 80−40414
polymers, viscoelasticity, calc. using relaxation and retardation spectra *(German)* 78−92290
polymers, Volterra eqns. approx. soln. 79−50614
polymers and polymer science in dentistry 79−83435
polymers in nonisothermal strain, thermomechanical coupling effect 79−86355
polymers with periodic deform., longitudinal flow 80−6008
polymers with various atomic composition and viscoelastic props., laser damage 80−104017
polymethacrylic acid, swollen networks, viscoelastic photoelastic behaviour 80−59366
polymethylpentene, visoelastic props., γ-irrad. influence *(Russian)* 78−88492
polyox dilute aqueous solns., flow resistance mechanisms in porous media 79−41747
polyoxymethylene-copolyamide blend melt, viscoelastic peculiarities *(Russian)* 78−38263
polypeptides, helical, conc. solns., rheological behaviour and liq. cryst. order 80−83771
polypropylene, audio freq. shear and Young's modulus determ. from torsional vibr. of laminated bar 77−62218
polypropylene, linear viscoelastic region, creep prediction using temp. pulse technique 78−68732
polypropylene, nonlinear viscoelastic effects 77−90401
polypropylene, shear stress/strain behaviour, press. effect 78−84936
polypropylene, stretching flow for film prod., stretching over canonical mandrel 78−71304
polypropylene glycol, Rayleigh-Brillouin spectra calcs. 79−47465
polypropylene melt, viscoelastic property measurement using improved design rheometer 79−37276
polystyrene, atactic, thermal behaviour above glass-rubber relax. temp. 77−39548
polystyrene, bimodal mol. wt. blends, recoverable compliance 80−66568
polystyrene, melts, stratified two-phase flow, interface deform. 77−11158
polystyrene, Millar interpenetrating network, viscoelasticity and phase domain form. 78−83749
polystyrene, ordered monodisperse latexes, viscoelasticity and flow props. 80−58992
polystyrene, oriented high-molecular, physicocomech. props. *(Russian)* 79−33028
polystyrene, partial draining of low-molecular weight polymers with flexible chains 80−23592
polystyrene, solns., nonlinear viscoelasticity, stress development at start of shear flow 77−3800
polystyrene, swollen network in benzene, pendent chains, influence on thermodynamic and viscoelastic props. 80−28481
polystyrene, viscoelastic, linearity conservation 80−108492
polystyrene amorphous film, cyclically fatigued, molecular behaviour 80−35310
polystyrene latex, ordered monodisperse, lyotropic liq. cryst., mech. props. 79−98676
polystyrene melt, linear viscoelastic props. influence of molecular wt. distrib. 80−19309
polystyrene melt, normal and shear stress relax., Rheometrics mech. spectrometer transient response 78−42577
polystyrene melt dynamic viscoelastic props., mol. weight distrib. 78−63407
polystyrene melts, low mol. mass, dynamic viscoelastic behaviour, alternating shear expts. 77−62226
polystyrene monofilaments, uniaxial extension, strengthening 79−8334
polystyrene polybutadiene polystyrene triblock copolymers, extension of contour plotting method for representing linear viscoelastic loss 77−32620
polystyrene solutions in decahydronaphthalene, viscoelastic props., time depend. *(German)* 79−77051
polystyrene-polyvinyl methyl ether blends, dynamic mech. and sonic vel. behaviour 79−34090
polystyrene-tricresyl phosphate solns., viscoelastic props., conc. depend. 80−76299
polystyrenes, blends, molten, rheology, dynamic viscoelastic props. in terminal zone 77−31268
polysulphonamide solutions, mech. props. during gelling *(Russian)* 77−19579
polysytrene melts, stresses and birefringence in intermittent shear flows 80−19308
polyurethane, filled, relation between static and dynamic deform. characts. 80−3137
polyurethane, glass ball rolling on adhesive viscoelastic material, contact area 79−52394

viscoelasticity continued
polyurethane, stress plate in contact zone with solid indentor 78−1624
polyurethane solid foams, creep laws *(German)* 80−65139
polyurethanes, crosslinked, effect of oligoglycol mol. wt. and SiO_2 filling on viscoelasticity and supermol. struct. *(Russian)* 79−34092
polyvinyl acetate, partial draining of low-molecular weight polymers with flexible chains 80−23592
polyvinyl acetate, struct. relax., enthalpy and elec. polarisation obs. 79−41978
polyvinyl acetate, torsional stress/strain meas., press. effect 78−84937
polyvinyl alcohol networks, swelling equil. with dil. salt solns., thermoelastic behaviour, hydroxyl group interact. 80−79667
polyvinylacetate melt, thermodynamic constitutive eqns., adiabatic deform. expts. 78−1620
polyvinylidene fluoride-PMMA blends, dynamic mech. props. and sonic velocity, cryst. phase transitions 78−26454
porous bodies, stresses induced by drying, elastoviscoplastic model, finite element anal. 80−23904
prefluorinated polymer, DuPont Krytox 143-AB, viscoelastic and dielectric props. 80−1503
pressure distribution in elastic hydrodynamic contact of cylinders 77−84208
protein dispersions, viscoelastic effects, shear viscosity and primary normal stress difference 80−87754
protein solution, propagation of surface shear waves 79−77146
pseudo-elastic analysis of plastics, validity in load-bearing appl. 78−39868
PTFE, partly crystalline, viscoelastic props., stressed state estimation 79−66099
PTFE, relaxational props. effect of temp. and hydrostatic press. *(Russian)* 77−44325
pulse propag., uniaxial, in viscoelastic medium, formulation using Boltzmann superposition integral 79−12619
pulsed NMR technique for meas. radiation effects in polymer 80−66051
PVC, antiplasticisation rel. to ageing and nonlinear viscoelasticity 78−52929
PVC, antiplasticised, linear-nonlinear viscoelasticity transition 79−5015
PVC, commercial tubes, photoviscoelastic investigation 79−34095
PVC, deform. temp.-time depend. props., viscoelastic linear and nonlinear regions comparative anal. 78−64600
PVC, filled, with varying plasticiser content, deformative props. in highly elastic state, temp. depend. 79−20099
PVC, mech. behaviour in nonlinear viscoelasticity range 79−4996
PVC, plasticised, fatigue, fractographic study 80−30101
PVC, plasticised, fatigue crack growth charact. 80−30100
PVC, plasticised, history-independent recovery, creep, stress relaxation 78−80607
PVC, plasticised film, defect form. study, turbidity and shrinkage meas. *(Russian)* 77−62490
PVC, plasticiser influence 79−52292
PVC, rheology, viscoelasticity, panel discussion 79−3984
PVC, rheology, viscoelasticity 79−3982
PVC, rigid, viscoelastic props. rel. to thermal, mech. history 79−5016
PVC melt, viscoelastic property measurement using improved design rheometer 79−37276
PVC plastisol, steady shear rheological behaviour 79−37274
PVC strip, viscoelastic props. from impact studies *(Russian)* 79−32289
quadrature representation of viscoelastic correspondence principle in frequency domain 79−46233
quartz, ceramic, elastic property changes on sintering 77−90301
quasioptimal approx. polynomials, appl. to soln. of problems 79−86349
quasistable and dynamic problems, reduction to soln. of algebraic eqns. *(Russian)* 77−57198
rate type constitutive eqns., free energy of viscoelastic and viscoplastic materials 80−79168
rate-dependent memory function model, admissibility 77−35105
Rayleigh problem, similarity soln. for totally automorphous model *(German)* 80−28426
Rayleigh wave dispersion in visco-elastic solid *(Japanese)* 77−17035
Rayleigh waves over isotropic half-space 77−68499
Rayleigh-Taylor instability of two viscoelastic superposed fluids 79−72869
rectal wall, mathematical anal. of passive viscoelastic props. *(French)* 77−66822
rectangular viscoelastic prism exposed to repeated stretching and contraction, thermomech. anal. 77−54896
red blood cells, viscoelastic study of aggregation 80−97960
red cell membrane, human, surface elasticity and viscosity 80−61608
red cell membrane, temp. dependence of viscoelastic recovery 80−40979
red cell membrane protein monolayers, viscoelastic props. 79−48224
reinforced hollow spheres, dynamic behaviour 78−1577
relativistic magneto thermo viscoelastic medium, effect of mag. and thermal fields on plane wave propag. 79−2637
relaxation function symmetry and monotonicity 79−75348
relaxation modulus, evaluation from response to constant strain rate followed by constant strain 80−74765
residual stresses when cooling, plate, sphere, cylindrical shell *(Russian)* 77−39234
resin slab, stress response, fluctuating external moisture (temp.) effects 78−55620
resonance vibrations in short viscoelastic cylindrical shell 80−58962
rheological relations invariance with rel. to orthogonal time depend. transform. of coords. 78−1623
rheometer, high freq., operation, calibration, appls. 78−83345
rheonomic viscoelastic materials, under prolonged loading, failure hypothesis 80−3180
rigid elastic body system, turning round fixed point, linear viscoelasticity theory *(French)* 80−69646
rigid ellipsoidal particles in external field, dil. suspension, rheological eqns. *(Ukrainian)* 80−48661
rigid indentor sliding over power law viscoelastic half space 79−27602
rigid indentor sliding over power law viscoelastic layer, anal. 79−7346
rigid punch motion at viscoelastic space boundary, dynamic contact problems *(Russian)* 79−81819
rigid slider, deformational contact and friction on viscoelastic substrates 79−50677
Rivlin-Ericksen flow past stretching plate, skin friction, heat transfer calc. 77−72272
Rivlin-Ericksen fluid, dispersion medium on rheological behaviour of dilute suspension of dipolar dumbbells, viscoelastic props. 80−99983

viscoelasticity continued
Rivlin-Ericksen fluids, unsteady flow through circular and coaxial ducts in radial mag. fields 78−42632
Rivlin-Ericksen viscoelastic fluid, unsteady flow through confocal elliptic cylinders 79−37354
rock specimens impulse response, estimation and viscoelastic solid model appl. 79−80049
rod, conical, nonlinear viscoelastic materials, soln. using generalised correspondence principle 80−38288
rod, dynamical behaviour, effect of thermomechanical conjugation under forced longitudinal oscillations *(Ukrainian)* 78−67074
rod, forced longitudinal oscillations, thermomechanical coupling effect 80−19274
rod, fundamental solutions of wave equations with delay time 79−27576
rod, hinge supported, parametric oscills. *(Russian)* 79−50624
rod, nonlinear waves and finite rod impact on rigid obstacle 79−41606
rod, numerical inversion of Laplace transform. by asymptotic extension 78−1576
rod, shock rel. to hard obstacle *(Russian)* 80−23911
rod analysis, using Boltzmann-Volterre memory theory, second-order approximate solution *(Russian)* 78−87278
rod driven by sinusoidal displacement, thermomechanical response 77−89056
rod with small nonlinearities, vibr. anal. 79−98657
rod with temperature-dependent properties, wave propag. 77−54822
rods with nonlinear elasticity relation and nonlinear internal friction, parametrically excited oscills. 80−99947
rolling, Newtonian or non-Newtonian liqs., two-roll mill problem 78−42616
rotational quasi-viscometric flows around a rotating sphere 79−60023
RQP method of inferring a mechanical relaxation spectrum 79−37195
rubber, fracture in viscoelastic systems under cyclic loading 80−81195
rubber, network, highly swollen, long time dynamics 80−38291
rubber, network entanglement contrib. 80−39203
rubber, rupture life calc. 77−59933
rubber bonded cylinder, Lagrange anal. of dynamic props. 79−14304
rubber network elasticity, mol. theory 80−38290
rubber under cyclic compression, heat generation and thermal conduction 79−52283
rubber-resin mixtures, viscoelasticity 79−43303
rubbers, swollen, low-freq. dynamics, optical and mech. props. 80−43626
San Andreas Fault, cyclic displacements. viscoelastic relaxation 79−20799
seismicity, viscoelastic stiffness model 79−20764
semiflexible and rigid particles in solution 79−94505
SH waves due to shearing-stress discontinuity in viscoelastic half-space, displacement 80−56405
SH-motion in general viscoelastic material overlying hard elastic matter 79−29715
shaft, whirling motion, stability analysis 78−13894
shear flow of heat conducting viscoelastic fluids, nonlinear temp. depend. 79−41675
shear waves, circular and elliptic polarised in viscoelastic fluid 79−60024
shearing motion, unidirectional simple, analysis of automorphous model 78−5718
shell, cylindrical, composite with viscoelastic filler, optimisation w.r.t. long-term stability 79−18760
shell, cylindrical, viscoelastic core, parametric vibrations 77−27489
shell, cylindrical composite, with viscoelastic filler, parametric oscills., dynamic instability *(Russian)* 78−38221
shell, multilayer, cylindrical, viscoelastic strain equations under axisymmetric load 77−80079
shell, orthotropic, vibrations in various media 77−27488
shell, spherical, interaction with acoustic medium, pressure δ-impulse *(Ukrainian)* 80−69681
shell, thick-walled, deform. in post critical stage 77−58566
shell, thin cylindrical, stiffened with viscoelastic rings, vibr. damping charcts. 80−28452
shell and plate, reinforced, viscoelastic and elastic, with transverse shear strain, stability 77−84171
shells, axisymm., transient vibrations 80−10179
shells, compressed viscoelastic orthotropic, stability 79−7305
shells, double layered cylindrical, damped axisymmetric vibrs., refined theory 79−75338
shifted Chebyshev polynomials, soln. of second kind operation eqns., convergence 78−62059
shock profiles, elastic discontinuities struct. 79−14330
shock wave structure, eqn. of state for viscoelastic medium 78−9594
shock-compressed, compression and rarefaction waves obs., 150-250 kbar 77−77535
silicon oil, separation of elastic and shear thining effects in capillary rheometer 78−42691
simple liquids, collective motion 80−24329
skeletal muscle mechanical props. and model, contractile force depend. *(Japanese)* 80−56091
skin components, rheological props. under compressive load 80−35945
skin mechanical properties, effects of split dose radiations 77−52842
skin rheological behaviour, expt. results and struct. model 80−16968
skull-brain system, human, prolate spheroidal viscoelastic shell containing viscoelastic fluid, axisymm. vibrs. 78−80901
small deform. superposed on finite deform. *(Russian)* 78−32679
small deformations superposed on large stretch, stress-deformation relns. 77−72187
smectic mesophases, viscoelastic properties and field instabilities 79−27904
sodium polystyrene sulphonate, solns., infinite dilution viscoelastic props. 79−14363
soft polymer, isotropic, viscoelastic behaviour in moderately large deformation 77−54944
soft viscoelastic material, complex modulus of elasticity determ. 77−62221
soil, two phase with viscoelastic skeleton, finite element anal. of consolidation 77−11138
sol, coagulated, viscoelastic props., elastic floc model 79−37270
solid, linear quasi-static theory, variational and minimum principles 80−10157
solid viscoelastic body, motion relative to centre of mass *(Russian)* 80−53649
sphere, rot. in compressible viscoelastic fluid, ang. vel. correlation function calc. 77−46977

viscoelasticity continued
sphere behaviour in non-homogeneous flow of viscoelastic fluid 77−68640
spherical particle, free-fall rate in immobile liq. 80−19302
spherical shell immersed in liquid, disturbances due to central explosion 79−81734
spine, intervertebral disc material, human, viscoelastic response obs. 80−51141
spinning, isothermal, of Newtonian and viscoelastic liq., draw reson. instability 79−60027
spring rod, vibration heating, amplitude depend. *(Ukrainian)* 80−38301
sputum, meas. using conventional dynamic and raised cosine pulse methods *(Japanese)* 80−67132
square well fuild, elastic modulus and viscosity coeff. 77−30086
stability of viscoelastic rods and shells under loads that decrease with time 80−69700
stability problems 80−27133
standard linear body, free torsional ascills. 80−99940
starch, glycerin impregnated, dynamic viscoelasticity *(Japanese)* 80−104203
steel, eutectoid and hypoeutectoid viscoelasticity under transformational superplasticity *(Japanese)* 77−52416
steel, stainless, global bending response analysis of elastic and viscoplastic nuclear shipping cask structures subjected to impact loading 80−76301
steel, stainless, type 304, viscoplastic behaviour, strain rate sensitivity, creep, relaxation, tensile tests 80−66727
steel casting, calc. method of thermal and thermo-visco-elasto-plastic processes *(German)* 80−79859
steel continuous casting, thermal, thermo-visco-elasto-plastic processes *(German)* 80−81044
steel ingot, state of viscoelasticoplastic stress deformation, in process of solidification *(Russian)* 80−45295
steel shell, mech. behaviour during solidification 80−81043
strain amplitudes, max. value for linear viscoelasticity theory 78−30252
strain wave propagation in visco.elastic bars due to longitudinal impacts anal. *(Japanese)* 80−96223
stratified material, compressed, stress determ. *(Rumanian)* 80−28434
strength, long term, generalized criterion 77−27477
strength and stability of viscoelastic structures, method of solving integral eqns. used 80−10167
stress anal. of viscoelastic bars subjected to impulsive loading 79−32305
stress clock function in viscoelasticity 80−99941
stress field for half-space in randomly varying temp. field *(Ukrainian)* 80−33467
stress relation to deformation, theory 79−59958
stress wave propagation in viscoelastic media 78−46910
stress waves focusing in viscoelastic solid cylinder *(Russian)* 79−27535
stress waves generated by internal heating in Voigt and Maxwell materials Laplace transform anal. *(Japanese)* 80−69693
stress-strain behaviour, mathematical simulation for viscoelastic material *(German)* 80−1442
stress/strain meas., by Moire method *(German)* 78−22309
stress/strain relationships, fluctuations 80−17802
strip, dynamic crack propagation due to antiplane loading 80−64464
strip, flat, stationary bending plane determ., under moving load *(German)* 80−1446
strip with circular hole, visco-elastoplastic stress conc. 77−68455
structure damping for noise control, evaluation of viscoelastic props. 80−43632
styrene butadiene rubber, dicumyl peroxide cured, behaviour in moderately large deform. 78−60692
styrene copolymer, props. rel to composition *(German)* 79−66291
styrene-acrylonitrile copolymer, amorphous, rubbery state, nonequil. tensile deform., effects of temp. and strain 80−40442
styrene-butadiene block copolymers, in 1-chlorohexadecane, rheological props., viscoelasticity 79−23288
styrene-butadiene block copolymers, in dil. soln., extrapolation methods for intrinsic viscosity 80−24636
styrene-butadiene uncrosslinked gum rubber, viscoelastic behaviour in moderately large deform. 77−89079
styrene-butadiene-styrene block copolymer, nature of melt rheological transition 78−75113
styrene-butadiene-styrene block copolymer, stress relax. following steady-state flow, residual shear stress development 80−83772
styrene-diene block copolymers, pressure sensitive adhesives, morphology and viscoelastic behaviour 77−52419
styrene-isoprene block copolymers, mol. wt. from frictional props. 78−90329
styrene/acrylic terpolymers, viscoelastic props. 80−64509
styrene/MMA copolymers, struct. and rheology 80−1444
subcritical growth of cracks in thin viscoelastic plates 80−28465
surface wave propagation in viscoelastic media 78−42555
surface waves, influence of gravity 77−81797
surface waves on clamped boundary 78−90767
surface waves on standard linear viscoelastic solid 80−28461
suspension, dilute, arbitrary-shape particles, time-depend. flow, Brownian rot. effect 78−26188
suspension, viscoelastic properties 79−92006
suspensions of spheres in viscoelastic media, alignment and aggregation effects, photographic obs. 77−80129
synovial fluid, normal and pathological 80−16966
T-jump expt., effect of finite rates of temp. change 77−72191
technical fabrics, viscoelastic compliance, appl. of stress-time analogy method 80−1497
Teflon, viscoelastic behaviour prediction of low temp., creep curves exam. 79−20141
temperature displacement and stresses anal. *(Russian)* 78−18194
tendon, viscoelastic deform. obs. 80−101211
tendon mechanics, discrete nonlinear viscoelastic model *(German)* 78−44525
tetrafluoroethylene-vinylidene fluoride copolymer, exporide-diphenyl-olpropane resin filled, viscoelastic and strength parameters 79−91730
tetrafluoroethylene-vinylidene fluoride mixture, in epoxide-diphenylene propane resin, exam. of temp. depend. of stress relaxation, viscoelasticity 80−11688
theory, existence of uniqueness of solution of integral and integrodifferential eqn. 77−62173
thermal stress state of viscoelastic bodies, with props. dependent on unsteady temp. 78−83229
thermally stimulated processes 78−10829
thermodynamic restrictions on relaxation function 77−75821
viscoelasticity continued
thermodynamics of relaxation and creep processes, viscoelastic materials with fading memory 78−71282
thermomechanical theory of viscoelasticity for incompressible material *(Russian)* 78−63327
thermomechanics, introduction, book 78−54187
thermoplastic elastomers, crosslinked by secondary valence interactions, elasticity and processing, crosslinking behaviour 80−40320
thermoplastic materials, flexure testing 77−86087
thermoplastic polymer, linear viscoelasticity, rel. to orientation, recoverable strain and mech. props. 77−56041
thermoviscoelastic laminate beam, stress anal. *(German)* 80−106727
thermoviscoelastic material, sensitivity of thermomechanical response to thermal boundary conditions and material constants 79−77001
thermoviscoelastic materials, thermodynamics of nonlinear single integral representations, appl. to one-dimensional wave propag. 77−68438
thermoviscoelastic media, dynamical problems, Volterra method generalisation 80−33481
thermoviscoelastic transient responses, stability and accuracy of finite element solns. 80−5951
thermoviscoelastic-plastic materials, constitutive reln. 80−58
thermoviscoelasticity, bound dynamical problems, approx. calc. methods for crit. thermal states *(Russian)* 78−28949
thermoviscoelasticity, heat liberation effect in deformable linear medium 80−33484
thermoviscoelasticity, linear bound, minimum principle *(Ukrainian)* 80−33468
thermoviscoelasticity, nonlinear universal functions, influence of temp. *(Russian)* 79−10495
thermoviscoelasticity, variational techniques *(Russian)* 78−13922
thermoviscoelasticity problems, numerical soln. processes, stability, convergence *(Russian)* 79−27536
thermoviscoelasticity theory, nonlinear, asymptotic soln. of problems 77−65695
thin plate, optimal cool down in linear viscoelasticity 80−79176
thin shell, swelling under const. loading 78−63326
thin walled systems, stability *(Russian)* 80−1452
thixotropic fluid, shear flow, oscillatory Couette flow, apparent viscoelasticity 79−90288
three-layer beams with viscoelastic cores, nonlinear vibrations, expt. 79−32341
three-layer elastic-viscoelastic beam damping characteristics *(Japanese)* 78−9575
thrust foundations, resulting vibrs. in viscoelastic bodies *(German)* 79−90177
time reversal and symmetry relations in finite linear viscoelasticity 80−102970
Timoshenko beam, steady state dynamic response to travelling loads 77−68457
transducer, viscoelastic, in-situ, Duomorph, appl. to polymeric materials 79−30463
transient wave propag. in viscoelastic bar 80−106745
transitional flow of viscoelastic medium, lag time eval. 80−38371
transverse impact method for studying the viscoelastic properties of materials *(Russian)* 79−32398
triangle pulse and delta function excitation response 79−55332
triblock copolymer, model for rheology 80−23979
trifluoropropylmethylsiloxane fluids, viscoelastic props., mechanical impedance, viscosity and density meas. 80−79249
tube, porous, nonlinear viscoelastic materials, soln. using generalised correspondence principle 80−38288
tube, viscoelastic, containing flowing fluid, bending vibrs. 79−94521
tube, viscoelastic-plastic, successive deformation under cyclic, temp. variation 80−92074
tube, viscous fluid wave propag., asymptotic formulae and numerical results 79−34595
tubes, liquid filled elastic and viscoelastic, longitudinal waves theory 79−64562
two-component materials, thermo-viscoelastic theory 78−73854
two-dimensional creeping flow of simple viscoelastic fluid through finite gap *(German)* 77−46979
two-dimensional wave problem, Volterra method solns. 80−69727
two-layered beam, vibrational analysis, with unconstrained viscoelastic layer damping *(Japanese)* 80−5968
underwater sound absorpt. in viscoelastic medium containing short cylindrical cavities 77−84049
universal quasi-static deformation for an incompressible isotropic body with memory *(Russian)* 79−81735
urethane prosthetic compound, dynamic mode determ. 79−48376
urethane rubber, viscoelastic disc, contact problem, photoviscoelasticity obs. *(Japanese)* 78−30202
urinary bladder passive props., collection phase model 79−34596
uterine muscle, isotropy and anisotropy during labour contract. 80−94257
van der Waals liq., statistical theory of viscoelastic relax. 77−68907
variational and minimum principle applications *(Japanese)* 80−48599
variational Lagrangian irreversible thermodynamics of nonlinear thermorheology 77−27467
variational Lagrangian thermodynamics, nonisothermal finite strain mechanics of porous solids, thermomolecular diffusion 77−65668
variational principle in general dissipative materials *(Japanese)* 77−23896
vibrating elastic solid due to scattering of elastic waves by pores 79−86372
vibration analysis of viscoelastic bodies with small loss tangent 77−65706
vibration damping treatments for viscoelastic materials, design evaluation 79−18799
vibration of viscoelastic cylinder with elastic shell when subjected to random forces 79−59941
vibration of viscoelastic orthotropic layered cylinderical shell in acoustic medium, numerical anal. 77−54828
vibration of viscoelastic plate with circular outer boundary and eccentric circular inner boundary 79−81760
visceral smooth muscles in vertebrates, viscoelastic and plastic props. 78−73169
visco-elastoplastic medium mechanical birefringence in loading and unloading processes 78−59314
viscoelastic bodies, adhesion and fracture mechanics, review 78−83336
viscoelastic fluid, flow anal. between 2-D surfaces subject to normal high freq. oscillations 80−16493

viscoelasticity continued
viscoelastic material, linear, creep function, information theory approach to its monotonicity, concavity and symm. 77−84156
viscoelastic properties dynamic evaluation for use in cardiac prosthetics 78−40405
viscoelastic reacting fluids flowing over flat plate, boundary layer anal. of surface deposition 78−42675
viscoelastic tube filled with viscoplastic media, unsteady motion 78−87366
viscoelastometer, dynamic, direct reading, automation, appls. to polymer films, fibres 79−3980
viscoelastoplastic deformation of isotropic body, tensor laws of behaviour *(French)* 77−62160
viscoplastic medium, optimum control of transient process under press. *(Russian)* 79−72821
viscoplasticity theory based on infinitesimal total strain and nonlinear viscoelasticity 80−79164
viscoplastoelastic material, plane wave propagation anal., upon shock loading 79−14336
viscous fluid under cyclic deform., self-heating, hydrodynamic thermal explosion 80−58993
viscous liquid, acoustic and thermal props., phenomenological models 79−82393
viscous liquids, US shear absorption, effect of pulse width 78−83878
vitreous humour, human, in vivo obs. 80−56077
vocal fold vibration, viscoelastic theory 77−25471
Voigt column, influence of elastic end support on stability 79−37238
Volterra eqn., growth estimates for solns., appl. to viscoelastic initial-boundary value problems 77−74195
water-in-oil cream, viscoelastic props. 77−58629
wave, spherical, propag. in viscoelastic half-space 77−75845
wave propag. in viscoelastic plate in liquid 78−79247
wave propagation, integration contour deform. for Laplace transform inversion 80−74801
wave propagation, nonperiodic, in compressible elastico-viscous fluid 80−43724
wave propagation, weak, in elastic-plastic and elastic viscoplastic solids with interfaces, Al calcs. 78−18216
wave-front method for dynamics of high damping bar 77−23895
wedge, plane, nonlinear viscoelastic materials, soln. using generalised correspondence principle 80−38288
Weissenberg effect, review of expts. 79−60025
wood-PMMA composites, temp. depend. of viscoelastic behaviour *(Japanese)* 77−77541
wood-polymer composite, dynamic viscoelasticity and modulus *(Japanese)* 78−59356
work done, estimates, nonsimple viscoelastic material, from later stress meas. 77−57190
Al, 2618, creep under step stress changes, viscous viscoelastic model 80−81138
Al alloy 2618, creep and recovery under combined stress, viscous-viscoelastic model representation 79−34117
Al-Mg-Si alloy, descriptive method for alloy creep tests by nonstationary loadings 78−23759
Al-SiC fibre reinforced materials, therm. stresses in unit cell 80−10160
Al_2O_3-Epon 828-Z, mixture, acoustic wave prop. characts., using differential-path US technique 79−42151
As-S-Tl, glass, viscosity and elastic props. 80−100180
C fibre reinforced epoxy resin, transverse creep compliance, time and temp. depend. *(Japanese)* 80−45358
C paste, viscoelastic props., depend. on coke grain size 80−1501
C, pyrolytic, high-temp. deform. under mech. loads 77−16644
$CaCO_3$ filled polymer melts, viscous props. 80−19311
Cu-Zn, amorphous, viscoelastic behaviour *(Japanese)* 77−86110
Cu-Zr, amorphous, viscoelastic behaviour *(Japanese)* 77−86110
Fe, commercially pure, viscoelasticity under transformational superplasticity *(Japanese)* 77−52416
Fe-P-C, viscoelastic behaviour of amorphous alloys *(Japanese)* 77−86110
LC-440, shear modulus and viscosity relax. near isotropic-nematic phase transition *(Russian)* 77−39543
LiCl, hypersonic relaxations studied by Brillouin light scatt. techniques, viscoelastic effects obs. 80−83375
Na_2O-P_2O_5 glass, elastic and viscoelastic props. by Brillouin scatt. 79−51972
$PbCrO_4$, paste, anomalous viscous flow 79−64617
Pd-Si, amorphous, viscoelastic behaviour *(Japanese)* 77−86110
Si_3N_4, hot-pressed, creep and strain recovery 80−100874
Si_3N_4, hot-pressed, viscoelastic strain recovery obs. 79−79042
Si_3N_4-MgO, compressive creep, source of viscoelastic effect 80−50675
SiO_2-glass, high-temp. strain relax., optical correlation spectroscopy 77−65951
W, viscoelastic wave propagation model at near-melt conditions, electron-photon impact energy deposition 79−77002
YIG, phonon viscosity effect on dislocation motion 80−24450

viscometers
see also viscosity measurement
acoustic technique for shear viscosity meas. 77−958
air-bearing viscometer, transient rheology study 80−59152
annular viscometer, measuring principle *(Japanese)* 78−59522
aperiodic industrial for non-Newtonian fluid *(Russian)* 80−53897
automatic capillary, accuracy one part in five million 80−87825
automatic recording capillary viscometer for study of polymeric reactions 77−27631
automatic rotating disc, with servomotor *(Russian)* 77−19649
automatic thermo-compensator stability improvement *(Russian)* 77−55114
blood sedimentation, at controlled shear rates 77−66877
blood viscometers and anticoagulants compared 79−83834
Brookfield viscometer adaption for use with slurries and suspensions 77−4884
capillary, for use with crosslinking polymer melts 79−7431
capillary, systematic error source identification 79−18982
capillary, Ubbelohde-type, surface tension effects for spherical fluid reservoir case *(German)* 79−86534
capillary, Ubbelohde-type and types with different reservoir bulbous form, surface tension effects calc. *(German)* 79−86535
capillary rheometer, viscous heating from power law fluid, perturbation expansion anal. 78−63519

viscometers continued
capillary type, for superheated liq. viscosity meas. at high press. 77−58823
capillary type with a feedback system, stabilization of press. difference 79−14502
capillary viscometer and obs. of low shear rate blood viscosity 80−98180
capillary viscometer for blood flow meas. 79−79671
capillary-type closed, stabilized flow 80−59156
capillary-type closed viscometer, effect of unsteady flow 78−9736
clinical capillary blood viscometer development 77−40844
closed-type capillary viscometer used without applying suction 77−19646
complex apparatus for viscous and elastic prop. meas. at high press. of liquids 78−9734
cone-plate viscometers, haemolytic secondary effects 79−62281
Couette, measurement error correction, non-Newtonian liquids appl. *(German)* 78−94868
Couette viscometer, shear rate determ. 77−68723
Couette viscometer for short time shearing of blood 80−98179
Couette viscometry, meas. of rheological props. of red blood cells 80−97992
Couette-type, capacitor assembly for meas. small rotational vels. 80−100046
diamond anvil pressure cell falling sphere viscometer, wall effects 79−82023
differential fluid viscometer *(Russian)* 79−90355
dilute polymer solution viscosity/pH meas. 79−68831
dynamic viscometer theory 79−77315
eccentricity of rotating cylinder, error calc. in viscosity meas. *(German)* 78−67291
electromechanical, with digital readout, biological fluid meas. appl. 78−28131
electrostatic, development based on investigation of damping of vibrating grid in viscous medium 80−38308
falling coaxial cylinder viscometer for wide range of shear rates 78−79393
falling cylinder viscometer, for meas. of viscosity of polymer melt under hydrostatic pressure *(German)* 77−55115
heat transfer in biconical and concentric spherical viscometers 79−55318
high pressure slit-viscometer, non-isothermal flow, thermal boundary conditions *(German)* 78−67292
high viscosity fluid continuous meas. device 78−5834
high-pressure, applic. up to 4 kbar and 300°C 78−59515
high-temperature melt, torsional cylinder oscills. type 80−79418
Hoppler, ball passage time meas. digital electronic circuit *(Polish)* 78−47075
hydrodynamic thermal explosion in power-law fluid flow 79−77158
immersion viscometer, exam. of design 79−52544
interfacial viscometers, surface shear viscosity determ. 79−23384
lifting liquid type, accelerated, theory and exptl. design *(Japanese)* 80−83870
lifting liquid type *(Japanese)* 79−82005
liquid multimatter blend viscosity measurement at high vapour pressure, Hoppler viscosimeter appl. *(German)* 78−94867
low shear rate viscometer, design and appl. *(Japanese)* 79−55432
manual, for industrial processing of liq. rubber *(German)* 79−27729
material functions for steady circ. shear in orthogonal rheometer 79−23385
multicapillary two-phase for polymer *(Polish)* 79−4097
Newtonian fluid, secondary flow in cone-and-plate viscometer 78−42692
one-bulb capillary type for polymer intrinsic viscosity meas. *(Polish)* 78−42687
oscillating cylinder, absolute, with digital data acquisition system, for high-temp. measurements 79−82003
oscillating disc viscometer, appl. viscosity meas. of CO_2 and propylene *(German)* 77−42954
oscillation type, capacitive transducer of torsional oscills. 80−64656
polymer melts, extensional rheometers, review 78−71302
portable field viscometer type RV-K74P 79−68829
power law fluid, rheology, data treatment from cylindrical viscometer 77−3893
Rankine-type capillary viscometer, for gases *(Japanese)* 80−14859
rheometer, high freq., operation, calibration, appls. 78−83345
rheometer, rot., inertial normal force correction 78−63520
rheometer, testing, transient shear, stiffness, drive shaft movement *(German)* 78−67166
rolling ball viscometer, calibration for meas. on organic liquids 77−69107
rotary, operational principles *(Russian)* 78−91039
rotary, with weight-driven rotor, rotation speed control attachment 79−50822
rotating disk, in liquid surface with adsorbed film, torque 78−32685
rotation, real flow curve determ., with wall effects *(Russian)* 79−64714
rotational interferometric viscometer for Newtonian viscosity measurements 79−50824
rotational viscometer, non-Newtonian fluid viscosity measurement 80−19529
sealed oscillating crucible viscometer for corrosive volatile liquids at high temp. 77−15140
shear viscosity of settling suspensions meas. 79−82011
skin friction meter using viscosity balance principle for metal surfaces 77−35266
small volume inclined falling ball viscometer 78−1772
solar radiation tracking sensor 80−86295
spinning drop interfacial viscometer, liquid-gas interface, surface viscosity meas. 80−44395
string viscometer with wide temp. range 78−26217
suspension, automated meas. of viscosity 79−37258
temperature meas. at fixed viscosity, instrum. 78−1764
torsional balance rheometer, viscometric functions of elastic liqs. 77−3851
torsional vibr. viscometer designed for meas. from 30 to 300 Hz *(German)* 78−67164
Ubbelohde suspended level capillary type, semiautomatic meas. *(German)* 79−94561
vibrating, for measurement of viscosity of slurries, assessment 80−28586
vibrating wire, adaptation for liquids 80−87827
viscometric data from Brookfield RVT viscometer, conversion to shear stress-shear rate relationship 80−1495
viscosimeter for three coeffs. of viscosity of liq. crysts. meas. 79−4095

viscoplasticity *see plasticity*

viscosimeters *see viscometers*

viscosity
see also electroviscous effect; internal friction; viscosity of gases; viscosity of liquids
accretion discs in close binary systems, viscosity and tidal torques 78−12296
acoustic field in stratified media of variable viscosity, Green's functions 80−4545
acoustic wave propagation in isotropic viscous weakly compressible medium, eqn. limits problem *(French)* 80−8808
acrylate adhesive coating on glass substrate, mech. props. determ. using transfer functions of US oscillations *(Russian)* 79−87644
acrylic dispersions, conc., shear thinning and thickening rheology 77−48691
acrylic dispersions, shear thinning and thickening rheology 77−52676
adhesive layer, high viscosity thermal resistance 77−1269
aerodynamics, high Reynolds number, global approach and coupling approach 80−48742
Aerosil-filled polyester, viscosity meas. under nonisothermal conditions with rotary viscometer 79−68664
alkali borate glasses, single and mixed, viscosities 80−92701
aluminosilicate glasses, effect of Al_2O_3 on viscosity if ternary aluminosilicates *(Japanese)* 78−83989
amorphous metals, struct. imperfections, review of expt. evidence 79−37630
anisotropic simple materials, transport coeffs., reciprocal relations 77−72708
approximate viscosity matrix, differential-difference representation 80−31518
asphalt, glass transition temp. and viscosity 79−77045
asthenosphere, kinematic viscosity rel. to median valley of Mid-Atlantic Ridge 80−90071
asthenosphere, nonlinear viscosity and stress propag. 79−16422
atmosphere, eddy viscosity coeff. var. 77−70737
atmosphere tides in joint presence of friction and rot., f-plane approximation 79−66847
atmosphere turbulent boundary layer, eddy viscosity coeff. for finite-element numerical modelling 80−77061
B_2O_3-SiO_2 glass, surface flattening kinetics by sinusoidal profile decay method *(Japanese)* 80−34284
Bianchi type-V universes, neutrino viscosity 79−9042
biomembrane drug tolerance, spin label study of ethanol effects 77−66799
biomembrane fluidity, influence on activity of bound enzymes, book contrib. 80−30688
biomembrane microviscosity measurement, light scatt. effects 79−39365
Bjerknes forces in viscous medium and acoustic coagulation of aerosols 77−68680
blood cells, stored, rheological behaviour obs. *(French)* 80−67110
borophosphate glasses, effect of F on props. 78−67657
boson system, multicomponent, transport coeffs., crit. behaviour, kinetic theory 77−2611
boundary layer turbulence, 3D eddy viscosity relations 77−84237
Boussinesq fluids, turbulent viscosity and conductivity in turbulent convection 80−98543
buried obstacle, interaction of shock wave rel. to bulk viscosity of subsoil *(Russian)* 77−89054
butadiene acrylonitrile copolymer, raw elastomer, containing crosslinked particles, flow behaviour 79−37359
butadiene-styrene latexes, viscosity and particle diameter distrib., ageing process *(Polish)* 79−70098
butadiene-styrene three-block copolymer, rheological props., 60-110°C *(Russian)* 79−23292
n-butanol, microemulsion, dynamical and structural props., by chem. physics method 79−79308
ε-caprolactam, after polymerisation under reduced press. *(Japanese)* 78−95929
cataclysmic binaries accretion discs, convection as viscosity source 78−93307
catalysts, heterogeneous, gas phase diffusion and reaction calcs., viscous flow importance 79−47970
cell membrane influence of lipid composition and procaine on hyperthermic cell death 78−27907
cell wall, Acetabularia, deform. rel. to genetic and geometric factors 77−56348
cell wall deform. and morphogenesis, local control of viscoelastic deform., Acetabularia 77−56349
cement pastes, flow behaviour, specific surface and conc. of solids influence 80−65132
cerebroside-lipid mixed films, surface viscosity 79−74601
cholesterol, adsorbed monolayer on aerosil, IR spectra 78−15753
clay suspensions, with negative thixotropy, hysteresis loops, deflocculant addition effect 79−52789
clays, heat treatment, effect on rheological props. of enamel slips 80−60809
close binary stars, tidal friction due to envelopes turbulent viscosity 77−57013
clusters of galaxies, viscosity rel. to intracluster gas heating 79−9011
coal tar pitch, containing mesophase, thixotropic changes occurring on reheating 79−90205
colliding bodies systems in gravit. field, effect of transversal viscosity 77−67026
compact stars, viscosity rel. to evolution of homogeneous ellipsoidal figures 77−33333
concentrated disperse systems, min. energy dissipation principle 77−72339
concentrated disperse systems, non-Newtonian shear viscosity in steady flows 79−81957
concentrated disperse systems, non-Newtonian viscosity model 79−77231
concrete, workability, predictions from viscosity-elasticity analogy, effect of aggregate volume conc. 77−25087
concretes, further development of 2 point test for workability and extension of its range 80−66728
confined acoustic beam in viscous medium, viscous energy losses near boundary 78−18092
constructional materials, creep, viscosity, resist. to inelastic deform. 80−89309
continuous medium eqns. of motion, fluid flow, vol. viscosity, Hamilton Jacobi eqn. *(Russian)* 77−46984

viscosity continued
convection rates of viscous fluid, Earth upper mantle and continental drift appl. *(Russian)* 80−1581
cosmological evolution, effect of viscosity *(Russian)* 77−45624
cosmological fluid, lepton era, transport coeffs., Weinberg-Salam model 78−32623
cosmological fluid, viscous phenomena and entropy in early universe 77−82337
cosmology, Friedman models, viscosity effects *(Russian)* 77−29969
crack propagation, fracture viscosity and plastic flow calc. *(German)* 77−54934
crystalline and amorphous solids, plastic behaviour in terms of defect motions 78−95104
cylinder, circular, wake of steady flow at different Reynolds numbers 80−38416
cytoplasm spherical drop with effective surface tension influenced by oscillating enzymatic reactions 80−108862
dental composite paste, rapid setting non-Newtonian viscosity eval. with parallel-plate plastometer 79−27610
detergent micelle microviscosity, rel. to photochem. activity of chlorophyll 77−21478
dipolar dumbbells in a viscoelastic Oldroyd liquid, dilute soln., electric field effect on rheological behaviour 80−6009
dislocation segments, pinned, effects of viscosity on quantum motion *(Russian)* 80−44207
disperse system, fluid interface, dynamic properties 77−25313
dispersed medium, effective viscosity and heat cond. coeffs. 80−89537
dissipative media, nonlinear, one-dimensional waves, theory 77−58592
drag on sphere accelerating rectilinearly in elastico-viscous fluid, Fourier transform technique 78−51145
Dynamic fluid interface displacement and prediction of air entrainment 78−2337
Earth, convective stability of upper mantle, viscosity jump effect 77−70620
Earth interior, anisotropic viscosity rel. to convection models having multiplicity of large horizontal scales 79−16430
Earth interior, shear heating rel. to viscosity and lithosphere-mantle decoupling 79−20790
Earth mantle, viscosity constraints on convection and Earth thermal history 79−16429
Earth mantle, viscosity rel. to Earth thermal evolution 80−89988
Earth mantle, viscosity-depth funtions rel. to flow one-dimensional modelling 79−39698
Earth mantle viscosity, rel. to Earth tides theory assuming Earth as viscoelastic body 80−67333
Earth upper mantle, viscosity, non-Newtonian fluid 79−79770
education, metallic glasses, phase transition and mech., elec. and mag. props. 78−36765
effective magnetic viscosity due to hydrodynamic turbulence in weak large scale mag. field 77−33340
elastico-viscous liquid flow in axisymmetric pipe of slowly varying cross-section 80−83774
emulsion, dilute, straining motion, effect of inertia on dynamic viscosity 80−87797
emulsion, relative drop-drop and drop-wall motions, slow 79−32641
emulsions, concentrated, rheological props. 80−99981
enamel, melted vitreous, for protective coating appls., gas generation in highly viscous phase *(Russian)* 77−73360
entangled polymers, viscoelastic props., transient network model 78−13918
epithelium of small intestine, mech. props. of intercellular contacts 78−53351
erythrocyte membrane fluidity, adult and neonatal human cells 77−36885
erythrocyte membranes, fluidity change after X-irrad., pyrene excimer fluoresc. obs. 80−72262
erythrocytes, membrane protein vertical displacement, rel. to microviscosity changes 77−44608
ethylene vinylacetate copolymers in paraffin, viscosity of conc. solns. 79−81835
exam. of glass forming region, properties and crystallisation 78−88454
extensional viscosity of a dilute suspension of spherical particles at intermediate microscale Reynolds numbers 80−106835
feldpsar in porcelain, melting behaviour and viscosity meas. *(German)* 79−90758
ferroelectric narrow walls, steady-state motion 80−11356
ferrofluids, dependence on magnetic polarisation *(Czech)* 77−16109
first normal stress difference prediction and dynamic moduli from steady flow viscosity 77−75868
flow curves determ. by method of representative viscosity *(German)* 77−68642
fluid, anisotropic, transport coeffs., perturbation theory 77−7497
fluid, steady rot. screw motion 79−50736
fluid film, approx. eqns. for long nonlinear waves 78−38346
fluid mixture, coeff. prediction 77−43361
free surface in uniform laminar stream 79−98678
friction coefficient, sliding, between liquid and solid, method for experimental det. 78−22307
gas flows, selfgravitating, thermodynamic processes and radiation, numerical method 80−14848
gas mixtures, high temp., transport prop. calc. *(Russian)* 79−37432
gelatin sol-gel transition, viscosity meas. method 80−85219
general physics and heat, book 79−25814
glass, crystallisation and opacity, exam. by high temp. viscometry and X-ray diffr. *(Polish)* 78−84875
glass, flat, dependence of creep, viscosity on cooling intensity, during quenching 80−20964
glass, internal friction in region of transition to viscous-flow state 79−66101
glass, solidification kinetic eqn., derivation from heat transfer and viscosity eqns. 80−25679
glass, viscous flow, examination of mechanism 78−87805
glass and glass-forming liq., viscoelastic properties, comparison with Lennard-Jones model 80−84983
glass formation influence *(French)* 77−55931
glass phase separating, interpretation of temp. dependence of transport process 78−87806
glass viscosity, as function of temp., computer calc. 79−29100
glass with frozen structure, viscous flow, valence configuration flow theory 80−39335

viscosity continued
glasses, commercial, viscosity and stress relax. in glass transition region 80−93589
glasses, industrial, temp. depend. at const. struct. temp. 80−65271
glassy state and highly viscous liq., rheology 80−70130
gravity waves, non-uniform free surface, superficial viscosity and tension *(French)* 80−48728
gyrotropic media, viscosity tensor decomposition calcs. 77−15153
hard sphere fluid, elastic modulus and viscosity coeff. 77−30086
hard-sphere mixtures, excess thermal cond. and viscosity 77−11292
hard-sphere suspension, viscosity, direct inter-macromolecular interactions effects 79−95199
heating of viscous and non-Newtonian fluids on a rotating disk 79−77095
heavy ions collision, liquid drop model generalisation *(Rumanian)* 78−58260
Hercules X-1, accretion disc viscosity determ. using slaved disc model 80−62110
heterogeneous system with chaotic structure, generalized conductivity coefficients, review 77−87708
high loaded contacts, influence of press. and temp. on effective viscosity during lubrication *(German)* 77−46974
hydroxyethyl cellulose, polymer segments, fluoresc. depolarisation on conjugated spin lables 80−91711
ice surface layer, viscosity, from thermal contraction meas., 0 to −50°C 80−49469
ice surface viscosity, activation energy, vacancy migration 80−107458
incompressible turbulence, statistical investigation of eddy viscosity 80−14675
incompressible viscous flow, numerical methods *(Chinese)* 77−82395
incompressible viscous fluid, slow motion of small sphere outside cylinder 80−96239
incompressible viscous Navier-Stokes eqn., numerical soln. by finite element of penalisation type 79−50747
index values, latitudes 77−62659
inelastic and viscoelastic fluid flow past sphere, creeping and boundary layer flow, drag coeff. 77−51090
inorganic glass, viscosity and free vol. 79−94916
interfaces, pure, thermodynamics and dynamics rel. to Spacelab 79−28910
interfacial viscometers, surface shear viscosity determ. 79−23384
interpolation formulae, extrapolatable, for data correlation *(Dutch)* 78−12661
interstellar gas, in disc galaxies, effects of dissipation on response to oval distortions 78−12355
intracellular membrane microviscosity, rat liver and hepatoma 27 80−30675
Invar N36 melt, cast metal struct. depend. on heat treatment, subgrain struct. *(Russian)* 80−40343
isotropic media, linear dynamical eqns. of state, general formalism 78−93639
Jupiter convective interior, turbulent viscosity and tidal Q 77−29713
kinematic, role of vertical natural flow, adjacent to surface transition limits 79−50726
kinetic theory of dense fluids, generalised Chapman-Enskog soln. 79−54033
Kolmogorov's −5/3 power law, statistical derivation by turbulent-viscosity approach 78−90837
laminar flow through rough wall cracks, friction factor formula *(Rumanian)* 80−69925
laminar viscous flow down an open inclined channel with naturally permeable bed 80−69764
lecithin, adsorbed monolayer on aerosil, IR spectra 78−15753
linear Newtonian viscosity, calculative props. 80−68048
liquid, simple kinetic model 78−55793
lithosphere, subducting, dynamic support of ocean trench outer rise 78−81116
low viscosity flows, hybrid vortex-ADI soln. of N-S equations 79−68718
LPDE melt, tensile stress overshoot in uniaxial extension, single integral constitutive eqn. 80−1507
lubricant, shear rheological behaviour at high press. 80−35342
lunar crust, viscosity from large impact structs. isostasy 78−12120
magnetic, ferromagnetic colloid system 78−15715
Mercury crust, viscosity from large impact structs. isostasy 78−12120
metallic glasses, atomic transport behaviour, review *(Japanese)* 79−94907
metallic glasses, flow behaviour, entropy model 77−24345
metals and alloys, polycrystalline, LF viscosity meas. 78−80576
methane, transport coeffs., statistical mech. calcs. 77−7494
methyl methacrylate, free radical polymerisation, viscosity effects 77−81404
methylhydropolysiloxanes, equilibration by catalysts *(German)* 78−35722
microemulsion, viscosity meas. *(French)* 78−61055
micropolar effects in liquids, characts. evaluation under rotating electric field *(Polish)* 79−55638
micropolar fluid drop in viscous fluid, flow, stream functions, velocities, spins, drag 80−53821
minerals, effect of viscosity on release adiabat meas. 80−51388
molecule, moving in compressible viscous fluid, hydrodynamic drag 79−27732
muscle, frog, spin-lattice relax. times for ^{13}C in isotope-enriched glycine 77−44605
muscle cell membrane fluidity rel. to fusion 77−77873
natural rubber, viscosity meas. when various accelerators were added *(German)* 78−30688
Navier-Stokes eqn. discontinuities, appl. of distributions *(French)* 80−6022
nearly viscometric glide bearing fluid *(German)* 79−81830
neurone membrane microviscosity, rel. to elec. activity modulation by Aplysia 78−7329
neutrino-electron mixture, influence of spin and Weinberg-angle on bulk viscosity 77−61223
non-Newtonian fluids oscillating pipe flow, shear dependent viscosity effects 79−77190
nondissipative viscous stresses 78−9741
nonisothermal flow of viscous or non-Newtonian fluids over rotors of centrifugal heat exchangers 79−77097
nuclear matter, thermodynamic model, shear viscosity temp. dependence 78−62499

viscosity continued
Nylon 6 film, prior high-press. treatment effects, weight swelling, density, IR crystallinity, X-ray and viscosity obs. 80−81025
nylon-6 fibre, chain rupture and tensile deform. viscosity-av. mol. wt. obs. 78−76714
ocean, vertical eddy viscosity effects on Rossby and Eady waves 80−51404
optical waveguides, inhomogeneous glass sintering, self stresses producing bulk flow 80−14448
oscillating cup expt., shear elasticity in liqs. digital computer simulation 77−72190
overthrust faulting, model of const. thickness overthrust on visco-plastic sole 80−51378
oxides at high temperatures, crystalline and non-crystalline, surface mass transport mechanisms obs. *(Japanese)* 80−54479
parabolic partial differential equations, operator compact implicit soln. methods 78−89348
parallel tube banks in transverse viscous flow, heat transfer and hydraulic drag *(Russian)* 79−10450
perturbed spherical flows 77−51105
phosphatidylcholine membranes, interaction of colchicine, spin-label study 77−86455
photoemulsions, gels, coloured component addition, struct. form., dynamic shear modulus, viscosity meas. *(Russian)* 80−7871
photographic emulsion 78−16866
photographic emulsions, high shear rate viscosity and dynamic surface tension 79−19495
plastics, extrusion props. prediction using capillary rheometer 79−90204
plug formation in plates, cylindrical projectile impact, nonlocal viscous fluid model 78−49653
PMMA, solvent cast, surface characts., chromatographic study 80−20020
polyamide-polyurethane copolymer dispersions, structurisation and relax. props., coating from props. 80−76559
polybutadiene, hydrogenation 80−26008
polybutadiene rubber, modified with oligoester acrylate, plastic-elastic and rheological props. *(German)* 80−19871
polycaprolactam characteristics dependence, at equilibrium state, on polymerisation conditions, in closed system *(Japanese)* 78−95928
polydimethyl siloxane-b-styrene-b-dimethyl siloxane block copolymer, morphology, mech. props. 80−64930
polyester resin, unsaturated, chalk filled, props. *(German)* 80−104228
polyethylene, high-density, mixed with gypsum, flow props. *(Japanese)* 77−7357
polyethylene, high-density, mixed with gypsum, flow props. *(Japanese)* 77−7358
polyethylene, low density foam production, viscosity meas., comparison with polystyrene *(Japanese)* 77−52276
polyethylene film, chain rupture and tensile deform., viscosity-av. mol. wt. obs. 78−76714
polyethylene oxide, polymer segments, fluoresc. depolarisation on conjugated spin lables 80−91711
polyethylene terephthalate, chain rupture and tensile deform., viscosity-av. mol. wt. obs. 78−76714
polyisoprene, rheological props., accelerator and temp. effects *(German)* 78−34101
polymer, filled, anomalous conc. depend. at low filler concs. *(Russian)* 77−44287
polymer, stiff, optimised Rouse-Zimm theory 78−46472
polymer homologue mixtures, viscosity, conc. depend. *(Russian)* 79−23761
polymer melting, during extrusion, integral energy-balance model 77−46899
polymer melts, particle filled 78−87319
polymer melts, rheological props., effects of hydrostatic press. 80−48663
polymer model, dynamic viscosity, simulation 78−55875
polymer mols., internal viscosity of kinetically flexible chains 77−50575
polymer solutions, dilute and moderately concentrated, intrinsic viscosity 80−48753
polymers, linear and ring, intrinsic viscosities, perturbation calc. 79−55914
polypropylene, film and fibre, chain rupture and tensile deform., viscosity-av. mol. wt. obs. 78−76714
polypropylene-bitumen mixture, thermomech. investigation changes in viscosity, ductility, elasticity, mol. wt. effects *(German)* 78−35454
polyurethane cement, viscosity and shear strength, components influence *(German)* 80−93729
polyvinyl dispersions, viscosity and particle diameter distrib., ageing process *(Polish)* 79−70098
porous medium immiscible viscous displacement, stability anal. 80−48799
primary normal stress function from shear viscosity data 77−68548
proportionate Coulomb and viscously damped isolation system 78−42561
propyl stearate monolayers, elasticity and viscosity determ. by laser light scatt. 77−72749
protein dispersions, viscoelastic effects, shear viscosity and primary normal stress difference 80−87754
protogalaxy, instability of gravitating rot. viscous gaseous systems rel. to ring struct. form. 77−17690
PTFE, rheological props. below m.p. with certain low molecular smectic states 79−87675
PVC, calendering, prediction of stress and torque 79−8266
PVC chlorinated, mol. parameters determ. 79−41974
PVC plastisol, flow behaviour at high shear rate *(German)* 80−92186
PVC plastisols characts. 79−86724
pyrene derivatives, micelle-embedded, rot. relax., time-resolved fluoresc. depolaris. obs. 80−58300
quantum mech. canonical approach to particle motion with dissipative forces 77−57227
quantum phenomenology 78−54298
quartz glasses, viscosity rel. to crystallisation 77−24386
reservoirs, turbulent viscosity and bottom friction of wind driven currents *(Russian)* 77−70700
resin impregnated glass tape, friction and rheological props. 77−63806
rheogoniometry, viscous heating and heat transfer 79−82013
rod external segment surface membrane, lateral diffusion of rhodopsin 78−15828
rubber, filled, viscosity anomalous conc. depend. at low filler concs. *(Russian)* 77−44287
sea ice deformation, viscous law as stochastic average of plasticity 78−16028

viscosity continued
second virial viscosity coefficient, temp. depend. 80−19543
semiflexible and rigid particles in solution 79−94505
silica, vitreous, effects on viscosity of impurity alkali oxide, OH, Al_2O_3 and Ga_2O_3 78−64580
silica, vitreous, vapour-synthesized, viscous flow 78−64581
silicate glasses, viscosity-temp. relation 80−2187
simple fluid shear depend. viscosity, central force interactions 80−79970
sintering, rheological and microscopical models, relationship 79−95963
skin friction measurement, comparison of viscosity balance and Preston tube methods 77−55109
slow viscous flow due to motion of sphere on axis of circular cone 80−14654
sludge, cohesive, dynamic props. *(Japanese)* 80−45580
smooth pipe flow, location of eddy viscosity maximum 79−81860
sodium dodecyl sulphate, microemulsion, dynamical and structural props., by chem. physics method 79−79308
sol near sol-gel transition, Rouse approx. *(French)* 78−61054
solar convection zone, turbulent viscosity rel. to mag. fields floating-up time and 11-year cycle 80−101580
solar convective zone, non-stationary mechanisms rel. to non-uniform ang. vel. distrib. maintenance *(Russian)* 79−96985
solid body-microparticle impact, cratering, viscous effects 79−66255
square well fuild, elastic modulus and viscosity coeff. 77−30086
SS 433, accretion disc viscosity determ. using slaved disc model 80−62110
stability analysis and characts. for two-phase flow eqn. systems with viscous terms 80−59103
stars, rigidly rotating, secular instabilities due to viscosity 80−4342
stars, rigidly rotating, secular instabilities in general relativity due to viscosity 80−4341
stars, rotating Newtonian, secular instability to gravit. radiation and viscosity 78−53922
statistical mechanics, response theory for systems nonlinearly displaced from equilibrium, graphical approach 80−22285
steel, austenitic Mn-Ni ageing , alloying element influence on struct. and mechanical props. *(Russian)* 80−35256
steel, martensitic low C, development and props. *(Russian)* 80−20933
steel, shock transition rise-time meas., limiting viscosity coeffs. 79−77680
steel EI736, creep, viscosity, resist. to inelastic deform. 80−89309
stellar accretion discs, viscosity determ. for Hercules X-1 and (SS 433) 80−62110
stellar models, secular instability of Maclaurin spheroids due to gravit. radiation and viscosity 77−17538
Stokes flow, attached and free eddies 80−48679
Stokes flow, eddy structure between two spheres with relative vel. 79−27647
Stokes flow, Faxen relations generalisation 79−32438
subsonic viscous flow, 3-D unsteady actuator disc theory 79−27615
Sun, two-dimensional eddy viscosity rel. to differential rot. problem 77−53518
Sun convective zone, anisotropic viscosity rel. to differential rot. mechanism 79−25556
suspended spheres, effective shear viscosity of regular array 78−51718
suspension, conc., of aggregable particles, viscosity calc. 79−7362
suspensions, effective viscosity, modified cell model approach 80−74944
suspensions, heavily filled, viscosity relations 80−48776
thermo-viscous materials, with hidden variables, shock waves and acceleration waves 80−74788
thermodynamics, relativistic, nonstationary, hidden variable approach 80−68097
thermoviscous solids with microstructures, irreversible thermodynamics 78−34005
thin pipe with thin linear elastic wall, viscous fluid motion model 79−64769
toluene, microemulsion, dynamical and structural props., by chem. physics method 79−79308
transient natural convection in curly viscous fluids, boundary layer approx. 79−77096
tube/fluid vibrations, effects of fluid viscosity 79−3967
turbine flowmeter, universal viscosity curve, errors 78−34243
turbulent jets and wakes, development and struct., variable eddy viscosity formula 79−37371
turbulent pipe flow, use of eddy viscosity expressions for vel. profiles in Newtonian, non-Newtonian and drag-reducing flows 80−83789
turbulent viscosity in stellar convection zones, effect of rot. 80−36612
two-dimensional shear flow, viscosity effects, microscopic model 77−89085
ultrasound resonance absorption by moving dislocation 80−54318
unsteady squeezing of viscous fluid from tube 79−90296
Van der Waals fluid near critical pt., transport props. 79−46537
vinyl alcohol-vinyl acetate copolymers, mol. architecture and physicochem. props. 80−44103
viscid-inviscid interaction of incompressible separated flows 77−19593
viscoelastic fluid flow past sphere, anomalous separation, wake formation 77−51091
viscoplastic material, mixing process, Bingham model, two-dimens. flow *(German)* 80−92076
viscous flow in a partially filled rotating horizontal cylinder, effect of speed of rotation on bubble position 79−77125
$e\bar{e}\nu_e\bar{\nu}_e$, reactive mixture, bulk viscosity 78−45565
Al, shock transition rise-time meas., limiting viscosity coeffs. 79−77680
Al-Cu, partially solidified, viscosity and struct. *(Japanese)* 79−14950
Al_2O_3-SiO_2 refractory, creep, viscosity, resist. to inelastic deform. 80−89309
As-Se-Te glasses, glass form., charact. temp., density, thermal expansion and dynamical viscosity, struct. model 78−26672
$(AsSe)_{1-x}Te_x$ glasses, thermal props. and viscosity, temp. and conc. depend. 77−76324
B_2O_3-SiO_2, optical waveguide glass, sintering kinetics 80−84898
$BaGeO_3$-$(0.25MgF_2.0.75YF_3)$-Ga_2O_3 glass, synthesis and props. 80−25648
BaO-La_2O_3-GeO_2, exam. of glass forming region, properties and crystallisation 78−88454
$Ba(PO_3)_2$-MgF_2=$0.4AlF_3.0.6CaF_2$ glass system, vsicosity and energy parameters of rheological props. *(Polish)* 79−73331
C mixes, rheological props. at very low shear rates using capillary rheometer 77−65691
C mixes, rheological props. using capillary rheometer, binder content depend. 77−65692

viscosity continued
CaO-Al_2O_3-SiO_2 based glasses, kinetic parameters of glass ceramic form. determ. 77−24385
Co_5Ge_3, solid and liquid, physicochemical props. and structure 80−39548
Cu, shock transition rise-time meas., limiting viscosity coeffs. 79−77680
(Fe,Co)PBAl, metallic glass, viscous flow, alloying effect 78−79793
Fe ore concentrate, sinter quality improvement *(Chinese)* 80−104089
$Fe_{40}Ni_{40}P_{14}B_6$, amorphous, steady-state creep rate, cryst. effect 80−81102
$Fe_{40}Ni_{40}P_{14}B_6$ metallic glass, isothermal viscosity and crystn. 80−49395
$Fe_{40}Ni_{40}P_{14}B_6$, Metglas 2826, acoustic emission during viscous flow 78−42915
H plasma, viscosity calcs. *(Russian)* 80−53953
$K_2(F,O)$-B_2O_3-SiO_2, effect of replacing B_2O_3 by Al_2O_3 or Ga_2O_3 78−63677
K_2O-Al_2O_3-P_2O_5 glass, low-temp. viscosity 80−39198
Kr, molecular dynamics simulations, three effective interactions 79−69224
LiF-$NaPO_3$-MeF_x (Me=Mg, Ca, Al) glasses, IR spectroscopy study 80−16042
Li_2O-Al_2O_3-SiO_2 glasses, viscosity, thermal expansion, glass transform. temp., and refr. index 79−42282
Li_2O-SiO_2 glass, water content effect on crystal nucleation and growth 79−55670
MgF_2, hot pressing in vacuum, compaction kinetics, selective recryst. 77−16517
MgO-CaO-Al_2O_3-SiO2(-TiO_2) systems, glass-ceramics, crystn. kinetics *(Russian)* 79−37626
NaO-B_2O_3-SiO_2, phase separated glass, viscosity and microstruct., heat treatment effect 79−99343
Na_2O-2CaO-3SiO_2 glass, cryst. nucleation and growth, viscosity, thermodynamic props. 80−84079
Na_2O-Al_2O_3-P_2O_5 glass, low-temp. viscosity 80−39198
Na_2O-CaO-SiO_2 glass, water content effect on crystal nucleation and growth 79−55670
Na_2O-CaO-SiO_2 glass, surface viscous flattening kinetics, sinusoidal profile decay method 79−79139
$2Na_2O$-CaO-3SiO_2 glass, cryst. nucleation rate, viscosity, heat treatment 80−84081
Na_2O-GeO_2 glasses, low temp. viscosity, as function of composition 78−38865
Na_2O-SiO_2 glass, OH^- content effect on mech. and other props. 80−89337
Na_2O-SiO_2-SnO_2 (TiO_2) glass, exam. of Na^+ self diffusion, elec. conductivity, and viscosity 78−87819
Ni alloy KhN56VMKYu, creep, viscosity, resist. to inelastic deform. 80−89309
Ni_5Ge_3, solid and liquid, physicochemical props. and structure 80−39548
NiPBAl, metallic glass, viscous flow, alloying effect 78−79793
PbO containing crystal glasses, viscosity, effects of Li_2O, BaO, ZnO, MgO and SrO 80−19973
PbO containing crystal glass, viscosity-temp. depend., glass transition, and softening point 80−24637
PbO-SiO_2, surface flattening kinetics by sinusoidal profile decay method *(Japanese)* 80−34284
Pd-Ni-P, metallic glass, viscous flow, alloying effect 78−79793
$Pd_{77.6}Cu_6Si_{16.5}$, metallic glass, viscosity meas. from rates of thermal transformations 78−26713
$Pd_{48}Ni_{32}P_{20}$, metallic glass, viscosity meas. from rates of thermal transformations 78−26713
Pt-Ni-P, metallic glass, viscous flow, alloying effect 78−79793
$Pt_{45}Ni_{30}P_{25}$, metallic glass, viscosity meas. from rates of thermal transformations 78−26713
Se, amorphous, correl. between mol. struct. and props. 77−11484
Se, amorphous, viscosity meas. using holographic technique 79−37263
Se amorphous films, structural relax., viscosity, creep, heat capacitors, and IR spectra meas. 79−42424
Se-Ge-Sb alloy glass, crystn. kinetics 77−20057
SiO_2, on Si, viscous flow meas., 960 to 1075°C 77−39729
SiO_2 powder filled epoxy resin, flow props. during curing *(Japanese)* 78−59355
SiO_2, vitreous, heat treatment effect on viscosity and struct. 80−19714
SiO_2, vitreous 80−103513
SiO_2-Al_2O_3-CaO-MgO-Na_2O-K_2O effect of partial substitution of Na_2O by K_2O, on crystallisation 80−10499
Sn-Pb (15 wt.%), partially solidified slurry, exam. of structure, viscosity 78−84793
Tb-Fe amorphous thin films, magnetic after-effect, Kerr magneto-optic effect obs. 80−97123
TiN, thermoplastic slips, viscosity, thixotropy, dilatance determs. 80−25633
UF_4-LiF(KF) molten binary mixtures, viscosity meas. 80−65270
ZnB_2O_4-MF_2 (M=Mg, Ca, Sr, Ba) glass system, physicochem. props. 80−34877

viscosity measurement
see also viscometers
acrylic bone cement viscosity characterisation 79−79690
air and water flows, measurement of skin friction using viscosity balance 79−64811
amalgam preparation without O_2, apparatus to measure viscosity 80−59150
automatic rotating disc viscometer with servomotor *(Russian)* 77−19649
blood, red cells, rheological props. meas. by Couette viscometer 80−97992
capillary rheometer, end correction for power-law fluids 78−91037
diamond anvil pressure cell, accuracy 78−83504
drop falling through liquid, for teachers 79−40331
dynamic viscometer theory 79−77315
elastic waveguide slow torsional wave sensors 79−46748
electrolyte solutions in glycerol, investigation by US shear strains 80−88266
ethylene-vinyl-acetate copolymer melt, viscosity 79−33105
extensional flow capillary rheometer for extensional viscosity meas. 78−55704
falling slug method, intensity fluctuation spectroscopy appl. 78−71408
fatty acid monolayers, light scatt. meas. 80−89011
film probes, flush-mounting, effect of probe-body temp. changes on stability 77−7482
flow injection analyser, microprocessor-based 80−33713

viscosity measurement continued
gas, Rankine-type capillary viscometer *(Japanese)* 80−14859
gas, vibrating disc method 78−71416
gas friction, detector using active permanent magnet suspensions 78−24829
high pressure viscosity meas. method 80−69955
high viscosity fluid continuous meas. device 78−5834
high-temperature viscosity measurements by gas percolation through porous medium 78−1781
holographic method, appl. to amorphous Se 79−37263
Hoppler viscometer ball passage time meas. digital electronic circuit *(Polish)* 78−47075
intermolecular potential energy in gas, determ. from viscosity meas. demonstration 77−13556
liquid, 25 to 100 C, up to 500 MPa, falling body instrument 80−103510
liquid, and solid particle shape factor, device employing Stokes' method 79−23382
liquid, complex apparatus for viscous and elastic prop. meas. at high press. 78−9734
liquid gas interfaces, contactless method 79−1277
liquid metal, meas. by torsional oscillation method, crucible size effect 77−51139
liquid metals, apparatus for 80−59759
liquids, capillarity method determ. 80−82619
liquids and gases, transient hot-wire technique 79−200
liquids under shear, Couette cell for birefringent, viscous and dielectric props. meas. 78−37034
lyotropic liquid crystals formed by phosphated polyoxyethylene surfactants, n-hexane, water, rheological props. meas. 77−54947
melt dynamic viscosity meas., vibr. method 77−90519
metal, liquid, viscosity determination by oscillating vessel method *(Japanese)* 80−70439
metallising slurry viscometer 78−59509
NaCl aqueous solutions, viscosity at high temps. and pressures, investigation 78−95175
Newtonian, using rotational interferometric viscometer 79−50824
Newtonian liquid between coaxial cylinders, end-effect correction of Margules eqn. 78−79399
non-Newtonian, aperiodic industrial viscometer *(Russian)* 80−53897
nonisothermal conditions measurement of fluid rheology with rotary viscosimeter 79−68664
oil films, interferometric methods 77−89214
oxide melts, at 1000 to 1750°C, methods survey *(Slovak)* 80−47079
parallel-plate plastometer, appl. to rheology of filled polymer melts 79−77036
phase vibration method appl. to large viscosity meas. 77−72375
photoreceptor membrane viscosity and component dynamics, recombination kinetics method 79−39366
piezoelectric method for fluids at 40 kHz 78−59519
planar piezoresonator shear vibration mode 77−19643
plastic extrusion process 77−27639
poly-ε-caprolactone, melt, crystallisation kinetics, shear effects 79−69021
polyethylene oxide, melt, crystallisation kinetics, shear effects 79−69021
polymer, multicapillary two-phase viscometer *(Polish)* 79−4097
polymer, one-bulb capillary viscometer appl. *(Polish)* 78−42687
polymer melt, viscosity, normal stress coeffs. determ. method *(German)* 79−7360
polymer melt, viscosity under hydrostatic pressure, falling cylinder viscometer *(German)* 77−55115
polymer melts, Brabender torque rheometer calibration and reading's interpretation 79−10620
polymer solutions, automatic recording capillary viscometer meas. 77−27631
polymers, conc. solns. in volatile solvents, high temps., method for viscosity meas. 80−19535
PVC, thermal stabilisation by triazine dithiols *(Japanese)* 80−108386
recorder with programmed dispensing unit for chemical reaction 77−89212
rolling bottle device, for measuring flow of liqs. and powders 80−6174
rotary viscometer operational principles *(Russian)* 78−91039
rotational viscometer, non-Newtonian fluid viscosity measurement 80−19529
simple fluid, light scatt. depolaris., shear viscosity meas. 77−27647
slurries using vibrating viscometers, assessment 80−28586
Stokes' law, school lab. course 77−87613
Stokes's law experiment correction, student lab. expt. 77−33800
structure-forming solutions, double light refraction and viscosimetry 79−94745
supercooled liquids, Couette-type viscometer with capacitor assembly for meas. small rotational vels. 80−100046
superheated liquid, viscosity meas. apparatus and technique for use at high press. 77−58823
temperature controlled water bath for glass capillary viscometers 78−59525
temperature meas. at fixed viscosity, instrum. 78−1764
thixotropic materials, characterisation via extrusion rheometer 77−63876
timer for plasma viscosity measurement 79−20690
torsion pendulum viscometer micro-processor assisted, high precision 79−50816
ultimate shear stress meas. by modified impact viscometer at high pressures 79−18980
viscoelastic fluid, steady shear viscosity meas. using falling ball viscometer 79−94565
viscoelastic liquid, second normal stresses meas. using rot. sphere viscometer 78−79391
viscometer, lifting liquid type *(Japanese)* 79−82005
viscometer automatic thermo-compensator stability improvement *(Russian)* 77−55114
viscometric data from Brookfield RVT viscometer, conversion to shear stress-shear rate relationship 80−1495
volatile liquid, boundary viscosity, meas. by blowoff method 79−11006
volatile liquids, boundary viscosity using blow-off method 79−23383
water, mobility in blood plasma, NMR determ., viscosity correl. to $1/T_2$ 80−67176
water, viscosity meas. behind shock wave front *(Russian)* 77−31707
water-fluidised bed, viscosity meas. by oscills. damping 78−59475
CO_2 and SF_6 on temp. at moderate densities 77−19653
Fe, cast, hypoeutectic, primary crystn. features by means of apparent viscosity meas. in early stages of solidification *(Japanese)* 79−43231
Fe-Al liquid alloys, apparatus for viscosity meas. *(Czech)* 80−29103

viscosity measurement continued
$Fe_{40}Ni_{40}P_{14}B_6$, metallic glass, glass transition, viscous flow and differential scanning calorimetry meas. 80−96635
Hg vapour, viscosity and thermal cond. meas., data anal., 694-1054K 80−19545
Hg vapours, vibr. disc method, 620-800K 80−19530
NaCl, using absolute oscillating cylinder viscometer, 810 to 930°C 79−82003
SF_6 viscosity, investigation 78−94884
Sn, viscosity meas. *(Italian)* 79−19137

viscosity of gases
acetic acid, viscosity of dissociating vapour 78−5840
n-alkane+Ar mixtures, intermol. pot. using Kihara model with spherical cores 77−54591
atmospheric wave propag., viscous diffusion, heat loss damping mechanism 80−56516
benzene, vapour, theoretical study 77−3904
binary gas mixture, kinetic theory collision integrals, generalised phase shift approach 80−83874
binary gas mixture, transport properties in applied mag. field 80−83873
binary mixtures, use of diffusion and second virial coeffs. to predict viscosities 79−14506
butane, gas, absolute viscosity 77−35299
n-butane, viscosity meas. at atm. press. and 25-195°C 79−86550
n-butane-isobutane mixtures, viscosity meas. at atm. press. and 25-100°C 79−86550
n-butane-N_2(CO_2) mixtures, viscosity, diffusion coeffs. 80−1722
butyric acid, viscosity of dissociating vapour 78−5840
critical exponent for shear viscosity of simple, binary and ternary fluids 78−83988
critical fluids, non-Newtonian effect and normal stress effect 80−49396
dense fluid, obs. rel. to Enskog hard-sphere transport theory 77−1254
dense gas, logarithmic density dependence of viscosity and thermal cond. 77−51150
dense gas mixtures, viscosity, composition depend. 77−35295
dense gases, density dependence of transport coeffs., viscosity 79−94757
dense gases, viscosity and thermal cond. 79−46415
diffusers, curved, performance, separation in subsonic, transonic channels *(French)* 78−94818
difluoromonochloromethane, parameters of Lennard-Jones 12-6, Stockmayer 12-6-3, 6-Exp, Kihary intermol. pots. 77−34711
dilute gas, transport props., simple pair pot. model 80−87835
dilute gas mixtures, transport props., calc. prog. 80−10342
dilute gas transport props., logarithmic term in softness expansion 80−83872
dilute hard sphere gas, effect of long mean free paths 77−42952
eddy, atmospheric flow over two-dimensional obstruction *(Italian)* 79−20956
ellipsoidal molecular models, transport props. determ. 77−68725
energy transference analysis, press. effects 78−51271
ethane, gas, absolute viscosity 77−35299
ethane, viscosity and thermal cond. of liquid and gas, correl. eqns. 78−26715
ethane-CO_2(N_2)(SF_6)(tetrafluoromethane) mixtures, viscosity, diffusion coeffs. 80−1722
ethylene, gas, absolute viscosity 77−35299
fluid, reacting spheres, kinetic theory 78−35668
fluids at evaluated pressures 80−2191
formic acid, viscosity of dissociating vapour 78−5840
gas ejector, with slotted nozzle, effect of viscosity on limiting performance 77−27572
gas flow, through ultrafine capillaries 80−6151
global existence theorems for soln. of viscous heat-conducting perfect gas *(French)* 77−68363
heat pipe, spectroscopic, operation 80−106708
homonuclear diatomics, dilute gas transport props. calcs. 77−72399
hydrocarbon, internal degrees of freedom, Eucken factor, effect on transfer props. 78−22445
inert gas, transport and equilib. props., using LJ (12-7) pot. 79−98849
inert gas binary mixture, unlike mol. force consts. from viscosity data, thermal cond. 78−33565
inert gases, viscosity, expt. and derived from statistical models *(French)* 77−35302
inert gases, viscosity rel. to ionis., skin friction of wetted oscill. disc 78−34252
interaction potential, direct determ. from gas viscosity meas. 78−37702
intermolecular pair pot. energy function from gaseous transport coeffs. 78−62870
intermolecular pair pot. energy function from gaseous transport coeffs., unlike monatomic interactions 78−62871
intermolecular potential energy in gas, determ. from viscosity meas. demonstration 77−13556
isobutane, viscosity meas. at atm. press. and 25-195°C 79−86550
kinetic theory, mol. gas viscosity coeff. 79−41784
low-pressure gas discharge, mean free path and viscosity, mag. field effects 80−24282
magnetoviscosity coefficient, polyatomic gases 79−55436
measurement using transient hot-wire technique 79−200
mechanism, in simple liquids and gases, interrelation *(Russian)* 78−67846
methane, gas, absolute viscosity 77−35299
methane, intermol. pair pot. energy function 77−10721
methane-ethane-propane-butane, binary and multicomponent mixtures, viscosity, diffusion coeffs. 78−94883
mixtures, one-fluid approx. transport coeffs., critical region behaviour 79−14951
mixtures, viscosities estimation, new simplified methods 77−80261
monatomic gases, quantum corrections to transport coeffs. 77−15148
monatomic gases, transfer coeffs., 100-3000K 79−82021
multicomponent mixtures, prediction by corresponding states law, meas. by oscillating disc instrument 77−31414
multicomponent mixtures of gases *(French)* 79−90363
nonlinear shear viscosity in steady Couette flow 80−28588
nonlinear viscous flow in 2-D and 3-D, kinetic theory 79−50694
nonstationary viscous flow of thermally conductive gas around semi-infinite plate, numerical anal. 80−6104
partly ionised gas, viscosity calc., simplified expressions 79−18983
perfect gas, blast wave with transport props., self-similar soln. 77−68621
phenol, vapour, viscosity coeff. and second virial coeff., conformity with Lennard-Jones pot. *(German)* 79−32732

viscosity of gases continued
polar gases, viscomagnetic effect 77−84384
polyatomic gas viscosity related to Cp and molal vol. 78−34248
polyatomic gas-inert gas mixture, viscomag. diffusion flux 78−47087
propane, gas, absolute viscosity 77−35299
propane, viscosity and thermal cond. correl., liq. and gas 140-500K 79−77332
propane-$N_2(CO_2)$, mixtures, viscosity, diffusion coeffs. 80−1722
propionic acid, viscosity of dissociating vapour 78−5840
propylene, viscosity meas. at 298 to 473K *(German)* 77−42954
pulmonary airway constriction localisation using gases of varying density and viscosity 77−12949
pulmonary resistance, lower, effect of gas phys. props. and flow 77−12945
pulmonary resistance distribution, effects of gas density, viscosity and flow-rate 77−12948
spinning drop interfacial viscometer, liquid-gas interface, surface viscosity meas. 80−44395
square well fluid, viscosity, transport processes 79−98847
standards for single substances and mixtures 78−14481
steam, dynamic viscosity, eqn. at −20 to 150°C 77−20103
steam, effective spherically symmetric pots., applicability to viscosity calc. 78−1779
steam, low and moderate density, compressibility factor and viscosity coeff. eqn. 80−33722
steam, viscosity, international formulation 78−26714
steam-air mixture, condensation, transport and thermodynamic props. *(Japanese)* 78−34251
subsonic laminar viscous gas flow in flat channels and in shadow regions *(Russian)* 79−50749
symmetric top molecules, viscosity and thermal cond. under simultaneous elec. and mag. field 80−6188
teaching, relax. approx. to Boltzmann eqn. approach 78−73804
temperature variation 77−89222
transition regime, tangential viscosity model, density depend., appl. to He 79−1280
two-dimensional rotational flow, large Reynolds no., numerical calc., discrete vortices with random walk 77−31312
velocity correlation functions, transport props. predictions, medium density 77−7500
viscosity and diffusion coeffs. 77−89225
viscous gas eqn., movable net difference scheme *(Russian)* 79−50838
viscous gas flow, subsonic and supersonic, simplified Navier-Stokes eqns. 80−31520
water, vap., averaged potential for complex polar fluids 80−48833
air, viscosity rel. to ionis., skin friction of wetted oscill. disc 78−34252
Ar and Ar-NH_3 mixtures, viscosity under press., density depend. and mol. assoc. 80−1727
Ar, bulk viscosity, density depend. calcs. 77−3903
Ar, dense gas, thermal cond. and viscosity coeffs., irreversibility and Kirkwood superposition hypothesis *(French)* 78−94881
Ar, force constant props., 12-6 pot. model 78−13563
Ar, interatomic pot. and transport props. 77−14519
Ar, shear viscosity determination under high pressure, using capillary viscometer 78−55708
Ar, transport props. with Lennard-Jones (12-6) pot., distance parameter 79−55437
Ar, viscosity, meas. up to 2000K by percolation through porous medium 78−1781
Ar, viscosity meas. at very high press. 80−59155
Ar-Kr, pair pot. energy functions, gas phase bulk property reproduction 77−27642
Ar_2, interatomic potential single parameter 80−48059
CF_4-CH_4-CO_2-SF_6, prediction by corresponding states law, meas. by oscillating disc instrument 77−31414
CF_4-He(Ne)(Ar)$(N_2)(CO_2)(CH_4)$ mixtures, viscosity and diffusion coeffs. 77−89225
CO_2, viscosity, density expansion near critical temp. 80−53909
CO_2, viscosity meas. at 298 to 473K *(German)* 77−42954
CO_2, viscosity meas. at low temps. 80−6193
CO_2, viscosity rel. to ionis., skin friction of wetted oscill. disc 78−34252
Cs, up to 1620K 77−1254
D_2O, gaseous, viscosity, 200-400°C, up to 300 bar 78−63527
F_2, viscosity coeffs., modified hard-sphere calcs. 77−11295
H_2, dissociated, viscosity, thermal cond., 1-1000 bars, 2000-10000K 77−39391
H_2, viscosity meas., 25-100°C, up to 120×10^5 Pa 79−32731
H_2-NH_3 mixture, viscosity meas., 25-100°C, up to 120×10^5 Pa 79−32731
H_2+alkali metal, exchange reactions and rot. transfer effects on transfer coeffs. 77−66749
HD+He, relax. and kinetic cross-sections, DWBA calcs. 79−41782
He, accurate empirical intermol. pot. 79−68291
He, coeff. from thermal conductivity, 400-2500K 77−54586
He, dense gas, transport eqns., shear viscosity and acoustic vel., quasi-particle kinetic eqn. calcs. 80−53906
He-Kr(Xe), scaling parameters for thermal diffusion factors, viscosity, mutual diffusion coeff. calcs. 77−35292
He+Ar, interatomic pot. well depth, SPFD pot., diffusion, viscosity and second virial coeff. 80−5599
Hg vapour, viscosity and thermal cond. meas., data anal., 694-1054K 80−19545
Hg vapours, viscosity meas. by vibr. disc method, 620-800K 80−19530
I_2, dynamic friction coeff. meas. by saturation spectroscopy, radiative lifetimes 78−18368
Kr, interatomic pot. and transport props. 77−14519
Kr, Lennard Jones (12,6) pot. distance parameter, transport props. calc. 80−79423
Kr mixtures, binary and ternary, viscosity meas. 78−18367
Kr, near solidification, 50°C, up to 6500 bar, meas. and simulation using Lennard-Jones pot. *(French)* 78−67301
Kr, shear viscosity determination under high pressure, using capillary viscometer 78−55708
Kr, viscosity, vibr. disc method meas. 80−75020
Kr, viscosity coeff., density expsn. 78−91054
N_2, dilute gas transport props. calcs. 77−72399
N_2, measurement using capillary-type closed viscometer, effect of unsteady flow 78−9736
N_2, measurements using oscillating disc type viscometer 78−51273
N_2, thermodynamic and transport props., consistent correlation using Lennard-Jones (12-6) and Buckingham (exp-6) pots. 78−91045

viscosity of gases continued
N_2, viscosity determ. up to 2000K 79−32730
N_2 viscosity meas., capillary method *(Japanese)* 77−35301
N_2, viscosity rel. to ionis., skin friction of wetted oscill. disc 78−34252
N_2-NH_3 mixture, measurements using oscillating disc type viscometer 78−51273
NH_3, measurements using oscillating disc type viscometer 78−51273
NH_3-Ar mixture, thermal cond., viscosity, Senftleben-Beenakker effect 80−100054
NH_3-He mixture, viscosity, Senftleben-Beenakker effect 80−100054
N_2O, and mixtures with CO_2 viscosity and thermal cond. coeffs. predictions, 180-900K, ≤23 MPa 77−84383
N_20, viscosity meas. at low temps. 80−6193
Na, vapour, viscosity meas., 1101-1186K, 0.2-0.8 bar 80−1723
Na, viscosity meas., 727-1109K 78−71416
Ne, interatomic pot. and transport props. 77−14519
Ne, Lennard Jones (12,6) pot. distance parameter, transport props. calc. 80−79423
Ne, shear viscosity determination under high pressure, using capillary viscometer 78−55708
O_2, rotational collision number, diffusion coeffs. 79−1281
O_2, shear viscosity coeff., 75-300K, up to 34 MPa 78−34253
O_2 viscosity coeffs., modified hard-sphere calcs. 77−11295
O_2, viscosity rel. to ionis., skin friction of wetted oscill. disc 78−34252
Rb vapour, viscosity rel. to thermal cond. 79−72982
SF_6, equilib. composition and transport props., 300 to 15000K 77−24051
SF_6 viscosity, investigation 78−94884
SF_6, viscosity meas. at low temps. 80−6193
SF_6-He(Ne)(Ar)$(N_2)(CO_2)(CH_4)(CF_4)$ mixtures, viscosity and diffusion coeffs. 77−89225
SF_6+H_2 mixture, equilib. composition and transport props., 300 to 15000K 77−24051
Xe, Lennard Jones (12,6) pot. distance parameter, transport props. calc. 80−79423
Xe, viscosity meas., 170-1300K, up to 1000 bar 78−42698
Xe+He(Ne)(Ar)(Kr), binary mixture viscosity and diffusion coeffs. 78−38443

viscosity of liquids
see also lubrication
acetate ion radicals, solns., pulse radiolysis, CIDEP, viscosity depend. 77−75189
acetic acid-acetone mixture, physical parameters 80−2716
acetic acid-H_2O, assoc. liq., struct. props., static and dynamic phys. props. meas. 79−70316
acrylamide aqueous solution, ultrasonic investigation *(Chinese)* 80−107371
acrylonitrile methallylsulphonate copolymers in DMF, polyelectrolyte behaviour 79−66351
acrylonitrile-butadiene-styrene terpolymers Sb_2O_3 effect of melt viscosity *(German)* 78−18265
acrylonitrile-styrene copolymer melts, rheological behaviour *(German)* 77−51012
air entrainment at solid/liquid/gas interface 77−1276
Al-Si (2.4 wt.%), liq. fluidity, solid-liq. coexisting zone *(Japanese)* 80−15175
albumin, bovine serum, macroion soln. viscosity and diffusion, quasielastic light scatt., electrostatic interaction 79−70508
alcohols, assoc. liq., viscous props. 80−2186
alcohols, H-bond system, liq., high-press. effect 80−49080
alcohols, US effects on shear viscosity 78−59184
alkali, chlorides, aqueous solns., high precision visocity meas. 80−10695
alkali halides, aq. solns., isomorphous salts viscosity investig. 78−95173
alkali halides, aqueous area solutions, conc., viscosity meas. 79−23759
alkali halides, molten, rigid sphere model 77−7946
n-alkane-dimethylsiloxane mixtures, shear viscosity press. depend. 78−30775
n-alkanes, obs. and anal. of depolarised Rayleigh doublet 78−35154
n-alkanes, oligomers, hydrodynamic behaviour, viscosity 77−559
n-alkanes, rel. to hypersonic attenuation, temp. depend. of Brillouin spectra 79−11426
N-alkylpyridium halides, molten, and mixtures with $AlCl_3$, density, elec. cond. and viscosity meas. 80−24630
alloy, binary liq., viscosity coeffs. by Enskog theory 80−1920
andesite melt, viscosity at high press. 77−29291
aniline-cyclohexane, viscosity conc. and temp. depend. in crit. mixing region 77−35686
anilines, substituted, in benzene, dielectric relax. and mutual viscosity, obs. 79−38449
apparent viscosity in viscometric flows 77−68920
p-aromatic poly(amide hydrazide), dimethyl sulphoxide solvent, dynamic birefringence, conform., viscosity *(Russian)* 78−39525
aromatic polyamides, rigid and nonrigid, ultrahigh modulus fibres 79−95992
atomic liquids, shear viscosity determ. by nonequilib. mol. dynamics 80−79971
auramine O, fluoresc. efficiency, solvent viscosity effects at high press. 78−9188
azo polyamide, solutions, spectra and viscosity 79−68340
azoxy compound, liquid cryst. mixture, nematic, elec., optical and viscoelastic props. 79−55803
basalt melt, viscosity at high press. 77−29291
BBB, polybisbenzimidazobenzophenanthroline-dione, solns., viscosity rel. to temp. 77−4137
BBOA, pretransitional shear viscosity divergence near smectic A-smectic B transition 79−33077
benzene, liq., mol. motion at high press. 80−103509
benzene-polystyrene, semidilute solns., viscosity and reptation time 79−99345
benzenes, isomeric substituted, viscosity near freezing pt. 79−51292
benzenes, nitrohalide substituted, microwave absorpt., mol. struct. 78−75522
benzenes, substituted, dense liq., mol. reorientation and shear viscosity 77−4213
benzophenone-Eu complex, triplet-triplet energy transfer, viscosity and temp. depend. 79−87847
bilayer membrane dynamics, combination of Rouse model and Marcelja liq. cryst. theory 79−100581
binary acid+base mixtures, excess vol. and viscosity 77−21408
binary alloys, excess viscosity 77−55380

viscosity of liquids continued
binary and ternary systems, pred. of isothermal vapour-liquid equilibria, heat of mixing, viscosity 77−31761
binary critical mixtures, shear viscosity, pseudospinodal curves and scaling 78−22844
binary fluid, crit. transport props., theory 78−14497
binary liquid mixtures, effectiveness of mixture eqns. 77−69109
binary liquid mixtures, viscosities, comparison of eqns. 77−59135
binary liquid mixtures, viscosity, Panchenkov model calcs. *(German)* 77−31797
binary liquid mixtures, viscosity isotherm classification *(German)* 77−28033
binary liquid mixtures, viscous flow props., mol. thermodynamic theory 78−2280
binary liquid system, viscosity calc. method 77−55318
binary liquid systems, apolar-apolar and polar-apolar, significant structure theory, appl. 80−1909
binary mixture, high-frequency sound absorpt. near crit. separation point 78−83881
binary mixture, viscosity, semi-empirical procedure, data correlation 78−34643
binary mixtures, viscosity rel. to thermodynamic excess functions *(German)* 77−35740
binary polymeric mixtures, soln. viscosities meas. 80−54423
biological cell saturation density, evidence against diffusion-limited process 78−48770
biomacromolecules, rigid, modelling approaches of hydrodynamic props. 80−61613
bitumens, oil sand, rheological props. 80−64506
blood, rheological parameters for viscosity, viscoelasticity and thixotropy 80−16963
blood, variation associated with hyperlipoproteinaemia rel. to cardiovascular risk factors *(German)* 78−57031
blood oscillatory flow, Fahraeus-Lindqvist effect 80−3668
blood plasma, reduced viscosity in joggers rel. to non-joggers 80−16967
blood plasma viscosity in sickle-cell anaemia 80−94250
blood rheology, clinical changes in peripheral vascular disease and smokers 80−16965
blood rheology, erythrocyte rigidity effects on viscoelastic dilatancy 80−61610
blood viscosity and red cell aggregation changes after haemodilution 80−97952
blood viscosity and red cell aggregation under near-zero gravity 80−3660
blood viscosity at low shear rate, capillary viscometer and obs. 80−98180
blood viscosity factors and functions, clinical appls. 80−3664
blood viscosity factors in severe nondiabetic and diabetic retinopathy 78−65069
bromides, and mixtures, molten, elec. cond., density, viscosity, surface tension, review 77−80638
4-bromo-m-thiocresol, liq., dielectric relax. mechanisms 79−42891
bubble columns, axial dispersion coeffs. rel. to fluid props. 77−3861
bulk viscosity, inverse power pot. 78−91466
butadiene-acrylonitrile copolymer liquid, viscosity *(Japanese)* 80−39334
capillarity method determ. 80−82619
capillary wave form. on gravity water waves, model eqn., surface tension, viscosity 78−83421
carbon tetrachloride, generalised transport coeffs., hydrodynamic eqn. 78−87803
carbon tetrachloride, transport coefficients for a fluid of square-well rough spheres 79−55634
castor oil, viscosity meas. under nonisothermal conditions with rotary viscosimeter 79−68664
CBOOA, liq. cryst., temp. depend. of apparent viscosity and density 78−18542
CBOOA, liq. cryst., twist viscosity and mech. props. near smectic A-nematic transition 78−95136
CBOOA, nematic and smectic, anisotropic shear viscosity meas. 77−15310
CBOOA, US attenuation near nematic-smectic A transition 78−87773
cellulose acetate butyrate, in soln., hydrodynamic behaviour 80−64876
cellulose trinitrate, in soln., gel-like aggregate form. rel. to configuration 77−31036
channel flow, plane, shear rate dependent viscosity, effect on stability *(German)* 80−87809
charged macromolecule soln., effective viscosity low-shear limit 79−69274
4-chloro-α-toluothiol, liq., dielectric relax. mechanisms 79−42891
2-chloro-p-nitroaniline, in benzene soln., dipole moment from solute relax. time-solvent viscosity relation 80−37905
chloroform, dense liq., mol. reorientation and shear viscosity 77−4213
o-chlorophenol-acetone (ethyl methyl ketone), thermodynamic and transport props. 80−92686
cholesteric liq. crysts., isotropic phase, pretransitional viscosity 80−84312
cholesteric liquid crystal, oriented, Newtonian capillary shear flow, effective viscosity 79−18957
cholesteric liquid crystals, viscosity coeff. at smectic-cholesteric transition 79−77791
cholesteryl 2-(2-ethoxy-ethoxy) ethyl carbonate, dynamics of isotropic-cholesteric transition, normal and blue phases 79−95134
cholesteryl oleate, isotropic liq. cryst., shear viscosity 78−26668
cholesteryl oleyl carbonate, isotropic liq. cryst., shear viscosity 78−26668
classical fluid, dynamic scaling for crit. viscosity 80−59689
classical liquids, microdynamics, book contrib. 79−60248
classical liquids, multiplicative renormalisation of anomalous shear viscosity 77−35739
classical simple liq., long-time anomalies suppression, Ar(Rb) appls. 80−24339
coating of flat sheet during withdrawal from wetting liq., meniscus shape, flow model 77−29044
COC, dynamics of isotropic-cholesteric transition, normal and blue phases 79−95134
collagen, enzyme- and alkaline-soluble, optical rot. dispersion and circular dichroism 77−70411
colloidal dispersion dynamics, review 80−71956
concentrated electrolyte, solutions, viscosity, mixture law 78−18818
condensed gases, diatomic and monoatomic, principle of corresponding states for viscosity 77−84959
convection in high Prandtl number fluid with strongly temp. depend. viscosity 77−3823

viscosity of liquids continued
coolants and index matching media for Nd:glass laser systems 80−33015
couple stress fluid pulsatile flow through circular tubes 79−62275
critical exponent for shear viscosity of simple, binary and ternary fluids 78−83988
critical fluids, non-Newtonian effect and normal stress effect 80−49396
crown ether-containing polymers, in alkali salt solns., complexation, viscosity obs. 80−64877
cryptocyanine, solns., fluoresc. lifetime, viscosity depend. 79−59497
crystal violet, fluoresc. efficiency, solvent viscosity effects at high press. 78−9188
crystallisation from solution, same complex effects 80−100189
cumene, films, thin, wetting, rheological characts. determ., capillary method 78−51788
cyclohexane, liquid, density effect on transport properties 80−65264
cyclohexane+toluene, binary liq., viscosity and excess free energy of mixing 78−51680
cyclooctane+toluene, binary liq., viscosity and excess free energy of mixing 78−51680
Czochralski growth simulation, influence of crystal rotation rate 77−85931
n-decane, films, thin, wetting, rheological characts. determ., capillary method 78−51788
dense fluid, obs. rel. to Enskog hard-sphere transport theory 77−1254
dense gas mixtures, viscosity, composition depend. 77−35295
dense gas transport calcs., Rice Allnatt theory 77−76590
dense hard core system, transport coeffs., entropy 77−62656
dense one-component systems, low-temp., kinetic phenomena, shear viscosity *(Russian)* 80−10694
dextran aqueous solutions, microviscosity investig. by square-wave polarography 79−95200
dextran fractions, production, characterisation and solution properties 80−59368
p-p′-dibutyl-azoxybenzene, nematic liq. cryst., elasticities and viscosities, light scatt. meas. 79−4245
dielectric, ionic-cond. and -dissociation under low elec. field 77−8089
dielectric liquid, cond. effect on electroviscosity 78−1751
dielectric polar liq., electroviscosity rel. to cond. process, EHD model 78−1750
1,1-diethyl-2,2′-dicarbocyanine iodide, solns., fluoresc. lifetime, viscosity depend. 79−59497
dilute polymer solns., origin of internal viscosity *(French)* 78−91465
dilute suspension of spheres in power model fluid, apparent stress deform. behaviour 78−42578
dimethyltetraphenylmethylphenylsiloxanes, density, viscosity, surface tension and crit. temps. 79−86830
diphenyl hexachloride, liq., imaginary compressional modulus (compressional viscosity) 77−76480
diquinolyl cyanomethane, fluoresc. quantum yields, viscosity effects 80−60646
DOBAMBC, chiral smectic C-phase ferroelectric liq. crystal film, classical X-Y system, props. 80−44123
DOBAMBC, ferroelectric liquid crystal film, freely suspended, polarisation, elastic consts. and viscosity meas. 79−55663
drop deformation and orientation in shear and extensional flow fields, dynamic interfacial props. 80−107611
drop dynamics in shear fields, role of dynamic interfacial effects 80−107612
drop falling through liquid, for teachers 79−40331
dye laser, pulsed, light polarisation, solvent viscosity effect 80−32977
dyes, substituted methane, press. effs. on viscosity-depend. fluoresc. 77−34672
dyes in organic solvents of high viscosity, diffusion coeffs. 78−10203
dynamic density measurement of body in a liquid, viscosity effects 79−6097
dynamic viscosity and heat cond. coeffs., linear relationship 77−7884
dynamic viscosity coeffs. *(Russian)* 78−47550
EBBA, pVT data and viscosity-press. behaviour 78−94989
elastic fluids, shear-thinning, Carreau viscosity eqn., creeping motion of spheres 80−87753
elastohydrodynamic contact, rheological model 80−33544
elastohydrodynamic lubrication at high press., mineral oils between disks 78−34094
elastohydrodynamic lubrication at high press., non-Newtonian behaviour 79−46350
elastohydrodynamic traction, granular behaviour 80−103008
elastohydrodynamics, solns. to steady-state problems 77−35107
electrolyte, dielectric dispersion and friction, viscous momentum transport and relax., ion mobility 78−27775
electrolyte conc. solns., conc. depend. 77−55378
electrolyte mixtures, in aq. soln., viscosity, individual electrolyte effects *(German)* 78−22881
electrolyte mixtures in aq. soln., viscosity contrib. coeffs. *(German)* 80−15287
1.1-electrolyte solutions, conc. aq. 77−72745
electrolyte solutions, fluctuations rel. to shear viscosity dispersion 77−15497
electrolyte solutions in glycerol, investigation by US shear strains 80−88266
electrolytes, conc. solns., viscosity temp. depend. 78−80749
electrolytes, in ethylene carbonate viscosity and conductance meas. at 40°C 79−28122
electrostatic drop formation, effects of conductive liquid props. 78−1122
electrostatic drop formation rel. to liquid viscosity 79−55024
emulsions, unstable water-oil type, rheological props. obs. non-Newtonian obs. 77−75866
erythrocyte deformability, viscometric flow and laser diffractometric technique 78−35879
ethane, viscosity and thermal cond. of liquid and gas, correl. eqns. 78−26715
ethanol, aq. soln., conc. fluctuations, shear and longit. relax., Brillouin scatt. and pulse techniques 78−71792
ethanol-water mixtures, specific volume, compressibility, viscosity, up to 3200 bar, 15, 25°C 78−10113
ethyl alcohol, US attenuation, for vol. viscosity, 0-60°C 78−63871
ethyl formate, liquid, temp. depend. of US absorpt. and volume viscosity 78−38776
ethyl n-dodecoate, photocapillary effect, temp. depend. *(Russian)* 78−34682
ethylbenzene+toluene, binary liq., viscosity and excess free energy of mixing 78−51680

viscosity of liquids continued
ethylene glycol., Brillouin freq. and linewidth, depend. on viscosity and mol. wt. 79−37609
ethylene methacrylic acid polymer and Na salt, ionic aggregation and melt rheology, H_2 bonding effect 78−67159
(ethylene-co-vinyl alcohol)-g-ethylene oxide graft copolymers, sol. behaviour 80−19682
ethylene-vinyl-acetate copolymer melt, viscosity 79−33105
ethylene-vinylacetate-copolymers charact. by gel chromatography, viscometry, osmotic meas. *(German)* 78−14496
extended Jones-Dole equation, for rel. viscosity of electrolytic solns. 78−10208
fatty acids, long chain, spread monolayers, rheological behaviour 79−95245
Fermi liquid viscosity in finite geometry 80−24702
ferrofluid US attenuation anomalies 79−55830
ferromagnetic suspension, bulk viscosity calc. *(Russian)* 77−81429
Ficoll, bacterial movement in viscous environments 79−43840
film, entrained, thickness, effect of surface induced gradual viscosity increase 78−83488
film, liq., flowing down inclined plane with heat transfer, interfacial shear, stability 79−37290
flavin aqueous solns., fluorescence quenching by iodide ions, temp. and viscosity effects 77−34673
flow birefringence, vel. and temp. profiles calc. in cone and plate rheometer 77−54945
flow in narrow channels, effect of surface induced gradual viscosity increase 78−83488
flow mechanism, for simple liq., Ree Eyring theory extension 77−31794
flow of purely viscous non-Newtonian fluid, Rayleigh problem, pseudosimilarity soln. *(German)* 79−37364
fluid, dense, chem. reacting, Enskog theory 78−35667
fluid, reacting spheres, kinetic theory 78−35668
fluidity model of Hildebrand, modification 79−37864
fluids, one and two dimensional, hydrodynamics, viscosity, heat conductivity, kinetics *(Russian)* 80−79972
fluids at evaluated pressures 80−2191
free coating of surface, effect of angle 79−46892
galactomannan aqn. soln., rheological props., role of molecular mass and conc. *(French)* 78−22312
gelatin gels, coloured component addition, struct. form., dynamic shear modulus, viscosity meas. *(Russian)* 80−7871
glass and glass-forming liq., viscoelastic properties, comparison with Lennard-Jones model 80−84983
glass devitrification, heat treatment parameters determ. from viscosity changes *(Polish)* 80−40404
glass fibre reinforced polyethylene melt, rheological props. 79−37273
glass fibre reinforced polypropylene, effect of injection speed on fibre orientation 79−4944
glass forming liquids, vol. relax. 80−96429
glass transition rel. to press. depend. of viscosity 80−34171
glass-forming, viscous flow and valence config. theory 80−14756
glass-forming melts, window, glass-transition temps. from viscosity temp. depend. 80−34113
globular protein rotatory mobility meas. by spin probe method, soln. viscosity 77−16902
glycerol, shear relaxation, KCl or NaBr additive effects 79−60537
glycerol solutions, diffusion coeffs., viscosity 78−51711
glycol solutions, diffusion coeffs., viscosity 78−51711
haemoglobin, human and Lumbricus terrestris, conc. depend. of self-diffusion 78−68984
haemoglobin, in salt soln., diffusion rel. to intermol. interactions, light scatt. investig. 77−44585
hard sphere macromolecule dil. soln. viscosity, Thorne-Enskog theory 78−91467
hard-sphere fluid, shear viscosity, nonequilib. molecular dynamics calcs. 79−68996
hard-sphere fluid, viscosity and self-diffusion coeffs. 78−51716
hard-sphere liquid, shear viscosity, from nonequilib. mol. dynamics 79−19132
HBAD, liq, cryst., temp. depend. of apparent viscosity and density 78−18542
heavy and ordinary water dynamic viscosity coeffs. relation in liquid phase 78−21759
heavy water dynamic viscosity coefficient in supercritical region of parameters of state, experimental investigation 78−67845
p-n-heptyloxybenzylidene-aminofluorenone/COOB mixtures, dynamic twist viscosity near polycrit. points 79−95133
hexadecane, liq. film, boundary viscosity using blow-off method 79−23383
n-hexane, viscosity meas. at 353 to 436K, and corresponding vapour press. 77−69107
n-hexane-cyclohexane mixture, 25 to 100 C, up to 500 MPa 80−103510
n-hexane-n-dodecane 'ideal' mixture, viscosity, theory *(German)* 78−22882
n-hexane-n-pentadecane mixtures, solns., mech. of US absorption and viscosity *(Russian)* 79−90732
n-hexane/acetone mixtures, electroviscous effect, AC and DC meas. 79−14949
hexanetriol 1,2,6, liq., light scatt. study of struct. relax., viscosity and dielec. relax. 79−86672
hexyl-azoxybenzene, liq. cryst., twist viscosity and mech. props. near smectic A-nematic transition 78−95136
high pressure viscosity meas. method 80−69955
Hildebrand's law, fluidity as a function of molar vol. *(French)* 78−63872
homonuclear diatomics, dense fluids, transport props. 78−75519
hyaluronate solns., cooperative phase transitions, review 80−45850
hydraulic charact. of liqs. flowing through porous metal fibre mats., permeability laws 78−67848
hydrodynamic thermal breakdown in viscous fluid, Couette flow between cylinders 78−83391
hydroxyethyl cellulose, microviscosity, mobility profile 80−91710
hydroxylpropylmethyl cellulose, aq. solns., turbulent flow charact., friction-reducing props. 78−94649
ideal mixture, viscosity, theory *(German)* 78−22882
inert gases, transport props. in mean spherical approx. 78−9927
Invar, Fe-Ni (36 wt.%), alloy 36N, effect of melting conditions on thermal expansion coeff. 80−65256
iodides and mixtures, molten, elec. cond., density, viscosity, surface tension 77−80638

viscosity of liquids continued
isobutyric acid and water, shear viscosity of critical mixture, amplitude ratios 80−2188
isobutyric acid-water critical mixtures, shear viscosity, pseudospinodal curves and scaling 78−22844
Kelzan dilute aqueous solns., flow in various geometries 79−41757
Kramer's chemical reaction model, barrier mediated diffusion, generalisation to include viscosity term 80−71890
laminar convection in vertical tube, thermophysical prop. temp. depend., effects 78−90895
Lennard-Jones fluid, nonequilibrium molecular dynamics, $t^{-3/2}$ long-time tail for stress-stress time correlation 80−70100
linear block copolymers, hydrodynamics 79−69273
lipid hydrocarbon chain, biomembrane, rot. motion and fluidity 80−76714
liquid crystal, colloid and surface chemical aspects 78−9950
liquid crystal, rotary motion about short axis, dielectric and splay viscosity meas. 77−43145
liquid crystal, viscosity, anomalous properties near N→S_A transition point *(Chinese)* 80−84052
liquid crystal, viscosity-pressure behaviour rel. to transition pts. 79−23707
liquid crystal cpds. incorporating trans-1,4-substituted cyclohexane ring system, synthesis and phys. props. 79−90543
liquid crystals, NMR spin-lattice relax. time near phase transitions 80−71222
liquid crystals, prep. and phys. props., book 80−105444
liquid theories, validity, agreement with pertinent experimental fact 80−38881
liquid-glass transition, free volume approach, thermodynamic behaviour 80−1940
lubricants, viscosity and density determ. up to 150°C and 150000 psig 77−59940
lysozyme aqueous solutions, viscosity and density 79−48208
lysozyme-salt water soln., critical mixing point, turbidity and viscosity meas. 77−86437
macromolecular liquids, dynamic viscosity, for static-oscill. vel. gradients superposition 77−76279
macromolecular solution, dil., assoc. influence on reduced viscosity 79−90518
macromolecular solution, flexible mols., mol. models for mech. props. 79−59957
macromolecular solutions, kinetic theory and rheology 77−7424
macromolecule, dynamic birefringence and volume effects, rigidity determ. *(Russian)* 77−42456
macromolecule liquid, translational friction coeffs. of rigid, symm. top mols. 80−6003
MBAB, twist viscosity, temp. depend. 77−35472
MBBA, and MBBA-EBBA mixtures, determ. of viscosity coefficients by torsional vibrs. 79−14953
MBBA, electroviscous effect 79−69010
MBBA, isotropic, de Gennes coeffs. 78−31207
MBBA, isotropic, obs. and anal. of depolarised Rayleigh doublet 78−35154
MBBA, nematic, viscosity coeffs., Onsager-Parodi relation validity 79−19147
MBBA, nematic liq. cryst., bend viscosity calc. 78−34423
MBBA, pVT data and viscosity-press. behaviour 78−94989
MBBA, shear modulus and viscosity relax. near isotropic-nematic phase transition *(Russian)* 77−39543
MBBA, with chiral impurities, cholesteric struct. shear flow normal to helical axis 79−86689
MBBA liq. cryst., free iminoxyl radical addition, domain struct. parameter depend. *(Russian)* 77−58948
MDBA, liq. cryst., temp. depend. of apparent viscosity and density 78−18542
mean spherical model approx. 78−75514
measurement complex apparatus for viscous and elastic prop. meas. at high press. 78−9734
measurement using transient hot-wire technique 79−200
measurement with oscillation type viscometer, capacitive transducer of torsional oscills. 80−64656
mechanism, in simple liquids and gases, interrelation *(Russian)* 78−67846
metal, ionic transport coefficient calculation *(Rumanian)* 79−60533
metal, liquid, viscosity determination by oscillating vessel method *(Japanese)* 80−70439
metal, meas. by torsional oscillation method, crucible size effect 77−51139
metal, phys. chem., conf., Konigstein, Germany (Mar. 1976) 77−1059
metal, rel. to NQR 77−1615
metal, viscosity anal. 78−91468
metallic glass, heat of crystn. and viscous behaviour 80−75166
metallic melts, viscous flow due to high overheating, quasipolycrystalline model 80−70110
metals, calc. using microinhomogeneous struct. model *(Russian)* 80−15284
metals, viscosity effect on cond. meas. by rot. mag. field method *(Russian)* 77−57349
methacrylic acid-methyl methacrylate statistical copolymer suspension polymerisation, stabilisation effects, viscosity 78−85157
methane, dense gaseous and liq., thermal cond.-viscosity correlation, up to 500 atm., 95-500 K 77−80657
methane, freq.-depend. shear viscosity 79−77798
methane-Ar, cryogenic fluid mixture, transport phenomena, shear viscosity *(Russian)* 80−29198
methane-Ar liquid mixture, viscoelastic props., acoustic relax. *(Russian)* 78−75736
methanol, liq., compressed, self-diffusion, NMR spin-echo meas. 77−77122
methanol, viscosity meas. at 353 to 463K and corresponding vapour press. 77−69107
methofas, degradation and viscosity meas., transition process 77−72258
4-methoxy-4′-azoxybenzene, nematic liq. cryst., elasticities and viscosities, light scatt. meas. 79−4245
methyl alcohol, US attenuation, for vol. viscosity, 0-60°C 78−63871
methyl cellulose, bacterial movement in viscous environments 79−43840
methyl formate, liquid, temp. depend. of US absorpt. and volume viscosity 78−38776
methyl iodide, dense liq., mol. reorientation and shear viscosity 77−4213

viscosity of liquids continued
methyl iodide, liq., mol. reorientation, dielec. and viscosity meas. 80−100157
methylcyclohexane, dense liq., self-diffusion and viscosity 80−15278
methylphenylsiloxanes, density, viscosity, surface tension and crit. temps. 79−86830
microemulsions, aerosol OT, inhomogeneous interior, fluoresc. and polarisation decay probes 80−50891
microemulsions, phase diagram and homogeneity gap, light scatt. and viscosity meas. 80−16736
mixed halide melts, elec. cond., surface tension, density and viscosity, tables 79−60531
mixed strong electrolytes, relax. effects in limiting law region, integral representation 77−86322
mixture, empirical formula, continuum theory and generalised Navier-Stokes system 78−14498
mixture, Hildebrand fluidity eqn., viscosity calc. 78−38867
mixture, of dense simple fluids, bulk viscosity, hard spheres appl. 80−14982
mixtures, liq., eqn. for predicting viscosity 77−39686
mixtures, one-fluid approx. transport coeffs., critical region behaviour 79−14951
molecules, spheroid-cylindrical, dynamics in dilute soln. 80−44090
molten salts, cellular convection near solidification point *(French)* 78−14004
molten salts, transport coeffs., integral representations 78−67842
motor oils, use of polymeric additives to increase viscosity index, exam. of mechanism 78−95816
mucus mechanical props. rel. to mucociliary transport, effect of pharmacologic interventions 80−3663
mullite-based dispersed refractory system, rheological props. at high temp. 77−16629
multicomponent liquid mixture, viscosity, Panchenkov model calcs. *(German)* 77−31797
NaCl aqueous solutions, viscosity at high temps. and pressures, investigation 78−95175
nematic and smectic liq. cryst., viscous and plastic behaviours 79−86686
nematic liquid crystal, isotropic phase, complex shear viscosity 77−39667
nematic liquid crystal, material consts., solute effects 77−1072
nematic liquid crystal, orientational electrooptic effects, time characts. 78−27191
nematic liquid crystal, rel. to ESR of symmetrical three-spin systems, slow motional spectra 77−36135
nematic liquid crystal, spin-lattice relax., viscosity effects, theory 77−4574
nematic liquid crystal, stress tensor nonlinearities, viscosity coeffs. 77−27831
nematic liquid crystal, twist viscosity, planar-model calc. 78−42893
nematic liquid crystal, viscometric flow, apparent viscosity 79−60265
nematic liquid crystal, viscosity, rotational, mol. statistical theory *(Portuguese)* 77−47351
nematic liquid crystal, viscosity depend. on order parameter, thermodynamic model 79−77503
nematic liquid crystals, apparent viscosity during simple shear flow 77−72549
nematic liquid crystals, MHD effect, high resolution NMR *(Russian)* 78−15040
nematic liquid crystals, shear flow, effect of mag. fields and boundary conditions, PAA example 77−7668
nematic liquid crystals, shear flow in presence of electric AC field, elastic and viscous const. determ. 77−43144
nematic liquid crystals, temp. dependent props., twisted nematic displays 79−32901
nematic liquid crystals, viscosity, rel. to order parameter *(Russian)* 78−91242
nematic-chiral mixtures, viscosity and electrooptical characts. 79−86682
nematic-isotropic mixture, dielec. props., phase diagram 78−52424
nematic-smectic A(C) phase transitions, contribs. to viscosities from order parameter fluctuations 79−60489
nematic-smectic A phase transition, sound attenuation and dispersion 79−82286
3-nitro-o-anisidine, in benzene soln., dipole moment from solute relax. time-solvent viscosity relation 80−37905
nitrobenzene, in acetone-isopropanol soln., Rayleigh scatt. and viscosity 80−5550
nitrobenzene, liquid and CCl_4 soln. shear waves and translation-rotation coupling obs. by depolarised Rayleigh scattering 80−71432
nitrobenzene, rot. relax. times of anisotropic mols., optical Kerr effect and viscosity expts. 77−79906
nitrobenzene-cyclohexane system, viscosity and activation energy 78−26615
nitrobenzene-n-hexane, liq. mixture, static and dynamic viscosities near crit. point 77−69108
nitrobenzene-n-hexane, shear viscosity, critical conc. fluctuation rate, verification of renormalisation prediction 78−47514
nitrobenzene-n-hexane critical mixture, shear viscosity meas. 77−72689
nitrobenzene/n-hexane (n-heptane), critical exponent β, phase coexistence curve anal., viscosity coeff. meas. 80−100327
m-nitrotoluene, pure and in soln., rot. relax. times of anisotropic mols., optical Kerr effect and viscosity expts. 77−79906
non-linear model, constitutive equation testing with free. vol. relax. spectrum 80−6011
non-Newtonian fluids, dissipation effects, critical eqns. *(German)* 79−27611
non-Newtonian fluids, mass transfer from cylinders to power law fluids 80−83826
non-Newtonian fluids, mass transfer from spheres to power law fluids 80−83825
non-Newtonian fluids in jacketed agitated vessel, heat transfer, viscosity correl. 78−75143
non-Newtonian liquids, Rayleigh classical equation generalisation 80−19444
nonisothermal flow of viscous fluid in pipes, crit. phenomena 80−103074
nonNewtonian fluid, shear rate calc. in coaxial viscometer, method comparison 79−4048
nuclear reactor core melt from LOCA, viscosity, thermal cond., specific heat 77−14247
Nylon 12, short-time adhesion, rel. to diffusion properties *(Japanese)* 79−70294
Nylon 12 melt, diffusion *(Japanese)* 79−95192

viscosity of liquids continued
4-n-octyl-4′-cyanobiphenyl, smectic A liq. cryst., shear-induced textures and rheology 78−91228
4-octyloxybenzoyloxy-4′-cyanostilbene, enantiotropic reentrant nematic behaviour at atmos. press. 79−60490
octyloxycyanobiphenyl, liq. cryst., twist viscosity and mech. props. near smectic A-nematic transition 78−95136
oil, density change meas. at high pressure, using impact viscometer 79−14872
oil droplets, motion and optical props. by interf. method 78−67893
oil film, viscosity balance method of skin friction meas., appls. to three-dimensional flow 77−19645
oils, viscosity and solidification press., 0-10^4 Pa, 20-180°C 77−43266
organic heat carriers, charact. *(German)* 78−79198
PAA, nematic phase, solubilisation of poly-ethylen-oxide chain, effect on twist viscosity 78−67642
parallel flow between parallel plates, substruct. distrib. and apparent viscosity 78−13983
p-n-pentyl p′-cyanobiphenyl, anisotropic viscosity, US meas. 77−31581
p-n-pentyl p′-cyanobiphenyl, isotropic phase, viscosity coeffs. 77−31582
pentyl-cyano-biphenyl, nematic, hydrodynamic parameters meas. with and without applied elec. field 80−100297
perfluorinated polymer, Krytox 143-AB, viscous, viscoelastic and dielectric properties 80−70440
perfluorocyclobutane, dense fluid, self-diffusion, shear viscosity, density, and temp. depend., NMR 77−36152
p-phenitidine, in benzene soln., dipole moment from solute relax. time-solvent viscosity relation 80−37905
phenolic resins, average molecular weight and viscosity of acetone solns. *(Japanese)* 79−65234
phenylcyclohexanes, nematic, low melting liq. crysts. with positive dielec. anisotropy, phys. props. 77−43148
phenylpyrimidines, liq. crysts., synthesis and phys. props. 78−1995
phosphatidylcholine bilayers, fluidity changes and phase transitions, intramol. excimer fluoresc. obs. 80−85342
photographic, film development kinetics of viscous solutions *(German)* 79−83482
photon correlation spectroscopy, liquid surfaces, effect of instrumental broadening 77−87852
piezoelectric determ. of viscosity at 40 kHz 78−59519
pinacyanol, solns., fluoresc. lifetime, viscosity depend. 79−59497
pitch and bitumen, viscosity, temp. depend. up to 500°C 80−92698
PMMA isotactic, syndiotactic stereocomplex formation in soln., composition, struct. 79−66292
PMMA soln. in toluene, diffusion, viscosity rel. to temp. *(German)* 79−42289
polar liquids, activation energy for viscosity, rel. to charge distrib. 79−37865
polar molecule/nonpolar solvent, dielec. relax. computation from viscosity data 80−11330
polar molecules, viscosity activation energy and relax. time, RF cond. meas. 80−96677
poly(γ-benzyl)-L-glutamate, viscosity behaviour in dioxane solvent, conc. depend., aggregation 79−82371
poly(aminiumphosphate)s, mol. wts., and cond. studies 80−14264
poly(azomethines), thermotropic mesophases *(French)* 79−77507
poly(methacrylic acid), aq. soln., gelation kinetics under shear stress 78−3387
poly N,N-diallyldimethylammonium chloride, soln. props., struct. 79−94861
poly-1,4-phenylene terephthalamide, in H_2SO_4, dilute soln. viscosity 78−75524
poly-1-olefin melts, steady-state and dynamic rheology 79−59956
poly-γ-benzyl-glutamate, conc. soln., rheology, liq. cryst. transition 79−94574
poly-γ-benzyl-L-glutamate, lyotropic liq. cryst., trifluoroacetic acid effect on viscoelasticity, susceptibility 77−84644
poly-γ-methyl-L-glutamate, conformational props., viscosity, osmotic press. meas. 77−31032
poly-L-glutamic acid-Na, cooperativity parameter determ. from viscometry 80−75147
poly-m-phenylene-isophthalamide in dimethylacetamide, flow birefringence *(Russian)* 80−66148
poly-n-benzamide, lyotropic liq. cryst., structural orientation *(Russian)* 77−31593
poly-N-benzamide, lyotropic liq. crystals, viscosity anisotropy 80−10693
poly-N-vinyl imidazole solution, light scatt., viscosity and dynamic birefringence, mol. wt. obs. *(Russian)* 79−33665
poly-p-chlorostyrene-propylbenzene soln., excluded vol. effect and transitional phenomena 79−77795
poly-p-tert-butylphenylmethacrylate, soln., viscometric behaviour 80−88016
polyacrylamide aqueous solution, ultrasonic investigation *(Chinese)* 80−107371
polyacrylamide dilute aqueous solns., flow in various geometries 79−41757
polyacrylamide solution, drag reducing, rheological props. meas. 79−37271
polyacrylamide solutions, viscous behaviour 80−2185
polyacrylamide-maltose syrup soln., meas. of viscoelastic flow props. 78−1622
polyamide mixtures, thermodynamically incompatible, composition-prop. relationship *(Russian)* 80−7872
polyarylate-arylenesulfone oxide block copolymer, glass transition, melt and soln. viscosity *(Russian)* 79−55915
polyazomethines, dil. soln. props. 80−19972
polybutadiene, dil. soln., viscosity, temp. depend., solvent effects 80−59686
polybutadiene, hydrogenated, linear and star branched, melt rheology 80−23978
polybutadiene-n-hexane-n-heptane soln., Rayleigh scatt., diffusion coeff., viscosity 78−15179
polydicarboxylic acids, electrophoretic and viscometric props. 80−66811
polydimethyl siloxane solns., limiting viscosity no.-mol. wt. relations 78−18267
polydimethylsiloxane oligomers, Brillouin scatt. obs. of hypersonic sound speed and loss, mol. wt. depend. 79−91457
polydimethylsiloxanes, linear, mol. wt. determ. from density and viscosity 79−81310
polydodecane amide soln., viscosity, mol. wt. *(Russian)* 79−51296
polyelectrolytes, translating, electrolyte friction theory 80−29194

viscosity of liquids continued
polyethylene, foam growth, thermomech. anal. 80−3416
polyethylene, high density, filled with pearlite, melt rheology *(Japanese)* 77−54942
polyethylene, linear, melt rheology 80−23976
polyethylene, low density, melt flow, mech. degradation *(Russian)* 79−50691
polyethylene, low density melts, temp. depend. of the elongational behaviour 80−6012
polyethylene, melt, low density, filler effect on viscosity and viscoelasticity 77−68546
polyethylene, standard reference material, limiting viscosity numbers 79−14952
polyethylene extruded melt, elongational viscosity, tensile props. 78−67163
polyethylene film-resin melts, rheological props., prep. method depend. 78−34099
polyethylene glycol, Brillouin freq. and linewidth, depend. on viscosity and mol. wt. 79−37609
polyethylene imine, oligomers, solns., linear struct., props. *(Russian)* 79−50177
polyethylene melt, flow with steady state and recurrent deform. 77−898
polyethylene melt, low density, filler effect on viscosity and viscoelasticity 78−46919
polyethylene melt, rheology and molecular struct., melt identification from mech. props. 77−11490
polyethylene melts, low-density, viscosity and viscoelasticity, filler effect 80−10222
polyethylene oxide, aq. salt soln., meas.-based thermodynamic quantities 78−75525
polyethylene oxide, aq. soln., nonlinear dynamic viscoelasticity 79−94576
polyethylene oxide, dilute aq. soln., laminar viscous tube flow, scale-depend. effect 79−7367
polyethylene oxide, solns. in toluene and ethyl benzene, phase equilib., struct. and thermodynamic stability *(Russian)* 79−86871
polyethylene oxide dilute aqueous solns., flow in various geometries 79−41757
polyethylene oxide fractions and blends, melt viscosity, thermal props. 78−83990
polyethylene solns., conc., viscosity, shear speed depend. *(German)* 79−27671
polyisobutylene melt, transient shear and elongational data 77−58631
polyisobutylene solutions, viscous behaviour 80−2185
polyisoprene, in cyclohexane soln., conform. transition *(French)* 79−7542
polymer, chain molecule, excluded vol. theory based on fifth-power eqns. for unperturbed mol. dimensions 77−50578
polymer, entangled, phenomenological consequences of Doi-Edwards viscoelasticity theory 80−79250
polymer, flexible ring, intrinsic viscosity 80−103511
polymer, liq., Brillouin scatt. and segmental motion, appl. to polypropylene glycol 78−91217
polymer, nondraining coils, first order excluded volume effect on intrinsic viscosity 78−55968
polymer, polydisperse, hydrodynamic invariants *(Russian)* 77−19580
polymer, random coil, nonzero thickness, suspension, shear viscosity conc. depend. 79−10238
polymer dilute solution, elongational flow, tensile viscosity 77−7486
polymer dynamics simulation, relax. rates and dynamic viscosity 78−91211
polymer in mixed solvents, viscosity data as function of mol. wt. 78−18266
polymer melt, polydispersity, estimation from rheological data 80−6535
polymer melt containing suspension, cell model theory of shear viscosity 80−103048
polymer melts, dynamics, self-diffusion const., relax. time and viscosity 80−64874
polymer melts, flow indices *(Japanese)* 80−79360
polymer melts and solutions, determ. by extrapolation method *(German)* 79−99347
polymer melts and solutions, rheological equations, review 79−86391
polymer mixtures, solns., viscosity *(Russian)* 79−65236
polymer solns., dilute, Hartree self-consistent field analysis 80−5648
polymer solns., not infinitely dilute, second-order fluid coeffs., conc. depend. 80−106771
polymer solution, bulk viscosity theory 78−22880
polymer solution, conc. 77−62229
polymer solution, diffusion, viscosity and dynamic struct. factor, dynamic scaling theory 79−64977
polymer solution, dil., rotating Couette flow, elongational viscosity and stability 79−27669
polymer solution, dilute, aq., appl. of Hildebrand's fluidity model, apparent viscosity temp. depend. *(German)* 79−37366
polymer solution, dilute, chain mol. dynamics and transport processes 80−14989
polymer solution, eqn. for dilute to moderate concs. 79−69276
polymer solution, excluded volume and intrinsic viscosity plots 77−89363
polymer solution, flexible mols., dynamic intrinsic viscosity, hydrodynamic interaction 78−47548
polymer solution, intermolecular interpenetration and entanglement, crit. concs. 79−27900
polymer solution, internal viscosity, rel. to dynamic behaviour 77−55379
polymer solution, intrinsic viscosity, mol. wt. and temp. dependence 80−34222
polymer solution, intrinsic viscosity 78−2281
polymer solution, normal stress effects 77−32867
polymer solution, Taylor-Gortler vortices, elongational viscosity effects 78−22379
polymer solution, US absorpt., internal viscosity-normal mode description 79−10899
polymer solution, viscosity v. molecular weight, linear plot 78−67844
polymer solution, zero-shear rate viscosity meas. 79−90293
polymer solution models and viscometric props., book contrib. *(French)* 77−84284
polymer solutions, concentrated, transport properties, hydrodynamic mean field theory of voscisity of sphere suspension 79−4422
polymer solutions, dil., coherent scattering law, continued fraction formalism 80−103234
polymer solutions, dil., dynamical props. 78−38608
polymer solutions, dil., dynamics, model 79−73086

viscosity of liquids continued
polymer solutions, dilute, internal viscosities, frictional coeffs. calcs. 78−6171
polymer solutions, dynamics and hydrodynamics, book contrib. 79−60261
polymer solutions, fluctuation-dissipation relations, viscosity, mol. wt. depend. 78−14266
polymer solutions, internal viscosity, in poor solvents, self-entanglements *(French)* 79−4229
polymer solutions, laminar flow, effect of capillary entrance *(French)* 78−87330
polymer solutions, rheology, finitely extensible nonlinear elastic dumbbell theory 78−9617
polymer solutions, rigid-chain, flow birefr., hydrodynamic and dynamic-optical props. 79−24286
polymer solutions, transport coeffs. and scaling laws in dil. regime *(French)* 79−82372
polymer solutions, transport properties, conc. effects 80−64875
polymer solutions, viscosity, intrinsic, friction coeff., porous sphere model 78−71301
polymer solutions, viscosity data represented as function of mol. wt. 78−26716
polymer solutions in nematic liquids, dilute 80−29199
polymer solutions viscosity rel. to mol. mass *(Russian)* 80−2190
polymeric solutions, viscous behaviour 80−2185
polymerisable mass, unsteady viscosity meas. method *(Russian)* 79−23293
polymerisation in flow-through reactor, low-temp. conditions 80−61092
polymers, conc. solns. in volatile solvents, high temps., method for viscosity meas. 80−19535
polymers, flexible, solns., shear flow, dielec. anisotropy, appls. 79−15393
polymers, flexible rings, nondraining, intrinsic viscosity, translational friction coeff. 79−18855
polymers in mixed solvents, viscosity data as function of mol. wt. 79−37866
polymers solns., cooperative phase transitions, review 80−45850
polymers with periodic deform., longitudinal flow 80−6008
polymethine cyanine dyes, viscosity depend. fluoresc. lifetime using synchronously operated ps streak camera 80−28041
polymethylene, short-chain molecules, hydrodynamic behaviour, extended Rouse-Zimm theory 77−558
polymethylsiloxane-polyarylate block copolymer, soln., viscosity, rel. to film mech. props. and microstruct. *(Russian)* 79−23762
polyoxyethylene, dil. solns., laminar flow in tubes, scale effect 79−86472
polyoxymethylene-copolyamide blend melt, viscoelastic peculiarities *(Russian)* 78−38263
polyoxymethylene-copolyamide mixtures, melt rheological props., extrudate microstruct. *(Russian)* 80−7530
polypeptides, helical, conc. solns., rheological behaviour and liq. cryst. order 80−83771
polyphenyl melts, viscosity near freezing pt., association 79−51292
polyphenylquinoxaline, soln., conform., equilib. rigidity *(Russian)* 79−55643
polypropylene melt, thermal stabilizer content effect on props., processing and ageing *(Polish)* 79−70099
polypropylene melt, zero-shear-rate viscosity, press. depend. meas. 78−43164
polypropylene solns., viscosity-mol. wt. relation 79−37867
polypropylene sulphide in athermal solvent, viscosity-temp. coeffs. 80−39333
polystyrene, in solns., intrinsic viscosity rel. to mol. wt., unperturbed dimensions 80−65268
polystyrene, melt, bulk diffusion, local diffusion *(Japanese)* 78−95170
polystyrene, monodisperse latex, shear US meas. 78−31711
polystyrene, polymer chain, internal friction range, HF viscosity theory *(French)* 80−79968
polystyrene, soln. in trans.-decalin, viscosity and thermodynamic props., press. depend. 79−69275
polystyrene blend, melt, bulk local viscosity determ. 77−31796
polystyrene conc. sols. in toluene, rheological behaviour *(German)* 78−55618
polystyrene in 1-chloroparaffins, perturbed chains, hydrodynamic interaction effects in intrinsic viscosity 79−99344
polystyrene in benzene or cyclohexane, zero shear-rate intrinsic viscosities 80−75376
polystyrene in mixed solvents, intrinsic viscosity 78−67843
polystyrene in solns., unperturbed dimensions rel. to temp., solvent composition 79−64132
polystyrene melt, carbon-black filled, rheological study 80−48665
polystyrene melt, local viscosity determ. rel. to temp. *(Japanese)* 77−31795
polystyrene melt, rheological props. 79−37273
polystyrene melt, viscosity, thermodynamic props. *(Russian)* 79−51295
polystyrene melt dynamic viscoelastic props., mol. weight distrib. 78−63407
polystyrene melts, flame-retardant high-impact, shear viscosity-temp.-shear rate relationships 80−59691
polystyrene monodisperse latex, anomalous viscosity in disordered state 80−74822
polystyrene solns., non-Newtonian flow curves, viscosity 30°C 78−83438
polystyrene solution, internal viscosity, model for Lamb-Matheson-Philippoff increment 77−62284
polystyrene solutions, viscous behaviour 80−2185
polystyrene-co-divinylbenzene microgels in dimethylformamide, diffusion coeff., viscosity and mol. wt. meas. 80−30286
polystyrene-cyclohexane soln., excluded vol. effect and transitional phenomena 79−77795
polystyrene-methylcyclohexane soln., excluded vol. effect and transitional phenomena 79−77795
polystyrene-mineral oil mixture, viscosity and normal stress coeff. 80−44349
polystyrene-tetrahydrofuran-water system, thermodynamic and hydrodynamic props. 79−96353
polystyrene/polyethylene blend, particle dimension as function of melt viscosity added graft copolymer conc. 77−52279
polystyrenes, blends, molten, rheology, dynamic viscoelastic props. in terminal zone 77−31268
polystyrenes, in toluene 79−1773
polysulfonamide, optically active, synthesised by interfacial polycondensation, mol. wt. determ. 80−99595

viscosity of liquids continued
polysulphonamide solutions, mech. props. during gelling *(Russian)* 77−19579
polythene melts of high density, viscosity meas., entropy and compressibility *(German)* 78−67162
polyurethane, branched soln., viscous reduction props. *(Russian)* 78−87807
polyvinyl acetate, and conc. solns., viscosity meas. 80−65269
polyvinyl imidazolium sulphobetaine, aq. soln. props. 79−32879
polyvinylacetate solution, long-chain branching characterisation, molar masses 79−94122
porous particles suspension, effective viscosity, flow 79−18929
potential flow with elliptical form free boundary, viscosity effect 78−42581
Prandtl number, eqn. of state analogy and linear relations with transport props. 77−59156
principle of corresponding states, dynamic props. 77−89358
propane, viscosity and thermal cond. correl., liq. and gas 140-500K 79−77332
propanes, substituted, dielec. relax. in liquid state 77−8500
1-propanol, low temp. pulse radiolysis, solvated electrons, absorpt. spectral changes 77−12813
protein dynamic states, role of geometry and elastic strains 78−48745
protein solution, limiting viscosity number determ. *(French)* 77−12874
pulmonary surfactant film, surface dilatational viscosity obs. 79−62278
PVA, liq., mobilities at const. temp., vol. 78−95174
PVC, flow behaviour, particulate and melting flow, rheology 79−3981
PVC, plasticised, foam growth, thermomech. anal. 80−3416
PVC, suspensions, melts, rheological props. rel. to struct. 79−3983
PVC dispersion, rheology, particle size effects 79−92007
PVC pastes, rheological, surface props. rel. to density of prep. foams *(Polish)* 78−85212
PVC plastisol, steady shear rheological behaviour 79−37274
PVC plastisols, high resin level, rheological behaviour, discontinuous viscosity 80−23980
PVC-polyacrylonitrile blends, compatibility determ. 79−4416
pyridine, compressed liq., self-diffusion coeffs., viscosity, density, temp. press. depend., NMR spin-echo 79−37862
pyridine, cyclohexane soln., depolarised Rayleigh scatt. 79−47467
pyridinium molten salts, ^{1}HNMR rel. to transport props. 77−73087
quartz glass-water suspensions, electrolytes effect on viscosity, pH and zeta pot. props. 79−34365
random copolymer solution, electrooptics of crystal-like mols. *(Russian)* 77−63396
resin mortar, flowability, viscosity meas. with rotational viscometer *(Japanese)* 78−11260
ribonuclease A, microviscosity, mobility profile 80−91710
ring polymers, internal viscosity, statistical theory 77−88610
salol, liq. and supercooled, VH light scatt. spectra *(French)* 77−1755
seawater, bulk viscosity and l.f. sound attenuation, Be and B influence 77−3696
semiconductor melts, estimate of positional component of entropy of fusion, cluster model 77−55349
semiconductors, meas. by rotating mag. field method viscosity effect *(Russian)* 77−57349
semiquantum liquids, viscosity and heat cond. temp. depend. *(Russian)* 80−34260
shear, orientational and translational motion coupling const. depend. in VH depolarised light scatt. 77−59584
shear viscosity of settling suspensions meas. 79−82011
shear viscosity via periodic nonequilib. mol. dynamics 77−62660
short-chain molecules, hydrodynamic behaviour, extended Rouse-Zimm theory 77−558
short-chain molecules, hydrodynamic behaviour, viscosity 77−559
silicate glass, high temp. microscopy investigation of softening temp., viscous flow, angle of contact *(Polish)* 77−55242
silicate slag melt, physicochemical optimisation 78−85112
silicone liqs., 0-10^4 Pa, 20-180°C, and solidification press. 77−43266
silicone oil, ionic behaviour, carrier mobility and viscosity 80−107453
silicone oil, props. determ. by harmonical shear vibr. *(German)* 78−67164
silicone oils, environmental stress cracking of polyethylene due to liq. viscosity 77−4863
simple fluids, fluctuation expressions for nonequilib. distrib. functions in adiabatic flows 80−92441
simple liquid, self-diffusion and viscosity near MP, hard sphere model *(Russian)* 77−66035
simple liquids, transverse mode, Maxwell relax. time 78−22622
simple liquids, viscosity, density depend., theory 77−20105
sodium dodecyl sulphate micelles, diarylalkane intramolecular excimer formation, microfluidity and fluoresc. meas. 78−80791
sodium polystyrene sulphonate, solns., infinite dilution viscoelastic props. 79−14363
sodium tetraborate glass, melt, temp. depend. of high viscosity property *(Russian)* 80−39336
soft sphere viscosity, numerical calc. using discrete hydrodynamics 79−90505
soft spheres binary mixtures, equilib. and non-equilib. radial distrib. functions 80−49074
soft-sphere dense fluid, bulk viscosity, nonequilib. and equilib. mol. dynamics calcs. 80−79663
soft-sphere mixture viscosity, nonequilib. mol. dynamics 80−19680
spermatozoa swimming in cervix, effects of dynamical interaction and peripheral layer viscosity 78−69126
spheres, porous, in a linear flow field, motion and rupture 79−64755
spinning drop interfacial viscometer, liquid-gas interface, surface viscosity meas. 80−44395
spirobenzopyran copolymer photochromic soln., photoviscosity effect 80−6536
square well fluid, viscosity, transport processes 79−98847
square-well fluid, viscosity below critical density, molecular dynamical calcs. 80−79661
stiff polymer chain dynamics, local and global mode interaction, dil. soln. viscosity, dielectric relax. 78−37776
stiff polymer dilute solutions, non-Newtonian viscosity 77−35103
trans-stilbene, soln., lifetime and anisotropic fluoresc., viscosity effects *(German)* 80−106352
Stokes problem for a suspension of spheres at finite concentrations 78−55967
stopped-flow spectrometer performance with viscous solutions 77−32852

viscosity of liquids continued
stratified flow, viscosity distribution effect on flow stream parameters along bottom surface, model *(Russian)* 78−22401
styrene divinylbenzene, viscosity meas. during radical copolymerisation 80−3344
styrene-butadiene block copolymers, in dil. soln., extrapolation methods for intrinsic viscosity 80−24636
styrene-isoprene block copolymers, dilute soln., conform. obs. 79−10774
styrene-p-chlorostyrene triblock copolymer, dil. soln., conform. behaviour, comp. depend. 78−42886
styrene-p-chlorostyrene triblock copolymers in dil. soln., conform. behaviour, temp. depend. 79−90519
styrene-vinylpyrrolidone block copolymer soln., conform. props., light-, X-ray scatt. and viscometry obs. *(Russian)* 78−37779
styrene/acrylic terpolymers, viscoelastic props. 80−64509
supercooled liquid, thermal conductivity and viscosity, mode-mode coupling 80−88370
superfluid viscous liq., hydrodynamics and transport coeffs. 77−69134
superheated liquid, viscosity meas. apparatus and technique for use at high press. 77−58823
surface, free, charged, isolated, exptl. study of deform. *(French)* 80−88240
surface oscillations, viscosity and surface tension relax. effects 77−62266
surface viscosities at high pressure gas-liquid interfaces 78−75907
surface wave due to shock wave interaction, viscosity effect 77−11202
suspension, Brownian rotational-translational particles, at finite conc., dynamics and hydrodynamics 79−7401
suspension, dil., of spherical particles in non-Newtonian liq., rheological behaviour 80−24058
suspension, effective viscosity, statistical theory 79−90290
suspension of nonharmonic dumbell mols., intrinsic viscosity 78−2282
suspension of spheres, effective shear viscosity theory 78−11565
suspension of spheres in non-Newtonian fluid, viscosity 78−90807
synovial fluid, pathological, rheological props. *(German)* 78−57032
TBBA, smectic phases, rot. viscosity, phase transitions 77−80418
temperature variation, rel. to molar entropy of vaporisation 77−31793
temperature variation 77−89222
ternary electrolytes, viscosity and ion-solvent interactions in dioxane-water mixtures 78−18817
ternary fluid, crit. transport props., theory 78−14497
ternary liquid mixtures, shear viscosity at plait points 77−35685
tetra-n-pentylammonium salts, molten, thermodynamic props., cation struct. 79−55639
tetraalkylammonium bromide soln., conductance and viscosity, temp. and concentration depend. 80−6531
tetrabutylammonium iodide, in aq. proline soln., elec. conductance investigation 80−10692
tetraglycine, aq. soln., density, viscosity and dielectric const., 0-60°C 78−47462
tetramethylammonium iodide, in aq. proline soln., elec. conductance investigation 80−10692
thermophysical properties rel. to compressibility 78−83964
thin film, viscous, between two nearly parallel walls, temp. distrib., convection effects 80−83801
thin interlayer, between ice and surface of quartz capillaries, viscosity meas. 79−55913
time constants from shear viscosity data 79−37275
toluene, diffusion, viscosity rel. to temp. *(German)* 79−42289
toluene, relationships between thermal cond., dynamic viscosity and density, high state parameters 78−83861
toluene, viscosity meas. at 353 to 463K and corresponding vapour press. 77−69107
toluene+ethylbenzene (cyclohexane) (cyclooctane), binary liq., viscosity and excess free energy of mixing 78−51680
transport coefficients for a fluid of square-well rough spheres 79−55634
transport properties, relationships between thermal cond., dynamic viscosity and density, high state parameters 78−83861
trifluoropropylmethylsiloxane fluids, viscoelastic props., mechanical impedance, viscosity and density meas. 80−79249
triglycine, aq. soln., density, viscosity and dielectric const., 0-60°C 78−47462
triphenylmethane dye soln., electronic relax., viscosity-depend., using picosec. flash photolysis 80−66258
unassociated liquids, estimate of props. 79−51232
unsaturated polyester resins, gelation, viscosity meas. *(Polish)* 80−59690
urethane elastomer, thermoplastic, dilute soln., viscosity and sedimentation 80−103512
van der Waals fluid, transport props., shear viscosity calcs. 77−35738
variable resistance boundary layers, frictional resist. effects on motion of bodies 80−96243
vibrating wire viscometer, adaptation for liquids 80−87827
vinyl copolymers containing biphenyl units in backbone, thermal props. and soln. viscosity, synthesis *(Japanese)* 77−90316
vinylpyrrolidone-tert-butylphenyl methacrylate copolymers, prep., soln. props. 79−18854
viscoelastic fluid, flow anal. between 2-D surfaces subject to normal high freq. oscillations 80−16493
viscoelastic fluid, steady shear viscosity meas. using falling ball viscometer 79−94565
viscoelastic fluid lubrication, slider-bearing config., non-Newtonian normal stresses 80−69753
viscoelastic non-Newtonian liquids, resist. to tensile stress 80−1505
viscous fluid, shear processes, local order theory 80−59687
viscous liquid flow through annular clearance over rotating inner cylinder 80−64626
Viton A fluoroelastomer-EPDM blends, melt viscosities 77−7781
volatile liquids, boundary viscosity, meas. by blowoff method 79−11006
water, dynamic viscosity, eqn. at −20 to 150°C 77−20103
water, films, thin, wetting, rheological characts. determ., capillary method 78−51788
water, liq., NMR proton spin-lattice relax. and shear viscosity press. depend., −15 to 10°C 77−40144
water, mag. treatment affecting props., proposed mechanism 78−84827
water, mobility in blood plasma, NMR determ., viscosity correl. to $1/T_2$ 80−67176
water, multiparameter viscosity-temp. eqns. analysis 80−15283
water, nonfreezing thin interlayer between ice column and quartz capillary 80−54475
water, relationships between thermal cond., dynamic viscosity and density, high state parameters 78−83861

viscosity of liquids continued
water, thermal activity coeff., rel. to density, heat cond., sp. heat and viscosity meas. 77−7883
water, transport and thermodynamic props. *(Japanese)* 78−34251
water, viscosity, 10-150°C, press. effects 78−51715
water, viscosity, −8°C to 150°C, anal. of data 78−95101
water, viscosity, international formulation 78−26714
water, viscosity meas. behind shock wave front *(Russian)* 77−31707
water viscosity changes close to quartz surface, fine capillary calcs. 80−54422
water viscosity changes effect on electrokinetic phenomena in capillaries 80−53867
water viscosity rel. to limiting equiv. cond. of alkali, Cl^- ions in aq. soln. 77−1252
water-alcohol mixtures, US attenuation meas., method of streaming 80−88272
water-methanol mixtures, viscosity at 25°C, isotope substitution effects 80−92700
water-toluene-sodium dodecyl sulphate-butanol 1 mixture, interface light scatt., interface tension meas. 80−76039
Widom-Rowlinson hard-sphere mixture model, transport props. 80−14981
xanthane, dilute solns., viscosity rel. to temp., shear rate *(French)* 80−39332
xanthene dyes in n-alcohols (ethylene glycol) (glycerol), rot. relax., time-resolved fluoresc. depolaris. obs. 80−58300
Ag chalcogenide melts, changes in short-range order struct. during heating 79−50973
Ag, temp. depend. *(French)* 78−59964
Ag-Ge alloy, temp. depend. *(French)* 78−59964
$AgSbSe_2(Te_2)$, exam. of kinematic viscosity of melts, and short range ordering 79−1383
Al, 600-1000°C *(Russian)* 77−59133
Al alloys, liquid, kinematic viscosity temp. depend., porosity, H solubility, supercooling *(Russian)* 80−54425
Al, liquid, kinematic viscosity temp. depend., porosity, H solubility, supercooling *(Russian)* 80−54425
Al, molten, viscous flow, H dissolution temp. depend. X-ray anal. 79−91628
Al soap solutions, viscous behaviour 80−2185
Al-Cu, liq. alloys, with zero superheat, fluidity 80−70289
Al-Cu dilute alloys, vein closing mechanism in fluidity tests 80−84924
Al-Si (2.4 wt.%), liq. fluidity in solid-liq. zone 80−108429
$AlBr_3$, specific and equivalent cond. of aq. solns., viscosity 77−35736
Al_2O_3, floating zone melting, forced convection, computer simulation 78−88422
Al_2O_3, floating zone melting, forced and free convection, computer simulation 78−88423
Al_2O_3, liq., viscosity determ., oscill. cup technique 79−23758
Al_2O_3-SiO_2-MgO-CaO, blast furnace slag, viscosity, MP *(Russian)* 77−25039
Ar, dense fluid, viscosity, gaussian memory function approach 80−28904
Ar, hole theory, compressional viscosity and vibrational relaxation 80−70311
Ar, kinetic phenomena, shear viscosity *(Russian)* 80−10694
Ar, liquid, shear viscosity correlation function 78−47460
Ar, liquid, shear viscosity coeffs., model calcs. 78−47549
Ar-Kr liquid mixtures, volume and shear viscosities *(Russian)* 77−84961
As-S, melt struct., orientation birefr., viscosity, refr. index, and density 80−84713
$Au_{0.77}Ge_{0.136}Si_{0.094}$, undercooled metallic melt, viscous behaviour 77−66037
$Au_{77}Ge_{13.5}Si_{9.4}$, heat of crystn. and viscous behaviour 80−75166
Ba, thermophysical properties, up to 1800K 78−30767
$BaPO_3F$-Al_2O_3-B_2O_3 glasses, viscosity in the softening region and crystn. range 80−29105
Bi_2O_3-Mo(W)O_3 melts, electrophys. props. 77−89817
Bi_2O_3-$SiO_2(GeO_2)$, metastable phases form., crystn. conditions, melt viscosity and density effects 80−35167
Bi_2O_3-Si(Ge)O_2 melts, phys. props. 77−89566
$3Bi_2O_3.5B_2O_3$, viscosity, molar volume of melt and enthalpy of fusion 79−10924
CO_2, viscosity near liquid-vapour transition point 80−2189
CS_2, in CCl_4, orientational fluctuations, depolarised Rayleigh relax. time obs., temp. and conc. depends. 79−4809
$CaCl_2$ aq. solns., viscosity meas. 79−77792
$CaCl_2$-KCl, binary melt, viscosity *(Japanese)* 78−10209
CaF_2, melts, elec. cond., surface tension, viscosity, density *(Russian)* 80−92758
CaF_2-MgO-SiO_2, melts, elec. cond., surface tension, viscosity, density *(Russian)* 80−92758
CaF_2-MgO(SiO_2), melts, elec. cond., surface tension, viscosity, density *(Russian)* 80−92758
$Ca(No_3)_2.3.91H_2O$-$NiCl_2$ melts, glass forming, transport behaviour 78−59963
CaO-SiO_2 melt, viscosity and polymerisation *(Russian)* 78−26712
CaO-SiO_2-MnO molten mixtures, struct. and phys. props. *(French)* 80−24635
CaO-SiO_2-NiO melt, viscosity and elec. cond., effect of NiO conc. *(Japanese)* 79−23760
$CdCl_2$, aq. solns., sound absorpt. and relax. phenomena 80−49311
$Cd(NO_3)_2 4.1H_2O$-$CoCl_2$, melt viscosity, equivalent conductivity, glass transition temp. 78−75855
$Cd(NO_3)_2 4.1H_2O$-$NiCl_2$, melt viscosity, equivalent conductivity, glass transition temp. 78−75855
Co, calc. using model potential obtained from X-ray expts. *(Russian)* 77−31580
Co, viscosity, up to 2100K, vibr. method 78−38866
Co(II)-containing aq. electrolyte soln., nucl. mag. relax., hydration shell *(Russian)* 80−54966
$CoSO_4$, aq. soln., viscosity meas., viscous flow activation energy, entropy *(Japanese)* 77−43363
Cr-Ge liquid and amorphous alloys, struct. props., cond., viscosity, surface tension *(Russian)* 80−54119
Cr_2O_3, slips and castings, rheological and technological props. 77−16779
Cs, liquid, neutron diffr. struct. anal., density and viscosity temp. depend. 80−6352
Cs, transport coeffs., temp. and press. depend., Enskog theory 78−6170
CsCl-UCl_3 melts, density, surface tension and viscosity 78−67764
Cu and Cu alloy 77−4138
viscosity of liquids continued
Cu tripolyphosphate complexes, electrolyte development for direct deposition of Cu 80−45246
CuCl, molten, struct. and transport props. 79−19134
$CuGaTe_2$, exam. of kinematic viscosity of melts, and short range ordering 79−1383
$CuInSe_2$-$CuInS_2$, melts, viscosity, elec. cond., density composition prop. graphs 79−14948
$CuInTe_2$, exam. of kinematic viscosity of melts, and short range ordering 79−1383
Cu_2S-Ni_3S_2, melt viscosity 77−51536
$CuSO_4$, aq. soln., viscosity meas., viscous flow activation energy, entropy *(Japanese)* 77−43363
$CuSO_4$, aq. solns., densities, viscosities, elec. cond. meas., 20 to 70°C 80−59688
$CuSO_4/H_2SO_4$ electrolytes, densities, elec. cond., viscosities 80−107455
D_2O, assoc. liq., viscous props. 80−2186
D_2O, compressed at low temp., mol. motions, spin-lattice relax., viscosity and self-diffusion 77−76287
D_2O, US attenuation, for vol. viscosity, 0-60°C 78−63871
D_2O, US excess absorption and compressional viscosity, temp. depend., hole theory 77−4157
DPM-4, electroviscous effect 79−69010
Dy_2O_3-K_2O-MoO_3, melt, viscosity meas. 79−99346
Eu^3He, statistical eikonal T-approximation *(Russian)* 79−21655
Fe, calc. using model potential obtained from X-ray expts. *(Russian)* 77−31580
Fe, effect of C, O, S, P additions *(Russian)* 77−59134
Fe, liquid, viscosity meas., temp. depend. *(German)* 77−55377
Fe melt, oscillating viscometer viscosity meas. *(Czech)* 80−29103
Fe, molten, impurities effect on viscosity 78−95172
Fe particles, dispersed in Hg, mag. props., aggregate form. 80−60375
Fe, viscosity, up to 2100K, vibr. method 78−38866
Fe-C, pre-eutectic melt, struct. anomalies *(Russian)* 77−28794
Fe-Si (0-6 wt.%) melts, viscosity *(Russian)* 80−15285
$Fe_{40}Ni_{40}P_{14}B_6$ glass, viscosity near T_g, using rapid heating, and fusion characts. 80−70438
FeO-Cr_2O_3, melt, exam. of viscosity and self-diffusion 79−95198
FeO-Fe_2O_3-SiO_2 system, molten, struct. by high temp. X-ray diffr. 80−49084
FeO-MnO-SiO_2 system, melts, viscosity rel. to temp., composition *(Czech)* 79−19387
FeO-SiO_2, molten, viscosity and density 78−59965
FeO-SiO_2 melt, viscosity and polymerisation *(Russian)* 78−26712
Fe_2O_3, flocculated suspension in ethylene glycol, intrinsic viscosity rel. to shear rate 80−1502
FeS-Cu_2S, FeS-CoS, FeS-Ni_3S_2, melt viscosity 77−51536
FeS-MnS(MnO), melt, exam. of viscosity and self-diffusion 79−95198
Fr, properties from melting point to 7500K, prediction *(Russian)* 80−44296
Ga, up to 1800K 77−1254
Ge-Se liquid solutions, glass-forming, viscosity 77−66036
GeO_2 melts, density, viscosity, struct., at high and low press. 79−87431
Ge_xSe_{1-x}, liq., kinematic viscosity, 300-600°C 77−31706
Ge_xSe_{1-x}, vitrification, liquid-solid phase diagram, viscosity var. *(French)* 77−72680
$HN(SO_2Cl)_2$, physical props. meas. 79−51293
H_2O, assoc. liq., viscous props. 80−2186
H_2O, US attenuation, for vol. viscosity, 0-60°C 78−63871
H_2O-ethanol-chloroform mixture, shear viscosity near plait point, non-linear effect 77−84960
H_3PO_4-H_2O, superviscous and glass, relax., ^{111}Cd TDPAC obs. 80−15831
He, accurate empirical intermol. pot. 79−68291
He, superfluid, viscosity, ion mobility and λ-transition 77−72731
^3He, A and B-phases, viscosity and superfluid density meas. 77−66063
^3He, A-phase, vortex-free slippage of phase, I vector oscill. *(Russian)* 78−63897
^3He, liq., hydrodynamic modes, macroscopic dispersion relations, two fluid model 78−10242
^3He, liq., hydrodynamic modes, microscopic dispersion relations, transport coeffs. 78−10243
^3He, liquid, polarisation potentials, viscosity, thermal cond., spin diffusion 80−88389
^3He, liquid, shear viscosity and thermal cond., s- and p-wave approx. 79−1535
^3He, sound propag. at elevated densities, 0.35 to 1.4K *(Russian)* 80−92741
^3He, superfluid, A-phase, viscosity tensor, generalised paramagnon model 80−39379
^3He, superfluid, B-phase, first-sound attenuation and viscosity 80−75401
^3He, superfluid, B-phase, transport processes at low temp. 77−55412
^3He, superfluid, B-phase, transport coeffs. 79−51342
^3He, superfluid, dynamic orbital effects, US propag. and viscosity, book contrib. 80−2235
^3He, superfluid, heat capacity, spin susceptibility, NMR and viscosity *(Danish)* 78−22921
^3He, superfluid, kinetic properties, model for calc. of helium-helium excitations cross-section *(Russian)* 78−56006
^3He, superfluid, mag. reson., electron cloud distortion, viscosity and density meas. 79−65277
^3He, superfluid, nonequilib. processes, shear viscosity 77−66068
^3He, superfluid, oscillation viscometer results of A- and B-phase resonances, and normal phase viscosity 79−51351
^3He superfluid, phys. props. *(Danish)* 78−2325
^3He, superfluid, quasiparticle transport eqn., shear viscosity 78−14531
^3He, superfluid, spin relax., transport, spin fluctuation dominance model 77−66052
^3He, superfluid, transport and relaxation properties, viscosity, thermal, cond. and normal fluid density relax. 78−79839
^3He, superfluid, transport parameters, Kubo formulae and BCS-Green's functions 80−88382
^3He superfluid A-phase, orbital relaxation viscosity coeff. 77−66066
^3He, superfluid B-phase, microscopic evaluation of transport parameters 79−51354
^3He, superfluid B-phase, shear viscosity calc. 77−51562
^3He, superfluid B-phase, shear viscosity, s-p-d wave approximation 80−96715
^3He superfluid B-phase, viscosity, T-matrix calcs. *(Russian)* 78−63895
^3He, superfluid B-phase, viscosity meas. to 1 mK 79−51360
^3He, superfluid density and viscosity meas. 77−66061

viscosity of liquids continued
^{3}He, viscosity of normal and superfluid phases 79−51357
^{3}He-^{4}He, liquid mixture, second sound, quantised vortex creation at constrictions, excitation model 80−44383
^{3}He-^{4}He, superfluid solutions, second sound attenuation and dissipation processes, 1.3-2.0K *(Russian)* 79−42335
^{3}He-^{4}He, viscosity behaviour props. *(Russian)* 80−44382
^{3}He-B, viscosity near superfluid transition 78−38903
^{4}He, ion radius anomaly near lambda transition 77−76634
^{4}He, liq., phase transitions, positive and negative ion mobilities meas. 78−87833
^{4}He, liquid *(Russian)* 80−44382
^{4}He, positive ion mobility, with large He I halos 77−43400
^{4}He, superfluid, normal density viscosity, meas. at different freq. *(Russian)* 79−33130
^{4}He, superfluid, rotating, pressurised, relaxation pheonomena, transition ^{4}He II 79−99381
^{4}He, superfluid, viscosity props. depend. on oscill. freq. 80−6576
^{4}He, superfluid, viscosity and thermal conductivity *(Russian)* 80−10720
^{4}He, viscosity and positive ion mobility near melting transition 78−10240
^{4}He, viscosity behaviour near superfluid transition 77−89605
^{4}He, viscosity near superfluid transition under press. 79−19413
^{4}He, viscosity near superfluid transition under press. 79−55959
Hf complex, Hf-EDTA 80−34837
Hf, liquid, viscosity at melting point, free energy *(Russian)* 80−92699
$HfOCl_2$, aqueous solns., rotational diffusion, TDPAC study 80−34837
Hg, liquid, ferromag., containing Fe particles, time depend. magnetisation 80−44877
Hg, thermophys. props. rel. to clustering in liqs. 77−1065
Hg, transport coeffs., temp. and press. depend., Enskog theory 78−6170
Hg-In (3, 15, 30, 45 at.%) amalgam, viscosity meas. near melting point 80−70441
Hg-Tl amalgam, viscosity meas. 80−88349
$InBr_3$, specific and equivalent cond. of aq. solns., viscosity 77−35736
$In(NO_3)_3$, specific and equivalent cond. of aq. solns., viscosity 77−35736
InP, fused, SRO structure changes on heating 77−89367
K_2BeF_4, aq. solns., isomorphous salts viscosity investig. 78−95173
KCl solution, nonfreezing thin interlayer between ice column and quartz capillary 80−54475
$K_3P(As)O_4$, aq. solns., isomorphous salts viscosity investig. 78−95173
$K_2S(Cr)O_4$ aq. solns., isomorphous salts viscosity investig. 78−95173
$K_2S(Se)O_4$, aq. solns., isomorphous salts viscosity investig. 78−95173
Kr, liq., US attenuation and bulk viscosity 80−49304
Kr, near solidification, 50°C, up to 6500 bar, meas. and simulation using Lennard-Jones pot. *(French)* 78−67301
Kr, viscosity, 130-1300K, up to 10^9 dyne cm^{-2} 79−60536
LC-440, shear modulus and viscosity relax. near isotropic-nematic phase transition *(Russian)* 77−39543
La, liquid, viscosity from 940 to 1220°C *(German)* 79−28123
Li, thermophys. props. rel. to clustering in liqs. 77−1065
LiBr soln., conductance and viscosity, temp. and concentration depend. 80−6531
$LiPO_3$ melt *(Russian)* 77−43362
$MgCl_2$-KCl, binary melt, viscosity *(Japanese)* 78−10209
$MnCl_2$-tetra-n-butylammonium halide melts, density, elec. cond., and viscosity 80−24631
$MnO-SiO_2$ melt, viscosity and polymerisation *(Russian)* 78−26712
$MnSO_4$, aq. solns., viscosity meas., viscous flow activation energy, entropy *(Japanese)* 77−43363
N_2, liquid, US absorpt., bulk viscosity and relaxation 77−35639
N_2, viscosity near liquid-vapour transition 79−77799
NH_3-metal, soln., thermophysical props., review 79−77758
NH_4Br soln., conductance and viscosity, temp. and concentration depend. 80−6531
NH_4NO_3-$LiNO_3$-NH_4Cl-water system, cond. and viscosity *(French)* 79−51286
N_2O, and mixtures with CO_2 viscosity and thermal cond. coeffs. predictions, 180-900K, ≤23 MPa 77−84383
N_2O_4, viscosity and thermal cond., approx. polynomials *(Russian)* 80−59739
Na, liq., transport coeffs., static struct. factor calcs. 77−7643
Na, thermophys. props. rel. to clustering in liqs. 77−1065
Na_2O-SiO_2-MgO glass, melt viscosity and IR meas. to study MgO behaviour *(Japanese)* 78−14495
$NaAlSi_2O_6$, jadeite, melt, changes in viscosity and struct. at high press. 77−29290
$NaAlSi_3O_8$, albite, melt, viscosity and struct. changes at high press. 79−29754
NaBr in hexantriol-1.2.6, structural relaxation shear and compressional viscous processes, electrolyte effects 79−94686
NaBr in hexantriol-1.2.6, shear relaxation 79−94687
NaCl-$AlCl_3$ melt mixtures, viscosity meas. 79−82368
NaCl-KCl electrolyte mixtures, in aq. soln., viscosity, individual electrolyte effects *(German)* 78−22881
NaCl-KCl mixed aq. solns., viscosity meas. 79−82370
NaF-AlF_3 melt mixture, viscosity meas. 79−82369
$Na_xH_2P_xO_{3x+1}$, conversion products in presence of orthophosphate effect on melt props. 77−25355
Na_2O-SiO_2-NiO melt, viscosity and elec. cond., effect of NiO conc. *(Japanese)* 79−23760
$Na_2S(Se)O_4$, aq. solns., isomorphous salts viscosity investig. 78−95173
$Na_2Si_2O_7$ melt, changes in viscosity at high press. 77−29290
Ni, calc. using model potential obtained from X-ray expts. *(Russian)* 77−31580
Ni, viscosity, up to 2100K, vibr. method 78−38866
Ni-Al, diffusion coeff. differences, rotating-disc determ. 80−39330
$NiCl_2$, aq. soln., viscosity meas., struct. props. 78−75863
$NiCl_2$-tetra-n-butylammonium iodide melts, densities and kinematic viscosities 79−77793
$(Ni_{0.5}Pd_{0.5})_{82}P_{18}$ amorphous alloy, liquid-quenched, crystn. kinetics, nucleation 80−100176
O_2 liquid, US absorpt., bulk viscosity and relaxation 77−35639
O_2, shear viscosity coeff., 75-300K, up to 34 MPa 78−34253
PMMA, polymer chain, internal friction range, HF viscosity theory *(French)* 80−79968
$POCl_3.SnCl_4$:Nd^{3+}, phosphor, laser parameters and physiochem. props. 77−14709
Pb, comp. and temp. depend., up to 500°C 79−65233
Pb, hard sphere diameter, interionic potential 79−77797
Pb, thermophys. props. rel. to clustering in liqs. 77−1065
viscosity of liquids continued
Pb-Sn, melt viscosity rel. to phase equilib. *(Russian)* 79−69272
Pb-Tl alloy, comp. and temp. depend., up to 500°C 79−65233
$PbO-B_2O_3$ glass-forming melt, specific volume and viscosity, temp. depend. 80−84073
$PbO-B_2O_3-Al_2O_3$ system melts and glasses, viscosity, phase separation, and supercritical fluctuations effects 79−65235
$PbO-MO-SiO_2$ (M=Ca,Mg,Ba,Ni,Co) system, melt, viscosity meas. in temp. range 950 to 1250°C *(Japanese)* 79−77663
$PbO-SiO_2$ melt, behavior of MgO and NiO *(Japanese)* 79−52746
$PbO-SiO_2$ optical glass melts, resistivity rel. to viscosity 77−76589
$PbO-SiO_2-TiO_2$, molten, viscosity *(Japanese)* 78−18819
Pb_xSe_{2-x} melts, viscosity and radial distrib. function for stoichiometric and peritectic comp. 80−1916
$Pd_{0.775}Cu_{0.06}Si_{0.165}$, undercooled metallic melt, viscous behaviour 77−66037
$Pd_{77.5}Cu_6Si_{16.5}$, heat of crystn. and viscous behaviour 80−75166
Pu, hard-sphere model, phys. prop. meas. interpret., adjacent solid phase implications 77−19866
Rb, liquid, freq. moment and viscosities calc. 80−88348
Rb, liquid, shear viscosity correlation function 78−47460
Rb, liquid, shear viscosity coeffs., model calcs. 78−47549
RbCl-UCl_3 melts, density, surface tension and viscosity 78−67764
Rn, calc. of critical density 80−59547
SF_6, viscosity meas., 230-800K and press. up to 5×10^8 dyn cm^2 78−95171
Se, shear viscosity relaxation rel. to US absorpt. 78−2202
Se, viscosity meas. by rot. cylinder method 80−88347
Se:Te, impurity effect, chain length role *(French)* 78−51717
Si, floating zone melting, forced convection, computer simulation 78−88422
Si, floating zone melting, forced and free convection, computer simulation 78−88423
SiO_2, molten, viscosity, 2300 to 2600K 79−37863
SiO_2-B_2O_3, viscosity meas. up to 1840°C *(French)* 80−79969
Sn-Cu film, spreading kinetics on Nb substrate in vacuum, 700 to 800°C *(Russian)* 77−80680
Sn-Se, melt, density, kinematic viscosity, struct., 900-1400K 78−14395
Te, liquid, meas. of viscosity, density and surface tension *(French)* 78−91371
Ti, liquid, viscosity at melting point, free energy *(Russian)* 80−92699
TiO_2, aq. suspension, flocculation effect on dilatant flow 79−61916
Tl, comp. and temp. depend., up to 500°C 79−65233
$TlNO_3$, Tl_2SO_4, TlOH, aq. solns., viscosities at 25°C 77−20104
Tl_2Te_3, exam. of electrical props., density and viscosity, for solid or liquid states 79−95431
Tl_2Te_3, exam. of electrical props., in solid, liquid state 80−54686
Tl_2Te_3:Ag(Sn), effect of dopant on electrical props., density and viscosity, for solid or liquid states 79−95432
U, hard-sphere model, phys. prop. meas. interpret., adjacent solid phase implications 77−19866
V, liquid, viscosity at melting point, free energy *(Russian)* 80−92699
Xe, sound propag. near critical pt. 79−82285
YIG, garnet, high temp. solns., shear viscosity meas., rel. to LPE 80−10697
Zn, liquid, viscosity determination by oscillating vessel method *(Japanese)* 80−70439
Zn-Cd liquid/Fe-Ni-Al mag. powder, effective viscosity of composites *(Russian)* 80−54424
$ZnCl_2$-LiCl(NaCl)(KCl)(CsCl), molten, US absorption coeffs. and bulk viscosity coeffs. *(Japanese)* 80−88271
$ZnCl_2$-Li(Na)(K)(Cs)Cl, molten, viscosity, 260 to 560°C *(Japanese)* 77−51537
$ZnCl_2$-MCl, (M=Li,Na,K,Cs), melt, viscosity meas. by oscillating cylinder method *(Japanese)* 80−10696
$ZnCl_2$-MCl_2 (M=Cd,Pb,Sn,Ba) system, molten, viscosity coeff. meas. *(Japanese)* 79−77662
$Zn(NO_3)_2$-$Cu(NO_3)_2$ glass forming melts, density and viscosity 79−77794
ZnO/Al_2O_3, microstratified mixing of suspensions, viscosity dependence 79−70023
$ZnSO_4$, aq. solns., viscosity meas., viscous flow activation energy, entropy *(Japanese)* 77−43363
Zr, liquid, viscosity at melting point, free energy *(Russian)* 80−92699

visibility
see also atmospheric optics; brightness; light transmission
acetylene smoke particles, agglomerated, optical extinction meas. at 0.5145 and 10.6 μm 80−48155
advection-radiation fog near Lake Michigan, visibility meas. 77−81996
aerosol particle growth and size distrib., humidity effects, effects on visibility 77−25321
area imaging CCD low light level performance 77−39089
artificial satellite visibility calc., explicit method *(Japanese)* 77−82104
astronomical observatories, dome seeing theory 80−12657
astronomical seeing, atmosphere surface layer optical inhomogeneities investigation by acoustic method 80−67434
astronomical seeing, influence of spatial resolution on Ca^+ K-line width and shift in solar prominence 80−77364
astronomical seeing, meas. at Kitt Peak 80−61899
atmosphere, Bombay Airport during 1974-75 and 1975-76 winters 79−21018
atmosphere, correct spectral weighting of meteorological visibility 79−21017
atmosphere, CW lidar meas. 78−40651
atmosphere, extinct. coeff. from distant contrast meas. 78−61730
atmosphere, extinction at 10.6 μm CO_2 laser wavelength, from meteorological records 79−39848
atmosphere, fog and haze microphysics, visual range obs. 80−109195
atmosphere, Harmattan dust deposition rel. to visibility, wind and solar rad. 80−94578
atmosphere, lidar meas., extinction coeff. extraction accuracy 78−24369
atmosphere, lidar meas. problems in hazy visibility conditions 77−9572
atmosphere, lidar returns from fog, doubly scatt. radiation contrib. 78−77326
atmosphere, light scatt. coeff. of marine boundary layer 80−82052
atmosphere, London, England, rel. to SO_4^{2-} aerosols long-distance transport 79−21015
atmosphere, meas. by modulated CW lidar, comment 77−64440
atmosphere, meas. by modulated CW lidar, reply to comment 77−64441
atmosphere, meas. using long-path laser transmissometer 78−85751

visibility continued
atmosphere, multiwavelength contrast telephotometry, aerosol extinction and visibility determ. 79−66842
atmosphere, O_3 conc. rel. to visibility reduction in Midwest 78−61507
atmosphere, poor visibility due to pollution at Bombay Airport during monsoon season 78−32225
atmosphere, reduction by aerosols, linear system theory of visual acuity appl. 78−11997
atmosphere, rel. to airborne soil particles mass conc. 77−73849
atmosphere, rel. to fog and clouds liq. water content 78−81404
atmosphere, scatt. coeff. as function of visibility and wavelength, empirical formula 79−34944
atmosphere, solar radiation absorpt. by aerosol, spectrophone meas. 79−80027
atmosphere, statistics rectification 79−5610
atmosphere, temporal vars. beside motorway, England 79−39852
atmosphere, transparency, meas. on Maidanak mountain during autumn and winter (1977 to 1978) *(Russian)* 80−72627
atmosphere, urban visibility degradation, multivariate statistical anal. 79−62579
atmosphere, visibility, turbidity and light scatt. obs. 80−105047
atmosphere, visibility at ground level, two meas. methods 80−82078
atmosphere, visibility correl. with solar insolation at Fort Hood, Texas 78−24333
atmosphere, visibility reduction by sulphates in photochemical smog 77−21904
atmosphere, visibility rel. to surface wind at Gutersloh, Germany, smoke pollution effects 79−29853
atmosphere, visual range and relative humidity relationship from aerosol meas. 77−56728
atmospheric experiments, definition weaknesses of visibility 79−8688
atmospheric haze effect on horizontal visibility range of objects 78−16161
atmospheric O_3 and aerosols, in St. Louis urban plume, form. and transport 77−5316
atmospheric water content and turbidity in Thailand, calc. 79−5580
Bombay Airport, visibility diurnal var. 77−53187
Canadian haze climatology 78−57304
cloud/fog extinction coefficients, spectral correls., theory 79−96812
colour contrast meas., haze method and apparatus 79−71508
comets, visibility conditions rel. to discovery probability and reality of concentration of perihelia 80−67660
definition, confirmation using marine optics data 80−23633
distance constancy mechanism, visibility of gradients and low spatial freq. sinusoids 78−65018
distant light visibility calc., colour and flash time corrections 79−83781
dust, airborne, worldwide data on reduced visibility 78−40662
dust storms, freq. and diurnal var. in contiguous United States 77−29353
equivalent sphere illumination, maximum contrast sensitivity publication proposal, advantages 79−9235
ferritin particle visibility in SEM with field emission gun 79−25174
fog effects on visibility *(French)* 77−81978
fogs, warm, haze droplets effects on visibility in natural and treated fogs 79−100951
foveal increment threshold, lateral effect of oscill. of peripheral luminance gratings 80−108904
S Germany, large scale weather conditions and flight conditions *(German)* 77−17178
grating, sine-wave, average-luminance surround effect 80−51092
haziness factor in image contrast of aerial landscape photographs *(Russian)* 77−37449
illumination system, optical design 80−64135
interference fringe visibility and spacing, atmospheric turbulence effects 80−51572
interference transfer function with quadratic detect., coherent illum. 80−78782
IR heat camera component developments for night vision *(German)* 79−49287
IR transmission under limited visibility conditions 79−39863
IR wavelengths extinction by aerosols in coastal fog 78−81400
isolated alphabetic letters and numerals, annotated bibliography 78−53411
Kitt Peak National Observatory, probability of clear daytime skies 80−12512
laser beacon visibility in fog, range extension technique 80−101434
laser propagation experiment in low visibility atm. 77−88829
laser propagation experiment in low visibility atmosphere 78−46703
Lidar visibility measurements, using Raman/aerosol ratio method 79−100953
meteors, effective field of view for line sources 78−36535
meter design, visibility concepts 77−87803
mountain shadow phenomena, spike seen by off-summit observer 80−78761
moving target visibility, effect of mental set 78−27957
Mt. Majdanak (1976 June-July), atmospheric extinction and night sky brightness *(Russian)* 79−39856
near-Sun objects, twilight visibility function calc. 77−5321
nephelometer visual range estimates, contrast brightness theory, operational theory 80−8424
Ondrejov laser satellite-tracking station, cloud cover data 78−36418
particulate pollution contribution 77−73852
phase contrast microscope attachment for weak phase object visibility 80−86396
photometric contrast as basic value for visibility meas. *(German)* 80−95118
pollution effects over SW.United States, historical database 80−21424
power plant plumes, visual impact, model 79−16664
radio sources, compact, visibility phase deduction and mapping from VLBI data 78−89266
radiographical visibility and sharpness of lung struct. at 90, 140 and 350 kV 80−98124
reduction by aerosols in Los Angeles air basin 78−16157
repetitive image visibility, two-dimensional Fourier spectrum description 77−58282
Sacramento Peak Observatory night sky conditions, cloud cover, seeing and precipitable water 80−51653
Sargasso Sea, optical props. of seawater *(Russian)* 80−94532
seeing at Chinese solar observatory testing sites *(Chinese)* 77−67032
slant meteorological visibility, definition, determ. and appl. 79−100954

visibility continued
southern stars, observability from S hemisphere observatories rel. to cooperative obs. 78−69681
spatial frequency tuning studies, psychometric curves description by probability summation 80−61576
St. Louis, visibility reduction and downwind aerosol evolution 79−53514
stars and point sources, visibility estimate using visual instruments, search coeffs. 79−7089
stellar visibility in optical instrument, effect of measuring mark parameters 78−61736
stratiform clouds, visibility range rel. to local characts. meas. *(Russian)* 77−53158
structure visibility change with contrast reversal 79−57664
transparent film on absorbing substrate, optimum angle of incidence for monochromatic interference 80−43254
trends in atmos. visibility due to air quality change, appl. of ridit anal. 80−82051
turbid media with coloured illumination 79−72489
underwater, basic controlling parameters 78−36196
E.United States, visibility distrib. in moving high pressure system 79−83664
urban aserosol comp. and mass, particle size depend., rel. to visibility level 77−91258
urban-suburban air pollutant transport, chemical and physical transformations 77−37399
visual instruments, optical component contamination, effect on visibility of extended objects 80−64137
AlGaAs DH injection phase-locked laser, coherence 80−102726
C aerosol visibility vs. particle size distrib. 78−88911

visible and ultraviolet spectra of inorganic solids
actinide compounds, spectroscopic techniques for electronic props. meas. 80−11427
actinolite, optical spectra obs. 77−40284
adsorption rel. to dopant admixture 78−95596
alkali, borate glass:S, blue and green coloration, absorpt. spectra 79−87470
alkali aluminometaphosphate glass, $MPO_3.Al(PO_3)_3$:U (M=Li,Na,K), vibronic excitation, absorption and emission spectra 78−52524
alkali halide: $Tl^+(In^+)(Sn^{2+})(Pb^{2+})(Cu^-)$, charge transfer absorpt. band 79−73977
alkali halide:Ag film, EPR and optical exam. of Ag impurity centres 77−85562
alkali halide:$CrO_4^{2-}(MoO_4^{2-})(MnO_4^-)(ReO_4^-)$, frozen solns., absorption spectra, 4.2-300K 79−87467
alkali halide:Cu^+, absorpt., emission and lifetime data, temp. depend. 77−4671
alkali halide:$H^-(D^-)$, local modes and colour centre absorpt. bands, analogy 80−60632
alkali halide:NH_2^-, paraelectric alignment, UV electroabsorpt. and Kerr effect 77−12413
alkali halide, chalcogen^{2-} vacancy centres, absorpt. and fluoresc. spectra 78−48204
alkali halide, polarization dichroism in the optical spectra of Jahn-Teller excitons 79−69435
alkali halide crystals, activated, physical phenomena and optical data processing appl. *(Russian)* 80−80819
alkali halides, absorption spectra, freq. and temp. depend. of vibr. bands 80−2787
alkali halides, doped, optical absorption and MCD spectra, Gaussian quadrature calc. 80−7367
alkali halides, emission band of F-centre 80−76071
alkali halides, F_A-centre optical absorpt., estimate using symmetry-adapted wave functions 80−11448
alkali halides, F-centres, optical pumping, spin-orbit and hyperfine coupling 77−16360
alkali halides, microcryst. powders, colour centres, refl. spectra 78−23493
alkali halides, off to on centre defect transitions under hydrostatic press. 78−15199
alkali halides, temperature dependence 78−92050
alkali halides, thermoreflect. spectrum, 5 to 9 eV, electronic struct. 77−81123
alkali halides, vacuum UV absorption spectra, exciton splitting rel. to exchange interaction 78−23494
alkali lime germanosilicate glasses, optical absorpt. of transition metal impurities 80−2784
alkali metal film, inert gas impurities, metal-insulator transition, optical absorption and cond. 77−24598
alkali metal film, inert gas impurities, optical excitation spectra obs. 77−24876
alkali metal film, inert gas impurities, optical spectra, rel. to inert gas solids 77−24878
alkali metal film, inert gas impurities, sharp pair spectra and excited states 77−24877
alkali metal halides, hole self-localization and capture, temp. depend. 80−92526
alkali metal halides, X-ray induced colour centre and halogen aggregate form. 80−96565
alkali metal metaniobates, electron spectra of polycrystals, 0.06 to 25 μm 77−20868
alkali metal metatantalates, electron spectra of polycrystals, 0.06 to 25 μm 77−20868
alkali metal salts with aromatic hydrocarbons, photoelectron emission and optical absorption *(Russian)* 78−80456
alkali metals, agreement with theory *(French)* 78−72558
alkali phosphate glass:Nd^{3+}, laser material evaluation 77−54715
alkali phosphate glasses, colour and absorption spectra of Fe 77−85752
alkali silicate:Nd_2O_3 glasses, coloured, dichroism *(Polish)* 79−99919
alkali silicate glass: Cu^+/Cu^{2+}, opt. absorpt. rel. to impurity redox equilib. *(Japanese)* 77−12824
alkali-trihalogeno-plumbates, $M[PbX_3]$, cryst. growth struct. and spectra *(German)* 79−90632
alkaline earth oxides with adsorbed CO, reflectance spectra obs. 79−28781
alloy, comp. modulation spectra, line shape 78−76491
alloy, electronic characts. from thermomodulation spectra 79−87421
aluminate glasses, new families, light transmission, 0.4 to 6 μm 77−24843
aluminophosphate glass:Mn:Mg(Sr), optical props. H_2O effects 77−28600

visible and ultraviolet spectra of inorganic solids continued
amethyst, Fe^{3+} diffusion, associated phenomena 77−36269
amorphous semiconductor, optical absorpt. edge shape, band edge fluctuations 77−20880
anthracene, Davydov splitting of lowest singlet exciton under high press. 77−72823
anthracene, O-O exciton absorption bands, thermomodulation study 78−39563
anthracene, single cryst., piezomodulated reflection spectra 79−61392
anthracene derivative films, Langmuir-Blodgett built-up multilayer, prep. and characterisation 79−95293
antiferromagnetic, crysts. with spin-forbidden transitions, two-photon light absorption *(Russian)* 77−48185
antiferromagnetic, noncollinear, exciton-magnon light absorpt. at $T \neq O$ *(Russian)* 78−23482
antiferromagnetic garnet, absorpt. and luminesc. spectra, cryst. field and exchange interactions 77−73154
benzene film, vacuum UV absorpt. spectrum, 1100-2500 Å, effect of deposition temp. 78−23542
beryl, channel constituents, electronic absorption spectra of Fe^{2+} 79−69863
bimetallic cluster, photoselective bimetallic aggregation, review 80−53182
biotites, optical absorpt. bands 80−7371
bis(p-toluene sulphonate)diacetylene, fully and partially polymerised, optical props. 77−1696
borate glass: Ni, absorption spectra, mag. props., coordination behaviour *(German)* 80−40147
boric oxide-alkali oxide glasses, use of optical spectral lines of Nd,Co,Ce as struct. changes *(Polish)* 77−68926
borosilicate glass, influence of Ti on absorption spectra of transition metals in glass 77−12403
borosilicate photochromic glasses, photosensitivity rel. to AgCl particle shape 78−31223
caesium uranyl propionate, low temp. absorpt., luminesc. spectra, intermol. interactions 80−2830
CaF_2:Na, Stark effect on Na disturbed F_2-centres 77−69279
CdS film, polycryst, optical spectra, 0.5-6.5 eV 80−55212
ceramic high-temperature transmission/wavelength characteristics *(French)* 79−7188
ceramic translucent systems, absorpt. and scatt. coeffs for visible light, Kubelka-Munk theory 80−60627
ceramics, piezoelectric, photoacoustic effect 80−84252
chalcogenide glass, optical transitions and electronic struct., review 77−76741
chalcogenide glass films, photostructural changes, photodarkening 80−49121
chalcogenide semiconductors, optical and elec. props., comparison with SiO_2 78−6721
chalcogenide vitreous semicond. films, photoinduced optical anisotropy, spectral responses 79−65948
chalcogenide vitreous semiconductors, reversible photoinduced changes in optical, physicochem. and contact props. 79−24378
chlorides, I^- or Br^- doped, optical investigation of atomic hydrogen centres 78−88351
1-chloro-9,10-anthraquinone crystal, electronic structure of lowest triplet state *(Japanese)* 79−8158
colour centre-phonon many-mode interaction, absorption band shape, adiabatic approx. 78−2883
9-cyanoanthracene, cryst., polarised refl. spectra at 2K, 360-460 nm, dielec. function 79−91461
D^- centre in strong magnetic fields, optical absorpt. spectrum 80−20670
diamond: Sb, ion implanted, defect study using optical absorpt. and EPR 80−24480
diamond, electron irradiation, vacancy charge states, optical absorpt. spectra 77−90177
diamond, elementary excitation in crystals, dielectric theory 78−60076
diamond, GR1 and UV band, fine struct. 80−20678
diamond, GR1 band, anal. of satellite lines by quadratic Jahn-Teller computing 80−97295
diamond, GR 2-3 absorpt. line, uniaxial stress effects 78−72563
diamond, irradiated, MCD spectrum of GR1 line, neutral vacancy model 77−69850
diamond, irradiated, optical spectrum 78−6719
diamond, irradiated, optical study of TR12 and 3H defects 77−85772
diamond, Jahn-Teller coupling at neutral vacancy 80−71453
diamond, linewidth of GR2-8 transition 78−60488
diamond, natural type IB, thermal conductivity anomaly, defects obs. 77−85003
diamond, optical absorption and luminesc. spectra, review 80−2848
diamond, optical absorption lines, GR4 and GR8, effect of uniaxial stress 80−34956
diamond, pseudo-Jahn-Teller effects in H3 vibronic spectrum 77−90182
diamond, radiation-induced optical absorption spectrum, 0.4-2.0 MeV electrons 77−84798
diamond, role of electron-hole interaction in optical spectra, review 80−45113
diamond, semicond., energy band struct., elec. and optical props., review 77−35862
diamond, type IB, electron irradiated, 2.367 eV vibronic absorpt. system, optical study 79−73975
diamond, type Ib, electron irradiated, migration of N, optical absorption meas. 78−56505
diamond, uniaxial stress splitting of E to E transitions at trigonal centres in cubic crystals 80−97312
diamond, UV absorpt. produced by substitutional N_2 pairs 80−29770
diamond, vacancy, mol. orbital theory of transitions 77−85757
diamond, vibronic bands at 2.498 eV (H4), 2.417 eV and 2.536 eV, absorpt. and luminesc. under stress 77−85758
diamonds, artificially coloured, spectroscopic diagnostic technique 78−65281
dielectric crystal, phase transitions, laser spectrometry, use of diamond anvil devices *(Japanese)* 80−49362
diethylammonium manganese chloride, antiferromag., magnon sideband exam. by absorpt. spectra 77−12108
direct semiconductors, picosecond absorption spectroscopy 79−47482
dye crystal, CTIP, exciton surface polaritons detect. by ATR spectra at 295K 79−4818
electrode surface, anisotropy of optical props. 80−60534
electrolyte, solid film, size-selective photochromism 79−99968
electronic states determ. using synchrotron radiation 77−20882

visible and ultraviolet spectra of inorganic solids continued
F-centre optical absorption bandshape calc. for transition to state with Jahn-Teller and spin orbit couplings 80−55135
ferrite spinels, magneto-optical refl. spectra by equatorial Kerr effect *(Russian)* 77−32400
ferrocyanide ion, electronic struct. and related props., calc. by SCF Xα-scattered wave method 77−15809
ferroelectric semiconductors, props., book 80−82590
ferromagnetic dielectric, magneto-optical near UV reflection-spectra, meridional and polar intensity effects *(Russian)* 78−39572
ferromagnetic metal, magneto-optical near UV reflection-spectra, meridional and polar intensity effects *(Russian)* 78−39572
ferromagnetic semiconductor, absorpt. edge and cond. band width, temp. and mag. field depend. 77−36267
films, amorphous, prep., struct., props., review, book contrib. 78−48321
fluoride coating materials, refractive index, spectroreflectometry meas. 250 to 2000 nm 79−32006
fluorochloroapatite, synthetic, defect struct. and colour centres obs. *(Russian)* 78−30612
frosts, Na and K doped, reflectance spectra and implications for Io surface 78−84561
GaP, reevaluation of bandgap and free exciton binding energy 78−60061
garnet, Fe^{3+} ligand field spectrum 79−78701
Gd, optical conductivity meas., 0.5-3.1 eV *(Russian)* 80−45100
gems and minerals, colour 77−37182
GG GaS_2, indirect exciton exam. 78−39029
glass:Cr^{3+}, absorpt. spectra, Fano antireson. and vibronic Lamb shift 80−71458
glass:Eu^{3+}, spectral line inhomogeneous broadening, electron excitation migration *(Russian)* 77−48200
glass:Nd laser materials, intensities of optical transitions 77−689
glass, coloured, toughening process, spectral charact. 80−43416
glass, multicomponent Schott, proton-induced colouring 80−9974
glass, photochromatic, induced colour by optical/thermal treatment 80−34954
glass, photochromic, spectral charact. control 80−16073
glass, trapped electrons, electron-phonon interaction 79−78697
glass fibre waveguide, γ-irrad., reversible optical bleaching of induced absorpt. 80−14462
glasses:Ce (III) and (IV), u.v. absorpt. 77−4658
glasses, elec., mag., and optical props., conference, Troy, NY, USA (Aug. 1979) 80−105417
glasses, electron scavenging, hopping controlled time-depend. reaction rates 80−108723
gradient index material models and exptl. verification 80−16002
granular metal, dielec. const., Maxwell-Garnet and effective medium theories 77−47760
graphite, highly oriented, pyrolytic surface, polarised reflectivity spectra at near normal incidence, surface prop. effects 79−15481
graphite, piezoreflectivity, 3 to 6 eV 79−47472
graphite, reflectance meas. in visible spectrum 77−77241
graphite intercalate with SbF_5 and AsF_5, optical reflectance 78−35163
graphite intercalation compounds, band struct. model, dynamical dielec. function, reflectivity 80−34348
graphite intercalation compounds, KC_8 and CsC_8 polarised reflectance 78−31213
graphite nitrate, $(C_{3.24})^+(NO_3)^-3HNO_3$, DTA, NMR and refl. meas., dynamical and electronic props. 77−59478
graphite-alkali metal intercalation cpds., electronic props. 80−45202
group V transition metal dichalcogenides, layered, thermoreflectance spectra 77−52120
halide crystals, 3p→4d transitions of transition metal ions, assignment from expts. on LiCl:Cu^+ 78−27272
halosodalites, synthesis, cathodochromism, reflectivity spectra 77−40399
hemicylinder-air-quartz system, semi-infinite crystal, dispersion of surface phonon polaritons 78−71939
ice, electronic structure investig. by XPS, UPS and UV absorpt. spectra 77−16452
II-VI and III-V cryst., excitons detect., precision method 79−19906
II-VI semiconductor, two-photon and two-step absorption of light 80−7389
II-VI semiconductor mixed crystal, comp. disorder-induced broadening for free excitons 79−15479
II-VI semiconductor mixed crystals, two photon absorption *(Russian)* 77−20875
II-VI semiconductors, photoreflection exciton spectra *(Russian)* 77−20874
II-VI semiconductors, zinc blende and wurtzite struct., two photon spectra, quantitative investigation 80−50373
III-V, tetrahedrally bonded, electronic density of states and optical spectrum 77−62797
III-V semiconductor, d core levels, electron-hole interaction 77−11880
inert gas, solid, dead layer effects in UV reflectance of excitons 78−72553
inert gas crystals, excitons exam. 78−51898
inert gas solids, core transitions, nonstructural theory of core excitons 78−84148
inorganic molecular crystals, metal complexes electronic spectra and intermolecular interactions 80−55137
IV-VI semiconductors, two photon spectra, quantitative investigation 80−50373
KCl, pure and Ba-doped, γ-irrad., point defect form. and interaction, X-ray and optical studies 79−65078
lanthanides, 4d spectra in atoms rel. to solids 79−31450
laser window material absorption obs. 79−14012
layer materials with stacking faults, fine structure splitting of ground state excitons 77−51665
layer metal particles, surface plasma oscillations 77−76765
layered compounds, book contrib. 77−44023
layered compounds, modulation spectroscopy, book contrib. 77−40267
leucosapphire, electronic band struct., optical props. 79−95329
leucosapphire, large cryst., UV transmittance 77−88876
leucosapphire, spectral absorpt. coeff., 1800K 78−27252
leucosapphire, spectral absorption coeff., 0.25-1.25 micron, up to 1800K, and 3.5-5.2, up to 1200K 78−27204
LiH, cubic, vibronic struct. and anisotropy of excitons, refl. and edge luminesc. spectra 78−23523
manganese aluminosilicate glass, insulating spin glass, exchange dipole optical transition 80−40136
mechanical surface excitons, interaction with radiation, refl. and transmission spectra 79−15098

visible and ultraviolet spectra of inorganic solids continued
metal, electronic characts. from thermomodulation spectra 79−87421
metal, electronic structure, optical absorption 79−38566
metal, light reflection, adatom characts. depend. 78−10918
metal, struct. induced surface plasmon polariton modes using ATR, theory 79−60890
metal film, disordered and amorphous, quench-condensed, optical cond. and band struct. 77−1746
metal film, optical props. as function of wavelength *(Russian)* 78−52591
metal film, structure-related optical characts. in visible and UV 77−55841
metal sphere, LF plasma reson., interband transitions effect 79−99906
metal sputtered film, compressive stress transition 78−10310
metal surface oxidation, refl. spectra obs. 78−39958
metal surfaces, adsorbate spectra, vac. UV differential reflectivity obs. 79−28783
metal-chalcogenide glass-metal structures, elec. field influence on opt. parameters, electrostimulated chem. transforms. 77−76950
metal-insulator composite films, optical props., rel. to solar collector appls. 78−72622
metal-insulator composite solar selective absorbers optical props. 79−52037
metallic aggregated system, optical props., interband transitions and optical cond. reson. 77−44016
metallic glass, prep. and phys. props. development 80−81003
metallic mirror coatings, protected and unprotected specular reflectance 79−76792
metallic thin film, structure-related optical characteristics in visible and UV 78−35217
metaphosphate glass: Ag dosimeter, optical absorpt. and radiophotolum., effect of temp. 78−40333
metaphosphate glasses, $n(M_2O.P_2O_5).(1-x)Y_2O_3.xTb_2O_3.3P_2O_5$, M=Li, Na, K, excitation and emission spectra 80−40150
3-methylpentane glassy matrix, localised electrons, cavity model 80−107743
microcline, continuous laser emission effects on surface, spectroscopic obs. 79−94271
microcrystals on C foil, size distrib. from electron micrograph obs., UV absorpt. spectra obs. 80−55121
mixed crystals with indirect band struct., no-phonon struct. from Wannier exciton model 78−43898
$Mn_{1-x}Cu_xSb$ films, $0 \leq X \leq 0.3$, magneto-optical props. 79−51981
nepheline, continuous laser emission effects on surface, spectroscopic obs. 79−94271
$NH_4Al(SO_4)_2.12H_2O:MnO_4^-$, visible and UV absorpt. spectra interpretation 80−45116
noble metal aggregated film, absorpt. peaks, collective oscills. of electrons 78−80428
nonmetal, impurity optical absorption and emission, anharmonic effects 78−56503
olivine, optical absorpt. spectra and radiative heat transport at high temp. 79−79818
optical fibres, glass and plastic, neutron irradiated, optical absorpt. spectra 0.7 to 1.1 μm 80−58762
optical glass attenuation and optical density spectral curves 79−50361
orthoferrites, magneto-optical refl. spectra by equatorial Kerr effect *(Russian)* 77−32400
orthovanadates, rare earth activated, spectroscopic props. 77−16363
oxide coating materials, refractive index, spectroreflectometry meas. 250 to 2000 nm 79−32006
oxide glass:Cr^{3+} absorption and emission 78−6774
oxide glasses:Sm^{3+}, optical transitions 79−61430
oxide semiconductor crystals, with forbidden energy gap, review of spectroscopic props. 78−2876
oxide surfaces, adsorbate spectra, vac. UV differential reflectivity obs. 79−28783
perylene, energy structure, photocond., photoemission and absorpt. spectra meas. 77−39895
phosphate glass: Ni, absorption spectra, mag. props., coordination behaviour *(German)* 80−40147
phosphate-tungstate semicond. glass, W (V) complex, EPR and electronic spectra interpretation 77−69682
photothermal absorber stacks on Ag, stabilisation 77−32459
pnictide amorphous semiconductors, absence of photodarkening 80−103970
polar glasses, aq. and alcoholic systems, trapped electrons, photocond., optical spectra 77−85742
polarised electronic absorption spectrum at 300 and 77K, phys. chem. lab. expt. 80−17774
poly-N-epoxypropylcarbazole layers, optical and photoelec. props. 77−39896
polydiacetylene, cryst., refl. spectra, Kramers-Kronig transforms 78−43889
polydiacetylene-toluenesulphonate, photocond. meas., 0.62-3.1 eV 80−70757
polynitramines, solid cyclic, luminesc. meas. 77−32424
polyvinyl acetate film, I_2 doped, optical absorpt. band, elec. cond. 77−85234
polyvinyl alcohol films activated, thermochromism *(Russian)* 79−91415
potassium halides, F-centres, optical pumping, spin-orbit and hyperfine coupling 77−16359
praseodymium ethyl sulphate, phase transition under pressure, absorpt. spectra *(Russian)* 80−92667
purple membrane films, absorpt. and circular dichroic spectra 79−83708
pyrene, single cryst., γ-irradiated, EPR and optical absorption meas. 78−72412
quartz, cryst. and fused, far UV optical consts. 77−81078
quartz, cryst. and melt, irrad., optical absorpt. spectra, computer calcs. *(Russian)* 78−92091
quartz, cultured cryst., vacuum UV transmittance before and after electron irrad. 78−83044
quartz, electron irradiated, optical and anelastic absorptions and resonator freq. 78−64385
quartz, fused, continuous laser emission effects on surface, spectroscopic obs. 79−94271
quartz, irrad., annealed optical absorpt. power *(Russian)* 77−36273
α-quartz, phonon polariton dispersion in reststrahlen bands 77−35647
quartz, pleochroic amethyst, optical absorpt. of d^4 ion Fe^{4+} 78−15201
quartz, radiation effects rel. to diffuse interstellar bands origin 77−13432

visible and ultraviolet spectra of inorganic solids continued
quartz, rose, charge transfer mechanism for origin of colour, EPR and optical expts. 78−52537
quartz, synthetic, discoloration rel. to lattice deform. 77−24872
quartz, transient absorption on pulse electron irrad. 79−1779
α-quartz electron states, self-consistent pseudopot. calc. 77−62823
quartz glass, spectral absorpt., 3000-4000K 80−25401
quartz resonator, electron irrad., optical absorpt. 77−8609
radiation damage tetragonal R2 centre, optical and EPR spectra 78−2888
rare earth cobalticyanides, $R(Co(CN)_6)n.H_2O$, (R=La to Lu), optical spectra 78−39566
rare earth complexes, formation and props., book contrib. 80−43204
rare earth compound, crystal field and Slater parameters and coordination 78−6771
rare earth element sulphides, condensates, struct. and optical transmittance 80−20727
rare earth garnets, cryst. field parameters for R^{3+} ions, exchange charge model 78−47747
rare earth ions, trivalent, in O-dominated host, high energy states, reflectance spectra 77−69849
rare earth metal film, optical cond., rel. to cryst. struct. and electronic config. 77−36303
rare earth oxide film, transmission of refl. spectra, opt. consts. and parameters 79−95864
rare earth oxide films, optical absorpt., refractive index, band gap and zone struct. *(Russian)* 78−76544
rare earth oxides, binary, struct. and props., book contrib. 80−45292
rare earth oxydiacetate, spectra, energy level patterns 79−38561
rare earth oxymolybdates and oxytungstates, R_2MO_6, spectroscopic props. and crystallochem. laws 77−36215
rare earth sulphides-1.8 Ga_2S_3 glasses, vibr. spectra, electronic transitions, short range order 77−69820
rare earth titanates, pseudoperovskite struct., nonlinear spectral and luminesc. characts. 80−29771
rare earth trifluoride film, optical props., 5 to 34 eV 79−38687
rare earth trifluorides, vacuum-UV excitation spectra of Nd^{3+},Er^{3+} and Tm^{3+} 78−80381
rare earth vanadites, X-ray fluoresc., IR and UV spectra 77−77206
rare earth-gallium sulphide glass, R_2S_3-1.8Ga_2S_3, vibr. and electronic spectra, short-range order 78−27228
rare-earth oxides, absorption spectra and energy levels of trivalent ions 77−63420
refractive index and extinction coeff. 79−78643
refractory metal films, evaporated, optical props., rel. to struct. 80−55211
rocks, metamorphic, visible and near IR spectra rel. to comp. 77−17087
rocks, sedimentary, visible and near IR spectra rel. to comp. 77−17086
rocks and minerals, colour values from diffuse reflectance spectra *(French)* 78−11881
rocks from Cr-rich areas, visible and near IR spectra, remote sensing appls. 80−4000
rocks of volcanic origin, refl. characts., 400-800 nm 80−90073
rubidium uranyl propionate, low temp. absorpt., luminesc. spectra, intermol. interactions 80−2830
ruby, Cr^{3+} ion doped, R-line region, absorpt. spectrum, dispersion rel. to mag. field 80−2732
ruby, luminescence, absorption of R and N lines, effect of mag. field 80−60550
ruby, optical free induction decay modulation and absorpt. line struct. due to superhyperfine interaction 80−33091
ruby, optical pair spectrum, Stark effect with AC elec. field modulation 78−10911
ruby, optical spectra freq. shifts press. depend., nonperturbative theory 78−23499
ruby, spectral absorpt. coeff., 1800K 78−27252
ruby, spectral absorption coeff., 0.25-1.25 micron, up to 1800K, and 3.5-5.2, up to 1200K 78−27204
ruby, Zeeman effect of R-absorpt. lines 79−47416
ruby colouring due to specific growth, annealing and irrad., exam. of visible, infrared and UV spectra 79−11440
sapphire, 14.8 MeV neutron damaged, optical vibronic absorption spectra 80−50384
sapphire, natural, origin of colour 79−70794
sapphire, synthetic and natural, optical spectra comparison and identification 80−40138
sapphire, vacuum UV spectra, Cr^{3+} impurity and anion vacancy conc. 78−84605
semiconducting alloys, comp. profile, second derivative wavelength modulation 80−103967
semiconducting films, exciton polariton attenuation, spatial dispersion effect 80−20097
semiconductor, direct gap, one-photon Keldysh absorption 77−8599
semiconductor, exciton absorption, electric field effect *(Russian)* 78−43902
semiconductor, hot carrier phenomena, optical obs. 79−95845
semiconductor, layered, direct and indirect two photon processes 77−40261
semiconductor, optical absorption by impurities, phonon-electron interaction 78−56502
semiconductor, optical and IR characterisation 79−95846
semiconductor, optical excitations, many particle effects 79−87046
semiconductor, photo-excited electron momentum distrib., hot luminesc. polarisation 77−16396
semiconductor, struct. induced surface plasmon polariton modes using ATR, theory 79−60890
semiconductor, tetravalent, fundamental absorpt. spectra, direct interband transitions 78−63972
semiconductor films, two-photon interband absorpt., quantum size effects 79−43054
semiconductor with nonspherical bands, absorpt. in crossed elec. and mag. fields 77−40264
semiconductors, amorphous, optical absorption, theory 80−80818
semiconductors, deep level carrier trapping and emission, transient spectroscopy, book contribution 80−80216
semiconductors, light absorption, amplification and luminescence, saturation effects *(Russian)* 78−13771
semiconductors, magnetic, electron spectrum, light absorpt. spectrum, calcs. 80−2793
semiconductors, modulation spectroscopy in far UV, electroreflectance and thermoreflectance 77−66516

visible and ultraviolet spectra of inorganic solids continued
silicate Fe activated glass, diffraction trating recording by UV laser 80−5842
silicate glass: Cr^{3+}, optical props., 88-273K, energy levels in crossing region 78−6709
silicate glasses:Cu^{+}, effect of UV irrad., absorption bands 78−31222
silicate glasses, model of struct. element, calc. of physicochem. props. 79−69016
silicate smokes, vapour-condensed, 800 to 130 nm extinction and interstellar extinction curve 80−82180
silicates, radiation effects rel. to diffuse interstellar bands origin 77−13432
single crysts. and thin films, absorpt. edge temp. depend., gap energy changes 79−42991
SmS film, metallic, interpretation of optical absorption spectrum 78−27344
sodium uranyl acetate (deuteroacetate) 80−2830
solid-liquid transition, optical reflectance spectra 80−24569
solids, XUV photoabsorpt. spectra, at. effects 80−2785
sphalerite, hydrothermal single crysts., feasibility of optical methods for quality control 80−89065
spinel transparent glass ceramics, colour centre form. due to alkali metal vapour and X-ray irradiation 79−87316
sputter-deposited materials, electrical and optical props. 79−47181
steel, stainless, hard, and mild, optical constant dispersion and emissivity, up to 900K 78−52464
stilbene, single cryst., triplet excitons, delayed fluorescence 78−63988
stilbene, single cryst. under pulsed electron excitation, triplet exciton luminescence and opt. absorpt. 79−7838
surface exciton polaritons, attenuated total reflection spectra 77−24867
synchrotron radiation, props. and appls., review 79−36830
tellurite glass, Cu^{2+} (Ni^{2+}) coloured, band-pass filter characts. 550-616 nm 78−66919
tetracene single crystals, exciton refl. spectra, 4.2 to 300K 79−47478
tetracyanoplatinates, energy band calcs. 77−39780
$(TMTSF)_2X$, ($X=PF_6^-$, AsF_6^-, SbF_6^-, BF_4^-, NO_3^-) highly conducting salts, props. 80−59969
transition metal, inner shell photoelectron and photoabsorpt. spectra 79−43091
transition metal chalcogenophosphates, intercalation with n butyl-lithium, possible appl. in Li batteries 80−71446
transition metal complex, $MX_a.b$(hexamethylenetetramine).nH_2O, optical reflection spectra, mag. suscept.. 79−56810
transition metal complexes, acetylacetonates, mag. susceptibility and optical reflection spectra 77−59381
transition metal compounds, intensity of Laporte forbidden transitions, ligand polarisation model 78−64378
transition metal dichalcogenides, layer type, reflectivity meas., 6-40 eV 77−55801
transition metal dichalcogenides, modulation spectroscopy obs. 78−80377
transition metal film, 4d, optical absorption meas. using synchrontron radiation, 20-250 eK 77−12457
transition metal ion 3d→4s transitions in crystals, obs. and interpretation 78−6339
transition metal ions, exchange-coupled in ionic crystals, optical spectra *(Rumanian)* 79−87474
transition metal monoantimonides, 3d-states, optical evidence for analogy with transition metals 77−62816
transition metals, BCC, thin films, optical props. 79−78781
transparent solids, absorpt. coeffs. by laser calorimetry, wavelength modulation spectroscopy 78−66876
tremolite, optical spectra obs. 77−40284
TTT_2-$(I_3)_{1+x}$, physical props., elec., mag. and optical meas. 80−24908
UV transparent materials, 355 and 266 nm absolute two-photon absorption coeff. obs. 79−18493
vanadyl phthalocyanine, exciton electroabsorpt., optical density spectra 77−85746
water cryofilm, on specular and diffusing surfaces, bidirectional reflectance 78−88274
X-irrad., optical absorpt. spectra and dichroism meas. 80−108239
zeolite-Y, continaing Ag atoms, ions and clusters, optical absorption spectra 79−36569
zincblende structure semiconductor in intermediate mag. field, exciton spectra 78−18969
$24BaO.V_2O_5.25P_2O_5$, ESR and absorpt. spectra, V(IV) ions conc. 78−64266
$24CaO.V_2O_5.25P_2O_5$, ESR and absorpt. spectra, V(IV) ions conc. 78−64266
ADP-type crystals, electrooptic effect in ultraviolet region 78−76431
Ag (111) electrodes, electroreflectance spectra meas. 77−59591
Ag, adsorption of O, dielec. perm., plasma surface vibr., modulation spectroscopy 77−48198
Ag, aggregated film, optical props., 0.35-1 μm 77−66548
Ag aggregates, matrix isolation spectra 78−46476
Ag, bonding of CN^-, electrorefl. exam. 77−80700
Ag, discontinuous film, light absorpt. spectra, dielec. function calcs. 79−51507
Ag electrode, emersed, electrorefl. spectra 79−28788
Ag, electroreflectance spectroscopy, longitudinal surface plasmons 80−40137
Ag film, bounded by dielectric slabs, attenuated total refl. angular spectra 78−92135
Ag film, evaporated, chemisorption effects on reflectance and elec. resist. 80−11495
Ag film, optical props. after thermal cycling, thickness and substrate temp. effects *(French)* 77−48263
Ag film, optical props. as function of wavelength *(Russian)* 78−52591
Ag film, optical props. in intermediate region between pure Drude and interband absorption 77−81170
Ag film, substrate surface structure effects on absorptance 78−19585
Ag films, underlayer effect on surface roughness, surface plasmon excitation meas. 79−51456
Ag foil interface with liquid, oxide props. from reflectance and scatt. light spectroscopy 80−60702
Ag foil-electrolyte boundary reactively formed oxide layers, differential reflectance 79−69856
Ag foils, surface plasma-wave reflectance and roughness-induced scatt. 80−66228
Ag halide doped photochromic glass absorption spectra *(Russian)* 78−60490

visible and ultraviolet spectra of inorganic solids continued
Ag halide photochromic glass, darkening mechanisms under pulsed laser excitation 78−25938
Ag halide photochromic glasses, optical properties, effect of Cu ions 80−93364
Ag halides, tetrahedrally coordinated, semiempirical band struct. model 77−51655
Ag, intraband optical conductivity, electron-electron scatt. 78−35166
Ag microcrystals, matrix isolation spectra 78−46476
Ag particles, lattice defect influence on size effect 78−88329
Ag particles, light scatt. spectra, size and shape effects 77−44015
Ag, single cryst. electrodes, electroreflectance obs. in aqueous solns. 80−25342
Ag surface, periodically modulated, radiative decay of surface plasmons excited by fast electrons 77−24599
Ag surface, sinusoidally modulated, light emission of nonradiative surface plasmons 77−1467
Ag surface layers, reflectivity, contrib. of longit. polarisation waves 79−83046
Ag surface layers on Au and Al substrates, reflectance spectroscopy 79−78780
Ag, surface plasma oscills., sinusoidal surface 77−73179
Ag, surface plasma waves, dispersion curves, attenuated total reflection spectra 78−88015
Ag, surface plasmon reson. interaction with dye monolayers 78−84674
Ag, thermomodulation spectra of high-energy interband transitions 80−108226
Ag, thermorefl. spectrum at room temp. 77−8601
Ag, thin layer on Al surface, surface plasmon ATR spectroscopy 79−78770
Ag-AgI island granular film, Weigert effect, anomalous dichroism 77−12455
Ag-Al_2O_3-Au structure, electrorefl. meas. *(French)* 80−50366
Ag-As-S system glass, struct., props. and vibr. spectra 79−65901
Ag-Cd dilute α-phase alloys, optical gaps, thermoreflectance meas. 77−66520
Ag-Cu, metastable alloy film, optical props. 77−12460
Ag-Cu, optical spectra, 0.5-6 eV, d-band struct. 77−48168
Ag-Hf(Ta)(Pt) film, optical absorption spectra meas. 77−85823
Ag-LiF, alternating plasma-dielec. five layer system, ATR angular spectra 79−19943
Ag-Zr(Nb)(Mo) film, dielec. const., optical props., DC resist. and thermoelec. power 77−85824
$AgAsS_2$, $AgSbS_2$ and $AgBiS_2$, cryst. and vitreous, refl. spectra, energy spectrum 77−8596
$AgAsS_2$, cryst. and amorphous, band struct., photoemission and refl. spectra obs. 77−66581
AgBr dispersion in gelatin, adsorbed S and Au, transient absorpt. spectra, latent image form. and decay 80−66837
AgBr, optical absorpt. of indirect exciton in high mag. field 78−60486
AgBr, Stark effect on I-bound exciton 79−28719
AgBr(Cl)(I) ultra fine grained photog. emulsions, impurity obs. spectra *(Russian)* 79−69871
AgCl, colloid centres induced by reactor neutrons at 20K 78−72560
AgCl microcrystals in sol., cryst. growth, optical absorpt. 77−12835
AgCl, molten and solid, visible absorption spectra *(Japanese)* 79−4816
AgCl, optical absorpt. of indirect exciton in high mag. field 78−60486
AgCl photochromic glass, additional absorpt. spectrum, ellipsoidal model of colour centres 80−40142
AgCl, spectral absorpt. coeff. obs. rel. to published data 79−73963
Ag_2CrO_4, investigation by diffuse reflectance spectroscopy 78−88326
$AgGaS_2(Se_2)$, press. depend. of energy gap, absorption edge obs. 77−12401
$AgGaSe_2$, two-photon absorpt. and short pulse stimulated recombination 80−89054
$AgGaSe_2$ wavelength-modulated reflectance, optical electronic transitions, 1.5-5.5 eV 78−35170
Ag_2HgI_4, preparation, optical and luminescence spectra 80−104064
β-AgI, 2H and 4H polytypes, exciton refl. spectra at 4.2K 79−69860
β-AgI (4H), visible spectra, reflected light phase and amplitude, exciton resonance 80−45110
β-AgI, exciton refl. spectra, optical activity *(Russian)* 78−64380
AgI film, crystallisation, exciton absorption spectra meas. 77−35483
β-AgI thin film, exciton spectrum 80−55216
$AgInS_2$, and $AgIn_5S_8$, spray pyrolysis, film struct., elec. and optical props. 80−71592
$AgInSe_2$, reflectvvity and XPS meas. 78−35165
$AgIn_5Se_8$, optical gap and low temp. depend. 79−99907
Ag_8MSe_6, M=Ge,Sn,Si, absorpt. edge under hydrostatic press. 77−85740
AgN_3, optical absorpt. spectra, and photoemission, electron band scheme 79−100015
$AgNa(NO_2)_2$, triplet absorpt. polarised spectra, near ferroelec. phase transition 79−47473
Ag_2O, quadrupole exciton transition and struct. of optical absorpt. edge 79−38569
AgPd, dil. alloys, electronic states, virtual bound states model test *(French)* 77−62809
Ag_2S, metal-nonmetal transition, crystallographic, optical, mag. and transport props. 78−6418
Ag_2SO_4:CrO_4^{2-}, polarised electron spectrum assignments, red colour explained 77−85753
$Ag_2S.HgI_2$ and $Ag_2Se.HgI_2$ thin films, transmission spectra and photochromism 79−52032
Al film, enhanced mirror, high-rate sputtering, reflectance and dispersion 77−42636
Al film, optical cond., energy derivative spectrum 77−66551
Al film, optical dielec. const. in visible region, 300 to 1.5K 77−90211
Al films, anodisation rate and augmentation factor, oxidation in ammonium tartrate 79−79152
Al mirror, with MgF_2 overcoating, reflective scatt. and reflectance meas. in vac. UV, moisture and oil vapour influence *(German)* 79−86227
Al oxide anodic film, colloidal metal, origin of colour, optical props. meas. 78−68571
Al, surface plasmon dispersion curves, splitting by Ag surface layers 78−60178
Al, surfaces, Au-coated and diamond turned, EUV reflection efficiencies 79−14073
Al thin film evaporated on quartz substrate, surface irregularities 79−90920
Al ultrafine particle film, size effects in optical absorption 79−99965

visible and ultraviolet spectra of inorganic solids continued
Al ultrafine particles, optical props., 0.3-2.5 μm 80−76020
Al-fuchsin-SnO_2 MSM structure, field depend. of electroabsorption spectra 77−40263
Al-Ge-SiO solar selective absorber surfaces, optical behaviour at high temp. 80−101130
AlAs-GaAs monolayer crystal, two-photon absorpt. spectrum 78−52589
AlAs-GaAs monolayered periodic cryst., optical props. 77−81079
$Al_2Be_3Si_6O_{18}:Cu^{2+}$, synthetic beryl, ESR, optical spectra and X-ray diffr. meas. 77−16166
AlF_3, disordered film, optical transitions as function of prep. conditions 78−27340
AlF_3 film, optical absorption meas. rel. to prep. conditions *(French)* 77−44078
AlF_3 films, electronic transitions near optical absorpt. edge, depend. on prep. conditions *(French)* 77−63429
$Al_{0.4}Ga_{0.6}As$:Te, saturable optical absorpt. of deep Te-complex centre 79−99917
$(Al_{0.42}Ga_{0.58})As$, LPE grown layer, optical absorpt. coeff. meas. 78−6801
$Al_xGa_{1-x}As$, press. coeff. of direct band gap from optical absorpt. meas. 80−11430
$Al_xGa_{1-x}As$:N, photoluminesc. and optical absorpt. spectra of N impurity bound-excitons 79−47496
$Al_xGa_{1-x}As$-GaAs, CW 300k quantum-well heterojunction laser, optical and injection pumping operation 80−5735
AlH_3, photoelectric effect spectra and kinetics, photochem. mechanism colour centres 78−56506
AlN, absorpt. edge shape interpretation, Wannier excitons absorpt. in charge impurity elec. field 80−66233
AlN, epitaxial, refl. spectra, 5-12.5 eV 79−99967
AlN epitaxial films, optical props. in vac. UV region 79−56872
AlN, excitation, luminescence, reflection spectra in fund. absorpt. region 78−10956
AlN film, chemical and plasmachem. vapour deposition, optical and other props. 77−28727
AlN, VPE by closed space vapour process, and optical absorpt. edge 78−88371
AlN:O, UV spectra of deep impurity centres, radiative recombination 79−87490
AlN-Si_3N_4 CVD film preparation and props. 77−77408
$AlNH_4(SO_4)_2:Cr^{3+}$, optical spectral, crystal field, spin orbit and exciton interactions 80−34958
α-Al_2O_3, additively coloured single crystal, luminescence *(Russian)* 80−55169
α-Al_2O_3, colour centres, AES, electron energy loss, and optical spectroscopy obs. 78−35176
Al_2O_3, corundum, γ-irrad., colour centres, growth method effect 77−1710
α-Al_2O_3, crystal defects from X-ray irradiation, F-centres, X-ray luminesc. obs. 80−55176
α-Al_2O_3, defects in unirradiated cryst., optical absorpt. spectra 79−61409
Al_2O_3 film, RF sputtered by planar magnetron, phys. props. 77−43448
Al_2O_3, neutron irradiated, electron centres, optical spectra exam. 77−63440
Al_2O_3, optical absorpt. and external photoeffect, 6 to 40 eV 77−55802
Al_2O_3, optical props. of F-centre 79−43003
α-Al_2O_3, polarised luminescence in neutron- and proton-irradiated single crystals 80−66271
Al_2O_3:Co, spectra, heat treatment and irrad. effects 77−4659
α-Al_2O_3:Co,H, Co and proton ENDOR, IR and optical spectra charge compensator nature and defect struct. 80−44956
$Al_2O_3:Cr^{3+}$, shock compression, absorpt. spectra 80−20675
α-Al_2O_3:Er(Cr), crystal defects from X-ray irradiation, F-centres, X-ray luminesc. obs. 80−55176
β-Al_2O_3:Mn(Co)(Ni), absorpt. and emission spectra, mag. susceptibility 79−87471
Al_2O_3:Ni anodised films, electrolytically coloured, spectrally selective surface 80−11490
Al_2O_3:Si, Ti, pure and doped, luminescence, optical absorpt. and colour centres 79−87501
Al_2O_3:Si(Ti)(V)(Fe)(Co)(Ni), gamma-irrad., low temp., induced absorpt. spectra 79−56820
Al_2O_3:Ti(Si), annealing, electron irrad., absorpt. spectra 77−20890
Al_2O_3:V, valency changes of V ions, γ irradiation, thermal cond. optical absorption and EPR meas. 77−80541
α-$Al_2O_3:V^{3+}(Cr^{3+})(Co^{3+})$, optical absorption spectra, DC and AC field effects 78−10925
α-$Al_2O_3:V^{3+}(V^{4+})(Co^{3+})(Co^{2+})$, optically and thermally stimulated reactions, absorpt. spectra 80−80825
Al_2O_3-B_2O_3-P_2O_5 glasses, formation and props. 78−83737
Al_2O_3-B_2O_3-SiO_2 sheet glass, solar energy appl., optical and mech. props. 80−87447
Al_2O_3-Na_2O, β and β'' phases, stability, cond., paramag. impurity effects obs. 77−84976
β-Al_2O_3-Na_2O, colour centers, AES, electron energy loss, and optical spectroscopy obs. 78−35176
β-Al_2O_3-Na_2O:Cr, absorpt. and emission spectra, mag. susceptibility 79−15495
Al_2O_3-Nd_2O_3, optical absorpt. spectrum and struct. of β-phase *(French)* 77−69848
Al_2O_3-$P_2O_5:Nd^{3+}$ glass, high Nd conc., spectroscopy and lasing obs. 78−46609
Al_2O_3-SiO_2-MO-Fe_2O_3 glass, M=Ca, Mg, Ba, Sr, UV and EPR absorpt. spectra 80−89018
AlP(As)(Sb), APW calc. of electronic structure and optical props. 79−99479
$AlPO_4$, synthetic berlinite, electron irrad. effects, ESR, ENDOR, optical spectral study 80−80608
Ar, adsorbed on Al, differential refl. spectroscopy, local field effect 80−80811
Ar, cryst., luminesc., absorpt. spectra, free, self-localised excitons coexistence *(Russian)* 78−31231
Ar, liquid and solid, absorpt. and luminesc. spectra of self-trapped excitons 79−65893
Ar:S_2, absorption spectra of matrix-isolated S_2 molecules 77−52139
$^{40}Ar:^{41}K$, matrix isolation model system 78−45722
As-Ge-S(Se), glass films, photostruct. changes 77−85822
As-Ge-Se system, synthesis and phys. props. of amorphous layers 77−52252

visible and ultraviolet spectra of inorganic solids continued
As-S glasses, acousto-induced structural changes, optical props. 80−49122
As-Se glass film, photoinduced absorpt. changes 79−87519
As-Se system glasses, opt. absorpt. edge shift on densification 77−77250
As-Se:^{197}Au, glassy, Au impurity influence, elec. cond., optical absorpt. and Mossbauer meas. 77−24558
AsF_5-graphite intercalation compound, metallic. optical reflectance meas. 78−6683
As_2S_3, As_2Se_3, optical props., electronic struct., photocond., book contrib. 77−44024
As_2S_3, cryst., vitreous or amorphous, nonlinear light absorption, temp. depend. *(Russian)* 77−48199
As_2S_3, cryst. and glassy, two-photon spectrum at room temp. 79−24334
a-As_2S_3, energy gap meas., by Faraday rotation 80−66161
As_2S_3 evaporated film, optical props., depend. on light exposure and heat cycling 78−68572
As_2S_3 glass, melt-quenched, reversible photostruct. change 77−68925
As_2S_3 glass, press. effect on optical props. 80−50363
As_2S_3, glassy, photoinduced defects, EPR and absorpt. spectra 80−59398
As_2S_3, glassy, X-ray induced paramag. colour centres 78−19327
As_2S_3, photoacoustic spectroscopy, app. of expt. system for powdered samples 77−87846
As_2S_3, two photon light absorpt. dispersion, induced linear light absorpt. *(Russian)* 80−66231
As_2S_3:Ag glassy films, optical transmission spectra, photodoping effect 80−66317
As_2S_5, amorphous, struct., vibr. and electronic spectra 80−64908
As_xS_{100-x} amorphous film, photoinduced changes in optical props. 80−50445
As_xS_{100-x} amorphous films, optical props. and photoinduced changes 80−60700
As_xS_{100-x}, chalcogenide glass thin films, absorption in range of large optical densities *(Russian)* 80−11428
$(As_2S_3)_{1-x}(As_2Se_3)_x$ and $(As_2Se_3)_{1-x}(As_2Te_3)_x$ pseudobinary glasses, comp. depend. of opt. props. 77−90157
$As_2S_{3-x}Se_x$, amorphous, picosecond relax. of optically induced absorption 80−97302
$As_2S_3(Se_3)$ evaporated films, optical absorpt. and thermally induced effects 79−42989
$As_2S_3(Se_3)$, X-ray induced paramag. states and luminesc. 78−95520
$As_{40}S_{25}Se_{25}Si_{10}$ glass film, transient photoinduced absorpt. 77−40295
$As_2S_{3-x}Te_x$, ternary chalcogenide glassy system, optical absorpt., mag. susceptibility and AC cond. meas. 80−55125
$As_4Sb_2Se_9$ glassy semiconductors, electronic props. 80−103712
AsSe film, light-induced light absorption changes 77−73181
As_2Se_3, amorphous, time resolved meas. of photoinduced optical absorpt. and photocond. 80−49807
As_2Se_3, cryst., electroabsorption on indirect gap 80−80812
As_2Se_3, glassy, Cu, Ag and O impurities influence on electronic energy spectrum and mol. vibr. spectrum 77−90181
As_2Se_3, glassy, X-ray induced paramag. colour centres 78−19327
As_2Se_3, lone-pair semiconductor, defect chemistry 80−25421
As_2Se_3, polarised light reflectance spectra, band struct. 78−63979
As_2Se_3, vitreous, elec. and opt. prop. changes on densification 77−11958
As_2Se_3-Ti_2Se (Tl_2Se_2) (Tl), glass, hot pressed, temp. dependence of optical absorption edge 78−88328
$As_{60}Se_{40}$, amorphous films, spectral characts. of photodarkening 78−76494
As_7Se_3 amorphous films, thermal relax. processes determ. by optical props. 77−15716
$(As_2Se_3)_{1-x}(As_2Te_3)_x$ amorphous films, changes in optical props. under elec. fields and optical excitation 79−61455
As_4Se_5Ge, glass, light irrad. induced changes in optical and elec. props. *(Japanese)* 78−68031
Au, aggregated film, optical props., 0.35-1 μm 77−66548
Au, dielectric const. by multiangle reflection meas., optical props. 79−95723
Au, discontinuous film, optical absorption 77−69927
Au, discontinuous film, optical transmittance 78−56529
Au discontinuous films, optical transmittance, effect of island morphology 78−84673
Au electrode, emersed, electrorefl. spectra 79−28788
Au film, modifications of optical and elec. props. as function of struct. during deposition 79−78777
Au film, optical dielec. const. in visible region, 300 and 2.5K 77−90211
Au film, self-supporting, thermotransmission meas. 1.8 to 3.5 eV 78−27343
Au film on Ag, optical constants, 4000-6000 Å, using surface plasmon optical excitation 77−69925
Au films, on Al, Ni, EUV reflection efficiencies 79−14073
Au, films on barrier-layer photocells, spectral distrib. of transmission coeffs. 77−1744
Au, high-resolution spectroscopy in far UV 77−66484
Au, intraband optical conductivity, electron-electron scatt. 78−35166
Au, ion implanted, ellipsometry, 1.8-5.5 eV, dielec. function 78−6697
Au monocrystals, anisotropic surface effects, electrorefl. spectra 79−8123
Au, optical props., dielec. function, void model, sample effects 80−76048
Au particles, light scatt. spectra, size and shape effects 77−44015
Au solar black, optical props., microstruct. influence 79−42937
Au, surface plasma waves, dispersion curves, attenuated total reflection spectra 78−88015
Au thermal modulation reflectance spectrum, temp.-dependent shift 77−81121
Au, thermomodulation spectra of high-energy interband transitions 80−108226
Au ultrafine particles, optical props. 78−19481
Au, Xe physisorption, electronically excited atoms coupling to cond. states 77−89642
Au-Ag, optical spectra, 0.5-6 eV, d-band struct. 77−48168
Au-Cr, cosputtered films, optical props. 0.2 to 6.1 eV 77−32454
Au-Cu, dielectric const. by multiangle reflection meas., optical props. 79−95723
Au-Cu, optical spectra, 0.5-6 eV, d-band struct. 77−48168
Au-Cu alloy, refr. index and absorpt. coeff., 1-5 eV *(Russian)* 78−60484
Au-Pd dil. alloys, electronic states, virtual bound states model *(French)* 77−62809
Au(Ag)(Cu)-Sn liquid, optical reflectivity spectra of virtual bound states 80−89021

visible and ultraviolet spectra of inorganic solids continued
AuBr, spectra and luminesc., 100 to 200K *(Russian)* 77−69911
$AuBr_3$, spectra and luminesc., 100 to 300K *(Russian)* 77−69911
$AuCu_3$, ordered, band struct. and optical props. at 30K 79−60696
$Au_{1-x}Si$ amorphous metallic films, optical props. as function of composition 79−95865
$Au_{1-x}Si_x$, amorphous film, spectra 0.01-6.2 eV, $0.13 \leq x \leq 0.5$ 78−68574
Ay, discontinuous film, light absorpt. spectra, dielec. function calcs. 79−51507
β-B, rhombohedral, localised states charact., review, book contrib. 78−47728
B:H amorphous CVD films, IR, visible, and near UV optical props. 80−50442
$B_{12}C_x$, phonon energies and electronic props., x depend., refl. spectra and thermoelec. power meas. 80−16052
BN, epitaxial, refl. spectra, 5-12.5 eV 79−99967
B_2O_3-M_2O:S_2 glass, (M=Li, K, Na), absorpt. spectra of S_2 mols. 79−24337
B_2O_3-SiO_2:Ce glasses, radiation resistance mechanism, optical absorpt. and luminesc. obs. *(Polish)* 79−86825
$BaAl_{12}O_{19}$, refr. index and optical absorpt. 80−66139
$BaBr_2$:Sm^{2+}, fluoresc., and vibr. and electronic absorpt. spectra 77−8627
$Ba_{15}Ca_{27-x}Nd_xAl_3Be_{27}F_{231+x}$, $0 \leq x < 8$, optical props. and vitreous domain 79−65820
$BaCl_2$:Pb, absorption and emission spectra *(Russian)* 78−23527
$BaCl_2$:Sm^{2+}, fluoresc., and vibr. and electronic absorpt. spectra 77−8627
$BaCl_2(Br_2)$, F-centre localisation, absorpt. spectra calc. and EPR spectra analysis 77−48203
$BaCrO_4$, investigation by diffuse reflectance spectroscopy 78−88326
BaF_2, U-centre, electronic struct. and optical transition energies, SCF MS Xα calc. 79−4532
BaF_2, ultralow loss optical fibre material, loss mechanism 80−78920
BaF_2, undoped, H-centre prod. by reactor neutron irrad., optical absorpt. meas. 77−59010
BaF_2, undoped and U-doped, neutron irrad., absorpt. band attributed to F_2- centres 80−7380
BaF_2:Pb^{2+}, band struct., Jahn-Teller effect, UV luminesc. and optical absorpt. spectra 80−66243
BaF_2:Pr^{3+}, wavelength and temp.-modulated UV absorpt. 80−2799
BaF_2:RF_3, cryst., absorpt. spectra, γ-ray effects 77−12409
BaF_2:U, absorption band spectra following neutron irrad. 80−29763
BaFBr, X- and γ-irrad., thermolum. and optical absorpt. spectra 79−95857
BaFCl crystals, F-centres, X- and γ-irradiation, thermoluminescence and optical absorption spectra 80−45155
BaFX, X=Cl, Br, I, absorpt. and refl. spectra 79−82994
$BaMnF_4$, struct. phase transition, optical parameters obs. 80−100328
$Ba_2NaNb_5O_{15}$, dispersion of quadratic optical susceptibility *(Russian)* 77−3635
$Ba_{2.09}Na_{0.72}Nb_{5.02}O_{15}$, cryst. growth, monodomenisation, detwinning, optical homogeneity, composition, dielec., spectral props. 77−44151
$Ba_{2.09}Na_{0.72}O_{15}$, ferroelec., photocond. and optical absorpt. spectra. 77−8149
$BaNb_x^{V}Ti_x^{III}Ti_{1-x}^{IV}O_3$, A and C-domain crysts., elec. cond. and absorption spectra 77−47805
Ba_2NiF_6, quadratic layer antiferromag., tetragonal optical spectra obs. 77−16326
BaO, logarithmic derivative reflectance spectra 80−11429
BaO, surface states, reflectance spectra, impurity effects 77−20873
BaO-Al_2O_3-B_2O_3-V_2O_5 glass, spectra, oxidation-reduction behaviour, DC cond. 77−76814
BaO-B_2O_3:UO_2^{2+}→Er^{3+} glass, energy transfer 78−2895
BaO-B_2O_3-V_2O_5 glasses, polaron hopping cond., optical absorpt. and ESR spectra 79−23966
BaO-B_2O_3-V_2O_5 glass, oxidation-reduction of V, thermodynamics 80−85169
BaO-B_2O_3-V_2O_5(Fe_2O_3)(Cu_2O), glass, resist. and activation energy, reduced valency 77−51749
BaO-M_xO_y-B_2O_3 glass, UV absorpt., inherent absorpt. wavelength and oscill. strength, cation effects 78−80374
$Ba(PO_3)_2$-WO_3, electron-absorpt. spectra and structure of W centres 80−88873
$Ba_{0.25}Sr_{0.75}Nb_2O_6$, ferroelec., photocond. and optical absorpt. spectra 77−8149
$Ba_{0.25}Sr_{0.75}Nb_2O_6$, spontaneous electroopticabsorption effect 78−19443
$BaTiO_3$ and $BaTi_{1-x}Fe_xO_{3-x}F_x$, electrical, optical and mag. props., photoelectrolysis 77−47856
$BaTiO_3$, paraelec. cryst., electro-optical absorpt. near Curie temp. 77−1657
$BaTiO_3$, photoelectron and optical spectra derived from self-consistent charge MO and band calcs. 80−96785
$BaTiO_3$, radiation spectra during pulsed repolarisation 79−95804
$BaTiO_3$, transport and optical props., small polaron hopping theory 79−47096
$BaTiO_3$, UV refl. spectra, optical consts. 0 to 32 eV Kramer-Kronig anal., band struct. calcs. 78−43903
$BaTiO_3$, vacuum UV spectra and electro-optical prop. *(Japanese)* 79−65900
$BaTiO_3$:Nb, ferroelec. and paraelec. phases, props. 79−42919
BaX_2, X=Cl, Br, I, absorpt. and refl. spectra 79−82994
(Be, Al)B_{12}, wide-gap semicond., elec. cond., refl. and absorpt. spectra 80−20188
$BeAl_2O_4$:Cr^{3+}, alexandrite, potential laser material, stimulated emission and absorpt. spectrum 79−33734
BeF_2 glass, IR and UV transmission spectra 80−89019
BeO, free film and Au substrate, transmission spectra and photoemission charact. 77−24925
Bi film, optical props. as function of wavelength *(Russian)* 78−52591
Bi-SiO_2 cermet films, elec. and optical props. 79−78775
$Bi_{12}GeO_{20}$, reflectivity spectrum and band struct. 79−47474
$Bi_{12}GeO_{20}$:Mn, Cr, reversible photochromic effects, absorpt. spectra before and after illum. 79−91471
$Bi_4Ge_3O_{12}$ crystals, doped with Dy^{3+}, Ho^{3+}, Er^{3+}, Tm^{3+}, Yb^{3+}, growth, spectral and laser props. 80−45115
$Bi_4Ge_3O_{12}$, fluoresc., absorption emission, excitation and decay time meas. 77−20910
$Bi_4Ge_3O_{12}$:Nd^{3+} and $Bi_4Si_3O_{12}$:Nd^{3+} crysts., absorpt. and luminesc. spectra, 4.2-300K 80−34957
BiI_3, band struct. determ. 77−15766
BiI_3 film, exciton peaks, temp. depend. 90-270K, and press. depend. up to 3500 atm. 77−36265

visible and ultraviolet spectra of inorganic solids continued
BiI_3, lamellar single cryst., absorpt. spectra and Urbach rule *(Russian)* 77−28606
BiI_3, layered compound, exciton spectra, surface and stacking fault effects 80−40134
BiI_3, layered single crystal, band-edge excitons, optical constant meas. *(Russian)* 77−90171
BiI_3, photoacoustic spectroscopy 79−42992
BiI_3 single crystals, refl., absorpt. and photoluminesc. spectra, exciton transitions 77−52164
BiI_3, structure, exciton states and physicochem. characteristics *(Russian)* 80−100435
BiI_3, UV reflectivity meas. 78−72545
Bi_2O_3, transmission spectra of thin films 78−76440
BiOI, UV reflectivity meas. 78−72545
BiSe, reflection spectra 77−16325
$Bi_{12}SiO_{20}$, film and single cryst., optical absorpt. edge and optical transitions 79−33730
$Bi_{12}SiO_{20}$, visible and UV refl. and absorpt. spectra 80−34950
$Bi_{12}SiO_{20}$:Mn, Cr, reversible photochromic effects, absorpt. spectra before and after illum. 79−91471
$Bi_{12}SiO_{20}$:Nd, light absorpt. and transmission spectra, photoluminescence spectrum, optical absorpt. coeff. 79−74001
$Bi_8T_7S_5$, thin crystal, optical consts. from transmissivity spectra, clas oscillator anal. 77−1748
BiTe, reflection spectra 77−16325
β′-$Cu_xV_2O_5$, mag. and spectroscopic study, semiconductor to metal tion 80−2628
C, amorphous, prepared by glow discharge method, elec. and optical props. 77−21036
C, arc evap. film, optical props., 0.6-3.8 eV 77−81166
C black, IR-, UV- and NMK spectra, props. after extraction with organic solvents *(Polish)* 79−70010
C film, amorphous, pseudogap determ. 77−20474
C smokes, vapour-condensed, 800 to 130 nm extinction and interstellar extinction curve 80−82180
CC GaAs, n- and p-types, optical consts., 2.5-3.5 eV, normal incidence reflectance meas. 79−15428
CO, chemisorobed on Ni(111), surface optical excitations, reflectance spectra, electron energy loss meas. 78−84064
CO, cryst. at 5K, absorpt. and emission spectra, exciton interpretation 79−87481
CO-Ar, cryst. at 5K, absorpt. and emission spectra, exciton interpretation 79−87481
CO-Ne, cryst. at 5K, absorpt. and emission spectra, exciton interpretation 79−87481
C_3PbCl_3, single crysts., X-ray and photoluminesc., and reflection spectra 77−69896
CS_2, electronic transitions, solid phase UV spectra 77−3380
CS_2^+, electronic transitions, solid phase UV spectra 77−3380
CU_2O high press. phase transforms, optical and X-ray studies 80−44313
Ca film, imaginary part of permittivity determ., 2-5.6 eV *(French)* 77−4694
Ca film, optical absorption and plasma reson. 77−40296
Ca film, optical consts. meas., 2 to 5.6 eV *(French)* 78−52586
Ca, optical props., 2-11 eV 78−15191
$CaCO_3$, γ-irrad. defects, absorpt. spectra obs. 77−63447
$CaCO_3$, Iceland spar natural crystals, optical charact. 77−10988
$CaCo_2(PO_4)_2$, reflection spectrum and mag. susceptibility meas. 77−59586
CaF_2, 0.36 μ absorptance/fluence dependence obs. 79−15506
CaF_2, bleaching characteristics of crystals coloured by low energy electrons 78−76497
CaF_2, F-centre growth by neutron irrad. 79−55788
CaF_2, fluorite crysts., lattice O^{2-} effect on thermal, elec., and thermoelec. props. 77−76599
CaF_2, hot pressed, dielectric, optical props. 79−56720
CaF_2, natural fluorite colouring, effect of impurities on absorpt. spectra 79−56822
CaF_2, U-centre, electronic struct. and optical transition energies, SCF MS Xα calc. 79−4532
CaF_2, undoped, H-centre prod. by reactor neutron irrad., optical absorpt. meas. 77−59010
CaF_2:CaO, optical scatt., absorpt. at 205 nm 80−20669
CaF_2:Ce^{3+}, absorpt. peaks in the lowest 4f→5d band, effect of conc. 80−2798
CaF_2:Ce^{3+}, thermally modulated UV absorpt. spectra, 90K 77−28602
CaF_2:Co, X-irrad., F-centre form., optical absorpt. spectra and dichroism obs. 79−42998
CaF_2:Co, X-irradiated, optical absorption spectrum 78−35173
CaF_2:Co^{2+}, designation of optical transitions near 5.40 nm, temp. evolution of absorption spectra meas. 77−55806
CaF_2:Co^{2+}, elec. field effect on spectra induced by odd vibrs. 79−73973
CaF_2:Co^{2+}, MCD spectra 77−28603
CaF_2:Dy, colour centres, antiresonance-type phenomenon in external fields 78−68529
CaF_2:Dy, TLD-200, thermolum. phosphor, photolum. and absorpt. spectra, thermolum. mechanisms 80−97321
CaF_2:Dy crystal with M centre, antiresonance line, mag. field effect 80−55138
CaF_2:Er, defect structure, quenching effect, dielec. relax. and optical absorption 80−65031
CaF_2:Er^{3+}, fluorite, defect equilibria cluster control 79−99231
CaF_2:Eu, oxidation and reduction of Eu, EPR and optical studies 80−25199
CaF_2:Eu^{2+}, two-photon absorpt. spectra exam. of excited state of Eu^{2+} 77−77261
CaF_2:Eu^{3+}(Sm^{3+}), VUV absorpt. spectra, dopant clustering 80−108230
CaF_2:Gd, triply ionised, lowest energy 4f-5d transition 79−24345
CaF_2:Ho^{3+}, site-selective spectroscopy 80−29791
CaF_2:M, M=Mn, Fe, Co, Ni, X-irrad., impurity effects on defect prod. 80−92525
CaF_2:M^{3+}, M=activator ion, redox processes during growth 77−85924
CaF_2:Mn, low temp. X-irrad., Mn centres, optical absorpt. and emission props. 80−60635
CaF_2:Na, single cryst., X-irrad., optical absorpt. and thermoluminesc. 80−34952
CaF_2:Na, tunable room temp. laser action of M-centres, luminesc. and absorpt. spectra 79−31907
CaF_2:Ni, X-irrad., optical absorpt. spectra and dichroism meas. 80−108239

visible and ultraviolet spectra of inorganic solids continued
CaF_2:Ni, X-irradiated, optical and EPR meas. 80−108235
CaF_2:Pb_xO, UV absorption, impurity centres 78−68534
CaF_2:Pb^{++}, band struct., Jahn-Teller effect, UV luminesc. and optical absorpt. spectra 80−66243
CaF_2:Pr^{3+}, wavelength and temp.-modulated UV absorpt. 80−2799
CaF_2:RF_3, colour centre prod. by γ-irrad., absorpt. spectra obs. 78−72565
CaF_2:Sm^{2+}(Eu^{2+}), cubic crysts., vibronic spectra, induced dichroism method 77−81131
CaF_2:Tb, spectra of radn.-induced defect form. 80−2801
CaF_2:U^{3+}, anomalous magnetooptic props., optical detection of ESR and cross-relax. resonances 80−93287
CaF_2:Y, absorpt. spectra, radiation defect formation energy, F to M centre conversion kinetics 79−65079
CaF_2:Yb^{3+} vacuum UV absorpt. spectrum, rel. to other rare-earth ions 79−43001
CaF_2-Ge(Si), cosputtered composite semiconductors, selective solar energy absorbers 79−56876
CaF_2-NaF crysts., F_A centres, 385 and 435 nm absorpt. bands of electron irrad. crysts. 78−2889
$CaF_2.3Ca(PO_4)_2$, apatite, fission damage detection, absorpt. spectra 78−84617
$Ca_3Fe_2Ge_3O_{12}$ garnet, light absorpt. spectral study 80−93322
CaO, absorpt. band identification of colour centres 77−40271
CaO, electron irradiated, photocond. and luminesc. meas., F-centre electronic struct. determ. 78−6409
CaO, neutron irrad., MCD, optical absorpt. lines 77−77255
$Ca_2PO_4Cl:MnO_4^{3-}$, polarised electronic spectrum 77−52137
CaS, absorpt. band identification of colour centres 77−40271
CaS, single crystal, reflectance and absorption spectra, at edge of fundamental absorption *(Russian)* 78−56499
$CaSO_4$ phosphors:Ce(Eu)(Dy)(Tm), gamma-irradiated valency conversions in rare-earth ions 80−55198
$CaSO_4$:Dy(Tm), thermolum. thermolum. phosphor, photolum. and absorpt. spectra, thermolum. mechanisms 80−97321
CaSe:Pb^{2+} phosphors, luminesc., refl., emission, and excitation spectra 79−11456
$CaWO_4$:Nd^{3+} absorpt. spectra, hypersensitivity of $^4I_{9/2}$ to $^4G_{5/2}$ $^2G_{7/2}$ transition 80−97309
$CaWO_4$:Pr^{3+}, anomalous hypersensitive $^3H_4 \rightarrow {}^3P_2$ transition 80−106296
$CaYAlO_4$:Nd^{3+}(Er^{3+}), absorpt. and luminesc. spectra 77−69901
$Ca_3Y_2Ge_3O_{12}$:Eu^{3+}, garnets, prep., struct., luminesc., absorpt. spectra, Eu^{3+} localisation 77−69884
$CaY_2Mg_2Ge_3O_{12}$:Nd^{3+}, optical absorpt. and fluoresc. intensities 80−29793
$Cd_{1-x}Mn_xTe$, exchange interaction, magneto-optical spectra 80−25348
Cd_3As_2 film, amorphous and cryst., transmission spectra, 0.6-15 μm 78−11013
Cd_3As_2, thermoreflectance spectra 78−6702
$CdBr_2$, optical refl. spectra, exciton bands obs. around optical gap 78−15192
$CdBr_2$:Co^{2+}, exchange-coupled Co^{2+} pairs, optical absorpt. and Zeeman studies 80−66242
$CdBr_2$:Cu^+, polarised absorption spectra 77−59594
$CdBr_2$:Fe^{2+}(Co^{2+})(Ni^{2+}), charge transfer near UV spectra, 4.2K, mag. circular dichroism 78−80378
$CdBr_2(I_2)$, exciton spectra, temp. and press. effects 77−20881
Cd(Ca)F_2:Co^{2+}, Jahn-Teller split $^4A_{2g} \rightarrow {}^4T_{1g}$(P) absorption band, elec. field effect 78−15202
$CdCl_2$, optical refl. spectra, exciton bands obs. around optical gap 78−15192
$CdCl_2$:Co^{2+}, optical absorpt. spectra, Zeeman study 78−6712
$CdCl_2$:Cu^+, polarised absorption spectra 77−59594
$CdCl_2$:Fe^{2+}, magneto optical study, ferromagnetically coupled Fe(II) pairs 78−6711
$CdCl_2$:Fe^{2+}(Co^{2+})(Ni^{2+}), charge transfer near UV spectra, 4.2K 78−80378
$CdCl_2$-$CdBr_2$, solid soln., luminesc., optical absorpt. 78−19538
$CdCr_2S_4$, $Cd_{1-x}X_xCr_2Se_4$, (X=Zn, Hg), optical and magneto-optical surface effects 79−82953
$CdCr_2S_4$, polycrystalline films, mag. semicond., spinel-type, magneto-optical effects *(Japanese)* 79−47415
$CdCr_2S_4$, thermoreflectance near Curie point 79−78659
$CdCr_2S_4(Se_4)$, thermoreflectance, photoconductance, Raman scatt. near mag. phase transition 80−97298
$CdCr_2Se_4$, crit. behaviour of optical absorption edge 78−35143
$CdCr_2Se_4$, energy structure, magnetooptic effects 80−71394
$CdCr_2Se_4$ film, absorpt. and Faraday effect 78−2936
$CdCr_2Se_4$ film, mag. linear and circular dichroism and Faraday rot. 79−99966
$CdCr_2Se_4$, mag. semicond., spinel-type, magneto-optical effects *(Japanese)* 79−47415
$CdCr_2Se_4$, magnetic red shift origin, specular reflectivity, band struct. 80−40127
$CdCr_2Se_4$, optical absorption due to transitions between bands and local levels 79−38537
$CdCr_2Se_4$, optical reflectivity, dielectric const. by expt. data Kramers-Kronig anal., spinel struct. 79−99903
$CdCr_2Se_4$, reflectance magneto-circular dichroism 77−81120
$CdCr_2Se_{4-x}S_x$, influence of anion substitution on red shift of optical absorption band edge 77−32399
CdF_2, UPS and XPS spectra, rel. to optical props. 80−66386
CdF_2:Co^{2+}, MCD spectra 77−28603
CdF_2:Cr^{2+}, orthorhombic Jahn-Teller distortion 78−19007
CdF_2:Eu, role of solution and precipitation phenomena on ITC spectra 80−7265
$CdGa_2S_4$, direct excitons, refl. spectra 79−90972
$CdGaS_4(Se_4)$, absorption and refl. spectra anisotropy, band struct. 77−69840
$CdGa_2S_4(Se_4)$, band struct., and optical spectra 78−19511
$CdGa_2S_4(Se_4)$ film, optical absorpt., and energy gaps 78−11012
$CdGa_2Se_4$, struct. of valence band, photocond. and reflection spectra meas. 80−6719
$CdGa_2Se_4$, thermoreflectance and visible absorpt. spectra, energy gap, cryst. field splitting 80−34945
$CdGu_2S_{4(1-x)}Se_{4x}$, opt. absorpt., elec. cond., spectral response, thermopower 77−72862
$Cd_xHg_{1-x}Te$, band struct. and optical props. 80−15450
$Cd_xHg_{1-x}Te$, film, optical props., struct. depend. 77−1751
CdI_2, UV reflectivity meas., band struct., LCAO calcs. 78−72545
CdI_2-Ni^{2+}, absorption and mag. circular dichroism, spectra, phonon density of states of CdI_2 deduced 79−19913
$CdIn_2S_4$ film, vac. deposited, growth, struct., optical and photoelectronic props. 80−10831
$CdIn_2S_4$, fund. reflectivity, 2 to 6 eV, band struct. implications 78−39574
$CdIn_2S_4$, fundamental optical constants 78−84549
$CdIn_2S_4$, photoconducting semiconductors, fundamental absorption edge 80−40130
$CdIn_2S_4$:Co, optical absorption meas. 78−64384
$CdIn_2S_4$:Cr, absorpt. and photoluminesc. spectra, Cr conc. depend. 79−78712
$Cd_{1-x}Mn_xSe$, fundamental optical props. 80−84751
$Cd_{1-x}Mn_xTe$, effect of Mn $3d^5$ states on band struct., exciton refl. struct. in mag. field 79−11094
$Cd_{1-x}Mn_xTe$ mixed crystal, fundamental absorption edge 78−10919
$Cd_{1-x}Mn_xTe$ mixed cryst., giant exciton Faraday rotation 78−27260
$Cd_{1-x}Mn_xTe$ mixed crystals, excitonic magnetoabsorption 80−40095
CdO-GeO_2:Tl_2O photochromic glass for optical information retention media 80−33108
CdO-P_2O_5 glasses, prep., density, elec. and optical props. 79−70033
CdO-SnO_2 film, DC reactively sputtered, transparent electrode props., optimum sputtering conditions 80−11116
CdO-SnO_2 film, DC sputtering prep., visible and near IR transmission, resist. 78−88049
CdO-SnO_2 film, prep. by RF sputtering, elec. cond. and transparency 80−7492
CdO-ZnO-P_2O_5 glasses, prep., density, elec. and optical props. 79−70033
CdP_2, two-photon light absorpt. dispersion, allowed-forbidden transition *(Russian)* 78−15193
$CdPS_3$, layered, organometallic intercalates, X-ray diffr., optical absorpt. and mag. props. 80−45103
CdS, $A_{n=1}$-exciton, reflectance and thermoreflectance spectra, spatial dispersion and angle of incidence effects 80−25409
CdS, A-exciton-polariton, time depend. optical spectrosc. obs. 78−80376
CdS, absorpt. spectra, 400-650 nm, electron irrad. defects and absorpt. edge shift 78−64382
CdS active surface, exciton stimulated emission and superradiance refl. spectra, props. 80−25411
CdS, additional waves and polariton dispersion, reflectivity, transmittivity spectra 80−71443
CdS, attenuation of transmitted light in exciton region, polarisation, coherence, scatt. 77−69852
CdS, chemically precipitated film, optical spectra, annealing effects *(Russian)* 79−11424
CdS, electron-hole liq., effect of excited electron states lifetime on gain spectra 77−85748
CdS, electron-hole liquid, non-equilib. transmission spectroscopy meas. 77−20883
CdS, electron-hole plasma, gain and refl. spectra study 80−66227
CdS, emission and transmission spectra, excitonic mols. effect 77−44062
CdS, energy transfer by normal modes in exciton reson. region 77−89705
CdS epitaxial layers on sapphire, exciton struct. of absorpt., photoluminesc. and photocond. spectra 80−89027
CdS, equivalent gap alteration by light scatt. by acoustic domains 77−85687
CdS, exciton absorpt. at low temps. *(Russian)* 78−48195
CdS, exciton obs. in thin surface layers, refl. spectrum *(Russian)* 78−2877
CdS, exciton optical and luminescence spectra characts. near dislocation slip bands 80−45111
CdS, exciton spectra anomalies, surface state effects 78−18974
CdS, exciton spectrum of high-density gas of nonequilib. carriers 79−38567
CdS, exciton-contrib. to reflection spectrum at high excitation intensities 78−43900
CdS, exciton-phonon interaction, interpretation of optical absorpt. data 79−14897
CdS, excitonic mol. transitions, optical gain and induced absorpt. spectra 80−11438
CdS, excitonic polariton reflectance, quantitative anal. in spectral range of A-exciton 79−15480
CdS, excitonic polariton reflectance, B-exciton and k-linear term 80−7369
CdS, excitonic region, nonlinear optical meas., 4.2K 78−68531
CdS film, crystallinity and optical props., effect of cation-anion ratio 77−76689
CdS film, high cond., high transmittance, growth by evaporation method, and characterisation 77−77386
CdS film, prep. by hot wall technique, morphology and semicond. props. 79−95292
CdS films, electrolessly deposited, annealing effect on optical spectra 80−2884
CdS, gain spectroscopy and plasma recomb. 78−88327
CdS, group velocity of light and polaritons, refl. and luminesc. spectra 77−24863
CdS, high intensity excited, exciton reflection spectra, reflection struct. 80−20692
CdS, highly excited semicond., linear optical response, electron-hole liq. 79−51980
CdS, induced absorption and gain from high density excitons 78−68533
CdS, induced absorption in energy ranges of exciton and exciton-biexciton transitions 78−72548
CdS, influence of Lamb US waves on exciton spectra *(Russian)* 80−7374
CdS, influence of surface states on absorption edge 77−16344
CdS, intrinsic exciton fine struct.; two-photon absorption 77−12397
CdS, irrad. with high doses of fast reactor neutrons, absorpt. spectra 79−73221
CdS, magnetoreflectance and magnetoluminesc. of A exciton 78−39597
CdS, optical modulation caused by acoustic domains 77−85689
CdS, optical props., spatial dispersion effect *(Russian)* 79−61404
CdS, photoplastic effect due to α, β dislocations, spectral depend. 77−90180
CdS, photorefl. in exciton region, surface layer influence 78−76489
CdS, pure and Al doped vacuum deposited film, photoelectric props. and optical absorption 78−60162

visible and ultraviolet spectra of inorganic solids continued
CdS, reflectance, transmittance and luminesc. spectra, light group vel. near exciton reson. *(Russian)* 77−69857
CdS, spectra of refl. and transmission coeffs. near exciton absorpt. line 80−88951
CdS, spontaneous optical activity in exciton spectrum *(Russian)* 78−35167
CdS sprayed film, prep., optical props., struct. and comp. 79−78875
CdS, stimulated emission and optical gain in dense exciton system 79−33731
CdS, thermoreflectance spectra, additional boundary conditions in terms of optical constants 79−15478
CdS, transition metal centres, first-harmonic electromodulation spectra 78−35116
CdS, transmission spectra, region of exciton reson., spatial dispersion effects 79−78704
CdS, two-photon absorpt., excitons *(Russian)* 78−39571
CdS:Cd,Cu crystal, formation and bleaching of optically-induced absorption bands 78−31221
CdS:Cu,Pb reflectivity of Ni-salt coated powder, pre-irrad. effect on defect form. 79−27973
CdS:Cu(In), two-photon and two-step absorption of light 80−7389
CdS:Li, anisotropy of the absorption by impurity centers in hexagonal crystals 78−88343
CdS:Li film, chemical bath deposited, photocond. and optical props. 80−2426
CdS:Li film, optical props. 80−2886
CdS:Ni_3 exciton reflection spectra 78−72557
CdS:Ni^{2+}, Zeeman effect at Ni impurities 80−60633
CdS:Ti^{2+}, linear electroabsorption due to Ti^{2+} centres 77−66525
CdS-ZnS(CdSe), film, light transmittance spectra, comparison with Schott GG 495 glass filter 78−33838
$3CdSO_4.8H_2O$, cryst., phonon assisted indirect transitions 78−72559
CdS(Se), magnetoreflectance spectra of anisotropic II-VI semiconds. by mag. field modulation 77−66519
CdS(Se), optical detection near absorption band edge 77−749
CdS(Se), optical spectroscopy, absorpt. coeff., lattice vibr. modes, band gap, acoustic approach 77−69822
CdS(Se), single cryst., band parameters from optical exciton spectra 79−47021
$CdS_{0.4}Se_{0.6}$, two-photon absorpt., effect of polarisation of laser radiation 77−69856
$CdS_{1-x}Se_x$, comp. disorder-induced broadening for free excitons 79−15479
$CdS_{1-x}Se_x$ gradient cryst., pseudointersection of dispersion curves n_o (λ) and n_e (λ) 79−15487
CdS_xSe_{1-x} mixed crystals, exciton spectra 78−92131
CdSe crystals, photocurrent and electrorefl. spectra, stoichiometry defects revealed by annealing *(Russian)* 77−52134
CdSe, electrorefl. and photocurrent of ground state excitons 79−99905
CdSe epitaxial layers, on GaP-CdS substrates, absorption and electroabsorption 80−40178
CdSe, excitonic mol. transitions, optical gain and induced absorpt. spectra 80−11438
CdSe film, as-deposited and recrystallised, struct. and fund. optical absorpt. 77−1753
CdSe, fundamental absorpt. edge, influence of laser radiation intensity *(Russian)* 80−71445
CdSe, hexagonal, Coulomb interaction at E_1 interband transition 78−19507
CdSe, high intensity excited, exciton reflection spectra, reflection struct. 80−20692
CdSe, magnetoreflectance and magnetoluminesc. of A exciton 78−39597
CdSe single crysts., exciton luminesc. and polarisation spectra under one- and two-photon excitation 79−65391
CdSe, thin films, exciton piezotransmission 79−24380
CdSe:Ag, In, cryst., photocurrent and electroreflection, 77 to 300K *(Russian)* 78−23136
CdSe:Cd, Cu, photo-induced changes in absorpt. spectra 78−80382
CdSe:Cl(In), photoluminesc. props. near fund. absorpt. edge, impurity conc. effects 79−52003
CdSe:Fe, exciton electroreflectance spectra, impurity effects 77−16335
$CdSiP_2$, optical activity near isotropic point, absorpt. spectra 79−69804
$CdSiP_2$, reflectance spectra at 300K 80−25407
$CdSiP_2$, thermoreflectance spectra 77−81122
$CdSnAs_2(P_2)$ single crysts., refl. spectra, band struct., dielec. consts. 77−44022
$CdSn_xO_y$, DC reactively sputtered film, elec. and optical props. 79−87022
$CdSn_xO_y$ films, transparent conducting, deposited by RF sputtering from CdO-SnO_2 target 80−76179
Cd_2SnO_4 film, optical transmission and reflection, evaluation for solar heat collectors 77−52191
Cd_2SnO_4 film, RF sputtered from powder targets, props. 77−43759
Cd_2SnO_4 selective coatings, optical absorpt. edge 78−83046
$CdSnP_2$, optical props., band struct. calcs., real space atomic potential parameters 79−95325
CdTe, energy bands and optical props. calc., tight-binding model with spin-orbit interaction 80−65448
CdTe film, exciton spectra, press. and temp. depend. 80−80886
CdTe film, low-resist., prep. by multi-source evaporation method, and characterisation 80−25582
CdTe, optical absorpt. coefficient, photovoltaic determ. 77−39890
CdTe, oscillatory magnetoabsorpt. spectra 80−40096
CdTe, picosecond absorption spectroscopy 79−47482
n-CdTe, single crystal, photoreflectance, temp. depend. of exciton spectra *(Russian)* 78−23488
CdTe, spatial dispersion rel. to exciton reflection spectra *(Russian)* 80−40126
CdTe, time-resolved spectra, carrier relax. time, phonon lifetime 80−11433
CdTe:Fe(Ni), luminesc. and refl. spectra, high temp. annealing effects 80−24472
CdTe:Mn^{2+}, exciton refl. spectra and mag. susceptibility 80−66253
CdTe:V,Cr, optical props. meas. 79−73969
CdTe-In_2Te_3, composition depend. of energy gap, optical absorpt. obs. 77−80728
CdTe-Te film, prep. by combined hot-wall-flash evaporation method, and characterisation 80−55296
$CdTiO_3$, refl. and absorpt. coeffs. 3-3.5 eV, and refr. index dispersion *(Russian)* 78−39561

visible and ultraviolet spectra of inorganic solids continued
$Cd_{1-x}Zn_xS$ 10 μm film optical and electrical characterisation *(French)* 78−64153
$Cd_{1-x}Zn_xS$ films, thermal evaporation prep., phys. props. 80−84410
$CeF_3:Pr^{3+}$, 400-700 nm, 78K, 22 kbar press. effects 77−81133
CeN, optical props. and valence mixture 78−56450
$CeO_2:Y_2O_3$, bias sputtering, film growth and charact. 77−40366
$Ce_{3-x}S_4$, $Ce_{3-x}Sm_xS_4$, elec. cond. mechanism, thermoelec. power, Hall and absorpt. coeffs. 77−24559
CeSe:Fe, long-wavelength fundamental absorpt. edge formation, role of Fe 77−16351
CfI_2 and CfI_3, cryst. struct. determ., X-ray diffr., optical spectra 78−75645
Co catalyst, magnetooptical investigation of mag. props. 79−69858
Co film, even magneto-optical transmission effects, 0.4-1.25 μm 77−32354
Co, HCP, low energy interband absorption, electronic struct. exam. 79−73930
Co Y zeolite, absorpt. spectra, Co^{2+} ions location upon dehydration 77−73152
Co-Fe-Si-B, ferromag., magneto-optical spectra in amorphous and cryst. states *(Russian)* 80−84749
$CoAl_xFe_{2-x}O_4$, Kerr effect, magneto-optical refl. spectra 79−82954
$Co_3(AsO_4)_2.8H_2O$, optical absorpt. spectra, spin orbit splitting and cryst. field parameters 79−38560
$CoBr_2$, UV reflectivity spectra for band struct. calc. 77−20878
$CoCO_3$, two-sublattice noncollinear antiferromag., exciton-magnon light absorpt. mechanisms *(Russian)* 80−89017
$CoCO_3$, weak ferromagnet, optic study of spin wave spectrum *(Russian)* 79−47263
$CoCO_3$, weak ferromagnet, light absorpt. dichroism and mag. config. *(Russian)* 79−87457
$CoCO_3$, weakly ferromagnetic, light scatt. accompanying spin system excitation by high microwave power *(Russian)* 78−2745
$CoCO_3$, weakly ferromag., light absorpt. dichroism and mag. config. 80−66223
$CoCO_3$-LiCl-H_2O system, complexing during cryst. growth, of spherocobaltite, electron diffr., neutron diffr. and spectroscopic obs. 77−44144
$CoCl_2$, electronic absorpt. spectra and coord. in cryst., soln. and melt 79−38570
$CoCl_2$, UV reflectivity spectra for band struct. calc. 77−20878
$CoCr_xFe_{2-x}O_4$, magneto-optical refl. spectra by equatorial Kerr effect *(Russian)* 77−32400
$Co_xFe_{3-x-y}Cr_yO_4$, epitaxial, magneto-optical props., effect of Cr^{3+} 78−52590
$Co_{1-x}Fe_xSi$, elec. and optical props. 80−49740
$Co_{1-x}Fe_xSi$, solid solution, optical props. 78−72556
$Co_xMg_{1-x}Al_2O_4$, struct., catalytic activity, Co^{2+} ion distrib. 78−30595
$Co_{1-x}Ni_xSi$, solid solution optical props. 78−72556
CoO-MgO-Cr_2O_3-Fe_2O_3-TiO_2, form. and colour of spinel solid soln. *(Japanese)* 80−16059
CoO-ZnO-MgO ternary systems, solid solns., struct. charact. 80−60629
CoP amorphous alloy, heat treatments influence on opt. props., struct. and DC resist. obs. 80−80892
CoP metallic glasses, elec. and optical props., annealing effects 79−38565
CoSi, absorpt spectrum, phase correction in Kramers-Kronig anal. 79−56815
CoSi solid solution, optical props. 78−72556
CoSi, thermoelectric and optical props. 78−91714
Cr black films, electrodeposited, visible and IR reflectance 77−81168
Cr complexes with glycilglycine, structure, optical, e.p.r. and mag. investig. 77−1103
Cr, emissitivty and reflectivity, oxide film thickness effect 79−82364
Cr, optical absorpt. spectrum 0.25-21 μm *(Russian)* 77−81118
Cr, ultrafine particles, coatings for selective absorpt. of solar energy, efficiency 78−18060
Cr-Co (4 wt.%) alloy, antiferromag. transitions effect on opt. props. 77−12371
Cr-Cr_2O_3, black chrome films, surface microstruct. rel. to optical props. in solar absorbers 79−52036
Cr-Cr_2O_3, black chrome solar selective absorber, microstruct. 79−56875
Cr-Cr_2O_3 black chrome, commercial, solar absorber coating characterisation 80−80111
Cr-Ni-Ti alloy and steel, emissitivty and reflectivity, oxide film thickness effect 79−82364
$CrBr_3$, reflectance and thermoreflectance meas. 77−24866
$CrBr_3$, reflectance and thermoreflectance spectra in paramag. and ferromag. phases 79−56770
$CrBr_3(Cl_3)$, two-dimensional mag. insulator, cryst. field splitting, spectroscopic g-factors 79−47059
$CrBr_3(Cl_3)$, two-dimensional mag. insulators, cryst. field spectra, mag. circular dichroism 79−47058
$CrCl_2$, optical absorpt. spectra, spin-allowed transitions 78−52527
$CrCl_3$, reflectance and thermoreflectance meas. 77−24866
CrO_2, optical conductivities and dielec. functions in 0.2-6 eV range, rel. to band struct. 79−42938
CrO_4^{2-} in halide salt aqueous solution, absorpt. spectra, 4.2 to 290K *(Russian)* 78−60499
CrO_n, mag. and optical obs., prep. by calcination of $CrCl_3$ 79−24736
Cr_2O_3, UV absorption spectra from reflectivity meas. 78−2879
Cr_2O_3/γ-Fe_2O_3/Pt electrode, two layer oxide surface film anal. by modulation spectroscopy *(Japanese)* 80−11491
$CrPS_4$, phys. props. and Li intercalates 79−19788
CrSb, optical props., 0.05 to 5 eV 77−48194
CrTe, film, attenuated total refl., magneto-optical effects 77−52196
Cr_7Te_8 film, optical and magneto-optical props., appl. as storage medium 78−23545
Cs, extreme UV absorpt spectra, threshold singularities of p-shell absorpt. 77−36261
Cs, UV absorpt. spectra 80−2780
CsAu, optical absorpt. in liq. and solid 79−61397
$Cs_3BiSbBr_9(Cl_9)$, ^{121}Sb Mossbauer chem. shifts, optical reflectance spectra, solid state band populations 77−40162
CsBr, F-centre absorpt., uniaxial stress effects 80−60634
CsBr, temp. depend. of Cs colloids absorption bands 80−40145
CsBr:Cu, polarisation study of tetragonal Cu^{2+} aggregate centres 78−39590
CsBr:Cu^+, excitation and absorpt. spectra 80−108255
CsBr:Cu^+, off-centre, optical absorpt. meas. 79−33740
CsBr:MNO_4^{2-}, optical and vibronic spectra 79−65909

visible and ultraviolet spectra of inorganic solids continued
CsBr:Th, absorpt., excitation, fluorescence spectra 79−43032
$CsCd(NO_2)_3$, pure and metal ion doped, cryst. struct., reflectance spectra and thermal decomp. 79−51081
CsCl(Br)(I), doped F_{Z1}-centre exam. 78−14341
$CsCl(Br)(I):NO_2^-$, vibronic and reson. Raman spectra of BCC cryst. 79−87468
$Cs_3Cr_2Br_9$, Cr (III) trigonal pair, exchange interactions, absorpt., MCD and Zeeman spectra 78−19009
$Cs_3Cr_2Cl_9$, optical absorpt., MCD, exchange interactions 78−10917
$Cs_3Cr_3Cl_9$, thermo-optical spectroscopy, detection by mirage effect 80−47116
Cs_2CrO_4, investigation by diffuse reflectance spectroscopy 78−88326
$CsCuCl_3$, cryst., gyrotropy, anomalous dispersion curves 80−2719
$CsCuCl_3$, phys. props. 77−62511
CsF, F-centre optical absorption bandshape calc. for transition to state with Jahn-Teller and spin orbit couplings 80−55135
$CsFeCl_3$, linear chain ferromag., optical absorpt. and dichroism in mag. field 77−77237
$CsFeS_2$, crystal ligand field theory, band assignment, absorpt. spectra study 80−20657
CsI, optical props. in vacuum UV 77−24861
CsI, pure and Na(Tl)-doped, luminesc. from bound excitons, UV absorpt. and EPR 77−77282
CsI, temp. depend. of Cs colloids absorption bands 80−40145
CsI, ultralow loss optical fibre material, loss mechanism 80−78920
$CsI:MnO_4^{2-}$, multiple-order Raman scatt., and absorpt. spectra 77−40229
CsI:Na, localised excitons, absorption and emission 77−32425
CsI(Br)(Cl), electronic struct. anal. by reflectance and thermoreflectance studies 79−69855
$CsMnF_3$, exciton-magnon interactions in optical transition, absorpt. and emission spectra meas. 80−70981
$CsMnF_3$, hexagonal antiferromagnet, light interaction *(Russian)* 77−36257
$CsMnF_3$, light absorpt. spectrum in mag. fields up to 300 kOe *(Russian)* 77−52115
$CsMnF_3$, mag. field- and temp.-depend. of light absorption spectra 78−52528
$Cs_2NaBiCl_6$, optical props. 78−68549
$Cs_2NaTbCl_6$, mag. circ. polarised emission, MCD, $^7F_J \rightleftarrows {}^5D_4$ transitions 77−77242
$Cs_2NaTmCl_6$, UV absorpt. spectra, mag. circular dichroism spectra, vibr. obs. 80−29758
Cs_2O-Ag photocathode, light absorption and photoemission 80−50510
Cs_2O-B_2O_3:Tl^+(Pb^{2+})(Bi^{3+}) glass, optical basicity, variation with probe ion and comp. 80−2800
$CsPbBr_3$, $CsPbCl_3$, ionic semiconductors, electronic and optical props. 79−38594
$CsPbBr_3$, electronic and optical props. 80−25414
$CsPbBr_3$, optical props. and electronic struct. 78−48198
$CsPbCl_3$, electronic and optical props. 80−25414
$CsPbCl_3$, electronic struct. and optical props. in fundamental absorpt. region 80−93367
$CsPbCl_3$, optical props. and electronic struct. 78−48198
$CsPbCl_3(Br_3)$, optical and photoelectronic spectra 79−24410
$CsPbCl_xBr_{3-x}$, optical meas., LCAO band scheme 80−25437
$CsPr(MoO_4)_2$, energy levels and mag. props. of Pr^{3+} ion *(Russian)* 79−7810
Cs_2ReF_6(-Cs_2GeF_6) cryst., $ReF^-{}_6$ ion electronic absorpt. spectra, Raman, visible, IR and UV, liq. H and room temps. 77−77193
Cs_2SnCl_6:$ReCl_6^{2-}$, luminesc. and absorpt. spectra, relax. processes 77−85779
$CsSrCl_3$:Tl, absorpt. and luminesc. spectra 78−72586
$CsUO_2(NO_3)_3$, absorpt. spectra, MCD and natural dichroism, UV and visible 79−69853
Cs_2ZrBr_6, $PtBr_4^{2-}$-$PtBr_6^{2}$ doped, mixed valence, absorpt. spectra, vibronic struct. 80−97308
Cu adsorbed atoms on Pt electrode, optical props., electronic struct. 77−69855
Cu, adsorbed mol. monolayers, UV-visible spectra 78−72619
Cu, aggregated film, optical props., 0.35-1 μm 77−66548
Cu alloy, comp. modulation spectra, line shape 78−76491
Cu, cluster and bulk, struct. and electronic props. 78−95592
Cu clusters, visible and near-UV spectra 78−19503
Cu complex, bis-L-tyrosinato copper(II) complex, electronic spectra and dichroism 79−41183
Cu complex, catena-μ-isothiocyanato-(N′-pyridylmethylene-N″-salicyloylhydrazinato-NN′O) copper (II), EPR and visible spectra 80−5566
Cu complex, Schiff-base, ESR and optical absorpt. in soln. and powder 79−65892
Cu complex phthalocyanine, optical density spectra, charge transfer states 79−95800
Cu complex with adenine, powder, physical properties obs. *(Japanese)* 77−43878
Cu complex with L-phenylalanine amino acid, ESR spectra and magnetic susceptibility measurement 80−34761
Cu, dielectric const. by multiangle reflection meas., optical props. 79−95723
Cu, discontinuous film, light absorpt. spectra, dielec. function calcs. 79−51507
Cu film, optical props. in intermediate region between pure Drude and interband absorption 77−81170
Cu halides, reflection spectra, 4.5-7.5 eV, bond struct. scheme 79−61402
Cu halides, tetrahedrally coordinated, semiempirical band struct. model 77−51655
Cu halides two photon spectra, quantitative investigation 80−50373
Cu, intraband optical conductivity, electron-electron scatt. 78−35166
Cu, metal cluster, optical spectroscopy, atom to bulk 78−95591
Cu particles, light scatt. spectra, size and shape effects 77−44015
Cu, single cryst. electrodes, electroreflectance obs. in aqueous solns. 80−25342
Cu, thermomodulation spectra of high-energy interband transitions 80−108226
Cu-alloys, dil., optical props. and electronic struct. 78−35164
Cu-Au film, optical props. of ordered and disordered alloys 77−20945
Cu-Cd-Cl stretched photochromic glass, polorisation effects 79−95729
Cu-Cu_xO film, numerical anal. of normal reflect. data 79−99457
Cu-Ga, ion bomard. effect on surface comp., reflectometry AES 77−81190

visible and ultraviolet spectra of inorganic solids continued
Cu-Ni, dil. alloy, optical reflectivity meas. virtual bound state model analysis 78−2873
Cu-Ni, optical absorption and photoemission spectra 80−45216
Cu-Pd dil. alloys, electronic states, virtual bound states model test *(French)* 77−62809
Cu-Xe film, metal-nonmetal transition, optical and resist. meas. 77−89818
$CuAlS_2$, reflectvvity and XPS meas. 78−35165
$CuAlS_{2x}Se_{2(1-x)}$, excitonic structure, phase-shift-difference spectra 78−2872
$Cu_{10}As_{31}Se_{38}O_{21}$, chalcogenide glass, exam. of electron mechanism of photo induced changes 78−87998
CuBr, biexciton dispersion, two-photon absorpt. 80−76045
CuBr, biexciton two-photon absorption 79−47480
CuBr, biexciton two-photon absorpt. 80−11432
CuBr, evaporated film, magneto-optical effects on exciton bands 78−72624
CuBr, exciton absorpt. band shape, dielectric const. real part derivatives *(Russian)* 80−25413
CuBr, multiplet struct. of P-excitons due to valence band degeneracy 78−39035
CuBr, P exciton fine struct. 80−20091
CuBr, piezo-optical effects on excitons, importance of k-linear terms 79−95802
CuBr, single oriented crystals., electroreflectance, exciton transitions 77−66517
CuBr, surface exciton polariton, ATR meas. 77−77236
CuBr-Ag system, spectral distrib. of photosensitivity *(Russian)* 78−56535
CuBr(Cl)(I), energy bands, relativistic KKR method, UV absorpt. spectra 80−39501
CuBr(I), reflectance and thermoreflectance spectra, electronic struct. 80−71444
CuCl, absorpt. coeff., 0.4-25 μm, band struct. determ. 77−73155
CuCl, biexciton first excited state, LO phonon assisted two-photon absorption 77−40260
CuCl, biexciton two-photon absorpt. 80−11432
CuCl, direct creation of high biexciton density at K=0, two-photon absorpt. and emission spectra 79−33727
CuCl, evaporated film, magneto-optical effects on exciton bands 78−72624
CuCl, excitons bound to neutral donor impurities, magneto absorption spectra 79−56816
CuCl, existence of charged excitons 78−76496
CuCl film, exciton absorption bands *(Russian)* 79−51985
CuCl, induced absorption due to exciton-biexciton transitions 78−15187
CuCl, nonlinear light absorpt., picosec. pulse, exciton-biexciton transitions 79−47483
CuCl, optical absorption under press. 80−34949
CuCl, optical consts. in exciton absorption region, spectral depend. *(Russian)* 77−81125
CuCl, phonon-assisted two-photon absorpt. of excitonic mol., bare-exciton approach 79−78702
CuCl, refl. spectra, 4.5-30 eV, vel. to band struct. 80−103969
CuCl, reson. coherent nonlinear scatt., biexciton autoionising states 79−51978
CuCl, surface exciton polariton, ATR meas. 77−77236
CuCl, time resolved exciton-biexciton transitions, UV excitation, luminescence spectra 79−69883
CuCl, two-photon absorpt. and luminesc., biexcitons 80−11434
CuCl, UV spectra, Γ_1 biexciton level, appl. of nonlinear spectroscopic technique 79−8156
CuCl:Ag system, light sensitivity spectrum, exciton struct. *(Russian)* 79−51985
CuCl-Ag system, photosensitivity spectrum in region of CuCl exciton absorpt. *(Russian)* 79−78707
CuCl(Br)(I), optical props., 4 to 30 eV, band struct. 77−90166
$CuFeS_2$ single crystal, optical reflectivity spectrum 80−40129
$CuGaS_2$, coloration, pure and Fe doped, EPR and optical absorpt. obs. 78−88336
$CuGaS_2$, press. depend. of energy gap, absorption edge obs. 77−12401
$CuGaS_2$, reflectvvity and XPS meas. 78−35165
$CuGaS_2$-$CuGaSe_2$ system, forbidden-band width 78−35280
$CuGaS_{2x}Se_{2(1-x)}$, excitonic structure, phase-shift-difference spectra 78−2872
$CuGa(S_xSe_{1-x})_2$, refl. spectra, comp. depend. 78−39570
$CuGaSe_2$ film, optical props. near and above fundamental absorption edge 78−35215
$CuGaSe_2$, temp. depend. of fundamental absorpt. edge 78−92090
$CuGaSe_2$ thin films, on GaAs substrates, structural and elec. props., photoluminesc. meas. 79−65564
$CuGaTe_2$, elec. and optical props. 80−6829
$CuGaTe_2$ film, flash evaporated, growth and optical props. 79−95296
γ-CuI crystalline film, excitonic spectra *(French)* 79−78771
CuI, single crysts., growth and optical props. 80−93470
CuI, thermoreflectance spectrum, 4-7 eV region 79−19904
$CuIn_{1-x}Ga_xSe_2$ mixed cryst., optical transmission spectrum and gap energy temp. depend. 79−65896
$CuInS_2$ films prepared by spray pyrolysis, elec., optical and struct. props. 79−73609
$CuInS_2$, fund. reflectivity, 2 to 6 eV, band struct. implications 78−39574
$CuInS_2(Se_2)$ film, vacuum deposited, absorpt. coeff. 78−72621
CuInSe, reflectvvity and XPS meas. 78−35165
$CuInSe_2$, energy gap, temp. depend., 15-300K, optical absorpt. obs. 77−36266
$CuInSe_2$ film, MBE growth, AES and optical absorpt. obs. 79−78903
p-$CuInSe_2$ film, prep. from vac. evaporation of $CuInSe_2$, optical and elec. props. 79−82697
$CuInSe_2$, influence of impurities and free carriers on optical props. 80−108225
$CuInSe_2$ semicond. films, optical props., 1-3 eV 78−27346
$CuInTe_2$, optical transitions from valence band states 79−87416
$Cu_xMg_{1-x}Al_2O_4$, spinel solid solns., solid-state and surface props. 77−66415
CuO-MgO system, Cu ions valence states, electronic refl. spectra 78−35168
Cu_2O, Cu inclusions and annealing, optical and IR absorpt. obs. 80−60630
Cu_2O, energy band interactions under uniaxial compression 80−25412

visible and ultraviolet spectra of inorganic solids continued
Cu_2O, even-parity excitons assignment, from two-photon spectrum 80−6731
Cu_2O film, reactively-sputtered, phase comp., resist. and optical consts. 79−95534
Cu_2O, optical absorpt. due to paraexciton in strong mag. field 77−28596
Cu_2O, relationship between interband transitions and spectrum of diag-magnetic excitons in moderate mag. fields 79−91412
Cu_2O, sample thickness depend. of exciton polariton absorption coeff. 80−34941
Cu_2O, yellow exciton series, 1s paraexciton levels, phonon assisted transitions, optical absorpt. edge 78−79934
Cu_2S, polycryst. thin films, struct., optical and elect. props. for solar energy appl. 80−10837
Cu_2S, rel. to band models of Cu_2S-CdS heterojunctions *(Japanese)* 78−23154
Cu_2S:Cd(Zn), effects of doping on elec. and optical props. 78−38743
$Cu_{2-\delta}S$, thin films, determ. of stoichiometry from optical props. 79−60656
Cu_xS, layers produced by reactive RF sputtering, struct., elec. and optical props. 79−90908
$CuSiO_3.2H_2O$, chrysocolla, electronic absorpt. spectra 78−92087
Cu_2ZnGeX_4, (X=S,Se), optical and electrical props. 77−35941
Cu_2ZnSiX_4, (X=S,Se), optical and electrical props. 77−35941
D_2, solid, fundamental absorption spectra, 10 to 40 eV at 2K, using synchrotron radiation 79−73967
$DyCrO_3$, Cr^{3+} exciton-Dy^{3+} spinflip absorpt. 77−73153
$Dy_2Ge_2O_7$, opt. absorpt. spectra, cryst. field parameters 77−48196
DyIG, magneto-optical absorption, near IR 80−40094
$Dy_2O_2SO_4$, antiferromag., mag. props. and Zeeman effect meas. 79−33464
Dy_2S_3, optical props. and electronic struct. in fund. absorpt. region 80−80817
Er, paramagnetic and antiferromagnetic states, optical absorption *(Russian)* 78−56497
$ErCrO_3$, mag. field induced spin reorientation, optical Zeeman absorpt. spectra 79−61398
$ErCrO_3$, spin-reorientation, optical obs. 77−63201
$ErFeO_3$, spin flip, Faraday effect and absorption spectrum meas. 77−43842
$Er_2Ge_2O_7$, opt. absorpt. spectra, cryst. field parameters 77−48196
$EsCl_2(Br_2)(I_2)$, prep., characterisation and decay of Es(II) 80−16727
Eu chalcogenide mag. semiconductors, modulation spectroscopy *(Japanese)* 77−24862
Eu-chalcogenides, magnetic exciton states optical props. 77−31948
EuO, crit. behaviour of opt. absorpt. edge 77−59418
EuO, ferromagnetic, mag. field effect on optical absorpt. edge, piezotransmission spectra 78−95578
EuO, nonstoichiometric film with excess EU, absorption band dispersion 79−8204
EuO, reflectivity spectra near absorpt. edge 79−47471
EuO, transmission and resistivity, stress modulation effect near Curie temperature 80−96874
$EuO_{1-\delta}$ films, Faraday effect dispersion rel. to electronic struct., visible and IR spectra 80−45162
$EuO_{1-\Delta}$, thin film, Faraday effect dispersion and transmission, 0.5-1.1 μ, 20.4 and 77K, anion vacancies 79−19945
EuO(S), ferromagnetic electronic structure, absorption, thermoreflection and thermotransmission spectra *(French)* 80−97300
EuO(S)(Se)(Te), phase transition spectroscopy 77−63426
EuS, absorpt. spectrum, change near mag. saturation using quasi-particle multi-band theory 79−61342
EuS film, thermoreflectance spectra below Curie temp. 77−66550
EuS films, ferromag., optical spectra and light scatt. from spin waves 80−16116
EuS, pure and Gd doped, electronic struct., mag. exchange and elec. transport props. 78−87974
EuS, thermo- and magnetorefl. spectra, dynamical spin fluctuation effect on exciton state 77−52126
EuSe, high field Faraday rot., 1.7-3 eV 77−52131
EuSe, mag. semicond., dielec. and optical props. 78−10824
EuSe, MnO-type antiferromag. spin order, Faraday rotation obs. 77−47974
EuSe, optical absorption exam., electron phonon interactions 78−10923
EuSe(Te), magnetic phase transitions, thermal modulation spectroscopy study *(French)* 80−97301
$Eu_{0.14}Si_{0.31}O_{0.55}$ glass, optical, magnetic, and magneto-optical props., chemical clustering 79−42951
$Eu_{1-x}Sr_xS$, exciton refl. spectra 80−2782
$Eu_xSr_{1-x}S$, magneto-optical redshift in absorpt. and photoluminesc., mag. short-range order 80−71388
EuTe, high field Faraday rot., 1.7-3 eV 77−52131
EuTe, optical absorpt. in high mag. field 79−28726
$(EuX_6)^{3-}$, (X=Br, Cl), spectral hypersensitive intensity, ligand polarisability contrib. 78−51946
$Eu_{1-x}Yb_xTe$, ($0<x<1$), mag. semicond., elec., mag. and optical props. 80−97070
(Fe, Ti) silicate glasses, optical absorption and Mossbauer spectra 80−55136
Fe absorption bands in glass fraction of lunar soil 77−49320
Fe, BCC, low energy interband absorption, electronic struct. exam. 79−73930
Fe complex, $Fe_4[Fe(CN)_6]_3$, $Fe_3[Fe(CN)_6]_2$ and oxidised $Fe[Fe(CN)_6]$, electron structs. and refl. spectra 77−55813
Fe complex, Fe(II) and Fe(III) cyanides-3d transition metal, mag. suscept., reflectivity spectra, cryst. field 79−56808
Fe complex, $K_3[Fe(SCN)_6].4H_2O$, optical reflection spectrum, mag. suscept., permittivity, dehydration temp. 79−56809
Fe film, even magneto-optical transmission effects, 0.4-1.25 μm 77−32354
Fe film bounded by dielec. layers, surface polariton in ATR angular spectra 79−15545
Fe granular deposits, plasma reson., rel. to interstellar dust extinction curve 79−21387
Fe, interband optical conductivity, self energy correction 80−2792
Fe, optical constant dispersion and emissivity, up to 900K 78−52464
Fe passive film AC electroreflectance and impedance obs. 78−7093
Fe-Al, optical props., comp. and order-disorder transform. depend. *(Russian)* 79−28852
Fe-Co alloy, optical characts., 0.073-4.92 eV, quantum absorption 79−56814

visible and ultraviolet spectra of inorganic solids continued
Fe-Co alloys, optical and spectrosc. props. *(Russian)* 78−72529
Fe-Co films, optical props. order-disorder transformation influence, absorpt. band existence *(Russian)* 79−65942
Fe-Cr, passivation films, modulation spectroscopy study 80−3244
Fe-Ni alloy, optical and electronic characts., 20-1750°C, comp. depend. *(Russian)* 78−84601
Fe-Ni-B(-P), ferromag., magneto-optical spectra in amorphous and cryst. states *(Russian)* 80−84749
$FeBO_3$, antiferromag., optical absorpt. spectra, role of local mag. mode 79−28785
$FeBO_3$, mag. linear dichroism and absorpt. spectra, Jahn-Teller effect 80−54662
$FeBO_3$, mag. linear dichroism and absorpt. spectra, exciton-magnon absorpt. mechanism 80−66160
$FeBr_2$, metamagnetic, optical study of mag. phase diagram 78−56312
$FeBr_2$, multicritical behaviour 77−4627
$FeBr_2$, optical props. around Neel temp. 79−78658
$FeCl_2$, light scatt., metamagnetic transition effects 77−4513
$FeCl_2$, optical props. around Neel temp. 79−78658
$Fe_{2-x}Cr_xO_3$, elec., optical and photocond. props. 79−56262
FeF_3, thin film, optical absorpt. meas. 79−15546
FeO, Fe_3O_4, Fe_2O_3, absorption spectra, 0.1-6 eV, one electron energy level diagram 78−52487
β-Fe_2O_3 film, CVD and characterisation 77−44172
Fe_2O_3, haematite, anal. of refl. spectrum by Kramers-Kronig relations 80−16058
α-Fe_2O_3, magneto-optical refl. spectra by equatorial Kerr effect *(Russian)* 77−32400
α-Fe_2O_3, photochem. props. of sintered and doped samples for solar photoelectrochem. cell appls. 80−89651
Fe_2O_3 sputtered films, optical transmission and reflection spectra depend. on substrate temp. 79−91517
Fe_2O_3-$B2O_3$-PbO glasses, visible and UV optical props. *(Rumanian)* 78−48196
Fe_3O_4, dielec. function and polar Kerr rotation, 0.5-3.6 eV 80−66221
Fe_3O_4, magnetite, charge carriers, optical props. 80−34874
Fe_3O_4, magneto-optical refl. spectra by equatorial Kerr effect *(Russian)* 77−32400
Fe_3O_4, optical props. in spectral range 0.03 to 12 eV 79−51977
$xFe_2O_3.(1-x)[3B_2O_3.PbO]$ glasses, diffuse refl. spectra 79−51982
$FeSiO_3$, UV and soft X-ray spectra, band gap determ. 79−61468
Fe_2SiO_4, fayalite, Czochralski growth under controlled O_2 fugacity conditions 80−84843
Fe_2SiO_4, UV and soft X-ray spectra, band gap determ. 79−61468
$Fe_{1-x}Zn_xF_2$, dil. antiferromag., electronic and mag. props., Raman scatt. and optical absorpt. study 80−108207
Ga film, optical props., 2-15 eV 77−77308
Ga, optical properties in 0.3 to 5 eV range 78−31196
Ga, optical props. in 0.5-60 eV range, dielectric const. and loss functions *(French)* 77−12353
Ga-group V semiconductors, electroreflectance spectroscopy using synchrotron rad. 78−10912
Ga-Xe film, metal-nonmetal transition, optical and resist. meas. 77−89818
$Ga_{1-x}Al_xAs$, epitaxial layers, reflectivity meas. by wavelength modulation spectroscopy *(French)* 77−59632
$Ga_{1-x}Al_xAs$, topographical stoichiometry determ. using electroreflectance 78−23483
$Ga_xAl_{1-x}N$ film, growth and props. 78−39702
n-GaAs, absorption tails in surface depletion layer and bulk 78−64379
GaAs, amorphous sputtered films, hydrogenated, photoinduced optical absorpt. 80−50362
GaAs anodic oxide, refl. and transmission, 0.01-6 eV 78−95613
GaAs anodic oxide, refr. index meas., Sellmeier eqn. 77−12454
GaAs anodic oxide film, optical props. 78−72626
GaAs anodic oxide films, optical studies using rot. light-pipe reflectometer 80−76096
n-GaAs anodised MOS, electrorefl. spectra 79−99901
GaAs, CC Ga-3d-excitation, high resolution reflectivity down to 15K 80−25415
GaAs, carrier conc. variations using electrolyte electroreflectance, topographical features 79−99562
GaAs, carrier concentration determ. using electroreflectance 78−23483
GaAs, deep level photoionisation, absorpt. by derivative surface photovoltage spectroscopy 79−99575
GaAs, deep trap study by free exciton refl. spectra 79−60761
GaAs, donor van der Waals interactions, spectral lineshapes 80−11450
GaAs epitaxial layers, polariton wave packet propag. in exciton reson. 80−2345
GaAs, exam. of magnetic susceptibility and absorption spectra 79−1778
GaAs, exchange interaction, analytical and nonanalytical parts, from polariton spectra in mag. fields 80−50367
GaAs, exciton parameters near absorption edge 79−73448
GaAs, exciton quenching, obs. at room temp. using electrolyte electroreflectance 80−60546
GaAs, exciton-polariton reflectance spectra, exciton impact ionization and illum. intensity effects 79−42943
GaAs, final state interactions in gain and absorpt. spectra of electron-hole liq. 78−43305
GaAs, fundamental absorption band, influence of phonons on long-wavelength wing 79−69857
GaAs, heavily-doped, band gap, magnetoabsorpt. oscills. obs. 78−18960
GaAs, high resist., linear electroabsorpt., characts., valence band splitting 77−44018
GaAs, impact ionisation of excitons 79−38079
GaAs, ion-bombarded, energy band struct., electrorefl. obs. 79−19517
GaAs, k-linear coupling, E_1' transitions 78−91583
GaAs, low-temp. absorption spectrum in presence of optical pumping 78−15188
GaAs, noncentrosymmetric cubic cryst., electrooptic effect dispersion of permittivity 79−69812
GaAs, one-photon absorption coeffs. calcs. 77−20884
GaAs, opt. consts. in 0.6 to 4.2 eV range 79−51928
GaAs, optical absorption near fundamental edge due to CO_2 laser pulses 78−39569
GaAs, optical absorption spectrum dynamics using sub-ps. optical pulses 80−11431
GaAs, optical inhomogeneity, physical basis 79−15430
GaAs oxide, anodic, optical props., 1.5-6.0 eV 77−90209

visible and ultraviolet spectra of inorganic solids continued
GaAs, oxide film growth, thermal oxidation, optical obs., model 77—56120
GaAs, photoabsorption and magnetoabsorption effects 77—16332
GaAs, photoexcited, carrier relaxation determ. from time resolved transmission spectrum changes 79—99583
GaAs, picosecond absorption spectroscopy 79—47482
n-GaAs, piezo-absorpt. meas. 79—87455
GaAs, reflection spectra, optical consts. *(Russian)* 79—38571
GaAs, Schottky barrier electrorefl. under uniaxial stress, band struct. 77—48193
n-GaAs, spectra, light induced, electrolyte and Schottky barrier techniques of meas. 80—76046
GaAs thin films, reactively sputtered, ESCA/XPS study 80—97430
GaAs, time-resolved spectra, carrier relax. time, phonon lifetime 80—11433
GaAs, valence band fine struct. from light mod. with nonequilib. opt. phonons 78—39568
GaAs:Co^{2+}, piezoabsorption meas. tunnel splitting and Jahn Teller effect in $^4T_1(P)$ state 79—15494
GaAs:Cr, luminescence and absorption spectra, temp. depend. of fine structure 80—6779
GaAs:Fe, profile of impurity optical absorption bands 78—56509
GaAs:O, annealing effects, optical absorpt. and I-V charcts. 80—29037
GaAs:O, optical characterisation of deep O implants 77—55294
GaAs:Se, ion implanted, surface state study from photoreflectance 79—91465
GaAs:Si, ion-implanted, annealing with Nd:glass laser 79—73194
GaAs:Te, amorphous, ion implanted layers, optical refl., 1.5-7.0 eV 79—8152
n-GaAs:Te, electron-irrad., absorpt. spectra *(Russian)* 78—15200
GaAs:Te, ion implanted optical transitions in modulated reflectivity spectrum 79—73972
p-GaAs:Zn, optical absorpt. spectra and photocond. after 2 MeV electron irrad. *(Russian)* 77—69859
GaAs-$Al_xGa_{1-x}As$ superlattice, mag. field induced dimensionality change 78—64381
GaAs-AlAs, epitaxial struct. with alternate layer comp. modulation, fabrication and characterisation 77—1322
GaAs-AlAs layered films, MBE prep., struct., rel. to optical props. 79—77950
n-GaAs-$Ga_{1-x}Al_xAs$, superlattice, subband struct. and optical spectra, self-consistent calc. 80—15443
GaAsP, composition dependence of phonon frequencies 78—75764
$GaAs_{1-x}P_x$, electron irrad., radiation defects annealing 80—29059
$GaAs_{1-x}P_x$ epi-wafer, comp. profile of heterogeneous struct., anodisation-electrorefl. meas. 78—26782
$GaAs_{1-x}P_x$ epitaxial layers, charge carrier conc. determ. from low-field electrorefl. spectra 77—85320
$GaAs_{1-x}P_x$, piezomodulation spectra of indirect gap, zero-phonon and phonon-assisted transitions 77—48192
$GaAs_{1-x}P_x$:N, photoluminesc. and optical absorpt. spectra of N impurity bound-excitons 79—47496
$GaAs_{1-x}P_x$:N epitaxial layers, absorption and photolum. spectra meas. 77—24894
$GaAs_{1-x}P_x$-GaP heterostructure, photomodulation spectroscopic exam. 77—40257
GaAs(P)(Sb), fine struct. in energy derivative reflectance spectra 79—78705
$GaAs_{1-x}Sb_x$ epitaxial n-n heterostructures, gap energies and interface pots., modulation electroabsorpt. meas. 79—11201
$Ga_{1-x}In_xAs$, VPE grown, refractive index, reflectance meas. 79—4780
$Ga_{0.08}In_{0.92}As_{0.18}P_{0.82}$, band struct., optical studies 79—47013
GaInP, composition dependence of phonon frequencies 78—75764
$Ga_zIn_{1-z}P$, piezomodulation spectra of cond. band struct. 77—48191
$Ga_{1-x}In_xSe$, energy bands near absorpt. edge, transmission and photoluminesc. spectra 79—83022
$Ga_{1-x}In_xSe$, energy spectrum and struct., X-ray diffr. and light absorption 79—11437
GaN, epitaxial, refl. spectra, 5-12.5 eV 79—99967
GaN epitaxial layers, exciton cathodolum. *(Russian)* 78—76543
GaN:Zn, VPE grown, optical cross sections, photoluminesc. and optical absorpt. meas. 80—55160
Ga_2O_3 film, growth by reactive vapour deposition, optical and elec. props. 77—48347
Ga_2O_3-R_2O_3:Nd^{3+} glass, prep., charcts., X-ray diffr., absorpt. and thermal anal. obs. *(French)* 78—19704
GaP, deformation potentials of direct and indirect absorpt. edges 79—69854
GaP, effective mass anisotropy at X_{1c} and X_{3c} minima of conduction band, optical absorpt. spectra 77—8021
GaP, effects of hydrogen incorporation during deposition by sputtering 79—69981
GaP, electron irrad., radiation defects annealing 80—29059
GaP, exam. of magnetic susceptibility and absorption spectra 79—1778
GaP, excited 1s-level of S-bound excitons 79—82996
GaP, fine struct. of indirect exciton 78—19509
GaP, hyperbolic singularity of dispersion law of excitons 79—42466
GaP, impurity-containing single crysts., refl. spectra 80—80823
GaP, indirect exciton fine struct. in absorpt. spectrum, stress effects 79—42986
GaP, indirect exciton fine struct. and effect of uniaxial stress 79—95805
GaP, ion-bombarded, energy band struct., electrorefl. obs. 79—19517
GaP, line shape and symmetry analysis of core-level electroreflectance spectra 77—8600
GaP, obs. of Γ-L indirect transition, phonon struct. 78—48194
GaP, optical inhomogeneity, physical basis 79—15430
GaP oxide, anodic, optical props., 1.5-6.0 eV 77—90209
GaP, refr. index, 100 to 420K, permittivity calcs. *(Russian)* 77—90156
GaP:Cu, elec. and optical props., rel. to doping and heat treatment 80—16056
GaP:Fe, optical absorption spectrum and Faraday effect 80—108245
GaP:Fe, profile of impurity optical absorption bands 78—56509
GaP:N(Te), ion implanted at 40 keV, refl. spectra, 210-2000 nm, annealing *(Russian)* 78—80386
GaP:Zn, light attenuation by impurity precipitates 79—11441
GaP-In LPE layers, carrier diffusion lengths and escape probabilities optical absorpt. and photoemission meas. 79—87559
GaP-InAs solid solns., energy band struct., edge absoprtion spectra 78—39018

visible and ultraviolet spectra of inorganic solids continued
GaP_xAs_{1-x}, exam. of magnetic susceptibility and absorption spectra 79—1778
GaP_xAs_{1-x} solid solns., edge absorpt. 77—16334
$(GaP)_x(ZnS)_{1-x}$ solid solutions, X-ray fluorescence spectra, photoluminescence *(Russian)* 79—74003
GaS, electrolum. and electroabsorpt., 77K 77—48247
GaS layer crystal, differential indirect exciton spectra 79—8159
GaS, optical absorption edge under hydrostatic press. 78—23487
GaS, reflectivity from 4 to 32 eV, Kramers-Kronig anal. 80—34943
GaS:Bi_2S_3, photocond. and optical obsorpt. 79—51634
α-Ga_2S_3, defect semicond., optical absorption meas. 78—15186
Ga_2S_3-La_2S_3-Nd_2S_3:Nd^{3+} chalcogenide glass, Nd^{3+} emission and absorption spectra, nonradiative relax. 77—40268
GaS(Se), absorpt. edge, exciton levels and Raman scatt., press. effects above 40 kbar 77—48187
GaS(Se), $GaS_{0.6}Se_{0.4}$, angle resolved UPS, energy band dispersion curves determ. 79—100022
GaS(Se), reson. Brillouin scatt. 80—89010
$GaS_{1-x}Te_x$, solid soln., single cryst., crystallography and optical props. 79—55711
GaSb, bound excitons at doubly ionisable acceptors 79—42459
GaSb, E_1 and $E_1+\Delta_1$ edges using electroreflectance, Franz-Keldysh oscills., high mag. fields 77—66518
GaSb films, amorphous and cryst., vac. evaporated, Elec. cond. thermoelec. power and optical absorpt. 80—2504
n-GaSb, fundamental absorpt. and energy relax., elec. field induced changes 77—1688
GaSb oxide, anodic, optical props., 1.5-6.0 eV 77—90209
GaSe, absorpt. and electroabsorpt. near indirect edge 77—20827
GaSe, absorpt. spectra, electron-hole system at high densities 77—69854
p-GaSe, back wall Schottky barrier cells, diffusion length, RT spectral response meas. 80—107806
GaSe, electron-phonon interaction and optical props. 80—34942
GaSe, excitation spectra and structural props., X-ray Laue diagrams and optical transmission *(French)* 80—50358
GaSe, exciton, excitation-induced absorption and luminesc. 78—60516
GaSe exciton absorpt., change under a pulsed dye laser 78—92088
GaSe, exciton absorption under intense excitation 77—77235
GaSe, exciton absorption spectrum, polariton effects 77—85747
GaSe, exciton spectra at 4.2K rel. to layer struct. 77—16336
GaSe, exciton-phonon bound state, photocond. and visible absorpt. spectra obs. 80—50369
GaSe, exciton-phonon quasibound states, photocond. and luminesc. study 80—96800
GaSe excitonic spectra fine struct., reflection and transmission spectra *(Russian)* 80—55126
GaSe, fine struct. of exciton spectrum 78—39567
GaSe, interlayer interaction and exciton spectra study 77—52165
GaSe, magnetoluminesc. at 4.2K 79—61345
GaSe, optical consts. at fundamental absorpt. edge 77—66471
GaSe, optical excitation, excitonic spectra, stimulated luminesc. 80—40132
GaSe, pressure-induced polytypic transforms. and edge absorpt., exciton lines 77—28595
GaSe, reflectivity from 4 to 32 eV, Kramers-Kronig anal. 80—34943
GaSe, refr. index 0.45 to 330 μm, interf. and refl. meas. methods 77—63387
GaSe thin films, electroabsorpt. spectra, exciton line splitting 80—107716
Ga_2Se_3, film, electrical and optical props. 77—1505
GaSe(Te), optical spectra in 2 to 50 eV range 78—10915
$GaSe_{1-x}Te_x$, energy bands near absorpt. edge, transmission and photoluminesc. spectra 79—83022
$GaSe_{1-x}Te_x$, room temp. electroreflectance meas. 77—12361
$GaSe_xTe_{1-x}$ mixed crystals, near-band-edge optical props., absorption edge spectra 79—61401
GaTe, exciton polariton effect on absorpt. edge, absorpt. and refl. spectra, 4.2 to 300K 80—20664
GaTe, exciton polariton effect on absorpt. edge, thickness depend. of absorpt. 80—20665
GaTe, excitonic absorpt. edge, transmission and refl. meas. 80—40133
GaTe, laser modulated reflectance meas. 77—63424
GaTe layer semiconductor, UV-visible wavelength derivative and thermorefl. spectra 78—6666
GaTe, reflectivity, 1-35 eV, electron props. determ. 77—20872
GaTe, single cryst. prep. and electroabsorpt. spectra investig. 80—103968
GaTe:Sn, electroabsorption spectra 79—19901
GaX_3, (X=Cl,Br,I), charge transfer spectra 79—76441
Gd, 4f-shell optical excitations, vacuum UV absorpt. meas. 77—1698
Gd, magneto-optical Kerr effect spectra in UV region using synchrotron radiation 77—52127
Gd, optical constants, reflectance meas. *(French)* 78—2869
Gd, optical consts. polarimetric meas., mag. ordering effects 78—15184
Gd, optical properties, 0.5-3.1 eV *(Russian)* 79—11432
Gd, thermoreflectance meas. 79—69816
Gd-Co amorphous thin film, mag. and optical props., conc. depend 79—19748
Gd-La alloy, optical freq. cond. in 0.5-3.1 eV range, paramag.-ferromag. transition 80—29761
$GdAlO_3$:Er^{3+}, $^4S_{3/2}$ to $^4I_{9/2}$ transition laser action, optical and luminescence spectra 80—16082
$GdBr_3$, frozen aq. soln., fluoresc. and absorpt. spectra 79—43022
$GdCl_3$, frozen aq. soln., fluoresc. and absorpt. spectra 79—43022
$Gd(ClO_4)_3$, frozen aq. soln., fluoresc. and absorpt. spectra 79—43022
GdFeBi, amorphous ferrimag. films, magneto-optical props., optical spectra 80—76008
$Gd_3Ga_5O_{12}$:Nd^{3+}, cryst. field anal. 78—64013
$Gd_3Ga_5O_{12}$:Nd^{3+}, optical absorpt. and fluoresc. intensities 80—29793
$Gd_2Gi_2O_7$:Nd^{3+}, spectroscopic props. 77—69866
$Gd_2(MoO_4)_3$, cryst. field parameters for Gd^{3+} 77—66142
$Gd_2(MoO_4)_3$, low temp. optical absorpt., external mag. field influence 78—43896
$Gd_2(MoO_4)_3$:Nd^{3+}, optical spectrum, free ion wavefunctions, radiative transition probabilities 79—24339
$Gd_2(MoO_4)_3$:Nd^{3+}(Dy^{3+}), cryst. field parameters 77—66142
GdP, electronic struct., mag. exchange and elec. transport props. 78—87974
GdS, electronic struct., mag. exchange and elec. transport props. 78—87974
Ge, amorphous sputtered films, hydrogenated, photoinduced optical absorpt. 80—50362

visible and ultraviolet spectra of inorganic solids continued
Ge, carrier conc. variations using electrolyte electroreflectance, topographical features 79−99562
p-Ge, carrier heating by weak electric field 77−11927
Ge, crit. points in E′ region from ellipsometric data 77−80726
n-Ge, direct identification of $L_3' \rightarrow L_1$ transition, electroreflectance 77−1689
Ge, E_1-optical struct. from electroreflectance spectra 78−43897
Ge, electrodeposited, X-ray, electrochem., and electrorefl. characterisation 78−14624
Ge, electron-hole drops, kinetics of spatial distrib. *(Russian)* 78−43312
p-Ge, electrorefl. spectra, 2.1 to 2.3 eV, influence of light beam 77−90169
N-Ge, electrorefl. spectra, light induced, electrolyte and Schottky barrier techniques of meas. 80−76046
Ge, electroreflectance spectra, meas. on Al-SiO_2-Ge struct. 77−1677
Ge, electroreflectance spectra, nonparabolicity effects of bands *(Russian)* 79−4791
Ge, energy-gap narrowing and state filling under laser irrad. 79−42441
Ge, exciton mol. by phonon-assisted two-photon absorpt., theory 78−48197
Ge film, A1-type and amorphous, complex refractive index and reflectance 77−52121
Ge film, amorphous and crystalline, optical props. 77−16412
Ge, lattice disorder influence on optical spectra in interband transition region 79−43006
Ge optical props. in 2.5-15 micron region 80−80775
Ge, piezoreflectance, at E_1 and $E_1+\Delta_1$ edges, high mag. field 77−77245
Ge, Schottky barrier electrorefl. under uniaxial stress, band struct. 77−48193
Ge, sum rule for intraband optical absorpt. of shallow acceptor impurities 79−28793
Ge-As-Se films, light irrad., heat treatment rel. to optical props. *(Russian)* 79−4858
Ge-Bi-S system, semicond., elec. cond., glass transition temp. and optical absorption meas. 77−16329
N-Ge-Bi-Se glass, elec. and optical props. 80−65550
Ge-Ga amorphous alloy, co-evaporated elec. and optical props. 80−70860
Ge-S-Ga(In) system glasses, photoinduced changes 80−24365
Ge-Se, amorphous, photocond., photo-induced ESR, optical edge shift 80−49809
Ge-Se glass film, photoinduced absorpt. changes 79−87519
Ge-Te alloy films, amorphous, semicond. props., refr. index, struct. study 78−26978
GeC_x, amorphous, prepared by glow discharge method, elec. and optical props. 77−21035
$GeFe_2O_4$, single crysts., elec. and mag. props, optical absorpt. spectra 80−54719
GeO amorphous film, hologram recording, photochem. props. 79−64186
GeO film, optical props., rel. to possible appl. in holography 80−29816
GeO:Cr, dielectric thin film, transmission and EPR spectra 77−69676
GeO_2, film, optical and electrophysical props. *(Russian)* 77−85821
GeO_2, tetragonal, exciton struct. in UV absorption edge 78−48199
GeO_2:Si, optical props. IR absorpt., UV reflection spectra 78−84619
GeO_2:V^{4+}, crystal field splitting from ESR and optical absorpt. results 79−47063
GeS, absorpt. spectra, electron-phonon interactions 80−80810
GeS, electron-hole interaction in d-electron excitations, photoelectron and optical spectra 78−34776
GeS, orthorhombic single cryst., fine struct. in reflectivity 79−19903
GeS, physical basis for Urbach's rule 80−93366
GeS_2 glass, melt quenched, reversible photostructural change, optical transmission spectra obs. 80−45109
GeS(Se), dielec. function, optical and electron energy loss spectroscopy 78−15189
$Ge_{100-x}S_x(Se_x)(Te_x)$, amorphous film, effect of alloying chalcogen atom on elec. cond., optical transmission and ESR 79−78101
$Ge_{20}Sb_{25}S_{55}$ glasses, optical props., absorption edge temp. depend. 80−2789
GeSe, optical absorption edge meas. 77−63430
GeSe, single crystal, optical absorption 80−25383
$GeSe_2$ amorphous film, laser induced light absorpt. oscillation, exciton model 80−50446
$GeSe_2$, amorphous film, photocond., photo-induced ESR, optical edge shift 80−49809
$GeSe_2$ evaporated films, optical absorpt. and thermally induced effects 79−42989
$GeSe_2$, exciton absorpt., transmission spectra of cryst., glasses and amorphous samples 79−15485
$GeSe_2$ film, light-induced light absorption changes 77−73181
$GeSe_2$, optical absorption edge 78−43901
$GeSe_4$ film, self-controlled laser beam chopping effect 78−31266
$Ge_{1-x}Se_x$ film, EPR, elec. and optical props. meas. 78−48038
$Ge_{1-x}Se_x$, photolum. and optical props. meas. 77−20908
Ge_xSe_{1-x}, amorphous, exponential absorpt. edge rel. to struct. 79−99902
p-GeTe, reflectance, and thermorefl. spectra 80−80814
Ge(111)2×1, oxide layer, surface states detect optical reflectivity obs. 80−50368
H_2, solid, fundamental absorption spectra, 10 to 40 eV at 2K, using synchrotron radiation 79−73967
H(D)CN(C^1A')→H(D)+CN($B^2\Sigma^+$), photofragment excitation spectra measurement 79−45777
$H_{1.6}MoO_3$, electronic props., mag. susceptibility and spectra 80−80266
H_xWO_y film, effect of struct. on optical and electrical props. 78−84671
HfO_2 film, CVD growth, struct., elec. and optical prop. characterisation 77−55891
HfS_2, intercalation-induced shift of absorpt. edge 79−82999
HfS_2, optical props., modulation spectroscopy 77−52117
$HfS_2(Se_2)$, vacuum UV reflectivity spectra, cond. band model 77−44012
Hg, reflection spectra, electronic density of states, calc. 80−66229
Hg-Xe solid films, optical absorpt., localised states 79−61452
Hg-Xe solid mixture, optical criterion for Mott transition 78−75996
$Hg_{2.86}AsF_6$, anisotropic linear-chain conductor, optical reflectance meas. 77−77247
$Hg_{0.75}Cd_{0.25}Te$, single crystal, reflection spectra 80−40140
$Hg_{0.75}Cd_{0.25}Te$, thermorefl. spectra, effect of excitons on E_1 and $E_1+\Delta_1$ structs. 80−16057
$Hg_{1-x}Cd_xTe$, mixed crysts., band struct. and optical transitions, distorted atomic orbitals 77−69224

visible and ultraviolet spectra of inorganic solids continued
$Hg_{1-x}Cd_xTe$, optical absorpt., quasilocal acceptor level effects, theory 80−92853
$Hg_{1-x}Cd_xTe$, surface topographic stoichiometry variations, electrolyte electrorefl. obs. 78−27249
$Hg_{1-x}Cd_xTe$, two-photon absorpt. spectra 80−20660
Hg_2Cl_2, cryst., birefringence and dichroism, 200-500 nm and far IR 78−27257
$HgCr_2Se_4$, optical and magneto-optical surface effects 79−82953
$HgCr_2Se_4$, thermoreflectance, photoconductance, Raman scatt. near mag. phase transition 80−97298
HgI_2, exciton study by wave length modulated reflectivity, band parameters 77−51667
HgI_2, excitons, spectral obs. 78−23492
HgI_2, phonon struct. in wavelength modulated refl. spectra and mag. circular dichroism 79−8125
$Hg_{1-x}Mn_xTe$, 1.7 to 3.5 eV, reflectivity spectra 78−43899
α-HgS, cinnabar, reson. Raman effect and luminesc. meas. 80−50338
α-HgS, polarised reflectance spectra, 2-5 eV, 77 and 293K 77−77243
$Hg_{2.91}SbF_6$, anisotropic visible and IR refl. rel. to metallic cond. 77−8602
HgTe, energy bands and optical props. calcs., tight-bonding model with spin-orbit interaction 80−65448
HgTe, optical absorption 77−28572
HgTe-HgSe film, optical spectra in fundamental absorption edge 79−74012
Ho_2O_3, photoacoustic spectra using Helmholtz reson. cells 80−9048
$Ho_2O_2SO_4$, antiferromag., mag. props. and Zeeman effect meas. 79−33464
$HoVO_4$, first excited doublet, zero field splitting 77−20870
I_2, absolute absorption spectrum measured by Fourier transform spectroscopy 79−75622
In film, polycrystalline optical transitions from d core states 77−85827
In, relativistic energy bands, density of states, and optical spectra, KKRZ calc. 79−51478
In-Bi, single crystal, vacuum UV optical props. 77−1697
InAs, absorpt. rel. to dopant admixture 78−95596
InAs:S(Mg), ion implanted, photocond., photo-EMF, and optical absorpt. spectra 80−70763
InAs:Zn, optical absorpt. and refl. spectra 79−91479
InAs(P)(Sb), fine struct. in energy derivative reflectance spectra 79−78705
$In_{1.9}As_{0.1}Se_3$, growth by chem. vap. transport, characterisation as photoelectrode 78−43994
$In_xGa_{1-x}As$, epitaxial solid soln. film, spectral depend. of transparency, absorpt. spectra calcs. 80−45161
InGaAsP-InP DH laser, optical gain meas., low-intensity luminesc. and absorpt. spectra 79−98356
$In_{0.79}Ga_{0.21}As_{0.54}P_{0.46}$, LPE layer, electroreflectance meas. 79−24290
$In_{1-x}Ga_xP$, quantitative characterisation of chemical disorder from wavelength-modulated no-phonon absorpt. 79−15482
$In_{1-x}Ga_xP_{1-z}As_z$, lattice matched to InP, electroreflectance obs. 80−93416
$In_xGa_{1-x}Se$ single crystals, exciton absorption spectra 80−20663
InI, orthorhombic, reflection spectra, exciton transition 79−24333
InN film, refl. and transmission spectra, band struct. 78−72625
InN film, specular reflection spectra, lattice parameters 80−7428
InO_3:Sn film, prep. by spray hydrolysis, struct., elec. and optical props. *(Japanese)* 79−42678
n-In_2O_3 film, RF sputter grown, substrate bias effect on elec. and optical props. 78−64150
In_2O_3 layers, chemically sprayed, prep. and intrinsic absorpt. in band edge 77−81169
In_2O_3, reactive ion plating onto insulating substrates, and elec. and optical props. 79−87588
In_2O_3:Sn, coating on polyester film, elec. and optical props. 79−99959
In_2O_3:Sn, transparent conducting films, prep. by $InCl_3$ thermal decomp., transmittance, resistivity 79−33944
In_2O_3:Sn films, RF reactive sputtered, optical props. rel. to band struct. 79−91515
In_2O_3-SnO_2 film, stress, and elec. and optical props. 78−51861
In_2O_3-SnO_2 thin film, effects of heat treatment on resist. and optical absorpt. 78−43495
InP, deep trap study by free exciton refl. spectra 79−60761
InP, exchange interaction, analytical and nonanalytical parts, from polariton spectra in mag. fields 80−50367
InP, exciton localisation at impurity pairs 79−37999
InP, excitons bound to neutral donors in VPE layers, luminesc. and absorpt. obs. 79−42460
InP, Faraday interband effect subjected to quantising mag. fields 80−97246
InP, free excitons in high mag. fields, band struct. 77−52129
InP, press. depend. of direct absorption edge 80−93365
InP, reflection spectra, optical functions, exciton peaks *(Russian)* 80−50372
InP, valence band fine struct. from light mod. with nonequilib. opt. phonons 78−39568
InP:Bi, isoelectronic impurity states, emission and absorpt. obs. 79−42491
InP:Bi, uniaxial stress effect on free and Bi-bound excitons 79−56854
InP:Fe, Hall and resistivity meas., optical absorpt. 80−10990
InP_xAs_{1-x}, absorption edge and band gap comp. depend., bowing effect 77−4653
$In_{2/3}PSe_3$, cryst. growth and characterization 77−77357
In_2S_3, film struct. and props. 77−80706
InSb, carrier conc. variations using electrolyte electroreflectance, topographical features 79−99562
InSb, film, E_0, E_1 absorption edge size quantisation, optical and electroreflectance spectra 80−34998
n-InSb, Landau emission spectra, influence of bakcground radiation 78−43935
InSb, one-photon absorption coeffs. calc. 77−20884
InSb, two-photon absorpt. spectra 80−20660
InSb-CdTe solid solns., electroreflectance spectra, Brillouin zone transitions 80−7330
γ-InSe, fundamental absorpt. edge 80−2781
InSe, large monocrysts. grown from nonstoichiometric melt, gap meas. 77−55882
InSe, opt. props. new fundamental absorpt. edge 77−16330
InSe, optical const. and interband transitions 77−20816
InSe, optical props. from 2-25 eV 80−29760

visible and ultraviolet spectra of inorganic solids continued
n-InSe, optical spectra, photocond. and resistivity 78−88321
InSe, photo-absorption of green exciton 80−80816
InSe, reflectivity and low energy absorption 80−34944
InSe, reflectivity from 4 to 32 eV, Kramers-Kronig anal. 80−34943
InSe, spin orbit split off valence bands, exciton transitions, Hopfield's quasicubic model, visible absorpt. spectrum 80−50370
InSe, wavelength modulated optical absorption above fundamental edge 78−27255
In_6Se_7 single crystals, absorpt. edge 79−87459
$In_{2-x}Sn_yO_{3-y}$ thin films, optical transmission and elec. resist. 77−69926
In_2Te_3 film thermal deposition, transmission spectra and elec. cond. *(Russian)* 80−49555
InX_3, (X=Cl,Br,I), charge transfer spectra 79−76441
Ir, electronic struct. determ. from optical refl. meas. 77−62812
IrF_6, in mixed crysts., Jahn-Teller effect, $\Gamma_{8g}(t_{2g})^3$ state, 6800 Å 78−76032
K, extreme UV absorpt. spectra, threshold singularities of p-shell absorpt. 77−36261
K salts, spectral refl. changes and luminesc. during 2-10 keV proton bombardment, implications for Io 79−96950
K smoke particles, optical props. 480 to 620 nm, rel. light scatt. cross sections meas. 80−97293
K, UV absorpt. spectra 80−2780
K-Cs, extreme UV absorpt. spectra 80−97294
K-Rb, extreme UV absorpt. spectra 80−97294
$KAl(SO_4)_2.12H_2O:MnO_4^-$, visible and UV absorpt. spectra interpretation 80−45116
KBr, colour centre form. under polarised UV irrad., dichroism in absorption spectra 80−107232
KBr, colour centres isothermal decay 79−51975
KBr, efficiency of V_k- and Ag^0-centres generation *(Russian)* 80−39080
KBr, electron irradiated, defect accumulation kinetics of low temps. 80−10577
KBr, energy of form. of Schottky defects 77−7714
KBr film, oblique incidence transmission spectra for polarised extreme UV radiation 78−39614
KBr, IR laser window appl., crystal growth, polishing and optical absorpt. 77−7102
KBr, m-crocryst. powders coloured in electrodeless discharge, reflectance spectra, thermolum. 78−15238
KBr, pulse radiolysis of metastable interstitial centre of high temp. 80−20658
KBr, pure and Sr^{2+} doped, X-irrad., hole Br_3^- centre creation and destruction 77−15411
KBr, quenched, absorpt. spectra, role of Schottky defects 77−59599
KBr, self-trapped exciton and F-centre form. 79−73443
KBr, UV two-photon absorpt. relative to known Raman cross section 79−81487
KBr, X-irrad. crysts., halogen aggregation, absorpt. spectra obs. *(Russian)* 80−66234
KBr:Ag, optical absorpt. spectra interpretation mol. orbital scheme 80−20671
$KBr:In^+$, B-band, optical absorpt. and mag. circular dichroism calcs. 80−29765
$KBr:In^+$, optical absorption and MCD spectra, Gaussian quadrature calc. 80−7367
$KBr:In^+(Ga^+)$, mag. circular dichroism meas. 79−42988
KBr:KI, microcrystalline powder, isothermal decay of colour centres 79−42995
$KBr:MnO_4^-$, vibronic spectra interpretation 79−37770
KBr:Na(Rb)(Cs), microcrystalline powders, isothermal decay of colour centres 80−2804
KBr:Sr, X-irradiated, first-stage F-centre production, absorption spectra 77−76395
KBr-KI:Tl, spectral, polarisational and kinetic characts. 78−80385
$KBr(Cl):OH^-$, cc U_2 to H_2O^- defects conversion after UV photodecomp. 80−107230
KCN, F-centre emission spectrum 77−12420
KCN-KCl mixed crystals, F-centre optical absorpt. half width 77−81134
$K^+CN_x^-Cl^-_{1-x}$, influence of structural disorder on exciton spectra 80−108224
K_2CO_3-D_2O, glassy matrix, absorpt. spectra after X-irrad., solvated electrons 79−65903
$KCaCl_3$, phase transitions, optical and dilatometric meas. 79−61394
KCl, absorption spectra of F-aggregate centres, 2K 77−48207
KCl, additively coloured photochromic crystals, spectral sensitivity *(Russian)* 80−91871
KCl and KCl:KBr, colour centres isothermal decay 79−51975
KCl and $KCl:NO_2$, X-irrad. crysts., Cl_3^- centres photodissoc., optical anisotropy and creation mechanisms *(Russian)* 80−66235
KCl, cryst., two-layer colloidal K and Cu colour centre light absorption 77−12408
KCl, doped, elec. conductivity and optical absorpt., quenching from 750°C 78−2289
KCl, electron irrad., F-centre absorpt., ellipsometric obs. 78−23501
KCl, energy of form. of Schottky defects 77−7714
KCl, F-centre phonon many-mode interaction, absorption band shape 78−2883
KCl film, oblique incidence transmission spectra for polarised extreme UV radiation 78−39614
KCl, γ-irrad., F-centre absorpt., flash-stimulated changes 80−92524
KCl, irrad., V_3-band in absorpt. spectra, model *(Russian)* 79−56821
KCl, irradiated crystal, determ. of oscillator strength of V_3-centre *(Russian)* 78−92095
KCl, luminesc. excitation spectra of F-aggregate centres, 400-900 nm. *(Russian)* 78−10980
KCl, m-crocryst. powders coloured in electrodeless discharge, reflectance spectra, thermolum. 78−15238
KCl, photo-induced F-centres, hologram recording 80−28174
KCl single crystals, F-band absorpt. and thermolum. under DC field and X-ray irrad. 79−65910
KCl surface, VUV irrad., colour centre layer, angle-of-incidence derivative ellipsometry and reflectometry 80−73420
KCl surface, vacuum UV radiation damage, spectroscopic study 78−71758
KCl, thermal and photothermal conversion of colour centres, after high-dose electronic interaction *(Russian)* 80−39156
KCl, ultralow loss optical fibre material, loss mechanism 80−78920
KCl, undoped and Pb- or NO_3^--doped, colloid centre formation, absorpt. spectra, 300-1000 nm 79−78710

visible and ultraviolet spectra of inorganic solids continued
KCl:Ag, optical absorpt. spectra interpretation mol. orbital scheme 80−20671
KCl:Au, EPR and optical absorpt. 78−39397
KCl:Ba(Sr), Z-centre, luminesc. and absorpt. spectra obs. 80−49221
KCl:Ca, optical studies of Z_4 centres 79−24336
KCl:Ca, thermolum. and optical absorpt. spectra of Z_1 centres 79−52029
KCl:Ca, Z_2-centres, optical absorpt. and ESR spectra 79−91480
$KCl:Ca^{2+}$, Z_1-centre thermolum. 80−80879
$KCl:CaCl_2$, KOH, complex form., U-centre influence, optical absorpt. bands 77−80502
KCl:Ca(Ba)(Mg)(Sr), microcrystalline powders role of Z centres in stabilising coloration, optical absorption 80−54227
KCl:Ca(Yb), Z_2 and Z_2^+ centres, excited state, magnetooptical spectra 80−108233
$KCl:Cu^-$, absorpt. and emission spectra, $3d^{10}4s^2 \rightarrow 3d^94s^24p$ bands 79−24343
$KCl:Cu^-$ excitation and absorpt. spectra 80−108255
$KCl:Cu^+$, exciton bands, optical absorpt. and MCD spectra 80−80821
$KCl:Eu^{2+}$, F centres and 220-nm optical-absorption band, creation by X-rays 79−55778
$KCl:Eu^{2+}$, lattice defect equilib. optical absorpt. and cond. studies 80−29767
$KCl:Eu^{2+}$, optical absorpt. meas. for Eu^{2+} conc. determ. 79−51137
KCl:I(Br), colouration under two-photon excitation, absorption spectra 78−84618
KCl:Li, $(F_2^+)_A$ centres, optical props. 80−89026
KCl:Na, absorption from relaxed excited state by F_A and F_B centres 77−44031
$KCl:Na^+$, self trapped excitons, optical absorption and emission 77−43503
KCl:Na(Ag), UV irrad. anionic H and D atoms, ESR and optical absorpt. expts. 79−99187
KCl:Pb, impurity valence, heat treatment influence, absorpt. spectra obs. 79−38574
KCl:Pb exam. of simultaneous effect of heat treatment, Pb concentration on state, phase diagram construction 79−96008
$KCl:Pb^{2+}$, γ-irrad., rel. to props. 78−31262
$KCl:Pb^{2+}$, highly doped, state of dispersion of Pb^{2+} 77−1144
$KCl:Pb^{2+}$, pure and doped, electrolytically coloured, elec. cond. and optical absorpt. meas. 80−100668
$KCl:Pb^{2+}$, X-ray irrad., electron-trapped centres, Pb^+ and Pb^0, optical absorpt. spectra 80−71461
$KCl:Pb^{2+}$(0.005% Pb), A band fine structure, electron-phonon interaction 78−60491
$KCl:Pr^{3+}(Sm^{3+})$, absorption spectra at 4.2 K, anal. 80−7378
KCl:Ru, absorption bands, complex. form. 77−1705
$KCl:SnCl_2$, Sn^+ centres, polarised luminesc. and EPR 79−65076
$KCl:SnCl_2$, X-ray irrad., polarised luminesc. and EPR study of Sn^{3+} centres 80−39868
$KCl:SrCl_2$, H_{Na} annealing, X-ray irrad., H centre capture by IV dipoles 78−10927
KCl:Tl, mixed phosphor, dimer absorption bands, 200-300 nm 79−73976
$KCl:Tl^+$, absorpt. spectra, electrolytic coloration, migration in electric field, heat treatment 78−23504
$KCl:Tl^+$, optical absorpt. spectra following X-irrad., F- and V-centres 79−99912
$KCl:Tl^+$ cryst., A band, mag. field effect 80−34897
$KCl:Tl^{2+}$, hole mechanisms of H- can F-centre production, thermolum. obs. 77−16407
$KCl:Tl^{2+}$, optical absorpt. spectra interpretation mol. orbital scheme 80−20671
KCl:Yb, Z_2-centres, optical absorpt. and ESR spectra 79−91481
KCl-KBr mixed crystals, sign reversal of piezo-optic birefringence 79−99849
KCl-KH, F- and U-centre redistrib. at end of proton tracks, microspectrophotometric anal. 80−10583
KCl-KI:Tl, spectral, polarisational and kinetic characts. 78−80385
KCl-Mg, thermolum. of Z-centre, optical absorpt. 80−55203
KCl-Mg, X-irrad. and F-bleached, optical and ESR spectra 77−48052
$KCl-Tl^+$,$Ca^{2+}(Sr^{2+})$, electrolytic colouring, colour centre form., optical absorpt. spectra 79−15497
KCl(Br), coloured, irrad. damage during positron bombardment 78−63791
$KCl_{0.5}Br_{0.5}$:Ca, X-ray irrad., Z_1-centres, thermoluminesc. and optical absorpt. meas. 80−16108
KCl_xBr_{1-x}, mixed crystals, thermolum. and optical absorption studies 80−104000
KCl(Br)(I) with alkali and halogen impurities, colour centre deformation induced nonradiative decay 80−7387
$KCl(Br)(I):Eu^{2+}$, single cryst. optical absorpt. spectra 80−45117
$KCl(Br)(I):Zn^+$, optical absorpt. bands rel. to charge transfer 80−66245
K_2CrCl_4, ionic ferromag., temp. depend. intensity in optical absorption 77−12399
$K_2Cr_5F_{17}$, monocrystal, cryst. field and mag. props., EPR and optical absorpt. spectra 79−19773
K_2CrO_4, solid and solution, investigation by diffuse reflectance spectroscopy 78−88326
K_2CsSb, evaluation as photocathode material 78−11072
$K_2Cu_{1-x}Mn_xF_4$, Cu-Mn exchange interaction, optical determ. 78−72551
$KD_{2x}H_{2(1-x)}PO_4$ crystals, $0<x<0.98$, light scatt. by polaritons 80−96802
KDP-type crystals, electrooptic effect in ultraviolet region 78−76431
KD_2PO_4, electronic struct., UV reflection spectra 79−38558
$K_5Eu(MoO_4)_4$, electric dipole transition cross section and effective site symmetry of Eu^{3+} 78−52556
KF, F_2+-centre excited-state absorption spectrum, rel. to H_2^+ model 80−16066
$KF:Pd^{2+}$, pure and doped, two-step photoionisation, laser-active F_2^+ centre form. 79−963
KF(Br)(Cl)(I), K^+3p core excitons, refl. spectra study, low temp. 80−29759
$KFeCl_3$, linear chain ferromag., optical absorpt. and dichroism in mag. field 77−77237
$KFeS_2$, crystal ligand field theory, band assignment, absorpt. spectra study 80−20657
KH_2AsO_4, electronic struct., UV reflection spectra 79−38558
KH_2AsO_4, ferroelec., electronic struct. study *(Japanese)* 79−87463
KH_2PO_4 and related substances, electronic structures study *(Japanese)* 79−87463

visible and ultraviolet spectra of inorganic solids continued
KH_2PO_4, electronic struct., UV reflection spectra and XPS 79−38558
KH_2PO_4, Pockels effect in UV region 77−12398
KH_2PO_4, vac. UV transmission 77−73150
KH_2PO_4, vacuum UV spectra and electro-optical prop. *(Japanese)* 79−65900
KH_2PO_4:Tl, 5.76 eV absorpt. band, temp. effects on doublet struct. 79−78713
KH_2PO_4:Tl, UV absorption bands obs. 78−27266
KI microcrystals, UV spectra by diffuse reflectance technique, surface electronic transitions obs. 80−75614
KI, optical bleaching of V_2 and V_3 bands 79−33739
KI, oscillator strengths of defects, Smakula eqn. generalisation 80−108232
KI, piezo-optical study of excitons 80−16055
KI, quenched, absorpt. and emission spectra, α-centres 80−11442
KI, self-trapped excitons and F-centres, picosec. range form., absorpt. bands 78−19515
KI, UV two-photon absorpt. relative to known Raman cross section 79−81487
KI, V-centres, optical and thermal bleaching of V_2 and V_3 bands 77−85751
KI:Cu^-, absorpt. and emission spectra, $3d^{10}4s^2 \rightarrow 3d^9 4s^2 4p$ bands 79−24343
KI:Cu^+, exciton bands, optical absorpt. and MCD spectra 80−80821
KI:$In^+(Tl^+)(Ga^+)$, mag. circular dichroism meas. 79−42988
KI:Pb_3 absorpt. spectra of Pb^{++} centres 80−76058
KI:Pb^{2+}, absorpt., excitation and luminesc. spectra 78−19519
KI:Pb^{2+}, UV absorpt. and mag. circular dichroism spectra 80−25418
KI:S^{2-}, photoinduced polarisation and depolarisation 79−33738
KI:Tl^+, phosphor, anomalous stress-induced dichroism 79−4828
KI-KCl:Cu^+ mixed cryst., off-centre Cu^+ 79−65112
KMF_3, M=Mg, Ni, Co, Mn, reflectivity, 8-60 eV, excitonic struct. 77−20871
$KMgF_3$, extreme UV spectra, 9-30 eV 78−23486
$KMgF_3$:Co^{2+}, γ-irrad. single cryst., visible and IR absorption, MCD, annealing data 78−10926
$KMgF_3$:$Co^{2+}(Fe^{2+})(Mn^{2+})(Ni^{2+})$, high energy absorption spectra interpretation 78−6716
$KMgF_3$:Eu^{2+}, Zeeman absorpt. and luminesc. spectra *(Russian)* 77−69872
$KMgF_3$:Mn^{2+}, exchange and spin-orbit interactions, optical spectra study 79−95817
$KMgF_3$:Sm^{2+}, absorpt. spectra and Zeeman effect, 3000-12000 Å, 4.2-295K 79−24341
$KMgF_3$:$V^{2+}(Cr^{2+})(Fe^{2+})$ 3d→4d absorpt. band exam. 77−63435
$KMnF_3$, exciton line and magnon satellite in UV spectrum at high press. *(Russian)* 79−4517
$KMnF_3$, Faraday effect mechanism in paramag. phase 80−60552
$KMnF_3$, stress-induced phase transition, optical props. meas. 77−20067
K_2NaCrF_6, Cr^{3+} optical spectrum open shell SCF MO cluster CI calc. 78−19501
K_2NaGaF_6:Cr^{3+}, mag. circular dichroism and absorption spectra 77−77254
$KNdP_4O_{12}$, laser emission cross sections, fluorescence spectra, radiative lifetimes, quantum efficiency 80−23694
$KNiF_3$, K_2NiF_4, antiferromag., two-exciton transition 77−32398
K_2NiF_4, quadratic layer antiferromag., absorpt. 77−16326
K_2NiF_4, two-dimensional antiferromagnet, fine struct. obs., 4.2K *(Russian)* 77−59587
K_2O-BaO-SiO_2:Nd^{3+} glasses, absorption and fluoresc. spectra, density 80−25417
$K_2PdBr_4.2H_2O$, visible and UV absorpt. spectra, 10-295K 79−38572
K_2PdCl_4, visible and UV absorpt. spectra, 10-295K 79−38572
$K_2Pd(SCN)_4$, visible and UV absorpt. spectra, 10-295K 79−38572
K_2PtBr_4, visible and UV absorpt. spectra, 10-295K 79−38572
$K_2Pt(CN)_4Br_{0.3}2.6H_2O$ crystal, quasi-one-dimensional, optical consts. and dielec. permittivity dispersion 77−1695
$K_2Pt(CN)_4Br_{0.3}.xH_2O$, conductivity and optical refl. depend. on water content 77−39828
$K_{1.62}Pt(C_2O_4)_2.2H_2O$, plasma resonance absorpt. from small particles 77−24841
K_2PtCl_4, visible and UV absorpt. spectra, 10-295K 79−38572
$K_2Pt(SCN)_4$, visible and UV absorpt. spectra, 10-295K 79−38572
K_2SO_4-$ZnSO_4$ glass, transition metal ion doped, visible spectra 79−51990
K_2SnCl_6:$ReCl_6^{2-}$, (K_2PtCl_6:$ReCl_6^{2-}$), luminesc. and absorpt. spectra, relax. processes 77−85779
KTb_3F_{10}, Faraday rotation, optical absorpt. spectra and refr. index 78−72542
KTb_3F_{10}, mag., optical, magneto-optical behaviour 78−68484
$KZnF_3$, exchange interactions of transition metal ions in orbitally degenerated excited states 80−65512
$KZnF_3$:Mn^{2+}, exchange and spin-orbit interactions, optical spectra study 79−95817
$KZnF_3$:Ni^{2+}, Mn^{2+}, interference transition electric dipole mechanism 80−34896
Kb_2S_3, condensates, struct. and optical transmittance 80−20727
Kr, film, absorpt. in exciton region 78−52529
Kr, liquid and solid, absorpt. and luminesc. spectra of self-trapped excitons 79−65893
Kr, solid, reflectivity, Kromers-Kronig anal. 77−73122
Kr:S_2, absorption spectra of matrix-isolated S_2 molecules 77−52139
La compounds, plasma light reflection by free charge carriers 80−11403
$LaAlO_3$, exchange interactions of transition metal ions in orbitally degenerated excited states 80−65512
$La_2Be_2O_5$:Nd^{3+}, optical absorpt. and fluoresc. intensities 80−29793
$LaCl_2$:$U^{3+}(5f^3)$, polarised absorption spectra and energy levels 80−16063
$LaCl_3$:Pr_I optical absorpt. and Zeeman spectra, zero mag. field splitting 79−91482
$LaCl_3$:Pr^{3+}, hyperfine struct. of 6011 Å line, laser-induced absorpt. line narrowing 78−15196
$LaCl_3$:U^{3+}, cryst., spectrum anal., cryst. field parameters 80−76057
LaF_3:Ho^{3+}, laser excited fluorescence absorption spectra, symmetry groups 78−60514
LaF_3:Pr^{3+}, optical transition, spin decoupling and magic angle line narrowing 80−28286
LaF_3:Pr^{3+}, ultrahigh resolution photon echo spectroscopy 80−28285
LaF_3:Pr^{3+}, ultraslow optical dephasing 80−58648

visible and ultraviolet spectra of inorganic solids continued
LaF_3:Pr(Nd)(Sm)(Eu)(Gd)(Dy)(Ho)(Er)(Tm), cryst. field anal. of triply ionised ion spectra 80−2796
La_3NbO_7, weberite-type, elec., mag. and opt. props. 77−85212
$La_{2-x}Nd_xTi_2O_7$, luminesc. and absorpt. props. 79−65928
LaOF, features of formation of band structure 79−33232
La_2S_3, optical props. and electronic struct. in fund. absorpt. region 80−80817
La_2S_3 single crystals, optical props. 79−87458
$La_{1-x}Sr_xVO_3$, high-temp. transport meas. and optical props. 77−11917
Li aggregated deposits, optical props., 1-6 eV 77−66549
Li deposits, optical consts., 0.5-10.7 eV, Kramers-Kronig anal. 77−40201
Li film, optical absorpt. spectra, rel. to phase struct. 77−4651
$Li_2Ag_{2-x}In_x$, optical props., struct., energy bands, interband transitions 78−72539
β-LiAl, optical dispersion, room temp. reflectance spectra 80−66195
LiBr:$Cu^{2+}(Ni^{2+})(Co^{2+})(Fe^{2+})(Mn^{2+})$, optical absorpt., charge transfer spectra 80−2797
LiC_6 intercalation cpd., synthesis method and reflectivity spectrum 79−15600
$Li_2Cd_{2-x}In_x$, optical props., struct., energy bands, interband transitions 78−72539
LiCl, refr. index, 300-700 nm., temp. coeff., 100-580K *(Russian)* 78−15142
LiCl:Ag, fluoresc. and UV absorpt. spectra 80−80844
LiCl:Cu^+, 3d→4p transitions, near UV absorpt. spectrum assignment 78−27272
LiCl:$Cu^{2+}(Ni^{2+})(Co^{2+})(Fe^{2+})(Mn^{2+})$, optical absorpt., charge transfer spectra 80−2797
LiCl-D_2O, aq. 10 M glass, optical absorpt. spectra after X-irrad., electron scavenging efficiency 79−83476
LiCl-D_2O glass, trapped and quasifree electrons optical transitions, bound-continuum character 78−6660
LiD, cubic cryst., exciton-phonon interaction and exciton anisotropy 78−72083
LiD(H), excitons and exciton-phonon interaction, refl. spectra meas. 4.9 to 5.3 eV 77−44019
$LiErF_4$, spectroscopic anal. Er^{3+} polarised absorpt. spectra, cryst. field parameters 79−95756
LiF, alkali ion implantation, migration, segregation, effect on optical props. 80−100269
LiF, coherent radiation generation in F_2-centres 78−50782
LiF, electron irrad., transport of valence band holes, optical absorpt. obs. 79−99188
LiF film, electronic excitations, inelastic electron scatt. spectra 77−32479
LiF, influence of neutron irrad. temp. on F-aggregate centre form. 78−72561
LiF, M-centre vibronic absorpt. spectra, elec. field, method of moments 78−27186
LiF, R core exciton thermotransmission and absorpt. spectra, line shapes, forbidden and allowed excitons 79−73968
LiF, TLD phosphor, Z_3 centre, thermolum. and optical absorption spectra 79−24374
LiF, TLD-100, trapping centres, optical absorpt. spectra defect and thermolum. mechanism models 80−50436
LiF, ultralow loss optical fibre material, loss mechanism 80−78920
LiF:Fe^{3+}, optical absorpt., 200-750 nm 78−39576
LiF:Mg, dependence of optical absorpt. on temp. during X-ray irrad. 80−66237
LiF:Mg, TLD-100, thermolum. phosphor, photolum. and absorpt. spectra, thermolum. mechanisms 80−97321
LiF:Mg, X-irrad., colour centres, ESR and UV asborpt. meas. 80−108069
LiF:Mg, X-irrad. induced sensitisation mechanism, optical absorpt. spectra 80−60637
LiF:Mg, Z_2- and associated Z-centres, elec. cond., ionic thermocurrent, and optical absorpt. meas. 80−107229
LiF:Mg,Ti, thermolum. related Z-centres, optical absorpt. bands 78−23540
LiF:Mg,Ti crystals, Z_3-centres, correlation of thermoluminescence and optical absorption 80−45154
LiF:$Mg^{2+}(CO^{2+})$, X-ray induced UV absorpt., band shapes, F- and Z-centers 77−20889
LiF:OH crystals, X-irradiated, H centres formation and annealing 80−54226
LiF:U_3O_8, X- and γ-irrad., U^{5+} luminesc. molecular centres, optical and ESR expts. 77−48224
LiF:U^{5+}, absorption and laser-excited fluoresc. 79−99927
LiF+UO_2^{2+}, optical spectra, 2000 to 6000 Å 77−81129
$Li_{0.5}Fe_{2.5}O_4$, magneto-optical Kerr effect, reflectivity spectra 80−66157
$Li_{0.5}Fe_{2.5}O_4$, magnetooptical spectra, polar Kerr rotation, dielectric tensor elements spectra 80−40091
$Li_{0.5}Fe_{2.5}O_4$, polar Kerr rotation spectra, 2-5.7 eV, comparative study with YIG 79−47413
$Li_{0.5}Ga_{0.85}Cr_{1.625}O_2$ spinel, tetrahedral coordination of Cr^{3+} ion, electronic spectra, X-ray and neutron diffr. *(French)* 79−65031
$Li_{0.5}Ga_{2.5}O_4$-$CuCr_2O_4$ system, phase diagrams, IR spectra, Cu^{2+} electronic spectra *(French)* 78−51461
LiH, cubic cryst., exciton-phonon interaction and exciton anisotropy 78−72083
LiH, excitons, reflection, cathodolum. and photocond.-excitation spectra 78−10989
LiH, formation and annihilation of Li colloids and H bubbles 80−107228
LiH, single crysts., refl. photolum., cathodolum., and photocond. meas. 77−52186
LiH(D), isotope effect on Wannier-Mott exciton levels 80−103633
$LiHoF_4$, spectroscopic anal., Ho^{3+} polarised absorpt. spectra, cryst. field parameters 79−95756
LiI crystal, irradiated at low temps., optical absorption spectra 80−45123
LiI, reactor irrad., absorpt. spectra 79−65902
LiI:Pb, absorpt. spectra of Pb^{++} centres 80−76058
LiI:Tl, absorpt. spectrum obs. 80−50378
$LiIO_3$, circular dichroism and UV absorpt. spectra, optical activity 77−20879
α-$LiIO_3$, energy band struct., nonlinear optical absorpt. obs. 79−64277
$LiIO_3$, visible and UV refr. indices 78−19439
$Li_{1-x}K_xI$, intrinsic optical absorpt. spectra 78−23500

visible and ultraviolet spectra of inorganic solids continued
Li_3N, optical absorpt. coeffs., exciton creation, optical anisotropy 79−95796
Li_3N, superionic conductor, cryst. growth and struct., phys. props., book contrib. 79−42308
$Li_{1-x}Na_xBr(I)$, intrinsic optical absorpt. spectra 78−23500
$LiNbO_3$, dispersion of quadratic optical susceptibility *(Russian)* 77−3635
$LiNbO_3$ doped with transition metal oxides, absorption spectra temp. depend. 77−90176
$LiNbO_3$, energy band struct., nonlinear optical absorpt. obs. 79−64277
$LiNbO_3$, exciton migration, laser time-resolved spectra obs. 79−69861
$LiNbO_3$, pure, two-photon photorefractive recording 78−31220
$LiNbO_3$, refractive index, temp. depend. over 300 to 620 nm *(Russian)* 78−56451
$LiNbO_3$, transition metal doped, photovoltaic effects, spectroscopic investigation 77−20365
$LiNbO_3$, two-photon and X-ray induced Nb^{4+} and O^- small polarons, ESR and optical absorpt. 78−76306
$LiNbO_3$:Co_x optical props. 78−64383
$LiNbO_3$:Cu^{2+}, EPR and optical spectra 80−20453
$LiNbO_3$:Fe, characts. for holographic storage appls. 77−23630
$LiNbO_3$:M, (M=Cr,Mn,Fe,Co,Ni,Cu), absorpt. spectra, 0.3-2.0 μm *(Russian)* 77−20898
$LiNbO_3$:Ni optical absorpt. spectra 80−71450
LiNd phosphate glass, spectral and generation props. 77−1700
$LiNdP_4O_{12}$, laser emission cross sections, fluorescence spectra, radiative lifetimes, quantum efficiency 80−23694
Li_2O, neutron irrad. effects, optical absorpt. spectra 80−75271
Li_2O-Al_2O_3-P_2O_5:V^{4+}, glass exam. of ESR spectrum of V^{4+}, optical spectra, and structure 78−88180
Li_2O-B_2O_3:Tl^+(Pb^{2+})(Bi^{3+}) glass, optical basicity, variation with probe ion and comp. 80−2800
Li_2O-B_2O_3-WO_3 glass, photochromic and electrochromic props. 79−28787
Li_2O_1 fund. optical absorpt. edge, number of displaced atoms from $^6Li(n,\alpha)^3H$ reaction 78−51594
(Li_2O-Al_2O_3-SiO_2):Fe_2O_3, glass, pyroceramic form., colour centres, magnetochem. investig. 77−16537
$LiRF_4$, R=rare earth, laser matrices prep. and characterisation 77−24945
$Li_{1-x}Rb_xI$, intrinsic optical absorpt. spectra 78−23500
$LiSO_4.H_2O$:Cr^{3+}, single cryst., EPR and optical absorpt. spectra 80−39855
$LiTaO_3$, single crysts., Czochralski growth in air and N_2, optical transmission curves 79−33922
$LiTbF_4$, $LiTb_{0.5}Y_{0.5}F_4$, and $LiTb_{0.25}Gd_{0.75}F_4$, Faraday rotation, optical absorpt. spectra and refr. index 78−72542
$LiTbF_4$, mag., optical, magneto-optical behaviour 78−68484
$LiTbF_4$, Tb^{3+} absorption spectra, 4000 to 25000 cm^{-1} 78−72550
$LiTmF_4$, spectroscopic anal., Tm^{3+} absorpt. spectra, cryst. field parameters 79−95757
$LiYF_4$, electron-irrad. induced defects, optical and EPR study, impurity effects 80−66238
$LiYF_4$ UV reflectance, transmission and photoluminescence obs. 79−15488
LuAG:Nd^{3+}, cryst. field anal. 78−64013
$LuAlO_3$:Er^{3+}, $^4S_{3/2}$ to $^4I_{9/2}$ transition laser action, optical and luminescence spectra 80−16082
$Lu_3Ga_5O_{12}$:Nd^{3+}, cryst. field anal. 78−64013
LuH_2, electronic struct., optical studies, 0.2-5 eV, 4.2-340K 79−78005
(Mg, Fe)SiO_3, orthopyroxenes, cation distrib., electronic and Mossbauer spectra 80−7370
$(Mg,Fe)_2SiO_4$, olivine, fayalite rich, single cryst., UV absorpt. spectra at high press. 78−85545
Mg, deposits of different roughness, refl. drops and surface plasmons 77−20392
Mg film, optical cond. energy derivative spectrum 77−66551
$MgAl_2O_4$, radiation damage, optical absorpt., F-centres 80−64994
$MgAl_2O_4$, spinel, γ-irrad. effect on optical absorpt. and thermolum. spectra 77−85759
$MgAl_2O_4$:Cr^{3+}, exchange parameters determ. from emission and luminesc. excitation spectra 77−52160
$Mg_xCd_{1-x}Te$, electroreflection spectra, comp. depend. 80−66230
MgF_2, 0.36 μ absorptance/fluence dependence obs. 79−15506
MgF_2, disordered film, optical transitions as function of prep. conditions 78−27340
MgF_2 film, optical absorption meas. rel. to prep. conditions *(French)* 77−44078
MgF_2 films, electronic transitions near optical absorpt. edge, depend. on prep. conditions *(French)* 77−63429
MgF_2, optical absortion following pulsed electron irrad., 100-500K 79−8164
MgF_2, transient absorption and luminesc. following electron beam excitation 77−69920
MgF_2, vac. u.v. transmission, anisotropy effect 77−797
MgF_2:Co^{2+}(Mn^{2+}), Coulomb and exchange interaction consts. optical spectra line assignment, new technique 80−45124
MgF_2/In/MgF_2 struct. surface plasma wave optical excitation in In 79−91516
$Mg(NH_4)_2(SO_4)_2.6H_2O$:Cr_2O^{2-}, optical absorption study, $Cr_2O_7^-$ and CrO_4^{3-} centres 80−55128
MgO, electron irrad., V^--centres, stress-induced optical dichroism, absorpt. spectra 79−61406
MgO, Fe^{2+} and Fe^{3+} conc. and valency, optical density, EPR and MCD obs. 77−89462
MgO, free film and Au substrate, transmission spectra and photoemission characts. 77−24925
MgO, ion irrad. induced vol. changes, optical absorpt. expts. 77−59053
MgO irradiated with Li^+ and K^+ ions, optical props. of metal aggregates 79−65907
MgO, neutron irrad., MCD, optical absorpt. lines 77−77255
MgO:Cr^{3+}, emission and excitation spectra 80−93387
MgO:Fe crysts., oxidised and reduced, optical absorpt. spectra at low temps. 77−63436
MgO:Fe^{3+}, Mn^{2+}, X-irrad. induced anion Frenkel defects, stabilisation by Fe^{3+}, optical and ESR obs. 77−68969
MgO:Ga, γ-irradiated, EPR and optical studies 79−73809
MgO:Li, $[Li]^0$ defect, high temp. and ionisation induced effects 78−34509
MgO:Li, $[Li]^0$ defect, stress induced optical dichroism 78−35179

visible and ultraviolet spectra of inorganic solids continued
MgO:Li, $[Li]^0$ defects, magneto-optical props. 77−12365
MgO:Li, mech. deformed crysts., imprinting of slip bands using Li impurities 80−59473
MgO:Li, oxidation and reduction up to 1700K, defect prod. 79−39013
MgO-Al_2O_3 spinel crysts., thermolum. spectra 79−65938
MgO-Fe^{2+}, shock compressed absorpt. spectrum, appl. to Earth mantle 80−90039
MgO-P_2O_5-Al_2O_3-$3P_2O_5$ glass, absorpt. shift, electron and hole traps, thermolum. meas. 79−65897
$MgSO_4.7H_2O$:$(Cu[H_2O]_6)^{2+}$, EPR and optical spectra anal. 79−38377
Mg_2SiO_4:Tb, thermolum. phosphor, photolum. and absorpt. spectra, thermolum. mechanisms 80−97321
$Mg_xZn_{1-x}Te$, band struct. refl. spectra meas. 80−80813
$Mg_xZn_{1-x}Te$, high purity, luminesc. and band gap 78−68553
$Mg_xZn_{1-x}Te$, spin orbit splitting, of electron energy levels, reflectivity meas. 79−69479
$Mg_xZn_{1-x}Te$, temp. depend. of energy gap, near band gap reflectivity spectra 79−28786
Mn ferrites, Fe-excess, charge carriers, optical props. 80−34874
Mn halogenides, optical spectra, metal-ligand bonds *(Russian)* 79−51986
MnAs, optical props., 0.3-14 eV 77−52122
$MnAs_{0.85}P_{0.15}$, optical props., 0.3-14 eV 77−52122
$MnAs_{0.88}P_{0.12}$, excitonic absorpt., derivative refl. spectra 80−25406
$MnAu_2$, helical antiferromagnetic compound, optical props. and electronic struct., visible and IR obs. *(French)* 80−45101
$MnAu_2$, helical antiferromag., optical absorpt., density of states 80−66224
$MnAu_2$, optical consts., 0.5-3.5 eV, intra-and interband absorpt. *(French)* 78−10916
$Mn(CN)_3.(H_2O)_{0.57}$, mag. interactions, theory 80−97085
$MnCl_2$, $MnBr_2$, mag. phase diagram, optical absorption meas. 77−4514
$MnCl_2.2H_2O$, magnetically ordered phase, $^6A_{1g}$ to $^4T_{2g}$ transition absorpt. lines, Zeeman effects 78−6699
$MnCl_2.2H_2O$, ordered, paramag. phases, optical absorpt. spectra, V-lines, Zeeman effects 78−6698
$MnCl_2.2H_2O$, paramag. phase, external mag. field depend. of $^4T_{2g}$(II) Kramer doublets of Mn^{2+} 78−6700
MnCuBi film, optical and magneto-optical props. 77−4695
$MnCu_{1-x}Dy_xBi_{0.86}$ film, mag. and magneto-optical props., appl. as storage medium 77−8550
MnF_2, MCD spectrum, Zeeman splitting of purely excitonic lines 77−40262
MnF_2, radiation damage, optical absorpt. and luminesc. expts. 78−2161
MnF_2, two-exciton many photon absorption, effect of statistical props. of light on intensity *(Russian)* 78−95589
MnF_2, zero-field splitting of Mn^{2+}, appl. of complete d-electron calc. 77−15799
$Mn_xFe_{3-x}O_4$, dielec. function and polar Kerr rotation, 0.5-3.6 eV 80−66221
$Mn_xFe_{3-x}O_4$, optical props. 80−20606
MnO, absorption line shape, magnon sidebands 77−52128
MnO, cubic antiferromag., magnon-phonon sideband in fine-struct. of optical absorption 77−59590
MnO, linear optical anisotropy meas. at antiferromag. transition 77−36205
MnO, magnon-sideband lineshape, exciton-phonon interaction effects 80−65846
MnO, optical absorpt. spectra fine struct. 77−32393
MnO-Al_2O_3-SiO_2 glass, optical spectra 78−68528
MnSb, optical props., 0.05 to 5 eV 77−48194
Mn_nSi_{2n-m}, thermoelectric and optical props. 78−91714
$MnSiF_6.6H_2O$, optical absorption spectra, 77-300K, assignments 77−36259
MnZn ferrite, optical refl. and electroreflection spectra obs. 78−27262
Mo complex, halogenoxomolybdenum (V), cryst. and electronic struct., reactivity 77−76369
Mo complexes, bis-carboxylate Mo(V), struct. and catalytic reactivity 77−77804
Mo complexes, dinuclear, chem. and spectroscopic props. 77−77239
Mo complexes with poly(iminoethylene)-dithiocarbamate polymer, synthesis and spectra 77−77189
Mo cpds, chemistry and uses, conf., Oxford, Eng., Sep (1976) 77−77749
Mo, thermoreflectance spectra, 0.3 to 6 eV rel. to band struct. calcs. 77−66521
MoO_2, optical conductivities and dielec. functions in 0.2-6 eV range, rel. to band struct. 79−42938
MoO_3 film, optical absorpt. after ion irrad., appl. to ion beam profile monitoring 79−26181
MoO_4^{2-}, in halide salt aqueous solution, absorpt. spectra, 4.2 to 290K *(Russian)* 78−60499
$Mo_6O_{19}^{3-}$, in Mo/SiO_2 supported catalyst system, EPR, UV-visible spectra 79−99764
MoS_2, excitons, mag. circular dichroism and wavelength modulated reflectance meas. 79−23900
$MoS_2(Se_2)$, effect of uniaxial stress on excitonic optical spectra 78−84606
$MoS_2(Se_2)(Te_2)$(2H) polytypes, Kramers-Kronig anal. of reflectivity spectra, 0-30 eV, band model 79−51976
MoS_2(2H), electro-absorpt. edge spectra, cryst. thermal modulation, exciton state field ionisation 79−61395
$MoSe_2$, exciton spectra 80−97296
$MoSe_2$, excitons, mag. circular dichroism and wavelength modulated reflectance meas. 79−23900
$(Mo_xV_{1-x})_2O_5$, mag. and spectroscopic investigation 80−25206
N_2 solid, refl. spectra, 500-1300 Å 79−33724
N_2, solid, UV spectra, phonon induced exciton fine struct. 79−15477
$NH_4Al(SO_4)_2.12H_2O$, CrO_4^{3-} centres, EPR and optical absorption spectra 79−91475
NH_4Br, thermorefl. spectra, band energy anal. 77−12402
NH_4Br:Cu^{2+}, ESR and absorpt. spectra, 300-1500 nm 78−60492
NH_4Br:Tl, absorption, excitation and fluorescence spectra 79−33824
NH_4Cl, thermorefl. spectra, band energy anal. 77−12402
NH_4Cl:$[MoOCl_5]^{2-}$, single cryst., struct. investigations 77−66524
NH_4Cl-TlCl, mixed phosphors, diffuse absorption spectrum 79−24342
NH_4ClO_4, formation of colour center by X-irradiation, optical absorption spectra 79−19247
NH_4ClO_4:Co^{2+}, optical absorpt. spectra 77−66523
$(NH_4)_2CrO_4$, investigation by diffuse reflectance spectroscopy 78−88326
$NH_4H_2PO_4$, electronic struct., UV reflection spectra and XPS 79−38558

visible and ultraviolet spectra of inorganic solids continued
$NH_4H_2PO_4$, ferroelec., electronic struct. study *(Japanese)* 79−87463
$NH_4H_2PO_4$, Pockels effect in UV region 77−12398
$NH_4H_2PO_4$, vac. UV transmission 77−73150
NH_4I, thermorefl. spectra, band energy anal. 77−12402
$(NH_4)_2SO_4:MnO_4^-$, X-ray irrad. damage, optical absorpt. spectra study 80−66246
$(NH_4)_2Zn(SO_4)_2:Ni^{2+}$, optical absorpt. spectrum, room and liq. air temp. 79−15499
$(NPCL_2)_3$, trimer and polymer, polycrystn., resistivity 77−51735
Na salts, spectral refl. changes and luminesc. during 2-10 keV proton bombardment, implications for Io 79−96950
Na, UV absorpt. spectra 80−2780
Na-Fe fluorophosphate glass, Mossbauer study, mag. and optical props. 80−16065
NaA zeolite:S, optical spectra 78−88342
$Na_6Al_6(Si_{0.99}Ge_{0.01})_6O_{24}.2NaBr$, Ge-doped sodalite powders, UV absorpt. band 80−71452
$Na_4Al_3Si_3O_{12}Cl:Br,Ge$, sodalite, reflectance and luminescence obs. 79−4839
$Na_8(Al_6Si_6O_{24})Cl_2$, sodalite, photochromism, ESR and optical spectra obs. 77−32407
$Na_6Al_6Si_6O_{24}.NaX_{(2-n)}$, (X=Cl, Br, I), X-ray irrad., thermal-erase cathodochromism and dihalide mol. centres *(Russian)* 80−66236
NaBr powder coloured in electrodeless discharge, reflectance spectra, thermoluminescence props. 78−6796
NaBr, Stark effect of F-centre obs. 77−1707
$NaBr:Ag^+$, UV absorption bands, temp. depend. 80−20672
$NaBr:Cu^+$, absorpt. spectra, pressure effects up to 6 kbar, comparison with $NaCl:Cu^+$ 79−4826
NaBr:Pb, absorpt. and emission spectra of Pb centres 79−78717
NaBr:V, covalency effects, EPR and optical spectra 77−85557
$NaBrO_3$, dispersion of Faraday effect 80−2731
$NaBrO_3$, single crystals, thermolum., optical absorpt., X-ray effect 79−95858
NaCl, absorpt. spectra, influence of elec. field 80−2794
NaCl, additively coloured, sensitised with O, photochromic props. 79−28792
NaCl crystals irrad. by high electron doses, annealing, colour centre prod., absorpt. spectra study 80−2074
NaCl, energy of form. of Schottky defects 77−7714
NaCl, F-centers, laser irrad. optical bleaching kinetics 80−66244
NaCl, gamma irradiated, optical bleaching of colour centres, F-aggregate centre form. 79−95813
NaCl, gamma irradiation, optical and thermal bleaching of colour centres, trapped electron centre form. 79−95814
NaCl, m-crocryst. powders coloured in electrodeless discharge, reflectance spectra, thermolum. 78−15238
NaCl, neutron irradiated, induced flow stress and optical absorpt. 77−62569
NaCl, photoemission exam. of Na^+-2p core excitons 78−43982
NaCl plates, γ-irrad., optical absorption spectra, hologram recording samples 78−17878
NaCl, thermoluminesc. and optical absorpt., simultaneous DC field and X-irrad. 79−99956
NaCl:Ag, absorpt. spectra, influence of elec. field 80−2794
NaCl:Au, EPR and optical absorpt. 78−39397
NaCl:Ca, Z_1 centre thermoluminescence study 80−16109
NaCl:Cu, UV absorpt., emission, excitation spectra, Cu^- centres 77−81127
$NaCl:Cu^+$, electrolytically coloured, electron trapping, optical absorpt. 80−100672
$NaCl:Eu^{2+}$, optical absorpt. meas. for Eu^{2+} conc. determ. 79−51137
$NaCl:Eu^{2+}$, single cryst. optical absorpt. spectra 80−45117
$NaCl:Mg^{2+}(Mn^{2+})(Ni^{2+})(Cd^{2+})(Pb^{2+})$, Z_4-like centre, absorpt. spectra obs. 78−76498
$NaCl:Mn^{2+}$, radiation-induced colouring, room temp. kinetics 79−55736
NaCl:NaOH, $NaNO_3$, oxygen colour centres, spectral absorpt. rel. to annealing 200-600°C 77−69862
$NaCl:NaOH(NaNO_3)$, absorpt. spectra and dielectric losses 78−19524
NaCl:Ni single crystals, VUV spectrum, ionic conductivity, X-ray diffr. 78−92097
$NaCl:O_2^-$, excitation and absorpt. spectra at 2K, O_2^- excited state field 79−56843
$NaCl:OH^-$, UV and IR absorpt. spectra, colour centres transformation 79−28791
$NaCl:Pr^{3+}(Sm^{3+})$, absorption spectra at 4.2 K, anal. 80−7378
NaCl:Ru, absorption bands, complex form. 77−1705
$NaCl:V^{2+}$, elec. field effect on Z-like centres spectrum 80−2802
$NaCl:Zn^+$, X-irrad., EPR and optical absorpt. 78−43642
NaCl-Cu^-, absorpt. and emission spectra, $3d^{10}4s^2 \rightarrow 3d^9 4s^2 4p$ bands 79−24343
$NaClO_3$, dispersion of Faraday effect 80−2731
$NaClO_3$, X-irrad., thermal stability of radiation damage products 79−34324
$NaClO_4$-D_2O, glassy matrix, absorpt. spectra after X-irrad., solvated electrons 79−65903
NaF, excess electron colour centre obs. 77−16343
NaF film on ZnSe plate, absorption coeff. ATR spectroscopy 80−35000
NaF, M-centre vibronic absorpt. spectra, elec. field, method of moments 78−27186
NaF, M-centres, dichroim absorpt., appl. to optical waveguide polariser 79−995
NaF, piezooptical coeffs., 200-600 mμ 77−69800
NaF, X-irrad., colour centres and thermolum. 80−84790
NaF: Mn^{2+}, VUV absorpt. spectrum and EPR 80−55142
NaF:LiF, γ-irrad., colour centre form., reflectance and thermolum. meas. 79−55739
$NaF:Mn^{2+}$, two-step photoionisation, laser-active F_2^+ centre form. 79−963
NaF-SrF_2-CrF_3, glass transition, crystn. and melting temps., optical transmission *(French)* 80−64910
NaI, refr. index, 300-700 nm., temp. coeff., 100-580K *(Russian)* 78−15142
$NaI:Cu^+$, luminesc. of iolated V_K-centres 78−84641
NaI:F, electron-lattice coupling of F-centres, optical props. 80−60641
NaI:Pb, absorpt. spectra of Pb^{++} centres 80−76058
Na_2KSb, evaluation as photocathode material 78−11072
$Na_2KSb(Cs)$, photocathode, optical props. 79−78827
$NaMO_2$, Stark shift of visible absorpt. of NO_2^- 78−19499

visible and ultraviolet spectra of inorganic solids continued
$NaMgF_3$, defects induced by X- and vacuum UV irrad., optical and elec. study 80−107319
$NaMgF_3$, extreme UV spectra, 9-30 eV 78−23486
$NaMgF_3$, optical absorpt. of radiation produced defects 77−28604
$NaMgF_3:Eu^+$, Zeeman absorpt. and luminesc. spectra *(Russian)* 77−69872
$NaMgF_3:Sm^{2+}$, absorpt. spectra and Zeeman effect, 3000-12000 Å, 4.2-295K 79−24341
$Na_2MoO_4(S_4)(Se_4)$ crystals, charge transfer spectra of MoX_4^{2-} complexes 80−54658
NaN_3, UV irradiated, polarised optical absorpt. of F_2^+-, F-centres 77−28605
$NaNO_2$, phonon side bands of triplet absorption 78−76488
$NaNO_2$, vacuum UV spectra and electro-optical prop. *(Japanese)* 79−65900
$NaNO_2$, X-irradiated IR, UV and visible absorption 79−95811
$NaNO_3$, pure cryst., NO_3^- singlet-triplet absorption, Stark effect obs. 79−8153
$NaNdP_4O_{12}$, laser emission cross sections, fluorescence spectra, radiative lifetimes, quantum efficiency 80−23694
Na_2O-Al_2O_3-B_2O_3-SiO_2, CuCl crystal activated photochromic glasses, absorpt. spectra 79−27353
Na_2O-B_2O_3 glass, covered with PbO film, deep penetration of Pb^{2+} ions 78−79535
Na_2O-B_2O_3 glass, γ- or UV-irrad., laser and thermal bleaching of colour centre, absorpt. spectra 79−33744
Na_2O-B_2O_3:Au glasses, Au solubility, oxidation state and opt. absorpt. 80−44321
Na_2O-B_2O_3:Cu^{2+}, glasses, ESR and optical absorpt. 80−34760
Na_2O-B_2O_3-CoO glass, Co^{2+}, ion activated, magneto-optical study 79−65844
Na_2O-B_2O_3-SiO_2:Fe_2O_3, effect of liquid phase separated structure on transparency in near UV and visible regions 79−4823
Na_2O-BaO-SiO_2:Nd^{3+} glasses, absorption and fluoresc. spectra, density 80−25417
Na_2O-CaO-P_2O_5:Co glass, bonding, symmetry meas. 79−46572
Na_2O-CaO-SiO_2 glass, optical props. characteris. in 0.006 to 22 eV region 77−16328
Na_2O-CaO-SiO_2 glass, electronic struct. and optical props. 80−2790
Na_2O-GeO_2-CoO glass, Co^{2+} ion activated, magneto-optical study 79−65844
Na_2O-P_2O_5, metaphosphate glass, active solute doped, absorpt. spectra of radiation products 78−64865
Na_2O-SiO_2 glass, electronic struct. and optical props. 80−2790
Na_2O-SiO_2 glasses, elementary electronic excitations, refl., luminesc., and photoemission meas. 80−84778
Na_2O-SiO_2:Cu^{2+} glass ESR and optical absorption 79−77526
Na_2O-SiO_2:CuO glass, gamma-irradiated, EPR and optical spectra 80−103885
Na_2O-SiO_2-B_2O_3 glasses, phase separation meas. by optical absorption spectra of VO^{2+} *(Japanese)* 79−70414
Na_2O-SiO_2-CoO glass, Co^{2+} ion activated, magneto-optical study 79−65844
Na_2O-SiO_2-$Pr_2O_3(Ho_2O_3)$ glass, magneto-optical props. 79−65894
Na_2O-WO_3 glass containing transition metal ions optical absorption 78−27254
NaOH ice, γ-irrad, ESR and absorpt. spectra of trapped electrons 79−66318
NaOH-D_2O, glassy matrix, absorpt. spectra after X-irrad., solvated electrons 79−65903
$Na_2O.3B_2O_3$, glass, effect of Fe_2O_3 conc. and temp. on UV absorption 77−16340
$Na_3Pr(C_4H_4O_5)_3.2NaClO_4.6H_2O$, absorpt., circular dichroism, and mag. circular dichroism spectra 80−97243
NaRhY zeolite, Rh complexes with CO and methyl iodide ligands, spectrosc. obs. 80−85159
Na_xWO_3, metallic, optical and electronic props. 80−24398
Na_xWO_3, optical props., analysis of free- and bound-electron contribs. 77−77248
Nb alloys, optical props., 0.1-25 eV, band models 78−10892
Nb anodic oxide films, reversible optical changes 78−35580
Nb, BCC lattice, optical prop. in range λ=0.265−18 μ, polarimetric meas. 79−15075
Nb, bulk, optical props., 6.6 to 23 eV 79−4815
Nb, electronic and optical properties 78−91612
Nb, electronic struct., thermoreflectance studies 80−76047
Nb, optical spectroscopy, for investigation of electronic struct. 78−91611
$Nb_3(AlSi)$ film, thermomodulation spectra, 1.1-2.8 eV 78−48250
$NbH_{0.453}$, influence of H on bulk band struct., optical absorptivity spectra obs. 77−89692
NbN, opt. consts. and physicochem. spectra 77−85677
NbN, optical props. and charact. electron energy loss spectra 79−52056
Nb_2O_5 anodic coatings, refr. index and spectral phase change, reflectance meas. 79−43052
$NbS_2Cl_2(Br_2)(I_2)_x$ absorpt. edge spectrum, fine struct. 80−66219
Nd, complex, Nd^{3+}-hexakis-antipyrine triiodide single crysts., polarised absorpt. spectra 78−10922
Nd:glass films for integrated optics, RF sputtering and optical charact. 79−46087
Nd:glass laser rod, piezoelectric detection of photoacoustic signals 78−54467
$NdMoO_4$, photoacoustic spectroscopy, dichroism meas. 78−62227
$Nd_2(MoO_4)_3$, thermo-optical spectroscopy, detection by mirage effect 80−47116
$Nd(NO_3)_3.6H_2O$, optical absorpt. spectra, 4.2K, single crystal, Stark levels 77−81119
Nd_3NbO_7, weberite-type, elec., mag. and opt. props. 77−85212
Nd_2O_3, A-type, optical absorpt. spectrum and paramag. susceptibility 79−56811
Nd_2O_3 powder, piezoelectric detection of photoacoustic signals 78−54467
Nd_2O_3, transmission and luminesc. spectra 79−65929
Nd_2O_3-Al_2O_3-SiO_2 glass, exam. of spectroscopic and luminescent props. 78−88364
Nd_2O_3-SiO_2 glass, exam. of spectroscopic and luminescent props. 78−88364
NdP_5O_{14}, spectral line intensity anal. 78−43888
Nd_2S_3, optical props. and electronic struct. in fund. absorpt. region 80−80817
$Nd_2Ti_2O_7$, transmission and luminesc. spectra 79−65929

visible and ultraviolet spectra of inorganic solids continued
$(NdX_6)^{3-}$, (X = Br, Cl, I), spectral hypersensitive intensity, ligand polarisability contrib. 78−51946
Ne, liquid and solid, absorpt. and luminesc. spectra of self-trapped excitons 79−65893
Ne, solid, bulk and surface excitons, transmission and refl. spectra obs. 79−95340
Ni, absorption spectrum anomalies, 2-3 eV, optical anisotropy *(French)* 78−43893
Ni catalyst, magnetooptical investigation of mag. props. 79−69858
Ni complex, 1,2-benzoquinonedioximates, refl. spectra, 0.5-2.5 eV, Young's modulus and internal friction 78−39562
Ni complex, Ni-hexamethylenetetramine, reflectance spectra 78−31218
Ni, emissitivty and reflectivity, oxide film thickness effect 79−82364
Ni film, even magneto-optical transmission effects, 0.4-1.25 μm 77−32354
Ni, interband optical conductivity, self energy correction 80−2792
Ni, magneto-optical Kerr effect in UV region, electronic struct. 77−52127
Ni, optical consts., influence of temp. and relation to bandstruct. 80−25403
Ni, optical spectrum, anomalous temp. depend. around T_c, band struct. 80−40128
Ni, surfaces, Au-coated and polished, EUV reflection efficiencies 79−14073
Ni Tulton salts, cryst. field spectra in visible and near IR regions, solid dilution effect 80−100666
Ni ultrafine particles for solar energy photothermal conversion 79−100538
Ni-Co(Fe)(V)(Ti), dil., optical absorpt., electronic struct. 80−108227
Ni-Cr, interband absorpt. and refractive index, photoconductivity dispersion function 77−36263
Ni-Cu alloy, optical absorpt. meas. 78−19518
Ni-Ge-SiO, solar selective absorber surfaces, optical behaviour at high temp. 80−101130
Ni-NiO_x-NiS_y, black Ni, struct.-depend. thermal and optical props., rel. to solar thermal conversion 79−79404
Ni-pigmented anodic Al_2O_3, for selective absorpt. of solar energy, optical and struct. props. 80−55892
β'-NiAl, electronic struct. and optical props. 80−97228
$NiAl_tFe_{2-t}O_4$, Kerr effect, magneto-optical refl. spectra 79−82954
NiAs, optical props., 0.05-5 eV 77−48194
$NiBr_2$, thermoreflectance meas. 77−24866
$NiCl_2$, thermoreflectance meas. 77−24866
$NiCr_xFe_{2-x}O_4$, magneto-otpical refl. spectra by equatorial Kerr effect *(Russian)* 77−32400
NiF_2 film preparation and characterisation 80−59815
$Ni(H_2V)_2(H_2O)_2$, synthesis and characterisation *(French)* 80−45225
Ni_3Mn thin films, transmission spectra, structural order depend. 80−66318
NiO doped glass, improved band-pass characts. 78−42394
NiO-MgO, ESR and refl. spectra, Ni^{2+} distrib. 79−33745
NiP amorphous alloy, heat treatments influence on opt. props., struct. and DC resist. obs. 80−80892
NiSb, optical props., 0.05 to 5 eV 77−48194
$NiSiF_6.6H_2O$, and hexadeuterate, optical absorption spectrum, 300 and 80K 79−73966
Ni_xZrS_2, fundamental optical absorption edge 79−99904
Ni(100) platelet surface optical and magneto-optic consts. 78−15151
α-O_2, antiferromagnetic polycrystal, splitting of exciton absorpt. lines in mag. field *(Russian)* 80−103943
α-O_2, cryst., exciton, exciton-magnon, and biexciton absorpt. at 1.5K 80−84750
α-O_2, cryst., exciton effects, spectra *(Russian)* 79−47481
O_2, cryst., polyexciton light absorpt. *(Russian)* 78−27251
α-O_2 crystals, absorption line biexciton polarisation *(Russian)* 80−89028
α-O_2 crystals, spin ordering effect on light absorpt. *(Russian)* 80−89029
α-O_2 crysts., absorption band at 1.3K, $^1\Sigma_u^- \leftarrow {}^3\Sigma_g^-$ transition *(Russian)* 77−48186
O_2, film, spectroscopy, using Lummer-Gehrcke interferometer 77−5898
PH_3, core-excited states, valence-Rydberg mixing and term values, XUV spectra and CI calc. 79−76444
PLZT ferroelectric thin films, epitaxial growth and optical props. 80−70543
PLZT, opt. spectra and luminesc. 78−76508
Pb film, polycrystalline, optical transitions from d core states 77−85827
Pb film, vacuum deposited, reflectance spectra, structural rearrangement effects 77−24905
$(Pb_{1-y}Ba_y)_{1-x}La_xNb_{2-x/5}O_6$, transparent ferroelec. ceramic, optical transmittance, electrooptic props. and Curie temp. 77−32395
$PbBr_2$, red luminesc., absorpt. spectra 80−2831
$PbBr_2$, reflectance spectra, exciton peaks 77−24870
$PbBr_2(Cl_2)$, exciton spectra, temp. and press. effects 77−20881
$PbBr_2(Cl_2)$, light sensitive material, regularities in exciton states 77−20885
$PbCl_2$:NaCl, trapped exciton states, absorption spectra 80−50383
$PbCl_{2-2x}I_{2x}$, orthorhombic, absorpt. spectra 77−59633
$PbCo_2(PO_4)_2$, mag. susceptibility, elec. cond. and optical refl. 79−56495
$PbCrO_4$, investigation by diffuse reflectance spectroscopy 78−88326
PbF_2 optical props. 77−32394
PbF_2-Na_3AlF_6, semitransparent wide band dielectric mirror synthesis using dispersive and absorbing materials 79−89986
PbFBr(Cl), reflectance spectra, exciton peaks 77−24870
$Pb_5Ge_3O_{11}$, light scatt. meas., central peak dynamics at ferroelectric transition 77−4606
$Pb_5Ge_3O_{11}$, uniaxial ferroelectric, optical activity dispersion 78−48141
$Pb_{1-x}Ge_xTe$, solubilities, elec. and optical props. 77−35940
PbI_2, complex dielectric and optical consts., ellipsometric determ. 78−23425
PbI_2 crystals, exciton condensation, excitation and luminesc. study 80−55182
PbI_2, exciton absorpt. band shape, dielectric const. real part derivatives *(Russian)* 80−25413
PbI_2, exciton spectra depend. on strong excitation, crystal transmission 79−69433
PbI_2, exciton states, high field magnetoabsorption 77−52130
PbI_2, excitons in spatially dispersive medium, absorption theory 80−54618
visible and ultraviolet spectra of inorganic solids continued
PbI_2, film, fundamental absorption edge, complex dielec. const. *(Russian)* 77−40266
PbI_2 film, highly excited, oscillator strength of excitons, absorpt. and emission spectra 78−76001
PbI_2 film, photolyzed, refr. index change 78−11010
PbI_2, film, spectral depend. of optical consts. on fundamental absorption edge *(Russian)* 77−16415
PbI_2, film exciton spectrum, Faraday rot. 77−20944
PbI_2, film intercalated with pyridine, UV absorpt. spectrum, Frenkel excitons 77−24864
PbI_2, first-order 2H-4H polytype transition, exciton spectroscopic study 80−59647
PbI_2, high-pressure phase transition, optical props. meas., 300K and 78K 77−51495
PbI_2 intercalated with organic donor mols., cryst. struct. and phys. props. 78−26543
PbI_2 laminar semicond., phase transition of first kind by exciton spectroscopy *(Russian)* 79−82334
PbI_2, layered compound, exciton spectra, surface and stacking fault effects 80−40134
PbI_2, optical props. 77−32394
PbI_2, photoexciton interaction, luminescence spectra, polariton dispersion diagram 80−93397
PbI_2, photolum. and reflectivity temp. depend., cryst. anisotropy effect on electron-phonon interaction *(Russian)* 78−15225
PbI_2, press. depend. of band-gap excitons, 77K, optical absorpt. spectra 79−8157
PbI_2, single cryst., luminesc., photocond. and absorpt. after thermal treatment 79−56855
PbI_2, two-photon absorpt. spectrum 77−52118
PbI_2, UV reflectivity meas., band struct., LCAO calcs. 78−72545
PbI_2, visible exciton spectrum, exciton-phonon interactions, dielectric const. and oscill. strengths 80−25405
PbI_2:KI, trapped exciton states, absorption spectra 80−50383
PbI_2:KI alloys, fundamental abs. edge, potential as solar convertor 80−101128
PbI_2-$PbBr_2$ mixed systems, cryst. growth, struct. and optical props. *(German)* 80−96499
PbI_2-$PbBr_2$, optical spectra, solid soln. struct. 78−48247
$PbMoO_4$, near-edge absorpt. band, fluoresc. and photocond. 77−44017
PbN_6, electronic transitions and energy band struct. 79−74053
PbO film, on vitreous SiO_2, interdiffusion reactions, UV spectroscopy obs. 78−51750
PbO film on Na_2O-B_2O_3 glass, interdiffusion layer 79−51318
PbO glass, reflection spectra 78−88325
PbO layers on Pb films, optical props. 79−83042
PbO, visible absorpt. spectra rel. to indirect exciton transitions 80−60628
PbO-B_2O_3:Cu^{2+}, glasses, ESR and optical absorpt. 80−34760
PbO-SiO_2 glass, electronic struct. and optical props. 80−2791
PbS epitaxial film, struct., optical and elec. props. 78−19583
PbS(Se), valence band struct. determ. by optical absorpt., size quantization effects 80−59871
$PbSe_{0.5}S_{0.5}$, valence band struct., absorpt. spectra, elec. props. 80−44505
$Pb_xSn_{1-x}I_2$, thin films, photosensitivity, ageing and annealing effects *(Russian)* 78−6804
$Pb_xSn_{1-x}O_2$ film, optical props. 78−39616
$Pb_{1-x}Sn_xTe$, electroreflectance, Faraday rot., elec. band struct. parameters 77−66113
$Pb_{1-x}Sn_xTe$ film, pure and Bi doped, polycryst., struct., elec., optical props. 79−42542
$Pb_{1-x}Sn_xTe$, reststrahlen band, reflection spectra 79−8162
$Pb_xSn_{1-x}Te$, RF-sputtered epitaxial single-cryst. films, thermorefl. spectra 77−63476
p-PbTe, thermorefl., 1.0-4-6 eV 78−76492
PbTe very thin epitaxial films, transmission and refl. spectra, 1 to 5 eV 80−7430
PbTe:Na, In, high temp. Fermi level position 79−90948
PbTe:Tl, absorpt. coeff. spectral depend. 80−93370
$PbTi_3O_7$, photocond. and optical transmission 78−64058
$PbWO_4$, Czochralski growth method, optical props. 78−60566
$Pb(WO_4)_{1-x}(MoO_4)_x$ mixed crystal, growth by Czochralski method, props. 78−60566
Pd complex, 1,2-benzoquinonedioximates, refl. spectra, 0.5-2.5 eV, Young's modulus and internal friction 78−39562
Pd, electronic struct. determ. by relativistic APW method, rel. to UV spectroscopy 77−4289
Pd, optical properties, 0.1 to 6 eV 78−92092
Pd, thermomodulation spectra of high-energy interband transitions 80−108226
$PdH_{0.65}$ film, thermoreflectance spectra 78−56463
PdIn, refractive index, reflectivity and band struct., APW calcs. 80−40139
PdO, optical props., 0.5-5.4 eV 79−56813
PdO, semiconductivity and stability, optical props. 78−43497
$Pd_{81}S_{19}$ and $Pd_{84}Si_{16}$, metallic glasses, optical refl. spectra and optical consts. 79−87464
Pr compounds, plasma light reflection by free charge carriers 80−11403
Pr IV salts, $4f^2$ config., semiempirical eqns. for deciphering spectrum 77−24874
Pr^{3+} hexa-antipyrene triiodide, single cryst., polarised absorpt. spectra 77−77234
$Pr(OH)_3$, low temp. heat capacity, thermophys. props. optical spectra, anal. of Schottky contributions, review 80−24611
Pt (100), (110), and (111), form. of Cu monolayer, optical and electrochem. studies 79−99419
Pt complex, 1,2-benzoquinonedioximates, refl. spectra, 0.5-2.5 eV, Young's modulus and internal friction 78−39562
Pt electrodes, chemisorbed H, anion effects on multiple states, reflection spectra obs. 79−43634
Pt evaporated film, optical props. meas. in VUV, 220 to 150 Å 80−45159
Pt, thermomodulation spectra of high-energy interband transitions 80−108226
$Pt(NH_3)_4SO_4$, cryst., absorption spectrum *(French)* 79−28784
PtO film, electrochemically formed, anisotropy of optical constants, reflection spectroscopy and Kramers-Kronig analysis 77−32456
PtO_2, sputtered film, optical props. under H_2 reduction 80−20728
Rb, extreme UV absorpt. spectra, threshold singularities of p-shell absorpt. 77−36261

visible and ultraviolet spectra of inorganic solids continued
Rb halides, high-resolution spectroscopy in far UV 77−66484
Rb, UV absorpt. spectra 80−2780
Rb_2AgCl_3 luminesc., absorpt. and excitation spectra 77−12424
$RbAg_4I_5$ superionic films, elec. cond. and optical absorpt. studies 79−99355
RbBr, UV two-photon absorpt. relative to known Raman cross section 79−81487
RbBr(I), parallel and perpendicular Stark effect of F-centre 77−1703
RbCN, ferroelasticity and F- and M-centres absorpt. 79−87475
$RbCaCl_3$, phase transitions, optical and dilatometric meas. 79−61394
$RbCaF_3$, optical absorpt. of radiation produced defects 77−28604
RbCl:Ag, phosphor, luminesc., absorpt. and excitation spectra 77−12424
RbCl:Au, EPR and optical absorpt. 78−39397
RbCl:Ca^{2+}, thermolum. and optical absorption studies 80−104002
RbCl:Eu^{2+}, optical absorpt. meas. for Eu^{2+} conc. determ. 79−51137
RbCl:Eu^{2+}, tetragonal sites, spin Hamiltonian parameters, EPR and UV absorpt. spectra obs. 80−50177
RbCl:Tl, absorpt. spectra, 210-300 nm 79−87473
RbCl(Br):Eu^{2+}, single cryst. optical absorpt. spectra 80−45117
Rb_2CrO_4, investigation by diffuse reflectance spectroscopy 78−88326
Rb_2CsSb, evaluation as photocathode material 78−11072
RbF-CsF, solid solution, fundamental absorption 79−11433
$RbFeCl_3$, linear chain ferromag., optical absorpt. and dichroism in mag. field 77−77237
$RbFeS_2$, crystal ligand field theory, band assignment, absorpt. spectra study 80−20657
RbI:AgI, thermal reorientation kinetics of I_2^-, decay of optical anisotropy 77−52138
RbI:Pb, absorpt. spectra of Pb^{++} centres 80−76058
Rb_2MnCl, layer antiferromag., optical absorpt., temp. and mag. field depend. 80−20661
Rb_3MnCl_4, quasi-2D-antiferromag., linear birefr. and optical absorpt. spectra 80−71385
$RbMnF_3$, Faraday effect mechanism in paramag. phase 80−60552
$RbMnF_3$, radiation damage, optical absorpt. and luminesc. expts. 78−2161
$RbMnF_3$, reflectivity, 8-60 eV, excitonic struct. 77−20871
$RbMnF_3$, triplet states, piezospectroscopy 79−38562
$RbMnF_3$:Er^{3+}, absorption, emission, excitation and lifetime meas. 80−71460
Rb_2NiF_4, quadratic layer antiferromag., absorpt. 77−16326
Rb_2SnCl_6:$ReCl_6^{2-}$, luminesc. and absorpt. spectra, relax. processes 77−85779
ReO_4^-, in halide salt aqueous solution, absorpt. spectra, 4.2 to 290K *(Russian)* 78−60499
Rh, electronic struct. determ. from optical refl. meas. 77−62812
Ru (11$\bar{2}$0), complex RI meas. in visible region 77−1650
Ru complex, Ru(2,2′-bipyridine)$_3Cl_2$-$6H_2O$, photocond., optical absorpt. and fluoresc. 77−80807
Ru complexes, $[Ru(bipy)_n(pq)_{3-n}]^{2+}$ mixed-ligand, electronic absorpt. and emission spectra meas. 80−71441
Ru, optical props. 79−24282
α-$RuCl_3$, reflectivity and absorpt. spectra, thermo-reflectance 79−47438
S, orthorhombic, photogeneration of charge carriers 80−107844
$(SN)_x$, electronic struct. and opt. props. 78−6256
$(SN)_x$, reflectivity calc. taking account of fibrous struct. 79−87462
$(SN)_x$, reflectivity spectra meas. by synchrotron radn. 79−91513
$(SN)_x$, single cryst., elec. anisotropy, polarised refl. spectra 77−36264
$(SN)_x$, temp. depend. of reflectance spectrum 77−85744
S_2N_2, cryst. and partly polymerised films, Raman scatt., optical absorption 77−8673
S_4N_4, Raman scatt. and opt. absorpt., press. and temp. depend. 77−36227
$(SNBr_{0.4})_x$, metallic, transport and optical props. 77−85724
SbI_3 film, exciton peaks, temp. depend., 90-270K, and press. depend., up to 3500 atm. 77−36265
SbI_3, layered compound, exciton spectra, surface and stacking fault effects 80−40134
SbI_3, refl. spectra of cryst., 300-800nm, and derived optical consts. 79−87456
Sb_2O_3-MgF_2, semitransparent wide band dielectric mirror synthesis using dispersive and absorbing materials 79−89986
Sb_2S_3, amorphous and crystalline thin films, optical consts. 79−91518
Sb_2S_3 film, amorphous and crystalline, optical props. 79−95867
Sb_2S_3, fundamental absorpt. edge, optical props. 79−56817
SbSBr, electronic and optical props. 78−34763
SbSI, band gap photoreflectance spectra near ferroelec. transition 79−38559
SbSI, electronic and optical props. 78−34763
SbSI, energy band struct. from modulation spectra 78−43892
SbSI, ferroelec. semicond., laser-modulated reflectance near T_c 78−72552
SbSI-GeS_2 system glasses with and without antireflection coatings, optical props. 77−8595
SbSeI, electronic and optical props. 78−34763
SbTe, reflection spectra 77−16325
Sc, band structure, density of states, absorpt. spectra, KKRZ calc. 80−70593
Sc, HCP, optical examination of electronic struct. 77−89694
ScH_2, electronic struct., optical studies, 0.2-5 eV, 4.2-340K 79−78005
ScH_2, optical interband struct. and low energy plasmons 78−31200
$Sc_2(WO_4)_3$:Er^{3+}, growth, solubility, absorption spectrum and thermal expansion meas. 77−36391
Se, A1 type metallic phase, optical consts. and refl. 77−32455
Se film, noncryst., controlled vapour deposition, crystn., and optical props. 78−39696
Se formed in chiral polymer matrix, circular dichroism 77−85685
Se, single crystals, fast neutron irradiated, annealing expts., dark conductance, reflectivity spectra 77−85266
Se, threads in natural mordenite channels, optical absorpt., cond. *(Russian)* 80−89022
Se, trigonal reflectivity and density of states press. depend., self-consistent pseudopotential calc. 77−31931
Se-Te-As-Ge glasses, absorpt. spectra, diffuse reflectivity loss correction 79−82995
$Se_{75}Ge_{25}$, obliquely deposited amorphous films, photo-induced optical effects 79−56871
$Se_{1-x}Te_x$, film, struct. and props. 79−99079
Si (111)7×7, dangling-bond surface states and O_2 adsorption, reflectometric study 79−99600

visible and ultraviolet spectra of inorganic solids continued
Si, absorpt. spectrum red shift, spectrum temp. depend. 79−78699
Si, amorphous, discharge produced, optical and photocond. props. 78−39147
Si, amorphous, doping and absorption edge 80−29042
Si, amorphous, photostructural changes, photodarkening 80−49121
Si, amorphous, pure and H doped, picosecond relax. of optically induced absorption 80−97302
Si amorphous film, film, glow discharge deposited, refl. spectra and dielec. function 80−50360
Si, amorphous film, glow-discharge, optical props. *(Japanese)* 79−65946
Si, amorphous film, RF plasma deposition from $SiCl_4$-H_2, characterisation 80−66435
Si, amorphous films, halogenated and hydrogenated, elec. and optical props. 80−97016
Si, amorphous hydrogenated, solar cell material 78−2565
Si, amorphous sputtered films, hydrogenated, photoinduced optical absorpt. 80−50362
Si, CVD prepared solar thermal absorber, temp. variation of absorpt. edge 80−12028
Si, carrier conc. variations using electrolyte electroreflectance, topographical features 79−99562
Si, continuum-exciton effect in optical spectrum 80−25416
Si, dielectric function spectra, ellipsometric determ., many-particle effects at E_1-transition 80−93363
Si, doped and amorphous, $L_{2,3}$ threshold spectra 77−69934
Si, electroreflectance, dielec. function, ellipsometric meas. 79−4790
Si, epitaxial film on sapphire, optical absorption and interface comp. profiles 77−12459
Si, exciton mol. by phonon-assisted two-photon absorpt., theory 78−48197
Si, film, amorphous, optical absorption at high press. 78−35216
Si film, electroreflectance spectra, 2.8 to 5.0 eV, ion bombard. effects 77−1752
Si film thickness meas. from visible refl. spectra 79−99960
Si, free carrier and interband absorpt. at 1.06 μm, temp. depend. 80−2783
Si, glow discharge amorphous film, reflectance and transmittance *(Japanese)* 80−34995
Si, glow discharge deposited, optical spectra, reflectance, dielectric function and oscillator strength 80−11492
Si, high dose self-irrad., spatial correl. between primary and secondary defect profiles 80−59536
Si, impurity doping influence on free-exciton absorpt. 77−69861
Si, ion irrad., temp. and dose depend. of defect profiles 80−29097
Si, ion-implanted, pulsed-laser annealing, dynamic behaviour by optical reflectance meas. 79−69122
Si, light reflection, effect of repeated oxidation 79−52402
Si, optical consts. by unpolarised incident radiation 80−76044
Si, optical excitations, many particle effects 79−87046
Si, optical spectroscopy, absorpt. coeff., lattice vibrs. modes, band gap, acoustic approach 77−69822
Si, optical spectrum, many particle effects, band struct. 80−89024
Si, reconstructed surface (111)2×1, polarization depend. of optical absorpt. spectrum 79−28396
Si, reflectivity time dependence during pulsed laser annealing 80−66214
Si, role of electron-hole interaction in optical spectra, review 80−45113
Si, surface roughness evaluation by UV refl. 80−39393
Si, thinly oxidised wafer reflectance at normal incidence, calc. 79−78641
Si, transition layer form., band struct., electroreflectance 77−16333
Si:Ar(B), implantation doped, electroreflection spectra 79−51983
Si:B amorphous film, CVD prep., EPR, elec. and optical props. 79−4558
Si:F,H, amorphous, elec. and optical props. 80−60031
a-Si:H, influence of H on optical props., H conc. and H bonds 80−76098
Si:H amorphous film, prop. by glow discharge deposition, and plasma parameter effects on props. 80−45240
Si:H amorphous films, photoinduced optical absorpt. and photocond. 80−50361
Si:H(B)(P), amorphous, UV absorpt. spectra 80−25420
Si:P, ion-implanted, optical refl. obs. of damage 78−55883
Si:P, temp. depend. of anomalous struct. in wavelength-derivative absorption spectra 77−52143
Si:P film, polycryst., heavily doped, mobility and carrier conc., optical determ. 80−66314
Si-Au amorphous system, optical absorpt., IR photocond. 79−42582
Si-H amorphous film, reactively sputtered, prep. and props. 79−78889
Si-SiO_2 interface, optical props. 79−99908
SiC (6H), semicond. with one-dimens. electron superlattice, interband optical absorpt. 79−15483
SiC, α- and β-types, electroreflection spectra of natural and low-energy ion-bombard. surfaces 79−61340
SiC, CVD, polished, total integrated vac. UV scatt. 77−62029
SiC film, amorphous, reactively sputtered, effects of S/C ratio and H content on elec. and optical props. 79−90906
SiC ion implanted, laser induced ordering and defects 80−84754
β-SiC, pyrolytic, optical and elec. props. 79−78093
SiC smokes, vapour-condensed, 800 to 130 nm extinction and interstellar extinction curve 80−82180
SiC, struct. of spectrum of excitons bound to neutral B atoms 78−19523
p-SiC:B (4H), absorption spectra of bound excitons 78−88338
α-SiC:H, prepared by reactive sputtering, layer props. *(Japanese)* 80−60695
SiC:Ti (6H), absorpt. spectra of n- and p-type cryst. 79−38581
SiC-Si struct. formation on ^{12}C ion implantation in Si, optical and photoelectric props. 79−91136
SiC_x, amorphous, prepared by glow discharge method, elec. and optical props. 77−21035
SiC(6H), ion-implanted, laser-induced recrystallization and defects 80−44221
Si_xGe_{1-x}:H, amorphous, photoinduced optical absorption 79−82973
Si_xGe_{1-x}(H) amorphous alloys, from glow discharge, optical properties 78−19510
SiH_4, core-excited states, valence-Rydberg mixing and term values, XUV spectra and CI calc. 79−76444
$Si_{1-x}H_x$ film, amorphous, RF sputtered, pure and P(B) doped, optical consts. 79−95866
SiN_x film, plasma deposited, comp. and characterisation, optical and elec. props. 80−15401
SiN_x, film by magnetron sputtering, composition, hardness and optical props. 78−3047

visible and ultraviolet spectra of inorganic solids continued
Si_3N_4, amorphous, $L_{2,3}$ threshold spectra 77−69934
Si_3N_4, CVD, struct., optical and mech. props. 77−1816
Si_3N_4 film, absorpt. meas. 79−78769
Si_3N_4 film, amorphous, optical props., band gap and surface roughness 77−32396
Si_3N_4 film, plasma-activated CVD, optical prop. depend. on growth conditions 77−55892
Si_xN_y, amorphous, prepared by glow discharge method, elec. and optical props. 77−21035
$Si_xN_yO_z$ film, band diagram, optical props. and elec. cond. meas. 78−84333
SiO_2, amorphous, $L_{2,3}$ threshold spectra 77−69934
SiO_2, amorphous, optical and elec. props., comparison with chalcogenide semiconds. 78−6721
SiO_2, electronic struct., review of spectroscopic and theoretical data 77−76749
SiO_2, fused, absorption edge meas. 78−43887
SiO_2, fused, as-received and irrad., dielectric props. 79−65786
SiO_2, fused, for sealed ampoule cryst. growth, thermal transmission function 80−84731
SiO_2, fused, γ-irrad., O-associated trapped-hole centres, optical absorpt. and ESR spectra obs. 79−65729
SiO_2, fused, high-temp. darkening and absorption spectra meas. 77−36258
SiO_2 glass, electronic struct. and optical props. 80−2790
SiO_2 glasses, opt. consts. in IR and vacuum UV 78−27238
SiO_2, optical absorpt. and external photoeffect, 6 to 40 eV 77−55802
SiO_2, RF sputtered, stoichiometry and atomic defects obs. 79−60647
SiO_2, stoichiometric condensate form. during electron beam evaporation of quartz, electrophysical props. 77−16496
SiO_2, thermally grown film, optical absorption and photocond. 78−64421
SiO_2, ultralow loss optical fibre material, loss mechanism 80−78920
SiO_2, vitreous, absorption edge, temp. depend. 77−20867
SiO_2, vitreous, H impregnated, γ radiation effects, hydride, hydroxyl formation 79−87874
SiO_2, vitreous, radiation behaviour of optical props. 78−21655
SiO_2-Al_2O_3-CaO-Na_2O:Fe^{3+}, optical absorpt. due to Fe^{3+} ligand field and charge transfer 80−89020
SiO_2-Al_2O_3-Li_2O:TiO_2(ZrO_2),Fe_2O_3, pyroceramic glass, coloration, absorpt. spectra obs. 77−8615
SiO_2-Na_2O-CaO:Fe(As)(Cr) glasses, optical absorpt. changes on heat treatment 78−31224
SiO_2-Na_2O-Nd_2O_3 glass, magneto-optical props., absorpt. spectrum 80−88969
SiO_2-PbO-K_2O glass, reflection spectra 78−88325
SiO_2-TiO_2-Na_2O glass, optical absorption coeff., 2.1-3.3 eV 77−77240
SiO_x, dielec. and optical props., chemical disorder effects 80−80815
Si_2Te_3, fundamental absorption and Franz-Keldysh effect meas. 77−1694
SiO_2:Ge, B, P, optical fibre, radiation induced optical absorpt. spectra, 0.4 to 1.7 μm region 80−58761
Si(111)2×1, oxide layer, surface states detec., optical reflectivity obs. 80−50368
Sm monochalcogenides, electronic struct., optical props. 0.03 to 12 eV 77−28594
Sm monochalcogenides, valence related optical and other studies, review 78−31215
$SmFeO_3$, orthoferrite, anisotropy of Faraday rotation 79−61341
$Sm_{1-x}La_xS$, press.-induced semicond.-metal transition, refl. and lattice compression meas. 77−62826
SmS, metallic, optical refl. investig. of valence fluctuations 77−63428
SmS, metallic, thermal modulation of reflectivity, 1.2-3.8 eV 79−99909
SmS, metallic, transmission, refl. and absorpt. spectra 78−19587
SmS, optical props. and electronic struct., Kramers-Kronig model anal. 79−69859
SmS, relative intensity of optical bands calc. 77−8603
SmS, semicond. thin film, absorpt. and refl. spectra, fine struct., cond. band extremum 79−69897
Sm_2S_3 films, refl. and transmission spectra at 300K 80−80889
Sm_2S_3-Sm_3S_4, valence related optical and other studies, review 78−31215
$Sm_{0.55}Tb_{0.45}FeO_3$ orthoferrite, optical and magneto-optical props. 79−61396
$Sm_{1-x}Y_xS$, press.-induced semicond.-metal transition, refl. and lattice compression meas. 77−62826
$Sm_{1-x}Yb_xS$, $Sm_{1-x}Tm_2S$ and $SmS_{1-x}As_x$, optical investig. of substitution effects on metal-semicond. transition 77−63427
Sn film, polycrystalline, optical transitions from d core states 77−85827
Sn film, vacuum deposited, reflectance spectra, structural rearrangement effects 77−24905
Sn film, white, optical props. between 2-15 eV 78−19584
Sn-Au(Cu), amorphous film, optical props. 79−69895
$(Sn)_x$, superconducting polymer, elec. cond., heat capacity and optical props. 80−7028
SnI_2 film, absorpt. spectrum *(Russian)* 79−43056
SnI_2, single crysts. and film, optical props. 77−32437
SnO_2 film, CVD using $SnCl_4$-H_2O and $SnCl_4$-H_2O_2 systems, elec. and optical props. 78−52686
SnO_2 film, optical and elec. props., rel. to stoichiometric deviation and struct. 77−47701
SnO_2 film, reactive ion-plasma sputtered, elec. and opt. props. 79−42677
SnO_2, reactive ion plating onto insulating substrates, and elec. and optical props. 79−87588
SnO_2, review 77−1673
SnO_2, rutile, band gap assignment by two-photon spectroscopy 79−19513
$Sn_2P_2(Se_xS_{1-x})_6$, ferroelec. tricrit. phase transform., light transmission study 80−71355
SnS, electron-hole interaction in d-electron excitations, photoelectron and optical spectra 78−34776
SnS_2, 2H and 4H, effect of press. on optical absorpt. edge 77−77238
SnS_2, crystal growth and optical props. in visible and IR regions 77−52114
SnS_2, optical props., modulation spectroscopy 77−52117
SnS_2, optical props. and band struct. 78−2880
SnS_2 press. effects on optical absorpt. edge 77−52119
SnS_2, refl. using Kramers-Kronig anal., optical functions 79−95798
SnS_2, UV reflectivity meas., band struct., LCAO calcs. 78−72545
SnS(Se), dielec. function, optical and electron energy loss spectroscopy 78−15189

visible and ultraviolet spectra of inorganic solids continued
$SnS_2(Se_2)$, optical transitions from d core levels 80−45105
SnS_xSe_{2-x}, thermal changes in optical props. 78−19504
$SnSe_2$, optical props., modulation spectroscopy 77−52117
$SnSe_2$, optical props. and band struct. 78−2880
$SnSe_2$, press. effects on optical absorpt. edge 77−52119
$SnSe_2$, refl. using Kramers-Kronig anal., optical functions 79−95798
$SnSe_2$, single crystal, reflectivity, XPS, UPS, and band struct. 78−6701
$SnSe_2$, thermorefl. spectra 77−90168
$SnSe_2$, UV reflectivity meas. 78−72545
$SrCl_2$:Cu^+, exciton bands, optical absorpt. and MCD spectra 80−80821
$SrCl_2$:Pb^{2+}, intracentre luminesc. *(Russian)* 77−16395
$SrCl_2$:S, S_2^- and S_3^- mol. paramag. centres, investigation using EPR, Raman and optical spectroscopy 79−51855
$SrCrO_4$, investigation by diffuse reflectance spectroscopy 78−88326
$Sr_{2x}Eu_{2-2x}NbO_4$, synthesis and props. 77−52265
SrF_2, 0.36 μ absorptance/fluence dependence obs. 79−15506
SrF_2, neutron irrad., role of F-centres in thermoluminesc. 79−19941
SrF_2, thin film, optical props., spectral dependence, 460-1000 nm 80−76094
SrF_2, U-centre, electronic struct. and optical transition energies, SCF MS Xα calc. 79−4532
SrF_2, UPS and XPS spectra, rel. to optical props. 80−66386
SrF_2, undoped, H-centre prod. by reactor neutron irrad., optical absorpt. meas. 77−59010
SrF_2:CeF_3(GdF_3)(TbF_3), absorpt. spectra of γ-irrad. cryst., 77K, 200-700 nm 78−84615
SrF_2:Na, tunable room temp. laser action of M-centres, luminesc. and absorpt. spectra 79−31907
SrF_2:Pb^{2+}, band struct., Jahn-Teller effect, UV luminesc. and optical absorpt. spectra 80−66243
SrF_2:Pr^{3+}, wavelength and temp.-modulated UV absorpt. 80−2799
SrFCl, thermolum. and optical absorption spectra 80−66309
SrFX, X=Cl, Br, absorpt. and refl. spectra 79−82994
SrO, logarithmic derivative reflectance spectra 80−11429
SrO, luminesc. band edge, 4-6.5 eV, optical absorpt., photoluminesc., cathodoluminescence, photocond. obs. 80−50411
SrO, surface states, reflectance spectra, impurity effects 77−20873
SrO:Ni, optical absorption spectra in visible and near IR region 80−45119
SrO:Ni^{2+}, linear Stark effect for zero-phonon optical absorpt. line 80−80830
$Sr_5(PO_4)_3Cl$:CrO_4^{3-}, polarised absorpt. spectra, visible and IR, ligand field transitions 79−95812
$SrSO_4$, celestite, colouring mechanisms 79−82998
$SrTiO_3$, absorption coeff., reflectivity, 293-853K 78−64342
$SrTiO_3$, energy band struct., two-photon absorption spectra study 80−15453
$SrTiO_3$, pure and Nb doped, heat treated, Hall effect, electrical cond., optical absorpt., defect states 78−47812
$SrTiO_3$, semicond., free carrier optical absorption and scatt. *(Korean)* 78−23489
$SrTiO_3$, UV refl. spectra, optical consts. 0 to 32 eV Kramer-Kronig anal., band struct. calcs. 78−43903
$SrTiO_3$:Fe^{4+}, opt. absorpt. 77−16349
$SrTiO_3$:Ni, photochromism, optical absorption spectra and EPR meas. 77−1708
SrX_2, X=Br, Cl, absorpt. and refl. spectra 79−82994
TGS-TGSe solid solution, temp. depend. of fundamental reflection spectra meas. 77−16337
Ta, and α-TaH_x, electronic struct., thermoreflectance studies 80−76047
Ta, density of unoccupied electronic states, UV isochromat spectra and SXAPS 79−77977
Ta, electronic props. and reflectivity, iterative empirical pseudopot. calc. 77−76745
Ta ion induced continuum emission 80−89025
Ta, optical spectroscopy, for investigation of electronic struct. 78−91611
Ta-W optical props., temp. depend., 4.2-1100K 78−2874
$TaH_{0.257}$, influence of H on bulk band struct., optical absorptivity spectra obs. 77−89692
Ta_2O_5, anodised film, nonuniformities, optical props., spectrophotometric obs. 78−2933
TaS, (1T), effect of CDW on optical spectra 79−95738
TaS_2 mixed coordination polytypes, optical props. 0.5-6.0 eV range, transmission spectra 79−15476
$TaSe_2$, 2H phase, CDW band struct. and IR and visible thermoreflectance meas. 77−28556
$TaSe_2$ (2H), effect of CDW on optical spectra 79−95738
$TaSe_2$ (2H), optical absorpt., band struct., plasmons, and CDW 80−45104
Tb complex, in $Cs_2NaTbCl_6$, f-f transitions, mag. dipole intensities, vibronic coupling model 80−25404
$TbAlO_3$:Nd^{3+}, absorpt. and luminesc. spectra 79−91470
$TbVO_4$, co-operative Jahn-Teller transition, low freq. dynamics, light scatt. study 80−88317
Te, synthetic, optical props. in visible spectrum and microhardness meas. *(French)* 77−28590
Te, trigonal, electronic and optical props., press. depend., self consistent pseudopotential formalism 79−65838
Te, valence band struct. under press., spin-orbit splitting, intraband absorpt. spectra 80−2330
TeO_2, paratellurite, optical absorpt. and refl. spectra, 80-500K, optical consts. determ. 80−50359
TeO_2, visible and UV refr. indices 78−19439
Th, interband structure and role of 5f electronic states, optical reflectivity meas. 77−76744
Th, optical reflectivity 80−16054
$ThBr_4$:U^{4+}, absorpt. spectrum, zero phonon line *(French)* 80−11443
Ti absorption bands in glass fraction of lunar soil 77−49320
Ti, and Ti alloys, surface layer, study using vac. UV spectrograph *(French)* 80−71987
Ti anodic oxide films, reversible optical changes 78−35580
Ti, clean and oxidised surfaces, refl., 2-25 eV 80−55123
Ti, oxidation kinetics, refl. interf. meas. of film thickness 77−90498
Ti-Ni, martensite transform. B2-B19′, optical props. and electron struct. *(Russian)* 80−34878
TiN, opt. consts. and physicochem. spectra 77−85677
TiN, optical props. at 300K 78−19466
TiO_2, deform. pot. meas. of direct forbidden transition 79−95806
TiO_2, electronic energy levels, electrorefl. spectra 77−24870

visible and ultraviolet spectra of inorganic solids continued
TiO_2 films, in Ti-TiO_2-electrolyte system, electroreflectance response 79−42945
TiO_2, fine struct. in intrinsic absorpt. edge 79−42987
TiO_2 optical coatings, deposition, performance 77−88896
TiO_2, resolved quadrupolar transition, absorpt. spectra obs., 1.6K 78−27259
TiO_2, rutile, deuteron and alpha-particle implantation, chemical effects, optical and cond. meas. 78−67755
TiO_2, rutile, optoelectronic props., band struct., theory 80−80175
TiO_2 single cryst., refl. and electrorefl. spectra 78−2870
TiO_2 single cryst., refl. and electrorefl., energy levels 78−2871
TiO_2, unambiguous assignment of fund. absorpt. edge 78−71817
TiO_2, uniaxial stress depend. of direct-forbidden and indirect-allowed transitions, absorpt. edge obs. 79−42990
TiO_2-SiO_2, semicond. glass, optical props. 78−60412
TiO_x, reactive sputtering, film prep. conditions rel. to stoichiometry 77−40370
Ti_2O_3, 3d-T_{2g} band optical transitions near conductivity transitions, temp. depend. 79−19900
Ti_2O_3, metal-semicond. transition, refl. spectra study 80−10880
Ti_2O_3, optical consts., polarisation dependent reflectivity 78−52531
TiS_2, nonstoichiometric, chem. transport reaction mechanism 77−8735
$TiS_2(Se_2)$, vacuum UV reflectivity spectra, cond. band model 77−44012
$TiSe_2$ (1T), effect of CDW on optical spectra 79−95738
Tl, band structure and fermi surface using relativistic APW calc., optical spectra interpretation 77−20231
TlBr, electromodulation spectroscopy of excitons 79−73444
TlBr, phonon struct. of forbidden-indirect transitions 79−61393
TlBr(Cl), electronic state of excitations and their phonon coupling 79−60719
TlBr(Cl), light sensitive material, regularities in exciton states 77−20885
TlCl, electromodulation spectroscopy of excitons 79−73444
TlCl, phonon struct. of forbidden-indirect transitions 79−61393
TlCl, role of electron-hole interaction in optical spectra, review 80−45113
TlCl-TlBr, KRS-6, ultralow loss optical fibre material, loss mechanism 80−78920
TlCl-TlBr mixed crystal, reflectivity spectra meas. 77−85743
$TlCl_xBr_{1-x}$, $TlBr_xI_{1-x}$, polymorphous mixed cryst. layers, opt. props. 78−23490
Tl_2CrO_4, investigation by diffuse reflectance spectroscopy 78−88326
$TlGaS_2$, optical and photoelec. props. 77−55571
$TlGaS_2$, optical and photoelectric exam. 79−11180
$TlGaS_{2x}Se_{2(1-x)}$, solid soln., fundamental optical absorpt. edge 80−25408
$TlGaS_xSe_{2-x}$, optical and photoelectric props., composition depend. 79−15183
TlI with CsCl struct., exciton magnetoabsorption 77−28593
$TlInS_2$ single crysts., three-dimensional exciton destruction, electroabsorpt. and transmission spectra 77−55803
$TlInS_xSe_{2-x}$ solid solution, optical and photoelectric props. 79−11179
$TlMnCl_3$, antiferromag., absorpt. spectrum, excitation-magnon-phonon process 79−87461
TlS_2, amorphous semiconductor, optical consts. 79−11400
TlSe, refl. spectrum in 4.2 to 8.0 eV range 79−51984
Tl_2WO_4, effect of heating on colour, reflectance spectra 78−38673
Tm, polycryst., optical props., temp. depend., photocond., relaxation parameters 78−84603
$TmAsO_4$, optical side bands, absorpt. spectra in mag. fields 77−52123
$TmCrO_3$, optical-absorption spectra of Tm^{3+} 80−20662
TmSe, metallic, optical refl. investig. of valence fluctuations 77−63428
α-U, polycryst., optical absorption meas. 0.15 to 2.0 eV 80−108223
UF_6, neat and mixed cryst. emission spectra, lowest charge transfer state, Jahn-Teller effect 78−67992
UF_6, UV spectra, electronic and vibronic states in gas and solid phases 77−14445
UO_2, 5f-magnetic semiconductor, spectroscopic data, review 80−97299
UO_2 and U_4O_9 single crysts., optical props. rel. to chem. bonding 77−28598
UO_2, electronic transitions, crystal field effects and phonons, phase transition 80−97303
UO_2, localised versus itinerant 5f electrons exam., reflectivity meas. 79−19905
UO_2, optical props. and electronic struct. 78−68527
UO_2, temp. depend. of 5f to $6de_g$ absorption edge and intra-5f transitions 79−24314
US, ferromagnet, electronic structure, reflectivity *(German)* 80−49567
US, optical props. and electronic struct. 80−25410
US(Se)(Te), electronic struct. and exchange band splitting, optical refl. meas. 80−66226
USb, localised versus itinerant 5f electrons exam., reflectivity meas. 79−19905
USb, reflectivity spectrum, band struct. 80−7368
USe (s) 80−16053
V, electronic struct., thermoreflectance studies 80−76047
V, optical absorpt. spectrum, 0.25-14 μm *(Russian)* 77−81118
VI_2, MCD spectra, interpretation rel. to mag. struct. 80−66222
VN, opt. consts. and physicochem. spectra 77−85677
VN, optical props. and charact. electron energy loss spectra 79−52056
VO_2, change in optical props. at semicond.-metal transitions 77−28597
VO_2, film, metastable metallic phase due to laser and electron beam irrad., refl. spectra 79−19944
VO_2 film, optical characts. of phase transition, ion bombardment effects 79−28281
VO_2, film, semiconductor-metal phase transition, fast laser kinetic studies 79−69419
VO_2, metal-insulator transition and electronic struct., ion bombard. effects 80−92948
VO_2, nonstoichiometry influence on electron struct. and metal-insulator phase transition 80−44507
VO_2, semicond. phase, optical spectrum, CNDO CI calc. 78−27258
VO_2, semicond.-metal phase transition, fast laser excitation, kinetics obs. 79−47018
VO_2, V_2O_3, film, absorption spectra, semicond.-semimetal transition 78−19512
V_2O_3, metallic differential refl. spectra and band struct. 77−1699
V_2O_5 electrochromism obs. and mechanism, thin film growth *(Russian)* 77−77249
V_2O_5 film, amorphous, thickness, density and refr. index determ. from reflectance interference spectra 80−55206

visible and ultraviolet spectra of inorganic solids continued
V_2O_5 film, optical absorption in 1.0 to 5.5 eV range 78−19586
V_2O_5, low dislocation density cryst. growth, opt. props. 77−63551
V_2O_5-B_2O_3-ZnO semiconductivity glasses, optical and modulated absorpt. spectra in band gap region 77−48189
V_2O_5-ZnO-B_2O_3 glass, sputtered, optical absorpt., band gap and Urbach tail 77−8597
V_6O_{13}, optical props. in metallic and semicond. phase 80−40135
VOCl, and $Li_{0.8}VOCl$ intercalation cmpd., magnetic, optical and electrical props. 79−95402
$mV_2O_5.(100-m)P_2O_5$, (m=100-2), V(IV) complexes conc., absorpt. and ESR spectra 78−64266
W, chemisorbed H, surface cond. and intrinsic surface states, surface refl. spectra 80−15378
W surface, (110), chemisorpt. effects on dielec. function, refl. spectra 80−75616
W, thermoreflectance spectra, 0.3 to 6 eV, rel. to band struct. calcs. 77−66521
W-Fe spin glass, optical props. and electronic states 80−20412
W-Re, optical props., temp. depend., 4.2-300K 78−2874
$W_xMo_{1-x}O_3$, absorpt. spectra and optical gap energies 79−91464
WO_2, optical conductivities and dielec. functions in 0.2-6 eV range, rel. to band struct. 79−42938
WO_3 amorphous layers, electrochromic absorpt. depend. on crystallinity and electron localisation 77−59589
WO_3 electrochromic absorption dependence on crystallinity 77−77314
WO_3 electrodes, vac. evaporation and anodic oxidation prep., electrochromic process kinetics 79−100390
WO_3 film, optical absorpt. after ion irrad., appl. to ion beam profile monitoring 79−26181
WO_3, polar, electrochromic absorpt. bands, small polaron theory 78−39528
WO_3, thin films, electrochem. coloration, optical and elec. props. 77−85345
WO_3:H^+, optical and elec. props., suggested band struct. model 77−4654
WO_3-B_2O_3-ZnO semiconducting glasses, DC cond. and optical absorpt. 80−107783
WO_3-MoO_3 film, amorphous, electrochromic optical absorpt., expt. results and model 78−27341
WS_2, excitons, mag. circular dichroism and wavelength modulated reflectance meas. 79−23900
WS_2 films, exciton peaks in absorpt. spectra, press. and temp. depend. 79−51496
$WS_2(Se_2)$, effect of uniaxial stress on excitonic optical spectra 78−84606
WSe_2, excitons, mag. circular dichroism and wavelength modulated reflectance meas. 79−23900
WSe_2, refl. spectra and photovoltaic effect, 1.5-3.2 eV, 4.1-300K 79−47470
Xe, crystalline, polariton effects, reflectivity, absorpt., and resonant luminesc. spectra calcs. 80−20095
Xe-MF_6, M=W, Mo, U, Re, Ir, charge transfer interactions, VUV and IR obs. 78−50664
Y film prepared in ultrahigh vac., optical meas. 6 to 14 eV 79−78767
Y, reflectivity spectrum, 3.5 to 30 eV dielectric function and plasmons 77−44014
Y-Er, surface, high-freq. elec. cond. dispersion function, effects of polishing and annealing 78−19506
YA-O_3:Er^{3+}, pulsed laser action, $^4S_{3/2}$ to $^4I_{9/2}$ transition laser action, optical and luminescence spectra 80−16082
YAG, colour centres conceived as bound polarons 78−63990
YAG, transient colour centres caused by UV radiation 77−84744
YAG:Ce^{3+}, excited-state absorpt. meas., tunable laser model system 79−42994
YAG:Cr^{3+}, optical absorption, cryst. field pot. expansion 77−36268
YAG:Cr^{3+}, radiation colour centres, absorpt. and thermolum. spectra 78−48206
YAG:Er^{3+}(Ho^{3+})(Tm^{3+}), oscillator strengths of impurities, 5000 to 30000 cm^{-1} 79−4830
YAG:Ge^{3+}, excited state absorpt. loss, 5d→4f rare earth lasers 78−90417
YAG:Mn, impurity-induced O^- colour centres, absorpt. and fluoresc. spectra 77−1709
YAG:Nd,Ce,Cr, effect of γ-rays, fast electrons on optical props., annealing and colour centre destruction 77−8608
YAG:Nd^{3+}, Ce^{3+}, sensitisation, luminesc., absorpt. and emission spectra *(Russian)* 78−10982
YAG:Nd^{3+}, cryst. field anal. 78−64013
YAG:Nd^{3+} and free Nd^{3+} ion, energy levels, absorption spectra 79−11076
YAG:Ti, crysts., colour centres, optical absorpt. spectra 79−65080
$YAlO_3$, $YAlO_3$:Nd, colour centre form. rel. to growth conditions, absorpt. spectra 79−90652
$YAlO_3$:Pr^{3+}, ultrahigh resolution photon echo spectroscopy 80−28285
$Y_3Al_5O_{12}$:Nd^{3+}, absorpt. spectra dependence on press. *(Russian)* 77−52183
$Y_2BiFe_{3.8}Ga_{1.2}O_{12}$ film, colour contrast between different domains 77−12166
$Y_2BiFe_{3.8}Ga_{1.2}O_{12}$ film, magnetooptic interference of light 77−32458
$YCrO_3$, mag. circular dichroism and Faraday rotation in R-lines region 79−28725
$YFe_{1-x}Co_{x/2}Ti_{x/2}O_3$, orthoferrite, anisotropy of Faraday rotation 79−61341
$Y_3Fe_{5-x}Ga_xO_{12}$, refr. index spectrum, visible region 79−73894
$Y_3Fe_{5-x}Sc_xO_{12}$, garnets, magnetooptical spectra, 15000-21000 cm^{-1} 77−90131
$Y_3Ga_5O_{12}$:Nd^{3+}, cryst. field anal. 78−64013
$Y_{1-x-c}Gd_xNd_cScO_3$, crystal, absorption, luminescence, stimulated emission spectra 78−15220
YH_2, electronic struct., optical studies, 0.2-5 eV, 4.2-340K 79−78005
YIG, Bi-substituted, LPE film, optical absorpt. changes due to impurity incorporation 77−1702
YIG, diamagnetic substituted, anal. of polar Kerr rot. spectra 78−68485
YIG films, MCD spectrum 79−28722
YIG, high field magneto-optical study 77−85749
YIG, magneto-optical Kerr effect, reflectivity spectra 80−66157
YIG, magnetooptical spectra, polar Kerr rotation, dielectric tensor elements spectra 80−40091
YIG, polar Kerr rotation spectra, 2-5.7 eV, comparative study with $Li_{0.5}Fe_{2.5}O_4$ 79−47413

visible and ultraviolet spectra of inorganic solids continued
YIG, pure and Ga-substituted diffuse refl. and thermorefl. spectra near Curie point 80−40131
YIG: Ca^{2+} epitaxial films, Fe^{4+} centres, MCD, optical absorpt., and thermoelectric power meas. 78−95595
YIG:Ca, oxidising effects of high temp. annealing in reducing atmosphere 80−66696
YIG:Ga(Sc), magneto-optical Kerr effect, reflectivity spectra 80−66157
YIG:Ru, optical absorpt. and MCD obs. of Ru^{4+} site occupancy 80−71456
Y_2O_3, reflection spectra, Kramers-Kronig anal. of optical charact. 79−8161
Y_2O_3 sintered pieces, optical transmittance 80−40561
$Y_2O_3:Eu^{3+}$, absorpt. spectra, fluoresc., electron beam excitation 78−92093
$Y_2O_3:Nd^{3+}$, absorpt. spectra, hypersensitivity of $^4I_{9/2}$ to $^4G_{5/2}$ $^2G_{7/2}$ transition 80−97309
$Y_{2-x}Pr_{0.2}Fe_5O_{12}$, magneto-optical props. 78−72489
YRBiFe garnets, epitaxial films, R=Gd+Yb, Faraday effect and phys. props. 77−69928
Y_3Se_4 powder, prep. and optical props. 77−28771
$Y_2Ti_2O_7:Nd^{3+}$, spectroscopic props. 77−69866
YVO_4, pure and Bi^{3+} doped, absorpt. and emission props., excitons 79−38592
$YVO_4:Eu^{3+}$, absorpt. spectra, fluoresc., electron beam excitation 78−92093
Zn-In-S thin layers, ternary phases, optical props. near long-wavelength intrinsic absorpt. edge 80−80887
$Zn_{0.1}Cd_{0.9}S$, two-photon and two-step absorption of light 80−7389
$Zn_xCd_{1-x}S$, forbidden band width, exciton refl. and luminesc. meas. 78−10947
$Zn_xCd_{1-x}S$ monocrystal, optical and nonlinear optical charact. *(Russian)* 79−98442
$Zn_xCd_{1-x}S$, reflectivity spectrum, excitons and energy band struct. 77−55804
$Zn_xCd_{1-x}S$ solid soln. films, reactive cosputtering, struct., comp. and opt. absorpt. edge *(French)* 78−6237
$Zn_xCd_{1-x}Se$, exciton reflection spectra anomalies *(Russian)* 80−97304
$Zn_xCd_{1-x}Se$, vacuum condensates, forbidden band width determ. from transmission spectra 77−8670
$Zn_xCd_{1-x}Te$ films, absorpt. spectra in 3.0 to 5.8 eV range 79−52034
$Zn_xCd_{1-x}Te$, reflection spectra, energy band struct. comp. depend. *(Russian)* 78−56500
$ZnCrO_4$, investigation by diffuse reflectance spectroscopy 78−88326
$ZnCr_2O_4$, antiferromag. spinel, absorpt. and luminesc. spectra 80−66225
$ZnCs_2(SO_4)_2.6H_2O:VO^{2+}$, optical absorpt. spectra obs. 80−40146
$ZnF_2:Mn^{2+}$, zero-field splitting, appl. of complete d-electron calc. 77−15799
$ZnGeP_2$ bandgap absorption edge, spectra, electron transitions *(Russian)* 80−97305
$ZnGeP_2$, single cryst., polarised light photocond., optical transparency anisotropy *(Russian)* 78−2518
$ZnGeP_2(As_2)$, reflectvvity and XPS meas. 78−35165
$ZnIn_2S_4$, fund. optical consts., Kramers-Kronig analysis, reflectivity spectra 78−39573
$ZnIn_2S_4$, fund. reflectivity, 2 to 6 eV, band struct. implications 78−39574
$ZnIn_2S_4$, III(a) polytype, absorpt. spectrum tail changes due to microstresses 80−2788
$ZnIn_2S_4$, layered semicond., reflectivity spectra 79−8155
$ZnIn_2S_4$ layered semiconductor, fundamental optical constants, comparison with band structure calcs. and PES 79−56757
$Zn_{1-x}Mg_xTe$, variation of fundamental edge, wavelength modulated reflectivity meas. *(French)* 77−81124
ZnO, ang. depend. of reflection spectra and directional dispersion of anisotropic exciton polaritons 78−31216
ZnO, attenuation of transmitted light in exciton region, polarisation, coherence, scatt. 77−69852
ZnO, band gap depend. on energy of zero-point vibrs., luminesc. obs. 79−73436
ZnO, electron-hole plasma, gain and refl. spectra study 80−66227
ZnO, electronic struct. calc., appl. of O nonlocal ionic pseudopot. 77−51659
ZnO, ellipsometric spectroscopy of nonpolar $(1\bar{1}00)$ surface 79−33651
ZnO, excitonic mol. transitions, optical gain and induced absorpt. spectra 80−11438
ZnO, excitonic molecule transitions, M-band emission 79−78742
ZnO, reflection spectra, exciton reflection at high excitation levels 77−69853
ZnO, single cryst. and film, emission band charact. *(Russian)* 77−52133
ZnO, surface exciton polaritons, ATR obs., book contrib. 79−42620
ZnO:Cu, H(D), OH and OD centres, IR-active absorpt. line spectra 79−15496
ZnO:Li, effect of LiOH mineraliser on struct. and optical props. 77−8737
ZnO:Ni^{2+}, Zeeman effect at Ni impurities 80−60633
ZnO-$B_2O_3:Cu^{2+}$, glasses, ESR and optical absorpt. 80−34760
ZnO(S)(Se), high field Faraday rotation, 6.5K 79−38522
ZnP_2, two-photon light absorpt. dispersion, allowed-forbidden transition *(Russian)* 78−15193
ZnP_2:In(Ga)(Ge)(S)(Se), doped and undoped, optical absorpt. spectra in range 0.5 to 2.2 eV 80−66250
Zn_3P_2, absorption edge meas. 78−80380
Zn_3P_2 bulk and thin film, UV reflectivity spectra, photovoltaic effects, optical consts. 80−25472
Zn_3P_2, direct and indirect optical transitions, metal-Zn_3P_2 contact photovoltage response 80−25402
Zn_3P_2, optical props., transition energies from transmission and refl. meas. 80−60532
Zn_3P_2 photovoltaic material and Schottky diode characteristics 78−64066
Zn_3P_2, single crystal, growth, electronic and device props. 80−25551
ZnS, cubic, direct and modulated refl. spectra, 165-360 nm 77−13807
ZnS evaporated film optical props. 160 to 2000 A 79−15544
ZnS film, dispersion charact. 77−59629
ZnS, high-resist., optical transmission thermal processing effects 77−63431
ZnS, natural and stress induced birefringence dispersion 78−6651
ZnS, plastically deformed, anisotropic cond. 78−56143
ZnS, reson. Brillouin scatt. and piezobirefringence 80−93348

visible and ultraviolet spectra of inorganic solids continued
ZnS, temp. coeffs. of charact. reflectivity struct. 77−85745
ZnS:Cu, spectral distrib., rise and decay behaviour *(German)* 80−60625
ZnS:Cu,Cl, exciton refl. spectra, hexagonal struct. 77−44021
ZnS:Cu^{2+}, Jahn-Teller effect, stacking faults and formation of polytypes, absorption and emission spectra 77−4660
ZnS:Ga(Cl), deep traps, impurity electroabsorpt. and photocond. meas. 78−6707
ZnS:Mn^{2+}, $^4T_2$ level, Zeeman splittings, Jahn-Teller effect 80−40141
ZnS:Mn^{2+}, heavily doped, anomalies in reflectivity 77−20891
ZnS:Ni, IR luminesc. and absorpt. spectroscopy 80−108261
ZnS:Ni^{2+}, Zeeman effect at Ni impurities 80−60633
ZnS:Tl(Al)(Zn), UV spectra of donor-doped single crysts. 77−12404
ZnS-Ag, broad band visible heat reflecting mirror 77−39017
ZnS-O, single cryst., fast neutron irrad., optical props. 78−27331
ZnS(Se), wavelength-modulated refl. spectra, 2.5 to 8 eV 77−20877
ZnS(Se):Ni, optical absorpt., impurity ionisation, optical phonon coupling 80−88505
ZnS_xSe_{1-x}, band gap, comp. depend., exciton refl. spectrum obs. 78−56071
ZnS(Se)(Te), thermoreflectance spectra, at energies from absorption edges to 9 eV *(Japanese)* 79−11436
ZnSe, absorpt. modulation of light, and its appl. to page composer 77−40258
ZnSe, attenuated total refl. spectra of surface exciton polariton 77−36262
ZnSe crystal, exciton reflection spectra, control of exciton-free surface layer thickness 80−7373
ZnSe crystals, doped and undoped, optical absorption edge 80−60626
ZnSe, cubic, magnetoreflectance of Γ_6-Γ_8 exciton ground state 78−23495
ZnSe, cubic, magnetoreflection of s-excitons 78−60426
ZnSe, effective mass parameter, two-photon absorpt., envelope-hole coupled exciton states 77−52124
a-ZnSe, elec. and optical meas., Mott-type model for amorphous semicond. 78−2414
ZnSe, electron irrad., short-lived optical absorpt. 79−51989
ZnSe, exciton-impurity complex, electroabsorption meas. 79−15484
ZnSe, laser induced modulation of opt. absorpt. 78−88324
ZnSe, reactor irrad., opt. props. 77−90137
ZnSe single crystal, exciton photolum. and refl. spectra, 4-90K *(Russian)* 77−66540
ZnSe, single crysts., opt. band gap and Mn^{2+} EPR, effects of prep. conditions 77−47730
ZnSe, temp. coeffs. of charact. reflectivity struct. 77−85745
ZnSe, two photon absorpt. by envelope-hole coupled exciton states, polarisation depend. 77−66522
ZnSe, two-photon absorpt., effect of polarisation of laser radiation 77−69856
ZnSe, two-photon and two-step absorption of light 80−7389
ZnSe:Cu, discovery of bound exciton, electroabsorption 80−45038
ZnSe:In, optical absorpt. spectrum, 0.4 to 0.7 μm 77−81136
$(ZnSe)_{1-x}(GaP)_x$, two-photon absorpt. at ruby laser freq., clarification *(Russian)* 79−15505
$ZnSnAs_2(P_2)$ single crysts., refl. spectra, band struct., dielec. consts. 77−44022
ZnTe, exciton localisation at impurity pairs 79−37999
ZnTe, excitonic effects at E_0 and E_1 gaps, wavelength modulated reflectivity spectroscopic study 79−61400
ZnTe film, exciton spectra, press. and temp. depend. 80−80886
ZnTe films, internal stress effect on fund. refl. spectra 80−60701
ZnTe, free exciton refl., surface layer effects 78−76493
ZnTe, refined, undoped, Cu acceptor, optical absorption and photoluminesc. meas. 80−34970
ZnTe, reflectivity meas., double beam wavelength modulated technique *(Korean)* 80−50365
ZnTe, shape of reflectance and thermoreflectance spectra 79−11430
ZnTe, single cryst., anomalous struct. of exciton refl. spectra 77−44020
p-ZnTe, single crystal *(Russian)* 78−23488
ZnTe, two-photon absorpt. line shape near direct band gap and critical point 79−65898
ZnTe, wavelength modulated reflectivity spectra *(Japanese)* 79−11435
ZnTe, wavelength-modulated reflectance spectrum, electron-phonon and exciton-phonon interactions 79−11434
ZnTe: group I element, absorption saturation *(Russian)* 78−35183
ZnTe:Ag, containing dislocation loops, optical absorption-edge fine struct. 78−43905
ZnTe:Bi, laser annealing, channelling, reflectivity spectra 80−66215
ZnTe:Cr(Mn)(Fe), exciton refl. spectra 80−2806
ZnTe:In(Al), pure and doped, Zn vacancy energy levels, elec. and optical props. 79−4827
ZnTe:Mn, exciton refl. band, giant mag. splitting *(Russian)* 78−56079
ZnTe:P, pure and doped, electron and exciton excited states of neutral donor 80−34393
ZrF_4-BaF_2-NdF_3 glass, vitreous domain, prep. and optical props. 78−27304
ZrF_4-ThF_4-$BaF_2:V^{3+}(Cr^{3+})$ glasses, absorpt. spectra *(French)* 79−99918
ZrN, opt. consts. and physicochem. spectra 77−85677
ZrN, optical props. and charact. electron energy loss spectra 79−52056
ZrN, optical props. at 300K 78−19466
ZrO_2, optimum sintering charcts., density, X-ray diffr., IR spectrum, UV spectrum obs. 78−76617
ZrO_2, stabilized, thermal barrier coating system, spectral emission and absorpt., 300 to 1590K 79−24672
$ZrO_2:Y_2O_3$, bias sputtering, film growth and charcts. 77−40366
ZrS_2, intercalation-induced shift of absorpt. edge 79−82999
ZrS_3, thermomodulated reflectivity and transmission 80−50357
$ZrS_2(Se_2)$, vacuum UV reflectivity spectra, cond. band model 77−44012

visible astronomical observations
2A 0311−27 optical counterpart, identification and spectroscopic obs. 79−25762
13 Egeria, occultation of SAO 92603, photoelectric obs. rel. to minor planet possible satellite 80−46460
108-76°1, new halo planetary nebula, chemical abundances 77−45510
145-IG-03, interacting galaxies, apparent luminous bridge 77−17681
0254−334/2, high-redshift QSO without Lyman α emission or absorpt., spectroscopic obs. 79−92886
0406+121, optical spectra 4950-7950 Å, of possible BL Lacertae object 80−51895

visible astronomical observations continued
0934.5+01, compact galaxy, optical variability 77−26051
0957+561 A, B, twin QSOs, spectroscopic obs. with multiple-mirror telescope 80−12827
0957+561A and B, twin QSOs, direct imaging rel. to gravit. lens interpretation 80−17686
1008−3814, southern ring galaxy in Vela, struct. and spectrum 79−58413
1308+32, BL Lacertae object, rapid optical outburst, 1980 June to July 80−98733
1309−216, probable BL Lacertae object with absorpt. red shift 1.49, optical spectrum 80−67856
1418+54, new violently variable BL Lacertae object, historical light curve 78−93410
1936 CA (Adonis), 1977 tentative rediscovery, elements and ephemeris 77−29703
1936 CA (Adonis), precise positions and magnitudes (1977 February 24 to March 22) 77−37552
1936 CA (Adonis), recovery confirmed and improved elements 77−25970
1947 XC=1979 XA, positions, UBV photometry and ephemeris continuation 80−31233
1947 XC=1979 XA, precise positions, 1979 December 18 to 1980 January 5 80−31238
1960 UA, recovery on 1977, June 16 77−60709
1963 UA, 1976 July 23 precise position 77−82151
1963 UA, precise positions (1976, November-1977, January) 77−29705
1963 UA, precise positions for 1976 June 26, 27 77−22132
1963 WA, precise positions (1976, October-1977, January) 77−53459
1966 S 2, positional obs., 1980 March 15 80−85893
1972 RA, Amor-type object, precise positions for 1979 Aug., approx. position for 1979 Sept. 79−92691
1973 NA, precise position (1973, August 1) 77−9694
1974OT, astrometric obs. 78−89107
1974OU, astrometric obs. 78−89107
1975 YA, precise positions and photographic magnitude (1976, June-July) 77−5486
1975 YA, precise positions for 1976 June 25 77−22132
1976 AA, position, elements and ephemeris (1977 Dec.-1978 Apr.) 78−12138
1976 AA, precise position (1976, December 27) 77−37553
1976 AA, precise position for 1977 Dec. 16 78−73673
1976 AA, precise positions 1976, June-Dec., ephemeris for 1977, Jan.-Apr. 77−17418
1976 AA, precise positions 1977, Mar. and Apr. 77−60710
1976 AA, precise positions and ephemeris extension (1977, Apr.-Dec.) 77−29706
1976 UA, improved orbital elements 77−17420
1976 UA, precise positions, 1976, Nov. 77−17417
1976 UA, precise positions 1976, Oct. 77−2365
1976 UA, precise positions 1976, Oct. 77−9696
1976 UA, precise positions (1976, October and November) 77−33392
1976 UA, precise positions and photographic magnitude (1976 October) 77−5487
1976 UA, precise positions for 1976 October-November period 77−9693
1976 WA, precise positions, ephemeris for 1977, Jan.-May 77−17419
1976 WA, precise positions 1976, Nov. and ephemeris for 1976/77 Dec.-Jan. 77−13278
1976 WA, precise positions 1976 Nov. and Dec. 77−9697
1976 WA, precise positions (1976, December) 77−37551
1976 WA, precise positions (1976, May and November) 77−53458
1976 WA (Object Schuster), positions, elements and ephemeris (1976 Dec.-1977 Jan.) 77−9695
1977 BA, approx. posn., improved elements and ephemeris (1979 Mch.-Apr.) 79−34904
1977 HA, astrometric obs. 78−89107
1977 HA, discovery, positions, elements and ephemeris (April-May) 77−45344
1977 HA, precise positions (1977, April) 77−53457
1977 HA, precise positions (1977 April-May) and improved elements 77−82153
1977 HA, precise positions for 1977 Apr. 22 77−45345
1977 HA, recovery, posns. and ephemeris (1979 June-July) 79−70986
1977 HB, discovery of fast-moving asteroidal object, positions 77−41348
1977 HB, positions, elements and ephemeris (1977, May-August) 77−49327
1977 HB, precise position for 1978 Apr. 10 78−73673
1977 HB, precise positions (1977, May 21) 77−67060
1977 HB, precise positions and possible ephemerides (1977, April-May) 77−56869
1977 HB, recovery, precise positions for 1978 May 9-10 78−53862
1977 HB asteroid, precise positions 1977 June 77−87310
1977 OA, discovery, 1977 July 18-19 positions 78−77518
1977 RA, positions, elements and ephemeris for Amor-type object 77−82152
1977 RA, positions, improved elements, and ephemeris 78−4137
1977 RA, precise positions, (1977 September 23 to December 8) 78−53860
1977 RA, precise positions, rot. period from light vars. 77−87309
1977 RA, precise positions 1977 Sept. 77−91466
1977 RA, precise positions (1977 Oct. 16) 78−20715
1977 UB, posn. in 1895 and improved orbital elements 78−20713
1977 UB, precise positions, 1977, Nov. 78−7915
1977 UB, precise positions for 1977 Nov. 13-18 period 78−12139
1977 UB, precise prediscovery positions 78−20716
1977 UB, prediscovery positions, improved elements, orbital stability 78−12140
1977 UB, prediscovery positions and ephemeris continuation 78−16331
1977 UB (Chiron), discovery, orbital elements 78−45264
1977 UB (Chiron), precise positions 1945 Apr. 16 and 1978 Jan. 9-10 78−49372
1977 UB (Chiron) astrometric obs. 78−89107
1977 UB (slow-moving Object Kowal), precise positions 1977 Nov. 9-10 78−7911
1977 VA, precise positions, 1977, Nov. 78−20717
1977 VA, precise positions, photoelec. obs., 1977 Nov. 78−12144
1977 VA, precise positions 1977 Dec. 78−49371
1977 VA, precise positions (1977 November 9 and 10) 78−7912
1977 VA (Object Helin-Shoemaker), discovery position 78−7908
1977 VA (Object Helin-Shoemaker), positions elements and ephemeris 78−7909
visible astronomical observations continued
1977 VB, discovery positions 78−7910
1978 CA, position, elements, ephemeris and B magnitude law 78−40860
1978 CA, positions 1978 Feb. 17-Mar. 8, photometric obs. 78−36487
1978 CA, precise positions, orbital elements, ephemeris 78−73672
1978 CA, precise positions 1978 March, ephemeris for 1978 Apr.-July 78−40862
1978 CA, precise positions (1978, March 7 to 12) 78−57486
1978 CA (Object Schuster), positions, elements and ephemeris (1978 Feb.-March) 78−36483
1978 CA and DA, photoelectric obs. of asteroid rotation periods 79−101106
1978 CA and DA, UBV photometry 78−36486
1978 DA, discovery, positions, elements, ephemeris and magnitude law 78−36484
1978 DA, position, elements, ephemeris and B magnitude law 78−40861
1978 DA, positions 1978 March 1-8, photometric obs. 78−36488
1978 DA, precise position for 1978 Apr. 9 78−73673
1978 DA, precise positions (1978, March 4 to 12) 78−57487
1978 DA, precise positions (1978 March 8 to 15) 78−45262
1978 P 1, speckle interferometric obs. (1980 June) 80−101553
1978 P 1, speckle obs. rel. to orbital radius and system mass and density 80−109394
1978 PA, discovery positions for probable Amor-type object 78−81579
1978 PA, semiaccurate positions, (1978 August 14 and 15) 78−81580
1978 RA, fast-moving asteroidal object approximate positions and photometry 78−85887
1978 RA (=1975 TB), precise positions, (1978 September 10 to 12) 78−93141
1978 SB, fast-moving object, discovery positions and magnitudes 78−93142
1978 SB, positions and UBV photometry 78−96422
1978 SB, precise positions, (1978 October 6 to 11) 78−93143
1978 SB, precise positions for 1978 Oct., orbital elements, ephemeris for 1978 Oct.-Dec. 78−96423
1979 BA, fast-moving object, discovery and precise positions, (1979 January 23 to 31) 79−35177
1979 BA, precise positions, (1979, February 28 and March 4) 79−40121
1979 J 1 discovery by Voyager 2 camera 80−77334
1979 J 1-3, satellite periods from Voyager 1 and 2 data 80−105196
1979 QA, fast-moving asteroidal object, discovery and precise positions (1979 August 22 to 23) 79−92692
1979 QB, Amor-type object, precise positions (1979 August 22 to 23) 79−92693
1979 QB, precise posns., elements and ephemeris (1979 Aug.-Nov.) 79−101108
1979 VA, discovery of fast-moving asteroid 80−12703
1979 VA, precise positions, (1979 November 15 to 16) 80−26776
1979 VA, precise posns., and rotation period from UBV photometry 80−17534
1979 VA, precise posns., elements and ephemeris (1979 Nov.-1980 Jan.) 80−26777
1979 XA, fast-moving asteroidal object in Aries, discovery 80−26771
1979 XA, precise posns. (1979 Dec. 15 and 19) 80−31235
1979 XA (=1947 XC), discovery and precise positions (1979 December 13 to 15) 80−26774
1979 XB, precise positions, (1979 December 11 to 15) 80−46458
1979 XB, very fast-moving asteroidal object in Eridanus-Fornax, discovery and positions 80−26772
1979 YA, discovery and approx. posn. (1979 December 16) 80−26775
1979 YA, posn. for 1979 Dec. 20 and comet-like appearance 80−31234
1980 AA, discovery of fast-moving object in Gemini 80−41756
1980 AA, precise positions, 1980 January 16, orbital elements and ephereris 80−36556
1980 LB, precise posns., orbital elements and ephemeris (1980 June-July) 80−82259
1980 PA, fast-moving asteroidal object, discovery and semi-accurate positions (1980 August 6 to 7) 80−94745
1980 PA, positions, 1980 August 8 to 17, improved orbital elements and ephemeris 80−98597
1980 PA, posns., elements and ephemeris (1980 August) 80−94746
1980 PA, precise posns., improved elements and ephemeris (1980 Sept.-Oct.) 80−101548
1980 QA, fast-moving asteroidal object in Capricornus, discovery and positions (1980 August 16 to 18) 80−98598
1980 S 10, precise positions, 1980 March 15 to 16, and relation to Dione 80−85893
1980 S 1, 3, 6, 25, new Saturnian satellites, positional obs., (1980 March 9 to 14) 80−94749
1980 S 3, 13, positional obs. (1980 March 15 and 16) 80−85893
1980 S 7 to 14, Saturnian satellites, obs. (1980 March 13 to April 8) 80−62068
2005+403, spectroscopic obs. of associated optical object, identification as quasar 77−2484
β Canis Majoris star, photometric obs. 80−17595
χ Cygni, Hα emission line profile obs. of long-period variable 79−25618
A0035, large southern ring galaxy, obs. 77−45559
A0535+26, transient slow X-ray pulsar, spectrophotometric survey 78−4263
A0620−00, transient X-ray source, optical counterpart, visible and IR obs. 80−101653
A0620−00, transient X-ray source, spectrophotometry 78−4400
A0620−00, X-ray nova, distance determ. from reddening 77−2495
A0620−00, X-ray nova, spectroscopic obs. 77−87417
A1742−28, transient X-ray source, optical counterpart, visible and IR obs. 80−101653
A194, cluster of galaxies, radial vels. 77−53691
2A 0042+323 (3U 0042+32) optical candidate, photometry and spectrum 78−54088
2A 0311−227, AM Herculis type X-ray binary, optical counterpart, radial vel. obs. 80−94890
2A 0311−227, complex emission line structure of spectroscopic binary 80−51915
2A 0311−227, high-speed photometry of AM Herculis-type binary 80−41912
2A 0311−227, new AM Herculis-type system, optical identification 79−101211
2A 0311−227, orbital period and polarisation obs. of optical counterpart 79−30151
2A 0311−227 optical counterpart, high speed photometry 80−82547

visible astronomical observations continued
2A 0311−227 optical counterpart, identification as AM Herculis type star 79−30149
2A 0311−227 optical counterpart, simultaneous photometric and spectroscopic obs. 80−90572
2A 0311-227 optical counterpart, spectroscopic and photometric obs. 79−101222
2A 0526−328, high speed optical photometry 80−51917
2A 0526−328, optical counterpart, eclipsing binary, visible emission line variability 80−73075
2A 0526−328, optical counterpart position and spectrum 79−5925
2A 0526−328 optical counterpart, radial vel. meas. and orbital period 80−90579
2A 0526−328 optical counterpart, spectroscopic obs. 80−77515
2A 0526−328 optical counterpart, X-ray emitting cataclysmic variable, spectrum and photometry 79−97103
2A 0526-328, optical photometry of assoc. star 80−22120
ZA 0536−328, AM Herculis-like star identification confirmed 79−40296
2 A 1052+606, X-ray and optical variability of RS CVn star 80−31331
2A 1219+305, high latit. X-ray source identification with BL Lacertae object 79−48960
A 1710−34, X-ray, optical and radio obs. 79−71158
2A 1822−371 optical counterpart, identification, photometry and spectrum 79−12545
2A 2251−179, X-ray quasar, UBV photometry 80−82349
A non 0945−30, intermediate luminosity X-ray galaxy, optical spectrum 79−2578
A- and F-type main sequence stars, scanner obs. 78−36563
A- and F-type stars, absolute energy distribs. 77−17554
A- and F-type stars in Selected Areas, photoelectric uvbyβ photometry 78−16412
A- and F-type visual binaries, uvbyβ photometry 79−21346
A-type bright supergiants in LMC, spectra, line intensities 77−22215
A-type central stars of planetary nebulae, radial vel. study 78−81629
A-type central stars of three planetary nebulae 79−17064
A-type stars, Ca II K line obs. 78−20830
A-type stars, obs. and calc. spectra, 3600-4200 Å region 78−12217
A-type stars, predicted and observed spectral energy distribs. 78−4208
A-type stars, quest for differential rot. 77−45409
early A-type stars, V/H abundance ratio from V II lines 79−21314
Abell 1146, photometry, isophotal magnitudes and luminosity function 79−67105
Abell 1367 galaxy cluster, obs. rel. to galaxies redshift-magnitude bands and evolution 78−54033
Abell 1781, photometry of field galaxies 78−77609
Abell 1831, statistical and photometric study of cluster of galaxies 80−51885
Abell 193 cluster of galaxies, BV photometry *(Russian)* 77−22319
Abell 2142, spectroscopic obs. of X-ray cluster (40 1556+27) 79−48940
Abell 2241, candidate X-ray cluster of galaxies redshifts 77−17699
Abell 262 cluster of galaxies, redshifts meas. 77−45579
Abell 2634, cluster of galaxies, luminosity function *(Russian)* 78−28801
Abell 2634 galaxy cluster, spectroscopic study and radial vels. 77−64857
Abell 2670, cluster of galaxies, luminosity functions 78−16545
Abell 30, Abell 78, planetary nebulae, unusual central struct. 80−51855
Abell 30 emission nebula, ejecta from central star 80−82474
Abell 399/Abell 401, X-ray binary galaxy cluster, mass 80−90546
Abell 401 cluster of galaxies, vel. dispersion meas. 77−26072
Abell 426 and 1367, surface brightness and colour distribs. of elliptical galaxies 78−81681
Abell 478, X-ray cluster of galaxies, redshift and optical struct. 78−8134
Abell 754, cluster of galaxies, radio and optical obs. 79−25737
Abell clusters of galaxies, photometric study 78−4370
accurate optical positions 77−29943
active galactic nuclei, envelope parameters and mass 79−35392
Adonis (1936 CA), precise positions (1977, February 26) 77−49326
ADS 148, visual binary speckle interferometry with linear digicon detector 77−78648
ADS 1538=Σ 168=BDS 1015, orbit of visual double *(French)* 78−8056
ADS 3358, speckle holography meas. of triple star 78−93120
ADS 4299, 8048 and 9352, parallaxes and masses for visual binaries 80−4402
ADS 5281, visual binary speckle interferometry with linear digicon detector 77−78648
ADS 7251, photographic obs. in 1962-73 period, orbital motion *(Russian)* 78−28726
ADS 7390 (ω Leonis), visual binary, spectroscopic obs. and removal of nodal ambiguity 77−13399
ADS 8887, photographically unresolved visual binary, parallax and orbit 78−57593
ADS 9476 (Aitken 14), possible astrometric companion *(French)* 79−44553
AE 1, He-rich variable, spectroscopy and photometry 80−41836
AFCRL sources, identification of southern objects 77−33682
AFGL 437, optical and IR obs., young star cluster embedded in nebulosity 78−4394
AFGL/CRL IR sources, spectroscopic obs. 78−32599
AGK2+81°266, hot subdwarf, spectral type 78−45323
AL0827+24, quasar, absorpt. lines in optical spectrum 78−4390
Algol type stars, H I α obs. 80−109484
887 Alinda, light curves and rotation period for Amor object 79−44401
Allegheny Observatory parallax program, astrometric constants for 47 stars 78−53923
Allegheny parallax program, stars in region of 91 and 92 Tauri, Lalande 20111, 18 Bootis and HD 187399 77−74037
Am stars, τ Ursae Majoris and 15 Vulpeculae, energy distrib. from spectral obs. 80−85949
Am stars, evolved, search for photometric variability on lower part of Cepheid instability strip 80−62145
Am stars, multicolour photometry Hα and O I obs. 77−67101
Am stars, photometric stability 77−56953
Am-stars, photometric study of three objects 79−40204
Am-stars, scanner obs. 79−5827
Amalthea (J V), UBV photoelectric photometry near greatest W. elongation 78−36493
Amor-type asteroids 1960 UA, 1977 RA, and 1977 VA, precise posns. for 1977 period 78−28570
visible astronomical observations continued
o Andromedae, Be star, radial vels. obs. 79−58355
o Andromedae, Be star, rapid spectroscopic variations 77−56970
o Andromedae, Be star, spectrographic obs. from (1967 to 1976) 77−71116
o Andromedae, Be star, spectroscopic evidence for new shell episode 80−90444
o Andromedae, Be-star shell spectrum changes, spectrograms 78−4245
FF Andromedae, BY Draconis variable, spectroscopic binary, orbit and active region model 77−33527
RT Andromedae, eclipsing binary, three-colour photoelectric obs. and improved ephemeris 80−22043
RT Andromedae, light curve anal. of short period eclipsing binary 80−46603
AN Andromedae, light curve of Am binary systems, possible third body 79−58374
BX Andromedae, period increase *(Chinese)* 78−36642
GP Andromedae, photoelectric photometry of RRs variable *(German)* 79−71044
σ Andromedae, rapid spectral line variability disproved 80−8625
SW Andromedae, RR Lyrae variable, uvbyβ photometry 78−12249
o Andromedae, shell star, lack of linear polarisation variability 80−62157
o Andromedae, shell star, UBV photometry 77−82227
BM Andromedae, spectroscopic and photometric obs. of T Tauri-type star 80−62130
λ Andromedae, spectroscopic binary, UV and optical obs. of chromospheric lines 79−30087
AC Andromedae, UBV photometry of triple mode variable star 78−93260
RT Andromedae, V photoelectric obs. and lightcurve 79−71073
λ Andromedae, V photometric obs. during 1976-77 period 78−40994
ET Andromedae (HR 8861), Ap star, light vars. and period 80−46571
ET Andromedae (HR 8861), spectrum variable, period from photometric measures *(French)* 77−17579
anomalous Cepheids in Draco dwarf galaxy, masses 77−2434
anomalous nova-like object in M31 79−80316
Anon 0050+72.8, peculiar emission line galaxy 77−91627
129 Antigone, photoelectric photometry and synodic rot. period 77−45343
AO 0235+164, Lacertid, optical and radio absorption line systems 78−16520
AO 0235+164, nature of nebulosity assoc. with BL Lacertae object 78−28778
AO 0235+164, nonthermal emission spectral break development 77−57092
Ap, Am and A stars, radii from observed energy curves 77−87403
Ap and Hg-Mn stars, spectrophotometric scans, search for broad continuum features 78−12247
Ap stars, Balmer lines *(Russian)* 77−17587
Ap stars, HD 27309, 119213, 170000, and 192913, ten colour photometry *(German)* 77−17584
Ap stars, long-term light variations *(German)* 77−17585
Ap stars, narrow band photometry of broad absorpts. 77−67095
Ap stars, new Δa-photometry and evidence for two-component struct. of 5200 Å feature 80−67734
Ap stars, obs. evidence for pulsational stability 79−21303
Ap stars, photoelec. obs. of light vars. *(German)* 78−20841
Ap stars, photometric peculiarity index 77−91550
Ap stars, photometry, photoelectric parameter of peculiarity 77−2433
Ap stars, Pt in magnetic sequence 77−45436
Ap stars, spectrophotometry of broad flux depressions and comparison with synthetic spectra 80−67735
Ap stars, UBV photometry, light curves, periods 78−32472
Ap stars in open clusters, rot. vels. and mag. braking 77−33500
Ap-stars, detection of 4200 and 5200 Å, continuum features 79−75215
Ap-stars, mag. field obs. using photoelec. method, visible spectra obs. 80−82373
Ap-stars, scanner obs. 79−5827
Ap-stars, spectral energy distrib., spectrophotometry in 3300 to 7100 Å region 80−85953
Ap-type stars, mag. fields and atmospheres struct. *(Russian)* 77−17594
S Apodis, R Coronae Borealis variable, visual magnitude estimates 77−53611
α Aquarii, Ca II K-line profile obs. rel. to chromospheric event 80−31299
AE Aquarii, cataclysmic variable, rapid light oscills. rel. to white dwarf oblique rotator model 80−36634
U Aquarii, R Coronae Borealis star, extraordinary comp. rel. to unusual s-processing event 80−17588
CY Aquarii, RRs type star, BV photometric obs. *(Italian)* 80−90449
α Aquarii, supergiant, Ca II H and K line variation 77−22227
R Aquarii, symbiotic long-period variable, spectrum of assoc. nebulosity 80−90450
EE Aquarii, UBV photometry of β Lyrae-type eclipsing binary 79−84817
R Aquarii, UBVRI polarimetric obs., orbital motion effect *(Russian)* 80−36646
U Aquarii, visual magnitude estimates 1976, Oct. 77−2429
σ Aquarii (A0 IVs), hot metallic-line star, spectrum and abundance anal. 80−90415
π Aquarii and other Be stars, light variations 77−45420
Aquila X-1, photometry and spectroscopy of optical counterpart, model 78−32614
Aquila X-1, UBV photometry during 1978 X-ray outburst *(Russian)* 79−101224
Aquila X-1 (3U 1908+00), faint flare star optical candidate 77−67141
Aquila X-1 (3U 1908+00), optical counterpart for flaring source 78−41089
Aquila X-1 (4U 1908+00), 1978 summer X-ray and optical outburst 80−73068
Aquila X-1 (4U 1908+00), optical outburst, obs. 78−69911
Aquila X-1 (4U 1908+00), optical outburst obs. 80−67909
Aquila X-1 optical counterpart, spectrum 78−77626
V794 Aquilae, AM Herculis-like brightness vars. 79−92804
U Aquilae, Cepheid variable, detect. as long-period binary by radial vel. spectrometer 80−51667
V342 Aquilae, eclipsing binary, period and light curve changes, (1966 to 1976) 80−67791
KO Aquilae, eclipsing binary system, UBV photoelectric study 80−62198

visible astronomical observations continued
V889 Aquilae, photometric obs. of eclipsing binary, apsidal motion 79−25640
TW V586 and V1079 Aquilae, photometry, photographic obs. *(Russian)* 78−20842
β Aquilae, single G-type subgiant, UVB photometry 79−62823
α Aquilae (Altair), 1941-77 astrometric obs. 79−12470
θ Aquilae (B9.5 III), spectrum and abundance anal. 80−90415
T Aquilae (Nova 1891), spectrophotometry of shell 80−72955
V603 Aquilae (Nova 1918), IUE obs. of periodic light vars. 80−105251
V603 Aquilae (Nova 1918), old nova, eclipses obs. 80−90476
V1301 Aquilae (Nova 1975), VBLUW photometry, absolute magnitude, distance and reddening 79−58342
387 Aquitania, slow spinning asteroid with rot. period of nearly one day, photometric evidence 80−17529
Ara OB1, NGC 6193 and Ara R1, young southern complex, UBVRI obs. 78−16473
V535 Arae, absolute characts. of W Ursae Majoris system 79−58373
Arakelian 120, optical and IR photometry of class 1 Seyfert 79−58423
Arakelian 120, Seyfert 1 galaxy, optical variability 79−40259
Arakelian 120, Seyfert 1 galaxy, UBV photometry, brightness and colour vars., models 80−26983
Arakelian galaxies, emission line spectra 77−74138
Arakelyan 120, Seyfert galaxy, spectrophotometry 79−62913
Arakelyan 120, Seyfert galaxy nuclei, optical variability, UBV obs. 80−73049
Ariel 0620−00, optical light curve and periodicity 77−13497
Ariel 1524=61, transient X-ray source optical identification 77−45611
Ariel 5 clusters, optical morphology and galaxy density 78−8135
β Arietis, Am star, spectroscopic obs. and curve of growth anal. 77−22237
56 Arietis, Ap star, spectrum vars. rel. to mag. field, precession and rot. 77−2432
κ Arietis, double-lined Am star, spectroscopic obs. and curve of growth anal. 77−22237
UX Arietis, RS Canum Venaticorum type binary, UBV photometry, 1974-5 period 77−91569
UX Arietis, RS Canum Venaticorum type star, UV excess, spectrophotometric obs. 78−8043
56 Arietis, spectrophotometry of Ap star, continuum features vars. 80−36638
UX Arietis, V photometric obs. during 1976-77 period 78−40994
asteroid, 1980 AA, position Jan 20-22 1980 and ephemeris until Feb. 21st 80−31239
asteroid, 1980 AA, rot. period observed photometrically 80−36558
asteroid 1976 AA, photometric obs. at 0.56 and 2.2 μ 77−82144
asteroid 1977 HB, precise positions 1977, May 77−53461
asteroid 624 Hektor, light curve indicating elongated shape 80−98600
asteroid families, obs. evidence for common origins 77−91468
asteroid position determination in April 1979, data reduction *(French)* 80−72845
asteroid positions in 1978, visible obs. 80−67630
asteroid satellites, discovery from occultations of stars 80−4286
asteroidal objects found during search for short-period comets 78−85907
asteroids, 1976 August obs. at ESO La Silla with GPO plus three discoveries *(French)* 78−45260
asteroids, absolute magnitudes 79−21219
asteroids, astrometric 1978 positions from ESO and GPO obs. 80−72841
asteroids, astrometry 1975-1978 from Uppsala southern station 80−85883
asteroids, astrometry in 1978 April, ESO obs. 80−85882
asteroids, Crimean obs. (1963-76) *(Russian)* 80−46456
asteroids, FK4 equinox corrections from meridian obs. 80−8519
asteroids, four objects found during Jupiter satellite study 79−75139
asteroids, improved orbits for ten objects rel. to quality of observations *(Russian)* 78−49369
asteroids, light curve survey of 9 objects during 1977 oppositions 79−53753
asteroids, light curve survey of faint objects 80−4283
asteroids, magnitudes and phase relations compilation 79−88617
asteroids, main-belt, photographic photometry of 110 objects 78−40859
asteroids, main-belt, positions 78−12135
asteroids, Minor Planet Circular 5333-5390, 623 precise posns. 80−77325
asteroids, Minor Planet Circulars, 3094 precise posns. 80−31241
asteroids, Minor Planet Circulars 4391-4424, 888 precise posns. 78−81578
asteroids, minor planet circulars 4425-4482, 2823 precise posns. 78−85886
asteroids, Minor Planet Circulars 4483-4520, 854 precise posns. 78−93140
asteroids, minor planet circulars 4521-4548, 669 precise posns. 79−2514
asteroids, Minor Planet Circulars 4583-4622, 901 precise posns. 79−16871
asteroids, Minor Planet Circulars 4623-4648, 682 precise posns. 79−25538
asteroids, Minor Planet Circulars 4649-4688, 674 precise posns. 79−35178
asteroids, Minor Planet Circulars 4689-4722, 1388 precise posns. 79−53754
asteroids, Minor Planet Circulars 4723-4746, 533 precise posns. 79−66953
asteroids, Minor Planet Circulars 4747-4788, 954 precise posns. 79−75136
asteroids, Minor planet circulars 4789-4844, 1438 precise posns. 79−84729
asteroids, Minor Planet Circulars 4845-4936, 4565 precise posns. 79−101107
asteroids, Minor Planet Circulars 4937-5016, 3390 precise posns. 80−8580
asteroids, Minor planet circulars 5017-5066, 669 precise posns. 80−17533
asteroids, Minor Planet Circulars 5137-5188, 2067 precise posns. 80−46459
asteroids, Minor Planet Circulars 5189-5248, 1389 precise posns. 80−67631
asteroids, Minor Planet Circulars 5249-5286, 1112 precise posns. 80−67632
asteroids, Minor Planet Circulars 5287-5332, 1045 precise posns. 80−67633

visible astronomical observations continued
asteroids, Minor Planet Circulars 5391-5422, 577 precise posns. 80−85884
asteroids, Minor Planet Circulars 5423-5454, 798 precise posns. 80−98599
asteroids, Munich meridian obs. (1941-61), orbital elements determ. *(German)* 80−77306
asteroids, Palomar planet-crossing asteroid survey, 1973-1978 period 80−36539
asteroids, photoelec. obs. by high school teachers 77−45347
asteroids, photoelectric photometry and rotation period for three large and dark objects 79−44402
asteroids, photoelectric photometry during 1975-77 period 78−61783
asteroids, photoelectric photometry of seven objects 79−35175
asteroids, photographic astrometry at Observatoria Nacional do Brasil (Sept. 1977) 79−70985
asteroids, photographic photometry with Schmidt telescope during 1977 and 1978 80−72844
asteroids, photometry in 0.56-2.2 μ range for 30 objects 78−69725
asteroids, position obs. at Sydney Observatory during 1975 77−53462
asteroids, positions meas. at ESO-La Silla during 1978 April 79−58293
asteroids, precise 1977 posns. for 7 objects, Sydney obs. 79−88618
asteroids, precise astrographic positions for 1958-1967 period 79−62786
asteroids, precise positions, (1977) 79−40117
asteroids, precise positions (August 1975 to May 1976) 78−12134
asteroids, precise positions for 18 objects meas. at Torino 78−69730
asteroids, precise positions for 35 objects 79−8873
asteroids, precise positions for nine selected objects in 1976-7 period 78−77514
asteroids, precise positions of 25 objects 79−58292
asteroids, precise posns. for 74 objects in 1977, Swedish obs. 80−62065
asteroids, precise posns. in 1975-6 period for 30 main belt objects 78−77515
asteroids, rotation period near 24 hours, problems 79−21220
asteroids, rotation rates, pole positions and shapes 80−17531
asteroids, Saratov obs. (1974 April-Oct.) *(Russian)* 80−46457
asteroids, survey for high-inclination minor planets 79−75156
asteroids, synodic rotation periods from photoelectric lightcurve 78−45259
asteroids, topocentric positions for 11 objects (Sept. 1977-Oct. 1978) *(German)* 80−46453
asteroids, Trojan group, discovery of new members, orbital elements and ephemerides 80−72847
asteroids, UBV photometry, shapes and rot. characts. 77−5484
asteroids, UBV photometry of 145 faint objects 78−69724
asteroids, UBV photometry of small and distant objects 77−82147
5 Astraea, photometric obs., pole orientation, rot. period 78−40858
astrometric obs. with Photographic Zenith Tube at Tokyo Observatory, anal. of errors 80−98547
astronomical diffuse objects, strip photometry appl. to globular clusters multicolour obs. 78−89229
Astronomical Engelhardt Observatory, latitude obs. *(Russian)* 78−4080
astronomical site testing, solar seeing and stellar scintillation obs. 77−29645
asymptotic giant branch stars in globular clusters, spectra 79−8913
atmospheric turbulence effects on optical and IR image form. *(French)* 80−46257
ϵ Aurigae, ^{7}Li I 6708 Å line and Li interstellar abundance 78−49494
59 Aurigae, δ Scuti star, light curves periodogram anal. 80−62141
WW Aurigae, Am eclipsing binary, spectrographic obs., radial vel. curves 77−33559
SX Aurigae, early-type semidetached binary, UBV photometric anal. 79−44521
ϵ Aurigae, eclipsing binary, astrometric study from Sproul 61-cm refractor plates 78−89219
ζ Aurigae, eclipsing binary, Ca I 6752 Å circumstellar line obs. 77−17619
ϵ Aurigae, eclipsing binary, distance from astrometric obs. 79−53859
SX Aurigae, eclipsing binary, light curves anal. by automated Fourier techniques 79−92798
NW Aurigae, eclipsing binary, photoelectric photometry 78−8052
LY Aurigae, eclipsing binary, photometric elements, masses, radii, luminosities 78−28723
IU Aurigae, eclipsing binary, two-colour photometry rel. to presence of third body 80−36669
IU Aurigae, eclipsing binary, variable light curve 77−17627
AR Aurigae, eclipsing binary Hg star, peculiar spectral var. during eclipse 80−98679
T Aurigae, eclipsing binary nova, times of minima 77−22267
IU Aurigae, light curve study of early-type close binaries in triple systems 78−89222
IU Aurigae, massive triple system, obs. 77−64798
KR Aurigae, optical spectrum, variability *(Russian)* 78−36597
CQ Aurigae, RS Canum Venaticorum type eclipsing binary, photoelectric obs. 79−40218
SX Aurigae, semidetached massive binary system, period changes 79−25637
θ Aurigae, short period Ap star, discovery of mag. field 77−33511
ϵ Aurigae, spectrum outside eclipse 77−71129
KW Aurigae (14 Aurigae A), pulsating ellipsoidal variable, blue light photometry rel. to tidal modes 79−97028
α Aurigae (Capella), Ca II lines obs. rel. to chromosphere model 78−40931
α Aurigae (Capella), orbital motion determ. using phase effect detect. at CERGA stellar interferometer *(French)* 80−36508
α Aurigae (Capella) AB, angular diams. by two telescope interferometry 78−8055
T Aurigae (Nova 1891), old nova, photometric and spectroscopic obs. 80−90446
AA Aurigae field, UBV photoelectric magnitude sequence 77−74073
63 Ausonia, BV photometric obs., light curve, rot. period 77−82150
AWM 4, redshifts for five galaxies in poor cluster 78−45415
B133, B134, B335, dark nebulae, star counts rel. to visual extinction 78−57612
B2 1101+38, BL Lacertae-type object UBV photometry 78−8114
B2 1225+317, IR and optical spectrophotometry, Hα/Lα ratio 79−25749
B2 1225+31, high-luminosity quasar, H emission line intensity ratios 79−25748
B2 1225+31, spectrum of bright quasar 78−93447

visible astronomical observations continued
B2 1308+326, BL Lacertae object, photometry and polarization during 1978 outburst 79−25718
B2 1308+326, optical and IR variability during 1978 outburst 80−51888
B2 1308+32 (CSVS 6997, OP 313), common identification as Lacertid 78−8128
B2 1523+29, Lacertid, optical variability from archival plates 77−26056
B2 1652+39, BL Lacertae-type object, photoelectric intraday photometric obs. 78−36681
B9 II to G0V stable stars, quantitative spectral classification *(Russian)* 79−44480
B, A and F stars, spectrophotometry, effective temps. 78−57546
B, A and F stars in selected areas, intrinsic uvby β indices, distances and colour excesses 78−89171
B I Ia-0 supergiants, spectra and mass loss 79−16948
B stars, seven new stars with Hα emission lines *(French)* 77−49391
B-type and Be-type stars, search for binaries 78−57551
B-type stars, CNO abundances in associations and general field 80−67702
B-type stars, optical counterparts of X-ray sources, luminosity class from O I 7773 Å triplet absorpt. 79−71031
B-type stars, radial vels. determined at Radcliffe Observatory 78−12225
B-type stars, search for weak interstellar lines in spectra 77−74124
B-type stars, uvby indices, empirical effective temps. and bolometric corrections 77−45429
B-type stars, wavelengths of neutral He lines 77−25999
B-type stars at intermediate galactic latitude, space distrib. 77−91535
B-type stars in young clusters and associations, He I 4026 Å line obs. and He/H ratio determ. 77−29887
late B-type stars small v sin i values, Ap star determ., visible spectra 80−77409
B-type supergiant stars, radial vel. vars. 79−21285
B-type variable star in LMC, possible identification with LMC X-3, spectral type 79−5923
Barnard's loop and evidence for associated expanding shell 79−53866
Barnard's star, spectrophotometry with Carnegie image tube 78−57466
Barnard 92, dark nebula, star counts rel. to visual extinction 78−57612
Barnard Loop, Hβ obs. 79−80346
barred spiral galaxies in Virgo cluster, surface photometry 77−13453
Basle catalogue of 1906 blue objects at high galactic latitudes 78−32360
BD+0°2989, late-type dwarf star, metal abundances 77−78779
BD+10°2179, C rich H deficient star, UBV photometric obs. 80−90437
BD+29°3805, K-type giant, spectroscopic binary orbit 80−67790
BD+39°3226, BD+34°1543, hot subdwarfs, spectral types 78−45323
BD+61°1211, optical counterpart of 2A 1052+606, RS Canum Venaticorum binary system 79−92803
BD−7°3007, nova-like variable, simultaneous spectroscopy and photometry 78−12250
BD +11° 4571=ADS 15010, subdwarf binary, history of astrometric obs. 79−62874
BD +1°4381, H deficient A-type star, effective temp. 79−40195
BD −9°4395, H deficient star, spectral photometry and quantitative anal. 77−56946
BD-3°5357, eclipsing binary with hot subdwarf component 77−91574
BDS 1269, visual binary, metal abundances and characts. of components 80−4397
BDS 1269 A, metal-poor δ Scuti star, pulsation periods from b-band photometry 80−105247
Be 94, UBV photometric obs. of young distant open cluster in Cepheus 78−61892
Be and shell stars, Balmer line polarisation meas. 77−56995
Be shell stars, Bβ high-resolution polarisation struct. meas. by digicon spectropolarimeter 79−44485
Be stars, discoveries in open clusters NGC 3766 and (IC 2581) 80−90445
Be stars, emission features rel. to luminosity class and spectral type 77−56969
Be stars, Hα survey 77−56967
Be stars, mag. fields determ. via linear polarisation spectrum *(Russian)* 80−90344
Be stars, photometric behaviour, UV excess, emission indices, galactic distrib. 80−36637
Be stars, rapid Hα variations 77−56971
Be stars, search for rapid Hα and Hβ line variability 77−26014
Be stars, spectroscopic obs. 77−56957
Be stars envelopes, observational study 77−13355
Be stars in galactic clusters, Hα study 77−56968
Be stars in open clusters, energy distrib. 78−85944
Be stress, bright, Hα emission variability 79−67027
Be-stars, echelle spectra 77−56989
Be-stars, Hα vars. in spectra of bright northern objects 79−35265
Be-stars, intrinsic polarisation 79−75213
Be-stars, spectra rel. to rotational hypothesis 77−56981
Be-stars, TV obs. of Hα and Hβ line profile rapid vars. *(Russian)* 79−16992
Be-type southern stars, photoelec. scanner meas. of Balmer emission line profiles 77−45452
776 Berbericia, slow spinning asteroid with rot. period of nearly one day, photometric evidence 80−17529
716 Berkeley, photographic photometry, light curves, magnitudes 79−12418
Berkeley 11, compact open cluster, UBV obs. 80−94840
1580 Betulia, Amor asteroid, photographic lightcurve 77−91465
1580 Betulia, broadband visual and 10.6 μ photometry 79−2511
1580 Betulia, UBV photometry and polarimetry 79−2512
binary central star in planetary nebula NGC 6853 from proper motion obs. 77−49434
binary galaxies, radial vels. and masses of 44 pairs 80−26990
binary star separation meas. using speckle interferometry 77−22102
binary stars, G and K-type giants, Ca II H and K lines emission intensity 80−82420
binary stars, meas. via speckle interferometry 77−71011
binary stars, obs. by speckle interferometry 80−90477
binary stars, speckle interferometry at 5200 Å for 30 objects 78−65656
binary stars, speckle interferometry meas. 78−85973
binary stars, speckle interferometry of 155 objects 79−17017
binary stars, speckle interferometry with 1 m telescope 78−69831
binary stars, spectroscopic and eclipsing, survey for intrinsic linear polarization 78−4288

visible astronomical observations continued
binary stars, visual, speckle interferometric meas. 77−78820
binary stars, visual obs. 79−35303
binary stars unresolved by speckle interferometry, epochs of obs., (1975-77) 78−73735
binary systems, speckle interferometric obs. with Haute-Provence 1.93 m telescope 80−90475
bipolar reflection nebulae, photoelec. polarization maps 78−28742
BL Lacertae-type objects, variable, IR and visible polarimetry and photometry 78−16528
blue compact Zwicky galaxies, spectroscopic survey 79−58417
blue objects and 5C3 radiosources optical counterparts obs. near M31 77−91526
blue star in SNR 1006, spectral features and UBV photoelectric meas. 80−41830
blue star-like objects in field of M31, photometric obs. 77−9744
blue stellar objects, from MC2 and MC3 catalogue, polarisation obs., BL Lacertae objects 79−48918
Bochum 15 stellar aggregate, photoelectric and spectroscopic obs. 77−87490
γ Bootis, Ap star, chemical element distrib. from spectrophotometry *(Russian)* 77−22238
γ Bootis, classical evolved δ Scuti star 79−75219
α Bootis, comparison of predicted and observed spectral energy distrib. 80−46546
AC Bootis, eclipsing binary, detailed photometric study 78−36637
44=i Bootis, eclipsing binary, variable light curve obs. and implications 78−61887
i Bootis, light curve and period vars. of W Ursae Majoris type star 80−4398
XY Bootis, photometric obs. of contact binary, light curves, mass ratio 78−4286
α Bootis, stellar gravity from metallic line profiles and effective temp. 77−64759
SS Bootis, UBV obs. and Fourier anal., eclipsing RS Canum Venaticorum binary 80−17613
TZ Bootis, W Ursae Majoris system, spectroscopic and photoelectric obs. 78−69832
AC Bootis, W Ursae Majoris system, V photoelectric photometry 77−64800
α Bootis (Arcturus), O and C abundances *(Russian)* 78−16420
α Bootis (Arcturus), obs. using image sharpening telescope 77−49295
α Bootis (Arcturus), spectral line asymmetry meas. rel. to Sun 80−51753
ξ Bootis A, late-type dwarf star, mag. field obs. 80−72949
Bordeaux Observatory, equatorial coords. for asteroids, planets and Moon in 1972-4 period *(French)* 78−81577
BPM 25114, hot magnetic white dwarf, image tube spectrophotometry 77−74051
BPM 25114, peculiar white dwarf, light vars., oblique rotator model *(Italian)* 78−93241
BPM 25114, southern mag. white dwarf, spectrophotometric obs. 79−92765
BPM 30551, ZZ Ceti type white dwarf, high-freq. oscills. 77−2445
BPM 30551, ZZ Ceti-type variable, light curves and power spectra 77−56948
BPM 31594, new southern hemisphere variable white dwarf 77−5531
BPM 4729, cool DA white dwarf with self-broadened Balmer lines 79−35255
bright galaxies, integrated magnitude and colours in UBV system, second catalogue 79−12509
bright galaxies, optical redshifts 78−89252
bright galaxies and compact galaxies apparent associations 78−41040
bright galaxy nuclei, optical and radio survey, sample selection and obs. 80−73039
bright nebulosities in opaque dust clouds 77−64668
bright O to G0 stars south of dec. +10°, photoelectric Hβ photometry 77−37600
bright quasars discovery program, preliminary results 77−17715
bright southern stars, Stromgren photometry rel. to spectral classification 79−88645
bright sporadic meteor, spectrum obtained with Wampler scanner 78−57508
bright zenith star obs., Poltava latit. differences interpretation 78−28488
Brno fireball (1977 Sept. 14), photographic data 80−41771
Butterfly Nebula M2-9 rel. to Be stars and protoplanetaries 79−48887
Byurakan 2, open cluster, UBV photometry 77−2345
5C1 radiosources, optical identification by photographic photometry and spectra 80−77503
3C273, spectroscopic obs. and redshift of associated galaxy 78−77606
5C4 radiosources, search for optical identifications 78−73767
3C 111, spectrum and redshift of luminous N-type galaxy 77−33666
3C 120, emission-line nebulosity morphology 79−80363
3 C 120, galaxy and nucleus, UBV photoelectric obs. 79−44601
3C 120, radio galaxy, vars. in optical spectrum *(Russian)* 80−90540
3C 120, Seyfert galaxy, spectrophotometric obs. of assoc. nebulosity 80−67890
3C 120, Seyfert galaxy nuclei, optical variability, UBV obs. 80−73049
3C 227 and 382 radiogalaxies, spectral-flux distrib. in 0.36-3.5 μ range 78−36710
3C 232, quasar, Ca II absorpt. lines due to galaxy (NGC 3067) 78−36719
3C 249.1, quasar, spectroscopic obs. of assoc. nebulosity 77−33677
4C 25.05, H_2 lines identification in spectrum of quasar *(Russian)* 78−69905
3 C 273, H I spectral line intensities *(Russian)* 79−88763
3C 273, rapid fluctuations of radio flux and circular polarisation and optical linear polarisation 77−91663
3C 273, spectrophotometry of QSO at optical and IR wavelengths 79−17123
3C 273, UBV obs., (1975 to 1979) 80−62309
3C 279, variable quasi-stellar source, IR and visible polarimetry and photometry 78−16528
3C 285, 3C 265, 3C 390.3, optical emission in radio lobes 78−57630
3C 285, double radio galaxy, discovery of optical emission in radio lobes 77−64866
3C 286, quasar, optical absorpt. lines detect., redshift 80−4454
3C 293, radio galaxy, radio and optical obs. 78−93418
3C 295 galaxy cluster, two-colour ISIT photometry rel. to galaxies evolution 78−24557
3C 303, double radiosource, radio struct. and optical field 78−16519

visible astronomical observations continued
3C 33, 98, 184.1 and 218, rotation axes 80−26997
3C 33, optical emission detect. in SW radio lobe 78−57665
3C 33, rot. axis. of assoc. optical galaxy 78−4355
3C 343.1, distant radio galaxy, spectroscopy and photometry, redshift 78−8123
3C 345, optical spectrum variability 80−8709
3C 345, quasar, optical variability 77−74157
3C 345, quasar relation between optical and radio VLBI 77−64876
3C 351, quasar, VLA maps and outer lobe optical emission search 80−105376
3C 351, search for periodic components in light variations *(Russian)* 79−53931
3C 371, BL Lacertae-type object, photoelectric intraday photometric obs. 78−36681
3C 382 (B2 1833+32), variability of optical counterpart 78−41053
3C 446, 1980 June outburst, UBV photometry 80−86010
3C 48, emission-line spectrum of quasar 79−71147
4C 55.27, quasar, redshift and spectrum 77−45596
3C 58, spectra of faint knots in SNR 78−93375
4 C 61.20, optically active extragalactic radiosource 77−17712
3C 6.1, 265 and 352, spectrophotometry of high-redshift radio galaxies 79−92876
3C 66 A, BL Lacertae-type object, photoelectric intraday photometric obs. 78−36681
5C 7 radiosources, optical identifications 79−67111
3C 98, 3C 178, 3C 192, 3C 327, narrow-line radio galaxies, optical spectra 77−33664
5C areas, optical identifications 77−37665
4C radio galaxies, structs. and optical identifications 79−71137
4C radiosources, optical identifications 77−26077
4C radiosources, search for variable quasars by image tube photography 77−22326
3C radiosources, systematic optical identification 78−36709
C- and M-type stars near globular cluster NGC 419 in SMC, cluster membership 80−26921
CA 0340−538 (3U 0328−523), southern cluster of galaxies, vel. dispersion and global parameters 78−36705
X Caeli, temp. and radius vars. 77−49395
California Nebula (NGC 1499), visual extinction uniformity across nebula 80−62225
53 Camelopardalis, Ap star, Ca II K and Hδ lines rapid vars. *(Russian)* 80−90458
53 Camelopardalis, Ap star, radial vels. and binary nature 79−80320
53 Camelopardalis, Ap star, surface mag. field distrib. 77−26015
Z Camelopardalis, dwarf nova, photometric obs. and light curve (1973-77) 80−56853
Z Camelopardalis, dwarf nova, spectrophotometry at standstill and in eruption 80−82366
SV Camelopardalis, eclipsing binary containing BY Draconis variable, motion round third component 79−67055
α Camelopardalis, O-type supergiant, spectroscopic study, model atm. anal. 78−28681
RU Camelopardalis, photometric behaviour, (1966 to 1977) 78−89206
53 Camelopardalis, photometric vars. 80−4367
AX Camelopardalis (53 Camelopardalis), Ap star, UBV photoelectric photometry and period of var. *(Italian)* 80−90448
α Camelopardalis (O9.5 Ia), variable Hα P Cygni profile 80−41818
38 Cancri, δ Scuti star, UBV photometric obs. of variability 80−22021
S Cancri, close eclipsing system, freq. domain anal. of light changes 77−53638
AH Cancri, contact binary in M67, spectrum and photometry 79−40222
WY Cancri, eclipsing binary, obs. rel. to absolute information derivation at lower end of main sequence 79−92799
UU Cancri, long-period eclipsing binary, radial vel. meas. 77−74096
RU Cancri, RS Canum Venaticorum type eclipsing binary, photoelectric obs. 79−40218
ζ Cancri, speckle holography meas. of double star 78−93120
49 Cancri, spectrophotometry of Ap star, continuum features vars. 80−36638
BT Cancri (38 Cancri) δ Scuti star, photometry rel. to radial and nonradial pulsation periods 80−85948
Canis Major R1, anomalous diffuse bands 80−51820
Canis Major R1, optical and IR props. of newly formed stars 78−93332
Canis Major R1 and OB1 associations, Fabry-Perot obs. of assoc. expanding gas shells 78−93336
R Canis Majoris, eclipsing binary, multiband photoelectric photometry 77−53633
UW Canis Majoris, eclipsing binary, photometry and primary component shape and atmospheric struct. 78−40992
CW Canis Majoris, eclipsing binary, UBV photometry 77−37615
YZ Canis Majoris, flare star, coordinated X-ray, optical and radio obs. 78−8012
29 Canis Majoris, massive hot binary star, spectrograms, mass loss 78−12299
α Canis Majoris, relative positions of components of visual binary 77−82274
27 Canis Majoris, spectroscopic obs. in 0.14-4.7 μ range 78−85957
α Canis Majoris (Sirius), astrometric study rel. to distance and components masses 79−5858
α Canis Majoris (Sirius), Ca II K line high resolution profile obs. 80−56830
α Canis Majoris (Sirius), Ca II K-line asymmetry, comments 79−30063
α Canis Majoris (Sirius), Ca II K-line asymmetry unconfirmed 79−30062
α Canis Majoris (Sirius), obs. using image sharpening telescope 77−49295
α Canis Majoris (Sirius), rot. vel. and Ba abundance 78−12218
α Canis Majoris (Sirius), search for surrounding nebulosity 78−93242
α Canis Majoris B, photoelectric obs. 78−4220
β Canis Majoris stars in southern hemisphere, photometric search 78−12243
β Canis Majoris variables, β photometry of early B-type stars 78−77562
YZ Canis Minoris, negative flares and dips of UV Ceti-type star 79−80317
YZ Canis Minoris, spectroscopic flare obs. 79−92780
α Canis Minoris (Polaris), interferometry, first fringe meas. 80−82215
α Canis Minoris (Procyon), CH and CN bands obs. rel. to CNO abundances 78−93222
R Canis sMajoris stars, photometric elements 79−58371

visible astronomical observations continued
4 Canum Venaticorum, δ Scuti variable, photoelectric photometry 77−53601
α^2 Canum Venaticorum, Ap star, surface mag. field distrib. 77−26015
4 Canum Venaticorum, BV photometry of δ Scuti star 79−35268
Y Canum Venaticorum, C star, $^6Li/^7Li$ atmospheric abundance 77−33523
TX Canum Venaticorum, cataclysmic variable, visible spectra obs. 80−105249
VZ Canum Venaticorum, eclipsing binary star, photometric elements and intrinsic variability 77−45487
TX Canum Venaticorum, evolution from cataclysmic to stationary P Cygni stage 79−12479
RS Canum Venaticorum, intrinsic linear polarization of eclipsing binary 80−4394
α^2 Canum Venaticorum, mag. Ap star high-resolution polarisation obs. inside spectral line 78−40951
α^2 Canum Venaticorum, magnetic field gradient in Ap-star atmosphere, Zeeman spectra 78−85953
AM Canum Venaticorum, orbital period increase 80−12765
RS Canum Venaticorum, out of eclipse light var. and comparison with similar stars 80−109489
RS Canum Venaticorum, spectrophotometric obs. of light curve wave distortion 77−33562
RS Canum Venaticorum, UV excess, spectrophotometric obs. 78−8043
RS Canum Venaticorum type binaries, Hγ line vars., chromospheric diagnostics 80−62181
RS Canum Venaticorum-type binaries, emission line vars. 78−24527
β Capricorni, 1977 October 20 lunar occultation results 79−44523
δ Capricorni, eclipsing binary, Am primary component metallicism var. 77−67115
β Capricorni, triple star, fundamental parameters from occultation astrometry and spectroscopy 79−40216
ν Capricorni (B9.5 V), spectrum and abundance anal. 80−90415
Carafe group of galaxies, spectroscopic and photographic obs. of peculiar galaxies 79−35387
Carina nebula, struct. and rel. to η Carinae 77−87520
Carina Nebula association, radial vel. study of WN stars and Of star 79−35261
Carina Nebula stars, interstellar λ4430 band obs. 78−32555
Carina OB 1 association, RI photometry, reddening law determ. 79−8957
Carina spiral arm, galactic struct. and star formation, spectrographic and photometric obs. *(French)* 78−89256
Carina spiral feature, photometry and spectra rel. to stars and interstellar dust distrib. 80−51871
χ Carinae, β Canis Majoris type variability discovery from UBV photometry 79−80326
l Carinae, Cepheid variable, Fourier anal. of light var. 80−90442
η Carinae, earliest spectroscopic obs. and interaction of star with Carina Nebula 77−45433
OY Carinae, eclipsing ultrashort periodic dwarf nova discovery 79−53823
η Carinae, evidence for circumstellar disc and asymmetric explosion *(Italian)* 79−53893
R Carinae, intrinsic linear polarisation narrow-band struct. 77−49397
η Carinae, optical and UV line emission of ionised Fe 77−13364
η Carinae, optical linear polarization map and outburst 79−67030
AG Carinae, P Cygni supergiant, spectrum of ring nebula 77−67100
θ Carinae, radial vel. of chemically-peculiar B-type star 80−8635
l Carinae, search for comparison stars, uvbyβ photometry, colour excess 80−62136
α Carinae (Canopus), periodic variable mag. field detect. 77−49381
QZ Carinae (HD 93206), massive multiple system in great Carina Nebula, spectral types and orbits 79−97027
QZ Carinae (HD 93206), O-type quadruple eclipsing system, spectroscopic and radial vel. study 80−105275
η Carinae and Carina Nebula, polarimetric study 79−67043
VY Carinae field stars, spectra and photometry rel. to cepheid absolute magnitude 77−64764
η Carinae nebulosity, proper motion meas. in complex outer shell 78−28687
558 Carmen, photoelectric light curves, synodic rot. periods, amplitudes of var. 79−53752
Cassiopeia, photoelectric UBV photometry 77−37598
Cassiopeia A, image tube spectrograms 78−16485
Cassiopeia A, supernova remnant, proper motion obs., expansion centre determ. 77−22289
Cassiopeia A supernova remnant, abundance inhomogeneities 80−12797
ρ Cassiopeiae, absolute energy distrib. in 3400-7100 Å range 78−49440
SX Cassiopeiae, Algol type binary, spectrophotometry 77−2454
TV Cassiopeiae, Algol variable, UBV photometric obs. 79−35306
γ Cassiopeiae, Be star, coordinated IR and optical obs., (in late 1976) 79−25616
γ Cassiopeiae, Be star, polarisation rapid vars. 80−22022
γ Cassiopeiae, Be star, rapid spectroscopic variations 77−56970
γ Cassiopeiae, Be star, spectrophotometric variability from UV and Hα obs. 79−5829
V523 Cassiopeiae, BV photometry of W UMa type system *(Russian)* 79−92807
SU Cassiopeiae, Cepheid variable, spectrophotometric determ. of effective temp. 80−90435
VX Cassiopeiae, early-type irregular variable, photometric variability *(Russian)* 80−72973
CW Cassiopeiae, eclipsing, binary, anal. of V light curve 77−57009
AO Cassiopeiae, eclipsing binary, intrinsic linear polarization, rel. to circumstellar envelope 77−17618
TV Cassiopeiae, eclipsing binary, period and UBV light curves 78−4287
RZ Cassiopeiae, eclipsing binary, spectroscopic orbit 80−22040
DO Cassiopeiae, eclipsing binary, three-colour photoelectric investigation 78−16462
MN Cassiopeiae, eclipsing binary orbital elements 77−71127
AB Cassiopeiae, eclipsing binary with δ Scuti primary, light vars. preliminary anal. 80−94831
VX Cassiopeiae, fast irregular variable, H_α and H_β lines obs. *(Russian)* 77−87400
γ Cassiopeiae, Hα and Hβ emission lines equivalent widths, scanner obs. 77−2430
γ Cassiopeiae, Hα linear polarisation in Be star 78−16425
TV Cassiopeiae, light curve and orbital elements of eclipsing binary 77−49430

visible astronomical observations continued
BM Cassiopeiae, long-period eclipsing binary, radial vel. meas. 77−74096
AZ Cassiopeiae, long-period eclipsing system, photoelectric obs. 80−46608
κ Cassiopeiae, OBC star, spectrophotometry, 3300-7100 Å region 79−67009
TU Cassiopeiae, periods and amplitudes from radial vels. 79−101159
WZ Cassiopeiae, semiregular variable star, variable CaCl absorpt. bands 79−88683
SU and TU Cassiopeiae, short-period Cepheids, photometry and spectra rel. to radius anomalies 80−26864
κ Cassiopeiae, spectral obs., coarse atm. anal. 77−33487
HT Cassiopeiae, spectroscopic obs. of dwarf nova 79−88668
6 Cassiopeiae, spectroscopic obs. of supergiant star, equivalent widths, microturbulence and radial vel. 80−22006
μ Cassiopeiae, subdwarf binary, spectroscopic orbit 78−8046
TU Cassiopeiae, third period in beat Cepheid 78−16424
γ Cassiopeiae, UV and optical spectral var. rel. to coronal emission 78−93251
o Cassiopeiae (HD 4180), Be star, Balmer emission lines vars. rel. to IR photometric vars. 79−58353
V509 Cassiopeiae (HR 8752), no emission at Hβ (1979 July 31) 79−92782
V509 Cassiopeiae (HR 8752), spectrum variable supergiant, Hα emission obs. 79−88672
SU Cassiopeiae region, field stars photometry rel. to Cepheid distance and pulsation mode 78−89204
V509 Cassioperae (HR 8752), light vars. during period of spectrum vars. 79−101161
cataclysmic variables, pulse timing meas., accretion disc models 79−62831
cataclysmic variables, visual continuum flux distribs. 80−36636
CD−42°14462, peculiar white dwarf, noneruptive close binary 77−53630
CD−42°14462 (V3885 Sagittarii), dwarf nova in permanent outburst 78−53966
CD−42° 14462, binary nature of nova-like variable 77−87435
CD −31°622 as metal-deficient subdwarf 78−65618
CD −33°12119, 3U 1727−33 candidate, UBV photometry 78−12251
cD galaxies in poor clusters, catalogue 77−22111
cD galaxies in poor clusters, photometry, spectra and redshifts 79−48907
cD galaxies in poor clusters, radial vel. meas. 79−8994
cD galaxy in Abell 2029, envelope spectra rel. to dynamics and struct. 79−92850
cD galaxy in Abell 401, spectral obs. of halo 78−32584
CD-31°622, spectroscopic obs. of DC white dwarf candidate 77−67090
186 Celuta, slowly spinning asteroid, photometry rel. to rot. period and comp. type 78−61782
V553 Centauri, C rich Cepheid, spectrum and photometry rel. to C and N abundances 80−4378
V553 Centauri, CH-type Cepheid, chemical comp. and luminosity 79−62849
Proxima=V645 Centauri, coordinated X-ray, optical and microwave study 79−5830
BV Centauri, dwarf nova, identification as spectroscopic binary 80−51775
V436 Centauri, dwarf nova, no periodic modulation in quiescent state light curve 79−88677
V436 Centauri, dwarf nova, photometry during superoutburst (May 1978) 80−46570
BH Centauri, early-type contact system in IC 2944 open cluster 77−33552
SZ Centauri, eclipsing binary, four-colour photometry, photometric elements, dimensions and He content 77−41391
V346 Centauri, eclipsing binary, spectroscopic orbit 79−58378
ω Centauri, globular cluster, search for new variables 78−61895
SV Centauri, period changes of β Lyrae-type eclipsing binary 77−33575
V78 in ω Centauri, radial vels. and circular orbit of eclipsing binary 79−97030
ω Centauri, SEC Vidicon photometry of main sequence 80−90491
ν Centauri, single-lined spectroscopic binary, β Cephei-type star 79−48821
UW Centauri, visual magnitude estimates, UBV photometry 78−40962
μ Centauri (B2 IVe), new circumstellar shell development, spectroscopic obs. (1980 June 10 to 12) 80−94808
V748 Centauri (Centaurus X-4?), high-latit. eclipsing system, VBLUW photometry 79−44529
V810 Centauri (HD 101947), yellow variable supergiant near Cepheid instability strip, VBLUW photometry 80−98672
V743 Centauri (HD 116994), light variability 79−97006
α Centauri A and B, Ca II k-line rel. to model chromospheres 77−13326
α Centauri and Proxima Centauri, space motions, masses 79−21348
α Centauri binary system, spectroscopic chemical anal. 80−62128
V645=Proxima Centauri optical flares during 1977 May, S.African obs. 78−32480
ω Centauri region, faint filamentary nebulosity obs. near globular cluster 80−56914
Centaurus cluster (HMS 1247−4102), galaxies redshifts meas. 77−45578
Centaurus galaxy cluster, spiral and elliptical galaxies distribs. rel. to Virgo cluster redshifts 78−54061
Centaurus I cluster of galaxies, redshift meas. and resolution into two vel. systems 80−77499
Centaurus X-3, spectroscopic obs. of Krzeminski's star 79−53934
Centaurus X-4, magnitude of optical counterpart 1979 June 14 79−75220
Centaurus X-4, SIT Vidicon spectra 79−80370
Centaurus X-4, spectroscopic obs. of visual counterpart, companion type 80−82545
Centaurus X-4, transient X-ray burster, optical counterpart discovered 80−67906
central star of Abell 46, eclipsing binary 80−73027
central star of planetary nebula NGC 7027, identification 79−67008
central stars of planetary nebulae, spectrogram analysis 79−97001
VV Cephei, 1976 November obs. in UBV rel. to eclipse start 77−9774
U Cephei, Algol type binary, spectrophotometry 77−2454
EI Cephei, Am eclipsing binary, light curve anal. 77−33560
ε Cephei, B photometry of δ Scuti-type star 79−44500

visible astronomical observations continued
EM Cephei, B-type eclipsing binary system, investigation of period and min. 80−17614
U Cephei, chem. comp. of secondary component of close binary system 79−35308
VV Cephei, complex close binary, linear polarisation during 1977 elcipse 78−40995
ER Cephei, contact binary in open cluster NGC 188, BV light curves 78−77580
VW Cephei, contact eclipsing binary, polarisation obs. 77−45489
VV Cephei, eclipsing binary, astrometric obs. at Sproul Observatory 78−4290
VV Cephei, eclipsing binary, distance from astrometric obs. 79−53859
CQ Cephei, eclipsing binary, narrowband photoelectric obs. *(Russian)* 77−22278
EM Cephei, eclipsing binary, spectroscopic obs. of shell *(Russian)* 78−57587
VV Cephei, eclipsing binary, UBV obs. 77−2456
CW Cephei, eclipsing binary in III Cephei association, photometry and distance 79−21326
δ Cephei, Hα radial vel. behaviour 80−51788
VV Cephei, Hα region spectra and system analysis 77−78823
δ Cephei, interstellar reddening 77−22243
β Cephei, linear polarisation obs. rel. to non-radial pulsations 79−40198
λ Cephei, linear polarization variability in emission line O star 78−36571
T Cephei, long-period variable, radial-vel. obs. 79−88684
μ Cephei, M supergiant, circumstellar shell and mass loss rate 77−45415
NY Cephei, massive eclipsing binary star, progress report from UBV photometry 80−67789
T Cephei, Me variable, Tc discovery 78−32483
VV Cephei, narrow band photometry during 1976-78 eclipse ingress 78−4296
19 Cephei, O-type supergiant, spectroscopic study, model atm. anal. 78−28681
EE Cephei, obs. of long period eclipsing binary *(Italian)* 78−93319
U Cephei, period changes in 1972-7 interval 80−8657
XY Cephei, photoelec. elements of semidetached binary system 80−31327
U Cephei, photoelectric obs. of recent eclipses 79−67061
U Cephei, primary eclipses obs., recent period behaviour 77−74087
RZ Cephei, RRc-type star, period var. *(Italian)* 77−91546
μ Cephei, semi-regular, supergiant, narrow-band polarimetry 79−25617
VV Cephei, spectroscopic obs. during 1976/77 eclipse ingress phase 78−45359
DI Cephei, spectrum vars. in T Tauri star 80−8628
ξ Cephei, triple system, spectroscopic study 77−22275
VV Cephei, UB photoelec. obs. 77−17633
EM Cephei, UBV, photometry rel. to constancy or variability of period 80−105286
VV Cephei, UBV obs. 80−17611
U Cephei, UBV photometry, light curve solns. 79−67054
VV Cephei, UBV photometry during ingress phase of 1976-78 eclipse 78−20862
U Cephei, UV excess, mass transfer in eclipsing binary system 77−33555
λ Cephei, variable outflow in Of star, spectroscopic obs. 79−35263
VW Cephei, W Ursae Majoris star, rot. line broadening rel. to shape and mass ratio 80−109494
17=ξ Cephei A, speckle interferometry, visual orbital elements 80−56874
β Cephei star search, northern photometric and spectroscopic obs. 77−74057
β Cephei stars, magnetic fields in nine variables 78−65631
β Cephei stars, photometric search of southern B-type stars 79−71040
β Cephei stars, search in open cluster NGC 4755, evolutionary stage determ. 79−8921
β Cephei stars, search south of declination −20°, B-type giants and subgiants 78−61863
β Cephei stars, vel./light curves for six objects 79−75214
VV Cephei system, distant, in Puppis, spectral classification, UBV photometry and polarimetry 80−51810
Cepheid variable stars, short-period, radial vels., BVRI photometry, radii 80−31309
Cepheid variables, VBLUW photometry rel. to intrinsic colours and physical props. 78−28696
Cepheid variables in Crux-Centaurus region, new objects 79−12477
Cepheids, binary star frequency from UBV photometry 77−45465
Cepheids, Hα emission in southern beating objects 79−21301
Cepheids, in LMC, BVI obs., period-luminosity-colour relation 79−71055
Cepheids, in Magellanic Clouds, UBV photometry, evidence for interstellar reddening 77−2435
Cepheids, in southern hemisphere, VBI photometry 77−53612
classical Cepheids, nonvariable supergiants and bright giants, spectrophotometric comparison 80−56837
Cepheids, short period, in N.hemisphere, UBV photometry rel. to search for double mode Cepheids 80−94814
Cepheids, southern, BVI photometry 77−60772
Cepheids between l=294° and 331°, UBV and 21 cm obs. 79−12478
Cepheids in Dunsink LMC II region, BV photographic photometry 78−45340
Cepheids in LMC and SMC, UBVRI obs. 77−71113
Cepheids in M31 (Andromeda galaxy), assoc. with interstellar gas and star complexes *(Russian)* 80−90455
Cepheus IV association, spectrophotometry of young stars 77−13328
Ceres, Belgian obs. and computed orbital elements *(French)* 77−71049
Ceres, diameter, interferometric meas. *(Russian)* 80−67634
Ceres, new reduction and collection of meridian obs. 77−13277
Cernis-Petrauskas (1980k), positions, (1980 August 10 and 17) 80−101556
δ Ceti, β Canis Majoris variable, period meas. and detect. of period decrease 80−105257
TV Ceti, F-type eclipsing binary, four-colour photometric obs. 79−40217
TV Ceti, light curves, photometric elements and He content 79−44526
δ Ceti, period changes of β Cephei type star 78−32487
T Ceti, semiregular variable, Tc I absorpt. line obs. 78−28689
TX Ceti, UBV obs., photometric elements of eclipsing binary star 79−8950
UV Ceti, variations of Hβ emission line during large flare 77−45456

visible astronomical observations continued
o Ceti (Mira), enhanced activity of B-type component at 1976 light minimum 78−81636
o Ceti (Mira), long-period variable, radial-vel. obs. 79−88684
o Ceti (Mira), mass loss rate determ. 79−48831
o Ceti (Mira), polarized Balmer emission lines, spectropolarimetry 79−21302
o Ceti (Mira), rapid light vars. of companion star during 1977 light min. 78−96492
o Ceti (Mira), spectrum of companion star 78−4253
o Ceti (Mira), strong TiO-related dia. vars. 78−16429
o Ceti (Mira) at 1978 max., spectropolarimetry 80−94799
o Ceti (Mira)-type stars, colour curves for Me and Se types 77−29857
ZZ Ceti stars, constraints on possible long-term variability 80−90428
ZZ Ceti stars search, photometric obs. of apparently quiescent stars 80−22005
UV Ceti-type flare stars, simultaneous 1420 MHz and optical obs. of flares 78−49464
RS Chamaeleontis, eclipsing binary, four-colour photometry rel. to photmetric elements, absolute dimensions and He abundance 80−67783
Z Chamaeleontis, monitoring of southern dwarf nova, 1954-76 period 78−93272
RS Chamaeleontis, uvby photometry of bright double-lined A-type eclipsing binary 78−69833
Charon (1978 P 1), posns. in 1980 April rel. to probable occultation 80−67651
Charon (1978 P 1), probable stellar occultation, 1980 April 6, min. dia. 80−62071
Charon (1978 P 1), satellite of Pluto, positions and dynamical parameters 80−62069
Charon (1978 P 1), stellar occultation obs., 1980 April 6, rel. to satellite dia. and struct. 80−94754
chromosphere, enhanced network, K-line obs. 77−78751
chromosphere, magnetic neutral lines, assoc. with X-ray arches 77−17511
chromosphere, Na distrib. and nonthermal motion vels. from D-line eclipse obs. 77−22200
chromosphere above sunspot umbrae, obs. of emission cores in Ca II H- and K-lines 78−53900
chromosphere flares, effective time of observations *(Russian)* 78−40893
Chu's object in Perseus, UBV photometry and spectrum rel. to identification as galactic star 80−62132
Ci 182354, astrometric anal. of unseen companion from 61 cm Sproul refractor plates 78−16459
α Circinids, meteor shower on June 4, Australian obs. 78−16359
Circinus galactic window, early type star obs. 77−13342
Circinus Sb galaxy, Mt. Stromlo Schmidt red plates *(Swedish)* 78−69877
Circinus X-1 (3U 1516−56), obs. of optical and radio counterpart 78−12414
Cirinus X-1, simultaneous radio and optical obs. during outbursts 79−17137
CL4 optical counterpart, accurate position 79−17116
Cl 0024, galaxy cluster, two-colour ISIT photometry rel. to galaxies evolution 78−24557
CL 4, radio source, optical detect. 79−71138
CL 4, radio source, optical identification and optical position 79−21453
classical Cepheids, light and radial vel. curves phase matching 77−17574
classical Cepheids colour excesses 77−22242
clock stars, R.A. correction, Melbourne obs. reduction *(Russian)* 79−92653
close binary stars linear polarisation 77−49435
close visual double stars, electronographic UBV magnitudes and separations 79−67056
cluster galaxies, alignment study 80−90516
cluster of galaxies 0122−688, spectrographic obs., redshift 80−41906
cluster of galaxies obs. at low galactic latit. 78−4373
cluster stars near IC 1805 (W4), spectral classes and photometry 80−62214
clusters galaxies, redshift determ. using Image Dissector Scanner, visible spectra 80−90544
clusters of galaxies, ang. size-redshift relation for nearby clusters 78−4372
clusters of galaxies, characteristic size as metric rod for determ. of q_0 78−36703
clusters of galaxies, number densities and radial cumulative distribs. 79−40278
clusters of galaxies, radial number-density distribs. 80−8697
clusters of galaxies, X-ray and optical study 78−28805
clusters of galaxies distance and local Hubble ratio 77−33661
Cn 3-1, planetary nebula, emission line obs. 77−33621
CoD−38°10980, white dwarf, photometry and spectroscopy rel. to gravit. redshift 78−24511
CoD −35° 10525, bright YY Orionis star, spectrum and UBV photometry 78−36566
Collinder 132a, b, UBVβ photometry of two sparse open clusters 78−32540
Collinder 140, nearby open cluster, UBV photoelectric photometry 78−53994
Collinder 140, young open cluster, spectroscopic and statistical study 80−62211
α Columbae, rapid spectral vars., cross correlation analysis 79−48808
Coma Berenices open cluster, spectral types 77−29886
Coma cluster, central regions struct. from equidensity diagrams 78−93435
Coma cluster, diffuse background light photographic meas. 77−91655
Coma cluster, new stellar standard sequence 78−93436
Coma cluster, photoelec. surface photometry, intergalactic gas luminosity upper limit 77−64858
Coma cluster field, accurate positions of faint optical objects in fields of radiosources 79−9015
Coma Cluster galaxies, photometry 78−12381
Coma galaxy cluster, luminosity function and struct. 77−45574
Coma/A1367 supercluster of galaxies and environment 78−65700
14 Comae, A-type shell star, spectroscopic obs. 78−7992
GQ Comae, low redshift, optically variable quasar discovery 77−33676
CC Comae, W Ursae Majoris star, proper motion 77−74099
CC Comae, W Ursae Majoris type, spectroscopic orbit 78−12300
CC Comae, W Ursae Majoris type binary, photometry and geom. elements 77−22272

visible astronomical observations continued
17 Comae A, Ap star, mag. field meas. and rot. period *(Russian)* 80−90457
17 Comae A, Ap star, Sr spots distrib. rel. to atmospheric mag. field *(Russian)* 77−17594
17 Comae A, magnetically variable Ap star, spectroscopic obs. 77−17595
GQ Comae Berenicis, QS0 or N galaxy, spectrophotometry obs. 80−77488
X Comae Berenicis, Seyfert galaxy, optical variability 77−74139
Comet, Bradfield (1979l), precise positions (1979 December 28 to 30) 80−31255
comet, probable discovery trail in Phoenix (1978 November 30) 79−25547
comet, unidentified object on Palomar Sky Survey (prints no.1267) 79−96974
Comet (1977c), discovery confirmed, 1977 February 23 obs. 77−25981
Comet Arend-Roland (1957 III), visible and UV spectra anal. *(Chinese)* 80−12709
Comet Bennett (1970 II), O(^1D) and H_2O^+ brightness profiles 79−35192
Comet Bowell (1980b), discovery posns., elements and ephemeris 80−51695
Comet Bowell (1980b), precise positions, elements and ephemeris (1980 March-July) 80−62075
Comet Bowell (1980b), precise posn. and orbital evolution 80−56770
Comet Bradfield (1974 III), nuclear brightness meas. using deconvolution technique 79−84745
Comet Bradfield (1974 III), precise positions 1974 April 7-May 12 period 77−91473
Comet Bradfield (1974 III), strip photometry 77−33412
Comet Bradfield (1975p), anti-tail photographic obs. 77−33410
Comet Bradfield (1975p), precise positions for 1976 Jan. 31-Feb. 1 77−17446
Comet Bradfield (1976a), precise position for 1976, Mar. 77−2371
Comet Bradfield (1976d), precise positions 1976 Mar. 27, 28 77−22140
Comet Bradfield (1978c), discovery positions and appearance 78−32397
Comet Bradfield (1978c), emissions from head 79−96971
Comet Bradfield (1978c), positions, elements and ephemeris 78−32401
Comet Bradfield (1978c), positions, improved elements and ephemeris 78−36514
Comet Bradfield (1978c), positions, magnitudes and UBV photometry 78−36521
Comet Bradfield (1978c), positions and appearance (1978 February) 78−32405
Comet Bradfield (1978c), positions and visual magnitude estimates 78−40873
Comet Bradfield (1978c), precise position, spectroscopic obs., total visual magnitude estimates 78−40879
Comet Bradfield (1978c), precise positions, 1978 (February 15 to March 12) 78−65551
Comet Bradfield (1978c), precise positions 1978 Feb.-Mar., total visual magnitude estimates 78−45288
Comet Bradfield (1978c), precise positions and magnitudes (1978 Feb.) 78−32404
Comet Bradfield (1978c), precise psoitions, (1978 February 28 to March 8) 78−40875
Comet Bradfield (1978c), semiaccurate position 1978 March 8 78−36529
Comet Bradfield (1978c) IR and total visual magnitudes (1978 March) 78−45283
Comet Bradfield (1978o), discovery and positions 78−93165
Comet Bradfield (1978o), precise position for 1978 Oct. 18 78−96439
Comet Bradfield (1978o), precise positions for 1978 Oct. 78−96433
Comet Bradfield (1979c), discovery, approx. positions 79−75158
Comet Bradfield (1979c), obs. of diffuse object (1979 September) 79−101120
Comet Bradfield (1979c), precise position for 1979 August 18 79−84751
Comet Bradfield (1979c), precise positions for 1979 Aug. 79−88624
Comet Bradfield (1979c), precise positions for 1979 Jun.-Jul., parabolic orbital elements 79−84746
Comet Bradfield (1979c), precise positions for 1979 Jun.-Jul. 79−80271
Comet Bradfield (1979c), precise posns., elements and ephemeris (1979 June-July) 79−75159
Comet Bradfield (1979c), precise posns. (1979 June 25) 79−70999
Comet Bradfield (1979c), total visual magnitude and coma diameter (1979 August 3) 79−80274
Comet Bradfield (1979c), total visual magnitude estimates, (1979 August 4 to 12) 79−88623
Comet Bradfield (1979c), total visual magnitude estimates (1979 August 17 to September 10) 79−92721
Comet Bradfield (1979l), 1980 March 4 magnitude and coma diameter 80−51696
Comet Bradfield (1979l), discovery posns. (1979 December) 80−31254
Comet Bradfield (1979l), obs. of precise position in 1980, 8th to 22nd Jan. 80−36572
Comet Bradfield (1979l), photographic obs. in 1980 23-4 Jan. 80−36574
Comet Bradfield (1979l), posns., elements and ephemeris (1980 Jan. 5-26) 80−31256
Comet Bradfield (1979l), precise props., orbital element and ephemeris (1979 Dec.-1980 Feb.) 80−26813
Comet Bradfield (1979l), spectra and visual obs. (1980 Jan.-Feb.) 80−41768
Comet Bradfield (1979l), visual obs. (1979 February 8 to 20) 80−46489
Comet Cernis-Petrauska (1980k), antitail, precise posns., parabolic elements and ephemeris 80−105206
Comet Cernis-Petrauskas (1980k), positions, 1980 August 2 to 16, orhital elements and ephemeris 80−98614
Comet Cernis-Petrauskas (1980k), total visual mag. and coma dia. (1980 Aug.-Sept.) 80−101561
Comet Chernykh-Petrauskas, discovery posn. (1980 July) 80−94756
comet discovery, 1977 July 18-19 positions 78−77518
Comet Fujikawa (1978n), discovery and positions (1978, October 9 and 10) 78−96431
Comet Fujikawa (1978n), precise position, (1978, October 10) 78−93166
Comet Fujikawa (1978n), precise position for 1978 Oct. 11 78−96434
Comet Fujikawa (1978n), precise positions, (1978, October 11 to 16) 79−5779
Comet Fujikawa (1978n), precise positions, (1978, October 13 to 14) 78−93168

visible astronomical observations continued
Comet Giclas (1978k), discovery report 78−85915
Comet Giclas (1978k), precise positions, (1978 September 10 to 12) 78−89122
Comet Haneda-Campos (1978j), discovery and initial posns. 78−85911
Comet Haneda-Campos (1978j), precise positions, magnitude, orbital elements, ephemeris for 1978 Sept. 78−85913
Comet Harlan (1976g), precise positions 1976, Jun.-Oct. 77−5506
Comet Harlan (1976g), precise positions 1976 Jul. 19, Sept. 18, Oct. 24 77−22139
Comet Helin (1977e), discovery, positions and appearance (April 16-18) 77−41359
Comet Helin (1977e), positions, appearance parabolic elements and ephemeris 77−49335
Comet Helin (1977e), precise positions, elements and ephemeris (April-May 1977) 77−45364
Comet Helin (1977e), precise positions, orbital elements, ephemeris 77−64700
Comet Helin (1977e), precise positions (1977, May) 77−49338
Comet Helin (1977e), precise positions (1977 April 18-29) 78−7935
Comet Helin (1977e), precise positions for 1977 April 18-22 period 77−41360
Comet Kobayashi-Berger-Milon (1975 IX), Irish amateur obs. (1975 July-Aug.) 79−75165
Comet Kobayashi-Berger-Milon (1975 IX), precise positions 1975 Aug. 4-14 period 77−91473
Comet Kobayashi-Berger-Milon (1975h), positions 77−13287
Comet Kobayashi-Berger-Milon (1975h), visual spectroscopic obs. 77−33424
Comet Kohler (1977 XIV), precise positions (1977 Oct.) *(German)* 80−46453
Comet Kohler (1977 XIV), precise positions for 1977 Sept.-Dec. from photographic obs. 80−4302
Comet Kohler (1977m), discovery obs. and position 77−82171
Comet Kohler (1977m), positions, elements, ephemeris and magnitude estimates 77−91484
Comet Kohler (1977m), positions, spectral emissions and magnitudes 78−7924
Comet Kohler (1977m), precise positions, (1977 October 5 to 19) 80−105203
Comet Kohler (1977m), precise positions, magnitudes, elements and ephemeris 77−87328
Comet Kohler (1977m), precise positions, orbital elements, ephemeris, total visual magnitude estimates 78−45286
Comet Kohler (1977m), precise positions 1977 Sept.-1978 Jan., total visual magnitude estimate 78−36518
Comet Kohler (1977m), precise positions (1977 Oct.-Nov.) 78−16355
Comet Kohler (1977m), precise positions (1977 September-October) 78−4155
Comet Kohler (1977m), precise positions and magnitudes 1977, Sept. 77−87331
Comet Kohler (1977m), precise positions and total magnitudes 1977, Sept. 77−87335
Comet Kohler (1977m), precise positions for 1977, Oct. to Dec. 78−20751
Comet Kohler (1977m), precise positions for 1977 Oct.-Dec. period 78−28590
Comet Kohler (1977m), precise positions for 1977 Oct.-Nov., total visual magnitude estimates 78−20743
Comet Kohler (1977m), precise positions for 1977 Sept. 7-18 period 77−87334
Comet Kohler (1977m), precise positions for 1977 Sept.-Dec., total visual magnitude estimates 78−20753
Comet Kohler (1977m), precise posns. for 1977 October-1978 March period 78−61806
Comet Kohler (1977m), total visual magnitude estimates, 1977 September 77−87329
Comet Kohler (1977m) precise positions (1977 October 13 to November 10) 78−7937
Comet Kohoutek (1972 XII), Swan Cloud, 1974 January 11, rel. to cometary plasma tails general morphology 80−98612
Comet Kohoutek (1973 XII), CN and C_2 spectrophotometry 78−20738
Comet Kohoutek (1973 XII), CN violet (0,0) spectra 80−82308
Comet Kohoutek (1973 XII), ion tail interaction with compression region of solar wind corotating stream 78−49267
Comet Kohoutek (1973 XII), spectrum interpretation by means of Franck-Condon factors, Rydberg-Klein-Rees method calc. *(French)* 77−17428
Comet Kohoutek (1973 XII), strip photometry 77−33412
Comet Kohoutek (1973 XII), tail shape and orientation 77−67069
Comet Kohoutek (1973 XII), visible spectra, band intensity var., electrospectrophotometer meas. 80−8588
Comet Kohoutek (1973XII), Swann band profiles 78−85909
Comet Kowal (1977f), discovery positions 77−45365
Comet Kowal (1977f), positions for 1977 May 17-19 77−53479
comet Kowal (1977f), precise positions 1977, May and orbital elements 77−53481
Comet Kowal (1977f), precise positions and possible ephemerides (1977, April-May) 77−53476
Comet Kowal (1979a), discovery report and positions, (1979, January 27 to 29) 79−25548
Comet Kowal (1979a), precise positions, (1979 February 1) 79−35195
Comet Kowal (1979a), precise positions 1979 Jan., orbital elements, ephemeris 79−25549
Comet Kowal (1979h), discovery and approx. posns. (1979 July) 79−92718
Comet Kowal (1979h), precise positions for 1979 Jul. 79−88625
Comet Lovas (1974c), precise positions, 1976, Aug.-Oct 77−5501
Comet Lovas (1974c), precise positions 1976, July 26-Sept. 18 77−17435
Comet Lovas (1974c), precise positions 1976, Oct.-Nov. and orbital elements 77−22145
Comet Lovas (1975 VIII), precise positions and ephemeris for (1977 May 17 to December 23) 77−37578
Comet Lovas (1975 VIII), precise posns. (1977 Aug. and Sept.) 78−12159
Comet Lovas (1976 XII), precise posn. (1978 February 4) 78−49386
Comet Lovas (1976k), discovery obs. 77−5500
Comet Lovas (1976k), precise position, orbital elements, ephemeris 77−64701
Comet Lovas (1976k), precise position 1976, Dec. 77−33421

visible astronomical observations continued
Comet Lovas (1976k), precise positions 1976, Dec., ephemeris for 1977, Jan.-Jun. 77−17442
Comet Lovas (1976k), precise positions 1976, Nov. 77−5505
Comet Lovas (1976k), precise positions 1976, Nov. and Dec. and improved elements 77−9709
Comet Lovas (1976k), precise positions 1976, Nov. and Dec. and improved elements 77−17434
Comet Lovas (1976k), precise positions 1976, Nov. and ephemeris for 1976/77 Nov.-Feb. 77−17433
Comet Lovas (1976k), precise positions 1976 Dec. 26-30 77−22141
comet Lovas (1976k), precise positions 1976/77 and ephemeris for 1978 Mar.-Jun. 78−24491
Comet Lovas (1976k), precise positions (1976 November 23) 77−9708
Comet Lovas (1976k), precise positions (1977, January) 77−29726
Comet Lovas (1976k), precise positons for 1977 Feb. 11, 19 and Mar. 14 77−53480
Comet Lovas (1977c), approx. position 1977, Feb. 77−33413
Comet Lovas (1977c), discovery report 77−29724
Comet Lovas (1977c), precise position, improved elements and ephemeris 77−82174
Comet Lovas (1977c), precise position (1977, March 12) 77−33417
Comet Lovas (1977c), precise positions, orbital elements and ephemeris 77−41358
Comet Lovas (1977c), precise positions, parabolic elements, ephemeris correction 77−33416
Comet Lovas (1977c), precise positions (1977, March-April) 77−49337
Comet Lovas (1977c), precise positions and corrected ephemeris 77−33415
Comet Lovas (1977c), precise positions for 1977 Feb. 28 and Mar. 19 77−37577
Comet Lovas (1977t), approx. positions for 1978, Jan. 78−24488
Comet Lovas (1977t), approx. posn. and stellar appearance 78−28591
Comet Lovas (1977t), asteroid-like appearance and orbit 78−28582
Comet Machholz (1978l), discovery report 78−89123
Comet Machholz (1978l), elliptical elements and total visual magnitude estimate 78−89129
Comet Machholz (1978l), positional obs., (1978, September 14 and 15) 78−89125
Comet Machholz (1978l), precise positions, total visual magnitude estimates, 1978 Sept. 78−89130
Comet Machholz (1978l), precise positions 1978 Sept.-Oct., magnitudes 78−93163
Comet Machholz (1978l), total visual magnitude estimates for 1978 Oct. 79−5785
Comet Machholz (1978l), total visual mags. and ephemeris continuation 78−93159
Comet Machholz (1978l), visual magnitude estimate (1978, September 19) 78−89126
Comet Meier (1978 XXI), photoelectric BV photometry rel. to opposition effect 80−31258
Comet Meier (1978 XXI), position from 1979 April 21 to 30, meas. and reduction *(French)* 80−72884
Comet Meier (1978f), discovery position, appearance and motion 78−49384
Comet Meier (1978f), positions, elements, ephemeris, magnitudes and spectrum 78−53881
Comet Meier (1978f), posns., elements, ephemeris and magnitudes 78−61801
Comet Meier (1978f), precise position, orbital elements, ephemeris and magnitude law 79−5781
Comet Meier (1978f), precise position, total visual magnitude estimate, 1978 Nov. 79−5789
Comet Meier (1978f), precise positions, 1978, April 30 to (May 8) 78−53884
Comet Meier (1978f), precise positions, (1978, May 2 to June 9) 78−69751
Comet Meier (1978f), precise positions 1978 Apr., spectroscopic obs. 78−49387
comet Meier (1978f), precise positions and magnitude estimates (1978 May-June) 78−69748
Comet Meier (1978f), precise positions for 1978 Apr.-May, total visual magnitude estimates 78−57505
Comet Meier (1978f), precise positions meas. at ESO, La Silla, in (April 1979) 80−105204
Comet Meier (1978f), precise posn. and visual mag. estimate (1978 Nov.) 79−5784
Comet Meier (1978f), precise posns. (1978 May-July) 78−77520
Comet Meier (1978f), precise posns. and total visual mag. estimates (1978 Apr.-May) 78−57504
Comet Meier (1978f), total visual magnitude estimates for 1978 July 78−85910
Comet Meier (1979i), discovery report and positions (1979 September 20 and 21) 79−92722
Comet Meier (1979i), precise positions (1979 September 22 to 28) 80−4306
Comet Meier (1979i), precise posns., orbital elements, ephemeris and magnitudes (1979 Sep.-Oct.) 79−101118
comet Meier (1979i) total visual mag. estimates (1979 Sept.-Oct.) 80−8590
Comet Mori-Sato-Fujikawa (1975 XII), precise positions 1975, May and June 77−53483
Comet Mori-Sato-Fujikawa (1975j), positions, 1975 Dec. 4-10 period 77−74012
Comet Mori-Sato-Fujikawa (1975j), precise position (1976, October) 77−29728
Comet Mori-Sato-Fujikawa (1975j), precise positions 1976, Mar.-Sept. 77−17438
comet on Palomar Sky Survey, discovery and semi-accurate position 80−77352
comet on Palomar Sky Survey print, posn. and daily motion 78−69752
Comet Russell (1979d), discovery posns. (1979 June) 79−71000
Comet Russell (1979d), precise posns., elements and ephemeris (1979 June-July) 79−71002
Comet Russell (1979d), semiaccurate positions, (1979 July 15 and 16) 79−80273
Comet Russell (1980l), discovery posns. and ephemeris (1980 September) 80−101557
Comet Russell (1980l), precise positions, 1980 September 6 to 8, and ephemeris 80−101559
Comet Sanguin (1977p), discovery, appearance and positions 77−91482

visible astronomical observations continued
Comet Sanguin (1977p), positions, elements and ephemeris 77−91486
Comet Sanguin (1977p), precise positions for 1977 October 78−4151
Comet Schuster (1975 II), precise positions, 1977, February 12 to 25, and orbital elements 77−37579
Comet Schuster (1975 II), precise positions 1977 Feb. and May 77−71065
Comet Schuster (1975 II), precise positions 1978 Jan. 78−40880
Comet Schuster (1975 II), precise posns. (1977 June) 78−12158
Comet Schuster (1976c), precise position and tail obs. (1977, January) 77−29727
Comet Schuster (1976c), precise positions 1976 July 28 77−17437
Comet Schuster (1976c), precise positions for 1976 Mar. 25 and Jun.2 77−22147
Comet Seargent (1978m), discovery, posns. and appearance 78−93158
Comet Seargent (1978m), ephemeris extension and magnitude estimate 79−44416
Comet Seargent (1978m), positions 1978 Oct. 78−93161
Comet Seargent (1978m), precise positions, (1978, October 2 to 4) 78−93164
Comet Seargent (1978m), precise positions (1978, October 6) 78−96432
Comet Seargent (1978m), precise positions for 1978 Oct. 78−96436
Comet Seargent (1978m), precise positions for 1978 Oct. 78−96438
Comet Seargent (1978m), total visual magnitude estimates for 1978 Oct. 79−5786
Comet Tago-Sato-Kosaka (1969 IX), tail structure (1969 Dec.-1970 Jan.) 79−44415
comet tails, H_2O^+ surface brightness rel. to CO^+ 80−72880
Comet Torres, discovery and positions, 1980 June 13 and 14 80−82306
Comet Torres (1979e), discovery and approx. posns. 79−71001
Comet Torres (1979e), precise position, 1979 July 31, and ephemeris 79−84749
Comet Torres (1979e), precise positions, (1979 July 3) 79−75161
Comet Torres (1979e), precise positions for 1979 Jun.-Jul. 79−84747
Comet Torres (1979e), precise posns., elements and ephemeris (1979 June-Aug.) 79−75160
Comet Torres (1980e), 1980 June 17 semi-accurate posn. 80−85898
Comet Torres (1980e), precise posns., elements and ephemeris (1980 June-July) 80−85900
Comet Tritton (1978d), discovery, appearance and positions (1978 Feb.) 78−32403
Comet Tritton (1978d), positions, elliptical elements, ephemeris and magnitude law 78−36522
Comet Tsuchinshan (1977q), 1977 November 8 precise positions and appearance 78−4154
Comet Tsuchinshan (1977q), discovery positions 78−7934
Comet Tsuchinshan (1977q), positions, elements, and ephemeris 78−16350
Comet Tsuchinshan (1977q), precise positions, elements and ephemeris 78−16353
Comet Tsuchinshan (1977q), precise positions (1977 December) 78−28584
Comet Tsuchinshan (1977q), precise positions (1978, January 3) 78−45284
Comet Tsuchinshan (1977q), precise positions for 1977 Nov.-Dec. 78−20746
Comet Tsuchinshan (1977q), precise posns. (1977 Nov.-1978 Jan.) 78−61804
Comet van den Bergh (1974 XII), precise position (1976, October 31) 77−29729
Comet West (1975n), Belgian obs. 77−41356
Comet West (1975n), edge-on nucleus configuration obs. 77−33409
Comet West (1975n), nucleus A precise positions, nuclei B and D separations and position angles 77−53478
Comet West (1975n), nucleus splitting, photography and narrow-band photometry 78−36512
Comet West (1975n), photography and narrow-band photometry 77−17429
Comet West (1975n), positions from photographic obs. 77−33411
Comet West (1975n), precise positions 1976 Apr. 1 and Jun. 2, orbital elements 77−17447
Comet West (1975n), precise positions of nuclei, 1976 May and September 77−9707
Comet West (1975n), scatt. phase function of cometary dust, 0.5 to 18 μ 77−29731
Comet West (1975n), spectrographic obs. 77−29730
Comet West (1975n), tail components orientation and struct. *(French)* 77−53475
Comet West (1976 VI), coma mols. and dust distrib., visible emission profiles 80−101562
Comet West (1976 VI), dust bursts, split nucleus, flare-ups, particle evaporation 79−30010
Comet West (1976 VI), dust tail striae, propagating inhomogeneities 78−61809
comet West (1976 VI), emission bands and continuum flux heliocentric depend. 80−36575
Comet West (1976 VI), photographic photometry near perihelion passage 79−35193
Comet West (1976 VI), polarisation of head 80−8587
Comet West (1976 VI), radiation polarisation obs. 79−62794
Comet West (1976 VI), spectrophotometry, emission bands and lines obs. 80−56768
Comet West (1976 VI), spectrophotometry after perihelion passage, emission features vars. 78−57503
Comet West (1976 VI), striated tail study 79−35194
Comet West (1978a), discovery, positions and spectral obs. 78−24489
Comet West (1978a), positions, parabolic elements and ephemeris 78−28583
Comet West (1978a), positions and ephemeris extension (1978 Jan.-July) 78−36516
Comet West (1978a), precise positions 1978 Jan., Mar. 78−49383
Comet West (1978a), precise positions for 1978 Jan.-May 78−61799
Comet West (1978a), precise posns. (1978 February-March) 78−40872
Comet West (1978a), precise prediscovery positions, hyperbolic elements 78−40878
Comet West (1978a), semiaccurate positions 1978, Jan. 78−24492
cometary nebula, remarkable structural change obs. 78−4333
cometary nebula near NGC 7023, brightening, stellar object visual magnitudes 78−20882
cometary nebula near NGC 7023, brightening and spectra 77−74118

visible astronomical observations continued
comets, Minor Planet Circular 5333-5390, 51 precise posns. for eight objects 80−77325
comets, Minor Planet Circulars, 42 precise posns. for eight objects 80−31241
comets, Minor Planet Circulars 4391-4424, 52 precise posns. for 15, objects 78−81578
comets, minor planet circulars 4425-4482, 26 precise posns. for eight objects 78−85886
comets, Minor Planet Circulars 4483-4520, 70 precise posns. for 13 objects 78−93140
comets, minor planet circulars 4521-4548, 190 precise posns. for 16 objects 79−2514
comets, minor planet circulars 4549-4582, 29 precise posns. for five objects 79−12421
comets, Minor Planet Circulars 4583-4622, 75 precise posns. for 14, objects 79−16871
comets, Minor Planet Circulars 4623-4648, 14 precise posns. for three objects 79−25538
comets, Minor Planet Circulars 4649-4688, 50 precise posns. for 11 objects 79−35178
comets, Minor Planet Circulars 4689-4722, 195 precise posns. for 23 objects 79−53754
comets, Minor Planet Circulars 4723-4746, 118 precise posns. for 14 objects 79−66953
comets, Minor Planet Circulars 4747-4788, 31 precise posns. for five objects 79−75136
comets, Minor planet circulars 4789-4844, 57 precise posns. for 14 objects 79−84729
comets, Minor Planet Circulars 4845-4936, 40 precise posns. for ten objects 79−101107
comets, Minor Planet Circulars 4937-5016, 122 precise posns. for 16 comets 80−8580
comets, Minor planet circulars 5017-5066, 42 precise posns. for 11 objects 80−17533
comets, Minor Planet Circulars 5137-5188, 41 precise posns. for seven objects 80−46459
comets, Minor Planet Circulars 5189-5248, 69 precise posns. for 13 objects 80−67631
comets, Minor Planet Circulars 5249-5286, 63 precise posns. for six objects 80−67632
comets, Minor Planet Circulars 5287-5332, 44 precise posns., for eight objects 80−67633
comets, Minor Planet Circulars 5391-5422, 64 precise posns. for eight objects 80−85884
comets, Minor Planet Circulars 5423-5454, 25 precise posns. for seven objects 80−98599
comets, precise posns. in 1974-6 period 80−46494
comets, recent, periodic, photometry rel. to gas and dust props. 79−70997
comets, short-period, with large perihelion distances, search, unidentified asteroids obs. 78−85907
Comets Kowal, two probable objects, discovery posns. and ephemerides 79−96973
compact and interacting southern galaxies with emission line spectra 78−41048
compact galaxies, mean surface brightness and integral brightness relation 78−93412
compact galaxies, spectroscopic and photometric obs. 78−77603
compact galaxies in compact cluster Shakhbazian 1, photometry *(Russian)* 78−93428
compact galaxies in fields near M3 and M92, selection, statistics and photometry with two telescopes 80−77485
compact galaxies in neighbourhood of Abell 193, list of 140 objects 79−88736
compact galaxies on UK Schmidt plates 78−81687
compact galaxy detect. method *(Russian)* 77−49302
compact groups of compact galaxies, morphology of 27 groups *(Russian)* 79−9008
compact groups of compact galaxies, ninth list 79−88751
compact nebulae, very-low-excitation, in Magellanic Clouds, spectra 78−32556
compact nonthermal sources, polarisation at cm., mm., IR and visual wavelengths 79−5913
comparison stars near OJ287 and ON325, variability, period determ. 80−26882
composite object 0246+18, bright galaxy with superposed variable star, UBV colours 79−71130
cool C stars, $^{12}C/^{13}C$ ratio calc. 78−4205
cool stars, CaCl bands obs. 77−53593
cool stars, neutral-ion spectral anomaly 78−7985
cool stars, polarisation wavelength depend. 77−2426
cool stars, polarization across TiO bands 79−97005
cool stars, Ti isotopic abundance ratios 80−26840
cool white dwarfs, spectrophotometric obs. 77−45422
Corona Austrina dark cloud, interstellar reddening law meas. 79−17050
Corona Austrina dark cloud complex, extinction distrib. 78−54001
Corona Austrina T1 association, UBV photometry of member stars *(Russian)* 79−17035
Corona Borealis cluster of galaxies, vel. dispersion 77−49487
S Coronae Austrinae, a bright southern YY Orionis star, spectroscopic obs. 77−29818
S Coronae Austrinae, identification of absorpt. lines, irradiated amethyst 79−25601
S Coronae Austrinae, line profiles in YY Orionis star 79−84808
ε Coronae Austrinae, polarimetric obs. of eclipsing binary 80−56888
S Coronae Austrinae, protostar, high dispersion spectroscopy, Balmer line profiles 77−64754
S Coronae Austrinae, spectroscopic and photometric vars. of YY Orionis star 79−48812
S Coronae Austrinae, T Tauri star, red-displaced absorpt. features obs. 78−4221
R, S, T Coronae Austrinae, T Tauri stars, long period vars. 80−82350
ε Coronae Austrinae, W Ursae Majoris type star, spectra, radii, masses 79−71069
R Coronae Borealis, 1977, February 17-26 magnitude fading 77−29854
β Coronae Borealis, Ap star, Ca II K and Hδ lines rapid vars. *(Russian)* 80−90458
B Coronae Borealis, Ap star, chemical element distrib. from spectrophotometry *(Russian)* 77−22238

visible astronomical observations continued
β Coronae Borealis, Ap star, Fe I spectrum rel. to atmospheric mag. field struct. *(Russian)* 77−17594
β Coronae Borealis, Ap star, high resolution polarization obs. 78−8011
β Coronae Borealis, Ap star, transverse Zeeman effect, oblique rotator model 77−13361
θ Coronae Borealis, Be star, strong shell line at Hα 79−67022
θ Coronae Borealis, Be-type star, shell line profile and radial vel. obs. 80−77426
R Coronae Borealis, decline 1977, Mar., visual magnitude esimates 77−37606
β Coronae Borealis, Hα line variability *(Russian)* 78−69815
ι Coronae Borealis, Hg-Mn star, spectroscopic binary, visible spectra obs. 80−72983
β Coronae Borealis, magnetic field gradient in Ap-star atmosphere, Zeeman spectra 78−85953
β Coronae Borealis, obs. with Zeeman analyzer system on McDonald 2.7 m telescope 80−62021
α Coronae Borealis, spectroscopic orbit determ. 77−22277
R Coronae Borealis in quiet state, spectral energy distrib. *(Russian)* 80−51781
R Coronae Borealis type variables and related objects, UBV photometric obs. 80−90437
R Coronae Borealis-type variables, B mag. and visual estimates 77−53609
coronal Fe XIV emission line intensity and profile, temporal variations 77−29767
coronal velocity fields, periodic oscillations, Fe XIV 5303 A line obs. 77−49362
cosmic dust in spiral galaxies, optical anal. method, visible obs. 80−101638
CPD−26°389, central star of NGC 1360, radial vel. obs. 80−4350
CPD−56°8032, emission line object, red and IR spectrum 78−4249
CPD −62° 1837 (HDE 308122), long-period variable member of triple 80−105260
CPD-26°389, central star of NGC 1360, spectroscopic binary within planetary nebula 77−45494
3CR, radio galaxies, spectrophotometry spectral energy distrib. 79−21413
3CR radio galaxies, redshifts, strong emission line spectra 77−33666
3CR radio sources, optical fields investigations to faint limiting magnitudes 78−54067
3CR radiosources, photographic obs., optical identifications 77−13481
3CR radiosources, source counts and V/V_{max} tests for complete sample 78−77613
3CR radiosources quasars and galaxies, optical identification 80−90555
Crab Nebula, emission region size, electron transport and mag. field models 77−17650
Crab Nebula, emission-line spectra of condensations 79−35327
Crab Nebula, optical linear polarization obs. from Durham 77−74126
Crab Nebula, photoelectric spectrophotometry of filaments, abundances 78−41006
Crab Nebula, search for associated and nearby extinction 77−67118
Crab Nebula, small-scale polarisation obs. 79−25656
Crab Nebula, spectrograms of filaments, faint forbidden lines 78−45388
Crab Nebula outskirts, remarkable spectra and element abundances 78−36662
Crab pulsar, proper motion 77−82269
Crab pulsar, resolution of peak of optical pulse 78−93292
crater morphology and size relation 77−41332
CRL 2688, Cygnus Egg Nebula, optical spectropolarimetry 77−33602
CRL 2688 (Egg Nebula), bipolar nebula, optical and IR polarimetry 78−36658
β Crucis, β Canis Majoris star, photometric obs. 80−17595
α¹ Crucis, improved spectroscopic orbit 80−67792
BI Crucis, new symbiotic star, spectrum 80−109442
25 G Crucis (HD 108250), orbital elements from spectrograms 80−82432
CSV 6110 in Taurus, *o* Ceti type variable, visible obs. 80−67745
CTB 80, peculiar supernova remnant, central radio source optical and H I obs. 80−56896
Curtis-Schmidt thin prism survey for extragalactic emission line objects, Univ. of Michigan list I 77−71012
65 Cybele, occultation of AGK3+19°599, 1979 October 17, obs. 80−31237
65 Cybele, occultation of AGK+19°0599, 1979 October 18, obs. using photoelectric photometer *(Chinese)* 80−105172
SS Cygni, 1896-1975 study of dwarf nova 79−16986
CH Cygni, 1977 April surge before September outburst 77−87412
CH Cygni, 5700-8700 A spectrograms 77−87415
29 Cygni, λ Bootis type star, photometric variability 77−64765
V1500 Cygni, (Nova 1975), emission line profiles during early nebular stage 79−53826
V1500 Cygni, (Nova 1975), photoelec. obs., period decrease, visual magnitude estimates 77−22252
V1500 Cygni, accurate position and praenova search 77−2440
α Cygni, anomalous spectral line contours of Fe II multiplet *(Russian)* 78−93243
31=o^2 Cygni, astrometric studies 78−69779
V389 Cygni, BV photometry of peculiar variable 79−44534
X Cygni, Cepheid, radial vels. 78−73723
SS Cygni, colour variations during dwarf nova outbursts 80−46576
χ Cygni, diameter of Mira-type star from speckle interferometry 80−67728
XX Cygni, dwarf Cepheid, composition and motion, visible photometric and spectrographic obs. 80−77424
SS Cygni, dwarf nova, outburst, visual magnitudes (1978 June 14 and 15) 78−65628
EM Cygni, dwarf nova, photographic study 77−33529
SS Cygni, dwarf nova, rapid optical oscills. phase variability 80−85947
SS Cygni, dwarf nova, spectrophotometry rel. to accretion disc models in erruption and at min. light 80−36635
31 Cygni, eclipsing binary, Ca I 6752 Å circumstellar line obs. 77−17619
CG Cygni, eclipsing binary, changing light curve obs. 79−48857
V388 Cygni, eclipsing binary, photoelectric obs. 77−37617
V367 Cygni, eclipsing binary, spectroscopic study 78−53984
GO Cygni, eclipsing binary, UBV photometry rel. to period changes 80−72999
V453 Cygni, eclipsing binary in cluster NGC 6871, photometry and distance 79−21326

visible astronomical observations continued
P Cygni, electron scattering in expanding atmosphere 79−21311
V1500 Cygni, expansion rate and distance 77−2439
V1057 Cygni, FU orionis type, UBVR photometry 78−12230
P Cygni, Hα and Hβ emission lines equivalent widths, scanner obs. 77−2430
P Cygni, H Balmer line profiles, accel.-decel. envelope, mass loss 79−40205
V1016 Cygni, image-tube spectrograms 80−8639
SS Cygni, light curve periodicity 79−21300
χ Cygni, long-period variable, radial-vel. obs. 79−88684
V1057 Cygni, mean B-band magnitude (1978 July 30 ± 2^d) 79−84792
CH Cygni, new active period, model, double system with accretion disc *(Russian)* 78−69813
V444 Cygni, orbital period var. rel. to Wolf-Rayet star mass loss *(Russian)* 79−101178
CH Cygni, outburst and spectral changes, 1977 August 31 obs. 77−82231
χ Cygni, P Cygni profiles obs. in Na I and K I reson. lines 77−13362
V389 Cygni, peculiar (Ap-type) binary, spectroscopic obs. 78−85975
CC Cygni, photometric obs. of RS Canum Venaticorum type binary, interpretation 80−62182
V1500 Cygni, post-nova light curve development, UBV and Hβ obs. 77−71115
α Cygni, radial vel. and line profile vars. in supergiant 80−22010
SS Cygni, radial vel. of dwarf nova 79−62833
V1331 Cygni, radial vels. of spectra lines in unusual T Tauri star 79−71045
V1500 Cygni, spectral development, visible and near IR obs. 78−4231
1500 Cygni, spectrophotometry of early phase with objective prism plates 77−17576
57 Cygni, spectroscopic binary, search for systematic radial vel. anomalies 80−17617
CI Cygni, spectroscopic obs. using multichannel analogue detector system 78−36461
CG Cygni, spectroscopic study of close eclipsing binary 79−97031
59=V832 Cygni, spectrum scanner obs. 80−94809
32 Cygni, supergiant eclipsing binary, λ6575 and λ4870 light curves anals. 79−88700
CH Cygni, symbiotic star, 1977 outburst, radial vel. and atm. struct. determ. 80−72969
CH Cygni, symbiotic star, binary model 80−62158
V1016 Cygni, symbiotic star, IR variability obs. from VJHKL photometry *(Russian)* 80−105263
CH Cygni, symbiotic star, rapid and slow light vars. 80−51792
CH Cygni, symbiotic variable, flickering obs. during outburst, binary model 79−8929
59=V832 Cygni, variable mass flux from spectroscopic obs. 80−41840
CH Cygni, visible and near IR spectra 77−82232
V1500 Cygni, visual magnitude estimates 1976, Nov. and Dec. 77−9758
β Cygni, visual obs. of brighter component close companion 80−8663
Cygni 1975 (V1500 Cygni), visual magnitude estimates (1977 Aug.-1978 Jan.) 78−32474
V645 Cygni (CRL 2789), bipolar nebula, O-type exciting star 78−4392
V1357 Cygni (Cygnus X-1), no long-term light vars. (1928-77) 80−41861
V1341 Cygni (Cygnus X-2), halo population binary 79−97099
V1341 Cygni (Cygnus X-2), shortest optical variability *(Russian)* 80−17695
V1341 Cygni (Cygnus X-2), UBV photometry and light vars. 79−5833
V1341 Cygni (Cygnus X-2), UBV photometry and possible 82-minute quasi-periodic bursts obs. *(Russian)* 79−17140
α Cygni (Deneb), Ca II K line high-resolution obs. 78−16408
α Cygni (Deneb), Ca II K-line core asymmetry 80−85981
α Cygni (Deneb), variable line profiles interpretation 77−64761
V1500 Cygni (Nova 1975), 3.35 hour 1978 light curve, rel. to possible double period 79−67039
V1500Cygni (Nova 1975), 3 hour photometric period stabilisation 79−92776
V1500 Cygni (Nova 1975), 3 hour var. 79−16966
V1500 Cygni (Nova 1975), Balmer line emission profiles evolution in early decline phase 80−82371
V1500 Cygni (Nova 1975), binary nature, spectral meas. 77−87446
V1500 Cygni (Nova 1975), brightness meas., (1917 to 1976) 78−36618
V1500 Cygni (Nova 1975), BV photometric obs. 78−36613
V1500 Cygni (Nova 1975), BV photometry 78−36619
V1500 Cygni (Nova 1975), distance and temp., visible spectral obs. *(Chinese)* 80−85955
V1500 Cygni (Nova 1975), flux distribs. rel. to shell electron temps. and densities 79−30068
V1500 Cygni (Nova 1975), Hα and Hβ emission line vars. 80−4389
V1500 Cygni (Nova 1975), H I emission line profiles vars., envelope ejection vels. determ. 79−35281
V1500 Cygni (Nova 1975), He abundance of ejecta 78−28691
V1500 Cygni (Nova 1975), light curve for 1975 Aug.-1977 July period 80−4372
V1500 Cygni (Nova 1975), line spectrum evolution 78−32493
V1500 Cygni (Nova 1975), linear polarization obs. 78−36601
V1500 Cygni (Nova 1975), model for spectrographic obs. 77−87444
V1500 Cygni (Nova 1975), multiband photometry 77−87445
V1500 Cygni (Nova 1975), obs. of magnitude and spectrum changes *(French)* 77−82258
V1500 Cygni (Nova 1975), optical polarisation obs. 78−36622
V1500 Cygni (Nova 1975), photoelectric obs. 78−36620
V1500 Cygni (Nova 1975), photometric and spectroscopic obs. 78−36604
V1500 Cygni (Nova 1975), photometric obs. 78−36616
V1500 Cygni (Nova 1975), photometry, light curves, magnitude estimates 78−85960
V1500 Cygni (Nova 1975), photometry rel. to 3.3 hour var. and flickering 78−36591
V1500 Cygni (Nova 1975), polarimetric and photometric obs. 78−36612
V1500 Cygni (Nova 1975), short-term light vars. 78−36609
V1500 Cygni (Nova 1975), small amplitude light var. 78−36608
V1500 Cygni (Nova 1975), spectral energy distrib. 78−36605
V1500 Cygni (Nova 1975), spectral evolution 77−87447
V1500 Cygni (Nova 1975), spectrographic obs. *(Chinese)* 79−16982
V1500 Cygni (Nova 1975), spectrophotometric study *(French)* 77−82259
V1500 Cygni (Nova 1975), spectroscopic data 79−16988

visible astronomical observations continued
V1500 Cygni (nova 1975), spectroscopic obs., three hour periodicity, nebular model 78−12235
V1500 Cygni (Nova 1975), spectroscopic studies, models for 3 hour profile vars. 79−8920
V1500 Cygni (Nova 1975), spectroscopic studies, nebular and central binary system 79−62830
V1500 Cygni (Nova 1975), spectrum variations 78−36607
V1500 Cygni (Nova 1975), three hour light var. 79−80314
V1500 Cygni (Nova 1975), TV photometry 78−36602
V1500 Cygni (Nova 1975), UBV photometry, short period variability 78−61862
V1500 Cygni (Nova 1975), UBVR Hα photometry and polarimetry 78−36611
V1500 Cygni (Nova 1975), UBVRI photometry and polarimetry 78−36614
V1500 Cygni (Nova 1975), visible and near UV photoelec. photometry 78−36610
V1500 Cygni (Nova 1975), visible and near UV spectrophotometric obs. 78−32492
V1500 Cygni (Nova 1975), visible and near UV spectrophotometry 78−32494
V1500 Cygni (Nova 1975), visible and UV spectra and light curve 80−12771
V1500 Cygni (Nova 1975), visible spectroscopy 78−36598
V1500 Cygni (Nova 1975), visible-band linear polarimetry 78−36621
V1500 Cygni (Nova 1975), visual magnitude estimates (1977 May-Aug.) 77−82230
V1500 Cygni (Nova 1975) photometric obs. at Skalnate Pleso Observatory 78−36617
V1668Cygni (Nova 1978), linear polarisation obs. 80−26875
V1668 Cygni (Nova 1978), multifilter photometry and polarimetry 80−90454
V1668 Cygni (Nova 1978), optical light curve, uvby photometry 80−62154
V1668 Cygni (Nova 1978), photoelec. photometry, rapid flickering 80−36640
V 1668 Cygni (Nova 1978), spectral development 80−51789
V1668 Cygni (Nova 1978), spectrographic obs. around max. brightness *(French)* 79−58343
V1668 Cygni (Nova 1978), spectroscopic and photometric obs., (1978 to 1979) *(Russian)* 80−109444
V1668 Cygni (Nova 1978), UBV light curve 80−46565
V1668 Cygni (Nova 1978), visual mag. estimate (1979 April 25) 79−53824
V1668 Cygni (Nova 1978), visual magnitude estimates, 1978 Nov.-1979 Apr. 79−48819
V1668 Cygni (Nova 1978), visual magnitude estimates, 1979 June 79−80324
V1500 Cygni (Nova Cygni 1974), periodicities and rapid line variability 77−33524
V1500 Cygni (Nova Cygni 1975), interstellar reddening and distance 78−4230
V1500 Cygni (Nova Cygni 1975), low resolution spectrophotometry 77−49403
V1500 Cygni (Nova Cygni 1975), shell phase obs. 77−49392
V1500 Cygni (Nova Cygni 1975), spectrophotometric obs. 77−49402
V1500 Cygni (Nova Cygni 1975), spectroscopic obs. of coronal line phase 77−33504
V1500 Cygni (Nova Cygni 1975), spectrum around max. light 77−87411
V1500 Cygni (Nova Cygni 1975), UBV photometry 77−33525
V1500 Cygni (Nova Cygni 1975), UBVRI photometry 77−33509
61 Cygni A, B, late-type dwarfs, metal abundances 77−78779
CI Cygni symbiotic star, UV and optical spectrum changes during eclipse 80−105258
Cygnus A, optical struct. 77−9802
Cygnus A, rot. axis of assoc. optical galaxy 78−4355
Cygnus A compact radiosource, astrometric obs. 77−74152
Cygnus Loop, fast shock wave detection, optical spectra 80−82467
Cygnus Loop, forbidden Fe XIV emission radial distrib. 78−32545
Cygnus Loop, radial distrib. of Fe X and XIV forbidden line emission 80−51828
Cygnus Loop, supernova remnant, high vel. gas obs. and filaments spectra *(Russian)* 78−41028
Cygnus Loop, supernova remnant, ionization struct. 77−87525
Cygnus loop remnant, radial vels. 77−17666
Cygnus OB2 number 12, spectral classification and membership of association 80−51760
Cygnus region, new optical supernovae remnant discovery 78−4330
Cygnus X H II region, maps of calibrated surface brightness of (Hα+N II) 77−78854
Cygnus X region, riddle of γ Cygni radio source resolved 78−28809
Cygnus X region, visual extinction map and radio brightness temp. 78−61929
Cygnus X-1, absence of 39 day period in non-UV data 78−8167
Cygnus X-1, discovery of synchronous binary polarization 78−41087
Cygnus X-1, extended secondary envelope with eclipsing region, V-polarization obs. 79−35433
Cygnus X-1, mean blue light curve feature 77−17718
Cygnus X-1, new period in X-ray binary system *(German)* 78−81712
Cygnus X-1, search for rapid optical periodicities 78−24573
Cygnus X-1, variable circular polarisation obs. 77−29952
Cygnus X-1 (HDE 226868), optical photometry, (1972-1976) 78−32609
Cygnus X-1 (HDE 226868) system, search for third star 77−45606
Cygnus X-1 (V1357 Cygni), narrow-band photoelec. obs. *(Russian)* 79−88767
Cygnus X-1 (V1357 Cygni), optical light curve vars. rel. to X-ray vars. 80−109560
Cygnus X-1 (V1357 Cygni), optical photometry (1980 May 25 to July 7) 80−90578
Cygnus X-2, binary, radial vel. and orbital elements from visible spectra obs. 80−77519
Cygnus X-2, optical magnitude variation *(Russian)* 77−26093
Cygnus X-2, optical variability upper limits 78−96564
Cygnus X-2, spectroscopic obs., orbital period, spectral-type var., X-ray heating 79−9036
Cygnus X-2, spectroscopic obs. *(Russian)* 77−26092
Cygnus X-2, TV photometer obs. of optical counterpart *(Russian)* 78−57697
Cygnus X-2, variable optical flickering 78−73773

visible astronomical observations continued
Cygnus X-2 optical candidate, high-speed photometry 77−13494
D and cD galaxies in poor clusters, struct. and photometry 78−32580
DA 240, radio galaxy, high-vel. gas in jet 78−28773
DA white dwarfs, H I Balmer γ line profiles and masses 80−77399
41 Daphne, photoelectric photometry and synodic rot. period 77−45343
dark cloud complexes, magnetic field struct. 77−17648
dark cloud complexes in Scorpius and Ophiuchus, extinction distrib. 78−54002
dark nebulae in M31, catalogue 80−72787
degenerate star candidates, photoelectric and spectroscopic obs. 80−12763
degenerate stars, photometry and spectra 78−12224
Deimos, 37 positional photographic obs. during 1973 October at Pulkovo *(Russian)* 78−28568
Deimos, loose material downslope movement obs. 80−94737
Deimos, photographic positional obs. with Ukrainian Academy 400 mm astrography *(Russian)* 79−44395
Deimos, photometry from Viking orbiter images 80−72838
Deimos, spacecraft imaging 78−89102
Deimos, spectral evidence for carbonaceous chondrite surface comp. 80−41754
Deimos, surface morphology, comp. and props. 78−89103
Deimos, surface photometry 77−29696
Deimos, Viking Orbiter imaging results 79−35170
HR Delphini, determ. of mass of ejected nebula 77−74068
δ Delphini, spectroscopic binary fine anal. 77−17620
HR Delphini (Nova 1967), cataclysmic binary spectrum 80−4359
HR Delphini (Nova 1967), emission line spectrum peculiarities 79−35280
HR Delphini (Nova 1967), emission lines at nebular stage *(Russian)* 80−17597
HR Delphini (Nova 1967), He I radial vel. var. 77−82249
HR Delphini (Nova 1967), photoionisation models of envelope in nebular stage, obs. data 78−61864
HR Delphini (Nova 1967), physical props. and element abundances in nebular state 78−36573
HR Delphini (Nova 1967), premax. and principal absorpt. line systems in spectrum 79−35279
HR Delphini (Nova 1967), short period light vars. from UBV photometry 80−67744
HR Delphini (Nova 1967), short period photometric vars. obs. 79−44503
HR Delphini (Nova 1967), spectra, line identification, radial vels. 80−17594
HR Delphini (Nova 1967), spectral evolution during decline 77−87440
Hr Delphini (Nova 1967), spectral evolution during decline period 78−40957
HR Delphini (Nova 1967), spectroscopic orbit 79−44510
δ Delphini stars in Michigan Spectral Catalogue, uvbyβ photometry rel. to spectral types 80−4377
349 Dembowska, rot. period and phase curve 79−35174
337 Devosa, unusual object with triple extrema in photoelectric light curve, rot. period 79−40116
78 Diana, astrometric obs. rel. to central path of occultation of SAO 75392, (1980 September 4) 80−101547
diffuse gaseous nebulae, Hα photoelectric photometry *(French)* 80−62240
diffuse interstellar bands in 6500-8900 Å region 79−21373
diffuse interstellar features at 6379 and 6614 A, high resolution profiles 78−4314
diffuse interstellar line at 6284 Å, obs. and relation to interstellar reddening 80−51843
diffuse moving object, discovery and precise positions for (July 1, 1976) 77−33423
diffuse object, detect., in galactic centre direction *(French)* 79−8959
disc galaxies in Virgo and Hercules clusters, sizes 79−75269
distant cluster of galaxies, photometry and red shift 78−12377
distant galaxy clusters, redshifts and photometry, rel. to Hubble diagram curvature 78−49515
distorted interstellar bubbles discovery around two stars 79−71088
diurnal latitude vars. spectra based on obs. at Gor'kii 79−35100
DO white dwarfs, spectrophotometry rel. to effective temps. and He abundances 79−35249
S Doradus, LMC Hubble-Sandage variable, IUE and ground based spectroscopic obs. 80−101595
30 Doradus, nebular complex, photographic obs. 77−33606
30 Doradus, supermassive nebula, motions of neutral and ionised material 77−71137
30 Doradus, uvbyR surface photometry 77−91600
S Doradus (HD 35343), luminous LMC supergiant, long time baseline VBLUW photometry 80−22007
S Doradus (HD 35343), luminous LMC supergiant, long time baseline VBLUW photometry 80−36630
30 Doradus central object (HD 38268), interstellar and nebular lines obs. 80−51839
30 Doradus direction, unique interstellar Ca II K-line profile obs. 80−51850
30 Doradus nebula, Balmer line photometry 79−62888
30 Doradus nebula, in LMC, interstellar Ca II and Na I obs. 80−46643
30 Doradus nebula, surrounding nebulous filaments 79−67076
30 Doradus nebula in LMC, optical obs. of bright core 80−67827
30 Doradus nebular complex, chemical comp. and struct. obs. 80−62226
30 Doradus region, in LMC, interstellar extinction and stellar population 78−96517
30 Doradus region, interstellar extinction and stellar population 77−13413
30 Doradus region, uvbyR surface photometry 78−81670
double galaxies, observational data on well-defined sample 80−17674
double Herbig-Haro object in Orion Nebula 77−26006
double spiral galaxies, UBV photometry, magnitudes and colour indices 79−62914
double star measures at Lick Observatory, Mount Hamilton, California 78−85979
double stars, Lick obs. of 254 pairs 80−8660
double stars, measures of 120 visual pairs 80−56878
double stars, micrometer obs. 78−57582
double stars, new discoveries at Nice, 15th series *(French)* 79−35304
double stars, Nice obs. of 267 objects *(French)* 79−44531
double stars, obs. using phase-grating stellar interferometer *(Russian)* 79−101070

visible astronomical observations continued
double stars, obs. with Herstmonceux 28-inch refractor, (1963-1970) 80−41863
double stars, photographic measures 78−57581
double stars, position angles and separation, Venezuelan obs. *(French)* 80−77450
double stars, separation and position angle obs. 80−98691
double stars discovered at Nice, 14th series *(French)* 77−78654
double-mode Cepheids, UBV photometry of four suspected stars 79−48825
DR15, H II region, optical emission assoc. with 408 to 2695 MHz radio sources 80−94881
Draco dwarf spheroidal galaxy, stellar colour magnitude diagram and proper motion 80−73029
Draconid meteors, number in (1972) 77−67077
K Draconis, Be star, search for short time scale vars. in Hα emission 80−109441
BY Draconis, binary, slow light variability anal. 77−53629
AR Draconis, BV light curves and orbital elements 79−101173
BS Draconis, BV photometry of eclipsing binary 79−44536
73 Draconis, CH lines in spectrum of Ap star *(Russian)* 77−56958
RZ Draconis, eclipsing binary, photoelectric light curve and orbital period study 80−109461
BY Draconis, flare star, Ca II emission variability 77−33528
BY Draconis, late-type flare star, metal abundances 77−78779
CM Draconis, low dispersion spectrum, metal abundance of eclipsing binary 79−25636
BY Draconis, magnitudes, colours and photometric period changes *(Russian)* 77−64771
AI Draconis, period and spectroscopic orbit of eclipsing binary 78−89221
WW Draconis, RS Canum Venaticorum type star, two-colour photoelectric lightcurves and elements 80−46606
φ Draconis, short period Ap star, discovery of mag. field 77−33511
BY Draconis, spectroscopic binary flare star, BVRI obs. 77−53595
73 Draconis, spectroscopic study and model atm. anal. of Ap star 77−33531
CM Draconis, spotted dM4e eclipsing binary flare star, absolute dimensions and masses 78−12289
BY Draconis, spotted flare star, spectra and photometry rel. to pre-main-sequence nature 80−36633
CR Draconis, UV Ceti variable, flares colour behaviour 80−22020
BV Draconis (ADS 9537A), W Ursae Majoris type star, photoelectric photometric obs. 79−35296
BW Draconis (ADS 9537B), W Ursae Majoris type star, photoelectric photometric obs. 79−35296
BY Draconis type variables, flare activity and quiescent variability 78−45338
BY Draconis type variables, photometry, amplitudes and phases 79−67038
BY Draconis-stars, ages from spectra *(Russian)* 77−64774
BY Draconis-type stars, Hα emission line profiles, rapidly rot. gaseous envelopes *(Russian)* 78−65625
BY Draconis-type stars, spectroscopic binary incidence 77−87401
BY Draconis-type stars of 1 M⊙, photoelectric obs. *(Russian)* 77−64772
dust distrib. in giant extragalactic H II regions 79−35320
dust free zone around Sun, search with Helios 1 solar probe 78−45277
dwarf galaxies NGC 5128 group 79−25738
dwarf irregular galaxies near Local Group and M81 group, photographic obs. 79−35363
dwarf irregular galaxy identified in Phoenix 77−26057
dwarf nova outbursts, colour vars. 80−46576
dwarf novae, eruption types and superhumps, obs. 79−75212
dwarf novae, period-amplitude relationships 77−91545
dwarf novae, photometry of rise to max. and decline 77−9753
dwarf novae, rapid brightness oscills. obs. 78−40968
dwarf novae, search for light oscills. during outbursts 78−40966
dwarf novae, spectra *(Russian)* 80−8638
dwarf novae, spectrophotometry, 1250-7500 Å region 80−46577
dwarf ring galaxy, discovery, luminosity, diameter and distance 77−49482
dwarf spheroidal galaxy in Draco, BV photometry 79−97076
dwarf spheroidal galaxy in Draco, foreground interstellar reddening 79−97077
dwarf stars, Ca II K and Hα profiles rel. to chromospheric models and activity 79−48773
dwarf stars, M-type, in South Galactic Pole direction, catalogue of 282 objects 79−5762
dwarf stars, metal-poor, abundance anals. of yellow spectra 79−92760
200 Dynamene, photoelec. light curve, rot. period, low spin rate object 78−32383
E3 (ESO-037-SC 01) dying globular cluster, photometry and stellar content rel. to tidal truncation 80−105291
E galaxies in Abell clusters, UR surface photometry 79−12525
E/S0 radio galaxies, ionized gas obs. 79−17105
early O-type star in SMC, discovery 79−5820
early type stars, intermediate-band photometry 77−49385
early type stars, photoelectric Hα line photometry 77−91528
early type stars, UBV photometry rel. to galactic plane discontinuity near (l=140°) 77−9797
early-type contact binaries, uvby beta photometry 78−53981
early-type emission-line stars, intrinsic and interstellar polarization components separation 79−30079
early-type stars, in Monoceros region, interstellar extinction determ. 77−9777
early-type stars, northern intermediate galactic latit., Hβ photometry, rel. to glactic struct. 80−36631
early-type stars, radial vel. meas. and standard wavelengths 77−17547
early-type stars, spectral classification, calibration using TV multichannel system 77−67091
early-type stars, suspected variability and line emission, Hα obs. 79−67036
faint early-type stars in neighbourhood of H II region RCW 38, UBV photometry 80−4352
early-type stars in Norma 80−62129
early-type stars in southern hemisphere, four colour photometry and spectral types 78−40945
early-type stars with six degrees of galactic anticentre direction, radial vels. 78−7990

visible astronomical observations continued
early-type ultra-short-period variable stars, new class identification and photometry 79−88662
Earth-Moon libration points, search for natural or artificial objects 80−98647
eclipses, pre-telescopic obs., uses in modern astronomy 79−96930
eclipsing binaries, corrected light elements for nine objects 77−37620
eclipsing binaries, UBV photometric programme at Palomar and Kitt Peak 77−64796
eclipsing binaries in Scutum-Vulpecula regions, visual minima obs., 1920-1950 period 77−33564
eclipsing binaries visual minima, Cracow Observatory obs. 77−74086
SW eclipsing binary, period study, photometry and spectra obs. 80−82424
eclipsing binary stars, V−R photometry rel. to distances, masses, radii and absolute magnitudes 79−44520
eclipsing variables in Magellanic Clouds, tabulated light curves 78−16536
effective field of view for line sources 78−36535
Elara radius and albedo 77−33399
354 Eleonora, rot. period and phase curve 79−35174
elliptical and S0 field and cluster galaxies, photometry, colour distribs. 79−17071
elliptical galaxies, ang. size determ., 2-D Fourier transform technique 79−35373
elliptical galaxies, in Coma cluster, surface brightness and colour distribs. 78−41063
elliptical galaxies, internal dynamics 79−53902
elliptical galaxies, isophotes struct. 78−41058
elliptical galaxies, normal, giant ellipsoidal shells discovery 80−86000
elliptical galaxies, optical posns. for identified radiogalaxies 79−97074
elliptical galaxies, photometric data on twists 80−56932
elliptical galaxies, rot. meas. rel. to oblate models 78−16529
elliptical galaxies assoc. with B2 radiosources, orientation 80−77501
elliptical galaxies in Virgo and Coma clusters, ellipticity profiles 78−28785
elliptical galaxy dwarf companions, Palomar plate search 77−33653
59 Elpis, photoelectric lightcurves and rotation period of asteroid 78−69729
182 Elsa, photoelec. light curve and rot. period of asteroid 80−56750
emission line galaxies, spatial distrib. rel. to clusters, visible spectra obs. 80−73046
emission line galaxies and quasars, classification system and list of 116 objects 77−22308
emission line object, spectral obs., possible planetary nebula 77−49451
emission line stars, spectrographic obs., 5650 to 8750 Å *(French)* 79−48815
emission line stars in LMC, spectroscopy and IR photometry 77−13348
emission nebulae, first obs. with optical multichannel analysis of Sao Paulo University 80−26743
emission nebulae with strong S II forbidden lines in LMC 77−29891
emission variable in Sagitta, magnitudes 77−17599
emission variable in Sagitta, photographic magnitudes from Harvard patrol plates 77−2431
emission-line galaxies, phys. conditions in nuclei *(Russian)* 79−80359
emission-line object candidate for 4U 1630-47, photometric and spectroscopic obs. 77−82324
emission-line stars in galactic cluster NGC 663, spectroscopic obs. 80−4363
emission-line stars of Sanduleak and Stephenson, classification spectra 78−93273
emission-line variable (No.86) in core of M 15, UBV photometry, probably W Virginis star 80−77458
283 Emma, light curves and rot. period 79−16868
Enceladus, near IR spectra and JHK photometry 80−56761
equatorial and southern bright stars, UVBYβ photometry 77−22205
equinox, position and motion during 250 yrs. 77−73935
δ Equulei, improved orbit for visual binary 78−45364
γ Equulei, magnetic field obs. of Ap-star 80−51782
δ Equulei, three-dimens. orbit 79−53852
CC Eridani, BY Draconis variable, Hα variations 77−87406
AS Eridani, eclipsing binary, photometric elements, masses, radii, luminosities 78−28723
CD Eridani, photometric soln. for eclipsing binary system 80−62185
66 Eridani, spectroscopic binary, search for light var. 78−32524
o^2=40 Eridani B, white dwarf, gravitational redshift 79−62868
WX Eridani light curves, period, orbital elements of eclipsing binary 80−26902
Eridanus, high galactic Hα filaments and evidence for associated expanding shell 79−53866
433 Eros, astrometric obs. during 1975 opposition 78−57485
433 Eros, Belgian obs. and computed orbital elements *(French)* 77−71049
433 Eros, brightness changes during major oposition 77−67061
433 Eros, photographic obs. at 1975 opposition 78−49373
eruptive blue variables at high galactic latit., spectrophotometry 78−32482
eruptive variable in Andromeda, posn. and mags. (1979 Sept.) 79−101163
ES type galaxies, UBV photometry obs. 80−73053
ESO 012-G21, Seyfert 1 galaxy, spectrum, redshift, UBV photometry and X-ray identification 80−8695
ESO 103-G35, Seyfert galaxy and possible X-ray source 79−88741
ESO 103-G35, type I Seyfert, optical counterpart of H 1834−653 X-ray source 78−96547
ESO 113-IG45, galaxy and/or quasar, spectrum, photometry and struct. 78−28782
ESO 113-IG 45, interacting galaxy, Type 1 Seyfert spiral with bright central quasar 78−8126
ESO 113-IG 45 (=Fairall 9), Seyfert galaxy, spectroscopic and multiaperture photometric obs. 80−31362
ESO 140-G43 (Fairall-51), new southern Seyfert 1 galaxy, discovery and red shift 78−54044
ESO 210-6A southern globule, nearby star formation 79−21399
ESO 263-PN 02, spectroscopic obs. of southern planetary nebula 80−101626
ESO/Uppsala galaxies, spectroscopic and photometric obs., second catalogue 78−77497
ESO/Uppsala survey of ESO(B) Atlas of southern sky, fifth list containing 2395 objects 78−20653

visible astronomical observations continued
ESO/Uppsala survey of ESO(b) Atlas of southern sky, fourth list, 2920 objects 77−26059
ESO/Uppsala survey of ESO (B) Atlas of southern sky, sixth list containing 3162 objects 79−8850
45 Eugenia, photoelectric light curves, synodic rot. periods, amplitudes of var. 79−53752
45 Eugenia, rot. period and photoelec. light curve determ. 80−72846
247 Eukrate, UBV photometry, light curve and rot. period 80−21942
15 Eunomia, close approaches to SAO stars, occultation prediction accuracy 79−30003
52 Europa, photometry and rot. period 78−12133
164 Eva, rotation period from photoelectric obs. 77−60707
Evershed flow in chromosphere-photosphere transition region 78−65593
exciting stars of Orion triple emission nebula, UBV photometry 77−13430
extended radiosource 1400+162, BL Lacertae object in group of galaxies 78−4339
extinction towards South Galactic Pole from A and F star reddening 77−60812
extragalactic background light, upper limit 79−17142
extragalactic background light at 5115 Å, upper limit 79−101225
extragalactic background light intensity at 5100 Å wavelength 78−4414
extragalactic emission line objects, third list from Curtis Schmidt thin prism survey 78−28538
extragalactic emission-line objects, second list from Curtis Schmidt thin prism survey 78−28537
extragalactic emission-line objects, Univ. of Michigan List IV 78−77494
extragalactic faint blue objects, nature and distrib. 80−82476
extragalactic nonthermal sources, spectral flux var. in 0.36-3.5 μ range 79−35412
extragalactic optically variable objects, calibration of photoelec. comparison sequences 77−87537
extragalactic radiosources, optical identifications 80−105373
extragalactic radiosources, optical variability 78−12396
extragalactic radiosources, optically violent variables, monitoring of long-term vars. 80−31376
extragalactic radiosources, spectroscopic obs. in 3200-5700 Å range 78−86032
extreme galactic B and A supergiants, light vars. 77−56927
extremely red stars at $l^{II} \approx 113°$, $-10° \leq b^{II} \leq +90°$, photometry and spectra 78−57554
extremely red stars on Palomar prints, optical variability search 78−57563
F and G stars, MK spectral types 79−66999
F and G-type supergiants, search for light vars. 79−88657
F corona, radial vel. obs. at 1979 February 26 solar eclipse 80−85914
F- and G-type stars, C and N abundances 77−91530
F- and G-type stars, props. determ. by spectral quantification 77−29791
F-type supergiants, southern, visible spectra obs. 80−98660
F-type supergiants in Magellanic Clouds, Ca abundances 80−98655
faculae, initial growth phase and development 77−74030
faint blue objects in field of open cluster M67, spectroscopic obs. 77−22329
faint blue southern stars, Hβ photometry, metallicity, luminosity 77−41381
faint blue stars, photometry, third list of southern stars 79−71030
faint blue stars, southern, UBV photometry 80−82349
faint blue stars, uvby photometry in northern hemisphere 78−16415
faint blue stars in high galactic latits., search of PSS fields near South Galactic Pole 80−46415
faint blue stars near galactic anticentre, spectral types 79−71021
faint blue stars near galactic anticentre, UBV photometry 78−40932
faint blue stars near North Galactic Pole, catalogue 77−49314
faint blue stars UVBY photometry, second list of southern stars 77−45424
faint galaxies radial vel. meas. from objective prism plates 77−45562
faint OB stars in Coalsack region 77−74047
faint proper-motion stars, spectra and photometry to very low luminosity degenerates deficiency 80−17575
faint quasars, spectroscopy and props. of CTIO 4 metre survey 78−32592
faint red stars, photoelec. photometry of complete sample, space density 79−71034
faint red stars at intermediate galactic latit., UBVR photometric obs. 78−32457
faint star clusters in LMC, survey, visible obs. 80−73011
faint stellar images, colour-magnitude diagrams and clustering correl. functions rel. to star populations 80−82360
faint stellar systems, discovery on ESO Schmidt plates 78−20887
Fairall 160, 182, UBV photometry 80−82349
Fairall 9=ESO 113-IG45, companion galaxy to Seyfert 79−44616
Fairall 9 and Fairall 51, spectrophotometry, Seyfert 1 class galaxies 79−17076
fast irregular variables, UBV and JHKL photometry *(Russian)* 78−28684
Feige 24, EUV star, spectrophotometry in 3800-8200 Å region 78−4280
Feige 24, hot white dwarf, OAO-2 photometry 77−9747
Feige 24, spectroscopy of EUV source, binary orbit, mass 78−93218
Feige 7, hot rotating magnetic white dwarf discovery 77−53589
Feige 7, mag. white dwarf, spectroscopic studies 79−25603
Feige 86, $^3He/^4He$ from He I 6678 Å obs. of He deficient blue horizontal-branch star 79−92774
Feige 86, horizontal branch star, chemical comp. 77−9745
field galaxies space distrib., redshifts and photometry of complete sample 79−21418
filamentary and diffuse nebulosity near giant nonthermal radio loop 78−93445
filaments surrounding RR Pictoris (Nova 1925), spectrophotometry, abundances, ionization 79−40194
fireball of 1977 September 14 over Czechoslovakia 78−32408
fireballs, occurrence freq. rel. to mass distrib. of massive meteoroids 77−45366
fireballs photographed in central Europe, trajectories, orbits and classification 78−36534
FK4 star coord. improvements using Ni2 astrolabe obs. *(German)* 80−26719
FK4 supplementary stars, right ascensions obs., definitive results 80−17473
FKSZ stars, differential catalogue of RA in 20-90° zone, Pulkovo obs. *(Russian)* 78−28644
visible astronomical observations continued
FKSZ stars, meridian circle obs. at Kiev University Observatory, (1972 to 1975) *(Russian)* 79−44336
flare star, near Orion Nebula, UBV obs. *(Russian)* 77−82223
flare star 2329−03, spectra, chromospheric emission 77−74070
flare star discovery obs. *(French)* 77−87409
flare star search in Cassiopeia region near W3 77−37603
flare stars, combined optical and radio obs., long-duration events 79−53827
flare stars, multichannel spectrophotometry 80−105256
flare stars, photoelectric monitoring (1974 to 1976) 79−44509
flare stars, photographic photometry, discovery of five new stars 77−56943
flare stars, photographic photometry of four new objects 78−89207
flare stars in Pleiades, photometric obs. *(Russian)* 77−91536
flare stars in Pleiades, UV and photographic obs. of flares *(Russian)* 77−13367
flare stars in Praesepe field, plate records and cluster membership 77−53652
flare stars in Scorpius-Ophiuchus region, discoveries *(Chinese)* 80−77418
Fornax cluster, membership determ. by photographic photometry 80−82523
Fornax cluster of galaxies, bright members surface photometry 78−96548
Fornax dwarf elliptical galaxy, giant branch colour-magnitude diagram 80−4431
Fornax dwarf galaxy, detection and props. of identified planetary nebula near centre 78−41005
Fornax galaxy, very red giant stars discovery 80−51768
Fourcade-Figueroa galaxy near NGC 5128, resolution, redshift and distance 78−73758
Fraunhofer lines and continuum, solar disc polarisation meas. 78−73688
FXP 0520−66, flaring X-ray pulsar, nature and optical identification *(Russian)* 80−77521
G127.1+0.5, central source of SNR 79−17067
G128-7, cool DA white dwarf, spectrophotometry rel. to atmospheric parameters and evolution 80−62126
G139-29, perturb. from rectilinear motion, astrometric red dwarf binary system with subluminous component 79−8910
G200-39, hot hybrid white dwarf, spectroscopic obs. 80−26852
G206.9+2.3 (=PKS 0646+06), supernova remnant, optical identification 78−36660
G206.9+2.3 (PKS 0646+06), supernova remnant, optical nebulosity discovery 78−96518
G24-16, parallax and astrometric orbit from Sproul plate series 78−53983
G262−21/22, subluminous stars in common proper motion binary 77−33491
G286.8−0.5, nonthermal radiosource in front of Carina Nebula, SNR 79−35355
G287.8−0.5, possible supernova remnant in Carina *(Italian)* 79−53924
G290.1−0.8, optical emission detect. from radio supernova remnant 79−30103
G290.1−0.8, optical SNR photographed 79−40249
G292.0+1.8, abundance anomalies, radial vels., possible Crab-like SNR 80−46628
G292.0+1.8, supernova remnant, optical identification and spectrum 79−84839
G292.0+1.8, young supernova remnant, high vel. material obs. 80−22064
G296.1−0.7, radio SNR in Crux, assoc. optical nebulosity 78−16499
G326.3−1.8, peculiar supernova remnant, optical identification 79−25675
G339.2−0.4, supernova remnant or planetary nebula, radio and optical obs. 80−22104
G35-26, high-velocity mag. degenerate, obs. 78−73709
G77-61, dwarf C star, proper motion 78−4209
G 208-44/45, possible double flare star, spectral obs. 80−67727
G and K-type giant stars, Li abundances 80−41819
G- and K-type giants, spectra and CNO abundances 77−5530
G- and K-type stars, space motions 77−45430
G-type dwarf stars, Mg II and Ca II emission line intensities 79−80306
G-type dwarfs, macroturbulence and age anticorrel. 78−93226
galactic anticentre, space distrib. of stars and dust *(Russian)* 78−73754
galactic bright nuclei, survey of 448 galaxies 78−32569
galactic centre field, planetary nebulae and Wolf-Rayet stars identifications 80−8674
galactic clusters in Cassiopeia, stellar photometry and proper motions obs. *(Russian)* 79−97042
galactic clusters observed in three colours, catalogue and distances 79−40089
galactic distrib. of interstellar absorpt. from Celescope catalogue, UBV and Hβ obs. 77−60810
galactic G-type supergiants, UBV photometry 80−41824
galactic globular clusters colour excess ratio, rel. to interstellar absorpt. law 78−28797
galactic Hα background emission, high spatial and spectral resolution pictures 80−56897
galactic halo, blue horizontal branch stars search on Schmidt plates 78−4362
galactic halo, density gradients in SA 82 and SA 107 fields *(German)* 77−60825
galactic halo C star possible association with Magellanic Stream, visible obs. 80−77411
galactic new H II regions and exciting stars, obs., rel. to spiral struct. 78−61900
galactic North Pole, NGC 4147 direction, halo density distrib., RGU photometry 77−37599
galactic novae, search for light echoes 78−12246
galactic nuclei, stellar population synthesis 78−36688
galactic plane, visible and near IR photographic survey 79−62911
S.Galactic Pole, astrometry of B<14 stars, UK Schmidt results 79−66929
galactic struct., in solar neighbourhood, Aquila direction, RGU photometry 77−91621
galactic structure around l=140°, b=0°results from stellar UBV photometry 78−24555
galactic structure from optical obs. *(German)* 79−17104
galaxies, absorption features radial gradients rel. to metallicity 79−40254

visible astronomical observations continued
galaxies, apparent luminosity function to 21st magnitude 80−31350
galaxies, automated faint object counts to J=24 mag. 79−71120
galaxies, bright, southern, of Las Campanas survey, new classification for 153 systems 79−71113
galaxies, bright, southern, photoelectric photometry 79−21436
galaxies, brightness distrib., decomposition of profiles into spheroid and disc components 78−8115
galaxies, compact and bright-nucleus, in S.hemisphere, spectroscopic survey 80−94725
galaxies, counts up to 25th apparent magnitude *(Russian)* 80−51879
galaxies, deep samples correl. anals. 79−67104
galaxies, diffuse [O I] emission and Hα lines, warm interstellar gas 78−4312
galaxies, distrib. in 36 square degree field near North Galactic Pole 79−40261
galaxies, dwarf irregulars IC 1613 and SMC, star cluster distribs. 79−62900
galaxies, E and S0, UBVR and JHK photometric obs. 79−58412
galaxies, early-type, photometric determ. of twists in three objects 79−25703
galaxies, early-type, rot. curves meas. 78−54034
galaxies, elliptical, extended radio sources, optical positions 80−105331
galaxies, elliptical, surface photometry 78−57625
galaxies, elliptical, vel. dispersions rel. to mass to light ratios 80−98707
galaxies, elliptical and S0, absorpt.-line strengths 80−4430
galaxies, elliptical and S0 colour-absolute magnitude relation 78−8108
galaxies, extended optical-rotation curves for spirals 79−97083
galaxies, faint, number magnitude counts 80−26976
galaxies, halos of spirals, photometry and mass-to-light ratios 79−5892
galaxies, interacting, luminosities and diameters 80−17677
galaxies, interacting, with compact components, UBV photometry 78−20888
galaxies, irregulars and blue compacts, chemical comp. and evolution from spectrophotometry 80−36711
galaxies, lenticular, photographic obs., morphology and H I content *(French)* 79−2570
galaxies, mag. fields from light polarisation obs. 78−69872
galaxies, morphology of 15 blue dwarfs on red Asiago plates 79−101200
galaxies, new colours, magnitudes and types for E and S0 objects 78−89246
galaxies, obscured, in Cygnus, photometric obs. 77−29922
galaxies, optical identifications for 2A X-ray sources 78−89273
galaxies, optical redshifts 80−56936
galaxies, radial velocities for 39 objects 78−45410
galaxies, radial vels. distortion by night sky spectrum 77−41406
galaxies, radial vels. for 42 southern objects 80−41902
galaxies, redshifts, vel. dispersions and line strengths meas. 77−29916
galaxies, redshifts for 196 bright objects 80−46661
galaxies, Sc I and II types, integrated B and V photometry 77−5559
galaxies, Sc I type, magnitudes and radial vels. rel. to vel. anisotropy, data 77−5560
galaxies, Sc-type, colours of nuclei *(Russian)* 77−13471
galaxies, southern, strong emission line spectra, characts. 79−21432
galaxies, southern, UBV photometry of 262 objects 79−35364
galaxies, southern, with broad emission lines 78−20891
galaxies, southern late type and irregular, visible survey 80−105334
galaxies, southern peculiar objects and pairs, spectra and radial vels. 78−45411
galaxies, spectrophotometric gradients *(Russian)* 79−92861
galaxies, survey of irregular and late-type southern objects, classifications 77−91618
galaxies, UBV photoelectric photometry and photometric parameters 80−67855
galaxies, with UV continuum, tenth list *(Russian)* 77−91445
galaxies angular diameter counts, determ. of selection criteria for deep Schmidt plates 77−91623
galaxies assoc. with QSOs, spectroscopic search 80−105355
galaxies compact groups, survey 77−22320
galaxies from ESO/Uppsala list, first catalogue of spectroscopic obs. 77−22113
galaxies in Abell 2255, red shifts 79−40276
galaxies in rich cluster at 00^h47^m, −29°46′, static props. using COSMOS meas. 79−40279
galaxies in rich clusters, morphological types 80−85872
galaxies in righ Abell clusters, photometry and luminosity functions 79−88752
galaxies in two fields near SGP, geometric props. 79−25739
galaxies interacting, radial vels. and luminosities 77−78874
galaxies near galactic plane between l=245° and 255°, catalogue 77−2346
galaxies near late-type spiral NGC 4945, radial vels. and BV photometry 80−109547
galaxies nuclei, vel. dispersions meas. 77−57083
galaxies of high surface brightness, spectra, redshifts absolute magnitudes *(Russian)* 77−49467
galaxies of high surface brightness, spectral obs. *(Russian)* 77−49466
galaxies of Virgo cluster, photographic surface photometry 77−78870
galaxies pair at low galactic latit., discovery 78−96536
galaxies surface distribution, comparison with galaxy fields stochastic simulation 80−90530
galaxies with active nuclei, spectroscopic and photometric obs. 77−37650
galaxies with radio jets, Hα and 450 nm obs. 80−51889
galaxies with UV continuum, photoelectric UBVR photometry *(Russian)* 80−36721
galaxies with UV continuum, twelfth list 80−67585
galaxies with UV excess, second list 80−67584
galaxies with UV excess, spectra and morphology of 58 objects 80−26968
galaxies with UV excess and double and multiple nuclei, spectral study 80−67848
galaxy, discovery of new Sculptor-type dwarf elliptical in Carina 77−82311
galaxy, dwarf irregular, in Sculptor, discovery by ESO 3.6 m telescope 77−22311
Galaxy, nuclear bulge, spectral scans 79−21415
galaxy clusters, nearby, galaxy content and evolution 79−17108
galaxy clusters near NGP, number-density distrib. 77−71149
galaxy group in Cetus with redshift discrepancy 78−36708
galaxy groups, radial vel. meas., membership, mass/light ratios and distances 77−33660

visible astronomical observations continued
galaxy groups and clusters, southern, redshift data 79−84861
galaxy morphology in rich clusters, implications for galaxies form. and evolution 80−62255
Galaxy nuclear bulge, stellar UBV photometry 78−53926
galaxy nuclei, stellar population models 77−2467
new galaxy of Local Group near NGC 6822, discovery 79−84852
galaxy pairs containing one Markarian and one normal galaxy, morphology 78−96535
galaxy pairs with Markarian components, spectroscopy *(Russian)* 77−37648
galaxy photometry, B system magnitudes, luminosity curves and photometric parameters 77−49469
galaxy photometry, magnitudes and colours from multiaperture UBV photoelectric photometry 77−49470
galaxy radial vel. meas. in clusters 77−64856
galaxy redshifts survey, data reduction techniques 80−22074
Galilean satellites, astrometric obs. in (1977) 79−48728
Galilean satellites, diameters from Pioneer data 78−85893
Galilean satellites, orbits from numerical integration *(French)* 80−26779
Galilean satellites, photometry of Io, Europa and Callisto, 1976 to 1979, possible solar variability detect. 80−98623
Galilean satellites, Pioneer 10 and 11 photographs 77−9699
Galilean satellites, spectral reflectivities in 0.32-0.86 μ range 79−35181
Galilean satellites, surface features from Voyager 2 obs. 80−72871
148 Gallia, UBV photoelectric lightcurves and rotation period 79−101105
gamma-ray sources, search for optical counterparts, supernova remnants 79−35429
Ganymede, phase curve and surface microstructure from Voyager 1 photopolarimetry 79−96958
GCl 0422−213, distant globular cluster in Eridanus, preliminary photometry and spectroscopy 80−17624
GD 154, new pulsating white dwarf, obs. 78−40928
GD 229, mag. white dwarf, spectroscopic studies 79−25603
Gd 428, variable star, photometry and spectrum rel. to nature of dwarf Cepheids 78−73720
GD 552, emission-line proper-motion star 78−85943
GD 90, magnetic white dwarf, circular polarisation obs. 78−16409
Geminid meteor shower, obs. over Waltair during 1961-66 period 78−40881
Geminids, flux in 1974, magnitude ratio and mass index 80−4307
U Geminorum, 1978 February magnitude estimates 78−36589
U Geminorum, dwarf nova, M-type dwarf companion spectral type 79−62851
U Geminorum, dwarf nova, radial vels. from emission line obs. 77−57029
U Geminorum, dwarf nova, visual magnitude estimates, (1979, March 23 to 24) 79−44501
U Geminorum, dwarf nova, visual magnitudes during outburst, (1980 May 6 to 9) 80−72978
YY Geminorum, eclipsing binary, photometry and orbital period study 80−105287
U Geminorum, eclipsing binary dwarf nova, times of minima 77−22267
U Geminorum, magnitude estimates for 1978 Oct. 78−96493
ε Geminorum, occultation by Mars, evidence for atm. tides 77−37550
ε Geminorum, occultation by Mars, struct. and extinction of Martian upper atm. 78−7898
ε Geminorum, occultation by Mars photometric obs. 77−91527
U Geminorum, radial vel. meas., rot. accretion disc and hot spot model 77−33561
U Geminorum, soft X-ray emission and visual magnitude estimates 77−91544
U Geminorum, V mag., primary eclipse and visual mag. estimates 79−44505
U Geminorum, visual magnitude estimates during outburst (1980 Oct.) 80−109439
U Geminorum, visual magnitudes for 1978 Jun. 78−65627
β Geminorum (Pollux), Ca II lines obs. rel. to chromosphere model 78−40931
1 Geminorum B, spectroscopic binary, orbit from photoelectric radial vels. 77−22269
ε Geminorum occultation by Mars, McDonald Observatory obs. 77−60702
giant and supergiant stars, atm. $^{12}C/^{13}C$ ratio 77−13337
giant E and cD galaxies, optical extent 77−45557
giant H II regions in Magellanic Clouds, monochromatic photographs 77−45516
giant H II ring in LMC, obs. and rel. to energetic stellar winds 78−77593
giant stars, G- and K-type, CNO abundances 78−7993
giant stars, nonthermal vels. in photosphere 78−4219
giant stars ang. diameters determ. from lunar occultation obs. 79−30054
giant stars in 47 Tucanae, cyanogen distrib. 79−71025
giant stars in globular star clusters, Ca II H and K-lines and abundance 80−72940
giant stars in M13, M92, NGC 6397 and M15, weak-G-band effect obs. 77−78778
GK giants in visual binaries, CN strengths, mixing and supermetallicity 77−56930
GK-type dwarf stars, Mg H lines obs. rel. to Mg isotopic abundances 80−51757
Gliese 815, dMe spectroscopic-visual triple 79−12493
Gliese 82, dM4e star, flare activity discovery 77−91539
Gliese 867, flares obs. on both components of visual binary 79−48861
globular cluster, discovery on ESO Schmidt plates 78−20887
globular cluster giant stars, blanketing differences meas. 80−4345
globular clusters, element abundance survey 77−87489
globular clusters, energy distribs. from Orbiting Astronomical Observatory photometry 80−73009
globular clusters, evidence for H II in cores 78−8065
globular clusters, H II optical search 78−12305
globular clusters, in M31, luminosity distrib. 80−36708
globular clusters, integrated UBV photometry 77−67116
globular clusters, metal-rich, TiO band strengths, reddening and metallicity determ. 79−40227
globular clusters, metal-rich, V, I_K photometry 77−45503
globular clusters, NGC 6440, 6541, 7099, surface brightness, star density and colour profiles 80−12783
globular clusters, radial UBV colour distribs. 79−25648

visible astronomical observations continued
globular clusters, southern, surface-brightness profiles rel. to struct. and stellar content 79−71078
globular clusters, spectral energy distrib. and Fe/H ratio 78−53937
globular clusters, star counts 77−33578
globular clusters, UBV photometry 78−16468
globular clusters, UBVR photometric obs., dust patches 78−81662
globular clusters (M3, M5, M13, M15), equidensity curve meas. *(Russian)* 79−97041
globular clusters evolved stars, CN strengths and UV excesses from DDO photometry 77−64753
globular clusters in Magellanic Clouds, masses determ. 79−5867
globular clusters in Virgo cluster of galaxies, distance modulus 77−74149
globular clusters in Virgo cluster of galaxies, luminosity distrib. 78−12308
globular clusters red giants, metal abundances in M92 and (M15) 79−92759
globular clusters rel. to gravitational disturbance 78−69849
globular clusters south of $\delta = -22°$, distance determ. 77−26030
globular star clusters, TiO band strengths in metal-rich clusters 78−49487
Gor'kii latitude observations, half-year nutation wave terms errors 79−62728
Great Comet of 1577, Tycho Brahe's obs. and deductions 78−32407
Greenwich Obs., Time Report (1976, Jan.-March) 77−45293
Greenwich Obs. Time and Latitude Service, Time Report (April-June, 1977) 78−69661
Greenwich Obs. Time and Latitude Service, Time Report (January-March 1977) 78−57431
Greenwich Obs. Time and Latitude Service, Time Report (January-March 1978) 79−25453
Greenwich Obs. Time and Latitude Service, Time Report (January to March 1979) 80−72749
Greenwich Obs. Time and Latitude Service, Time Report (July-September 1976) 78−20624
Greenwich Obs. Time and Latitude Service, Time Report (July-September 1977) 78−73619
Greenwich Obs. Time and Latitude Service, Time Report (July-September 1978) 79−62729
Greenwich Obs. Time and Latitude Service, Time Report (October to December, 1977) 78−89046
Greenwich Obs. Time and Latitude Service Time Report (April-June 1979) 80−72750
Greenwich Obs. Time and Latitude Service Time Report (October-December 1976) 78−24443
Greenwich Obs. Time and Latitude Service Time Report (October-December 1978) 79−101053
Greenwich Observatory, 1976 April to June time report 77−70581
X Gruis, Algol variable, mean light curve and photometric solution 77−64799
RS Gruis, RRs variable, photoelectric radial vels. 77−5533
Gum nebula, Balmer alpha photographic obs. and interpretations 78−24545
Gum Nebula, cometary globule obs. 77−2464
Gum Nebula, evidence for star form. triggered by nebula expansion 77−29821
Gurzadyan's clustering in Auriga, spectral types 79−21366
GX304−1 (4U 1258−61), shell spectrum of optical counterpart 80−46582
GX 17+2 (3U 1813−14), photometry of optical candidate 78−28849
GX 17+2 (3U 1813-14), optical search 77−2485
GX 1+4, search for Hα pulsations 78−86037
GX 1+4 optical counterpart, symbiotic star, spectrophotometry 77−33498
GX 304−1, shell star optical counterpart 78−93471
GX 339−4 (4U 1658−48), possible black hole binary, optical studies 79−101220
H1-36 (3U 1746-37), emission line object, radio and optical spectra 77−82239
H 0544-665, optical candidate for LMC X-ray source 80−36737
H 2155−304, highly luminous BL Lacertae object, spectral obs. 80−4459
H 2155−304, optical counterpart position and spectrum 78−93478
H 2252−035, optical counterpart photometry and spectrum 80−101651
H 2252−035, spectrophotometry, no periodic linear polarization (1980 Sept.) 80−105401
h 3556, triple star, binary orbit and masses and third component relative motion 79−88701
h 4866 B, vars. in spectral type and radial vel. 78−32518
H-H 28, H-H 29, large proper motion Herbig-Haro objects, astrometric obs. 79−71022
H-H 2, condensation H, spectrophotometric data 79−62826
H-H 7 and 11, spectrophotometry of very low-excitation objects 80−46549
halo population near Sun, intermediate-band photometry 79−44473
halo stars, cool, Al abundance from spectral obs. 80−105232
Haro 15, spectrophotometry and morphology of galaxy with UV excess *(Russian)* 78−93387
Harriot, Thomas, 1560-1621, biography, astronomical instruments and obs. 79−35512
HBV 475 (V1329 Cygni), high-excitation emission lines obs. 78−40955
HD 101065, peculiar star, spectroscopic obs. rel. to presence of Fe 77−45455
HD 101065, Przybylski's star, element identification 78−4233
HD 101065, Przybylski's star, light variability freq. anal. 80−62152
HD 101065, search for light vars. 78−69812
HD 101205 region, spectrographic and photometric obs. of stars and interstellar medium 77−49383
HD 101947, yellow supergiant star, Cepheid with 125 day period 79−88671
HD 10380, Population I giant, chemical anal. and comparison with high vel. stars 80−82352
HD 105056, ON supergiant, radial vel. study 80−90427
HD 105902 (ADS 8448), Ba star in visual binary, spectra and photometry 77−78805
HD 108078, spectroscopic binary orbit from photoelec. radial vel. meas. 80−77451
HD 108102 (T111), possible RS Canum Venaticorum system in Coma star cluster 79−67020
HD 108, Of star, spectral vars. due to solar wind 79−35262

visible astronomical observations continued
HD 111133, Ap star, 5200 Å flux depression variability *(German)* 79−44496
HD 11579, spectroscopic binary orbit from photoelectric radial vels. 80−41862
HD 116458, Ap-star, photometry, spectrum and orbit 77−64767
HD 116890, Ap star, 5200 Å depression index and light variability 77−64767
HD 116890, Si Ap star, UBV photometry, periodicity 79−80318
HD 116994, uvby photometry, var. period determ. 77−13358
HD 118246, new Be star at high galactic latit., photometry and spectrum 78−73721
HD 120640, spectrophotometry and quantitative anal. of B star 77−60758
HD 122563, metal-deficient giant, atm. $^{12}C/^{13}C$ ratio, mixing 78−4201
HD 124224, He Si variable, spectroscopic obs., starspots, oblique rotator model 78−12239
HD 127617 (Bidelman's high latitude Be star), photometric and visible spectra obs. 80−77420
HD 128279, cool halo star, abundances, reduction procedure and equiv. widths 77−49384
HD 129041, new δ Scuti star, period and amplitude 79−2547
HD 129494, new pulsating δ Delphini star, photometric obs. and luminosity 80−67750
HD 129708, new bright short-period Cepheid variable with unusual spectrum, photometric obs. 80−67751
HD 133461, spectroscopic binary orbit from photoelec. radial vel. 77−57016
HD 134439/40, high vel. stars, parallaxes, proper motions and positions 77−71128
HD 137126 spectroscopic binary orbit from photoelectric radial velocities 79−84824
HD 13738, spectroscopic orbit from photoelec. radial vels. 78−12297
HD 137613, C rich H deficient star, UBV photometric obs. 80−90437
HD 138403, emission line spectrum 77−67100
HD 139216, unusual Balmer lines in M-type giant 79−80310
HD 143313, orbit for double-lined spectroscopic binary from radial vels. 79−62873
HD 147508, spectroscopic binary, orbit from photoelectric radial vels. 78−69839
HD 149499B, hot white dwarf, continuous spectrum, H deficient 79−48795
HD 14969, IAU radial-velocity standard star, orbit from photoelectric radial vels. 80−56884
HD 151932, single WN 7 type star with var. He I envelope 79−44493
HD 152667, =OAO 1653−40, photometry, spectrum and physical parameters 79−17021
HD 152667 (V861 Scorpii), phys. props. and orbital parameters, supergiant star with black hole companion model 79−71067
HD 153747, freq. anal. of early-type δ Scuti star 79−71053
HD 153882, obs. with Zeeman analyzer system on McDonald 2.7 m telescope 80−62021
HD 153919, Of supergiant, X-ray binary 3U 1700−37 optical counterpart, light curve anal. 78−32470
HD 153919, Of X-ray binary, narrow band photoelectric photometry 77−60761
HD 153919(3U 1700−37), coronal emission line search 79−35302
HD 153919 (3U 1700−37), binary X-ray source, radial vel. data in blue spectral region 78−61888
HD 153919 (3U 1700−37), forbidden Fe XIV emission detect. 78−16571
HD 153919 (3U 1700−37), further spectroscopic obs. 80−4358
HD 153919 (3U 1700−37), X-ray binary, spectrum variations 78−8158
HD 153919 (3U 1700−37), X-ray binary uvby photometry 77−17624
HD 153919 (3U 1700−37), X-ray eclipsing binary, VBLUW photometric obs. 79−17135
HD 153919 (3U 1700-37), binary X-ray source, radial vels. in blue spectral region 78−49556
HD 153919 (3U 1700-37), X-ray binary, five colour photometry 77−29877
HD 153919 (4U 1700−37), optical oscills. obs. 78−96572
HD 154368, interstellar species, excitation temps. and column densities in direction of supergiant 79−8981
HD 155989, spectroscopic binary, orbit from photoelectric radial vels. 79−21355
HD 159176, spectroscopic binary, radial, vel. obs., orbit and masses 79−25644
HD 159378 (Tr 27-102), yellow variable supergiant near Cepheid instability strip, VBLUW photometry 80−98672
HD 161480 in open cluster IC 4665, peculiar star study 77−33530
HD 161698, Hg-Mn star, chemical elements identification in spectrum 79−58354
HD 165052, O-type binary, spectroscopic obs., masses and radii 78−93308
HD 165590, spectroscopic-visual triple system 77−67113
HD 165590, visual binary with spectroscopic binary component 78−32519
HD 165590 triple system, spectroscopic obs. 79−84825
HD 166734, Of star, spectroscopic binary orbit determ. from visible obs. 80−82414
HD 167771, O-type binary, spectroscopic obs., masses and radii 78−93308
HD 168607 (B9 Ia$^+$), S Doradus type star candidate, spectral line profiles *(Russian)* 80−90456
HD 170899, possible halo population giant star 80−26859
HD 174209 (ADS 11719C), photoelectric radial vel. 78−32517
HD 174237, periodic radial vel. changes, interacting binary with var. mass transfer 79−53818
HD 175742, spectroscopic binary, orbit determ. with CORAVEL photoelectric radial vel. spectrometer *(French)* 80−36671
HD 17576, UV subdwarf companion discovery from uvbyβ photometry 78−96479
HD 179558, spectroscopic binary, orbit from photoelectric radial vels. 79−101177
HD 181330, spectroscopic binary, orbit from photoelectric radial vels. 78−93320
HD 184279, B-type subgiant, variability 79−84804
HD 18474, G-type giant, rare earth's abundance *(Spanish)* 79−25605
HD 184905, H I line strength var. in Ap-star 79−16987
HD 184905, variable Ap star, radial vels. for Si II and Ca II lines 77−22251

visible astronomical observations continued
HD 184927, He variable star, spectroscopic props. 80−51790
HD 184927, He variable star, spectrum obs. 77−22249
HD 185332, new δ Scuti star, photometric and spectroscopic obs. 80−90451
HD 186205, He star, fine abundance anal. 77−87408
HD 187299, spectroscopic binary orbit from photoelectric radial vels. 77−91575
HD 187299 B, spectroscopic detect., late B-type main sequence star 79−48860
HD 187399, spectroscopic binary, spectral obs. *(Russian)* 77−49427
HD 188209, O-type supergiant, spectrophotometry, 3300-7100 Å region 79−67009
HD 188753, close visual binary with spectroscopic binary component 77−57015
HD 191639, B-type main sequence star, variability 79−84804
HD 192163, 191765, Wolf-Rayet stars, optical interstellar spectra obs. 80−17640
HD 192273, optical spectral obs. of proposed EUV source 79−35256
HD 192913, Si Ap-star, lanthanide abundances, spectral identifications 78−45345
HD 193077, probable single WN 5 star with absorption lines 80−56834
HD 193793, Wolf-Rayet binary, visible and near IR spectra 78−8023
HD 193793, Wolf-Rayet star, photometric evidence for C-rich dust cloud 80−26861
HD 193857, metallic-line binary star, orbital elements 79−75250
HD 195592, obs. of interstellar K I 4044 Å line 78−24533
HD 196517, new δ Scuti type variable star 78−49462
HD 197406, Wolf-Rayet spectroscopic binary, radial vels. and orbital elements 80−51812
HD 199892, spectrographic binary, spectrograms and orbital elements 79−21359
HD 200120, Be star, emission features *(French)* 77−56977
HD 200428/9, spectroscopic binary orbit from photoelectric radial vels. 77−5547
HD 200775, Be star, optical and UV extinction by dust in (NGC 7023) 80−109515
HD 200775, possible protostar in reflection nebula NGC 7023, optical polarization and IR spectrum 80−85944
HD 200925 radial vels. of new short period δ Scuti star *(French)* 80−90441
HD 203631, spectroscopic binary orbit from photoelectric radial vels. 80−105285
HD 206860, G0 V star, UBV and IUE obs. of active region 79−92766
HD 20722, peculiar nebula surrounding K-type giant 79−58407
HD 214419, Wolf-Rayet spectroscopic binary, light and vel. changes, common envelope model 79−53856
HD 214686, double-lined spectroscopic binary, orbital elements and masses 79−58376
HD 215038, Ap star, line identification list 78−32484
HD 215441, Ap star, line spectrum variations 78−4232
HD 215441, effective mag. field meas. and field geometry 78−53950
HD 216533, Ap star, spectral variation obs. 78−4244
HD 22007 (primary of ADS 16681), spectroscopic binary, radial vel., orbit elements 80−67793
HD 221568, Ap star, light var. period 80−56856
HD 223969, spectroscopic binary orbit from photoelec. radial vels. 77−82279
HD 22403, spectroscopic binary with Ca II emission, orbital elements *(French)* 79−53854
HD 224085, spot-covered red dwarf, light curves 77−74093
HD 226868 (Cygnus X-1), periodicity in optical light curve during X-ray flare 78−81652
HD 2343, spectroscopic binary, orbit from photoelectric radial vels. 80−8656
HD 26676, unusual radio star, not close binary 78−73707
HD 27507 and escape vel. from Galaxy 78−85935
HD 30466, double wave photometric variable Si star 77−87410
HD 31908, freq. analysis of δ Delphini star 80−46581
HD 33579, 35343, HDE 286757, 269006, most luminous LMC supergiants, long time baseline VBLUW photometry 80−22007
HD 33579, HD 35343 (S Doradus), HDE 268757, HDE 269006, most luminous LMC supergiants, long time baseline VBLUW photometry 80−36630
HD 34452, Si Ap star, spectroscopic study 78−65634
HD 3473, A2p star, spectrograms, Si and rare earth elements overabundance 77−74071
HD 3580, 187473, 212432, Si stars, uvby photometry and periods 78−96487
HD 38268, in 30 Doradus, unique interstellar Ca II K-line profile obs. 80−51850
HD 3980, late Ap star, photometric and mag. variability obs. 80−56845
HD 39937, 101379, 155555, 174429, southern RS Canum Venaticorum stars candidates, radial vel. study 80−98686
HD 4174, peculiar M-giant, magnetic field 80−8631
HD 4174, symbiotic star, spectroscopic obs. 80−85945
HD 43930, photoelec. radial vels. and spectroscopic binary orbit 77−33574
HD 45088, BY Draconis binary, surface activity from high rot. vel., visible obs. 80−77425
HD 45088, reticon obs. in red of dK3 spectroscopic binary 80−67778
HD 47129 (Plaskett's star), massive O-star binary system, variable linear polarisation obs. 78−53989
HD 47732, double-lined binary, spectroscopic orbit 78−57574
HD 47732, young close binary in NGC 2264, photometry and struct. 78−57575
HD 49798, H-deficient subdwarf O-type binary, non-LTE spectral anal. 79−16978
HD 50169, Ap star, uvby photometric obs. 77−22236
HD 50896, WN5 star, variable emission-line spectrum obs. 80−51791
HD 50896, Wolf-Rayet star, detect. of polarisation struct. across emission lines 79−97008
HD 50896, Wolf-Rayet star, linear polarisation periodic vars. rel. to binary star nature 80−72972
HD 51480, shell star, spectroscopic obs., atmospheric struct. and distance 80−31305
HD 51585, B[e] star, visible and near IR spectrum 77−45445
HD 52788, freq. anal. of δ Delphini star 79−35276
HD 63791, probable metal-poor halo G-type giant field star 80−26859
HD 65750, photometric vars. of red giant, obs. of surrounding refl. nebula IC 2220 78−36567

visible astronomical observations continued
HD 67084, new southern spectroscopic binary, radial vels., orbital elements 78−57592
HD 67198, new southern spectroscopic binary, radial vels. 78−57592
HD 698, massive spectroscopic binary, spectral obs., evolutionary state, mass loss 78−57590
HD 72968, low amplitude photometric double wave Ap star, light curve 78−28697
HD 77581 (3U 0900-40), X-ray binary, spectroscopic orbit and masses of components 78−16461
HD 77581 (4U 0900−40), optical pulsations from eclipsing binary 79−48951
HD 77581 (Vela X-1), discovery of optical pulsations 77−82327
HD 77581 (Vela X-1), four colour photometric obs. and light curve anal. 77−17621
HD 77581 (Vela X-1), optical pulsations discovery 78−20911
HD 77581 (Vela X-1), X-ray binary, photometric obs. 77−41392
HD 77581 (Vela X-1), X-ray obs. and UBV photometry 78−65722
HD 77581 and 153919, polarimetric obs. of massive X-ray binaries 80−98688
HD 80383, UBV photometry of β Cephei type star 80−36644
HD 84903 and 184711, differential anal. of extreme metal deficient stars rel. to halo star HD 122563 79−80302
HD 8781, freq. anal. of low-amplitude δ Scuti star 80−46575
HD 87892, central star of NGC 3132, obs. of visual companion 78−20859
HD 88230, dM0 star, high-dispersion photometric atlas from 3900 to 6000 Å 78−7996
HD 88661, Be star, photometry and light vars. *(French)* 78−57562
HD 90657, Wolf-Rayet spectroscopic binary, spectroscopic obs. 77−13357
HD 91619, 96919, B-supergiants, peculiar H_α profile variations 77−17577
HD 91805, spectrum anal. rel. to nature of Bidelman-MacConnell weak G-band stars 78−49432
HD 92664, Ap star, photometric variability and period from uvby photometry 79−40199
HD 92740, spectroscopic binary WN7 star, spectroscopy and photoelectric photometry 79−8924
HD 93162, probable single WN7-type star in Trumpler 16 cluster 78−85946
HD 93250, O3 massive star in η Carinae complex, non-LTE analysis 80−77398
HD 93521, high galactic latit. peculiar O-type star, spectrum 77−78784
HD 93521, Population II O-type star, spectroscopic obs. 79−16961
HD 94033 ultra short period cepheid, obs. 80−22024
HD 96953, spectroscopic binary orbit from photoelectric radial vels. 80−56887
HD 97048, pre-main-sequence star, spectral changes 77−74055
HD 97048 (=HM 18), pre-main sequence star, unidentified IR features obs. 80−85943
HD 97950, central star in NGC 3603, interstellar spectral lines, visible obs. 80−101586
HD 9996, Ap star, spectrsocopic obs. 78−77558
HDE 226868 (Cygnus X-1), Hα emission in (1977) 80−51919
HDE 226868 (Cygnus X-1), He II 4686 Å emission in spectrum 79−21328
HDE 226868 (Cygnus X-1), long-term circular polarisation variability 79−9031
HDE 226868 (Cygnus X-1), orbital period and Hβ light curve 79−48952
HDE 226868 (Cygnus X-1), orbital period and inclination 78−16579
HDE 226868 (Cygnus X-1), variable linear polarisation, 1974-1975 obs. 77−9810
HDE 228766, evolved Of system, spectroscopic obs. 78−12237
HDE 232078, variable mass loss in metal deficient red giant 79−67010
HDE 245770, optical counterpart to A 0535+26, dimens. spectral type and luminosity visible obs. 80−72976
HDE 245770, possible counterpart of variable X-ray source A 0535+26, line and continuum vars. 80−17600
HDE 245770, spectroscopic obs. of X-ray nova Ariel 0535+26 optical counterpart 77−45450
HDE 245770 (A0535+26), Hβ var., general props., spectral obs. 78−4247
HDE 245770 (A0535+26), spectroscopy and orbital periods 78−93306
HDE 245770 (A0535+26), UBV photometry during X-ray outburst 79−67024
HDE 245770 (Ariel 0535+26), 1977 spectrum, objective prism study 78−61866
HDE 245770 (Ariel 0535+26), optical spectrum of Be star 78−4227
HDE 245770 (Ariel 0535+26), photoelectric UBV photometry 78−36592
HDE 245770 (Ariel 0535+26), UBV photometry during X-ray flare-up 78−28705
HDE 283048, hot subluminous star, spectrum 78−20823
HDE 313846, most extreme Of star, spectroscopic obs. and mass outflow 79−88682
HDE 326333, new β Canis Majoris star, photometric obs. 80−17595
He2-442, UVRK photometry and spectroscopic obs. *(Russian)* 80−94817
He 1-3, planetary nebula, misidentification correction 79−62895
He 2-111, planetary nebulae, giant halo with very high vels. discovery 79−25691
He 2-467, yellow symbiotic star, emission lines and continuum 80−62155
He-3 1863, unusual high latit. Be star, spectral obs. 77−87418
head-tail radio galaxies in poor clusters, radio and optical obs. 78−96530
head-tail radio galaxies velocities with respect to intracluster medium 78−49516
6 Hebe, dimensions as result of occultation obs. 79−92694
6 Hebe, occultation of γ Ceti, 1977, Mar. 77−33407
6 Hebe, phase functions 77−64689
6 Hebe, size from 1977 March 5 γ Ceti A occultation obs. 78−53856
624 Hektor, nature of Trojan asteroid 79−35176
Helix Nebula, abundance anomalies in planetary nebula 78−86001
Henize 715 (4U 1145−61), Be-type star, colour and luminosity vars. (1976-1980) 80−72979
Henize 787 (SAO 251905), five-colour photometry 77−29846
Henize 788 (Wray 977), counterpart of 3U 1223-62, five colour photometry 77−29846

visible astronomical observations continued
Henize S22, emission line star in LMC, spectrophotometric study 78−69803
103 Hera, photoelectric light curves, synodic rot. periods, amplitudes of var. 79−53752
Herbig Ae/Be stars, Hα profiles 78−16410
Herbig Ae/Be stars, multicolour linear polarization meas. 79−25607
Herbig Ae/Be stars, multicolour polarimetry 78−49445
Herbig Ae/Be stars, spectrophotometry 78−93258
Herbig-Haro object 1 exciting star, identification as T Tauri star 80−17633
Herbig-Haro object 24, emission/reflection nature 80−41829
Herbig-Haro objects, nearby IR sources optical spectra 80−67720
Herbig-Haro objects, new, spectroscopic obs. 79−5763
Herbig-Haro objects, spectrophotometry and radiating shock waves 78−85936
Herbig-Haro objects associated with NGC 2264 young cluster 79−71026
Herbig-Haro objects in Gum Nebula, spectrophotometry 78−36565
Herbig-Haro objects in Orion Nebula 80−77397
Hercules supercluster, basic redshift data 80−36725
Hercules supercluster, evidence for intracluster medium 80−22092
Hercules supercluster, galaxy distrib. in field 78−93437
Hercules X-1 (HZ Herculis), Bowen fluorescence mechanism evidence 78−53985
Hercules X-1 (HZ Herculis), coordinated optical and X-ray pulsations obs. 80−51909
532 Herculina, occultation of SAO 120774, discovery of 1978 (532) 1 possible satellite 78−69734
532 Herculina, photoelectric light curves, synodic rot. periods, amplitudes of var. 79−53752
HZ Herculis, 0.8 day periodicity in line emission 77−74089
HZ Herculis, abnormal N III emission lines in 1978 Aug. spectrum 78−81661
AK Herculis, atypical W Ursae Majoris type, BV light curves 78−28719
14 Herculis, C/Fe ratio of K-type dwarf 78−93227
α^2 Herculis, circumstellar absorpt. lines rel. to absolute mass loss scale for red giants 78−7997
AC Herculis, curve-of-growth analysis of RV Tauri variable 80−22026
DY Herculis, dwarf Cepheid, radial vel. and radius 79−58358
DY Herculis, dwarf Cepheid, uvbyβ photometry and evolutionary status 79−58357
AH Herculis, dwarf nova, changes in rapid oscills. during outburst 79−88686
AH Herculis, dwarf nova outburst, rapid oscills. evolution 80−94805
u Herculis, eclipsing binary, phase-locked polarization 78−4281
DI Herculis, eclipsing binary, photometric obs. anal. rel. to relativistic motion of periastron 80−94830
AD Herculis, eclipsing binary, spectroscopic obs. and orbital elements 78−73738
DQ Herculis, eclipsing binary emission line eclipse phenomena, visible spectra obs. 80−94800
u Herculis, eclipsing variable, two new light curves 80−90472
DQ Herculis, emission lines phase depend. in accretion disc 77−74095
DQ Herculis, He II 4686 Å line phase shift from spectrophotometry 79−21296
AM Herculis, high speed photometric obs., 186 min. var., dwarf nova model 77−64806
AM Herculis, high-speed circular polarimetry 79−25629
AM Herculis, IR and visual monitoring, model constraints 79−17018
OP Herculis, irregular variable, Tc I absorpt. lines obs. 78−28689
88 Herculis, light and colour vars. of shell star 79−53817
V396 Herculis, low redshift, optically variable quasar discovery 77−33676
AM Herculis, low-mass X-ray binary, radial vels. and line intensities 77−78826
α Herculis, M supergiant, circumstellar shell and mass loss rate 77−45415
52 Herculis, magnetic, spectral and photometric vars. of Ap-star 78−85952
AM Herculis, multicolour photometry, slow optical pulsar 78−28693
AM Herculis, narrow-band photoelectric obs. *(Russian)* 78−77565
HZ Herculis, nonperiodic optical flickering obs. 78−53988
ι Herculis, nonradial pulsations (1975-77) 79−5823
AK Herculis, photoelec. obs. and period study, possible visual companion 79−67065
AM Herculis, photometric and polarimetric obs. 78−65657
AM Herculis, photometric and spectrographic obs. 77−45492
DQ Herculis, photometric study of light curve 71 s oscill. 78−93259
AM Herculis, possible cataclysmic variable of Z Camelopardalis type 77−33497
AK Herculis, R and I light curves, B and V light curves comparison, starspot 79−67064
AC Herculis, RV Tauri star, UBV obs. 80−56857
4 Herculis, shell star, Balmer intensity profiles 77−56973
4 Herculis, shell star, photometric obs. rel. to binary star hypothesis 77−91538
BL Herculis, short-period Population II variable, chem. comp. determ. 79−8923
HZ Herculis, spectrograms, radial vels. and equivalent width meas. 77−74094
AM Herculis, spectrophotometric obs. at min. light min. light 80−98692
AM Herculis, spectroscopic obs., H lines and He II 4686 Å line intensities 78−57589
AM Herculis, UBVRI light curves 78−85972
AM Herculis, visual magnitude estimates (1977, April-May) 77−53642
AM Herculis, visual magnitude estimates (1980 March-June) 80−82428
AM Herculis, X-ray binary, emission lines, radial vel. var. 77−33567
AM Herculis, X-ray binary, obs., slow rotator model 78−12408
AM Herculis, X-ray binary, optical light curve 77−33566
AM Herculis, X-ray binary, optical variability 78−53952
AM Herculis, X-ray binary, polarization obs., mag. compact star discovery 77−33569
AM Herculis, X-ray binary, spectroscopy and photometry, model 77−33568
AM Herculis, X-ray binary, vel. curves for emission lines broad and sharp components 78−32513
AM Herculis, X-ray eclipsing binary, UV and visible spectra anal. 80−109563
AM Herculis (3U 1809+50), multicolour linear and circular polarisation obs. and geometrical model 78−8053

visible astronomical observations continued
AM Herculis (3U 1809+50), polarimetry and spectrophotometry rel. to mag. field 80−94835
AM Herculis (3U 1809+50), simultaneous three-channel photometry rel. to optical flickering mechanism 80−82411
AM Herculis (4U 1813+50), narrow-band photoelec. obs. *(Russian)* 79−88767
AM Herculis (4U 1813+50), rapid light variability obs. *(Russian)* 80−8662
AM Herculis (=3U 1809+50), near IR and violet mag. obs. 77−53643
HZ Herculis (Hercules X-1), optical and UV obs. 80−109487
HZ Herculis (Hercules X-1), optical behaviour, 1976 Aug.-1977 Nov. 79−53855
HZ Herculis (Hercules X-1), optical behaviour in (1976) 78−32603
HZ Herculis (Hercules X-1), optical pulsations spectrum meas. 77−33685
HZ Herculis (Hercules X-1), Sonneberg photographic obs. 77−37618
HZ Herculis (Hercules X-1), UBVR photometry during 1977 Jul.-Aug. *(Russian)* 79−17028
DQ Herculis (Nova 1934), extended nova shell spectra 78−93253
DQ Herculis (Nova 1934), masses of interactive binary 79−97029
V533 Herculis (Nova 1963), periodic light oscills. obs. 78−93285
α Herculis A, M-type supergiant, Li abundance in atmosphere *(Russian)* 80−72950
944 Hidalgo, UBV obs. of rotation and CN band not in spectra 77−5485
high velocity giant stars, detailed chemical anal. 80−82352
high-latitude blue variables, slit spectra 79−21312
high-latitude reflection nebulae illuminated by the galactic plane 77−17647
high-resolution astronomical imaging, results 80−82225
high-velocity stars, southern, radial vels. 80−21988
high-velocity stars, southern, UBV colours 80−21989
Himalia, radius and albedo 77−33399
Hodge 11, in LMC, colour-magnitude diagram, metal abundances 78−69850
Hodge 11 star cluster in LMC, electronographic photometry and colour-magnitude diagram 79−40230
horizontal-branch A-type stars, astrophysical parameters determ. 79−62829
TU Horologii, ellipsoidal variable, UBV photometry 78−4292
TU Horologii, period and spectroscopic orbit of ellipsoidal binary system 79−58372
hot white dwarfs, luminosity function, spectral type anal. 80−90418
Houck atlas of Milky Way 77−37510
HR7922, B-type spectroscopic binary, orbital soln. 80−26910
HR8891, B-type spectroscopic binary, orbital soln. 80−26910
HR 1099, Ca II H and K emission enhancement during February 1978 radio flare 79−21341
HR 1099, Hα region spectrophotometry during February 1978 radio flare 79−21344
HR 1099, H and Ca II, emission during February 1978 radio outburst 79−21340
HR 1099, new bright RS Canum Venaticorum variable, spectrum 77−9754
HR 1099, optical ephemeris and photometric wave minimum phase 78−36641
HR 1099, optical linear polarisation meas. 78−53958
HR 1099, photometric and spectroscopic obs. 1978 Feb. 78−40998
HR 1099, radio emitting variable star, photoelectric photometry 77−53602
HR 1099, RS Canum Venaticorum binary, Hα profile obs. 79−21343
HR 1099, RS Canum Venaticorum binary, optical spectrophotometry during major flare outburst 79−21342
HR 1099, V photometric obs. during 1976-77 period 78−40994
HR 1099 (V711 Tauri), RS Canum Venaticorum star, Hα line variability, visible spectra obs. 80−105277
HR 1170, δ Scuti-type star, light and colour curves 77−74058
HR 1170, HR 7331, nonradial δ Scuti pulsators, photometry multiperiod anal. 79−88663
HR 1217, Ap star, spectrum and light vars. relationship 80−26878
HR 1225, δ Scuti star, photoelectric study and periodogram anal. 80−109436
HR 1300 spectroscopic binary Am star, orbital elements 77−49438
HR 2081, double-lined spectroscopic binary, radial vel. orbit and min. masses 80−51811
HR 2172, double-lined binary, radial vels. and equivalent widths *(French)* 77−17625
HR 2317, spectroscopic binary orbit from photoelectric radial vels. 79−40225
HR 2557, light vars., luminous δ Scuti-type star 78−32490
HR 3089, He-rich star, spectrum anal. 77−9751
HR 3126, peculiar M giant in reflection nebula, mass loss 77−17558
HR 3153, young cluster M giant, mass loss 77−17558
HR 3413, Ap star, photometric vars. and period *(French)* 78−32471
HR 432, 515 and 8006, δ Scuti stars, spectrographic obs. 80−36639
HR 4594, freq. anal. of low-amplitude δ Scuti star 79−35275
HR 4594, pulsating marginal metallic line (Am) star, obs. 78−49448
HR 4665, spectroscopy of bright long-period RS Canum Venaticorum system 80−36665
HR 5049, Co II in spectrum of southern magnetic Ap-star 80−82384
HR 5153, Ap star, rot. vel. and light vars. period 77−17593
HR 5161, spectroscopic binary star, radial vel. orbit 80−12781
HR 5597, irregularly variable magnetic star 77−74061
HR 5999, variable shell star, VBLUW photometry 78−28701
HR 5999 (V856 Scopii), multicolour photometry, circumstellar dust shell 79−48828
HR 6127, chemically peculiar star, spectral lines and equivalent width lists, visible obs. 80−82387
HR 6388, spectroscopic binary, orbit determ. from photoelec. radial vels. 78−49482
HR 6392, double star with very high luminosities, photometry, and spectra 77−45493
HR 6659, spectroscopic binary, radial vel. obs. 80−82430
HR 6684, β Cephei-type variable, radial vel. var. 78−45344
HR 6766, weak G-band star, light-element abundances 78−57548
HR 6940, spectroscopic binary orbit from photoelectric radial vels. 78−4294
HR 7083, spectroscopic binary, orbit from photoelectric radial vels. 78−32517

visible astronomical observations continued
HR 7331, δ Scuti star, relation between radial vel. and light vars. 77−9752
HR 774, Mg isotopes and s-process elements in Ba star 79−25594
HR 8102, uvby anal. of δ Scuti type star 78−53965
HR 8210, freq. anal. of low-amplitude δ Scuti star 79−35275
HR 8210, pulsating marginal metallic line (Am) star, obs. 78−49448
HR 8752, binary supergiant, emission feature variability, visible obs. 80−109463
HR 8752, spectrum var. of G-type supergiant 79−62828
HR 8752 (HD 217476), superluminous superiant, line spectrum changes rel. to expanding shell 79−80308
HR 8752 (V509 Cassiopeiae), emission-line spectrum rapid changes 80−36645
HR 9049, (HD 224113), eclipsing spectroscopic binary star, period determ. 80−46609
HR 9070, Be star, spectral vars. obs. 80−12773
HR 9076 (ε Tucanae), Hα shell profile 78−36583
HR 96, Ap-type star, atm. parameters and stellar comp., visible obs. 80−67740
Hyades, BVRI photometry of new possible cluster members 78−32533
Hyades, lunar occultations, 1978 September 22 reappearance events 79−40185
Hyades cluster, possible members BVRI photometry 80−51821
Hyades cluster, shape and luminosity distrib. 80−17622
Hyades stars, Hα and O I 7774 Å photometric obs. 77−22286
Hydra I cluster, photometric obs. of brightest galaxies 77−33659
Hydra I cluster of galaxies, ram-pressure sweeping, optical evidence 78−93429
EX Hydrae, 2:3 period ratio in light curve 80−46580
TT Hydrae, absolute dimensions of β Persei type eclipsing binary 80−62184
VX Hydrae, dwarf Cepheid, uvbyβ photometry 77−29856
EX Hydrae, dwarf nova, IR and optical light curves 80−67747
EX Hydrae, dwarf nova lightcurve, periodic and secular vars. 80−77413
χ^2 Hydrae, eclipsing binary, four-colour photometry, orbital elements, dimensions and He abundance 78−65653
EZ Hydrae, eclipsing binary, photometric obs. and primary min. ephemeris 78−73737
EX Hydrae, eclipsing binary dwarf nova, times of minima 77−22267
AI Hydrae, light curves and photometric elements of eclipsing binary 78−65652
EX Hydrae, spectra of dwarf nova 80−98670
TT Hydrae, UBV photometry, improved light elements 78−69837
χ^2 Hydrae, uvby light curves of double-lined eclipsing binary 78−40996
AI Hydrae, uvby photometric obs. of eclipsing F-type binary 78−69835
VW Hydri, colour variations during dwarf nova outbursts 80−46576
WX Hydri, dwarf nova, obs. of superhumps during supermaximum 79−88677
VW Hydri, dwarf nova, short period light oscills. 78−20837
VW Hydri, light curves of dwarf nova 78−12245
VW Hydri, outbursts of dwarf nova, long and short eruptions comparison 79−88669
Hyperion, near IR spectra and JHK photometry 80−56761
HZ 43, visual binary, photographic measures 77−5548
Iapetus, brightness and B−V colour index 77−60719
Iapetus, normal reflectance from lunar occultation obs. 78−85897
Iapetus, radius from 1974 March 30 lunar occultation 78−36505
Iapetus, visible and IR obs. rel. to relative reflectance at 1.6 and 2.2 μm 80−98607
IAU 13S6A, strong southern radiosource, optical identification 77−64865
IAU Radial Velocity Standard stars, radial vels. meas. *(French)* 80−51743
IC 1318, giant H II region, large-scale line splitting discovery 78−96521
IC 1318 b and c and 5070, N II 6584 Å forbidden line profiles of giant H II regions 79−67081
IC 1318 nebular complex in Cygnus X region, light extinction 80−51835
IC 1613, galaxy, colour-magnitude diagram and luminosity function for brightest stars 77−5561
IC 1613, structure and content of Local Group dwarf galaxy 78−86006
IC 1795 (W3), N II forbidden line unusual profiles over giant H II region 80−46645
IC 2149, planetary nebula, absolute spectrophotometry, in visible and near IR 77−17669
IC 2581, young open cluster, ratio of total to selective extinction determ. 79−5870
IC 2944, stellar aggregate surrounding HD 101205, spectrographic and photometric obs. 77−17636
IC 310, galaxy, outer structure from electronographic obs. 78−16521
IC 342, Scd galaxy, discovery of companion 80−36712
IC 3568, planetary nebula, struct. and internal extinction 80−31338
IC 361, open cluster, preliminary photometry 78−89228
IC 418, planetary nebula C abundance from visible and IUE obs. 80−82451
IC 418, planetary nebula structure from electronographic data 79−35339
IC 4329A, Seyfert galaxy, photographic photometry and optical spectrum 80−36706
IC 4329A, spectrophotometry of extreme Seyfert, possible quasar 79−101190
IC 443, fast filaments and high vel. gas, Hα obs. of SNR 79−30106
IC 443, supernova remnant, detect. of gas at 10^6K 79−53875
IC 443, supernova remnant, Hα inteferometric obs. of fast filaments and high vel. gas 79−75258
IC 4593, planetary nebula, absolute spectrophotometry in visible and near IR 77−17669
IC 4593, planetary nebula, emission line obs. 77−33621
IC 4756, open cluster, uvby β photometry, distance modulus 78−53997
IC 4997, O III 4363 Å forbidden line/Hγ intensity ratio vars. 78−86003
IC 4997, O III 4363 Å/Hγ ratio reversal in spectrograms of planetary nebula 79−92821
IC 4997, [O III] 4363 Å line intensity in variable planetary nebula 78−8100
IC 5146, young star cluster, polarisation of starlight 77−5550
IC 5152, low-luminosity barred galaxy, struct., rot. curve and redshift 80−56950
image degradation, contrib. of lower atmospheric layers, use of photodiode array 79−21019

visible astronomical observations continued
Imbrium sculpture and lunar basin radial texture, evidence for sedimentary origin 77−37526
ε Indi, late type dwarf star, spectrum rel. to model atmosphere and comp. 80−90425
ε Indi moving group, detailed anal. of members HD 40409, HD 102365 and λ Aurigae 78−85982
Innisfree meteorite, fireball photograph, recovery on Earth 78−61821
Innisfree meteorite fireball Canadian camera network record and orbit determ. 78−65563
173 Ino, photometric vars., light curves and rot. period 79−16869
intergalactic dust obs. near NGC 300 77−45553
intergalactic optical surface brightness in Coma cluster, photometry 77−87550
Interkosmos 7, photometry of eclipses observed in situ 77−91408
intermediate Population II stars, Strömgren uvby photometry 77−60757
International Latitude Service obs., errors 77−45324
International Time Bureau obs. for continental drift meas. 77−13072
interstellar $^{12}CH^+/^{13}CH^+$ abundance ratio, meas. towards 20 Tauri, ξ Persei and ζ Ophiuchi 80−67809
interstellar absorption lines of Na I, K I, Ca II, in stellar spectra rel. to galactic gas distrib. 80−26963
interstellar CH^+ 3957 A line towards ζ Ophiuchi rel. to $^{12}C/^{13}C$ ratio 77−87529
interstellar CH^+ upper limit towards τ Scorpii 78−4309
interstellar dark clouds, visual extinction meas. and CO/H_2 ratio 78−96513
interstellar faint optical emission lines, limits on temp. and ionization state of emitting gas 77−37634
interstellar grains, interaction of light with small-particle system 77−74111
interstellar K I, 4044 Å line obs. 78−24533
interstellar large globules, absorpt. meas. rel. to struct. and dynamics 80−62246
interstellar lines towards Cepheus OB2 association, anal. 80−22052
interstellar lines towards stars of low reddening 78−57603
interstellar low mass dust clouds in solar vicinity, photometric survey results 80−36512
interstellar matter in front of χ Ophiuchi, optical obs. 79−25673
interstellar matter in Magellanic Clouds, giant and supergiant shells obs. 80−94858
interstellar matter towards Orion OB1 assoc. stars ε Orionis and π^5 Orionis, Copernicus obs. 80−22050
interstellar Na I and/or Ca II lines, obs. towards 47 stars 79−25676
interstellar Na I lines hyperfine struct. in α Cygni direction 78−24542
interstellar reddening in direction of low latit. globular clusters 77−22299
interstellar reddening in high-latit. field around ω Bootis 79−101185
interstellar reddening law from normal and Be star energy distribs. 77−74109
Io, active volcanic eruptions and hot spots, Voyager 1 discoveries 79−40131
Io, albedo stability and colour markings, historical meas. 79−96951
85 Io, astrometric obs., 1865-1977, and definitive orbit 80−4284
Io, brightness increase after eclipse, colour TV obs. 77−87318
Io, currently active volcanism discovery 80−26789
Io, IR refl. spectra, 2.8-5.2 μm 80−56756
Io, long term light vars. *(Italian)* 78−93147
Io, morphology of Na emission region 77−49329
Io, Na cloud, first photographs 78−32389
Io, Na cloud direct images 78−61792
Io, Na I D_2 emission line profiles, var. with orbital phase angle and mag. latit. 78−4139
Io, Na I D-line emission synoptic obs. 77−13281
Io, periodic variations obs. in Na and K clouds 78−4138
Io, pictures of Na cloud 79−12425
Io, post eclipse brightening, BV photometry 77−37560
Io, reflectance spectrum, evidence for sublimates and adsorbates 79−92707
Io, search for colour changes and brightening upon eclipse reappearance 77−91469
Io, surface composition, comparison of observed and lab. reflectance spectra 77−60716
Io, visible spectrum, search for new features 79−35185
Io Na cloud, monochromatic imaging using filters, slitless (multislit) spectrograph, and interferometers 79−8840
Io Na cloud, obs. rel. to Jupiter magnetosphere thermal electron density 79−40133
Io Na D-line emission, comparison of observed and theoretical line profiles 78−93145
IR bright stars in region of galactic centre, catalogue and photometry 80−77299
IR source assoc. with Sh 2-149, spectral type and luminosity class 78−73772
IR sources, photometric histories of six objects 79−5916
IR sources embedded in molecular clouds, optical spectrophotometry 78−96520
IRC+30219, variable C star, optical emission-line phase obs. 80−90569
7 Iris, photometry rel. to rot. and pole orientation 77−74004
Irkutsk prism astrolabe obs. programme *(Russian)* 78−4114
42 Isis, photoelectric light curves, synodic rot. periods, amplitudes of var. 79−53752
isoplanatism and turbulence of the upper atmosphere 79−96810
JL 76, spectroscopic obs. of DC white dwarf candidate 77−67090
Juno, occultation of AGK3 +0°1022, obs. 80−26773
Juno, occultation of AGK3 +0°1022 re-analyzed 80−41757
Jupiter, absolute reflectivities and limb darkening, 4100-8300 Å Si vidicon imaging 78−7916
Jupiter, Amalthea and Galilean satellites, 1976-8 absolute and relative posns. 79−62789
Jupiter, astrolabe obs., 1976-77 winter period *(French)* 78−32387
Jupiter, astrometric obs. of faint satellites during 1975-6 opposition 79−75139
Jupiter, atm. H_2 content from spectral line equivalent width *(Russian)* 78−12143
Jupiter, atmosphere, equatorial belt, spectrophotometry in 0.6-1.1 μm range 79−96960
Jupiter, atmosphere, zonal vel. and texture from Voyager 1 images 79−92711
Jupiter, atmosphere constituents, comparison with Saturn, visible spectra obs. *(French)* 80−101550

visible astronomical observations continued
Jupiter, atmospheric absorption in blue and UV 79−40125
Jupiter, atmospheric dynamical activity in 1975, photographic and photoelec. obs. 79−21224
Jupiter, atmospheric methane and ammonia abundance photoelectric obs. 77−33397
Jupiter, C/H, $^{12}CH_4/^{13}CH_4$ ratios determ. from near-IR spectra 77−9698
Jupiter, cloud features, pre-Voyager velocity data 79−92710
Jupiter, cloud structure and vel. fields 79−92712
Jupiter, colour filter obs. in 1975-76 period 77−91470
Jupiter, equatorial atmosphere, Voyager obs. of small-scale waves 79−92713
Jupiter, fast moving bright spot obs. in North Temperate Current C 80−67640
Jupiter, Galilean satellites, 1975-6 astrometric obs. 80−4288
Jupiter, Great Red Spot and South Temperature Belt white spots motion and struct. 77−67065
Jupiter, ground-based imaging rel. to Pioneer and Voyager cloud configurations interpretation 80−26787
Jupiter, H_2 quadrupole lines in spectrum 79−70990
Jupiter, Hα auroral activity obs. 77−45350
Jupiter, H Lyman-α brightness, longit. asymm. 80−72852
Jupiter, HD search at 6045 Å, D/H ratio upper limits 78−85892
Jupiter, IR and visible spectrum, C/H ratio 79−48729
Jupiter, lightning flashes, first results, geometric reduction 79−96952
Jupiter, longitude measurements for surface details, phase exaggeration effect *(French)* 78−36497
Jupiter, magnetosphere, S nebula 77−87315
Jupiter, methane and NH_3 bands, longitudinal variability, visible obs. 80−82270
Jupiter, methane and NH_3 bands spectropolarimetry, 6800-8200 Å 79−66955
Jupiter, methane band photometry, absolute reflectivity, centre-to-limb vars. 79−53759
Jupiter, methane band photometry, SEB and STrZ reflectivity, atm. models 79−53760
Jupiter, Na I emission from region C_2, Na transport from Io 79−53758
Jupiter, near IR spectral albedo 80−31242
Jupiter, NH_3, spatial distrib. from optical band strengths and curves of growth 80−46386
Jupiter, NH_3 6450 A absorption band obs. 77−33396
Jupiter, NH_3 abundance from visible obs. 80−82269
Jupiter, NH_3 atmospheric abundance 78−12142
Jupiter, obs. of light and dark spots in equatorial regions 78−57493
Jupiter, Pioneer 10 and 11 photographs and Earth-based obs. 77−67064
Jupiter, Pioneer 10 imaging data for prominent belt and zone, haze particles 78−45269
Jupiter, polar regions limb darkening obs. and atmospheric props. 79−62790
Jupiter, reflectivities during 1976 opposition 79−40124
Jupiter, ring system, Voyager 2 obs. 80−12707
Jupiter, S II forbidden line emission from thermal plasma 78−93146
Jupiter, S II forbidden line emission nebula studies 80−67636
Jupiter, S II forbidden line emission round planet, distrib. and intensity 80−85885
Jupiter, S II ring, var. in characts., link with Io, visible obs. 80−90360
Jupiter, S II torus, longitudinal asymmetry visible spectra 80−82271
Jupiter, satellites, diameters from lunar occultation meas. 78−45272
Jupiter, satellites 1979 J 1 and 2, Voyager 1 imagery analysis 80−67639
Jupiter, South Equatorial Belt disturbance, discovery 79−58295
Jupiter, south temperate belt white spot annual oscills. obs. 79−70991
Jupiter, spectrophotometric and polarimetric obs. *(Russian)* 77−71050
Jupiter, spectrophotometry in 0.6 to 1.1 μ region, Jovian atmosphere optical parameters latit. vars. 80−46468
Jupiter, upper atmosphere aerosol content from Ganymede eclipse obs. 77−41349
Jupiter, Voyager 1 mission photographs 79−84698
Jupiter, Voyager 1 obs. 79−96948
Jupiter, Voyager 1 photographic obs. of atmosphere ring and major satellites 80−26788
Jupiter, Voyager colour photographs of planet, Amalthea and Galilean satellites *(German)* 79−96959
Jupiter, wind vector, eddy mmtm. and energy conversion obs. 80−72851
Jupiter's satellites, mutual phenomena (1973 Sept.-1974 Jan.) 79−40129
Jupiter's satellites, precise positions during 1973 77−17421
Jupiter and Galilean satellites, astrometric position determ. (1977) *(French)* 80−77326
Jupiter and Galilean satellites, astrometric position determ. 80−77327
Jupiter and Galilean satellites, positions obtained in 1978 at ESO-La Silla *(French)* 80−21943
Jupiter cloud zones, near IR obs. 77−29712
Jupiter faint satellites, astrometric obs. during 1976 to 1977 opposition 80−26778
Jupiter faint satellites (VI-XIII), astrometric obs., (1974 to 1977) 78−89107
Jupiter Galilean satellites, Amalthea, Voyager 1 results 80−4293
Jupiter magnetosphere, S II obs. rel. to S plasma discontinuities 80−4291
Jupiter measures of photographs of 1974/75 apparition 77−60717
Jupiter ring, Voyager 1 detection 79−40131
Jupiter tropical and temperate belts, 0.6 to 1.1 μm spectrophotometry, brightness distrib. and atmosphere optical parameters 79−92715
Jupiter XIII, precise positions during 1975-76 opposition 77−64691
K1082, in globular cluster M15, suspected ultrashort period variable star 80−26883
K3-50, ionized gas, IR and optical spectrophotometric meas. of compact H II region 79−53870
K648, halo planetary nebula, Ar III line obs. and low Ar abundance meas. 80−82443
K648, halo planetary nebula, spectrophotometry and element abundances 78−41011
K giants and GK supergiants, circumstellar Ca II lines rel. to mass loss 77−56928
K-type giant stars, colour excesses, interstellar dust grains distrib. determ. 79−40251
K-type giant stars, evidence for circumstellar shells from 0.4 to 20 μm photometry 80−90420
K-type giant stars at South Galactic Pole, DDO photometry rel. to CN anomalies and distances 80−8622

visible astronomical observations continued
K-type giants, multivariate anal. of spectrophotometry rel. to atmospheric characts. 77−78772
K-type stars, spectral profiles, macroturbulence rel. to luminosity 79−96997
22 Kalliope, light curves, phase function, pole and dimensions 78−53857
22 Kalliope, pole coordinates from photoelectric photometry 80−31230
K-type stars, spectroscopic investigations in 4500 to 7500 Å region 80−109430
Kepler's SN 1604 remnant, spectrum 80−85982
Kepler's SNR, distance from interstellar absorption determ. 80−46651
Kitchener daylight fireball of November 4, 1977, no meteorites 79−16892
Klemola 44, cluster of galaxies, X-ray, optical and radio obs. 77−74150
Klemola 44, X-ray cluster of galaxies, redshifts and vels. 78−45414
216 Kleopatra, photometry rel. to comp., diameter, elongated shape and possible stellar occultations 80−94743
Kobayashi-Berger-Milon (1975IX), Swann band profiles 78−85909
Kottamia Observatory site, seasonal atm. extinction due to aerosol 80−46253
Kron 3, SMC globular cluster, identification with X-ray source (4U 0026−73) 79−5919
Kuiper 41, orbit and flare activity of visual red dwarf pair 79−97032
Kustner 1082 in globular cluster M15, hot ultrashort period Cepheid *(Chinese)* 77−67096
KUV09313+4052, variable UV excess object, discovery, position and photometry 80−62159
L19-2, low-amplitude ZZ Ceti type variable, UBV colours, period determ. 78−4242
L19-2, ZZ Ceti-type variable, light curves and power spectra 77−56948
L973, red giant in globular cluster M13, curve of growth anal. 79−48796
Lacerta OB1 association, uvby photometry 77−22285
Lacerta OB1 association stars, spectral classification and distances 77−37626
SW Lacertae, contact eclipsing binary, polarisation obs. 77−45489
BL Lacertae, coordinated obs. 1979 September 19-25 period 79−80354
AR Lacertae, double-subgiant eclipsing binary, spectra, abundances 78−8044
AR Lacertae, eclipsing binary, photometric obs., intrinsic variation 77−22271
BL Lacertae, existence of periodic components in light vars. *(Russian)* 79−101205
EV Lacertae, flare star, photometry and spectrum rel. to starspots and rot. period 80−98665
AR Lacertae, Hα spectrogram following radio outburst, results 77−49432
EV Lacertae, high-speed five-colour photometry of flare star 77−56956
10 Lacertae, nonradial pulsations (1975-77) 79−5823
5 Lacertae, obs. of second max. for long period spectroscopic binary 78−57591
BL Lacertae, optical monitoring by three-colour photographic photometry 78−16525
BL Lacertae, photoelectric intraday photometric obs. 78−36681
BL Lacertae, polarisation at visible and IR wavelengths 77−9803
12=DD Lacertae, radial vel. and line profile var. 77−78797
AR Lacertae, RS Canum Venaticorum type star, UV excess, spectrophotometric obs. 78−8043
EW Lacertae, shell spectrum change, 1978 Dec. radial vels. 79−21306
10 Lacertae, spectral line studies using LTE-method *(Russian)* 79−92769
BL Lacertae, spectrum and magnitude of associated galaxy 78−24552
BL Lacertae, spectrum and redshift 77−26055
AR Lacertae, times of minima, photoelec. obs. 77−57012
EV Lacertae, UV Ceti variable, flares colour behaviour 80−22020
12=DD Lacertae, vel. curves and period charge, spectrograms 77−26016
SW Lacertae, W Ursae Majoris star, photoelectric obs. and epochs of min. light 80−62196
12 Lacertae (DD Lac), spectral variations 77−71114
BL Lacertae object 0109+22, optical and radio props. 78−32567
BL Lacertae objects, polarisation, visual and IR photometry and polarimetry 80−77480
BL Lacertae objects, search for rapid brightness variability 80−90567
BL Lacertae type objects, linear optical polarisation study *(Russian)* 78−57640
BL Lacertae type objects, southern, optical monitoring 80−56969
393 Lampetia, long rotation period from photoelectric lightcurve 79−40120
Landolt celestial equatorial UBV standard stars, spectral classifications 79−75199
late B-type stars, Ca II K-line profiles 78−73722
late B-type stars, rot. and incidence of HgMn stars 78−89199
late B-type stars, spectroscopic obs. rel. to duplicity 78−57547
late type stars, Ca II H and K lines and nearby continuum photoelectric calibration 80−36617
late-type dwarf stars, BVRI photometry, metal abundance index and galactic evolution 77−60754
late-type field stars in S.hemisphere, radial vel. study rel. to possible duplicity 80−98686
late-type spectroscopic binary stars, search for Ca II H and K lines 77−33551
late-type stars, intermediate band photometry in Geneva system 78−12231
late-type stars, obs. of emission lines in Ca II H and K wings, line width-luminosity relation 77−78766
late-type stars, OH emission time var., correl. with visual magnitude 77−60764
late-type stars, spectrophotometry, incident and emergent flux calc. 78−4200
late-type stars in stellar groups, intermediate band photometry 78−4300
late-type stars intermediate-band photometry, calibration of indices 78−49424
late-type stars photometry, photoelectric MgH+Mgb index meas. 80−12753
late-type supergiants, C, N and O abundances for G AND K Ib stars 78−24509
late-type supergiants, luminosity effects in spectra 77−60753
LB 3459, O-type subdwarf plus hot white dwarf eclipsing binary, photometry, anal. 79−48859

visible astronomical observations continued
LB 3459, short period eclipsing binary system containing two O-type subdwarfs, uvby photometry 78−53987
LDS 678B (EG 131), white dwarf, spectrum 78−40946
LDS 785A (EG 153), DB white dwarf, discovery of H 77−45425
Leda (Jupiter XIII), precise positions for 1976 Nov. 2 and Dec. 13 77−22135
Leo I dwarf galaxy, 23 new variables discovered 78−53953
Leonid meteor shower, struct. and activity, 1971 Nov. 15-19 obs. 77−67075
Leonid meteor shower, struct. and relative activity of radiants, 1972 November 78−45291
Leonid meteors, spectral analysis 79−16890
AS Leonis, flare star, chromospheric emission lines in nonflare red spectrum 79−21294
AD Leonis, flare star, Hα emission short-period variability limits 79−48807
XY Leonis, light curve synthesis for contact binary 79−12494
AQ Leonis, light var. anal. of RR Lyrae star 77−56941
87 Leonis, lunar occultation ang. diameter 79−25599
ρ Leonis, non-anomalous diffuse interstellar absorpt. features 78−16418
20 Leonis, possible eclipse obs. in triple system 78−12298
R Leonis, strong TiO-related dia. vars. 78−16429
20 Leonis, triple system with a δ Scuti variable, spectroscopic obs. 77−49440
AD Leonis, UV Ceti variable, flares colour behaviour 80−22020
CW Leonis (IRC+10216), IR C star, intrinsic polarisation obs. and origin 80−67730
υ Leonis (SAO 138298), angular diameter from lunar occultation obs. 78−45332
π Leonis lunar occultation obs. giving angular diam. 77−33493
T Leonis Minoris, Algol-type semi-detached binary system 77−91580
19 Leonis Minoris, spectroscopic binary, orbital elements and mass ratio 80−62197
68 Leto, rot. period and photoelec. lightcurves determ. 80−98594
48 Librae, Be star, shell spectrum line profiles 80−62146
AP Librae, BL Lacertae object, emission line obs. in (1976) 77−29932
EH Librae, dwarf Cepheid, BV photometry 77−82226
AP Librae, extended source obs. by photoelectric photometry 78−4348
48 Librae (FX Librae), Be star, search for short time scale vars. in Hα emission 80−109441
48 Librae (FX Librae), shell star, spectroscopic study 78−96486
limb darkening in 3033-7297 A range 77−53507
Lk Hα 120, T Tauri star, spectrum 77−74052
LMC, catalogue of 302 C stars 78−20654
LMC, dynamics of giant interstellar shells from line profiles 80−46674
LMC, four super-giant H II shells obs. 78−86012
LMC, integrated photometric props. 78−54054
LMC, interstellar 4428 Å feature 79−35335
LMC, probable nova discovered 1978 March, position and magnitude 78−45341
LMC, space orientation and translational motion *(German)* 77−53684
LMC, stellar photoelectric UBV photometry *(German)* 80−21932
LMC, tilt determ. from Cepheid obs. 79−53912
LMC, yellow star search from low-proper-motion stars 77−5576
LMC, yellow stars UBV photometry and LMC members number 78−93417
LMC central regions, stellar count-brightness ratios rel. to population struct. 78−89245
LMC disc, underlying stellar component photometry rel. to population struct. 77−33633
LMC interstellar extinction, visible and UV obs. 80−51877
LMC OB and supergiant stars, deep objective prism survey catalogue 79−40090
LMC supergiants, BVI photometry 77−33490
LMC supernova remnants N49 and N63A absolute photometry 77−74116
LMC X-1 optical candidate, spectrum and semi-accurate position 80−67908
LMC X-2, spectrogram confirms optical counterpart 79−21463
LMC X-2 optical candidate, UBV photometry and variability 79−17136
LMC X-4, possible optical counterpart 77−13502
LMC X-4, possible optical counterpart OB star 77−29959
LMC X-4, spectroscopic obs. and orbit 79−9028
LMC X-4 optical candidate, binary nature 77−64879
LMC X-4 optical counterpart, photometric and spectroscopic obs. 77−49431
Lo 807, open cluster, two-colour photographic photometry 78−96512
Local Group, discovery of three new members, dwarf galaxies 79−5907
long period Cepheids, UBVRI photometry and classification 77−71112
long-period close binaries, general relativistic periastron advances 77−91564
long-period variable stars, maser activity rel. to Hδ emission, obs. 79−88685
long-period variable stars, radial vel. obs. 79−88684
long-period variable stars in S.hemisphere, narrowband polarimetry 80−98666
loose open cluster search in southern Milky Way, UBV photometry 77−64814
loose stellar clusterings in southern Milky Way, continued photometric studies 80−36679
low amplitude variables in Cepheid instability strip, photoelectric photometry 77−17580
low galactic latitude stars, proper motions, UBV photometry and mean secular parallax 78−57542
LP182-44, faint high-vel. degenerate star with probable C features, photometry and spectrum 79−67007
LP 131-66, new cool red degenerate star 79−48780
LP 182-44, faint blue star with large proper motion, discovery 78−49439
LP 701-29, lowest luminosity degenerate star with heavily blanketed spectrum 78−36562
LP 790-29, southern mag. white dwarf, spectrophotometric obs. 79−92765
LS55° −8, high-speed photometric obs. of new nova-like variable 78−57565
LS 630, subdwarf O star, spectrum and absolute magnitude 77−17561
LS I+61°303, radio, optical, X-ray, gamma-ray Be star, optical and radio obs. 79−88755
LS I +61°303 as optical counterpart for GT 0236+610 source 78−36568
visible astronomical observations continued
LS II+33°5, new H deficient B-type star, spectrum 78−93265
LS IV −14°109, H deficient A-type star, effective temp. 79−40195
LSI+61°303, possibly optical counterpart of GT 0236+610, absence of variability 78−49438
LSI+61°303, supergiant Be star, radio emission and radial vel. periodic vars. 80−62149
LSS 1916, 3371, new VV Cephei stars, spectra and colours 79−35299
599 Luisa, photoelectric light curve 78−16328
luminous C stars in LMC, photometry 78−28670
luminous composite stars in the Large Magellanic Cloud 79−58375
luminous obscured galaxy assoc. with G127.11+0.54, optical spectroscopy and photometry 80−31371
luminous stars in M31 80−36622
luminous stars in NGC 6822 and IC 1613, visible spectra and photometry 80−82345
lunar crater arcs, catalogue and distribs. 77−41333
lunar crater rim topography, radial variation 77−60633
lunar laser ranging, McDonald Observatory results 77−64678
lunar laser ranging, orbital dynamics and selenodetic results 77−29672
lunar laser ranging obs., universal time meas. results 78−85854
lunar mare grounds relative spectral reflectivity 80−12695
lunar occulation events, 1974 to 1977, photoelectric obs. summary 79−88642
lunar occultations, obs. at Sydney Observatory during (1974-1976) 78−69658
lunar occultations, photoelec. obs. 79−5819
lunar occultations, photoelectric obs. at McDonald Observatory 77−2331
lunar occultations, reaction times in obs. *(French)* 79−88607
lunar occultations, TV camera appl. *(French)* 79−58263
lunar occultations from University of Illinois Prairie Observatory (1977-1978) 80−105148
lunar occultations of stars, 1969-72, Sofia Observatory obs. 79−29979
lunar occultations of stars, diameter meas., photoelec. obs. 80−72920
lunar occultations of stars, double and multiple stars obs. 78−4079
lunar occultations of stars, summary of obs. 78−7982
lunar occultations of stars (1943 to 1971), catalogues 79−88606
lunar occultations of stars and planets, obs. at Cracow in 1974-75 period 77−33363
lunar surface, topography of sinuous rilles in Harbinger Mountains region 77−78683
lunar surface brightness fluctuations, photometric and polarimetric obs. 77−78681
lunar surface colour differences, Tycho and Alpine valley areas 78−20663
lunar surface features mapping at Kottamia obs. 80−12691
lunar total eclipse, 1974 November 29, in Ussuriisk 77−67051
lunar total eclipse, 1975, May 24-25, UBV photometry 77−22126
lunar total eclipse, 1975 November 18, obs. in Tadzhikstan 77−67052
RR Lyncis, Am eclipsing binary, photometry and spectroscopy, abundances 77−33558
SW Lyncis, close binary, orbital elements 77−74090
Lynds 134, optical extinction and surface brightness obs. of dark nebula 80−17627
Lynds 1778/1780, optical extinction and surface brightness obs. of dark nebula 80−17627
Lynga 6, open cluster, photometry rel. to reality and membership of Cepheid TW Normae 77−87491
Lynga 6, open cluster, relation of long period Cepheid TW Normae 77−17639
ι Lyrae, Be star, Hα emission disappearance 79−5834
δ^2 Lyrae, M-type supergiant, Li abundance in atmosphere *(Russian)* 80−72950
β Lyrae, eclipsing binary, intrinsic linear polarisation in Hα, Hβ emission lines 77−41390
β Lyrae, narrow-band photometry in (1971) 80−46605
β Lyrae, photoelectric photometry rel. to orbital period variability 80−72997
α Lyrae (Vega), absolute calibration 79−40193
α Lyrae (Vega), Coude spectroscopy of emission lines 79−21290
α Lyrae (Vega) rot. rate determ. from line profile photoelec. obs., Fourier transforms 80−77408
RR Lyrae star in globular cluster NGC 6717, photometric investigation 80−46624
RR Lyrae stars, Ca and Fe decoupling 79−30069
RR Lyrae stars, in 47 Tucanae, membership and metallicity 80−62206
RR Lyrae stars, in Baade's window region, metal abundances 77−9749
β Lyrae, high time-resolution spectroscopy at Hα 77−13388
β Lyrae, optical and IR photometry, gaseous disc electron density distrib. 78−28722
β Lyrae, photoelectric photometry (in 1971) 78−12294
MV Lyrae, polarisation and spectrum obs., polar class candidate *(Russian)* 78−93322
α Lyrae (Vega), Ca II H and K lines high resolution profiles 78−85939
RR Lyrae blue variables in M22, photometry 78−85945
RR Lyrae stars, atlas of light and colour curves 77−82228
RR Lyrae stars, in southern hemisphere, VBI photometry 77−53612
RR Lyrae stars, VBLUW photometry rel. to reddening and blanketing 79−48806
RR Lyrae stars in ω Centauri, UBV photometry rel. to comps. 78−73719
RR Lyrae stars in galactic bulge, spectra and comp. 77−26012
RR Lyrae stars in globular cluster M4, metal abundances 79−58351
RR Lyrae stars in IC 4499 globular cluster, periods and light curves 79−44490
RR Lyrae stars in LMC, list of 76 objects 77−91549
RR Lyrae stars in M4, UBV photometry 77−78802
RR Lyrae stars in M 15 globular cluster, period behaviour 77−45444
RR Lyrae variables in ω Centauri cluster, spectroscopic obs. 79−5824
RR Lyrae variables in globular cluster NGC 6121 (M4), UBV photometry 80−22018
RR Lyrae variables in N.Galactic Pole fields, periods, light curves and metal abundances 79−88660
RR Lyrae variables in NGC 1851, periods and light curves 78−73714
M101, Mars model from gas kinematics 79−35371
M101, spectra of H II regions, comp. gradient across spiral galaxy 78−65683
M104, galactic-scale magnetic field from optical polarisation obs. 77−22313
M104 (Sombrero), radial distrib. and total number of globular clusters 77−74140

visible astronomical observations continued
M104 (Sombrero galaxy), mass spectrum of star form. 77−17675
M10, M12, M71, M92, globular clusters, radial vels. from meas. of stars in fields 78−41004
M11, open cluster, internal motions from stellar proper motions 77−22280
M11, open cluster, stellar proper motions rel. to membership 77−17641
M13, central region, colour-magnitude diagram 77−53656
M13, globular cluster, astrometric obs. for stellar proper motions and membership probabilities 79−75252
M13, globular cluster, two colour photographic photometry of variable stars 77−87492
M15, faint stars photometry rel. to main sequence intrinsic width and luminosity function 77−78834
M15, globular cluster, core, Hα and continuum obs. 79−17031
M15, globular cluster, optical struct. of core 77−13412
M15, nucleus brightness profiles of X-ray globular cluster 78−69848
M15, possible second planetary nebula detect. in Hα 77−17655
M15, surface brightness distrib. from electronographic obs. of globular cluster 78−85981
M15, X-ray globular cluster, search for O III 5007 Å forbidden line emission 78−36644
M15-K1082, two-hour variable UV-bright star in NGC 7078 (M15), spectra 79−88681
M16, O III 5007 Å forbidden line profiles from core of H II region 79−8976
M17, large-scale vel. components, insect-eye Fabry-Perot obs. 78−93380
M1-2 central star, possible eclipsing binary in planetary nebula 80−105239
M1-67 possible H II region, internal motions 79−92841
M1-76, possible forbidden line BQ star rather than planetary nebula 79−84847
M1-78, emission nebula, optical position and 15.4 GHz struct. 78−41025
M22, comparison with ω Centauri, spectroscopic evidence 80−46617
M22, globular cluster, membership and other problems 78−32537
M25, young open cluster, UBV obs., photoelec. calibration, distance, reddening 79−8956
M25 (IC 4725), open cluster, stars four colour and Hβ photometry 78−8067
M2 (NGC 7089), globular cluster, faint stars photometry and colour-magnitude diagram 80−101623
M31, disc colour gradient photoelec. surface photometry obs. 80−73032
M31, gas-to-dust ratio determ. 78−8120
M31, globular clusters colour indices, rel. to interstellar absorpt. law 78−28796
M31, Hα survey, catalogue of 981 H II regions 78−40840
M31, inner nuclear regions, spectral features and dwarf content 78−86005
M31, M51, nuclei, isophotometry 79−71114
M31, open star clusters obs. rel. to spiral struct. 79−75270
M31, position angle of major axis of nuclear region 77−53682
M31, radio continuum survey at 2695 MHg comparison with optical data 77−57085
M31, rotation of nuclear region from spectra 78−45395
M31, search for globular clusters in disc and minor axis fields 78−32568
M31, semistellar nucleus, possible M-dwarf enrichment 80−51862
M31, UBV photometry of star clusters *(Russian)* 79−17034
M31, UBV photometry of star clusters 79−62879
M31, vel. dispersions in nucleus and bulge 77−26049
M31 field, van den Bergh variables 77−74056
M31 nuclear bulge, rotational vels. meas. 80−41888
M32, photoelectric scanning of elliptical galaxy *(Italian)* 79−21435
M32-1, planetary nebula in M32, spectrophotometry and filter photometry 79−25664
M33, density wave motion obs. evidence from star form. and evolution 77−45552
M33, detection of SNRs, by strong S II forbidden line emission 78−36665
M33, emission regions catalogue 80−46416
M33, ionisation of interarm medium 77−67131
M33, radio and optical obs. of supernova remnants *(Italian)* 79−53890
M33, supergiants distrib. rel. to spiral struct. and star form. 79−21437
M33, warped optical plane obs. 80−56944
M34, open cluster, spectral types of brightest stars 78−12311
M34, open cluster, UBV photoelectric photometry 78−12307
M36, photographic obs., mass, radius, central density, stellar vels. of open cluster *(German)* 80−31333
M37, open cluster, luminosity function 77−13419
M39, open cluster proper motion membership 77−91588
M3, globular cluster, luminosity function 77−57069
M3, inner structure of globular cluster, photoelec. scanning method *(Italian)* 78−93343
M3, photoelectric radial vels. of individual stars rel. to cluster dynamics 79−75251
M42 and M43, optical linear polarisation 78−86004
M43, small diffuse nebulae in Orion complex, optical linear polarization map 80−46644
M49, globular clusters space distrib. 78−93393
M4, globular cluster, colour-magnitude diag. 77−37629
M4-18, emission line spectra of peculiar planetary nebula 79−84846
M4-18, spectroscopic obs. of compact planetary nebula 80−67829
M51, ionized gas velocities 79−75268
M55, globular cluster, colour-magnitude diagram 77−64812
M5, globular cluster, bright variable star obs. 77−91590
M5, M13, M3, globular clusters, giant stars chemical comp. 80−67695
M5 giant branch, spectroscopic survey 78−16467
M67, open cluster, stellar proper motions rel. to membership 77−22281
M69, metal-rich globular cluster, photometric calibration 77−91592
M81, enigmatic dark lines identified as galactic high latit. nebulosity 80−56947
M81, kinematics of gas in nuclear disc 77−9795
M82, irregular galaxy, colour distrib. 77−37653
M82, optical polarisation wavelength depend. 80−67861
M82, surface photometry and gross struct. of irregular galaxy 80−31367
M82, UBV colours and surface brightness distrib. of galaxy 79−9006
M82 as exploding radiogalaxy, image tube spectrogram evidence 78−69880
M82 central regions, kinematics 78−45394

visible astronomical observations continued
M83, H II regions spectral characts. and chemical abundances 80−56927
M87, central regions luminosity distrib., isothermal core, point source or black hole models 79−71110
M87, dynamical evidence for central mass concentration 78−49529
M87, emission-line filaments and active accreting nucleus in giant elliptical galaxy 80−56931
M87, evidence for supermassive object in galaxy nucleus from SIT and CCD area photometry 78−49528
M87, luminosity profile and outer corona 78−41035
M87, photographic surface BV photometry of giant elliptical galaxy 78−69867
M87, photometric structure of jet in galaxy 79−92848
M87, spectroscopic obs. of galaxy nucleus 79−92858
M87 jet, radiation from knots rel. to model *(Russian)* 80−36719
M87 jet knots, polarisation and spectroscopic props. 80−12817
M89, elliptical galaxy, associated optical jet discovery 79−25731
M8, Dragon dust cloud obs., isophotometry 78−36673
M92, globular cluster, membership and internal motions 77−17634
M92, globular clusters, luminosity function 77−57068
M 1-2, planetary nebula, emission line obs. 77−33621
M 1-92, Minkowski's Footprint, optical spectropolarimetry 77−33602
M 2-9, planetary nebula structural changes (1952-78) 80−82456
M 31 spiral structure, morphological approach 78−65690
M-type dwarf stars, spectrophotometry with Carnegie image tube 78−57466
M-type dwarf stars near north galactic pole, scanner obs. of MgH band 77−78789
M-type dwarfs, Hα emission line var., stellar surface phenomena 79−21313
M-type giants, temp. sequence based on TiO spectra *(Russian)* 78−2083i
M-type giants and supergiants, circumstellar envelopes, observational study 78−53939
M-type giants and supergiants, circumstellar gas and dust shells, optical and IR obs. 79−21281
M-type stars, classification from spectral scans 80−62127
M-type stars, in Orion population, CaH and TiO band strengths 78−12227
M-type stars, observations in wavelength range 370 to 550 nm, energy distribution 79−84798
M-type stars, TiH band identification 79−48789
M-type stars in direction of N galactic pole, photometry and spectroscopy 77−37594
M-type supergiants, in LMC, MK spectral types, luminosities 79−62820
M-type supergiants, photoelectric two-dimensional spectral classification 78−53936
M-type variable stars, obs. in DDO photoelec. system, spectral classification 78−32463
Magellanic Cloud supernova remnants, Hα photometry rel. to optical emission from shocks 79−92831
Magellanic Clouds, chemical comp. of planetary nebulae 77−37632
Magellanic Clouds, H II regions chem. comps. 78−93381
Magellanic Clouds, lists of planetary nebulae 79−58405
Magellanic Clouds, planetary nebulae, identification, luminosity function and numbers 80−67815
Magellanic Clouds, spectrophotometry of nebulae suitable as standards 78−12350
Magellanic Clouds stars, photoelectric (B, V) magnitude sequences 77−53592
main sequence B-type stars, physical parameter determ. from uvbyβ photometry obs. 80−72952
main sequence stars, chromospheric var. from Ca II line obs. 77−56936
main sequence stars, chromospheric vars. 79−16931
main sequence stars with variable Ca II H and K emission, starspot hypothesis 79−58328
main-sequence stars, F to M-type, comparison of activity cycles to old and young stars 80−105235
major planets, positions determ. with Odessa meridian circle, (1974 to 1975) *(Russian)* 79−44394
Markarian 132, spectrum and redshift systems 78−89248
Markarian 185, 186, UBV surface photometry *(Russian)* 77−91614
Markarian 205, electronographic and spectroscopic obs. rel. to distance 79−97058
Markarian 231, Seyfert 1 galaxy, optical variability 79−40259
Markarian 231, Seyfert galaxy, substructure with UV excess, UV and visible obs. 80−82512
Markarian 290, multicolour photometry of Seyfert galaxy *(Russian)* 77−64848
Markarian 298 (=IC 1182-4), multicolour photometry *(Russian)* 78−57641
Markarian 325, irregular galaxy, emission clumps observational props. 80−67869
Markarian 335, Seyfert galaxy, spectroscopic investigation *(Russian)* 79−101204
Markarian 348, Seyfert galaxy, spectrophotometry 79−88735
Markarian 374, Seyfert galaxy, spectra of double nucleus components 78−69882
Markarian 3, class 2 Seyfert, visible spectra obs. 80−85999
Markarian 421, optical and radio obs., identification with 2A 1102+384 X-ray source 79−5899
Markarian 421 and 501, polarisation data for BL Lacertae objects 78−93406
Markarian 464, 766 and 841, historical light curves for Seyfert galaxies 79−58425
Markarian 501, optical variability 77−78867
Markarian 509, brightness variability meas. *(Russian)* 77−17671
Markarian 59 , supergiant H II region in SBm galaxy NGC 4861 spectrum and struct. 80−98705
Markarian galaxies, emission line intensities depend. on colour index *(Russian)* 77−17672
Markarian galaxies, morphological and colorimetrical obs. 77−37646
Markarian galaxies, nature from photometry and classification 78−28781
Markarian galaxies, spectroscopic obs. *(Russian)* 77−49465
Markarian galaxies 508 to 700, optical positions 79−21417
Markarian galaxies in poor cluster ZwCl 1122.3+6317, radial vels. 80−26989
Markarian galaxies with broad emission lines, spectroscopic obs. *(Russian)* 77−45567

visible astronomical observations continued
Markarian II, 180 and 421, spectra of stellar population 78−54047
Markaryan 372, Hβ profile of Seyfert galaxy 80−26972
Mars, 1877-1971 dust storms and polar cap recession rate correl. *(Italian)* 77−91461
Mars, 1973, dust storm, maps from hourly photographs 77−5477
Mars, aeolian environment, differential redistrib. rates 79−44399
Mars, astrolabe obs., 1975-76 winter period *(French)* 78−32378
Mars, astrolabe obs. from Paris Observatory (winter 1977-78) *(French)* 79−70982
Mars, atmosphere opacity, 1977 obs. from Viking 80−41753
Mars, atmospheric dust, Viking Orbiter obs. of opposition effect 79−25536
Mars, atmospheric oblateness from ε Geminorum occultation obs. 77−5483
Mars, atmospheric opacity during July-November 1976, Viking orbiter obs. 78−20676
Mars, cloud formations, reflectivity time var., visible photometry obs. 80−72840
Mars, cloud obs. by Mars 2 in 0.36 to 1.38 μ range 77−53450
Mars, cloud positions during 1907-73 period, topographic control 78−36479
Mars, crater streaks in Chryse Planitia region, early Viking results 78−65534
Mars, diurnal props. of clouds over Tharsis volcanoes 80−94738
Mars, dust and ice hazes, Mariner 9 TV limb obs. 79−5772
Mars, dust storm obs., 1978, Jan. 78−24482
Mars, dynamical phenomena during June-November 1976, Viking orbiter imaging results 78−20675
Mars, extratropical cyclones, Viking Orbiter 1 obs. during summer season 79−44398
Mars, geological obs. in Cydonia region from Viking 78−20674
Mars, geology of Chryse Planitia 78−20673
Mars, highland and lowland units relative ages, Viking contribs. to Mariner studies 78−65529
Mars, impact craters, emplacement of ejecta by surface flow 78−20671
Mars, Noctis Labyrinthus-Valles Marineris regions, structure pattern anal. 77−29694
Mars, north polar cap, 1975-1978 photographic obs. 80−72823
Mars, north polar cap, 1977-1978 regression obs. 80−72825
Mars, north polar region, Viking 2 orbiter imaging 77−56864
Mars, obs. with Algiers astrolabe (winter 1973) *(French)* 78−61775
Mars, obs. with Danjon astrolabe of San Fernando Observatory *(French)* 78−57483
Mars, occultation of ε Geminorum, atmosphere temp. profiles 79−2508
Mars, occultation of ε Geminorum, obs. at Princeton 78−57482
Mars, occultation of ε Geminorum, planetary atm. temp. struct. determ. 77−87306
Mars, occultation of E Geminorum (1976 April 8), preliminary results 77−37545
Mars, opposition effect, Viking Orbiter 1 obs. of Chryse-Acidalia region 79−44397
Mars, orbit determination on basis of radar and visible observations 80−90323
Mars, Paris Observatory astrolabe obs. *(French)* 77−49322
Mars, permafrost features obs. by Viking orbiters 78−20670
Mars, phase function, July to November 1976, Viking orbiter photometric obs. 78−20677
Mars, photographic position meas. *(Russian)* 78−93137
Mars, photographic positional obs. with Ukrainian Academy 400 mm astrograph *(Russian)* 79−44395
Mars, photographic positions in 1973 and 1974, Pulkovo normal astrograph obs. *(Russian)* 78−28567
Mars, photographic zenith tube obs. during 1975 and 1978 oppositions 79−40109
Mars, photometric imaging in 0.35-1.10 μ range 1973 opposition 77−71044
Mars, polar regions, Mariner 9 and Viking obs. of layered deposits 78−7899
Mars, position obs. with Paris astrolabe (1975 to 1976) *(French)* 78−61776
Mars, positional photographic obs. with Pulkovo double short-focus astrograph, (1973 to 1974) *(Russian)* 79−96944
Mars, positions, with Danjon astrolabe at San Fernando Observatory (Jan. to Feb. 1978) *(French)* 80−94736
Mars, positions (1975-6), Paris Astrolabe obs., corrections *(French)* 79−44393
Mars, positions and ephemeris corrections from Paris astrolabe obs. *(French)* 79−101103
Mars, rot. period determ. from transits of albedo stations across central meridian (1659 to 1971) 80−98588
Mars, spiral clouds, Viking Orbiter images during 1978 northern summer 79−75133
Mars, surface, Viking obs. 78−61779
Mars, surface colour change at Viking landing site 80−72829
Mars, surface features, Viking 1 lander photographs 77−13267
Mars, surface markings, change in opinion on nature, 1877 to 1914 period 79−80406
Mars, surface struct. from optical and IR refl. spectrum and thermal props. 77−29690
Mars, Tempe area, detection of abnormally light area 78−28569
Mars, topography, photogrammetric portrayal 80−67609
Mars, variable surface albedo features study during Viking primary mission 78−20678
Mars, Viking 1 orbiter imaging of Valles Marineris and geological anal. 78−20672
Mars, Viking 1 orbiter photographic obs. 77−2363
Mars, Viking 2 landing site, photographs 77−17396
Mars, Viking lander photographs 77−2360
Mars, Viking lander sample field obs., current status 80−67626
Mars, Viking orbital colorimetric images 77−17414
Mars, Viking orbiter and lander photographs 77−17397
Mars, Viking orbiter images IPL processing 78−20679
Mars, Viking orbiter imaging expt., preliminary results 77−17401
Mars, Viking-1 photography rel. to tectonics and volcanism *(Russian)* 79−48726
Mars, visual characts. of rough planar surfaces from Viking Orbiter images 80−98589
Mars atmosphere dust, Viking orbiter imaging obs. 79−84707
Mars bright spots in 1971 dust storm, multiple light scatt. in craters 77−60705

visible astronomical observations continued
Mars dust storm of 1971, cloud form., multicolour TV photometry obs. 80−101546
Mars northern plains, polygonal troughs obs. and origin 80−98590
Mars occultation of ε Geminorum, obs. from C.E. Kenneth Mees Observatory 78−53853
Mars polar landscapes, perennial ice cover and dust storms interplay rel. to evolution 79−84721
Mars S polar cap, seasonal recession as seen by Viking 79−84715
Mars surface, global colour vars. obs. 78−65527
Mars surface, Viking landers imaging obs. during one Mars year 79−80265
Mars surface physical props., Viking 1 lander preliminary results 77−17402
Mars upper atmosphere, temp. struct. from ε Geminorum occultation obs. 79−53749
Martian channels, Viking data rel. to classification and form. time 78−20669
Martian volcanic features, obs. from Viking orbiters 78−20668
maser stars, late supergiants and long period variables 80−77410
MC2(3) radio sources, optical positions from Palomar Sky Survey 80−31375
MC2 and MC3, optical identifications, 11^h28^m to 17^h00^m right ascensions 78−20900
MC2 and MC3 sources, radio spectra and optical identification 77−33670
MCG−6-30-15, type 1 Seyfert galaxy, X-ray and optical obs. 80−82479
MCG 8-11-11, Seyfert galaxy inside error box of 2A0551+466, optical spectra 77−74130
MCG 8-11-11, X-ray Seyfert galaxy, recent optical activity in nucleus 79−25701
MCG 8-11-11 (2Ariel 0551+466), Seyfert galaxy, brightening of nucleus 78−41053
MCG -5-23-16, spectroscopic obs. of possible X-ray source 78−45404
MCG-5-9-22, galaxy, red shift rel. to supernova absolute magnitude 78−81644
MCS 141, 232, 275, quasars, spectra interpretation 80−90562
MD 101065, effective temp. and atm. electron press. 77−45468
Me, globular cluster, stellar proper motions, membership and cluster internal motions 80−8665
dMe stars, survey of BY Draconis syndrome 78−16428
Me-type dwarf stars, long-term variability 78−93254
Medium-Amplitude Red Variables, UBVRI photometry 77−45438
56 Melete, photoelectric light curves, synodic rot. periods, amplitudes of var. 79−53752
Melotte 66, oldest open cluster, colour-magnitude diagram rel. to age 80−17621
Melotte 66, very old open cluster, BV photometry rel. to broad giant branch 78−32538
18 Melpomene, occultation of SAO 114159; discovery of 1978 (18) 1 possible satellite 79−16870
18 Melpomene, occultation of SAO 114159, photoelectric obs. 79−12420
18 Melpomene, occultation of SAO 114159, secondary extinction event obs. rel. to 1978 (18) 1, possible satellite 80−56749
18 Melpomene, occultation of SAO 114159 on 1978 Dec. 11, revision obs. 79−12423
18 Melpomene, rot. period from photoelec. obs. 80−82258
Merate Observatory, time and latit. results of astrolabe obs. (1977) 79−40061
Mercury, bright patches in several large craters, possible physico-chemical alteration process 78−32375
Mercury, intercrater plains, Mariner 10 obs. 77−9685
Mercury, regolith containing Fe^{2+}, refl. spectra, 0.65-2.5 μm 80−56736
Mercury, transits in 1677-1973 period, collected obs. of internal contacts 77−25964
Mercury transit, 1973, November 10, photographic obs. *(German)* 77−22127
Mercury transit, 1973 November 10, photographic obs. at Pulkovo *(Russian)* 78−28562
Merope nebula, uvby photometry and dust grains phase function in UV 78−32553
metal-poor dwarfs, Fe/H abundances from red spectra of nine objects 80−51751
metal-poor stars, abundance anals. of high-vel. dwarfs blue spectra 78−53933
metal-poor stars, C/Fe ratio from CH features 79−16945
metal-poor stars, spectra and Al/Fe ratios 78−57549
metal-poor stars, spectral energy distrib. and Fe/H ratio 78−53937
metallic line stars, spectral energy distrib. *(Russian)* 80−72975
meteor, fast sporadic spectrum 78−93170
meteor bright line spectra, study via astronomical TV system 78−61817
meteor counts, test for registration independence 80−8594
meteor data from visual obs., rigorous method of normalization and analysis 79−88627
meteor trajectories, orbits 80−72887
meteoric material influx rate from photographic obs. of bright meteors 79−21233
meteoroid albedo and size distrib. in 0.3-4.8 AU range 78−36539
meteors, magnitude errors and magnitude scales of observers in Sweden and Czechoslovakia 78−36533
meteors, N_2^+ 4278 Å bands in spectra, quantitative anal. 78−45290
meteors, NASA-NMSU meteor observatory trajectories and orbits 77−22152
meteors, optical brightness rel. to ionised trail props. 80−77354
meteors, photographic altitudes 80−8593
meteors, television photographs photometry 78−96441
meteors, trajectories and orbits from NASA-NMSU Meteor Observatory 77−74014
meteors, TV obs. 77−87339
meteors (comet debris) studies, video techniques appl. 79−80241
meteors from Periodic Comet Griff-Skjellerup (1977b) Florida results 77−53484
meteors television spectra, prod. and study 77−67076
methane 6819 Å line interpretation rel. to inhomogeneous scattering models for Uranus and Neptune 78−53871
9 Metis, pole coordinates from photoelectric photometry 80−31230
9 Metis, UBV photometry, light curve and rot. period 80−21942
9 Metis occultation of SAO 80950, Guianan obs. 80−31236
ZZ Microscopii, radius of dwarf Cepheid from BV photometry 78−77560
Milky Way atlas using super-wide-angle photographs 77−74145

visible astronomical observations continued
Milky Way northern region surface brightness, R photometry *(Russian)* 78−93388
minor planets, 1978, April, astrometric positions determ., ESO GPO obs. 80−77319
minor planets, meridian obs. (1974 to 1977) 78−69660
minor planets, positions from Torino Observatory (1977-1979) 80−94739
minor planets, positions in August 1977 from Observatorio Nacional, Rio de Janeiro *(French)* 80−94740
minor planets, precise positions obs. at Sydney Observatory during (1976) 78−69735
Mira variables, light and colour variations 77−64770
Mira variables, observations in wavelength range 370 to 550 nm, energy distribution 79−84798
Mira variables, polarisation variation detect. in absorption features 77−33496
MK spectral types for 67 early type stars 77−33473
MKW 3s, poor galaxy cluster, redshifts obs. rel. to cD galaxy extended X-ray emission 80−51884
Molonglo catalogues sources, optical obs. 77−60840
Molonglo radiosources optical counterparts, spectrophotometric obs. 78−4375
Monoceros Loop, supernova remnant, high vel. gas, Na I lines obs. 78−12348
Monoceros Loop, supernova remnant, narrow band photography, shock wave model 78−32547
Monoceros Loop, supernova remnant, photographic obs. of diffuse and filamentary nebulosity 78−32548
Monoceros OB2 association, evidence for supernova-induced star form. 80−31334
Monoceros R2 association, stellar UBV photometry and spectra 77−13409
19 Monocerotis, β Canis Majoris variable, photometric obs. 80−4379
1 Monocerotis, δ Scuti star, oscillation modes from photoelectric radial vels. and BVRI photometry 80−51787
1 Monocerotis, δ Scuti star, photometry and anal. 78−32495
21 Monocerotis, δ Scuti type star, freq. anal. 77−49398
V616 Monocerotis, A0620−00, transient X-ray source, spectrophotometry 77−33684
R Monocerotis, bipolar nebula, optical and IR polarimetry 78−36658
CV Monocerotis, Cepheid variable in anon. open cluster 79−58349
AU Monocerotis, eclipsing binary, cyclic variation in period 77−33565
VV Monocerotis, eclipsing binary, orbital elements and dimensions *(French)* 78−89225
R Monocerotis, Fe II forbidden line intensity changes *(Russian)* 79−8907
AU Monocerotis, mathematical anal. of photometric peculiarities 80−77448
VV Monocerotis, RS Canum Venaticorum type eclipsing binary, photoelectric obs. 79−40218
V616 Monocerotis, spectroscopic obs. of X-ray nova, Ariel 0620−00 optical counterpart 77−45450
R Monocerotis, T Tauri star, long period vars. 80−82350
V616 Monocerotis (A0620-00), light curve 77−64777
V616 Monocerotis (A 0620−00), UBV photometry 80−56846
R Monocerotis (NGC 2261 cometary nebula), spectrophotometry *(Russian)* 77−49446
V616 Monocerotis (Nova 1975=A0620−00), 8-day modulation from photoelec. photometry 77−87442
V616 Monocerotis (Nova 1975=A0620−00), spectroscopic obs. 77−82257
V616 Monocerotis (Nova 1975=A0620−00), X-ray and visible light curves 77−82331
V616 Monocerotis (Nova 1975), photographic photometric obs. 78−36587
Moon, 1978 March 24 total eclipse, S.African obs. 79−44384
Moon, Aristarchus crater obs. in 1975-6 period 77−33367
Moon, disc brightness distrib. rel. to photometric props. and dimensional scatt. indicatrix 80−101538
Moon, first telescopic obs. by Galileo (December 1609) 77−29978
Moon, free librations determined from laser range meas. 77−37521
Moon, Heiligenschein and albedo differences at zero phase angle 79−21205
Moon, Kazan heliometric obs. (1895-1958), new reduction *(Russian)* 79−92688
Moon, Linne controversy, possible variations rejected 77−78680
Moon, marginal zone relief maps from stellar occultation obs. *(Russian)* 77−73984
Moon, Mosting A posn. determ., plate reduction *(French)* 78−20661
Moon, multispectral maps and ratio images of nearside 79−40099
Moon, partial eclipse of 1977, April 3-4, amateur obs. reports 77−73985
Moon, photometric and polarimetric obs., 1976 April to 1977 December 80−51677
Moon, photometric anomalies from 1962 obs., possible transient phenomena 80−67587
Moon, positional photographic obs. at Pulkovo with long-focus horizontal telescope *(Russian)* 78−28533
Moon, selenodetic coord. system based on Kazan heliometric obs. *(Russian, English)* 80−41738
Moon, spectral photometry during max. solar activity 77−37522
Moon, transitory, phenomena obs. during lunar eclipses 78−61770
Moon, young crescents, obs. and photographs 77−73986
MR 2251−178, nearby QSO in cluster of galaxies 80−67900
MR 2251−178, X-ray QSO, spectrophotometric obs. 79−17122
MRK 80, Lacertid, optical variability from archival plates 77−26056
multiple stars, parallaxes and proper motions, Sproul 61 cm refractor astrometric meas. 77−9768
multiple stars, visual obs. 79−35303
α Muscae, β Canis Majoris type variability discovery from UBV photometry 79−80326
θ Muscae, Wolf-Rayet binary, spectrum and photometry 77−22235
MWC 17, emission line star, dense planetary nebula like object 77−45449
MWC 342, emission line spectrum in 1974-75 period 78−57558
MWC 349, IR source optical identification with reddened high-luminosity star 80−56971
MWC 349, separate spectra of components of visual binary 79−48858
MX0053+60 assoc. with γ Cassiopeiae, Be star 77−22250
MXB1637−53, X-ray burster, optical candidate 77−67140
MXB 1636−53, X-ray burst source, simultaneous X-ray and optical bursts obs. 79−92893

visible astronomical observations continued
MXB 1636-536, binary nature from simultaneous X-ray and optical obs. 80−82548
MXB 1728−34, X-ray burster, search for optical counterpart 77−33694
MXB 1735−44, optical bursts discovery 78−81708
MXB 1735−44, optical bursts obs. 78−61937
MXB 1735−44, X-ray burst sources, 3 s delay in optical burst 79−58442
MXB 1837+05(Serpens X-1), simultaneous optical and X-ray bursts obs., 1978 Sept. 79−35435
MXB 1837+05 (Serpens X-1), detect. of optical burst coincident with X-ray burst 80−27013
MXB 1837+05 (Serpens X-1), optical obs. of X-ray bursts 79−30153
Mz 3 (p-K 331−1°1), obs. of bipolar nebula, possible protoplanetary 78−45376
N132 D, SNR in LMC, rapidly moving material, visible and UV solns. 80−82449
N132D, supernova remnant in LMC similar to Cassiopeia A, photographic and spectroscopic study 78−93345
N51D, bubble-like nebula in LMC, internal motions obs. 80−105295
N51D, giant filamentary shell in LMC, nature and dynamics 80−105343
N70, giant filamentary shell in LMC, Ca II K absorpt. line profile rel. to dynamics 80−90511
N 59, nebular complex in LCM, filter photography 79−17052
N-type galaxies, optical spectra 79−40258
NAB 0137−01, quasar, UBV photometry and brightness vars. 80−56967
NAB 0137−01, spectrophotometry of possible X-ray quasar 77−13490
nearby bright galaxies 79−97062
nebula near radiosource CL4, discovery 77−91601
nebulae, photoelectric spectrophotometry of compact objects 78−89236
nebulae, polarisation maps obtained with electronographic camera 77−57081
nebulosity in region of S.Celestial Pole, obs. and origin 79−92839
128 Nemesis, long rotation period from photoelectric lightcurve 79−40120
128 Nemesis, photoelectric light curve 78−16328
287 Nephthys, photoelectric photometry and rot. period 79−84727
Neptune, limb brightening in 7300 Å methane band, photometry obs. 80−82297
Neptune, methane 6825 Å band obs. 77−78715
Neptune, obs. by Galileo, (1612 and 1613) 80−105485
Neptune, photometric var. in 1953-76 period 78−85901
Neptune, rot. period determ. and effects of seeing on reflected spectrum 80−46479
Neptune, rot. period from spectral line tilts 78−20726
Neptune, rotation period determ. 79−16878
Neptune, secular brightness increase, 1972-76 period 78−16346
Neptune, stellar occultation obs. (1980 August 21) 80−109395
NGC 1023, SB0 galaxy, surface photometry, brightness distrib. 77−22316
NGC 1052, active elliptical galaxy, radio and optical study 78−65693
NGC 1052, elliptical galaxy, electron density and N II/Hα line intensity ratio in nucleus 77−33642
NGC 1055, 681, 4594, galaxies, rot. curves and mass distribs. *(Russian)* 80−90541
NGC 1068, light polarisation in Seyfert galaxy 78−54046
NGC 1068, Seyfert galaxy, forbidden O III lines high-resolution profile 80−46665
NGC 1068, Seyfert galaxy, UBV photometry 77−67132
NGC 1068, type 2 Seyfert, recombination spectrum and reddening 80−90519
NGC 1084, NGC 7331, spiral galaxies, surface photometry and mass distrib. 79−40265
NGC 1087 and 1090, surface B photometry and mass distribs. in spiral galaxies 80−46676
NGC 1097, jets on image-processed plates of galaxy 78−61922
NGC 1199 and silhouetted compact high-redshift object 78−41031
NGC 1261, globular cluster, colour-magnitude diagram 80−17623
NGC 1265, galaxy, outer structure from electronographic obs. 78−16521
NGC 1275, double nucleus, radio and emission line obs. *(Russian)* 79−21439
NGC 1275, ionization and excitation mechanisms in surrounding filaments 79−71107
NGC 1275, multicolour photometry of Seyfert galaxy *(Russian)* 77−64848
NGC 1275, nucleus, daily vars. in optical continuum flux 79−71118
NGC 1275, photometric and spectrum vars. 80−22075
NGC 1275, Seyfert galaxy, emission line variability and nucleus conditions 77−37649
NGC 1275, Seyfert galaxy, nucleus, emission line intensities rel. to gas and radio source structs. *(Russian)* 79−48936
NGC 1275, Seyfert galaxy, optical outbursts *(Russian)* 77−82301
NGC 1275, Seyfert galaxy, radio and optical variability of nucleus 78−28793
NGC 1275, Seyfert galaxy, search for regular optical brightness vars. of nucleus *(Russian)* 77−60828
NGC 1275, Seyfert galaxy, spectrograms 77−22314
NGC 1275, Seyfert galaxy, spectroscopic obs. *(Russian)* 77−17670
NGC 1275, Seyfert galaxy, vars. of emission line spectrum and conditions in nucleus envelope 77−17688
NGC 1275, spectroscopic and photometric obs. 77−33630
NGC 1275, stellar populations, visible UV obs. 77−91628
NGC 1275, vel. field mapping 78−81680
NGC 1275 (3C 84), Seyfert galaxy, optical and 3 mm radio vars. similar struct. 79−67102
NGC 1275 (Perseus A), correl. between optical and radio variability *(Russian)* 80−77505
NGC 1275 as pair of interacting galaxies, spectra and structure 80−26969
NGC 128, S0 galaxy, rot. curve 77−33631
NGC 1291 and 1326, kinematics of lenticular galaxies 79−53908
NGC 1313, barred spiral galaxy interferometric study 77−49474
NGC 1313 barred spiral galaxy, asymmetric rot. *(French)* 79−97082
NGC 1316 (Fornax A), optical study of giant radiogalaxy 80−77479
NGC 1365 and 1386, IR and optical props. of emission-line galaxies 80−51867
NGC 1411, discovery of SN in elliptical galaxy 77−67104

visible astronomical observations continued
NGC 147, Local Group galaxy, identifications and radial vels. of planetary nebulae 77−33596
NGC 1499 (California Nebula), Hα obs., ξ Persei as exciting star 77−33622
NGC 1512 and 1510, interacting galaxies, optical and H I study 79−80348
NGC 1566, Sbc galaxy, spectrophotometry of nucleus and nine H II regions 80−51824
NGC 1569, irregular galaxy, optical linear polarization obs. from Durham 77−74126
NGC 157, spiral galaxy, surface photometry and mass distrib. 79−40264
NGC 1672 and 2997, nuclei morphology, Hα obs. 80−67867
NGC 1809 rel. to PKS 0502-696, no connection 79−30129
NGC 1817, UVB photometry of open cluster, distance, age 77−91587
NGC 1851, 6624, globular cluster, abundance gradients spectroscopic investigation 80−82437
NGC 1851, globular cluster, radial vel. of evolved star UV5 as X-ray source candidate 77−74158
NGC 1851, Hα absorption of UV5 and core of globular cluster 78−61896
NGC 1851, X-ray globular cluster, central region struct. 77−45501
NGC 1854, LMC blue globular cluster, photographic photometry 77−74107
NGC 185, Local Group galaxy, identifications and radial vels. of planetary nebulae 77−33596
NGC 1868 in LMC, BV photometry of metal-poor intermediate-age cluster 80−51814
NGC 188, old open cluster, photographic photometry 77−53430
NGC 188, open cluster, BV photographic photometry with PDS microdensitometer 79−88600
NGC 1904, globular cluster, BV photometry 77−13415
NGC 1904 (M79), UBV photometry, colour-magnitude diagram of halo globular clusters 78−32528
NGC 1961, rotation curve for massive spiral 79−62898
NGC 1999, electronographic imaging polarimetry obs. of reflection nebula 80−26964
NGC 1999, reflection nebula, optical polarisation map and struct. 80−94856
NGC 2169, open cluster, spectral types of brightest stars 78−12310
NGC 2231, star cluster in LMC, electronographic photometry and colour-magnitude diagram 79−92813
NGC 2243, metal abundance of old open cluster 78−93333
NGC 2243, old open cluster, UBV photometry 77−78835
NGC 2244, young open cluster, uvby Hβ photometry, colour excess, distance, age 78−32532
NGC 2264, H II region, classification of optical, IR and radio obs. data 80−67818
NGC 2264, N II forbidden line unusual profiles over giant H II region 80−46645
NGC 2264, open cluster, reddening, blanketing and metallicity from spectroscopic obs. 80−26916
NGC 2264, young open cluster, differential reddening due to intracluster dust clouds 78−53996
NGC 2281, open cluster, UBV photometry, binary star freq., luminosity function 78−81663
NGC 2287, open cluster, UBVRI photometry, distance, age, metal content 79−12498
NGC 2359, radial vels. and internal motions in ring-type nebula 78−81678
NGC 2362, very young open star cluster, photographic star counts *(German)* 78−16472
NGC 2366 H II region visible and radio obs. 80−77475
NGC 2403, Sc III type, surface photometry 78−32581
NGC 2419, globular cluster, variable star obs. 77−60804
NGC 2420, old disc cluster, photometry and spectra rel. to stars chemical comp. 80−46620
NGC 2420, PDS photometry of old open cluster, colour-magnitude diagram 78−57600
NGC 2420 and 47 Tucanae comparison rel. to galactic evolution 77−45499
NGC 2439 association, photometric and spectroscopic study 78−16470
NGC 2467, H II regions complex, internal motions 77−22304
NGC 2477, photographic obs., mass, radius, central density, stellar vels. of open cluster *(German)* 80−31333
NGC 2516, proper motions in the region 79−88706
NGC 2516, spectroscopic binaries, radial vels. from objective prism plates *(German)* 78−45360
NGC 2527, galactic cluster, UBV photometry 78−16479
NGC 2536, spiral galaxy, radial vars. of emission line ratios 80−82497
NGC 253, barred spiral galaxy, detailed surface photometric study 80−105327
NGC 253, spiral galaxy, gas outflow from nucleus rel. to nucleus stellar population 78−28776
NGC 2571, open clusters, UBV anal. 79−58386
NGC 2639 companion galaxy, redshift and assoc. UV excess objects 80−56965
NGC 2685, geometry of flattened galaxy 79−12511
NGC 2685, polarization of peculiar galaxy *(Russian)* 79−35390
NGC 2715, 5033, 5055, rot. curves and orientation parameters 79−12517
NGC 2742, spiral galaxy, rot. and mass. *(French)* 78−89255
NGC 2776, rotation and mass from image-tube spectra of Sc galaxy *(French)* 79−101199
NGC 2782, peculiar hot-spot nucleus galaxy, vel. field 78−4357
NGC 2818, open cluster, photoelec. sequence 77−91595
NGC 2903, photometric obs. of bright patches in spiral arms *(Russian)* 77−64847
NGC 2903, spiral galaxy, nucleus identification and visual energy distrib. 80−62273
NGC 2997, late-type galaxy, rot. and mass 79−21409
NGC 2997, morphology and hot spots around nucleus of galaxy 80−62282
NGC 2997 and 5128, morphology of galaxies from ESO 3.6 m telescope obs. 79−97063
NGC 300, NGC 1365, southern galaxies, H II regions comp. 80−4441
NGC 3079, rotation and mass from image tube spectra *(French)* 77−29931
NGC 3105, young open cluster, photoelectric UBV obs. 77−64811
NGC 3114, open cluster, objective prism radial velocities *(French)* 79−48868

visible astronomical observations continued
NGC 3115, lenticular galaxy, photometry and struct. 80−36707
NGC 3115, s0 galaxy, photometric obs. 77−29917
NGC 3115, S0 galaxy, rotation and mass of inner 5 kiloparsecs 80−105326
NGC 3201, globular cluster, BV photometry 77−2458
NGC 3201, globular cluster, UBV photometry of bright stars 77−60803
NGC 3227, Seyfert galaxy, photoelectric and spectroscopic study and comparison with galaxy chain (VV 150) 80−98724
NGC 3247, RGU photometry of open cluster, catalogue of 129 stars *(German)* 77−82290
NGC 3256, peculiar galaxy, kinematics 78−96537
NGC 330, young cluster in SMC, radial vels. of individual stars 80−67803
NGC 3312 in Hydra I cluster, ram-pressure sweeping of interstellar medium 78−93429
NGC 3324, very young open cluster in Carina spiral feature UBV β photometry 77−22282
NGC 3372, H II region, forbidden O III emission obs. rel. to η Carinae location 80−4383
NGC 3379, elliptical galaxy, spectroscopic obs. rel. to rot. and vel. dispersion 78−49529
NGC 3379, elliptical galaxy as luminosity distrib. standard 80−22073
NGC 3379, surface photometry, computerised analysis 78−12101
NGC 3448, optical and H I 21 cm line obs., peculiar nucleus 78−36696
NGC 3516, SBO type Seyfert galaxy, extended nebulosity, UV and visible obs. 80−82487
NGC 3516, Seyfert galaxy, search for regular optical brightness vars. of nucleus *(Russian)* 77−60828
NGC 3516 Seyfert galaxy, optical spectrum 77−26052
NGC 3532, relative proper motions, cluster membership 79−35318
NGC 3532, southern galactic cluster, stellar photoelectric sequences 77−45502
NGC 3532, southern open cluster, UBV photometric study 80−46621
NGC 3603, luminous young cluster, UBV photometry 78−36643
NGC 3603 stars, interstellar λ4430 band obs. 78−32555
NGC 3620, southern emission-line galaxy at low galactic latitude 78−86022
NGC 362, globular cluster, BV photometry 77−13416
NGC 3631, galaxy, H II regions and spiral struct. 77−45538
NGC 3672, high luminosity spiral galaxy, extended rotation curves 78−8124
NGC 3686 galaxy quartet, surface photometry, mass distribs. and group stability 80−62297
NGC 3898 and 4036, B photographic photometry of bright galaxies 78−54045
NGC 3928 C (Markarian 190), identification as miniature spiral galaxy 80−105347
NGC 4038-9, giant H II regions in interacting galaxies 79−97053
NGC 4088, rotation curve and mass of spiral galaxy *(French)* 78−36698
NGC 4103, open cluster, membership determ. from proper motions, visible obs. 80−67802
NGC 4151, galaxy, outer structure from electronographic obs. 78−16521
NGC 4151, optical polarization of Type 1 Seyfert 79−53906
NGC 4151, Seyfert galaxy, companion galaxy and spiral arm obs. 78−16522
NGC 4151, Seyfert galaxy, optical and X-ray variability correl. *(Russian)* 79−21440
NGC 4151, Seyfert galaxy, optical polarimetry, circumnuclear dust envelope 78−61916
NGC 4151, Seyfert galaxy, optical variations of nucleus 77−82305
NGC 4151, Seyfert galaxy, periodicity of optical variations 78−41047
NGC 4235, Seyfert galaxy, spectrum and radial. vel. 78−49536
NGC 4278, possible visual obs. of supernova 77−29865
NGC 4314, barred spiral galaxy, UBV surface photometry of central region 80−77482
NGC 4321, IUE UV and visible obs. of supernova (1979 April) 79−53834
NGC 4321, UV and visible obs. (1979 April-May) of supernova 79−58363
NGC 4321 (M100), interstellar Na I and Ca II absorption in supernova spectrum 80−51847
NGC 4378, anaemic Sa galaxy, extended rot. curve 79−8990
NGC 4449, emission nebulae content of galaxy 79−84848
NGC 4472 and 5846, luminous giant ellipticals, B−V colour appl. 80−51865
NGC 4473, flattened elliptical galaxy, spectroscopic obs., dynamics 78−57631
NGC 4565, edge-on spiral galaxy, grid photography of halo 80−62261
NGC 4565, spiral galaxy, minor axis brightness profile rel. to massive halos problem 78−93409
NGC 4565, spiral galaxy, optical halo detect. 78−12364
NGC 4590, metal poor globular cluster, BV photometry 77−64813
NGC 4593, Seyfert galaxy, spectrophotometry 80−51878
NGC 4594, search for O I 6300 Å forbidden line from warm neutral interstellar medium 79−71129
NGC 4594, Sombrero galaxy, H I content, stellar rotation curve, mass-to-light ratio 77−53680
NGC 4755, southern open cluster, Balmer line photoelectric photometry 80−56892
NGC 4762, S0 galaxy, rot. curve and dynamics 78−28774
NGC 4833, southern globular cluster, BV photometry of variable stars 78−4304
NGC 488, Sb galaxy, rotation curve from emission line spectra 80−62266
NGC 4945, late-type spiral galaxy, excited gas kinematics, obs. 80−109547
NGC 5012, B and R imagery of S0 galaxy 79−92847
NGC 5053, haloglobular cluster, photometric study 77−74103
NGC 5102, lenticular galaxy, dust and young stars obs. 79−44609
NGC 5102, peculiar SO galaxy, UBV photometry 77−13452
NGC 5128, Centaurus A, stellar population and dust lane 78−20890
NGC 5128, inner structure of optical jet 79−12516
NGC 5128, NE halo, compact emission regions and BSOs 79−17095
NGC 5128, struct. and evolution from multicolour photography 79−53913
NGC 5128 (Centaurus A), globular clusters deficiency 80−26986
NGC 5128 (Centaurus A), high-resolution spectroscopy and tubelike model of dust band 80−56945

visible astronomical observations continued
NGC 5128 (Centaurus A), narrow band photography 79−92854
NGC 5128 (Centaurus A), struct. and evolution from photographic and spectroscopic obs. 80−4429
NGC 5128 (Centaurus A) optical struct., picture processing anal. 79−53907
NGC 5128 (lentaurus A), image tube spectrograms 80−41892
NGC 5195, companion of M51, rot. and relative mass 77−22306
NGC 520, Irr II galaxy, new photographic and spectroscopic obs. 80−41889
NGC 520, tidal interaction in peculiar galaxy 79−48916
NGC 5236, spiral galaxy peculiar nucleus continuum and reddening 80−73031
NGC 5253, surrounding star clusters, fossil evidence for star form. burst, visible obs. 80−77489
NGC 5291, massive gas-rich peculiar lenticular galaxy in IC 4329 cluster 79−71127
NGC 5383, barred spiral galaxy, kinematic study *(French)* 77−71141
NGC 5383, barred spiral galaxy, optical surface photometry 79−9000
NGC 5406, 1977, March 28 photovisual magnitude of Lovas' supernova 77−57002
NGC 5416 cluster, redshifts, morphologies and photometry 79−58434
NGC 5506, X-ray Seyfert, spectra 78−93411
NGC 5506 (3U 1410−03), probable X-ray galaxy, optical spectrum and morphology 77−13466
NGC 5617, open cluster, photoelec. and photographic photometry of member stars 79−17032
NGC 5662, open cluster, photoelec. and photographic photometry of member stars 79−17032
NGC 5728, barred spiral, vels. and mass distrib., spectral obs. 80−94863
NGC 5823, open cluster, photoelec. UBV sequences for north and south regions 77−82293
NGC 5866, edge-on galaxy, luminosity obs., BV photometry 80−82511
NGC 5907, rotation and mass of edge-on galaxy from spectra *(French)* 78−77595
NGC 6025, open cluster, nonmember identification from proper motions 77−53653
NGC 604, giant H II region in M33, SNRs rel. to content of high mass stars 80−31340
NGC 604, H II region in M 33, Hβ photometry and Fabry-Perot interferometry rel. to core-halo struct. 80−85984
NGC 604 in M33, [S III] obs. and N/S abundance gradients 78−8083
NGC 6067, open cluster, photographic, obs. *(German)* 77−53650
NGC 6087, galactic cluster, four-colour and Hβ photometry 80−62208
NGC 612, rotation of lenticular radio galaxy 80−51874
NGC 612 (PKS 0131−36) radio galaxy with disc, radio and optical structs. 79−2568
NGC 6144, globular cluster, and neighbouring region, photometric obs. 80−51816
NGC 6166, cD galaxy, B−V profiles 80−51865
NGC 6200, loose young open cluster in Sagittarius arm extension 77−87493
NGC 6210, 6543, 6572, planetary nebulae, spectroscopic obs. using multichannel analogue detector system 78−36461
NGC 6210, planetary nebula, absolute spectrophotometry in visible and near IR 77−17669
NGC 6217, spectra of galactic nucleus *(Russian)* 79−92869
NGC 6221 and NGC 7213, optical spectrophotometry of X-ray galaxies 79−35377
NGC 6224, X-ray globular cluster, photometry of nucleus 77−37628
NGC 6231, open cluster, spectral types 80−90492
NGC 6231, young open cluster, main sequence stars photometry and spectra 79−88709
NGC 6235, globular cluster, obs. of variable stars 78−4305
NGC 6240, unusual radio galaxy, radio and optical, obs. 80−4440
NGC 6240 (=VV 617+MCG 0-43-4), interacting Seyfert with reddening *(Russian)* 79−58426
NGC 6251, radio galaxy, CCD photometry rel. to central supermassive object 80−26966
NGC 6256, probable galactic globular cluster, BV photometry 78−77583
NGC 6266, globular cluster, colour magnitude diagram, distance and metallicity 78−61894
NGC 628, evidence against discrete states of redshift 77−60820
NGC 6302, line profiles from ionised and neutral gas in peculiar nebula 78−12341
NGC 6302 chem. composition of planetary nebula 78−96525
NGC 6306, active galaxy, spectrophotometry and morphology *(Russian)* 78−28768
NGC 6334 and 6357, H II region distances from early type star photometry 78−85998
NGC 6356, photometric obs. of Mira variables in globular cluster 78−32530
NGC 6366, metal-rich globular cluster, BV photometry and colour magnitude 77−5462
NGC 6383, photometry and spectral classifications, age and distance of open cluster 78−93342
NGC 6383, young open cluster, central core stars obs. 78−41003
NGC 6397, globular cluster, metal poor late-type stars and early A-stars, radial vels. 77−17638
NGC 6397, globular cluster, vel. dispersion meas. using TV detector and cross-correl. techniques 78−16305
NGC 6397, metal-poor globular cluster, BV photometry of 399 stars 77−82292
NGC 6440, globular cluster, surface photometry of cluster core 80−82436
NGC 6494 (M23), open star cluster, membership from astrometry with PDS microdensitometer 80−98697
NGC 650/1, planetary nebula, emission line profiles and internal kinematics 80−17639
NGC 6528, globular cluster, colour-magnitude diagram for field stars 77−87483
NGC 6528, metal-rich globular cluster, colour-magnitude diagram from UBV photometry 80−4406
NGC 6530, open cluster, broadband photometry 77−45504
NGC 6530, UBV photometry of variable stars in open cluster 77−74106
NGC 6530, young open cluster, UBV photometry, magnitudes, reddening, distance, age 78−93341
NGC 6535, photometric study of variable stars in globular cluster 78−32529

visible astronomical observations continued
NGC 6541, globular cluster, UBV photometry, metallicity and distance 79−35316
NGC 6543, planetary nebula, electronographic data rel. to struct. 78−20869
NGC 6543, planetary nebula, emission line obs. 77−33621
NGC 6546, open cluster, assoc. with Cepheid AV Sagittarii disproved 79−58387
NGC 654, young open cluster, membership obs. 77−29885
NGC 654, young open cluster, UBV photometric study 80−109502
NGC 654, young star cluster, polarisation of starlight 77−5550
NGC 6584, new variable stars in globular cluster 80−62137
NGC 6604 and 6704, UBV photometry of open clusters 78−53993
NGC 660, barred spiral galaxy, photometry and spectroscopy 77−5566
NGC 6611, young open cluster, UBV magnitudes and colours, reddening, distance, luminosity 80−31332
NGC 6618, polarimetric obs. of nebula and neighbouring stars *(Russian)* 78−49491
NGC 6624, optical counterparts of X-ray burster in core of globular cluster 80−67801
NGC 6624, optical studies of X-ray globular star cluster 78−93335
NGC 6624, UBV photometry of X-ray globular cluster 78−93337
NGC 6633, open cluster, stellar spectral types 77−74108
NGC 6638, globular cluster, Mira and RR Lyrae variable obs. *(French)* 78−16475
NGC 663, UBV photometry of open cluster, distance 79−5869
NGC 6656, metal-poor globular cluster, BV photometry of 374 stars 77−82291
NGC 6717, globular cluster, colour-magnitude diagram, distance and metallicity 80−46624
NGC 6720, O III 5007 Å forbidden line obs., vel. structure of planetary nebula 78−61909
NGC 6720 (Ring Nebula), monochromatic isophotometry 77−53673
NGC 6720 (Ring Nebula), strong forbidden N II emission and element abundances 77−26035
NGC 6745, peculiar ring-like galaxy, struct. *(Russian)* 79−25732
NGC 6752, first giant branch, C/N abundances in globular cluster 80−67719
NGC 6752, globular cluster, blue horizontal-branch stars photometry 78−49488
NGC 6752, globular cluster, main sequence from UBV photometry 79−71079
NGC 6822, new compact H II regions discovery 80−51854
NGC 6822, struct. and content of irregular galaxy 77−41405
NGC 6822, UBV photometry of dwarf irregular galaxy 79−62903
NGC 6823, UBV photometry and spectra, extinction study of young open cluster 80−4407
NGC 6853, planetary nebula, spectroscopic obs., element abundances 77−53667
NGC 6853 (Dumb-bell Nebula), complex motions of neutral and ionised gas 78−24539
NGC 6853 (Dumbbell Nebula), ionization and abundances 78−45390
NGC 6872, remarkably large barred spiral galaxy 80−31358
NGC 6888, circumstellar nebula, spectroscopic investigations 77−57076
NGC 6888, emission nebula, forbidden N II/Hα ratio 79−8964
NGC 6888, ring nebulae around Wolf-Rayer star HD 192163, spectra of filaments and smooth gas *(Russian)* 80−90515
NGC 6902, H I rich southern supergiant spiral galaxy, opticals studies 80−8680
NGC 6910, uvby Hβ photometry of open cluster 77−91586
NGC 6913, uvby Hβ photometry of open clusters 77−91586
NGC 6913 galactic cluster, photoelec. photometry of brighter stars, variability obs. 80−46625
NGC 6914b, surface brightness and UBV colorimetry *(Russian)* 77−13446
NGC 6946, spiral galaxy, N overabundance in nucleus *(French)* 78−89257
NGC 7000, N II 6584 Å forbidden line profile of giant H II region 79−67081
NGC 7000 (North America Nebula), visual and rocket UV imagery 80−82440
NGC 7000/IC 5070 (North American/Pelican) nebular complex, obscuration and excitation 78−36667
NGC 7009, spectral comparisons of ring and ansae 79−71101
NGC 7023, refl. nebula, surface brightness study 80−56903
NGC 7027, interstellar extinction 164-2170 nm obs. of planetary nebula 79−67082
NGC 7027, planetary nebula, continuum obs. and electron temp. 77−2462
NGC 7027, planetary nebula, position meas. with small Schmidt telescope 78−73749
NGC 7027, planetary nebula, struct. from electronographic obs. 80−12789
NGC 7027 and NGC 7293, spectral obs. of planetary nebulae *(Russian)* 78−61897
NGC 7213, S0 galaxy with Seyfert nucleus, spectra and direct obs. 78−86024
NGC 7217, spiral galaxy, extended rot. curve, mass distrib. 79−21414
NGC 7293, Helix Nebula, O III 5007 Å forbidden line splitting 79−25694
NGC 7293 (Helix Nebula), planetary, obs. of [O I] λ6300 vel. field 78−12340
NGC 7293 planetary nebula (Helix Nebula), microstructures *(Russian)* 78−93344
NGC 7380, young cluster, interstellar polarization obs. 77−17649
NGC 7385, optical-radio knot obs. in elliptical galaxy 79−35362
NGC 741, 1316, 7626, radio galaxies, optical spectra and dynamics 80−94871
NGC 7469, Seyfert galaxy, spectrum 77−57089
NGC 7479, barred spiral, surface photometry, struct. 78−81690
NGC 752, DDO astrophysical study 79−48864
NGC 7541, rotation curve and mass distrib. in spiral galaxy *(Russian)* 80−94874
NGC 7603, Seyfert galaxy, spectrum variations 77−13463
NGC 7635, Bubble Nebula, line intensities 77−33605
NGC 7654 (M52), open cluster, stars four colour and Hβ photometry 78−8067
NGC 7723, dynamics of barred spiral galaxy 79−5893
NGC 772, galaxy, false companions identified as refl. nebulosities *(Russian)* 80−36723
NGC 7743, barred spiral, surface photometry, struct. 78−81690

visible astronomical observations continued
NGC 7789, open cluster, DDO and UBV photometry 77−53648
NGC 7793, galaxy, Hα interferometry 77−53683
NGC 7793, late-type galaxy, ionized gas phys. conditions and mass-luminosity distrib. 80−26967
NGC 7822 (W1) optical studies of kinematics rel. to supernova remnant struct. 78−54028
NGC 931, interacting Seyfert galaxy, struct. and spectra 79−25716
NGC 935-IC 1801, close pair of spiral galaxies, rot. curves and mass distribs. 77−45556
NHC 4594 (Sombrero Galaxy), H II regions and ionised interarm gas detect. 78−36685
Norma dark cloud region, stellar photometry rel. to cloud struct. 78−16494
Norma nova-like X-ray source, search for optical candidates 77−82322
GU Normae, Cepheid, BVI photometry and assoc. with (NGC 6067) 77−45464
IM Normae (Nova 1920), recovery, spectral obs. of faint candidate stars 79−71058
North America and Pelican Nebular Complex, struct., visual extinction map 80−22063
north galactic pole stars, radial vels. 77−22207
northern early-type stars at intermediate galactic latits., UBV photometry and MK spectral classification 77−82221
northern FK4 stars, radial vel. meas. 80−26848
northern sky photographic optical IR survey 79−21198
Nova, Aquilae 1975 (V1301 Aquilae), IR development 77−17570
nova, probable, in LMC, discovery and spectrum 79−8931
Nova Centauri 1979, UBV photometry and spectrum, identification with X-ray transient 79−62842
Nova Cygni 1975, continuum periodic variability 77−13365
Nova Cygni 1975, Hα, Hβ emission lines equivalent widths, scanner obs. 77−2430
Nova Cygni 1975, photographic obs. 77−5535
Nova Cygni 1975, polarisation obs. *(Chinese)* 77−67097
Nova Cygni 1975, rapid vars. of emission line profiles 77−45434
Nova Cygni 1975, speckle interferometry with linear digicon detector 77−78648
Nova Cygni 1975, spectrophotometric exam. *(French)* 77−22240
Nova Cygni 1975, spectroscopic obs., detect. of diffuse enhanced spectrum 77−29850
Nova Cygni 1975, spectrum obtained with small image-intensifier spectrograph 78−73647
Nova Cygni 1975 (V1500 Cygni), light curve 77−2437
Nova Cygni 1975 (V1500 Cygni), minute time scale flickering and 6.6 hour light period 77−17582
Nova Cygni 1975 (V1500 Cygni), spectral features during early decline phase 77−22245
Nova Cygni 1975 (V1500 Cygni), spectroscopic developments and kinematics 77−45446
Nova Cygni 1978, discovery report 78−85962
Nova Cygni 1978, photoelectric obs. and visual magnitude estimates 78−89214
Nova Cygni 1978, photometric obs., light vars., IR obs. showing dust form. phase 78−96494
Nova Cygni 1978, prediscovery mags. and 1978 September spectral features 78−93282
Nova Cygni 1978, rapid flickering and UBV photometry (1978 Sept.) 79−16985
Nova Cygni 1978, spectra, polarisation, photometry and visual magnitude estimates 78−93283
Nova Cygni 1978, spectrum, distance and absolute magnitude 78−89212
Nova Cygni 1978, spectrum, polarisation and visual magnitude estimates 78−89213
Nova Cygni 1978, spectrum and visual magnitude estimates 78−89210
Nova Cygni 1978, UBV photometry, brightnesses and distance 78−93284
Nova Cygni 1978, UBV photometry and short-period vars. 79−5835
Nova Cygni 1978, V photoelectric and visual magnitudes (1978 Sept.-Nov.) 79−5837
Nova Cygni 1978, visual magnitude estimates (1978 September 10 to 12) 78−85963
Nova Cygni 1978, visual magnitude estimates for 1978 Oct. 78−93286
Nova Delphini 1967, emission line spectrum *(Russian)* 78−16440
Nova Delphini 1967, spectrophotometry in 3400 to 6500 A range 78−16430
Nova Delphini (1967), photoelectric and spectrographic obs. 78−20844
Nova Gygni 1978 79−67035
nova in LMC, discovery confirmation, magnitude, photometric obs., pre-max. spectra 78−49456
nova in LMC, discovery obs. 77−33513
nova in LMC, photometric obs. 77−60769
nova in LMC near HV 12080 (1977, February 20), discovery 77−37605
nova in Magellanic Clouds (LMC), premaximum spectrum 79−62853
nova in NGC 5272 (=M3), discovery, V mags. and spectrum 79−71050
nova in Sagittarius, discovery of probable declining nova (1978 March) 80−4376
probable nova in Sagittarius (1978), magnitudes (1978 June 30 to October 3) 79−101164
Nova LMC 1977b, photometry, light curves, distance modulus 78−8019
Nova LMC 1977b, VBLUW photometry, absolute magnitude, distance and reddening 79−58342
Nova Monocerotis 1975 (Ariel 0620−00), linear polarisation obs. 77−13351
Nova Ophiuchi 1976, precise position 77−2444
Nova Ophiuchi 1977, identification with X-ray transient 77−91540
nova outbursts, shell ejection before max. 77−2441
Nova Sagittae 1977, discovery obs. 77−9759
Nova Sagittae 1977, precise position, photographic and visual magnitudes 77−17602
Nova Sagittae 1977, spectral obs., visual magnitude estimates 77−22253
Nova Sagittae 1977, visual magnitude estimate 77−17601
Nova Sagittae 1977, visual magnitude estimates 77−60768
Nova Sagittae 1977, visual magnitude estimates (1977 Aug.-Oct.) 78−8021
Nova Sagittae 1977, visual magnitude estimates (1977 November 6 to 1978 January 7) 78−36593
Nova Sagittarii 1974 (V3888 Sagittarii), line identifications and radial vels. 77−22246
Nova Sagittarii 1977, discovery report 77−33516
Nova Sagittarii 1977, early spectrum 78−32496

visible astronomical observations continued
Nova Sagittarii 1977, image-tube spectra (April 1977) 77−41384
Nova Sagittarii 1977, photometry, spectrum, absolute magnitude and distance 78−53955
Nova Sagittarii 1977, position and visual magnitude estimates 77−33519
Nova Sagittarii 1977, visual magnitude, UBV and Hα obs. (1977, March) 77−33517
Nova Sagittarii 1977, visual magnitude estimates 77−60766
Nova Sagittarii 1977, visual magnitude estimates (1977, Aug.-Oct.) 78−4246
Nova Sagittarii 1978, discovery on 1978 April 7, position, Balmer emission lines 78−45342
Nova Sagittarii 1978, precise position, visual magnitude estimates 1978 Apr. 78−49458
Nova Scuti 1975, spectrum, line identifications 78−45335
Nova Scuti 1975, UBVRI photometry 77−33520
Nova Serpentis 1978, discovery obs. 78−36594
Nova Serpentis 1978, image tube spectrograms, emission lines 78−40964
Nova Serpentis 1978, IR magnitudes and BVR photometry 78−65629
Nova Serpentis 1978, precise position, spectra, visual magnitude estimates 78−36596
Nova Serpentis 1978, UBV photometry, visual magnitude estimates, spectrographic obs. 78−40963
Nova Serpentis 1978, UBV photometry and magnitude estimates 78−40959
Nova Serpentis 1978, VBLUW photometry, absolute magnitude, distance and reddening 79−58342
Nova Serpentis 1978, visible and IR photometry rel. to dust shell evolution 80−90430
Nova Serpentis 1978, visual magnitude estimates 1978 Mar.-Apr. 78−49457
Nova Serpentis 1978, visual magnitude estimates (1978 April) 78−53959
Nova Serpentis 1978, visual magnitude estimates (1978 April-June) 78−61873
Nova V3888 Sagittarii (1974), UBV and uvby photometry during decline stage 78−20836
Nova Vulpeculae 1976, Hα emission line profile variations *(Russian)* 77−74074
Nova Vulpeculae 1976, magnitudes and photoelectric obs. (1976 October-November) 77−5538
Nova Vulpeculae 1976, photoelec. obs., visual magnitude estimates 77−33533
Nova Vulpeculae 1976, photoelectric V measures and visual magnitude estimates 1976, Dec. 77−17600
Nova Vulpeculae 1976, polarisation meas., reddening and distance 77−29855
Nova Vulpeculae 1976, spectra and light 77−33510
Nova Vulpeculae 1976, spectra in range .38 to 1.12 microns *(French)* 77−53606
Nova Vulpeculae 1976, spectrograms and photoelectric V obs. 1976, Oct. and Nov. 77−2443
Nova Vulpeculae 1976, visual magnitude estimates 1976 Nov.-Dec. 77−17598
Nova Vulpeculae 1976 (NQ Vulpeculae), light, colour and vel. curves 78−28708
Nova Vulpeculae 1979, photoelectric obs., (1979 April 21 and 25) 79−53822
Nova Vulpeculae 1979, photometric history (1898 to 1978) 79−53819
Nova Vulpeculae 1979, prediscovery obs. and visual magnitude estimates 79−48817
Nova Vulpeculae 1979, slow nova, pre-maximum light curve 80−4364
Nova Vulpeculae 1979, spectroscopic and photometric obs., (1958 and 1968) 79−58344
Nova Vulpeculae 1979, spectroscopic and photometric obs., possible exceptionally slow nova 79−48820
Nova Vulpeculae 1979, visual magnitude estimate, (1979, May 2) 79−58348
Nova Vulpeculae 1979, visual magnitude estimates, 1979 Jun. 79−75221
nova-like stars, cyclotron line search in optical spectra *(Russian)* 80−67753
nova-like variables, photometric obs. 77−82245
novae, Li/Na ratio upper limit 79−101156
novae, visual magnitude estimates (1977, April-May) 77−53610
novae, visual magnitude estimates (1977, June-Aug.) 77−74064
novae, visual magnitude estimates (1977 January-February) 77−29853
novalike object in NGC 5272, photometry and identification as W Virginis variable 79−75224
novalike object in Vulpecula, 1980 May-June spectra and magnitudes 80−82392
novalike object in Vulpecula, light curve, photometric and spectroscopic obs. 80−67758
novalike object in Vulpecula, photoelectric UVB obs. (1979 June 9 to 15) 79−80323
novalike object in Vulpecula, photometry, June 1980, and spectral classification 80−94807
novalike object in Vulpecula, UBV photometry (1979 August 6 to September 20) 80−8644
novalike object in Vulpecula, visual and red photographic magnitudes 79−92784
novalike object in Vulpecula, visual magnitude estimates 79−88673
novalike object is Vulpecula, visual magnitude estimates (1980 February 2 to May 9) 80−72980
novalike variable in Virgo, discovery, approximate positions and magnitudes, (1980 July and August) 80−98674
NP 0532, Crab pulsar, pulsed and unpulsed light 79−17005
NQ Vulpeculae (Nova 1976) spectroscopic obs. 79−21316
NRAO 5 GHz and 4C catalogues, optical spectra and redshifts 78−8145
NRAO 5 GHz S2 and I surveys, radiosource identifications 78−54062
null circular polarisation meas. 78−96478
44 Nysa, pole coordinates from photoelectric photometry 80−31230
O3 to O5.5-type stars, spectra 77−33481
O and B0 supergiants in Magellanic Clouds, spectral classification 77−78777
O to F type stars, Balmer lines and mean electron density 77−17564
O-B stars, Fourier transform spectroscopy in 4800-10200 Å range 79−16993
O-B stars, spectrophotometric and UBV colorimetric parameters *(Russian)* 77−17569
O-type binary and stellar wind search 78−89197

visible astronomical observations continued
O-type planetary nuclei, spectral classification, magnitudes, distances 78−4203
O-type stars, in LMC, uvby photometry 77−60756
O-type stars, radial vels. and K-term 77−56922
O-type stars, rotational vels., V sin i and macroturbulence 77−45411
O-type stars and T Tauri objects, Hα, O I photometry 77−67092
OA 184, supernova remnant, interferometric obs. in Hα line, expansion vel. *(Russian)* 79−88728
OA 33, variability of optical counterpart 78−45421
OAO 1653-40, 38 s X-ray pulsar, optical counterpart, spectroscopic search 80−73072
OB stars, in LMC, spectroscopic obs., galaxy distance determ. 79−71111
OB stars, in Vela region, list of 166 objects 77−87280
OB stars in Circinus-Norma region, search for faint objects 80−62121
OB stars in M31 77−37601
OB-type southern stars, UBV, Hβ and polarisation meas. 77−26007
OB-type stars, C III 5696 Å and He II 4686 Å obs., C III transition from absorpt. to emission 79−67006
OB-type stars in SA 98, UBV photoelectric meas. 80−46535
OB-type stars in vicinity of long period Cepheid VZ Puppis, UBV β photometry 78−45339
Oberon, near IR spectra and JHK photometry, mass and dia. measurement 80−56761
Object Kowal, positions, indeterminate orbit, elements and ephemeris 78−7907
object Kowal, slow-moving asteroid discovery and positions 78−4136
object Schuster, approx. positions, 1976, Nov. 77−5489
Object Schuster, discovery and positions for fast-moving Apollo-type object 78−32385
object Schuster, fast moving asteroid, discovery obs. 77−5488
Object Sebok, fast-moving asteroidal object, discovery and positions 77−17416
objective prism spectra of stars, computer classification *(German)* 77−49304
OBN, OBC stars, radial vels. and short period binaries frequency 78−53951
occultations, lunar, photoelectric obs. at Dominion Astrophysical Observatory (DAO) 79−75198
occultations, photoelec. obs., diffraction, stellar diameters and double stars 78−7866
occultations of stars by Moon, 1965-71 events recorded at Poltava *(Russian)* 78−4083
UV Octantis, VBRI obs. of RRab star, radius determ. 79−8928
UZ Octantis, W Ursae Majoris system, UBV light curves 80−22042
OE 110, Lacertid, optical variability from archival plates 77−26056
Of stars, raxial vel. meas. 78−4226
Of stars, search for rapid Hα and Hβ line variability 77−26014
OF-024 optically active extragalactic radiosource 77−17712
Of-type stars, HD 150958, 152386 and 163758 in blue region 79−5825
Ohio radio sources, optical identification using radio and optical positions meas. by Texas interferometers 78−28808
OI090.4 and OJ−131, BL Lacertae objects 78−4359
OJ 287, BL Lacertae object, case for synchronous optical-radio outbursts 80−8679
old halo stars, chemical comp. rel. to nucleosynthesis in Galaxy 78−65616
old novae, search for rapid photometric oscills. 78−4251
open cluster containing Wolf-Rayet and Of-stars 77−64810
open cluster reddening, polarimetry and field star photometry of M67, Hyades and Coma cluster 80−62222
open clusters, diam. and luminosity functions from starcounts 77−91589
open clusters, spectroscopic obs., search for Ap stars 78−45367
open clusters near η Carinae, RGU photometry 77−37631
171 Ophelia, binary asteroid evidence from light curve 80−4287
ζ Ophiuchi, 1980 March emission episode, Hα and He I line behaviour 80−62151
V2051 Ophiuchi, AM Herculis-type variable, spectrum scans 77−45492
Y Ophiuchi, anomalous Cepheid, evidence for duplicity 78−53990
χ Ophiuchi, Be star, rapid spectroscopic variations 77−56970
χ and 66 Ophiuchi, Be stars, search for short time scale vars. in Hα emission 80−109441
V1010 Ophiuchi, early-type contact system, two-colour light curves 77−33553
V566 Ophiuchi, eclipsing binary, period change, UBV photometry 77−29883
U Ophiuchi, eclipsing binary, photometric anal. 77−53628
XX Ophiuchi, emission-line star, near IR spectrum 77−49404
U Ophiuchi, massive eclipsing binary star, spectrophotometry 80−26900
ζ Ophiuchi, obs. of interstellar K I 4044 Å line 78−24533
RZ Ophiuchi, orbital elements for eclipsing binary from new obs. 79−21327
V566 Ophiuchi, photoelectric obs. of eclipsing binary 77−71130
RS Ophiuchi, recurrent nova, spectrum obs. 79−62848
V1010 Ophiuchi, short period close binary, radial vel. curve 77−29884
ζ Ophiuchi, spectral vars. related to rot. 80−22000
ω Ophiuchi, UBV photometry of Ap star, periodicity in luminosity vars. *(French)* 78−57559
ζ Ophiuchi (HR 6175), O-type star, emission line episode 80−72953
70 Ophiuchi A, late-type dwarf star, mag. field obs. 80−72949
Ophiuchus-Scorpius region, ZB flare stars and nebular variables *(Chinese)* 78−28702
optical counterparts of 5C radiosources and blue objects, spectrographic obs. 79−101212
optical counterparts of extended radiosources, improved optical positions 78−93444
optical flashes from burst X-ray sources, obs. 77−41420
optical identifications rel. to cosmological evolution of extragalactic radiosources 77−17728
optical quasars, radio and optical obs., redshifts, luminosity function 78−49552
optical studies from space, Soviet, review 78−85815
OQ 172, H_2 lines identification in spectrum of quasar *(Russian)* 78−69905
OQ 172, quasar, H_2 lines in absorpt. spectrum 80−36734
OQ 208, red shift difference between broad and narrow emission lines 79−67100
Orion I OB assoc. and evidence for associated expanding shell 79−53866
Orion Nebula, C abundance from visible and IUE obs. 80−82451
Orion Nebula, chem. comp. from emission line obs. 77−49456
visible astronomical observations continued
Orion Nebula, fine-struct. lines obs. and elemental abundances 80−4410
Orion Nebula, forbidden line and optical continuum electron temps. comparison 79−30105
Orion Nebula, forbidden line wavelengths *(French)* 77−64829
Orion Nebula, high vel. emission object obs. 77−22296
Orion Nebula, high-vel. features driven by stellar wind from θ^2 Orionis A 79−8978
Orion Nebula, large proper motions of nebular features and faint star 78−12349
Orion Nebula, linear polarisation obs. 78−45392
Orion Nebula, macroscopic motions from atomic line vels. 80−62243
Orion Nebula, nebular condensations found with S20 photocathodes assoc. with Lallemand electronic camera *(French)* 79−44592
Orion Nebula, optical evidence for stellar wind bubbles 79−88724
Orion Nebula, optical linear polarisation meas. 77−45536
Orion Nebula, photoelectric photometry of central region 77−33624
Orion Nebula, photographic obs. in Hα, Hβ and He I 10830 Å lines 78−81669
Orion Nebula, physical conditions from optical and radio lines obs. 77−45524
Orion Nebula, spectrophotometric obs., ion abundances, and thermal balance 77−67121
Orion Nebula, temps. and abundances in outer part 79−53868
Orion Nebula cluster, MK spectral types 77−22283
Orion Nebula cluster, search for expansion 77−74102
Orion Nebula peripheral regions, spectrum obs. rel. to element depletion and ionisation 80−36686
Orion Nebula stars, wavelength depend. of polarisation, rel. to intracluster dust and circumstellar shells 77−78839
Orion OB1 association, stellar spectral types 78−32539
Orion OB 1 association, photometric study 77−82128
Orion population stars, variables light curve characts. and emission line intensities 80−67721
Orion region, survey of extremely red stars with Schmidt telescope *(Japanese)* 78−20833
δ Orionis, apsidal motion of spectroscopic binary 79−8952
κ Orionis, B0.5 Ia star, Hα profile variable 79−101146
ζ Orionis, C III line obs. 77−87387
θ^1 Orionis, eclipsing binary, period determ. 77−2455
UX Orionis, fast irregular variable, H_α and H_β lines obs. *(Russian)* 77−87400
U Orionis, H I emission lines rapid variability *(Russian)* 79−16989
ε Orionis, interstellar K-line, photographic obs. 79−16956
α Orionis, M supergiant, circumstellar shell and mass loss rate 77−45415
χ^1 Orionis, new solar-type astrometric binary, parallax and orbital elements 78−73740
22 Orionis, nonradial m-mode changes in 53 Persei variable 80−72939
α Orionis, polarized light scattered by dust shell 79−12473
η Orionis, quintuple system, spectroscopic orbit from speckle interferometry 77−22276
α Orionis, reconstructed images using stellar speckle interferometry 77−22222
ζ Orionis, Reticon obs. of Hα P Cygni profile 80−82365
α Orionis, speckle interferometry diameter, limb darkening 77−91525
YY Orionis, spectroscopic and photometric obs. 78−93225
δ Orionis, spectroscopic binary, spectrophotometry *(Russian)* 77−64802
α Orionis, supergiant variable, mass loss, visible spectra obs. 80−67755
α Orionis, vel. fields in shell from Fe II emission line obs. 79−101144
χ^1 Orionis (SAO 077705), ang. dia. from occultation obs. 78−20825
θ Orionis A, eclippsing binary, photographic photometric obs. 79−58380
θ^1 Orionis A, UBV photoelec. obs. of primary eclipse 77−91576
δ Orionis A, UV spectrophotometry and optical polarimetry, stellar wind variability 79−21277
λ Orionis association, photometric props. of young cluster 78−16478
σ Orionis E, He star, radial vels. 77−45443
σ Orionis E, mag. field discovery 78−93268
σ Orionis E, peculiar eclipsing binary, linear polarization obs. 78−32508
σ Orionis E, period and luminosity stability from uvby β photometry 78−8017
θ^1 Orionis E, suspected variable, photographic photometric obs. 79−58380
YY Orionis stars in Chamaeleon T-assoc. 79−30064
OX+029, nearby extended variable object 79−67096
P-K 164+31°1, spectroscopic obs., identification of planetary nebula 77−74123
Pal 12, metal-rich globular cluster in outer galactic halo, optical and IR obs. 80−105290
49 Pales, binary asteroid evidence from light curve 80−4287
Pallas, 1978 May 29 occultation of SAO 85009, diameter determ. 79−44400
Palomar 5, remote globular cluster in galactic halo, chem. comp. 77−87482
55 Pandora, photometric vars., light curves and rot. period 79−16869
471 Papagena, rotational period and photoelectric lightcurve *(German)* 78−4134
471 Papagena, rotational period and photoelectric lightcurve 78−4135
parallax and proper motion meas. for seven stars 80−62109
parallax stars in Herstmonceux programme, second list 78−77498
parent galaxies of supernovae, redshifts 79−44612
Paris astrolabe observations, time and latitude (1976) *(French)* 77−78078
Paris astrolabe time and latitude obs. for 1977-8 period *(French)* 79−101051
Parkes 2700 MHz survey, optical identifications 77−49489
Parkes 2.7 GHz selected area survey sources optical identifications 77−17701
Parkes radiosources with flat spectra, optical identifications 78−4382
Parsamyan 21, colorimetry of cometary nebula *(Russian)* 79−8960
Parsamyan 22, surface brightness and UBV colorimetry *(Russian)* 77−13446
partial solar eclipse, 1976 April 29, obs. in Poltava 78−45201
γ Pavonis, C and N abundances 77−91531
MW Pavonis, eclipsing binary, UBV light var. and orbital elements 77−49429
peculiar A and B stars, Y abundances 77−33503
peculiar and interacting galaxies in southern sky, emission line obs. of 37 objects *(Russian)* 78−49511
peculiar bright southern stars, identification and spectral types 77−82225

visible astronomical observations continued
peculiar central stars of planetary nebulae, spectroscopic characts. 77−87405
peculiar extragalactic sources, multiaperture UBV photometry 78−28772
peculiar galaxy system in Hydra 79−58433
peculiar giant galaxies with fragmentation *(Russian)* 77−26063
γ Pegasi, β Cephei star, dynamics of photosphere and shells 78−49447
AU Pegasi, binary Type II cepheid, photometric and spectroscopic study 80−26866
BB Pegasi, BV photoelectric lightcurve analysis of eclipsing binary 80−62194
DY Pegasi, dwarf Cepheid, revised ephemeris, period decrease 79−67040
RU Pegasi, dwarf nova, rapid and ultrarapid light vars. 77−53596
AW Pegasi, eclipsing binary, photometric elements, masses, radii, luminosities 78−28723
o Pegasi, hot Am star, spectroscopic obs. and curve of growth anal. 77−22237
57 Pegasi, long-period pulsating variable, spectrographic and photometric obs. 79−21305
BX Pegasi, photoelectric photometry of totally eclipsing W Ursae Majoris systems, 1978 Oct. to Nov. *(Chinese)* 80−31330
κ Pegasi, radial vel. meas., visual binary with spectroscopic binary component 78−32520
RU Pegasi, radial vel. of dwarf nova 79−62833
θ Pegasi, rapid spectral line variability disproved 80−8625
AG Pegasi, symbiotic binary system, UV and optical spectrum rel. to nature of components 80−109449
1 Pegasi, visual binary, radial vel. meas. 79−21347
EQ Pegasi (BD+19°5116), flare active binary system 78−61868
II Pegasi (HD 224085), surface-active binary star, spectroscopic obs. 80−90480
118 Peitho, rot. period and light curve from photoelectric obs. 80−46454
554 Peraga, photoelectric photometry and rot. period 79−84727
Period Comet Brooks 2 (1980f), recovery, positions and perihelion passage correction 80−85899
Period Comet Wolf-Harrington (1977j), independent recovery in Japan 77−71067
Periodic Comet Arend-Rigaux (1977k), position and tail obs. (1978 March 5) 78−40874
Periodic Comet Arend-Rigaux (1977k), positions, appearance and spectrum 78−12157
Periodic Comet Arend-Rigaux (1977k), precise positions 1977 Aug. 77−91477
Periodic Comet Arend-Rigaux (1977k), precise positions 1977 Oct.-1978 Jan., total visual magnitude estimates 78−36517
Periodic Comet Arend-Rigaux (1977k), precise positions for 1977 Nov.-Dec. 78−20745
Periodic Comet Arend-Rigaux (1977k), precise positions for 1977 Oct.-1978 Mar. 78−65548
Periodic Comet Arend-Rigaux (1977k), recovery and ephemeris continuation 77−74013
Periodic Comet Arend-Rigaux (1977k), recovery and positions 77−82172
Periodic Comet Ashbrook-Jackson (1977g), 1978 April precise posns. from ESO La Silla *(French)* 79−101117
Periodic Comet Ashbrook-Jackson (1977g), magnitude estimates (1978 Aug.-Sept.) 78−85912
Periodic Comet Ashbrook-Jackson (1977g), precise position (1977 Oct. 13) 78−20749
Periodic Comet Ashbrook-Jackson (1977g), precise position for 1978 Apr. 5 78−53887
Periodic Comet Ashbrook-Jackson (1977g), precise positions (1977 May and Sept.) 77−91485
Periodic Comet Ashbrook-Jackson (1977g), recovery, appearance and positions 77−49334
Periodic Comet Ashbrook-Jackson (1977g), spectroscopic obs. 78−96437
Periodic Comet Ashbrook-Jackson (1977g), total visual magnitude estimate for 1978 July 1 78−73679
Periodic Comet Ashbrook-Jackson (1977g), total visual magnitude estimates 1978 July 78−77519
Periodic Comet Ashbrook-Jackson (1977g), total visual magnitude estimates 78−93169
Periodic Comet Ashbrook-Jackson (1977g), total visual magnitude estimates for 1978 Oct.-Nov. 79−5787
Periodic Comet Ashbrook-Jackson (1977g), visual magnitude estimates (1978 September 7 and 10) 78−89128
Periodic Comet Ashbrook-Jackson (1978 XIV), precise positions *(German)* 80−46453
Periodic Comet Ashbrook-Jackson (1978 XIV), precise posns. (1978 April) *(French)* 80−41767
Periodic Comet Ashbrook-Jackson (1978 XIV) 80−31258
Periodic Comet Borrelly (1980i), recovery and approximate positions, (1980 July 9 and 21) 80−94755
Periodic Comet Chernykh, precise positions and magnitudes (1977 Sept.-Oct.) 78−7926
Periodic Comet Chernykh (1977l), approx. positions (1977 Sept. 1-2) 77−82169
Periodic Comet Chernykh (1977l), discovery obs. and appearance 77−82168
Periodic Comet Chernykh (1977l), precise positions, improved elements and magnitudes 78−7932
Periodic Comet Chernykh (1977l), precise positions 1977, Sept. 77−91475
Periodic Comet Chernykh (1977l), precise positions 1977, Sept. and Oct., ephemeris to 1978 Apr. 78−7941
Periodic Comet Chernykh (1977l), precise positions 1977 Aug.-1978 Mar. 78−53886
Periodic Comet Chernykh (1977l), precise positions 1977 Dec.-1978 Jan. 78−49379
Periodic Comet Chernykh (1977l), precise positions 1977 Sept.-Dec. 78−24490
Periodic Comet Chernykh (1977l), precise positions (1977 November 17 to 1978 January 8) 78−32400
Periodic Comet Chernykh (1977l), precise positions and ephemeris for 1977 Aug.-Oct. 77−82170
Periodic Comet Chernykh (1977l), precise positions and visual magnitudes 1977, Aug. and Sept. 77−87330
Periodic Comet Chernykh (1977l), precise positions for 1977 September 77−82173
Periodic Comet Chernykh (1977l), precise positions for 1977 Sept. 6-19 period 77−87333

visible astronomical observations continued
Periodic Comet Chernykh (1977l), precise positions for 1977 Oct.-Dec., total visual magnitude estimates 78−20755
Periodic Comet Chernykh (1977l), precise positions for 1977 Sept. 79−25546
Periodic Comet Chernykh (1977l), precise posns., improved elements and ephemeris 78−69747
Periodic Comet Chernykh (1977l), precise posns. (1977 Sept.-Nov.) 78−16351
Periodic Comet Clark (1978g), recovery on 1978 Apr. 13, positions Apr. 13-30 78−49388
Periodic Comet Comas Sola (1977n), recovery obs. 1977, Sept. 77−87332
periodic Comet Comas Sola (1977n), tentative obs. (1978, November 29) 79−16889
Periodic Comet Comas Sola (1977n), total visual magnitude estimate, (1978, October 8) 78−96435
Periodic Comet d'Arrest (1976 XI), nucleus light curve and rotation 78−53877
Periodic Comet d'Arrest (1976 XI), tail photometry rel. to meteoroids characts. 78−53876
Periodic Comet d'Arrest (1976e), precise positions, 1976, Aug.-Nov. 77−5503
Periodic Comet d'Arrest (1976e), precise positions 1976, July-Oct. 77−17441
Periodic Comet d'Arrest (1976e), precise positions 1976 Aug. 14-23 period *(French)* 77−91474
Periodic Comet d'Arrest (1976e), precise positions (1976, July-August) 77−37571
Periodic Comet d'Arrest (1976e), precise positions and antitail 77−37580
Periodic Comet d'Arrest (1976e), precise positions for 1976 Oct. 15, Nov. 14, Dec. 23 77−22151
Periodic Comet d'Arrest (1976e) precise positions 1976 Jun.-Aug. and total visual magnitudes 77−2372
Periodic Comet Daniel (1979b), recovery on 1979 Feb. 2, precise position, ephemeris 79−30013
Periodic Comet Denning-Fujikawa (1978n), precise positions, (1978, October 28 and November 2) 79−5780
Periodic Comet Encke, photometry rel. to large dust grains emission 78−85908
Periodic Comet Encke, position for 1977 July 14, visual magnitude estimate, coma diameter 77−78719
Periodic Comet Encke, postperihelion interference filter photometry 79−2519
Periodic Comet Encke, precise positions, 1977, Aug. to Oct. 78−7942
Periodic Comet Encke, precise positions, 1977, Sept. 77−91476
Periodic Comet Encke, precise posn. for 1980 Oct. 8 and perihelion passage correction 80−109398
Periodic Comet Encke, semiaccurate position, CN production rate and ephemeris correction 77−67070
Periodic Comet Encke, semiaccurate posn. and appearance (1980 August 8) 80−94758
Periodic Comet Encke, total magnitude estimates (1977 September) 78−7925
Periodic Comet Faye (1976i), precise position, total visual magnitude estimates and coma diameters 77−22150
Periodic Comet Faye (1976i), precise position for 1977 Feb. 19 77−82166
Periodic Comet Faye (1976i), precise positions (1976, September-1977, January) 77−45362
Periodic Comet Faye (1976i) precise positions 1976, Jul.-Oct. 77−13289
Periodic Comet Forbes (1980a), recovery obs. and corrected ephemeris 80−46490
Periodic Comet Gehrels 3 (1975o), 1976, Oct.-Dec. precise positions 77−25982
Periodic Comet Gehrels 3 (1975o), precise positions, (1977 November 18 to 1978 March 5) 78−40876
Periodic Comet Gehrels 3 (1975o), precise positions 77−60726
Periodic Comet Gehrels 3 (1975o), precise positions for 1978 Feb.-Mar. 78−73677
Periodic Comet Gehrels 3 (1975o), precise posns. for 1978 March-April period 78−49385
Periodic Comet Giacobini-Zinner (1978h), recovery, positions for 1978 Apr. 30 and May 1 78−49389
Periodic Comet Giclas (1978k), precise position, (1978, September 14) 78−85916
Periodic Comet Giclas (1978k), precise positions 1978 Sept., elliptical elements, ephemeris 78−93162
Periodic Comet Giclas (1978k), spectroscopic obs. 78−96437
Periodic Comet Griff-Skjellerup (1977b), precise positions 1977 Jan. 21-26 77−22143
Periodic Comet Grigg-Skjellerup (1977b), precise positions, magnitudes and coma diameters (1977, March-April) 77−49339
Periodic Comet Grigg-Skjellerup (1977b), precise positions, total visual mag. estimates, coma diameters 77−60729
Periodic Comet Grigg-Skjellerup (1977b), precise positions 1977, Apr.-May and meteor activity 77−71064
Periodic Comet Grigg-Skjellerup (1977b), precise positions (1977 Jan.-Aug.) 78−7928
Periodic Comet Grigg-Skjellerup (1977b), precise positions and ephemeris, 1977, Mar.-Apr. 77−33414
Periodic Comet Grigg-Skjellerup (1977b), precise positions and appearance (1977, April) 77−45360
Periodic Comet Grigg-Skjellerup (1977b), visual magnitude estimates (1977, March) 77−33418
Periodic Comet Gunn, position, osculating elements and ephemeris for 1977/8 77−33420
Periodic Comet Gunn, precise positions, 1976, Jul.-Oct. 77−17432
Periodic Comet Gunn, precise positions, Aug., Sept. and Oct. 78−12155
Periodic Comet Gunn, precise positions for 1977 Oct. and Dec. 78−69750
Periodic Comet Halley, rotation period from halo diameter meas. 80−51694
Periodic Comet Haneda-Campos, precise positions, (1978 August 11 to September 5) 78−89121
Periodic Comet Haneda-Campos (1978j), precise position for 1978 Sept. 29 78−93167
Periodic Comet Haneda-Campos (1978j), precise positions, (1978 September 2 and September 8) 78−89124

visible astronomical observations continued
Periodic Comet Haneda-Campos (1978j), precise positions 1978 Aug.-Sept., ephemeris for 1978 Sept.Oct. 78−89131
Periodic Comet Haneda-Campos (1978j), precise positions (1978, September 6 and 8) 78−85914
Periodic Comet Haneda-Campos (1978j), precise positions (1978, August 10 to September 12) 78−89127
Periodic Comet Harrington (1980m), recovery and precise positions (1980 September 4 to 9) 80−101558
Periodic Comet Holmes, recovery and precise position (1979 July 20) 79−80272
Periodic Comet Honda-Mrkos-Pajdusakova (1980c), independent recovery 80−67658
Periodic Comet Honda-Mrkos-Pajdusakova (1980c), recovery and positions (1980 May 1 and 6) 80−67656
Periodic Comet Jackson-Neujmin (1978q), recovery, and ephemeris for 1978 Nov.-1979 Feb. period 79−12435
Periodic Comet Klemola (1976j), positions for 1976 Aug. 25-1977 Jan. 21 period 77−78718
Periodic Comet Klemola (1976j), precise positions 1976, Aug. and Sept. 77−2370
Periodic Comet Klemola (1976j), precise positions 1976, Oct. 77−17431
Periodic Comet Klemola (1976j), precise positions for 1976 Sept. 16-19 77−17445
Periodic Comet Kohoutek (1980j), recovery and approximate positions (1980 August 6 and 7) 80−94757
Periodic Comet Kojima (1977r), precise positions 1977 Dec.-1978 Jan. 78−36519
Periodic Comet Kojima (1977r), precise positions (1977 Dec. 5, 20) 78−20748
Periodic Comet Kojima (1977r), precise positions for 1978 Jan. and Mar. 78−65549
Periodic Comet Kojima (1977r), recovery posns. and earlier obs. 78−20739
Periodic Comet Kopff (1976b), precise positions 1977 June, July, Sept. 77−91478
Periodic Comet Kopff (1976b), precise posns. (1977 June-Oct.) 78−16356
Periodic Comet Kopff (1976b), precise posns. (1977 Oct. and Dec.) 78−28587
Periodic Comet Kowal 2 (1979a), precise positions, (1979, February 1 to 28) 79−40140
Periodic Comet Kowal 2 (1979a), precise positions (1979, March 1 to 28) 79−48739
Periodic Comet Kowal (1977f), positions, orbital elements, ephemeris 77−64699
Periodic Comet Kowal (1977f), precise position for 1977 June 13 77−82164
Periodic Comet precise positions, 1977, Jul. 77−71061
Periodic Comet Reinmuth 1 (1979j), recovery obs. 80−8589
Periodic Comet Reinmuth 2 (1980n), recovery posns. and appearance (1980 Sept.) 80−101560
Periodic Comet Russell (1979d), precise posns. (1979 June-July) and improved elements 79−84748
Periodic Comet Sanguin (1977p), positions, improved elements and ephemeris 78−16352
Periodic Comet Sanguin (1977p), precise positions 1977, Oct. to Dec. 78−20752
Periodic Comet Sanguin (1977p), precise positions (1977 October 11 and 19) 78−7936
Periodic Comet Sanguin (1977p), precise posns. (1977 Nov.-1978 Jan.) 78−73685
Periodic Comet Sanguin (1977p), prediscovery position, elliptical elements, and ephemeris 78−4153
Periodic Comet Schuster, (1977o), positions, orbital elements and ephemeris 77−91481
Periodic Comet Schuster (1977o), confirmation and semiaccurate posns. (1977 Oct.) 78−7929
Periodic Comet Schuster (1977o), discovery and positions (1977 October) 78−7927
Periodic Comet Schuster (1977o), precise positions, 1977 October 16 and (1978 January 2) 78−65550
Periodic Comet Schuster (1977o), precise positions 1977, Nov. 78−12156
Periodic Comet Schuster (1977o), precise positions (1977, October 9-17) 77−91483
Periodic Comet Schuster (1977o), precise positions (1977 September) 78−7933
Periodic Comet Schuster (1977o), precise positions and ephemeris for 1977/78, Dec. to May 78−7940
Periodic Comet Schuster (1977o), precise positions for 1977 Sept.-Dec. 78−20754
Periodic Comet Schuster (1977o), precise posns. (1977 Dec.-1978 Jan.) 78−36524
Periodic Comet Schuster (1977o), precise posns. (1977 Nov. and Dec.) 78−20741
Periodic Comet Schwassmann-Wachmann 1, 1976 Nov. 17 outburst obs. 77−5502
Periodic Comet Schwassmann-Wachmann 1, 1978 September 13-14 magnitude 78−93160
Periodic Comet Schwassmann-Wachmann 1, appearance (1978 Nov.-Dec.) 79−12436
Periodic Comet Schwassmann-Wachmann 1, appearance and total magnitude (1979) December 80−36571
Periodic Comet Schwassmann-Wachmann 1, CO^+ obs. near minimum brightness 80−82305
Periodic Comet Schwassmann-Wachmann 1, coma obs. (1979 October 31) 80−8591
Periodic Comet Schwassmann-Wachmann 1, compact condensation obs. 79−25550
Periodic Comet Schwassmann-Wachmann 1, magnitudes (1979 February) 79−40139
Periodic Comet Schwassmann-Wachmann 1, new outburst, spectrum and visual magnitude estimates 79−53774
Periodic Comet Schwassmann-Wachmann 1, obs. on 21st and 22nd Jan. 1980 of coma dimensions 80−36573
Periodic Comet Schwassmann-Wachmann 1, outburst, total visual magnitude estimates, 1978 March 6-8 78−36527
Periodic Comet Schwassmann-Wachmann 1, photometric and polarimetric obs. during 1976-77 outbursts *(Russian)* 79−80276

visible astronomical observations continued
Periodic Comet Schwassmann-Wachmann 1, precise positions, 1978 January 1 to 16, and outburst date 78−32399
Periodic Comet Schwassmann-Wachmann 1, precise positions, (1978 February 27 to March 12) 78−49381
Periodic Comet Schwassmann-Wachmann 1, precise positions 1976, Oct. and magnitudes for Dec. 77−17439
Periodic Comet Schwassmann-Wachmann 1, precise positions 1976 Oct. 30-Dec. 27, visual magnitudes 77−22138
Periodic Comet Schwassmann-Wachmann 1, precise positions 1977 Dec.-1978 Feb., total visual magnitude estimates 78−36520
Periodic Comet Schwassmann-Wachmann 1, precise positions (1976, Sept.-Nov.) 77−29725
Periodic Comet Schwassmann-Wachmann 1, precise positions and magnitudes (1976 Oct.-Nov.) 77−5498
Periodic Comet Schwassmann-Wachmann 1, precise positions and magnitudes 1976/77 Nov.-Feb. 77−37574
Periodic Comet Schwassmann-Wachmann 1, precise posns. (1977 Dec.-1978 March) 78−69746
Periodic Comet Schwassmann-Wachmann 1, precise posns. (1977 March and Aug.) 78−16354
Periodic Comet Schwassmann-Wachmann 1, precise posns. and magnitudes (1977-8) 78−28585
Periodic Comet Schwassmann-Wachmann 1, total visual magnitude estimates for 1978 Oct. 79−5788
Periodic Comet Schwassmann-Wachmann 1, total visual magnitude estimate, (1979 February 4) 79−30011
Periodic Comet Schwassmann-Wachmann 1 (1974 II), outburst and CO^+ detect. spectrophotometric obs. 80−72881
Periodic Comet Schwassmann-Wachmann 2 (1979k), recovery posns. and ephemeris 80−26811
Periodic Comet Schwassmann-Wachmann 3 (1979), discovery report and precise positions 79−88622
Periodic Comet Schwassmann-Wachmann 3 (1979g), precise position for 1979 August 19 79−84750
Periodic Comet Schwassmann-Wachmann 3 (1979g), precise position (1979 August 22) 79−92719
Periodic Comet Schwassmann-Wachmann 3 (1979g), precise positions (1979 August 19 to 22) 79−92720
Periodic Comet Shajn-Schaldach (1978i), recovery positions 78−73678
Periodic Comet Smirnova-Chernykh (1975e), precise position 1976 June 4 77−33426
Periodic Comet Smirnova-Chernykh (1975e), precise positions (1976, May-June) 77−37572
Periodic Comet Stephan-Oterma (1980g), recovery positions, elements and emphemeris 80−82307
Periodic Comet Stephan-Oterma (1980g), total visual magnitudes and coma diameters, (1980 September 7 to 11) 80−109397
Periodic Comet Taylor (1916 I = 1977a), precise positions, orbital elements, ephemeris 77−22142
Periodic Comet Taylor (1977a), precise and prerecovery positions 77−45363
Periodic Comet Taylor (1977a), precise position 1977, Jan. 77−22144
Periodic Comet Taylor (1977a), precise positions (1977, February-March) 77−49340
Periodic Comet Taylor (1977a), precise positions (1977, March-April) 77−64702
Periodic Comet Taylor (1977a), precise positions and prediscovery obs. (1976 Nov.-1977 Feb.) 77−33419
Periodic Comet Taylor (1977a), precise positions for 1977 Jan. 14 77−22146
Periodic Comet Tempel 1 (1977i), precise position 1977, June 77−71062
Periodic Comet Tempel 1 (1977i), recovery on 1977 April 12, precise positions 77−60728
Periodic Comet Tempel 2, optical spectrophotometry at 3 AU distance, albedo, nucleus radius 80−26814
Periodic Comet Tempel 2 (1977d), BV photometry, (1979, January 28 and 31) 79−30012
Periodic Comet Tempel 2 (1977d), precise position 1977, April 77−71063
Periodic Comet Tempel 2 (1977d), recovery obs. (1977, March 27) 77−37576
Periodic Comet Tritton (1978d), positions, elements and ephemeris 78−36531
Periodic Comet Tritton (1978d), precise positions 1978 March 78−40877
Periodic Comet Tsuchinshan 1 (1978e), precise position (1978 March 8) 78−45285
Periodic Comet Tsuchinshan 1 (1978e), recovery, precise position 1978 Feb. 4 78−36526
Periodic Comet Tsuchinshan (1978p), recovery and semiaccurate posns. 79−5783
Periodic Comet Tuttle (1980h), recovery and precise position (1980 July 14) 80−85901
Periodic Comet Tuttle-Giacobini-Kresak (1978r), recovery and semiaccurate positions 79−12434
Periodic Comet Van Biesbroeck (1977s), precise positions 1977 Dec. and 1978 Mar. 78−45289
Periodic Comet Van Biesbroeck (1977s), precise posns. (1978 April-May) 78−73686
Periodic Comet Van Biesbroeck (1977s), precise posns. (1978 Jan.-May) 78−61802
Periodic Comet Van Biesbroeck (1977s), recovery position 78−20740
Periodic Comet Whipple (1977h), confirmed recovery and positions (1977, May) 77−56876
Periodic Comet Whipple (1977h), precise positions 1977, Jul. and Aug. 78−24487
Periodic Comet Wild 2, (1978b), precise positions, (1978 February 8 to April 12) 78−53885
Periodic Comet Wild 2 (1978b), discovery and precise posns. (1978 January) 78−28586
Periodic Comet Wild 2 (1978b), positions, appearance and magnitudes (1978 Jan.-Mch.) 78−36530
Periodic Comet Wild 2 (1978b), positions, elements, ephemeris and magnitude estimates 78−36515
Periodic Comet Wild 2 (1978b), positions, elements and ephemeris 78−28589
Periodic Comet Wild 2 (1978b), precise positions 1978 Feb.-Mar., total visual magnitude estimates 78−45287
Periodic Comet Wild 2 (1978b), precise positions (1978 Feb.-Apr.) 78−53880

visible astronomical observations continued
Periodic Comet Wild 2 (1978b), precise positions (1978 January 27) 78−32398
Periodic Comet Wild 2 (1978b), precise positions for 1978 Jan.-Feb. 78−32402
Periodic Comet Wild 2 (1978b), precise positions for 1978 Mar.-May 78−73676
Periodic Comet Wild 2 (1978b), precise posns. (1978 February-April) 78−73681
Periodic Comet Wild 2 (1978b), precise posns. and magnitudes (1978 Jan.-May) 78−61803
Periodic Comet Wild 3 (1980d), discovery posns., orbital elements and ephemeris (1980 April-June) 80−67657
Periodic Comet Wild 3 (1980d), precise positions, (1980 May 9 to 17) 80−72885
Periodic Comet Wolf-Harrington (1977j), precise position 1978 Jan. 3 78−36528
Periodic Comet Wolf-Harrington (1977j), precise positions (1977, July-August) 78−7931
Periodic Comet Wolf-Harrington (1977j), recovery and positions 77−67071
X Persei, 13.9 minute periodicity, 3U 0352+30 optical counterpart 77−22247
AX Persei, 1978 Jan.-Feb. outburst of Z Andromedae-type object 78−36588
X Persei, 580 day and other periodicities 78−16435
ζ Persei, ^{7}Li I 6708 Å line and Li interstellar abundance 78−49494
21 Persei, Ap star, chemical element distrib. from spectrophotometry *(Russian)* 77−22238
X Persei, Be star, coordinated IR and optical obs., (in late 1976) 79−25616
ϕ Persei, binary Be star, He II emission obs. rel. to components masses 80−12768
AW Persei, binary cepheid variable, radial vel. meas. 77−74072
X Persei, BV magnitudes 77−91542
X Persei, distance determ., 3U 0352+30 optical counterpart *(Chinese)* 78−69836
KT Persei, dwarf nova, brightness oscills. during two outbursts 77−2438
UV Persei, dwarf nova, characts. of outbursts 79−71052
X Persei, eclipsing binary, gaseous ring struct., H I alpha obs. 80−109482
RY Persei, eclipsing binary, spectroscopy and physical parameters of atmospheres 80−101618
RT Persei, eclipsing binary, V light curve 77−53636
RY Persei, eclipsing binary, visible spectral obs., model 80−67795
AG Persei, eclipsing binary in II Persei association, photometry and distance 79−21326
21 Persei, magnetic variable, Fe, H_γ and H_δ obs. *(Russian)* 77−49388
12 Persei, masses and luminosities from speckle interferometric obs. 78−93305
AG Persei, massive eclipsing binary star, spectrophotometry 80−26900
IW Persei, metallic-line close binary star, photometric and spectroscopic obs. 80−62186
53 Persei, nonradial mode identification 80−8632
53 Persei, nonradical pulsator, light var. rel. to line profile changes 80−4362
β Persei, partially eclipsing binary, freq. domain light curve anal. 77−53639
X Persei, photometric behaviour, 1964 to 1979, and binary star model 79−53820
1 Persei, photometric variability, possible eclipsing binary 78−32489
21 Persei, spectrophotometry of Ap star, continuum features vars. 80−36638
S Persei, supergiant light curve rel. to maser emission var. 78−49461
AG Persei, two-colour photometry of eclipsing binary system, apsidal motion 78−96504
RW Persei, UBV photometry of semidetached binary system 79−25639
53 Persei, undulations of B-type star 78−89201
X Persei, V-band polarization variability 78−49455
7 Persei, visual binary, radial vel. meas. 79−21347
20 Persei, visual binary, radial vel. obs. 78−73736
Gk Persei, visual magnitude estimates (1978 July) 78−69809
X Persei (2U 0352+30), photoelec. obs., light vars. 78−40999
X Persei (2U 0352+30), spectral line variations *(Russian)* 78−65655
X Persei (3U 0352+30), photometry, search for optical 13.9 minute period 78−16426
X Persei (3U 0352+30), simultaneous X-ray and ground-based optical obs. 80−17591
X Persei (4U 0352+30), light vars., tidal distortion by massive unseen companion 78−36640
β Persei (Algol), detection of B component, mass determ. 78−65654
β Persei (Algol), minimum light obs. rel. to orbital period (1964 to 1978) 79−58377
β Persei (Algol), orbital inclination and masses determ. from speckle interferometry 80−36668
β Persei (Algol) type semi-detached binaries, rotational vels. 78−89220
GK Persei (Nova 1901), visual magnitude estimate for 1978 July 78−69807
GK Persei (Nova 1901), visual magnitude estimates for 1978 Jul. 78−73718
V400 Persei (Nova Persei 1974), photoelectric obs. 78−4252
α Persei cluster, OAO 2 photometry 78−93331
γ Persei cluster, stellar membership determ. by proper motion meas. 80−56890
α Persei cluster, stellar spectral types 79−58385
β Persei field, Asiago Schmidt obs. and new variables *(Italian)* 77−91547
α Persei star cluster, polarisation wavelength depend. 79−48865
β Persei-type eclipsing binaries, red spectra, element abundances and neutrinos 77−57041
Perseid meteor shower, television obs. 80−4309
Perseus, spectrophotometric survey of stars along Milky Way 78−45403
Perseus cluster field, accurate positions of faint optical objects in fields of radiosources 79−12527
Perseus galaxy cluster, obs. rel. to galaxies redshift-magnitude bands and evolution 78−54033
Perseus OB2 association, spectroscopic survey of B- and A-type stars 77−91585
PG 0026+129, spectrophotometry of QSO at optical and IR wavelengths 79−17123

visible astronomical observations continued
PG 1115+08, triple QSO, spectroscopic obs. and gravit. lens model 80−86012
PG 2337+12, high latitude blue variable, possible old nova 77−22241
phase-sensitive detection, representation of observable signals in Chebyshev polynomials 79−89857
PHL 1092, narrow line quasar, discovery of extreme Fe II emission 80−77508
PHL 957, Lyman α emission halo upper limit 77−33678
PHL 957, quasar, H_2 and CO absorpt. lines obs. *(Russian)* 79−101216
PHL 957, quasar, upper limits on Lyman α halo 80−51907
Phobos, 20 positional photographic obs. during 1973 October at Pulkovo *(Russian)* 78−28568
Phobos, composition, evidence for carbonaceous chondrite surface from spectral anal. 78−49365
Phobos, evidence for carbonaceous chondritic composition from multicolour obs. with Viking lander cameras 78−49366
Phobos, first encounter by Viking Orbiter-1, mass and density determ. 78−49364
Phobos, Marsshine and shape/size determ. 79−44396
Phobos, photometry and origin of dark markings on crater floors 79−16861
Phobos, photometry from Viking orbiter images 80−72838
Phobos, spacecraft imaging 78−89102
Phobos, surface density of impact craters 77−37547
Phobos, surface morphology, comp. and props. 78−89103
Phobos, surface photometry 77−33389
Phobos and Deimos, preliminary results from Viking obs. 78−20681
Phobos and Deimos, Viking imaging, primary mission overview 78−20680
Phobos and Deimos, Viking photographs, surface features 79−21218
Phobos transit of Mars viewed by Viking cameras 78−69723
Phoebe, near IR spectra and JHK photometry 80−56761
SX Phoenicis, dwarf cepheid, spectrum 77−49405
AI Phoenicis, orbital elements and dimensions of eclipsing binary *(French)* 79−71074
SX Phoenicis, short period dwarf Cepheid, UBV photometric obs. 78−57561
SX Phoenicis, simultaneous photometric and polarimetric obs. 78−49451
ρ Phoenicis, temp. vars. of δ Scuti type star 78−53960
AE Phoenicis, W Ursae Majoris type system, orbit 78−85970
AE Phoenicis, W Ursae Majoris-type star with elliptical orbit 77−57010
SX Phoenicis light curve, colour effect obs. 78−93248
Phoenix group of galaxies, example of plate processing via two-dimensional digital filtering 79−16835
photoelectric astrolabe type II, accuracy, time and latit. obs. *(Chinese)* 77−22063
photoelectric occultation observing, techniques and apparatus 78−4117
photoelectric UBV photometry of comparison stars in fields of extragalactic sources 77−5562
photographic four-colour sky atlas 78−24472
photographic obs., mass, radius, central density, stellar vels. of open cluster *(German)* 80−31333
photographic zenith tube obs. for time and latit. determ., meas. errors estimation 77−56816
photometry, total magnitudes and colours in BV from Holmberg photographic photometry 77−49471
photosphere, magnetograph meas. and high resolution mapping of coronal mag. field 77−56892
photosphere brightness fluctuations, two-dimensional spectral anal. of disc centre granulation 77−53520
photosphere faculae intensity, centre to limb var. 80−21967
photosphere magnetic field patterns, evolution during Skylab 78−20798
photospheric convective vels. from granule contrast profiles in Fe I 6569.2 A line 77−17507
photospheric facular granules, morphological props. and origin 77−78744
photospheric network, dark component, Ca I 6103 line scan 77−29759
photospheric oscillations, search for long period modes 77−41370
Pictor A, powerful radio galaxy, photographic and spectrophotometric obs. 77−49481
Pisces group of galaxies, redshifts meas. 77−45579
53 Piscium, confirmed β Canis Majoris type variable 79−44492
TX Piscium, disc brightness distrib. and envelope obs. from lunar occultation meas. 80−67725
64 Piscium, double line spectroscopic binary, orbital elements *(French)* 79−35305
SS Piscium, RRc variable uvbyβ photometry 77−33526
SZ Piscium, RS Canum Venaticorum star, photometric obs. rel to starspot model 80−109490
UV Piscium, short period eclipsing binary, light and colour curve obs. 79−88697
RZ Piscium, UBV photometry, light minima *(Russian)* 78−93323
Pismis 6 and 8, open clusters, photometry and spectra rel. to proximity to (Wat 6) 79−88712
PK 108−76°1, 49+88°1, halo planetary nebulae, Ar III line obs. and low Ar abundances meas. 80−82443
PK 181+1.1, very low surface brightness planetary nebula near galactic anticentre, discovery 79−17049
PK 60−7°1, nebula around FG Sagittae, spectrophotometric study 79−40240
PK 6-2°1, southern planetary nebula, N and He overabundance 77−78849
PKS 0211−47 and 0634−20, giant radiogalaxies, optical and radio obs. 78−81702
PKS 0237−23, absorpt. spectrum obs., absorpt. lines origin 78−41074
PKS 0438−43, high radio luminosity quasar, identification 79−17124
PKS 0521−36, BL Lacertae object, radio and optical props. 79−84854
PKS 0528−250, neutral stellar object with no emission and rich absorption 78−49551
PKS 0537−286, high-z QSO with extreme Lyman continuum cutoff 79−12538
PKS 0548-322, surface photometry of X-ray emitting BL Lacertae object 80−22069
PKS 0735+178, B mag. brightening of BL Lacertae object 77−37654
PKS 0735+178, BL Lacertae object, spectrum, multiple components in z=0.424 absorpt. system 79−25707
PKS 0735+178, BL Lacertae-type object, brightening and linear polarisation obs. 77−22318
PKS 0736+01, optical spectrum variability 80−8709
PKS 0837−12, resolved optical structure of low-redshift quasar 78−81704

visible astronomical observations continued
PKS 1157+014, spectral obs., of QSO with no Lα emission 80−31384
PKS 1158+007, redshift from QSO spectrum 79−58440
PKS 1345+12, radio galaxy, optical spectrum 78−4341
PKS 1402+044, dissector scanner obs. of red object with 3.20 redshift 78−65710
PKS 1718−649, galaxy, radio and optical study 77−45564
PKS 1954−388, brightening 78−77615
PKS 2126−158, absorption spectrum, high resolution study 79−53928
PKS 2134+004, highly luminous QSO, historical light curve 78−54072
PKS 2135−14, photographic obs. of quasar, assoc. faint optical features 79−9026
PKS 2155-304, BL Lacertae object, no evidence for redshifted forbidden O III emission 80−73035
PKS 2201+04, compact galaxy, optical variability 77−26051
PKS 2322-12, narrow-line radio galaxy, optical spectrum 77−33664
planetary meridian obs. with photoelectric multislit micrometer, disc centre determ. 77−53443
planetary nebula, faint new object discovered near NGC 6401 globular cluster 77−49461
planetary nebula and diffuse objects, detect. in galactic centre direction *(French)* 79−21434
planetary nebula central stars, He II 4686 Å emission evidence for stellar winds 78−57608
planetary nebula central stars, spectral types and absolute magnitudes 77−87504
planetary nebula evolution, analytical survey of spectrophotometric data 77−26045
planetary nebula in irregular galaxy NGC 6822, spectrophotometry and He, N, O and Ne abundances 80−41867
planetary nebula in Monoceros, new identification 78−86002
planetary nebula obs. in red globular cluster NGC 1852 in LMC 77−17668
planetary nebulae, absolute flux densities for emission lines in 6000-11000 Å range rel. to physical parameters 80−51857
planetary nebulae, bipolar, photographic photometry *(Russian)* 77−13447
planetary nebulae, emission line intensities for small ang. size moderate excitation nebulae 79−21407
planetary nebulae, emission line obs. and He enrichment 79−21380
planetary nebulae, Fabry-Perot interferometry 78−4323
planetary nebulae, forbidden line and optical continuum electron temps. comparison 79−30105
planetary nebulae, interstellar extinction determ. 77−22295
planetary nebulae, low excitation, of small ang. size, spectral studies 80−17646
planetary nebulae, moderately bright, spectroscopic study 79−84835
planetary nebulae, new discoveries on plates taken with UK 1.2 m Schmidt telescope 77−45530
planetary nebulae, nuclei parameters for 8 objects, evolutionary stage *(Russian)* 79−21404
planetary nebulae, O/H ratios meas. rel. to Galaxy O enrichment 80−105328
planetary nebulae, optical positions rel. to radio identification improvements 77−5551
planetary nebulae, photoelec. filter photometry of 25 objects 77−9781
planetary nebulae, photoelectric spectrophotometry of emission lines, abundances 78−81677
planetary nebulae, S abundance from IR and visible line meas. 80−82444
planetary nebulae, southern, red-sensitive objective-prism survey list of suspected objects 78−77496
planetary nebulae, spectrophotometry, emission line intensities physical conditions 78−36651
planetary nebulae central stars, Cassegrain image-tube scanner obs. 77−22214
planetary nebulae central stars, visible and near IR spectra 77−78785
planetary nebulae discoveries with low surface brightness 78−16496
planetary nebulae in M31 (Andromeda galaxy), astrometric catalogue 79−40087
planetary nebulae in M31 (Andromeda galaxy), identifications and photometry 78−28737
planetary nebulae in southern hemisphere, new discoveries 77−64667
planetary nebulae kinematics, radial vel. meas. 80−46633
planetary nebulae near peculiar supernova remnant G326.3−1.8, discoveries 79−25675
planetary obs. from space probe *(German)* 77−53445
planetary position determ., Mars, Jupiter, Saturn, Jovian satellites *(French)* 80−72809
planets, astrometric and radiometric methods, tests of general relativity 78−45552
planets, meridian obs. (1974 to 1977) 78−69660
planets, Munich meridian obs. (1941-61), orbital elements determ. *(German)* 80−77306
planets, solar activity effects on brightness 79−75177
planets, strong scintillation at Earth's night horizon, Salyut 4 obs. 77−9590
planets and asteroids, positional catalogue from photoelectric meridian obs. 77−91453
planets and conjunctions, Mayan obs. in AD 293-1237 period 77−17392
planets and natural satellites position meas. 78−81573
plate reduction study of stellar photographs taken with a TV camera *(French)* 77−17330
Pleiades, Hα and O I photometry 79−35315
Pleiades, spectral classification of brightest stars, Ap, Am and shell stars 78−57601
Pleiades central field, stellar proper motions rel. to cluster internal motions 79−88711
Pleiades stars, wavelength depend. of polarisation 77−45500
Pleione (28 Tauri), envelope behaviour in 1976, spectroscopic obs. 80−8636
Pleione (28 Tauri), metallic-line shell spectrum anal., (1973-1976) 80−8637
Pluto, 1978 P 1, discovery of possible satellite, ephemeris 78−69744
Pluto, 1978 P 1, possible satellite, direct visual obs. 78−93152
Pluto, 1978 P 1, possible satellite, Pluto image elongation obs. 78−81586
Pluto, 1978 P 1, satellite, obs. 78−85900
Pluto, appulse on 1980 Qpril 6, no occultation from S.England 80−67650
Pluto, astrometric posns. (1975 May-1978 May) 79−70993
Pluto, astrometry (1973 to 1979) 80−85894

visible astronomical observations continued
Pluto, diameter meas. by speckle interferometry 80−41763
Pluto, geocentric positions for the 1974-8 period 80−46478
Pluto, image tube spectra, 6800-9000 Å, search for possible atm., methane upper limit 79−16880
PN 108-76°1, halo planetary nebula, spectrophotometry and element abundances 78−41011
PN 173+3.1, planetary nebula near galactic anticentre, coords., radial vel. and orbit 80−105309
PN 49+88°1, halo planetary nebula, spectrophotometry and element abundances 78−41011
308 Polyxo, photoelectric lightcurves and rotation period 80−46455
32 Pomona, photoelectric photometry, composite light curve and synodic period of rot. 77−9691
Population II Cepheids and RR Lyrae stars in globular cluster M19, photographic obs. 78−41002
possible comet, discovery 77−17436
possible comet, discovery 78−20747
Praesepe, photometry in BVRI colours 80−26917
Praesepe stars, Ca II K-line photometry and metal abundance rel. to Hyades 77−57064
pre-main-sequence A and F stars in NGC 2264, nature of IR excesses 78−32461
790 Pretoria, C-type asteroid, light vars. obs. and rot. period 80−21941
196 Prokne, photoelectric photometry and rot. period 79−84727
proper motion stars, catalogue of stars with $m_V<15$, annual motion $>1''$ 79−58275
26 Proserpina, photoelectric photometry and rot. period 79−84727
Przybylski's star (HD 101065), β photometry and period determ. 80−41835
PSR 0531+21, Crab pulsar, light curve, 1973 to 1976 period *(Russian)* 78−12263
PSR 0531+21, Crab pulsar, optical light curve changes in 1970-7 period 80−36654
PSR 0833−45, Veal pulsar, optical pulses detect. 77−49417
PSR 0833−45, Vela pulsar, optical pulse profile 80−46593
PSR 0833−45, Vela pulsar, pulsed and unpulsed light 79−17005
PSR 1913+16, binary pulsar, companion star possible optical obs. 79−84823
PSR 1913+16, binary pulsar, digital area photometry 77−49410
PSR 1913+16, binary pulsar, optical pulses upper limit 77−26020
PSR 1913+16, optical candidate, astrometry and high-speed photometry 80−101609
PSR 1913+16, optical candidate discovery, position, magnitude 78−69819
16 Psyche, opposition effect and surface structure *(Russian)* 80−67635
pulsars in S.Hemisphere, obs. of optical pulsations 78−77569
VV Puppis, AM Herculis type binary, accretion column absorpt. spectrum obs. 79−101176
VV Puppis, AM Herculis type binary spectrophotometric obs. 79−5860
VV Puppis, AM Herculis-type variable, spectrum scans 77−45492
VV Puppis, brightening, emission line spectrum 78−40960
VV Puppis, brightening of magnetic variable (1978 March) 78−36595
ρ Puppis, chromospheric activity and atm. dynamics of δ Scuti star 77−17581
VV Puppis, dwarf nova, spectroscopic obs. during active phase 79−80322
V Puppis, light curve study of early-type close binaries in triple systems 78−89222
ρ Puppis, line profile variable, pulsational mode-typing 80−90432
VV Puppis, linear and circular polarisation during active phase 77−37621
VV Puppis, obs. in faint state 79−25643
ζ Puppis, of supergiant, mass flow var., visible and UV obs. 80−90431
RX Puppis, peculiar emission-line object, spectrum and UBV photometry 79−44497
VV Puppis, photometric activity, flickering 77−67112
VV Puppis, proper motion meas., distance and luminosity 78−96510
ζ Puppis, Reticon obs. of Hα P Cygni profile 80−82365
L_2 Puppis, semiregular variable, Ca I uneven distrib. from narrowband polarimetry 80−98666
VV Puppis, spectroscopic obs., broad absorpt. features discovery 79−44502
ρ Puppis, temp. and radius vars. 77−49395
ζ Puppis, visible and UV spectroscopy of stellar wind var. 79−16949
R Puppis (HD 62058), G-type supergiant, UBV photometry and variability confirmation 80−41824
Puppis A, Fe X and XIV forbidden line emission 79−44580
Puppis A, Fe XIV coronal line and filamentary emission 79−84843
Puppis A, optical spectral obs. of filaments *(Italian)* 79−53883
Puppis A supernova remnant, optical and radio comparison 78−28760
TY Pyxidis, light curve of RS Canum Venaticorum type binary 79−25641
T Pyxidis, recurrent nova, photoelectric obs. 78−4252
PZT stars, mean posns. and proper motions for 304 stars, obs. at Ondrejov 80−82175
Q0002−422 and 0453−423, QSO absorption spectra, high resolution study 79−62925
Q0353−383, QSO abundance anomalies, UV and visible spectral obs. 80−82532
Q0453−423, quasar, absorption line spectrum 78−8144
Q0957+561, double quasar, components brightness ratio var. 80−77509
Q2227.6−3928, highest redshift quasar from Tololo deep survey 78−12403
Q2228.1−4033, high redshift quasar from Tololo deep survey 78−12403
Q 0002−422, QSO with $z_{abs} \ll z_{em}$ 78−16565
Q 0932+501, bright quasar with broad absorption features 80−46697
Q 0957+561, double quasar, intervening galaxy obs. rel. to gravit. lens hypothesis 80−27005
Q 1246−057, absorpt. line spectrum, presence of outflowing material 78−93453
Q 2240.9-3702, Q 2238.9-4115, optically selected QSOs with broad-lined absorpt. systems spectra 80−4456
QSO 0242+622, spectrum and luminosity of low redshift object 78−93451
QSO 0957+561, double quasar, visible spectrophotometry, gravitational lens interpretation 80−82533
QSO 1038+528 A,D, close pair of radio-emitting quasi-stellar objects, radio and optical obs. 80−51902
QSO 1756+237, absorbing regions, physical conditions from visible obs. 79−71146

visible astronomical observations continued
QSO absolute spectral energy distrib. in 0.3−10 μ range 79−62926
QSO absorbing regions, extended Lyman α emission obs. 79−44631
QSO absorption line spectra for six high-redshift objects 78−93449
QSO candidates, spectroscopic obs., indentifications 80−31385
QSO candidates and radio galaxies, optical spectroscopy 80−56966
QSO pairs, spectroscopic obs. 77−5587
QSO redshifts and field galaxies 78−89271
QSOs, catalogue of 403 objects 77−26080
QSOs, compact group in Leo 80−27006
QSOs, high-redshift, Image Dissector Scanner (IDS) spectrometry and redshifts 80−22111
QSOs, Lyman α/Hβ intensity ratio 77−45600
QSOs, optically selected, accurate positions 79−9022
QSOs, permitted Fe II emission, obs. 79−35361
QSOs, redshifts for 19 objects 79−97060
QSOs, redshifts for 24 optically selected objects 78−54073
QSOs, survey of optical variability of compact extragalactic objects 79−101215
QSOs near S.Galactic Pole, photometry and 5000 MHz emission 79−88761
QSOs of small and intermediate emission redshift, absorpt. lines homogeneous survey results 80−31218
quarsars, magnitude estimation from Palomar Sky Survey prints 80−36510
quasar, strong emission line, with redshift z=0.189, spectrum and photometry 80−8710
quasar 0420−01, correlated time-delayed radio-optical outburst 79−25750
quasar near companion galaxy NGC 5296, photometry and redshift 77−13489
quasars, absorpt. line spectra and redshift systems 77−13488
quasars, absorpt. lines statistics and line-locking 78−57681
quasars, CTIO Curtis Schmidt survey −40° zone, discoveries and spectrophotometry 80−73064
quasars, CTIO surveys of large redshift objects 78−57692
quasars, emission-line, survey, new discoveries and faint quasars number limits 79−92884
quasars, faint emission line spectroscopy 78−8146
quasars, from $\delta<-45°$ zone, accurate positions 77−87566
quasars, high-luminosity, space distrib. 78−8147
quasars, high-redshift, emission-line spectra rel. to radio or optical selection 77−53696
quasars, long time scale optical variability 77−22328
quasars, low redshift X-ray selected, visible spectra and UDVR photometry 80−105397
quasars, low-red shift, photoelectric UBV photometry *(French)* 80−51904
quasars, low-redshift, optical struct. 78−32596
quasars, Lyman α absorpt. line distrib., intergalactic origin 80−67899
quasars, Mg II 2798 Å and Hβ emission, line profiles 80−12807
quasars, optical surveys, electronographically recorded low-dispersion slitless spectra 78−57467
quasars, optically selected, with $3.0<z<3.5$, spectrophotometry rel. to absorpt. line problem 79−25746
quasars, otical variability, survey of objects from 17-22^h RA 78−41079
quasars, redshifts of 24 southern objects 77−13491
quasars, search for rapid brightness variability 80−90567
quasars, southern, optical monitoring, data reduction 79−58439
quasars, southern, optical monitoring 80−56969
quasars, spectral characts. of three high redshift objects 80−4455
quasars, spectral props. of 85 objects from spectrophotometry 80−51897
quasars, with $2.5<Z<3.1$, emission line spectra 77−9806
quasars 0957+561 A, B, twin quasistellar objects or gravit. lens theories 79−67114
quasars absorption line features of Fe II and Mg II 78−16559
quasars assoc. with compact radio sources, apparent magnitude-redshift relations for resolved and unresolved sources *(Chinese)* 80−105380
quasars in CTIO 4 m survey, visible and UV spectrophotometry 80−86009
quasars in field fo 3C 345, optical variability meas. 77−78886
quasars in region of NGC 1629 companion galaxy, spectra and redshifts 80−56965
quasars in spiral arms of galaxy NGC 1073 79−53904
quasars M87 and 3C 273, imaging polarimetry 78−41076
quasars near peculiar pair of galaxies NGC 7714−7715, spectra and redshifts 78−28835
quasars of Michigan-Tololo survey, spectrophotometry 80−22105
quasars with absorption redshifts greater than emission redshifts, spectroscopic study 77−45595
quasars with high redshift, discovery and spectroscopic obs. 77−45594
quasi-stellar objects, low-redshift, spectra, absorpt. lines obs. 79−21459
quasi-stellar objects, luminosity indicators in emission-line spectra 77−57103
quasi-stellar objects, variable, photometry and completeness of faint blue objects in Sandage-Luyten field 78−54069
quasi-stellar objects, variable, photometry and completeness of faint blue objects 78−93446
quasi-stellar objects with low-redshift absorpt. systems, search for nearby faint objects 79−17121
quasi-stellar radio sources from 4C and Parkes catalogues, spectra and photometry 78−65714
quasisteller objects in 13^h+36° field, optical variability from blue magnitudes obs. 79−40291
quiescent prominences, Ca^+, H and He line emission 77−29750
quiet Sun, activity, microspicules obs. in Hα and He I D_3 line 79−66983
quiet Sun, limb darkening coeffs., integrated spectrum 78−24498
R548, pulsating white dwarf, photometric obs., light curve anal. 78−32488
R548, pulsating white dwarf, photometric props. 77−9742
R 136, central star in 30 Doradus, nebula, variability *(German)* 77−45448
radio and cD galaxies, optical props. 78−93413
radio galaxies, broad-line Mg II 2798 Å and Hβ emission, line profiles 80−12807
radio galaxies, elliptical, minor axes orientations rel. to radio sources orientations 80−82527
radio galaxies, narrow-lined, spectrophotometry 78−93391
radio galaxies, new complete sample, struct., redshifts 79−17096
radio galaxies, optical emission in radio lobes 78−57630
radio galaxies, optical emission-line spectra 78−57643

visible astronomical observations continued
radio galaxies, optical spectra, morphological classification rel. to spectroscopic classification 78−41038
radio galaxies in Coma cluster, optical obs. 78−12358
radio galaxies with radio jets, optical spectra of nuclei 79−84859
radio sources, optical identifications using accurate radio and optical positions 77−37660
radio sources, optical positions 77−78881
radio sources, position coincidence optical identifications using Texas Interferometer radio positions 79−88753
radio sources, precise optical positions in FK 4 system, pilot programme results 78−65709
radio sources from B2 catalogue, optical identifications and 5 GHz flux meas. 79−40283
radio sources from Molonglo Deep Survey, optical spectra 78−69900
radio sources in globular clusters, optical identifications 79−62923
radio sources in south polar cap, optical identifications 79−75284
radio sources of Parkes 2700 MHz survey, identifications from Palomar Sky Survey prints 79−75121
radio sources of Parkes 2700 MHz survey, new optical identifications 79−75289
radio sources south of declination −75°, optical identification 77−64863
radio tail galaxies in clusters, redshift determs. 78−69889
radiogalaxies, colour and space density, redshift dependence 79−75278
radiogalaxies, faint southern objects, identification and spectrophotometry 80−56935
radiogalaxies, redshifts for three objects 79−97060
radiogalaxies, spectrophotometry of three objects 78−54066
radiogalaxies from B2 Catalogue, optical identification, radio positions and redshifts 80−86005
radiosources, catalogue of 347 sources obs. at 610 MHz, source parameters, identifications 78−40838
radiosources, coordinated photometric and spectroscopic observations of strong extragalactic 90 GHz sources 78−93440
radiosources, flat spectrum, optical identification of complete sample 79−5911
radiosources, galaxies and quasars, optical counterparts, astrometry 80−90551
radiosources, in fields of five unidentified high latit. X-ray sources, list of 249 objects 77−87281
radiosources, optical identifications, spectrophotometric obs. 79−92879
radiosources, spectroscopic identification of three southern PKS sources 79−25744
radiosources from 13th part of Parkes 2700 MHz survey, optical identifications 78−20901
radiosources in 3rd Westerbork survey, optical identification 79−58436
radiosources in 5C3 field, optical identifications *(German)* 79−30140
radiosources in 5C 6 survey, optical identifications 79−48949
radiosources with flat or inverted spectra, optical and radio props. 78−81697
RCW 107 (NGC 6164/5), ionisation struct. of southern H II region 77−45526
red and nebulous objects in dark clouds, survey, catalogue of 150 objects 80−56904
red compact galaxies, surface photometry 77−53679
red degenerates, eleventh list 79−25596
red dwarf stars, VI photometry rel. to space density 77−5524
red dwarf stars near north galactic pole, vel. dispersion 78−7989
red giant stars in globular clusters M92 and NGC 6397, C abundances 79−48785
red giants, in Draco dwarf galaxy, metal abundance determ. 79−17078
red giants, spectra, TiO bands obs. and theory 78−96480
red giants and supergiants, mass loss, spectroscopic obs. 77−9743
red giants in Galactic nuclear bulge, spectroscopy 77−26058
red giants in globular cluster NGC 6752, DDO photometry and spectra 79−71079
red giants in globular clusters, mass loss 78−93238
red giants in M13, Na abundance var., protocluster gas inhomogeneities 80−82439
red giants in M5 (NGC 5094), intermediate band electronography 78−49490
Red Rectangle, refl. nebula assoc. with HD 44179, spectrum interpretation 77−49462
red stars at north galactic pole, proper motions 78−4214
red stars survey in 30 Doradus region of LMC, list of 298 stars 79−48794
red supergiants in Magellanic Cloud clusters, spectral types 79−40190
red variable star, possible optical candidate of 2S 1702−363, spectroscopic obs. 78−77566
red variable stars in globular cluster M22, light curves 77−64808
red variable stars in M13, photometric investigation 77−74104
red variable stars in SMC OB association NGC 371, periods 78−53961
Reticon spectrophotometer at Cima Ekar Observatory, first obs. 79−58254
Reticulum globular cluster, structure, star counts 78−12309
Rhea, normal reflectance from lunar occultation obs. 78−85897
Rhea, planetary, 1976 to 1979, rel. to possible solar variability detect. 80−98623
rich clusters of galaxies, study of 1889 clusters from Abell's catalogue 77−87556
rich galaxy cluster 0004.8−3450, bri photometry 80−46685
Rosette Nebula, internal vels. from Hα emission line profile study 79−53869
Ross 614, parallax, orbit and mass of astrometric binary 77−91565
Ross 640, H-poor white-dwarf, H abundance determ. 77−87388
Ross 657, metal deficiency obs. 77−5532
Rst 4036, red-dwarf binary star, orbital period and total mass 80−12780
Rubin-152, possible massive O-type star on galactic fringe, spectroscopic obs. 80−98656
2S0921−630, discovery and optical stellar identification 79−21466
S0 galaxies, luminosity distrib. perpendicular to plane of discs rel. to struct. and origin 80−36705
S0 galaxies, surface photometry, luminosity struct. 80−62258
S147, kinematics of old SNR 79−44585
S88B, Hα knot, optical radio and IR obs. of vicinity 77−74115
2S 1702−363 optical counterpart, BV photometry and spectrum 78−54082
2S 1702−363 optical counterpart, UBV photometry 80−82349
2S 1822-371, optical photometry of assoc. star 79−92894
S stars, photometric obs. of unidentified spectral bands 77−22226
S-type stars, CeO band identification, new s-process mol. 77−33488

visible astronomical observations continued
S-type stars, molecular spectral atlas 78−77554
S-type stars, revised spectral classification system in red 80−46541
S-type stars in Southern Milky Way, objective prism survey and BVI photometry 78−61754
SA 133 field near galactic centre, three-colour stellar photometry *(German)* 80−36618
HM Sagitaae, emission-line star, UBV photometry and spectral obs. in (1978) *(Russian)* 80−36648
FG Sagittae, 1975-8 spectral obs. of peculiar variable 80−72959
WZ Sagittae, 1978-9 outburst of dwarf nova, spectra 80−94801
U Sagittae, Algol type binary, spectrophotometry 77−2454
WZ Sagittae, B mags. and total visual magnitude estimates 79−21308
WZ Sagittae, BV photometry and magnitudes (1978 Nov.-Dec. outburst) 79−12484
HM Sagittae, continuum spectrum, model, dense nebular around hot star *(Russian)* 78−69814
UU Sagittae, eclipsing binary, central star of Abell 63 planetary nebula 78−93304
U Sagittae, eclipsing binary, elements determ. from light changes anal. in freq. domain 77−53637
HM Sagittae, emission variable, optical spectrograms and IR magnitudes 77−67098
HM Sagittae, emission variable as embryonic planetary nebulae 77−56950
HM Sagittae, emission-line star, polarimetry, (1977 to 1978) *(Russian)* 80−36649
HM Sagittae, emission-line star, spectrum vars. (1978 to 1979) 79−58347
FG Sagittae, Fe-peak and s-process elements abundance *(Russian)* 78−12253
WZ Sagittae, image-tube spectroscopic obs. of 1978 Dec. outburst 80−72958
V Sagittae, light curve coherent oscills. 78−8022
FG Sagittae, light vars. rel. to photometric radius and pulsation mass 78−36576
HM Sagittae, near emission-line object, optical and IR obs. 78−36575
FG Sagittae, nonstable star, spectrophotometric obs. 78−28683
WZ Sagittae, period change and magnitudes (1978 Dec.-1979 Jan.) 79−21309
HM Sagittae, photometric and spectroscopic obs. rel. to proto-planetary nebula mass ejection 78−85947
U Sagittae, photometric study of eclipsing binary 77−22270
FG Sagittae, planetary nebula central star, radial vel. meas. rel. to binary star model 80−98664
HM Sagittae, planetary nebula excited by Wolf-Rayet star, spectrum 78−54003
HM Sagittae, possible proto-planetary, nebula, emission line widths 78−45389
WZ Sagittae, recurrent nova, photometric study at minimum light 78−24513
WZ Sagittae, recurrent nova, spectroscopic obs. and model for superhump phenomena 80−82368
WZ Sagittae, recurrent nova, spectroscopic obs. during 1978 outburst 80−26862
WZ Sagittae, recurrent nova, spectroscopic study during 1978 outburst 80−56849
U Sagittae, secondary mass from vel. curve 79−97025
FG Sagittae, spectral type and element abundances *(Russian)* 78−93281
WZ Sagittae, spectroscopic obs. (1978 December 1 and 2) 79−16983
WZ Sagittae, spectroscopic obs. and photoelectric V-magnitudes 79−16984
FG Sagittae, spectrum of assoc. nebula 78−49498
HM Sagittae, symbiotic star, IR variability obs. from VJHKL photometry *(Russian)* 80−105263
WZ Sagittae, time of minimum light, period, magnitudes 79−21353
WZ Sagittae, time-resolved broadband obs., optical pulsations, period 79−92781
HM Sagittae, UBV changes and planetary nebula emission lines 77−71120
HM Sagittae, UBV photometry and spectral obs. (1977) *(Russian)* 79−16991
FG Sagittae, UBV photometry and spectroscopic obs. 77−71119
WZ Sagittae, UBV photometry and spectroscopy of 1978 Dec. outburst 79−12483
WZ Sagittae, visual magnitude 1979 April 8 79−44508
WZ Sagittae, visual magnitude estimate 1979 June 20 for recurrent nova 79−84800
WZ Sagittae, visual magnitude estimates, 1978 Nov., 1979 Jan.-Feb. 79−30075
WZ Sagittae, visual magnitude estimates, (1978, November 28 to December 11) 79−12481
HM Sagittae, visual magnitude estimates 77−87416
V1500 Sagittae, visual magnitude estimates 1977, Feb. and Mar. 77−37607
Sagittae 1977, visual magnitude estimates 1977, FEb. and Mar. 77−37607
HS Sagittae (Nova 1977), visual magnitude estimates, (1978, August 5 to September 3) 78−89209
HS Sagittae (Nova 1977), visual magnitude estimates 78−61872
HS Sagittae (Nova 1977), visual magnitude estimates 1978 June 78−85961
XZ Sagittarii, Algol system, UBV photometric investigation 80−22041
μ Sagittarii, binary star, obs. of eclipse of unseen companion 80−4401
AQ Sagittarii, C star, ang. dia. from lunar occultation meas. 80−22008
V1357 Sagittarii, case for eclisping binary, visible obs. 80−77452
AV Sagittarii, Cepheid, assoc. with open cluster NGC 6546 disproved 79−58387
RY Sagittarii, decline and magnitudes (1977 September-August) 77−87414
V3955 Sagittarii, field RV Tauri/SRd variable 79−88665
V1647 Sagittarii, light curves, photometric elements and apsidal motion 77−60795
ξSagittarii, lunar grazing occultation, 1974, October 21 obs. 77−33368
ξ^2 Sagittarii, lunar occultation obs. giving angular diam. 77−33493
W Sagittarii, magnetic field from Zeeman meas. 78−4240
RY Sagittarii, magnitude estimates for R Coronae Borealis-type star 77−78800
V356 Sagittarii, massive eclipsing binary star, spectrophotometry 80−26900
RY Sagittarii, pulsating R Coronae Borealis star, visible and IR photometry 77−45462
MV Sagittarii, R Coronae Borealis variable, brightness decline obs. and UBV photometry 80−8641
V1017 Sagittarii, recurrent nova, decline obs. 77−82233
RY Sagittarii, spectra near min. light 80−36642
RY Sagittarii, visual magnitude estimates, 1977, Sept. 77−91541
RY Sagittarii, visual magnitude estimates (1977 Oct.) 77−91543
RY Sagittarii, visual obs. of 1977 Sept.-Oct. minimum 78−49463
V4021 Sagittarii (Nova 1977), visual magnitude estimates for 1978 May and July 78−69806
Sagittarius dwarf irregular galaxy, discovery on ESO Schmidt plates 78−20887
Santiago astrolabe, time, latit. and radius obs. (1968 to 1971) 78−12077
Santiago astrolabe observations from 1972 to 1976, results 80−46363
SAO 015338, optical counterpart of 2A 1052+606, RS Canum Venaticorum type binary 79−21352
SAO 015338 (2A 1052+606), Hα emission and analysis of possible identification 78−32608
SAO 114159, duplicity detect. from occultation by 18 Melpomene 79−16870
SAO 158687, occultation by Uranus, 1977 March 10, obs. at Tokyo Astron. Obs. 78−61716
SAO 158687, occultation by Uranus, 1977 March 10 77−87322
SAO 158687, occultation by Uranus and satellite belt 77−29718
SAO 158687, occultation by Uranus rings, 1977 March 10 photoelec. obs. and anal. *(Chinese)* 78−69657
SAO 158687, occultation by Uranus satellite rings 77−37568
SAO 85009, occultation by Pallas, 1978 May 29, corrected prediction, photoelec. obs. 78−57430
Saturn, 1978 opposition astrometric obs. of satellites 79−75149
Saturn, 1979 S 3, discovery of possible satellite 80−26802
Saturn, astrolabe obe. at Paris (1971-6) *(French)* 78−85896
Saturn, astrolabe obs., 1977 Jan.-April *(French)* 78−32390
Saturn, astrometric results from 1974 lunar occultations of satellites 78−36506
Saturn, atm. H_2 content from spectral line equivalent width *(Russian)* 78−12143
Saturn, atmosphere constituents, comparison with Jupiter, visible spectra obs. *(French)* 80−101550
Saturn, D-ring (1973 September) 79−96966
Saturn, E-ring density and satellite posns. (1966 Dec. and 1980 Mar.) 80−94750
Saturn, E-ring radial structure, 1980 March CCD obs. 80−105201
Saturn, echelle spectrogram 78−96426
Saturn, F-ring and new satellite, Pioneer II discoveries 80−8585
Saturn, H_2 quadrupole lines in spectrum 79−70990
Saturn, HD detect. at 6063.88 Å, D/H abundance ratio calc. 78−57495
Saturn, HD search at 6045 Å, D/H ratio upper limits 78−85892
Saturn, long term variation of H_2 and methane absorpt. 77−71058
Saturn, near IR spectral albedo 80−31242
Saturn, NH_3 abundance from visible obs. 80−82269
Saturn, obs. of possible new satellite 78−7921
Saturn, obs. with Algiers Observatory Danjon astrolabe (1969 to 1974) *(French)* 78−61794
Saturn, obs. with CERGA Observatory Danjon astrolabe, (1974 to 1976) *(French)* 78−61793
Saturn, obs. with Paris astrolabe (1975-1976) *(French)* 78−89115
Saturn, outer ring and five possible new satellites discovery 80−46472
Saturn, outer ring search, 1979 November obs. 80−17543
Saturn, ring A, Encke division, photometric confirmation from Iapetuo eclipses 78−45273
Saturn, rings, four colour phase curves, analysis 80−4295
Saturn, rings, International Planetary Patrol obs. and data reduction 80−4294
Saturn, rings optical thickness, nearby faint satellites obs., possible new satellite 79−16876
Saturn, satellite analyses and electronographic obs. (1980 March) 80−77346
Saturn, satellites, 1980 March Pic du Midi obs. 80−67646
Saturn, satellites, astrometric obs. from McCormick Observatory (1977) 80−105200
saturn, satellites 1966 S 2 and 1980 S 15-18, separations 80−67645
Saturn, satellites 1980 S 24 and 1966 S 2, 1980 April obs. 80−82280
Saturn, satellites and rings, imaging, photometry and polarimetry obs. from Pioneer 11 probe 80−82289
Saturn, satellites I-IX, astrometry obs. from McDonald Observatory (1975-1976) 80−105199
Saturn, UBV photoelectric pinhole scans of disk 79−40135
Saturn, visual mapping and photometering, 1973-4 period 77−87321
Saturn's rings, anisotropic optical scatt. 77−41352
Saturn's rings, azimuthal brightness vars., obs. at intermediate tilt angle 78−4145
Saturn's rings, structure from refl. sunlight polarization obs., disc of rock bodies 79−53767
Saturn's satellites, precise positions during 1973 77−17421
Saturn A and B rings, surface brightness obs. *(Russian)* 80−72872
Saturn and its satellites, positional photographic obs. at Pulkovo, (1971 to 1974) *(Russian)* 79−96965
Saturn B-ring, optical reflectance polarimetry (1958-76 obs.) 79−44408
Saturn D-ring methane 890 nm band obs. 79−44407
Saturn E-ring, obs. during (March 1980) 80−67647
Saturn globe and rings, optical reflectance polarimetry and interpretations for B-ring 80−31248
Saturn innermost satellites, separations and times of elongation, (1980 February 29 to March 18) 80−56762
Saturn NH_3 atmospheric abundance 78−12142
Saturn ring A profile from stellar occultations 79−35187
Saturn ring system, low tilt angle photometry and thickness 79−35186
Saturn ring system, optical polarimetry during 1979 opposition 80−36570
Saturn rings, five-colour photometry 78−36504
Saturn rings, new ring detection by focal coronograph *(French)* 80−72772
Saturn rings, photometric determ. of thickness 79−66959
Saturn rings azimuthal brightness vars., obs. at tilt angle (B∼11.°5) 79−48732
SB 21, extremely He rich subdwarf O-star, spectrum 80−98659
Sc galaxies, nuclear regions stellar content 77−9793
Sc galaxies, rot. props. from major axis visible spectra obs. 80−90517

visible astronomical observations continued
SchuWe-3, spectroscopic obs. of southern planetary nebula 80−101626
U Scorpii, 1979 March outburst, visual magnitude estimates 79−44504
3 Scorpii, He weak star, mag. field discovery 79−88676
V866 Scorpii, linear polarization obs., wavelength depend., circumstellar dust envelopes 79−53809
β Scorpii, lunar occultation obs., magnitudes for five components 77−87471
β Scorpii, lunar occultation obs., magnitudes for three components 77−87472
α Scorpii, M supergiant, circumstellar shell and mass loss rate 77−45415
V879 Scorpii, M-type long period variable, visible obs. *(Chinese)* 80−85956
U Scorpii, magnitudes and UBVRI photoelectric obs. of 1979 June outburst 79−71049
β Scorpii, multiple star, lunar occultation astrometry 78−57583
β Scorpii, occultation by Jupiter, turbulent atmosphere obs. 77−37562
τ Scorpii, photospheric vel. fields 78−28672
U Scorpii, probable identification of recurrent nova at minimum 78−45343
U Scorpii, recurrent nova, 1979 March outburst unconfirmed 79−44506
U Scorpii, recurrent nova, spectroscopic and visual magnitude obs. during outburst 79−75225
V703 Scorpii, RRs variable, photoelectric radial vels. 77−5533
V861 Scorpii =OAO 1653−40, photometry, spectrum and physical parameters 79−17021
α Scorpii (Antares) nebula, spectrum 78−41014
V861 Scorpii (HD 152667), X-ray binary, behaviour of Hα 79−101171
V861 Scorpii (HD 152677), Hα emission features vars. 78−77579
β Scorpii A, spectroscopic orbit 79−67059
α Scorpii AB, mass loss and circumstellar absorption lines 79−8916
Scorpius region, UBV surface brightness photometry of Milky Way from Helios 1 78−57634
Scorpius X-1, light and colour curve of periodic variation 77−49497
Scorpius X-1, optical magnitude variation *(Russian)* 77−26093
Scorpius X-1, rapid variability simultaneous X-ray and optical obs. 80−62322
Scorpius X-1, worldwide study plan (1980 April) 79−97104
Sculptor dwarf galaxy, photoelectric sequence and preliminary colour-magnitude diagram 77−53429
RT Sculptoris, close eclipsing binary, uvby light curves 77−60798
VY Sculptoris, novalike variable, precise position 80−101597
VY Sculptoris, novalike variable, spectrum during faint state 80−98675
AI, WZ and XX Sculptoris, southern δ Scuti stars, photoelectric study 80−90452
RY Scuti, β Lyrae system, optical and radio spectra 79−30090
RY Scuti, eclipsing binary, ephemeris and UBV obs. 80−94832
δ Scuti, line profile variable, pulsational mode-typing 80−90432
δ Scuti, temp. and radius vars. 77−49395
V373 Scuti (Nova 1975), VBLUW photometry, absolute magnitude, distance and reddening 79−58342
δ Scuti variables, photometric search of Hyades cluster 80−36677
δ Scuti variables, photometric survey of α Persei cluster 78−93246
δ Scuti variables, southern survey 78−96489
δ Scuti variables, spectrographic obs. of σ Andromedae, θ Pegasi and 2 Lyncis 78−61867
δ Scuti-type stars, chromospheric activity and atom. dynamics 77−17581
seeing, meas. at Kitt Peak 80−61899
seeing, wavelength depend., atm. inhomogeneity effects 78−92979
semi-Ba and Ba stars, heavy element abundance effect on spectroscopic luminosities 77−53586
Serpens X-1 (4U 1837+04), burster optical binary counterpart visible spectra and photometry 80−94891
41 Sextantis A, new metallic line spectroscopic binary 78−53982
Seyfert 1 galaxies, O I 8446 Å emission excitation mechanism, visible and IR obs. 80−85991
Seyfert 1 galaxies, permitted Fe II emission, obs. 79−35361
Seyfert 1 galaxies, spectrophotometry 78−4346
Seyfert 1 galaxy 1224+04, discovery from spectrophotometry obs. 80−77488
Seyfert 2 galaxies, spectrophotometry 78−93391
Seyfert 2 X-ray galaxies, nucleus spectra and photometry obs. 80−98712
Seyfert and emission-line galaxies, UBV obs., light vars. 79−30134
Seyfert galaxies, accurate optical positions 78−89254
Seyfert galaxies, depend. of emission line intensity on colour index *(Russian)* 78−28769
Seyfert galaxies, exploratory obs. of gas near nuclei 79−48906
Seyfert galaxies, Mg II 2798 Å and Hβ emission, line profiles 80−12807
Seyfert galaxies, nearby, photographic study of morphology 80−82478
Seyfert galaxies, optical emission-line spectra 78−57643
Seyfert galaxies, survey of 80 objects based on large-scale image-tube plates 77−45323
Seyfert galaxies, type 1, nuclei props., UV emission, colour index *(French)* 79−48923
Seyfert galaxies and quasars, Fe II emission obs., spectrophotometry 78−4347
Seyfert galaxies from lists of Markarian galaxies, spectroscopic obs. *(Russian)* 79−80360
Seyfert galaxies from Zwicky lists, spectrophotometry 79−75274
Seyfert galaxies nuclei, optical variability from U, B, V and Hα photometry 78−96543
Seyfert galaxies with large z, electronographic survey 77−91624
Seyfert galaxy nuclei, spectroscopic obs. 77−9792
Seyfert nuclei, absolute spectrophotometry 79−12508
Seyferts in 12th list of galaxies with UV continuum *(Russian)* 80−17659
Sh2-156 (IC 1470), morphology, excitation and structure of bright galactic nebula 80−67826
Sh 2-158 (NGC 7538), bright high excitation galactic nebula, morphology, excitation and kinematics 79−40241
Shahbazian 1 group of galaxies, dynamics from spectroscopic, obs. 80−67878
Shakhbazian I, cluster of galaxies, photoelectric V magnitudes 77−17700
Shakhbazian I, cluster of galaxies, photographic photometry 77−33662
Shapley-Ames southern galaxies, Las Campanas survey and classifications 78−45409
Sharpless 176, large nearby planetary nebula, radius and distance determ. 77−87503
Sharpless 235A, optical, radio and IR obs. of H II region 80−4415

visible astronomical observations continued
Sharpless 254, 255 and 257, triple emission nebula in Orion, obs. 77−13430
Sharpless 88A-B and 106, compact H II regions, optical obs. 79−8969
shell nebulae in Magellanic Clouds, survey in S II, N II and O III forbidden lines and Hα 79−67085
short-period Cepheid blue variable in M22, photometry 78−85945
Simeiz 147, filamentary nebula, supernova remnant, optical obs. 77−13445
SIMS, C and SC stars, new discoveries on southern, red-sensitive objective-prism plates 80−36511
140 Siwa, C-type asteroid, light vars. obs. 80−21941
Sk 160, optical counterpart of SMC X-1, VBLUW photometry 77−82277
sky brightness, zenith photoelectric measurements during annular solar eclipse (1976, April 29) 78−3900
SMC, abundances in 10 H II regions 78−4320
SMC, atlas of variable stars, clusters, emission regions and supergiant stars, book 79−44619
SMC, faint planetary nebulae identification 79−17081
SMC, photoelec. UBV and RI sequences 77−82307
SMC, photometric study of wing and eastern halo 78−86011
SMC, stellar content of NE outer arm and halo 78−86013
SMC, stellar populations, distrib. and evolution 80−94868
SMC, structure from supergiant distrib. 77−45549
SMC, UBV photoelectric photometry *(German)* 78−77594
SMC, UBV photometry of open, intermediate and globular clusters 79−17033
SMC Cepheids, five-colour obs. and comparison with galactic Cepheids 77−29923
SMC probable members and foreground stars, spectral types and UBV, photometry 79−40091
SMC star clusters catalogues, identifications and coordinates 78−89086
SMC stars, Herschel catalogue rel. to CPD 79−44337
SMC wing, photoelectric UBV sequence 78−69874
SMC X-1, VBLUW photometry, evidence for accretion disc 78−12409
SMC X-1, X-ray binary, 5 colour photometry 77−17622
SMC X-1 (SK 160), spectroscopic orbit and masses 78−4285
SMC X-2, 14th magnitude OB star 0.5′ from source position 78−4411
SMC X-2, colours, spectral type and position of optical candidate 78−12421
SMC X-2, obs. of optical candidate 78−8162
SMC X-2, optical identification with main sequence Be-star 79−40301
SMC X-2, SMC X-3 optical counterparts, spectra 78−93469
SMC X-3, colours, spectral type and position of optical candidate 78−12421
SMC X-3, obs. of optical candidate 78−8162
SN 1006 optical remnant, peculiar spectrum obs. 79−21371
SN 1181 (3C 58), discovery of optical counterpart 78−32546
SN 1181 optical remnant assoc. with 3C 58 discovered 78−65678
SN 1604 (Kepler's supernova), optical remnant expansion time scale, brightness, reddening 78−28747
SN 1970g, in M101, spectra of type II supernova 78−8030
SN 1970j, 1971l and 1971u, spectra and type identifications 77−22255
SN 1972e in NGC 5253, spectrum 80−41844
SN 1972e in NGC 5253, Type I, spectrum after 365 and 435 days 78−4255
SN 1973f in NGC 4944, photometric obs. 79−21318
SN 1973r in NGC 3627, photometric and spectroscopic obs. 77−49407
SN 1974g, type I, in NGC 4414, post-maximum spectral obs. 77−78806
SN 1979C in M100 (NGC 4321), precise position 80−85962
SN 1979c in M100 (NGC 4321), spectrophotometry 80−62166
SN 393, no optical nebulosity near nonthermal radiosource posns. 79−58366
SN in anonymous galaxy in Canes Venatici, discovery obs. 80−67759
SN in anonymous galaxy in Centaurus, discovery, posn. and magnitude 80−85961
SN in MCG −3-34-61, Type I spectrum revealed (1980 June) 80−82401
SN in NGC 1199, mag. 17 object, 1979 Sept. obs. 80−41846
SN in NGC 3733, discovery of mag. 15 supernova (1980 March 17) 80−51793
SN in NGC 3913, B magnitude and spectrophotometry 79−44513
SN in NGC 5854, discovery of mag. 15 Type I supernova (1980 March 20) 80−51793
SNRs, coronal line emission obs. and shock-heated plasma temp. determ. 78−65676
SNRs in Magellanic Clouds, direct photography 77−91612
SNRs in Magellanic Clouds, spectroscopic study 77−91613
solar active region, 1978 April to May, morphological features *(Chinese)* 80−8613
solar active region, mag. and vel. fields study 77−17486
solar active region McMath 14943, optical obs., 1977 Sept. 79−48766
solar active regions, vel. field assoc. with sunspot form. 77−2396
solar activity in 1973, short-term periodicity, BAA Solar Section obs. 77−78741
solar annular eclipse of 1976, April 29, Moon's shadow in Sahara, NOAA-4 picture 77−33464
solar atmosphere, evidence for trapped gravity waves 80−72898
solar atmospheric oscillations, power, phase and coherence spectra 79−8897
solar aureole photographs, 309 to 640 nm, validity of aerosol single scatt. 77−5448
solar Ba II 4554 A line, extreme limb obs. 77−53506
solar background corona, Skylab study near solar minimum 78−28616
solar Ca II K-line, search for global oscillations 78−7959
solar Ca II K-line network in coronal holes 77−78752
solar Ca II line width, Wilson-Bappu effect 79−12464
solar chromosphere, Balmer lines intensity fluctuations 79−53793
solar chromosphere, Hα obs. close to limb 78−28628
solar chromosphere, Hα spicules, spectra, props. 79−25563
solar chromosphere, He I D_3 line obs. of spicules, photoionisation model 78−65592
solar chromosphere, high resolution spectroscopy, space-time vars. 77−53498
solar chromosphere, waves in lower regions, energy transport 79−62804
solar chromosphere limb flare, 1959 July 25, spectrum rel. to physical conditions 80−105227
solar chromosphere network pattern, identification with 1.35 cm radio-granulation *(Russian)* 78−40897

visible astronomical observations continued
solar chromospheric network, evolution during active regions development *(Russian)* 78−57531
solar chromospheric plages, Ca II obs. rel. to physical props. models 78−89153
solar chromospheric waves, oscill. mode and vel. amplitude 79−21263
solar corona, 1973 June 30, polarised brightness distrib. rel. to N.polar hole density model 80−98627
solar corona, Alfven waves above sunspots from forbidden line obs. 77−78732
solar corona, colours during eclipse and dust composition 80−51730
solar corona, compact and diffuse clouds rel. to 1971 Dec. 14 type II-IV radio bursts 77−22193
solar corona, Fe XIV 5303 Å emission line obs. of polarisation 77−49352
solar corona, green line polarisation obs. at 1973 June 30 total eclipse 79−66969
solar corona, Hα obs. of fine chromospheric structs. *(French)* 78−28607
solar corona, mag. loops and downflows obs., rel. to convection 78−93175
solar corona, photoelectric obs. of Fe XIV depletion (1976, April 20) 78−28617
solar corona, physical props. of polar coronal hole from 2 to 5 $R_\odot$ 77−45372
solar corona, structure during 1976, October 23 eclipse, predictions v. obs. 77−25990
solar corona, white light polarisation during 1973 June 30 eclipse 78−20786
solar corona mass ejection events, outward vel., Skylab obs. 77−22197
solar corona polarisation obs. at 1970 March 7 eclipse 77−33462
solar corona polarisation obs. during 1973 June 30 total eclipse 77−13313
solar corona white light polarisation obs. at 1973 June 30 total eclipse *(French)* 77−74027
solar coronal 5303 Å emission line, photoelectric meas. by automatic coronal photometer 79−12454
solar coronal and chromospheric spikes obs. during 1973 June 30 eclipse, photometric anal. 77−17520
solar coronal emission line at 5303 Å rel. to activity in 20th cycle 79−66985
solar coronal holes, obs. in Fe XIV 5303 Å line, assoc. with recurrent geomag. disturbances 79−16762
solar coronal line profiles above active regions, statistical anal. 78−7968
solar coronal loop transients, magnetic driving 78−61842
solar coronal polar rays obs. during 1973 June 30 eclipse 77−17470
solar coronal red line, more precise wavelength *(Russian)* 78−40899
solar coronal streamer motions and mass changes 78−65594
solar coronal streamers, electron densities from K-coronameter polarisation meas. 78−4182
solar coronal structure overlying type III burst producing active region, Skylab obs. 80−21976
solar coronal transient, 1973 August 21, radio and white light obs. 79−71010
solar coronal transient and eruptive prominence, importance of Hα emission 77−2389
solar coronal transient event, 1973 Sept. 14-15, material motions and mag. field 77−17529
solar coronal transients, freq. rel. to solar activity indices 77−22181
solar D abundance from SSO spectrograms 79−66982
solar differential rotation and giant cell circulation of Ca^+ network 77−17508
solar differential rotation meas., 1978, from recurrent and non-recurrent sunspots 79−84780
solar direct radiation var. during 1976 April 29 annular eclipse 79−84781
solar disc centre visible continuum emission, absolute meas. *(French)* 78−96453
solar eclipse, 1973 June 30, spectroscopic obs. by Dutch expedition 80−8614
solar eclipse, 1973 June 30, spectroscopic obs. by Dutch expedition 80−8615
solar eclipse, 1976, October 23, totality obs. from Zanzibar and Australia 77−33463
solar eclipse, 1977 October 12, photographic obs., cloudy weather 78−45315
solar eclipse, 1977 October 12, photographic obs. from North America 78−45314
solar eclipse, 1977 October 12, ship-borne, expeditions in NW.Pacific 78−32434
solar eclipse 1919 May 29, gravitational deflection of light, obs. reexamined 80−67553
solar eclipse of 1979, February 26, an illustrated record from N.American obs. 80−4328
solar eclipses, ancient Chinese obs. 80−72916
solar elements i and Ω determ. from Doppler vel. meas. of solar plasma 78−28599
solar ephemeral region flares and supergranulation network diffusion 79−21265
solar equatorial K-corona, temporal evolution 78−28618
solar eruptive prominence and surge, Skylab X-ray and Hα obs. 77−78755
solar eruptive prominence of June 8, 1974 Hα filtergrams 77−22182
solar extreme limb spectrograms, 4545-4579 Å, during 1970, March 7 eclipse 77−17472
solar faculae, line profiles and models 77−45375
solar faculae, mag., vel. and brightness struct. 79−25557
solar faculae, photographic obs. model, lifetime calc. 79−48761
solar faculae and sunspots, direct photographs with balloon-borne 10 cm telescope *(Japanese)* 79−80292
solar faculae excess brightness, wavelength depend., rel. to solar oblateness 78−7955
solar Fe I line spectrum, photosphere Fe abundance determ. *(Russian)* 80−12720
solar fibrils, lifetime and evolution 77−29760
solar filament features Hα contrast profiles 77−2402
solar filament obs. with multi-channel subtractive double pass spectrograph 78−12189
solar filaments, short-lived, differential rotation 78−28642
solar filaments disparitions brusques, evidence for role of mag. field *(Russian)* 80−51726

visible astronomical observations continued
solar filaments symm. location, example of giant convective cells 77−29779
solar five-minute oscillations, observational search for large-scale organisation 78−65589
solar flare, 1973 June 15, Hα, magnetic and X-ray morphology 78−4173
solar flare, 1978 February 11, Hα, Hβ and VHF obs. 78−93187
solar flare magnetic fields and microwave burst spectra 78−7970
solar flare of 1975, August 10, magnetic field reconstruction 77−13302
solar flare prominence, 1979 March 27, photographic obs. *(Chinese)* 79−92744
solar flare-loop prominence system, 1972 May 24, optical and X-ray obs. 79−30045
solar flares, Ca II K-line obs. rel. to temp. min. region struct. and flare heating mechanisms 79−12458
solar flares, Hα, hard X-ray and microwave emissions in impulsive phase 78−77540
solar flares, H spectral lines obs. rel. to mechanism investigation *(Russian)* 79−16925
solar flares, microwave and optical emissions comparison 80−31284
solar flares, Na I D-line emission and position rel. to mag. field *(Italian)* 78−96456
solar flares, nonthermal plasma wave elec. fields meas. using Stark effect 78−12193
solar flares, observation by optical and radio techniques 79−48765
solar flares and prominences, mag. fields meas., photographic method *(Russian)* 78−65584
solar flash spectrum, obs. at 1979 February 26 eclipse 80−67687
solar flux distribution, comparison with stellar flux distribs. and solar B−V and U−B colours determ. 79−66970
solar flux in Venus atmosphere, meas. by Pioneer Venus multiprobe mission radiometer expt. 79−48718
solar Fraunhofer lines, east-west asymmetry of central residual intensities and other parameters 78−53916
solar granular velocity vertical component, height depend., spectral obs. 79−66980
solar granulation, dark dot form. in cell 80−31274
solar granulation, discovery and history 77−2382
solar granulation, lifetime from balloon-borne imagery 78−28601
solar granulation, one-dimensional speckle interferometry 78−45299
solar granulation, photometric props. from balloon-borne imagery and digital image enhancement 78−7956
solar granulation, power spectrum calibration by Michelson stellar interferometry 77−17464
solar granulation structure, vertical motions spatial and temporal behaviour obs. 80−85912
solar granule/intergranule brightness contrast, new determ. 78−20797
solar Hα macrospicules, identification with EUV macrospiculs and X-ray bright point flares 78−16361
solar Hα post-flare loops dynamics, 1973 July 29 flare 80−31286
solar He I 5876 Å line emission, height distrib. in middle chromosphere 77−17525
solar Hf abundance from HF II spectral lines obs. 77−17518
solar images quality, influence of atmospheric thermal disturbances *(French)* 77−53532
solar inner corona electron density distrib. from Fe XIV 5303 Å line intensity obs. 78−61843
solar inner corona polarization meas. at 1972 July 10 eclipse 77−82197
solar large-scale magnetic field, Stanford obs. compared with Hα synoptic charts 78−28612
solar limb brightness oscills. obs. 79−62798
solar limb darkening function at 5012 Å, possible vars. 80−67677
solar limb effect, Fe I line contours and shifts 77−13309
solar loop prominence kinematics 79−84774
solar luminosity variation, Ca H and K behaviour at solar minimum and cycle 21 onset 79−16907
solar mag. field intensity determ. for nonspot mag. regions 78−96452
solar magnetic field var. during class 2b flare, meas. and anal. 78−89160
solar magnetic fields, meas. by Mt. Wilson magnetograph, effects of ang. resolution 77−22082
solar magnetic tubes, gas oscills., spectral line obs. 79−25564
solar mean magnetic field, 1968-74 period, obs. method, rel. to interplanetary mag. field 77−71082
solar mean magnetic field, contrib. of background mag. field and fields of active regions and spots *(Russian)* 78−57530
solar metallicity and UBV colours from spectral quantification 78−65577
solar Mg I 4571 A line, extreme limb obs. 77−53506
solar neutral sheet obs. in corona during 1973, June 30 total eclipse 79−84757
solar obs. with CERGA astrolabe *(French)* 77−45380
solar observations during 1969 at Kodaikanal Obs. 78−61833
solar oscillations, PEPSIOS spectrometer obs. 78−93203
solar oscillations, search during 1974-76 period 78−93190
solar oscillations with 160 min. period, magnetograph obs. 79−40156
solar p-mode oscillations, tracer of radial differential rot. 79−35221
solar photosphere, brightness field near disc centre, two dimens. spatial spectrum 78−7964
solar photosphere, C I 5380 Å line sensitivity to temp. changes 77−60743
solar photosphere, centre-to-limb var. of RMS granular contrast 78−4176
solar photosphere, gas motions in single sunspot *(Russian)* 78−65582
solar photosphere, granular brightness fluctuations centre to limb var. 79−66971
solar photosphere, granular vels. around sunspots 77−29776
solar photosphere, granulation statistical properties and seeing, speckle interferometry obs. 79−88634
solar photosphere, intensity, vel. and temp. fluctuations in upper regions 77−56886
solar photosphere, large-scale velocities, research programme 77−71101
solar photosphere, line profile vars. with heliographic latit. 77−2383
solar photosphere, linear hydrodynamical eqns. coupled with radiative transfer, Mg I 5172 Å line interpretation 78−77529
solar photosphere, metallic line profiles var. with heliographic latit. 78−61837
solar photosphere, microturbulent motions 79−75189
solar photosphere, small scale structures correl. depend. on resolution 79−84769

visible astronomical observations continued
solar photosphere, struct. compared with chromosphere 77−29777
solar photosphere, wave propag. obs. 77−22162
solar photosphere, wavelength depend. of granulation, 0.38-2.4 μm region 78−12188
solar photosphere-chromosphere transition region emission, spectral obs. in Hα region 79−35233
solar photospheric faculae, contrasts at solar disc centre using filigree pictures 78−12181
solar photospheric granulation, speckle interferometric obs. *(French)* 80−46523
solar photospheric network, mag. fluxes and field strength meas. 77−71083
solar photospheric network structure from Mn I lines obs. 79−30039
solar photospheric oscillations depth depend. 80−31275
solar photospheric velocity field and Hα filaments spatial correl. 77−2401
solar plage region magnetic points, vertical vel. fluctuations 77−71084
solar polar true average field strengths 77−78743
solar polar vortex, spectroscopic search 79−5801
solar prominence, 1969, October 15, Ca^+ lines obs. rel. to macroscopic motions 79−40167
solar prominence loop, 1973 Nov. 3, H I, He I and He II emission line spectra 77−64736
solar prominence model based on spectral obs. 80−31287
solar prominence outer regions, temp. and microturbulence *(French)* 77−53510
solar prominence spectra taken at Ondrejov Observatory, inclined spectral features obs. 80−62098
solar prominences, fine struct., small scale Doppler shifted features 77−78754
solar prominences, flocculi and Hα filaments, obs. during 1969 at Kodaikanal obs. 78−61832
solar prominences, polarisation of D3 emission line 77−29746
solar prominences fine structure, obs., Hα filtergrams 77−17523
solar proton events and coronal mass ejections 78−77545
solar pulsations at periods from 7 to 70 minutes, observational search 78−93180
solar quiescent prominence, influence of spatial resolution on Ca^+ K-line width and shift 80−77364
solar quiescent prominence spectra, meas. of Ca^+ 8542 and 8498 Å He 4471 Å and Ti^+ 4468 Å 80−90373
solar quiescent prominences, Hα and Hβ emission line profiles 79−71011
solar quiescent prominences, Hβ, He D_3 and Ca II 8542 Å line emission meas. 78−32427
solar quiescent prominences, spectra meas. 78−40886
solar quiet chromosphere, velocity waves propag. 77−22198
solar rotation, 1966-1978 period 79−66977
solar rotation, determ. using sunspot spectra 79−92745
solar spectra, appl. to stellar photographic equivalent widths calibration 78−73658
solar spectra, balloon meas., stratospheric N_2O vertical distrib. determ. 78−61493
solar spectra, gap in 5250 Å region, spectrogram 77−49360
solar spectra, lines curvature meas. via automatic comparator 77−82123
solar spectral lines, high-resolution meas. using scanning Fabry-Perot interferometer 80−77298
solar spectrum, absorpt. lines asymmetry *(Russian)* 80−72901
solar spectrum registration using double-pass spectrophotometer with digital registration, precision *(Russian)* 79−96917
solar supergranulation study with diode array magnetograph 77−2384
solar surge of 1961, Sept. 1, rotational and turbulent motions 77−91496
solar surge producing short-lived filament 77−33458
solar surge prominence, 31 May, 1971, observation as continuum event 77−22183
solar Ti abundance from weak spectral lines obs. 77−29778
solar Type III-RS bursts of 1975, August 12, Hα obs. 77−29774
solar velocity fields, large-scale, from Doppler line shift obs. 80−12730
solar-type stars, metal abundances, microturbulence, spectroscopic data 78−40943
solar-type stars, photoelec. scanner obs., search for solar spectral analogues 78−40938
southern Ap stars, photometric vars. *(French)* 79−16981
Southern Coalsack, dark nebula, conspicuous globule obs. 77−33614
southern compact and bright nucleus galaxies 77−74136
southern compact and bright-nucleus galaxies, spectroscopic survey 79−84683
southern dark clouds, survey for Herbig-Haro objects and Hα emission stars 78−28536
southern dark dust clouds, catalogue 77−56844
southern dwarf novae, image tube spectra 77−56960
southern galaxies with strong emission lines spectroscopic obs. 77−17679
southern groups and clusters of galaxies, catalogue 78−28539
southern interacting galaxies with emission lines 77−91653
southern late-type and irregular galaxies, survey, morphology, luminosity 79−21420
southern metal-poor stars, UBVRI photometry and UV excesses 80−56828
southern OB stars, MK spectral classifications 78−12221
southern peculiar A-type stars, spectra and atmospheric anals. 78−24517
southern peculiar emission-line stars, observational data rel. to mass ejection 80−41843
southern peculiar galaxies and galaxy pairs, morphologies, spectra and redshifts 78−32579
southern planetary nebulae identifications 77−22302
southern quasars and quasar candidates, UBV photometry 78−32595
southern radiosource identifications 77−45591
southern radiosources, red shifts for 32 Parkes objects 79−44627
southern radiosources, redshift meas. 77−26075
southern rich clusters of galaxies, finding list for 474 clusters 78−24470
Southern Sky Survey, role of European Southern Observatory 80−12658
southern standard stars, 320-880 nm energy distrib. 80−62125
southern subdwarfs, UBV photometry, UV excesses 79−5818
southern visual double stars, meas. at Cerro Tololo Observatory 78−8057
speckle, interferometric measurements of binary stars 79−71065
spectral energy distribution for 50 stars, 3200-7550 Å region *(Russian)* 78−65620
spectroscopic binaries, G-type dwarfs and early type FK4 stars, uvby Hβ photometry 77−82275

visible astronomical observations continued
spectroscopic binaries discovered from composite spectra 78−69826
spectroscopic binaries in open cluster NGC 6475, radial vels. 77−87488
spectrum variables, He weak and He strong stars 78−4243
spherical compact galaxy pairs, UBV obs. 77−37645
spicules, simultaneous K and D3 line obs. *(French)* 77−29763
spiral and irregular galaxies, brightest superassociations as distance indicators 80−62260
spiral galaxies, comp. gradients rel. to density wave theory 77−2468
spiral galaxies, early-type, absolute magnitude-colour relation 77−74133
spiral galaxies, early-type, multiaperture UBV photometric props. 80−98706
spiral galaxies, optical surface photometry rel. to local mass-to-light ratio 80−31361
spiral galaxies, rot. direction determ. by means of edge-on systems *(Russian)* 80−36722
spiral galaxies, UBVR surface photometry and mass distrib. 79−71123
spiral galaxies bulges, vel. dispersions meas. 80−26965
spiral galaxies nuclei, spectra and stellar population 80−56926
spiral galaxies studied at Westerbork, optical surface photometry 80−17655
spiral galaxies with large redshifts, optical obs. 77−29933
spiral sunspots, flares and prominences photographic obs., 1972 October *(Chinese)* 78−69761
SS 433, associated filamentary optical nebulosity detect. 79−88723
SS 433, B V photometry and short-term light vars. (1979 July 23 to September 17) 79−101165
SS 433, discrepancy between optical and radio positions 80−31303
SS 433, emission line wavelength changes 79−48816
SS 433, enormous periodic Doppler shifts obs. 80−17593
SS 433, Hα blue component wavelength obs. and weak lines interpretations 79−67023
SS 433, IR and visible obs., IR excess and emission processes 80−4387
SS 433, IR light curves from BVIJHK photometry, period and ephemeris 80−8642
SS 433, light curves, double peak and binary-like period, photometry 80−94804
SS 433, light minimum epoch and period 80−26886
SS 433, near IR (600 to 1100 nm) spectra, 1979 June and September 79−97009
SS 433, nearby faint, highly-contorted nebular filament discovery 80−94855
SS 433, no 6-day periodicity in 1978 June-1980 Feb. obs. period 80−62150
SS 433, no short period vars. from high-speed photometry 79−58346
SS 433, photometry, 1979 July to October, and 6.5 day period identification 80−8643
SS 433, radial vel. curve low amplitude section, visible spectra anal. 80−67737
SS 433, radio and optical obs. 79−88661
SS 433, radio and optical positions coincidence 80−56840
SS 433, short term Hα central intensity increases 80−4375
SS 433, spectroscopic obs. and probable binary nature 80−51780
SS 433, V band photometry and broad min. prediction (1980 April-May) 80−82390
SS 433, visible and IR photometric and polarisation obs. 79−80321
SS 433, visible and IR photometry rel. to IR variability 80−98676
SS 433, visible and JHKL photometry and light vars. periodicity 79−53821
SS 433 in SNR W50, relativistic jets interaction with interstellar medium 80−101629
standard stars defining near two-colour photometric system for near IR, obs. 79−62759
standard stars for uvby photoelectric photometry south of declination +10°, obs. 77−2347
standard stars for VRI photometry with S25 response photocathodes, obs. 77−2422
star cluster hidden in ghost image of Sirius on Palomar Sky Survey, discovery 80−109501
star clusters, faint, discoveries and descriptions 79−25651
star colours, refr. corrections for atmospheric spectral transmission changes 78−28535
star density distribution of red and blue globular clusters of LMC 79−92811
star formation, observational studies conclusions 79−25592
star image at telescope focus, quality, rel. to photoelectric obs. efficiency 80−62034
star pair latitude obs. anal., mean pole position calc. 80−21892
star proper motions rel. to galaxies, systematic errors in photographic obs. *(Russian)* 79−16941
star sequences, BV photoelectric photometry and reliability in variable star fields 79−97039
starfield in direction to Scutum Cloud, RGU photometry 79−35242
starlight deflection by Sun, daytime obs. by photographic astrometry 79−8797
stars, 313 nearly low galactic latitude objects, linear polarization meas. 80−46641
stars, aberration of light rel. to spectral type *(German)* 78−73702
stars, absolute positions determ. by Sanders-Raimond method 77−53404
stars, absolute proper motion meas. in M31 area *(Russian)* 77−71106
stars, AGK3R declinations improvement using Toepfer meridian circle obs. *(Russian)* 78−28645
stars, angular diameter meas. with large altazimuth telescope *(Ukrainian)* 79−96925
stars, bright, nearby, astrometric anals. from Sproul 61 cm refractor plates 80−61991
stars, Ca II emission from chromospheres of late-type objects 79−30061
stars, CASF 3 astrolabe catalogue of San Fernando *(French)* 77−78653
stars, catalogue of photometric parameters meas. in Geneva Observatory system 77−73974
stars, DDO photometry, accuracy of derived two-dimensional spectral classes 78−16395
stars, diffuse interstellar band at 5780 Å, photoelectric meas. 78−93350
stars, early-type, in northern Milky Way fields, UBVβ photometry 77−2424
stars, first astrolabe catalogue of San Juan 77−13253
stars, luminous, in Monoceros, photometry rel. to galactic struct. 77−9799
stars, new UBV photoelectric sequences in Puppis (l=250°, b=0°) 77−45426

visible astronomical observations continued
stars, parallax and proper motion anals. of Sproul long-interval plate series 79−71015
stars, photometry in Geneva seven colour system, second catalogue 77−13252
stars, polarisation meas. near N.Galactic Pole rel. to interstellar extinction 79−62814
stars, right ascension determ. with Sukharev horizontal meridian circle *(Russian)* 78−28646
stars, Shanghai astrolabe and diurnal latitude and longitude var. *(Chinese)* 77−67025
stars, UBV photometry, influence of Balmer discontinuity on reductions 77−74046
stars, variable velocity, previously observed at David Dunlap Observatory, radial vels. 79−101141
stars, Walraven VBLUW photometry 77−17377
stars, young, in galactic anticentre direction, photometry and spectra rel. to outer Galaxy struct. 80−22079
stars, Zeeman and Doppler shifts in spectrograms meas. 78−36467
stars, zero polarisation standards list 79−40187
stars in 37 southern open clusters, MK spectral classifications anal. 79−88644
stars in 3U 1538-52 field, photometric search for optical candidates 78−12412
stars in dust clouds with bright nebulosities 80−56893
stars in field centred at $\alpha = 2^h17^m.9$, $\delta = +58°59'$, BV magnitudes and spectral classes *(Russian)* 78−40841
stars in Magellanic Clouds and Milky Way, five-channel photometric obs. 78−16398
stars in Pleiades region, radio and optical obs. of flares *(Russian)* 78−93245
stars in southern hemisphere, trigonometric parallaxes 78−69780
stars in vicinity of PSR 1913+16 binary pulsar, astrometry and photometry 78−93219
stars in X-ray source fields, transmission grating spectroscopy, optical condidates 79−21283
stars near South Galactic Pole, UBV photometry of 51 stars 78−4216
stars near southern open clusters, relative radial vels. *(German)* 80−94724
stars occulted by rings of Uranus, 1977-1980, colours and magnitudes 78−16277
stars of Carina-Crux-Centaurus region, UBV photometry rel. to interstellar extinction 79−40242
stars of solar neighbourhood, chromospheric Ca II H and K emission survey 80−109423
stars of upper Scorpius region, spectrophotometry 79−88647
stars optically misidentified with extragalactic radio sources, photometry and spectra 78−73708
stars trigonometric parallaxes, determ. by Yerkes Observatory 40 inch refractor 78−89168
stars with peculiar interstellar polarisations, interstellar lines and grains props. 77−53659
stars with planets, astrometric photoelectric detection obs. 80−56882
stars within 25 pc of Sun, polarisation obs. 78−12202
Stein 2051, orbital motion, evidence for triple system 78−4289
Stein 2051B, temp. and radius of cool white dwarf 77−13338
stellar, speckle patterns and plane scintillation, statistics 79−100948
stellar absorption bands in O, B and A type objects 79−8915
stellar BVRI photometry, secondary standards 79−70962
stellar BVRI photometry, with photometer using Si diodes as light detectors 78−20651
stellar Ca II emission line, V/R ratio rel. to mass loss 78−93208
stellar Ca II H and K emission, flux meas. by four-channel photon-counting spectrophotometer 78−73646
stellar clusters in LMC, instrumental colour-magnitude diagrams 77−22279
stellar colours influence on β-index meas. 79−21270
stellar digital speckle interferometry 77−53641
stellar electronographic BVR magnitude sequences, for UK 1.2 m Schmidt plates calibration 79−88703
stellar flux distributions, comparison with solar flux distrib. and solar B−V and U−B colours determ. 79−66970
stellar formation and evolution, role of UV obs. *(Italian)* 78−32446
stellar image spatial freq. modulation, atm. correlation scale meas. 78−40661
stellar iris diaphragm photometry, nonuniform background correction 80−12680
stellar low-dispersion objective prism spectra from UK 1.2 m Schmidt telescope 77−45311
stellar oscillations, PEPSIOS spectrometer search 78−93203
stellar parallaxes, need for space-borne and ground-based obs. 79−66992
stellar parallaxes, US Naval Observatory data 80−72788
stellar photoelectric photometry at Hvar Observatory, colour systems and extinction meas. 77−78643
stellar photoelectric photometry at Wise Observatory, performance assessment 78−73657
stellar photoelectric UBV sequences, in fields of eight low-red shift quasars *(French)* 80−51904
stellar photometric obs. for Earth atm. aerosol content determ. 78−92976
stellar photometry, extinction oscills. caused by atmospheric disturbances 80−56606
stellar photometry, UBVR sequences around globular clusters (NGC 5946, 6440 and 6624) 79−88702
stellar proper motions and parallaxes, meas. at Van Vleck Observatory 77−37595
stellar radial velocities, correl. meas. in stellar field at galactic latitude $b^{II} = -30°$ *(French)* 78−89173
stellar radial velocities, Radcliffe Cassegrain d-camera meas. for vel. system determ. 78−73645
stellar scintillation aperture averaging effects, photon counting meas. 77−91519
stellar secondary spectrophotometric standards, obs. in 5840-10800 Å range 79−29995
stellar space density and interstellar extinction in Ophiuchus region 77−64839
stellar speckle interferometry, lens-atmosphere modulation transfer function meas. 79−101078
stellar speckle interferometry and holography, isoplanicity and temporal correl. meas. *(German)* 79−75116
stellar speckle pattern statistics, photon counting techniques 79−25324

visible astronomical observations continued
stellar spectra, atlas 78−20657
stellar spectra, photographic equivalent widths calibration against solar photoelectric equivalent widths 78−73658
stellar spectral energy distribution in 3500 to 7500 Å region, absolute calibration 80−67710
stellar spectral energy distributions, results from Fourier transform spectrometry 77−82215
stellar spectrophotometric standards, obs. rel. to extinction monochromatic coeffs. on Terskol Peak *(Russian)* 79−44246
stellar spectrophotometric standards, spectral energy distrib. determ. of eight stars 79−35147
stellar spectrophotometry at Moscow and Alma-Ata, comparison 79−58273
Stepanyan's star, eclipsing binary, eclipses obs. and orbital period refinement 80−62195
Stepanyan's star, obs. of G8 V absorpt. spectrum and emission spectrum 80−67788
Stepanyan's star, spectrophotometric and photometric obs., 228-min period 80−56883
Stepanyan's star found to be eclipsing binary, possibly cataclysmic 80−51806
Stephenson's planetary nebula, optical, near IR and radio obs., position 79−67086
Stephenson-Sanduleak 433, emission-line star/X-ray source/radiosource assoc. with W50 SNR 79−8930
Stephenson-Sanduleak 433, Hα emission object, hot spot detect., rot. vel. and spectrum vars. 79−8933
Stephenson-Sanduleak 433, moving emission features, dynamical models 79−67034
Stephenson-Sanduleak 433, spectral variability 79−62839
Stephenson-Sanduleak 433, Thomson scatt. lines in spectrum, relativistic gas motions 80−22019
Stephenson-Sanduleak 433, unusual optical spectrum changes of Hα-emission object 79−5838
Stock 16, Basel 18, 19, Cr 272 and NGC 5168, open clusters, RGU photometry 78−16474
subdwarfs, old disc population, CaH and TiO band strengths 78−40930
subdwarfs in 47 Tucanae, CN vars. 80−94794
563 Suleika, rot. period and photoelec. lightcurves determ. 80−98594
Sun, 1966, May 20, partial eclipse contacts from Belgian obs. *(French)* 77−71074
Sun, 1973, June 30 total eclipse, photographic photometry of K- and F-corona 78−89140
Sun, 1978 May 7 events, radio, optical and geophysical manifestations *(French)* 80−8611
Sun, apparent diameter long period oscills., obs. 78−89138
Sun, asymmetry of selected Fraunhofer lines 78−4175
Sun, atmospheric waves, vertical propag., phase delay obs. 79−96981
Sun, Ba II 4554 Å obs. rel to five-minute oscills. horizontal energy flows struct. 80−62103
Sun, Ba II 4554 Å obs. rel. to five-minute oscills. in temp. min. region 79−62808
Sun, blue continuum flares and D3 preflare shell obs. 80−51709
Sun, C I, 5380 Å response to solar luminosity vars., effects of granular convection 80−85910
Sun, C I 5380 Å line obs. rel. to luminosity vars. and global oscills. 77−53487
Sun, CA II K-line, centre-to-limb obs. of K_2 component *(French)* 80−82331
Sun, CH photospheric lines and $^{12}C/^{13}C$ atmospheric ratio determ. 77−5518
Sun, chromosphere filaments and flare obs. 1967-9, Hα monochromatic light 78−61836
Sun, chromosphere impulsive flares space-time relation to centimetre wave bursts *(Russian)* 79−16924
Sun, chromosphere line profiles from OSO-8 satellite 80−67690
Sun, chromospheric feature lifetime rel. to rotation 79−44442
Sun, chromospheric rotation during 1972-73, years of declining activity 78−4186
Sun, coronal obs. with Solwind coronagraph 80−82325
Sun, coronal oscillations above active region, Fe XIV spectra obs. 80−41794
Sun, coronal streamers and ribbon structures rel. to IMF three-dimens. structure 79−5778
Sun, coronal transients at high latitude, 1979 September 27 Solwind obs. 80−94774
Sun, diameter from photoelectric driftscans 78−4169
Sun, differential rot. and giant cell circulation of Ca II network 77−53546
Sun, differential rot. of photospheric mag. fields assoc. with coronal hole 77−22167
Sun, differential rotation of Ca II network and photospheric plasma 79−25585
Sun, equator-crossing spot, development and motion 80−90394
Sun, exploding granules, evolution pattern 78−89164
Sun, fast var. in rotation during 19th and 20th cycles 77−53552
Sun, Fe I line meas. of gravitational red shift 80−90391
Sun, Fe I line profiles and magnetic field in quiet network regions of photosphere 78−69758
Sun, fibril changes in small flare, high resolution obs. 79−44452
Sun, flare spectrum, H lines rel. to metal emission 77−49353
Sun, flare spray on solar disc during radio bursts 79−80294
Sun, Fraunhofer line profiles for 1973 period *(Russian)* 79−92743
Sun, Fraunhofer lines, profiles in 4226-7700 Å range *(Russian)* 78−28606
Sun, global rotation rate determ. using 1967-74 sunspot data 80−90387
Sun, granulation seeing at Chinese solar observatory testing sites *(Chinese)* 77−67032
Sun, granule fragmentation, morphological study in Ca II K-line 80−56799
Sun, H_α high resolution obs. of active regions *(Japanese)* 78−89163
Sun, Hα activity and Fe I 5250 Å line magnetogram rel. to radio brightness *(Russian)* 77−64724
Sun, Hα flocculi in 1971, January-April, flare correlation *(Chinese)* 77−67081
Sun, Hα patrol film and spectrograms rel. to microwave flux decreases 77−25989
Sun, Hα plage formation after flare 79−44445
Sun, Hα spicules, dynamics at various heights, spectral obs. 80−90392
Sun, Hα-flares rel. to radio bursts and sunspots 80−41803

visible astronomical observations continued
Sun, He I D_3-line profile meas. with birefringent filter 78−4177
Sun, hedgerow prominences, fine structure from spectral obs. 78−40906
Sun, high-resolution obs. by Skylab Hα telescopes 77−60604
Sun, large-scale vel. features, magnetograph obs. 79−35224
Sun, light absorption in photospheric layers, eclipse limb darkening obs. *(French)* 80−8612
Sun, limb emission lines near Ca II H and K and spatial intensity vars. 80−51720
Sun, line profile families of faculae and pores 78−49408
Sun, loop prominence knots, motions, Hα line filtergram obs. 80−67693
Sun, loop type coronal transients, mass flow 79−44450
Sun, magnetic and vel. field evolution of sunspot group 78−89143
Sun, magnetograms from Kitt Peak National Observatory 60 cm vacuum telescope *(Norwegian)* 77−60613
Sun, mean mag. field obs. at Stanford 78−20800
Sun, meas. of Fraunhofer lines asymmetry *(Russian)* 78−40892
Sun, Mg I and II line profiles comparison with theoretical spectra, visible obs. 80−82320
Sun, morphological analysis of 1972 October large group *(Chinese)* 78−28603
Sun, nonradial p-mode oscills. 78−32428
Sun, nonthermal vels. in photosphere 78−4219
Sun, north-south brightness asymmetry, obs. 78−45303
Sun, O emission lines, Draper's 'discovery' and subsequent debate 77−37706
Sun, oscillations of 160-min. period, no terrestrial atmospheric extinction effects 80−105216
Sun, oscills. period obs. rel. to internal struct. 80−105226
Sun, photosphere, solar rot. from Doppler obs. 80−105219
Sun, photospheric granulation, 2-dimens. power spectrum analysis, data processing 80−101570
Sun, plage development rel. to spectra and models *(Russian)* 77−64725
Sun, polar mag. fields strength 79−12446
Sun, positions in 1976, CERGA astrolabe obs. *(French)* 78−69760
Sun, prominences, emission line intensities rel. to model calcs. 79−44447
Sun, reson. line polarisation, non-mag. polarisation, centre-to-limb var. 80−67678
Sun, rotation, background vel. fields, anal. and instrumental effects, visible obs. 80−72915
Sun, secular diameter decrease, Tobias Mayer obs. refute hypothesis 80−90389
Sun, sidereal equatorial rotation rate, KI 7699 Å line meas. 79−44441
Sun, size, struct. and strength of small-scale mag. field 77−78738
Sun, spectral line asymmetries, radial movement effects 80−41792
Sun, spicule inclinations statistical study 77−91508
Sun, structure from global studies of 5-min. oscills. 80−26838
Sun, study of June 30, 1973 transpolar coronal hole 77−53526
Sun, sunspot analysis for 1943-1977 period, Catania obs. 79−25584
Sun, sunspot umbral dots, dynamic and struct. behaviour for photometry obs. 80−109409
Sun, Ti I lines meas. and solar Ti abundance 77−29743
Sun, total eclipse of 1976 October 23, contact timing expt. 78−36547
Sun, Tycho Brahe's obs. 79−88785
Sun, white light faculae 1972-7 obs. 79−16920
Sun, young active regions, filaments, and flares 80−72910
Sun , total eclipse of 1976 October 23, in-flight obs. near Victoria, Australia 78−36548
Sun annular eclipse, 1976, April 29, photographic obs. for ephemeris time correction determ. *(German)* 79−44335
Sun magnetic field intensity and Hα line behaviour 78−57522
sunset obs. from Apollo-Soyuz, atmospheric light refr. study from space *(Russian)* 78−65383
sunspot chromosphere, radial vel. and brightness oscills. regimes *(Russian)* 80−51727
sunspot groups, small pores proper motion meas. 80−12733
sunspot intensity meas., correction for stray light during 1973 June 30 eclipse 78−28596
sunspot light bridges fine structure 79−66984
sunspot magnetic fields higher rot. rate at photosphere, Doppler meas. 80−46516
sunspot moats, lifetimes from magnetograph obs. 80−21966
sunspot penumbrae, fine struct. of mag. field and brightness 77−22179
sunspot structure from Solar Stratospheric Observatory obs. 79−25574
sunspot umbra, bright points morphology and intensity *(French)* 78−89146
sunspot umbrae, mag. field gradient from echelle spectrograms 77−33456
sunspot umbrae, material motions obs. 77−45374
sunspot umbral brightening assoc. with two-ribbon flare 80−41804
sunspot umbral dots, improved obs. 80−26831
sunspot umbral spectrum, TiO rot. lines, temp. determ. 78−96451
sunspot umbral spectrum in 6812-6898 Å range 79−101136
sunspots, photoheliographic results, (1968 to 1971) 79−2487
sunspots, struct. and dynamic props. of large group of 1972 August 78−49409
sunspots, umbral flares 79−25579
sunspots, Wilson effect *(Chinese)* 80−12721
sunspots magnetic fields and proper motions, 1968 October 20-27 complex group obs. *(Russian)* 78−65583
sunspots penumbral vortical pattern anal., 1972 August *(Chinese)* 77−22157
sunspots umbras, outward wave propag. and motions in mag. tubes 79−16927
supergiant, B-type, assoc. IR source GL 2636, IR and visible obs. 80−105302
supergiant elliptical galaxies nuclei, CCD photometry rel. to supermassive object in (NGC 6251) 80−26966
supergiant OH maser sources, optical radial vels. 77−49378
supergiant stars, B2 to G0, small amplitude light vars. 78−32469
supergiant stars, in LMC, long-term light vars. 78−45326
supergiant stars, in SMC, radial vels. 78−93237
supergiant stars in LMC, spectral types and magnitudes, catalogue of 1882 objects 78−32361
supergiants, metal abundances of G- and K-type Ib stars 77−33482
supergiants, photometric histories of three highly reddened blue objects 79−5916
supergiants, semi-period of variation for B2 to G0 type stars 78−61854
supergiants assoc. with groups of luminous OB stars, photometry and spectra 77−17555

visible astronomical observations continued
supergiants in LMC, spectra, diffuse interstellar 4430 Å feature 80−73033
supergiants in SMC, MK classifications 77−87390
supernova, possible, in Virgo galaxy cluster, discovery, position and spectrum 80−90460
supernova, remnants, O, N and S abundances, optical emission from shock waves 77−49447
supernova, type I, in ESO 290-G50, spectral obs. 78−96496
supernova, Type V, in galaxy MCG 43223, spectrum obs. 78−93288
supernova discovery in anon. galaxy in Grus, position 78−93289
supernova discovery in anonymous galaxy in Camelopardalis, photographic magnitude 79−5849
supernova discovery in MCG 10-16-117 78−69817
supernova discovery in NGC 4647, magnitude 79−25619
supernova in anon. galaxy, discovery obs. 78−20846
supernova in anonymous faint spiral galaxy, discovery obs. 78−8031
supernova in anonymous galaxy, discovery report 79−2549
supernova in anonymous galaxy in Centaurus, magnitude (1980 June 30) 80−85962
supernova in anonymous galaxy in Cygnus, photometric and spectrophotometric obs. 79−5847
supernova in anonymous galaxy in Cygnus, UBV photometry and spectrum 79−5846
supernova in anonymous galaxy in Grus, discovery and magnitudes (1980 May 23 to July 12) 80−94820
supernova in anonymous galaxy near k Centauri, discovery and magnitudes 80−85962
supernova in ESO 153-G27, discovery and magnitudes (1979 August 19 to October 15) 80−26892
supernova in faint ScI galaxy, discovery and position 77−22257
supernova in galaxy MCG-5-9-22, discovery 78−81643
supernova in IC 5201, discovery report 79−44514
supernova in M100 (NGC 4321), discovery of possible type II object before max. 79−48835
supernova in MCG 10-16-117, classification and spectrum 78−69818
supernova in MCG −3-34-61, discovery of 17 mag. object 80−72989
supernova in MCG -4-32-23, precise position, photographic magnitude 78−57568
supernova in MCG-4-32-23, discovery and magnitude 78−53968
supernova in MCG-5-9-22, spectrum and absolute magnitude 78−81644
supernova in NGC 1411, spectral obs. and precise position 77−82266
supernova in NGC 3226, discovery, magnitude 77−33537
supernova in NGC 3733, spectrophotometry (1980 March 22) 80−62164
supernova in NGC 3780, possible unusual variable 79−5848
supernova in NGC 3780, spectrophotometry of type II object 79−17000
supernova in NGC 3913, discovery report 79−44512
supernova in NGC 3913, type I characts. and likely max. magnitude 79−48834
supernova in NGC 4321, spectrograms (1979 April) 79−48836
supernova in NGC 4321, spectrophotometry, type II characts. 79−67044
supernova in NGC 4321, spectrum, lightcurve and magnitude of type II object 79−71061
supernova in NGC 4321, type II characts. and 1979 April UBV and visual obs. 79−58364
supernova in NGC 4321, UBV photometry, light curve and type 79−67045
supernova in NGC 4321, UBV photometry 79−53835
supernova in NGC 4321, UBVR photometry 80−77428
supernova in NGC 4321, visual magnitude estimates, 1979 May-Jun. 79−75229
supernova in NGC 4340, discovery obs. 77−22256
supernova in NGC 4647, classification and time since maximum 79−25620
supernova in NGC 4902, discovery and magnitude (1979 August) 79−88693
supernova in NGC 5406, discovery of 14th magnitude object 77−33535
supernova in NGC 977, discovery obs. 77−17606
supernova in Zw 310-31 = VV 11-10-52 faint galaxy NE of nucleus 78−4259
supernova remnant candidates, spectroscopic survey in 6000-6800 Å region 77−60815
supernova remnant discovery in southern sky 77−45518
supernova remnant in Cygnus, high vel. gas obs. *(Russian)* 79−21403
supernova remnant with broad optical emission lines near NGC 4449 irregular galaxy 79−17057
supernova remnants, evolution of line intensity ratios in Galaxy and LMC 77−17656
supernova remnants, Fe X and XIV forbidden line emission 79−44580
supernova remnants, filamentary vels. *(Italian)* 79−53889
supernova remnants, galactic, new optical obs. 80−17636
supernova remnants, galactic, systematic search for optical nebulosity 79−29998
supernova remnants, Hα emission of optical filaments, shock waves interaction with interstellar medium 78−8103
supernova remnants, in LMC, obs. in O III and S II forbidden lines 77−91607
supernova remnants, kinematics and evolutionary sequence in cloudy interstellar medium, interferometry obs. 80−67823
supernova remnants, low surface brightness, optical and radio obs. 79−88717
supernova remnants, optical, candidates in M33 central region 79−21402
supernova remnants, optical filament form. problem, observational approach 78−45384
supernova remnants in Large Magellanic Cloud, high-resolution mapping in coronal [Fe XIV] emission 79−97051
supernova remnants in M33, catalogue and spectroscopic survey 80−41734
supernova remnants in M33, optical identification 79−62894
supernova remnants in M33, spectra, element abundances 79−35354
supernova remnants in Magellanic Clouds, optical obs. review 79−75259
supernovae, BV magnitudes, spectroscopic obs., brightness, distance 79−16999
supernovae, light curves and spectra obs. at Asiago Astrophys. Observatory 77−87457
supernovae, pre-telescopic obs., uses in modern astronomy 79−96930
supernovae, Type II, O I absorpt. lines obs. in spectra *(Russian)* 77−45474
supernovae, Type II, photometric classification and observed characts. 79−25621
supernovae, visual hunting by amateur astronomers, prospects 77−91556

visible astronomical observations continued
supernovae at great distance, luminosity and temporal var. as cosmological probes 80−94821
supernovae in anonymous galaxies, three new discoveries 80−46589
supernovae in NGC 488 and NGC 977, UBV photometry 79−62857
supernovae in NGC 7723, NGC 1325, NGC 4402, UBV photometric obs. 78−16444
supernovae stellar remnants, spectroscopic search 80−26890
87 Sylvia, UBV photometry, light curve and rot. period 80−21942
symbiotic C star (UKS-Ce1), spectrum 77−67094
symbiotic stars, obs. of unidentified bands at 6830 and 7088 Å 80−46573
symbiotic stars, unidentified emission line obs. at 7090 Å 77−33522
symbiotic stars and recurrent novae, high speed photometry 77−60799
Sz 80, southern emission-line galaxy at low galactic latitude 78−86022
T626, red giant in open cluster M67, curve of growth anal. 79−48797
TASV 030645, possible new variable star in Perseus 78−69810
44 Tauri, δ Scuti star, light curves and periods, least squares determ. 79−62850
68 Tauri, Am star, photoelectric UBV obs. of magnetic field *(German)* 77−17586
γ Tauri, ang. diameter determ. from lunar occultation obs. 80−62119
41 Tauri, Ap star, Ca II K and Hδ lines rapid vars. *(Russian)* 80−90458
ζ Tauri, apparent wavelength depend. of v sin i 78−12240
45, 97 and 102=ι Tauri, astrometric studies 78−69779
SU Tauri, brightness increase, visual magnitude estimates 77−29852
V471 Tauri, BV photometry of white dwarf eclipsing binary, light curve vars. 78−96508
V711 Tauri, change in nature of light curve, and flare, 1979 October to December 80−26906
α and θ^1 Tauri, diameters from Hyades lunar occultations 79−75253
θ^1 Tauri, double star, lunar occultation obs. 79−67052
RW Tauri, eclipsing binary, elements determ. from light changes anal. in freq. domain 77−53637
RW Tauri, eclipsing binary, gaseous ring struct., H I alpha obs. 80−109482
λ Tauri, eclipsing binary, photometric elements, masses, radii, luminosities 78−28723
CD Tauri, eclipsing binary star, intermediate-band photometric anal. 77−13389
SU Tauri, emission lines at min. and BV photoelectric photometry 80−8640
T Tauri, H_α line profile, fast variations obs. *(French)* 78−61859
T Tauri, Hα line profile vars. 78−40944
DL Tauri, Hα profile in T Tauri type star *(French)* 78−8003
DR Tauri, highly variable young star, spectrometric and photometric obs. 78−20829
δ Tauri, Hyades giant, identification as spectroscopic binary 77−64794
51 Tauri, Hyades spectroscopic binary, speckle interferometry 77−29876
T Tauri, integral brightness and Hα emission vars., 1971-77 period *(Russian)* 78−61852
T Tauri, linear polarization obs., wavelength depend., circumstellar dust envelopes 79−53809
λ Tauri, massive eclipsing binary star, spectrophotometry 80−26900
V471 Tauri, period var. and light curves of eclipsing binary system 80−22038
DR Tauri, pre-main-sequence star, brightening, 1970 to 1979, and historical light curve 80−31297
SU Tauri, R Coronae Borealis variable, brightening after long minimum, 1980 August to September 80−109438
SU Tauri, R Coronae Borealis variable, fading, visual magnitude obs. 79−92785
T Tauri, rapid Hα vars. nonconfirmation 78−73706
ζ Tauri, shell star, Balmer intensity profiles 77−56973
DR Tauri, T Tauri star, Balmer line profile changes and inverse P Cygni profiles 80−101591
BP Tauri, T Tauri star, He I triplet-to-singlet ratio 78−28680
DR Tauri, T Tauri star, mass flow var. in envelope, visible spectra 80−85939
RW Tauri, UBVRI light curves of Algol-type eclipsing binary 77−91577
SU Tauri, visible and IR photometry and polarimetry *(Russian)* 78−61860
Su Tauri, visual magnitude esimates 77−37606
α Tauri (Aldebaran), angular diameter from lunar occultation 79−40185
α Tauri (Aldebaran), Ca II K line high-resolution obs. 78−16408
α Tauri (Aldebaran), Ca II lines obs. rel. to chromosphere model 78−40931
α Tauri (Aldebaran), radius from 1978 Aug. 26 occultation fast photometry 79−67005
α Tauri (Aldebaran), Ti isotopic abundance ratios 77−22212
V471 Tauri (Bd+16°516), Ca II H and K and Hα line vars. 79−67063
V711 Tauri (HR 1099), 1978 photometry during radio outburst 79−21338
V711 Tauri (HR 1099), RS Canum Venaticorum star, BV light curve during (1978-79) 80−105279
V711 Tauri (HR 1099) and related Ca II emission binaries, Hα emission survey 79−21339
20 Tauri (Maia) and related stars, photometric constancy 79−58338
BU=28 Tauri (Pleione), envelope during shell phase, 1972-75 period 78−28707
BU=28Tauri (Pleione), spectral var. during 1969-1975 period 77−33532
BU=28 Tauri (Pleione), spectrum vars., 1938-75 period 78−36578
BU Tauri (Pleione), UV photometry during shell phase 77−64768
28=BU Tauri (Pleione) Be shell star, 3167 to 4924 Å spectrum atlas 80−98673
RV Tauri and yellow semiregular variables, photometric investigations 80−26865
T Tauri star, extremely young, and assoc. nebula, fading 78−93236
T Tauri stars, gas flow from line profiles 79−67004
T Tauri stars, Hα and Na I D lines high-resolution profiles 80−62116
T Tauri stars, photometric and spectral props. 79−21282
T Tauri stars, photometric vars. 77−9741
T Tauri stars, radial vels. and spectral types 77−56921
T Tauri stars, seven-colour TV photometry, obs. methods *(Russian)* 77−64756
T Tauri stars, seven-colour TV photometry, variability *(Russian)* 77−64757
Taurus Cloud region, flare stars *(Chinese)* 80−85957
Tautenburg objective prism survey objects, high-resolution spectra and redshifts 80−4436

visible astronomical observations continued
RR Telescopii, slow nova, evolution of nebular spectrum 77−60771
BL Telescopii A, yellow variable supergiant near Cepheid instability strip, VBLUW photometry 80−98672
terrestrial longit. determ., without time, from obs. of lunar altitude 78−85836
Terzan 2, globular cluster, identification with X-ray burst source XB 1724−31 79−5919
17 Thetis, opposition effect and surface material, UBV photometry *(Russian)* 79−58294
88 Thisbe, photoelectric light curves and rotation 80−17528
115 Thyra, astrometry and orbit improvement *(German)* 80−85881
time and latitude, astrolabe obs. at Merate Observatory for (1976) 78−12078
Titan, Kuiper bands detect. in spectrum 78−85898
Titan, long term light vars. *(Italian)* 78−93147
Titan, NH_3 atmospheric abundance 78−12142
Titan, normal reflectance from lunar occultation obs. 78−85897
Titan, secular brightness increase, 1972-76 period 78−16346
Titan, spectral reflectivity in 0.32-0.86 μ range 79−35181
Titan (Saturn VI) eclipse, 1979 December 20, photometric obs. 80−31250
Titan eclipse by Saturn, light curve obs. rel. to Saturn upper atmosphere struct. 80−90362
Titania, near IR spectra and JHK photometry, mass and dia. measurement 80−56761
Tokyo Astronomical Obs., Time and Latitude Bulletins (1976 April-June) 77−64619
Tokyo Astronomical Obs., Time and Latitude Bulletins (1976 Jul.-Sept.) 77−70982
Tokyo Astronomical Obs., Time and Latitude Bulletins (Apr.-June 1978) 79−101052
Tokyo Astronomical Obs., Time and Latitude Bulletins (April-June 1977) 78−45203
Tokyo Astronomical Obs., Time and Latitude Bulletins (April/June 1979) 80−72752
Tokyo Astronomical Obs., Time and Latitude Bulletins (December 1975) 77−2335
Tokyo Astronomical Obs., Time and Latitude Bulletins (Jan.-March 1976) 77−70983
Tokyo Astronomical Obs., Time and Latitude Bulletins (Jan-Mch. 1978) 80−17476
Tokyo Astronomical Obs., Time and Latitude Bulletins (January-March 1977) 78−45202
Tokyo Astronomical Obs., Time and Latitude Bulletins (Jul-Sep 1979) 80−82177
Tokyo Astronomical Obs., Time and Latitude Bulletins (July-September 1977) 78−73618
Tokyo Astronomical Obs., Time and Latitude Bulletins (July-Sept. 1978) 80−4239
Tokyo Astronomical Obs., Time and Latitude Bulletins (November 1975) 77−2334
Tokyo Astronomical Obs., Time and Latitude Bulletins (Oct.-Dec. 1976) 77−87242
Tokyo Astronomical Obs., Time and Latitude Bulletins (Oct.-Dec. 1978) 79−84646
Tokyo Astronomical Obs., Time and Latitude Bulletins (October 1975) 77−2333
Tokyo Astronomical Obs., Time and Latitude Bulletins (October-December 1977) 79−5736
Tokyo Astronomical Obs., Time and Latitude Bulletins (September 1976) 77−2332
Tokyo Astronomical Observatory Time and Latitude Service, Bulletin (January to March 1979) 80−72751
Tokyo meridian circle obs., true external errors, from SAO 158687 occultation by Uranus 78−28487
Tololo emission line galaxies, size, morphology and spectroscopy, visible obs. 80−73044
Tololo emission-line galaxies, nature from photometric and spectroscopic obs. 78−49531
Tololo list of emission line galaxies, spectroscopic and radio survey 77−64851
Tololo quasars, follow up visible spectroscopy for five candidates 79−17125
Ton 1542, Seyfert galaxy, electronographic photometry *(French)* 77−45547
Ton 1542, Seyfert galaxy nucleus, optical polarisation *(French)* 77−26053
Tr 22, open cluster, photoelec. and photographic photometry of member stars 79−17032
Tr 27-102 (HD 159378), possible long-period Cepheid, light vars. obs. 78−45336
Trapezium type multiple systems, relative proper motions *(Russian)* 78−93314
R Trianguli, Mira variable, narrow-band polarimetry 79−25617
RW Trianguli, nova-like binary star, eclipse timings 79−21357
α Trianguli, radial vel. vars. from microdensitometer scans of photographic spectra 79−25642
RW Trianguli, short-period close binary, circumstellar material size and brightness vars. 78−32512
U Trianguli Australis, UBVRI obs. of beat Cepheid 79−53833
trigonometric parallaxes, proper motions, magnitudes and colours for 44 stars 79−35235
trigonometric parallaxes of 14 stars 79−5808
Triton, diameter and reflectance, spectral and radiometric obs. 80−17546
Triton, image tube spectra, 6800-9000 Å, search for possible atm., methane upper limit 79−16880
Triton, narrow band spectrophotometry 79−16879
Trojan asteroids, radii and albedo 77−33399
Trumpler 1, open cluster, UBV photometry 77−74105
Trumpler 27, heavily-reddened young open cluster, spectra and photometry 77−78836
Trumpler 27 star 28, obs. of WC9-type star with large IR excess 80−67738
Trumpler 37, young open cluster, stellar UBV magnitudes and MK classifications 77−22284
47 Tucanae, colour-magnitude diagrams for inner regions 78−57598
AQ Tucanae, eclipsing binary, UBV photometry, light curves 79−8951
47 Tucanae, globular cluster, photometry and spectra rel. to stars chemical comp. 80−46620

visible astronomical observations continued
47 Tucanae, globular cluster, UBV photometry 77−37630
47 Tucanae, metal-rich globular cluster, UBV photometric study 77−57065
47 Tucanae, spectral inhomogeneities in faint globular cluster stars 78−93340
47 Tucanae cluster, abundance gradients from spectroscopic obs. 79−40228
Tycho's supernova (SN 1572), unsuccessful search for optical stellar remnant 80−101603
Tycho's supernova optical remnant, expansion obs. 79−8962
Tycho's supernova remnant, filaments spectrum 78−73747
Tycho secondary craters, morphology and ejecta deposits 77−29670
Tycho SNR spectrum, model of optical emission from fast shock wave 80−46631
Tycho supernova remnant, search for fossil Stromgren sphere 78−36661
type I supernovae, photographic and spectroscopic obs. 77−57000
4U 0115+634, X-ray binary, 1980 Aug. photometry and spectroscopy 80−101650
4U 0241+61, optical and radio identification, luminous low-redshift QSO 78−61940
3U 1247-41, Centaurus X-ray cluster, vel. dispersion 77−74148
4U 1258−61, spectrum change in optical counterpart 79−71154
4U 1538−52, binary X-ray pulsar, early B-type supergiant as counterpart 78−93472
4U 1538−52, obs. of optical candidate 78−41093
4 U 1538−52, optical light curve of X-ray binary 79−35431
4U 1538−52, spectrograms of optical candidate, confirmation of identification 78−41094
4U 1538-52, optical counterpart spectroscopy and system parameters 79−5924
4U 1538-52 optical counterpart, discovery of reddened Be-type star 78−36727
4U 1543−62, optical candidate obs. 78−77625
4U 1608−52, optical identification and transient source outburst 78−41088
4U 1626−67, 7.7-second X-ray pulsar, simultaneous X-ray and optical obs. 80−51914
4U 1626−67, discovery of optical pulsations from proposed candidate faint blue star 79−9034
4U 1626−67, light pulses from optical counterpart 80−51916
4U 1626−67, pulsed optical emission detect. 79−62934
4U 1626−67, X-ray pulsar, optical candidate photometry 78−12418
4U 1626−67 optical counterpart, photometry 79−67120
4U 1626-67 optical candidate, optical pulsations discovery 78−65720
4U 1636−53 (MXB 1636−53), X-ray burster, optical candidate photometry 78−12418
4U 1658−48 optical counterpart, identification and semi-accurate position 78−69908
3U 1735−44, optical identification 77−60852
3U 1735−44, spectral obs. of optical counterpart 77−64882
4U 1735−44 (MXB 1735−44), optical identification and similarity to (Scorpius X-1) 78−93468
4U 1735−44 (MXB 1735−44), X-ray burster, optical candidate photometry 78−12418
4U 1755−33, optical candidate obs. 78−77625
4U 1837+04, UBR plates of Davidson optical counterpart 78−81714
4U 1837+04 (Serpens X-1), obs. of optical candidate 78−41093
4U 1837+04 (Serpentis X-1), absorption spectrum of counterpart 78−69912
4U 1907+09, optical identification using HEAO-1 scanning modulation collimator position 80−82542
3U 1956+11 optical counterpart, photometry and spectrum 78−49554
4 U 2129+47 optical counterpart, spectrum and photometry rel. to 80−17693
UBV photometry of southern galaxies 79−101198
UBV photometry of stars in field of IC 1795 (W3) 77−57082
UBVRGI photometric measurements of 1297 stars, catalogue on mag. tape 78−40839
UK Schmidt Telescope, obs. 79−48680
Umbriel, near IR spectra and JHK photometry, mass and dia. reassessment 80−56761
Universal Time observations, short period terms anal. *(Chinese)* 79−8589
unresolved visual binaries, suspected, reexamination 78−40993
Uranus, astrolabe obs. during 1977 at Santiago, Chile 79−58298
Uranus, astrometric obs. with Danjon Astrolabe of Santiago during 1975 and (1976) 78−12151
Uranus, atmospheric D/H ratio meas. 78−57497
Uranus, D/H ratio from visible spectra obs. 80−82296
Uranus, disk structure in 7300 methane band 80−17544
Uranus, evidence for satellite belt from SAO 158687 occultation 77−29718
Uranus, geometric oblateness from digitized photography, Stratoscope II balloon obs. 80−67649
Uranus, H_2 quadrupole lines detect. in spectrum 78−93149
Uranus, HD detect. at 6063.88 Å, D/H abundance ratio calc. 78−57495
Uranus, limb and polar brightening at 7300 Å 77−56873
Uranus, limb brightening, visible spectrum 78−61797
Uranus, limb brightening within methane 7300 Å band 78−85902
Uranus, lunar occultation, 1977 February 10, radius, limb darkening and polar brightening at 6900 Å 80−17545
Uranus, methane 6825 Å band obs. 77−78715
Uranus, methane absorpt. band in spectrum 78−45275
Uranus, methane band limb-brightness obs. 79−84742
Uranus, new satellite occultation of SAO 158687, Kavalur obs. 77−53473
Uranus, photometric var. in 1953-76 period 78−85901
Uranus, rings, possible obs. by William Herschel 79−48733
Uranus, rot. period, modified spectroscopic technique 78−16345
Uranus, rot. period determ. and effect of seeing on reflected spectrum 80−46479
Uranus, rot. period from spectral line tilts 78−20726
Uranus, rot. period meas. 78−7920
Uranus, rot. period spectroscopic determ. 80−51691
Uranus, rotation periods rel. to methane band strength var. 78−49376
Uranus, rotation velocity determ. 78−36508
Uranus, SAO 158687 occultation obs. rel. to upper atmosphere temp. struct. 79−62791
Uranus, satellite rings, KAO obs. of SAO 158687 occultation 77−53471
visible astronomical observations continued
Uranus, satellite rings occultation of SAO 158687, discovery accounts 77−74009
Uranus, secular brightness increase, 1972-76 period 78−16346
Uranus, whole-disc optical polarization meas. 77−45356
Uranus and Neptune photometric obs. for solar luminosity monitoring 77−53500
Uranus occultation of SAO158687, obs. possibilities in methane bands 77−29719
Uranus occultation of SAO 158687, 1977, Mar. 77−33407
Uranus occultation of SAO 158687, obs. rel. to upper atmosphere mean temp. and temp. vars. 80−46477
Uranus occultation of SAO 158687, planetary radius and ellipticity determ. 80−67648
Uranus ring system, obs. of occulation of (SAO 158687) 77−67068
Uranus rings, geometric albedo upper limit 78−36510
Uranus rings, occultation of SAO 158687, 1977 March 10, photoelec. obs. 79−30007
Uranus rings, radii and widths from 1978 April 10 occultation of SAO 158687 79−8878
Uranus satellite belt, numbers and positions from SAO 158687 occultation 77−33408
Uranus satellite ring system, new features from Kavalur photoelectric record of SAO 158687 occultation 78−12152
Uranus satellite rings, identifications and sizes from SAO 158687 occultation by 77−45358
Uranus satellites, astrometric obs. 80−67654
Uranus satellites, narrow band spectrophotometry of Ariel, Umbriel, Titania and Oberon 79−16879
Uranus stellar occultation, 1980 August 15 to 16, reality of additional occultations questioned 80−109396
Uranus upper atmosphere, struct. from SAO 158687 occultation obs. 80−17547
RU Urase Minoris, photometric obs. of contact binary 77−74088
Ursa Major stream, spectral types 78−85984
UX Ursae Majoris, anomalous 1977 period change for nova-like eclipsing binary 78−85956
γ Ursae Majoris, Ap star, chemical element distrib. from spectrophotometry *(Russian)* 77−22238
CQ Ursae Majoris, Ap star, UBV photometry, light curves, colour indices 78−49454
CQ Ursae Majoris, Ap star, UBV photometry, light vars., period determ. 79−88667
VV Ursae Majoris, BV photometry and elements of eclipsing binary 77−26026
TX Ursae Majoris, close eclipsing system, freq. domain anal. of light changes 77−53638
W Ursae Majoris, contact eclipsing binary, polarisation obs. 77−45489
XY Ursae Majoris, eclipsing binary, light curve changes, starspot activity 77−57044
XY Ursae Majoris, eclipsing binary, observational evidence for large-scale spot activity on primary component. 80−109491
XY Ursae Majoris, eclipsing binary, polarimetric obs. 78−28718
UX Ursae Majoris, eclipsing binary, time series photometry 80−77446
XY Ursae Majoris, eclipsing binary, variable light curve 77−91568
AN Ursae Majoris, emission lines and radial vel. curve 77−33514
AW Ursae Majoris, light curve anal. of contact binary 80−56875
AN Ursae Majoris, nova-like variable, extremely high circular polarisation obs. 78−8018
AN Ursae Majoris, polarisation meas. of nova-like object 77−29851
AN Ursae Majoris, polarisation of AM Herculis-type nova-like binary 78−85958
SU Ursae Majoris, probable 1980 March super outburst 80−51785
AN Ursae Majoris, steady low luminosity state 79−40219
W Ursae Majoris, vars. of period and light curve of eclipsing binary *(Italian)* 78−93318
α and β Ursae Minoris, astrometric obs. (1953-61) for Pulkovo large transit instrument orientation parameters determ. *(Russian)* 79−96910
α Ursae Minoris, coherence interferometer obs. for atmospheric modulation transfer function estimation *(Russian)* 79−16715
γ Ursae Minoris, high dispersion spectroscopy 80−41853
RT Ursae Minoris, photoelectric obs. of eclipsing binary 77−82276
α Ursae Minoris (Pole Star), stellar parallax meas. by Flamsteed and aberration 79−88786
α Ursae Minoris B (Polaris B), spectral type and interstellar reddening 78−8005
α Ursae Minoris region, field stars uvbyβ photometry rel. to reddening of Polaris 79−58356
UV5, in globular cluster NGC 1851, He abundance determ. 78−49441
UV and X-ray sources, objective prism spectrophotometry 78−8150
UV galaxies, double nuclei, visible spectra obs. *(Russian)* 80−77495
V 65 in ω Centauri, cluster membership determ. 78−73743
V 78 in ω Centauri, cluster membership determ. 78−73743
Valinhos astrolabe obs. (April 1974-December 1977) *(French)* 79−70944
van Bueren 62, 117, 121, dwarf stars in Hyades, spectroscopic orbits 79−5862
variable compact object discovery in Perseus, bright blue N-galaxy, photometry and spectrum 79−12524
variable emission-line star in core of M15, spectrum, photometry and position 79−5840
variable star discovery in M33, light curve, magnitude 78−73717
variable stars, 3-colour photoelectric obs. at Mt. Kobau (1970-3) 77−56955
variable stars, BAV results for 1973-5 period *(German)* 77−71118
variable stars, in globular cluster NGC 2298, photometry 77−13353
variable stars, Scorpius-Ophiuchus region, discoveries *(Chinese)* 80−77418
variable stars, UBV photometry at geographic latit. 69°22′ north 79−44376
variable stars in globular cluster NGC 1261, Oosterhoff type I system 77−53651
variable stars in globular cluster NGC 5286, B photometry, cluster membership 78−32534
variable stars in globular cluster NGC 5986, periods and light curves 79−5868
variable stars in globular cluster NGC 6934, photometry 80−56891
variable stars in Sculptor dwarf spheroidal galaxy, catalogue, of 602 stars 79−58431
variable stars in southern hemisphere, discovery *(Spanish)* 77−64782
variable UV excess object, discovery 79−40280

visible astronomical observations continued
variable UV excess object in Bootes, UGR photometry, position 79−48942
VB10, spectrophotometry rel. to low luminosity M-type dwarfs optical spectral classification 79−58339
Vela, spatial distrib. of young stars, UBV obs. 77−37597
Vela X-1 (HD 77581), X-ray binary, uvby obs. 77−37668
γ^2 Velorum, bright Wolf-Rayet binary, optical light curve 77−56945
AI Velorum, BVRI photometry and photoelectric radial vels. rel. to nature of variable star 80−94815
AI Velorum, dwarf Cepheid, nature from uvbyβ photometry 77−78801
CV Velorum, light curves, photometric elements and absolute dimensions 77−60796
AH Velorum, radius, delta luminosity and pulsation mode of δ Cepheid 80−46572
AI Velorum, RRs variable, photoelectric radial vels. 77−5533
γ_2 Velorum, Wolf-Rayet binary, orbital element determ. from spectral obs. 80−85950
γ^2 Velorum, WR binary, photometry and polarimetry 77−29847
Venus, atm. H_2O content from narrow band photometry data 79−62779
Venus, atmospheric, scattering coeff. from Venera 9 and 10 photometry 80−8572
Venus, atmospheric net radiation meas. by Pioneer small probe 80−46435
Venus, atmospheric struct. and comp. from refl. sunlight polarisation calc. and obs. 80−36533
Venus, cloud cover obs. and recording 78−49355
Venus, cloud layer model, Venera-10 optical meas. interpretation *(Russian)* 79−21215
Venus, cloud optical properties and atmos. layered struct. 80−51681
Venus, cloud particles phase function, Mariner 10 data 79−40105
Venus, CO_2 7883 Å band, high-dispersion spectroscopic obs. near superior conjunction 78−53851
Venus, dust ring possibility from Venera 9 and 10 spectroscopy 80−8573
Venus, exosphere, hydrogen Lyman α emission 80−105188
Venus, infrared spectra near superior conjunction, CO_2 bands 80−56740
Venus, night airglow excitation, O_2 Herzberg II bands 77−41340
Venus, nightside ionosphere, formation process, ionization, mixing ratios 80−41751
Venus, photographic position meas. *(Russian)* 78−93121
Venus, photographic position meas. *(Russian)* 78−93135
Venus, photographic posns., Fk4 corrections 79−8851
Venus, photographs from Pioneer Venus mission 79−84698
Venus, Pioneer nephelometer expts. results 80−46430
Venus, positional observations at UKrainian Main Astronomical Observatory, (1972) *(Russian)* 79−44390
Venus, positions, photographic obs. (1967-72) from Nikolaev *(Russian)* 79−92689
Venus, regional polarization, 1950-77 obs. 80−8570
Venus, sunlight absorption in atmosphere, Pioneer radiometer meas. 80−46434
Venus, surface dust detected by Venera 9 and 10 radiant flux obs. 80−72803
Venus, surface panorama and atmosheric boundary layer structure, Venera 9 and 10 obs. 77−78688
Venus, UV markings contrast spectral depend. 79−62783
Venus, Venera 9 and 10 panoramas and surface features *(Russian)* 77−25967
Venus, winds, spectroscopic obs., techniques and data reduction 79−75130
Venus and Mercury, Mariner 10 images, digital processing 77−78647
Venus atmosphere, H_2SO_4 aerosols characts. from isophotes, spacecraft obs. 78−81575
Venus atmosphere, lighting conditions in 0.5-1.1 μ range, Venera 9 and 10 meas. 77−78696
Venus atmosphere, retrograde rot., Fabry-Perot meas. 78−65525
Venus atmosphere, scattered solar radiation, day sky spectrum, Venera meas. 80−56573
Venus atmosphere, Venera-8 optical meas. interpretation 79−8864
Venus cloud layer, struct. according to Venera 9 televised pictures 80−67604
Venus cloudy layer, TV observation of UV and violet region from Venera station orbiter *(Russian)* 79−53747
Venus day sky spectrum, Venera 11 and 12 spectrophotometric obs. *(Russian)* 79−66949
Venus motion, numerical theory using radar, optical and Venera satellite obs. data 78−16325
Venus polarisation, wavelength depend. obs. rel. to UV cloud model 80−82250
Venus stratosphere, retrograde rotation meas. with Fabry-Perot radial vel. spectrometer 79−44389
Venus surface, Venera 9 and 10 landers, visible radiation 80−46425
Venus surface panoramas, photometric analysis of Venera 9 and 10 obs. 77−78686
Venus surface relief, Venera 9 and 10 contrast evaluation 77−78687
very red stars on Palomar Sky Survey prints 77−26008
Vesta, ang. diameter from speckle interferometry 78−20712
Vesta, diameter, interferometric meas. *(Russian)* 80−67634
Vesta, UBV photometry and lightcurve 80−36546
VI Cygni (Cygnus OB2) association, interstellar λ4430 band obs. 78−32555
Viking 2 landing and first photographs of Mars' surface 77−9689
BF Virginis, β Lyrae-type eclipsing binary, light curves 77−13395
32 Virginis, A-type main-sequence and Am-type star components 79−30091
32 Virginis, Am star, spectroscopic obs. and curve of growth anal. 77−22237
β Virginis, chemical composition and age 78−61855
α Virginis, decline of β Canis Majoris pulsation 79−12482
EQ Virginis, dK5e star, new absorpt. line obs., possible infalling gas 77−37602
AH Virginis, eclipsing binary, photometry rel. to period and light curve vars. 77−78822
ϵ Virginis, equivalent widths of Fe lines for spectral anal. 77−78771
CU Virginis, He I 4026 Å line var., photoelectric meas. 78−77555
EQ Virginis, late-type flare star, metal abundances 77−78779
78 Virginis, magnetic Ap star, high resolution polarisation obs. inside spectral lines 80−51772
78 Virginis, magnetic field gradient in Ap-star atmosphere, Zeeman spectra 78−85953

visible astronomical observations continued
AR Virginis, RR Lyrae variable, photographic photometry and mean light curve *(Russian)* 80−12769
CU Virginis, short period Ap star, discovery of mag. field 77−33511
CG Virginis, soln. of photoelect. light curve of eclipsing binary *(Chinese)* 79−53857
ψ Virginis (SAO 139033), ang. dia. from occultation obs. 78−20825
θ Virginis A, pulsating star of unknown type 79−44555
W Virginis stars, in southern hemisphere, VBI photometry 77−53612
Virgo cluster, UBV sequences for bright galaxies 77−13476
Virgo cluster of galaxies, new velocities 78−86028
Virgo cluster of galaxies, total magnitudes from Byurakan surface photometry 77−17698
visual binaries, orbital elements for 15 pairs 78−85969
visual binaries, radial vel. meas. 79−21347
visual binaries with variable components, orbital elements, visible obs. *(Russian)* 80−77455
visual binary stars, astrometric obs. rel. to gravit. const. var. *(Russian)* 79−44537
visual binary stars, parallaxes, mass ratios and masses for six pairs 77−64795
visual binary stars, southern, new obs., orbits and masses 78−96502
visual double stars, ang. separation and position angles, photographic obs. 78−40997
visual double stars, astrometric meas. at Nice *(French)* 78−89224
visual double stars, meas. at Las Campanas Observatory, Chile 78−8058
visual double stars, micrometer obs., (1975 to 1977) 78−89218
visual double stars, photographic meas. of position angles and separations 80−26909
visual double stars, photographic measures 79−17024
visual double stars, photographic obs., ang. separations and position angles 78−20860
visual double stars, southern, measures 79−21360
visual double stars, spectral classification and UBV photometry 77−74084
visual double stars measured at Las Campanas Observatory, Chile 78−85978
VRO 42.05.01, Hα inteferometric obs. of fast filaments and high vel. gas 79−75258
VRO 42.05.01, high vel. gas expansion in supernova remnant *(Russian)* 79−17069
Vulpecula OB2 stars, photometry and spectra rel. to membership of 67 day Cepheid S Vulpeculae 80−41831
15 Vulpeculae, Am star, photoelectric UBV obs. of magnetic field *(German)* 77−17586
WW Vulpeculae, fast irregular variable, H_α and H_β lines obs. *(Russian)* 77−87400
21 Vulpeculae, new luminous long period δ Scuti star, photometry 80−31306
BS Vulpeculae, photoelec. photometry of eclipsing binary, light curve, period 79−21351
15 Vulpeculae, radial vel. from spectrograms 77−56952
BW Vulpeculae, V photometry, light curve, quadratic ephemeris 80−26881
NQ Vulpeculae, visual magnitude estimates 1977, Feb. and Mar. 77−37607
ER Vulpeculae, W Ursae Majoris star, rot. line broadening rel. to shape and mass ratio 80−109494
Vulpeculae 1976, polarization and magnitude obs. 1976, Nov. 77−2442
LV Vulpeculae (Nova 1968 No.1), spectroscopy 77−87438
NQ Vulpeculae (Nova 1976), Hα emission line profiles in 1976 November to December *(Russian)* 78−40971
NQ Vulpeculae (Nova 1976), Hα var. 79−58352
NQ Vulpeculae (Nova 1976), spectral evolution 78−89205
NQ Vulpeculae (Nova 1976), UV and visual spectra analysis *(Chinese)* 80−12770
NQ Vulpeculae (Nova 1976), visual magnitude estimates 77−22254
NQ Vulpeculae (Nova 1976), visual magnitude estimates for 1978 Aug.-Oct. 79−5839
NQ Vulpeculae (Nova 1976), visual magnitudes, 1977 Nov.-1978 Jun. 78−65626
NQ Vulpeculae (Nova 1976), visual magnitudes (1978 June 29 to July 13) 78−85959
NQ Vulpeculae (Nova Vulpeculae 1976), photoelectric obs. 78−4252
NQ Vulpeculae (Nova Vulpeculae 1976), photometric obs., visual magnitudes 77−60767
NQ Vulpeculae (Nova Vulpeculae 1976), spectroscopic obs. of slow nova 78−85955
NQ Vulpeculae (Nova Vulpeculae 1976), visual magnitudes (1977 Aug.-Nov) 78−16434
VV 126, multicomponent interacting galaxies, visible spectroscopy obs. *(Russian)* 80−77494
VV 150, galaxy chain, photoelectric and spectroscopic study 80−98724
VV 493 (UGC 07910), unusual extragalactic object, morphology and spectrum rel. to probable nature 80−98718
VV 5-32-63/64 in Abell 1775, supermassive double galaxy, radial vels. 80−8693
VV 5-42-11(=Zw 171-20), probable supernova in interacting galaxy 77−53615
VV 617 (NGC 6240), obs. of nucleus in type II Seyfert *(Russian)* 79−67103
VV 794 H II regions, photographic and spectral obs. *(Russian)* 80−77493
VV 8, galaxy, rot., mass and surface brightness obs. *(Russian)* 79−48937
VV interacting galaxies search for clumpy irregular galaxies 79−101201
0846+51W1, eruptive BL Lae object with high z, visible and radio obs. 79−62899
W1 (S171), optical supernova remnant radial vel. field 80−62250
19 W32, 43 and 109, galactic centre planetary nebulae search 80−90506
W3/W4/W5 region, heavy optical obscuration obs. 80−62301
W50, supernova remnant, N II emission enhancement and distance rel. to assoc. with (SS 433) 79−92783
W50, supernova remnant, optical filaments spectra rel. to SS 433 mass loss rates and lifetime 80−12804
W50, supernova remnant, optical spectrum 80−90557
W50, supernova remnant, spectrum of optical nebulosity 80−51851
W50, supernovae remnant, associated filamentary optical nebulosity detect. 79−88723
W50 (SS 433), supernova remnant, optical filamentary nebulosity discovery 80−56916

visible astronomical observations continued
W51, first optical detection, rel. to galactic spiral struct. 78−61900
W851, high-velocity star, parallax and tangential vel. 77−49387
W92, possible gravit. contracting binary system in NGC 2264 young cluster 78−32462
Walker No.67 in NGC 2264, interstellar linear polarisation meas. rel. to circular polarisation existence 78−12223
Wat 6, open cluster, photometry and spectra rel. to proximity to (Pismis 6 and 8) 79−88712
weak absorpt. features in Ca II H and K wings rel. to nonthermal broadening in photosphere 77−60735
weak G-band stars, CH and NH band strengths, atm. material from CNO cycle 79−8917
weak-G band giant stars, Li abundance determ. 78−53948
Westerbork 1415 MHz survey of background radiosources, optical identifications 77−49488
Westerbork 1415 MHz survey of background radiosources, optical identifications 77−64867
white dwarf C_2 stars, spectrophotometry 77−29824
white dwarf stars, rot. and gravit. redshift 77−29816
white dwarfs, multiperiodic light curves, g-mode rotation 78−4210
white dwarfs, search at south galactic pole 79−21274
white dwarfs, southern, Stromgren photometry 78−32456
white dwarfs, spectra of 47 southern stars 78−16417
white dwarfs, spectrophotometry with Carnegie image tube 78−57466
white dwarfs, spectroscopic survey using Luyten catalogues 78−7998
white dwarfs, visual surface brightness relation appl. 78−81624
white dwarfs in globular cluster NGC 6752, UB photometry 78−93233
white dwarfs in open clusters, obs. rel. to progenitor stars upper mass limit 80−51738
white dwarfs with He lines, spectrophotometry 77−53588
wide visual double stars, B, A and F type, uvbyβ photometry 79−17025
wind effects on latitude obs. at Poltava *(Russian)* 78−3915
WLM galaxy (A2359), BV photometry 77−82302
Wolf 1062, astrometric anal. of unseen companion from 61 cm Sproul refractor plates 78−16459
Wolf 1062, red dwarf, astrometric perturbation 77−49439
Wolf 922, nearby red dwarf, evidence for low-mass unseen companion 80−51809
Wolf-Rayet stars, faint, photometry and spectrography 79−40200
Wolf-Rayet stars, in M33, spectral obs. 77−64779
Wolf-Rayet stars, near IR spectra emission line characts. 79−53825
Wolf-Rayet stars, search for rapid Hα and Hβ line variability 77−26014
Wolf-Rayet stars, search in SMC 79−67014
Wolf-Rayet stars, short-lived changes of emission lines *(Russian)* 80−72977
Wolf-Rayet stars, WC9, optical spectropolarimetry and spectrophotometry 77−64778
Wolf-Rayet stars discovery in 30 Doradus nebula in LMC 79−16980
Wolf-Rayet stars in galactic-centre field, new discoveries from spectroscopic obs. 80−8674
Wolf-Rayet stars in LMC, new discoveries, positions, spectra and magnitudes 80−46569
Wolf-Rayet stars in LMC, new discoveries 79−67018
Wolf-Rayet stars in SMC, spectral classification 78−73716
WRA 977, B-type supergiant, spectroscopic obs., X-ray source identification 79−101148
WRA 977 (4U 1223−62), lightcurve and radial vel. curve 79−21307
Wray 977, optical counterpart to X-ray binary pulsar, 4U 1223−62, optical spectra 80−72984
Wray 977 (4U 1223−62), B-type supergiant, spectral classification 79−80305
X-ray and gamma-ray sources, optical counterpart identification using proper motion data 78−93457
X-ray burst sources, optical monitoring 78−77622
X-ray bursters, 1980 plans for simultaneous optical/X-ray obs. 80−8716
X-ray bursters, spectroscopic study of optical counterparts 80−46699
X-ray clusters of galaxies, gas stripping from spirals 78−32586
X-ray clusters of galaxies, radial distrib. of morphological types of galaxies 78−8129
X-ray clusters of galaxies, X-ray luminosity correl. with galactic content 78−32585
X-ray source fields from Einstein Observatory, RI photometry with CCD camera 80−62315
X-ray sources, linear optical polarisation obs. *(Russian)* 77−64880
yellow semiregular and RV Tauri variables, photometric investigations 80−26865
Yerkes poor cluster members, reshifts 80−51858
young emission-line stars in S Hemisphere, image tube spectrograms 78−8016
young open clusters, UVBYβ photometry rel. to bimodal star form. 77−49374
young Orion stars, scanner K-line photometry 77−33579
ZB 33, RR Lyrae type star, light curve study *(Chinese)* 80−8633
zodiacal light, Helios 1 and 2 obs. 78−24483
zodiacal light, source function from Helios A and Pioneer 10 photometric obs. 78−36539
zodiacal light Fraunhofer lines Doppler shift, interplanetary dust dynamics 78−45278
zodiacal light photopolarimetry, brightness annual vars. rel. to zodiacal cloud symmetry plane 78−45276
zodiacal light spectrum, Doppler shifts meas. 78−85904
zodiacal light surface brightness meas. by AE-C satellite 80−17548
II Zw 136, Seyfert galaxy nuclei, optical variability, UBV obs. 80−73049
I Zw 1727+5015, redshift and spectra of BL Lacertae-type object 78−41044
I Zw 18, dwarf blue compact galaxy, blue star emission spectra 77−37593
III Zw 2, quasar, spectrophotometry of assoc. galaxies and nebulosity, redshifts 79−21460
II Zw 40, dwarf blue compact galaxy, blue star emission spectra 77−37593
VII Zw 421 and II Zw 67, spectrophotometry of S0 galaxies 80−51866
VII Zw 466, ring galaxy, UBVR photometry 79−8991
II Zw 70, optical and radio obs., evidence for star form. 79−16935
I Zw 92, III Zw 77, compact galaxies with broad emission lines, spectra 78−73760
ZwCl 1710.4+6401, BV photometry of member galaxies *(Russian)* 77−87555
Zwicky compact galaxies, spectroscopic survey 79−17074

visible astronomical observations continued
μ Draconis (ADS 10345), radial vel. var. from spectra in visible 80−17612
1228, nearby red dwarf, evidence for low-mass unseen companion 80−51809
20,986, new unresolved astrometric binary 78−57594
Ba 0 stars, abundance anal. 77−17557
Ba, CH and R-type carbon stars, spectrophotometry 77−17575
Ba II giant stars binary nature from visible radial vel. obs. 80−82355
Ba stars, DDO system photometry, luminosity anomaly 79−35246
C star, variable, in open cluster, Stock 8, spectroscopic and photometric obs. 79−84791
C stars, $^{12}C/^{13}C$ abundance ratio 77−33494
C stars, in LMC, VRI photometry, optical spectroscopy and evolutionary implications 79−71019
C stars, spectral clssification by photoelec. photometry of line strengths 78−73711
C stars, spectrophotometry, C/O and $^{12}C/^{13}C$ ratios calc. 77−91533
C stars, violet opacity 78−53940
C stars in Cygnus, new discoveries and BV photometry 80−46551
C stars in NGC 419, SMC globular cluster, photographic photometry 78−53962
C stars in red globular clusters in Magellanic Clouds 79−101143
C_2 absorption bands in stellar spectra, 876 nm obs. 80−12805
CH in diffuse interstellar medium, optical and radio obs. 78−93356
CH star in M22 globular cluster, CH and CN anomalies 78−8001
CH stars in south galactic cap, radial vels., photometry 77−87396
Ca II H and K lines in F0 to M2-type stars, high resolution absolute flux profiles 80−26842
Fe III in astronomical sources, multiplet table 80−41732
H deficient and He weak stars, uvby photometry, variability 80−46579
H I and Mg II absorpt. lines obs. in QSOs and BL Lacertae objects 78−28838
H II condensation in NGC 2175, obs. of involved stars 78−20883
H II region vel. dispersions rel. to linear diameters 77−33595
H II regions, abundance gradients from photoelectric spectrophotometry in 3700-7400 Å range 78−41036
H II regions, chemical comp. of galactic and extragalactic regions 78−93359
H II regions, giant, extragalactic, vel. dispersions from Hα line widths 79−44606
H II regions, unusual large-scale motions 78−16509
H II regions, weak emission lines spectrophotometry using image tube *(French)* 79−88601
H II regions as extragalactic distance indicators, obs., struct. considerations 79−40231
H II regions in barred spiral galaxies NGC 1313, 5236 and 7552 visible obs. 80−82510
H II regions in Perseus arm, spectrophotometry and reassessment of galactic abundance gradients 80−22055
H II regions near nucleus of spiral galaxy NGC 3310, exploratory investigation 80−62235
H I+molecular/H II shells from 1 to 1200 pc dia. in LMC, obs. and origin 79−25678
H_2O^+, interstellar, unsuccessful search and abundance upper limit 78−69860
Hα emission line star obs. rel. to star formation 79−58333
Hα emission objects in Coalsack direction, finding list 77−22115
Hα emission stars, optical scanner data 80−56827
Hα emission stars in and near NGC 7000, obs. 77−13363
Hα emission stars in Milky Way, catalogue of new discoveries 77−64665
Hα emission stars in southern dark clouds, UBVR photometry 78−81633
Hα emission stars in young cluster NGC 2264, UBVRI obs., pre-main sequence stars 79−35267
Hα-emission stars in Perseus OB1 assoc. region 80−56855
He rich stars, intermediate and extreme, spectral atlas in 3700 to 4600 Å range 80−94806
He strong stars, mag. fields meas. 79−44486
He weak and He strong stars, spectrum variability 79−40201
He-weak stars, photoelectric meas. of H Balmer lines 79−16994
^{3}He stars, spectroscopic search, diffusion hypothesis 79−35264
Hg-Mn spectroscopic binaries, high-dispersion spectrograms 77−17629
HgMn stars, spectrophotometry 80−26867
Io, Na I, Ca I, Fe I, and Mg I emission lines in spectrum 79−21223
RR Lyrae stars in Sonneberg fields near north galactic pole, distances, density distrib. 77−82229
Mn-Hg stars, differential curve-of-growth analyses 79−16971
N deficient supergiants in loose assoc., LTE and non LTE abundance anals. 79−44478
NaH, interstellar, search in diffuse clouds 78−4325
τ Scorpii, spectral line studies using LTE-method *(Russian)* 79−92769
Tc stars, search for TcO spectral bands 78−40935
U stars and related objects, spectroscopic study 78−49465

vision
see also colour vision; eye; vision defects; visual perception
aberration tolerances for visual optical systems 77−73529
accessory optic projections upon oculomotor nuclei and vestibulocerebellum 80−3643
accessory optic system in the rat 80−21470
accommodation, reaction and response times obs. 80−67073
accommodation as a function of object form 79−11930
accommodation compensation for visual instrument astigmatism 79−34563
accommodation cues in distance judgment, chameleon 77−52791
accommodation dynamics, range nonlinearity 79−83770
accommodation in infants, photorefractive study 80−56028
accommodation microfluctuations, IR optometer recorder *(French)* 78−7463
accommodative responsiveness rel. to contrast sensitivity for sinusoidal gratings 80−61552
acoustic seeing aid for blind *(Polish)* 80−8215
acuity, infant, underestimation as near threshold gratings are not preferentially fixated, expt. obs. 80−56053
acuity and contrast sensitivity, goldfish 79−62264
acuity assessment by evoked pots., temporal depend. of spatial freq. selectivity 78−64995
acuity assessment through linear extrapolation to threshold of bar grating evoked responses 80−67080

vision continued
acuity asymmetry in opposed semi meridians *(French)* 80−16936
acuity charts, suitable illumination sources 80−12079
acuity development in infant monkeys during early postnatal weeks 78−61180
acuity for letters in rows or columns, advantage to rows 80−89761
acuity in cats with central retinal lesions 78−40158
acuity in human infants, assessed with stationary stripes, phase-alternated checkerboards 79−48261
acuity in human infants, review and comparison of studies 79−53112
acuity in infants and its meridional variation 79−53113
acuity screens, reflectance obs. 80−67178
acuity test letters, with and without serifs, comparitative expts. 79−34564
acuity tests, comparison of STYCAR and Lighthouse tests for preschool children 78−35851
acuity tests, near-point, type-size variability 78−48802
adaptation, afterimages and cone saturation 78−56978
adaptation, technique for estimating the contrib. of photomech. responses 80−85547
adaptation 78−15834
adaptation mechanisms, length-selective and non-length-selective, properties 79−20541
adaptation to patterns containing 2-dimens. spatial struct. 78−40160
adaptation to sine wave gratings, subharmonics 78−69073
adaption model evaluation for vestibulo ocular reflex 79−11931
adaption to bright lights gold fish, 'silent period', behavioural confirmation expts. 79−2064
aftereffects derived from inspection of orthogonally moving patterns 80−104589
airport control tower cab, optical design 80−58661
alcohol effect on visual recovery from glare, rel. to target acquisition 78−11660
Alopex process: Visual receptive fields by response feedback, trigger features 80−61546
alpha-contingent visual stimulation, detect. of cerebral lateralisation of function 80−94190
anisotropy, development in late childhood, 5 to 11 years 77−60213
annelid worms, deep-sea and surface types 77−86496
annular artificial pupils, props. 80−41356
aperiodic stimulus detection by probability summation among narrowband channels 77−48802
apparent contrast matching, narrow-band spatial mechanism 80−61571
aquatic eyes, retinoscopy, refractive error considerations 80−61750
artifical vision machine for blind people *(Korean)* 79−66583
artificial sight and hearing, appl. of microcircuits 78−20311
associative learning model, voltage-dependent Ca^{2+} and K^{+} conductances 80−72166
astronaut light flash observation on Skylab 4, role of nucl. stars 77−5089
attention operating characteristic, visual search examples 79−57641
auditory deprivation effects on vision, common intermodal and intramodal factors 80−89754
aviation medicine, visual, auditory and vestibular fitness standards (report) 79−11920
axon-bearing horizontal cells, teleost retina, functionality obs. 80−51084
bacteriorhodopsin, 13-cis and trans isomers, photochem. and dark equilib. 77−90798
bar pattern detection, effects of subthreshold inducing fields 78−15840
barnacle photoreceptor visual response rel. to metarhodopsin transitions 78−69050
barnacle photoreceptors, initiation of light adaption, intracellular recordings 79−20542
barnacle photoreceptors, lateral vs. median, elec. props. and early receptor pots. 77−44651
bathoproducts of rhodopsin, isorhodopsin I, and isorhodopsin II 80−51088
behaviour monitoring system, EMG triggered photographic technique 78−31919
bibliography, British university dissertations and theses, 1972-7 80−105449
bifoveate retina of lizard, light microscopic study 80−101165
binocular, constant curvature assumption, theory 80−94214
binocular competition in cats, behavioural study 77−12916
binocular detection of disparate light flashes 77−60212
binocular disparity initial appearance and singleness of vision 78−40161
binocular eye movements during accommodation vergence 78−61186
binocular flicker stimulator using polarisers 78−24075
binocular interactions, role in development in cat 80−12117
binocular interactions, suprathreshold, effects of prolonged monocular occlusion 80−67085
binocular summation, contrast sensitivity, visual acuity and recognition 78−61188
binocular summation, fusion and tolerances 80−104588
binocular summation and the binocularity of cat visual cortex 80−16946
binocular summation in normal and stereoblind humans 77−60211
binocular vergence dynamic components step stimulation 79−79550
binocular vision deprived humans, binocular interactions tuned to size and orientation 80−81606
binocularity and stereopsis in the evolution of vertebrate vision 80−12144
binoculars, preferred dioptric settings for high and low light levels 77−21528
biomedical stimulus device for characterizing temporal MTFs in man 80−51204
blind boy with visual assoc. cortex destruction, pattern-evoked occipital pots. 78−40145
blink reflex, peripheral electrical stimulation inhibitory effect, abolition by naloxone *(French)* 80−35880
blinking and suppression of visual stimulation 80−97909
Boll, Franz, (1849 to 1879), investigator of retinal pigments, biography 78−20927
brain, complex visual stimuli representation 78−88709
brain, mag. evoked field mapping 80−104705
brain functional organisation, methodical approach *(Russian)* 78−35824
brain mechanisms of vision 79−96557
brain potentials, visually evoked, meas. of signal components 77−40946
brain signal processing *(German)* 78−48792
brightness contrast simultaneous induction in pigeons 78−48804
Broca-Sulzer effects, asymmetry in brightness and darkness effects 80−101185

vision continued
n-butyl retinal Schiff bases, absorpt. spectral props., rel. to bathochromic shift in visual pigments 78−40117
callosal neurones selection, effect of visual experience, cat 79−79524
car drivers, work spectacles and functional visual fields *(Italian)* 80−108875
carotenoids related to visual chromophore, electronic struct., band shape model 78−20142
cat, Siamese, abnormal visual resolution 77−16931
cat binocular vision, eye alignment development 78−27955
cat superior colliculus, neuronal network charact. 78−31808
cat visual acuity and near point of accommodation 77−60214
cataractous lens, optical transmission at 430 nm and blue field entoptoscopy 80−45883
category detecting nerve cells formation, mathematical theory 78−80859
cerebral cortex, mammalian, visual areas, book contrib. 79−96560
cerebral potential sources location for visual field impairment assessment in humans 80−30922
checkerboard pattern generator electronic 77−40801
checkerboard-evoked multichannel pot. fields, reference-free components identification 80−108887
chemical synapse, feedback mechanism model through elec. current 78−96043
chromatic response of human eye, Karhunen-Loeve analysis of landscape multispectral data 80−48164
chromophore, optical spectra of related polyenes 77−29102
chromophore electronic structure 78−15764
chromophore rhodopsin photon absorption, probing by picosecond spectroscopy 79−8507
circadian rhythms in humans, role of light, bibliography 77−48985
clinical optotypes, high-pass spatial frequency letters 79−2063
clinical perimetry, glossary of basic information *(Italian)* 79−39413
coarse pattern detection with minimum contrib. from rods 77−48803
cognitive processes, anal. by meas. of visual fixation points 78−31816
comparison with hearing, broadcasting appl. *(Japanese)* 78−73155
compensatory eye movements to miniature rotations, rabbit, retinal image stability implications 80−45890
complex pattern discrimination, learning by young kittens, expt. obs. 80−56049
complex receptive field of cat visual cortex, spectral charact. of stimuli and responses 77−16927
complex shaped objects, visual resolution and recognition, vibr. influence *(Russian)* 80−45909
complexity estimation of visual search, for objects against nonuniform backgrounds 80−67086
composite photographic-human visual system, spatial-freq. filtering effects in performance 78−4725
compound eye, Dipteran, small signal phototransduction 80−35882
compound gratings, phase and detect. obs. 80−61558
computed tomography of the visual pathways 80−56178
cone, computer-driven hardware model, response obs. 80−72402
cone system, attenuation during rapid dark-adaption, frog 79−62253
cone voltage-current relationships, turtle, origin of non-linearity 79−74659
cones, single and double, intraspecific evidence for function in teleost retina 79−62248
conference, Houston, USA, (March 1977) 80−8736
contact lens fabrication, spincasting using polyhydroxyethyl methacrylate 77−795
contact lenses, hard, dimens. stability of different materials 78−77150
contact lenses, thickness definition 80−46094
contingent negative variation and accuracy of time estimation. A study on cats 80−26216
contingent negative variations, rel. to distraction-arousal hypothesis 77−5002
contrast, successive and simultaneous obs. 80−76742
contrast detection thresholds of moving sine wave patterns, perimetry, far peripheral field 78−69070
contrast detection thresholds of moving spatial sine wave patterns, perimetry, near peripheral field 78−69069
contrast detection thresholds of moving spatial sine wave patterns, perimetry 78−69071
contrast detection thresholds of moving spatial sine wave patterns, perimetry 78−69072
contrast evoked potential, invariance with retinal illuminance changes 80−51085
contrast sensitivity, low spatial freq. and low number of cycles at low luminance 78−65021
contrast sensitivity as a function of position on the retina 80−61561
contrast sensitivity function 77−25442
contrast sensitivity function rapid meas. 78−56975
contrast sensitivity of 6 month old infant meas. by evoked pot. 77−12913
contrast sensitivity rel. to stimulus onset and image motion 80−16938
contrast sensitivity to narrow-band CRT phosphors 79−11933
contrast threshold for sinusoidal gratings, functional area for summation 78−65002
contrast threshold response of human eye based on Tiffany data anal. 80−51093
contrast thresholds for patterns of dynamic visual noise 79−100611
contrast thresholds versus border enhancement, scatt. light effect 80−94213
corneal lens, soft radius of curvature meas., using autostigmatic microscope 77−60198
corrective saccades, effects of altering visual feedback 78−40150
cortex, cat, functionally characterised neurones morphology and intracortical projections 79−74655
cortex, cat, tuning of receptive fields 79−57646
cortex, circuitry changes gated by postsynaptic activity, kitten 79−74652
cortex afferent geometry and neuronal trigger features generation, primates 78−35842
cortex area 19 cells, cat, classification by connectivity and photic responsiveness 80−35886
cortex functional specialisation of rhesus monkey 78−80873
cortex local spectral anal., image description model 78−40143
cortex neural circuitry model for orientation sensitivity 79−11927
cortex neurones, rabbit, organisation of background activity 78−69044
cortex neurons, cat, mechanisms underlying receptive field props. 79−74662
cortex receptive field organisation and spatial freq. charact. 78−69068
cortical, critical period interaction, kitten 78−56972

vision continued
cortical area 19 of cat, periodic complex cells 78−56974
cortical cell spatial resolution and nonlinearities, cat 77−9187
cortical changes in uncrossed retinotectal projection after one eye removed at birth 79−57650
cortical desynchronisation detected by power meas. of scalp EEG 77−81494
cortical effects of early visual experience 80−12119
cortical electrical phosphene props. 80−12112
cortical evoked potential, normal humans, main chapters of research 79−20537
cortical muscarinic acetylcholine receptor and acetylcholinesterase increase on exposure of dark-reared rats to light 78−24069
cortical neurone orientational prop. recovery and ocular motility in dark-reared kittens 78−53396
cortical neurone reaction patterns to const. illum. 78−80871
cortical neurons, optimality of bar and grating stimuli 80−85391
cortical orientation selectivity, of partially visually deprived cats 80−26230
cortical pattern evoked pots. and single unit responses, cat 78−27947
cortical pattern evoked visual pots., estimation of rat eye refr. 77−70455
cortical periodic complex cells, cat, spatial freq. selectivity 78−69057
cortical plasticity in monocularly deprived immobilized kittens, eye movement dependence 80−81588
cortical plasticity rel. to local perfusion of noradrenaline 78−35847
cortical potentials associated with detect. of visual events 77−52782
cortical projections of area 18 in owl monkeys 77−60207
cortical receptive field binocular differences in kittens after rotationally disparate binocular experience 77−90784
cortical slow negative waves following non-paired auditory and visual stimuli 80−3650
cortical visual evoked potential, normal humans, bibliography of research 79−5278
crayfish, coding and decoding of steady state information by patterned pulse trains 80−12105
critical duration changes during dark adaptation 80−51094
critical flicker fusion freq., river lamprey 79−74663
crustacean eyes and polarisation sensitivity 78−7350
Curculionidae head capsule transmission of long-wavelength light, rel. to visual cues 77−64030
cyclofusional response, human, effect of stimulus size 78−61187
dark adaptation, rod-cone interaction 77−32891
dark adaptometer for student use and optometric practice 78−48912
dark-adapted retina, absolute threshold 77−90788
dark-adaption, comments on the testing of 2 prominent hypotheses 80−108896
defocus, psychophys. and electrophysiological effects 77−90768
detection, effect of photon noise 80−61559
detection and resolution, effects of target size 79−48259
detection of stationary structs., role of eye movements, theoretical model 80−81594
detective quantum efficiency of human eye 78−56976
detective quantum efficiency reduction due to lateral neural interactions 78−53395
diabetic blindness prevention with ophthalmic photography 80−16920
difference thresholds modelling, appl. of ordered topological vector spaces 80−104587
dioptric corrections of age dependent isopters 79−20539
dipteran giant visual interneurone response props., rel. to optomotor control 78−27940
direction selectivity in visual cortex, neural network model 79−48251
direction sensitivity in visual cortex, neural net model 79−48248
direction-selective adaptation with very slow motion 79−92218
direction-specific adaptation, 2D anal. 80−61555
discrimination between small objects and large textured backgrounds 78−11652
disinhibition in visual aftereffect adapting to two orientations 80−97921
distance constancy mechanism, visibility of gradients and low spatial freq. sinusoids 78−65018
distortion measure in image processing context, visual system model 78−65015
dual input nonlinear system characterisation using impulse trains 78−31761
dynamic functions, objective and automatic meas. 77−1989
EEG, event-related potential changes in chronic alcoholics 80−67076
EEG, operant conditioning of brain steady potential shifts in man 80−21466
EEG, pattern stimulated pots., dipole localisation 80−26235
EEG, pattern-evoked potentials and nerve conduction vel. in family with adrenoleucodystrophy 80−45875
EEG alpha rhythm blocking, absence in visuobehavioural deprivation 78−27944
EEG alpha-detection system, feedback stimulation and data analysis system 79−29642
EEG analysis methods and activation techniques *(Croatian)* 78−44666
EEG background activity during one-second photic stimulation on/off effects 78−69047
EEG photic flash response, quantitative approach 80−30923
EEG visually evoked responses in children, intermittent photic stimulation *(French)* 79−16201
effect of vibration on reading numeric displays 80−104582
electric responses in geniculo-striate and pulvino-extrastriate systems, squirrel monkeys 77−40667
electro oculography, computerised diagnostic system 80−21566
electro-optical imagery display efficiency study using human visual system model 77−73531
electron-optical convertor resolution, static and dynamic eye characts. 77−7204
electronic eye for blind people, implementation through the optical nerve *(Croatian)* 80−109060
electrophysiological examinations for selection, ophthalmological surveillance of flying personnel 79−11929
electrophysiologoal techniques for exam., of visual function in man, review 78−35843
electroretinogram, adaptation-overlap model, response to laser stimuli 79−74650
electroretinogram, E- and b-wave analogue model, retinal expression of inductive reactance 77−48797
electroretinogram, elicited with sinusoidal flicker, component anal. 79−74660
vision continued
electroretinogram, human, nonlinearities reflected by Wiener kernels 79−34556
electroretinogram, photopic, freq. response characts. meas. with synchronous detect. 77−48796
electroretinogram e-wave, frog, rel. to ganglion cell activity and rod responses 79−48254
electroretinogram of albinos 79−53099
electroretinogram P III component model, luminance variations 77−81495
electroretinographic response rel. to vars. of visual performance during day 78−77051
electroretinographic species difference within the leopard frog complex 79−62254
electroretinography, human, psychophysical appl., review 78−35859
energy uptake in the first step of visual excitation 80−30724
epilepsy, photosensitive, role of pattern in TV viewing 80−26214
epileptic subjects, background illumination effect obs., intermittent stimulation 80−98009
epiphysis, frog, characts. of slow pots. 80−56029
equivalence classes of visual stimuli, model neural network 78−69064
equivalent background and retinal eccentricity 79−43898
ERG, human corneal, frequency domain anal. 80−45888
ERG, rabbit, dynamic light-dark adaptation 80−35887
ERG, suprafusion, theoretical retinal anal. 80−56020
ERG, Wiener kernels and freq. response functions, human retina, obs. 80−45887
ERG B-wave of ground squirrel, spectral components 80−51082
ERG photostimulus calibration by standard photometer and photodiode 80−8222
ergo-ophthalmology and ergo-optometry *(Italian)* 80−26223
event related potentials of the late positive complex in visual discrimination tasks 79−39416
evoked brain potentials, comparison of signal components in auditory and visual pots. 78−44513
evoked cortical potential, rel. to dark adaptation, human 77−9192
evoked cortical potential, removal of alpha by selective averaging 77−81766
evoked cortical potential meas., signal optimisation using Kalman filter *(Japanese)* 80−72348
evoked cortical potentials, transient response, techniques reviewed 78−35844
evoked cortical potentials in men during compression and saturation in $He-O_2$ 78−61173
evoked cortical potentials in renal failure, latency changes 79−16200
evoked cortical pots. during binocular rivalry 78−40153
evoked cortical response obs., infants and adults 79−43873
evoked cortical responses, monocular study 80−3640
evoked elec. and mag. response simultaneous recording 78−53558
evoked electrocortical response rel. to microwave-induced hyperthermia, guinea pig 80−61627
evoked neural activity intensity and structure, rel. to visual system modelling 77−25426
evoked potential, cortical, normal humans, bibliography 79−39414
evoked potential, man, early oscillatory pots. 79−70549
evoked potential, microsecond sensitivity of human system to irregular flicker 80−81586
evoked potential, N1-P2 correls. of reaction time at the single trial level 80−85389
evoked potential, nonstationary EEG, anal. using max. entropy method 80−26397
evoked potential, steady state latency determ. 77−21516
evoked potential, theoretical investigations and clinical appl. 80−26234
evoked potential amplitude rel. to pattern displacement amplitude 77−90778
evoked potential analysis, on-line signal optimisation using minicomputer 77−5112
evoked potential analysis *(Japanese)* 80−12090
evoked potential augmentation/reduction by cortical mechanisms, cat 78−27945
evoked potential data, appl. of low-pass linear filters 79−84032
evoked potential distribution, half-field pattern-reversal and pattern-onset stimuli 77−12912
evoked potential evidence of adaptation to spatial Fourier components in humans 78−69051
evoked potential late components in man, effects of selective attention 77−70445
evoked potential latency, steady-state, phase versus time analysis 78−11643
evoked potential maturation in normal child *(French)* 78−24068
evoked potential on-line evaluation by sliding average form. *(German)* 78−85402
evoked potential recording in high-noise environment, biphasic 60 Hz synchroniser cct. 78−24155
evoked potential recovery, cumulative inhibitory effect of repetitively flashed stimuli 78−69048
evoked potential registration methods *(German)* 78−48916
evoked potential rel. to sensory discrimination task 80−3645
evoked potential scalp topography in auditory and visual go/nogo tasks 78−31818
evoked potential spectrum, short-term vars. 77−48795
evoked potential to search in short-term memory, late components 78−61172
evoked potential waveform, effects of head support *(Japanese)* 80−3642
evoked potentials, amplitude and degree of event-related desynchronisation 80−12087
evoked potentials, appl. in brain mechanism studies and diagnosis *(German)* 80−61535
evoked potentials, average, microprocessor-based system for studying 80−56150
evoked potentials, averaged, long-term changes after X-irrad., rabbit 78−11704
evoked potentials, changes in P3 waves with event repetition 79−70550
evoked potentials, classification for visual stimuli discrimiuation 79−92414
evoked potentials, cortical extracted pattern response with bipolar and monopolar recordings 77−12919
evoked potentials, during hypothermia, prolonged circulatory arrest 79−16204
evoked potentials, event-related, in normal, mentally retarded and autistic children 80−85388

vision continued
evoked potentials, human scalp topography 77−40669
evoked potentials, interlab. vs. intralab. and intersession vs. intrasession variability 77−70570
evoked potentials, latency and reaction times as power functions of luminance in peripheral field 79−11928
evoked potentials, latency and wave form obs. 80−97907
evoked potentials, monocular, recording under binocular conditions 78−81035
evoked potentials, n-hexane induced changes, ERG of industrial workers 80−45886
evoked potentials, recording and evaluation procedure for neurophysiology and medical diagnostics *(German)* 80−26404
evoked potentials, single-trial classification using stepwise discriminant anal. 80−85387
evoked potentials, size-specific information channels and selective attention 79−62246
evoked potentials, size-specific interocular suppression, rel. to human binocular vision 78−31810
evoked potentials, spectral band analysis, contrib. to attentional processes study *(French)* 80−61721
evoked potentials, steady-state, effects of meridional variation 80−56033
evoked potentials, transient, in man, size and orientation specificity 78−69056
evoked potentials, transient, real-time filtering 78−31940
evoked potentials, use in intracranial pressure estimation 80−26398
evoked potentials, use in pediatric diagnosis 80−26407
evoked potentials, usefulness in multiple sclerosis diagnosis *(Italian)* 79−34555
evoked potentials and EEG freq. in patients undergoing haemodialysis and kidney transplantation 78−61160
evoked potentials and excitability cycle during simulated diving at −610 m in O_2-He 77−5000
evoked potentials and sensory dimensions 80−61548
evoked potentials from occipital and precentral cortex in visually deprived humans 78−3479
evoked potentials in discrimination tasks, scalp topography 77−52797
evoked potentials in monkeys 80−45885
evoked potentials in the first 6 years of life 80−97905
evoked potentials rel. to pattern reversal stimulus frequency *(German)* 79−16322
evoked potentials steady state, recording and appls., review 78−35823
evoked potentials to electronic pattern reversal, latency variations 80−94202
evoked potentials to sine wave modulated light in normals and patients, interhemispheric relationships 78−77049
evoked potentials to stimulus trains, normative data and photosensitive seizures appl. 80−94204
evoked pots., polarity inversion obs. 79−100602
evoked response, automated EEG system 77−90936
evoked response, central visual field contribs. 80−108881
evoked response, digital inverse filtering 79−53098
evoked response, multiplexing system for multichannel signal averaging 80−36165
evoked response, simultaneous recording to flashes at different retinal locations. 80−72279
evoked response, standard normal determ. 77−1995
evoked response, visual function assessment using signal averaging 77−44655
evoked response meas. using computerised rapid random flash 79−83776
evoked response meas. using versatile pattern-reversal stimulator 80−17177
evoked response of humans, nonlinear anal. 78−92622
evoked response shape self-regulation in man 78−31809
evoked response test goggle system using liquid crystal shutters 79−79676
evoked response to sinusoidal gradients, latency changes, humans 78−7349
evoked response to sinusoidal gratings, latency obs. 80−16933
evoked responses, peripheral versus foveal, multiple sclerosis early diagnosis appl. 80−67276
evoked responses, statistical detect., evaluation of Woody's adaptive filter 77−81757
evoked scalp pot., random within-set design for sampling 80−3842
evoked scalp potentials, human, equiv. dipoles in visual cortex 78−92613
evoked scalp potentials, spatiotemporal mapping for human 78−35845
evoked-response data acquisition system, specification and design 80−56165
excitatory-inhibitory visual system organisation evidence from oversaturation *(French)* 77−12922
extended object visual detection 78−15839
external geniculate body, cat, geometric props. of space of description of images 80−94203
external geniculate body, metric of space of description of images 80−30716
external geniculate body receptive field of cat, space-time wt. function 78−64989
external geniculate body receptive fields, neuronal network model 78−64990
extra-retinal photoreceptor model for Aplysia californica 78−44506
extrafoveal spectral sensitivity during dark adaptation 80−45896
extraocular photoreceptors in invertebrates 77−44648
eye, chemical and physical aspects *(Dutch)* 77−9188
eye, holography application *(Japanese)* 79−79515
eye accommodation, temporal stability of the dark focus 79−43867
eye corrective saccadic movements, for refixation amplitudes of 10° or less 79−43886
eye motion kinetics in moving target pursuit, oculomotor abnormalities in neurological disorders detect. 80−108888
eye movement research, data collection using on-line computers 80−41329
eye movements, vel. precision in smooth pursuit 79−57656
eye optical system, retina contrib. to modulation lowering, aerial images *(French)* 79−34553
eye protection filter small dioptric powers local variation determ. *(German)* 78−27937
eye torsion in response to tilted visual stimulus 80−45891
eye vergence movement of rabbits in visuomotor behaviour 79−43892
eye-specific tecta termination bands, three-eyed frogs 79−62251
falconiform eye, depression in deep fovea acting as telephoto lens system 78−88705

vision continued
far point dependence on target size, expt. data 79−79517
field displacements evoked by intense sound exposure, humans 78−85332
filter performance, inhomogeneous and anisotropic 80−76738
fish, adaption to underwater light spectral composition 78−3485
fixation changes in transverse plane at eye level, Hering's law of equal innervation 78−61184
fixation disparity rel. to rapid prism adaption 80−16929
fixation distance changes, ecular translation and cyclotorsion obs. 80−89752
fixation stability observations, proprioceptive information and autokinesis considerations 80−51086
flash evoked potentials following unilateral electroconvulsive therapy 80−97906
flashed gratings, temporal responses rel. to human transient and sustained channels 77−70475
flicker, vel. specificity to pattern sensitivity ratio, human vision 80−101181
flicker and transient responses, nonlinearity 79−29526
flicker critical frequency independent of wavelength *(Spanish)* 79−24989
flicker fusion phenomena, expt. studies of random neural nets 80−12077
flicker sensitivity in primates, psychophysics and electrophysiology 77−29150
fly, movement discrimination rel. to S/N ratio 77−48801
fly visually guided flight head and body movements 77−40664
foveal fixation, functional test based on differential cone directional sensitivity 80−85399
foveal vision central mechanisms, monkey 80−12108
frog, Rana esculenta, under-corrected lens rel. to comparable aerial and underwater vision 78−7344
functional visual field 80−81578
fundus reflex luminance rel. to increased cognitive processing 78−35849
geniculate neurone spatial resolution, impaired by monocular deprivation in kittens 77−21518
giant neuron of fly, performance, spike generation 80−108886
glare, adverse consequences in aviation 79−11932
glare source position and BCD brightness relationships under uniform field brightness, expt. *(Japanese)* 80−35889
glasses, prescription meas. 80−67981
glial smooth endoplasmic reticulum acid phosphatase transport into damaged axons, role of microtubules 80−85381
gloss appearance by means of moire patterns, connection to binocular vision *(German)* 80−52300
GMP, cyclic, proposed role in visual cell function 78−64997
goldfish, absolute visual sensitivity 79−48258
grating, sine-wave, average-luminance surround effect 80−51092
grating adaptation decay 78−40159
grating detection, patterns of temporal interaction 77−81497
grating free scanning, production of patterned retinal exposure obs. 80−56034
grating generating by microcomputer, appls. to human visual system 79−2172
grating induction, a new type of aftereffect 80−72175
grating patterns, moving digital technique for generation on oscilloscope 77−40957
gratings moving in opposite directions, summation and discrimination 80−72169
GTP hydrolysis in intact rod outer segments, rel. to transmitter cycle in visual excitation 79−83773
guided locomotion, psychophysical evidence for neural mechanism sensitive to flow patterns 80−51107
head holder, orientable, for use in visual research 79−2171
head movements of mealworm beetle, props. and role 80−76772
head movements of mealworm beetle, responses to rotating panoramas 80−76773
hemi-retina evoked average multichannel EEG pot. fields, latency differences between upper and lower hemi-retina 78−24067
hierarchical detection structures in vision 79−79523
historical paper by Jean Mery written in 1704 80−57050
horizontal cell response in carp to monochromatic light, dynamic model, pattern recognition appl. 78−44507
housefly flight torque and lift responses to single strip in visual field 78−85311
human, pattern detection and recognition, review 77−73527
human retinal image processing, two-channel model 80−94215
human vision, texture discrimination and Fourier anal. 78−96051
human visual analyser, contrast sensitivity 79−5284
human visual system, MTF *(Japanese)* 77−73526
human visual system, transient characteristic using masking experiments 80−41009
hydrophilic contact lenses, meas. and laboratory-stated parameters 78−77149
hyperacuity, spatial configurations 77−81498
hyperacuity decision model 79−5294
hypsorhodopsin, squid, form., picosec. spectrosc. obs. 79−39183
identification of objects by neuronal system with references 77−36919
illumination and reflection edges, recognition by human visual system 80−94209
image defocus detection by human infants 78−7354
image degradation by irregular retinal mosaic 78−20177
image evaluation, psychophys. and visual aspects, conf., Rochester, USA, (Oct. 1977) 78−65016
image formation, ocular optics and evolution 77−1991
impedance, nonlinear integral equation 79−100599
increment thresholds, luminance, brightness 78−15838
incremental threshold function, additive eqn. 77−70466
infant acuity meas. from pattern reversal evoked pots. 78−40149
infants, 6 to 45 days, maturation of evoked pots. and visual preference 77−70456
information coding, adaptation and differential sensitivity in system of detectors 77−56367
information processing, bandpass channels, zero crossings 79−83779
information processing, multi-input system representation, polynomial algorithm properties 80−101145
information processing, review *(German)* 77−64034
information processing within retina and lateral geniculate nucleus 79−74648
inhomogeneous model predictions, detect. of local, extended spatial stimuli 80−45894

vision continued
insect compound eye, internal desynchronisation of bilaterally organised circadian oscillators 78−80875
insect optical cells anal. using microcomputer *(German)* 77−86724
insect visual neurones, sexual differences 80−41010
insects, pathways possibly underlying neural adaptation and lateral inhibition 77−48792
insects which turn and look 77−90769
instrument focusing to take account of eye accommodation 80−101811
intensity discrimination capacity of tree shrew retinal ganglion cells 80−61556
intraocular lenses, literature review 1976-1977 79−96707
IR nonlinear perception in 800-1355 nm range 80−12123
IR recording retinoscope for accommodation monitoring 80−36055
iris coloboma, selective atrophy in lateral geniculate nucl., cat 78−3471
isorhodpsin, resonance Raman spectra 79−92148
kinescope spot size, relation to picture quality 77−44675
kinetics of visual pigment systems, bistable system measurements appl. 78−92624
kinetics of visual pigment systems, mathematical anal. 78−92623
Kuhne, Friedrich Wilhelm, (1837 to 1900), chem. processes in retina, biography 78−20928
large field early light adaptation, rod and cone activities 79−53117
laser low-level prolonged exposure effects on visual function 80−3714
laser scanned visual displays, pulsed light data extrapolation 80−3713
lateral displacement as response cue in Titmus Stereo test 78−56983
lateral geniculate body, types of receptive fields and freq. characts. 77−25424
lateral geniculate nucleus, cat, electrophysiological classification of X- and Y-cells 78−64996
lateral geniculate nucleus, monkey, cell size changes in undeprived laminae after monocular closure 80−16927
lateral geniculate nucleus in cat, struct. of identified X and Y cells 80−26231
lateral geniculate nucleus of cat, oscillatory neural activity entrainment 79−92216
lateral geniculate nucleus of cat, periodic stimulation, neural activity transient persistence 80−56021
lateral geniculate nucleus postnatal development in humans 80−12114
lateral geniculate nucleus X-cell early development, kitten 78−27946
lateral impedance theory, Markov processes appl. 79−2046
lateral inhibition as mechanism of movement detect., forward inhibition 78−20176
LED true checkerboard pattern reversal stimulator for visually evoked pots. study 80−61658
lens, human and calf, light scatt. and reversible cataracts 80−56019
lens, light scatt., appl. of random density and orientation fluctuation theory 79−62241
lens accommodation, interpositus neuron control obs. 80−21469
lens aperture, rel. to depth of focus, appl. to reading with relaxed eye 78−12489
lens testing, simplified Talbot interferometers 77−757
LF electric current stimulation of auditory and visual sensations 78−40261
LF sine-wave target visibility depend. on number of cycles and surround parameters 78−69075
Lie group representation, computational results 78−27939
light adaptation, multiple intracellular contribs., Limulus ommatidia 79−43896
light adaption in a normal and a rod monochromat, psychophysical and VEP increment obs. 80−16939
light adaption model and Weber's law 79−8508
light adsorption, recovery of retina sensitivity of silver carp *(Chinese)* 79−2056
light sources, psychophysical luminous efficiency *(Polish)* 80−33110
light-adapted photoreceptors, sensitivity changing mechanisms evaluation 79−79543
lighting conditions in work place, Swedish report on manual casting *(Swedish)* 77−77896
lightness normalisation with rods and cones 79−100609
lizard, visual acuity as function of pupilar diaphragmation 77−70453
loss, in objective determ. of human $+G_z$ accel. tolerance, ultrasonic blood flow meas. method 78−3619
luminance and opponent colour contribs. to visual detect., temporal and spatial integration 79−8509
luminance and opponent colour contribs. to visual detect., temporal and spatial integration 79−8510
luminance changes, discrimination and detect. 80−101171
luminance difference threshold, Holladay's principle *(Japanese)* 78−65000
luminance difference threshold as contrast threshold, rel. to inhibitory interaction in spatial summation 77−60210
luminance difference thresholds of foveal vision, uniform surrounding luminance effects *(Japanese)* 79−24988
luminance edge thresholds under stabilised viewing conditions, eye movement role 80−81589
luminance increment detectability, superimposed random fluctuation effect 77−32890
lumirhodopsin, photoconversion at 77K, quantum efficiency estimation 80−67081
M-cells, logic cct. model to account for CNS inhibition features 78−64917
Macular pigment, role in polarised light detect., meas. technique 80−61560
magnetic response of brain, monitoring using SQUID 77−29231
magnetophosphenes, quantitative anal. of thresholds 80−72184
magnetophosphenes, quantitative determ. of thresholds 80−61620
magnification in striate cortex and retinal ganglion cell layer of owl monkey 78−40146
masking-induced sensitivity changes in Limulus photoreceptors 80−41024
matched filter model of brightness change detect. 78−65001
metarhodopsin I-II transition obs. by absorpt. changes of eriochromblack T 77−44593
metarhodopsin transition, triggering of light-induced change in Ca binding, rod disk membranes 80−94211
microcomputer-controlled visual stimulator for eye movement and visual evoked pots. study 80−41350
microelectrode studies of single neurons, rel. to problems of vision *(German)* 78−53397
microprocessor-controlled contrast sensitivity measurements 79−92327
vision continued
microsaccades, role in high acuity observational tasks 80−108893
microsaccades during finely guided visuomotor tasks 77−9198
microtubules in optic nerves of temperature acclimated goldfish, electron microscopy 80−85395
microwave exposed monkeys, skilled visual-motor performance obs. 80−61634
midbrain, similarities between overlapping visual and tactile maps in mammals and reptiles 80−61550
minicomputer system, automatic visual stimuli, hand and eye movement monitoring *(French)* 79−34682
mobility aid for blind people based on US sensing 80−56290
model using optical engineering theory concepts 79−96555
modelling, straight line recognition algorithm 79−34562
modulation transfer function, modification by presaccadic gratings 79−48245
molecular basis of vision 80−108876
molecular mechanism for initial process of visual excitation 80−51089
molecular mechanisms and dynamics exam. by tunable laser resonance Raman spectroscopy 77−56378
monocular astigmatism effects on kitten visual cortex development 78−7345
monocular deprivation, morphological effects on different classes of neutrons in lateral geniculate nucleus 77−52781
monocular deprivation, unequal, alternating, cause of asymmetric visual fields in cats 80−104584
monocular light exclusion, reduction of retinal directional sensitivity obs. 80−81592
monocular occlusion, alternating, effects on cat visual cortex 80−16932
monocular vergence movements produced by external visual feedback 80−108883
monosynaptic reflex, influence of visual input 77−60197
motion and vision, stabilised spatio-temporal threshold surface 80−16926
motion flow perception, conditions for in dynamic visual noise 80−72174
motor systems, eye and hand, optimal response in pointing at visual target 80−56079
motor systems of eye and hand, optimal response in pointing at a visual target 80−61567
movement detection mechanism spatial characts., achromatic vision 80−89753
movement-detecting neurons, fly, contrast sensitivity obs. 80−72163
moving objects localisation, cats 80−76736
MTF versus image quality 77−86487
multiple sclerosis diagnosis using cerebral evoked response and optokinetics 80−36183
Myctophidae, lantern fish, bioluminesc. in response to light intensity, by visual monitoring 77−16953
neocognitron, self-organising neural network model, pattern recognition mechanism unaffected by shift in position 80−76745
nerve signals derivation from contrast flash data 80−108885
nervous activity monitoring in Drosophila by [^{3}H]deoxyglucose 80−56024
nervous mechanism for visual information processing *(Japanese)* 80−97908
neural discharge phase-locking to periodic stimuli 79−83775
neural information processing, primate visual system appl. 80−30722
neural light intensity analyser model 79−57648
neural network dynamical response, effect of boundaries, Limulus retina 80−30717
neural representation of visual space 77−40670
neural superposition compound eye of male Bibionidae expt. obs. 79−43874
neuromagnetic response latency of human visual cortex 78−40151
neuron receptive field mapping with visual stimulus generator 79−74817
neuron response to light stimulus, computer monitored method 77−86725
neuron simulation using analogue and digital electronic circuit *(Spanish)* 78−27942
neuron specificity acquisition and loss in visual cortex, theory 79−83772
neuron-discharges in eye movements 80−12099
neuronal organisation within mammalian visual thalamus 78−27948
neuronal properties underlying visual information processing in barnacle 78−88710
neuroscience annual review, book 79−96540
non-spiking visual interneurone, spike response 78−11645
nonlinear receptive field model 78−27951
nonlinear visual processing in cat's retina, model 80−85385
nonlinearity, analytical derivation 80−67082
occipital evoked potential meas. of contrast sensitivity and acuity of conscious cat 78−48803
ocellus of phalangium opilio, electrical response 79−53095
octopus brightness preference as function of background brightness, expt. 78−20178
ocular dominance shift failure after monocular occlusion in kittens, brain catecholamines 77−1998
ocular peripheral saccades, latency obs. 80−12089
ocular physiology review 80−56023
oculomotor control system, expt. set-up for clinical investigation, visual, acoustic, vestibular stimulations 78−80990
ophthalmic lens distortion display 78−7338
ophthalmic lenses, basic principles of fracture testing 79−96233
ophthalmic lenses, thin, chemtempered, static load strength testing 80−5812
ophthalmology and vision research, appl. of lasers, holography 80−12210
optic nerve fibre arrangement in cat, non-retinotopic 80−30720
optic nerve fibre topography in tectum retinal projection, cichlid fishes 79−48250
optic nerve fine structure in lamprey 77−60201
optic tectum, goldfish, fine struct. 80−85396
optic tectum, IR and visual integration in rattlesnakes 78−69054
optic tectum, pigeon, single cell spatial- and temporal-freq. selectivity 80−41016
optic tectum, pigeon, single-neuron responses to moving sine-wave gratings 80−41015
optic tectum extracellular recording, reproducible manufacture of metal-filled microelectrodes 78−69263
optic tectum model of various vertebrates *(Spanish)* 78−40144
optic tract fibers, cat, Markov properties of nonstationary spike trains 80−51077
optic tract fibre spike trains, cat, nonstationary anal. on Markov props. *(Japanese)* 77−90780

vision continued
optic tract fibres, physiologically characterised, projection patterns, cat obs. 80−101167
optic tract fibres, receptive field props., tree shrew 79−48252
optic tract of self-respiring fish, method for obtaining single cell response 77−56545
optical line spread width judgement, merits of Gaussian moment 80−16924
optical mechanism of image formation in Limulus eye 79−83767
optical scan system for encoding and tabulation of visually scored sleep data 80−8197
optics conference, Madrid, Spain (Sept. 1978) 80−77547
optokinetic reactions, rabbit, rel. to visual streak 79−43884
optokinetic reactions in man elicited by localised retinal motion stimuli 80−45889
optokinetic stimulation device, expt. and clinical appls. 80−3844
optometric education in Nigeria, three year programme 79−25781
optometry, future of public and community health 80−12084
optometry, interdisciplinary course with vision training specialisation 79−40311
optometry as remediation and education 80−12082
optometry conference, Anaheim, USA (Dec. 1979) 80−90602
optometry opportunities, trends in higher education and health 80−8756
otpical line spread width judgement, merits of Gaussian moment 80−16923
outer isopter perimetric response variability obs. in old subjects 80−108894
owl, effect of monocular deprivation on binocular neurones of visual Wulst 77−16929
owl, tawny, Strix aluco, absolute visual threshold and scotopic spectral sensitivity 77−77899
owl, visual Wulst, neurons selective for orientation and binocular disparity 77−1996
owl monkey, Aotus trivirgatus, spatial contrast sensitivity 77−70464
parallel visual pathways review 80−89751
particle induced visual phenomena in space 78−20297
pattern and movement detect. in man and rabbit, separation and comparison of occipital pots. 78−48805
pattern evoked pots., implicit time in infants, spatial vision maturation index 80−16928
pattern reversal generator for visually evoked responses studies 80−46004
pattern rotation system for a visual stimulator 80−98061
pattern thresholds for moving and stationary gratings during smooth eye movement 78−61178
pattern visual evoked pots., age-dependent latency change obs. 80−85390
pattern-evoked cortical pots., human infants, spatial and temporal interaction 80−101169
pattern-evoked potential, modifications rel. to stimulated part of visual field 80−26225
patterns having the same coordinates pre- and post-saccades, interaction 80−61551
performance after blue light exposure, rhesus monkey 79−53114
perimetric examination in visual physiology *(Italian)* 79−62244
perimetry, automated, history, theory and practical application 79−92402
perimetry by visual evoked pot. recording limitations 78−69049
peripheral, size and luminance discrimination obs. 80−101172
peripheral contrast sensitivity for sine-wave gratings and single periods 80−61562
peripheral critical flicker frequency 80−41039
peripheral luminance gratings, lateral effect of oscill. 80−108903
peripheral retinal optical image quality variation obs. 79−83766
peripheral vision photopic contrast sensitivity rel. to cortical magnification factor 78−24071
phase selectivity of spatial frequency channels 80−45895
phasic pupillary light reflex and visual evokes potentials, simultaneous anal. 80−26226
phenomena induced by relativistic $^{6}C^{+}$ ions, with and without Cherenkov radiation 79−24991
phosphenes, X-ray induced, mech. of formation, electrophysiological obs. on albino rats 80−104675
photic sensitivity of macaque monkey and pulvinar neurons 80−12106
photoconvertible pigment states and excitation, prolonged depolarising afterpot., blowfly 80−8060
photographic image detection and recognition visual factors, optimal viewing conditions 78−4724
photokeratoscopic technique for corneal image study 77−1993
photomicrography, low-power critical focusing 80−13165
photon counting microspectrophotometer for study of single vertebrate photoreceptor cells 80−12323
photon detection with optimum counting processor 78−27956
photopic contrast sensitivity without foveal vision 78−73161
photopigment and receptor props. in Drosophila compound eye and ocellar receptors 80−8063
photopigment depletion effects on brightness and threshold 78−56977
photopigment rapid conversions in blowfly visual sense cells, effect on receptor pot., pupillary response 80−8062
photoreception, relevance of Halobacterium photosensory mechanism 77−90738
photoreceptor, barnacle, conditioning light effect modification by metarhodopsin absorpt. of light 80−8064
photoreceptor, barnacle, effects on prolonged depolarising afterpot. of Mn^{2+}, Ca^{2+} 80−8051
photoreceptor, barnacle, props. of on-transient of intracellular response 80−8052
photoreceptor, barnacle, upper limit on translational diffusion of visual pigment 80−8053
photoreceptor, invertebrate,, basic mechanisms of excitation and adaptation 80−81593
photoreceptor bleaching and adaption reversal by microsecond flashes 79−79542
photoreceptor cell disk membrane, photoinduction of pot. 79−70548
photoreceptor cells, daily rhythms and vision research 78−61176
photoreceptor diameter and spacing for highest resolving power 77−70452
photoreceptor directional sensitivity, coherence and polarisation obs. 79−100610
photoreceptor electric response, in invertebrates and vertebrates, quantitative model 77−44656
photoreceptor fluorescence rel. to UV sensitivity, fly 79−92219
vision continued
photoreceptor membrane fragment modified artificial lipid membranes, effect of light 77−77898
photoreceptor membrane interfacial pots., light-induced 80−72161
photoreceptor noise suppression, rel. to incremental intensity thresholds 79−43895
photoreceptor optics, angular sensitivity 80−61541
photoreceptor optics, formalism and excitation 80−61540
photoreceptor rod cells, vertebrate, visual transduction, book contrib. 79−96561
photoreceptor sensitivity increase following light illumination, frog expts. 80−51095
photoreceptor transduction, determ. of pigment transition or state coupled to excitation 80−8054
photoreceptor transduction mechanism, conf., Julich, Germany, Oct., (1976) 77−90774
photoreceptor voltage signal at visual threshold 77−16930
photoreceptors, bullfrog, effect of temp. on rapid dark adaptation 79−43883
photoresponse suppression during anoxia, role of Ca^{2+}, Limulus 79−62252
photostable pigments, function in fly photoreceptors 80−8058
photostimulator, LED fibre optic, for research on visual nervous integration 80−67302
photostimulator for visual electrophysiology 78−35846
phototransduction dynamic props. in fly, Phormia regina, light adaptation effect 79−53109
physical and biological sciences, conf., Japan (Mar. 1979) 80−17714
physiology and psychology, development, contrib. of Joseph LeConte 80−86063
picosecond relaxation meas. of primary visual processes, book contrib. 77−64166
picosecond spectroscopy using ultrashort laser pulses, appls. 79−54195
picture distortions compensation of moving patterns typical for time filters 80−76731
pigeon, accessory optic system, projection of displaced retinal ganglion cells 77−90781
pigment, model system, spectroscopy and photochem. 77−32871
pigment absorption spectral band shapes, lognormal distribution curve description 79−53110
pigment responses to prolactin in trout, effect of thiourea 78−69065
pigment retinal chromophore, role of protein in photochem. 78−15772
pigment spectra nomograms, wavelength depend. 77−25430
pigment unprotonated chromophore-protein bond, ^{13}C NMR spectra 78−11607
pigmentary retinal epithelium of trout, chromatographic detect. of indolic cpds. *(French)* 79−53115
pigmented biomembranes, photoelec. and magneto-orientation effects, review 77−48766
pigments, slow flash photolysis using conventional spectrophotometer 78−68904
pigments in solution, flash photolysis kinetics, effect of prep. 77−32892
pineal unitary response to light stimulation in frog central nervous system 77−52780
plasticity, effect of early avoidance training on brain development in kittens 79−83734
polar coordinate data Fourier anal. 78−56988
polarisation vision, functional similarity with colour vision 78−3497
polarised light detection by humans 80−16934
polynomial models for research and clinical use 77−48804
preferred orientation, variability due to methodology 80−56032
prelumirhodopsin, psec. kinetics, primary photochem. event in vision, proton translocation 78−44508
primary visual cortex, orientation selectivity development models, normally and dark reared kittens 80−41007
primary visual cortex orientation selectivity development kinetics, normally and dark reared kittens 80−41006
primate, subdivisions and interconnections 80−12110
prosthetic device, bioengineering and biomedical aspects of focal surface model 78−48942
proton transfer, rel. to initial photochem. process 77−1999
psychophysical evidence for sustained and transient channels in the monkey visual system 80−35896
psychophysical functions in fish with respecified retinotectal connections 80−12152
psychophysiological techniques applied to aircraft design and other operational problems 80−26384
pupil diameter of observer's eye, effect of electron-optical convertor screen luminance 80−35890
pupil light reflex simulation model 77−70462
pupil response as indicator of visual function, pupilometry equipment 78−40154
pupillary escape, positive off-diagonal kernels as correlates of dynamic process 80−26229
pupillary response to light, gekkonid lizards 79−57653
pupillary system, human, same-signed 1st and 2nd degree kernels 80−26228
pursuit after-nystagmus 80−41018
quanta coincidence model for absolute threshold vision, Ricco's law deviations 79−53118
radiation detectors, sensitivity, informational threshold, rel. to human vision 77−87838
radiographic viewbox information capacity, viewbox improvements 79−74746
rapid flicker detection by rod photoreceptors 77−48800
reaction times, for functional exploration of sensory, sensory-motor and auditory routes *(French)* 77−37077
reaction times in observation of lunar occultations *(French)* 79−88607
readaptation after dazzle, multidimensional functional model *(German)* 79−16208
reading through pinholes, for teaching 80−17765
reading without a fovea 80−76748
receiver operating characteristic curves for Poisson signals 79−83778
receptive field props. of neurones in visual cortex of cat 80−26227
receptive field types in lateral geniculate body and functional model 78−69046
receptive fields in area 17 of cat visual cortex, linear and nonlinear properties 80−104583
recognition system with thinking, model for humans 80−76744
reduced eye, expts. in life science labs. 80−82617
refraction estimate dependence on visual task 79−62237

vision continued
refraction measurement, illum. spectral comp. effect 77−1990
research, the place of the library 80−30711
research and future trends *(Japanese)* 80−97899
research laboratory, clinically oriented, tasks and goals 80−12083
response function models, psychophysical tests 79−79557
response properties of fly visual systems 80−41021
retina, cat, contrast gain control 79−79536
retina, cat, transfer function for spatial freqs. *(Spanish)* 79−62247
retina, cephalopod, dark adaption dynamics 79−79541
retina, excitation and interaction, review, book contrib. 79−5282
retina, frog, GABA and lateral spread and tonic activity 79−74661
retina, frog, near IR transmission of rods rapid light-induced changes 79−74658
retina, goldfish, X-like and not X-like cells obs. 79−43837
retina, lateral spread of light adaptation, rat 77−44659
retina, pigeon, antidromic invasion of ganglion cells 79−43881
retina, pigeon, graded pots. accompanying antidromic invasion 79−43882
retina, pigeon, non-directional and directional ganglion cells 79−57655
retina, rat, rod elec. model, early receptor pot. generation 79−57647
retina, roach, post-receptoral neurons, adaption effects in elec. responses 79−79534
retina, snapping turtle, mixed rod-cone responses in horizontal cells 79−79533
retina electrical activity and lipid peroxidation 79−43885
retina photoreceptor membrane, light and GTP-regulated GTPase interaction 80−45897
retinal, all-trans, reson. Raman excitation profile 78−73137
11-cis-retinal, donor energy effects on triplet-sensitized isomerization 78−3353
retinal, highly polar excited electronic states, electron transfer 78−48757
trans-retinal, picosecond photophysics 77−9169
all-transretinal, two-photon spectrum, rel. to photophysics of vision 79−41159
retinal anatomy and physiology, reprint of 1877 paper 78−20932
retinal b-wave currents, frog 79−57652
retinal bipolar cells, dogfish, visual signal transmission near absolute threshold 79−79535
retinal cells of cat, spatio-temporal model 78−92621
retinal chemical processes, reprint of 1879 paper 78−20933
retinal chromophore transition dipole moment, orientational changes obs. 80−41023
retinal diffusion and eye optics quality, OTF and light scatt. characterisation 80−41004
retinal distribution of illuminance, universal mathematical expression *(German)* 79−92214
retinal excitation, molecular mechanism for initial process 79−100598
retinal ganglion cell functional pathways, book contrib. 79−96559
retinal ganglion cell layer, cat, newly identified presumptive microneurones population 80−67077
retinal ganglion cell of frog, excitatory and inhibitory processes giving rise to delayed response 79−2055
retinal ganglion cell on and off processes, spatial distrib., anal. of receptor inputs 79−100606
retinal ganglion cell response props. in Siamese cat 80−12115
retinal ganglion cell responses in dark-reared rats 79−53102
retinal ganglion cells, orientation bias, cat expts. 80−94206
retinal ganglion cells, responses to stationary and moving stimuli 80−51080
retinal ganglion cells, scotopic increment thresholds 79−79558
retinal ganglion cells, suppression of maintained activity 79−79537
retinal ganglion cells action pots., goldfish, function of lighting conditions 79−43888
retinal ganglion cells in the galago, size and tropographic arrangement 80−67078
retinal ganglion cells of a tree shrew, definition of neural response and incremental sensitivity 80−41011
retinal horizontal cell receptive field centre/surround interaction model 77−86497
retinal horizontal cells, nonlinear characts. of spatial summation in receptive field, model 80−26232
retinal image disparity, fusional response central and motor components 77−25457
retinal image light and dark contrast component processing 78−24070
retinal image stabilisation 80−12088
retinal image stabilisation quality during small body rotations in man 79−100595
retinal isomers, dark equilib. and photochem. 78−15771
retinal L-type horizontal cells, dynamic interaction in receptive field 80−26233
retinal L-type horizontal cells, nonlinearity in dynamic characts. 79−100603
retinal light intensity 2-dimens. profiles from laser-irrad. monkey eye 78−40141
retinal mechanisms of visual latency in Bufo marinus, electroretinogram obs. 79−48255
retinal model, layered visual processing 80−16925
retinal neurons, catfish, spatiotemporal testing and modelling 80−41005
retinal neurons, spatio-temporal receptive field meas. 79−57649
retinal photoreceptors, response increase and noise decrease by circadian clock in Limulus brain 80−94210
retinal pigment epithelium phagocytosis, RCS rat 79−34561
retinal processing, nonlinear, generalised model 79−53107
retinal receptor directional sensitivity, flicker effects 80−8057
retinal receptors, weakly anisotropic waveguide model 77−79929
retinal response, expected waiting time 80−51091
retinal responsivity compression, V-log I functions and increment thresholds 78−61181
retinal rods, thermal activation of visual transduction mechanism 79−74651
retinal Schiff bases in lipid bilayer membranes, photoelec. effects *(Japanese)* 78−7322
retinal Schiff-base, photochem. step of vision, H-bonds, intermol. associations 78−31812
retinal stimulation by Ra 79−71213
retinal streak, turtle, orientation of horizontal cell axon terminals 79−74653
retinal synaptic transmission effectiveness, neurone regulator model 79−57645
retinal-entrapped membrane, photo-induced potential 78−20148
retinas, goldfish, dorsal rel. to ventral areas obs. 79−43880

vision continued
retino-suprachiasmatic tract, evidence for in the rat 80−21471
retino-tectal mapping using microprocessor controller 78−31995
retinoscopic and subjective measurements, discrepancy, effect of age 79−34550
retinoscopic artifact obs. in rabbits 79−48247
retinoscopy, near and cycloplegic, in early primary schoolchildren 80−8047
retinoscopy artefact in rat and rabbit eyes, origin at retina/vitreous interface obs. 80−51075
retinotectal pathway, uncrossed, development rel. to plasticity studies, rat 80−56025
retinotectal projection development, Gierer-Meinhardt eqns. appl. 80−56022
retinotectal projection development, mathematical model *(Japanese)* 80−21467
retinotectal projection in goldfish to an inappropriate region with a reversal in polarity 80−72153
retinotectal projection orderly compression following partial tectal ablation, newborn hamster 79−74656
rhodopsin, bathochromic shift origin 78−31767
rhodopsin, bathorhodopsin and isorhodopsin, mech. of photoconversion 78−53336
rhodopsin, bovine, conform. in situ and solubilised with detergent 77−44587
rhodopsin, bovine, kinetics of intermediate photolysis processes 79−43608
rhodopsin, bovine, mol. wt. determ. by monolayer method 77−81492
rhodopsin, bovine, photochem. cis-trans isomerisation at liq. He temps. 78−64939
rhodopsin, cattle, phosphorylated, isoelec. focusing 78−15766
rhodopsin, cis-trans isomerisation on psec time scale 77−86498
rhodopsin, coherent states of flexible macromol., mol. basis of vision 79−79472
rhodopsin, isorhodopsin, photochem. on picosecond time scale, bathorhodopsin form. 79−83706
rhodopsin, photo- and thermo-bleaching rel. to heterogeneity problem 80−41114
rhodopsin, presence of two closely arranged SH groups in mol. 78−53323
rhodopsin, primary photophys. and photochem. processes in visual excitation 78−15773
rhodopsin, resonance Raman spectra 79−92148
rhodopsin, solubilised, photoinduced conform. changes, spin-label method 77−81496
rhodopsin, transient light-induced conform. changes 78−15774
rhodopsin, vertebrate, chromophore orientation obs. 80−40959
rhodopsin, visual pigment, mag. anisotropy estimation 80−51137
rhodopsin and bathorhodopsin, theoretical analysis of optical activity 77−52783
rhodopsin and intermediates, absorpt. spectra and orientational change of chromophore 78−7321
rhodopsin and its photoproducts, directional absorpt. props. obs. 80−51090
rhodopsin and photoproducts, temp. and wavelength effects on photochem. 78−11612
rhodopsin and thermal intermediates, fast struct. fluctuations in protein component 80−72137
rhodopsin conformation, spectral studies 78−15765
rhodopsin flash photolysis, rabbit retina 78−76996
rhodopsin in model membranes, charge displacements in interfacial layers 77−52785
rhodopsin $P499_1$ and porphyropsin $P522_2$, paired visual pigments in goldfish 79−53111
rhodopsin phosphorylation as possible mechanism of visual adaptation 78−15836
rhodopsin photoproduct kinetics in frog retinas, rapid scanning microspectrophotometer meas. 78−92763
rhodopsin photosensitivity, thermal stability and metarhodopsin prod., extractant effects 78−7355
rhodopsin thermal stability in photoreceptor membrane and Triton extracts, squid rhodopsin 77−32893
rhodopsin visual pigment, photochemical transformations 79−66472
rhythms in animals, role of light, bibliography 77−48986
rod, amphibian, dark adaptation processes 78−15835
rod and cone signals interaction, temporal sine stimulation 78−11651
rod disc membrane phosphodiesterase control 79−79527
rod ERG, human, dark-adapted a-wave response function obs. 80−56036
rod outer segment birefringence gradient, struct. interpretation, 3-dielectric layer model 79−83771
rod outer segment phagocytosis obs., rat 79−62249
rod outer segments, spread of activation and desensitisation 80−35881
rod outer segments membrane current fluctuations 79−79530
rod outer segments membrane current obs. 79−79529
rod outer segments pots., frog, local stimulation and adaption obs. 79−79528
rod outer sements, isolated, photoresponses, frog 79−43890
rod photoreceptor membrane, pot. regulation by cyclic GMP 79−74654
rod photoreceptors, response to light 79−92220
rod photoreceptors, vertebrate, opposing effects of Ca^{2+} and Ba^{2+} 79−24990
rod threshold, human, influence of cones stimulated by contrast flashes 78−69074
rod threshold, neighbouring cone influence 79−53116
rod-cone interaction, spatial patterns 80−16930
rod-cone interaction obs. 79−100607
rod-cone interrelationships at light onset and offset 80−41022
rods, frog, bleaching and background adaption 79−79532
rods, role in iconic storage 79−24987
rods, threshold rel. to pigment in Xenopus 79−79526
rods, toad, effects of Ba^{2+} on dark-adapted intensity-response curve 79−79531
rods, toad, spontaneous quantal events induced by pigment bleaching 80−108895
saccade-related unit activity in monkey superior colliculus 80−12101
saccades, primary and secondary for goals defined by instructions 79−43878
saccades, small, lack of useful purpose considerations 80−61553
saccadic eye movement, accompanying pots. 80−12102
saccadic eye-movement system, processing of direction and magnitude obs. 80−56035

vision continued
saccadic suppression, exogenous and endogenous contribs. 77−40671
saccadic suppression by corollary discharge in the locust 79−92217
saccadic system, anal. by double step stimuli 80−41014
scalar fields structure, two dimensional, vision appls. 79−100594
scanning eye movement target point selection 78−24066
scotomata, effect on responses to pattern reversal in one half visual field 79−39417
scotopic light flash reaction time 78−77053
scotopic reaction time, peripheral area-intensity interaction 78−3484
screening-pigment migration in retinula cells of crayfish, spectral sensitivity 80−72165
search, effects of target, background and observer variables 80−101187
search field size effect on visual search efficiency 77−9195
sensitisation effect, rectilinear stimuli 79−2062
sensitivity, resolution and Rayleigh matches following monocular occlusion for one week 80−104585
sensitivity and adaption, conf., Guildford, England (Sept. 1978) 79−79516
sensory evoked potentials in nervous system clinical disorders, book contrib. 79−2029
sensory substitution system, trends *(Japanese)* 79−66470
shark visual system 78−15824
shift effect, discovery *(German)* 79−57651
shutter control system, rapid cycling, for expts. 80−41358
signal detection, 1 of M, asymptotic equiv. of likelihood ratio and multiband models 78−71045
signal detection by simultaneous observation through multiple channels, decision behaviour 77−90791
simulator of human visual system *(Russian)* 80−76877
simultaneous vision, model using binocular gate neuron 79−5275
single optic nerve fibres in Limulus brain, innervation patterns, modified Co staining technique 79−53096
smallest channel in early human vision 80−101178
spatial, threshold, four mechanism model 79−43897
spatial adaptation rel. to prolonged inhibition 77−44661
spatial contrast sensitivity in albino and pigmented rats, behavioural obs. 80−41013
spatial frequencies, systems for detect. of high and low freqs. 78−65022
spatial frequency and bar width selectivity in cat visual cortex 78−40152
spatial frequency channel, human, space domain props. 79−2060
spatial frequency channels, inhibition between, complex gratings adaptation 80−72160
spatial frequency channels, interactions 79−2059
spatial frequency characteristics of receptive field of cat visual cortex, rel. to stimulus speed 78−20174
spatial frequency characts. of complex receptive fields 78−20175
spatial frequency processing rates modification with multiple freq. stimuli 79−53101
spatial frequency psychometric discrimination thresholds in different orientations 80−81590
spatial frequency responses of human visual system *(Japanese)* 79−8502
spatial frequency tuning studies, psychometric curves description by probability summation 80−61576
spatial impulse adaptation, rel. to Fourier transform models of visual processing 77−9191
spatial localisation during pursuit eye movements 80−51081
spatial separation acuity as function of stimulus size 78−69087
spatial summation, fovea, asymmetrical effects of longer and shorter dimensions 79−2061
spatial summation and light adaptation in goldfish visual system 77−77897
spatial summation at threshold level human peripheral retina, psychophys. expts. 77−70476
spatial summation for complex bar patterns 80−61557
spatial vision, psychophysical investigation, normal and reeler mutant mouse obs. 80−41032
speckle movement in laser refraction 80−41001
spectacle lens test facility complex 79−39603
spectacle lenses, scatt. light meas. *(German)* 78−46746
spectral eye fatigue, school lighting effects 80−76732
spectral luminous efficacy maximum, definition *(German)* 78−54333
spectral luminous efficiency of human eyes, approximate representation by Gauss-function *(German)* 80−81591
spectrally-opponent responses in ground squirrel optic nerve 80−35883
speech perception, auditory and visual contribs. 77−16939
speechreading ability, visual-neural correlate 78−64992
stabilisation of visual world rel. to voluntary nystagmus and saccadic suppression 80−101184
static campimeter with CRT display 77−90941
stereo disparity, cooperative computation algorithm 77−5005
stereoacuity in mentally retarded and intellectually normal adolescents 78−77055
stereopsis clinical test 80−61566
stereopsis in toads 77−52792
stereoscopic acuity for moving retinal images 78−69084
stereoscopic images, image reconstruction of 3-dimens. gamma ray source, 3 methods 79−5365
stereoscopic threshold and viewing time with random-dot stereograms 78−35850
Stiles-Crawford function, specification of directionality 80−45907
stimulator, computer-controlled, for electrophysiology expts. 78−69230
stimulus deflector for eye movement, three-dimens. system 78−48945
stimulus detection, freq.-of-seeing and sensitivity-duration obs. 79−74664
stimulus onsets and offsets, response of visual mechanisms 80−16937
stimulus sequence with uniform freq. of ordered pairs 78−56966
striate cortex, cat, differential responses of 'simple' and 'complex' cells during saccades 80−85394
striate cortex, cat, inhibitory sidebands of complex receptive fields 80−67079
striate cortex, cat, movement direction detect. and contrast reversal effects, cell response obs. 80−72155
striate cortex cat, orientation selectivity of single cells 79−2053
striate cortex single cell response, effects of interacting visual patterns, cat 78−7346
striate neurons in area 17 of Siamese cats, response props. 80−12116
striate visual cortex, spatial freq. rows 77−32888
sunglasses, commercial, UV and IR windows, transmission meas. 0.3 to 0.85 μm 77−36915
superior colliculus and its sensory inputs, primate 80−12100

vision continued
superior colliculus directional selectivity in hamster rel. to strobe-rearing and dark-rearing 78−69052
sustained and transient mechanisms in human vision, temporal and spatial props. 78−40171
tactile stimulation and processing of images for visual prosthesis *(French)* 79−100788
tapetum lucidum, cat, morphology obs. 80−108878
target tracking, eye movement evaluation using EOG 80−109057
tectal cells, frog, intracellular recordings 79−79525
tectal units, goldfish, centre-surround organisation and receptive field interactions 79−79538
tectum opticum neuron response characts., Salamandra 79−53092
telescopes, light vergence and accommodation 78−24065
temporal characteristics revealed by reaction time to double pulses of light, humans 77−44688
temporal properties of human visual nervous system 78−7353
temporal visual resolution, annotated bibliography 77−60199
testing instrument, determ. of visual acuity and depth perception threshold 78−81007
threshold, effect of stimulus presentation rate 77−40672
threshold, transient increase due to combined changes in propagation direction and polarisation plane 80−51096
threshold effects of active and passive image displacements 78−27952
threshold spatial vision, sensitivities to complex gratings and aperiodic stimuli 80−35888
threshold vision model incorporating visual field inhomogeneity 77−44660
tracking, target vel. signals in vermal Purkinje cells, monkey obs. 80−56026
transducer noise in locust photoreceptor, intracellular responses 79−34560
transduction in photoreceptors with bistable pigments, prolonged depolarising afterpot., obs. 80−8050
transient mechanism in the human system, spatiotemporal characterisation 80−72159
transient sensitisation by a contrast flash 80−72162
twin-flash response as a function of flash diameter 79−48257
two eyes constituting separate visual channels, expts. 80−97923
UV light detection by homing pigeon 78−40157
variability and periodicity, bibliography 78−27936
veiling reflections and reflected glare from glossy paper, lighting conditions for visual comfort 80−76733
velocity discrimination by pigeons 78−61179
velocity matching during smooth pursuit of different targets on different backgrounds 78−61189
ventral photoreceptors, Limulus, excitation by photons and fluoride ions 80−8065
vergence accommodation meas., dynamic optometer 78−35852
vergence control, role of spatial freq. tuned channels 80−101170
vernier readings, visual acuity *(German)* 78−31814
vertebrate retinas, outer segment layer, light-induced Ca fluxes 80−94207
vertical fusional response in humans 78−48816
vestibular adaptation to long-term stimuli 79−88075
vestibular nystagmus, Alexander's law model 80−35878
vestibulo-ocular reflex, horizontal, linear system anal. appl. to alert rhesus monkey 79−100600
vestibulo-ocular reflex gain in monkey at high rot. freqs. 78−56973
vibration effects on acuity 78−61168
vibration effects on continuous manual control 78−61169
visibility of isolated alphabetic letters and numerals, annotated bibliography 78−53411
visual acuity threshold variation, study of research literature *(French)* 79−5283
visual and auditory systems modelling *(Japanese)* 79−66474
visual angle increase, optical devices, geometrical and physiological optics *(Hungarian)* 78−20312
visual chromophores, two-photon absorptivities, SCF-PPP-CI calcs. 79−31631
visual cortex, geometry of orientation columns 79−100601
visual cortex development model, mammal 78−3483
visual development, environmental effects 79−11926
visual field investigations, recent developments 79−96552
visual field plotting using eye movement response 80−8045
visual pattern recognition, models *(Japanese)* 80−97920
visual pigment, steady-state composition in rainbow trout 80−51097
visual pigment chromophores, models, spectroscopic and photochemical studies 80−30723
visual pigment composition of rainbow trout 79−43899
visual pigment processes and prolonged pupillary responses in insect photoreceptor cells 80−8061
visual pigment regeneration studies, use of [15^3-H]all-trans-retinal tracer 80−41357
Visual pigment systems, implications of bistability 80−8059
visual pigments, conf., Florence, Italy (Sep. 1978) 80−4468
visual pigments, resonance Raman studies of the primary photochemical event 80−41020
visual target discrimination, illumination effects 79−5292
visual Wulst retinotopic organisation in nocturnal and diurnal raptors 80−12098
visual-vestibular interaction during body rotation in man, nonlinear model 80−76735
visual-vestibular interactions, model of cerebellar influence 78−40156
visuomotor mechanisms of monkey parietal lobe, visual input 78−27943
vitamin A, visual chromophores, two-photon spectra, lowest excited state 78−64934
vitamin A deprivation rel. to behavioural threshold and rhodopsin content in rat 77−70463
whistling ducks, retina structure rel. to feeding habits 78−53391
working position illumination, factors affecting good vision and efficiency *(Spanish)* 80−3638
X-ray image transmission system response rel. to X-ray diagnosis 78−35941
X-ray phosphenes, mech. of formation, photochem. investigations 80−108877

vision defects
see also contact lenses
100-Hue response, scotopic axis 80−26236
aberrations, high-order, subjective meas. 77−1994

vision defects continued
accommodation microfluctuations, IR optometer recorder *(French)* 78−7463
accommodation orthoptics, objective assessment of dynamic insufficiency 80−45884
acuity at ages 16 to 90, effects of luminance and contrast 78−3495
acuity deterioration in acquired colour vision deficiencies 80−56040
acuity reduction, pattern and movement detect. 78−56979
aids for the blind, review 77−29227
albino humans, asymm. of visual evoked response, brain abnormality 80−94208
albino rabbit, eye optokinetic movement inversion in anterior visual field 78−77052
amblyopes, monocular fixation and acuity 78−48801
amblyopia, acuity and contour interactions across the visual field, expt. obs. 80−56038
amblyopia, human, differences in neural basis, effect of mean luminance 80−72156
amblyopia, interocular comparison of eye movements while reading 78−53393
amblyopia, lack of normalcy of dominant eye 80−97898
amblyopia, monocular, prevalence among anisometropes 80−67071
amblyopia, neural function and dysfunction, activity within an amblyopic channel 80−108890
amblyopia, neural function and dysfunction, co-operative activity of amblyopic channels 80−108891
amblyopia, ocular rivalry suppression, effect of 9 Hz flashing light 79−34566
amblyopia, speedy evoked pot. methods for vision assessment 80−61661
amblyopia, strabismic and anisometropic, visual evoked response, effects of check size and retinal locus 78−61171
amblyopia, visual acuity and contrast sensitivity rel. to stimulated region of the retina 80−45893
amblyopia, visual development in humans, animal models 80−12118
amblyopia patients, random-dot-stereogram performance 79−83785
amblyopia related research, extrafoveal vision, vernier acuity and apparent target depth 79−39420
amblyopic children, determ. of visual acuity before and after treatment *(Italian)* 79−20540
amblyopic eyes, reliability of visual acuity meas. 78−65011
ametropia, expt. obs. of speckle motion in laser refraction 80−45879
ametropia determination with laser refractor 78−35907
aniseikonia, artificial, geometrical explanation of induced size effect, binocular vision 80−72173
aniseikonia, eikonic lens design for minus prescriptions 80−46095
anisometropia, artificially induced, effect on separable binocular processes 80−45906
anisometropia, cortical evoked potentials, electrophysiological correlate of perceptual suppression 79−53105
anisometropic amblyopia, increment threshold spectral sensitivity 77−44670
anisometropic amblyopia, physiological basis, expts. on kittens 79−24986
anomalous trichromacy, single pigment shift model 78−11654
aphakia, best retinal focus for various fixation distances 80−108882
aphakia, intraocular lens implant evaluation 78−81061
aphakia and aberrations 77−29146
astigmatic amblyopia, study 79−11922
astigmatism, acuity development in normal and astigmatic infants 80−12151
astigmatism, etiology of 79−16199
astigmatism, recognition threshold and sharpness threshold 78−27950
astigmatism, refractive, evaluation and control of DuraSoft contract lenses 79−34706
astigmatism and orientation preference in human infants 80−61542
astigmatism in infants 79−57642
astigmatism in infants meas. by photorefraction 79−62242
astigmatism induced by pterygium 78−40139
astigmatism of central and peripheral cornea, asymm. meas. by photokeratoscopy 78−64981
astigmatism of oblique rays and TiO glass lenses *(Italian)* 80−56278
Bausch and Lomb Autoplot tangent screen standardisation, for visual field meas. 78−64976
bifocal lens designs, marginal aberrations 78−48927
binocular oculomotor problems, phoria, vergence and fixation disparity 78−35835
binocularity affected by sectioning of corpus callosum, of cat 80−97922
blind aid, image conversion to a tactile presentation 80−94414
blind mobility aid, computerised instrumentation system for simulation and evaluation 79−12045
brain damage patients, 'extinguished field' information processing 80−30728
cataract, cold, form. in young rat lens, phase separation of protein-water mixture 78−11640
cataracts, visual acuity obs. *(Italian)* 79−79539
cerebral blindness recovery, evoked pot. and psychophys. meas. 77−40668
chromatic aberration, effect of yellow ocular filter, fish eye 80−8046
chromatic aberration meas. with chromoretinoscopy 80−81581
chromatic aberration rel. to accommodation, meas. using dynamic laser speckle pattern 80−81582
colour, exchange threshold method of anal. in humans 80−12129
colour, Roth 28-hue test 78−3494
colour blindness and opponent-colours theory 80−12133
colour defects, X-chrom lens *(Italian)* 80−17186
colour navigation light judgement by colour defective men 79−53119
colour vision, congenitally defective, increment thresholds for white and spectral lights on white background 77−90792
colour vision, normal and dichromatic, vector model 80−51099
colour vision defective patients, anarchic versus random 100-hue responses 79−62257
colour vision testing, colorimetric assessment of Holmgren wool test 78−53409
concomitancy testing, new method 80−94305
congenital colour defectives, colour discrimination obs. for different illuminants 79−79544
congenital colour defectives across young Sardinian population 79−62255
constant esotropia with anomalous correspondence, home visual therapy 80−8207
contact lens, soft, base curve radius selection, sagittal depth considerations 80−46096
vision defects continued
contact lenses, ultra-thin, corneal-edema response 79−34552
corneal edema with contact lenses under closed-eye conditions 79−96553
corneal scattering, contact lens wear, border-enhancement spread, subjective monitoring method 79−29641
dark adaptation, normal and pathological data-distinguished by dark adaptomer 80−41019
demyelinating diseases, visual evoked response as a diagnostic tool 79−20538
demyelinating optic neuritis, provoked visual impairment by visual evoked response 79−16202
deuteranomalous trichromats, locus if unique green 78−53400
diabetic retinopathy, impairment of colour discrimination 78−15841
dichromat long-wavelength-sensitive photoreceptor spectral sensitivity determ. by border percept elimination 78−69092
dichromats, large-field substitution Rayleigh matches 80−101173
disc vascularity in Down's Syndrome 80−67069
diseases of optic nerve, tracts and visual cortex, annual review of ophthalmic literature 78−3475
divergence excess, prevalence and management 80−35877
divergence excess strabismus, optometric therapy 80−97902
divergence paralysis, association with papillar oedema *(Italian)* 79−79520
dyschromatopsias, hazards in aviation 79−11934
dyslexic visual perception and aculomotor performance 79−83769
electro-oculogram light-induced amplification, quantification in clinical practice 77−90771
electro-oculographic amplification induced by macular light adaptation in various retinal diseases 77−90773
electro-oculographic response, comparison between binocular and monocular recordings 77−48791
electro-oculographic response, diagnostic tool for principal ocular disorders *(Italian)* 79−5391
empty-field myopia correction on dark-focus of accommodation basis 79−53131
ergo-ophthalmology and ergo-optometry *(Italian)* 80−26223
evoked potentials in neurological disorders 79−24981
exotrope, intermittent, of divergence excess type, panoramic viewing, visual acuity and anomalous retinal correspondence 80−51076
extinction photometry, entoptical scatter, model 80−51087
eye movement phase plane meas., antiaircraft tracking operator performance anal. 78−15825
eye strain and chromatic asthenopia rel. to affectations of optic pathways *(Italian)* 80−56041
field modifications in ocular and neuro-ophthalmological pathology, perimetry glossary *(Italian)* 79−79540
fixation disparity and stereopsis 78−56984
Friedmann quantitative analyser for study of posterior pole disease *(Italian)* 80−17172
Fuchs's endothelial dystrophy, optometric management 79−83994
fusional amplitude deterioration in diabetic people 80−26224
glaucoma, early diagnosis by meas. of internal eye pressure 79−25140
glaucoma, optic disc changes meas. using retinal stereophotogrammetry 80−3757
globe defects, evoked pots. from occipital and precentral cortex in visually deprived humans 78−3479
Haidinger's brushes, recent explanation and their clinical use 80−45880
hemianopia, new mirror design for detect. 80−108992
heterophoria, prism-induced, oculomotor adaption 80−108880
Hudson-Stahli line of the cornea, prevalence obs. 80−35876
human eye defects rel. to visual nondestructive testing *(German)* 77−86488
hypermetropia rel. to chromatic aberration in small animals 78−40140
hyperopia, induced, effects on intelligence test performance 79−43868
hyperopic eye functional visual acuity at intermediate range 78−48791
jerk nystagmus, some new findings 80−67074
keratoconus, position of corneal apex 80−94200
lateral geniculate nucleus in dark-reared cats, Y cell loss without cell size changes 80−3644
lateral spatial interaction in humans with abnormal visual experience 78−7363
lens protein composition obs. during senile nuclear cataract development 79−62236
meridional amblyopia 80−12150
meridional disparity effect on depth perception 79−53133
myopes, accommodation with rigid and flexible contact lenses 78−48787
myopia, corrected and uncorrected, effect of pupil size on visual acuity 80−45882
myopia, environmental, annotated bibliography 79−39418
myopia, extreme, produced by modest change in early visual experience 79−53085
myopia, Prentice Memorial Lecture [optometry] 80−27089
myopia, spherical error of refraction, statistical anal. of biological theory 80−45881
myopia, supernormal visual capacity 80−81612
myopia and eye enlargement after neonatal lid fusion in monkeys 77−29145
myopia associated with incipient cataract *(Italian)* 79−62238
myopia in developing chicks following monocular and binocular lid closure 80−61543
myopia incidence changes following classroom environment changes 80−12080
myopic and typical eyes, first order optics 78−44499
night convergence and presbyopia *(Spanish)* 80−89746
night myopia at automobile luminances 79−48246
nystagmus, congenital, orientational detect. modification obs. 80−56039
ocular albinos, human, visual anomalies meas. by evoked pots. 79−43875
ocular dominance, changes induced by stimulation with rotating gratings, lambs 79−34559
ocular motility test in strabismus and amblyopia evaluation, computer administration and analysis via PAL8 program 78−48784
ocular pathology patients, random-dot-stereogram performance 79−83785
oculomotor deficiencies, association of symptoms with meas. 79−96556
ophthalmic correcting cylinder axis, ophthalmometric prediction 80−98174
ophthalmology and physics, review 79−53084
optic nerve, tracts and visual cortex diseases, ophthalmic literature review 79−83762
optic-nerve head, congenital malformations 79−92213

vision defects continued
optokinetic nystagmus, computer graphic optokinetic stimulus pattern 79−44008
optometer, refractive error correction optical system with continuously variable spherocylindrical power 79−62385
orthokeratology, refr. error rel. to corneal power 78−48786
paradoxical sleep, occipital spikes and eye movement activity, visually defective children 79−16185
partial sight, acuity rel. to illum., contrast and distance 78−53398
perimeter localising, for visual field study and retinal tear location 78−85442
photocoagulation using ruby laser, colour discrimination time variability 78−53401
post-retinal disease, visual fatigue 77−60209
presbyopia, visual response experiments after awakening from sleep 77−90790
primary glaucoma etiopathogenesis 80−12086
protanopes and deuteranopes, large-field trichromacy 77−56379
pseudophakic patients, binocularity evaluation 80−51106
pupil, human, normal and diseased, model for computer simulation 77−77895
pupillary response meas., use of black light stimulation 78−64977
red-green deficiency, validity of Pinckers' 100-hue version of Panel D-15 78−3493
refraction meridional differences and illum. depend., sharpness and recognition thresholds of defocused targets 80−16922
refraction scotomata rel. to eye chromatic aberration 79−62239
refractive error, meas. using modified Foucault knife-edge test 77−4999
refractive error, simplified anal. of meridional refr. data 78−65149
refractive error meas. using dynamic laser speckle pattern 80−81583
refractive error measurement by Ophthalmetron, cycloplegia effect 80−41002
refractive keratoplasty, theory and computations of optical modification to cornea 80−35875
refractor, remote subjective device employing continuously variable sphere-cylinder corrections 77−1992
Refractor III system, computer-assisted eye examination 79−34698
resolution abnormalities in cats reared in stroboscopic illumination 79−83788
retinal degeneration, defective phagocytosis of isolated rod outer segments by RCS rat pigment epithelium 78−11647
retinal degeneration, hereditary, cone inputs to ganglion cells 80−8056
retinal degeneration in RCS rats raised under ambient light levels 79−43887
retinal diseases, literature review (1975-76) 78−35836
retinal function, laser interference fringes meas. *(German)* 77−12910
retinal images, defocused and spatially filtered, stereoscopic acuity 80−101177
retinal injury mechanics, laser exposure limits 79−66485
retinal lesions, incidence prior to retinal detachment *(Italian)* 79−79514
retinal research and study, selected review 80−108874
retinal spectral-response characteristics model, light propag. through human eye 79−92215
retinal-image movement rel. to eye rotation, contact lens/spectacle system for correction 79−53281
retinitis pigmentosa, visual field expander 78−65148
retinitis pigmentosa, vitamin A receptors in retina 77−21514
retinitis pigmentosa and night blindness, Generation II aid 77−21660
retinopathy, nondiabetic and diabetic, blood viscosity factors 78−65069
retinoscopy, theory including aperture stops 78−85308
retinoscopy of infants at distance, limits of normal and anomalous reflexes 78−61170
retrolental fibroplasia, A-mode ultrasonography and oculometry 80−89816
saccadic ocular dysmetria simulation using sampled-data model 77−56373
scotopic axis in 100-Hue response of congenital defectives under high press. Na illum. 80−16940
scotopic vision deficits in young monkeys exposed to Pb 77−56377
senile macular degeneration, colour discrimination rel. to visual acuity 80−108897
serous retinopathy, monolateral central, colour discrimination in 23 patients 79−5286
sharpness corrective devices and apparatus *(Hungarian)* 78−15823
signal transmission by visual pathways, distortions of retinal images 80−85400
soft contact lenses, future developments 80−12310
spectacle lens design, computation of unwanted sphere and cylinder in periphery 78−48928
spectacle test lenses, large set 79−92427
spheroidal degeneration of cornea and conjunctiva, pathology 80−12085
squint, optically induced, in kittens, effect on binocularity 79−79556
squint angle estimation, Hirschberg test, eye axial length meas. 79−34551
stereoblind humans, residual binocular interaction 80−89764
stereoblindness, rel. to binocular summation 77−60211
strabismic amblyopes, stimulus field size assessment 78−11649
strabismic amblyopia, influence of field size for periodic stimulus 78−65003
strabismic amblyopia, luminance-dependent nature of abnormality 79−2058
strabismic amblyopia, optical aberrations rel. to visual loss 78−48788
strabismic amblyopia, relationship between pattern and movement perception 78−65027
strabismic amblyopia, threshold contrast sensitivity function 78−7352
strabismic amblyopia in infants 80−30715
strabismus, fusional convergence ranges using random dot stereograms, operant conditioning 80−108900
strabismus and amblyopia, eye movement analysis by computerised ocular motility test system 80−41299
strabismus patients, random-dot-stereogram performance 79−83785
stress, functional consequences, annotated bibliography 80−26222
technical aids for compensating defective vision and blindness 78−85451
testing, using screen image divider 78−57114
therapy of strabismus, amblyopia and learning disorders, rel. to visual deprivation studies 80−12081
time-varying response anomalies 80−16935
transient tritanopia, expts. in blue cone monochromacy 79−16209
tritanomaly detection, optimisation of a Rayleigh-type equation 80−56044
uniocular macular scotoma, central versus peripheral vision 79−83777
vision defects continued
vertical fixation disparity, correction by horizontal prism 80−67281
vestibular nystagmus, computer analysis method *(German)* 77−40663
visual cortex, altered connections in Siamese cat 80−12091

visual auroras *see aurora*

visual perception
100-hue test, validity of Pinckers' version of Panel D-15 78−3493
aberrations, high-order, subjective meas. 77−1994
absolute distance estimation, monocular and binocular viewing with no optical reference 77−60216
accommodative, bias towards intermediate viewing distances, Mandelbaum effect 79−79518
achromatic channel, nonlinearity of minimum-border and flicker matches 78−65028
acuity at ages 16 to 90, effects of luminance and contrast 78−3495
acuity development in normal and astigmatic infants 80−12151
acuity experiments, image viewed through a rotating mirror 79−76790
acuity meas. computer-aided system *(German)* 79−2144
adapting effects and complementary afterimages of steady and flickering light 78−69083
adaptive filters and eye movements 79−53153
adjacency principle, relative weighting of information 78−92634
after-image blurring not due to diffusion mechanism 78−69099
aftereffects of changing-size and motion-in-depth 79−100621
ambiguities, non-resolvable, model 79−34567
analyser space-frequency filter harmonisation with statistics of images 80−30726
angiography, visual perception limits 78−85313
angiography visual perception limits 78−73231
anisometropia, cortical evoked potentials, electrophysiological correlate of perceptual suppression 79−53105
apparent brightness rel. to contrast threshold on photopic background 77−9200
apparent contrast enhancement of flashed sinusoidal gratings 79−43915
apparent movement perception, psychophysical optimum condition analysis expt. 77−81510
apparent movement perception, psychophysical optimum condition analysis applications 77−86504
apparent vernier offset, actuity obs. 80−16949
apparent vertical rel. to vertical horopter 79−100619
artificial stereo, enhancement aid for human perception 79−31806
astronaut visual working capabilities, rel. to external conditions logical approach *(Russian)* 77−5088
asynchronous gratings summation obs. 80−35901
auditory-visual perception of speech with reduced optical clarity 80−35919
autokinesis suppression by proprioceptive information about target location 78−7370
background effect on foveal and parafoveal cone dark adaption 79−43914
bandwidth compression effect on military target observers' detection and recognition performance 80−106484
bandwidths of orientation channels in human vision 79−79551
behaviour modelling, using catastrophe theory 79−83784
Bezold-Brucke hue shift meas., effects of psychophys. procedure and stimulus duration 77−32901
binocular colour fusion limit 79−57659
binocular cross-correlation in time and space 78−40173
binocular depth discrimination, spatio-temporal aspects, Mach-Dvorak effect 80−12149
binocular depth mixture with non-symmetric disparities 78−56991
binocular depth perception, model suggested by neurophysiological evidence 77−21527
binocular depth perception scheme suggested by neurophysiological evidence 77−44671
binocular eyepiece nonparallelism influence 79−72665
binocular grating perception, contrast effects 77−70473
binocular image perceived direction 79−43923
binocular interactions, spatial freq. masking in human vision 79−83787
binocular masking-level differences, influence of bandwidth and temporal props. of spatial noise 77−44681
binocular rivalry and sighting dominance 79−16210
binocular rivalry between after-images illuminated intermittently 77−36935
binocular rivalry sensitivity to nondominant stimulus changes 79−62263
binocular rivalry suppression inhibitory effect, orientation independ. 78−61185
binocular summation, eye accommodative-vergence state rel. to binocular instrument collimation 78−53417
binocular vision, artificial aniseikonia, geometrical explanation of induced size effect 80−72173
binocular vision, effect on separable processes of artificially induced anisometropia 80−45906
binocular vision, frog ipsilateral retino-tectal pathways 80−85401
binocular vision, fusional vergence eye movements rel. to fixation disparity 80−56031
binocular vision, population study of fixation disparity, heterophoria and vergence 79−96563
binocular vision, visual sensitivity of one eye 79−20544
binocularity affected by sectioning of corpus callosum, of cat 80−97922
binocularity evaluation of pseudophakic patients 80−51106
binocularity in kittens reared with optically induced squint 79−79556
bionic image analysis using lines and edges 77−36931
biphasic optokinetic response in crab, anal. 80−101175
bistable stroboscopic motion display, factors controlling competing sensations 79−43920
blue-sensitive cones, apparent saturation at colour-opponent stage 79−57661
blur detection sensitivity in optometric tests 79−11935
book retinoscopy, brightness changes 78−61183
border contrast enhancement as index of contact lens performance 78−3492
border enhancement, brightness vs. darkness effects 78−7366
border enhancement, effect of scatt. light 78−11658
brain damage patient, 'extinguished field' information processing 80−30728
brightness, demonstration of nonlinearities using luminance profiles 77−56380
brightness detection, midbrain reticular stimulation, Rhesus monkey 79−43919

visual perception continued
brightness enhancement mechanism 78−69061
brightness exponent for periphery in Bloch region 78−69081
brightness generation, colour-brightness, contrib. of cortical colour channels to brightness sensation 78−11657
brightness increase effect due to direction of light polarisation 80−41041
brightness metacontrast, foveal and spatial props. 77−40677
brightness perception and retinal rivalry in binocular vision, integrated model 80−101180
brightness under contrast, psychophys. functions 78−57000
Broca-Sulzer effect, combined temporal and spatial unified model 80−35893
Broca-Sulzer effect, spatial, at brief stimulus duration 77−36940
Broca-Sulzer effect and its spatial analogue, decrement versions 79−43921
Broca-Sulzer effect in a Ganzfeld 79−53151
Broca-Sulzer effect under scotopic viewing conditions 77−12924
Broca-Sulzer phenomenon, effect of retinal eccentricity 78−69102
cerebral dominance 78−7372
cerebral lateralisation effects in visual half-field expts. 78−3496
changing size perception, effect of object size 80−51108
chromatic, human, colour picture signal transmission system model, math., treatment 77−25441
chromatic backgrounds, dual role in colour perception 79−53126
chromatic border perception, by R and G cones in trichromatic eye 79−57658
chromatic border perception, role of red- and green-sensitive cones 78−69091
chromatic input to stereopsis, calcs. 80−16948
chromatic stereopsis, opposition of photometric and dioptric factors *(Italian)* 78−56986
chromatostereopsis, 28 annotated references covering 166 years 79−5290
classical optics, failure to account for observed phenomena 79−5289
cognitive processes and eye fixations 77−25438
coherent motion and stereopsis in dynamic visual noise 77−86503
colour, exchange threshold method of anal. in humans 80−12129
colour, Roth 28-hue test 78−3494
colour aftereffects, spatial frequency contingent range 79−2071
colour appearance specification, terms and formulae 78−56995
colour changes due to distance and lighting, direct assessment using Natural Colour System 78−57004
colour contrast, inductive math. modelling *(Russian)* 77−52793
colour differences scaled by chromatic modulation sensitivity functions 79−53121
colour flicker, lateral interactions and rod intrusion 77−81503
colour images, rate distortion coding simulation for colour images 78−7361
colour Mach bands, definitions 78−69096
colour perception, human, graphic model *(German)* 78−57005
colour perception and Stiles' π mechanisms, humans 77−44683
colour perception fundamentals 78−77054
colour signals from incremental and decremental light stimuli 77−21526
colour TV images, effect of luminance contrast on chromatic blur 79−39419
colour vision model 80−81604
colour vision perception in Greek literature 80−22184
colour vision zone fluctuation model, nonlinear processing at receptor level 80−81601
colour-coding properties of sustained and transient channels, human 77−25440
colour-contingent motion positive aftereffects, interocular transfer 78−69100
coloured afterimages, interactions with simultaneous contrast 79−2069
coloured field, effect of subtense and surround luminance 78−57003
colourfulness, new concept 78−56996
complementary image, site of origin obs. 79−70552
complementary images, time-course of induction 79−2070
complex shaped objects, visual resolution and recognition, vibr. influence *(Russian)* 80−45909
complex stimuli viewed in light and dark surrounds, perceived saturation 77−70468
component letter perceptibility rel. to gross vision of word, quantitative model 79−53145
composite stimulus detection, rel. to grating and line detectors 78−3487
computer-based testing system 79−74769
consonants auditory and visual similarity rating patterns anal. 78−48807
conspicuity, search and fixation tendencies of eye 77−21530
constancy limits, colour, and colour perception 80−41025
continuity perception in stroboscopic motion, temporal freq. anal. 79−74674
contour interaction in human vision, inhibition 77−12926
contour perception, implications of spatial summation models 78−69094
contrast, edge-induced, Crack-O'Brien effect 80−35894
contrast constancy and linearity of contrast sensitivity 77−9201
contrast detection, linear models, convexity theorem for subthreshold stimuli 78−69085
contrast effects on smooth-pursuit eye movement velocity 79−43891
contrast increment detection of square-wave third harmonic 77−36924
contrast perception, suprathreshold response obs. 80−30729
contrast reduction by small localised stimuli, above-threshold orientation-selective masking 77−40676
contrast reversals in backward masking 78−48817
contrast sensation, stimulus contrast obs. 80−41040
contrast sensitivity, achromatic and colour, instrument for testing 78−73275
contrast sensitivity, orientation anisotropy in rhesus monkey, behavioural study 80−45912
contrast sensitivity and acuity, goldfish 79−62264
contrast sensitivity during saccadic eye movements 79−48270
contrast sensitivity enhancement by spatial freq. adaptation 78−7364
contrast sensitivity of human infant for moving and static patterns 78−7351
contrast sensitivity over first 3 months of life in human infant 78−3486
contrast threshold difference between spatial sine- and square-wave gratings 79−74679
contrast thresholds of random patterns 78−65020
contrast thresholds versus border enhancement, sensitivity to retinal defocus 80−30725
convergence micropsia rel. to retinal eccentricity 77−44682
convergent disparity discriminations in narrow-band-filtered random-dot stereograms 79−43917

visual perception continued
cooperative stereo algorithm, empirical approach 79−100615
cooperative stereo algorithm anal. 78−53413
Cornsweet illusion, edge-induced visual contrast and spatial freq. interaction 78−11659
cortical evoked potentials by dynamic random-dot stereograms 79−43876
cortical neurones, pattern selective adaptation, cats 79−53090
countercolour system and colour vision eqns. for arbitrary colour *(German)* 78−57007
counting, role of small saccades 77−25456
Craik-O'Brien effect in human visual system, temporal depend. 80−81608
Craik-O'Brien-Cornsweet illusion for visual depth 78−48815
critical flicker freq. for sensitivity difference meas. of retina *(Japanese)* 79−8512
critical flicker fusion in normal and binocularly deprived cats 80−35898
cross-modal and intramodal matching tests, tape construction method 80−41334
CRT/observer interface development trends 78−24076
defect analysis, remote subjective refractor using sphere-cylinder corrections 77−1992
defocus psychophys. and electrophysiological effects 77−90768
depth information from binocular delay obs. 79−74675
depth perception, binocular and monocular motion parallax, geometric and physiological aspects 78−80877
depth perception, meridional disparity effects 79−53133
depth perception, visual sensitivities to cues, TV broadcasting appl. *(Japanese)* 78−48808
depth perception and size constancy *(Japanese)* 80−97918
depth perception by motion, instability 80−35895
depth perception from spatial freq. difference 80−41033
depth perception in terms of hypotheses 78−80878
depth perception in young cats, effect of neonatal section of corpus callosum 80−61572
depth perception rel. to visual fixation points 77−86502
depth perception threshold and acuity determ. by vision testing instrument 78−81007
depth vision in aviation 79−11938
diagnostic imaging systems, image quality assessments 77−90890
diagnostic radiographic video system psychophysical evaluation 79−74751
dichoptic pattern masking, effect of stimulus luminance 77−44680
dichromat long-wavelength-sensitive photoreceptor spectral sensitivity determ. by border percept elimination 78−69092
dim light, seen as uniform light not isolated flashes due to photons 78−96052
Dipteran fly neural superposition eye, rhabdomere visual axis misalignments 77−64032
directional scanning biases and shifts of apparent visual direction 77−44687
discontinuous tests, temporal integration obs. *(Spanish)* 79−24992
discrimination, chromatic and achromatic, field separation, gap effect 77−25446
disparity processing in human binocular vision 78−40179
displacement thresholds, foveal and peripheral, rel. to stimulus luminance, line length, movement duration 80−101183
display design, visual psychophysics appl. 78−65017
display systems *(Japanese)* 79−70551
distinctness of borderline rel. to Natural Colour System 78−57002
distortion, oblique line in presence of abutting vertical line 79−2072
dot pattern locally parallel structure computation 78−65012
dot pattern perception process simulation 77−21532
dynamic random-dot stereograms, computer generated, binocular depth perception 78−80879
dynamic theory of visual perception 79−74681
dyslexic visual perception and aculomotor performance 79−83769
echocardiography, binocular stereoscopic display system 79−48297
edge and colour discriminations, retinal neurons network 79−48256
edge coding and detection using directional masks 78−42289
edge effect reversal for increment threshold with small background 77−60219
edge induced visual contrast phenomena, exptl. anal. 79−20545
EEG contingent negative variation rebound effect, visual and auditory simuli 80−3648
efferent commands, perceptually monitored and unmonitored, smooth pursuit eye movements 79−53104
egocentric distance, oculomotor rel. to motion parallax cues 80−45914
egomotion and relative depth map from optical flow 80−76743
electro-optical system image evaluation, subjective effects of electronic and turbulent noise 78−65023
electronic imager observer performance rel. to display S/N ratio 77−40679
electronic imaging systems, detection thresholds 79−11936
emmetropic observers, perceptual effects of low-power plus lenses 80−67084
empty-field myopia correction on dark-focus of accommodation basis 79−53131
entoptic phenomena 79−53106
equal saturation contours for surface colours 78−57001
evoked potentials, luminosity and chromatic responses in man, subjective hue estimates 80−97903
experience neural correlates in single units of cat visual and somatosensory cortex 80−12120
exposure duration influence on spatial channel tuning 79−43922
extrafoveal vision, vernier acuity and apparent depth for targets of different hues 79−39420
extrafoveal visual and vernier acuity rel. to receptor field, expt. 79−62260
extrafoveally perceived displacement, illusory reversal 80−56048
eye movement amplitudes, information used by the perceptual and oculomotor systems 80−35885
eye movement role in hand movement control 80−26237
eye saccades, counting accuracy obs. 79−43889
face scanning and eye contact in early infancy 78−40169
Fechner-Benham colour effect, hue reversal following white light adaption 80−51112
Fechner-Benham subjective colour 77−44685
field size utilised by human visual system, static and dynamic conditions 80−12135
field strength in monocular and binocular perception, threshold luminance meas. *(Japanese)* 78−40166

visual perception continued
field testing, three-channel optical system *(Spanish)* 79−24993
fields, computer appls. 80−45892
figure perception, role of eye movements 80−101186
figure recognition, small-size, comparison of halftone and colour scales 78−48785
figure-ground discrimination by relative movement, fly appl. 80−56046
figure-ground discrimination by the visual system of the fly 79−2065
fine-grain movement illusion, rod- and cone-mediated interactions 77−25455
fixation points rel. to depth perception 78−69101
fixation-sensitive areas in the eyes of the walking fly, Calliphora erythrocephala 79−43904
flicker perception study using fluorescent TL tubes 77−86501
flicker sensitivity, two-stage retinal diffusion 79−74657
flicker sensitivity meas. with intermittent stimuli, temporal gradient detection comparison with De Lange curves 79−79553
flicker sensitivity meas. with intermittent stimuli, threshold depend. on stimulus duration 79−79552
flicker-induced asymmetries in border enhancement, brightness and darkness perception 80−67083
fluorescent lamps, high colour rendering, visual clarity investigation 78−48809
form detection, complexity effects 77−44678
form identification in peripheral vision 77−25444
form recognition, scale invariant, in man and machines 78−40176
form vision, role of geniculocortical system, behavioral anal., cat 80−12137
Fourier analysis by visual system or by visual investigator determ. 79−53089
foveal vision, mental scanning mechanism 79−2066
foveally viewed yellow target, chromatic uncertainty effect on detectability 78−65005
foveation system, afferent part, computer simulation model 77−25437
frequency gradient pattern threshold visibility 78−11662
fusional power and reserve determ. instrument 79−88148
generation and display of visual stimuli, psychology experiments, microprocessor based system 80−41328
geometrical illusion, math. anal. based on perceptual field *(Japanese)* 77−44676
geometrical illusions analysis in terms of perceptual field 77−2002
global feature processing in texture discrimination, psychological evidence 79−79554
global peripheral excitation, local foveal inhibitory effects 79−88076
gloss perception, model using binocular cells in lateral geniculate body 80−72167
grating acuity of the wild European rabbit 80−35900
grating contrast judgements, Wiener anal. 79−5293
grating contrast judgment 77−32902
grating detectability, aberration effect evaluation in visual instruments 79−55073
grating detection and resolution thresholds, role of cones and rods 78−92626
grating duration perception, effects of colour specific adaptation 77−21529
grating perception at threshold, noise masking expt. technique 80−72171
grating summation in fovea and periphery 78−69097
gratings, coloured, perceived duration, interocular effects of adaption 80−56051
gray scale optimisation for photoscanners 79−79555
grey toad, colour perception constancy, role of background in recognition of blue stimuli 78−15844
grey-out elimination, roles of spatial waveform, freq. and phase 79−43910
grouping, new approach 80−12142
halftone image coding rel. to visual performance characteristics 77−58280
hallucination patterns, mathematical theory of neuronal activity 80−35892
haploscope, automated miniaturised device for testing binocular visual function 77−2004
haploscopic apparatus for study of colour perception under different adaptation conditions 78−56997
Hermann grid illusion, detection thresholds 79−2076
hue change with eccentricity, rod and cone contribs. 80−45904
hue change with rod intrusion during dark-adaptation 80−51104
hue substitution, wavelength latency effects 77−44684
human eye characteristics exploitation in colour television tubes design 77−56372
human picture distortion ratings compared with objective error measures 78−44510
human psychophysics: functional interpretation for contrast sensitivity versus spatial frequency curve 79−48265
human visual system models for image enhancement and display design 77−58279
human visual system spatial characts. nonlinear model 77−12929
human visual system spatial sinewave/squarewave grating contrast threshold difference 79−57662
hyperacuity, integration regions 77−21524
iconic memory, temporal characts. 77−52790
iconic persistence and perceptual moment as determinants of temporal integration 79−53147
iconics and image processing 79−94173
illuminance dependence of 100-Hue response for normal subjects of different ages 77−90794
illuminated scene, visual clarity, theory and expt. 78−48810
illusion of flying clouds involving visual capture and distance reversal 77−12927
illusions and visual functions 80−12143
illusions due to interactions of stabilised retinal patterns and spatial visual noise 79−100620
illusory motion in depth, aftereffect of adaptation to changing size 78−48814
illusory movement perception obs. 80−21473
image coloration psychophysics 78−65025
image contrast and its dependence on luminosity, physical model *(Italian)* 79−62261
image defocus detection by human infants 78−7354
image matching with the eye, effects of pictorial noise 80−51113
image number in neuron structure, multilayer determined neuron network appl. 77−44674

visual perception continued
image processing in animals and man, visual capability factors 78−61190
image quality data rel. to realistic visual task prediction 78−53415
image quality descriptor relationships using signal detect. theory 78−71050
image quality psychophysics, research methods and strategies 78−65024
image sharpness thresholds 78−65019
image size in neuron structure, neuron matrices apparatus appl. 77−44673
image transformations, human factors, algorithm 78−58939
image transmission techniques, conference, San Diego, USA (Aug. 1976) 77−79773
infants, reaching responses to visually presented objects 77−2005
information capacity of eyes 78−11661
information display technology, symposium, San Francisco (1978) 79−9209
information evaluation 79−29534
insect visual system elementary movement detectors 77−2001
instantaneous/durable perception, electrophysiological correlates 77−25451
instantaneous/durable perception, psychophys. study 77−25450
intensity response, simple expt. for teachers 79−71203
interference in peripheral recognition of embedded letters *(Japanese)* 80−61569
intermittent monochromatic light saturation 79−53138
interocular transfer of luminous flux discrimination, rabbit 77−25448
Johansson effect stability, psychological expt. *(Japanese)* 78−96049
kinetic depth effect, amplitude, freq. and phase determinants of perceived rotations and rigidity 80−76746
kinetic induction produced by light simulation in humans 77−44689
lateral inhibition process modelling by semi-group theory 78−65010
lateral masking in foveal and eccentric vision 78−56993
lateral spatial interaction in humans with abnormal visual experience 78−7363
lateralisation effect in reading Chinese characts. 80−30727
lateralised perception of bilateral chimaeric faces by normal subjects 77−66815
learning-set formation, monkey eye movements 78−77057
length illusions rel. to interactions between orientation detectors 77−70472
light adaptation in cone photoreceptors, dark glasses model 80−12122
light deprivation and maturation, bibliography 78−15843
lightness perception rel. to perceived spatial arrangement 77−36932
line spread function meas., implications for channel bandwidths 78−65030
line-spread function, human, near fovea, quantitative charact. 79−2073
local adaption effect simulation with nonlinear spatial filters 77−44657
local organising processes and motion schemas *(Spanish)* 78−69086
long-lasting afterimages caused by neural adaptation 77−70474
looming detectors in human visual pathway 78−65029
low luminance vision in aviation 79−11937
luminance-brightness comparisons of LED alpha-numeric sources at suprathreshold levels 78−92625
luminescent material choice, psychophys. considerations, in book contrib. 77−73172
luminous efficiency functions determined by successive brightness matching 79−43906
Mach patterns, incremental and decremental thresholds 78−77059
Mach-Dvorak illusion, onset to onset rule for binocular integration 78−7367
mammalian visual cortex development model 77−44672
mammographic screen-film systems, comparison of laboratory and clinical evaluations 78−69187
masking independent of both separation and spatial frequency 80−16947
matching information to brain, problems 80−51114
McCollough aftereffects, calorimetric matches 78−65026
McCollough effect, classical conditioning model 77−36937
McCollough effect retention in darkness, storage vs. enhanced read-out 77−36936
McCollough effects, binocular interactions during establishment 79−48271
mealworm beetle visual edge fixation and negative phototaxis 77−16933
medical display system perceived dynamic range evaluation from receiver operating charact. curves 78−44662
medical image lesion contrast and photon count density rel. to D-log E curve 78−69195
mental scanning mechanism in foveal vision, expts. 79−5280
metacontrast, perceptual changes, variables quantification 79−43912
metacontrast and paracontrast suppression of contourless area 79−53150
metacontrast as function of spatial freq. composition of target and mask 79−48267
metacontrast as function of spatial separation with narrow line targets and masks 78−7369
metacontrast masking rel. to luminance transients 77−81506
metacontrast with black and white stimuli, inhibition of on- and off-sustained activity 79−53139
microcomputer controlled haploscope for binocular experiments 80−46091
minimally distinct border, temporal analogue 78−40174
mirror symmetry detection in random dot displays, versatility and absolute efficiency 80−16944
missing fundamental illusion, var. of spatio-temporal characts. with dark adaptation 77−81507
monocular depth structure analysis, psychophysical approach 79−57663
monocular rivalry, spatial frequency, orientation specificity of simultaneous and successive inhibition 79−53140
monocular rivalry of complex waveform, perceptual instability 79−53148
monocular space perception and visual stability, math. model 80−45910
motion, subjective Lorentz transformations 78−69082
motion after-effect theory, perception mechanism 78−35862
motion and form information, dissociation and interaction 79−53141
motion flow perception, conditions for in dynamic visual noise 80−72174
motion illusions of rotating gratings of high contrast and different spatial freqs. 79−43907
motion in depth, binocular and monocular stimuli, review 80−61570
motion in depth, information processing 80−21474
motion perception, analogous illusion in man and fly 79−48266
motion perception, form in formation is necessary 80−16950
motion perception, functional difference between central and peripheral vision *(Japanese)* 80−61568

visual perception continued
motion perception, role in smooth pursuit eye movements 79−100618
motion perception, role of colour 78−85312
motion perception, smooth eye tracking in absence of real movement 79−2075
motion perception rel. to smooth pursuit eye movements 80−3649
motion smear 80−56047
motion/disparity aftereffect 77−12925
movement detecting neural element in fly visual system, performance 79−43871
movement detection, model investigations of lateral inhibition 79−53127
movement detection, one-way, in fruitfly visual system 79−39415
movement detection, performance of a wide-field element in the blowfly visual system 80−89763
movement detection, upper-velocity threshold 80−8067
movement detection by foveal and parafoveal retina, effects of background struct. and target size 80−85403
movement detector angular orientation acting on flight lift response in flies 79−43905
movement direction perception, effects of adaptation in analyser 78−96050
movement illusion and tracking movements of eye 77−86500
movement illusion interactions, motion aftereffects and induced movement 77−9199
movement parallax, asymptotic function of amplitude and vel. of head motion 78−69088
movement processing in the visual system model 79−66473
movement-selective mechanisms in human vision sensitive to high spatial frequencies 78−92632
moving pattern interaction, subjective standstill 78−11664
moving patterns, perceptual anal. 77−29152
moving target visibility, effect of mental set 78−27957
moving targets, highly specialized nerve circuits 77−81501
multidimensional scaling 78−64979
Munsell colours, principal hue components 78−56999
myopia, supernormal visual capacity 80−81612
Necker cube perceptual reversal, absence of accommodation 80−41037
negative aftereffects and use in investig. of perceptual systems 77−48807
negative colour afterimage and McCollough effect, comparable retention times 79−53146
neural network finding binocular correspondence, inference 79−34557
neuronal network analysis using statistical signals, feline visual system 79−43872
night vision equipment matching to human observer 77−40937
noisy photographic images, threshold contrast, parametric model of observer *(Russian)* 77−52794
nuclear medicine image processing, clinical quality meas. 77−86626
object fixation and spontaneous pattern preferences in Drosophila melanogaster 79−43903
ocular rivalry suppression, effect of 9 Hz flashing light 79−34566
ocularity domains and growth behaviour of axon terminals 79−48249
off-foveal retinal images, accommodative convergence response 79−29532
ontogenetic change in human colour vision, developmental pseudocyananopsia 78−35854
opponent chromatic mechanisms predict hue naming 80−12132
opponent-colour channel spectral sensitivity 78−7359
opponent-colours theory and colour blindness 80−12133
opposite colour difference and anti-colour, humans 77−70471
optical instrument image evaluation by multitarget array detection 80−1362
optical system quantitative tolerance specification and standard development 80−48384
optical system specification and test procedures 80−48385
optokinetic nystagmus, induced by stereoscopic contours 79−48269
orientation detector colour inputs, human visual system 77−25435
orientation discrimination, facilitation effect 79−48272
orientation discrimination 80−12141
orientation discrimination by young infants 80−61573
orientation sensitivity of visual movement detection system activating landing response of blowflies 80−101176
orthogonal combination of three visual channels 78−3491
orthogonal systems generating hypersensitivity, colour and depth 78−80881
parafoveal stimuli, spectrally different, psychophysical tests of equiv. luminance 78−53414
patter perception, functional diff. between central vision, peripheral vision *(Japanese)* 79−29533
pattern classification, systems analysis using detection expts. 77−36929
pattern detection, absolute efficiency, humans 80−12138
pattern detection and discrimination at low spatial freqs. 77−70465
pattern discrimination, phase-dependent interaction of widely separated spatial freqs. 80−45913
pattern induced flicker colours, effect of time delays 77−48808
pattern induced flicker colours, sensory process sensitivity to short time delays 78−96048
pattern matching, human performance, spatial freq. anal. model 78−40177
pattern perception time integration, tactile mode comparison 79−53143
pattern recognition, transformation and relational-struct. models, random-dot pattern tests 79−53130
pattern recognition by assignment of invariant features and feature-relations 77−25445
pattern recognition from psychological view-point *(Japanese)* 80−97919
pattern recognition functional mechanisms in humans 80−81609
patterned stimuli adaption, condition for Weber's contrast law 79−48260
patterns, drifting contrast, electronic device for generation 80−26421
perceptual analysers underlying visual texture discrimination 78−53412
perceptual stability law, abstract foundations 79−5291
perspective distortion in photography, eye as simple lens 80−17734
phantom-motion aftereffect 78−31815
phase-specific adaptation, independ. of black and white 77−32903
photochromatic interval estimation for peripheral vision 78−27954
photographic image threshold luminance detail value, effect of target and photographic parameters 78−56989
photoreceptor noise suppression, rel. to incremental intensity thresholds 79−43895
pictorial depth sensitivity development 78−77058
pictorial noise pattern subjective effects 77−90799
pigeon visual search, hunt and peck method 77−77900
polarisation and colour vision, functional similarities 78−3497

visual perception continued
polarized light incident on cornea, transient adaptation 80−81596
position constancy loss during pursuit eye movements 78−40170
predators, visual detect. of cryptic prey by blue jays 77−40675
primate sensory projection spatial mapping 77−25436
prismatic adaptation, single and multistate, long-term retention by humans 78−40168
pseudoscopic image restored by a hologram, peculiarities of visual perception *(Russian)* 79−50255
psychometric measures for specifying colour appearance 80−76747
psychophysical analysis of the 'sensation of reality' induced by a visual wide-field display 80−108901
psychophysical function, harmonisation of Fechner and Stevens 80−8068
psychophysical stimuli, generalised, generation by large format optical display 79−44072
psychophysics as method of meas. of biosystems *(Japanese)* 78−53591
psychophysiological function of the human eye *(Czech)* 80−21472
Pulfrich effect study device, versatile, multi-input 80−8221
Pulfrich stereophenomenon, spatial freq. effect 77−40678
pursuit eye movements, perceptual vs. retinal stimulus 77−9196
pursuit eye movements, smooth tracking 77−9197
pursuit movements in absence of target, perceptual effect 78−73162
quantum fluctuations and adaptive spatial interactions 79−16206
radiographic decision making and phys. image props. 78−69189
radiographic image formation, perceptual eval. of phys. parameters, computer-simulated images 80−41222
radiographic image quality comparison for different screen/film combinations by subjective judgments 78−73229
radiographic images, threshold mechanisms in presence of visible noise 77−86624
radiographic observer performance meas. and characterisation, free response approach 78−69200
radiography, computed, contrast-detail-dose evaluation 80−41221
radiography, detection of bars and discs in quantum noise [radiography] 80−41042
radioisotope imaging device assessment, psychophysical approach 77−86625
random dot pattern density change detect. efficiency 78−69089
random pattern generation using coherent optical spatial filtering, for vision research 79−98462
random-dot pattern texture discrimination 78−65013
random-dot texture discrimination 78−65014
random-dot-stereogram performance of optometric patients 79−83785
Rayleigh Match, spatio-temporal characts. 77−32900
reaction time as a measure of suprathreshold grating detection 79−53144
reaction time measurements, spatial summation exam. 79−92223
reaction times, square-wave gratings of different spatial frequency and contrast *(Italian)* 79−39421
reading, span of recognition 78−40172
receiver operating characteristic anal., generalisation to detect. and localisation tasks in scintigraphy 77−40745
receiver operating characteristic and diagnostic benefit determ., visual detect. performance in medicine 77−86563
receptive field-like properties, human psychophys., anal., dichoptic props. of Westheimer function 77−9203
receptive field-like properties, human psychophys. anal., dichoptic props. of transient-like function 77−9204
red-green opponent spectral sensitivity, meas. methods disparity, perceptual basis 79−53120
red/green matching portable filler anomaloscope for genetics study 77−5004
reflected light common and relative components as information about illum., colour and 3-dimens. form 78−56982
relative motion extraction, neural mechanism model *(Japanese)* 78−56987
relative motion extraction model 78−48794
relative motion induced between stationary lines 79−53149
remoteness of point light source in space with no optical reference, visual estimate accuracy 80−104590
repetition perception in quasi-random patterns, visual echoes 77−25453
repetitive images, two-dimensional Fourier spectrum description 77−58282
resolution abnormalities in cats reared in stroboscopic illumination 79−83788
resolution and contour interaction in the fovea and periphery 80−51109
retina, significance of antidromic potentiation and induced activity 80−12092
retinal image displacements and saccadic eye movements, adaption to altered relationship 79−43911
retinal images, defocused and spatially filtered, stereoscopic acuity 80−101177
retinex systems' role in colour perception 80−81598
reversible perspective figure, factors affecting fluctuation rate 77−60215
road user, testing using liquid crystal device *(French)* 77−36930
rod contribution to colour information, using scotopic luminosity function and colour mixture data 78−35855
rod ERG, human, rel. to psychophysical responses in light and dark adaptation 78−69063
rod photoreceptor model sensitivity, depend. on level of background light intensity 78−20179
rod receptor orientation local variations 78−40175
rotating three dimensional object geometric properties perception 79−83786
saccadic eye movements, small, perceptual function 80−61577
saccadic eye movements and visual stability 79−2068
saccadic movements during changes in fixation to stimuli at different distances 77−32895
saccadic omission, grey-out obs. 79−43909
search image formation in blue jay (Cyanocitta cristata) 79−83789
selective attention, role of inferotemporal cortex, monkey obs. 79−100616
selective chromatic adaptation at different spatial freqs. 78−65006
sensitivity, within-species vars. in squirrel monkey 78−7358
sensitivity changes during metacontrast 79−43913
sensitivity during successive chromatic contrast, interactions between photopic mechanisms 77−25449
sensitivity to controlled motion of line or edge 79−53142
sensitivity variations, contrast resolution and eye movements 79−53088
sensory information processing, parallel and sequential *(French)* 77−12873

visual perception continued
sentence information processing, EEG evoked response and CNV obs. 79−57626
short-term visual storage mediation rel. to spatial freq. 78−35861
signal transmission by visual pathways, distortions of retinal images 80−85400
simulation and image realism, seminar, San Diego, USA (Aug. 1978) 80−3639
simulators of auditory and visual impairment, development project 79−83982
simultaneous colour contrast, deviations of induced colours from directions of complementary colours 78−56998
single stroke figures, influence of visual field size on perception 80−101179
sinusoidal line stimuli, orientation effect 77−25452
sinusoidal luminance gratings, 1- and 2-dimens., visual processing 77−44677
size, shifts after adaptation to gratings 80−85398
size and brightness difference equivalence of honeybee *(German)* 79−53128
size change perception, selectively sensitive neurons in cat visual cortex 79−100608
size constancy, failure below half a degree 80−45911
size constancy, visual angle constancy of subjective checkerboard pattern 80−16945
size illusion opposite to Craik-O'Brien illusion 77−81508
size of one object among many, expt. obs. 80−81607
size of perceptive fields fovea and periphery, light- and dark-adapted obs. 80−61574
size preference of frogs for prey, effect of viewing distance 78−7362
solid shape, internal representation with respect to vision 79−74671
spatial aftereffects, role of afterimages 78−7365
spatial and temporal information separation model 78−40167
spatial characteristics of human system, nonlinear model 77−25439
spatial contrast visual detection, influence of location in visual field, target extent and illuminance level 79−2067
spatial extent, effect of saccadic recalibration on visual perception 77−48806
spatial filtering constrained by biological data 80−30731
spatial Fourier transform model 79−11940
spatial freq. responses and multi-channel theory *(Japanese)* 80−97916
spatial frequency, accommodation response dynamics 79−53134
spatial frequency, perceived shift at orientations orthogonal to adapting gratings 80−51110
spatial frequency analysers, lateral inhibitory interaction 78−7371
spatial frequency analysis of visual environment, anisotropy and carpentered environment hypothesis 79−53137
spatial frequency and light spread description of visual acuity, hyperacuity 77−52789
spatial frequency channel interactions in human visual system 80−12140
spatial frequency channels, human, masking by sine and square waves 77−2000
spatial organisation of human visual system at detect. threshold, status of research 80−12139
spatial phase, sensitivity obs. 80−72172
spatial phase sensitivity, sinusoidal grating targets 79−2077
spatial probability summation and disinhibition 79−74678
spatial resolution for detect. of real and apparent pattern and movement 78−48806
spatial sensitisation as function of delay 78−11663
spatial separation acuity as function of stimulus size 78−69087
spatial summation effects on two-component grating thresholds 78−69080
spatial vision, cat 80−12136
spatio-temporal modulated stimulus, directional and nondirectional coding 79−74676
spatio-temporal stimulation in lightness and colour *(Japanese)* 80−97917
spatiotemporal contrast detection invariances, humans 80−85402
spatiotemporal contrast detection threshold surface is bimodal 79−29535
speckle motion in laser refraction, apparent speed obs. 80−45879
speech, visual vowel and diphthong perception from two horizontal viewing angles 80−35923
speechreading, visual perception of syllables and sentences, age effects 80−16943
speed-accuracy tradeoff in visual detect., appls. of neural counting and timing 77−32894
stereoacuity in mentally retarded and intellectually normal adolescents 78−77055
stereoblind humans, psychophysical evidence for a monocular visual cortex 79−43908
stereomovement from interocular delay in random visual noise, random spatial disparity hypothesis 78−24074
stereopsis, absolute thresholds as meas. by crossed and uncrossed disparities 80−45908
stereopsis, contrast disparity obs. 80−41034
stereopsis, fusion at site of ghosts 78−69090
stereopsis, limit of single vision, depend. on contour sharpness 78−88711
stereopsis, obs. of independent channels for different extents of spatial pooling 80−56052
stereopsis, orientation and position disparities 80−12145
stereopsis, review 78−77056
stereopsis, rivalrous texture stereograms 77−2003
stereopsis, role of colour contours 79−74677
stereopsis, synkinetic interaction of convergence accommodation and accommodative convergence 80−51111
stereopsis and binocular rivalry from dichoptic stereograms 78−56990
stereopsis assessment with operant conditioning in young children 79−83783
stereopsis by harmonic analysis 79−43918
stereopsis facilitation by texture contours 79−100617
stereopsis in human infants 80−89762
stereopsis in monkeys using random dot stereograms, effect of viewing duration 80−41038
stereopsis mechanisms 80−12148
stereopsis with and without monocular contours 77−81505
stereopsis without binocular correlation 79−2074
stereoscope vergence, convergence and divergence independence obs. 80−30714
stereoscopic acuity interference, spatial, temporal and disparity tuning 79−53136
visual perception continued
stereoscopic depth, effect of vertical disparity 78−56994
stereoscopic depth channels for position and for motion 80−12146
stereoscopic depth effects in dichoptic perception of gratings 78−69093
stereoscopic depth perception, underlying neural mechanisms in visual cortex of cat 80−12147
stereoscopic localisation with eyes asymmetrically converged 78−56985
stereoscopic vision spatial limitations 78−80880
stereovision in SEM 80−73532
Stiles Crawford I effect using polarized light 80−81595
Stiles-Crawford function at 35° in temporal field, foveal peak stability 79−62262
Stiles-Crawford hue shift following photopigment depletion 79−57660
stimulation apparatus, stepper-motor shutter drive using monostables 78−35860
stimulus effect on surrounding visual space, induction field effect *(Japanese)* 80−8066
stimulus perceived difference in honeybee, contrib. of individual parameters *(German)* 79−53129
stimulus subjective offset and total persistence obs. 80−56056
strabismic amblyopia, relationship between pattern and movement perception 78−65027
strabismic amblyopia, threshold contrast sensitivity function 78−7352
striate cortex, spatial mapping approach to perceptual coding 80−101168
striate cortex functional architecture quantitative model 80−89747
stroboscopically illuminated moving noise patterns, movement and spatial periodicity dual percept 80−81605
structure visibility change with contrast reversal 79−57664
subjective contours shape and model for generation, filling-in gaps 77−16932
subjective performance, noise and quality influence 78−53416
superior colliculus, cat, neuron response to stationary and moving visual stimuli 79−43893
suprathreshold contrast perception and complex random textures 78−69103
suprathreshold information transfer, brightness match profiles of high contrast gratings 78−56992
suprathreshold sinusoidal flicker perception obs. 79−57665
surface blacks and whites 79−74673
sustained/transient channel interactions, form inhibits motion in human visual system 78−48812
symbol discrimination, human visual performance predictor 78−40178
Talbot's law failure, foveal vision of discontinuous test 80−81611
target discrimination rel. to colour of illumination 79−53135
target edge sharpness and temporal brightness enhancement 79−53152
target localisation during smooth eye movements 79−74680
target smooth pursuit, effect of luminance on oculomotor performance 79−48268
telescopic visual search time rel. to field of view 79−27363
temporal brightness enhancement determ. by luminance, chromatic stimuli 79−74672
temporal discriminations of brief pulse intervals 79−43916
temporal facilitation with stroboscopic motion 79−53132
temporal noise, detectability of power fluctuations 78−48811
temporal order in adjacent visual stimuli 77−81502
temporal resolution of chromatic stimuli, with or without luminance transients, exam. 78−35856
temporal sensitivity of human visual system to sinusoidal gratings 80−97915
temporal square-waves, apparent contrast from light- and dark-phase matching data 77−36939
temporal stereopsis and dynamic visual noise 78−7368
textural resolution limit investigation 77−12928
texture discrimination, rel. to Fourier anal. in human vision 78−96051
texture discrimination, underlying perceptual analysers 78−85310
texture discrimination 79−43902
texture discrimination using random-dot patterns 78−11650
texture similarity judgments, spatial frequency bases 80−30730
textures, discriminable, with identical Buffon needle statistics 79−34568
thermal images, data processing and optimal projection to human eye 78−38038
three dimensional imaging, conf., San Diego, USA (Aug. 1977) 78−78971
three dimensional vision, collimated one position illumination 77−36933
three-dimensional objects machine visualisation via skeletal transformations 77−40674
threshold changes near light-dark border, real vs. equivalent background lights 77−25454
threshold conditions, quantum coincidence theory 80−81610
threshold vision and light quanta, rel. to history of visual science 77−25443
threshold vision aspects of picture encoding 77−81509
tilt after-effect magnitude, colour and contour rivalry influence 78−69098
tilt aftereffect, clinical assessment apparatus and obs. 79−83954
tilt effect due to viewing large, patterned rotating field 80−41035
tilt illusion, repulsion and attraction effects in oblique meridian 77−44679
tilt illusion and tilt aftereffect, linear summation 80−35897
tilt illusion during binocular rivalry 77−36938
tilt illusion magnitude, influence of colour and contour rivalry 80−61575
time frequency response of visual analyser and linearity eval. *(Russian)* 80−41031
trichromacy, large-field, in protanopes and deuteranopes 77−56379
TV picture quality and coding limitation 77−12923
two movement directions of intermingled dot fields, mutual repulsion 80−56050
US imaging light intensity perception charact., stochastic noise influence 80−98053
vergence eye movement role in stereoscopic perception of space 78−85315
vernier acuity, effect of contrast, edge-gradient and target line width 77−25447
vernier acuity targets, metacontrast masking distribution, sustained channels inhibit transient channels 79−53094
vernier acuity with dot test objects 79−62265
vernier-horopter and colour 78−65007
vertical fusional vergence ranges of the rhesus monkey 80−35899
vertical movement elementary detectors of fruitfly 79−34558
vertical perception, Listing's law and eye position sense 77−44686
vestibular nuclei visual-vestibular convergence in cat 80−85420

visual perception continued
video displays, conventional or stereo, operator performance for perceptual tasks 78−80882
video displays, conventional or stereo, operator performance for perceptual tasks 78−85314
violet effect, strongly saturated subjective colour induced by flicker light *(German)* 79−53125
visibility reduction by atm. aerosols, linear system theory of visual acuity appl. 78−11997
vision, brightness subjective evaluation rel. to object and adaptation luminances *(Japanese)* 78−44509
visual forms interactions prediction using Lie operators 77−5003
visual problems raised by low altitude high speed flight 79−11939
waterfall illusion in an insect visual system, expt. obs 80−56055
whiteness perception, individual differences and common trends 79−100612
word recognition, global attributes, contrib. of word length 77−9202
Zollner and related illusions, expts. using matching technique 78−48813

visualisation, particle track *see particle track visualisation*

vitreous state
see also electron energy states of amorphous solids; glass; glass transition
abietic acid, transverse US wave propag., glass and liquid transition region 80−79883
abietic acid glass, corona-charged, TSC curves 77−55744
alchohols, glassy, spectra shift of trapped electrons, after γ-irrad. 79−78709
alcoholic glass, 4.2K, trapped electron photocond. and optical spectra following radiolysis 79−29378
alkali borates, vitreous and cryst., vibr. spectra and struct. comparison 78−23470
alkali glasses, rapidly quenched, alkali ion cond. 80−107559
alkali metal polyphosphates, vitreous, mol. weight distrib. determ. by gel-chromatography 79−50173
alkali metal polyphosphates, vitreous IR spectra 80−16043
alkali metal-hexamethylphosphoramide, low temp. glass, EPR of solvated K, Cs and Rb 78−91927
alkaline glassy state, aq., density determ., radiation chem. 80−42197
alkanes, liq. and glassy, semicontinuum model with structured first solvation shell for excess electrons 77−90711
anthracene glass, excess electron optical absorption spectrum model, band shape 78−33500
anthracene-2-methyltetrahydrofuran, glassy solution, site-selective impurity phonon coupling 77−81142
aqueous conc. solns., ionic hydration and secondary dielec. relax. 79−24882
aqueous glass, 4.2K, trapped electron photocond. and optical spectra following radiolysis 79−29378
aqueous glasses, electron trapping reaction kinetics, non-Gaussian diffusion model 78−34843
n-butanol, glassy and crystalline forms, trapped electrons, conc. of mol. vacancies determ. 77−65948
ceramic 22KhS, glass phase, valence state of Ti and Mn ions, ESR determ. 77−43871
ceramic suspension, rheological properties, effect of grainy filler ceramic suspensions 80−43685
ceramics, glassy phase, struct. study through electron-beam induced ionisation effects, HVEM obs 80−14978
ceramics, vitreous, slow neutron irradiation effect *(Spanish)* 80−57816
chain molecular amorphous solids, stat. thermodynamics and mol. theory 78−26442
chemical bond stiffness, rel. to thermodynamic and kinetic props. *(French)* 77−72561
conference on noncrystalline solids, Clausthal, Germany (Sept. 1976) 78−22654
copper salicylaldoxime, vitrified solution, additional absorpt., in axially symmetric ESR spectra 77−16151
9-cyanoanthracene excimer emission, in glassy and cryst. matrices 79−11445
decalin, liq. and glass mol. motion, kinematic and electrodynamic solns. 80−25293
dichloromethane-decalin glass, mol. dynamics, from dielec. loss meas., 107-148K, 293K 78−76379
dicyano bisphenol polycarbonate, crazing, polar group incorporation 78−85017
dielectric relaxation, theory, appl. of derived dielec. loss formula 80−50262
diffusion of radical-ion pairs, spatial distrib., electron spin echo obs. 80−29622
1,3-diphenyl-5-(p-chlorophenyl)-2-pyrazoline, singlet excitation energy migration in cryst. and glassy states 79−95831
EBBA, orientational order in glassy and nematic phases, IR dichroism meas. 80−64891
elastomer, relaxation processes, statistical description *(Russian)* 79−23229
electron spin echo, nuclear modulation 78−2727
electron trap relaxation model, for glassy polar matrix 80−15470
epoxide polymer, cellular, in vitreous state, creep 79−96092
ethanol, glassy matrix, absorpt. spectra after X-irrad., solvated electrons 79−65903
ethanol, polymorphic forms, mol. motion, NMR obs. 80−88885
ethanol glass, trapped and solvated electrons produced in presence of applied electric field 80−7379
ethanol-d_1(d_2)(d_3), glassy state, solvated electron geometry, electron spin echo modulation obs. 80−66009
ethylene glycol-water glass, γ-irrad., temp. depend. photobleaching of trapped electrons 79−66320
eutectic mixture, glassy nematic phase, complex permittivity tensor 79−91336
ferroelectric, microscopic model 77−40191
general theory development 79−41971
glass-forming systems, structure *(Russian)* 80−38925
glass-forming systems, structure and thermodynamics *(German)* 80−38924
glass-metal bonding, review of physical properties *(German)* 79−83167
glassy C electrodes for photogalvanovoltaic and photovoltaic cells 80−89630
glassy-C, irradiation induced dimensional changes 80−65052
glycerol, cryst. and glassy states, sp.ht. 80−2176
glycerol, liq. and glass, thermal diffusivity meas. 79−82394
vitreous state continued
glycerol($-d_3$), single cryst., glassy, and supercooled, polarised Raman spectra, anharmonic multiphonon interactions 79−91419
glycerol-D_2O:Tb^{3+}, Nd^{3+} soln. and frozen glass, energy transfer 78−60509
hydrocarbons, γ-radiolysis in glassy and polycryst. states, EPR spectra 77−52658
ice, sp. ht., entropy and 'glass transition' 77−51520
ill-condensed matter, summer school, Les Houches, France (July-Aug. 1978) 80−82561
induced crystallisation in glass-forming systems, heterogeneous nucleation 80−64903
internal friction and relaxation in vitreous solids *(French)* 77−72651
internal parameters, ordering parameters, history function, rel. to glass transition 78−30738
ionicity and coordination, tight binding calcs. 80−49129
Lennard-Jones, glass, Raman spectrum calc. 78−48165
liquid-glass transition, glass transition depend. on heating and cooling rates 80−79920
liquids, glass-forming, viscous flow and valence config. theory 80−14756
local motions, dielec. losses and relax. phenomena 80−108154
lunar regolith fine fraction, Luna-24 slow positron probe 80−26762
mathematical models of disordered systems, book 80−1878
MBBA, frozen nematic glass, EPR spectra of copper and cobalt triazene-1-oxide complexes 80−88871
MBBA, orientational order in glassy and nematic phases, IR dichroism meas. 80−64891
MBBA, Raman spectra in cryst., frozen glassy, and liq. cryst. states 80−60601
MBBA, solid phase polymorphism and phase transforms., IR spectra obs. 79−8128
MBBA-EBBA eutectic mixture, vitrified orientation of Cr(III) acetyl acetonate in liquid cryst. 77−16152
melts, glass forming, exam. of isobaric-isothermal pots. in glass transition interval 79−7681
metallic glasses, formation, structure and thermal stability, review *(German)* 78−83747
methanol, glassy matrix, absorpt. spectra after X-irrad., solvated electrons 79−65903
methanol glass solvated electrons, EPR, ^1H spin flip satellites, geometrical model 80−7146
methylcyclohexane, trapped electron charge distribs., optical transitions 77−28139
3-methylpentane, glassy soln., Hg sensitised UV photolysis, radical production 79−52720
3-methylpentane, trapped electron charge distribs., optical transitions 77−28139
3-methylpentane glass, electron-ion pair polarisation, γ-irrad. induced current and IR photocurrent 77−69768
2-methyltetrahydrofuran glass, 77K matrix ENDOR line shape model and expt. 78−6600
2-methyltetrahydrofuran glass, solvated electrons by electron spin echo modulation spectra 79−88991
methyltetrahydrofuran-methanol glass:β-naphtholate, electron solvation, laser flash photoionis. compared with pulse radiolysis 79−74405
2-methyltetrahydrofuran-methanol mixed glasses, annealed, γ-ray produced electrons transfer from IR to bisible traps 80−11440
microscopic theory 80−44137
molecular fluoresc., phosphoresc., and ODMR line narrowing in solids 80−43084
molecular glass, density of states for IR active internal modes of tetrahedral mols. 78−75788
nylon 6, oriented glassy, mol. wt. influence on cryst. rate 80−44156
nylon-1 polymers and copolymers, mech. props. rel. to glass transition 77−11625
obsidian, Japanese, ^{57}Fe Mossbauer spectra of naturally occurring glasses 80−67364
one-dimens. disordered solid, anomalous specific heat 79−23746
one-dimensional disordered harmonic system, heat capacity from spectral moments 79−28107
optical oscillator strengths and excitation energies in liquids, solids and mols. 78−6648
organic glass, electron-cation recombination; charge distrib. simulation and luminesc. kinetics 80−2855
organic glass, photochem. of trapped electrons 79−52722
organic glasses, low temp. mol. mobility, NMR T_1 meas. 80−60439
organic polymers, total fracture surface energy, theory 79−43406
PET, glassy polymer, local struct. determ. 80−33904
phosphoric acids, glass transition temps. 77−4050
physiological support medium+NaCl+cryoprotective agent, equilib. and nonequilib. behaviour 77−16561
PMMA, craze growth, expt. and model 78−15520
PMMA, glassy, photoelasticity 80−45034
PMMA based plastics, specific fracture energy depend. on crack growth rate., mol. struct. effect 80−66639
polar glasses, aq. and alcoholic systems, trapped electrons, photocond., optical spectra 77−85742
poly(alkyl methacrylate), vitreous state, thermal cond., hole theory of liqs., press. 78−84013
poly(ethyleneterephthalate)-p-hydroxybenzoic acid copolyester, liquid crystalline, X-ray scatt. obs. 78−9949
poly(spiro[2,4]hepta-4,6-diene) molecular characterisation, glassy state props. 80−64928
poly-N-n-alkylmaleimides, glass transition temp. 77−65956
polyacrylonitrile glassy polymer, energetics of gas sorption 80−29270
polyalkylmethacrylates, vitreous, thermal cond., press. and temp. depend. 78−2315
polybutene-1 glass, Raman spectra, low temp. crystallisation *(French)* 79−99875
polycarbonate, glassy, temp. drop during deform. 78−15456
polycarbonate, glassy polymer, energetics of gas sorption 80−29270
polycarbonate, glassy state, enthalpy relax., thermal density fluctuations 80−59678
polycarbonate, magic-angle ^{13}C NMR, relax. times, motions 79−4739
polyethylene terephthalate, crystallisation kinetics from glassy state 78−75579
polyethylene terephthalate, glass conversion zone determ. from DTA *(German)* 77−20059
polyethylene terephthalate, glassy, energetics of CO_2 sorption 80−29270
polyethyleneterephthalate, ordering, thermal pretreatment at vitrifying temp. effect *(German)* 79−65006

vitreous state continued
polyimides, glassy aromatic, plastic deform. 77−48494
polymer, amorphous, enthalpy relax. rel. to T_g 77−52278
polymer, glassy, power law relationship between yield stress and shear modulus 78−15467
polymer, glassy, sheets and spheres, gel diffusion with discontinuous swelling 80−44354
polymer, glassy state, ^{13}C NMR *(German)* 80−93188
polymer, isobaric vol. and enthalpy recovery, transparent multiparameter theory 80−24375
polymer, Rayleigh-Brillouin spectroscopy 79−38556
polymer, solvent osmotic stresses, prediction of Case II transport kinetics 80−26049
polymer, thermoluminescence data numerical anal., glass-rubber transition temp. spread 77−52189
polymer films and sheets 78−80590
polymer glass, isothermal struct. relax., in high elasticity transition region, mol. model *(Russian)* 78−87629
polymer glasses, aged, enthalpic state determ. by scanning calorimetry 80−6528
polymer glasses, enthalpy relax., scanning calorimetry technique 80−90851
polymer glasses, struct., review of expt. results 79−37636
polymer relaxation in glassy state, free vol. fluctuation effects 79−69022
polymer-filler system, glass transition *(Japanese)* 77−51479
polymeric glasses, non-elastic deformation, thermodynamic and kinetic anal. 78−64604
polymers, amorphous, semi-cryst., mech. motions, review 77−32616
polymers, cholesterol containing, struct. and liq. cryst. props. *(Russian)* 78−38622
polymers, glassy, craze surface displacements, model 80−93651
polymers, glassy, sorption of solvents, sample-dimension effects 79−52766
polymers, glassy, structural acoustic relaxation 79−95088
polymers, specific heat rel. to rate of heating *(Russian)* 77−85986
polymers, vitreous, quasibrittle fracture 80−21094
polypropene-alt-1,4-butadiene and hydrogenated derivative, mol. relaxations in glassy state 80−53177
polystyrene, craze and fracture surface morphology 77−12682
polystyrene, craze growth, expt. and model 78−15520
polystyrene, crazing, fracture, polymerisation route and internal lubricant effects 77−12683
polystyrene, fracture surface, formation and struct. of striations 77−28892
polystyrene, glass transition temp. meas. reproducibility using differential scanning calorimetry 77−15563
polystyrene, glass-like, intermol. interactions temp. depend., IR spectra *(Russian)* 79−51967
polystyrene, glassy, light scattering, quenching effect 80−20649
polystyrene, glassy atactic, struct. anal. from small-angle X-ray scattering 79−73109
polystyrene, glassy state, relax., free vol. fluctuations effect 80−19722
polystyrene, n-heptane and methanol crazes, micromechanics 77−12680
polystyrene, n-heptane and methanol crazes, structure 77−12681
polystyrene, sorption of organic vapours, glassy-state relaxation induction and meas. 80−44415
polystyrene, struct., X-ray scatt. and conformational analysis 78−26449
polystyrene networks, glass networks, glass transition temp., mol. wt. depend. 77−11680
polystyrene-b-isoprene and hydrogenated derivative, mol. relaxations in glassy state 80−53177
polystyrene-tetrachloroxylene(tetrachlorobenzene) glassy solns., additive morphology rel. to mech. props. 79−65007
polyurethane, TSD rel. to glass transition dipole relax. activation *(Russian)* 77−20793
n-propanol, glassy and crystalline forms, trapped electrons, conc. of mol. vacancies determ. 77−65948
N-p-propoxybenzylidene-p-pentylaniline, orientational order in glassy and nematic phases, IR dichroism meas. 80−64891
PVC, mech. behaviour in nonlinear viscoelasticity range 79−4996
PVC, sorption of organic vapours, glassy-state relaxation induction and meas. 80−44415
quartz, irradiated, fused, crystalline, absorpt. spectra, colour centres 80−7384
quartz glass, boron-containing, struct. investig. using ESR spectra 77−7673
quartz glass, Si^+O^- defect bands, Raman intensities, thermal treatment effects 79−15444
quartz surface, in vacuum, mechanism of appearance of elec. charges 79−69743
quartzite, vitrified, and quartzite based refractory concretes, prep. and props. 80−89188
rare earth glasses, R_2O_2S-Ga_2S_3, (R=La to Nd), exam. of preparation and props. *(French)* 78−80504
rare earth metaphosphates, glasslike, spectral intensity, effect of number of 4f electrons 78−84602
rare earth vitreous dielectric, electronic energy transfer to impurity OH^-, luminesc. kinetics *(Russian)* 79−47509
real liquids, quenched to glassy state, struct., one dimens. Ising model appl. 80−54134
rheology of glassy state and highly viscous liq. 80−70130
semitransparent material, destruction at critical point in radiative gas stream *(Russian)* 79−32910
silica, effects on viscosity of impurity alkali oxide, OH, Al_2O_3 and Ga_2O_3 78−64580
silica, vitreous, Nd^{3+}-activated, multitype opt. centre 78−68558
silica, vitreous, vapour-synthesized, viscous flow 78−64581
silicate glaze, diffusion of Sn(IV) 80−49417
solid electrolytes, conductance mechanism cc AgI/Ag oxysalt system, vitreous solid electrolytes, conductance mechanism 80−107560
structure, isobaric variation, phenomenological theory *(French)* 80−59393
styrene acronitrile copolymer, glass transition temp. determ. by elec. meas. 78−47506
styrene-acrylonitrile copolymer swelling, glass transition and crazing, polar group incorporation 78−85017
styrene-isoprene triblock copolymer, mol. relax. in glassy state 80−53177
styrene-methacrylic acid copolymer, glass-like, intermol. interactions temp. depend., IR spectra *(Russian)* 79−51967
tektites and natural glasses, Mossbauer anal. 80−21952
tektites-irgizites, Fe ions state rel. to form. conditions 78−61420
vitreous state continued
o-terphenyl, dipolar solutes, reorientational motions, dielectric relax. below glass transition 80−19706
tetrahydro-2-methylfuran glass, γ-irrad., spin trapping of radicals by BNB, EPR obs. 78−10776
N,N,N′,N′-tetramethyl-p-phenylenediamine, TMPD, glassy soln., photoionisation, recombination isothermal luminesc. *(French)* 77−16404
thermal conductivity, 1.5 to 30K *(French)* 77−39704
thermal devitrification *(French)* 77−72563
thermodynamics of glassy state with multiple order parameters 78−14283
1,3,5-triaryl-2-pyrazolines, glass-forming props. 77−11677
triphenylamine in 3-methylpentane and ethanol glasses, γ-radiolysis, IR spectra, trapped electron 77−16842
viscoelastic materials, glass-transition temp., thermodynamic criterion 77−59783
viscous liquid, glassy state, effect of fictive temp. on dielec. relax. 79−24256
Ag-As-Se system, glass-forming 79−65001
AgI-Ag oxosalt systems, solid electrolytes with glass-like struct., thermodynamic and electrochem. props. 79−10978
AgI-Ag_2O-MoO_3, comparison of ionic conductivity between glassy and crystalline solid electrolytes 78−30786
$Ag_7I_4AsO_4$ vitreous electrolyte, ionic cond. 79−77807
Al_2O_3-SiO_2 refractory, SiO_2-rich glassy phase, deconvolution of microprobe conc. profiles 77−52606
$Al(PO_3)_3$, vitreous struct. 78−26443
As-Ge-S(Se), glass films, photostruct. changes 77−85822
As-S-Tl, glass, viscosity and elastic props. 80−100180
As_2O_3, cubic and glassy, phase shift calcs. for EXAFS 77−48275
As_2O_3, glassy, intermediate range order from polarised features of Raman spectrum 80−49113
As_2O_3, vitreous, local struct. and vibrational spectra 80−55091
As_2O_3, vitreous, X-ray diffr. study of struct. 80−92464
As_2S_3, crystalline and vitreous, nonlinear absorption of ruby laser radiation *(Russian)* 78−22165
As_2S_3-HgS, phase diag., IR spectra 77−36479
AsSI, X-ray diffr. study in vitreous and fused states 77−7675
As_2Se_3, effect of gamma-radiation on solution kinetics 77−19986
As_2Se_3, short-range structure, neutron diffr. in high momentum transfer region 77−4045
AsSeI, X-ray diffr. study in vitreous and fused states 77−7675
B_2O_3, glassy, influence of annealing on transition region 80−44145
B_2O_3, Raman cross sections, rel. to appl. in fibre Raman lasers 78−31176
B_2O_3, struct. obs. using small-angle X-ray scatt. 79−41966
B_2O_3, vitreous, struct. and bonding determ., NMR obs. 77−39545
B_2O_3, vitreous, struct. study using small-angle X-ray scatt. 80−84071
B_2O_3, vitreous, struct. study using ^{10}B NMR 80−84658
B_2O_3, vitreous and crystalline, Raman spectra exam. 77−66491
B_2O_3 vitreous and liq., ^{11}B NMR line shape and spin-lattice relax. meas. 77−4575
B_2O_3-K_2O-Na_2O-Rb_2O-Cs_2O glass, small angle X-ray scatt. exam. of struct. 80−38922
BaO-Fe_2O_3 system, splat cooled phases struct., magnetisation and susceptibility 300-1100K *(French)* 77−48017
BeF_2, aq. glass, 76K, solvated electron spectrum evolution, following ns radiolysis 78−88295
BeF_2 glass, glass transition temp. and thermal expansion 80−64902
BeF_2, ionic transport and defect struct. 80−107472
BeF_2, vitreous, band limits and vibrational spectra 79−73935
BeF_2, vitreous, IR and reduced Raman spectra, weak Raman bands 78−68498
BeF_2, vitreous, Raman and IR spectra 78−39549
BeF_2, vitreous, Raman spectra meas. 77−20858
BeF_3, water free vitreous, preparation and props. 79−66033
C, directional O ion beam etching, compared with reactive ion etching 80−71781
C film, sputtered glassy, prep., mech. and struct. props. 77−66588
C, glassy, crack form. during prod., propag. by thermal stress 79−11700
C, glassy, electrolytic durability 80−66809
C, glassy, LMSC process prepared, exam. of props. by TEM and X-ray anal. 78−63675
C, glassy, negative magnetoresist. 78−23118
C, glassy, struct. evolution due to thermal treatment at 1000 to 2700°C, layers evolution 77−68923
C, glassy, struct. evolution due to thermal treatment at 1000 to 2700°C, tridimens. config. 77−68924
C, glassy, struct. parameter var. with heat treatment temp. 77−11488
C, glassy and fibrous, density of states, magnetoresistance theory appl. 80−44620
C, glassy foam, props. 77−24976
C, glassy reticulated struct., low temp. thermal cond. meas. 79−86938
C, low temp. sp. ht., thermal cond. and US vel. meas. 78−47533
C, prep. from liq. phenolformaldehyde resin, TEM obs. 79−83145
C, vitreous, wetting by Cu-Sn-Ti alloys 78−71904
$CaCl_2(Br_2)(I_2)$, glassy aqueous soln., LF region Raman spectra 80−84729
$Ca_{1-x}La_xMgAl_xSi_{2-x}O_6$, crystalline and vitreous phase comp. and props. 77−44221
$Ca(No_3)_2$-H_2O system, induction period supercooling depend. meas. 80−19918
CaO-Al_2O_3-SiO_2 glass-$MoSi_2$ filler, vitreous composite prod. 77−90313
CaO-SiO_2 glass, solid reactions, study by hot stage electron microscope *(Japanese)* 78−12798
Co enamel, vitreous, objective colour evaluation, rel. to firing parameters *(Czech)* 80−42252
Co-Si interface, metal-semiconductor transition, rel. to first compound nucleation 80−24771
D_2, solid, quadrupolar glass ordering NMR adsorption line shapes 80−7178
Fe, realistic relaxed struct. model pair distrib. function 78−30544
$GaCl_3$, Raman spectral differences from liquid to glassy state, ionic equilib. interpretation 80−20619
Ge-Se-Tl, vitrification region 77−43154
GeO_2, glassy high freq. vibr. bands, central force model 80−49330
GeO_2, new high-pressure modification 78−75825
GeO_2, Raman cross sections, rel. to appl. in fibre Raman lasers 78−31176
GeO_2, structural analysis, using fluorescence excitation *(German)* 80−38923

vitreous state continued
GeO_2, tetrahedral glass, Raman studies 78−71823
GeO_2, vitreous, band limits and vibrational spectra 79−73935
GeO_2, vitreous, LO vibrational modes, Raman and IR spectra 77−7819
GeO_2, vitreous, struct., contrasted with EXAFS obs. of $ZnCl_2$ liq. and glass struct. 80−70133
GeO_2, vitreous, struct. study using small-angle X-ray scatt. 80−84071
GeO_2, X- and γ-irrad., thermolum. and paramag. centres 77−63472
$GeSe_2$, exciton absorpt., transmission spectra of cryst., glasses and amorphous samples 79−15485
H_2, solid quadripolar glass, relax. time and low temp. sp.ht., computer simulations 80−49377
HNO_3-H_2O, liq. and glass, mol. assoc., ion pairs, Raman obs. 79−28749
$HNO_3.H_2O$, devitrification crystallisation, fast Raman and wide-line NMR obs. *(French)* 79−73915
$HNO_3.H_2O$ glassy form, stochastic rot. motions 79−7551
H_3PO_4-H_2O, superviscous and glass, relax., ^{111}Cd TDPAC obs. 80−15831
K_2CO_3-D_2O, glassy matrix, absorpt. spectra after X-irrad., solvated electrons 79−65903
$Kr.2SiO_2$, props. of vitreous deposits 78−22664
La_2O_3-B_2O_3-P_2O_5, glasses, struct. changes during heat treatment, NMR obs. 77−7672
(Li,Na,K) (Nb,Ta)O_3, pseudo-binary and ternary systems quenched metastable glassy and cryst. phases 80−29935
Li salt based solid electrolyte, synthesis and characterisation, secondary cell appl. *(French)* 80−72034
$(Li_2B_4O_7)_{1-x}(WO_3)_x$ dipolar glass, space charge injection, thermally stimulated depolarisation currents 80−66103
LiCl, and LiBr, glassy aq. solns., Raman spectra, rel. to amorphous ice and liq. water 79−47423
LiCl, aqueous glass, neutral matrix for EPR studies of radiation damage to biomols. 79−96632
LiCl-D_2O, aq. 10 M glass, optical absorpt. spectra after X-irrad., electron scavenging efficiency 79−83476
LiCl-Li_2O-B_2O_3 system of vitreous electrolytes *(French)* 78−27767
LiCl-Li_2O-P_2O_5 glass system, vitreous domain, struct., elec. cond. *(French)* 80−70135
LiCl(Br)(I), glassy aqueous soln., LF region Raman spectra 80−84729
$LiNbO_3$, vitreous, anomalous dielectric behaviour and reversible pyroelectricity 77−85658
$LiNbO_3$:Cr^{3+} glass, roller quenched, crystn. kinetics 80−44143
Li_2O-Al_2O_3-SiO_2, study of elastic props. 80−104205
$LiTaO_3$, vitreous, anomalous dielectric behaviour and reversible pyroelectricity 77−85658
xMnO.(100−x)[19TeO_2.PbO], EPR studies of Mn^{2+} ion distribution 80−71167
MoF_5, mol. and electronic struct., vitreous, liq., and tetrameric states, ^{19}F NMR obs., mol. mobility 80−34787
N_2, liq. and glassy state, spin density and current correl. functions, computer simulation 79−14661
$NaClO_4$, aq. glass, formation of trapped H-atoms and electrons on X-irrad. 80−35559
$NaClO_4$-D_2O, glassy matrix, absorpt. spectra after X-irrad., solvated electrons 79−65903
NaF-SrF_2-CrF_3, glass transition, crystn. and melting temps., optical transmission *(French)* 80−64910
NaOH aqueous glassy systems, 77K, γ-irrad., struct. stabilisation 79−91976
NaOH-D_2O, glassy matrix, absorpt. spectra after X-irrad., solvated electrons 79−65903
Na_2S-GeS_2, glass, synthesis, elec. cond., Raman spectra, temp. and composition depends. *(French)* 79−14962
$NpBa_6Zr_{12}F_{64}$ glass, Mossbauer spectrum, evidence for charge states 3+ and 4+ *(French)* 78−88231
P-Se system, glass form. props., effect of P concentration *(Russian)* 78−2019
P_2O_5, pure vitreous, Raman spectra and struct. 79−69838
P_2O_5, Raman cross sections, rel. to appl. in fibre Raman lasers 78−31176
Pb ceramic glaze, Cu^{2+} doped, Pb^{2+} release 80−49101
$PbGeS_3$, vitreous and cryst., IR and Raman spectra *(Russian)* 78−72527
$PbMnFeF_7$ and Pb_2MnFeF_9, vitreous, insulating, evidence of spin-glass transition 80−97112
PbO-SiO_2 glasses, high temp. ESR of Fe(III) 80−60410
$PbO.2B_2O_3$, vitreous, structural aspects studied by Raman scattering 77−8575
$PbSiO_3$ and Pb_2SiO_4, vitreous, free energy of form. at elevated temps. 79−43195
Sb-O-Cl(Br)(I), glass-forming regions 80−88057
Sb_2O_3 glass, X-ray diffr. anal. of struct. 78−87621
Se, crystn., optical microscope obs. 77−84659
Se, elastic coeffs. about glass transition temp. US study *(French)* 80−19865
Se, glass transition temp., enthalpy rel. to annealing, DSC 77−15561
Se, glassy, pure and K-doped, photolum. and optically induced ESR 80−50398
Se, glassy, structural excitation energies of defects, pseudopot. approach 80−107061
Se, mech. props. at temps. <300K, uniaxial compression tests *(French)* 78−55908
Se, trigonal, vitreous and red amorphous, phonon density of states comparison 80−54329
Se, trigonal and vitreous, sp. ht. and thermal cond., 3 to 300K 80−59676
Se, vitreous, darkened films, thermal and optical bleaching, light transmission obs. 80−50447
Se, vitreous, micromech. props., anelastic behaviour, internal friction *(French)* 77−72652
Se, vitreous, temp. depend. of sound vel. 77−84855
Se:Ge(Si)(Sn), vitreous, crystn. kinetics study by elec. cond. meas. 79−65526
Se:P, stabilisation of cond. 77−11910
Se:P, vitreous, crystn. kinetics study by elec. cond. meas. 79−64998
Se-Te-$Ge_{0.5}Sb_{0.5}$, DTA, critical cooling rates determ. *(French)* 77−72682
SiC fibre, development from organosilicon polymers by heat treatment 80−81014
$Si_{1-x}H_x$, noncrystalline film, struct., interatomic distances, SRO 80−107053

vitreous state continued
SiO_2, charged defect centres 80−107745
SiO_2, compaction dependence on ionisation dose 78−67738
SiO_2, cryst. and vitreous, struct. sensitive expansivity 78−22873
SiO_2, D_2 diffusion and solubility, 0-800°C, interaction with structural OH 77−89585
SiO_2, D-impregnated, radiation induced isotope exchange 79−99240
SiO_2, dielec. absorpt. saturation, 0.4-8K 78−23394
SiO_2, effect of high-dose X-rays and reactor radiation 80−19838
SiO_2, electron irrad. effect on sp. ht. 79−65212
SiO_2 films, growth on Si, role of defect structure 80−65403
SiO_2, fused, as-received and irrad., dielectric props. 79−65786
SiO_2, fused, broken bond defect generation mechanisms 80−88044
SiO_2, fused, ion beam induced luminescence 80−40166
SiO_2, fused, irrad., O_2^- radical defect centres, ESR obs. 79−61222
SiO_2, fused, shear-wave Brillouin scatt. intensity from photoelastic consts. 79−91454
SiO_2, fused, structural analysis, using fluorescence excitation *(German)* 80−38923
SiO_2, fused, US study by harmonic generation, elastic consts., Gruneisen parameters 78−83735
SiO_2, glass, ^{29}Si hyperfine struct. of E′ centre, microwave saturation props. 80−7165
SiO_2 glass, low press. plasma treatment, paramag. defect form. *(German)* 78−23341
SiO_2 glass, optical props. of colour centres, intrinsic and modified defect states 79−60756
SiO_2, glassy, small-angle neutron scatt. obs. 77−7677
SiO_2 glassy-amorphous system, struct. *(German)* 78−38626
SiO_2, hydrated vitreous, spectrum of low-energy dipolar states, dielec. const., dielec. losses and relax. 77−90098
SiO_2, impurity C determ. by isotopic spectral method 80−26093
SiO_2, intrinsic surface phonons, Raman scatt. and IR refl. 80−24728
SiO_2, irrad., EPR of Al E_1' centres 80−11268
SiO_2, low temp. thermal props. and intrinsic defects 80−29057
SiO_2, multiphonon IR absorpt. 80−25381
SiO_2, new high-pressure modification 78−75825
SiO_2, noncryst., MOS structure, ionic impurities motion, trapping layers 78−30999
SiO_2, noncryst., radiation-induced defect centres, ESR spectra and struct. 78−23343
SiO_2, paramag. centres associated with bonding defects 80−80609
SiO_2, pure and Ge doped, luminescence centres at 396 and 280 nm 80−103996
SiO_2, Raman cross sections, rel. to appl. in fibre Raman lasers 78−31176
SiO_2, resist. to NaOH 80−21143
SiO_2, semi-empirical mol. orbital model, appl. to radiation compaction 79−73433
SiO_2, struct. and phonon spectra 80−50324
SiO_2, struct. models 79−37628
SiO_2, substrate for PbO film, interdiffusion reactions, UV spectroscopy obs. 78−51750
SiO_2, tetrahedral glass, Raman studies 78−71823
SiO_2, thermophoretic deposition of small particles in MCVD process 79−52123
SiO_2, transient electrical transport, general and unified treatment 80−59977
SiO_2, valence-attenuation pair defect, states, IR and Raman spectra 79−91442
SiO_2, viscosity meas., review 80−103513
SiO_2, vitreous, band limits and vibrational spectra 79−73935
SiO_2, vitreous, effect of neutron irrad. on low temp. dielec. susceptibility 79−73878
SiO_2, vitreous, existence of gap in low-energy density of states 79−60769
SiO_2, vitreous, fast neutron irrad. effect on struct., interstitials role 78−26599
SiO_2, vitreous, fast neutron irrad., low temp. US meas., two-level systems role 78−30703
SiO_2, vitreous, H impregnated, Raman spectroscopy 77−36230
SiO_2, vitreous, H impregnated, γ radiation effects, hydride, hydroxyl formation 79−87874
SiO_2, vitreous, He solubility, 100 to 1350 atm., 5 to 80°C 79−4414
SiO_2, vitreous, heat treatment effect on viscosity and struct. 80−19714
SiO_2, vitreous, hydroxyl free, reaction with H, diffusion, absorpt. spectra 80−85210
SiO_2, vitreous, III-V analogues and bonding topology 79−73102
SiO_2, vitreous, intrinsic radiation defects, nonbridging O 80−19837
SiO_2, vitreous, irradiated, EPR exam. of H_2 hyperfine spectra 79−28611
SiO_2, vitreous, LO vibrational modes, Raman and IR spectra 77−7819
SiO_2, vitreous, laser-annealed surface, characterisation by ellipsometry 80−103544
SiO_2, vitreous, low temp. sp. ht., effect of heat treatment 78−59955
SiO_2, vitreous, low temperature heat capacity enhancement model 80−75369
SiO_2, vitreous, neutron irrad. effects on heat capacity, thermal cond., US velocity temp. depend. 78−83851
SiO_2, vitreous, neutron irrad., luminescence nature and ESR signals correl. 79−43038
SiO_2, vitreous, non-bridging O centre, optical props. and energetic struct. 80−34976
SiO_2, vitreous, photoelectric and photoluminescent props. in fundamental absorpt. region 78−39596
SiO_2, vitreous, quant. X-ray anal. of cristobalite 80−88049
SiO_2, vitreous, Raman active defects, thermal equilibration 80−55092
SiO_2 vitreous, Raman spectrum, bound OH, Si-O stretch vibr. 78−19462
SiO_2, vitreous, Suprasil-I, spectral diffusion at 0.5K, acoustic hole burning expts. 79−60439
SiO_2, vitreous, Suprasil-W, short time scale transient temp. profiles, time-depend. sp. ht. 79−60519
SiO_2, vitreous, Suprasil-W, thermal diffusivity, 16 mK-2.3K 79−60563
SiO_2, vitreous, US velocity, freq. and temp. depend. 78−63812
SiO_2, vitreous and cristobalite, interstitial struct. anal. from gas solubility data, review 79−23525
SiO_2, vitreous and neutron irrad., thermal cond., heat treatment effect 79−90837
SiO_2 vitreous film on Si, defect struct. comparison with crystalline SiO_2 and Si-O bond nature 80−54557
SiO_2, vitreous films on Si, channel and network defects 80−54142
SiO_2, vitreous layers, thermal growth on Si 80−93675

vitreous state continued
SiO_2, X-ray compaction efficiency 80−65044
SiO_2:Ag, luminescence and colour centre props. 78−10954
SiO_2:Ag, X-ray induced EPR and luminesc. centre 80−65043
SiO_2:Al, vitreous state, EPR of Al defects 78−91951
SiO_2:Fe, absorption spectra and structural state of Fe^{3+} ion 80−16071
SiO_2:Nd^{3+} films, cathodoluminesc. 80−20717
SiO_2-based glassy layers, passivating Cu at 500°C 80−3246
SiO_2+H_2 reactions, rate controlling processes for H_2 transport in vitreous silica 78−26733
SiO_{2-x} system, model for paramagnetic E′-centre 78−35034
Sn (IV) in glassy aq. soln., Mossbauer spectra 80−15894
Te-Ge eutectic alloy, glassy, crystn. mechanism 78−22836
Te-Si glassy alloys, IR transmission and sp. ht. changes in glass interval, vibr. modes, struct. models 78−23474
TeO_2, structure simulation of some tellurite and chalcogenide glasses quasi-crystalline structural diffusion method *(Russian)* 80−54147
TeO_2-NaCl(-NaBr), condition diagram, thermographic obs. *(Russian)* 80−55377
Tl_3AsS_4, crystal growth by Bridgman-Stockbarger method, exam. of props., glass formation 79−11506
$TlAsS_2(Se_2)(Te_2)$, vitreous, crystn. kinetics 80−64918
YIG, amorphous, ionic glass, hard-sphere random-packing model 80−24369
YIG, vitreous electric-field-gradient distrib., Mossbauer quadrupole splitting meas. 80−75901
$ZnCl_2$ glass, glass transition temp. and thermal expansion 80−64902
$ZnCl_2$, glassy and liq, EXAFS obs. of struct., comparison with vitreous GeO_2 80−70133
ZrF_4 based glass, elec. and dielec. props. in freq. and temp. ranges 5-500 kHz and 130-280°C *(French)* 79−23772
ZrF_4 based glasses, solid electrolyte, conductivity and activation energy 80−70464
ZrF_4-BaF_2-MF_n (M=Na, Ca, Ln, Th, n=1, 2, 3, 4), vitreous phases, network formers, modifiers and stabilisers *(French)* 80−64909
ZrF_4-BaF_2-NdF_3 glass, vitreous domain, prep. and optical props. 78−27304
$ZrSiO_4$, heavy ion irrad., metamict zircon form. 80−2088

vitrification
acoustic emission obs. during heating through glass temp. 80−84253
alkali silicate glasses, struct. and thermal props. 80−84075
aluminate glasses, new families, light transmission, 0.4 to 6 μm 77−24843
Araldite AW106/Hardener HV953U epoxy resin, thermal props. at high press., glass transition 77−59160
bone china body, MgO effect on vitrification mech. props. *(Japanese)* 79−78922
Ω-caprolactam-ε-caprolactam polymers, vitrification, fusion, crystallisation *(Russian)* 77−47561
ε-caprolactone-γ-(tert-butyl)-ε-caprolactone copolymers, dynamic mech. props., glass transitions 77−25086
carbon tetrachloride, prep. of glassy state, DTA 77−24388
ceramics, consisting of quartz, feldspar, and kaolin, compaction press. during firing effects 80−29909
chain molecular amorphous solids, stat. thermodynamics and mol. theory 78−26442
chalcogenide materials, glass form. theory 79−86713
chalcogenide melts, glass form. regions calc. using empirical theory of glass form. 80−33894
chalcogenide melts, glass-forming, miscibility criteria and phase separation 77−76569
commercial glasses, viscosity and stress relax. in glass transition region 80−93589
communal entropy and glass transition, theory 80−70131
configurational properties of liquids near glass transition 78−26662
creep analysis of canisters for radioactive waste vitrification 78−86648
critical cooling rate for glass form., crystn. and nucleation 80−84078
crystallisation of melts and glasses, nonisothermal, kinetics 79−94914
determ. of glass phases, phys. props. meas. 79−23526
determination using ruby fluoresc. spectra shift in high press. cell 77−26321
epoxy resin, cure history effect on dynamic mech. props. 80−54356
ethanol, plural glass-transitions, thermodynamic functions 78−38820
fission product treatment, continuous process, industrial scale *(French)* 77−23228
fission products, concentrated solns., continuous vitrification *(French)* 77−361
fission products solutions at Marcoule, description and hot operation results 80−5270
fluoride systems, fundamental condition for glass formation 80−44135
glass, ancient samples, trace element anal. by neutron activation, rel. to corrosion and devitrification 78−12801
glass, electrothermal props. in structural transform. zones *(French)* 80−88047
glass, structure, influence of thermal history *(German)* 80−38930
glass formation, models 78−2012
glass formation and effect of nucleating heterogeneities 77−11487
glass forming and props. 80−19717
hard-sphere fluid, eqns. of state, transport data, glass transaction 77−4182
hard-sphere liquid, glass transition, computer mol. dynamics simulation 77−11674
inorganic glass, specific heat in anomalous region near vitrification temp., simple relax. model 77−43341
internal parameters, ordering parameters, history function, rel. to glass transition 78−30738
Lennard-Jones liquid, mol. dynamics studies of glass form. 80−38896
liquid-glass transition, free volume approach, thermodynamic behaviour 80−1940
melt, nucleation and cryst. growth in glass-forming melt 78−2016
metal metal system, glass formation 80−64921
metallic alloy, prediction of glass-forming ability 79−23524
metallic glasses, formation, stabilities, and props. 80−64912
metallic glasses, formation and rapid quenching techniques 80−76214
metallic glasses, glass transition temp. 79−99081
metallic glasses, review *(German)* 79−41962
metallic glasses formation, review 77−66606
$(Mg_{0.88}Fe_{0.12})_2SiO_4$, natural peridot, shock-prod. olivine glass, TEM 78−10178

vitrification continued
molecular liquids and their binary solns., glass transition temps. 79−51239
noncrystalline solids conf. Lyon, France (Dec. 1976) *(French)* 77−72560
nonmetallic compounds, type A_xB_y, glass form. from melt 80−44140
nylons, glass transition temp., thermal, mech. meas. 77−31758
oxychalcogenide glasses, phase separation 77−8803
phase separation and glass structure concept changes, review 77−65955
phosphate system, containing halogens glass formation 80−103254
polyester-organic solvent mixtures, phase diagrams, eutectic props., devitrification, crystn. *(French)* 80−3015
polyethylene terephthalate, thermal diffusivity, conductivity meas., crystallisation rel. to glass transition 77−47632
polymer, amorphous, under press., glass transition phenomena, model 79−23706
polymer melt, flow-induced orientation freezing-in by vitrification, appl. to processing 79−23531
polymers, mol. struct. rel. to bulk props. 77−32553
polystyrene, amorphous, press. effect on glass transition and glassy state 78−26674
polystyrene films, amorphous, X-ray small angle scatt. near glass transition, struct. *(Russian)* 77−31606
polystyrene-polyisoprene block copolymers, low mol. wt., glass transition temp., DSC investig. 77−7854
polyvinylacetate films, amorphous, X-ray small angle scatt. near glass transition, struct. *(Russian)* 77−31606
pot vitrification of fully radioactive fuel reprocessing wastes 77−61547
Purex solvent extracting system, monitoring and control instrumentation 80−37566
PVC, uniaxially stretched, mol. orientation, birefringence, effect of plasticizers, draw ratio 77−48500
quartz, dislocations, electron irrad. induced vitrification 80−107252
quartz, shock-loaded, IR spectroscopic studies, solid-state glass prod. 79−19157
radioactive high level liquid waste, container design and specification 77−61541
radioactive high level wastes at Karlsruhe nuclear research centre 77−61545
radioactive liquid high level waste solidification 78−21669
radioactive liquid waste, thermal decomp. of Harvest feed slurries 80−52757
radioactive liquid waste from nuclear reprocessing, vitrification, durability 78−54852
radioactive waste, continuous vitrification of fission product solns. 77−61544
radioactive waste, Harwell inactive vitrification pilot plant 77−61543
radioactive waste, high level, vitrification, industrial scale plant, France 77−365
radioactive waste, high-level, stability of phosphate and borosilicate glasses used for solidification *(Russian)* 77−61560
radioactive waste, high-level, thermal, chemical and radiation stability *(Russian)* 77−61559
radioactive waste, high-level, thermal and radiation effects on borosilicate glasses 77−61557
radioactive waste, high-level liquid, vitrification, full scale in-can melting 79−59213
radioactive waste, liquid solidification processes, problems 77−364
radioactive waste, Magnox, development and radiation stability of glasses for vitrification 77−61554
radioactive waste, phosphate vitrification, KS-KT-100 plant *(Russian)* 77−61552
radioactive waste, reprocessing, solidification vitrification of liquid waste, review 79−9762
radioactive waste, thermal decomp. of nitrates and additives in glass-making *(Korean)* 78−86638
radioactive waste, UK solidification facilities 77−61542
radioactive waste, vitrification using in-can melting process 80−83204
radioactive waste calcination and vitrification 77−61546
radioactive waste conversion to glass, exptl. joule-heated ceramic melter 80−18471
radioactive waste immobilisation using continuous glass melter 80−83199
radioactive waste immobilization, continuous glass melter 79−59214
radioactive waste solidification to phosphate glass-metal matrix blocks 77−61550
radioactive waste solns., French techniques *(French)* 77−67835
radioactive waste vitrification system design 77−54340
radioactive waste vitrification without precalcination, radionuclide behaviour *(Russian)* 77−61553
rare earth-gallium sulphide system glasses *(French)* 77−19877
selenide systems, binary, glass transition behaviour, model, comp. depend. 78−26673
semiconductor, crystal-glass transition influence on local struct., Mossbauer and X-ray spectra 77−36163
silicate glasses with high oxide modifier concs., property-comp. relns. 78−67655
structural transformations, temp. effect on chem. equilib. 79−94912
thermal devitrification *(French)* 77−72563
thermodynamical and model-statistical treatment 78−26661
thermosetting materials, formation and props., phase diagram and torsion pendulum anal. 80−55381
1,3,5-triaryl-2-pyrazolines, glass-forming props. 77−11677
vitreous matrices for high level Purex waste containment 77−360
X-ray scattering at small angles study of glasses containing no modifying oxides 80−84071
Ag-As-Te system, vitrification region, physiochem. props. 79−41960
Ag-Sb-S, prep. and props. of glasses in the system 77−20053
AgX-Ag_2O-P_2O_5 (X=I, Br, Cl), glass formation and ionic conductivity 80−65290
amorphous, Raman scatt. investig. of irreversible thermostruct. transform. 77−48163
As-S, amorphous, glass transition and specific heat, intermolecular bond saturation 80−15011
As-S-Te, vitrification, density and elec. cond. measurements 79−7645
As-Sb-S-I system glasses, vitrification and volt-ampere characts. 77−31756
As-Se, amorphous, glass transition and specific heat, intermolecular bond saturation 80−15011
As-Se system glasses, structural and electronic transitions 77−76890

vitrification continued
As-Se-Te glasses, glass form., charact. temp., density, thermal expansion and dynamical viscosity, struct. model 78−26672
As-Te-In, glass-forming, density and microhardness 80−103257
As_2S_3, thermal capacity, 300 to 600K 80−103492
As_2S_3-Tl_2S, As_2Se_3-Tl_2Se and As_2Te_3-Tl_2Te systems, vitrification and reaction characts. 77−15560
As_2Se_3, thermal capacity, 300 to 600K 80−103492
As_2Se_3-InI_3, glass system, IR spectra 78−64365
$(AsSe)_{1-x}Te_x$ glasses, thermal props. and viscosity, temp. and conc. depend. 77−76324
As_2Te_3, $As_4Te_5I_2$, $TlAsTe_2$, local struct. changes on crystal-glass transition, Mossbauer spectra 77−36157
As_2Te_3, thermal capacity, 300 to 600K 80−103492
B_2S_3-Tl_2S system, phase diagram and verification 80−35165
BaB_2O_4-RF_2, R=Mg, Ca, Sr, Ba, glass form., struct. and props. 80−84077
$Ba(PO_3)_2$-AlF_3-CaF_2, elec. cond. and IR spectra 80−89005
$Ba(PO_3)_2$-AlF_3-MgF_2, elec. cond. and IR spectra 80−89005
$Ba(PO_3)_2$-MgF_2, vitrification region 77−35676
BeF_2 glass, glass transition temp. and thermal expansion 80−64902
Bi-Sb-S-I system glasses, vitrification and volt-ampere characts. 77−31756
$Ca_{0.65}M_{0.35}$, glass transition temp., comp. depend. 80−79702
$Ca(NO_3)_2$-H_2O solns., ice I homogeneous nucleation temp., slow vitrification mechanism 78−26666
$Ca(No_3)_2.3.91H_2O$-$NiCl_2$ melts, glass forming, transport behaviour 78−59963
CaO-Ga_2O_3, spectroscopic and petrographic anal. 77−15556
CaO-Ga_2O_3-Bi_2O_3, vitrification regions 77−15557
CaO-MnO-SiO_2 system glasses, vitrification and crystallisability 77−7853
CaO-SiO_2, melt, effect of cooling rate upon glass transition, X-ray analysis 79−27920
$CdAs_2$, cryst. struct. and vitrification capacity 80−88126
$CdGe_{1-x}Sb_xAs_2$ system, amorphous and cryst. phases, DTA and microhardness obs. 78−22835
Cu-Ag-Ge, Hume-Rothery glass form. 80−96449
Cu-Sb-I system, glass form., struct. and IR spectra 80−64915
$Cu_{56}Zr_{44}$ metallic glass, devitrification and its effect on mech. props. 80−33893
Fe-B(−Ni), chemical ordering, crystallisation and glass transition temp. 79−90563
Fe-C-X, glasses and metastable cryst. phases, third element effect 80−75171
$Fe_{83-x}M_xB_{17}$ and $Fe_{78-x}M_xSi_{10}B_{12}$ (M=refractory metal), glass form. and thermal stability 80−79703
$Fe_{78}Mo_2B_{20}$ glass, thermal expansion, glass transform. and crystn. temps. 80−2183
$Fe_{32}Ni_{36}Cr_{14}P_{12}B_6$ glass, thermal expansion, glass transform. and crystn. temps. 80−2183
$Fe_{32}Ni_{36}Cr_{14}P_{12}B_6$ metallic glass, effect of pre-ageing on glass transition temp. 80−100326
$Fe_{40}Ni_{40}P_{14}B_6$ glass, thermal expansion, glass transform. and crystn. temps. 80−2183
Ge-Bi-S system glasses, opt. props. and glass transition temp. 77−77224
Ge-S-Se, glass formation 80−103251
Ge-S-Se system, glass-forming, struct. and props. 80−19713
Ge-S-Te system, glass forming 80−19718
Ge-Si-S system, glass formation, transition temp., crystallisation and melting 80−100178
Ge_2S_3, glass form. and characterisation *(German)* 80−64913
$GeSe_2$-As_2Se_3-Sb_2Se_3 system glasses, vitrification and elec. cond. 79−50996
$GeSe_2$-$SnSe_2$-As_2Se_3, GeSe-SnSe-As_2Se_3, Mossbauer investigation 77−20052
$GeSe_2$-Te, phase diagram and vitrification region determ. by DTA, SEM, X-ray diffr. *(French)* 77−72565
Ge_2Se_3, glass form. and characterisation *(German)* 80−64913
Ge_xSe_{1-x}, vitrification, liquid-solid phase diagram, viscosity var. *(French)* 77−72680
In-As-Se-I system, glass form. obs. 77−77466
KCl melt, effect of cooling rate upon glass transition, X-ray analysis 79−27920
KCl microcrystal, computer simulation of melting and glass form. 79−65173
KF-BeF_2-DyF_3, crystalline and vitreous phases of cross sections 78−44096
KF-BeF_2-DyF_3, phase diagrams, intensification region 78−44097
KF-BeF_2-DyF_3 system, KBe_2F_5-DyF_3 cross section phase diagram, vitreous phases struct. 77−24383
$3KNO_3-2Ca(NO_3)_2$, glass form. from liq., struct. transform., Raman spectrum obs. 80−64916
$3KNO_3-2ZnCl_2$, glass form. from liq., struct. transform., Raman spectrum obs. 80−64916
K_2O-Al_2O_3-P_2O_5-Nb_2O_5 glasses, struct. role of Nb 78−67653
$K_2O.3CaO.BaO.xSiO_2$, property-comp. relns. 78−67655
LaF_3-BaF_2-ZrF_4(-MF), M=Na, Li, glassy transition, refr. index, density and molar refr. 80−1937
La_2O_3-GeO_2-$Ta_2O_3(HfO_2)(ZrO_2)$, vitrification, crystn. 77−15559
La_2O_3-WO_3, melt, glass formation on rapid quenching 77−20055
$La_2O_3GeO_2$-$Ga_2O_3(B_2O_3)$, vitrification and crystallisation 77−15558
Li_2O-GeO_2 glass, synthesis, Ge coordination state 77−24271
M_2O-MnO-B_2O_3 glasses, M=Li, Na, K, glass-forming region and physicochem. props. 78−63678
$M_2O(MF_y)$-BeO-P_2O_5 glasses, M=alkali metal, alkaline earth, Cd or Zn, glass-formation 78−67656
MgO-SiO_2, melt, effect of cooling rate upon glass transition, X-ray analysis 79−27920
Na-A zeolite, struct. obs. by high-resolution electron microscopy 80−84175
NaCl melt, effect of cooling rate upon glass transition, X-ray analysis 79−27920
NaF-SrF_2-CrF_3, glass transition, crystn. and melting temps., optical transmission *(French)* 80−64910
Na_2O-$2SiO_2$, melt, effect of cooling rate upon glass transition, X-ray analysis 79−27920
Na_2O-B_2O_3-SiO_2, containing halogens glass formation 80−103254
Na_2O-P_2O_5-SiO_2 glass, metastable liquid immiscibility 80−100331
Na_2O-PbO-SiO_2 glass-ceramic composite, directionally crystallised 80−107058
Na_2O-SiO_2 glass containing halogens glass formation 80−103254
$Na_2S_2O_3.5H_2O$, glass transition, anal. of large stable supercooling 77−51477
Nb-Ir(Rh) system glasses, form., crystn. and microhardness, resist. obs. 80−89178
Nb-Ni amorphous alloys, glass transition and ductility, O additions effect 80−75168
$Nb_{0.4}Ni_{0.6}$, amorphous, pair distrib. function, temp. depend., rel. to glass transition 80−24368
$Ni_{78-x}M_xSi_{10}B_{12}$ (M=refractory metal), glass form. and thermal stability 80−79703
P-S, amorphous, glass transition and specific heat, intermolecular bond saturation 80−15011
P-Se, amorphous, glass transition and specific heat, intermolecular bond saturation 80−15011
P-Se glass system, IR spectra 78−64365
P-Se-Te system glasses, vitrification region 78−51425
P_2O_5-GO_3-CaO(Nd_2O_3) systems, vitrification regions and physicochem. props. of glasses 77−11673
$PO(SCN)_3$:Nd^{3+} solns., spectroluminesc. props. 77−16362
P_2Se_xSy glass, vitrification temp., elec. props. and hardness meas. *(Russian)* 77−28177
PbO-B_2O_3 glass-forming melt, specific volume and viscosity, temp. depend. 80−84073
PbO-GeO_2 glass, synthesis, Ge coordination state 77−24271
Pd-Cu-Si, glass form., crit. cooling rate 80−75169
$Pd_{77.5}Cu_{6.0}Si_{16.5}$ metallic glass, glass transition temp., cooling rate depend. 80−75181
$3RbNO_3-2Ca(NO_3)_2$, glass form. from liq., struct. transform., Raman spectrum obs. 80−64916
Sb-O-Cl(Br)(I), glass-forming regions 80−88057
SbSBr glass, IR reflectivity spectra 80−71403
Se, amorphous, US wave attenuation and vel., near glass transition 77−89501
Se and Se-As, amorphous, dipolar activity at glass transition temp., AC method 77−66454
Se, glass transition temp., enthalpy rel. to annealing, DSC 77−15561
Se-Ge-Sb alloy glass, crystn. kinetics 77−20057
Si-Ge-Te system glasses, structural and electronic transitions 77−76890
SiO_2 based glass, high SiO_3 radioactive waste fixation 79−49708
SiO_2, crystobalite form. in evacuated silica ampoules, cryst.-amorphous transform. 77−68933
SiO_2 fused powder, difference between white and black silica, devitrification rates 80−28918
SiO_2-Al_2O_3-CaO-MgO-TiO_2 system glasses, phase separation and crystn. 77−24384
SiO_2-$NaAlSiO_4$ glasses and devitrificates, prep. and vibr. spectroscopy study *(Polish)* 80−93530
SiO_2(-TiO_2) glass prep., melting *(Polish)* 80−40316
SnSe-$GeSe_2$-As_2Se_3 glasses, vitrification region and elec. cond. 80−15008
$SnSe_2$-$GeSe_2$-As_2Se_3 system glasses, vitrification and elec. cond. 79−50997
SrO-Ga_2O_3, spectroscopic and petrographic anal. 77−15556
SrO-Ga_2O_3-Bi_2O_3, vitrification regions 77−15557
Ta-Ir(Rh) system glasses, form., crystn. and microhardness, resist. obs. 80−89178
$Tb_{0.8}Yb_{0.2}(PO_3)_3$, cooperative sensitisation of luminesc., order-disorder transition effect 77−36283
Te-Si glassy alloys, IR transmission and sp. ht. changes in glass interval, vibr. modes, struct. models 78−23474
$Te_{80}Ge_{20-x}A_x$ glasses, rapid melt cooled, glass transition and stability range 80−75170
TeO_2-Cr_2O_3 system, phase diagram and vitrification 79−83182
TeO_2-NiO system, phase diagram and vitrification 79−83182
Ti-Ni amorphous alloys, glass transition and ductility, O additions effect 80−75168
TiO_2-containing slag-glasses, phase separation and glass-ceramic formation 78−51424
TiO_2-SiO_2 glass form. by low temp. chem. polymerisation 80−84899
TiO_2-Ti_2O_3-P_2O_5, glass form., struct. and elec. props. 80−44592
Tl-B-Se system, vitrification region, primary crystallisation fields 77−15321
Tl-Ge-S system, glass forming 80−19716
Tl-Ge-Te, glass formation 80−103255
$TlAsTe_2$, local struct. changes on crystal-glass transition, Mossbauer spectra 77−36157
Tl_2Se-As_2Se_3-SnSe system alloys, covalent component of chem. bond effect in vitrification processes, Mossbauer obs. 77−36156
$(Tl_2Se)_{3x}$-$(Sb_2Se_3)_{1-x}$ system, phase diagram 77−16558
U-Co(Ce)(Fe)(Mn)(Ni)(V) metallic glasses, glass form. and thermal stability 80−75183
Y_2O_3-SiO_2-Al_2O_3 system, composition depend. of refractive index in vitrification region 77−24812
ZnB_2O_4-RF_2, R=Mg, Ca, Sr, Ba, glass form., struct. and props. 80−84077
$ZnCl_2$ glass, glass transition temp. and thermal expansion 80−64902
ZnO-SnO_2-M_xO_y, M_xO_y=glass-forming additive, I-V characts., heat treatment effects 77−43595
Zr-Cu, metallic glasses, glass transition temp., crystallisation temp., exothermal relaxation effect 79−52747
Zr-Cu amorphous alloys, glass transition and ductility, O additions effect 80−75168
Zr-Cu(Ni)(Co)(Fe) metallic glasses, glass form. and thermal stability 80−75177
$Zr_{0.475}Cu_{0.475}M_{0.05}$, glass transition temp., comp. depend. 80−79702
(ZrF_4-BaF_2-ThF_4)-EuF_2 system, glass forming region, prep. and props. 79−91633

Vlasov equation
adiabatic compression of ion rings and associated plasma, kinetic theory 79−46469
Alfven-Carlquist double layer theory of solar flares 78−77526
Bernstein modes in electron cyclotron heating of Tokamak, Vlasov dispersion eqn. 80−33809
Chirikov-Taylor model, turbulent diffusion calc. 80−79469
coherent state approach, quantum effects calcs. 78−1803
crystal thermodynamics in statistical theory, density Fourier coeffs., stress tenser, internal energy 80−13025
cubic crystals, temp. series in statistical theory 80−17895

Vlasov equation continued
cyclotron maser, theory of solid-state device 79−41361
cyclotrons resonance maser, Vlasov-Maxwell eqns., guided wave field theory 80−14309
cylindrical rotating P-layer, electrostatic stability props. 79−64851
cylindrical shells, boundary conditions in Vlasov theory 80−69660
diamagnetic boundary layers, kinetic theory, rel. to solar wind 77−9642
dilute electron plasma kinetic eqns. in coherent region 78−75264
direct interaction approximation and plasma turbulence theory 79−19036
dispersion eqn. from linearised Vlasov eqn. with local approx. for laser produced plasma instabilities 80−38687
dispersion function for anisotropic longitudinal waves 80−14891
disturbance propag. in relativistic Vlasov plasma 77−72426
drift instabilities, density grad., oblique propag. at zero beta 78−71470
drift wave stabilisation by HF applied electric field 77−19701
E layer, nonrelativistic nonneutral, Vlasov equilib. and electrostatic stability 77−7580
electron beam, relativistic, Vlasov equilib. 77−51225
electron gas with external mag. field, Vlasovs equation with mollified density 80−1756
electron rot. relativistic beam in magnetised plasma, Vlasov equilib. *(Russian)* 77−84452
electrostatic ion cyclotron electron drift instability anal. using linear Vlasov dispersion reln. 80−1780
electrostatic temperature and gradient drift instabilities, linear Vlasov dispersion relation 79−90400
electrostatic Vlasov turbulence, iterative soln. 80−10375
field reversed ion layer in background plasma, stability props. 79−77370
Fokker-Planck-Vlasov eqn., weak solns., uniqueness and stability 79−92951
high freq. rad. field in turbulent plasma 80−38648
high-beta plasmas, energy anisotropy instabilities, comparison of various kinetic and fluid descriptions 79−1310
hot nonuniform magnetised plasma wave propag. theory, Vlasov eqn. perturbation expansion 80−33768
instabilities in ion beam-plasma system *(Japanese)* 78−91124
integration in configuration space 77−7512
ion acoustic wave, self excited, in hot plasma, dispersion theory 80−92283
ion beam with rotational and axial motion, thermal equilibrium props. 80−53934
ion-acoustic wave, phase velocity 80−103147
Langmuir system, kinetic theory of mag. field generation 80−69974
Langmuir wave evolution, three dimensional kinetic model, Vlasov eqn. calcs. 80−43923
Langmuir waves in Vlasov plasma, nonlinear theory, wave-particle interaction 80−64701
Langmuir waves in Vlasov plasma, nonlinear theory, wave-wave interaction 80−64700
laser radiation, nonlinear scatt. by fast ion waves in plasma 80−106916
laser-fusion regime, plasma transport, extension of Braginskii system of fluid equations 80−53935
light neutral leptons, dynamical role in cosmology 79−35407
linearised collisionless eqn. soln. for plasma oscillations 78−30423
linearised form of Vlasov plasma, optimal control 80−53920
linearised Vlasov-fluid model for sharp boundary screw pinch 79−60168
liquids, simple classical, vel. correl. and relative diffusion 78−14262
magnetised plasma, numerical integration of Vlasov eqn. 77−68744
magnetised plasma, Vlasov theory coherent state approach 80−64675
Maxwell-Vlasov equations, in region exterior to perfectly cond. infinite cylindrical antenna 78−1843
Maxwell-Vlasov system, boundary value problem 79−19001
Maxwellian local velocity distribution, Vlasov equilib. 80−87928
Migma-type solutions of the Vlasov equation in cylindrical coordinates 79−81082
model connection, hydrodynamic, water bag and Vlasov models 79−4107
N-particle classical system, Vlasov dynamics and fluctuations in 1/N limit 78−130
non-linear transport equations: Properties deduced through transformation groups 80−4680
nonlinear electron transport in vac. diode 77−13718
nonlinear oscills. in warm plasma with initial vel. perturbations 77−15179
nonlinear plasma wave, freq. shift, initial damping 77−19695
numerical integration in phase-space, splitting scheme determ. 77−68745
numerical solution, with filtering in time 79−82036
one-dimensional inhomogeneous plasma, ion and electron vel.-space distribs. 78−51281
parametric excitation of charge density fluctuations in classical and quantum electron-hole plasmas 79−50856
parametric plasma instability, saturation in a strong electromagnetic field *(Russian)* 78−22475
plasma, coherent four-wave scatt., appl. to plasma diagnostics 80−28681
plasma, method of solving Vlasov kinetic eqn. 78−14133
plasma, one-component, dilute, kinetic eqns. and fluctuations in μ space 77−89230
plasma, renormalised Vlasov turbulence 80−19579
plasma, skin effect of microwaves and transverse pseudowaves 78−59600
plasma, two-dimens. turbulence 77−58862
plasma, Vlasov and water-bag models, self similar solns., simulation 78−26242
plasma bump-on-tail instability, single-mode saturation, Vlasov-Poisson eqn. 77−7525
plasma column, ultra-high current, electron collisionless motion 79−64824
plasma oscillations, Vlasov theory, linear approx., electron distrib. initial value problem 77−84423
plasma sheath, integro-differential eqns., nonlinear, nonlocal, soln. formalism 80−43936
plasma turbulence, quantum mechanical Vlasov eqn. 78−83566
positive and negative ion beams nonlinear interaction, math. simulation and expt. 77−595
propagation of a wide ion beam into a magnetic barrier, Vlasov equilib. model anal. 79−90439
realistic Vlasov slab equilibria with magnetic shear 79−90440
relativistic, nonlinear EM wave propag. in plasma 77−47209
relativistic collisionless plasma, EM perturbation of relativistic Vlasov-Maxwell eqns. 79−90449
relativistic electron beam, Vlasov eqn. in plasma medium 80−14910
Vlasov equation continued
relativistic magnetised Vlasov-Maxwell plasma, current responses 79−90450
relativistic particle ring, coherent oscillations, Vlasov eqn. 78−55060
renormalized kinetic theory of nonequilibrium many-particle classical systems 79−82038
screw pinch, sharp boundary Vlasov fluid stability anal. 77−24071
screw-pinch configs., collisionless, hybrid-kinetic stability props. of high-beta plasmas 80−43871
sharp boundary Vlasov-fluid screw pinch, free and forced m=0 oscillations 80−38636
sideband instability, growth rates 77−19696
soliton formation in warm magnetised Vlasov plasma 79−90396
splitting schemes for numerical soln. of two-dimens. Vlasov eqn. 78−67310
statistics, time asymptotic, nonlinear turbulence eqns. 77−65835
stochastic equations of motion for plasma particles 80−38551
system interacting via, vel. depend. interactions and pair-wise central pot. 78−34270
theta pinch, rigidly rotating, Vlasov fluid stability 80−28794
theta-pinch implosions, ion refl., hybrid Vlasov-fluid model 77−15229
transverse plasma oscillations, linearised Vlasov-Maxwell eqn. solns. 79−90398
trapped particle instability in Tokamaks, book 78−83562
two dimensional Vlasov eqn., numerical soln., multistep technique 78−1795
two-dimens. Vlasov eqn., multistep technique for numerical soln. 77−27648
universal drift instability, magnetic gradient effects 79−60117
unmagnetised plasma, quasilinear theory of parametric processes 79−94787
velocity space ring plasma instability, magnetised ion interaction, Vlasov theory 79−77368
Vlasov stability, particle reson. effects in axisymm. field reversal config. 78−83553
Vlasov-Maxwell eqns., existence and uniqueness theorem 79−94775
Vlasov-Maxwell equilibria, exact solns. with sheared mag. fields 77−3977
Vlasov-Poisson eqn., space-time approach 78−83523
Bi, Bernstein waves, electrostatic wave dispersion relation in mag. field 80−34471
V_2O_5-P_2O_5 semiconducting glasses *see amorphous semiconductors*
vocoders
see also speech synthesis
32 channel multiplex audio response system based on formant vocoder principle *(German)* 80−96133
4800 bps, voice excited predictive coder based on improved baseband/sub-band filters 79−64448
automatic coded digital speech transmission, pitch extractor features 79−41530
Bengali vowels format struct., tracking loop formant extraction system 80−106673
C-CD discrete Fourier transform processors for channel vocoder 80−53568
deaf speech and hearing aids, vocoders, frequency lowering and lipreading cues 80−12309
digital, optimization by exploiting human auditory masking 80−33356
digitizers for present day and for mid 1980s, practical implementation 80−33357
diphone synthesis for phonetic vocoding 79−64440
discrete time acoustic tube vocoder 79−59885
formant representations of parameters for channel vocoder 80−83709
linear predictive coded speech digitisers, background noise spectral subtraction 80−96140
linear predictive coding vocoders, performance in noisy environment 79−64416
linear predictive coding voice digitizer with background noise suppression 79−64417
linear predictive vocoder with new pitch extraction and exciting source, experimental model 79−59884
log likelihood ratio interpretation as measure of waveform code performance 80−83706
low bit-rate robust vocoder with special envelope estimator and pitch estimator 79−59883
microprocessor based real-time speech processor 79−64437
minimum phase homomorphic 79−90090
mixed-phase homomorphic vocoder 79−59882
mixed-source model for speech compression and synthesis 79−14200
multimicroprocessor implementation of all-digital speech synthesizer 80−96143
pole-zero modelling of speech 80−83716
portable, tactual, design, hearing aid appl. *(Japanese)* 78−44691
real-time speech high-performance processor design 80−96144
signal models for low bit-rate coding of speech 80−106674
speech digitisation and bandwidth compression techniques, ADPCM and ADM *(Korean)* 79−59876
speech noise suppression filter for narrowband vocoder 80−91977
speech processing, automatic, approaches, models and appls. *(German)* 79−50532
speech waveform coders, objective quality meas. equipment and method 80−91981
tactual vocoder, max. information transmission, time-invariant stimulation *(Japanese)* 80−41317
time-domain algorithms of speech signals, harmonic bandwidth compression 79−46125
visual speech vocoder as teaching aid for deaf 78−36069
voice *see speech*
voice coders *see vocoders*
voice communication
acoustic noise suppression in speech using spectral subtraction 79−46124
acoustic noise suppression using spectral subtraction algorithm 79−64413
acoustics, speech and signal processing, IEEE international conf., Washington, DC, USA, 1979 Apr. 79−55275
aircraft, operational noise environment, expt. study 79−81662
articulation rate and pitch modification using constant-Q transform 79−68515
automatic coded digital speech transmission, pitch extractor features 79−41530
automatic speech recognition, speaker authentication and data entry 79−94419

voice communication continued
Bengali vowels format struct., tracking loop formant extraction system 80−106673
digital multiplex system, acquisition performance of frame synchronisation system 80−99901
digital speech interpolation system called adaptive DPCM with time assignment speech interpolation 80−99903
digital voice processing techniques 79−81663
feedback suppression during acoustic irradiation, adaptive method *(German)* 80−106676
forward and backward prediction in adaptive differential PCM over nonideal channels 80−99902
frequency warping for nonuniform talker normalization 79−59894
high noise environment, intelligibility and S/N ratio *(Japanese)* 77−73533
interval modulation semiconductor laser communication system 78−9331
intervocalic consonants, intelligibility in noise 79−68514
IR torch using semiconductor DH laser diode 77−39101
laryngeal dynamics, effects of Teflon injection 79−70560
linear prediction of formants for low bit rate digital speech transmission 79−59880
linear predictive vocoder with new pitch extraction and exciting source, experimental model 79−59884
loudness function of artificial speech, for reference equivalent meas. 80−79068
low bit-rate robust vocoder with special envelope estimator and pitch estimator 79−59883
man-machine voice communication, speech production mechanisms and models *(Spanish)* 80−87665
microprocessor based real-time speech processor 79−64437
narrowband linear predictive coding speech transmission over noisy channels, vocoder 79−55276
narrowband speech algorithm eval. 79−64450
narrowband systems, frequency domain noise cancelling preprocessor 79−68511
parametric coding of speech spectra, computer studies 80−96137
parametric coding of speech spectra 80−96136
person-machine speech communication systems, speech recognition using dialogue process 79−64423
pitch contour transfer between utterances with differing lexical content 79−81652
signal models for low bit-rate coding of speech 80−106674
SIRENE, computerized speech training aid 79−70701
SPAC speech processing system using autocorrelation function, operation and characts. 79−68510
speech digitization and bandwidth compression, ADPCM and ADM *(Korean)* 79−55273
speech processing, automatic, approaches, models and appls. *(German)* 79−50532
speech processing system using autocorrelation function, 8 kbits/sec. 79−59893
speech training aid system tri-normalized speech processor 79−70700
sub-band coding with adaptive bit allocation 80−28386
through-water diver communication system Wet-Phone, voice or switch operated, 31.5 KHz carrier, 1350 m range 80−38187
transform coding of speech, analysis/synthesis frameworks. appls. 79−59886
transmission channel quality determining physical method 80−33369
verbal communication aid for nonvocal patients 79−57816
vibration pick-up-type ear microphone and two way communication device 78−1535
vocal output and preferred listening level rel. to ambient noise 79−68500
He speech investigations, intelligibility and unscrambling *(Japanese)* 79−81657
He speech unscrambler using charge-transfer devices 79−98559

voids (solid)
alloy, overaged and dispersion hardened, dislocation bowing computed from Orowan relations 77−19949
alloy, substitutional solid soln., irradiated creep rate enhancement theory 77−63739
alloys, intergranular precipitate effect on diffusion growth of creep voids 79−34041
alloys, irradiated, effect of defect trapping and solute segregation, on defect recombination rates and void swelling 78−47369
alloys, irradiated, segregation, inverse Kirkendall effect, effect of constitution on void swelling 78−91472
amorphous thin films, crack networks of voids 78−2399
artificial voids, partial discharges, electro-optical obs. 78−87558
benzil cored fibres, void-free cryst. growth, X-ray diffr. and optical microscopy study 80−71586
biaxially stretched sheets, exam. of void growth and local necking 78−90735
bounded media, dislocation loop growth and void swelling by charge particle damage 78−6110
α-brass, dezincified specimen, effect of voids on positron annihilation 79−15553
α-brass, metallographic and fractographic study of void formation during creep 80−16449
brass, soft 70/30, density changes, void growth in biaxial stress fields, plastic deformation 80−71692
α-brass, with few inclusions, shear mode of ductile fracture 77−36652
brass wire, US inspection, immersion method 80−66757
CANDU fuel bundle design with reduced void effect 78−25277
cavities under stress at high temps., rel. to metal creep 77−32625
cavity growth, creep mechanisms, independent and sequential 80−55480
cavity growth diagram, for high temp. creep 80−65140
cavity location, computer program 78−18481
cavity size distrib. functions evolution, numerical study for 1 MeV electrons 80−2072
ceramic, stress intensity factor estimates for a peripherally cracked spherical void and a hemispherical surface pit 79−29196
coalescence kinetics in cryst. with dislocations and volumetric generation of point defects 77−68996
coated, capture efficiency 80−96515
composite materials loaded in, uniaxial tension under pressure, tensile strength eval. 78−19828
copolyimide glass based on benzophenone tetracarboxylic acid dianhydride 77−63720
crack tip, moving, void growth, coalescence, finite element anal. 78−1609

voids continued
creep, swelling and growth, radiation induced, bias factors estimated from self-consistent model 80−88249
creep crack growth, diffusion and deformation controlled 80−79867
creep damage and the remaining life concept 80−59574
creep voids, diffusional growth, review 78−71720
defect clusters, nucleation and growth due to energetic particle radiation, chemical rate reaction theory, computer program 80−49263
delamination wear, subsurface void nucleation mechanism 78−3230
densities, interpretation from critical radius arguments 79−23657
detection, thermal NDT of delamination and inclusion flaws, ID anal. 80−71820
diffusive cavitation of grain interfaces, non-equilib. models 79−46668
m-dinitrobenzene cored fibres, void-free cryst. growth, X-ray diffr. and optical microscopy study 80−71586
divacancies, in void swelling 79−99236
ductile fracture, quantitative study of inclusions taking part in process 78−27630
ductile fracture, strain hardening and damage relationship 80−108564
ductile fracture in random distrib. of voids, computer simulation 79−90723
ductile fracture topography, geometrical contribs. and H_2 effects 79−83310
ductile intergranular fracture, discussion on mechanism 79−73250
ductile metals, spontaneous void growth in elastic and elastic/plastic media 80−48567
dye penetrant method using sorption developer, developer indications/single void diameter relation 79−70287
dynamics of void lattice *(Russian)* 77−80594
EBR-II, multiaxial in-reactor creep in presence of significant void swelling 79−55818
elastic wave scatt., appl. of matrix method of optimal truncation 80−62480
elastic wave scatt. from localised defects in solids, long-wavelengths 79−87794
elastic wave scattering, Born approx. 77−79984
elastic waves, multiple scattering by elastic ellipsoidal inclusions, self-consistent approach 78−63372
electron microscopy technique for small voids obs. 78−34403
epoxy treeing breakdown, slit model 80−15970
evolution, of void and interstitial loop evolution in pulsed fusion reactors 80−84217
fast reactor materials, fast neutron damage 78−10093
FBR fuel cladding alloys, phase instabilities and swelling behaviour 79−54500
FBR fuel pin failure, fuel porosity and crack effects on transient overpower analysis 80−71760
FCC metals, dislocation loops and voids, growth kinetics, role of divacancies 79−99196
ferrites, void, conc. and dimensions determ. by acoustic charact. 80−35472
ferromagnet containing void, Gibbs free energy, numerical calc. 80−29597
fibre reinforced composite, containing voids, elastic consts. and US velocity, theory 77−89498
filled polymers, cumulative internal damage, US assessment 79−57180
film, microporosity described in terms of vacancies and voids 80−24769
fission reactor materials, void swelling calculations using FACSIMILE VSI 80−42782
fluorene, γ-irrad., void form. 80−2068
Fokker-Planck continuum description 78−87707
Fokker-Planck eqn. describing evolution of interstitial loop microstruct. during irradiation 80−107215
formation energy, pseudopot. calc. 77−68961
fracture, computational models for one and two dimens. wave propag. 77−11628
fracture, ductile intergranular, problem of nucleation of voids 79−79110
fracture, intergranular, at elevated temps. 77−48545
fuel element modelling, interpreting and predicting irradiation creep 77−42058
fusion materials, heavy ion irradiation, swelling theory 80−34090
fusion reactor first wall material, mobile He inclusion in void swelling rate theory model 80−34069
fusion reactor metals, irradiated, defect cluster nucleation, He injection effect 80−34091
fusion reactor metals and alloys, microvoid form., gaseous impurity atom effects, positron annihilation study 80−49275
fusion reactors, inertial confinement, first walls, void growth, analytical model 80−63377
gas atoms per bubble of inert gas in solid 77−76468
gas bubbles in solids, simultaneous hetero- and homogeneous nucleation model 80−2066
grain boundary, stress induced drift diffusion, appl. to creep and growth of grain boundary voids 78−72811
grain boundary drift diffusion under influence of stress fields 79−77835
grain boundary sliding and intercrystalline fracture in high temp. creep *(Czechoslovakian)* 77−32642
granular materials, influence of void compaction and material nonuniformity on acceleration waves 77−68472
granular materials, void compaction and material nonuniformity, influence on acceleration waves, addendum 78−83280
granular medium, shear modulus, rel. to void ratio *(Japanese)* 79−32401
graphite, pyrolitic, oriented ellipsoidal voids, small-angle X-ray scatt. 78−64429
graphite nucleation, role of pre-heat treatments *(Japanese)* 80−35220
graphite pebble bed system, meas. of neutron wave propagation *(German)* 77−6481
growth, defect theory and processes, review 80−2009
growth, rel. to intrinsic point defect properties 78−47315
growth and incubation, stress effect 79−51147
growth kinetics, effect of surface energy barriers 79−51146
Hastelloy C-4, loaded at high temp., useful life 80−40523
Hastelloy-X, electron irrad., void swelling 79−14822
heterogeneous materials, cavities development *(Russian)* 79−55812
high alumina cement pastes, accelerated conversion, acoustic emission 77−36726
hydrogen embrittlement due to H-inclusion interaction 78−30664
initiation in random distrib. of spherical particles 79−46650
intergranular fracture during power-law creep 79−96105
interstitial cluster nucleation at the onset of irradiation 78−79635

voids continued
ion bombardment, electron microscopical anal. of surface effects and volume defects, review *(Rumanian)* 80−29093
ion exchange resins, macroporous rapid method of rating total void volume 80−21208
IR crystals, optical imaging of growth defects 80−64988
irradiated dilute alloys, kinetic model for solute redistrib. to sinks and void growth 79−78973
irradiated material, heterogeneous void nucleation 77−51415
irradiated materials, cascade damage and self-ion injection effects on swelling 78−34549
irradiated materials, point defect trapping and void growth 79−7626
irradiated metals, model simulation of photon energy band, low energy photon diffr. 79−78795
irradiation creep, temp. depend. 77−43252
irradiation creep due to dislocation and glide 77−69009
irradiation effects, low dose, void incubation, rate theory approach 79−77635
irradiation effects, void nucleation, swelling, creep, rate eqns. 80−49274
irradiation-induced swelling, and creep, effects of pt. defect trapping and solute segregation 79−79040
isotropic medium, elastic wave scatt. from flaws, long-wave approx., appl. to ellipsoidal voids and inclusions 79−86368
joints, visualisation using transmission-type scanning acoustic microscope 77−90511
Kevlar 29 and 49, aramid fibres, microvoid obs. 80−38960
layered structure, spherical voids determ., APL program 77−27872
lenticular, thermal gradient migration 80−2216
LMFBR reactor materials, simulation of void swelling and radiation-induced creep 78−8907
long elastic wave scatt., inverse problem 79−55819
metal, cavity growth in irrad. sample under stress 79−73211
metal, effects of large scale voids on thermal magnetoresist. 80−10946
metal, excitation by fast electrons of surface plasmons on spherical voids 77−11975
metal, formation energy of spherical cavities 77−80499
metal, He deposition and promotion of void nucleation during accelerator expts. computer simul. 79−23658
metal, He migration and defect interactions, role in radiation damage processes 77−28041
metal, heavy ion bombard., void conc., effect of implanted He *(Russian)* 80−88213
metal, heavy irradiation damage at high temps., void swelling problems *(Japanese)* 77−59049
metal, irrad., containing pre-existing dislocations, interstitial loop form. kinetics 80−65040
metal, irrad., peak void swelling temp. 77−72608
metal, irradiated, ordered arrangement of micropores on dislocations 77−19943
metal, irradiated, surface plasmon modes of voids 79−60617
metal, irradiated, void nucleation theory 79−1464
metal, NDT using positron annihilation technique 78−3294
metal, nonlinear electron density distribution around point defects, applications 79−19549
metal, nonlinear electron density distribution around point defects, formulation 79−19548
metal, oxidation of high temp. material, lattice vacancy effect 77−70203
metal, pure, vacancy injection during oxidation, reexamination of evidence 78−60864
metal, radiation damage effects, neutrons and heavy ions, rel. to reactor technology, review 77−43255
metal, simple, density profile, potential for spherical voids 79−11077
metal, surface plasmons size effect, RPA calcs. 77−80823
metal, trapping of H, book contrib. 80−24491
metal, void growth in irrad. sample, fully dynamic rate theory 79−73212
metal, void lattice, plasma oscill. 78−10382
metal, void surface topology 77−89424
metal, void swelling and dislocation loop growth on fast particle irrad. *(Russian)* 77−59047
metal, X-ray excitation of surface plasmons on spherical voids 77−11974
metal couple, porous homogeneous vacancy migration and void form. 77−55401
metal ductile fracture, void growth stress/strain relations *(French)* 80−19280
metal film, void size and number prediction 79−28256
metal surface-void van der waals interaction energy 78−10036
metals, compensated and uncompensated, effect of spherical voids on electrical magnetoresistivity 80−65531
metals, ductile, spall damage accumulation theory 77−70153
metals, influence of a surface coating, on void formation 78−47416
metals, irradiated, validity of rate theory, point defect diffusion eqns. 79−55777
metals, irradiated, void growth, appl. of Langevin method 79−77632
metals, irradiation induced swelling, bias factor 80−2062
metals, point defect and microstruct. behaviour during irrad., appl. to fusion reactors 79−23638
metals, radiation effects, ion beam study, review 79−10883
metals, radiation effects on elasticity and elastic moduli, yield stress 80−2078
metals, swelling during pulsed irrad., model, void growth exam. 78−47436
metals, thermal magnetoresist. and cylindrical voids 78−91658
metals, void growth and time-lag, statistical theory 80−88208
metals, void lattice form, spinodal decomp. of vacancies 78−92234
metals, void swelling, depth dependent, by self-ion irradiation, generalized model 79−14856
metals and alloys, irradiated, solute segregation and precipitation effects on void swelling 78−67741
metals irradiated general rate theory model of void swelling 79−23655
Metglas 2826 ribbon, voids formation during crystallisation 80−108428
microvoids as pigments in polymeric materials, review 79−52617
momentum transfer and damage energy gradient effects on He permeability 78−10102
neutron and heavy ion damage correlation, predicted temp. shift on swelling with radiation dose rate change 79−7630
neutron damage simulation, using HVEM, state-of-the-art 77−51417
neutron radiation induced, small angle scattering facility at SAFARI-1 reactor 79−50951
neutron-irrad., void annealing, positron annihilation obs. 77−76469
Nimonic, irradiated, void nucleation, numerical evaluation 80−70252
Nimonic 80A superalloy, contrast from cavities in HVEM 80−79780

voids continued
Nimonic PE16, He injected, bubble-void transitions in Ni ion bombard. 80−34095
Nimonic PE16, Ni ion irradiated, Ni segregation to voids 79−28020
Nimonic PE-16, electron irrad. in HVEM, void growth, vacuum environment influence 80−107323
non-metallic materials, flaw detection by tomodensitometry *(French)* 79−20295
nuclear fuel, quantitative metallographic anal., computer program, QMA 79−15951
nuclear fuel, transport phenomena under severe temp. gradient 80−615
nuclear reactor materials, depend. of evolving cavity distrib. functions on cavity growth kinetics 79−3206
nucleation, effect of mobile He 77−51405
nucleation and growth, effect of point defect trapping on impurities 79−23637
nucleation of defect clusters in crystalline solids 79−42051
nucleation rate determ. from size distrib. 78−10035
nucleation theory with Maxwell demons 77−85054
oxide fuels, in-pile densification by vacancy boil-off and vacancy knockout, model 79−8259
phase stability under irradiation, theory 79−77634
phthalic anhydride+8-hydroxyquinoline, solid-state reaction kinetics 77−36746
plastic deformation, necked bar, void growth, finite element anal. 80−64383
plastic powder compact rheological characteristics *(Japanese)* 78−95770
PMMA, oriented, hypersound propag., elastic props. 78−75737
point defect diffusion in stress field of edge dislocation of irrad. solid 78−51720
point defect production in irradiation, swelling, cascade diffusion theory 80−34044
point defect reactions, conc. depend. of rate const. for diffusion or reaction controlled reactions 79−7625
point defect sink strength in irradiated materials 77−51368
point-defect recombination, role of in theory of void swelling 79−42105
polycrystalline material, diffusional growth of cracks *(Russian)* 78−91376
polycrystals, intergranular void stability during diffusion growth *(Russian)* 80−10540
polyethylene, artificial voids, partial discharge charact. *(German)* 78−92023
polyethylene, electric breakdown, effects *(Korean)* 78−2799
polyethylene, solid, heterogeneity investigation by small angle neutron scattering 78−14298
polyethylene, ultrahigh modulus, drawing temp. effect on void form. and modulus 80−35241
polyethylene insulation of HV cables, water-treeing, environmental stress cracking phenomenon of elec. origin 80−40575
polyethylene spherulites, thermal expansion 78−2268
polymers, filled, cumulative internal damage, US assessment 80−97653
polypropylene monofilaments, tensile props., orientation degree depend., IR dichroism obs. 78−3163
polystyrene, high-impact type, deformation and microvoid form. 78−80602
polystyrene filament, melt spun, struct. and mech. props., effect of drawing, twisting, annealing, untwisting 80−45331
polystyrene-wood, polymer composite, dielec. props. at low temperature range *(Japanese)* 78−95541
polytrioxane, γ-irrad., layer-like void formation 78−22760
polyurethane, void detection by neutron gauging 78−23910
polyurethane foam, fast-neutron gauging for void detection 78−7157
porous ductile media, rupture by void nucleation and growth, criteria and flow rules 77−52492
porous metals, plasticity, stress-strain curves, yield stresses, strain vectors 80−83738
porous rigid-plastic material containing rigid inclusions, yield function, plastic potential, void nucleation 78−64612
porous solid, shear stress enhancement of void compaction 79−69182
precipitate hardened material, intergranular cavity growth inhibition 80−50677
pulsed radiation effect on void growth and swelling 80−34043
radiation cascades in void generation 79−73210
radiation creep and void swelling, bias factors in reaction-rate-theory anal. 79−46700
radiation effects, distrib. functions of point defects and moving gas filled holes 77−55302
radiation effects, sink strength of random array of voids, steady-state diffusion problem, variational technique 80−49266
radiation induced segregation of impurities to voids, kinetic model 77−43245
rate theory of void swelling, effect of recombination on sink strengths 78−87712
reactor fuel element defects, loss of cladding tightness, anal. of fuel element exploitation *(Czech)* 80−52736
reactor materials, radiation-induced embrittlement and swelling due to void form, ASTM research 78−13231
reactor materials, void swelling simulation, review 78−8906
refractory fusion reactor materials, neutron irrad., microstruct., voids, nucleation TEM study 80−29065
sapphire filament, grown by laser-heated floating zone method, microvoids obs. 77−32518
sapphire ribbon crystal, interface growth feature rel. to voids 78−34456
sapphire ribbon crystals, EFG growth and charact., voids, grain boundaries and dislocations 80−103283
sapphire ribbon EFG prod., substrate for heteroepitaxial Si, sheet and distrib. microvoids 80−108342
sapphire ribbon microvoid distribution control in edge-defined film-fed SOS growth 77−77370
SEM of sintered materials, qualitative and quantitative study of voids 80−16212
semiconductor DH lasers, three dimensional thermal problems 77−75554
silica optical fibres, surface flaws obs., fracture strength 77−14793
sintering, appl. of stereological charact. of interface interaction 77−63589
size distribution during irradiation and annealing, time depend. computation 78−30674
solidification in space environment, bubbles thermal migration and interaction with solidification interfaces 79−47670
solidification interface in reduced gravity, bubble interactions 78−84787
sphere tangent to four spheres, APL soln. 77−27773

voids continued
spherical, annular crack initiation, stress intensity factor estimates 80−106757
spherical voids, elastic wave scatt. at long wavelengths 80−48480
spinodal decomposition of vacancies, void lattice formation 79−10845
stainless steel, void characts. from ultrasonic scatt. data 79−79188
steady state nucleation, spatial correl. effects 78−67705
steel, AISI 316, fast reactor irradiated, solution treated, struct. 77−69008
steel, Al killed, density changes, void growth in biaxial stress fields, plastic deformation 80−71692
steel, alloy, forgings, H precipitation kinetics, diffusion to voids, effect on shattercrack formation 80−16344
steel, austenitic, annealed, Ni ion bombardment, swelling temp. depend. effect of He implantation 80−29080
steel, austenitic, cold worked, derivation of simple void-swelling equation 79−7631
steel, austenitic, gas implantation effects, fusion reactor first wall damage simulation 80−29079
steel, austenitic, hot isostatically pressed superalloy A286, fracture path 78−23824
steel, austenitic, Ni-Cr, neutron-irradiated solute segregation and void swelling 79−60407
steel, austenitic, tempering cavity condensation *(French)* 80−55442
steel, austenitic, type En58B, martensite formation and reversion, effect on void swelling 80−11641
steel, austenitic, type FV548, irradiated, Ni and Si rich phase, energy dispersive X-ray anal. voids and precipitation, TEM study 79−66063
steel, austenitic, type M316, martensite formation and reversion, effect on void swelling 80−11641
steel, austenitic 316, displacement energy determ., HVEM obs. and electron bombardment 78−6100
steel, austenitic stainless, deformation induced cavitation, exam. 79−43363
steel, austenitic stainless, HVEM irrad., point defect trapping influence on void swelling 79−23652
steel, austenitic stainless, type 316, irradiated with 46.5 MeV Ni^{6+} ions, soluble C effect on void swelling and low dose dislocation structs. 80−49280
steel, austenitic stainless, type 347 and 316, voids at grain boundaries near creep fracture surfaces 79−83311
steel, austenitic stainless, type FV 548, 20% cold worked irradiated with 22 MeV C^{2+} ions or 46 MeV Ni^{6+} ions, study of void swelling 79−37744
steel, austenitic stainless, V alloyed, creep mechanism 77−48514
steel, austenitic stainless FV548, neutron irradiated, Si-rich phase occurrence of M_6C phase 80−15156
steel, austenitic type 316, continuous gas generation effects in neutron and simulation environments 80−34068
steel, C, ductile fracture, role of hydrogen 79−57103
steel, C, ductile fracture under cold forming conditions, press. effect 78−52938
steel, C, quenched and tempered, ductility, effect of hydrostatic press. 78−44190
steel, cold worked FV548, electron irradiated, void swelling after 10 ppm He preinjection 77−19989
steel, continuously cast billets, influence of hot working on internal cracks 79−83242
steel, Cr-Mo:P (2.25, 1 wt.%), stress relief cracking, effect of P segregation 80−89324
steel, Cr-Ni (18%, 12(8)%), martensite formation and reversion, effect on void swelling 80−11641
steel, ferrite-pearlite, ductile fracture, pearlite colony morphology and hydrostatic press. effect *(Japanese)* 78−15510
steel, ferritic, FV607, void swelling, theory 78−71763
steel, ferritic, FV607, void swelling in 1 MeV electron irradiation 78−71762
steel, ferritic, void swelling during irradiation, suppression mechanisms 80−6441
steel, ferritic alloy and martensitic stainless, void swelling response after fast reactor irradiation 80−6437
steel, high C, ductile fracture, role of second phase particles 79−52359
steel, low alloy ferritic, sub-micron cavity nucleation, SEM obs. 78−95753
steel, low-C, kinetics of void development in fracturing A533B tensile bars 80−76357
steel, low-C, S10C and 520C, tensile fracture at low temps. *(Japanese)* 80−81163
steel, medium C, deformed, H_2 enhanced load relaxation 79−61635
steel, mild, and cold-rolled, diffusion, permeation, and accumulation of H_2 *(Japanese)* 77−39692
steel, mild, tempered and quenched, dynamic fracture toughess 77−36665
steel, neutron irrad. induced, reduction of void size by cold working, TEM 78−79636
steel, Ni-Cr-Mo and Cr-Cu-Mo and sintered, ductile fracture, microvoid effects *(Japanese)* 80−108542
steel, nonmetallic inclusion, effect on hot ductility 80−29999
steel, nuclear reactor press. vessel, radiation induced embrittlement, slow neutron small angle scatt. study *(German)* 77−34390
steel, pearlitic, creep-induced micropore healing kinetics of 12MKh and 15Kh1M1F, TEM obs. *(Russian)* 80−71690
steel, Si, electron irrad. in HVEM, void swelling, Si role 80−54285
steel, spheroidized, shear mode of ductile fracture 79−61714
steel, spheroidized AISI 1095, ductile fracture of U-notched bend specimens 79−24616
steel, stainless, 304, void form., effect of sequential and simultaneous He implantation 78−71719
steel, stainless, cc Cr-Ni (20, 18 wt.%), effect of tensile stress on growth of He bubbles 79−55796
steel, stainless, depth distrib. of swelling, TEM exam. 80−15165
steel, stainless, dose rate and cascade collapse effects on swelling 79−23656
steel, stainless, electron irrad. in HVEM, radiation damage obs. 77−50233
steel, stainless, fracture toughness, −20 to +22°C, of type UNS-S 15500 79−70145
steel, stainless, He effects on microstruct. in ion-irrad. 80−29078
steel, stainless, He ion bombard., in situ electron microscope examination 80−34094
voids continued
steel, stainless, HK40 and HP, centrifugal cast tube, creep damage estimation from creep void obs. *(Japanese)* 79−87687
steel, stainless, ion bombardment, primary recoil energy spectra characts. 78−10103
steel, stainless, irradiated, void nucleation, numerical evaluation 80−70252
steel, stainless, irradiation creep and swelling, microstructural modelling 77−52407
steel, stainless, laser fusion reactor first wall, void growth charact. 80−34042
steel, stainless, neutron irrad., point defect cond. and void radius change, appl. of model for void growth 78−47436
steel, stainless, neutron irrad., pore annealing kinetics 77−72638
steel, stainless, neutron irradiated, stress effects on microstruct. 77−47490
steel, stainless, solution treated, irradiated to low doses with 22 MeV C^{2+} and 46.5 MeV Ni^{6+} ions, interstitial loops 79−14855
steel, stainless, solution treated FV 548, irradiated with 22 MeV C^{2+} and 46.5 MeV Ni^{6+} ions void swelling 78−22771
steel, stainless, spatial regularity of electron irrad. induced voids, impurity effects 77−47487
steel, stainless, type 304, void swelling 200 keV C^+ bombardment, dose and temp. depend. 77−55309
steel, stainless, type 304L, fast neutron irradiation, voids nucleation 79−77644
steel, stainless, type 316, influence of preirrad. thermal-mechanical treatment on phase stability and swelling 79−55792
steel, stainless, type 316, irradiated, numerical simulation of void nucleation 79−73208
steel, stainless, type 316, neutron irrad., Ni ion bombard. effects of injected interstitials on void volume 80−34092
steel, stainless, type 316, neutron irrad. damage simulation using HVEM, surface effect on void swelling 78−29572
steel, stainless, Type 316 and 321, irradiation-induced creep following 4 MeV H^+ bombardment 78−14390
steel, stainless, type 316 electron irradiated, void swelling 78−55891
steel, stainless, used as reactor cladding material, void swelling obs. by HV electron microscope *(Japanese)* 79−42108
steel, stainless, void growth kinetics, effect of surface energy barriers 79−51146
steel, stainless, void shrinkage during electron irrad. 78−34540
steel, stainless, void swelling, Si point defect trapping, interstitial loop growth rate temp. depend. obs. 80−49270
steel, stainless, void swelling obs., under HV electron microscope *(Japanese)* 80−54218
steel, stainless, voids, TEM, diffr. contrast 80−75218
steel, stainless 316, Fokker-Planck eqn. describing evolution of interstitial loop microstruct. during irradiation 80−107215
steel, stainless 316, irradiated void swelling incubation period, stress effects 78−6105
steel, stainless 316, soln. annealed, cavity alignment and precipitation during dual ion bombardment 80−70273
steel, stainless AISI 316, fast neutron void swelling simulation dose and dose rate effects 77−15457
steel, stainless austenitic, neutron irrad., swelling due to gamma prime and $M_{23}(C,Si)_6$ form. 78−51590
steel, stainless type 316, effect of damage rate on void growth, point defect conc., microstruct. development 79−73209
steel, type 1045, hydrogen enhanced nucleation of microvoid as function of local plastic strain 79−79053
steel, type FV548, 1 MeV electron irradiated, influence of pre-injected He on void nucleation and growth 80−34054
steel, types 60G, ShKh15, structural changes near holes and inclusions due to pulsed currents *(Russian)* 80−108459
steel austenitic stainless, Cr-Ni 316 type, electron irradiated, void swelling 79−42104
steel welds, bead-on-plate, H_2 diffusion and trapping 80−96697
steel wire, US inspection, immersion method 80−66757
steels, C, H_2 embrittlement after patenting and cold deform. *(Russian)* 79−29175
superconducting composites, Kirkendall void elimination by solution anneals 80−7520
superconductor, flux pinning summation curves 78−52165
superconductors, multifilamentary, voids growth obs., via hot stage SEM 80−70089
superplastic alloys, cavity growth 80−93627
superplasticity, cavity growth anal. 80−60923
swelling, bulk recombination role 78−83847
swelling, effect of recombination of sink strengths in rate theory 79−14851
swelling, nucleation theory 80−65038
swelling, rel. to in-pile precipitation 78−70595
swelling, simulation, effect of self ion injection 78−22772
swelling, simulation, theoretical evaluation of dual beam irradiation expts. 78−79646
swelling, volume, errors in determ. by TEM 80−84208
swelling and irradiation induced creep 77−44297
swelling depth distribution produced by 5 MeV Ni ions 77−7771
swelling in metals and alloys under irradation, theory 78−75692
swelling rate, vacancy dislocation loop effect 80−2084
swelling transition from gas bubble to void growth 78−14383
TEM contrast, aid void vol. determ. 80−75217
TEM contrast of void arrays in crysts. 80−14975
TEM observation of cavities, review of techniques 80−14974
tension creep, finite element anal. of void growth 79−18739
tetrahedral semiconductor, interstitial type dislocation loop form. by vacancy precipitation 78−67715
thermoplastics, structural changes during deformation, rel. to impact resistance 80−25800
trapped species in host lattice, teaching 78−16594
type II superconductor, fluxoid-void interaction 79−7950
US testing, automatic *(German)* 79−83406
Van der Waals energy between voids and particles, from asymptotic to close contact 80−80351
void lattice, displacive stability of void 78−14335
void sink strength depend. on mutual recombination, point defect loss to fixed sinks 80−33995
void-containing materials, ductile fracture, conditions for shear localisation 78−79663
void-swelling, response to temp. changes 79−65116

voids continued
wire rope NDT, EM field perturbation by internal void in conducting cylinder 79−34213
X-ray, and neutron small-angle scattering, structural defect studies, review 79−10752
Zircaloy-2, irradiation-induced creep following 4 MeV H^+ bombardment 78−14390
Ag film, void growth, TEM obs. 80−59833
Ag thin films, deposited by cathodic sputtering using high-resolution electron microscopy, voids obs. 80−49557
Ag wire, ultrapure, cryst. forms of hillocks and voids formed by electromigration 77−31811
Al, Al ion irradiated, void swelling and annealing of voids, electron microscopy study 80−88216
Al alloy, dil., neutron irradiation 78−22766
Al alloy, void form. in defeated targets 77−15403
Al alloy 2024-T4, ductile fracture, microvoid effects *(Japanese)* 80−108542
Al alloys, neutron irradiated, suppression of radiation damage microstruct. by trace impurities 79−77643
Al and Al-Mg alloy N4, irradiation with 100 and 400 keV Al ions, obs. and analysis of damage struct. 77−4133
Al, annealed and neutron irrad., exam. of positron lifetimes in voids and other defects 78−47426
Al, commercial purity, density changes, void growth in biaxial stress fields, plastic deformation 80−71692
Al, effect of microvoid size on positron annihilation and residual resist. 77−48272
Al, high purity, neutron irradiated, void annealing kinetics 80−44234
Al, neutron damage, positron annihilation 80−65056
Al, neutron irradiated, direct obs. of radiation induced coated cavities 77−47493
Al, neutron irradiated, void surface props. determ., anisotropic small-angle neutron scatt. 78−10095
Al, positron annihilation in small voids, self consistent calc. 77−20952
Al, positron trapping at voids, temp. depend. 79−61464
Al, pure, electron irradiation damage 77−19988
Al, recovery features, TEM and positron lifetime meas. examination 78−80611
Al-Al_2O_3 alloys, dilatometric method for studying relaxation of conc. of defects 77−55288
Al-Cu (4 wt.%), effect of semicoherent precipitation on void swelling, when neutron irradiated 79−42115
Al-Cu-Mg/mica particulate composite mech. props. 80−100919
Al-$CuAl_2$ eutectic, deformed, thermal stability 77−52348
Al-Cu(Ag), tensile ductility, effect of ageing and impact velocity *(Japanese)* 78−15465
Al-In alloy, dilute, electron irradiation, interstitial dislocation loop obs. 78−18681
Al-Mg, fracture during superplastic flow 78−60729
Al-Mg, Si alloy, void form. under different precip. conditions, after Al ion irrad. 80−59529
Al-Mg (0.1 at.%), neutron damage, positron annihilation 80−65056
Al-Mg alloy A99, intercrystalline fracture during US treatment 79−15795
Al-Mg-Si alloys, ductile intergranular fracture mechanisms, void formation and nucleation 80−108578
Al-Si alloy, dilute, electron irradiation, interstitial dislocation loop obs. 78−18681
Al-SiO_2-Si, void form. in Al interconnection lines at Si-SiO_2 boundaries 80−2476
Al-Zn-Mg, cavitation during superplastic deform. *(Japanese)* 78−15464
Al-Zn-Mg superplastic alloy, cavity growth under creep conditions 80−60940
AlB_2 flake reinforced composites, prep., props. rel. to aspect ratio, book contrib. 78−48366
n-$Al_xGa_{1-x}As$, Au-based ohmic contacts TEM obs. 80−34509
Al_2O_3, composite film, barrier layer, ellipsometric meas. 78−67918
Al_2O_3 composite films, elec. instability 78−68452
Al_2O_3, cylindrical voids, exam. of instability 78−79603
α-Al_2O_3, sintered or hot-pressed, porosity effect on positron mean lifetime 78−27463
Al_2O_3 void formation by fast neutron irradiation, TEM exam. 78−51591
Au, as deposited film prepared by vap. deposition 77−69194
Au, epitaxial film, on NaCl substrate, electrotransport inferred from void growth rate *(German)* 80−10699
Au film, effect of high DC density stressing on pre-existing voids 80−24770
Au film, excess vacancy diffusion to free surfaces and voids, resist, decay 79−65237
Au film, low temp. void growth and resistivity decay 78−10302
Au film, void growth in early stages of ageing and electromigration 78−38991
Au film, void size and number prediction 79−28256
Au, optical props., dielec. function, void model, sample effects 80−76048
Au wire, ultrapure, cryst. forms of hillocks and voids formed by electromigration 77−31811
Au/Pb thin film couple, room temp. interdiffusion study 79−28154
B fibre, fracture, Griffith criterion appl. 77−12684
B fibre, proximate void origin and initial growth stages 77−80498
B fibre, US inspection, immersion method 80−66757
B_2O_3-SiO_2-Na_2O phase-separated glass, creep fracture morphology 80−81151
$BaTiO_3$ surface voids, Auger spectrochem. anal., organic contamination 79−24467
C fibre, structural and mech. characts. 77−28737
C fibre derived from mesophase-pitch, Young's modulus and tensile strength, struct. flow elimination 80−80995
C fibre reinforced plastic, shear props., effects of flaws and voids 77−44334
C fibres, pitch and lignite based, exam. of microvoids by X-ray scatt., heat treatment and stretching effects 79−20091
C, glassy, struct. parameter var. with heat treatment temp. 77−11488
CaF_2, anion-void superlattices *(Danish)* 79−14796
CaF_2, electron irrad. defect aggregates, ordering, U and Th impurity effects 80−75216
CaF_2, fine-grained, forging and bulk optical props. 80−33103
CaF_2, fluorite, electron irrad., {100} faceted anion voids 79−51153
$CaWO_4$, Czochralski grown, distrib. coeffs., cavity form., cellular struct. 77−11492
CdS single cryst., vaporization and form. of negative whiskers 80−92659

voids continued
CdTe, laser window material, vap. deposition, mech. props. 77−46776
CdTe:P, annealing induced lattice defects, TEM obs. 80−2010
Co-Ga β' quenched single crystals, annealing-out of point defects 80−55426
Cu alloy, superplastic, microscopic examination of internal void formation 80−16383
Cu, cracks in fatigue early stages, direct obs. of substruct. by electron microscope *(Japanese)* 78−7028
Cu, dlectron irrad. at 130K, positron lifetime investig. of stage III recovery mechanism 77−47484
Cu, electron irrad., void swelling and dislocation loops 79−99206
Cu, electron irradiated, void nucleation, Monte Carlo simulation method *(French)* 77−59046
Cu, grain boundary morphology effect on void form. 78−48533
Cu, high purity, small-angle neutron scatt. from pores in high temp. fatigue 79−14795
Cu, polycryst., creep and fracture behaviour, effects of prestrain and O 80−97544
Cu, prestrained, tough pitch and sintered, ductile fracture, voids *(Japanese)* 77−52472
Cu, sintered, appl. of stereological charact. of interface interaction 77−63589
Cu, sintered, residual voids, quantitative anal. of morphological changes by metallography 79−47854
Cu, surface tension at intermediate and high temps., influence of additional elements 78−15476
Cu, surface tension cct. cavities under Cu^+ ion irradiation, O_2 and He effects *(French)* 77−35611
Cu, tough pitch wire, cupping fracture surface, SEM study *(Japanese)* 79−79087
Cu, void growth and localisation of shear in plane strain tension 78−64613
Cu-Fe (1.5 wt.%), precipitation-effect on void formation during electron irradiation 80−84211
Cu-Fe (1.5 wt.%) alloy, void form. during irrad. in HVEM, reactor irrad. simulation and ageing effects 80−107327
α-Cu-Zn, whiskers, X-ray topography, substruct. 77−11831
Fe alloys, swelling, correlation with number of bonding d electrons 77−47491
Fe and Fe alloys, fast neutron irradiated at high temps., mech. props. 79−51157
Fe, annealed and cold-rolled, diffusion, permeation and accumulation of H_2 *(Japanese)* 77−39692
Fe, BCC, void nucleation following electron irrad. 80−29054
α-Fe, cavity formation at grain boundary-subboundary interactions 77−86040
α-Fe, irradiation induced void swelling, Cr additions effect 80−55408
Fe, microcracks formed by H_2 precipitation, SEM and TEM obs. *(Japanese)* 79−70071
Fe, oxidation at elev. temp., scale/metal interface charact. 79−74286
Fe, pure, ductile fracture, effect of nonmetallic inclusions 78−64660
Fe, pure, hydrogen-charged, initial cracking obs. 80−108580
α-Fe, TEM on struct. round fatigue cracks 77−12699
α-Fe, void swelling during irradiation, suppression mechanisms 80−6441
α-Fe, void swelling response after fast reactor irradiation 80−6437
α-Fe whiskers, pure, ductile fracture, microscopic obs. of initiation mechanism 80−85044
Fe-Cr, irradiation induced void swelling, Cr additions effect 80−55408
Fe-Cr-Ni (12, 15 wt.%) austenitic alloy, Ni^{6+} irradiated, void swelling and phase stability, Si and Ti effects 80−65055
Fe-Cr-Ti-Mo-TiO_2 (13, 3.5, 1.5, 2 wt.%) dispersion hardened, void swelling 80−65046
Fe-Cu (0.34 wt.%), neutron irradiated, field-ion microscope detection of ultra-fine defects 79−42116
Fe-Mn (32.5 and 38.3 wt.%), steel sheet, exam. of form limit diagrams and damage 78−48461
Fe-Ni-C (31, 0.1 wt.%), metastable austenite, fractography 77−59919
Fe-Ni-Cr, pulsed HVEM irrad., effect on microstruct. evolution 80−34053
Fe-P (0.14 wt.%), cavity formation at grain boundary-subboundary interactions 77−86040
$Fe_{80}B_{20}$, metallic glass, Doppler broadening of positron annihilation γ-radiation and elec. resist. 80−66321
$Fe_{78}Mo_2B_{20}$, metallic glass, Doppler broadening of positron annihilation γ-radiation and elec. resist. 80−66321
$Fe_{32}Ni_{36}Cr_{14}P_{12}B_6$, metallic glass, Doppler broadening of positron annihilation γ-radiation and elec. resist. 80−66321
GaAs, LPE layers, voids and depressions in facet and terrace growth 78−38974
Gd-Co, sputtered film, growth induced anisotropy 77−16123
$Gd_3Ga_5O_{12}$, Czochralski grown, effect of melt flow phenomena on perfection 78−88419
Ge, amorphous, pure and H doped, voids, atom probe FIM 80−49107
Ge, amorphous thin films, fast crystn. and void precipitation in laser pulse annealing, TEM exam. 79−56086
H assisted cracking, mechanisms, review 80−50721
H_2 transport by dislocations to fracture initiation sites, inclusions, microvoids 77−21263
In, linear magnetoresistance increase by artificial voids 79−60799
In wire, linear magnetoresist., effect of voids 78−51974
InSb, ion implanted, efficient void form., TEM obs. 80−44237
interstitial cluster nucleation, effect of trapping at onset of irradiation 79−78974
IrO_x, electrochromic, oxidation state changes and struct. 80−100950
KCl crystals, Eu^{2+} concentration effect on lattice parameter and density of crystals 80−88169
Li ferrites, porous, porosity effect on saturation of magnetisation 80−108036
LiF, radiation induced voids, formation on dislocations 80−15159
LiF single crystal, void disappearance 78−55864
LiF single crystals, exam. of void morphology effects on their disappearance kinetics 79−10843
$LiY_{0.416}Er_{0.5}Tm_{0.067}Ho_{0.017}F_4$, Stockbarger single cryst., charact. of solidification behaviour 77−24948
Mg, neutron irrad. damage, TEM obs. 79−46713
Mo, BCC, void nucleation following electron irrad. 80−29054
Mo, damage profile resulting from Ni^{2+} and He^+ ion bombardment 78−10100
Mo, effect of microvoid size on positron annihilation and residual resistivity 77−48272

voids continued
Mo, He ion irradiated, ordered arrangement of micropores on dislocations 77−19943
Mo, high-temp. neutron irradiated, annealing study by positron lifetime 77−51413
Mo, ion bombardment, damage profile, void size and density, TEM 78−47451
Mo, ion bombardment by Ni^{2+}, TEM study of damage depth distrib. 78−10101
Mo, irrad.-induced voids and dislocations, annealing, theory *(Russian)* 78−47418
Mo, microstruct., swelling induced by ion bombard., He injection effects 80−29083
Mo, neutron irrad., radiation anneal hardening mechanism 80−71678
Mo, neutron irradiated, relationship between void size and positron lifetime 77−15454
Mo, neutron irradiated, small angle X-ray scatt. and TEM study of voids 79−14849
Mo, neutron irradiated, void swelling and shrinkage, TEM study 80−34079
Mo, neutron irradiation induced voids, irrad. temp. determ. from void lattice const. 77−46289
Mo, neutron radiation-induced shrinkage of voids 79−51158
Mo, neutron-irradiated, high-temp., positron annihilation charact. meas. 77−89480
Mo, neutron-irradiated, positron lifetime study 79−23654
Mo, ordered void obs. 79−86786
Mo, positron investig. of neutron irrad. induced voids 77−8679
Mo, positron lifetime meas. of neutron irrad. induced voids 77−7766
Mo, proton irradiated, annealed and rolled, void form. 78−22774
Mo tips, film coated characterisation by atom probe FIM, atomic clusters, voids 80−33863
Mo, vacancy diffusivity from width of grain boundary void denuded zone 77−47615
Mo, void containing, positron annihilation charact. 80−80898
Mo, void lattice and depend. of vacancy porosity on irradiation dose *(Russian)* 79−27972
Mo, voids, effect of impurities on positron lifetime 77−15453
Mo wire, US inspection, immersion method 80−66757
Mo-Ti (1 wt.%), fast neutron irradiated, direct obs. of solute segregation to voids 79−78971
Mo-Ti-Zr (0.5, 0.1 wt.%), neutron irradiated, void swelling and shrinkage, TEM study 80−34079
Mo-Ti-Zr alloy, neutron radiation-induced shrinkage of voids 79−51158
Mo-Zr, heavy ion irradiated, void swelling, phase instability 80−29084
$MoSe_2$ and other layer structs. containing hohlstellen, electron diffr. 77−80397
$MoSe_2$, TEM exam. 77−35548
$Na_8Al_6O_{24}Cl_2$, radiolytic radiation damage, Cl^- voids and Cl gas bubble formation 79−7628
Na_2O-B_2O_3-SiO_2 glass-Ni compact, indented, strength and fracture toughness 80−93636
Na_2O-CaO glass, shear deform. under pyramidal indentations 80−84989
Nb and Nb alloys, superconductor, flux pinning under heavy ion irradiation 78−52167
Nb and Nb-Zr (1 wt.%), ion irradiated, void ordering 78−22770
Nb, BCC, void nucleation following electron irrad. 80−29054
Nb, flux pinning by voids during neutron irrad. 77−40008
Nb, irradiated superconductor, fluxoid defect interactions 78−52166
Nb, neutron irrad., microvoid form., ang. correl. and yield strength meas., TEM obs. 78−88381
Nb, TEM, elastic side band imaging 80−75219
Nb:O, type II supercond., radiation-induced flux pinning 78−80106
Nb-Ge, compounds with A15 structure, films, TEM study *(French)* 80−80135
Nb-Ge-Si, compounds with A15 structure, films, TEM study *(French)* 80−80135
Nb-Si, compounds with A15 structure, films, TEM study *(French)* 80−80135
Nb-Ti, void volume fraction reduction, Ni^+ ion irradiation 79−51162
Nb-Zr, type II supercond., radiation-induced flux pinning 78−80106
Nb-Zr (1%), He bubbles and voids with ringed images SEM and TEM exam. 78−51529
Nb_3Sn superconductors, Kirkendall voids, effects on mech. and supercond. props. 79−33429
Nb_3Sn, thin film, TEM microanalysis 80−104491
Ni alloys, swelling, correlation with number of bonding d electrons 77−47491
Ni, anodically oxidised, 100 keV proton channelling investig. of oxide layer struct. 77−84820
Ni, cavity coalescence following $^4He^+$ irrad. 80−70272
Ni, cavity evolution in 500 keV $^4He^+$ irrad. 80−29082
Ni coating, electron beam evaporated, ductility and struct. 78−11439
Ni, cold-worked, impurity-induced vacancy clustering 79−99972
Ni, He^+ irradiated, cavity depth distrib. determ. technique 79−51161
Ni, ion irrad. with 20 and 500 keV $^4He^+$, depth distrib. of cavities and dislocation damage 80−107346
Ni, irradiated, numerical simulation of void nucleation 79−73208
Ni, irradiated with Cu and Ni ions, depth depend. damage profile 79−14857
Ni, irradiation-induced creep following 4 MeV H^+ bombardment 78−14390
Ni, irradiation-induced creep, mechanism for large transient strains 78−14391
Ni neutron and heavy ion damage correlation, dose rate and He injection effects 79−7629
Ni, neutron irrad., void formation, C interstitial effects 77−76471
Ni, pure, heavy ion irradiated, dendritic void growth 78−14386
Ni, self-ion irradiated, He effect on void form. 78−6112
Ni, vacancy diffusivity from width of grain boundary void denuded zone 77−47615
Ni, void annealing and void formation energy 77−68962
Ni, void swelling caused by neutron and self-ion bombardment, 573 to 873K 78−14387
Ni, void swelling rates in self-ion irrad. sample 80−29081
Ni-Al, ion irradiated, dendritic growth of voids 77−11605
Ni-Al (42 at.%), Al_2O_3 growth, form. of voids at metal-oxide interface 78−53030
Ni-Al solid solns., N_2^+ irrad., void ordering 78−79644
Ni-Al(Cr)(Ti), ion irradiation induced void swelling and defect microstructs., TEM obs. 79−51164
voids continued
Ni-Co-Cr-Al-Y, plasma-arc-sprayed, metallurgical charact. and oxidation behaviour 80−40618
Ni-Si, proton irrad., γ' precipitation, early stages 80−34096
NiAl, quenched and annealed, void formation 79−46652
NiSb, dilute alloy, impurity-induced vacancy clustering 79−99972
PbS film, vac. deposited, optical and phys. props. 80−2315
$Pb_xSn_{1-x}Te$, grown by vap. transport in closed system, quality improvement 77−40341
PbTe thermoelectric materials, microstructure anal. using SEM X-ray microanalysis 80−107211
Pt, neutron damage, positron annihilation 80−65056
PuO_2-UO_2 mixed oxide fuel, plutonia particle behavior during sintering in Ar-H_2 (8%) atmosphere 79−8258
Si, amorphous, hydrogenated, small angle X-ray scatt., void distrib. 80−15087
Si amorphous film, annealing behaviour of void network 78−18551
Si, ion implanted, voids, electron microscopy 78−67757
Si, powder compact, Ar-sintering, microstruct. changes 77−90306
Si:Ar, ion-implanted, epitaxial regrowth by laser annealing, microstruct. 80−84404
n-Si:Cs, ion implanted, minority carrier lifetime and defect struct., annealing effect 78−6395
Si:H, amorphous films, plasma-deposited, defect states, IR, ESR, and refractive index meas. 79−65944
Si-Al-O-N ceramic, grain boundary desegregation and intergranular cohesion 80−100872
Si-H, amorphous, random network model 80−1932
Sn/Au thin film diffusion couples, Kirkendall void form. 80−96698
Ta, ion irradiated, ordered void arrays 78−34553
Ta, neutron irradiated, microstruct. and swelling 77−69006
Ti coated Nb, reduction of void number density and size by ion irradiation 78−51600
Ti-Al (14.4 at.%), void form. and solute segregation under Ni ion irradiation 79−42122
Ti-Al-V (6, 4 wt.%), void formation and growth, tensile fracture, exam. 78−80637
Ti-Al-V (6,4 wt.%), heavy ion irrad. effect on microstructure 79−10884
Ti-Al-V (6,4 wt.%), ion irradiated, microstruct. study using TEM 80−96572
Ti-Al-V (6,4 wt.%), microstruct. effect of base metals on diffusion welding *(Japanese)* 80−89296
Ti-Fe-C-N, ion irradiated, microstruct. study using TEM 80−96572
Ti-Mn (0.4 and 12 wt.%), bonding between α-β interfaces, subsequent deform. 78−14517
TiC, electron irrad. damage, electron microsc. study 80−84210
TiC hard coating on Co, effect of martensitic transform. in substrate causing cracks 79−29060
$(U,Pu)O_2$, mixed oxide fuel elements, lenticular pore movement 78−78460
α-U, strain rate effect on flow and fracture 80−100887
UO_2, lenticular void migration rate in thermal gradient 78−21642
UO_2-U_4O_9, thermal cond., effect of microstruct. and microcracking 79−97810
V, He preinjected, void swelling on neutron irradiation 77−7765
V, neutron irradiated, void swelling, O_2 effect 78−6106
V, purification and plastic props. 80−25810
V, superconducting props., effect of voids 78−52168
V, void formation from 200 to 700°C following heavy-ion irradiation 78−10104
V:N, ion bombard., void form. 80−34097
V:O, neutron irrad., void form., 673-1073K 80−29066
V-Cr (wt.%), 3.5 MeV $^{51}V^+$ irrad. induced void swelling and solute segregation 79−7637
V-Ni, ion bombard., void form. 80−34097
V-O (1 to 4 at.%), solid soln., void swelling, V ion beam irradiation, 550 to 905°C 78−63795
V-O alloy, temp., dose and conc. depend. of void form. following V^+ ion beam irradiation 78−10105
W, doped wire, secondary recrystallisation temp., bubble parameter effects 77−32596
W fibre reinforced Cu composites, correl. between thermal cycling-induced microstructural changes at interphase boundaries and tensile behaviour *(Japanese)* 80−71674
W, high temp. strength and ductility 77−52406
W, ion irradiated, defect clusters obs. 80−2089
W, vacancy-defect clustering, due to annealing and quenching, TEM and elec. cond. exam. 78−47344
W wire, AKS-doped, second phase particle obs. by TEM, SEM and atom probe microanalysis 80−108457
W wire, US inspection, immersion method 80−66757
W-Mo, vapour deposited, long-term strength and thermocyclic creep 80−16405
WC-Ni hard alloy composite, sintered, void healing 80−60821
Zn, electron momentum distrib., neutron-induced defects, positron annihilation study, for single cryst. 80−71508
Zn-22 wt.% Al superplastic eutectoid alloy tensile deformation obs. *(Japanese)* 79−90714
Zn-Al (22 at.%) eutectic, superplastic, microscopic examination of internal void formation 80−16383
ZnS-CdS:Ag(Ni)(Co), electron-irradiated phosphors, void formation mechanism 79−55780
ZnSe, single crysts., grown from melt under Ar pressure, defects form. 79−4312
Zr, void swelling during electron irrad., HVEM study 80−92559
Zr-base alloys, annealed specimens, irradiation growth 80−49276
Zr_3Al, ordered polycrystals, ductile fracture 78−64641
$ZrH_{1.9}$, neutron irrad. induced defects, nature and thermal stability 77−50246

Voigt effect *see magneto-optical effects*

volatilisation *see vaporisation*

volcanology
1923 to 1957, volcanic eruptions effects on atmospheric transmission, Smithsonian Astrophysical Observatory meas. 80−17374
1974-1975 eruptions, rel. to southern hemisphere stratospheric aerosols 79−48551
N.Aegean region, volcanology rel. to crustal shortening 77−53028
aerosol, rel. to tropospheric mean temp. 77−33168
aerosols, in stratosphere, from Agung eruption, solar radiation absorpt. estimation 77−87072

volcanology continued
Afar depression, Ethiopia, volcanism rel. to Atlantic type continental margin development 77−21692
Afar region plate tectonics, seismic and volcanic evidence 80−21700
Afar triangle, November 1978 fissure eruption rel. to seafloor spreading 79−57912
African plate, volcanism rel. to mantle convection pattern and stress system 77−81859
airborne particle and gas emissions, meas. 79−2203
airborne particles in stratosphere, effect on radiation reaching Earth surface 80−82035
Aiyansh Volcano, British Columbia, ages of eruptions 78−92811
Alae lava lake, Hawaii, numerical analysis of cooling 77−64248
SWAlaksa, episodic accretion and plutonism 80−101346
Aleutian and Alaskan volcanoes as tectonic stress orientation indicators 77−91087
Aleutian and Pribilof Islands, Alaska, Pb and Sr isotopes in volcanic rocks 78−57185
Aleutian Ridge explosive volcanism episodes 78−53636
Aleutian subduction zone seismicity, volcano-trench separation, rel. to great thrust-type earthquakes 80−21655
alkali basalts, Nd, Sr isotope geochemistry rel. to metasomatically veined mantle heterogeneities 80−56420
altered volcanic rocks at Matagami, Quebec, geochemistry and geothermal model for massive sulphide genesis 78−77231
Andean subduction zone, intermediate aseismicity and recent andesitic volcanism 77−49055
Andean Wadati-Benioff zone morphology, andesitic volcanism, Nazca plate tectonic features 78−32039
central Andes, plate tectonics rel. to Plio-Quaternary tectono-magmatic zonation 77−29273
andesites, Andean region, petrogenetic composition variations 80−8313
andesitic volcanism and crustal evolution 78−85524
Antarctic Peninsula igneous rocks, transverse geochemical vars. rel. to calc-alkaline magmas genesis 80−56466
Antarctica, seismicity rel. to volcanic activity 77−86803
arc-trench volcanism, magmatic evolution, generalised models 78−65241
Archaean Dalembert tuff, Rouyn-Noranda, Quebec, Canada, petrography, and eruption mechanism 79−62472
Archaean layered greenstone from Pilbara Block, age of volcanics 78−53627
Archaean lithospheric/crustal thickness from volcano spacings 78−65225
Archaean volcanic centres, effects on ocean chemistry and biological evolution 77−56653
Archaean volcanism, high-temp., rel. to evolution of lunar orbit 77−29671
central Arizona, reversal chronology from volcanic sequence rel. to ocean floor polarity record 80−72419
Asal-Ghoubbet rift zone, Afar, 1978-9 geodetic survey after seismo-volcanic activity 80−46164
Asama, Japan, Fe-Ti oxide minerals in 1973 eruption 77−17065
Asama and Kusatsu-shirane Volcanoes, Japan, Bouguer anomaly and gravity changes *(Japanese)* 79−70733
Asama Volcano, Japan, amg. and elec. obs. *(Japanese)* 79−70736
Asama volcano, Japan, distrib. of gamma radioactivity 79−66696
Asama Volcano, Japan, geodimeter survey during 1977, ground deform. *(Japanese)* 79−70732
Asama Volcano, Japan, groundwater chem. vars. rel. to volcanic activity *(Japanese)* 79−70814
Asama volcano, Japan, in situ gamma ray radiometry appl. *(Japanese)* 79−66824
Asama Volcano, Japan, joint geophys. and geochem. obs. in 1977 *(Japanese)* 79−70771
Asama Volcano, Japan, precise levelling surveys *(Japanese)* 79−70731
Asama Volcano, Japan, remote meas. of SO_2 emissions *(Japanese)* 79−70772
Asama Volcano, spectral studies of explosion earthquakes assoc. with 1973 eruptions *(Japanese)* 80−67340
Asama-yama Volcano inactivity rel. to Matsushiro earthquake swarm, Japan 77−70599
ascending andesitic magma, cooling model 78−65239
ascending magma, heat and mass transfer 79−34768
ash, SEM examination, examples of devitrification and early diagenesis 80−81860
ash, terrestrial vs. extraterrestrial 77−2134
ash generated by ignimbrite/sea water explosions 80−26480
ash particles, influence of shape on atmospheric settling vel. 79−84364
ash-flow tuffs, Lake Precambrian in E. Newfoundland 79−84258
ashfall, pollen influx obs. of Mazama and Glacier Peak, Montana 78−24275
Askja Caldera, Iceland, imaging radar obs. rel. to surface roughness 79−16426
N.Atlantic recent sediments, volcanism effects on mineral comp. 78−44802
N.Atlantic Tertiary volcanic province, basalt magma sources during ocean opening 79−100821
Atlantic-type continental margins, igneous activity rel. to geodynamic development 77−21737
Atlantis II Deep geothermal system, changing hydrothermal activity 78−85532
atmosphere blow-off mechanism 77−29524
atmosphere temp. drop due to airborne volcanic dust 80−85726
atmospheric dust veil index since 1665, statistical anal. of effect on temp. changes 79−8680
atmospheric volatile elements enrichment by volcanic activity, Augustine volcano example 79−39796
Australia, tectonic, igneous and metallogenic provinces rel. to mantle convection and subcrustal stresses 80−72484
Azorean lavas, REE and LIL element compositions 77−25669
Azores, evidence for mantle plume from Sr isotope geochemistry in Central North Atlantic 77−5179
Azores, K-Ar age of oldest volcanics, volcanic history 80−46158
Azores, volcanism controlled by earthquake rupture direction 80−104911
Baikal rift zone, petrochem. of Cenozoic basalts and assoc. rocks 78−36171
basalt, erupted at Reykjanes Ridge crest, vesicularity 78−73351
basalt flows from Absaroke Mountains, Wyoming, palaeomag. study 77−86765
basalt glasses from FAMOUS area, Mid-Atlantic Ridge, regional var. and petrogenesis 80−31041

volcanology continued
basalt glasses from Mid-Cayman Rise spreading centre, geochemical var. and petrogenesis 80−101364
basalt petrogenesis, role of dynamic partial melting 80−46179
basaltic andesite dykes, Iritono, central Abukuma plateau, plagioclase grain size 78−7618
basaltic lava flows, degassing effects on rheology 79−12115
basaltic magmas classification, use of Ti, Zr, Y, Sr, K, P and Nb distribs. 77−5150
basaltic pillars, in collapsed lava pools on deep ocean floor 80−3991
basaltic volcanism rel. to mid-ocean ridges thermal struct. and kinematics 78−77210
basalts, open system cryst. fractionation and incompatible element var. 77−66916
basalts, origin rel. to rare earth fractionation patterns in peridotite partial melts 77−37198
basalts, Palaeocene, of Mull and Skye, immobile trace elements rel. to palaeotectonic affinities 79−34816
basalts of Iceland and Reykjanes Ridge, F contents and outgassing 79−57900
Basin and Range province, bimodal volcanic centres rel. to tectonic extension thermal effects 79−70763
Bataan Peninsula, volcanoes exhibiting no seismicity 80−81827
Belgium, possible volcanic anomalies 80−21691
Benue Trough, Nigeria, early Cretaceous basalt volcanism and initial continental rifting 78−61417
N.Black Hills, S.Dakota, evidence for late Tertiary volcanic activity 77−78142
Bogoslof Island, E.Aleutian arc, alkalic rock suite 77−70660
NE.Brazil, Post-Palaeozoic volcanism and tectonic significance 77−21735
S.British Columbia, tectonics rel. to Mesozoic-early Cainozoic activity 77−81852
British Tertiary igneous province, Arran dykes palaeomagnetism and ages 78−73306
Cainozoic volcanic centres of N.Africa, gravity links rel. to E.African Rift 79−34722
California, volcanism rel. to earthquake swarms and crustal spreading along strike-slip faults 79−66645
California, volcanism rel. to geometry of triple junctions related to San Andreas transform 79−57904
California coastal region, Neogene volcanism 80−21702
Campanian tuff ash layer (Y-5) in E.Mediterranean, age, origin and volcanology 80−56444
Canadian hotspot under young submarine volcano J. Tuzo Wilson 77−37165
Cantal continental volcanic system (France), ^{87}Rb-^{87}Sr constraints on genesis and evolution 79−88327
carbonatite and kimberlite magmas, generation rel. to mantle peridotite petrogenetic grid 77−5137
carbonatites, geographical distrib. rel. to so-called impact structs., implications 79−34825
carbonatites, geological aspects of calcite microstructure 79−57933
carbonatites, origin by liq. immiscibility 79−57928
carbonatitic igneous rocks, apatite comp. vars. 79−57929
E.Carpathian volcanic rocks, rare earth elements and Y, Rb, Sr, Cs, Ba, Pb, Th, U, Zr, Hf and Sn concs. 77−5151
Cascade Range, volcanic evolution 79−5466
Cenozoic explosive volcanism recorded in deep sea cores, tectonic effects, climatic implications 77−49052
Cenozoic volcanic rocks, SE.California, regional stratigraphy, K-Ar ages and tectonics 79−70798
Central American andesites petrogenesis, Sr isotope evidence 79−20833
Cerro Galan, NW.Argentina, Sr isotope evidence for crustal contamination of calc-alkaline volcanic rocks 80−98318
Cerro Galan Caldera, NW.Argentina, tectonic setting 78−85523
Chaine des Puys, France, lava flow-baked sediments ages and palaeomag. field strengths 79−44100
Chile, Quaternary volcanism 78−44980
China, volcanism rel. to active faulting and tectonics 77−86848
cinder cone fields, struct. and emplacement 80−76949
Clarno Formation, central Oregon, volcanism on thin continental margin 77−29296
climate change acting as trigger to volcanism 80−81858
climate change due to climate activity, ^{14}C and historical records 80−98442
climate variability, effects of volcanoes, pollution and CO_2 78−28292
clinopyroxenes from deep-sea basalts, statistical anal. of chemistry 80−41437
Coast Plutonic Complex of S.British Columbia, Canada, volcanism and geothermal resources 79−70429
Coldbrook Group in Caledonia Highlands of S New Brunswick, stratigraphy, palaeogeography and tectonic setting 77−91128
Colima Volcano, andesitic pyroclastic flows, 1975 Dec.-1976 Apr. eruption 77−29269
Colorado Plateau, age and extent of potassic volcanism 79−66668
composite volcanoes morphometric evolution 78−77205
Concepcion Bank, off Morocco, crustal struct., tectonic unit of volcanic origin 79−39689
continental and oceanic basalts, $^{143}Nd/^{144}Nd$ ratio vars., rel. to magma sources and mantle struct. 77−21708
continental volcanics, $^{143}Nd/^{144}Nd$ and $^{87}Sr/^{86}Sr$ ratios 78−53635
continental volcanism, role of ancient lithosphere 77−2133
convective heat transfer model for lithospheric thinning and crustal uplift 79−84199
convergent plate margins, volcanic activity rel. to great earthquakes 78−7588
Coso Range, California, Late Cainozoic volcanism 80−90049
crustal fracture, fluid-filled, mechanical interaction with Earth surface 79−79779
crustal rifting and volcanism relative timing and tectonic implications 78−81129
Dalradian metabasaltic rocks, petrochemical affinities 77−5202
Dalradian metabasaltic rocks, petrochemical affinities 77−5203
deep-sea basalts, He and Xe as measure of magmatic differentiation 80−31040
degassing of Earth, rel. to atm. comp. 79−70775
Dellwood knolls, volcanic activity age rel. to role in triple junction tectonics off northern Vancouver Island 80−90067
Denchai Basalt, N.Thailand, paleomagnetism, age and geochemistry 80−41421

volcanology continued
Diablo Plateau region, W.Texas, intracrustal magmatic activity rel. to tectonic uplift 80−72481
dike pattern rel. to stress state near Spanish Peaks, Colorado 77−91095
Dinarides, Yugoslavia, middle Triassic volcanism rel. to peri-Mediterranean tectonics 78−77238
Duncansby volcanic neck, NE.Scotland, palaeomag., K/Ar ages, tectonic implications 78−61369
dust, effects on climate, statistical evidence from long-term temp. records 78−69439
dust loading of atmos., 1923-54, pyrheliometric and circumsolar sky radiation obs. 80−46240
dust veil index, correl. with N.Hemisphere average temps. during Little Ice Age 80−82050
dust veil index of volcanic activity, apparent periodicity 79−92514
dust veil index rel. to N.Atlantic climatic change 77−78402
Early Tertiary lava flows from Greenland rel. to Baffin Bay-Labrador Sea evolution 77−17020
earthquake swarms in volcanic areas, model 77−44934
Eastern Rift, Africa, volcano spacings and lithospheric attenuation 77−5167
Eifel fields, pliocene and quaternary volcanic phases, K/Ar age determ. 80−46160
Emperor Seamounts, confirmed extension of Hawaiian volcanic chain *(German)* 78−96189
Eolian Islands, S. Thyrrenian Sea, basement structural trends from aeromagnetic and gravimetric data 78−40519
episodic plutonism in magmatic arcs, rel. to arc-trench gap accretion 80−76956
Erebus volcano, glass inclusions rel. to anorthoclase megacrysts *(French)* 77−9388
eruption cloud dispersion in stratosphere, lidar and numerical models for Vulgan Fuego and Augustine 77−56682
eruption clouds in Guatemala, atmospheric studies 80−41505
eruption energetics and dynamics, control of cloud column heights 78−61381
eruption mechanisms, gas pressures, new theory 79−34784
eruption risk mapping 78−11856
eruptions beneath glaciers, landforms rel. to Mars 80−67616
eruptions clusters, as course of abrupt palaeoclimatic events 80−51531
eruptions effects on stratospheric minor constituent chem. 79−84437
eruptions prediction, overview and recommendations 79−8703
eruptive gases, thermodynamic and isotopic studies 78−69316
SW.Ethiopia, dating of volcanic and rifting history 80−51369
Etna, 1973 November seismicity 77−44956
Etna, 1975 sub-terminal lavas, compound lava field formation 77−25670
Etna, activity and implications 80−31017
Etna, SO_2 emission fluctuations during 1977 eruptions 79−39694
Etna volcanic magma, ^{222}Rn daughters emission and enrichments 77−21736
Etna volcano, shallow geological struct. by elec. sounding 80−41419
European territory, tectono-magmatic processes rel. to heat flow 79−96751
explosive eruption column behaviour; magma props. and conduit geom. influence 80−109128
explosive volcanic activity, role in causing glaciations 79−20961
external ballistics of volcanic eruptions 80−46159
Fishguard Volcanic Group, SW.Wales, rhyodacitic pillow lava and isolated-pillow breccia 80−12389
Fogo seamounts, assoc. with anomalous upper mantle struct. 78−85515
fractional crystallisation of periodically refilled magma chamber, geochemical evolution 77−41016
Fuego, post-eruption stratospheric aerosol layer, lidar meas. 77−56679
Fuego 1974 eruption, effect on aerosol conc. at Mildura, Australia 77−5276
Fuego eruption, aerosol emission, density, temp. and particle content determ. 80−90050
Fuego eruption, stratospheric aerosols long term vars., lidar obs. 79−16597
Fuego volcano eruption, O_3 and Aitken nuclei meas. in stratosphere 77−49141
fumarole B isotope composition, Satsuma Iwo-Jima, Japan 80−67358
Galapagos Inner Rift, 86°10′W, struct., tectonics and volcanism 79−79808
Galapagos Rift at 86°W, regional morphological and struct. anal. 80−26491
Galapagos Rift at 86°W, sealed topography and magmatic episodes 80−21681
Galapagos Rift at 86°W, volcanism struct. and evolution of rift valley 80−21707
Galapagos Rift hydrothermal fields, struct. and morphology of seafloor 80−72489
gases emitted by Volcano Mihara, meas. using automatic recording instrument, comparison with tremors 77−66899
geophysical timescales from absolute-dated ice cores from Greenland *(Danish)* 79−34776
geothermal exploration in Iceland, volcanological methods 79−74877
Geronimo lavas from Quaternary in S.E. Arizona 80−8303
Glacier Peak tephra comp. var. rel. to stratigraphy 79−57897
Glacier Peak tephra in North Cascade Range, stratigraphy, distrib., rel. to glacial events 79−25247
glass inclusions in volcanic rocks, samples of early magmatic liquid 77−37202
Gondwanaland break-up rel. to flood basalt volcanism and subduction 78−65251
Gran Canaria/Tenerife mag. discordance rel. to NW.African continental margin form. 78−85478
granite magmatism initiation and thermal diversity 78−65240
E Greenland, struct. of coastal dyke swarm and assoc. plutonic intrusions 80−56467
W.Greenland Cretaceous-Tertiary volcanic region, magma traps theory appl. 79−70776
Greenland Ice Sheet impurities, past volcanism record 78−11855
greenstone belts, numerical models of vertical Archaean tectonism 80−81861
Hakone volcano, Japan, thermal structure and energy balance 79−74878
Hawaii Geothermal Project, groundwater geochem. study 80−72567
Hawaii xenolithic dunites, excess ^{129}Xe and high $^3He/^4He$ ratios 79−34814
Hawaiian basalt, petrologic data from silicate melt and other inclusions in olivine 77−2146

volcanology continued
Hawaiian glaciation chronology, K/Ar and ^{14}C ages 77−33113
Hawaiian lava flows, geomagnetic palaeointensities and Pacific nondipole low 78−61324
Hawaiian lavas, contamination evidence from ^{230}Th-^{238}U data 77−5166
Hawaiian volcanoes, rift zones as expressions of plume generated radial stress fields 80−90051
Higashi-Izu monogenetic volcano group, Japan, geology *(Japanese)* 78−96176
Himalayan geothermal belt *(Chinese)* 79−79759
hot spots and island arcs, rel. to mantle plumes 77−91081
hydraulic transients, as seismic sources in volcanoes and glaciers 79−100816
hypersthenic magmas, water contents 80−72507
Iceland, coastal shelf and slope, central volcanoes 77−73698
NE Iceland, dyke swarms rel. to geomag. anomalies (ΔZ) 80−89951
Iceland, geothermal activity rel. to geological struct. 78−61376
Iceland, lateral magma flow within rifted crust 78−73339
N.Iceland, major rifting episode with intense earthquakes, ground deform. and magmatism 77−37175
N.Iceland, plate boundary rifting, 1975-78 period 79−84210
Iceland, sea floor morphology to south and west rel. to recent volcanic activity 80−90068
Iceland, Skagi and Langjokull volcanic zones, petrology and structure 79−2195
Iceland, Skagi and western neovolcanic zones, geochemical vars. 78−96171
Iceland, statistical anal. of damaging earthquakes and volcanic eruptions, (1550 to 1978) 80−89975
SW Iceland, stratigraphy and palaeomagnetism of Esja, Eyrarfjall and Akrafjall mountains 80−89950
Iceland, tectonic spreading, problems and mechanism 78−36137
Iceland, Tertiary lava pile struct. props. rel. to continuum model of crustal generation 80−90059
N Iceland, volcanic activity rel. to height meas., (1965 to 1977) 80−89931
N.Iceland fissures, relative movements and tile changes 80−90062
Iceland Krafla, activity history 80−21694
NE Iceland neovolcanic zone, geodetic meas. and horizontal crustal movements 80−89930
W.Iceland shelf, central volcanoes, magnetic and gravity evidence 77−37180
Icelandic columnar basalt, anisotropy of mag. susceptibility vars. 77−86859
Icelandic rhyolites, generation by melting of plagiogranites in oceanic layer 77−86885
Icelandic subglacial volcanisms, thermal and physical studies 80−101350
Icelandic volcanism, rift zones as expressions of plume generated radial stress fields 80−90051
ignimbrites with low aspect ratio, characts. 80−41423
ijolitic igneous rocks, apatite comp. vars. 79−57929
immiscible picritic liquids, Ni partitioning 78−32069
E.Indian Ocean, volcanoclastic material in Quaternary deposits 77−78154
intra-plate volcanism during Cainozoic, rel. to mantle convection 80−98293
intraplate seismicity, zones of weakness, alkaline magmatism and tectonism 79−74882
intraplate volcanism, geological and geophysical parameters 78−65243
intraplate volcanism, magma flow through lithospheric fractures, tensional tectonics 78−65242
ionospheric plasma disturbance due to earthquakes and volcanic eruptions 80−36453
island arc development, obs. expts. and speculations 80−98298
island arc lavas, sources as indicated by Nd and Sr isotopic studies 78−32044
island-arc volcanism, magma formation and ascension due to sinking of tectonic plates 79−100823
islands of S.Atlantic, 1975 Soviet expedition results *(Russian)* 77−25668
Italy, heat flow in volcanic areas 79−70769
NE.Japan, Quarternary magmas H_2O contents lateral vars. 79−57899
Japanese islands, lateral var. of phenocryst assemblages in volcanic rocks 77−86886
Jbel Boho, Precambrian-Cambrian boundary from zircon radiochronology *(French)* 78−61359
Kambalda (W.Australia) komatiite sequence, precious metals values in interflow sedimentary rocks 79−20830
Kamchutka, tectonic tilt meas. rel. to volcanic activity 80−3984
Kapuho lava, Hawaii, olivine phenocrysts excess ^{129}Xe and high $^3He/^4He$ ratio 79−34814
Karmutsen volcanic rocks, burial metamorphism, N.E.Vancouver Island 77−17063
Kauai shield-building volcanism, age and Hawaiian Island chain volcanism linear migration 80−36281
KBS Tuff, E.Turkana, Kenya, K-Ar age estimate 80−56433
KBS Tuff, N.Kenya, fission track age and assoc. hominid remains 80−56432
Kenya, palaeomag. results from Narosura and Magadi volcanics 79−79740
Kerguelen Islands igneous rocks, Nd isotopic study rel. to enriched oceanic mantle sources 80−98319
Keweenawan volcanism, rel. to protoceanic rift system and foundered basin sequence in Michigan 79−39712
Kilauea, Hawaii, ground Rn survey of Puna geothermal area is lower east rift 80−85657
Kilauea, Hawaii, heat transfer meas. in 1977 lava flow 80−85632
Kilauea, Hawaii, volcanomagnetic effect discovery using improved signal discrimination 79−92629
Kilauea fumaroles, He/CO_2 ratios as premonitors of volcanic activity 80−26482
Kilauea Iki, shallow magma reservoir seismic props. 78−73338
Kilauea volcano, Hawaii, three-dim. crust and mantle struct. 78−28205
Kilauea volcano, incrustations and fumarolic condensates 77−29271
kimberlite pipes, as source of mantle rock specimens 79−2205
kimberlite pipes, exploration geophysics appl. 80−51393
kimberlites, micaceous, chemistry of micas 79−16465
Kirishima volcanoes, Japan, geothermal survey *(Japanese)* 80−67357
Klamath Mountains, Oregon, Jurassic island arc sequence identification in Rogue and Galice formations 79−100836

volcanology continued
Klyuchevskaya Sopka volcano (1974), volcanic bombs and lava, chem. anal. 80−101351
komatiite generation and greenstone belt models, thermal aspects 79−70762
komatiite magma, olivine and molten sulphide fractionation, model 78−96177
komatiite-derived tholeiites in Proterozoic of New Quebec 80−8305
komatiites and high-MgO lavas, origin, crystallisation 78−65312
Krafla, Iceland, 1978 July deflation, magma intrusion rel. to seismic activity 80−90054
Krafla caldera, N Iceland, gravity and height vars. during present rifting episode 80−90060
Krafla Caldera, NE Iceland, gravity and elevation changes caused by magma movement 80−90052
Krafla fissure swarm, Iceland, surface deform. in rifting events 80−90061
Krafla volcano area, N. Iceland, subsidence events, (1975 to 1979) 80−90053
Kusatsu-shiran Volcano, Japan, geothermal survey *(Japanese)* 79−70760
Kusatsu-shirane Volcano, Japan, 1976 steam explosion, geophys. obs. *(Japanese)* 79−70773
Kusatsu-shirane Volcano area, Japan, geomag. total force intensity meas. *(Japanese)* 79−70737
La Soufriere, Guadeloupe, gravity changes around volcano 79−92468
La Soufriere, Guadeloupe, seismic profiles of superficial structs. *(French)* 80−76932
Lake Van, E.Turkey, volcanism evolution and plate interaction 77−29270
Laki (Iceland) eruption, 1783 no Hg contrib. to Greenland Ice Sheet 78−65349
Lassen Park volcanic gases, He isotope ratios 79−16425
lava flow terrain, radar imaged by satellite 80−98285
lava flows, Quaternary, age determ. via thermoluminescence dating of volcanic plagioclases 80−98475
lava flows, thick layered peridotite-gabbro, Munro Township, Ontario 78−36168
lava flows of Mt. Etna, partial self-reversal and NRM 80−46126
lava lake cooling model, numerical analysis method 77−64247
lava lakes of Kilauea, Hawaii rel. to mantle magma 80−26483
lava temp. meas. techniques and apparatus on Etna 77−25800
Lesotho kimberlite pipes, isotopically light C in diamonds 79−48487
Lesser Antilles island arc, palaeomagnetic and geochronological survey 80−8265
Lesser Antilles volcanic island arc, geochemistry 78−7598
Lokbatan, mud volcano complex, violent eruption, 1977 October *(Russian)* 78−73340
Long Valley Caldera, California, implications of mag. model 77−86846
Longonot volcano, Central Kenya, geology, question of volumes of volcanic products 80−85633
magma chamber, fluid dynamics model of differentiation and layering 80−76939
magma genesis, mineral phases and parental rocks, $^{87}Sr/^{86}Sr$ ratios 77−25671
magma genesis conditions, H_2O and CO_2 solubility, petrological implications 78−11886
magma migration beneath ocean ridge mantle convection 80−12366
magma mixing, petrological process and volcanological tool 77−37201
magma mixing as acid explosive eruption triggering mechanism 77−53027
magma mixing at mid-ocean ridges, DSDP data 78−77209
magma pockets, stressed state rel. to destruction *(Russian)* 78−69315
magma series erupted in different marine tectonic settings, trace element anal. 80−21667
magma traps, lithostatic control theory 79−66669
magmagenesis 79−12103
magmas, influence of volatile components 80−41418
magmas, thermal history, low press. reference point 78−65244
magmatic rocks, anchieutectic comp. 80−12381
magnetic spherules in Arctic Ocean sediments, volcanic origin from Ti content 80−26488
major eruptions and volcanic dust rel. to N.Hemisphere temp. changes 78−36258
Makaopuhi lava lake, Hawaii, influence of augite on plagioclase fractionation 80−12390
Malartic Group, Abitibi, Archaean volcanism, petrography and geochemistry of lavas 80−17258
mantle degassing, rel. to oceanic Cl and Br origin 78−65342
mantle plume, fluid-dynamic model of ascending flow 80−12370
Marcus-Necker Ridge, volcanic rocks comp. and stages of development 80−36282
Marda calc-alkaline suite, rare earth elements, Archean geochem. analogue of Andean-type volcanism 78−11898
Mariana Island arc and trough, volatiles content of submarine volcanic rocks 79−92535
Marydale Formation, Kheis Group, South Africa, Rb-Sr age 78−32088
Massif central, France, basalt xenoliths rel. to upper mantle struct. and geodynamics *(French)* 79−48424
Mauna Loa, air quality obs. as meas. of volcanic activity 80−76950
Mauna Loa, venting rel. to Observatory CO_2 record short-term disturbances 78−88879
Mauna Loa, volcanically related secular trends in atmospheric transmission 79−62585
E.Mediterranean gravity anomalies, volcanic activity rel. to tectonic development 78−69318
Mediterranean region, struct. and tectonics, conf., Haifa, Israel (Aug.-Sep. 1976) 78−69306
Mesozoic pillow lavas from French Alps, clinopyroxenes comp. trends, cooling rate effects 77−5154
Mesozoic volcano-tectonic rift zone and back-arc basin development, South America 79−29762
Mesozoic-Cainozoic volcanism of Australia 78−96178
metabasalts from Point Sal ophiolite, California, rare earth and trace element geochemistry 78−32092
lower metadiabase from Michigan Basin basement, alkaline affinities from petrological study 80−4009
E.Mexico tectonic significance of alkaline volcanism 77−78143
Michigan Basin deep hole metagabbro, mineralogy and geochemistry compared to seawater hydrothermal alteration 79−39710
Mid-Atlantic Ridge, ocean-bottom seismograph obs. near 45°N rel. to magma intrusion 78−96157
mid-ocean ridge basalts, comparison with lunar mare basalts 79−16424
mid-ocean ridge basalts, density var. rel. to magma mixing and primitive lavas scarcity 80−56460
mid-ocean ridges, obs. and implications of ridge crest hot springs 80−98304
mid-plate hot-spot swells, thermal origin 79−8619
midocean ridge basalts, source evolution from Bay of Islands ophiolite complex Nd and Sr isotopic study 80−85651
Midway volcano, Hawaiian volcanic chain, age determ. 78−32041
Miocene-Pliocene lava sequence at Bassastadaa, E.Iceland 77−17046
Montana de Fuego, Lanzarote, volcanic zone temp. distrib. *(Spanish)* 77−70627
Mount Agung 1963 eruption, volcanic dust influence on N.American high arctic climate change and glacier mass balance 78−36214
Mount Agung eruption as test of global climatic perturbation 78−69440
Mount Etna, large ground deform. from precise levelling obs. 77−37172
Mount Etna, Sicily, heavy metal chem. of atm. particulate matter 78−61491
Mount Etna, SO_2 discharge meas. 77−78141
Mount Mazama ash falls, two eruptions during Holocene 79−62473
Mount Shasta, magnetisation implications for virtual geomag. poles determ. from seamounts 79−39637
Mount St. Helens, Washington, electron microprobe anal. of glass shards from set-W tephra 78−24274
Mt. Baker, new fumarolic activity, obs. during 1975 April-July period 77−37174
Mt. Etna, stress effects on volcanic rock magnetic props. 77−37192
Mt. St. Augustine, 1976 eruption, ash cloud trajectory 77−2234
mud volcano in Trinidad, gravity anomaly model 80−56442
mud volcanoes, Copper River Basin, Alaska, composition of emitted gases 79−84308
mud volcanoes in W.Caspian Sea area *(Russian)* 77−64281
Mull lava succession palaeomag. study rel. to Eurasian Plate motion 77−48995
Mynbulak, hydrovolcanoes *(Russian)* 77−60361
Namafjall geothermal field, Iceland, volcanic eruption through borehole 79−53332
Nasu zone, NE.Japan, trace element vars. in volcanic rocks 79−88317
Nauru Basin, basalt composition rel. to Cretaceous intra-plate eruptions 80−94499
Nazca group volcanic rocks, Peru, volcanic history 80−12357
Neogene explosive volcanicity, temperature and glaciation 80−26481
Neogene volcanism in Rumania and thermal spring water *(Rumanian)* 78−20451
Neogene-Quaternary volcanogenic formations, Dzhavakhet highland, palaeomag. 79−74834
New England Seamounts, submersible observations 78−20383
New Hebrides, geochemisty and origin of Quaternary volcanism 78−20375
New Zealand, plate tectonics developments 79−84208
New Zealand continental and orogenic volcanism, magma traps theory appl. 79−70776
E Newfoundland, Proterozoic volcanism rel. to NW Gondwanaland tectonics 79−57908
NW.Nigeria, calc-alkaline volcanics and possible Pan-African suture zone 78−32086
oceanic basins, volcanic evolution of marginal and interarc basins 80−8271
oceanic lithosphere flexure and uplifted atolls, comment 80−26486
Onverwacht Group, Transvaal, sedimentology rel. to early Earth volcanism 78−44812
Onverwacht Group Volcanics, southern Africa, Sm-Nd dating 79−62469
ophiolite genesis, tectonic regimes 79−57898
ophiolitic metabasalts in Mediterranean area, clinopyroxene comp. 79−57925
Ordovician volcanic rocks, N.Maine, magmatic affinity and tectonic significance 77−44984
organic compound synthesis on primitive Earth, volcanic processes 77−64434
orthopyroxene, occurrence and origin in some lavas from the French Massif central 78−96203
Oshima Island, Japan, anomalous secular variation, rel. to earthquake or volcanicity *(Japanese)* 80−41369
Oshima Volcano, Japan, elec. resist. changes and 1978 Jan. 14 earthquake *(Japanese)* 80−46132
Oshima Volcano (W.Hokkaido), eruptions at time of 1741 tsunami *(Japanese)* 80−67345
Oshima Volcano seismic activity prior to Jan. 1978 Izu-Oshima-kinkai earthquake *(Japanese)* 80−46138
P-wave abnormal delays in The Geysers-Clear Lake geothermal area, California 79−74860
S.Pacific, neoformation and weathering of assoc. volcanosedimentary levels *(French)* 78−73353
Pacific island and seamount ages rel. to volcanic chains origin 77−64242
Pacific Ocean, volcanic processes rel. to seismic props. of layer 2A 77−29260
Pacific plate, central stress fields delineated by linear volcanic chains 77−17068
E.Pacific Rise, hydrothermal vents on seabed issuing H_2 and methane 80−41422
E.Pacific Rise, struct. of crust, volcanism periodicity and magma flow 80−17243
E.Pacific Rise, young cratered volcanoes pairs 80−12374
E.Pacific Rise near 3°25′S, structural geomorphology of fast-spreading rise crest 78−44799
Pacific-Nazca plate boundary, volcanism in fast slipping transform fault zone 79−25226
Paluweh 1928 explosive eruption rel. to obs. climate change 79−2204
Pantelleria peralkaline lavas, glass inclusions in quartz and anorthoclase *(French)* 77−9389
Papua New Guinea, delayed partial melting of subduction-modified mantle 78−57183
Papua New Guinea, Late Cainozoic geotectonics and volcanism 80−51372
past volcanism from atmospheric turbidity determ. 78−88912
peralkaline rhyolites, assoc. with andesitic arcs of SW.Pacific 78−32043
Permo-Triassic volcanic arc terrane, Oregon-Idaho, spilite and keratophyre petrogenesis 79−20826

volcanology continued
central Peru, Eocene volcanism rel. to coastal batholith uplift and unroofing 79−2199
Peru-Chile Trench granulitic basement, Sr isotope ratios of calc-alkaline volcanism 78−28204
Peruvian Coastal Batholith, ring complexes, subvolcanic regime 77−5143
Phanerozoic tectonics and volcanism rel. to pulsation and expansion of Earth *(Russian)* 79−2202
Philippine Islands, tectonic struct. revealed by seismicity and volcanicity 80−94511
piezomagnetic anomaly field, Kilauea volcano, Hawaii 77−2089
piezomagnetic field, assoc. with Mogi model of surface displacements around volcanoes 80−67334
pigeonite, occurrence and origin in some lavas from the French Massif central 78−96203
E.Pilbara Block, W.Australia, Archaean shallow-water volcanic-sedimentary facies 79−57926
pillow lava, spreading cracks props. 79−79780
Pinacate volcanic field, Mexico, cinder cone struct. and eruptions 80−56443
Pinacate volcanic field (Mexico), genesis of phenocrysts and megacrysts in basaltic lavas 77−81881
Piton de la Fournaise volcano, SE.Reunion Island, gravity survey *(French)* 80−56334
plagioclase, zoned, of different magmatic environments, preliminary ion-microprobe anal. 79−34815
Pleistocene explosive eruptions in NW.America, surface albedo increase 80−61789
Pleistocene glaciation on Daisetsu volcano, rel. to Lake Biwa stratigraphy 78−24323
Late Pleistocene tephra in South Island, New Zealand, identification and significance 80−8306
pleistocene volcanism and glacial initiation 77−91088
Ploskii Tolbachik volcano, night observations *(Russian)* 79−84205
Poas volcano, pyroclastic sulphur eruption, Costa Rica 80−51370
point-density measurements using WANG 2200C minicomputer with digitiser 77−33072
prebiological compounds, form. in volcanic processes 78−40667
primitive Earth, volcanic processes role in organic compounds evolution 78−32230
Proterozoic anorogenic magmatism, rel. to analogous apparent polar wander loops 80−56360
pumice from KBS Tuff, East Rudolf, Kenya, $^{40}Ar/^{39}Ar$ dating 77−5160
pumice from KBS Tuff, East Rudolf, Kenya, fission track dating 77−5159
pyroclastic flow deposits, utilisation 80−12365
pyroclastic flows, mobility 78−7604
pyroclastic flows by eruption column collapse 78−61380
quarks, search for occurrence in seawater, ocean sediment deposits and volcano lava *(Russian)* 77−64288
Quaternary basaltic volcanism in Coso Range, California, rel. to geothermal anomaly 80−90002
Quaternary lavas, Snake River Plain, Idaho, mineralogy and petrology 78−20402
Quaternary volcanic ashes, petrography, Laguna de Fuquene, Colombia 79−84206
Quaternary volcanic rocks across NE.Japan, trace element contents, lateral variation 80−104926
rare earth element, abundances in layered Komatiite lava flow, Ontario, Canada 79−29764
rare gases in volcanic rocks, isotopes mass fractionation as indicator of gas transport to or from magma 80−98292
Recent andesites in Ecuador and N.Chile, Sr isotope data 78−32042
Red Wine alkaline province, central Labrador, chronology 78−11842
Reventador 1929 explosive eruption rel. to obs. climate change 79−2204
Reykjanes Ridge and Iceland, Cl and Br degassing by volcanism 78−36136
Reykjanes Ridge crest, morphology near 62°N 80−90070
riftward younging of volcanic units in Ethiopian rift valley 79−84204
Ririwai ring complex, Nigeria, heat flow meas. 79−57894
Roberts Arm Group, Newfoundland, age rel. to phases of volcanism 80−12354
Roccamonfina Volcano, geochronology and palaeomag. *(Italian)* 77−49036
Roccamonfina volcano, Roman comagmatic region, Italy,, potassic igneous rocks O isotope geochemistry 80−41420
Roccamonfina volcano caldera wall, petrochem. of pumiceous layers *(Italian)* 77−49051
rocks evolution in island arc, batch fractionation model, example from Japan 79−34818
rocks from W.Pacific island arcs, $^{87}Sr/^{86}Sr$ ratio 77−33031
Sakurajima volcano, ^{226}Ra-^{222}Rn disequilib. and pumice radioactivity 77−33033
San Juan volcanic field, S.Colorado, palaeomagnetic poles 78−32002
San Miguel Island, Azores, heat flow and mid-Atlantic rift volcanism 77−86844
Santa Maria volcano, Guatemala, evolution 77−70629
Santorini (Thera), tephra from 1450 BC eruption discovered at Rhodes 80−109129
Santorini (Thera) and Minoan tephra from bronze age eruption 78−24272
Santos Basin, Brazil, volcanism rel. to bordering continental rifts system 77−21768
Sao Miguel, Azores, quantitative study of volcanism, tephrochronology 78−61382
sapphirine-bearing rocks with sedimentary and volcanogenic protoliths from Arunta Block, Australia 79−44185
NW Scotland Tertiary continental volcanics, Nd and Sr isotope evidence for crustal contamination 79−66693
sea mounts, S.Indian Ocean, gravity models *(French)* 79−74884
seismic waves diffraction by finite crack, appl. to location of magma lens 79−16416
shackanite and related analcite-bearing lavas in British Columbia 79−57921
shape of volcanoes and subordinate vents position 77−53026
shear cracks nucleation and initial propag. 79−81804
Sheveluch volcano, explosion energy and depth determ. 77−17064
Shikoku Basin, off-ridge volcanism and seafloor spreading 78−65256
E. Sicily, genetic implications of isotope and trace element variations 78−11893
Sierra Leone Rise, equatorial Atlantic, alkali-rich volcanics 79−2215

volcanology continued
silicate liquids high-temp. props., rel. to basic magma equilib. and ascent 77−86868
silicate magmas, liquid immiscibility in K_2O-FeO-Al_2O_3-SiO_2 system 77−13076
S.Kivu, Zaire, basaltic flows on Idjwi Island *(French)* 77−64246
S.Kivu, Zaire, study of Tshibinda-Kalehe volcanic chain *(French)* 77−64245
Slate belt, volcanic evolution, possible primitive oceanic island arc 78−81125
Soufriere Crater Lake, use as calorimeter, erupted lava heat loss rate calc. 78−28207
Soufriere eruption, April-June 1979 activity 80−21693
W.South America, volcanism, seismicity and anelasticity interrelationships 77−33044
South Novo-Tolbachinsky volcano, flowing lava elec. cond. 80−72498
spilitic rocks, rare earth element mobility and geochem. charact. 77−86887
spilitic rocks from Michigan Basin deep drill hole, petrology 79−39711
St. Augustine volcano, Alaska, particles in eruption cloud, (Jan. to Feb. 1976) 78−57186
St. Augustine volcano, Alaska, search for atmospheric ice nuclei production 77−13110
St. Augustine volcano, nuee ardente obs. 77−78140
St. Augustine Volcano, ruby lidar meas. of stratospheric dust 77−29431
St. Augustine volcano eruptions, airborne meas. and obs. 77−49053
St. Lucia, Sulphur Springs geothermal field model 80−94494
stratosphere chemistry, quantity of injected sulphur and halogens 80−51474
stratospheric post-volcanic aerosol decay, lidar meas. 79−53444
stress accumulation in lithosphere 77−17071
stress corrosion cracking theory, geophys. appls. 77−62212
Stromboli, Italy, energy budget 79−70774
strong volcanic earthquakes assoc. with lateral eruptions, dynamic focal parameters 78−61347
subduction zone, ascending flow between descending lithosphere and overlying asthenosphere 78−40531
subduction zone, thermal model with downgoing slab dehydration rel. to island arc volcanism 79−79784
submarine geothermal resources, seafloor spreading centres and volcanic areas 77−37171
Suiko seamount, Emperor seamount chain, palaeomagnetism and relation to Hawaiian hot spot 78−57162
Sumatra, explosive volcanism ages rel. to late Cenozoic clockwise rot. 77−60363
Takayama volcanic area, Japan, upper mantle S-wave anisotropy 80−90024
Tambora, Indonesia, 1816 eruption rel. to year without summer (New England, 1816) 80−4089
tephra, late Holocene, from British Columbia and Alberta, identification 78−36167
tephra attributed to Glacier Peak, Washington, electron microprobe data 78−24273
tephra deposits, dating of ancient events 80−36283
terrigenous and volcanogenic deep sea bottom sediments chem. comp., Sea of Japan 77−21758
Tertiary basalts, of E.Greenland continental margin, biostratigraphic ages, plate tectonics implications 77−5153
Thera eruption and Late Minoan-IB destructions on Crete 77−66898
Thetford Mines ophiolites, Quebec, palaeomagnetism 80−61757
tholeiitic basalts, rare earth elements behaviour during submarine weathering 78−73369
Toba, N. Sumatra, late Pleistocene eruption K-Ar age 79−16427
Tolbachik volcano, Kamchatka, satellite obs. of 1975 eruption 77−33032
Tolbatchik volcanic area, weak shock waves in eruption column 77−56612
trace element behaviour in magmatic processes, quantitative models 78−65214
trace metals emission, contents in Antarctic snows (1914 to 1974) 79−34867
Troodos Massif, Cyprus, metallogenesis along Arakapas fossil oceanic fracture zone 79−29769
Turkish-Iranian Plateau, post-collisional tectonics, comparison with Tibet 80−3986
Tuscan anatectic magmatism, eastward migration due to Apennines anticlockwise rot. 79−16428
Twillingate Granite and Herring Neck Group, Notre Dame Bay, Newfoundland, geochronology 77−17049
W United States, Cenozoic igneous activity rel. to plate interaction and absolute motion 79−2207
Upper Cenozoic volcanism, central Andes, ages and volumes 79−29730
Upper Jurassic pyroclastic rocks in Skye, W.Scotland 77−29297
Volcan de Fuego (Guatemala), 1975 eruption rel. to stratospheric dust 78−73445
Volcan Poas, Costa Rica, subaqueous S lake 78−28206
Vulcano Island neighbourhood, heritage and neoformation in volcanic and hydrothermal sediments *(French)* 79−62482
water, isentropic decompression from crustal and mantle press., thermodynamics 79−79769
water-air and water-steam mixtures, sound speed rel. to fluid flow 77−84029
Wesleyville area, Bonavista Bay, Newfoundland, plutonic evolution 77−17095
xenolith transport in magmas 77−81853
Y-5 ash layer in E.Mediterranean, age, origin and volcanology 80−56444
Yellowstone caldera, Wyoming, USA, vertical crust movement 80−81859
Yellowstone caldera thermal struct. and Yellowstone Lake heat flow meas. 78−48997
Yellowstone Group, palaeomag. of welded tuffs 78−48967
Yellowstone Lake, seismic refl. and refr. surveys and palaeomag. study 78−49049
Yellowstone Park hot spot, volcanic and tectonic evolution 80−56472
Yellowstone Park volcanic gases, He isotope ratios 79−16425
Yellowstone volcanic plateau, conf., USA (1974) 78−49004
CO_2, isentropic decompression from crustal and mantle press., thermodynamics 79−79769
$^{13}C/^{12}C$ ratio in magmatic gases of Afar ridge volcanism 80−21732
Fe-Ni sulphide deposits, possible volcanic-exhalative origin 77−17097

volcanology continued
Hg emission rel. to Hg-sensitised UV photoreactions in abiogenetic organic synthesis on primitive Earth 77−37173
N_2O emission, rel. atmospheric N_2O sources, sinks and vars. 78−85631
SO_2 emission, rel. to stratospheric aerosol event of (1974-1975) 77−45084
SO_2 emissions in Mediterranean region, remote meas. 79−20987
$^{34}S/^{32}S$ ratio in magmatic gases of Afar ridge volcanism 80−21732
U province, N.Sweden, evolution rel. to Svecofennian orogenesis and subsequent volcanics 79−84271
U redistribution and mobility during metamorphism of volcanogenic formations 77−64283
W, abundances in volcanic rocks 79−16468

volt-ampere meters
see also power measurement; wattmeters
Coulombmeter, solid electrolytes appl. *(Czech)* 77−77779
multiplier wattmerer, appl. to VA and VAR meas. 77−53930
pointer-type, automatic testing, digital representation errors 77−53937

Volta effect *see contact potential*

voltage *see electric potential*

voltage comparators *see comparators (circuits)*

voltage control
action potential clamp to probe effectiveness of space clamp in axons 78−40441
automatic bias control cct. for injection lasers 78−71110
automatic radiographic system and HT generator, for gastrointestinal tract exam. *(Japanese)* 79−88167
automatic RF sputtering system for multicomponent film production 78−52672
coulometer, controlled-pot., design, operation, anal. appls. 77−25335
coulopotentiograph system, automatically controlled, for trace analysis of metal ions 79−92026
dual slide projector fader control cct., using a triac dimmer 80−69489
electrochemical voltage indicators, production, voltage response, resist. 77−1936
electroconvulsive therapy, servo-controlled volt. machine 78−77148
electrolysis, transductor and thyristor appl. *(Dutch)* 77−63925
electron microscope, UHV, const.-load tensile device and appls. to materials science 78−11462
electrostatic high voltage generator for TEM, stability improvement *(French)* 78−62268
flash tubes, electronic, power supply with volt. and capacitance control 77−67518
fusion reactors, Wendelstein VII and ASDEX, neutral beam injectors, HV power supply system, thyristor control 80−99332
HV pulse controller and temp. monitor microcomputer-based, Kerr effect study appl. 79−6103
HV stabilised supplies for 25 kV SEM *(Czech)* 79−21858
Langmuir probe, control system for maintaining prone at plasma potential 78−5943
lipid bilayer hydrophobic ion interactions, inner volt. clamping method 78−28129
low-noise preamplifier, output stabilisation by pole-zero cancellation in feedback cct. 77−61088
mass spectrometer, spectrum sweep using HF pickup voltage supply control 77−13812
microelectrode current and voltage clamp cct. for central nervous system neurons 78−24191
microtron voltage control system using thyristor convertors 77−14280
multicellular preparations, volt. clamp method 77−40955
MW impulse generator system, for ion cyclotron heating, fusion reactor 78−70635
nanosecond pulse generators, wave processes 77−18730
neutral beam source 8 MW voltage series regulator, for fusion reactor 78−70631
potentiostat, rapid response, construction, operation and evaluation 79−52678
potentiostat for corrosion studies 79−96237
RF sputtering, bias voltage control circuit 77−28720
sodar system tone-burst protector, cct. design, micrometeorological appl. 79−18641
steel, mild, corrosion rate meas. in H_2SO_4 using microprocessor controlled potentiostat 80−71798
storage ring, feedback-stabilised, resonator wall instability caused by ponderomotive forces 80−5418
X-ray tube anode voltage compensation under dropping power condition, digital compensation system *(Bulgarian)* 79−35902

voltage-controlled oscillators *see variable-frequency oscillators*

voltage controllers *see voltage regulators*

voltage distribution
see also electric breakdown; overvoltage; surface discharges; transients
arc voltage gradient in fully-developed turbulent air flow 78−71597
body surface ECG potential mapping, data acquisition system 79−29653
body surface potential distribution map recording and processing 78−57116
body surface potential image recording and processing methods 79−20704
chloroform HV polarisation and space charge obs. *(Russian)* 80−25277
electrosurgical passive grounded electrode/patient equivalent circuit analysis 77−78025
epicardial and body surface potential distributions related by geometric transfer coeffs. 77−21671
methylene chloride HV polarisation and space charge obs. *(Russian)* 80−25277
MIS structures with semiconductor layers of critical thickness, potential distrib. and capacitance calc. 78−95381
photomultiplier absolute spectral sensitivity in photon-counting mode 79−67383
plasmatron, linear, 3-phase, current and voltage charact. *(Russian)* 77−84535
rotationally symmetric periodic electrostatic focusing system field distrib. 79−76574
SEM potential distribution mapping technique 79−21857
surface potential distribution meas. by vibrating electrode 79−67340
Ag-Cu_2O-Ag bistable switching devices, freq. distrib. of threshold voltage 77−32091
Na-S cells, S electrode potential distrib. model 79−96435

voltage dividers
see also autotransformers; potentiometers
2 MV resistive voltage divider for measurement of pulsed voltages in vacuum 80−31803
analogue divider for heart ratemeter 78−40368
commutable circulator, with increased mean-power level 78−4637
for current and voltage measurement in pulsed X-ray devices *(Japanese)* 78−93788
EHV choke coil measuring bridge *(German)* 77−18047
electro-optic, capacitor type, current meas. appl. *(Italian)* 77−26339
high voltage supply for X-ray equipment, low-power devices 78−21309
HV instrument transformer calibration system based on LV inductive voltage divider 77−82567
HV peak value meas. techniques *(Dutch)* 77−67472
inductive, calibration methods comparison, between 10 kHz and 100 kHz 80−13100
Josephson, voltage standard, resistive divides *(Japanese)* 79−63266
Josephson voltage standard system, influence of voltage divider 78−74027
photomultiplier stable running using voltage dividers *(German)* 79−68172
resistive voltage-ratio standard for 10 kV DC meas. 77−5873
standard capacitor, simple calibration method 77−82571

voltage doubler rectifiers *see voltage multipliers*

voltage drop *see electric potential*

voltage measurement
see also potentiometers; voltmeters
9 V range, successive LED indication, variable voltage power supply appl. 77−53950
AC, average-value voltage transducer error anal. *(Russian)* 78−45649
AC, by analogue transducers, checking and calibration methods in USSR 80−98872
AC, matching measurement sensing method to application 80−47072
AC, multijunction thermal convertor, meas. errors 77−18033
AC, precision direct meas. facility 78−49863
AC, small, combined meter checking 80−13057
AC, small low-freq. voltage ratio meter 79−17440
AC, standard apparatus using thermoelectric convertors, 20 Hz to 1500 MHz 77−18036
AC, transistorised voltmeter type TF 2600B 77−53934
AC high voltage meas., confirmation of voltage ratios up to 200 kV 78−74018
AC measurement, using digital instruments 78−93726
AC measuring equipment checked against DC voltage, thermoelectric voltage convertor technique 77−53942
AC potentiometer, features and ccts. *(Polish)* 78−29128
AC voltage calibrators, testing standards 79−35786
AC voltage unit standard, USSR, 20 Hz to 30 MHz range 78−93734
AC/DC, Measurement Standards Laboratory, capability improvement 78−54332
accumulator cells, galvanostatic potential meas. system 77−30185
AF, high accuracy, using AC-DC comparator 77−18024
alternating voltage unit, 20 Hz to 30 MHz, USSR special standard 77−30180
amplitude meas. of signals up to microwave freqs. using Ge diodes 77−37905
arc axial potential meas., wall stabilized Ar arcs 78−30499
arcs parameters determ., natural fluctuations of voltage and emitted light correlation *(French)* 80−19654
automated controlled-current system, for coulometric, potentiometric and galvanostatic meas. 77−70353
automated measurement of noisy voltages with preset confidence level 77−37906
automatic potentiometer, microprocessor-controlled for nanovolt meas. 79−21771
automotive distributor, arc initiating processes, EM radiation reduction 80−19665
calibration service in 0.1 to 10 Hz range using AC voltmeter/calibrator 80−22385
calibrator using band-gap voltage reference, oscilloscope appl. 78−65941
combustion calorimetry, use of DC comparator apparatus 79−75529
contact pot. in compression couplings, pot. simulation using polarisation optical method *(Russian)* 79−78156
contact potential, at Hg-polymer surface, charge exchange obs. 80−75642
contact potential, H_2 and O_2 concentration determ. appl. *(Czech)* 79−70386
contact potential difference meter, IC, for meas. work function of electrons 79−35780
contact potential meas., surface pot. jump effect of spots, coatings and cryst. faces 77−51805
corrosion rate of ship basal layers, cathodic protection method *(Dutch)* 78−3297
CRO calibrator, Y amplifier, cct., constr., amateur radio appl. 77−30183
cyclotron dee voltage calibration using an intrinsic Ge X-ray detector 80−99359
data logger, 16-channel with multiplexing, and voltage pulse measurement 80−42203
data logger, peak and trough voltage waveform measurement 77−22575
DC, HV, transducers using solid-state sensors 79−44916
DC, low voltage in high ohmic circuits, using op amp based anxiliary equipment *(Czech)* 78−4664
DC, parity circuit design for voltmeters 77−142
DC and AC analogue voltmeter calibration using digital voltmeter *(Polish)* 78−45655
DC digital voltmeter, high-speed, precision 78−8420
DC nanovoltmeter input circuit set-up and choice *(Polish)* 77−49743
DC potentials in low temp. ccts., superconducting chopper amplifier for meas. 77−26306
DC potentiometer for 100 mV-10 nV range, circuit diagram *(Polish)* 78−41332
DC voltage instability meter 79−2790
DC voltage monitor for standard cell using AC Josephson effect 77−82552
decade potentiometer, method for linearised readings 79−21765
dielectric thin-film breakdown voltage and self-healing effects mag. method 79−87388
dielectrics, radiation method for electric potential distrib. meas. 77−41640

voltage measurement continued
diffusion pump power line, voltage monitoring by CMOS cct. 77−5855
digital DC voltmeter, general purpose, description *(Russian)* 77−65047
digital dynamic method for precise meas. of static characteristics 78−54389
digital multimeter, general-purpose, design practice 77−57348
digital multimeter, type Shch68003, with printer output, features 77−74437
digital multimeter technology and future development 77−57345
digital multimeters, MOS/LSI, mains/battery operated, construction and performance *(French)* 77−61090
digital panel meters, noise resist and CMRR improvement, power source interference elimination 80−211
digital voltmeter, AC with double integration, speed increase method *(Russian)* 77−2642
digital voltmeter, amateur construction project *(German)* 77−82542
digital voltmeter, universal, type Shch68001, features 77−74435
digital voltmeter type AD2037 79−58684
digital voltmeter with intermediate freq.-pulse conversion *(Russian)* 77−71347
digital voltmeter with plug-in convertor, type Shch68002, 1 microvolt-1 kV range 77−74436
divider calibration, inductive, between 10 kHz and 100 kHz, international comparison of calibration methods 80−13100
double AC Hall effect system for profiling semicond. impurities 77−37924
DVMs, microprocessor controlled, programmable 78−93720
electric double layer capacity, chronopotentiometric meas., reversible electrochem. reaction effects 78−80753
electrically conducting surface coating, of linear induction accelerator tube, beam losses and coating inhomogeneity 78−5066
electrochemical potentiostatic measurements, automatic resist. polarisation compensator 77−21393
electrometer, high-sensitivity, with modem amplifier 77−74447
electrometers, high-speed general-purpose, features 77−74448
electron microscopes high-voltage supplies, capacitive meas. of slow fluctuations 77−13826
electrostatic precipitator flashover voltage meas. method principle and results *(Polish)* 77−67471
epicardial potential derivation from torso skin potential obs. 77−64148
frequency-voltage convertor using Nb-oxide-Pb tunnel junctions, design 77−82555
gas adsorption on metal film, cct. for surface potential changes meas. by static capacitor 80−62691
glow discharges, high-pressure, electro-optical meas. of current and voltage 78−37033
heater, miniature, for thermo-emf meas. using SiC heating element 79−2764
HF high voltage meas. by electro-optical effect 78−86301
high precision, automatic error correction using iterative method *(Russian)* 78−70089
high voltage sphere gap tech., influence of neighbouring surfaces *(German)* 78−29880
high-accuracy AC voltage standard 77−13771
high-speed SEM voltage contrast waveform display 79−67432
HV electrical meas. by optical methods 78−24822
HV fluctuations, measurement using Mollenstedt electron spectrometer 79−67434
HV measurement using quartz electrogyration effect 77−41656
HV nanosecond transient meas. from pulsed low inductance gas discharge, Kerr effect 78−51380
HV peak value techniques *(Dutch)* 77−67472
HV power supplies, voltage testing techniques 77−74422
hyperaldosteronism screening test with rectal potential difference probe *(German)* 79−16323
IC local voltage measurement by SEM 79−54156
indicator, quadrature, current and voltage, errors components determination 77−74442
inductive voltage divider, calibration by step-up method up to 1 MHz 77−18031
integrating digital voltmeter, for DC bipolar LV meas. 77−37922
integrating recorder of a slowly varying voltage 79−93124
intestinal mechanical and electrical activity recording transducer 77−44862
intramembrane potential jump meas. by potentiodynamic method 80−81778
Josephson devices, voltage standard *(Japanese)* 77−51851
Josephson effect voltage standard, BIPM, France 77−82484
Josephson effect voltage standard, commercial prototype 79−26068
Josephson element principles, applications to precision meas. of electric potential and magnetic flux at high freq. *(Norwegian)* 80−80447
Josephson multiple junction generated higher voltage standard 79−26069
Josephson voltage standard system, influence of voltage divider 78−74027
Josephson voltage standards, future of superconducting instruments in metrology 79−26020
Josephson voltage standards, recent advances 77−18023
Josephson-effect voltage standards, BIPM-and NLP-standard comparison 79−21778
Josephson-effect voltage-standard instrument, features 78−93729
Kelvin method contact PD meas. manipulator 78−57979
laser light measuring techniques *(Japanese)* 80−86342
laser sensing system for elec. and mag. fields in power transmission 77−45870
linear rotary potentiometer nonlinearities compensation 78−45646
low voltage meas. in DC cct. at liquid He temp. 77−37919
maintenance, renovation and repair procedures for multimeters including Avo model 8 79−35795
microphone sensitivity, AC voltage level measuring system 79−50545
microwave voltmeter, broad-band based on hot carrier thermoelec. effects, features 78−21166
MIS structure capacitance-voltage charact. gauge 77−37923
molten semiconductors in strong electric fields, method of plotting volt-ampere characts. 77−87787
MOS structure semicond. surface potential, quasistatic meas. 79−56323
MOS structures, instantaneous characts. meas. *(French)* 77−55616
MOSFET electrometer amplifier type MDM 77−79106
moving-coil expt. for meas. of current and EMF, vel. control technique 80−98939
multilayer Ni deposits, simultaneous thickness and electrochemical potential determination for individual layers 80−71813

voltage measurement continued
multimeter, automatic storage, for DC and AC signals *(German)* 77−10044
multimeter, microprocessor controlled *(French)* 77−74433
nanosecond probe, passive, transmission line model 77−26331
neuronal membrane DC resting pot., automatic offset cct. 77−40940
nitrobenzene, temp. depend. of electro-optic Kerr coeff. 80−2725
nonsinusoidal waveform measurement using analogue multimeters 78−16809
NPL standard voltage monitoring system based on AC Josephson effect 77−82554
NPL voltage standard based on Weston cells, computer control meas. 77−82572
optogalvanic spectroscopy, analytical appls., elec. meas. 78−62231
peak amplitude detector for LV waveforms 77−2666
peak reading RF probe 77−10063
penetrameter cassette, multiple exposure, for meas. of effective kilovoltage of diagnostic X-ray beams 80−61662
photomagnetoelectric effect, contactless measurement apparatus, operation analysis using equiv. cct. 77−41655
photovoltaism of solid discs and flakes, cell designs with variety of contacts 78−24816
plasma potential measurement using scanning multiple collector electrostatic analyzer 79−73046
potential microprofile in electrophotographic films 77−45913
potential-drop meas. system for fatigue crack detection of steel specimens 79−34225
potentialograph, electrical circuit 78−4638
potentiometer, microprocessor-controlled, for nanovolt meas. 78−89502
potentiostat principles and construction *(Dutch)* 77−77856
precision meas. systems for meas. from high impedance sources 78−54402
precision peak and trough detector using operational amplifiers 77−87792
pulse continuous RF signal amplitude and phase difference measuring device 78−12719
pulsed high voltages in vacuum using 2 MV resistive voltage divider 80−31803
in pulsed X-ray device, voltage divider and Rogowski coil *(Japanese)* 78−93788
pulses, HV probe system with subnanosecond rise time 77−10061
ratio/detection system, flexible, for comparing DC voltage developed by AC Josephson effect 79−21774
ratios, in two-bridge gas analyser 80−50907
recording potentiometer, 2-coordinate, method for accomplishing time scanning 77−61080
reference voltage on signal generators, testing with B3-24 compensation valve voltmeter *(German)* 79−54155
reproduction of volt at German ASMW 80−98944
resistive channel, perturbation of homogeneous current path by stub 77−43677
resistive ratio standard, for DC voltage meas. to 10 kV 77−18028
resistive voltage-ratio standard for 10 kV DC meas. 77−5873
RF accurate voltage meas., review 77−18043
RF signal level reference, for instrument calibration 77−115
RF sinudoidal voltage, up to 1 GHz, power meter and bolometer methods 77−82561
RF voltage standard, precision, using thermistor bridge, HF-UHF range 78−89504
RF voltage standard, precision, using thermistor bridge, HF-UHF range 79−21772
RF voltage standard system for voltages from microvolt to 1 V *(Japanese)* 78−89491
RF waveform weighting measuring heads, DC millivoltmeter URV appl. 77−53946
RMS measurement, error estimation in voltmeters 80−22381
RMS measurement errors quantified 80−57274
RMS value meas. devices and theory *(Dutch)* 77−87791
rocket carrying electron gun, electrical potential determ. device 79−21146
selfcalibrating AC potentiometer, theory 77−82570
SEM, min. measurable voltage estimation 77−82646
SEM, voltage meas. system improvement 77−49813
SEM, voltage meas. via new electron energy analyser 77−54019
SEM stray field reduction for voltage contrast meas. 79−67431
SEM voltage contrast mode at semiconductor surfaces, anal. of conditions *(Czech)* 79−35897
semiconductor, current and voltage fluctuation determ. by noise spectral density meas. 80−15577
semiconductor, molten, quartz cells for elec. cond. and thermo-EMF meas. 77−74439
semiconductor contact potential and conductivity simultaneous automatic meas. 78−21118
semiconductor differential thermal EMF measurement device for solid, fusion region and melt states 78−12716
semiconductor film, cell for measuring electrophys. parameters over wide temp. range 77−51830
semiconductor-liquid junctions, differential capacitance measurement by desk calculator controlled system 79−78170
semiconductors, airtight cell for simultaneous conductivity and thermo-EMF meas. 78−21168
small DC voltage, to ±15 nV, CMOS analogue gates at low temp. 79−35776
standard, cryogenic comparator for Josephson standard 77−18030
standard cell, combination type, composite amalgam electrodes, low temp. coeff. 77−18026
standard cell, temp. controlled enclosure with 25 μK stability 77−18027
standard cell calibration, using supercond. junction device 77−18029
standard cell calibration against Josephson voltage reference 77−5874
standard cell EMF stability testing, thin-film tunnel Josephson function method 77−67468
standard cell group enclosure monitored by AC Josephson effect 79−26076
standard cells, low resistance differential potentiometer appl. *(Polish)* 78−29127
standard cells combination with low temp. coeff. for Josephson voltage standard maintenance 80−101788
standard cells with low temp. coeff., characts. 80−101090
standard representative of ohm and volt, January 1977, France *(French)* 79−26077
standard using Josephson effect *(German)* 78−93722

voltage measurement continued
standard volt by BIPM since 1932 77−82566
student experiment, establishing V=L(dI/dt) directly 77−37688
subcellular particle membrane pot. difference, compensation meas. method 77−56547
superconducting magnet, pulse loss and voltage meas., elec. method 77−37949
surface balance, monolayer parameters meas. in radiation field 78−82092
surface potential distribution meas. by vibrating electrode 79−67340
surface potential meas. in high vac., vibrating capacitor method modification 77−71343
surface potentials visualisation and meas., using SEM 80−68307
system for use with Josephson device in maintaining voltage standard 78−93730
thermal EMF in ultrahigh, vacuum electron microscopy 79−26184
thermo-EMF coeff., non-steady-state method 79−85150
thermoelectric voltage across relay contact for different metals *(German)* 79−26040
transducer with unified output for measuring effective value of AC voltage 78−74028
transients, fast digital technique *(Polish)* 80−86340
tree root potential meas. electrode earthing method *(Russian)* 80−26420
true RMS measurement using electronic methods 78−24819
true RMS voltage indicator system 78−12713
unit voltage comparison with working standards, Josephson effect 77−53941
utilising Josephson effect, voltage reference system *(French)* 77−67470
valve voltmeter, static HV, for DC/AC peak-voltage measurement *(German)* 79−58757
vector voltmeter used for microwave measurements with the aid of high speed sampling 78−8418
volt dissemination method and standard cell enclosure design 80−98876
volt realization, method and equipment based on fundamental physical consts. and superconductivity phenomenon 80−98943
voltage cell using Josephson junction, computer simulation 79−93089
voltage standards, using Si reference diodes 80−62619
voltage transfer standard based on AC Josephson effect, standard cell calibration appl. 77−82553
voltage-time derivative, determ. from slowly varying voltages 77−82546
voltage/pH convertor, using operational amplifiers *(French)* 79−63267
voltmeter, analogue, with storage cct. *(German)* 79−12814
voltmeter, LF, fast response, microprocessor-based, for true RMS value 78−89503
voltmeter frequency error reduction using eccentric and elastic transducer *(Bulgarian)* 77−61082
wideband current and voltage comparators 77−57356
X-ray system tube, high security 79−35794
X-ray tube kVp meas. with Si p-i-n photodiode *(German)* 79−232
AgBr crystals, electrical potential distrib. near interface, recording using automatic device 79−24759
Ca-selective membrane electrodes, asymmetric, potentiometric meas. 77−77785
Cd-Sn-Pb composite amalgam electrode standard cells and combinations 77−5871
Ce^{4+}/Ce^{3+} dosimeter, adsorbed doses, potentiometric determ. 78−94146
O^{2-} low partial press., thermogalvanic meas. using O^{2-} ion conductors 80−73389
Pb-Pb_xO_y-Pb Josephson junction, long-term stability at liq. N_2 temp., voltage standard 77−72945
SF_6 breakdown voltage at high pressure meas. *(German)* 77−55181
Si-insulator structures, contact pot. meas., vibr. condensor method *(German)* 79−11232

voltage multiplier rectifiers *see voltage multipliers*

voltage multipliers
see also potential transformers
IC use in wattmeter 77−53930

voltage quadrupler rectifiers *see voltage multipliers*

voltage reference diodes *see avalanche diodes; Zener diodes*

voltage regulation *see voltage control*

voltage regulator diodes *see avalanche diodes; Zener diodes*

voltage regulators
see also voltage control
commutqable source of reference voltages in ionospheric plasma probe meas. 80−31192
dental pain reliever with increased stabilisation of working current 77−48922
electrostatic high voltage generator for TEM, stability improvement *(French)* 78−62268
high-voltage DC stabiliser 78−4642
intensity regulator for 5 to 50 keV electron guns *(French)* 78−54499
laser primary regulated dual power supply 79−98396
neutral beam power supply, series switch/regulator system, 40 kV, 80 A, 10 ms, for fusion reactor 78−66366
neutral beam source 8 MW voltage series regulator, for fusion reactor 78−70631
phototransducers in tide-recording equipment, voltage and light output ratio stabilisation *(Russian)* 78−88949
power-supply block for ion source with electron bombardment 78−8467
precision measuring ccts., large, small current filters, semiautomatic testing DC instrument appl. 77−53940
pulse-operated voltage stabiliser 78−4641
reference cct. with adjustable temp. coeff. 79−30407
solar array shunt regulator hot spot problem and countermeasures 79−96460
stabilised voltage supply, 2000 V and 2×200 V, current-carrying, for ion source *(Czech)* 77−5963
stabiliser attachment circuit 78−57981
tuned limiter for receiver amplifier in a fast-recovery pulsed NMR spectrometer 78−70173
US flaw detector supply, portable 77−90573
wire chamber powering, current-limiting technique 77−54424
X-ray electron spectrometer appls. 78−21307

voltage stabilizers *see voltage regulators*

voltage transformers *see potential transformers*

voltage transients *see transients*

voltammetry (chemical analysis)
see also polarography
AC, on-line digital FFT faradaic admittance data acquisition 78−61118
acetate aqueous soln., polarisation curve anal., Pt electrode *(Japanese)* 79−34319
anodic oxidation mechanism obs., of ethyl alcohol and acetaldehyde 79−57247
anodic stripping semidifferential electroanal. with Hg film electrode 79−79324
anodic stripping voltammetry, standard addition method, evaluation and optimisation 79−16058
automatic controller for voltammetric anal., design, operational sequence 80−71968
bipotentiostat of simplified design 80−35589
blood, thin layer differential pulse voltammetric anal. 78−20089
catalyst surface characterisation by cyclic voltammetry, review 78−40092
ceramic glazes, Pb, Zn and added chromogenic ions release, as function of colouring oxide mill additions, voltammetric exam. 78−39920
chronocoulometry, square root of time mark generator using TTL digital ccts. 80−35588
chronopotentiometry, programmed current, electrode process followed by chem. reaction 80−35595
coulometer, controlled-pot., design, operation, anal. appls. 77−25335
coulometry, potential scanning, chem. react. appls. 77−25281
coulopotentiograph system, automatically controlled, for trace analysis of metal ions 79−92026
cyclic, for accelerated corrosion life tests of PbO_2 electrode 78−31582
cyclic and linear scan voltammetry 77−48711
cyclic differential pulse, computerised instrumentation 78−85235
cyclic staircase voltammetry, expt. evaluation 79−74434
cyclic voltammogram, effect of slow two electron transfers and disproportionation 78−56938
cyclic voltammograms at spherical electrodes, switching pot., drop size effects, digital simulation technique 80−40766
data treatment, extrapolation of forward current to back peak pot. 78−61076
differential cathode ray polarograph, exam., determination of Cd, Zn 78−56930
differential pulse anodic stripping voltammetry, in thin-layer cell 77−36812
differential pulse anodic stripping voltammetry at hanging Hg drop electrode, multiple cell system 77−32847
differential pulse voltammetry, stationary electrodes, computer based instrum. appls. 77−36809
differential pulse voltammetry at dropping Hg electrode, computerised instrumentation 79−79326
digital signal generator for rapid scan differential pulse voltammetry 80−61182
diminished electrolyte, semi-integral electrolysis using voltammetry 79−70339
electrode reaction, number of electrons involved determ. method 80−35596
electrode surface, partially covered, eqns. for chronopotentiometry 78−85236
electrode-electrolyte interface, solid film props., review of expt. techniques 77−77780
electrodes for inversion voltamperometry with alternating current 79−70333
environmental sample, anal. by anodic stripping voltammetry 79−11836
heavy metal ion concentration, detection in water by electrochemical methods *(German)* 79−92039
intermodular AC phase-selective 77−29057
Kalousek polarography, computerised high accuracy 79−52792
Kel-F-graphite composition electrode, voltammetric appls. 78−92489
linear sweep, appl. to electrode mechanisms *(Italian)* 77−16871
linear sweep anodic stripping voltammetry, recursive estimation evaluation 80−26067
linear sweep voltammetry, charge transfer, diffusion control 80−45583
liquid chromatography, use of electrochemical detection methods 80−50906
micromolar analysis by ring electrodes shielding at rot. ring-disc electrode 79−92018
microprocessor-assisted flow-through anodic stripping voltammeter for oceanographic appls. 78−36324
natural water chem. anal., modulated polarographic, voltammetric techniques 77−37253
organic compounds, classification from voltammetric data, computerised pattern recognition 79−16057
oyster, thin layer differential pulse voltammetric anal. 78−20089
pattern recognition techniques, for interpretation of severely overlapped data, theory 78−7254
pattern recognition techniques, for interpretation of severely overlapped data, expt. 78−7255
phase selective anodic stripping voltammetry, review 80−40788
pigments, photochemical ionisation reactions in soln., automatic conductimetric instrument for kinetic studies 77−4971
potentiostat, double probe compensation system, resist. characts., slope optimisation 77−44568
pulse polarograph, with stationary electrodes, rapid scanning modifications 78−3402
solid electrodes, behaviour in normal and differential pulse voltammetry 78−73055
soy bean, thin layer differential pulse voltammetric anal. 78−20089
square wave voltammetry, at dropping mercury electrode, exptl. appls. 78−35734
square wave voltammetry, at dropping mercury electrode, theory 78−35733
staircase voltammetry, microcomputer-controlled polarograph appls. 80−66895
staircase voltammograms, synthesis, anal., convolution, devolution 77−25336
static mercury drop electrode 80−97740
steel, C, potentiodynamic behaviour, in conc. NaOH, cyclic voltammetric obs. 79−16006
thin layer electrochemical cell *(French)* 77−12854

voltammetry continued
thin layer potential sweep voltammetry, regeneration mechanisms 78−53291
thin-layer differential pulse anodic stripping voltammetry 78−20089
thionine-coated electrode for photogalvanic cells, electrochem. and XPS anal. 80−72071
p-tricyanovinylphenyldicyanomethide ion, donor props., cyclic voltammetry and π-complex form. 80−88520
ultratrace analysis by differential pulse anodic stripping voltammetry, new technique 78−40100
Ag halide microcrystals, electron acceptoring props., chronovoltammetry 79−20441
CdTe electrode, redox reaction due to complex $M(CN)_6^{3-/4-}$ *(French)* 80−89482
Cu, cyclic and anodic stripping voltammetry, appl. to natural waters anal. 79−74446
Cu-rare earth oxide-Y composite coatings, oxide and Y effect on coating precipitation 80−55554
H, adsorption on Pt electrode surface, exam. by triangular sweep cyclic voltammetry 79−70342
Hg, determ. in sea and inland waters, differential pulse anodic stripping voltametry method 77−70361
Hg electrode, membrane coated, continuous voltammetric anal., appls. 77−25341
Hg, rotating thin film electrodes, staircase voltammetric stripping anal. 77−12843
$Li/SOCl_2$ primary cell, cyclic voltammetric and coulometric obs. of $SOCl_2$ reduction 80−30440
$NaCl-AlCl_3-CrCl_3$, molten, electrochemical exam. of Cr 78−56939
O_2 concentration meas. in tissue, pulse-mode method, equipment 78−7551
Pb complex, $Pb(C_2O_4)_2^{2-}$, stoichiometry, form. const. determ., teaching appl. 79−84916
$Pb-H_2SO_4$ cells, Sb alloying effect on solid Pb electrochemical properties 80−55668
Pt (100), (110), and (111), form. of Cu monolayer, optical and electrochem. studies 79−99419
Pt electrode, in Na_2SO_4-NaCl melt, polarisation meas., reactions 78−68898
Pt electrode (100), (111), polycryst. surfaces, comparison of electrochem. activity 78−61015
Pt, low index surface, adsorption of O_2 reduction intermediates at steps 79−70343
Ru electrodes, adsorption and surface reactions, cyclic voltammetry and X-ray emission spectrometry 78−61018
WO_3 electrodes, vac. evaporation and anodic oxidation prep., electrochromic process kinetics 79−100390
$Y_2Ti_2O_7$, precipitation from oxalates, carbonates, exam. 80−55641
Zn, electrode in alkaline soln., exam. of surface state by potentiodynamic voltammetry 80−85187
$ZnSO_4$ electrolyte, simultaneous determ. of Pb, Tl by anodic stripping voltammetry 77−12844
$ZnSO_4$, electrolyte evaluation by cyclic voltammetry and SEM 77−29076
$ZnSO_4$ electrolytes containing Ge and Co, polarisation charact., exam. by cyclic voltammetry 80−104444
ZnTe electrode, redox reaction due to complex $M(CN)_6^{3-/4-}$ *(French)* 80−89482
ZrO_2:Cu, point defects, electrochem. characterisation 80−35599

voltmeters
see also digital voltmeters; potentiometers
AC, ambiguity, in equivalent noise bandwidth approximation 78−4662
AC, calibration, standard apparatus using thermoelectric convertors, 20 Hz to 1500 MHz 77−18036
AC, lock-in, for small voltage meas. *(Czech)* 77−13779
AC, transistorised, type TF 2600B 77−53934
AC voltages, small, combined meter checking 80−13057
analogue, with storage cct. *(German)* 79−12814
checking using UPMA-3, extension of meas. limits 80−13058
circular-scale 240° moving-iron AC ammeters and voltmeters 77−57360
CMOS operational amplifier applic., to 50 V in four ranges 77−41653
DC, low voltage in high ohmic circuits meas., using op amp based auxiliary equipment *(Czech)* 78−4664
DC electro-optic voltmeter, direct reading, with high input resist. 78−245
DC microvoltmeter, electronic, design and operation *(Czech)* 77−61092
DC microvoltmeter based on modem 80−31798
DC microvoltmeter with 3, 10, 30 and 100 μV ranges *(Russian)* 78−8422
DC nanovoltammeter based on modem 80−31797
DC nanovoltmeter input circuit set-up and choice *(Polish)* 77−49743
digital type AD2037 79−58684
electrometric voltmeter input capacitance absorption meas. 77−79107
electronic, checking at HF 79−67343
electrostatic kilovoltmeter errors in unearthed circuits 77−13773
error estimation and use 80−22381
femtovoltmeter and voltage tunable heterodyne receiver based on DC resistive SQUID 79−63276
FET voltmeter with high input impedance *(Spanish)* 77−37934
field mill, electrostatic field meas., school use 78−16613
frequency error determination over wide range 80−4734
frequency error reduction using eccentric and elastic transducer *(Bulgarian)* 77−61082
frequency measurement applications *(French)* 80−22331
galvanostatic potential meas. apparatus for automatic accumulator testing 77−30185
generating voltmeter, appl. to ion beam energy meas. of Van de Graaff accelerator 78−58508
HF millivoltmeter, 50 KHz to 50 MHz range, cct., construction details *(German)* 78−4630
high impedance, using DC amplifiers, student laboratory appl. 78−12505
impedance multiplier circuit 77−41649
kilovoltmeter for X-ray equipment 80−13191
kilovoltmeters and HV scale convertors, certification using highly accurate test apparatus 79−80606
LF, fast response, for true RMS 2 mV-10 V range 79−21770
LF, fast response, microprocessor-based, for true RMS value 78−89503
LF millivoltmeter, range 0-100 mV at frequencies from 20 to 100 KHz *(Spanish)* 80−13060

voltmeters continued
maintenance, renovation and repair procedures for multimeters including Avo model 8 79−35795
microwave, broad-band, based on hot carrier thermoelec. effects, features 78−21166
microwave measurements made by vector voltmeters with the aid of high speed sampling 78−8418
millivoltmeter, for 5 mV DC and 2 mV AC 77−37932
millivoltmeter, high sensitivity amplifier attachment, LF operation appl. *(German)* 78−74032
millivoltmeter, instantaneous peak value response, biomedical appls. 80−42208
millivoltmeters, chemical analysis appl., 1978 exhibition in Munich *(German)* 79−20482
minivoltmeter electronic, 500 μV to 100 V, current meas. in 10 nA range *(Spanish)* 78−54408
NMR absorption peak voltmeter cct. error analysis *(Russian)* 79−26079
pyrometric, temp. meas. of rotating object, non-contact method 79−35742
RF, types and uses 79−80639
RF accurate voltage meas., review 77−18043
sample-and-hold voltmeter for time-related meas. 77−57347
SQUID, DC, circuits, optimisation 80−13056
SQUID, DC, noise limitations 79−21784
SQUID picovoltmeter operating in mag. fields up to 3.2 T 79−58698
transistor, high-Z input, 10 mV to 400 V, using operational amplifiers 79−80646
true RMS voltage indicator system 78−12713
true RMS voltmeter with IC 78−86288
valve B3-24 compensation voltmeter for testing reference voltage on signal generators *(German)* 79−54155
valve voltmeter, static HV, for DC/AC peak-voltage measurement *(German)* 79−58757
wide range, AC and DC, construction project 78−12724
wideband AC electronic voltmeter *(Spanish)* 78−86304
wideband electronic voltmeter testing installation 77−79119
ZnS:Cu,Cl, electrolum. voltmeter design, accurate high-voltage meas. 78−24813

volume control
cation-exchange sorption microcalorimetry, automatic micro-injection system 78−24777
circulatory assist apparatus, stabilisation of gas vol. in pneumatic transmission unit 80−3863
posthaemorrhage blood volume control model for intravenous fluid therapy 77−40697

volume control (gain) *see gain control*

volume diffusion *see diffusion in solids*

volume measurement
abdominal fluid accumulation meas. using electric impedance 77−48912
alloys thermal expansion coefficient, and volume effect anomalies during transformations, review of differential dilatometric error sources *(Russian)* 79−34223
anatomic deadspace meas. in mechanically ventilated patients, using N_2 washout 79−96694
anatomical feature or lesion volume estimation algorithm 80−98080
apparatus volumetric calibration by cryogenic Xe gas transfer 78−93653
arterial impedance plethysmographic signal quantitative interpretation 79−57742
beat-to-beat stroke volume estimation from pulmonary arterial pressure contour 79−53178
biomedical volume estimation, computer algorithm 80−98043
body organ volume determination by US scanning 80−17034
body organs, in vivo meas. using computer-based u.s. echography 77−2033
bubbles, acoustical meas. of gas bubble volumes and gas flow rates 80−62633
calibration of nuclear materials accountability tanks 80−68829
capacitance sensors for phase percentage determ. in multiphase pipelines 80−62625
capillary, differential capacitance manometer for fast volume determ. 77−87734
cardiac left ventricular ejection fraction meas., scintigraphic count-volume and geometric methods compared 79−83896
cardiac stroke volume meas. from impedance, rel. to aortic flow waveform 77−86522
cardiology, radioisotope sequential meas. of ventricular vols. and cardiac output 80−94319
complex shape bodies, pneumatic-freq. method using air compression *(Polish)* 79−49199
dental moulding volumetric variation meas. holographic interferometry 79−88214
dielectrography methods and apparatus, recording capacitance changes due to blood vol. fluctuations 78−57046
differential dilatometer for detecting volume changes in specimen under H_2 attack 79−17395
dilatometer, high-temp., for meas. shrinkage kinetics of liquid-containing ceramic materials 79−17396
dilatometer, meas. thermal dilatation of metallic amorphous ribbons 80−86258
dilatometer for PVT meas. of liquids and plastic crystals at low temperature 80−68208
dilution dilatometer for excess vol. meas. 77−48678
dynamic measurements of liquid quantities, international harmonisation 79−68840
flow, CW NMR to determining volume fractions and flow rates of component mixtures 80−33710
fluid volume evaluation in spherical vat with deformable metal diaphragm 77−57310
gas, forbidden volume, van der Waal's gas equation 77−60864
gas parameter determ. using total internal reflection 77−58839
gas volume counter calibration, gravimetric standard method *(German)* 77−55112
gas-dynamic gauge, infrasonic, with pressure pulsations stabilisation 77−5806
gas-liquid mixtures, flowing, gas conc. meas., acoustic method 78−59448
glass capacity measures testing, measurement standards, appl. 79−6085
heart imaging from computerized tomography 78−88741
iceberg volume meas. using photogrammetric techniques 77−82048
impedance plethysmography, influence of erythrocyte vel. 78−61238

volume measurement continued
laboratory practices, devices repair and checking *(German)* 78−32803
left ventricular volume rel. to QRS voltage and Frank vectorcardiogram 79−44029
lung closing volume meas. using acoustic He analyser 78−61223
lung volume, online calc. by digital computer 80−72351
lung volume estimation method, constant inflation pressure 80−67306
lung volume measurement from supine portable chest radiographs 80−81703
measuring bell jar pressure and flow rate constancy under rapid shift 77−58825
medical, algorithm based on polyhedral approx., using US or CT data 80−104790
metallic bellows dilatometer, calibration 77−82487
nuclear materials accountability, tank volume calibration algorithm 80−83159
nuclear materials accountability tanks, automated calibrator 80−83158
pneumatic devices, internal gas volume measurement based on Boyle-Mariotte's rule *(Hungarian)* 79−49196
pneumotachograph, for flow and vol. meas. in normal and dense atm. 77−5120
polymer, volume dilatometer design 78−5706
porosimeter−volumetric apparatus *(Hungarian)* 79−40531
pulmonary diffusing capactiy, anatomic dead space meas. 77−25502
pulmonary gas volume using acoustic pneumograph 77−48913
pulmonary volume calculator, automatic analogue device, performance in hospitals *(French)* 78−31930
pulmonary volume meas. by closed-cct. He mixing method, reproducibility 77−48904
rapid and accurate meas. apparatus for press. and vol. 79−88972
respiration remote meas. instruments, appl. to studies in centrifuge 77−77996
respiratory flow-volume integrator 77−48914
respiratory monitor and histogram computer for rodent studies 77−52944
respiratory test performance indicator for subject motivation 79−57797
sensor for conductive liquids using array of point sensors 80−68177
solution component quantity determination using two-coordinate potentiometer 78−93657
steel, stainless volume changes during phase changes, meas. using low temp. differential scanning dilatometer *(Russian)* 79−34224
stereological method for rapid volume ratio estimation 79−80571
timber volumetric meter *(Russian)* 80−57253
two-phase systems, volume fraction determination using helical capacitance sensors 79−75516
US bladder volume sensor, pocket-size 80−36034
US renal volumetry in children, accuracy and simplicity of the method 80−98044
vacuum vessels, volume ratio determ. by successive expansion method 79−172
vectorcardiographic P loop correlation with left atrial volume echocardiogram 79−44025
ventricular volume determ. from indicator dilution curves, dog expts. 79−57696
Ar, compressed gas, PVT meas. at high press. 80−98927
Fe based porous metals, exam. of volume change under high pressure 78−52906
Ni based porous metals, exam. of volume change under high pressure 78−52906
V_3Si volume changes during phase changes, meas. low temp. differential scanning dilatometer *(Russian)* 79−34224

vortex flow *see vortices*

vortex flow (superconductivity) *see flux flow*

vortex lattice pinning *see flux pinning*

vortex state (superconductivity) *see mixed state*

vortex structure (superconductivity) *see flux-line lattice*

vortexes *see vortices*

vortices
see also cavitation; turbulence
acoustic destabilization of vortices 79−32533
acoustic noise emission in flow past vibrating rigid bodies 79−23310
acoustic radiation from bodies in unsteady flows 80−69799
acoustic streaming in air, vorticity determ. *(French)* 79−59858
acoustic wave scattering by temp. and vel. inhomogeneities 79−50491
acoustic-vortical turbulence struct. 78−83373
acoustically excited jet, discrete noise spectrum, vortex pairing 80−74847
aeroacoustic source distribution, integral representation, general theory 79−50492
aerodynamic flow, vortex-induced side force on slender bodies 79−14408
aerodynamic flow round wing section with two vortex sources, calc. *(Russian)* 77−31318
aerodynamic sound generation by unsteady subsonic flows around rigid bodies 80−69798
aerodynamics, discrete vortices method and multidimensional singular integral eqns. theory 80−19421
aerofoil, oscillating, viscous incompressible flow, finite element anal. 80−38427
aerofoil, thin, windward surface shock layer, hypersonic flow 78−34158
aerofoil in unsteady airstream, two-dimens. viscous flow, numerical predictions 78−75166
aerofoil in unsteady viscous flow, numerical soln. procedures 78−75165
air, damp, working characteristics of vortex tubes *(Russian)* 80−74903
air, vortex ring interaction along parallel axes 77−27537
air vortex radius during liquid flow in centrifugal atomizer 77−80201
aircraft vortex wakes, neutral atmospheric effects on dissipation 79−32528
aircraft wake, vortex interactions and decay 77−58695
aircraft wake vortices, tracking system based on acoustic refr. scatt. 77−46840
airfoil trailing edge noise, near-wake struct. and unsteady pressures at trailing edge 80−69794
airscoops, vortex filament-shock front interference, vortex dissipation 80−10253
Alboran Sea, mesoscale oceanic vortex, drifting buoy and satellite meas. *(French)* 79−16473
alternating vortices in presence of wall *(Italian)* 77−54998
annular fluid jets, small inner diameter, investigation of vortices by schlieren photography 80−74935
annular jet inner regions, jet and wake vortices 79−86479
annulus with inner rot. tube, heat transfer 79−1204

vortices continued
aortic and mitral valve prostheses, in vitro flow visualisation 77−86703
arc, axial flow stability, cathode emission mechanism change effect 78−83638
arteries with longit. ridges, flow field and mass transport anal. 77−44702
artificial membrane lung, fluid vortices and mass transfer 77−52919
Atlantic Ocean, cyclic currents system as plane vortex with elliptical nucleus 77−53466
atmosphere, boundary layer structure of axisymm. vortex, lower boundary condition effect 79−25298
atmosphere, convective vortex model, unsteady two-cell similarity soln. 79−16626
atmosphere, divergence and vorticity from observed winds over India during monsoon 78−7695
atmosphere, eddy viscosity in two and three dimensions 77−5289
atmosphere, effect of subjectively enhancing initial vorticity field in short-range numerical forecast 80−82008
atmosphere, global vorticity budget over tropics and subtropics at 200 mb during northern summer 78−40640
atmosphere, interlatitudinal angular momentum exchange 79−39834
atmosphere, low vortex over S.E. Chinghai-Tibetan Plateau, annulus expt. simulation *(Chinese)* 77−70787
atmosphere, meridional fluxes of pot. vorticity *(Russian)* 77−81960
atmosphere, oscill. model of action centres, vortices interactions *(Russian)* 80−4075
atmosphere, sailplane flights through funnel clouds 78−69396
atmosphere, spiral bands in linear model of cyclonic vortex 77−25736
atmosphere, surface layer, meas. using acoustic echo sounder array 78−7810
atmosphere, topographic influence on surface wind 78−81266
atmosphere, vorticity conservation as criterion for evaluation of barotropic schemes *(Russian)* 77−64369
atmosphere, vorticity dynamics anal. of two and three dimensional turbulent flow 78−69395
atmosphere flow, vorticity eqn. rel. to aperiodic trajectories and stationary points 77−5287
atmosphere global scale transport processes *(Dutch)* 78−3889
atmosphere large-scale eddy transports, linear parameterisation 80−17361
atmosphere tropical belt, local vortex propag., numerical expts. *(Russian)* 77−21847
atmosphere vorticity area index, correl. with solar plages 78−73459
atmospheric, potential vorticity conservation by finite difference eqns. in generalised vertical coordinates 80−26576
Atmospheric Cloud Physics Laboratory simulation, vorticity transport eqn. solns. 80−94690
atmospheric thermally driven vortices, numerical model, dust-devil dynamics appl. 77−17191
atom and mol. wavefunction nodal topology, quantised vortices and paramagnetism 77−46476
axial flow fans, aeroacoustic mechanism for rotor-vortex interactions 79−3849
axial turbomachine, cascade and through-flow theories as inner and outer expansions 78−75148
axially symmetric flow between coaxial circ. cylinders 79−64669
axially symmetric form of biharmonic eqn., elec. analogue technique for approx. soln. 77−27502
axisymmetric flow in slot between coaxial cylinders *(Russian)* 78−14019
axisymmetric laminar boundary layer, swirling flow through conical hydrocyclone, heat transfer 79−98733
axisymmetric starting vortices, visualisation using laser-induced fluoresc. 77−35283
backwash vortex under waves running up sloping bed 80−100001
Barotropic fluid in semi-Riemannian manifold, classical and relativistic vorticity 78−65842
Benard Karman street of vortices generated in asymmetric fluid field *(Italian)* 78−83406
Bianchi universes, magnetic fields and fluids with conductivity 80−83864
bifurcation in steady flows of viscous fluid, expt. 78−30267
bifurcation in steady flows of viscous fluid, theory 78−30266
biharmonic equation, analogue technique, cylinders falling between parallel walls 78−55628
biphase liquid, vortex flow, calc. of discrete component motion velocity and distrib. *(Russian)* 79−90320
biphase liquid cylindrical vortex, mass force effect on dispersion phase distrib. *(Russian)* 80−79388
blades, three-dimens. annular array, aerodynamic forces with nonsteady flow 80−99991
Blasius flow, horizontal, heated from below, longitudinal vortices onset 78−71342
blood flow in branching vessels, visualisation using water model 77−25477
bluff bodies, cavitating, constrained flow, drag and vortex shedding 78−47006
bluff bodies in shear flow producing vortex streets 79−59987
bluff cylinder vortex shedding, universal wake Strouhal number 78−46976
bluff cylinders, vortex shedding freqs. at low Reynolds no. 77−35147
body of revolution, slender, nonlinear normal forces, Reynolds no. influence *(German)* 78−51191
body of revolution, tail region flow vorticity calcs. 80−69845
body-propeller combination, numerical soln. including swirl and data comparisons 80−19407
boiling, mechanism model based on rotating vortex model with spatial heating 80−14694
Bose systems, free, infinite, condensation region 80−73259
boundary layer, nonstationary, with self-induced press. 78−34164
boundary layer, transitional, oscills., stability waves, vortices 78−38287
boundary layer flow, atmospheric, turbulent modelling, predictor-corrector multiple iteration 77−91237
boundary layer flow on end wall of vortex chamber 77−7403
boundary layer form. in inviscid flow with vorticity 78−14022
boundary layer temperature fluctuation space correlation coeff. in turbulent core *(Russian)* 78−14001
boundary layer turbulence, quantitative model for momentum exchange by coherent motions 79−7372
boundary layers, incompressible, vortex sheet approx. 78−67201
boundary layers beneath pot. vortex, finite-difference schemes 77−14982

vortices continued
bounded container, statistical mechanics of two-dimens. vortices 77−3831
bounded turbulent shear flow mechanism obs. 78−90854
breakdown flowfields, spectral characts. in water 80−19408
breakdown regimes, in rot. cylindrical cavity, identification 79−50731
breakdown structure, book contrib. 78−59407
breaking gravity-wave flow near tip, time-dependent free-surface flows 80−83808
buoyancy induced flow over inclined heated porous surface, vortex instability 80−33601
buoyant surface jets analysis for heated plume characts. prediction 77−15087
burning vortex ring, turbulent, acoustic emission 78−94676
bursting phenomenon in bounded turbulent shear flow, streamwise vortices 80−1600
cambered wings, vortex lift predictions 77−31311
cascade, with large-deflection oscills., unsteady aerofoil theory, numerical soln. *(Japanese)* 78−67211
cascades with different trailing edge thicknesses, vortex shedding freq. determ. 78−75152
cavity, square, 2-D, recirculating flow of incompressible fluid, large Re, convergence of finite-difference schemes 80−33611
cavity flow, broadband noise generation, vortex model 77−75900
cavity flow, columnar vortices 80−24037
cavity flow past cylindrical induces in venturi 77−31347
centrifugal instabilities in finite containers, periodic model 80−106783
channel, annular, with vortex generators, and uniform (nonuniform) heat injection length, crit. heat flux *(Russian)* 78−83397
channel, curved rectangular, secondary flow, Taylor-Gortler vortex pattern 80−106849
channel, laminar boundary layer, Gortler vortices 80−64572
chaotic flows of autonomous dissipative systems 80−73176
chaotic Taylor vortex flow, dynamic instabilities and transition 79−94630
chordwise variation in vorticity, approxs. for use in panel methods 78−18306
circular cylinder, impulsively started, time-depend. flowfield 77−3826
circular cylinder, turbulent crossflow in vortex zone 80−10252
circular cylinder flows, coherence function method 80−96068
circulatory viscous incompressible liquid flow, momentum eqn. anal. *(Russian)* 79−59992
closed stationary cavity form containing homogeneous vortex motions of ideal incompressible liquid *(Russian)* 79−64671
closed torus in Stokes flow, eddy-type motion and vortices 77−42850
cloud, motion of a large dusty buoyant thermal with a vortex ring 79−48561
cloud vortex and eddy formation over California coast 77−70732
coaxial jets, correl. covariance meas. in initial region 77−84289
combination of potential and vortex flows, boundary value problem for incompressible liquid *(Russian)* 77−68595
combined free and forced convection, periodic vortex formation 80−74878
combustion chamber, acoustic mode excitation by vortex shedding 80−19150
compressible boundary layer flows, curvature near separation 78−55661
compressible free vortex flow, boundary-value problem 78−26139
compressible nonadiabatic gas flow in tube, eqns. system numerical integration *(Russian)* 78−83427
concentration interface in turbulent mixing layer, visual growth 80−38392
condensed Bose system, roton spectrum 79−63133
conditional eddies in isotropic turbulence, higher order estimates 80−92119
conference, computation fluid dynamics, Rhode-Saint-Genese, Belgium (March 1977) 77−80134
confined vortex flow characts., expt. 78−5749
confined vortex oscillator, mathematical model 78−14104
conical surface, boundary layer due to swirling flow with throughflow 77−47024
convected turbulence, vortex shedding influence on noise generation 77−3830
convection, forced, turbulent, in square cavity, shear effect 79−1180
convection, free, 2D flow, steady state, finite element anal. method 77−75910
convection, time dependent, double diffusive, stability in inclined slot 78−5744
convection currents in axisymmetric cyclone 80−77084
convection in channel downstream of constriction, local transfer coeffs. augmentation 78−5800
convective diffusion problems, finite element solns., Navier-Stokes eqns. 80−1583
convective instability in thermal entrance region of heated channel 77−42812
convergence, vortex methods for Euler's equations 80−33614
cooling tower plumes 79−20950
corner, three-dimens., Navier-Stokes eqn. soln., numerical code 78−30314
cosmology, early evolutionary stages of universe spatially inhomogeneous models *(Russian)* 80−4467
Cosserat continuum, analogy between disclination rank and vortex line invariant *(French)* 78−1977
Couette-Taylor flow, laser Doppler velocimetry obs. of transition to turbulence 80−92163
counter gradient flow downstream of two different diameter cylinders *(French)* 80−43693
cross flow induced vibrations, vortex shedding in a heat exchanger tube bank 79−3957
cross stream-jet mixing, near field influence on mass, momentum and vorticity fluxes 77−39320
crossflow developing in boundary layer during longit. flow around right dihedral angle 80−59049
curved semicircular duct laminar flow, secondary vortex flow 80−106847
curved tube, wall shear rates in entry region, vortex struct. 79−81972
curved wall power fluidics characts. 80−103053
cyanine dyes, J-aggregates, swirl-induced optical activity 78−72482
cyclone centre location using kinematical determinant 80−56535
cyclone development along weak thermal fronts, model soln. 80−81994
cyclone forecasting applications to typhoons 77−25801
cyclone formation mechanism for monsoonal mid-troposphere 79−34913
cyclone genesis in Mediterranean and Ligurian Sea *(French)* 79−48534
vortices continued
cyclone in Arabian Gulf, 1977 June, development and severity 78−69429
cyclone interaction, NCAR objective analysis v. subjective analysis 77−86985
cyclone waves and front development, surface friction effects 77−86966
cyclone-anticyclone couplets, vorticity budget 80−8391
cyclone-anticylcone couplets, quasi-Lagrangian kinetic energy budgets 77−66958
cyclones, pressure drop reduction using deswirler 79−12176
cyclonic storm, Arabian Sea, 1976 June, diurnal var. and secondary vortices form. 79−20915
cylinder, axisymmetric, with slanted base, near-wake flow 80−74886
cylinder, circ., near-wake obs. by temp. fluctuation meas. 78−51168
cylinder, circ., oscillating in turbulent water flow, press. fluctuations 79−59995
cylinder, circular, wake of steady flow at different Reynolds numbers 80−38416
cylinder, circular, with slit, flow characts., control, patterns, wake flow, vortices 78−83404
cylinder, forced convective heat transfer, sound wave effects 80−43699
cylinder, perforated, circ., finite-aspect-ratio, drag coeff. 79−23360
cylinder in cross flow, skin friction and vortex shedding freqs. 78−94758
cylinder in flow close to plane boundary, boundary turbulence and vortex shedding 79−32484
cylinder in unbounded fluid, Oseen flow calc. at low Reynolds number 79−77117
cylinder wakes, vortex periodicity criterion, separated flow region 80−19399
cylinders, circ., various arrangements, flow interference, review 78−46985
cylinders, smooth and roughened, in crossflow near plane surface, vortex shedding 79−81911
cylinders, square cross section, oscills., vortex shedding freq. 78−46983
cylindrical annulus, rotating, transition to Taylor vortices, Ekman layers 80−87776
decay mechanism, for laminar and turbulent vortices and swirls 79−50732
decaying vortex core, boundary layer dynamics, atmospheric appl. 79−55394
definition problems, proposal based on pathlines, book contrib. 80−1605
detached flow around bodies with local vortex sheets 80−87778
detached flow around wing in ideal fluid, vortex sheet break-up 77−11200
detached flow round thin wings, vortex struct. 80−38421
developed flow in curved channels, vortex formation *(German)* 80−1689
die entry flow, kinematics and stability 79−60026
diode, used as outflow valve in pulsatile blood pump 78−44724
discrete frequency sound generation by fluid flows 80−69812
discrete vortex method for flow representation including separated regions 77−80172
disrupted states, vortex flow and breakdown 77−89131
divergent duct, vortex flow breakdown, group vel. criterion 80−87807
double row of moving vortices near a wall, stability condition *(Italian)* 78−83407
driven cavity problem, numerical methods in Navier-Stokes eqns. 79−1202
drop deformation, shear and vorticity effects 80−87795
drop deformation dynamics, vortical flow Lagrange function *(Russian)* 77−55007
dual jet discharged into rectangular duct, flow and heat transfer 80−43751
duct, turbulent air flow, small streamline curvature effects 79−60064
duct flow with oscill. plate, numerical soln. 79−50794
duct wall cavities, heated bottom surface, forced convection heat transfer 80−6048
ducted impeller, unsteady press. field anal. 79−46326
dust cyclone, 1975 obs. at Ashkhabad *(Russian)* 77−29396
dust devils, boundary conditions for subsynoptic vortex flow models 77−87041
East Australian current anticyclonic eddy struct. 77−17134
East Australian Current eddy, sound propag. 78−65322
eddies in viscous liquid 79−14412
eddy detection scheme 79−96834
eddy flow attachment ideal fluid, partial differential eqn. soln. method 78−5752
edge interaction, low frequency component generation mechanisms 80−53795
edgetone, fluid mechanics of vortex street 78−13835
education, topological solitons in physics, vortices and mag. monopoles as examples 79−25793
EHD vortex convertor, power jet distrib. stage anal. calcs. *(Russian)* 77−7470
Ekman layer of circular vortex 79−46324
elastic fluids, thermodynamic effects on shock waves and vorticity jump 77−15061
electrically cond. fluid, vortex suppression by mag. field 77−35249
electrically-induced vortical flow from hemispherical electrode 79−94733
electrovortical flow in corrugated tube *(Russian)* 78−26205
ellipsoid freely suspended, rotation about a slow viscous flow's vorticity axis 78−38386
elliptic, motion of solid spherical particle *(Russian)* 79−90261
elliptic cylinder about axis perpendicular to flow, autorotation 80−103033
elliptic cylinder unsteady aerodynamics and vortex induced oscillations, test results 78−94746
elliptically rotating liquid, generation of vortical perturbations as atm. model *(Russian)* 77−49146
enclosed rotating cone with superimposed throughflow, frictional resistance, Taylor vortices effects 80−43717
energetics of a linear array of hollow vortices of finite cross-section 80−92157
energy balance in vortex trail 77−58705
energy production and control of atmospheric vortices 78−61510
Euler equation in two dimens., numerical approx. *(French)* 80−48715
exhaust jet, swirling, noise and flow characts. obs. 77−75950
external disturbance transformation into boundary layer waves 80−28523
fans, low tip speed, axial flow, vortex shedding noise 77−80014
ferromagnetic superconductors, self-induced vortices, magnetisation, Gibbs free energy 80−70916

vortices continued
finite area vortex regions, contour dynamics for the Euler equation in two dimens. 79−37326
finned plate surface, convective heat transfer, vortex flow and turbulence intensity 77−72296
fire tornadoes, Japan, max. wind speed estimation 78−36255
fire whirl phenomenon, model 79−72958
flame advection and propagation in fluid 80−59097
flat bodies with blunt tail sections, subsonic flow and wake obs. 77−68616
flow, through a surface 78−38341
flow around obstacles, in reactor cooling system, Strouhal criterium appl., vibr. excitation *(Czech)* 78−66331
flow behind aircraft 79−32535
flow effects on structures, conf., New York, USA, (Dec. 1976) 78−46927
flow measurement, plane mixing layer vortex digital image processing 80−103095
flow noise past rod, wind tunnel expts. 78−50978
flow over body, Fredholm integral eqn., spline fit approx. 79−37302
flow past axially uniform viscous vortex, tornado mathematical model 78−59405
flow past circular cascade of arbitrary profiles 77−39303
flow phenomena within vortex sink rate sensor, numerical study 78−63436
flow rotational speed meas. instrument 77−80247
flow separation, unsteady, behind normal plate, discrete-vortex model, velocity-point scheme *(Japanese)* 80−79330
flow separation, unsteady, behind normal plate, discrete-vortex model, modified velocity-point scheme *(Japanese)* 80−79331
flow separation experiments, galloping and vortex induced oscillations 80−43750
flow through porous media, eddy motion charact. 80−6136
fluid mechanics, mathematical introduction, book 80−66
fluid with constant vorticity, motion in singly-connected region, Kirchhoff's elliptical vortex 80−6067
fluidised bed, numerical soln. to 20 unsteady diffusion eqn. for vortex flow 77−84320
fog devil, photographic obs., New South Wales, Australia 77−81985
forced convection in flows through rows of surface protrusions 78−94732
formation during large air bubble ascent in water 78−83410
formation from downdraught in rotating environment, appl. to cloud. mech. 80−8399
formation in mixing layer downstream of a separation in near wake of body *(French)* 80−48716
forward facing step, neutrally stable atmospheric flow, shear layer, separation, vortices 80−48685
four-vortex integrable and chaotic motions 80−103035
free convective flow in porous medium, longit. vortices, onset, linear stability anal. 78−94813
free stream vorticity adjusting to flat plate, Laplace eqn. soln. 78−59406
free vortices behind stationary wing as energy source for wind turbines 80−40820
friction losses, vortex chamber end walls, Kantorovich method 77−47021
fully developed laminar flow with internal heat generation between horizontal parallel plates, thermal instability 78−90899
fully developed steady turbulence, intermittency exponent determination, maximum principle 79−98691
furrowed channels with pulsatile flow, observed flow patterns, separation and vortices 80−33673
gas, ideal dissociating, differential effects of shock waves on flow parameter behind shock 77−15135
gas, perfect, vortex sheet, separation from smooth body at large Reynolds number *(French)* 80−74908
gas, turbulent boundary layer vel. distrib., probabilistic statistical approach, vortices 80−92123
gas flow meas. with vortex meter and microcomputer *(German)* 80−92241
gas flow round porous axisymm. body with injection, vorticity *(Ukrainian)* 77−75923
gas jet, wall impact model, subsonic 78−34176
gas separation, energetic, influence of vortex-tube configurations and length 77−7400
gas separation in vortex tube, theory and expts. *(Japanese)* 79−4021
gas tunnel, vortex, applic. of concept to high temp. plasma production 77−84459
gas turbine annular vortex shedding acoustic resonance analysis *(Japanese)* 80−14526
gasdynamic three dimensional flow, vortex conservation *(Russian)* 77−35157
Gifting propeller operation charact. by computer aided numerical anal. 80−6068
Gortler stability at rigid and elastic plane plates *(Russian)* 80−79261
Gortler vortex type perturbation profiles in boundary layers problem on curved surface *(Russian)* 80−74834
Gortler vortices, high value eigenstates, stability diagrams, book contrib. 80−1606
Gortler vortices, nonlinear analysis 77−11198
Gortler vortices in the nonlinear region, book contrib. 80−1607
gravitational collapse in perfect fluid, vorticity, general relativity theory 77−11282
gravity waves on rot. fluid, numerical method 77−51071
Gross Pitaevskii eqn., generalised solns. 80−49437
Gulf Stream, anticyclonic eddy obs. in slope water aboard CGC Evergreen 80−72546
Gulf Stream, cyclonic rings, potential energy distribution 77−56651
Gulf Stream cold core ring, observed formation 78−44862
Gulf Stream cyclonic eddies, Sargasso Sea hydrology *(Russian)* 78−85589
Gulf Stream ring, coalescence with Gulf Stream off Cape Hatteras 79−79872
Gulf Stream ring, frontal zone asymmetric disturbances 79−2267
Gulf Stream Rings, linear quasigeostrophic dynamics appl. 77−86917
gyre in Alboran Sea, laboratory simulation 79−100846
harmonic oscillations of annular wing in steady ideal fluid flow 79−94552
Hartmann flow in heated channel, thermal instability 77−7461
head-on collision of two vortex rings 78−26125
heart valves, blood flow, vortex-grid method 80−41105
heat exchanger radial tube bank vibration in transverse liquid flow *(Russian)* 79−81973
heated air mass in stratified atm., vortex ring form. 79−84365
Heisenberg planar model, two dimens., renormalisation vortices, and symmetry breaking perturbations 78−10638
helical gas stream from nozzle, quasi-one dimens. theory 79−64734
helicopter rotor, nonlinear mathematical simulation of unsteady flow past rotor 79−86442
Helmholtz instability of vortex sheet, effect of background vorticity *(Japanese)* 80−10254
Helmholz's vortex eqn., Cauchy problem, diff. approx. soln. *(German)* 80−1608
high gradient magnetic separation at moderate Reynolds number 80−38500
Hill's spherical vortex, response to axisymmetric disturbance 79−10566
hollow vortex enclosed in cylindrical vessel, internal disturbances 79−77122
homogeneous turbulence, uniform distortion, generation of pressure fluctuations 77−27519
horizontal funnel cloud over Shawnee, Oklahoma (1976 June 29) 79−66747
hurricane Eloise 1975, double diffusive convection in boundary layer 77−70738
hurricane formation, tropical storm control by cloud seeding *(German)* 80−90207
Hurricane Gladys (1975), subcloud layer energy transformations 80−77089
hurricane rainbands, possible form. mechanism 79−8658
hurricane rainbands, vertical struct., interaction with mean vortex 79−8659
hurricane surge potentials over SE.Louisiana, forecast model 80−46216
hurricane-intensity extratropical storms, satellite forecasting, comments and reply 77−17249
hurricanes, forced secondary circulations 79−84387
hurricanes, formation and structure rel. to tropical circulation 79−88462
hurricanes, inertia-buoyancy waves 78−7705
hurricanes, interaction between symmetric mean vortex and shearing steering current rel. to spiral bands excitation 80−56538
hydraulic resistance in vortex, tangential self-oscills. effects 80−87775
hydraulic vortex amplifiers, two-stage shear-modulated 77−53237
hydroacoustics, role of surface shear stress fluctuations 80−69808
hydrodynamic effect on contour 79−86438
hydrodynamic instabilities, transition to turbulence, Couette flow, vertex streets, Rayleigh-Benard instability 78−83362
hydrodynamic instabilities and turbulence, flow states, examples and meas. methods 80−92116
hydrodynamics of point vortices on sphere *(Russian)* 79−32529
hydromagnetic stability of a vortex sheet in compressible, perfectly conducting fluids 80−14831
hydrophone wake, mounting configuration rel. to vortices and infrasonic flow noise 77−47119
hypersonic boundary layer over slender sharp cone, turbulent shear stresses, heat transfer 77−23989
hypersonic viscous shock layer, leeward vortex-induced heat transfer 77−80179
ideal fluid separated flow, turbulent wakes and vortices locations 79−98732
ideal vortex motion, two dimens., symms., conservation laws 78−87349
impulsively started circular cylinder, initial flow, separation, vortices, wakes and boundary layers 80−19401
impulsively started flow about circular cylinder, two-dimens. vortex shedding, inviscid model 80−19400
inclined body of revolution, vortex wake effects of nose config. and free stream velocities *(Japanese)* 78−30299
inclined hot-wire response equations, for flow field having dominant tangential velocity component 78−14105
inclined surface, natural convection flow, transition, vortex system, meas. method 79−27632
incompressible flows, 2-D, potential flow past aerodynamic body, subsurface panel method 80−74901
incompressible fluid flow vorticity-streamfunction computation 77−47018
incompressible fluid in circular cylinder, vorticity dynamics in spin-up from rest 79−77130
incompressible laminar planar flow between parallel plates, ang. vorticity formulation 80−64643
inhomogeneous turbulent flow scale charact., vortex struct. relationship 80−53754
instability zones due to acoustic pulse striking a vortex sheet on a supersonic stream 79−64689
integrals of hydrodynamic equations, for vortex motion Helmholtz 1858 paper 79−9072
intensive air flow round thin and sharp axially symmetric bodies *(Russian)* 79−37330
interaction of multi-vortex rings, flow visualisation *(Japanese)* 77−42846
interactions, book contrib., review 80−19410
interface between two fluids, vortex sheet discretised evolution with buoyancy and surface tension effects 77−27579
interfacial gravity waves, form. by submerged vorticity regions and fluid inhomogeneities 79−64682
internal structure of vortex breakdown 78−55651
inviscid, 3-dimens. incompressible flow, spontaneous singularity, Taylor-Green vortex 80−48720
inviscid barotropic vorticity eqn., soln. by finite difference, finite element and pseudospectral method 80−43687
inviscid flow, 2-D, weakly sheared, past circular cylinder 80−74893
inviscid flow through wide-angle diffuser with actuator disk 79−37325
inviscid fluid, accelerating flow horizontal divergence, turning vorticity eqn. anal. 80−77013
inviscid fluid, approach of symmetrical vortex pair to plane surface 79−68721
isolated nonlinear vortex evolution 80−81910
isotropic turbulence, conditional flow struct., anal. 80−19335
isotropic vorticity theory, appl. to adverse pressure gradient flow 80−59047
jet, axisymmetric, modelling of large eddies, harmonic forcing effect 78−90957
jet, circ., controlled perturbation, smoke visualisation 78−90956
jet, finite disturbances and growing vortices 77−47055
jet, impinging, eddy struct. effect on heat transfer 79−1227
jet, large scale struct. and vortices, linear stability theory 78−26179
jet, subsonic, of gas, vortices, flow visualisation patterns 78−63471

vortices continued
jet, turbulent mixing layer, wave dispersion on vortex pairing 79−32612
jet in cross flow, injection angle effect on vortex props. 78−94779
jet mixing in transverse subsonic crossflow, vortex strength 79−14447
jet mixing layer, large-scale turbulence and vorticity 79−32611
jet noise generation, role of vortex pairing 80−69807
jet noise source characterisation, conditional sampling 79−41722
jets, axisymmetric, large eddies, numerical model 80−79375
jets, axisymmetric subsonic and supersonic, in parallel stream, turbulence meas. 77−31349
jets, subsonic coaxial, initial region, vortices 77−80191
Josephson junction, long, driving of single vortex 77−63034
Josephson junction line, vortex motion *(Japanese)* 78−91824
Josephson tunnel junction, nonresonant vortex motion 80−97037
Joukowski airfoil, unsteady viscous flow, bound-vorticity distrib., numerical anal. 78−51169
Jupiter, Great Red Spot as plane vortex with elliptical nucleus 77−53466
Jupiter, vortices buoyancy rel. to atmosphere differential rot. 80−46467
Kamchatka Current, satellite obs. of eddies 78−81182
Karman vortex air flow system *(Japanese)* 80−38417
Karman vortex street behind circular cylinder, series truncation method, Navier-Stokes eqns. solns. 78−79325
Kelvin-Helmholtz instability in supersonic and super-Alvenic fluids 80−87816
Kelvin-Helmholtz-like instability of a shear layer subject to free boundary conditions 79−68726
Kovasznay type vorticity probe, influence of fluctuating vel. components 79−72973
Kutta condition, unsteady 78−90917
laminar boundary layer, elongational viscosity and secondary instability 77−23997
laminar boundary layer, vorticity genesis 78−1630
laminar boundary layer along concave wall, vortex instability analysis 77−55000
laminar boundary layers on concave curved walls, heating effect on stability 77−65745
laminar boundary-layer flows with swirl and large suction 80−1519
laminar compressible boundary layers, Taylor-Gortler instability 78−26140
laminar incompressible flow past rot. elliptic cylinders 77−27538
laminar to turbulent boundary layer shear flow, three-dimens., stability eqns. 78−38284
laminar wing flow, tip vortex stability 77−19611
Langmuir circulations, controlled laboratory expts. 79−23330
leading edge vortices, flow meas. 78−63433
Linderstrom-Lang vortex tube, gas separation perform. 77−27536
Linderstrom-Lang vortex tube, gas separation performance 77−47019
line vortex pair, interaction with ground plane 78−1669
liquid, oscill., spherical particle free fall, eqn. of motion 77−3859
liquid crop falling into still liq., vortex ring formation 78−90946
liquid crystals, subcritical region, vortex penetration length, cct. behaviour 79−55662
liquid fuel droplet heating with internal circulation 78−75194
liquid metal-gas two-phase MHD generator, pot. loss mechanisms, rel. to fluid dynamic processes 77−39359
LMFBR subchannel coolant flow behind blockage, temp. noise obs. 79−13389
local mass-transfer coeffs. meas. by holographic interferometry, vortex instability effect 78−75234
log-normality of vorticity at fluid particle 78−26129
longitudinal counterrotating vortices, wall boundary layer of flow with ang. momentum *(German)* 77−75922
magnetosphere, plasma vortices, satellite meas. 79−40021
Mars, extratropical cyclones, Viking Orbiter 1 obs. during summer season 79−44398
material lines in viscous and elastic flow between eccentric co-rot. cylinders 77−23966
Maxwell fluid, diffusion of vortex line in stagnation point flow 80−74892
Maxwell toroidal vortex, analogs and extensions 80−28510
Maxwellian fluid, line vortex diffusion *(French)* 77−65765
MBBA, nematic film, with two free surfaces, EHD flow 79−98817
merger, in two-dimens. mixing, statistical theory 78−42618
mesoscale eddies in mid-ocean, simulated dynamic balances, model 80−26525
mesoscale synoptic eddy, POLYMODE results for NW Atlantic *(Russian)* 78−85588
mesoscale vortex area in central Atlantic, meteorology *(Russian)* 78−85658
metal ribbon, amorphous, fluid-flow-temp. model for casting by melt extraction 79−56942
meteorology dynamical topics, vorticity and divergence 79−12226
MHD, in container, induced by rapidly alternating or rot. mag. field 79−64785
MHD charged gas flow, multicomponent eqns. *(Russian)* 79−14488
MHD equilibria, by secondary bifurcation, rectangular boundary conditions 78−42673
MHD nonviscous flow equations, steady plane, plane radial, and vortex flow 79−32697
MHD shear invisual flow, vortex sheet stability 80−28571
MHD shock waves with heat addition 79−55427
MHD viscous flow, stability in curved channel 78−9720
MHD vortex flow generation, viscous fluid with spherical boundary, by AC EM field 78−5804
MHD-gravity waves, over-reflection in stratified flow 77−11207
microconvective heat, mass transfer processes 79−86435
micropolar unidirectional plane flow, spin-vorticity relation 77−19584
Mid-Ocean Dynamics Experiment maps, potential vorticity and conservation 77−41043
MINI-OTEC ocean thermal energy conversion plant test 80−45727
mixing layer, free, axisymmetric, turbulent spot, vorticity and Reynolds stress 80−79281
mixing layer vortices, numerical simulation 78−90853
mixing length determination, from turbulence characts. meas., in tubes and boundary layers *(Russian)* 78−83371
mixing process induced by the vorticity associated with the penetration of a jet into a cross flow 79−7396
models of atmospheric random vortices 78−28265
momentum horizontal transport, cumulus-scale, in monsoon depression over India 78−44961
vortices continued
monsoon depression, vorticity budget and vertical vel. distrib. 77−78321
motion of three point vortices 79−41695
multiple fluid in three dimensions, vortex theory 80−14709
mutual slip-through of a pair of vortex rings 79−77129
mutual slip-through of vortex pair 78−42619
natural convection, heat transfer in enclosed cavity 77−51056
Navier Stokes eqn., explicit numerical soln., effects of initial boundary conditions, vorticity 79−81839
Navier-Stokes eqns., general finite difference formulation, appl. to vorticity eqns. 77−39269
Navier-Stokes equation, operator version, convection propagation and convected curl operators, Lie algebra 80−46812
Navier-Stokes equation soln. method, finite element anal., 2D unsteady viscous flow 77−89088
Navier-Stokes equations, stream function-vorticity formulation incorporating no-slip conditions, variational principle 78−38267
Navier-Stokes equations, vortex flow, new exact solutions 78−38340
Navier-Stokes solvers, efficiency, vorticity-stream function form 77−58632
NDT, thermal, vortex tube appl. 80−89453
nematic liquid crystal, two-dimensional, Kosterlitz-Thouless phase transitions 79−7680
nematic suspended films under AC and DC fields 77−11470
neutron stars, rotating, form of quantum vortex filaments 80−67770
Newtonian fluid containing rigid particles, peristaltic pumping at low Reynolds number 79−10604
noise generated by an eddy *(French)* 80−19363
nominally planar turbulent boundary layer, spanwise nonuniformity and vortices 80−53762
nominally two-dimensional boundary layer, spanwise nonuniformity, uniformalisation 77−72283
non-Gaussian probability distribs. for vortex fluid 77−47023
non-Newtonian flow, finite difference numerical solns 78−9661
noncirculating regions in axial zone of vortex cell 79−14411
nonlinear problems, discrete vortex element methods 78−30302
nonviscometric flow, drop suspension model, deformation and vorticity 79−60022
nonviscous perfectly conducting gas, vorticity adiabatic flow, theoretical study 78−91023
nozzle, Laval, vortical helical ideal gas flow, asymptotic series soln. 79−81943
nozzles, convergent, swirl effects on mass flux and thrust 80−74936
nuclear fluid dynamics 78−33131
numerical weather prediction, difference scheme for vorticity eqn. soln. *(Chinese)* 79−20951
obstacle in potential flow, vortical and entropic distortions 79−32532
ocean, admixture diffusion in vortex flow 79−2277
ocean, baroclinic synoptic eddies, evolution model *(Russian)* 78−85599
ocean, deep synoptic eddy zone, structure of homogeneous layer *(Russian)* 78−85601
ocean, deformed eddy shape, with varying Coriolis force 79−66708
ocean, intense mesoscale eddy containing Mediterranean water off Bahamas 79−74902
ocean, Langmuir circulations and wind drift currents, Langmuir vortices, struct. 77−49074
ocean, mesoscale eddy generation, available potential energy *(Russian)* 78−85598
ocean, topographically bound vortices theory 79−57956
ocean, topographically generated eddies 77−2153
ocean, topographically trapped vortex on Norwegian continental shelf 80−31046
ocean, wind driven, new class of steady solns. to wind-driven ocean problem 80−85667
ocean currents, synoptic-scale, numerical model 80−12424
ocean currents in synoptic eddy, periodic components *(Russian)* 78−85593
ocean cyclonic mini-eddy obs. near Blake Escarpment, W. Atlantic 77−9437
ocean cyclonic rings, warm saline water/cooler fresher water mixing 78−44861
ocean eddy effect on inertial oscillations 77−33082
ocean eddy fields in N.Atlantic and N.Pacific, geographic var. of intensity 77−9431
ocean eddy formations, hydrochemistry *(Russian)* 78−81215
ocean internal waves and mesoscale eddies, weak interaction 77−9433
ocean synoptic eddy, current meas. *(Russian)* 78−85590
ocean synoptic eddy area, temp. disturbances, vertical structure *(Russian)* 78−85600
ocean thermohaline structure of water masses in vortex formation *(Russian)* 78−85592
ocean vortex formation, dynamical structure *(Russian)* 78−85591
ocean vorticity transport, diffusion parameterisation of mesoscale eddy effects from numerical expt. 79−48508
oceanic eddy formation in Somali Current, wind effects 80−26523
oceanic layer vortex formation from barotropic Rossby wave *(Russian)* 79−100859
oceanic mesoscale eddies generation, numerical simulations with two and three layer quasigeostrophic models 79−57950
open channel thermally stratified flow, eddy diffusivity buoyancy effects, obs. 78−90904
open pipe exits, flow during acoustic resonance, vortices and boundary layers 80−92224
ovalling oscillations of cylindrical shells in cross flow, comments 80−59045
N. Pacific, midlatitudes, zonal variability in eddy energy distrib. 77−60397
pair trajectories near orifice, two-dimens. pot. flow 77−55005
partially cavitating hydrofoil, linearised theory, singularity method *(Japanese)* 78−14050
particle flow behaviour in branching vessels models, vortices in 90° T-junctions 80−16971
particles suspension in turbulent vortices, meas. of small sphere motion in rot. vel. field 77−58771
passing-through of vortex ring pair 78−83409
perfect fluids expanding with both vorticity and shear, cosmological appl. 79−48669
perforated screen, sound diffraction, vortex shedding influence 80−69849
periodic oscillations beating in vortex collapse *(Russian)* 77−58697
periodic wake, beind circular cylinder 79−94626

vortices continued
permeable shells with pole hole, pot. nonseparational inviscid flow *(Russian)* 77−75972
phase space quantisation of interacting vortices in two demensions 80−4634
phase turbulent impinging jet, struct., vortex stretching 79−32476
pinning in nucleopores, effect on second sound resonators 80−49439
pipe, heated, straight, free-forced convection in entry region 78−90883
pipe, horizontal, straight, heated, entry flow 79−32675
pipe-jet system in crossflow, turbulent vortex shedding modes 80−10274
piston-cylinder assembly with open annular port, unsteady flows 80−79329
planar magnets, quasi-two-dimensional, dynamics of vortices 80−71066
planar shock wave, annular vortex damping *(Russian)* 79−10667
plane flow of second grade fluid through contraction 77−3870
plane incompressible perfect fluid, equilibrium states, Euler equation 80−53791
plane jet curvature in bounded cross flow with stagnant zone 79−46355
plane mixing layer, two-point LDV meas., vorticity distrib. 80−38506
plane Poiseuille flow, stability numerical computation 79−10549
plasma, ion vortex from baroclinic vector 80−79501
plasma, two force-free vortices interaction 79−37469
plasma depolarisation of EM waves, astrophysical appls. 77−17358
plasma generator arc chamber, hydrodynamic struct. 80−1817
plasma vortex formation by baroclinic vector in laser-pellet interaction 79−14580
plate, Kirchhoff-Rayleigh flow, separation, wakes and vortices 80−69839
plate, thick, parallel flow, with separation and reattachment, local and average mass transfer *(German)* 78−22339
plate, yawed, flat, leading edge vortex induced 3-dimens. turbulent boundary layer 78−90856
plates, flat, rotating stratified flow, boundary layers 80−53793
point heat source, natural convection in rotating environment 79−10445
point vortices in regular polygons, reson. instability of steady states 77−62262
Poiseuille flow, convective instability and heat transfer, viscous dissipation effects, vortex onset 77−31295
Poiseuille flow, horizontal plane, heated from below, axial heat cond. effects on thermal instability 77−42825
polyatomic fluids, nonsymmetric pressure tensor 79−75350
polyethylene melt, vortices in die entry region and viscosity meas. 78−1700
polymer admixtures influence on origin of vortices in wake behind cylinder 77−58744
polymer solution, Taylor-Gortler vortices, elongational viscosity effects 78−22379
polymer solution, viscoelastic, in annular die entry, upstream flow charcts., instability onset 79−60036
polymer solution, vortex inhibition, velocity profile meas. 77−19628
polymer solutions, viscoelastic, tubular entry flow, vortex charcts. in stable flow 79−32428
polystyrene melt, vortices in die entry region and viscosity meas. 78−1700
porous tube array, flowfield struct., turbulence and vorticity distribs. 77−27589
potential flow, surface source and vorticity panel method 79−46278
potential flow about boundary shape, method of singularity with spline fit distrib. 78−22324
potential flow over wing with free vortex 78−63444
potential vorticity in jet stream-frontal systems role of turbulence 80−77044
Prandtl-Batchelor closed streamline theory, 3-dimens. analogue, helical streamline flow 79−81895
profile cascades, hydrodynamic interaction, vortex wake form. 77−89129
profile with jet flap, discrete vortex method *(Russian)* 79−77201
profiles, mixed inverse problem 79−94634
protogalactic medium, vortex generation 80−62360
pulsar nucleus, superconducting vortex systems *(Russian)* 79−8935
pulsar-type superfluid system, rotating, dynamics of Onsager-Feynman vortices *(Russian)* 77−82270
pulsars, superfluid liquid rotation, theory, relativistic effects in vortices *(Russian)* 78−61876
pulsatile Hiemenz flow struct., wall shear stress temporal var. near stagnation point 77−75929
quantum, dynamics 80−59758
quantum fluid, hydrodynamics equations in presence of vortices *(Russian)* 79−33141
quantum fluids, vortex formation and dynamics, Magnus force *(Russian)* 80−10719
quasi-standing-wave phenomenon due to oscillating internal flow, vortices in shear layer 80−106809
radial source flow between parallel disks, vorticity transport eqn. 78−42615
radiating gases, flow parameter vorticity and gradients for an optically thin gas 79−4089
random vortex methods for two dimens. large Reynolds number flow, errors 78−42614
Rank vortex effect theory 77−58699
reattaching laminar and turbulent separated flow, three-dimens. heat and mass transfer 77−65759
rectangular cavities, end effects, vortex flow and wall jet 80−10309
rectangular cavity in viscous gas flow, numerical anal. of acoustic resonance 79−64378
rectangular elbow, 3-dimens. turbulent compressible duct flow, stagnation pressure losses, vortices 80−64640
rectilinear vortex pairs ejected from slits 77−15037
resonance tube driven by subsonic jets, aerothermodynamic charcts. vortex shedding 78−51208
resonant gas oscillations in open pipes due to moving piston 79−68805
respirator based on jet-flow vortex-type components *(Russian)* 79−79683
rigid circular cylinder in confined flow, fluctuating lift and drag forces 77−15118
ring, constant vorticity, instability to short azimuthal bending waves 78−22354
ring, passage through circ. aperture, max. dimensions 77−84262
ring, visualisation, smoke wire technique *(Japanese)* 77−35264
ring evolution in stratified and shearing environment 78−30303
ring formation at tube and orifice openings 79−41696
ring vortex instability, wave formation dependence on vorticity distrib. 78−34146
vortices continued
ring vortices under water, vel. and momentum rel. to form. parameters 77−62257
rings, expts. 77−68596
rings, growth and breakdown *(Japanese)* 77−75926
rising core, at centre of vortex, analysis for laminar flow 78−1666
river bend fluid flow behaviour, simulation 79−100885
roll up calculations of two dimens. vortex sheets 78−71340
rolled vortex sheets, viscous diffusion 79−46325
rolled-up vortex sheets, asymptotic struct., double-scale technique 77−23968
rollup and pairing, energetics 80−38419
Rossby wave critical layer, evolution, vorticity outward diffusion 78−79329
rotating Bernoulli surfaces in compressible inviscid flow, vorticity transport 80−19403
rotating blades, vortex noise radiation 78−38143
rotating cylinders, Taylor vortex form. and spectral props. of boundary value problems 79−90262
rotating disc boundary layer transition regime, spiral vortices 80−59040
rotating fluid, vortices formation near reson. for elastoid-inertia waves 80−12473
rotating stratified fluids, vortices theory and atmospheric appls. 79−39814
rotating superconductors, Ginzburg-Landau equations *(Russian)* 77−40009
rotor, Savonious, two-dimensional vortex sheet model 79−83552
NESargasso Sea, large cold core cyclonic current rings 78−49031
Saturn, vortices buoyancy rel. to atmosphere differential rot. 80−46467
sea straits and wide estuaries, geostrophic adjustment, theory and lab. expt. 79−20847
secondary convective flows in plane inclined layer *(Russian)* 77−80153
secondary flow in cascades, theory *(Japanese)* 78−83412
secondary flows in curved ducts of rectangular cross-section 77−84323
secondary polyvortex currents in rotating elliptical cylinders *(Russian)* 78−38338
secondary vortices in wake of cylinder *(French)* 79−46323
secondary vorticity in internal waves 79−72899
semi-infinite porous medium bounded by horizontal surface, mixed convective flow, vortex instability 80−79304
separated flow around flat plate, influence of vortex diffusion 77−19613
separated flows, three-dimens., with vortex filaments, num. simulation 77−58706
separated flows, upwind and central difference schemes 80−28539
separated flows around circular cylinder, numerical solns. 77−3815
separated unsteady flows around bodies, streamline and steakline photographs 78−1634
separating laminar boundary layer, horsehoe vortex 80−19405
separation flow over a disc, accel. influence 79−86443
separation zone, closed, stationary, form. as Re→∞ 79−81846
servo force-balance instrum. for wall shear stress meas. 79−1273
severe thunderstorms internal struct., dual-Doppler radar meas., tornado generation 78−61504
shaped edge cylinders in oscillatory flow, separation and vortex shedding forces 80−53825
shear flow, vortex sheet Helmholtz instability 79−37328
shear instability, vortex nutation, amplitude oscill. 78−51171
shear layer, 2-dimens., large, disturbed, final self preserving state 78−90851
shear stress determination, in laminar and Taylor vortex flows, using flush-mounted hot film probe 80−28486
shear turbulence, vorticity transfer theory *(Russian)* 79−50719
shedding, influence of grazing flow on the acoustic impedance of a cylindrical wall cavity 80−69784
shedding, interaction of induced sound with flow past a square leading edged plate in a duct 80−69783
shedding behind circular cylinder 77−15033
shedding by cylinders in steady currents 78−14021
shedding flowmeter, stabilisation in low Reynolds number range 80−83865
shedding from inclined flat plate in shear flow, simulation 77−80170
shedding from inclined flat plate in uniform flow 77−80169
shedding noise of aerofoils in smooth flow 77−80147
shedding of vortices, flow meas. *(German)* 80−79419
sheet core theory, appl. to wings *(French)* 78−1674
sheet formation simulation, buoyancy and surface tension effects 78−9643
simulation of flow, vortex methods, review 80−106801
singularity spontaneous appearance in shape of evolving vortex sheet 79−18897
sink, vortex formation, phase transition in nonequilibrium open system 79−1200
sink flow in a rotating basin, Ekman layer 79−94629
sink-vortex flow in compressible medium, book contrib. *(German)* 80−1603
slender bodies and wings, vortex asymmetries 78−9644
slender delta wing with leading edge vortices, thickness effect synthesis 79−98734
slender profile, wake effects in finite amplitude nonsteady motion 77−23963
slender-body vortices 78−26124
small particles suspended in turbulent fluid, convection, mass transfer 80−87793
solar polar vortex, spectroscopic search 79−5801
solid body with vortex filling, canonical eqns. of motion *(Russian)* 79−63034
solid in plane-parallel vortex flow of ideal incompressible liquid 79−14414
sound attenuation in low Mach no. nozzle flow 79−50721
sound diffraction by perforated screen, low Mach number grazing flow 80−53805
sound emission by turbulent layer over inhomogeneous boundary 77−68297
sound generation and simulated emission by vortex flows 80−69797
sound generation by flow-acoustic coupling 80−69793
sound generation by head-on collision of two vortex rings 80−69801
sound generation by vorticity waves in swirling duct flows 77−62261
sound production in moving stream, Lighthill's acoustic analogy, jet noise 78−79313
sound radiation from linear vortex over plane with projecting edge 77−811

vortices continued
spatial decay of vortex array at grid 77−19610
spatial vorticity distrib. meas. technique 78−67289
sphere, conducting, proous in uniformly conducting fluid flow 78−34204
sphere, transient flow, unsteady matched Stokes-Oseen soln. 79−32448
sphere, vorticity dynamics *(Russian)* 78−34143
sphere, vorticity dynamics 79−68716
sphere in current carrying liq., convection mass transfer, num. anal. 80−83851
sphere or disc sinusoidally vibrating in liquid, flow pattern obs. *(Japanese)* 79−94631
sphere rotating in viscous fluid, induced flow 77−15036
spherical vortices, theoretical generalisations 79−68723
spinning cone, spin rate effect on side force 78−71349
spiral vortex flow characteristics at high Taylor numbers 80−1598
spiral vortex flow stability, experimental investigation 80−79327
square cavity, recirculating flow, finite element results 79−64764
square cavity recirculating flow R=400 to 1000, hybrid vortex-ADI solution for flows of low viscosity 79−68718
square cylinders, smooth/turbulent lift, drag, vortex shedding 77−89109
stability criteria for time-dependent flows 78−79305
stability of body-centered polygonal configurations of ideal vortices 78−71341
stability of cylindrical vortex sheet 79−10567
stability of plane vortex sheets in an ideal fluid 78−63437
stable flow past a wing, appl. of method of discrete vortices 80−74889
stable solutions for vortex systems 79−98735
stable solutions for vortex systems 80−33613
stably stratified medium, plane free convection from local heat source 80−96253
stagnation flow, stability to three-dimens. disturbances 78−30265
stagnation flow, two-dimens., stability, longit. vortices, perturbation method 78−75146
stagnation flow turbulence about circular cylinder, visual study 80−96248
standing vertex-pair behind flat plate, normal to uniform viscous fluid flow 79−14406
standing vortices behind cylinder in glycerin-water solns., visualization 80−59151
standing waves on hollow core vortices 80−106807
stationary V-states, interactions, recurrence, and breaking 78−42620
statistical dynamics of chaotic flows 80−106786
steady translating vortex pair family with distributed vorticity 80−92158
steady viscous flow past circular cylinder, numerical study, vortices and separation 80−92108
steady vortex driven by heat line source, math. anal. 79−23329
stenotic flow models, fluid dynamic wall interactions 77−56414
stochastic properties of a four-vortex system *(Russian)* 79−4022
stochastisation, configurational temp. range in which quasiperiodicity is absent *(Russian)* 79−77132
Stokes flow, eddy structure between two spheres with relative vel. 79−27647
Stokes flow, viscous wake development for spherical particle near large obstacle 77−89126
Stokes flow between two spheres, flow separation 77−11176
Stokes flow past plane with cylindrical ridge or trough, separation 78−55653
Stokeslets and eddies in creeping flow, review, book contrib. 80−96265
stratified flow, Coriolis force blocking attenuation, wakes, baroclinic vorticity and boundary layers 80−6129
stratified flow past three-dimens. obstacles 78−71383
stratified fluid, vortex rings, unsteady motions and distorted ring obs. 77−15091
stratified fluid flow over stationary obstacle in channel, vortex shedding freq. 78−79321
stratified fluid with free surface, near field disturbance due to slender body 78−59443
stratified liquid, convective flow struct. after lateral heating *(Russian)* 77−11232
stratified rotating fluid, mass transfer between layers causing vortex 80−12401
stratosphere, potential vorticity rel. to polar stratosphere-troposphere exchange in summer 80−72599
streaklines in a shear layer perturbed by two waves 80−59055
stream swirling, effect on laminar flow struct., heat exchange in round tube 77−11265
streaming, past axisymmetric bluff bodies, approx. theory 77−84217
streamline pattern in confined vortex flow 77−51063
streamwise vortex separation and stability *(German)* 80−6069
streamwise vorticity meas. in swirling flows 79−60074
streets, stability on curved surface with reflection symmetry 80−46810
sub and transonic flow over wing, flow separation, vortex struct., shock wave shape *(French)* 80−14733
subsonic flow around delta wing, vortex breakdown pt. stabilisation 77−39305
subsonic jet, injected into subsonic cross flow, laser-Doppler meas. 77−42893
suction vortex formation, surface roughness effects, simulation 78−7704
summer monsoon, mid-tropospheric cyclones 78−40636
Sunray tornado, photographs showing evolution 77−25731
superconducting film, vortices, static and dynamic interaction with periodic pinning potential 78−52170
superconducting film containing single flux vortices, tunnelling 77−59360
superconducting mixed state, vortices, transport entropy theory 78−43534
superconducting vortices, interaction energy using constrained var. calc. 79−78256
superconductor, nearly pure, flux line motion, semiphenomenological theory 78−52171
superconductor, type II, peak effect, static and dynamic crit. currents obs. *(Russian)* 77−85399
superconductor, type II, vortex motion, and elec. cond., in weak mag. field 77−59362
superconductor with paramag. impurities, transport entropy of vortices 77−20506
superconductors, type II, vortex pinning at edge dislocations, electrostatic mechanism 80−103802
supercritically flowing water, upstream propagation of waves *(German)* 79−68727
superfluid, rotating, continuous model of vortex oscills. 80−70490
vortices continued
superfluid, rotating, vortex oscills., continuum model 78−34669
superfluid, Vortex formation near protuberances on a solid surface and the structure of the Ginzburg-Pitaevski equations 79−86947
superfluid rot. speedups accompanying ang. deceleration 80−10738
superfluidity, quantised vortices nucleation in small channels 79−37891
supersonic, leeside flowfields of planar delta wings, Reynolds number 79−60003
supersonic conical flow, without axial symmetry, numerical method 77−89147
supersonic flow, inviscid, over external axial corner, shock wave and vortical singularities 77−42866
supersonic flow field meas. of slender cone at high angle of attack 79−77177
supersonic flow over hemisphere-cylinder at incidence up to 19° 78−59419
supersonic flow past slender cone at high incidence 78−90932
supersonic vortex flow, with adiabatic index $\gamma=2$ 77−901
suspended particles, influence on turbulence struct. in tube flow 77−75969
swirling convective boundary layer, vorticity dynamics 80−59048
swirling flow, breakdown of tornado-like vortices 77−55003
swirling jet from vortex filament, Navier-Stokes eqn. soln. 80−38470
swirling jets, confined, axisymmetric viscous incompressible flow, numerical prediction 77−84286
swirling viscous flow with applied mag. field, differential eqns. for boundary layer 78−22428
symmetric and asymmetric vortices on inclined bodies of revolution 79−46322
symmetric Couette and Taylor flow between rotating coaxial cylinders, Navier-Stokes eqn. solns. *(German)* 78−94750
symmetric finite-amplitude rotational waves, streamfunction soln. 77−41044
symmetric vortex wake shedding from a cylinder in confined flow 79−50730
Taylor 80−59044
Taylor cells hydrodynamics instability and vortex currents in Couette flow 80−64571
Taylor column, vortex shedding 79−14407
Taylor vortex flow, eccentricity effects on torque and load 78−71339
Taylor vortex flow, effect on development length in concentric annuli 80−1597
Taylor vortex flow, effect on radial forces in an eccentric annulus with axial oil flow 78−94749
Taylor vortex flow, finite difference transient implicit method, stability 79−14404
Taylor vortex flow, flow study by shear stress meas. 79−77126
Taylor vortex flow, heat and mass transfer with const. axial flow rates 77−15035
Taylor vortex flow with imposed laminar axial flow and isothermal surface heat transfer, velocity profiles 80−103031
Taylor vortices, finite difference numerical computation 77−62259
Taylor vortices above higher instability points 78−75150
Taylor vortices in Couette flow, temporal development 79−64672
Taylor vortices in rotating fluid, temporal development 79−77131
Taylor vortices near instability point, amplitude, mode-coupling theory 77−68598
Taylor vortices near oscillating cylinder, subharmonic destabilisation 80−92162
Taylor-Couette flows at very high Taylor number, marginal instability 80−1599
Taylor-Gortler instability of boundary layer with suction and blowing 77−27512
Taylor-Green vortices, numerical study 78−67204
Taylor-vortex flow, mathematics in finite length cylinders 80−100002
Taylor-vortex flow between rot. cylinders, amplification rates and torques 77−42848
teaching, superfluid He, charged trapped vortex ring 77−45650
temperature gradient effect on stability of flow between concentric rotating cylinders 80−79263
thermocapillary convection, unevenly heated liq. stream near gas bubble 78−59460
thermodynamics of discrete line vortex fluids 77−3919
thin cylindrical body acceleration in viscous fluid 79−10571
three-dimensional flow in highly-loaded axial turbomachine, vorticity effects 78−26130
three-dimensional flow over wings with leading-edge vortex separation 80−74927
three-dimensional gasdynamic flows, variational principle in Euler description, vortex conservation 80−48731
three-dimensional vorticity eqn., conservative form, numerical soln. 77−55011
Tollmien Schlichting wave, two-dimens., flat plate downstream flow field 78−38357
top-hat jet core, stability 77−19612
topographically induced, in homogeneous rot. flow, free surface effect 78−42612
tornado, contrib. of vortex-stabilised arc to energy 78−53711
tornado clouds, expected lidar returns 77−21901
tornado cyclone, wave-CISK model for convective mesosystems 77−45081
tornado flowfield struct., laboratory expts. 80−56566
tornado life cycle, photographic sequence 80−41537
tornado missile hazard, synthesized windfield model 79−31239
tornado type wind energy system, wind and solar energies effect of line heat source 79−87959
tornado vortex model, appl. to nuclear plant design 78−17444
tornado vortex simulation at Purdue University 78−40677
tornado warnings, Indiana alerting systems 79−5549
tornado wind speeds required to drive splinters into wood 77−17174
tornado-like boundary layer flow, two-eqn. simulation 77−35151
tornado-like vortex, laboratory expt. of swirl ratio effect 80−61862
tornado-like vortex dynamics, calculations 79−86440
tornado-parent storm relationship from dual-Doppler radar anal. 77−21830
tornadoes, Huntsville, AL, luminous electrical phenomena 77−45060
tornadoes, multiple vortex phenomenon, inertial instability 79−53454
tornadoes, nearby magnetometer data 77−9467
tornadoes, numerical simulation of lab. vortex expts. 78−69411
tornadoes, stochastic vorticity-augmentation, theory 77−45100
tornadogenesis, numerical model of vortex growth 78−49114

vortices continued
tornadogenesis, precipitation and rotating wind, comments and reply 77−66963
tornadogenesis in rotating thunderstorm, numerical model 79−79970
tornados, vorticity and divergence fields from dual-Doppler radar obs. 77−17172
torus, added-mass coefficients 78−32683
tracers, near buoyant particles, motion in vortex flow 77−89216
trailing edge vortices behind rectangular wing, expt. study *(German)* 77−72305
trailing vortex, shed from lifting wing tip, decay, injected air jet modification 78−63434
trailing vortex wake downstream of lifting wing, vel., vorticity and press. distribs. 77−47017
trailing vortices, ang. momentum eqn. 78−14024
trapped vortices in rotating flow 78−55650
trench flow, square section, viscous liquid, laminar and turbulent conditions obs. 77−75981
tropical cyclone, nested grid for 3-dimens. 3-level model 78−28342
tropical cyclone model vortex motion with and without current 78−28266
tropical cyclone motion 77−53146
tropical cyclone rainband microstructure 79−100927
tropical cyclone recurvature forecast from temperature wind-height data 77−64380
tropical cyclones, convective fluxes 78−28267
tropical cyclones, preferred mode of Ekman conditional instability of second kind (CISK) 80−72617
troposphere, circulation intensity assoc. with solar mag. sector boundary transits 79−74936
tube, round, vortex streams, radius of separation *(Russian)* 80−69841
tube, severely-contricted, symmetric, separating flow 79−50697
tube arrays in cross-flow, flow induced vibrs. 78−46984
tube bank, in-line, acoustic reson. generation mech. 78−46958
tube banks in air crossflow, hydrodynamic vibration models *(Russian)* 78−46981
tube bundle in crossflow at low Reynolds nos., heat transfer 79−98712
tube input parameters, effect on rate of rotation of flows *(Russian)* 80−96264
turbomachinery ring chamber, oscillatory behaviour of confined ring vortex 80−6075
turbulence, 2-D, hydrodynamic and plasma applications, dynamical eqns., diffusion, MHD, superfluidity, review 80−69769
turbulence, free-stream, near semiinfinite flat plate, vortex array representations interaction 78−90842
turbulence, fully developed, origin of intermittency 77−58658
turbulence, homogeneous vel. and temp. fields, statistical transfer coeffs. 77−7375
turbulence, large scale struct., discrete vortices merging, vortex rings in jets 78−90847
turbulence, models, two-dimens., vortex and Fourier mode 78−46945
turbulence caused by slender bodies, high angles of attack to medium of travel *(French)* 80−59041
turbulence generation, vortex interpretation of Landau's theory *(Russian)* 79−77077
turbulence modelling, large eddy simulation technique for high R turbulence flows 79−64639
turbulence separation, subsonic and supersonic, ultra-short duration visualisation *(French)* 78−75128
turbulent boundary layer, eddy viscosity 77−31289
turbulent boundary layer, source of pressure fluctuations field, model 77−27515
turbulent boundary layer, two-dimens., spanwise nonuniformity, effect of streamwise vortices 77−23964
turbulent boundary layer, viscous sublayer temp. fluctuation spatial correlations *(Russian)* 78−34114
turbulent boundary layer on flat plate mainstream turbulence, vorticity effects 78−83408
turbulent channel flow, meas. of vorticity and turbulence prod., pattern recognition method 78−26194
turbulent end-wall boundary layers, numerical anal. 77−80168
turbulent flow, two-dimens., evolution of point vortex energy spectrum *(Russian)* 77−39300
turbulent flow between rot. cylinders, model eqns. calc. 78−90852
turbulent flow downstream of sudden expansion 79−32472
turbulent flow noise generation, role of tornado-like vortices 80−69811
turbulent flow simulation with three-dimens. vortex in cell method 80−19330
turbulent flow vortex region boundaries during sudden expansion *(Russian)* 77−31310
turbulent free convection in mag. field, statistical characts., vortices 80−79310
turbulent gas flows, conservation props. 79−18876
turbulent horseshoe vortex 80−103016
turbulent jet flow, simulation by discrete eddy system, statistical characts. 79−98771
turbulent jets, vortex-street structure 80−10280
turbulent line vortices 79−27649
turbulent liquid flow, at wall, physical model 77−27514
turbulent mixing layer, numerical simulation via vortex dynamics 80−19362
turbulent mixing layer, quasi-two-dimens. eddy-struct., vortex rolls 79−81896
turbulent mixing layer, two-dimens., initial conditions effect 78−90848
turbulent mixing layer description from transient vortex flow results 80−1533
turbulent motion in vortex ring 77−35148
turbulent pressure fluctuations on jets, long range effects, book contrib. 80−1663
turbulent round jet, incompressible flow, numerical prediction 79−1171
turbulent shear flows, vorticity transfer theory, re-examination 77−31291
turbulent structure near wall 78−26106
turbulent Taylor vortex flow in long fluid columns 79−81898
turbulent vortex flow meas. by laser Doppler anemometer, meas. of turbulent vortex flow 80−79412
turbulent vortex ring motion analysis 77−51061
turbulent vortex rings, turbulent motion and heat transfer *(Russian)* 77−55008
twisted air flow in permeable tube, local heat transfer 78−71338
two circumferences in flow field of unit intensity isolated vortex *(Ukrainian)* 78−55648

vortices continued
two dimensional, statistical mechanics 78−30304
two dimensional convective transport, vorticity at wall with suction, finite difference representation 80−10255
two dimensional turbulent mixing layer, spanwise struct., vortices 80−69771
two dimensional vorticity eqn., soln. using difference methods *(Chinese)* 79−72895
two dimensional vorticity equation soln., difference method *(Chinese)* 79−50729
two vortex interaction in fluid with lower stagnation press. 77−51067
two-dimensional rotational flow, large Reynolds no., numerical calc., discrete vortices with random walk 77−31312
two-dimensional turbulence in square region, inviscid Navier-Stokes eqn. calcs. 78−16656
type II superconductor, cylindrical, rotating in mag. field, dissipation determ. 77−28309
type II superconductor, mag. props. phase transition around H_{c1} at finite temp. 77−4472
typhoon havens research program at the Naval Environmental Prediction Research Facility 79−5616
typhoons, intensity change with cloud-plume outflow aloft 77−45107
typhoons, positive vorticity advection rel. to transform in northern latits. 78−92947
uniform potential vorticity flow, wave interactions and turbulence theory 79−8655
uniform potential vorticity flow, wave interactions model 79−12196
unstable boundary layer, streamwise vorticity growth 77−58700
unstable flow past cavity, three-dimens. nature, obs. 80−59053
unsteady airfoil, Kutta condition *(Japanese)* 80−92155
unsteady airfoil stall in laminar boundary layer, water tunnel visualisations 80−53745
unsteady flow, axisymm., Navier-Stokes eqns. in vectorial form 79−68724
unsteady flow, vorticity meas. technique and data acquisition 80−19525
unsteady flow damping by compliant boundaries 77−31274
unsteady high Reynolds number flow through circular aperture 79−50735
unsteady high Reynolds number flows, inclusion of vorticity in numerical anal. 78−75151
unsteady mixed convection heat transfer from a horizontal circular cylinder 79−81879
unsteady motion on transversely sheared mean flow, scatt. and distortion 79−59997
unsteady self-similar rolled-up vortex sheet, large-scale struct. 79−32531
unsteady separated flow, aerodynamic characts., vorticity field 80−38457
unsteady transversely sheared mean flow characts., gusts 78−26142
unsteady viscous separated laminar flow, numerical modelling 78−46933
US meas. of vortices in wind tunnel expts. 80−10334
V-grooved rotating cylinders, vortex motions and mixing performance 80−43714
velocity decomposition method, pot./complex-lamellar method, turbulent shear layers 79−32481
velocity field measurements of a laminar thermal 79−68674
velocity of circular vortex ring with thin elliptical core 80−48719
velocity potential generated by localised vortex distrib. *(French)* 79−77134
velocity profile and state of gas in vortex tube *(German)* 77−89138
Venus, vortex circulation, Mariner 10 polar stereographic UV images 79−35167
vertical axis wind turbine, flow field exam. using vortex model 80−61267
vibration mechanism, vortex-excited, of cylindrical struct., photographic evidence 79−46406
vibrations due to vortex shedding induced on two cylinders, one in wake of other 77−58589
vibrations of several obstacles within the two dimensional flow of an incompressible fluid *(French)* 80−69846
viscoelastic fluid, creeping flow through tapered contraction 77−55050
viscoelastic fluid tubular entry flow, velocity field in stable flow 79−50757
viscoelastic liquid, boundary layer anal. of oscillating cylinder flows 77−65771
viscous flow, 2nd order upwind scheme critique 78−94744
viscous flow, between concentric rot. spheres, visualisation and meas. 77−15038
viscous flow, numerical boundary conditions 77−23929
viscous flow, time-dependent, integral representation approach to simulation 80−38375
viscous flow, unsteady, around elliptic cylinder, heat transfer, finite difference method *(Japanese)* 80−69831
viscous flow computations, boundary approx. and accuracy 79−64621
viscous flow past circular cylinder, two coord. systems description 77−58643
viscous flow past solid body at large Reynolds number, spiral form. 77−42799
viscous flow past two-dimensional bluff body, new approx. theory 77−918
viscous fluid, vortex dipoles 80−48718
viscous fluid surface, Navier-Stokes eqns. 79−77123
viscous gas flow, subsonic and supersonic, simplified Navier-Stokes eqns. 80−31520
viscous two-dimens. incomp. flow with separation at cascade inlet edge, num. calc 79−90232
vortex collapse *(Russian)* 79−98736
vortex filament form. from ascending flows over evap. liquid 78−63440
vortex filament with decaying vortical core and axial velocity 79−14415
vortex flow aerodynamics, review of developments rel. to design 79−77140
vortex flowmeter calibration data and appl. 78−34231
vortex flowmeter for student laboratory use 79−7424
vortex layer of small thickness, eqn. of motion, appl. to long waves 78−83414
vortex motion of a compressible liquid *(Russian)* 79−77124
vortex pair, mutual slip-through 79−27650
vortex pairs, turbulent, neutral surroundings, verification of similarity soln. 78−26127
vortex ring core, turbulence struct. 80−33615
vortex ring formation and initial motion 79−77139
vortex ring formation at a circular nozzle, rolling-up and circulation prod. 79−50738

vortices continued
vortex ripples 77−27544
vortex sheet roll up, appl. of Cloud in Cell technique 79−64670
vortex sheets, calculation of three-dimensional unsteady flows *(French)* 78−14025
vortex sheets, instability mechanism of rolled sheets *(French)* 79−81901
vortex sound at low Mach number, appl. to various flow fields 78−46978
vortex stretching, due to shear layer instability 77−65776
vortex tube efficiency, hot end inner rifling influence 79−94462
vortex zone from turbulent jet impinging on external stream plane surface 79−90301
vortex-excited vibrations, energy constraints 79−37327
vortex-induced wake buffeting and its suppression 80−103030
vortical momentum of bounded ideal incompressible fluid flows 80−59051
vortical momentum of incompressible fluid 79−10568
vortical ring, interaction with shock wave 79−94650
vortices, merging, in wind tunnel, laser velocimeter surveys 79−32718
vorticity vector, rot. theory 80−82604
wake, jet, vortex struct. rearrangement in ideal fluid calc. *(Russian)* 78−5780
wake around circular cylinder, steady flow 77−27533
wake behind circular cylinder, two-dimens. vortex shedding 78−75149
wake flow behind cone placed on flat plate, separation and vortex form. 77−72302
wake flow behind wedge, two-dimens., press. distrib. and vortex shedding freq. 77−72301
wake of sphere, visual flow obs. 78−34141
wake of sphere drawn through stratified fluid, vortex struct. 77−42896
wake of two-dimensional bluff body, rel. to axisymm. case 77−42844
wake vortices, flow visualisation *(Japanese)* 77−89128
wake vortices, interactions and water tank obs. *(Japanese)* 80−28514
wake vortices of axisymmetrical bodies, vortex-pair obs. *(Japanese)* 80−28513
wakes, implicit finite-difference procedure 78−14018
wall boundary layer, induced turbulence influence from jet and vortex generator *(Russian)* 79−59970
wall jet, radial, linear stability 78−22392
warm core cyclone over North Sea, conditional instability *(German)* 78−16118
water, friction factors in 2-D flow with relative large roughnesses 78−30357
water, large-scale, nonstationary model *(Russian)* 79−72955
water, surface gravity water propag., wave action and set-down on shear current 78−90920
waterspout of 3 March 1977 at Iraklion, Crete *(German)* 78−16121
wave-induced flow, through sharp-edged orifice, starting mechanism 77−75925
wavy vortices in flow between two long eccentric rot. cylinders, linear theory 77−51064
wavy vortices in flow between two long eccentric rot. cylinders, nonlinear theory 77−51065
wedge like sharp edge starting vortex, flow visualisation expts. 80−59046
wind energy generator system, tornado-type, latent heat from moist air, effect on vortex 80−30365
wind over ocean surface, horizontal divergence and vertical vorticity 77−81974
wind power considerations 78−79327
wind tunnel, wall interference, two-dimens., correction method, examples *(French)* 78−67293
wind turbine, vertical-axis (Giromill), vortex sheet analysis 79−83553
wind turbine flow analyses, Tornado-type 79−83555
wing, trailing line vortices, axial flow 79−32534
wing of finite span, free vortices 79−64685
wing-tip vortex cavitation, vapour core characteristics eval. by asymptotic expansion 80−106825
wings, delta, for supersonic aircraft, lift with leading-edge vortices, at low speeds 79−14422
wings, low aspect ratio, computation of nonlinear characts. 79−41690
X-Y model, two-dimens., vortex formation in Monte Carlo calcs. 77−63224
X-Y model, vortices and low temp. struct. 78−49777
X-Y model classical, Monte Carlo study 79−63168
yawed circular cylinders, vortex excited oscills. 78−46982
He, film, Brownian motion, boundary layers and quantised vortex prod. 80−6579
He film, jump in superfluid density 80−44387
He, flowing superfluid, hydrodynamics of vortex generation 77−1272
He II, ion velocity shift in vortex resonance 77−35771
He II, motion in rapidly rotating bucket 77−31817
He II, rot., vortex-disc interaction 78−10237
He II, superfluid, rotating with vortices, defect hydrodynamics *(Russian)* 80−49445
He II rotating, Poisson brackets and continual dynamics of vortical lattice *(Russian)* 79−73359
He II superfluid, turbulence during rotation, critical lengths 80−49443
He, superfluid, thermal counterflow in rot. flow, vortices and turbulence 79−86946
He, superfluid, turbulence, steady homogeneous counterflow 78−87836
^{4}He films, vortices and superfluid decay 80−96710
He-I, liquid, Taylor vortex instability in Couette flow 79−98683
^{3}He, A-phase, in rotating bucket 78−2328
^{3}He, A-phase, phase slippage without vortex cores 77−31831
^{3}He rotating A-phase, periodic structure of peculiar vortices *(Russian)* 77−35784
^{3}He, superfluid, A phase, phenomenological model of collapsed superflow and orbital relax. 79−51348
^{3}He, superfluid, A-phase, screening effect and nucleation of coreless vortices, in stationary and rotation containers 79−69311
^{3}He, superfluid, A-phase, vortex ring without singular cores 79−11001
^{3}He, superfluid, singularities investig. by homotopic topology methods *(Russian)* 77−69140
^{3}He, superfluid A and B phases, vortex solns. *(Russian)* 77−11762
^{3}He, superfluid A phase, planar textures 78−79837
^{3}He, superfluid A-phase, coreless vortices, in presence of heat flow 79−14980
^{3}He, superfluid A-phase, linear singularities and structures 77−51564
^{3}He, superfluid A-phase, new phase-transfer decay mechanism for persistent currents 80−6586
^{3}He, superfluid A-phase, orbital motions 79−19416

vortices continued
^{3}He, superfluid A-phase, rotational textures 79−11002
^{3}He, superfluid A-phase, rotating, vortex lattice detectability 80−29240
^{3}He, superfluid A-phase, topological struct., nucleation and screening effect 79−1537
^{3}He-^{4}He mixtures, quantised vortex lines and lifetime of negative ions trapped by vortices 78−84022
^{3}He-^{4}He mixtures, rotating, ion trapping on vortex lines 79−28169
^{3}He-^{4}He rotating solution, vibrating disc meas. *(Russian)* 77−24464
^{3}He-A, superfluid, vortex ring without singular cores 78−67880
^{3}He-HeII solutions, van der Waals molecular dimers $(^3He)_2$, bound states *(Russian)* 80−49454
^{4}He film, superfluid, dynamics 80−59748
^{4}He film, vortex pair prod., boundary layer problem 79−99378
^{4}He, isotopically pure superfluid, vortex nucleation 80−44378
^{4}He, liq., Venturi level differences 80−24698
^{4}He, liq., vortex rings, neutron elastic scatt. cross section calc. 79−4443
^{4}He, liquid, second sound, quantised vortex creation at constrictions, excitation model 80−44383
^{4}He, rotating, superfluid vel. distrib. in intervortex regions *(Russian)* 77−43398
^{4}He, rotating superfluid, vortex patterns and energies 80−6578
^{4}He, superfluid, capillary flow props., instabilities and vortex motion 77−55408
^{4}He, superfluid, current flow effects *(Dutch)* 79−1534
^{4}He, superfluid, fluctuations in turbulent counterflow, vortex line density fluctuation power spectra 80−84335
^{4}He, superfluid, freely suspended, rot. vel. nonregular variation *(Russian)* 80−88376
^{4}He, superfluid, generalised two-fluid eqns., canonical form, vortex transport 77−20144
^{4}He, superfluid, hydrodynamic stability of vortex ring in counterflow 79−86944
^{4}He, superfluid, ion escape from vortex rings at press. up to 2.5 MPa 77−31821
^{4}He, superfluid, ion motion along vortex lines, in RF elec. field 79−51323
^{4}He, superfluid, isotopically pure, roton-driven mech. for nucleation of negatively charged vortex rings 80−59746
^{4}He superfluid, laminar flow through capillary tubes 79−55949
^{4}He, superfluid, negative ion vortex nucleation rate for ions whose drift vels. are limited by roton emission 79−55969
^{4}He, superfluid, negatively charged vortex rings, nucleation near solidification press. 78−55997
^{4}He, superfluid, nonrotating, vortex states 78−55996
^{4}He, superfluid, pressurised, vortex nucleation by neg. ions, thermal roton influence 80−10721
^{4}He, superfluid, quantized vortices and dielec. const. splashes in crossed fields *(Russian)* 79−19410
^{4}He, superfluid, rot., second sound vel., mutual friction 78−51766
^{4}He, superfluid, rotating, vortex critical creation vels., equilib. vortex density *(Russian)* 79−19408
^{4}He, superfluid, rotating, vortex free energy 79−51329
^{4}He, superfluid, rotating, effect of hysteresis, second sound attenuation meas. *(French)* 79−55965
^{4}He, superfluid, rotating, pressurised, relaxation pheonomena, transition ^{4}He II 79−99381
^{4}He, superfluid, rotating, Tkachenko waves 80−39376
^{4}He, superfluid, rotating, vortex position photography technique 80−96708
^{4}He, superfluid, rotating freely, spontaneous accel. as manifestation of new type of quantum phase transition 79−55971
^{4}He, superfluid, rotating under high press. collectivisation ang. speed shift of vortex oscills. 79−51326
^{4}He, superfluid, self-diffusion of turbulence through porous media 79−55961
^{4}He, superfluid, slowly rotating, spontaneous acceleration, phase transition in system of macroscopic quantum vortices 79−33131
^{4}He, superfluid, spherically confined, quantised vortices *(Russian)* 80−70487
^{4}He superfluid, stability, interaction two vortex lines 78−47621
^{4}He, superfluid, stationary vortex arrays, obs. with TV/photographic method 79−77851
^{4}He, superfluid, superflow, healing and relax. in He II flows, rectilinear vortex struct. 79−14976
^{4}He, superfluid, superflow dissipation near lambda point 79−55947
^{4}He, superfluid, thermal counterflow, vortex line drift velocity effects on temp. diff. data anal. 78−51765
^{4}He, superfluid, thermal counterflow, fluctuating forces meas. 79−42330
^{4}He, superfluid, thermorotation effects 78−79832
^{4}He, superfluid, thermorotation effects 79−55966
^{4}He, superfluid, threshold first sound amplitudes for vortex line generation 79−55970
^{4}He, superfluid, trajectories of quantised vortex rings near orifice 78−55995
^{4}He, superfluid, turbulent counterflow, vortex line density by second sound burst technique 79−55963
^{4}He, superfluid, US generated quantised vorticity 78−38893
^{4}He, superfluid, uniformly or nonuniformly rotating, vortex motion, eqns. *(Russian)* 78−87838
^{4}He, superfluid, vortex form., crit. vel. depend. on oscill. period *(Russian)* 80−92732
^{4}He, superfluid, vortex lattice form. relax. times in two-valued vessel subjected to ang. accelerations *(Russian)* 80−92731
^{4}He, superfluid, vortex nucleation inhibition by strong electric fields 80−92735
^{4}He, superfluid, vortex photography progress report 79−55968
^{4}He, superfluid, vortex pinning, surface roughening effects 80−88381
^{4}He, superfluid, vortex quantisation and Higgs mechanism 78−2321
^{4}He, superfluid, vortex ring energy and momentum for large core radius 77−4231
^{4}He, superfluid, vortex ring transition 77−4234
^{4}He, superfluid, vortex tangle dynamics, turbulence theory 77−35777
^{4}He, superfluid, vortex-induced torque on porous disc, quantum calc. 78−51762
^{4}He, superfluid, vortex-line density fluctuations 77−80666
^{4}He, superfluid, vorticity threshold and vortex-core parameter near T_λ, second sound probe meas. 77−85007
^{4}He, superfluid, vorticity fluctuations in turbulent counterflow 79−33138
^{4}He superfluid film, dissipation by pinned vortex lines 77−80662

vortices continued
^{4}He, superfluid film, dynamics of vortex pairs using Fokker-Planck equation 79−69313
^{4}He superfluid film, energy dissipation rate meas. 77−80663
^{4}He, superfluid film, on oscillating planar substrate, energy dissipation 78−47620
^{4}He, superfluid film, superflow decay, vortex pinning effects 80−84332
^{4}He, superfluid flow through pinhole, vortex generation 77−72730
^{4}He, superfluid flow through 2 μm-diameter orifices, obs. of quantised vorticity 79−19412
^{4}He, superfluid mechanics for high density of vortex lines 78−54290
^{4}He, superfluid rot. film, melting of two-dimensional vortex lattices 80−2539
^{4}He, superfluid turbulence, vel. and temp. depend. from thermal resist. meas. 80−20003
^{4}He, superfluid vortex lattice collective oscills. *(Russian)* 78−51759
^{4}He, superfluid vorticity, nondissipative two-fluid eqns. 79−7724
^{4}He, surface profiles, evidence of large superfluid vortex 78−18857
Hg, liq., turbulent channel flow, in mag. field, spatial correl. and vorticity *(Russian)* 77−3876
Pb superconducting film, interaction between crystal lattice and vortices 77−28307
Pb-Cd, oriented lamellar superconductor-normal composite, supercond. 79−1650
rotating system, equilibrium Onsager-Feynman vortex lattice ^{4}He, superfluid, rotating system, equilibrium Onsager-Feynman vortex lattice *(Russian)* 80−29234
Sn, molten rotating stream, vortical filament generation during solidification *(Russian)* 78−88460
$Ta_{70}Nb_{30}$, Abrikosov vortex formation kinetics *(Russian)* 80−93055
unsaturated films, decay of persistent currents obs. ^{4}He superfluid, 80−75397

vulcanisation
butyl rubber vulcanisation with resins, use of organic accelerator *(Polish)* 79−74129
elastomers, continuous radiation vulcanisation *(German)* 78−92231
epoxy resin, plastic deform. mechanism 80−97534
fibre reinforced polymer, soaking, wetting and compounding of materials during production *(German)* 80−93535
glass fibre reinforced poly- and vinyl ester thermoset moulding, cure cycle effect on mech. props. 80−45369
mixtures in range of reversion, vulcametry, cross-linking model *(German)* 80−104113
natural rubber vulcanisate, network changes during physical testing 80−60936
poly(dimethylsiloxane) rubber, filled with modified silica, cross-linking 79−95990
polyester-polyurethane interpenetrating polymeric network glues, props. 80−16640
polymer chains, critical percolation exponents 79−61557
polymer chains and vulcanisation, discrete Hamiltonian in Potts model 79−95991
PVC-g-butyl rubber grafted copolymer, tensile strength increased by S_2Cl_2 curing 79−95993
rubber, natural vulcanizates, vulcanization temp. and vulcanization systems effect on struct. and props. 78−19705
rubber vulcanisation using sulphenamide accelerator, use of *N*-(cyclohexylthio) phtalimide as retarder 79−83169
rubber-metal facings, vulcanisation degree determ., γ-ray method 80−61043
rubbers, radiation cured, phys. props. 77−69003
structural kinetic method, of formation of crosslinked polymeric compositions *(Russian)* 79−34303

waiting line theory *see queueing theory*

wakes
aerodynamic wake roll-up rel. to steady incompressible flow over aerofoil 77−42859
aerofoil cascade with sinusoidal vibr., induced vel. *(Japanese)* 77−15031
aerofoil in unsteady airstream, two-dimens. viscous flow, numerical predictions 78−75166
aerosol in cylinder wake, local particulate vel. 77−11238
aft-loaded airfoil, boundary layer displacement effect and wake near trailing edge 78−22366
air, hypersonic wake, electron recomb. coeff., temp. depend. meas. 79−27834
air wake, hypersonic, ionised, free electron attachment coeff. meas. 79−27835
air wall-jet immersed in uniform flow, aerodynamic forces on circular cylinder 77−62287
airborne dusts transport in near wakes of bluff bodies 79−4064
aircraft, vortex interactions and decay 77−58695
aircraft vortex wakes, neutral atmospheric effects on dissipation 79−32528
aircraft wake vortices, tracking system based on acoustic refr. scatt. 77−46840
airfoil trailing edge noise, near-wake struct. and unsteady pressures at trailing edge 80−69794
airfoil wake region, lift prod. by rotating cylinder 77−7401
airfoils and cascades, unsteady wakes meas., rel. to predictions 77−72300
annular jet inner regions, jet and wake vortices 79−86479
arbitrary body, unsteady separated inviscid incompressible flow, numerical soln. 80−28509
artificial satellite molecular wake shields of various shapes for vacuum expts. 79−88966
asymptotic, supersonic, 2-dimens. turbulent wakes, fully developed mean flow criteria 80−14706
Atmosphere Explorer C (AE-C) satellite, near-wake struct. parametric investigation 79−53647
axisymmetric afterbodies, separated turbulent flows, wakes, exhaust plume effects 80−74885
axisymmetric bluff body flows, near wake props. 77−58694
axisymmetric jets and wakes, calc. with turbulence model 78−67239
axisymmetric transonic turbulent base pressures 80−19425
axisymmetrical wakes, velocity fluctuation probability distrib. 79−98804
ballistic device, hypersonic wake, anomalous dispersion meas. 79−82014
base flow at supersonic vel., rockets and re-entry vehicles appl. 78−67243
bidimensional flow past symmetric profile 77−60942
binary stars, interstellar material accretion wakes 79−21358

wakes continued
bird flight, wake behind finch 80−81629
blades in transonic flow, shocks and boundary layers, time marching method 79−4036
blown flap, upper surface, trailing edge wake flow and sound generation 77−75902
bluff bodies, cylindrical, flow visualisation investig. of wakes at low Reynolds number 78−83405
bluff body, laminar incompressible flow, separation, reattachment, eddies, drag 79−59964
bluff body, turbulent near wake, vel. correlation struct. 78−30298
bluff body, two-dimens., drag and wake *(Japanese)* 78−55647
bluff cylinder vortex shedding, universal wake Strouhal number 78−46976
bluff cylinders, vortex shedding freqs. at low Reynolds no. 77−35147
blunt body, boundary and wake, supersonic viscous gas flow, numerical soln. 80−38441
blunt body, wake flow field meas. using laser Doppler anemometry 77−35262
blunt body problem in nonuniform flow fields 78−5748
blunt cone hypersonic and supersonic flow, near wake Reynolds number effects, interferometric obs. 80−43733
blunt-based axisymmetric body, subsonic turbulent near-wake 78−94740
body of revolution, flow interaction near tail, iterative procedure 77 35128
body of revolution, iterative soln. for flow within and exterior to boundary layer and wake 77−35129
body of revolution, low-drag, thick axisymmetric turbulent boundary layer and near wake 80−19352
body of revolution, turbulent wake and asymm. hydrodynamics 77−89127
body of rotation in supersonic turbulent flow, base press. 79−86455
boundary layer in stratified medium, shear flow 79−64736
bubble and droplet-type contactors, wake shedding 79−4060
cascade wake pattern with trailing-edge slot or surface suction 78−90909
cascades with different trailing edge thicknesses, vortex shedding freq. determ. 78−75152
cavitation erosion intensity in hydrodynamic wakes *(Russian)* 80−53790
channel flow, influence of rarefaction and compression waves on base pressure *(Russian)* 79−27656
channel height effect on nearcritical flow past circular cylinder, pressure distrib. in wake 80−14818
chlorobenzene drops falling freely through water, breakup 80−69899
circular cylinder, impulsively started, time-depend. flowfield 77−3826
circular cylinder, turbulence distortion, wake and velocity fluctuations 79−68712
circular cylinder flows, coherence function method 80−96068
circular cylinder near wake in turbulent crossflow, expt. techniques 80−14705
circular cylinder with tripping wires, heat transfer, flow and wakes *(German)* 80−1589
coherent structures in coflowing jets and wakes, strobing laser beam visualisation 79−32610
cone, interference study of hypersonic near wake 79−64665
cone placed on flat plate, separation and vortex form. 77−72302
core recirculation bubbles, adverse press. gradient, wind tunnel visualisation *(French)* 77−54997
counter gradient flow downstream of two different diameter cylinders *(French)* 80−43693
cross stream-jet mixing, near field influence on mass, momentum and vorticity fluxes 77−39320
cylinder, axisymmetric, with slanted base, near-wake flow 80−74886
cylinder, circ., near-wake obs. by temp. fluctuation meas. 78−51168
cylinder, circ., separated wake stagnation pt., 2nd order boundary-layer soln. 78−63432
cylinder, circ., wake in nearly homogeneous turbulent stream 79−1197
cylinder, circular, wake of steady flow at different Reynolds numbers 80−38416
cylinder, circular, with slit, flow characts., control, patterns, wake flow, vortices 78−83404
cylinder, circular with boundary layer suction, wake changes 80−53785
cylinder, forced convective heat transfer, sound wave effects 80−43699
cylinder, heated, turbulent temp. and thermal flux characts. using four-wire probe 80−19541
cylinder, vel. and temp. probability distrib. in mixing layer and wake 79−68711
cylinder in flow close to plane boundary, boundary turbulence and vortex shedding 79−32484
cylinder in incompressible flow, finite element anal., wake development and stability 79−14364
cylinder in inviscid conducting fluid flow, non-aligned mag. field distortion 77−27597
cylinder in low Reynolds number flow, vortex shedding mechanism 79−32525
cylinder in unbounded fluid, Oseen flow calc. at low Reynolds number 79−77117
cylinder wake, external turbulence effects 78−94665
cylinder wakes, vortex periodicity criterion, separated flow region 80−19399
cylinders, circ., various arrangements, flow interference, review 78−46985
cylinders, closely spaced row, average drag force 77−68591
cylinders in turbulent flow, heat transfer 79−1198
cylinders placed in turbulent plane mixing layer, time-averaged aerodynamic forces 80−28524
Darrieus rotar windmill arrays, wake interaction, wind tunnel simulation 80−61245
Darrieus rotor, aerodynamic analyses comparison 80−61264
dichloroethane drops falling freely through water, breakup 80−69899
diffusion boundary layers, with surface reactions, laminar or turbulent regimes, thermal simulation method 77−75912
disc in rarefied plasma flow, external mag. field effect on wake electrostatic field struct. 79−10648
disc wake, cavitating flows with perturbations 80−92190
discrete frequency sound generation by fluid flows 80−69812
drag prediction, of bodies of revolution, importance of near wake 77−23962
EBR-II building complex, wake and dispersion models rel. to released material 77−91186

wakes continued
EM waves scattering by turbulent flows in wake of artificial satellites 79−8730
entrainment mechanism 78−1649
fan wakes, turbulent structure 78−79322
flame, V-gutter stabilised, laser anemometry and schlieren photography meas. 77−35263
flame holders, two-, three-dimensional, wake struct. 80−53786
flame stabilisation behind bluff-body flame holder *(Japanese)* 78−67284
flat bodies with blunt tail sections, subsonic flow and wake obs. 77−68616
flow separation, unsteady, behind normal plate, discrete-vortex model, velocity-point scheme *(Japanese)* 80−79330
flow separation, unsteady, behind normal plate, discrete-vortex model, modified velocity-point scheme *(Japanese)* 80−79331
fluid flow and heat transfer around two circular cylinders of different diameters in cross flow 80−14687
fluidised bed, three-phase, bubble wake solids content 78−42660
fluidised beds, three-phase, containing fine/light solids, contraction or expansion 80−28557
formation caused by shock wave descending from plate edge *(Russian)* 79−14402
free boundary layer turbulence, calc. of mean and fluctuating characteristics 79−72885
free shear flow, appl. of multiscale transport model *(French)* 79−50763
free stream turbulence and shear effects on boundary layer and wake structs. 78−26112
free turbulent mixing in streamwise press. gradients, linearised k-ε anal., wakes 80−59039
galactic wake turbulence, rel. to head-tail radio sources form. 80−36703
galaxies, accretion wake model of radio jets *(Japanese)* 79−84857
gasdynamic laser nozzle wake, flowfield props. boundary layers 80−24027
granular materials, flow around heated cylinder, thermal wake and separation point 77−31302
heat transfer augmentation, convective, effect of mech.-produced unsteady boundary layer flow 78−71261
heat transfer in steady and pulsed flow *(French)* 79−1188
heated cylinder, detailed similarity in wake 78−67200
heated flat plate plane wake, intermittency in free turbulent shear flows 80−19348
heated round turbulent jet, in coflowing stream, vel. and temp. profiles 77−27569
high-temperature supersonic jet, noise spectrum 79−94691
higher-order nonlinear interaction among spectral components in a wake 79−72894
hot-film anemometer for cylinder wake pattern with spray cooling 78−34238
hydrophone wake, mounting configuration rel. to vortices and infrasonic flow noise 77−47119
hypersonic, free electron distrib., RF method 79−27833
hypersonic flow field behind blunt body, approx. calc. and electron density in wakes *(Russian)* 79−86461
hypersonic laminar near wake of blunted cone, convective heat and mass transfer 79−98752
hypersonic sphere in air, obs. with open microwave resonator 79−77301
hypersonic wake, excitation temp. meas. by atomic spectral line relative intensities 80−43732
hypersonic wake of blunt body, physicochem. perturbed throat region 79−68743
ideal fluid separated flow, turbulent wakes and vortices locations 79−98732
impulsively started circular cylinder, initial flow, separation, vortices, wakes and boundary layers 80−19401
inclined body of revolution, vortex wake effects of nose config. and free stream velocities *(Japanese)* 78−30299
instability and laminar to turbulent transition 78−38337
integral relns. for jet in wake flow *(Russian)* 79−77202
intermittency determ. from probability density function of passive scalar 77−3827
intermittency determination from passive scalar probability density function 78−42611
inviscid bluff-body model, far-wake displacement effect 77−68590
ionosphere satellite wake, assessment ion current distrib. 80−101527
jet, free, streamlines and local velocities in rarefied atm. 77−42884
jet, two-dimensional turbulent, in moving stream, preferential entrainment 80−1660
jet-flap flows, near wake region, mean and fluctuating vels. 79−4051
Jupiter magnetosphere, Ganymede wake turbulence rel. to field-aligned current obs. 77−25975
kerosene drops in crystallising $MgCl_2$ brine, direct contact cooling 79−1053
laminar, of thin flat plate set parallel to stream, centre line vel. variation 78−14042
laminar, vel. distrib. of flat plate 78−34140
laminar boundary layer induced wake behind cylinder attached to plate 80−43712
laminar flow, wake pattern behind airfoil, noise generation 77−42842
laminar two-dimens. wake of incompressible pseudoplastic fluid 77−51089
laminar wake formation in shock wave prod. from plate edge 79−77120
laminar-turbulent transition, artificial control by external sound 78−34139
laminar-turbulent transition zone 78−94739
large eddies in wake and turbulent boundary layer, vel. fluctuations 80−24036
large-scale coherent structures in the wake of axisymmetric bodies, unsteady flow 79−77121
laser, elec. discharge type, flow generated by an array of eccentric porous tubes 79−965
Lavrentiev wake model and cascade 77−35145
liquid jet air wake boundary layer eqns. 77−75954
LMFBR, maximum wake temp. and Nusselt number behind blockages in Na-cooled bundles 79−31026
LMFBR pin bundle, model to correlate wake residence time meas. behind blockages 79−31027
LMFBR subassembly, central blockage wake anal. 78−29556
low density magnetised plasma wake, perturbations 79−41808
magnetically suspended cones, laminar near wake meas. probe interference 77−84257

wakes continued
main eddies of recirculating zone induced by impulsively started cylinder, origin *(French)* 80−53784
mean dynamic field downstream of two identical cylinders with weak source interaction *(French)* 78−87347
momentumless wakes, similarity and decay laws 80−53789
natural convection flow interaction over heated body 77−51059
near wake of disc, annular jet, vel. characts. 78−38336
near-wake for slender cone, Mach number depend. of laminar transition 77−62277
near-wake phenomena, with and without external compression, axial and radial air injection effects 80−10273
negative wake behind bubbles in non-Newtonian liquids 79−64716
noise generated by single wake cutting aerofoil *(French)* 77−917
non-Newtonian power law fluid, laminar far wake flow 80−53824
nonequilibrium turbulent flows near wall, matching problem 80−96250
nonlinear stern wave production in pot. flow past flat bottomed body 80−38425
nozzle in different jet regimes, internal and external flows, separation and wakes 80−100023
oscillating wings, three-dimensional nonlinear unsteady potential flow calcs. 79−41689
Oseen velocity distributions in the wake of a flat plate 80−53788
particles in a fluid, convective diffusion and mass transfer, wakes, chemical reactions 80−38394
particles moving in reactive, dispersive system, mass transfer interaction 79−64738
perforated plate generators in wind tunnels, wake, shear flow and isotropic turbulence prod. 80−69770
periodic, beind circular cylinder 79−94626
periodic flow, wake of circular cylinder, laser Doppler correl. technique 77−35278
photon correl. velocimetry, turbomachinery and industrial burner velocity and turbulence profiles 79−60083
photon correlation technique, appl. to sinusoidally perturbed flow characts. meas. 77−42945
pipe-jet system in crossflow, turbulent vortex shedding modes 80−10274
plane turbulent wakes, intermittent bulges, spanwise struct. 78−42610
plasma, low-density, electrostatic field struct. in wake of sphere 77−60509
plasma, model for fast moving body, turbulence and instability 79−77353
plasma electron obs. in Venus wake 78−77510
plasma wake in rarefied flow, electrostatic field struct. 77−91402
plasma wake in rarefied flow around bodies, ion density computation accuracy 79−50849
plasma wake of dipole antenna entering planetary atmosphere, cylindrically stratified model 79−48647
plate, Kirchhoff-Rayleigh flow, separation, wakes and vortices 80−69839
plate, with temp. and vel. profile nonuniformities, laminar flow and heat transfer 77−75913
polymer admixtures influence on origin of vortices in wake behind cylinder 77−58744
polymer solution, laminar wake, behind cylindrical body 79−37355
polymer solution, turbulent flow investig. using laser Doppler velocimeter 77−58822
poorly streamlined body wakes, analogy to sudden flow expansion in tank *(Russian)* 77−31310
porous tube array, flowfield struct., turbulence and vorticity distribs. 77−27589
profile cascades, hydrodynamic interaction, vortex wake form. 77−89129
propane flame, wake stabilized, response to sudden accel. or deceleration of free stream 80−61096
propeller wake, stalling conditions, 3-dimens. flow field obs. 78−46972
rarefied magnetised plasma, wake of rapidly moving body 78−67330
reacting particle in fluid, convective diffusion, nonlinear surface reaction kinetics 80−106854
rectangular cylinders, 2-dimens., drag coeff., correction method comparison 80−64568
relaxing wakes behind surface-mounted obstacles in rough wall boundary layers 79−94625
rotating disc, viscous flow near edge *(Russian)* 77−72303
secondary vortices in wake of cylinder *(French)* 79−46323
separated flows, three-dimens., with vortex filaments, num. simulation 77−58706
separated flows around circular cylinder, numerical solns. 77−3815
sharp-edged disc, semiempirical anal. of cavitation in wake 77−35188
ship model wake meas. in wind tunnel, laser anemometer autocorrelation *(German)* 79−60085
ships, hull form evaluation by wake pattern analysis and compilation *(Japanese)* 79−27644
slender body, axisymmetric wake, transition and instability 79−32524
slender profile, wake effects in finite amplitude nonsteady motion 77−23963
slightly heated cylinder, turbulent wake, conditional sampling study, turbulence struct. 80−6063
slightly heated small perturbation jets and wakes in press. grad., self-preservation 80−96290
space vehicles, use of vacuum for conducting expts. 78−74013
spectrally local disturbance evolution in grid generated nearly isotropic turbulence 80−48681
sphere, visual flow obs. 78−34141
spherical cap bubbles and solid spherical caps, fluid dynamical properties 77−65787
square cylinders, smooth/turbulent lift, drag, vortex shedding 77−89109
square prism in uniform flow, wall press. of separation-reattachment flow 78−26123
square prism separation-reattachment wall press. 79−98704
steady transonic flow past aerofoil, viscous effects, prediction model 80−14732
steady viscous flow past circular cylinder, numerical study, vortices and separation 80−92108
stochastic self-oscillations and turbulence, review 80−4537
Stokes flow, asymm. streaming, past spherical cap, wakes, drag, torque 77−15032
Stokes flow, effect of separation on drag and torque 80−106818
Stokes flow, viscous wake development for spherical particle near large obstacle 77−89126
Stokes flow between two spheres, flow separation 77−11176
Stokes flow past smooth cylinder 78−55627

wakes continued
stratified flow, Coriolis force blocking attenuation, wakes, baroclinic vorticity and boundary layers 80−6129
stratified flow, wakes, book contrib., review 80−19473
stratified fluid confined between horizontal planes, flow due to object motion 77−51097
stratified fluid flow over stationary obstacle in channel, wake struct. 78−79321
stratified fluid in channel, wake collapse in the thermocline and internal solitary waves 80−53787
stratified fluid with free surface, near field disturbance due to slender body 78−59443
stratified nondiffusive flow, over horizontal flat plate, boundary layers and wakes 77−47058
structure in separated flow around flat plate, influence of vortex diffusion 77−19613
submersion of a body into a fluid *(Ukrainian)* 80−33610
subsonic base pressure fluctuations on axisymmetric blunt-based body, Mach no. depend. 80−19423
subsonic bluff body wakes, measurement of fluctuating pressures 80−10249
supercavitating blocked flow, finite cavity, anal. for wake displacement thickness 78−18322
supersonic, of transverse circ. cylinder, laminar to turbulent transition, external noise effect 78−38367
supersonic field, wave equation generalised axial radiation soln., flow patterns, wakes *(German)* 78−14043
supersonic flow, self-induced oscills. 78−67215
supersonic flow, wake of axisymmetric body, ideal gas, numerical anal. 78−59420
supersonic gas flow around sphere, wake struct. 79−77119
supersonic jet, nonsteady interaction with barrier, math. model of oscillatory cycle 80−19462
supersonic jet, turbulent wake, laser velocimeter meas. 78−26173
supersonic near wake, mass transfer 78−9650
surface-mounted cube in uniform and turbulent streams 77−27535
swirling recirculating reacting turbulent jets passing through diffusers 79−50764
symmetric vortex wake shedding from a cylinder in confined flow 79−50730
symmetrical airfoil, transonic flow, inviscid and turbulent flow props., wake 80−48736
symmetrical wake calc., two-dimens. laminar and turbulent flows 80−14707
tandem cylinders in motion, mathematical model for aerodynamic forces, aeroelastic appls. 77−62270
Taylor column, vortex shedding 79−14407
temperature fluctuations in wake of linear heat source 79−77118
temperature pulsations in wake behind linear heat source *(Russian)* 79−14401
thermal convection in step wake with pulsating jet *(French)* 80−10240
thermal turbulent wake studied by 3-beam holographic interferometry *(French)* 77−62316
thermal wake of flat plate with one heated face, turbulence 78−94741
thin flat plate parallel to supersonic stream, laminar near wake, centreline velocity 79−55392
trailing vortex wake downstream of lifting wing, vel., vorticity and press. distribs. 77−47017
transport in near wake regions of surface-mounted cubes 79−12183
tube, cylindrical, coaxial, effect of array of spheres on mass transfer rate to tube wall 80−74884
tube bank, heat transfer and flow around second cylinder of three cylinders in cross flow 77−15025
turbine blade arrays, turbulence characts. of stream, obs. 78−71319
turbulence memory in self-preserving wakes 79−32527
turbulence separation, subsonic and supersonic, ultra-short duration visualisation *(French)* 78−75128
turbulence wakes behind isolated circular cylinder, determination of probe-length requirements for wind-tunnel investigations 79−68688
turbulent, behind slender propeller-driven bodies 78−38335
turbulent, development and struct., variable eddy viscosity formula 79−37371
turbulent, external compression effects 79−32560
turbulent, meas. with pulsed-wire and hot-wire anemometers 77−11288
turbulent, power law, rel. to marginal instability principle 79−32458
turbulent, two-dimens., influence of upstream history 78−59400
turbulent, two-dimens., second-order closure anal. 77−39364
turbulent, vel. and temp. distribs., conditional averaging *(Russian)* 78−38296
turbulent axisymmetric near wake behind bluff-base bodies 78−1665
turbulent axisymmetric temperature wake, final decay period modelling 77−3828
turbulent boundary layer, complete vel. profile, wake deficit and inner layer terms 77−51048
turbulent boundary layer, mean flow meas., mildly curved surface 77−58661
turbulent boundary layer, supersonic, wall temp. effect 78−94765
turbulent boundary layer with separated flow, integral method 80−1547
turbulent diffusion from sources near obstacles with separated wakes, eddy diffusivity model 79−81865
turbulent diffusion from sources near obstacles with separated wakes, conc. meas. near cylinder 79−81866
turbulent energy and length scale eqn., mean vel., similar solns. 77−89102
turbulent heated wake, interface statistics 79−27645
turbulent jet, trailing edge noise mechanism 79−41720
turbulent near wake, modelling using interaction hypothesis 78−63431
turbulent near wake, of flat plate trailing edge 77−89125
turbulent near-wake behind step with supersonic jet 79−14448
turbulent separating boundary layer, subsonic, integral prediction method 80−1623
turbulent shear flow from two cylinders, negative production 78−94666
turbulent shear flow without solid boundaries, effect of polymeric additives 79−77084
turbulent shear layers, modified law 77−35146
turbulent skin friction at subsonic and supersonic speeds, wake component influence 80−19340
turbulent temporal decay, final period struct. elements 78−94653
turbulent thermal wake, behind asymmetrically heated plate 79−64664
turbulent wake, 2-dimens., large scale struct. 78−90847
turbulent wake, cylinder generated, interface position 78−94742
wakes continued
turbulent wake, fluctuations in boundary 79−27646
turbulent wake, in two-dimens., scalar field evolution eqn. 78−94669
turbulent wake, numerical simulation using Navier-Stokes eqn. 78−94743
turbulent wake of axial flow turbomachinery rotor blades, numerical anal. 80−1596
turbulent wake of heated cylinder, interface statistical props. 77−19608
two circular discs in tandem, drag reduction, wakes 80−106795
two dimens., vorticity transfer theory, re-examination 77−31291
typhoon Tess wake vertical struct. in upper layer of Pacific Ocean 80−26538
unsteady quasiperiodic flows, self-synchronising Schlieren flow visualisation, near wake 80−19527
variational methods, book contrib. 79−32456
vehicle hypersonic wake, radiation from injected small particles, free molecular regime 80−64650
velocity field measurements of a laminar thermal 79−68674
vibrations due to vortex shedding induced on two cylinders, one in wake of other 77−58589
vibrations of several obstacles within the two dimensional flow of an incompressible fluid *(French)* 80−69846
viscous drag of two-dimensional contours moving in a weak polymer solution 80−100014
viscous flow, unsteady, around elliptic cylinder, heat transfer, finite difference method *(Japanese)* 80−69831
viscous flow around circular cylinder, steady flow 77−27533
viscous flow around circular cylinder, unsteady flow 77−27534
viscous flow past circular cylinder, two coord. systems description 77−58643
viscous flow past two-dimensional bluff body, new approx. theory 77−918
viscous mixing at trailing edge 78−1635
vortex breakdown flowfields, spectral characts. in water 80−19408
vortex collapse, periodic oscills. *(Russian)* 77−58697
vortex shedding behind circular cylinder, wake 78−75149
vortex shedding from smooth and roughened cylinders in crossflow near plane surface 79−81911
vortex sheet, highly rolled, core theory appl. to wings *(French)* 78−1674
vortex sheet roll up, appl. of Cloud in Cell technique 79−64670
vortex struct. in wake of sphere drawn-through stratified fluid 77−42896
vortex structure rearrangement in wake and jet, ideal fluid calc. *(Russian)* 78−5780
vortex wake of two-dimensional bluff body, rel. to aixsymm. case 77−42844
vortex wakes, implicit finite-difference procedure 78−14018
vortex-induced wake buffeting and its suppression 80−103030
vortex-stress, turbulent plane mixing layers, growth rate, structure measurements 79−50716
vortices, interactions and water tank obs. *(Japanese)* 80−28514
vortices formation in mixing layer downstream of a separation in near wake of body *(French)* 80−48716
vortices of axisymmetrical bodies, vortex-pair obs. *(Japanese)* 80−28513
wake vortices, flow visualisation *(Japanese)* 77−89128
wake-induced flutter of cylinder in wake of another 77−80167
wall jet, 3-dimens., surface layer props. computation 80−1667
wedge, two-dimens., press. distrib. and vortex shedding freq. 77−72301
wedges, high Reynolds number flow, base pressure in near wake 80−59038
windmill arrays, wake interaction, theory and preliminary results 80−61246
wings, low aspect ratio, computation of nonlinear characts. 79−41690
wings near ground, nonlinear unsteady one dimensional theory 80−79344
yawed slender wings, Abel integral eqns. for wake strength 79−32552
H_2O channel flow, heat transfer from cylinder oscill. in cross flow 79−55386

Walsh functions
see also encoding; filtering and prediction theory; signal processing
edge image analysis, Walsh functions used in Fourier transforms 79−72507
EEG anal. appl. 79−12020
EEG signals, Walsh power spectra estimation 77−40823
evoked potential optimal filtering in sequential range *(German)* 78−85401
fast Walsh transform configuration program derivation, appl. to seismic data processing *(Chinese)* 80−21853
holographic memory with controlled transparency, associative access to data 79−31841
image invariant Walsh spectrum definition and calc. *(Russian)* 79−94156
lens optimisation, FEE-based criterion 78−79097
mixed Fourier Walsh transforms, appl. to seismic array processing 77−81819
nuclear reactor optimal control using Walsh function variational synthesis technique 77−38347
nuclear reactor time-varying reactivity reconstruction method 78−671
optical imagery appls., polar co-ords. 77−23626
optical processing, performance of generalized two-dimensional linear transforms 80−9824
real time image restoration through Walsh filtering 77−27264
signal processing, matrix relationship with discrete Fourier transformation *(Russian)* 78−26
surface texture assessment 80−36995
transform, light pulse processor, filter appl. *(Japanese)* 77−78449
Very Large Array, phase switching, radioastronomy appl. 78−81539

Wannier functions
band structure calcs., optimised LCAO version, appl. to Wannier states results for Cu 79−33220
Bloch electron in mag. field 77−80906
Bloch electrons in uniform mag. and electric field, effective Hamiltonian 77−69207
Bravais-lattice operator in one band of solid 80−10519
Coulombic interaction summation in Gaussian basis 80−70575
crystal in static elec. field, true width of electron levels 77−66145
crystals, bonding, superlattices and diffraction 79−19535
cubic crysts., perfect, nonBloch electron state density 80−75487
diamond semiconductors, electronic structure, self consistent local description 80−20067
dislocated lattices, scattered wave functions 78−6326

Wannier functions continued
disordered alloy, Blackman-Esterling-Berk approximation, rederivation and proof of analyticity 78−10318
electron-phonon coupling, Frohlich-Mitra modified tight-binding approx. 77−69253
elemental semiconductor, electric susceptibility from chemical-bond approach 78−51922
elemental semiconductor, local field effects in static response 78−76010
excitons, single site theory in disordered semiconductors, general consideration 79−99486
excitons, tightly- and weakly-bound, unified treatment, Wannier representation 78−43301
excitons, Wannier, electronic spectrum, in quasi-two-dimensional structures 80−65460
excitons, Wannier and Frenkel, simple model for unified treatment 79−69422
ferromagnet, itinerant electron, surface spin waves, tight-binding Hubbard model 80−39763
film, Wannier excitons 79−69426
Gaussian functions distributed over lattice, analytical transform. into Wannier functions 78−32768
generalized lattice representations using generalized Bloch and Wannier functions 80−22300
graphite, Wannier functions and density matrix determ. in terms of localised orbitals 78−2408
III-V semiconductors, ionic tetrahedral, electrical susceptibility, chemical bond approach 78−87931
impurity electron level position depend. on interaction with bands, Wannier representation calcs. 80−54653
interface energies, appl. to stacking faults 79−19547
lattice, deformable, local and global stabilities of electron 80−54620
localised Wannier functions, numerical calc. from ab-initio Hartree-Fock wave functions 79−60671
metal, density matrix, using Wannier functions 77−69210
metal, doubly occupied Wannier functions, constructive definition 80−75492
metal, electron density surrounding impurity, Wannier function calc. 77−20262
one-dimensional lattice, impurity perturbed electronic struct. using generalised Wannier functions 79−69468
perturbed crystals in k q representation, in presence of homogeneous electric field 79−69386
perturbed crystals in kq representation, in presence of uniform mag. field 78−30856
polar, layered material, quenching of excitonic diamag. shifts 79−19526
polar crystal, effective electron-hole interaction for intermediate and strong electron-phonon coupling 77−80735
polar semiconductor, exciton, energies, oscillator strengths, and phonon side bands 80−44512
polyacetylene, bond length alternation and energy gap, intermediate exciton formalism 80−29305
polyene, infinite, electronic states under local perturbation 77−57878
semiconductor, dielec. response function, local field effects 79−51505
semiconductor, dielectric liq. of Wannier-Mott excitons 80−65458
semiconductor, Wannier excitons, fine structure, lineshape and dispersion, review 80−44520
semiconductors, Fourier transformed X-ray Compton profiles 80−35004
spatially dispersive media, optical boundary value problem 80−45024
spin susceptibility, inter- and intra-atomic electron interactions 77−62789
surface bands, lattice and symmetrical description 80−70785
symmetry-adapted Wannier functions, variational procedure 80−2323
tails, role of singular points, multipole wave functions, Cu cond. band appl. 79−37956
transition metal surface, electronic perturbations 78−95334
transition metal-H systems, energy and electron density of states, improvements to theory 80−70636
Wannier-Stark ladders of finite crystal, level shifts 78−30895
Ar, valence electron distrib., pseudopotential calcs. 80−2335
BN, Wannier functions and density matrix determ. in terms of localised orbitals 78−2408
Be, X-ray scattering, Wannier function calcs. 80−87988
CdS, Wannier exciton and Wannier-exciton-ionised-donor complex, binding energies of lowest excited states 80−34363
Cu, surface, (111), (100), (110), energy band parameters, EHT calcs. 78−34883
GaAs, self-consistent localised electronic struct. 79−42445
Ge, self-consistent localised electronic struct. 79−42445
Ge-Si, electronic structure, short-range order effects, calc. 80−92861
H, atomic crystalline phase, ground state energy calc. *(Russian)* 79−19426
H, metallic, variational calc., energies, electron densities 77−15740
hexamethylphosphoramide:Li glass, metallic condensation of Wannier-Mott impurity states 78−2420
InSe, energy band structure, chem. bond polarity, photoemission, semiempirical tight binding method 80−44504
MgO, valence electron distrib., pseudopotential calcs. 80−2335
Na, BCC, doubly occupied Wannier functions, constructive definition 80−75492
NaCl, valence electron distrib., pseudopotential calcs. 80−2335
Ni, paramag., generalised Wannier functions to fit MAPW band struct. 79−19509
Si, ab initio self-consistent calcs., charge density and band struct. 79−69409
Si, phonon induced intervalley transitions, violation of selection rules 78−30875
Si, total energy calcs. by r-space method, Wannier functions 80−88503
Si, vacancy, local energy levels in Wannier approx. 77−20264
Si, valence bond Wannier functions calcs. 78−60053
Si:Sb(P)(As), shallow donor states with strong central cell perturbation theory 78−51933
TlCl, ground-state props., Wannier functions, and electronic struct., ab initio self-consistent calc. 80−80178
TlCl(Br), Wannier exciton-ionised donor complexes, binding energy calc. 80−49609
ZnSe, self-consistent localised electronic struct. 79−42445
ZnSe, two-photon absorpt. spectra, spin Hamiltonian for Wannier excitons 77−52124

warning systems *see alarm systems*

waste disposal
see also radioactive waste
actinide burner, fusion-driven, design of superconducting toroidal coil 77−27693
actinide recycling, neutron multigroup cross sections 77−23237
actinides, fast reactor recycle as waste management alternative, performance calcs. 78−13269
actinides, short lived, neutron cross sections for transmutation, Van de Graaff accel. study 79−85713
activated sludge aeration, galvanic dissolved O_2 sensor improvement 77−70364
activated-sludge process control, biological solid-retention time method 77−25699
alpha bearing and high level wastes management 79−26597
Antarctica, radioactive waste disposal, glaciological aspects 77−61523
Antarctica, radioactive waste disposal site 77−61522
Asse salt mine, disposal of radioactive waste 77−65308
atactic polypropylene waste, pyrolytic conversion to fuel oil 80−35627
Atlantic nuclear waste disposal site, radionuclide redistrib. 80−85309
bentonite clay, Na enriched, buried radioactive waste isolation material appl. 79−81029
Biblis nuclear power station, waste production, storage and disposal 80−68903
bilge water oil pollution monitoring system development 77−5246
calcining facility, construction material anal. 78−86647
CANDU irradiated fuel storage, concrete canister programme, heat transfer and shielding effectiveness 78−58388
CANDU nuclear stations, decommissioning 77−74973
CANDU reactor waste disposal, development programme 79−13494
CANDU wastes, disposal options in Canada 78−41826
cellulosic, municipal, ethanol production 80−61502
cemented radioactive wastes, stability improvement method 80−57869
cinematographic liquid-waste, treatment in laboratories *(Japanese)* 79−54209
coal combustion wastes, resource materials recovery using combination sinter-dilute acid leach methods 79−48063
commercial LMFBR spent fuel shipping system 79−9821
concrete canister spent fuel storage facility, conceptual design study 79−45378
conference, radioactive waste management, Vienna, Austria (Mar 1976) 77−61530
contaminated groundwater zone control by underground impermeable wall, radioactive waste site *(Japanese)* 79−34446
CTR central power station waste management 78−773
Czechoslovak Rez Nuclear Research Institute airborne radioactive release monitoring 78−89991
decommissioning of commercial power reactors, technical feasibility, cost, environmental effects 79−67902
decontamination and waste management at shutdown reprocessing plant, experience 78−66354
deep ocean sediment thermal conductivity meas. platform rel. to nuclear waste storage 80−46175
deep sea waste disposal *(German)* 78−24311
effluent monitoring, purpose and value 78−89986
electricity generation, technological and economic aspects 79−48066
electronics manufacturing plant waste treatment facility 77−73780
Environmental aspects of nuclear power *(Japanese)* 77−83112
environmental protection, radioactive waste from power plants in USSR 79−26601
environmental radioactivity control, relevance to control of other environmental contaminants 79−9889
environmental research, bibliography of AECL publications 79−34444
environmental risks associated with radioactive waste management 79−26604
fast reactor role in limitation and control of Pu prod. 79−9758
fibre-optic glass manufacture using polypropylene sump pumps 80−14410
fission product waste solidification, high-level, for final storage *(German)* 80−22958
fission products, concentrated solns., continuous vitrification *(French)* 77−361
fission products, continuous vitrification process, industrial scale *(French)* 77−23228
fission reactor, radioactive waste disposal 77−74954
fluid radioactive waste, processing plant for long-term storage rel. to ocean dumping 80−5279
fluidised bed containing biomass, expansion 80−14803
fuel production, refuse derived fuels, pyrolysis, hydrolysis, fluidised beds 80−66920
fuel reprocessing and waste treatment at Karlsruhe nuclear research centre 79−31143
fusion reactor transmutation waste management program effectiveness, ^{90}Sr disposal case 77−34460
geologic nuclear waste disposal, pathway anal. review 79−22424
geologic repositories, characteristics for radioactive waste acceptance criteria 80−18486
geologic repositories for commercial nuclear waste, feasibility study of basalt formations 80−18479
geologic repositories for nuclear waste isolation 80−18584
geologic repositories for radwaste, feasibility study of granite formations, Stripa, Sweden 80−18481
geologic repositories for radwaste, US Earth Science Technical Plan 80−18482
geologic repositories of radioactive waste, US Geological Survey Program [for nuclear waste geologic repositories] 80−22989
geologic repository for nuclear waste at Nevada Test Site 80−18480
geologic repository for radioactive waste, status report on Waste Isolation Pilot Plant 80−18478
geological and ocean nuclear waste disposal programme in UK 78−41829
geological disposal of high-level radwaste, chemical factors controlling environmental actinide sorption 80−13713
geological long-term disposal of high-level radwaste, Sweden 80−13712
ground waste disposal, sorption and migration studies for ^{90}Sr, ^{137}Cs 79−54523
hazard indices for nuclear high-level waste in underground repository, rel. to naturally occurring toxic minerals 78−15913
high activity waste immobilisation, potential solidification material properties 79−49790

waste disposal continued
high level liquid radioactive waste, denitration with formic acid, Pt group effects 79−36339
high level nuclear reactor waste immobilisation in SYNROC 79−43794
high level radioactive liquid waste, disposal options, fuel reprocessing 79−49703
high level radioactive waste, disposal options 79−26610
high level radioactive waste management, safety and protection aspects *(French)* 79−26656
high level radwaste management, storage, transportation, disposal, review 79−54522
high level waste reprocessing, management in France *(French)* 79−26598
high-level nuclear waste management from nuclear fuel reprocessing 77−65309
high-level radioactive waste, ultimate disposal on seabed, rel. to oceanographic circulation 78−13273
high-level radioactive waste disposal on seabed following reprocessing, feasibility study 78−13271
high-level radioactive waste management 80−37470
high-level radioactive waste storage, distribution calc. *(German)* 79−81014
high-level tritiated aqueous waste, immobilization in polymer-impregnated concrete 78−13265
high-level waste solidification plant, contribs. to risk evaluation 78−17356
high-level-waste disposal on ocean floor, prospects of international cooperation 78−13272
hospitals, radioactive liquid waste elimination, math. model for decay pond design *(Italian)* 79−48345
hot cell for reprocessing of spent nuclear fuel samples 78−58364
HTGR, at Peach Bottom, gamma scanning the primary circuit at end-of-life 77−46419
hydrometallurgical plant effluent waters, Mo and W determ. by activation analysis with low-power neutron sources 78−7279
immobilised nuclear waste, disposal centre conceptual design 80−52774
incinerator for transuranic contaminated waste 79−49718
industrial chemical waste at deep water dump site, acoustic monitoring 79−34466
industrial odorous pollution rel. to perceived sensory discomfort 77−37391
industrial use of sink-and-float test *(Japanese)* 80−55948
industrial wastes, determ. of Mn (II), (III), Cr (III), (VI) 78−61105
inorganic chemicals industry, water pollution and solid waste disposal 77−70704
Iranian solar town conceptual development 80−35645
irradiated fuel elements recycling plant design modifications and safety of used nuclear fuel during storage and disposal *(German)* 80−99219
irradiated nuclear fuel, long range storage, American proposals *(French)* 79−49709
irradiated nuclear fuel storage, waste management implications 79−31079
irradiated nuclear reactor fuel rod components, EM separation, feasibility 80−99224
Lac du Bonnet batholith, Canada, geological reconnaissance for nuclear waste disposal 80−73977
leachate collection system design for lined landfill site 77−78283
leaching of solidified radioactive waste, rel. to diffusivity const. 78−5055
liquid radioactive waste, disposal in deep aquifers, USSR approach 79−29489
liquid radwaste system at Santa Maria de Garona nuclear power plant 77−42140
liquids, flash point meas. for safe disposal 80−47051
LMFBR spent-fuel shipment cask, radiation shields 77−46313
LMFBR spent-fuel shipping, organics as coolants 77−46312
long-lived fission product waste transmutation by spallation and neutron reactions using linear accelerator 78−13268
low level radioactive waste disposal site, trench water study 79−52963
low level radioactive waste volume reduction and cost savings 79−36360
low-level radioactive waste, impact of decay daughters 79−52964
low-level radioactive waste management complexity and cost-effectiveness 78−94117
low-level waste burial facility at West Valley, correl. of water accumulation to operating practices 78−13266
low-level waste burial facility at West Valley, remedial work for trench water accumulation 78−13267
LWR and coal power stations, effects on ambient media from mining to waste disposal *(Spanish)* 77−75005
LWR fuel cycle, high level waste, management 77−359
LWR fuel fabrication plant, cost of controlling inorganic chemical releases 78−5003
LWR nongaseous radwaste, collection, treatment and storage 79−54572
LWR spent fuel elements, disposal in geologic isolation, feasibility study report 80−106140
LWR spent-fuel processing and packaging options, for disposal in geologic repository 80−18485
LWR waste, leach tests of cement containers under high hydrostatic press. *(Japanese)* 79−63761
marine pollution in Kuwait, meas. 79−5510
marine waste disposal information reliability 79−12275
metallurgical, with heavy metal ions, influence on flotation of $PbSO_4$ with sodium hexadecyl sulphate *(Japanese)* 80−55701
Mississippi Pascagoula Estuary water quality planning using Gauss-Seidel iterative technique 78−73402
multistage counter current extraction with HDEHP, rare earth distrib. ratios calc. 79−49705
municipal refuse, utilisation of heat energy 80−66919
municipal sludge, disinfection by high energy electrons 79−24922
national energy programme of USA, nuclear power, fuel enrichment and waste disposal 79−26686
New Waste Calcining Facility process filter remote handling 79−9820
nuclear, ecological problems solution *(German)* 77−54344
nuclear, permanent home search discussion 77−42113
nuclear, spent fuel storage racks, decontamination and disposal 78−21731
nuclear fission waste storage in glass and salt *(Dutch)* 78−29587
nuclear fuel centre, fuel and waste facilities, safety, protection and socioeconomic aspects 78−58395
nuclear fuel cycle wastes, solidification and burial techniques, USSR *(Russian)* 79−31081
nuclear fuel disposal safety in Switzerland *(German)* 78−74455

waste disposal continued
nuclear fuel reprocessing, radioactive waste elimination by nuclear transmutation *(Spanish)* 80−5298
nuclear fuel reprocessing and waste disposal, public issues 77−46375
nuclear fuel reprocessing in West Germany, case against suspension *(German)* 80−32418
nuclear fuel storage facility, German Government responsibility, legal aspects *(German)* 78−86701
nuclear fuelled electric power supplies, radioactive waste handling *(Spanish)* 77−67821
nuclear generating station, waste disposal and licensing *(German)* 80−99222
nuclear material disposal planning and difficulties *(German)* 78−86630
nuclear plant and lab. operations, radiation protection and waste handling 77−65338
nuclear power, radioactive waste management 79−9763
nuclear power plant laundry drain treatment system development 79−9788
nuclear power plant zero liquid discharge considerations 79−9858
nuclear power plants, safety research in Europe, role of Joint Research Centre 77−65299
nuclear power programme radioactive waste management 78−13258
nuclear power station, radioactive waste management 77−74974
nuclear power station decontamination, chelating agent appl., aspects 78−50280
nuclear power stations, fuel circuit review, radioactive conditioned waste final storage *(German)* 80−799
nuclear power stations, licensing procedure, public participation under Atomic Energy Act *(German)* 80−102256
nuclear power stations, waste management principles modifications *(German)* 80−102255
nuclear process liquid waste containers, stress corrosion cracking 77−46311
nuclear reactor gaseous effluents reprocessing, radionuclide management 79 76078
nuclear spent fuel disposal in Germany *(German, English)* 79−9771
nuclear spent fuel storage for Pacific Basin nations 78−86659
nuclear waste, interaction with hydrologic cycle 78−94103
nuclear waste, problems and safety 78−86636
nuclear waste, synthesis of nuclear waste monazites, actinide hosts for geologic disposal 79−22406
nuclear waste, treatment and storage problems *(French)* 77−23227
nuclear waste constituents, stabilisation in Portland cement 80−13630
nuclear waste disposal, geological aspects 79−9759
nuclear waste disposal, migration in geologic formations 78−4994
nuclear waste disposal, social criteria 77−30652
nuclear waste disposal problem and soln. *(French)* 79−93740
nuclear waste disposal problems, present and future trends 78−66350
nuclear waste disposal R & D programmes by OECD countries 78−41823
nuclear waste incineration for destroying actinides, costs and risks 78−41825
nuclear waste isolation plant design studies in USA 78−46151
nuclear waste management, R and D concept, in W.Germany 77−61509
nuclear waste management problem, R&D efforts 78−4991
nuclear waste management research, UKAEA programme for Iran 78−4992
nuclear water solutions, radioactive ion removal by electrodialysis 79−36338
nuclear weapons testing, radionuclide distributions in oceans and marine sediments 78−13344
ocean coastal zone, stratified water circulation forecasting for water quality management planning 79−5543
ocean disposal in Mid-Atlantic Bight control measures 79−5511
ocean dumping surveillance and data recording system 77−5247
ocean-disposed waste drift, satellite and current drogue studies 78−3824
ocean-dumping studies, strategies and tools 79−12138
offshore disposal of dredged material, sediment props. as tracers 77−5245
particle accelerator decommissioning, radioactive waste management 80−18720
Phenix fast breeder reactor fuel dismantling hot cell 77−50274
pollution of underground water supervision, w.r.t. biochemical degradation processes *(French)* 78−24316
polychlorinated biphenyls waste disposal by pyrolysis, plasma torch appl. 80−76487
polymers, synthetic, radiative degradation, chem., phys., environmental, technological effects, review 80−40948
programme in W.Germany *(German)* 78−8954
PWR and BWR systems and fuel cycle in USA 79−26687
PWR spent-fuel shipping, neutron multiplication and shielding 77−46418
pyrolysis, waste reduction in controlled atmosphere 78−35658
radiation and isotopes appl., development trends 78−55041
radio-nuclide transport in soil, conc. profile in groundwater, waste storage problems *(German)* 79−74556
radioacrive material, high level and α-bearing, international co-operative research programmes 79−36363
radioactive, actinide elimination by nuclear transmutation 77−61569
radioactive, arguments against actinide partitioning 77−61570
radioactive, Austrian research and development *(German)* 77−10473
radioactive, bitumenisation development *(German)* 77−10474
radioactive, calcined simulated high level waste, prep. and characterisation of singered glass-ceramics 77−28770
radioactive, CANDU spent fuel, containment in concrete canisters, UO_2 oxidation 77−6539
radioactive, cask concepts for spent-fuel storage 80−5284
radioactive, commercial burial site, radionuclide dynamics and health implications 77−61618
radioactive, confinement in glass, stability charact. *(French)* 77−61556
radioactive, Czechoslovak Research Institute activities *(Slovak)* 80−83188
radioactive, development in Hungary *(Hungarian)* 78−13249
radioactive, disposal in Asse salt mine, Germany, results and future developments 77−61575
radioactive, disposal methods in German Democratic Republic, use of abandoned salt mine 77−61574
radioactive, disposal of high-level and long-lived waste 78−29610
radioactive, disposal using linear accel. 79−67980
radioactive, dose to rodent inhabitants 78−85383
radioactive, dry spent fuel cask handling system and transport 78−17348

waste disposal continued
radioactive, from nuclear power plants *(Russian)* 79−30966
radioactive, geochemical aspects of radionuclide migration from waste repositories 80−13711
radioactive, German Waste Management Centre, technical project design phase status *(German)* 79−13432
radioactive, heat treatment, effluent gas purification techniques *(French)* 77−23230
radioactive, high level, vitrification, industrial scale plant, France 77−365
radioactive, high level waste glass, field leach test 77−6541
radioactive, high-level, evaluation of products for solidification 77−61555
radioactive, high-level, fixation in glass ceramics 77−61558
radioactive, high-level, leaching of radioactivity from glass blocks buried below water table 77−65312
radioactive, high-level, long-term storage and disposal in geological formations 79−93764
radioactive, high-level, stability of phosphate and borosilicate glasses used for solidification *(Russian)* 77−61560
radioactive, high-level, thermal and radiation effects on borosilicate glasses 77−61557
radioactive, high-level, ultimate disposal in salt domes, waterproof geometry on safety aspect 77−61576
radioactive, high-level, vitrified, thermal, chemical and radiation stability *(Russian)* 77−61559
radioactive, high-level and actinide contaminated, from fuel reprocessing, long-term radiotoxicity problems 77−61571
radioactive, high-level vitrified waste, risk anal. of repository in geologic salt formation 78−17362
radioactive, in geologic formations *(French)* 77−88230
radioactive, in mines, Dutch policy *(Dutch)* 80−671
radioactive, in vault, preliminary assessment of temp. distrib., model simulation 79−636
radioactive, laundry waste treatment system 78−17338
radioactive, liquid, solidification processes, problems 77−364
radioactive, long-lived, disposal in Trisaia clay formation, Italy 77−61573
radioactive, long-lived, final disposal in underground clay formation, Belgium *(French)* 77−61572
radioactive, long-term risk assessment of waste disposed in geologic formation 78−17361
radioactive, low- and intermediate-level waste, risk anal. of road transport in Netherlands 78−17359
radioactive, low- and medium-level, surface and concrete-lined trench storage, seven years experience report *(French)* 77−61579
radioactive, low-level, developments and studies for marine disposal 77−61578
radioactive, low-level commercial disposal sites, trench water survey 79−85629
radioactive, medium-level, and spent solvent, expts. on treatment, bituminisation 77−61563
radioactive, medium-level, from power plants, cementation and bituminisation methods of solidification 77−65313
radioactive, medium-level, from PWR, direct bituminisation technique *(French)* 77−61562
radioactive, medium-level, incorporation into heat-hardened resins *(French)* 77−61566
radioactive, medium-level, sedimentation method of bituminisation, thermogravimetric characts. of products 77−61561
radioactive, medium-level and low-level, incorporation in polymer impregnated cement 77−61564
radioactive, non-fuel bearing components, engineered transport and burial system 77−61580
radioactive, oceanic and geological, environmental impact assessment *(Japanese)* 80−9346
radioactive, of low and moderate activity, bituminisation, French experience *(French)* 77−26852
radioactive, of low and moderate activity, conditioning by thermosetting resins *(French)* 77−23229
radioactive, off-shore discharge, safety aspects *(French)* 77−18678
radioactive, pilot plant concept for New Mexico site, deep salt form. 77−61577
radioactive, programme in Switzerland *(German)* 78−8953
radioactive, proliferation, resource conservation and waste management *(German)* 79−13500
radioactive, Pu-contaminated, at fuel facilities, management techniques 77−61568
radioactive, public acceptance 78−41824
radioactive, public issues 77−33822
radioactive, reprocessing of irradiated fuels, French and European policies *(French)* 80−809
radioactive, risk analysis for management system, safe design 78−17351
radioactive, risk estimation, evaluation, and management 78−17350
radioactive, Rocky Flats waste packaging 77−6536
radioactive, safety and regulations *(German)* 78−54836
radioactive, Sandia solidification process for high level aqueous wastes 77−61551
radioactive, solidification of ion exchange resins in polystyrol, transport and storage *(German)* 77−23217
radioactive, Swedish project on safety *(Swedish)* 77−38341
radioactive, transport to reprocessing plant and final storage *(German)* 77−34403
radioactive, underground storage, geological aspects *(German)* 79−13431
radioactive, US Federal disposal programs, 1978 status 79−36374
radioactive, US prospects 79−49792
radioactive, use of ceramic encapsulation process, based on powder metallurgy *(German)* 78−33281
radioactive, vitrification using microwave power, industrial process appl. 79−18008
radioactive, West German solution *(German)* 77−38338
radioactive acid digestion test unit, nonradioactive startup operations 79−49717
radioactive bitumen-salt mixtures, thermal stress behaviour *(German, English)* 77−65290
radioactive calcined waste solid spillage, recovery of U, erosion in solids transport system 78−13264
radioactive dry solid waste, effectiveness of commercial compactor in university health centre setting 77−66860
radioactive emission meas. and control *(German)* 77−79484

waste disposal continued
radioactive fuel and waste, review of treatment handling, storage and disposal *(Italian)* 79−63753
radioactive fuel waste, deep underground disposal, Canadian programme 79−22423
radioactive high level waste, ceramics for solidification and storage 77−6542
radioactive high level waste, retrieval system design, Hanford 79−45380
radioactive high level waste disposal risk assessment 77−6532
radioactive high level wastes at Karlsruhe nuclear research centre 77−61545
radioactive high-level waste management 77−34412
radioactive high-level waste solidification products, composition, struct., props. *(Russian)* 79−31082
radioactive ion exchange resin, embedding in bitumen 77−10475
radioactive liquid, bituminisation process, physical and chem. props. of products 77−57727
radioactive liquid high level waste solidification 78−21669
radioactive liquid scintillation counting waste vol. reduction by distillation 78−78556
radioactive liquid waste from decontamination processes *(German, English)* 77−38345
radioactive liquid waste from nuclear reprocessing, vitrification, durability 78−54852
radioactive liquid waste with T contamination, packaging 77−6538
radioactive liquid wastes, solidification 77−83046
radioactive low-level, solid, land burial experience report 77−61581
radioactive low-level waste, industrial processes for treatment and storage 80−5280
radioactive low-level waste disposal in Japan, research and planning 78−86657
radioactive nuclear reactor waste disposal rel. to fuel reprocessing 77−67853
radioactive nuclear reactor waste solidification 77−67836
radioactive solidified high level wastes, storage in stainless steel bins, corrosion meas. 77−6535
radioactive spent fuel elements of HTR, continuation store *(German, English)* 77−65289
radioactive spent ion exchange resins from power plants, bituminisation and cementation 77−61565
radioactive waste, conditioning and storage costs estimation *(Italian)* 78−25303
radioactive waste, continuous vitrification of fission product solns. 77−61544
radioactive waste, decision anal. 80−18488
radioactive waste, disposal by bituminisation, fire safety and explosion prevention 79−71920
radioactive waste, disposal methods, risk assessment 79−41021
radioactive waste, final disposal possibilities, waste conditioning, storage and safety, review 79−26554
radioactive waste, geologic repository, site search and qualification process 80−18474
radioactive waste, geological disposal, Canadian program 77−3140
radioactive waste, geological disposal, Netherlands programme 79−26609
radioactive waste, geological storage and disposal in partially serpentinized ultramafic rock 77−61524
radioactive waste, Harwell inactive vitrification pilot plant 77−61543
radioactive waste, high level, disposal in deep-sea bed, New Zealand 78−705
radioactive waste, interim storage and final disposal, French experience 77−38344
radioactive waste, land disposal, repository, packaging and cost estimate *(Japanese)* 78−66351
radioactive waste, leach-migration experiments to determine the mobility of radionuclides in geologic media 80−18487
radioactive waste, liq., decontamination by ion exchange and electrodialysis 79−71926
radioactive waste, long term hazards of transuranic elements, removal requirements *(French)* 77−26848
radioactive waste, low-level solute and gas transport from burial site 79−85628
radioactive waste, Magnox, development and radiation stability of glasses for vitrification 77−61554
radioactive waste, management of U mining and milling waste, N.Australia 79−31076
radioactive waste, national programmes, aspects 78−697
radioactive waste, phosphate vitrification, KS-KT-100 plant *(Russian)* 77−61552
radioactive waste, pool systems for spent-fuel interim storage facilities 80−5283
radioactive waste, radionuclide adsorption by Mn oxides in soil 78−69349
radioactive waste, reprocessing, solidification vitrification of liquid waste, review 79−9762
radioactive waste, reprocessing philosophy, German waste management *(German)* 79−54565
radioactive waste, rock salt storage, γ-radiation effects *(Dutch)* 77−88232
radioactive waste, site selection and eqpt. planning at Gorleben, FRG *(German)* 80−68855
radioactive waste, solidification using urea-formaldehyde resins, technical eval. 79−67875
radioactive waste, solidified, radionuclide migration in aerated zones, ^{90}Sr leaching from cement *(Japanese)* 77−42109
radioactive waste, sorption of ^{106}Ru and ^{59}Fe on natural sorbents *(Russian)* 77−38370
radioactive waste, thermomech. impact around rock salt borehole 80−5278
radioactive waste, transceramic, from nuclear power plants, storage vessels and methods *(Dutch)* 80−68845
radioactive waste, transportation and burial 79−54574
radioactive waste, UK solidification facilities 77−61542
radioactive waste, underground repository, design and operation 79−26589
radioactive waste, vitrification, industrial scale plant, under construction in France 78−78478
radioactive waste beneficial utilisation, programmes in 1977 78−8950
radioactive waste burial, study of natural convection in porous media with heat generation 77−51114
radioactive waste by incineration in shaft furnaces *(German)* 80−47584
radioactive waste by Julich incineration process *(German)* 80−47583

waste disposal continued
radioactive waste calcination and vitrification 77−61546
radioactive waste calcining at Idaho Chemical Reprocessing plant, design criteria 77−61549
radioactive waste calcining facility, remote maintenance equipment 78−13263
radioactive waste disposal, conf. Montreal, Canada, 1973, Oct. 77−61520
radioactive waste disposal, hard rock repositories, soln. 78−78477
radioactive waste disposal, popular assumptions, critical examination 80−106141
radioactive waste disposal, Spanish programme *(Spanish)* 79−31074
radioactive waste disposal and deep sea biology 79−29638
radioactive waste disposal by solidification, evaluation of various techniques 79−31080
radioactive waste disposal by solidification and burial, geological aspects 80−63316
radioactive waste disposal criteria proposals by EPA and NRDC, review 80−18484
radioactive waste disposal following decommissioning of nuclear facilities *(French)* 80−13736
radioactive waste disposal in geologic formations, site selection criteria 80−106142
radioactive waste disposal in geological formations 79−31070
radioactive waste disposal in hard rock, slow crack growth anal. of granite 79−89452
radioactive waste disposal into deep ocean, hazard assessment 77−88233
radioactive waste disposal into internationally important waters, limit evaluation *(Russian)* 79−29488
radioactive waste disposal options, modelling studies 78−41830
radioactive waste encapsulation at Hanford 77−6534
radioactive waste final disposal in asphalt products, safety evaluation *(Japanese)* 77−50254
radioactive waste fixation in glass, laboratory expt. 77−74957
radioactive waste fixation in high-SiO_2 glass matrix prod. by porous glass process 79−49708
radioactive waste geologic disposal, migratory props. of waste elements 79−67893
radioactive waste geologic disposal, safety anal., functional relations of risk to input data uncertainties 80−83189
radioactive waste geologic repositories, computer anal. of long-term radiation hazards 80−18483
radioactive waste handling at Swedish nuclear power plants 79−26612
radioactive waste in geological formation, general considerations *(German)* 79−9757
radioactive waste interactions with surrounding rock at disposal sites 78−54853
radioactive waste management, and plutonium, Swedish approach 79−31075
radioactive waste management, closed nuclear fuel cycle, W.Germany 79−619
radioactive waste management, goals and criteria 79−31072
radioactive waste management, India's programme 79−26606
radioactive waste management, industrial aspects, Western Europe 79−31071
radioactive waste management, Japan Atomic Energy Research Institute 79−26608
radioactive waste management, research programmes 77−67824
radioactive waste management, review of new technical standards in Japan *(Japanese)* 79−67880
radioactive waste management, storage, disposal, safety 77−65291
radioactive waste management 77−10476
radioactive waste management alternatives 77−46367
radioactive waste management and disposal methods and policies 79−93757
radioactive waste management and environmental impact 77−86897
radioactive waste management and its role in Canadian fuel cycle 79−89393
radioactive waste management at Point Lepreau nuclear power station 78−29600
radioactive waste management from nuclear fuels and power plants in Canada 79−26600
radioactive waste management in Belgium *(French)* 79−26607
radioactive waste management in Canada 77−61521
radioactive waste management in West Germany 79−31073
radioactive waste management practices in selected European countries 80−37471
radioactive waste management scheme involving actinide transmutation 79−26611
radioactive waste management schemes, criteria for assessing societal, moral and political implications 78−13270
radioactive waste pot vitrification 77−61547
radioactive waste processing, consequences of separation of long-lived α-emitters *(Czech)* 80−5251
radioactive waste repository, shale investig. and vermiculite role 80−32354
radioactive waste solidification, composition, structure and properties of final product obs. *(Czech)* 78−66353
radioactive waste solidification in concrete, polymer impregnation 77−6537
radioactive waste solidification to phosphate glass-metal matrix blocks 77−61550
radioactive waste solidification using a drum drier, FIPS method 77−61548
radioactive waste storage, high-level waste glass 77−6540
radioactive waste storage, materials considerations 77−6533
radioactive waste storage, rock salt structure design *(Dutch)* 79−30953
radioactive waste storage glass properties, improvements, R&D in United Kingdom 79−59181
radioactive waste storage in crystalline rock, temp. distrib. calc. *(German)* 78−86631
radioactive waste storage in monitored containers in a controlled underground tunnel environment 79−97820
radioactive waste storage in salt domes, conceptual design 80−106143
radioactive waste study, groundwater vel. estimation 80−82111
radioactive waste transportation in Japan 78−86658
radioactive waste treatment and disposal *(French)* 80−99221
radioactive waste underground disposal, solutes movement through aqueous fissures in porous rocks 80−94553
radioactive waste underground repository, geotechnical assessment, hydrogeology, rock mechanics 79−26590
waste disposal continued
radioactive waste underground repository, summary of study feasibility 79−26591
radioactive wastes, disposal in sea 80−37472
radioactive wastes, glass containment, effect of α-emitters *(French)* 77−26849
radioactive wastes, leach behaviour of hydrofracture grout 77−10478
radioactive wastes, long term disposal facility failure hazards, preliminary examination 79−54533
radioactive wastes, methods and risks, survey *(French, English)* 77−83064
radioactive wastes from nuclear power stations 77−363
radionuclide disposal, GARD computer program for geochemical assessment 79−31068
radionuclide migration from low-level waste burial site 78−21671
radionuclides in soils and sediments, Co and actinide adsorption by Mn and Fe oxides 79−66422
radwaste, operation of a pilot solid waste incinerator 80−22990
reactor waste, storage, reprocessing and disposal, book 79−63780
reactor waste disposal in geological form., long term risk assessment 78−58387
reclamation industry, use of liquid N_2 79−58712
regional wastewater management systems, chance constrained approach 79−57513
residual waste treatment technology, review 80−40932
review of energy resources, reactor accidents, radioactive waste disposal 78−50413
safe nuclear waste disposal route, Swedish utilities design 78−41827
safety assessment of radioactive waste disposal into salt deposits, fault tree anal. appl. 78−55046
salt formation, high radioactive waste disposal *(German)* 79−54566
salt mine waste disposal, experience in West Germany 78−41828
sea disposal of low level radioactive waste, preparations *(Japanese)* 79−9768
septic tile field, groundwater pollution 77−29338
sewage effluent along Israel coast, nearshore sediment pollution by trace metals 78−44882
sewage outfall siting with dye-buoy remote sensing of coastal circulation 78−65438
sewage sludge land disposal, Mo hazard 77−33115
shale fracturing for radioactive waste disposal at ORNL 77−88251
sludge dehydration using Funda filter *(Japanese)* 77−88234
sludge disposal in coastal waters, Philadelphia study 78−3823
society effects of nuclear power developments 80−47590
solar town in Iran, conceptual development 79−57408
solid radwaste combustion, development of wire cloth filter for flue gas scrubbing 79−71919
solid waste utilization in integrated community energy systems 79−100359
spent fuel storage and disposal and plant building and operating legislature *(German)* 80−99223
spent LWR fuel storage in Pacific Basin at Palmyra Island, decision making methods 80−27763
spent nuclear fuel, long term storage, United States' scheme 79−45355
spent nuclear fuel, storage alternatives 78−74456
spent nuclear fuel shipping cask containment and accident impact limiters 77−46314
spent nuclear fuel shipping casks, R and D sea going vessel requirements 79−31083
spent nuclear fuel stored in basalt, chances of reintroduction into biosphere, analysis 80−106144
spent nuclear fuel transport problems *(Russian)* 79−31084
spent reactor fuel, risk analysis of alternatives from reactor pool until final disposal 78−17355
storage and shipment of spent fuel elements INFCE Working Group 6 *(German)* 80−102257
Tarapur Atomic Power Station radioactive waste discharge monitoring 78−89989
thermal analysis of irradiated nuclear fuel transport flasks 80−5281
thermal reactor stations in USSR, fuel reprocessing and waste disposal *(Russian)* 79−26592
transportation of nuclear waste material, risk analysis 78−17357
transuranic nuclear waste management, evaluation of alternatives 80−18490
transuranic waste, retrieval of buried wastes and long-term management 79−49719
transuranic waste disposal classification system 79−93763
Tsuruga power station radioactive waste treatment system *(Japanese)* 78−74442
underground high level radioactive waste disposal 79−9760
underground repositroy of high-level radwaste, water intrusion scenario studies, anal. and re-eval. 80−73950
underground solidified high-level radioactive waste retrieval system development 79−9818
urban solid wastes, energy production appl. viability assessment *(Spanish)* 79−57419
USA Energy R&D Administration role in low-level waste management 78−94114
USA Environmental Protection Agency activities in radioactive waste management 78−94115
USA Geological Survey low-level radioactive waste burial site selection 78−94116
USA Nuclear Regulatory Commission low-level waste management programme 78−94113
vitreous matrices for high level Purex waste containment 77−360
vitrified high level liquid waste, container design and specification 77−61541
vitrified high-level radioactive waste, associated hazards 78−13259
vitrified high-level radioactive waste, rail transportation, fault tree anal. and accidental release 78−17358
vitrified high-level waste, calcs. of radioactivity release due to leaching in final disposal 78−17360
waste management, legal aspects 77−88229
waste management in the Federal Republic of Germany. A survey of policy and research and development 79−26599
water disinfection and oxidation, ClO_2 appl. 80−12032
water reactor fuel, reprocessing, waste disposal 79−36395
Zircaloy hulls, conversion to zirconate ion exchange materials for waste stabilisation 78−702
Am retention by rock 77−71679
^{60}Co leaching in cement composites 77−61508

waste disposal continued
^{60}Co removal from waste water, adsorption on activated charcoal with oxine 78−58365
^{137}Cs adsorption by sediments near water-cooled nuclear reactors 77−78281
^{137}Cs immobilisation in cement-waste composites 78−82466
^{137}Cs leaching from ion-exchange resin incorporated in polyethylene or cement composite 77−65275
Hg emissions from wastes stored near Cl manufacturing plant 77−66938
I radioactive waste, solidification in conrete, leach rates 78−703
Pu retention by rock 77−71679
Pu-contaminated solid waste, operational techniques for minimisation, segregation and accounting 77−61567
Rn emanation from α-emitting waste, expts. 80−98314
RuO_4, catalytic reduction in radioactive liquid waste processing 79−76092
SiO_2 based glass, packaging of radio-active waste appl. *(French)* 79−71910
T transport, storage and disposal, charact. of metal tritides 77−54343
^{99}Tc, reduction and sorption in granitic bedrock, biological hazard estimation 79−79415
Th-contaminated waste water, decontamination with soap *(German)* 77−26846
Th-U spent fuel, disposal of long lived α-emitters 77−26855
U and UF_6, mining, manufacture and purification processes, safety and waste disposal *(Spanish)* 79−63785
U, milling waste management in USA 79−31077
U mills, radioactivity release meas. 78−82479
U mining, U refining and decay processes, radioactive mining waste disposal *(Dutch)* 80−21418
U, Vitro Mill Tailings at Salt Lake City, Utah, remedial action 77−46315

water
see also groundwater; heavy water; hydroxonium ion; ice; moisture; seawater; steam
α-particle stopping power and straggling in water and tissue-equivalent liquid 80−23274
absorption by rigid foamed polyurethanes, effect of cellular struct. 80−39416
absorption coefficients meas. using far IR laser source 77−5932
absorption on Na_3AlF_6 film on Si, fused quartz substrates, IR anal. 80−75446
absorption on ZnS film on Si, fused quartz substrates, IR anal. 80−75446
abundance and distrib. in glassy rims of submarine pillow basalts 79−12111
acetonitrile-water mixture, electrolyte transfer, thermodynamic props. 80−3395
acetylcholine, nonenzymatic hydrolysis, Raman obs. 79−29505
acoustic nonlinearity parameter meas., comparison with seawater 78−75727
acoustic rad. from ionising particles 78−71793
acoustic relaxation in critical region *(Russian)* 80−92609
acoustic waves, laser-induced 78−25996
action potentials in single axons, effects of hyperbaric air and hydrostatic press. 80−56007
adhesion to muscovite mica model high surface energy solid 77−55435
adiabatic expansion of water vapour from the saturation line in Laval nozzles 78−79356
adsorbed, effect on elec. cond. of amorphous Si:H film 78−88048
adsorbed, surface-induced NMR line splittings and augmented relax. rates 78−64288
adsorbed gas, on glassy AsSe, surface cond., photocond. 78−80038
adsorbed in kaolinite dispersions, PMR exam. *(Russian)* 78−35058
adsorbed in monolayer hydrate of halloysite, NMR obs. of mol. motion 78−95226
adsorbed layer, polymolecular, on quartz surface, IR absorption spectra 80−9595
adsorbed layer on NaCl surface, absorpt. and thickness meas. 80−16001
adsorbed layer on powdered quartz, thermal effects on DTA 79−100161
adsorbed layers on Pt(100), bonding, electron energy loss spectra 80−34311
adsorbed molecule in pores of zeolites, intermed. state of enhanced mobility 78−60027
adsorbed molecules, interaction with surface hydroxyls, IR spectra 78−43244
adsorbed multilayers on quartz, surface forces 80−6597
adsorbed on Al_2O_3, Raman spectroscopy study 80−65358
adsorbed on cellulose, mech. relaxation at low temps. 77−43277
adsorbed on cellulose, NMR relaxation times 79−78552
adsorbed on IR optical elements, effect on laser breakdown threshold 77−79886
adsorbed on kaolinite, vol. expansion, lattice deform. 80−45555
adsorbed on kaolinite clays, dielec. props. 78−76381
adsorbed on lunar fines, effect of annealing temp. on water etching 77−60632
adsorbed on microcrystalline WC, mol. dynamics 78−71941
adsorbed on porous glass, proton spin-lattice relax. meas. by pulse NMR 78−84053
adsorbed on proteins, new programme for NMR study of diffusion 79−92139
adsorbed on silica, low temp. thermally stimulated depolarisation spectra fine struct. 79−78611
adsorbed vapour, effect on liq. water flow in Pyrex glass capillary tubes 80−92759
adsorption, by MoO_3 79−77898
adsorption, detection of OH groups for adsorption centres in plant tissues, dielectric relaxation *(Japanese)* 80−7999
adsorption, O_2-induced and reaction with other adsorbates on Ag(110) 80−55714
adsorption, on Fe_xO_y, oxidation and reduction effects on adsorption 78−43237
adsorption, on SiO_2, surface treatment and methylation effects 78−84058
adsorption, on $ZnSO_4.7H_2O$, meas. of water physically adsorbed rel. to water of crystallisation *(Japanese)* 80−6622
adsorption anomaly in SnO_2, effects of cryst. growth of solid 80−10779
adsorption by Au electroplate on Cu 77−69168
adsorption by Na montmorillonite, meas. at −5°C 78−65540

water continued
adsorption in cement and tricalcium silicate paste NMR relaxation exam. 78−48354
adsorption of β-lactoglobin 78−60009
adsorption of bovine serum, meas. at interfaces by drop volume technique 78−60009
adsorption of lysozyme, meas. at interfaces by drop volume technique 78−60009
adsorption on α-Fe(111) under the influence of 2.5 keV electrons 79−28199
adsorption on β-AgI surface, effective pair pot. model 80−100394
adsorption on Ag and Pb halide surfaces, mol. studies of ice-forming capabilities 77−31872
adsorption on Al_2O_3, energetics, effects of adsorption temperature on surface processes 78−60028
adsorption on amorphous, porous, hydrophilic P-doped SiO_2 80−80061
adsorption on Au, work function change 77−7966
adsorption on biopolymers, effects on origin and mobility of charge carriers 79−92461
adsorption on CaF_2 surface, IR internal reflection spectra 79−77920
adsorption on Cu (100) surface, EELS study 80−2260
adsorption on Fe, Co, Ni, Pt, Cu, and Au films, work function changes 80−44705
adsorption on GaAs(110) surface, UPS study 80−6632
adsorption on GaAs (110), surface photovolt. spectroscopy 80−49499
adsorption on Ge, neutralization of surface recomb. and fast capture centre 79−33184
adsorption on Ge (111) surface, surface recomb. centre neutralization 79−38147
adsorption on Hg, critical anal. of expt. data *(Spanish)* 79−82435
adsorption on In, AES study 79−82451
adsorption on lunar soil 15081,2, microcrystallinity determ. 77−87292
adsorption on MgO at high temps., IR spectra 77−47687
adsorption on MgO during α-irrad., thermostimulated surface cond. obs. 80−34499
adsorption on Ni (100), combined XPS/LEED/SIMS exam. 79−83075
adsorption on Ni film, change in work function *(German)* 79−42365
adsorption on North Ray Crater lunar soil (Apollo 16), rel. to soil maturity 77−87287
adsorption on plasma deposited a-Si:H, effect on cond. 80−49749
adsorption on Pt, reaction between H_2 and adsorbed O 80−49514
adsorption on Pt (111), thermal desorption, UPS, and XPS study 80−80088
adsorption on Pt surfaces, D_2O+H, $D_2{}^{16}O+{}^{18}O$ exchange reacts. 77−80695
adsorption on pure Co surfaces, decomp. phenomena *(German)* 80−26054
adsorption on quartz, appl. of Hill-de Boer eqn. 79−15008
adsorption on rare earth metal films, oxidation, XPS obs. 77−31888
adsorption on Re(0001), XPS, UPS and temp. programmed desorption 80−71574
adsorption on Si, surface charging during illumination, effect of various surface treatments 79−51651
adsorption on silica, stepwise multilayer adsorpt., 130-150°C 78−14574
adsorption on silica gel, effect on pore struct. 79−52786
adsorption on SiO_2, neutron scatt. study 79−60643
adsorption on SiO_2 films, sintering effects investig. 79−66031
adsorption on SiO_2 rel. to EPR relax. time *(German)* 79−95645
adsorption on SnO_2, adsorption anomaly rel. to pretreatment 79−28194
adsorption on SnO_2, isotherms 78−56038
adsorption on TiO_2, IR spectra 78−14577
adsorption on U, XPS study 80−7473
adsorption on W(100) surface, adsorbate density determ. 77−1320
adsorption-desorption kinetics on Si and Ge surfaces 77−47684
adsorpton on SiO_2:Co(II), coord. lifetime, surface effect, NMR obs. 80−34299
aerated, laser beam focusing by vertical temp. gradient 78−33661
aerated tap, limiting detect. range in optical transmitter-receiver system 77−78461
aerosol, evaporation during transport through atmosphere *(Russian)* 79−88408
aerosol, propagation of intense radiation at 10.6 μm 80−5692
aerosol with fine droplets, laser radiation intensity fluctuations at 630 nm 80−4109
AES, chem. state effects, for water and simple organic cpds. 78−72687
AES, chemical-state effects 78−92566
affinity for $Li^+(Na^+)(K^+)$, ab initio SCF calcs. 80−58125
aggregates, dimer and octomers, dipole moments, polaris. model calcs. 79−77482
air pollution water vapour effect, damp air and plumes *(Dutch)* 77−70823
air-water, two-phase mixtures, vertical downward flow, void fraction 77−11235
air-water choked flow in short pipes 77−84314
air-water separated critical flow *(Japanese)* 78−42650
air-water surface, lecithin bilayers spontaneous form. 79−74603
air-water two-phase flow in vertical pipe, heat transfer *(Japanese)* 77−24011
alcohol/water mixtures, NMR and IR obs., low temp., shifts, interpretation 77−52065
alkaline electrolysis, chrysotile asbestos corrosion in KOH, effect of SiO_3^{2-} on electrode overvoltages 80−30433
alkaline electrolysis using inorganic-membrane-electrolyte for H_2 prod. 80−72092
alpha particle stopping power, 0.5-8 MeV 78−40334
alpha-particle, stopping power and straggling, spectrometer design 78−82563
amorphous solid, low density, IR spectrum, OH stretching region 79−11411
amorphous solid, low density, Raman spectra, OH stretching region 79−11410
amorphous solid, low-density, OH stretching spectrum 79−11413
amorphous solid, spontaneous electric polarisation rel. to solid struct., 20 to 100K 79−65791
amplified spontaneous emission in spherical and disk-shaped laser media 80−1177
analysis by X-ray spectroscopy 77−52689
anion-water H-bonds, nature, from IR and Raman OH(OD) splittings 78−62811
annular mist flow in tube, wall film mass flow rate 80−69905

water continued
anomalous compressibility to 1-9 kbar, correl. with supercoding 79−65134
anoxic pore waters in sediments, effects of oxidation during sampling on silicate content 78−61394
aqueous solns., max. density temp., structural interpretation 77−58933
aqueous solns., max. density temp., structural interpretation 77−58934
Arctic sea ice, water drag 77−21781
association, in superheated vap., equilib. consts., H bond vibr. 77−66750
asteroid Ceres, evidence for water of hydration 78−32386
asteroids, search for water of hydration from IR reflectance spectra 80−77318
atmosphere, abundance determ. by analysing solar spectra 78−85643
atmosphere, dimer conc. in H_2O vapour at different temps. and vapour press. *(Chinese)* 80−109237
atmosphere, liquid water content from Nimbus 6 scanning microwave spectrometer data parameterisation 79−58047
atmosphere, precipitable water meas. as Sacramento Peak Observatory 80−51653
atmosphere, vapour concs. above mesopause 77−73898
atmosphere, vapour contamination of Lyman-α ion chambers 79−8731
atmosphere, vapour-phase complexes, rel. to anomalous submm. spectra 78−16156
atmosphere, water vapour absorption in 8 to 13 μm spectral region 79−39855
atmosphere, water vapour and liq. water in Typhoon June (1975), scanning microwave spectrometer meas. 78−73436
atmosphere, water vapour data for astronomical IR sites 79−21181
atmosphere, water vapour polymers rel. to absorpt. in IR window 77−45145
atmosphere, water vapour transport to Antarctica rel. to fallen snow O isotopic comp. 78−36237
atmosphere, weak spectral absorpt. of vap. in visible and near IR 80−82062
atmosphere H_2O, vibrationally excited, collisional emission rel. to new diffuse bands in twilight 80−72662
atmosphere H_2O molecules, allowance for IR absorpt. effect on stellar radiation *(Russian)* 78−40832
atmosphere precipitation, D-^{18}O relationship global climatic interpretation 80−17331
atmosphere vapour, transport between troposphere and stratosphere implications for pollutant transport 80−105034
atmosphere water vapour, IR continuum absorpt. calc. *(Russian)* 78−96293
atmosphere water vapour of extraterrestrial origin, possible role in Sun-weather relationships 78−69416
atmosphere water vapour variations, baseline results from Smithsonian obs. 78−32197
atmospheres of Uranus and Neptune, estimation of ammonia and water vapour contents 80−90366
atmospheric, IR attenuation, lab. study of role of molecular and aerosol contribs. *(Russian)* 79−34945
atmospheric, probabilistic models for objective anal. of hydrometeorological fields *(Russian)* 77−56697
atmospheric, rel. to ultrafine particle form. and ion mobility 77−25742
atmospheric droplets, sources and effects of surface organic monolayers 78−69412
atmospheric precipitable water, computation from upper air data 79−34886
atmospheric vapour, absorpt. of CO_2 laser beam, optoacoustic detector meas. 77−9512
atmospheric vapour, IR attenuation meas. in W.Europe 78−53698
atmospheric water vapour, IR radiometry, clear air turbulence detect. 77−73890
atmospheric water vapour and aerosol optical depth determ. by remote sensing 78−65389
atom-atom and mol. correlation functions, electron diffr. 77−80405
autoadsorption and surface entropy in 20-50° temp. range 77−28065
backscatter and absorption coeffs., simultaneous determ. 80−82074
ball lightning explanation by water electrolysis and combustion 78−69436
benzene-ethanol-water, shear viscosity at plait points 77−35685
bioclimatic coefficients and water consumption coeff., change with respect to climatic zones *(Russian)* 77−53169
biological cell, NMR *(French)* 77−90739
biological cells, classical diffusion to explain ^{1}H spin relax. in NMR obs. 79−83721
biological cells, mechanism of dehydration on thawing 77−81478
at biological interfaces, struct. and functional aspects 78−40121
biological samples, PMR, fast-exchange model interpretation via differential kinetics clarified 80−67033
biological systems, NMR 78−56952
biophotolysis, living electrode of algae as long-lived photoconvertor 80−104510
biosystem, diffusion meas. by pulsed gradient NMR, cell struct. size determ. 78−77159
bladder, toad, temp. dependence of ADH-induced water flow and intramembranous particle aggregates 80−61520
boiling, crit. heat flux in low press. region 78−90663
boiling, free-convection, critical heat flux density 80−48691
boiling, from porous coated surface 79−76946
boiling, heat transfer around single nucleation site 77−24394
boiling, natural convection mechanisms on horizontal tube 77−24396
boiling, on Cu surface, natural boiling site cavities, SEM obs. 77−31763
boiling, on Cu surface, rel. to methanol 78−90654
boiling, pool type, produced by distrib. internal heat sources, in homogeneous nucl. reactor 78−90685
boiling, subcooled and low quality flow film, at atmospheric pressure 80−32324
boiling, subcooled nucleate flow, void fraction, incipient boiling pt. 77−39203
boiling, transition boiling under forced convective conditions, reactor accident condition 78−89961
boiling, under increased gravitation, heat exchange mechanism, review 77−46895
boiling and heat transfer on horizontal pipes with annular fins 80−74855
boiling at finned wall, heat transfer simulation 77−42817
boiling at subatmospheric press., heat transfer rate, heating surface effects 80−69630
boiling crisis in swirled flow of water in pipes 79−90241
water continued
boiling critical heat flux density, free motion conditions, 1-205 bar *(Russian)* 79−68560
boiling curves, subcooled and forced convective conditions 79−14230
boiling in annuli under forced convection, boiling noise 79−1062
boiling in Laval nozzles, discharge and dynamic characteristics 80−19470
boiling in round tube, temp. field anal. 77−42818
boiling in tube, critical heat flux 78−83232
boiling in vertical channel 78−9544
boiling on finned surface, heat transfer crisis 78−9540
boiling superheat, maximum, of drop submerged under immiscible liquid layer 80−79928
boundary conditions for numerical simulation, book contrib. 79−60247
Bremsstrahlung distrib. from 22 MeV electron irradiation 78−59840
bremsstrahlung spatial distribution in water and water-iron by 22 MeV electron bombardment, meas. with activation detectors 77−57754
Brillouin light scatt., temp. gradient induced 80−100663
brine-dodecane-sodium octylbenzene sulphonate pentanol, phase diagram *(French)* 79−82339
bubble growth in superheated water at reduced pressures, finite difference anal. *(Japanese)* 80−92150
buoyancy induced flow, adjacent to horizontal surfaces 79−23316
t-butanol-water, X-ray scatt. intensity composition depend., soln. struct. 78−6005
BWR, air clearing in H_2O-type press. suppression systems, scaling laws 79−54563
BWR, air clearing in H_2O-type press. suppression systems, scaling laws 79−54564
BWR, design and operation, review of water chemistry, in feed water, coolant and steam systems 79−36311
BWR, water chemistry characterisations 78−21635
BWR water chemistry characterisation 78−21658
calorimeter for absorbed dose meas. 80−76836
VY Canis Majoris, OH and H_2O microwave maser emission obs. 78−53949
canopy interception, measure of loss from hydrologic budget 78−11928
capillary tube, spontaneous movement rate 79−65295
capillary wave form. on gravity water waves, model eqn., surface tension, viscosity 78−83421
carbon tetrachloride, liquid, under high press., refr. index vs. density 79−28712
carbon tetrachloride-I_2-water system, mass transfer in pulsed perforated plate column 78−71385
carbon tetrachloride-n-octanol-water miscible liq. systems, isopiestic vapour press. meas., activity coeffs. determ. 77−48679
R Cassiopeiae, late-type giant, possible H_2O thermal emission identification 78−81628
catalytic surface activity, $LaNi_5$ surface segregation *(German)* 80−51008
cave waters, stable isotope geochemistry rel. to climatic change, 230000 to 100000 BP 79−2234
cavitation, gas supersaturation thresholds under high press. 77−16861
cavitation due to ultrasound, radn. force balance method 80−24063
cavitation expts. in steel Berthelot tube 80−87788
cavitation expts. using shock tube 80−87789
cavitation nuclei conc., holographic and hydrodynamic obs 78−83440
cavitation nuclei content 77−31346
cavitation strength, statistical anal. 77−11227
cell water permeability during freezing and thawing, cryomicroscope multiple nonlinear regression analysis 79−92197
cellulose, mobility of adsorbed water, NMR pulse obs. 80−108835
central force model, appl. to mol. dynamics simulation of NaCl aq. soln. 80−49077
central force potentials, struct. and dynamics 78−38607
μ Cephei, late-type supergiant, possible H_2O thermal emission identification 78−81628
ceramics, porous, frost resistance under 1-d cooling, pore size distrib. effect *(Japanese)* 78−44069
channel blockage and turbulence influence on water transverse flow past cylinder *(Russian)* 80−79401
channel flow, heat transfer from cylinder oscill. in cross flow 79−55386
chemical analysis, dosing of vapour in vac. system to calibrate analysers 77−32850
chemical analysis, review 80−7877
chemical attack on float glass, behaviour of Al tracer *(French)* 80−89378
chemical exchange, proton spin-echo NMR 77−9053
chemical processes induced radiolytically in well defined aqueous systems 80−66823
chemical reaction with pyrolitic graphite surface 78−15707
chemisorbed on α-alumina, electron binding energies, UPS, SCF-Xα-SW calcs. 77−69169
chemisorbed on Hg, Ag, Pb, Ga, Fe, Pt, effect on surface props. 78−60187
chemisorbed on metal surface, molecule struct., interband angle 80−59787
chemisorbed on Pt (111), EELS spectra, vibr. freqs. 80−80920
chemisorbed on Ru(001), conformation, electron stimulated desorption ion ang. distribs. 77−89637
chemisorbed phases on TiO_2 and $SrTiO_3$, UPS meas. 78−10285
chemisorption, on Ni catalysts, dynamics, neutron spectrosc. obs. 80−59778
chemisorption, on Si (III) surface, appl. of UPS ultra high vacuum apparatus *(Japanese)* 80−37125
chemisorption, on TiO_2(ZnO), differential heat of chemisorption 78−84052
chemisorption on Ni, neutron inelastic spectroscopy 79−69353
chemisorption on reduced and stoichiometric $SrTiO_3$(111), UPS and XPS studies, illum. effects 80−71572
chemisorption on Rh (111), effect of adsorbed O, H, or CO, LEED and thermal desorption meas. 80−75435
chemisorption on Si (111) 7×7 surface 80−10792
chemisorption on TiO_2, electron stimulated desorption, AES and charact. loss spectra 78−22963
chemisorption on TiO_2 (100), electron spectroscopy, evidence for Ti^{3+} photogeneration 78−38940
chemisorption on ZnO, cond. and ESR meas. 79−56072
chlorophyll a-water interaction, NMR obs. in CCl_4 and trichloromethane 79−34501

water continued
chloroplast, EPR signal II and Mn-water splitting, factors influencing stability 78−24038
chloroplast, mag. relax. of water protons and state of water photodissociation system 80−51133
cholesterol+water, interaction in organic media, dielec. and NMR spectroscopy 78−76979
chromatophores of photosynthesising purple bacteria, sorption and desorpt. of water 78−69012
clay-water systems, NMR, substrate struct. and H_2O mol. relax. 78−7247
cloud and rain drops, accel. to terminal vel. 77−78334
cloud drop spectrum evolution rel. to collision efficiency 78−69415
cloud droplet coalescence growth, fast computational method for Telford's theory 78−69486
cloud droplet spectrometry using light scatt. technique 77−41219
cloud droplets, stochastic collection eqn., computational instability in numerical soln. 77−2211
cloud drops collision efficiency, elec. charges and vertical external elec. field effects 77−25738
cloud liquid water content measuring devices 77−41223
cloud particle size distrib. meas. by optical array probes 77−41220
clouds, ice and water content from Nimbus 6 IR sounder data 78−92925
clouds, ice-bearing cumulus evolution, numerical simulation and obs. 77−2216
clouds, liquid water and ice contents rel. to radiative props. parameterisation 80−56601
clouds, liquid water content measuring device 79−88489
clouds, over Sierra Nevada, liquid water content meas. 77−2213
clouds, phase discrimination with polarisation diversity lidar 78−96269
cluster evidence from phase transition changes in IR mol. absorpt. coeff. 79−10100
cluster interpretation of IR water vapour continuum, comments 79−12262
cluster ions, collision-induced dissoc. at high press. 77−83679
cluster ions and D-region, mass spectrometer results analysis 78−61659
cluster ions formation in D-region rel. to mesospheric temp. 77−21842
cluster ions in mesopause region during winter anomaly, temp. and NO density vars. effect 79−21087
cluster ions production in quiet daytime D-region 77−45242
clusters, struct. and props. 80−39304
clusters around alkali metal ions, secondary emission obs. 77−63518
coadsorption with Br, on Cu(100), Helmholtz layer model system 80−92777
coherent Raman ellipsometry, vibr. stretching region and liq. struct. obs. 80−93341
cold water, tensile strength expts. 79−10539
collagen-water system, phasic transition invesitgation by calorimetry and NMR 79−62167
collective excitations in 10^8 cm^{-1} momentum range, neutron scatt. expt. 78−43087
collision-induced far IR absorpt., depolarised Rayleigh scatt. 77−81100
column, shock wave generation by impinging piston, waveform, propag. mode and state change 77−58733
combustion flow, passive optical diagnostics 77−44527
comet nuclei, water dominated, vaporisation rel. to lifetimes and orbits 80−56772
complex dielectric constants, meas. at 10 GHz using cavity perturbation method 78−24815
complexes with HF(HBr)(HCl), in supersat. soln., Raman spectra assignments 78−70840
compressed, supercritical, NMR ^1H relax. 78−60349
compressed, thermodynamic props., evaluation by statistical error anal. 80−92685
compressibility modulus 78−75701
Compton profile, electronic energy calc. 80−37822
Compton profile, exptl. determ. 77−32460
Compton profile, H-bond contrib., HFS Xα model 78−17726
Compton profile meas., non-additivity of elastic and inelastic X-ray scatt. 78−43953
computer simulation, intermolecular potentials 80−38890
concentration in lower stratosphere, far IR spectroscopy, quantitative anal. 79−39790
concentration in stratosphere, simultaneous inference using inversion algorithm 80−82000
condensation, thermodynamics of nucleation on charged centres 79−20955
condensation number, from micron size drop evaporation and growth rate determ. 79−90774
condensation on AgI aerosol particles, implications for ice-forming activity 80−101406
condensation on charged centres 78−51791
condensation onto ice, deposition coeffs. 80−6507
condensation via rarefaction wave 78−71847
condensation via rarefaction wave 79−46796
condensed gas films, thermal radiation absorpt. 78−32824
condensed multilayers, electron bombard. effects, AES line-shape anal., XPS, and desorption meas. 80−7450
contact angle measurement, effect of acoustic energy 78−95207
contact angle on polystyrene, cause of hysteresis 78−95206
content of porous materials, rapid thermal method of determ. 77−86258
continuity of state between liquid and amorphous solid, IR obs. 79−8130
convection, free, from horizontal cylinder to air (water) (Si oils), correlation eqns., viscous dissipation 78−5632
convection onset in horizontal layer, with max. density effects, nucl. plant waste heat storage 79−46164
convective heat transfer, free, with density inversion, in confined rectangular vessel *(German)* 79−18671
cooling system, fluid relay responding to flow rate 77−37879
corrosive effect of distilled water on Al evaporated films, ellipsometric obs. 77−48590
Crepis seed, influence of post irradition moisture alteration on biological after-effect 79−20581
critical flow states through pipe, modified Bernoulli theory 78−30345
critical mixture of water and isobutyric acid, shear viscosity, amplitude ratios 80−2188
critical mixture with 2,6-lutidine, spinodal decomposition, Rayleigh scatt. 80−70416
cryofilm, on specular and diffusing surfaces, bidirectional reflectance 78−88274
water continued
crystallisation, in magnetic field, crystal size reduction *(Russian)* 77−11670
crystallisation front, repulsion of macroscopic particles by gas layer 78−18568
crystallisation front movement, water and gas bubble distrib. 78−22830
CW and flash photoelectrolysis using ferroelectric photoanodes 80−81339
cyclohexane-acetic anhydride, crit. resistivity, H_2O impurity effect 79−51565
cylinder heat transfer to turbulent cross-flow of water at critical Re *(Russian)* 78−34132
decomposition by solar energy conversion for H_2 production 80−97813
decomposition H production by thermochemical and thermoelectrochemical cycles 80−26029
decomposition into H and O using solar energy, one-step effusional process 78−15672
deionised filtered, attenuation coeffs. meas. by split-pulse laser method, visible region 79−17505
dendritic ice formation in flowing water pipes, blocking mechanism 77−47092
density, effects of isotopic comp., temp., press., and dissolved gases, review 78−26616
density, meas. of small difference by elastic vibrator method *(Japanese)* 80−27272
density maximum points meas. 78−57900
density relation for pure and saline comp. 78−2185
depressurisation, early response 79−30908
desorption rate, effects of method of return to atm. press. for pressure vessel *(French)* 80−42233
detection of bacteria and algae by resonance Raman spectroscopy 80−94418
determination, in gases, mass spectroscopic method, prep. techniques 77−40587
determination, in organic solvents, IR spectrophotometric method 78−31731
determination in rocks and minerals by inorganic gas chromatography 80−85767
2,2-dichloro-1,1,1-trifluoroethane, redeuteration H-D exchange with water 79−64112
dielectric breakdown with picosecond laser pulses, SHG sharp increase 80−102769
dielectric constant of bonded lattice model 78−23386
dielectric effects, high field, Piekara factor meas. 78−68441
dielectric insulation for electron accelerators and impulse current generators *(Russian)* 78−75430
dielectric relaxation in plant tissues 78−88692
dielectric relaxation of compressed liquid at 17.613 GHz using microwave refl. meas. method *(German)* 80−71306
dielectric relaxation rate 79−78619
dielectric relaxation spectroscopy of polar fluids in microwave region, double beam interferometry method *(German)* 80−71309
diemthyl sulphoxide-H_2O-NaCl system, DTA exam. of primary ice phase field 78−48382
diethyl ether-ethanol-water, shear viscosity at plait points 77−35685
diffusion const. in presence of large background gradients, modified pulsed gradient technique 80−31831
diffusion in wheat grain endosperm tissue, ^1H NMR obs. 80−8001
diffusion of H and water transport in concrete, neutron radiography study, results review 78−59961
diffusion of O_2, N_2, H_2 and Ar, laser interferometric study 77−76584
diffusion through narrow pores of biomembranes, ^1H NMR obs. 79−92194
diffusive motions near 1°C 78−43156
dimer, coherent X-ray scatt. profile calcs. 77−61765
dimer, difference electrostatic mol. pot. contour maps, basis set superposition effect 80−102462
dimer, electron affinity, ab initio SCF calcs. 79−76343
dimer, intermolecular pot. functions from ab initio calcs. 80−5473
dimer, isotopic forms, Ar matrix isolated IR spectra, assignments, config. 77−6780
dimer, meteorological implications 80−8418
dimer, partially deuterated, microwave spectra and struct. 80−74212
dimer, props., influence on tropic meteorology 79−2349
dimer, stability, CNDO/2 and STO-3G calcs. 79−760
dimer, struct. from mol. beam elec. reson. spectra 77−54555
dimer, struct. studied by CNDO/2 method 80−69081
dimer, tunnelling-rotational energy levels, group theoretical classification 77−54549
dimer config., vib.-rot. band intensities, rel. to 8-13 μm atmospheric extinction 80−9610
dimers, and H_2O.Ne, excited, first order interaction energy, ab initio calc. 80−32598
dimers., IR spectra, in N_2 matrix, assignments and force consts., isotope effects 77−61744
dimers, IR spectra in N_2 matrix, temp. and IR irrad. effects 77−61745
dimethylsulphoxide-water-0.9 m $NaClO_4$, salt effect on vap.-liq. equilib. 79−51245
dioxan-$H_2{}^{16}O(H_2{}^{18}O)(D_2{}^{16}O)$, solns., FP determ., equilib. method 77−20048
p-dioxane-water mixtures, adiabatic compressibilities and sound vels., temp. depend. 79−28044
dioxane-water mixtures, compressiblity, density, US vel. rel. to temp., conc., struct. *(German)* 77−43263
p-dioxane-water system, excess molar heat capacities, 298.15K, US vel. obs. 80−6523
direct and indirect action of constant magnetic field on biological subjects 79−34580
discrete chemistry, new approach to water analysis 78−88674
disperse systems, flotation of fine particles by group of bubbles, kinetics 78−53261
dispersed medium freezing, origin of water aspiration 77−60130
dissociation by polynaphthoquinone-SO_2-I_2 system for H_2 prod. 80−16825
dissociation by S-I cycle for thermochem. prep. of H_2 80−16823
dissociation by Sb-I-Ca process for thermochem. prod. of H_2 80−16824
dissociation on Pt(111), identification of adsorbed OH species 80−49509
dissociation under solar illumination, band bend of surface of n-TiO_2 photoanode 78−91765
dissociation using solar energy for H prod. 80−30597
dissolved CO_2 Raman spectra 77−65467

water continued
distilled, surface tension, AC field influence calc. comparison with exptl. data *(Russian)* 77−55417
DNA, water localisation in a DNA mol. by differential Fourier synthesis 80−94164
DNA interaction, single and double helix DNA 80−30646
DNA water salt solns., microcalorimetric investigation of phase transition and eutectic fusion 79−79448
Douglas fir, evapotranspiration determ. using weighing lysimeter 77−64353
drainage, by capillary flow *(Japanese)* 78−95208
drinking water, Finland, internal radiation doses due to radioactivity 80−109029
drinking water, Finland, natural radioactivity 80−108819
drop, collisions on elastically deformable media, simulation of erosion by rainfield 77−56113
drop breakup, catastrophic, free flight meas. of particle sizes 77−31361
drop evaporation by 10.6 μm laser radiation 77−75589
drop fragmentation by laser 79−7169
drop impact on rigid surface 77−85084
drop interaction expts., review 78−11974
drop size in nozzle flow of moist water vapour 77−42904
drop thermal explosion by high-power laser radiation 77−75590
drop vibration analysis in near-zero gravity 77−7426
droplet, explosive vaporisation on 10.6 μm radiation exposure, inhomogeneous internal heat evolution 80−29162
droplet, IR emissivity 80−36394
droplet, laser induced evaporation, diffusion coeff. temp. depend. 77−20062
droplet aerosol interaction with EM radiation, temp. field and refractive index distrib. model 78−3899
droplet clouds, rate of evaporation, stability 79−52782
droplet coalescence in turbulent clouds 77−45114
droplet collision and coalescence for small Reynolds numbers 77−78326
droplet conc. and size determ. from cloud liquid water content and extinction meas. 80−51579
droplet evaporation, heat transfer characts., on heated surfaces 78−59269
droplet evaporation, modelled by wet porous sphere, heat-transfer meas. 78−59268
droplet evaporation and microclimatic modification 77−17248
droplet forced convection and heat transfer rel. to vapour conc. *(Chinese)* 79−23185
droplet growth rel. to condensation coeff. *(Russian)* 79−34901
droplet interactions, expts. for educational use 78−4441
droplet size distrib. spectra in cumulus clouds *(Russian)* 80−81991
droplet vaporisation in moderately-high temp. stationary media, Chang model 78−34609
droplet-graphite surface hypervel. impact simulation, using high-power pulsed laser 77−44094
droplet/ice crystal clouds, angular depolarisation and multiple scattering of polarised laser light 80−41549
droplet/ice crystal clouds, angular scattering of polarised laser light 80−41548
droplets, ebullition under steady-state superheated conditions 80−74928
droplets, ebullition under transient superheated conditions 80−74929
droplets, evaporating in vert. hot air tunnel, radiative transfer effect 79−46400
droplets, initiation of optical breakdown in air 80−10352
droplets, small, weakly absorbing, motion in bounded laser beam 79−12269
droplets, subcooled, nucleation in Ar-H_2O vapour mixture, rate const. 80−61131
droplets in mists, clouds, size, density distrib. meas., laser remote sensing technique *(Japanese)* 78−49175
droplets in Wilson cloud chamber, light scatt., ripple struct. of extinction coeff. 77−34821
droplets size distrib. in cloud bases 78−73458
droplets size distrib. in mist, vol. extinction coeff. at visible and IR wavelengths 77−37287
droplets suspended in turbulent flow, evaporation rate rel. to $Ca(CO_3H)_2$ soln. drops 79−90771
drops, acting as capacitors in corona discharge *(Russian)* 77−62420
drops, coalescence, theoretical model of approaching drops 78−32207
drops, coalescence problem, efficiency 78−32208
drops, collisions, coalescence efficiency, expt. evaluation 78−32206
drops, collisions with spherical particles, impaction and electrical effects 78−28272
drops, crystallisation on CuS aerosol prepared by burning pyrotechnic mixture 78−96279
drops, in methylphenyl silicone oil, intermittent elec. field heat transfer augmentation 78−94872
drops, interpretation of foil impactor impressions, rel. to hail research 78−57356
drops, on brass surface, Leidenfrost pt., press. effect 78−87784
drops, on DC transmission conductors, corona discharge and elec. charge 79−82114
drops, optical props., comparison with atmospheric aerosols *(Russian)* 78−77328
drops, optically dense, motion in laser radiation field 78−50842
drops, size meas., evaluation of direct methods 77−22527
drops accel. to terminal vel., drag coeff. 78−61506
drops collision efficiency in atmosphere 77−29378
drops crystallisation under influence of AgI-type reagents, kinetic parameters *(Russian)* 77−81963
drops in PMMA, effect of drop size on contact angle 80−2245
drops in subsaturated air, aerosol particle collection efficiency 78−28273
drops of water, ice or mixed phase, backscatt. at 633 nm 77−64426
drops on HV overhead power lines, expt. 80−33851
dynamic viscosity coeffs. *(Russian)* 78−47550
effect of graphite-$FeCl_3$ intercalation compound formation *(German)* 79−52634
elastic wave propagation in thick water layer between solid plates 77−4158
electric breakdown for applied electric fields in range 200-500 kV/cm in the 2-10 microsecond time domain 80−71316
electric breakdown mechanism, high speed photography expts. 79−91367
electric breakdown processes, obs. of prebreakdown during electrohydraulic forming *(Japanese)* 77−24977
electric breakdown strength of water transmission line 78−9897
electrification during laminar flow in metal pipe 80−6954

water continued
electrochemical splitting, solar energy assisted, on MoS_2 layer cryst. surface 77−90612
electrode-solution interfaces, role of water 78−40058
electrokinetic and rheological parameters in single capillary 80−10220
electrolysis, design and operation of advanced H_2O electrolysers for H_2 prod., review 80−61449
electrolysis, H_2 production, module design, geometry, capacity, operating temps., pressures, electrode types 80−72098
electrolysis, H thermoelectrochemical prod. using H_2SO_4-SO_2 cycle, electrochem. aspects 80−35776
electrolysis, limiting conditions for use of nuclear reactor heat in thermoelectrochemical cycle *(Russian)* 78−46183
electrolysis, nucleate boiling, vapour bubble behaviour, heat and mass diffusion 80−67013
electrolysis, photoassisted, Fe_xO_y electrodes prep. and characts. 78−15683
electrolysis, S cycle H prod. process, laboratory prod. model and electrolyser development 80−30602
electrolysis, solid polymer electrolyte, H_2 technology 80−67012
electrolysis and recombination, teaching demonstration 77−9843
electrolysis at Hg cathode, $H^+(D^+)$ discharge activation energies in $H_2O(D_2O)$ 80−40707
electrolysis at high temp. for H prod. 80−30439
electrolysis H_2 production, onsite, for electric generator cooling 80−72097
electrolysis in fused NaOH for H_2 prod. 80−76660
electrolysis with solid polymer electrolyte, for H_2 production 80−61442
electrolyte solns., aq., water struct., differential IR spectral investig. 77−52651
electrolytic decomposition in acid molten electrolytes at 220 to 320°C for H prod. 80−45769
electrolytic dissociation using solar energy and TiO_2 electrode *(Czech)* 77−29014
electron absorpt. at high energy 78−881
electron attachment to O_2 and H_2O in flames, kinetics 80−3349
electron degraded 1 keV energy spectra in water vapour and C foil 80−9474
electron diffraction 78−83686
electron elastic and inelastic interactions with liq. water 80−9477
electron energy deposition, effect of 21.4 eV plasmon, model 77−4135
electron energy loss, Monte Carlo anal. 77−31703
electron energy loss spectra, yield calcs., biological implications 79−7641
electron slowing down in water, spatial correlation of energy deposition events 80−9473
electron slowing down spectra in X and γ irradiated water 80−12197
electron spatial absorbed-dose distrib. for 25 MeV beam 77−88289
electron stopping power, continuous slowing down approx., range difference for 0.2 to 10 MeV electrons 80−39187
electron track end effects in water 80−11932
electron transport simulation in liq. water, appl. to microdosimetry and radiobiology *(French)* 80−12202
electronic component package, H_2O content determ., plasma chromatograph-mass spectrometer applic. 78−86379
electronic structure investig. by XPS, UPS and UV absorpt. spectra 77−16452
electrostatic interactions and the structure of water, conf. Brussels, Belgium (1972) 78−26413
electroviscous effect, mechanism in DC and AC fields 79−51294
empirical potential model EPEN/2, parameterisation testing 79−54933
empirical potential model EPEN/2 for conform., intermol., solvation studies 79−50102
emulsion, water-in-oil-in-water, multiple phase, prep. technique 77−1953
emulsions, dielec. props. obtained after crystallisation/melting cycle 77−86381
enthalpy of ionisation, 273 to 323K, from HCl neutralisation meas., sp. ht. changes 77−48676
enthalpy of ionisation, meas. by reaction-solution rotating-bomb calorimeter 80−4717
epoxy resin, destruction by diffused water 78−48511
equation of state, between 350 and 1000°C (0 to 10 GPa) and between 100 to 350°C (200 MPa to melting curve) 80−15214
equation of state, perturbed-hard-sphere, applicable to sub- and supercritical temps. 79−19350
equation of state determ. from sound speed eqn. 77−47538
equations of state in uniform and two-phase states, thermodynamic model interpolation 80−24565
erythrocyte membrane, pulse NMR meas. of water exchange 79−43826
erythrocyte membrane water permeability defect in human epilepsy, NMR 77−29122
erythrocytes, human, effect of hydration on water content 77−16921
ethanol-benzene-water-$(NH_4)_2SO_4$, liq. mixture, near tricrit. pt., light scatt. and sum rules 80−34933
ethanol-H_2O, liq., Compton profile at 60 keV 79−47535
ethanol-water mixture, saturated, min. film boiling temp. on horiz. stainless steel and Cu surfaces 78−90692
ethanol-water mixture, Soret coeff. determ. 79−19386
ethanol-water mixtures, specific volume, compressibility, viscosity, up to 3200 bar, 15, 25°C 78−10113
ethanol-water system, metastable states, hydrates existence and props., low temp. 78−71835
ethanol-water-chloroform mixture, light scatt. near plait point 78−72532
ethylene glycol-water, glass, 4.2K, trapped electron photocond. and optical spectra following radiolysis 79−29378
ethylene glycol-water, uninhibited soln., corrosion of Al 79−70222
ethylenediamine-H_2O mixtures, inhibition of Ps form. by NO_3^- ions 78−95988
ettringite, expansion by H_2O adsorption, exam. 78−64806
evaporation, rate var. with vap. press. 78−18758
evaporation, surface cooling, apparent evaporation coeff. 80−2148
evaporation coefficient, reply to comments 78−75912
evaporation coefficient, variation with observation conditions 78−75909
evaporation coefficients, comments 78−75910
evaporation coefficients, comments 78−75911
evaporation from nonsaturated surfaces, parameterisation 79−53372
evaporation through monolayer free and monolayer covered surfaces, temp. gradients meas. 80−88402
evaporation variation with salinity and temp. 77−53083
evaporative water loss meas. from small animals by dew-point hygrometry 78−20326

water continued
evapotranspiration calc. using planetary boundary layer theory 77−25716
exploration, geophysical methods, International School 1st course proc. (Erice, Italy, 1975 April 15-26) 77−9526
eye, proton relax. in normal and cataractous cryst. lens 77−60203
eye cataractous lens, NMR study of state of water *(Hungarian)* 78−64986
eye lens, normal and senile cataractous, PMR study of state of water 78−64987
eye lenses, crystalline, of humans, fish and birds, state of water, NMR meas. 79−48212
far IR transmission spectrum 77−38041
far IR transmission spectrum 78−4713
fast neutron angular penetration spectra, comparison with Monte Carlo calcs. 77−23303
fast neutron penetration spectra 78−29535
fatigue crack plasticity of low C steel, effect of water vapour 78−64678
feldspar/water O isotope exchange, effect of fluid press. 78−57204
film, between muscovite sheets, permittivity change meas. method, 20-70°C 80−55009
film, on slightly rough quartz surface, ellipsometric thickness meas., error estimation 78−32856
film, vaporisation in rot. pipes 79−14228
film, wavy laminar flow down vertical plate at high surface tension numbers 79−94587
film adsorbed on CaF_2, internal reflection spectroscopy 79−15549
film condensation inside pipes, heat transfer, general correlation 79−46312
film crossflow around cylinder, local heat transfer 79−98711
film flow behaviour and effect on cocurrent air flow, press. distrib. along rigid wavy structures 77−55029
film on Teflon surface, boiling heat transfer 79−90124
film shape on mosaic surface of solid *(Russian)* 79−51395
films, subcooled, flowing down vertical tube, heat transfer 80−79318
films, thin, wetting, rheological charact. determ., capillary method 78−51788
finite water assemblies, steady state thermal neutron spectra, space and ang. depend. 77−50187
fission reactor coolant, water chemistry *(Japanese)* 80−68737
flame gas, electron-neutral energy exchange in AC field 77−42519
flat plate multiple pass solar collector using aqueous optical properties 80−7957
flat rectangular channel turbulent water flow, free stream and viscous sublayer temp. fluctuations 78−83369
floods in United States and their management 77−41073
flow, 1st normal stress difference meas., rel. to polymer solns. 79−98829
flow, annular, air-water, interfacial drag and wall layer height 77−39324
flow, around rod bundle with helical spacers, air distrib. 79−30894
flow, forced laminar convection in horizontal pipe, density inversion effects, numerical anal. 78−90900
flow, pipe, local heat transfer to turbulent flow, superposition principle, expt. 78−83479
flow, vertical boundary layer convection, salinity and press. depends. 79−37316
flow around cylinder, thermophys. charact. rel. to friction and heat transfer *(Russian)* 78−38328
flow boiling and pool boiling critical heat flux, effect of flow passage geometry 77−62250
flow in capillaries, Washburn eqn. 79−64767
flow in heated tubes, with near critical parameters, turbulent flow, heat transfer 80−59022
flow rate through cylindrical channels, determ. 79−90339
flow through circular pipe, pulsed NMR study 80−28566
flow through inhomogeneous porous media, analytical theory 77−62301
flow through rock specimen, average pore vel. meas. 79−5473
flow with air contents, partially- and super-cavitating hydrofoils in cascade, analysis method *(Japanese)* 80−14763
flowing water erosion, bed scallops and ripples sizes 79−27628
foams, shock wave propagation 79−64737
fog and clouds, liq. water content rel. to atm. visibility 78−81404
forced convection of supercritical press. water in heated small bore tubes 77−65739
form drag of in-line tube banks in water cross-tlow *(Russian)* 79−7412
formaldehyde-water, heuristic intermol. pot. function, ab initio MO calcs. 78−33566
formation, during Fe oxide reduction, kinetics 79−83449
formation on O_2 exposure of hydrides of intermetallic cpds. 80−97727
formic acid-water polymers, gas phase, H-bonded complex struct. from elec. dipole moment obs. 78−74791
free boundary problems of the steady water cone in the well of a petroleum reservoir *(Chinese)* 79−50699
free convective heat transfer with density inversion of water between two concentric cylinders 77−42836
free energy calcs. by random network model 80−92688
free energy of liq. water, ab initio Monte Carlo calc. 78−83975
free surface, metastable effects associated with press. pulse refl. 80−6463
freezing, cylindrical and two-dimens. with varying wall temp. 77−1217
freezing, production of stimulated coherent radiation 78−83920
freezing and melting behaviour in capillary, dilatometry, elec. cond. meas. 78−75908
freezing drops, ice envelope splitting *(Russian)* 77−27982
Freon-12 and water, flow boiling crisis in horizontal tubes, fluid-to-fluid modelling 80−48785
freshwater, precipitation processes, study by particle site anal. 80−50883
friction factors in 2-D flow with relative large roughness 78−30357
frost properties, rel. to frost formation types 77−80614
frozen soil, water and ice envelope pressure potentials 77−78286
furfural-water interface, anomalous mass transfer, coupling of heat and mass transfer 77−80626
fusion reactor-high temperature electrolysis system for H_2 prod. 79−18041
galactic H_2O vapour sources, maser phase duration galactic distrib. 79−35343
gamma-ray buildup factors 80−27822
gamma-ray buildup factors for Pb/H_2O stratified radiation shields 80−86994
gas, electron-ion recombination, at 292K, three-body interaction 79−46418
gas and vapour bubble nucleation on brass surface in water 78−71845

water continued
gas laser pumped by electronic-vibr. energy transfer, transitions 7 to 7.7 μm 77−31094
gas-phase radiolysis of ethane, inhibition of free radical prod. 79−39178
in geological conductors, influence on elec. props. *(German)* 79−5472
in glacier, influence on sliding on plane strewn with hemispherical obstacles *(French)* 79−8640
glass fibre reinforced epoxy resin, destruction by diffused water 78−48511
glass fibre reinforced epoxy resin, destruction by freezing or boiling of phase separated water 78−48512
glass water resistance, rapid meas. method 79−61812
glass-transition temperature, crystn. temp., and dielec. const. 80−15229
glycerine-water drops, collision dynamics, ang. of incidence influence *(Russian)* 78−83461
glycerine-water mixture, cylinder oscillating in viscoelastic fluid, secondary flow 79−60037
granitic magmas, water content 77−5187
gravitational wave absorption by water mols. 80−82189
gravity wave, steady, numerical soln. using Riemann Hilbert method 80−33618
gravity waves in water of variable depth 79−48514
gravity-free environment, evaporative loss by man 79−57779
ground level abundances of N_2O, CO_2, CO and H_2O, simultaneous determ. 78−11969
ground water level fluctuations, influence of outer water level variations, basic investigations 78−53663
gypsum hydration water, isotopic comp. 79−20829
H-bonded dimers, PCILO calc., energies, geometries 78−37557
heat capacity and structure, isomerisation reaction role 79−33097
heat emission of a rough-surfaced tube in turbulent water flow *(Russian)* 80−74837
heat of ionisation, calorimetric meas. on enthalpies of reaction of I_2O_5 79−70359
heat of vaporisation, student lab. meas. method 79−30175
heat pipe working fluid, crit. heat/mass transfer 78−42517
heat pipes, exptl. obs. *(Chinese)* 78−30171
heat transfer and flow through hydraulically induced fracturesin hot dry rock 79−34424
heat transfer and power expenditure in agitated vessels with bare (finned) tube baffles 79−1052
heat transfer coefficients, heater plate thickness effects 78−34124
heat transfer correlation for subcooled water films on horizontal tubes 79−77114
heat transfer of rough cylinder in transverse water flow *(Russian)* 79−10449
heating, by natural circulation solar system, with linear and nonlinear temp. distribs. 77−75778
heating at microwave freqs. and complex permittivity meas. for specific purities and salt. soln. 80−60480
heavy and ordinary water dynamic viscosity coeffs. relation in liquid phase 78−21759
heavy charged particle/water interaction, dose distrib. due to electrons, delta rays 80−13937
heavy ion beam propag., energy loss and fragmentation of nuclei 79−54755
heterogeneous systems, NMR, substrate struct. and H_2O mol. relax. 78−7247
1-hexene-water(-D_2O), field-induced surface reactions, field ionis. mass spectra obs. 78−95949
high pressure properties and structure, mixture model 77−84612
high pressure steam/water mixture flow through cylindrical channels, obs. 80−79404
high-pressure Raman spectra, bending and librational bands 78−68499
humid atmosphere, water droplet vaporis. model with natural convection 78−33999
hydrate librational modes in IR spectra 78−48161
hydration kinetics, microwave obs. 79−34255
hydration of surfactant micelles, H_2O penetration 80−45572
hydrationally active phases, electron structs. and props. of anions 77−44574
hydraulics of water flows, terrestrial equivs. of Martian outflow channels 79−40112
hydrocarbon drops levitated in water, acoustically forced shape oscill. 79−47987
hydrogen bond breaking by negative pion capture *(Russian)* 79−94866
hydrometeors, radiative props. at microwave freqs. 79−20940
hydrometeors in clouds, size, conc. and struct. meas. 77−41218
hydrophobic effect, dil. soln. struct. and thermodynamic props., semi-empirical model 78−20060
hydrophobic interaction, of two Xe atoms, mean force determ. 80−54114
hypersound phase vel. and damping by high resolution Brillouin spectroscopy 77−69845
hypersthenic magmas, water contents 80−72507
ice, crystalline, localised excess electrons yield studied as function of dose rate 80−97712
ice-water interface, dynamic light scatt. during freezing 79−33074
ice-water interface, local temp. meas. and convective flow 79−73293
ice-water interface, surface tension meas. by grain boundary groove method 77−24481
ice-water interface struct., fluctuations during solidification 78−59935
imaging systems in water, point and beam spread functions 78−5426
impurity in SiO_2 based optical fibre waveguides, water impurity 77−68270
incipient boiling characteristics at atmospheric and subatmospheric pressures 78−90688
infiltration in dry soil 77−78279
infiltration into frozen soils, numerical modelling 79−39772
infiltration into horizontal sand column, flow charact. 77−78280
injection of gases through porous plate, squeezing out of liq. 80−64622
interaction with Cl and Cl_2, surface reactions at low temps. 79−79288
interaction with Zn (0001) surface, UPS meas. 78−76585
intercalation in β-Al_2O_3-Na_2O, effect on ionic cond. 79−99364
interface with Al_2O_3 layer on stainless steel, leaky wave generation 80−75419
interface with Bi electrode, halide ion adsorption parameters, zero charge pot. conc. depend. 80−40706
interface with fatty acid solid monolayer, model 80−54505
internal press. isobars, anomaly short-range order influence 77−65944
interstellar, high abundance in Orion, dynamical explanation 79−48876

water continued
interstellar diffuse clouds, search for H_2O, Copernicus UV obs. 79−40233
interstellar H_2O, 183 GHz line emission obs. 80−41869
interstellar H_2O, abundance and column density in post-shock gas 80−56911
interstellar H_2O, synthesis in interstellar clouds by radiative association reaction $H+OH \rightarrow H_2O+h\nu$ 80−90509
interstellar H_2O maser, in shock-induced star form. region in (NGC 281) 79−25688
interstellar H_2O maser emission, new sources detect. 80−62298
interstellar H_2O maser features, high-velocity, in W3(OH), obs. 80−31339
interstellar H_2O maser in H II region complex (RCW 48-49) 77−57102
interstellar H_2O maser in H II region NGC 281, obs. 78−28740
interstellar H_2O maser in Orion A, giant outburst 80−8703
interstellar H_2O maser source in Orion A, obs. of outburst *(Russian)* 80−105320
interstellar H_2O maser sources, near IR pumping 77−78862
interstellar H_2O masers, influence of dust on collisional pumping 78−54030
interstellar H_2O masers assoc. with mol. clouds, VLBI aperture synthesis obs. 79−21368
interstellar H_2O masers in H II regions, time vars. obs. 79−88725
interstellar H_2O masers in NGC 6334, positions and spectra rel. to star form. 80−73025
interstellar H_2O masers near type I OH masers, obs. 79−25671
interstellar maser emission increase in W3(OH) 77−53672
interstellar maser lines intensity vars. due to induced Compton scatt. 78−4319
interstellar maser lines very-high-velocity satellite features generation by stimulated Raman scatt. 78−73746
interstellar maser source near NGC 2071, discovery 78−73768
interstellar masers, 22 GHz obs. with resurfaced Parkes radiotelescope 77−33347
interstellar masers, collisional pumping in circumstellar shock wave 77−53675
interstellar masers, radial vel. struct. 77−33617
interstellar masers, survey in southern hemisphere 77−91599
interstellar masers, weak OH maser emission detect. 77−33618
interstellar masers assoc. with compact H II regions, model 78−81666
intracellular water, effect of paramag. impurities on proton spin-lattice relax. 80−51134
ion $(H_2O)_n+H_2O \rightleftarrows ion(H_2O)_{n+1}$, standard free energies of reaction 79−34348
ion-water interactions, survey of diffr. studies 80−24347
ionisation energy at 298.15K 78−3364
Iowa lakes, water transparency survey 79−2308
IR absorpt. spectra, band profile temp. depend. 77−30869
IR absorption spectra in 8-14 μm region, water cluster interpretation 79−98081
IR emission due to latent heat of transform. 77−31754
IR spectrum, influence of Cu^{2+} ions 78−72501
irradiated by photons up to 2 MeV, initial energies of Compton electrons and photoelectrons 80−108320
isentropic decompression from crustal and mantle press., thermodynamics 79−79769
Ising lattice model with directional bonding, renormalisation group study 80−28894
Ising model and config. heat capacity 79−33096
isobutyric acid+water, thermal expansion near upper crit. soln. temp. 77−29031
isobutyric acid-water, crit. mixture, conc. fluctuation mean relax. time, US absorpt. and vel. meas 80−29163
isobutyric acid-water binary fluid system, crit. props. 77−76563
isobutyric acid-water critical mixtures, US and hypersonic study 80−88268
isobutyric acid-water mixture, electrical conductivity near crit. pt. 77−15612
isobutyric acid-water mixtures, phase separation, light scatt. 78−84592
isobutyric acid-water mixtures, spinodal decomposition, light scatt. 77−72688
isobutyric acid-water near-critical liquid mixture, nucleation 80−92664
isobutyric acid-water system, liq.-liq. critical pts., Ising exponents, extended scaling 77−20072
isothermal flows behind shock wave in water 77−89159
S.Israel, isotopic comp. of formation waters from deep drillings 77−86945
jet, destruction of rock, theory based on drag force on grains in permeable medium 78−55691
jet, round, impinging, heat transfer in interference zone of film flow along wall 77−58750
jet, turbulence fine struct., polymer addition effects, high speed photography 78−26178
jet atomisation of Fe-C melts, Fe powder production 79−100090
jet streaming, planar and cylindrical, instabilities rel. to glassy alloy casting 80−35129
jets, two-dimensional, effects of applied sound *(Japanese)* 78−79353
jets, under gravity, cross-section shape 77−3854
Jupiter, interior models, water and rock abundances 77−33398
Jupiter magnetosphere, contrib. of water products from Galilean satellites 78−45268
Kerr const., 280 to 350K temp. depend. 78−35113
Kerr constant, meas. at 30°C and 441 and 633 nm 77−55771
kidney, tissue water freezing study, ^1H NMR obs. 80−8027
laminate, fibre reinforced composites, moisture diffusion, 3-D Fick's law 78−10218
laser backscattering from turbid mixtures 80−1129
laser breakdown, photoacoustic and photohydrodynamic parameters 78−52597
laser induced breakdown, comparison with D_2O 78−68453
laser produced cavitation, behavioural study by holo-cinematography *(German)* 78−87371
laser propagation in water, multiple scattering effects *(Japanese)* 78−78915
laser spectroscopy using an optothermal receiver 80−37810
laser-induced ionisation, quantum yield, temp. and wavelength depend. 80−11924
lattice fluid model on 2D quadratic lattice 79−93056
lattice gas model, phase transitions 79−80535
water continued
layer, semiinfinite, cooled (heated) from below, convection onset, density anomaly influence *(German)* 78−22350
leakage neutron spectrum meas. in light water using time of flight technique 78−62592
light scattering, ratio of Brillouin to total scatt. intensity 78−52515
light scattering from water surfaces *(French)* 79−27171
light water, cold neutron interactions, total cross-section meas. 77−67786
linear electrooptic effect 77−16283
liquid, and glycerin soln., heat transfer in oscillating liquid-filled cylinders 80−10117
liquid, broad band vibr. struct., polarisation CARS obs. 79−85963
liquid, Compton profile at 60 keV 79−47535
liquid, critical heat flux of saturated natural convection boiling with heating from below 80−10114
liquid, diamagnetism, temp. dependence, NMR chemical shift calcs., molecular interactions data 80−75707
liquid, electrical breakdown in μs regime with Cu, brass, steel and Al electrodes 80−103917
liquid, electron solvation dynamics 80−85205
liquid, equations for mag. susceptibility, electric polarisability 80−75708
liquid, far IR optical consts. meas. with optically pumped laser 80−40082
liquid, force bias Monte Carlo simulation 79−77487
liquid, H bond distrib., Monte Carlo simulation calcs. 80−54106
liquid, H-bond networks, percolation process 79−69001
liquid, intermol. coupling, isotope and salt effects, Raman spectra 78−90169
liquid, IR spectral investigations of assoc. 79−65847
liquid, mag. treatment affecting props., proposed mechanism 78−84827
liquid, Monte Carlo-Metropolis computer simulation, convergence charcts. 80−10485
liquid, physical props., two-state model approach 80−75144
liquid, proton NMR chem. shift, press. depend. 77−8428
liquid, proton spin-lattice relax. by slow proton exchange 80−60437
liquid, pulsed electric field applied to sharp point, prebreakdown field 80−6308
liquid, Raman and IR spectrum in overtone OH stretching region 80−58263
liquid, relax. compressibility and heat capacity 80−92580
liquid, single 1.06 μm picosecond pulse superbroadening, concurrence with dielec. breakdown 79−86223
liquid, single-particle motions 79−1385
liquid, solubility in compressed air 78−34631
liquid, solvated electrons, photon-induced electron transfer transitions 79−8154
liquid, struct. relax. time in 2-state model, 0-100°C 80−1914
liquid, thermal conductivity at high pressures, meas. with Ag co-axial cylinder cell *(Japanese)* 80−80007
liquid, UV absorpt. spectra 80−76043
liquid, viscosity, −8°C to 150°C, anal. of data 78−95101
liquid, viscous props. 80−2186
liquid, visible absorpt. meas., pulsed dye laser optoacoustic spectroscopy 80−11426
liquid, zeroth order random network model 79−68993
liquid interface, mol. orientation and surface pot. at 4°C 80−15339
liquid intermol. force model, used to compare Monte Carlo and mol. dynamics calc. methods 80−14984
liquid layer beneath ice crust on Europa, model 80−26780
liquid mixtures, with methanol(ethanol)(acetic acid), Verdet const., pulsed mag. field meas. 80−16012
liquid properties representation, by modified Redlich-Kwong eqn. of state 78−34590
liquid structure, group freqs. appl. 79−98057
liquid structure, Monte Carlo studies, review 80−54101
liquid structure potential energy function, appl. to ice lattice energy 79−73125
liquid water, PVT props., density meas., 150-350°C, saturation to 1 kbar 78−34594
liquid water content meas. of lab. supercooled clouds, instrument design 78−96316
liquid-solid phase transition, photoacoustic detection 78−75810
lithium perfluoro-octanoate-water, liquid crystal, ^{19}F multipulse NMR obs. 80−34795
lithium perfluoro-octanoate-water system, liq. cryst. struct., self-diffusion, NMR 78−15036
living body, water exchange dynamics in normal and pathological conditions 78−64914
LMFBR steam generators, leak detection of steam or water into sodium 79−13434
localised excess electrons, semicontinuum models 78−73129
long range forces in mol. dynamics calcs. 78−79517
low freq. Raman spectra, isotope shifts, ice-like struct. 79−28732
2,6-lutidine-H_2O, phase separation, hydrodynamic effects 78−83960
2-6-lutidine-water, anomalous supercooling near critical point 80−70384
2,6-lutidine-water, fluid film, crit. phenomena, scaling, law of corresponding states 79−90787
2,6-lutidine-water, fluid film, crit. temp. shift, crossover temp., coexistence curve amplitude, fluid-boundary interaction 79−90788
2,6-lutidine-water, spinodal decomposition, light scatt. obs. 78−34625
2,6-lutidine-water thick films, interferometric obs. of crit. behaviour 80−93266
LWR, thermal neutron steady state spectra in pure and poisoned water 79−36306
LWR mixed oxide fuels, determ. of H_2O, Hz content by hot extraction methods *(German)* 79−49808
lyotropic phase orientation, ^{17}O and ^2H NMR study 78−27905
lysozyme bound water, thermally-stimulated press. and current 78−15757
lysozyme hydration, correl. of diverse types of meas. 80−61507
lysozyme spin-labelled preps., water-protein layer microstruct. study by mag. relax. 78−76980
lysozyme-water mixture, phase separation, rel. to cold cataract form. in young rat lens 78−11640
machine simulation, book contrib. 79−60249
in magmas, influence on physical props. and comp. 80−41418
mammalian cells, NMR relax. time meas. of bulk water 80−21454
marine advection fog, water distrib. rel. to droplet size, salt particle nuclei 79−5570
Mars, atmosphere model and water vapour distrib. 79−40113

water continued
Mars, consequences of liquid water saturated regolith in early Martian history 78−65538
Mars, crust, possible fossil H_2O liquid-ice interfaces 78−65539
Mars, northern summer ice cap, Viking 2 water vapour obs. 77−53454
Mars, polar ice discovery 77−22130
Mars, water vapour obs. from Viking orbiters 78−20682
Mars atmosphere, water vapour global seasonal var. and implications for permafrost 79−84714
Mars atmosphere, water vapour vertical distrib. 79−84713
Mars regolith, implications of abundant hygroscopic minerals 78−65541
maser emission from cool stars, catalogue of 82 objects 79−8909
maser emission from Mira and semiregular variable stars, microwave and IR obs. 79−67037
maser emission in W49N, W51 and Sagittarius B2, high vel. features 77−9779
maser emission search from globular star clusters 79−30094
maser near RT Serpentis, obs. 79−8932
maser sources near Herbig-Haro objects 7-11, 22 GHz obs. 80−73019
in maser stars, search for absorpt. lines 77−78804
masers, Herbig-Haro objects and interstellar bullets 79−35329
masers, in dense interstellar mol. clouds, high sensitivity survey 78−85988
masers, interstellar, in mol. clouds assoc. with small Hα emission regions 79−17042
mass spectrometric chem. anal. of D, ^{17}O and ^{18}O from natural waters of Mt. Everest *(Chinese)* 80−77016
maximum density, free convective flow, past infinite porous plate with const. suction 78−42606
measurement standards for H and O stable isotopes 78−32246
medical nebulizer produced, droplet size distrib., evaporation effect 78−24084
medical phantom, absorbed dose calibration of high-energy X-rays 79−8548
melting ice layer, heated, free convection onset criterion, density anomaly effect *(German)* 78−22351
meltwater, from Alpine glaciers, ion exchange influence on dissolved load 78−81228
membrane, water swollen, rapid prep. technique, obs. using SEM with cryo-unit 79−89047
membranes for ion exchange, ion and water transport eqns. 78−68930
mesosphere, water vapour line at 22.2351 GHz, hyperfine structure 79−8666
metals determ., in water and organic materials, flameless atomic absorpt. spectrometry with wire loop atomiser 80−45586
metastable liquid, US vel. under atmospheric press. 79−10897
metastable state, fundamental equation 80−103447
metastable states, phase diagram *(Russian)* 78−95129
metastable superheated water, specific vols. and P-V-T props. 80−92032
in meteorites, low temp. condensation rel. to H and O isotope study 80−36518
methanol-H_2O, liq., Compton profile at 60 keV 79−47535
methanol-H_2O matrix, 77K, electron solvation and presolvation, electron spin-lattice relax. 79−57260
methanol-H_2O mixture, evaporating droplets in air, temp. modelling *(German)* 80−2243
methanol-water, assoc. mixture, rot. barrier solvent effect, CNDO/2 calc. 78−29861
methanol-water (propylene glycol), proton medium effects, ferrocene redox couple reference obs. 77−77786
methanol-water-air mixing, in perforated disc type stirring cascade, power dissipation, mechanism and correlation 79−1238
methyl propionate-H_2O mixtures, in DMSO, acetonitrile solns. IR, assoc., solvent, catalytic effects *(French)* 79−87827
MHD free convection flow past infinite porous plate 80−33703
MHD motion meas. by microfluxmeter 78−79384
microemulsion, H_2O-toluol-sodium dodecylsulphate-alcohol, diffusion coeff., light scatt. data 78−15722
microemulsion, water-in-hexadecane, dielectric behaviour, Cole-Cole type relax., temp. depend. 78−56426
micropolar effects in liquids, characts. evaluation under rotating electric field *(Polish)* 79−55638
microwave absorption by biological material, role of water 80−17004
migration capacity of As, effect of acid-alkaline conditions 77−37244
mineral type, Na, Cl, I and S determ. by neutron activation and X-ray fluoresc. analyses 78−3428
mixture with toluene-sodium dodecyl sulphate-butanol 1, interface light scatt., interface tension meas. 80−76039
mixtures with formic acid, acetic acid, propionic acid, and n-butyric acid, PMR relax. obs., mol. assoc. 79−33553
mobility, sorption by epoxy resin, low resolution PMR method 80−11276
model membrane systems, structural element, structural changes in lecithin-water system 78−96023
modified droplet model, mean droplet interaction below T_c 80−70363
molar heat capacity under high press. near solidification point 78−51695
molecular beam apparatus, appl. as target for storage ring 77−6586
molecular diffusion and 180° flips in solids 77−15327
molecular diffusion of air, experimental determ. of coeff. 77−28029
molecular dynamics, computer simulation, intermolecular potentials 80−38890
molecular dynamics of H_2O, D_2O, anal. by inelastic neutron scatt. 77−35462
molecular energy quantities from localised charge densities, dependence on geometry and basis set 80−63525
molecular geometry, vibr. anharmonicity effects 79−50159
molecular hyperpolarisability in associating mixtures, SHG 77−552
molecular interactions, nonadditive pot. model, quantum mech. data fitting 78−1047
molecular ion, H_2O^+, sub-Doppler laser spectroscopy using fast ion beams 80−9655
molecular nonrigidity effect on line shift 77−50473
molecular one-electron props., review of expt. and theoretical data, Hartree-Fock calcs. 77−67980
molecular photodissoc. ionis., 16-41 eV 77−18995
molecular photodissoc. with OH($A^2\Sigma^-$) radical form. 79−57270
molecular photodissociation, vibr. excitation of OH 77−75242
molecular reorientation, free from H-bonding, IR absorpt., dielectric loss 77−36233
molecular static polarisability, ab initio SCF wave functions 80−74106
molecular structure and dynamics, water on inorganic surfaces 77−31873
water continued
molecular vibration, kinematic anharmonicity in exact and approx. coords. 78−17653
molecular vibration, radial distrib. function of vibr. excited mol. 79−85951
molecular vibration in crystal lattice, model calc. 78−75741
molecule, 78−82616
molecule, 1s shake-up spectrum, ab initio equiv. cores, improved virtual orbital and CI calcs. 77−46597
molecule, 22 GHz rot. transition relax. rate consts. 79−18180
molecule, $4\nu_2$ band, hot vap., Fourier transform spectrum, rot. consts. 80−32712
molecule, $\nu_1+\nu_3$ combination band, evolution with temp. 78−66548
molecule, (e,2e) separation energy spectra, valence orbital electron momentum distribs. 77−38736
molecule, ab initio calcs., VSEPR model and Pauli exclusion principle 79−31380
molecule, ab initio SCF CI calcs., ground state energy, config. and force consts. 77−18782
molecule, ab initio VB and localised HF MO hybridisation 77−57852
molecule, and ^2H, ^{18}O isotopic derivatives, vibr. freqs. using MINDO/3 force consts. 77−71793
molecule, and D_2O, Feshbach-reson. and dissoc. electron attachment 79−41246
molecule, and D_2O, local model vibrs. 79−76414
molecule, and dimer, mag. shielding rel. to hydrogen bonding 77−14348
molecule, and ion, excited states, pot. energy curves w.r.t. bond ang., one-centre expansion approx. 79−6886
molecule, and monopositive ion, ab initio SCF study of low lying electronic states 79−49946
molecule, and P_2O, T_2O, inertia defects and dipole moments by kinetic consts. method 80−928
molecule, anharmonic pot., determ. of zeroth approx. 77−75255
molecule, anharmonic vibr. spectroscopic coeffs. contribs. 78−86846
molecule, Balmer radiation production by electron impact 0-2000 eV 79−76521
molecule, binding energy, MO momentum distrib., electron impact coincidence spectrometer obs. 77−61869
molecule, bond bending, bond orbitals rel. to nucl. motion 80−95513
molecule, bond dissociation, MCSCF LMO calcs. 77−57886
molecule, bonding electron pairs, size and shape parameters, Gaussian basis set MO calcs. 80−27935
molecule, centrifugal distortion 77−57974
molecule, centrifugal distortion anal. of ground vibr. states 78−70834
molecule, CI, high-order many-body perturbation theory 77−88397
molecule, CI calc. extrapolation, using perturbation theory natural orbitals 79−85907
molecule, CI calcs. using modified virtual orbitals 80−58163
molecule, collisionless multiphonon ionis. 77−65517
molecule, Compton profile, directional, polarisation functions 79−36706
molecule, config. interaction calcs. for SCF basis sets 78−58593
molecule, core 1s shakeup study, XPS and Xalpha calcs. 80−69064
molecule, core ionis., single orbital relax., LCAO MO SCF calcs. 78−29739
molecule, core ionis. pot. of O, basis set depend. 78−17821
molecule, correl. energy, fourth order diagrammatic, many body Rayleigh Schrodinger perturbation theory 80−63556
molecule, correlated wavefucntions 78−70755
molecule, correlation energy, many-body Rayleigh-Schrodinger perturbation theory calc. 78−894
molecule, correlation energy, quadruply excited configs. effects 79−54773
molecule, cubic anharmonicity constants, normal coord. ab initio calcs. 79−36595
molecule, dipolar correlation factor and dipole moment, in ice III 79−77548
molecule, dipole moment derivatives, MINDO/3 semiempirical calcs. 77−75055
molecule, dipole oscill. strength distribs., sums 78−21975
molecule, dipole properties and dispersion energies additivity, using atoms and small mol. models 80−53091
molecule, dissoc. excitation by electron impact, multiple scatt. effect 79−89793
molecule, dissociative electron attachment 77−42431
molecule, dissociative excitation by electron impact, Born approx. *(Japanese)* 77−42425
molecule, dissociative excitation by electron impact Glauber approx. *(Japanese)* 77−42426
molecule, double excitation wavefunctions, multiconfigurational SCF method 77−10604
molecule, double hole states POCI calc., Auger spectrum 78−78630
molecule, double SCF method for electron correl., stretching force const. 78−17575
molecule, elec. and mag. props., equations of motion method calcs. 77−83513
molecule, elec. and mag. props. in static fields, perturbed Hartree-Fock calcs. 78−50462
molecule, elec. dipole polarisability, coupled and uncoupled Hartree-Fock calcs. 77−34539
molecule, electro-optical harmonicity of OH bond 77−34634
molecule, electro-optical parameters determ. *(Russian)* 77−14466
molecule, electroionisation 79−22849
molecule, electron affinity, mol. geom. effects calcs. 78−82618
molecule, electron binding energies calcs. 78−86768
molecule, electron collision cross sections behind shock wave in plasma 77−11309
molecule, electron density, basis set, electron correl. effects 78−74581
molecule, electron density, generalised Berlin diagram, internal modes 79−98001
molecule, electron impact, dissoc. excitation, core pot. correction 78−25724
molecule, electron impact, H,D(2s,2p) prod. 78−42230
molecule, electron impact, inelastic scatt., 4-6 eV energy loss region 78−90277
molecule, electron impact, vibr. excitation, effective range theory 80−83485
molecule, electron impact dissoc., H atom sublevel excitation 77−14593
molecule, electron impact dissoc., OH($A^2\Sigma^+ \rightarrow X^2\Pi_i$) emission spectra, crossed-beam investigations 80−83504
molecule, electron impact dissoc. excitation, Balmer-α emission obs., Doppler profile meas. 79−31706

water continued
molecule, electron impact dissoc. excitation cross sections 77−61861
molecule, electron impact partial absolute ionis. cross section, 20-350 eV, rel. to H_2 and NH_3 *(French)* 79−861
molecule, electron impact reson. observed in $A^2\Sigma^+ \rightarrow X^2\Pi$ radiation of OH 78−46455
molecule, electron pair interactions calcs. 80−23298
molecule, electron propagator theory for mol. electron binding energies and photoionis. intensities 80−47848
molecule, electronic ground state, SCF HF and CI calcs, pot. energy hypersurface, spectroscopic consts. 78−50473
molecule, electronic states, oscill. strengths calcs. 78−9095
molecule, electronic structure SCEP theory calcs. 77−10579
molecule, emission detection in galaxy NGC 253 at 22.235 GHz 78−16534
molecule, energy levels, triat. large amplitude vibrs. model appl. 80−23392
molecule, energy levels and mol. vibr., internal coord. model 79−799
molecule, equilibrium structure, general valence force field, SCF ab initio calcs. 77−3265
molecule, ESCA and soft X-ray emission, vibr. excitation 80−23433
molecule, ESCA peak intensity, sudden approx. calc. 79−54911
molecule, excited states, generalised Brillouin theorem multiconfig. method 77−67993
molecule, excited states, SCF scheme 79−6885
molecule, excited stretching vibrs., quantum mechanics. 80−91535
molecule, fast electron impact, secondary electron energy distrib. 77−58148
molecule, floating spherical GO calcs. of electron momentum distribs. and Compton profiles 77−30933
molecule, force consts., ab initio calcs. with differentiated estimation of integrals 77−67974
molecule, force consts., ab initio CI calcs. *(French)* 78−90093
molecule, force consts., vibr. freqs., CNDO/2 and MINDO calcs. 77−14607
molecule, fragment ion formation on photoionisation, energetics and mechanism 77−501
molecule, generalised overlap amplitudes, (e,2e) spectroscopic determ. 77−61862
molecule, geom. and electronic struct., ab initio SCF calc. 79−76331
molecule, geometry, SCF and CI calcs., basis set effects 78−62715
molecule, geometry optimisation, using bond function augmented basis sets 78−905
molecule, ground state, CI calcs. on triply and quadruply excited configs., basis set effects 80−95549
molecule, ground state, cond. energies, higher-order excitation contribs. 80−58166
molecule, ground state, energy, bond parameters, diagrammatic perturbation theory calcs. 78−25414
molecule, ground state correlation energy, diagrammatic perturbation theory 80−18774
molecule, ground state props., coupled cluster and MBPT methods appl. 80−47881
molecule, H bonding, electronic struct., geometries, moments, dimerisation energies, charge distrib., pseudopotential calcs. 80−27942
molecule, H-X bond position, correlation with electronegativity 78−9069
molecule, harmonic and anharmonic matrix elements comparison, appl. to vibrational energy transfer 80−63760
molecule, harmonic force consts., vibr. freqs., integrated intensities, MINDO/3 method 80−58411
molecule, harmonic vibrations of nine unsymmetrical isotopic forms calc. 77−452
molecule, Hartree-Fock perturbation theory, first-order, symmetry calcs. 79−6854
molecule, heavy nucleus isotope shift calcs. 78−86917
molecule, higher ro-vibr. levels., high resolution flame spectra 77−58033
molecule, homeomorphism, structural, between nuclear pot. and electronic charge density 80−42968
molecule, hydration to formamide, point charge model 77−34569
molecule, in D_2O ice I_c, decoupled vibr. spectra 80−52984
molecule, in native starch, transverse PMR, temp. effects *(German)* 77−60186
molecule, inelastic electron scatt., geometrical parameters determ. 77−88585
molecule, interaction with AgI surface clusters, CNDO calc. 77−4254
molecule, intermolecular interaction energies calcs. using minimal basis sets 80−78681
molecule, ionis. pot., quark influence, ab initio SCF calc. 79−10058
molecule, ionisation energies, self-consistent-charge Hartree-Fock-Slater calcs. 77−6687
molecule, ionisation pot., CI and perturbation methods 79−31734
molecule, ionisation pot., quasidegenerate many body perturbation theory calcs. 77−50346
molecule, IR and band strengths, 5000-5750 cm^{-1} 78−5292
molecule, IR and Raman spectra, bonding, vibr., band shapes 79−6938
molecule, IR line intenisties and widths, ν_2 rot.-vibr. band 78−9200
molecule, IR spectra, 5030-5640 cm^{-1}, line centre positions, $H_2{}^{18}O$, $H_2{}^{17}O$ 78−5220
molecule, IR spectra, 6974-7387 cm^{-1}, line centre positions, $H_2{}^{18}O$, $H_2{}^{17}O$ 78−5221
molecule, IR spectra, linewidths 79−59454
molecule, IR spectrum, rot. anal., isotope effects 78−78694
molecule, IR spectrum rot. nonequilib. *(Russian)* 79−50023
molecule, isotope derivatives, mech. anharmonic problems, spectroscopic consts. 79−63983
molecule, isotope effects, ^{17}O NMR 77−34663
molecule, isotopic species, far IR spectra, assignments, moments 77−6761
molecule, iterative natural orbital procedures, convergence props. 78−46257
molecule, iterative natural orbitals for CI using perturbation theory 77−79549
molecule, KLL Auger electron spectrum, semi-internal correl. 80−48038
molecule, large amplitude vibrs. model 79−41150
molecule, laser Stark and IR-RF double reson. at 6 μm 79−45760
molecule, line strengths and intensities, ab initio calcs. 79−72300
molecule, linear response function, diagonal ARPA calcs. 78−74594
molecule, linewidths and press. shifts, in N_2 and air, Anderson theory and quantum many-body theory 78−74708
molecule, local mode structure 78−29770
water continued
molecule, localisability in MO calcs., measured by absolute overlap and 2nd moment dispersions 78−74557
molecule, localised MO, basis set depend. 79−36525
molecule, lone pair orbital explicit representation, augmented contracted Gaussian basis set 78−25423
molecule, lone pair stereoactivity, bond geometry model 79−45649
molecule, low-lying excited states, improved virtual orbital calcs. 77−14372
molecule, mag. shielding consts., coupled HF perturbation theory 79−6863
molecule, mag. susceptibility, HF perturbation method 77−79702
molecule, many body perturbation theory fourth order calc. of correl. energy 80−14087
molecule, many electron Green's function calcs. optical pot. 80−58126
molecule, many-body Green's function, electronic mol. props. 78−25417
molecule, maser emission from OH/IR sources 78−16432
molecule, maser emission from stellar sources, bright IR star monitoring at 2.7 μm 78−16433
molecule, matrix isolation spectra, vibr.-rot. lines, nucl. spin interconversion 78−46336
molecule, matrix of rotational energy Hamiltonian, calc. *(Russian)* 78−37622
molecule, MC-SCF theory, modified one-electron Hamiltonian, iteration convergence 79−6871
molecule, mean amplitude of mol. vibration, approx. calc. method 79−13697
molecule, microwave absorpt. coeff. 77−64378
molecule, minimal basis set localised orbitals, conjugate gradients method calcs. 79−6849
molecule, minimal Slater basis set VB calcs. 78−46272
molecule, mol. Rydberg $S_1 \leftarrow S$ and $S_1 \leftarrow T$ transitions, semi-empirical SCF MO calc. 80−91453
molecule, multi-root config. interaction calcs. 80−102451
molecule, multiphoton absorpt. and dissoc. 80−99530
molecule, multiphoton UV photodissoc. 78−50602
molecule, multiplet states, SCF theory 80−69062
molecule, multipole expansion of diatomic overlap, MEDO calcs. 78−46264
molecule, nucl. elec. shielding tensor calcs. 80−83296
molecule, nucl. mag. shielding and susceptibility, SCF calcs. 77−14351
molecule, nucl. spin-spin coupling consts., finite perturbation and sum-over-states calcs. 79−85893
molecule, nucl. spin-spin coupling consts. geometric approx. 79−59380
molecule, nuclear spin-spin coupling, ab initio SCF perturbation theory 78−33525
molecule, nuclear spin-spin coupling consts., finite perturbation-CI calcs. 80−5563
molecule, O muonic X-ray spectra, H(D) isotope effects 77−75344
molecule, one-electron props., SCF Xα SW functions 78−62719
molecule, open-shell SCF calcs. with model pot. method 77−57875
molecule, orbital relax. energy for single and double ionis. from valence shells 80−106253
molecule, orbitals calcs., using modified Adams-Gilbert eqn. 77−34542
molecule, oscillator strengths, 10-60 eV, for photoabsorpt., photoionis. and fragmentation 78−42133
molecule, perfect pairing valence bond model, ab initio SCF calcs. 77−6689
molecule, photoabsorpt. cross section, 10 to 50 nm 77−61797
molecule, photoabsorption, Stieltjes-Tchebycheff calculations, Hartree-Fock calcs. 79−18238
molecule, photoassisted decomposition at room temp. with activated C over Pt/TiO_2 80−55703
molecule, photoassisted decomposition at $SrTiO_3$ surface 80−85202
molecule, photodissoc., H Lyman-α emission 79−10158
molecule, photodissoc. resonances, converged 3-dimens. quantum mech. calcs. 80−106366
molecule, photodissociation, atomic hydrogen Lyman-α, Balmer series 79−45775
molecule, photoelectron ang. distrib. asymmetry parameter for 30.4 nm photons 79−98151
molecule, photoelectron spectra, 21.2-151.4 eV and soft X-ray, ionis. cross-section 78−37683
molecule, photoionis. cross section by atomic extrapolation method 79−81242
molecule, photoionis. cross sections, for YMζ and ZrMζ lines, HF vs OPW methods 77−42353
molecule, photoionisation cross sections and asymmetry parameters, SCF Xα scatt. wave calcs. 80−63542
molecule, polarisability, elec. dipole, near Hartree-Fock value, using EFV GTOs 77−88591
molecule, polarisability and mag. susceptibility calc. by SCF and CI method 80−99443
molecule, polarisability tensor components, virial theorem calcs. 80−53087
molecule, polarised photofluoresc. excitation spectra, VUV photodissoc., excited state lifetimes 78−5261
molecule, Politzer's k and V/T variations, mol. geom. effects 79−54766
molecule, pot. energy surface, many-body methods using STO 79−85921
molecule, pot. energy surface by MS Xα method and mol. geometry 79−13656
molecule, pot. surface, modified LEPS, ground state 78−17584
molecule, proton mag. shielding const., HF perturbation theory 78−46258
molecule, pseudopotential calculations, parameter fitting scheme appls. 78−41928
molecule, pseudospectral dipole oscillator strength distribs. 78−50503
molecule, quantum mech. pot. surface, power series expansions 77−34577
molecule, quenching of laser-excited O_2 80−99515
molecule, radiative damping of rot. 77−18907
molecule, Raman scatt. activity and IR intensity, finite field method 79−59462
molecule, relative ionisation energies, Tamm-Dancoff approx. calcs. 80−83243
molecule, relaxation by IR and microwave coherent transients 80−28092
molecule, reorientation and diffusion in Xe hydrate and other structs., PMR and dielec. relax. 77−36142
molecule, rot. consts. for ground state and (110) and (011) interacting states 78−21902

water continued
molecule, rot.-vibr. Schrodinger eqn. soln., bond lengths and angles, force consts. 79−41151
molecule, Rydberg states, visible spectra 78−9162
molecule, SCF calcs. using cusped Gaussian basis sets, polarisation effects 80−74118
molecule, SCF energy optimisation with regard to Slater's exponents *(French)* 79−49936
molecule, self assoc., intermolecular interactions, matrix isolation vibr. spectra obs. Raman and IR spectra 80−52995
molecule, semi-empirical INDO calc. of electronic struct. 80−32611
molecule, semiempirical CNDO/2 wave functions, pair density anal., environmental effects 80−91451
molecule, separated electron pair theory, numerical calcs. 80−87049
molecule, separated electronic pair functions, direct minimisation of energy functional, LCAO-MO SCF, density matrix formalism 79−31392
molecule, shape, electrostatic force study with floating wavefunction 78 - 37545
molecule, shape as function of O-H separation 80−43203
molecule, singlet states, CI calc. 77−46502
molecule, slow electron scatt., rigid mol. model with exchange and polarisation 80−43194
molecule, spectra, pure rot. band, exponential wide band parameters 79−31498
molecule, spectroscopic consts., rot. energy levels 77−10663
molecule, sum rule props., SCF optimizations of MO and VB calcs. 78−5156
molecule, theoretical IR transition matrix elements 79−85953
molecule, threshold PES, OH^+ fragment obs. 80−78647
molecule, time-resolved IR single-shot absorpt. spectra 79−58808
molecule, total electrostatic pot., Thomas-Fermi eqn. soln. 79−10034
molecule, triple-dipole energy calcs. using pseudo spectral theory 78−46418
molecule, ultrahigh resolution IR absorpt. spectra using tunable PbTe laser diode 79−75628
molecule, uncoupled state in palygorskite lattice, isotropic dilution IR obs. 77−8568
molecule, unimolecular reactions, rate theory 79−74348
molecule, UV and VUV spectra, 180-790 Å, absolute photoabsorpt. cross-section 77−75182
molecule, vac. UV absorption spectra, Rydberg series vibr. anal. 78−42093
molecule, valence shell electron pair interactions, VSEPR theory test 79−31393
molecule, vapour, mol. association entropy and enthalpy, thermal cond. meas. 80−7777
molecule, vapour phase spectrum, 8050-9370 cm^{-1}, vibr., rot. anal. 79−72308
molecule, variationally deorthogonalised localised molecular orbitals, electronic struct. 79−97968
molecule, VB minimal Slater basis set calcs., comparison with H_2O, MO calcs. 79−36536
molecule, vertical ionis. pot., many-body Rayleigh-Schrodinger perturbation theory 78−9063
molecule, vertical ionis. pot. calc. from one-body Green's function 77−42440
molecule, vertical ionisation pots., CI calcs. 79−13645
molecule, vertical valence ionis. pot., many-body Green's functions 78−22051
molecule, vertical valence ionis. pot. calc. by pertubation, CI and CPA techniques 80−69263
molecule, vibr. anal., normal coord. calcs., nucl. corrections to mol. props. 77−88441
molecule, vibr. energy levels, semiclassical trajectory method calcs. 78−58660
molecule, vibr. freq. shifts in polyatomic solutes 78−58654
molecule, vibr. freqs. from anharmonic ab initio/empirical PE functions 79−76406
molecule, vibr. motion, local- vs. normal-mode description 80−5521
molecule, vibr. Raman scatt. signature in flames 78−25539
molecule, vibr. relax. at high temps. 77−79681
molecule, vibr. transition moment and band intensity 79−27036
molecule, vibr.-rot. intensities of $3\nu_2$, $\nu_1+\nu_2$, and $\nu_2+\nu_3$ bands of $H_2{}^{16}O$ 78−5291
molecule, vibrational excitation by electron impact, threshold structs. 78−22038
molecule, VUV photodissoc., vibr. and rot. distribs. 80−87191
molecule, X^1A_1 ground state, large-amplitude Hamiltonian for vibr.-rot. 78−25511
molecule+Ar, collisional energy transfer in unimol. reaction, classical trajectory calcs. 78−62882
molecule+atom, quasielastic H atom ejection *(Russian)* 78−37712
molecule+$Kr(^3P_1)$, decomposition, $OH(A^2\Sigma^+)$ internal energy distrib. 79−10183
molecule+molecule, medium distance interaction, SCF LCAO MO, supermol., perturbation and MCF calc. 79−837
molecule+$N_2{}^*\rightarrow N_2+H_2O^*$ 80−87212
molecule+positive ion, inelastic scatt., 4-6 eV energy loss region 78−90277
molecule+positive ions, reaction rate consts., product distrib., ICR obs. 79−8428
molecule bond distribution functions, anharmonicity effects on electron diffr. pattern 80−69234
molecule core 1s and 1b, photoelectron bands, vibr. excitations, ab initio calc. 80−63543
molecule ground state ionis. pots., generalized Mo theory 80−52907
molecule in α-oxalic acid dihydrate, H_2O proton shielding tensor, multiple pulse proton NMR obs. 80−63655
molecule in $CuCl_2.2H_2O$ or $CaSO_4.2H_2O$, intramol. force field cals. 79−51229
molecule nonlinear optical polarisability meas. 79−54991
molecule polarisabilities, finite-field calc., perturbation correlation 79−72249
molecule surface mobility on phospholipid membrane 79−79450
molecule-lysozyme, interaction, intermol. pot. calcs. 77−75250
molecules, charged, model for form. and stabilisation of clathrate 80−91714
molecules, dispersion energy consts., dipole oscill. strength, refractivity 77−50492
molecules, hydration, reorientational motion, quadrupolar relax. of ^{27}Al in aqueous soln. 77−85601
water continued
molecules, isotopic, vibr. intensities, ab initio and empirical calcs., band strengths 80−78593
molecules, isotopic vibr. intensities, ab initio and empirical calcs. 80−78592
molecules, quadrupolar relax. of ^{27}Al in aqueous soln., formulation of relax. rate 77−85600
molecules in biological systems, relax. rel. to vol., pulse NMR obs. 80−40960
molten glass/water thermal interaction, nucl. reactor appl. 78−46149
molten reactor fuel-coolant interaction simulation, water-molten Sn reaction 78−58363
monolayer, ordered, adsorbed on KCl (100), secondary ion mass spectra 77−76660
monolayer of alcohol on water, eqn. of state 78−6195
monomer and dimer, isotopic forms, Ar matrix isolated IR spectra, assignments, config. 77−6779
monomer on ice I_h basal plane, static interaction 78−18891
Monte Carlo simulation, convergence of new algorithm 78−63649
Monte Carlo simulation 80−54113
Monte Carlo simulation of isothermal-isobaric ensemble 78−30530
Monte Carlo simulation of struct. and thermodynamic props. 80−88017
muon stopping, diamag. shielding of muon-substituted cpds. 79−57279
muonium atoms and intraspur reactions 79−70358
muscle, mouse, ^1H NMR anal. above and below freezing 80−56073
muscle, of barnacle, transverse nucl. mag. reson. relax., bounds on bound water 77−4989
muscle water, frog, varied mag. field, multiple-pulse and magic-angle spinning ^1H NMR obs. 80−51135
muscle water, study of spin-lattice and spin-spin relax. times of ^1H, ^2H, and ^{17}O 80−21443
muscle water transverse and longit. NMR relax. rates 78−35810
n-state configurational excitation model, diagnostic thermodynamic props. 80−10481
naphthalene anion radical+H_2O, react., H_2 prod. 78−92460
natural, trace metals, energy dispersive X-ray fluoresc., at absorpt. anals. comparison 77−60175
natural convection at density extremum 78−94696
natural convection heat transfer from horizontal ice cylinder, anal. and obs. 77−27521
natural fracture water identification by radiological parameters 77−78245
natural reservoirs, average age rel. to average transit time 78−81239
natural water surfaces cooling, impact of atmospheric CO_2 79−92569
near-critical fluids in turbulent flow through tubes, heat transfer num. prediction method 77−42832
neutron activation analysis for determ. of selected elements and heavy metals 80−76580
neutron diffusion across absorpt. discontinuity 78−21620
neutron diffusion in water containing 1/v and non-1/v absorbers 79−30879
neutron irradiation and mag. field effects on cavitation and nuclei spectra 77−62568
neutron number and dose albedo 79−93681
neutron scattering, book contrib. 79−60232
neutron transport, 2-D benchmark expt. 78−58318
neutron transport at thermal energies, effect of 1/v absorbers 78−29532
NGC 4945, galaxy, water vapour emission obs. 78−93427
NMR proton spin-lattice relax and shear viscosity press. depend., −15 to 10°C 77−40144
NMR shielding constants of ^1H and ^{17}O, paramag. contrib., triple perturbation theory 79−10127
NMR studies of water in biological systems 80−3886
non-Boussinesq convective struct. near 4°C 79−18886
non-Faraday electrolysis, at low current density 79−70340
non-flowing boiling water films, critical breakup thicknesses 79−94468
non-uniform water-bearing rock formations, evaluation via DC resistivity sounding method 78−40474
nonelectrolyte addition effect on struct. 78−9937
nonelectrolyte-water, X-ray scatt. intensity composition depend., soln. struct. 78−6005
nonelectrolytes, aqueous, excess heat capacity, H bonding 78−3362
nonylphenol diethylene glycol ether-water-p-xylene system, liquid crystal stabilization of multiple emulsions 79−16046
nuclear magnetic relax. of protons at identically oriented planar interfaces 77−36148
nuclear power station, hot water leakage from first loop, 22.8 MPa initial pressure, flow characts. 78−66357
nuclear power stations, corrosion damage, influence of water chemistry 79−54517
nuclear water-cooled reactor systems, water chemistry 79−93694
nucleate and transient boiling in narrow space between disks 77−84115
nucleate boiling heat transfer, press. factor 77−69080
nucleate pool boiling, bubble freq. model, surface effects 78−90651
nucleation, heterogeneous, on ions, atomistic model 77−62612
nucleation on ions, molecular model 77−1222
nucleic acid-water interactions, review 78−44448
nucleic acids nitrogeneous bases, thin films, water content determ. using quartz resonator 79−92439
octane-water interface, electron transfer in presence of chlorophyll 77−81474
octane-water interface, water photo-oxidation in presence of adsorbed porphyrins 78−64933
oil on surface, spreading patterns, surface contamination effects 79−43795
oil-water emulsions, pool boiling heat transfer 79−55378
oil-water interface, electroadsorption and electrocapillarity 80−44393
oil-water interface, fatty alcohol adsorbed layer phase transition, high-press. effect 79−99395
oligomers, H-bonding, PCILO calcs. 77−83500
optical absorption coeff. 79−82992
optical absorption coefficient at 488 and 541.5 nm, adiabatic laser calorimetry 77−73123
optical constant submillimetric wave meas. 79−33656
optical constants, 400-5000 cm^{-1}, 1, 16, 27, 39 and 50°C, rel. to intermol. struct. 77−66469
optical constants, 6-450 cm^{-1}, 19°C 78−6649
optical constants, 70 to 450 cm^{-1}, reflection dispersive Fourier transform spectrometric obs. 77−40203
optical consts., absorpt. and refr. index 0.1 Å-1 m 78−48139

water continued
optical fibres, diffusion of OH in core and H_2O in cladding, transmission props. 78−42420
optical properties, 250-600 nm 77−52035
optical props. of Lake Ontario coastal waters 80−36337
optical props. under press., molecular polarisability depend. on thermodynamical state 78−80312
optical spectra of solvated electrons, band resolution 79−78698
oscillatory flow, rolling motion of sphere on plane boundary 77−3834
oscillatory motion around bottom ripples, theory *(Polish)* 77−70686
osmotic permeability of red cell membranes 79−34528
oxidisability determination using titrometric liquid analyser 79−79441
pair pot. near H bonded equilib. config., amorphous and crystalline solid and liq. 80−64946
partition function ratio, reduced, generalised finite polynomial approx. H_2O rel. to D_2O 78−66529
penetrative convection instabilities *(French)* 79−46304
n-pentane-water interface, nucleate boiling 78−2342
peridotite-H_2O-CO_2 system, phase relationships, rel. to planetary mantles 78−77506
permeability of cellulose acetate membranes at low press., nature of flow 77−73467
permeability of cellulose acetate membranes at low press., temp. var. 77−73466
permeation in polytetrahydropyran 2,6 diyliminocarbonyl hydrophilic membrane 79−74419
permittivity at mm wavelengths 80−66098
petroleum-acetylene-O_2 combustion products, seeded, elec. cond., for MHD power plant 78−34256
petroleum-water-gas mixture, in inclined stratum, nonstationary filtration, including gravity 78−1729
phase boundaries, spline representation, for pressurised water reactor use 77−23207
phenol-water mixture, pure and KCl-doped, electrical conductivity near crit. pt. 77−15612
photo-oxidation at $BaTiO_3$ electrodes 77−12000
photo-oxidation in phospholipid bilayers containing chlorophyll a 77−16917
photoacoustic effect, nsec. and psec. laser pulse induced 78−38777
photoassisted electrolysis, EPR of VO_{aq}^{2+} ions 78−11540
photoassisted electrolysis using Fe_2O_3 semicond. electrolyte 77−77771
photoassisted electrolysis using semicond. oxide anode 77−69413
photoassisted oxidation at TiO_2:Be electrodes 80−30502
photocatalysis on TiO_2 using solid C, appl. to H prod. 80−26150
photochemical dissociation utilising solar energy for H_2 prod., review 80−61452
photochemical oxidation, using TiO_2 electrode with dye sensitisation 79−91964
photodecomposition of gaseous H_2O over TiO_2 and TiO_2-RuO_2 surfaces 80−85194
photodecomposition over Pt/TiO_2 catalysts 80−81337
photodesorption from TiO_2, pulsed-laser-dynamic-mass-spectrometer study 80−35568
photodissociation, semiclassical approach to abnormal rotation of $OH(A^2\Sigma^+)$ 78−40069
photoelectrochem. H prod. using hybrid electrodes 80−45775
photoelectrochemical evolution of O_2 using manganese chlorophyll electrode 79−83719
photoelectrolysis, of water, efficient electrode materials 79−29478
photoelectrolysis, semicond. electrode requirements and props., book contrib. 79−65547
photoelectrolysis, stable cells prod. 77−44484
photoelectrolysis, suitability of $FeTiO_3$, Fd_2TiO_4 and Fe_2TiO_5 anodes 77−63920
photoelectrolysis, using Fe_xO_y-coated n-Si heterostruct. photoanode 80−61384
photoelectrolysis, using n-GaAs photoanodes 77−77789
photoelectrolysis, using semiconductor electrodes, electronegativity effects 77−44482
photoelectrolysis, WO_3 electrode behaviour 77−66757
photoelectrolysis at high current density, using TiO_2 and $SrTiO_3$ photoanodes 78−15679
photoelectrolysis by irradiation of platinized n-type semicond. $SrTiO_3$ and $KTaO_3$ 77−86332
photoelectrolysis for solar energy conversion, TiO_2 and $SrTiO_3$ electrodes 79−52959
photoelectrolysis in sunlight, using sensitised TiO_2 electrodes 78−19143
photoelectrolysis using semiconductor electrode, surface state charge transfer 79−28405
photoelectrolysis using semiconductor electrodes, appl. to solar energy conversion 79−29477
photoelectrolysis using TiO_2 electrodes 79−74407
photoelectrolysis with semicond. materials 78−2562
photoelectrolysis with TiO_2 catalyst 80−60755
photoelectrolysis with TiO_2-covered solar-cell electrodes 77−1928
photoelectrolysis with transition metal doped TiO_2, $SrTiO_3$ anodes 79−74531
photoelectrolytic decomposition by visible irrad. of p-GaP electrode 77−77778
photoelectrolytic H prod., recent advances, review 80−45774
photolysis, applic. of Au-coated n-Gap electrode photoelectrochem. behaviour 77−21399
photolysis, for H_2 prod. using chlorophyll photocatalysts 80−61458
photolysis, for H fuel prod. *(French)* 80−55776
photolysis, for photoelectrochem. H_2 production using solar energy and Zn(Mg)(Cr)(Ni) phthalocyanine dyes *(French)* 80−55936
photolysis, H_2 and O_2 determ. by gas chromatography 78−61089
photolysis, Si catalyst, I-V model 80−108721
photolysis, using solar energy for H_2 prod., feasibility of large scale generation 80−72095
photolysis for H prod., using fission pumped gas lasers 80−45810
photolysis in n-TiO_2-KOH-Pt cell, H_2 partial press. 78−64858
photolysis using biological and artificial catalysts for H prod. 80−61444
photolysis using Pt/(chlorophyll a.$2H_2O$) reaction for H_2 production 80−89663
photolysis with n-TiO_2 anode 78−2563
photon correlation spectroscopy, liquid surfaces, effect of instrumental broadening 77−87852
photooxidation, at α-Fe_2O_3:TiO_2 electrodes 78−15684
photooxidation by α-Fe_2O_3 electrodes 78−76886

water continued
photosensitised decomposition, electron transport across phospholipid vesicle walls 78−80787
phototaxis in walking fly, water balance and phototactic response 79−20577
β-picoline-water solution, light scatt. spectra, ultra- and hypersonic absorpt. *(Russian)* 80−93353
pipe flow, turbulent shear struct. 77−3872
PIXE elemental anal. 78−20127
plane-parallel convective flow instability near 4°C 80−92137
planetary satellite Io, H_2O loss and anhydrous surface form. 79−53756
plant content meas. using high-sensitive impedance meter *(Japanese)* 77−5125
plasma impurity in N_2 RF capacitative discharge, effect on heating 80−59312
plasma water shifts during thermal dehydration 80−67044
plasmochemical decomposition using nuclear energy source for thermochem. H_2 production 80−61436
PMR, direct observation in rotating frame *(Russian)* 78−39422
PMR, in presence of nonreson. field, interpretation *(French)* 78−72421
PMR obs. in obligately halophilic blue-green alga 79−96526
PMR spin-lattice relaxation in hydrated biological systems, cross-relax. effects 79−34496
polarisation fluctuations, effective freq. calcs. 77−90093
polarisation model, appl. to hydrated Li^+, review 80−54115
polarisation model, water and ionic dissoc. products 78−91216
polyarylate, F-2 influence of water on mech. props. *(Russian)* 78−88513
polyoxyethylene dodecyl ether/water system, lamellar liq. cryst., solubilized hydrocarbon effect on struct. and dislocation pattern 79−94885
polyvinyl alcohol, absorption of H_2O mols. from liq., Raman spectrosc. technique 79−42364
polywater, discovery, production and appls. 78−30529
pool nucleate boiling heat transfer thermodynamic investigation *(Chinese)* 79−72783
porous medium, homogeneous, deep evaporation characterisation *(French)* 78−59468
porphyrin-water interface, photoinduced charge separation 77−81408
positronium formation, isotope effects 80−93432
potential evaporation from soil, water and crop surfaces, eqn. adaptable to remote sensing use 77−64334
prebreakdown stage fundamental charact., calc. *(Russian)* 80−49019
precipitable vapour in atmosphere with temp. inversion 77−78330
precipitable water amounts meas. using integrated absorption in atmospheric 1.38μm band 80−4108
preconcentration, for X-ray fluoresc. anal., using ion exchange filter membranes 78−7228
propylene glycol-water (methanol), proton medium effects, ferrocene redox couple reference obs. 77−77786
protein hydration dynamics, quasi-elastic neutron scattering 79−16127
protein-water interactions in aq. solns., Raman spectroscopy 77−6792
protein-water system dynamic model 77−21470
proton affinity, many-body Rayleigh-Schrodinger perturbation theory 78−92497
proton beam dosimetry, miniature Si dosimeter 80−47733
proton mag. moment in Bohr magnetons, g-factor ratio determ. 78−33526
proton relay model systems, reaction field theory of solvent effects 78−44346
puddle water, nighttime disappearance with ice needles growth and daytime reappearance 77−29334
pulsating air bubbles in water, stability using optoelectrical method *(German)* 77−27578
pulsating flow in heat exchanger effect of pulsations on heat transfer 79−94614
pulsed NMR studies of biological water 80−35930
pulsed opto-acoustic spectroscopy 80−62743
pumping, by means of flat solar energy collectors *(French)* 80−55902
pure, interaction of muonium with radiolysis products, OH. scavenging by tert-butyl alcohol 79−24806
pure water PVT properties, use and misuse for lake waters 77−49095
purification system for at. absorpt. anal. 77−52688
PWR, in-reactor loop expts. on corrosion product transport and water chemistry 78−58335
pycnometer, precision hydrostatic, density comparison, influence of isotropic comp. and dissolved air 78−45597
pyrex-H_2O system, electrokinetic coeff. determ. from sedimentation pot. 80−3365
pyridine-H_2O, bonding, double quadrupole reson. obs. 80−32749
pyridine-water soln., reorientational relax. and activation energy of pyridine, depolarised Rayleigh scattering 80−76037
pyrolysis, computer thermodynamic anal. and optimisation of thermochem. cycles for H prod. 80−45766
pyrolysis, for H prod., development of two new thermochem. cycles at ORNL 80−35780
pyrolysis, for H prod., optimum temp. conditions utilizing HTGR nuclear heat 80−35781
pyrolysis, for thermochem. H_2 prod. 80−55928
pyrolysis, H prod. using the Mark 13 process, status report 80−30606
pyrolysis, thermodynamics, solar-H_2 energy systems 80−61448
pyrolysis, utilising solar energy for H_2 prod., thermodynamics, review 80−61450
pyrolysis by Mg-I cycle for thermochem. H prod. 80−35786
pyrolysis by S-I cycle for H prod. 80−35769
pyrolysis for H prod., equilibrium effects in high press. prod. 80−35775
pyrolysis for H prod., HBr decomposition using $FeBr_2$ and Fe_3O_4 80−35778
pyrolysis for H prod. using S-I cycle 80−35770
pyrolysis using Br-Ca-Fe cycles for H production 80−35784
pyrolysis using Fe-Cl thermochem. cycle for H_2 prod., chem. engineering anal. 80−97811
pyrolysis using S-cycles for H prod. thermochem. anal. of energy balance 80−35779
quality trends, statistical tests for dependent obs. 77−29513
quark affinity to water molecule, centre expansion SCF calcs. 80−43213
quartz, synthetic and natural, water content determ. 77−86401
Quaternary magmas of NE Japan, H_2O contents lateral vars. 79−57899
quenching rates on hot surfaces, wetting of outer tube walls by water 77−82996
radial distribution functions, for liqs. and amorphous substances, analytical computation method 80−24301

water continued
radiation stratified cooled, temperature structure *(German)* 79−41687
radiolysis, excitation, ionisation processes *(Rumanian)* 77−48666
radiolysis, hydrated electron absorbance, spur overlap 77−86328
radiolysis, mathematical modelling for kinetics in operating reactors 78−61036
radiolysis, $O(^3P)$ atom yield 80−35556
radiolysis, positronium form. inhibition by NO_3^- electron scavenger 79−66325
radiolysis and effects upon in-reactor zircaloy corrosion 77−12817
radiolysis of H_2O vapour, H_2 production by thermoradiation dehydrogenation using nuclear power, kinetic anal. 80−67010
Raman bands, influence of paramag. rare earth cations 78−15157
Raman scattering of ν_1 vibr., in liq. and gas phases, transverse cross-section 78−82739
Raman spectra, liq. state, depolarisation ratios, libration and translational spectra 79−4797
Raman-line splitting, surface waves of liquid drop in EM field 77−69826
random network model, entropy calc. 80−64870
random network model, liq. and ice polymorphs enthalpy and heat content 80−64869
Rayleigh-Brillouin scattering and compressibility 79−91455
reaction between water droplets and molten sodium 78−71263
reactor H_2O-graphite system, neutron rethermalisation 79−97806
recoil T atoms+H_2O, neutron effects, apparent phase effect 77−63935
refractive index, temp. depend., relationship to mol. polarisability 78−56448
renography, comparative study in hydration and dehydration *(Japanese)* 80−81726
reserviors, suspended load sedimentation, analysis and prediction method 78−53664
river water temp. forecasting, Fourier series and communication theory techniques 77−25718
$tRNA_{yeast}^{phe}$, Fourier transform PMR in aq. soln., ^1H exchange and relax. rates meas. method 78−15049
rock permeability and penetrating water zone propag. 78−7671
roto-vibrational structure, correlated bender theory 78−37627
in Russian tektites, water conc. 77−87346
salts, aq. solns., mechanical and electro-optical anharmonicity *(Ukrainian)* 78−2830
sapphire-H_2O interface, SiO_2 sputtered film performance as acoustic antireflection coating 80−106686
saturated liquid, boiling onset, film boiling transition, crit. heat flux densities *(Russian)* 78−83234
saturated steam/water system, thermodynamic data tables 78−26679
saturated vapour condensation, comparison with saturated air vapours 77−11780
saturated water vapour pressure standardization 80−26596
seasonal reservoir, optimal releases, deterministic case 80−8362
self diffusion, high-press., low-temp. spin-echo NMR obs. 77−8446
self diffusion in frog muscle 80−8037
self-diffusion, flow meas., 25-65°C 78−2278
self-diffusion, pressure and temp. depend., NMR spin-echo obs. 80−65266
self-diffusion −31°C to 350°C 78−2275
self-diffusion coeff., pressure and temp. depend. meas. by proton spin echo 80−39328
self-diffusion coeff. meas. in aq. electrolyte solns., NMR spin-echo method 78−80243
self-diffusion coeffs. in pure water and aq. electrolyte solns., tracer meas. 78−95169
self-diffusion in porous membranes, ionic solns., struct. props. 79−52765
serine, neutral and zwitterion, water solvation, Monte Carlo simulation 80−76707
sessile drop impinging on heated surface, heat and mass transfer mechanism 78−90908
sessile water drops on inclined plane surfaces, shape 78−67891
shielding of 14 MeV neutrons using iron-water combination 77−61614
shock compression at high press. *(Russian)* 80−92608
shock compression at press. approaching 1 Mbar *(Russian)* 80−79851
shock waves, in pure vap. vibr. relax. time at low density 79−98761
simulated water, cooperative effects importance 80−28906
simulation, Monte-Carlo method, 1 g cm^{-3}, 300K, using Rahman Stillinger ST2 pot. 77−51290
simultaneous boiling and forced convection heat transfer from horizontal cylinder to water in crossflow 77−15018
skin, normal, heat and H_2O migration, unsteady state 79−92155
skin stratum corneum, human, linear meas. of water content using microwave probe 80−21518
snow, liq. water content investigation by radiometry in 3 to 60 mm wavelength region 80−72561
snow, water content meas., calorimetric method *(Japanese)* 80−31142
snow, water equiv. of dry snowpack, active and passive microwave response 80−72563
snow water pressure in ripe snowpacks 79−53384
snow wetness, active and passive microwave response 80−67382
sodium decanoate-n-decanol-water system, lamellar G-phase, orientational-order, EPR investigation 80−24355
soil, cohesionless, strength, influence of high pore-water press. 77−25678
soil, nonsaturated, water infiltration, positive head effect *(French)* 79−2296
soil, water content effects on N_2O emission 79−83672
soil erosion processes meas. in German area of Moselle river valley 77−81937
soil moisture profile development during water redistrib. after infiltration 77−29344
soil water, flow regimes near porous cup water samplers 77−66942
soil water, hysteretic steady state profiles 77−91172
soil water, nonlinear diffusion eqn. via perturbation, iterative and optimal techniques 77−66943
soil water, percolating, sampling using plastic suction lysimeter 77−29498
soil water, saturated-unsaturated flow in deformable porous medium, numerical model 77−91181
soil water, seepage boundary-value problems soln. by direct variational method 78−83331
soil water absorption with exponential diffusivity, infiltration and perturbation methods 77−66944
soil water content, estimation via total solar reflectance and spectral band ratioing 77−60479
water continued
soil-root system, transient analysis, water transport 77−5269
soil-water system, γ-ray transmission studies, calibration 80−26629
solar photochemical decomposition for H_2 prod. 80−16822
solar-heated water system for a photographic processing laboratory 80−40837
solubility and transport behaviour, dissolution during oxidation of Si 80−93801
solubility in CaO-Al_2O_3 melt at 1600°C 78−51687
solubility under magma genesis conditions, petrological implications 78−11886
solute hydrophobic interaction, mol. aggregation, free energy, entropy and enthalpy, scaled particle theory 77−84609
solutions in organic solvents, IR spectra and struct. 79−38534
solutions molecular properties, one dimensional solubie models 79−46536
solvated electron, polaron coupling const. from dipolar plasmon freq. 77−89720
solvated electrons, optical absorpt. spectra. temp., isotope effects 80−55124
solvated electrons, optical spectra and model potentials 80−30318
solvent, structure, ESR spin probe obs. 77−59460
solvent properties, electrochem. adsorpt. of tetraethylammonium bromide from H_2O, D_2O solns. 79−83459
sonoluminescence, from water containing dissolved gases 77−85818
sonoluminescence generation by US therapy equipment 77−77930
sonoluminescence spectrum in visible region *(French)* 79−33855
sorbed on DNA, temp. anomaly, IR spectroscopic obs. 80−51046
sorption and desorption on DNA and lysozyme, thermal-stimulated press. and thermogravimetric anal. 80−8008
sorption by polycarbonate, effect on dielec. behaviour 79−11383
sorption in polysiloxane dizwitterionomers 80−49506
sorption into polysiloxane dizwitterionomers, effect on dielec., mech. relax. 80−50261
sorption on Fe, visualisation using THO and autoradiography 78−26761
sorption on Si(111), EELS 78−14571
sorption on ThO_2 sol-gel for nucl. applics. 77−4940
sound wave generation in water by laser pulse interaction 77−50812
spark, high voltage, resistive phase 78−67453
specific heat determ. in tunnel theory 79−33095
spectrum, 4200 to 5000 cm^{-1} 77−58005
spray, air atomised, dispersion characts., orifice shape depend. 78−34182
squeezed boiling, internal characts. 78−90655
ST2 discrepancy between Monte Carlo and mol. dynamics calc. using truncated pot. anal., internal energy determ. 80−95702
ST2 solution, hydrophobic hydration around apolar species pair, Monte Carlo simulation 80−6336
ST2 solution of nonpolar spheres, hydrophobic interaction Monte Carlo simulation 80−6335
statistical mechanics of aq. fluids, book contrib. 79−60250
steam bubbles direct contact condensation in water at high press. 77−39202
steam-water, flow characts. at high press. 78−94805
steam-water annular dispersed flow, liq. distrib. between core and film 77−75971
steam-water counterflow in porous media, model, geothermal systems appl. 79−79879
steam-water mixture, intensive drop condensation, flow boundaries 77−35204
steam-water mixture, upward flow in tube, liq. film-core mass transfer, liq. distrib. 78−75189
steam-water mixture, with high vap. content, annular flow, heat transfer, press. loss 78−75193
steam-water systems, two-phase press. drop correlations 77−82995
steam-water two phase mixture, relative vel. of vapour phase, determ. of void fraction 78−5791
steam-water-ice system, two-dimens. triangular lattice model, matrix calc., props. 77−27975
steep gravity waves in water of arbitrary uniform depth 77−70683
stellar H_2O maser emission, new sources detect. 80−62298
stellar maser emission, circumstellar shell model 77−60765
stellar masers, detect. of new sources 78−32466
stellar masers, time vars., 22 GHz obs. 79−30077
stimulated Raman scattering of psec. pulse train, dynamics 79−64286
stratified atmosphere, nonadiabatic heat dynamics with mass exchange and water phase transitions 79−58004
stratiform clouds, local water contents and particle characts. *(Russian)* 77−53158
stratosphere, H_2O abundances rel. to HF/HCl ratio 79−16568
stratosphere, H_2O mixing ratio, in-situ obs. using NOAA UV fluoresc. instrument 80−90137
stratosphere, thunderstorms as micrometeorological sink 79−84385
stratosphere, water vertical transport rel. to atmosphere HT and HTO 79−2347
stratosphere composition, mixing ratio profiles from IR solar spectra obs. 80−105015
stratosphere water vapour, meas. via balloon-borne IR instrument 79−8718
stratospheric composition, in situ obs. of H_2O 80−105077
stratospheric H_2O, maintenance of extreme aridity, review 80−105028
stratospheric ion chemistry, H_2O reactions with $O_2^+.O_3$ 79−2343
structural changes due to hydration of monat. ions, stoichiometric mixture, thermodynamic props. 78−7225
structure, liq. theory, review, book contrib. 77−39525
structure, review *(French)* 78−26424
structure, theory based on quasi-component distrib. functions 78−38606
structure and motion at high pressure 78−87606
structure and props., minimal basis set description 80−6347
structuring and protein adsorpt. on surface of hydrophilic polymers, ESCA evaluation 80−108758
subcooled, choked expansion and the isentropic homogeneous equilib. model for 2-phase flow 78−91034
subcooled, flashing flow in convergent-divergent nozzles 77−80195
subcooled film boiling heat transfer from spheres 78−51047
submerged cylinders, forced oscills. test in water 78−5728
subsea permafrost, interstitial water convection rel. to heat and mass transport 79−2302
subsurface drainage and irrigation, expt. evaluation of theoretical solns. 78−61465
sum rules for connecting vibr. freq. parameters of H_2O, D_2O and T_2O 79−36615

water continued
sunlight transmission through uniform waterdrop atmosphere study 78−36244
superbroadening, by self-focused picosec. laser pulses 77−75612
supercooled, Brillouin scatt. 78−43884
supercooled, dispersed within emulsions, freezing, differential scanning calorimetry meas. 77−15552
supercooled, hypersonic sound vel., thermodynamic interpretation 78−59860
supercooled, I^- charge transfer to solvent spectra, water struct., solvated electron 77−50447
supercooled, LF sound velocity and related thermodynamic props. 79−73255
supercooled, longit. proton relax. times, press. and temp. depend. 77−85598
supercooled, polychromatic correlated site percolation 80−22296
supercooled, probability of ice nuclei form. 78−3909
supercooled, sound vel. dispersion, struct. relax. effect, Brillouin scatt. obs. 80−107375
supercooled, US vel. and attenuation *(French)* 79−90730
supercooled drops, hydrodynamic behaviour, interaction with columnar ice crystals 78−32205
supercooled emulsified droplets, relative permitt. and cond., Maxwell-Wagner interfacial polarisation 78−52423
supercooled high-pressure H_2O and D_2O, density max. 77−1162
supercooled liquid, high freq. sound vel. and absorpt., thermodynamic singularity, 228K 77−76489
supercooled to −33°C, sound vel. determ. by acoustic levitation method 80−88269
supercritical, heat transfer and pressure drop in horizontal tubes *(Japanese)* 79−14399
supercritical water flow in curved channels, heat transfer and drag 79−90246
supercritical water flow in tube under very high press., heat transfer charact. *(Japanese)* 77−42840
superheated, specific heat estimation 77−24413
superheated liquid, growth of spherical bubbles, anal., numerical calcs. 77−24399
superheated water, Brillouin scatt., sound velocity meas. 80−95631
superheated water, flashing kinetics, γ-radiation effects 80−92025
supersaturated solns. of ethanol and water, bubble nucleation, contact angle effects 79−94702
supersaturated solns. of nitrogen and water, bubble nucleation, contact angle effects 79−94702
surface, spreading vel., rel. to mol. struct. *(German)* 78−95209
surface boiling in tubes, heat transfer 78−9541
surface dipolar plasmons, nonradiative, dispersion relations 78−6308
surface EM wave excitation 79−13893
surface energy, electrostatic contrib. 80−20014
surface structure, single ion hydration energies 78−26752
surface subjected to laser radiation, repulsion of bodies, optically generated vapour cushion 79−10339
surface tension, press. effects, adsorpt. of hydrocarbon gases and CO_2, 0-50°C 78−56024
surface tension, temp. coeffs. meas. 78−43216
surface tension, Thakur-Hickman meas. 77−85019
surface tension and energy, Fowler model 80−10754
surface tension from Skeleton table *(German)* 80−75407
surface tension in air, effect of air diffusion and interface struct. 77−4246
surface waves, nonlinear propagation, effect of random inhomogeneities 77−11204
surfactant-water liquid crystal phases, review 80−28913
swelling of PVA, sorption of $TiCl_4$ from benzene solns. *(Polish)* 79−4471
tap water, tension pulse propag. in column 79−69176
temperature of maximum density, solute effects and partial molal expansibility 77−24256
tensile strength, theoretical prediction 79−42131
tension effects, Berthelot-Bourdon tube method 80−88238
tension pulse transmission 79−68750
thermal activity coeff., rel. to density, heat cond., sp. heat and viscosity meas. 77−7883
thermal boundary layer near air-water interface, fine struct. *(Russian)* 78−22332
thermal conductivity, at 25-350°C, 0.1-245.3 mN/m^2 77−51556
thermal conductivity, meas. by transient hot wire method 77−30144
thermal conductivity equation, 0 to 800°C, triple pt. press. to 1000 bars, crit. region 80−39364
thermal conductivity in crit. region 77−89599
thermal conductivity in region of 4°C *(German)* 77−20136
thermal excitation of acoustic waves by periodic sequence of nanosecond laser pulses 79−95084
thermochemical cycles of high temp. decomposition, thermodynamic method of research *(French)* 79−96295
thermochemical decomposition, based on $CeTiO_3$ for H_2 prod. 80−55929
thermochemical decomposition by Ce-Cl cycle for H production 80−35783
thermochemical decomposition for H prod., impact of thermal burdens and kinetics 80−35787
thermochemical decomposition for H prod. using S-Br cycle, development of lab.-scale plant 80−35774
thermochemical decomposition using General Atomic S-I cycle for H prod. 80−55941
thermochemical decomposition utilising solar heat for H_2 prod. 80−61451
thermochemical H production using SO_2-I_2 water splitting cycle 80−30600
thermochemical water splitting cycle for synthetic fuel prod. at fusion reactors 78−58458
thermochemical water-splitting cycles based on Ce and alkaline earth phosphates for H_2 prod. 80−55945
thermodynamic activity in Dead Sea brine 78−31673
thermodynamic props., computer programme calcs. *(French)* 80−54409
thermodynamic props., numerical calc. program *(French)* 77−69101
thermodynamic props. at high pressures from US vel. 79−94474
thermolysis, solar furnace, thermodynamic analysis 79−83625
thermoosmosis through cellulose acetate membranes 79−52768
thermoosmotic flow, filtration, in porous glasses 78−53248
thermophysical properties rel. to compressibility 78−83964
thin layer between quartz plates, IR absorption spectra 79−56773
water continued
tissue microwave dielectric props. rel. to rot. mobility of tissue water 77−29092
tissue molecular dynamics and freezing phase transition studied by proton spin relax. 78−68983
total transmittance of solar radiation through absorbing black liquid H_2O 79−34441
trace element anal. by ESCA 77−66779
trace metal anal. by energy dispersive X-ray fluoresc., enrichment procedures 77−60174
transcapillary water movement resulting from non-oncotic osmotic forces 78−44548
transient heat transfer (0-220°C, 1-10 bars) *(Russian)* 78−38183
transient heat transfer during natural convection *(Russian)* 77−68367
transient natural convection in horizontal pipe with const. cooling rate through 4°C 77−42828
transition flow boiling heat transfer to water in verticle annulus, BWR LOFA appl. 77−23182
transmittance, in laser radiation field effect of thermal defocusing *(Russian)* 79−1745
transport and thermodynamic props. *(Japanese)* 78−34251
transport in biomembrane, NME determ. methods *(Rumanian)* 80−94435
transport phenomena in cellulose diacetate membranes, hydration and dialysis coeffs. 80−76556
transport properties, relationships between thermal cond., dynamic viscosity and density, high state parameters 78−83861
triethylamine-H_2O, crit. phenomena, US vel. and absorpt. 78−91382
triethylamine-water, near crit. soln. pt., sp. ht. at const. press. and crit. conc., −1-22°C 78−38847
triethylamine-water critical mixtures, US absorpt. 79−28045
trimer, geometric config. energies, SCF LCAO MO calcs. 80−63551
trimethylamine-water critical fluid, ratio of sound dispersion to attenuation 79−55826
triple point as temp. fixed point 80−59626
triple point cell prep. for calibrating thermometers 78−204
tritiated, activity monitoring with flow cell type detector 78−82524
tritiated, inhalation hazard from open containers 80−8240
tritiated water intake, calc. of committed dose equiv. 79−16311
tritium in rabbits after ingestion of freeze-dried tritiated food and tritiated water 80−21549
troposphere, ^3H in water vapour, rel. to reactor release detect. 78−11988
troposphere, tritiated water vapour natural fluctuation rel. to environmental radiation surveillance 77−88287
troposphere humidity, new insight with Meteosat water vapour channel 79−25292
tube bank streamlining in critical flow regime with heat transfer *(Russian)* 78−14009
tumour-bearing mouse tissues, proton T_1 study of water coverage parameter changes 79−24953
turbid natural waters, spectral scatt. props. 80−72560
turbulence, free-stream, control by means of honeycombs 77−35122
turbulence effects heat transfer from cylinders in crossflow at critical Reynolds no. 79−98707
turbulent flow in tube, critical heat flux meas. *(Russian)* 79−10558
turbulent heat transfer downstream of unsymmetric blockage in tube 79−55377
turbulent water optical propag., refr. index spectrum of temp. or salinity fluctuations 79−5487
two-phase flow patterns, high pressure water in heated four rod bundle 78−89938
ultimate tensile strength estimated 77−7779
ultrapure water electrolytic conductivity meas. 79−24755
underwater electric discharge, acoustic, hydraulic and total efficiency 78−51388
underwater spark discharge, vapour-gas cavities generation and space-time evolution characts. 80−19650
unsaturated flow within porous materials, obs. by NMR imaging 79−98840
unsteady critical heat flux during boiling 77−23946
unsteady heat transfer to water at supercritical press. 80−48692
unsteady transient heat transfer with phase transitions 80−48693
in upper atmosphere, electron impact yield spectra 78−28401
upper atmosphere, H_2O prod. from H-implanted interplanetary dust grains 78−65445
upper atmosphere, water vapour rel. to winter radio absorpt. and Na nightglow 77−33239
US assisted radiant heat transfer into water and air 79−46169
US attenuation, for vol. viscosity, 0-60°C 78−63871
US attenuation temp. depend. in associated liq. 77−51441
US vel. and adiabatic compressibility determination, 25 to 80°C 80−88265
US vel. meas. by Brillouin scatt., supercooled to boiling range 77−15495
US velocities in superheated ordinary and heavy water, thermodynamic props. 80−65156
US velocity in crit. region 80−59582
UV lines oscillator strengths, rel. to water abundance in interstellar clouds 78−90104
Van der Waals interaction, Kramers-Kronig eqn. with full spectral data vs. oscillator model approx. 78−5998
Van der Waals polymer molecules, negative ions formed in nozzle expansion 78−90296
vapor in flames, coherent anti-Stokes Raman spectrum 79−36652
vaporisation, latent heat, student expt. 80−27081
vaporisation and thermoelastic press. due to CO_2 laser pulse 80−84227
vapour, 118.6 μm radiation absorption by H_2O vapour, temp. and press. effects meas. 78−75255
vapour, 2-D laminar boundary layer 80−19492
vapour, absorpt. at 7.1 cm^{-1}, temp. depend. 78−82722
vapour, absorpt. coeffs. at HF laser wavelengths 79−80010
vapour, absorpt. lines at ruby laser wavelengths, saturation effect 80−4098
vapour, absorption at 1 to 8 μm, rel. to atm. spectra 78−81402
vapour, absorption line profile, N_2 induced broadening 78−20516
vapour, absorption near 4250 cm^{-1} 78−82729
vapour, absorption spectrum, LiF F_2^+-centre laser intracavity spectroscopy appl. 80−32999
vapour, adsorbed, reaons for CH_4 release from graphite, desorption study 79−51420
vapour, adsorbed on polyvinyl acetate film, effect on charge retention, TSC obs. 77−32321

water continued
vapour, adsorbed on quartz, effect on surface cond. 77−85297
vapour, adsorbed on ZnO, effect of annealing and grinding 78−68656
vapour, adsorpt. on Al_2O_3 79−73398
vapour, adsorpt. on NH_4Cl, NH_4I powders 79−1545
vapour, adsorption, on montmorillonite, specific surface area 79−29406
vapour, adsorption on Cu and Cu_2O and desorption, relative humidity effects 80−49505
vapour, adsorption on Ge films, IR spectra 80−6628
vapour, adsorption on NiO, prepared by thermal decomp. of $Ni(OH)_2$, effect on microporosity 80−80060
vapour, adsorption on polymer carbons, porosity and surface chem. 79−52753
vapour, adsorption on SnO_2, desorpt. and cond. meas. 80−10790
vapour, adsorption on SnO_2 gas sensor, effect on cond. 78−76067
vapour, adsorption on TlCl and TlI, 273, 283 and 293K 78−56035
vapour, adsorption on transition metal hydroxide surfaces, gas chromatography study 79−66343
vapour, alpha-particle stopping cross section, 0.3 to 2.0 MeV 77−55313
vapour, anal. of skin evaporimeter performance 80−56256
vapour, atm. absorption line parameters, AFGL, compilation update 79−21013
vapour, atm. attenuation, meas. with IR hygrometer 79−34943
vapour, atm. conc. meas. by laser absorpt. techniques 78−61595
vapour, atmospheric, 460 μ absorpt. determ. 78−96295
vapour, atmospheric, effects on turbidity 77−78420
vapour, atmospheric, IR transmissivity 78−11998
vapour, atmospheric, laser sounding by reson. method *(Russian)* 77−33185
vapour, atmospheric, microwave absorpt. at 0.869 mm *(Russian)* 77−5277
vapour, atmospheric, microwave meas. of absolute values of absorpt. 79−66773
vapour, atmospheric, narrowing of collision shape of mol. absorpt. line in powerful laser field 79−29860
vapour, atmospheric, spectral transmission at wavelengths 0.7 to 1 μm 78−85685
vapour, attenuation of 10.6 μm radiation, role of $(H_2O)_2$ dimers 78−13741
vapour, attenuation of HF/CO_2 laser beam 80−61905
vapour, averaged potential for complex polar fluids 80−48833
vapour, chemical transport of GaAs, growth kinetics of epitaxial layers 77−16500
vapour, chemisorbed on $MgCr_2O_4$, mobility of water vapour mols. 77−51595
vapour, chemisorption on Fe film, XPS obs. 77−48587
vapour, chemisorption on TiC (001) surface, change in work function 80−29461
vapour, condensation from moist air in curved channels, mass and heat transfer 79−90251
vapour, condensation in presence of H_2SO_4 and HNO_3 pollutants 78−81343
vapour, continuous detection during thermal decomposition reacts. 80−3440
vapour, continuum absorpt. press. depend., 3.5-4.0 μm region 79−63992
vapour, continuum IR absorpt. near near 1200 cm^{-1}, temp. depend. 78−85687
vapour, depolarised Rayleigh scatt., rot. Raman spectra, mol. polarisability 78−33513
vapour, desublimation in vacuum, heat and mass transfer and duration 77−11687
vapour, dimerization, from thermal cond. meas., 373K 78−44359
vapour, dissoc., thermodynamic props. *(Japanese)* 77−80263
vapour, dissociating, composition and thermodynamic props., initial at. method 78−40034
vapour, dissociative and mol. adsorption on Re *(French)* 79−69344
vapour, distrib. in stratosphere 77−45112
vapour, effect on contact resist. of ZnO:NiO-Li_2O n-p heterojunction 80−34506
vapour, effect on motion of Ag particles supported on graphite 78−34695
vapour, effect on struct. and amorphous-cryst. transition of pyrimidine bases 77−70408
vapour, electron irrad. induced corrosion of Al and Mg 77−81343
vapour, electron stimulated interaction with Ni surface, AES obs. 77−31902
vapour, emissivity, data extrapolation method 77−7506
vapour, far IR absorpt. coeffs. by H_2O laser meas. 80−9599
vapour, H-D isotope exchange, mass spectroscopic sensitivities and equilib. const. 77−42434
vapour, HDO depleted, continuum absorpt. meas. 3.5 to 4 μm 77−87075
vapour, high-altitude profile on Mars 79−8869
vapour, in atmosphere, attenuation of 8-13 μm radiation *(Russian)* 78−88915
vapour, in Mars atmosphere, comparison of spacecraft meas. 79−8871
vapour, in mesosphere, ground-based microwave obs. 77−33161
vapour, in tropical atm., IR cooling rate rel. to CO_2 78−81405
vapour, initial reaction probability with Ba getter film, AES obs. 80−61153
vapour, initial reaction with Fe (001) surface 77−69173
vapour, interaction with Er and ErD_2 thin films 77−40575
vapour, intracavity laser spectroscopy sensitivity, saturation absorpt. influence 79−63312
vapour, ion mobilities, liq. droplet model failure 79−60097
vapour, ion mobility, 20 to 70°C 78−75252
vapour, ionis. coeffs. and dissociative electron attachment 80−43833
vapour, IR absorpt. spectrum, contrib. by molecular clusters 80−9598
vapour, IR bands transmission functions 80−106324
vapour, i.r. CO laser beam absorpt., optoacoustic meas. 77−2241
vapour, IR continuum absorpt. due to librational mode of dimer 78−66542
vapour, is atm., 10.6 μm laser beam attenuation, meteorological factors 77−2242
vapour, large-scale irregularities in troposphere, effects on radioastronomical seeing 78−24339
vapour, latit. distrib. in lower stratosphere, aircraft meas. 78−32173
vapour, line shape functions in absorpt. coeff. calc. 80−9600
vapour, low density flow temp. and density meas. by submillimetre spectroscopy 80−43816
vapour, meas. in stratosphere using UV fluoresc. hygrometer *(French)* 78−65401
water continued
vapour, microwave absorpt., spectral line press. broadening theory 77−30864
vapour, microwave breakdown, 20 mtorr-22 torr 79−72983
vapour, partial press. meas., student expt. 79−44685
vapour, perturbed-hard-sphere eqn. of state 80−96331
vapour, photodissoc., production cross section meas. for $OH(A^2\Sigma^+$ to $X^2\Pi)$ fluoresc. 78−25604
vapour, photoinduced nucleation 79−10934
vapour, photoinduced nucleation expt. 80−2149
vapour, polar mols. interaction, Wooley pot., 2nd virial coeff., dimer form. 77−65831
vapour, pressure broadened absorpt. in 10 μm region, O_2 addition effects 78−92975
vapour, pulse radiolysis, OH $(C^2\Sigma^+)$ time resolved emission 79−10138
vapour, radiance spectra, nonisothermal band models 77−62329
vapour, radiation absorption capacity 80−14873
vapour, Raman lidear meas., daytime atmosphere 80−85718
vapour, refr. index calc. and dispersive Fourier transform spectrometry 79−32736
vapour, remote conc. meas. using tunable IR laser 77−87118
vapour, role in thermal oxidation of Si, ellipsometry meas. 78−27656
vapour, rot.-vibr. levels, nonperturbative multimode model, 2 interacting Morse oscills. 78−9135
vapour, rovibr. Raman spectrum, ν_2 and $2\nu_2$ vibrs. 77−58022
vapour, rovibrational Raman spectrum 78−90174
vapour, saturated (subcooled), crit. discharge through differently shaped channels 78−55681
vapour, slow neutron scatt., effect of pressure total interaction cross section 78−17273
vapour, solar radiation absorpt. in troposphere, including multiple scatt. 78−61553
vapour, sorption by cobalt phthalocyanine film, AES obs. 78−91531
vapour, spectral line broadening by N_2, CO_2, Ar, intraresonator laser spectroscopy method 79−54863
vapour, spectral line shape changes in vapour with buffer gas *(Russian)* 78−46402
vapour, spectral line wave number, intensity and width near 5.3 μm *(French)* 77−50432
vapour, spectrochem. anal., effect on HF torch discharge *(Japanese)* 77−44554
vapour, spectrophone meas. of isotopes at selected CO, CO_2 laser wavelengths 78−57310
vapour, submillimetric high-resolution Fourier transform spectra 79−31509
vapour, supercrit. temp., electron localisation, density fluctuations, mol. orient. 78−38446
vapour, thermal cond., 375-600°C, 250 mPa 79−90367
vapour, tropospheric mixing ratio and influence on tropopause over India 77−53123
vapour, vars. in Mars polar areas, model 78−49363
vapour, visible absorpt. spectrum, fine struct. acoustooptical determ. 80−86450
vapour, wet, boundary layer in compressible flow 80−10295
vapour, Xe sensitized radiolysis, primary product yield 79−57265
vapour absorpt. bands, long distance meas. of cloudy atm. by radiometry 80−90196
vapour absorpt. in 10-12 μm atm. window 78−20513
vapour adsorption and outgassing by solder sealing glass, ultramicrogravimetric meas. using ultrahigh vac. system 79−80580
vapour adsorption isotherm, improved measurement method *(Japanese)* 78−6220
vapour and HCN mixtures, adsorption by activated and impregnated C 80−39412
vapour and liquid, atm. remote sensing with Nimbus 5 microwave spectrometer 77−49129
vapour and liquid determ. in atm. and clouds by microwave radiometry 78−93007
vapour and liquid far IR spectroscopy 80−60610
vapour at saturation, droplet nucleation by ions, ion mobilities 79−46794
vapour bands, 2.7 and 1.9 μm, adiabatic pressure depend. 78−33509
vapour channel, atmospheric transmission function, cloudless radiances 80−46256
vapour circulation in human organism, model *(Russian)* 79−2093
vapour condensation in rarefaction waves, homogeneous nucleation case 77−42869
vapour continuum absorpt., 4.5-5.0 μm 80−36395
vapour continuum absorption, 3.5 to 4.0 μm region 78−92973
vapour continuum absorption (3.5 to 4 μ) temp. dependence obs. 80−61903
vapour dielectric constant, rotational part, engineering method of calc. 78−40717
vapour electron stopping power and energy degradation 80−23276
vapour emissivity, simple parameterisation 77−42958
vapour etching of GaAs, rate 80−16519
vapour images from Meteosat, comparison to tropical steamline analyses 80−8384
vapour in air-water interfacial layer, isotopic distrib. rel. to bulk evaporation coeffs. 78−85576
vapour in troposphere under stable anticyclonal conditions, CO_2 laser radiation absorpt. 78−20515
vapour ionised by He^+ and He^{2+}, secondary electron emission yield obs. 80−102562
vapour IR continuum absorpt., appl. to aerosol IR spectrometry theory 80−101428
vapour laser, CW, characts. at 118 and 28 μm 79−81411
vapour laser, CW 28 μm, operating characts. and discharge conditions 80−69369
vapour laser, pulsed oscill., elongation by admixture of He 78−87039
vapour layer, heat cond., radiation interaction 79−55307
vapour line 724 nm differential absorption lidar at 724 nm water vapour 80−17384
vapour maser turn-on in H II region W3(OH) 78−36677
vapour modification of silica gel skeletal struct., thermal analysis obs. 78−88659
vapour nucleation on AgI target, mol. beam investig. 77−52212
vapour plasma, electron energy distrib. function, electron sink and plasma resist. effect *(Russian)* 80−106987
vapour press. formulation in range 0 to 100°C 77−69078
vapour pressure behaviour, generalised treatment 78−2227
vapour pressure meas. at triple point 77−43338

water continued
vapour RF discharge, low press., afterglow, spherical plasmoid, optical diagnostics 78−38568
vapour sorption by cured commercial epoxies 79−82454
vapour submillimetric-wave absorption obs. with photoacoustic cell 80−61901
vapour vertical profile in stratosphere *(French)* 80−77033
vapour-N_2, absorption at CO_2 laser frequencies 79−50011
vapour-N_2, nonstationary rarefaction wave, nonequilib. condensation obs. 77−75937
vapour-soot-CO_2 mixture, in luminous flames and smoke, IR mean absorption coeffs. calc. procedure 78−91061
Venus atmosphere; wager vapour mixing ratio from Pioneer Venus IR radiometer expt. 79−48719
Venus lower atmosphere, water vapour detect. by Pioneer Venus 79−48720
vertical infiltration of water in unsaturated soils, analysis 77−29346
vertical tube with laminar combined convection, water, finite difference anal. 78−90894
viscosity, 10-150°C, press. effects 78−51715
viscosity, dynamic, eqn. at −20 to 150°C 77−20103
viscosity, international formulation 78−26714
viscosity, multiparameter viscosity-temp. eqns. analysis 80−15283
viscosity changes close to quartz surface, fine capillary calcs. 80−54422
viscosity changes effect on electrokinetic phenomena in capillaries 80−53867
viscosity measurement behind shock wave front *(Russian)* 77−31707
viscosity rel. to limiting equiv. cond. of alkali, Cl^- ions in aq. soln. 77−1252
vortex large-scale, nonstationary model *(Russian)* 79−72955
VUV reflectance, refr. index, absorpt. coeff., isotope effects 78−6695
warm fog and steam clouds, emission spectra variations, evidence for clusters in vapour phase 79−39849
water:Cu(II) adsorbed on silica surface, EPR spectrum, freezing props. of water 77−4555
water+glycine(serine) zwitterions, interaction pots., ab initio SCF LCAO calcs. 78−48747
water mobility in blood plasma, NMR determ., viscosity correl. to $1/T_2$ 80−67176
water photoelectrolysis, rel. to charge transfer via surface states of semicond. 80−75636
water-2-propanol, density, US vel. meas. 78−18529
water-air and water-steam mixtures, sound speed rel. to fluid flow 77−84029
water-air interface, overall heat transfer coeffs., humidity and density profiles, turbulent pulsations *(Russian)* 78−22349
water-air plug-train system, press. wave propag. characts. 80−59058
water-alcohol mixtures, US attenuation meas., method of streaming 80−88272
water-carbon tetrachloride soln., fundamental H_2O IR spectrum, liq. struct. 80−23419
water-cetyltrimethylammonium bromide-haxanol system, ^{13}C NMR, catalysis in micellar and liq. cryst. phases 79−61909
water-dioxan mixtures, positron annihilation, o-positronium pick-off quenching 79−24386
water-dioxane(acetone) systems, electro-optical Kerr constant meas. at 632.8 nm 79−4788
water-dye solution, light scatt. effects on photoacoustic spectroscopy 80−95144
water-ethanol, inversion of Kirkwood-Buff theory 78−27807
water-ethanol, vapour-liquid equilibrium, transpiration method meas. 79−99305
water-ethanol mixture, nonlinear acoustic coeff. meas., 0-50°C *(French)* 80−34142
water-ethanol mixture, solid and liq., US vel., −80 to 20°C, 1-5 MHz 78−59933
water-ethanol mixtures, hydrophobic interaction, scaled particle theory 78−22625
water-ethylene diamine, liq.-solid equilibrium *(French)* 79−51236
water-fluorocarbon mixture, phase equilibria and critical phenomena at high press. 78−51648
water-imidazole, H bond interrupted chain, cooperative effects, STO-3G ab initio calcs. 80−63535
water-in-dodecane microemulsions, dielec. study of phase transition 79−28668
water-in-dodecane microemulsions, struct. transitions in liq. cryst. phase, dielec. props. 79−28669
water-isobutyric acid, crit. mixture 80−24601
water-isobutyric acid (2,6-lutidine) mixtures, critically quenched, phase separation and coalescence 80−24581
water-isobutyric acid critical mixtures, shear viscosity, pseudospinodal curves and scaling 78−22844
water-isobutyric acid mixture, heat of transport, crit. exponent 80−15277
water-isobutyric-acid, crit. fluid, refr. index, α and Δ components 79−82940
water-methanol, heat of mixing, high-press. calorimetric obs. *(German)* 78−16797
water-methanol(formamide), permeability of cellulose membrane 78−11557
water-methanol (n-propanol), binary mixtures, nucleation 80−44305
water-methanol mixture, nonlinear acoustic coeff. meas., 0-50°C *(French)* 80−34142
water-methanol mixtures, viscosity at 25°C, isotope substitution effects 80−92700
water-methanol vapour, condensation in presence of inert gas 77−80051
water-methanol-(ethanol), vapour-liquid equilibrium, transpiration method meas. 79−99305
water-nitrobenzene interface, mechanoelectrical energy conversion using interfacial tension changes 79−14982
water-oil microemulsions, optical matching 80−61157
water-p-dioxane at 11 and 25°C, US absorption 80−65171
water-petroleum emulsions, mean particle diameter and conc. determ. by light scatt. 80−89538
water-polystyrene spheres (highly charged), solid- and liq.-like phases, soft core liq. theory 77−63963
water-propylene 1.3-diamine, liq.-solid equilibrium *(French)* 79−51236
water-steam mixture, upflow in heated tubes, void fraction 77−62296
water-triethylamine, crit. fluid, refr. index, α and Δ components 79−82940
water continued
wave amplitude measurement, surface standing, using capacitance meas. circuit 79−50833
wave damping, effect of large grooves 77−11209
wave diffraction by 3-D bodies, hybrid element method 78−38344
wave stability, linear theory approach 77−51068
waves, electronic instrument for precise meas. 78−86294
waves, Mach reflection from wall *(Polish)* 77−70684
waves, nonlinear, dynamic properties stochastic modelling 79−23332
waves, viscous attenuation of mean drift 77−58710
waves in narrow channels: faster capillary waves 79−18905
weirs and flumes for flow measurement, book 80−1717
wetting angle of quartz meniscus movement depend. 79−37899
wetting of Au, hydrocarbon contaminant effect, macroscopic continuum model 77−85018
wind waves in shallow water, statistical model *(Polish)* 79−25260
wind-generated waves, airflow separation 77−70734
X-irradiation, O prod., rel. to hypoxic cell radiosensitivity 77−25514
X-ray attenuation, 5-40 MV, rel. sensitivities of materials for half-value-layer meas. 77−45927
X-ray scatt. curve anal. 79−10785
yeast cell membrane, water transport study, pulse NMR obs. 80−40981
yeast cells, translational mobility of water, pulsed NMR obs. 79−57612
zeolite-water desorption, complex reaction interphase boundary kinetics 79−57203
Zircaloy-4, cyclic nature of corrosion in 633K water, optical and electron microscope study 79−66207
π energy dependent mean free path length for star formation 77−23393
Al hydration, in vap. phase, rel. to upper atmosphere chemiluminesc. 79−29362
Ar-$N_2(Cl_2)(F_2)(H_2O)$ laser, energy pathways by proton excitation 78−5459
Ar+HCN(H_2O), electron excitation of Ar* and Ar_2*, fluoresc. and dissoc. energy transfer collisions 77−14580
BF_3-H_2O mixtures, vapour density and dissociation, 150-400°C 77−7491
BN, cubic, water catalysed form. 78−53199
B_2O_3, molten, reaction with water, reactor fuel-coolant interaction simulation 78−58363
$Ba[Fe(CN)_5NO]_2.2H_2O$, NMR, H_2O orient. *(French)* 78−52366
$Be^{2+}+H_2O$, mol. complex struct. and interaction energy, CI calc. 79−18133
Bi_2O_3, molten, reaction with water, reactor fuel-coolant interaction simulation 78−58363
$Br(H_2O)_n^-$, geometric and electronic struct., CNDO/2 calcs. 77−79542
$Br(4^2P_{1/2})+N_2O$, electronic-vibr. energy transfer obs. 78−55220
C-H-O(-N) gas mixtures, high temp. emissivity, 4.8 μ region, shock waves 77−76027
CO-H_2O-NH_3-methanol, solid mixture vibr. modes, IR spectra 80−90504
CO-He-O_2-H_2O laser discharge, stability, influence of recombination and ion chem. 78−17915
CO_2-N_2 gasdynamic laser, amplification coeff. rel. to water vapour content *(Russian)* 77−7057
CO_2-N_2-H_2O fast flow discharge laser, output power time depend. 80−99697
CO_2-N_2-H_2O gas mixture, method for obtaining vibrational population inversion 79−94210
CO_2-N_2-H_2O gasdynamic laser, water vapour condensation and mol. relax. processes 79−13946
CO_2-N_2-H_2O gasdynamic laser, small signal gain and vibr. wall accomm. 79−98340
CO_2-N_2-H_2O mixture, unstable-oscillatory expansion *(Russian)* 78−1637
CO_2-N_2-Ne-H_2O mixture IR laser *(Russian)* 79−10323
CO_2-O_2-H_2O, mixture, mol. negative ions, photodissoc. and photodetachment cross section 77−27129
CO_2-O_2-H_2O, photodissoc. and photodetachment of negative ions 80−14182
CO_2-water, saturated two phase flow system, non-equilib. state transient process 80−59096
CO_2-water vapour mixtures, 2.7 micron band absorption, 1000 to 2200K, 0.25 to 3 atm. 77−58006
CO_2-water vapour slug flow, radiative and convective transfer interaction 77−58529
$CaCl_2$-$BaCl_2$-H_2O ternary system, 45°C isotherm *(French)* 79−96004
$Ca(NO_3)_2$-H_2O solns., ice I homogeneous nucleation temp., slow vitrification mechanism 78−26666
Cd, determ. in sea and fresh waters, interlaboratory comparison 78−81209
$CdCl_2$-KCl-H_2O, water activity, 0 and 50°C, conc. depend. *(Russian)* 78−31679
CdO thin film conductivity, H_2O and CO adsorption effects 79−56340
^{252}Cf neutron source for water-steam mixture void fraction meas. 79−26762
Co^{2+} ion removal in high temp. water using TiO_2 79−89376
$CoCl_2$-LiCl-glycerin-water system, Co^{2+} ion coordination transition, spectral investig. 79−42953
CsPFO/H_2O(D_2O) system, nuclear mag. relax. of water at identically oriented planar interface 77−36148
D_2O-H_2O, IR absorption spectra, statistical charact., continuous model of liq. struct. confirmation 78−6671
D_2O-H_2O mixtures, US vel. at 298.15K, adiabatic compressibility 78−10127
D_2O-H_2O-HDO, gaseous mixture, absorpt. meas. by Michelson inclined mirror interferometer, high spectral resolution 80−9023
DOD, vibr. intensities, ab initio and empirical calcs. 80−78592
DOD, vibr. intensities, ab initio and empirical calcs., band strengths 80−78593
$D_3O^+(H_2O)_{0,1,2}+H_2O$ reactions, SIFT studies, review 80−58435
ethanol-water system, complex dielec. permitt. in UHF region and NMR spectra *(Japanese)* 80−100620
$EuCl_3$-$NaPO_3$-H_2O system, Eu polyphosphates form. at 0°C 80−35515
Fe, influence of acid Na_3PO_4 soln. in tap water as a corrosion inhibitor 80−45424
Fe-H_2O laminated radiation shield, fast neutron transport 80−13931
Fe-water multilayer radiation shielding design optimisation, conversational procedure 77−14273
Fe+H_2O, clean surface oxidation and passivation by H_2O vap., XPS 77−81424
H production, thermochem. H_2O decomposition using S compounds, feasibility anal. 80−35768

water continued
H-bonded dimers involving NH_3 and HF, PCILO study 79−72238
H-bonded structure, IR spectra, assignments 78−62800
H-bonding, multiple, from lower crit. soln. pt. theory of aq. mixtures 79−4415
$H^+ + H_2O(N_2)$, UV and visible band emission cross-sections 77−16847
H_2 and O_2 production from H_2O using solar energy, eval. of a hybrid process 80−104519
H_2-$H_2O(Cl_2)$, diffusion in stratified positive column, impurity effects 77−11320
$H_3+H_3O^+ \rightarrow H+H_3O^+$, reaction kinematics 78−31625
HCl-H_2O, p-V-T relations up to 773K and 1500 bars 78−43096
HCl-KCl-H_2O mixed electrolyte solns., elec. transport 80−3355
$HClO_4$-H_2O, aq. soln., IR and Raman spectra, conc. depend. *(Russian)* 80−53002
$H^+(D^+)$ exchange rates, ^{17}O NMR linewidths, pH depend. 80−91661
HDO, beam maser double reson., hyperfine struct. D quadrupole coupling 77−65493
HDO, interactions with myosin, intermolecular spin diffusion study 80−18951
HDO, line strengths and intensities, ab initio calcs. 79−72300
HDO molecules, stretching vibrs., freq. meas. in hydrates 78−29772
HDO molecules in solid hydrates, D quadrupole coupling consts., O-H and O-D stretching freqs., H bond distances 78−29773
$H^+(H_2O)_c$ ion-induced water clusters, mass spectra, IR continuum absorpt. 80−87257
$H^+(H_2O)_n$, secondary electron emission from charged clusters on 2.4 keV Ar bombarded surfaces 79−15580
HNO_3-H_2O, liq. and glass, mol. assoc., ion pairs, Raman obs. 79−28749
HNO_3-water, homogeneous nucleation, relative humidity depend. 78−71846
H_2O, $(D_2O)(HDO)$, photoelectron spectrum, Franck-Condon, factor calc., geometry and vibrs. *(French)* 77−83652
H_2O, config. and vibr. heat capacities, H-bonds 79−99331
H_2O dimer, continuum absorpt. spectra in 8-13 μm range *(Chinese)* 80−109237
H_2O photodissociation, $OH(A^2\Sigma^+ \rightarrow X^2\Pi_i)$ yields 80−71927
H_2O vapour under point corona discharge, microprocessor control for vapour generator and EHD phenomena 80−106852
H_2O^-, ab initio calcs., electron affinity, stability 77−42239
H_2O^-, in γ-irrad. Y-type zeolite, alternative EPR triplet assignment to NO_3^{2-} 78−11534
H_2O^-, trapped in γ-irrad., Y-type zeolites, ESR obs. 77−9099
H_2O^+, ab initio potential energy surface study by CI techniques, equilibrium conform. determ., mol. dissoc. pathways 80−78550
H_2O^+, airglow emissions from cometary inner comas 78−45282
H_2O^+, electronic spectrum 77−473
H_2O^+, in Comet Bennett (1970 II), brightness profiles 79−35192
H_2O^+ in cometary tails, surface brightness rel. to CO^+ 80−72880
H_2O^+, interstellar, unsuccessful search and abundance upper limit 78−69860
H_2O^+, pot. energy surface, linear approach 78−41978
H_2O^+, pot. energy surface from $O^+ + H_2$ reaction 80−47922
H_2O^+, states geometries, electronic vibr. coupling consts. HF calcs., comparison with Xalpha calcs. 80−27946
H_2O^{2+}, singlet state orthogonality constrained SCF calc. 77−26962
$H_2{}^{16}O$, 6.3 μm region hot bands, intensities 77−75156
$H_2{}^{16}O$ and $H_2{}^{18}O$ samples, vap. press. isotope effects, 0-170°C 78−18757
$H_2{}^{16}O$, $H_2{}^{18}O$, isotope fractionation, H-bonds, force consts., liq. water struct. 77−76288
$H_2{}^{16}O$, $H_2{}^{18}O$, molecular vibration-rotation, determ. of line intensities *(French)* 79−18186
$H_2{}^{16}O$, $HD^{16}O$, $H_2{}^{18}O$, mol. diffusivities in N_2, isotope effects 79−1282
$H_2{}^{16}O$, interacting vibr. states, energy level fitting 78−78618
$H_2{}^{17}O$, $H_2{}^{18}O$, Stark spectra with CO laser, Lamb dip spectra of ν_2 band 78−62840
$H_2{}^{18}O$, chemisorption on $SrTiO_3$, oxidation and reduction, isotope exchange study 80−104461
$H_2{}^{18}O$, $H_2{}^{17}O$, rot. spectra, 650-50 cm^{-1} 77−65458
$H_2{}^{18}O$, interstellar, detect. in Orion mol. cloud and DR 21(OH), H_2O abundance estimate 78−57621
$H_2{}^{18}O$, line positions and intensities, $\nu_1+\nu_2$ and $\nu_2+\nu_3$ bands 78−74656
$H_2{}^{18}O$, self-diffusion, pressure and temp. depend., NMR spin-echo obs. 80−65266
$H_2{}^{18}O$, vibr. relax. rate consts., fluoresc. method determ. 78−17762
H_2O/D_2O electrolysis, Pd electrodes, H/D isotope separation factors, and exchange efficiency 79−50149
H_2O-acetic acid, liq. mixture, thermodynamic excess functions, calorimetric meas. 77−52666
H_2O-acetic acid-silver acetate, ternary liq., elec. cond. and density 78−91464
H_2O-air, two phase upflow across horizontal tube bundles, void fraction and flow pattern 80−92201
H_2O-alcohol microemulsion, elec. cond. and struct. 79−20471
H_2O-CO_2, IR radiation transfer 79−80028
H_2O-CO_2-N_2 gas mixture, oscillatory nonequilib. in planar supersonic nozzle flow 78−1758
H_2O-CsCl-1-glyceryl 1-octanoate, Cs^+H_2O interaction in lamellar phase, NMR quadrupole splitting and chemical shift 80−50209
H_2O-D_2O mixing, diffusion meas. using neutron radiography 77−15605
H_2O-decahydronaphthalene (tetrahydronaphthalene), liq.-liq. phase equilib., crit. phenomena 78−18764
H_2O-ethanol-chloroform mixture, shear viscosity near plait point, nonlinear effect 77−84960
H_2O-ethylene (H_2O) nonbonded interactions, pot. energy curves, CNDO/2, INDO and extended Huckel calcs. 77−27140
H_2O-formaldehyde complex, IR spectrum in solid Ar, N_2 matrix 80−43042
H_2O-formyl-triglycyl amide, analytical pot., ab initio calc. 79−48206
H_2O-H_2 cooling in supersonic nozzle, submillimetre wave generation 80−48229
H_2O-H_2O_2, isolation of singular component for heat capacities of supercooled H_2O 80−107437
H_2O-H_2S complexes, equilib. config., H-bond energies and electron densities, CNDO/2 method 80−14084
H_2O-H_2S supersystem, ab initio LCAO MO SCF calcs. of H bonding 79−89607
H_2O-H_2SO_4, mixtures, transient nucleation, stochastic theory 77−1221
H_2O-H_2SO_4 system, nucleation, aerosol form. 77−70327
H_2O-HF, H-bonded complex, cubic force consts. calcs. 80−47868
water continued
H_2O-HF, microwave spectroscopic investigations of hydrogen-bonded complexes 78−62794
(H_2O)-HF complexes, (x=1 or 2), geometry, CNDO/2 calc. 79−36531
H_2O-HF heterodimer, H bonding, microwave rot. spectrum, mol. geometry and moment 80−99501
H_2O-HNO_x-NO_x^- clusters, gas phase, thermodynamic quantities, mass spectra obs. 80−50875
H_2O-isobutyric acid, crit. mixture, partial molar vol., temp. depend. 78−18800
H_2O-Li^+ complex, charge transfer theory, Mulliken population, ab initio calc., multiconfiguration scheme 80−106392
H_2O-Li(Al), mol. complex, electronic struct. calcs. 78−66465
H_2O-liquid metal stratified flow, horizontal co-current, interface heat transfer, turbulence model 80−92131
H_2O-methanol, liq., zero-angle X-ray scatt., conc. depend. 79−27897
H_2O-N_2H_4, isolation of singular component for heat capacities of supercooled H_2O 80−107437
H_2O-NaCl-sucrose, phase diagram determ., appls. in cryobiology 78−15777
H_2O-O_2-CO_2, gas mixture, photodetachment and photodissoc., mass spectra meas. 77−500
H_2O-SO_2-alkane gaseous mixture, photoinduced nucleation and quantum yields 79−96348
H_2O-trifluoracetic acid, molecular dynamics simulation of chemical reactions in solution 80−40673
H_2O+ methane, pairwise interaction pot. function, ab initio SCF MO calc. 79−22786
H_2O+Ar^+, thermal-energy charge transfer, H_2O^+ product internal and kinetic energy 80−16654
H_2O+Ar(Kr), $(^3P_{0,2})$ state quenching cross sections 78−70912
H_2O+CO_2, photoassisted reaction on $SrTiO_3$ (111) face, methane form. 78−76878
H_2O+Cl_2O=HOCl, equilib. const., Fourier transform IR determ. 80−7765
$H_2O+Cl_2O \rightarrow 2HOCl$, equilib. const., UV spectrum investig. 79−79238
H_2O+Cs(K), ionising collisions in crossed-beam systems 78−48641
H_2O+D_2, isotope exchange on Pt, CO poisoning effects 79−11824
H_2O+D_2, isotope exchange on Pt over hydrophobic support 79−11823
$H_2O+D_2O \rightleftharpoons 2HDO$, vibr. anharmonicity effect on equilib. 79−74410
$H_2O+D_3O^+(D_2O)_n$, binary reactions, rate coeffs. and product ion distributions determ. 80−81305
$H_2O+H_9(F^-)(CH_4)$, interaction energy calc. using minimal basis sets 80−9678
H_2O+H_2O, interaction energy, MCF and perturbation calculations 77−27139
H_2O+H_2O, vibr. relax. near room temp. 78−86939
$H_2O+H_2O(He)(Ar)(N_2)(O_2)(CO_2)$, vibr. energy transfer temp. depend. 80−63763
$H_2O+H_2O(Na^+)(K^+)(NH_4^+)$, supermolecule calcs. with additive procedure, intermolecular interactions and binding energy 80−52880
$H_2O+H_3O^+H(H_3S^+)(HCNH^+)(HCNO.H^+)$, proton transfer, rate and equilib. consts. 78−48636
H_2O+H^+, 0.3 to 1.5 MeV, electron ejection, energy and ang. distrib. meas. 77−71851
H_2O+HDO, isotope exchange in liq.-vapour system, r.i. and thermal cond. obs. *(German)* 77−4902
H_2O+HF, mol. electrostatic pot., H-bonds, CNDO/2 calc. 77−61822
H_2O+H(n=3), $O(3p^3P)$, radiation quenching in pulse radiolytically excited water vap. 79−89738
H_2O+He, collisional excitation of interstellar molecules, rate consts. 80−67816
H_2O+He, differential scatt. cross-section, intermol. pot. 79−36728
H_2O+He, rot.-translational energy transfer, nonlinear vs. linear rotors, surprisal anal. 79−76492
$H_2O+He^+(O^+)(N_2^+)(O_2^+)(Ar^+)$, 50 to 250 keV, OH radical form. 78−56890
H_2O+He(Ne), metastable, chemi-ionisation and secondary ion reactions 77−40531
H_2O+He(2^3S), energy transfer processes, reaction products, UV and visible obs. in flowing afterglow 78−85138
H_2O+inert gas ion, thermal energy charge transfer 78−37739
H_2O+Li^+, ab initio GTO calc. of vibr. intensity changes of spectroscopic parameters 78−58583
H_2O+methanol-d_0(-d_1)(-d_4), D exchange reaction, thermodynamics 78−94328
H_2O+methyl ion, ternary association reaction in energy range 0.04-0.1 eV 80−71896
H_2O+N_2, vibr. relax., holographic interferometric meas. 78−66631
H_2O+N_2, vibr.-translation relax. cross section in glow discharge plasma 77−43092
$H_2O+N_2{}^*$, deactivation, from laser-induced CO_2 fluoresc. obs. 80−63776
$H_2O+N_2{}^*$, vibr. excited quenching temp. depend. flowing afterglow 77−54595
$H_2O+N_2(CO_2)$, collision broadened H_2O absorpt. line, laser radiation intensity effects 77−83661
$H_2O+N^+(O^+)(Ne^+)$ symmetric collisions, double K-shell ionisation, two-electron-one-photon transitions 77−19067
$H_2O+NH_2^+(NH_3^+)$, bimolecular reactions, product. distrib., rate consts. 78−11513
$H_2O+NH_3^{\cdot+} \rightarrow NH_4^+ + OH^{\cdot}$ 78−15660
H_2O+Ne, hollow-cathode discharge, Ne spectral intensity 79−4202
H_2O+Ne^+, thermal energy, reaction rate coeffs. and product distrib. 79−29333
H_2O+Ne*, pot. energy surfaces, MO and CI calcs., Penning ionisation electron spectra 80−106376
H_2O+Ne(He), Penning ionis. electron spectroscopy, energy peak shifts and shapes 77−42392
H_2O+O, rot. excitation, classical Monte Carlo calcs. 77−34727
$H_2O+O^{n+}(Xe^{n+})(Pb^{n+})$, 50 keV, multiple scatt., target at.+energetic ion spatial correlation influence 79−27062
H_2O+OH, mean collision cross sections from microwave spectroscopy 80−1046
H_2O+OH, rot. inelastic collision, microwave spectra 79−45806
$H_2O+OH(A^2\Sigma^+)$, quenching rates and fluoresc. efficiency, rel. to atmosphere 80−14199
$H_2O+O(^1D)$, direct reaction in flow system 80−3333
$H_2O+O(^1D)$, rate coeff., atm. OH prod. 79−58009
$H_2O+O(^1S)$, product channels 78−46422

water continued
$H_2O+O(2^1D_2)$, collisional deactivation meas., 295K, rel. to atmospheric processes 80−16663
H_2O+SO_2, collisional quenching of $^3B_1$ state, 8-1300 torr 78−86906
H_2O+SO_2, rot. linewidths (intensities) of $^{32}S^{16}O_2(^{34}S^{16}O_2)$, 91.5-95.5 GHz 78−42044
$H_2O+SO_2+O_2(N_2)$(Ar), condensation nuclei form., ion polarity and age depend. 79−39220
$H_2O+SO_3 \rightarrow H_2SO_4$, gas phase kinetics, CNDO/2 calc. of H_2SO_4 and $SO_3.H_2O$ struct. 78−76840
$H_2O+Sc(La)(Y)$, O atom abstraction, product internal state distrib., fluoresc. study 78−48643
H_2O+T, energetic reactions, hard sphere excitation functions 79−1963
$H_2O^+ + H_2$, ion-molecule reaction detection of laser-induced ion spectrum, rot. components 78−74671
$H_2O^+ + NH_3$, bimolecular reactions, product. distrib., rate consts. 78−11513
$H_2O^+ + NO_2(O_2)(NO)(CO)(H_2)$(ethylene)(methane), rate constants determ. as function of relative kinetic energy 80−81292
$(H_2O)_2$, accurate atom-atom potential 78−21990
$(H_2O)_2$, and isotopic species, Ar isolation IR spectra, band assignments, struct. 77−3364
$(H_2O)_2$, and isotopic species, Ar matrix IR spectra, Xe, HCl, $(CH_3)_2O$ doping, struct. 77−3365
$(H_2O)_2$ dimer intermolecular pot., liq. struct. mol. dynamics simulation 78−71657
$(H_2O)_2$, electrostatic mol. pot. curves, proton transfer and bridging pot., CNDO/2 calc. 79−94054
$(H_2O)_2$, energy decomp. anal. of H-bonding, ab initio MO calcs. 77−57868
$(H_2O)_2$, exchange forces, Hellmann-Feynman theorem calc. 77−54589
$(H_2O)_2$, H-bonding and indirect exchange ('superexchange') in 79−93912
$(H_2O)_2$, photoionis., H_2O proton affinity 78−17731
$(H_2O)_3$, core and valence ionis., nonempirical LCAO MO SCF calcs. 77−67973
$(H_2O)_n$, n=8, 64, cluster thermodynamics calcs. using Monte Carlo method 77−58219
HOD, DOD, HOT, TOT, IR band intensities estimation 78−86916
HOD, HOT, vibr. intensities, ab initio and empirical calcs. 80−78592
HOD, IR band intensities in ice and water 79−3443
HOD, IR spectra in D_2O, combination vibr. 80−9609
$H_2O(D_2O)$, VUV absorption spectra, Rydberg series, rot. line shapes, quantum defect 78−5244
HOH, HOD, HOT, vibr. intensities, ab initio and empirical calcs., band strengths 80−78593
$HO_2.H_2O(NH_3)$ complex form., ab initio calcs., min. energy configs. 77−14340
$H_2O.H_2S$, IR spectra of complex in solid nitrogen, 20K 79−10102
$H_2O...HF$ complex, force field, vibr. freqs., equilib. geometry bond energy, ab initio calc. 77−65450
$H_3O^+.nH_2O$ cluster ions, stability, assoc. and dissoc. 77−60055
$H_2O(ads)+H(ads) \rightarrow OH+H_2(g)$, H_2 formation mechanism 80−6628
H_2SO_4/H_2O aerosol formation, growth simulation using general dynamic eqn. 79−47990
H_2SO_4-H_2O, aerosol form., nucleation calcs. 78−31709
H_2SO_4-H_2O, vapour mixture, temp. depend. of nucleation, aerosol form. 77−86350
H_2SO_4-H_2O aerosols nucleation rate in presence of ionisation source 80−104464
H_2SO_4-H_2O-ion aerosol particles, ultrafine, stratospheric form., ion-induced nucleation 80−72608
H_2SO_4-water, homogeneous nucleation, relative humidity depend. 78−71846
HTO, rain scavenging 79−16563
^3H measurement, deep electrolytical enrichment, behaviour of phosphate pickled mild steel cathodes 80−93764
$H^*_2+H_2O(SF_6)$, ionis. collisions 79−64088
He+water (cyanomethane), afterglow, excitation and quenching reactions, optical pumping 78−35690
Hg determ. in sea and fresh waters, interlaboratory comparison 78−81209
Hg determination, error anal. 78−69519
Hg, thermodynamical Gruneisen parameter, press. depend. 78−14479
Hg+water systems, drop fragmentation rel. to thermal explosion detonation requirements 78−71368
hydrocarbon-water, emulsions, superheated, bubble nucleation 78−61056
$I(H_2O)_n^-$, geometric and electronic struct., CNDO/2 calcs. 77−79542
IR, absorpt. in regions of weak absorpt., lab. meas. rel. to atm. windows 79−64005
$I^*+H_2O(D_2O)$(HDO), $5^2P_{1/2}$ electronic to vibr. energy transfer, quenching and time resolved IR fluoresc. 79−3537
$I(5^2P_{1/2})+H_2O(D_2O)$(HX)(DX), collisional quenching, isotope effects 77−34583
$K_2HgCl_4.H_2O$, cryst., IR spectra, water mol. struct., H-bonding 77−81089
K_2O-Ga_2O_3-P_2O_5-H_2O, reactions, 150-500°C 80−35514
$La_2(SO_4)_3.9H_2O$, and isotopic forms, water librations, Raman obs. *(French)* 79−28754
Li/H_2O, surface complex form., obs. using photoelectron spectra 79−69359
$Li+H_2O \rightleftharpoons LiOH+H$, equilib. consts., ab initio SCF and CEPA calcs. 78−3361
Li_n, at. cluster with H_2O mol. attached, MO study 79−76541
LiCl aqueous soln., ion-water clusters, electronic struct., Compton profile 78−47227
Mg removal from interstitial waters in reducing environments 79−66673
Mg vermiculite, adsorbed water mol. orientation, elec. pot. calc. 78−26763
$Mg(PO_4)_2.xH_2O$, x=8, 22, dehydration and water bonding 77−44456
N_2 and methane boiling on water, initial water temp. effect 77−19606
N_2-CO_2-H_2O gasdynamic laser mixture, electron beam diagnostics 77−83845
N_2-H_2O plasma state, partial equilib. with reaction invariants *(French)* 79−52739
NH_3-H_2O, solar absorption refrigeration system, Seoul, Korea *(Korean)* 78−51052
NH_3-water system, vapour-liquid equilib., thermodynamics 79−42246
NH_3+H_2O, collision-induced energy transfer, IR-microwave double reson. obs. 78−42171
NH_3+H_2O coolant for solar refrigeration *(French)* 79−24911
water continued
NH_4NO_3-$LiNO_3$-NH_4Cl-water system, cond. and viscosity *(French)* 79−51286
$(NH_4)_2SO_4$-ethanol-benzene-water, liq. mixture, near tricrit. pt., thermodynamic model and sum rules 80−34196
$N_2O/N_2/H_2O$, CW gasdynamic laser, numerical anal. 78−29935
N_2O_4-NO-H_2O, distrib. coeff. for N_2O_4 on liquid-vapour equilib. *(Russian)* 80−55699
$N_2O_5+H_3O^+$, rate consts. 78−56879
^{13}N species formed by proton irradiation of water 80−45532
$N_2^*+H_2O$, vibr. deactivation rate, hard core calc. 79−31651
Na-H_2O reaction testing in large leak test rig 78−86577
Na_2^+-$(H_2O)_n$ clusters, gas phase, high press. mass spectrometry, atmospherical implications 80−58436
NaCl, mass transfer from sedimentary deposit layer to stationary water region *(Japanese)* 77−25700
NaCl-KCl($MgCl_2$)-H_2O mixed electrolyte solns., elec. transport 80−3355
NaCl-water-tetrahydrofuran system, heat. of soln. meas. using Calvet microcalorimeter *(French)* 77−44504
Na_2O-B_2O_3-SiO_2, optical waveguide glass, molar absorptivity of water 80−80066
Na_2O-SiO_2 glasses, water reactions at elevated temps. and press. 80−81312
Na_2SO_4-$CoSO_4$-H_2O, phase equilib., activities, Pitzer eqn. calcs. *(Russian)* 80−65190
O_2 bubbles, rising in water, dissolution mass transfer coeffs. 79−41737
O_2+H_2, 118750 GHz transition, press. broadening 77−75136
$O(^1D)+O_2(N_2)(CO_2)(O_3)(H_2O)$, 100-350K, reaction rate consts. 77−21355
OH+H_2O, OH linewidth rot. depend. on UV transitions 80−91606
$P_4+H_2O(D_2O)$, vapour, chemiluminesc., transient emitting species 77−1926
RbCl-KCl(H_2SO_4)-H_2O, water activity, 0 and 50°C, conc. depend. *(Russian)* 78−31679
RbX-CdX_2-H_2O, X=Cl,Br,I, Gibbs free energy, H_2O activity, 25°C *(Russian)* 78−31678
SO_2-H_2O microwave absorption, 94 GHz by mol. interaction 79−31507
T concentration meas. with electrolytic enrichment cell and reduction system 78−20128
THO, prediction of flux from air to plant leaves 80−26381
TOT, vibr. intensities, ab initio and empirical calcs. 80−78592
TOT, vibr. intensities, ab initio and empirical calcs., band strengths 80−78593
Ti complexes, cryst., amorphous, coordinated H_2O, mol. force field ellipses, mol. force consts. 77−34609
$Ti(OH)_x$, amorphous, dehydration and crystallisation 77−43150
U, conc. determ. by fission track registration technique 80−12565
U-light water slab, meas. of space depend. ang. thermal neutron spectra 77−14208
^{133}Xe solubility coefficients in water, saline, dog blood and organs 80−56331
$ZnAs_2$-H_2O, Schottky diodes, elec. and photoelec. props., excitons 80−65653
ZnP_2-H_2O Schottky diodes, elec. and photoelec. props., excitons 80−65653
ZnSe/water, interface, laser-induced damage in ZnSe 80−102746

water boilers *see boilers*

water conditioning *see water treatment*

water cooling towers *see cooling towers*

water pollution
see also water pollution detection and control
acid mine drainage in impoundments, computer simulation 77−37260
acid precipitation effects, Norwegian SNSF-project on forest and fish 77−37411
acid rain, neutralization in Hubbard Brook ecosystem 79−74922
acidification of Canadian lakes, effects on fish populations 77−37259
acidification of headwater stream, New Jersey Pinelands 80−81945
active pollutant dispersion in shallow sea, model 77−29324
acute fish toxicity and absorption tests of an experimental detergent builder, trisodium carboxymethyloxysuccinate 79−57184
Aegean Sea, Cu, As and Hg conc. determ. 79−2292
aeration system optimal design for polluted streams 77−37251
NW.Africa, snowfield acidity (1977-79) 80−98370
air pollution transfer into water bodies, model 77−33118
aircraft effects, Canadian environmental policy 78−33950
Amoco Cadiz oil spill, preliminary report 79−12147
aquatic ecosystems, acid precipitation effects, review 77−37257
aquifers, pollutant prop., experimental study *(French)* 77−41105
Arabian Sea, petroleum hydrocarbon conc. in shelf regions and adjacent waters 79−48190
Argo Merchant wreck site, oil and sediment hydrocarbons, gas chromatography 79−83645
N.E.Atlantic, heavy metals and petroleum products 78−3827
N.Atlantic surface water, T and ^{90}Sr conc. and distrib. 78−65345
N Atlantic water columns, trichlorofluoromethane (F-11) exploratory anals. 78−88847
atmospheric transport of pollutants, new direction in hydrometeorology 78−96240
Baltic Sea, heavy metals pollution and ferromanganese nodules accretion rate 77−81864
Bantry Bay, Ireland, oil spill from tanker Betelgeuse, initial effects 80−3540
Bay of Naples, bottom sediment contamination 79−16519
bay with currents, soln. of two-dimens. dispersion convection eqn. 77−91157
Bedford Ouse River, systems model of stream flow and water quality 80−81956
benzo(a)pyrene in lake sediment, western USA 80−61476
biological material analysis, As and Hg determ. by neutron activation anal. 80−36216
biological process models in water quality system, identification 79−5540
biological waste water treatment by activated sludge at Haguenau City water treatment plant *(French)* 80−61473
Black Sea, quantitative distrib. of suspended matter 78−3818
Bombay, coastal pollution physicochemical studies 80−104522
Bombay Harbour sediments, elemental concs. 77−73709
bromate, sunlight-induced form. in chlorinated seawater 77−49088
buoyant contaminant in shallow channel, longitudinal dispersion 77−21805

water pollution continued
California harbours, vessel-related contamination by Cu and other metals 79−88010
Cambay drinking water, metal contents 79−20899
Caspian Sea, T content 79−34858
chemicals, protocols for evaluating effects on aquatic life 78−53604
Chesapeake Bay, impact on anoxia on Mn fluxes 79−92099
Chesapeake Bay pollution, data importance 80−3544
chloroform, production from polyelectrolytes 77−78252
Clyde Sea Area, Scotland, ^{134}Cs and ^{137}Cs contamination, water and sediment tracer species 80−3541
coal-fired power station, heavy metal fallout to nearby pond 80−76667
coastal, monitoring by neutron activation analysis 77−41068
coastal aquifer of Israel, nitrate and chloride pollution, single-cell model 77−5265
coastal environments, vulnerability to oil spill impact 79−57509
coastal inlet water temp. change due to artificial heat input 79−16506
coastal marine environment, pollutant dispersal and deposition, Th isotope analogue expts. 80−81927
coastal marine sediments, ^{14}C ages rel. to pollution, fossil C effect 80−98308
coastal sediments, Pu and ^{137}Cs contents 79−57974
coastal zones, chlorophyll a distrib. mapping 79−2294
Cochin backwater, India, estuarine water, particulate heavy metal content 80−7964
Cochin backwaters, India, organic pollution effects on hydrographic features 77−91156
Cochin backwaters, industrial pollution, impact on water quality and hydrographic features 80−76668
conference, Rochester, NY, USA (May 1979), polluted rain 80−82585
contamination of marine sediments, trace metals from wastewater 79−83643
convection-diffusion equation, 1-D, finite elements method, weighted residuals 80−53775
cosmogenic and artificial radioisotopes distrib. in ocean, turbulent exchange intensity determ. *(Russian)* 79−39744
Cs accumulation in muscle tissue of marine fishes 80−35797
Danube water and sediments, radionuclides detec. during 1977 79−12158
deep sea waste disposal *(German)* 78−24311
Derwent Reservoir, N.England, Zn, Cd and Pb in water, sediments and submerged plants 79−25286
Dickinson Bayou, Texas, water quality survey 77−60437
diffusion-convection, finite element method soln. 78−90888
dispersion in channels with non-uniform vel. distrib. 79−16556
dispersion in turbulent shear flow 77−41090
dissolved pollutants photolysis rates, suspended sediments effects 79−100546
drainage water from spruce trees, acid content determ. method 77−37448
dredger spoil, dumping ground obs., motion of fine particles with current 80−17287
drinking water, Finland, internal radiation doses due to radioactivity 80−109029
Duluth-Superior Harbour, thermal pollution rel. to ice growth 79−2299
dynamic models synthesis, finite-difference method 77−81950
ecological disturbances caused by coastal pollution source, math. model 77−78232
effluent P standards impact on eutrophication control 79−88015
English Channel, actinide concs. and transfer into S.North Sea 79−48519
environmental effects from nuclear energy, effects of small radiation doses 79−2312
environmental pollution by nuclear fission products 78−85607
environmental radioactivity meas. in the EEC, 1977, for air, deposition, water and milk 79−62162
estuaries, contaminants, long-term dispersion 77−78229
estuarine density fronts, effects on coastal pollutants 78−7659
estuarine salt marsh, micro-organisms and trace metals 80−55950
estuarine water-quality model in an oscillating constant-volume reference frame 79−34871
estuary, chlorination of drinking water affecting organic colloids 80−97824
estuary and river sited power plants, water discharge and chlorination, simulation 78−96250
estuary pollution model development, wind and freshwater flow influence 78−81207
estuary sediment containing lead pollution, rel. to flood control measures, California 80−76670
estuary sediment heavy metals, Mosquito Lagoon, Florida 80−76671
estuary thermal impact of multiple power plant operations 78−96232
estuary water quality models, finite difference and finite element methods 78−77375
fallout in sediments, mixing and accumulation study 80−81864
fallout on Taiwan, 1971 to 1975 period 77−90918
filtration parameters of polluting miscible fluids through porous aquiferous phreatic media 80−53855
flow in open channel, buoyancy effects on lateral contaminant dispersion 79−50775
fluvial geomorphology, rate law for relaxation times 77−33098
forced plume characteristics 78−18286
forest soils, effect of acid precipitation 77−73771
formaldehyde, concs. in rain water and on atmospheric aerosol 78−57243
Fraser River (British Columbia) deltaic sediments, heavy metals content 77−33048
freshwater ecosystems in Norway, acid precipitation effects 77−37258
freshwater food chains contamination by ^{60}Co, direct water borne contamination of organisms *(French)* 79−20688
gas-oil mixtures trapped under ice, stable config. obs., energy meas. 80−108818
geothermal energy, environmental problems, air and water pollution, subsidence, induced seismicity, blowouts, noise, review 80−55797
global sea pollution, ecological aspects 78−3826
Gran's plot, acid-base titration 79−79432
Great Lakes water quality, remote sensing data interpretation 80−98364
Great Lakes, sediment chemical composition, anthropogenic loadings 77−37256
Great Lakes, toxic substances 80−55949
ground water pollution at Dharwar, India 78−69380
groundwater, phosphate leaching from agricultural soils 79−20901
water pollution continued
groundwater, two-dimens. contaminant transport simulation 77−78287
groundwater contaminant arrival distribs. as general evaluation requirements 79−16533
groundwater contaminant arrival distribs. for steady flow in heterogeneous systems 79−16535
groundwater contaminant arrival distribs. in transient flow systems 79−16536
groundwater contaminant location/arrival time/outflow distribs. for steady flow 79−16534
groundwater from geologic repositories, computer anal. of long-term radiation hazards 80−18483
groundwater in Grant Mineral Belt, New Mexico, effects of U mining and milling 77−56657
groundwater pollution from septic tile field 77−29338
W Gulf of Mexico, ^{90}Sr in water, coral, hermit crabs and molluscs 77−81590
E. Gulf of Mexico, black magnetic spherule fallout rel. to micrometeorite studies 77−37242
Gulf of Thailand, currents and particulate matter movements 77−49090
halocarbons, meas. in W. Europe 78−36272
heavy metal ion removal in clay suspensions 77−86955
heavy metals, adsorption on inorganic minerals 78−49006
heavy metals, content in water and sediments in reservoir reservoir supplying major mining centre 80−30617
heavy metals in non-industrial river, baseline study of northern New England, USA 80−61477
high-level radioactive waste, ultimate disposal on seabed, rel. to oceanographic circulation 78−13273
hospital radioisotope release to environment, model and meas. 78−96105
Hudson River estuary, man-made radionuclides and sedimentation 77−2183
Humboldt Bay, California, offshore current meas. rel. to proposed outfall 78−44876
humic acid and fulvic acids chemistry as pollution indicator 80−76688
hydrometeors, pH detailed struct. 79−92111
hydrophobic pollutants, sorption on natural sediments 79−83651
hydrospheric trace elements, water pollutants 78−85266
impurities dispersion in river, model *(Dutch)* 79−88011
in situ leach mining, environmental considerations rel. to water quality 80−3543
N.Indian Ocean, dissolved petroleum content 80−98361
inland aquatic ecosystems, chemical effects 77−70706
inorganic chemicals industry, water pollution and solid waste disposal 77−70704
Iowa lakes, water transparency survey 79−2308
Israel coast, nearshore sediment pollution by trace metals derived from sewage effluent 78−44882
in Kakogawa River basin, multiobjective optimisation 79−57993
kinematic parameter estimation for transport of pollutants in overland flow 79−52971
Kingskettle, Scotland, phenol and cyanide leaches into groundwater from gasworks site 79−88020
Kuskokwim River drainage, Alaska, Hg dispersal from lode sources 78−40600
Kuwait, marine pollution 79−5510
Kuwait Bay, organic matter in sediments rel. to pollution 79−62154
Laccadive Sea, absence of Hg pollution determ. from total Hg concs. meas. 80−104996
lake, microcystis removal ship, Seimei, Japan *(Japanese)* 77−56753
Lake Constance, eutrophication effects on sedimentation 79−79889
Lake Erie, sedimentary record of heavy metal pollution 79−83644
Lake Huron, shore contamination from radioactive fallout 77−86897
Lake Michigan, sulphate deposition in stable atmos. conditions 80−81494
Lake Michigan, trace element input by aerosol deposition 80−76672
Lake Monona, Wisconsin, Cu environmental chemistry 79−44214
Lake Naini Tal, India, metal pollution in water and sediment 80−97828
Lake Ontario water quality near Port Granby radioactive waste storage site 80−97829
lake sediment records in New York State 80−85311
lake surface, crude oil spill spreading 78−16079
Lake Toya, Japan, acid mine drainage, pH effect 79−34449
Lakes Superior and Huron, sediment composition, anthropogenic inputs 79−79419
land use influence on water quality 77−33117
liquefied natural gas spilled on water, spreading and evap. investig. 78−26748
liquefied natural gas spills on land and water, dispersion hazard 77−45141
LWR irradiated fuel pellets, leaching in deionized water, sea brine and typical groundwater 79−26581
main drainage systems, contamination due to cinematographic film processing, analysis techniques *(Russian)* 79−89023
mapping discharge conditions in catchment areas *(French)* 77−33105
marine environmental impact due to Cu mining activities, Chile 79−12140
marine pollution, dynamically passive impurity propag. in sea surface layer 80−31063
marine radioecology, radiobiological protection aspects *(French)* 78−11744
marine sediments, presence of azaarenes 77−37181
Mediterranea, floating plastic debris obs. 80−104999
Mediterranean Sea, petroleum aggregates distrib. in hyponeustal zone 77−49085
E.Mediterranean sediments, heavy metal content, off Lebanon coast 80−97830
Mediterranean surface water oil pollution, 1974 meas. *(Russian)* 77−60430
Mersey estuary, H_2S effect on methyl Hg in sediments 79−2295
Messina harbour, annual cycle *(Italian)* 77−25697
migration obs. near South Carolina coastal front 80−45831
Minch waters and sediments, Windscale effluent 77−91158
mineral dusts, electron microscope anal., environmental monitoring 77−81877
mineral dusts in environment, health hazards 77−87068
mirex in lake Ontario sediments, circulation simulation 80−26556
mixed spot spreading in stratified saline soln., expt. investigation *(Russian)* 78−40595
Moscow river water pollution modelling *(Russian)* 77−29328
mountain watershed, ski basis impact, heavy metals pollution 79−20903

water pollution continued
municipal sludge, disinfection by high energy electrons 79−24922
natural temp. and man-made variations *(Dutch)* 79−83642
natural waters, heavy metal-organic matter interactions 77−60439
near-field model for dissolved O_2 and other water quality parameters 78−81261
Netherlands, chlorophenols in surface waters, 1976-7 obs. 80−16858
Neva Bay, Leningrad, modelling of dynamic transport of pollutants 77−78220
New York Bight, ^{228}Th-^{228}Ra radioactive disequilib. rel. to coastal pollution 79−29784
nonpoint pollution continuous simulation 79−52967
N.North Sea, actinide activities in inflowing water 79−16520
North Sea, Ekofisk Bravo blow-out, petroleum hydrocarbons in water, fish and sediments 79−74559
North Sea, southern, pollution patches evolution modelling 77−45018
North Sea and Baltic pollution, natural and man-made influences *(German)* 79−5508
nuclear industry, radiation doses, health risks from various power sources 80−57899
nuclear plant cooling, effluent dispersion, thermal and radioactive, math. model *(Spanish)* 77−74908
nuclear power plant chronic aq. releases, calc. rel. to meas. doses 79−54605
nuclear power stations, long term radioactivity values, meas. in marine life *(Spanish)* 80−7962
nuclear power stations, radioactive emissions, heat emissions, other environmental effects 79−22491
nuclear waste, interaction with hydrologic cycle 78−94103
nuclear waste ponds and streams, Hanford, ecological search for radiation effects 80−89804
numerical simulation of pollutants releases in shallow sea 77−78234
ocean, chem. fields dyanmic equilib. and balance anal. 77−64328
ocean, concentration probabilities from stationary point source of passive admixture *(Russian)* 77−78231
ocean, discharged conservative substances long term conc., estimation technique 78−44885
ocean, particular trace metals transport by bubbles 79−57940
ocean circulation and hydrography in power plant vicinity 77−41039
ocean data collection 80−3545
ocean dumping of high level radioactive waste 80−32376
ocean floor hot spring created by drill hole 80−55951
ocean pollution, appl. of data and information services 78−69463
ocean subsurface oil-rich layer at 200 metres, obs. in Carribean and N.Atlantic 80−56498
ocean surface layer, dye plumes diffusion, expt. 78−44871
oil, on sea surface, optical characts., 0.4-15 μm, rel. to photosynthesis suppression 79−52968
oil film on sea, retardation of O_2 exchange with atmos. 80−109175
oil from World War II tanker, potential drift directions along N. Mid-Atlantic Bight 78−40566
oil on sea surface, spray comp. and aerosol generation 77−29325
oil on sea surface, thermal radioemission spectral characts. 80−85686
oil on surface, spreading rel. to surface contamination 79−43795
oil patch probable movement from Bombay High region 78−81219
oil pollution, estimation of aromatic hydrocarbons in seawater in Gulf of Mexico 78−44880
oil pollution, review of effects on water and marine life *(French)* 79−48193
oil pollution on sea surface, effect on radio location signals *(Russian)* 77−78230
oil slick burning in Arctic, adverse atm. effects during clearing of spills 80−16875
oil spill, dynamics in fractured ice field in Buzzards Bay, Massachusetts 78−40596
organic compound isolation using liq. chromatography 77−1957
organic pollutants, influence of detergents on hydrosolubility and suspension *(French)* 80−7961
organic pollution of ocean, rel. to dissolved free amino acids conc. in seawater 78−44883
organochlorine residues in rainwater 78−73495
Ottawa River, multidisciplinary research project on pollution 80−21421
palaeohydrologic phenomena recorded by lake sediments 77−66936
Pascagoula River basin estuary, model for water quality planning 77−64343
Passaic River, New Jersey, nitrification, historical and expt. investigation 80−7968
passive contaminant dispersion in oscillatory fluid flow 78−44881
Perch Lake Basin, Ontario, hydrological and geochemical studies conference, Chalk River, 1978 April 25 to 26 80−51955
Persian Gulf and approaches, oil pollution, 1978 obs. 80−105000
pesticides in USSR rivers, 1973-1976 period 80−81495
phenol, ^{60}Co and ^{137}Cs fixation on natural sorbents 79−57506
phosphate facility, evaluation of ^{226}Ra and ^{222}Rn concs. in nearby water 80−45827
phosphate fertilisers, geochemistry rel. to world rivers natural U content 79−44208
Puget Sound, oil migration, mixed Lagrangian-Eulerian model 80−45830
PWR steam generator operations, Westinghouse, benefits of contaminant control 79−93818
QUAL II river model soln. algorithm characts. 78−65348
quality indices, statistical anal. 80−8368
quality standards, geometric mean 79−16539
radioactive, use of box model method *(Japanese)* 80−9346
radioactive contamination in aquatic organisms, evaluation by statistical and information theory 78−53535
radioactive effluent discharges, European Community, 1972-76, radiological aspects 79−41019
radioactive liquid waste disposal in deep aquifers in USSR 79−29489
radioactive pollution by reactor organic coolant, environmental effects 79−66425
radioactive pollution consequences from liquid pathways due to reactor core meltdown accident 80−104778
radioactive transport in the aquatic ecosystem, foodweb model 80−104777
radioactive waste, computer anal. of relative potential hazards 80−21422
radioactivity in Arizona water, baseline values 78−81230
radioactivity of Bulgarian spring waters *(Russian)* 77−41098
radioisotope environmental dispersion models, evaluation of uncertainties 80−46074
water pollution continued
radionuclide accumulation by marine organisms, sediment and sea water influences 78−80981
radionuclide accumulation by oysters in reactor effluent, math. model 77−81589
radionuclide chain migration in groundwater 78−85616
radionuclide concentration by marine organisms, temp. effect 77−90920
radionuclide distribution among green alga, marine sediments and sea water 78−53534
radionuclide distributions in oceans and marine sediments from nuclear weapons testing 78−13344
radionuclide migration from low-level waste burial site 78−21671
radionuclide migration in groundwater from accelerator earth shields 79−48194
radionuclide migration in seawater and marine sediments *(French)* 78−11916
radionuclide redistrib. at Atlantic nuclear waste disposal site 80−85309
radionuclides, artificial and natural, tracers of large-scale ocean circulation *(Russian)* 79−39742
radionuclides in sample soil and water, environmental effects 77−13092
radiosotope behaviour in sediments in laboratory-scale aquatic ecosystem 78−3831
rainwater chemical composition 30 km downwind from industrial complex 77−37395
regional water quality management, goal programming approach 79−57514
regional water quality management, pilot study 79−57515
resource problem, water, with multiple objectives, interactive optimisation, Yodo River basin, Japan appl. 79−57516
river, Danube, radioactive pollution meas. 1972 to 1975 by γ-spectrometric anal. *(Bulgarian)* 79−88019
river, dissolved oxygen and biochemical oxygen demand, random signal anal. applic. 77−45047
river and ground water pollution due to drought in England and Wales, 1975-6 period 78−88868
river basin, Monongahela, acid mine drainage problems treatment via QUAL II simulation 79−29806
river flow prediction by multiplicative model 79−53399
River Main, County Antrim, N and P loads meas. by discrete and intensive sampling 79−44213
river pollution dilute capacity at tributary confluence, mathematical model *(French)* 79−8646
river quality study, Streeter-Phelps models sensitivity anal. 77−70715
river sediments, P content, bonding form., in Elbe, Trave, Eider, Schwentine *(German)* 79−34868
river systems, water quality models, Monte-Carlo anal. 80−8367
river water quality management, stochastic programming model 79−57507
river water quality system, recursive estimation techniques appls. 79−5538
river water quality vars. operational forecasting from streamflow vars. 77−78265
rivers, influence of industrial effluents and sewage on thermal regime 79−29793
rivers, pollutant dispersion, boundary conditions effect 78−85611
rivers, thermal discharges, unsteady temp. distrib. modelling 77−5264
rivers, transverse mixing in meandering nonuniform natural channels 77−5263
rivers, wind effects on pollutant dispersion capacity 77−21808
runoff from land receiving animal wastes, pollutant transport, review 80−97831
Saguenay fjord sediments, distrib. and partition of Co, Ni, Cr and V 77−33100
Saruhashi river, anal. of heavy metal ion concs. and DO, BOD, SS and NH_4^+ values *(Japanese)* 79−34447
Saruhashi River, Japan, heavy metal pollution *(Japanese)* 78−40599
sea, semi-bounded dispersion from point-source with and without chem. reaction 77−64329
Sea of Azov, seawater self-purification from pollutants 77−53076
sea pollution simulation, higher accuracy predictor-corrector method 79−66431
sewage sludge land disposal, Mo hazard 77−33115
sludge disposal in coastal waters, Philadelphia study 78−3823
snow meltwater chemistry, conc. changes during melting 79−53388
soil, humid temperate zone, potential effects of acid precipitation 77−73772
soil acidification by precipitation, increased by S and N filtering by trees 77−73775
soil chemical process changes caused by acid precipitation 77−73773
soil pH and base saturation of exchange sites, and precipitation effects 77−73774
solid pollutants in marine and estuarial environments, radioactive tracing 77−41069
statistics, in France, 1974 *(French)* 77−25777
stochastic model, internalization 78−61455
stream draining agricultural watershed P input, sampling 77−33116
stream sediment trace metals, downstream of Pb smelter 80−61475
stream-pollution model with random deoxygenation and reaeration coefficients 79−70472
streamflow meas. in remote catchments, natural pollution loads estimation 77−70714
streams, inorganic pollutant meas. by nuclear techniques 77−41102
Streeter-Phelps type model, parameter estimation 79−5539
subsurface environments, fate of pollutants, math. modelling 77−56658
surface runoff, New Zealand, P transport, effect of fertiliser and grazing cattle 77−53094
surfactants affecting temp. of skin-layer, for oil slick studies *(Russian)* 80−109172
Tagus Estuary, water quality study *(French)* 79−66706
Tehran groundwater pollution by detergents 78−61453
Texas impoundments, critical levels of P and N_2 78−11929
Thailand, water pollution problems 78−88853
thermal, due to power plants water effluents, power engineering and water conservation viewpoints *(Czech)* 79−57505
thermal, nuclear power station cooling water impact on water surface temps. and ice conditions *(Finnish)* 79−20868
thermal pollution, simple non-linear cooling models for well-mixed rivers 79−20902
thermal pollution by discharges into waterways, mixing problems 79−8645
thermally stratified acid water in snowmelt 77−73770

water pollution continued
Tolo Harbour, Hong Kong, untreated waste entering via streams 80−89685
trace element detection by activation analysis *(French)* 77−41067
trace element meas. by neutron activation analysis 77−41103
transfer charact. evaluation using tracers *(French)* 77−41104
underground repositroy of high-level radwaste, water intrusion scenario studies, anal. and re-eval. 80−73950
undersea resources and related topics, world-wide survey 80−35622
NE.United States, soil Al leaching by acid precip. in high-elevation watersheds 80−12442
Urazoko Bay, ^{60}Co radioecology, levels in sargassoes and marine sediments 77−9448
urban catchment flow and water quality model predictive accuracies 77−37279
urban runoff, effects of storm freq. on pollution 78−53667
urban runoff pollution analysis, continuous and single event simulations compared 77−37271
urban runoff pollution rel. to land use 79−5530
urban storm water in Sydney, Australia, quality charact. 77−64357
Velsao and Colva beaches, Goa, India, water quality charact. 78−81218
Venice lagoon, effect on contaminant residence time of modified tide regime 80−12431
volatile pollutants, second virial coefficients, empirical correl. 79−52965
Walker Branch Watershed, atmospheric input and origin of elements 77−86956
waste disposal from electronics manufacturing plant 77−73780
waste products discharge supervision w.r.t. biochemical degradation processes *(French)* 78−24316
wells of Greater Chicago area, dead water, ^{3}H anal. 78−16062
^{241}Am concentrations concs. in drinking water and organic fertiliser 77−56488
As, inorganic, in freshwater environment, stability and solubility theoretical aspects 79−16553
As, migration capacity, effect of acid-alkaline conditions on hydrogeochem. 77−37244
CO, radioactive and stable, determ. in marine biological materials 80−36157
CO_2 from fossil fuel, marine calcite dissolution, effect of sediment mixing 78−81212
CO_2 from fossil fuels, effect on ^{14}C, concs. in Florida annual coral rings 79−16513
^{14}C, bomb-produced, concs. in Florida annual coral rings 79−16513
^{14}C in Atlantic from nucl. weapons tests 80−89683
^{113}Cd^{m}, in marine organisms and sediment around Marshall Island nucl. test site 80−109174
Cl^- ion concentrations in river, spring waters in Okinawa Honto, origin *(Japanese)* 79−39324
^{60}Co, fixation on natural sorbents from phenol-polluted water 79−57506
Cs, radioactive, dynamics in herons inhabiting contaminated reservoir system 78−28092
^{137}Cs accumulation and elimination by naturally contaminated wood ducks 77−66865
^{137}Cs adsorption by sediments near water-cooled nuclear reactors 77−78281
^{137}Cs distribution in watersheds of Eastern USA 77−25701
^{137}Cs, fixation on natural sorbents from phenol-polluted water 79−57506
^{137}Cs movement and loss in small lake 78−24317
^{137}Cs, radiotracer studies in equatorial Indian Ocean *(Russian)* 79−39743
^{137}Cs, runoff coeff. from surfaces of river basin soils 79−44212
^{137}Cs, seasonal cycling in reservoir 79−100881
Cu, rate of loss and speciation in lakewater 80−7967
^{3}H, environmental surveillance, sensitivity to natural fluctuation of tritiated water vapour in troposphere 77−88287
^{3}H, environmental transport from atm. release of mol. ^{3}H 78−11987
^{3}H kinetics in freshwater marsh, simulation model 78−24318
Hg concentrations in seawater, ^{203}Hg tracer and ^{75}Se tracer 80−21420
Hg contamination of sediments in semienclosed bay, Norway 78−81220
Hg emissions from geothermal power plants 77−73838
Hg emissions from wastes stored near Cl manufacturing plant 77−66938
Hg, in fish and waters of Irish Sea and other United Kingdom fishing grounds 78−36204
Hg in Gulf Stream 80−7965
Hg levels in soil and water in Israel and Sinai 77−29337
Hg loss rate from contaminated estuarine sediments 80−85310
Mn nodule mining, environmental effects 77−33096
N_2O, concs. in Michigan waters and USA municipal waters 78−57223
N_2O, losses from agricultural land dissolved in drainage water 79−43797
^{237}Np in invertebrate tissues, uptake from water 79−74765
P, atmosphere contrib. to aquatic system 79−100545
P in streams draining from agricultural watershed 80−61474
Pb, contamination, rel. to traffic density *(German)* 79−70470
Pb in hydrosphere, global and regional distrib. 79−16517
Pb in lakes, rel. to boating activities and sediment interaction 80−104523
Pb in subalpine pond sediments, anthropogenic source var. 80−85315
Pb pollution, rel. to atmospheric tetraalkyllead natural source 79−2367
^{210}Pb, ^{210}Po, concs., physico-chem. states and residence times in marine and estuarine waters 78−11913
^{210}Pb, balance in Long Island Sound 79−20861
Pu, A=239, 240, concs. in drinking water and organic fertiliser 77−56488
Pu accidental release at Thule, Greenland, environmental behaviour 77−56656
Pu, concs. in stream near Argonne National Laboratory, ^{239}Pu and ^{240}Pu 77−45037
Pu ecological export from reprocessing waste pond 78−53533
Pu from fallout in alkaline, saline lakes 80−97826
Pu, in Irish Sea, oxidation state 79−16516
Pu, industrial effluent, behaviour and transport in Great Miami River, Ohio 78−16061
^{237}Pu IV and VI oxidation states, relative uptake from water by bush beans 78−73266
^{238}Pu^{4+}, ^{238}Pu^{6+}, ^{239}Pu^{4+}, ^{239}Pu^{6+}, alga uptake rel. to isotope and oxidation state 80−30692
^{239}Pu, ^{240}Pu, concs. in fish and seawater from Kwajalein Atoll 80−26380
^{A}Ra, A=226, 228, content in groundwater of Fall Line aquifers 80−89682
water pollution continued
^{226}Ra, assessment of quantities in North Carolina drinking water supplies 80−45826
^{226}Ra in Taiwan buffalo bone and environmental samples of N. Taiwan power reactor site 77−64142
^{226}Ra leaching from contaminated soils, investigation of Ra bearing soils from Port Hope, Ontario 79−20900
^{222}Rn concentration in N.Carolina groundwater supplies rel. to stomach dose and conc. standards 78−85612
S isotope variations as pollution index in lakes near Sudbury, Ontario 78−57228
SO_2 low core, equilibria between air and water 78−16137
Se concentration in seawater, ^{75}Se tracer and ^{203}Hg tracer 80−21420
Se in estuarine water in Solent area 78−57230
^{90}Sr concentration in freshwaters of USSR 79−39770
^{90}Sr, content in E.Sivash waters *(Russian)* 78−77282
^{90}Sr diffusion from instantaneous point source in ocean, numerical calc. *(Russian)* 78−69372
^{90}Sr, runoff coeff. from surfaces of river basin soils 79−44212
T concentration in natural waters of N.Italy *(Italian)* 80−40933
T in deep N.Atlantic current, from weapons tests 80−101380
T, in Pacific Ocean, source function for transport models 78−32122
U environmental distribution and movement, agricultural product distrib., Japan 77−90921
U, in situ mining, Wyoming State regulations and environmental monitoring 79−88510
V, meas. by neutron activation analysis 77−41239
Zn pollution in British coastal waters, photosynthesis inhibition 79−24921

water pollution detection and control
see also water treatment
activated sludge control parameter, oxygen uptake rate 80−35798
activated-sludge process control, biological solid-retention time method 77−25699
American detection, research and enforcement program 78−45002
analytical methods comparison 77−90685
Arctic oil spillage response techniques 80−46204
arsenic in freshwater fish traced to fly ash leachate using neutron activation analysis 80−97827
artificial aeration optimization, in river networks 78−36203
artificial radioactivity migration in environment, survey of models 79−96487
asbestos mining area river pollution meas. by proton-induced X-ray emission 79−100556
askarels, environmental pollution reduced using biodegradation *(Slovene)* 78−7663
automated measuring systems, sampling, anal. and results 77−21885
automated multisample-stream chemical monitoring system 77−44531
automated profiling water quality sensing system 78−45052
automated rapid system for anal. of dissolved organic N in natural waters 78−93014
automatic sampling buoy for accumulation of dissolved and particulate organic material in seawater 78−49149
automatic water monitoring system, Finland 80−67026
Beaufort Sea, environmental risk of oil spills, management tool 77−81920
benzo(a)pyrene, determ. in water using spectrofluorimetry 80−7997
Bikini lagoon, coral alpha emitters, solid-state track detection 78−53661
bilge water oil pollution monitoring system development 77−5246
biological nitrification systems, control strategy 80−35799
biological specimen pattern recognition via matched spatial filtering 78−69261
Black Sea, heavy metal conc. meas. by charged particle induced X-ray anal. 78−24312
BOD values, short time determ. methods comparison *(Japanese)* 79−48192
borehole vertical groundwater flow as aid in pollution study 80−81938
BWR with forward-pumped heater drains, water quality performance 79−67918
capillary gas chromatography of chlorophenols in surface waters 80−16858
catchment areas, large, jet flow similitude *(French)* 79−66423
chemical flocculation plant at Ahrensburg, in West Germany, water treatment appl. *(German)* 78−40601
Chesapeake Bay, pollution history 79−34445
chloride, nitrate, nitrate and NH_3 simultaneous automated determ. 77−29511
chronic radioactive release assessment, models and computer codes 80−13710
cine film processing wastes, environmental pollution control of industrial plants *(Russian)* 79−44964
coastal, remote sensing appl., Italian methods *(Italian)* 78−3828
coastal currents and pollution, satellite, aircraft and drogue studies 77−37206
coastal waters, meas. and sampling techniques 79−12137
coastal waters sensitivity to anthropogenic trace metal emissions 79−43796
COD distribution of Mikawa Bay, numerical expt. 79−57512
coke-plant effluents, second-stage activated sludge treatment 79−92102
combined sewer system detention storage, real-time control algorithm 77−37281
component selection for continuous pH measurement, pollution abatement appl. 77−73767
SW Connecticut, detect. of nonpoint pollution of small streams 77−33099
contaminated groundwater zone control by underground impermeable wall, radioactive waste site *(Japanese)* 79−34446
continuous oil-in-water meas. by towed fluorometer 80−45846
coring and squeezing technique for study of subsurface water chem. 78−57332
Danube River, distrib. of artificial radionuclides at mile 34, 1976 79−39323
decision anal. appl., Rhine river study 77−66946
diatom recognition and counting, matched-filter and statistical method 80−101304
dielectric props. and determ. of microwave emissivity 80−101142
dinitrotoluene isomers, occurrence and determ. in seawater 80−7966
dissolved forms of trace elements in streams, dialysis cell meas. 80−97851
dissolved O_2 in water, automatic analyser *(Japanese)* 80−35812

water pollution detection and control continued
distributed parameter system, multiple shooting and sweep algorithm 77−25728
effluent monitoring in environmental control 79−79443
electrochemical porous flow-through electrodes, mass and charge transfer and cell design *(French)* 80−16697
emulsion containing water from crack detection processes using penetrating agents, purification *(German)* 79−5517
energy disperion X-ray analysers, evaluation 78−48712
environment materials, multielement anal. by rotrode direct reading spectrometry 77−70355
environmental chemistry, anal. techniques, conf., Barcelona, Spain, (Nov. 1978) 80−88038
environmental measurement, conf., Gaithersburg, Maryland, USA (Sept. 76) 78−69504
environmental monitoring, the role of electronic system in India 77−41146
environmental monitoring instruments 80−45825
Environmental Protection Agency requirement for underground injection in solution mining of U ore 79−92101
environmental radioactivity prior to the Kori nuclear power plant operation 79−6773
environmental samples, X-ray fluoresc. anal., particle size correction method 78−48705
equipment for metals industry 79−66432
estuarine dynamics, mass balance eqn., longitudinal dispersion function estimation 77−37262
estuarine fronts remote sensing, behaviour study, pollutant effects 77−78470
estuarine sediments, heavy metal pollution detection 78−73546
estuary, Jamaica Bay, New York, dissolved O modelling 77−17146
estuary, volatile petroleum hydrocarbons contrib. to organic C budget 79−70473
estuary water quality management for P treatment 77−21823
fertilizers, nitrogenous and phosphate, pollution problems from manufacture 79−34450
Finnish river water pollution monitoring network 80−89686
fission reactor coolant decontamination *(Spanish)* 79−45345
floating barrier, zone of action surface vels., pollutant spread prevention *(Russian)* 79−88009
fluidised bed containing biomass, expansion 80−14803
fluorescence microscopy, water pollution abatement, self-cleaning capacity of epipelic bicenoses 79−79702
fluorometric dye meas. background variation expts. 80−45844
fluorometric techniques and instrumentation 80−45845
Fourier transform gas chromatograph-IR system, trace organic pollutants detect. 78−68967
freshwater acidification meas. 79−43802
fungicides, detect. by laser excited reson. Raman spectroscopy 78−31732
fuzzy equations, water pollution control appls. 79−57523
gas chromatography/mass spectroscopy analysis of volatile organic compounds in water supplies 79−12151
geothermal waste water, environmental effects on river system 79−29487
Great Lakes coastal waters, thermal plume meas. systems 78−44891
groundwater, chemical pollutants convective dispersion reln. 80−16855
groundwater contamination, Holt County, Nebraska, USA 80−12033
groundwater pollutants from underground coal gasification 78−92865
groundwater restoration, reduction of environmental impact of U solution mining 79−88012
groundwater system, transport of chain decaying radionuclides 80−51019
Gulf of La Napoule in France, pollution abatement attempt, results from dredgings 80−16857
hard water, trace element determ. by multielement ICP-AES method 78−23992
hazardous chemicals detection using resonance Raman spectroscopy in flow-through system 79−74581
heavy metal ion concentration, detection in water by electrochemical methods *(German)* 79−92039
heavy metals, distrib. and speciation in aquatic systems, analytical techniques 78−69390
heavy metals and organic C conc. in surface microlayer, physical processes effects 79−57978
heavy metals distrib. in Gulf of Fos, NW Mediterranean 79−12141
high mountain stream water quality modelling, Bishop Creek, California 78−53666
high-level liquid waste, damage to organic extractant in positioning process 80−9345
human health aspects of water pollution in developing nations 77−29339
humic acid and fulvic acids chemistry as pollution indicator 80−76688
hydrocarbon pollution detection, caution on use of Niskin sampling bottles 78−45039
hydrocarbons, comp. and sources in Severn Estuary 79−12148
hydrocarbons, detect. in water and sediment of wilderness lake, Canada 79−12155
hydrodynamic dispersion of chemical in soil *(Italian)* 77−41071
hydrometallurgical plant effluent waters, Mo and W determ. by activation analysis with low-power neutron sources 78−7279
industrial chemical waste at deep water dump site, acoustic monitoring 79−34466
industrial liquid waste, purification and by-product recovery 79−83648
industrial surface treatment water residues *(French)* 80−16528
industrial waste water and wastes, conf., Stockholm, Sweden (Feb. 1975) 77−70703
industrial wastes, determ. of Mn (II), (III), Cr (III), (VI) 78−61105
industrial wastewater, automatic potentiometer monitoring station 78−56932
industrial wastewater, techniques for removing oil and grease 79−83646
information transducing sensor using electrokinetic effects, appl. to water quality control 79−70349
instrumental photon activation analysis of lyophilized seawater, multielement conc. of heavy-metal contaminants 80−16892
instrumentation maintenance problems 78−77366
intertidal ecosystems, ecological effects of petroleum, field expts. 79−66420
Isar River, Bavaria, trace elements distrib. in sediment, suspension and water samples by neutron activation analysis 78−3834
Jamaica Bay, NY, estuarine P model parameter estimation 77−21777
lake biochemical and physical model interfacing 77−21822
Lake Erie, elutriate-primary productivity bioassays of dredge spoil disposal 79−88016
lake eutrophication modelling and control 77−21820
water pollution detection and control continued
Lake Huron, wet and dry deposition of P 79−57991
Lake Ontario tributary waters, N and P conc. determ. 79−79418
lake quality monitoring, multidate Landsat data extraction progrm 80−17299
lake sediments as indicators of heavy-metal pollution 77−25710
lake Superior, organic C as nonspecific water quality indicator 79−25287
Lake Superior, remote determ. of chem. loading due to spring runoff 78−96243
Lake Windermere, catchment area, dissolved Hg conc. meas. 79−24924
lakes, suspended solids, anal. using Landsat multispectral data 79−16523
LANDSAT data digital chromaticity mapping for water quality anal. 79−29872
large fuel reprocessing plant, anticipated chem. emissions 78−5004
laser fluorosensor performance, sea-state effect 78−92990
laser image printer for IR scans of ocean surface *(French)* 80−72119
laser polarimeter for active spill detection 77−21938
laser spectroscopy, remote determ. of impurity conc., calibration by Raman scatt. 79−16090
leachate collection system design for lined landfill site 77−78283
liquid activity meas. instrumentation in Czechoslovakia 79−49873
LWR fuel fabrication plant, cost of controlling inorganic chemical releases 78−5003
LWR stowaway fuel cycle effluent projections 78−94110
maintenance-free water test stations, design and installation *(German)* 78−65403
marine chlorophyll a analysis, using aircraft multispectral scanners 80−77164
marine drilling contamination, seawater Ba content as pollution indicator 77−2180
marine mining, environmental effect meas. 79−12305
marine oil pollution surveillance, microwave remote sensing technology *(Japanese)* 80−76685
marine particulate plume density and distrib., acoustic assessment 80−45843
marine pollution, N cycles investigation 77−25698
marine pollution bioassay using fertilised mollusc eggs *(Japanese)* 79−52969
marine pollution monitor, automatic, shipboard, oil conc. obs. 78−53662
marine sediment analysis and pollutant detection by X-ray fluorescence 77−5361
marine waste disposal information reliability 79−12275
mathematical modelling aspects, book 78−73418
matrix isolation Raman spectroscopy, water pollution detect. appl. 80−108829
Mediterranean Action Plan 79−62156
Merrimack River Basin, water pollution abatement benefits, survey results 78−61456
metals monitoring, instrument survey 79−74580
methyltin compounds, separation and determ. in environmental samples 79−79416
Mississippi Pascagoula Estuary water quality planning using Gauss-Seidel iterative technique 78−73402
modelling, filtering and control 79−57520
modular system for monitoring of temp., pH, dissolved acids, turbidity and colour *(German)* 80−26186
monitoring and instrumentation 79−12301
monitoring at source and in environment, equipment and law enforcement 77−91263
monitoring systems in Taiwan 79−57511
Moscow River basin, automated surface water quality monitoring system 77−78266
multielement analysis of environmental sampelsdby samples by X-ray fluoresc. spectrometry 78−69513
multielement analysis using inductively coupled plasma atomic emission spectrometry 79−83520
multielement instrument neutron-activation analysis, ecology appl. 80−40946
municipal water treatment levels differences 79−83649
national environmental monitoring system 78−77329
natural, furnace at. absorpt. anal., computer-assisted, turnkey data system 77−77829
natural water chem. anal., modulated polarographic, voltammetric techniques 77−37253
nephelometric turbidimeters, Rome's metropolitan water board appls., control systems *(Italian)* 77−81953
Netherlands water quality monitoring 79−24920
neutron activation analysis of Cr after preconc. on activated C 78−3993
nitrate determ., improved hydrazine reduction method 79−34467
nitrate determ. in estuarine waters, UV absorption technique 79−16719
nitroglycerine, in waste water, monitoring continuous electrochem. analyser 77−60147
nondestructive neutron activation analysis of environmental samples using low-energy photon spectrometry 78−3995
North Sea, microwave meas. using SLAR 78−77245
North Sea pollution detection, remote sensing project *(Dutch)* 78−36202
nuclear power plant, impact and fate of released Cu on aquatic environments 78−7665
nuclear power plants, effect on chem. quality of surrounding surface- and ground-water 78−7679
nuclear power plants, hydrobiological studies, conception and data obtained *(French)* 80−76665
nuclear power station effluent analysis methods for environmental monitoring 79−13556
nuclear power station thermal plume monitoring by drogues 77−3192
nuclear power station using seawater for condenser cooling, radiation monitoring 78−29552
nuclear reactor cooling water, control of radiochemical contamination *(Korean)* 78−54820
nuclear techniques in hydrology, survey 77−37419
ocean acid waste dump, particulate Fe mapping 80−56497
ocean coastal zone, stratified water circulation forecasting for water quality management planning 79−5543
ocean colour remote sensing, pollutant location due to dumping 77−78460
ocean dumping surveillance and data recording system 77−5247
ocean industrial waste dumping, dispersion meas. technique 78−44884
ocean meas. capability improvement using advanced engineering technology 79−12303

water pollution detection and control continued
ocean surface pollutants, microwave detect. of adsorpt. and spreading films 79−5690
ocean surface water, global radioactive contamination levels determ., math. method 78−7816
ocean surface wind wave related turbulence meas. by impellor current meter array 80−46301
ocean surveillance by US Coast Guard using remote sensing techniques 78−45004
ocean water quality instrumentation system test 77−41066
ocean-disposed waste drift, satellite and current drogue studies 78−3824
ocean-dumping studies, strategies and tools 79−12138
oceans, waste disposal in Mid-Atlantic Bight control measures 79−5511
Oceans 1976 conference, Washington (Sept 1976) 77−5241
offshore disposal of dredged material, sediment props. as tracers 77−5245
offshore environmental monitoring program for proposed nuclear power plant in Islote, Puerto Rico 78−11917
oil, remote characterisation by time-resolved laser fluorosensors, lab. expt. 78−73097
oil contaminated waste water treatment by foam fractionation 79−92104
oil contaminations on sea surface, radar detect. *(Russian)* 77−49089
oil detect. using scanning lidar system *(Russian)* 78−32123
oil detection, appl. summing luminescence spectrometer with polychromator and spatial filter 77−74517
oil detection, in water, using combined GaAlAs laser and fibre optic bundles 78−96301
oil film on sea surface, microwave radiation characts., expt. *(Japanese)* 78−92854
oil films thickness meas. on polluted water from oil fluoresc. props. 79−79437
oil fractional analysis by high-performance liquid chromatography *(Japanese)* 80−81936
oil on sea, remote sensing using laser radar 78−77373
oil polluted sea surface, atmosphere-ocean system apparent contrast 79−25265
oil pollution indicator, ocean wave effects on remote sensing ability, model study 77−17255
oil recovery, polymer additives in reservoir flooding 80−72100
oil slicks, use of FFT in evaluation of laser Raman and fluoresc. decay times 78−81444
oil slicks on sea surface, petroleum products content determ. 77−64330
oil spill, Amoco Cadiz, obs. during 1978 March-May 79−62155
oil spill, extinction coefficient meas. using coaxial dual channel laser system 80−73425
oil spill analysis with gas chromatography 78−7294
oil spill detection by airborne laser fluorosensor 80−67024
oil spill remote detection by laser radar 79−25332
oil spill simulation in Florida Gulf outer continental shelf 78−73406
oil spill trajectory modelling, advancements 79−5509
oil spills, in ocean, polyurethane foam plastics as sorbents 79−53011
oil spills in ocean, recovery of oil by skimming 78−81222
oil spills in ocean, role of Scarlet Prawn in separating hydrocarbons 78−81221
oil spills remote detection using laser-excited Raman backscatt. and backscatt. fluoresc. 78−32242
oil spills remote monitoring, computer controlled laser radar system *(Japanese)* 78−92994
oil thickness on wavy water surface, light sensitive gauge 79−8720
oil traces, on water surface, continuous detect. system *(German)* 80−72115
optical methods of water quality determ., turbid waters spectral scatt. props. 80−72560
optical processor, real-time, for pattern recognition of biological specimens 78−40454
organic C meas., new approach 79−74582
organochlorine, pesticide residual levels, pollution in Sathiar reservoir water, mud and organisms 80−45828
organonitrogen wastes 80−35796
organophosphorus pesticide residual levels, pollution in Sathiar reservoir water, mud and organisms 80−45828
Par River estuary, India, pollution transport and abatement methods 80−104521
particulate matter, conc. on membrane ultrafilters, neutron activation anal. 79−52841
pelagic tar ocean distribution and surface circulation 80−16856
pesticides, detect. by laser excited reson. Raman spectroscopy 78−31732
petrochemical industry, prevention of water pollution 77−70705
petroleum, weathered, source identification using IR spectra and correl. coeffs. 78−15153
petroleum oil pollution at sea, detection by CO_2 laser radar 77−91324
petroleum spills on water, control using gellants 80−61496
petrols, optical consts. in 0.25 to 25 micron region, sea pollution detection appl. *(Russian)* 78−76976
phosphorus removal system, automation 80−76669
physical methods, continuous, in tubular columns, probes utilisation *(French)* 78−3836
PIXE anal. of drinking water in cities of Iran 77−49096
pixe analysis of water with detection limits in the ppb range 79−48005
plastic ocean distribution and surface circulation 80−16856
polarography, amalgam, film, with accumulation, appl. to micro-, macro-object anal., review 78−61098
polluter discriminant analysis using statistics data base 77−5244
portable computerised laboratory for water quality monitoring 80−61472
potentiostatic measurements for pollutants analysis in waste waters *(German)* 80−26185
prediction, finite element method appls. 78−93019
purity meas. by coulometric method *(Japanese)* 78−45769
quadrupole mass spectrometry applics., book contrib. 77−25622
quality, surveillance, optimal sampling freq. selection, autocorrel. techniques 79−53001
quality management alternatives, equity measures 77−25715
quality modelling, Kalman filter theory and practice 78−45058
quality monitoring system CAD 77−41100
radiation treatment of waste water. process control techniques appl. 79−96489
radio buoy for tracking oil slicks 78−45034
radio-nuclide transport in soil, conc. profile in groundwater, waste storage problems *(German)* 79−74556
radioactive Cs contamination, removal agent efficiencies *(Slovak)* 78−24319

water pollution detection and control continued
radioactive effluent release reduction, Japanese LWRs 79−31078
radioactive emission meas. and control *(German)* 77−79484
radioactive tracer methods for treatment process anal. and mixing patterns in streams 77−25711
radioactive tracing of hydrological pollutants *(French)* 80−7995
radioactive waste, liquid effluents, aquatic radiological impact anal., radiocaesium transport in sediment 80−95486
radioactive waste disposal, retention of Am and Pu by rock 77−71679
radioactive waste disposal into deep ocean, hazard assessment 77−88233
radioactive waste disposal into internationally important waters, limit evaluation *(Russian)* 79−29488
radioactive waste in deepsea disposal sites, environmental surveys using submersibles 77−61617
radioactivity meas. appl. *(Hungarian)* 77−36840
radioactivity standards for environmental monitoring, prep. 78−80816
radiochemical analysis for Rn in groundwaters appl. to Christchurch artesian wells 77−82039
radionuclide accumulation in marine organisms, computer kinetic modelling 79−53261
radionuclide adsorption on hydrated MnO, ^{137}Cs and ^{90}Sr 78−3822
radionuclide sorption from shallow land disposal of low level radioactive waste 80−16851
radionuclides in seaweeds, environmental significance 79−43798
rainwater, multielement anal. 78−69512
Raman spectroscopy, tonic organic substances detection 80−30616
recycling and urban water conservation 79−79892
regional wastewater treatment system, computer appl. 77−41064
regional water pollution control, energy anal. 80−26180
regional water quality management, optimisation model 77−66945
remote detection by laser-induced luminesc. techniques 78−81442
remote sensing, environmental potential survey in Japan 78−57374
remote sensing appls. *(Japanese)* 80−94122
remote sensing techniques for ocean surveillance used by US coastguard 79−34991
reservoir sedimentation process and detention structure model 78−44892
river aeration system subject to random disturbances, optimal control 78−16078
River Periyar, S.India, pollution profile 79−57510
river pollution, dynamic behaviour of distributed systems *(Dutch)* 80−3542
river pollution distribution determination by remote sensing, study 80−81512
river quality assessment, Willamette River basin, Oregon, implications of a prototype project 79−20896
river quality models near effluent outfalls 79−62157
river quality monitoring, sampling freq. 79−53380
river stream observer-based water quality controller 77−81938
river system, robust decentralised control of water quality 79−57522
river systems, water quality modelling and operational control 79−16555
River Tiber, physical processes related to discharge into sea, aerospatial obs. 80−108831
river water, field sampling unit using ion exchange resin to concentrate radioactive ions 77−9532
river water, Na determ. by flame emission meas. 77−36850
river water exam., L65 turbidity meter description *(Dutch)* 77−27332
river water quality, math. deterministic model, Blackwater catchment appl. 79−66732
river water quality, math. deterministic model, formulation and description 79−66731
river water quality, modelling and control problems, review 79−57519
river water quality monitoring, pollution sources estimation 79−52970
riverine and coastal effluents, remote sensing of thermal alterations and circulation patterns 79−57524
rivers, multielement anal. 78−69511
rivers downstream pollution, one-dimensional transient model for short-term prediction 80−81496
RWE environment protection organisation outline and functions *(German)* 80−101552
Safe Drinking Water Act, microbiology, QC for the Water Supply Lab., USA 79−74558
saline water, trace element determ. by multielement ICP-AES method 78−23992
sample analysis, automatic, pH, conductivity, alkalinity, process water treatment appl. 79−12287
sampling program for water quality 78−69388
sampling programme for trace elements in Po river bed sediments 78−69389
Saronikos Gulf, Greece, sediments, trace elements analysis by neutron activation 78−3825
satellite techniques, equipment Conf. on Earth resources electronics Rome, Italy (Mar.77) *(Italian)* 77−82056
Sava River, influence of water pollution on ranney wells in Belgrade 78−40602
sea, wind-ruffled, sunlight glitter pattern, time-averaged intensity calcs., oil pollution detect. appl. 79−53349
sea and beach persistent oil spill identification methods 80−90101
sea area surveillance using side looking airborne radar system *(Dutch)* 80−12560
sea surface oil pollution detect. by lidar *(Russian)* 77−45019
seawater, rapid determ. of radioactive Cs using Cs selective resin 78−85609
seawater pollution studies, laser appls. *(Polish)* 78−20528
seawater radioactive contamination, rapid determ. of levels of ^{54}Mn, ^{59}Fe, $^{58,60}Co$ 78−85608
sediment graph model based on instantaneous unit sediment graph 79−53394
sewage sludge, ocean-dumped, 200 kHz acoustic tracking 77−2182
shipboard pollution monitoring system, automatic Beckman Model 915 organic carbon analyzer 79−16521
silt double-labelling technique for radioactive tracing of physio-chemical behaviour of Zn $(OH)_2$ *(French)* 80−7994
sludge systems, nitrifying activated, design and control 77−5243
soft water, trace element determ. by multielement ICP-AES method 78−23992
soil water, percolating, sampling using plastic suction lysimeter 77−29498
Storm Water Management Model for runoff prediction 77−37275
stormwater runoff from various land cover types, characterisation and impact 78−88852

water pollution detection and control continued
stream dissolved O concentration optimisation using instream aeration 77−17153
stream pollution controller design via pole assignment 77−60434
submerged particle detection, sonar, diffusion and scattering theory *(Italian)* 77−91335
sulphate residues of fresh waters, elemental, anal., spectrographic technique *(Russian)* 77−12868
sulphate turbidimetric determ., nonsegmented continuous flow method 79−70405
sulphates, isotopic tracing of pollution *(Italian)* 77−53078
surface water continuous analysis by NH_4^+-sensitive plastic membrane electrode 80−89701
surface water pollutants, airborne monitoring by fluorescence spectroscopy 79−2397
surface-active agents, determ. in waste waters, review 79−53007
suspended sediment conc. meas. with sampling bottles accumulators 79−53552
suspended solid analysis by single-particle scatt. 79−79435
Susquehanna River system, use of ^{210}Pb as heavy metal tracer 78−49046
systems analysis appl. 80−26182
Tahoe-Truckee system water-quality simulation 77−37261
tanker oily discharge at sea, deballasting monitoring system appl. 77−45020
tin inorganic compounds, separation and determ. in environmental samples 79−79416
titrometric liquid analyzer for determining oxidisability of water 79−79441
total organic carbon measurements for industrial water and wastewater 80−26071
trace analysis of pollutants using automated HPLC 79−96384
trace elements, meas. accuracy using neutron activation anal. 78−69509
trace elements determination using routine neutron activation analysis 78−3992
trace metal anal. by energy dispersive X-ray fluoresc., enrichment procedures 77−60174
trace metal analysis in water, accuracy in AAS and AES using graphite furnace 78−69510
trace metal conc. in waste water, spectrochem. anal. 78−61106
trace metals, energy dispersive X-ray fluoresc. at absorpt. anals., comparison 77−60175
trace organic pollutants in water, conc. and gas chromatographic determ. methods 79−52854
transition metal, determination in estuarine and sea water by at. absorpt. spectra 79−74557
trihalomethanes, determ. in water, comparison of dynamic and static head space and solvent extraction techniques 79−92114
tritiated water, fixation in silica gel, zeolite, leaching in cement 79−97851
ultrapure water, trace metal determ. 80−81394
underground coal gasification, potential impacts on groundwater quality 79−87949
United States, history of pollution control 77−33818
upstream control effect on water supply reservoir 79−57508
urban bulk precipitation and streamflow quality relationships 79−88382
urban runoff, Hg and chlorinated organics conc. meas. 79−24923
USA coastal zone water quality monitoring, aircraft vs. spacecraft 77−78233
USSR environmental pollution obs. and monitoring system 80−85322
USSR Hydrometeorological Service, automation of data collection and processing 79−34994
USSR metrological provisions for water conservation 79−96495
vegetable washers, effluents meas. via plexiglass HS flumes 77−62321
vinyl chloride, trace determ. in water by direct injection GC/MS 78−35739
volatile fission products from nuclear fuel cycle and power stations, pollution effects *(Russian)* 79−31152
volatile organohalogen analysis in water purification processes 79−21080
waste water disinfection and oxidation, ClO_2 appl. 80−12032
waste water of sulphate cellulose prod., radiation treatment *(Russian)* 80−55688
waste water treatment plant, BASF, operating experiences with special meas. and control *(German)* 79−66424
wastewater treatment, activated sludge, process control model 77−17154
wastewater treatment, distributed digital processing and closed loop computer control 80−45824
water organic spill detector, computerised, development and appl. 77−41070
West German nuclear power plant liquid radioactive effluent control 79−13550
West German nuclear power plant liquid radioactive effluent monitoring 79−13554
world water resources, prospects and problems 79−39779
X-ray fluorescence, preconcentration using ion exchange and precipitation 77−12864
X-ray fluorescence analysis of natural water, preconc. technique 78−61620
X-ray spectroscopic method 77−52689
zero liquid discharge considerations 79−9858
Zuari estuary, Goa, India, environmental parameters monitoring 78−81214
^{137}Cs, conc. variations in Baltic Sea 1973 to 1975 79−92100
As conc. meas., column chromatography versus flameless atomic absorption spectrophotometry 80−55969
B, dissolved, in water, determ. via azomethine H colorimetric method 79−92115
Br_2 in environmental water samples, determ. by neutron activation, isotope exchange 77−44550
^{14}C, bomb-produced, distrib. in equatorial Atlantic, upwelling rate estimation 79−39726
Cd determ. in drinking water by graphite furnace at absorpt. anal. 80−55733
Cd sorption and accumulation in sediment of Tama River 79−52972
Cd sorption and accumulation in sediment of Tama River 79−74924
Ce in marine sediments, determination method 80−104543
^{137}Cs conc. meas. in ocean, sorbent props. *(Russian)* 79−39763
^{137}Cs leaching from ion-exchange resin incorporated in polyethylene or cement composite 77−65275
$^{137}Cs/^{134}Cs$ radioisotopes in seawater, Cs-selective resin determ. 80−94137

water pollution detection and control continued
Cu, cyclic and anodic stripping voltammetry, appl. to natural waters anal. 79−74446
Fe, characterisation in environmental samples by Mossbauer technique 79−66433
^3H, conc. in atmospheric precip., rivers, and seas, USSR 79−74560
^3H, environmental anal. by mass spectrometric meas. of ^3He 77−9447
^3H, low-level meas., inter-laboratory comparison 78−44888
Hg conc. determ. in Arabian Sea waters 79−25268
Hg, determ., in fresh and saline waters, automated UV digestion-AAS method 78−44414
Hg, determ. in drinking water, surface water and sewage effluent 79−92103
Hg, determ. in sea and inland waters, differential pulse anodic stripping voltametry method 77−70361
Hg determination, error anal. 78−69519
Hg flux meas. in South Atlantic Bight 80−4046
Hg in surface waters in seas around the UK 78−7664
Hg, neutron activation anal. for low levels in water 79−70503
I^-, anal. in groundwater by X-ray fluorescence spectrometry 80−45829
I_2 in environmental water samples, determ. by neutron activation, isotope exchange 77−44550
IO_3^-, determ. in rainwater by neutron activation anal. 78−76953
^{125}I thyroid dose calc., air and water conc. limits 79−88195
^{54}Mg, removal from waste water by oxine-impregnated activated charcoal 80−9344
Mn determination in environmental waters by neutron activation anal. 79−74584
N contamination assessment by use of differential temp. calcs. 79−66730
N, total content trace anal. by isotopic dilution and optical spectroscopy 77−5253
NO_3^-, determ. in waste and treated waters by laser Raman spectroscopy 79−92113
N_2O, determ. in water using electron capture detection gas chromatography, multiple equilib. 80−76566
NaCl, mass transfer from sedimentary deposit layer to stationary water region *(Japanese)* 77−25700
P control in estuaries, parallel shooting models, Corpus Christi Bay (Texas) and Jamaica Bay (New York) appls. 79−57521
P determination, automated procedure 80−81517
P, reactive, in natural waters, low concs. automated determ. in presence of As, Si and $HgCl_2$ 79−44277
P, removal process modelling and control by multivariate time series method 79−74561
PO_4^{3-}, removal kinetics in small alkaline lakes, natural and artificial processes 79−79417
P_2O_5, determ. in Jordan Gulf of Aqaba 79−12142
Pb, conc. determ. in estuarine waters, Raritan and Lower New York Bays 79−12139
Pb, conc. in coastal waters of North and South Lebanon 79−12146
Pb, determ. in aqueous solns. by Delves Cup technique and flameless atomic absorpt. spectrometry 78−68973
^{210}Pb determination in sediment core from ocean floor off Californian coast 80−72101
Pu and Am inventory of ecosystem near a nuclear facility 80−97820
^{226}Ra, determ. of tap water pollution *(Czech)* 79−34675
^{226}Ra determination in water, sampling and meas. methods 77−9278
^{226}Ra in public water supplies, conc. determ. *(German)* 80−94138
^{222}Rn concentration in water, meas. by gamma counting 78−53733
^{222}Rn concentrations in water, rapid meas. with commercial liq. scintillation counter 78−28339
^{222}Rn determination in air and water, sampling and meas. methods 77−9278
Se determ. in environmental water by preconc. on charcoal, neutron activation anal. 77−44551
^{90}Sr and T in N.Pacific surface water during 1974, conc. meas. 80−26181
^{90}Sr, conc. variations in Baltic Sea 1973 to 1975 79−92100
T concentration reduction for aquifer 80−21423
T enrichment in water by electrolysis for low-level T activity meas. 78−17536
T, sampling and meas. in environmental samples using gas-filled proportional counters 78−86699
U determ. in natural water by ion exchange separation, delayed neutron counting 77−36847
U determination in environmental waters by epithermal neutron activation 79−53010
U determination in sea water by preconc. on Chelex 100 and neutron activation 79−53009
V determ. in sea and surface water, preconc. on charcoal, neutron activation anal. 77−44549
Zn and Cu levels in Belfast Lough 80−3539

water purification *see water treatment*

water supply
see also dams
agricultural land urbanisation hydrologic impact, distributed watershed model 77−37277
agricultural water demand information, remote sensing 79−2315
alluvial aquifers, relations between geophysical and hydraulic parameters *(Italian)* 77−53079
Andhra Pradesh, aridity and its fluctuations 77−56661
annual flow regulation, appl. of probability and statistical methods *(Chinese)* 79−96778
Antarctic iceberg melting 78−88863
aquifer, viscoelastic model appl. to subsidence due to pumping 77−91175
artesian wells drilled in permafrost, temp. field, efficiency of heaters for ice plugging prevention 77−78242
Baghdad insolation and meteorological data for flate plate collector design 79−62092
bounding wells to counteract preexisting groundwater movement effects 79−2324
Box-Jenkins modelling advances, model construction 77−87632
budget modelling and effects of spatial var. of soil hydraulic props. 77−73779
Cambay drinking water, metal contents 79−20899
cascade static stability and critical velocity *(German)* 78−79306
centralized management systems for Kagawa Prefecture irrigation-water system *(Japanese)* 80−89684
chloroform, production from polyelectrolytes 77−78252

water supply continued
Cleveland, Ohio, organics in water 79−16550
climate and climatic change, effects on water supply 78−49044
Derwent Reservoir, N.England, Zn, Cd and Pb in water, sediments and submerged plants 79−25286
domestic system, hydraulic noise control by energy absorption technique appl. 77−19487
domestic water, ^{222}Rn conc. meas. by gamma counting 78−53733
drinking water exam., L65 turbidity meter description *(Dutch)* 77−27332
Environmental Protection Agency requirement for underground injection in solution mining of U ore 79−92101
erosion and sedimentation, problems rel. to water supply, research needs 78−61444
Finnish river water pollution monitoring network 80−89686
flood forecasting in river, by unit hydrograph method 77−5254
flow-through reservoir, vel. and temp. fields, num. simulation 77−17152
Galal Badra Basin, Iraq, water deficit 80−26565
ground water, Canterbury, New Zealand, aquifer simulation 77−53093
ground water supplies in Himalayan region of Uttar Pradesh, influence of droughts 77−56708
groundwater, computer assisted management *(German)* 79−57989
groundwater and surface water management by decomposition 77−64345
groundwater and surface water resources, effects of 1975-6 drought on development 78−88869
groundwater exploration in hard rock terrain and best well locations 77−41075
groundwater management, system response function hierarchy 77−64346
groundwater occurrence in trappean terrain of Sholapur district, Maharashtra, influence of groundwater divide 79−8649
groundwater quality in GFR, survey results *(German)* 79−62539
groundwater recharge in Ganges Basin, alternative methods for water supply 80−81952
horizontal-axis wind-turbine system for pumping duties in Third World agriculture, design 80−61259
hot springs in Kohu City, Japan, fluorine content analysis *(Japanese)* 79−70821
hot water springs in N.Spain, trace elements concs. *(Spanish)* 77−49097
hot water supply using solar collectors *(Dutch)* 80−7954
hydrogeomorphic controls rel. to floods and morphometry in small drainage basins 77−29340
hydrologic information needs and remote sensing 77−56665
hydrological system statistical modelling *(German)* 78−96246
hydrometeorology, appls. to hydrology and water management 78−96240
icebergs, melting in environment with salinity gradient, rel. to fresh water supply 78−24305
icebergs from Antarctica for Saudi Arabia water supply 77−81949
India, surface water resources overall assessment by water balance method 77−56662
interactive lake survey programme for water resource surveillance 78−81257
Iraq, frost phenomena and damage 77−73795
irrigation, centralised water management control system *(Japanese)* 79−53373
irrigation and groundwater salinity, river basin salt balance management 77−78276
Israel, water shortage and supply, long-run policy for agriculture 78−61454
Kingskettle, Scotland, phenol and cyanide leaches into groundwater from gasworks site 79−88020
leaky aquifer, flow in fractured porous media 77−91173
Lithuanian water resource distrib. optimisation, informational preconditions *(Russian)* 79−92555
Malawi solar energy utilisation prospects 79−57379
Maneri Bhali Hydel hydroelec. scheme, stage I, model, India 77−9452
Manic 3 reservoir, Quebec, induced seismicity 79−66636
Masulipatam (Andhra Pradesh), water balance in drought years 77−56663
metal pipelines corrosion, fundamental criteria *(Russian)* 79−1921
metrological servicing in USSR ministry of land reclamation and water management 79−96496
multi-inflow reservoirs, flow dynamics 78−20452
natural channel flow simulation by computer-controlled RC network 77−45046
network anal. using node recording algorithms and admittance matrix 78−85613
network anal. using sparse matrix and successive linearisation methods 78−85614
nonstationary flows, slowly varying, calc. via method of characteristics with fixed net *(German)* 79−5515
open channels with weirs and flumes, discharge measuring structs. 79−68874
optimal water distribution systems design 78−61457
pixe analysis of water with detection limits in the ppb range 79−48005
polyacrylamide, additive to water supply, effect on cavitation and erosion in pipes 78−83441
purification processes, volatile organohalogen analysis technique 79−21080
quality standards, geometric mean 79−16539
radioisotope applications in agriculture, hydrology, medicine industry etc., booklet 78−35947
recycling and urban water conservation 79−79892
regional water quality management, optimisation model 77−66945
reserviors, suspended load sedimentation, analysis and prediction method 78−53664
reservoir, discrete representation of storage for stochastic optimisation 77−64354
reservoir management, dynamic programming and release rules 77−73776
reservoir operation under conflicting objectives 77−73777
reservoir optimisation, information value 78−49060
reservoir sedimentation process and detention structure model 78−44892
reservoir storage capacity, small sample expectation of population and adjusted ranges 78−61468
reservoir storage capacity, small sample expectation of rescaled population and adjusted ranges 78−61469
reservoir storage for Australian streams, preliminary estimation 77−86947
reservoir storage size sampling error 78−61466
water supply continued
reservoir supplying major mining centre, water and sediments heavy metals content 80−30617
reservoir surface area from LANDSAT imagery 79−66834
reservoir under random sediment yield, Bayes design 78−11933
reservoir with inclined bottom, gas motion under press. penetration *(Russian)* 77−81952
reservoirs, effluent P standards impact on eutrophication control 79−88015
reservoirs, tectonic and tectonophysical conditions for occurrence of induced earthquakes 77−81802
reservoirs with Markovian inflows, modelling 78−16080
resource research using Pennsylvania State Univ. reactor 79−12159
resource system, Monte Carlo simulation, variance reduction techniques 78−81244
resources management, systems anal. and modelling techniques appl. 79−5518
resources planning, use of multiattribute utility theory 78−11932
resources planning and management, appropriate model choice 79−83650
resources policy, scientific and technological considerations 79−8642
river and ground water pollution due to drought in England and Wales, 1975-6 period 78−88868
river basin water resource, Pareto region, stochastic multicriterial problem in control 80−4055
river management operational system development using weather radar 78−40718
river water quality vars. operational forecasting from streamflow vars. 77−78265
Rome's Metropolitan water board, water pollution control *(Italian)* 77−81953
run off at Syr Darya hydroelectric power station, recording aspects *(Russian)* 77−86942
Russia, hydrology in tenth five-year-plan period 77−78262
satellite remote sensing appls. 77−25788
Sava River, influence of water pollution on ranney wells in Belgrade 78−40602
seasonal forecasting models, Akaike's information criterion 80−67386
Sierra Nevadas, snowcover, satellite obs. during 1977 Californian drought 78−65352
solar plant for hot water supply *(Rumanian)* 80−97766
storage reservoir analysis, mass-curve techniques, systems and perspective 80−8457
subsurface environments, fate of pollutants, math. modelling 77−56658
Sundesert Nuclear Plant water supply 79−9862
trace element determination, by multielement ICP-AES method 78−23992
Tsimlyansk Reservoir, hydrometeorological studies 79−39784
turbidimetry instrumentation, light scattering techniques appl. 79−12150
Turkey, karst water resource development 80−61821
underground water resources in Belgium *(French)* 77−25712
United States, history of pollution control 77−33818
United States municipal waters, N_2O concs. 78−57223
unsteady flow to pumped well in fissured aquifer with maintained free surface level 79−16547
upstream control effect on water supply reservoir 79−57508
urban hydrology and sediment control, symposium, Lexington (1976) 77−37266
usage regions in Lithuania, multi-image classification *(Russian)* 78−16069
utilisation system, area wide multimodal system; nonlinear goal programming model 79−57518
Volga water management system, effectiveness of spring flood long-range forecasts 78−3837
water power, potential, regional analysis method 79−83557
water resource management, gaming-simulation appl. in Hunter River Valley, New South Wales 79−57517
water table level sensing, using strain gauge load cells 77−21802
world water resources, prospects and problems 79−39779
B determination in nuclear power station waters, flame photometer method 78−45672
Fe, determ. in waters, colorimetric-acid digestion method 78−61088
^{226}Ra in public water supplies, conc. determ. *(German)* 80−94138

water treatment
see also desalination
activated sludge wastewater process control model 77−17154
aeration of natural waters, effluents, O_2 bubble mass transfer coeffs. 79−41737
aeration system optimal design for polluted streams 77−37251
Arizona Nuclear Power Project waste water reclamation for cooling 79−9861
askarels, environmental pollution reduced using biodegradation *(Slovene)* 78−7663
biological waste water treatment by activated sludge at Haguenau City water treatment plant *(French)* 80−61473
biological wastewater treatment system using photosynthetic energy conversion 80−30510
boiler feedwater pH meas. apparatus improvements 79−79341
chemical flocculation plant at Ahrensburg, in West Germany, appl. *(German)* 78−40601
chlorination of wastes, as source of N_2O in Michigan waters and USA municipal waters 78−57223
coke-plant effluents, second-stage activated sludge treatment 79−92102
condensate at BWR power stations, pulver resin on-floating method, construction and initial startup aspects *(Hungarian)* 79−76116
dispersed particles precipitation on fibre in elec. field 78−53262
dissolved O_2 in rivers, reliability parameter in probabilistic programming models 80−26179
drinking water ozone concentration automatic chemi-luminescent meas. *(Russian)* 77−66784
electrochemical porous flow-through electrodes, mass and charge transfer and cell design *(French)* 80−16697
electronics manufacturing plant waste treatment facility 77−73780
fission reactor coolant decontamination *(Spanish)* 79−45345
fission reactor heavy water purification by deuterated ion exchange resins 78−8897
fluidised bed containing biomass, expansion 80−14803
galvanic dissolved O_2 sensor, improved, activated sludge aeration appl. 77−70364

water treatment continued
gas chromatography/mass spectroscopy analysis of volatile organic compounds 79−12151
high-level liquid waste, damage to organic extractant in positioning process 80−9345
hydrodynamic dispersion of chemicals of soil *(Italian)* 77−41071
industrial liquid waste, purification and by-product recovery 79−83648
industrial wastes, Mg recovering, use of sink-and-float test *(Japanese)* 80−55948
industrial wastewater, techniques for removing oil and grease 79−83646
ion chromatography appl., on-stream, impact on energy conservation 80−55737
ion-exchange wash water recycling system, photographic processing laboratory appl. 80−42277
magnetic, HF combined *(Russian)* 79−15682
municipal sludge, disinfection by high energy electrons 79−24922
municipal treatment levels differences 79−83649
municipal wastewater plants, air pollutants monitoring 79−80050
municipal wastewater treatment plants, mathematical modelling of electrical energy consumption and heating requirements 80−26194
nuclear power plant laundry drain treatment system development 79−9788
nuclear power station decontamination, chelating agent appl. 78−50280
oil contaminated waste water treatment by foam fractionation 79−92104
osmosis appl., reverse, using sulphonated aromatic polysulphone, expt. results 77−44508
Palisades Plant steam generator operation rel. to water chemistry 79−9854
phosphorus removal system, automation 80−76669
pollution control equipment for metals industry 79−66432
pollution control modelling, book 78−73418
polymer manufacture, radiation treatment of waste-water, feasibility *(Russian)* 78−46181
primary and secondary water chemistry of PWR power stations, European experience 80−106110
purification, granular charge inhomogeneity effect on head losses 77−75976
PWR power station secondary water chemistry study, progress report 80−106108
PWR steam generator eddy-current inspection results 79−9855
PWR/BWR power stations, waste-water treatment plants, engineering experience 77−6543
radiation treatment of waste water. process control techniques appl. 79−96489
radiative purification of waste waters of paper manufacture *(Russian)* 78−61035
radioactive, low-level, ^{60}Co removal by ferric hydroxide coagulation-flocculation, improvement using diethyldithiocarbamate 78−37415
radioactive liquid waste processing by ion exchange at Westinghouse Waltz Mill Site, USA 77−54345
recycling and urban water conservation 79−79892
regional wastewater management systems, chance constrained approach 79−57513
regional wastewater treatment system, computer appl. 77−41064
removal of H^+, NH_4^+, Cu^{2+} and Cd^{2+} by using Itaya-Zeolite *(Japanese)* 78−95951
sample analysis, automatic, pH, conductivity, alkalinity, process water treatment appl. 79−12287
sewerage wastewater, heat recovery system at Green Bay plant 79−83610
sludge systems, nitrifying activated, design and control 77−5243
solar energy concentrator thermoreceivers, waste water sediments disinfection 79−83624
solar photodecomposition, redox reaction thermodynamics 80−35697
sterilisation by high-energy electron beams 77−70507
suspended solids measurement standard, macerated glass fibre filter paper appl. 79−8454
tap-water purification for home dialysis *(German)* 79−2160
total oxygen demand measurement in waste-water treatment plant 79−96399
trace metal conc. in waste water, spectrochem. anal. 78−61106
turbidimetry instrumentation, light scattering techniques appl. 79−12150
UV irradiation, water sterilisation unit design and appl. 79−57713
waste water treatment plant, BASF, operating experiences with special meas. and control *(German)* 79−66424
wastewater treatment, distributed digital processing and closed loop computer control 80−45824
wastewater treatment, instrumental anal. 79−74432
water distillation using basin-type solar stills, use of wood charcoal beds 80−7924
Westinghouse steam generatcr experience with all volatile treatment 79−9853
wind powered brackish water purification by electrodialysis and reverse osmosis 80−35630
Zion Generating Station steam generator operating experience 79−9851
As salt toxic effect on activated sludge micro-organisms *(Chinese)* 79−24919
B determination in nuclear power station waters, flame photometer method 78−45672
B salt toxic effect on activated sludge micro-organisms *(Chinese)* 79−24919
ClO_2 appl., waste water disinfection and oxidation 80−12032
^{24}Mg, removal from waste water by oxine-impregnated activated charcoal 80−9344
O_3 concentration in water, chemiluminescent meas. method 77−60159
P reduction in sewage effluent by electrochemical process 80−104445
P removal process modelling and control by multivariate time series method 79−74561
Pu(VI) in drinking water, max. permissible conc., chlorination effects 79−34448
S salt toxic effect on activated sludge micro-organisms *(Chinese)* 79−24919
Si salt toxic effect on activated sludge micro-organisms *(Chinese)* 79−24919

watthour meters
see also power measurement
No entries

wattless power *see reactive power*

wattmeters
see also power measurement; volt-ampere meters
AC digital type F4860, operational principles *(Russian)* 78−70158
analogue, appl. for specific core loss meas. or elec. steel sheets *(German)* 80−13099
battery self-discharge process assessment by microcalorimetry 80−30935
calibration, (3+3)-phase voltage and current source of high stability 77−18038
calibration, at zero power factor using digital sinewave generator 77−18039
CW CO_2 laser power meter, thin film bolometer, NaCl monocrystal divider, 0 to 500 W range, digital output *(Russian)* 77−37992
defibrillator energy meters, traceable calibration methods 80−30928
differential, analogue, adiabatic calorimeter and liquid chromatograph appl. *(Czech)* 78−23979
differential thermal wattmeter, for AC/DC transfer of power 77−18041
digital, for compact electronic equipment 80−209
electronic loss meas. apparatus for supercond. coils 77−26361
electrostatic, with automatic voltage feedback for torque balance 77−82569
errors, systematic and random, in wattmeter apparatus for measuring unit losses in electrical steel sheet 80−71858
heat receivers with moving heat carrier, freq. characts. 80−4733
withIC multiplier, use in model power system 77−53930
in-line, based on SWR bridge, for transmitter output power monitoring 77−79103
multiplier unit for acoustic and electronic wattmeters 77−79118
ponderomotive microwave power meter, frequency range 8.5 to 12 GHz, power range 0.5 to 100 W, VSWR up to 1.1 *(Russian)* 77−37939
power measurement in three-phase AC cct. *(German)* 77−74458
reactive acoustic field, complex wattmeter meas. 79−41535
static, for use in educational establishments 78−45656
steel, electrical sheet, wattmeter unit for measuring specific losses, system errors 79−91893
superconducting magnets excited by AC, energy loss meas. device 79−2796
test instrument survey *(German)* 78−8394
waveguide wattmeters, ponderomotive and bolometric types, standard, comparison 77−71345

wave analysers
see also spectral analysers; transient analysers
automatic mass ECG analysing computer 77−81600
EEG waveform detection by microprocessor 77−73610
seismic microvibration frequency analysis by 50 m interferometer 80−109276
whistler occurrence rate and dispersion real-time analyser 77−87129

wave digital filters
eEG transient detection by matched inverse digital filtering 80−85506

wave equations
see also Dirac equation; Schrodinger equation
aberrating Gaussian beam, free-space propagation, wave eqn. solns. 78−87008
absorbing boundary conditions for num. simulation of waves 77−87638
abstract wave equations, solns., large-time behaviour 78−77723
acoustic wave eqns., spectral theory, generalised Neumann boundary conditions 78−59173
action at a distance and relativistic wave equations for spinless quarks 79−36030
ADI difference of schemes, high order, wave eqn. soln. 79−66
aerodynamically generated noise, especially jet noise *(French)* 78−14002
anharmonic oscillator system, hierarchy of evolution eqns. 80−68053
asymmetric systems described by a pair of local covariant wave equations 79−75391
asymptotic forms of radial wavefunctions and Jost functions for cutoff potentials 79−71278
asymptotic solns. using methods of averaging and two-timing 78−59
atomic resonant states, wavefunctions of complex coord. method 80−106282
axially symmetric Helmholtz eqn., fundamental solution 78−77722
Backlund transform. derivation in inverse scatt. formalism 80−8810
Backlund transformation, simple structure of superposition formula, 79−12616
Backlund transformations as canonical transformations 78−81855
Bargmann-Wigner eqns., SO(4,2) covariant formulation 78−37126
Benjamin Ono eqn., exact multi-soliton soln. 79−40379
Benjamin-Ono eqn., conservation laws 80−31524
Benjamin-Ono eqn., multi-soliton like solns. 78−28960
Benjamin-Ono eqn., props. 79−63050
Benjamin-Ono equation, Backlund transform. and conservation laws 80−4540
Benjamin-Ono equation, higher order, solns. 80−62482
Benjamin-Ono equation, internal wave solitons, linear stability 80−53802
Benjamin-Ono equation, meromorphic solutions 80−31980
Benney's long wave eqns., Hamiltonian formalism 80−31525
Benney's long wave equations, conservation laws and Lax representation 80−14719
Bernoulli equation, wave motion in relaxing gas 80−90681
Bhabha equations, diagonalization *(Russian)* 77−79004
Bhabha first order relativistic wave eqns., historical development 78−14
Bhabha first-order, Foldy-Wouthuysen transformations, solns. 77−30254
Bhabha first-order, summary of results in series of six papers 77−30255
bi-local field interaction with external field 78−66030
bilinear soliton equations, method of constructing generalised soliton solns. 80−4541
bilocal field, and mechanical model 78−29241
black holes, rotating, electromagnetic perturbations 78−12279
Bloch waves, low freq., for wave eqn. of periodic type 79−17243
Bloch waves, periodic variations in shape 77−31926
boson field in external potential, instability, Klein paradox, particle creation 77−6017
bosons in weak external EM field, as one-particle problem 78−12462
Bossinesq equation, similarity solutions and Backlund transformation 80−68056
Boussinesq type eqn., reduction to modified Hirota eqn. 80−8804
Bremmer series decomposition of solns. to lossless wave eqn. in layered media 78−53738
Burgers equation, relationship to differential stochastic eqn. 80−36869
canonical transformations theory for nonlinear evolution eqns. 77−29993

wave equations continued
catastrophe theory, anal. of wavefront dislocations 80−8812
Cauchy problem, linear eqns. with const. coeffs., absolute instability, 3-dimens. 79−12622
causality of a wave equation and invariance of its hyperbolicity conditions 80−91000
linear Chapman-Enskog procedure, evolution equations of hydrodynamic variables 80−49075
characteristic cone data, soln. of wave eqn. in R^{n+1} 78−57807
charge current density of Pauli eqn. using vel. operator method, nonrelativistic derivation 78−73872
chemical, for ionic system reactions 78−15653
chemical reactions in multicomponent system with diffusion, nonlinear wave equations 78−19991
circular duct with hyperbolic horn, sound radiation modes 80−96096
Claerbout equation, alternative derivation 79−84135
classical, cross-section generating solutions of field equations 79−97488
classical V-A theory and non-conservation of the dynamical parity 79−54014
completely integrable class of mech. systems, Korteweg-de Vries eqns., multicomponent Schrodinger eqns. particle motion 78−54218
completely integrable operator evolutionary eqns., Schrodinger Korteweg-de Vries, KdV eqns. 79−97248
completeness value for eigenfunctions of second order differential eqns. 80−31564
conference, nonlinear problems in theoretical physics, Jaca, Gain 1978 80−4478
conference on solitons and condensed matter physics, Oxford, England (June 1978) 79−75364
confined solutions of multidimensional inversion equations 78−77678
conformal invariance of relativistic equations for arbitrary spin particles 79−30649
conservation laws for the classical Maxwell-Dirac and Klein-Gordon-Dirac equations 79−49066
conserved densities, Hamiltonian systems 80−90682
constants of motion of nonlinear equations in an extended Poisson formalism 79−49061
continuous spectrum decay, sine-Gordon eqn., nonlinear optics appl. 78−71143
continuously stratified liquid, linear wave theory, internal wave operator solution 80−43759
coupled bilinear eqns., exact one- and two-periodic wave soln. 80−68050
coupled nonlinear evolution eqns., L-operator factorisation 79−44751
coupled spherical wave equation system for relativistic 2 particle interaction *(French)* 79−35549
covariant perturbed wave equations in arbitrary type-D backgrounds 79−30314
covariant wave equations, Galilei group and mag. moment of electron 77−64955
curved space-time, compact and noncompact sources 80−73571
cylindrical KdV equations, soln. asymptotic behaviour (in t), Cauchy problem 80−98803
cylindrical vector waves expansion in terms of spherical vector waves, EM scatt. appl. 77−10817
damped wave equation, Copson's appl. of Reisz's method 77−53742
de Broglie wave packet, nondispersive 78−36858
de Sitter space-time, QFT, relativistic wave eqns. *(German)* 77−82666
de Sitter space-time, wave eqns. for arbitrary spin 77−30234
deep water gravity waves, two-dimens. nonlinear wave eqn., exact envelope soliton solns. 80−43725
delta wing equations, high freq. solns. 79−46337
deuteron relativistic wave equation in EM fields *(Russian)* 79−89248
diatomic lattice, solitary wave solns., ϕ^4 kink, struct. phase transition, phonon dispersion curves 79−80544
diatomic molecule, vibr.-rot. states, high accuracy wave functions and energies 80−74159
dielectric waveguide modal props., one-dimens. wave eqn. analysis 79−81537
difference method for extended stability range 80−4538
diffracted wave fronts 80−82652
diffusion, nonlinear waveshapes generated by possibly finite initial disturbances 78−36948
diffusion with wave fronts, definition *(French)* 77−67386
Dirac operators, conformal group representations 77−33895
Dirac-Coulomb functions, asymptotic expansions of radial integrals 79−308
dispersive nonlinear wave eqn., soliton like solns. 78−93538
dispersive nonlinear waves, conservation laws group theoretic aspects 77−30016
dispersive systems, nonlinear, possible model eqn. for long waves 77−67296
dispersive wave equation, spatial discretisation effect on steady state and transient solns. 77−30014
dispersive waves, nonlinear interaction between strong and weak waves 79−17242
dispersive waves, nonlinear model eqn., parametric growth rate 79−12615
with dissipation, growth and instability theorems, appl. to continuum mechanics 78−36839
domain with moving boundaries, difference schemes on non-uniform grid *(Russian)* 77−22380
double sine Gordon equation, exact multiple soliton solutions 78−20978
dynamic stability of solitons and general nonlinear wave phenomena *(German)* 80−4544
eikonal eqn., underlying geom. struct. 77−60957
electron spin equations of motion in external field 80−18102
electronic wavefunctions in a space of constant curvature 80−5466
electrons in Kerr geometry, one dimens. wave eqn. 78−12622
EM moments of spin J-1 particles, and equivalency of wave eqns. *(Russian)* 77−65113
energy loss of a modified Korteweg-de Vries solitary wave in a varying medium 80−90683
evolution eqns. with given set of conserved densities, algorithm 79−71257
evolution equations, impulse and distributed control *(French)* 80−68049
evolution equations, nonlinear, inverse spectral transform, generalisation of Klein-Gordon problem 80−68055
evolution equations, unknown control dates, periods and type, optimal control, existence theorem *(French)* 80−62478
evolution systems and convection-diffusion, stiffness and stability, Gershgorin theory 80−77626
wave equations continued
evolutionary problems, error anal. of finite difference, finite element and spectral methods 80−46815
extended hadrons, de Sitter fibre bundle, gauge theory of strong interactions 77−18189
extension of nonlinear evolution equations of the K-dV (mK-dV) type to higher orders 80−105508
exterior Neumann problem for reduced wave eqn. in spherically symm. medium, constructive methods of soln. 77−50799
ferromagnet, magnetostriction is magnetic field, sound-spin wave coupling 79−15334
fibre optic structures, multimode coupling 79−37033
field statistical moments in medium with large-scale inhomogeneities 80−37953
field theory, massless equations, first-order, conformally covariant 78−29265
Field-Koros-Noyes chemical wave equation, asymptotic solutions 80−66857
fields solution using transmission line matrix, random walks appl., Monte Carlo approach 79−53991
finite difference approximation, using cubic spline technique 79−49
finite element Laplace transform soln. 78−4488
finite-band solutions to the duality equation on S^4 and two-dimensional relativistically invariant systems 80−42349
first-order relativistic, Foldy-Wouthuysen transformation, explicit construction 77−30253
first-order relativistic, relationship between Lorentz and Foldy-Wouthuysen transformations 77−30252
FitzHugh-Nagumo equations, perturbation anal. of slow periodic wave soln. 78−24060
fluids of finite depth, exact one- and two-periodic wave solns. 80−53797
fluids of finite depth, N-soliton soln. of higher order wave eqn. 80−48724
forced van der Pol oscillator, frequency entrainment 78−57794
four body equation 77−17857
Fourier-Laplace transform asymptotic behaviour, wave eqns. with memory, oscillatory integrals *(Russian)* 79−92990
free Klein Gordon fields, conservation laws 80−340
freely gravitating charge, radiation, in field of weak plane gravitational wave *(Russian)* 78−89381
Galerkin methods applied to some model equations for non-linear dispersive waves 79−53985
Gegenbauer functions, expansion formulas and addition theorems 77−5634
Gel'fand-Levitan equations with comparison measures and comparison potentials 80−12931
Gelfand-Levitan eqn., variational principle 78−32708
general light cone frame, from Galilei group to Lorentz group, appl. to Schrodinger-Pauli eqn. 77−61187
general nonlinear differential-difference equations, integrability by inverse scattering method 79−12575
general system quantisation, rigid sphere appl., wave eqn. using correspondence principle 78−57801
generalised sine-Gordon eqn., Backlund transformation, nonlinear σ model 80−4844
geophysics, finite-difference migration for steep dips 79−92620
Godel universe, scalar perturbations 78−57709
gravity waves, interfacial and internal long, dissipation, Korteweg-de Vries eqns. 80−90686
Green's function discontinuities across characteristic surfaces of field eqns. 79−93279
Green function expansion into eigenfunction set 80−22205
Green tensor expansions for harmonic vector wave eqn. in spheroidal coord. systems 78−41171
gyrotropic absorbing crystals, nonorthogonal eigenwave refl. 80−99624
gyrotropic medium, Green's function and field of moving charges 80−58445
harmonic oscillators, vibr.-vibr. energy transfer, perturbed wave eqn. soln. 80−1051
harmonically bound radiating electron, nonrelativistic wave equation 79−40701
heat and mass transfer, simultaneous, in moving media, wave equation 79−44747
helical curve motion and soliton eqns., scaling invariance 78−49667
Helmholtz eqn., test of Born and Rytov approx. using Epstein problem 78−63212
hidden symmetries in dynamical systems 80−37168
higher order Benjamin-Ono equation, N-soliton and N-periodic wave solns. 80−12915
higher order Korteweg de Vries eqn., Backlund transform 80−105510
higher order modified KdV eqns., bilinearisation 80−105509
homogeneous isotropic viscoelastic medium, wave propagation eqns. with time lag 79−35573
Hurley's field equation for arbitrary spin, covariant matrices, transition matrices 77−6034
Huygens, principle on curved space-time, validity 78−21024
Huyghens' principle, validity for spinor field eqns. *(French)* 77−41487
hyperbolic conservation laws; initial and initial-boundary value problems, large-time behaviour 77−74233
hyperbolic conservation laws, Glimm scheme for solving, deterministic version 78−20972
hyperbolic mixed problems, leading wavefront propagation 78−36836
hyperboloids, wave eqn., O(2,2) symm., separation of variables 78−77679
hypergeometric functions, two-variable, Lie theory and separation of variables 80−73189
hypoelastic compressible rate-sensitive material flow, integrable generalized wave eqns. 78−38213
incompressible irrot. flow, water waves and Korteweg-de Vries eqns. 80−69850
infinite component, soliton solns. 77−26180
infinite component wave equations, composite system internal struct. 77−65102
infinite crystal, surface states determ. by complex extension of tight binding 78−80032
infinite-component relativistic wave eqns., perturbation theory 77−61184
inhomogeneous media, wave eqns. props. 79−63055
initial value problem, several space dimensions, Rothe method 80−82651
integrable nonlinear evolution equation, soliton soln. from inverse scatt. method 80−73186

wave equations continued
integral transform groups for differential operators from Lie algebras 80−4887
internal waves with finite fluid depth, inverse scatt. problem, Backlund transformation 80−31517
invariance groups for class of countable systems of first-order partial differential eqns. 78−49635
invariance groups of Dirac and Kammer-Duffin-Petiau eqns. 77−67320
invariant bedding, numerical solution of drift wave equations 80−10374
inverse problem for random sources 79−97214
inverse problems of determination of an arbitrary set of point sources 79−17241
inverse scatt., generalised problem prolongation structs., soliton solns. 77−3833
inverse scattering method, commutator representation of Painleve type ordinary differential eqns. 80−68052
inverse scattering transform eqns., survey of developments 78−57795
inverse source problem of scalar waves, acoustic and EM examples 77−30015
ion-acoustic Korteweg de Vries solitary waves in plasma with density, temp. gradients 78−55720
iterated waves, singularities of elementary soln. of limit problems in half-space *(French)* 77−60944
Jaulent-Miodek family of nonlinear evolution eqns., Hamiltonian formulation 80−31511
Kadomstev-Petviashvile eqn., reduction to Painleve transcendents 79−92954
Kadomtsev-Petviashvili dispersive systems, 2-D lumps 79−92955
Kadomtsev-Petviashvili eqn., appl of variation of action method of one field solitons 80−331
Kadomtsev-Petviashvili eqn., inverse scatt. problem, separation of variables 78−62087
Kadomtsev-Petviashvili equation, two-dimensionaL solitons and their interaction 78−12575
Kadomtsev-Pyatviashvili eqn., asymptotic behaviour of solns. (two-dimensional Korteweg-de Vries eqn.) 80−52036
Kadyshevsky eqn. in relativistic space, deep bound states 77−54044
KdV, Backlung transform. for pole movement *(French)* 79−12711
KdV eqn., particular N-soliton soln. 80−31971
KdV equation, perturbative expansion and initial value problem 80−62487
Kemmer-Duffin equation with proper time, diagonalisation *(Russian)* 77−61200
Kerr-Newman background space, nonstatic nuclear forces, meson field at black hole event horizon 78−61880
Klein Gordon, nonlinear generalisations, exact solns. 79−35569
Klein Gordon eqn., appl. to hadronic atoms in momentum space 79−872
Klein Gordon eqn. (1+4)-dimensional invariant expansion of soln. in orthogonal coord. system *(Russian)* 77−13875
Klein Gordon equation, equivalent variational integral, numerical soln. by finite element method 78−78064
Klein Gordon equation, massless, bound states in Kerr metric 79−35600
Klein Gordon lattice field eqn. in 4-D space-time, Lorentz covariance 78−54184
Klein-Gordan equations with logarithmic nonlinearities, classical theory 79−5996
Klein-Gordon, exact soln., coherent states of relativistic particle in external EM field 77−2721
Klein-Gordon, instabilities of massive scalar perturbations of rotating black holes 79−54026
Klein-Gordon, Lorentz and Dirac eqns., exact solns. *(Russian)* 77−79205
Klein-Gordon, with nonconstant coeff., Riemann's function derivation 77−57153
Klein-Gordon and Dirac equations, relation between quantum defects and phase shifts *(Russian)* 77−79207
Klein-Gordon eqn., asymptotic growth of L^p norm *(French)* 80−73178
Klein-Gordon eqn., essential spectrum selfadjointness and invariance 77−18157
Klein-Gordon eqn., meson masses calc. using harmonic oscillator pot. 79−93392
Klein-Gordon eqn., nonlinear interactions of counter-travelling waves 80−77627
Klein-Gordon eqn., path integrals representation 77−67553
Klein-Gordon eqn., perihelion precession rate in system of two charged masses 78−73897
Klein-Gordon eqn., relativistic particle motion in standing wave fields 79−58910
Klein-Gordon eqn., stochastic derivation 77−61185
Klein-Gordon eqn. and Poincare group 78−62292
Klein-Gordon eqn. for particle in const. elec. field with plane EM wave 77−30297
Klein-Gordon eqn. in stationary space times, positive and negative frequency solns. 78−29002
Klein-Gordon eqn. of tachyons, nonrelativistic reduction and interpretation 77−74262
Klein-Gordon eqn. on fibre bundle $P(M_4,G)$ 77−17864
Klein-Gordon eqn. soln., appl. to Green function construction for scalar QED *(Russian)* 79−54288
Klein-Gordon eqn. with step nonlinearity, jetlike solutions 80−17813
Klein-Gordon eqns., nonlinear, with localised solns. 78−89620
Klein-Gordon equation, identical motion in relativistic quantum and classical mechanics 77−61177
Klein-Gordon equation, inverse spectral transform 80−68055
Klein-Gordon equation, Lie-Backlund transformation group 80−68371
Klein-Gordon equation, potential interaction using a metric space 80−82879
Klein-Gordon equation, spinor and scalar fields in 4-D non-Euclidean momentum space, eqns. of motion, vacuum momentum 80−68379
Klein-Gordon equation, stringlike solns. 78−82114
Klein-Gordon equation, time-independent, relativistic Stark effect, resonances 80−62890
Klein-Gordon equation with light-cone data 78−93789
Klein-Gordon equation with optical potls. of strong interaction 77−5990
Klein-Gordon equations, nonlinear model, particle-like piecewise analytical soln. *(Russian)* 77−30228
Klein-Gordon field in naked-singularitiy background 78−70274
Klein-Gordon kinks with fourth order derivative self coupling 78−32970
Klein-Gordon nonlinear eqn., generalised susceptibility of solitary wave 79−75357
wave equations continued
Klein-Gordon nonlinear eqn., solitary wave exist. in higher dimens. 77−74232
Klein-Gordon nonlinear equation, numerical soln. 78−89352
Klein-Gordon nonlinear problems, existence of standing waves *(French)* 79−63339
Klein-Gordon operator, one-component factorisation 77−13625
Klein-Gordon particles, massless bound state, Coulomb potential 80−37188
Klein-Gordon particles in deep square wells 80−31982
Klein-Gordon theory, classical limit in coherent state representation, holomorphic solns. 79−49372
Klein-Gordon-Fock equations, invariance with respect to Poincare group 77−57456
Klein-Gordon-Schrodinger coupled eqns. 79−35955
Korteweg de Vries, soln., connection with two-dimens. Ising model 77−65004
Korteweg de Vries eqn., asymptotic soln. 79−58555
Korteweg de Vries eqn., conserved densities 79−2636
Korteweg de Vries eqn., periodic multi-soliton solns. and Toda lattice 77−30109
Korteweg de Vries eqn., second modified, exact multi-soliton soln. 80−73180
Korteweg de Vries eqn., self similar solns. and pots. with trivial S-matrix 79−30266
Korteweg de Vries eqn., similarity soln. and related Painleve transcendent 78−49674
Korteweg de Vries eqn. equivalence transformations 77−74196
Korteweg de Vries equation, second order non-linear dispersive wave eqn. as alternative 78−57791
Korteweg de Vries equations, higher order, soliton solns., inverse scatt. problems 77−45741
Korteweg de Vries integrals and Poisson's theorem 79−69
Korteweg de Vries modified eqn., quantum corrections for interacting phonon system 79−60454
Korteweg de Vries modified eqn., solitary wave solns. 80−46818
Korteweg de Vries soliton, collapse into weak noise shelf 78−57792
Korteweg-de Vries, and conservative evolution eqns., generalization of potential operators and variational principles 79−75352
Korteweg-de Vries, Backlund and inverse scatt. transform 79−63067
Korteweg-de Vries, complex modified eqn., dispersion, self-propagation in anisotropic medium 79−75371
Korteweg-de Vries, cylindrical eqn., soln. asymptotic behaviour 80−31526
Korteweg-de Vries, generalised Hamiltonian dynamics, appl. to nonlinear field theory 79−75678
Korteweg-de Vries, Hirota and inverse spectral methods 80−71
Korteweg-de Vries eqn., explicit solns. without scattering data 79−67167
Korteweg-de Vries eqn., Fourier expansion soln. 80−46814
Korteweg-de Vries eqn., generalised, conserved quantities 80−68054
Korteweg-de Vries eqn., higher order, prolongation struct., Lie algebra, soliton solns. 78−8249
Korteweg-de Vries eqn., polynomials soln. 78−69991
Korteweg-de Vries eqn., quasi-solitary wave soln. 80−70
Korteweg-de Vries eqn., slowly varying solitary wave solns. 80−72
Korteweg-de Vries eqn., variation principle 78−32708
Korteweg-de Vries eqn., weak dissipation effect on two soliton soln. 80−27143
Korteweg-de Vries eqn. 78−16661
Korteweg-de Vries eqn. and 2nd Painleve transcendent, boundary value problem in plasma theory 80−69971
Korteweg-de Vries eqn. difference analogue 78−55
Korteweg-de Vries eqns., nonresonant mode coupling 80−27142
Korteweg-de Vries eqns., perturbed solns. and soliton production 80−42074
Korteweg-de Vries equation, algebraic soliton 77−9858
Korteweg-de Vries equation, discrete version with x-dependent coefficients 79−17239
Korteweg-de Vries equation, higher-order, Backlund transforms. 80−77631
Korteweg-de Vries equation, modified, N-soliton soln., matrix trace method 80−36871
Korteweg-de Vries equation, numerical methods of solution, difference and transform schemes, accuracy 80−46833
Korteweg-de Vries equation, perturbation theory 77−33852
Korteweg-de Vries equation, soliton soln. using matrix trace 80−36870
Korteweg-de Vries equation, solns. for slowly decreasing boundary conditions 80−36872
Korteweg-de Vries equation and nonlinear waves 79−92956
Korteweg-de Vries equation prolongation Lie algebra 80−62501
Korteweg-de Vries equation solns. 79−84964
Korteweg-de Vries equation with loss and nonuniformity terms, N-soliton solns. 77−13600
Korteweg-de Vries equations, N-soliton soln., functional integral representation 80−4542
Korteweg-de Vries generalised systems, rels. 79−58551
Korteweg-de Vries solitary wave, energy loss 80−62489
Korteweg-de Vries solitary waves for cylindrical and spherical symmetric ion acoustic waves 79−77371
Korteweg-de Vries soliton solutions, perturbations 80−105511
Korteweg-de Vries type eqns., group-theoretical interp. 80−77624
Korteweg-de Vries-Burgers' eqn., asymptotic soln. for monotone shock wave 79−35568
Korteweg-de Vries-Burgers equation, self-similar solns., quasi-solitons 78−93537
Korteweg-de-Vries and Schrodinger eqns., oscill. water surface wave solns. 78−26131
Korteweg-de-Vries eqn., exact soln. via a generalisation spectral transform 78−65786
Korteweg-de-Vries eqn., solitons and rational solns. 79−67
Kortweg de Vries (Burgers) nonlinear long waves, mathematical modelling 80−8791
Lagrangian-Hamiltonian systems, partial quantisation *(Portuguese)* 80−77653
Langmuir soliton formation with ion-acoustic densiton emission 78−75328
Langmuir solitons, prolongation struct. 79−88814
Laplace eqn., axisymmetrical Koshi problem *(Russian)* 80−101713
Laplace operator in 2-D, coordinate transform., for teachers 78−61999
Lie group framework for soliton eqns., Lund-Regge model generalisations 79−17605

wave equations continued
Lie theory and semisubgroup coords. 77−33873
Lie theory and space-time wave eqn., Lorentz group 77−26179
Lie theory and wave eqn. in space-time, SO(4,C) group 79−12968
light rays, commutator relation of ray operators and wave equation, relation 80−36877
lightlike wave function and wave eqn. on null-plane using Bethe Salpeter eqn. 78−41412
linear differential systems, multidimensional inversion formalism as compatibility condition 79−84961
linear equation associated with solitons, Green's function using scatt. theory 78−4507
linear supersonic flow round a yawed elliptic cone *(German)* 77−65762
linear waves, asymptotic behaviour and wave patterns construction *(Czech)* 80−69
linearization of relativistic nonlinear wave equations 80−62837
Lippmann-Schwinger equation, uniqueness of solns. 79−17643
local spin-$^1/_2$ wave equations and harmonic confinement 80−4926
long wave, in nearly uniform channel of approx. rectangular cross section 77−35111
long waves in dispersive media, solitary wave interaction 80−59062
long-range scattering, existence of wave operators 77−74244
Lorentz invariance, rel. to Galilean invariance of diffusion eqns. 79−17276
lossless, in layered media, canonical Bremmer series decomposition 77−91064
lossless layered media state space models 77−91065
magnetic gap, soliton bound states in Ising model, quantum double sine Gordon eqn. solns. 79−78288
massive particles with any spin. consistent eqns., Klein-Gordon divisor, review 80−73577
massive spin-2 fields, nonuniqueness 77−65075
massless boson fields, group theory 77−34098
massless particles wave eqns., positive freq. solns., generally covariant defn. 77−49644
massless scalar field in a de Sitter universe and its thermal flux 79−127
matrix relativistic wave eqns. 78−367
meromorphic solutions of nonlinear partial differential equations and many-particle completely integrable systems 80−31523
meson model based on superposition of Klein-Gordon eqns., ϕ, f', F, K spectrum 78−58121
meson spectrum, quark-antiquark relativistic two-body wave eqn. bound states 77−30328
meson three-dimens. wave eqn. from Bethe-Salpeter eqn., comment 77−65136
method of potentials in the mixed problem for the wave equation 79−40381
microncausal Euclidean wave functions for hadrons, virtual mesons in deuterons 78−41408
migration of seismic records, solution by phase shift method 79−84132
mirages, form., wave eqn. calcs. 77−33749
Miura's transform. of modified Korteweg deVries eqn. 79−75356
Miura transformation, Backlund transform. and problem of collision 77−9881
Miura transformation of Kaup and Mikhailov eqns. 80−57103
mixed boundary value problem for reduced wave equation on sphere 77−64927
mixed problem for vectorial wave equation, with dissipative energy *(French)* 79−49058
modal properties of dielec. waveguide, one dimens. wave eqn. analysis 79−27398
modified Korteweg-de Vries eqn., N-soliton solns. 80−36876
modified Korteweg-de Vries solitary wave in a slowly varying medium 80−36873
modulated normal wave interaction 79−21563
molecules resonant states, wavefunctions of complex coord. method 80−106282
Moller wave operators, existence and completeness 80−82649
monodromy- and spectrum-preserving deformations. I, soln. of nonlinear differential eqns. 80−98802
multi-soliton soln. construction, direct method for sine-Gordon and Zakharov-Shabat eqns. 79−75360
multimode cylindrical surface wave excitation, multiple impedance boundary condition simulation 78−26000
multisoliton formula for completely integrable two-dimensional systems 79−67166
multisoliton solutions of nonlinear Klein-Gordon eqns. 79−12617
N-soliton solns. of nonlinear evolution eqns., Wronskian representation 79−25867
n-space dimensions, approx. integration formulae 78−16659
new conservation law *(Russian)* 77−78989
non-Abelian gauge group theory, relationship with solitons 80−4549
non-linear wave equations in a curved background space 78−65827
non-linear wave motion, one-dimensional 79−64
noncausal effects in relativistic wave eqns., Wightman fomulation 77−41750
nonconservative hyperbolic systems, gradient catastrophe in soln. 78−69992
nonlinear, comparison of statistical linearisation, diagrammatic expansion, and projection operator methods 78−54306
nonlinear, constrained harmonic motion 80−77625
nonlinear, in Hilbert space, bounds for solns., appl. to nonlinear elastodynamics 77−13618
nonlinear, soliton and appls. *(Japanese)* 79−80418
nonlinear, soliton solutions, inverse scattering method 80−12919
nonlinear, soliton solutions and their applications 80−8813
nonlinear, symm. of solitons and general solns. 79−85210
nonlinear, travelling waves, stability *(Russian)* 77−30019
nonlinear 3-wave eqns. in 3 spatial dimensions, solns. 79−97212
nonlinear dispersive systems, 2-D lumps 79−92955
nonlinear dispersive waves, statistical theory, based on Korteweg de Vries eqn. 78−16662
nonlinear dissipative, asymptotic stability of bounded or almost periodic soln. 77−67295
nonlinear evolution eqn., Cauchy problem 79−75353
nonlinear evolution eqns., conserved densities 79−71256
nonlinear evolution eqns., multi-soliton solns. 79−58556
nonlinear evolution eqns., prolongation structs. 78−24637
nonlinear evolution eqns., prolongation structs. in two-dimens. 77−36
nonlinear evolution eqns., soliton connection 78−16661
nonlinear evolution eqns., solitons and rational solns. 79−67
wave equations continued
nonlinear evolution eqns., solitons on moving space curves 77−74254
nonlinear evolution equation, exact two-periodic wave soln. 80−12914
nonlinear evolution equation class solvable by spectral transform technique 79−75370
nonlinear evolution equation soln., spectral transform method, cylindrical KdV eqn. 79−2657
nonlinear evolution equation soln. by spectral transform, conservation laws, cylindrical KdV eqn. 79−2658
nonlinear evolution equations, connection with Painleve type ordinary differential eqns., inverse scatt. transform 80−62486
nonlinear evolution equations, conservation laws by spectral transform 79−5985
nonlinear evolution equations, integrable, inverse scatt. method 80−12913
nonlinear evolution equations, reverse scattering method, Hamilton's structure and Beklund's transformations *(Russian)* 80−86090
nonlinear evolution equations and conservation laws, spectral transform method 80−62488
nonlinear evolution of three-wave interactions in inhomogeneous medium 77−74272
nonlinear evolution of waves in free shear layers, effects of critical layer structure 80−83809
nonlinear field equations, scattering theory 80−4882
nonlinear hydrodynamical eqn. of Kaup, periodic and N-soliton solns. *(French)* 80−31521
nonlinear hyperbolic eqn., approx. periodic soln. 77−17778
nonlinear hyperbolic waves, Poincare-Lighthill-Kuo method secular term elimination 78−41166
nonlinear Klein Gordon eqns., localised nondissipative stationary solns., quantum droplets 78−12819
nonlinear Klein-Gordon eqn. related to Riemannian geometry, localised solns. 79−26223
nonlinear Klein-Gordon eqns., non-dissipative character, confinement principle 78−62361
nonlinear Klein-Gordon equation, solitary wave collisions 79−80761
nonlinear Klein-Gordon equations, three dimens. multiple soliton-like solns. 78−49955
nonlinear long waves, mathematical modelling 80−8791
nonlinear media, Poincare normal form method 80−36875
nonlinear partial differential eqns., interactions between short and long waves 77−67299
nonlinear partial differential eqns., pure soliton solutions 77−82368
nonlinear Schrodinger equation solns., recurrent motion in continuum dynamical systems 80−22235
nonlinear standing waves, evolution in bounded media 77−49607
nonlinear string dynamics, rigid body motions, space curves, prolongation structures, fiber bundles, and solitons 79−97213
nonlinear three wave interactions, space-time evolution in homogeneous medium 79−84966
nonlinear three wave interactions, space-time evolution in inhomogeneous medium 79−84967
nonlinear transmission line, solitary waves 80−4543
nonlinear wave and spinor eqns., causal solns. by regularisation 77−33872
nonlinear wave envelope equations for plasma physics, Fourier's method convergence 79−55463
nonlinear wave eqns. and covariance 78−49715
nonlinear wave eqns. in n-dimensional space, periodic solns. 78−93540
nonlinear wave equation, periodic solutions 80−73188
nonlinear wave phenomena, numerical and theoretical study 78−81851
nonrelativistic limits for Klein-Gordon and Dirac eqn. 80−330
nonrelativistic wave eqn., second order in time, EM interaction 79−80774
nonseparable wave equations, multidimensional perturbation theory 79−58576
nuclear matter as optical medium, nonlinear phenomena, possible investigation methods 77−2924
numerical integration by digital integrators 77−53760
numerical soln. to wave eqn., Laplace transform and FFT 78−57763
numerical solution for real or complex eigenvalues 77−33877
numerical solution of problems in unbounded regions, use of coord. transforms 78−8219
oblique derivative for wave operator in half-space, singularities of elementary soln. *(French)* 77−60943
oblique derivative problem *(French)* 78−36837
oblique differential problem, comment *(French)* 79−21556
ocean random gravity wave mathematical representation 80−46198
off energy two body t-matrix in the R-matrix theory *(Russian)* 80−22780
one-dimensional, asymptotic formulae for eigenvalues *(Japanese)* 79−25869
one-dimensional field, complex, solitary-wave soln. 77−5707
optic fibre light propagation, review of analytic methods of study *(French)* 79−90001
optical fibre, graded index, wave eqn. for propag. fields 80−58757
optical fibres, graded index, soln. of wave eqns. using modal approach 79−36995
optical film, non-homogeneous, oblique light incidence *(Russian)* 79−13905
optically thin phase grating, comparison of optical path and differential eqn. methods 80−102823
Painleve second transcendent, numerical and asymptotic approx. 78−49675
parametric interaction of three dimens. wave packets, exact solns. 77−13635
particle density operator, phonons in many-particle system 77−53830
partition of energy for uniformly propagating systems 77−67303
Pauli eqn., algebraic struct., from geometric interp. of Heisenberg's commutation rule 78−93549
perturbed wave eqn., Pettis integration initial-value problem 79−71285
phase memory, necessary conditions 80−22206
plane interface transmission, singularities in elementary soln. *(French)* 77−71217
plane stratified media, mixed problems for wave eqn., singularities of Riemann functions 77−30017
plane stratified media, mixed problems for wave eqn., singularities of Riemann functions 77−30018
plane wave interference in inverse scatt. theory 78−57
plane wave propagation, general theorems, self-adjoint differential operators of order 2n 78−36842

wave equations continued
plane wave solns., rel. to const.-identity 3-dimens. wave 80−17749
plane-fronted gravitational waves, integrals of wave equations in space time *(Russian)* 78−89380
Poincare invariant differential equations for particles of arbitrary spin 79−30689
Poisson's formula for two dimens. wave eqn., direct soln. by Fourier transform 77−37727
Poisson brackets and related evolution equations 79−30263
Poisson relation for the wave equation in an unbounded open set *(French)* 80−73179
polarised spin-1 nuclei or mesons, elastic scatt., relativistic spin and wave eqn. EM interaction 77−50104
polycrystal, US scatt. by grains 80−2122
polynomial field theories, nonlinear Klein Gordon eqn., exact multiple solution solns. 78−45773
progressive waves in dissipative media, long range ray theory *(French)* 80−42070
prolongation struct. of nonlinear eqns. of self-induced transparency 79−44752
propagation anal., wave-kinetic method, phase-space path integrals 78−62088
pulsons, two space-dimensional, dynamics of collisions in ϕ^4 field theory 78−8250
quantisation of free fields in stationary space times 77−67335
quantisation of soliton solution of a generalised discrete non-linear equation 79−17261
quantised frictional forces, nonlinear wave equation solutions 79−85
quantised many-body problem, dissipative system wave eqn. 80−86104
quark model, wave eqns. for mesons and baryons *(Chinese)* 78−86444
quasi-linear initial value problems, variational formulation 77−13579
quasiclassical approx. in scatt. problem, wave function representation by functional integral 78−87
quasilinear partial differential equations, separability 78−65784
quasipotential eqns., Levinson theorem violation, S-matrix 78−54576
quaternionic EM wave equation and dual charge-filled space 77−57209
R-separable solutions of wave eqn. ψ_{tt}-$\Delta_3\psi$=0 78−62293
radial, Bremmer series soln., for eqn. with spherically symmetric velocity function 78−28973
randomly perturbed one dimens. wave eqn., multiple-scales space-time anal. 78−8247
real ray tracing when ray direction is complex 79−9126
reduced wave eqn., parabolic approx., asymptotic solns. 78−78908
reduced wave equation, exterior problems, numerical solns. 78−89351
reduced wave equation, fixed incident field, inverse problem 80−62484
reducible relativistic wave eqns. 79−45003
Reggeon quantum mechanics, Hamiltonian formulation, S-matrix, pomeron Green functions 78−16951
regularised long wave equation, anelastic collision of solitary waves, numerical anal. 78−77724
regularised long wave equation, solitary wave solns. 77−13616
relativistic, algebraic structure, Lie algebras 79−67460
relativistic, coupled to external fields, constraints problems 80−86549
relativistic, curved space-time, generalised quaternion formulation 78−366
relativistic, noncausal effects 77−45939
relativistic 20-component spin-1/2, props. 77−45962
relativistic field eqns., two-soliton solns. 78−74124
relativistic field equations for same spin, equivalence 78−74132
relativistic Hamiltonians, connection between unitary transformations and reduction 77−30262
relativistic Hamiltonians, diagonalisation of Dirac and Sakata eqns. with const. mag. field 77−34081
relativistic infinite-component wave eqns., space-like solns. 77−61183
relativistic linear wave eqn., kinematical interpretation of subsidiary conditions 77−2737
relativistic radial equations for two spin 1/2 particles with static interactions 78−32699
relativistic symmetry group of spin and particle number 77−64971
relativistic three-body wave equation for Dirac particle+two Klein-Gordon particles, preon model 80−73574
relativistic wave eqn., criterion for reducibility 77−57439
relativistic wave equation, Poincare group, extended particle model 78−41414
relativistic wave equations derivation, elementary domains theory, stochastic quantisation procedures 77−41502
relativistic wave equations without Velo-Zwanziger pathology 78−24927
rigid sphere quantisation, appl. to charged sphere in EM field, Pauli eqn. 79−82
rotating plane-fronted waves and their Poincare-invariant differential geometry 80−332
saturation theorems connected with the abstract wave equation 79−14207
scalar and EM wave eqn. solns. in gravit. and EM waves metric 78−8307
scalar field, complex, one-dimens., with fourfold phase anisotropy, solitary-wave solns. 79−58553
scalar Helmholtz eqn. in 3-D, finite element soln. 77−30002
scalar partial differential eqns., variational principles 79−30255
scalar potential inter-relation between non-relativistic and relativistic wave eqns. 78−58110
Schrodinger type partial differential equations, principal fundamental soln. using integral eqn. approach 78−81806
second order hyperbolic equations with small nonlinearities 79−49063
second-quantised Dirac and Klein-Gordon eqns., external fields 77−26472
seismic inverse problem appl. of control theory 79−2402
seismic SH wave equation soln. for scattered field near plane boundary 77−86788
semilinear, superexponential decay of solutions 79−84963
semilinear wave equation, bifurcation of periodic solns. 79−80449
shallow water waves with quasi-periodic boundary conditions, eigensolutions of elliptic problem 80−83804
simple wave description by particle displacement 79−12623
simultaneous Wiener-Hopf equations, solvability in boundary condition case 79−44750
sine Gordon equations, complex solitons and poles 79−30264
sine Gordon theory, derivation based on infinite set of coupled pendula 79−92962
sine-Gordon, two-dimens. eqn., reduction to Painleve transcendents 79−92954
wave equations continued
sine-Gordon chain, evidence for breather excitations 79−63054
sine-Gordon chains, role of breather solns. in statistical mechanics 79−85212
sine-Gordon eqn., geom. prop. of Backlund transform. 79−12620
sine-Gordon eqn., inverse method for solving differential-difference and difference-difference eqns. 80−105513
sine-Gordon eqn., return effect for rotationally symmetric solitary wave soln. 79−5986
sine-Gordon eqn., separability 78−65784
sine-Gordon eqn., soliton creation-annihilation operators as canonical transformation 77−30041
sine-Gordon eqn., solitons and separable elliptic solns. 79−97215
sine-Gordon eqn. and Laplacian invariant, separable solns., complex solitons 80−90680
Sine-Gordon eqn. in 3-D, diffusion theory *(French)* 77−61174
sine-Gordon eqn. separable solutions in terms of Painleve transcendent 80−52037
sine-Gordon eqn. two dimens. solns., Josephson junction phase calcs. 79−82725
Sine-Gordon eqns., differential geometry appls., soluble relativistic field theories *(Russian)* 78−74162
sine-Gordon equation, 3 and 4 dimens., exact solns. 80−86091
sine-Gordon equation, approx. treatment of two soliton solns. 79−88838
sine-Gordon equation, Backlund transform., physical space-time solitons 80−77629
sine-Gordon equation, Backlund transformations and Dirac factorisation 80−73185
sine-Gordon equation, classical solns. of field eqns., moving t'Hooft-Polyakov monopole *(Russian)* 78−16935
sine-Gordon equation, difference analogue 78−20976
sine-Gordon equation, double, multidimensional multisoliton kink solutions 80−73184
sine-Gordon equation, exact mass spectrum, WKB approx. 77−33896
sine-Gordon equation, nonlinear, constrained harmonic motion 80−77625
sine-Gordon equation, nonlinear field equations, quantum inverse scattering transform method, 2-D ice and ferroelectric lattices 80−68348
sine-Gordon equation, one dimens., group of invariance, dimens. anal. method 78−54528
sine-Gordon equation, regular solns. using surfaces of const. negative curvature *(Russian)* 78−20980
sine-Gordon equation, separability, variable transforms 80−57102
sine-Gordon equation, soliton solns. and appl. to solid state physics *(Japanese)* 77−30025
sine-Gordon equation, two soliton solutions, breather solution 80−12945
sine-Gordon equation, two-dimensional, separable solns. 78−89614
sine-Gordon equation in 2+1 dimensions, particular solns. 79−85211
sine-Gordon equations with multisoliton solutions, polynomial conserved densities 77−9887
sine-Gordon field theory, two dimens., second order phase transition, lattice model 78−78095
sine-Gordon field theory Coulomb gas equivalence, classical gas with logarithmic pot. 80−4850
sine-Gordon kinks, nonequilib. props. using mol. dynamics techniques 79−12737
sine-Gordon massless quantum eqn. in 2 space time dimens. 78−32754
sine-Gordon perturbed equation, soliton mass formulae 80−22200
sine-Gordon problem, soliton mass, renormalisation 79−40678
sine-Gordon solitons, dynamics, in presence of perturbations 77−37751
sine-Gordon supersymmetric eqn., inverse scatt. 80−47165
sine-Gordon system, solitons and bion dissoc. 79−63048
sine-Gordon system, strings and vortices with soliton solns. 77−5674
singular hypersurfaces, asymptotic regularisation as alternative to distrib. 80−36923
SL(2,*C*), new nonlinear realisations 79−88828
slowly varying medium, multiple time scale method 78−8248
small amplitude plane waves in quasilinear dissipative medium *(French)* 79−25866
Smoluchowski equation in presence of hydrodynamic interactions, Chapman-Enskog method 80−46979
SO(n) groups, (n>5), representation theorem 78−86407
solar magnetoatmospheric waves, inhomogeneous wave eqn. 77−82189
solitary waves, damping by weak dissipation 79−63053
soliton dynamics in nonintegrable systems, classical solns. 78−28996
soliton equation, geometrization 79−75358
soliton evolution of modified Korteweg-de Vries eqn. under action of perturbations 79−84970
soliton formation, mth order parametric interaction, using Klein-Gordon eqns. 80−12917
soliton history in mathematics of solns. to nonlinear evolution eqns. 79−75365
soliton inelastic interaction, examples and Boussinesq. eqn., computer investigation 78−51
soliton perturbations and nonlinear focusing, anal. method for fluid dynamics 79−75369
soliton resonant production in regularised long wave eqn. 79−97216
soliton studies in mathematical physics 79−75366
solitons, cylindrical, exact solutions to equation 79−75359
solitons, in dispersive media, nonlinear evolution eqns. soln., review 78−60
solitons, nonlinear self dual network, with saturable property Korteweg-de Vries eqns. 79−21560
solitons, nonlinear wave equations solns., classical, quantal, appls. 78−57793
solitons, numerical studies, historical review 79−75367
solitons, phase-locked solutions, comparison of single and double sine-Gordon solns. 79−58552
solitons, review of concepts and methods in theory *(Polish)* 80−68057
solitons amplification in modified Korteweg-de Vries eqn. 80−27145
solitons and SL(2,R) 78−57748
solitons as particles, oscills., singular perturbation theory 78−73882
solitons in condensed matter, propag. and decay due to interactions with medium 79−25871
solutions decaying at prescribed rate with respect to time 77−58230
solutions of eqn. in $S'(R_{n+1})$, props. 77−41474
sound generation and propagation in flows, inhomogeneous convected wave equation 80−69813
space-time, homogeneous, isotropic, with const. curvature, wave eqn. of nonrelativistic spin-s particle, Galileian limit 78−32740
spatially nonhomogneous, nonmonochromatic solns. based on WKB approx. 78−86179

wave equations continued
special relativity, transport equation for discontinuity wave amplitude *(French)* 80−90667
spectral and scatt. theory for class of non-selfadjoint operators 77−60972
spectral transform, nonlinear discrete evolution equations 80−4553
spectral transform and nonlinear evolution equations 80−4551
spectral transform method for nonlinear evolution eqns. from Zakharov Shabat linear problem 78−65785
spectral transforms, nonlinear evolution equations 80−4552
spherically symmetric scalar waves, gravitational self-interaction *(Russian)* 79−9165
spin 1/2 wave equations irreducible under Poincare group, degenerate to Dirac eqn. 78−21332
spin 3/2 wave eqn. 77−71231
spin $^3/_2$ massive/massless particles, field theory, wave eqns. and actions 79−75687
spin-1/2 tachyons, quantum mechanics 77−5693
spin-s tachyons and tachyon wave propag., book contrib. 79−58890
spinless particle interaction with electromag. field, path integrals, Klein-Gordon eqn. 78−58144
spinning particles interacting with external fields, invariance groups of relativistic eqns., SU_3 symm. 78−49962
stability of wave fronts defined by eikonal equations, elementary catastrophes 80−73187
stochastic medium, propagation of mean field 80−73177
stratified fluid with finite depth, internal wave eqn. governing long gravity waves 79−97217
string vibrations, linear and nonlinear, physical discretisation 78−45480
SU(3) wave eqns. for quarks 80−57571
superposition of solitons from same nonlinear differential eqns. 80−67
supersonic field, wave equation generalised axial radiation soln., flow patterns, wakes *(German)* 78−14043
supersymmetric Liouville and sine-Gordon eqns., method of inverse scatt. and Backlund transforms. 79−2951
symmetry approach to exactly solvable evolution equations 80−82648
symplectic operators and hereditary symmetries, applic. to soliton eqns. 80−82650
tachyon wave propag. and spin-s tachyons, book contrib. 79−58891
tachyons, spinless, propagator determ. 77−74263
Teitler's higher-spin field eqns. 77−22637
Thomas-Fermi-Dirac eqn. nonlinear problem 77−22483
three-frequency soliton solns. in second approximation *(Russian)* 78−57789
time dependent Hartree Fock solns. for heavy ion scatt., wave packets to stationary waves 78−62558
time periodic solutions of a semilinear wave equation 79−17246
Toda equation, difference analogue 78−20975
Toda lattice, wave behaviour in nonlinear LC equivalent circuit 80−105577
Toda lattice equation, nonlinear, constrained harmonic motion 80−77625
transfinite ordinals as axiom no. symbols for unification of quantum and EM wave functions 77−5688
translationally invariant nonrelativistic Hamiltonian, for atom 77−5700
transversely inhomogeneous slab, modal wave propag. with gain or loss variations 80−48122
travelling waves, memory effects in random walk process 80−27232
trilocal structures, secular eqn. 80−90776
two-body equal-time wave eqn., quark-antiquark system 78−32992
two-body relativistic wave eqns. 79−63358
two-fermion relativistic eqns with form factors, anomaloys mag. moment interactions 78−372
underwater sound, comparison of two normal-mode solns. based on different branch cuts 77−84044
Unimoment method, simplified matrix element representation 77−74207
vector product formulation of special relativity and electromagnetism 80−105496
vector wave equation, depolarisation term anal. 80−8814
vertically polarized waves in inhomogeneous media, full wave solns. 77−6980
viscoelastic rod, fundamental solutions of wave equations with delay time 79−27576
wave front set of soln. of simple initial boundary value problem with glancing rays 77−41458
Whitham eqn. for two-layer finite depth fluid, multi-soliton solns. 78−55621
Wick equation soln. *(Chinese)* 77−71435
WKBJ approx. for classical particles with spin in external field 78−32692
Yang-Mills theory, 4-d Minkowski space general theorem for absence of finite energy nonsingular solns. 78−21318
d breakup into Δ resonances, probability, isobar model, static NN-ΔΔ mixing pot. 78−29438
2 NN̄ system, bound state energies, Faddeev method *(Russian)* 79−49407
ψ_{tt}-$\Delta_3\psi$=0, R-separable solns. 78−4489
$(\bar{\psi}\psi)^2$ two dimensional model, equivalence to sine Gordon systems, conservation laws 79−2917
Ca_2, vibr.-rot. states, high accuracy wave functions and energies 80−74159
H atom, Dirac and Klein-Gordon relativistic eqns., energy level splitting 80−77938
H, low density atomic gas calculation, for dilute hard-sphere Bose-gas model 80−87194
He, superfluid B phase, spin wave breathers, double sine-Gordon equations 80−15329
^{3}He, superfluid, soliton solns. for spin orbital freedom wave eqns. *(Japanese)* 78−38904

wave functions
see also orbital calculation methods
alkali fluorides mol. Compton profiles, parallel-perpendicular anisotropies 79−94038
alkali halide, polarisation energy for core states 80−10903
alkali halides, F_A-centre optical absorpt., estimate using symmetry-adapted wave functions 80−11448
alpha-particle, internal wave functions, higher configs. effect on probabilities of α-transitions in spherical nuclei 78−17155
analytic radial orbitals, optimisation on variational parameters 80−42941
angular momentum coefficients in relativistic atomic struct., Fortran program MCP75 77−10605
wave functions continued
anharmonic oscill., interpolative perturbation scheme 78−32720
antisymmetrization wave function by method of group functions 77−3278
any-spin, 1st-order, single replacements from complete CI root function 79−81144
asymptotic form for system of N charge particles in external Coulomb field 77−71871
atom, of first row, cluster expansion for spin density, pseudo-orbial calcs. 77−54502
atom, one-electron density, spherically averaged, upper bounds calc. 78−25415
atom, outer shell ionisation, ang. distribs. and polaris. of charact. X-rays and Auger electrons 79−10205
atom, relativistic calcs., perturbation theory approach 79−31422
atom, screened Coulomb pots., anal. perturb. theory for relativistic case 78−21861
atom+atom, resonance energies, complex, diverging wave functions, least squares bivariational method 78−17741
atom+diatom, energy correction of infinite order sudden approx., improved phase shift approach 80−95710
atom+polyatom systems, rotation-vibration symmetry correlation 80−61074
atom and mol. wavefunction nodal topology, quantised vortices and paramagnetism 77−46476
atom Breit interaction between electrons, calc. angular coeffs., computer program 80−18779
atom electron scattering length calc. with imprecise target wave function, variation principle 79−72375
atom or ion, wave function asymptotic coeff. for electron 79−26871
atom scattering by corrugated potential wall, appl. to diffr. by cryst. surface 80−42104
atomic, exponential decay of sub-continuum wave functions 77−46477
atomic, Z=20 to 90 $K\alpha_1/K\beta_1$ X-ray intensity ratio rel. to at. number 77−23457
atomic collisions, approximate wavefunctions, radial couplings calcs. 78−42163
atomic collisions, mol. approach, radial couplings between approx. wavefunctions 77−38713
atomic collisions, quasiclassical theory, transition between spatially degenerate levels 80−43150
atomic collisions, two-state approximation in the adiabatic and sudden-perturbation limits 79−22780
atomic eigenfunctions, nodal structure 80−57122
atomic electron scatt. length, target ground-state wave function imprecisely known, variational principle 77−58164
atomic electronic 4s, 3d energy levels, textbook diagram, teaching 78−73801
atomic energy spectra calc. using trajectory integrals 78−21838
atomic exact wave functions, many electron operators, upper bounds 78−50459
atomic model potentials soluble in closed form 80−23287
atomic orbitals, hydrogen-like, shape, teaching appl. 78−93496
atomic resonant states, wavefunctions of complex coord. method 80−106282
atomic struct., numerical HF radial function during SCF iteration, convergence 78−58574
atomic wave functions, weighting factors determ. from g-factors 79−98237
atomic wavefunctions collapse 78−70733
atomically centred, point charge models, magnetic susceptibilities, Frost-model Lewis basis sets calcs. 79−54761
atoms, approximate and exact state wavefunctions, ionisation potentials, energy difference calcs. 79−97967
atoms, light absorption, subtractive stimulated emission theory 79−59396
atoms, singly excited states, oscillator strengths, ab initio calcs. 80−920
atoms and ions, central analytic potential with three parameters 77−71737
B-S wave function for generalised four-dimens. harmonic oscill. *(Chinese)* 78−64
baryon wave functions, SU_n representation transformations and phase *(Chinese)* 79−93313
Be, Rayleigh-Schroedinger perturbation calculations 78−9064
binding energy of nuclear matter, corelated basis functions method appl. 78−45998
Born-Green-Yvon equations, for strongly interacting Fermi systems 79−49161
Born-Oppenheimer, scaled and unscaled crude-adiabatic 77−88371
Born-Oppenheimer electronic wave function, density matrices, electronic and nucl. motions separation 79−59332
Born-Oppenheimer nuclear motion wave function determ., incl. conical intersections and identical nuclei 79−54932
Bose system, Jastrow wavefunction, hypernetted chain method 80−17866
Boson system, hard spheres, condensed phase, Jastrow wave function 78−84018
bound state problems, scattering theory calc. 79−92979
Brueckner condition for MO selection in correlated orbitals 77−23436
catastrophe and fractal regimes in random waves 80−8811
catastrophe and stochasticity in semiclassical quantum mechanics 80−8861
catastrophe theory, anal. of wavefront dislocations 80−8812
charge exchange, quantum mechanical and impact parameter capture amplitude 80−87226
charge transfer, variationally consistent approximation scheme 79−22825
charged particle near mag. monopole *(Chinese)* 77−67600
chemical bond transferability, group or loge functions 78−41939
CI methods for improving unrestricted Hartree-Fock spin densities 80−32617
CI wavefunction, terms selection for pot. energy surface 77−88401
closed-shell atoms, Jastrow wave functions, var. calcs. 80−83249
cluster expansion, electron correlations, SAC and SAC CI calcs. 80−18802
cluster expansion electron correlations, SAC and SAC CI theories 80−18801
cluster expsn. of wavefunction, closed-shell orbital theory 79−10004
coherent states and Pippard networks of Dingle functions 77−20218
coherent states of relativistic particle in external EM field, Klein-Gordon, Dirac eqns. solns. 77−2721
commutation symmetry for system of identical particles *(Russian)* 80−12944

wave functions continued
Compton scattering, γ-rays off bound electrons, nonrelativistic form factors, Fortran program 77−10252
cond. electron wave function, lattice symm. depend. 77−85844
confining potentials, order of levels theorem, two body nonrelativistic interacting system 77−49634
confining potentials, peculiar prop. of wavefunctions 80−46863
construction method for Bohr's model *(Russian)* 77−13638
continuum function expansion on resonance wave functions and amplitudes, nuclear struct. calcs. 79−13215
copper dichloride dipyridine, ground state wave function and superexchange interaction 79−42752
correlated, graphical unitary group approach, abelian point group symmetry utilisation 79−68193
correlated electronic wavefunctions, Schrodinger eqn. variational form, generalised k-particle Brillouin conditions 79−81146
correlated wave functions anal. gradients from two particle density matrix and unitary group 80−78548
correlation coefficient and electron correlation 80−78552
Coulomb problem, zero-energy 78−62097
Coulomb wave function, in u representation 79−58584
Coulomb wave functions, completeness in quantum mechanics 78−89278
coulombic potentials, two virial theorems 77−3429
cranked deformed harmonic oscillator, wave functions, matrix elements, high spin nucleus appl. 78−25131
cranked Hartree-Fock-Bogoliubov wave functions, ang. momentum distribs. at band crossings 78−93956
cranking model wave function, investigation w.r.t. angular momentum 79−483
curved space-time quantum stochastic processes, covariant Kolmogorov-Klein-Fock eqn. 80−18083
Davydov splitting theory, excitonic parameters, split absorption bands, organic molecular aggregates *(Spanish)* 79−59437
dechannelling (aligned-to-random beam transition), WKB approx. 80−34109
delocalisation, static and dynamical aspects 77−30761
density functionals in unrestricted Hartree-Fock theory 79−89583
deuteron, EM form factors relation to wave functions 78−37210
deuteron wave functions, relativistic 80−22595
diatomic ionic-molecular systems, two centre mol. wave function 77−65524
diatomic mol., X-ray scatt. intensities, vibr. averaging 78−74722
diatomic molecule, electron scatt., low energy, multichannel variational calcs., static exchange approx. 80−83483
diatomic molecule, vibr.-rot. states, high accuracy wave functions and energies 80−74159
diatomic molecule, wave functions and intensity factors, using effective Hamiltonian *(French)* 78−5114
diatomic one-electron mols., wavefunction calc., collision matrix elements, computer program 78−50457
diatomic radicals, wavefunctions, populations and orbital energies, Roothaan calcs. 78−86773
diatomic systems, nonadiabatic coupling matrix elements by Hellmann-Feynman theory and HF 80−83263
diatomics, spin coupled theory of mol. wavefunctions, struct. and props. 77−50337
dipole absorption oscillator strengths, simple approx. method for computing radial wave functions 78−62111
Dirac particles, massless bound state, Coulomb potential 80−37189
Dirac relativistic wavefunctions, momentum representation 79−13650
Dirac-Slater wave functions, electronic structure of light actinides 77−28108
discontinuous approx. mol electronic wave functions, ab initio LCAO and VB ZDO appls. 77−50340
disordered system, one-dimens., density of states and wavefunction shape, periodic boundary condition influence 80−80223
double excitation wavefunctions, multiconfigurational SCF method 77−10604
eccentric spheres, interior and exterior boundary-value wave problems 77−75384
Eckart wave function, generalised 77−57231
education, multiple scattering theory, target nucleus wave function antisymmetry 77−49523
education, nonspreading wave packets, physical interpretation of Berry Balazs wave function 80−57040
education, renormalisation rule for WKB-type wave functions 78−69944
effective hamiltonians, pseudopotentials and applics. 77−30754
Einstein paradox 78−32730
elastic-scattering in several coordinate dimensions, global nature of semiclassical wavefunctions 79−63092
electron+ion scattering, Schwinger's variational principle, Rydberg states 80−78713
electron correlation problem, unitary group approach, matrix element evaluation 79−31411
electron density and density matrix approximations using potential energy error bounds 78−94180
electron distribution, Hylleraas-type wavefunction transform. to momentum space 79−54757
electron elastic scatt., by spatially bounded mag. field 77−13834
electron exchange matrices calcs., spin function recoupling method 77−47782
electron in magnetic field, rotator approximation *(Russian)* 77−30032
electron liquids, inhomogeneous, variational approach, appl. to metallic H_2 79−38013
electron momentum distribution, study by means of Compton effect *(Polish)* 78−48252
electron wave function pair Fourier transforms, at., mol. and solids, by (γ,2e) and (e,3e) *(Russian)* 77−71878
electronic, MRD-CI method 78−46278
electronic piecewise polynomial wavefunctions, for HF calcs. 78−5115
electronic system, props. without antisymmetrisation 80−32586
elementary particles, physical fields, symmetry, causality props. 79−6270
energy functional, direct minimisation in LCAO-MO density matrix formalism 78−5118
equations of motion-Green's function methods, wave function approach 77−65416
excitation energy, eqn. of motion method calcs., approxs. and error anal. 79−36501
excited states, oscill. strengths calcs., influence of wave function determ. method 80−99478
excited states, perturbation and SCF calcs. 80−102455
excited states, wavefunction calcs., symmetry-adapted cluster expansion method 79−9994
expansion of MO wave functions into VB work functions 78−74580
exponential potential and mass dependence 80−73199
factorized wave function, appl. to He 79−3355
Fadeev integral eqns. for 3 particles in boundary condition model, wave function determ. 78−54248
Fermi system, Jastrow wavefunction, hypernetted chain method 80−17866
fermions, quantum mechanics of ground state 80−82713
ferrohaemoglobin excited state wave functions *(Japanese)* 79−8475
few electron atoms, compact and accurate integral-transform wave functions 77−75066
field wavefunction, analytic properties in optics 80−1138
form factors for atoms and ions with $Z \leq 54$ 77−10582
formaldehyde, $^3A_1$ and $^1A_1$ states, electrostatic mol. pot., basis set and wave function calcs. 79−10020
four nucleon wave functions, Taylor series method 78−66223
four-body problem, K-matrix formalism, bound state scatt. theory 77−17858
free electron in external field, wavefunctions, nonrelativistic treatment 80−99611
free relativistic electron in external field 80−99612
Frost-model, computation of long-range molecular interaction coeffs. 77−23533
generalised hydrogen-type, momentum representation 77−6674
generalised perturbation theory, quality of first order wave function 77−67963
geometric quantisation and wave functions 77−17869
geometrodynamics, inclusion of observer in wave function 78−54234
global wavefunctions, appl. to scatt. theory 78−41179
hadrons, one-gluon corrections, hadron EM characteristics, bag model *(Russian)* 79−93380
hadrons and their constituents, wave-particle quality 80−9136
half-integral spin particle wave function, 720° rot. effect, teaching models 79−62958
harmonic oscill. covariant wavefunctions, chiral config. mixing 77−49913
harmonic oscillator wavefunctions, asymptotic behaviour 80−67979
Hartree problem, iterative diagonalisation soln. 79−6829
Heisenberg ferromagnet, dil., mag. excitations, localisation, wavefunctions 78−60275
Hellmann-Feynman theorem for limited CI wave function, 1st-order props. 79−59329
HF subsystems, long range induction and dispersion interactions 80−53092
HF wavefunctions, restricted and unrestricted, convergence problem 77−418
high-Z elements subshells, photoelectron angular distribution 80−99487
higher order modified pot. for effective phase integral approx. 79−44779
highly charged ion, $1s^22s^22p^53d$ configuration, energy spectra in relativistic approx. 80−14082
highly ionised atoms, relativistic effects, book contrib. 78−74588
hybrid orbitals and Runge-Lenz vector, matrix elements 77−38606
hydrazones, protonation energy and basic strength 80−37719
hydrocarbon, conjugated, nonlinear susceptibility, extended basis set calcs. 79−27107
hypervirial scaling iterative method 80−73196
hypervirial theorem, scaling problem 77−23408
hypervirial theorems and symmetry, optimal variational wave function 80−17841
inert gas atom, photoionis. cross sections of excited levels, quantum defect method calcs. 80−37795
inhomogeneous Airy function, Gi(3) and Hi(3) 80−43259
inhomogeneous electron gas at jellium surface, exchange energy 80−10901
integral equations of scattering theory, close coupling method *(Russian)* 77−74268
integrated spatial electron populations, evaluations for simple mols. 80−78524
ion+atom collisions, coupled state equation 79−50109
ion+polar molecule collision, low-energy, rot. state approach 80−74224
ions, positive and negative, Hartree-Fock-Roothan wavefunctions with 3d and 4d electrons 78−17569
isoelectronic sequence, E1 and E2 oscillator strengths, MCHF calcs. 80−106292
iterative scheme for simultaneous calc. of m 1st eigenstates of real symmetry matrix 79−85888
Klein-Gordon equation applic. to quasi-classical wave function, conservation laws for ensemble of noninteracting particles 77−64962
labial muscle EMG analysis and feature extraction by Hanning Cosine Modulated wave function 77−81605
lepton, bound in Coulomb field of nucleus 79−94115
lightlike wave function and wave eqn. on null-plane using Bethe Salpeter eqn. 78−41412
linear harmonic oscillator on lattice, wave functions, energy eigenvalues, Pade approximant method 78−57817
lipid hydrocarbon chain, biomembrane, rot. motion and fluidity 80−76714
Lippmann-Schwinger approach to elastic scatt. by semiinfinite crystals 78−47687
local multigaussian FSGO one-determinant wave functions, energy gradient expression 80−23282
local scaled Schrodinger relations and the virial theorem, kinetic energy operator 80−78527
localisation approach, applic. to additive props. 77−30752
localised electrons, single particle wave function random field calcs. *(Russian)* 80−34397
logarithmic perturbation expansions, appl. to H in multipole field 80−37720
loge theory and wave function calcs. 77−30753
Lowdin's α-function, symmetry property 77−23413
Lowdin's projection operators for ang. momentum 78−62689
many-body system, effect of increasing N *(French)* 78−37539
many-body theory, short-range asymptotic wave function method, appls. 78−24727
many-body wave function (N>3), unique soln. 78−86190
many-electron atom-unbound electron system, normalisation of wave function 77−68123
many-electron atoms, generalised spherical functions 77−46483

wave functions continued
many-electron atoms, orthogonal multidimensional ang. functions 79−13628
many-electron atoms, use of generalized spherical functions 77−38601
many-electron atoms with different coupling types, transform. of wave functions 77−67956
many-electron system, time reversal, spin-adapted wave functions 77−26961
many-electron systems, time depend., complex scaling and resons. calcs. 79−22612
many-particle wave function, hyperspherical expansion, singularities at partial wave origin 77−74264
matrix elements of $\delta(r_1)$, approx. wavefunction 80−47860
MCSCF and CI wave functions, two-particle density matrix and graphical unitary group approach 80−63558
MCSCF method improvement 80−52857
meson structure wave functions, instantaneous interaction approx. straton-+antistraton pair *(Chinese)* 77−10216
meson structure wave functions in relativistic straton model, Bethe-Salpeter eqn. *(Chinese)* 78−50011
meson wave functions, straton model, Bethe-Salpeter eqn., SU_6 symm *(Chinese)* 77−34125
meson wave functions, SU_n representation transformations and phase *(Chinese)* 79−93313
meson wave functions in 1+1 dimens. QCD 78−54559
mesonic wave functions at zero point, decay processes $\pi\rightarrow\mu\mu$, $K\rightarrow\mu\mu$, $1^-\rightarrow e^+e^-$ *(Chinese)* 77−10242
methane, harmonic and anharmonic matrix elements comparison, appl. to vibrational energy transfer 80−63760
micrononcausal Euclidean wave functions for baryons by assuming 'Yukawa type' couplings and G′-parity 79−45030
mode finding, experimentally, when several contribute to a reson. 78−83310
molecular, charge and current densities 77−3261
molecular, transcorrelated method 77−61678
molecular ab initio CI pot. curves, mol. wavefunctions and vibr. freqs. comparison of methods 80−27956
molecular deuteron quadrupole coupling freqs. calc. 78−29801
molecular electron scattering, continuum wave functions, discrete basis set method 79−22829
molecular Hartree-Fock calcs., symmetry adapted Fock matrices construction algorithm 77−23424
molecular image, effects of dynamical scattering, in high resolution electron microscopy 78−14255
molecular ionisation energies, self-consistent-charge Hartree-Fock-Slater calcs. 77−6687
molecular quantum mechanically calculated observables, reliability determ. 80−63505
molecular scattering wavefunctions, algebraic approx. 78−78780
molecular spectra, generator coordinate method, nonadiabatic mol. dynamics 79−31495
molecular static polarisability, ab initio SCF wave functions 80−74106
molecular vibrational wave functions, semiclassical Gaussian basis set method 80−9583
molecule, generalised overlap amplitudes, (e,2e) spectroscopic determ. 77−61862
molecule, multiconfiguration wave functions, optimisation 77−23406
molecule, polar, electron scatt. symmetry 80−32834
molecule, polar, slow electron capture and rot. excitation 79−81287
molecule, single spin-config. singlet states, wavefunctions, energies 77−83505
molecule electron density distrib. maps, graphical construction from MO LCAO calculated wave functions 77−83480
molecules, approximate and exact state wavefunctions, ionisation potentials, energy difference calcs. 79−97967
molecules, interacting, rigid, HF, self-consistent nonorthogonal group function approx. 79−31430
molecules, light absorption, subtractive stimulated emission theory 79−59396
molecules, method of moments, criteria for good weight functions, appl. to correlated wave functions 77−23415
molecules, multiconfigurational wave functions, optimization scheme 77−57889
molecules, transition probability evaluation in double asymmetric pot. well 80−69120
molecules, two-particle density determ., energy and density matrix *(French)* 77−88368
molecules resonant states, wavefunctions of complex coord. method 80−106282
momentum eigenfunctions in complex momentum plane, Hartree Fock functions 80−63517
momentum wave function determ. in atomic, molecular and nuclear systems 77−88556
momentum-dependent nuclear potential, group-theoretical derivation of matrix elements 77−26588
monopole pot., wave function for electron motion *(Chinese)* 78−77768
moving electron in field of two Coulombic ions fixed in space, rel. to H_2^+ line spectrum 80−42083
multicentre multielectron system, wave function construction 78−893
multiconfiguration wave functions, optimisation 78−33411
multidimensional systems, semiclassical calc. of bound states 80−963
multipole expansion, choice of orders and density partitioning techniques 77−61677
muonic atoms, Dirac-Fock method, light to heavy ions 78−74805
N-body scatt., wave function components within linked-cluster formalism 79−45040
n-electron atomic wavefunction, Schrodinger inequalities, many-electron densities 78−94191
n-electron molecular wavefunction, Schrodinger inequalities, many-electron densities 78−94191
N-electron zero-momentum energy expressions, approx. wave function accuracy assessment criterion 79−3348
N-representability, Fock coordinate wave function and spin separation 77−64967
neutron ^{13}C-^{12}C+n spectroscopic factor from $^{12}C(^{13}C,^{13}C)^{12}C$, 12 MeV 77−65194
neutron spinor wave function, 4π-periodicity factor using perfect cryst. interferometer 78−45515
neutrons, ultracold, storage in plane, quantum effects *(Russian)* 79−9658
nodeless wave function quantum theory 80−57119
wave functions continued
non-closed shell many-electron-theory at. charge wavefunctions, Be through Ne and Si 77−57849
non-orthogonal wavefunctions, complex systems, and relative X-ray intensities 77−83477
nonlinear triatomic molecule, wave functions, Born-Oppenheimer approx. adiabatic correction 77−83485
nuclear, approximate short-range correls., appl. to ^{19}F parity mixing 77−285
nuclear collisions, TDHF calcs. using separable three dimens. wavefunctions, $^4He+\alpha$ appl. 78−50111
nuclear matter, variational techniques, review 80−22748
nuclear momentum-space wavefunctions via nucleon knockout reactions, off shell effects 77−88122
nuclear octupole vibration, collective, wave functions, spherical harmonics 80−68532
nuclear proton-neutron model, translationally invariant wave function, U(3(n-1)) scheme appls. 77−41906
nuclear shell and cluster model wave functions 78−29412
nuclear wave function struct. at relativistic values of nucleon momenta *(Russian)* 78−89805
nucleon, three relativistic quarks bound state on light cone *(Russian)* 77−6085
numerical study of phase-integral connection formula 77−71230
off-energy-shell generalisation 80−18257
one-body alpha-decay widths and resonance states 79−13259
one-dimensional particle-in-the-box problem, perturbation theory illustration using champagne bottle situation 80−36816
one-electron atomic systems, ionisation energies determ. from optimised one-electron wave functions 77−38599
one-electron atomic systems, optimisation effectiveness 77−34538
one-electron atomic systems, optimisation procedure, isoelectronic series of Li, Be, B, and C 77−38598
one-electron atomic systems optimisation procedure 77−38597
open shell, self-consistent electron pair theory 78−25408
optical absorption spectrum of D^- centre in strong magnetic field 80−20670
orbital-optimised, instability, rel. to positive orbital energies 80−58109
orthogonality, radial orbitals, energy invariance 78−84
oscillating Hermite-Gaussian wave functions for harmonic oscillator Schrodinger eqn. 78−70004
oscillator, circ., Cartesian and polar wave functions connection, rel. to dynamical O(3) symmetry *(Russian)* 79−49073
oscillatory parameters of self-consistent wave functions *(Russian)* 78−21506
p-block ats., energy levels, position orbital calcs., electron repulsion integrals, teaching appl. 78−93494
pair density analysis, applics. 77−30751
path integral formalism, barrier penetration effects on wave functions and energy spectrum 78−62117
perturbation theory, variational methods, evaluation of second-order matrix elements 80−12936
perturbational molecular orbital analysis, hybrid lone pairs problem 79−89608
perturbed ladder operator method, wavefunctions, matrix elements, closed form expressions 80−73203
phase, relationship with Green's function 80−105543
phenanthrene-pyromellitic dianhydride, single cryst., charge-transfer triplet excitons, spin polaris. 79−11069
phonons, coupled rotational band approach, zero-rank operators 80−47341
photoemission, many-electron theory, in electron spectroscopy book 78−17714
photon, Dirac-like eqn., transform. props. 79−58914
photon, invariant struct. 77−71475
photon emission by N-independent excited atoms 77−57895
planar defect 'on edge', electron wave function in vicinity 80−88002
point charge model approach to intermol. interaction coeffs. 80−18897
point charge model approach to mol. elec. polarisability 80−18797
polar molecule, excited state MCSCF wave functions, BeO appl. 80−47916
Politzer-Parr partitioning, electron correl., isoelectronic, isonuclear, spin and excitation aspects 80−78522
polyacenes, linear, open-shell ground state wave functions 79−762
Polyakov-'t Hooft monopole and dyon, quantum theory *(Russian)* 78−392
polyatomic molecule, vibr. struct. of electronic spectra, FORTRAN programs 80−32699
polycyclic aromatic ring systems, localised MOs and wave functions 79−31398
position space LCAO wave function, momentum space variation approx., many centre integrals 80−27926
positive ions, electron impact ionisation, Coulomb-Born approx. 80−74249
positronium decay, theory and relativistic wave function corrections 77−10791
predissociation, and preassociation, two-state model, uniform semiclassical wave function approach 78−90241
primitive wave function in theory of intermolecular interactions 80−95703
projection of wave functions on states with definite ang. momentum 78−12590
prolate spheroidal radial function of third kind, asymptotic formula 80−42077
proteins, role in electron transport at large distances, donor and acceptor mol. wave-function 79−34480
pseudopotentials from self-consistent atomic calcs., appl. to band struct. determ. 80−59846
pseudostates wave functions determ. in modified close-coupling calcs. 80−99572
quantal particle, inverted Morse pot. barrier, transmission, reflection coeffs., phase-integral approx. 77−53801
quantisation, geometric, representation spaces 78−36869
quantum bundles, group actions, relationship to group representations 80−17837
quantum dynamics, sensitivity anal., Green's function method 79−67178
quantum dynamics semiclassical approximation 80−12927
quantum field theory, multilocal, Fock-space technique, particle creation effects 80−77945
quantum mechanical particle in random potential, inverse participation ratio in $2+\varepsilon$ dimens. 80−36908

wave functions continued
quantum mechanical system of identical particles 78−49756
quantum mechanics, development and Heisenberg's role *(Polish)* 78−89291
quantum mechanics, molecular, book 77−79538
quantum system, jarring and corresponding stimulated transitions 80−17839
quantum transition concept in undergrad. courses, explanation of photon creation and absorpt. 80−36807
quark model of nucleons, ground state wave functions, O(3)×SU(6) symmetry 78−62352
quark model relativistic generalisation minimal boosting of SU(6) scheme, meson, baryon props. 77−41814
quartz resonators, parameter calc. with energy trapping *(Russian)* 78−30141
quasi-discrete states in complex pots., Schrodinger eqn. with Woods-Saxon pot. *(Russian)* 78−86194
quasibound state wavefunctions for particles inside Coulomb barrier, computation 77−2914
quasipotential eqns., for QED eqns. by Fock-Podolsky method 77−65127
radial Coulomb eqn., soln. by double Chebyshev expansion technique 77−37768
radial integrals calc. in Coulomb approx., use of semiclassical wavefunctions 80−43025
radial wave functions, approx. relativistic corrections 77−421
rare earth atoms, Gaussian basis sets calcs. 80−63541
rare earth elements, extended orbital calculation method 77−6667
rare earth orthovanadates, covalency, chemical bonding and opt. spectra 77−80442
Rayleigh-Schrodinger, appl. of Pade approximants 78−65806
real-time approach to instanton phenomena, multidimensional pots. with degenerate absolute minima 78−78067
relativistic amplitudes as wave functions, invariant diagram technique *(Russian)* 79−2957
relativistic atomic wave functions, Hartree-Fock calcs. 79−10009
relativistic average of config. wavefunctions, applicability to at. and ionic intermediate coupling props. 78−17574
relativistic effects in central field approximation, RELAC method and use 80−9520
relativistic scattered wave theory, normalisation and symmetrisation 78−62694
relativistic theory, quantum defect phase shift relationship 79−771
relativistic three-particle bound states, wave function calcs. 78−8558
relativistic wavefunctions, approx. near turning point, WKB calcs. for $Z>137$ 80−86598
rotated coordinate method use, rel. to stabilisation method 80−37845
rotation in phase space, Fourier transform method 77−33744
s-state, probability density calc. 78−57812
Saito potential, off-energy-shell unitarity 80−18207
scattering, algebraic theory, existence of wave operators *(French)* 78−24692
scattering, multichannel, optimised Kohn method 79−49108
scattering, single-channel, optimised Kohn method 79−49107
Schrodinger eqn. with double-minimum potential, numerical integration 78−58573
Schrodinger equation, exactly soluble with bistable pot. 80−67950
Schrodinger equation, new type, evolution of wave function with respect to position 80−27178
Schrodinger equation, normalisation consts., Poschl-Teller and B_0 tan h z-U_0 cos $h^{-2} z$ pots. 78−65818
Schrodinger equation for three charged nonrelativistic particle system, wave functions and generalised wave operators 79−75398
Schrodinger wave functions at pot. discontinuities, continuity conditions, for teaching 80−27077
Schwarzschild space-time, radial wave functions, global prop., irregular singular point 77−2567
second-row atoms, SCF loge localised wave functions 78−41932
seismic wave, reflection at free surface, appl. of Huygens' principle 78−7594
self consistent electron pair theory, perfect pairing valence bond generalisation 80−63532
semiclassical, regular and irregular 78−20998
semiconductor, screened impurity in mag. field ground state energy of bound electron 78−72107
semiconductor, wave functions and optical cross sections associated with deep centres 78−34801
Serber-type spin eigenfunctions, generation by projection operator method 77−30028
Serber-type spin-adapted wave functions and time reversal 78−5117
shell model matrix elements, two-body, by Taylor-series method 80−32212
Siegert wavefunctions, partial widths calcs. 80−5507
single-term atomic state props., variationally optimised local central pot. calcs., $2<Z<55$ 79−41123
SO(2N+1) operator representation and wave functions of fermion many-body systems 78−41227
solvated electrons, wavefunctions, approx. single parameter var. calcs. 78−66467
spin depend. wave functions and band parameters 77−72818
spin wavefunction matrix element expansion 78−41185
spin-extended Hartree-Fock method, approx. variant 77−79531
square integrable function determ. problem 78−93548
static screened Coulomb potential, high-accuracy eigenvalues 79−40403
stationary state, standing de Broglie wave, Aharonov-Bohm effect 80−22228
straton model, near-flat-bottom interaction pot., wave function of pseudoscalar meson *(Chinese)* 78−82167
structure, complex coord. method 78−94190
SU(2) gauge field, ground state wave functionals 78−74142
superfluid model, isotopic invariance and pairing energies 80−22687
superheavy atoms from heavy ion collisions, electronic binding energy, wave functions 78−46252
superposition state in regular and irregular spectrum, time evolution, intramolecular dynamics 80−83335
symmetry breaking, wave function choice, effect on predictions, DKP formalism view 80−9120
symmetry restricted multiconfiguration annihilation of single excitations calcs., applic. to methylnitrene 78−62695
symmetry-adapted-cluster expansion, variational determ., open-shell orbital theory applic. 78−54213
T matrix, $^1S_0$ two-nucleon, interior wave function 77−14038

wave functions continued
three particle nuclear molecular states, Schrodinger eqn., wave functions and energy spectrum *(Russian)* 78−86497
three particle reactions, S-matrix theory kinematic props. 78−54578
three pion states, permutation group S_3 irreducible representation 79−17635
three-body eigen wave function of a continuous spectrum, asymptotic form 79−5994
three-body problem in one dimension 80−82655
three-body system, ground state determ. 78−62710
three-nucleon system, fractional-parentage construction of wave function 77−14041
total angular momentum body frame radial wavefunction, coupled states and infinite order approxs. 78−25641
transition metal ion, superposition of quasidegenerate configurations, principal quantum number N=3 80−14079
translationally invariant wave function of many-body system bound by harmonic forces 77−61018
trial wave functions, by off-diagonal hypervirial theorem 79−22578
triatomic molecules, vibr. energies, wavefunctions, ab initio calc. 78−17652
trinucleon, analysis of shape 77−18434
trinucleon properties, one-boson-exchange potentials 77−18433
triton, virtual dissociation into deuteron and neutron, mean square radius *(Russian)* 79−3092
two centre one-electron system, continuum wave functions 79−93915
two electron atoms, three-body problem 80−83286
two or three electrons, interacting with localised mag. moment, wave function determ. *(French)* 79−12636
two-body correls., variational approach 80−91455
two-centre continuum Coulomb wave functions in entire complex plane 77−23403
two-centre integrals evaluation using α-functions 77−23412
two-dimensional multichannel scattering, wavefunction corrections averaging method 78−9060
two-electron atom, momentum distrib. and Compton profiles, Fourier integral calcs. 77−3276
two-electron atom, trial wave function for ground state 80−78510
two-electron wave functions with monopole interaction, asymptotic forms 80−78528
two-nucleon reduced widths in symmetric two-centre shell model 80−32213
two-particle collective excitations, energy and wave function calcs. 80−20098
unified theory of atoms and atomic aggregates, self consistent theory 80−102418
unimolecular dissociation dynamics, collinear triat. system, R-matrix method 79−70315
unrestricted Hartree Fock wave function, spatial symmetry recovery by spin projection 80−58150
valence nucleons, muonic atom analysis 80−27530
variation-iteration principle for wave functions, bound and scatt. states 78−54227
variational, stability, continuity, symmetry 77−23409
variational localised site cluster expansion, wave function higher ansatze, linear Heisenberg model 79−7959
variational localised site cluster expansion, wave function ansatze, many body theory 79−6827
Waller-Hartree pure spin-state wave functions, many-electron theory 77−38600
Wigner's (2n+1) rule in MBPT 80−42095
with definite ang. mom., matrix elements and cross-section calcs. 77−30839
WKB wave function, systems with many degrees of freedom, solitons and pseudoparticles 78−29255
x^4 potential, associated ground state wavefunction, sum rules 79−45036
Young's double beam interference experiment with spinor and vector waves 78−89363
zero-radius potential, regularised model for multicomponent systems 79−27052
(d,p), effects of d deformation and D-state influence, wave functions 79−13201
d, 6 quark system, wave function, elastic form factor, NN forces, spectroscopy *(Russian)* 78−50015
d, form factors relation to wave functions 78−70462
d, short-range behaviour 77−50065
d, six-quark model, form factors and struct. functions 78−45871
d wave function with $\Delta\Delta$ reson., effect on EM form factors 77−18486
e+atom wavefunction by solving coupled second order integro-differential equations, computer programs 80−18924
e+ion wavefunction by solving coupled second order integro-differential equations, computer programs 80−18924
$e^+e^-e^-$, two-electron at., three-body problem, binding energy 79−3372
$\eta(549)$, $\eta'(958)$ with inert component, gluon bound state 78−74226
(γ, e) reaction, determ. of atomic wave function, electron energy levels *(Russian)* 78−957
NN bremsstrahlung amplitude, sensitivity of observables to short and intermediate distance wavefunctions 78−62449
π Bethe Salpeter wave function in ladder model, light cone behaviour 77−18176
πD elastic scatt., 47.5-256 MeV, single scatt. contrib. 77−67671
ψ, particle, wave functions and partial decays in SU_4 model *(Chinese)* 77−65152
ψ, ψ', quark model, relative magnitudes of wave functions at origin calc. 77−87947
t, unnatural parity transitions in (p,t) reactions 77−67750
t wave function, asymptotic normalisation 77−10384
Ag_2, AgAu, AgCu, AgH, AgLi, VB calcs. 77−57883
AlO, A-X transition, Franck-Condon factors computation, iterative method compared with Langer's method 78−86762
AlO, Franck-Condon factors and r-centroids for $D^2\Sigma$-$X^2\Sigma$ transition 79−94037
Ar XV, wavefunctions and oscill. strengths, CI calcs. 80−23317
Au, inner electron wavefunction, meas. using Bragg scatt. of 412 keV gamma-radiation 79−14734
Au_2, AgAu, AuCu, AuH, AuLi, VB calcs. 77−57883
B, ground state wave function, 2s-2p electron promotion effect 78−86779
B^+, Hund's first rule, new interpretation 78−78620
$B^{3\bar{2}}$, few-parameter two-electron wavefunction of ground state 77−75051
BH, CI wavefunction, terms selection for pot. energy surface 77−88401

wave functions continued
BH, SCF and CI wavefunctions for electronic struct. and one-electron props. 77−67978
BH_3-ethylene complex, semiorthogonalised orbitals, integral approx. scheme 80−83262
B_2H_6 and $B_2H_5NH_2$, electronic struct. and bonding, comparative calcs. 79−31397
$B_nH_n^{2-}$, n=5-12, localised orbitals, bonding, PRDDO calcs. 78−13431
$B_xN_xH_{x+3}$, energy levels and wave functions, π-electron approx. 77−38608
Be, atom, ground state, accurate CI wavefunction 77−42245
Be, Hund's first rule, new interpretation 78−78620
Be isoelectronic series, excited states, oscill. strengths calcs., influence of wave function determ. method 80−99478
Be^{2+}, few-parameter two-electron wavefunction of ground state 77−75051
^{8}Be, γ-decay strength of isovector M1 transition, microscopic wave function 78−62503
C, optical oscillator strengths, independent particle model, excited state wave functions, LS coupling and Born approx. 80−32674
C, theoretical ionis. energies and oscill. strengths, excited s-, p- and d-levels 78−86823
C^{2+}, Hund's first rule, new interpretation 78−78620
C^{4+}, few-parameter two-electron wavefunction of ground state 77−75051
C_3, Renner effect, vibronic levels and wavefunctions, ab initio variational method 80−14127
$C_2B_{n-2}H_n$, n=5-12, localised orbitals, bonding, PRDDO calcs. 78−13431
CO, one-electron props., corrections, Moller-Plesset perturbation theory calc. 80−95519
$^{12}C(\pi^+,\pi^+)$, phase shift equivalent optical pots., π wave function constraint 79−9629
Ca XVII, wavefunctions and oscill. strengths, CI calcs. 80−23317
Ca_2, vibr.-rot. states, high accuracy wave functions and energies 80−74159
$CaCO_3$:Li, CO_3^{3-}-Li^+ centre, irradiated synthetic single crystal, bond angle and wave function 77−81006
Cs I, atomic wavefunctions collapse 78−70733
Cs_2^{2+}, low-lying states, MC SCF+CI 80−69053
Cu^{2+} complexes, ground state wave functions, g-factor anisotropy, lattice structs. 77−24536
Cu^{2+}, dopant, ground state wavefunctions and Δg 78−64012
Cu^{2+}, g-anisotropy and ground state wave functions in crysts. *(German)* 78−23065
Cu^{2+}, in Zn (II) complex, ground state ion wavefunction calcs. 78−895
Cu^{2+} ions, ground state wave functions, cryst. field effect, ESR data anal. 78−23060
Cu-like ions, E1 transitions, wavelengths, oscillator strengths and transition probabilities, data tables 80−37780
Cu_2, AgCu, AuCu, CuH, CuLi, VB calcs. 77−57883
Eu, electron impact excitation cross section, Born and Ochkur approx. 80−87230
EuO, cryst. field parameters due to $4f^{N-1}5D$ configs. 80−80230
Fe group ions, pair excitations in refinement of d^N-shell calc., multiconfig. approx. 77−42248
Fe XXII, allowed transition CI wave functions, oscill. strengths and transition probabilities 80−32664
Fe XXIII, wavefunctions and oscill. strengths, CI calcs. 80−23317
GaAs, energy bands and wavefunctions, localised orbital description 78−18942
n-GaAs-$Ga_{1-x}Al_xAs$, superlattice, subband struct. and optical spectra, self-consistent calc. 80−15443
P- Ge, acceptor wavefunctions in spherical approx. and piezoresist. 80−29405
Ge, energy bands and wavefunctions, localised orbital description 78−18942
H atom, variations, quantum theory calcs., generator coord. calcs. 80−41987
H, elastic electron scatt., pseudostates wave functions determ. in modified close-coupling calcs. 80−99572
H, first-order wave functions, computer calcs. using Green's functions 78−41934
H, in static multipole field, logarithmic perturbation expansion 80−91431
H, Stark and photoabsorption spectrum, density of oscillator strengths, atom c.f. semiconductor spectra 80−83318
H, Stark spectrum and field ionisation, density of continuum states, normalised wavefunctions 80−83317
H, wavefunctions, parabolic, polar, unitary transform. coeffs. *(Russian)* 79−3344
H^-, ground state electron correlation visualisation 79−3367
$H+H_2$, scatt. wave function modal struct. and global behaviour 80−81307
H+methane, abstraction and exchange reaction, barrier height calc. using POL-CI wave functions 80−81304
H^++H, charge transfer cross section calc., up to 100 keV 78−55235
H_2 $^1\Sigma_g^+$ ground state, hybrid Slater-Gaussian-type 1s orbital calcs. 77−38605
H_2, $^3\Sigma_g^+$ state, improved adiabatic energy, dissoc. energy 79−10011
H_2, approx. wave function accuracy criterion, reduced local energy 77−50348
H_2, channel coupling theory of covalent bonding, dissoc. energy 78−13419
H_2, D_2, photoionisation, body-frame Hund's case b description 78−94295
H_2, electron wave function calc. with Weinbaum function supplemented by floating function 79−26882
H_2, electronic energies of $D'\Pi_u$ and $B''\Sigma_u^+$ states, wave functions 77−23438
H_2, four-body system, adiabatic representation 80−91530
H_2, polarisabilities, higher, static, calc., wave-function quality depend. 80−18814
H_2^+, electron scatt. eqns. convergence, H_2 continuum states, appl. to photoionis. 78−66663
H_2^+, exchange perturbation theory 80−63518
H_2^+, exponentially small part of wave function *(Russian)* 80−9497
H_2^+, extended LCAO method, $1s\sigma g$ orbital *(Russian)* 79−93922
H_2^+, mol. props. in intense mag. fields 79−81169
H_2^+, nonexponential wavefunctions for $1s\sigma_g$ and $2p\sigma_u$ states 77−415
wave functions continued
H_2^+, nonexponential wavefunctions for $2p\pi_u$, $3d\pi_g$ and $3d\delta g$, $4f\delta_u$ states 77−416
H_2^+, one centre partial wave treatment, Coulomb versus electron exchange intermol. forces 79−6839
H_2^+, one-electron wavefunction calcs., expectation values 77−83483
H_2^+, polarisability, internuclear distance depend., excluding continuous spectrum 77−10581
H_3^+, photofragmentation vibr. energy levels and wavefunctions calcs. 78−42143
HCN, Fermi and Coulomb correl. holes, SCF and CI wave functions 80−69085
HCN, vibr. energies, wavefunctions, ab initio calc. 78−17652
HCl, electric field gradient at Cl, two- and one-centre wavefunction expsn. 78−17561
HCl, electrostatically interacting mols., CI multipole function calcs. convergency 80−91458
HCl, one-electron props., corrections, Moller-Plesset perturbation theory calc. 80−95519
HF, Auger spectra, correl. effects, energies and wavefunctions, ab initio CI calc. 80−14125
HF, electrostatically interacting mols., CI multipole function calcs. convergency 80−91458
$H_2(H_2^+)$ and isotopes, expectation values, Born-Oppenheimer, adiabatic and non-adiabatic results 78−82624
H_2O, correlated wavefucntions 78−70755
H_2O, excited stretching vibrs., quantum mechanics. 80−91535
H_2O, generalised overlap amplitudes, (e,2e) spectroscopic determ. 77−61862
H_2O, harmonic and anharmonic matrix elements comparison, appl. to vibrational energy transfer 80−63760
H_2O, multiplet states, SCF theory 80−69062
H_2O, semiempirical CNDO/2 wave functions, pair density anal., environmental effects 80−91451
H_2O, valence shell electron pair interactions, VSEPR theory test 79−31393
H_2S, valence shell electron pair interactions, VSEPR theory test 79−31393
$^1H(n,\gamma)^2H$, relativistic invariant approach, parity violation 79−3147
^2H, D-state wave function calc. 78−8740
^2H, from $^2H(N,N)$ scatt. and NN potential 77−18418
$^2H(p,p)$ cross section, d wave function with spin at light front *(Russian)* 79−85478
^3H binding energy, D-state percentage of deuteron, wave function shape 77−2902
H_2^*, energy and occupation curves, wave functions, natural spin orbital anal. 77−83493
He, $1s^2$ ground state piecewise polynomial CI natural radial orbitals wave functions 80−18805
He 2^3S-3^3S electron impact excitation, first Born and Glauber cross sections 78−55243
He, electron elastic scatt., 50-500 eV, optical model semiclassical wavefunction approx. 78−22030
He, exchange and correlation pots., density functional theory 80−52848
He, fine structure, 2nd order contribs. from all intermediate states 79−3354
He, generalised oscill. strength, variational determ., extremum principle appls. 78−94213
He, ground state, explicitly correlated wave functions 78−17566
He ground state, Hylleraas six parameter wave function, minimisation method 80−27925
He, ground state electron correlation visualisation 79−3367
He isoelectronic sequence, few-parameter wavefunctions of ground state 77−75051
He, isoelectronic sequence, 2^1S states, analytic wave function 80−9525
He isoelectronic sequence, $\delta(r_1)$ matrix elements using spatially distrib. operators 80−102445
He, mesoatoms, π^-, μ^-, K^-, p^- atoms, energy spectra, wave functions *(Russian)* 78−55264
He metastable state, two- and three-photon ionisation 80−91518
He, muonic three-particle system with Coulomb interaction, correl. wavefunctions calcs. 77−68144
He^-, reson. calcs. with correlated target state wave functions, complex coord. method 79−26939
He^-, wave function structure, complex coord. method 78−94190
He-He, Born Oppenheimer pot. using Hylleraas-type electronic wave functions 80−91442
He-He, Born-Oppenheimer pot. using Hylleraas-type electronic wave functions 79−31438
He-He, energy and interaction potential of two ground-state atoms 80−63740
He-like ions, H^- through Mg^{10+} 1^1S state variational wave functions 77−34545
He-like ions, He through Mg^{10+}, 2^1S, 2^3S, 2^1P and 2^3P states variational wave functions 77−34546
He-like two electron atoms, three-body problem 79−3372
$He+H_2$, adiabatic distorted-wave infinite order sudden approx. 80−99558
He_2^{2+} $^1\Sigma_g^+$ ground state, hybrid Slater-Gaussian-type 1s orbitals calc. 77−38605
HeH^+, excited states, variable screening models, natural spin orbital analysis of wave functions 80−37747
HeH^{2+}, lowest 20 states, eigenvalues, electronic wavefunctions, w.r.t. internuclear separation 77−18811
HeH^{2+}, pot. energy curves for $2p\pi$ and $3d\delta$ excited states 78−29756
$HeLi^{4+}$, pot. energy curves for $2p\pi$ and $3d\delta$ excited states 78−29756
^3He, asymptotic normalisations for S-state wave-function component 77−74777
^3He, correl. pairing theory 78−10247
^3He, D-state effects in $(d,^3He)$ reactions 78−4948
^3He wave function, D-state component from tensor analysing power of (d, ^3He) reactions 78−54769
$^3He(p,t)\Delta^{++}$, 850 MeV, search for $(\Delta^{++},2n)$ in the ^3He wave function 78−82345
^4He ground state wave function in translationally invariant oscillator basis 77−6262
^4He, liquid, condensed phase, long-range order of one- and two-body density matrices 80−10726
^4He, liquid, three body correlation 78−87834
^4He system, O^+ states, microscopic wave function 80−463

wave functions continued
Hg, electron impact excitation, spin polaris. and differential cross section 78−17800
Hg, positron scatt. at low energy 80−91670
HoF_3, single cryst., Ho^{3+} energy level spectrum calc. 79−1586
p-Hz, quantum diffusion of O-H_2 impurities 80−96719
K, Pauli susceptibility and Knight shift meas., electron wave functions 80−44937
Li, ^2S ground state calc. using Hylleraas-type wavefunctions 78−33418
Li ground state, HFS 80−91699
Li, ground state, radially correl. wave functions 77−75066
Li isoelectronic sequence of three electron atoms, pair correlation study 80−74096
Li isoelectronic series, wave functions, effective pots. and energy values 79−68182
Li, lowest $^2P^0$ and $^4P^0$ states, variational Hylleraas-type wavefunction 79−10023
Li, mesoatoms, π^-, μ^-, K^-, p^- atoms, energy spectra, wave functions *(Russian)* 78−55264
Li, optical oscill. strengths calcs. 80−91495
Li_2, potentials and wave functions of electrons *(Russian)* 78−47688
Li^+, few parameter two-electron wavefunction of ground state 77−75051
LiCl, aqueous soln., self consistent wavefunctions, HFS Xα pot. in cluster model, Compton profile calc. 79−78783
LiH, dipole moments and transition moments, semi-rigorous bounds, error limits 78−78635
LiH, one electron props., Xα multiple scattering wave functions 80−42945
LiH, variational Hylleraas-type wavefunction, correl. 78−9082
LiH^{3+}, pot. energy curves for 2pπ and 3dδ excited states 78−29756
LiNC type molecules, Born-Oppenheimer approx. applicability 80−32603
^{6}Li, three-body model using hyperspherical harmonics 78−29411
^{7}Li, cluster model wave function and r.m.s. radius 78−70442
^{2}M+hadron→proton+X, polarised d, S and D wave functions, nuclear core hypothesis 78−62417
Mg IX, wavefunctions and oscill. strengths, CI calcs. 80−23317
Mo, electron states, localised and itinerant features using mixed-basis representation of crystalline wave functions 79−60748
N^-, continuous absorption coeffs., from elastic e-N scatt. data, target wavefunction effect 78−9128
N^{5+}, few-parameter two-electron wavefunction of ground state 77−75051
NH_4F, cryst. struct., mol. wavefunction calcs. of struct. factors 77−62507
Na isoelectronic series, wave functions and effective pots. of valence electron 80−47873
Na, potentials and wave functions of electrons *(Russian)* 78−47688
Na_2 molecular electronic struct. for lowest $^3\Sigma_u^+$, $^1\Sigma_u^+$, $^3\Sigma_g^+$, $^1\Pi_u$, $^1\Pi_g$, $^3\Pi_u$ and $^3\Pi_g$ states 80−63738
Ne atom with 1s-hole, wave function calcs. using radial orbitals, orthogonality 77−67971
Ne, Auger spectra, correl. effects, energies and wavefunctions, ab initio CI calc. 80−14125
Ne I, wave functions, weighting factors determ. from g-factors 79−98237
Ne II, III, and IV ground state, photoionis. cross sections, close coupling calcs. 80−5513
^{58}Ni, charge density, single particle struct., using proton wave functions 78−45995
^{58}Ni(e,e′) 5.125 MeV $J^\pi=6^+$ state excitation, isoscalar character 79−22227
O isoelectronic sequence, optical oscillator strengths 80−63589
O_3, wave function calc. rel. to energy separation, cyclic and open isomers 79−93929
^{16}O, binding energy, wave function of ground state, orthogonal schema model 79−63582
^{16}O, Hamiltonian matrix analysis, base model of orthogonal scheme for 0^+ state 79−63610
^{16}O, two nucleon emission following bound pion absorption 78−82395
$^{16}O(0^+) \rightleftarrows {}^{16}N(0^-)$, nucl. wave functions and mesonic exchange currents 79−40887
^{18}O, low-lying positive-parity states 77−6239
P_4, allowed multiplets, coordinate wavefunctions 78−33444
Pd, phonon linewidths and electronic mass enhancement, electron-phonon contrib. 79−95099
S IV, P-, D-, S-states, oscillator strengths, transition strengths, CI calcs. 80−922
SO_2, harmonic and anharmonic matrix elements comparison, appl. to vibrational energy transfer 80−63760
^{32}S, ground state, comparison of cluster and two-centre shell models 79−6444
Sc I, oscill. strength calc. 80−78571
Si, donor ground state wave functions 78−87937
Si, energy bands and wavefunctions, localised orbital description 78−18942
Si IV radial wave functions of discrete spectrum calcs., dipole and quadrupole polarisation 80−5476
Si isoelectronic sequence, CI calcs. of oscillator strengths, L-S framework 80−14089
Si, localisation of wave functions of surface states 79−69574
Si XI, wavefunctions and oscill. strengths, CI calcs. 80−23317
Si_2, electronic struct. and bonding, atomic effective pot. appl. 80−95745
SmO, cryst. field parameters due to $4f^{N-1}5D$ configs. 80−80230
^{203}Tl, ^{205}Tl, core excitations to low-lying states, e.m. props., hyperfine splittings, isomer shifts 78−89794
V^{4+}, cryst. field effect on ESR parameters 77−36116
V^{4+} ion complexes in diamagnetic crystals, ground state wavefunctions, hyperfine interaction parameters, EPR meas. 78−19311
W, electronic states, localised and itinerant features using mixed-basis representation of crystalline wave functions 79−60748
Yb, electron impact excitation cross section, Born and Ochkur approx. 80−87230
YbO, cryst. field parameters due to $4f^{N-1}5D$ configs. 80−80230
Zn (II) complex, β-diketonate, 5-coord. adducts, Cu^{2+}, ground state ion wavefunction calcs. 78−895
Zn, isoelectronic sequence, oscill. strength and MCHF wavefunctions, outer correl. 80−91505
^{A}Zr, A=90, 92 and 94, charge densities and single-particle structure 80−9224

wave mechanics
see also wave equations; wave functions
bispectrum and nonlinear wave coupling for three-wave coupling 80−52038
Bose-like oscillator, one dimens., wave mech. representation using Wigner commutation relations 78−36872
de Broglie relationship rel. to covariance principle 77−13543
de Broglie wave, relativistic Doppler shift for teaching 78−49613
de Broglie wave packet for a simple stationary state 80−17810
de Broglie waves, dispersion relations 80−67949
de Broglie waves explanation of length contraction and time dilatation 77−60932
differential equations representation of wave processes, ordinary-type *(Russian)* 78−81850
education, three dimens. wave packet tumbling motion 77−82340
Einstein-Podolsky-Rosen paradox, de Broglie's physical waves, solitons 80−90710
elastic rod, nonlinear modulation of torsional waves 77−62195
electron atom collision, radial wave packets, appl. to target distortion 80−87234
electron in coherent EM field, null-plane formulation, Volkov soln. expansion 77−13898
electron wave packet in uniform electric field for teachers 78−61983
fermions, charged relativistic, semi-classical, two-body problem, new approach 78−29284
Feshbach-Villars transformation, bosons, fermions 77−87647
forced harmonic oscillator, Hamiltonian for time-depend. damping, for teachers 79−21495
gauge invariant wave mechanics and the Power-Zienau-Woolley transformation 80−99073
group velocity, four-dimensional 80−17814
Huygens' principle, formulation of quantum and classical mechanics *(French)* 78−36851
infinite component wave equations, composite system internal struct. 77−65102
invention, Schrodinger-Einstein correspondence 79−84898
inverted biharmonic oscillator potential, exact penetrability calcs. 77−2554
Kemmer-Duffin eqn., additional symmetry 78−89
locality principle, governed by Schrodinger eqn. 79−88834
Louis de Broglie's thesis, conceptual background, comment 77−87620
Louis de Broglie's thesis, conceptual background, reply 78−13
model-space effective operators construction 78−4508
multidimensional wave packet motion in quadratic potentials with and without friction: oscillation and barrier penetration 78−65804
nonlinear-wave mechanics and particulate self-focusing 80−105520
nonMarkovian stochastic model of non-relativistic wave mechanics *(French)* 77−82450
optimisation theory approach *(French)* 77−13598
origin, pedagogical approach *(Portuguese)* 80−22166
particle interactions with infinite and semi-infinite periodic potentials 78−28991
phase and group velocity, oscilloscope expt. for undergraduate teaching 78−61993
photon variable mass across anisotropic medium *(French)* 77−13624
potential scattering 77−74248
propagation of wave packets in quasiclassical approx., tunnelling *(Russian)* 77−33905
quantum numbers as hidden parameters, in causal interpretation of wave mechanics *(French)* 80−68062
Rarita-Schwinger eqn., additional symmetry 78−89
Rayleigh scattering, classical and wave mechanical theory 77−31067
reciprocal mass tensor 79−12635
reflection, from moving and rotating barriers, math. anal. 78−93539
relativistic, hypothesis on origin of quantum potential *(French)* 78−86405
relativistic, optimal control 79−40660
relativistic wave mechanics, stochastic model *(French)* 78−86404
resonant interaction, three-wave, separable initial-value problem of initially nonoverlapping envelopes 80−68058
scattering by several fixed scatterers, integral eqn. approach 77−78996
Schrodinger's route to wave mechanics 80−17783
Schrodinger's wave dynamics, global mobility 78−45512
sine-Gordon equation, two soliton solutions, breather solution 80−12945
spinless particles through one dimens. pot. barrier, formal series method, refl. coeff. 78−32700
square well bound states of particle, for teachers 79−35478
statistical theory of the calculus of probability, wave mechanics 78−54301
step in amplitude of d.c. pulse on wave packet, for teachers 79−97137
tachyon and tardyon causal and noncausal wave propag. 77−49593
tautomeric transform., quantum-statistical model 77−38739
thermoelastic materials, heat conducting, relativistic theory of wave propagation 80−83748
three-particle scattering, unitary regularization *(Russian)* 78−28999
tunnel effect, inner energy storage by wave mech. system 78−36857
two-centre problem with realistic potentials, single particle energies, wave functions 77−82887
wave packet dynamics, classical S-matrix limit 77−17836
wave-packet motion in Eckart and quadratic pots., appl. to H interstitials in transition metals 80−52067
weak evolution operators with constant coefficients and spreading of wave packets 79−85004
H, excited state interaction with photon field, simultaneous eqns. 78−66481
H, self-interaction of excited at. with radiation field 78−86794

wave power generation
asynchronous system for electrical generation, from randomly varying input 79−48081
ball screw type wave power generator, design, eqns. of motion, digital simulation 80−35632
buoy, Japanese *(German, English)* 79−83558
contouring (Cockerell) raft development, large-scale power generation feasibility 79−43736
conversion systems for ducks, design 79−43727
convertor, fully submerged model design and experimental testing 79−92059
convertor using three vertical floating plates 79−43730
Coriolis ocean turbine energy system status 80−45628
duck generator appl., Salter, Loch Ness expts. 79−43738

wave power generation continued
economic optimisation, optimum annual load factors estimation 79−43732
economic viability aspects 79−43728
efficiency meas. and optimisation 80−21370
electric generator, wave activated, design 79−20866
electrochemical gas concentration cells for the conversion of ocean wave energy 80−40821
energy accounting study 80−76589
energy analysis 79−48083
energy exchanger in advanced power cycle systems 80−35633
energy from the sea [tidal and wave power], research in United Kingdom 79−79371
energy potential of ocean surface waves, currents and tides as renewable energy sources 80−30371
energy resources and technologies, Conf., Chicago, IL, USA, Nov. (1978) 80−23123
engineering and economic assessment 79−34422
future energy concepts, Conf. London, England (Jan.-Feb. 1979) 79−43709
generator design constraints, directly driven 79−43725
hydrodynamics of energy absorption 79−43726
hydroelectric potential of the Zaire River, specifications and cost estimates of proposed plants 80−30375
inexhaustible energy resources, research and development in Britain *(German)* 80−72000
Isaacs wave-energy pump, field tests around Hawaii 79−57354
Kaimei, air-turbine coupled to AC generator 80−72010
large-scale, connection to Public Electricity Supply System, problems assessment 79−48082
materials aspects of wave energy convertors, review 80−85262
nonlinear energy transfer in a narrow gravity-wave spectrum 79−100873
ocean current power plant, vertical axis turbine, design and anal. 80−61272
ocean swell and wave energy conversion system, feasibility 80−55795
ocean wave energy conversion techniques and subsystems 80−45627
offshore float device, prototype design and expt. results 80−26107
operating efficiency, Salter duck, two-pontoon system, comparison 78−94591
options and constraints, 1978 state and development trends 79−48080
oscillating water column wave-energy device 79−39274
'passive' Mauritius wave energy project, electro-mechanical aspects 79−43724
pneumatic wave-energy convertor, performance study *(Russian)* 80−76600
renewable energy sources and the environment 79−79411
small scale generators, design criteria and wave characts. 80−55796
submerged sphere as an absorber of wave power 80−26108
Sweden, review of possible developments *(Swedish)* 80−93847
system optimization by diffraction theory 79−20867
UK potential, current status of research 79−43722
United Kingdom development, system reliability analysis 79−43739
utilisation prospects 80−61269
vertical energy absorbing plates hydrodynamic properties analysis 79−39273
weatherproof submersible ocean wave energy convertor 80−45626

wave propagation
see also acoustic wave propagation; electromagnetic wave propagation
acceleration wave propagation, modification in theorem of Bailey and Chen 79−12621
acceleration waves in anelastic bodies, propag. conditions 77−1169
acoustic field in stratified media of variable viscosity, Green's functions 80−4545
in active and passive periodic structures, review 77−3504
Alfven waves in solar photosphere, refl. rel. to sunspots cooling 79−5799
analytic signal in oscillation theory, review 79−5988
anharmonic chain with nearest neighbour interaction, periodic permanent waves 79−150
anisotropic random medium, scatt. in depth direction 79−2635
arterial system, elastic non-uniformity using hydraulic model 77−29164
arteries, pulse wave propag., initial stresses and muscle activity effects 80−12172
atmosphere acoustic-gravity waves, theoretical props. 77−33270
atmosphere gravity waves, meanflow interaction theory rel. to radar obs. 78−81282
atmosphere stationary planetary waves, propag. in longit.-depend. basic wind flow *(German)* 80−56526
atmospheres, wave propag. with high radiation pressure 80−26729
attenuation factor in pulsating turbulent gas flow in channel 77−42852
axial radiation reception from point source within axially symmetric medium 77−64948
axisymmetric disturbance due to shearing stress discontinuity propag. in elastic medium 78−67075
bar semi-infinite prismatic, elastoplastic wave propag., intense load-release wave existence *(Russian)* 78−24671
barotropic Rossby wave drag due to isolated shallow topography 77−78323
Barre granite, prop. determ. and wave propag. 77−56617
barrier theory based on half-barrier penetration, reflection and transmission coeffs. 80−98801
Beltrami-Michell and Beltrami-Michell type eqns. in static and dynamic elasticity 77−53782
bending vibrations in their plates, layer potential method of solution *(French)* 78−59336
bimaterial interface, wave propagation in non-uniform motion of displacement discontinuities 80−19264
Bloch waves, low freq., for wave eqn. of periodic type 79−17243
bodies with initial stresses, elastic wave propag., review 80−38323
body waves, short period, propag., isotropic scatt. model including wave conversions 78−40510
book, physics of vibrations and waves 77−41494
boundary friction effects on elastic wave propag. 79−46242
boundedness and periodicity criteria for wave motion in the Eulerian formulation 80−101720
bursting phenomena in excitable membranes 79−66455
calcite rock, compression wave studies 78−81151
chemical composition centre waves, periodic chaotic, Pade approximant scheme 78−80716
circular semi-infinite liquid jet, harmonically forced at nozzle, instability and wave propagation 79−32618

wave propagation continued
classical mechanics, logical drawbacks 80−17799
coherent three-wave interaction, phase integral 79−60127
composite processing, appl. to reflected wave complex spectra *(Russian)* 79−84531
composite semi-infinite rod, wave propagation 80−10180
composites, fibre reinforced and particulate, mechanical model 78−51105
compressible hyperelastic solids, spherical wave propag. analysis 77−58588
compressional and shear wave vels. in rocks, temp. depend. 78−7579
compressional and shear waves in saturated rock during water-steam transition 80−30995
compressional impulse interaction with slot normal to surface of elastic half space 79−50626
compressional wave vel. temp. depend. in anisotropic dunite 78−77224
compressive and tensile wave propagation in fluid column 79−18901
connectivity theory for formally symmetric operators 78−49651
constant Q-wave propagation and attenuation 80−30996
continuous and discrete systems, eqns., props. 79−5
continuously stratified liquid, linear wave theory, internal wave operator solution 80−43759
convergent cylindrical shock wave parameters meas. in metals by elec. methods 79−46407
Cosserat medium, hemitropic, propag. of plane, cylindrical and spherical waves 78−20968
couple stress effects on wave prop. in elastic layer immersed in infinite liquid 79−1126
cylinder, nonhomogeneous anisotropic, wavefront propag. analysis 77−68492
cylindrical ang. spectrum, van Cittert Zernike theorem 77−78988
cylindrical anisotropic waves propagation in nonhomogeneous material 79−32364
degenerative dispersion laws, motion invariants and kinetic equations 80−90684
diatomic gases, oscill., relaxing and radiating, propag. of small disturbances *(Russian)* 77−27625
diatomic solids viewed as directed media, generalised continuum model, longit. wave propag. 77−69051
diffractals (wave interaction with fractals) 79−58549
diffraction problem, non-homogeneous media, non-stationary problem 80−22211
diffraction problems at smooth unbounded wavy surfaces in inhomogeneous medium, direct method *(Russian)* 79−75363
diffraction stationary problem in non-homogeneous media 80−68
diffraction theory, infinite systems of eqns. *(Ukrainian)* 79−49060
discontinuity wave propagation in elastic body with dislocations 79−18787
discontinuity waves, reflection and transmission through shock wave, general theory, characteristic shocks 79−76908
dispersive wave trains, near-linear, two-time procedure for higher order modulation 78−65788
dispersive waves, nonlinear mixing 77−22428
dissipative and nonequilibrium media, pulse spreading 80−94961
dissipative and/or dispersive systems, perturbative and reductive method *(French)* 80−36868
dissipative gas of massless particles, wave propag. *(French)* 79−63047
dissipative rubberlike material rod, nonisothermal nonlinear waves 79−86380
disturbances in viscoelastic medium due to impulsive forces on spherical cavity 78−67076
duct, hard-walled, wave propag. in gas 79−41753
dusty gas, weak wave, general decay law 78−5785
dynamic and static high-pressure event differences 79−21557
E_s-layer, Langmuir wave propag. and enhanced plasma line 79−29928
early Universe, EM and gravit. Green's functions 78−73786
effects on Omega, anal. *(French)* 78−24672
EHD flow, nonstationary, with charge diffusion, nonlinear and linear wave processes 80−59124
elastic, controllable, finite deformations, cylindrical shell 77−7329
elastic deformed material, speed of propagation of waves 78−54201
elastic fibre reinforced composites, wave guide-type propag., microstruct. theory 78−83279
elastic half-plane, wave propagation for non-uniform motion of displacement discontinuities 80−1478
elastic half-space over circular pressure zone with non-uniformly changing radius 80−92080
elastic laminated composites, transient wave propagation 79−50630
elastic longitudinal wave propagation in circular cylinder with Cauchy's initial stress 79−37217
elastic materials, strongly anisotropic, wave propagation 79−14300
elastic plane progressive waves in linear elastic material binary mixture 79−32357
elastic plastic half-plane under movable loads, propag. of plane waves *(Russian)* 78−5685
elastic short waves grazing incidence on slender cavity 80−5983
elastic wave, transverse, reflection from cylindrical defect 78−47472
elastic wave propag., one-dimens., finite element anal. *(Japanese)* 78−28961
elastic wave propag. in cylindrical coord. systems 78−88798
elastic wave propag. in DNA film, vel. *(Russian)* 77−51511
elastic wave propagation in anomalous layers, variational approach 79−44260
elastic wave propagation in quarter plane, finite difference scheme stability 79−14310
elastic wave propagation rel. under model and natural conditions, similarity criteria in comparative anal. 79−96742
elastic wave propagation when negative slope region in stress/strain diagram *(Russian)* 78−79255
elastic waves, anisotropic materials, propag. from spherical and cylindrical cavities 77−72213
elastic waves, in oceanic model sediments 77−44966
elastic waves, multiple scattering by elastic ellipsoidal inclusions, self-consistent approach 78−63372
elastic waves, spurious reflection in nonuniform finite element grids 79−14303
elastic waves at frictional boundary, transmission (reflection), approx. anal. method 78−63371
elastic waves in anisotropic media, asymptotic equipartition of kinetic and strain energy 80−92081
elastic waves in discrete random medium 77−19554

wave propagation continued
elastic waves in two-phase media, interaction model 78−18213
elastic waves in vertically inhomogeneous media 77−73675
elastic waves on circular wire, nonlinear mode coupling 77−79990
elastic waves propagation in highly scattering medium, diffusion approach 77−86804
elastic-plastic wave propagation, transmission of elastic-plastic boundaries 77−62188
elastico-viscous fluid, compressible, nonperiodic wave propag. 80−43724
elasto-plastic medium, compressible, coupled dilatational and shear waves, proagation speeds 77−893
elastodynamic diffraction, two-dimens., by cracks, matched asymptotic expansions 80−1468
elastoplastic half-spaces interface, oblique refr. of plastic wave, self-similarity problem *(Russian)* 78−20974
electroelastic plane wave propagation in piezoceramic medium *(Russian)* 77−55752
elliptical cavity, wave diffraction 80−38320
energy flux for plane waves in linear conservative systems 78−12574
engineering problems, numerical anal. based on finite element method *(Japanese)* 78−28928
Eulerian computation technique for domains with moving boundaries 77−53779
evolution and propagation of waves in self-gravit. medium, astron. appl. *(Chinese)* 79−80211
evolutionary isotropic radiation 79−2638
exact transport eqn. for randomly perturbed focusing medium 79−81344
exceptional, in continuous medium, finite deform., evolution of discontinuities, elastic pot. determ. *(Italian)* 78−54202
excitation and proagation of elastic waves, book 80−94937
explosive instability upon interaction of localized and nonlocalized waves 80−31530
exponential amplification in gravitational field of ultrarelativistic rotating body 78−93594
F_2-layer, MHD waves ducted propag. 77−2299
ferroliquid, magnetoelastic oscills. 79−94639
fibre composites, orthogonally reinforced, wave propagations 78−41168
fibre reinforced composites, dispersive behaviour of time harmonic waves 77−859
fibre reinforced composites, ultrasonic vibrs. propagation velocity, dependence on composites elastic props. 80−5975
films as two-dimensional continua, dynamics, wave propagation and stability 79−68568
finite, exponential waves, solitons formation through nonlinear coupling 79−5967
finite-amplitude deep-water waves on currents 79−92958
flood wave propagation in channels with storage areas, diffusion eqn. 79−25277
fluctuations of intensity at two wavelengths in turbulent medium 80−87318
fluid impregnated solids, elastic and dynamic response regimes 78−90713
in fluid saturation porous medium *(French)* 78−86165
fluid-structural interactions, one-dimensional networks, MULTIFLEX code 80−13535
forced nonlinear waves, associated instabilities 79−58554
free waves, in helical spring of small pitch 78−9598
frictional attenuation, amplitude depend., rocks appl. 80−31034
in galaxies, density wave propag. through disc 78−20894
galaxy, disc shaped, global dispersion reln. for density waves 79−62916
gas, dissociating, relativistic flows, growth and decay of weak waves, shock wave formation 80−69949
gas, relaxing, in thermodynamical state of weak equilib., Bernoulli equation 80−90681
geophysical sounding, wave propag. functions for horizontally stratified Earth 77−21918
granular material, finite amplitude 1-D pulses 80−43642
granular materials, void compaction and material nonuniformity, influence on acceleration waves, addendum 78−83280
granular medium, body waves propag. 77−23909
gravitation wave propagation in expanding universe 78−73787
gravitational waves, dispersion in cold matter 80−12967
gravitationally unstable propagation, rot. and streaming effects 79−37293
gravity waves, propag. of spectra in thermosphere 79−66848
gravity waves observed during tornado outbreak (1974, April 3), upper atmosphere propag. 78−85753
gravity-capillary travelling surface waves, on liq. film falling past permeable bed 78−87351
Green function expansion into eigenfunction set 80−22205
group velocity, W.R. Hamilton's investigation 80−17815
harmonic, in viscous fluid in thin orthotropic cylindrical shell *(Russian)* 77−23969
head injury model with viscoelastic brain tissue, mech. response 78−69117
Helmholtz's reciprocity theorem, invalidity for scalar wave field propag. 80−31527
Helmholtz eqn. integral formulation for inhomogeneous media 80−81919
Helmholtz eqn. within wedge, Green's functions 79−9130
hidden symmetries in dynamical systems 80−37168
high strain rate processes, review 80−84864
holographic interferometry, transient wave motion obs. from single doubly-exposed hologram 78−25825
homogeneous anisotropic medium, propag. of wavefront produced by non-stationary source *(Russian)* 77−41489
homogeneous isotropic viscoelastic medium, wave propagation eqns. with time lag 79−35573
homogenised medium, with periodic structure, wave diffraction *(French)* 79−49057
hydraulically induced crack, mapping by point source signals diffr. meas. 79−48572
hydromagnetic waves in high β plasmas, propag. and damping 80−17482
hydromagnetic-inertial-gravity waves, propag. in magnetic-velocity shear 79−55422
hyperbolic differential equations, difference and finite element anal. methods 79−49059
hyperbolic mixed problems, leading wavefront propagation 78−36836
hyperbolic systems, high-order methods, dynamic problems 80−68033
hyperdetonation shock wave propagation in a nonhomogeneous medium 79−23236
I-beams, dispersion relations for normal modes 78−9597

wave propagation continued
ideal elastic fibre-reinforced slab, dynamic flexural deformations, flexural wave propag. 80−33510
ideal string, extremal solutions of inverse eigenvalue problems with finite spectral data 80−101712
impact and axisymmetric wave propag. in short length bars 78−5683
impacted solids, compression and shear wave propag., modelling 80−83755
impedance matching interface layer synthesis *(Russian)* 78−77728
imperfectly periodic structures, random evolution approach 79−14339
incompressible liquid oscills. in variable cross section viscoelastic tube due to pulsating press. 80−31519
incremental deformations of initially stressed media with couple stresses 78−62077
independent random sine waves in additive Gaussian noise 79−68497
infinite elastic bar, induced oscills., normal and associated wave propagation 80−5980
infinite medium with cavities, response to impact load 77−50945
infinite n-dimensional medium with resistance a discontinuous function of velocity *(Italian)* 79−17231
inhomogeneous anistropic elastic media, cylindrically symmetric waves, propagation and reflection 79−21559
inhomogeneous media, backscatter folding series *(Russian)* 78−73862
inhomogeneous media, determ. of structure from plane wave reflection response, numerical approx. 80−73183
inhomogeneous media, determ. of structure from plane wave reflection response, direct problem 80−77628
inhomogeneous viscoelastoplastic media, wave propagation *(Russian)* 79−32337
interfacial waves launched by an explosive line-source in a submerged elastic half-space 78−75088
internal state variables materials, thermomech. wave propag. 77−3760
interplanetary two-fluid shock waves propag., model 80−26711
inverse problem, finite difference method calcs. 80−17809
inverse problem for seismic wave eqns. in one dimens. *(French)* 79−44138
inverse problem soln. using J-fraction expansion 78−11819
inverse scalar wave scatt., statistical estimation *(Russian)* 78−54200
ionosphere, MHD wave propag. characts. 77−2298
ionospheric ions and electrons, collision cross-section 80−26666
irregular dispersion of waves and group acceleration 78−89354
isotropic medium, propag. crit. of accel. waves 77−62190
Kadomtsev-Pyatviashvili eqn., asymptotic behaviour of solns. (two-dimensional Korteweg-de Vries eqn.) 80−52036
KdV equations, general similarity soln. in terms of second Painleve transcendents 79−63051
Korteweg-de Vries, complex modified eqn., dispersion, self-propagation in anisotropic medium 79−75371
Lagrangian-mean flow, exact theory of nonlinear waves 79−37331
laminated composites, mechanics of homogenisation and random evolutions 80−28423
laminated composites, simulation of effect of bonding materials on dynamic behaviour 79−46216
laminates, periodic and disordered, complex transfer matrix approach 77−42768
layered hyperelastic half-space, one-dimens. propag. of weak discontinuities 78−30226
layered media, modified modal theory of transient response 79−71255
layered media with lateral inhomogeneities, modal methods 77−73676
LF tunnel waves propag. through subcrustal lithosphere, numerical expt. 77−49025
linear elastic continuum, book 79−25862
linear propagation in rotating fluid, critical level absorption and valve effects 80−106805
linear wave motions study using FFT, NDT appl. 80−92038
linear wave theory, conservation eqns., aeroacoustics appl. 78−9476
linear waves, asymptotic behaviour and wave patterns construction *(Czech)* 80−69
linearised inverse problems, variational approach 79−71259
liquid-filled porous solid, first strain gradient theory of thermoelasticity 77−53783
LMFBR, dynamic response of containment vessel and coolant wave propag., REXCO-EUR code manual 78−58349
long internal Rossby waves, nonlinear propag. 80−81896
long wave-short wave interactions, an exact solvable model 79−49062
longitudinal wave scattering by sphere-like bodies of revolution *(Ukrainian)* 80−22202
longitudinal wave vel. and absorpt. in rocks and minerals at high press. and temp. 79−39704
lossless wave supporting system, distributed parameters from boundary meas. 78−16658
Love wave scattering matrix for continental margin, theory 78−20360
Love wave scattering matrix for continental margin model 78−48982
Love waves, propag. in bodies with initial strains *(Ukrainian)* 79−30258
Love waves transmission through laterally varying structure 77−56592
Love-type SH waves, propag. in nonhomogeneous internal stratum between two semi-infinite elastic media 78−32016
magnetogasdynamic spherical shock waves, propag. in exponential medium 79−84664
magnetogravity waves, propag. in isothermal conductive atmosphere 79−92670
magnetothermoelastic plane Lamb's problem in initially stressed conducting medium 78−67077
magnetothermoleastic waves, propag. in initially stressed conducting layer 79−63
material containing rigid spheres, dynamic model for wave propagation 79−51199
matrix approach to propagation in piecewise continuous stratified non absorbing media 79−75355
media with bulk viscosity under shock loading, nonstationary plane wave propag. 78−94611
medium with high radiation press., basic eqns. for homogeneous media 79−88581
medium with hysteresis type damping, signal propag. *(Russian)* 79−53986
mesosphere internal gravity waves, propag. range *(Russian)* 79−16575
MHD, in anisotropic media, electrical dissipation effects *(Japanese)* 78−87445
MHD waves, vertically propagating, in isothermal atm. with horizontal mag. field 80−6162

wave propagation continued
micropolar elastic cylinder, free vibrs., wave propag., asymptotic anal. 78−51111
modelling, on oscillograph screen *(Russian)* 79−21558
molecular dynamics method in statistical physics, longitudinal and shear waves, dense systems, review 80−18895
mono-coupled periodic systems with single disorder, general method for free wave propag. 79−37225
mono-coupled periodic systems with single disorder, response to convected loadings 79−37226
multi-dimensional space, reductive perturbation method for wave modulation *(Japanese)* 77−41472
multidimensional magnetogasdynamic flows, shock wave propagation and breaking 79−98818
multidimensional wave radiation from source with Gaussian time variation and Gaussian approx. distrib. about spherical sheet 78−45487
multiple ray reflections in spherical isotropic Earth model, normal mode representations 78−48981
multiple scatt. in 1-D 79−44754
multiply scattering medium, intensity fluctuation spectra, theory 80−46819
neutron wave propagation in couple core Argonaut reactors 80−27752
non-linear dispersive wave, coupled modes approach, effect of dissipation on recurrence 78−49670
non-linear wave motion, one-dimensional 79−64
noncausal, in spin-O theories with external field interactions 77−41770
nonhomogeneous medium, reflectionless shock wave 78−54197
nonhomogeneous plastic polytropic medium, plane shock wave propagation, closed form soln. *(Polish)* 79−32350
nonhomogeneous viscoelastic media, propag. of initially plane waves 77−11145
nonlinear, extension math. principles of linear theories *(French)* 77−42647
nonlinear 1-D lattice, wave propagation theory 77−30105
nonlinear aftereffect medium, longitudinal one-dimens. wave propagation 80−5974
nonlinear deform. wave propagation in dissipative medium, interaction and reverse problems 78−53
nonlinear deformation waves in nonhomogeneous medium *(Russian)* 79−50642
nonlinear dispersive wave ensemble asymptotic dynamical eqns. 80−4547
nonlinear dispersive wave eqns., modulational instability and envelope solns. 78−54199
nonlinear effects upon waves near caustics 79−92957
nonlinear elastic dispersive media, interaction of solitary waves *(Russian)* 80−42076
nonlinear evolution equations simulating pair production and annihilation, solitary wave solns. 78−86167
nonlinear hyperbolic partial differential eqns. and mathematical models 78−77729
nonlinear interaction of dispersive waves with equal group vel. 77−75607
nonlinear lattice, nonlinear partial differential eqn. 77−13707
nonlinear media, theory of generation, amplification and damping of waves *(Russian)* 79−75361
nonlinear multiphase wave interactions, instabilities and solitary envelope soln. 77−9888
nonlinear standing waves, evolution in bounded media 77−49607
nonlinear viscoelastic wave propag., effect of time dependent compressibility 77−39244
nonlinear wave and soliton propagation, arbitrary density profile, adiabatic approx. 78−49676
nonlinear wave packets propagation, finite depth effects 79−48510
nonlinear wave process in a finite dissipative region *(Russian)* 79−17240
nonlinear wave propagation, spectral and pseudospectral methods, turbulent sound wave appl. 77−5672
nonlinear wave propagation in relativistic continuum mechanics 80−22203
nonlinear wave theory 80−36874
nonlinear waves, effect of discontinuities on statistical characts., anal. *(Russian)* 77−37762
nonlinear waves, fixed intensity approximation *(Russian)* 78−9410
nonlinear waves, modified conservation laws *(Russian)* 77−45706
nonlinear waves, propag. in unstable media, reductive perturbation technique 78−57796
nonlinear waves in dissipative or dispersive media 78−49672
nonspreading wave packets 79−44672
nuclear matter, elongated soliton type wave solutions, finite amplitude wave propagation *(Russian)* 80−13397
ocean long waves scatt. at mouth of estuaries bordered by continental shelf 77−9442
ocean wave groups, vels. and refr. laws verification 78−85575
one-dimensional medium, with space-time fluctuations, spectral correlation field characts. 79−71260
P- and S-waves diffracted around core, attenuation 79−53312
P- and S-waves diffracted around core, rel. to mantle base vel. struct. 79−53313
P-wave to Rayleigh-wave conversion coefficients for wedge corners: model experiments 79−14309
parabolic wave theories and applications 80−51436
paraboloids of revolution, internal fractures due to stress wave focusing 80−83762
parametric interaction of three dimens. wave packets, exact solns. 77−13635
parametric interactions in inhomogeneous medium with abrupt boundaries 77−49606
particulate suspensions, weak wave propagation 77−80207
path integrals for waves in random media 79−63049
perfect fluid, accel. waves and second sound 79−25865
perforated screen, sound diffraction, vortex shedding influence 80−69849
periodic elastic media, wave dispersion 79−17244
periodic fluctuations in nonuniform media, mathematical conditions for existence 77−13617
periodic surface, uniqueness theorems for scattering *(Russian)* 78−49677
periodic waveguides, smooth boundary waves 79−84969
periodically layered medium, wave propag. normal to layering, viscoelastic analogy 80−48636
permanent wave structs. on an open two layer fluid 78−59411
phase and group velocity, oscilloscope expt. for undergraduate teaching 78−61993
wave propagation continued
phase-space projection identities for diffraction catastrophes 80−27162
pipe conveying fluid, wave propag. and vibration response 78−9592
plane elastic wave diffraction by wedge, three dimensional nonstationary problem 80−69723
plane periodic waves, nonlinear propagation in relaxing gas, numerical anal. 80−92170
plane stratified media, mixed problems for wave eqn., singularities of Riemann functions 77−30017
plane stratified media, mixed problems for wave eqn., singularities of Riemann functions 77−30018
plane wave diffraction by smooth cylindrical surfaces *(Russian)* 78−12577
plane wave motions, energy partition in refl. and refr. 78−77727
plane wave propagation, general theorems, self-adjoint differential operators of order 2n 78−36842
plane wave propagation in thermoelastic solids with Tolotti's isothermal pot. 79−18786
plane wave scatt. by lossless penetrable obstacles, low freq. expansions 77−26211
plane wave scatt. by moving obstacle 79−71254
plane waves, group vel. in inhomogeneous media *(Russian)* 78−5755
plane waves in generalised thermoelasticity, stability and propagation 79−50618
planning plate with high speed in regular waves, pitching and heaving *(Chinese)* 80−43721
plastic longitudinal dynamic wave propagation, impact end 79−14294
plastic wave speeds in isotropically work hardening materials 77−65711
plastic wave theory, comparison of predictions with impact expts. 80−83742
point pulse source in elastic anisotropic half-space, propag. of vibrs. 78−57174
polarisation state of waves, theory 80−56525
polarised radiation transport theory, charact. eqn. 80−4678
polychromatic wave, refl. from absorbing layer, coeff. minimisation 77−82396
polytropic gas, initial pressure effect on stationary shock wave propagation 79−50753
polyurethane foam, press. wave propag. and refl. characts. 77−35634
porous medium during gas blow through, exothermal reaction wave propagation 79−79222
pressure pulse propagation in two-component slug flow 79−77235
prestressed nonlinear elastic solids, exact relativistic theory of wave propag. 79−1124
probabilistic model for the reflection of waves from a rough surface 79−40380
progressive waves in dissipative media, long range ray theory *(French)* 80−42070
pseudostationary wave, anal. 80−82605
pulsatile pressure waves of finite amplitude in elastic tubes, water expt. 77−27596
pulse propag. in media with freq. dependent Q, theory 80−72438
pulse propagation in spatial and temporal random medium 79−25868
pulse wave propagation in turbulent media, analytical theory 79−58550
pure harmonic tide in canal, eqns. of motion quadratic resistance term linearisation 78−69369
PWR, MULTIFLEX code, anal. of hydraulic force with hydro-structural interactions during LOCA 78−58373
PWR LOCA, subcooled decompression, multidimensional wave prop. with FLASH-genre codes 79−59194
quasilayered elastic strip, modulated propagating normal wave transform. 80−74800
radiating gases, sonic wave propag., wave front curvature effects, shocks 80−87784
radiating instabilities and resonant overreflection 79−53433
radiation attenuation in inhomogeneous media, effective coeff. 79−64181
radiation damping in general relativity 78−8310
radiation pressure, force exerted by a propagated wave on an obstacle 78−78869
radiation problems transport eqns., using Wigner distribution 80−168
radiation propagation in nonlinear media problems, decomposition method 79−84971
random linear systems and temporal homogeneity 78−32691
random media, oceanic appls. 79−5987
random media propagation, use of physical concepts in multiple scatter problems 79−21561
random stationary medium, Helmholtz equation, Karhunen-Loeve representation, analysis *(French)* 77−41492
random wave propag., mean power transmission determ. by using cumulant expsn. 78−36841
randomly imperfect periodic laminated composites, wave propagation, diffusion approx. 79−98659
randomly inhomogeneous layer, statistical moments of wave field, strong fluctuations of wave intensity 80−57107
randomly loaded elastic body dynamics, probability characts., of solns. to boundary-value problems *(Russian)* 77−41490
ray paths in a fluctuating environment 79−9129
Rayleigh channel waves propag. in coal seams, model seismic expt. *(German)* 78−40513
Rayleigh waves transmission and reflection through a step 78−44775
reaction-diffusion eqns., axi-symmetric time periodic solns. 78−81930
reaction-diffusion systems with explicit traveling wave and transient solutions 80−22207
real ray tracing when ray direction is complex 79−9126
rectification string, pulsation states *(Russian)* 79−30260
rectilinear rarefaction waves, systems of first-order quasi-linear hyperbolic equations 80−90679
reflection from an asymmetric inhomogeneous medium 79−44753
reflection in slowly varying medium 78−81856
reflexion by real potentials, phase integral treatment 79−49084
relativistic fluid with vibrational relaxation, growth and decay of weak discontinuities 80−69948
relativistic heat conducting inviscid fluid, exceptional waves *(French)* 77−53824
relativistic monatomic gas, propagation eigenmodes, Marle's 14-moment description 77−27626
relativistic self-inductive radiative fluid 79−41772
relativistic thermo-viscous fluid dynamics, heat conduction and wave propag. 80−24107
resonant wave triad, nonlinear evolution eqns., exact solns., singularities 78−81853

wave propagation continued
resonant wave triads, weakly nonlinear, space and time evolution, pump wave approx. 78−81852
rods, elastic with multiple wave speeds, wave propagation 79−72850
rods, quasi-bifurcation within axial plastic compressive wave 79−10513
rods and clad rods, elastic waves anal., tutorial review 78−94608
Rossby wave packet, vertical propag. in dissipative medium *(German)* 78−36220
rotary shear waves in initially stressed neo-Hookean material, radial propag. 77−35071
rotating fluid of spherical configuration 80−106804
S-waves, type II, refl. and refr. in elastic and anelastic media 77−52986
sandstone, determination of Biot parameters using static tests exam. of procedure 79−20299
scalar partial differential eqns., variational principles 79−30255
scalar wave diffraction by two parallel slits in plane 78−49671
scalar wave propagation, coherent scalar field in pair correlated random distribs. of aligned scatterers 78−32690
scalar wave scatt. by slender body of revolution 78−81857
scalar waves, high freq. scatt. by plane boundary stratified medium 77−67297
scalar-wave propag. in random elastic layer 80−83754
Schwarzschild black hole, elastic scatt. and absorption of waves 79−5857
second harmonic generation, nonequilib. media 78−77726
seismic attenuation in rocks, role of grain boundary friction 79−34755
seismic body waves, Earth-flattening approx. from geometric ray theory 77−64229
seismic body waves, focusing at epicentre antipode 79−16399
seismic body waves attenuation in layered anelastic solid 77−25647
seismic body waves in anisotropic media, propag. through layer 77−49020
seismic body waves in upper mantle, parameters in Crimea-Vrancha-Bohemia geological traverse *(Russian)* 79−53316
seismic data migration, collocation formulation of wave equation migration 80−4126
seismic high-frequency Pn,Sn phases on ocean bottom seismographs, high efficiency propag. 79−16400
seismic multiple ScS waves, attenuation beneath Japanese Arc 79−92508
seismic Rayleigh waves, inversion of global average group vels. and attenuation coeffs. 79−12090
seismic Rayleigh waves attenuation and group vel., regionalisation and pure path models 79−12091
seismic Rayleigh waves in mantle, phase vel. and Q 79−74846
seismic refraction method appl. to faults prospecting, model expt. and features of seismograms *(Chinese)* 79−12286
seismic S_n waves, propag. through Bering Sea and NW.Pacific Ocean 80−51346
seismic SH-waves propag. in stratified medium with local inhomogeneities, finite element treatment *(Russian)* 79−34763
seismic shear waves, vel. struct. for spherically averaged Earth 79−92504
seismic surface or interface P-waves, propag. in earthquake near field 79−66628
seismic surface waves, theory and obs., review *(German)* 77−64227
seismic surface waves propag., ray tracing appls. 79−66630
seismic transverse waves in rocks, propag. expts. 77−21682
seismic wave, reflection at free surface, appl. of Huygens' principle 78−7594
seismic wave attenuation, role of intrabed multiples 79−16393
seismic wave attenuation in partially saturated rocks 80−3997
seismic wave propagation in nonplanar struct., high-freq. glorified optics technique 79−66629
seismic wave propagation velocities in subsurface soil layers 79−62460
seismic waves, dynamic poroelasticity fundamental soln. rel. to pore fluid effects 79−74847
seismic waves, impulsive, propag. in spherically symmetric model 79−74849
seismic waves, integral spectrum parameters appl. to geological section prediction *(Russian)* 79−8705
seismic waves, long distance propag. in layered transition zone between mantle and core *(Italian)* 79−12071
seismic waves, one-dimensional, in elastic inhomogeneous media, inverse solns. 78−40518
seismic waves, propag. rel. to oceanic crust deep profiling using refl. meas. *(Russian)* 79−39966
seismic waves, ray paths and relative intensities in one- and two-dimens. vel. models 77−25649
seismic waves, refl. refr. and diffr. in media with elliptical vel. depend. 79−5454
seismic waves, screening in media with inclined boundaries *(Russian)* 78−92794
seismic waves, through spherical body with linear vel. function, intensities and travel times 77−56582
seismic waves, volume and surface sources due to layers laterally varying boundaries 79−16397
seismic waves in ellipsoidally anisotropic media, refl. and transmission coeffs. 79−84136
seismic waves propag. in medium with randomly distrib. inhomogeneities, attenuation and scatt. *(Hungarian)* 77−86791
seismic waves velocities investigation, new methods using common-point obs. *(Russian)* 79−74981
self-focusing of waves on deep water surface *(Russian)* 80−94536
semi-infinite elastic strings, interactions between stretching and deflection waves 77−45703
semiclassical wave propagation matrix method, appl. to surface transparent pot., Bloch waves 79−101
set of point sources determ. 79−88816
SH wave propag. in two-layered heterogeneous medium 78−48976
SH waves diffraction by rectangular impenetrable wedge 77−86780
SH waves refl. and refr. at plane boundary 80−12339
SH-wave propag. in heterogeneous media over homogeneous half-space 79−62446
SH-waves refl. and refr. in presence of slip and friction 79−46243
shallow seas, nonlinear stationary internal and surface waves propag. 80−17292
shallow water in polygonal bottomed tank, wave motion, initial condition influence 79−50746
shear modes in anisotropic systems, dispersion curves 78−36107
wave propagation continued
shear wave propagation in layered elastic medium, dispersion eqn. 79−17245
shear waves, horizontally polarised, finite crack in linear elastic media 79−68652
shear waves computation by ray method 79−53532
shell, cylindrical, inhomogeneous, thermoelastic torsional waves 79−92952
shell, cylindrical, Rayleigh wave propag. using elasticity theory *(Russian)* 80−38307
shell, orthotropic cylindrical, interacting with a fluid, nonaxisymmetric elastic wave propag. 80−33518
shell, spherical, with rigid core, deform. under effect of plane press. wave *(Ukrainian)* 77−31239
ship waves, hybrid integral eqn. method 79−32540
shoaling of finite-amplitude surface waves on water of slowly-varying depth 80−69853
shoaling waves, breaking invariants 78−85577
shock wave decay in elastic rods 79−41603
shock wave dispersion on plane layer *(Russian)* 80−33628
shock waves, astrophysical, post-collisional propag. and amplification *(Russian)* 79−44360
shock waves, cylindrical relativistic propag. in presence of mag. field 79−53708
shock waves, plane, relativistic, propag. 79−53707
shock waves, plane, relativistic, propag. in slowly moving medium 80−62005
shock waves in isotropic elastic space 80−28448
shock waves in optically thin grey atmosphere 80−53810
slender body, wave radiation, charact. wavelength 79−2640
slinky wave demonstrator, folding apparatus 79−44684
slowly varying wavetrains, dissipation and dispersion effects 80−64573
small amplitude plane waves in quasilinear dissipative medium *(French)* 79−25866
solar atmosphere, propag. of MHD shockwaves 78−24503
solar atmosphere, resonance, theory 79−84768
solar atmosphere, struct. of turbulent shock wave propagating across mag. field 79−40166
solar atmosphere five-minute oscills., obs. in temp. min. and propag. into chromosphere 79−62808
solar chromosphere, sinusoidal compressive waves radiative dissipation 79−84770
solar corona, fast mode waves evanescence 78−89147
solar photosphere, nonadiabatic radial wave eqn. rel. to solar oscills. detect. 79−5800
solid, surface stress effects on plane wave propag. 77−3761
solid particle suspension, wave propagation *(French)* 79−46361
solid particle suspension in compressible fluid, wave propag. 80−69858
solids, inhomogeneous linearly elastic, parabolic theory of stress wave propagation 78−38243
solitary wave propagation in 3-dimensional lattice 80−8929
soliton, dimensioned profile for propagation *(French)* 77−35155
soliton gas, turbulence due to weak dispersion, stochastisation of soliton motion 78−41169
Sommerfeld's diffraction problem 80−12916
space charge wave propagation along rotating relativistic electron beam 79−55047
spectral broadening of waves propagating in a random medium 80−94960
stability criterion for feedback control of unstable waves 77−5671
stable baroclinic Rossby wave propag. through mean shear flow 80−81895
stationary waves, teaching 80−67999
stellar collapse, adiabatic hydrodynamics and shock wave propag. 80−56861
stellar interior, semiconvection as occasional breaking of weakly amplified internal waves 79−48778
step in amplitude of d.c. pulse on wave packet, for teachers 79−97137
stochastic medium, propagation of mean field 80−73177
stochastic self-modulation in nonequilib. media *(Russian)* 79−98902
strain wave propagation in visco.elastic bars due to longitudinal impacts anal. *(Japanese)* 80−96223
strain waves, in solids, third approx. effects, asychronous interactions and self-action 77−1171
strain waves in anisotropic cylindrical crystal, theory 77−11062
stratified fluid, modified finite depth fluid eqn., exact N-soliton soln. 80−28517
stratified media, matrix anal. 79−12618
stratified media, wave interactions *(Russian)* 77−11231
stratified medium, reflectionless shock wave passage 78−54196
stress wave propagation calcs., effect of material constitutive models 78−90769
string, pulse vel. derivation without calculus, for teaching 78−24610
strong discontinuity wave in initially strained elastic medium 79−14301
sunspot umbral flashes and overstable magnetoacoustic modes 80−12734
superdetonation waves, in air, propag. towards laser beam, vel. meas. *(Russian)* 77−35159
superfluid scatt. problem associated with wave propagation 79−55948
superluminal wave propagation, causality criteria 78−73861
surface waves, inhomogeneous liq.-vap. interface, origin 78−75158
surface waves in vertically inhomogeneous elastic halfspace with horizontal inhomogeneity 77−52998
surface waves propag. in crystalline media 78−2350
surface waves propagation over liquid and crystalline layers, elastic consts. of crysts. 80−76924
surface waves propagation over liquid and crystalline layers, theory 80−76925
surface-wave dispersion in inhomogeneous medium, investigation by finite difference method 79−66631
tachyon and tardyon causal and noncausal wave propag. 77−49593
temperature compensation and travel times of waves 80−69731
temperature waves, flat, in semitransparent absorbing-scattering medium 78−90683
temperature waves in rigid heat conductor 77−14892
temperature waves in rigid materials with memory 79−17238
thermal wave propagation in nonlinear absorbing medium 80−96183
thermoelastic layer, gravity influence on wave propag. 79−94544
thermoelastic surface waves in micropolar elastic solid medium 77−72206
thermoelastic-plastic coupled medium, accel. and shock wave propag. 77−58578

wave propagation continued
thermoelasticity, coupled problems, effect of second order time derivatives 77−42772
thermoelasticity models taking account of a finite heat propagation rate 79−94541
thermosphere, tidal and planetary wave propag. 77−87147
thermoviscoelastic media, non-homogeneous, discontinuity propagation 80 102972
three-frequency wave interaction, waveguide and soliton solns. 78−41167
three-wave dissociation process, attenuation coeff., nonlinear increase 79−7654
tibia flexural wave propagation, discontinuous model and in vitro study 77−29169
time dependent Poisson queue and moving boundary problems for the heat and wave equation 79−63172
Toda lattice, poles, soliton solns. 79−75368
torsional wave diffraction by penny shaped crack, in axial mag. field 79−24206
torsional waves in two-layered circular cylinder with imperfect bonding 77−14948
transient and impulse responses of one-dimens. linearly attenuating medium, analytical results 78−32687
transient and impulse responses of one-dimens. linearly attenuating medium, parametric study 78−32688
translational relaxation at shock wave front in gas mixture 80−74917
transmission coefficients for generalised propagation problems 79−68
transmission through pressure duct, analysis and experimental results *(Italian)* 78−36838
transverse pulse propagation along hanging chain, teaching 78−28898
transversely isotropic layered media, reflection and transmission of seismic waves 77−91025
trapped waves around circular island, amplitude relation 79−7380
travelling pressure induced over a stepped depth change *(Russian)* 80−79335
travelling waves in hyperelastic rods 79−49051
truss, pin-jointed, plastic wave propag. *(German)* 77−35069
truss joints, elastic and plastic wave distrib. *(German)* 79−18769
tsunami, anal. by finite element method 78−92848
tsunami simulation, Hawaii, open boundary reflection interference 80−17232
tsunamis propagation, finite difference simulation, book contrib. 80−3956
turbulent medium, four-point field coherence function 79−98279
two-dimensional, method of characteristics 78−73863
two-dimensional periodic plates, free wave propagation 80−19268
two-way transmission 78−20977
unidirectional fibrous composite, mixture theory for longitudinal wave propagation, formulation 79−50631
unidirectional fibrous composite, mixture theory for longitudinal wave propagation, computational procedure 79−50632
unidirectional wave motions, book 78−77730
unidirectional wave propagation in one-dimensional first order Hamiltonian systems 80−86092
unified wave propagation theory, tenuous random medium 78−4491
upper atmosphere, acoustic-gravity waves diffr. around spherical Earth 78−4016
Van der Pol diffusion coupled oscillators, wave self-focusing and self modulation 80−90685
Van der Pol oscillators, diffusion-coupled active medium, nonlinear waves 80−4546
variational equations solved one as function of other *(French)* 77−41493
velocities and refr. laws of wave groups, comment 79−70811
vibrational energy propag. in thin elastic plate of const. width 78−9599
vibrations and waves in physics, undergraduate text book 78−54203
viscoelastic bar, transient wave propag. 80−106745
viscoelastic cylinders, dynamic torsion and nonstationary wave propagation *(Russian)* 79−50634
viscoelastic fibre-reinforced composites, wave propag. 79−76992
viscoelastic half-space, spherical wave propag. 77−75845
viscoelastic layer, plane transient wave propag. interaction of deformation fields with temp. *(Ukrainian)* 79−30259
viscoelastic layered composites, wave propag., dispersion and dissipation effects 80−102982
viscoelastic media, surface wave propagation 78−42555
viscoelastic medium, formulation of uniaxial pulse propag. using Boltzmann superposition integral 79−12619
in viscoelastic plate in liquid 78−79247
viscoelastic wave propagation, integration contour deform. for Laplace transform inversion 80−74801
viscoelasticity linear, isotropic integro-differential models *(French)* 79−80443
viscoplastic medium, plane wave propag. and scatt., similarity condition 77−35072
viscoplastic wave propagation, inversions for const. vel. case 79−12614
water, long wave propag. over water of lowly varying depth 77−49073
water, long-period, finite difference-element integration scheme 78−75157
water, surface gravity water propag., wave action and set-down on shear current 78−90920
water wave, partial reflection by nonuniform adverse currents 79−64681
water wave packet evolution, Schrodinger and Korteweg-de Vries eqn. models 79−72902
water wave propag. over circular shoal, parabolic eqn. method 80−14717
water waves propagation over deformable sea floor 79−57966
water-air plug-train system, press. wave propag. characts. 80−59058
water-wave transmission through barriers with small gaps 77−15046
wave beam self focusing with plateau-like intensity distributions *(Russian)* 79−89976
wave diagrams, weak shock wave diffraction and reflection *(Chinese)* 79−64692
wave propagation in a random medium, statistical properties *(French)* 80−52040
wave scattering, second order approx. in planar linear sheet 80−17812
wave-packet self-modulation, in nonlinear dispersive medium 78−41192
wavefront curvature in layered medium, seismology appls. 79−29712
wavefront dislocations, incoherent Gaussian random waves 78−16660
weak discontinuities evolution law for hyperbolic quasilinear systems 80−4548
weak shock propagation in liquid-filled tubes 78−26004
wave propagation continued
weak spherical shock waves, propagation from arbitrary piston motions 80−22204
weak wave propagation in elastic-plastic and elastic viscoplastic solids with interfaces, Al calcs. 78−18216
weakly nonlinear wave propagation due to dispersion and dissipation. long wave approx. 80−57104
whispering gallery waves near inflection point of boundary 77−60945
W, viscoelastic wave propagation model at near-melt conditions, electron-photon impact energy deposition 79−77002
wave scattering *see scattering*
waveform analysis
see also spectral analysis
acoustic radiation and scatt. anal., use of linear system theory 77−75729
analog signal processing, book 80−86047
analogue multimeters, used for nonsinusoidal waveform measurement 78−16809
arrhythmia detection by RR-interval comparison *(Bulgarian)* 78−15919
arterial haemodynamic transfer function calc. from Doppler US flowmeter waveforms 78−61235
atrial electrical activity, triaxicardiometric analysis 79−39585
Auger spectroscopy, tailored waveform modulation calc. for integral spectra 77−32860
blood vel. waveform for arteries obtained from US flowmeter, transfer function modelling 78−61225
classification problems of discrete and stationary stochastic signals 79−63002
compressible hyperelastic solids, spherical wave propag. analysis 77−58588
earthquake foreshocks, waveform anal. rel. to differentiation from earthquake swarms *(Japanese)* 80−67342
earthquake swarms, seismic waveform anal. rel. to differentiation from foreshocks *(Japanese)* 80−67342
ECG pattern recognition and representation by finite Haar transform 78−3654
EEG computerised analytical method *(Slovenian)* 78−28113
electrophoretic waveform analysis for blood serum protein composition determ. 78−64928
EMG, interactive minicomputer system for anal. of twitch waveforms of human motor units *(Japanese)* 78−28103
exercise ECG processing reproducibility rel. to waveform recognition and lead system 78−7513
exercise ECG quantitative analysis system *(Japanese)* 79−29652
exercise ECG repolarisation phase, T-wave amplification obs. 79−43845
generalized ray and reflectivity methods of waveform synthesis, comparison 79−84501
human scalp, olfactory evoked brain pot., correl. anal. of recorded waveforms *(Japanese)* 80−97946
ischaemic cardiac disease determ., heartbeat interval analysis and questionnaire evaluation 79−39580
ischaemic myocardial reactions, triaxicardiometric obs. 79−43844
layered system, spectral function, waveform determ. at depth 78−16172
multidimensional contour resolution into components 79−84941
multiunit spike train separation techniques evaluation criteria 78−85422
neutron spin-echo integral transform spectroscopy 80−4748
optical wavefunctions, inversion of integral equation for system distorted by aberrations 79−98304
polarography, DC wave automatic anal., minicomputer appl. 77−25333
pulse picosecond waveform meas. 78−57923
real time wavefront anal. automatic method for interferograms 79−75585
resonator loaded with periodically inhomogeneous active medium, spatial struct. of field 79−81462
seismic deconvolution and wavelet estimation 78−20542
seismic exploration, technique and processing, book 80−51975
seismic incident and reflected wave forms, inverse problems *(Russian)* 79−34762
seismic waves, multi-segment traces deconvolution and synthesis 80−77162
seismic waves from Oroville earthquake, California, 1975, focal mechanism determ. 77−9346
shock-loaded solids, wave profile measurement 79−94564
sonar, linear-period-modulated waveforms for rel. estimation 77−54825
spectral analysis using programmable pocket calculator, Simpson's rule appl. *(Spanish)* 78−86121
speech analysis, glottal-area waveform estimation via nonlinear inverse filtering technique 77−56390
time-domain finite length digital filter, exact wave-shaping, geophys. appl. 77−2266
US Doppler signal analyser, real-time, multichannel, blood vel. meas. appl. 77−73551
uterine contraction waveform online digital processing system 78−15916
vectorcardiogram computer interpretation method, prototype system 77−90954
volume holograms, coupled wave analysis, effect of second order derivatives 80−53232
wavefront-reconstruction imaging *see holography*
waveguide antennas
active-passive array for plasma wave excitation 80−48911
biological microwave exposure source, compact light-weight Gaussian-beam launcher 78−96119
diffraction by semi-infinite parallel-plane waveguide in anisotropic plasma 78−1845
far IR antennas for 0.1 to 3.0 mm range, review 80−69553
focused spot-size controlled Gaussian-beam launcher for microwave exposure studies 80−89920
Gaussian beam launcher, for selective partial body exposure of biological substances 79−29578
waveguide attenuators
fibre-optic band-pass attenuator 79−37003
fibre-optic variable attenuator 79−64328
Helmholtz resonator array for attenuation of zeroth normal mode in tubes 80−87602
rotary-vane type, automatic calibration on modulated subcarrier system 77−18022
waveguide components
see also circulators (microwave); directional couplers; optical waveguide components; strip line components; waveguide attenuators; waveguide couplers
chirped-grating multiplexers in dielectric waveguides 77−58445

waveguide components continued
dielectric discs in rectangular waveguides, permittivity measurements, EM wave scattering *(Russian)* 77−18050
dielectric resonator, trapped mode, coupling and tuning for laser beam modulation 78−55389
feedthrough waveguide resonator Q-factor meas. 77−10053
ferrite rod phase shifter, azimuthally magnetised, soln. of differential eqns. in terms of Bessel and Neumann functions 79−55025
linear accelerator, waveguide bunchers, nonlinear anal. 77−378
microwave optical radiation modulator, $LiNbO_3$ cryst. 77−27353
phase shifter, multilayer dielec. waveguide struct., for submillimetre waves, theory 77−34003
precision cells, for lossy liquids permittivity meas. at 70 GHz 78−37032
PVF_2 pyroelectric device for homodyne MM wave detect. at 100 GHz, high-sensitivity *(Japanese)* 79−97432
quarter wave absorbers, C-band, NiZn ferrite appl. 79−38386
rectangular to circular waveguide transition, for use with discharge lamp, 60 to 90 GHz range 79−26074
resonators, RF breakdown, rel. to lower hybrid reson in Tokamak plasma 78−26364
TE_{on}-mode filters for VLA radiotelescope circular waveguide system 79−66922

waveguide connectors *see waveguide couplers*

waveguide couplers
see also directional couplers
cavity variable coupling, with solid construction, for EPR spectrometer 77−13790
commutable circulator, with increased mean-power level 78−4637
microtron waveguide, coupling coeff. with resonator rel. to high-freq. path 77−65367
optical, coupling coeff. meas. by detuning 78−30066
optical, thick dielectric grating on asymmetric slab waveguide, scattering losses approximate theory 77−68257
optical fibre coupling techniques *(German)* 80−28330
planar waveguide structure for integrated optics, props. *(Czech)* 80−96018
RF coupling gaps in plasma filled waveguide, mutual interaction 77−58867
RF coupling loops, transmission line approx. 80−28672
SAW bandpass filter using fanned multistrip coupler 77−50837
SAW multistrip coupler, superposition model 80−74674
scattering matrix and radiation characts. of junction between monomode waveguides 77−34946
surface EM wave coupling efficiencies 77−19391
surface EM waves, excitation efficiency of prism and grating coupling techniques 77−61902
tapered fibre coupler for optical pulse backscatter meas. 77−7212
US clad-rod waveguides, with sinusoidally perturbed core-cladding interface, torsional modes coupling 77−79999

waveguide joints *see waveguide couplers*

waveguide junctions *see waveguide couplers*

waveguide theory
see also guided electromagnetic wave propagation; optical waveguide theory
acoustic, Bleustein-Gulyaev waveguides with gratings, anal. 80−1391
acoustic and liquid wave propag. in slowly-varying guides 78−4490
acoustic cylindrical waveguide, parametric sound generation theory 77−50849
acoustic signals in randomly inhomogeneous waveguides, spatial coherence 77−58521
acoustic tubes with wall-mounted resonators, sound attenuation 77−11063
acoustic wave characteristics rel. to EM waves *(Japanese)* 78−46858
acoustic wave propag. and damping, in ducts with flow, section discontinuity effects *(French)* 77−6576
acoustic waveguide in ocean, internal waves influence on sound propag. 77−14837
anisotropic media, gyroelectric or gyromagnetic, rectangular waveguide, wave propag. *(French)* 77−10813
arbitrarily shaped dielectric body inside waveguide, three-dimensional anal. 78−71005
artron effect (self-reson. electron deceleration) 77−6991
charge radiation in waveguide with transversally moving walls, anal. *(Russian)* 79−888
charged filament moving in iris-loaded plane waveguide EM radiation 80−23609
complex waves in a circular dielectric waveguide 79−81337
composite waveguide, continuum modelling of EM wave propag. 79−55031
corrugated cylindrical waveguide, propagation characts. *(Italian)* 79−17235
cylindrical inhomogeneity in homogeneous medium of infinite extent, guided EM field numerical computation 80−14274
cylindrical waveguide filled with uniaxial, collisional, hot and moving plasma, dispersion for TE and TM modes 80−106934
degenerate TM mode scattered by impedance step 79−64160
dielectric jet with plane laminar flow, waveguide effect stability, anal. *(Russian)* 77−7546
dielectric rod waveguide in magnetoplasma, TM mode propag. 78−51314
dielectric screened three-layer waveguide, cut-off characteristics and modal inversion screened three-layer waveguide, cut-off characteristics and modal inversion 80−1303
diffraction application of minimum autonomous block method 79−68362
diffraction at inclined dividing boundary between dielectric materials in rectangular waveguide 79−885
diffraction at waveguide corner with mirror *(Russian)* 77−19396
diffraction of EM waves on slots in plane waveguide walls *(Russian)* 78−29884
diffraction of waveguide fields by small disks and apertures located at nodes 79−55036
discrete modes of a system subject to an inhomogeneous, high-frequency force 80−43237
Earth-ionosphere waveguide parameter determ. by VLF transitional route meas. 77−91234
eccentric spheres, interior and exterior boundary-value wave problems 77−75384
elastic waveguides with elliptical cross-section, numerical anal. by mode-matching method 79−23109
electric waveguide, step discontinuity, radiation loss 77−42588

waveguide theory continued
electrically and mag. polarised matter in waveguide, EM field, Green's function method 78−1123
electrodynamic boundary problems, method for solving 80−95773
electrodynamics, projection methods, applicability limit 80−91734
electron autoreson. motion, effect of longitudinal wave field *(Russian)* 79−7063
electron beam in circ. waveguide electrostatic instability in rippled magnetic field 80−19588
elliptically polarised modes in gyrotropic waveguides 77−10815
EM field penetration into conductive spherical cavity 78−86990
EM scattering by spherical shell with arbitrarily located circular aperture, anal. 78−62989
EM transmission structures, relativistic foundation and network formalisms 80−58446
EM wave diffr. by periodic waveguide gratings, reson. effects *(Russian)* 79−887
enclosed dielectric microstrip, analysis of losses, Schelkunoff method *(Spanish)* 80−45005
far IR waveguides for interferometers measuring electron density in Tokamak plasma 79−73034
ferrite rod phase shifter, azimuthally magnetised, soln. of differential eqns. in terms of Bessel and Neumann functions 79−55025
ferroelectric film, appl. and props. at microwave frequencies 77−1632
flanged parallel-plate waveguide, diffr. theory 79−45891
fluid-filled waveguide with transverse resistivity, mode-selective sound transmission 78−1452
H_{10} mode scatt., in rectangular waveguide, by cylinder with longitudinal slot 80−43238
Huygens' principle and equivalence principles 80−1106
inhomogeneous circular waveguide, asymptotic eigenvalues 80−53442
inhomogeneous dielectric filled uniform waveguides, EM wave propag. 80−83666
inhomogeneous planar waveguide, propag. charact. of guided waves, numerical method 79−76554
liquid waveguide, sound generation by absorpt. of modulated laser radiation 78−1539
low-loss dielectric tube leaky waveguide, transmission characts. 80−95999
microstrip anisotropic electrostatic field problems, Green's function technique 78−70998
microstrip waveguide, theory of radiated waves using asymptotic wave diffr. theory 79−18339
microwave EPR self-induced transparency in free radical powder, theory, expt. 77−24747
modulated normal wave interaction 79−21563
muffin-tin structure, deflecting modes *(French)* 79−45469
multilayer dielectric waveguide struct., phase shifter for submillimetre waves 77−34003
multilayer lossless dielectric loaded waveguide, transient field distribution 80−23604
nonlinear lower-hybrid waveguide in plasma, stability 80−19578
nonparabolic graded-index medium, wave propagation 79−18516
nonparallel dielectric waveguides, degenerate mode coupling 79−37006
open-ended, finite element method for unbounded field problems 80−23600
periodic waveguides, wave propagation 79−84969
planar, bounds on soln. of Helmholtz equation 80−14507
planar dielectric waveguide, interacting discontinuities, anal. 79−27445
planar dielectric waveguide with interacting step discontinuities, field and network anal. 79−55214
plane wave at skew incidence on right-angled impedance wedge 78−90346
plane-parallel plasma waveguide iris admittance 77−84447
plasma filled waveguide, electron beam interaction, spatial evolution of complex EM modes, collision effects 79−14556
plasma heating, lower hybrid waves, backscatter, effect of waveguide boundary conditions 80−64709
plasma-filled cylindrical waveguide, nonlinear EM wave propag. 77−991
polarised matter in co-axial waveguide, general cross-section, EM field 78−1124
quantisation of radiant energy, teaching appl. 78−36757
radially inhomogeneous waveguide modes, vector wave characts. 80−78960
radiation pattern of open ended waveguide in air core surrounded by annular plasma column 78−67366
rectangular waveguide, blackbody radiation, EM fluctuations 79−41309
rectangular waveguide, partially filled, appl. to solid, liquid multilayer dielec. consts. meas. 79−2791
rectangular waveguide partially loaded with magnetised planar ferrite, e.m. wave propag. 77−576
reflection and transmission at interface between elastic waveguides, variational soln. 77−84027
reflection from moving boundary between two dielectrics in waveguide 77−584
reflective arrays, coupled mode vector anal. and flowchart 79−7241
relativistic electron beam in iris-loaded waveguide, limiting current 78−5879
relativistic electron beam in waveguide, slow cyclotron waves 80−106983
relativistic free-electron wave generators, electrically pumped 80−91742
RF coupling gaps in plasma filled waveguide, mutual interaction 77−58867
RF plasma heating, effect of wall corrugations on lower hybrid wave spectrum 80−33787
rib wave guides, field expansion analysis, measurements at mm-wavelengths, approx. solutions comparison 77−54778
scattering and mode conversions by circular cylinder, slab waveguide guided modes 80−9791
scattering matrix and radiation characts. of junction between monomode waveguides 77−34946
shear wave propag. in trilaminated waveguides, continuum mixture theories 78−33935
singularity extraction in kernel function rel. to rectangular cavity dyad 78−66728
slow-wave system, phase motion of particles in beam-excited self consistent field 79−10253
sound, LF, in waveguide with irregular boundaries (Arctic underwater model) 77−11079
sound transmission through double partition, exact soln. 77−7233
static field problems of dielectric objects, moment formulation 77−3512
strain waves in anisotropic cylindrical crystal, theory 77−11062

waveguide theory continued
surface wave line, dielec. obstacle on impedance jump 78−18063
three-frequency wave interaction, waveguide and soliton solns. 78−41167
TM mode-conversion at terminator for anisotropic ionosphere, param. study *(German)* 80−46333
translational invariance and normal modes, for teachers 79−25
transversally nonhomogeneous waveguide EM wave propagation, using variational methods *(Czech)* 80−33155
two-dimensional waveguide transition theory 78−12576
undulator radiation from bunches in waveguide *(Russian)* 79−76561
US clad-rod waveguides, with sinusoidally perturbed core-cladding interface, torsional modes coupling 77−79999
wave scattering by ideally conducting bodies in rectangular waveguide *(Russian)* 79−884
X-ray propagation through capillaries, surface roughness influence 79−49349

waveguides
see also acoustic waveguides; circular waveguides; dielectric-loaded waveguides; dielectric waveguides; optical waveguides; plasma filled waveguides; rectangular waveguides
acoustic wave propagation as guided modes, parabolic approx. 80−43506
atmosphere, radio propag. in natural waveguides 77−78328
buncher waveguides, engineering design 77−83399
charged particle self-reson. motion in EM wave with varying propag. vel. 77−75399
coaxial waveguide wave impedance, USSR special standards 77−30182
conference, IR and MM waves and appls., Miami Beach, USA (Dec. 1979) 80−57009
DC superconducting magnets, pot. damage due to HF EM wave propag. 78−50371
Earth mantle, seismic S_n waves propag. through Bering Sea and NW.Pacific Ocean 80−51346
Earth-ionosphere waveguide excitation by low-freq. sources in inhomogeneous ionosphere 79−66873
Earth-ionosphere waveguide model, inverse propag. problem soln. 79−58154
electron beam, relativistic, high-current, in microwave linear accelerator, transient behaviour 80−32541
electron radiating in waveguide, self-reson. radiation 79−55040
electron waves in plane periodic system, linear theory 80−48130
EM syringe for injecting energy into deep-lying tissues 78−53545
far IR waveguides for interferometers measuring electron density in Tokamak plasma 79−73034
ferrite ring, 2000 NN type, self-accel. caused by high-current electron beam interruption 80−4809
ferrite-filled waveguide, chopped electron beam, self-accel. theory 77−54660
ferromagnetic metal polycrystals, model for EM generation of US guided waves 78−22236
fibre reinforced composite waveguides, axisymm. elastic vibrs. 80−102995
frequency-voltage convertor using Nb-oxide-Pb tunnel junctions, design 77−82555
gas-filled, ion acceleration by electron beam, in mag. field 78−9316
Gaussian-beam launcher for microwave exposure studies, dielectric hemisphere-loaded scalar horn 80−12206
group vel. direct calc. from dispersion curve 77−27407
impedance meter verification scheme 78−37035
inhomogeneous waveguide system, self-consistent beam dynamics 78−9009
ionosphere, role of near-critical rays in distant HP propag. 79−53619
ionosphere VLG guide over Atlantic Ocean, obs. of shadow of mesosphere O_3 on D-region 79−58161
iris loaded waveguide relativistic electron beam interaction, electron energy distrib. space charge effects 78−46190
iris-loaded waveguide, inhomogeneous ferrite filled, autoacceleration 78−79441
linear accelerator, resonantly coupled RF power manifold 77−38497
magnetoelastic waves, shear, horizontal, integral representation 77−90009
microwave discharge, supersonic flow in waveguide, electron densities, possible laser 80−38842
microwave radiation effects on cells in vitro study using waveguide exposure chamber 79−5327
microwave system for chronic exposure of small animals 80−56318
multimode square waveguide applicator, for microwave therapy 79−34630
open-ended waveguide probe/applicator combination *(French)* 80−3820
power meas. at higher microwave freq., conf., London, England, (Jan 1979) 79−26082
radiating electron in strong monochromatic wave at open waveguide 79−55039
reflection maser, tunable, using ruby-filled waveguide 78−5443
relativistic electron beam generation in coaxial vacuum waveguide, mag. self insulation breakdown *(Russian)* 78−1145
relativistic electron beam interacting with EM wave, dielec. filled channel 79−59622
self excitation of active noise suppression in a waveguide 78−18109
self-made oscillatory semicond. waveguide, EM beam self-focusing 79−18488
space-time processing of acoustic signals in waveguides 80−5878
surface resistivity, evaporated Au at 890 GHz 77−34004
tropospheric, numerical comparison of ray method and normal wave method 80−21858
two-dimensional diffraction by parallel-plane waveguide in anisotropic plasma 78−5880
UHF microtron system with ferrite gate, frequency responses 77−46430
X-ray, planar, self-imaging 80−57443
X-ray light pipe, transmission meas. at 5.9 and 14.4 keV 77−193
CO_2/N_2O waveguide laser design 80−33025
Cr, film, trivalent, cathodic deposition, as bonding interface between Cu and polyethylene, dielec. lined mm waveguide appl. 80−76201

wavemeters
see also frequency meters
absolute calibration of grating spectrograph for laser wavelength meas. 78−90528
digital wavemeter for CW lasers 78−89447
Fizeau wavelength meter, laser and other monochromatic sources, digital display 78−89450
fringe-counting wavemeter, based on compact spherical interferometer 80−42255
interferometer, two-channel, based on prismatic dividers, energy factor analysis, using model of coupled multi-terminal networks *(Russian)* 80−52302
lambdameter, improved design based on moving mirror Michelson interferometer, accuracy tests 79−63194
laser beam interferometric wavelength measurements through post-detection signal processing 80−42254
laser CW digital wavemeter, moving cube-corner interferometer system 78−50840
laser wavemeter, inexpensive broadband optics and minicomputer interface 78−89448
microwave, calibration using spectrometer *(Polish)* 78−29866
moving carriage Michelson interferometer, 1 in 10^7 laser wavelength meas. 78−89452
servocontrolled Fabry-Perot interferometer, 3 in 10^{11} laser wavelength meas. 78−89452
traveling Michelson interferometer with phase-locked fringe interpolation 78−89451

waves
see also charge density waves; elastic waves; electromagnetic waves; gravitational waves; gravity waves; liquid waves; magnetohydrodynamic waves; magnetostatic waves; ocean waves; oscillations; plasma waves; spin density waves; spin waves; surface waves (fluid); wave propagation
action, conservable quantities measuring wave activity 79−37332
aerodynamic noise from wave-turbulence interaction 80−14679
aerodynamic wave drag, nonplanar singularity distribs., Hayes' algorithm extension 77−84271
air, weak nonlinear waves, struct. and propag., effect of vibr. relaxation 79−64683
air flow above sea surface, wave components rel. to eddies transfer rate *(Russian)* 79−16578
air-water flow, periodic instability related to continuity waves 78−1716
amplitude vacillation in baroclinic flow, model 78−69407
annual review of fluid dynamic, book 80−94927
approximate solution in gasdynamics 80−92174
asymmetrical fluid, thermoconvection wave propagation, microinertial and couple stress effect 80−19446
atmosphere, effect of terminator boundary slope on disturbance prod. 77−91208
atmosphere, five-day wave rel. to coherence of ionospheric absorpt. and 30 mb temp. 77−33275
atmosphere, instability theory of tropical large scale disturbances 77−5302
atmosphere, Kelvin-Helmholtz waves under subtropical jetstream 79−66781
atmosphere, large amplitude Rossby waves 79−62567
atmosphere, large-scale wave transport of stratospheric O_3 to Pacific Ocean 80−72600
atmosphere, mean motion induced by transient inertio-gravity waves 80−105029
atmosphere, nonlinear stationary waves theory *(Russian)* 78−16089
atmosphere, obs. of Lamb waves originating in nongeostrophic disturbances 77−45085
atmosphere, planetary wave heat and momentum fluxes rel. to stratosphere and mesosphere meridional circulations 80−109219
atmosphere, Rossby waves stability *(Russian)* 78−44923
atmosphere, solitary Rossby waves theory 80−56539
atmosphere, trough-ridge systems as slantwise convection 79−79993
atmosphere, upper westerly waves interaction with intertropical convergence zone rel. to Zambian weather during rainy season 80−90175
atmosphere baroclinic waves, numerical modelling of instability *(Russian)* 78−44922
atmosphere features of topographic wave clouds in central and northern Urals 80−101413
atmosphere frontal waves development, numerical simulation accounting for mountain ridges effect *(Russian)* 78−53701
atmosphere general circulation, eqns. of kinetic and available pot. energy evolution in wave-number freq. space 80−109227
atmosphere jet stream, fronts and wave disturbance compared with Gulf Stream 79−2268
atmosphere large and meso-scale baroclinic waves, influence of boundary layer *(Russian)* 77−33140
atmosphere planetary waves, tropospheric-stratospheric interaction during stratospheric warming event 80−4074
atmosphere Rossby-Haurwitz waves, rel. to sunspots influence on weather 77−91238
atmosphere short internal waves, nonlinear instability *(Russian)* 77−49107
atmosphere unstable baroclinic waves, downstream and upstream development 80−56540
atmospheric fronts, wave development anal. employing two-layer model *(Russian)* 77−53109
autowave processes in distributed kinetic systems, review 80−101721
backwash vortex under waves running up sloping bed 80−100001
baroclinic finite amplitude instabilities, book contrib., review 80−19328
baroclinic instabilities of deep fluid 78−79307
baroclinic waves, amplitude vacillation theory 77−29382
barotropic waves, resonance and energy variation 79−84445
Benjamin-Ono equation, periodic wave and soliton solns. 79−35570
Benjamin-Ono equations, two-parameter Miura transform. 80−14720
Benney's long wave eqns., Hamiltonian formalism 80−31525
Benney's long wave equations, conservation laws and Lax representation 80−14719
bispectrum and nonlinear wave coupling for three-wave coupling 80−52038
boat wake effects on shoreline of Lake Manapouri 79−25278
boundary layer, nonlinear wave development during laminar to turbulent transition *(Russian)* 77−80173
boundary layer on flat plate, two-dimens. waves 77−84263
boundary layer stability, nonlinear effects 78−1636
bubble collapse in liquid, pressure wave, nonequilib. vapour condensation effects 80−59060
δ Cephei, atmospheric vel. field 79−25611
channel, constant depth, wave field from uniform movement bidimensional source *(French)* 80−79332
channel flow, influence of rarefaction and compression waves on base pressure *(Russian)* 79−27656

waves continued
chemical waves, multiple, induced by electric field 79−92047
chemically reactive flow, wave head of gasdynamic disturbance 77−62309
closed tube, nonlinear resonant acoustic oscillators, finite rate theory 80−92171
collisional drift waves, nonlinear evolution, bifurcations to chaotic state 80−14666
combined convection flow along vertical surface, fluctuating boundary layers 80−96254
compressible atmospheres, waves on axisymm. mean flows, generalised Eliassen-Palm and Charney-Drazin theorems 78−81306
computational fluid mechanics, book 80−1517
conducting non-Newtonian liq., shear disturbance propag., mag. field effect *(Russian)* 77−65809
conduit with variable gradient, rapidly flowing incompressible liquid, short waves 80−92219
convergent supersonic jet, wave struct. in interaction with infinite 2-dimens. obstruction 77−55064
craters, coherently overturned flaps produced by hydrodynamic type wave motion 78−57209
deep water waves, instabilities, review, book contrib. 80−96274
density waves in disc around Uranus, as explanation for 'rings' 78−4148
density waves in galaxies, energy and lifetime rel. to galaxies classification and spiral struct. 80−98715
density waves in galaxies, maintenance of spiral struct. and discrete spiral modes 77−33638
density waves in M33, evidence from H I distrib. and spiral struct. 80−56948
density waves in self-gravitating disc, accretion-induced overstability 78−73752
density waves in spiral galaxies, finite spiral arm inclination regime in stellar dynamics 78−49534
diatomic gas, weak nonlinear wave propag., effect of convection, vibr. relax. 77−27623
diffusive instabilities in rotating elec. conducting compressible layers 80−38379
disc galaxies, density wave solns. rel. to masses and mass-luminosity ratios 77−78871
dissipative media, nonlinear, one-dimensional waves, theory 77−58592
divergent duct, vortex flow breakdown, group vel. criterion 80−87807
drag of three-dimensional body in hypersonic Newtonian flow *(Russian)* 78−22369
ducts, one-dimensional models for transient gas-liquid flows 80−64614
dynamo action associated with random waves in a rotating stratified fluid 80−33687
eddy heat fluxes and temp. variances in baroclinic waves, weakly nonlinear theory 80−8390
energy transport by waves without spatial damping, dissipative media 80−31531
exothermic, in gas flows 77−68709
finite amplitude wave propagation in nearly parallel flow 80−74899
finite depth stratified fluids, internal wave solitons, infinite depth limit 80−64574
flame, laminar long wave stability, EHD problem anal. 80−53866
flood wave propagation in channel *(Italian)* 80−28564
flow, parallel, role of negative energy waves in some instabilities 79−59967
fluid layer heated from below, thermal disturbance propag. 79−32464
fluid mechanics, mathematical introduction, book 80−66
free shear layer in viscous critical layer regime, nonlinear stability 80−33576
freely interacting laminar boundary layers in channels 79−81981
galactic density waves, excitation at Lindblad and corotation resons. by external potential 80−22072
galactic tightly wound density waves, nonlinear self consistent theory 79−101206
galaxies, corrugation waves in differentially rotating gas layer 77−5571
galaxies, spiral, non-linear corrugation waves numerical computations 80−67859
galaxies, spiral density wave caused by orbiting retrograde companion 78−96533
galaxies, spiral density waves, loosely wound, hydrodynamic model 79−101207
galaxies, spiral density waves, tidal disturbances of material arms and star clusters *(German)* 79−17086
galaxies density waves, non-linear effect on gravit. instability for adiabatically deformed case 78−20864
galaxies density waves, spiral struct. variability in numerical models 79−25725
galaxies discs, spiral waves nonlinear interaction with stars near corotation radius *(Russian)* 80−62289
galaxies spiral density waves, response near corotation radius to central bar 77−17689
Galaxy, density wave model rel. to struct. around l=140°, b=0° 78−24555
Galaxy spiral density waves, illustrated by periodic stellar orbits superposition 79−84828
gas filled tube, radial resonances excitation, boundary layer considerations 79−98808
gas system entropy waves dissipation, power plant appl. 80−19395
gas-liquid annular two-phase flow, wave and interfacial friction characts. 78−67249
gas-liquid mixture, press. perturbations propag. 78−34186
gaseous density waves in barred spiral galaxies, steady-state gas-dynamical study 80−12819
geophysical fluid dynamics theory, book 80−105443
gradually varying channel, solitary wave evolution, KdV eqn. soln. 80−24040
granular cohesionless material, gravity flow in chutes and channels 79−64753
gravitating disc, rotating, nonlinear stability theory 80−17488
head on collisions between two solitary waves 80−87780
heavily damped, method for determ. wave number and damping coeff. 78−63557
high subsonic nozzle flows, pressure waves from convection of temp. disturbances 80−6125
hurricanes, spiral bands excitation by interaction between symmetric mean vortex and shearing steering current 80−56538
hydrodynamic wave excitation at tangential discontinuity by high-intensity US beams 80−58851
waves continued
hydrostatic mountain waves, terrain shape effects for stratified fluid 80−21804
hyperbolic system, simple wave growth, charact. shock instability, fluid appl. *(French)* 77−68623
ice-water interface, wave formation, heat transfer in presence of turbulent flow 80−103015
inclined surfaces, wave instability of laminar mixed convection flow 80−69837
incompressible stably stratified fluid, internal waves, Brunt-Vaisala freq. 80−79343
incompressible viscous liquids, dynamic anal. 80−48729
inertial waves, produced by obstacle in deep rotating container 79−59993
inertial waves and an initial-value problem for a thin spherical rotating fluid shell 78−55656
interacting, amplitude distrib. function, effect of large-amplitude wave 79−7654
internal linearized waves propagating in a stably stratified system, props. 78−34149
internal wave motion in a periodic stratification 80−1672
internal waves at surface between two fluids, velocity potentials for singularities 78−90926
internal waves excited by travelling forcing effects, compressibility influence 78−61495
interstellar medium, wave-wave interactions in rotating gravitating gas cloud 80−105154
inverse scattering solution for three dimens. three-wave resonant interaction 80−77633
ionosphere, travelling (wave) disturbances of absorpt. near 100 km height 79−25392
ionosphere travelling disturbances, detect. by auroral zone incoherent scatter radar 79−48610
irrotational waves at the limit of breaking *(Italian)* 80−24039
jet, circ., free shear layer transition wave development 78−94643
jet, horizontal five-layer, instability 78−79348
jet, stationary rotationally symmetric supersonic, wave struct. *(German)* 79−86483
jet, turbulent axisymmetric, spatial waves 77−19630
jet exhaust noise, role of shear-layer instability waves 77−47054
Kelvin-Helmholtz billows, finite amplitude, evolution 78−81293
Kelvin-Helmholtz wave, large amplitude, in atmosphere, struct. determ. from altocumulus billows 80−72621
laminar to turbulent boundary layer transition, nonlinear wave interaction, numerical calc. 78−38281
laminar to turbulent boundary layer transition prediction, linear stability theory 78−38279
Langmuir waves, modulated, nonlinear Landau damping effect 78−81849
Larunar boundary layer, low free stream perturbations influence, hydrodynamic waves 79−98738
lee waves, Longs model radiation condition extension to 3-dimens. *(French)* 79−64674
Lee waves classical theory, asymptotic approx., upper boundary condition role 80−12472
linear waves, asymptotic behaviour and wave patterns construction *(Czech)* 80−69
linearly stratified fluid, gravitational collapse of mixed region 80−33653
liquid with gas bubbles, steady-state perturbations, wave propag. 78−5788
long wave-short wave resonance equations, complete soln. for fluid mechanics and plasmas 79−37334
M31 density wave model for spiral arm pattern, M32 gravit. effects 79−21408
Mach reflection of solitary wave 80−79340
Mandel'shtam and nonlinear oscillations and wave theory, review 80−105515
Mars atmosphere, baroclinic waves rel. to surface meteorology 78−89096
mesosphere, Southern hemisphere, wind speed quasi 2-day wave obs. 80−109207
MHD, generalised polar diagrams of plane-parallel stationary simularity flows, waves 80−96314
mixed fluid, nonlinear internal wave formation from gravitational collapse 80−33619
modified Benjamin-Ono eqn., N-periodic wave and N-soliton solns. 80−28518
modulational instability expt. using nonlinear transmission line 77−82397
multiple scattering, theoretical analysis *(German)* 79−75362
multiple three-wave interactions, integrability 79−67168
multistable self-wave media 80−86094
neutral waves in a barotropic zonal jet 79−46333
non-rotational waves at the limit of breaking *(Italian)* 80−24038
nonaxisymmetric wave in pipe flow 79−46390
nonlinear interaction of two waves in boundary-layer flows 80−59016
nonlinear media containing chaotic inhomogeneities, equation closure for average field 79−81601
nonlinear wave effects in a closed tube 79−90332
nonlinear wave fields, diffusion of action 78−81854
nonlinear wave modulation in strongly dispersive systems with random field 78−36840
nonlinear wave phenomena in a closed tube *(Russian)* 78−87353
nonlinear wave resistance theories for 2-dimens. press. distrib. 80−87781
nonlinear wind waves, theoretical model using nonlinear Schrodinger eqn. 79−77154
nonresonant second-order interaction of waves, generation of deeply penetrating gravity-like oscill. 78−28508
normal mode linear initialisation on sphere 80−77042
paraffin wax, solar energy storage heat transfer characts. 80−55921
periodic solution above level bottom 80−57099
photodissociation wave in atmosphere, transparency channel form. 78−79407
planar sonic nozzle, three dimens. wave struct. of nonstationary gas outflow 77−55068
plane periodic waves, nonlinear propagation in relaxing gas, numerical anal. 80−92170
plane shear waves in viscoelastic fluids as motions with proportional stretch history 79−64613
plane wave growth eqn. in polytropic heat cond. relativistic fluid *(French)* 80−28580

waves continued
plane wave-plane shock interaction in magnetofluiddynamics 80−69931
planetary wave, radiatively damped, in middle atmosphere, interaction with zonally averaged circulation 80−109217
planetary waves, vertical propag. rel. to lower ionosphere VLF transmission disturbances 80−8485
pneumatic wave-energy convertor, performance study *(Russian)* 80−76600
Poiseuille flow, nonlinear Tolmin-Schlichting waves, self-excited oscillation stability 79−90263
polythermal glaciers, flow, surface wave anal. 80−46210
potential waves in one dimens. 77−30013
propagation in active and passive periodic structures, review 77−3504
quadratic path solns. for initial-value problem 77−67298
quasi-standing-wave phenomenon due to oscillating internal flow, vortices in shear layer 80−106809
rate type plastic material with general work hardening, acceleration waves 79−37211
rectilinear rarefaction waves, systems of first-order quasi-linear hyperbolic equations 80−90679
recurrence formulas for phases and amplitudes of free wave spherical functions 78−56
relativistic hydrodynamics, thermal waves and growth eqn. *(French)* 80−28579
relaxing gas flow, discontinuity growth 80−28525
resonance tube, oscillation excitation from supersonic jet *(Japanese)* 80−24116
resonant interaction of long and short waves, envelope pulse solitons and breather state 80−1616
resonant three-wave process, Backlund transform. 77−68609
resonant wave triad, nonlinear evolution eqns., exact solns., singularities 78−81853
resonant wave triads, weakly nonlinear, space and time evolution, pump wave approx. 78−81852
roll-wave stability on thin laminar flow down inclined plane wall 80−28488
rolling waves on vertical fluid film 77−84264
Rossby, nonlinear, stochastic closure 77−89133
Rossby small amplitude wave stability in channel 77−56684
Rossby solitary waves, theory 78−1678
Rossby wave, critical layer evolution 78−79329
Rossby wave forced on uniform shear, critical layer evolution 78−42622
Rossby wave interactions and stability in rot. two-layer fluid on β-plane 80−10257
Rossby waves, barotropic, instabilities 78−55654
Rossby waves in rot. two-layer fluid on β-plane, reson. interactions 79−77145
Rossby waves in rotating annulus, laboratory and theoretical study *(Russian)* 80−19509
rotating stratified channel, low-freq. waves 77−47030
rotating stratified fluid, appl. of radiation condition for a source 79−64676
rotating stratified fluid, internal and inertial waves 78−67245
Schwarzschild black hole stationary spherical accretion flow, travelling wave perturbations 80−51800
self-gravitating fluid column, modulational instability 80−85848
semi-infinite body, two-dimensional linear and nonlinear stern waves, separation point 80−69852
shell, elastic, containing ideal fluid, anharmonic vibr. 80−5978
short cylindrical channel, laminar axisymmetric nonstationary viscous gas flow, oscillations 80−38495
small amplitude waves, scale selection in phys. modelling *(Ukrainian)* 77−51069
snow driven by moving body, plastic wave generation *(Japanese)* 77−84186
solar atmosphere, model of centimetric and millimetric emission oscills. 77−22175
solar corona, slow waves rel. to slowly moving disturbances in X-ray corona 80−21971
solar five-minute oscillations, horizontal energy flows struct. 80−62103
solar photosphere, wave propag. obs. 77−22162
solar photosphere, waves and convective motions determ. from spectral lines asymmetry *(Russian)* 80−72901
solar wind, long-period waves upstream from Earth bow shock rel. to wind deceleration 80−98528
solitary Rossby waves in two-layer system, theory 80−17293
solitons, instability, self-refraction *(Russian)* 77−11212
some lecture demonstrations on the statistical properties of wave fields 79−67130
spectral evolution of strongly interacting waves 79−77144
spiral density waves in galaxies, non-linear theory 78−32576
spiral galaxies density waves, appl. of hydrodynamic flow theory near Lindblad resons. 78−96527
stability of convective motion in two-dimens. vertical fluid layer with permeable boundaries 77−55086
standing waves on hollow core vortices 80−106807
steady rotating flow over topography, steady β-plane channel, quasi-linear theory 80−92159
steam generator tubes, forced and natural circulation, inception condition correlations 80−74868
stellar atmospheres, waves effect on spectral line anal. 79−44465
Stokes wave, high wavenumber instabilities 79−81907
stratified fluid, finite depth, wave motion due to periodic pressure, uniform asymptotic anal. 78−55673
stratified fluid in channel, wake collapse in the thermocline and internal solitary waves 80−53787
stratified fluid of finite depth, exact multi-soliton soln. for nonlinear waves 80−22199
stratified heavy incompressible fluid, waves in presence of mag. field 78−59495
stratosphere, annual and semi-annual waves obs. using Nimbus 5 selective chopper radiometer data 78−81315
stratosphere, effect of planetary waves on Lagrangian motion of air parcels 80−109215
stratosphere, travelling planetary waves 80−105030
stratosphere, wave-mean flow interaction rel. to sudden warmings, numerical model 77−5297
stratosphere, zonal mean winds vars. rel. to planetary wave props. and links with troposphere 80−109225
stratosphere long waves, comparison of thermal struct. in N. and S. Hemispheres 77−5296
waves continued
student laboratory exercise, simple harmonic motion, to waves 77−60880
subsonic turbulent jet, entry zone flow wave struct., eddies 80−14773
sunspots umbras, outward wave propag. and motions in mag. tubes 79−16927
superposed fluids, Taylor instability nonlinear theory for wavenumbers near linear cutoff value 79−55355
superposition, computer programs for high-school expts. 78−86094
supersonic compressed boundary layer on two-dimens. plate, unstable localised disturbance characts. 77−55031
supersonic flow past slender body, wave system 78−34155
supersonic underexpanded jets, discharging into opposing supersonic stream, wave structure anal. 80−19461
surface waves, derivation from general boundary theory 79−1442
suspension, transversal undostatic forces prod. by border effects 77−72316
suspension, wave motion in flow down inclined plane *(Ukrainian)* 79−77220
thermoconvective waves in a conducting and radiating fluid 80−19415
thermoconvective waves in stratified compressible fluid, stability criterion contradiction 80−19414
thermosphere, equatorial, wave propag. rel. to density perturbations during geomag. atom *(French)* 79−96846
thermosphere, winter, evidence for long wavelength propagating tidal modes in S. hemisphere meteor region 80−109287
thermosphere neutral waves, direct meas. 77−9581
thermosphere waves generation by southward midnight surge in F-layer wind 77−33233
thin body in nonsteady longitudinal motion, wave resistance in finite depth liquid 80−33616
three-soliton interactions, resonant triads of Korteweg de Vries eqn. 78−67207
three-wave decay interaction, steady-state turbulence spectrum 80−96249
three-wave resonance interaction of disturbances in a boundary layer 79−90264
Tollmien-Schlichting wave packet formation and nonlinear evolution in unstable parallel flow *(French)* 79−50739
Tollmien-Schlichting wave packet produced by turbulent spot in laminar boundary layer 79−68733
Tolman-Schlichting waves in boundary layer effected by external perturbation 79−90265
Tolmin-Schlichting waves, nonlinear interaction in shear flow *(Russian)* 77−58708
toothlike wave dispersion due to turbulent viscosity *(Russian)* 78−1676
transient gas flows with vibr. relaxation, acceleration wave growth and decay 80−1610
transient thermal convection in horizontal rectangular spaces heated from below, waves 80−1566
transversal undostatic forces prod. by border effects 77−72316
trapped nonlinear waves near sonic type singularity 80−24041
trapped waves around circular island, amplitude relation 79−7380
tropical middle atmosphere, wave/zonal flow interaction rel. to semiannual oscillation 80−109216
troposphere, Sun-induced large-amplitude standing planetary waves 78−36236
troposphere planetary pressure waves, transient coupling with D-region short wave absorpt. vars. 77−33162
turbulence in rot. layer, convective wave motion *(Russian)* 77−58670
turbulent boundary layer generation in unsteady flow 78−90828
turbulent flow, interaction of external disturbance, stability 77−54977
turbulent gas flows in channels with high freq. press. oscillations, heat transfer 80−24024
turbulent interface layers, viscous and capillary-gravity waves 78−71323
turbulent jet, wavelike eddies 77−89175
two layer shear flow, radiation field and baroclinic eddy development in β-plane 79−81897
two-layered flow, internal waves at interface, statistical props. *(Japanese)* 80−1673
two-phase stratified horizontal flow, averaged and local instantaneous formulations, stability 80−64613
upper atmopshere, comparison of waves in OH emission layer and F_2-layer 78−45065
upper atmosphere, irregular wavelike motions prod. by lower atmosphere jet streams *(Russian)* 78−96333
upper atmosphere, wave struct. between 50 and 120 km rel. to winter anomaly 78−45193
upper atmosphere, wavelike perturbations vertical propag. rel. to OH, Na D-line and O I 5577 Å nightglow 79−80067
upper atmosphere, waves obs. during 1973, June 30 solar eclipse 77−53302
upper atmosphere wave structure, obs. by Illinois University meteor radar 77−41205
upper atmosphere waves during winter anomaly, results of meteor obs. from Sheffield 78−45070
upper troposphere easterlies, waves rel. to monsoon over Kerala 77−56706
viscoelastic tube filled with viscoplastic media, unsteady motion 78−87366
viscous compressible fluid, wave perturbations *(Russian)* 78−75161
viscous fluids with hidden variables and hyperbolic systems, exceptional waves 80−103037
viscous incompressible liquid, vibrational displacement, wave mechanism 80−43777
vortex layer of small thickness, eqn. of motion, appl. to long waves 78−83414
vortices in flow between two long eccentric rot. cylinders, linear theory 77−51064
vortices in flow between two long eccentric rot. cylinders, nonlinear theory 77−51065
water boundary layers, Tollmien-Schlichting waves and transition 79−81845
wave transport in stratified, rotating fluids 78−89192
wave-transition spectra and vacillation in open rotating cylinder 78−14020
waving plate, external flow of perfect fluid, pressure field *(French)* 80−38426
weak nonlinear waves in compressible fluid, higher order approx. 80−92165
Weddell Sea, planetary wave modes rel. to bottom water variability 80−67366

waves continued
CO_2, weak nonlinear waves, struct. and propag., effect of vibr. relaxation 79−64683
N_2O, weak nonlinear waves, struct. and propag., effect of vibr. relaxation 79−64683

waxes
blooming of rubber 80−104109
carnauba wax, and rosin mixtures, hetero- to homocharge transition, temp. depend. *(Japanese)* 78−35082
carnauba wax, electret states, role of crystallites 80−2686
carnauba wax, magnetoelectret state, mag. anisotropy, quantum mech. effect 77−59379
carnauba wax, orientation prod., by mech. press. or US waves 78−64314
carnauba wax, polarised, simultaneous variation of dielec. const. and discharge current, room temp. to beyond melting point 80−11314
carnauba wax, thermoelectret, lattice parameter changes at elevated temps. 80−29674
carnauba wax, thermoelectret orientation parameters, solidification with different cooling rates 79−38444
carnauba wax and rosin thermal electret, elec. charge studied by TSC 80−7286
carnauba wax electret, effective charge rel. to polarisation tmep. 78−15086
carnauba wax electret, electric charge studied by TSC *(Japanese)* 78−6626
carnauba wax electrets, residual strain and crystal size of orienting crystallites and their effect on charge behaviour 80−11319
carnauba wax magneto-electret, Struve function 78−76287
carnauba wax thermoelectret, charge behaviour 80−7276
carnauba wax thermoelectrets crystallite orientation, X-ray diffr. obs. 78−43774
ceresin wax magnetoelectret, X-ray diffr. pattern 78−6014
Fischer-Tropsch wax, NMR investigation 80−7186
halocarbon, thermoxidative stability study, hybrid microcircuit appl. 79−100271
impurity in polyethylene film electrets, influence on polarisation props. *(French)* 80−44999
paraffin wax, elec. cond., 33-55°C and 1-2 kV cm^{-1} 79−99555
paraffin waxes, melting point determ., automatic analyser, based on dilatometry 79−14223
Parowax, thermal energy storage, phase change material, time variation of storage and release 80−67008
polychlorotrifluoroethylene wax, thermoxidative stability study, hybrid microcircuit appl. 79−100271
polyethylene wax characterisation by gel chromatography, osmotic meas. and scattered light meas. *(German)* 77−86420
polyethylene-paraffin wax, blends, rapid cooling processing techniques 80−84905
shellac and bee's wax, orientation solidification in mag. field, magnetoelectrets, X-ray diffr. 77−12299
sisal wax, electronic conduction and persistent internal polarisation 78−80277
Takiwax film, hologram recording at 10.6 μm, image reconstruction 78−17868
Takiwax films for pulsed IR holography 79−18363
wax-graphite composite, specific capacitance, temp. and grain size depend. 80−50286
WC vacuum sintering furnace systems 78−84737

waxing *see polishing*

weak ferromagnetism
see also canted spin arrangements; Morin temperature
alloys, nearly and weakly ferromagnetic, mag. clusters, unpolarised neutron diffuse scatt. 78−39297
alloys, two-component, electron interactions and spin-wave stiffness const., very weak ferromagnetism limit 77−1548
antiferromagnet, rhombohedral, spin-reorientation phase transition *(Russian)* 80−93122
antiferromagnet, second-order phase transition, weakening of effect of fluctuation in order parameter near crit. point 79−15316
chains of classical spins, weak ferromagnetism 79−15268
cobaltous acetate tetrahydrate, weak ferromag. obs. below 85 mK 79−73695
collective excitations in transverse mag. field, AFMR spectrum 80−93100
copper formate tetrahydrate, antiferromag. phase, neutron diffr. study 80−93085
copper oxalate, two-dimensional antiferromag. PMR study 77−28453
critical temperature region, boson field analysis 77−51911
crystal field model of Invar effects in weak and strong ferromagnets 79−56484
dialkylammonium copper tetrachloride, ferromagnetic layer compound, magnetostatic mode excitation 80−29538
dipropylammonium manganese tetrachloride, two-dimens. weak ferromagnet, AC susceptibility 80−65823
domain structure theory, for antiferromagnet with weak ferromagnetism 78−47997
domain wall dynamics, nonlinear waves, mag. solitons *(Russian)* 80−75793
$Fe_xCo_{1-x}Ti$, ferromag., high-field and high-press. mag. behaviour 78−91919
garnets, crystal and static mag. props. 79−99166
hexagonal antiferromags., ground states antiferromag. vectors, ferromag. moments *(Russian)* 78−27040
high-frequency props. of weak ferromagnets and antiferromagnets, singularities *(Russian)* 80−50196
hysteretic phenomena 78−27059
Invar alloys elastic and magnetoelastic effects 79−56589
Invar behaviour in crystalline and amorphous alloys 79−56489
itinerant electron system, weakly ferromagnetic ground state, Fermi liquid theoretical study 79−4646
Landau-Lifshitz eqn. solutions, moving domain walls, struct. *(Russian)* 80−100596
manganese stearate, literally two-dimensional magnet, mag. ordering, EPR 79−28597
manganese stearate, mag. two-dimensional system, mag. susceptibility 78−10669
manganese stearate, two-dimensional mag. struct. 80−108040
metal, nearly and weakly ferromag., freq. depend. elec. cond., Drude's formula deviation 79−47091

weak ferromagnetism continued
metals, HF polar spin waves, phenomenological theory *(Russian)* 77−89938
one-magnon Raman processes in weak ferromagnets with single-ion anisotropy 78−27234
orthoferrite plate, domain boundary crit. velocity *(Russian)* 78−35015
orthoferrites, single ion anisotropy contrib. 80−25126
paramagnons, appl. of fundamental exns. of Femi liq. theory 77−61015
rare earth cobalt alloy, RCo_2, itinerant system 78−52191
rare earth orthochromites, mag. interactions and weak ferromagnetism 78−52220
rare earth vanadites, RVO_3, mag. props 77−32190
rare earth-Co intermetallics, RCo_2, itinerant ferromag., magnetovolume effects 79−8038
soft phonons and mag. phase transitions 80−54889
third-order invariants *(Russian)* 78−95435
transition metal alloys, electronic specific heat, near and weak ferromagnetics 78−80158
transition metal alloys, magnetovolume effects near crit. conc. for ferromag. 79−56591
transition metal magnetic alloys, dilute, props., review of theory 79−15282
uniaxial ferromagnet, with easy plane anisotropy correl. functions and magnetisation, temp. depend. *(Russian)* 80−84581
uniaxial weak ferromagnet, energetic spectrum *(Russian)* 79−51762
weak itinerant electron ferromagnet, spin fluctuation curvature of Arrott plot 79−8012
$BaMn_{0.99}Co_{0.01}F_4$, magnetoelec. phenomena, dielec. behaviour near Neel temp. 80−71151
$BaMnF_4$, phase transitions, review 79−78378
$BaO\text{-}Mn_2O_3\text{-}B_2O_3$, amorphous mag. oxide, field-cooling effect *(Japanese)* 80−84615
CeFeSi, mag. susceptibility, weak ferromag. at temps. below 470K *(Russian)* 78−56290
$CeFe_2Si_2$, mag. susceptibility weak ferromag. at temps. below 700K *(Russian)* 78−56290
$CoCO_3$, antiferromagnetic reson. and two-magnon absorpt. *(Russian)* 80−29627
$CoCO_3$, light scatt. by thermal magnons and magnons excited by antiferromag. reson. 79−82965
$CoCO_3$, long wave IR spectrum, high freq. antiferromag. reson. *(Russian)* 78−31115
$CoCO_3$, weak ferromag., antiferromag. reson., phenomenological theory 78−60339
$CoCO_3$, weak ferromagnet, optic study of spin wave spectrum *(Russian)* 79−47263
$CoCO_3$, weak ferromagnet, light absorpt. dichroism and mag. config. *(Russian)* 79−87457
$CoCO_3$, weakly ferromag., light scatt. on spin waves *(Russian)* 78−72419
$CoCO_3$, weakly ferromag., light absorpt. dichroism and mag. config. 80−66223
Cr, δ- and BCC, fine particles, mag. props. 78−52314
Cr-Mn alloys, antiferromag. and weak ferromag., elec. props. 79−56514
$CrTe_{1+x}$, thermal expansion and spontaneous magnetostriction *(Russian)* 78−48017
$\alpha\text{-}Cs_xVF_3$, mag. props., 4.2-550K *(French)* 77−80933
Cu complex, strong antisymmetric exchange 78−34976
Cu_xS, $1 \leq x \leq 2$, quantum temp. size effect and magnetism *(Russian)* 80−103764
$DyFe_{0.998}Co_{0.002}O_3$, mag. transition, NMR meas. 78−27036
$DyFe_{0.998}Co_{0.002}O_3$, orthoferrite, domain struct. near mag. transitions 80−2599
$DyFe_{1-x}Co_xO_3$, thermal expansion and magnetostriction anomalies close to curie point 77−8383
$DyFeO_3$, mag. field induced intermediate state 77−55672
$DyFeO_3$, mag. intermediate state obs. by visual polarisation method *(Russian)* 77−40059
$DyFeO_3$, spin reorientation near Morin temp., magnetooptical exam. 78−68284
$DyFeO_3$, spin reorientation transitions induced by magnetic fields, Mossbauer study 80−71246
$DyFeO_3$, weak ferromagnet, μSR study 80−93226
$ErCrO_3$, field-induced spin reorientation relax. 79−78402
$ErCrO_3$, magnetisation, NMR freq. temps. depend. weak ferromagnetic-antiferromagnetic spin reorientation transition 80−29631
$ErFeO_3$, high freq. props. in ordering region of spin system, antiferromag. reson. study *(Russian)* 80−2644
$ErFeO_3$, weak ferromagnet, μSR study 80−93226
$Eu_{1-x}Sr_xVo_{3-0.1x}$, metal-insulator transition and mag. susceptibility 77−47816
Fe base amorphous alloys, Invar and Elinvar characts. 80−29592
$FeBO_3$, antiferromag., optical absorpt. spectra, role of local mag. mode 79−28785
$FeBO_3$, basal mag. anisotropy, antiferromag. reson. *(Russian)* 79−47338
$FeBO_3$, Brillouin scatt. from parametrically excited phonons 79−73956
$FeBO_3$, FMR instability, parametric excitation of phonons, Brillouin scatt. obs. 79−78529
$FeBO_3$, magnon dispersion by light scatt. and ferromag. reson. 77−55668
$FeBO_3$, single cryst., weakly ferromag., Mossbauer study *(Russian)* 77−81038
$FeBO_3$, spin wave dispersion at small wavevectors, Brillouin scatt. and ferromag. reson. 78−47962
$FeBO_3$, spin-reorientation phase transition *(Russian)* 80−93122
$FeBO_3$, weak ferromag., mag. field influence on crit. behaviour of susceptibility 78−14942
$FeBO_3$, weak ferromagnet, spin wave band struct. and microwave props. 79−1661
Fe_3BO_6, canted mag. struct. near Neel point, Mossbauer meas. 78−35073
Fe_3BO_6, Faraday rotation and birefringence 80−100650
Fe_3BO_6, mag. struct. determ. by Mossbauer method 77−40164
Fe_3BO_6, spin reorientation by mag. field, Mossbauer meas. 78−35074
Fe_3BO_6, spin-reorientation, elec. resist. and microwave absorption 78−14751
Fe_3BO_6, weak ferromag., growth of bulk single cryst. by vapour phase reaction 77−24939
Fe_3BO_6, weak ferromag., mag. reson. 77−69706
$Fe_xCo_{1-x}Si(Ti)$, magnetic props., sp. ht. and resist. meas. 79−61120

weak ferromagnetism continued
$Fe_xCo_{1-x}Ti$, high press. mag. props. 78−23271
FeF_3, NMR of ^{57}Fe nuclei 79−95676
α-Fe_2O_3, H-T phase diagram 79−87258
Fe_2O_3, haematite, optical indicatrix deform. and rot. during field induced phase transition 78−68482
Fe_2O_3, haematite, weak ferromag. to pure antiferromag. transition, X-ray diffr. study 77−51904
Fe_2O_3, hematite, transverse galvanomag. parity effects anisotropy *(Russian)* 80−49770
α-Fe_2O_3, hematite, weakly ferromag. domain struct., X-ray topography obs. 79−28551
α-Fe_2O_3, Morin transition, Mossbauer spectra meas. 78−31071
Fe_2O_3, natural haematite, weakly ferromag., Hall effect *(Russian)* 77−11937
Fe_2O_3, natural haematite, weakly ferromag., magnetoresist. *(Russian)* 78−23110
Fe_2O_3, shocked hematite, Mossbauer exam. 78−64304
α-Fe_2O_3:Al^{3+}(Ga^{3+})(Cr^{3+})(In^{3+}), substitution effect on Morin transition, neutron diffr. study 80−44827
Fe_3O_6, O_2 annealed, optical absorpt., spin struct., polaronic absorpt., cryst. field transitions 78−68493
α-FeOOH.nH_2O, hydrogoethites, national, weak ferromagnetism 77−53042
$Fe_xPd_{82-x}Si_{18}$ metallic glass, mag. phase diagram, weak ferromagnet-spin glass transition 80−54893
$Fe_xPd_{82-x}Si_{18}$ metallic glass, mag. transitions, weak ferromagnetism 80−100583
$FeTh_2S_5$, mag. struct. and props., neutron diffr. and mag. meas. 80−60201
Fe_2TiO_4, ulvospinel, mag. props. weak ferromag. in 4-200K temp. range 78−56351
$GdCrO_3$, EPR linewidth, Neel point to 700K 80−39849
$GdCrO_3$, Faraday rotation and linear birefringence meas. 77−77180
$GdSn_3$, Neel temp., hydrostatic press. depend. 80−29549
$(Ge,Pb)_{1-x}Mn_xTe$, mag. and elec. props. meas. 80−29534
^3He, superfluid, A-phase weak ferromagnetism and peculiarities of superfluid transition *(Russian)* 78−67885
$Ho_{0.5}Dy_{0.5}FeO_3$ orthoferrite, domain wall struct., stability conditions, Morin transition, anisotropy const. 80−34684
$KMnF_3$, mag. props. and struct. transitions, antiferromag. reson. meas. 79−8052
$KMnF_3$, soft phonons and mag. phase transitions 80−54889
α-K_xVF_3, mag. props., 4.2-550 K *(Russian)* 77−80933
$MnAs_{0.97}P_{0.03}$, orthorhombic, mag. anisotropy 77−43832
MnB_2, polycryst., magnetoresist. and mag. props. *(Russian)* 80−92907
$MnCO_3$, weak ferromag., antiferromag. reson., phenomenological theory 78−60339
Mn_3Ge, triangular spin ordering, weak ferromagnetism 79−47237
Mn_3Ge_2, elec. props. and mach. of antiferromag. - weak ferromag. transition 77−76792
MnSi, μ^+ Knight shift, temp. depend. 78−80270
MnSi, weak itinerant ferromag., mag. excitations, neutron scatt. obs. 78−34969
MnSi, weak itinerant ferromagnet, mag. excitations 79−7985
Mn_3Sn, triangular spin ordering, weak ferromagnetism 79−47237
NH_4CoF_3, mag. props. 77−85432
α-$Na_3Fe_2(PO_4)_3$ orthophosphate, cryst. and vitreous, Mossbauer spectroscopy and mag. susceptibility *(French)* 80−80657
β-$Na_xV_2O_5$, antiferromag. props. and weak ferromagnetism 79−78337
$NdFeO_3$, mag. transition, NMR meas. 78−27036
$NdSn_3$, Neel temp., hydrostatic press. depend. 80−29549
$Nd_{1-x}Sr_xVo_{3-0.1x}$, metal-insulator transition and mag. susceptibility 77−47816
Ni-Pt alloys, mag. props. under hydrostatic press. 78−6556
Ni-Ru (3.3 at%), magnetisation, magnetocrystalline anisotropy, magnetostriction and elastic consts., thermal variations 79−28563
Ni-V(Mo)(Ru)(Cr), weak ferromag., stiffness const., low-temp. meas., rel. to RPA-CPA theories 78−31063
Ni-Y, amorphous, resist. and magnetoresist. meas., weak itinerant ferromagnet 78−68018
$NiCl_2.2H_2O$, mag. phase diagram and exchange parameters 77−77054
NiF_2, weak ferromag., antiferromag. reson., phenomenological theory 78−60339
NiFe, spin wave exchange stiffness const., tendency to weak ferromag. 77−4510
$Ni_{1-x}Fe_xS_2$ (x=0 to 0.075), weak ferromag. exam. 79−51755
NiS_2, anomalous magnetoresist. 79−78121
NiS_2, high press. effect on mag. transition temps. 78−91866
NiS_2, mag. torque curve 79−47305
NiS_2, model for weak ferromag. 79−65632
NiS_2, pure and Co doped, ferromag. props. 79−91227
NiS_2, single cryst., weak ferromag., elec. and mag. props. 77−85226
NiS_2, weak ferro- and antiferromag., magnetisation and neutron diffr. meas. 80−65794
NiS_2, weak ferromagnet, galvanomagnetic effect 79−11148
Pd-Mn, Curie temp. and magnetisation, vol. depend. 80−34629
Pd-Ni, disordered alloy, onset of ferromagnetism, effect of press. 79−61111
$PrSn_3$, Neel temp., hydrostatic press. depend. 80−29549
Pt-Co alloys, crit. neutron scatt. in crit. conc. region for onset of ferromagnetism 78−72347
Pt-Fe alloy, low field AC susceptibility 79−73698
$RbFeF_3$, Mossbauer spectra, mag. phases 80−15878
$RbMnCl_3$, antiferromag. static mag. props. *(Russian)* 78−60270
$RbMnF_3$, cubic antiferromag., existence of weak ferromag. 79−69693
$RbNi_xMn_{1-x}F_3$, powder, mag. props. 80−2560
α-Rb_xVF_3, mag. props., 4.2-550K *(Russian)* 77−80933
$Sr(Fe_{0.766}W_{0.234})O_3$, cryst. growth, mag. and Mossbauer studies 79−42743
$SrNd_2Fe_2O_7$, mag. struct., neutron diffr. determ. *(French)* 78−52224
$SrO.Eu_{1-x}Sr_xVo_{3-0.1x}$, elec. and mag. props. 77−89819
$SrO.Nd_{1-x}Sr_xVo_{3-0.1x}$, elec. and mag. props. 77−89819
$TbFeO_3$, magnetisation studies 77−24681
$TiBe_{1.8}Cu_{0.2}$, ferromag., magnetisation density 80−103817
$TiFe_xCo_{1-x}$, thermal expansion and magnetoelastic effects 80−80585
$TlMnCl_3$, weak ferromag. and mag. struct., temp. depend. 78−19219
UPt, magnon heat capacity, magnon magnetisation and mag. entropy 77−24685
UPt, valence bands, XPS spectra 80−50520
$V_xCr_{3-x}S_4$, elec. and mag. props. 79−28523

weak ferromagnetism continued
Y-Ni amorphous alloy, spontaneous magnetisation, Curie temp. and paramag. susceptibility 78−68189
$YCrO_3$, EPR linewidth, Neel point to 700K 80−39849
$YCrO_3$, magnetisation, NMR freq. temps. depend. weak ferromagnetic-antiferromagnetic spin reorientation transition 80−29631
$YFe_{1-x}Mn_xO_3$ orthoferrite, spin reorientation, mag. torque meas. 78−47979
$YFeO_3$, domain boundary dynamics *(Russian)* 79−73768
$YFeO_3$, hydrothermal synthesis and mag. struct. 77−47972
$YFeO_3$, induced spin reorientation near Neel point 78−19267
$YFeO_3$ orthoferrite, weak ferromagnet domain struct. near Neel temp. 79−99739
$YFeO_3$, weak ferromagnet, domain wall motion and velocity *(Russian)* 80−54917
$YFeO_3$:Co^{2+}, single ion anisotropy contrib. 80−25126
YFe_2O_4, parasitic ferrimagnetism 79−4703
$YbFeO_3$:Co, mag. struct. factors, neutron diffr. study 79−47248
$Zr(Fe,Al)_2$, weak itinerant ferromag., mag. anisotropy effects on mag. isotherms 80−11187
$Zr(Fe_{1-x}Co_x)_2$, mag. props. and Mossbauer effects 79−91322
$ZrZn_2$, high purity, mag. props., pulsed fields up to 17 T 78−64198
$ZrZr_2$, itinerant electron ferromag., effect of spin fluctuations, NMR 77−16192

weak interactions, elementary particle *see elementary particle weak interactions*

weapons
electro-optical sensors use, prediction of atmospheric effects 79−53522
EMP radiation, nuclear explosion 77−54366
Laser ballistic missile destructor and weapons technology 77−50710
LMFBR fuel cycles that reduce nuclear weapon material proliferation 80−106105
military fibre-optic communication systems progress 78−1425
neutron bombs, effects *(German)* 78−814
neutron weapons, physical and military problems *(Norwegian)* 79−81091
nuclear, global consequences 77−57148
nuclear weapons testing, radionuclide distributions in oceans and marine sediments 78−13344
target and hunting gun optical sights 79−72664
Weapons Neutron Research Facility initial target/moderator configuration 79−9933
^{235}U, recovery from enrichment plant tailings by laser isotope separation, non-proliferation of nuclear weapons aspects 80−83212

wear
see also abrasion; hardness
abraded surfaces, topography rel. to contact area and abrasion mechanism 80−58986
abrasive and impact abrasive wear testing equipment for materials at elevated temps. 78−7136
abrasive wear mechanism, grit size effect 80−16501
abrasives, granular composition changes due to wear *(Russian)* 79−79115
acoustic cavitation erosion, amplitude-spectrometric study 77−52505
acrylic resin wear and cutting surface against brass *(Japanese)* 78−56779
adhesive, in presence of magnetic field model 77−28913
adhesive wear and friction, state of the art 77−8955
alloy, friction and wear, effect of oxides 79−20203
alloy testing for use in heat treatment furnace, disc tribometer with high temp. pin 78−95900
alloys, ion implantation in tribology and corrosion science, overview 79−14830
alloys, metalloceramic, hard, estimation by measuring magnetic permeability 77−90558
alumina, wear, effect of liquid environment, use of pendulum scratching sclerometer *(Russian)* 77−16693
alumina ceramic artificial hip joint wear tests *(German)* 79−8567
analytical surface tools, review 78−64718
antifriction materials, device for wear testing 80−21223
apparatus, for adherence, wear resist. and thermal shock meas. of thin films 78−72943
arc electrodes, heat exchanges obs., dependence on electrode material and cooling conditions *(French)* 80−19655
Armco iron, wear resistance in liquid Sn and Bi *(Russian)* 77−59941
articular cartilage, in vitro studies of wear against stainless steel 79−74714
asbestos-reinforced friction materials, wear and thermal processes 80−40559
asperity deformation models, slip-line field anal., wear and friction regimes 79−87739
aspheric axisymmetric lens figuring, wear pattern prediction 77−27398
Auger electron spectroscopy of wear surfaces formed in lubricant testing machine 77−40452
bearing materials, rolling, steel, WC and Si_3N_4, effects of high temperature operation 80−21124
bearing surfaces, appl. of Markov processes theory *(Russian)* 77−59943
belt grinding, struct. transformations 80−30169
bend erosion, particle size effect 78−11346
body rotating in viscous abrasive medium *(Russian)* 79−79114
boronised coating on steel, sliding and abrasive wear, corrosion resist. 78−11428
boundary lubricated surfaces, wear initiation 79−34157
brass, α-β phase transformation caused by friction 80−76378
brass, abrasive wear, critical grit size effect *(Japanese)* 80−11783
brass, comparison of liquid impact erosion and cavitation erosion 80−104302
brass, frictional wear, effect of alloying and metal oxide compounds *(Russian)* 78−31541
brass, sliding contact in magnetic field, model for cross diffusion 79−79121
brass 63, recrystallisation textures, and deformation formed by dry sliding against steel 79−91698
brass on steel, cyclic wear behaviour 79−52380
brass rings, sliding against mild steel, prow formation processes *(Japanese)* 80−35336
brass/steel couple, wear results from talysurf traces 79−52392
brittle, non metallic materials, wear chart, exam. *(German)* 78−35521
brittle material, wear, acoustic emission obs., effect of ion aggregates in Rebinder-Westwood environment 78−48536

wear continued
bronze, Al, wear on 13% Cr steel in presence of aviation fuel 80−11781
bronze, Al and Ti, sintered frictional material, wear resistance, effect of matrix struct. 77−28911
bronze, sintered, Zr addition effects on struct., hardness, wear resistance *(Russian)* 77−70019
bronze bearings, TEM exam. of wear debris 77−77595
bronze casting, graphite dispersed, graphite particle size effect on wear *(Japanese)* 79−15804
bronze scrapers, wear by rubber 79−66173
bronze-on-steel contact, lubricated, effect of zinc di-n-butyl dithiophosphate on wear 79−20219
built-up edge form., direct SEM obs. 80−104303
capillary wear effects in interfacial tension meas. with Lippmann electrometer 78−26751
cast Fe (3% C), erosion in cavitating venturi 80−108602
cathode spots of the first kind, erosion rate resistivity and thermal cond. depend., explosive model 79−14630
cavitation damage prediction 79−74265
cavitation erosion, observation of eroded surface by SEM 78−15536
cavitation erosion intensity in hydrodynamic wakes *(Russian)* 80−53790
cavitation-produced stress in solid 77−24354
cavitational corrosion of materials in molten metals on const. mag. field appl. *(Russian)* 80−60987
cemented carbide tools when turning grey cast Fe 79−43442
cemented carbides, indentation fracture, surface fracture toughness nature 78−60849
ceramic artificial hip joint, wear and friction tests *(German)* 79−8568
ceramics, erosion in high temp. steam and H atmosphere 80−35334
ceramics, microstructure dependence of mechanical behaviour 78−88533
ceramics and brittle solids, abrasive wear, role of plastic deform. and fracture 80−108594
cloth materials, nucleonic NDT instrument 78−53171
coal conversion plant material, corrosion and wear 78−53012
coatings for wear and lubrication 79−19494
coaxial plasmatron, Cu electrode degradation by arc spot, thermal shock and surface cracks 79−14629
composite friction and bearing materials, development, friction and wear theory, review 80−60979
composite materials, water lubrication, wear studies 80−60984
computer industry, review of wear problems 79−20210
conference, Dearborn, MI, USA (April 1979) 80−105426
conference, St. Louis, USA (April 1977) 78−64717
contact, frictionally heated, thermoelastic deform. 80−83764
contact planform effect, roughness, friction and wear 80−64497
contact stress anal. involving fretting fatigue loadings, computer soln. 78−34096
contacting asperities, theoretical analysis of elastic-plastic deformation 79−95076
contacting bodies, roughness and Poisson's ratio effect on deform. 79−79122
continuous recording of wear of specimens on friction machine 80−55604
correlation function appl. in meas. 77−28914
corundum-based refractory lining, wear resistance in combustion gas flow *(Russian)* 79−8370
cumulative damage model 79−44736
cumulative damage stochastic model, fatigue and wear life test data anal. 79−18823
cumulative damage stochastic model 79−18822
curved pipe carrying gas particle mixture, erosion 80−16498
cutting fluids testing rel. to tool wear, thin layer activation technique 80−55619
cutting tools, diffusive wear, mag. field effect 80−60985
debris anal., quantitative methods 78−64912
debris anal. and condition monitoring review 78−68854
delamination theory, review 78−3229
delamination theory implications for minimization 78−3238
delamination wear, macroscopic effects 80−35343
delamination wear, mechanics of crack propag. 78−3231
delamination wear, subsurface void nucleation mechanism 78−3230
diamond, friction in contact with W, temp. depend. *(Russian)* 77−73350
diamond, polycrystalline tool, wear in rock removal processes 78−64724
diamond, segmental wheel, wear resistance 78−48539
diamond, wear during hard rock drilling, effect of chemomechanically active fluids 79−15802
diamond tools on steel, wear due to clean surface reactions 78−85008
diamond wear during hard rock drilling, effect of chemomechanically active fluids 79−15803
die steels for cold plastic working, powder metallurgy, charact. 78−68649
die wear during wire drawing, review 80−30113
dimethacrylate resins dental composite, abrasion and wear props. 79−96710
dressing effect on grinding performance, review 80−16502
droplet impact, high-speed, effect of gas medium on dimensions of contact area 77−28942
dry sliding wear, role of dynamic recrystallisation 80−108599
ductile erosion, prediction, mechanistic model 77−12709
ductile metals, velocity depend. of erosion by solid particles, at low incidence angles 78−87311
Duraluminium, surface erosion due to US activation *(German)* 79−57122
EBR-II subassemblies, 61-pin wire-spaced, exptl. confirmation of design to minimize vibr. and wear 79−67825
elastic half-space, with crack inside, determ. of stress intensification factors 80−99964
elastically deformable media, liq. drop collisions, simulation of erosion in rainfield 77−56113
elastomeric bearings, high-capacity, laminated, finite-element anal. 80−96197
elastometric materials, friction testing using reciprocating friction and wear tester 80−76451
elbor, friction in contact with W, temp. depend. *(Russian)* 77−73350
electroboronizing, Al effects on hardness and wear resistance *(Korean)* 77−73356
electrode erosion in pulse discharge breakdown of multiple medium *(Russian)* 79−95707
electromagnetic device for loading and measuring wear in vacuum 78−56841
wear continued
EM sensor window materials, particulate erosion 80−38080
energy transform. process 79−18838
entropy production model 80−74815
epoxy resin, filled, wear props., SEM obs. 80−16500
epoxy resin, stresses arising during high-speed droplet impact 80−71764
epoxy resin wear and cutting surface against brass *(Japanese)* 78−56779
epoxy-steel system, friction and wear 78−44229
erosion, book contrib. 78−11350
erosion damage due to cavitation, expt. studies in plasticine 80−1490
erosion tests, comparison of results from various methods and sources 79−61819
erosion with plain jets and jets with cavitation inducers 79−15805
erosivity and mechanoluminescence *(German)* 80−25873
evaluation, ferrography method *(Polish)* 79−79197
examination, appl. of small cyclotrons *(Hungarian)* 78−70656
exoelectron emission for tribomechanical surface treatment *(German)* 77−4870
fatigue life dispersion in rolling contact, new model 78−59349
Fe, cast, mechanism of boundary lubrication with zinc dithiophosphate 79−79120
ferrographic particle separation technique 79−70395
Ferrography, use to predict wear, for maintenance 78−3303
ferrography of polymer form. under lubricated nibbing contact 77−21292
fibre reinforced composite, wear mechanisms, quantitative model 79−47786
fibre reinforced plastic, wear mechanism against mild steel 78−56782
fluoro epoxy resins, surface props., appls., wear resistance and friction 78−64713
fluorocarbon polymer thin films for lubrication of Au contact surfaces 80−89157
four ball test re-examination for lubricants 78−60964
fracture mechanics appl. to wear 80−11792
fretting effect on fatigue 80−16482
fretting effects on fatigue 77−16688
fretting expt. slip meas., high resolution optical method 79−61830
fretting fatigue, device for investigation in contact zones between shaft and embracing part 79−57171
fretting fatigue 77−4152
fretting fatigue cracks 80−35345
fretting fatigue in vacuum apparatus for investigation 78−15640
fretting fatigue mechanism, environment effect 79−61775
fretting on polycarbonate, influence of experimental conditions on wear 78−44228
fretting wear, slip amplitude effects *(Japanese)* 80−96237
Fretting-induced damage between contacting steel-polymer surfaces 78−15539
friction, lubrication and wear, review of papers published 1974 to 1976 79−15806
friction and wear, material aspects in manufacturing processes 80−81210
friction and wear theory, new charact. of asperity interactions 77−16697
friction machine for wear tests, plastic lubricant attachment 78−3273
friction surfaces, wear meas. using profilograph, mould producing material quality factors 78−7116
frictional electromagnetic clutch material, sintered, friction, hardness, wear props. 78−11339
frictional heating and oxidational theory 80−44255
gas lubricated bearings, test equipment to examine friction and wear, exam. of design 79−52522
gas turbine airfoils, protective coatings, degradation charact. and methods of application 79−24670
glass, wear, acoustic emission obs., effect of ion aggregates in Rebinder-Westwood environment 78−48536
glass fibre reinforced PTFE and polyacetal, friction and wear against glass and steel 78−56783
glass materials, rain erosion mechanisms 79−34154
glass/MoS_2 reinforced PTFE, fibre orientation effect on friction and wear 79−79125
glasses, high vol. low cost, as solar reflectors, compositions and weathering effects 80−106589
graphite, fibre reinforced epoxy, fibre orientation effect on friction and wear 79−79125
graphite, radiation damage effect on erosion by H 78−21640
graphite, sliding against C, dusting wear regime 80−97595
graphite, surface erosion by 100 keV $^4He^+$ and 200 keV H_2^+ 78−23569
graphite, surface erosion by ion bombardment crystal anisotropy effect 78−23845
graphite, thin layer activation meas. technique, assessment 78−92366
graphite dispersed Al-Si, wear charact. *(Korean)* 80−93658
graphite fibre reinforced, Cu-Sn exam. of high speed tribological props. in friction expts. against steel 79−15809
graphite fibre reinforced metal, fibre orientation effect on wear 79−87744
graphite fibre reinforced metals, tribological behaviour, fibre origin effects 79−96158
graphite fibre reinforced polyimide composites 79−52381
graphite filled PTFE, carbon aspect ratio effect on friction and wear charact. 77−59945
graphite reinforced Al, wear volume/sliding time relationship 79−61743
grinding wheel life modelling, group method of data handling 80−58987
hard alloy insert jig brushes, wear resist. *(Russian)* 80−60977
hard-facing alloy, assessment method 80−15186
hardfacing alloys in impact abrasive loading, wear resistance, temp. effects 79−87737
Haynes Stellite 6B, Al_2O_3 particle erosion of surface, SEM obs. 78−88545
Haynes Stellite 6B, particle erosion damage, TEM obs. 78−88546
heat exchanger, liquid-fluidised bed, scale control and corrosion tests, geothermal power plant appl. 79−48090
hip joint, wear of plastic material 77−21661
history, factors affecting, relation to other mech. props. 79−92916
holographic technique with computer aided anal. for wear meas. 80−87345
human joint, ferrography applic. 79−34694
hydraulic liquids, cavitation-erosion props. assessment using ultrasonic dispergator 80−71832
impact, abrasion, wear, review *(German)* 78−88536
impact interaction of microroughnesses of rubbing surfaces *(Russian)* 79−100265

wear continued
impact wear, book 78−48544
Inconel 718, high temp. fretting fatigue, fatigue and fretting wear 80−3197
Inconel 718, superalloy, wear of superhard tool during cutting, SEM and metallographic obs. 78−64720
interface erosion rate meas. using pulse-echo US method 78−182
ion-implanted alloys, surface props. effects and appls. 80−79824
joint prosthesis materials, wear meas., test machine design 79−20716
Kevlar fibre reinforced epoxy, fibre orientation effect on friction and wear 79−79125
laboratory measurement method using Ferrography, study of diesel engine wear 78−3304
liquid cavitation and droplet impact erosion, predictability of prototype machine from lab. tests 78−64723
LMFBR materials, exam. of material requirement 78−50256
low-alloy steel, abrasive wear resistance, effect of C content, annealing quenching 77−56115
lubricant evaluation, using four ball friction machine 80−25951
lubricant wear debris examination, oil anal. techniques, appl. to plain bearing materials study 80−97596
lubricated, contrib. to theory 80−88257
lubricated contacts, adhesive wear 80−16491
lubricated elastomers in contact with regularly spaced sliders, frictional dynamics 79−20213
lubricating oils, spectrographic anal. of wear metals 78−20114
lubrication mechanism, by surrounding gas molecules in adhesive wear 79−42143
machine tool wear resistance, accelerated testing *(Russian)* 80−40543
magnesite-dolomite refractories, tar bound, fracture and wear 80−104287
martensitic steel, abrasive wear resistance, effect of tempering strain martensite 77−56116
materials and lubrication media, for frictional pairs, choice by energy criteria *(Russian)* 78−31541
materials selection for wear resistance 80−21120
materials under complex stress, with local dynamic loading, strength 79−91768
materials under melting, intensity calc. 80−103416
measurement, thin layer activation technique 78−72945
measurement by surface replication 77−12771
measurement by thin layer activation 78−60932
mechanical treatment in aq. salt soln., material transport rel. to wear 80−16506
mechanism review 78−72891
metal, abrasive wear resistance rel. to physicomechanical props. 79−91804
metal, cavitation erosion resist., increase by case hardening, possible mechanism 80−11845
metal, coated abrasive belt grinding, relation between wear of grain cutting edge and material removal 80−16507
metal, dimensional anal. 77−70193
metal, ductile, jet-impingement solid-particle erosion testing, halo effect 80−76376
metal, erosion by high speed particles, temp. effects 80−40556
metal, erosion damage, temp. effects 79−34156
metal, erosive wear by impinging SiC particles, surface hardness and material props. effect 77−66705
metal, FCC, cavitation erosion 77−86191
metal, friction pair, seizure centres on contacting surface *(Russian)* 77−70185
metal, hard, brittle, correlation between wear, crack resistance and stress intensity factor *(German)* 77−36666
metal, impact abrasive wear, anal. 79−43443
metal, internal stresses during rolling friction and their evaluation 77−28912
metal, nonferrous, unlubricated wear data interpretation 79−38989
metal, oxidation, oxide thickness and oxide transfer in wear 77−16755
metal, particle erosion meas. 77−66703
metal, plastic deform. and sliding friction 79−87743
metal, polymer coated, wear and friction 77−21328
metal, sliding wear, surface topography and integrity effects 78−3235
metal, soft film, initial wear rate 80−11795
metal, steady state rate calc. from profilometric traces 77−77592
metal, surface layer transform. and failure, kinetic charact., under dry friction 77−52506
metal, wear, grinding and erosion, microsphere form. mechanism 79−79123
metal, wear charact., mechanisms 77−32697
metal erosion by microparticle impact, strain rate effect 77−80577
metal erosion by solid particles, high-speed photography 78−39919
metal near surface microstructure effect 78−64730
metal sheets, frictional surface damage during press forming 78−76768
metal sheets sliding on dies under plane strain drawing, sliding surface damage obs. *(Japanese)* 77−44369
metal surface, AES anal. in adhesion, friction and wear 78−53179
metal surface, exoelectron emission as observation technique 77−81202
metal surfaces, factors influencing contact behaviour 80−92092
metal surfaces, laser heat treatment, wear resist., corrosion protection, hardening, review 78−72939
metal wear energy balance under abrasive and boundary friction, expt. 78−85006
metal-ceramic containing diamond, impact hardening 79−15828
metal-glass mats. alloyed with Cu, powder prep. and props. 78−72912
metal-metal metal-polymer sliding, wear mechanisms, review 79−70174
metal-polymer contacts, methods of decreasing wear 79−20209
metallic ion plated soft film, friction and wear 78−15549
metallic materials, erosion resistance, eval. of role of mech. props. 79−83328
metallic wear debris, morphological anal. 80−76453
metallographic micro of worn balls, prep. method 78−3274
metallography of worn surfaces, exptl. difficulties, delamination theory implications 79−34253
metals, abrasive wear and impact and arc erosion, exam. of comparative tendencies of metal loss 79−15811
metals, antiwear action of Zn di-n-butyl phosphate 80−11782
metals, cavitation erosion 78−48538
metals, empirical linear wear law 78−60851
metals, FCC, texture changes in running surface as result of frictional stress 79−91699
wear continued
metals, friction and wear rel. to comp., struct. and props., review 80−25872
metals, in sliding contact, glow discharge effect 79−83333
metals, ion-implanted, friction and wear, review 80−40555
metals, method for rapid determ. of resistance 77−25210
metals, transition, of IV-VI and VIII groups, in intense laser radiation *(Russian)* 77−12702
metals and alloys, abrasion wear testing 77−40493
metals and alloys, finishing, use of ion implantation techniques, effect on wear and corrosion props. 79−34204
metals and alloys, laser erosion, influence of metallic target temp. *(Russian)* 79−39028
methyl α-n-alkylacrylate methyl methacrylate copolymer, friction and wear 77−63809
MHD generator, cathode spot erosion, thermal conduction-diffusion 78−5955
mineral oil lubricants, behaviour in line contact and oscillatory movement *(Spanish)* 79−98671
Mossbauer spectroscopy appl. to friction, lubrication and wear studies 80−40547
multilayer interference film, mass production by roll coating *(Japanese)* 79−81577
multispeed tool life tests with radioactive tools 78−44338
Mylar film sliding against polyethylene and PVC , material transfer 78−64726
n-octadecyl methacrylate methyl methacrylate copolymer 77−63809
natural flow and US cavitation erosion comparison 78−59435
nitrided steel surface wear-related topography 78−60847
noble metals (Ru, Rh, Pd, A, Re, Os, Ir, Pt, Au), wear coefficients determ. using pin-on-cisc apparatus 80−76366
non-magnetic material wear in presence of magnetic field 80−60982
nonferrous metals, unlubricated wear data 80−16510
nozzle erosion, ion implantation effects, ion beam anal. 79−48011
oils, antiwear props. determ. method in tests on friction machines 78−60915
optical materials rain erosion mechanisms 78−83049
optical surface shaping, contact problem soln. 80−33260
orthopaedic implants, SEM study of wear 78−15926
palliative treatments for fretting fatigue, review 80−21126
particulate ablation of solid, appl. of erosion slowness theory to surface contour generation prediction 79−87740
percussive impact wear, development of theory 78−94623
periclase refractories, props. after testing at over 2000°C 80−104317
Permalloy, magnetic head wear resistance and surface charact. against magnetic tape *(Japanese)* 80−35335
Permalloys, wear by magnetic tape, AES *(Japanese)* 78−39916
Permendur 49, ordered and disordered, clean mild wear 80−16508
PFTE, combined rotating and linear motion effects on wear 80−3201
phosphate esters, scuffing resistance 79−38990
physicochemical processes during frictional contact leading to H_2 generation *(Russian)* 77−52496
plant condition monitoring in nuclear power generating industry, review 80−47612
plastics, materials testing, application-oriented test standardisation *(French)* 78−85061
PMMA, rain erosion behaviour, exam. 78−53001
polyacetals with fusible alloy fillers, adhesive wear behaviour *(Japanese)* 79−70173
polyamide resin wear and cutting surface against brass *(Japanese)* 78−56779
polycarbonate-steel surfaces, changes in morphology induced by fretting 78−15538
polyethylene: (Dy_2O_3), mech. props. and transfer to steel surfaces 80−16496
polyethylene, friction and wear with lubrication by thermooxidative destruction products 77−52504
polyethylene, high density, wear mechanism at steel surface, SEM, TEM and DTA 78−64727
polyethylene, ultra high mol. wt., knee prosthesis, in vivo wear props. 80−17204
polyethylene, ultra high molecular weight, wear limit, γ-irradiated and unirradiated *(Japanese)* 78−27649
polyethylene, ultra-high mol. wt., wear mechanisms in total joint replacement 77−52929
polyethylene, ultrahigh mol. wt., wear props. 79−84001
polyethylene, ultrahigh molecular weight, wear, rel. to replacement hip joints 77−17008
polyethylene based compositions, filled with Fe, Al_2O_3 powder, effect of filler particle size on wear resistance 78−44226
polyethylene film sliding against PTFE, PVC, PP, PMMA, material transfer 78−64726
polyethylene terephthalate, joint prosthesis fragment dispersal meas. *(German)* 79−8566
polyethylene wear against dry stainless steel in unidirectional motion 79−20212
polyethylene wear debris from simulated service as total hip prosthesis, quantitative recovery 79−48378
polyethylene-glass fibre composites, gamma-irradiated filler 80−66840
polyimide, carbonized layer form., friction, wear *(Japanese)* 77−52502
polyimide films, effect of atm. and temp. on wear, friction and transfer 78−85003
polymer, adhesive 78−56781
polymer, reciprocating impact wear testing apparatus, results 78−15639
polymer, stress distribution after action of rough surface indenter 79−52471
polymer, wear testing of bearing material, new sliding bearing test facility 78−95862
polymer endoprosthetic joint, fatigue life 80−40521
polymer film, surface profile obs. and nature of contact by multiple beam interferometry 77−1878
polymer viscoelasticity and strength characterisation, advanced light scatt. techniques 80−11857
polymer-metal sliding, wear eqn. in terms of fatigue and topography of sliding surfaces 80−108597
polymer-polymer and metal-polymer sliding wear mechanisms, review 79−70174
polymeric composites, sliding wear mechanisms at metal surfaces, microscope obs. 79−87742
polymeric joint replacements, problem of wear 79−83999
polymeric transfer film form. mech. in wear 78−64729

wear continued
polymers, abrasive wear resistance rel. to physicomechanical props. 79−91804
polymers, friction and wear, role of mech. props. 78−52998
polymers, wear in thermally stressed state 80−3202
polymers for artificial joints, wear testing 78−31981
polyoxymethylene, wear mechanism at steel surface, SEM, TEM and DTA 78−64727
polyphenyl ether fluid operating in elastohydrodynamic contacts, IR emission spectra 79−91807
polyphenylquinoxalines, graphite filled, behaviour during friction 80−40553
porcelain, correlation between wear, crack resistance and stress intensity factor *(German)* 77−36666
powders, ultra fine prod. by rotating friction mill, mechanism in initial wear region *(Japanese)* 80−25589
problem areas, unsolved, review 77−4858
prostheses articulating surfaces, holographic interferometry exam. 78−40415
prosthesis wear, holographic studies using optical contouring 80−67288
PTFE, sliding charact., friction and wear *(Japanese)* 78−56778
PTFE, transfer layers produced by rubbing, apparatus for study 79−47861
PTFE, wear, sliding speed, contact press. and rubbing surface temp. 80−76372
PTFE, wear mechanism at steel surface, SEM, TEM and DTA 78−64727
PTFE+metal, fluoride prod., DSC and XPS anal., rel. to polymer wear 80−11889
PTFE-metal interaction, X-ray photoelectron spectroscopy obs. 80−11788
PVC, filled with SiC particles, abrasion resistance *(Japanese)* 78−7055
PVC, wear props. *(Japanese)* 79−96151
pyrex, plates, exam. of friction, wear and elastic constant mechanisms 78−87309
pyridine, ethyl pyridine, heat of adsorpt. on sponge Fe, Fe_2O_3, CuO, adhesive wear, flow calorimetry 78−85193
reactor component-support impact dynamics, elastic anal. by model expansion method 79−45343
Rebinder effect rel. to wear, chemomechanical interaction 80−21121
reciprocating impact wear testing apparatus 78−15639
recording head wear by magnetic tape, wear meas. using Knoop diamond indentations 77−70192
Relite-base alloy compositions wear caused by sliding abrasive material stream 78−95813
replica technique study 79−20329
resistance, surface treatments, selection procedure, review 78−72892
resistance rel. to specific fracture energy for various materials *(Russian)* 78−85005
resistance testing of hard alloys by mag. loss on polarity reversal 77−59879
resistant material, US welding effect on struct. *(Slovak)* 79−74185
Reynolds equation, numerical soln. with slip boundary conditions and large bearing number 79−90197
rolls in hot strip mills, contact fatigue failure 80−60950
rough surfaces in contact, stochastic approach to deform. mode 77−59950
rubber, graphite filled, performance assessed against steel structures under water lubrication conditions 80−21123
rubber, sliding wear mechanism 77−63810
rubber, wear mechanisms, optical microscope obs. *(French)* 77−21285
rubber mixtures, device for determining wear 80−21226
sandpaper, standardised, for Taber abraser, influence of relative humidity an abrasive quality *(Japanese)* 79−8369
sapphire, wear chart, exam. *(German)* 78−35521
satellite, hardness and erosion resistance to aqueous SiO_2 slurry 79−43441
sealing materials, friction and wear tests *(German)* 79−38987
self-lubricating, struct. and props. 79−100267
self-protection of high wear materials, compacted wear debris films 79−96149
SEM specimen chamber use for dynamic expts., state-of-the-art review 78−23918
Sendust alloy, magnetic head wear resistance and surface charact. against mag. tape *(Japanese)* 80−35335
signature response, for friction and wear 80−40541
simulative testing, systems analysis data sheet for friction and wear tests 77−28967
simulative wear study critically reviewed 77−28968
sintered parts for frictional units 78−11342
Sitall, microcrystalline glass, exam. of frictional props. under end-end rubbing 80−16488
slide calipers, bench for production testing of wear resistance 80−8959
sliding contact, friction, wear, temp. anal. 80−93659
sliding contact problems, heat conduction, temp. and heat source distribs. 79−98588
sliding contact seal, thermoelastic instabilities 78−18257
sliding wear test apparatus, design and statistical evaluation, polymeric restoratives evaluation 80−21237
soft metal used as solid lubricant, compatibility effects 77−21291
sound absorption materials, effects of outdoor exposure 77−88985
sound absorption materials, effects of outdoor exposure on absorpt. coeffs. 77−88985
spark gap electrodes, erosion charact. 80−103204
spark switches, high repetition rate, with Al and brass electrodes, surface ageing 80−106997
spherical indentation mechanics, appl. to reversible and irreversible contact between rough surfaces 78−13976
sputtered refractory carbides, adhesion to metal substrates, improved 80−76481
stainless steel, design fix for vibr. induced wear in fuel pin bundles 77−42094
steady, mechanism anal. by fatigue theory as stochastic process 80−11789
steady state sliding, elementary results of dimensional analysis 77−12711
steel, 12Kh18N9T-TiB_2, eutectic alloy, high temp. props. 78−84931
steel, 40Kh, heat-treated, wear during friction under extreme conditions 78−85007
steel, 4130, annealed, fretting, material removal mechanism 79−20217
steel, adhesive wear, heat treated load effect 78−11344

wear continued
steel, AF 1410 against stainless steel, repetitive impact, microstruct. effect 79−74263
steel, AISI 1045, laser transform. hardening, fatigue and wear rates 79−70198
steel, Al-Cr-Mo, nitride hardened roller, surface fatigue failure under pure rolling and sliding rolling contacts 79−79183
steel, Al-Cr-Mo, nitride hardened rollers, surface fatigue resistance under pure rolling and sliding-rolling contacts 79−79184
steel, alloy, electroslag remelting effect, an impact-abrasive wear resistance 80−55541
steel, alloy, friction surface and lubricant nature, effect on adsorption and temp. stability of lubricant layers 78−15544
steel, alloy, rolling wear study of misaligned cylindrical contacts 80−108590
steel, alloy, surface quality improvement, thermomech. treatment 80−61020
steel, alloy, U20Kh6T2D, structural transformations during heat treatment, and wear resistance 78−88484
steel, alloy, wear particles, spheroid form. by cavitation erosion 79−52382
steel, ATSI 9310, fretting, selected fretting resistant surface treatments 79−29223
steel, austenitic, friction in vacuum of type U8 steel under microshock loading *(Russian)* 80−108583
steel, austenitic, high Mn, abrasive wear resistance *(Korean)* 77−25162
steel, austenitic, martensitic transform. effect on hardening kinetics and fracture resist. of friction surface of 45Kh12G8 and 110G13 *(Russian)* 80−50727
steel, austenitic, precipitation hardenable, friction and wear under abrasive conditions *(German)* 77−59951
steel, austenitic stainless, cavitation erosion resistance, martensitic transform. effect *(Russian)* 78−35524
steel, austenitic stainless, flow cavitation erosion, initial part of incubation period 78−44224
steel, austenitic stainless, fretting wear in air and CO_2 at elevated temps. 80−21119
steel, austenitic stainless, metastable, Si effects, unlubricated adhesive wear, oxidation resistance, solid soln. hardening 77−59949
steel, austenitic stainless, unlubricated, friction, wear and microstruct. of types 304, 316 and Nitronic 60 80−108589
steel, ball bearing with modified chem. comp., improved rolling contact fatigue 78−64732
steel, borided, 45, 20Kh, 30KhGSNA and Kh12F1, relative wear resistance 77 73351
steel, C, 45, surface wearing ability, surface finishing method and running-in effects 80−11794
steel, C, annealed, rolling wear under dry contact conditions 79−52391
steel, C, austempered, exam. of running in and wear 80−16485
steel, C, cavitation erosion, exam. of mechanism and rates 79−5063
steel, C, erosion-corrosion in aqu. H_2S soln. up to 120°C, 1.6 MPa press. 80−21155
steel, C, fretting fatigue damage, SEM exam. 78−88541
steel, C, hard patch of rubbed surface, tempering effect *(Japanese)* 78−7054
steel, C, induction hardened, surface durability, optimum case depth 80−30137
steel, C, ion nitriding, wear resistance *(Japanese)* 77−63828
steel, C, rolling wear study of misaligned cylindrical contacts 80−108590
steel, C, spinning machine ring, increasing wear resist. by boriding 80−21115
steel, C, struct. changes in centres of galling 79−38985
steel, C, wear charact. of worn surface layer under lubrication *(Japanese)* 78−35526
steel, C, wear during impact, effect of C content 79−38986
steel, C, wear of Cr, Zn protective coatings, exam. using nuclear radiation excited X-ray fluorescence 80−21206
steel, C, wear resistant, review of abrasive adhesive and rolling wear *(Korean)* 79−24624
steel, C and alloy, wear resistance, change through hardened layer 79−96153
steel, C and Cr, surface damage during friction, struct. effect 80−35339
steel, carburized, point contact sliding microhardness testing, microscopic exam. 79−87738
steel, contact rapid meas. tech. for electrical contact resistance applied to lubricant additive studies 77−16698
steel, Cr, carburising with high-activity carburiser 80−76412
steel, Cr plated, factors influencing durability 80−108643
steel, Cr with metastable austenite, wear resist., temp. effect 80−76370
steel, Cr-C (18, 0.9 wt.%), cavitation, abrasion resistance, effect of unstable austenitic struct. *(Russian)* 77−16695
steel, Cr-Ni, case hardened rollers, surface fatigue failure under pure rolling and sliding rolling contacts 79−52472
steel, Cr-Ni-Nb, LKh16N4B, high temp. frictional charact. 80−21118
steel, effect of compressive stress, methods of investigation 77−25208
steel, electrospark alloying with TiC-Ni-Mo alloys 77−59998
steel, eutectoid, activation energy of oxidation in wear 77−52507
steel, eutectoid, wear due to impulsive friction, device for exam. 80−25957
steel, fatigue, impact loading, friction, wear in surface active media *(Russian)* 79−29268
steel, fatigue strength of 30 KhGSNA, 12 KhN3A, effect of friction in abrasive medium after hardening 78−35507
steel, fretting against polymers, composition effect on metal surface wear 78−60848
steel, friction and wear during hot forging 80−89358
steel, gas boronized, sliding wear charact. 80−16499
steel, gas nitrosulphurized, in temp. range 813-903K, wear props., surface and cross-sectional hardness, X-ray diffr. and SEM study *(Japanese)* 79−29224
steel, grinding effect with Elbor wheel 78−48540
steel, high C and mild, roughness and wear characteristic of spark-eroded surfaces 79−52390
steel, high Mn mandrels, wear resist., surface layer chem. comp. influence *(Russian)* 79−52444
steel, high speed, irradiated, absolute tool wear determ. by γ-γ coincidence counting of radiotracers 77−73352
steel, high speed, tool, charact. 78−48542
steel, high speed, wear resistance of white layer formed by vacuum oil quenching *(Japanese)* 78−11336
steel, high speed tool, diffusion wear model 79−29230

wear continued
steel, high speed tool, roughness and wear characteristic of spark-eroded surfaces 79−52390
steel, high speed tool, sliding contact in magnetic field, model for cross diffusion 79−79121
steel, high speed tool, wear, effect of magnetisation on tool life 80−89361
steel, high speed YXM62, heat treatment, mech. props., wear, fracture toughness for cutting tool 78−19864
steel, high temperature strength, corrosion-erosion effect of gas metal mixtures stream *(Russian)* 78−35576
steel, high-speed, grain size effect on wear characts. 77−59944
steel, HSLA, V effect on mech. props. *(Korean)* 80−29987
steel, ion nitrided, rolling wear props. *(Japanese)* 77−48554
steel, ion plated Pb film covered, Hertzian contact expt. 77−52511
steel, ion-softnitriding of type S15C with N_2-H_2-CH_4 mixture, mech. props. of surface *(Japanese)* 79−61780
steel, low alloy, medium C, sliding interfaces, division of heat and surface temp. rel. to oxidative wear 78−64712
steel, low C, surface layer struct. under sliding friction 79−52393
steel, machining, adhesion mechanism of built-up edge and layer on rake face of cutting tool 79−47784
steel, maraging, 18 wt.% Ni, annealed surface damage during machining, lubricated conditions 77−59948
steel, maraging, 18 wt.% Ni, solution heated and aged, surrface damage during machining, unlubricated 78−15599
steel, maraging 18 wt.% Ni, annealed, surface drainage during machining, unlubricated conditions 77−59947
steel, mechanism of boundary lubrication with zinc dithiophosphate 79−79120
steel, medium C, behaviour under combined fatigue and wear 78−3236
steel, medium C, drilling in liq. Sn-Zn eutectic, cutting conditions rel. to tool parameters *(Russian)* 79−34187
steel, medium C, fretting fatigue, microstructural and environment effects 78−64734
steel, medium C, interface temp. meas. in fretting 78−64741
steel, medium C (0.42 wt.%), wear charact. in unidirectional and reciprocating friction *(Japanese)* 79−100266
steel, medium C quenched, tempered, relation between wear and work surface layers *(Japanese)* 77−52499
steel, metallic coated, sliding wear resistance 77−12708
steel, metallography of worn surfaces, exptl. difficulties, delamination theory implications 79−34253
steel, mild, cavitation erosion rate, effect of stress level 78−15545
steel, mild, conical rider on Cu surface, SEM exam. of plastic deformation and wear at friction junction 78−88542
steel, mild, point contact sliding, microhardness testing, microscope exam. 79−87738
steel, mild, sliding contact in magnetic field, model for cross diffusion 79−79121
steel, mild and stainless, fretting wear, role of adhesion and delamination 78−35533
steel, Mn, solutioning of castings in salt baths 78−23871
steel, N_2, wear resistant, review of abrasive adhesive and rolling wear *(Korean)* 79−24624
steel, N_2 implantation, nitride form., wear rate reduction 78−27149
steel, Ni-G rollers, case hardened, surface durability in pure rolling and sliding-rolling contacts 79−61739
steel, nitriding, mag. field effect 79−57153
steel, pearlitic, wear behaviour rel. to basic material props. 80−108592
steel, punch, for blanking tools, method of wear resist. determ. 80−55600
steel, rail, fracture rough exam. of wear in rollers, subject to creep 79−15808
steel, scoring and scuffing on lubricated sliding surfaces, Mossbauer study 80−7690
steel, sheet structural changes during rolling influence of lubricants on friction and wear 78−95815
steel, Si-Cr-Mo-W-V (2,4,1,3,2 wt.%), heat treatment and props. 80−16349
steel, Si-Mn-C (1.6-2.0, 0.4-0.6, 1.1-1.4 wt.%), cast graphitised, heat treatment effects on mech. props. and wear resist. 79−96050
steel, sintered, diffusion treatment with B, Si, Cr and C, corrosion and wear improvement 77−77642
steel, sintered bearing material, standardisation, wear and friction props. 78−19901
steel, sintered type M2 high speed, heat treatment response and cutting props. 78−15336
steel, sliding wear reduction by metallic coatings 77−21331
steel, stainless, 316, erosion in cavitating venturi 80−108602
steel, stainless, annealed 310, deform. at erosion sites, TEM and SEM studies 78−64725
steel, stainless, austenitic, CC Ni-Al, γ-phase, fracture mechanical aspects of abrasive friction, wear, chip formation 78−72865
steel, stainless, cavitation-erosion in fresh water, electron microscope and electrochem. study 80−55580
steel, stainless, erosion by coal ash particles 79−61745
steel, stainless, improvement of props. by ion implantation 80−16601
steel, stainless, stress distribution effect on chipping of blanking punch *(Japanese)* 78−31543
steel, stainless, type EP838 ion irradiated, surface structure changes during post-irradiation heating *(Russian)* 80−75272
steel, stainless, wear in dibenzyl disulphide-containing oil, X-ray photoelectron spectroscopy of surface chemistry 78−64736
steel, stainless 310, erosion at 975°C in combustion gas atoms. 77−66704
steel, stainless AISI 304, single phase FCC, stacking fault energy and delamination wear 78−3239
steel, stainless AISI 304, wear at high sliding speed 78−3237
steel, stainless wear by magnetic tape, Auger spectroscopy exam. *(Japanese)* 78−39916
steel, surface wearing ability, finished surface direction effect on wearing ability 80−11793
steel, tool, abrasive wear rate rel. to fracture toughness and microstructure *(German)* 79−29232
steel, tool, high speed, multispeed tool life tests with radioactive tools 78−44338
steel, tool, improvement of props. by ion implantation 80−16601
steel, tool, maraging, based on N12M10, exam. of hardening, crack resistance and wear *(Russian)* 79−34047
wear continued
steel, tool, thermal treatment effect on abrasive wear resistance 78−92369
steel, type Kh12M, rel. between structural inhomogeneity and wear resist. *(Russian)* 80−66672
steel, unhardened, grinding by Si_3N_4-based abrasive material 78−35529
steel, unlubricated sliding wear, effect of N ion implantation 79−74261
steel, W-Mo, tool, hydrostatic extrusion and tempering, wear resistance effect 80−50728
steel, WC reinforced surface layer, serviceability improvement by Ni, Cu-Ni, V alloying additions 77−21290
steel, wear characts. of burnished machined surfaces 80−108595
steel, wear due to paper and printer ribbon exam. 79−15812
steel, wear loss, using $^{56}Fe(p,n)^{56}Co$ and loss of activity meas. 77−4881
steel, wear meas. by ^{56}Co activity reduction 79−57166
steel, wear mechanism review 78−72891
steel, wear mechanisms, metallographic data 77−59942
steel, wear produced by polyisoprene polybutadiene, rubber 79−15810
steel, wear resist., effect of rolling friction strengthening, oil abrasive environment *(Russian)* 79−15799
steel, wear resist., mech. props. and struct. effects 80−35338
steel, wear resistance during abrasive wear, comp. and struct. effects 80−35337
steel, wear resistance in liquid Sn and Bi *(Russian)* 77−59941
steel, wear resistance of 30KhGSA and 40 kHNMA after thermal and thermomech. treatment 77−70087
steel, wear resistance of broaching bits in relation to boriding and heat treatment 78−85051
steel, wear resistance of low temp. nitriding treatment 80−89357
steel, wear testing in oils containing organosulphur cpds., XPS obs. of surface comp. rel. to wear 77−36668
steel, with brass inserts, Whittemore gauge length meas., reliability 77−36669
steel 35KhN2VL, deoxidation effect on fatigue and endurance limit in wear tests varying P and S content *(Russian)* 78−35523
steel 40 kH, wear resistance in oil abrasive environment, various grinding methods *(Russian)* 77−70184
steel 45, hardened layers, struct. and composition, after electrospark doping *(Russian)* 77−70213
steel 9Kh18, wear resistance during friction, effect of retained austenite 77−21288
steel (alloy)-TiC (70, 30 wt.%) composite, sintered, wear resist. 80−100815
steel AISI 1020, wear at high sliding speed 78−3237
steel austenitic stainless, cold working type, heat treated, tool wear during cutting 79−47782
steel bearing balls, exoelectron emission for surface fatigue wear testing 78−39960
steel gas nitrosulphurising, S25C, wear property 80−50729
steel hardfaced, effects of quenching on structure and wear resist. 77−21175
steel jig brushes, wear resist. *(Russian)* 80−60977
steel matrix-bronze surface, water lubricated bearing material, manufacture, friction, corrosion and erosion 78−11341
steel medium C, type 45, electroerosion, white-layer structures detection method 79−52485
steel scrapers, wear by rubber 79−66173
steel ShKh15, high C, wear tests in fuel oil, O_2 conc. effect in oil *(Russian)* 77−16694
steel ShKh15, physiomechanical props., hydroextrusion effects 77−21287
steel surface deformation by oblique impact of square plates 77−66701
steel-cast Fe cam-roller pair, wear resistance after strengthening treatment *(Russian)* 78−31542
steel-polymer wear mechanism during fretting corrosion 78−35522
steels, C, friction in liq. Sn, Rebinder effect *(Russian)* 79−29269
strength parameter dispersion/inhomogeneity of microscopic damage relation 77−86122
strongly anisotropic rough surfaces, statistics 79−91805
styli of electrical surface roughness meas. instrums., electron microscopic examination of wear *(German)* 80−101782
superficial plastic deformations by particles *(French)* 80−40540
surface coatings, materials conservation and optimum tribological performance 80−34130
surface contact fatigue onset, mag. detection system 79−20330
surface contacts, tribological props. 79−19469
surface damage, plastic deformation cause in fatigue, wear, fretting and rolling fatigue 80−40537
surface erosion, nonuniform incident flux effect 79−39003
surface erosion by ion bombardment *(Russian)* 78−23567
surface roughness effect on abrasive wear 77−28915
surface strength in friction, structural and energy conditions *(Russian)* 77−56111
surface texture assessment, Walsh function method 80−36995
surfaces in sliding contact, surface temp. effects 77−77594
synthetic diamond drills, improved durability 80−87573
systems analysis, and description of wear processes *(German)* 80−103417
Teflon-4, gamma irrad., wear resistance and antifriction props. 80−7691
temperatures reached during sliding 80−16505
test friction machine, exam. of design 79−52526
test specimen, metallographic technique 80−35496
test system, low temp., exam. of design 79−52523
testing device, cyclic load and temp. var., to 800°C 80−66718
testing equipment for use at high temp. in air 78−56839
testing in various media, device 79−29319
theory, metallography of worn surfaces 80−35346
thermodynamic aspects of wear and tear, entropy and negentropy *(German)* 79−3907
thermoelastic transition from line to point contact 80−83768
thermomechanical approach *(Ukrainian)* 77−68537
thin layer activation, appl. to wear and corrosion meas., surface treatment and sputtering 79−87810
three-body abrasive wear classification, design of new tester 80−108682
Tokamak, recycling and surface erosion processes 80−33805
tool, during machining, solid state reactions 79−79126
transition metal borides, abrasive props. 77−63808
transition metal nitrides of group IV-V, laser irrad. action, erosion strength *(Russian)* 77−56112
transition metals and their compounds, shaping by laser radiation, erosion resistance increase obs. *(Russian)* 77−53871

wear continued
Tribaloy 700, hard surfacing in Na, friction, wear and corrosion 79−24628
tribological system and wear factors, worn vol., load and sliding distance calc. 80−21122
tribology, review of current understanding 77−59066
tribology study reactor fuel element, PEC type, in Na at high temps. *(Italian)* 78−58362
uniform and nonuniform smoothly varying water stream, erosional capacity, rel. to particle size of granular bed material 77−84316
US erosion testing based on Al foil damage using light scatt. 77−36695
US shock waves emitted by cavitation at rotating perforated plate, wear, thickness effects 77−27565
vacuum metallised surfaces, protection by clear coatings 80−35392
vibration test rig for wear meas. of granules 78−56840
white cast Fe, abrasive wear 80−108587
wing pump using flash-resistant hydraulic fluids *(German)* 79−83331
wire for high-speed matrix printers *(Japanese)* 80−55540
wood chip refiners, cavitation effects in two-phase flow 80−35348
zinc dialkyldithiophosphate surface film, prep. and nature 80−104300
Zircaloy-4, techniques of impact and sliding wear study 79−74337
AG, wear, recrystallisation as controlling process, FCC metal 77−56117
Ag alloy, wear resistance, internal oxide effect *(French)* 77−52503
Ag alloys, erosion rate and props. of cathode spot 79−79119
Ag, electrical contact material with liquid lubricant, prod. and appl. 78−10559
Ag, sliding charact., friction and wear *(Japanese)* 78−56778
Ag, wear under reversed friction, temp. effect 80−108588
Ag-Zn, internally oxidized, elec. contact charact., alloying additions effect *(Japanese)* 80−88619
AgMgO for LV switchgear contacts, properties *(Slovak)* 78−56603
Al alloy 7075-T7351, fretting fatigue crack form. 80−35344
Al alloy matrix, reinforced with fibrous and particulate nonmetals, wear, friction 77−4758
Al alloys, erosion by ball bearing impact 79−61740
Al alloys, impact wear, microstruct. effect 80−11791
Al alloys 7075-T6 and 2024-T3, crack propag./wear rate relationship 78−3232
Al and Al-Cu(Mg), comparison of liquid impact erosion and cavitation erosion 80−104302
Al, cavitation erosion considering bubble collapse and pulse height spectra 80−16503
Al, cavitation erosion in water flow, initial stage 78−27648
Al, erosion by coal ash particles 79−61745
Al, erosion by solid particle impingement at normal incidence, SEM obs. 80−104304
Al, reactive electro-erosion under pulse electric discharge 79−52686
Al, single phase FCC, stacking fault energy and delamination wear 78−3239
Al, sliding wear in NaCl of varying pH 78−3240
Al, soft, type 1100-0, erosion tests in cavitating venturi 80−35347
Al, surface deformation and wear track obs. using analytical electron microscope 80−108687
Al, surface erosion due to US activation *(German)* 79−57122
Al, surface subjected to friction, wear, exoelectron emission, rel. to O_2, H_2O, gaseous adsorpt. 79−1816
Al, tribological investigation using two-cylinder tribometer *(German)* 77−25164
Al, wear, recrystallisation as controlling process, FCC metals 77−56117
Al, wear particles, spheroid form. by cavitation erosion 79−52382
Al, wear under reversed friction, temp. effect 80−108588
Al, wear volume/sliding time relationship 79−61743
Al-Cu type 2024 alloy, erosion in cavitating venturi 80−108602
Al-Cu-Mg (4, 1.5 wt.%), mica dispersed, wear characts. and bearing performance 80−108591
Al-Cu(Mg), age-hardenable, US cavitation erosion mechanisms, effects of comp. and heat treatment 78−53002
Al-Cu(Mg), liquid impact erosion 80−108598
Al-graphite particulate composite, exam. of friction, wear and tensile props. 78−72890
Al-Si alloy, as-cast binary, wear characteristics against steel 79−96156
Al-Si cast alloy, flank wear of carbide tool during machining *(Japanese)* 78−19900
Al-Si casting alloys, graphite-dispersed, mech. props. and wear resist. 77−4857
Al-Si hypereutectic alloy, wear resistance 77−77593
Al-Si-Cu-Ni alloy casting, thermal props. 78−95814
Al-Zn-Mg-Cu alloy 7075-T651, adiabatic shear localisation and erosion 79−96157
Al_2O_3, abrasive, wear in simulated hot grinding 78−56784
Al_2O_3 hard anodic coatings, effects of cellular structures 78−11448
Al_2O_3, sintered, correlation between wear, crack resistance and stress intensity factor *(German)* 77−36666
Al_2O_3, wear chart, exam. *(German)* 78−35521
Al_2O_3(-TiO_2) coatings, detonation deposited on steel, prep., wear resist., antifriction props. 78−60877
Au film, ion plated, defect growth structs., SEM obs., and effect on mech. props. 80−24768
Au, sliding charact., friction and wear *(Japanese)* 78−56778
Au, wear, atmos. press. effect, rel. to fatigue 77−70189
Au-In, electrodeposited from acid cyanide electrolyte, exam. of wear and corrosion resistance 78−80482
Au-plating, additive-free, electronic appls. props. 80−108718
β-B, abrasive props. 77−63808
B filled elastomer mould, surface coating for wear prevention in mould 78−64728
B-S compounds, relative antiwear efficiency 78−35532
BC, sintered and hot pressed, friction and wear, 20 to 1500°C 78−60844
BN, cubic, sintering technology and cutting performance of tools 80−29919
C fibre reinforced C matrix composites, wear, oxidation contribution 79−52383
C fibre reinforced PTFE and polyacetal, friction and wear against glass and steel 78−56783
C fibre reinforced polyethylene matrix, ultra high molecular weight, wear limit, γ-irradiated and unirradiated *(Japanese)* 78−27649
C fibre rubbing on rotating cylinder, friction and wear 77−52498
C, glassy, surface erosion by ion bombardment crystal anisotropy effect 78−23845
C, hard, surface wear characts. 80−108596

wear continued
C, isotropic pyrolytic, for biomedical devices, mech. props. 78−65150
C steel, abrasive wear resistance, effect of C content, annealing, quenching 77−56115
$(CF_x)_n$ rubbed films applied to different finished surfaces, obs. 79−83332
Cd film, dry lubrication on C steel, tribological behaviour 80−89364
Cd, wear under reversed friction, temp. effect 80−108588
^{252}Cf fission fragment implantation for wear meas. 79−87765
Co alloys, wear resistance, struct. effect 79−29229
Co base alloys, unlubricated, adhesive wear study 80−108593
Co, single crystal, cavitation erosion, role of twinning 80−107272
Co, superalloy, attritious wear in grinding 77−32696
Co-Cr-Mo alloy shoulder prosthesis, wear and fatigue tests 80−26415
Co-Cr-WC, corrosion and corrosive wear in sea water 78−92408
Co-Mo-Cr-Si Laves phase, sputter deposited, struct. and wear props. 77−40477
Co-WC, corrosion and corrosive wear in sea water 78−92408
CoB-based boride coatings on Co base alloys, microstruct. and mech. props. 78−11427
Cr film, on mild steel, hardness and protective props., rel. to grain size 78−11436
Cr, sliding charact., friction and wear *(Japanese)* 78−56778
Cr-AlN, dispersion hardened, erosion resistance 77−12637
Cr-Ni steel, carburised, effect of atm. during heating to quenching temp. on austenite decomp. 77−56157
Cr-Ti/MgO-NbC(TaC) dispersion-strengthened, high temp. wear and oxidation resist. 80−25877
Cr-Ti/NbC(TaC) dispersion-strengthened, high temp. wear and oxidation resist. 80−25877
CrC, wear mechanism in abrasive particle stream 77−12703
Cr_3C_2, plasma sprayed wear resistance coating, exam. of wear behaviour 20 to 1000°C 80−16487
Cr_3C_2-Ni, friction and wear, 20-1000°C 80−30112
$Cr_3Si_2(C_2)$, sputtered films, microstruct. and wear props. 78−64733
Cu against Pyrex glass, steady wear mechanism, expt. study to confirm theoretical anal. 80−45404
Cu and Cu-Al(Sn), wear, recrystallisation as controlling process, FCC metals 77−56117
Cu and Cu-Sn(Zn)(Al) alloys, wear, effect of Mn_5Si_3 content *(Japanese)* 78−35525
Cu, erosive wear mechanisms, combined TEM and SEM obs. 80−108601
Cu film, ion plated, defect growth structs., SEM obs., and effect on mech. props. 80−24768
Cu, gas content and temperature effects in vibratory cavitation tests 79−61744
Cu pin, heavily deformed surface layer after dry sliding against steel ring, TEM obs. 77−60033
Cu pin against steel ring, dry sliding wear, role of dynamic recrystallisation 80−108599
Cu pin-on-disc friction and wear under boundary lubrication, dissolved O_2 effect 80−76365
Cu, plastic strain meas. due to sliding wear 78−64731
Cu, recrystallisation textures, and deformation formed by dry sliding against steel 79−91698
Cu, sliding charact., friction and wear *(Japanese)* 78−56778
Cu solid soln., wear 78−3233
Cu solid solutions, single phase FCC metal, stacking fault energy and delamination wear 78−3239
Cu surface subjected to friction, wear, exoelectron emission, rel. to O_2, H_2O, gaseous adsorpt. 79−1816
Cu, tribological investigation using two-cylinder tribometer *(German)* 77−25164
Cu, wear, atmos. press. effect., rel. to fatigue 77−70189
Cu, wear under reversed friction, temp. effect 80−108588
Cu, wear volume/sliding time relationship 79−61743
Cu-Ag solder composite, plastic deform. below worn surfaces 77−36670
Cu-Al(Sn), effect of Al and Sn on friction and wear 78−11348
Cu-C bushings, powder metallurgically prepared, exam. of friction and wear charact. 79−15813
Cu-Cr, precipitation hardened, wear 78−3234
Cu-ferrous alloy, hard inclusion composite exam. of wear resistance props. 79−34153
Cu-graphite brushes, friction and wear under severe sliding conditions against steel 79−38991
Cu-graphite starter brushes, effect of high velocities, current densities on wear, friction 78−88544
Cu-M alloys (M=Zn,Al,Sn,Mn,Pb), diffusive redistrib. during friction *(Russian)* 78−52999
Cu-Ni, erosive wear by impinging SiC particles, surface hardness and material props. effect 77−66705
Cu-Sn, graphite dispersed, wear, effect of graphite content *(Japanese)* 77−56114
Cu-Sn-P (5, 1-5 wt.%), effect of P on friction and wear characts. 80−16494
Cu-Sn-Pb-Fe-graphite, bronze-based, sintered alloy, silica additions effect 77−63807
Cu-TiC precipitation hardened composite, struct. effect on friction 78−11337
Fe alloy granule reinforced Cu M2 wear resistance in rubbing with lubrication 80−16490
Fe alloy granule reinforced Cu, friction in vacuum 80−25880
Fe alloy granules in Cu binder, exam. of wear characteristics without lubrication 79−96154
Fe alloys, wear resistance, struct. effect 79−29229
Fe and Fe-C, (0.8 wt.%), sintered, hot forging ahd chemicothermal treatment, effect on wear resistance 80−25606
Fe and Fe-Cr alloys, friction behaviour in oxygen, development of wear-protective oxides and influence on sliding friction 80−30111
Fe base alloy, particle erosion meas. 77−66703
Fe, carburised sintered and pressed specimens, wear resistance 77−77590
Fe, cast, cavitation erosion rate, effect of stress level 78−15545
Fe, cast, effect of heat treatment, on wear resistance, 78−44148
Fe, cast, grey, abrasive wear rate rel. to fracture toughness and microstructure *(German)* 79−29232
Fe, cast, grey, martensitic, lamellar, internal notch effect on abrasive wear *(German)* 79−29231
Fe, cast, hardness, wear resist. and struct., electron irrad. effects 79−96126
Fe, cast, high Cr, wear resistance improvement 77−70186

wear continued
Fe, cast, high Mg content (0.33%), exam. of phase composition charact. 78—84780
Fe, cast, high strength, wear resist., electrocontact surface facing influence *(Russian)* 79—52385
Fe, cast, Mn, wear resist. and hardening, struct. effect 79—87734
Fe, cast, nitrided, wear resistance *(Korean)* 80—21178
Fe, cast, point contact sliding, microhardness testing, microscope exam. 79—87738
Fe, cast, sintered, friction and wear 79—91806
Fe, cast, steel cam-roller pair, wear resistance strengthening treatment *(Russian)* 78—31542
Fe, cast, surface temperature effect on dry sliding wear 80—60983
Fe, cast, wear, effect of vibrations 79—52389
Fe, cast, wear mechanism of friction couples 79—83329
Fe, cast, wear mechanisms, metallographic obs. 77—59942
Fe, cast, wear resist., effect of rolling friction strengthening, oil abrasive environment *(Russian)* 79—15799
Fe, cast, white Cr alloyed, wear resistance, effect on abrasive hardness 78—64722
Fe, cavitation erosion, exam. of mechanism and rates 79—5063
Fe, comparison of liquid impact erosion and cavitation erosion 80—104302
Fe, ductile, with different secondary struct., abrasive wear *(German)* 80—25871
Fe, friction in liq. Sn, Rebinder effect *(Russian)* 79—29269
Fe, grey cast, friction and wear, phosphating effect 77—70190
Fe, sintered, friction and wear 77—59946
Fe, surface subjected to friction, wear, exoelectron emission, rel. to O_2, H_2O, gaseous adsorpt. 79—1816
Fe, wear of surface due to friction, surface hardening 78—44227
Fe, wear sliding track, deformation 77—12707
Fe-based materials, wear resistance, surface hardening processes, review 78—72894
Fe-based sintered friction material, wear rate, depend. of phase struct. 79—15801
Fe-based sintered friction material, wear rate depend. of phase struct., conf., Haifa, Israel, (July 1977) 79—15683
Fe-C-Mo-Nb-Al-Ti-B (0.015, 5.75, .7, 1.6, 2.5, 0.1 wt.%), TZM sheet, wear resistance, effect of surface hardening 77—59985
Fe-Co-Ni-W alloy, 45KKhVN, plastic deform., electron microscope obs. *(Russian)* 78—80584
Fe-Cr, friction and wear in controlled environment, effect of sliding mode and specimen geometry 78—15542
Fe-Cr (13 wt.%)+polycarbosilane, powder metallurgy, charact. 77—85962
Fe-Cr (5 wt.%), friction and wear in controlled environments, oxide film effect 78—15546
Fe-Cu-Ni-Cr_3C_2-C based sintered friction material, wear, surface geometry and struct. effects 80—25875
Fe-glass porous material, wear resist. under dry friction 80—25876
Fe-Mn-C (11.5, 0.2 to 1.6 wt.%), water quenched, effect of C on phase composition, abrasion, plasticity *(Russian)* 78—35445
Fe-P, sintered frictional material, friction and wear rubbing pair under moderate load 77—21208
Fe-P base frictional material, sintered, friction and wear under moderate load 77—12704
Fe-P-S composite sintered bearing materials manufacture, wear intensities 80—20881
Fe-P(S) sintered materials, antifriction props. 79—24626
Fe-TiB_2, eutectic alloy, high temp. props. 78—84931
Fe-X-MoS_2 (X=WC, HfC, Al_2O_3, ZrO_2, HfB_2, ZrB_2), self lubricating coatings, exam. of props. 79—96217
Fe_2O_3, plasma sputtered coatings, oxide dissociation, coating props., struct. and composition *(Russian)* 80—54577
Ge, erosion by rain at subsonic velocities 77—70191
HfC-HfB_2 alloys, wear in vacuum, role of boride phase 80—21113
In film, friction and fear in ultrahigh vacuum, effects of speed, film thickness and substrate surface roughness 79—20202
InAs-FeAs, eutectic, growth from melt, electrical props. 77—11911
Mg cast iron, effect of heat treatment on phase comp., microstruct., wear resistance 77—56006
MgF, polycryst., quartz particle impacts no. effect on erosion in elastic-plastic response regime 80—81209
MgO, cryst., cumulative deform. by softer sliders 77—4154
MgO single cryst., impact wear charact. 80—76374
MgO single cryst., impact wear damage 80—76375
MgO single crystal, wear and friction on sintered Al_2O_3 in vacuum 77—12710
MgO, single crystal, wear damage, surface cracks 78—68825
MgO single crystal on low C steel disc 78—15541
MgO, sintered, refractories, props. after testing at over 2000°C 80—104317
Mn cast Fe, W effect on transform. in thin surface layers during dry sliding friction 77—21289
MnZn ferrite, abrasive wear *(Japanese)* 78—39917
Mo sintered composite, MoS_2 containing, friction and wear props. 80—11786
Mo, wear resistance, effect of surface hardening 77—59985
Mo-AlN, dispersion hardened, erosion resistance 77—12637
Mo-Cu, electrical erosion resistance during electrospark machining 78—35531
Mo-Zr-Ti (0.5, 0.1%), adhesive wear polishing of 25 mm spheres 80—89397
Mo_2B_5-based alloys, mech. props., rel. to appl. as electrodes in electrospark machining 80—21174
MoS_2, self-propag. high-temp. synthesis, props. 80—2975
MoS_2, sliding charact., friction and wear *(Japanese)* 78—56778
MoS_2 solid lubricant, antifriction and elec. props. depend. on oxidation temp., dopant influence 80—108584
$MoSi_2$, sputtered films, microstruct. and wear props. 78—64733
Na_2O-CaO-SiO_2 glass, high-vel. liq. impact, oblique impact anomaly 80—89329
Na_2O-CaO-SiO_2 glass, hot erosion plastic flow and fracture 80—89354
NbC, deformation behaviour during rubbing in wide temp. range 80—16486
$NbSe_2$ solid lubricant, antifriction and elec. props. depend. on oxidation temp., dopant influence 80—108584
Ni alloys, wear resistance, struct. effect 79—29229
Ni and Ni-Cr(Mo), wear tracks, TEM obs., tested in simulated face seal 77—52508
wear continued
Ni base alloy, particle erosion meas. 77—66703
Ni base alloys, unlubricated, adhesive wear study 80—108593
Ni, cavitation-erosive wear in surface-active media, dislocation struct. and fracture study by FMR *(Russian)* 79—52384
Ni, erosive wear mechanisms, combined TEM and SEM obs. 80—108601
Ni, in unlubricated sliding, mechanical aspect 77—12706
Ni, single phase FCC stacking fault energy and delamination wear 78—3239
Ni, sliding charact., friction and wear *(Japanese)* 78—56778
Ni, surface subjected to friction, wear, exoelectron emission, rel. to O_2, H_2O, gaseous adsorpt. 79—1816
Ni, wear, atmos. press. effect, rel. to fatigue 77—70189
Ni, wear, recrystallisation as controlling process, FCC metal 77—56117
Ni-(W,Cr)C, corrosion and corrosive wear in sea water 78—92408
Ni-based-Ta(Cn,N) hard metals, isostatic hot pressing influence on mechanical properties 78—92219
Ni-Cr (20 wt.%), high temp. frictional charact. 80—21118
Ni-Cr (20 wt.%) alloy LNKh, room-temp. friction charact. 80—25874
Ni-Cr-B-Si, hard faced with WC, exam. of abrasion and wear props. 79—34202
Ni-Cr-Mo-C hardfacing alloy, hardness and abrasive wear resistance 79—79117
Ni-Cr-W-C(Si) hardness, corrosion resistance, wear resistance tests in 10% HCl *(German)* 78—92368
Ni-P (8 wt.%), protective coating for wear and corrosion resistance of steel 77—21329
Ni-Zn ferrites, hot-pressed, key props. 78—15348
NiCr-AlY sintered fibre metal struct. abradable seal material, friction and wear 78—56785
$(Ni_{0.47}Zn_{0.53})_{1-x}Fe_{2+x}O_4$, recording head medium 77—86187
Pb film, friction and fear in ultrahigh vacuum, effects of speed, film thickness and substrate surface roughness 79—20202
Pb, friction, wear in supercond., normal states *(Russian)* 78—39914
Pb ion plated soft film, initial wear rate 80—11795
Pb, recrystallisation textures, and deformation formed by dry sliding against steel 79—91698
$Pd_{781}Cu_{55}Si_{164}$, liquid quenched metallic glass, wear resistance 79—66079
Pt-Pt mechanical contact, FIM obs. of contact area 78—35527
Se, amorphous, friction and wear under lightly loaded contact 78—64740
Si, near (111) slices, scratches made by diamond stylus 77—12726
SiC, abrasive, wear in simulated hot grinding 78—56784
SiC, abrasive paper, variables affecting degradation 79—43444
SiC, attritious wear in grinding 77—32696
SiC, reaction-bonded, impact erosion by ang. Al_2O_3 particles 80—89362
SiC, single cryst., friction and wear behaviour in sliding contact with various metals 80—21112
SiC single cryst., reaction-bonded and hot pressed, hardness and wear behaviour 79—38970
SiC single crystal, friction and fracture in contact with itself and Ti 80—11780
SiC surface, H^+, D^+ and Ar^+ bombardment, 5 to 15 keV, meas. of erosion yield 78—79647
β-SiC/Si abrasive resistant material, prep. and props. 80—20878
SiC-B_4C eutectic, directional solidification, growth and mech. props. 79—91638
SiC-Si, wear resist., props. under abrasion and corrosion 80—100927
Si_3N_4, reaction-bonded and hot pressed, hardness and wear behaviour 79—38970
SiO_2 reinforced decorative laminates, abrasion resistance, abrasive paper deterioration 77—16696
Sn bronze, extruded atomized powders, struct. and props. 79—38763
Sn, ion plated soft film, initial wear rate 80—11795
Sn, recrystallisation textures, and deformation formed by dry sliding against steel 79—91698
TaC-TaB_2, exam. of high temp. friction and wear, and deformation behaviour 79—34152
Ti alloy, fretting wear, role of adhesion and delamination 78—35533
Ti alloy VT1-0, wear resistant coated, metallic and intermetallic, electrospark applied *(Russian)* 79—1916
Ti alloys, lubrication by chloroparaffins, friction and wear *(Russian)* 80—93657
Ti alloys. wear under conditions of rolling stress 79—20211
Ti, antifriction props. 77—90467
Ti diffusion coated cast Fe, wear resistance 79—52459
Ti electrodes, RuO_2 coated, corrosion during O evolution rel. to electrode prep. *(French)* 80—76420
Ti, erosion by coal ash particles 79—61745
Ti metal-metal interface, adhesion energy, surface treatment and ion implantation effects 80—107660
Ti, reactive electro-erosion under pulse electric discharge 79—52686
Ti, tribological investigation using two-cylinder tribometer *(German)* 77—25164
Ti, wear at high sliding speed 78—3237
Ti, wear under conditions of rolling stress 79—20211
Ti-Al-V (Mo-Sn)(Zr), environmental effects in alloy fretting, effect on fatigue props. 78—56787
Ti-Al-V (6, 4 wt.%), cavitation induced erosion, under mill annealed, soln. treated and aged, and beta annealed conditions 79—8371
Ti-Al-V (6,4 wt.%), fretting fatigue behaviour of temps. up to 600°C 80—21104
Ti-Al-V (6,4 wt.%), high temp. fretting fatigue, fatigue and fretting wear 80—3197
Ti-Al-V alloy, friction coeff. reduction on injection with TiC particles 80—85086
Ti-Cr, sintered, friction and wear, structural factors 78—60843
Ti-Cr-TiC, sintered, friction and wear, structural factors 78—60843
Ti-Mg-ZrC(HfC)(TiC)(TiB_2) sintered, friction and wear props. 79—70019
Ti-TiC system, sintered, friction and wear, structural factors 78—60843
TiB_2, electrode, hot pressed, erosion resistance, struct. and porosity effects 78—3228
TiC coated high speed steel, machining of steel 4340, tool life 78—11435
TiC, deformation behaviour during rubbing in wide temp. range 80—16486
TiC film, Au-dispersed, struct., hardness and wear rate 77—77493
TiC, frictional charact. and contact-zone deform. in homogeneity range 80—66673
TiC reactively sputtered coatings on Ni-Cr-Mo-Ti (19,11,3 wt.%), adherence, XPES and wear study 80—25565

wear continued
TiC-Au film, prep. by activated reactive evaporation, struct. and mech. props. *(Japanese)* 78−3252
TiC-Ni-Mo hard alloy, wear resistance under end face friction cond. 78−60846
TiC-TiB_2, friction characts., comp. depend., 20-1000°C 80−3203
TiC-TiB_2, strength and antifriction props. over wider range of concs. 80−50673
TiC-TiB_2 alloys, composition effect on surface layer rupture at various temps. 80−25879
TiC-TiB_2 alloys, wear in vacuum, role of boride phase 80−21113
$Ti(CN)_x$, reactively sputtered, erosion props. 79−47779
TiO_2, plasma-sprayed coating against grey cast Fe 79−34155
(W, Mo)C, hard-facing applications, effect of Mo on struct and hardness of WC 80−108474
W-Cu, electrical erosion resistance during electrospark machining 78−35531
W-Pt mechanical contact, FIM obs. of contact area 78−35527
W_2B_5-based alloys, mech. props., rel. to appl. as electrodes in electrospark machining 80−21174
WC, deformation behaviour during rubbing in wide temp. range 80−16486
WC, roughness and wear characteristic of spark-eroded surfaces 79−52390
WC-Co alloy, hard metal, resistance of cavitation erosion *(Japanese)* 80−16575
WC-Co alloys, P additions, effect on hot pressing, hardness and wear resist. 78−11162
WC-Co cermet, dynamic SEM wear obs. 77−36667
WC-Co hard metal, stress conc. factor and stress intensity factor, rel. to wear *(German)* 78−11335
WC-Co sputter deposited film, friction and wear 78−72918
WC-TiC(TaC, NiC)-Co, hard, homogeneity and wear resistance estimation, by magnetic method 77−90558
WS_2, self-propag. high-temp. synthesis, wear props. 80−2975
WS_2 solid lubricant, antifriction and elec. props. depend. on oxidation temp., dopant influence 80−108584
WS_2-NbS_2 system, compds., elec., antifriction props. 79−38066
WSe_2, lubricant, prep. by self-propagating high-temp. synthesis, technological characts. 78−35338
Zn, wear under reversed friction, temp. effect 80−108588
ZnS, hot pressed, water drop impact damage, SEM exam., IR transmission 78−88543
Zr alloys, wear due to fretting and periodic impacting 80−16509
ZrC based cermets, strength and gas-abrasive wear resistance 77−25163
ZrC-ZrB_2, friction characts., comp. depend., 20-1400°C 80−3203
ZrC-ZrB_2, strength and antifriction props. over wider range of concs. 80−50673
ZrC-ZrB_2 alloys, wear in vacuum, role of boride phase 80−21113
ZrO_2, metastable, tetragonal, erosive damage depth, martensitic transform. effect 79−61738
ZrO_2, wear chart, exam. *(German)* 78−35521

wear, abrasive *see abrasion*

wear resistant coatings
alumina on stainless steels and Inconel, gasless ion plated films 77−40476
apparatus, for adherence, wear resist. and thermal shock meas. of thin films 78−72943
ball bearing surface CVD coating expts. 79−83366
bituminous surfaces, review of aggregate selection critera for improved wear and skid resist. 80−7689
boride, diffusion soaking effect on struct. 78−18846
boride coatings, technology, props., book contrib. 78−48574
boride on stainless steel, mech., elec. props., boronising sintering method investig. 78−60594
boronised coating on steel, sliding and abrasive wear, corrosion resist. 78−11428
boronising, titanium alloys, effect on wear 78−19903
bronze powders, electric-pressure sintering onto cylindrical parts in fluidised bed 80−100960
brush plating, for wear resist. appls. 80−66443
cemented carbide ion plating, high-speed steel tools, cost and cutting performance 80−30174
clear, protection of sputtered metal layers 80−35392
composite material deposition by electrolysis *(French)* 77−73375
corundum-based refractory lining, wear resistance in combustion gas flow *(Russian)* 79−8370
cutting tool coating by cubic BN reactive vapour deposition 80−40545
CVD, appl. to tribology 78−64743
diamond coatings, for increased wear resist. 80−76371
diamond containing electroless Ni coatings, fabrication and props. 79−47795
diamond-based, fabrication and wear resist. 80−40576
dielectric hard transparent coatings 77−36678
dielectric overcoating on Al and Ag mirrors, polarisation effects 77−72055
electron beam deposition, principles and technology 79−24439
electroplated coatings for wear resistance, survey 78−72913
electroplated diamond-composite abrasion-resistant coatings 79−61737
electrospark coating improvement by laser action *(Russian)* 79−15850
electrospark-applied, metallic and intermetallic, on Ti alloy *(Russian)* 79−1916
engineering component ion implantation 79−83360
Fe, cast, high Cr, hardfacing of roll, wear resistance and thermal durability 80−7686
finishes for wear reduction, data sheet 79−91814
fretting corrosion control using coatings and surface treatments 80−35368
fretting fatigue prevention for steel/Ti-Al-V mating surfaces 78−64721
glazes with improved abrasion resistance *(German)* 80−11798
hard coating deposition by sputtering 80−40544
hard coating on metal surfaces, abrasive wear resist. meas. 79−20327
hard metal powders, electric-pressure sintering onto cylindrical parts in fluidised bed 80−100960
hardfacing, review 78−72937
hardness and ductility 79−87025
high temp. materials conf., Reutte, Austria, (May 1977) 79−57124
impulse discharges treatment, of machine bearings coatings *(Russian)* 79−1917

wear resistant coatings continued
ion implantation, surface treatment process in production engineering 80−34028
Ioncote coating process, using field emission systems for corrosion and abrasion protection *(German)* 80−76205
IR segmented composite window design 80−106621
lubricant additive effects on surface wear, Auger electron spectroscopy appl. 77−44445
lubricating coating, solid, elemental anal. by proton-stimulated X-rays 78−88687
materials selection, relation between materials properties and wear 80−21120
mechanical failure prevention, conf., Caithersburg, USA (Oct. 1975) 77−21327
metal coatings on steel for watch part finishing, ion plating *(French)* 78−23879
metal flame spray coating acceptance factors and tests in steelworks environment 79−83397
metal surfaces, chemical conversion coatings for wear resist., review 78−72893
metal-dielectric bilayer system, optical, mechanical and corrosion props. 77−32707
metal-dielectric codeposited film, optical, elec., mechanical and corrosion props. 77−32708
metal-metal bilayer system, optical, mechanical and corrosion props. 77−32707
metallographic exam. of sprayed-on coatings *(German)* 78−19981
metals, oxide coated, environment-sensitive mechanical behaviour 77−32722
Nichrome-silicate glass-CaF_2 multicomponent self-lubricating coating, prep. by plasma spraying, and props. 80−40604
optical coating abrasion resistance characterisation test 79−14129
palliative treatments for fretting fatigue, review 80−21126
parylene coating for $Ga_{1-x}Al_xAs$ laser diode end facet protection 79−36921
Permalloy, solid boriding for mag. head appl., wear resist. and microhardness 80−21172
photographic migration images, liquid developed, fixing and abrasion resistance 80−4792
planar magnetron sputtering developments and applications 77−77379
plasma arc spraying, operating principles and applications *(French)* 80−76418
plasma arc spraying using N_2 shielding gas, other prod. process improvements 77−21296
plasma sprayed coating consolidation by laser remelting 80−93697
plasma spraying technique appl. *(Japanese)* 80−55558
plastic optical components, flexible rapid curing abrasion resistant coated film 78−66890
polycarbonate ophthalmic-prescription lens series, scratch-resistant coatings 79−81501
polymer composition coatings for rubbing mechanisms for optomech. instruments 78−29198
polymer films, between contacting surfaces, effect of contact pressure and temp. 78−60842
polymer powdered coatings, guide element fabrication of cine cameras 78−78021
polymeric coatings, wear resist. props. 78−72914
protective coatings, role in mechanical failure prevention, conf., Caithersburg, USA (Oct. 1975) 77−21327
protective coatings for metals, chemically vapour deposited 78−44261
rain erosion resistant antireflective coatings for IR windows 78−83050
refractory carbide, silicide and boride RF sputtered wear-resistant coatings, XPS study of adherence 79−34191
refractory compound hard coating, electron beam evaporation in reactive atm. 77−44396
refractory wear-resistant coatings, composite struct. develop., props. 77−63618
Relite-base alloy compositions wear caused by sliding abrasive material stream 78−95813
rough surface modelling and online monitoring 79−80576
self-protection of high wear materials, compacted wear debris films 79−96149
semiconductor, implantation of Si, Al, Hf, Ta into InP and GaAs, form. of protective oxide 78−79622
silica hard coating for magnetic surfaces 80−7715
silica-alumina hard coating for magnetic surfaces 80−7715
silicide base coating for steel parts 78−72936
silicide coatings, on steel, exam. of fracture processes 78−44206
static evaluation of surface coatings for compliant gas bearings in an oxidizing atmosphere to 650°C 79−20201
steel, alloy U8, wear resistant diffusion coatings of B-Cr(Si) 78−56823
steel, ATŚI 9310, fretting, selected fretting resistant surface treatments 79−29223
steel, cutting cemented carbide grade, HfN coating 79−24667
steel, diffusion coatings, carbide and boride, props. *(Russian)* 79−52443
steel, high alloy ledeburitic, wear and corrosion resistant coating by chemical vapour deposition 78−92403
steel, high-C, boriding, boride case struct. 79−24665
steel, medium C, 45, deposition of composite, wear resistant Ni-B-Cr coating 78−11420
steel, medium C, 45, fatigue strength increase by plasma steel coatings, fretting corrosive cond. 79−15875
steel, roller-bearing, high-temp. wear resistant coating treatment *(German)* 79−24629
steel, sliding wear reduction by metallic coatings 77−21331
steel, stainless, liquid boronizing, wear resistant coating *(Korean)* 79−43475
steel, surface treatment protective coatings for scuffing and adhesive wear resistance 77−86217
steel, tool, TiC coated by CVD, wear resistance 79−34196
steel casting surface alloying feasibility trials 79−83395
steel Kh12, impact abrasive wear improvement by TiC coating 77−70187
surface coatings, materials conservation and optimum tribological performance 80−34130
vacuum furnace fusion requirements for self-fluxing overlays 79−83367
vapour deposition of wear resistant coatings 77−21307
vapour deposition of wear-resistant surfaces, review 78−72938
vapour deposition on steel 79−56935
vinyltrimethoxy silane, plasma polymerised, abrasion resist. antirefl. coating for polycarbonate 77−42635

wear resistant coatings continued
Ag, electrospark applied, on Ti alloy, frictional characts. obs. *(Russian)* 79−1916
Al, ion plating on Ti, graded interface form. 78−11442
Al powders, electric-pressure sintering onto cylindrical parts in fluidised bed 80−100960
Al_2O_3 hard anodic coatings, effects of cellular structures 78−11448
Al_2O_3, wear characteristics, comparison or coated and uncoated WC hard metals 78−92365
α-Al_2O_3, wear resistant coatings on cemented carbide machine tools *(German)* 79−74297
Al_2O_3-(TiO_2) coatings, detonation deposited on steel, prep., wear resist., antifriction props. 78−60877
B coating on steel 45, effect of abrasive particle size on wear 78−44225
B filled elastomer mould, surface coating for wear prevention in mould 78−64728
B-Cu(Al) coating on steel 45, effect of abrasive particle size on wear 78−44225
BN-based, fabrication and wear resist. 80−40576
BP coatings, on Mo by CVD and their composition and microhardness 79−28942
Be-B, ion implanted surface hardened layer on Be 80−16604
C diamondlike layers, RF plasma deposited, frictional props. 80−71762
C films, vacuum-vapour-deposited for prosthetic coatings, wear behaviour 79−43440
C, ion-plated, on metal, deposition method, graphitic struct., and tribological props. 78−11440
Co, electrodeposition using insoluble anode 77−8772
Co-Cr-Ta(Al) alloy, high temperature wear resistant coatings, CrO_2 hardened 79−24677
Co-Cr-W-C, hardfaced coating for high temp. liquid Na service, deposition and wear 77−32724
Co-Cr-W-C, wear-resistant coating alloy, carbide form. and decomp. 77−32711
Co-Mo-Cr-Si, plasma and detonation coatings, Laves- and carbide-strengthened, comparative props. 78−15562
Co-Mo-Cr-Si Laves phase, sputter deposited, struct. and wear props. 77−40477
Co-Ni-Cr-B, centrifugally cast metallurgical coatings for wear resistance in plastics molding machines 79−29285
Co-Ni-Cr-B, X-306 centrifugally cast cylinder lining alloy, compatibility with hardfacing alloys 77−32726
CoB-based boride coatings on Co base alloys, microstruct. and mech. props. 78−11427
CoO deposition on glass using laser beam 79−83364
Cr, CVD protective coating on steel, struct. and carbide form. 77−40387
Cr diffusion coating of steel types 45, 50, U8, U10, ductility 79−43357
Cr, electroplate, effect on props. of substrate 77−21330
Cr electroplated steel, laser treatment 80−21191
Cr, electrospark applied, on Ti alloy, frictional characts. obs. *(Russian)* 79−1916
Cr, on mild steel, hardness and protective props., rel. to grain size 78−11436
Cr plated steel, factors influencing durability 80−108643
Cr-C, deposited by hollow cathode discharge, characterisation 78−11371
Cr-N, deposited by hollow cathode discharge, characterisation 78−11371
CrAl, electrospark applied, on Ti alloy, frictional characts. obs. *(Russian)* 79−1916
CrC electrophoretic coating, electric field strength effect on deposition rate 78−19677
CrC, plasma sprayed coating 78−68835
Cr_3C_2 (Cr_7C_3) based coatings, detonation deposited, wear resist., 20-1000°C 80−11843
Cr_3C_2, $Cr_{23}C_6$, plasma sprayed coatings for gas-cooled reactor appl. 79−24676
Cr_3C_2, plasma sprayed wear resistance coating, exam. of wear behaviour 20 to 1000°C 80−16487
Cr_7C_3 CVD coating on steel 79−83393
Cr_xC_y-Cr-Ni-Mo wear resistant coating prep. by laser beam melting, and props. 80−40607
Cr_2O_3, RF sputtered coating for wear appls., on Inconel X-750 foil, prep. and props. 80−40605
$Cr_3Si_2(C_2)$, sputtered films, microstruct. and wear props. 78−64733
Cu-Sn industrial bronzes, Sn diffusion in deform. zone influence on wear resistance, friction *(Russian)* 80−108582
Fe and Fe-Cr alloys, friction behaviour in oxygen, development of wear-protective oxides and influence on sliding friction 80−30111
Fe, cast, white martensitic, centrifugally cast metallurgical coatings for wear resistance in plastics molding machines 79−29285
Fe, grey cast, friction and wear, phosphating effect 77−70190
Fe-base wear resistant dispersion hardened electrolytic coating, annealed and sintered 78−35593
Fe-based sintered friction material, wear rate, depend. of phase struct. 79−15801
Fe-Ni-Cr-B, X-101 centrifugally cast cylinder lining alloy, compatibility with hardfacing alloys 77−32726
Fe-X-MoS_2 (X=WC, HfC, Al_2O_3, ZrO_2, HfB_2, ZrB_2), self lubricating coatings, exam. of props. 79−96217
FeB, and Fe_2B, diffusion saturation and formation on high strength cast Fe 78−53032
FeB_x coatings on steel, formed by B diffusion, pack cementation process, microstruct. and mech. props. 78−15592
Fe_xN_y, on ion-nitrided C steel, microstruct. hardness, and wear resist. *(Japanese)* 77−63828
Fe_2O_3 films, DC reactively sputtered, for selectively semitransparent photomasks, struct., mech. and chem. props. 80−59835
Mg cast iron, effect of heat treatment on phase comp., microstruct., wear resistance 77−56006
$Mn_3(PO_4)_2$ coating on steel, wear resistant appl. 80−16609
(Mo,W)C-$(Mo,W)_2C$, hard facing alloys 79−24667
Mo coating on EN8 C steel, fretting wear and fatigue strength assessment 78−88583
Mo flame sprayed coatings, comp., microstruct. and mech. props. 80−16598
Mo, plasma-sprayed, powder characts. 78−48548
MoS_2, RF sputtered layers with variable stoichiometry, lubrication props. 80−40557
MoS_2, RF sputtered lubricant, wear life, sputtering parameter effects 80−40558
$MoSi_2$, sputtered films, microstruct. and wear props. 78−64733

wear resistant coatings continued
NbC coating on C steel and Armco Fe, deposition, struct. and props. 79−52462
Ni, B-containing multicomponent diffusion layer formation *(Russian)* 77−44400
Ni coating, heat treated, as plated, electrochemical study of corrosive wear 80−16536
Ni coating, self lubricating containing oxides, carbides and borides on steel 80−21189
Ni-base wear resistant dispersion hardened electrolytic coating, annealed and sintered 78−35593
Ni-Cr-Fe-Si-B wear-resist. and corrosion-resist. coatings by furnace melting 80−35428
Ni-Cr-W-C(-Si), struct. and props. of corrosion and wear resistant alloys 79−24627
Ni-Mo-Cr-Si, plasma and detonation coatings, Laves- and carbide-strengthened, comparative props. 78−15562
Ni-P (8 wt.%), protective coating for wear and corrosion resistance of steel 77−21329
Ni-SiC coating, heat treated, as plated, electrochemical study of corrosive wear 80−16536
Ni-SiC composite coatings, phase composition calc., wear resistance *(Russian)* 79−11709
Ni-SiC(WC), dispersion hardened coating, chemically deposited using electroless baths, exam. of protection props. 79−34208
Ni-W-C, X-800 centrifugally cast cylinder lining alloy, compatibility with hardfacing alloys 77−32726
Ni-WC, dispersion hardened, centrifugally cast metallurgical coatings for wear resistance in plastics molding machines 79−29285
NiAl, electrospark applied, on Ti alloy, frictional characts. obs. *(Russian)* 79−1916
Re coating on cemented carbides, CVD, hardness *(German)* 78−64777
Si-C amorphous wear-resistant coating 79−34165
SnO_2 coating, scratch resistance and suitability for glass artificial heart valves *(German)* 79−12028
steel, Hadfield, hollow cathode sputtering 78−11433
TaC-NiC, powder for plasma arc spray coating appl. 78−15591
Ti diffusion coated cast Fe, wear resistance 79−52459
Ti, wear and corrosion resistance, effect of surface alloying with Nb and Si *(Russian)* 77−25191
Ti-Zr-Nb-Si, Nb and Si surface alloying effects on wear and corrosion resistance *(Russian)* 77−25191
TiAl, electrospark applied, on Ti alloy, frictional characts. obs. *(Russian)* 79−1916
TiB_2, on Ti and Ti alloys 79−20290
TiB_2, on WC-Co alloy cutting plates, hardness and struct. 80−21175
TiC abrasion-resistant coatings, glow discharge assisted CVD 79−83392
TiC, activated reactive evaporation and sputter deposition, friction and wear characts. 77−44394
TiC, activated reactive evaporation and sputter deposition, ancilliary props. 77−44395
TiC base hard metals, N_2-containing surface wear resistant layers, struct. anal. *(German)* 78−92405
TiC coated high speed steel, machining of steel 4340, tool life 78−11435
TiC, coated WC cutting rools, frictional characts. 79−20218
TiC coated WC-Co cemented carbides, fracture toughness 80−85046
TiC coatings, RF sputtered, on 440-C steel, adherence, friction, and wear props. 79−47823
TiC, form. by activated reactive evaporation, wear resistant props. 77−44411
TiC, laser CVD, coating characterisation 80−93494
TiC layers, on steel and cemented carbides, load-bearing capacities 80−40606
TiC, on WC-NbC-Co, ion plating, and cutting tests 79−24678
TiC, TiVC, on steel, sputter deposited, adhesive quality 77−12531
TiC, wear characteristics, comparison or coated and uncoated WC hard metals 78−92365
TiC-Au film, prep. by activated reactive evaporation, struct. and mech. props. *(Japanese)* 78−3252
TiC-Ni composite coatings, form. and wear resistant props. 77−63602
Ti(CN) coating for steel, abrasion resist., CVD parameter depend. 77−40471
TiC(N) overlay coating on stainless steel, Ti or Al, effect on physicomechanical and wear props. 80−40603
Ti(N,C,O), coating for cemented carbides and high speed steels by CVD 78−92406
TiN coated WC cutting rools, frictional characts. 79−20218
TiN coating on steel for watch part finishing, ion plating *(French)* 78−23879
TiN decorative coating, ion plating on steel and Stellite, and abrasion resist. 78−11441
TiN, form. by activated reactive evaporation, wear resistant props. 77−44411
TiN, hard coating on soft Al alloy, tribological anal. 80−108600
TiN, on WC-NbC-Co, ion plating, and cutting tests 79−24678
TiN, vapour deposited coating on cemented carbide tools, deposition parameter effects on wear 77−63563
TiN wear resistance coatings, reactive evaporation and activated reactive evaporation *(French)* 79−57126
W, CVD, for components in contact with HTR-He 79−626
WC, plasma sprayed coating 78−68835
WC, sputter deposited, elec. resist., mag. susceptibility and adhesion meas. 77−44395
WC-Co, sputter deposition, friction and wear characts. 77−44394
WC-Co (15 wt.%), alloy VK15 coating on Ti-Al, detonation sprayed, antifriction props. 80−21188
WC-Co (15 wt.%), detonation sprayed on Cr-Ni steel with automatic powder feed 80−25558
WC-Co particles electrophoretic deposition, on metal surfaces *(German)* 80−2969
WC-Co sputter deposited film, struct. and comp. 78−72023
WC-Co sputter deposited film, friction and wear 78−72918
WC-Ni detonation sprayed coating, wear resistant 78−35594
WC-TiC, powder for plasma arc spray coating appl. 78−15591
WC-TiC-Co, powder for plasma arc sprayed coating 78−15591
WC-TiC-TaC, powder for plasma arc spray coating appl. 78−15591
W_2C, W_3C, chemical vapour deposited coatings, low temp. form., on steel substrate 78−92404
Zn, effect of surface-active substances in electrodeposition on props. *(Russian)* 78−11359

wear resistant coatings continued
Zn thin metal primer systems for steelwork 79−79148
ZnS, on ZnSe substrate, erosion-resistant composite window fabrication and evaluation 78−71211

weather *see meteorology*

webs (membranes) *see membranes*

weighers *see balances*

weighing
accuracy class increase, using several standard weights of equivalent mass *(Rumanian)* 80−47022
accurate method for mass meas. using analytical balances with built in weights *(German)* 78−45596
adjustment of weights to OIML conditional density, single pan balance method 77−41572
air, ultrapure, molar density at 298.15K for mass transfer buoyancy corrections 79−88917
air density determining, by weighing two bodies, for aerostatic-force correction calc. 77−9984
air density direct determination in balance through artifacts characterised in evacuated weighing chamber 79−88916
air density equation and mass unit transfer 79−88918
airborne particulate matter collected on filters, chamber for weight determ. 79−57552
analytical balances with weights adjusted to conditional density *(Rumanian)* 78−49800
animal and organ, automatic balance *(Japanese)* 79−25173
attesting weights of different classes of accuracy 79−49206
automatic, application in ceramics industry 80−95074
automatic, Russian balances types 900VN and 959DN, accuracy improvement 80−52166
Autoweigh system, electronic weighing device for premature infants 78−44632
balance, microprocessor based, capabilities 80−13067
balance meas. instruments, system accuracy *(Slovak)* 78−49798
balances with weight and cost read-out *(Polish)* 80−90820
British trade weights and measures activities 80−27267
conventional, protection w.r.t. air buoyancy *(German)* 77−53863
Czochralski crystal growth, automatic, weighing method 77−85929
Czochralski crystal growth, automatic, weighing method 77−85930
digital weighing systems, error estimation *(German)* 77−74365
dynamic weighing method using transducer 80−17926
electronic scales and precision instrum. *(German)* 78−70100
electronic using load cells, advantages 79−12772
electronic weigher, explosion proof design and appl. *(Hungarian)* 77−41571
electronic weighing system, digital transducer instruments 80−95076
ferrous alloy melting, chromatogravimetric equipment for redox studies 78−40097
FFTF element measuring system 79−9729
flow measurement weighing techniques 77−84365
force standard machines and measurement, 0.5 to 30 MN 79−35727
free-piston manometer comparison, weight relocation method 80−90831
gravimetric measurement of sorption isotherms, errors 78−67905
hydrostatic, for porosity determ. of coatings 80−66714
hydrostatic, solid density standards 80−77758
hydrostatic method, for diffusion rate determ., metallic materials in Al melts 79−86913
hydrostatic weighing, treatment of suspension wire *(Japanese)* 79−82006
hygroscopicity of dusts, contaminants and corrosion products using instrumental gravimetric method 78−74118
industrial weighing, gyroscope appl. 80−42217
irradiated nuclear fuel reprocessing streams, remote anal. techniques 79−13510
liquid, programmable precision digital equipment *(Hungarian)* 78−32795
liquid density measurement, displacement sphere method *(German)* 80−52168
load cell, automatically controlled using capacitive and US sensors *(German)* 79−35715
load cell pattern approval, France 80−42199
load cells and indicators for weighing machines, permissible number of digits *(German)* 79−35681
load transducer parallel operation tests *(German)* 77−79079
loose and pulverised materials in motion, design and operation *(Polish)* 78−12673
LPE source materials, weighing method 80−66439
magnetic suspension, simultaneous weight and torque meas. in controlled atmospheres 78−65907
mass, force and weight, relationship and measurement of weight 80−27273
mass change meas., automatic recording system, exam. 78−57901
mass comparator, high precision, using bonded strain gauge load cell 80−57261
microbalance system, detection of minimum weight difference *(Japanese)* 79−26032
microprocessor based electronic scale 77−74421
microweighing in vacuum and controlled environments and use of beam microbalance, book 80−62401
nuclear fuel elements, in-cell element weighing system of HFEF 77−54298
ore body total mass and coords. determ. from gravimetric anomaly *(Russian)* 77−86746
oxide melts, specific weight determ. at 1000 to 1750°C, methods survey *(Slovak)* 80−47079
patient weight monitoring, continual in-bed method 78−48910
preliminary assigned values, (dosage), determ. method 77−71299
self-balancing bridge as a micro-balance 77−2644
sensitivity limitations on force and weight meas. in vac. 78−65908
shipboard weighing techniques 78−45595
SI units fundamentals *(French)* 80−95059
single-pan analytical balances, liquid density meas. using solid density standards *(German)* 80−52167
small weight, automation problems *(Polish)* 78−70099
substance amount measurement and dosage determ. 80−31717
systematic effect caused by interactions between realizations of ampere and kilogram with fundamental constants 79−85127
thermogravimetric system for investigating gas-metal reactions at elevated temps. 80−229

weighing continued
thermogravimetry, balance inclination and specimen temp. error sources 80−98887
torsion balance, sat up by welding fused quartz rods and fibres *(Japanese)* 80−31738
ultrahigh vacuum system for ultramicrogravimetric study of samples loaded in controlled environment 79−80580
weighbridge and heavy-goods weighing machines, changes in standards 79−6096
weighing apparatus for hydraulic lysimeter in the Western Australian cereal belt 79−12276
weights and measures, conference, Washington (1978) 80−27260
Al, film, initial oxidation, AES, work function and gravimetric meas. 78−7087
BN, degree of conversion from cubic to hexagonal, determ. method 79−15887
La_2S_3-LaS_2, p-T-x phase diagram of La-S system 77−21112
O_2, chemisorbed on metal films, active sites, chemiluminesc. and vacuum microbalance obs. 78−22950
U in safeguards, automated gravimetric titrator 79−85609

weighing machines *see balances*

weight, atomic *see atomic mass*

weight, molecular *see molecular weight*

weight indicators *see balances*

weight measurement *see weighing*

weightlessness experiments *see zero gravity experiments*

Weinberg model
$\Delta I = 1/2$ dominated weak decays of strange hadrons, Weinberg-Salam scheme 80−27499
$\Delta I = 1/2$ rule 77−22676
$\Delta S = 1$ nonleptonic weak decays, $\Delta I = 1/2$ rule, quark models and current algebra 80−47282
antiquark sea role in determ. of $\sin^2\theta_W$ from total neutron cross sections *(Russian)* 80−4910
asymptotic freedom predictions for neutral and charged current neutrino interactions 78−8581
atom parity breaking, implications for unification of weak and EM interactions 77−57479
Cabibbo angle and quark masses in the Weinberg-Salam model 79−93332
Cabibbo angle calcs., mass matrices in Weinberg-Salam model 80−86674
Cabibbo angle in the $SU(2)_L \times U(1)$ gauge theories 79−35991
Callan-Symanzik and Weinberg equations: frame dependence of fixed points 80−4838
charged Higgs boson properties; Weinberg Salam model 79−40719
chiral unified gauge model based on nonlinear chiral hadron Lagrangian 80−42378
classical stationary solution of gauge invariant Lagrangian of Weinberg-Salam model *(French)* 77−2784
colour-flavour symm., renormalisation effects in guage theories 78−33018
cosmological constant, broken gauge theories and 3K black-body radiation 78−28870
cosmological fluid, lepton era, transport coeffs., Weinberg-Salam model 78−32623
CP violation in gauge theories, valence quark hypothesis 79−12940
CP violation via Higgs boson exchange, Weinberg-Salam model anal. 79−63384
D_5 group, 2 values of Cabibbo angle, 4 quark flavours 80−68405
discrete symmetries, natural flavor conservation and weak mixing angles 79−49438
divergence cancellations, in Weingberg-Salam model 80−32052
duality invariance, simple gauge theories including EM-type fields with sources 80−27440
dynamical Higgs mechanism, weak $\Delta I = 1/2$ rule, sum rules, heavy quarks and leptons 80−27442
dynamical scaling violations, evidence from neutral current anomalies 79−17664
dyon solutions 78−66066
effective Lagrangian in spontaneously broken gauge theories 79−17653
effective potential of Coleman-Weinberg Lagrangian, simple computation 78−8543
eight quark model by adding horizontal SU(2) gauge to Weinberg-Salam model 79−71682
electric charge, critical value in classical model *(Russian)* 80−13256
electro-weak interactions, neutral currents, W and Z-bosons 80−73638
electro-weak interactions concept and Weinberg-Salem model verification *(Czech)* 80−22549
electron mass, calc. in left-right-symmetric model 79−26282
electroweak force, grand unification and superunification 79−93333
electroweak mixing angle, sequential triplets scheme of fermions 80−86650
EM and weak interaction unification, bearing of Weinberg model and gauge invariance *(German)* 80−32054
fermion and Higgs boson mass constraints 79−49437
fermion asymmetry of the Universe and the W condensate, Weinberg Salam model *(Russian)* 80−73087
fermions, charge density phase transitions in gauge theories with spontaneous symmetry breaking *(Russian)* 79−2969
flavor unification, τ decay, and b decay within the six-quark-six-lepton Weinberg-Salam model 79−35990
flavor-changing effective neutral-current couplings in the Weinberg-Salam model 80−86649
flavour symmetry breaking and isovector parity-violating potentials 79−80780
gauge Bosons struct., quark-antiquark pair 77−30308
gauge model of weak and electromag. interactions, polarised lepton scatt. 78−45901
gauge model with spontaneous P-violation, anal. of spontaneous CP violation 77−38113
gauge theories, an introduction for experimental particle physicists 78−82119
in gauge theories applied to weak interactions, review 77−26479
gauge theories of weak, EM, and strong interactions, book contrib. 79−30694
gauge theory, renormalisation of ghost and Goldstone fields and ghost symmetries 80−90987
Glashow-Weinberg-Salam model, one-loop corrections to vector boson masses 80−57548

Weinberg model continued
gluon exchange diagrams, effect on parity violating weak interactions 79−97565
graded Lie algebra structure, derivation from lepton Lagrangian 79−49440
grand unification E_8 theory, Weinberg-Salam model reproduction *(Russian)* 80−4909
hadronic matter, Pomeron and critical temp. 80−22566
hadronic weak decays in asymptotically nearly-free theories 77−65154
Han-Nambu and SUB quark models, modified, appl. to Weinberg-Salam unified gauge model 80−22562
heavy atoms, P-odd effect suppression in unified gauge theory, l-N scatt. P-odd asymmetry *(Russian)* 77−61300
heavy Higgs boson decay in Weinberg-Salam model 80−95241
heavy muon in minimal gauge scheme as possible cause of $e\mu$, $\bar{\nu}_\mu$ anomalies 77−61241
heavy vector mesons, decay into Higgs particles 78−12908
heavy Weinberg-Salam type neutral Higgs boson, possible LEP prod. 79−75718
hierarchy in asymptotic reconstruction of spontaneously broken isotopic symmetry *(Russian)* 79−2968
Higgs boson, mass, upper and lower limits *(Russian)* 78−4795
Higgs Boson nature, test in $e^+e^-\rightarrow HHZ$ 79−63405
Higgs bosons, photoproduction 80−22558
Higgs bosons, Weinberg model, input mass scale 80−22554
Higgs coupling constraints from axionatics, Weinberg-Salam model Higgs extension 79−40706
Higgs doublets, CP violation, $\Delta I=1/2$ rule 77−65132
Higgs doublets, massless, particle masses, perturbation constraint 80−57541
Higgs fields and the determination of the Weinberg angle 79−40709
Higgs induced neutral currents, symmetries leading to flavour conservation, Cabibbo angle 79−63407
Higgs mechanism, unification of weak and EM interactions *(French)* 80−77999
Higgs meson mass and decay of metastable vac. state. 78−4819
Higgs-boson exchange P and CP violation 78−8575
Higgs-induced neutral processes, natural-flavour conservation, K-symmetries 80−57539
high energy lepton pair prod. with pol. hadrons, P and C violations 80−99068
high energy neutrino physics, recent expt. results 80−4982
high energy neutrino-hadron collisions, dilepton mass spectrum, V-A and Weinberg interaction calcs. 79−3010
inclusive lepton pair prod., P violation, quark-parton model in Weinberg-Salam theory, QCD 80−37217
intermediate boson production in pp($\bar{p}$) collisions, single lepton inclusive cross sections from decay 77−41868
ladder approx., relativistic repulsive effects in nonrelativistic systems 79−35972
Lee-Weinberg model of weak and EM interactions, string-like solns., vortices 80−47231
left-right symmetric model with global symmetry 79−17657
left-right symmetry and quark-lepton unification extension 80−78002
lepton mixing matrix, sequential Weinberg-Salem theory, CP conservation 80−47238
lepton number non-conservation in Weinberg model with two Higgs doublets 77−67585
leptonic interaction gauge model in SU_3 with 30° Weinberg angle 80−4903
light Higgs boson, appl. of current algebra 78−45835
mass differences in Weinberg model, upper limit determ. 77−61245
minimal anomaly-free electroweak model for several generations 80−4906
mixing angles of leptons in an extended Weinberg-Salam model 79−71679
multidimensional unified theory of gravit., EM and weak interactions 78−41462
muon number conservation spontaneous breakdown, off-diagonal neutral currents 77−49889
muon number nonconservation effects in gauge theory with V+A currents and heavy neutron leptons 78−8573
muon number violation, Weinberg model extension 77−67610
neutral current anomalies, differences between dynamical scaling violations and slow rescaling 77−49896
neutral current constraints on gauge models of weak and EM interactions 78−45831
neutral current couplings in neutrino-hadron interactions 78−24993
neutral current effects in Berthe-Heitler pair prod. 78−33022
neutral current effects in positron annihilation baryon-antibaryon effects 77−18310
neutral current P-violation, gauge flavours, Weinberg model testing 77−61240
neutral currents, flavour-changing, Wienberg-Salam model 80−22553
neutral currents and quark charge origin 78−21373
neutral currents natural flavour conservation, determ. of Cabibbo angle 79−22015
neutral currents properties and structure, gauge theory predictions, obs. 78−12856
neutral-current coupling, high-energy ν interactions 78−66104
neutrino + nucleus reactions, using shell model and Weinberg model to describe currents 79−93605
neutrino pair bremsstrahlung and number of lepton generations 80−101978
neutrino-electron mixture, influence of spin and Weinberg-angle on bulk viscosity 77−61223
non leptonic hyperon decay amplitudes, calc. without arbitrary parameters 80−13300
non-Abelian gauge theories, local covariant operator formation, quark confinement 80−47190
nonAbelian gauge theories, topological configurations, magnetic poles on flux strings 79−49368
nonleptonic decays, Weinberg-Salam and harmonic oscillator quark model 80−102048
nonlinear Lagrangians and spontaneous symm. breaking 78−70303
nucleon weak interaction pots. in the Weinberg-Salam model *(Russian)* 80−13258
orthopositronium decay into axions 78−78125
parity non-conserving processes, weak interaction theory, review 78−50002

Weinberg model continued
parity nonconservation in heavy atoms and weak magnetism in neutral currents *(Russian)* 80−82932
parity violating neutral currents, radiative corrections, Weinberg-Salam and left-right symmetric models 80−52451
parity violation in atoms induced by radiative corrections 78−78108
polarised resonance, lepton pair decay, charge asymmetry calc., W-S model test 79−17716
QCD, sum rules for light quarks *(Russian)* 78−45812
quark mass, current, induced isospin violations 80−32069
quark masses from Weinberg-Salam model renormalisation group eqns. 80−42377
quark-lepton correspondence, multigeneration $SU(2)_L\times U(2)$-based model 80−22584
quarks, flavour number determination using Higgs scalar particle 80−13288
quarks-antiquarks system, effect on neutral currents *(Russian)* 77−6078
reformulation, for lepton scheme with 4-component ν-effects of Higgs scalar bosons *(Russian)* 79−80784
relativistic kinetic theory of $e\nu_e$ and $e\nu_\mu$ systems, transport coeffs. 79−21680
renormalisation effects on Weinberg angle 78−62344
restrictions on weak interaction models, Salam-Weinberg $SU(2)\times U(1)$ gauge theory framework 77−41801
right handed colour octet currents in $\nu(\bar{\nu})$ reactions, agreement with Weinberg model 78−93874
sequential Weinberg-Salam model, neutral current flavour conservation, fourth generation 79−97561
$\sin^2\theta_w$, grand unified gauge theories and proton decay 80−73634
six quark model, quark mixing angle bounds 79−71686
six quark model without right handed currents 77−6081
spin projection operators for fields of any spin *(Japanese)* 78−32733
spontaneous CP violation 77−26480
spontaneous symmetry breaking dynamics 80−32060
stellar core collapse, neutrino trapping 78−32437
stellar matter, neutrino opacity, pure neutral vector boson contrib. 78−53928
Sterman-Weinberg formula for quark jets and gluon jets, leading log version, master equation 80−22552
Sterman-Weinberg jet formula 79−6325
Sterman-Weinberg jets, leading log derivation 79−63413
strange particle nonleptonic decay, asymptotic freedom, light quarks and $\Delta T=1/2$ rule 77−38164
string-like configurations in Weinberg-Salam theory, Regge trajectories of excitations 78−16966
strong CP problems, soln. in Weinberg-Salam model, colour group extension 79−75699
$SU_2\times U_1\times U'_1$ electroweak model, Weinberg-Salam intermediate bosons 80−105831
$SU(2)_L\times SU(2)_R\times U(1)$, CP invariance, global chiral U(1) symmetry, axion-quark coupling 79−22009
$SU(2)_L\times U(1)$, mass hierarchies and Cabibbo angle formula 79−63420
$SU(2)_L\times U(1)$, nonlinear realisation of Weinberg-Salem model for chiral $SU(4)\times SU(4)$ meson theory *(Russian)* 79−30693
$SU(2)_L\times U(1)$ gauge group, axial-vector isosinglet neutral hadronic current coupling to ν and e 79−63371
$SU(2)_L\times U(1)$ gauge model, mixing angles and CP violation 80−73648
$SU(2)_L\times U(1)$ theory, radiative corrections, simple renormalisation framework 80−101973
$SU(2)_L\otimes SU(2)_R\otimes U(1)$ gauge models confronting neutral current data 79−22013
$SU(2)_L\otimes U(1)$ gauge Weinberg Salam model, lepton number bound 80−82927
$SU(2)_L\times SU(2)_R\times U(1)$ gauge models, neutral current sector, natural parity conservation 79−9324
SU(2), unification of isospin and hypercharge, electroweak interactions of leptons 80−27439
$SU(2)\times U(1)$, allowed supersymmetric vacuums of Yang-Mills theory 78−4783
$SU(2)\times U(1)\times G$ Weinberg-Salam extension, possible neutral current struct. at PETRA/PEP and LEP 79−89096
$SU(2)\times U(1)\times U'(1)$ extension, new neutral current structs. 79−58920
$SU(2)\times U(1)$ gauge model, eigenvalue condition for Weinberg mixing angle, new leptons and quarks 78−41463
$SU(2)\times U(1)$ gauge model predictions for neutral current reactions 77−71424
$SU(2)\times U(1)$ Weinberg-Salam model, possible classical solns. 80−86644
$SU(2)\times U(1)$ Weinberg-Salam model, weak mixing angle, grand unified gauge theories 79−89093
$SU(2)\otimes U(1)\otimes U'(1)$, anal. in neutral current interactions, parity nonconservation in ed scatt. 79−17731
SU(2/1) supergroup, irreducible gauge theory of a consolidated Salam-Weinberg model 79−40707
$SU(3)\times U(1)$ gauge theory of weak and EM interactions 78−70317
superconductivity, gauge invariant model, local, collective excitations 77−87902
superconductivity model of weak and EM fields, self-interacting lepton field Lagrangian 77−41800
superconductivity unified model of weak, EM and strong interactions 77−49888
superheavy Higgs particles, proportional renormalisation corrections to W and Z mass, Weinberg-Salam model 79−276
supersymmetric, Lagrangian, invariant under SU(2/1) gauge group and rotations, in 6-D graded space 80−57537
supersymmetric extension of Weinberg-Salam model, lepton interactions, low energy 77−49887
supersymmetric Weinberg-Salam model 79−67490
superweak gauge theory of CP-invariance violation 79−75710
torsion potential, coupling strength, experimental bounds 80−73249
transition amplitudes and probabilities for $\nu\nu$, $\bar{\nu}\nu$, $\bar{\nu}\bar{\nu}$, νe, $\nu\bar{e}$, $\bar{\nu}e$, and $\bar{\nu}\bar{e}$ scatt. 78−21415
twistor theory in Weinberg-Salam and Georgi-Glashow SU(5) model 80−73651
two-electron atoms, autoionisable states decay, parity violation effects 79−72231
two-electron ions, autoionisable states decay, parity violation effects 79−72231
$U(1)\times U(1)(\mathrm{loc})\times SU_2(\mathrm{loc})$ invariant Weinberg Lagrangian, hypercharge group 79−71680
U(1) as the minimal horizontal gauge symmetry 79−80753
unified field theory, quantisation 78−89646

Weinberg model continued
unified lepton-quark model of Nambu-Jona-Lasinio type for weak, EM and strong forces 77−30304
unified theories, mass scales, alternatives to SU(5) 80−27441
unified theories of strong+weak+EM interactions, Weinberg angle, dynamical symm. breaking *(Russian)* 78−413
unified vectorlike gauge theory based on group SU(6) for quarks+leptons 78−4818
uniqueness of the Weinberg-Salam gauge model 79−35989
universality and weak isospin of leptons, nucleons, quarks 78−70273
V(e)V(q)+A(e)A(q) neutral currents in SU(2)×U(1)×U(1) theory 79−17667
(V-A) model, mixing between ordinary and heavy leptons, neutral current reactions 78−41472
vacuum instability, appl. to Goldstone and Weinberg models 77−65107
vacuum instability, cosmology and particle mass constraints for Weinberg-Salam model 80−78007
vacuum instability and Higgs scalar mass, appl. to Weinberg model 77−10178
vacuum instability and new constraints on fermion masses in Weinberg-Salam model 79−45045
vectorlike theory with parity violating neutral current and natural symmetry 77−13909
weak interaction theory, review 78−4822
weak interaction theory satisfying high energy unitary bounds, Weinberg model appl. *(Chinese)* 79−320
weak interactions, exptl. test *(Russian)* 79−97564
weak neutral current struct., ν and $\bar{\nu}$ interactions hadronic energy distrib., Weinberg-Salam model 79−35993
weak neutral currents unveiled 80−73658
weak-EM interference, neutral currents, P-violation, in polarised e-scatt. and e^+e^- interactions 79−63404
Weinberg angle determ. in reformulation of Weinberg model to Yang-Mills theory 79−35984
Weinberg-Salam model, gauge ambiguity effects 80−4908
Weinberg-Salam SU(2)⊗U(1) gauge theory effective Lagrangian, neutral current results 79−35992
Weinberg-Salem model, sequential, quark mixing angs., new generalised Cabibbo fit appl. 79−17655
Yang-Mills theory, Higgs particle 80−4905
zero-fermion modes in models with spontaneous symmetry-breaking 80−18105
β-decay modes and weak interaction fundamental nature *(Hungarian)* 77−26482
D-meson, gauge theoretic formulation of $SU_2\times U$, model, mass limit 78−70316
eD, 19.4 to 22.2 GeV, unpolarised target, parity violation in inelastic scatt. of polarised electrons 79−63482
ed, polarized scatt., parity violation Weinberg-Salam model without parton model 79−40787
ed deep inelastic scatt., p-violating asymmetries, neutral current couplings, sea quark contrib. 79−97630
ed→eX, polarised deep inelastic scatt., test of Weinberg-Salam model 79−22006
ee elastic scatt., possible weak interaction effects, Weinberg-Salam model estimates 79−75755
e^-e^+ inelastic scatt. 78−82194
$e^-e^+\rightarrow\mu^-\mu^+$, high energy total cross sections, Salem-Ward-Weinberg model 79−22086
e^+e^-, $SU_L(2)\times U(1)$ and $SU_L(2)\times SU_R(2)\times U(1)$ predictions at high Q^2, neutral currents, Z-bosons 80−63029
$e^+e^-\rightarrow\mu^+\mu^-\gamma$, neutral current effects and hard photon correction 79−13096
e^+e^- annihilation, charged Higgs boson prod. signatures, Weinberg-Salam parametrisation 80−57620
e^+e^- annihilation channel, differential dispersive theory of ψ/J 78−45933
$e^+e^-\rightarrow b\bar{b}$, heavy quark masses and C- and P-odd asymmetries, Weinberg-Salam model *(Russian)* 80−102060
e^+e^- collisions, weak neutral current effects, unified theories of dimension *(Hungarian)* 79−9326
$e^+e^-\rightarrow e^+e^-$, Bhabha scatt. one loop radiative corrections in Weinberg model 80−13310
$e^+e^-\rightarrow\mu^+\mu^-$, 40-200 GeV, cross section, one loop corrections in Weinberg model 80−18139
$e^+e^-\rightarrow\mu^+\mu^-$, radiative corrections around Z^0, Weinberg-Salam model 80−99103
$e^+e^-\rightarrow\mu^+\mu^-X$, possible Higgs boson detection in missing mass plot 80−4977
$e^+e^-\rightarrow\nu_e\bar{\nu}_e\gamma$, gauge theory analysis, Weinberg-Salem model, ang. and energy distribs. 78−12894
$e^+e^-\rightarrow pX$, weak neutral current, polarisation effects, asymm. parameters *(Russian)* 78−459
$e^+e^-\rightarrow q\bar{q}$, high energy total cross sections, Salem-Ward-Weinberg model 79−22086
$e^+e^-\rightarrow q\bar{q}g$, gluon bremsstrahlung, neutral current and beam polarisation effects 80−99106
$e^+e^-\rightarrow W^+W^-$, charact. of μe events anal. in Weinberg model 77−71478
$e^+e^-\rightarrow W^+W^-$, polarisation amplitudes 80−42484
$e^+e^-\rightarrow W^+W^-$, radiative, corrections in Weinberg model 80−52512
$e^+e^-\rightarrow Z^0\gamma\rightarrow\mu^+\mu^-\gamma$, Weinberg model anal. of Z^0 decay ang. distrib. 80−47275
$e^+e^-\rightarrow ZZ$, polarisation amplitudes 80−42484
$e\bar{e}\nu_e\bar{\nu}_e$ mixture, covariant transport eqns., collision terms from Weinberg Salam theory 77−74315
$e\bar{e}\nu_e\bar{\nu}_e$-mixture, reactive collisions influence on bulk viscosity 77−74637
$e\mu$ elastic scatt., possible weak interaction effects, Weinberg-Salam model estimates 79−75755
eN, deep inelastic scatt., heavy lepton mixings, Weinberg-Salam model 80−62992
eN→eX, $SU(2)_L\times U(1)$ gauge theory distinguished from $SU(2)_L\times SU(2)_R\times U(1)$, neutral currents, z-bosons 80−62908
eN elastic scatt., pol. e, nucleon form factors, P violating symmetry, Weinberg-Salam calcs. 80−68461
ep, high Q^2, QCD corrections to parity-violating asymmetries 80−22618
ep deep inelastic scatt., p-violating asymmetries, neutral current couplings, sea quark contrib. 79−97630
ep→eX, polarised deep inelastic scatt., test of model 79−22006
η, neutral weak current effect on decay mode Weinberg-Salam model, P-violation contrib. 78−86450

Weinberg model continued
γ circular polarisation, neutral current effect in bremsstrahlung and pair production 80−73655
$\gamma e^-\rightarrow e^-\nu\bar{\nu}$, energy spectra of recoil fermions, Weinberg-Salem model 78−12895
$\gamma N\rightarrow l^+l^-X$, pol. γ, neutral current effect, Weinberg Salam model calcs., p violation 80−5000
$\gamma N\rightarrow l^+l^-X$, polarisation effects on P-violating asymmetry in Weinberg-Salam model 80−32055
$\gamma N\rightarrow$lepton pairs, weak neutral currents anal. 78−8670
$\gamma p\rightarrow$ lepton pair, P violating asymmetry 80−105901
$K\rightarrow 3\pi$, CP violation, current algebra anal., six quark Weinberg-Salam model 80−47281
$K^-\rightarrow\pi\mu\nu$, μ polarisation and T-odd correlations, Weinberg model of CP violation *(Russian)* 80−62969
$K^+\rightarrow\pi^+\mu^+\mu^-$, radiative corrections in Weinberg model *(Russian)* 77−38163
$K_L\rightarrow 2\gamma$ or $\pi^+\pi^-\gamma$, Weinberg-Salam model, weak radiative decays, large dist. contribs. *(Russian)* 77−82740
$K_L\rightarrow 2\gamma$ or $\pi^+\pi^-\gamma$, Weinberg-Salam model, weak radiative decays 78−41541
K_L and K_S mass difference in asymptotically free gradient theory *(Russian)* 77−30333
$K_L\rightarrow\mu^+\mu^-$, and nλZ vertex in Weinberg-Salam model *(Russian)* 77−2821
$K_s^0\rightarrow\pi\pi$ in terms of spectral function integrals, short distance approach 77−61242
l(l̄)N, P-odd asymmetries in deep inelastic scatt. of polarised l and l̄ *(Russian)* 79−49527
$\mu\rightarrow ee\bar{e}$, Weinberg-Salam model with neutrino mixing *(Russian)* 77−38114
$\mu\rightarrow e\gamma$, Weinberg-Salam model with neutrino mixing *(Russian)* 77−38114
$\mu\rightarrow e\gamma$ in Weinberg Salam model, spontaneously broken μ-like charge symm., heavy leptons *(Chinese)* 78−82191
μ magnetic moment, weak coupling contribution, Weinberg-Salam model 80−22607
μ-e mass quotient, modified Weinberg-Salam model calcs. *(French)* 80−82926
μ-e universality, very large Higgs mass limit 77−87935
μ-e universality and spontaneous μ-e mass splitting 77−30302
μ^- to e^+ conversion in nuclei, mediation by Majorana lepton 80−22547
μN, deep inelastic scatt., heavy lepton mixings, Weinberg-Salam model 80−62992
NN parity-violating π-exchange pot. 77−65133
NNπ amplitudes, parity violating, QCD calc. in Weinberg-Salam model and SU(4) flavour symmetry breaking 79−67520
NNπ coupling, parity violating, quark, model calc. in Weinberg Salam model 79−35987
NNρ couplings, parity-violating, QCD and MIT bag model, $1/2^-$ resonance contribs., $SU(6)_w$ symmetry 80−57540
np→dγ process, weak interaction between nucleons *(Russian)* 79−63513
np→dγ radiative capture, relativistic effects, parity violation, Weinberg-Salam model *(Russian)* 80−32120
ν, $\bar{\nu}$, inclusive neutral current interactions 78−25036
ν EM form factors and mag. moments, neutral currents, astrophysics applics. *(German)* 80−62904
ν interactions, dimuon prod., high y-anomaly, extended minimal Weinberg model 77−26510
ν neutral current couplings and νe^- weak neutral current coupling constraint, fermionic assignments 80−4915
$\nu(\bar{\nu})$N elastic scatt. cross sections in Weinberg model of neutral currents 77−10240
$\nu(\bar{\nu})$N neutral current interaction, charm prod. in quark parton model 77−61246
$\nu(\bar{\nu})N\rightarrow\nu(\bar{\nu})\gamma X$, hadron neutral current, Weinberg-Salam model *(Russian)* 78−45910
$\nu(\bar{\nu})$+N, neutral to charged current inclusive cross-section ratio determ. 77−26511
$\nu(\bar{\nu})$e, differential cross-section calc. in gauge theories, W-boson exchange 77−82728
$\nu(\bar{\nu})$p elastic scatt. and neutral currents, by polarised proton target *(Russian)* 77−26507
$\nu_e(\bar{\nu}_e)$e, charged and neutral current interference, test of Weinberg-Salam model 80−42385
ν_e-ν_μ universality corrections for neutral current interactions in Weinberg-Salam model 79−54292
$\nu'\rightarrow\nu\gamma$, Weinberg-Salam model with neutrino mixing *(Russian)* 77−38114
$\bar{\nu}_e$+e inelast. scatt. total and differential cross sections in Weinberg-Salam theory *(Bulgarian)* 79−85254
νd→νnp, photon-neutrino coupling theory, Weinberg-Salam model comp. 79−13102
$\nu_\mu d\rightarrow p n\nu_\mu$, neutral current induced neutrino reactions, differential and total sections 79−17708
$\nu e\rightarrow\nu e\gamma$, radiational scatt., polarisation effects *(Russian)* 77−46038
νe scattering, weak lepton structure analysis, Weinberg-Salam model *(Russian)* 78−25039
$\nu e^-\rightarrow\nu e^-\gamma$, energy spectra of recoil fermions, Weinberg-Salem model 78−12895
$\bar{\nu}_e$e annihilation in Weinberg-Salam model, number of quarks and leptons *(Russian)* 80−102041
ν_μe (and $\bar{\nu}_\mu$e) scatt., log. order α electromag. corrections 79−63467
νl interactions, differential and total cross sections *(Russian)* 77−6112
νN and $\bar{\nu}$N elastic and quasi-elastic scatt., determ. of Weinberg angle 77−54064
νN→hadron+hadron neutral current prod., cross sections, Weinberg angle *(Russian)* 77−6111
νN interactions and consquence of model, general survey *(German)* 77−22729
$\nu n\rightarrow\mu^- p$, Higgs boson exchange effects on second-class currents 80−91075
$\nu N\rightarrow\nu X$, $SU(2)_L\times U(1)$ gauge theory distinguished from $SU(2)_L\times SU(2)_R\times U(1)$, neutral currents, z-bosons 80−62908
$\nu n\rightarrow\nu n\pi^0$, neutral current induced one-pion production, Weinberg-Salam structure 80−52454
$\nu n\rightarrow\nu p\pi^-$, neutral current induced one-pion production, Weinberg-Salam structure 80−52454
ν_lN deep inelastic scatt., radiative correction inaccuracies, quark-parton and Weinberg-Salam theories *(Russian)* 79−93403

Weinberg model continued
νp elastic scatt., implications for weak interaction models 77−6108
νp elastic scatt., neutral current struct. anal. 77−61273
νp inclusive interactions, ratio of neutral current to charged current cross sectins 77−79263
$\bar{\nu}p \rightarrow \mu^+ n$, Higgs boson exchange effects on second-class currents 80−91075
$\nu p \rightarrow \nu n \pi^+$, neutral current induced one-pion production, Weinberg-Salam structure 80−52454
$\bar{\nu}p \rightarrow \bar{\nu}p$, energy spectra of recoil fermions, Weinberg-Salem model 78−12895
$\nu p \rightarrow \nu p \pi^0$, neutral current induced one-pion production, Weinberg-Salam structure 80−52454
Ω^- nonleptonic decay branching ratios from Weinberg-Salam and MIT bag models 80−37261
pN, dilepton production by pol. protons, parity violating, asymmetry, Weinberg-Salam calcs. 80−42488
$p\bar{p}$, hadronic jets, possible intermediate bosons 80−18149
$\bar{p}p$, pp, $SU_L(2)\times U(1)$ and $SU_L(2)\times SU_R(2)\times U(1)$ predictions at high Q^2, neutral currents, Z-bosons 80−63029
pp and $p\bar{p}$ collision, intermediate vector boson production 80−9186
$\bar{p}p \rightarrow e^+e^-$ annihilation, weak neutral current effects *(Russian)* 80−105837
$pp \rightarrow N\Delta$, parity violation in Weinberg model 78−8701
$pp(\bar{p}) \rightarrow W^{\pm}(Z^0)X$, QCD perturbation theory struct. function predictions 80−42505
pp scatt., <300 MeV P-odd asymmetry for pol. ρ *(Russian)* 80−102063
$p\bar{p} \rightarrow W^{\pm}X$, front back asymmetry in QCD and Weinberg-Salam model 79−97579
$p\bar{p} \rightarrow Z^0 \rightarrow l\bar{l}$+anything, cross section for Z^0 production, Weinberg model *(Russian)* 77−10296
$p\bar{p} \rightarrow Z$+anything, front-back asymmetry differential cross section, $W^{\pm}$ prod. 79−6352
π^0, neutral weak current effect on decay mode Weinberg-Salam model, P-violation contrib. 78−86450
$\pi^{\pm}$ decay, gauge theory, radiative corrections to μ-e universality 77−10244
πN coupling, parity violating, weak and EM interaction model anal. 79−67599
ψ' decay, Higgs bosons, five-quark model, P and T nonconservation 77−74686
$\Sigma^0 \rightarrow \Lambda e^+ e^-$, parity violating effects, standard and pure vector Weinberg Salam model 79−36075
$\Sigma^+ \rightarrow p\gamma$, $1/2^-$ resonance poles to parity-violating amplitude, two-quark weak transitions 80−78062
t-quark mass from discrete symmetries 79−63462
$\tau(1.8)$, charged lepton anomalous mag. moment, Weinberg-Salam model effects 79−13126
W boson e^+e^- prod. calcs. in Weinberg-Salam model 77−30301
W boson magnetic and quadrupole moments 77−30383
W-production via Z-decay in Weinberg-Salam model 80−101979
W^{+or-} bosons, lowest order g-2 Weinberg-Salam model, Feynman diagrams 80−47291
Z^0 flux loops, more heavy particles in the Weinberg-Salam model 78−82136
$Z^0 \rightarrow H^0 l^+ l^-$, leptonic decay into light Higgs boson, grand unification test 80−42381
Bi, parity non-conserving optical rot., Weinberg-Salam relativistic central field theory vs. obs. 78−953
Bi, parity nonconserving optical rot. upper limit, obs. vs. Weinberg-Salam theory 78−952
Bi weak charge, $SU(2)\times U(1)$ model anal. 79−26281
H simultaneous mag./elec. microwave resonance transition, parity nonconservation, Weinberg-Salam theory test 77−54066
$^2H(\gamma,n)p$, parity violation expts. review, weak NN interaction 80−73792
^4He production, nonzero neutrino rest mass effects 80−105413

Weissenberg cameras *see cameras; X-ray crystallography apparatus*

welding
see also electric welding; electron beam welding; laser beam welding; lead bonding; ultrasonic welding
alloys, variable composition, errors in deriving empirical relationships using accelerated methods 80−25980
austenitic stainless steel, ultrasonic tests, false indications, cause and influence 78−31599
austenitic stainless steel weld metal defect detection, shear-wave polarisation effect 78−44337
austenitic steel neutron-irradiated weld toughness rel. to ferrite content 79−83327
austenitic steel transformation temp. and crack prevention in weld cooling 79−83200
austenitic welds, US inspection 80−71821
bimetal rolling, calc. of strains by variational method *(Polish)* 80−45323
bimetallic welded joints, heterogeneous, metallographic anal., etcharts and etching regimes 80−40635
Br.AZhNMts 7-2.5-1.5-9 bronze, Mg-Al, type, fatigue and stress corrosion cracking, welding effects 80−3233
breeder reactor fuel pin end closures, pulsed magnetic welding 79−93806
bronze-steel, phase composition and struct. of diffusional interlayer in fusion zone, X-ray analysis 78−56821
butt joints, calc. of temp. field for nonideal thermal contact *(Russian)* 80−10121
butt welded joint dynamic strength, partial penetration and slag inclusion effects 79−83288
butt welds inspection, using multielement US probe 77−90569
cellular and cellular dendritic growth, general microsegregation eqn. 80−84921
Colmonoy, self-weldability in high temp Na *(Japanese)* 80−89392
composite material, manufacture by explosive welding *(German)* 79−43171
continuous drive fraction welding process, selection of welding conditions 77−114
crystal units, vacuum system for cleaning and cold welding *(Polish)* 80−31776
crystalline particles at sphere-plane contact, nondiffusional deform. under capillary forces 78−15329
cylindrical welded rod with interlayer of lower elastic modulus, stresses in tension 79−24557
defects, NDT 79−79192
defects, toughness, crack growth anal. 79−43429
electrical contacts in switching equipment, welding resistance meas. 77 57353
electroslag welding, electromechanical and thermal flow phenomena 79−11758
engineering structures, exam. of fracture processes 78−60777
fatigue strength, low cycle steels and welds, relationship to static tensile props. 78−64684
fatigue strength of welds 80−3179
ferritic steel, characterisation of non-planar defects by ultrasonic testing 79−87812
fission reactor pressure vessel and circuit development, conf. report 80−47541
flash welded joints, fatigue strength obs., under heating and cooling cycles, microstructures influence 79−15760
flaw detection in welded joints, X-ray television systems appl. and characteristics 77−81380
flaw study using ultrasonic holography *(Dutch)* 78−68855
flaws detection, by acoustic emission monitoring, with aid of microcomputer 80−11866
friction welded joints, strain distrib. and fatigue cracks of joint's subjected to repeated torsion *(Japanese)* 79−8350
furnace welded pipe inspection unit for above 1000°C 78−53134
fusion reactor vacuum vessel welds, ultrasonic scanner 80−99288
hard-alloy/U8 C alloy steel weld, local internal stress region boundaries 77−59846
Hastealloy X, relations between weld heat affected zone cracking and microstruct., Gleeble test *(Japanese)* 78−52858
heat affected zone of weld, extraction and testing of flat, microtensile specimens *(German)* 77−9017
heat source, high energy density, appl. to welding, review *(Japanese)* 79−29329
high temperature deformations during welding, measurement, new strain gauge characteristics 77−67417
hip total replacements, welds in stems of cast Co-Cr femoral components 78−44697
impact welding, wavy interface characts. and formation 80−97680
impact welding process, fundamental parameters 80−97679
Inconel 706 and 718, relations between weld heat affected zone cracking and microstruct., Gleeble test *(Japanese)* 78−52858
inspection system for Space Shuttle external fuel tank, automatic, interim report 80−76463
irradiated fuel rods, in-cell welding techniques 80−22956
joint, reflection of ultrasound from irregularities 79−39086
joint, welded, through defects, study using vacuum bubble method of airtightness inspection 79−52599
joints, radiographic inspection, real flaws detectability evaluation 80−81266
lengthwise seam, US inspection of cylindrical testpieces 79−39087
liquid metal alloys solidification temp. range meas. technique 79−12799
LWR, effect of small pipe weld types on personnel exposure 78−4996
material selection w.r.t. brittle fracture strength *(German)* 78−15534
materials testing by grain struct. comparison *(German)* 77−86273
metal, diffusion welding, migration of oriented intergranular boundary with pores *(Russian)* 80−84943
metal, microplasma welding, heat propagation in parent metal *(Russian)* 78−15642
metal, weld pool solidification under EM agitation 79−24510
metal, welded joints, pore formation mechanism evaluation, rel. to solidification 80−3017
metal strips, welded, aged, reduction of deformations *(Russian)* 80−97508
metal to ceramic reaction welding, interfacial noble-metal corrosion 78−53035
metall, thin section fusion weld, US inspection 79−15916
metals, coating with H-transparent Pd layers, spot welding technique 79−47816
microwave surface wave plasma at atmospheric press., production and appls. 79−50868
monitoring in-process, with acoustic emission 80−16620
multipass welds, high temp. internal deformations development and effects on crack formation 80−81082
noble-metal tubes, cold-weld sealing 80−41556
nuclear reactor components, weld seam inspection, steam supply system, quality assurance *(German, English)* 77−83052
oblique entry US inspection of welds, defect coord. meas., error anal. 78−40008
permanent joining techniques 80−82782
PETRA electron-positron storage ring, vacuum system techniques and problems 78−17452
pipeline girth weld, determ. of acceptable defect level 79−34143
pipeline inspection, welding flaw detect., NDT 78−19984
pipes, large-diameter, US testing of welds 78−3267
pipes, welded branch, stresses calc. 80−108493
pipline girth welds, NDT of defects 78−27704
plate, complex shape, temp. field during welding with moving heat source *(Russian)* 79−68553
polypropylene, neutron irradiation effect on weldability and adhesion *(Japanese)* 79−60405
pressure vessels weld quality assessment, NDT methods and equipment 78−56871
PWR twin header bore welded steam generator design 79−93813
radiographic inspection of welded joints, effectiveness investigation 78−56872
radiographic weld testing between tubes and tube-plates in heat exchangers *(German)* 78−7151
rail joint, thermit-welded, US flaw detection probe 78−56852
residual stress formation in explosive welding 79−83285
residual stresses, evaluation by Barkhausen noise meas. 80−76436
seam defect parameters, measurement using TV-computer unit 79−67451
sheet metal, deep-drawn, for implant device encapsulation, mech. and metallographic props. *(German)* 79−8564
small diameter pipe weld, gamma radiography using enriched ^{169}Yb source 79−83399
soft-interlayer welded joint bending and torsion endurance, residual stress effects 79−83287
solar cell welds, nondestructive tech. system selection 78−35629
solar cells, NDT for mechanical strength evaluation 78−35630

welding continued
spot welding process, acoustic emission signals, anal. *(German)* 78−44296
stainless steel type 316 weld metal with controlled residual elements, creep behaviour 77−8902
of stainless steels, brittle fracture resistance improvement by N content reduction 78−95788
steel, 24Kh2NMFA, weldments, heat-affected zone struct. 79−24552
steel, acoustic emission associated with phase conversions 79−70275
steel, alloy, sheet, crack-propag. resist. in heat-affected zone in presence of H, rolling direction and preliminary plastic tensile strain effects 80−60971
steel, alloy 10G2S1 welds, fracture, subjected to low-temp. fatigue 80−89350
steel, ASTM A588, fatigue test of fillet weld, practical aspects of anal. 78−64682
steel, austenitic, fracture toughness meas. by Charpy impact testing, welding, heat treatment, neutron irrad. effects 79−5062
steel, austenitic, high-temp. crack resist., B and Mo influence *(Russian)* 80−16435
steel, austenitic, Ni-Cr, corrosion tests with stray currents after manufacturing operation and welding *(German)* 77−86274
steel, austenitic ferritic weld metal, austenitising and ferritising effects of elements 79−87614
steel, austenitic stainless, effect of autogenous welding on chloride pitting corrosion 79−91842
steel, austenitic stainless, ferritic, single phase ferritic solidification in welds, exam. 80−7546
steel, austenitic stainless, liquation cracking during welding, comp. influence 80−66645
steel, austenitic stainless, welded joints, cold working effects on mech. and corrosion props. *(Hungarian)* 78−52838
steel, austenitic stainless, welds, exam. of austenitic solidification mode 80−7545
steel, austenitic stainless weld, US inspection, focusing probe significance *(German)* 77−73397
steel, brittle fracture resistance, welding and heat treatment effects 80−50723
steel, C, cold rolled sheet, spot welded joints, static fracture appearance 80−55538
steel, CC Ni-maraging weld metal, increasing fracture toughness by heat treatment 78−72871
steel, Cr-Mo weld metal, reheat cracking, residual elements and microstruct. influence 80−66553
steel, Cr-Mo weld metal, trace element embrittlement suppression by creep strength effects 80−66656
steel, Cr-Mo-V low-alloy, mech. props. and stress relief cracking, effects of impurities and deoxidation practice 80−66599
steel, CrNiMoV, weld metal, hot cracking resistance during electroslag welding, effects of Cr 79−87732
steel, development and results of an instrumented restrained cracking (IRC) test *(German)* 78−85060
steel, dispersion hardening type 0Kh12NDL, cast, resistance to cold crack formation during welding 79−87731
steel, electroslag welded sheet, impact strength and toughness, welding effect *(German)* 77−86139
steel, fatigue crack propag. in weld 77−81324
steel, fatigue life prediction for fillet welded attachments, under service loadings 78−64683
steel, ferritic, Cr-Mo, containing less than 12 wt.% Cr, sensitisation during welding, to intergranular corrosion 78−88566
steel, ferritic weldment, US testing of defects, charact. and size 78−7104
steel, H effect on weldability 80−50720
steel, herringbone specimen weld stresses rel. to heat-affected zone rigidity 79−29130
steel, high strength, fine grained, quenched and tempered, residual welding stresses, stress relieving temp. *(German)* 78−72793
steel, high strength, weld zone resistance to welding induced cold cracking, preliminary heat treatment effects 79−91720
steel, high-speed, shiny nonfusion rings in friction welding, origin 78−23872
steel, HSLA, HAZ microcrack study in multilayer welding *(Chinese)* 79−100172
steel, HSLA and Low C, weldment, AE monitoring 79−87800
steel, interpretation of weld radiographs 79−91861
steel, low alloy, 10KhSND, 16G2AF, welded joint low-cycle fatigue during crack form. and propag. during biaxial bending 79−11704
steel, low alloy, high strength, fatigue crack growth, in presence of welding residual stresses *(Russian)* 80−71739
steel, low alloy, softening of heat affected zone under postweld tempering 77−21196
steel, low alloy, welded joints, cracking during heat treatment 80−7724
steel, low alloy type 14Kh2GMR, high strength, welded joint, impact toughness, welding thermal cycle and tempering effects 80−3157
steel, low alloy-high strength, deforms. during cold crack developments in welded joints 80−81142
steel, low-alloy sheet, welded hydraulic turbine volute chamber, strength and toughness 78−68820
steel, maraging, 18 Ni, welded joints ageing props. obs. *(Japanese)* 80−40401
steel, maraging influence of H content on γ-α transform. during welding *(Russian)* 79−78962
steel, microstructure control in flash butt welding 79−91715
steel, mild Cr welding, 550°-850°C heating effects on structure and toughness 79−24540
steel, mild explosively welded, 0.1% C tube to 0.2% C plate, microstructure 77−70221
steel, oxidation reaction of Si and Mn during CO_2-O_2 arc welding 77−60116
steel, plates, thin, welding residual stresses calc., elastoplastic thermal stress anal. 78−83262
steel, stainless, austenitic, explosively welded, orientation relationship in martensitic transform. 80−104158
steel, stainless, Cr(-Mo)(-Ni), self-weldability in high temp Na *(Japanese)* 80−89392
steel, stainless, LWR appl., US and AE testing of welds 79−36330
steel, stainless, type 304 welded, low temp. sensitisation, nucleation of CR carbide nuclei along grain boundaries TEM, SEM study 79−38851
steel, stainless, weld overlaid, creep-rupture props. 78−13230
steel, stainless/Nb interaction in vacuum percussion welding, Ni interlayer effect 79−29061
steel, tempered StE70, water quenched, residual strain field in centrally welded plates *(German)* 78−72794
steel, weld, morphology, effect of ferrite content 77−36521
steel, welded joint brittle fracture susceptibility test 79−29168
steel, welding residual stresses, sources, X-ray meas. *(German)* 77−86265
steel, welds obs. at high temperature, by moire photography 79−74336
steel butt weld structure and mech. props., explosive treatment effects 79−24541
steel plates, plastic coated, RF welded, quality and strength *(German)* 79−34185
steel weld fatigue life estimation, multichannel NDT monitor 78−56846
steel welded joint impact strength, preheating and tempering effects 79−24542
Stellite, self-weldability in high temp Na *(Japanese)* 80−89392
strain measurements, transient longitudinal strain changes 80−16332
stress measuring device design and application 80−68194
structural joints, low cycle fatigue anal. 77−3789
submerged arc weld metals, chevron cracking, metallographic study 78−56761
TEM, welded crystals, grain boundaries in Si 80−103364
thermal stresses and metal movement, computer simulation 78−34002
thin hemispheres, deform. during making of circular welded joints, special features 79−90155
Ti alloys, gas-saturated layer effect on cracking 77−44359
tube, spirally welded, pressure-test apparatus 77−52583
tube to tubesheet welds, X-ray and isotropic techniques for boroside radiography 77−86261
ultrasonic and eddy current testing of welded titanium tubes *(Japanese)* 80−108651
ultrasonic examination of welds, book 78−48608
ultrasonic flaw detection, in USSR, survey 79−87768
ultrasonic flaw detector, automatic, for butt welds *(Japanese)* 80−25976
ultrasonic inspection, welded joints in sugar extraction diffusion apparatus 80−93703
ultrasonic testing of welds, techniques review 77−74899
underwater plasma weld cooling 79−1932
underwater wet plasma wetting in pressurized water 78−7090
US applied to weld testing, creativity aspects *(German)* 77−73426
US defectometry, reliability for welds in 22K steel 78−56858
US defectoscope, echo-pulse, testing of annular welds 78−53090
US imaging for weld inspection 77−86254
US inspection probe for joint 78−92426
US monitoring of welds in nuclear power station fuel rods 79−5116
US testing of austenitic welds, metallurgical noise reduction 80−76466
US testing of electron beam closure weld on press. vessel 77−40480
US testing of electroslag welds, using tandem probe techniques 78−27692
US weld inspections with freq. scanned SH waves 80−76465
wear resistant material, US welding effect on struct. *(Slovak)* 79−74185
weld joint of high-pressure vessel, radiography inspection 79−100313
weld quality testing, US, in spiral-welded gas pipes 77−90550
weldable clad metal interlayer growth kinetics model 79−24493
welded component fatigue life and crack propag. analysis with internal stresses 77−77576
welded dissimilar cylindrical shells under service loading, stress/strain calc. and expt. 79−83284
welded pipe joint, efficency of various methods of NDT 79−39103
welded pressure vessels, residual stresses determination 78−40014
X-ray inspection of welded seams in heavy engineering using Philips MG 420 and MG 300 systems 79−93269
Zircaloy-4, resistance-welded, microstruct. of weld region 80−66549
Al alloy, weld metal structure and hot cracking susceptibility 79−24595
Al alloy welded joint, microstructural and chemical heterogeneity 79−29096
Al alloy welded joints, hot cracks in mutual solidification zone 79−24594
Al alloys AMg6M, AMg6, 5083, weld at cryogenic temps., mech. props. 79−66136
Al foil, alloying additions (Si, Mg, Y, Se, Sc) effect, on tensile strength, weldability 80−55475
Al plates with air gap, temp. field for microplasma welding of edge joints *(Russian)* 80−7755
Al-Be-Mg (30, 5wt.%) alloy, weld solification parameters 79−24511
Al-Mg (2.5wt.%) sheet, surface oxide state and weldability 80−59769
Al-Mg alloy AMg5, welded structures, machine for fatigue life investigation 79−52566
Al-Mg weldment, US testing, defect acceptance criteria, electron strength 77−70239
Al-Mg-Zn, granulated, degassing atm. effect on mech. props. of semifinished products 80−7720
Al-Zn-Mg alloy, welded, solute profiles at weld bead/parent metal interface 78−19942
Ar purifier, portable, 0.3 m^3/h, design and appl. *(Polish)* 79−12781
Be, welded acoustic emission 78−39976
Cr effect on carbon steel weld metal hot cracking resistance 79−79061
Cu, diffusion welding, tensile fracture strength *(Japanese)* 80−7663
Cu, impact welding, viscous energy dissipation 77−70058
Cu, poly and single crystalline, solid phase bonded interface, behaviour exam. *(Japanese)* 78−48611
Cu-Cr-Zr-Ti-B alloy system, solidification cracks formed during welding, reduction by microalloying with B 79−96148
Cu-mild steel explosively welded interface, SEM examination *(German, English)* 80−96746
Cu-Ni diffusion couple, diffusion bonding process, fracture surface exam. *(German)* 77−35762
Fe, cast, nodular graphite, welded, struct. exam., heat treatment effects 78−80703
MgO bicrystals, formed by welding single crystals with H_3PO_4, exam. 78−56796
Mo and Mo alloy TZM, solid-state bonding, tensile strength of bond *(German)* 79−47756
Mo, deformed, dislocation-free channels prod. by heat pulses, electron microscope obs. and hardness meas. *(Russian)* 79−52251
Mo/Nb welded joints in sheet metal, detect. and exam. of cracks, initiation, development 77−73385
Mo-B alloys, B distrib. in welds, nuclear track autoradiography study 79−43282

welding continued
Nb-Ti superconductor, for fusion facility, cold-pressure-welded joints 78−62630
Ni alloys, liquation cracking during welding, comp. influence 80−66645
Ni alloys, welding crack resist. during welding, heating, stress reduction by hardening 79−24618
Ni, diffusion welding, migration of oriented intergranular boundary with pores *(Russian)* 80−84943
Ni-Cr, ERNiCr-3 weld metal, strain-rate effects on high temp. behaviour 79−93726
Ni-Cr, self-weldability in high temp Na *(Japanese)* 80−89392
$Ni_{40}Fe_{40}B_{20}$ glass alloy, rapidly quenched, explosive welding to A516-70 steel and to itself 78−39954
NiO_2 single crystals, welding, optical and SEM study 79−65097
Ta capacitor, stress wave emission anal. in resistance welding 79−11739
Ti alloy TA6V, superplastic behaviour of welded specimens 77−86100
Ti-Al-V (6,4 wt.%), microstruct. effect of base metals on diffusion welding *(Japanese)* 80−89296
TiI_4:C, deep doping during ion-beam welding, microhardness meas. 79−19294
V-Nb(MO) alloys, effects of welding on mech. props. 77−21176
W-ThO_2 composite, struct., lamination tendency, effects of method of manuf. 78−68653
WC-Co hard alloy-steel welds, effect of intermediate layer composition on structural changes and mechanical properties 78−60616
Zr-Nb (2.5 wt.%), seam welding tubing, microstruct. in weld region 79−61621
Zr-Nb (2.5 wt.%), transforms. during annealing of welded joint, after thermal cycling *(Russian)* 80−29984

welding electrodes
arc welding electrode metal drop free surface calc., MHD anal. *(Russian)* 78−5822
bimetallic electrodes for plasma torches, Cu to W joining methods 80−24266
cellulose-coated, plasma flow effect on weld pool obs. 79−7496
coated arc electrodes, identification of types and brands using SEM with energy-dispersive X-ray detector 80−81400
manual metal arc electrode constitution effect on AISI 316 weld metal mech. props. 80−66601
piezoceramic microwelding transducer component oscillation amplitudes 79−26046
C rods, for resistance welding of metals with high elec. and thermal cond. 77−79077

welding equipment
shielding technique development, torches with ring nozzles operation modelling 79−7497

Wentzel-Kramers-Brillouin calculations *see WKB calculations*

Wertheim effect *see Wiedemann effect*

wetting
adhesion, of liq. to solid surface, contact angle rel. to dielectric constant 80−10741
adsorbed film and capillary layer, transition layer 79−23807
and adsorption, unified theory using Percus-Yevick eqn. for hard spheres with surface adhesion 77−31879
adsorption isotherm and solute activities from spreading pressure-surface charge data 78−14576
adsorption of liq. mixture on solid, equilib. thermodynamics 78−84045
advancing front struct. of spreading liquid 77−31844
air entrainment at solid/liquid/gas interface 77−1276
air temperature sensors, aircraft borne, wetting in cloud rel. to entrainment overestimates 79−53483
alloy, binary, atomic roughness and chemical adsorption at solid-liquid interface *(French)* 78−51787
angle determ. method for adhesive and material to be joined *(German)* 77−62709
binary mixture, nucleate boiling, bubble growth, saturation press.-temp. relation 77−46892
blood compatibility of isolated veins and synthetic biomaterials, surface props. 77−56522
boiling, solid quenching in subcooled water, propag. of wetting front *(French)* 79−77108
boiling curves for fission reactor core reflooding after LOCA 79−67814
boiling heat transfer during rewetting, one-dimens. cond. model 79−598
caffeine in aq. electrolyte, adsorpt. isotherm and solute activities from spreading pressure-surface charge data 78−14576
capillary flow, initial stage analysis, relax. model 80−74977
cemented carbides, physical and chem. nature 80−76265
cladding, three-regions rewetting model with decay heat generation and inlet subcooling 80−22965
clastic rock softening characteristic tests *(Japanese)* 78−49013
collective heterogeneous boiling nuclei formation, statistical dynamic model using wettability 77−89531
concrete, creep during drying and wetting 79−52319
condenser efficiency and performance enhancement, evaporative cooling *(German)* 79−72781
conduction controlled surface rewetting, general 1-D model 77−83011
conduction-controlled rewetting of hot surface, two-parameter relation 77−19605
conduction-controlled rewetting with precursory cooling, two-dimens. analysis 77−15019
contact angle, ionic crystal surfaces 80−10746
contact angles meas., aq. ethanol (glycerin) solns.-metal surfaces, 20-70°C 78−56025
contact reaction between graphite and electrolytic Mn, Co, Ni and Fe 80−15342
cooling wave on hot surface, development, method of weighted residuals 80−27767
critical point wetting, three phase junction 77−59177
cryogenic liquids, nucleate boiling, influence of thermal props. of heating surface material 77−46888
cumene, films, thin, wetting, rheological characts. determ., capillary method 78−51788
n-decane, films, thin, wetting, rheological characts. determ., capillary method 78−51788
deformable solid surfaces, thermodynamics 78−34694
dense fluid monolayer, eqn. of state, appl. to alcohol monolayer on water 78−6195
Disjoining pressure of thin layers of binary solutions 78−15716
drop, surface wetting, motion anal. 78−22934
drop spreading on solid surface, initial stage charact. 80−59761

wetting continued
E-glass textile filaments, wetting characts. 80−80030
edge effect, inhibition of liq. spreading 77−55430
elastically deformable bodies, influence of vol. deform. of solid 79−11008
elastically deformable bodies, reduction of effects of deformation to line tension 79−11007
electrode, wetproofed, pore filling degree with electrolyte and liq. reactant 80−40702
electrolyte solutions, aq., wetting angle rel. to rate of meniscus movement capillary rise 79−65292
electrospark machining, bronze, spreading and form. of surface layer, in solid-alloy-liquid-metal systems, kinetics *(Russian)* 78−27668
entrapped liquid lenses at elastomer-glass interface, formation and geometry 77−85021
ethanol-water mixture, saturated, min. film boiling temp. on horiz. stainless steel and Cu surfaces 78−90692
ethylenic polymer films, highly fluorinated, exam. of wetting props. 78−60856
evaporating menisci of wetting fluids 80−29248
falling evaporating thin film, interfacial phenomena effect on interline region on hot spot rewetting 79−86321
falling film rewetting 78−75906
Fe, melt, wettability of CaO-MgO refractory *(Russian)* 78−10257
Fe base alloy, with metallic coating, oxidation effects, wetting, adherence 78−7085
fibre reinforced polymer, soaking, wetting and compounding of materials during production *(German)* 80−93535
filament and cluster crystals, liqs. in ultrathin channels, rel. to supercond. materials development 79−19162
film, kinetics of rupture 79−56045
film, thermodynamic theory of clustering and percolation transitions 77−47697
film, thickness on rough substrates 79−56044
film boiling, effect of adsorption characts. on minimum temp. 80−79114
film boiling destabilisation, liq. drop falling onto hot liq. surface 78−94588
film pressure of insoluble monolayer at air/water interface, effects on wetting at solid surface 77−85017
fin and tube heat exchanger, heat transfer, water spray effects 79−193
finely grooved solid surface, apparent contact angle of liquids, SEM study 77−51573
flat sheet withdrawn from wetting liqs., coating, meniscus shapes, flow model 77−29044
Freon-113 vapour environment, rewetting of hot surfaces, two-phase high pressure flow simulation 80−32358
glass, surface props. and contact angle after treatment with glow discharge and heating 80−21139
granular material, thermal conductivity, wetting effect 78−47611
graphite, fibre reinforced Sn-Pb investment castings, tensile strength 77−48487
graphite, surface, wettability, surface tension, contact angles of liqs. 79−37901
graphite crucibles, oxidation loss and wettability of inorganic fluxing materials *(Japanese)* 78−84755
graphite materials, by pyroceramic melt, lining material 77−1831
heated tubes, alternate dry and rewet, flow boiling, obstruction effects 79−1181
horizontal crystal ribbon growth, meniscus stability 80−103281
horizontal surface, silicone oil drop spreading 80−2250
hydrophobic powder, wetting props. 79−33162
ice, rel. to particle engulfment, theoretical model 80−54351
imbibition equation, similarity solutions, wetting abilities of immiscible fluids 80−43773
immiscible liquids, binary system, wetting hypothesis, validity, Antonow's rule appl. *(French)* 80−49462
infiltration in homogeneous isotropic porous medium, moisture profiles and wetting 78−18336
irrigating films, laminar, entry zone length for vertical plate wetting 80−53742
liquefied natural gas spilled on water, spreading and evap. investig. 78−26748
liquid alkali-metal solid metal interfaces, chemistry and physics 77−51576
liquid crystal films, disjoining pressures isotherms *(French)* 79−99401
liquid films, wetting, on solid surfaces, isotherms of disjoining press., meas. methods 78−51804
liquid meniscus in capillary, dynamics, wetting 77−85023
liquid surface, spreading vel., rel. to mol. struct. *(German)* 78−95209
liquid-liquid interfaces in isolation, and in interaction, review 77−47651
liquids on liquids, spreading kinetics 77−72748
low melting, metals, on Cu surface, spreading kinetics 80−10742
manometers, liq., sensitivity, wetting hysteresis effect 80−98926
maximum speed of wetting, experimental results 80−29253
meniscus profile, contact angle, differential interference method 79−56039
meniscus shape in rot. vertical tube 78−51797
meniscus-film-vapour equilibrium, generalised Young equation at low or zero contact angle 79−65298
metal fibre mats., porous, struct., hydraulic characts., liq. permeability 78−67848
metal supported crystallites, wetting in sintering and redispersion 80−24751
metal wettability, using macroscopic theory of mol. forces *(Russian)* 77−66073
metal-liquid surface energy, effect of lubricants, plasticity during cold working stresses *(Russian)* 77−55419
methacrylic polymer films, highly fluorinated, exam. of wetting props. 78−60856
microscopic approach, multilayer wetting related to multilayer adsorption 77−47650
microspreading on rough surfaces by SEM 77−72746
mineral, disperse, with small specific surface, heat of wetting determ. 77−29050
mixture, binary, nucleate boiling heat transfer, conc. depend. 78−87249
molecular dynamics, mechanism 78−51789
nonwetting liq. drop formation in capillaries and bores *(German)* 78−87370
oil drop spreading and wetting on submerged solid substrate, forced spreading 79−46887

wetting continued
oil drop spreading and wetting on submerged solid substrate, dynamics 79−46885
oil drop spreading and wetting on submerged solid substrate, static profiles 79−46884
oil drop spreading and wetting on submerged solid substrate, drop dynamics 79−46886
pendant drop, glass spheres attachment, wetting perimeter 80−2251
periodic capillary tube, two phase fluid flow and hysteresis 80−107615
periodic capillary tube, two phase fluid flow and hysteresis 80−107616
platelet adhesion to solid surfaces, effects of plasma proteins and substrate wettability 78−35814
poly(vinyl pyrrolidone), silicone grafted, for contact lenses, surface props. and stability of thin tear film 80−17194
polyester tapes, dynamic wetting behaviour 77−39723
polyethylene, environmental stress cracking at high stress, liquid wetting props. effects 78−92383
polyethylene, high-press. melt, spreading index on Cu, Al, glass, PTFE 79−37902
polyethylene, linear, melt props. correl. with chain length distribs. *(Russian)* 80−37920
polyethylene terephthalate fabric, surface struct., props. rel. to plasma surface treatment 78−95831
polyethylene terephthalate film, surface modification by corona discharge, adsorption and wettability 77−86212
polyfluoroethylene resin, porous, wetting angles with cyclohexanone and isopropyl alcohol meas., porosimetry method 77−1278
polymer, adhesion phenomena and influence of various factors, work of adhesion *(Polish)* 80−3292
polymer, wetted by insulating liq., under elec. field, charge transport and absorpt. 80−6534
polymer drop wetting solid surface, spreading index for polymer surface props. *(Russian)* 78−51802
polymers, quality control method based on solid surface wetting 79−52534
polystyrene melts, wetting kinetics for spreading of viscous sessile drops 80−15338
porous media wetting, capillary rise, contact angle effect *(German)* 78−84033
powder-water-oil system, cohesion of powder particles with water, rheological prop. *(Japanese)* 80−14647
quartz, dynamic wetting angle of dry lyophilic surface 80−88405
quartz, wetting by Au-Si eutectic melt 77−31840
quartz slit, wetting angle by water, aq. solns. of electrolytes 79−37899
quenching rates on hot surfaces, wetting of outer tube walls by water 77−82996
refractory carbides, borides and nitrides, wetting by and interactions with liq. metals 80−54473
refractory oxides, wettability of single crysts. by liquid metals *(Russian)* 77−43408
rewetting model using generalised boiling curve 79−9675
rewetting temperature in vertical channel coolant flow 79−59117
rigid solid, by simple fluid, work of adhesion, statistical mech. treatment 77−89618
rotating disc apparatus, thin-film, minimum irrigation density determ. 77−47125
silicate glasses, surface energy calc. from wettability data 77−35804
size effect accompanying wetting *(Russian)* 80−6596
slip velocity during wetting of solids 77−47649
soda-lime glass, chemically modified, water contact angle, adhesional wetting 77−55426
solid bodies, capillary interaction 78−51792
solid surface roughness, effects on wetting, expt. study 80−34275
solid-fluid interface, wetting and adhesion, thermodynamic aspects 80−89525
spray cooling, characts. and minicomputer control *(French)* 79−3889
spreading from binary surfaces, thermodynamics 78−6197
Spreading of liquid TiO_2 over refractory metals under the influence of surface forces 78−26749
spreading phenomenon in dry powder electrophotography 78−63904
static drop on inclined plate, shape, finite element method anal. 80−29245
steel, interfacial tension in phase boundary with MnO-TiO_2-SiO_2(Al_2O_3) *(Czech)* 78−63907
steel, mild wettability, effect of relative humidity 78−18872
steel, molten, wettability of aluminosilicate refractories 79−82415
steel, molten interfacial tension in phase boundary molten CaO-SiO_2-Al_2O_3-CaF_w2 slag *(Czech)* 78−63908
steel-(MnO-SiO_2-ZrO_2) slag system, molten, interface, wetting angles, surface tension *(Czech)* 79−19432
surface energy, theory and appls., symposium, New York, USA (Apr. 1976) 77−55422
surface roughness effects 77−59178
surface tension, review of theory 79−77866
surfaces, invertible, wetting angle protein replica form. 79−37900
sytrene-tetrahydrofuran block copolymer, H_2O contact angle and surface struct. *(Japanese)* 78−79861
temperature depend. of wetting angles near critical temp. 78−63905
testing, technological processes *(German)* 77−62710
tetradecane, wetting on solid substrates, disjoining pressure isotherms 78−51794
turbulent water film, with different initial flow conditions and high temp. gradients, heat transfer 78−90862
uracil in aq. electrolyte, adsorpt. isotherm and solute activities from spreading pressure-surface charge data 78−14576
vertical plate, wetting by a liquid, model 78−22319
vinyl polymer mixed monolayer behaviour 77−85020
viscoplastic medium, formation of contact with solid surface under pressure 79−69320
viscous liquid creeping on surface, asymptote to free surface and vel. depend. of contact angle 80−6600
water, films, thin, wetting, rheological characts. determ., capillary method 78−51788
water, hot, film, wavy laminar flow down vertical plate at high surface tension numbers 79−94587
water film shape on mosaic surface of solid *(Russian)* 79−51395
water surface, spreading vel., rel. to mol. struct. *(German)* 78−95209
wetting by molten silicate, applied polarization potential effect *(Japanese)* 79−51394
wetting of refractory oxide single crysts. *(Russian)* 77−43408
wetting continued
wetting tension depend. on meniscus curvature, adjacent liquid film disjoining press. isotherm 80−2247
wood in water, heat of wetting *(Japanese)* 77−76646
Ag clusters on Si substrates, opt. spectra investig. of struct. *(German)* 80−25492
Al alloys, contamination, automated nondestructive inspection 80−16629
Al, liquid metal embrittlement by Ga 78−64653
Al-graphite adhesion and contact angle, effects of metal additives *(Japanese)* 78−60008
Al-Sio_2, reactions and wetting behaviour 77−15664
AlN, wetting by Ni alloys 78−80710
Al_2O_3, wettability of single crysts. by liq. metals *(Russian)* 77−43408
α-Al_2O_3, wetting by Au-Si alloy and Si 77−85022
Al_2O_3, wetting by Cu-Sn-Ti alloys 78−71904
Al_2O_3, wetting by Cu-Ti ternary alloys 80−107617
Au, by water, hydrocarbon contaminant effect, macroscopic continuum model 77−85018
B fibres, plasticizing and wettability-enhancing coatings 79−29252
B_4C, reaction kinetics with liq. Al, Si, Ni and Fe 80−84344
B_4C-Ti(V)(Cr), contact reaction with liq. Ni 80−55707
B_2O_3 containing glasses, wetting and reactions on Pt, effect of C and water 77−7951
Bi, epitaxial growth, decoration of Sb surface 79−28227
C fibre reinforced Al composite, CVD fibre coating, diffusion barrier and wetting agent 77−40458
C fibres, plasticizing and wettability-enhancing coatings 79−29252
C fibres, wettability, relative, evaluation 78−43209
C, vitreous, wetting by Cu-Sn-Ti alloys 78−71904
C, vitrified, surface, wettability, surface tension, contact angles of liqs. 79−37901
CaO-SiO_2-Al_2O_3-Na_2O-CaF_2 melts, surface tension and limit wetting angle in contact with C and CrNi steels *(Czech)* 79−37908
Cd, spreadability on Cu and brass plates *(Japanese)* 80−29252
Cu, corrosion and wetting in presence of thiol reagents 80−11822
Cu, meas. of contact angle between melt and cryst. during Czochralski growth 77−28708
Cu, spreading and form. of surface layer, in solid-alloy-liquid-metal systems, kinetics *(Russian)* 78−27668
Cu-Sn binary system, wettability and interaction between solids and liqs. *(Japanese)* 80−92760
Cu-to-glass adhesion 77−44386
Fe, high C, interfacial tension in phase boundary with MnO-TiO_2-SiO_2(Al_2O_3) *(Czech)* 78−63907
Fe-C (graphite), adhesion and wettability of graphite *(Russian)* 80−20008
γ-Fe_2O_3, densified, rheological and mag. props. 80−44873
GaAs, surface wetting with Hg, doping degree influence 80−92762
Ge surface, wetting by Sn, Pb rel. to cryst. orientation 78−43211
LaB_6-Cu, form. by wetting of LaB_6 with Cu 80−100813
Li falls. liq., for Tokamak reactors, film wetting props. 77−38412
MgO, wettability of single crysts. by liquid metals *(Russian)* 77−43408
MgO-Al_2O_3-ZrO_2, wetting with liquid Fe and Al 78−22936
Mo wetting by Cu-Ag-P alloy 79−82417
Na, at high temps. in pure vapour atmos. 77−76645
Na, heat pipe meas. with gas plug containment up to 720°C 80−23878
NaCl-LiCl mixed crystals, Au decoration study of solid-melt interface, phase separation 80−15026
Na_2O-B_2O_3 glass, wetting and adherence on Au 80−24714
Na_2O-CaO glass, wettability, effect of cleaning procedures 80−65336
Nb, spreading of Sn-Cy alloy films in vacuum, 700 to 800°C *(Russian)* 77−80680
Nb wetting by Cu-Ag-P alloy 79−82417
Ni, spreading and form. of surface layer, in solid-alloy-liquid-metal systems, kinetics *(Russian)* 78−27668
Ni-O, liquid alloys, surface tension and wettability of Al_2O_3 *(Japanese)* 79−99398
Pd-C (graphite), adhesion and wettability of graphite *(Russian)* 80−20008
Pt-C (graphite), adhesion and wettability of graphite *(Russian)* 80−20008
Rh-C (graphite), adhesion and wettability of graphite *(Russian)* 80−20008
Si surface, wetting by Pb, Sn, Ge in H_2+HCl 78−43210
β-SiC crystals, wetting by Si and growth by vap.-liq.-solid mechanism 78−3005
SiC fibres, plasticizing and wettability-enhancing coatings 79−29252
SiC, self bonded, wetting by Si, effect of phase composition 79−33161
A-SiC, self-bonded polycryst., wetting by Si, base plate surface roughness effect 79−23809
SiC, wetting by Cu-Ti and Cu-Sn-Ti melts 78−68664
β-SiC, wetting by fused Ge, Sn and Pb 77−85016
SiC whiskers, wetting of surface by Fe-Si-C melt and its influence on growth stability 77−39756
Sn-Pb solder, wettability on Cu and mild steel plates *(Japanese)* 80−89244
Sn-Pb solder on Cu plate, spreadability, effect of fluoride and iodide addition to $ZnCl_2$ flux *(Japanese)* 80−29251
Ta wetting by Cu-Ag-P alloy 79−82417
Ti^{4+} hydroxide, coagulation struct. effects on particle size of TiO_2 78−52732
Ti-molten glass system, interactions and wetting, EPR anal. 78−14542
TiC, wetting by Cr-Ni-Mo-Mn alloy steel, expt. planning investigation 80−60822
TiC-Ni powder compact, wetting problems in sintering 80−11596
TiC-steel compact prod. by sintering in vacuum and in Ar or H_2 atmos. 77−63616
TiC-VC(Nbc)(YaC), comp. depend. 77−28772
TiO_2, wettability of single crysts. by liquid metals *(Russian)* 77−43408
UO_2 and UO_2-Ni, surface, grain boundary and interfacial energies 78−21649
UO_2 cracked fuel pellets, by molten stainless steel, in LMFBR transient undercooling accident 78−4993
W surface wetting by liquid Cu depend. on preliminary surface treatment *(Russian)* 80−35388
WC-Co, sintered hard alloy, mechanism of penetration of liquid metals 78−60619
Zn, liquid metal embrittlement 78−64653
Zr-ZrO_{2-x} composite, wetting charact. 77−44207
ZrO_2 refractories, wettability with Fe and Al melts 77−89619

whiskers (crystal)
alkali halide, X-irrad., elec. breakdown, temp. and F-centre conc. depend. *(Russian)* 77−8504
CdSe whiskers, growth in H_2 80−15425
central-force interatomic pot. construction from whisker deform. data 79−56103
corundum *(Russian)* 79−65352
elastic strains producing device, at He temperatures in magnetic field 80−50788
epoxy C plastics, under tensile stress, effect of whiskerization of polymer matrix on creep resist. 79−87699
field electron emission microscope atomic resolution exam. 78−32929
field emission cathode, single crystal, activation efficiency improvement 78−27377
film, thermal strain, strain relax. above room temp. 80−59841
growth, cellulose acetate membrane appl., vector mass transport appl. 79−96360
growth, new mechanism for the blistering of surfaces in complex radiation environments 78−95093
growth by vapour-liquid-solid mechanism, book contrib. 79−69383
gypsum whisker, produced by desulphurisation *(Japanese)* 77−76712
ion emitters for field mass spectrometer 77−18132
layered structures, single-crystal growth methods, review 77−59680
magnetometer, for meas. of mag. props. of whiskers 79−63284
mass transport and assoc. failures 80−59694
mechanical properties, method for investigating in complex stressed state 80−3264
metal, 1/f noise 79−38193
metal, 1/f noise theory 78−34872
metal, growth axes determ., rapid X-ray technique 77−11830
metal whisker point contact junctions, tunnelling and rectification characts. 80−6955
metal whisker thickness meas. using MII-4 microinterferometer 78−166
metal whiskers, quantum oscills. of mag. moment 79−15280
metallic whisker single crystals, low temp. magnetometer for mag. moment meas. 79−88986
open-structure submillimetric-wave mixer props. 79−30551
phthalic anhydride, whisker crystals, vapour growth and morphology 77−35841
phthalic anhydride, whisker growth in closed cryst.-vapour system 78−34734
single crystals under large loads, theoretical elastic behaviour, review and appl. 80−71681
sodium acetate trihydrate, whisker growth on membrane in aq. soln. 78−30854
steel fibres, polycrystalline, Mossbauer spectroscopy 80−44959
tensile strength, dislocation density depend. *(Russian)* 78−19820
vapour-liquid-solid growth mechanism *(Russian)* 80−107074
whisker crystal growth, radial periodic instability mechanism *(Russian)* 80−107682
Ag/α-Ag_2S, interface, electrochemical transfer across phase boundaries 78−73046
α-Ag_2S whiskers, growth in VLS system, SEM and X-ray diffr. anal. 79−46989
Al, diffusion of Zn, temp. depend. 77−85122
Al, stability and strength of FCC metal using Morse pot. 80−59430
AlN whiskers, strength rel. to growth conditions using vapour-liquid-solid method 79−11052
Al_2O_3, alumina, whiskers growth by hydrolysis of AlF_3 79−28260
Au film, epitaxial growth, whisker form. 77−76713
Au film, whisker growth due to high current densities 77−69191
BaO whiskers, electromech. effect 79−65800
Bi, de Haas van Alphen oscills., 4.2K, meas. using magnetometer 79−63284
Bi, elec. resist. under strain *(Russian)* 79−91164
Bi, electron transition on simple extension, elec. resist. and magnetoresist. meas. *(Russian)* 80−29422
Bi, excess 1/f noise, 50 to 350K 80−92951
Bi, persistent metallic behaviour, elec. resist. meas. 80−75544
Bi, whiskers, hardness, elec. props. *(Russian)* 78−51874
Bi whiskers, thermopower, temp. depend., 77 to 300K phonon drag effect 79−82615
Bi wire, elastically bent, elec. resist. in mag. field 80−44568
Bi-Sb (6 at.%), persistent metallic behaviour, elec. resist. meas. 80−75544
C whisker formation by Ar ion bombardment 78−30851
CaF_2, whiskers and crysts., flux growth and charact. by morphology and fracture strength 79−19987
$CaSo_4$, growth on CaF cryst. face etched in H_2SO_4, etch pit morphology 80−6408
Cd, supercond. crit. temp., stress depend. 77−39989
CdS single cryst., vaporization and form. of negative whiskers 80−92659
CdS:In, vapour deposition 78−75969
CeO_2, single cryst. whiskers, electron field emission 78−27378
Cr, crystal growth incorporated with field electron emission 80−44458
Cu and α-Cu-Zn alloy, whisker growth in Zn reduction, morphological change to dendrites 79−28261
Cu, current induced 1/f noise 77−32058
Cu, H_2 reduction of CuI, growth mechanism 78−30853
Cu whisker blades, RF size effect, expt. technique and line shapes 79−65511
Cu, whiskers, Ar^+ ion implanted, X-ray study on lattice defects *(Japanese)* 79−99230
Cu whiskers, Bragg case diffr. curves by X-ray triple cryst. diffr. method 79−51461
Cu, whiskers, hardening during uniaxial extension, preliminary torsion deform. *(Russian)* 78−15420
Cu-Ni crystals, growth, H_2 reduction of CuI-$NiBr_2$ mixture, habit study by X-ray difr., optical and SEM 79−60665
α-Cu-Zn, substruct., X-ray topography 77−11831
Fe, 90° walls, stable orientations, theory and X-ray observations *(Japanese)* 80−60359
Fe, [111] oriented whisker, mag. domain struct. and approach to saturation 79−82814
Fe ⟨100⟩ whiskers, inverse Wiedemann effect 77−90001
Fe, AC susceptibility, critical slowing down of mag. fluctuations 77−69594
Fe, domain wall interaction with mobile impurities 77−12145
Fe, elastically and plastically deformed, mag. domain structs. 80−15752
Fe, elongation induced struct. distortion, X-ray topographic investig. 77−85121

whiskers continued
Fe, ferromag. domain theory, quasi-dislocation theory appl. *(Japanese)* 80−60358
Fe, grown from $FeCl_2.4H_2O$, exam. of growth morphology 78−72051
Fe, H_2 effect on deform. 78−68755
Fe, inverse Wiedemann effect, torsional strain and azimuthal mag. field influence 80−108045
Fe, mag. anisotropy, magnetisation and temp. depend. near T_c 80−39766
Fe, mag. crit. phenomena, size effects 78−68258
Fe, mag. memory function at crit. temp. 77−24714
Fe, magnetoresistance, deviations from Kohler's rule 80−70673
Fe, optimisation of magnification of magneto-optic Kerr effect by interference layers 79−51808
Fe, polycryst., FIM obs. of struct. 78−84111
Fe, polycryst. whisker, microstruct. SEM and TEM 77−39755
Fe polycrystalline whiskers, H_2 embrittlement 79−100259
α-Fe single crystal whiskers, controlled growth by H reduction of ferrous halides, X-ray and SEM exam. of crystals 78−60554
Fe, soft mag. material, AC response near Curie temp. 78−64223
Fe whisker, magnetic aftereffect in 180° mag. bowed Bloch walls 79−78432
Fe whisker, magnetisation curve meas. using SQUID system 80−86347
Fe whisker crystals, domain walls, interaction with dislocation bundle, X-ray topography obs. 79−87282
Fe, whisker growth, added C black effect 78−30852
Fe whisker growth, on wustite, Wagner's mechanism 80−10847
Fe, whisker single crystals, ferromag. reson. and surface anisotropy 80−71187
Fe whiskers, cryst. morphology and dislocation struct. study using optical and SEM, X-ray diffr. topography 79−23876
Fe whiskers, dynamics of mag. freq. response near Curie point 80−34648
Fe whiskers, galvanomag. size effects 78−14709
Fe, whiskers, H_2 effect on mech. props. 80−108556
Fe, whiskers, high strength, polycrystalline, microstruct. obs. 79−33214
Fe whiskers, magnetisation in small mag. fields, investigation using Kerr magneto-optic effect 80−2603
Fe, whiskers, polycrystn., Mossbauer study 80−20571
α-Fe whiskers, pure, ductile fracture initiation, macroscopic obs. of deform. history and failure 80−85043
α-Fe whiskers, pure, ductile fracture, microscopic obs. of initiation mechanism 80−85044
Fe whiskers, struct., dislocations, mag. domains *(Polish)* 79−33210
Fe whiskers, undeformed, X-ray topographic study 77−80716
$Fe_{1-x}O$ wustite whiskers form. 79−77972
Fe_2O_3 whisker growth from $Fe_{2-x}SiO_4$ oxidation 78−84113
FeS_2, pyrite, whiskers growth by chem. vapour transport, surface struct. and morphology 79−23550
Ga whisker growth from GaN/Ga layered films 80−92800
GaAs, epitaxial, polycryst., monocryst. layers and whiskers growth by CVD, SEM obs. electron diffr. study *(French)* 79−43150
GaAs, growth by thermal decomp. method 77−55875
GaAs ribbon whiskers, photopumped, laser action 80−91801
GaAs, vapor-phase etching, mechanisms and kinetics 80−100934
GaAs:Zn optically pumped ribbon-whisker laser, picosecond pulses 80−99771
GaAs-Br_2(-Zn) system, filamentary cryst. prep. 78−52650
GaN, photoluminesc. spectra, energy distrib. 80−97339
GaP ribbon waveguide, vapour-grown, phase-matched SHG 80−48339
GaP, vapor-phase etching, mechanisms and kinetics 80−100934
GaP:Ni, whisker growth on surface 79−33212
Ge, amorphous whisker growth 78−2400
Ge, whisker growth from vapour phase 80−15426
Ge, whiskers nucleation, effect of machining support surface *(Russian)* 79−65352
In, and alloys, supercond. crit. temp., stress depend. 77−39988
In whiskers from Sn-In alloys, current carrying, superconductivity breakdown 80−60133
KBr, whiskers, F-centre accummulation and track effects due to X-ray irrad. 80−39484
KBr, X-irrad., defect form., thermolum. and ionic cond. obs. *(Russian)* 78−84666
KCl, whiskers, F-centre accummulation and track effects due to X-ray irrad. 80−39484
KCl, X-irrad. induced deform. effects, glow curves *(Russian)* 79−52022
LaB_6, chemical vapour growth of whiskers, and single crystals 78−72710
MnAs, single cryst. whiskers, morphology and cryst. orientation, SEM and X-ray diffr. study 79−60664
$MnAs_{1-x}P_x$ whiskers, thermoelectric power, 5 to 350K, phonon drag effects and mag. transitions 79−28363
Mo, crystal growth incorporated with field electron emission 80−44458
$NH_4H_2PO_4$, surface effects on strength of whiskers and microcrysts. *(Russian)* 78−51864
NaCl, plastic deformation influence on shape recovery effects 80−6684
NaCl, plastically deformed, internal friction amplitude depend. 77−15727
NaCl whiskers, plastification in elec. field *(Russian)* 80−21010
NaCl whiskers, X-irrad., stress oriented dislocation loop nucleation 79−33213
NbN, Nb_4N_3-NbN, Nb_2N-Nb_4N_3, Nb_2N, cryst. growth parameters and morphology of chem. vapour deposition, X-ray diffr. and SEM study 79−23861
Nb_2O_5, single cryst. growth by chem. transport reactions involving $TeCl_4$ 77−36382
Ni, diffusion parameters of Zn, 750 to 950°C 77−66101
Pb, growth from metallic vapour phase, $<10^{-14}$ torr, elec. resist. 78−47686
Pb, third-order elastic consts. combinations 80−92585
$PbCO_3$ whiskers, growth kinetics in silica gel 78−75971
PbTe single crystals, growth from vapour phase under micro-gravity conditions 80−80957
Sb, quantum oscills. of magnetoresist. *(Russian)* 78−60145
Sb whisker crystals, magnetoresist., size effects *(Russian)* 79−7821
SbSI, reversible characts. of generation of second microwave harmonic 78−39509
SbSI, vapour phase growth on seeds 78−11090
Se-Te whisker crystals, growth 79−99464
$Se_{90}Te_{10}$, chem. and thermal etching 77−15417
Si, (111) oriented, FIM and atom-probe FIM obs. 80−10473
Si, amorphous, growth method for field desorption mass spectrometry 79−28262

whiskers continued
Si, amorphous whisker growth characts. by SiH_4 thermal decomposition 80−34342
Si, as basis for low-temp. sensors of temp. and deformation 79−5095
Si, as basis for strain resistors 79−5094
Si crystal whiskers for use as photoconvertors 79−67386
Si, growth by thermal decomp. of SiH_4 79−69970
Si p-type single-crystals for thermoanemometers 78−3975
Si whisker, amorphous, meas. of Young's modulus 78−83865
Si, whisker, growth by reduction of $SiCl_4$ in H_2 gas current 77−15726
Si whisker coated C fibres for composites, shear strength improvement 78−3093
Si whisker field desorption ion source, Cu, Sn, Ag, Te, Cd and Sb isotope abundance ratios 80−11975
Si, whisker growth in amorphous state, in SiH_4-Ar atmosphere, visual obs. 78−84112
Si whisker indirectly-heated thermoresistor 78−86255
Si whiskers, polytypism and amorphousness 78−26801
Si whiskers, radial growth rates anisotropy, steps on {112} faces 79−60666
Si, whiskers nucleation, effect of machining support surface *(Russian)* 79−65352
Si:Au(P)(B) whiskers, impurity inhomogeneity 80−39145
β-SiC, atom-probe FIM expts. 78−35275
SiC microtubes, formation by carburisation of Si whiskers 80−81011
β-SiC whisker, failure and defects 79−96145
SiC whisker coated C fibres for composites, shear strength improvement 78−3093
SiC whisker reinforced Ag composite, prep. aboard Skylab, and characterisation 78−84741
SiC whiskers, wetting of surface by Fe-Si-C melt and its influence on growth stability 77−39756
Sn, and alloys, supercond. crit. temp., stress depend. 77−39988
Sn, supercond., current carrying 78−72304
Sn, supercond., current induced phase transition 78−10600
Sn, supercond., current-carrying, mutual influence of voltage steps in V-I characts. 78−10601
Sn, supercond. whiskers, HF radiation effects on current-voltage characts. 79−65619
Sn wire, elastically bent, elec. resist. in mag. field 80−44568
Sn-In, dil., supercond., current-induced resistive state 79−51712
SrN, impurity activated whisker growth by CVD 79−66010
TiC, growth rate for CVD 77−47704
TiC, TF electron emitters props. obs. 80−66403
TiC whiskers, growth by CVD, catalytic effects of various metals and refractory oxides 79−33211
TiN(C) whisker growth in CVD 80−59843
TiP whiskers growth, on gold drops in VLS growth 79−4497
W, AC and DC electrochem. etching 78−43278
W, crystal growth incorporated with field electron emission 80−44458
W, energy spread meas. of thermal field-emitted electron flow 78−92168
W, monocryst. particles and whiskers, reduction of vap. deposited WO_3 77−52249
W needle crystal growth, discharge-induced decomp. of hexacarbonyltungsten mols. 80−84414
W needles produced by $W(CO)_6$ decomp. 79−95302
W-Ni, MBM diode, resist. depend. of detected signals 80−2482
Zn aerosol condensation, prismatic and spherical particle form. 77−9135
Zn, supercond. crit. temp., stress depend. 77−39989
Zn whiskers, quantum oscills. of mag. moment 79−15280
Zn wire, elastically bent, elec. resist. in mag. field 80−44568
Zn-Al eutectoid alloy, straining at elev. temp., whisker crystal 79−29087
ZnO, hollow crystals, growth by oxidation of ZnSe vapour, mechanism 78−34733
ZnO, precipitation from gas phase 78−6025
ZnS, vaporisation, negative whisker form. by solid-liq.-vapour mechanism 77−35684
ZrC, CVD on Ni, catalytic effect 78−51865
ZrC_x, nonstoichiometric, synthesis by CVD 79−28941
ZrN(C) whisker growth in CVD 80−59843

whistlers
see also ionospheric electromagnetic wave propagation; magnetospheric electromagnetic wave propagation
Alfven kinetic wave parametric excitation by whistler waves 77−27668
Alfven wave turbulence, interaction with whistler wave turbulence 80−64728
amplification at freq. > upper cut-off freq. 78−40763
analysis methods, ground-based obs. *(French)* 78−36398
analysis methods, theoretical whistlers *(French)* 78−40762
antenna radiation patterns in laboratory plasma in whistler wave regime 77−27685
auroral electron beam, whistler mode electrostatic noise generation 78−85759
auroral hiss, nearly reson. whistler amplified Cherenkov radiation, limitations 80−101482
auto and cross-correlation analysis techniques on-board spacecraft *(French)* 79−70925
automatic observation 78−89014
avroral ionosphere, whistler mode radiation, generation by parametric decay of Bernstein waves 77−76095
banded struct. origin, on refl. from ionosphere 80−101476
beam-plasma system, instability due to whistler mode EM waves 79−14564
beam-plasma system, unstable, whistler wave propag. along reson. cone, diagnostics 77−31484
Cerenkov interaction between obliquely propagating whistler wave and electron beam, computer simulation 80−43937
coherent nonlinear interaction dependent on wave amplitude 80−72715
coherent VLF signal injection into magnetosphere, threshold power for growth 80−101496
CW whistler, influence on magnetospheric noise 77−82087
damping near electron gyrofreq. due to cold-plasma injection, rel. to magnetosphere 80−28659
detection, multichannel filter and shift register obs. system 78−93031
deuteron trans-equatorial whistlers, in topside ionosphere 80−77203
dipole antenna in magnetoactive plasma EM field distrib. 80−100079
direction finding on whistler mode signals, initial results from tracking receiver system 78−77429
dispersion, automatic meas. by phase locked loop discriminator *(Japanese)* 77−91312

whistlers continued
dispersion, group delay automatic meas., ionosphere and magnetosphere electron density 78−93050
dispersion characteristics, of whistlers observed at Sofia during decreasing solar activity period 79−8779
dispersion characts. of low latitude whistlers, effect of ions 78−20575
dispersion measurement using five channels phase-locked loop discriminator *(Japanese)* 80−31143
Doppler shifts on whistler received at Siple Station, Antarctica 78−28429
Dowden-Allcock approximation, generalisation and comparison with Bernard approximation 80−51607
ducted whistler mode signals, Pc 4-5 pulsation effects on Doppler shift 78−4040
ducted whistlers, simultaneous ground and satellite reception 77−87204
ducting in plasmasphere, ray-trace study 80−72704
ducts in outer plasmasphere, form. 78−57407
Earth-ionosphere waveguide propag., effect on whistlers polarisation and arrival angles 79−100924
Earth-ionosphere waveguide propagation effect on polarisation and arrival angles 80−36457
echo induced suppression of coherent VLF transmitter signals 77−87191
electric fields in quiet plasmasphere, dynamo origin, whistler data 78−77426
electron beam-whistler wave nonlinear interaction, computer simulation 77−3938
electron interacting with whistler in magnetosphere 80−46349
electron plasma oscillation bursts correl. with whistlers 80−72703
electron whistler, transform into ion-cyclotron whistler in multicomponent plasma during quasilongit. propag. 78−73572
electron whistler transform. to ion-cyclotron whistler in multicomponent plasma 79−53661
electrostatic lower hybrid wave, nonlinear decay to whistler and Alfven wave pair 78−26275
electrostatic noise damping by warm auroral electrons 80−41668
ELF/VLF ground-based obs. at high latits. during GEOS-1 and ISEE-1 and -2 passes 79−29949
equator obs. confirming that whistlers do not propagate to Earth surface 80−77216
excitation of high-frequency waves with mixed polarization by streaming energetic electrons 80−1773
extrapolation, comparison of systematic errors in different methods 77−53334
fine structure modulation, source regions 77−87203
finite amplitude whistler wave solitons and filaments, properties and propagation 79−41836
focusing and interference of whistler-mode waves in spatially varying mag. field 78−65465
group velocity, in two-ion plasma 78−87452
high power level plasma waveguide mode excitation 79−41839
hydromagnetic whistlers, stimulated excitation in near-Earth plasma by pulsed radio emission 79−58192
incoherent scattering of radio waves by whistler mode oscills. 78−45135
ion cyclotron beam-whistler mode instability in parallel shocks 78−14148
ion cyclotron whistlers, topside ionosphere, complex ray tracing study 78−96346
ionosphere, anomalous dispersion, ray propag. in middle latits. 77−33253
ionosphere, channel lower hybrid resonance excitation by superthermal particle streams *(Russian)* 78−4025
ionosphere, propag. characts. of ground observed VLF waves after emerging from ducts 79−8741
ionosphere, propag. theory, ray-tracing 78−49216
ionosphere, VLF waves, natural and elecron-beam producted, rocket obs. 78−7829
ionosphere, whistler-mode pulse propag. between two satellite at medium freqs. 78−69605
ionosphere propagation, equatorial anomaly affecting ground reception 80−51601
Jupiter inner magnetosphere, whistler mode noise 78−89112
Jupiter magnetosphere, discrete whistlers obs. by (Voyager 1) 80−26795
Jupiter magnetosphere, electron pitch-angle diffusion by whistler mode waves near Io plasma torus 80−4290
Jupiter magnetosphere, Io plasma injection rel. to whistler made waves and Jovian diffuse aurora 80−4289
large amplitude oscillation by high power microwaves 80−43913
LF ion acoustic perturbation emission in presence of stationary whistler turbulence 77−49242
linear wave transformation in ionosphere and ion whistler formation *(Russian)* 78−65449
low latitude whistler characteristics, correlation with geomagnetic activity *(Japanese)* 79−16769
low latitude whistlers, lower and upper freq. cut-off explanation 80−82131
low latitude whistlers, rel. to cloud distribs. in conjugate area 77−2309
low-latitude, conditions of duct trapping 79−84586
low-latitude coordinate observation system using direction finder and real-time analyser 80−67479
low-latitude propagation limit 80−82152
low-latitude types in the ionosphere, measurement of wave-normal directions 78−4023
low-latitude whistlers characts. observed at Okinawa, Japan 78−73576
lower oblique whistler resonance cone, interference struct. in Maxwellian magnetoplasma 80−59219
magnetic storm low-latitude whistlers, for magnetosphere elec. field 80−85817
magneto-acoustic solitons, macroscopic instability *(Russian)* 77−47200
magnetoplasma, modulation instability of whistler waves 77−72450
magnetosphere, critical electron pitch angle anisotropy for chorus generation 77−2308
magnetosphere, elec. field induced instability 77−70942
magnetosphere, electrons resonance interactions with whistlers, bunching effect 78−45146
magnetosphere, EM instabilities in anisotropic loss-cone plasma 77−87185
magnetosphere, instabilities of the whistler mode 79−88551
magnetosphere, key-down signals amplitude pulsations 77−29598
magnetosphere, non-ducted propag. 78−36402
magnetosphere, parallel elec. field effect on whistler mode instability 80−26700
magnetosphere, particle precip. caused by single injected whistler-mode wave 77−56797

whistlers continued
magnetosphere, polar region, VLF noise generation by electron beams 78−4039
magnetosphere, trigger VLF emission theory 77−17294
magnetosphere, use of trigger VLF emission for plasma diagnostics 78−45149
magnetosphere, VLF coherent waves stimulated growth 77−33291
magnetosphere, VLF wave propag., bouncing period, plasma inhomogeneity effect 77−53319
magnetosphere, VLF whistlers assoc. with low energy electron enhancements 77−33285
magnetosphere, VLF whistlers propag. in directions near reson. cone rel. to electron temp. 77−82086
magnetosphere, whistler duct struct. and formation 80−94659
magnetosphere, whistler effects in controlled VLF phase reversal expt. 77−25866
magnetosphere, whistler instability in anti-loss-cone plasma 77−64545
magnetosphere, whistler mode chorus generation by energetic electrons during substorms 78−96356
magnetosphere, whistler mode mag. field amplitudes rel. to very weak pitch angle diffusion 78−28399
magnetosphere, whistler wave trapping phenomena 77−15195
magnetosphere chorus, occurrence patterns and normalised freq. 77−9625
magnetosphere coherent VLF waves, nonlinear pitch angle scatt. of energetic electrons 78−89011
magnetosphere examination of VLF whistler pulse analysis 80−17441
magnetosphere meas. of occurrence rate of whistlers during geomagnetic storms 80−12621
magnetosphere whistlers, meas. via remote unmanned ELF/VLF goniometer receiver in Antarctica 80−21854
magnetosphere-cusp interface, EM and electrostatic emissions during substorms 79−66880
magnetospheric ducts formation and lifetime 78−61684
magnetospheric plasma, whistler propagation 80−90294
magnetospheric whistler duct obs. by ISIS satellites 77−22020
magnetospheric whistler parametric instability, pitch-angular electron scatt. *(Russian)* 78−77420
magnetotail, whistler mode mag. noise bursts obs. 77−29592
man-made whistler-mode signals, spacecraft obs. near electron gyrofrequency 78−28418
measurement with microprocessor control *(Japanese)* 80−31144
MHD whistler source location and generating proton spectra 77−64542
modulational instability of whistler-mode signals 78−85774
monochromatic whistler wave, nonlinear evolution in nonuniform mag. 80−43912
nature, types and observations, review 80−36458
non-nose whistlers, parameters determ., unknown causative atmospherics 77−22002
nonlinear self-distortion in magnetoplasma 79−40031
nonresonant interaction with electrons in plasma 78−9792
nose whistlers, extrapolation via linear-Q anal. and extrapolation factor, systematic errors 77−53333
obliquely propagating modes in cold plasma permeated by anisotropic plasma 77−80288
occurrence rate and dispersion real-time analyser 77−87129
occurrence rate variation with geomagnetic latitude 79−40010
parallel electric field affecting thermal damping 80−41663
parametric decay, nonlinear wave interactions 77−19716
parametric excitation of backward ion cyclotron wave with a pump in the lower hybrid range 79−37490
pararesonance (PR) whistlers, features 80−67455
partly ducted whistlers over Europe, propag. theory 78−65463
PL whistlers, simultaneous ground and satellite reception 77−87205
plasma, dense, dispersion and attenuation of whistler waves 78−63570
plasma, electrostatic wave decay near lower hybrid freq. 77−977
plasma, EM wave beam self-focusing 78−75357
plasma, magnetised, whistler wave damping, dipole antenna obs. 78−34327
plasma, nonlinear quasioptics in DC mag. field *(Russian)* 79−98914
plasma, parametric decay of non-ducted whistler-mode signal 80−6239
plasma, scattering decay of electron whistler-ion quasimode parametric coupling 78−18401
plasma, self-channelling of whistler waves 77−47208
plasma, self-focusing and filamentation of Gaussian whistlers 77−47206
plasma, wave packet propag. at ang. to mag. field, nonlinear evolution *(Russian)* 79−98886
plasma, whistler pulse self-distortion 79−46456
plasma, whistler wave ducting caused by antenna actions 78−59586
plasma, whistler wave trapping in density crest 80−53984
plasma in external mag. field, electron beam-whistler soliton interaction, appl. solar wind 77−11360
plasma ion heating, by nonlinear ion-sound waves, excited by whistlers and Alfven waves *(Russian)* 79−27783
plasma shock waves, collisionless, ion cyclotron beam whistler turbulence 77−7540
plasma whistler wave, filamentation instability due to ponderomotive force 79−14538
plasma-ion beam interaction in external mag. field, instability and shock wave struct. 77−42994
plasmapause, whistlers and VLF noise propag. 78−40749
plasmapause location rel. to Pc 1 propagation paths and whistler obs. 77−9604
plasmasphere, guidance of whistler-mode waves 78−93054
plasmasphere, horiz. inhomogeneities, whistler obs. 80−4168
plasmasphere, nightside, whistler obs. of substorm electric fields 79−40009
plasmasphere, outlying struct. from whistler obs. 77−2304
plasmasphere, VLF ducts modelling 79−58202
plasmasphere, whistler data on electron density solar cycle, annual and diurnal vars. 78−88985
plasmasphere, whistler duct positions 77−53301
plasmasphere structure from whistler records at Belsk, Poland 78−20581
polarisation and arrival direction meas. at low latit. 77−45240
polarization, external transverse elec. field effects 78−28427
precursor whistler mode plasma turbulence formation in parallel shock waves 80−24172
precursors, catalytic role of power line radiation 78−12056
precursors, possible mechanism 77−25869
precursory emissions, newly observed monochromatic precursor starts 80−85809

whistlers continued
prolongitudinal mode whistlers, raytracing in transition level gradient model 78−4042
propagation at low latits., review 78−73586
propagation characts. at low latitudes 79−80078
propagation in magnetoplasma, interpretation of 6-component measurements 80−83921
propagation in narrow density trough 80−38629
propagation in nonuniform mag. field, test particle correlation, simulation, magnetosphere appl. 79−37486
propagation theory 77−45261
protonosphere, electron conc. inhomogeneities meas. by whistler method 77−67011
QT mode whistlers, LHR effect 77−70923
randomly phased, modulated by kinetic Alfven and ion quasimodes 77−80293
rays and foci in a magneto-ionic medium with linearly varying magnetic field, theory 80−105135
real time whistler analyzer 77−87119
resonant particle effects in Langmuir and whistler waves, long-time-scale plasma simulation 78−42796
review 80−46348
scattering, nonlinear, by lower hybrid and ion Bernstein modes 80−43929
self-modulation, two-dimens. nonlinear 77−80295
semiautomated analyser, using spectrum analyser and programmable tracking filter 79−74975
side-band mutual interaction of whistler-mode waves 80−82148
solar type IV meter bursts, whistler modulation rel. to continuous radiation microstruct. 77−53534
solar type IV meter bursts microstruct., modulation of continuous emission by whistlers wavepackets 77−78761
solar wind, electron beam energy gain due to interaction with whistler soliton 77−9649
solar wind, heat flux regulation by whistler instability 77−45277
solar wind, stability against whistler mode, anal. of proton to α-particle vel. ratio 79−2453
solar wind, whistlers electrostatic mode instability criterion 79−96877
solar wind, whistlers model for small-scale inhomogeneities 78−45173
solitons, classification of descriptions 78−75286
sonograms, anal. of quasiperiodic struct. 77−53316
spectral-temporal analysis, digital methods 80−4175
stability of whistlers and pearl type waves in magnetosphere 78−12051
stationary turbulence stability and evolution 77−45259
substorm electric fields in plasmasphere, model based on whistler data 80−41661
super whistler, theory and anal. 80−26688
supersonic large amplitude electron whistler-wave-ion density perturbation coupling, solitons 77−58854
temperature anisotropy and beam type instabilities 77−3937
trapping in narrow density trough 79−64870
triggered VLF emissions and detrapped electrons 78−77421
turbulence, nonlinear interaction of magneto-sound waves 78−45134
turbulence effects in the cyclotron resonance of monochromatic whistlers 79−16759
two-frequency direction finder development 79−53674
Varanasi, India, low-latitude whistler recordings 77−29600
very low dispersion whistlers, non-ducted low latit. VLF path model 79−44301
VLF direction-finding techniques comparison for determ. whistlers exit point at ionosphere 80−26631
VLF hiss in plasma penetrated by electron beam 78−26293
VLF non-ducted whistler-mode signals at low latitudes 78−61658
VLF radiation during simultaneous magnetospheric substorm and thunderstorm, rel. to elec. fields and electron precip. 80−67392
VLF signals, time-varying, determination of wave normal directions *(French)* 79−70927
VLF subionospheric propag., whistler-induced anomalies 80−26668
VLF waves triggered by natural whistlers 80−98521
VLF whistler emissions, simultaneous obs. at Brorfelde, Chambon-la-Foret and Moshiri 78−81509
VLF whistler mode signals, simultaneous phase and group path meas. 78−49234
VLF whistler obs. of radial plasma drift and coupling to ionosphere 80−77239
VLF whistler-mode transmissions, Pc 3 micropulsation obs. 79−8781
VLF whistlers, magnetosphere cold plasma densities meas. comparison with ULF waves meas. 78−28436
wave modulation, nonlinear theory 80−26686
wave radiation in plasma *(Russian)* 78−36400
whistler propagation times eqn., inversion via spectral expansion 80−8495

white dwarfs
2A 0311−227, AM Herculis type binary star, IR photometry and polarimetry 80−77517
2A 0311−227, AM Herculis type X-ray binary, optical counterpart, radial vel. obs. 80−94890
2A 0311−227, complex emission line structure of spectroscopic binary 80−51915
2A 0311−227, high-speed photometry of AM Herculis-type binary 80−41912
2A 0311−227, new AM Herculis-type system, optical identification 79−101211
2A 0311−227, optical counterpart, AM Herculis type eclipsing binary, V-band obs. 80−101617
2A 0311−227, soft X-ray emission from AM Herculis-type system 79−101219
2A 0311−227 optical counterpart, binary star, light curve Fourier anal. 80−82549
2A 0311−227 optical counterpart, possibly AM Herculis type white dwarf 79−35434
2A 0311−227 optical counterpart, simultaneous photometric and spectroscopic obs. 80−90572
2A 0311-227 optical counterpart, spectroscopic and photometric obs. 79−101222
2A 0526−328, optical counterpart, eclipsing binary, visible emission line variability 80−73075
Abell 46, planetary nebula, eclipsing binary nucleus, hot component UV continuum obs. by IUE 80−98693

white dwarfs continued
accreting compact object in binary system, magnetosphere theory, X-ray sources 80−46394
accreting magnetic degenerate dwarfs, X-ray and UV emission 80−41826
accreting magnetic white dwarfs, cyclotron emission 77−45427
accretion belts, rel. to nova phenomena 78−36582
accretion of rotating fluids by barytropes 77−33486
apsidal motion in highly evolved stars 77−45483
AE Aquarii, cataclysmic variable, rapid light oscills. rel. to white dwarf oblique rotator model 80−36634
R Aquarii (M7+pec), white dwarf component identification from IUE obs. of circumstellar emission 80−82370
V603 Aquilae, accretion disc radiation of cataclysmic binary 77−91537
Ariel 0620−00, transient X-ray source, white dwarf spherical model 78−12415
atmosphere structure rel. to composition in hot stars 80−98658
atmospheres chem. evolution, diffusion and accretion 80−36628
atmospheric models and peculiar objects, conf., Rome, Italy (Sep. 1976) *(Italian)* 78−93239
Balmer line formation in rotating white dwarfs 79−30059
BD+66°1066, nucleus of planetary NGC 6543, lightcurve oscills. 79−75223
BD−7°3007, nova-like variable, simultaneous spectroscopy and photometry 78−12250
binary star, white dwarf outer layer C and O enrichment from companion 80−109465
binary stars, rapid mass accretion on to white dwarfs and extended envelope form. 80−67723
binary stars with single optical component, ellipsoidality effect on light vars. 79−92806
in binary systems, accretion disk flux distrib. and colours 80−94778
in binary systems, surface nucl. reactions and origin of mag. fields 80−101616
birth rate, rel. to planetary nebulae, distance scale 78−20867
bloated dwarf model of nova light curves 77−82251
BPM 25114, hot magnetic white dwarf, image tube spectrophotometry 77−74051
BPM 25114, peculiar white dwarf, light vars., oblique rotator model *(Italian)* 78−93241
BPM 25114, southern mag. white dwarf, spectrophotometric obs. 79−92765
BPM 30551, ZZ Ceti star, high freq. oscills. 77−2445
BPM 30551, ZZ Ceti-type variable, light curves and power spectra 77−56948
BPM 31594, new southern hemisphere variable white dwarf 77−5531
BPM 4729, cool DA white dwarf with self-broadened Balmer lines 79−35255
α Canis Majoris, EUV obs., Sirius B model atm. 77−33489
α Canis Majoris (Sirius) B, story of its discovery 79−84932
α Canis Majoris (Sirius B), EUV obs., evidence against photospheric origin of 0.25 keV flux 78−49481
α Canis Majoris (Sirius B), spectral energy distrib. 80−8629
α Canis Majoris B, acoustically heated corona rel. to X-rays 77−60755
α Canis Majoris B, photoelectric obs. 78−4220
α Canis Majoris B (Sirius B), corona model constraints 79−2543
α Canis Majoris B (Sirius B), effective temp. rel. to soft X-ray obs. 79−44477
α Canis Majoris B (Sirius B), mass and radius from astrometric study 79−5858
α Canis Majoris B (Sirius B), minimum flux H coronal model rel. to X-ray emission 80−8626
α Canis Majoris B (Sirius B), search for far UV emission 79−5821
α Canis Majoris B (Sirius B), search for surrounding nebulosity rel. to historical mass loss 78−93242
ζ Capricorni, Ba star, white dwarf+giant, UV spectra obs. 80−105284
OY Carinae, white dwarf cataclysmic, eclipsing binary, parameter determ. 80−82385
cataclysmic binaries, masses and evolution 77−57031
cataclysmic variables, pulse timing meas., accretion disc models 79−62831
cataclysmic variables, short-period light oscills. rel. to non-radial oscills. of rot. stars 78−32477
cataclysmic variables, theoretical UBV colours of accretion discs 78−61865
CD−42°14462, peculiar white dwarf, noneruptive close binary 77−53630
CD-31°622, spectroscopic obs. of DC white dwarf candidate 77−67090
o Ceti AB, IUE obs. of UV spectrum 80−22027
ZZ Ceti stars, constraints on possible long-term variability 80−90428
ZZ Ceti stars, southern hemisphere survey 77−56948
ZZ Ceti stars and pulsations, physical props. 79−48781
ZZ Ceti stars search, photometric obs. of apparently quiescent stars 80−22005
Z Chamaeleontis, cataclysmic binary, masses radii, and mass exchange rel. to gravit. radiation 80−4386
Z Chamaeleontis, eruptive binary, model from photoelectric data anal. 80−72961
cluster white dwarfs, numbers rel. to progenitor stars upper mass limit 80−51738
CoD−38°10980, gravit. redshift meas. 78−24511
cold degenerate stars, immiscibilities rel. to luminosities and comps. 78−69798
collision with main sequence star, physical processes and results 77−64758
collisions with main sequence, stars in dense galactic nuclei 78−65621
conservation of energy equation from scale covariant gravitation theory 80−73216
convection zones in λ4670 white dwarfs 77−17559
convective mixing and accretion 77−5529
cool, IR photometry, atm. comp. 79−16950
cool DA white dwarf and subdwarf discrimination by spectroscopy and photometry 78−7999
cool white dwarfs, spectrophotometric obs. 77−45422
core, Coulomb collisions in degenerate plasma in quantising mag. field, photon absorpt. *(Russian)* 78−55715
coronae, low-temperature, contrib. to EUV background 80−62324
critical accretion flow of gas into compact stars, rel. to X-ray sources 78−20817
crystalline physiology, model for non-chemical form of life 77−90978
white dwarfs continued
cyclotron self-absorption in accretion columns of magnetic degenerate stars, X-ray sources appl. 80−12760
SS Cygni, accretion disc radiation during dwarf nova outburst 77−91537
SS Cygni, dwarf nova, white dwarf mass from rapid optical oscills. obs. 80−85947
ss Cygni, hard X-ray source, obs., accretion onto white dwarf 79−30078
Cygnus X-2 as spherically accreting nonmagnetic degenerate dwarf 80−46703
DA stars, atmospheric parameters and mass distrib. 79−88655
DA stars, H I Balmer γ line profiles and masses 80−77399
DB-type white dwarfs, model atmospheres 80−51761
deflagration front, slow, propagating into degenerate star, struct. and evolution 79−84790
degenerate accretion disc model 79−25467
degenerate cores, thermomagnetic instability conditions 80−77395
degenerate equilibrium configurations with frozen-in mag. field 78−8008
degenerate magnetic white dwarfs, critical parameters estimation 78−65622
degenerate mass in bimetric theory of gravitation *(Russian)* 79−12466
degenerate relativistic electron gas, electron collisions, thermal conductivity 80−109355
degenerate star candidates, photoelectric and spectroscopic obs. 80−12763
degenerate star surface, slow deflagration front stability 80−67729
degenerate star-red giant interacting binary stars, compressible fluid flow, accretion 80−67779
degenerate stars, spectrophotometry and spectra 78−12224
degenerate stars, UV spectrophotometry, IUE obs. 79−53810
degenerate stars with H atmospheres, props. rel. to theoretical models 80−17576
degenerate stars with He atmospheres 77−13335
diffusion time scales 79−92761
discovery and research *(French)* 77−41380
DO white dwarfs, effective temps. and He abundances 79−35249
dwarf novae, soft X-ray emission 77−45457
dwarf novae, white dwarf radiation rel. to light vars. 77−9753
o^2=40 Eridani B, gravitational redshift 79−62868
40 Eridani B, no X-ray or 4885 MHz image 80−105282
40 Eridani B, possible X-ray emission 79−97035
eruptive blue variables at high galactic latit., spectrophotometry 78−32482
evolution, mass loss 77−74044
external layers, models rel. to spectra interpretation 79−62824
faint 10 pc stars, sequence extension 79−8914
faint blue stars, southern, UBV photometry 80−82349
faint blue stars in young cluster fields 79−21291
faint blue stars proper motions near galactic anticentre 77−87386
fast nova model evolution from pre-explosion to decline 79−35273
Feige 24, EUV obs., temp. determ., interstellar H I density calc. 78−16422
Feige 24, EUV star, spectrophotometry in 3800-8200 Å region 78−4280
Feige 24, hot white dwarf, OAO-2 UV photometry 77−9747
Feige 24, intense EUV source in Cetus 77−9746
Feige 24, spectroscopy of EUV source, binary orbit, mass 78−93218
Feige 4, hot white dwarf, identified with bright EUV source 78−89200
Feige 7, hot rotating magnetic white dwarf discovery 77−53589
Feige 7, mag. white dwarf, spectroscopic studies 79−25603
force-free magnetic fields in degenerate stars, stability 78−49425
formation, effects of stellar mass loss 80−77281
formation and evolution 79−48799
formation in binary systems 79−44483
formation in large star clusters 79−48866
formation rate in globular clusters 80−4346
formation rate in stellar systems 78−28674
G128-7, cool DA white dwarf, atmospheric parameters and evolutionary consequences 80−62126
G200-39, hot hybrid white dwarf, spectroscopic obs. 80−26852
G35-26, high-velocity mag. degenerate, obs. 78−73709
G 165−7, metallic line white dwarf, model atm. code anal. of spectrum 80−85940
gamma ray bursts from magnetic white dwarfs, model *(Chinese)* 80−12831
GD229, cyclotron absorpt. 79−53813
GD 154, new pulsating white dwarf, obs. 78−40928
GD 229, mag. white dwarf, spectroscopic studies 79−25603
GD 40, spectrum anal., Ca abundance determ. 77−87385
GD 428, extreme dwarf Cepheid 77−78798
GD 552, emission-line proper-motion star 78−85943
GD 90, magnetic white dwarf, circular polarisation obs. 78−16409
general relativistic stellar evolution code 79−58317
gravitational collapse, numerical integration of general relativistic eqns. 77−17568
gravitational radiation, from neutron stars and white dwarfs 78−65646
Grw +70°8247, polarised radiation rel. to mag. field and magnetosphere struct. 77−2428
H 2252−035, spectrophotometry, no periodic linear polarization (1980 Sept.) 80−105401
H 2252−035, X-ray flux modulation, compact star rotation 80−101652
H 2252−035 cataclysmic variable, white dwarf rot. period from photometry and spectrum 80−101651
hard X-ray emission from white dwarf binary systems, obs. 78−36732
HD 149499 B, IUE obs. of hottest white dwarf 80−41828
HD 149499B, hot white dwarf, continuous spectrum, H deficient 79−48795
HD 49798, strange composite sdO star, possible existence of white dwarf companion 78−49435
heavy ion diffusion in envelopes 80−51754
Henyey-type evolution code appl. to mass accretion stage 78−61848
AM Herculis, accretion onto highly magnetised white dwarf 79−92764
φ Herculis, Hg-Mn star, corona search, UV obs. 80−72986
AM Herculis, high-speed circular polarimetry 79−25629
AM Herculis, highly magnetised, accreting white dwarf 77−49396
AM Herculis, IR spectroscopy, period, mass function 79−71066
AM Herculis, IUE UV obs. 79−67051
AM Herculis, multicolour photometry, slow optical pulsar 78−28693
AM Herculis, OSO-8 X-ray obs., 2-250 keV energy range 79−71075
AM Herculis, photoelectric obs. rel. to accretion struct. around degenerate star *(Russian)* 78−77565
DQ Herculis, polarised radiation rel. to mag. field and magnetosphere struct. 77−2428

white dwarfs continued
AM Herculis, UBVRI photometric and polarimetric obs. 79−5861
AM Herculis, visual magnitude estimates (1980 March-June) 80−82428
AM Herculis, X-ray binary, obs., slow rotator model 78−12408
AM Herculis (3U 1809+50), binary star model 77−71155
AM Herculis (3U 1809+50), IR light curves 78−28727
AM Herculis (3U 1809+50), multicolour linear and circular polarisation obs. and geometrical model 78−8053
AM Herculis (3U 1809+50), polarimetry and spectrophotometry rel. to mag. field 80−94835
AM Herculis (3U 1809+50), single accretion column model 78−57578
AM Herculis (3U 1809+50), UV spectrum obs. 80−67782
AM Herculis (4U 1814+50), X-ray emitting mag. white dwarf binary, review of props. 80−105403
DQ Herculis (Nova 1934), white dwarf rot. period rel. to nova remnant shape 80−105244
AM Herculis objects, linear polarisation model 78−16460
AM Herculis type binaries, cyclotron self-absorption in accretion columns of magnetic degenerate stars 80−12760
AM Herculis/3U 1809+50 X-ray binary, rot. mag. white dwarf model 77−33571
high-luminosity degenerate stars with He burning near surface, pulsational props. 77−5519
homogeneous ellipsoidal stars, evolution 77−33333
hot degenerate stars in steady-state accretion, thermal stability 78−40929
hot He- and metal-poor white dwarfs as thermal soft X-ray sources 78−57553
hot white dwarfs, effective temps. 79−25602
hot white dwarfs, EUV flux interstellar absorpt., local clumpiness factor determ. 80−36627
hot white dwarfs, luminosity function, spectral type anal. 80−90418
HR-diagram and luminosity function determ. *(Chinese)* 80−77403
VW Hydri, dwarf nova, almost corotating mag. white dwarf model 79−16977
VW Hydri, outbursts of dwarf nova, long and short eruptions comparison 79−88669
HZ 29, binary white dwarf system, evolution and gravit. radiation 77−57030
HZ 43, EUV obs., temp. determ., interstellar H I density calc. 78−16422
HZ 43, He abundance and stellar struct. from soft X-ray spectra 80−72944
HZ 43, self-consistent model atm. anal. 77−22220
HZ 43, ultra soft X-ray spectrum 78−85941
HZ 43, UV spectrum obs. by International Ultraviolet Explorer (IUE) 78−96474
ideal Fermi gas, thermodynamics and eqn. of state 77−30117
integrated polarisation of H lines in string magnetic field 77−17563
interior, nuclear crystals form. *(Polish)* 77−17355
JL 76, spectroscopic obs. of DC white dwarf candidate 77−67090
L19-2, low-amplitude ZZ Ceti type variable, UBV colours, period determ. 78−4242
L19-2, ZZ Ceti-type variable, light curves and power spectra 77−56948
LB 3459, O-type subdwarf plus hot white dwarf eclipsing binary, photometry, anal. 79−48859
LDS 678B, null circular polarisation meas. 78−96478
LDS 678B (EG 131), spectrum 78−40946
LDS 785A (EG 153), DB white dwarf, discovery of H 77−45425
linear radial and nonradial modes of oscillation 78−4213
low-luminosity dwarfs, rel. to Dirac cosmology 77−22334
LP182-44, faint high-vel. degenerate star with probable C features, photometry and spectrum 79−67007
LP 131-66, new cool red degenerate star 79−48780
LP 145-141, C_2 white dwarf, spectrum, strong UV absorpt. obs. by IUE 80−67715
LP 182-44, possibly low-luminosity white dwarf 78−49439
LP 701-29, heavily blanketed white dwarf, spectrum synthesis 78−32455
LP 701-29, lowest luminosity degenerate star with heavily blanketed spectrum 78−36562
LP 790-29, southern mag. white dwarf, spectrophotometric obs. 79−92765
LP 790-29 mag. degenerate with heavily blanketed energy distrib., obs. 79−5815
luminosity function, of Population I white dwarfs in SA 51, SA 57 and (SA 68) 80−98648
luminosity function depend. on progenitor masses 78−65614
luminosity functions, comparison between observed and theoretical 77−5528
luminosity in scale covariant theory of gravity 79−80303
M67, distrib. of white dwarfs rel. to mass loss 77−13408
M-type dwarf stars, spectrophotometry with Carnegie image tube 78−57466
magnetic, spectra, review 77−50383
magnetic DA white dwarfs, calc. and obs. spectra 79−71032
magnetic DA white dwarfs, spectral line and circular polarisation profiles 80−62123
magnetic field, Faraday effect and depolarization of optical emission 79−97002
magnetic fields, effect of vacuum birefringence on X-ray emission polarisation 78−4408
magnetic fields in superdense stars, cyclotron reson. emission 79−75207
magnetic flux distrib., radiative/conductive equilib. models 79−53811
magnetic white dwarf in binary system, collapse, mass ejection, nova mechanism 78−32485
magnetic white dwarfs, Hα polarisation and line profiles, theory 77−2427
magnetic white dwarfs, line and continuum spectra 78−4207
magnetic white dwarfs, relative freqs. among cool stars and hot stars 79−84788
magnetic white dwarfs, source of polarised radiation 77−2428
magnetic white dwarfs, unexplained spectral features theory 80−82187
magnetic white dwarfs spectra, cyclotron absorpt. features theory 80−4351
magnetic X-ray binaries, synchronous rotation appl. to AM Herculis 79−62867
magnetised, accretion, role of electron conduction 80−82358
magnetised white dwarfs, mass accretion theory 79−92764
magnetobremsstrahlung and optical polarisation, theory 77−45417
magnetospheres of accreting compact stars possessing multipole magnetic fields 79−97020
white dwarfs continued
mass, main sequence star max. mass for white dwarf evolutionary stage 80−105237
mass accretion onto massive white dwarfs, rel. to thermonuclear runaways 80−41822
mass distribution, rel. to stellar mass loss rates and galactic evolution models 80−46548
mass-accreting white dwarfs, evolution 80−77281
mass-radius relation, constraints on gravit. const. 79−25464
masses, rel. to planetary nebulae ejection by He shell flashes and planetary distance scale 78−24540
masses and radii of H-rich and He-rich stars 79−35245
massive accreting white dwarfs in close binary systems, H shell flashes 79−75203
meridional circulation caused by stellar rot., general rel. eqn. 79−62818
mixing processes and elements separation in envelopes 78−12222
model atmospheres, masses and radii 77−33485
model atmospheres and synthetic spectra, effective temps. 5000-7000K *(Italian)* 78−93240
models, thermodynamic inconsistency of modified Saha eqn. at high press. 78−36450
multiperiodic light curves, g-mode rotation 78−4210
neutrino retention, influence on stellar mass and radius 79−62817
in NGC 6752, globular cluster, UB photometry 78−93233
nonejecting novae as EUV sources 78−12238
nonradial nonadiabatic oscillations, models with H and He rich envelopes 77−56925
nonradial oscillation mode splitting, effects of differential rotation 78−4211
nonradial oscillation modes in presence of slow rot., quasiadiabatic anal. 79−12462
nonradial oscillations of degenerate dwarfs, theoretical review 77−87398
nonradial oscillations of slowly rotating models 80−4348
nova outburst, CNO abundances and hydrodynamics, 1 M⊙ models with small mass envelopes 79−12475
novae, effect of binary companion on outburst 80−82394
novae, effects of white dwarf rot. on remnants shapes 80−105244
novae, low-temp. photonuclear p-nuclei nucleosynthesis in degenerate H burning zones 78−57540
novae, outbursts, accretion model 79−88680
novae review 77−78799
one-component plasma, crystallized, dynamics and energy, self-consistent-phonon theory 80−107384
oscillations, junction conditions across perturbed contact discontinuities 80−94787
RU Pegasi, dwarf nova, white dwarf nonradial pulsations rel. to ultrarapid light vars. 77−53596
GK Persei, X-ray outburst detect. from old nova 79−67033
PG 1413+01, white dwarf-red dwarf eclipsing binary, photometry and spectral types 79−8944
photometry, calibration 78−85938
RR Pictoris, accretion disc radiation of cataclysmic binary 77−91537
planetary companions, detection by direct photometry from space telescope 79−71076
planetary nebulae central stars, evolution to white dwarf stage 78−12325
planetary nebulae central stars, UV radiation meas. 78−28679
planetary nebulae local space density and formation rate 77−17652
planetary nebulae nuclei, spectral type evolution *(Russian)* 79−58361
planetary nebulae nuclei, temps. rel. to masses and nebulae evolution 80−82344
prewhite dwarfs, UV radiation effect on intergalactic medium temp. and ionisation struct. 77−13455
pulsed UV radiation from hot spots on accreting white dwarfs 77−13343
VV Puppis, AM Herculis type binary, accretion column absorpt. spectrum obs. 79−101176
VV Puppis, AM Herculis type binary, optical absorpt. spectrum, cyclotron intepretation and models 80−73003
VV Puppis, AM Herculis type binary spectrophotometric obs. 79−5860
VV Puppis, circular polarimetry in active state and evidence for two accreting poles 79−48854
VV Puppis, proper motion meas., distance and luminosity 78−96510
VV Puppis, spectroscopic obs., broad absorpt. features discovery 79−44502
R548, pulsating star, photometric obs., light curve anal. 78−32488
R548, pulsating white dwarf, photometric props. 77−9742
radial oscill. mode of hot white dwarf, nonlinear calc. 80−67713
radiative heat transfer in presence of mag. field *(Russian)* 77−87247
rapidly rotating, oscills., numerical calc. 80−46554
rejuvenation due to interstellar accretion 77−17550
relativistic degenerate electron plasma, dielectric response in mag. field, plasma oscillations 80−54022
review, structure and evolution, luminosities, spectra and non-radial oscills. 80−82356
review of physics of structure and evolution 79−25606
rigidly rotating white dwarfs, critical ang. vel. 77−5525
Ross 640, H-poor white-dwarf, H abundance determ. 77−87388
Ross 640, He-rich star, Ca, Mg, S and Fe abundances from UV spectra 80−94790
rotating magnetic white dwarfs, equilib. struct. 78−49433
rotation and gravitational redshift meas. 77−29816
WZ Sagittae, eruptive binary, model from hot spot eclipses anal. 80−72962
WZ Sagittae, recurrent nova, physical parameters, present state, past and future evolution 78−85948
secular instabilities of rigidly rotating stars in general relativity, theoretical formalism 80−4341
secular instabilities of rigidly rotating stars in general relativity, numerical results 80−4342
seismology, effects of crystalline core on nonradial oscills. freqs. 80−17577
slow nova, evolution of model with Z=0.03 envelope from pre-explosion to extinction 78−32468
slow nova, hydrodynamic study of outburst 78−40954
slow nova with 1.25 M⊙ white dwarf model 77−82264
slow nuclear deflagration, mechanism for mass ablation from degenerate stars 79−35248
slow rotation in collapsed stars, effects of mass loss 78−49426
solar neighbourhood, white dwarfs freq. distrib. rel. to stellar integrated colours 79−44460
south galactic pole, search for white dwarfs 79−21274
southern white dwarfs, Stromgren photometry 78−32456

white dwarfs continued
space density of hot dwarfs, EUV and soft X-ray sources 78−61856
space motions and luminosity function 77−45413
spectra obtained with low-dispersion Fehrenbach prism, computer simulation 78−57468
spectra of 47 southern stars 78−16417
spectra of magnetic dense stars, theoretical anal. of atomic spectra 80−105160
spectra of very cool dwarfs, abundance change effects 77−29829
spectral classification of cool dwarfs 77−29828
spectral evolution and accretion from interstellar clouds 79−35252
spectroscopic survey using Luyten catalogues 78−7998
spherically symm. accretion near Eddington limiting luminosity 79−16809
SS 433, binary star model including mag. white dwarf 80−4385
SS 433, ultra-close black hole-degenerate dwarf binary system model 80−4384
stability, of white dwarfs undergoing spherically symmetric steady-state accretion 80−77402
Stein 2051B, temp. and radius determ. 77−13338
structure, parameters of polytrope of index three 79−62819
structure rel. to giant planets 79−16955
supercritical accretion discs winds struct. and appearance, numerical models 80−21984
superdense matter eqn. of state, nuclear size correction to relativistic Thomas-Fermi model 78−29413
superflares, model for cosmic gamma-ray bursts *(Chinese)* 77−22021
supernova, type I, explosions, contrary evidence from radial distrib. in spiral and elliptical galaxies 80−62163
supernovae, Type I outbursts 79−58367
surface accretion, C enhancement mechanism for fast nova occurrence 80−85936
surface accretion, thermal runaway, nova phenomenon 77−82222
surface accretion of interstellar matter 80−51734
in symbiotic star systems, evolution *(Russian)* 77−17616
symbiotic stars, accretion rates rel. to subclasses 80−62144
symbiotic stars, binary model with super-critical accretion 77−45458
V471 Tauri, BV photometry of white dwarf eclipsing binary, light curve vars. 78−96508
V471 Tauri, white dwarf eclipsing binary, IUE UV spectra 80−26912
V471 Tauri (Bd+16°516), Ca II H and K and Hα line vars. 79−67063
V471 Tauri (BD+16°516), eclipsing binary white dwarf, spectroscopy and photometry rel. to evolution 77−57028
thermal emission of an optically thick plasma containing a strong magnetic field 79−25469
thermal pulses in nuclear shell burnings, finite amplitude, general theory 79−80299
thermonuclear runaways, theory 78−40937
thermonuclear runaways in white dwarf envelopes 77−56961
time evolution of hot white dwarfs with masses over Chandrasekhar limit 77−17567
triple close approaches effect on stellar system evolution, one-parameter family appl. 80−17618
two-colour diagram, calcs. rel. to white dwarfs masses and radii 80−46547
AN Ursae Majoris, nova-like variable, circular polarisation rel. to white dwarf mag. field 78−8018
uvby photometry of 112 southern objects 80−8624
van Maanen's star, astrometric study of Sproul plate series, radial vel., gravit. redshift 78−40936
variable DA white dwarfs, kinematics rel. to nonvariable DA stars 78−53947
variable white dwarfs, multiple periodicities 77−87434
very low luminosity degenerates, deficiency from faint proper-motion stars obs. 80−17575
vibrating, ultra-short var. 79−21287
virial theorem, energy content and mass-radius relation 78−45327
visual surface brightness relation appl. 78−81624
VV Puppis, 3470 Å emission as cyclotron line 80−36673
Weedman 2, star misidentified with radio source, identification as white dwarf 78−73708
X-ray bursts during passage through dense clouds 77−78896
X-ray sources with repeating bursts, magnetospheric accretion model 77−5597
X-rays from spherically symm. accretion onto degenerate dwarfs 77−78781
XUV emission, possibility of detect. *(German)* 80−109372
zero-temperature degenerate stars with subnuclear densities, radial oscills. 78−12219
C-O dwarf, H and He burning in degenerate envelope *(Russian)* 80−17585
C-O white dwarfs, C-O eutectic model 80−77405
C_2 (4670 Å band) stars, evolutionary status 80−4355
C_2 stars, spectrophotometry 77−29824
CNO nuclei enhancement in nova progenitors 77−33484
Fe I 3719.94 Å line broadening by He, line width and shift meas., lab. expt. 77−73942
H burning shells, thermal stability 78−4212
H, He white dwarf atmospheres, minimum-flux coronal models 80−8626
H I Balmer line strengths, profiles and equivalent widths 79−96998
H line asymmetries and gravitational redshifts 77−17556
Hβ line profiles for dwarfs with dipole and quadrupole magnetic fields 78−8004
He flash and nova evolution 80−72938
He lined white dwarfs, spectrophotometry 77−53588
He rich stars, intermediate and extreme, spectral atlas in 3700 to 4600 Å range 80−94806
He rich white dwarfs, elec. fields influence on accretion and stellar winds 79−48772
He rich white dwarfs, origin rel. to He stars post-giant evolution 77−56947
He shell burning, thermal pulses in accreting white dwarf 80−22009
He white dwarfs rejuvenation by mass accretion 78−73712
He-rich, convective mixing 79−71018
He-rich, coronae 78−85940

white noise
acoustic white-spectra stimuli, place clues rel. to direct use of time information in hearing 77−90803
attenuated white noise statistical gravity model 80−30977

white noise continued
auditory localisation, behavioural compensation limits in earmuff listening conditions 77−36947
axon membrane white noise, stimulation, strength-freq. relationship, squid 78−3466
binary image in noise corruption by additive Gaussian noise 79−36848
biological system, white noise analysis 79−1995
biological system identification, quasi-white random signals optimal use 77−73502
biological system identification, quasi-white random signals optimal use, appl. 77−73528
bistable optical system, phase transitions induced by white noise 79−18388
charged particle track reconstruction, fitting procedures, multiple scatt. effects *(German)* 78−74091
coherence improvement in anal. by use of repeated random sequence generator 80−36203
computerised tomography, reconstruction noise rel. to detectability 78−69213
crayfish stretch receptor repetitive firing behaviour nonlinear systems anal. 78−80853
cubic semiconductors, bulk hot-electron props., review 79−99553
disordered system, four-dimensional, electrons 77−8039
electrochemical noise generated by anodic dissolution or diffusion 77−25277
electroretinogram, human, nonlinearities reflected by Wiener kernels 79−34556
film grain noise, spectral density estimation, in electron microscopy *(French)* 80−9075
Fourier spectroscopy, spectral smoothing under white and background-noise-limited expts. 79−35861
function, distorted by noise, resolution into sum of exponentials 80−77707
functional analysis, Volterra expansion, zero-mean Gaussian process 79−86296
Gaussian in telex-communication system, reduction *(Rumanian)* 77−27427
generalised Brownian functionals epxressed as generalized multiple Wiener integrals 79−30370
hot plasma, white noise excitation, sum of ion acoustic waves 78−42736
Langevin equation, modified, functional integral and operator formalisms 79−63152
laser designation system spot motion model identification 79−94277
laser generated plasma, stochastic (white noise) anal. of resonant absorption 79−50874
linear structure, lightly damped, white noise generated non-stationary random vibrs. 78−90742
Markov fields and local operators, difference between Gaussian and Poisson white noise 80−57186
Markovian integro-differential master eqns., Langevin description 80−31676
nematics, EHD instabilities, white noise effect 80−70115
neuron, spatially distributed, response to white noise current injection 79−83728
neuron population, local, model performance 79−20531
neutron density fluctuations in on-off controlled reactor, exact stochastic anal. 79−36308
nonlinear Langevin eqn. for Markov processes with white Gaussian and generalised Poisson noise, Kramers-Moyal form of master eqn. 79−21653
nonlinear second order system, eigenfunction expansion solutions of Fokker Planck eqn. 80−73172
oil exploration seismic data processing, white noise estimators 78−3973
oscillating irregular field, effective potential 79−75457
power and temp. fluctuations for reactor with temp. feedback, exact statistical anal. 79−36309
probability theory of the white noise direct product *(French)* 79−44858
relaxation spectrometry, injected white noise as soln. of phase problem 78−76830
remote transducer optimal signal correction with internal fluctuating white noise *(Russian)* 79−6107
repetitive firing computer models nonlinear systems anal. 78−80854
retinal neurons studies, appl. of white noise anal. *(Japanese)* 79−66471
ripple noise pitch detection by human, adaptive model 78−73166
seismic data, single-channel white-noise estimators for deconvolution 78−77345
speech intelligibility, temporal interruptions with and without intervening noise 77−32911
stellar spectroscopy, linear filtering theory for case of white noise *(Italian)* 80−90340
stochastic approx. procedures in continuous time 78−69969
stochastic stability of dynamic multi-nonlinearity systems, action of white noise 80−68135
thermal viewing system, image integral scanning effectiveness 79−50402
two-dimensional white noise problem and inversion layer localisation 78−84271
viscoelastic beam, constrained, flexural vibrating, response to random excitation of white noise and turbulent boundary layer type 80−53671
Au/Pt-Ir contact, spectral characts. of VLF noise allowing for logarithmic creep *(Russian)* 77−85301
GaAs, epitaxial layers, low freq. current noise between 4.4 and 300K 78−95388
H maser autotuning system analysis 79−55101

wideband amplifiers
300 W wideband pulse amplifier 78−86302
isolated for biological signals, cct. 78−57089
low-noise charge pre-amp., spectroscopy with Si surface barrier detectors 77−54467
NMR pulsed spectrometer wideband preamplifier 79−71502
stochastic beam cooling expts., low-noise wide-band power amplifier system 80−58011
US tumour irradiation, closed-loop energy and temp. control 79−83874
us vibration propag. vel. meas. in solids using broadband amplifier 78−1521

Widmanstatten structure
brass, Widmanstatten α-precipitates, edgewise growth 77−77481
stability principle for plate growth 80−84939
steel, alloy type, photoemission electron microscope obs. of high temp. precip. behaviour 80−108456

Widmanstatten structure continued
steel, austenitic stainless, ferritic, single phase ferritic solidification in welds, exam. 80−7546
steel, C, relax. resist. rel. to struct. 78−23788
steel, C, weldable, ferrite-pearlite, Widmanstatten structs., resist. to fracture 79−29203
steel, hypoeutectoid, fracture toughness, effect of Widmanstatten ferrite 80−35315
steel, hypoeutectoid Widmanstatten struct. form., contrib. to the laws *(Slovenian)* 78−84817
steel, medium C, Ni-Cr-Mo, overheated, fractographic study *(Chinese)* 80−66616
steel, SiO_x inclusion formation on introduction of solid SiO into molten steel *(Russian)* 78−80530
steel, V, precip. and transform. kinetics, effect of N 80−97485
Zircaloy-2, hot-pressed, influence of diffused C on structure and oxidation 80−61016
Zircaloy-4, resistance-welded, microstruct. of weld region 80−66549
Cu-Ti (4 wt.%), isothermal transformation, electron and optical microscopy obs. of microstructure 80−16307
Fe-Cu-Ni (2, 5 wt.%), interphase precipitation obs. in assoc. with Widmanstatten ferrite lateral growth 80−40365
Fe-Ni meteorite, STEM/X-ray microanalysis across α/γ interface 80−105212
Fe-V-C (0.3, 0.05 wt.%), interphase precipitation obs. in assoc. with Widmanstatten ferrite lateral growth 80−40365
α-β Ti alloy interfaces, elastic interact. stresses, effect on plastic flow onset 80−104218
$\alpha+\beta$Ti alloys, colony size effect on fatigue crack growth on Widmanstatten struct. 80−30094
α-βTi alloys, high strength, heat-treated weldments, intergranular fracture 80−21097
Ti-Al-Mo-V (8, 1, 1 wt.%), Widmanstatten colonies, fracture toughness 80−85031
Ti-Al-V (6.4 wt.%) cast alloy, with improved microstruct., mech. props. *(Japanese)* 80−71701
Ti-Al-V-Sn (6, 6, 2 wt.%) weldments, heat treated, transangular fracture 80−40524
α, $\alpha+\beta$, β-Ti-Mn alloys, Bauschinger effect during cyclic straining 79−43310
Zr-Al (8.6 wt.%), dimensional stability struct. and mech. props, effects of neutron irrad. 80−92563

Wiedemann effect
Fe ⟨100⟩ whiskers, inverse Wiedemann effect 77−90001
Fe whiskers, inverse Wiedemann effect, torsional strain and azimuthal mag. field influence 80−108045
$Fe_{40}Ni_{40}P_{14}B_6$, amorhpous ribbon, influence of torsion on mag. props. 80−7138
Ni wire, polycryst., inverse Wiedemann effect for low torsional stress 79−11332
Ni wire, polycryst., magnetoelastic hysteresis with torsion, inverse Wiedemann effect *(Spanish)* 77−73064
$Tb_{0.27}Dy_{0.73}Fe_2$, LF magnetoelastic effects 78−68348
$Tb_{0.27}Dy_{0.73}Fe_2$, perpendicular suscept., magnetomechanical coupling and shear modulus 78−91918

Wiedemann-Franz law *see Lorenz number*

Wien effect
dilute aqueous solutions, EHD liquid motion, interference with second Wien effect 79−94735
electrolytes, Gauss's divergence theorem in Onsager's theory 79−47934
electrolytes, mixed solns. 78−75856
Mathematics of Wien dissociation for weak electrolytes 78−3343
perturbation solution of Wien dissociation in weak electrolytes 78−23950
stepwise-dissociating acids, bases, salts, high field conductance 77−40551
tetra-n-butylammonium picrate, soln. in benzene, field dissoc. effect on ion pairs 79−91061

Wigner coefficients *see Clebsch-Gordan coefficients*

Wigner crystal
alloy, heat of formation within density functional formalism 79−57283
CDW of two-dimensional electrons, in strong mag. fields 78−43316
conductivity of cryst. on liq. He surface *(Russian)* 80−6594
density-functional theory of Wigner crystallization 79−42477
electron crystal, appearance of crystallised layer in superfluid He *(French)* 79−73364
electron gas, classical and two-dimens., self-diffusion theory 80−141
electron gas, diamagnetism and surface currents 80−88496
electron gas, Wigner distribution for cylindrically symmetric system 80−65475
electron gas Wigner transition, bifurcation theory 79−97297
electron sheeet on liquid He surface, liq. to cryst. transition 79−42341
electrostatic energy, correction to Fuchs' calc. 79−73130
electrostatic energy, Fuchs calc. 80−79743
electrostatic energy, Fuchs method, Wigner solids and Coulomb lattices, theory 80−79745
electrostatic energy, Fuchs method 80−79744
electrostatic stability of Wigner and Wigner-Dyson lattices 78−84162
fermion one-component plasma ground state, two and three dimens. Monte Carlo study 79−33248
ferromagnetism, itinerant electron. of two dimensional system 77−24666
H-stability and energy in one component plasma, numerical anal. 77−66129
interacting electron gas in mag. field, parquet eqns. 79−90980
inversion layers, mag. field induced Wigner transition 77−89869
jellium, static dielectric function exam., Wigner distrib. function 77−66132
lattice quantum oscills. in mag. field, specific heat, mag. moments *(Russian)* 80−49636
localisation of electrons in a magnetic field 79−60752
long-wavelength excitations in strong mag. fields 79−82533
many-electron system, Wigner cryst., electron chain and CDW in strong mag. fields 78−60067
melting curve, approx. theory 79−82535
melting curve of Wigner electron crystal 79−19531
melting temperature calc., dislocation theory 78−43207
MOS structures, two-dimensional electron crystallisation induced by strong mag. field 77−28253
one-component plasma model, crystallised, dynamics 80−107384
phenomenological theory of first- and second-order metal-insulator transitions at absolute zero 79−69420

Wigner crystal continued
quasi-one-dimensional systems, charge distrib. and lattice distortion 78−6317
semimetallic film, Wigner crystal in high magnetic field 79−73456
TCNQ, dimer gas model 78−87926
TCNQ, generalised Wigner lattices and band motion effects 80−24815
TCNQ salt, $MEM(TCNQ)_2$, phase transition electronic struct. interpretation 80−24781
TCNQ salt, NMP-TCNQ, electronic struct., SCF calc., total energy polarisation effects 80−15469
TCNQ salts, electron arrangement in ground state, optical spectra interpretation 78−47715
TCNQ salts, quasi-one-dimensional, Wigner cryst. model 78−47273
TCNQ salts, Wigner crystal model 79−42008
three-dimensional Wigner crystal in magnetic field, vibr. freq. 79−73457
three-dimensional Wigner lattice, possible light scatt. expt. for detection 77−36254
TTF-TCNQ, antiferroelectric ordering of TCNQ ion elec. polarisation 80−20598
TTF-TCNQ crystal, antiferroelec. ordering of electronic polarisation, simple model anal. 78−92028
two dimensional electron gas in strong mag. field 78−60005
two-dimensional, formation in strong mag. field 78−60072
two-dimensional, melting temp., quantum effects 80−88491
two-dimensional, melting temp. in strong mag. fields, quantum effects 80−88492
two-dimensional, phase diagram in mag. field *(Russian)* 79−38008
two-dimensional, phonon coupling with second surface sound in liq. He *(Russian)* 80−92756
two-dimensional, possible re-evaporation at extremely low densities 78−56085
two-dimensional crystal in magnetic field 80−2350
two-dimensional electron solid, melting 78−83921
two-dimensional electron system, high- and low-density limits 77−76761
two-dimensional electron system in strong mag. field, crystallisation 78−30966
two-dimensional Wigner crystal, static and dynamic props. 77−43293
two-dimensional Wigner crystal in strong mag. field, classical and quantum theory 78−79948
two-dimensional Wigner glass in strong mag. field, numerical study 78−63993
two-dimensional Wigner-crystal-liquid-surface system, eigenmodes and instability of charged liq. surface 80−10896
α-AgI, superionic conductor, struct. and dynamics, two-dimens. mol. dynamics model 80−49413
CdS:Cl, heavily doped, fluoresc. spectrum upper threshold calculated 78−52568
EuTe, magnetic impurity states, mag. and transport props. 80−96913
GaAs-$Al_xGa_{1-x}As$ multilayers, two-dimens. transport at high mag. fields 80−65724
$Gd_{3-x}\square_xS_4$, transport and mag. props., mag. Wigner localisation 80−97069
Ge, electron-hole-liquid, high-field phase transition to two-dimensional Wigner cryst. 79−60720
He, liq., surface, two-dimens. Wigner cryst., electron-ripplon reson. anomalies *(Russian)* 80−92754
He, liq., two-dimensional lattice, on surface, reson. linewidths 79−86949
He liquid surface, localised electron states 78−60007
He, parametric excitation of electrons *(Russian)* 79−37892
HgCdTe, Magneto transport anomalies at low carrier densities, Wigner crystallisation 80−20222
n-InSb, long-wavelength excitations in strong mag. fields 79−82533
PbSnTe, Magneto transport anomalies at low carrier densities, Wigner crystallisation 80−20222
PbTe, Magneto transport anomalies at low carrier densities, Wigner crystallisation 80−20222
Si inversion layers, phase diagram in strong mag. fields 80−88492
Si inversion layers, temp. depend. of magnetoconductivity in ground Landau level 77−39914
Si MOS inversion layer, Anderson localisation and Wigner crystal form. *(Japanese)* 77−69425
SmB_6, valence fluctuating state, sp. ht. 80−20127

Wigner effect *see radiation effects*

Wigner lattice *see Wigner crystal*

Wilson cloud chambers *see cloud chambers*

Wimshurst machines *see electrostatic generators*

wind
acoustic Doppler and angle of arrival wind detect., comparison with direct meas. 79−39884
acoustic noise, wind-generated noise produced by implant of spray with ocean surface 80−106655
acoustic radar method for wind measurement *(Chinese)* 80−46290
acoustic wave refraction by nonuniform wind, error in Rayleigh's theory 79−72743
acoustic-microwave Doppler radar system, wind and wind shear meas. at Dulles Airport 78−32233
Adriatic Sea, meteorology contrib. to high tides prediction 77−86906
Adriatic Sea, southern wind induced surges, numerical model 77−53059
aeolian sedimentation on Earth and Mars, comparisons 80−31042
aerodynamic drag of sea surface, role of high freq. gravity waves 80−26536
aerodynamic roughness as function of wind direction over asymm. surface elements 78−92890
aerodynamic roughness length for complex terrain 79−53475
aeroelastic stability of wide span surface structs., wind vels., flutter, binary divergence 78−26083
aerosol sampling thin-walled tube aspiration coeff. 77−37460
SE.central Africa, wind flow patterns in relation to rainfall 79−84460
N.W.African continental shelf, wind, current and temp. meas. 77−86923
E.African low level jet stream, theory 78−40632
air composition at Barrow, Alaska, influenced by wind direction 80−85704
air flow above water waves, numerical model 77−81912
air pollution, concentration pattern determ. in one wind direction *(Dutch)* 77−70821
air pollution, impurity concentration meas., sampling error statistical anal. *(Dutch)* 77−70828
air pollution concentration pattern determ. over long period *(Dutch)* 77−70822

wind continued
air pollution emission, transmission and immission, fundamentals *(Dutch)* 77−70820
air pollution meas. errors, sampling method improvements *(Dutch)* 77−70827
air pollution measurements, wind depend. rel. to interpretation via pollution roses 78−81379
air pollution survey vehicle measurements *(Dutch)* 78−81365
air-sea interaction, surface drift current speed and direction calc., geostrophic wind factor 78−61422
air-sea interface, momentum flux determ., wind-wave interaction method 77−33130
air-sea interface, oceanic variability obs. during Project BOMEX 78−69362
air-sea interface, wind speed rel. to cooling water boundary layer thermal state *(Russian)* 78−81192
air-water exchange reactions, wind-wave interactions *(Dutch)* 78−3785
air-water interface, energy transfers at high wind speeds, effect of spray 78−85574
airborne Doppler radar meas., bias error determ. 78−3879
aircraft effects of thunderstorm-induced low-level wind variation 77−91217
aircraft meteorograph, design, appls., accuracy *(Chinese)* 80−17387
airflow over bell-shaped mountain, cloud model 80−77049
airflow regime influence on Rn content, rel. to lower atmosphere vertical stability determ. *(Spanish)* 79−92560
airflow turbulent kinetic energy, budgets in mountainous terrain 80−105022
airports, averaging time for along-runway and across-runway components reports 77−17177
alpine tundra habitats, effects of phys. habitat factors and plant morphology on ^{137}Cs contamination 77−37058
ambient air/water interface, frictional coefficient at low wind strength, obs. *(French)* 78−16020
Amderma region, winter wind speed increase prediction *(Russian)* 77−21852
N.America west coast, wind stress rel. to sea level alongshore correl. 78−73381
Ampere Glacier, Kerguelen Is., heat balance in ablation area 77−64335
ancient Mesopotamia, city wall and street orientation rel. to winds 78−49074
anemometer design using transistors, wind sensor for portable battery operated instrument 79−71420
Antarctica, wind struct. up to 80 km altitude 80−81992
Antarctica and equatorial India, atm. struct. during southern summer 77−53121
Apennine valley day breezes, Parma, Italy 80−26589
Arabian Sea, wind stress, sensible and latent heat fluxes, ISMEX-73 data 78−85627
Arctic Basin, ice movements, external factors 80−26541
Arctic Basin, plane nonstationary model of wind-driven circulation 77−21789
S.Asia, monsoon circulation, role of mountains 77−49121
Asian summer monsoon, simulation by general circulation models 78−40637
astronomical telescope, anal. of frame-type mount under wind load 78−28518
N.Atlantic, sea surface temp. response to atm. forcing 78−73399
E.Atlantic, trades and Harmattan rel. to aeolian dusts 77−64327
NE.Atlantic circulation, climate and oceanic var., Little Ice Age 80−8422
N.Atlantic easterly gales, 1881-1970 period 80−77101
W Atlantic Ocean, increased wind stress rel. to E Atlantic equatorial adjustment 78−88836
Atlantic Ocean, trade winds seasonal vars. rel. to upwelling in Gulf of Guinea 78−88837
N.Atlantic westerlies strength rel. to climatic change 77−78402
atmosphere surface layer, features of organised motion rel. to local wind vel. 80−72602
atmospheric surface boundary layer, hot-wire meas. on S.W. Kansas, Denmark, expt. 77−9458
auroral F-region ionosphere form. role. of neutral winds and particle precip. 79−44296
auroral NO densities, horizontal winds effects 80−26656
auroral oval, dayside, neutral wind profiles obs. between 115 and 175 km altitude 80−98494
auroral zone neutral wind vels. near tropopause using Chatanika UHF Doppler radar 77−5274
N.Australian coast, tropical cyclone guest speeds 77−86997
E.Australian coast, wind stress generation of shelf waves 77−37234
availability data in high plain regions of S.W. USA 77−37343
balloon meas. in boundary layer, wind vel. determ. *(German)* 79−84421
Baltic and North Sea water exchange, barotropic model wind effects 77−73742
SW Baltic Sea, wind-driven circulations 79−5490
Baltic Sea region, wind meas. rel. to atmospheric heat and moisture balance 77−87057
Banks Island, Canada, deposits and aeolian processes *(French)* 78−36163
baroclinic boundary layer structure 78−81326
baroclinic instabilities in deep fluid model 77−49113
baroclinic waves, influence of static stability and wind shear time changes 80−109226
barotropic-baroclinic instability of mean zonal wind during summer monsoon 78−40638
basin response to fluctuating winds and mesoscale motions in ocean 79−57965
W.Bay of Bengal, 1978 southwest monsoon effects. on wave characts. 80−109152
Bear River Range, north-central Utah, wind direction rel. to cirque characts. 80−72510
beaufort scale data, conversion to wind vel. study *(German)* 80−8407
Beaufort scale rel. to wind and sea state 79−2354
Beaufort Sea, geostrophic wind rel. to ice movements (1973-1975) 77−45011
Beaufort Sea, winds and surface temps. rel. to August ice cover vars. 80−101366
Beaufort Sea Coast, Alaska, sea breeze processes 80−41485
Belgium, weather in 1975, review 77−25747
Belgium, weather in 1977 79−58049

wind continued
Belgium, wind speed and direction, 1963-1972 obs. *(French, Flemish)* 77−87053
Belgium, wind speeds rel. to air pollution increases 78−81374
S.Benguela Current, upwelling site, wind effects and biology 80−104987
Benguela Current, wind regime rel. to anomalously high waves region 80−51434
bidirectional vane, response characts. 79−66814
blocking of mid latitude westerly winds by planetary waves 80−105036
blocking stability in barotropic channel flow 79−96785
bora, rel. to N.Adriatic Sea circulation 78−40556
bora, screening of ships in port of Novorossiisk 77−78365
Boston Basin, areal parameters and vertical structure of sea breeze 79−88396
boundary layer, birefringence under wind speed gradient shear 78−69453
boundary layer, bulk model for wind and pot. temp. 80−77030
boundary layer, clear air wind perturbs., dual Doppler radar obs. 79−53462
boundary layer, diurnal var., diffusion eqn., theory 79−48540
boundary layer, dynamic structure in urban areas, numerical simulation 79−66741
boundary layer, effects of ocean long waves 77−45005
boundary layer, friction vel. and temp. scale from temp. and wind vel. profiles 78−81268
boundary layer, horizontal trajectory computation based on surface geostrophic wind 77−37284
boundary layer, lateral coherence of isotropic turbulence and wind 80−72575
boundary layer, log-linear profile relationship over rough terrain during stable conditions 77−60444
boundary layer, longit. wind vel. component meas. 77−78369
boundary layer, lower, influence of built-up area on turbulence *(Russian)* 78−44925
boundary layer, mean horizontal wind profiles about block building 77−73789
boundary layer, nonstationary, under influence of strong wind, engineering model *(Russian)* 77−5280
boundary layer, nonstationary advective, resistance law hypothesis 77−60441
boundary layer, obstacle in weakly stratified flow, upstream influence, theory 80−56527
boundary layer, roughness length and zero-plane displacement, wind and temp. profiles 78−24329
boundary layer, spectral scale of wind fluctuations 78−20481
boundary layer, speed and turbulence characts. near ground over escarpments 78−44897
boundary layer, stably stratified, wind meas. rel. to turbulence and internal waves spectra *(Russian)* 78−81297
boundary layer, stratified and oscillating, driven by surface temp. grad. 80−51515
boundary layer, unstably stratified wind profiles rel. to turbulent energy dissipation rate *(Russian)* 77−64372
boundary layer, wind obs. and anal. over nonuniform terrain 77−17195
boundary layer, wind shear fluctuations downwind of surface roughness elements 78−92918
boundary layer, wind shears and inversions *(German)* 78−81336
boundary layer at nighttime, vertical struct. obs. 80−61848
boundary layer depth and vertical wind profile 77−9462
boundary layer flow over gentle curivlinear topography with sudden change in surface roughness 77−45110
boundary layer fluxes determ. over natural grassland, aerodynamic method 78−73480
boundary layer jetlike wind over open coast, mesoscale nocturnal phenomena 80−81971
boundary layer measurement system, for wind and temp. struct. *(German)* 80−94616
boundary layer model, two-dimens., appl. to Nanticoke region, Lake Erie north shore 79−66750
boundary layer probing by acoustic sounder 77−17243
boundary layer profile meas. using acoustic Doppler sounder 78−65413
boundary layer structure during light wind, water vapour IR absorpt. meas. 77−91197
boundary layer top, appl. of meteorological data to regional evapotranspiration determ. 77−91171
boundary layer turbulence and wind coherence meas. 77−91201
boundary layer wind shear hazard, radar detection feasibility 80−90256
boxplot, graphic display of speed and direction data 77−91310
breeze characteristics, statistical model 80−85737
upland Britain, wind chill 80−41546
lowland Britain, wind chill anal. 79−66782
calm wind situations, pollutant dispersion analytical modelling 78−81385
canopy flow, higher order closure model 78−44944
Cape Canaveral sea breezes, elliptical clockwise diurnal oscill. 79−100921
Caspian Sea shallow areas, wind waves freq. spectra *(Russian)* 79−16477
Chesapeake Bay, atm. forcing effect on subtidal sea level var. 80−26530
Chesapeake Bay, water surface laser radar refl. as function of wind speed 77−41034
Chesapeake Bay and Potomac River, nontidal variability, nonlocal atm. forcing 78−92829
Chicago area lake breeze, numerical study 78−7682
Chinook effects on Calgary air quality 80−16876
chinooks, effect on urban heat islands and air pollution 78−61534
NE.Chukchi Sea, wind effects on coastal currents 78−32107
circulation change during 1976/77 winter 77−78391
circulation in closed basins, rigid-lid model 78−32131
circulation over Antarctica, seasonal vars. 77−21829
clear air, FM-CW Doppler radar obs. 78−57271
cloud motion estimates, aircraft verification expt. 78−16113
cloud motion fully automated method, Meteostat data comparison with gradient winds 80−109244
cloud motion vectors and moored buoy wind measurements, comparison 79−84394
cloud motion wind data, meas. improvement 80−8386
cloud motion winds from ATS 6 images comparison with coinciding SMS 1 winds 79−79954
cloud winds over oceans, satellite obs. technique 80−85764
cloud-motion winds derivation, Meteosat image data 80−46270
clouds, stability anal. of deep streets 79−2335

wind continued
coastal boundary layer with friction, wind stress forcing, time depend. model 79−34861
coastal breezes, dispersive, monostatic acoustic sounding system *(French)* 78−7683
coastal zone, local thermal wind-field disturbances freq. statistical forecasting 80−36371
coastal zone, wind regime influence on marine aerosols influx into atmosphere 79−29818
coastal zone of non-uniform sea, wind effect on steady circulation *(Russian)* 78−16038
NE.Colorado convective storm, Doppler radar meas. of turbulent kinetic energy dissipation 77−29388
Concorde sonic booms as probe of atm. temp.-wind parameters 77−91323
Coningsby, Lincolshire, surface wind assoc. with snow rollers form. (1979 January 2) 80−72568
continental shelf south of Cape Hatteras, wind stress and Gulf Stream rel. to water flushing 78−81183
convecting columns interaction over linear heat sources, wind effect *(Russian)* 78−55637
convective boundary layer slab model, study using Air-Mass Transformation Expt. data 79−57995
convective systems, life cycles, GATE data 79−53440
cotton canopy aerodynamic features 77−45105
crop damage by hail, effect of wind and shelter by trees 77−45097
Cross Fell, England, severe low level turbulence occurrence and synoptic situation 79−79962
cross-wind velocity meas., interference fringe visibility and spacing, atmospheric turbulence effects 80−51572
crosswind profiles, remote sensing using correlation slope method 80−31131
cumulonimbus motion and splitting, role of downdraught, numerical simulation 79−44227
cumulus cloud motion as indication of air flow vel. 80−98418
cumulus congestus cloud unmixed updraught cores, ice initiation 80−81997
cup anemometer meas. of mean wind speed at sea, rain-induced errors 78−61485
cyclones, ring of max. wind, centre location using kinematical determinant 80−56535
D-region, neutral winds meas. via payload B I rocket-borne expt. package 78−45190
D-region, time vars. in winds and electron densities at Sastakoon, Canada 79−25389
D-region, winds rel. to radio wave propag. during Western European Winter Anomaly Campaign (1975/76) 78−45123
data acquisition and processing for wind power site evaluation 79−66400
daytime neutral winds in lower thermosphere and mesosphere, meas. during winter anomaly 78−45071
Deer-Sloan Creek watershed, rainfall vars., wind and topography influence 77−2212
diabatic surface layer, wind prediction model 80−77032
diffusion, steady state 3-D model, numerical anal. *(Japanese)* 79−79984
direction consistency index 79−12166
direction determ. from rime deposits 80−98428
direction fluctuation statistics and lateral dispersion 80−56577
direction fluctuations characts. in surface layer 79−79913
direction gauge based on pulse height analyser 79−25351
direction meas., wind vane motion 80−90264
direction meas. with vane, graphic recording and averaging 80−82098
direction measurement, electronic method *(Croatian)* 77−41181
directional wind wave spectrum meas., role of dispersion reln. 79−20860
dispersing plume, crosswind geometry, second-order reaction 80−61480
dispersion ellipticity over ocean surface, N. Atlantic example 78−61528
dispersion expts. in Sydney region using SF_6 as tracer 80−67389
diurnal and semidiurnal variations over tropical island 78−24332
diurnal variation in SW lower Michigan, lake breeze and general lake effects 79−39809
divergence theorem for wind velocity *(Spanish)* 80−36376
divergent wind component in initial state, effect on primitive eqn. model initialization 77−86974
Doppler crosswind relations, beam-swinging expt. on troposcatter link 77−5303
Doppler radar data analysis 80−41564
Doppler sodar antenna configs. for horizontal wind meas. 78−65410
Doppler-radar techniques for wind meas. 80−26645
double theodolite measurement of wind speed and direction, control of inherent uncertainties 80−77160
downdraught caused by nimbostratus rainfall evaporation, numerical anal. 80−8400
downslope severe windstorm and aircraft turbulence event induced by mountain wave 78−73431
drag coefficients for marine regime, shipboard evaluations 79−5494
Drake Passage, wind rel. to Antarctic polar frontal zone variability during summer (1976-1977) 78−85579
dry snow and bare ice surface, interaction with wind 80−109181
dual Doppler radar and vel. azimuth display of subsynoptic-scale vertical wind 80−109263
dual-Doppler radar measurement, coverage area as function of meas. accuracy and spatial resolution 80−82093
dual-Doppler radar obs. rel. to kinematic models of dry convective boundary layer 77−37292
dust haze of African Harmattan wind, 1962-1973 visibility obs. 80−61900
dust storms, Great Plains, USA, lessons 79−29486
dust storms, types, locations and mechanisms 77−9481
dust transport in Maricopa County, Arizona 79−70824
dustfall from isolated cement works, implications for residential development 77−37403
dynamo region, long-period winds, effects on surface geomag. field elements 77−2090
dynamo region, wind systems rel. to mag. vars. during reverse equatorial electrojet events 78−36368
E_3-layer clouds drift directions, effect of neutral winds 79−44298
E_s-layer, prod. by wind shear effects on meteor ions 77−25837
E_s-layer formation, unified theory, neutral wind and elec. field effects 79−5710
E_s-layer formation and variations at midlatit., wind contrib. 77−29544
E_s-layer in Brazilian geomag. anomaly, winds rel. to particle ionisation source 77−78558
wind continued
E_s-layer occurrence at temperate latits., small and large wind shears effects 77−29556
E-region, equatorial, dynamics rel. to neutral wind vars. 78−36369
E-region, midlatit. nighttime model including metallic ions 77−45249
E-region, neutral winds, comparison of Chatanika radar and optical meas. 78−32272
E-region, temperate latit., dominant winds from E_s-layer backscatter obs. 78−85761
E-region, winds and elec. fields meas. over Malvern 78−49206
E-region auroral zone neutral wind and current meas. by incoherent scatt. radar 77−70927
E-region neutral wind, simultaneous obs. by different techniques at low and mid-latits. 77−53303
E-region valley, nighttime neutral wind vels. from ionisation layers obs. 77−29569
E-region winds, no correl. with seasonal var. of equatorial ionosphere radio waves absorpt. 78−85762
Earth annual wobble, affected by wind stressed sea level 80−36221
Earth rotation variability, meteorological and oceanic causes and consequences 77−56571
Earth surface winds, correl. with Jupiter winds questioned 79−25290
effect on ocean currents, regression coeffs. and bottom stress anal. 80−8320
effect on winter 1975 circulation in Chesapeake Bay 80−36313
effects, 8th meeting of US-Japan Panel (Gaithersburg, MD, 18-21 May 1976) 77−78395
effects on latitude obs. at Poltava *(Russian)* 78−3915
elastic structures, quadratic transformation of Gaussian process applied to stochastic dynamics *(French)* 77−54917
electric generators, wind-powered, potential output calc. for USA 77−2205
electric power generation for high rise flats, application *(German)* 77−70739
empirical eigenvector anal. of vector obs. 77−86990
energy, prospecting in Prince Edward Island, programme overview and status report 80−61243
energy anal., use of wind fabric diagrams 77−91230
energy conversion, variance anal. of wind characts. 78−49100
energy pattern factor meas., analogue technique appl. 77−81964
energy potential determ. for wind power plant site evaluation 79−66399
energy potential in Karnataka State, in India 80−108782
energy source for mesoscale motions in oceans 78−40625
energy survey anemometer and recording instrumentation 77−33222
energy transfer to ionosphere from lower atmosphere 78−28381
energy transfer to near-inertial ocean waves, calc. 80−4017
SE.England, NW winds in summer of 54 BC 77−49149
SW.England and S.Wales, gale force winds and blizzard (1978 February 18 to 19) 80−12507
England and Wales, 1975-76, zonal winds assoc. with dry period 77−56700
environmental impact assessment, air pollution problems 78−49124
equatorial currents in two-layer ocean driven by wind *(Russian)* 79−25255
equatorial electrojet, effects of gravity wave winds and wind shears 77−5388
equatorial electrojet, equivalent circuit anal. of neutral wind effects 78−57392
equatorial electrojet, neutral winds and phase vel. of instabilities 78−57388
equatorial mesosphere and stratosphere, vertical vel. determ. from Diurnal Experiment 80−77047
equatorial ocean response to periodic monsoon winds 78−3773
equatorial stationary zonal circulation, numerical calcs. 80−85732
equatorial trough zone occurrence and struct. in Venezuela 79−79974
equatorial waves in upper stratosphere and mesosphere, rel. to zonal wind semiannual oscill. 79−5575
equatorial westerlies over E.Africa and Lake Naivasha level changes 80−61819
erosion threshold velocities, tests with portable wind tunnel 79−70826
erosive action on sub-Antarctic Marion Island 80−31093
erosiveness in New Zealand, index 79−5579
error estimation of OMEGA-derived wind measurements 79−29916
error predictions for Omega stations, smoothing improvement factor 78−7719
escarpment wind profile 79−12217
estuary pollution model development, wind and freshwater flow influence 78−81207
evaporation calc. using measured wind, temp. and humidity profiles 77−17194
evaporation from Earth surface, wind influence *(Spanish)* 78−44965
extratropical cyclones, real-time wind meas. by Doppler radar, colour display system 78−61594
extreme wind speed probability, mixed wind climates 78−28295
extreme wind speeds, prediction from parent distrib. 77−56690
F_2-region neutral winds, Navier-Stokes eqns. *(French)* 79−35031
F-region, artificially-injected gases dispersal in night-time atm. 78−65460
F-region, high latit., equatorward neutral wind rel. to Fe^+ ions distrib. 79−16736
F-region, midlatitude wind source, energetic neutral atom precipitation 79−70913
F-region, neutral wind during dayside aurora 80−90273
F-region, neutral winds from ionosonde meas. of hmF2 at low latit. mag. conjugate regions 78−81477
F-region, neutral zonal winds rel. to interhemispheric ion transport 80−98509
F-region, zonal wind computed bounds during Joule heating 79−21084
F-region at night time, negative correl. of wind to elec. field 80−41603
F-region height neutral air wind, servo model of ionosphere 80−101486
F-region thermosphere wind, southward midnight surge obs. by Chatanika radar 77−33233
F-region wind affecting O^+ and H^+ equal ionisation level 80−90280
F-region zonal winds, estimation during Joule heating using incoherent scatter techniques 78−36344
fast gusts occurrence freq. inside corn canopy 79−100917
fields derived from dual-Doppler radar meas., error estimation 77−17171
fjord, Norway, wind-driven circulation 79−20848
fjord fronts, effects of winds and tides 79−57953
flow around tall buildings 78−36256

wind continued
flow field determination, comparison of interpolation methods for sparse data 80−51575
flow over isolated hill of moderate slope 80−12515
flow over surface obstructions, numerical soln. 77−33173
flow over wavy boundary, water waves 77−73792
force on windbreaks *(French)* 79−53418
forcing effect on infinite β-plane ocean model 80−4031
forecasting for offshore operations 79−2353
forecasting method for weather assoc. with western disturbances 79−100903
forecasting of surface winds, statistical method *(German)* 77−64475
funnel clouds, charcts. from obs. during sailplane flights 78−69396
gale damage, 1976 January 2-3, Lincolnshire, England 77−2207
galloping of rectangular prisms in smooth and in turbulent flow 77−75840
general circulation, interannual var. from northern hemisphere upper winds 77−25740
geomorphological processes, conf., Louvain, Belgium (Apr. 1976) 77−81923
Georgia shelf, current, temp. and coastal sea level response to atm. and Gulf Stream forcing 79−70804
geostrophic balance of horizontally periodic motions 79−39824
geostrophic correlation of initial geopot. and wind fields *(Russian)* 79−100899
geostrophic flow over shallow topography 80−90120
geostrophic wind field evaluation from Nimbus-6 soundings 78−53695
geostrophic wind speed rel. to momentum exchange, global maps *(German)* 78−44955
Germany, tower meas. of wind speed freq. distrib. *(German)* 78−16120
global ocean wind fields mapping using satellite scatterometer SeaSat-A 78−73529
global roughness length distrib. rel. to energy dissipation on ground *(German)* 77−64388
gravity wave induced wind field determ. using phase path meas. 78−16178
Great Britain, northerly gales of (1978 January 11 to 12) 80−12508
ground level and geostrophic frequency distribution, topographic influence 80−17346
ground level trajectory of diffusing cloud, wind vector turning effect 79−12232
ground level wind departure from geostrophic wind, effects of orography, stability and baroclinity *(German)* 79−66771
ground surface roughness change, affecting air flow charcts. 80−51501
Gulf Coast, USA, boundary layer speed and direction 80−101404
Gulf of Alaska, Seasat comparison data set 80−94570
Gulf of Alaska, SeaSat scanning multichannel microwave radiometer results 80−46248
N.Gulf of Alaska, wind stress rel. to coastal flow meas. by drogued drift buoys 80−51431
NE.Gulf of Alaska continental shelf, wind, current and bottom pressure 77−25741
Gulf of Alaska SeaSat Experiment 14.6 GHz scatterometer surface wind obs. 80−46200
Gulf of Genova, effect of low freq. winds on sea level and currents 80−8322
Gulf of Lions, wind-induced upwellings 79−79870
W.Gulf of Maine, wind rel. to gulf winter circulation 80−51430
NW Gulf of Mexico, near-bottom cross-shelf currents, response to wind forcing 78−3780
Gulf of St. Lawrence, wind-driven inertial currents in Magdalen Shallows 79−20845
gust front evolution and tornado genesis, Doppler radar obs. 77−91219
gust front of thunderstorm, wind shear meas. using pulsed lidar 80−67415
gust recorder, digital 77−56762
gusting effect on rain-induced polarization, theoretical model *(French)* 78−53678
gusts, local forecasting method *(German)* 78−85727
hail and crop damage, wind effects and hailcube meas. 77−17173
HAPP investigation for high-altitude platform operation feasibility 80−17369
Harmattan dust deposition, N.Nigeria, rel. to wind speed 80−94578
heat and mass transfer, wind-induced, over large bodies of water 77−11186
heat balance of upper ocean under light winds 78−69355
heat budget of upper ocean under light winds 77−41055
heat transfer of boundary layer with ocean, reef effects, AMTEX 1975 obs. 80−26567
S.Hemisphere polar front jet, prod. of ground level gravity waves in SE.Australia 78−73439
HF radio acoustic sounder, atm. wind and temp. remote meas. 78−32235
high-altitude wind measurement, radiowave drifts technique 80−31137
hill affecting airflow, in boundary layer, overspeed effect 80−72577
hill affecting turbulent diffusion from point source in stratified flow 80−56505
Himalaya, wind and storms during summer 80−72620
Holocene palaeo-winds, evidence from palynology in Baffin Island 78−57262
horizontal wind field in frontal system, determ. from single-Doppler radar 79−21057
horizontal wind meas., airborne system automatic calibration *(French)* 78−24386
horizontal wind profiles, comparison of Doppler radar and rawinsonde balloons meas. 78−44916
horizontal winds and temp. structure rel. to atmospheric tidal oscills. 78−20457
human hearing, wind noise expts. 78−92648
hurricane, barotropic ocean response 78−36191
hurricane and typhoon forecasting appl. of Kalman filter 77−64409
hurricane Camille, wind speed and direction, ocean wave height and barometric press. meas. 78−36254
hurricane dection by Doppler radar for coast of U.S.A. 80−67414
Hurricane Gloria, ocean wave patterns, obs. with airborne synthetic-aperture radar 78−44873
hurricane model-ocean model integration, mutual response 80−4032
hurricane over Arabian Sea, surface wind and sea waves 77−53159
hurricane sea surface wind speed, L-band radar backscatt. obs. 80−56561
hurricane season activity analysis, N.Atlantic (1886-1974) 80−101427
wind continued
hurricanes, forced secondary circulations 79−84387
hurricanes, interaction between symmetric mean vortex and shearing steering current rel. to spiral bands excitation 80−56538
hurricanes and tropical meteorology 79−39785
hurricanes in the USA, speed determ. by Monte Carlo method 80−90209
hydrodynamics, vertical eqn. of motion and wind eqns. 78−69428
immature cyclonic storm struct. in Bay of Bengal revealed by radar 78−85628
incoherent scatter results for co-ordinated special intervals at St. Santin (France) 79−2416
India, November 1977 Andhra Pradesh cyclone and associated storm surge 80−51499
Indian monsoon rel. to equatorial stratospheric westerlies 77−29370
Indian Ocean, equatorial currents during NE.monsoon 79−2270
W.Indian Ocean, low-level cross-equatorial jet stream 78−44959
W.Indian Ocean, METEOSAT obs. of low-level airflow 79−44222
Indian Ocean, monsoon effects on Somali Current 77−53063
W.Indian Ocean, SE. trades local vars. 78−32150
Indian Ocean, sea levels in western equatorial region rel. to tides, meteorology and ocean circulation 80−4018
Indian Ocean response to change of monsoon *(German)* 77−17138
Indian summer monsoon, influence of Arabian Sea 78−81333
Indian summer monsoon, oscill. with one month period 77−53118
Indian summer monsoon cyclogenesis and variability 78−81319
Indian summer monsoon meteorology 79−74938
Indian summer monsoon rel. to tropospheric flow patterns over southern hemisphere 78−81334
induced airflow caused by wind blowing over snow cover *(Japanese)* 78−88854
industrial aerodynamics, conference, Aachen 80−17712
inhomogeneity transfer velocity meas. by 10 cm radiowave propagation correlation *(Russian)* 78−77297
intertropical convergence zone cloud cluster, wind field behaviour 80−17322
intertropical convergence zone struct. over GATE area 78−57283
ionosphere, current and wind systems, influence of magnetospheric convection 77−5386
ionosphere, current and wind systems generation by motion of plasmasphere material 77−13161
ionosphere, equatorial, elec. fields generated by gravity wave winds 77−53283
ionosphere, equatorial, zero and maximal vel. contours rel. to mid-latit. absorpt. 80−12597
ionosphere, influence on drift of magnetically oriented inhomogeneities *(Russian)* 79−29926
ionosphere, inhomogeneities drift in geomagnetic field 79−88546
ionosphere, large-scale horizontal winds in presence of vertical rel. 77−78561
ionosphere, lower, wind obs. by Kyoto meteor radar 80−67444
ionosphere, meas. by self-contained tethered balloon sounding system 78−28343
ionosphere, midlatitude, dynamical model for 100-1000 km altitude range 78−53768
ionosphere, neutral wind rel. to enhanced O I 6300 Å prod. by ionospheric modification expt. 77−33263
ionosphere, nighttime equatorial, Rayleigh-Taylor and wind-driven instabilities 79−96855
ionosphere, polar wind profiles latit. var., Alouette II data 78−69588
ionosphere, semidiurnal winds seasonal var. in dynamo region 78−93033
ionosphere, tidal wind elec. field rel. to F_2-layer global electron-density distrib. 77−64514
ionosphere dynamo region, wind fields expansion rel. to electrostatic fields 78−36387
ionosphere EM wave absorpt. rel. to wind and temp. struct., winter 1975/6 obs. 80−36438
ionosphere tidal winds, mixing freq. components in electron content data 79−29929
ionosphere vertical wind causing equatorial counter electrojet 80−85795
ionosphere winds, rel. to geomag. field elements annual line component 79−20752
Iowa, wind-aligned drainage in loess 80−41467
IR Doppler wind-sensing system, spaceborne, atmospheric effects 79−96828
Irish Sea, backing of W. and N.W. winds rel. to differential heating 78−24340
island wind shadows, stable thermal stratification 77−45062
isolated convective storm, three-dimens. numerical model, variable ambient wind shear 79−5574
NW.Italy, large-scale winds rel. to coastal waters oceanographic conditions during 1977 spring 79−34827
Japan, fire tornadoes, max. wind speed estimation 78−36255
Japan, wind charcts., field obs. and lab expts. 78−36253
jet stream, different, theory 80−46242
jet stream, mesoscale var., Sunset 40 MHz Doppler radar obs. 79−53477
jet stream, VHF radar obs. 80−90187
jet stream and associated O_3 enhancement *(Russian)* 80−94568
jet stream generation of Kelvin-Helmholtz instability 80−90165
jetstream, correl. with ionospheric gravity wave obs. at S. hemisphere mid-latit. station 79−21096
Kamloops fjord lake, wind forcing of internal Kelvin waves 78−73411
katabatic wind model, hydraulic approach 80−17321
katabatic wind observations 80−56587
Kuroshio current, wind-stress curl. rel. to surface vel. vars. in East China Sea, (1956-75) *(Chinese)* 80−31049
Lagrangian and Eulerian fluctuations 80−41519
Lagrangian wind and current vectors very close to short-fetch windswept sea surface 80−72553
lake, variable depth circular model, time dependent response to wind stress 78−24320
lake, wind-induced circulation and water level changes, two-dimensional finite difference model 78−77287
Lake Balkhash, wind driven water level vars. 78−81237
lake circulation models, wind driving 80−85688
Lake Constance, heavy storms and wind strength and direction *(German)* 77−56695
Lake Erie, three-dimens. circulation, free-surface and rigid-lid models 79−20894
Lake Lebsko water level analysis and wind effects *(Polish)* 77−70708

wind continued
lake Michigan, W. shore, breeze circulation cell 79−88445
Lake Ontario, north shore coastal boundary layer response to storm 78−24322
Lake Ontario, wind-induced intermittent full upwelling 77−33110
Lake Ontario atmosphere turbulence, vel. and scalar statistics 77−33128
Lake Superior, coastal upwelling/downwelling cycles 78−44889
Lake Suwa, wind driven currents, obs., numerical calcs. *(Japanese)* 77−37254
Lake Tahoe, California-Nevada, surface wind stress rel. to coastal front 79−2301
Lake Vanern, Sweden, wind, fetch and water depth rel. to sediment distrib. 77−66934
lakes, circulation, seiches, tides and storm surges, finite element methods, book contrib. 79−34876
lakes, wind effect eqns., finite difference schemes 79−12163
lakes, wind effects on surface to bottom fronts 79−2261
lakes Langmuir circulations prod., controlled laboratory expts. 79−23330
lakes thermal structure, modified wind speed influence 78−11943
lakewide wind-driven circulation, numerical models 77−37243
land and sea breeze simulation along complex coastline 80−36364
land and sea breezes at Sepik River coast, Papua New Guinea 78−85642
land-breeze sea-breeze circulation asymmetry, comments 77−70784
land-sea breeze around island of Sylt 77−91236
Langmuir circulations, driven by wind, laboratory studies in wave tank 78−85582
laser beam propag. in evap. liq. drop medium, wind refr. 77−5322
lidar and anemometer meas. of wind vel., comparison 79−39885
lidar for global wind meas., computing simulation of satellite-borne equipment 79−58231
lidar velocimeter detect. of atm. aerosol flow 77−13127
Ligurian Sea continental shelf, wind and current autumnal data series anal. 80−85675
loading of large reflector antenna, structural design 78−57448
local climatic wind, use of trees as indicator 80−82007
local mesoscale circulation over Venice due to mountain-sea interaction 79−88401
local weather prediction, hydrodynamic methods 78−61521
London Weather Centre, urban influence on wind directions 77−73817
longitude dependent wind flow, stationary planetary waves propag. theory *(German)* 80−56526
longshore pressure gradients caused by offshore wind 80−67370
low-level air flow in central valley, Maui, Hawaii 79−20929
low-level jet, struct. investigations *(German)* 78−69422
lower atmosphere, VHF coherent radar sounding, wind and refractivity turbulence struct. 78−28281
lower atmosphere, wind and O_3 obs. (1976 January 5 to March 31) *(French, Flemish)* 77−33174
lower atmosphere, wind and O_3 vertical distrib. meas. (1977, April 1 to June 29) *(French, Flemish)* 78−11966
lower thermosphere, dynamical processes connection with troposphere and stratosphere processes *(Russian)* 78−24401
lower thermosphere gravity wave obs., 5-90 minute period 80−61930
lower trade-wind circulation, downstream variation 77−78381
mapping for windpower development programme in Sweden 80−61237
marine atmosphere, climatic comparisons of estimated and measured winds from ships 80−105020
marine atmosphere, mean wind speeds and turbulence 80−98406
marine atmosphere, wind vel. rel. to oceanic whitecaps and sea state 80−72554
marine surface wind, numerical prediction *(Chinese)* 80−46212
mass consistent atmospheric flux model (MASCON) for complex terrain regions 78−92964
mass consistent model for wind fields over complex terrain 78−92906
mathematical model for diagnosis and prediction of surface winds in mountainous terrain 78−3871
Mauna Loa Observatory, southerly airflow correl. with CO_2 record short-term disturbances 78−88879
maximum wind speeds, calc. from parameters of truncated distrib. curve *(Russian)* 77−53157
mean direction, influence on sea surface wave development 79−48511
mean zonal circulation in meteor zone above France and Sweden 79−75003
mean zonal wind in middle atmosphere, calc. from numerical model of zonal mean circulation 80−109218
meanflow-gravity wave interaction, indication in upper atmosphere radar obs. 78−81282
measurement, continuous, using VHF Doppler radar, preliminary results 80−8444
measurement by tethered aerodynamically lifting anemometer for WTG siting 80−48830
measurement in severe storms using airborne pulsed Doppler lidar system 79−66812
measurement via sea wave measurement using HF radio scatter 77−25789
measurement with propeller vane devices, dynamic props. 80−31138
meridional geostrophic wind along 50°N 80−101399
mesopause, prevailing wind altitude-latit. struct., 80-100 km altitude 79−29829
upper mesopause region, wind systems behaviour in winter and winter/summer conditions transition 79−44220
mesopause wind from ionospheric drift meas., geomagnetic storm effects 79−35025
mesophere, mag. storm effects at mid-latitudes 80−61970
mesoscale downdraughts, assoc. with cool ocean surface waters, GATE results 78−69365
mesoscale flow over complex terrain during Eastern Tennessee Trajectory Expt. (ETTEX) 78−49101
mesoscale intense convective storm, Oklahoma, objective anal. 78−32168
mesoscale trade wind field, role of advective acceleration 77−70793
mesoscale wind circulation in land-sea breeze 78−65354
mesoscale wind fields, satellite-derived, covariance anals. 80−82013
mesoscale wind radar mapping, receiver bandwidth effect on refl. and Doppler vel. estimates 79−53549
mesoscale winds aloft, numerical prediction models, verification 78−16110
mesosphere, comparison of neutral winds determined by rocket techniques with partial refl. drifts 77−87019
mesosphere, equatorial, waves and winds over Jicamarca from multiheight radar obs. 78−36230

wind continued
mesosphere, Southern hemisphere, wind speed quasi 2-day wave obs. 80−109207
mesosphere, wind systems behaviour during transition from summer to winter conditions 78−49097
mesosphere, wind variance rel. to eddy diffusion models 80−109198
mesosphere, winds and waves over Jicamarca, 1974 May 23-24 VHF radar obs. 80−12497
mesosphere, winds rel. to mid-latit. internal gravity waves 77−5298
mesosphere neutral winds, incoherent scatter spectrum meas. in 60 to 90 km region 79−16569
mesosphere periodic temp. and wind fluctuations 77−78361
mesosphere winds at equatorial latits., observational aspects review 78−36229
mesosphere zonal wind obs., long-period waves at 60-90 km altitude 80−77056
meteor region winds, periodic fluctuations of recurrent nature 80−90266
meteor region winds at 45°N latitude, 95 km altitude 80−46330
meteor trail distortion studies 80−85870
meteor trails, atmospheric ambipolar diffusion coeff. meas. errors 78−88952
meteor wind, oscills. rel. to travelling quasi 2-day wave 78−81480
meteor wind automatic meas. set, drift obs. accuracy *(Russian)* 77−41248
meteor wind automatic meas. set, programming and systems interaction *(Russian)* 77−41247
meteor wind data, tidal winds and poleward momentum transport 80−12581
meteor wind data for global comparisons 79−2413
meteor wind profile comparison with electron density obs. 77−9587
meteor wind radar, semiautomatic display and photographic recording system 79−8712
meteor winds over Sheffield, radar obs. 79−2415
meteor zone, wind height struct. by statistical method *(French)* 80−51589
meteor zone wind speed and O I 5577 Å airglow wave vars. 79−62637
meter, digital, speed and direction indication 80−207
microprocessor-controlled 64-cell pulsed optical receiver for crosswind sensing 77−18096
microwave link cross-polarisation effects 79−66736
microwave radar for wind meas. 77−33195
microwave radar measurements in clear air 77−13136
middle atmosphere, VHF radar obs. 80−105032
minimum wind stress for wave inception 78−57285
Mistral over Gulf of Lions, turbulent surface layer structure *(Russian)* 79−39734
Mohliner Feld (east of Basle), influence of wind on topoclimate *(German)* 80−61890
MONEX, monsoon experiment 1979, objectives 79−8665
monitoring by remote automatic station on radio link 78−85726
monostatic Doppler sodar system, meas. method, wind obs. appl. *(German)* 79−16710
SW monsoon, effect of waves in equatorial stratosphere 79−8664
monsoon, horizontal wind effects on moisture eqn. in digital simulation of evaporation phase 77−56712
monsoon depression, Bay of Bengal, tropospheric vertical wind shear 79−8670
monsoon depression formation, effect of wind shear 79−84461
monsoon depressions, life history, struct. and movements 78−44963
SW.monsoon over India, onset and northern limit 78−49102
monsoon reversal effects on Somali current 78−92833
monsoon squalls over Goa, India 79−48546
monsoon system oscillations, spectral anal. of obs. records 77−33148
monsoons and Indian Ocean equatorial currents variability, modelling *(Russian)* 78−44839
morning evolution of wind profile, semi-empirical model of evolution *(French)* 79−84399
Mount Kenya, wind speed rel. to condensation nuclei concs. 80−82012
mountain drag meas. 79−53452
mountain in airflow, 2-D numerical simulation *(Russian)* 80−81986
mountain waves and severe downslope windstorms, theory 80−56551
mountain-assoc. infrasound, source mechanism 77−78324
multimodal Doppler spectra in terms of sub-beam scale motions 77−29385
near water atmospheric layer, mean wind vel. meas. 77−9461
neutral atm. disturbances, reaction of midlatit. ionosphere 77−25805
neutral atmospheric motions effects on two-stream irregularities in equatorial electrojet 79−16742
neutral upper atmosphere, density, temp. and winds 79−75006
neutral upper atmosphere, magnetospheric convection effects on global wind field 77−29525
neutral wind in upper atmosphere, rel. to magnetospheric disturbances in aurora borealis zone *(Norwegian)* 78−24399
neutral wind obs. during equatorial electrojet 77−45210
neutral wind profile following surface roughness change, calc. 78−73483
nighttime thermospheric winds at high latitudes 79−74999
nocturnal jet at dawn 78−20479
noise abatement acoustic barrier performance, scale model studies of effects of wind 77−23806
nongeostrophic winds, excitation of atmospheric Lamb waves, obs. 77−45085
nonlinear wind-wave system, model and expt. 79−34846
nonuniform shear effect on mountain waves refl. and intensification 80−90127
North Sea, wind fields during gales 78−96272
North Sea, winds rel. to sea surface temp. year to year changes, (1948 to 1974) 80−67367
northern hemisphere, stratosphere, winds for 1957-65 period 78−24350
nuclear power stations, tornado missile hazard, synthesized windfield model 79−31239
numerical prediction, methods and results 78−69393
observation system, low latit., First GARP Global Expt. 79−39983
ocean, advective mixed-layer model with imposed surface heating and wind stress 80−12395
ocean, Langmuir circulations and wind drift currents, Langmuir vortices, struct. 77−49074
ocean, local wind stress curl rel. to Cayman Sea and Gult of Mexico circulation 79−48495
ocean, monomolecular slicks drift response to wind and wave action 78−69364

wind continued
ocean, two-layer, stable wind-driven equatorial currents theory *(Russian)* 78−61427
ocean, underwater, wind noise ambient levels, freq.-freq. correls. 77−64302
ocean, wind circulation in two-dimens. dynamical model *(Russian)* 78−40557
ocean, wind driven currents in inshore region deep water 80−81925
ocean, wind effects on surface to bottom fronts 79−2261
ocean, wind field variability relationship with internal waves 80−31052
ocean, wind long-term fluctuations rel. to ocean nonlinear coastal and equatorial jets 80−51427
ocean, wind speed meas. 200 km from land rel. to air-sea heat transfer coeffs. 80−72552
ocean, wind stress and buoyancy flux effects on continental shelf circulation 80−72540
ocean, wind vel. rel. to distrib. and steepness of ripples on carrier waves 80−72548
ocean, wind-driven flow in zonal channel with stratification and bottom topography 80−51402
ocean, wind-induced turbulence energy distrib. rel. to mixed layer evolution *(Russian)* 80−94529
ocean baroclinic Rossby waves generation by meteorological forces 77−86916
ocean boundary layer wind flow, determ. from phase speeds of upwind and downwind travelling waves 80−98332
ocean circulation, modelling expts. with wind stress 79−57952
ocean circulation driven by wind, finite element anal. 80−56487
ocean continental shelf wave forcing in Florida current 77−73758
ocean current flow, wind-induced, in upper Hudson Shelf Valley 79−34840
ocean current flow at planetary boundary layer, wind induced, temp. profiles, model 80−26526
ocean current regime in Gulf of Kutch, NW.India 78−36184
ocean currents driven by large scale atmos. disturbances 80−109159
ocean drift currents, Langmuir circulation, theory and averaged current 77−37210
ocean dynamic response to atm. disturbances 77−13084
ocean forcing, mixing mechanism in upper ocean, Langmuir circulation instability 80−104970
ocean gravity wave growth by modulated wind stress 77−17119
ocean inertial oscills. radiation damping, wind mixed layer turbulence 79−39730
ocean interaction, wind-driven equilib. Langmuir circulation model 80−101381
ocean internal wave generation by advecting atmospheric fields 77−53066
ocean internal waves generation, exptl. study *(French)* 79−62518
ocean oil spill trajectory modelling, wind and current forcing functions 79−5509
ocean over North America eastern continental shelf, wind stress meas. 78−3776
ocean ripples, wind-generated, gravity waves effects, Doppler meas. 77−62264
ocean storm wave heights, statistical distrib. 78−73390
ocean surface, heat flow conditioned by wind pulsations *(Russian)* 77−60414
ocean surface, microwave emission at 37 GHz, wind effects 80−12414
ocean surface, microwave radiometric determ. of wind speed during BESEX 77−29479
ocean surface, radar backscatter rel. to wind speed and fetch 78−77247
ocean surface, speed determ., microwave radiometric meas., Bering sea expedition 77−17158
ocean surface, speed meas., SeaSat-A scatterometer 77−29626
ocean surface, wind stress and roughness length over breaking waves 78−24299
ocean surface intrusions, fronts and internal waves, wind stress effects 79−2262
ocean surface microwave emissivity, model of wind roughening 80−46184
ocean surface mixed layer, energy and momentum transfer by wind 78−44856
ocean surface wind and pressure fields during TROPEX-72 near Equator 77−37320
ocean surface wind and waves, radar meas. techniques 78−81418
ocean surface wind field mapping, high-resolution, skywave radar 77−17159
ocean surface wind obs., SeaSat scatterometer/scanning radiometer/altimeter comparison 80−46249
ocean surface wind speed, meas. via microwave radiometry 78−81415
ocean surface wind speed meas. from HF sea scatter by skywave radar 77−17160
ocean surface wind wave related turbulence meas. by impellor current meter array 80−46301
ocean surface winds, HF radio obs. 78−77241
ocean upper layer, conc. and size distrib. of wind-produced air bubbles 77−17143
ocean wave prediction using parametrical wind-sea model 80−17272
ocean wave radar monitoring, ground wave and sky wave sensing techniques 80−109256
ocean waves directional spectrum, new meas. method, description 79−16706
ocean waves directional spectrum, new meas. method, lab. wind waves meas. 79−16707
ocean waves growth and var. for weak wind, linear theory *(Russian)* 79−16475
ocean waves travelling against wind, HF radar obs. 78−77242
ocean wind forcing variations, sea surface temp. response 79−48505
ocean wind wave elevation sensor array system 80−46322
ocean wind wave generation in water of finite depth 77−64314
ocean wind wave period and height forecasting at Digha, India 77−53064
ocean wind waves, directional slope and curvature distribs. 77−31316
ocean wind waves generation theory, dynamical eqns. *(Russian)* 78−44840
ocean wind waves growth stochastic form. 79−16499
ocean wind-driven circulation, effect of islands and depressions 78−3799
ocean wind-driven circulation effects of bottom topography *(Polish)* 77−73743
ocean wind-driven currents, bottom friction 77−13089
wind continued
ocean wind-driven quasigeostrophic water movements near fast ice edges 78−49026
ocean wind-generated linear and nonlinear Kelvin waves along irregular coastline 78−11908
ocean wind-generated surface waves, HF spectrum meas. 78−44857
ocean wind-generated wave profile, transform. of wind rel. profiles and drift current *(Russian)* 78−61429
ocean wind-generated waves, power spectrum, wave height calc. *(German)* 77−17137
ocean wind-waves in finite water depth, freq. spectra *(Russian)* 78−44843
ocean-atmosphere interaction parametrisation for storm conditions, atm. circulation models appl. *(Russian)* 78−65359
ocean-atmosphere system, interannual variability 79−2330
oceanic boundary layer, effect on pack ice drift, model 80−26528
oceanic coastal upwelling frontogenesis, simulation, isopycnic coord. model 79−34843
oceanic eddy formation in Somali Current, wind effects 80−26523
oceanic wind fields, high resolution mapping using skywave radar 77−29480
oceanic wind speed and stress estimation from ambient noise meas. 79−74963
oceanic wind speed meas. using HF skywave radar sea scatter 77−29481
oceans and lakes, Langmuir circulations, generation by instability mechanism 77−64304
oceans Langmuir circulations prod., controlled laboratory expts. 79−23330
off-shore meas. by HF Doppler ground-wave radar 78−77295
offshore wind power model estimates 80−61244
Okhotsk Sea, wind rel. to pack ice drift radar meas. *(Japanese)* 78−96224
Okhotsk Sea coast of Hokkaido, wind rel. to ice field divergence and rot. meas. *(Japanese)* 78−96223
Ontario air poliution incidents and wind variability 79−70822
optical scintillometer, finite aperture, for profiling wind and refr. index struct. parameter 79−25331
optical wind and precipitation sensors *(Japanese)* 78−16207
Orange Lake, Florida, wind vel. fluctuations rel. to lake latent and sensible heat fluxes prediction 80−72562
Oregon Coast, wind and current data, rotary cross-bispectra and energy transfer functions 78−44858
Oregon-Washington continental shelf, ocean barotropic response hindcast during 1972 summer 79−48497
orography, influence on atmospheric movement with Coriolis force included *(Russian)* 80−94565
overdetermined windfinding systems, error anal. 80−17399
Pacific, E.equatorial, long wave obs. from geostationary satellite, rel. to SE. trade winds 78−24308
N.Pacific, South China Sea and Indonesian Seas, regional energetics during winter 78−44960
N.Pacific, wind drag and relative separations of undrogued drifters 79−79866
NW Pacific, wind-wave tropical cyclone model, parametrisation characts. 78−24301
N.Pacific and N.Atlantic, wind field temporal and spatial scales 79−79942
Pacific interior wind stress changes rel. to El Nino 77−17124
Pacific Ocean, equatorial, easterly wind stress rel. to 14°C isotherm slope annual var. 80−72537
N. Pacific Ocean, interior midlatit., main thermocline seasonal cycle, wind driven model expt. 79−48499
N.Pacific Ocean, tropical, wind forcing of annual Rossby wave 80−51421
Pacific Ocean, wind forcing rel. to oceanic circulation around New Zealand 80−72538
tropical Pacific Ocean, wind rel. to thermocline displacement, simple Ekman-type model 79−48498
N Pacific Ocean, wind stress fluctuations rel. to water temp. anomalies vertical struct. 78−73394
Pacific trade wind fields, time and space scales, 1950-72 period 77−70754
Paradip Coast, India, surface wind directions rel. to wave characts. 80−41450
particulate pollution in Delhi due to Indraprastha power plant 79−21000
Pasquill stability classification for coastal site 79−16610
passive remote crosswind sensor 78−7773
Peruvian oceanic upwelling system near 15°S, wind obs. 80−101377
Philippines, high wind study 78−36257
photochemical oxidant transport, mesoscale lake breeze and synoptic-scale aspects 77−2232
planetary boundary layer, 3-D field obs. width radar 80−90183
planetary boundary layer at Tamara Island wind structure, balloon obs. 77−45052
point discharge current, effect of windspeed 79−88409
polar F-region, winds and drifts 77−33274
polar ionosphere, neutral winds and ion drifts 77−87173
pollutant dispersal, Gaussian plume model parameters for ground-level and elevated sources 80−82010
pollutant trapping by local circulation, obs. 77−37397
pollutants concentration equation, wind speed averaging 78−57307
pollutants long distance transport, time-averaged wind field for analytical diffusion model 80−94125
pollution of industrial area, occurrence affected by wind direction 80−89691
pollution transport, air quality models development for limited wind fetch 80−104533
power calc. and monitoring 77−33171
power from wind and Sun, meteorological aspects 78−36250
power resources, statistics 77−70765
power transmission lines, mathematical model for aerodynamic forces, and aeroelastic appls. 77−62270
pressure, omnidirectional probe *(French)* 79−25349
pressure data acquisition system, microprocessor based 79−70888
pressure distribution variations in geostrophic wind 80−17348
pressure field, use in solenoidal wind velocity component, forecast 80−82034
principal components analysis of vector wind measurements 79−39807
probe for static pressure sensing in 2D flow, wind effect on buildings 79−71403
profile determ. X-band solid-state radar system 78−12028

wind continued
profile meas. disturbance by slim mast 77−73790
profile power-law exponent var. as function of surface roughness and stability profile power-law exponent var. as function of surface roughness and stability 79−88387
puff pollutant dispersion model with wind shear and dynamic plume rise 79−57996
quasibiennial oscillation, an unusually large westerly amplitude 79−88439
radar backscatter from water waves, induced current effects on microwave backscatter, expt. 77−25688
radar detection of wind shear, for airport use 80−51565
radar determination of winds at sea 80−26644
radar observation of vertical component of lower atmos. wind 80−72642
radar reflectivity variations with height due to wind shear on rain cells *(French)* 78−53682
radar technique for tropo- and stratosphere wind measurement 80−90257
radio meteor wind data, anal. using finite element approximation 78−81475
radio meteor wind facility at Christchurch, New Zealand 79−2387
radio meteor wind meas. over Atlanta 79−2411
radioactive dust captured by wind from Earth's surface, radioactive fallout *(Russian)* 80−16869
radioactive release, cloud dose data file fast correction for changes in dispersion parameters 78−80969
radiotheodolite windfinding system of USA National Weather Service 80−17379
radiowave propagation, raindrop canting angle as function of wind velocity, crosspolarisation 78−3855
radiowave wind obs. of waves during 1976 over Saskatoon 79−79935
recorded obs., freq. isopleth diagram 77−73892
remote forcing of Somali Current, cross-equatorial inertial jets model 79−88357
remote measurement of wind speed, single particle correlation by laser backscatt. 77−91302
remote measurements, individual particle scatt. and single-burst digital correl. 79−100980
remote probing by line-of-sight MM wave and optical methods, spatial filtering concepts 80−36426
remote sensing, laser beam wave case, book contrib. 79−34959
remote sensing from Earth orbit using microwave technique 80−41573
remote sensing in Irish and Celtic Seas using MF radar 79−16725
resistance above hilly terrain, universal functions in resist. law 77−25732
Riso, Denmark, 1975 direction fluctuations 77−53148
rivers, wind effects on stream flows 77−21808
Rock of Gibraltar, wind-tunnel simulation at 1:5000 scale, compared to meteorological meas. 78−28284
rocket sounding methods since World War II 80−17398
Rome, effect of urban heat island on wind flow during summer season 80−85717
Ronsard radar for investigation of vertical rising winds *(Dutch)* 78−81447
rough surface affecting momentum transfer of flow 80−51511
rough terrain mass-consistent flow fields, derivation method using wind obs. 80−105013
runner's forward motion, effects of wind assistance and resistance 80−101204
Sahel rainfall 1975-6, D, T and ^{18}O evidence and regional winds *(French)* 80−21809
Sahel region, general and regional circulation effects on climate *(French)* 79−20962
saltation, Magnus effect, lab. expt. 77−70764
sand barrier beach shoreline accumulative section, protective dune ridge morphodynamics *(Russian)* 80−36287
sand barrier beach shoreline transit section, protective dune ridge morphodynamics *(Russian)* 80−36286
Santorini (Thera) eruption, 1450 BC, evidence for northwesterly winds from tephra discovery at Rhodes 80−109129
Scotian shelf (N.Atlantic Ocean), wind-induced sea level changes 80−72531
sea and land breeze obs. over Goa, India 78−32155
sea and land breezes direction rot. rate 78−69408
sea breeze, numerical results, truncation errors 79−10447
sea breeze circulation over Bombay 78−32160
sea breeze forecasting at Eskmeals 78−69418
sea breeze fronts, inland penetration in England 77−45103
sea breeze numerical model, heat convection parameterization 79−12223
sea breeze occurrence in hilly terrain, Wales 77−78388
sea breeze over gulf or lake, numerical model 77−49115
sea breeze rel. to pollution over gulf region 78−11977
sea ice, wind stress meas. *(Japanese)* 78−88842
sea level nonperiodic vars. of synoptic freq. on tidal sea shelf *(Russian)* 78−65320
sea level oscillations, low-freq. wind-induced, along N.America east coast 79−84286
Sea of Azov, storm surges calc. 78−96231
sea state, surface wave prediction model for varying wind fields 80−12408
sea state and wind sensing by HF skywave radar 78−24396
sea surface, wind-ruffled, isophotes of sunlight glitter 77−45001
sea surface drift induced by wind and waves 80−81914
sea surface effects of wind near Belgian coast *(French)* 78−65372
sea surface reflection of radar signal, spatial intensity fluctuations 80−109170
sea surface signal interpretation and energy transfer calc. 78−28241
sea surface stress measurements 79−66701
sea surface tension variability with mean wind speed 78−7656
sea surface velocity meas., microwave radiometer for Nimbus-G and SeaSat-A 77−29625
sea surface wind fields, SKYLAB 1.4 GHz radiometric meas. 78−65338
sea surface wind speed, retrieval from scanning multichannel microwave radiometer obs. 80−90261
sea surface wind speed and significant wave height measurement using pulsed radar 77−29477
sea surface wind-driven flow 80−46187
sea surface wind-generated waves, elevation, vel. and accel. statistical distrib. 77−25695
sea temp. microwave radiometry, effect of wind, obs. at 2.65 GHz at Chesapeake Bay 77−29314
sea waves influence on wind profile 78−92895
wind continued
sea waves interaction, similarity theory appl. *(Polish)* 77−21795
sea-breeze front passages at Cambridge, England 78−44973
sea-surface, radar backscatter meas. at 13.9 GHz from Skylab 77−91304
sea-surface wind stress determination using SEASAT-A microwave scatterometer, algorithm 79−39883
SEASAT-A satellite microwave scatterometer for wind sensing 77−5417
seasonal var. of semi-diurnal neutral wind components 77−70895
sediment movement behaviour effects *(French)* 77−78151
sediment transport during dust storms, Slims River Valley, Yukon territory 79−5552
semiannual zonal wind oscillation, westerly phase, role of Kelvin wave 79−88429
semidiurnal tide in the meridional wind at F region heights at low latitudes 79−53596
severe thunderstorms internal struct., dual-Doppler radar meas., tornado generation 78−61504
shallow sound, energy balance and wind effects 79−2243
shallow water basin, wind-driven current, eddy viscosity, bottom friction 78−65319
shallows of water body, wind-induced currents *(Russian)* 77−29329
shear, effect on acoustic backscatter in GATE 80−85709
shearing instability mechanism model, effect of horizontal differencing 80−26578
shearing up to 700 m rel. to daytime and diffusion class *(German)* 78−44954
shelf waves with wind-generated effects, resonant interactions 78−44835
shoreline escarpment affecting boundary layer turbulence, wind profile etc. 80−109243
Sierra Leone, monsoon characts. 78−7693
Simpson Lagoon, Arctic Ocean, wind and current patterns 77−37237
simulation, air jets perpendicular to wind-tunnel stream 77−56691
simulation in Oxford University wind tunnel 78−22443
simulation in wind tunnels, roughness element geometry anal. 78−47079
slopewash and wind action, Quaternary morphogenesis in Belgium 77−81924
SMS images during GATE, wind field determ. accuracy 77−53147
snad grain surface texture rel. to wind vel. conditions 80−41443
over snow surface, effects on Pb and sulphate deposition vels. 77−2231
snow surface and wind interaction 79−84356
Snowdonia, anabatic wind 79−100934
soil erosion, wind tunnel simulation, effects on fine dust production 79−20834
solenoidal wind velocity component, forecast from known press. field 80−82034
Somali coast, wind stress, spatial and temporal var. 78−49092
Somali jet, planetary boundary layer model 80−72591
sound measurement affected by rain and wind in trees 79−76926
sound propagation outdoors, effect of wind speed distrib. *(Japanese)* 79−1018
Southern Ocean, wind stress and bottom topography effects in two layer model 78−81181
southern trade winds, rel. to oceanic upwelling processes during last 75000 years 78−57217
space-time kinetic energy spectra in mid-latitudes 78−7707
spectra determ. from propeller anemometer and thermistor meas. *(French)* 79−16708
spectral kinetic energetics, diagnostic study 77−41117
speed, freq. distribs. of hourly meas. 80−94554
speed, interannual and monthly vars. 80−51490
speed, rel. to maximum sensible heat flux in stable boundary layer 80−17345
speed and direction from automated environmental monitoring system 80−81513
speed and direction meas., pulse height analyser appl., automatic distrib. meas. system 79−96839
speed and direction meas., review of cup, propeller and laser anemometers 80−90264
speed and direction meas., using digital anemograph *(Czech)* 80−77174
speed and direction prediction, empirical eigenvector method *(German)* 79−34924
speed and direction prediction, statistical analysis of ground wind vector 80−17347
speed and direction prediction using empirical eigenvector method *(German)* 77−87030
speed and temp. profiles over melting glacier, log-linear model fitting 79−79912
speed anomaly in surface layer in Po Valley 80−17313
speed freq. distrib. determ. for lowest 200 m 79−21052
speed frequency distrib. near surface 79−79946
speed frequency distrib. using monthly average and fastest mile data 77−78331
speed from Geos 3 data 80−4079
speed in cloudy atm., long distance meas. by radiometry 80−90196
speed intensity distrib. anal. using pulse height analyser 78−88937
speed limits to work under hot enviornments for clothed men 80−8030
speed meas. from orbit using lidar system 80−4114
speed measurement using laser velocimeter 78−32251
speed near ground, spectral anal. 78−11950
speed remote meas., single-particle correl. techniques, aerosol condition, meas. rate 79−62609
speeds in stable boundary layer 77−73786
speeds required to drive splinters into wood during tornado 77−17174
sporadic-E layer, electron density explained by wind shear acting on metallic ions 80−46338
sporadic-E layer, equatorial formation, electric fields and neutral winds effect 78−12045
squall line formation, nonlinear process 78−81323
squall lines, radar obs. during GATE 78−20474
St. Louis, urban-rural wind differences, tower meas. 80−51487
St. Louis downwind plume, thermodynamic props. and aerosol patterns 79−16603
stability category determ. for airborne radionuclide release assessment 78−73504
stability classification schemes applied to non-homogeneous terrain coastal region 80−8379
stationary planetary waves and zonal wind, southern hemisphere 78−28276
steady wind incidents rel. to air quality management in Pittsburgh 77−49155

wind continued
steering wind rel. to precipitation line orientation 77−45093
steppe meteorology, boundary layer universal profiles in rainy season *(German)* 79−84420
stochastic predictors of site wind, AR and ARMA models 80−67400
storm surge prediction at Milford Haven, wind-induced motion models 79−66743
storm turbulence, characts. near top of spruce forest 80−17349
storms, wind-wave height max. in storm, determ. 79−12125
stratified flow around three-dimens. barrier 80−48769
stratified fluid density interface, wind-wave interaction 77−62291
stratified inlet, anal. of wind influence on surface layer 77−41051
stratified inlet, obs. of wind influence on surface layer 77−41050
stratified lakes, temp. distrib. seasonal var., two-dimens. model, wind-induced currents effects 77−29327
strato-mesosphere, seasonal relation with LF radiowave absorpt. 79−62645
strato-mesosphere dynamics, rel. to medium and short radiowaves seasonal absorpt. courses 79−58149
stratosphere, annual and semi-annual waves obs. using Nimbus 5 selective chopper radiometer data 78−81315
stratosphere, correl. with mesospheric electron densities and drifts 77−9470
stratosphere, diurnal variation of wind and temp. in equatorial region 80−82022
stratosphere, internal waves interaction with mean flow, rel. to quasi-biennial oscill. 78−69404
stratosphere, lower, power spectral anal. of meteorological data 78−40616
stratosphere, lower, winds, full-day radar meas. over Jicamaca 79−25308
stratosphere, periodic temp. and wind fluctuations 77−78361
stratosphere, seasonal climate, numerical simulation, zonal temp. and wind 79−5566
stratosphere, temperatures and geostrophic winds during 1973-74, Nimbus 5 radiance meas. 79−79976
stratosphere, tropics, upper winds, data clustering technique 77−91225
stratosphere, vertical wind shear from Lagrangian wind field obs. 80−82032
stratosphere, warming of 1976-77, temp. and wind fields 77−56699
stratosphere, wind monitoring using Concorde-generated infrasound 80−51492
stratosphere, zonal mean winds vars. rel. to planetary wave props. and links with troposphere 80−109225
stratosphere, zonal wind cycle in southern hemisphere 79−79977
stratosphere, zonal wind speed oscills., solar cycle influence 80−94562
stratosphere, zonal wind speed rel. to long wave characts. 77−5296
stratosphere, zonal winds effect on Earth rot. 80−81804
stratosphere and mesosphere, UHF radar echoes, for wind and turbulence obs. 77−33135
stratosphere and mesosphere, wind and temp. diurnal and semidiurnal oscills., rocket meas. 79−5556
stratosphere and mesosphere winds, 20-80 km 1975/6 obs. of W.Europe 80−36359
stratosphere wind phenomena affecting troposphere circulation pattern 80−82021
stratosphere zonal winds variation, correl. with 27-day solar rot. 78−88878
stratospheric warming, 1976-77, dynamical development 79−79968
stress over sea surface for short fetches *(German)* 79−29808
strong gales in E.Atlantic region, jet stream effects in subtropical latits. *(Spanish)* 78−44966
strong wind shear, obs. using pulse compression radar 78−32193
subsoil behaviour in Potsdam rel. to storms and atmospheric pressure *(German)* 79−62425
summer monsoon circulation aspects 80−8413
summer monsoon over S. Asia, break and active phases 78−3912
summer monsoons over Africa and India, comparison 78−32149
Sunray tornado, photographs showing evolution 77−25731
surface air flow, in influence on geoelectrical field obs. at North Pole-22 drifting station *(Russian)* 79−48537
surface flow over equatorial oceans, dynamics and climatology, 1911-70 period 79−58061
surface gravity wave, wind-wave generation, bispectral contrib. 78−49033
surface layer, discrete turbulent gust concept 78−44907
surface layer, drag coeff. rel. to intermittent convection 78−44898
surface layer wind profile curvature rel. to Richardson number 80−81974
surface ocean current response, quadratic and linear laws 80−26529
surface speed over drifting pack ice from surface weather charts 80−41476
surface stress estimation, mathematics of vel. scaling parameter 80−61849
surface waves, wind-generated in deep water, Rayleigh method *(Russian)* 78−36178
surface wind, algorithm for wind speeds using Geos 3 measurements 80−4078
surface wind at Trawsfynydd Power Station, N.W.Wales, rel. to topography 77−60440
surface wind field over ocean, evidence for S_3 atmospheric tide 78−44911
surface wind of Arizona cool season, correl. to press. gradients 80−98379
surface wind over ocean, horizontal divergence and vertical vorticity 77−81974
surface wind speed data, appl. to hourly mixing depths estimation 80−51482
surface wind speeds run duration anal. for energy appl. 79−100916
surface wind strength estimation methods 79−88392
surface wind time series statistical structure 77−78370
surface winds, small-scale, vars. over water surface, computation model 78−61480
surface winds, topographic influence 78−81266
surface winds of Alaska, mountain barrier baroclinity effects 80−90118
suspended dust deposition, wind speeds and particle concs. 78−40623
symmetric instability of stratified geostrophic flow 80−98425
synoptic windfinding, satellite imagery of cloud drift 80−17397
synoptic windfinding technique, Loran and VLF navaids used with radiosondes 80−17392
synoptic windfinding using Omega VLF navaid, atmos. radiowave propag. 80−17309
synoptic windfinding using tropical constant-level balloon system 80−17395
tethersonde system for remote meas. of wind and temp. 79−80038
tetraalkyllead in air, depend. on wind direction rel. to natural source 79−2367
thermosphere, circulation systems, northern hemisphere, 80-100 km altitude 78−81481
thermosphere, diurnal vars. in temp., comp. and winds 77−87141
thermosphere, eddy diffusion vars. and assoc. transport processes 77−33226
thermosphere, electric field momentum coupling characts. 78−88958
thermosphere, equatorial, neutral winds determ. from O I 6300 Å nightglow Doppler shifts 78−81473
thermosphere, excitation of transverse motions of ionospheric atomic and mol. ions 77−13155
thermosphere, gravity waves and winds *(French)* 77−53256
thermosphere, ion-drag effects 80−17432
thermosphere, ionospheric model effects on horizontal wind calcs. 78−36345
thermosphere, large-scale waves, obs. during mag. storms 79−35021
thermosphere, lower, dynamics, incoherent scatt. radar technique appl. 79−8734
thermosphere, lower, mid-latitude winds meas. *(Russian)* 78−36340
thermosphere, lower, wind regime rel. to stratospheric and mesospheric processes 78−4019
thermosphere, lower, wind variance field rel. to eddy diffusion models 80−109198
thermosphere, mass spectrometric meas. 78−28359
thermosphere, meridional wind and O depletion at high latitudes 78−28353
thermosphere, meridional wind divergences at midlatitudes 79−70901
thermosphere, mid-latitude, lower, winds meas. 79−53587
thermosphere, midlatitude F-region winds and temps. during 1976 March 26 magnetic storm 79−53594
thermosphere, midlatitude winds rel. to storm time disturbance change rate 79−12323
thermosphere, N Polar Cap winds 80−67445
thermosphere, neutral wind response during August 1972 mag. storms 77−25858
thermosphere, nighttime, energy balance 79−35022
thermosphere, nighttime, winds rel. to neutral atmosphere parameters var. *(Portuguese)* 80−41584
thermosphere, nighttime meas. during mag. storms 77−9585
thermosphere, nighttime winds from Atmosphere Explorer C 78−28354
thermosphere, O_2 thermal and wind-induced var., AE-D meas. 79−53592
thermosphere, O global distrib., dynamical effects 79−74996
thermosphere, polar, wind vel. meas. by using artificial luminous clouds, disturbed and quiet times 79−62634
thermosphere, seasonal var. of diurnal winds over Millstone Hill during solar cycle max. 77−53267
thermosphere, temps., wind vels. and emission intensities from O I 630 nm airglow 79−58144
thermosphere, temps. and winds from O I 630 nm line profiles in nightglow 79−58143
thermosphere, tidal struct. at equinox, temp. and vel. fields predictions 78−81476
thermosphere, tidal winds in 100-200 km altitude region, Arecibo obs. 77−82074
thermosphere, vertical winds and turbulence from Ba cloud release over Thumba 78−49188
thermosphere, wind enhanced thermal escape, collisional modifications 77−49204
thermosphere, wind flow directions from ionosphere nighttime total electron content meas. 77−25829
thermosphere, wind regimes rel. to turbopause altitude vars. during night 77−78548
thermosphere, winds and temps. determ. from ionospheric obs. using numerical simulation 77−53268
thermosphere, winds rel. to mid-latit. internal gravity waves 77−5298
thermosphere, winds rel. to O and O_2 density vars. 77−37470
thermosphere, winter, prevailing winds in S.hemisphere meteor region 80−109287
thermosphere and exosphere, neutral temperature and winds, geomag. disturbances effects 80−26658
thermosphere and mesosphere solar semidiurnal tidal wind rel. to airglow var. 77−21965
thermosphere circulation, seasonal and solar cycle variation 80−56661
thermosphere midlatitude winds, simultaneous meas. at 105°W and 79°W longit. 79−16727
thermosphere neutral and ion winds in polar region 77−45209
thermosphere neutral wind, midlatitude meas. during ALADDIN programme 80−31153
thermosphere neutral winds, tidal modes rel. to low latit. dynamo currents seasonal vars. 80−8479
thermosphere neutral winds deduced above Millstone Hill, mathematical model, uncertainties and results 79−39995
thermosphere neutral winds deduced above Millstone Hill, seasonal vars., (1970 to 1971) 79−39996
thermosphere nighttime winds and temps., monthly vars. during solar min. 78−32263
thermosphere strong east winds, investigation by reflected natural infrasound obs. 79−21089
thermosphere temperature and wind measurement Fabry-Perot-interferometer imaging system appl. 80−101441
thermosphere wind influences on F-region TIDs 80−109305
three-dimensional spectrum at Karlsruhe using vector vanes *(German)* 77−5305
Thumba, India, temp., circulation and struct. 77−78362
thunderstorm, electric field and wind profile, balloon meas. 78−85636
thunderstorm density currents, wind shear obs. 77−13109
thunderstorm gust front detection, sensitive pressure-jump sensor design 78−57357
thunderstorm wind gusts in Australia, statistical study 77−86996
tidal energy distrib. with altitude, wind field influence *(Russian)* 78−69402
tidal wind system in upper atmosphere rel. to ionospheric sporadic layer vertical motion 79−100993
time variability of wind and temp. vertical profiles, uncorrelated standing waves *(Russian)* 77−91215

wind continued
tornado, 1978 January 3, at Newmarket, England 79−39812
tornado, contrib. of vortex-stabilised arc to energy 78−53711
tornado, math. model, flow past axially uniform viscous vortex 78−59405
tornado, simulated, feasibility of flow meas. via three-dimensional anemometers 77−17244
tornado activity rel. to precipitation, assessment 80−61882
tornado flowfield struct., laboratory expts. 80−56566
tornado funnel formation, simulation expt. 77−21853
tornado in Cheyenne, USA, 16th July 1979, storm damage 80−77029
tornado interpretation of 1646 East Anglian meteorite 80−68009
tornado missile transport analysis 79−12205
tornado outbreaks, automated 12 to 36 hour probability forecasts 80−77062
tornado over Delhi, of 1978 March 17, sodar obs. 80−109188
tornado over Punjab, 1975 March 10, synoptic situation and meteorological conditions 79−96793
tornado simulation, core radii and peak vels. in modeled vortices 80−90130
tornado threat in United States, distrib. 78−69397
tornado vortex, barotropic instability theory 80−51458
tornado-like vortex, laboratory expt. of swirl ratio effect 80−61862
tornado-parent storm relationship from dual-Doppler radar anal. 77−21830
tornado-producing cumulonimbus, 1973 June 4, Oklahoma, USA 77−17202
tornadoes in UK, rel. to solar mag. sector crossing, 1957-77 period 80−77094
tornadoes probing with pulse Doppler radar 78−20558
tornadogenesis, numerical model of vortex growth 78−49114
tornadogenesis, precipitation and rotating wind, comments and reply 77−66963
trade wind, coeffs. of mechanical resist. law over tropical ocean 77−45066
trade wind field over Pacific Ocean 77−2206
trade winds in Pacific rel. to El Nino, numerical simulation 77−17123
trade winds of Indian Ocean basin, rel. to intertropical convergence zone cloud clusters features 79−29822
trade-wind boundary layer, thermodynamic structure, model appls. 79−88433
trade-wind boundary layer, thermodynamic structure, theoretical formulation and sensitivity tests 79−88432
trajectories changed by nocturnal jet *(German)* 79−66769
tramontane effect on sea-shore circulation near Cap Leucate 77−37227
transverse vel., remote meas. using laser Doppler velocimeter 80−4115
tree-covered surface scattered radio signal spectral density obs. 77−87049
tropic winds meas. by Arecibo 430 Mhz radar 79−100975
tropical Atlantic Ocean, influence on water surface IR emissivity *(Russian)* 77−60384
tropical atmosphere, Taifun-75 data from equatorial Pacific area, typhoons 79−58052
tropical circulation, role of horizontal friction forces *(Russian)* 78−65360
tropical cloud clusters, wind and dynamic fields 77−29405
tropical cyclone, model of ocean-atmos. boundary layer interaction 80−109231
tropical cyclones, radius and frequency of 15 m s^{-1} (30 kt) winds 80−105025
tropical cyclones in Bay of Bengal and Arabian Sea, max. wind speed calc. 77−53124
tropical E.Atlantic, press. and wind fields from TROPEX data 80−82040
tropical hurricane, wind field rel. to main ocean waves *(Russian)* 78−16021
tropical region, wind roses of freq. and stability appl. to pollutant dispersal 80−97846
tropical stratopause, 2-day oscill. of meridional wind 80−56557
tropical troposphere, three-dimens. wind struct. around cumulus clouds over island 79−5588
Tropical Wind, Energy Conversion and Reference Level Experiment (TWERLE), results 78−40605
tropical winds, anal. and data listings 79−39787
troposphere, diurnal var. in GATE region 79−29826
troposphere, equatorial, contrib. to theory of circulation 79−29821
troposphere, equatorial, response to heat sources 79−29832
troposphere, flow periodicities during NE monsoon season 79−20917
troposphere, middle-upper latits. westerlies rel. to Sun-induced standing planetary waves 78−36236
troposphere, N.Hemisphere wintertime disturbance, transient disturbance 80−51459
troposphere, upper mean zonal wind determ. with allowance for turbulence heat fluxes *(German)* 78−32137
troposphere, variance spectrum over E.Europe 80−8397
troposphere, wind rel. to near-surface internal gravity waves *(Russian)* 77−33141
troposphere, wind-height data for tropical cyclone recurvature forecast 77−64380
troposphere and stratosphere, radar meas. of winds in Arctic region 78−49172
troposphere velocities and irregularities, VHF radar studies using spaced antenna techniques 79−16701
troposphere wind at 300 mb, scale-interaction study with horiz. filtering method 80−98423
troposphere winds, evidence for solar cycle signal 80−72604
troposphere winds, radar obs. made at Kwajalein Atoll, equatorial Pacific 80−90188
troposphere-stratosphere wind profile, using Poker Flat MST radar 80−72579
upper troposphere/lower stratosphere winds, rel. to satellite-derived radiance gradient 80−98447
tropospheric studies, microbarographs, sodar, FM-CW radar, review 77−91332
trough-ridge systems as slantwise convection 79−84456
Tsumeb, S.W.Africa, boundary layer profiles for dry season in steppe *(German)* 79−34923
turbines, spacing in large arrays 77−73797
turbulence intensities rel. to cup anemometer overspeeding 77−53241
turbulence structure over water in high wind 80−12502
turbulent wind structure on hill crest 80−85722
wind continued
two-dimens. flow in forest canopy layers, numerical studies 77−37290
two-dimensional turbulent flow past rectangular cylinder 78−1645
typhoon and hurricane areas, distrib. models of press. and wind over sea surface 79−62570
typhoon characteristics over South China Sea 79−25309
Typhoon Della, weather conditions in eye of storm 79−29828
typhoon June, 55 GHz meas. of winds 79−100906
Typhoon June (1975), surface wind speed meas. by scanning microwave spectrometer 78−73436
typhoon movements expt. simulation *(Chinese)* 79−84449
typhoon prediction by barotropic primitive equation model using splines *(Chinese)* 80−4063
typhoon Tess wake vertical struct. in upper layer of Pacific Ocean 80−26538
typhoon track prediction, appl. of multiple-category discriminant anal. *(Chinese)* 77−66967
typhoon tracks near Taiwan, forecasting using simulations 80−90200
typhoon trajectories seasonal activity rel. to subarctic frontal zone position over NW.Pacific 78−61526
typhoons, detection and appl. of associated acoustic waves *(Chinese)* 79−34996
typhoons anomalous tracks, over East China Sea, mechanism *(Chinese)* 80−82043
typhoons structure over Soviet Far East during transformation of decay 77−78378
uniform shear, Rossby wave critical layer evolution 78−79329
United States, extreme winds, damage 79−62571
United States, recorded and predicted wind speeds 79−88457
United States, synoptic weather situations assoc. with major wildland fires 78−61499
United States E. coast, storm rel. to narrow warm water tongue intrusion in Sargasso Sea 78−73382
upper atmosphere, artificial satellite laser ranging 77−64485
upper atmosphere, dynamical properties 79−75005
upper atmosphere, effects on propag. of auroral infrasonic wave emission 77−29534
upper atmosphere, infrasound refr. by winds 77−33229
upper atmosphere, meteor wind obs. from Sheffield during January 1976 winter anomaly 78−45070
upper atmosphere, meteor wind study at Kyoto University 79−48595
upper atmosphere, neutral waves determ. from AE satellite meas. 79−58139
upper atmosphere, neutral wind rel. to F_2-layer hemispherical differences 78−69603
upper atmosphere, OH emission, waves and winds, 80-100 km altitude 78−93025
upper atmosphere, seasonal winds rel. to vars. in disturbances latit. struct. 78−32264
upper atmosphere, temp. and wind distrib. between 100 and 120 km altitudes *(Russian)* 77−29527
upper atmosphere, vertical winds effects on medium scale internal gravity waves propag. 79−75004
upper atmosphere, wind shear effects on neutral gas diffusion time-depend. model 79−66846
upper atmosphere, wind shear rel. to E_s-layer form. at middle latits. 77−13157
upper atmosphere, wind wavenumber regions rel. to meteor trails electron density fluctuations 78−73687
upper atmosphere, winds and aerodynamic lift effects on S3-1 satellite orbit inclination 77−53262
upper atmosphere, winds determ. from China 2 rocket (1971-18B) orbit 80−4231
upper atmosphere, zonal winds from satellite orbit anal. 77−13143
upper atmosphere disturbances 90-100 km altitude, rel. to stratospheric warmings *(German)* 77−70894
upper atmosphere neutral wind gradients, meteor radar obs. 80−41575
upper atmosphere neutral winds and nighttime F-region maintenance 77−29555
upper atmosphere tidal wind variations, upper mesopause region, ionospheric reflection height *(German)* 77−87139
upper atmosphere tides and winds meas. from meteor radar obs. 79−66851
upper atmosphere wind, solar eclipse obs. at 80-100 km altitude 80−46327
upper atmosphere wind and temperature meas., laboratory discharge lamp source appl. 80−4148
upper atmosphere wind meas. errors from meteor trails 77−49202
upper atmosphere winds from Cosmos 408 rocket orbit 78−73559
upper atmosphere winds from satellite 1973-101A orbit 78−73560
upper atmosphere winds observed by radio meteor drift, 80-100 km altitude 80−46328
upper atmosphere zonal wind speeds determ. from satellite 1966-51C orbit anal. 77−56786
upper atmosphere zonal winds, var. with height and local time, satellite orbit anal. 77−56785
upper atomsphere daytime neutral winds, Li release tracking by photometer 79−39871
upper mesopause, diurnal variation of zonal and meridional components 80−109284
upper troposphere, wind fluctuations meas. rel. to mesoscale turbulence *(Russian)* 78−16090
Uppsala urban meteorology project 79−53419
urban areas, atm. stability classification schemes 77−49127
urban mixed layer, persistent horizontal rolls revealed by dual-Doppler radar 79−12203
urban mixing layer, mesoscale perturbs. on airflow 79−16602
urban wind structure near city centre 79−66758
urban-rural complex, air pollution effects, two-dimens. numerical simulation 78−81369
urban-rural vel. differences 77−91187
urban-scale wind fields, three-dimensional, construction, objective anal. technique 80−101407
Urbana Meteor Radar observations during GRMWSP/CTOP periods 79−2412
urbanization effect on wind at Bombay Airport 79−48547
Ursat'evsk wind, air flow struct. 77−70792
US Federal wind energy programme, wind charact. programme element, overview 80−61242
USA-Japan studies on wind and seismic effects, conf., Tokyo, Japan (May 1975) 78−36252

wind continued
uw covariance in lower atmosphere, corrections 77−64381
valley ventilation by cross winds 80−48771
variability of wind and temp. fields in cyclonic and anticyclonic conditions *(Russian)* 77−29394
vegetative canopies, secondary wind speed maxima 78−3868
velocity, diurnal variation, harmonic anal. *(Rumanian)* 79−21009
velocity, remote meas. using video equipment for pollution monitoring *(French)* 80−7990
velocity, transverse, single-beam laser meas. 78−53747
velocity and direction meas. by laser sounding, correl. method *(Russian)* 77−29474
velocity and temp. flux-profile relationships 77−70735
velocity components, power spectra *(Russian)* 79−88403
velocity determ. from laser intensity fluctuation meas. *(Russian)* 78−36302
velocity determ. from pressure field using Navier-Stokes type eqns. 77−78374
velocity effects on amplitude scintillations of mm waves 78−61496
velocity estimation via optical signal processing 77−41107
velocity fluctuations in 95-100 km altitude region rel. to lower atm. wave processes *(Russian)* 77−29523
velocity gust factors, analytical approach 78−88897
velocity gust factors, analytical expression and wind tunnel simulation 80−31107
velocity magnitude and persistence, probability models 79−5583
velocity meas. near wind power plant in Sweden 80−61883
velocity meas. system, computerised 77−56742
velocity meas. using acoustic sounders, review 79−53528
velocity measurement, by time-of-flight laser anemometer 78−69469
velocity measurement, spatial filtering of lidar signal 79−29901
velocity over water area, underwater noise level *(Russian)* 79−34834
velocity sensors, crossed hot-film anemometers, compensating for non-ideal geometry 80−31122
velocity spectra, determ. from cup anemometer meas. *(Russian)* 77−13102
velocity spectra from hot-film anemometer and gust-probe meas. 77−78339
Venetian region, advection-diffusion model for for real-time forecasting of air pollution episodes 80−77096
Venice, Italy, spectral anal. of wind and SO_2 conc. 77−73824
vertical air velocity, airborne meas. system 80−77159
vertical cross-section analysis based on cylindrical projection, kinematic estimations 79−84549
vertical profile, high-altitude meas. with IR radar 79−70865
vertical profile fine structure over sea in near-shore zone 77−60445
vertical profile in subcloud layer of thunderstorm from lightning photographs 77−87013
vertical profiles sounding, acoustic Doppler extraction by adaptive lienar-prediction filtering 77−64453
vertical velocity, acoustic Doppler power spectra comparison with direct meas. 79−57999
vertical wind shear, modification of gravity waves trapeze instability 77−5301
Virginia Beach, Virginia, winds rel. to coastal sea currents and assoc. sand stream 78−73392
visibility rel. to surface wind at Gutersloh, Germany, smoke pollution effects 79−29853
Wangara expts. and wind profile relationships 77−21857
warm frontal region, wind and precipitation struct., Doppler radar study 80−81995
water bodies, contained, wind-induced drift 79−48512
water bodies, cooling from surface under free and forced convection regimes *(Russian)* 78−36179
water circulation patterns, wind-generated, in Fox Chain of Lakes, Illinois 79−53391
water surface, drag coeff. rel. to gust factor in light wind *(French)* 78−44905
water surface, free, roughness determ., from air flow struct. anal. 78−63441
water surface roughness rel. to air flow *(Russian)* 77−70669
water surfaces, new evaluation of wind stress coeff. 80−72603
water wave generation, airflow separation 77−70734
water wave generation, Phillips-Miles theory 78−79328
water wave interaction, numerical model calcs. 77−922
water waves, duration-limited, 1-dimens. spectra of growth 78−46990
water waves, long-term parameter distrib. function 78−81202
water waves generation, spatial correls. rel. to freq. independent phase vels. 80−98333
waterspout frequencies along USA East and Gulf Coasts 77−78329
wave damping in medium with natural turbulence *(Russian)* 77−41058
wave motions and daily neon winds, 52-110 km altitude, at midlatits. 79−5565
wave tank, microscopic and macroscopic surface structs. growth and decay rates 80−48726
wave-slope spectra in capillary-gravity range, increasing wind, laser beam meas. 77−3836
wave-wind interaction, two-layer flow, numerical simulation 78−92823
waves, calc. 79−14418
waves, wind-induced, exptl. investig. of freq. spectrum components dispersion ratio *(Russian)* 79−10581
waves generated by wind obs. on variable current 77−41053
waves in shallow water, statistical model *(Polish)* 79−25260
weather conditions for long gliding flights over England 79−58048
weather forecasting scheme, determ. of initial wind field 79−39833
weather maps, for present weather, wind, and ceiling, examples, forecasting use *(German)* 80−4081
Weddell Sea drift ice, pushed north by barrier winds 80−26514
Weibull statistics use to characterize wind speed distribs. 78−92928
Weibull velocity distrib. estimation method 78−92908
Weibull velocity distrib. parameters, vertical extrapolation formulae, errors 78−92916
westerlies rel. to zonal and meridional circulation in N. Hemisphere middle latitudes 77−49130
wet plume rise from cooling towers in strong winds 77−33182
whirlwind, ring-shaped, onset caused by rising air in stratified atmosphere *(Russian)* 78−77298
wind and seismic effects, conf., Tokyo, Japan (May 1977) 79−62569
wind-field analysis methods 80−105038
windblown dust in planetary atmospheres 77−45083
wind continued
windchill maps of lowland Britain, calc. from instantaneous data 80−61893
winter thunderstorms, anomalous of Hokuriku coast, wind shear rel. to dipole struct. 78−73443
zonal surface wind, rel. to baroclinic instability on sphere 77−5286
zonal wind in tropical middle atmosphere, observational evidence of semiannual oscillation 80−109216
zonal winds at 95 km altitude, correl. with radar meteor echo rates 80−56775
^{41}Ar dose distributions due to atm. release from HWR, including wind effects 77−14271
O_3 affected by sea breeze, Wallops Island, Virginia 80−51473
SO_2 gas pollution of Osaka city, optimal discharge control 79−52993
SO_2 regional transport, three-dimensional grid model 77−37375

wind energy *see wind power*

wind power
AEROSOLEC, combined solar-wind power station for telecommunication appls. 80−61306
alternative versus conventional energy sources, economic comparison *(German)* 80−72002
anemometer, low level wind meas. for WTG siting 80−48830
assessment, wind energy resource survey methodology 80−76594
assessment of wind energy systems in a utility framework 80−30369
availability, analysis of the potential of wind energy conversion systems 80−30363
Belgium, wind energy *(French)* 79−29445
brackish water purification by electrodialysis and reverse osmosis, wind powered-processing 80−35630
complementary nature of wind and solar energy at a continental mid-latitude station 79−92062
conference, Amsterdam, Netherlands (Oct. 78) 80−61235
conference, London, 21 Nov. 1979 80−55790
Cycloturbine, straight-bladed vertical axis wind turbine with cyclically pitched blades 80−61263
Darrieus rotor, aerodynamic analyses comparison 80−61264
Darrieus vertical axis wind turbines 80−76599
desalination appl. reverse osmosis, expt. installations *(French)* 80−55807
design and development of small systems at 1-2 kW, 8 kW and 40 kW 80−55784
development, availability, and storage possibilities *(French)* 80−89587
development as alternative energy source, c.f. nuclear power, book 80−45624
development programme in Sweden 80−61237
developments and improvements, energy data at Danish stations *(Norwegian)* 80−30364
domestic applications, review 79−52889
domestic premises heating appl., low-cost conversion system development 79−43716
domestic use in United Kingdom, Cambridge project 79−48076
domestic wind power system including storage, simulation analysis 79−92058
education, wind energy as alternative energy source, energy science course material 78−61973
electric power generation, economic potential 79−61941
electrical energy production from solar energy, techniques and systems 79−96424
electricity production, windmill construction *(French)* 80−66925
electrolysis of brine using wind energy 80−30368
energy accounting study 80−76589
energy conversion system, electricity storage using batteries 80−72008
energy output analysis of small scale generation systems using local climatological data 80−55787
energy production and control of atmospheric vortices 78−61510
energy resources, overall view *(French)* 80−40804
energy resources, review of alternatives to fossil fuel *(Italian)* 80−66917
energy strategy, soft vs. hard energy technologies, review 79−24885
experiment, test of kinetic theory, for teachers 78−81770
exploitation, programmes in Tanzania 80−61240
exploitation on large scale, physical planning aspects in Holland 80−61241
flexible blade windmills 80−66930
flow over complex terrain, wind tunnel simulation 80−76596
fluid dynamic aspects, turbulence, review 80−7909
flywheel system for storage and conversion of energy from wind turbine 80−30572
future energy concepts, Conf. London, England (Jan.-Feb. 1979) 79−43709
generation in combination with conventional system, economics *(German)* 79−66398
harnessing tomorrow's energy sources, prospects 79−100484
Hawaii, 1977 survey 79−29454
Hawaii, wind and insolation as alternative energy resources 80−45623
heating of residential house, in combination with solar power, Danish design 79−57411
hollow tower vortex generator, tower aspect ratio 79−74484
hollow tower vortex generator, turbine vortex jet interaction 79−74485
horizontal axis wind turbines, 100 to 2500 kW, development status 80−76597
horizontal-axis wind-turbine system for pumping duties in Third World agriculture 80−61259
India's wind energy potential and utilisation, as supplement to solar power 79−61942
industrial utilisation of energy, book 80−61222
Iran, rural electrification program utilising wind power 80−55789
Ireland, assessment of actual wind power availability 80−21366
irrigation plant appl., comparison with solar power, w.r.t. cost, maintenance and reliability 79−70425
limits to wind power utilization 80−7908
local and mesoscale weather, impact 78−81358
mean wind isowind maps for many parts of the world showing sites suitable for wind power plants *(Italian)* 80−89586
measuring instrument design 79−57404
meteorological aspects, resource assessment, site selection, US R and D program 80−76593
MOD-2 wind turbine system, 300 ft diam. 2.5 kW, development program 80−35631
New Zealand, wind energy prospects in Otago region 80−76595

wind power continued
North Sea windmill deployment for 20% of UK's needs 80−97759
off-shore based wind turbine systems for Sweden, systems concept study 80−61261
offshore wind energy systems for the UK 80−55794
offshore wind power model estimates 80−61244
Pacific Northwest, potential 79−83549
plant design in MW range 80−55788
potential estimation using power laws 78−92912
potential in Karnataka State, in India 80−108782
power plants, experimental projects in progress, design problems and results achieved *(Italian)* 80−72007
Prince Edward Island, evaluation of system worth to electrical grid 80−50932
probability models 79−5583
prospecting in Prince Edward Island, programme overview and status report 80−61243
pumps, development programme 80−55792
pumps appl., economic comparison with solar pumps 79−74507
R&D in United Kingdom 79−79370
recent developments aid economic aspects 80−61238
remote communities novel energy concepts, technical and economic aspects 79−48078
renewable energy sources, Rumania *(Rumanian)* 80−35639
renewable energy sources and the environment 79−79411
research and developments, future trends as to viability as energy source 80−66924
research programme, in Holland 80−61236
resources evaluation for use in rural areas, w.r.t. economic and social aspects 79−70416
review of the US Wind Energy Programme 80−50929
Savonius rotors, wind-tunnel air-speed corrections 80−61255
seawater desalination by wind power, anal. 80−108781
shrouded wind turbine, pilot plant construction 80−66931
site evaluation, estimation of wind characteristics using COMPLEX model 80−101075
small wind energy conversion systems, commercialisation, R and D program 80−76598
solar photovoltaic-wind hybrid alternative energy system 80−30409
status and development trends, in late 1970s 79−57347
storage systems simulation model, SIMWEST program package 79−52872
surface wind speeds run duration anal. for energy appl. 79−100916
systems technology, R and D review 80−76592
tornado type wind energy system, wind and solar energies effect of line heat source 79−87959
tornado-type generator system, latent heat from moist air, effect on vortex 80−30365
turbines, bicycle rotors for vertical axis wind turbines, design and performance 80−30367
United Nations energy program for solar and wind energy appls. 80−3496
urban development of small-scale wind power systems in New York City 80−55786
US Federal wind energy programme, wind charact. programme element, overview 80−61242
utilisation, machine dynamics, geometry, economics and social acceptance 80−45625
utilisation prospects 80−61269
vertical axis wind turbine, flow field exam. using vortex model 80−61267
vertical axis wind turbine, operation and anal. 80−30366
vertical axis wind turbines, design, construction, testing and manufacturing 80−66929
vertical axis windmill with variable geometry, development 80−61254
vortex augmentor concept., wind power distribution, control and conversion 79−83554
vortex wind power 78−79327
wave energy convertor array power available 78−81216
Weibull wind speed distrib. parameters, estimation using Weibull prob. paper and percentile estimators 80−50931
wind heat system utilising wind turbine driven heat pump 80−66926
wind scarer appl., for orchards and grain fields in tropical countries 79−70423
wind turbines, rotational dynamics, eval. of turbine response to wind speed changes 80−55785
windmill arrays, wake interaction, theory and preliminary results 80−61246
windmill arrays, wind-power conversion limits, simple formulas 80−3485
windmill for use in irrigation, with horizontal axis sail 80−21368
windmill using sail-type Savonius rotor, low-cost water pumping appl. 80−21367
windmills, max. power extraction, theory 79−58482
windmills in closely spaced arrays, performance 80−40819
windpump ITDG development program, for small-scale manufacture and use in under-developed arid regions 80−26106

wind power plants
10 MW, large-scale generation potential 79−43713
30 kW aerogenerator performance prediction and meas. 79−43720
60 kW experimental wind power plant in Sweden, test results 80−61253
60 m diameter wind turbine generator, design concept 80−61262
200 kW Gedser windmill in Denmark, performance and structural response meas. 80−61431
200 kW generator, design features and details of parallel operation with diesel engine driven plant *(Italian)* 80−101074
200 kW vertical axis wind turbine, preliminary test results 80−66928
AEROSOLEC, combined solar-wind power station for telecommunication appls. 80−61306
Aldborough aerogenerator design and construction 79−48074
assessment of wind energy systems in a utility framework 80−30369
Australian wind-powered generator potential and requirements 79−29444
Chinese windmill, Campbell, vertical-axis, low-cost design 79−61939
control and stabilization of the DOE/NASA Mod-1 two megawatt wind turbine generator 80−30370
control of horizontal-axis conversion system, on-line, performance in turbulent wind environment 79−48069
control strategy for variable speed wind power generator *(French)* 80−76591
convertor efficiency increase, by load matching improvement 79−48079

wind power plants continued
Cretan windmills, high rate energy extraction from low speed winds 80−30362
desalination plant utilising reverse osmosis, 6 kW convertor 80−61282
design, atmospheric turbulence structural influences 80−61247
design and development as alternative energy source, c.f. nuclear power, book 80−45624
design of plant in MW range 80−55788
development, safety, reliability and quality assurance, low cost approach 80−61268
developments and improvements, energy data at Danish stations *(Norwegian)* 80−30364
developments in Japan 80−61239
domestic wind, solar, wind and solar heating systems, performance and economic evaluation 79−43744
economic assessment of future potential 79−61941
electricity production, in Denmark from 1900 to 1950 80−16778
energy accumulators appl., flywheel, stationary, economic assessment *(German)* 80−35757
experimental projects in progress, design problems and results achieved *(Italian)* 80−72007
fixed-pitch propellor, water heating appl. 80−61260
furnace systems, advanced, for residential and agricultural heating and power supply 79−48070
generator, 1 kW, vertical axis, design and development 79−61940
generator oscillation modes in large power systems 79−29446
high temperature storage for a wind energy system 80−55920
Indian development of windmills, vertical-axis and horizontal-axis types, for rural appl. 79−70419
integration into existing power systems, implications 80−61258
integration of wind-driven generators, into power system 79−48077
joint operation, with solar plant, exptl. investigation 79−39278
Magdalen Islands wind turbine, nine months operating experience report 80−66927
MOD-2 wind turbine system, 300 ft diam. 2.5 kW, development program 80−35631
network of wind generators, wind power depletion 79−43721
offshore systems for United Kingdom, feasibility assessment 79−48075
parameters for rational and economic installation *(Italian)* 80−89586
performance evaluation method 80−61248
power system that includes wind energy generators, model based regulation 80−61256
power transmission, epicyclic gear design 80−61252
research and developments, future trends as to viability as energy source 80−66924
review of the US Wind Energy Programme, MOD-1 and MOD-2 machines 80−50929
site evaluation at Whangaparaoa, data acquisition and processing 79−66400
site evaluation at Whangaparaoa, wind energy pot. 79−66399
siting statistical evaluation, based on longitudinal correlation 79−70422
small scale wind energy systems, design charact. and appls. 80−55791
small wind energy conversion systems, commercialisation, R and D program 80−76598
South Africa schemes feasibility, with and without energy storage 79−43714
toroidal accelerator rotor platforms appl., performance and economic viability analysis 79−48073
turbine generator system, optimum selection 80−40818
urban development of small-scale wind power systems in New York City 80−55786
utilisation, solar energy model anal. to 2010 *(German)* 80−26109
value to electric utility, economic model 80−61257
velocity meas. near wind power plant in Sweden 80−61883
vertical-axis windmill, tilting blade, for use in rural areas in India 79−70424
vortex augmentor concept., wind power distribution, control and conversion 79−83554
windmill, vertical axis, aerodynamic design and testing 79−43717
windmill blades materials and design 79−43719
windmills, horizontal axis, cost effectiveness evaluation 79−70421
windmills arrays, directional 79−43718
windmills for rural use, based on Savonious rotor, Indian development 79−57353
windmills in closely spaced arrays, performance 80−40819

wind tunnels
3-D laser Doppler velocimeter 80−10331
acoustic equation time transform., flow effects on sound field, wind tunnel noise meas. appl. 78−87198
adaptive-wall, convergence to interference-free conditions 78−38419
adaptive-wall wind tunnel, iterative anal. of subsonic flow 78−22364
aerodynamic design, wind tunnel tests and numerical methods compared 77−27635
aerodynamic design of blower tunnels with wide-angle diffusers 78−1771
aerodynamic heating test, use of melting liq. crysts. 79−77299
aerofoil dynamic stall tests, effect of freestream fluctuations 78−75164
airport fencing for air pollution reduction, wind-tunnel expt. *(Japanese)* 80−12034
architectural and industrial aerodynamics 4×2 m tunnel, Oxford University 78−22443
atmospheric boundary layer, model scale factor, full- or part-depth simulation 78−28285
atmospheric motion simulation, wind tunnel charact. review *(Italian)* 80−4156
balance, 6-component, using load cell techniques *(German)* 79−37268
blockage rel. to flow over two-dimensional surface mounted flat plates 78−59381
calibration by shock standoff distance computation up to Mach 1.2, schlieren method 77−27557
cascade deviation, prediction and measurement 80−24049
CERT-T_2 injector driven wind tunnel, performance flow quality *(French)* 77−24044
channel height effect on nearcritical flow past circular cylinder 80−14818
closed return config., for industrial aerodynamics, atm. shear flow simulation 77−55110
contraction section, smoothly varying nozzle construction method 78−47081
cross-sectional shock shape meas. using columnar and plane discharges 79−27666

wind tunnels continued
cryogenic, real gas effects 78−94760
cryogenic wind tunnel, induction-driven, preliminary tests *(French)* 79−27730
digital data filtering in continuous wind tunnels 80−10336
Doppler-difference laser anemometry, appl. to wind tunnel meas. 79−7421
dynamic drag and lift co-eff. determ. in wind tunnel, transducer device 79−40558
dynamic force balance, two-component, for mounted flying insects 80−22350
European high Reynolds number transonic cryogenic wind tunnel *(French)* 79−32714
European transonic wind-tunnel project for testing at cryogenic temps. 79−58713
facility for study of cross-flow induced vibrations in heat exchanger tube bank 79−3957
flow separation experiments, galloping and vortex induced oscillations 80−43750
flow visualisation in wind tunnel, appl. bubbles around bluff body 77−80238
fluctuating pressure meas. of drag reduction spike 78−30310
graupel formation and growth, cloud simulation 80−17324
human hearing, wind noise expts. 78−92648
Hurst phenomena in grid turbulence 78−46947
hypersonic wind tunnel, flow core relative area, nozzle similitude ratios 80−48747
infra-sound reduction from auxiliary compressors of large wind tunnels 79−81628
interference assessment of boundary meas. 78−71403
intermittent high Reynolds no. wind tunnel 78−18361
inviscid free air flow simulation using perforated walls in wind tunnels 79−90276
ionised air as wind tunnel tracer 79−37428
ionized air as tracer 78−22435
IR camera for separated flow regions diagnosis in wind tunnels 80−10335
laser anemometer photon correlation techniques 77−80256
laser velocimeter for wind tunnel measurements, principles 78−71405
laser velocimeter meas., principles and techniques 77−80252
low density wind tunnel for rarefied gas dynamics 80−96285
low speed wind tunnel contractions, optimum design 79−77157
low velocity, low turbulence intensity, at Karlsruhe University, charact. *(German)* 78−26224
low-Reynolds-number turbulent boundary layers 80−1556
Ludwieg tube with downstream valve, starting process 79−72965
Mach t tunnel, fluctuating disturbances 78−1761
nozzles, low-speed, effect of inflow nonuniformity *(German)* 78−71382
open cct., exptl. procedures to improve charact. *(Japanese)* 80−19528
particle and droplet field holography 79−76642
plane jet curvature in bounded cross flow with stagnant zone 79−46355
pollution distrib. obs., aerodynamic aspects *(German)* 79−8686
pressure fluctuations, freestream 78−14102
pulsed-wired anemometer for low vel. air flow investigation *(Japanese)* 77−62319
reflected-beam laser anemometry using photon correlator 80−106861
roughness effects of multiple windbreaks 77−72285
roughness element geometry required for atmospheric wind simulation 78−47079
Savonius rotor, aerodynamic performance testing in wind tunnel 80−61266
Savonius rotors, wind-tunnel air-speed corrections 80−61255
shear flow production using curved wire gauze screen 77−3805
shear flow turbulence with artificial roughness anal. 77−42809
shear layer acoustic refraction theories, comparison, parameters for open jet wind tunnel shear layer correction 78−90556
shear layer turbulence structure obs., thermally stratified *(Japanese)* 79−41731
ship model wake meas. in wind tunnel, laser anemometer autocorrelation *(German)* 79−60085
smoke tunnel, school and undergraduate use 78−16614
sound source location, using acoustic mirror as directional microphone 78−30372
square prisms, interaction in two flow fields 78−9632
stack plume simulation, necessary height for stack close to building 77−2225
stepped rod in wind tunnel, flow separation downstream 77−58718
strain gauge, wind tunnel dynamometer, five component 78−54361
subsonic wind tunnels with slight perforation 79−68738
supersonic, Mach 5 quiet tunnel development 78−38437
supersonic flow, meas. turbulence using modified hot-wires and hot films 79−90356
supersonic flow over hemisphere-cylinder at incidence up to 19° 78−59419
supersonic wind tunnel, wall cavity, effect on starting charact. 77−58827
swirling flow managment, appl. to wind tunnel and duct flows 79−41754
test program for determining effect of spin on boundary-layer transition at Mach numbers 5 and 8 on 9-deg. cone configurations 80−14864
testing and numerical methods, conference, Rhode-St-Genese (1976) 77−27634
three-dimensional flow field graphic representation 77−27636
torque meter, sensitive, wing rolling moment meas. appl. 77−53891
transonic flow, wind tunnel wall and viscous effects, numerical simulation 77−27552
transonic flow simulation by tracking and blowing *(German)* 80−6081
transonic test section wall interference minimisation *(French)* 77−27550
transonic wind tunnel, noise level effect on model charact. *(French)* 78−71411
transonic wind tunnel laser velocimeter meas. interpretation 77−31324
turbine blade and nozzle guide vane, transient cascade, heat transfer meas., wind tunnel 78−94768
turbulence around Rock of Gibraltar, simulation at 1:5000 scale 78−28284
turbulence generators in combination with barriers and/or roughness, charact. 79−94598
turbulent boundary layer struct. with low external flow turbulence *(Russian)* 79−68689
turbulent boundary layers on rough surfaces, simple roughness elements, natural wind simulation 80−69774
turbulent dispersion concentration valves, system for wind tunnel meas. 79−5191
unsteady aerodynamics research, data acquisition using minicomputer 80−10337
unsteady pressure coefficients digital measuring unit *(French)* 80−68169
unsteady pressure measurement, large signal/noise technique 79−94743
ventilated wind tunnel, modern developments 77−31405
viscosity balance measurement of skin friction var. with Reynolds number, improved tunnel 77−72377
vortices, merging, laser velocimeter surveys 79−32718
vortices in wind tunnel expts. meas. using US pulses 80−10334
wall effect on bluff body eddy props. 79−59964
wall interference, two-dimens., correction method, examples *(French)* 78−67293
wall interference reduction using adaptable walls *(German)* 79−77320
walls effect on flow past cylinders and cooling tower models 78−46930
water droplet size distrib. interferometer 79−80673
windmill design and testing, vertical axis 79−43717
N_2, cryogenic, shock wave-boundary layer interaction *(German)* 78−71370

wind turbines
5 kW, low-cost, for isolated appl., design, construction and proving 79−43715
5 kW AC generator, with automatic load matching device, field testing 79−70418
30 kW aerogenerator performance prediction and meas. 79−43720
100 kW, experimental, developed in USA, design and experiences 79−48067
200 kW, NASA development under DOE direction, design and performance 79−48068
200 kW vertical axis wind turbine, preliminary test results 80−66928
aerodynamics, machine performance and rotor aerodynamics 80−74904
aeroelastic behaviour, large Darrieus rotors derived from behaviour of 5.5 m rotor 80−61251
bicycle rotors for vertical axis wind turbines, design and performance 80−30367
control, on-line, of horizontal axis wind energy conversion system, performance in turbulent wind environment 79−48069
control and stabilization of the DOE/NASA Mod-1 two megawatt wind turbine generator 80−30370
Cycloturbine, straight-bladed vertical axis wind turbine with cyclically pitched blades 80−61263
Darrieus rotar windmill arrays, wake interaction, wind tunnel simulation 80−61245
Darrieus rotor, aerodynamic analyses comparison 80−61264
Darrieus vertical axis wind turbines 80−76599
Darrieus wind turbine system, parametric performance analysis by digital simulation 80−40817
design and development of small systems at 1-2 kW, 8 kW and 40 kW 80−55784
diffuser augmented, improved conversion approaches 79−83556
diffuser augmented concept, expt. demonstration 79−48071
domestic use in United Kingdom, Cambridge project 79−48076
economic assessment of future potential 79−61941
efficiency, Lanchester-Betz limit 80−97758
energy effectiveness of arbitrary arrays of wind turbines, calc. 80−97755
flexible blade windmills 80−66930
fluid dynamic aspects, turbulence, review 80−7909
fluids engineering, Conf. San Francisco, CA, USA (Dec. 1978) 79−83550
flywheel system for storage and conversion of energy from wind turbine 80−30572
free vortices behind stationary wing as energy source 80−40820
generator dynamic stability, digital simulation 79−96415
generator system, optimum selection 80−40818
Giromill, vortex sheet analysis 79−83553
horizontal axis, interaction with wind field calc. 79−83551
horizontal axis wind turbine blades, aeroelastic stability and response 80−61250
horizontal axis wind turbines, 100 to 2500 kW, development status 80−76597
horizontal-axis wind-turbine system for pumping duties in Third World agriculture, design 80−61259
irrigation pump Rankine cycle solar engine and wind turbine comparison 79−57448
large, aeroelastic stability 80−61249
Magdalen Islands wind turbine, nine months operating experience report 80−66927
MOD-2 wind turbine system, 300 ft diam. 2.5 kW, development program 80−35631
off-shore based wind turbine systems for Sweden, systems concept study 80−61261
offshore wind energy systems for the UK 80−55794
offshore wind energy systems for United Kingdom feasibility assessment 79−48075
power extraction from wind, theoretical study 79−58482
reciprocating water pump, stroke adjusting mechanism for rotor speed control 80−50930
review of the US Wind Energy Programme, MOD-1 and MOD-2 machines 80−50929
rotational dynamics, eval. of turbine response to wind speed changes 80−55785
rotor blade, 3-degree flap-lag-feather, nonlinear dynamic response 79−81771
Savonius rotor, aerodynamic performance testing in wind tunnel 80−61266
Savonius rotors, wind-tunnel air-speed corrections 80−61255
shrouded wind turbine, pilot plant design and construction 80−66931
Tornado-type, flow analyses 79−83555
UK field measurements collaboration [wind turbines] 80−55793
variable geometry vertical axis windmill development 80−61254
variable pitch vertical axis, investigation 80−61265
vertical axis, high-efficiency and high-output design 79−70417
vertical axis wind turbine, flow field exam. using vortex model 80−61267
vertical axis wind turbine, operation and anal. 80−30366
vertical axis wind turbines, design, construction, testing and manufacturing 80−66929

wind turbines continued
vertical axix, tilting using overspeed control 80−97757
vertical-axis, as alternative resources, 1978 status and development 79−70420
vertical-axis, electricity generation in dwelling, independent of servicing network 79−61943
vertical-axis, torque ripple, analytical and expt. results 79−48072
vortex augmentor to increase power, test model results 80−97756
wind heat system utilising wind turbine driven heat pump 80−66926
wind scarer appl., for orchards and grain fields in tropical countries 79−70423
windmill, vertical axis, Savonious rotor type, two-dimensional vortex sheet model 79−83552
windmill arrays, wake interaction, theory and preliminary results 80−61246
windmill arrays, wind-power conversion limits, simple formulas 80−3485
windmill blades, planform shape and twist for maximum power output 79−87957

winding (process)
coil winding stress mathematical model 77−73430
fibre reinforced composites, zonal winding pattern analysis, thin spherical shells 80−38253
fusion reactor, Large Coil Program, coil winding development support 80−106190
fusion reactor coil insulation and winding techniques 79−31210
glass fibre reinforced plastic, tubular specimen manufacture, apparatus 79−15906
glass fibre reinforced plastics, winding device for mech. test specimens prep. 78−7138
JET Tokamak toroidal field coil manufacture 79−31206
Nb_3Sn filamentary hexapole magnet construction and testing 79−30503

windings
see also coils; machine windings
CERN Proton Synchrotron focus control, pole face winding design and field correction 79−31299
electromagnet windings with constant current density, maximum permissible mag. field 78−57990
Helmholtz coils, optimisation, critical current rel. to mag. induction 79−67353
inductance measuring instrument for windings with steel magnetic yoke *(Bulgarian)* 79−88976
MHD, moving conducting fluid inductive interaction with external main windings, config. effects *(Russian)* 78−75225
solenoid inductance, minimisation, mag. induction optimum profile 79−31769
superconducting composite media, effect of axial conduction and metal-helium heat transfer on local stability 78−91832
superconducting magnet, transient heat transfer to liq. He from bare Cu surfaces 78−83219
superconducting solenoid, Al stabilised design and construction, for CERN intersecting storage rings 77−46428
toroidal field coil construction and appl. *(German)* 78−54877
Al strips used in accelerator coils instead of Cu 79−72126

wire telephony *see carrier telephony*

wires (electric)
see also conductors (electric); insulated wires
aging process investigation natural and accelerated, Cu wire leads with Sn60Pb coating appl. *(Polish)* 80−35231
cold formed wire connector 79−88929
compensating for heat flow along current-carrying leads 77−7299
conductivity, quantum size effect, theory 77−35907
die wear during wire drawing, review 80−30113
electrical conductivity of thin wires, Kubo formalism 79−56191
electromagnetic field, anomalous behaviour of near fields calculated by method of moments 79−89829
explosion, electrical, investigation of resulting particles *(Russian)* 79−37558
ferromagnetic, Fe alloy, torsion stress influence on magnetisation obs. *(Slovak)* 77−90468
grounded horizontal wire of arbitrary length, EM fields 79−27130
International wire and cable symposium, Cherry Hill USA (Nov. 1978) 79−37018
long metallic tethers in ionospheric plasma, electrodynamics 78−69652
metal wire and bar NDT, electrical and EM methods 80−11865
metallic thermal connectors for use in nuclear refrigeration, elec. resist. meas. 78−224
pacemaker, lead wire fracture 78−57134
pacemaker implantable lead performance evaluation, status report 78−57135
properties of high-conductivity copper and copper alloy wires *(Japanese)* 79−91665
semiconductor thin quantised wire, with charged defects, interband light absorption *(Russian)* 77−59593
steel-Al bimetallic wire for overhead lines, manufacturing methods 80−16247
superconducting, magnetisation rel. to field orient. 78−52151
superconducting threads of mixed materials containing many filaments, stability and transverse conductivity meas. *(French)* 79−73629
surface scatt., electric field integral eqn. formulation 77−38784
thermoelectrode material nonuniformity data analysis 77−61065
thermoelectrode wire classification standard samples 77−5865
thin wire antenna coupling with human body 77−21563
Al, eddy current effects on NMR 80−2645
Cu, gas-cooled, for superconducting dipole magnets, experimental study 79−67995
Cu, growth of diffusion layer in Sn coatings due to ageing effect *(Polish)* 80−34227
Cu, hard drawn wire, stress corrosion cracking *(Japanese)* 77−25193
Cu, stranded and solid wire, rel. stability of thermal EMF in cryogenic environment 78−60111
Cu/SbF_5 intercalated graphite/Cu composite wires, elec. cond. 80−44687
Fe wires, catalytic, electrically heated, steady state temp. multiplicity, resist. meas. 77−32828
InPb-covered manganin wire, level detector, depth gauge, demonstration of superconductivity 79−35751
NbTi supercond. threads in Cu matrix, struct. composition and props. *(French)* 79−73649
Ni pulsed heater wire, appl. to high-press. heat capacity and thermal cond. meas. 77−41613

wires continued
Pd-Ag microwires, electrical resistance, influence of gaseous environment in heat treatment *(Russian)* 80−20146
V_3Ga superconducting multifilamentary wires, effect of low temp. neutron irrad. 77−32132
W, hot emitter, surface struct. change during baking above 2000K 79−65971
W, wire, elec. resistance, low-temp. continuous and cyclic heating effects, compared with W-Re 78−92370
W-Re, wire, elec. resistance, low-temp. continuous and cyclic heating effects, compared with W 78−92370

wiring
see also printed circuits
IC wiring tools for laboratory use 78−86073

wiring diagrams *see circuit diagrams*

WKB calculations
(2+1) dimensional compact QED, combined WKB-variational method, vacuum tunnelling 80−101960
ϕ^4 system, metastable state, decay rate calc. 80−22301
accretion onto compact gravitating object, travelling sound wave behaviour WKB anal. 80−67551
acoustic wave propagation in bilinear medium, mode theory, WKB approx. 77−7229
anharmonic oscillator, 3-term recursion relations and quasienergies, WKB method, quantisation rules 79−97257
anharmonic oscillator with polynomial pot., asymptotic forms of energy eigenvalues 78−45509
anharmonic oscillators, single and coupled, with quartic coupling energy levels for large n, WKB type calcs. 79−35587
atmosphere acoustic-gravity waves, theoretical props., WKB solns. 77−33270
atom-surface 3-9 interaction, bound state vibr. spectrum 78−14615
atom-surface scatt., inelastic, energy transfer and sticking coeff., classical and quantum treatments 80−40209
atomic spectral lines, foreign gas broadening, WKB approx. for satellite bands 78−46304
Bertotti-Robinson metric, pair production, semi-classical treatment 79−2702
bound states, semiclassical, in one-dimension, perturbation formalism 80−12937
bound states, WKB approx. from Heisenberg matrix mechanics 78−32717
bound states in quantum mechs. and AFT, eqns. of motion, variational principles, WKB approx. 78−54540
central potentials, wave function at origin for large-n S-wave levels 79−35585
collisionless drift wave in Vlasov plasma, nonlocal anal. 80−43910
complex potential energy surface systems, nonradiative processes, WKB calcs. 80−45133
complex WKB method, asymptotic behaviour of phase integrals 77−67332
continuum Dirac electron, Coulomb field, simple asymptotic wave function 78−41455
cosmological particle creation classical analogue, WKB approx. 79−30160
cosmological particle production 80−27023
coupled second order eqns., adiabatic expansions of solns. 79−71226
dechannelling (aligned-to-random beam transition), WKB approx. 80−34109
defective dielectrics, EM heating with time depend. param., WKB calcs. 80−71367
diffusion in bistable potential, systematic WKB treatment 80−46975
Dirac eqn., quasistationary levels in lower continuum, energy calc. *(Russian)* 78−45826
Dirac equation, WKB approximation at Z>137 79−17650
distorted crystal, X-ray intensity mode oscills., two wave WKB approx. calcs. 80−28876
education, hadronic atom strong interaction induced level widths and shifts, WKB calc. 77−78923
education, renormalisation rule for WKB-type wave functions 78−69944
eigenvalues, asymptotically exact, upper and lower bounds 77−3250
EM beam self-focusing in semiconductor 79−18488
EM waves in two-dimensionally inhomogeneous media 79−41302
energy levels determ. via path integral 78−77763
expansions in curved spaces, functional integrals, higher order corrections 79−71280
fermion interactions, eigenvalue spectrum 77−8035
flow stability between concentric cylinders 77−51120
four term WKBJ approx., appl. to Varshni V and Lennard-Jones pot. 80−58113
free boson gas in weak external pot. 80−86203
free particle propagator covarient WKB expansion in Riemannian space 80−68100
generalised WKB method simplification 79−7767
graded index fibre, error estimates fo first order WKB calc. method 80−87488
graded-index fibres, propag. consts. and group delays of guided modes 79−98464
graded-index slab waveguide TE mode analysis 77−72087
gravitational waves dispersion in cold matter 80−12967
hadron nonlinear string model 77−87901
hadronic amplitudes in scaling region for e^+e^- and e^-+hadron 78−41484
hadrons, string state, WKB-like wave functional and path-dependent phase factor, colour flux 80−52481
hard core potential scattering, semiclassical phase shifts, WKB calcs. 78−86178
heavily doped semiconductor, density of eigenvalues, localisation, general disordered system 78−56109
heavy ion scattering cross-sections, WKB calcs., unphysical reflection phenomena 80−27656
Hellmann-Feynman and virial theorems, WKB approx. and scaling behaviour 78−86193
Helmholtz eqn., 1-dimens., refined Maslov-WKB technique appl. 80−90795
high frequency gravitational and electromagnetic wave coupling 78−8304
higher order corrections, general case 79−84999
hydrogenic atom, one dimensional, in electric field, solid state appl. 77−43764

WKB calculations continued
hydrogenic partition function, compensation of bound and scatt. state contribs. 77−61012
inhomogeneous circular waveguide, asymptotic eigenvalues 80−53442
inhomogeneous dielectric waveguide propagation, generalised WKB solns. 77−75385
inhomogeneous dielectric waveguides, generalized WKB approach 78−1359
inorganic molecules with polytopic bonds, motion of nuclei 79−41125
instanton phenomena, real time approach, multidimens. potential with continuous symmetry 79−2922
ionospheric, electron density profile determ. from rocket-based 40 kHz propag. obs. *(Japanese)* 78−24403
Jahn-Teller problem, $T\times e_g$, spin-orbit allowed tunnelling splitting, zero-phonon line splitting 78−19006
JWKB approximation for multiple-humped fission barriers, ^{234}Th appl. 78−585
JWKB phase integrals, higher order, evaluation 80−87195
JWKB quantisation condition, appl., breakdown and near-dissoc. behaviour 78−58571
large order expansions in perturbation theory 78−54525
laser-assisted inelastic collisions, impulse approximation theory and other short wavelength approximations 80−18904
lattice quantum theory; WKB approx. 80−32009
Lennard-Jones mol., WKB vibr. energy level calc. 78−9057
light caustic, phase shift, WKB approx. 77−19166
lower hybrid wave, linear amplification and absorption 80−28673
lower hybrid waves, ray trajectory and ion absorpt. in Tokamak 80−28667
luminescence kinetics 79−33810
magnetosonic and Alfven waves, transfer by solar wind 80−67490
massive gauge theories, with instantons, wave functions, energies, vacuum and heavy quarks, WKB Schrodinger eqn. 79−35951
massive Gross-Neveu model, semi-classical quantisation by inverse scatt. method 79−2924
membranes, linear laminated media, permeation, sorpt. 79−1966
metal clad diffused optical waveguides, charact. of propag. modes, WKB anal. 79−3768
metal-semiconductor-metal junction, tunnelling phenomena in terms of exact method and WKBJ approx. 80−20329
modal dispersion in optical fibres with any numerical aperture and doping profile 78−1391
molecule, asymmetric double-min. pots., tunnelling 77−6660
molecule, quartic potential function with finite BE, props. 79−26913
multidimensional bistable potential, diffusion, WKB calc. 80−101770
multidimensional WKB wavefunctions, local and global semiclassical approximations 78−73880
multimode fibre bandwidth computation from measured index profiles 80−58740
multimode optical fibre bandwidth computation from refractive index profiles 79−76815
neutron dynamical diffraction, gravitational and mag. field effects 80−59345
non-functional approach *(Russian)* 77−13627
non-functional approach *(Russian)* 78−36861
nonlinear birth and death processes, relaxation mode anal. 77−49681
nuclear Coulomb excitation, accuracy of WKB approx. determ. 77−65216
numerical anal. to large order, one dimensional Schrodinger equation 78−16688
numerical integration leading to Bohr-Sommerfeld formula, alternative to JWKB calcs. 80−86119
one-dimensional field theories with odd-power self-interactions 79−254
optic fibre light propagation, review of analytic methods of study *(French)* 79−90001
optical fibre, GRIN, leaky modes, WKB method 77−7180
optical fibre, multimode graded profile, characteristic eqn., WKB method *(Italian)* 78−83080
optical fibre, power-law refractive index profile, scalar modal eigenvalues and group delays 80−28322
optical fibre, transmission charact. of graded-index fibres with lossy outer layer 78−55437
optical fibre bend radiation calc., WKB method 78−59130
optical fibre waveguide, inhomogeneous multimode, analysis 79−59833
optical fibres, non-circular graded index, leaky modes 79−1003
optical graded index fibre propag., expt. and theory 78−90496
optical graded index waveguide, pulse broadening, cladding effect 77−79924
optical step-index fibres with microbending, bandwidth 80−23775
optical W-fibre, leaky mode struct. and attenuation 77−79928
optical waveguide, multilayered, attenuation and tunnelling coeffs. for leaky rays 78−38002
optical waveguide, planar graded-index, TE and TM modes, WKB analysis accuracy 78−50925
optical waveguides, accuracy of WKB approx. 77−34947
optical waveguides, graded-index anisotropic, WKB analysis of guided and semileaky modes 79−27416
optical waveguides, multimode, step index limit of power law refr. index profiles 79−10387
optical waveguides to integrated optics, mode anal., prism coupling method 78−66947
phase integral approximations, advantages over JWKB approx. 80−87027
phase memory, necessary conditions 80−22206
phase shifts produced by repulsive, strongly singular, inverse power pots., high-energy behaviour 79−97233
phase space path integrals, without limiting procedure 78−32718
planar ion exchange waveguides, TE and TM mode analysis 78−9444
plasma, inhomogeneous, Langmuir waves, parametrically excited 77−76073
plasma, one dimens. screening 80−65478
plasma drift waves, collisionless, in Vlasov plasma 79−4139
plasma waves, longit. to EM wave conversion, varying plasma 78−18389
polarisation effects in penetration of barrier with applied mag. field, relativistic corrections 79−78852
polarisation effects in penetration of nonrelativistic electrons through potential barrier with appl. mag. field 78−11084
potential determ. from elastic scatt. phaseshifts, generalised WKB method 77−58116
potential problems, non-local, Perey effect, WKB method 80−68077
WKB calculations continued
potential reconstruction by differential scatt. cross section, WKB approx. *(Russian)* 78−45818
potential scatt., semiclassical off-shell T-matrix elements, repulsive local pots. 77−17845
potential scattering, JWKB phase shifts, using Gauss-Mehler quadrature formulas 78−46411
predissociation, multichannel, and inelastic scatt., uniform WKB theory 79−72404
prism-waveguide coupling efficiency for waveguides with arbitrary refr. index profile, WKB approx. 79−7231
pseudo-first-order phase transitions in one dimension 80−22270
pseudoparticle contrib. to energy spectrum of 1-D system, comparison with WKB result 78−4517
quantum mechanical multidimensional problems, WKB approx. 77−82412
quarkonium, quantum mechanical applications, masses and leptonic widths of ψ and Υ 80−27484
quartic oscillator, semi-classical expansion 80−31592
radial integrals calc. in Coulomb approx., use of semiclassical wavefunctions 80−43025
radial wave eqns., Bremmer series soln., for eqn. with spherically symmetric velocity function 78−28973
radial wave functions, JWKB connection with bound-state/free-state duality 80−62950
radiowave propagation in critical coupling media, comparison of generalised WKB and Katsenelenbaum's methods 80−91728
radiowaves in stratified ionosphere 77−13177
ray and wave optics of integrable and stochastic systems, WKB method 80−59244
real-time approach to instanton phenomena, multidimensional pots. with degenerate absolute minima 78−78067
relativistic wavefunctions, approx. near turning point, WKB calcs. for $Z>137$ 80−86598
rigid rotor, asymmetric, semiclassical energy levels determ., tunnelling 78−37624
Robertson-Walker universe, pair-creation of particles 80−22265
scalar Yukawa$_2$ field theory, vacuum energy density in large order perturbation theory 79−17620
Schrodinger eqn. one dimens. pot. finite interval, semiclassical eigenvalues 78−28978
Schrodinger equation, numerical integration, using WKB approx., eigenvalue estimates 78−12486
Schrodinger equation for central potentials, energy levels and level ordering 79−80463
self-consistent WKB calculation in a model nucleus with Skyrme interaction 79−45186
semiclassical approxs. for heavy-ion transfer reactions 78−94021
semiclassical expansion of the anharmonic-oscillator propagator 79−63072
sine-Gordon equation, exact mass spectrum, WKB approx. 77−33896
single-barrier penetration of electrons, Eckart pot. 79−44788
singular potentials, bound states, WKB approx. 77−82402
slab waveguide, inhomogeneous step-index and WKB anal. 78−66923
soliton free energies calcs., WKB approx. failure 80−42073
solitons and pseudoparticles, systems with many degrees of freedom 78−29255
spectral and scattering inverse problems 79−17282
stationary path integrals appl., bound state energies and wave functions 78−12587
step-index fibres, pulse responses investig. using WKB approx. 80−91898
stochastic diffusion in a periodic potential 80−12994
SU(2) Yang Mills multi-instanton paths, tunnelling pots. and WKB wave functionals 79−248
supercritical nuclei, $Z>137$, WKB method appl. *(Russian)* 79−49587
surface electron states, in 1-dimens. cryst., semiclassical treatment 78−52046
TCNQ, salt, $Me\phi_3As(TCNQ)_2$, nonOhmic elec. cond., tunnelling model and expt. 79−99558
meso-tetraphenylporphine, potential parameters of H migration tunnel rates calcs. 80−5600
third-order JWKB approximation method applic. to absolute continuity criteria derivation, approx. operators construction 78−12591
third-order JWKB approximation method applic. to absolute continuity criteria derivation, approx. operators and estimates 78−12592
three-dimensional generalised WKB method, separation of variables *(Russian)* 77−26194
three-dimensional generalised WKB method, soln. *(Russian)* 77−13626
Tokamak machines, Vlasov plasmas, geometrical optics approach, Tokamak appl. 80−14902
transverse waves propag. along axisymm. mag. field in nonhomogeneous plasma, WKB kinetic theory 78−42740
Trivelpiece-Gould mode propagation in axially inhomogeneous plasma column 78−75317
two-well oscillator, eigenvalues, scaling properties, WKB approx. 79−25897
variable parameters systems, variation of oscillation phase and amplitude *(Russian)* 78−81799
Varshni V and Lennard-Jones pots., 3rd order WKBJ eigenvalues 79−6982
vertically polarized waves in inhomogeneous media, full wave solns. 77−6980
water wave, partial reflection by nonuniform adverse currents 79−64681
wave equations, spatially nonhomogneous, nonmonochromatic solns. based on WKB approx. 78−86179
wave propagation in stratified media, matrix anal. 79−12618
WKB method for systems of integral equations 80−98787
WKBJ five term approx. 80−31569
WKBJ method, deductions from artificial RI profiles, based on elementary functions 77−38778
$Z>137$, WKB approximation for Dirac's equations, spontaneous positron production *(Russian)* 78−78123
Al-I-Pb tunnel junction, clean and doped, tunnelling conductance, WKB calc. fitting 79−15232
Al-insulator-Pb, clean and doped tunnel junctions, barrier profiles 79−56445
Ar+HCl, inelastic scatt. exponential perturbation theories 80−74217
Ar+N_2, inelastic scatt. exponential perturbation theories 80−74217
ArBr, pot. curves, population distribs. and chemiluminesc. for B(1/2) and C(3/2) electronic states 80−45509

WKB calculations continued
ArHX, (X=F,Cl,Br,I) van der Waals mols. vibr. and thermodynamic props., WKB calcs. 77−71740
Ba I, quasi-Landau spectrum, semiclassical strong field mixing models 80−63847
Ba_2^{2+}, very long lived vibr. states, lifetimes, WKB calc. 80−78560
CO, analytic RKR pot. including higher-order WKB approx. effects 77−57901
H, Stark broadened line shape, unified Franck-Condon-JWKB method 77−10635
HF, analytic RKR pot. including higher-order WKB approx. effects 77−57901
He vapour, low-temp. positive ion mobility by absorptive model, WKB calcs. 79−77333
$He+H_2$, inelastic scatt. exponential perturbation theories 80−74217
KBr:Tl, nonradiative transitions in colour centres, WKB approximation 77−85803
KI:Tl^+, A_T emission, mag. circular polarisation, WKB approx. for nonradiative transition rate 80−55180
KI:Tl, A_T emission, linear polarisation, appl. of semi-classical WKB formalism 80−45134
KI:Tl, nonradiative transitions in colour centres, WKB approximation 77−85803
KrF*, oscillatory bound-free emission spectra, semiclassical anal. method 80−7799
LiNC, metal atom motion, WKB calcs. 78−82623
Na_2, laser-induced atomic fluoresc., semiclassical intensity calc., transition moments 77−18838
$(O_2)_2$, van der Waals mol., WKB vibr. eigenvalues 78−33498
$^{208}Pb+^{136}Xe$, double octupole phonon excitation, coupled channel WKB approx. 78−4960
$^{122}Sn+^{120}Sn$, 630 MeV, multipair transfer calcs. for superfluid ions, coupled channel WKB approx. 78−37373
Sr I, quasi-Landau spectrum, semiclassical strong field mixing models 80−63847
$U^+ + U(U^+)(U^{2+})$, elastic scatt. in plasma, interaction pots. and momentum transfer 80−38534
YIG rod, inhomogeneously magnetised, propag. characts. of magnetoelastic wave 78−15006

wolfram *see tungsten*

wood
N.American trees, cellulose D/H ratios rel. to palaeoclimatology (9500-22000 BP) 77−60462
analysis, quantitative, spectral appl. of microdensitometry *(Czech)* 79−30524
balsa, cryogenic insulation, exam. of strength specifications, props. 80−25819
boiler fuel, sawdust waste of timber mills *(German)* 80−40805
burning, wood vs. fossil fuel as source of atm. CO_2 excess 77−53162
cell wall, fine struct. *(Japanese)* 79−96283
chipboard, creep data, 3- and 4-element response curve fitting 77−90395
clean cut surface preparation for SEM studies 78−15935
coatings, electron-beam curing 77−70200
combustion in heating plants, calorific values *(German)* 80−40815
cracked beam, mode II stress intensity flow 77−73325
cutting, stress distrib. and frictional coeff. at tool-chip interface, specific gravity effect *(Japanese)* 80−1492
dimensional stabilisation, with 2-hydroxyethyl methacrylate and MMA *(Japanese)* 80−7532
dimensional stability, and hygroscopicity, with ethylene glycol and isocyanate *(Japanese)* 80−2982
Douglas fir, crack front width effect on fracture toughness 77−56060
electronic moisture gauge 79−70279
energy in W.Virginia 80−72006
epoxy bond system, cleavage fracture toughness *(Japanese)* 77−77574
fibre reinforced Portland cement composite, strength 80−100822
filled polystyrene exam. of reversible elastic deformation 78−48437
flash pyrolysis, in cyclone, solar gas-solid chemical reactor *(French)* 80−61296
forest productivity study using LANDSAT data, computer training, USA 77−78527
Forest Service, digital terrain model appls. 79−84086
fracture toughness variations with specimen size, statistical approach 80−100889
friction between wood and metal 77−1167
gasification of wood wastes using flash pyrolysis and concentrated solar energy *(French)* 80−61226
gasification using fluidized bed wood gasifier 80−30348
heat of wetting in water *(Japanese)* 77−76646
impulse method of determining moduli of elasticity, shear moduli 77−77661
Japanese red pine seedlings, tensile strength *(Japanese)* 77−77538
laser processing capacity using CO_2 laser 77−5820
materials and processing *(Japanese)* 77−77728
particle board, method of mech. testing, elastic deform. meas. 78−56837
plywood, strength geometry 77−70123
plywood shallow shells, orthotropic, mech. charact., effect of restraint of sliding or expansion *(Japanese)* 77−77522
PMMA composites temp. depend. of viscoelastic behaviour *(Japanese)* 77−77541
polymer composite, dynamic viscoelasticity and modulus *(Japanese)* 78−59356
poplar, hybrid, direct hydrogenation to liq. and gaseous fuels 79−87945
prestrain effect on dynamic modulus of elasticity and attenuation coeff. in nonconducting materials 80−29110
radioactivation of shielding materials Fe, Benelex by fast neutrons, γ-ray spectra, decay rates 79−682
rupture mechanism exam. *(German)* 78−52976
screw, effects of crest and pilot hole in withdrawal resist. *(Japanese)* 80−3290
set, force induced from moisture recovery of drying set *(Japanese)* 77−77537
softwoods, flow paths *(Japanese)* 80−3288
softwoods, transverse Poisson's ratio and Young's modulus *(Japanese)* 80−2111
stress distrib. in cell wall subject to tensile force in transverse direction *(Japanese)* 77−77539
stud walls, rel. between maximum compressive load and width *(Japanese)* 80−3124

wood continued
thin plate perforated by hard missile, energy dissipation prediction 79−8361
timber, determ. of critical Rice integral *(French)* 80−16412
timber butt-joint, with metal plate connectors, rotating bending fatigue *(Japanese)* 80−3175
timber frame constructions, sound insulation of wood joist floors 78−87203
tree form energy plantations, woodchip transport and handling 80−30327
tree rings, ^{14}C radial flow and chemical pretreatment for ^{14}C meas. 78−28346
tree rings, climatic information from $^{18}O/^{16}O$ in cellulose, lignin and whole wood 78−24355
tree rings, long term environmental pollution histories, neutron activation analysis 79−92107
tree rings, reconstruction of climate vars. since (1602) 80−51528
tree trunk, modified hole drilling technique for determining residual stresses *(Japanese)* 77−77683
trees, US pulse echo method for flaw detection 80−66731
urea-formaldehyde resin/wood materials, book 80−73114
vapour phase reaction of 2,4-tolylenediisocyanate *(Japanese)* 77−77603
vibratory cutting, behaviour of chip and effect on cutting force *(Japanese)* 77−77540
waterlogged woods, props., conservation problems *(Japanese)* 80−3289
wood, load bearing capacity, and deformability, evaluation of timber structure safety *(German)* 78−39983
yield stress, strain-rate theory, moisture effects 77−16646
^{13}C record in tree rings, vars. in N.hemisphere trees during last 150 years 80−17363
^{14}C dating of geological and archaeological samples 78−92993
^{14}C meas. on submerged forest floating chronologies, rel. to atm. ^{14}C vars. 79−48563

wood processing
see also paper industry
chip refiner, steam flow anal. 79−50787
gasification processes, theoretical model 79−61937
hydrolysis, ethanol production as alternative energy resource 79−48039
lignin, chemical conversion, practical utilisation *(Japanese)* 77−32537
polysaccharide components dissolved into chlorite liquor according to the variation of treating conditions *(Japanese)* 80−3291
timber dryer, forced-air, for tropical latitudes, solar heating appl. 80−21384
waste, fuel gas production, gasifier design and construction 80−7895

word processing
see also data preparation
semantically accessible communication aid development trends 80−8218

work function
see also electron emission; Schottky effect
absolute determ. method for metals and semiconductors 77−28697
adatoms, electronic state, depend. on conc. 78−72001
adsorbed layers, order-disorder transition, effect on work function 80−59791
adsorption system surface properties variational calcs., binding energy, Lang model 80−29279
alkali halides, heterogeneous adsorption, photoelec. work function changes 77−69175
alkali metal, flat surface, inhomogeneous strain effects, jellium model calcs. 77−72907
alkali metal chemisorbed layers, changes in work function due to charge transfer 78−18900
alkaline earth oxide cathodes with In_2O_3 additions, effect on emissive props. 77−48298
alloy, binary, surface segregation prediction using bulk alloy variables 79−65300
anthracene, solid, electronic struct., comparative ESCA study of polyacenes 78−52631
atomic electronegativity scale rel. to work function 78−64096
benzene, solid, electronic struct., comparative ESCA study of polyacenes 78−52631
caesiated surface, negative ion emission *(French)* 80−108314
cathode, oxide coated, emission local nonuniformities 77−20978
cathode material choice methodology to obtain low work function 80−100500
chemisorbed layer, depend. of work function in order-disorder phase transition 79−19460
chemisorption on metals, appl. of field emission techniques 78−35255
contact potential difference meter, IC, for meas. work function of electrons 79−35780
crystal surface discrete dipole layer effect on surface barrier shape 79−95468
crystallographic point groups, Cauchy symm., elastic work functions 77−72644
cubic metals, anisotropic relation between work function and melting temp. 79−37813
Davisson line retarded field data determ. of thermionic consts. 79−87555
DC method for continuous meas. of work function changes 80−84503
defects role, review 78−14551
density functional formalism compariosn of Hartree Fock and X_α formalism 77−76900
diamond, semiconducting, electron-hole liquid formation conditions and parameters 79−78013
Einstein theory of stimulated emission of radiation *(Hungarian)* 79−89880
electron binding energies reference level problem in photoelectron spectra of solids and adsorbates 78−63936
electron gas, neutrally charged with surface, props. 79−38144
electron-hole drops, size effects, work function determ. 78−72077
elements, work function periodicity 78−19124
elements, work functions and sublimation entropies 79−56283
fast variation meas., photoelectric method 79−91561
FEM, local field strength and work function rel. to field emitters, analogue simulation on Teledeltos paper 77−41731
ferromagnetic anomaly of electron work function at Curie point, Vonsovsky-Sokolov model 77−12142
film semiconductor work function var. meas. using single pulses 77−76898
Fowler-Nordheim slope variation with cryst. plane size, FEM-FIM obs. 78−27383

work function continued
high-current multirod cathode, influence of absorption effects on characts. 80−20756
II-VI semiconductors, thermoemission of positive ions in simple gas atoms *(Russian)* 77−28676
inhomogeneous surface work functions, use of Kelvin method *(French)* 79−78155
insulators, XPS, binding energy, surface pot. and work function calcs. 80−89113
interstitial compounds, electronic structure and useful phys. props. 77−89683
ionic crystal, surface parameter calc. by pseudopotential method *(Russian)* 78−76130
jellium metal, surface props. in linear pot. approx. 77−43689
jellium metal, surfaces props., statistical calc. 80−24987
jellium metal, work function changes on single crystal planes 79−99604
jellium metal surface, work function calc. 79−65536
jellium surface props., statistical calc. 79−60897
measurement method for use in inert medium 79−49250
measurement of changes, method of continuous meas. by AC variation of diode technique 79−33328
metal, contrib. of John Bardeen 80−57057
metal, electronic work function under tension, 20 to 1200°C 80−76448
metal, free electron contrib. 78−56208
metal, periods IV, V, and VI, work function depend. on plasmon energy 78−18986
metal, rel. to alloying tendencies and impurity heats of soln. 79−28102
metal, surface charge density prod. in satic electrification 78−14797
metal, surface dipole barrier, calc. 80−96958
metal, surface dipole barrier, semi-empirical calc. 80−39659
metal, surface energies and work function, simple analytic model 80−49862
metal, surface pot. drop and contact pot. difference in terms of orbital electronegativity 78−2546
metal, with terraced surface, calc. 80−6950
metal, work function, pseudopot. calc. 80−96970
metal, work function changes due to absorpt. 77−7972
metal interface of unlike metals, secondary ion-ion emission 78−11050
metal mirrors, for high-power appls., multithreshold damage analysis 77−88884
metal oxides, nonstoichiometric, work function, high temp. meas. using dynamic condenser 78−64097
metal oxides, nonstoichiometric, work function and near-surface chem. diffusion 80−80034
metal substrate, adsorption systems, relationship between work function and degree of adsorption coverage 79−83092
metal surface, change-in-SCF theory 78−84282
metal surface, expts. on photoelectric effect, apparatus 78−81745
metal surface, ground state, variational self-consistent-method 78−56204
metal surface, influence of submonolayer films on props., calc. *(Russian)* 80−2273
metal surface, ion bombarded, secondary negative ion emission 79−28879
metal surface, work function change on simultaneous adsorption of atoms of two different elements 78−60184
metal surface props., Rayleigh-Ritz variational calcs. 79−69570
metal surface props. in square barrier and linear one electron potential model 79−19645
metal surfaces, dipole barrier and work func. calc. 79−15208
metal work function temp. depend. 79−78154
metal-barium stearate-metal structs., internal voltage work function meas. 79−82684
metal-insulator interface, catalytic reactions studied by work function meas. 80−55711
metal-metal contacts, use as prevention H escape from metals 80−24595
metal-semiconductor boundary, deposited metal atomic number barrier height depend. 77−12002
metallic and nonmetallic solids, Fermi energies 80−2451
metallic atom chemisorption, work function variations 79−46936
metallic clusters, small size fluctuations of work function 78−14792
metallic granules, electron work function interrelation with granule size 80−39660
metallic surface, self-consistent electron theory, review 80−88616
metallic thin films, absolute work function meas. by field-emission retarding-pot. device 77−59322
metallic thin films electrostatic interaction of charges with metal surface in size-quantised film 80−24996
metals, chemisorption of gases, book 79−69370
metals, multiphoton phenomena in photoelectron emission at high laser intensities 79−28886
MIM structures, thermal dielec. relax. 79−11237
mirror electron microscopy, appl. to work function variation meas. 80−86505
MIS negative barrier contact for induced back surface field solar cell 80−101101
MOS p-channel transistors, metal-semicond. work function 78−34903
Mulliken electronegativities, rel. to work function 78−9096
multialkali antimonide photocathodes, emission and work functions 79−78836
naphthalene, solid, electronic struct., comparative ESCA study of polyacenes 78−52631
negative correction for positive surfaces 78−84281
negative ion formation, by sputtering, work function depend. 78−39645
nontransition metals, electron density, bulk and surface props. relation 80−103609
nucleic acids and related compounds, photoemission rel. to absorpt. and luminesc., 120 to 250 nm 77−81466
pentadecanoic acid, monolayer on water, surface pot. meas. in coexistence region 77−28236
photocathodes exhibiting negative electron affinity, model and GaAs expt. *(French)* 77−8724
photoelectric, depend. on light freq. *(Russian)* 77−32066
physicochemical surface processes investigated by alpha-particle effect on electron work function 78−2547
poly-N-vinylcarbazole, electrophotographic film, dark discharge 78−34864
polypropylene thin film conduction mechanism, expt. obs. 77−28271
porous metal cathodes, emission props., work function 80−100502
probe, vibrating capacitor type, for surface and adsorption studies 78−10274
work function continued
quartz powders, CaO soln. chemisorpt. rel. to lattice parameters, work function 79−37918
rare earth element submonolayer films, electronic phase transitions, heat of absorption 80−24736
rare earth hexaborides, low work function thermionic electron emitters, props. 79−33884
rare earth hexaborides, thermoelectronic props. rel. to surface state *(French)* 79−69950
rare earth metals, electron work function by contact pot. difference method *(Russian)* 79−60913
rare earth oxide, cathode material, influence of surface and bulk effects 78−11065
rare gas, crystal, quasi-atomic and quasi-molelcular exciton states *(Russian)* 80−103628
refractory materials, emission and adsorption props., rel. to electronic struct., review 77−76899
refractory metals, work function, ionising radiation effects meas. method 80−6951
retarding potential method of measurement in axial magnetic field using miniaturised electron gun 79−80719
Schottky barrier formation, chemical effects 78−91753
Schottky barrier heights, semi-empirical tight-binding calc. 79−28408
semiconductor, electron emission from surface subband, reduced work function 80−60757
semiconductor substrate, work function rel. to AES *(French)* 80−50479
semiconductor-metal boundary, Schottky barrier form., chem. mechanisms 80−49869
silicide Schottky barriers, elemental description 80−60085
single crystals with lowered work function, secondary and Auger electron emission anisotropy 80−100716
solids, photoemission, book contrib. 79−61495
stainless steel, austenitic, surface, interaction with O_2, AES and work function obs. 80−65364
submonolayer films on metallic surface, struct. and props. review 78−38972
surface electron states, electric field sustained, δ-well crystal 78−10528
surface microstructure determ. and microanalysis by ultrahigh vacuum field emission gun SEM 80−96423
surface potential and work function meas. from secondary electron emission energy in SEM 80−66343
surface-atom polarisability derivation from field-ion energy deficits 80−76155
tetracene, solid, electronic struct., comparative ESCA study of polyacenes 78−52631
thermionic, convertor, V-I charact., collector material depend. 77−7606
thermionic electron emission from surface with adsorbed atom islands 80−7462
transient ion desorption, work function, evap. rate, ion heat of adsorption 77−20198
transition metal carbides, adsorption of Cs(K), adsorpt. energy, thermionic emission 77−7978
transition metals, 3d, absolute $2p_{3/2}$ core binding energies and work functions 78−15253
TSEE, role of surface pot. 77−8732
wide-gap semiconductors, thermionic emission current, surface states effects 79−15581
Ag (111), adsorpt.-desorpt. props. and surface struct. chem. of Cl 77−89648
Ag, adsorption on W, substrate temp. effect on relation between work function and coverage, FEM obs. 80−2272
Ag, determ. from electron interferometry meas. of Au-Ag contact PD 77−32069
Ag, effect of Hg adsorption 77−7966
Ag, evaporated layer, secondary electron energy distrib. and work function *(French)* 79−99993
Ag film, enhancement of electron photoemission by excitation of surface plasmons *(French)* 77−63524
Ag photocathode work function, decrease due to adsorbed alkali halides 79−78824
Ag, surface props. rel. to adsorbed O_2, H_2O vapour, work function determ. 78−60187
Ag, thin film deposited on Si, work function *(French)* 80−80353
Ag, UPS, expt. methodology aspects 77−90245
Ag, vac. deposited films, surface pot. and work function rel. to thickness 79−42672
Ag-O-Cs surface, oxidation, role of Cs suboxides in low work function surface layers, XPS 80−76131
$AgAsS_2$, cryst. and amorphous, band struct., photoemission and refl. spectra obs. 77−66581
Ag_3SbS_3, pyrargyrite, thermoelec. and photoelec. work functions, Fermi level and electron affinity *(Russian)* 77−15939
Al (111), chemisorpt. of O 78−14593
Al, chemisorption of O_2, on (111) and (100) faces, AES and work function obs. 77−35822
Al, etched, electronic props. of surface *(Russian)* 78−15569
Al, evaporated layer, secondary electron energy distrib. and work function *(French)* 79−99993
Al, film, adsorption of O_2 and N_2 77−24486
Al, film, initial oxidation, AES, work function and gravimetric meas. 78−7087
Al, initial interaction of O with single cryst. faces, LEED, AES and work function study 80−84392
Al, low temp. electronic work function, temp. depend. 77−47928
Al surfaces, interaction with O_2, work function changes and ellipsometric parameters 79−47831
Al, thin film deposited on Si, work function *(French)* 80−80353
Al-dimethyl terephthalate contacts, effect of elec. field on contact electrification 79−19660
Al-SiO_2-Si system with reactively sputtered SiO_2, work functions difference 80−6987
Au, effect of water or Hg adsorption 77−7966
Au, evaporated layer, secondary electron energy distrib. and work function *(French)* 79−99993
Au film, work function changes upon water contamination 80−44705
Au, stepped surface, edge atom dipole moments 78−14791
Au, surface dipole moment calc. 80−60060
Au, UPS, expt. methodology aspects 77−90245
Au, vac. deposited films, surface pot. and work function rel. to thickness 79−42672

work function continued
Au, X-ray cathode, secondary electron energy distrib. excited at 277 and 1487eV 77−8716
β-B, rhombohedral, photon energy depend. of work function 78−19637
Ba, adsorbed layers on W, Auger and work function meas., impregnated W cathode model 79−43073
Ba, adsorbed on 4d or 5d metal, O_2 coadsorption effects, thermionic emission obs. 78−11064
Ba film, growth on (111) face of Ir covered with graphite monolayer 78−26791
Ba film, monatomic, conc. depend. of characteristic loss spectrum 77−15938
Ba film, multilayer and monolayer, an W substrate, AES and work function meas. 77−24921
Ba film, structure effects on work function, electron micrographs and photoemission meas. 79−83107
Ba film, work function and struct. 78−80040
Ba-O system, adsorbed layers on W, Auger and work function meas., impregnated W cathode model 79−43073
BaB_6, work function, thermionic and field emission retarding pot. meas. 77−90233
BaB_6, work functions from thermionic and field emission retarding pot. methods 79−65537
BaO, epitaxial, on Ir, low energy electron spectra, electron affinity, conduction band edge position 78−14790
BaO epitaxial films, cathode poisoning due to O_2, CO_2, and S, surface anal. 79−42600
BaO, film, emission props. in relation to struct. 80−100501
BaO film, multilayer and monolayer, on W substrate, AES and work function meas. 77−24921
BaO films on Ir, thermionic props., Auger, LEED, and emission microscopy 79−43089
BaO, monolayer on W (110), film struct. and electron state 80−100498
BaO-Ba coated cathode, role of surface donor centres 78−11063
$BaTiO_3$, adsorption of $O_2(H_2)$, effect on work function and spontaneous polarisation *(Russian)* 78−6211
$BaTiO_3$, electron exoemission unipolarity associated with phase transitions 80−97415
Be (0001) surface, work function and purity, AES, LEED and photoelectron spectra meas. 78−68606
Be film, on W (110), growth mode, work function, thermal desorption, and struct. 80−75477
Bi film, evaporated on W, work function obs. by field emission method 78−6834
Bi-Sb alloys, electron work function determ., contact pot. difference method 77−39920
Bi_2O_3, oxide film on polycrystalline Bi, exam. of oxide film growth rate using XPS *(German)* 79−11041
Bi_2S_3 film, evaporated on W, work function obs. by field emission method 78−6834
C, black, surface acidity effects on work function 78−2548
C, film, work function, heat treatment 78−64563
Ca film, structure effects on work function, electron micrographs and photoemission meas. 79−83107
Ca films, thin and ultrathin, vac. deposited, struct. and photoemission meas. 80−11538
CaO epitaxial layer, on Mo, secondary electron emission, struct. effects, LEED and AES expts. 78−2959
Cd-Bi alloys, electron work function determ., contact pot. difference method 77−39920
$CdGa_2S_4$ double surface-barrier diodes, current-voltage characts. 80−92972
CdS-Au structure, work function of {0001} faces of CdS, effect of piezoelec. props. 78−23164
CdS-metal interface, chemical reactions and local charge redistrib. workfunction and band-bending changes 79−19661
CdSe-As_2S_3($AsSbS_3$) heterostructure, energy bands and interface props., photoelectron spectroscopy 78−2551
CdSe-metal interface, chemical reactions and local charge redistrib., work function and band bending changes 79−19661
CdTe-metal contact, surface barrier exam. 78−64111
CeB_6, crystal preparation, elec. resistance, phase transitions 80−97427
CeB_6, single cryst. work function, thermionic emission, evaporation 77−24922
CeB_6, thermionic emission rel. to surface state 78−39654
CeB_6, work functions from thermionic and field emission retarding pot. methods 79−65537
$CeBr_6$, work function, thermionic and field emission retarding pot. meas. 77−90233
CeO_2, single cryst. whiskers, electron field emission 78−27378
Co (0001), chemisorption of O_2, surface oxidation and CO oxidation 79−60631
Co ($10\bar{1}2$), struct. and CO chemisorption obs. 79−4474
Co film, texture and adsorption of CO *(German)* 77−24485
Co film, work function changes upon water contamination 80−44705
Co, pure surfaces, adsorpt. of water and decomp. *(German)* 80−26054
CoO, and Co_3O_4, surface reequilibration kinetics 77−55449
Cr (100), adsorption of O_2 and initial oxidation at room temp. 80−20034
Cs film, work function theory, size effect 78−43460
Cs ion source, thermionic emission in SF_6 mol. gas 80−71557
Cs, photoelectron energy distrib. curves, depend. on light polarization 79−15591
Cs suboxide film, work function theory, size effect 78−43460
Cs/W, work function measurement in SEM 80−80918
Cs-O, low work function surface, prod. by Cs_2CO_3 decomp. and emission characts. 77−85882
Cu (100), coadsorption of O_2 and Cs, effect of O_2 on Cs work function 79−15014
Cu (100), electronic struct., self-consistent local-orbital calc. 80−80348
Cu (100), three-layer film, work function and density of states, self-consistent calc. 77−35978
Cu, (100) and (111) faces, by response function with d orbital effects on electronic screening 77−62977
Cu (100) surface, interaction with O_2, AES, EELS, LEED and work function studies 80−24731
Cu (111), adsorpt.-desorpt. props. and surface struct. chem. of Cl 77−89648
Cu (111), chemisorpt, of CO on differently prepared surfaces 78−6223
Cu (111), Cs adsorption system, electronic surface band energy 80−2443
work function continued
Cu (111) surface, self-consistent electronic struct. calcs. on bulk and thin films 79−1614
Cu adsorption of O_2, N_2O on (100) surface, reaction with CO 80−103583
Cu, electrodeposited, heating temp, influence 79−33331
Cu, electronic work function, temp. derivative from 2.9 to 6.2K 79−56284
Cu, evaporated layer, secondary electron energy distrib. and work function *(French)* 79−99993
Cu film, pure and CO covered, work functions 79−91570
Cu film, work function changes upon water contamination 80−44705
Cu films, adsorption of O, study of gravimetric uptake and work function 79−33179
Cu films on Ru (0001), growth, struct. and electronic props. 79−77958
Cu, influence of cryst. orientation on work function, with and without adsorbed S *(French)* 78−76134
Cu, low temp. electronic work function, temp. depend. 77−47928
Cu, secondary electron emission, temp. depend. 77−32067
Cu-Cd(In)(Sb), electron work function, contact pot. difference meas. 78−80041
Cu-dimethyl terephthalate contacts, effect of elec. field on contact electrification 79−19660
Cu-Ni alloy surfaces, chemisorption of CO, LEED, AES, thermal desorption, and work function meas. 79−90879
Cu(100), adsorption and incorporation of O_2 78−56042
Cu(110), adsorption of O_2 and its reaction with CO 80−15373
Cu(111), adsorption of Cs, struct. and electronic props. 78−23147
Dy, surface ionisation on W (110) 79−87142
Er, film, evap., CO effect on work function 78−39188
Er film, work function, effects of O_2 sorption 78−19125
Er-H_2 system, work function changes correlated with phase changes, elec. resist. meas. 77−11828
$Eu_xLa_{1-x}Al_2$, binding energy and workfunction charges using XPES 80−33928
Fe (100), adsorption of Br_2, AES, LEED, work function, and thermal desorption study 80−15375
Fe (100), adsorption of carbon tetrachloride, AES, LEED, work function, and thermal desorption study 80−15376
Fe (100), adsorption of Cl_2, AES, LEED, work function, and thermal desorption meas. 79−82465
Fe (100), adsorption of I_2, AES, LEED, thermal desorption, and work function study 80−15374
Fe (100), adsorption of tetrabromomethane, AES, LEED, work function, and thermal desorption meas. 80−39422
Fe (110), adsorption and decomposition of ammonia, LEED, AES, UPS, work function and desorption meas. 79−69345
Fe (110), adsorption of K, LEED, AES, UPS and XPS meas. 79−77919
Fe (111) surface, S segregation, LEED, AES and work function changes 80−15350
Fe, adsorption of CO, resistance changes, work function change and thermal desorption meas. 79−19450
Fe, coadsorption of CO and H, effect of preadsorption of one on adsorption of other 79−19451
Fe film, work function changes upon water contamination 80−44705
Fe, polycrystalline, H_2 adsorpt. and embrittlement, work function changes 80−96741
Fe surface, (111) and (100), adsorpt. and decomp. of NH_3 78−40077
Fe surface, H_2 chemisorption LEED, UPS, thermal desorption spectroscopy, work function meas. 78−14566
Fe, surface props. rel. to adsorbed O_2, H_2O vapour, work function determ. 78−60187
FeO_x, work function, high temp. meas. using dynamic condenser 78−64097
$Fe_{1-x}O$, wustite phase, surface elec. props. 78−76133
Ga, electron work function meas., dynamic capacitor method 77−39919
Ga, surface props. rel. to adsorbed O_2, H_2O vapour, work function determ. 78−60187
Ga, work function, electrochem. determ., rel. to In-Ga alloys 77−44489
GaAs (110), clean, cleaved, surface states, work function meas. 80−49847
GaAs (110), struct., elec. props., effects of illumination, O_2 absorpt., electron bombard. *(French)* 78−34690
n-GaAs (110) surface, Cs adsorption, work function meas., adsorption site model 79−23839
GaAs epitaxial thin films with neg. electron affinity, photoelectron energy distrib. 80−100755
GaAs, MBE (001) layers, work function meas. 80−49870
GaAs, photocathodes exhibiting negative electron affinity *(French)* 77−8724
n-GaAs, photoemission and work function of (111A) and (111B) surfaces, energy states 77−20980
GaAs Schottky-barrier diode, elec. props. 77−59331
GaAs surface, clean and O_2 covered, work function and photovoltage meas. 77−1446
GaAs, surface segregation of implanted alkali metals, photoemitter prep. and characts. *(French)* 78−60544
p-GaAs/rare earth metal contacts, surface pot. barrier 80−60086
GaAs-metal Schottky barrier height rel. to chem. reactivity 80−25008
GaInAs, photocathode with negative electron affinity, photoemission, influence of strong elec. field 79−8227
$Ga_{1-x}In_xAs$, photocathode, work function depend. of photoelectric emission 78−68071
n-GaP films, reduced work function, energy spectra of secondary electron emission 79−28867
GaP, luminesc. from electron-hole drops, 2 to 77K 79−11454
GaP-metal Schottky barrier height rel. to chem. reactivity 80−25008
GaSb surface, temp. depend of work function *(French)* 80−6949
Gd, surface ionisation on W (110) 79−87142
GdB_6, crystal preparation, elec. resistance, phase transitions 80−97427
Ge (100) with Cs and Cs+O_2 overlayers, negative electron affinity surface, thermal stability of work fn. 78−92167
Ge (111), adsorption of K and Cs, effect on surface elec. props. 79−90880
Ge (111) coadsorption of K and O_2, rel. to work function, K thermodesorpt. spectra 78−79874
Ge (111) surface, clean, O_2 adsorption rate and electron work function 80−59779
Ge, (111) surface, clean and O_2 adsorbed, photoemission yield spectroscopy of electronic surface states 79−91122

work function continued
p-Ge (111) surface, Cs adsorption, work function meas., adsorption site model 79−23839
Ge, adsorbed metal atoms effect on surface electron props. 77−55597
Ge, bound exciton complexes, density functional calc. 80−10890
Ge, size effects in small electron-hole drops 79−82530
Ge strain-confined large electron-hole drop characteristics 80−65469
Ge, work function, meas. by thermionic emission 78−19628
Ge:Na (111) surface, O_2 adsorpt., work function, surface cond. changes meas. 78−79875
He, liquid dielec. breakdown voltages, depend. on work function of cathode surface 80−2695
$HfSi_2$, work function rel. to phys. props. 77−47887
Hg drop electrod in MOS struct., Na-induced work function shift 79−42652
Hg, surface props. rel. to adsorbed O_2, H_2O vapour, work function determ. 78−60187
Hg, work function, temp. coeff. from electrochem. data 78−60186
$Hg_{0.8}Cd_{0.2}Te$-ZnS MIS struct., nonparabolic bond semicond., surface state studies, capacitance measurements 79−78190
HgSe/CdSe lattice-matched heterostructs. as Schottky barriers, CVD epitaxial growth and elec. props. 80−49877
II-VI semiconductor-electrolyte boundaries, electrolyte boundaries, photo e.m.f. meas., semicond. energy bands 77−1481
In-Ga, work function, electrochem. determ. rel. to Ga 77−44489
InAs, oriented single crysts., photoemissive props., photoelec. thresholds 77−59666
n-InP (100), photovoltage transients by retarding pot. electron beam techniques 77−24586
InP surface, interaction with Cl, electron spectroscopic obs. 78−56036
n-InP-metal surface barrier struct., props. 79−11223
InSb, external photoelec. effect 78−27366
InSb, irrad. real and clean surfaces, work function 78−95336
Ir (100)-1×1 surface struct. and reconstruction kinetics, LEED, UPS and work function meas. 79−90851
Ir (111), desorption of Ba, conc. depend. of kinetic characts. of thermal desorption 78−2377
Ir, adsorption of H_2, influence of surface steps and clusters, field emission investig. 77−28698
Ir, field emission spectrosc. from (111) flat and stepped planes 80−76157
Ir, with adsorbed Xe, 5p photoemission, local surface struct. influence 80−2920
Ir, work function meas. rel. to O_2, H_2 adsorpt. 77−66094
Ir(111), chemisorption of O_2, LEED-Auger expts. 77−20191
K (001) surface, electronic struct. by density matrix method 79−60900
K single crystals on W tips, field emission from individual planes 78−27385
KCl film, porous, injection mechanism for transmission secondary electron emission 78−19643
KCl:Tl, thermoemission of positive ions in simple gas atoms *(Russian)* 77−28676
KF/Pt thick layer/substrate system, thermal positive and negative ion emission, surface prop. non-uniformity effect 79−28882
(La, Y, Sc)B_6 solid solns. electron work function, thermal emission technique 80−20755
La, adsorbed on 4d or 5d metal, O_2 coadsorption effects, thermionic emission obs. 78−11064
LaB_6 (001) surface, struct., initial oxidation, XPS, UPS, LEED, AES, work function meas. 79−99403
LaB_6 (100), (110), and (111), surface structs. and work functions 80−70512
LaB_6 (100) surface, O_2 adsorption, UPS and LEED study 80−49519
LaB_6 (210) surface, work function, struct. and chemisorpt. stability, XPS, UPS and LEED 80−65344
LaB_6, adsorption on Ta 80−20039
LaB_6, and related cpds., thermionic props. *(French)* 78−60541
LaB_6 cathodes, single crystal, of <100> and <110> orientations, brightness meas. from 1500 to 1950K 80−62808
LaB_6, clean and oxidised (100) surface, LEED, AES, work function, evaporation meas. 78−71989
LaB_6, field emission and FIM expts. 77−90255
LaB_6, high temp. interaction with 0_2, AES and mass desorption expts. 80−7698
LaB_6 single cryst. tips with [100], [110], [111] and [210] orientations, thermionic emission patterns 80−66379
LaB_6, single cryst. work function, thermionic emission, evaporation 77−24922
LaB_6 single crystal needles, thermal field emitted electron total energy distribution spread 80−45218
LaB_6, single crystals, thermionic work function meas. 78−11067
LaB_6, sintered, work function and Richardson const., Mo poisoning effects 79−52070
LaB_6 surface stoichiometry, thermionic emission B conc. effects 79−87556
LaB_6, synthesis and props. *(Japanese)* 80−40255
LaB_6, thermionic emission characts., jellium model 77−8710
LaB_6, thermionic emission rel. to surface state 78−39654
LaB_6, work function, thermionic and field emission retarding pot. meas. 77−90233
LaB_6, work functions from thermionic and field emission retarding pot. methods 79−65537
LaB_x, phase relationships, chemical activity and work function obs., thermionic appls. 77−90234
LaB_x x=4.24 to 29.2, thermoelectric electron emission, work function, 1400-2100K 78−60539
LaB_6(001) surface, struct. and initial oxidation, UPS, XPS and work functions meas. 77−86195
$LaCrO_3$-MgO, LC20M electrode material in open cycle MHD systems, thermionic emission characts. 80−97394
$LiNbO_3$, effect of spontaneous polarisation on thermionic emission 78−35245
MgO, adsorption of Cs and Li, AES, LEED, work function, and secondary electron emission meas. 80−44407
MgO secondary emitter, increasing of efficiency by coating with Cs or Li film 78−2960
MgO secondary emitter efficiency improvement for low primary electron energies 79−69931
Mo (011) face, adsorption of Sr and La, influence of substrate electronic struct. on props. 78−60032
Mo (100), adsorption of O_2, AES, LEED, work function, and desorption meas. 80−6654
Mo (100), early stage condensation of Cu and Ag, comparison with W (100) 80−80072
Mo (100), effect of metallic adsorbates on surface reson. 79−65983
Mo (100), emission and work function, K adsorption effects 78−11060
Mo (110), of Cs and O_2, common adsorption, work function and thermal stability by contact pot. method 80−44427
Mo, (110) and (111) faces, joint adsorption of Cs and O, and emission props. 78−2364
Mo (111), work function temp. coeff. 80−100499
Mo, (112) face, Sr submonolayer adsorption 80−2271
Mo (112) surface adsorption of Li film, LEED and contact pot. method 80−10794
Mo, adsorpt. of NH_3, and catalytic decomposition, field emission study 78−14596
Mo, adsorption of K, surface coverage depend., field emission microscopy 77−11788
Mo, coadsorption of O_2 and Cs, electron emission props., thermal stability 80−66878
Mo, effect of Hg adsorption 77−7966
Mo field emitter, adsorption of Te on single cryst. faces 78−34714
Mo film, work function, effects of O_2 sorption 78−19125
Mo, surface, electron-stimulated desorption of negative ions, work function 78−72654
Mo, thermionic emission, work function in atmospheric pressure gases 78−76575
Mo-Ca, ion implanted, range distrib. of Ca^+ ions, work function and AES obs. 78−27365
Mo-dimethyl terephthalate contacts, effect of elec. field on contact electrification 79−19660
Mo-Mo_2C-La_2O_3-Pt cathode, Pt effect on work function *(German)* 79−74048
Mo-TiC(ZrC)(HfC), thermionic emission, surface structural characts. after prolonged use, work function variation 80−20758
MoS_2, adsorption of Cs and O_2, LEED, Auger and work function meas. 78−71994
Mo(001), H chemisorbed, self-consistent electron struct. 80−44693
Na_3AlF_6 film, evaporated, electron bombard. effect on secondary electron emission, Auger peak shifts 80−2903
Na_xWO_3, x=0.6 and 0.8, surface characts. 80−39392
Nb (110), adsorption of O_2, variation in work function, retarding field and thermionic emission meas. *(French)* 79−78823
Nb, adsorption of O_2, continuous meas. of surface pot. variations using mirror electron microscope 77−47680
Nb, superconducting transition effect on electronic work function 77−47928
Nb-H, electron work function, 300 to 600 degrees C, contact potential difference meas. 80−29462
Nb-Mo-Ti-Zr-C, work function temp. and phase depend. *(Russian)* 80−2449
$NbC_{0.86}$, single crystal work function, thermionic emission and contact pot., microhardness and binding 79−19649
NbC_x, monocrystal, work function anisotropy of electrons *(Russian)* 79−73568
$NbSe_2$, adsorption of Cs and O_2, 200-300K 78−26767
Nd film, on W(100), struct., electronic and dynamic props. *(Russian)* 77−76702
Ni (001), O_2 overlayer struct. and theory of electron struct. 79−65319
Ni (100), adsorption of CO, EELS and concomitant surface anal. 80−7453
Ni (100), dissociative chemisorption and mol. adsorption of NO 80−65373
Ni (100), initial oxidation, electron energy loss spectra, LEED, AES, and work function meas. 79−61795
Ni (100) surface, adsorption of H_2, LEED, work function meas. and thermal desorpt. obs. 79−23843
Ni (100) surface, electron binding energies of core levels in adsorbed Cs 78−18896
Ni (110), chemisorption of O_2 and initial oxidation, AES, EELS, and work function meas. 80−54523
Ni (111), adsorption sites of CO using IR reflection-absorption spectroscopy and work function meas. 79−69355
Ni (111), adsorption sites of CO, LEED, AES, thermal desorption, work function, and IR system meas. 79−77903
Ni (111), chemisorption geometry of H, LEED, thermal desorption, and work function meas. 80−39433
Ni, (111), chemisorption of H, geometry, order and disorder 79−65311
Ni (111) surface, adsorption of Cl, LEED, AES, work function and flash desorption meas. 77−85069
Ni (111) surface, with O_2, Se, S and Te adsorbed layers, bonding geometry and electronic struct. 79−77909
Ni, adsorption of ethylene at room temp., surface complex vibr. from electron energy loss spectroscopy 79−73404
Ni alloys, thermionic electron emission into Cs vapour 78−60540
Ni clusters, electronic props. and implications for chemisorption 79−23886
Ni film, interaction with O_2, AES, EELS, work function, and gravimetric meas. 80−75433
Ni film, work function change during water adsorpt. *(German)* 79−42365
Ni film, work function changes upon water contamination 80−44705
Ni films, CO-covered, adsorpt. of H, isotherms, resist., work function changes 78−75926
Ni monolayer and submonolayer films, on ZnO, UPS study 80−7472
Ni surface, (111), chemisorbed CO, bond energies 80−100398
Ni-Cu diffusion couple surface, epitaxial, chemisorption of CO and AES work function changes 77−31891
Ni-H, ferromag., H impurities and μSR, self-consistent calc. 80−84447
NiO, nonstoichiometric, near-surface and bulk chem. diffusion 80−80035
NiO, undoped and Li_2O doped, surface reequilibration kinetics 77−55449
Ni(111), adsorption of acetylene, evolution of adsorber species, rel. to vibr. spectra 78−95952
O adsorbed on Ni (111), order-disorder transition 79−82447
Pb, electron field emission, temp. effect 80−60756
Pb, surface props. rel. to adsorbed O_2, H_2O vapour, work function determ. 78−60187
Pd (100), adsorption of Xe and CO, lateral interactions, effect on work function, UPS, and IR spectra 79−77904

work function continued
Pd (111), chemisorption of Cl_2, LEED, AES, thermal desorption, and work function meas. 80−75444
Pd (111), electronic states calc. and adsorbate-induced photoemission struct. interpretation 78−60179
Pd film, work function changes due to adsorbed H_2, surface and interface dipoles 80−96972
Pd ribbon, H_2 adsorption, thermal desorption and work function meas. 80−70538
Pd-Pt, with adsorbed Xe, 5p photoemission, local surface struct. influence 80−2920
Pd-TiO_2 Schottky barrier, work function depend. on adsorbed species 80−54782
Pd-ZnO Schottky-barrier diode, H_2 sensitivity 80−11085
Pd-Zr alloy, activity coeff. rel. to electronic props. *(German)* 77−20084
Pd(110) surface, adsorption of Xe, work function study 80−6633
Pt (100), adsorption of S, obs. 78−14606
Pt (111), adsorption and desorption of H_2, obs. by dynamic meas. of work function 79−77915
Pt (111), adsorption of CO using XPS, UPS, TDS and dynamic meas. of work function 79−65322
Pt (111), adsorption of CO, XPS, UPS, thermal desorption, and work function meas. 79−77905
Pt (111), at. steps role in H interaction 77−15690
Pt (111), chemisorption of Cl_2, LEED, AES, thermal desorption, and work function meas. 80−75444
Pt (111), chemisorption of mol. O_2, XPS, UPS, EELS, and work function meas. 80−76139
Pt (111) stepped surface, adsorption of O_2, CO, C_2N_2 and ethylene 78−71992
Pt (111) surface, of CO, LEED, desorption and work function meas. 77−72781
Pt, adsorption and decomp. of ethylene, 90 to 500K 79−46933
Pt, adsorption of H, face specificity, field emission probe-hole microscope obs. 77−11783
Pt, adsorption of water, H_2 and reaction between H_2 and adsorbed O 80−49514
Pt, Cs adsorption field-emission microscopy 78−51822
Pt film, work function changes upon water contamination 80−44705
Pt, stepped surface, edge atom dipole moments 78−14791
Pt, surface dipole moment calc. 80−60060
Pt, surface props. rel. to adsorbed O_2, H_2O vapour, work function determ. 78−60187
Pt-Ba alloy, elemental comp. and chem. state of surface during thermal activation, AES obs. 78−2345
Pt-Zr alloy, activity coeffs. rel. to electronic props. *(German)* 77−20084
Pt(111), adsorption of Br, irreversible order-disorder transition, LEED AES, thermal description and work function meas. 79−69361
RE, adsorption of K, work function changes, FEM obs. 77−72772
Rb_2Te film electron affinity and photoelectron work function obs. 79−69959
Re, adsorpt. of Au, on low index planes 78−14597
Re, adsorption of k on (10$\bar{1}$0) surface, electron-adsorption props. 79−33192
Re, effect of Hg adsorption 77−7966
Re, polycryst., on adsorpt. of C, CO, H_2 and C_2H_4 *(French)* 77−28075
Re, thermionic emission, work function in atmospheric pressure gases 78−76575
Re, thermionic work function of low index planes 80−55255
Re:C, work function, graphitic layer formation 80−96966
Rh foil, work function determ. rel. to heat treatment temp., extrinsic photoeffect meas. 77−39918
Ru (001), electron stimulated desorption of CO, correl. with other meas. 78−47658
Ru (110), adsorption of H_2S, H_2, and S, UPS and work function change meas. 79−78834
Ru field emitter, adsorption of H_2, field-induced redistrib. processes 79−78854
Ru, NO chemisorpt. and decomp. 78−18903
Ru, with adsorbed Xe, 5p photoemission, local surface struct. influence 80−2920
Ru(110), adsorption of H_2S, H_2, and S, UPS and work function meas. 79−99424
Sb-In, electronic work function, contact pot. difference meas. 77−85299
Sb-Sn, electronic work function, contact pot. difference meas. 77−85299
Sb-Zn, electronic work function, contact pot. difference meas. 77−85299
SbSI, adsorption of $O_2(H_2)$, effect on work function and spontaneous polarisation *(Russian)* 78−6211
Sc, adsorbed on 4d or 5d metal, O_2 coadsorption effects, thermionic emission obs. 78−11064
Se, amorphous film-metal system, contact pot. distrib. and photo-EMF, work function 77−76925
Si (100) with Cs and Cs+O_2 overlayers, negative electron affinity surface, thermal stability of work fn. 78−92167
Si (111), adsorpt. of Cs, LEED, work function and thermal desorpt. 78−14590
Si, (111), struct. depend. oxidation, high resolution photoemission yield spectroscopy 77−1305
Si (111), with chemisorbed Al, electronic struct., self-consistent pseudopotential calc. 78−34880
Si, adsorbed metal atoms effect on surface electron states 77−55597
Si, amorphous, hydrogenated, work function and Auger spectroscopy of initial oxidation 78−76132
Si, electron-hole drops, thermodynamical parameter determ. from luminescence data 80−2845
Si film, on W (100) struct. and work function, LEED meas. 77−66096
Si, metal contacts to O_2 contaminated surfaces, Schottky diodes 79−56309
Si photofield cathode, BaO adsorbed layer, work function and emission props. *(Russian)* 78−68608
Si, work function and Auger spectroscopy of initial oxidation 78−76132
Si:Al(B)(P), bound multiexciton complexes, work function thermodynamic determ. 78−72078
p-Si/rare earth metal contacts, surface pot. barrier 80−60086
p-Si-As_2S_3 isotype crystalline-amorphous heterojunctions, electrophysical props. 79−24063
a-Si-metal Schottky barrier, I-V characts., barrier heights 77−8191
Si-metal Schottky barriers, surface states and barrier heights 77−80838
Si-SiO_2 surface states, influence of Φms(T) 79−99597
p-Si-SiO_2 system, C-V meas. using Au/Hg probe, work function difference between probe and Si 80−2450

work function continued
Si(111), adsorption of HBr(Cl), AES, electron energy loss spectra and electron impact desorption exam. 78−43243
SmB_6, crystal preparation, elec. resistance, phase transitions 80−97427
SmB_6, work function, thermionic and field emission retarding pot. meas. 77−90233
SmB_6, work functions from thermionic and field emission retarding pot. methods 79−65537
Sn-Pb alloys, electron work function determ., contact pot. difference method 77−39920
Sr film, photoemission, action of elec. field 77−48317
Sr film, structure effects on work function, electron micrographs and photoemission meas. 79−83107
SrO epitaxial layer, on Mo (110), secondary electron emission and struct., LEED and AES expts. 78−2958
Ta (112), oxidised, emission and work function, K adsorption effects 78−11060
Ta, adsorption of K, surface coverage depend., field emission microscopy 77−11788
Ta, adsorption of O_2, FEM obs. of work function changes 78−26771
Ta autocathode, influence of electric field and heating on work 80−7478
Ta film, vacuum-deposited, gas adsorpt. effects on photoelec. props. 78−15298
Ta, photo field emission spectroscopy of band structure by He-Ne laser irrad. 80−55276
Ta-H, electron work function, 300 to 600 degrees C, contact potential difference meas. 80−29462
TaC surface, effect of C oxidation on work function, 1250-2000K, AES 79−24054
Tb, surface ionisation on W (110) 79−87142
Th film, coating on Rh layer, work function rel. to degree of coverage *(Czech)* 78−80039
Ti (0001) film, with adsorbed H (1×1) monolayer, electronic struct., surface geometry 80−54750
Ti film, chemisorption of N_2, O_2, CO and CO_2, changes in work function 77−59221
Ti, film, evap., CO effect on work function 78−39188
Ti film, work function, effects of O_2 sorption 78−19125
Ti, interaction with O_2, resist. and work function changes obs. 80−45431
Ti, ion-surface bombard. optical radiation emission by excited atoms 78−39652
Ti, polycryst., chemisorption, of N_2, O_2 and CO, secondary electron yield spectrum obs. 78−38933
TiC (001) surface, change in work function with chemisorption of O_2 and H_2O 80−29461
TiC single crystal, work function, field emission characts. *(Japanese)* 78−19641
TiO_2, (100) surfaces, ionisation of sputtered-atomic particles 80−20750
Ti_xSi_y, work function rel. to phys. props. 77−47887
U, field emission microscopy, emissive props. 78−88409
V (100), sorption investig. using total current spectroscopy of slow electrons 77−8694
V-H, electron work function, 300 to 600 degrees C, contact potential difference meas. 80−29462
V_2O_5 single crystals, contact-limited conduction 79−95493
V{100}, Au(Au) layer growth, total current spectroscopy 77−36329
W,(100) and (111), methane adsorption effect 78−38963
W (011), adsorption of Ag, LEED, AES, and work function meas. 79−86990
W (011) face, adsorption of Sr and La, influence of substrate electronic struct. on props. 78−60032
W (100), adsorbed La, depend. of work function, heat of adsorpt. on surface coverage, contact potential study 78−67912
W (100), adsorpt. of acetylene, room temp., electron spectroscopy obs. 79−7749
W (100), adsorption of CO, thermal desorption and work function meas. 80−29273
W (100), adsorption of O_2, AES, desorption, LEED and work function obs. 77−1317
W (100), adsorption of O_2, surface struct. and thermally stimulated reaction 77−55451
W (100), adsorption of Zr, AES, LEED, thermal desorption, and work function meas. 80−39444
W (100), chemisorption of Hg, AES, LEED, work function and thermal desorption expts. 78−34709
W (100), coadsorption of Zr and O_2 at high temp. 80−6653
W (100), early stage condensation of Cu and Ag, comparison with Mo (100) 80−80072
W (100), effect of metallic adsorbates on surface reson. 79−65983
W (100), reconstruction in presence of O half monolayer, struct. props. 80−44421
W (100), surface reconstruction kinetics in presence of O half-monolayer 80−65375
W (100) photocathode, monitoring of Cs and O_2 coadsorption 77−55862
W (100) surface, adsorbed Au, Cu layers, electron field emission revealing unmasked surface reson. 79−15595
W (100) surface, chemisorption of CO_2, NO, UPS studies, work function behaviour 79−23841
W (110), (112), of Cs and O_2, common adsorption, work function and thermal stability by contact pot. method 80−44427
W (110), adsorption of N_2, thermal desorpt. and work function meas. 77−1294
W (110), coadsorption of Ba and Cs, work function of surface under equilibrium conditions 79−15025
W (110), codeposition of Cs and O, Cs_2O form. 80−44425
W (110), dipole moments of single 5d metal adatoms field emission meas. 77−47674
W (110), Fowler-Nordheim studies 80−34501
W (110), O_2 diffusion, coverage-distance plots, diffusion coeff. 77−62755
W (110), oxygenated and oxidised, Cs absorption 80−44424
W (110) and (100), adsorption of Xe and coadsorption with O, work function and thermal desorption meas. 80−39448
W (110) plane, adsorption of CO, electron impact desorption, thermal desorption and work function meas. 77−85064
W (110) surface, adsorbed Pd, growth, struct., stability, desorption 80−59794
W (110) surface, adsorption of O_2, LEED, AES and thermal desorption meas. 78−38957
W (112), adsorption of La, contact pot. difference, LEED and field emission microscopy *(Russian)* 78−14618

work function continued
W {001} (1×1)→($\sqrt{2}\times\sqrt{2}$)R45° surface struct. transition, LEED, AES, and work function meas. 79−42348
W, adsorption and early stages of condensation of Ag and Au on single cryst. surface 78−6212
W, adsorption of Au, field emission microscopy exam. of work function, correlation with LEED and RHEED meas. 78−35276
W, adsorption of Fe *(Japanese)* 78−91536
W, adsorption of Ga, In and Sn, field emission, FIM 77−16470
W, adsorption of Gd in field ion microscope *(Russian)* 77−47662
W, Ag adsorption on (001), (011) and (111), work function changes 77−62757
W, coadsorpt. of Ni and K, average work function change 79−28190
W, coadsorption of La and B, field emission meas. 78−47662
W, coadsorption of La and B, field emission and field ion microscopy 80−104049
W, coadsorption of Th and H, FEM exam. 79−90869
W, effect of La-O surface layer *(Russian)* 77−35816
W, electronic work function, self-consistent calcs. 78−76135
W epitaxy on W(110) substrate, work function meas., LEED investigation 80−80103
W faces, simultaneous adsorption of Ba and Cu atoms, work function changes 80−65378
W field emitter, adsorption of Cu, field emission energy distribs. 77−59677
W field emitter, adsorption of Te on single cryst. faces 78−34714
W field emitter, effect of Au adsorption on (110) and (211) planes 77−12503
W film, adsorbed Th layer, work function, temp. depend. 77−28701
W, impregnated thermionic cathode, surface props. exam. using AES and work function meas. 77−8715
W, ion induced secondary electron emission, probe for adsorbed O 80−55251
W, joint adsorption of Ba and Ti, work function meas. 80−100411
W, K atom beam impact on gas-covered surface, K^+ ion current peculiar decay 79−74045
W, low-index planes, adsorption of Pb, probe-hole field emission microscopy obs. 77−47677
W, monolayer of Ga(In)(Sn), field ion image qualities and work function 78−35272
W, photo field emission spectra of optical transitions, band struct. 77−16467
W, regularly stepped single crystal surfaces, work function determ. by thermionic emission 77−59665
W single cryst., dislocation effects on thermionic emission and work function 80−76129
W, stepped surface, edge atom dipole moments 78−14791
W stepped surface, O adsorption and desorption obs. 77−47675
W, surface dipole moment calc. 80−60060
W, surfaces (100) and (110), adsorbed O electron stimulated desorption, combined method using LEED and AES 79−33181
W, thermionic emission, work function in atmospheric pressure gases 78−76575
W, thermionic emitter, work function rel. to output characts., in arc regime 77−52213
W tip, Cu covered, field ion microscopy study 78−23587
W, V adsorption effect, surface struct. depend. 77−51607
W, work function, field emission meas., Te and Cs surface film effects 78−19645
W, work function measurement in SEM 80−80918
W:La, B coadsorption and work function, FEM and FIM obs. 79−52087
W:Os coated dispenser cathode, chemical and physical process obs. 79−28885
W-dimethyl terephthalate contacts, effect of elec. field on contact electrification 79−19660
W-O system, surface elect. cond. of oxides in equilib. with gas phase 79−61791
W-Ti, Ti addition effect on heat resistance and radiative props. *(Russian)* 80−25515
W-Tic(ZrC)(HfC), thermionic emission, surface structural characts. after prolonged use, work function variation 80−20758
W-Zr, Zr addition effect on heat resistance and radiative props. *(Russian)* 80−25515
W-Zr-C, Zr and C addition effect on heat resistance and radiative props. *(Russian)* 80−25515
W-ZrC (25 wt.%), eutectic alloy, thermionic emission and adsorption props. 79−69951
(W-Au)-SiO_2-Si:B MOS transistor, ion implantation effect on threshold voltage 78−34903
W(001), surface states and surface resonances, self-consistent electronic struct. 80−96960
W(100), clean thermally induced c(2×2) surface struct. 77−62714
W(100) surface resonance, effect of Cu adsorption 77−59201
W(110), Cs and O_2 coadsorption, surface anal. 77−89656
W(110), effect of chemisorpt. of CO and O_2 78−71986
W(110) surface, Ba monolayer, struct. transformation stages 77−47681
W(211), adsorption of Be, work function changes and scatt. electron energy losses 79−46947
W{100}, adsorption of N_2, surface disorder effects on work function change 77−20192
W{100} surface, co-adsorption of Cu and O_2, AES, thermal desorption, LEED and work function meas. 78−38950
Y, adsorbed on 4d or 5d metal, O_2 coadsorption effects, thermionic emission obs. 78−11064
Y single crystal, thermionic emission work function 78−2971
ZnO $10\bar{1}0$ surface, reaction of O_2, AES, LEED, EPR, desorpt., surface cond. and work function expts. 78−95950
ZnO $(000\bar{1})$ and $(10\bar{1}0)$ surfaces, clean and contaminated, reactivity to Cl_2 79−61904
ZnO accumulation layers, Hall mobility and work function, correl. 78−60185
ZnO, low energy cathodolum., surface effects 78−60522
ZnO, polar surfaces (0001), $(000\bar{1})$ specificity, field emission, H adsorption 77−21009
ZnO, prismatic surface, O_2 interaction obs. 77−31899
ZnO surfaces, work function, band bending, and electron affinity 79−47145
ZnO-Cs, fabrication, UPS meas. 78−15279
ZnS, surface, work function and luminesc. phenomena, effect of H,H_2,O and O_2 adsorpt. 78−10538
ZnS-metal Schottky barrier height rel. to chem. reactivity 80−25008

work function continued
ZnSe-metal Schottky barrier height rel. to chem. reactivity 80−25008
Zr, adsorption and absorpt. of CO, NO, N_2, O_2, and D_2, dissoc. and diffusion 80−80085
ZrC, effect of H_2 adsorpt., thermionic emission expts. 78−2970
ZrC, pure and with Y additions, thermionic emission, hot pressed or CVD 77−12484
ZrC work function, sorbed O_2 effect, thermionic emission and thermal desorption obs. 79−56285
ZrC-W, thermionic emission current density, cathode operating time and comp. depend. 77−8714
$ZrC_{0.84}$, single crystal work function, thermionic emission and contact pot., microhardness and binding 79−19649
ZrC_x, monocrystal, work function anisotropy of electrons *(Russian)* 79−73568
$ZrSi_2$, work function rel. to phys. props. 77−47887

work hardening
see also cold working
alkali halide doped angle crystals, latent hardening 78−51607
alloy, dispersion hardened, temp. depend. of work-hardening due to Orowan loops 79−91668
alloy, dispersion hardened, work hardening due to Orowan loops, temp. depend. *(Japanese)* 80−66534
alloy, ordered, conservative jog slip on superpartial screw dislocations, work hardening 77−7731
alloy, space lattice types A_1, A_2 and A_3, strain hardening function *(German)* 80−20955
alloys, hot plastic strain, stress- strain-time dependences *(Russian)* 80−40430
alloys, $L1_2$-type superstruct., anomalous temp. depend. of deform. characts. *(Russian)* 79−20109
alloys, Ll_2, superstructure, dislocation link strength and strain hardening at high degrees of deform. *(Russian)* 78−39792
alloys, single cryst., work hardening phenomena and screw dislocation dipole clusters 80−100845
anisotropic elastic state, plastic-strain mechanism 78−42530
austenitic steel, mechanical properties, effect of high temp. thermomechanical treatment and post-deform. ageing *(Russian)* 78−39809
bar of linearly work hardening material, critical load *(Russian)* 77−89053
Bauschinger AE peak detection of back stress component in flow stress *(Japanese)* 78−6977
BCC metals and alloys, glide and work hardening, review *(German)* 79−34067
BCC metals and alloys, glide and work hardening review *(German)* 79−29089
BCC metals and alloys, review of plastic deformation and work hardening *(German)* 78−84946
bitumen, rheological model of Maxwell-Norton type *(French)* 79−64614
block copolymers, morphology rel. to stress/strain props., deform. hardening effect, birefringence meas. 77−48501
bounded metalworking process, iterative numerical anal. technique 79−83212
brass, adsorpt. of Hg, effect on mech. strength, creep, fatigue, embrittlement, work hardening, roller burnishing effects *(Russian)* 79−29267
α-brass, Bauschinger AE peak detection of back stress component in flow stress *(Japanese)* 78−6977
β-brass, bicrystal and tricrystal stress strain behaviour 77−36607
brass, cold rolling, inhomogeneous texture 80−89251
brass, crack opening displacement, rel. to flow stress 78−68810
α-brass, fatigue crack propag., role of dislocation substruct. 80−60963
brass, fatigue hardening and high cycle fatigue under reversed bending 79−20180
α-brass, single crystal, deform. and ductility at elev. temps. *(Japanese)* 79−5012
α-β brass, two phase bicrystal, deform. and fracture at 450K 80−16409
β-brass, uniaxial tension and compression, cyclic stress-strain behaviour 80−97551
brass (37%Zn), workhardened thin specimens, fracture, anisotropy coeff. role *(French)* 80−104276
bronze P, heavily cold rolled, yield strength enhancement mech. 77−36539
cantilever postcollapse behaviour, strain hardening effects on large plastic deformation 79−46232
cell wall and lattice misorientation origin during deform. 80−71712
cement based materials, fatigue hardening 79−29086
ceramic nuclear fuels, mech. props. at compressive deformation 80−651
clad sheet metal, optimum combination of composing sheets for deep drawing 77−81241
composite, lamellar, matrix strain hardening mechanism *(Russian)* 77−59801
composite superconductor, flux jumps and training 80−70911
concrete, endochronic model for nonlinear triaxial behaviour 78−51095
constitutive eqns. of work hardening-recovery type, numerical integration, improved method 78−6949
Cr, strain hardened metal and microalloys, low temp. brittleness 79−96140
crack opening displacement, interrelation with J-integral 79−50648
cracktip under incipient creep deform., stress field and modified J-integral *(Japanese)* 80−103411
creep, effect of interstitial and vacancy dislocation loops *(Russian)* 77−81271
crystalline materials, in situ deform. by high voltage electron microscopy 80−103352
Cu, formation of double twist boundaries during plastic deform. *(Russian)* 77−81295
Cu-Al, FCC, study of dipoles using weak-beam electron microscopy 78−22724
cubic single crystals, hardness meas. by spherical indentation 80−16622
curves, critical points 79−43263
cyclic inelastic behaviour of metals, friction stress method 77−4855
cyclic plasticity for nonproportional paths, comparison with prediction of three incremental plasticity model 78−92308
deformable solids, fracture and hardening kinetics 80−35210
deformation broaching of difficult-to-form metals 80−108473
diamond-metal strip, strength props. 79−61678
discrete structures under dynamic loading, work hardening adaptation 80−74726
dislocation interaction, force between dislocation, and misfitting ordered particle, calc. 78−83815

work hardening continued
dislocation train moving through dislocation forest, loop formation 80−107238
dislocations model, compatibility with transient and steady state creep *(Italian)* 80−33487
ductile fracture, J-integral estimates 77−89064
ductile fracture, strain hardening and damage relationship 80−108564
ductile single crystal, geometric effects in inhomogeneous deform. 79−46741
Duralumin, adsorpt. of Hg, effect on mech. strength, creep, fatigue, embrittlement *(Russian)* 79−29267
easy glide, computers modelling, range of permissible parameters *(Russian)* 78−47375
edge crack, elastic-plastic stress distrib. near flat surfaced notch with cycloidal tip 77−35084
elastic plastic body, model, and analogy with liquid vapour phase equilib. 77−84155
elastic structures, work hardening deflection stability 79−27528
elastic-plastic models, integration algorithms 80−5959
elastic-viscoplastic frames, dynamic responses, strain hardening effects 80−79178
elasto-plastic material, crack tip stress and strain fields and fracture behaviour 78−22304
elastoplastic strip or half-plane under moving load, residual stresses and plastic zones 80−53645
elastoplastic struct. with kinematic hardening, cyclic loading *(French)* 78−42537
elastoviscoplastic system, work hardening due to residual stresses constitutive eqns. for rates *(French)* 77−70068
electrotechnical steel, quality significance on energy and materials savings in magnetic circuits *(Czech)* 80−20947
fatigue crack propag. and strain softening under hydrostatic press. 77−16691
fatigue crack propagation, crack closure, effective stress range factors 80−100924
fatigue crack propagation model for strain hardening materials 78−18236
fatigue review 77−4150
FCC crystal, grip effect and bend gliding during uniaxial tensile deform. *(Japanese)* 79−52314
FCC metals and alloys, deform. behaviour 77−8892
fibre reinforced composites, thermal cycling, elastoplastic strain calc. under action of external stresses *(Russian)* 79−38896
fibre-reinforced rigid-plastic beam with end supports, impulsive loading 77−80095
filler metal, deformation mechanism at brazed joint 78−80616
finite distortional latent hardening in single crysts., perpetuation of slip 78−3144
finite strain work-hardening theory for rate independent elasto-plasticity 79−76983
forming limit curve for bending processes 80−7627
fracture stress obtained from the elastic crack tip enclave model 80−71730
galvanic coatings, adhesion after strain hardening, test device 80−71837
heteroplastic material, plastic rate, effect of strain hardening *(French)* 77−63718
high-temp. behaviour of inelastic metals 77−4830
hot twisting, shearing stresses, anal. determ. 78−60900
hypo-elastic materials with internal variables, shear 77−31221
hypoelastic materials with internal variable, work-hardening, hysteresis, fracture law 77−62177
ideal fibre reinforced, rigid plastic cantilever beam, impulsive loading, subsequent motion 77−80096
ideal fibre reinforced rigid plastic beams, impulsive transverse loading, control impact 77−80094
Inconel 600, mechanisms of dynamic strain ageing and jerky flow 79−79024
Inconel 718, low cycle fatigue at 298 and 823K 77−86151
indentation hardness to yield stress ratio glide processes 77−40426
isotropic strain hardening theory *(Russian)* 80−38279
kinematic hardening models, use in multi-axial cyclic plasticity 80−25717
material indentation analysis 79−8308
metal, anisotropic, description of history dependent plastic flow behaviour 80−11732
metal, computation of strain hardening curve 77−90363
metal, fatigue fracture-stacking fault energy correlation *(Russian)* 78−15499
metal, FCC or BCC, dislocation annihilation during tensile and cyclic deform. and limits of dislocation densities 80−34007
metal, FCC polycrystalline, work hardening, plastic deform *(Hungarian)* 77−77504
metal, finite elastic-plastic deformation at high temp., work hardening rule 77−4828
metal, hardening and softening during absorption fatigue in surface active medium, governing laws 77−86230
metal, nonlinear mech. response, Swift effect 78−35433
metal, plastic, work hardening, sintered, porous, irreversible deform. 78−19849
metal, plastic anisotropic hardening pot., stress/strain relation under combined axial load/torsion 78−52896
metal, polycryst., Bauschinger effect and mutual restriction between grains 78−52895
metal, polycrystalline, strain hardening, dislocation link length model 80−84953
metal, sheet, numerical anal. of tensile tests 77−86101
metal, space lattice types A_1, A_2 and A_3, strain hardening function *(German)* 80−20955
metal, strain hardening relation, method of error rectangles 77−55980
metal, surface layer dissolution, effect of rate on softening during plastic strain 78−39957
metal, work-hardening, plastic, sintered, porous, irreversible deform. 78−35459
metal and alloy, deformation strengthening and anisotropy prediction *(Russian)* 78−27533
metal sheet, circular, impulsive press. by underwater wire explosions, dynamic plastic deform. 80−84866
metal sheet, strain propag. under non-uniformity distributed load 77−16653
metals, cold forging, upset tests anal., stress-strain law determ. appl. *(French)* 79−20064
work hardening continued
metals, deformability, quantitative determ. in drawing 79−52229
metals, FCC, slip dislocation reactions at coherent twin boundaries, effect on work-hardening 79−1431
metals, FCC, yield threshold at 4.2K, effect on strain-hardening curve *(Russian)* 80−50671
metals, hardening response in small deform. 79−47719
metals, porous, plastic flows, microscopic frictional effects, J_2-flow potential and yield function 80−64384
metals, research at Birmingham, (1945-55) 80−62444
metals, strain hardening, creep, stress relaxation correlation with high temp. processes *(Russian)* 79−34053
metals, work-hardening, dislocation multiplication model 79−61608
metals and alloys, criteria for evaluation of strain hardening 77−55982
metals and alloys, yield criterion, rheological interpretation *(Russian)* 80−21014
metals with mixed hardening, finite element anal. of elastic-plastic materials 79−27543
micromechanical constants of statistical model interpetation of anisotropic work hardening *(Bulgarian)* 79−100169
microstrains distrib. in macroinhomogeneous fields *(Russian)* 80−21018
model comprising work hardening and solid solution hardening 79−34051
montmorillonite, mech. props. at high press., rel. to fault behaviour 79−84234
multiple-mode plastic straining, numerical anal. uniqueness 77−62166
necking and tensile instability in material with strain hardening and strain-rate hardening 78−23717
Nimonic cylinder, stress redistribution obs. 77−4831
nonisothermal theories, of plastic flow and theory of work hardening in creep 79−57077
nonlinear hardening model, appl. to cyclic loading phenomena simulation 77−21158
notch tip stress distrib. in strain hardening material 79−3927
one dimensional plastic materials with work hardening, acceleration waves 79−32339
one-dimensional plastic material with work hardening constitutive eqns., stress-strain relations 79−32296
Orowan loop storage capacity, system containing ellipsoidal particles 77−76402
oxides, interaction between point defects and dislocations, cryst. plasticity 80−15149
parabolic curve appl. 79−43264
perforated plates, finite element elasto-plastic anal. 80−10168
phase transformation, $\alpha \rightleftarrows \beta$, influence on mech. props. *(Russian)* 78−68681
plane stress crack problems, fully plastic soln. and large scale yielding estimates 77−19573
plane-strain work hardening, meas. and anal. 80−81073
plastic and viscous hardening of materials, steady and cyclic loading 77−4793
plastic asymmetric edge crack under longitudinal shear 77−80117
plastic constitutive equations with work hardening *(Japanese)* 80−25718
plastic deformation, cyclic, exam. of reversible strain, effect on dislocation motion 78−84892
plastic dielecs. with general work-hardening, phenomenological theory 79−8113
plastic material, rate type, with kinematic work hardening 78−15450
plastic material, work-hardening model evaluation 77−77500
plastic material, work-hardening model evaluation 77−77501
plastic rate type materials with general work hardening 78−42548
plastic torsion elongation, fibre rot. with anisotropic work hardening *(German)* 77−72184
polycrystalline metals, stored energy and strain hardening 79−82276
polyethylene, extruded high-density fibres, deformation and strain hardening 79−70035
polyethylene, high density, hydrostatic extrusion behaviour 80−50649
polyoxymethylene, rolled, prediction of yielding behaviour 77−73306
porous materials, approx. solns. of problems of plastic working 78−68643
Portevin-Le Chatelier effect and inverse strain-rate sensitivity 79−1476
Prandtl Reuss plastic material, with kinematic work hardening, consitutive equations *(Japanese)* 77−77502
Prandtl Reuss plastic material with isotropic work hardening, loading and unloading *(Japanese)* 77−8854
Prandtl-Reuss plastic material, with kinematic work hardening, steady simple extension *(Japanese)* 77−77503
Prandtl-Reuss plastic material with isotropic work hardening, constitutive equations *(Japanese)* 77−4789
Prandtl-Reuss plastic materials, with general work hardening, constitutive equations *(Japanese)* 78−92276
properties of high-conductivity copper and copper alloy wires *(Japanese)* 79−91665
PVC, orientation hardening 78−76662
quartz, thermoluminescence sensitivity change due to stress 77−59627
rate-type plastic material with scalar and tensor internal variables 77−68449
refractory metal, disturbed layer depth on abrasive lapping with TiC, NbC, WC micropowders 77−44391
rheological analysis of stress change experiments during high temperature creep 79−37193
rigid plastic continua, adaption under dynamic loadings 79−27548
rigid work hardening structures optimum design 78−13917
sapphire, work hardening 77−16604
shakedown analysis, numerical, circular plates subjected to press and temp. cycles 77−3749
sheet material, method for strength meas. under biaxial tension 80−66717
sheet metal forming, material behaviour 78−95787
sheet metal forming, strain hardening and strain rate sensitivity 78−7000
sheet metals, ductile, shearing process 78−84841
sheet metals, strain-induced changes in mech. props. and press formabilities 78−19781
sheet-metal laminate effect of interstage annealing on stretch formability 77−55917
shot peening residual stress effects on plastic microstrain in isotopic media *(French)* 79−77675
simulation of inelastic material behaviour in struct. anal. 78−34041

work hardening continued
slip, primary coplanar, role in deform. of FCC crystals *(Japanese)* 77−52412
slip and twinning relns. *(Russian)* 77−65982
soil, cohesionless with curved yield surfaces, elastoplastic stress-strain theory 78−18186
soil, plastic flows, microscopic frictional effects, J_2-flow potential and yield function 80−64384
solid soln., ductility, comp. effect *(Japanese)* 79−43334
steady state response of systems with hardening hysteresis 78−60680
steel work hardening parameter determ. 77−77495
steel, 0Kh16N15M3B, irradiation effects on resistance to cyclic elastoplastic deformation 79−91767
steel, 12Kh1M1F, pipe with axial surface crack, resistance of failure in plastic deform. 79−100235
steel, 30CH2GMT and 35CHG2SV, thermomechanical hardening *(Czechoslovakian)* 77−32602
steel, 40Kh, plastic-strain mechanism for work hardening 78−42530
steel, 45KhN, hardening by loading 77−86050
steel, $\alpha \rightarrow \gamma$ transformation during rapid heating of N18K9M5T and N25 77−59788
steel, alloy, cyclic strength after strain hardening and tempering, precip. hardened 40FT and 40 78−52988
steel, alloy, martensitic transforms. during deform. of types N28, N29, N30 and N31 78−56639
steel, alloy, softening process in deformed type 15GYuT, metallographs *(Russian)* 78−52840
steel, anisotropic sheet, strain hardening, stress state depend. 80−55421
steel, austenite, carbide strain hardened, strength and plasticity, effect of Mn content *(Russian)* 80−97500
steel, austenite hot deformation influence on phase transformations 80−7606
steel, austenitic, 0Kh14AG12M, temp. depend. of mech. props. and kinetics of phase transforms. *(Russian)* 78−92297
steel, austenitic, 45Kh2N12GS, post deformation holding at deform. temp. effect on struct. and strength of austenite and martensite *(Russian)* 79−1880
steel, austenitic, 800H, effect of aging and cold working on fatigue behaviour 78−84846
steel, austenitic, high Mn, abrasive wear resistance *(Korean)* 77−25162
steel, austenitic, Mn strain hardening at room and low temps. *(German)* 79−38845
steel, austenitic and ferritic stainless, fatigue, effect of struct. and work hardening rate *(French)* 77−63783
steel, austenitic and martensitic, structural sensitivity of Bauschinger effect *(Russian)* 79−52303
steel, austenitic stainless, 08Kh18N10T, hot-worked precipitation kinetics and struct. of dispersed phases, Ti effect 80−29964
steel, austenitic stainless, AISI 316 L, viscoplastic deformation under hot working conditions, struct. model 79−83278
steel, austenitic stainless, martensitic transform. effect during static and fatigue loading 77−52325
steel, austenitic stainless, strain hardened containing N_2, low temp. props. 79−66128
steel, austenitic stainless, types 304L and 316L, work-hardened, electrochem. and corrosion behaviour in acid solns. 80−50757
steel, austenitic stainless recrystallisation *(Japanese)* 77−52346
steel, austenitic-martensitic, phase comp., struct. and mech. props. 80−29974
steel, C, crack opening displacement, rel. to flow stress 78−68810
steel, C, deformation strength and strain rate depend. under plain strain state *(Japanese)* 80−30028
steel, C, low temperature strength, preliminary plastic deform. effect 80−81128
steel, C, plastic deform., −150 to 200°C, effect on loading surface 79−66130
steel, C, rotating bending fatigue strength, high tensile load effect during stress cycling *(Japanese)* 77−52477
steel, C, strain ageing and fatigue limit 80−40378
steel, C, strain ageing contribution to fatigue hardening 78−23817
steel, C, X-ray line fitting by Gram-Charlier distrib., appl. to tension test *(French)* 79−15689
steel, C(0.2 wt.%), explosively strengthened, cause of anomalous increase in H_2 of low cycle endurance *(Russian)* 77−16729
steel, C (0.1 to 1.15 wt.%), fatigue, mean stress effects *(German)* 78−56721
steel, C (0.1-1.15 wt.%), fatigue under reversed tension-compression stresses, photoelasticity investig. *(German)* 78−31493
steel, C content effect on annealing texture, plastic anisotropy and mechanical props. 80−29976
steel, C-Mn, corrosion in acidic soln., metallurgical factor effects 79−70206
steel, C-Mn-Si, dual phase, stress-strain curves, deformation behaviour 79−52324
steel, cast, type 20, exam. of strain characts. in premelting temp. range *(Russian)* 79−29140
steel, CK10, structural, temp. and freq. depend. of stress-strain behaviour under cyclic loading *(German)* 79−38888
steel, cold deformation hardening, effect of C content and cementite shape 78−92277
steel, cold rolled high strength sheet, with high drawability, fabrication process 77−73288
steel, Cr-Mn, strain hardening, 4.2 to 293K 80−81076
steel, Cr-Mo (2.25, 1 wt.%), creep and high temp. low-cycle fatigue tests 80−85061
steel, Cr-Mo (2.25, 1 wt.%), strain hardening shakedown load during bending 80−20958
steel, Cr-Ni, strain hardening, 4.2 to 293K 80−81076
steel, deform. resist., softening effects, analytical depend. calcs. *(Russian)* 80−49293
steel, deformability characts. in surface-active medium at decreasing temp., mech. working effect *(Russian)* 77−59851
steel, deformation and fracture resistance due to low-cycle fatigue in plane bending 79−66166
steel, deformation at large plastic strains, work hardening rate 79−20065
steel, deformation under mutual indentation in contact with Li melt *(Russian)* 77−59853
steel, deformed eutectoid C_2 back stress decrease on annealing and H embrittlement 80−20981
steel, ductile struct., crack propag. 78−68805
work hardening continued
steel, fatigue strength on combined surface strain-hardening and tempering *(Russian)* 77−59900
steel, ferritic, cleavage fracture toughness, temp. and strain rate depend. 80−85028
steel, grain boundary strengthening mechanism 80−35207
steel, high Si dual-phase, mech. props and microstruct. anal. 80−40444
steel, high strength, low alloy, response to cyclic plastic deform. 78−7035
steel, high strength, surface work hardening effect on life 77−70234
steel, high-strength, low cycle fatigue, hysteresis loops, cyclic strain curves, fatigue diagrams *(Polish)* 80−66638
steel, intermediate class Kh16N6, structural aspects of work hardening 77−90369
steel, low alloy, hot deform. behaviour and modified ausforming *(Japanese)* 78−11244
steel, low alloy, strengthening by strain tempering, deform. effects 78−15424
steel, low alloy structural, type 30KhGSA, effect of thermomech. treatment on strength, fracture toughness and fatigue props. 80−11676
steel, low C, cyclic stress-strain response under spectrum loading *(Slovak)* 78−19886
steel, low C, dynamics of cyclic plastic deform. and fatigue life at low temps. 77−16670
steel, low C, dynamics of cyclic plastic deform. at low temps. *(Czechoslovakian)* 77−32679
steel, low C, gas nitrocarburized, cyclic stressing 79−57098
steel, low C, high strength, thermomech. treatment, strengthening mech. 79−57014
steel, low C, initial stages of plastic deform. *(Japanese)* 80−93618
steel, low C, instability obs. by large strain compression 80−35253
steel, low C, low cycle fatigue props. with variable strain ranges *(Czech)* 80−45390
steel, low C, Mn, strain hardening parameters, electron microscope obs. 77−63690
steel, low C, normalised, plastic deform., using microhardness and grain strain meas. 77−4810
steel, low C, quenched, hardening during explosive forming 79−87650
steel, low C, rimmed, structural damage in sheet metal forming 78−64614
steel, low C, strain ageing, effect of prestrain *(Korean)* 77−8865
steel, low C, stress-controlled and strain-controlled tests, S/N curves comparison *(German)* 80−40476
steel, low C, type En3, high strain deform., struct. and props. 80−89301
steel, low or medium alloy, work hardening effect on martensitic transform. cond. *(French)* 80−16329
steel, low-alloy, bearing, mech. props., carbide behaviour effect *(Korean)* 80−93615
steel, low-alloy, props. with nitride and Cu hardening at low temps. *(Russian)* 80−40372
steel, maraging, and HY-80, deform., hydrostatic pressure effect 77−36596
steel, martensitic, 28Kh3SNMVFA, strain hardening at high temps. *(Russian)* 79−74174
steel, martensitic, medium alloy, quenched state, deform. hardened, ageing effects *(Russian)* 77−21179
steel, medium C, microflow and strain hardening under cyclic loading 80−104182
steel, mild, adiabatic viscoplastic deform. at high strain rate, negative strain hardening *(French)* 77−21212
steel, mild, annealed, plastic flow under proportional and non-proportional straining 80−40465
steel, mild, fatigue crack initiation 77−86163
steel, mild, plate, explosive hardening of one end 77−36531
steel, mild, tubes between rigid plates, lateral compression, strain hardening effect 78−48422
steel, mild, work hardening and strain ageing during fatigue *(Japanese)* 77−8931
steel, Mn (13.5 wt.%) hardening mechanism during friction 79−96152
steel, Mn-Cr, blank hardened, shot peening effect on bending fatigue strength *(German)* 78−35402
steel, Ni-Cr-Ti, thin bands, cold working, props. and struct. of 36NKhTYu 79−78994
steel, Ni-Mo, sintered, martensitic transformation due to cold working, metallographic study 78−44127
steel, non-alloy, effect of shearing *(French)* 78−15423
steel, notched bar impact test specimens, strain hardening distrib. *(German)* 77−60004
steel, perforated bent sections, microstruct. near holes 78−23725
steel, plastically deformed or hardened, X-ray diffr. data anal., moment method *(Czech)* 78−31593
steel, quench-hardened, exam. of anomalous plasticity when deformed *(Russian)* 79−11663
steel, quenched and tempered 52100 bearing, plastic deform. in compression 77−40437
steel, railroad rail, effect of cold worked layer on Rayleigh wave dispersion 79−1014
steel, sheet, effects of strain rate and deformation heating in tensile testing 78−85089
steel, sheet, rapid test for props. assessment 80−40650
steel, spheroidized, Bauschinger effect and work hardening 78−64596
steel, spheroidized, medium C, strain hardening 78−52845
steel, stainless, 304, annealed and 9% prestrained, cyclic hardening and softening, room temp. 77−52483
steel, stainless, anelastic and nonlinear viscoplastic behaviour relations at low homologous temps. 77−63742
steel, stainless, deformation temp. determ. for high yield strength 78−44177
steel, stainless, even elongation and relative hardening in martensitic, transition and austenitic 78−52926
steel, stainless, intrinsic stacking fault energy, effect on cyclic hardening 79−11638
steel, stainless, type 304, viscoplastic behaviour, strain rate sensitivity, creep, relaxation, tensile tests 80−66727
steel, stainless, type Kh17N13M2T, strengthening by plastic deformation and cold working *(Russian)* 78−52839
steel, stainless, wire, axial texture after electroplastic drawing, X-ray struct. investigation *(Russian)* 80−104177
steel, stainless, wire, cold drawing 80−50650
steel, stainless 304, cyclic plasticity, exponential stress-strain law 77−25157

work hardening continued
steel, stainless 304 sol. of annealed and thermally-aged, high-cycle fatigue behaviour 80−100923
steel, stainless SUS 304, Bauschinger AE peak detection of back stress component in flow stress *(Japanese)* 78−6977
steel, stainless type 304 L, mech. behaviour under constant stress associated with cyclic strain 80−25767
steel, stainless type 316, monotonic and cyclic biaxial loading at room temp. 78−52928
steel, strain hardening, weakening factor 1273-1473K *(Russian)* 79−78990
steel, strain-hardened subsurface layer, residual stress change in fatigue 80−81185
steel, stress relaxation, short-term, creep and strain hardening *(Russian)* 80 30005
steel, structural, fatigue softening, temp. and load freq. influence *(German)* 79−61614
steel, structural martensitic, corrosion resist. under stress effect of strain ageing with hydroextrusion *(Russian)* 79−38853
steel, tensile prestrained strength of anisotropic rolled steel, rot.-bending fatigue tests, slip bands 78−27590
steel, TRIP, warm extrusion, process control and tensile props. 80−16338
steel, tube eversion, effect of materials and geometrical parameters, conf., Haifa, Israel, (July 1977) 79−15683
steel, type 15Kh2NMFA, strain ageing effect on strength and toughness, susceptibility to strain hardening 79−57028
steel, type 20Kh deformed, austenite grain size, inheritance effect with quenching and tempering 80−60881
steel, type 28Kh3SNMVFA, strain hardened martensite, resist. to tempering, exam. 80−16348
steel, type 4340, deformation study, positron lifetime and hardness correlation 79−87649
steel, ultrahigh strength, monotonic and cyclic stress strain curves 80−35268
steel, work hardening modulus and malleability in static tension 77−77496
steel, X-ray and microhardness meas. at high strain rates *(German)* 78−3184
steel 03Kh12N10MT, mech. props. at low temps. 77−16615
steel 1Kh17N2Sh, fatigue failure, surface finishing influence 80−60972
steel austenitic stainless, fatigue, low cycle, temp. and strain rate effects *(Japanese)* 79−29198
steel bar deformation meas. by holographic interferometry using four point bending machine 78−60721
steel components, residual stress distrib. on surface cold working *(Russian)* 77−59975
steel fatigue in surface active media, adsorption facilitation mech. 80−55586
steel fibre reinforced concrete, tensile strength and ultimate strain *(Polish)* 80−21027
steel Kh, work hardening under nonisothermal loading 79−57005
steel mild, plastically deformed, X-ray meas. of stress and TEM 77−48496
steel tube eversion, effect of material and geometrical parameters 79−15690
steels, 110G13 and 40Kh10G10, hardening and structural transformations during friction *(Russian)* 77−52527
steels, heat-treated, nature of high sensitivity to stress raisers 80−21051
steels, hot plastic strain, stress- strain-time dependences *(Russian)* 80−40430
strain hardening structures under repeated loading, deflection analysis 78−63313
strain rate gradient development 79−46219
strain tempering by rapid heating and cooling of cold drawn wires *(Japanese)* 78−84863
stress/strain relation, rate and temp. depend., analytic formulation 80−40466
stretch zone width and striation spacing. The comparison of theories and experiments 80−85051
superplasticity rel. to strain diag. *(Russian)* 77−59854
tensile creep and early failure, model 80−15185
tensile stability, effect of crack and cavitation generation 77−16659
tensile test piece, profile of contracted part after the beginning of necking *(German)* 77−86269
tensile test specimen contour, expt. and calc. comparison *(German)* 77−86233
thin metal strip, effects of hardening and anisotropy on plane strain compression 77−80083
αTi, work hardened in tension, developed of internal strain *(French)* 78−76716
α and $\alpha+\beta$Ti alloy of different stability, exponential law use for anal. of strain hardening process 79−15697
torsional strain curves plotting 80−40638
transverse isotropic inelastic work hardening constitutive model, numerical implementation 78−42547
Tresca type plastic material, simple shear deform. with combined work hardening *(Japanese)* 80−35206
tubes between rigid plates, lateral compression, strain hardening effect 78−48422
uniaxial stretching curve data anal. using creep with anisotropic hardening theory *(Russian)* 79−76981
US strengthening of cryst. mats., instrument for US attack at low temp. 77−49732
viscoplastic materials, dynamic convergence theorem for strain and work hardening 80−96199
viscoplastoelastic material, plane wave propagation anal., upon shock loading 79−14336
yielding of plates with hardening and large deformations 78−59311
Zircaloy, annealed, neutron irradiated, inhomogeneous deform. behaviour 80−85014
Zircaloy-2, martensitic transform. contrib. to strength and work hardening, and martensite flow props. 78−84842
Zircaloy-2 fuel tubes, low cycle fatigue studies at room temp., 300 and 350°C 80−93637
Zircaloy-4, H_2 effect on mech. props. *(Korean)* 79−70123
Ag, cold rolling, inhomogeneous texture 80−89251
Ag plastically deformed crystal, exam. of dislocation dynamics during strain rate changes 78−88506
Ag, plastically deformed crystals, exam. of dislocation dynamics during strain rate changes 78−88507

work hardening continued
Ag-Cu (5 at.%) solid solution, pre-fatigued, strain hardening at high temp. 78−15426
Al, acoustic emission under plastic deform., spectral anal., dislocation mean free path 78−84934
Al alloy, adiabatic viscoplastic deform. at high strain rate, negative strain hardening *(French)* 77−21212
Al alloy, deformation and fracture resistance due to low-cycle fatigue in plane bending 79−66166
Al alloy, deformation at large plastic strains, work hardening rate 79−20065
Al alloy 2017, corrosion fatigue strength, tensile prestrain effects *(Japanese)* 78−56819
Al alloy 2024-T3, work hardening in surface layers and bulk during fatigue 78−48428
Al alloy 2029-0, circular plates with work hardening, nonlinear behaviour, experimental deflection and strain data 79−38893
Al alloy 5182-0, punch stretching, strain and strain rate hardening effects at elev. temps. 79−56998
Al alloy 7075, fracture toughness, hydrostatic press. depend., tensile ductility 78−3209
Al alloy RR58, low cycle fatigue at 423K, prior treatment effect 80−104254
Al, Bauschinger AE peak detection of back stress component in flow stress *(Japanese)* 78−6977
Al bicrystal, plastically deformed, slip heterogeneities 80−79858
Al, cold rolling, inhomogeneous texture 80−89251
Al, commercially pure, stress-strain curves, cyclic loading initial stage *(Japanese)* 80−93617
Al, deform. enhanced photoemission meas. 77−32511
Al, deformed, thermal recovery, microstruct. and stress-strain relations 80−16325
Al, FCC, strain hardening and recovery by pure metal mode, high temp. deform. *(Japanese)* 78−52843
Al FCC single crystal, crystal rotation accompanying scratch deform. *(Japanese)* 79−15733
Al, fatigue hardening at various test freqs. 79−24539
Al, initial stages of plastic deform. *(Japanese)* 80−93618
Al, isotropic hardened, yield condition 79−61653
Al, non-elastic deformation, phenomenological model with solute strengthening effect incorporation 78−39832
Al, oriented single crystal, plastic deform. *(Japanese)* 79−43336
Al plate, explosive hardening of one end 77−36531
Al, polycrystalline, acoustic emission energy release, grain size and flow stress depend. 80−11722
Al, prestrained, isotropic hardening rule, rel. to stress/strain curve 78−23772
Al rods, waveform variation of reflected acoustic shock pulse due to work hardening 77−21167
Al, single cryst., latent hardening *(Japanese)* 78−44135
Al single crysts., elastoplasticity, dislocation model, work hardening, tensile tests, stress/strain curves *(Japanese)* 77−52410
Al, surface fatigued single crystal, inhomogeneous positron trapping 77−90216
Al, US fatigue crack propagation obs. 77−40451
Al, use in design of composite superconductors in elasto-plastic region 77−28851
Al, work softening, microstruct. interpretation 77−32593
Al, workhardened thin specimens, fracture, anisotropy coeff. role *(French)* 80−104276
Al-(Mg)(Fe), pure (dilute), large wire drawing plastic deform. 80−108508
Al-Ag (15 wt.%), precipitation hardenend cyclic stress-strain response 78−35412
Al-Al_3Ni eutectic composite, substructural matrix hardening *(Russian)* 77−21162
Al-alloys, precipitation hardening, effect on dynamic strain ageing and jerky flow 80−20945
Al-Cu, alloys under tension at 1.6-300K 79−38842
Al-Cu, Bauschinger effect 79−61646
Al-Cu, type 2036-T4, plane-strain work hardening, meas. and anal. 80−81073
Al-Cu (4 wt.%), supersaturated and aged conditions, high strain deform. 80−60907
Al-Cu (4 wt.%), with θ' precipitates, relation between elastic limit and hardness *(French)* 79−5018
Al-Cu-(Mg), precipitation strengthened, Bauschinger effect 77−36585
Al-$CuAl_2$ eutectic, heat treatment and interlamellar spacing effect on tensile deformation 80−29979
Al-Mg (1 wt.%), mechanisms of dynamic strain ageing and jerky flow 79−79024
Al-Mg (2 wt.%), hardening and fracture characts., β-phase dissolution role 80−81178
Al-Mg alloy AMg6, mech. props. of welded joints, impurity effects 78−95789
Al-Mg alloy under tension at 1.6-300K 79−38842
Al-Mg_2Si(1.42 wt.%), aged, dislocation structs. caused by plastic deformation 80−25786
Al-Mg-Si, type 6010, microstruct. characts. influence on formability, heat treatment 80−81090
Al-Ni (6 wt.%), fine-grained, deform. in tension and torsion 80−85008
Al-Ni(Cd)(Fe)(Si), cold worked, struct. and props. 80−71666
Al-rare earth alloys, granules, rolling to form foil, exam. 80−20825
Al-Si (1.2 and 0.6 wt.%), single crystal, dispersion hardened with SiC, Bauschinger effect and work hardening 79−43360
Al-Si (1.2 wt.%), dispersion hardened, temp. depend. of work-hardening due to Orowan loops 79−91668
Al-Si (1.2 wt.%), dispersion hardened, work hardening due to Orowan loops, temp. depend. *(Japanese)* 80−66534
Al-Si crystals, work hardened, softening and creep rates on annealing 80−11663
Al-Ti alloy for use in aircraft, mechanical props. improvement *(French)* 80−97502
Al-Zn alloy, under tension at 1.6-300K 79−38842
Al-Zn-Mg, precipitation strengthened, Bauschinger effect 77−36585
Al-Zn-Mg(3.2, 2.2 wt.%), deform. strengthened by Guinier Preston zones 77−52343
Au, work hardened, Hasiguti peaks, spectrum and recovery, impurity effects *(French)* 77−66670
Be, deformation strengthening, microstruct. and impurity effects 77−4791

work hardening continued
Be, strain hardened metal and microalloys, low temp. brittleness 79−96140
Bi, low temp. plasticity, temp. effect on strain hardening, slip *(Russian)* 77−31713
Bi, strain hardening curve correlation with slip band nucleation stress spectra 80−70217
β-brass, nonisoaxial bicrystal, simultaneous hardening and softening 77−36606
α-brass, serrated yielding, tensile tests and TEM obs. 79−34110
α-brass, solid soln., ductility, comp. effect *(Japanese)* 79−43334
C steel, strain hardening parameters, determination from stress-strain curves 78−80562
CaF_2, plastic deform, work hardening regions, TEM obs. 80−3140
Cd, Cottrell-Stokes law, 4.2 to 300K, forest dislocations and other obstacles 77−43269
Cd, hardening resulting from pyramidal glide 77−48495
Cd single crystal, low-temp. work hardening 78−3138
Cd-Zn (Ag), annealed, work softened, exam. of crystallographic texture, hardness 78−80559
Cd-Zn single crystal, plasticity, 4 to 50K 79−43362
Co, influence of FCC phase retained at room temp. on mech. props. 79−47677
CoO single crystals, strain rate deform. characts., yield stresses and work hardening 77 to 1400K 80−60939
Cr, diffusion coating strengthening by plastic deformation, controlling physical factors *(Russian)* 77−25187
Cu alloys, strain hardened, struct. factor effect on stress relaxation *(Russian)* 80−25748
Cu and Cu-Si, deformation and fracture under dynamic loading 78−35442
Cu, annealed, cyclic plasticity under cyclic nonproportional strain histories, cyclic hardening, memory erasure, strain hardening 78−88510
Cu, annealed O free, high cond., proportional biaxial cyclic hardening 78−84844
Cu, Bauschinger AE peak detection of back stress component in flow stress *(Japanese)* 78−6977
Cu, bicrystal, {110} ⟨112⟩, deform. *(German)* 77−48513
Cu bicrystals, effect of grain boundary on tensile deformation *(Japanese)* 78−88495
Cu, condensates of different thicknesses, polycrystalline, mech. props. 79−65350
Cu, cyclic hardening and saturation behaviour of single crystals 78−64555
Cu, cyclic hardening role in crack nucleation at high strain amplitude 78−64633
Cu, cyclic strain hardening under deform. at various temps. 79−43273
Cu, cyclic work hardening during frequency change fatigue tests *(German)* 79−34068
Cu, cyclic work hardening frequency effects *(German)* 79−29090
Cu, dislocation content at large plastic strains 79−74224
Cu, electrical conductivity, effect of cyclic strains and work hardening at 4.2K 78−91655
Cu electrodeposit, US agitation effect on hardness, porosity and grain size, work-hardening 77−60075
Cu, FCC single crystal, crystal rotation accompanying scratch deform. *(Japanese)* 79−15733
Cu, fatigue crack propag., role of dislocation substruct. 80−60963
Cu, fatigue hardening and failure at intermediate life 77−48548
Cu, fatigue hardening and high cycle fatigue under reversed bending 79−20180
Cu, fatigue of single crystals and low const. plastic strain amplitude 79−20174
Cu, isotropic hardened, yield condition 79−61653
Cu, meas. of stored energy by work hardening and dislocations *(French)* 77−44273
Cu, parabolic curve appl. 79−43264
Cu, polycryst., surface layer hardening by multiple impact 80−108469
Cu, polycrystalline, Krupkowski's formula for strain hardening curve, physical interpretation 79−100158
Cu, prestrained, tough pitch and sintered, ductile fracture, voids *(Japanese)* 77−52472
Cu, recrystallised, inhomogeneous deform. due to texture changes *(German)* 79−29158
Cu, shock loaded, work hardening and press. depend. of dislocation arrangement and density 78−48429
Cu single crystals, dispersion strengthened, low temp. recovery of work-hardening and creep 79−83211
Cu single crystals oriented along [100] and [111], exam. of slip line length 78−76664
Cu, strain hardening parameters, 4.2 to 300K *(Russian)* 79−20063
Cu, strengthening by dislocation substructures 77−36538
Cu, stress hardening anal. 78−56652
Cu, swaged, inhomogeneous work hardening *(German)* 80−76267
Cu, US fatigue crack propagation obs. 77−40451
Cu, whiskers, hardening during uniaxial extension, preliminary torsion deform. *(Russian)* 78−15420
Cu, wire, axial texture after electroplastic drawing, X-ray struct. investigation *(Russian)* 80−104177
Cu wire, mech. props. and struct. after high-speed recrystallisation *(Russian)* 79−47704
Cu, work hardening curves, critical points 79−43263
Cu X-ray and microhardness meas. at high strain rates *(German)* 78−3184
Cu-Ag solder composite, plastic deform. below worn surfaces 77−36670
α-Cu-Al, single crystal, low cycle fatigue 79−43405
Cu-Al (10 at.%), single crystal, orientation depend. of work hardening near [111] axis 77−12646
Cu-Al (10 at.%) alloy, work hardening at high temp. 77−32589
Cu-Al (15 at.%), single crystal, steady state deform. with ⟨001⟩ axis at high temp. *(Japanese)* 78−6980
Cu-Al (5.8 at.%) dislocation multipoles, weak-beam electron microscope obs. 79−73171
Cu-Al alloys, strain hardening parameters, conc. and temp. depend., 4.2 to 300K *(Russian)* 79−20063
$Cu-Al_2O_3$ dispersion hardened wires, drawn, substruct. and strength 78−35405
$Cu-Al_2O_3(SiO_2)(TiO_2)$ alloys, internally oxidised, plastically deformed, influence of particle form on primary loop nature *(French)* 80−103344
Cu-Al(Si), single crysts., latent hardening study by meas. of flow stress on secondary systems *(Japanese)* 79−24538

work hardening continued
Cu-Be (2 at.%), plastic deform. and dislocation substruct. 80−76307
Cu-Fe, precipitation kinetics study by thermoelectric power measurement *(French)* 79−20050
Cu-Fe, single crystal with coherent γ-Fe particles, precipitation hardening 78−31416
Cu-Ge, primary coplanar slip, role in deform. of FCC crystals *(Japanese)* 77−52412
Cu-Ge (8.7 at.%), pulse duration effects in shock hardening 77−12644
Cu-Ge (8.7 wt.%) pulse duration effects on shock hardening 78−80561
Cu-Ge (8.7 wt.%) shock hardening behaviour at very short pulse durations 78−80560
Cu-Nb multifilamentary composite, dislocation resistivity 80−70671
Cu-Ni (10 at.%), hardening, recovery, and struct. changes during high temp. creep *(Russian)* 80−89288
Cu-Ni-Sn (10, 6 wt.%), temp. depend of yield stress and work hardening 80−21026
Cu-Ni(Al), strength and substruct., strain point influence *(Russian)* 79−52233
Cu-Si (6.5 at.%) alloy, easy glide deform., obs. and mechanism 77−8887
$Cu-SiO_2$ (0.0052 vol. fraction), work hardened, low temp. softening, particle size effects 77−52342
α-Cu-Sn, cyclic work hardening frequency effects *(German)* 79−29090
A-Cu-Sn, cyclic work hardening during frequency change fatigue tests *(German)* 79−34068
Cu-Sn solid soln. steady state deform. *(Japanese)* 78−19832
Cu_3Au, disordered [001]-orientated single crysts., plastic deform., TEM and slip line studies 80−97541
Cu_2MnAl, Heusler alloy, single crystal, plastic deform. 77−44308
β-(CuNi)Zn, anomalous strengthening 77−48503
$Cu_2S(Te)$, microstructure, work hardening in polymorphic transform. and subsequent annealing effect 79−52199
Cu_2TE, annealing and deform. of defects induced by phase work hardening during thermal cycling 79−52230
Cu_2Te, microstructure, work hardening in polymorphic transform. and subsequent annealing effect 79−52199
Fe and alloys, softening effect *(French)* 77−63875
Fe and Fe_3Si, hardening and softening during adsorption fatigue in surface active medium, governing laws 77−86230
Fe, Armco, microflow and strain hardening under cyclic loading 80−104182
Fe, Armco, texture role in prestrain embrittlement 78−60796
Fe, BCC, strain hardening and recovery by pure metal mode, high temp. deform. *(Japanese)* 78−52843
Fe, cast, contact deformation, reverse slipping effect *(Russian)* 80−97591
Fe, cast, increase in yield strength, after phase transformations 78−44125
Fe, cast, Mn, wear resist. and hardening, struct. effect 79−87734
α-Fe, cavitation and sliding distrib. changes during creep at 500°C 78−6991
Fe, deformed, dislocation structure determ. from magnetic props. 78−55874
Fe, high purity large single crystal sheet prep. method *(French)* 77−77375
Fe, high purity single crystals, dislocation density rel. to work hardening *(German)* 77−32590
Fe, isotropic hardened, yield condition 79−61653
α-Fe, low cycle deform., strain rate and depressed temp. effect 79−61660
Fe, low temperature deform., strain-rate cycling and stress relaxation tests *(Japanese)* 78−52876
Fe, model for Luders band formation and plastic instability related with strain softening due to Johnston-Gilman-Hahn theory 79−61676
Fe, pure, magnetoelastic damping at low shear stress amplitudes *(French)* 77−59441
Fe, quenched-in hydrogen, yield stress decrease of prestrained specimens 80−16454
Fe, single crystals, work hardening and behaviour and dislocation struct. during simple shear tests 78−95762
Fe, single crysts, increase in initial work hardening as result of hydrostatic pressure 79−38887
α-Fe, single crysts., work hardening *(German)* 80−50652
Fe, strain hardening and rate sensitivity, effect on ductile-brittle transition temp. 78−39900
Fe-Ag (50 vol.%), two-phase system, plastic deformation *(French)* 78−39831
Fe-Al (0.069 and 0.158 wt.%), internally oxidised, low temp. deform. *(Japanese)* 78−52876
Fe-C-Cr-Mo(Ni)(V), white cast, effect of abrasion on carbide microstructure *(German)* 78−88540
Fe-Co-Cr-Mo (20, 15, 5 wt.%), maraging, stainless alloy fracture toughness 77−73326
Fe-Mn (1 at.%), strain age hardening 80−108472
Fe-Mn-C, structural var. during warm deform. in $\gamma \rightarrow \varepsilon$ transform. region *(Russian)* 77−81293
Fe-Mn-Cr-C, twinning and strain induced FCC to HCP transform. 77−44248
Fe-N, neutron irrad. effects on mech. props. 79−4338
Fe-Ni-C (27, 0.23 wt.%), work hardening and martensitic transform. at 263K 79−100143
Fe-Ni-Cr-Ti-Al, with thermoelastic control coeff., comp. and heat treatment influence on props. *(French)* 80−81074
Fe-Ni-Mo, inhomogeneous solid solns., annealed and work hardened states, X-ray K-absorption spectra *(Russian)* 78−56544
Fe-Si, microflow and strain hardening under cyclic loading 80−104182
Fe-Si (3 wt.%), single crystal, plastic deform., 473 to 1000K 77−73310
Fe-Si (3.12 wt.%), brittle fracture, work hardening effect at notch tip 78−44220
Fe-Si(Ni), strain hardening and rate-sensitivity, effect on ductile-brittle transition temp. 78−39900
Fe-W-Cr-Mo-Co (18,12,3,x wt.%) alloy, cold working, effect on magnetisation and hardness obs. *(Japanese)* 77−40428
Ge, doubly deformed, dislocation interaction obs. 79−73172
KBr:divalent cations, minimum work-hardening rates in compression and shear 79−74175
KCl, strain hardening during relax. of deforming stresses 77−7786
KCl:Sr, mechanical props. as function of dopant conc., dislocations 77−69027
LiF single crystals, glide band sources, work hardening 80−34126

work hardening continued
LiF, strain hardening curve correlation with slip band nucleation stress spectra 80−70217
LiF, strained, mean mobile dislocation velocity 78−18657
Mg, cyclic hardening of single crystal 78−64552
MgO, compressive stress-strain behaviour at high temps. 80−25774
MgO, cryst. preliminary processing rel. to deform. curve parameters, slip line struct. 77−52421
MgO, lattice misorientation and displaced vol. for microhardness indentation 78−64617
MgO, single crysts., work hardening and creep 79−43262
Mo alloy MT, strain hardening depend. on temp. and structural state *(Russian)* 79−91664
Mo and Mo superalloys high temperature properties 78−44173
Mo, defect struct. in plane strain deformed single crystal 77−63751
Mo fibre reinforced Cu, rule of mixtures of deform. parameters in stage III 80−97532
Mo fibre reinforced Cu with weak interfaces, stability of tensile deform. 80−97533
Mo, hardened sub-structure, high-temp. radiation resist. *(Russian)* 78−56654
Mo, high purity single crystal doped with C, low temp. mech. props. 77−77544
Mo, plastic deformation during rolling at 293K, crystallography of slip *(Russian)* 77−32588
Mo, single and polycrysts., struct. change during work softening, HVEM 80−103336
Mo single crystal, effect of prior ultrasonic working on hardness, crystal orientation and creep resistance *(Russian)* 79−34056
Mo, single crysts., work hardening and softening in cyclic strain 80−20957
Mo, sintered, pure, work hardening 77−16607
Mo, strain hardened metal and microalloys, low temp. brittleness 79−96140
Mo, US working effect on single cryst. during deform., strengthening effect, plasticity resource *(Russian)* 79−34107
Mo-Cr-V-P, load curves, structure states boundaries and strain hardening *(Russian)* 80−89241
Mo-Ti (3.5 wt.%), load curves, structure states boundaries and strain hardening *(Russian)* 80−89241
Mo-V-C, hot-worked, substructural hardening and high-temp. strength *(Russian)* 80−25731
Mo-Zr-C (0.063, 0.06 wt.%) alloys, ageing, effect of cold deform. by hydrostatic extrusion 79−57001
NaCl, damage process preceding semi-brittle fracture in depend. on deform. microcrack development 77−44272
NaCl, deformed, dislocation densities, TEM 77−43219
NaCl, plastically deformed, recovery of work hardening *(German)* 77−35626
NaCl, plastically deformed [001] oriented single crystals, TEM 77−36579
NaCl, work hardening, acoustic emission 79−100167
NaCl:NaBr crysts., dislocation motion under work hardening, transmission electron microscopy 77−51381
NaCl:Sr, mechanical props. as function of dopant conc., dislocations 77−69027
Nb, internal friction peaks, induced by work hardening, low temp. relax. spectra *(French)* 77−1844
Nb, single crystal, surface oxide softening, TEM obs. 77−40462
NbC, deformation behaviour during rubbing in wide temp. range 80−16486
Nb_3Sn fatigue effects in unidirectional composites, computer simulated model 80−35289
Ni, deformed, work-hardening, dislocation and mosaic struct., X-ray and electron microscopy 77−35625
Ni, lattice defects, formation kinetics, work hardening and resistivity study *(Russian)* 80−10557
Ni, polycrystalline, strain hardening, dislocation link length model 80−84953
Ni, pure and alloyed, and fibre reinforced, at elevated temps. 77−52353
Ni, shock loaded, work hardening and press. depend. of dislocation arrangement and density 78−48429
Ni, shock loaded, work softening 78−27537
Ni single crystal, compressed, strengthening and dislocation cells *(German)* 80−66536
Ni transient creep stress doped at $T<T_{0.2MP}$, strain-hardening coeff. depend. *(Russian)* 77−48482
Ni, work hardening, grain size effects 77−16605
Ni-Al-Cr, strain hardening, participation of various slip systems *(Russian)* 79−24536
Ni-alloys, precipitation hardening, effect on dynamic strain ageing and jerky flow 80−20945
Ni-Cr-Al-Ti-Mo, low temp. mech. behaviour, precipitation 78−39860
Ni-Mo (5.8-24 at.%) solid soln. struct. and strength characts. *(German)* 79−4975
Ni-SiO_2 composite film, influence of hardening phase on yield stress *(Russian)* 79−5001
Ni_3 (Al.Ti), flow stress and work hardening, exam. of temp. depend. by tensile tests 78−84839
Ni_3Al and Ni_3(Al,Ti), deformation characts., temp., strain rate and orientation depend. 77−44320
Ni_3Al, noncoherent second phase particle effect on strain-hardening parameters *(Russian)* 79−47703
Ni_3Al, overshooting while testing in tension 78−44189
Ni_3Fe, mono- and polycrysts., strain hardening, test temp. effects *(Russian)* 80−66531
Ni_3Fe, nondislocation origin friction stress in alloys, deformation hardening 80−21050
Ni_3Fe, ordered and disordered states, strain hardening characts., temp. depend., multiple slip case *(Russian)* 78−15421
Ni_3Fe, single crysts., long range order degree influence on strain hardening *(Russian)* 80−11660
Ni_3Ga, temp. depend. of mech. props. *(Russian)* 79−38895
Ni_3Ge single crystals, orientation and temp. depend. of flow stress 79−5008
Ni_3Ge, temp. depend. of mech. props. *(Russian)* 79−38895
Ni_3Mn, dislocation struct. after heat treatments, TEM *(Russian)* 77−8848
Pb, hardening in intermediate state 78−47917
Pb, sample length effect on plasticity 78−44179
Pb, strain hardening and recovery, during primary creep 78−39799
work hardening continued
Pb, work hardening, and recovery rates during steady state deformation, temp. and stress effect 80−45319
Pb:Ni, paramag. impurity effect on work hardening at superconducting transition *(Russian)* 77−47915
Pb-2n, work hardening in mixed state *(Russian)* 79−42707
Pb-In (5%), supercond. mobile dislocation density, instantaneous flux change meas. 80−15670
Pb-Sn, eutectic alloy, plastic deform., work hardening *(German)* 78−92279
Pb-Sn(Cd)-Te, microhardness meas. as function of applied load, elec. props. exam. 78−48493
PbTe, microhardness meas. as function of applied load, elec. props. exam. 78−48493
Pd-Cu-Ga, cold work and annealing-induced hardening, X-ray diffr. anal. and metallographic exam. *(Russian)* 79−38844
Pd-H system, controlled H phase-induced strain hardening *(Russian)* 79−1878
$Pd_{77.5}Cu_6Si_{16.5}$ metallic glass wire, cold drawing 80−50650
Pr, mech. props. from 78 to 525K 77−21165
Re, metallo-ceramic, deform. and cold working by cold rolling *(Russian)* 78−56655
Si, single crystals, dynamical recovery and self-diffusion 78−87816
Sn plate, rapid test for props. assessment 80−40650
Sn, single cryst., plastic deform., 1.6-300K *(Russian)* 78−3179
Ta, evidence for slow strain-rate embrittlement due to O_2, SEM study 79−79109
Ta, internal friction peaks, induced by work hardening, low temp. relax. spectra *(French)* 77−1844
Ti alloy TA6V, fatigue, low cycle, and microfractography *(French)* 77−70168
Ti alloy TA6ZrSD, low cycle fatigue at 450°C *(French)* 79−70169
Ti alloy VT3-1, fatigue failure, surface finishing influence 80−60972
Ti alloys, texture strengthening 78−23724
α-Ti based alloys, deform. twinning effect on mech. props. at low temps. *(Japanese)* 78−6979
Ti, commercial purity, cyclic behaviour and delayed softening 77−36641
Ti, dynamic annealing, effect on dynamic strain ageing phenomena 80−7594
Ti, grain size effect on yield stress and work hardening at 295 and 575K 78−64593
α-Ti, plastically deformed by rolling, optical and electron microscope obs. 79−91666
Ti-(Al)-Zr-Si (5, 0.5 wt.%), creep 77−36595
α-Ti-Al, stress/strain curves 77−63738
Ti-Al-Cr-Mo-Zr hard alloy VK15, shot blasting in strength improvement 77−81272
Ti-Al-Mo(Cr)(Fe), thermomechanical treatment effect on mech. props., strengthening mechanisms 80−55441
Ti-Al-V (6,4 wt.%) superplastic alloy, maximum attainable ductility 80−60919
α, α+β, β-Ti-Mn alloys, Bauschinger effect during cyclic straining 79−43310
β−Ti-Mo, thermal instability, hardness and tensile deform. *(Japanese)* 80−71703
Ti-V, cyclic stress-strain response 78−60700
Ti-Y(Er), dispersoid effect on deform. 79−24530
Ti_3Al, cyclic deform., dislocation struct. 78−7003
TiC, deformation behaviour during rubbing in wide temp. range 80−16486
α-U, mech. behaviour, strain rate influence, 300 to 550°C 79−38907
U_3Si, tensile ductility from 25 to 320°C 79−74225
V, polycryst., O_2 effects on strength and ductility 77−36529
V, slip geometry and dislocation struct., rel. to degree and temp. of deform. *(Russian)* 78−38717
V, strain hardening, screw dislocations and microtwinning *(Russian)* 80−29971
V-Fe (5.0 at.%), work softening at elevated temps. *(Japanese)* 77−52347
V-H, H effect on fatigue crack propag. 78−48516
V-Ta (5 wt.%), strain hardening, screw dislocations and microtwinning *(Russian)* 80−29971
W fibre reinforced Cu composite, work hardening 77−52341
W, US working effect on single cryst. during deform., strengthening effect, plasticity resource *(Russian)* 79−34107
W-Re alloy, elec. resistivity meas. near conc. anomaly, 300 to 1200K 77−35911
W-Re alloys, anomalous conc. depend. of elec. resistivity 77−35917
WC, deformation behaviour during rubbing in wide temp. range 80−16486
WC-Co hard alloy, preheating influence on explosive shock hardening *(Russian)* 79−29083
α-Zircaloy, strain ageing at 1000K 79−47725
Zn, compatible bicrystal, plastic deform. *(Japanese)* 78−31460
Zn, Cottrell-Stokes law, 4.2 to 300K, forest dislocations and other obstacles 77−43269
Zn crystal, $\{11\bar{2}2\}\langle 11\bar{2}3\rangle$ slip system, deform. stress, dislocation density depend. *(Russian)* 80−103353
Zn, deforming stress under basal slip, contrib. of forest and primary dislocations 78−3186
Zn, hydrostatically compressed single crystal, work hardening studied by stress relax. method 79−20069
Zn, incompatible bicrystals, effect of grain boundaries on mech. props. *(Japanese)* 78−39798
Zn, oriented polycrystals, tensile behaviour under hydrostatic press. *(Japanese)* 77−52417
Zn particulate composite, mech. props., microstruct. correlation, at low and high temps. 77−32624
Zn single crystal, rel. to discontinuous creep *(Russian)* 77−81292
Zn, strengthening by electroplastic strain, surfactant effect *(Russian)* 80−20953
Zn, work hardened crystal, jump-like plastic deform., dislocation struct. instability 79−96094
Zn-Al (10,22,50wt.%), low temp. mech. props. plastic deformation, glissile dislocation nucleation *(Russian)* 80−11695
Zn-Al-Cu casting alloys, mech. props. and dendritic morphology, Al content effect *(Korean)* 80−93612
Zr alloys, acoustic emission during tensile testing 77−90433
α-Zr, polycrystalline, cyclic deformation *(Japanese)* 78−68757
α-Zr, strain ageing at 1000K 79−47725

work hardening continued
Zr, tensile deformation behaviour, neutron irrad. effects, dislocations, twinning inhibition 77−90393
Zr-Cu, dil. martensites, struct. and strength 79−29077
Zr-Nb (1 wt.%), tensile props., 295 to 773K 79−8318
Zr-Sn (1.5 wt.%), martensitic transform. contrib. to strength and work hardening, and martensite flow props. 78−84842
Zr_3Al, $L1_2$ phase, work hardening 78−23718
Zr_3Al, ordered, strengthening by fast neutron irrad. 78−84838
workers *see personnel*
wrapping *see packaging*
Wratten filters *see optical filters*
X^0 meson resonances *see eta meson resonances*
X-ray absorption
see also X-ray absorption spectra
α-alumina soft X-ray absorpt. and EXAFS on K edge 79−99981
absorbed dose unit, 1 to 5 J/kg, USSR special standard 77−32956
absorption correction, optimisation *(French)* 79−68973
absorption factor, determ. for single cryst. of any shape in inclined X-ray diffractometer 79−64959
aerosol loaded filters, X-ray fluoresc. anal., absorpt. corrects. calcs. 78−7311
aerosol loaded filters, X-ray fluoresc. anal., filter absorpt. correction 77−60166
attenuation measurements on Y tong shielding material *(German)* 80−98145
azimuthal scanning method, allowance for X-ray absorpt. in single-crystal diffractometry 80−38874
benzyl mercury chloride, cryst. struct. and absorpt. calcs. 80−84166
biological materials, extrapolation of linear attenuation coefficients from diagnostic energies to megavolt range 78−24145
biological X-ray microanalysis 80−41349
bone mineral content meas. after successful renal transplantation 77−48854
bone mineral measurement using polychromatic X-rays, correls. 78−53478
brain, experimental oedema, serial meas. of specific gravity and computerised tomography attenuation 80−98005
bremsstrahlung intensity distrib. at origin in thick W target by attenuation anal., 60 to 140 kV 77−34060
capillary porous body, drying, X-ray absorption obs., radiometry, temp. control 78−67023
characteristic absorption, study using diffractometer DRON-2,0 80−20733
computed tomography 78−65125
computerised tomographic scan evaluation, partial vol. phenomenon effects on linear attenuation coeffs. 80−41176
computerised tomography, attenuation coeff. absolute values 79−83918
computerised tomography, beam hardening artifact explanation 79−83931
corrections in single cryst. diffractometry, FORTRAN program 77−11438
crystal, ionic, K-absorption, fine struct., relative hole mobility influence *(Russian)* 79−47542
diffraction expt., incident beam intensity meas. by absorpt. method 80−68333
diffusion equation model for kilovolt electron transport at X-irradiated interfaces 79−24388
dosimetry, restricted energy absorption coefficients 78−80971
effective coeff. determ. for soft X-rays 78−49950
electron probe anal., corrections, quantitative, effect of electron incidence angle 79−39270
energy dispersive filtration for simultaneous energy and wavelength dispersive analysis 79−12918
environmental samples, X-ray fluoresc. anal. absorpt. corrections 77−60169
fusion reactor, first wall, thermal response to X-rays, effect of inert gases 79−85776
fusion reactor first wall, hydrodynamic response of Xe protective buffer gas after absorbing target debris 79−85777
graphite, X-ray attenuation coeffs., in range 0.40 to 1.54 Å 79−32855
gypsum wallboard, attenuation characts. 79−70651
half-value layer determ., analytic method 80−66747
high energy photon absorption cross section for matter review *(Japanese)* 78−74506
history, J phenomenon of Barkla, scientific controversies 79−62983
Hounsfield number definition and computerised tomography number conversion 78−35952
HTR, pyrocarbon coated fuel, C density determ. by X-ray absorpt. 80−5301
intense scatterers, at low angles, absorpt. correction and normalisation of X-ray small angle scattering data 80−19671
interstellar photoabsorpt. cross-sections for dense clouds and intercloud regions 78−12327
Lexan, on polypropylene window of soft X-ray proportional counters, for eliminating UV sensitivity 79−74273
linear accelerator primary and leakage radiation attenuation in concrete 79−63823
mass absorption coeffs., meas. using X-ray diffractometers and fluoresc. spectrometers 80−18063
medical equipment, physical characts. of radiation 80−26334
particle size analysis using ^{55}Fe X-ray source and sedimentation cell 79−75491
particle size effects in X-ray absorpt. anal. 77−16882
pattern, recognition with spatially modulated X-rays 78−45761
PIXE, low energy mass absorpt. coeff., meas. technique 78−7309
plasma electron temp. determ., semi-analytical eqn. for X-ray absorpt. curve 77−27722
prescription lenses, attenuation of diagnostic X-rays 79−92395
proportional counter, wall effect elimination, method 78−4753
radiographic screen characteristic X-ray reabsorption calc. 79−74753
radiography, dose distribution description by X-ray quality monitoring *(German)* 80−41251
reflection coefficient of absorptive single cryst. 78−9898
sample cell for extended X-ray absorption fine structure meas. up to 1000°C 80−57454
selective X-ray absorption microanal. using synchrotron radiation, transition metals in Mn nodules 78−68957
self-absorption effects in X-ray fluoresc. anal., Monte Carlo simulation 77−60165

X-ray absorption continued
semi-empirical law, for mass absorpt. coeff. determ. 77−32468
Si wafer, anomalously transmitted X-ray intensity enhancement by asymmetric diffr., appl. to microstructure 79−14647
solar photosphere, hard X-rays photoelectric absorpt., approx. formula 77−22187
spectral distribution, evaluation of method of estimation from attenuation data *(Japanese)* 80−95207
stopping power, cavity theory verification by ionisation chamber 80−9476
tissue, dual-beam absorptiometry, iterative method for K_β filter elimination 77−70533
US resonance suppression of anomalous X-ray transmission *(Russian)* 77−89347
water, rel. sensitivities of materials for half-value-layer meas., 5 to 40 MV 77−45927
water irradiated by photons up to 2 MeV, initial energies of Compton electrons and photoelectrons 80−108320
X-ray filter assembly for fluorescence measurements of X-ray absorption fine structure 80−31961
Al, K X-ray absorption, K-emission spectrum, band struct. using APW method 80−97380
Al, polycrystn., X-ray attenuation and photoelec. coeffs. in range 0.3 to 1.3 Å 79−99979
Al, rel. sensitivities of materials for half-value-layer meas., 5 to 40 MV 77−45927
Al, soft X-ray absorpt. and EXAFS on K edge 79−99981
Al ultrasoft X-rays, phys. props. and Chinese hamster cell expts. 77−86542
Au-Si (polyethylene) interfaces, algorithm for energy deposition of X-rays 77−28648
^{57}Co, disintigrating nucleus, energy absorpt. by mol. environment 78−80775
Cs, soft X-ray outer-shell absorption and emission, one-electron calc. 79−69904
Cu, rel. sensitivities of materials for half-value-layer meas., 5 to 40 MV 77−45927
Ge, dislocation free single crysts., six wave diffr. of X-rays, interf. absorpt. coeffs. 79−14650
Ge, X-ray attenuation coeffs. 25 to 50 keV, energy dispersive method 77−66557
Ge, X-ray attenuation coeff., anomalous scattering factors and dispersion corrections rel. to photoeffect cross section 79−99980
Ge, X-ray linear absorpt. coefficients, in energy range 5 to 50 keV 79−73066
H_2, gas, X-ray attenuation coeffs. meas., 6 to 25 keV 77−75233
K, soft X-ray outer-shell absorption and emission, one-electron calc. 79−69904
Mg polycrystn., X-ray attenuation and photoelec. coeffs. in range 0.3 to 1.3 Å 79−99979
MgO-NiO, STEM microanal., absorpt. effects 80−80902
Mn, extended X-ray finestruct. obs. 80−25482
NbO_2, rutile phase, energy levels, momentum density, and Compton profile, embedded cluster model 80−50453
Pb, rel. sensitivities of materials for half-value-layer meas., 5 to 40 MV 77−45927
Pb-Bi, X- and γ-ray attenuation obs. 79−61457
Rb, soft X-ray outer-shell absorption and emission, one-electron calc. 79−69904
Se, X-ray sensitivity, induced photocurrents, xeroradiographic meas., pair creation energy 80−22490
Si, X-ray attenuation coeffs. 25 to 50 keV, energy dispersive method 77−66557
Si, X-ray attenuation coeff., anomalous scattering factors and dispersion corrections rel. to photoeffect cross section 79−99980
Si, X-ray linear absorpt. coefficients, in energy range 5 to 50 keV 79−73066
Si, X-ray mass attenuation coeff. meas. 77−31556
Si, X-ray rot. polarisation, absorpt. crystal orientation effects 78−47206
Sn, rel. sensitivities of materials for half-value-layer meas., 50 to 40 MV 77−45927

X-ray absorption spectra
α-alumina soft X-ray absorpt. and EXAFS on K edge 79−99981
actinide compounds, spectroscopic techniques for electronic props. meas. 80−11427
actinides, 3d X-ray spectra, 4f and 5f states 78−84681
adsorbate-substrate characterisation using EXAFS 77−43430
adsorbates, photoexcitation theory rel. to angle-resolved UPS and surface EXAFS 80−39426
adsorbed species, relax. shifts, line shapes and satellites in XPS and X-ray absorption spectra 77−90242
Al, one-electron calcs. of X-ray absorpt. and emission, jellium model 78−56543
alkaline earth zirconate perovskite type, X-ray K-absorpt. edge, chem. shift 79−91529
alloy, X-ray self-absorpt. spectroscopy method for unoccupied valence states obs. *(Russian)* 77−81175
amorphous, EXAFS, evidence for inequivalent environments of Ga and As 79−15558
amorphous materials, X-ray K-absorption edge chemical shifts 80−80904
amorphous solids, inorganic, struct., review 80−15004
amorphous solids, Raman intensities, connection with EXAFS Debye-Waller factors 80−108214
astronomical, sources, mechanisms, detection techniques 77−22061
atom, deep level X-ray absorption cross section modulation by optical field 77−14399
atom, resonance formation, role of surrounding potential 78−9168
atom Breit interaction between electrons, calc. angular coeffs., computer program 80−18779
atomic inner shell ionisation phenomena, conf., Freiburg, West Germany (Mar.-Apr. 1976) 77−27040
atomic X-ray absorption cross section enhancement by intense laser field 77−34582
atoms, mass absorpt. coeffs. in ultrasoft region, spectral depend. 77−10622
atoms in compounds, study of 4d excited states 77−26989
biological molecules, metalloproteins, review, book contrib. 79−5436
blood cell K^+ ion X-ray absorpt. edge fine struct., frog 79−66459
book on X-ray spectroscopy 80−2899

X-ray absorption spectra continued
caesium hydrogen tartrate, Cs L_{III}-edge anomalous X-ray scatt., meas. by synchrotron radiation 79−24389
chloroperoxidase, ferric form, X-ray absorpt. fine struct., Fe-N and Fe-S lengths 79−48213
CO_2 ferrite, crystal structure, X-ray absorpt. spectra, chemical shifts 80−88118
complex material atomic structure study, laboratory extended X-ray absorpt. fine structure technique 79−17589
computerised tomography, noise factor of a polyenergetic X-ray beam 80−56204
continuous X-ray radiation due to picosecond ruby laser plasma heating *(Russian)* 80−75079
core-hole lifetime effects in deep-level spectroscopies 78−48283
critical absorpt. energies, mass absorpt. coeffs. calc. evaluation of mathematical expressions 77−29065
cubic crystals, calc. of binding energy of X-ray excitons 78−2435
cytochrome c, absorpt. edge fine struct. of active site haem 79−24945
cytochrome c oxidase, oxidised and reduced, X-ray absorpt., edges, using synchrotron radiation 78−48758
cytochrome P-450, ferric form, X-ray absorpt. fine struct., Fe-N and Fe-S lengths 79−48213
data acquisition system for EXAFS and photo-electron spectroscopy expts. 78−62676
density of states in K excitation spectra of solid and liq. phases 78−19601
diamond:Ni, synthetic, X-ray absorpt. fine structure study of impurities 80−55133
disordered alloys, interatomic distances, coord. numbers, and mean relative displacements, EXAFS anal. 80−89087
dispersed metal catalyst clusters, EXAFS obs. 79−91530
DNA calf thymus binding to cis- and trans-dichlorodiammineplatinum(II) extended X-ray absorpt. spectra 78−85291
dosimetry materials, attenuation coeffs. meas., fluoresc. X-rays, low energy 78−84680
dynamical calculations 80−55227
edge singularities of relaxed-out bound states and relaxed-in band states 78−92173
edge-shifts, empirical relations, effective ionic charge for isoelectronic series 78−55136
electron energy loss spectra, threshold potentials and X-ray absorption, band struct. determ. *(Russian)* 78−39009
electronic states determ. using synchrotron radiation 77−20882
EXAFS, and complementary techniques, muon spin rotation and Mossbauer spectroscopy 80−39912
EXAFS, atomic origin of struct. 78−31277
EXAFS, determ. of struct. of disordered regions *(French)* 80−80905
EXAFS, fluorescence detection, sensitivity enhancement for dil. species and thin films 77−85843
EXAFS, for disordered solid struct. determ. 79−37624
EXAFS, multiple scatt. corrections 77−16427
EXAFS, new horizon in struct. determs. 79−19949
EXAFS, one-dimensional model calc. 77−20957
EXAFS, phase shift calc., fine struct. of As_2O_3 77−48275
EXAFS, theory and technique appl. in atomic environment *(French)* 79−26927
EXAFS amplitudes, many-body effects 80−97379
EXAFS amplitudes, wave function relaxation and chemical effects 78−46365
EXAFS and surface EXAFS from X-ray refl. meas 80−71512
EXAFS beats, determ. of differences in bond lengths 78−23552
EXAFS in molecules and crystals, method for calc. of atomic phase shifts 77−48276
EXAFS in photoelectron yield spectra 80−16123
EXAFS in photoelectron yield spectra and optimisation of the photon glancing angle 78−80435
EXAFS measurements, appl. to local struct. anal. *(Japanese)* 79−38691
EXAFS technique, struct. information around absorbing atom 78−91198
EXAFS-Auger process for surface struct. anal. 77−51580
EXAGS, and surface EXAFS studies in soft X-ray region using electron yield spectroscopy 79−47544
extended X-ray absorption fine structure using real space transform, struct. determ. technique 78−23553
ferrimagnetic materials, ionic state, and using X-ray K absorption edge of Fe 78−35226
filter assembly for fluorescence EXAFS meas. 80−90971
Fluorescent EXAFS data using solid state detector, for metals in dilute biological systems 78−66595
fluoromethanes, soft X-ray absorpt. spectra, fine struct. above K-edge of C 78−42096
glass, struct. determ. using EXAFS 80−45169
glass local structure exam. by EXAFS 80−108301
graphite, C K-absorpt. edge, EELS meas. 78−56551
graphite, C K-edge fine struct. 80−66325
graphite, X-ray emission and absorption, XPS, electronic struct. 77−16431
graphite intercalates with K, staging classical model variations, EXAFS results 80−45166
graphite-Br_2 intercalation cpds., EXAFS study 80−71515
haemoglobin Fe-N distance determ. by EXAFS 78−68989
II-IV-V_2 semiconductor, electronic struct. determ. 77−76751
III-V semiconductor, electronic struct. determ. 77−76751
Invar, X-ray K-absorpt. spectra, depend. on composition and temp. changes *(Russian)* 80−55226
K-emission satellites, low and high freq. origin 80−80900
lanthanide atomic vapours, (Sm, Eu, Dy, Ho, Er, Tm, Yb,) photoabsorption spectra 77−88417
Lytle potential, modified, for extended fine struct. of X-ray absorpt. edge 77−85839
mammography X-ray beam filtration 78−69207
many body effects 78−27374
metal, core spectra, independent-electron metal calc. 79−83056
metal, effects of correlation interaction of electrons with deep holes in X-ray spectra 78−31279
metal, narrow-band extra-atomic relax. and X-ray spectra 77−24928
metal, plasmon struct. in X-ray absorpt. spectra 79−38692
metal, X-ray self-absorpt. spectroscopy method for unoccupied valence states obs. *(Russian)* 77−81175
metal, XPS and X-ray absorption spectra, thermal broadening of core levels, many-electron effects 78−31284

X-ray absorption spectra continued
metal catalysts, structural exam. of monometallic and bimetallic systems 79−95264
metal film, mass absorption coeff. meas. using proton induced X-rays 78−2942
metallic glass, bulk and surface properties, review 80−44147
metalloproteins, site symmetry, X-ray absorpt. spectra using synchrotron radn. 78−64938
metals, exciton effects on X-ray absorption edges 80−108298
metals, narrow-band, and simple, edge singularities in spin-depend. final-state interactions 78−6810
metals, X-ray edges theory, review 77−66556
metals, X-ray spectra, final state pot., one-electron theory 80−55230
metals and alloys, review of X-ray spectroscopy 77−55849
methane, and -d_4, soft X-ray absorpt. spectra, fine struct. above K-edge of C 78−42096
molecular inner-shell photoabsorpt., shape resonances, extended X-ray absorpt. fine struct. 77−18979
molecule, X-ray absorption spectra, method of coupled differential eqns. 77−88466
molecules, highly symmetric, and complexes, theory of X-ray absorption spectra for central atoms *(Russian)* 78−50559
molecules, use of synchrotron radiation from storage ring 77−27199
narrow band metals, extra-atomic relax., X-ray spectra 77−36312
non-crystalline materials of low atomic number, X-ray Raman edge extended modulation for struct. study 80−49111
optical fibre preforms, refractive index distribution measurement using X-ray absorption measurements *(Japanese)* 80−87506
organic substances, determ. of heavy elements 77−2075
photoabsorpt. spectra, band struct., at. ionisation mechanisms, electron energy loss spectra 77−24909
photoelectric cross section calculation, from X-ray absorption data 78−56562
photoelectric cross-section at K-edge measurements 78−2983
plasmas, laser produced, as X-ray source for extended X-ray absorption fine-structure spectroscopy 80−320
PMMA, shock wave compression meas. *(German)* 78−95618
polyacetylene:AsF_5, X-ray absorpt. meas. of mol. struct., orientation and charge transfer 80−25486
polyacetylene, AsF_5 doped, X-ray absorpt. meas., 5K to room temp. 80−71516
polyacetylene, doping with AsF_5, mechanism, effect on elec. cond. and spectra 80−24473
polystyrene, film, optical props. from near IR to X-ray, sum rules 77−48195
PVC, shock wave compression meas. *(German)* 78−95618
α-quartz, correlation between cryst. perfection and refl. intensity for analyser cryst. 78−48259
rare earth alloys, RCo_5, X-ray absorpt. spectra, electronic struct. 80−16122
rare earth alloys, RCo_5, X-ray chemical shift and atomic charges 77−44085
rare earth germanides, X-ray emission, absorption and photoelectron spectra *(Russian)* 80−11509
rare earth metal, heavy, Lα and Lβ satellites, explained using EXAFS data 79−52045
rare earth metals, X-ray chemical shift and atomic charges 77−44085
rare earth sulphides L-X-ray absorpt. spectroscopy, conc. of ions with various numbers of f electrons 77−28646
rare earth-Pt intermetallics, chem. shifts of L_3-absorpt. edge of Pt 79−78789
rare earths, 3d X-ray spectra, 4f and 5f states 78−84681
(rare-earth)Al_2Ga_2, synthesis, NMR and X-ray absorpt. studies 80−108083
rare-earth oxides, R_2O_3, (R=Dy,Ho,Tm,Yb,Lu), EXAFS and chemical shift 77−81176
remote fine structure, multiple-scatt. model 77−28644
semiconducting cpds., average valence-⟨4⟩ X-ray K-absorpt. edge shift and electronegativity 77−16424
silicate glasses, local order around Fe, exam. using X-ray absorpt. spectrometry 80−79701
simple metals, X-ray threshold anomaly, exponents in theory 77−85838
single crystals, use of polarised radiation 78−8481
soft, meas. by photoelectron anal. 80−73557
soft X-ray thresholds, exchange effects, renormalisation group theory 78−31280
specular reflection meas. of photoabsorpt. 79−15561
superionic conductor, EXAFS investigation of struct. and ion motion 80−108302
superionic conductors, EXAFS studies of struct. and cond. process, book contrib. 80−25485
surface atomic and electronic struct. studied with synchrotron radiation 80−80945
surface characterisation, physical methods, review *(French)* 80−7889
surface EXAFS study of adsorbate Auger electron intensity on single cryst. surfaces 78−66562
surface reactions, EXAFS obs. 80−108735
surface struct. anal. using extended X-ray absorpt. fine struct.-Auger process 77−11768
synchrotron radiation, appls. 78−74825
synchrotron radiation, props. and appls., review 79−36830
synchrotron radiation applications, review 79−67448
ternary compounds, and complex systems, chemical shift in X-ray absorpt. spectra, effective changes 78−6811
transition elements, first-group, K-emission satellites, quasi-stationary states and origin 80−80903
transition metal, 4d, photoabsorption spectra near K-edge 78−92144
transition metal, Fe group, BCC struct., X-ray absorption spectra, Mossbauer spectra, comparison *(Russian)* 78−64299
transition metal binary alloys, X-ray K-absorpt. spectra *(Russian)* 79−1796
transition metal chlorides, origin of 'white' line in K absorption 77−8685
transition metal germanides, X-ray emission, absorption and photoelectron spectra *(Russian)* 80−11509
transition metal phosphides, valence electron energy spectrum, deduced from X-ray spectra and XPS 79−99984
transition metal-Al, X-ray spectra, electronic structure 79−78793
transition metals, 3d-, 4d-, 5d-, band struct. from spectral data and theoret. calcs. *(Russian)* 77−8013
transiton metal oxide perovskites, UPS, XPS, X-ray absorpt. spectra, band struct. study 79−56885

X-ray absorption spectra continued
vanadyl bisacetylacetonate, polarised X-ray absorption and double refraction 80−50459
Ag (111), adsorption of I_2, surface EXAFS exam. 79−82446
Ag (111) surface, adsorbed I, geometry and bond length, surface EXAFS 78−71952
Ag and Ag_2O, X-ray absorption, discontinuities and limits, chem. combination effects 80−93435
Ag halides, tetrahedrally coordinated, semiempirical band struct. model 77−51655
Ag, I_2 adsorption site on Ag(111), X-ray anal. 78−84679
Ag, K-edge photoabsorption spectra, linear APW calc. 78−43960
AgI, EXAFS investigation of struct. and ion motion 80−108302
AgI, position and dynamics of Ag ions using EXAFS, jump-diffusion cond. model 77−59643
α-AgI, superionic, anal. of Ag K-EXAFS data 80−97377
Al, (111) surface, adsorbed O, surface struct., LEED and SEXAFS data 80−92782
Al, chemisorption of O, O-Al and O-O bond lengths, surface extended X-ray absorpt. fine struct. 80−29267
Al, chemisorption of O, unoccupied extrinsic surface resonances and site struct. determ. by soft X-ray absorpt. 79−73403
Al film, thermomodulation of Al $L_{2,3}$ absorption edge 79−91533
Al, many-body response in X-ray absorption, emission and photoemission spectra 80−16124
Al oxidised surface, EXAFS in soft-X-ray region 79−37921
Al plasma, X-ray photoabsorpt. coeff. 79−27754
Al, plasmon struct. obs. in K photoabsorpt. spectra 79−38693
Al, shock wave compression meas. *(German)* 78−95618
Al, soft X-ray absorpt. and EXAFS on K edge 79−99981
Al, soft X-ray emission and absorpt. edges, self-absorpt. studies 80−40183
Al, struct. in 1s soft X-ray appearance pot. spectrum 79−33862
Al, surface, single cryst. unoccupied surface resonances, surface soft-X-ray absorption spectroscopy 79−28862
Al, surface relaxation using surface EXAFS 79−23816
Al, X-ray absorpt. and emission edges, one-electron and many-body effects 80−25484
Al, X-ray threshold anal. 78−31281
Al^{3+} ion, plasma in fast evolution, time-resolved soft X-ray absorpt. transitions 77−18827
Al-Al_2O_3, local struct. and interface states using surface soft X-ray absorpt. and photoemission spectroscopy 79−69595
Al-based 3d-transition metal alloys, soft X-ray absorpt., electronic struct. 79−38690
Al-Cu (1.9 at.%), solute fluctuations, EXAFS study 80−79949
Al-Cu alloys, dil., EXAFS spectra 80−2898
Al-Zn changes in inner-electron binding energies during ageing, electronic spectra study 77−28816
AlF_3, $L_{II,III}$ fine struct. of XAS 80−11508
Al_2O_3 monolayer, core excitons and inner well resonances in surface soft X-ray absorpt. spectra 80−40187
Ar, nonempirical calc. of X-ray K-absorpt. spectra 77−88465
As, X-ray absorption edge, chem. shift, electron binding energy in compounds 78−62822
As, X-ray K absorpt. edge, effective ionic charge and bonding schemes 80−29827
As, X-ray K-absorpt. edge shifts 77−4701
As_2O_3 crystalline and amorphous, EXAFS study of struct. 80−19776
$As_2S_3(Se_3)$ evaporated films, struct. and thermally induced effects 79−41963
$As_3(Se,Te)_3$ glasses, X-ray absorption and photoelectron spectroscopy study 80−7463
As_2Se_3, struct. determ. in amorphous and liq. state using EXAFS meas. 77−89366
Au, 4f X-ray photoabsorpt. structs. 77−18826
Au and Au_2O_3, X-ray absorption, discontinuities and limits, chem. combination effects 80−93435
Au, core-electron excitation edges 80−66345
Au, EXAFS at L-edges of heavy elements 79−47543
Au, L_{III}-edge X-ray absorpt. reson., chem. environment effects 79−72256
Au, $L_{2,3}$ EXAFS, determ. of s and d contrib. 77−44086
Au, M_5 absorpt. limits 78−6812
Au, thin foil, enhanced electron energy deposition heated, soft X-ray vacuum UV spectra 80−80901
B, amorphous, X-ray Raman edge extended modulation for struct. study 80−49111
Ba plaster, X-ray absorption coefficients, from 100 to 400 keV 78−31283
$Ba_{1-x}Sm_xS$, electron config. of Sm ions, X-ray L-absorpt. spectroscopy 80−60715
$BaTiO_3$, K-edge X-ray absorpt., cond. band states 80−97382
Be inorganic compounds, ultrasoft X-ray spectra 77−27086
Be, soft X-ray emission and absorpt. edges, self-absorpt. studies 80−40183
Be, X-ray spectra, separation of K-emission and absorpt. edges 79−33864
Bi and Bi_2O_3, X-ray absorption, discontinuities and limits, chem. combination effects 80−93435
Bi, chemical shift of X-ray L-absorption edge 79−52044
Bi halides, X-ray L_{III}-absorption edges 78−82750
Bi, M_5 absorpt. limits 78−6812
Br_2 adsorbed on Grafoil, EXAFS investig. 77−51602
Br_2 adsorbed on graphite, EXAFS 77−43430
Br_2, extended X-ray absorption fine struct. amplitude 79−59489
Br_2, extended X-ray absorption fine struct. amplitude attenuation, rel. to XPS satellites 80−37821
Br_2-graphite systems, adsorbed and intercalated, EXAFS 78−72638
CO, K-absorpt. spectra, reson. obs., near fine struct. 80−37817
CO, photoabsorpt. cross-section, 50-340 Å, as sum of empirical at. cross-sections 78−58718
CO, X-ray K-absorpt. spectra, vibr. fine struct., ab initio restricted HF calc. 78−86883
$CaCO_3$, X-ray Ca K-edge meas. 79−6950
CaF_2, EXAFS, intrinsic UV luminesc. excitation spectra 78−52567
$Ca_{1-x}Sm_xS$, electron config. of Sm ions, X-ray L-absorpt. spectroscopy 80−60715
$CdGeP_2$, electronic struct. at cryst./vitreous transition, X-ray K-absorpt. and emission 78−15248
Cd_3P_2, band struct., X-ray spectra determ. 78−35225

X-ray absorption spectra continued
$CdSiP_2$, electronic struct., X-ray spectroscopic investigation 80−108300
Ce, 4d-absorption spectra, similarity for atomic and metallic states 77−12463
$CeNb_3O_9$, $CeNbO_4$, $CeNbO_{7.6}$, electron config. of Ce ions, mag. sucept., L_3 absorpt. edge, resist. 79−43063
CeO_2, 4d absorpt. edge region, chem. binding effects 77−12467
Cl_2, absorption in ultrasoft X-ray region 78−90187
Cl_2, inner shell excited states, X-ray absorpt. spectra, HF calcs. 80−78536
Co and its cpds., X-ray K-absorpt. edge shifts, plasmon energies correlation 80−20734
Co complex, Co-thiourea compounds, X-ray K-absorpt. edge, effective nuclear charge 80−35006
Co complex, with p-amino salicylic acid, X-ray K-absorpt. discontinuity, shape, chem. shifts 79−47545
Co complex, X-ray K-absorpt. edge, ligand field splitting, spectrochemical series 77−10688
Co complexes, EXAFS obs. 80−998
Co complexes, $K_3[Co(CN)_6]$, $Na_3[Co(NO_2)_6]$, and $(NH_4)_2[Co(NCS)_4]$, X-ray Co K absorpt. edge struct. 77−20956
Co compounds, X-ray K-absorpt. edge, effective nuclear charge 80−35006
Co, EXAFS and shape of K absorption discontinuity 77−20955
Co, liq., soft X-ray band spectra 77−52199
Co, nearest-neighbour atom displacements derived from EXAFS spectra, temp. depend. 79−87524
Co oxides, effective atomic charge rel. to chemical shifts in transition metal compound XAS 79−78788
Co ternary compounds, chemical shifts of K X-ray absorption discontinuities 78−19599
Co, X-ray K-absorpt., edges, plasma oscills. effects 77−59640
Co, X-ray K-absorpt. edge shifts 77−4701
Co, X-ray K-absorption spectrum 80−97378
Co, X-ray refl. near $L_{2,3}$ absorpt. edge 80−71513
Co-Al, X-ray K-absorption spectrum 80−97378
$Co_3(AsO_4)_2$ X-ray K-absorpt. edge shifts of Co and As 77−4701
$CoCr_2X_4$ (X=O,S), K absorpt. discontinuity chem. shift, bonding parameters 77−77318
Cr and its cpds., X-ray K-absorpt. edge shifts, plasmon energies correlation 80−20734
Cr, X-ray K absorpt. discontinuities 78−60532
CrO_4^{2-}, electronic struct. determ. from X-ray spectra 78−86885
Cs, extreme UV absorpt spectra, threshold singularities of p-shell absorpt. 77−36261
CsX, (X=F, Cl, Br), absorpt. fine struct. at Cs^+ 4d threshold 77−18940
Cu (111) and (110), adsorption of I_2, surface EXAFS exam. 79−82446
Cu and Cu oxides, X-ray absorption, discontinuities and limits, chem. combination effects 80−93435
Cu, and Cu-Al disordered alloys, interatomic distances, coord. numbers, and mean relative displacements, EXAFS anal. 80−89087
Cu and its cpds., X-ray K-absorpt. edge shifts, plasmon energies correlation 80−20734
Cu, at. cluster, EXAFS study of bond length and binding energy 79−81317
Cu complex, bis-(alkylammonium) (11) tetrachloride, perovskite, lattice perfection 78−87633
Cu complex, Cu(II) acetylacetonates, X-ray K-absorpt. edges, edge widths and shifts 78−50556
Cu complex, mixed-valence, X-ray K-absorption spectra 79−33863
Cu complexes, dimeric carboxylate complexes, X-ray K-absorption edge position and EXAFS 77−85841
Cu complexes, EXAFS obs. 80−998
Cu complexes, involving metal-metal exchange interaction, shifts in X-ray K-absorption edge 77−16422
Cu complexes, N ligands, X-ray K-absorpt. edge, expt. 80−89084
Cu, core-electron excitation edges 80−66345
Cu EXAFS, with conventional X-ray source 77−69933
Cu, EXAFS Debye-Waller factors 80−45168
Cu extended X-ray fine struct., lattice consts. 80−89085
Cu film, EXAFS determination using high-pass photocathode X-ray ionization chamber 79−68164
Cu film, EXAFS meas. by total refl. 80−55228
Cu, film, partially oxidised, EXAFS studies on superficial regions 80−75474
Cu film, ultra thin, EXAFS 79−15559
Cu halides, tetrahedrally coordinated, semiempirical band struct. model 77−51655
Cu II complex, extended X-ray absorpt. fine struct. study 80−104011
Cu, nearest-neighbour atom displacements derived from EXAFS spectra, temp. depend. 79−87524
Cu, orbital energies and X-ray K-absorpt. spectra 80−69060
Cu, oxidation, EXAFS obs. 80−71808
Cu ternary compounds, chemical shifts of K X-ray absorption discontinuities 78−19599
Cu, thermal disorder, EXAFS determ. 80−45167
Cu, X-ray absorption edge, chem. shift, electron binding energy in compounds 78−62822
Cu, X-ray K-absorpt. edges, plasma oscills. effects 77−59640
Cu, X-ray K-absorption discontinuity, extended fine struct. 78−76556
Cu-Br bond length, EXAFS determ. for $CuBr_2$ 78−52593
Cu-N bond length, EXAFS determ. for $[Cu(NH_3)_4]^{2+}$ 78−52593
Cu-O bond length, EXAFS determ. for CuO, Cu_2O, $CuSO_4.5H_2O$, $Cu(OH)_2$ and $Cu(NO_3)_2.3H_2O$ 78−52593
$Cu_{0.7}Al_{0.3}$, chemical effect on valence electronic states, AES and SXAPS meas. 79−47558
$CuAlS_2$, X-ray spectroscopic study 78−39626
CuBr, superionic behaviour at high temp., EXAFS study 80−107496
$CuBr_2$, highly conc. aqueous soln., local ordering, extended X-ray absorb. fine struct. spectra 78−79520
CuCl, band struct., OPW calc. and X-ray spectra meas. 80−75506
CuCl, superionic behaviour at high temp., EXAFS study 80−107496
$CuCl_2(Br_2)$, aq. solns., EXAFS meas. 80−60714
$Cu_{0.5}Co_{0.5}Cr_{2-x}Rh_xS_4$, K absorpt. discontinuity chem. shift, bonding parameters 77−77318
$CuCr_2O_4$, spinel, K X-ray absorption spectrum 78−19600
$CuCr_2S_4$, spinel, K X-ray absorption spectrum 78−19600
$CuCr_2Se_4$, spinel, K X-ray absorption spectrum 78−19600
$CuCr_2Te_4$, spinel, K X-ray absorption spectrum 78−19600

X-ray absorption spectra continued
$CuCr_2X_4$ (X=O,S,Se,Te), K absorpt. discontinuity chem. shift., bonding parameters 77−77318
$CuFeS_2$, X-ray spectroscopic study 78−39626
$CuGaS_2$, X-ray spectroscopic study 78−39626
CuI, EXAFS investigation of struct. and ion motion 80−108302
CuI, superionic cond., EXAFS study 80−50462
$CuInS_2$, X-ray spectroscopic study 78−39626
CuO, mol. orbital energies and X-ray K-absorpt. spectra 80−69060
Cu_2O, mol. orbital energies and X-ray K-absorpt. spectra 80−69060
$Cu_{0.75}P_{0.25}$, chemical effect on valence electronic states, AES and SXAPS meas. 79−47558
$Cu_{0.67}S_{0.33}$, chemical effect on valence electronic states, AES and SXAPS meas. 79−47558
$CuSO_4.5H_2O$, EXAFS, rel. between Debye-Waller factor and thermal parameters meas. by neutron diffr. 80−84803
$Cu_{82.5}Sb_{17.5}$, X-ray K-absorption discontinuity, extended fine struct. 78−76556
$Cu_{0.9}Si_{0.1}$, chemical effect on valence electronic states, AES and SXAPS meas. 79−47558
Dy, bidirectional orbital interpretation of L_{III} absorption discontinuity shape 77−16423
Dy, EXAFS, white lines, interatomic distances 77−40302
$DyCo_3$, X-ray absorpt. edge shifts 80−25483
$DyFe_2$, amorphous, struct. determ. EXAFS exam. 78−51421
Er, bidirectional orbital interpretation of L_{III} absorption discontinuity shape 77−16423
$Er_3Fe_{5-x}In_xO_{12}$, lattice consts., T_c, mag. saturation, K-absorpt. and Mossbauer spectra, 80K *(Russian)* 77−20954
Eu compounds, X-ray L-absorption spectra, 'white line' absorpt. maximum, chem. shifts 77−58042
Eu I, 4d→f transitions in absorpt. spectra in 40-300 Å range 77−3298
Eu solid solutions with lanthanides, monosulfides, and oxides, vacant d states, X-ray absorpt. 80−103623
EuB_6, valence state of Eu, X-ray line displacement meas. 80−70633
$EuCu_2Si_2$, mixed valence system, X-ray absorption spectroscopic study 80−80906
EuO:Yb(Sm), electron transition and valence state of impurities, X-ray spectroscopy and structural anal. 78−39064
EuS:Yb(Sm), electron transition and valence state of impurities, X-ray spectroscopy and structural anal. 78−39064
$Eu_{1-x}Sm_xS$, electron config. of Sm ions, X-ray L-absorpt. spectroscopy 80−60715
$Eu_{1-x}Sm_xS$, electronic transition in Sm impurity ions, rel. to exchange interactions, L absorpt. spectra 77−59644
Fe, BCC and FCC struct. X-ray absorption spectra, Mossbauer spectra, comparison *(Russian)* 78−64299
Fe, EXAFS Debye-Waller factors 80−45168
Fe, far fine struct., multiple scatt. terms contrib. 80−40184
Fe, liq., soft X-ray band spectra 77−52199
Fe monomers and dimens. in solid Ar, EXADS study 80−97381
Fe oxides, effective atomic charge rel. to chemical shifts in transition metal compound XAS 79−78788
Fe rich micas, X-ray absorpt., heat treatment effects, chem. and struct. interpretation 80−84806
Fe, X-ray absorpt. spectra, effective co-ordination charges 80−84805
Fe, X-ray K absorpt. discontinuities 78−60532
Fe, X-ray K-absorpt. spectra, depend. on composition and temp. changes *(Russian)* 80−55226
Fe-compounds, K-absorption edge energy shift 79−4870
Fe-Cu (75 ppm), internal oxidation, local struct. determ. by EXAFS 80−25916
Fe-Ni-Mo, inhomogeneous solid solns., annealed and work hardened states, X-ray K-absorption spectra *(Russian)* 78−56544
$Fe_{70}Cr_{30}$, disordered, X-ray spectra study of electronic struct. 77−77324
$Fe_{36}Cr_{32}Ni_{14}B_{12}B_6$, amorphous X-ray absorpt. spectra, effective co-ordination charges 80−84805
FeF_2, EXAFS at high press., bond compressibility, at. spacings 78−39628
$(Fe_xMn_{1-x})_3C$ in steel, X-ray K-absorpt. spectra *(Russian)* 78−6813
$Fe_{40}Ni_{40}B_{20-x}P_x$ metallic glasses, local struct. and dynamic disorder of Fe and Ni, EXAFS obs. 80−89088
Fe_2O_3, X-ray absorpt. spectra, effective co-ordination charges 80−84805
Fe_3O_4, X-ray absorpt. spectra, effective co-ordination charges 80−84805
Fe_xO, X-ray absorpt. spectra, effective co-ordination charges 80−84805
FeS_2, EXAFS at high press., bond compressibility, at. spacings 78−39628
$FeSiO_3$, UV and soft X-ray spectra, band gap determ. 79−61468
Fe_2SiO_4, UV and soft X-ray spectra, band gap determ. 79−61468
Ga, anisotropy of white line in K-absorption spectrum, EXAFS mechanism 80−89086
Ga, K-EXAFS, orientation depend. at 5K 79−52043
Ga, X-ray K absorpt. edge, effective ionic charge and bonding schemes 80−29827
GaAs (110), O chemisorption, surface EXAFS meas. 80−50460
GaAs amorphous film, EXAFS, optical and elec. props. 80−49547
GaAs, X-ray K absorpt. edge, effective ionic charge and bonding schemes 80−29827
GaP amorphous film, EXAFS, optical and elec. props. 80−49547
Gd and cpds., L_3 X-ray absorpt. discontinuity 77−85840
Gd, bidirectional orbital interpretation of L_{III} absorption discontinuity shape 77−16423
Gd, X-ray absorpt. edge, plasmon excitation 80−7437
$GdCo_3$, X-ray absorpt. edge shifts 80−25483
Ge, EXAFS, in real space, struct. determ. 77−15273
Ge, EXAFS at high press. 80−97376
Ge, nearest-neighbour atom mean-square relative displacements, EXAFS spectra 79−91532
Ge-Ni, amorphous, struct., EXAFS study 80−49110
Ge-rare earth alloys, nature of chemical interaction, X-ray emission, absorpt. and photoelectron study *(Russian)* 80−55261
GeF_4, ($GeCl_4$), X-ray absorpt. spectra struct. 80−37819
GeS, anisotropic EXAFS, cryst. struct. determ. 80−66323
GeS(Se)(Te)(O_2), K X-ray spectra, Ge atoms effective charge, energy-gap widths 77−28657
$GeSe_2$ evaporated films, struct. and thermally induced effects 79−41963
HCl, K-emission and -absorpt. spectra, vibr. struct., ab initio calcs. 77−79629
HCl, nonempirical calc. of X-ray K-absorpt. spectra 77−88465
HF, K-emission and -absorpt. spectra, vibr. struct., ab initio calcs. 77−79629
X-ray absorption spectra continued
HF, nonempirical calc. of X-ray K-absorpt. spectra 77−88465
Ho, bidirectional orbital interpretation of L_{III} absorption discontinuity shape 77−16423
Ho, EXAFS, white lines, interatomic distances 77−40302
Ho, white line struct. in X-ray L_{III} absorption edge 79−15560
$HoCl_3$, white line struct. in X-ray L_{III} absorption edge 79−15560
$HoFe_2$, amorphous, struct. determ., EXAFS exam. 78−51421
Ho_2O_3, white line struct. in X-ray L_{III} absorption edge 79−15560
I_2, adsorbed on Ag(111), Cu(111), and Cu(110), surface EXAFS study 80−40186
InP, III-V semicond., electronic struct. of valence and conduct. bands 77−28110
Ir, L_{III}-edge X-ray absorpt. reson., chem. environment effects 79−72256
K, extreme UV absorpt. spectra, threshold singularities of p-shell absorpt. 77−36261
K, soft X-ray emission and absorpt. edges, self-absorpt. studies 80−40183
KCl, fine structure of X-ray absorption spectra 80−71514
KCl:Tl, effective cross sections ratio of charged and neutral centres for holes and electrons *(Russian)* 79−28319
$KMnO_4$, cryst., bond lengths and coordination numbers, EXAFS meas. 79−51043
K_xZrS_2, intercalation cpd., X-ray K absorption edges 78−39627
$K_3[Fe(CN)_6]$ X-ray Fe K absorption edge struct. of $[Fe(CN)_6]^{3-}$ meas. 78−43959
$K_4[Fe(CN)_6].3H_2O$, X-ray Fe K absorption edge struct. of $[Fe(CN)_6]^{4-}$ meas 78−43959
La-Sm-Au, amorphous, surface effects on Sm valence, XPS and X-ray absorption meas. 80−108325
$LaFe_{1-x}Co_xO_3$, UPS, XPS, X-ray absorpt. spectra, band struct. study 79−56885
$LaNi_{1-x}Fe_xO_3$, UPS, XPS, X-ray absorpt. spectra, band struct. study 79−56885
$LaNi_{1-x}Co_xO_3$, UPS, XPS, X-ray absorpt. spectra, band struct. study 79−56885
Li I, II, absorption spectra in grazing incidence region, 215-160 Å 78−5164
Li K edge, exchange effects 77−4702
Li, one-electron calcs. of X-ray absorpt. and emission, jellium model 78−56543
Li, X-ray absorpt. and emission edges, one-electron and many-body effects 80−25484
Li, X-ray edge spectra, phonon broadening 77−77279
Li, X-ray emission and absorpt. edges, temp. depend. 78−31282
Li, X-ray K-edge transitions, band theory 77−16426
Li, X-ray threshold, improved compatibility relations 77−8684
Li, X-ray threshold anal. 78−31281
LiF dispersing crystal, X-ray source, synchrotron-like intensities, EXAFS expts. 78−86398
LiF film, electronic excitations, inelastic electron scatt. spectra 77−32479
$LiNbO_3:Fe^{2(3)+}$, X-ray absorpt. 80−108299
Lu, absorption discontinuity, energy separation of orbitals 78−76557
Mg, one-electron calcs. of X-ray absorpt. and emission, jellium model 78−56543
Mg, plasmon struct. obs. in K photoabsorpt. spectra 79−38693
Mg, soft X-ray emission and absorpt. edges, self-absorpt. studies 80−40183
Mg, X-ray absorpt. and emission edges, one-electron and many-body effects 80−25484
Mg, X-ray threshold anal. 78−31281
$(MgAl_2O_4)_x(AMn_2O_4)_{1-x}$, A=Mg,Mn,Zn,Cd, $0<x<1$, mixed oxide spinels, chemical shifts of Mn K-absorpt. edge 80−29828
$MgAl_ySc_xFe_{2-x-y}O_4$, X-ray spectra Mossbauer spectra, electronic struct. of Fe and Sc 77−28647
$MgCl_2$, electronic structure by intersecting spheres model, X-ray absorption spectra interpretation 79−99482
$MgM^{3+}{}_xFe_{2-x}O_4$, M=In,Al,Cr,Sc, comp. effects on ferrite characts. 78−52305
$MgSiP_2$, electronic struct., X-ray spectroscopic investigation 80−108300
Mn and Mn oxides, K X-ray absorpt. discontinuity, shape and extended fine struct. 80−66324
Mn, BCC and FCC struct., X-ray absorption spectra, Mossbauer spectra, comparison *(Russian)* 78−64299
Mn compounds, single and complex, X-ray absorption near edge structs. 80−104013
Mn oxides, effective atomic charge rel. to chemical shifts in transition metal compound XAS 79−78788
Mn-compounds, K-absorption edge energy shift 79−4870
MnO_4 , bond lengths and coordination numbers, EXAFS meas. 79−51043
MnO_4^-, electronic struct. determ. from X-ray spectra 78−86885
$(MnO_4)^-$ type ions, metal X-ray K absorption spectra, low energy maxima interpretation 79−74019
MnP, metallic, band struct., X-ray spectral obs. 78−11019
Mo, K-edge photoabsorption spectra, linear APW calc. 78−43960
Mo, X-ray absorption edge, chem. shift, electron binding energy in compounds 78−62822
Mo, X-ray L_1, L_2 and L_3 absorption limits 77−90218
N_2, K-absorpt. spectra, reson. obs., near fine struct. 80−37817
N_2, K-photoabsorpt. cross-section, 400-450 eV 78−94257
N_2, photoabsorpt. cross-section, 50-340 Å, as sum of empirical at. cross-sections 78−58718
N_2, X-ray K-absorpt. spectra, vibr. fine struct., ab initio restricted HF calc. 78−86883
$NH_4H_2PO_4$, correlation between cryst. perfection and refl. intensity for analyser cryst. 78−48259
NO, photoabsorpt. cross-section, 50-340 Å, as sum of empirical at. cross-sections 78−58718
N_2O, photoabsorpt. cross-section, 50-340 Å, as sum of empirical at. cross-sections 78−58718
Na, impurities and photoexcited ions 80−39523
Na, K-absorpt. edge spectra 79−81177
Na, one-electron calcs. of X-ray absorpt. and emission, jellium model 78−56543
Na, soft X-ray L_{23} emission and absorpt. spectra 79−43064
Na, X-ray absorpt. and emission edges, one-electron and many-body effects 80−25484
Na, X-ray edge shape, band struct. role 77−16425
Na, X-ray threshold anal. 78−31281

X-ray absorption spectra continued
NaBr, EXAFS at high press. 80−97376
NaCl, excitons at $L_{II,III}$ absorption edge of Cl^-, decay characts. thermolum. meas. 77−28121
NaF, quasimolecular struct. characts. of $NaL_{II,III}$ absorpt. edge 80−93436
Na_2O-SiO_2-Fe_2O_3, glass, X-ray absorpt. spectra, effective co-ordination charges 80−84805
Na_2SiF_6, struct. of continuous X-ray absorpt. near $L_{2,3}(2p)$ ionisation threshold of Si 79−99983
NaX, (X=Br,Cl,F,I), X-ray absorpt. near Na^+ K edge 79−99982
Nb complexes, F-containing, X-ray K absorption edges, chem. interpretation 78−74676
Nb_3Ge film, EXAFS meas. 78−2935
$Nb_{0.5}Mo_{0.5}$, soft X-ray spectra, theoretical considerations 80−11511
$NbSe_2$ intercalated with Rb, EXAFS 80−2897
$NbSe_2$, intercalated with Rb, EXAFS meas. 80−40185
Nd, threshold pot. spectra, $N_{4,5}$ absorpt. widths 79−69578
NdO, mag. props., lattice consts., and X-ray absorpt. spectra 80−44798
Ne, nonempirical calc. of X-ray K-absorpt. spectra 77−88465
Ni (100), with absorbed O_2 monolayer, surface EXAFS, secondary electron yield meas. 79−47544
Ni and its cpds., X-ray K-absorpt. edge shifts, plasmon energies correlation 80−20734
Ni, at. cluster, EXAFS study of bond length and binding energy 79−81317
Ni, BCC and FCC struct., X-ray absorption spectra, Mossbauer spectra, comparison *(Russian)* 78−64299
Ni, core-electron excitation edges 80−66345
Ni, L_{III}-binding energy, absolute determ. from self-absorpt. meas. 80−71519
Ni, liq., soft X-ray band spectra 77−52199
Ni, $M_{2,3}$ edge, temp. depend. 80−50463
Ni, X-ray absorption and emission K and L spectra, APW calc. 78−68579
Ni, X-ray K-absorpt. spectra, depend. on composition and temp. changes *(Russian)* 80−55226
Ni-Al, ferromag. solid sol., electronic struct., X-ray absorpt. spectra meas. 79−69653
β-Ni-Al, X-ray absorpt. spectra meas., Fermi level location 80−35005
$NiCl_2$, aq. soln., Ni^{2+} coordination from extended X-ray absorption fine struct. 80−1913
$NiCl_2(Br_2)$, aq. solns., EXAFS meas. 80−60714
$Ni(NO_3).6H_2O$, Ni(II) coordination in aq. soln., EXAFS 77−85837
O_2 molecule, soft X-ray photoionisation cross-sections, 6 to 22 Å 77−14499
O_2, photoabsorpt. cross-section, 50-340 Å, as sum of empirical at. cross-sections 78−58718
Pb and Pb oxides, X-ray absorption, discontinuities and limits, chem. combination effects 80−93435
Pb, chemical shift of X-ray L-absorption edge 79−52044
Pb I, interchannel interactions and series quenching in 5d and 6s spectra 77−88418
Pb, M_5 absorpt. limits 78−6812
Pb, photoionisation cross section of atomic and final state effects on 5d core levels 78−84699
Pb, X-ray absorption edge, chem. shift, electron binding energy in compounds 78−62822
$PbCl_2$, photoionisation cross section of atomic and final state effects on 5d core levels 78−84699
PbS(Se), photoionisation cross section of atomic and final state effects on 5d core levels 78−84699
$PbZrO_3$, perovskite type, X-ray K-absorpt. edge, chem. shift 79−91529
Pd, K-edge photoabsorption spectra, linear APW calc. 78−43960
Pd-Ge glass, short range order obs. for $Pd_{80}Ge_{20}$ and $Pd_{78}Ge_{22}$, EXAFS expts. 78−55815
Pd-Ge metallic glass, appl. of EXAFS methods for struct. determ. 79−37624
$PrCo_5$, EXAFS and shape of K absorption discontinuity of Co 77−20955
PrO, mag. props., lattice consts., and X-ray absorpt. spectra 80−44798
Pt, catalyst, dispersed onto silica support, EXAFS meas. 78−48258
Pt clusters, supported on Y-zeolites, X-ray absorpt. spectrosc. obs. 79−24390
Pt complexes, X-ray absorpt. spectra, mol. orbital interpretation 78−42097
Pt, core-electron excitation edges 80−66345
Pt, EXAFS Debye-Waller factors 80−45168
Pt, L_{III}-edge X-ray absorpt. reson., chem. environment effects 79−72256
Pt, small particles, contraction and relax. of interatomic distances using EXAFS 79−47546
Pt, white line at L_3 edge 77−36313
Pu, α and δ phases, 5f states modification obs. 77−28649
Pu, K-absorption edge energy, accurate determ. using γ attenuation 77−59642
Rb and Rb compounds, X-ray K absorption edge, fine struct. 77−77319
Rb, extreme UV absorpt. spectra, threshold singularities of p-shell absorpt. 77−36261
$RbAg_4I_5$, EXAFS, RDF studies 79−87526
RbCl, nearest-neighbour atom displacements derived from EXAFS spectra, temp. depend. 79−87524
RbF(Cl)(Br)(I), chem. shift in X-ray absorpt. spectra, correl. with ion contrib. to bond 78−76559
Rb_xZrS_2, intercalation cpd., X-ray K absorption edges 78−39627
Re, extended X-ray abs. fine struct., L_α, L_β satellites 79−33861
$RhBr_3$, bond distances exam. by EXAFS 78−26525
Ru catalysts, chemisorption of O_2, EXAFS obs. 78−15708
Ru-Cu clusters, EXAFS study 80−84804
SF_6, X-ray absorption spectra *(Russian)* 78−50559
$(SN)_x$, brominated, X-ray absorpt. meas., 5K to room temp. 80−71516
$(SN)_x$:Br, X-ray absorpt. meas. of mol. struct., orientation and charge transfer 80−25486
SO_2, $L_{II,III}$ absorpt. edge, fine struct. 78−62823
$SbCu_2Si_2$, mixed valence system, X-ray absorption spectroscopic study 80−80906
Sc and Sc_2O_3, photoabsorpt. spectra, at. ionisation, band struct. mechanisms, electron energy loss investig. 77−24909
Sc-[Co,Ni,Cu]-Ga, phase equilibria, diagrams of state, X-ray, microstructural study *(Russian)* 80−55356
ScGa and Sc_5Ga_3, exam. of X-ray K spectra of pure Sc, Ga in alloys *(Russian)* 79−15562

X-ray absorption spectra continued
Se, amorphous, trigonal and monoclinic, 2p photoabsorpt. spectra 78−23551
Se, amorphous and cryst., X-ray K-shell absorpt. discontinuity 79−61467
Si (111), chemisorbed O_2 bonding geometry, electron yield EXAFS meas. 80−50461
Si, (111) surface, EXAFS of oxidation stage, O-Si bond length 79−95876
Si, amorphous and cryst. K X-ray spectra of band struct. 79−87525
Si, doped and amorphous, $L_{2,3}$ threshold spectra 77−69934
Si, X-ray linear absorption coeff. 78−26384
Si:As, amorphous, appl. of EXAFS methods for struct. determ. 79−37624
Si-H:As alloy, amorphous film, coordination of impurities, EXAFS of data 77−84780
SiC, Si X-ray absorption K-edges, charact. parameters *(Russian)* 79−47541
SiF_4, ($SiCl_4$), ($SiBr_4$), X-ray absorpt. spectra struct. 80−37819
SiH_4, $L_{II,III}$ continuous absorpt. spectrum of Si 80−95645
Si_3N_4, amorphous, $L_{2,3}$ threshold spectra 77−69934
Si_3N_4, CVD on Si (111), EXAFS 79−95876
Si_3N_4, N K-edge EXAFS, secondary electron yield meas. 79−47544
Si_3N_4, Si X-ray absorption K-edges, charact. parameters *(Russian)* 79−47541
SiO, Si X-ray absorption K-edges, charact. parameters *(Russian)* 79−47541
SiO_2, amorphous, $L_{2,3}$ threshold spectra 77−69934
SiO_2 monolayer, core excitons and inner well resonances in surface soft X-ray absorpt. spectra 80−40187
SiO_2, on Si (111), EXAFS 79−95876
SiO_2, Si X-ray absorption K-edges, charact. parameters *(Russian)* 79−47541
Si(111), surface density of states from soft X-ray absorpt. spectra 80−40187
Sm-Au, amorphous, surface effects on Sm valence, XPS and X-ray absorption meas. 80−108325
Sm_4Bi_3, mixed valence system, X-ray absorption spectroscopic study 80−80906
$SmCo_5$, EXAFS and shape of K absorption discontinuity of Co 77−20955
$SmCo_5$, X-ray K absorpt., chem. shift 79−91531
$SmCu_5$, X-ray K absorpt., chem. shift 79−91531
SmO, mag. props., lattice consts., and X-ray absorpt. spectra 80−44798
$Sm_{0.75}Y_{0.25}S$, mixed-valence, electron-lattice correlations, EXAFS studies 80−76103
$SrBr_2$, aq. solns., EXAFS meas. 80−60714
$SrS(F_2)(Cl_2)$, nearest-neighbour atom displacements derived from EXAFS spectra, temp. depend. 79−87524
$Sr_{1-x}Sm_xS$, electron config. of Sm ions, X-ray L-absorpt. spectroscopy 80−60715
$SrTiO_3$, K-edge X-ray absorpt., cond. band states 80−97382
Ta resonance absorpt. at L edges and white line 79−61469
IT-TaS_2, layered cpd., anisotropic X-ray absorption 78−39629
Tb, bidirectional orbital interpretation of L_{III} absorption discontinuity shape 77−16423
$TbCo_3$, X-ray absorpt. edge shifts 80−25483
$TbFe_2$, amorphous, struct. determ., EXAFS exam. 78−51421
ThF_4, 5d X-ray spectra 78−88382
ThO_2, 5d X-ray spectra 78−88382
Ti, EXAFS from L edge, 200-1000 eV 79−69903
Ti, X-ray refl. near $L_{2,3}$ absorpt. edge 80−71513
Ti+S ion, KL^n X-ray satellites, intensity distrib., photoabsorpt. effects 78−78657
TiO_2, rutile, K-edge X-ray absorpt., cond. band states 80−97382
TiO_x, X-ray Ti K spectra and band struct. 77−77320
TiP, metallic, band struct., X-ray spectral obs. 78−11019
Tl, M_5 absorpt. limits 78−6812
Tm, EXAFS, white lines, interatomic distances 77−40302
$TmCo_5$, covalent electron number, from chem. shift of Co X-ray absorption spectra 77−59641
TmSe, mixed valence, X-ray absorption study 80−76102
U compounds, meas. of energy shifts of K absorption edge and K X-rays 78−11020
UO_2, 5d X-ray spectra 78−88382
UO_2, electronic distributions by X-ray spectroscopy 80−97407
UO_3, 5d X-ray spectra 78−88382
V, electronic structure, X-ray spectra and XPS meas. 77−85842
V, X-ray band spectra calcs. 79−33860
VB_2, energy shift and struct. of K-absorpt. edge of V 79−38694
VC, energy shift and struct. of K-absorpt. edge of V 79−38694
VF_3, energy shift and struct. of K-absorpt. edge of V 79−38694
VN, energy shift and struct. of K-absorpt. edge of V 79−38694
VO_4^{3-}, electronic struct. determ. from X-ray spectra 78−86885
V_2O_3, effect of metal-insulator transition on V K-absorption spectrum 79−19950
V_xO_y, energy shift and struct. of K-absorpt. edge of V 79−38694
VS_3, energy shift and struct. of K-absorpt. edge of V 79−38694
VSi_2, energy shift and struct. of K-absorpt. edge of V 79−38694
2H-WSe_2, layered cpd., anisotropic X-ray absorption 78−39629
X-ray absorption K-edges in crystalline Si, SiO, SiO_2, SiC, Si_3N_4 *(Russian)* 79−47541
Xe like ions (I^-, Cs^+, Ba^{2+}, La^{3+}) $3d^94f$ config., collapse of 4f electron, X-ray spectral obs. *(Russian)* 80−58204
Y and Y_2O_3, photoabsorpt. spectra, band struct., at. ionisation mechanisms, electron energy loss spectra 77−24909
Y, K-satellite origin, Hayasi model of quasi-stationary states 77−1762
YCo_5, covalent electron number, from chem. shift of Co X-ray absorption spectra 77−59641
$Y_3Fe_{5-x}In_xO_{12}$, K absorpt. and Mossbauer spectra *(Russian)* 77−32467
Yb, EXAFS, white lines, interatomic distances 77−40302
$Yb_{1-x}Sm_xS$, electron config. of Sm ions, X-ray L-absorpt. spectroscopy 80−60715
Zn and its cpds., X-ray K-absorpt. edge shifts, plasmon energies correlation 80−20734
Zn single crystal, EXAFS, using linearly polarised synchrotron radiation 78−2943
Zn XIX, XX, spectral lines 20 to 50 Å 77−18822
Zn_3As_2, determ. of ionicity by X-ray absorption method 78−31278
$ZnBr_2$, aq. solns., EXAFS meas. 80−60714

X-ray absorption spectra continued
$ZnCl_2$, glassy and liq, EXAFS obs. of struct., comparison with vitreous GeO_2 80−70133
ZnF_2, X-ray absorpt. spectrum polarisation depend. 80−104012
$ZnGeP_2$, cryst., electronic struct., X-ray K-absorpt. and emission 78−15248
Zn_3P_2, determ. of ionicity by X-ray absorption method 78−31278
$ZnSiP_2$, electronic struct., X-ray spectroscopic investigation 80−108300
Zr, and its cpds., X-ray K-absorpt. spectra 78−76558
Zr complexes, X-ray K-absorption edge, shift and width meas. 77−8683
Zr, K-edge photoabsorption spectra, linear APW calc. 78−43960
ZrO_2, perovskite type, X-ray K-absorpt. edge, chem. shift 79−91529
ZrO_2-$YO_{1.5}$ solid solutions, ZrO_2 rich side, X-ray spectroscopic study 78−95617

X-ray analysis
see also electron probe analysis; X-ray chemical analysis; X-ray crystallography; X-ray diffraction examination of materials; X-ray spectroscopy
analytical electron microscope optimization of X-ray microanalysis, instrum. problems 80−73540
biological X-ray microanalysis, principles 80−73566
computer-aided anal. of X-ray data 77−67416
electron probe microanalysis for calcification studies of bone and cartilage 80−76885
energy selective, appls. in TEM 80−84036
environmental particulate exposure in humans, documentation 80−76886
gas proportional counter, for X-ray analysis, atomic K-lines *(Czech)* 79−31323
human body components, anal. by X-rays, developments 80−3810
industrial X-ray installation, spectroscopic anal. *(German)* 80−97668
microparticles, quantitative anal. with electron beam instruments 79−21866
molecules, electron distrib., ab initio anal. 80−47866
NDT, X-ray flash methods and equipment *(German)* 80−97669
optimised energy dispersive X-ray microanalysis 80−4811
peak-to-background method for quantitative anal. of single particles, with electron probe, developmental progress 80−73541
plasma diagnostics, PLT and PDX Tokamaks 80−75104
polyphase X-ray quantitative anal. method for nonpure samples *(Chinese)* 79−80737
prevention of losses and damage 80−73567
pulsed X-ray tubes, reduction in acquisition time 79−54239
residual stress anal. using X-rays, theory 77−84200
scanning electron microscopy; pellet mould for bulk specimen anal. 80−95191
scanning electron probe microanalyser, development of x-ray microanalysis 80−37139
SEM, cryogenic stage for sample preparation for X-ray microanalysis 80−42306
soft X-ray analysers for pulsed-source emissions 80−31957
soft X-ray microscopy, high resolution, appl. to biological materials 77−87889
spatial resolution in STEM 80−84039
steel, C hot dipped aluminised, phase composition anal. of alloy layer by X-ray, electron probe and hardness meas. 79−34192
superheavy elements, X-ray anal. of monazite inclusions in mica 77−25685
transition energy data, rel. to theory 79−76378
Al coated steel, porosity evaluation, micro X-ray spectral anal. *(Russian)* 80−35389
Cd distribution in bullfrog skin, determ. by electron probe X-ray microanalyzer 79−79707
NbTi composites, cryogenic stability due to boundary resistance between filament and matrix 79−58748

X-ray apparatus
see also biomedical equipment; X-ray crystallography apparatus; X-ray monochromators; X-ray spectrometers; X-ray tubes
analyser for soft X-ray spectroscopy of excitation potentials 79−21882
angiographic universal setups for general hospital with vascular surgery facility 79−92336
angiography, free arc, with film changer and image intensifier mounted on U-arm 77−86601
anode, rotating, temperature distribution, various types comparison 79−2901
astronomical, polarimeter, for solar and extrasolar obs. 78−57454
automatic radiographic system and HT generator, for gastrointestinal tract exam. *(Japanese)* 79−88167
axial tomography of skull, modified technique 77−86600
bent glass optics 78−45767
biological sample analysis, nanosec. X-ray diffr. pattern techniques 80−26429
biological specimen microscopy, flash X-ray method 80−51310
biomedical, motor-tilted diagnostic examination device Model UV-5B 80−85479
biomedical collimators, semi-automatic and automatic, manufactured by Medicor Works 80−85475
biomedical equipment, state of the art 80−81688
biomedical image storing equipment of Medicor Works 80−85476
biomedical scanners, fast, incomplete scan geometries 80−26330
biomedical spot-camera of Medicor Works 80−85477
blazed gratings in extreme off-plane mountings, X-ray efficiencies 77−82656
camera, 5-frame, for charged particle, inertial confinement fusion studies 80−57453
camera, attachment for aimed investigation of fractures 80−85102
camera, photocathodes, characts., for X-ray diagnostics of laser-induced plasmas 77−54031
camera for low angle diffraction expts. with synchrotron radiation 77−87888
camera for structural anal., high temp. system, for examining liquid metals 80−25950
cameras, subpicosecond resolution, progress report 77−5951
capacitor discharge mobile X-ray apparatus *(Japanese)* 79−88165
cardiac work, practical aspects of apparatus 79−96659
catoptrical crossed-mirror imaging at grazing incidence 80−77923
cerebral angiography routine enlargement system, Poly Diagnost N 77−86602
Chirana cylindrical cameras modification for Seemann-Bohlin focusing method *(Czech)* 79−26192
cinematographic systems for ballistics diagnosis 80−13194

X-ray apparatus continued
circular waveguides, transmission in curved Pb glass capillaries 78−86395
collimator, parallel X-ray beam generation and appl. to testing collimators 78−28526
collimators, for astronomical soft X-ray meas. 77−5436
computed tomography, principles, reconstruction, equipment and dose 78−53481
computerised tomography, dynamic spatial reconstructor, high temporal resolution scanner 80−51235
computerised tomography equipment, for intracranial diagnosis 78−31884
conducting pipe, transmission meas. of 5.9 and 14.4 keV 77−193
coronary arteriography, current techniques and equipment 78−35940
corrosion sutdy apparatus, cell for in-situ corrosion in high temp. water 80−90936
cosmic ray emulsion chambers, electron-photon cascade energy determ. errors 79−84613
cryostat for low-temp. X-irradiation of solid samples 80−86321
cylindrical articles of small diameter, monitoring by automatic X-ray apparatus 79−70280
Debye-Scherrer camera conversion to back reflection camera 80−99024
Delta Scan, computerised entire body transverse scanner, technical description 77−44781
densitometer with high sensitivity and quantum flux for gas shock wave meas. 79−26031
diagnosis and therapy, Soviet medical requirements, review 77−37032
Diagnost C for gastro-enterological X-ray diagnosis 77−86599
diagnostic apparatus optimal operating conditions 80−30847
diagnostic equipment, method and algorithm for adjusting 80−30852
diagnostic isocon imaging system 77−40760
diagnostic sets, operation of optical centreing systems 80−30831
diagnostic sets with automatic exposure relays, switching delays 77−48903
diagnostic table, computer controlled, multidirectional, CASSETTELESS spotfilm device *(Japanese)* 78−61278
diagnostic X-ray equipment power supply design 77−21608
diamond turned optics 77−27400
differential energy absorpt. X-ray cassette, radiographic image contrast enhancement 78−20264
diffraction from solid wedge, ghost source theory 79−2900
diffraction gratings, blazed, photofabrication 77−5966
diffraction gratings, VUV and XUV, simple selection rules 78−55435
diffraction stress analyser, for large structures *(Japanese)* 77−48599
dose compensation filter design using megavoltage radiography 80−3785
Einstein X-ray observatory, HEAO-2, results to date 80−56692
electrical circuit fault classification 77−21604
electronic radiography, computerised, for early detect. of vacular disease 80−41226
electrophotetic X-ray imager, self-contained instant display erasable 80−22491
electroradiographic image laser readout 80−41225
ellipsoidal lens for sub keV X-ray imaging 77−26444
endoscopic roentgenography appliance users' experience 77−25544
equipment safety in diagnostic X-ray departments 79−48346
equipment selection for intensive care unit 79−92346
European Molecular Biology Laboratory synchrotron radiation X-ray camera designs 78−66700
EXAFS system, tunable 80−57452
external beam therapy, 4 MeV linear accelerator, dosimetric aspects 80−17140
fan-beam scanners, suppression of ring artefacts by software algorithm 79−5394
field type X-ray stress analyser, applicability *(Japanese)* 77−52591
filter assembly for fluorescence EXAFS meas. 80−90971
flash radiography, high energy, for dynamic NDT 78−15624
flash source, high-intensity, appl. of electron-photon cascade model 77−68157
flash X-ray machine, distributed pulse power system anal. using SCEPTRE circuit code techniques 80−68336
flow detectors, radiation type, electron bremsstrahlung irrad. field dia. calc. 78−56857
focusing mirror for synchrotron radiation 80−90961
frame recording method for intermittent X-ray TV to reduce exposure dose in fluoroscopy *(Japanese)* 78−89607
generators, acceptable latitudes in the specifications 80−37137
generators, meas. of peak voltage with PIN-photodiodes 80−105754
goniometer, portable *(German)* 77−194
gratings in GMS mount 79−75664
grazing incidence optics, total transverse aberration function 78−45765
grazing incidence system, primary aberrations 77−88644
grazing incidence X-ray microscopy, of laser fusion targets 78−47178
GUR-5 goniometer for small-angle X-ray scattering meas. 78−74115
hard X-ray imaging collimator 77−5437
hard X-ray imaging instrument, for solar and cosmic sources 78−49332
high resolution X-ray optics, for astronomical and laboratory sources 78−45766
high-voltage low-power devices 78−21309
holographic microscopy *(Russian)* 78−12799
image amplifier, 14 inch, clinical appls. *(Japanese)* 79−92355
image converting panel, EL-PC type, X-ray TV system appl. *(Japanese)* 77−67551
image intensification in medical and industrial radiology *(French)* 77−30223
image intensifier, design aspects 77−38070
image intensifier, dual mode caesium iodide screen 78−21311
image intensifier, phys. principles 79−6247
image intensifier freq.-contrast charact. curves determ., biomedical appl. 78−7427
image intensifier noise evaluation, digital method 80−98097
image intensifier output screens 78−4755
image intensifier performance, image quality, and development trends 80−36124
image intensifier TV X-ray detector, high sensitivity, biological structure diffr. study appl. 78−89609
image intensifiers, electron-optical conversion factor 79−6248
image intensifiers, new generation, characts. *(Czech)* 77−18153
image intensifiers, quantum noise meas. 80−46033
image magnification technique 80−18054
image receptor, large area, with electrophoretic display 80−98091

X-ray apparatus continued
image-forming reflection system testing by grazing-incidence Linnik interferometry 79−76891
imaging devices, for laser fusion programme 78−47173
imaging system, surface roughness and scatt. effects 80−77921
imaging systems using aplanatic mirror pairs 77−5967
imaging techniques, conf., Reston, USA (Apr. 1977) 78−45762
industrial X-ray inspection systems for welded seams in heavy engineering, Philips MG 420 and MG 300 79−93269
intensified minification camera for low dose radiography 78−20262
intensifier, CCTV viewing system 77−9251
interferometer, three beam *(German)* 78−8483
interferometer, using quartz crystal *(Russian)* 79−44995
interferometers, two block types, effect of deformation due to heating on diffraction focusing *(Russian)* 77−41743
kilovoltmeter for X-ray equipment 80−13191
Kratky compact small-angle X-ray collimation system 80−105757
kymography, motion picture apparatus 80−30851
leakage radiation charact., 18 MeV, clinical linear acceleration 79−5379
Lexiscope, portable pocket size X-ray imaging system for medical/dental radiography 78−92701
liquid sample holder, adjustable, X-ray absorption study appl. 79−6252
LLL type interferometer, interfering beam phase rels. 80−90973
low-intensity X-ray imaging scope, Lixiscope, principle, appls. 79−30637
macroradiographic X-ray diagnostic table *(Japanese)* 79−88166
magnifier, for radiographic image magnification 79−17592
mammographic imaging, historical review in terms of image quality and reduced radiation dose 80−41229
mammographic X-ray screen sensitivity and resolution 78−7449
mammography, detective quantum efficiency anal. of electrostatic imaging and screen-film imaging 80−41232
mammography techniques comparison, in vitro studies of breast microcalcification detectability 80−41230
mammography with magnification and grids: detail visibility and dose measurements 80−41231
medical equipment, physical charact. of radiation 80−26334
medical X-ray and fluorographic film sensitometry 77−48858
micro-Fresnel zone plates for coded X-ray imaging of laser produced plasmas 78−42814
microbeam scan system with interactive display terminal *(Japanese)* 77−81563
microchannel plate X-ray image intensifier, image resolution 78−35937
microfocus equipment, for NDT 77−9008
microfocus rod anode system, 150 kV, for nondestructive testing 78−95881
microscope, aplanatic grazing incidence, design and performance 77−18147
microscope, axisymmetric grazing incidence, for laser fusion diagnostics, imaging charact. 78−75422
microscope, review in development, 10 nm resolution *(German)* 77−38077
microscope, using holographically made zone plates and gratings 78−37855
microscope, with high time resolution X-ray streak camera *(French)* 78−42823
mirror, for HEAO-B X-ray telescope, design, fabrication and expected performance 78−49330
mirror profile meas. machine 80−69496
mirrors, vac. UV and soft X-ray, for synchrotron radiation 78−83071
modulation collimators, design and construction 77−5434
multigrid collimators, design and fabrication 77−5435
multilayer mirrors for X-ray and far UV, optimum refl. 77−23725
MWPC, Xe filled X-ray imaging, counter, spatial resolution improvement by pulse height selection 77−18744
Neuroscope, for multiprojectional isocentric fluoroscopy and angiography 78−40292
neurosurgical intraoperative X-ray equipment use 79−92344
one- and two-dimensional spectra spatial resolution recording by spherical crystal analyser 78−74114
operating theatre X-ray installation planning 79−92339
optical systems, construction and appls. 79−17582
output rating, equivalent DC power standard *(German)* 78−3650
paediatric X-ray examination equipment assessment, point system 77−21603
pellicle stack, γ-ray family from cosmic-ray hadron reactions, accelerated scanning method 78−78546
penetrameter cassette, multiple exposure, for meas. of effective kilovoltage of diagnostic X-ray beams 80−61662
penetrameter for measuring peak kilovoltage of dental X-ray sets 80−41171
phase analysis, using DRON-1 diffractometer 80−22489
phosphor screens, use in mammography, speed and resolution 77−90883
photofluorographic camera with electro-optical image intensifier 80−36128
photograph comparator with sliding calliper 78−86397
picture transmission, CCTV system *(Hungarian)* 78−21306
pinhole camera, hole size required for no distortion 80−46028
pinhole photography of target pellet in laser fusion *(Chinese)* 79−97458
plasma diagnostics, soft X-ray imaging instrument for the Alcator A Tokamak 80−73563
polarimeter, design and appls. 79−6251
polarimeter Bragg crystal, using position sensitive proportional counter 78−74117
portable stress analyser using position-sensitive scintillation detector 80−13190
portable X-ray analyser for residual stresses, design, operation and testing 78−53058
portable X-ray imaging system for small-format applications 79−21886
portable X-ray unit, RAPS-1, for quality control, defectoscopy 79−44998
preamplifier with pulsed drain feedback 79−6249
proportional counters, position-sensitive, RC-line encoded, using low-resistance, metal wire anode and active load capacitance 79−54745
quantameter, ETL-type for angular distribution measurement 80−91367
radiation safety, diffraction and fluorescence anal. equipment 79−12017
radiation safety standards, baggage anal. equipment, Canada 79−2139
radiographic $CaWO_4$ intensifying screen, meas. of X-ray induced light photons emitted 80−41218
radiographic contrast improvement using fore-and-aft rotating aperture wheel device 80−41227

X-ray apparatus continued
radiographic equipment survey in hospital and preventive medicine establishments 77−21602
radiographic image-forming systems, reciprocity-law failure 79−53229
radiographic phantoms for testing X-ray imaging performance 80−51229
radiographic testing equipment, device charact. *(German)* 80−76438
radiographical subtraction device for daily practice and vascular procedures 80−36090
radiography, computed, low-dose X-ray imaging system 80−98092
radiography, exposure meas., energy depend. of correction factors for Victoreen 570 Condenser R-meters 78−3597
radiography, micro-dose system 80−51233
radiography, panoramic tomograph users' experience in exam. of teeth and jaws 77−21605
radiography, rare earth oxysulphide intensifying screens, resolution and dose 77−21597
radiography, working places incorporating Medicor equipment 78−35942
radiography equipment, idealised, for routine chest exams., specifications and requirements 80−46034
radiography equipment safety and preventative maintenance in rural community hospitals 77−40758
radiography instrument calibration, energy depend. of correction factors for Victoreen 666 Survey System 78−3596
radiography of breast, recent techniques *(French)* 77−81564
radiography screen-film combination selection 80−46047
radiotherapy hard X-ray machine, RT 305, phys. aspects and appl. 80−81709
radiotherapy high energy X-ray machines, effect on tumour cure rate 80−36067
random array grid collimators 80−62817
rapid process frame-by-frame registration 80−47159
rare earth phosphor intensifying screen speed gain 78−7447
rare-earth X-ray intensifying screens, calibration in 15-70 keV energy range 77−26446
reflectometer, for optical efficiency and scatter meas. 79−17590
reoentgenokymographic unit, physical and operational charact., plate thickness optimisation 79−57747
resonator based on successive refls. of surface wave 80−99021
review of X-ray optics in 1 to 300 Å wavelength range 78−29221
Roentgen-video computed tomography for 3D dynamic imaging by heart lungs and circulation 80−17112
rotating disk device for slit radiography of the chest 80−98116
RUM-20 apparatus, obs. on improving roentgenogram quality 80−30850
scanning system, fast 3D, using limited tilting angle 77−73556
screen-film system evaluation, intensity vs. time scale sensitometry 80−41219
screen-film system evaluation, sensitometric method 80−41220
screens consisting of scintillating crystal fibres, NDT appl. 79−6244
Seeman-Bohlin X-ray camera, sample holder construction 77−67418
semiconductor detector for industrial intensitometry 79−67452
semiconductor film X-ray and electrical characteristics meas. chamber 78−86396
slow scan SIT detector for X-ray diffraction studies using synchrotron radiation 79−48382
small angle scattering camera for synchrotron radiation X-rays, description and results 78−66020
soft X-ray imaging experiments with CCD, astronomical appls. 79−35138
soft X-ray synchrotron radiation focusing using toroidal mirror 78−45760
spark chamber X-ray camera, AR filled, device description and performance evaluation 79−13598
spectroscopy processor X- and γ-ray, active zero-pole cancellation feedback loop 79−9972
status monitor, for Elliot rotating-anode X-ray source 79−35908
STATUS X for canine teeth localisation 77−90881
steel, stainless 1Kh18N9T, flaw detection by X-ray television system 79−5120
stereo X-ray comparator, Zeiss StR 1-3, analytic system for 3D X-ray picture meas. *(German)* 78−92691
stereoradiology, single monitor systems using PLZT electro-optic shutters 77−60247
stereoscopic X-ray unit for medical diagnostic sets 80−85467
storage ring, soft X-ray microscopy/lithography branch line at SSRL 80−91344
streak camera, calibration using Au 77−4713
streak camera, for obs. of tightly pinched relativistic electron beams 77−49818
streak camera for subpicosecond laser fusion diagnostics 77−18122
superheavy primary cosmic ray nuclei, obs. with solid-state track detectors and X-ray films *(Japanese)* 78−61688
telescope, Wolter I type, paraboloid-hyperboloid combination, imaging props. 77−45310
Therac 6 linear accelerator, computer controlled evaluation for X-ray therapy 79−5363
Therac 6 linear accelerator, field elongation effects on depth-dose curves, central-axis output of X-rays 79−5361
thermographic installation, for temp. recording up to 1500°C 78−74003
thickness gauge, factors affecting measurement errors 79−88911
time-resolved coded aperture imaging system, for nuclear fuel motion HCDA conditions 78−45764
tissue-equivalent compensators for 4-MV X-rays, basic data 80−98069
tomography, computerized, NDT appls. *(German)* 80−76439
toroidal mirror fabrication for soft X-ray imaging 78−41384
transmission grating efficiencies for wavelengths between 5.4 Å and 44.8 Å 79−40077
transmission grating efficiencies in 50 to 250 Å range 79−98466
transmission grating for X-ray diffr. into orders, efficiency 80−47157
transmission X-radiographic development trends *(German)* 78−15636
tuneable polarisers using multiple Bragg reflections in grooved crystals 80−315
TV display systems, transmission charact. *(German)* 79−53215
TV installation for projection of high-resolution X-ray images *(German)* 79−57751
TV radioscopic system, for 400 kV X-rays, using microchannel plate image intensifier *(French)* 77−38071
two-phase flows, high-intensity X-ray system for stochastic measurements 79−93791
vacuum dependent scientific instruments, hydrocarbon contamination 79−63259
waveguide, planar, self-imaging 80−57443

X-ray apparatus continued
X-ray diffr. residual stress meas. method using parallel beam optics 78−5717
X-ray imaging, MOS solid-state detector arrays 78−47180
x-ray television using an image pick-up tube *(Chinese)* 79−54243
XUV mirror reflectivities from 50-150 eV 80−90966
zone plates, fabrication using electron beam and X-ray lithography 80−68335
Au coated surface, reflectivity in soft X-ray range 78−45221
Au, grating, extreme off-plane mounting, X-ray efficiency calc. 78−45757
BaFCl:Eu X-ray intensifying screen 78−11735
CsI:Tl powdered phosphor screen for X-ray image intensifier 79−6246
LaOBr:Tb phosphor X-ray mottle reduction by multilayer screen construction 78−4756
Re-W/C multilayer films for X-ray mirrors 79−44992
Xe-filled MWPC for hard X-ray imaging with sub-mm spatial resolution 80−99418

X-ray applications
see also radiation therapy; radiography
aerospace guidance computer failure anal., coverseal particle detection 78−21313
biological X-ray microanalysis 80−41349
blood flow meas., instantaneous, X-ray imaging using cine/video densitometric data 79−34598
bone mineral measurement using polychromatic X-rays, correls. 78−53478
Buddha sculpture survey using X-ray computed tomography *(Japanese)* 80−101915
cancer X-ray sensitivity increased by 434 MHz EM irradiation 78−24180
cast turbine blade microporosity tests 77−86276
cerebral tissue perfusion rate determ. from ^{15}O activity decay after photon activation 80−26341
cinematographic obs. of gas injection into liquid metals 79−49360
cinematography, brazing mechanism obs. appl., high-temperature, kinetics of filling capillary gaps 77−5954
cineradiography, with continuous X-ray source 78−44341
coded-aperture image deconvolution, single-emulsion-layer holographic inverse filters 79−76647
computerised tomography, axial, principle and medical diagnosis appl. *(Spanish)* 79−20698
computerised tomography, functional principles and applications *(French)* 79−70691
contact projection of micro-objects by X-ray synchrotron radiation 79−26193
contrast improvement by use of filter between specimen and film 77−5968
counter method as X-ray microbeam diffraction technique and its application to stress concentration problems *(Japanese)* 79−39077
crack inspection in foam insulation 80−76440
crystalline substances, deformation and stress meas. using X-ray elasticity method 79−43506
CW X-ray preioniser for high-repetition-rate gas lasers, appl. to HF pulsed laser 80−64037
defectoscopy, X-ray films sensitivity increase, 77−90552
diamond soft X-ray source for high-resolution lithography 79−21884
duralumin, elastic-plastic stress anal. by photoelasto-plastic method and X-ray method *(Japanese)* 78−13978
electrodeposition, stress measurement, of sphere by X-ray in depositing method 77−36409
field of 420 kV X-ray equipment including metal-ceramic tube *(German)* 78−4747
flash microscopy, appl. of electron beam-sliding spark device 78−5974
flaw detection, electroluminescent storage screens, expt. results 77−77722
flaw image produced with high energy scattered radiation, scattered radiation effects 79−34239
flow measurement, intact circulation, haemodynamics appl. 77−52822
fluorescence, for static or dynamic organ studies *(French)* 77−37033
gas flow diagnostics, temp. field determ. *(Russian)* 77−19648
gauging system for precision manufactured components quality control 77−10156
high speed photography, in aeroballistic range, track facilities of von Karman gas dynamics facility 78−37094
hologram recording, optimal conditions *(Russian)* 79−93266
holography, appls. and theory review, background and current status 78−74866
holography, intensity requirements at 1 Å, unfeasibility 77−42504
holography, X-ray synchrotron radiation, coherence props. and power 77−75442
hot gas flows, diagnostics of density distrib. *(Russian)* 77−19647
human body components, anal. by X-rays, developments 80−3810
image quality evaluation, visual and objective methods 77−25543
industrial radiography, X-ray emulsions *(French)* 77−38069
industrial radiography and radioscopy, basic physical principles, survey 77−38067
industrial TV radioscopy, applied to solid propellant motors *(French)* 77−38072
industrial X-ray defectoscopy, devices to improve X-raying conditions 77−73405
instructional program in X-ray science, survey of former students 79−9
internal cavities in objects, exam. by scanning with ionising radiation beams, from radioactive sources 78−40003
lithography for microfabrication for guided-wave optical devices 80−58812
lithography using synchrotron radiation 77−22628
macro X-ray fractography, fatigue failure anal. *(Japanese)* 78−11464
mammalian cells, replicon sizes estimated by X-ray plus bromodeoxyuridine photolysis method 79−16353
materials testing, Intel 8080A for data evaluation *(Hungarian)* 79−43522
mechanical anisotropy of texture effect on X-ray stress measurement *(German)* 79−29091
microscopy and lithography using X-rays, techniques, appls. 77−34059
microscopy of biological specimens, flash X-ray method 80−51310
mineral particles settling in liq., X-ray photography 79−20469
multipurpose radiation service centre, AEG, Germany 77−59796
muscle contraction kinetics obs., time-resolved diffraction diagrams recording with aid of computer *(Japanese)* 80−56291

X-ray applications continued
NDT, microfocus equipment 77−9008
NDT, X-ray flash methods and equipment *(German)* 80−97669
neutron activation anal. with X-ray registration, reduction of background using mag. field 80−16738
nuclear power plant components, acceptance tests, using X- and gamma ray images *(German)* 78−44297
oscillation apparatus for X-ray diffraction 79−63329
patient diagnosis, equipment development trends *(German)* 80−3751
photographic exam. of paintings, method for optimal contrast *(Russian)* 79−97459
photographs, determ. of structural and quantum granularity 80−35477
photography, using Polaroid film 77−67161
photolithography, fabrication of submicrometer period gratings with precisely defined profiles for integrated optics applications 80−58814
photolithography and microprobe, scanning X-ray microsource 79−9266
picosecond optical range gating 77−81549
picture examination TV equipment 77−21607
plasma diagnostics, emission spectrum of plasma focus, use of Ross filters and Si detectors 80−59273
pneumatic tyre inspection, in automated production line *(French)* 77−5969
polychromatic X-ray stress meas. *(Japanese)* 78−7143
porous materials, stress determ. by X-rays *(German)* 77−44436
quality control, automatic exposure relay 78−95893
radiography, X-ray TV systems, parameter estimation 77−73404
railways materials characterisation 77−11436
residual stress, X-ray evaluation, treatments for nonlinear distribs., review 80−25966
roentgenographic method of crankshaft bush checking 78−53149
scanning electron probe microanalyser, development of x-ray microanalysis 80−37139
scattered radiation characteristics, local approach to determination of the coordinates of an interface with air 80−86540
soft X-ray microscopy and lithography using synchrotron radiation 78−66018
speed-granularity relations for X-ray and γ-ray exposures 79−21828
steel, austenitic, X-ray elasticity constants *(German)* 80−30004
steel, austenitic stainless, deformed plate, X-ray line profile anal. *(Japanese)* 78−7144
steel, ball, fatigue life prediction, fully automatic X-ray diffr. apparatus *(Japanese)* 79−39076
steel, C, elastoplastic stress anal. by photoelasto-plastic method and X-ray method *(Japanese)* 78−13978
steel, C, X-ray diffraction correlation between cyclic loading and residual stress *(German)* 78−48583
steel, ferritic-pearlitic, X-ray elasticity constants *(German)* 80−30004
steel, hardened, stress determ. from X-ray meas. by fixed time method 78−90801
steel, hardened, X-ray elasticity constants *(German)* 80−30004
steel, residual stress determ. by X-ray integration *(German)* 79−52551
steel, residual stresses, X-ray appratus for meas. 77−60016
steel, welding residual stresses, sources, X-ray meas. *(German)* 77−86265
strain meas. in extremely soft material, embedded marker method 79−57162
stress anal., recent German activities 77−81359
stress anal., using position-sensitive proportional counter 80−1498
stress anal. of strongly fluorescing specimen 80−1499
stress analysis *(German)* 79−34269
stress determ., three axial stresses of general orientation *(German)* 77−9020
stress meas., nondestructive 78−68853
stress meas., statistical study improvement in precision by fixed time method 78−90801
stress measurement, error caused by side declining angle of counter scanning plane *(Chinese)* 80−52373
stress measurement, X-ray technique by side inclination method without $-\eta$ inclining incident angle *(Chinese)* 78−15608
stress measurement method, appl. to practical materials *(Japanese)* 80−52379
synchrotron radiation applications, review 79−67448
synchrotron radiation appls., characts. and sources 78−74960
tensometric measurements, reliability *(Czech)* 80−27382
thermistor bolometer failure anal. appl. 78−24795
thickness monitoring by fluorescence method during coating of steel with Sn or Zn 77−55884
tomography, computerised, dose, detectivity and information content 79−25141
topographic mapping, use of monochromatic, point source X-ray emission *(Russian)* 79−30416
transaxial tomography, simple rotational photographic method 79−93242
TV-computer unit for measuring defect parameters in weld seams 79−67451
vidicon TV combined with X-rays for instant inspection of precision parts 79−74321
welded joint non-metallic inclusions anal. 77−76245
X-ray acoustic resonance, investigation of dispersion surface of X-radiation in Si perfect crystal 79−41908
X-ray television system, based on vidicons, used for defectoscopy 78−72977
X-ray tensometry, residual macrostresses of artificial graphite 77−16642
Ni, residual stress determ. by X-ray integration *(German)* 79−52551
α-β-Ti alloys, stress anal. of strongly fluorescing specimen 80−1499
Ti-C coating on steel, structural study *(Bulgarian)* 77−24242

X-ray astronomical observations
see also X-ray sources (astronomical)
1732−303, 1745−248, new X-ray burst sources, discovery and identifications with globular clusters (Terzan 1, 5) 80−98739
4U 1608−52, steady X-ray source assoc. with Norma X-ray burst source, Uhuru obs. 77−5593
γ195+5, >100 MeV γ-ray source, X-ray emission obs. 79−97101
A0535+26, 1978 August outburst of recurrent transient, Ariel 5 obs. 78−86038
A0535+26, SAS-3 obs. of strong outburst (1977, May) 77−49498
A0538−66, outbursts and proximity to LMC X-4 position, Ariel 5 obs. 77−82321
A0538−66, recurrent X-ray transient source in LMC 78−54085
A0620−00, intensity variations and evidence for 8 day period 77−13496

X-ray astronomical observations continued
A0620−00, X-ray nova, Ariel V crystal spectrometer/polarimeter obs. 77−2494
A0620−00 (V616 Monocerotis=Nova 1975), X-ray and visible light curves 77−8233!
A1540−53, X-ray pulsator near 3U 1538−52 77−33696
2A 0042+323 (3U 0042+32), periodic behaviour rel. to binary nature 78−54089
2A 0251+413, identification as AWM 7 galaxy cluster by HEAO 1 80−90573
2A 0311−227, optical counterpart identification and X-ray meas. 79−30149
2A 0311−227, soft X-ray emission from AM Herculis-type system 79−101219
2A 0311−227, variable soft X-ray source discovery 79−35434
2A 0311−227, X-ray flux modulation period from HEAO obs. 80−77516
2A 0526−328, X-ray emitting cataclysmic variable, X-ray obs. 79−97103
2A 0526-328, location and identification with blue emission line star 80−22118
A 0535+26, transient X-ray source, flare obs. by (Prognoz 6) *(Russian)* 80−51920
A 0538−66, recurrent transient LMC X-ray source, precise position, supergiant star counterpart 79−62933
A 0538−66, X-ray burster position and optical candidate in LMC 80−73076
2A 1052+606, location and identification with late type emission line star (SAO 015338) 80−22118
2 A 1052+606, X-ray and optical variability of RS CVn star 80−31331
2A 1102+384, soft X-ray emission obs. 78−49564
2 A 1102+384 (Markarian 421=B2 1101+38), soft X-ray flux discovery 79−25721
2A 1102+384 (Markarian 421) BL Lacertae object, low-energy X-rays detect. 78−54083
2A 1219+305, high latit. X-ray source identification with BL Lacertae object 79−48960
2A 1251−290, high-latit. X-ray source, X-ray spectrum and variability 78−32611
2A 1348+700, 1415+255, 1410−029, Seyfert galaxies, X-ray spectra and variability 78−32611
A 1710−34, X-ray, optical and radio obs. 79−71158
A non 0945−30, galaxy, X-ray detect. and intermediate luminosity X-ray galaxies contrib. to background 79−2578
Abell 1060 galaxy cluster, X-ray spectrum obs. by (HEAO A-2) 80−82518
Abell 2029 galaxy cluster, radio and SAS 3 X-ray obs. 80−82519
Abell 2319, cluster of galaxies, X-ray and radio obs. 77−53692
Abell 478, cluster of galaxies, X-ray and radio obs. 78−8133
Abell clusters 401 and 399, possible gravitationally bound system, diffuse X-ray emission 79−25736
Abell clusters and superclusters, search for X-ray emission 78−54091
Abell clusters of galaxies, X-ray survey, HEAO 1 1-10 keV obs. 80−51882
Algol, eclipsing binary, spectral obs., description and interpretation 80 - 105283
AO 0235+164, search for X-ray emission from BL Lacertae object 79−17106
Aquila X-1, intense X-ray flare obs. 77−33687
Aquila X-1, nature of X-ray outbursts 78−20909
Aquila X-1, recurrent X-ray outbursts, Ariel V ASM obs. 77−26088
Aquila X-1, X-ray outburst obs. (1978 June 14 to 22) 78−65721
Aquila X-1, X-ray outburst of recurrent transient, 1979 March 79−44638
Aquila X-1 (3U 1908+00), flaring activity obs. 77−22332
Aquila X-1 (4U 1908+00), 1978 summer X-ray and optical outburst 80−73068
Aquila X-1 (4U 1908+00), X-ray outburst obs. 80−77514
Ariel 0327+43 new X-ray source near Nova Persei 1901, discovery 78−69910
Ariel 0535+26, periodic transient source, hard X-ray pulse profile 77−29951
Ariel 0535+26, transient source, refined position meas. and pulse period data 79−44635
Ariel 0535+26, X-ray outburst on 1978 April 10, SAS-3 obs. 78−45433
Ariel 0535+26 (HDE 245770), recurrent X-ray transient, further outburst 79−40300
Ariel 0620−00, transient source, X-ray spectra obs. with Bragg crystal spectrometer 79−12542
Ariel 0620−00, transient X-ray source, obs. using OSO-8 Bragg cryst. spectrometer 78−12426
Ariel 0620−00 (Nova Monocerotis 1976), Ariel 5 obs. of decay 77−29950
Ariel 1540−53, eclipsing X-ray binary pulsator 78−8151
Ariel 1540−53, X-ray flux 8.8 min periodic var. obs. 77−49502
Ariel 1850−08, identification with NGC 6712 globular cluster 77−13414
Ariel 5 hard X-ray observations 79−58444
Ariel 5 obs. of Circinus X-1 and galactic plane sources (1976 Nov.) 77−9818
Ariel V rotation modulation collimator experiment, 10 new X-ray sources obs. 77−49501
UX Arietis (H0324+28), RS Canum Venaticorum system as coronal X-ray source 79−16979
α Aurigae (Capella), intense line emission in soft X-ray spectrum 78−93228
α Aurigae (Capella), X-ray line emission obs., corona models 80−26905
AWM 4, poor galaxy cluster, extended X-ray emission detect. surrounding cD galaxy (NGC 6051) 80−51884
B-type stars, XUV obs. and constraints 78−93232
background radiation fluctuations and X-ray source counts at high galactic latit. 79−67119
background radiation isotropy, 2-18 keV energy range 80−46709
η Bootis, soft X-rays detect. with imaging X-ray telescope 79−48953
burst, spectral evolution 77−29958
burst sources, SAS 3 obs. (1977, July and August) 77−74160
burst sources, search for correlated X-ray and radio emission 78−57695
burst sources in Aquila, discovery 77−13500
bursting radio sources, search for 2-60 keV emission 80−17679
bursts, 2-20 keV, OSO-8 obs. 77−5601
bursts, Ariel V RMC expt. sky coverage and sensitivity 77−13204

X-ray astronomical observations continued
bursts of hard X-rays, SAS-3 detect. 1976, Nov. 77−2499
3C273, HEAO 1 (A4) obs. of 13-120 keV X-rays 79−44633
3C 120, Seyfert galaxy, X-ray emission detect. 77−78890
3C 273, X-ray spectrum, 2-60 keV 80−12824
3C 273, X-ray variability, spectrum and position 79−62929
3C 273, X-ray variability of quasar 79−67112
3C 390.3, 3C 273, 3C 111, 3C 129, extragalactic radio sources, search for hard X-ray emission 77−29939
3C 58, supernova remnant, soft X-ray flux upper limits 80−56915
YZ Canis Majoris, flare star, coordinated X-ray, optical and radio obs. 78−8012
RS Canum Venaticorum, quiescent X-ray emission obs. 78−81659
RS Canum Venaticorum systems, X-ray obs. and coronal model development 80−56873
η Carinae, soft X-ray results from OSO-8 Wisconsin Expt. 78−36722
ν Carinae, X-ray emission obs. from star and surrounding nebula 80−26876
Cassiopeia A, SNR, high-resolution X-ray obs., struct., expansion phase, mass 80−26960
Cassiopeia A, SNR, X-ray spectrum, line emission obs. 80−26961
Cassiopeia A, supernova remnant, search for X-ray line emission 78−57607
Cassiopeia A, supernova remnant, X-ray struct. 77−41401
Proxima=V645 Centauri, coordinated X-ray, optical and microwave study 79−5830
proxima=V645 Centauri, dMe flare star, quiescent corona, transition region, and chromosphere obs. 80−56850
α Centauri, soft X-ray emission 79−16951
Centaurus X-4, possible new outburst, identification with optical novalike object 79−62842
Centaurus A, X-ray struct., radio-lobe energy source evidence 80−26978
Centaurus A, X-ray variability, OSO-8 obs. 78−41082
Centaurus A (NGC 5128), detect. of X-ray emission from giant radio lobes 78−41055
Centaurus A (NGC 5128), radio and X-ray var. of nucleus 78−36711
Centaurus cluster, Fe XXV and Fe XXVI line emission obs. in X-ray spectrum 77−45580
Centaurus galaxy cluster, X-ray spectrum obs. by (HEAO A-2) 80−82518
Centaurus transient source, 1979 May obs. and possible Cen X-4 identification 79−53938
Centaurus X-3, accretion disk evidence from month-long X-ray obs. 79−44636
Centaurus X-3, long-term studies with Ariel 5 All-Sky Monitor 79−30146
Centaurus X-3, neutron star characts. from correlated spin-up and X-ray luminosity meas. 80−101648
Centaurus X-3, periodicity of extended lows 78−24526
Centaurus X-3, pulsation period and orbital elements 77−49494
Centaurus X-3, search for X-ray polarization 80−4457
Centaurus X-4, X-ray burst from novalike object 79−62935
Centaurus XR-4, bright transient X-ray source, assoc. with NGC 5824 globular cluster 78−12420
VW Cephei, W Ursae Majoris star, identification with faint X-ray source 80−51913
π Ceti, late B-type star, X-ray emission obs. 79−101160
CG 176-7, 189+1 and 195+4, X-ray emission associated with γ-ray source 80−31393
chromosphere, magnetic neutral lines, assoc. with X-ray arches 77−17511
Circinus X-1, Ariel 5 X-ray and IR brightness meas. 77−82325
Circinus X-1, binary model, orbital eccentricity from X-ray and radio obs. 80−98735
Circinus X-1, continuation of anomalous X-ray behaviour 78−32606
Circinus X-1, intense X-ray flares obs. 77−33687
Circinus X-1, ms X-ray bursts, possible black hole 78−4404
Circinus X-1, peculiar flaring episode detect., 1979 Jan. 79−21465
Circinus X-1, periodic X-ray emission, COS-B obs. 77−53705
Circinus X-1, semiperiodic pulsations 79−48963
Circinus X-1, X-ray and radio flux meas. 77−2498
Circinus X-1, X-ray flare obs., 1977, Sept. 77−82328
Circinus X-1 and Cygnus X-1, time variability comparison 80−56974
clusters of galaxies, detection of large X-ray halos 79−5909
clusters of galaxies, distances from X-ray and microwave obs. 79−71134
clusters of galaxies, large-scale struct. 80−82524
clusters of galaxies, large-scale X-ray struct. 80−8700
clusters of galaxies, origin of X-ray emission 78−57660
clusters of galaxies, OSO 8 X-ray spectra discussion 79−25734
clusters of galaxies, search for extended hot gas halos in Perseus, Virgo and Coma clusters 80−56953
clusters of galaxies, X-ray and microwave obs., cosmological deceleration parameter determ. 79−21476
clusters of galaxies, X-ray and optical study 78−28805
clusters of galaxies, X-ray spectra and relationship to other cluster props. 80−22093
clusters of galaxies, X-ray spectra in 2-20 keV range, OSO 8 obs. 79−5908
clusters of galaxies, X-ray temps. meas. rel. to other cluster props. 77−91668
clusters of galaxies observed by HEAO 1 scanning modulation collimator, X-ray locations and sizes 79−97090
Coma cluster, X-ray emission monitoring by Ariel V Sky Survey 77−2491
Coma cluster of galaxies, soft X-ray structure 79−62918
Coma cluster of galaxies, structure of diffuse X-ray emission 79−92874
Coma galaxy cluster, low energy X-ray absorpt. obs. 78−86025
compact X-ray sources, Ariel 6 and Copernicus obs. 79−58443
cool stars, HEAO 1 search for coronal soft X-ray emission 79−101140
σ Coronae Borealis (HD 146361), spectroscopic binary, soft, X-ray obs. with (HEAO-1) 80−56886
coronal emission line spectrum 13.3 to 13.8 Å 77−45389
coronal holes, locations, sizes and evolution during June 1973 to January 1974, EUV obs. 77−56893
coronal soft X-ray bright points, lifetimes distrib. 77−17512
COS B gamma-ray sources, 26-1200 keV hard X-ray obs. of error boxes 78−73774
cosmic exploration by X-rays, 1978 Bakerian lecture 79−48964
cosmic gamma-ray bursts, hard X-ray spectra 78−7846
cosmic ray and electron-induced background, HXX results from ANS in Earth orbit 78−81716

X-ray astronomical observations continued
cosmic X-ray bursts, OGO-5 satellite obs. 77−13492
cosmological objects, Einstein X-ray observatory appl. 80−105171
Crab Nebula, emission region size, electron transport and mag. field models 77−17650
Crab Nebula, extended soft X-ray emission obs. 77−13438
Crab Nebula, hard X-ray spectrum 79−62891
Crab Nebula, high energy X-ray spectrum, OSO-8 obs. 78−12315
Crab Nebula, imaging by balloon-borne X-ray telescope *(Japanese)* 79−80220
Crab Nebula, interstellar O edge in X-ray spectrum 79−67079
Crab Nebula, obs. by gamma-ray telescope with modulating anticollimator *(Russian)* 79−16832
Crab Nebula, polarimetry with OSO-8 X-ray polarimeter 78−12426
Crab Nebula, possible line feature at 73 keV, intensity and width 79−92829
Crab Nebula, search for thermal X-ray line emission 78−8095
Crab Nebula, X-ray line emission, balloon-borne obs. 80−41884
Crab Nebula, X-ray polarization, precision meas. without pulsar contamination 78−41086
Crab Nebula X-ray source lunar occultation obs. by balloon *(Japanese)* 77−82319
SS Cygni, dwarf nova, ANS detection of both soft and hard X-ray emission 78−36579
SS Cygni, dwarf nova, identification as hard X-ray source by HEAO 1 scanning modulation collimator 79−2548
SS Cygni, dwarf nova, soft X-ray pulsation obs. 80−46563
SS Cygni, dwarf nova, X-ray polarisations discovery 78−65628
ss Cygni, hard X-ray source, obs., accretion onto white dwarf 79−30078
Cygnus A, giant cD radio galaxy, extended X-ray source 79−67109
Cygnus Loop, ANS obs. of SNR 80−82455
Cygnus Loop, search for O VII X-ray line emission 78−93379
Cygnus Loop, SNR, soft X-ray spectra emission line features obs. 80−94849
Cygnus Loop, supernova remnant, imaging X-ray obs., temp. struct. 80−41876
Cygnus Loop, X-ray image 79−25663
Cygnus Loop SNR, soft X-ray image *(Italian)* 79−53895
Cygnus OB2 association (VI Cygni), soft X-ray emission sources discovery 80−26918
Cygnus region, soft X-ray sources and supernova remnants 78−4397
Cygnus X-1, absence of 39 day period in non-UV data 78−8167
Cygnus X-1, accretion disk round black hole, temp. var. 80−109561
Cygnus X-1, extended-bandwidth X-ray obs. 80−17689
Cygnus X-1, hard X-ray intensity and spectrum short term changes 77−9814
Cygnus X-1, hard X-ray spectrum 79−71156
Cygnus X-1, hard X-ray spectrum during 1975 November transition 77−2496
Cygnus X-1, high-energy X-ray spectra, 0S0-8 obs. 79−71151
Cygnus X-1, intensity transitions obs. by OSO 8 77−64886
Cygnus X-1, obs. during high state (1980 June 11 to 27) 80−86017
Cygnus X-1, polarimetry with OSO-8 X-ray polarimeter 78−12426
Cygnus X-1, rapid X-ray flaring obs. 77−57105
Cygnus X-1, Salyut-4 obs. in 0.2-10 keV range *(Russian)* 77−57109
Cygnus X-1, search for X-ray polarisation 78−4406
Cygnus X-1, short-term time variability, shot noise model 78−36721
Cygnus X-1, short-term time variability 78−93466
Cygnus X-1, short-term variability in hard X-ray region *(Japanese)* 79−80369
Cygnus X-1, submillisecond meas. of low state 77−45607
Cygnus X-1, temporal and spectral var., X-ray rocket obs. 78−8163
Cygnus X-1, transition from high X-ray state to low X-ray state, 1980 June to July 80−98738
Cygnus X-1, X-2 and X-3, long-term-studies with Ariel 5 All-Sky Monitor (ASM) 80−17688
Cygnus X-1, X-ray flux time variability struct. *(Russian)* 80−51921
Cygnus X-1, X-ray variability in high state 78−28855
Cygnus X-1 (HDE 226868), 78.4 day period search in X-rays and optical polarisation 79−75297
Cygnus X-1 (X-2, X-3), X-ray polarisation obs. from OSO 8 80−90571
Cygnus X-1 and Circinus X-1, time variability comparison 80−56974
Cygnus X-2, 3-8 keV obs. of possible degenerate dwarf 80−46703
Cygnus X-2, Ariel 5 SSI obs., modulation rel. to 79−21464
Cygnus X-2, polarimetry with OSO-8 X-ray polarimeter 78−12426
Cygnus X-3, 34.1 day period, 2-12 keV obs. by COS-B 80−94897
Cygnus X-3, 4.8 hour modulation period change disproved 80−8713
Cygnus X-3, 4.8 hour periodicity in spectra 79−5920
Cygnus X-3, 50-400 keV obs., power law spectrum 80−41913
Cygnus X-3, continuous period change obs. in 2-12 keV range 79−9033
Cygnus X-3, COS-B X-ray obs., 4.8 hour modulation 78−28856
Cygnus X-3, evidence for X-ray Fe line emission obtained with cryst. spectrometer 78−8153
Cygnus X-3, hard X-ray spectrum obs. 80−31388
Cygnus X-3, observational constraints, on models 78−16567
Cygnus X-3, period derivative 79−48955
Cygnus X-3, period derivative and asymmetric X-ray light curve from HEAO 2 obs. 80−105394
Cygnus X-3, X-ray Fe line emission meas. with Bragg crystal spectrometer 79−12544
Cygnus X-ray superbubble 80−90575
diffuse soft X-ray background, three-band obs. rel. to thermal emission models 77−45604
diffuse soft X-ray background enhancements 77−29953
diffuse soft X-ray emission, brightness distrib. 79−53942
diffuse X-radiation background above 20 keV, balloon obs. 78−54096
diffuse X-ray background, spectrum from 3 to 50 keV 80−41916
diffuse X-ray flux in 2 to 7 keV range, galactic component obs. 80−98745
AD Draconis, flare star, coronal soft X-ray emission obs. by (HEAO 1) 79−101140
dwarf novae, hard X-ray emission from 47 objects 78−93275
dwarf novae, HEAO-A2 soft X-ray survey during optical outburst 80−46574
early type stars, luminosity determ. X-ray obs. 80−105241
Einstein X-ray observatory, HEAO-2, results to date 80−56692
emission-line galaxies, high-excitation, HEAO 1 X-ray obs. 79−62907
40 Eridani, triple star, X-ray emission discovery 79−97035
40 Eridani A ($=o^2$ Eridani), evidence of corona on X-ray image 80−105282
40 Eridani C, X-ray image of dM4e flare star 80−105282

X-ray astronomical observations continued
ESO 012-G21, type I Seyfert galaxy, Ariel V X-ray spectra 80−90539
EUV/soft X-ray background, Apollo-Soyuz sky survey results 79−71160
Feige 24, hot white dwarf, soft X-ray obs. and stellar charact. 77−9746
flare obs. from Norma region, in position of 4U 1608−52 recurrent transient source 79−30152
flare-up of X-ray source, SAS-3 obs. 78−20915
FXP 0520−66, flaring X-ray pulsar, nature and optical identification *(Russian)* 80−77521
FXP 0520−66, flaring X-ray pulsar in Dorado, Venera 11 and 12 obs. 80−27018
G287.8−0.5, supernova remnant, X-ray emission obs. 77−2488
G65.2+5.7, soft X-ray spectrum and structure of SNR 79−71093
galactic bulge X-ray sources, precise positions from SAS-3 obs. 78−16575
galactic centre, Prognoz-6 obs. of X-ray fluxes and energy spectra *(Russian)* 80−109562
galactic centre, X-ray activity 79−58419
galactic centre, X-ray emission 79−17102
galactic centre and Cygnus region, spectral charact. of X-ray sources 78−54079
galactic centre region, high-energy X-ray detection 80−67854
galactic centre sources, positions meas. by Ariel-5 RMC expt. 78−4407
galactic centre X-ray burst sources 77−13499
galactic nucleus, high-resolution 2-10 keV rocket obs. of discrete X-ray sources 78−65692
galactic strong X-ray sources, ANS obs. of intensity and spectral vars. 79−17127
galactic X-ray sources, $320° < l^{II} < 340°$, positions 78−28860
galactic X-ray sources, $55° < l^{II} < 320°$, positions 78−61938
galactic X-ray sources, −20° to +6° galactic longit., positions 78−54094
galactic X-ray sources, Ariel 5 positions 79−58446
galactic X-ray sources, classification and Ariel 5 obs. 79−58445
galactic X-ray sources, long-term variability 79−2579
galactic X-ray sources, obs. from on board (Salyut 4) 77−91665
galactic X-ray sources, optical identifications 77−87573
galactic X-ray sources, OSO-7 obs. 78−32600
galactic X-ray sources, periodic modulation search 77−5592
galactic X-ray sources, position meas., radio and optical identifications 77−91671
galactic X-ray sources, precise positions 77−87574
galactic X-ray sources, unidentified, positions with HEAO-1 scanning modulation collimator 80−105395
galaxies, X-ray spectrum and variability of active objects 79−58420
galaxies compact groups, X-ray emission obs. 80−90574
Galaxy, diffuse soft X-rays distrib. and energy spectrum 78−28853
galaxy cluster, soft X-ray spectra, constraints on models for Coma Berenices and Perseus clusters 78−36702
galaxy clusters, structure and evolution 80−26994
galaxy clusters, X-ray spectra 80−26996
galaxy clusters at cosmological distances, X-ray emission detect. 80−26993
galaxy rich clusters and superclusters, and clusters extended halos, X-ray emission search 80−26988
galaxy superclusters, X-ray emission, Uhuru meas., intergalactic gas 78−41064
U Geminorum, HEAO 1 obs. of hard X-rays 79−21299
U Geminorum, HEAO obs. of low-energy X-ray emission 79−21298
U Geminorum, soft X-ray emission and visual magnitude estimates 77−91544
globular clusters, X-ray obs. with ANS 77−26029
globular clusters, X-ray sources locations 79−97102
GX9+1, lunar occultation position 77−45612
GX 13+1 (3U 1811-17), X-ray and radio obs. 78−41081
GX 17+2 (3U 1813-14), X-ray and radio obs. 78−41081
GX 301−2, spectra and pulse period vars. 77−2486
GX 301−2 (4U 1223−62), SAS-3 obs. of 1978 January brightening 78−28858
GX 304−1 (3U 1258−61), discovery of 272 second period var. 78−8152
GX 339−4, black hole candidate 79−48962
GX 339−4, variable X-ray source identification with faint blue object 79−40294
GX 3+1, X-ray bursts obs., (1980 July 19 to August 18) 80−98739
H0118+067, identification with RS Canum Venaticorum star UV Piscium, X-ray obs. 80−101654
H0630+82, identification with RS Canum Venaticorum star SV Camelopardalis, X-ray obs. 80−101654
H1122−59 near Centaurus X-3, new source, MSH 11−54 coincidence 78−28859
H1207−52, soft X-ray emission detect. from southern SNR 78−77620
H1616−51, soft X-ray emission detect. from southern SNR 78−77620
H2027+19, Delphinus soft X-ray source, model 80−90576
H2309+59 near Cassiopeia A, new source, V Cassiopeia coincidence 78−28859
H 0622−529, obs. of highly variable source 79−48959
H 1538−32, new extended soft X-ray source detect., possible old supernova remnant 80−51912
H 1743−32, transient source, detect. 78−45431
H 1743-32, transient X-ray source, HEAO-1 position obs. 77−87572
H 1908+050 (SS 433), X-ray obs. 79−71153
H 2155−304, positions and optical counterpart identification 78−93478
H 2156−304, intense high-latit. soft X-ray source and possible new BL Lacertae object 79−92891
H 2252−035, X-ray flux modulation, compact star rotation 80−101652
hard X-ray sources, obs. by spectrometer on Kosmos 428 satellite 77−64640
hard X-ray sources discovered by HEAO A-2 expt. 80−17690
HB3, supernova remnant, X-ray emission obs. 78−81679
HB 3, supernova remnant, soft X-ray obs. 80−56915
HB 9, soft X-ray emission obs. from old SNR 80−36697
HD 77581 (4U 0900−40), apsidal motion test of eclipsing binary 80−51908
HDE 226868 (Cygnus X-1), X-ray and UV spectra from HEAO 2 and IUE 80−82543
HEAO A-1 expt. survey 79−58246
HEAO-1 spacecraft, pointed obs. of selected sources 78−7856
Hercules supercluster, Ariel V X-ray obs. 77−60832
Hercules supercluster, evidence for intracluster medium 80−22092
Hercules X-1, 23 day low state, Uhuru obs. 77−5594

X-ray astronomical observations continued
Hercules X-1, 2-6 keV pulse profiles, Uhuru data 79−17129
Hercules X-1, eclipsing binary, X-ray spectra from Ariel V satellite 80−90580
Hercules X-1, Fe line emission discovery in low-state spectrum by (HEAO-1) 79−5922
Hercules X-1, hard X-ray line feature obs., cyclotron emission 78−81709
Hercules X-1, hard X-ray pulsation obs. 78−12293
Hercules X-1, hard X-ray spectrum, strong cyclotron line emission 78−41085
Hercules X-1, heliocentric pulse period, OSO 8 obs. 77−91573
Hercules X-1, high-energy pulsed X-ray spectrum from OSO 8 obs. 79−92888
Hercules X-1, high-energy X-ray spectrum 78−93473
Hercules X-1, long-term studies with Ariel 5 All-Sky Monitor 79−30146
Hercules X-1, orbital precession from Doppler modulation of pulsation arrival times 77−13398
Hercules X-1, pulse phase spectroscopy, 6-60 keV 79−84870
Hercules X-1, pulse profile in hard X-rays 77−9811
Hercules X-1, search for X-ray polarization 80−4457
Hercules X-1, X-ray pulsation obs. by SAS-3 during 1975, July 77−60793
Hercules X-1, X-ray spectra, Fe line fluoresc. from subrelativistic shell 78−4405
Hercules X-1, X-ray spectra, pulse phase depend. on high-energy continuum 79−17128
Hercules X-1, X-ray spectra near turn-on in 35 day cycle 77−60794
Hercules X-1, X-ray spectrum of pulse 78−8154
Hercules X-1 (HZ Herculis), coordinated optical and X-ray pulsations obs. 80−51909
Hercules X-1 (HZ Herculis), Copernicus and Ariel V obs. 77−45609
Hercules X-1 (HZ Herculis), hard X-ray obs. 78−36728
Hercules X-1 (HZ Herculis), soft X-ray results from OSO-8 Wisconsin Expt. 78−36722
ϕ Herculis, Ap star, X-ray emission obs. 79−101160
AM Herculis, evidence on nature of soft X-ray source from HEAO 1 obs. 79−17134
AM Herculis, hard X-ray spectrum 79−17022
AM Herculis, OSO-8 hard X-ray obs. 78−4409
AM Herculis, OSO-8 X-ray obs., 2-250 keV energy range 79−71075
AM Herculis, X-ray light curve 77−45491
DQ Herculis, X-ray obs. from Ariel 5 satellite 77−37671
AM Herculis (3U 1809+50), soft X-ray results from OSO-8 Wisconsin Expt. 78−36722
high galactic latitude ($|b|>10°$) X-ray sources, Ariel V (SSI) catalogue 78−32362
high-latitude X-ray sources, Uhuru satellite obs. 77−9808
high-sensitivity X-ray survey, discrete source contrib. to extragalactic background 80−27016
HR 1099, quiescent X-ray emission obs. from RS Canum Venaticorum star 78−81659
HR 1099, RS Canum Venaticorum star, 4U 0336+01 optical counterpart 78−32475
HR 1099, X-ray outburst obs. from RS Canum Venaticorum star 78−81658
HR 976, Am-type star, soft X-ray source obs. 78−81634
EX Hydrae, soft X-ray emission during optical quiescence, HEAO-A2 obs. 79−71054
β Hydri, nearby subgiant star, XUV radiation upper limit 79−12471
HZ 43, ultra soft X-ray spectrum of hot white dwarf 78−85941
IC 3575, peculiar galaxy possibly 4U 1232+07, HEAO 1 obs. 80−12832
IC 4329 A, X-ray obs. of extreme type 1 Seyfert 79−12515
IC 443, supernova remnant, X-ray spectrum and structure 77−49453
IC 443, X-ray images of SNR 79−48889
imaging by HEAO-2 satellite, obs. 79−92892
Jupiter, X-ray flux upper limits 77−5491
Kepler's SNR, weak soft X-ray emission detec. 79−58403
Kepler's supernova remnant, X-ray obs. from Einstein Observatory 80−82465
Klemola 44, cluster of galaxies, X-ray, optical and radio obs. 77−74150
HK Lacertae, RS Canum Venaticorum type variable, soft X-rays detect. 78−45362
BL Lacertae objects, high-energy X-ray obs. 80−31353
BL Lacertae objects, X-ray emission obs. by HEAO 1 scanning modulation collimator expt. 79−48921
late-type main-sequence and subgiant stars, HEAO 1 obs. of active coronae 80−72925
AD Leonis, X-ray emission from flares, HEAO 1 obs. 80−41837
LMC, SNRs identification from Einstein Obs. X-ray meas. 80−26980
LMC, X-ray survey using HEAO 1 scanning modulation collimator 80−17648
LMC bar, soft X-ray source identification 80−82491
LMC X−1, luminous extended X-ray source obs. 78−16570
LMC X-1, X-2 and X-3, positions from HEAO 1 modulation collimator 79−5923
LMC X-4, Ariel 5 obs. of eclipses and identification confirmation 77−74161
LMC X-4, discovery of X-ray eclipses 78−24572
LMC X-4, obs. of X-ray eclipses 78−24571
LMC X-4, X-ray variability obs. 78−4398
LMC X-ray source light curves, Ariel V obs. 77−74164
LS I+61°303, variable binary radio star (B1 Ib), X-ray emission detect. 80−105400
Lupus flare source, Ariel 5 ASM obs. (1979 October 25) 80−8715
Lupus Loop, supernova remnant, soft X-ray emission detect. 79−53876
Lupus Loop, X-ray spatial extent and spectrum of SNR 80−82457
Lupus region, soft X-ray structure 79−71085
AY Lyrae, soft X-ray emission detect. from dwarf nova, H1839+37 79−75227
MV Lyrae, soft X-ray emission from nova-like object 79−92787
α Lyrae, soft X-rays detect. with imaging X-ray telescope 79−48953
M31, X-ray sources, obs. 80−26979
M42 (Orion Nebula), X-ray obs. by Astronomical Netherlands Satellite 78−28852
M86, elliptical galaxy, X-ray evidence for hot gas retention 80−90535
M87, high-resolution X-ray spectroscopy, O VIII emission line detect. 80−26977
M87, search for hard X-ray emission 77−29939
M87 region, Fe XVII-XXIV X-ray line complex obs. 79−21425

X-ray astronomical observations continued
M87/Virgo cluster X-ray source spectrum, 1.1 keV Fe line emission discovery 79−25758
Markarian 421, X-ray spectrum change in BL Lacertae-type object 79−101196
Markarian 421 and 501, X-ray obs. in 2-60 keV band 79−17094
Markarian 464, type I Seyfert galaxy, Ariel V X-ray spectra 80−90539
Markarian 501, UV and X-ray obs. of BL Lacertae-type object 80−36717
Markarian 541, massive X-ray halo around Seyfert 79−35369
MCG−6-30-15, type 1 Seyfert galaxy, X-ray and optical obs. 80−82479
MCG 5-23-16, galaxy, X-ray emission detect. 78−41052
MCG 8-11-11, Seyfert galaxy, hard X-ray emission detect. 80−46660
MCG 8-11-11, X-ray obs. of Seyfert 1 galaxy 80−105344
MCG -6-30-15, X-ray emission in 2-10 keV range 78−45405
AT Microscopii, X-ray emission from flares, HEAO 1 obs. 80−41837
MIT/OSO 7 catalogue of X-ray sources, intensities, spectra, long-term vars. 79−80243
Mk 421, BL Lacertae-type object, X-ray emission detect. from 2A 1102+384 optical counterpart 78−57698
MKW 3s, poor galaxy cluster, extended X-ray emission detect. surrounding cD galaxy (NGC 5920) 80−51884
Moon, surface chemistry, weighted-filter imaging technique appl. to X-ray fluoresc., data 78−12124
MR2251−178, X-ray QSO discovery, 2 Ariel 2251−179 optical counterpart 78−24567
MSH 11-54 (H1122−59), supernova remnant, X-ray obs. 80−82463
MSH 14−63, probable remnant of A.D. 185 supernova, X-ray emission obs. 78−45427
MSH 14-63, supernova, remnant, soft X-ray emission obs. 77−37636
MSH 15-56=GX 326.3−1.8, soft X-ray emission detect. 79−44639
MXB0512-40, X-ray burst obs. 77−71153
MXB1637−53, 9 X-ray burst obs. 77−9822
MXB1730−335, MXB1728−34 rapid bursters, SAS 3 obs. 77−91666
MXB1730−335, rapid burster, turn-off obs. 1977, May 24 77−57107
MXB1730−335, rapid X-ray burster, dual charact., X-ray bursts classification 78−32613
MXB1730−335, SAS-3 obs. on 1978 Apr. 15-16, no burst activity 78−49563
MXB1730−335, X-ray bursts, Ariel 5 obs. 77−57106
MXB1730-335, rapid X-ray burster, turn-on 77−82330
MXB1916−05, X-ray burst obs. 77−64883
MXB 1636−53, simultaneous radio and X-ray obs. of X-ray burst source 79−48961
MXB 1636−53, X-ray burst source, SAS-3 obs. 78−8156
MXB 1636−53, X-ray burst source, simultaneous X-ray and optical bursts obs. 79−92893
MXB 1636-536, binary nature from simultaneous X-ray and optical obs. 80−82548
MXB 1659−29, identification with faint UV stellar object 78−61936
MXB 1659−29, nearby single burst on 1978 March 8 analyzed 78−36731
MXB 1659−29, persistent X-ray emission obs., (1978 March 6 to 9) 78−41090
MXB 1659-29, burst source identification with faint blue object 79−40294
MXB 1706−43, X-ray bursts obs. 78−8161
MXB 1728−34, bursts spectra, intensity and repetition rate 77−49504
MXB 1728−34, type I X-ray burst obs. by (HEAO-1) 80−17692
MXB 1728−34, X-ray bursts obs., (1978 March 8 to 10) 78−41091
MXB 1728-34, X-ray bursts discovery 77−5596
MXB 1730−333, no burst activity in 1980 July-Sept. period 80−105402
MXB 1730−333, Rapid Burster, possible X-ray emission 79−84868
MXB 1730−335, bursts obs. by SAS-3, 1978 March-April 78−45434
MXB 1730−335, further analysis of SAS 3 obs. of rapid burster 79−30145
MXB 1730−335, HEAO obs. of X-ray burst 79−17139
MXB 1730−335, new mode of X-ray bursts 80−41915
MXB 1730−335, rapid burster, position determ., HEAO 1 obs. 78−49561
MXB 1730−335, rapid burster, SAS-3 obs., (1979, March 3 to 4) 79−40299
MXB 1730−335, rapid burster, search for X-ray bursts, (1978 March 8 to 10) 78−41091
MXB 1730−335, rapid X-ray burster, long-term behaviour 78−32602
MXB 1730−335, rapid X-ray burster, SAS-3 obs. 79−9037
MXB 1730−335, rapid X-ray bursts obs. by SAS-3 77−53707
MXB 1730−335, SAS-3 obs. of 1978 March burst activity 78−45432
MXB 1730−335, SAS-3 obs. of burst activity, 1978 Oct. 78−96573
MXB 1730−335, variability of X-ray burst source 78−77621
MXB 1730−335 (Rapid Burster), steady X-ray emission obs. 80−22119
MXB 1730-335, anomalous bursts obs. from rapid X-ray burster 77−49496
MXB 1735−44, coincident X-ray and optical burst obs. 78−61937
MXB 1735−44, rapid X-ray bursts obs. by SAS-3 77−53707
MXB 1735−44, X-ray burst sources, 3 s delay in optical burst 79−58442
MXB 1837+05, X-ray bursts obs. by SAS-3 77−49500
MXB 1837+05(Serpens X-1), simultaneous optical and X-ray bursts obs., 1978 Sept. 79−35435
MXB 1837+05 (Serpens X-1), detect. of optical burst coincident with X-ray burst 80−27013
MXB 1837+05 (Serpens X-1) simultaneous radio and X-ray obs. 79−21467
N49 SNR in LMC, X-ray obs. of gamma-burst field 80−27019
N-galaxies as new class of X-ray sources 79−2572
NGC 1851, NGC 1904, globular clusters, radio and X-ray obs. 77−26028
NGC 3783, possible X-ray emitting Seyfert galaxy 77−13467
NGC 4151, OSO 8 X-ray obs. of flare in Seyfert galaxy 79−17093
NGC 4151, Seyfert galaxy, hard X-ray emission detect. 80−46660
NGC 4151, Seyfert galaxy, optical and X-ray variability correl. *(Russian)* 79−21440
NGC 4151, Seyfert galaxy, repeated X-ray flaring obs. 80−90534
NGC 4151, Seyfert galaxy, Uhuru obs. 78−12411
NGC 4151, Seyfert galaxy, X-ray absorpt. increase 78−12367
NGC 4151, X-ray emission monitoring by Ariel V, evidence for flare 77−2491
NGC 4151 (3U 1207+39), Seyfert galaxy, high-energy X-ray obs. with balloon-borne telescope 77−45610

X-ray astronomical observations continued
NGC 4151 (4U 1206+39), Seyfert galaxy, hard X-ray spectrum 78−49537
NGC 4410a/b, interacting pair, possible HEAO 1 obs. 80−12832
NGC 4593, var. X-ray emission from bright type 1 Seyfert 79−84856
NGC 5128 (Centaurus A), X-ray structure 78−24569
NGC 5128 (Centaurus A), X-ray variability, Ariel V Sky Survey obs. 78−16574
NGC 5506, Seyfert 2 galaxy, detect. of flare in X-ray emission 80−17656
Norma, novalike source, refined SAS 3 position 77−78893
Norma X-ray burster, Uhuru obs. 77−2487
North Polar Spur, SNR, soft X-ray spectra emission line features obs. 80−94849
North Polar Spur, X-ray features, supernova remnant 77−45554
North Polar Spur (Radio Loop 1), X-ray obs. 80−105370
nova at $\alpha=1^h14^m$, $\delta=+64.4°$, discovery obs. 78−24515
Nova Ophiuchi 1977, X-ray intensity on 1978 Mar. 9 78−40961
Nova Ophiuchi 1977, X-ray transient, positions and independent discoveries 77−82234
Nova Ophiuchi 1977 (H1705−25), X-ray light curve 78−49453
Nova Ophiuchi 1977 (H1705−25), X-ray nova, HEAO 1 obs. 78−49452
Nova Vulpeculae 1976, X-ray emission upper limits, Ariel V data 77−64781
novalike object in Centaurus, possibly Centaurus X-4, X-ray obs. and optical identification 79−62842
NP 0532, Crab pulsar, pulsed X-ray emission obs. during lunar occultation 78−8032
NP 0532, Crab pulsar, search for X-ray polarisation 79−5851
NP 0532, Crab pulsar, transient structure of high-energy X-ray emission 77−33541
OAO 1653−40, HEAO obs. of X-ray pulsations 79−44637
OAO 1653−40, pulsating hard X-ray source detect. 79−67118
OAO 1653−40 38 s pulsating X-ray source position and optical search 80−73072
OAO 1653−40 area, 38.22 second X-ray pulsations discovery 80−27014
observational test of cosmological particle production theories 80−109574
V843 Ophiuchi (Kepler supernova 1604) remnant, soft X-ray emission detect. 79−40244
ρ Ophiuchus dark cloud region, soft X-ray obs. 80−26947
Ophiuchus flare source near 4U 1708-23, Ariel 5 obs. 77−82323
Orion Nebula, low-luminosity X-ray sources obs., assoc. with star form. 80−26959
Orion Trapezium 79−35348
periodic pulsating X-ray sources discovery, Ariel 5 obs. 77−64885
β Persei, soft X-ray image 77−53627
GK Persei, X-ray outburst detect. from old nova 79−67033
X Persei, X-ray spectra, binary model 79−25757
X Persei (3U 0352+30), simultaneous X-ray and ground-based optical obs. 80−17591
X Persei (4U 0352+30), balloon obs. of hard X-ray flux variability 79−48803
X Persei (A 0535+26), Prognoz-6 obs. of X-ray fluxes and energy spectra *(Russian)* 80−109562
β Persei (Algol), X-rays detect. 77−9773
Perseus Cluster, compact and diffuse X-ray sources in core 78−49545
Perseus cluster of galaxies, energy-dependent map of X-ray emission, SAS 3 obs. 78−65702
Perseus cluster of galaxies, soft X-ray map 77−5579
Perseus cluster of galaxies, soft X-ray struct. 79−9009
Perseus galaxy cluster, low energy X-ray absorpt. obs. 78−86025
Perseus region, hard X-ray obs. 77−13493
PKS 0548−322, BL Lacertae object, X-ray spectrum 80−17654
PKS 0548−322 (H0548−32), X-ray obs. in 2-60 keV band 79−17094
PKS 0548-322, possible BL Lacertae object, low-energy X-rays detect. 78−89270
PKS 1209−52, soft X-ray emission detect., evolutionary phase 79−62892
PKS 2155−304, BL Lacertae object, rapid X-ray variability obs. 80−73035
PSR 0531+21 X-ray pulse ground-based obs. 77−91444
PSR 0833-45, Vela pulsar, pulsed soft X-ray flux, upper limits 80−105268
pulsar NP 0532, COS-B satellite obs., appl. of X-γ synchronisation to non-parametric anal. 78−73729
pulsating X-ray sources, accretion flow and neutron star structure from X-ray timing obs. 79−5917
CP Puppis (Nova 1942), soft X-ray emission detect. 79−80325
Puppis A, O VIII 18.97 Å resonance line emission detect. 77−45535
Puppis A, X-ray images of SNR 79−48889
Puppis A supernova remnant, X-ray spectrum and struct. 78−20876
quasars, HEAO-2 data, open Universe supported 79−62946
quasars, new obs. 79−62930
quasars, X-ray properties from Einstein Observatory obs. 80−27004
radio quasars, deep search for X-ray emission by Ariel V 78−12402
radio supernova remnants, X-ray obs. by ANS 79−92833
RCW 103, soft X-ray emission detect., evolutionary phase 79−62892
2S0921−630, discovery and optical stellar identification 79−21466
2S 0114+650, X-ray source discovery obs. 78−12423
2S 1254−690, galactic X-ray source, position and identification 79−12545
2S 1636−536 (MXB 1636−53), X-ray burst source, position 78−12419
2S 1728−337 (MXB 1728−34), X-ray burst source, position 78−12419
2S 1735−444 (MXB 1735−44), X-ray burst source, position 78−12419
Sagittarius, Ariel V obs. of X-ray nova (1979 October-November) 80−12834
satellite obs. of various X-ray sources 77−26087
SC 0627−544, Fe XXV and Fe XXVI emission lines in X-ray spectrum 79−48941
scanning modulation collimator instrument for HEAO-A satellite 77−71003
V861 Scorpii, upper limit on X-ray emission, and non-coincidence with (OAO 1653−40) 80−73072
V861 Scorpii, X-ray emission from unseen companion 78−89226
V861 Scorpii (OAO 1653-40?), simultaneous UV and X-ray obs. 80−17616
Scorpius X-1, binary star, X-ray spectrum 20-75 keV, high sensitivity determ. 80−98741
Scorpius X-1, binary star X-ray obs. from 20 to 250 keV 80−94893
X-ray astronomical observations continued
Scorpius X-1, emission var., Salyut 4 obs. in 0.2-2 keV range *(Russian)* 77−33702
Scorpius X-1, extended X-ray obs. with Bragg crystal spectrometer 79−12543
Scorpius X-1, high energy X-ray and SHF radio obs. 80−73067
Scorpius X-1, high energy X-ray obs. with Ariel V 80−17694
Scorpius X-1, linear X-ray polarisation obs. 79−101221
Scorpius X-1, linear X-ray polarisation upper limit 77−49503
Scorpius X-1, linear X-ray polarisation upper limit 78−49557
Scorpius X-1, mag. field determ. via linear polarisation spectrum *(Russian)* 80−90344
Scorpius X-1, Prognoz-6 obs. of X-ray fluxes and energy spectra *(Russian)* 80−109562
Scorpius X-1, rapid variability simultaneous X-ray and optical obs. 80−62322
Scorpius X-1, Salyut-4 X-ray spectrometry *(Russian)* 77−26091
Scorpius X-1, worldwide study plan (1980 April) 79−97104
Scorpius X-1, X-ray energy spectrum in 0.2-50 keV range, rocket obs. 78−57696
Serpens X-1, Ariel 5 obs. and models of spectrum and time var. 78−81707
Serpens X-1, no IR bursts assoc. with Type I X-ray burst 80−98742
Seyfert 1 galaxies, HEAO 1 scanning modulation collimator, obs. 80−51859
Seyfert 1 X-ray emitting galaxies, HEAO 1 spectra 80−51860
Seyfert galaxies, Type 1, obs. with HEAO-1 scanning modulation collimator 79−92864
Seyfert galaxies detected as X-ray sources by Ariel V satellite 78−49540
Seyfert galaxies X-ray emission, Uhuru obs. 78−93392
Skylab photographic X-ray images, analysis 78−49341
SMC, deep X-ray survey 79−25702
SMC, lack of absorption of 1 keV diffuse X-rays 79−35381
SMC X-1, pulsation period and orbital period decrease 77−49499
SMC X-1, pulse profile and refined orbital elements 78−8148
SMC X-1, soft X-ray emission detection, 2-day flaring period 79−35432
SMC X-1, spin-up rate meas. 78−41083
SMC X-1 (Sanduleak 160) binary source, X-ray pulsations, orbital elements and masses 77−9815
SMC X-2, SMC X-3, discovery, hard spectra, high luminosity rel. to galactic X-ray sources 78−49559
SMC X-2 and SMC X-3, variable X-ray sources, SAS-3 obs. 78−20914
SMC X-2 and X-3, SAS 3 discovery of new sources 77−91667
SN 1006, soft X-ray emission detect. 79−53876
SN 1006 remnant, Ariel V X-ray obs. 79−40250
SN 1006 remnant, X-ray spectrum 80−82457
SNR in Cygnus, soft X-ray emission detection 78−54013
SNRs, electron-ion equilib. and ionization nonequilib., X-ray evidence 80−41879
soft X-ray background, spatial struct., OSO-8 obs. 78−16580
soft X-ray diffuse background flux, southern galactic hemisphere 78−8170
soft X-ray emission from unidentified high galactic latit. source 77−5598
solar active region, comparison of 9.1 cm and soft X-ray emission 77−22180
solar active region and flare plasmas, electron density from Fe IX lines intensity ratio 78−20771
solar active region loops, evidence for opposed currents 77−2403
solar active regions, imaging with Fresnel zone plates 78−49342
solar active regions, open mag. fields 78−28631
solar active regions, preflare characts., soft X-ray obs. 79−84776
solar active regions, Skylab obs. of pre-flare X-ray morphology 77−17481
solar active regions and X-ray bright points, birthplaces 80−12739
solar active regions height struct., X-ray obs., OSO-8 limb crossing obs. 80−31280
solar active regions McMath 12472 and 12474, interconnecting transequatorial loops 77−71090
solar bright X-ray arcs and mag. flux emergence regions 78−12174
solar chromosphere flares, soft X-ray heating effects 79−40170
solar corona, active regions X-ray emission, evidence for mag. energy storage 77−17478
solar corona, activity complex development, Skylab soft X-ray obs. 78−12191
solar corona, Fe IX lines obs. for plasma density determ. 79−44429
solar corona, Fe XVIII X-ray emission lines, obs. and anal. 78−36542
solar corona, interconnecting loops sudden brightenings morphology 80−21972
solar corona, mag. fields interaction and energy release 77−17482
solar corona, physical conditions for bipolar magnetic region 78−77534
solar corona, plasma parameters in long-duration X-ray event, Skylab obs. 77−29741
solar corona, polar plume X-ray anal. 79−12455
solar corona, soft X-ray images from Skylab, atlas 79−21197
solar corona, soft X-ray obs. of large-scale active region brightening 78−20806
solar corona, temps. and temp. gradients from OSO-7 spectroheliograms 77−17506
solar corona, X-ray enhancements assoc. with Hα filament disappearances 77−22184
solar corona, XUV emission lines obs. rel. to Fe abundances and temps. determ. 78−4180
solar corona above active region McMath 12628, struct. rel. to solar atmosphere equilibria 78−53902
solar corona above active regions, soft X-ray and cm wavelength obs. 79−44431
solar corona abundances from X-ray obs. 77−56887
solar corona obs., holes as source of solar wind 77−2394
solar coronal active regions, anal. of soft X-ray photographs taken with Fresnel zone plates 78−77538
solar coronal active regions, Ni XIX spectrum 77−2390
solar coronal arch system, long-lived, X-ray obs. 77−71091
solar coronal hole, birth, Skylab soft X-ray obs. 78−7967
solar coronal hole, physical parameters defining changing struct. 78−20770
solar coronal hole boundaries short term evolution 78−61844
solar coronal hole boundary brightness in Fe XV 284 Å radiation 79−84775
solar coronal holes, atlas of boundary positions (1973, May 28 to November 21) 77−2349

X-ray astronomical observations continued
solar coronal holes and large-scale structures, plasma parameters from soft X-ray obs. 78−4161
solar coronal loops, obs. evidence of continual heating 78−61841
solar coronal obs. with Skylab 77−56891
solar coronal X-ray arch expansion into outer corona 77−22196
solar coronal X-ray bright point and small active region fine struct. rapid vars. 80−12741
solar eruptive prominence and surge, Skylab X-ray and Hα obs. 77−78755
solar filament eruptions and nonflaring coronal transients assoc. with non-thermal electrons 78−65595
solar flare, 1973 August 9, decay phase, X-ray and UV obs. 79−53780
solar flare, 1973 June 15, Hα, magnetic and X-ray morphology 78−4173
solar flare, 1973 June 15, high temp. plasma evolution 78−28636
solar flare, 1973 June 15, multiple loop activations and continuous energy release 78−28637
solar flare, electron density determ. from X-ray spectra obs. 80−82326
solar flare, energy storage and deposition obs. 77−17480
solar flare, EUV and X-ray obs. of thermal phase 79−8886
solar flare, hard X-ray emission, shot-noise character 79−96983
solar flare, hard X-ray obs. with 100 ms time resolution 77−71093
solar flare, multiple loop activations and continuous energy release, Skylab obs. 77−82209
solar flare energetics depend. on flare volumes 79−25566
solar flare second-stage X-ray emission, spectrum beyond 200 keV 80−51710
solar flare spatial structure in soft X-rays and cm wavelengths 77−17524
solar flare X-ray spectra, laboratory reproduction in region of Fe XXV-XXVI reson. lines 80−18819
solar flare-loop prominence system, 1972 May 24, optical and X-ray obs. 79−30045
solar flares, 1972 August 2 and 11, hard X-rays obs. 79−8900
solar flares, EUV and hard X-ray bursts interrelationship 78−61845
solar flares, EUV and hard X-ray sources relationship 80−46512
solar flares, Fe line X-ray emission 78−32426
solar flares, forbidden Fe XIX, Fe XX and Fe XXI lines obs. 78−57519
solar flares, Hα, hard X-ray and microwave emissions in impulsive phase 78−77540
solar flares, hard X-ray polarization 80−41787
solar flares, high-resolution X-ray spectra obs. 80−26837
solar flares, impulsive EUV and hard X-ray emission 78−65578
solar flares, nonthermal particle prod. during buildup and in absence of flares 77−17492
solar flares, obs. of lines between 171 and 630 Å 78−49406
solar flares, particle acceleration, X-ray and gamma-ray obs. 80−31265
solar flares, XUV electron density diagnostics 79−88633
solar flares energy release and transfer, Skylab X-ray obs. 77−82208
solar flares nonthermal X-ray emission directivity meas. 77−33461
solar flares X-ray spectra, Fe XXIV-XXV lines wavelengths in 1.85-1.87 Å region 80−21973
solar full-disc fluxes, 250-1940 Å rocket obs. 77−87360
solar hard X-ray flares, high time resolution anal., ESRO TD-1A satellite obs. 77−22185
solar hard X-rays, source height and anisotropy determ. 79−25568
solar impulsive flares, X-ray spectra rel. to adiabatic heating 78−93176
solar impulsive X-ray burst from coronal source, obs. 80−26836
solar intense compact subflare, physical parameter anal. 79−62802
solar ionising radiation, meas. during 1973 June 30 eclipse 79−8901
solar limb flares struct. and evolution, Skylab soft X-ray telescope obs. 77−82199
solar loop prominence system, flare assoc., high temp. corona 79−53782
solar multiply impulsive bursts, hard X-ray and microwave spectral evolution 80−26828
solar proton events and coronal mass ejections 78−77545
solar quiet corona, X-ray spectrum of highly ionised O and N 78−45297
solar radio and X-ray bursts positions and sizes 77−33459
solar soft X-ray flare kernel obs. by Skylab 77−29772
solar soft X-ray flares, emission measure 79−30047
solar soft X-ray limb flares from Skylab 78−4164
solar spectrometric obs. from Prognoz satellites 79−21127
solar spectrum, Ni IX to Ni XII transitions identifications from laboratory wavelengths 80−99474
solar subphotospheric activity assoc. with large flares, X-ray data 79−35225
solar X-ray active regions temp. and emission measure rel. to coronal mag. fields 80−12745
solar X-ray bright point emergence patterns spatial and temporal vars. 77−29782
solar X-ray bright points, obs. rel to globally variability in solar mag. flux emergence 80−51716
solar X-ray bright points, short-term temporal vars. 80−12740
solar X-ray bright points anticorrel. with sunspot number, 1970-78 period 79−53789
solar X-ray coronal cavities, prominence-related, config. and dynamics 79−25565
solar X-ray emitting active region, early evolution 78−28621
solar X-ray emitting features, energy or press. of plasma determ. from single filtergram 77−22186
solar X-ray flare kernel, site, size, spatial stability and energetics 79−25555
solar X-ray flares, 1974 July 5 and 6, polarisation obs. 77−2397
solar X-ray flares, Skylab obs. rel. to physical parameter profiles 80−17561
solar XUV He I and He II emission lines, intensities and gross centre-to-limb behaviour 78−40888
source positions, meas. by scanning modulation collimator on (HEAO 1) 78−93459
sources similar to Scorpius X-1, observational study 77−13498
southern Milky Way X-ray sources, Ariel V obs. 77−2492
spectroscopic binaries, single-line, nature of secondary stars from X-ray obs. 80−31329
stellar coronae, evidence for existence from X-ray and UV obs. 80−12756
stellar X-ray sources at high galactic latit., location with HEAO 1 scanning modulation collimator 80−22118
Stephenson-Sanduleak 433, X-ray emission obs. 79−12480
strong sources, graphite cryst. spectrometer obs., sensitivity to line emission 77−13238

X-ray astronomical observations continued
Sun, 1973 August 14 loop prominence, XUV emission and density 80−56807
Sun, 1973 June 15 flare in active region NOAA 131 (McMath 12379) 78−53913
Sun, 1979 March 25 flare 80−85915
Sun, active region coronal loops, gyroresonance absorption evidence 80−56792
Sun, active region McMath 12628, EUV and X-ray obs. 80−67692
Sun, comparison of He II 304 Å and He I 10830 Å spectroheliograms 78−20799
Sun, coronal and transition zone plasma evolution during 1973 August 9 compact flare 79−5792
Sun, coronal bright points, soft X-ray images 77−53557
Sun, coronal flare-like events, soft X-ray data from Skylab 78−61827
Sun, coronal hole evolution by sudden large scale changes 78−40910
Sun, coronal holes and assoc. solar wind, sunspot cycle 20 survey 78−40911
Sun, coronal long-decay X-ray enhancements, physical parameters 79−44448
Sun, coronal loops brightened by flares and transients, decay 78−40907
Sun, coronal loops in an active region, physical props. XUV obs. 80−90376
Sun, coronal X-ray transients rel. to hole evolution 79−12459
Sun, EUV spectroheliograms from Apollo Telescope Mount expt. S082A 77−60597
Sun, Fe XIX-XXII blend at 1.9 Å in flare X-ray spectra 79−96979
Sun, flares, X-ray emission (50-100 keV) directivity 80−105218
Sun, flaring X-ray bright points, assoc. with type III bursts 80−67681
Sun, gamma-ray lines from flare, HEAO 1 obs. 80−67682
Sun, hard X-ray spectrum of flare impulsive phase, OSO 7 obs. 79−12440
Sun, He I and He II XUV emission lines intensity ratios and distrib. functions 78−57516
Sun, He II 304 Å and Si XI 303 Å line profiles 79−12452
Sun, impulsive X-ray and radio bursts obs. 78−93174
Sun, Mg XII resonance line at 8.42 Å, new satellite line structure 78−53912
Sun, obs. by S056 X-ray telescope expt. on Skylab Apollo Telescope Mount 77−60596
Sun, purely coronal hard X-ray event obs. 78−93177
Sun, Si X-ray line emission from flares and active regions 79−25580
Sun, slowly moving disturbances obs. in X-ray corona 80−21971
Sun, soft X-ray bursts, statistical distrib. 80−26839
Sun, soft X-ray flux, Skylab obs., temporal oscills. 78−53904
Sun, X-ray and 2.8 cm coordinated obs. of active regions *(Italian)* 79−21254
Sun, X-ray emission rel. to solar cosmic-ray intensity preflare enhancements 78−45166
Sun, X-ray photometry from Prognoz satellites 80−17462
Sun, X-ray radiation rel. to radio waves anomalous absorpt. during sudden ionospheric distrubances 79−96857
Sun, X-rays from flares, Prognoz and Explorer satellite obs. of directivity in 4-24 keV range 78−69768
Sun, XUV spectra obs. by grazing incidence spectrograph on Skylab 77−60601
Sun, young active regions, filaments, and flares 80−72910
Sun EUV image, obs. by Skylab Apollo Telescope Mount TV monitor 77−60600
Sun instantaneous XUV images, obs. and recording on ATM television monitors 77−60605
supernova remnants, obs. of X-ray emissions 79−58404
supernovae, extragalactic, X-ray bursts search using HEAO-1 satellite 80−46585
transient events with precursor pulses, SAS 3 obs. 78−49562
transient short-lived source at high galactic latitude, ANS obs. 78−96563
transient source in Norma, precise position determ., HEAO 1 obs. 78−49560
transient source in Pictor, HEAO-1 A-2 expt. obs. 78−32607
transient X-ray sources in the galactic plane 78−93460
Tycho's SNR, HEAO 1 obs. and structure study 80−51842
Tycho supernova remnant, Type I SNR, elemental abundances from X-ray spectrum 80−46635
Tycho supernova remnant, X-ray line emission obs. 80−46636
4U0134−11, galaxy supercluster candidate, no X-rays from hot gas 78−8164
4 U1145−61, two X-ray periodicities from Ariel V obs. 78−81711
4U 0041+32, hard X-ray outburst, 1970 obs. 80−56976
3U 0042+32, SAS-3 meas. of position during flaring activity 77−37670
3U 0042+32, variable mid-latitude X-ray source, accurate position 77−78897
4U 0115+63, 3.6s X-ray pulsations discovery 78−61939
4 U 0115+63, absorption line in pulsed hard X-ray spectrum, HEAO 1 obs. 80−27017
4U 0115+63, orbital elements and nature of hard X-ray transients 78−93470
4U 0115+63, transient X-ray binary, absorpt. feature discovery at 20 keV 78−69909
4U 0115+63, transient X-ray source, accurate positions 78−24570
4U 0115+63, transient X-ray source, obs. 79−92890
4U 0115+63, X-ray transient, position and pulse profile 78−93467
3U 0328−52 region, X-ray emission from galaxies, Ariel V sky survey obs. 77−5599
3U 0352+30, evidence for 581 day modulation in X-ray pulse period 77−53708
3U 0352+30 (X Persei), OSO-7 hard X-ray obs. 77−26085
3U 0527−05, improved position and possible optical identifications 77−33691
3U 0614+09, case for X-ray burst 78−32610
2U 0832-45, extended X-ray source centred on Vela pulsar 78−41095
3U 0833−45, Vela pulsar X-ray flare obs. 77−22260
4U 0900−40, pulsating X-ray binary, search for periodic behaviour 79−84865
3U 0900-40 (HD 77581), increase in pulsational period 77−64877
3U 1118−60 (Centaurus X-3), hard X-ray obs. 77−2493
4U 1145−61, bright active source, SAS-3 monitoring 78−57699
4U 1145−61 (HD 102567), X-ray periodicity and orbital motion 78 -8160
4U 1206+39 (NGC 4151), hard X-ray variability of Seyfert galaxy 80−17647

X-ray astronomical observations continued
3U 1223−62, binary X-ray pulsar, Ariel V obs. 78−96566
4U 1223−62, pulsating X-ray binary, search for periodic behaviour 79−84865
3U 1223-62 (GX 301-2), hard X-ray obs. 77−2493
4U 1232+07, HEAO 1 obs 80−12832
3U 1247-41, Centaurus X-ray cluster, vel. dispersion 77−74148
4U 1249−28, location and identification with dwarf nova EX Hydrae 80−22118
3U 1254−69, hard X-ray obs. 77−2493
3U 1258−61 and 1626−67, X-ray obs. from satellites 77−37671
3U 1538−52, Ariel 5 obs. 77−49498
3U 1538−52, binary X-ray pulsar, orbital elements 78−16573
4U 1538−52, eclipsing binary pulsating system, position meas. by HEAO-1 78−96570
4U 1608−52, 1977 Oct. decline, all-sky-monitor obs. 78−4412
4U 1608−52, 3-6 keV flux during 1977, Sept. 77−82329
4U 1608−52, burst activity since Hakucho launch (1980 April) 80−62321
4U 1608−52, obs., identification with MXB 1608−52 78−69914
4U 1608−52, X-ray bursts obs. 79−48958
4U 1626−67, 7.7-second X-ray pulsar, simultaneous X-ray and optical obs. 80−51914
3U 1626−67, X-ray pulsar, 7.68 sec. periodicity, SAS-3 obs. 78−8157
4U 1626−67, X-ray pulsar, HEAO 1 obs. 79−92889
3U 1626−67, X-ray pulsar, X-ray position and optical candidate 77−67139
4U 1630−47, obs. of recurrent transient source 78−41092
4U 1630−47, recurrent transient, Ariel 5 SSI obs. of 1978 May-June flare 78−61935
3 U 1630−47, recurrent transient source, Uhuru and Ariel V obs. 77−5595
4 U 1630−47, recurrent transient X-ray source flaring episode obs. 79−2580
4U 1642−45 and 1630−47, X-ray flare detect. 78−12422
4U 1651+39, identification with BL Lacertae object Markarian 501 by HEAO 1 modulation collimator 79−5918
4U 1658−48, X-ray flare obs. 78−69908
4U 1700−37, 97 minute periodicity discovery 79−5921
3U 1700−37, further Copernicus X-ray obs. 78−96568
4U 1700−37, SAS-3 obs. of 97 minute periodicity 78−36730
4U 1700−37, search for X-ray flux short time-scale periodicity 79−71157
4U 1700−37 (=HD 153919), eclipsing binary, X-ray obs. 80−86016
4U 1700−37 (HD 153919), X-ray binary, high-energy X-ray obs. 80−86014
4U 1702-36, Scorpius X-1 like source, high energy X-ray obs. with Ariel V 80−17694
3U 1727−33, X-ray flux periodic behaviour 77−9816
4U 1755−33, exclusion from flaring transient source error box 77−82326
3U 1820−30 in globular cluster NGC 6624, recurrent X-ray bursts 77−60806
4U 1822−37, 2129+42, X-ray fluxes modulation periods from HEAO obs. 80−77516
4U 1907+09, optical identification using HEAO-1 scanning modulation collimator position 80−82542
4U 1907+09, X-ray flare obs. during 1980 Jan. period 80−41914
3U 1915−05, X-ray burst source discovery 78−8155
4U 1916−79, high-latit. X-ray source, X-ray spectrum and variability 78−32611
3U 1957+40 (Cygnus A region), X-ray obs. with ANS 77−53700
4 U 2129+47, position and optical identification, evidence for X-ray heating and binary period 80−17693
4U 2129+47, X-ray light curve and binary model 80−46704
4U catalogue of X-ray sources 79−40088
Uhuru sources, energy spectra of 43 objects, 2-20 keV 77−60851
ultrasoft X-ray background, obs. in S galactic hemisphere 77−45615
SU Ursae Majoris, soft X-ray halo around dwarf nova 80−98677
variable X-ray sources, Ariel 5 obs. 77−82320
Vela pulsar, nature of assoc. X-ray source 79−17138
Vela supernova remnant, X-ray maps 80−51838
Vela X-1, long-term studies with Ariel 5 All-Sky Monitor 79−30146
Vela X-1, OSO 8 extended obs. 78−49555
Vela X-1 (3U 0900−40), Ariel V Sky Survey instrument obs. 77−45495
Vela X-1 (3U 0900−40), X-ray obs. and UBV photometry 78−65722
Vela X-1 (HD 77581), binary source, spectral obs. 80−94892
Vela XR-1 (3U 0900−40), balloon obs. 78−69913
Vela-Puppis, low-luminosity X-ray source obs. 78−93458
Virgo, Coma and Perseus clusters of galaxies, soft X-ray morphology 77−2474
Virgo, Perseus and Coma clusters, X-ray obs., spectral evidence for hot evolved gas 77−17695
Virgo cluster, structure of extended X-ray source 78−4410
Virgo cluster, X-ray emission, Ariel V SSI obs. 79−12528
Virgo cluster, X-ray obs. of galaxies, rel. to dynamical evolution 80−26995
Virgo cluster, X-ray source struct. 78−54090
Virgo galaxy cluster, low energy X-ray absorpt. obs. 78−86025
W44, ANS obs. of X-ray emission from SNR 78−54010
weak X-ray sources, ANS meas. 80−46701
white dwarf binary systems, hard X-ray obs. 78−36732
WRA 977 (4U 1223−62, GX 301−2), binary star orbit determ., SAS 3 obs. 80−90570
X-ray burst sources, average props. of 10 objects 78−81710
X-ray bursters, 1980 plans for simultaneous optical/X-ray obs. 80−8716
X-ray events with long decay times, morphology and statistics 77−60733
X-ray source in Norma, novalike increase, SAS-3 obs. 77−67142
III Zw 2, type I Seyfert galaxy, X-ray emission detect. 78−20895
III Zw 2, X-ray and radio emission from compact galaxy 78−65691
SS Cygni, soft X-ray emission detect. during optical outburst 80−46574
U Geminorum, soft X-ray emission detect. during optical outburst 80−46574
O VII, emission line obs. in diffuse soft X-rays from Hercules N_H minimum region 79−25759
Si XIII and Si XIV line emission search with ANS crystal spectrometer 79−17131

X-ray astronomy
see also X-ray sources (astronomical)
80 cm X-ray telescope, facilities and observational possibilities *(German)* 80−109358
1975-6 advances 77−9817
2A catalogue and supplementary results from Ariel 5 sky survey 79−58276
actively shielded hard X-ray telescope 78−81540
Advanced X-ray Astrophysics Facility, results obtained 80−109366
Apollo Telescope Mount and solar instruments of Skylab, overview 77−60593
Apollo Telescope Mount television monitors, obs. and recording of instantaneous images 77−60605
Ariel 5 Bragg spectrometer, calibration data 77−5441
Ariel 5 satellite, design and performance of high energy X-ray detector 78−53826
Ariel V RMC expt. sky coverage and sensitivity to X-ray bursts 77−13204
Aryabhata satellite project 79−84638
automodulation collimator telescope, for point X-ray source imaging *(Russian)* 80−62018
background emission from quasars and clusters of galaxies 80−105405
background radiation spectrum, effects of evaporation of primordial black holes 79−88695
balloon payload, microprocessor-controlled, for hard X-ray obs. 79−62716
balloon-borne X-ray telescope, for Crab Nebula imaging *(Japanese)* 79−80220
Bent Crystal Spectrometer for solar X-ray spectroscopy 79−25489
Bhaskara, India's X-ray satellite 79−70943
bremsstrahlung source spectra anal. in terms of integral moments, solar hard X-ray burst appl. 79−16810
broad-band X-ray imaging systems, physical parameter method 78−49414
coded aperture imaging, predicted performance of uniformly redundant arrays 79−18351
coded aperture imaging with uniformly redundant arrays 78−37812
coded mask X-ray telescope for rocket appls., optimum design 77−13239
collimators, for astronomical soft X-ray meas. 77−5436
coma-free two-mirror systems, astronomical appls. *(Russian)* 77−64641
conference (La Jolla, CA, 12 to 14 September 1978) 79−53937
conference proc. (Innsbruck, 1978 May 29-June 10) 80−36775
cosmic exploration by X-rays, 1978 Bakerian lecture 79−48964
cosmic ray electrons, X-ray transient radiation detection, comparison with theoretical predictions *(Russian)* 79−66896
crystal spectrometer, new type, for cosmic X-ray studies 77−5443
curved crystal X-ray spectrometer, for HEAO-B satellite 78−49331
deep X-ray surveys, predictions and strategies 78−96567
dielectronic recombination spectra, appls. in astronomy 80−46391
diffraction grating, transmission efficiencies on EUV and soft X-rays 77−60621
diffraction grating, X-ray spectroscopy appl. 77−10155
diffuse background meas. using nondirectional detectors 77−73968
diffuse cosmic X-ray component separation in balloon borne meas. 78−28862
diffuse X-ray background, rel. to intergalactic matter 80−109543
diffuse X-ray background intensity, implications of uniformity of quasars radial distrib. in chronometric cosmology 80−105409
diffuse X-rays component, separation method using growth curves 79−25512
Einstein X-ray observatory and obs. of cosmological objects 80−105171
emission lines from Seyfert galaxies and QSOs, hard X-ray effects 80−26974
equipment, large-area gas scintillation proportional counter 78−49322
EUV solar image TV monitor on Skylab Apollo Telescope Mount 77−60600
EUV spectroheliographic, in Apollo Telescope Mount experiment S082A 77−60597
EUV spectroheliometer on Skylab Apollo Telescope Mount, photometric calibration 77−60595
EUV/soft X-ray background, Apollo-Soyuz sky survey results 79−71160
extragalactic sources, review 78−73776
extraterrestrial sources X-ray emission meas., equipment on (Salyut-4) 78−28521
focusing Fe line crystal spectrometer for Spacelab 79−25500
focusing gas scintillation proportional counter 77−83461
galactic centre, search for X-ray pulsations 79−44617
galaxy clusters, X-ray line spectroscopy 78−36701
gas scintillation counter X-ray spectrometer performance figures astronomy appl. 79−48673
gas scintillation proportional counter, large-area focusing, for X-ray astronomy 79−25494
gas scintillation proportional counter development for satellites 77−71004
gas scintillation proportional counter for first Spacelab mission 79−25488
gas scintillation proportional counter of large area for X-ray astronomy 79−80222
gas scintillation proportional large area counter, X-ray astronomy appl. 79−45556
gas scintillation spectrometer for X-ray astronomy, performance characteristics 80−56709
graphite crystal X-ray spectrometer on OSO-8 satellite 77−13238
grid telescope for imaging hard X-rays 79−25501
Hadamard transform X-ray telescope, charact. *(Japanese)* 80−94714
Hadamard transform X-ray telescope *(Japanese)* 79−84672
Hard X-Ray Burst Spectrometer on Solar Maximum Mission 80−51658
hard X-ray camera for study of gamma ray burst sources 79−25502
hard X-ray detection, risetime discrimination appl. to pressurised Xe gas proportional counter *(Japanese)* 79−80219
hard X-ray experiment for long-duration balloon flights 79−25493
hard X-ray imaging collimator 77−5437
hard X-ray imaging instrument, for solar and cosmic sources 78−49332
Hard X-ray Imaging Spectrometer on Solar Maximum Mission 80−51659
HEAO 1 scanning modulation collimator, X-ray source positions meas. 78−93459
HEAO A-1 expt. survey 79−58246
HEAO B, scheduled launch and observing opportunities 78−69647
HEAO programme outline 77−78595
HEAO-1 Cosmic X-ray experiment (A-2) 79−58248

X-ray astronomy continued
HEAO-1 prospects 79−62722
HEAO-1 spacecraft, pointed obs. of selected sources 78−7856
HEAO-2, Einstein X-ray Observatory, hardware, instruments performance characts. 79−70941
HEAO-2, X-ray pictures from space 79−92892
HEAO-2, X-ray telescope description, obs. and sources 80−12643
HEAO-2 Observatory, protective design considerations, system reliability 80−61983
HEAO-2 quasar data, open Universe supported 79−62946
HEAO-A 79−25445
HEAO-B, focal plane crystal X-ray spectrom. 78−40825
HEAO-B, high-energy astrophysical satellite lab., X-ray observ. facilities *(Dutch)* 80−61986
HEAO-B, imaging proportional X-ray counter 78−40823
HEAO-B, solid state X-ray spectrom. 78−40824
HEAO-B monitor proportional counter instrument 78−40822
HEAO-B spectrometer, high voltage power module and charge amplifier design 78−40826
HEAO-B X-ray Observatory 79−25446
HEAO-B X-ray telescope, focal plane transport assembly controls 79−48677
HEAO-B X-ray telescope, gas control system 78−40827
HEAO-B X-ray telescope, high resolution imaging instrument 78−40821
HEAO-B X-ray telescope, mirror design, fabrication and expected performance 78−49330
HEAO-B X-ray telescope, observing program 78−57443
HEAO-B X-ray telescope 78−40820
HEAO-B X-ray telescope orbiting observatory, aspect system providing absolute referencing to celestial sphere 78−40791
High Energy Astronomy Observatory (HEAO) programme 79−44368
High Energy Astrophysics Division of Am. Astron. Soc., meeting (Cambridge, MA, 28-30 Jan. 1980) 80−36761
high pressure gas scintillation spectrometers for X-ray astronomy 80−105166
high resolution imaging X-ray detector, for astronomical meas. 78−49333
high resolution X-ray optics, for astronomical and laboratory sources 78−45766
high-temperature plasma, X-ray spectroscopy 77−31434
hot interstellar medium 79−25699
image data processing system, Skylab X-ray solar obs. appl. 77−60619
image processing techniques for Ariel 5 rot. modulation collimator 79−80236
image reconstruction, from incomplete and noisy data 78−53837
imaging detector for hard X-rays/soft γ-rays 79−58250
imaging gas scintillation counter for X-ray astronomy 80−98551
imaging scintillation detectors, design 79−25511
imaging soft X-ray telescope for Spacelab 79−25498
imaging system, real-time, for solar coronal X-ray obs. from sounding rockets 80−41725
intergalactic C model abundance, X-ray absorpt. effects 80−62270
International Sun-Earth Explorer C spacecraft 78−85787
interstellar gas heating and ionization by X-ray photoelectrons 80−46383
interstellar soft X-ray photoabsorpt. cross-sections 78−12327
inverse-Compton emission from radiosource electrons and microwave background photons, prospects for X-ray detect. 79−71144
LAMAR facility for high sensitivity obs. 79−25497
large scale telescopes for high resolution obs. 78−93114
large-scale universal inhomogeneities, X-ray background evidence 79−75299
Leicester solar coronal Bragg spectrometer, wavelength calibration and resolution 77−5442
Lixiscope, X-ray and gamma-ray telescope system 80−62020
lunar occultations of point-like X-ray sources, anal. for source positions 79−88567
microchannel plate, X-ray quantum efficiency 78−45768
mirror objectives, tests with soft X-rays from plasma mirror of electroionisation CO_2 laser 78−85850
mirror X-ray telescope, on Salyut-4, gas-filled proportional photon counter 78−86746
modulation collimator, X-ray imaging device 79−25510
modulation collimators, design and construction 77−5434
multigrid collimators, design and fabrication 77−5435
multiple-grid telescopes, diffr. effects 79−44367
Multipurpose Utility Pointing and Stabilisation System *(Italian)* 77−82114
MWPC, for cosmic drift X-ray imaging 79−41063
MWPC, high press., for X-ray astronomy 79−5748
MWPC, large area, high-background rejection 78−93108
negative electron affinity III-V photocathodes for soft X-ray detection 78−93110
neutron stars, redshift determ. of X- and γ-ray lines rel. to strong principle of equivalence 78−40814
new developments, review 77−71154
non-solar studies, review 77−33698
optical systems, construction and appls. 79−17582
optimum coded mask X-ray telescope, design 79−66923
parallel X-ray beam generation, appl. to testing collimators 78−28526
parameter estimation using max. likelihood 79−62752
Penning source, continuous discharge, with 50 Å to 300 Å emission lines 79−50363
phoswich-type scintillation detector system for X-ray astronomy 78−49328
photon position determination using microchannel plates, X-ray imaging for HEAO-B 79−45555
point summation technique, appl. to faint X-ray sources detect. near COS-B γ-ray positions 78−54093
point-like X-ray sources positions determ., lunar occultation optimisation 79−92652
polarimeter, for solar and extrasolar obs. 78−57454
polarimeter, mosaic graphite, on OSO-8 satellite, design, preliminary results 79−25490
polarimeter, Thomson-scatt., satellite-borne, for solar obs. 79−25491
polarimetry, calibration of Bragg X-ray analyser crysts. 77−64664
position sensitive detectors appls. 79−25496
proportional, low-background counter for X-ray astronomy 78−29705
pulse shape analysers for phoswich detectors in space borne hard X-ray expts. 80−36501
quasar number counts and X-ray background 79−75294

X-ray astronomy continued
relativistic astrophysics *(German)* 79−80213
remote sensing spectrometers, data analysis system for planetary mission appl. 79−12411
review, 1960-1980 period 78−49567
review 78−32604
review of methods including electronic image processing *(Italian)* 79−16826
rocket-borne expts., effects of atmospheric X-rays from magnetospheric electrons 78−61640
rotation collimators, positively constrained imagery 77−9665
S056 X-ray telescope expt. on Skylab Apollo Telescope Mount 77−60596
SAS-3 Group program and obs., Ariel 5 obs. 77−49498
SAS-3 X-ray observatory 77−2329
satellite microchannel X-ray image convertors *(French)* 78−24436
satellite-borne instrument development problems and solns. 77−82111
satellites and missions associated with study of X-ray sources 79−8793
scintillation proportional large area gas counter for X-ray astronomy 78−49321
sealed position sensitive hard X-ray detector having large drift region for all sky camera with high angular resolution 79−48675
single photon X-ray detection with a CDD image sensor 79−35836
sky survey project EXUV 10-1000 Å waveband, proposed mission 80−82165
Skylab, experience, with Schumann-type XUV film 77−60599
soft (0.15-2 keV) sources, review 77−26094
soft X-ray polychromator for Solar Maximum Mission 80−51660
soft X-ray spectrometer, for diffuse cosmic sources 77−5440
solar and cosmic high resolution spectroscopy, instrumentation 77−13243
solar flare, transient plasma X-ray spectra, electron density and temp. diagnostics 80−77368
solar flare plasma, Langmuir turbulence spectrum estimate from X-ray obs. 80−82329
solar flares, transient plasma X-ray lines, rate coeff. determ. 80−72903
solar flares, X-ray line spectra from transient plasma 80−98626
solar X-ray images, quantitative interpretation by filter ratio anal. 79−40085
solar X-ray imaging techniques, past and future, review 79−25495
solar X-ray photometer, rocket-borne, construction details *(Polish)* 79−58247
solar X-ray photometer on Prognoz satellites, description and meas. method 80−17462
solar X-ray spectrograph, cylindrical-crystal, design and characteristics 79−29990
solar X-ray spectrometer and imager, Space Shuttle 80−17495
solar XUV, grazing incidence spectrograph on Skylab 77−60601
source position determ., parameter estimation method 78−61748
sources and processes 77−26084
space astronomy, new instrumentation, conference (Tel Aviv, 7-18 June 1977) 79−25473
Space lab integrated UV and X-ray astronomical payload proposal *(Italian)* 77−82112
space optics, imaging X-ray optics workshop, Huntsville, Alabama (1979 May 22 to 24) 80−62384
Space Shuttle, instrums. and expts. 80−109363
Spacelab facility for X-ray source spectroscopy and polarimetry 78−32314
spectra, direct deconvolution method 80−85867
spectra restoration 79−25515
spectral line studies, via gas scintillation counter 77−13247
spectral observations, value 77−5455
spectral reduction technique 79−96924
spectrometer, bent crystal, for solar X-ray spectroscopy 78−7881
spectrometer on Kosmos 428 satellite, for hard X-ray sources obs. 77−64640
spectrometer-telescope system for solar corona studies 80−105168
spectroscopy, fabrication of transmission gratings 80−14490
spectroscopy, solar and cosmic, symposium, Holmburg, England (May 1975) 77−5433
spectroscopy, transmission grating behind grazing incidence telescope 77−64654
spectroscopy in X-ray range 77−71009
superconducting superheated granules as X-ray and γ-ray imaging detectors 79−25504
supernova remnants *(Italian)* 79−53894
telescope, appl. of lobster eye optical configuration 80−17491
telescope, simultaneous optical and X-ray imaging 77−82121
telescope, SO56, energy throughput variation with off-axis angle 77−60592
telescope on Skylab, S-054 expt., for solar obs. 77−60616
toroidal mirror fabrication for soft X-ray imaging 78−41384
transition radiation from relativistic intergalactic dust grains 79−75272
transmission grating, facet-type, aberrations for cosmic X-ray and XUV spectroscopy 78−85851
transmission grating efficiencies for wavelengths between 5.4 Å and 44.8 Å 79−40077
transmission grating efficiencies in 50 to 250 Å range 79−98466
transmission gratings, aberrations, testing 79−25508
transmission gratings, expt. and theoretical props. 79−25509
transmission gratings for 7-304 Å operation, efficiency and resolution 80−82195
two-mirror system with zero spherical aberration *(Russian)* 77−64645
UTEX, integrated UV and X-ray astronomy facility on Spacelab 79−25475
wide field camera, design, sensitivity and performance 80−85863
Wolter type I telescope for rocket appl., X-ray optical props. 79−25499
X-ray bursters, 1980 plans for simultaneous optical/X-ray obs. 80−8716
X-ray imaging, conf., Reston, USA (Apr. 1977) 78−45762
XUV astronomy, review *(German)* 80−109372
XUV solar flare kernels, electron density meas. 79−16913
XUV solar telescope and white light coronagraph, CCD camera systems and support electronics 80−62023
XUV telescope/white light coronagraph expt., quadratic A/D converter 80−62024
Au coated surface, reflectivity in soft X-ray range 78−45221
CdTe spectrometers for hard X-ray astronomy 77−13206
CsI(Na) scintillating crystals in cosmic X-ray detectors, growth of deactivated layers 77−10554
Ge spectrometers, cooled, for X-ray and gamma-ray astronomy 77−5438

X-ray astronomy continued
H-like ions, scaled Coulomb-Born-Oppenheimer collision strengths 79−22839
Mg XII, resonance line, atomic parameters calc. for dielectronic satellite lines 80−42983
NaI(Tl) large area multi-crystal detectors for X-ray and gamma-ray astronomy 77−22070
Si:Li detector system for X-ray astronomy rocket expt. 77−5439
Si:Li X-ray astronomical spectroscopy 77−5460

X-ray characteristic temperature *see Debye temperature*

X-ray chemical analysis
see also electron probe analysis; X-ray diffraction examination of materials; X-ray fluorescence analysis
absorption detector use in gas chromatography, determ. of SO_2 in gas mixtures 77−29069
absorption function parameters determ. using exptl. intensity ratios 77−52698
absorption-edge fluoroscopy, spectral considerations 77−21618
advances, techniques and instrumentation, conference, Denver, USA (Aug. 1978) 80−3447
aerosol elemental composition in particle size fractions, human respiratory uptake 77−48726
aerosol samples, X-ray diffraction compound analysis 77−49176
air analysis 77−52689
air particulate deposits, particle-induced X-ray emission anal., 2 MeV protons 80−45833
air pollution monitoring, PIXE and NRA studies using lichen indicator 80−61744
alkali borosilicate glasses, observation of phase separation using SEM-EDX technique 80−76224
alloys, liq., composition determination during electron bombardment furnace fabrication, X-ray emission spectrography *(French)* 78−3427
alloys, thin foils, data correction for absorpt. effects 80−85255
alloys, X-ray fluorescence correction in thin foil analysis 80−85256
alpha-induced X-ray emission, thin-layer anal. 78−20132
aluminosilicate refractories, X-ray struct. determ. of quantitative phase contents 77−52707
amosite in calcium silicate matrix, detection limit in X-ray diffr. analysis 77−84578
anodic oxide superficial layer, X-ray emission spectrometry and ion backscattering *(French)* 80−49482
applications, conf., Denver, CO, USA, July-Aug. 1979 80−90613
atmospheric aerosols, chem. characterisation by X-ray absorpt. spectrosc. 80−61501
atmospheric aerosols, chem. characterisation by X-ray absorpt. spectrosc. 80−72121
atmospheric aerosols, composition, PIXE anal. 79−53004
atmospheric aerosols, quantitative anal. of high vol. filter samples 79−70501
atmospheric background aerosol, elemental conc. and particle size distribs., PIXE anal. 77−49139
automated X-ray microanalysis with electron microprobe and SEM 78−27840
bielemental thick samples, atomic comp. determ., H^+ and He^+ induced X-ray anal. 79−5223
biological fluids, ultramicroanal., by energy dispersive X-ray spectrometry 78−92768
biological frozen-hydrated specimens, in SEM, X-ray microanal. 77−56552
biological material, electron microscope autoradiography and X-ray microanalysis of diffusable substances using ultrathin frozen sections 77−60314
biological material, prep. for X-ray microanal. of diffusible elements, methods of drying ultrathin cryosections 78−77166
biological material, proton induced X-ray chem. anal., Fe and minor elements concs. 78−23989
biological material, X-ray microanalysis, graphite grids 80−8232
biological material prep. for X-ray microanal. of diffusible elements, rapid freezing and ultrathin section prep. 78−77165
biological materials, ion beam anal. in few MeV range 77−81768
biological microanalysis of thin specimens, quantitation problems 79−25164
biological object element anal., proton-induced X-ray emission method *(Russian)* 77−40939
biological samples, low temperature prep. using biochamber for X-ray microanal. 79−39628
biological samples, thick, PIXE anal., elimination of charging 78−88775
biological specimens, electron probe analysis, effects of electron irrad. of sample 79−43969
biological specimens, elemental anal. by proton excitation of charact. X-ray emission 79−1976
biological specimens, hydrated, bulk-frozen, prep. for X-ray microanal. 79−39629
biological specimens, X-ray micro anal., iso-atomic droplets as models 78−53598
biological thin sections, electron probe microanalysis 77−25620
Black Sea, heavy metal conc. meas. by charged particle induced X-ray anal. 78−24312
blood, elemental variations following gamma ray injury of mice, PIXE anal. 77−48973
blood, human, proton-induced X-ray emission anal. for Cu, Zn and Fe 79−53291
broadband X-ray excitation, quasi-fundamental correction methods 80−321
bulk material, determ. of impurity parameters from depth distrib. of foreign atoms 79−4331
bulk mode analysis using energy-dispersive X-ray fluoresc. spectrometer 77−60140
calibration facility of Lawrence Livermore Laboratory 79−49354
carbide-forming elements, K_α C line mass absorpt. coeffs. *(Czech)* 78−64905
carlfriesite, cryst. struct., chemical formula revision, and synthesis 79−55709
cast Fe, grey and ductile, subsurface defects, SEM and EDAX study 80−44400
cellulose, proton and photon induced X-ray emission anal., depth sensitivity 78−23988
charged particle induced X-ray emission 77−4967
coal, computer controlled technique 80−71994

X-ray chemical analysis continued
coal ash characterisation with X-ray photoelectron spectroscopy 79−1977
coated arc electrodes, identification of types and brands using energy-dispersive X-ray anal. 80−81400
compositional analysis with inner-shell ionisation by radioisotopic β-rays 79−57323
computerised control of powder diffractometer 80−3453
corrosion in H_2SO_4, estimated from weight loss meas. at 270°C and 56 bar *(French)* 80−85080
corrosion products, computer searching of JCPDS X-ray powder diffr. file 77−70390
crystal analyser optical alignment for X-ray fine spectral structure study 77−18148
crystalline compounds, computer identification techniques using X-ray powder diffr. file 77−70389
crystallites, concentration variations, X-ray diffraction line profile anal. 78−75491
cyclotron X-ray spectroscopic analysis of elements from Ti to Cs 79−100474
diffraction, single cryst. automated technique, comparison with powder method 77−70386
diffraction anal., historical review 77−70383
diffraction anal. on milligram samples collected on Ag filters 77−63972
diffraction analysis of cryst. powder using exptl. mass absorpt. coeffs. 78−3390
digitally controlled scanning microprobe for trace element analysis 79−52801
electrically conductive coating influence on X-ray microanalysis accuracy 80−11988
electron beam particulate analysis of air samples 80−40785
electron microprobe, automated, evolution of quantitative elementary point anal. in geosciences *(French)* 78−78046
electron microprobe analysis X-ray interferences correction, graphical method 79−43707
electron microprobes and scanning electron microscopy, conf., Orsay, France, Dec. (1978) 80−11979
electron microscope with facility for X-ray microanal. 79−12887
electron probe, feldspar minerals from Mt. Rokko 80−31038
electron probe analysis, spatial resolution in thin foils 80−101065
electron probe analysis, ZAF-correction procedures for biological bulk specimens 79−44073
electron probe dispersion influence on spatial resolution in STEM 80−85257
electron probe X-ray microanalysis, instrumentation and techniques, review *(Chinese)* 79−34415
electron probe X-ray microanalysis, quantitative investigation of thin specimens 80−101068
electron spectroscopy, for bulk and surface microscopy and microanal. 80−52367
element analysis, using nuclear-physical methods *(German)* 77−25347
elemental analyser, diffractometer based 80−318
elemental analysis, quantitative, using energy-dispersive X-ray spectrometer 80−104840
elemental analysis by means of X-ray attenuation measurements 80−50912
elemental concentration, estimations, in small particles using X-ray anal. in SEM 79−16098
elemental mapping techniques in microscopic domain 78−24013
EM6G TEM, modification for X-ray microanalysis 79−74470
energy despersive analysis, simplex spectral deconvolution method 79−80722
energy dispersive, STEM microanalysis of precipitates in Ni-base superalloy 80−104492
energy dispersive analysis, without need for standards, empirical table for fluoresc. yields 77−44543
energy dispersive spectral analysis, using semicond. detectors, review 80−85237
energy dispersive spectrometry, appl. to mineralogy *(French)* 79−5630
energy dispersive spectroscopy, quantitative, computer program 79−43689
energy dispersive X-ray diffraction method, annotated bibliography (1968-78) 80−36794
energy dispersive X-ray microanalysis, improved reproducibility by normalization to the background 78−48727
energy dispersive X-ray spectra, anal., computer techniques 79−43690
energy dispersive X-ray spectrometry, qualitative and quantitative analysis problems 80−85249
energy-dispersive X-ray microanalysis, background reduction due to backscatt. electrons 78−20121
epon sections, after O plasma microincineration 79−17584
ferrous metal, energy dispersion X-ray spectrometry *(French)* 78−85281
ferrous metallurgy use, review 79−39242
field emission gun STEM 80−85260
film profiling using proton excited X-rays 79−4490
films, orientation effects in quantitative X-ray microanal. 80−85259
fluorapatite, proton and photon induced X-ray emission anal., depth sensitivity 78−23988
fluorescence analysis 77−5063
fluorescence spectrum deconvolution method 79−74453
fly ash, depth composition determ. by XPES 78−68943
fly ash particles, effect of chem. variability on cell exposure 79−16172
forensic materials anal., problems influencing sample handling 80−3448
gall bladder stones, human, X-ray anal. 80−36081
gas atmosphere quantitative analysis adsorption chamber 80−85234
gas density measurement, high speed, using proton-induced X-rays 79−52805
Ge-Si sandwich struct., sputter profiling, combined Auger-X-ray anal. 80−66909
geological samples, chem. microanal., by X-ray microscopy near absorption edge with synchrotron radiation 78−20527
glass bubbles, form., condensate trace quantities determ., spectral anal. techniques *(Russian)* 77−36852
grain boundary segregation, X-ray spectral analysis method, for element distrib. determination 80−21337
graphite core, of fission reactor, impurity migration, proton microprobe obs. 79−52803
Guinier camera projects, microcomputer automation 80−3454
hair, human, PIXE analysis, correction factor, rel. to pollution monitoring 80−61743
Hastelloy X-R, reaction with sintered Li_2O pellets 79−39137

X-ray chemical analysis continued
heavy ion induced emission, role of automation 77−77863
heavy ion induced X-ray emission anal. 77−48727
HIXE, metal vapour targets production 78−80822
HIXE, theory and appls. 79−48006
Incoloy 800, reaction with sintered Li_2O pellets 79−39137
Inconel 600, reaction with sintered Li_2O pellets 79−39137
Inconel 625, nitriding in N_2-H_2 glow discharge 80−16590
interface composition determ. methods 79−70396
ion beam surface anal., UV vacuum sample chamber 77−4970
ion beams, use in material analysis by nuclear reactions and scatt. and ion-induced X-rays 77−4968
ion induced optical emission for surface and depth profile analysis 79−4333
iron oxides, core line X-ray photoelectron spectra 78−7263
Istra wall paintings in Yugoslavia, X-ray identification of pigments 77−16876
k-shell ionizations in proton induced X-ray emission analysis 80−101054
kidney stones, human, X-ray anal. 80−36081
light element anal. by 2 MeV, 150 keV proton and photon induced X-rays 78−53295
light element detection, meas. near detectability limits with a horizontal cryst. spectrometer 79−21877
light elements, principles of quantitative microanal. *(French)* 80−11980
light elements, ultrasoft X-ray spectroscopy, local anal., electron-microprobe excited radiation 80−99027
liver tissue, proton-induced X-ray emission anal. for Cu, Zn and Fe 79−53291
low alloy steel, alloying constituents, XES determ. 78−73126
low energy proton-excited X-radiation, composition anal. appls. 79−20498
low-temperature biological SEM and X-ray microanalysis 79−74818
lubricating coating, solid, elemental anal. by proton-stimulated X-rays 78−88687
material analysis by electron beam bombardment *(Japanese)* 77−86416
material characterisation, in a scanning electron microscope environmental cell 79−17577
metal surface, soft APS analysis to evaluate reactive plasma cleaning 77−44409
metallurgical and mineralogical specimens, energy dispersive analysis 77−60152
Metglas 2826A, direct meas. of decomp. on crystn. by X-ray microanal. in STEM 79−48025
microanalysis, in TEM up to 1000 kV 80−101063
microanalysis, quantitative, microcrystal standards and excessive background 77−36842
microanalysis of electron microscope extraction replicas, steel separations estimation *(Bulgarian)* 78−40012
microanalysis of solid matter in a scanning electron microscope *(Czech)* 79−8465
microbeam anal., conf., Ann Arbor, MI, USA (June 1978) 79−39258
microchannel intensity amplifier for electron microscope images during X-ray spectral anal. of light elements 77−12848
microchemical analysis, optimising conditions, analytical electron microscopy 80−101067
microscopic β-active particles, together with SEM autoradiography 77−57425
microscopy, high resolution, with synchrotron radiation, for chem. microanal. 80−81416
mild steel, alloying constituents, XES determ. 78−73126
mine concentrator appl. 78−35778
mineral fibre characterisation using energy dispersive X-ray spectrometry in TEM *(French)* 80−82857
mineral processing isotope on-stream anal. 78−35777
mineralogical use of energy dispersive X-ray spectrometry with Si(Li) diodes *(French)* 80−85251
minicomputer driven microprobe *(French)* 78−74111
minimum depth electron probe X-ray microanalysis for determining S content of human hair surface 80−22500
mullite, quantitative X-ray anal., standardisation, texture *(German)* 78−11176
multicomponent analysis, computer program using fundamental parameters and empirical coeffs. 78−44416
multiphase unknowns, identification by computer methods and quality of X-ray powder data 80−3452
mussel trace element monitoring appl. 80−30954
NBS low alloy steel standard, electron induced X-ray spectrosc., detection sensitivity anal. 79−5229
NBS low alloy steel standard, PIXE detection sensitivity anal. 79−5229
Nilomag alloy 771 coloured, X-ray photoelectron spectroscopy of surface film 78−64899
Nimonic 105, quantitative STEM chem. anal. using standard and standardless programs 79−17578
nozzle erosion, ion implantation effects, ion beam anal. 79−48011
nuclear fuels, elemental and isotopic conc. anal. using nondestructive assay 79−49691
nuclear materials, actinide determ. review of procedures at Rockwell Hanford Operations 79−81050
ore dressing X-ray spectrometric analysis centre 80−86541
organic substances, determ. of heavy elements by X-ray absorpt. 77−2075
Pacific marine aerosol, continental component identification by combined neutron activation and SEM with X-ray anal. 78−3990
particle size effects in X-ray absorpt. anal. 77−16882
particles, new method for X-ray micro-anal., based on peak to background meas. 79−24881
phase identification by powder diffr. anal., manual, computer search techniques, comparison 77−70387
phosphosilicate glass coatings, measurement of P content using SEM and energy-dispersive X-ray analyser 80−76588
phosphosilicate glass passivation layer P content, SEM analysis and interpretation 78−35759
phosphosilicate glasses, P content determ. by Rutherford backscatt., PIXE, and activation anal. *(Hungarian)* 80−85233
photoelectron spectrometer, X-ray excited, analyser brightness determ. 77−25331
photoelectron spectroscopy, factors affecting quantitative determ. 78−7249
photoelectron spectroscopy, hydrocarbon contamination reduction 77−44542
X-ray chemical analysis continued
photon activation analysis, nondestructive, X-ray spectroscopy applic. 77−90689
pigments of Minoan painted pottery, XRF-XRD analysis method 80−35586
PIXE, anal. of S and trace metals in nonurban and marine aerosols 77−49136
PIXE, appl. of protons from 3 MV Dynamitron accelerator 77−81453
PIXE, appl. of wavelength dispersive spectrom. 77−48735
PIXE, appl. to bioenvironmental anal. 77−48976
PIXE, appl. to primate trace element retention 80−81792
PIXE, applications 79−48007
PIXE, atmospheric aerosol, absolute element concs., PIXE and AAS, comparison 78−85237
PIXE, biological applications 79−48008
PIXE, external beam elemental anal. method, sensitivity obs. for biological samples 79−5227
PIXE, impurity depth determ. 77−48725
PIXE, influence of matrix effects on absolute anal. 77−48721
PIXE, procedure for thick target yield data anal. 79−8455
PIXE, synaptic vesicle ion content determ. 78−61166
PIXE, trace element anal., medical appl. 77−48865
PIXE, trace element anal. with triggered beam pulsing 77−46453
PIXE, trace element determ. in bovine retina rod outer segments and disc membranes 79−48012
PIXE, uncertainties in elemental quantitative anal. 79−39254
PIXE, use of external proton beam for multielement anal. 77−48719
PIXE, use of liposomes to reduce enhancement-absorption effects 80−101053
PIXE anal., appl. to environmental samples 77−48730
PIXE anal., enhancement 77−48722
PIXE anal., review of target backings and specimen preparation 77−48979
PIXE anal. in viticulture and oenology 77−48733
PIXE anal. of biological samples 77−48972
PIXE anal. of drinking water in cities of Iran 77−49096
PIXE anal. of meteoritic samples 77−49344
PIXE anal. of monazite inclusions in search for superheavy elements 77−49066
PIXE anal. of St. Louis aerosol, variation of elemental composition with particle size 77−49137
PIXE anal. of thick and thin targets of biological materials 77−48723
PIXE anal. of trace elements in ashed human tissues, correl. with diseases 77−48866
PIXE anal. of trace elements on liquids 77−48732
PIXE anal. of urban aerosols on heavy loaded membrane filters 77−49138
PIXE anal. with REX computer program 77−52714
PIXE analysis, MX-ray correction factors calcs., internal standard methods 80−45614
PIXE analysis of atmospheric gases, cryogenic conc. technique 79−53005
PIXE analysis of trace elements in environmental samples *(Chinese)* 79−61925
PIXE appl. to design and evaluation of catalysts 80−61201
PIXE appl. to trace element anal. 77−48717
PIXE applications, conf. 77−48715
PIXE data handling, statistical techniques 77−52715
PIXE spectra, computer code trace 77−52713
PIXE spectra, wavelength dispersion anal. 77−48736
PIXE spectroscopy, trace element analysis 77−48718
PIXE system, automated anal. of environmental samples 77−48716
PIXE system for air pollution meas. in South America 77−49157
pollutant particles, characterised by AES and XPS 79−43694
pollution samples, X-ray anal., absolute sensitivity and detection limits 78−7261
poly-ε-caprolactone-PVC blends, morphology 79−69019
polynuclear aromatic hydrocarbons, analysis by X-ray excited optical luminescence technique 80−66891
pottery manufacturing techniques, classification by X-ray anal. 78−354
powder diffr. anal., computer search/match methods evaluation, manual search comparison 77−70391
powder diffr. anal., reference intensity ratios determ. methods, errors 77−70385
powder diffraction patterns, quantitative matching 77−70384
powders, spray drying to minimize preferred orientation 80−3098
precipitate free zones, X-ray microanal. 80−108768
protein quality of leguminous plants, proton induced radiation anal. 77−48978
proton beam diffusing system for PIXE analysis 79−85848
proton beam trace element anal. at atmospheric press. 77−81454
proton induced X-ray emission, K or L shell ionisation cross section meas., comparison with theory 79−5226
proton induced X-rays, impurity atom depth determ. 77−11582
proton microbeam analysis in air 77−9311
proton microprobe, X-ray and γ-ray, appls. 79−48010
proton microprobe for nondestructive trace element analysis 78−64911
proton-induced X-ray emission anal. of single human hair roots 77−90973
pulmonary fibrosing disease diagnosis, histological section SEM and energy-dispersive X-ray microanalysis 80−72314
PVC, chlorinated, X-ray photoelectron spectra investig. 80−3469
qualitative, with automated X-ray spectrometer 80−22497
quantitative, of solid phases *(German)* 80−3446
quantitative trace analysis, using ion and proton induced X-rays *(German)* 78−64900
α-quartz, collected on PVC membrane filters, X-ray diffr. determ. 77−70392
quartz, quantitative X-ray anal., standardisation, milling effect on degree of disorder *(German)* 78−11176
quartz glass, Ge and B dopants, OH impurities, preform material and fibre optic waveguide struct. 80−64173
radioactive materials, X-ray diffr. studies 80−3450
radiographic microanalysis, sample sandwiched between anode and converter *(French)* 79−74471
radioisotope excited X-ray fluorescence, anal. of solns. 79−52835
radiometric analyser, appl. of expt. planning 80−61186
rat liver, trace element anal. using PIXE 77−48975
refractories, castable, X-ray powder diffr. meas. of phase composition, and flexural strength 80−3449
regression line derivation, low stability conditions 77−73486

X-ray chemical analysis continued
research and quality assurance appl. 80−73556
review 78−23981
review of literature, 1976-1977 78−83646
review of literature 1975-1977 78−85219
scanning electron microscope appl., energy dispersive vs. wavelength dispersive concepts 80−16739
scanning electron microscope with field emission gun for solid surface studies *(Czech)* 79−6240
scanning microprobe microscopy, conf., Paris, France (Oct. 1979) 80−82569
selective X-ray absorption microanal. using synchrotron radiation, transition metals in Mn nodules 78−68957
SEM/energy dispersive X-ray spectrophotometry, carousel stage for multisample anal. 77−40611
sensitivity, quality assurance, and cost in automated analysis via ion induced X-rays 79−5222
serum, trace element anal. by PIXE 79−48008
serum samples, trace element anal., automatic data acquisition, on-line method 78−48726
SIMS-AES-X-ray photoelectron spectral analysis system, for solids anal. 79−39268
skeletal muscle cells in culture, microanal., calibration 79−100798
small particles, characterisation and microanal. by STEM combined with other techniques 80−50901
smelting dust in oxygen blowing of Martin bath, phase comp. determ. 77−52705
solid, backscattering coeff. meas. of 15 to 60 keV electrons at various angles of incidence, rel. to X-ray microanal. 80−80919
solid surface characterisation techniques, review 78−22945
solutions, conc. changes, proton induced X-ray emission obs. 77−25325
SOS, quality evaluation using soft X-ray rocking curve 77−80711
spatial resolution, for SEM and STEM specimens, Monte Carlo methods 80−101066
spatial resolution, use of STEM 80−104490
specimen cup for X-ray anal. in a TEM 77−12851
specimen particles dimensions effect on X-ray intensity excited by protons 80−85238
spectra analysis, energy-dispersive, with aid of computer 80−3433
spectral analysis of minerals, calibration method 79−87904
spectral line superpositioning, calc. 80−85240
spectrometer, anal. of large samples in geochem. oceanography 79−16711
spectrometer, basic oxygen furnace, process monitoring 79−17586
spectrometers, Cauchois focusing with oblique-cut quartz analyser cryst. 79−52815
stainless steel, alloying constituents, XES determ. 78−73126
stainless steel, quantitative STEM chem. anal. using standard and standardless programs 79−17578
statistical anal. of data 77−70395
steel, Al-Cr, $FeO.(Al_xCr_{1-x})_2O_3$ inclusions, thermodynamics 80−60831
steel, austenitic, Cr-Ni, nonmetallic inclusions modification using rare earth metals *(Russian)* 80−40369
steel, austenitic, Cr-Ni-Mn-V, X-ray anal. of carbide phases formed during ageing *(Russian)* 80−20936
steel, austenitic, non-oxidising, B and by secondary ion emission and X-ray microanal. *(French)* 80−11985
steel, austenitic, type FV548, irradiated, Ni and Si rich phase, energy dispersive X-ray anal. 79−66063
steel, austenitic stainless, X-ray microanalysis of C *(French)* 80−11981
steel, austenitic stainless FV548, neutron irradiated, Si-rich phase occurrence of M_6C phase 80−15156
steel, commercial alloy ferritic, meas. of alloy and impurity elemental distrib. using STEM 80−35601
steel, Cr-Mn with increased N content, X-ray spectral microanalysis *(Bulgarian)* 78−53304
steel, Cr-Mo:P (2.25, 1 wt.%), stress relief cracking, effect of P segregation 80−89324
steel, ferritic stainless, Cr-Mo (12,1wt.%) microstructure influence on localised corrosion behaviour 80−61018
steel, low alloy, Mn determ. by AES and APS 79−48001
steel, stainless, coloured, X-ray photoelectron spectroscopy of surface films 78−64899
steel, stainless, ferritic, passivity in 1N HCl, X-ray photo-electron spectroscopic study 80−11817
steel, stainless, ground surface ion bombardment, in DC glow discharge 78−95098
steel, stainless, proton and photon induced X-ray emission anal., depth sensitivity 78−23988
steel, stainless, Type 304, surface analysis by SXAPS *(Japanese)* 77−70231
steel, W and Mo, quantitative anal. of carbides formed during tempering 78−64571
steels, obs. and anal. of sulphides, using non-aqueous electrolyte-potentiostatic etching method *(Japanese)* 80−89433
STEM, appl. to materials science 80−103228
STEM, structural and chemical analysis, appls. 80−88003
STEM appl., statistical variation limitation 80−61208
surface anal. tools review 80−103540
surface analysis, review of ESCA technique, instrumentation, and appl. 78−68947
surface and bulk microanalysis, electron spectroscopy apparatus *(French)* 80−47151
surface layers, methods, results of studies of atomic states and elemental composition 77−29063
surfaces and interfaces, analysis by combined Auger, X-ray and SEM studies 80−81413
surfaces and thin film studies by combined system of SIMS, AES and XPS 80−86536
synchrotron radiation, appls. 78−74825
system for elemental analysis using SEM-WDS combination 79−12917
target preparation of aqueous samples for XFA and PIXE 79−87915
TEM, exptl. and theoretical X-ray prod. 80−85258
thick samples, PIXE anal., detect. limit and sensitivity 79−52802
thick specimens, proton and electron induced X-ray spectrometry, detect. sensitivities 78−20087
thin film, sputter profiling, combined Auger-X-ray anal. 80−66909
thin foil, energy dispersive X-ray microanal. 77−60153
thin foil, X-ray microanalysis in electron microscope *(French)* 80−61191
thin foil, X-ray microanalysis in scanning transmission electron microscope, limitations 78−20122
thin foil microanalysis using XPS and STEM, surface film effects 78−35789
thin foils, chem. anal. by electron microscopy *(French)* 80−50899
thin samples, mass thickness and chem. composition determ., by TEM and X-ray anal. 80−103227
thin specimens quantitative analysis, effects of absorpt., fluoresc. and beam spreading 78−35787
tissue, dual-beam absorptiometry, iterative method for K_β filter elimination 77−70533
tissue, trace element anal. by PIXE 79−48008
tissue sample elemental comp., muonic X-ray analysis at LAMPF 79−53216
tissue-equivalent materials, low-Z elements, nondestructive determ. by muonic X-ray method 78−44417
trace analysis of thin specimen layers, substrate background radiation effects 79−29436
trace element, small proton accelerator suitability obs. for X-ray emission excitation *(German)* 77−25348
trace element anal. by charged particle induced X-ray meas. *(Japanese)* 77−1959
trace element analysis, by heavy ion induced X-ray emission 77−36808
trace element analysis by X-ray emission spectroscopy, excitation modes comparison 78−20113
trace element analysis using neutron activation and high-resolution X-ray spectrometry, beta-particle interference elimination 77−90688
trace element transport meas. during haemodialysis by PIXE 80−36102
transPu elements, chem., phase anal., X-ray powder diffr. techniques 77−70388
tubes, for diffr. anal., spectral purity, quantitative determ. *(Chinese)* 80−57444
tumour in rat, concentration of Ga, Yb, Tl, anal. by proton induced X-ray spectroscopy 77−5122
ultramicroanalysis, single grain oscillating crystal method *(Chinese)* 80−21332
ultrasoft X-ray microanalyser detector using secondary electron multiplier 77−21446
ultrasoft X-rays, detection with variable geom. proportional counter fitted to TEM 77−48712
water analyses 77−52689
water pollution, energy disperion X-ray analysers, evaluation 78−48712
X-ray fluorescence, Ar ion induced, for surface anal., preliminary obs. 79−5228
X-ray microanalysis, in TEM at high accelerating voltages 78−36078
X-ray phase analysis, rapid phase anal. methods, using DRON-1 diffractometer 80−22489
X-ray spectrometer control, interactive program for data collection, manipulation 78−7312
XPS source area minimisation, appl. to 30μm trachelomonas cell surface anal. 79−48037
ZAF corrections, quantitative X-ray anal. programs 79−21878
α-particle induced X-ray emission, K or L shell ionisation cross section meas., comparison with theory 79−5226
β-ray quantitative microautoradiograhy, by X-ray emission microanal. 78−20545
AgCuAg sandwich target, proton induced K-shell X-ray yield ratios 77−48724
Al alloy, anodic finish exam. by SEM and electron probe micro anal. obs. 79−96278
Al brass condenser tubes, XPS study of protective layers 80−35383
Al, sputter deposit PIXE expt. 80−61196
Al surface, porous anodic films, cell walls anal. by STEM and energy dispersive X-ray anal. 79−19476
Al-Zn-Mg-Ag, detection of small amounts of Ag by energy dispersive X-ray anal. 77−60154
Al_2O_3, sintering temperature effect of titanate additions 80−60808
Al_2O_3 thin film used in inelastic electron tunnelling spectroscopy, X-ray photoelectron spectrum 80−108319
Al_2O_3:MgO, grain boundary segregation of Ca and Mg X-ray spectrosc. and STEM study 80−107269
^{241}Am and $Pu/^{241}Am$ ratios, environment meas. using X-ray spectrometry 77−60265
Au-Cu-Cr, thin layer, deposited on glass or Si substrate, X-ray microanalysis *(French)* 80−50902
$BaO\text{-}GeO_2\text{-}Na_2O\text{-}H_2O$ system, hydrothermal crystn., phase formation laws 79−46636
$BaTiO_3$, epitaxial vacuum condensates struct. 79−95290
$BaTiO_3$:$BaTi_3O_7$, dielec. props. and microstruct. 80−60481
$\alpha\text{-}Bi_2O_3+KCl$, quantitative anal. of multocomponent powders, full-profile refinement of Guinier-Hagg X-ray film data 79−39249
$Bi_2Te_3\text{-}Sb_2Te_3$ solid solns., plastically deformed by hot extrusion, diffusion meas. using micro-X-ray spectrum anal. 79−14954
C, graphite content, quantitative X-ray phase analysis 79−52820
C-S-H gel, formed in hydration of C_3S pastes, chem. comp. 79−79346
$CaF_2+SiO_2+Mg(OH)_2$ matrix, quantitative anal. of multocomponent powders, full-profile refinement of Guinier-Hagg X-ray film data 79−39249
CaO, determination of contents in sintering charge, using X-ray spectral anal., assessment of error 79−52823
$(CaO)_3SiO$ cement pastes, electron microsc. anal. 80−108761
$Ca_x(PO_4)_y(OH)_z$, nonstoichiometric, wet-process formation from $\alpha\text{-}Ca_3(PO_4)_2$ *(Japanese)* 78−84752
CdS(Se)(Te), evap. onto electron bombarded NaCl substrates, epitaxial growth and characts. 79−28948
CdTe, trace anal. by heavy ion induced X-ray emission and SIMS 80−55755
Cl, in Ir catalysts, determ. by X-ray photoelectron spectroscopy 77−9146
Cr-Fe-Ga system, phase obs. at 800 and 820°C *(Russian)* 78−23662
Cs-Sn alloy, peritectic reactions, phase diagram *(Russian)* 80−40784
Cu, corrosion inhibition, chem. nature and struct. of protective films 77−60001
Cu, sputter deposit PIXE expt. 80−61196
Cu whisker, H_2 reduction of CuI, growth mechanism 78−30853
Cu-metal thin film couples, room temperature interactions 80−96699
Cu-Ni-Nb (30, 0.9 at.%), precipitate free zones, X-ray microanal. 80−108768
$CuInS_2$, homogeneity region and intrinsic dopant mechanism 78−34630
Es compounds, X-ray powder diffr. 80−2002

X-ray chemical analysis continued
Eu-B-C ternary and binary boundary systems, preparation techniques, X-ray analysis 80−60840
Fe alloy, corrosion inhibition, chem. nature and struct. of protective films 77−60001
Fe, cast, spheroidal, segregation investigation by X-ray spectral analysis *(German, English)* 77−63993
Fe-Ni (3 wt.%) alloys, embrittled, microanalysis of grain boundary segregation using STEM 78−35633
$^{59}Fe/^{55}Fe$ activity ratio of blood, meas. using semicond. detector 80−17062
Ga-Al-Sb, liq. phase epitaxy, phase diagram, X-ray microanal. 79−19491
$Ga_{1-x}Al_xAs$ based layer structures, optimum growth conditions, comp. and struct. perfection 80−104069
GaAs oxide film, thermal and anodic, in-depth profiles, XPS expts. 78−84086
GaAs, thick sample, atomic comp. determ., H^+ and He^+ induced X-ray anal. 79−5223
$GdCl_3.6H_2O$, thermal decomp., X-ray emission luminesc. *(Japanese)* 80−55763
H, determ. by simultaneous heavy-ion induced nuclear reacts. and at X-ray emission 78−85240
Hg lamps, RF-excited, dark film anal. 80−92789
I, stable, tissue determ. by X-ray photographic method 77−70540
InP, Zn diffused single-crystal, substitutional dopant and hole conc. meas. 80−75260
InSb, film, analysis by attenuation of substrate X-ray fluoresc. 78−27872
$K_2Mg_4Mo_4O_{16}.(OH)_2(H_2O)_2$, dehydration processes rel. to stoichiometry *(French)* 79−24734
$LiBO_2$-In_2O_3, phase composition, mag. props, elec. cond. 80−55365
Mg-Si-Al-O-N, grain boundary segregation, combined X-ray microanal. and lattice fringe imaging determ. 79−15681
MgO-NiO, STEM microanal., absorpt. effects 80−80902
Mn nodules, deep-sea, diagenetic features, X-ray spectral and SEM anal. 79−16099
Mn nodules, distrib. of transition metals by X-ray absorption microanal. 78−68957
Mn-Zn ferrites, grain boundary exam. using TEM and AES 80−107268
Ni alloy, STEM microanalytical techniques comparison for precip. comp. determ. 78−35790
$NiAl_3$, quantitative STEM chem. anal. using standard and standardless programs 79−17578
Ni_3Al-Ti(Cr)(Fe)(Zr)(Mo)(W), powder, X-ray spectral analysis exam. 80−16239
Pb compounds identification in urban aerosols, rel. to health hazard 78−44991
Pb content in blood, PIXE determination 80−51228
Pb_2NbYbO_6, X-ray structural investigation 79−65060
PbTe, thick sample, atomic comp. determ., H^+ and He^+ induced X-ray anal. 79−5223
Pd-Ag, thin layer, deposited on glass or Si substrate, X-ray microanalysis *(French)* 80−50902
$Pu/^{241}Am$ ratios, environmental meas. using X-ray spectrometry 77−60265
S aerosols characts. in Florida, PIXE anal. 79−21030
S content of plant materials, PIXE anal. 77−48977
Si wafers, channelling dips for K L X-ray prod., PIXE and Rutherford backscatt. anal. 79−4363
Si-Al-O-N ceramics, grain boundary segregation determ. by X-ray microanal. and lattice fringe imaging 79−15681
Si-SiN mixtures, X-ray diffr. powder anal. method, integrated intensities peak height approx. 77−56323
Si(Li) detectors, escape peak losses 80−27383
Si(Li) energy dispersive X-ray spectra, computer anal. 79−1981
SiO_2-base cores, for superalloys, high temp. characterisation 80−10640
Si_3O_7 layered stacks, polymorphism, cryst. chem. anal. 79−60301
SnO, disproportionation, thermoEMF, Mossbauer spectroscopic, X-ray diffr. anals. 79−11776
$Sn_{1-x}Pb_xSe(Te)$ films, oxidation rel. to annealing temp. and time, Mossbauer spectra, X-ray and microstruct. obs. 80−104311
SrO-Al_2O_3-B_2O_3-SiO_2, glass, corrosion by Cs vapour or liq. 77−16706
Ta film, reactively sputtered, N content determ. from Fourier anal. of X-ray diffr. profile 77−76693
thin film and surfaces, quantitative anal., He^{2+} induced X-ray emission technique 79−43548
Ti alloys, X-ray phase analysis, quantitative description of new method 79−52222
TiB form., kinetics investig., X-ray diffr. anal. using internal standard, dilution methods 77−70393
Ti_3O_5-Al_2TiO_5 ($MgTi_2O_5$), solid solubility, X-ray phase and optical microscopic exam. 80−59657
U ore, U content determ., radioisotopic X-ray technique using Compton scatt. 77−70357
V-Ti-C, elemental anal. of second phase carbides using electron loss spectroscopy 79−20500
Ve-Fe-Ga system, phase obs. at 800 and 820°C *(Russian)* 78−23662
$Y_{2.3}Gd_{0.6}Fe_{4.7}Al_{0.4}O_{12}$ garnet, Gd/Fe concentration ratio across pretransformed nucleus 79−11624
YIG, energy dispersive X-ray microanalysis, improved reproducibility by normalization to the background 78−48727
Zn on Be, zincating conditions, film characts. 77−40397
ZnSe, evap. onto electron bombarded NaCl substrates, epitaxial growth and characts. 79−28948
ZnTe, thick sample, atomic comp. determ., H^+ and He^+ induced X-ray anal. 79−5223
ZrC_x, micro X-ray spectral anal. of boundary zones 79−8301
ZrO_2, partially stabilized, processing defects 80−97558

X-ray crystallography
For results of structure analysis see crystal atomic structure
see also X-ray crystallography apparatus; X-ray crystallography calculation methods; X-ray crystallography technique
absorption factor, cylindrical specimen, perpendicular to cylindrical synchrotron radiation beam of same radius 78−76988
absorptive single crystal, X-ray refl. coeff. 78−9898
amorphous and gaseous states, philosophical problems in struct. determ. 78−50665
amplitude-modulated structure, general treatment of diffr. geometry *(Chinese)* 78−87589

X-ray crystallography continued
anomalous dispersion correction determ., use of photoelec. attenuation meas. 80−84026
anomalous transmission at three-wave diffraction (220;202) *(Russian)* 78−34393
anomalous transmission at three-wave diffraction (220;202) *(Russian)* 78−34394
anomalous X-ray scattering 80−54075
asymmetric Bragg case of grazing incidence, theory 77−4020
asymmetric Bragg case with small incidence angle *(German)* 79−23493
asymmetric Bragg condition for thick real crysts., applic. to dislocation networks *(German)* 78−67607
asymmetric crystal diffraction exam. of theory 79−50934
asymmetric Laue case, theory 77−1043
atom form factors of different atomic models, fitting theoretical struct. factors by varied temp. factors 80−1882
binary alloys, inhomogeneous, diffr. profile calc. 78−67609
block disorientation determination, in distorted crysts. by diffr. in divergent beam of X-rays 79−55607
bonding electrons, scattering of X-rays 79−99026
book, X-ray optics, appls. to solids 78−42859
book 78−59721
book 78−94949
Bormann effect, multiwave, expt. detect. for Si 79−14648
Bormann topograms, diffr. effects obs. during X-ray transmission through a cryst. with dislocations in slip planes 79−4310
Borrmann diffraction, simultaneous four-beam 77−19823
Borrmann effect in symmetrical cases of simultaneous diffr., photoelec. absorpt. 77−19825
Bragg case, Bragg angles of $\pi/2$ 79−86646
Bragg diffraction under uniform strain gradient, dynamical theory 78−79492
broadening of X-ray reflections from cryst. containing excess of dislocation walls of same sign *(Russian)* 79−7509
coherence length 78−26388
coherent scattering by crystal, photon model 80−24309
coherent scattering factors for neutral atoms with Z up to 54 *(Japanese)* 77−43103
computer simulation of topographs 78−30513
conference, Crystal XII, Canberra, Australia (Jan.-Feb. 1980) 80−62388
conference, International Crystallography Congress, Warsaw, Poland (Aug. 78) 79−23481
crystal assessment by X-ray topography using synchrotron radiation 77−84586
crystal optics, review of Ewald's papers from 1912 to 1968 79−23479
crystallites, elliptical, numerical anal. of X-ray diffr. 79−19122
crystallites, Scherrer consts., review and variation with hkl, contour map representation 78−42854
cubic crystal system, symmetry restrictions, on 2nd order tensor components, error correction in International Tables for X-ray Crystallography 79−73120
Debye solid, amorphous and disordered harmonic, struct. factors 78−9954
Debye-Scherrer line profile intensity distribution *(German)* 77−55201
defects classification according to influence on radiative diffraction *(Russian)* 80−70189
deformation density approach to cryst. orbital calc., transferable integrals, X-ray crystallographic meas. 80−38993
diamond structure crystals, forbidden Bragg refl., electron distrib. 77−51265
diamond type structures, three and four wave X-ray diffr. 78−67608
diffraction by coherent sound wave 77−84860
diffraction distortion distribution behaviour from mixing near low Fourier orders *(German)* 79−37583
diffraction enhancement of symmetry, simple and double enhancement 77−51257
diffraction focusing of X-rays by perfect cryst. *(Russian)* 78−75500
diffraction in asymmetric Bragg case *(German)* 79−10746
diffraction lines distorted profile, determ. of maxima positions 80−24307
diffraction peak broadening caused by substitutional disorder 79−77454
diffraction symmetry enhancement rel. to Patterson function 79−73068
diffraction topography, introduction *(Chinese)* 80−1883
diffractive focusing of spherical X-rays *(Russian)* 79−4207
diffuse scattering, effect of correlation 78−71640
dislocation density, rocking curve half-width obtained by double X-ray crystal spectroscopy in single crystal 78−2131
dislocations, contrib. of diffr. to the contrast in X-ray topography 79−23485
disordered crystals, 2H to 6H solid state transformation, deformation mechanism, X-ray diffraction study 80−33921
disordered crystals, 2H to 6H solid state transformation, layer displacement, X-ray diffraction study 80−33920
disordered cylindrical lattices, diffracted X-ray intensities 78−79493
distorted crystallites, aggregates, X-ray diffr. intensity, extinction effects 79−77452
dynamic diffraction by cryst. with periodic displacement field *(Russian)* 79−94843
dynamic symmetry, appl. for interpretation of X-ray diffr. patterns 78−47265
dynamical scattering, theory, methods and results, book 78−71628
dynamical theory, flat, focusing and distorted crysts., Abeles matrix method 77−19831
effective atomic charge rel. to electronegativity and ionicity 77−24287
elastic deformation effect on lattice-parameter determ. 77−72524
elastically bent cryst., intensity of diffracted beams in general case of diffr. 79−50935
elastically bent crystal, dynamic scatt. in quasiclassical approx. 77−4022
elastically bent crystal, dynamical Bragg diffr. of X-rays 79−14639
elastically bent crystal, integrated intensity of Laue diffr. 78−34383
elastically deformed crystals, infringement of Friedel law 77−31554
electron and magnetisation densities in molecules and crystals, Arles, France (Aug. 1978) 80−105428
electron density distribution, and other densities in crysts., problems of resolution and bias in experimental determ. 79−23490
electron density mapping in mols., cyrsts., conf., Rehovot, Israel, (Apr. 1977) 78−71622
electron scattering of X-rays, basic theory 78−71623
energy-dispersive diffractometry meas. on large crysts., expts. on GaAs 80−1888
Ewalds theory, X-ray crystal optics historical review *(German)* 79−50932

X-ray crystallography continued
EXAFS, in real space, struct. determ., appl. to Ge 77−15273
extremely asymmetric case, dispersion surface and dynamical theory, eqns. *(German)* 78−59717
extrinsic faulting in FCC crystal, diffraction model 77−19818
FCC crystal, extrinsic faults, X-ray diffr. matrix intensity eqn. 78−38575
fibrillas, crystallite shear deforms. rel. to small-angle X-ray scatt. pattern *(Russian)* 78−71690
films, multilayers, periodic and near-periodic, small-angle interferences of reflected X-rays 79−94846
four-wave diffraction, anomalous X-ray passage *(Russian)* 77−35437
Fourier transform, elimination of finite-range effect on block-size distrib. 77−31547
Fourier transforms of Gaussian orbital products 78−38573
generalised X-ray scattering factors, two-centre case with Slater type orbitals 78−79491
HCP lattice, Huang diffuse scatt. from interstitials 80−88142
high energy resolution X-ray spectroscopy, review 80−14959
history, 62 years of X-ray crystal optics, diffraction topography and interferometry *(German)* 79−46508
homogeneously bent crystal, general dynamical theory of X-ray Laue diffr. 77−31548
ideal anharmonic crystal, X-ray diffuse scatt. asymm. *(Russian)* 77−47300
ideal crystal, anharmonicity contrib. to X-ray scatt. 77−58920
III-V quaternary-binary heterojunction, X-ray characterisation of defects 78−95239
imperfect crystals, asymmetric limits of X-ray scattering in Bragg case 80−33853
indexing reliability, of X-ray diffraction powder patterns 80−87990
infinitely thick crystal, solution dispersion surfaces of two-beam dynamical Bragg reflection 78−75488
integrated intensities, in secondary extinction theory 80−49043
interferometry, comparison of X-ray and neutron interferometry 79−50952
internuclear density units, temp. factors, exptl. accuracy 77−55206
internuclear density units, temp. factors, theory in harmonic approx. 77−55205
introduction, structure and structuring of solids, book contrib. 78−42860
ion implanted layers, strain and damage distribs., X-ray diffr. model calcs. 79−69116
kinematical (Universal limit), and freedom from extinction 79−23486
laser optical simulation of diffr. from distorted lattices 79−23612
lattice dynamics and X-ray diffr., early work by I. Waller 80−62439
Laue case of grazing incidence, extremely asymmetric X-ray diffr., calc. for Si 78−51392
Laue case rocking curves, oscillatory struct. expt. determ., theoretical analysis 78−9899
Laue diffraction, exam. of energy flow in X-ray wavefields 79−50933
Laue patterns, cylindrical, flat transmission or flat back-reflection Laue photographs, calc. of crystal orientation 80−19670
Laue patterns, stereographic projections for noncubic crystals *(Ukrainian)* 79−32851
Laue patterns and stereographic projections, Laue back-reflection techniques, plot program PLOMAC 80−19669
Laue three beam cases, experimental observation and theory 79−50946
line broadening, fragmented crystal containing blocks *(Russian)* 79−86643
line-shape anal., simplifications using Fourier series, appl. to Mo film on Si 79−82123
mass attenuation coeffs. and anomalous dispersion corrections for wavelengths $IK\alpha_1$-$CuK\alpha_1$ 77−31559
multilayer close-packed structures, identification possibilities, X-ray and electron diffr. patterns 78−94951
multiple diffraction, theory of Bragg refl. 79−94842
multiwave X-ray diffraction theory, anomalous transmission in six-wave case 77−51264
N-beam dynamical diffr., number of permitted modes of propag. 79−73059
nongaussian random field from independent sources in discrete lattice *(Russian)* 77−72523
normalised structure factors, values of ε 77−51259
normalized structure factors, values of ε 77−19826
one-electron density functions, many-centred finite multipole expansions 78−71624
optical simulation using two dimensional grating 77−38802
order-disorder transformations, critical scattering of neutrons and X-rays, meas. techniques 79−55609
ordered superlattices, X-ray studies, rel. to microstructure 79−94844
paracrystal theory appl. to cryst. struct. investig. *(German)* 77−39552
partial structure factors, freq. modulated X-ray diffr. 77−35440
Pendellosung fringes, meas. of real part of anomalous scatt. in Si 78−26381
perfect crystal Bragg case, errors due to Zachariasen approx. 78−38574
perfect crystals, Bragg reflection, depend. on geometrical factors 79−7510
phase analysis, quantitative, methods of mixing 80−24317
philosophic concepts and implementation 79−94932
plane-polarised X-rays, coherent splitting, interaction with perfect crysts., synchrotron radiation topography 78−5989
polarisation plane diffr. rot. *(Russian)* 77−27787
polarisation states, of dynamically diffr. X-ray beams in Laue case 80−28878
polycrystalline aggregate, diffr. broadening of X-ray lines 78−94950
polycrystalline material, substitutionally disordered, domain size rel. to diffr. 80−28871
polycrystalline materials, partial texture index and meaning of Williams approx. *(French)* 77−58919
polycrystalline materials, size and angular spread of coherently reflecting regions, X-ray microdiffraction method 80−24311
powder diffraction data, American Crystallographic Association recommendations for standardisation *(Czech)* 80−24306
powder diffractometry, quantitation and calculated data 79−14636
powder pattern indexing, evaluation and reliability, criterion for rating diffr. patterns, F_N 79−37576
powder patterns for tetragonal and hexagonal polycrystalline materials, improved indexing method 80−24312
powder reflections, an error in several published tables of the multiplicities for Laue class $\bar{3}1m$ 79−14720
pulse scattering from two-dimensional crystals 79−60218
quartz, bent perfect crystal, diffractional focusing, X-ray spectroscopy *(Russian)* 80−54076
random binary alloy, charge and spin struct. factors, CPA theory 77−28374
random stacking model scatt. intensity, appl. to tetrahedrally bonded amorphous semicond. 78−9953
random structure refinement 77−51261
Renninger diagrams, ambiguity in indexing, distinction between some opposite directions in cubic cryst. 79−1370
review, rel. to appl. to materials science 79−10752
review, role of Fourier transforms in struct. determ. 77−27772
review of literature, 1976-1977 78−83646
scattering factors of ions in crysts., Watson sphere model, Hartree Fock Roothan method 80−49046
scattering of finite length X-ray wave train, dynamical theory *(Russian)* 79−4208
secondary extinction theory, high order correlations of lattice phase factors 79−23482
semiconductor, Bragg X-ray diffr. in elastically bent cryst. 80−24310
semiconductor film, X-ray diffraction in thin cryst. with linear variation of lattice period 78−26373
single crystal for devices with multiple crystal arrangement, X-ray characterisation 78−83651
six-beam anomalous transmission, interpretation from eigensolns. for Ge cryst. 77−19832
six-wave diffraction, augmentation of anomalous transmission, expts. on dislocation-free Ge 79−14650
small angle scattering, rel. to elec. resist. 79−19125
small-angle scattering, of X-rays and neutrons, (fourth international conf., Gatlinburg, USA (Oct. 77)) 79−10745
small-particle-size effect 77−31550
spectral instability of four wave coplanar X-ray diffr. *(Russian)* 80−33855
spherical particle of nonuniform electron density, small-angle X-ray scatt. 77−7631
spherical X-ray diffr. with many wave scatt., dynamical theory 78−91194
spherical X-ray wave, diffraction focusing effect *(Russian)* 79−23500
spherical X-ray wave, dynamics theory of diffr. 78−26372
square-section parallelepiped, primary extinction 78−38572
stacking fault contrast in X-ray section topography 79−77453
stacking fault insertion effects on diffraction pattern 79−86803
standard X-ray diffraction powder patterns, for 112 substances 79−60223
standard X-ray diffraction powder patterns 80−64839
standing waves obs. at Si cryst. surface 80−96417
structural defects, effect on dynamical scatt. of X-rays *(Russian)* 79−64960
structure amplitude phases, statistical-thermodynamic determ. 80−84028
structure amplitudes and intensities, fractional difference probability distrib. for 2 related crysts. 77−68893
structure factors, mapping of electrostatic props. 79−94841
substitution order-disorder, study by X-ray and electron diffr., book contrib. 79−68983
superlattice, 1D, kinematic and dynamic X-ray diffr. 80−33854
superlattices, one- and two-dimens., possibility of X-ray and electron diffr. struct. determ. 80−54560
synchrotron radiation appl., energy-dispersive powder diffr. 77−24245
synchrotron radiation applications 77−51283
textured materials, diffraction broadening studies, coherent domain size and microstrain 79−73060
texturised materials, orientation distrib., demonstration of ghost effect 80−70080
theory *(Chinese)* 80−44072
thermal diffuse scatt. effects on atomic parameters and electron density distrib. 77−19819
thick crystals, X-ray diffr. process, layer model, reflectivity, polarisation *(German)* 77−51262
thick crystals, X-ray diffr. process, layer model, reflectivity, polarisation *(German)* 77−51263
thin films, $I \sim \sin^2 x/x^2$ intensity eqn. verification *(German)* 80−19668
three beam diffraction, phases of X-ray reflections from single crysts. 79−23483
topographic image, dynamical contrast, obs. of polychromatic interference fringes 77−55204
topographic image, dynamical contrast, polychromatic interference fringes 77−55200
total external reflection of X-rays, differential eqn. calcs. 78−71625
two-crystal system with non-diffracting zone, X-ray interferogram fine struct. 80−1887
vibrational averaging of X-ray scatt. intensities 78−74722
von Laue diagrams, of X-ray scattering, and constant intensity curves of crit. scattering 79−99024
wave-train length, three-wave method for meas. 77−43105
X-N maps, room temp., errors due to non correction for thermal diffuse scatt. 78−75487
X-ray analysis, appls., conf., Denver, USA (Aug 1975) 77−56307
X-ray interferometer, temp. gradient influence on fringe pattern 80−1896
Zachariason's theory of extinction, critique 77−19828
Ge (111) plate, multiple X-ray diffr. expt., ambiguity in indexing Renninger diagrams 79−1370
Ge, anomalous X-ray transmission in the presence of four-wave diffraction (111, 200, 311) 78−79494
Ge, six-beam anomalous transmission pattern, computer anal. 77−4021
Ge, six-wave diffraction, intensification of anomalous transmission 77−7635
Ge, X-ray linear absorpt. coefficients, in energy range 5 to 50 keV 79−73066
Si, Bragg-case X-ray thin cryst. rocking curves, theory and expt. comparison 78−55785
Si, elastically bent crystal, with large strain gradient, X-ray diffraction study 80−44073
Si, Pendellosung fringes in synchrotron X-ray topographs 79−32858
Si, perfect cryst., X-ray acoustic reson. 79−27873
Si, X-ray linear absorpt. coefficients, in energy range 5 to 50 keV 79−73066
Si, X-ray linear absorption coeff. 78−26384
Si, X-ray mass attenuation coeff. meas. 77−31556

X-ray crystallography apparatus
see also goniometers; X-ray diffractometers; X-ray monochromators
aberrations correction, expt. criteria for use of deconvolution methods 78−18492
acid phthalate curved crystal spectrograph, diffraction efficiency calc. method 80−79630
air-sensitive crystal mounting, portable apparatus 77−51281
air-stream cooling device for precession photography of proteins 77−27781
automated diffractometers, free specimen selection and angular marking synchronization 78−18496
automatic data collection system for powder X-ray diffractometry 77−24244
automatic flat-bed microdensitometer for X-ray crystallography use in molecular biology lab. 77−35438
Automatic Guiding of Reflexion Position (ANRES-system) *(German)* 78−63637
automatic scanning system for multiple-sample Guinier X-ray powder diffraction films 80−22492
automatic system for low temp. studies of phase transitions 77−15281
back-reflexion camera 78−32962
Beurger precession camera, diffuse X-ray scatt. meas. *(Japanese)* 80−49049
Bonse-Hart X-ray diffractometer, asymmetrically cut, comparison with Kratky camera 80−77917
Bragg spacing comparator, accuracy of 3 parts in 10^8 for lattice spacing meas. 78−75489
camera, 10 cm diam. back-reflexion focusing, design and fabrication 78−18489
camera, Kossel X-ray technique, for obtaining crystallographic data in the SEM 78−34391
camera, low-angle, monochromatisation of primary beam on Borrmann principle 78−5985
camera, topographic 80−84029
camera for convergent beam recording of single cryst. 77−43113
camera for orientation of large monocrystals 78−22600
camera for topographic study of Si epitaxial layers 79−28221
capacitance-based micropositioning system for X-ray rocking curve measurements 80−205
cassette for synchrotron topography, automated 78−18494
cell, for high temperature X-ray anal. of reactive substances *(French)* 79−68978
cell device for analysis of reactive alloys 77−51272
collimators, design 79−23497
colour display of Laue patterns with scanning X-ray beam 80−87991
comparator for meas. cutoff angle of piezoelec. quartz wafers 80−105755
conference, International Crystallography Congress, Warsaw, Poland (Aug. 78) 79−23481
convergent beam camera for struct. anal. of microcrystals 78−22602
cooling, gas stream method 78−219
cryogenic X-ray topography, using synchrotron radiation 77−39507
cryostat, liq. He, for collection of 3-dimensional X-ray intensity data down to 20K 80−22369
crystal cooling device with heat exchanger 78−42850
curved X-ray position sensitive detector 78−63635
detectors, energy-sensitive, simplified calibration procedure 77−38548
diamond anvil, oscillating device for high press. X-ray diffr. 79−4209
diamond anvil device for X-ray diffraction on single crystals to 100 kbar 77−68896
diamond anvil high-press. X-ray cameras, uniaxial stress component 78−38584
diamond cell, single cryst., revised operating method, NaCl struct. refinement at 32 kbar 78−67610
diamond-anvil high pressure cell used in automatic diffractometer up to 90-kilobars 78−54387
diamond-anvil high-pressure cell, for X-ray diffraction studies 78−30514
diamond-anvil press. cell for X-ray diffr. obs. with solid-state or proportional counter 80−75119
diffraction curves, device for centre of gravity determ. 77−51271
diffraction lens, image form. 77−10154
diffractometer, automatic triple-crystal, precision meas. of Bragg and Huang intensity distribs. 78−18491
display systems for X-ray topographic images, review 77−68899
double crystal spectrometer, appl. to semicond. defect struct. *(German)* 77−72527
double focusing X-ray camera, use with synchrotron radiation 80−313
doubly curved crystal point focusing X-ray monochromator 77−82657
dynamical scattering, theory, methods and results, book 78−71628
energy dispersive X-ray diffractometery, technique, apparatus, data processing, computer profile fitting 77−68892
Fabry-Perot-type interferometer 79−86653
filament lifetimes, in rotating-anode X-ray machines, increasing using beam-deflecting magnet 80−77918
focal site lengthening, in Elliott rotating-anode X-ray sets 80−77919
furnace, using thermal image technique, for high temp. molten salt diffr. studies 77−15280
Gandolfi attachment, for Debye-Scherrer camera 79−37590
Gandolfi camera, modified for easy cryst. centring 79−14646
goniometer, for precise X-ray powder diffraction with temp. control *(French)* 80−79631
goniometer, for producing accurately oriented cryst. faces 79−37591
goniometer, for stress measurement in single crysts. and coarse-grained specimens 80−64837
goniometer, GUR-5, for small-angle X-ray scattering meas. 78−74115
goniometer for cutting single crystals 80−86275
goniometer system for X-ray diffr. exam. of large specimens 77−76248
goniometers, crystal mounting on ends of fibres using a controlled method 78−93663
graphite bonded channel design of simple construction 77−15282
grating, astronomical spectroscopy appl. 77−10155
Guinier-type focusing cameras, powder diffr. line profiles 79−58856
heating equipment, gas-flame, temps. up to 2600K for 4-circle diffractometer 79−60222
high brilliance sources and generators, soft and pulsed X-ray generators, book contrib. 78−42861
high pressure equipment for polymer studies, calibration of diamond anvil cell, 0-15 kbar 77−41635
high pressure equipment for polymer studies, in diamond anvil cell 77−74418

X-ray crystallography apparatus continued
high temperature, for X-ray diffr. exam. of ceramic minerals *(French)* 79−96234
high-pressure diffraction at liquid He temps., apparatus 77−11442
high-pressure energy dispersive X-ray diffr., miniature piston-cylinder apparatus 80−38870
high-pressure X-ray diamond-anvil cell, improved beryllium diamond support 78−30515
high-temperature X-ray topography system, for investigation of semiconductor single crysts. 77−76261
high-temperature X-ray unit, for polycrystalline specimens investigation 77−39503
hot microdeformation, and simultaneous X-ray topography apparatus *(French)* 80−38871
indexing device for Weissenberg photographs of single cryst. 77−43113
instrumentation and data analysis development, in X-ray and neutron small-angle scattering, review 79−10750
interactive graphics display system 77−22536
interchangeable Si(Li) detector on four-circle single-cryst. diffractometer 77−51278
interferometer with divergent polychromatic beams 79−27867
Lang camera X-ray diffraction theory *(Japanese)* 79−86648
Lang topography, automatic Bragg angle correction, extremum control *(German)* 78−59718
lattice parameter temp. depend. meas., Bond's method for single cryst. 77−24243
lattice period determ. by axial X-ray camera 79−68974
Laue camera, real-time back-reflection 79−37589
Laue camera, universal, using air press. differences for film adhesion *(Czech)* 78−71629
locking window shutter and collimator coupling to comply with Health and Safety at Work Act 77−39505
low temperature, classification of methods 77−51282
Lucke texture goniometer with computer control X-ray pole figure plotting appl. 78−18500
microcamera for analysis of cryst. defects in glasses 77−60002
microdensitometer for crystallographic investigations 79−54241
microfurnace for single-crystal diffr. meas. 78−32817
microscope resolution power, influence on estimation of basic method spatial struct. parameters 79−52543
monochromator, bicrystal, of moderate wavelength resolution for use with X-rays or thermal neutrons 77−76254
monochromator, double-mirror modified, for rotation photography of large-unit-cell crysts. 79−9269
monochromator, focusing, for small-angle diffr. studies with synchrotron radiation 77−39508
monochromator for high-angle double-cryst. diffr. 77−43111
monochromator for synchrotron radiation using three wave Bragg diffr. 80−87993
monochromator system, curved-crystal 78−66017
multi-anvil apparatus for high press. X-ray diffr. 78−1950
multiwire proportional chamber, two-coordinate detector for X-ray struct. investig. 77−1045
MWPC, flat area detector data acquisition system for X-ray crystallography 80−91381
MWPC, spherical drift chamber area detector for X-ray crystallography 79−41073
one dimensional curved wire chamber for powder X-ray crystallography 79−4210
optical adjustment of bent-crystal monochromators 79−14645
opticomechanical adjustment of single crysts. 77−43113
plasma focus chambers for X-ray diffr. studies of polycrystalline materials, nanosecond exposure times 77−89348
polarisation ratio, of two graphite monochromators, use of jig for X-ray beam polarisation 79−37588
polarisation ratio of crystal monochromators, method eliminating its relevence 78−55775
position sensitive detector for fast X-ray powder diffr. 80−319
position-sensitive detector, appl. to high pressure X-ray diffr. using diamond-anvil cell 80−79632
powder camera, for low temp. photography 79−58099
powder camera, high temp. focusing, new features 79−50942
powder diffraction, computer automation 80−1899
powder diffraction system, computer-controlled, with automatic sample changer 77−84577
powder-film calibration device 80−84030
precession camera, resolution, transformation equation between reciprocal space and X-ray film 79−49313
reciprocal lattice photographing with axis of film cylinder intersecting cryst. rotation axis at 45° 77−51274
rotating-anode X-ray tube apparatus 78−58100
rotation camera data, empirical method correction for absorpt. and decay effects 80−14962
sample cell, for small angle X-ray scatt. expts., temp. stabilisation 77−13830
sample holder for diffractometric studies of specimens with curved surfaces 78−22601
semiconductor detector uses and problems *(French)* 80−84031
shielding arrangement, for diffr. equipment 80−849
single crystal heater for kappa diffractometer 77−51280
single crystal X-ray diffractometery using 50 kilobar gasketed diamond anvil cell, appl. to Sb 77−31560
small angle scattering camera for synchrotron radiation X-rays, description and results 78−66020
small angle X-ray camera, using synchrotron radiation 77−43108
small-angle X-ray scattering camera, ORNL 10-metre 78−32961
spark erosion machine for cutting X-ray-aligned dielectric crystals 79−80592
spectrometer, DRON-1, with valve voltmeter, for heterogeneous struct. obs. 77−39504
spectrometer, with diffractional focusing 78−5988
spectrometer using 3 crystals for structural perfection study 77−19837
standing wave field excitation, meas. apparatus, appls. 77−15285
status monitor, for Elliot rotating-anode X-ray source 79−35908
synchroton radiation source and multichannel detector 78−47210
synchrotron radiation, X-ray optics and monochromators 77−54027
television area detectors, macromolecular structural studies with synchrotron radiation sources 79−55610
three beam interferometer, total refl. using Bragg diffr. 77−47302
topogram visualisation raster tube with shoot-through target 80−31956

X-ray crystallography apparatus continued
topographic camera, high-sensitivity double-crystal, lattice parameter meas. 80−77915
topography, new on-line system 80−79638
topography settings, white beam X-ray, for cryst. defects, synchrotron radiation 2-axis spectrometer 78−67619
tubes, for diffr. anal., spectral purity, quantitative determ. *(Chinese)* 80−57444
TV system for polymer deform. obs. 78−15610
two crystal spectrometer, small angle X-ray scatt. obs. 80−54077
Weissenberg goniometer, integrating, for X-ray structural analysis of single cryst. 77−43113
X-ray topographical chamber for work by the Lang extinction method, appl. to quartz *(Russian)* 78−83649
X-ray topography camera, high speed, semiconductor lattice defects exam. appl. 77−11443
LiF cell, for X-ray struct. investigations 80−64829
LiF curved crystal spectrograph, diffraction efficiency calc. method 80−79630

X-ray crystallography calculation methods
absorbing perfect crystal, temp. depend. of X-ray reflection intensity near absorpt. edge 80−1889
absorption, in single-crystal diffractometry, calc. program 80−38874
absorption correction, and normalisation of X-ray small angle scattering data for materials producing intense scattering at extremely low angles 80−19671
absorption correction, optimisation *(French)* 79−68973
absorption corrections in diffractometry of single cryst., cryst. shape and size determ. 78−1954
absorption corrections in single cryst. diffr., SHAPE and GAUSAB programs 78−67622
absorption factor, determ. for single cryst. of any shape in inclined X-ray diffractometer 79−64959
absorption-extinction correction technique 78−9903
absorption-weighted mean path lengths for spheres 78−75485
acid phthalate curved crystal spectrograph, diffraction efficiency calc. method 80−79630
Airy diffr. intensity profile integrals in topography of spike diffuse reflexions 77−84581
algorithms, mol. fragment recognition in E maps and electron density maps 78−55772
alignment correction when calculated adjustment exceeds allowed movement on one arc 78−18495
amorphous materials, smoothing and fast Fourier transformation of data 77−58928
p-anisidine, crystal structure determination with DAR-UM+BESM-6 automatic system 77−76386
anisotropic temperature factors, anharmonic motions 78−9902
anisotropic thermal scattering, correction of integrated Bragg intensities 78−67614
aspherical-atom formalism, testing refinements on small molecule data sets 79−7516
atomic scattering factors from Patterson syntheses 78−18498
band profile from exptl. profile of superimposed bands *(French)* 77−39506
Bayesian three stage model 78−91192
bent crystal, X-ray Laue diffraction, integrated intensity 79−23492
Bijvoet difference measurement, in crysts. with heavy atoms, stat. method for selecting reflections 79−50923
binary alloys, FCC lattice, mean distrib. of vacancies, computer program 77−62444
biological molecules, improved method for calc. the contrib. of solvent to X-ray diffr. pattern 79−16355
Bond method, of meas. lattice parameters, asymmetric Bragg reflections appl. 80−38861
bonding electrons, density distribs., simple refinement, appl. to bond charges in urea and thiourea 78−55782
Born-Oppenheimer approximation, X-ray Bragg scattering 79−32850
Bragg reflection in case of multiple X-ray scatt. 80−100127
Bragg reflection in case of multiple X-ray scatt. 80−100128
Bragg reflection multiplicities for any space group, computer program 77−55213
Bragg reflections, ang. positions calcs. by computer program 80−38863
Bragg reflections, profile measurement analysis 78−42855
Bragg reflections, ratio of integral intensities, determ. struct. perfection of single crystals 80−87987
broadening errors, in deconvoluted X-ray diffr. line profiles 80−38862
centrosymmetric electron density distributions, direct determ. by maximising integrated cube of electron density 80−10453
charge deformation, vibr. smearing 78−71634
charge deformation density refinement, computer program 78−71639
charge density, spatial partitioning 78−71638
charge density analysis techniques, appl. to s-triazine 78−38578
charge numbers-bond orders determ. from diffr. data 78−14306
close-packed crysts. with chaotic subtraction packing defects, general soln. of diffr. problem 80−92422
close-packed structures, with faults, anal. soln. for X-ray diffr. integrated intensities 80−100256
coherent single crystals, angle intervals of incident and reflected X-rays, calcs., meas. *(German)* 77−43104
collagen triple helical struct. study using Fourier transform 78−7318
complete structures, appl. of phase refinement, use of statistical information in tangent-formula refinement 79−7511
complex contour resolution into components, Fourier method 77−31561
complex structures, phase refinement, random approach to struct. determ. 79−10747
complex structures, phase refinement using magic determinants 79−7512
composite multidimensional function decomposition into its components 80−79625
composite X-ray powder patterns, computer generation 79−50931
computer simulation, of X-ray traverse topographs, on basis of Green function method 80−49044
computer simulation methods in X-ray topography 79−23484
concentration variations, diffr. strudies 79−42322
concentration wave method, appl. to complex oxide powder patterns 78−51393
constrained refinements, discussion 79−68972
coordinates calculation from distance information 78−38581
correction for interplanar spacings from Guinier powder photographs 78−63636

X-ray crystallography calculation methods continued
corrections for crystal-to-film distance variations in Laue photographs of α-SiC 77−43114
corundum, spherical ground samples, extinction effects, inhomogeneous mosaicity 78−75494
crystal atomic structures, computer-aided graphical representation of projections onto planes 79−60217
crystal orientation determ. by Laue method, computer calc. *(Chinese)* 79−32853
crystal setting, and data reduction, on a PW 1100 diffractometer, program using simple method based on real space 80−59342
crystal structure analysis, separation of unknown parameters 80−28869
crystal structure determ., optimal selection method on starting reflexion set *(Chinese)* 80−84025
crystallites, curved with layer shifts, diffracted intensities 80−28879
crystallites, needle shaped, X-ray powder reflection profiles calc., principles 80−100124
crystallites, X-ray peaks width and mutual overlapping determ. 79−86649
crystallography, electron densities, thermal smearing, limited resolution effects 78−71635
crystallography, electron distributions, aspherical-at. least squares refinements combined with Fourier methods 78−71633
cube, correlation function, intersect distrib. and scattering 80−59338
curved-crystal, X-ray monochromatising and focusing efficiency 79−55612
dead time, correction for counting losses in single cryst. X-ray diffractometry *(French)* 79−37587
Debye-Waller factor measurement, role in anal. of diffuse scattering data 79−23494
defect contrast numerical calc. in X-ray transverse topographs 77−84572
deformation density and valence density maps, errors, scale factor contrib. 78−38580
deformation density model of multipole terms, appl. to diamond 78−38656
deformed crystal, theory of X-ray scatt. *(Russian)* 80−70077
derived intensity statistics, X-ray reflection variances 77−1042
diamond, directional Compton profiles, X-ray scattering factors and 1-electron density matrix 80−10458
diatomic molecular form factors, vibr. average, study of convolution approx. 79−50926
difference density distributions, effects of incorrect phases, appl. to thiourea 78−55783
difference Fourier refinement using minicomputer, appl. to DIP-trypsin 77−58924
diffraction, extremely asymmetric Laue case, small incidence angle 77−84567
diffraction and spectral line breadth, anal. method using Voigt function 78−34387
diffraction by crystals with planar faults, struct. anal. using microtwins 78−91343
diffraction line broadening, of crysts. containing small angle boundaries, Warren-Averbach anal. 79−37578
diffraction lines smoothing appl. to separation of $K\alpha_1 K\alpha_2$ doublet *(French)* 77−15274
diffraction-profile Fourier analysis, determ. of microstruct. parameters 80−49042
diffractometer data, profile anal. using computer program 79−37580
diffractometer line profile location in X-ray stress anal. 78−5711
diffractometer reflexions, information content of unobserved and nonsignificant reflexions 79−50936
diffuse scattering, direct methods of anal., review 79−94845
direct methods, matrix formulation for finding strongest starting set of reflections 79−73065
direct methods, survey as number and kind of solved acentric equal atom structs. 80−38865
direct methods, use of centric projections 78−9900
direct procedures, triplet and quartet rels. 80−24305
disordered crystals, 1D, structure in formation from diffuse reflexions *(German)* 80−10459
dispersion corrections for at. scatt. factors 77−19827
distorted crystal, X-ray intensity mode oscills., two wave WKB approx. calcs. 80−28876
divergent beam diffr. phenomena, computer generation of identification 78−30520
double Patterson function of first kind, false maxima in struct. locating cross sections 78−47202
double reflection peaks, indexing methods 78−38586
drift and lattice const. determ., graphic method *(Chinese)* 80−87985
dynamic electron densities, anharmonic contribs. from large molecular librations 79−97971
dynamic electron density distribution, calc. from static and mol. wave functions 77−27776
dynamic scattering, asymm. Laue case, attenuation effects calcs. 77−7633
dynamic scattering, crystal with equidistantly bent reflecting planes, eqns. *(Russian)* 80−70079
dynamic scattering theory, quasiclassical approx., VKB applicability test *(Russian)* 78−71627
dynamic theory of scattering, crystal with equidistantly bent reflecting planes *(Russian)* 80−70078
elastic X-ray scattering, by thermodynamic average electron-charge density 80−100123
elastic X-ray scattering from solids containing non-rigid pseudoatoms 78−26378
electron charge densities, coherent X-ray and neutron diffr., review 77−76260
electron density analysis, exponent refinement, appl. to melamine 78−38579
electron density distrib. in crysts. and mols. from diffr. data 77−7632
electron density representations, topographical features 78−71637
electron distribution models, appl. to Si 78−38657
energy dispersive diagrams, eval. using small computer on-line techniques 80−92423
energy dispersive X-ray diffractometery, technique, apparatus, data processing, computer profile fitting 77−68892
epitaxial layer lattice consts. determ. 79−19479
epitaxic derivatives, program (AIDED) for automatic indexing, appl. to graphite lamellar compounds 79−50927
equivalent reflections averaging, using small computers 80−79634
error analysis of 2θ powder data for cubic or uniaxial phases 78−67615

X-ray crystallography calculation methods continued
errors in coordinates, bond lengths and angles 79−27870
external crystal adjustment, for Lang topography *(German)* 78−59719
extinction correction, in white X-ray and neutron diffr. 80−100120
extinction corrections, applicability 77−19829
extinction corrections, modified Zachariasen's method 77−43107
fast-rotation function representation in polar coordinate system 77−19813
FCC crystal, containing extrinsic stacking faults, X-ray scatt. intensity calc. 78−91193
FCC crystals, containing extrinsic stacking faults, X-ray diffr., derivation from theory 79−33005
fine structure characteristics of polycrystalline materials, problem of accurate calc. by central moments method 78−5984
FORTRAN program, FIREBIRD, X-ray powder refls. positions calc. 77−62443
FORTRAN program for Fourier coeffs. of assoc. generalised Legendre polynomials of generalised spherical harmonics in texture analysis *(French)* 77−15279
Fourier analysis of diffr. profile for N content determ. of sputtered Ta films 77−76693
Fourier series coefficients of X-ray diffr. lines, approx. methods *(French)* 77−31549
Fourier series termination and thermal smearing, estimation of effects on peak heights 77−62441
Frevel ZRD-SEARCH-MATCH program, for powder diffr. anal., generalisation 80−59341
Gauss-Seidel least-square refinement, procedure with rigid-group and parameter restraint capabilities 80−10455
generalised scattering factors, one-centre case with Slater-type orbitals 77−62442
generalised temperature-factor formulation , with appl. to CdS and other wurtzites 78−26383
generalized inverse matrices 78−9910
Green's functions numerical calc. for dynamical X-ray scatt. 77−80396
haemoglobin, sickling deer type III, macromol. struct. refinement by restrained least-squares and interactive graphics 80−28870
heavy atom location in struct. from Patterson function, computer aided 77−11439
high order refinements of H atoms, theoretical approach 79−19121
Hirshfeld type deformation functions, and elec. field gradients calcs. by Fourier series 79−73479
imaging of atoms, three dimensional molecular structure reconstruction, opto-digital computing 77−39510
imperfect solids, anal. of X-ray diffr. profiles, appl. of convolution relations 78−34386
imperfect spherical crystals, a priori estimates of errors in intensity 79−23489
indexing powder diffraction patterns of crysts. of orthogonal symmetry 77−47298
information retrieval system for X-ray phase analysis 78−79501
information theory aspects of struct. determ. 77−51258
instrumental aberrations correction, expt. criteria for use of deconvolution methods 78−18492
integral transforms, X-ray crystallography appl. 77−5633
integrated intensities, from a noncentrosymmetric cryst. near absorpt. edge, thermal vibr. effect 80−1884
integrated intensities, in secondary extinction theory 80−49043
integrated intensities in Bragg and Laue geometries 77−31553
integrated reflected X-ray energy, derivation 79−73063
integration method, extension of $\sin^2\psi$ method *(German)* 80−92420
intensities variation, effect of dispersion and higher symmetries 79−7520
intensity distrib., and integrated intensity in topography of crysts., Laue cases, statistical dynamic theory 80−107014
intensity errors, due to beam inhomogeneity and imperfectly spherical crysts. 79−99029
intensity measurements of twinned or grown together cryst. 77−51275
interatomic crystal vector calcs., non Fourier method 79−86652
interbranch scattering fringes, contrast *(Russian)* 80−64835
interference pattern, influence of medium inhomogeneities on nature and intensity *(Russian)* 80−64834
isomorphous replacement and anomalous scattering diffraction, data for macromol. cryst. combining method 77−19822
isomorphous replacement data, new statistical model for describing errors, case of one derivative 79−50920
isovector structure, relationship between basic and vector point systems 80−79626
Jacobi polynomial, augmented, sign 78−22599
Kα doublet separation by statistical processing method 79−10760
Kabsch's procedure, program BMFIT for matching of rigid bodies 79−50930
Karle-Hauptman determinants, use for small struct. determ. 79−7513
Kossel diffraction, source pt. location, ionic-fitting procedure 77−84576
lamellar structures, deconvolution method for evaluating small angle X-ray scattering 79−10756
lamellar structures, effects of distortions, small angle scattering, finite cluster model 79−10814
lamellar systems, collimation correction for non-isotropic small-angle X-ray scattering curves 79−10755
lattice parameter determ. by X-ray multiple diffr. study, analytical and graphical methods *(Russian)* 80−10460
lattice parameter program, least squares method 79−64958
Laue method, rapid indexing of spot pattern, computation method *(French)* 79−37575
Laue patterns, indexing back-reflections by computer 79−14644
Laue photograph indexing and monocrystal orientation determination by computer, new approach *(Chinese)* 80−79636
Laue photographs, back reflection, orientation, computer simulation 77−55199
layer sequence analysis for crysts. with stacking faults, method of structural models 77−19824
layer structures, intensity calcs. of diffr. product bands *(French)* 80−59339
LCAO calculation, of temp. effects on X-ray scattering factors of crysts. 80−10454
least squares, full matrix and block diagonal refinement 78−26375
least squares analysis, method for optimizing relative weights 78−9909
least squares refinement for powder film profile anal. 77−27778
least squares refinement technique based on fast Fourier transform algorithm 78−91197

X-ray crystallography calculation methods continued
least-squares structure refinement, weighting scheme, using Chebyshev polynomial 79−73067
line profile analysis, direct determ. of Fourier coeffs. by least squares method *(French)* 77−27775
line profile analysis, in theory of fine structures 80−33852
line profile analysis, on-line computer routine 78−79498
line profile analysis, separation of Kα_1 and Kα_2 components 77−76255
line profiles, corrections for angle depend. of Lorentz, polarisation and structure factors 77−72526
linearly disordered crystals, matrix method appl. for calc. of diffuse scattering 79−99023
linked-atom least-squares reciprocal-space refinement system, LALS, incorporating stereochemical restraints 78−26377
liquid crystal, X-ray structural analysis, computer program for analysing expt. data 78−1956
low angle X-ray diffr., pore or particle size distrib. calc. 77−39512
macromolecular structures, struct. factor least squares refinement procedure 77−84573
macromolecules, cryst. struct. refinement by simultaneous minimisation of energy and R factor 79−7517
MAGIC, multisoln. direct methods procedure 79−73062
magic integer generation 78−79497
magic integer phase representation for complex structs., MULTAN program soln. 77−84571
MDKS formula, test of behaviour 77−55207
mean squares smoothed Fourier transforms, method for crystallite size distrib. in polycryst. materials 77−27777
membrane systems, partially disordered, X-ray scatt., anal. method 78−91196
metals, cubic, crystallographic orientations distribution function, computer calc. 80−64827
microfibril dimensions, from small-angle X-ray scattering 79−37574
microstrain values from diffr. line profiles, error correction procedure 78−14244
misfit boundary, X-ray diffr., general soln. 78−51562
misfit boundary, X-ray diffr., special cases 78−63776
misfit boundary crystals, reflection curves 80−92421
molecular charge density projection into spherical atoms, appl. to X-ray diffr. data 78−91187
molecular charge density projection into spherical atoms, density basis functions for first row atoms 78−91186
molecular crystals, thermal diffuse scattering, errors in X-ray diffr. intensities and atomic parameters 79−73155
molecular fragments, oriented, use of struct. factors to find origin 77−51266
molecular packing plotter program 77−15272
molecular replacement method, translation function 77−19820
monoclinic substances, trial and error indexing program for powder patterns 78−34390
Monte Carlo method for phase determ. 79−27869
mosaic crystal, polarisation of diffracted X-rays, Stokes parameters *(French)* 78−9907
multi-beam dynamical diffr. of X-rays, permitted models of propag. 80−107015
multi-solution general form in Patterson method for low symm. system *(Chinese)* 80−107016
multilayered structures, planar, small-angle X-ray data processing, theory 79−37582
multiphase X-ray scatterers, randomness in two- and three-phase systems 80−19667
multiple reflection, correction of single-cryst. intensities for average values 79−23488
multiple-solution direct methods, appl. of magic integers 78−34384
needle crysts., very small, X-ray powder reflection profiles calc., principles 80−100124
negative intensity observations, treatment method 78−75486
non-centrosymmetric structures, statistical props. of normalised-structure factors 79−99028
one-dimensional convolution square roots, fast converging refinement 78−91189
one-dimensionally disordered cryst., X-ray scatt. intensities, disorder parameter reduction 77−84569
one-phase semiinvariants, practical aspects and appls. of probabilistic formulae 80−100119
one-phase structure semiinvariants, of first rank, estimation by generalised second representations 80−107013
optimized conjugate gradient solution for least-squares equations 78−79495
orientation distribution determ. from incomplete pole figures, computer program 78−64804
orientation distribution function analysis from incomplete pole figures normalised by iterative method 80−59344
orientation functions, experimental determ., appl. to diffr. band calc. *(French)* 79−86642
orientationally disordered structures, orientation and position correlations of a mol. 80−14966
orientationally disordered structures, positive definiteness of orientational distrib. functions 80−14958
oscillation diffraction data, processing, for very large unit cells with automatic convolution technique and profile fitting 79−50929
oscillation method, for cryst. with large unit-cells, determ. of relevant parameters 80−14961
overlap electron density, orientation-dependent scatt. factors 78−91190
overlap electron density scatt. factors 78−91191
overlapping Patterson peaks and direct methods, cryst. struct. of prostratin derivative solved 78−55779
P2 space group, compensation of excess intensity 80−107088
paracrystalline materials, weakly absorbing, method for normalising diffr. spectra 79−60220
partial Patterson function, use for superlattice reflection phase determ. 80−79627
particle dimension determination, by direct Fourier cosine transformation, of expt. SAXS data 80−79624
particle dimension distributions calc., general analytic method using scattering data 79−10753
particle-size distribution functions, determ. from SAS data by indirect transformation method 80−38860
pattern representation and manipulation *(Japanese)* 77−55208
pattern-recognition procedure for scanning oscillation films 77−84582

X-ray crystallography calculation methods continued
Patterson anal. ambiguity, direct method treatment *(Chinese)* 78−67611
Patterson function, three-phase invariants derivation method 79−27868
Patterson functions, identification of double peaks, P$\bar{1}$ space group 79−32859
Patterson maxima shape calc., program in AKIT 78−5987
Patterson method, multiple solutions for low symm. systems *(Chinese)* 80−87986
Patterson peak identification in presence of multiple peaks 77−35436
Patterson superposition technique, modified, using multiple vectors 79−32856
Patterson synthesis, partial, derivation of 57 black-and-white symmetry groups, interpretation 79−60296
Patterson vectors in centrosymmetric crystals, symbolic method for identification 78−1952
perfect crystal, disturbed surface layer, X-ray diffr. 77−85038
perfect crystals, X-ray diffr. for finite duration *(Russian)* 80−64825
phase composition, quantitative anal. 77−52709
phase determination of triple products from Bijvoet inequalities 77−55203
phase determination physical significance of triplets in direct methods 78−55776
phase extension, and refinement 80−14963
phase problem, new approach *(French)* 77−51260
phase refinement by Fourier transformation of difference electron density peaks 77−19821
phase relationships, appl. to complex struct., choice of reflexions 78−26380
phase relationships, appl. to complex struct., use of magic integers in phase determ. 78−26379
phase relationships, method of representations 78−9904
phase relationships applic. to complex structures, MAGLIN, successor to MULTAN 77−19816
phase relationships determ. from refl. intensity distrib. 77−84585
β-phycoerythrin crysts., twinned by merohedry, diffr. data treatment 80−108845
polarisation factor, for cryst.-monochromated radiation, weighted scheme for products 80−100122
polarisation factor errors, for cryst.-monochromated X-radiation 80−100121
polycrystal Debye-Scherrer line profile analysis moment methods using Fourier representation *(German)* 77−55202
polycrystal Debye-Sherrer line profile analysis, moment methods using convolution integral *(German)* 77−58923
polycrystalline material, substitutionally disordered, domain size rel. to diffr. 80−28871
polycrystalline materials, deformed, use of statistical regularisation material in X-ray diffr. study of structs. 79−46511
polycrystalline materials, lattice parameter meas., systematic errors 79−10749
polycrystalline materials, phase analysis data, algorithmic processing 78−1953
polymers, processing of small-angle X-ray patterns *(Russian)* 78−71642
polytypic structure with stacking faults, anal. by X-ray powder patterns 78−38577
powder diffraction data, search-match system 80−28874
powder diffraction identification optimisation, vector model 77−15278
powder diffraction patterns of heterogeneous materials, program for separating high-symmetry components 78−1955
powder diffraction system, computer-controlled, with automatic sample changer 77−84577
powder diffractometer patterns, appl. of pattern fitting struct. refinement method 77−76251
powder least-squares program, POWLS 80−1892
powder pattern, intensity distribs. calculation 79−14642
powder patterns, LAZY PULVERIX computer program 77−27784
powder photograph indexing program for orthorhombic crysts. 77−31563
powder reflections, computer program for determining multiplicities, correction for 31m Laue symmetry 79−10759
powder reflections, multiplicity determ., computer program 77−39509
powder samples, peak positions determ. from step-scanned X-ray powder diffr. data 80−103217
powder statistics, line profiles in diffr. spectra of identical crysts. and Gaussian samples, cryst. size distrib. 79−7508
powder statistics, Lorentzian line profiles of Bernouillian samples 78−91188
powder technique, trial struct. generating program for determ. of crystal struct. 80−28881
powder X-ray diffraction data, cubic lattice parameter, Fortran program 77−11440
preferred orientation, in tetragonal powders, X-ray intensity corrections 80−1880
primary extinction, for cylindrical finite crysts. 80−24300
profile analysis, influence on struct. parameters and deformation density distribs. 79−73064
profile fitting method, high-speed X-ray analysis 78−75492
profile-fitting refinement, applic. to cation distrib. determ. in $Zn_2Mg(PO_4)_2$ 77−76376
programmable calculator use for students in crystallographic comput. 80−36811
projection topograms for crystal with dislocations, calc. 79−86647
projection topographs, calc. of intensity profiles for dislocation images 79−14638
protein, min.-variance Fourier coeffs. from isomorphous replacement method by least squares anal. 77−52938
protein data measured on oscillation camera, collection and reduction method 79−29672
protein structures, Fourier refinement 80−51037
proteins, minimisation of functions of many variables appl. to X-ray struct. anal. 80−3589
proteins X-ray scattering data, Soule-Porod plots 77−51273
pseudo Kossel patterns, analysis and appl. *(Japanese)* 77−47301
quartet invariants in space group P1, least-squares analysis 77−84570
quartet theory, probabilistic approach 77−19808
quartz, spherical ground samples, extinction effects, inhomogeneous mosaicity 78−75494
quintets in P$\bar{1}$ and related phase relationships, probabilistic theory 78−9905
quintets use in direct procedures 78−9906

X-ray crystallography calculation methods continued
radial autocorrelation function, significance in X-ray diffr. patterns 80−51048
radial distrib. anal., computer program 80−28875
radial distribution function analysis, improved transformation procedure 79−73061
radial distribution functions, for liqs. and amorphous substances, analytical computation method 80−24301
radial distribution functions, quasi-crystalline model 80−1879
radial part of wave function determ., allowing for electron density distrib. anisotropy 77−4023
reciprocal lattice construction, Weissenberg photographs, axial coords. of diffr. spots 78−5983
reciprocal squares of lattice parameters, determ. by solving linear eqns. *(German)* 80−10452
recurrence relationship, for rapid relocation of misplaced molecules 79−99021
reduced cell for use in cryst. materials identification 77−15271
refinement, modified least-squares formalisms for overcoming the free-atom bias 78−71632
refining the phases of structure amplitudes, automated procedure 78−26376
reflection set generation, computer program 78−18485
reflection sets, unique, computer program for generation, for all space groups 78−18501
residual stress anal., computer controlled, software, precision 78−5712
rotation camera data, empirical method correction for absorpt. and decay effects 80−14962
saddle point method, for SAXS anal., error reduction 80−38868
satellite tobacco necrosis virus struct., detect. and idealisation procedures of non-crystallographic symmetry with phase refinement appl. 80−108840
scattering, small angle, curves calcs., of conc. polymer solns. 79−10783
scattering curves, optimisation of smoothing procedures, polynomial fitting and modified frequency filtering 79−60215
scattering data, calc. from variety of models, computer program using fast Fourier transform algorithm 77−76256
scattering density variance minimisation criteria for Fourier synthesis 78−55774
scattering factors for O^{2-} and N^{3-} in crysts. 79−7521
segment description, of unique set of reflections to data collection and data reduction 80−1881
semiconductor thin film, lattice parameter meas. 78−59720
shift-type packing defects, involving dislocation representations, influence on diffr. pattern 80−107239
short-range order parameters, AC-BD, X-ray diffr. determ. 80−38875
single-crystal diffractometry, peak searching, crystal setting and determining automatic cell constants 80−6319
SIR program, use of negative quartets 80−24304
six-wave diffraction, swinging fringes, expts. on dislocation-free Ge 79−14649
Slater-type orbitals, Z centre case, generalised X-ray scattering factors and Fourier transforms 79−99020
slit correction functions, exact soln. of slit-height correction problem in small angle X-ray scattering 80−79622
slit height smearing intensity correction factor program for small angle X-ray scatt. 79−86645
slit height smearing intensity correction program 79−86644
slit length correction, in small-angle X-ray scattering using the slit function 79−10754
slit-height correction in small-angle scatt. without spherical symmetry, numerical calc. 78−18490
small angle data, least squares method for evaluation without desmearing 78−42851
small angle scatt. curves, comparison of two smoothing methods *(German)* 77−89346
small angle scatt. depend. on divergence *(French)* 80−49045
small angle scattering, collimation correction for finite slit width case 78−79500
small angle scattering, curve anal., by triaxial body models using graphic display model 80−28873
small angle scattering, radial electron density distrib. calcs. indirect Fourier transform method 77−76246
small angle scattering, slit-height correction, exact soln., general method 78−42852
small angle scattering, slit-height exact soln., arbitrary slit transmission functions 78−42853
small angle scattering curves, collimation corrections 78−67623
small angle X-ray scatt., slit height smearing correction prog. 80−10456
small angle X-ray scatt., slit height smearing correction prog. 80−10457
small angle X-ray scattering curve desmearing, FORTRAN program 77−84587
small crystal particles, diffr. intensity calc. method 79−27871
small crystal particles, diffr. profiles calc. 79−27872
small-angle scattering, data evaluation method 77−84580
small-angle scattering, information content and error anal., Shannon sampling 80−59340
small-angle scattering problems, multiple scattering treatment 80−100125
software package to aid diffraction expts., SPADE 79−63195
spectral dependence of integral X-ray refl. coeff., calc. for stearic acid salts 77−11437
sphere tangent to four spheres, new fast direct soln. 79−99019
spherical crystals, mean path length of X-rays weighted by absorpt. 80−28877
spherical X-ray wave, dynamic diffr. theory, numerical results 80−38867
spherical-atom X-ray refinements, net atomic charges and molecular dipole moments, rel. between atomic charges and shape 79−27866
spot broadening, resolution, X-ray and electron beam diffr. patterns *(German)* 80−84033
stacking faults, diffr. pattern calc. 77−31552
step-scanning, determ. of integrated intensities *(French)* 79−37577
stereographic projections, of expt. electron density distrib. 78−91185
stressed polycrystals, X-ray diffr. line broadening, cryst. anisotropy effects *(Russian)* 77−19830
structural fragment, automatic construction, taking account of attainable chem. bond lengths 80−92419
structural fragments located by digital computer on basis of interatomic vector functions, automatic anal. 78−1947
structure amplitude determ. real part, from almost intrinsic refl. curve 77−31562

X-ray crystallography calculation methods continued
structure amplitude phases, statistical-thermodynamic determ. 80−84028
structure amplitudes, data averaging 78−47211
structure factor determs., data processing 78−71631
structure factors, accuracy assessment 78−71636
structure factors from electron density, test on model crystal 78−47204
structure factors from electron density distrib., theoretical foundations 78−47203
structure invariant phase probability, von Mises distribution 78−9901
structure semi-invariants, representations method 80−79724
structure-factor residuals, statistical analysis 78−1948
STRUKTURA, program system for cryst. struct. investigations 80−44071
superlattice, 1D, kinematic and dynamic X-ray diffr. 80−33854
symmetric peak approx. by Pearson type VII distributions 77−27783
$2F_0$-F_c synthesis, theoretical comparison with β and γ' synthesis 79−99018
tangent-formula development, and refinement and Fourier synthesis, theoretical weighting scheme 79−99027
tetragonal powders, X-ray intensity corrections for preferred orientation 80−1880
texture anal. three dimensional, computer simulation of errors 78−64805
texture analysis, numerical calc. of generalised spherical harmonic function *(French)* 78−18484
texture analysis by vectorial method *(French)* 78−18483
texture of materials, data acquisition and processing 80−64828
texture samples, orientation distrib. function reproducibility from pole figures 79−55611
thermal diffuse scattering corrections, choice of elastic constants in evaluation 79−32849
thermal factor refinement procedure, restrained-parameter 80−79628
thermal-motion correction for bond angles, harmonic approx. 78−55777
three-dimensional texture analysis, data processing, subroutines 77−25240
transition metal d-orbital occupancies refinement, from X-ray diffr. data 79−68971
transmission factor calc. 77−84574
triclinic materials, estimating unit-cell vol. from powder diffr. pattern 77−76250
triple products, direct phase determ. from Bijvoet inequalities, probabilistic approach 78−55778
truncation errors in single-cryst. diffractometry, correction formula 77−51267
twinned and clustered crystals, method and program of establishing UB matrices of single cryst. individuals 79−37586
unit cell volumes estimation from powder diffr. data, computer program for triclinic case 77−15277
unitary relation, use to solve phase problem in X-ray struct. anal. 79−90496
unobserved reflexions, simple statistical method for estimating, appl. to organic substances 79−50937
valence electron distribution, in crysts., diffr. data processing 80−92418
Vavilov-Cerenkov parametric effect, to use in cryst. struct. investigation 80−1895
Warren-Averbach method averaging *(German)* 77−58922
Warren-Averbach method verification, distortion model calc. *(German)* 77−58921
wave packet polarisation, in X-ray monochromators, dynamic theory *(Russian)* 80−64826
Weissenberg photographs, triclinic cell parameter determ. from one cryst. setting 79−7518
X-ray crystallography, book 78−94949
X-ray line profile anal., crystalline-diameter distrib. function 77−51277
X-ray line profile anal., unfolding diffr. profiler 77−51276
YZARC, multisoln. direct methods procedure 79−73062
Al {111}, X-ray Huang diffuse scatt. from dislocation loops 80−79797
Be, X-ray scattering, Wannier function calcs. 80−87988
Cu Laue X-ray back reflection pattern solving, algorithm and statistical error analysis 79−99030
Cu, struct. factor f(220), importance of extrapolation to zero extinction 79−19123
Ge, directional Compton profiles, X-ray scattering factors and 1-electron density matrix 80−10458
Li sites, determ. in cryst. structs. using method based on bond-strength calcs. 79−7514
LiF curved crystal spectrograph, diffraction efficiency calc. method 80−79630
LiH crystals, temp. effects on X-ray scattering factors in LCAO calcs. 80−10454
$Rb_2O.SrO.4B_2O_3.12H_2O$, real Patterson function determ., method of rhombs. 78−5986
Si, directional Compton profiles, X-ray scattering factors and 1-electron density matrix 80−10458
Si, multiphonon and one phonon X-ray scattering, and temp. depend. of Debye-Waller factors, shell model calcs. 79−99022
Ti alloy, phase reflex calc. on theoretical roentgenograms of immobile monocrystals 79−23491
Ti-S system, nonstoichiometric, containing stacking faults, X-ray diffr. intensity distrib. calc. 80−28872
ZnS, cubic crysts., having substitutional elastic distortion centres, diffuse X-ray scattering 80−24302
Zr alloy, phase reflex calc. on theoretical roentgenograms of immobile monocrystals 79−23491

X-ray crystallography technique
alloy powder, plasma remelting, spherical monocrystals for X-ray work obtained 78−47205
amorphism, techniques for determ. very short room temp. lifetimes 80−84981
amorphous solids, atomic scale determ., direct methods, review 79−37623
applications in industrial research *(Hungarian)* 78−18486
asymmetric Bragg diffraction from Si, effect on X-ray photoelectron yield *(Japanese)* 77−43110
asymmetric Bragg reflection and extinction-free meas. for optically flat surface 77−65929
attenuation coefficient meas., utilising angle-setting capability of diffractometer 77−1044
Automatic Guiding of Reflexion Position (ANRES-system) *(German)* 78−63637

X-ray crystallography technique continued
azimuthal scanning method, allowance for X-ray absorpt. in single-crystal diffractometry 80−38874
back-reflection pseudo-Kossel technique, appl. to determ. of lattice parameters of talc. 79−82124
biological structures, X-ray and neutron small-angle scattering 79−11889
biophysical data collection from X-ray film, using flatbed autodensitometer, error analysis 77−52937
Borrmann effect, production of nearly monoenergetic X-rays 77−61170
Borrmann transmission topography, for quantitive depth meas. of dislocations 79−86795
broad beam technique with increased resolution 79−86650
broadly divergent X-ray beam method, possibility of obtaining diffr. patterns from polycryst. specimens 80−107020
channeling technique using anomalous transmission, appl. to Si microdefects induced by heat treatment 79−19124
coherent single crystals, angle intervals of incident and reflected X-rays, diffractometry meas. *(German)* 77−43104
combining X-ray and neutron diffr. for charge density distrib. obs., book contrib. 79−60227
composition profile determ. for small diffusion zones, diffr. line broadening 78−67612
crystal centering, and diffractometer alignment errors calcs., appl. to high pressure crystallography 80−22494
crystal monochromators, determ. of polarisation ratio 80−99018
crystal setting, and data reduction, on a PW 1100 diffractometer, program using simple method based on real space 80−59342
crystal transfer, rapid and precise method for preserving orientation 77−76257
crystallite size distrib. meas. in polycrystalline mat. 77−27777
crystallite size distributions, from X-ray line profile anal., smoothing and validity 78−34389
curved monochromator focusing of synchrotron rad., expt. data interpretation 78−75496
data collection measuring procedure, X-ray four circle diffractometer with high pressure cell 78−75495
Debye-Scherrer line profile determ. of particle size and distortion moments *(German)* 78−62182
Debye-Scherrer method, lattice parameter determ., influence of specimen absorption and beam divergence 77−76249
diffraction intensity measurements, meas. time optimisation 78−75490
diffraction pattern parallel meas. 79−94848
diffraction pattern recording on photographic film, student expt. 78−41130
diffraction rotation method for thin layer structure *(Polish)* 79−55608
diffractometric procedure for junction polycrystalline structure study 77−20406
diffractometry and tomography for observation of semiconductor crystal growth and defects 80−73546
diffuse scatt. of X-rays by single crysts, appl. to semiconductor mixed crysts. *(German)* 78−30517
diffuse scattering close to reciprocal lattice points, high-resolution technique 77−39511
diffuse X-ray scatt. meas. by stationary use of Buerger precession camera *(Japanese)* 80−49049
dislocation image contrast, elastic anisotropy influence, appl. to feldspars 78−26573
dislocation image in X-ray plane wave topography, computer simulation 80−54234
dislocation microstress fields, study by X-ray dynamic focusing 79−23613
dislocation obs. using plane wave topography 78−91342
disordered crystals, 1D, structure in formation from diffuse reflexions *(German)* 80−10459
divergent beam scanning of crystal for investig. of imperfections and crystallographic props. 77−7634
divergent X-ray beam technique for noncubic cryst. struct., defect investigs. 77−76259
divergent-beam technique, precision lattice parameter meas. 79−10758
doping method, in quantitative X-ray diffr. phase anal. 79−50941
double-crystal method using nonparallel setting for lattice mismatch meas. between epitaxial layers and substrates 79−28235
dynamic diffraction focusing by elastically cambered crystal 77−15275
dynamical scattering, theory, methods and results, book 78−71628
elastically vibrating single crystal, simultaneous diffr. effect on rocking curve 80−107019
electron density studies, experimental problems 78−71630
electron-density matrix extraction from X-ray diffraction data 77−65930
electronic stationary picture method for cryst. with large unit cell 78−38582
energy dispersive diffractometry, semicond. detector uses and problems *(French)* 80−84031
energy dispersive X-ray diffraction, determ. struct. of amorphous alloys 80−84063
energy dispersive X-ray diffraction method, annotated bibliography (1968-78) 80−36794
energy dispersive X-ray diffractometery, technique, apparatus, data processing, computer profile fitting 77−68892
energy-dispersive diffraction, preferred orientation influence 78−22603
energy-dispersive diffractometry, influence of incident beam polarisation on integrated intensities 78−26382
energy-dispersive diffractometry, intensity meas. on large crystals 77−19834
energy-dispersive diffractometry, optimum resolution 78−42857
energy-dispersive diffractometry, using solid-state detector and continuous X-rays, appl. to Debye temp. determ. for Ag particles 79−50944
energy-dispersive diffractometry for quantitative determ. of preferred orientation 77−25241
energy-dispersive diffractometry using synchrotron radiation 78−18487
energy-dispersive powder profile refinement using synchrotron radiation 78−67613
epitaxial binary diffusion couples, chemical interdiffusion, X-ray diffr. line profile anal. 79−1527
epitaxial film, X-ray topographic measurement, local variations in spacing and orientation of lattice plane *(Japanese)* 78−38585
extended deformation fields, X-ray diffr. meas. method sensitivity 80−28880
extended growth defect characterisation, review 78−30649
extended X-ray absorption fine structure using real space transform, struct. determ. technique 78−23553

X-ray crystallography technique continued
external crystal adjustment, for Lang topography *(German)* 78−59719
extinction elimination by temp. gradient 78−38583
extinction-free measurements with plane-polarized X-rays 77−19849
fibrous polymers, crystallinity and crystallite size meas. 78−30549
film on single cryst. substrate, X-ray method for stress meas. 78−51860
film structure, X-ray and electron diffr. methods comparison *(Czech)* 77−47696
focusing, with (n,m)-positioning of crystals 80−87989
foil, preparation apparatus, for X-ray diffr. study of lattice defects 79−37585
Gandolfi method, lattice parameter meas. in epitaxic layers 79−11040
grain boundary thickness, meas. using X-ray techniques 80−34011
Guinier powder patterns, diffr. line profile function 79−23499
harmonic-free X-ray beams produced using thiourea dioxide crysts. 77−15284
high angle double crystal diffractometry, improvement for meas. temp. depend. of lattice constants, pt.I 80−1890
high angle double crystal diffractometry, temp. depend. of lattice constants, pt.II 80−1891
high pressure X-ray diffraction *(Chinese)* 78−26385
high temperature-high pressure X-ray diffr. study, appl. to press. calibration above 100 kbar *(Japanese)* 78−24809
high-pressure diffraction at liquid He temps., apparatus 77−11442
high-pressure X-ray diffr. patterns, nonuniform line broadening 80−79629
holographic computing step for image display 78−91199
holographic image processing, resolution improvement and three-dimens. reconstruction 77−10862
image digitising system for computer input of crystallographic structure models 79−50939
imaging and diffraction techniques, (book) 79−67441
in situ composites, crystallographic relation determ. by texture goniometry 79−86654
incident beam intensity meas. by absorpt. method 80−68333
indexing of selected area diffr. pattern, graphical technique, for teaching 78−54132
inelastic X-ray scattering 77−55406
instrumentation and data analysis development, in X-ray and neutron small-angle scattering, review 79−10750
interbranch scattering fringes, contrast *(Russian)* 80−64835
interferometer diffraction pattern, amplitude modulated beam 78−63641
interferometry, principles, techniques and appls., book contrib. 78−42862
interferometry with divergent polychromatic beams 79−27867
isomorphous derivative data collection, strategy with oscillation method 80−79633
Kossel diffraction application developments for SEM 78−34405
Kossel X-ray technique, for obtaining crystallographic data in the SEM 78−34391
Lang technique, image forces and dislocation config. 77−27785
large monocrystal X-ray reflection/scanning and transmission topographic methods 80−96415
laser alignment of crystal face perpendicular to axis of rot. 77−15283
lattice constant measurement of single crysts. with $K\alpha_1$-$K\alpha_2$ doublet in two-cryst. spectrometer 79−50938
lattice defects determ. from initial slopes of Fourier coeff. v. order curves for X-ray diffr. 77−7710
lattice deformation determ. from X-ray Pendellosung fringes 78−18499
lattice deformations, determ. by pendellosung X-ray fringes 80−54078
lattice strain distrib. obtained by X-rays, linear and nonlinear *(German)* 78−91200
Laue measurements, variable path and extinction 77−31555
Laue pattern interpretation method for cubic crystals 77−51270
Laue reflections splitting and defects image contrast form. *(Russian)* 80−64833
limited range step-scan method, for rapid X-ray diffr. data collection 79−73069
limited topogram technique for investigation of dislocation distrib., appl. to Si 79−23496
line defects, X-ray topography *(French)* 78−79502
live topography, diffr. pattern on TV screen, book contrib. 78−42864
low quartz crystal setting, enantiomorphism 78−79496
low-angle scattering with C Kα radiation 77−84579
macromolecular crystallography, method for preventing cryst. slippage 77−76258
macromolecular diffraction data collection, FORTRAN program 77−51279
magnetic domains observed by X-ray topographic technique in antiferromag. fluorides 78−14981
metal, FCC, with fibre texture, X-ray method of twin fault probability determ. 79−87817
metal fibre stress/strain curves determ. using X-ray goniometer *(German)* 78−92413
metal whisker, growth axes determ., rapid X-ray technique 77−11830
micellar dimensions determ., small angle X-ray scatt. *(French)* 77−29053
microcrystal size meas. 80−38872
microscopy, possibility of utilizing holographic schemes 79−36861
monochromation using ω/θ scan 78−9908
mosaic structure determ. in large single crystals, rapid X-ray method 79−37584
multiple diffraction, single crystals, studied by X-ray energy dispersive method 78−75499
multiple scattering, secondary reflections and their interference 80−33856
multiwave scattering using two-block P-interferometer 77−62446
nuclear emulsions, use in X-ray topography, development method improvements 79−50940
optical alignment of crystal analyser 77−18148
optical filtration methods, processing of X-ray images 80−87992
orientation of single cryst., diffractometer technique 78−42856
oscillation apparatus for X-ray diffraction 79−63329
oscillation camera data, processing and post-refinement 80−24316
oscillation method, for cryst. with large unit-cells, determ. of relevant parameters 80−14961
particle size meas. of crystallites in soln. by line-broadening meas. 78−18488
Peondellosung fringes, intensity distrib. 77−19836
perovskites with space group I4/mcm, determ. by cryst. struct. 78−75643
phase analysis of minority phases *(German)* 78−26387

X-ray crystallography technique continued
phase determ. in synchrotron radiation X-ray crystallography by anomalous scatt. techniques 78−67618
phonons and struct. transforms., comparison of neutron and X-ray scatt., book contrib. 77−89518
photograph simulations, on storage display, appls. to X-ray topography and TEM 79−14637
β-phycoerythrin crysts., twinned by merohedry, diffr. data treatment 80−108845
plate crystal, simple procedure to vary effective radius of curvature 78−42858
polycrystals, problems of X-ray determ. of dislocation density from one diffraction line *(German)* 78−2129
polymer crystallinity, Hermans-Weidinger graphic technique *(Russian)* 78−75582
polymer films, crystallinity degree estimate by diffraction pattern anal. 78−75555
polymers, crystalline, homophase and heterophase, small-angle neutron, X-ray and light scattering, recent developments 79−10751
polymers, non-crystalline, experimental separation of coherent component of X-ray scattering prior to RDF anal. 80−64838
powder, Guinier camera, film densitometry and pattern search-match procedures appls. 80−3454
powder camera films, calibration method 80−79635
powder diffraction data, search-match system 80−28874
powder diffraction technique appl., in research and quality assurance, impact of computerised data handling 80−73556
powder diffractometry, energy-dispersive, for phase analysis *(German)* 77−24246
powder intensity measurements, struct. factors accuracy 78−9911
powder samples, peak positions determ. from step-scanned X-ray powder diffr. data 80−103217
protein crystallography, synchrotron radiation appl. 77−52936
protein data measured on oscillation camera, collection and reduction method 79−29672
proteins, minimisation of functions of many variables appl. to X-ray struct. anal. 80−3589
quantitative diffraction analysis of cryst. powder using exptl. mass absorpt. coeffs. 78−3390
quantitative structural studies by means of the energy-dispersive method with X-rays from a storage ring 80−24314
quantitative X-ray diffr. anal. of anatase, rutile 79−32857
quartz, resonator, X-ray double crystal topographic assessment of defects 79−50943
Raman scattering edge, atomic struct. and extended modulation 79−99031
randomised X-ray powder diffraction patterns, adjustable sample holder 80−6317
reciprocal lattice construction, Weissenberg photographs, axial coords. of diffr. spots 78−5983
reciprocal space limitations, chart of accessible regions for limited beam-crystal surface angle 78−18493
reflection section topography, technique to determine kinematically reflecting region depths, use in crystal defect obs. 79−50945
review, X-ray and neutron diffraction techniques, advances, book contrib. 79−67453
Rietveld profile refinement method, anal. 80−24315
ring Laue diffr., X-ray struct. anal. method *(Russian)* 80−96416
rotation camera data, empirical method correction for absorpt. and decay effects 80−14962
sample preparation methods, survey 80−1898
Schulz reflection technique for texture meas., effect of X-ray linewidth on defocus correction 77−86255
section topograph technique, high resolution, applicable to synchrotron radiation sources 80−57449
section topography, cryst. dislocation and planar defect images, book contrib. 78−42863
semi-automated system for identifying cryst. materials with powder diffr. data 77−15276
sheet material, ideal texture determ., rapid method using colour slides 77−25226
signal peak recorded profile, influence of integration time const. *(French)* 77−5798
silicate mineral, identification and asbestiform varieties, election optical and X-ray techniques 80−8446
single crystals, lattice parameter determ., modified ratio method 77−43106
single-crystal plates deformations meas., using four-crystal X-ray spectrometer 80−49048
small angle soft X-ray scatt. using synchrotron radiation 77−21425
small-angle scattering of particles and micron-range structures, appl. to erythrocytes *(German)* 78−35812
small-angle X-ray scattering, calibration of absolute intensities, international project 78−67616
SOS substrate quality evaluation by X-ray rocking curve technique 77−76262
spectrometer crystal, isochromat spectroscopic method for 2d value determ. 77−65933
specular reflection coefficient, influence of X-ray beam parameters on meas. accuracy 80−107022
spherical crystal marking for identical remounting 78−18497
strain measurement by Pendellosung effects, expt. on P ion irrad. Si 78−55773
structure factor determs., data processing 78−71631
structure factor phase and intensity correlation, Goldberger technique evaluation, 2D 78−34392
substitutional solid solution comp. from X-ray integral intensities 77−84584
superstructure reflection determ. from pseudostruct. reflections *(Chinese)* 79−10748
surface relief of single crysts. using epitaxial replicas 77−51577
symmetric crystal, semi-empirical absorption-correction technique 77−65931
symmetric crystal, semi-empirical absorption-correction technique for arbitrary orientation 77−65932
synchrotron radiation, props. and appls., review 79−36830
synchrotron radiation applications, review 79−67448
synchrotron radiation appls., characts. and sources 78−74960
synchrotron radiation from electron storage rings, appl. to X-ray topography 80−64830

X-ray crystallography technique continued
synchrotron radiation source for electronic states and struct. anal. *(Chinese)* 80−44075
synchrotron radiation topography, appl. to mag. domains in Fe-Si 78−67620
synchrotron radiation topography for recrystallisation obs. 79−8411
synchrotron X-ray topography dynamic expts. 78−67621
texture, crystallographic, meas. by X-ray diffr. 78−22604
texture topography *(German)* 80−1894
textures materials, residual stress evaluation by X-rays *(German)* 80−40670
thermal gradient problem minimisation for proteins 77−27781
time-resolved X-ray diffr., using position sensitive counter 77−13831
time-resolved X-ray diffraction data collection by position sensitive detector 77−51269
topograph recording, of large cryst. slices, geometrical conditions 80−38869
topographic patterns, spectral sensitivity of TV system for visualisation *(Russian)* 80−62814
topography, new on-line system 80−79638
topography, oscill. technique for cryst. coarse perfection investigs. 78−30518
topography developments, review 80−64836
topography settings, white beam X-ray, for cryst. defects, synchrotron radiation 2-axis spectrometer 78−67619
triple-crystal diffractometer appl. to dynamical and kinematical diffr. from perfect and damaged crysts. 78−55784
twinned and clustered crystals, method and program of establishing UB matrices of single cryst. individuals 79−37586
two-dimensional solid, diffr. arrangement 78−75498
US resonance suppression of anomalous X-ray transmission *(Russian)* 77−89347
Vavilov-Cerenkov parametric effect, to use in cryst. struct. investigation 80−1895
very perfect crystals, topography and goniometry 78−30516
Weissenberg photographs, triclinic cell parameter determ. from one cryst. setting 79−7518
white radiation methods using synchrotron sources 80−44076
X-ray interferometry in multiwave case *(Russian)* 77−1041
X-ray interferometry preliminary results for crystallography, Si lattice constant 79−7522
X-ray line profile anal., crystalline-diameter distrib. function 77−51277
X-ray line profile anal., unfolding diffr. profiler 77−51276
X-ray topography, contrast of images of defects, book contrib. 79−68979
X-ray topography, principles *(Japanese)* 79−82125
X-ray topography, techniques and interpretations 79−67454
Cu, single crystal sintering model evaluation, Kossel interference and digital graphic simulation appl. *(German)* 80−2980
GaP VPE layers, precision lattice parameter meas. by Umweganregung method 79−65047
Si bent crystal gamma diffractometer, X-ray topographic study of large crystals 77−57805
Si, extinction fringes and Burgers vector determ., single-crystal interferometric technique 79−95013

X-ray detection and measurement
see also X-ray spectrometers
absolute low energy system and pulsed high intensity source 77−38531
absorbed dose unit, 1 to 5 J/kg, USSR special standard 77−32956
actively shielded hard X-ray telescope 78−81540
analyser for soft X-ray spectroscopy of excitation potentials 79−21882
angular distribution measurement by ETL quantameter for X-ray emission from thick targets 80−91367
area exposure product monitor, DQ-20 *(Japanese)* 77−73578
area photon detectors evaluation using detective quantum efficiency method 78−37519
astronomical Hadamard transform X-ray telescope 78−53828
astronomy, Ariel 5 satellite, design and performance of high energy X-ray detector 78−53826
attenuation measurements, effects of meas. apparatus 77−38587
autoradiographic inventory methods for nondestructive assay of reactor fuels and fuel assemblies 80−71875
Baldwin-Farmer chamber response at mammographic energies 78−28040
Bayesian deconvolution, appl. and algorithm implementation 78−70103
beam time saving technique for measuring excitation functions in heavy ion reactions 78−70721
betatron, radiation protection meas. 79−29636
bone-seeking radionuclide skeletal burden determ. from in vivo scintillation meas. of head 78−15915
Bragg analyser crystal polarimeters for X-ray astronomy, calibration 77−64664
C-CD array, X-ray sensitivity 77−71413
calorimeter for X-ray pulse dose determ. 77−21628
calorimeters, for meas. of ions, X-rays and scattered radiation in laser-fusion expts. 78−16800
calorimetric measurements, method to distinguish between electromagnetic and hadronic showers 79−748
CAMAC, 2-D anal. of spectroscopic data, electronics 80−5460
cavity chamber, model for determ. of ionisation when exposed to soft X-rays 78−17482
channel plate electron multipliers, detection of hard X-rays (10-140 keV) 77−88322
channelplate detector for SXAPS at primary electron currents >10 μA 79−49362
charge-coupled image sensor, direct soft X-ray response 77−74565
coded aperture imaging with uniformly redundant arrays 78−37812
coincidence intensity meas., tailing convections 79−81141
coincidence meas. of α, X, and γ-rays 79−26851
collective heavy ion electron ring accelerators, X-ray particle beam diagnostics 80−102358
composite X-ray and γ-ray detectors 79−9890
compositional analysis with inner-shell ionisation by radioisotopic β-rays 79−57323
computed tomographic reconstruction noise, effect on detectability 78−40296
computerised tomography, effective photon energy and linearity meas. 80−30841
computerised tomography, expt. dual XE detectors for quantitative CT and spectral artifact correct. 80−76825
computerised tomography, software balancing of multiple detectors during CT scanning 80−46026

X-ray detection and measurement continued
computerised tomography dosimetry, exposure meas. techniques 78−69212
computerized tomography field measurement utilising the partial vol. effect 80−89865
constrained model-based representations of X-ray detector efficiency curves 79−49897
continuous angular scanning meas. system 79−6787
coordinate gas counters for vacuum UV and ultrasoft X-ray spectra 79−89014
cosmic ray electrons, X-ray transient radiation detection, comparison with theoretical predictions *(Russian)* 79−66896
coumarin aqueous system as low-range chemical dosimeter 79−79659
crystal diffraction spectrometers 79−72183
crystal spectrograph with active readout 80−4826
curved crystal X-ray spectrometer, for HEAO-B satellite 78−49331
cyclotron dee voltage calibration using an intrinsic Ge X-ray detector 80−99359
data acquisition using position-sensitive counter *(Japanese)* 78−88774
dental X-ray unit kVp meas. 77−40767
detector calibration in 183 to 932 eV range 77−71717
detector calibration using low energy X-ray sources 77−75016
detector loss meas., synchrotron radiation, from electron storage rings 78−86752
diagnostic radiology, detector sensitivity and image conversion improvement 77−25546
diamond tissue-equivalent dosimeter, for X-rays and gamma-rays 77−56477
diamond-anvil press. cell for X-ray diffr. obs. with solid-state or proportional counter 80−75119
differential energy absorpt. X-ray cassette, radiographic image contrast enhancement 78−20264
dose mean value of specific energy, variational meas. 80−12276
dose rate meter, use as X- and γ-ray secondary protection-level standard 77−81579
dosimeter, for routine meas. with X-ray therapy equipment between 10 and 250 kV 78−28084
dosimeter, low-energy, direct-reading, correction factor energy depend. 78−24144
dosimetry, appl. of cavity theory 80−13947
dosimetry of long-wave X-ray radiation by thermoluminescent method 79−6768
double proportional counter for measurement of radioisotope Auger electrons and X-rays 79−81129
drift chamber based detector for X-ray scatt. expts. 80−58045
drift chambers, spherical large aperture X-ray imaging chamber 77−30721
dual proportional counter for recording transition radiation 80−63458
EAS arrival direction distributions 78−28471
electron-optical streak camera for picosecond pulse detect., book contrib. 77−61138
emulsion blackness-exposure curves for low energy X-rays 79−21842
emulsion chambers, characteristic curves of photographic emulsions 79−49905
energy deposition measurement by thin film resistors 78−29719
energy-dispersive detector, simplex method for fitting Gaussian profiles 79−722
energy-sensitive detectors, simplified calibration procedure 77−38548
exposure rate and absorbed dose meas. for 6-7 MeV 79−26766
extraterrestrial sources, X-ray emission meas. equipment on Salyut-4 78−28521
Farmer ionisation chamber, absorbed dose conversion factors C_λ and C_E 78−40341
film, versatile X-ray detector 78−45763
flat-response subkiloelectronvolt X-ray detector with subnanosecond time response 78−86741
fluorescence spectra, detector response function approach in least squares anal. 80−11989
fluorescence spectra in secondary target energy dispersive spectrom., background reduction 79−100471
focusing Fe line crystal spectrometer for Spacelab 79−25500
focusing gas scintillation proportional counter 77−83461
free air chamber for X-ray exposure standardisation at high quantum energies 80−14053
gas discharge converters of X-ray pictures with Ne filling, memory time 79−26827
gas filled proportional photon counter, for mirror X-ray telescope on Salyut-4 78−86746
gas scintillating proportional counter, for X-ray imaging, performance in medical appl. 79−2153
gas scintillation counter, for high count rate X-ray detection 80−14052
gas scintillation counter X-ray spectrometer performance figures astronomy appl. 79−48673
gas scintillation drift counter for fast X-ray detection 80−888
gas scintillation proportional counter, burst length discrimination system 78−21824
gas scintillation proportional counter, large-area focusing, for X-ray astronomy 79−25494
gas scintillation proportional counter development for satellites 77−71004
gas scintillation proportional counter of large area for X-ray astronomy 79−80222
gas scintillation proportional counter using a photomultiplier tube array 79−76294
gas scintillation proportional counters, props. in soft X-ray detection 79−13600
gas scintillation proportional large area counter, X-ray astronomy appl. 79−45556
gas-filled electroluminescent detector for soft X-rays, constr. and charcts. 80−32569
gas-scintillation proportional counters, high resolution, for X-ray astronomy, developments 77−54439
gaseous discharge proportional counters, ageing mechanism 78−78574
Geiger coordinate counters for UV and X-ray photons 80−69026
grid telescope for imaging hard X-rays, astronomical appl. 79−25501
hard X-ray experiment for long-duration balloon flights 79−25493
hard X-ray imaging instrument, for solar and cosmic sources 78−49332
HEAO-B X-ray Observatory 79−25446
high current relativistic electron beam, X-ray emission, pulsed dosimetry 79−81099

X-ray detection and measurement continued
high density proportional counter, medical imaging of e^+ radioisotope distrib. 79−5399
high resolution gas scintillation proportional counter for studying low energy cosmic X-ray sources 80−58052
high resolution imaging X-ray detector, for astronomical meas. 78−49333
image intensifier, fibre-optic coupled, large-area contrast 77−70534
imaging scintillation detectors, design, astronomical appl. 79−25511
imaging soft X-ray telescope for Spacelab 79−25498
industrial X-ray installation, spectroscopic anal. *(German)* 80−97668
inert gas photoelectron counter, XUV intensity meas. 78−32842
interferometric chopper for neutrons and X-rays 78−82088
ionisation chamber, parallel-plate, collection efficiency in pulsed X-ray field 80−99407
ionisation chamber for X, gamma rays, performance monitoring of radiation shielding 79−6797
ionization chamber, high-pass photocathode, for surface EXAFS 79−68164
K_β X-ray width meas. with bent crystal spectrom. 77−30697
Keithley diagnostic ion chambers, energy depend. of correction factors 78−53507
kVp indirect determ. using digital readout device 78−53486
LAMAR facility for high sensitivity astronomical obs. 79−25497
large M0 K X-ray, anisotropy from Ne on Al foil 78−55254
laser-fusion diagnostics, subpicosecond X-ray streak camera 78−42822
laser-fusion program, LLL, X-ray diagnostic instrumentation 77−76213
leakage radiation meas., effective energy determ. 78−28089
lightning, thermoluminescent dosimetry measurement of radiation 80−36361
limiting accuracies in multiwire proportional and drift chambers 79−3298
luminescent dosimetry 79−8542
lyoluminescence dosimetry using saccharides 77−52881
macromolecular structural studies, with synchrotron radiation, X-ray television area detectors 79−55610
metal photocathodes, for absolute intensity meas. in soft X-ray and vac. UV region 77−71412
metal screen-film detector MTF at megavoltage X-ray energies 80−30868
metal screen-film detectors, radiographic contrast obs. 80−30866
microchannel plate, response to hard X-rays 78−47181
microchannel plate, X-ray quantum efficiency 78−45768
microchannel plate image intensifier, quantum detection efficiency 77−83462
microdensitometer for crystallographic investigations 79−54241
modulation collimator, X-ray imaging device, astronomical appl. 79−25510
molecular biology, time resolved X-ray scatt. expts., rapid data collection systems 80−61740
multichannel semiconductor detectors for X-ray transmission computed tomography 80−58058
multicrystal detection system for localisation and meas. of photon emitters without external collimation 77−32959
multielement proportional counters for low-level ^3H and ^{14}C counting 79−76287
muscle contraction, time-resolved X-ray diffr., data-collection system *(Japanese)* 80−46108
MWPC, anode modulation effects of X-ray beam positions 79−76282
MWPC, appl. to radiation localisation problems in medicine and biology, review 79−5432
MWPC, cylindrical, soft X-ray detection in $p\bar{p}$ spectroscopy 79−3279
MWPC, localisation of X-ray quanta 78−62678
MWPC, Xe filled X-ray imaging, counter, spatial resolution improvement by pulse height selection 77−18744
MWPC appl. high count rate X-ray detection 79−3292
MWPC appl. to molecular biology 79−5433
MWPC avalanche initial angular width determ. 79−31327
MWPC gridded drift chamber for X-ray detection 78−70694
MWPC on cube lattice 79−93875
MWPC X-ray drift chamber for soft X-ray detection 79−18071
neutron activation analysis, X-ray meas. 78−74101
nuclear emulsions, use in X-ray topography, development method improvements 79−50940
one-coordinate detector for rapid multisnap recording on X-ray pictures 78−62282
optical/X-ray framing camera tube 78−37121
organic scintillators, saturation effects to nanosec. pulses of low energy X-rays 79−93880
orthovoltage X-ray therapy, TLD dose intercomparison 80−12272
parallel grid imaging proportional counter optimized for detection of low brightness stellar XUV-sources 80−58049
parallel plate imaging proportional counter and its performance with different gas mixtures 79−45533
pattern, recognition with spatially modulated X-rays 78−45761
penetrameter cassette calibration to 400 kV and extra-focal radiation effects in X-ray tube filtration meas. 78−20242
phosphorescent detectors and X-ray convertors, Symposium, Riga, USSR (Oct. 1966) 79−6243
phoswich detector, field monitoring of alpha-emitting contaminants in environment 78−70646
phoswich detector, reduction of low energy background 77−23369
phoswich detector for ^{147}Pm in-vivo meas. 78−28087
photodiode array, self-scanning, direct X-ray response 77−54032
photoelectric diode with Al photocathode, calibration 77−54033
photographic film, soft X-ray, sensitometry 2.1 to 21.6 Å *(German)* 77−10126
photographic film dosimetry by low energy photon transmission 79−45433
photographic film response to 25 MV X-rays, sensitometric curves, relative dosimetry 80−52376
photon collimation problems, Monte Carlo anal. 78−70724
picosecond X-ray chronoscopy 78−38546
pinhole camera, resolution improvement by image processing 77−30222
plasma electron temp. meas. by soft X-ray energy anal., pulse pileup effects 79−64910
plastic scintillation fast-slow coincidence spectrom., K-shell photoelectric cross section meas. 78−86754
plastic scintillator, neutral radiation incident spectrum determ. 77−54398
polymer films as ultrasoft X-ray counter windows *(Chinese)* 78−82083

X-ray detection and measurement continued
portable X-ray imaging system for small-format applications 79−21886
position sensitive counter, appl. for time-resolved X-ray diffr. 77−13831
position sensitive counter, kinetic X-ray diffr. 78−62283
position sensitive detectors, astronomical appl. 79−25496
position sensitive detectors, conference on synchrotron radiation instrumentation, Orsay, France (Sept. 1977) 78−62999
position sensitive detectors, linear, circular, two-dimens. 78−62281
position sensitive detectors, read-out systems *(Japanese)* 78−33397
position sensitive gas scintillation proportional counter for X-ray astronomy 80−58053
position sensitive parallel plate avalanche detector for heavy-ion X-ray coincidence meas. 77−30719
position sensitive X-ray detector 78−12800
position-sensitive detector, appl. to high pressure X-ray diffr. using diamond-anvil cell 80−79632
position-sensitive detector incorporating self-scanning Si photodiode array 80−52831
position-sensitive scintillation detector for portable stress analyser 80−13190
powder diffractometer proportional counter detector system, digital readout 78−4751
primary standard for determination of absorbed dose in water for X-rays generated at potentials of 7.5 to 30 kV 80−5354
proportional chamber, single coord., synchrotron radiation scatt. method in biopolymer solns. 78−65155
proportional chamber X-ray detection 78−86739
proportional counter, position sensitive, for steel residual stress meas. 77−56211
proportional counter, pulse shape discrimination technique *(Chinese)* 79−93867
proportional counter, wall effect elimination, method 78−4753
proportional counter background reduction by leading-edge discriminator 78−78561
proportional counter design and characts. *(Polish)* 78−41388
proportional counter with slight pulse amplitude shift for X-ray fluorescence anal. *(German)* 78−46213
pulsating potential X-ray machines, filter method for peak volt. and inherent filtration meas. 78−73201
pulsed radiation intensity meas. by counting delayed pulses produced in Geiger-Muller counter 77−46407
pulsed X-ray thermionic tube intensity and dose angular distrib. obs. 79−67450
quantum counters, dead time determ., accuracy estimation 80−99022
radiation quanta, comparison of least-squares and maximum likelihood estimates for counts which follow a Poisson distrib. 79−23487
radiography, diagnostic, X-ray spectra determ., high intensity 80−41217
radiography, exposure meas., energy depend. of correction factors for Victoreen 570 Condenser R-meters 78−3597
radiography, quality assurance meas. for diagnostic X-ray systems 77−40763
radiography beam characteristic time vars. meas. using solid state devices 80−46048
radiography instrument calibration, energy depend. of correction factors for Victoreen 666 Survey System 78−3596
radioisotopes low energy radiation meas. by X-ray detector, absolute method 78−878
radionuclide disintegration rates determ. for EC isotopes 77−57804
radiotherapy, high-energy accelerators, mixed photon-neutron field meas. 80−51267
scanning modulation collimator instrument for HEAO-A satellite 77−71003
scintillating imaging proportional counter as X-ray to light image convertor 77−65063
scintillation detectors appl., using inert gases *(Czech)* 78−86727
scintillators, organic, temporal characteristics and saturation effects for low energy X-rays 79−81125
screen-film detectors, megavoltage OTF meas. technique 79−80736
sealed position sensitive hard X-ray detector having large drift region for all sky camera with high angular resolution 79−48675
secondary-electron multipliers for soft X-ray (60-190 Å) detection 77−21446
self-scanning Si diode array, appl. to plasma diagnostics 77−41739
semiconductor detector for ionising radiation dosimetry, anisotropy of dose sensitivity 78−70705
semiconductor detectors for energy dispersive X-ray spectral analysis, review 80−85237
semiconductor radiation detector, cooled preamplifier systems *(Slovak)* 78−21813
semiconductor spectrometers for elemental anal. in electron microscope 79−11838
semiconductor X-ray detectors, energy depend. efficiency response modelling 79−45560
sensitometry of Kodak RAR 2490 film, for laser plasma expts. 77−35383
Si(Li) detector efficiency for 0.7-6 keV X-ray energy region 79−97928
single photon X-ray detection with a CDD image sensor 79−35836
slow scan SIT detector for X-ray diffraction studies using synchrotron radiation 79−48382
soft, Lexan coating on polypropylene window to eliminate UV sensitivity 79−74273
soft X-ray sealed gas electroluminesc. detector, design and characts. 79−733
soft X-ray spectrometry at high count rates 79−31310
soil samples, meas. trace radionuclide L X-ray detection 78−49020
solid state devices, algorithm for energy deposition at Au-Si (polyethylene) interfaces 77−28648
solid state electrophotographic imaging with ionic dielectric X-ray receptors 78−16899
solid state ionisation current comparator 77−23383
solid-state beam monitor 79−36431
spacecraft instrumentation, induced background radiation 78−85821
spectral energy distribution of diagnostic X-ray beams 77−70530
spectral quality of radiotherapy beams, photoactivation ratios, 15 to 40 MV 77−21619
spectral quality of radiotherapy beams, photoactivation ratios 4 to 15 MV 77−21620
spectrograph for single pulse detection 78−846
spherical drift chamber for meas. ang. distrib. of soft X-rays 77−54423
streak camera, high time resolution, with X-ray microscope *(French)* 78−42823

X-ray detection and measurement continued
streak camera electrode design using plasma simulation code 79−30632
subnanosecond X-ray framing camera, fibre array technique 78−41394
subpicosecond proximity-focused streak camera, for X-ray and visible light 77−79183
superconducting superheated granules as X-ray and γ-ray imaging detectors, astronomical appl. 79−25504
superheavy element data from monazite, background re-evaluation 77−33077
survey instruments, automated calibration and recordkeeping system 77−37876
thickness measurement, determ. by continuum integration 80−31713
thyroid fluorescent scanning system of concentric source-detector design 77−40738
time varying X-ray fields, digital acquisition system 77−57828
TLD, energy and directional response of Harshaw TLD-100 in diagnostic X-ray range 78−11738
TLD, X-ray quality and output determ. in diagnostic range 77−60241
TLD with BeO, for low exposure of personnel, sensitivity, accuracy 77−29209
transition radiation spectra from polyethylene foam interfaces, particle discrimination 78−21805
transitional emission detector, electron identification in cosmic ray background, X-ray detection study 80−4213
transuranic element meas. in vivo at CRNL 77−77993
two channel method with one special counter, X-ray intensity meas. *(German)* 77−6644
two-coord. X-ray detector 78−62284
ultrafast scintillators, response 78−41393
ultrasoft X-ray burst fluence, using fast, large-signal, free-standing foil bolometer 80−4770
Victoreen 555 integral and rate exposuremeter, digital display plug-in module 77−405
wave train length meas. with three-beam case interferometer 78−21310
Wolter type I telescope for rocket appl., X-ray optical props. 79−25499
X-ray anal., conf., Denver, USA (Aug. 1976) 77−70382
X-ray analysis, appls., conf., Denver, USA (Aug 1975) 77−56307
X-ray fluorescence anal. by total reflection *(German)* 80−30314
X-ray imaging, conf., Reston, USA (Apr. 1977) 78−45762
X-ray stream camera, ultrafast X-ray diagnostics for laser fusion experiments 77−79185
xeromammography exposure timing 78−40291
XTR-detector, Monte-Carlo simulation, 0.5-5 TeV cosmic ray hadron interactions *(Russian)* 79−49564
Ar-N_2 gas scintillation MWPC for high-intensity 5-10 keV X-rays 78−82575
Au, X-ray cathode, secondary electron energy distrib. excited at 277 and 1487eV 77−8716
$Bi_{12}SiO_2$ Pockels readout optical modulator, X-ray response 79−64313
$Bi_{12}SiO_{20}$ photoelectret, in optical processing and X, γ ray imaging 80−23764
$CaSO_4$:Dy Teflon TLD discs, metal filters for compnesation of photon energy depend. 80−30901
$CaSO_4$:Tm composite TLD for γ-rays, X-rays, β-rays, and thermal neutrons 78−28076
CdS monocrystalline sputtered X-ray transducer characteristics *(Russian)* 80−47162
CdTe detectors, portable miniature scanner, bone mineral meas. using ^{125}I X-rays 77−44750
CdTe detectors, X-ray fluorescence escape peaks in X-ray spectra 80−9448
CdTe detectors in nuclear medicine, capabilities, limitations, X-ray transmission tomography appl. 77−44748
CdTe photovoltaic mode γ- and X-radiation dosimeters 79−13594
CdTe, use in X-ray detectors 78−86745
CdTe X-ray detectors, energy resolution 77−71722
^{252}Cf fission fragment β-decay, X-ray-β particle coincidence technique 80−74094
CsI photocathodes, efficiency evaluation for soft X-ray diagnostics 80−57442
CsI(Na) scintillating crystals in cosmic X-ray detectors, growth of deactivated layers 77−10554
CuI photocathodes, efficiency evaluation for soft X-ray diagnostics 80−57442
Ge coaxial detectors, n-type high purity, construction and performance 79−41075
Ge, efficiency at very low energies by X-ray double method 79−3286
Ge intrinsic detector, use in borehole sonde for U exploration 77−9547
Ge low energy X-ray detectors, entrance windows 77−71718
Ge planar detector array for Pu detect. in lungs 77−17004
Ge X-ray detector, Au contact layer thickness meas. 80−62627
Ge X-ray detector, efficiency meas. 77−23368
Ge(Li) detector, comparison with Ge(Li)-NaI(Tl) Compton suppression spectrometer for low level activity meas. *(Slovak)* 78−21814
Ge(Li) uncollimated detector, parametric representation of efficiency curves for X-rays 77−18740
Ge(Li)-NaI(Tl) Compton suppression spectrometer for low level activity meas., rel. to Ge(Li) detector *(Slovak)* 78−21814
^3H conc. meas., scintillation detector appl., bremsstrahlung from β-rays 78−55042
HgI_2 detectors, fabrication, appl. to X- and gamma-ray detection 77−83459
HgI_2 detectors, room temp. X-ray spectra of Na and Mg 78−78049
HgI_2 detectors for X-ray, computerized tomography, evaluation 80−89837
HgI_2 in vivo medical probe, DC and pulse counting meas. 78−44593
HgI_2, nuclear detectors, high X-ray fluence irrad., DC currents 77−54415
HgI_2, photoelectronic props. 78−41897
HgI_2 X-ray luminesc., emission band characts., use as X-ray detectors 77−55815
^{123}I assays, coincidence counting of γ- and X-rays 77−14320
^{123}I source sumpeak calibration absolute activity 77−57785
^{123}I two-crystal coincidence counting 78−13394
Kr photo-ionization proportional scintillation chamber 80−58056
LiF TLD for radiotherapy dosimetry in accordance with section 13 of X-ray regulations *(German)* 78−20289
LiF TLD response to high-energy X-rays and electrons rel. to ^{60}Co photons 78−40332
LiH-LiF(Cl), mixed cryst., thermolum., appl. as X-ray detectors 79−6794

X-ray detection and measurement continued
Mg_2SiO_4:Tb TLD, response to X-ray and electron irrad. 79−3285
Mg_2SiO_4:Tb TLD, supralinearity of response to electrons and X-rays *(Japanese)* 78−78503
NaI:Tl scintillator response, γ-ray, (X-ray) rel. $^1/_2$-width energy depend., undergrad. expt. 78−49600
NaI(Tl) detector response using X-ray monochromator 79−93876
NaI(Tl) large area multi-crystal detectors for X-ray and gamma-ray astronomy 77−22070
NaI(Tl) linear response photon counter 79−45567
$^{92}Nb^m$, production and impregnation in polystyrene microspheres for X-ray detector calibration 80−74065
^{103}Pd inhalation studies, derivation of X-ray counting efficiencies for lung Pu 78−85391
Pu-Am survey instrument, β-α-γ-X-ray scintillation detect. probe 78−33376
^{239}Pu, lung burden X-ray counting efficiency, from inhaled ^{103}Pd studies 78−85391
Se, X-ray sensitivity, induced photocurrents, xeroradiographic meas., pair creation energy 80−22490
Si high-resolution X-ray spectrocopy, portable system 79−81117
Si microelectronic p-n junction photon detector 79−26815
Si photodiode array, position-sensitive photon detector for the UV or X-ray range 80−90970
Si:Li detector, escape peaks and internal fluoresc., general geometry case 77−18150
p-Si:P semiconductor detector in radiometric inspection problems 80−62819
Si-Li surface-barrier detectors for electron and soft X-ray spectrometry 80−882
Si(Li) detector, appl. to Am and Pu low conc. meas. in earth samples 78−58505
Si(Li) detector, β-ray background removal in X-ray meas. 78−55091
Si(Li) detector efficiency meas. 78−55108
Si(Li) detector response function approach in least squares anal. of X-ray fluorescence spectra 80−11989
Si(Li) detector system, discrepancies in X-ray excitation efficiencies 80−9450
Si(Li) detector system response to microphonics 79−31333
Si(Li) detectors, escape peak losses 80−27383
Si(Li) detectors, X-ray detection efficiency at off centre point 77−57811
Si(Li) high resolution spectrometer, with thermoelectric cooling 79−26813
Si(Li) photopeak efficiency meas., 0.52-8.04 keV 80−27889
Si(Li), relative photoionisation determ. from X-ray meas. 78−33369
Si(Li) uncollimated detector, parametric representation of efficiency curves for X-rays 77−18740
Si(Li) X-ray detector, Au contact layer thickness meas. 80−62627
Si(Li) X-ray detector, efficiency calib. in range 1-5 keV 77−79504
Si(Li) X-ray detector, efficiency calibration in 1.5 to 60 keV energy range 80−47823
Si(Li) X-ray spectrometer, development, and interdisciplinary appl. *(Hungarian)* 80−18056
^{231}Th, L2/L3 vacancy ratio for internal conversion by γ-X-ray coincidence technique *(Spanish)* 79−97682
X-ray dosimetry, intercomparison and standardisation 80−12270
Xe curved wire proportional chamber for powder X-ray crystallography 79−4210
Xe filled gas scintillation proportional counter in space environment, background radiation rejection efficiency 78−21819
Xe gas hard X-ray detector, risetime discrimination 78−90031
Xe gas proportional counter for astronomical hard X-rays detect., risetime discrimination appl. *(Japanese)* 79−80219
Xe high pressure proportional, scintillation camera for X-and γ-ray imaging 80−99412

X-ray diffraction
see also X-ray crystallography; X-ray diffraction examination of materials; X-ray diffractometers; X-ray scattering
applications, conf., Denver, CO, USA, July-Aug. 1979 80−90613
channelled charged particles, diffr. of emitted radiation 78−75699
cyclic X-ray monochromators, with perpendicular dispersion planes, emission coherence 80−90974
diagnostic radiography, diffr. phenomena on using Al attenuation-equalising filters 79−39486
diffraction from solid wedge, ghost source theory 79−2900
flash X-ray tube for diffraction studies on 2-stage light gas gun 80−86537
Fraunhofer diffraction symmetry, series expansion of Fourier transform 79−50212
generalities and classical methods *(Italian)* 80−87984
grating optimal blazing configuration calc. 80−105762
phase-matched nonlinear interaction of X-rays, possibility in ideal crystals 79−41416
retinal rod photoreceptor membrane orientation in intact eye 77−48790
by sound wave in coherent state 77−84860
strain meas., non-destructive testing method *(French)* 78−15626
synchronous nonlinear interaction between waves on Bragg diffr. in media with periodic struct. *(Russian)* 80−14399
time resolved, muscle contraction kinetics obs., appl., with aid of computer *(Japanese)* 80−56291
zone-plate coded imaging of laser-produced plasmas 77−55167
zone-plate coded imaging on microscopic scale 77−54673

X-ray diffraction examination of liquids
see also liquid structure
acetic acid, liquid, atomic pair correlation functions 79−7596
acetonitrile, mol. pair correl. functions, scatt. intensities, statistical mechs. calcs. 79−1382
acetonitrile, mol. pair-correl. function, X-ray and neutron diffr. 78−26420
alkali chlorides, aq. soln., ion-solvent and solvent-solvent interactions, X-ray obs. 80−44107
alkali halides, molten, ionic radii and X-ray diffr. patterns 78−59732
alkali halides, molten, struct. determ. by X-ray scatt. 78−87609
alkali metal iodide (bromide), molten, struct. by X-ray diffr. 77−4033
2-[4-n-]alkylphenyl-5-[4-n-alkyloxyphenyl]-pyrimidines, X-ray study of smectic modifications 79−32882
aqueous nonelectrolytic soln. microheterogeneous struct., X-ray diffr. study 78−87608
azobenzenes, p-acryloyl- and p-methacryloyl-oxy-p′-substituted, monomers and polymers, liq. cryst. props. 79−99065

X-ray diffraction examination of liquids continued
p-p′-azoxy di-n-undecyl α-methylcinnamate, smectic C layer thickness meas. by X-ray scatt. 78−94986
azoxybenzenes, p-acryloyl- and p-methacryloyl-oxy-p′-substituted, monomers and polymers, liq. cryst. props. 79−99065
benzene X-ray diffr. pattern and liq. models using C-H group scatt. factors 78−6004
benzene-hexa-n-alkanoates and benzene mixture, disc-like mesogens, thermotropic mesophases 79−86699
benzylideneanilines, ordered smectic phases, X-ray diffr. meas. 77−89375
binary melts, short-range order, X-ray and neutron scatt. *(German)* 78−14272
BPBAC, smectic B phase, neutron diffr. and X-ray obs. 78−94973
t-butanol, melting point, structure function, H-bonded hydroxyl groups 79−99053
t-butanol-water, X-ray scatt. intensity composition depend., soln. struct. 78−6005
N-(p′-butoxybenzylidine)-p-n-octylaniline, order parameters in nematic and smectic phases, X-ray diffr. meas. 79−94874
butyloxybenzylidene octylaniline, two- and three-dimensional smectic B liq. cryst. film, long range order 80−96442
butyloxyphenylnonyl oxybenzoate, smectic C layer thickness meas. by X-ray scatt. 78−94986
carbon tetrachloride, mol. struct. factors, X-ray diffr. 77−76291
CBOOA, liq. cryst., nematic to smectic A transition, high resolution X-ray scatt. exam. 78−94984
CBOOA, smectic A phase, specific volume and layer spacing, X-ray diffr. and dilatometry meas. 79−55659
CBOOA, smectic A-nematic transition, X-ray and light scatt. obs. 79−95129
CBOOA, smectic-A reentrant nematic transition under press., X-ray obs. 80−59637
CBOOA/4-cyanobenzylidene-4′-n-octyloxybiphenyl mixture, reentrant nematic phases 79−41953
chloroform, X-ray diffr., struct. of mol. in liq. 78−26421
cholesteryl acrylate, mono- and polymer, liq. cryst. order 78−9942
cholesteryl methacrylate, mono- and polymer, liq. cryst. order 78−9942
cholesteryl methyl carbonate, liq. cryst., low-ang. X-ray diffr. obs., solid and liq. 80−49093
cholesteryl p-acryloyloxybenzoate, mono- and polymer, liq. cryst. order 78−9942
chromatin, reversible conformational transition obs. 79−62179
collimation distortion, effect on diffr. curves 78−34388
colloidal particles, in a flowing solution, SAXS 80−61163
COOB, smectic A-nematic transition, X-ray and light scatt. obs. 79−95129
critical multiple scattering, X-ray induced η 77−76525
α-crystallin, of calf eye lens, small angle X-ray scattering study 79−11891
cyano biphenyl-substituted benzoates, exhibiting reentrant nematic behaviour, polymorphism and X-ray diffr. 79−94890
cyano derivatives, smectic layer spacings 79−46561
4-cyano-4′-octylbiphenyl, nematic-smectic-A transition, high-resolution X-ray and light scatt. study 79−73297
N-p-cyanobenzylidene-p-octyloxyanilene, second order nematic-smectic-A phase transition 77−72681
cyanooctylbiphenyl, smectic A phase, X-ray diffr. study 80−79690
trans-1,4-cyclohexane-di-4′-n-alkoxybenzenes, synthesis and mesomorphic props. 79−94887
trans-1,4-cyclohexane-di-n-octyloxybenzoate, struct. of smectic phases, X-ray diffr. meas. 79−86702
dectran hydrolyzates in soln., branching assessment using small-angle X-ray scatt. 79−41926
dextrans, branched, in soln., cross-section factor correction in small-angle X-ray scatt. data 80−84048
4,4′-di(p,n-alcoxybenzylideneamino)diphenyls, X-ray diffr. study of smectic polymorphism *(French)* 77−76299
α,ω-diarylperfluorpolienes, X-ray spectra, phase transition temp. depend., struct. and mesomorphic props. *(Russian)* 78−38621
dichloromethane, mol. struct. factors, X-ray diffr. 77−76291
dipalmitoyl lecithin bilayer, mol. tilt, X-ray diffraction obs. in gel phase 80−84059
DNA, double-helical model, sedimentation coeff., X-ray scatt. 77−14629
DOBAMBC, smectic, ferroelec. transition mechanism obs. by X-ray scatt. 79−77515
dodecylcyanobiphenyl, pretransitional behaviour of isotropic to smectic A phase transition 79−60487
electrolyte solutions, diffraction expts. and theory *(German)* 78−95935
electrolytes, aq. solns., X-ray, neutron diffr. data, termination errors, Fourier anal. 77−47299
ethylene-propylene copolymer, melt struct., X-ray diffr. obs. *(Russian)* 79−23533
ferrofluids, conc. depend. mag. grain correls., small angle X-ray scatt. study 80−61160
furnace, using thermal image technique, for high temp. molten salt diffr. studies 77−15280
globular proteins, in solutions, new method using X-ray diffuse scattering for investigation of conformation changes 79−12054
HBAB soln. in CBOOA, re-entrant nematic phase 79−14674
HBT, liq. cryst., phase transitions, quenching effects obs. 78−22833
4,4′-di-heptyloxyazoxybenzene, diffuse X-ray scatt. near smectic C-nematic transition 79−95139
p-heptyloxybenzylidene p'-heptylaniline, smectic C layer thickness meas. by X-ray scatt. 78−94986
N-p-n-heptyloxybenzylidene-p'-n-pentylaniline, X-ray diffr. of smectic phases 77−51318
4-n-hexyloxybenzilidene-4′-n-propylaniline, liq. cryst. phases, thermal and structural studies 78−1989
p-n-hexyloxybenzylidene-p-aminobenzoic acid, liq. cryst. phase transitions, X-ray diffr. and DSC meas. 79−86877
HOAB-cholesteryl benzoate mixture, twisted smectic-C and twisted nematic phases, optical and X-ray investig. 77−84634
HxBPA smectic phases, X-ray diffr. and Raman spectra 78−6012
IBPBAC, cryst. struct. and struct. of ordered smectic phases, X-ray diffr. obs. 79−86780
IBPBAC, order parameters in nematic and smectic phases, X-ray diffr. meas. 79−94874
IBPBAC, smectic B phase, neutron diffr. and X-ray obs. 78−94973
industrial wastes, Mg recovering, use of sink-and-float test *(Japanese)* 80−55948

X-ray diffraction examination of liquids continued
intermolecular correlation effects on liquid props. 77−27799
ion-water interactions, survey of diffr. studies 80−24347
ionic liquids, struct. determ., summer school lecture series 80−6349
lecithin/ethylene glycol and lecithin/water systems, lyotropic liq. crysts., X-ray diffr. and microscopic obs. 79−60266
liquid crystal, high resolution X-ray and light scatt. obs. 80−92460
liquid crystal, small-angle X-ray scatt., interpretation of data *(Russian)* 78−59752
liquid crystal, thermotropic, X-ray diffr. obs. of struct. 79−27905
liquid crystal, X-ray structural analysis, computer program for analysing expt. data 78−1956
liquid crystals, X-ray diffr. studies, review 80−100166
low-temperature topography, specimen stage with vacuum chamber *(Japanese)* 79−35901
lyotropic mesophase, mag.-oriented, X-ray diffr. obs. 80−1921
lyotropic nematic liquid crystals, mag. susceptibility, mol. aggregation meas. 80−19690
macromolecules in solution, density contrast, cross verification of X-ray scatt. and pycnometry expts. 79−10757
MBBA, calc. of order parameter from X-ray diffraction data 79−69009
mesogenic materials, tails or smear effects in X-ray diffr. photographs 80−96438
mesophase pitch, magnetically-oriented, phys. props., mol. struct. 80−64885
metal,-density determ. by X-ray diffr. *(Russian)* 78−75529
methanol, Compton profile meas., non-additivity of elastic and inelastic X-ray scatt. 78−43953
methanol-H_2O, liq., zero-angle X-ray scatt., conc. depend. 79−27897
2-methyl-1-propanol, liq. struct. at 20°C 79−32873
4-2′-methyl-butylphenyl-4′-n-octyloxybiphenyl-4-carboxylate, smectic F phase, characterisation and struct. 79−86707
nematic liquid crystal mixtures, binary, induced smectic phases, X-ray diffr. obs. 78−94987
neopentane, liq. struct. by X-ray diffr., −17-150°C 79−27898
4-nitrophenyl 4′-decyloxybenzoate, mol. struct. rel. to mesomorphic props. 77−89372
4-nitrophenyl-4′-alkoxybenzoates, incommensurate smectic A phase 80−10647
nonelectrolyte aqueous solns., X-ray diffr. meas. of struct., scatt. curves 79−10785
p-n-nonyloxybenzylidene-p-aminobenzoic acid, liq. cryst. phase transitions, X-ray diffr. and DSC meas. 79−86877
octyl-cyanobiphenyl, smectic A-nematic transition, X-ray and light scatt. obs. 79−95129
4-n-octyloxybenzoyloxy-4′-cyanostilbene, re-entrant polymorphism, nematic-smectic A-nematic-smectic A, X-ray study 80−34172
octyloxycyanobenzylidene, smectic A, anomalous ordering, Landau-Peierls system 78−30538
octyloxycyanobenzylidene, smectic A liq. cryst., high resolution X-ray scatt. exam. 78−94984
organic liquid, simple, struct. exam. and scatt. data interpret. 80−54096
paradiheptyloxyazoxybenzene, mol. cryst., characts. of mesomorphic transition to smectic phase 79−14920
partial structure factors, freq. modulated X-ray diffr. 77−35440
PBABA, skewed cybotactic nematic phase, X-ray diffr. obs. 79−77504
n-pentyl 4-(4-n-dodecyloxybenzylidene-amino)-cinnamate, X-ray studies in smectic I phase 80−70119
4-n-pentyl-phenylthiol-4′-n-octyloxybenzoate, smectic A-smectic C phase transition, high-resolution X-ray study 80−79921
4-n-pentylbenzenethio-4′-n-octyloxybenzoate, liq. cryst. phase transitions, press. and temp. depend. 79−77730
4-pentylphenyl-4′-benzoyloxybenzoate/TBBA system, smectic A_1-smectic A_2 transition, X-ray diffr. obs. 80−44303
poly(ethyleneterephthalate)-p-hydroxybenzoic acid copolyester, liquid crystalline, X-ray scatt. obs. 78−9949
poly(n-dodecyl L-glutamate), thermotropic polymorphism, low-angle X-ray diffr. *(French)* 78−34601
poly-γ-benzyl-L-glutamate, mag. oriented liq. cryst. solns., order parameter 77−15305
poly-(p-alkoxy-phenyl-p-acryloylbenzoates), nematic polymer, struct. determ. 79−99064
poly-(phenyl-p-acryloyloxybenzoate), nematic polymer, struct. determ. 79−99064
polybutadiene-poly-α-methylstyrene copolymers, struct. obs., prep. *(French)* 80−59401
polydisperse fluid, of hard or permeable spheres, scatt. function 79−86664
polyethylene, melt struct., X-ray diffr. obs. *(Russian)* 79−23533
polyethylene single-crystal suspensions, small-angle X-ray scatt. lamellar thickness determ. 79−10784
polyisobutene solns., X-ray scatt., Kratky cone collimation 80−19681
polyisocyanides, solns., struct. and acidification 80−19915
polymer melt, review of expt. results 79−37636
polymer solutions, at intermediate concs., small-angle X-ray scatt. 79−10779
polymer solutions, small-angle neutron, X-ray and light scattering, recent developments 79−10751
polymeric thermotropic liq. crysts., mesogenic elements and flexible spaces in main chain 79−60269
polyoxyethylene dodecyl ether/water system, lamellar liq. cryst., solubilized hydrocarbon effect on struct. and dislocation pattern 79−94885
polystyrene chain conformations, in conc. solns. and in bulk, small-angle X-ray scatt. 79−10781
polystyrene-polydimethylsiloxane, block copolymer micelles, small angle X-ray scatt. 79−69003
polystyrene-polyisoprene two-block copolymer soln., conformation, small angle neutron scattering, X-ray diffraction, review *(Rumanian)* 80−6348
1-propanol, X-ray diffr. study of struct. at −25°C 77−55227
proteins in solution, small angle scattering anal. using synchrotron radiation and energy dispersive techniques 79−12051
radial distribution functions, method of reducing termination errors 80−24332
rare earth ions, aquo complex form., in aq. chloride soln., coord., X-ray diffr. obs. 79−64975
rare earth metals, struct. factors, high temp. X-ray diffr. obs. 79−7544
rare earth metals 77−76294
review, role of Fourier transforms in struct. determ. 77−27772
review, time-depend. distribs. 77−43102
semiconductor alloy, pseudobinary, phase diagram calc. 78−52786

X-ray diffraction examination of liquids continued
smectic B mesophase, series anal. of steric interaction models, X-ray scatt. calc. 79−86701
smectic B phases, interlayer correlations 79−77502
smectic C* liquid crystal under press. *(French)* 79−99061
smectic C phase, tilt angle determ. by field-induced Freedericksz transitions and X-ray meas. 79−94884
smectic liquid crystals induced phases of liq. cryst. mixtures *(German)* 78−94995
soap system, C_{18} mono-cis-unsaturated, lyotropic liq. cryst., X-ray diffr. and EPR meas., Monte Carlo simulation 78−94981
sodium undecanoate/water system, lyotropic liq. cryst. struct. change due to polymerisation of amphiphilic component 80−59386
spherical particle of nonuniform electron density, small-angle X-ray scatt. 77−7631
statistical mechanical models in X-ray and neutron diffraction data interpret 77−31551
TBBA, liq. cryst., smectic A-nematic transition, cybotactic cluster form., X-ray obs. 78−95138
TBBA, mesophase identification by X-ray diffr., review 80−100166
TBBA, order parameters in nematic and smectic phases, X-ray diffr. meas. 79−94874
TBBA, phase transitions involving ordered biaxial phases, X-ray diffr. study 79−95136
TBBA, smectic C layer thickness meas. by X-ray scatt. 78−94986
TBBA, smectic polymorphism *(French)* 77−35470
TBBA liquid crystal, monoclinic cell parameters of solid, smectic and metastable phases, temp. dependence 80−70122
TBPA, liq. cryst., smectic F phase, X-ray diffr. obs. 80−44122
terephthalylidenebis-4-n-pentylaniline, smectic F phase, characterisation and struct. 79−86707
terphenylene mesophase, X-ray diffr. meas. 79−41946
tetrachloromethane, liq. struct. temp. depend., X-ray meas. 79−77478
trichloromethane, liq., radial pair distrib. function determ. 79−77476
trichloromethane, mol. struct. factors, X-ray diffr. 77−76291
urea, aqueous solutions, mol. associations, X-ray diffr. meas. 77−76290
water, Compton profile meas., non-additivity of elastic and inelastic X-ray scatt. 78−43953
X-ray scatt. intensity composition depend., soln. struct. 78−6005
Ag-Tl, eutectic liquid alloy, structural features, interatomic interaction *(Russian)* 79−77494
$AgNO_3$, molten, X-ray diffr. structural anal. 78−42887
Al, liq., X-ray diffraction analysis 79−4232
$AlCl_3$, aq. solns., order phenomena, X-ray diffr. obs. 80−1915
$Al(NO_3)_3$, aq. soln., X-ray diffr. obs. 77−72541
Al_2O_3, molten, structural, conform. and solidification 77−36491
$AlPO_4$, high temp. behaviour up to liq. state, phase relations, X-ray diffr. and therm. anal. study *(French)* 80−10660
Ar, liq., critical exponent, η, X-ray scatt. 80−92660
Ar, liq., struct. determ. by X-ray diffr., pair pot. calcs. 78−6003
Ar, pair correlation decay rate exponent, small-angle X-ray scatt. obs. 77−76293
AsI_3, molten, X-ray intensity curve, short-range order 77−4034
AsSI, X-ray diffr. study in vitreous and fused states 77−7675
AsSeI, X-ray diffr. study in vitreous and fused states 77−7675
Au-Co, liquid alloys, struct. determ. by X-ray diffr. 78−6006
Au-Co melts, struct., compressibility, X-ray and neutron diffr. 77−11614
Bi, struct. factor, interat. interaction pot., X-ray diffr. obs., 280-800°C *(Russian)* 78−14270
Br_2, struct., X-ray diffr. obs. 78−59733
CS_2, liq., S partial struct. factor, 20°C, from X-ray and neutron diffr. data 77−80407
CS_2, X-ray scatt., reference-site-interaction model, intermol. pot. function 77−11459
$CaCl_2.6H_2O$, liq., structural order 80−33871
$CaO-SiO_2$, molten binary, X-ray exam. of struct. 78−38610
Cd, interference function temp. depend. from X-ray diffr., elec. resist. calc. 77−47332
Cd, liq., X-ray diffr. meas. and interatomic interaction pot. calc. *(Russian)* 78−59735
Cd, small-ang. X-ray scatt., at. microgrouping depend. *(Russian)* 78−14271
Ce-Ni, struct., charge transfer effect 77−62465
$CeO-SiO_2$, molten and glassy state, X-ray diffr. determ. of struct. *(Japanese)* 78−9936
Co melt, struct. charact. time depend. in X-ray studies *(Russian)* 80−24350
Co, near-order struct., X-ray scatt. meas. 77−55231
Co particles, ferromagnetic colloids in toluene, small-angle X-ray scatt., interparticle correlations 79−11831
Co, struct. factor and radial distrib. curves, X-ray determ. *(Russian)* 77−31580
Co-Ge, liq. alloy, structure studied by X-ray diffr. *(Russian)* 79−77493
$Cr(H_2O)_6Cl_3$, aq., solute structuring 77−15298
$Cr(NO_3)_3$, aq. soln., X-ray diffr. obs. 77−72541
Cs, struct. factors, X-ray transmission diffr. expts. 77−47337
$CsNO_3$, molten, X-ray diffr. structural anal. 78−42887
Cu, liq., X-ray diffraction analysis 79−4232
D_2O, atom pair correlation functions, X-ray, electron and neutron diffr. data 77−80406
$EuCl_3$, coord. in aq. Cl^- soln., X-ray diffr. obs. 80−92445
Fe, liq., short-range order struct., O impurity influence *(Russian)* 80−38901
Fe, near-order struct., X-ray scatt. meas. 77−55231
Fe, struct. factor and radial distrib. curves, X-ray determ. *(Russian)* 77−31580
Fe, structure factor near transform. to amorphous solid, X-ray diffr. *(Russian)* 77−31579
Fe-C alloys, struct., neutron and X-ray diffr. meas. 77−51306
Fe-C melt structure, X-ray diffr. study *(Russian)* 80−19685
Fe-Co melt, volumetric characts., molar volume conc. depend. density *(Russian)* 80−33873
Fe-Do alloys, struct. determ. *(Russian)* 77−80409
Fe-Ge melts, struct. determ. 79−41940
Fe-Ni melt, short-range order, m.p. to 1750°C *(Russian)* 78−94966
Fe^{3+}-Fe^{3+} distances, in aq. NO_3^- and ClO_4^- solns., from small-ang. X-ray diffr. maxima 78−42880
$FeCl_3$, solns. and hydrated melts, complexes form., X-ray diffr. obs. 80−24342
$Fe(ClO_4)_3$, soln., struct., X-ray scatt. obs. 78−34421
$Fe(NO_3)_3$, aq. soln., Fe (III) hydration shells, X-ray diffr. 79−29337

X-ray diffraction examination of liquids continued
$Fe(NO_3)_3$ conc. aq. solns., and nonahydrate melt, struct., X-ray scatt. investig. 77−31576
$FeO-SiO_2$, molten, X-ray diffr. exam. of struct. 79−46543
$Fe_2(SO_4)_3$, aq. soln., solute struct. by X-ray scatt., Fe(III) sulphate complexes 79−32875
Ga, interference function temp. depend. from X-ray diffr., elec. resist. calc. 77−47332
Ga, liq., struct., X-ray diffr. obs. 77−84619
Ga, X-ray diffr., 323 and 203K *(French)* 77−84575
Ga, X-ray diffr. exam. of struct. at 203 and 323K *(French)* 78−14268
Ge alloys, molten binary, struct. and charact. of interatomic interaction, X-ray diffr. meas. *(Russian)* 77−1070
Ge-Sn(In) melts, short-range order, radial atomic distrib. functions 79−86673
^{3}He-^{4}He mixtures, structure factor determ. 79−60591
^{4}He, fluid struct. factor meas. in range 5.5 to 7.0K 80−80011
^{4}He, liq., nonsuperfluid, dynamic struct. factor, neutron scatt. meas. 79−46545
^{4}He, liquid, inelastic X-ray scatt. 77−55406
^{4}He, structure factor, momentum transfer meas. 78−22912
Hg, liq., struct., X-ray diffr. obs. 77−84619
Hg, liq., X-ray diffraction analysis 79−4232
Hg, liq.-vap. interface, density profile near triple point, X-ray refl. 78−75821
Hg, liquid structure, X-ray diffr. obs., 173-473K 80−14997
Hg, struct., −30 to 290°C, X-ray diffr., and appl. to electron transport props. 79−46551
Hg-K, liquid, structure factors, X-ray scatt. *(Japanese)* 80−54122
Hg-Na, liquid, structure factors, X-ray scatt. *(Japanese)* 80−54122
In, direct pair correl. function 78−38613
In, liq., X-ray diffr. meas. and interatomic interaction pot. calc. *(Russian)* 78−59735
In, small-ang. X-ray scatt., at. microgrouping depend. *(Russian)* 78−14271
In-Te alloys, atomic struct., X-ray diffr. meas. 79−41934
In-Tl, exam. of magnetic susceptibility in solid and liquid states, and X-ray data *(Russian)* 79−28503
K, struct. factors, X-ray transmission diffr. expts. 77−47337
KI-KCl(CsI) melt, X-ray diffr. struct. determ. 79−41925
KNO_3, molten, X-ray diffr. structural anal. 78−42887
K_2SO_4, molten, struct. analysis using X-ray scatt., correl. with cryst. struct. 80−10486
$LaCl_3$, aq. soln., H_2O coordination of metal ion, X-ray diffr. 79−69000
Li-NH_3 solution, small angle X-ray scatt. meas. 79−14667
LiCl, molten, struct. anal. by X-ray diffr. 78−94961
LiCl-$PbCl_2$, molten, struct. anal. by X-ray diffr. 78−94961
$LiNO_3$, molten, X-ray diffr. structural anal. 78−42887
Li_2SO_4, molten, and molten Li_2SO_4-Na_2SO_4 mixtures, struct. anal. by X-ray diffr. 78−63660
methanol-water mixture, Compton profile meas., non-additivity of elastic and inelastic X-ray scatt. 78−43953
Mg-Bi (30 at.%), molten, short range order and partial struct. factor, neutron and X-ray diffr. 78−9941
Mg-Bi melt; X-ray and neutron diffr., conc. depend., correl. number and nearest neighbours 80−49091
Mg-Cd melts, atomic struct., short range order and melting *(German)* 78−14273
$MgCl_2$, aq. solns., X-ray diffr. study 79−37608
$MgCl_2CaCl_2$, aq. soln., hydration, X-ray diffr. 77−43126
$Mg(NO_3)_2$, aq. soln., ionic coordination by X-ray diffr. 79−29338
$MgO-SiO_2$, molten binary, X-ray exam. of struct. 78−38610
$MnCl_2$, molten, struct. anal. by X-ray diffr. 78−63661
N_2, liq., atom pair pots., X-ray diff. 80−100158
NH_3, mol. correlation functions 77−62459
NH_4NO_3 conc. aqueous soln., X-ray scatt., NO_3^--H_2O interactions 78−42881
$(NH_4)_2SO_4$, aqueous soln., SO_4^{2-}-H_2O interaction, X-ray scatt. 79−77479
Na, struct. factors, X-ray transmission diffr. expts. 77−47337
Na-Cs, struct. factors, X-ray transmission diffr. expts. 77−47337
Na-Cs alloys, conc. fluctuations, X-ray transmission meas. 77−47329
Na-K liquid alloys, struct., X-ray and neutron diffr. meas. 80−107041
Na-NH_3 solution, small angle X-ray scatt. meas. 79−14667
NaCl, aqueous soln., Lennard-Jones parameters, mol. dynamics and X-ray obs. 78−9939
NaCl-KCl(CsCl) melt, X-ray diffr. struct. determ. 79−41925
$NaNO_3$, aqueous soln., X-ray diffraction, radial functions and positional correl. 80−79665
$NaNO_3$, molten, X-ray diffr. structural anal. 78−42887
Na_2SO_4, molten, and molten Li_2SO_4-Na_2SO_4 mixtures, struct. anal. by X-ray diffr. 78−63660
Na_2WO_4, molten, struct. by X-ray radial distribution anal. 78−83717
$Na_2W_2O_7$, molten, struct. anal. 79−41927
$NdCl_3$, aq. soln., H_2O coordination of metal ion, X-ray diffr. 79−69000
Ni melt, struct. charact. time depend. in X-ray studies *(Russian)* 80−24350
Ni, near-order struct., X-ray scatt. meas. 77−55231
Ni, struct. factor and radial distrib. curves, X-ray determ. *(Russian)* 77−31580
Ni-P, molten alloy, struct., X-ray scatt. 78−22640
$NiCl_2$, aq. soln., diffusion and struct. 78−14488
$PbCl_2$, molten, struct. anal. by X-ray diffr. 78−94961
Pd-Ni(Si), melt, struct. and physical-chemical props., thermodynamic props. *(Russian)* 78−18536
$Pd_{82.5}Si_{17.5}$, struct. compared with amorphous state 77−24275
$PrCl_3$, aq. soln., H_2O coordination of metal ion, X-ray diffr. 79−69000
R^{3+} ions, coord. in aq. Cl^- soln., X-ray diffr. obs. 80−92445
$RbNO_3$, molten, X-ray diffr. structural anal. 78−42887
$SbCl_3$, liquid, neutron X-ray diffraction pattern and models 80−38893
$SbCl_3$ liquid, X-ray and neutron diffraction study at 80°C 79−4230
SbI_3, molten, X-ray intensity curve, short-range order 77−4034
SiO_2, molten, struct., X-ray radial distrib. anal. 78−67651
$SmCl_3$, coord. in aq. Cl^- soln., X-ray diffr. obs. 80−92445
Sn, interference function temp. depend. from X-ray diffr., elec. resist. calc. 77−47332
Sn, liq., X-ray diffraction analysis 79−4232
Sn, small-ang. X-ray scatt., at. microgrouping depend. *(Russian)* 78−14271
Sn, structure factor meas. by X-ray diffr., interaction pot. *(Russian)* 77−7655

X-ray diffraction examination of liquids continued
TBBA, liq. cryst., evidence for cybotactic cluster pretransition formation, X-ray diffr. meas. 78−10179
TE, small-ang. X-ray scatt., at. microgrouping depend. *(Russian)* 78−14271
Te-Tl, eutectic liquid alloy, structural features, interatomic interaction *(Russian)* 79−77494
Tl-Te alloys, atomic struct., X-ray diffr. meas. 79−41934
Zn, interference function temp. depend. from X-ray diffr., elec. resist. calc. 77−47332
Zn, liq., X-ray diffraction analysis 79−4232

X-ray diffraction examination of materials
for results of crystal structural analysis see crystal atomic structure see also X-ray chemical analysis; X-ray diffraction examination of liquids; X-ray diffraction examination of microstructure; X-ray diffraction examination of molecular structure
β-eucrypite, glass-ceramics, internal stresses 79−15770
β-spodumene, glass-ceramics, internal stresses 79−15770
acid phthalate crystals, diffr. props., 0.1-2 nm 77−41740
acrylonitrile-vinylacetate(styrene) copolymer films, gas permeation, chem. struct. effects *(Japanese)* 78−31691
p′-acryloyloxyozoxybenzenes, substituted 79−1494
actinide pnictides, single cryst. and film growth by CVD 80−16165
adamantane, Ising, diffuse scatt., hard-core correl., weak-graph method 80−49137
adamantine ceramic, structural, thermophysical and electrophysical props. 80−6918
Ag-Cu fibre composites, highly deformed, lattice defects, X-ray interference lines anal. 80−10559
Agave cantala natural fibre, small-angle X-ray scatt. of densely packed colloidal system, scatt. inhomogeneities 80−76565
α-$AgSbS_2$, X-ray diffr. study of phase transitions in quenched samples 77−15577
air, analysis of dust in AFA filter 77−41142
Al, interstitial clustering following electron irradiation at low temp. 79−19243
aliphatic polymer fibres, supermol. struct., X-ray diffr. and acoustic methods 78−75570
aliphatic-aromatic block copolyamides, synthesis, struct. and dynamic viscoelasticity, DTA and X-ray anal. *(Japanese)* 78−31377
alkali alkanoates, solid-state transitions, diffractometric and conductometric meas. 79−60507
alkali metal hexacupronitrates, incommensurate Jahn Teller phase transitions 79−95156
alkali metals in graphite, organic molecule effects, aromatic hydrocarbons *(French)* 78−27433
p-alkoxy-phenyl-p-acryloyloxy benzoate polymers, mesomorphic struct. 80−38905
n-alkyl 4′-n-alkoxybiphenyl-4-carboxylates, smectic polymorphism, X-ray diffr. and miscibility meas. 79−27912
p-alkylbenzenesulphonate mixed micelles, dimens. determ., small angle X-ray scatt. *(French)* 77−29053
allanite, metamict, phase changes on heating, age determ., x-ray fluoresc. anal. 77−51493
alloy, cold-worked, particle size and strain determ. from X-ray diffr. profiles 78−88588
alloys, concentrated, local atomic arrangements, associated with ordering, review 80−50632
alloys, machining damage, depth of surface layers determ. 80−85094
alloys elastic const. meas. technique 78−7164
Alnico 8 permanent magnet, magnetic props. rel. with crystallographic texture 78−95483
alumina deposition by activated reactive evaporation, struct. obs. 77−44176
ammonium hydrogen oxalate hemihydrate, X-ray TDS effects on at. parameters and electron density distribs. 77−19819
amorphous alloy, and metastable phases, cryst. kinetics, review *(Japanese)* 80−38912
amosite in calcium silicate matrix, detection limit in X-ray diffr. analysis 77−84578
amphiphilic-polymer liquid crystal, NaCl conc. influence on struct., X-ray diffr. study 80−44126
amylopectin, glycerin impregnated, dynamic viscoelasticity *(Japanese)* 80−104203
amylose, glycerin impregnated, dynamic viscoelasticity *(Japanese)* 80−104203
and UO_2-Gd_2O_3 solid soln., high temp. thermal expansion, 298-1700K 78−83979
andalusite, shock-loaded, deform. 80−19873
aniline-HBr, ferroelasticity, orthorhombic to monoclinic phase transition, X-ray scatt. 80−39276
argyrodites, new family of tetrahedrally close-packed structs. 79−60300
Armco iron specimen, elastic const. meas., X-ray diffr. technique 78−5714
aromatic polymer fibres, supermol. struct., X-ray diffr. and acoustic methods 78−75570
asbestos, airborne, X-ray diffr. anal., calibration standards 78−69517
asbestos, chrysotile, crushed, temp.-induced changes in struct. 77−24305
asbestos fibre, identification techniques 77−60018
astigmatic X-rays, diaphragm for investigating materials by this method 80−25935
autunite, random layer structure by grinding, X-ray powder patterns 77−78174
back reflection Kossel patterns, anal. 77−57432
badde-leyite-corundum refractories, qualitative X-ray phase anal. 78−7112
benzalazine, thermal expansion, lattice consts. meas. 78−47539
benzene, phase transform. process, energy-dispersive X-ray diffractometry 80−96631
benzil cored fibres, void-free cryst. growth, X-ray diffr. and optical microscopy study 80−71586
2-benzyl-5-benzylidenecyclopentanone, and substituted form, topochem. single-cryst.-to-single-cryst. photodimerisation 80−66819
(2,2′-bi-2-thiazoline) iron thiocyanate, high spin to low spin transition, X-ray diffr. and Mossbauer obs. 79−38418
biological sample analysis, nanosec. X-ray diffr. pattern techniques 80−26429
biological specimens, use of semiconductor spectrometer SERP-1(M) 79−53288
biological structural determinations using synchrotron X-rays 80−46112

X-ray diffraction examination of materials continued
biological structure, using high sensitivity image intensifier TV X-ray detector 78−89609
biological structures in native form, selection of radiation 78−81087
biomembrane, egg lecithin+myelin protein (N-2), expt. obs. 79−57601
biomembrane struct. parameters determ. method 80−30948
biomembrane system egg lecithin+myelin protein (N-2) 79−57600
bis-(p-toluene-sulphonate) of 2,4 hexadiyne 1,6 diol, X-ray scattering obs. of polymerisation mechanism and phase transition *(French)* 80−70399
bis-p-toluene sulphonate of 2,4-hexadiyne-1,6-diol, X-ray scatt., incommensurable modulated struct. obs. 80−70185
bone, X-ray and neutron diffr. meas. of apatite cryst. orientation and growth, effect of chem. and heat treatment 79−39431
bone tissue crystals, effect of compression 77−25492
borate laser glasses, Cl^- coordinated, Tl^+, Mn^{2+} and Nd^{3+} impurities, absorpt. and X-ray obs. 79−38575
brass, cold worked, surface composition anal. oxidation, sulphidation by X-ray photoelectron spectroscopy 78−11423
α-βbrass, interface struct. of two-phase bicrysts. made by solid state diffusion couple method, X-ray Laue and TEM study 79−28214
brass, stress corrosion cracking, in ammoniacal atmosphere, surface stress change and crack growth *(Japanese)* 77−59986
α-β-brass, two phase bicrysts., deform. and fracture at 150K 80−16388
brass (70:30), cold rolled, optical, X-ray and TEM exam. of deformation struct., and textures 78−88500
brass coated steel wire, surface composition, oxidation, sulphidation, study by XPS 78−11423
α-brasses, cold worked, atomic diffusion kinetics to stacking faults, Laplace transformation method 80−19977
butadiene-styrene block copolymer, oriented, isotropic, struct. changes during deformation *(Russian)* 78−88512
caesium hydrogen tartrate, Cs L_{III}-edge anomalous X-ray scatt., meas. by synchrotron radiation 79−24389
caesium propanoate, solid state transitions and melting process, diffr. and conductometric meas. 80−10670
carbon tetrachloride, phase transform. process, energy-dispersive X-ray diffractometry 80−96631
carbon tetrafluoride+SiC(Si), reaction, metastable C phase prod. 79−29393
carnauba wax, thermoelectret, lattice parameter changes at elevated temps. 80−29674
carnauba wax, thermoelectret orientation parameters, solidification with different cooling rates 79−38444
carnauba wax electrets, residual strain and crystal size of orienting crystallites and their effect on charge behaviour 80−11319
carnauba wax thermoelectret, charge behaviour 80−7276
carnauba wax thermoelectrets crystallite orientation, X-ray diffr. obs. 78−43774
casted steel macroinclusion phase anal. *(Slovenian)* 77−70269
[CC] Ag−(100)InP, metal-semicond.cathode contact, metallurgical, physical, chemical processes 80−107911
cellulose, fibres crystallised from hydrazine, texture by X-ray diffr. 79−69030
cellulose, in Valonia, pole figures and orientation functions 77−86439
cellulose fibres, from jute, crystallinity percentage, estimation by X-ray methods 79−7553
cellulose II, paracrystalline lattice disorder, X-ray diffractograms 78−83751
cement, hot pressed, type III, role of admixtures on pastes and H_2O cured cement, exam. 78−44073
ceramic building materials, breakdown kinetics by X-ray diffr. 80−108526
ceramic mineral, exam. by X-ray diff. at high temp. *(French)* 79−96234
ceramics, local atomic arrangements, associated with ordering, review 80−50632
ceramics, structural stress meas. using X-ray diffr. meas. *(German)* 78−52744
ceresin wax magnetoelectret, X-ray diffr. pattern 78−6014
Ceylon graphite, randomised X-ray powder diffraction patterns, adjustable sample holder 80−6317
charge density, X-ray scatt. factors, gas phase electron diffr. 78−930
Chevrel type compounds, single crystals, growth, stoichiometry, elec. resist. 78−92187
chinaware, vitreous, elimination of crazing by repeating glost firing *(Japanese)* 79−20236
chloritoid, topotactical dehydration, X-ray diffr. and TEM study 79−51057
2-chloronaphthalene, order disorder transition, 253 to 309K, X-ray diffr., calorimetry study 78−75829
cholesteric-type liqiud crystals, small-angle X-ray scattering, mol. ordering determ. 79−60274
cholesterol crystal, polymorphic transition 77−1229
cholesteryl acetate, phase transitions and solid polymorphs 78−2255
cholesteryl propionate, struct. in characteristic phase, X-ray diffr. obs. 79−32891
cholesteryl vinyl succinate (fumarate), polymer+monomer systems, liq. cryst. phase states 79−1494
clay, isotropically consolidated sample prep. with random fibres 77−90531
clay minerals, interstratified, X-ray scattering 79−66685
clay sample preparation for X-ray diffr. anal. 80−97647
clinoptilolite, natural zeolite, ion-exchange, struct. rel. to heating 79−39145
coesite-stishovite transition determ. by in-situ X-ray meas. 77−17092
coke, imbedded in epoxy, X-ray diffr. 79−90495
collagen, rat tail, small angle scattering anal. using synchrotron radiation and energy dispersive techniques 79−12051
collagen fibril, mol. cryst. model as basis for struct. 77−48751
collagen fibril, probabilistic aspects of struct. 78−27886
collagen fibril cross-striation, thermodeform., electron microscopy and X-ray diffr. 77−86438
collagen in skin, selection of radiation 78−81087
collagen investigations, expt. confirmation technique for calc. phases and electron density profile 79−62408
collagen structure in cartilage of intervertebral disc 78−56951
collagen triple helical struct. study using Fourier transform 78−7318
colloidal particles, in a flowing solution, SAXS 80−61163
composite materials, crack growth, conc. criterion 80−65146
composite structure, strain meas. in 10 μm spots, rel. to IC failure 78−86262

X-ray diffraction examination of materials continued
computer-aided system of X-ray stress meas. *(Japanese)* 80−104366
copolyester, melting temperature changes due to heat treatment *(Japanese)* 79−70096
copper (I)-butyrate, dimorphism, X-ray diffr. and fluoresc. *(German)* 79−51090
cord reinforced rubber laminate, interlaminar-shear-strain meas. 79−57043
cordierite, thermal expansion 78−6165
cordierite glass-ceramic, effect of crystn. on thermal diffusivity 79−33127
corneal stroma, small angle X-ray and neutron diffr. study 79−11923
coronene, in n-heptane, Shpol'skii effect multiplets, struct. obs. by ESR and X-ray diffr. 77−62513
corundum, hydrostatic compression, X-ray diffr. meas. 79−99269
corundum, packing errors in structure, X-ray diffr. obs., charact. features 79−46655
cotton fibres, specimen clamps for X-ray angle-tensile meas. 78−4603
crystal, residual stresses with gradient determ. based on method for oblique recording 77−28944
crystalline materials, struct. of grain boundaries using diffr. techniques 80−59478
crystalline substances, deformation and stress meas. using X-ray elasticity method 79−43506
crystallites, concentration variations, X-ray diffraction line profile anal. 78−75491
$Cu_{1.8}Mo_6S_8$, superconducting state, triclinic struct., X-ray powder diffr. anal. 80−6388
cubic polycryst. materials, texture determ. method, X-ray diffr. technique 77−68897
cyano compounds, liq. cryst. phases, incommensurate coexistent density fluctuations 80−79691
cybotactic nematic mesophase 80−92454
cyclohexanol, glassy cryst., diffuse X-ray scatt. study 80−100171
cylindrical curved surfaces, X-ray diffraction meas. of axial stress, geometrical effect anal. 78−63403
cylindrically curved surfaces, tangential stress meas. using X-ray diffractometer 78−87590
DL-cysteine, phase transition obs. at 10°C *(French)* 80−49355
n-decylammonium cadmium chloride, perovskite-type layer cmpd. n-decylammonium chain dynamics 79−99313
degummed silk fibres, mol. motion and fine struct., X-ray, thermal, mech., dynamic loss tangent meas. *(Japanese)* 78−59765
desert varnish, importance of clay minerals 77−86893
detects in materials, direct observation and characterisation 78−88617
4,4'-di(p,n-alcoxybenzylideneamino)biphenyl series, smectic polymorphism, molecular area and tilt angle *(French)* 77−43139
diacetylene monocarboxylic acids, multilayers, struct. phase transitions and polymerisability 80−80129
dialkyl ammonium manganese chloride, phases and structural phase transitions, DSC and X-ray diffr. meas. 77−47574
diamantane, structural changes within plastic phase 79−14929
diamond, extra-reflections on X-ray diffr. patterns obs. 77−59042
diamond, optically active defects, anomalous X-ray scatt. 77−89434
diamond, superhard, dynamic characts. *(Russian)* 77−80593
diamond, synthetic, semiconducting, X-ray exam. of inclusion 77−84788
diamond, synthetic monocrystals, inclusions phase comp., radiographic method 80−100978
diamond, ultradisperse, ESR, particle size and lattice microdistortions 80−97140
diamond (113), scattering factor, Bragg reflection Pendellosung interference study 80−1885
diamond and zinc blende struct. bonding charges 77−76356
diamond anvil cell, high press. diffr., pseudo-Kossel lines 80−79623
diamond composite with Cu-Ti matrix, microstresses, X-ray diffr. exam. 78−56679
diamond powders, Mo coated, X-ray diffr. study 80−100936
diamond synthesis by graphitisation of carbon materials at high press. and temp., Ni influence 80−60795
dibenzoyl, X-ray TDS effects on at. parameters and electron density distrib. 77−19819
1,5-dichloroanthraquinone, solid state transformation, X-ray powder anal. 79−51251
p-dichlorobenzene, mol. cryst., martensitic phase transitions 77−19891
dickite, unusual crystal habit, structural disorder 80−59445
dielectric crystal, dislocation detection by divergent polychromatic beam method 77−35568
dielectric materials, amorphous high permittivity *(Japanese)* 79−73876
p-dihalobenzene series, cryst., chem. perturbation and lattice instability, X-ray and Raman scatt. 77−39654
p-diiodobenzene, polymorphic phase transformation 79−46591
m-dinitrobenzene cored fibres, void-free cryst. growth, X-ray diffr. and optical microscopy study 80−71586
dioctadecyl hydrogen maleate crystals, X-ray spectroscopic true $2d_{cr}$ value, 'effective' 2d value concept of Bragg spectrometer crystals 80−70081
dioleoyl-phosphatidylcholine/dipalmitoyl-phosphatidylcholine bilayer membranes, phase transitions 79−39367
dipalmitoyl lecithin dihydrate, phase transforms., 20 to 70°C, X-ray diffr. obs. *(French)* 78−91436
1,2-dipalmitoylglyceride, DTA and X-ray diffr., polymorphism *(French)* 78−43008
divalent Sr, Ba, Ca, Zn, Cd iodates, complex salts, phase transitions, cryst. struct. *(Chinese)* 80−70171
DNA calf thymus binding to cis- and trans-dichlorodiammineplatinum(II) extended X-ray absorpt. spectra 78−85291
dunite-dolomite mixtures, sintering and minerogenesis 77−66613
E-$Dy_2Si_2O_7$, single cryst. flux growth 79−52097
EABAC, liq. cryst., smectic and nematic, distrib. functions by X-ray diffr. 79−99072
electrodeposition stress in plate, X-ray methods 79−29298
electrolytic Fe based composite metal-powder coating structure *(Russian)* 79−83170
emerald, artificial single crystal, distrib. of Cr^{3+} impurity 80−59505
enstatite-type glass-ceramic, crystn. kinetics and mechanism 77−55241
environmental particulates, anal., X-ray techniques 77−56322
erythrocyte ghost membrane, human, electron density, small-angle X-ray diffr. 77−73510
erythrocyte membrane, phys. state of lipids 78−80835
erythrocytes, X-ray small-angle scatt. *(German)* 78−35812
esters, long-chain, X- and Y-type multilayers, form. conditions and struct. characterisation 80−80127

X-ray diffraction examination of materials continued
ethanol-water system, metastable states, hydrates existence and props., low temp. 78−71835
ethylene oxide, cryst. symmetry, X-ray diffr., far IR and Raman spectra 78−35123
ethylene-vinyl alcohol (<36.3 mol.%) copolymer, elastic moduli of crystalline region *(Japanese)* 79−15715
ethylene-vinyl alcohol (>40 mol.%) copolymer, elastic moduli of crystalline region *(Japanese)* 79−15716
ethylidene-N,N'-diacetamide, interpretation of X-ray diffr. patterns, applic. of dynamic symmetry 78−47265
ettringite, expansion by H_2O adsorption, exam. 78−64806
explosively formed coatings, macroscopic and microscopic stresses, X-ray diffr. exam. 77−44407
FCC crystal, containing extrinsic stacking faults, X-ray scatt. intensity calc. 78−91193
FCC metal, Debye-Waller factor determ. from X-ray data 77−1205
Fe-Cr-Co-Si-Mo, plastic deform. influence on structure and mag. props. *(Russian)* 79−70176
ferrite spinel films, LPE growth and props., SIMS, X-ray diffr., and spin wave reson. obs. 80−34323
ferrite spinels, normal and inverse, solid state chem. expts. for students 80−36815
ferrocene, noncryst. state struct., Willis disorder model *(French)* 78−83732
ferroelectric liquid crystal, new ordered smectic phases 78−51407
ferroelectric tetragonal ceramics, 90° domain-rot. fraction after polarisation, X-ray determ. 80−75992
ferromagnetic, uniaxial, remanent magnetisation from X-ray pole figure data 79−91252
film, thermal strain, strain relax. above room temp. 80−59841
films, X-ray technique for struct. evaluation, device appls. 78−75949
flavocytochrome b_2, rotation function study using X-ray data 79−51035
fluorochloroapatite, synthetic, defect struct. and colour centres obs. *(Russian)* 78−30612
2-fluoronaphthalene, disordered form, thermal expansion, neutron and X-ray diffr. study 80−24621
fracture mechanics anal. and NDT/destructive test correlations 77−90526
freeze-fracture electron microscopy freezing method evaluation by low temp. X-ray diff. 78−57145
frequency modulated X-ray diffr. for multi-element disordered system struct. 77−72525
GaAs-$Ga_{1-x}Al_xAs$ DH crystals, <110> oriented dark line defects 77−80510
gall bladder stones, human, X-ray anal. 80−36081
gehlenite glass, crystallisation kinetics 79−4251
gem stones, synthetic prep. X-ray studies for optimum conditions of heat treatment 80−45263
glass, cryst. defects analysis, microcamera development 77−60002
glass, struct. determ. using EXAFS 80−45169
glass fragments, classification into window and non-window types 80−81401
glass struct. study using small-angle X-ray scatt. 80−84071
glass structure, review 77−65954
glass workpiece, US drilling, structural alterations 78−48555
glass-plumbite-treated cotton, form. of coating at interface 79−15058
glasses, inorganic, struct. by X-ray scatt. diffr. obs. 80−84069
graphite, atomic thermal motion comparisons at 300K based on X-ray neutron and phonon spectrum data 79−7657
graphite, Cs-intercalated, melting and staging, X-ray scatt. obs. 79−19180
graphite, electrochemical insertion of $BF_3(C_2H_5)_2O$ *(French)* 78−27438
graphite, ground natural, Raman spectra, grinding influence 79−42956
graphite, thermal vib. amplitudes from integrated intensities corrected for TDS 78−67780
graphite fluorides, $(CF)_n$ and $(C_2F)_n$, prep., struct., discharge characts., electrode props. 80−89502
graphite intercalation compound, RbC_8, first stage intercalation cpd., X-ray crystallographic obs. *(French)* 79−32966
graphite intercalation compound $C_{24}K$, order-disorder transition, X-ray study 80−33922
graphite intercalation compounds, low energy optical transitions, refl. spectra, and X-ray diffr. 80−25371
graphite intercalation compounds, X-ray struct. factor meas. applications 80−54207
graphite intercalation compounds with K and tetrahydrofuran *(French)* 78−26692
graphite nitrate, structural ordering in intercalation compounds 78−26539
graphite nitrate intercalate, X-ray obs. *(French)* 78−27440
graphite salts, $C_8^+MF_6^-$, (M=Os,Ir,As), struct. and elec. props. 80−70183
graphite surface (002), phase diagram of adsorbed O_2 monolayer 79−73401
graphite-alkali metal-benzene ternary intercalation compounds thermal and X-ray anal. *(French)* 78−27434
graphite-AsF_5 intercalated species, fractional ionisation and identification 80−97397
graphite-$FeCl_3$ intercalation compounds, form. kinetics and microstruct. *(German)* 79−43560
graphite-like materials, orientation, exam. of preferred functions 80−1945
graphite-metal chloride intercalation compound, reduction 78−27821
graphite-$TlCl_3$ intercalation *(German)* 79−43562
graphite/epoxy laminates, stress meas. by X-ray diffr. from fillers 79−43331
graphitic Ceylon and California, occurrence carbyne forms of C, X-ray and SEM anal. 79−77450
graphitised C fibres, intercalation of Br_2 and ICl and its removal 79−43561
halide compounds ABX_3 with perovskite struct., cryst. chem., X-ray diffr. anal. 78−95042
Hastelloy-X, Ni-Cr-Fe-Mo, cyclic oxidation resist. improvement by high temp. etching treatment 80−97627
heart muscle, behaviour of myosin projections during staircase phenomenon 78−53362
p-n-heptyloxybenzylidene-p-aminobenzoic acid, smectic C to nematic transition 79−33076
n-hexatriacontane, cryst. struct., γ-ray effects obs. 78−43048
high energy resolution X-ray spectroscopy, review 80−14959

X-ray diffraction examination of materials continued
high moleculer weight, fibril structure induced by oriented crystallisation *(Japanese)* 79−90575
high pressure diamond anvil for X-ray diffr. up to 100 kb and down to 1.5K 79−73070
high pressure studies using split-octahedron type pressure apparatus 79−49246
high-temperature polycrystalline specimens, X-ray diffr. meas. 77−39503
histidine decarboxylase, determ. of molecular wt. and radius of inertia 79−53025
HOAB, liq. cryst., smectic and nematic, distrib. functions by X-ray diffr. 79−99072
hollandites, cryst. growth and structural props. 80−89129
hollandites, ionic cond., impedance, struct. 78−67856
HxBPA, liq. cryst., transitions, DSC and X-ray diffr., 170-380K 77−15314
ice, Antarctic deep core, X-ray diffr. topographic studies 78−63803
ice, cryst. Ic and Ih phases, diffr. patterns and far IR spectra, isotope effects 78−6662
ice, edge dislocation dipole form. by heat treatment, X-ray diffr. topography 79−99203
II-VI semiconductors, thin epitaxial layer, direct synthesis *(German)* 80−104070
III-V epitaxial pseudobinary compounds, lattice deform. determ. by X-ray diffraction 78−6242
ilvaite, Fe temp. depend. oxidation states, electron hopping, Mossbauer spectra, X-ray diffr. obs. 78−2779
image intensification of X-ray diffr. patterns from biological structures 77−66878
images processing, CALTIX system description *(French)* 77−4872
Inconel 600, PWR primary corrosion products 80−13578
Inconel X, X-ray study of stress meas., elastic const. *(Japanese)* 79−66092
insulation layers of magnetic laminations, FeO, Fe_2O_3, and Fe_2O_4 *(Polish)* 77−12743
Invar, effect of deform. by cold rolling 77−48556
Invar, Fe-Ni (36 wt.%), alloy 36N, effect of melting conditions on thermal expansion coeff. 80−65256
Invar, magnetic and thermal anomalies 80−34603
inverse scattering in Rayleigh-Debye approx., diameter distrib. for thin circular discs 79−24840
inverse scattering in Rayleigh-Debye approx., length distrib. for thin cylinders 79−24839
inverse scattering problem, soln. in Rayleigh-Debye approx. for thin spherical shells 77−48694
ionic radii, limiting values, rel. to crystallochemical radii 79−14730
ionised ethylene-acrylic acid copolymer, heterogeneous ionomer, dynamic mech. props. *(Japanese)* 77−59843
isopropyl ammonium chloroplatinate and chlorostannate, ferroelastic transition, thermal, optical, and elastic meas. 79−28096
isotactic polypropylene/butene-1 copolymers, soln. grown crystals, props. 77−55247
junction polycrystalline structure study 77−20406
kaolinite to mullite reaction series, reexam. of solid state phase transformations 78−64535
kaolinite-mullite thermal sequence, structural analysis and transition phases 77−36484
KCl, pure and Ba-doped, γ-irrad., point defect form. and interaction, X-ray and optical studies 79−65078
Kevlar fibres, effect of crystallinity and orientation on mech. props., Rulands X-ray method *(Japanese)* 79−38952
kidney stones, human, X-ray anal. 80−36081
Langmuir multilayer assembly film structure 77−39740
lapped paper and plastic insulated cable butt gap distribution and spliced joints study 77−77726
lead-containing stabilisers in PVC, degradation obs. using X-ray diffr. *(German)* 79−34297
lecithin cryst. growth rel. to mol. bilayer props. 78−31780
lipid bilayer, site of action of general anaesthetics 78−77008
lipid bilayer structure, X-ray refl. phases from oriented model membrane systems 78−96022
lipid thermotropic clustering in Tetrahymena endoplasmic reticulum membranes 80−85363
liquid crystals, struct. and optical props., neutron and X-ray diffr. obs. 80−24323
lithium ammonium tartrate monohydrate, spontaneous shear strain, X-ray obs. 78−56433
LMFBR, Na test of bellows expansion joints, metallographic study *(Japanese)* 79−67850
lunar regolith particles in Earth's atmosphere, variation in chemical composition in surface layers *(Ukrainian)* 80−12685
lunar regolith samples from Lunar-24, X-ray diffr. and thermogravimetric obs. 80−67598
lysozyme and complex with trisaccharide inhibitor, struct. in soln. and in cryst. 77−81465
α-lytic protease, predicted model rel. to X-ray struct. 79−62178
magnesite refractories, spinel bindal, with reduced thermal cond. 79−83162
magnetic amorphous alloys, atomic struct., energy dispersive X-ray diffr. meas. 79−73100
magnetic material, low texture patterns 77−43109
manganese stearate, Langmuir-Blodgett layers, high resolution X-ray diffr. 80−80126
manganese stearate monolayer, two-dimensional mag., prep. and characterisation 78−31097
margaric acid, evaporated film, X-ray diffr. anal. and mass-spectrography 77−15718
martensite crystal, struct. X-ray diffr. study 78−79565
materials failure and corrosion, microstructural aspects, obs. 79−52610
materials problems and basic research needs rel. to energy resources and storage 78−86703
membrane electron density profiles, determ. method on an absolute scale 79−16358
metal, cold-worked, particle size and strain determ. from X-ray diffr. profiles 78−88588
metal, DC reactive sputtering, glow discharge mass spectrometry and X-ray diffr. 79−38701
metal, textured cubic, residual stress evaluation 80−89435
metal crystallites of supported catalysts, size distrib. from wide-angle X-ray meas. *(German)* 77−84566

X-ray diffraction examination of materials continued
metal-metalloid amorphous systems, thermal instability, crystn. characts. 77−4044
metal-semiconductor interactions, low temp. cpds. form., backscatt. and X-ray obs. 79−28217
metallic glass, bulk and surface properties, review 80−44147
metallic layer, vapour deposited, struct., resist. component manufacture appl. *(German)* 77−55467
metallomacrocytes, mixed valent, cofacial assembly, cond. polymeric material 80−70143
metals, centre of gravity determ. of X-ray diffr. curves 77−51271
metals and alloys, crystn. process, X-ray fluoroscopic obs. 80−50620
meteorite, Cape York, Fe, Mossbauer and X-ray spectra of ordered Fe-Ni phase 77−78727
meteorite, Santa-Catharina, Fe-Ni alloy detection *(French)* 79−16895
meteorite Zaisho, Japanese pallasite, mineralogical and petrographical study 80−46509
N-methacryloil-ω-aminolauric acid cholesterol ester, liq. cryst. polymers, copolymers, structuring *(Russian)* 79−55665
5-methyl-1-thia-5-azacyclooctane-1-oxide perchlorate, single cryst. transform., evidence for intermediate state 80−88078
methylammonium chromium selenate, lattice consts. and ferroelec. props. 79−33641
methylammonium gallium selenate, lattice consts. and ferroelec. props. 79−33641
4,4′-methylenebis(1,3,5-trimethyl-4-imidazolin-2-one), cryst. and mol. struct. 80−107201
$Mg_{1.34}Fe_{0.16}Al_{0.12}Ti_{0.38}OBO_3$, warwickite, cation distrib. from X-ray struct. and Mossbauer spectra anal. 79−1424
$Mg_{70}Zn_{30}$, amorphous alloy 77−27835
mica, defects effect on epitaxial film struct. 78−26794
microparacrystallites, small angle X-ray scattering 79−10813
minerals, thermal annealing of ion tracks 78−20604
mixed-chain silicates, new ordering schemes 79−99142
mixes, ordered, characterisation 80−16215
Mo-Ni powder mixtures, form. using electric discharge sintering 77−12563
modulated structures, X-ray diffr. 77−39502
montmorillonite, physicochemical and engineering props., k-fixation effect *(Japanese)* 78−31366
multiphase material, X-ray determ. of elastic moduli *(German)* 79−91876
multiphase system, second phase vol. fraction determ. using incomplete pole figures 79−11741
multiphase unknowns, identification by computer methods and quality of X-ray powder data 80−3452
muscle, active frog skeletal, isometric tension, slow stretch effect, X-ray diffr. study 78−80906
muscle, frog skeletal, time resolved X-ray diffr. obs. during isotonic twitch 79−83836
muscle, myosin regulated, changes in crossbridge attachment 78−53361
muscle, myosin subfragment-1 attachment to actin, effect on equatorial X-ray refls. 78−27880
muscle, vertebrate striated, camera for low angle diffraction expts. with synchrotron radiation 77−87888
muscle contraction process, 10 ms time resolution X-ray diffr. 80−61741
muscle thin filaments, method for anal. of X-ray diffr. patterns 79−39348
muscovite mica, annealing of latent tracks of heavy ions *(French)* 79−19290
myelin, frog nerve, comments on the paracrystalline nature 79−16161
myelin, paracrystalline nature 77−52748
myelin membrane, frog, with paracrystalline lattice distortions, X-ray determ. of electron-density profile 79−11903
myelin swelling and meas. of forces between membranes 79−62204
myosin heads movement during a heart beat 79−48207
myosin muscle filaments, crustacean, struct. of backbone 79−20512
naphthalene, mag. polarised electret, X-ray diffr. obs. 78−43775
nematic binary mixture, smectic phase form. 78−26670
nematic liquid crystal with lateral substituents, mol. struct. effect 78−51411
nerve myelin, phasing the small-angle diffr. pattern 79−57588
neutron-bombarded, diffuse X-ray scattering *(Russian)* 80−92560
nickeliferous limonites, pressure leaching for Ni extraction, using H_2SO_4 78−39717
nitrobenzene, anion radical, in benzoate crysts., EPR and X-ray diffr. obs. 77−1597
NMP-TCNQ, X-ray diffuse scatt., and cond. study 80−49701
non-crystalline materials, pair distrib. functions determ. 77−72522
noncrystalline metals, struct. determ. by X-ray diffr. method *(Chinese)* 79−82126
p′-nonylhydroxybenzoic acid, struct. characts., cylindrically symmetrical interatomic-distance function 77−11482
nosean identification, in sodalite and conversion of nosean sodalite 80−84907
nucleosome core particles of chromatin, struct. 77−86440
nylon 66, doubly oriented, annealing of drawn and rolled samples, struct. 78−52859
nylon 66, polymorphism 79−14694
nylon 6, oriented glassy, mol. wt. influence on cryst. rate 80−44156
Nylon 6, small-angle X-ray scatt. struct. changes w.r.t. thermal and mech. history 79−41976
Nylon 6, solution crystallization 79−86719
Nylon 6 film, prior high-press. treatment effects, weight swelling, density, IR crystallinity, X-ray and viscosity obs. 80−81025
nylon II, high-press. X-ray structural study 78−14296
nylon-11, folded-chain crystal, pressure-induced crystallisation from melt, annealing 77−84671
Nylon-12, hydrostatic extrusion, struct. change *(Japanese)* 79−15693
Nylon-12 film, casting conditions effect on polymorphism 80−84903
nylon-6, pressure-crystallised, morphology and structure 77−84669
Nylon-6, shish-kebab struct., obtained from quiescent soln. by self seeding 80−15017
Nylon-6 fibre, crystal struct., WAXS obs. 80−15015
nylon-6 pressure-crystallised, annealing under pressure 77−84670
nylons 6, 66, 610, change in cryst. struct. with temp. 77−15324
obsidian, Lipari and Teotihuacan origin, Mossbauer, magnetisation, X-ray diffr. and fluoresc. study 80−46173
n-octadecanol, growth of high temp. α-phase crystals in γ phase single crystals 78−71700

X-ray diffraction examination of materials continued
octadecylacrylamide films, oriented ultrathin, radiation-induced solid state polymerisation 80−80128
olivines, lunar, Weissenberg photographs, reciprocal lattice from diffr. spots 78−5983
one-dimens. ionic conductor, modulation and incommensurability 80−19980
one-dimensional conductor, CDW in random pot., diffuse X-ray pattern *(Russian)* 77−69264
OOAB, liq. cryst., smectic and nematic, distrib. functions by X-ray diffr. 79−99072
order-disorder structures, X-ray powder patterns features 80−38864
orientationally disordered cryst., diffuse scatt., hard-core correl., weak-graph method 80−49137
orthosilicate chloritoid, layered, disordered, electron microscopic and X-ray anal. 78−75511
oxamide, thermal expansion tensor, calc. from lattice constant changes with temp. 77−76582
p-n junction struct., X-ray topography visualisation during prep. *(Russian)* 78−26386
palmitic acid, evaporated film, X-ray diffr. anal. and mass-spectrography 77−15718
para-polyamide based fibres, struct. deform. props. 80−60928
paradiheptyloxyazoxybenzene, mol. cryst., characts. of mesomorphic transition to smectic phase 79−14920
parallel cylinders radial size distrib. 79−100450
partially film coated crystal, strain field, deform. model and X-ray topography *(German)* 78−83653
pentaerythritol, Bragg reflection, thermal diffuse scatt. meas. *(German)* 78−75509
peptide linkages, H bonding effects, review 77−10783
perfect crystal, disturbed surface layer, X-ray diffr. 77−85038
perlite, low temp., processes occurring during firing 80−11607
Permalloy RF sputtered films, struct.-sensitive mag. props. 80−34705
perovskite, Re containing, new seignettomagnets and ferroelectrics 78−19425
PET, amorphous, intrinsic birefringence calc. from wide angle X-ray scatt. 80−108178
PET, crystallised in liquid environment, exam. of crystallisation kinetics and X-ray scattering 79−41980
PET, stress induced crystallisation, X-ray and light scattering obs. 79−99083
PET fibres, amorphous, exam. of birefringence 80−11360
petroleum, study of colloidal nature using automated Bonse-Hart X-ray small-angle scatt. unit 79−16044
phase analysis, quantitative, optimisation *(German)* 77−84583
phase form. and relations, phys. props. 79−43218
α-phenazine, multiple scattering, secondary reflections and their interference 80−33856
p-phenyl-benzylidene-p'-alkylaniline, ordered smectic B phase, mol. length, influence on characts. *(French)* 79−14671
phloroglucinol dihydrate crystals, growth characts., X-ray diffr. and optical microscopic study 79−19986
phospholipid bilayers, direct obs. of hydrocarbon chain tilt angle 79−34481
piezoelectric crystal, X-ray refl., oscill. elec. field effects 79−78625
piperidine solution of PbI_2, crystn. of intercalation cryst. 80−16170
plastic deform. and fracture *(Japanese)* 79−66117
plastic deformation incompatibilities, resulting from moderate cold drawing, X-ray line broadening determ. *(French)* 79−43265
plastic solid state nuclear track detectors, sensitivity and struct. variation 79−49912
plastic zone at tip of fatigue cracks 77−56058
PMMA, amorphous, electron microscope and small angle X-ray studies 77−84666
PMMA, atactic, elastic strain detection by X-ray scatt. 80−25751
poly(1-butene), melting and annealing behaviour, X-ray diffr. and DTA 79−28083
poly(γ-n-amyl L-glutamate), crystal transition, X-ray diffr. exam. of structure 80−24374
poly(γ-n-butyl L-glutamate), crystal transition, X-ray diffr. exam. of structure 80−24374
poly(γ-n-ethyl L-glutamata), crystal transition, X-ray diffr. exam. of structure 80−24374
poly(γ-n-propyl L-glutamate), crystal transition, X-ray diffr. exam. of structure 80−24374
poly(chlorotrifluoroethylene) films, crystalline superstruct., mol. orientation, X-ray diffr., depolarised light scatt. 78−71685
poly(dimethyl siloxane), networks formed by gamma irradiation, crystallisation 77−51330
poly(L-alanine) fibres, mol. motion and fine struct., X-ray, thermal, mech., dynamic loss tangent meas. *(Japanese)* 78−59765
poly(m-xylylene adipamide), crystallisation induced by water absorption *(Japanese)* 79−90573
poly(N-vinylcarbazone), charge transport and struct., bromination effect 78−11516
poly(p-phenylene terephthalamide), crystallised during polymerisation, morphology *(Japanese)* 77−51328
poly(paraphenylene terephthalamide), nematic structure by optical and X-ray methods *(French)* 77−31584
poly(tetramethylene terephthalate), struct., X-ray obs. 80−19725
poly(vinylidene fluoride) films, piezoelec. response depend. on phase I vol. fraction 80−20593
poly(vinylidene fluoride) films, poled, piezoelec. activity and field-induced cryst. struct. transitions 80−20592
β-poly(vinylidene fluoride) films, single cryst. orientation, piezoelec. 80−20591
poly 2,3-dichlorobutadiene, struct., morphology, polymorphism 79−65008
poly-1-butene, annealing and melting behaviour 79−38871
poly-ε-caprolactone-PVC blends, morphology 79−69019
poly-m-phenylene isophthalamide-ε-caprolactam, complex polymer cryst. 78−9967
poly-n-benzamide, lyotropic liq. cryst., structural orientation *(Russian)* 77−31593
poly-p-benzamide fibre, supermol. struct., X-ray diffr. and acoustic methods 78−75570
poly-p-phenylene terephthalate, high modulus fibre, struct. obs. 78−75564
poly-Schiff bases, thermotropic smectic B mesophase *(French)* 79−27911

X-ray diffraction examination of materials continued
poly-[1,2-bis-(p tolylsulphonyloxymethylene)-1-butene-3-inylene], defect imaging 77−15418
polyacetylene:I charge transfer complex, struct. 79−74052
trans-polyacetylene, bulk crystallinity, small-angle X-ray diffr. study 80−103263
polyacetylene-I_2, highly conducting, Raman, XPS and X-ray diffr. obs. 78−80454
polyacrylonitrile, copolymerisation with poly-2-hydroxyethyl methacrylate rel. to crystallinity 80−38935
polyacrylonitrile, new model for structure, small-angle X-ray scattering and TEM study 79−77531
polyacrylonitrile, single cryst. formation, during soln. polymerisation, struct. determ. 80−38938
polyacrylonitrile, struct. of heat treated fibres, X-ray diffr. 78−83752
polyalkane imides, crystallisability, supermol. and crystalline structures 80−84100
polyamide, aromatic, fibre, high modulus, mol. and supramol. struct. 80−79710
polyamide blends, formation by injection moulding, structs. *(Russian)* 80−44155
polyamide-6, fibrillar struct. and annealing, small-angle X-ray diffr. 78−75565
polyarylate organosiloxane polyblock copolymer, struct., props., phase conversion *(Russian)* 79−65010
polyaryloxyphosphazene copolymers, thermal, morphological and rheological props. 80−103265
polybutadiene-poly-α-methylstyrene copolymers, struct. obs., prep. *(French)* 80−59401
polybutene-1 film, deform. mechanism, rheo-optical meas. 80−21041
polybutene-1 film, tubular-extended, anal. of orientational and form birefringence 80−29712
polybutylene terephthalate, melt crystallised, solvent crystallised films and moulded bars, morpholigical obs. 80−84101
polybutyleneterephthalate, drawn annealed, struct. and props., X-ray scattering 79−7552
polycaproamide, oriented filaments, mech. props. 80−66550
polycaprolactam film, subjected to 9 kV elec. discharge, X-ray obs. *(Russian)* 79−23536
polycarbonate, amorphous, electron microscope and small angle X-ray studies 77−84666
polycarbonate, bisphenol A, WAXS pattern, temp. effect and thermal history 80−93583
polycarbonate, highly hot-drawn, mechanical prop. and phys. struct. changes 78−14293
polycarbonate, struct. ordering changes after annealing 79−94921
polycarbonate fibre, highly-oriented, drawing behaviour and mech. props. 78−76708
polyconjugate system, interrelation between physicochem. props. and microstruct. 78−55816
polycrystalline materials, deformed, use of statistical regularisation material in X-ray diffr. study of structs. 79−46511
polycrystalline materials, size and angular spread of coherently reflecting regions, X-ray microdiffraction method 80−24311
polycrystals, single phase, stress strain relations by X-ray diffraction *(Russian)* 80−5999
polycrystals containing defects with Coulomb displacement fields, X-ray scatt. *(Russian)* 78−38576
polydioxolan, crystallisation, morphology and melting props. 78−14297
polyester filaments, solvent-induced crystallisation 78−83754
polyesters, thermotropic, quiescent crystn. 80−38937
polyethylene, γ-irrad., asymmetric 002 X-ray line profiles, analysis 80−96567
polyethylene, {110} twinning mode, X-ray obs. 77−35572
polyethylene, adhesion to Cu, reactions of CuO with Cu or polymer 79−39118
polyethylene, amorphised by γ-irrad., interchain ordering, X-ray obs. 78−30545
polyethylene, amorphised by γ-irradiation, radial distribution function anal. for degree of interchain ordering 79−23530
polyethylene, amorphous-cryst., highly oriented, plastic deform. rel. to supermol. struct. *(Russian)* 79−51010
polyethylene, crystn. under high pressure 80−38946
polyethylene, doubly oriented, low density, deformation and structure, exam. 80−11705
polyethylene, fibrillar, high mol. wt., oriented crystallisation, heat treatment effect *(Japanese)* 80−25738
polyethylene, fibrous samples, struct. obs. by low-angle X-ray diffr. 78−34445
polyethylene, high density, cold-drawn, IR spectroscopy and X-ray diffr. 77−4764
polyethylene, high density, solid-state extruded, pole figure anal. 78−18556
polyethylene, high press. phase, US, DTA, and X-ray diffr. study 80−75188
polyethylene, high- and low-density, crystallinity degree, comparative obs. *(Polish)* 80−1943
polyethylene, high-density oriented, lamellar struct. obs. 77−55244
polyethylene, high-press. phase transforms., X-ray diffr. obs. 77−80617
polyethylene, lamellar two-phase systems, interface distrib. function determ. small-angle scatt. 79−10812
polyethylene, linear, cold-deformed, texture and molecular chain mobility 78−19805
polyethylene, linear, crystallised from melt, effect of crystallisation time on density, mech. props., X-ray scattering 80−25680
polyethylene, linear, glass transition temp. 80−15225
polyethylene, low density, α mgch. dispersion in relation to spherulite deform. mech. 80−25781
polyethylene, low density, deformed in tension, lamellar reorientations 78−84914
polyethylene, low-density, temp. changes in large period structure *(Russian)* 77−31603
polyethylene, low-temp. relax., effects of chem.- and electron irrad.-crosslinking 79−4990
polyethylene, melt-crystallised fractions, surface and full-strand melting, small-angle X-ray scatt. obs. 80−84279
polyethylene, nascent, electron microscope study 80−38940
polyethylene, observation of deformation process with X-ray TV system 78−15610
polyethylene, oriented, high temp. deform. X-ray diffr. expts. 77−56028

X-ray diffraction examination of materials continued
polyethylene, oriented, stress-strain curve, analogy with van der Waals isotherm 77−59869
polyethylene, roll oriented, superstructural change during uniaxial extension *(Japanese)* 77−52422
polyethylene, solid-state extruded, exam. of props. 80−11669
polyethylene, structural changes induced by high elec. field *(Japanese)* 79−23532
polyethylene, structure change on uniaxial compression *(Russian)* 79−34119
polyethylene, supermolecular structure, polymerisation at low pressure *(Russian)* 79−64126
polyethylene, terephthalate, amorphous, electron microscope and small angle X-ray studies 77−84666
polyethylene, ultra-high-strength filaments, soln. spun/drawn, mech. and thermal props. 80−40440
polyethylene, ultrahigh modulus linear, annealing effects on mech. stiffness and struct. 79−91717
polyethylene, welded, exam. of neutron irrad. effects on tensile characts. *(Japanese)* 78−84918
polyethylene, X-ray diffr. at press. up to 14000 kg cm^{-2}, 298K 77−35492
polyethylene, X-ray scatt., models for stacks of lamellae 79−37638
polyethylene, Young's modulus, crystallite thickness 78−76689
polyethylene cryst., unit cell variations with temp. and high press. 78−47250
polyethylene crystal, longitudinal growth in flowing soln., melting of continuous fibrillar crystal 80−19917
polyethylene fibre, high-strength high-modulus, morphology and tensile prop. relations 80−103264
polyethylene fibres, high density, ultra oriented, physical, mech. props. 80−25649
polyethylene fibril, high mol. wt., high melting point crystal *(Japanese)* 80−38954
polyethylene films, uniaxially and doubly oriented, crystallite size determ., microparacrystallite lamellar surface identification 78−48431
polyethylene high press. phase, struct., phase diagram and compressibility 78−9961
polyethylene melt spinning, extensional flow induced crystallisation 78−55818
polyethylene oxide, nascent and annealed, X-ray study of crystal structure 80−64922
polyethylene oxide 2000-200 mixtures, Raman scatt., small-angle X-ray scatt. 77−52089
polyethylene oxide-polystyrene-polyethylene oxide triblock copolymer, surface and full-strand melting, small-angle X-ray scatt. obs. 80−84279
polyethylene terephthalate, fibre, melting in crystn., intermediate and amorphous phases 77−84898
polyethylene terephthalate, glass-rubber transition determ., small-angle X-ray scatt. 78−95145
polyethylene terephthalate, glassy and partially cryst., X-ray scatt., differential radial distrib. function 79−14704
polyethylene terephthalate, mech. props., influence of cryst. arrangement and noncryst. region struct. 78−76707
polyethylene terephthalate, oriented, amorphous, stress-induced crystn., shrinkage meas. 80−92466
polyethylene terephthalate, shear compliances meas. of oriented sheet 80−104363
polyethylene terephthalate, uni- and biaxially drawn films, preferred planar orientation 78−80590
polyethylene terephthalate film, deformation band studies 77−52420
polyethylene terephthalate film, X-ray diffr. exam. of morphology 78−18558
polyethylene terephthalate-co-isophthalate, gelation and crystallization 80−24377
polyethyleneterephthalate, crystallised from thin layer melts, temp. depend. of morphology 80−54149
polyhexamethylene adipamide, calorimetric, X-ray and IR study 80−10512
polyimides, DFOPF and DFOB, X-diffr. exam. of structure and elasticity 80−6370
polyisobutylene fibres, stretched, crystn. kinetic study using synchrotron radiation 80−33909
trans-1,4-polyisoprene crystals, press. effect on melting temp. and lamellar thickness, press. crystn. 80−88302
polymer, amorphous, bulk, structure models and exptl. methods, review 78−22671
polymer, amorphous, segmental distrib., light-, neutron- and X-ray scatt., piezooptical and dielec. meas., review 78−51444
polymer, amorphous, struct. determ. by small-angle X-ray and neutron scatt. 77−84668
polymer, amorphous state struct., conf., Atlantic City, USA (Sept. 1974) 77−76327
polymer, loaded, mech. of macrocrack generation and propag., photometric and X-ray meas. 77−4886
polymer, molten or amorphous, chain conform. determ. by diffr. 77−80429
polymer, oriented, amorphous-crystalline low ang. X-ray diagrams, supermol. struct. models, schematic representation *(Russian)* 78−87630
polymer, oriented, under load, crystallite stability 77−70126
polymer, shear-induced crystallisation, optical study 78−14289
polymer, short-range order, radial distrib. functions from X-ray diffr. 77−76330
polymer, solid, orientation meas. and characterisation methods uing X-rays 78−75559
polymer, soln.-grown cryst., diffr. line-broadening, bending contrib. 78−75574
polymer blends, morphology and compatibility, X-ray and optical obs. 79−69026
polymer concretes, hydrothermally stable, hydraulic cement-type fillers 80−85144
polymer crystal, paracrystallinity, mosaic block concept 77−84673
polymer crystallinity, Hermans-Weidinger X-ray diffraction determ. technique *(Russian)* 78−75582
polymer film, supermolecular structure and mech. stress distrib. among chem. bonds 78−75562
polymer films, crystallinity degree estimate by diffraction pattern anal. 78−75555
polymer glasses and melts, struct., review of expt. results 79−37636
polymer liquid-crystalline solns., struct. 80−103235

X-ray diffraction examination of materials continued
polymer spherulite, cryst. lattice strains, mech. behaviour, X-ray diffr. detect. 80−59558
polymeric materials, stress meas., X-ray diffr. technique, review 78−5713
polymers, cryst. density, X-ray diffr. determ. 78−91273
polymers, diffuse boundary thicknesses, determ. by small angle X-ray scattering 80−38947
polymers, Fourier anal. of X-ray diffr. patterns 80−15016
polymers, glassy, improvement of alignment in diffuse fibre diffr. patterns 77−55243
polymers, multicomponent-multiphase, bulk struct. by rheo-optical techniques 78−91267
polymethylene, intramol. scatt. function calc. 77−38761
polymethylpentene, isotactic, crystal struct. 78−67663
polymethylsiloxane-polyarylate block copolymer, soln., viscosity, rel. to film mech. props. and microstruct. *(Russian)* 79−23762
polyoxymethylene, drawn, extra meridional reflections 80−24376
polyoxymethylene, ultrahigh modulus oriented, exam. of true crystal modulus, from −150 to 20°C 80−11687
polyoxymethylene diacetate, bulk cryst. and melting, polyoxyethylene additive effects 79−32921
polyoxymethylenes, determ. of crystalline fraction from X-ray diffraction 80−44150
polyoxymethylenes, dielectric relaxation, molecular mechanism *(Russian)* 80−88923
polypentamethylene terephthalate, oriented fibres, struct. anal. of two cryst. phases 79−73108
polypropylene, change of crystn. forms during purification 77−55934
polypropylene, isotactic, shear induced β-form crystallisation 78−18555
polypropylene, monofilaments, drawing behaviour, melt-induced orientation effects 78−84922
polypropylene, oriented, annealing, mol. mechanisms 77−12642
polypropylene, preoriented isotactic sheet, mol. behaviour in uniaxial drawing *(Japanese)* 77−68928
polypropylene, quenched form, struct., X-ray obs. 78−67661
polypropylene, structure change on uniaxial compression *(Russian)* 79−34119
polypropylene, thermoplastic, supramolecular struct. and frictional props. of surface layers 77−70188
polypropylene fibers, and films, and their hard elastic precursor small-angle X-ray diffr. studies 79−10815
polypropylene fibre, hard elastic, macroscopic deforms. in lamellae 79−96097
polypropylene fibres, homologue mixtures, props. 78−76709
polypropylene film, effect of crystallinity on deformation mechanism of biaxial stretching 77−80426
polypropylene systems, elastomeric impact modifiers rel. to morphology 79−66154
polypropylene-lignin system, X-ray diff., EPR exam. of interaction 78−68668
polypropylene-nylon 11 fibres, bimodal cryst. texture, X-ray diffr. and electron microscopy 78−75567
polypropylene-PMMA graft copolymer, X-ray meas. of crystallinity of component polymer *(Japanese)* 77−58962
polysiloxane dizwitterionomers, morphology, ionic aggregation 80−49130
polystyrene, high-impact type, deformation and microvoid form. 78−80602
polystyrene, isotactic, orientation of remaining amorphous chains during crystallisation 80−10506
polystyrene, soln. grown isotactic crystals, degree and distrib. of crystallinity, thermal stability 78−9964
polystyrene, solution grown isotactic crystal, thermal change kinetics study by X-ray diffr. 78−9965
polystyrene amorphous film, cyclically fatigued, molecular behaviour 80−35310
polystyrene blends, isotactic and atactic, small-angle X-ray scattering 78−55817
polystyrene chain conformations, in conc. solns. and in bulk, small-angle X-ray scatt. 79−10781
polystyrene filament, melt spun, struct. and mech. props., effect of drawing, twisting, annealing, untwisting 80−45331
polystyrene films, amorphous, X-ray small angle scatt. near glass transition, struct. *(Russian)* 77−31606
polystyrene latexes, soft X-ray scatt., struct. determ. 78−51395
polytetrahydrofuran, line-broadness in X-ray diffr. 77−19878
polytetramethyl-p-silphenylene siloxane, morphology and mech. behaviour 78−84885
polytetramethylene terephthalate, comparison of crystn. structs. in relaxed and strained forms 77−84675
polyurethane foam, X-ray exam. *(German)* 78−75596
polyurethane-polyurethane acrylate network, microinhomogeneities and props. *(Russian)* 78−51452
polyvinylacetate films, amorphous, X-ray small angle scatt. near glass transition, struct. *(Russian)* 77−31606
polyvinylidene fluoride, biaxially stretched film, corona charging and piezoelec. effect 78−88256
polyvinylidene fluoride, direct obs. of cryst. transform. process under high press. 78−38630
polyvinylidene fluoride, poling by corona charging, pyroelec. effect 78−19423
polyvinylidene fluoride, relax., influence of monomeric unit conform. and supermol. struct. *(Russian)* 79−23537
polyvinylidene fluoride, struct. study, piezoelec. and pyroelec. props. 80−7300
polyvinylidene fluoride, X-ray diffr. evidence for ferroelectricity 78−60399
polyvinylidene fluoride, X-ray high press. study 80−6369
polyvinylidene fluoride film, stretched, struct. and elec. props. 79−90572
polyvinylidene fluoride film, uniaxially stretched and corona poled, piezoelec. meas. 80−25311
polyvinylidene fluoride X-ray diffr. pattern changes due to corona charging 78−14285
portland cement, doped with ZnO, struct. and props. 80−60914
Portland cement-fly ash, physico-mech. props., SEM and X-ray diffr. anal. 79−74239
potassium oxalate, anhydrous, phase II, vibr. spectra and cryst. struct. 80−34901
powder examination using sealed cell 79−35906
powder specific surface, X-ray determ. method 80−47012

X-ray diffraction examination of materials continued
powdered mixture, stress-strain determ. by high press. X-ray diffr. 77−7792
powders, phase analysis by external standard method 79−68976
prosthesis block copolymers, non-thrombogenic, struct. and mech. props. 77−52925
proteins, globular, crystalline, intermol. interactions, denaturation, DSC and X-ray diffr. obs. 80−16897
proteins, X-ray crystallography, book contrib., review 77−40958
PTFE, NMR and X-ray diffr. investig. of press. induced III-I transition and mol. motion 77−51969
PTFE, struct. effects in stress-strain relations at elev. temps. 78−31484
purple membrane asymm. struct. 77−73512
PVC, amorphous-cryst., highly oriented, plastic deform. rel. to supermol. struct. *(Russian)* 79−51010
PVC, exam. of microstructure, using X-ray and light scattering 79−41983
PVC, glass-rubber transition determ., small-angle X-ray scatt. 78−95145
PVC, injection moulded, compression moulded and drawn samples, X-ray diffr. 78−83755
PVC, oriented mouldings, struct. order 80−60896
PVC, rigid, microdomains, small angle X-ray scattering study 80−28930
PVC-poly-ε-caprolactone blends, crystallinity and gas permeation 79−4433
PVDF, film, polymorphism induced by poling and annealing 80−24372
pyrazine, thermal expansion tensor determ. 77−15600
pyrimidine bases, water vapour effect on struct. and amorphous-cryst. transition 77−70408
pyrocarbon, lamellar material, thermal expansion meas. appl. of interlayer spacing X-ray diffr. technique *(French)* 77−20096
pyroceramic plate surface quality obs. after mechanical polishing 79−72732
pyrochlore, high temperature chlorination 78−11180
quantitative analysis software package for use with the APD 3500 79−50947
quartz, hydrothermally grown single crystals, real struct. investig. of rhombohedral faces *(German)* 78−2348
quartz, impact structs., peak shock press., X-ray diffr. investig., lunar rock bombard. appls. 78−7002
α-quartz, piezoelec. consts. determ. from dynamical X-ray diffr. curves 77−77153
γ-quartz, reaction, with NaCl-kCl melt, exam. of struct., IR absorption spectra 80−55706
α-quartz, Renninger effect, forbidden X-ray reflections 80−64980
quartz, synthetic, growth sector boundary between −X and Z sectors 78−59774
quartz, synthetic, growth sector boundary between −X and Z sectors 78−59775
quartz, synthetic, lattice distortions, optical inhomogeneities by X-ray topography and optical birefringence meas. 78−55887
quartz, synthetic, line defects, etch tunnels and X-ray topography 77−76406
quartz, synthetic local variations meas. in spacing and orientation of lattice plane, X-ray anal. 79−52099
quartz c-axis orientation in Saxony Granulites, petrofabric anal. by optical and X-ray diffr. studies 80−21740
quartz crystals, Bragg reflection enhancement due to X-ray irradiation under high elec. fields 79−14643
α-quartz dislocation free and low dislocation, prep. by hydrothermal crystallisation 78−72712
quartz plates, acoustic reson. vibr., Berg-Barrett X-ray diffr. method 80−40063
quinuclidine, cubic phase disorderd struct., X-ray diffr. study 79−69037
radiation induced defects, review *(Japanese)* 80−15152
radioactive materials, X-ray diffr. studies 80−3450
radioactive materials, X-ray diffraction sample holder 79−80738
radioactive waste, solidified, composition, structure and properties of final product obs. *(Czech)* 78−66353
rare earth chalcobismuthites, $RBiTe_3$, prep., elec. props., and crystallographic date 80−59981
rare earth compounds, $R_2V_2O_7$, (R=Tm, Yb, Lu), physical props. 78−39320
rare earth fluorides, as antirefl. coatings, evaluation 77−61963
rare earth garnets, preparation, substrate and epitaxial layer surface quality control, X-ray topography *(German)* 77−55432
rare earth hydrides, form. by rare earth reaction with H_2O vapour 80−76504
rare earth intermetallic, RNi_4AlH_x, Hz absorpt. and cryst. struct. of hydride 78−34487
rare earth intermetallics, RFe_2, spontaneous magnetoelastic distortion, X-ray diffr. expts. 77−63253
rare earth metal silicide thin film formation on (100), (111)Si substrates, backscattering study 80−70542
rare earth metals and some alloys, X-ray diffraction obs. of magnetostriction and phase transitions 77−73068
rare earth mixed molybdates, $R_2(MoO_4)_3$, $R_{2(1-x)}R'_{2x}(MoO_4)_3$, cryst. growth and crystallographic data, X-ray diffr. anal. 79−43132
rare earth orthovanadites, RVO_3, magnetic and cryst. struct., Jahn-Teller effect 77−32169
rare earth oxyphosphates, x Ln_2O_3.y P_2O_5, synthesis, characterisation and thermal stability 80−16256
rare earth thiohafnates, thermal stability and oxidation products in air 79−83346
rare earth $Zr_{1-x}O_{2-x/2}$ growth from skull melting, directional solidification 78−60567
rare earth-Fe_2, mag. props. changes due to H_2 absorption, unit cell vol. 77−63178
refractories, castable, X-ray powder diffr. meas. of phase composition, and flexural strength 80−3449
refractories, sintered, X-ray diffraction method for assessing local stress levels 79−96265
refractory coatings, deposited by electron evaporation, struct. and props. 79−23871
refractory metal films, evaporated, optical props., rel. to struct. 80−55211
residual pseudo-macrostress, X-ray meas. errors due to plastic deform. 77−68544
residual stresses in thin specimens, layer-by-layer X-ray diffr. analysis, additional strains and corrections 78−39964
residual stresses measurement 79−97484

X-ray diffraction examination of materials continued
residual stresses rel. to grinding and cutting directions, X-ray diffr. obs. *(Japanese)* 78−23847
review, time-depend. distribs. 77−43102
review *(Czechoslovakian)* 77−28958
review of literature 1975-1977 78−85219
rhombic distortion of cryst. lattice at low temp. 78−2253
ribosomes, E. coli, complexes of individual components, small angle X-ray scatt. study 79−11895
Rochelle salt, crystal, X-ray topographic obs. of localised vibr. 79−24264
roll surface damage eval. by X-ray diffr. technique *(Japanese)* 80−25892
rough surfaces, effect of 1° glancing angle on penetration depth 79−35665
rubber, X-ray scatt., differential radial distrib. function 79−14703
rubidium propanoate, solid state transitions and melting process, diffr. and conductometric meas. 80−10670
rubredoxin, Fe-containing protein, synchrotron radiation appl. 77−52936
sapphire, Czochralski crystals, formation of low angle grain boundary macrostruct. 78−47392
sapphire ribbon crystals, EFG growth and charact., voids, grain boundaries and dislocations 80−103283
sarcoplasmic reticulum hydrated oriented multilayers, lamellar X-ray diffr. 78−11614
SAW X-ray topographical representation 79−47870
scaffold, in bacteriophage λ head formation, small angle X-ray scatt. study 79−11896
schorl tourmaline, elastic const. 78−68718
seed materials subjected to mag. field, X-ray diffr. patterns. 80−89721
semiconductor alloy, pseudobinary, phase diagram calc. 78−52786
semiconductor crystal lattice defects, using high speed X-ray topography camera 77−11443
semiconductor single crystals, investigation via high-temp. X-ray topography system 77−76261
shellac and bee's wax, orientation solidification in mag. field, magneto-electrets, X-ray diffr. 77−12299
Si crystal, elastically bent, strain distrib. determ. by X-ray intensity meas. 79−50928
Sialon, prep. and charact. of ultrafine powders 80−11604
SiAlON X-phase, X-ray diffr. data 80−49198
silicate glasses, polishing, surface charact. using grazing X-ray reflection *(French)* 80−65353
silicate mineral, identification and asbestiform varieties, election optical and X-ray techniques 80−8446
silk fibroin films, conformational changes induced by water immersion 80−10498
single crystal, anomaly in electron and photon emission and scattering *(Japanese)* 79−37581
single-phase domain boundary identification by X-ray diffraction line broadening 78−1949
sintered frictional material, environmental effects on props. 78−11338
slurries, solids content determ. by X-ray scatt. 80−3467
small particles, cause of reduction in lattice spacing *(Russian)* 80−38967
sodium acetate trihydrate, whisker growth on membrane in aq. soln. 78−30854
sodium pentadecyl sulphonate, lyotropic liquid crysts., X-ray study of domain structure *(Russian)* 77−62469
solid solutions, decomposition, two-phase. X-ray diffr. anal., exam. of method 79−52510
solid-state reactions at elevated temps. 77−47303
SOS, cryst. perfection rel. to MOS transistor mobility 78−75956
spacecraft materials failure, metallurgical exam. 80−71868
sphingomyelin-cholesterol interaction in oriented bilayers, X-ray diffr. exam. 77−44603
β-spodumene-mica glass ceramics, phase evolution and TiO_2, MgF_2 additive effects, exam. 78−44089
sputtered coating, oxidation during metallic sputtering in inert atm. with uncooled cathode 78−3041
sputtered coatings, metallurgical characterisation 79−15056
stacking fault X-ray topograph, computer simulation 78−30513
standing wave field excitation, meas. apparatus, appls. 77−15285
starch, glycerin impregnated, dynamic viscoelasticity *(Japanese)* 80−104203
stearic acid, vacuum evaporated film, for low-loss capacitors 80−71317
steel, 1045, elastic const. meas., X-ray diffr. technique 78−5714
steel, alloy, 37KhGSTF and 44KhGSTF, quenched X-ray diffr. testing of heat treatment 78−56834
steel, alloy, high C, amorphous, produced by rapid quenching from melt, hardness and strength 78−59764
steel, alloy, type HSLA, exam. of NbCN precipitation by elec. resistivity meas. 78−84822
steel, alloy, type Kh16N11M3, struct. changes during thermocyclic working, dislocation struct. *(Russian)* 80−54243
steel, alloy type 25KhN3MFA, tempering of bainitic structure 80−20983
steel, austenitic, Cr-Ni (20, 25 wt.%), containing B and Ti additions, splat quenching, X-ray and TEM study 79−74186
steel, austenitic, hydrogenation effect, different stability charact. 78−35383
steel, austenitic stainless, Cr-Ni (18,8 wt.%), X-ray meas. of residual stress in ground surface layer *(Japanese)* 77−48491
steel, austenitic stainless, ferrite volume fraction, high-speed determ. by XDXRD 78−76628
steel, austenitic stainless, H_2 induced strain in single crystal *(Japanese)* 77−48530
steel, austenitic stainless, high temp. oxidation, high temp., in low O_2 press., surface anal., impurity diffusion effects 77−56142
steel, austenitic stainless, Ni-alloyed, Cr_2N precipitation, interface struct. and morphology 80−11644
steel, austenitic stainless, phosphide analysis using nonaqueous electrolyte potentiostatic etching method *(Japanese)* 80−89221
steel, austenitic stainless, unlubricated, friction, wear and microstruct. of types 304, 316 and Nitronic 60 80−108589
steel, austenitic stainless, welded explosively, induced martensites morphology 80−104153
steel, austenitic stainless, X-ray elastic constants, determination by ψ_0 oscillation method *(Japanese)* 78−64575
steel, austenitic stainless, X-ray stress meas., accuracy and method of data treatment *(Japanese)* 80−104365
steel, C, failure mechanisms in impact fatigue 80−40493

X-ray diffraction examination of materials continued
steel, C, phosphide analysis using nonaqueous electrolyte potentiostatic etching method *(Japanese)* 80−89221
steel, C, rubbed surface, continuous hard layer *(Japanese)* 77−52501
steel, C, X-ray diffraction correlation between cyclic loading and residual stress *(German)* 78−48583
steel, C, X-ray stress meas., appl. of position sensitive proportion counter *(Japanese)* 78−64791
steel, C (0.21 wt.%), loading wave shape effect on deform., failure, impact tensile strength of smooth specimen *(Japanese)* 79−29146
steel, C-Cr(MO)(W), high-C, amorphous crystn. behaviour *(Japanese)* 79−94911
steel, C-Cr-Mo(Cr-W)(Mo-W)(Cr-Mo-W), high C, amorphous crystallisation behaviour *(Japanese)* 79−94911
steel, carbon, fastener holes, cold-worked, residual stress meas. 78−7163
steel, carburised, with non martensitic microstruct. at surface, fatigue *(Japanese)* 77−48535
steel, cold-rolled, good and bad paintability, AES, SEM and X-ray diffr. characterisation of surfaces 79−42344
steel, continuously cast slabs, formation of longitudinal midface cracks 79−83315
steel, Cr ferritic stainless, meas. of alloy and impurity elemental distrib. using STEM 80−35601
steel, Cr-C, structural, struct.-prop. resl., high strength and toughness design criteria 80−97491
steel, Cr-Mn, metastable constitution diagram and phase transforms. *(Russian)* 80−50590
steel, Cr-Mn with increased N content, X-ray spectral microanalysis *(Bulgarian)* 78−53304
steel, Cr-Mo, high tension, delayed fracture, fundamental study *(Japanese)* 77−48531
steel, Cr-Mo (10-14, 2-6 wt.%), heat-resist., creep-rupture strengths 80−104271
steel, Cr-Mo (2.25, 1.0 wt.%), temper embrittlement, effect of P, Sn, comp. and carbide precip. 80−85036
steel, Cr-Mo (2.25, 1.0 wt.%), temper embrittlement, effect of Mn, Si, comp. and carbide precip. 80−85037
steel, Cr-Mo low alloy ferritic, meas. of alloy and impurity elemental distrib. using STEM 80−35601
steel, Cr-Mo-V, low alloy, V effect on creep *(Czech)* 77−86088
steel, fatigue crack tip plastic deform., X-ray diffr. investigation *(Russian)* 80−104251
steel, Fe-Al-C alloy, redistribution of C during tempering *(Russian)* 77−90371
steel, ferritic stainless, phosphide analysis using nonaqueous electrolyte potentiostatic etching method *(Japanese)* 80−89221
steel, gas nitrosulphurized, in temp. range 813-903K, wear props., surface and cross-sectional hardness, X-ray diffr. and SEM study *(Japanese)* 79−29224
steel, heat treated high strength, X-ray diffr. anal. of residual stress 80−3200
steel, high C, plate, rolling residual stress meas. by X-ray diffr. *(Japanese)* 79−66081
steel, high C, type 7KhFNSh, plastic deform. influence of X-ray interference line breadth *(Russian)* 80−93599
steel, high-speed tool, splat quenching, props. and struct. 80−76294
steel, HSLA control-rolled, surface residual stress meas., X-ray diffractometer 78−5716
steel, low C, deformed, comp. of precipitated carbonitrides, X-ray diffr. anal. *(Russian)* 79−20051
steel, low C, electroboronising by superimposed cyclic current, Na_2CO_3, B_4C, NaCl, NaOH activator studies 80−85081
steel, low C, influence of cold rolling reduction on elastic stored energy 79−91731
steel, low C, initial stages of plastic deform. *(Japanese)* 80−93618
steel, low C fatigued, appl. of microbeam X-ray technique to plastic zone size evaluation 80−3199
steel, low C rimming, effect of addition of Al to Zn on phase composition and morphology *(Polish)* 78−53014
steel, low C structural, fracture toughness and X-ray diffr. obs. of surface *(Japanese)* 80−66634
steel, maraging stainless, phase transformation and mech. props. rel. to heat treatment *(Chinese)* 80−66501
steel, martensitic, age hardening with Cu, Nb additions, exam. of hardness 80−7681
steel, medium C, ground, residual stresses, X-ray evaluation 80−79863
steel, mild, AISI 1009 and 1018, corrosion incipient processes in hypersaline geothermal brine at 90°C 80−50753
steel, mild, elastic stress meas. using X-ray diffraction, wavelength effect 77−84202
steel, mild, fatigue strength, effect of grinding surface *(Japanese)* 77−48533
steel, mild, origin of spherical particles on fatigue fracture surfaces and ferrograms 79−79112
steel, mild, X-ray meas. of conc. stress at crack tip *(Japanese)* 77−77570
steel, Mn, form. of twinned struct. *(Russian)* 78−64542
steel, Mo and Cr-Mo, X-ray elasticity constants at high specimen temp. *(German)* 80−35239
steel, N32, $\alpha \rightarrow \gamma$ transform., struct., texture conc. var. depend. on plastic deform. *(Russian)* 79−66050
steel, Ni, 11.6%, quenched cylinder residual stresses, boring/turning and X-ray diffr. obs. *(German)* 80−93586
steel, Ni, N22, X-ray diffr. study of austenite lattice near martensitic transform. *(Russian)* 79−1868
steel, Ni-Mn (16, 2 wt.%), 40N16G2, single crystal, stabilisation and destabilisation mechanisms *(Russian)* 78−23732
steel, plain C, type 304 and type 316 stainless, fatigue damage indicators, non-desructive 80−25932
steel, plain C, X-ray diffr. study of low cycle fatigue damage 77−66700
steel, powder forged, fatigue, surface treatment effect 80−85048
steel, quenched, tempering treatment, ultimate tensile strength and yield point *(Russian)* 77−32599
steel, quenched and low-annealed, X-ray determ. of macroscopic stresses 77−77660
steel, Si-Cr-Mo-W-V (2,4,1,3,2 wt.%), heat treatment and props. 80−16349
steel, Si-Mn-P-S-Ni-Cr, residual stress meas. by X-ray diffr. 80−71688
steel, stainless, austenitic, H_2 induced transformation obs. *(Japanese)* 80−11640
X-ray diffraction examination of materials continued
steel, stainless, Cr-Ni, maraging, effect of Mo, Co additions on hardening 78−84835
steel, stainless, fixing pins for fractured bones, strength, ultrasound effect 80−71710
steel, stainless, hydrogenation different stability characts. 78−35383
steel, stainless, PWR primary corrosion products 80−13578
steel, stainless, spatial distribution of limiter material and impurities on the first wall of TFR 400 79−651
steel, stainless, two phase, X-ray stress meas., by monochromator method *(Japanese)* 78−64792
steel, stainless, type 316, microstruct. changes in creep ductility, SEM, TEM, optical microscopy and X-ray diffr. study 79−38927
steel, stainless, wire, axial texture after electroplastic drawing, X-ray struct. investigation *(Russian)* 80−104177
steel, stainless type 316, $M_{23}C_6$ carbide precipitation, intermetallic phases, X-ray diffr. study 80−7586
steel, surface deposit of ZrC, exam. of composition *(Russian)* 79−34201
steel, surface Si reinforced type U8, metastable phase, composition, struct. *(Russian)* 80−92599
steel, textured, X-ray stress meas. 77−46975
steel, transformers, inhibitory phase *(Russian)* 78−3139
steel, type Kh13N9D2MT martensitic aged, struct. and mech. props. *(Russian)* 80−93600
steel, W, high C, amorphous, rapidly quenched from melt, mech. and thermal props. 79−38874
steel, W-Mo, types R6M5 and R6M5K5, decarburising layer evaluation 80−21164
steel cylinder, electrodeposition internal stress meas. 78−27693
steel St 52, textured, rolled, REK and lattice strain distrib. *(German)* 79−29095
steel surfaces, machined, X-ray diffr. residual stress meas. methods, comparison 77−56212
steels, high-purity and commercially based, containing 10 wt.%W or 5 wt.%Mo, tempering behaviour 80−7600
steels, KW12M and 40G5, X-ray diffr. study of austenite lattice near martensitic transform. *(Russian)* 79−1868
stishovite, compression to 100 kbar, eqn. of state from bulk modulus 77−17085
stress determination, by X-rays, texture effect 79−91701
stress meas., residual, use of position sensitive proportional counter *(Japanese)* 80−11853
stress meas. by microbeam technique, appl. to fatigue crack growth *(Japanese)* 78−64793
stress measurement by counter method, statistical anal. 78−27694
stress/strain distrib. meas. inside plastic zone of notched sheet, fatigue crack propag. *(Japanese)* 78−6981
substitutional solid solution comp. from X-ray integral intensities 77−84584
succinonitrile, plastic, diffuse scatt., hard-core correl., weak-graph method 80−49137
superalloys, phase extraction, chemical and X-ray diffr. anal. 78−72951
surface roughness assessment, X-ray scattering and differential interference contrast microscopy 79−30410
surfaces, machined, X-ray diffr. residual stress meas.. methods, comparison 77−56212
Tanane, ferroelec. ferroelastic transition, X-ray and optical expts. 78−15110
TaS_2, amine intercalation, water effects, X-ray diffr. meas. 80−44178
1T-TaS_2, nearly commensurate phase, harmonics effect on phase transitions 78−14462
TBK-3, ferroelectric ceramic, 90° electric domain processes, mech. stress, X-ray diffr. 78−72478
TCNQ complexes with ferrocenes, charge transfer type, struct. and mag. props. 80−24439
TCNQ salt, $(NMe_3H)(I)(TCNQ)$, one-dimens. semicond. with metal-like cond. 80−24909
TCNQ salt, $(TSeF)_x(TTF)_{1-x}$-TCNQ, struct., elec. and mag. props., review 80−20158
TCNQ salt, NMP-TCNQ, X-ray diffuse scatt. rel. to charge transfer 77−80496
TCNQ salt, TSeF-TCNQ, CDWs, X-ray study 79−28301
TCNQ salt, TSeF-TCNQ, Peierls transition and CDW ordering, X-ray study 80−20101
TCNQ salts, modulated struct., dynamical processes, X-ray and neutron scatt. 79−95155
TCNQ-HMTSeF, X-ray diffuse scatt., one-dimens. distortion in phonon spectrum and interpret. 78−10144
TCNQ-HMTTF, struct. evidence of CDW 78−51912
TCNQ-K, X-ray exam. of phase transitions 78−55933
TCNQ-Na, X-ray exam. of phase transitions 78−55933
TCNQ-Rb, X-ray exam. of phase transitions 78−55933
Teflon foils, cryst. struct. and texture changes due to polarisation process *(Polish)* 80−35209
telechelic polybutadiene-methacrylate acid copolymers, X-ray study *(French)* 78−18553
tendon, calcified, of turkey leg, collagen-mineral axial relationship 77−32872
ternary alloy, metastable miscibility gap determ. by small angle scatt. 77−28780
tetraethylammonium iodide-Ag_nI_{n+1}, ionic conductors, electrochem., props. 77−31808
tetramethyl-p-silphenylene siloxane/dimethyl siloxane, block copolymer, morphology and mech. behaviour 78−84885
tetramethylammonium tetrachlorozincate, X-ray study of incommensurate phase 80−71351
tetraoxane crystals, growth and perfection by evaporation of solns., X-ray topography 79−61510
textured sheet metals, X-ray diffr. anal. 80−6316
TGFB, deuterated, effects of deuteration on lattice parameters and Curie temp. 79−24422
TGS, domain boundaries, X-ray topographic study 78−48136
TGS, domain boundaries, X-ray topography 78−60409
theory, rel. to X-ray topography data 78−64254
thermoplastics, structural changes during deformation, rel. to impact resistance 80−25800
thin film characterisation 78−22991
thin films, anisotropy props., X-ray characterisation 79−23874
thin foils, chem. anal. by electron microscopy *(French)* 80−50899

X-ray diffraction examination of materials continued
thiourea, commensurate-incommensurate phase transition, X-ray diffuse scatt. meas. *(French)* 79−19856
thiourea, ferroelectric transition, X-ray scatt. 79−47398
thiourea, incommensurate phase transition, X-ray and neutron scatt. study 80−75963
thiourea-cyclohexane inclusion compound, crystal, low temp. diffr. pattern, atomic structure determ., phase transitions 78−31116
time-resolved X-ray scatt. method for molecular biophysics 79−62409
TiO, single cryst., short range ordering of vacancies, X-ray anal. 79−73163
Tishomingo Fe meteorite, microstructural study 79−16898
tobacco mosaic virus, data quality collected using modified mirror monochromator for rotation photography 79−9269
torbermorite study by X-ray line profile anal. *(Japanese)* 80−33984
transition metal complexes, dimethylglyoxymate films, prep. and physical props. 79−90923
transition metal disilicides, chem. linkage, enthalpy, above 1200K 77−90324
transition metal oxalates, crystal growth in silicate gel, characterisation 77−4724
transition metal-metalloid glasses, struct. and plastic flow, review 80−84090
transition metal-nonmetal glasses, with defined local coordination, struct. model 80−84092
transition metal-Si-B ternary and quaternary amorphous alloys, effect of comp. on crystn. *(Japanese)* 79−94910
transition metal-W-O system, phase relations in dioxide-trioxide region, 1373K 78−11212
transition metals, Y to Pd, intensities measured in temp. range 100 to 370K 78−18731
transuranic chalcogenides and pnictides, prep. and cryst. chem. 80−16255
transverse deformation theory, development to fourth stage *(Russian)* 77−56027
triamantane, phase transistions, X-ray diffr. meas. 79−14930
s-triazine, low temp. phase, reconciliation with NQR measurements 79−46798
s-triazine, structural phase change, sp. ht. meas. 78−55944
tridymite, thermal expansion meas. 80−59682
triglycine fluoberyllate, deuterated, dislocation line defect X-ray topographic analysis 80−59465
trimethylammonium cadmium chloride, $(CH_3)_3NHCdCl_3$, struct. phase transitions 79−1502
tropomyosin, cryst. struct. and molecular interactions 79−48210
trypsin, bovine, activation, activity and inhibition *(German)* 79−79465
TSeF-TCNQ, Kohn anomaly of metallic state, X-ray diffuse scatt. meas. 80−19887
TSeF-TCNQ, X-ray diffuse scatt., one-dimens. distortion in phonon spectrum and interpret. 78−10144
TsTS-23, ferroelectric ceramic, 90° electric domain processes, mech. stress, X-ray diffr. 78−72478
$TTF_{0.4}TSeF_{0.6}$-TCNQ, $2k_F$ and $4k_F$ CDWs, X-ray study 80−65474
$TTF_{0.97}Se_{0.03}$-TCNQ, Peierls-superlattices and soft phonon anomalies, X-ray scatt. meas. 78−75795
TTF_x $TseF_{1-x}TCNQ$ solid soln., DC conductivity, struct. 78−10423
$TTF(SCN)_{0.588}$, Peierls instability, strain coupled charge density waves, X-ray scatt. obs. 78−79949
$(TTF)Cl_x$, disorder transition, cond. decrease and commensurate charge density waves 80−70153
TTF-Cu bis-dithiolene, dimer, mol. displacements at 4.2K 80−10539
$TTF\text{-}CuS_4C_4(CF_3)_4$, quasi-one-dimens. antiferromag., spin-lattice dimerisation, X-ray scatt. obs. 77−85464
TTF-TCNQ, $4k_F$ anomaly, explanation 77−35875
TTF-TCNQ, and related cpds., partial charge transfer and CDW modulation 79−95349
TTF-TCNQ, Kohn anomaly and Peierls-type transition, X-ray obs. 78−14435
TTF-TCNQ, low-temp. modulated lattice, Peierls distortion, Kohn anomaly 78−10033
TTF-TCNQ, near commensurability, longit. cond. meas. and X-ray scatt. 79−78084
TTF-TCNQ, neutron and X-ray diffuse scatt., phase transitions, one-dimens. behaviour and interpret. 78−10381
TTF-TCNQ, Peierls-superlattices and soft phonon anomalies, X-ray scatt. meas. 78−75795
TTF-TCNQ, phonon anomalies and superstructures, Peierls transition, X-ray diffuse scatt. obs. 77−27962
TTF-TCNQ, spin waves, scatt. at $4k_F$, spin-Peierls fluctuations 78−72093
TTF-TCNQ, X-ray exam. of $2k_F$ and $4k_F$ anomalies 78−10162
turquoise, crystalline, Nogales Mexico, SEM and TEM study 79−29760
tveitite, X-ray powder and single cryst. electron diffr. study *(German)* 79−99160
twinned and clustered crystals, method and program of establishing UB matrices of single cryst. individuals 79−37586
urea, density distributions of bonding electrons 78−75616
urea, low temp. phase transition, X-ray diffr. expts. 79−1501
urea-n-paraffin adducts, order-disorder transition, thermal anal., X-ray diffr., and NMR 79−33084
vacuum deposited films, mech. props. 78−75968
vanadocene, order-disorder phase transition, sp. ht. and crystallographic study *(French)* 80−84131
vitreous china, crazing tendency, rel. to thermal expansion and quartz and cristobalite content *(Japanese)* 78−44243
VPE, growth processes, in-situ obs. *(Japanese)* 80−35104
weak X-ray scatt. interpretation by automated diffractometer 79−68977
wear debris anal., quantitative methods 78−64912
wear study, analytical surface tool, review 78−64718
wood-polymer composite, dynamic viscoelasticity and modulus *(Japanese)* 78−59356
wrought metals, plastic deform. testing, X-ray line profile anal. *(Hungarian)* 80−97663
X-ray anal., conf., Denver, USA (Aug. 1976) 77−70382
X-ray scattering from small defects in very perfect crysts. 78−47395
YIG, hot spraying to give fine, free flowing, sinterable powder 80−20865
zeolites, Na, Cs, Sr types, processing radioactive waste soln., thermal transform. 77−10477
zeolites, type Y, containg catalysts, cryst. struct., IR spectra 79−42958
Zircaloy, PWR primary corrosion products 80−13578

X-ray diffraction examination of materials continued
Zircaloy tubes, grain struct., texture, dislocation density effect on irradiation creep, X-ray diffr. and optical microscopy anal. 79−74208
Zircaloy-2 tubing, quantitative charact. of crystallographic texture 78−21647
ZnO, film, reactively RF sputtered, anal. of texture 78−67921
α-Zr, ω phase proportion during high press. deform. *(Russian)* 79−74147
$3CaO.Al_2O_3$, hydration retardation by $CaSO_4$ 79−61856
Ag, colloidal, lattice defects, X-ray diffr. and electron microscopy exam. 78−51567
Ag, Debye temp., X-ray diffr. determ., anharmonic parameters of pot. function 80−100320
Ag, Debye temperature correlations at high temp. 80−15210
Ag, Debye Waller determ. from modified Cheveau model 78−59918
Ag electrodeposition, on (100) face of single crystal Ag in presence of sulphadiazine 80−89161
Ag electrodeposits, dendritic growth inhibition by tartaric acid and tartrates *(French)* 78−87894
Ag film, vacuum-deposited, removed from substrate, internal strain *(Japanese)* 78−22872
Ag fine particles, X-ray Debye temp. determ. using solid-state detector and continuous X-rays 79−50944
Ag halide film physical props., effect of gelatin structure 80−97715
Ag ion plated film on permalloy, Cu and Vicalloy substrate, AES, SEM and X-ray study *(Japanese)* 78−11128
Ag powder, ultrafine, sintering, coalescence growth stage 80−89174
Ag, vacancy formation energy, thermal expansion meas. 79−14798
Ag, vacuum deposited on Al substrate, recrystallisation 78−60044
Ag vacuum-condensed films, on glass substrate, X-ray texture study 79−83226
Ag/Al thin film couples, diffusional alloying, Kiessig X-ray interf. obs. 80−10713
Ag-Al, short-range order, X-ray and electron diffr. study 80−54173
Ag-Al polycryst. thin-film couples, interaction process 79−51443
Ag-Bi-S, ternary phase diagram, DTA and X-ray diffr. investigation 80−84917
Ag-CdO cermets, coprecipitated carbonates and hydroxides, physicomech. props. 80−25706
Ag-Cu metastable solid soln., form. by ion-beam mixing 80−75244
Ag-Ga(In) thin film couples, room temp. interactions, X-ray powder patterns 80−2220
Ag-Ge, thermal expansion, X-ray determ. 78−26697
Ag-Ge-S glasses, X-ray determ. of struct. *(Japanese)* 80−10501
α-Ag-In solid solutions, lattice dynamics parameters *(Russian)* 80−96477
Ag-InP interface, AgP_2 formation during sintering 80−65309
Ag-Mg (15 at.%), disordered, short-range order, X-ray diffr. obs. 79−95176
Ag-Sn (6(8.2)(11) wt.%), splat-quenched, X-ray line broadening 80−40397
Ag-Zn alloy, electrodeposited under controlled potential, spontaneous transformations obs. 78−51853
$Ag_xAu_{1-x}Zn$, resistivity and X-ray diffr. 78−47283
AgBr-NaBr, phase diagram, miscibility, binodal curve and demixing kinetics, X-ray meas. 80−96659
$AgGaS_2$-$AgGaSe_2$ system, phase diagram, lattice consts., and IR spectra 80−60841
$Ag_4Ga_2S_5$, formation mechanism, X-ray and isotope exchange anal. 79−87591
Ag_5GaS_4, form. in Ag-Ga-S system 79−87618
α-AgI, cation distrib. and anharmonic thermal vib. 77−66005
β-AgI, phonon-induced X-ray scatt. from lattice dynamical model 79−37790
AgI solid electrolyte α-phase stabilisation 80−29209
α-AgI, superionic phase, struct., X-ray scatt. anal. 80−28983
B-AgI, X-ray diffuse scattering 80−14964
AgI-$Ag_2Mo_2O_7$($Ag_2Mo_4O_{13}$), solid, intermediate compounds with fast ion transport 77−43371
AgI-$Ag_2O.B_2O_3$ system, ionic cond., struct., electrochem. prop. in galvanic cell 78−95181
AgI-Ag_3AsO_4, AgI-$Ag_2Cr_2(Mo_2)O_7$ systems, solid electrolyte stability 77−15619
AgI-AuI, pseudo-binary phase diagram 78−76637
AgI-HgI_2, solid electrolyte, ionic and electronic cond., phase composition determ. 78−2296
$AgInS_2(Se_2)$-$SnS_2(Se_2)$, degree of solid solubility and phases charact. 78−35377
$Ag_xMo_3S_4$, chevrel phase, charge transfer and valence electron conc. 78−6029
$AgNO_3$, ESCA contrib. to X-ray struct. determ. *(French)* 77−62508
Ag_2O, phase transitions at press. up to 39 kbar 77−31770
Ag_2O, thermal expansion, lattice parameter determ., 150-250K 78−2267
α-Ag_2S whiskers, growth in VLS system, SEM and X-ray diffr. anal. 79−46989
Ag_2S-Ga_2S system, phase diagram, DTA and X-ray diffr. meas. 77−15544
$Ag_2S+Ln_2S_3$, powdered mixtures, reaction rate, production of ionic semiconductors 80−93741
Ag_3SBr, ionic conductivity in temp. range 93-573K, X-ray diffr. and DTA 80−79988
βAg_3SI, anharmonic thermal vibr. of cations 80−65214
Ag_3SI, ionic conductivity in temp. range 93-573K, X-ray diffr. and DTA 80−79988
Ag_3SI, superionic cond., phase transition and cryst. structs., sp. ht., neutron and X-ray diffr. obs. 80−10662
β-$AgSbS_2$, phase transitions, electrophysical props. 80−44316
α-Ag_2Se, superionic cond., X-ray diffr. study 77−84719
Ag_2Se, X-ray determ. of inclusion function 77−76559
$Ag_2Te_xSe_{1-x}$ system, solid solns. of substitution existence, X-ray phase obs. 79−43217
$AgZr_2(PO_4)_3$ system, phase charact. at different temps. 80−29936
(Al,Ga)As/GaAs, LPE grown heterostructures, X-ray diffr. exam. of interfacial elastic strains 78−72019
Al alloy, residual stress relax. rel. to temp., load cycling, aircraft struct. appl. 78−7053
Al alloy anodic oxide film hardness, effect of pH and metallic additives *(Japanese)* 77−56146
Al anodising, porous films formed in chromic acid 80−100966
Al binary alloys, rapid quenching, struct. and decomp. 80−76244

X-ray diffraction examination of materials continued
Al, cold rolled, X-ray diffr. and optical microscope exam. of fatigue damage *(Japanese)* 78−84976
Al, cold rolled and annealed, substruct. near fatigue crack tip, X-ray microbeam technique exam. *(Japanese)* 78−64621
Al crystal, lattice rotation during tensile deform., X-ray diffr. meas. 80−49231
Al, Debye temp., X-ray diffr. determ., anharmonic parameters of pot. function 80−100320
Al, Debye Waller determ. from modified Cheveau model 78−59918
Al, deformed, struct. and recrystallisation transmission Kossel diffr. obs. 77−52340
Al, dislocation substructure formation under hydrostatic extrusion 78−56696
Al electrolytes, X-ray determ. of cryolite ratio 78−3417
Al, fast neutron irradiated, struct. of defect cascades, diffuse X-ray scatt. study 80−39167
Al, fatigue damage, test temp. effects *(Japanese)* 77−52475
Al filings, interrelation between dynamic and static distortions, X-ray diffr. meas. *(Russian)* 77−43305
Al film, He^+ irrad., overpressurised bubble obs. 79−51165
Al film, MBE and field emission deposition on III-V semiconductors, comparative study 79−87016
Al film, struct. and props., effect of ion implantation 79−77936
Al film, vacuum deposited, 7 to 65 μ thick, morphology and purity determ. 77−76699
Al foil, modification of texture by fatigue, X-ray diffr. exam. 78−88477
Al, initial stages of plastic deform. *(Japanese)* 80−93618
Al, microrupture singularities in low stress range at elevated temp. *(Russian)* 79−29172
Al, orthogonal cut surface, effect of cutting condition on residual stress *(Japanese)* 78−85035
Al, polycryst., recrystn., synchrotron X-ray topography dynamic expts. 78−67621
Al, powder, X-ray at scatt. factors at 80K 78−2065
Al, pure, hydroextrudates, incomplete axial orientation *(Russian)* 80−20949
Al single crystals, relation between axial orientation rotating and deform. banding 80−104206
Al, surface fatigued single crystal, inhomogeneous positron trapping 77−90216
Al, surface strengthening of single crysts. on coating with evaporated films 77−8972
Al, vacancy formation energy, thermal expansion meas. 79−14798
Al, vacuum deposited, structural singularities and porosity *(Russian)* 78−75950
Al/NiSi/Si system, high temp. interaction study, elec. and struct. charcts., X-ray line spectra 79−24075
Al/Pd thin film couples, thermal reactions 80−59830
Al-Ag, discontinuous decomposition *(Polish)* 78−52808
Al-Ag, low-conc. alloy, spinodal curve and metastable miscibility gap 77−63680
Al-Ag_2Al, eutectic alloy, exam. of terminal solid solubility limits 78−76633
Al-Ag-Zn, ring diffuse X-ray scatt. phenomena *(Russian)* 77−16538
Al-$Al_{21}Pt_5$ eutectic alloys, unidirectionally solidified, struct. study 80−108394
Al-alloy, type 2024, fatigue life prediction, X-ray diffr. method 80−25837
Al-alloy plates, type VAD23, thermomech. parameters effect on struct. and props. 80−20988
Al-Cu, type 1100, synchrotron radiation microradiography 80−85121
Al-Cu film bilayers, growth kinetics of θ phase, He^+ backscatt. and X-ray exam. 78−84105
Al-Cu films, deposition rate, mol. beam incidence angle influence on struct., film props. *(Russian)* 79−60646
Al-Cu-Mg/mica particulate composite mech. props. 80−100919
Al-Cu-Mn, type 2219, synchrotron radiation microradiography 80−85121
Al-Cu-Zn alloy, ageing, X-ray and electron diffr. meas. *(Russian)* 78−39806
Al-Cu-Zn system, solid-phase reactions, phase diagram 80−50603
Al-Ge (0.2 at.%), exam. of interstitial trapping by X-ray diffuse scatt. 78−47363
Al-Ge (100) interfaces, MBE prep. and geometrical struct., total refl. X-ray diffr. study 80−49531
Al-Ge(001) interface, struct., total-reflected X-ray diffr. 80−88441
Al-Mg, ageing process, effects of Ag additions and pressure *(Russian)* 80−45321
Al-Mg, rapidly solidified, metastable phases *(German)* 79−34011
Al-Mg alloys, initial decomposition exam. by X-ray diffr. *(Russian)* 77−77482
Al-Nb-R system, R=rare earth, X-ray diffr. obs. of phase equil. *(Ukrainian)* 77−32560
Al-Si, ion plated contacts *(Rumanian)* 78−88029
Al-Si-N-O system, comps. corresponding to β'-sialon phase reaction hot-pressing 80−84891
Al-Si(Cu)(Zn-Mg-Cu), extraction and phase anal. 79−15673
Al-Sn-U alloy, phase equilib. exam. by metallographic and X-ray anal. 77−21102
Al-W(Mo)(Nb), struct. and props. of alloys obtained from granules 80−50717
Al-Zn, discontinuous decomposition *(Polish)* 78−52808
Al-Zn (10 at.%), ring diffuse X-ray scatt. phenomena *(Russian)* 77−16538
Al-Zn (10 wt.%), solute conc. fluctuation effects on ageing at low temp. 79−57023
Al-Zn (15 at.%), structural changes during post ageing between 125°C to 215°C 80−40399
Al-Zn (15 at.%), supersaturated alloy, growth and decomposition kinetics 80−29965
Al-Zn (5.05 at.%), comparison of X-ray and neutron small-angle scatt. 79−15647
Al-Zn-Mg, age-hardenable, precipitation and dissoluton processes, positron annihilation and X-ray small-angle scattering comparison 80−89238
Al-Zn-Mg, metastable miscibility gap determ. by small angle scatt. 77−28781
Al-Zn-Mg, precipitation mechanism, effect of Mg additions *(French)* 77−52330
Al-Zn-Mg (4.5, 2 to 3 at.%) solid state reactions by interrupted continuous heating 80−25737

X-ray diffraction examination of materials continued
Al-Zn-Mg (4.5 at.%, 2 or 3 at.%), decomposition behaviour during continuous cooling, XSAS and TEM examination 80−16264
Al-Zn-Mg (4.5 at.%, 2 to 3 at.%), decomp. behaviour during continuous heating 80−29922
$Al_{20}As_{40}Te_{40}$, amorphous alloy, radial distribution function anal., X-ray diffr. *(Spanish)* 80−28915
$Al_2Be_3Si_6O_{18}:Cu^{2+}$, synthetic beryl, ESR, optical spectra and X-ray diffr. meas. 77−16166
$Al_4C_3.3Be_2C$, X-ray difr. and TEM study 80−14973
Al_4Ca, phase transformation, struct. and orientation relationships 79−78963
AlF_3 based glasses, chem., thermal and optical props. *(French)* 80−70139
AlGaAsSb LPE growth, lattice-matched to GaSb, characterisation 80−60794
$Al_xGa_{1-x}P$, LPE, crystallographic obs. and electrolum. 80−88445
Al_3Mg_2, diffusionless phase transformation 80−104150
AlN film, oriented c-axis, low temp. deposition by reactive magnetron sputtering 80−76180
AlN, X-ray diffuse scattering 80−14964
β-AlO_3-$(Na,Li)_2O$, NMR, Raman and IR spectra, and X-ray diffr., heat treatment induced changes 80−107508
Al_2O_3, amorphous anodic film, struct. anal. 79−51452
Al_2O_3 anodic oxide film colour and structure obs. 78−11450
α-Al_2O_3, CVD-grown, cryst. perfection by transmission X-ray diffr. topography 79−65337
Al_2O_3, crystallite size and lattice distortion, determination using X-ray line broadening analysis, appl. to ceramic powders 79−8261
Al_2O_3, explosively compacted powder, struct. and annealing 77−55926
α-Al_2O_3, grain boundary segregation, electron microscopy 80−103361
Al_2O_3, hot pressing, microstruct., texture 80−40299
α-Al_2O_3, sapphire lamellar crystal, growth twinning investig. 77−4113
β-Al_2O_3-Ag_2O, stoichiometric and nonstoichiometric, structure comparison, phase transitions in stoichiometric compound *(French)* 80−60856
β-$11Al_2O_3$-Ag_2O, sublattice phase transition, stoichiometric 79−42241
Al_2O_3-Cr_2O_3, crystalline soln., microstrain rel. to lattice energy and strain energy 77−24411
Al_2O_3-Cr_2O_3, microstrain correction 78−59852
Al_2O_3-Cr_2O_3, solid soln., thermal expansion anisotropy, lattice consts. 80−54411
Al_2O_3-Cu composite, vapour deposition, microstruct., texture and surface topography 77−70001
Al_2O_3-Dy_2O_3, phase diagram at high temps. *(Japanese)* 79−38810
Al_2O_3-Dy_2O_3, phase diagram at high temps. *(Japanese)* 80−50619
Al_2O_3-Gd_2O_3 system, phase diagram at high temp. *(Japanese)* 80−45290
Al_2O_3-glass mixture, microstructural changes and shrinkage during sintering 80−25640
β-Al_2O_3-H_2O, stability and dehydration 78−51693
β-Al_2O_3-H_3O^+ protonic cond., struct. investig. 79−19213
β-Al_2O_3-$H^+(H_2O)_n$, p-type conductor, stability *(French)* 79−38063
β-Al_2O_3-M_2O, M=Ag, K, Rb, Na, Eu, X-ray diffuse scatt. 78−71725
β-Al_2O_3-NH_4^+, p-type conductor, stability *(French)* 79−38063
β-Al_2O_3-NH_4^+, protonic cond., struct. investig. 79−19213
β-Al_2O_3-NH_4^+, single cryst. characts. and AC cond. obs. 80−107514
Al_2O_3-Na_2O, β and β'' phases, formation by solid state reaction between $NaAlO_2$ and γ-Al_2O_3 80−29912
Al_2O_3-Nd_2O_3, phase diagram at high temps. *(Japanese)* 77−63649
Al_2O_3-Pr_2O_3, phase diagram at high temps. 77−63648
Al_2O_3-Pr_2O_3, phase diagram at high temps. *(Japanese)* 78−88449
Al_2O_3-SiO_2 system, andalusite and kyanite powders, shock induced transformations 80−45301
Al_2O_3-SiO_2-P_2O_5, refractory glasses, exam. of liquid immiscibility and crystallisation 78−55814
Al_2O_3-Sm_2O_3, phase diagram at high temp. *(Japanese)* 78−92253
$Al(OH)_3$, precip. from solns. containing Li ions, X-ray diffr. patterns and comp. determ. 80−76502
$Al_2O_3(H_2O)_3$, gibbsite, synthetic, crystallinity and topotactic reactions, X-ray diffr. obs. 78−63851
$Al(OOH)_3$, formed by reaction of methyl esters and $Na_2Al_2O_2$, exam. of props. 78−48346
$3.5Al_2O_3.2SiO_2$, mullite, decomposition by SiO_2 volatisation 80−61082
$Al_2O_3.3H_2O$-H_3PO_4-CaO(ZnO), phase equilib., $AlPO_4$ solid soln. 79−11586
$Al_2O_3.3P_2O_5.5H_2O$-SiO_2 composite, binding and struct. 79−66030
$AlPO_4$, high temp. behaviour up to liq. state, phase relations, X-ray diffr. and therm. anal. study *(French)* 80−10660
$Al_4Si_2C_5$, synthesis, X-ray diffraction pattern, lattice constants 80−50581
Al_2SiO_5, solid state reaction with $Ca_2P_2O_4$ *(Japanese)* 78−19702
$Al_{0.23}Te_{0.77}$, amorphous semicond., radial distrib. anal. by X-ray diffr. 78−71678
Am, high press. form, cryst. struct., X-ray diffr. obs. up to 14 GPa 80−24399
Am, phase transformation at high press. 80−107422
Ar, solid, density at melting and isochoric equations of state 78−83915
Ar, solid, lattice parameter determ. at melting 78−10174
AsF_5 intercalation with graphite and benzenoid systems, EPR, NMR and X-ray diffr. obs. 80−19775
As_2O_3, vitreous, X-ray diffr. study of struct. 80−92464
As_2O_5-$Rb_2O(Rb_2CO_3)$ system, phase diagram, polymorphic transform. 79−83181
$As_{2-x}S_{3+x}$, hydrogenated chalcogenide glasses, prep. by plasma decomposition 80−49735
As_2S_3, amorphous film, photodissolution of Ag, struct. changes 77−11815
As_2S_3 glass, at. struct. changes due to irrad., comp. variations and annealing 77−76323
As_2S_3 glasses, quasi-eutectic structure, X-ray and IR investig. 77−15320
As_2S_3-HgS, phase diag., IR spectra 77−36479
As_2S_5, amorphous, struct., vibr. and electronic spectra 80−64908
As_xS_y, bulk and vapour deposited films, comparison of struct., X-ray diffr. meas. 77−69195
As_xS_y vapour deposited film, struct. determ., X-ray and neutron diffr. correl. functions 79−60654
$(As_{0.4}S_{0.6})_{100-x}Cu_x$, glassy, struct. and elec. cond. study 80−59399
AsSI, X-ray diffr. study in vitreous and fused states 77−7675
$As_{2-x}Se_{3+x}$, hydrogenated chalcogenide glasses, prep. by plasma decomposition 80−49735
As_2Se_3-Sb_2Se_3, phase relns. 77−21118

X-ray diffraction examination of materials continued
AsSeI, X-ray diffr. study in vitreous and fused states 77−7675
$As_{60}Se_xTe_{40-x}$ glasses, crystallisation 77−35488
As_2Te_3-Tl_2Te system, phase diagram 77−16559
Au, Debye Waller determ. from modified Cheveau model 78−59918
Au, electrodeposited and sputtered, hard, reactive softening, X-ray diffr. studies 80−100414
Au, electron irradiated, low temp., Frenkel defects, diffuse X-ray scatt. study *(German)* 79−23601
Au film, epitaxially grown, struct., LEED, AES, resist. and X-ray diffr. analysis 77−59223
Au film, interface reaction with n-type $Ga_{0.7}Al_{0.3}As$ and GaAs 80−39482
Au film, MBE and field emission deposition on III-V semiconductors, comparative study 79−87016
Au film, on corundum, with intermediate Cu and Cr layers, struct. obs. 77−28084
Au, fine particles, gas evaporation technique for prep., X-ray diffr. study 80−75327
Au, fine particles, gas evaporation technique of prep., X-ray diffr. study, charact. temp. 80−75328
Au powder, ultrafine, sintering, coalescence growth stage 80−89174
Au, thin foil, spatial resolution of X-ray microanalysis 80−101065
Au/Pt interface, diffr. studies of conc. variations 79−42322
Au/Sn evaporated film, interdiffusion, X-ray diffr. and ion backscatt. obs. 79−33121
Au-Cu alloys, short-range order and energy of ordering, diffuse X-ray diffr. meas. *(Russian)* 77−43174
Au-Fe solid soln., props. during preparation by diffusion heating 77−12260
Au-Fe-Ni layer coating, Fe and Ni conc. meas. by X-ray diffr. *(German, English)* 80−34330
Au-Ge system, struct. of metastable phases *(German)* 80−108430
Au-Ge-Te ternary system, solid soln. in vicinity of GeTe, phase diagram *(French)* 77−85994
Au-Mn alloys, equiatomic region of phase diagrams crystallographic and mag. exam. 78−52755
Au-Pd-Zn system, quasibinary section phases investig. 77−12596
Au-Sn evaporated films, comp. and annealing behaviour, 20-400°C 77−76695
Au-Zn, (55 to 88 at.%), equilib. diagram, X-ray diffr. obs. 80−25660
(Au-Ge)-Ni film, for contacts to n-GaAs, metallurgical investigation using inert substrate 77−85313
(Au-Ge)-Pt film, for contacts to n-GaAs, metallurgical investigation using inert substrate 77−85313
AuAl formation by thin film interactions, identification by X-ray diffraction 79−99442
Au_3Cd, order-disorder phase transform., X-ray diffr. anal. *(Russian)* 80−45297
AuCu-Al thin film bilayer system, phase formation, backscattering spectra 80−96728
Au(Pd)-Zn, martensitic transformation, Hall coeff., specific elec. resistivity and X-ray powder diffraction 78−72774
$Au_4Si.m$, metastable phase, substruct. unit cell *(German)* 80−88091
$AuSn_4$-Sn, unidirectionally solidified, X-ray diffr. anal. of crystal struct. 78−91308
α-Al_2O_3, thermoluminescent trap stability, 450 to 1400°C 79−24372
B dispersed fractionated powder, struct. obs. 80−19703
B fibre reinforced Al, X-ray investigation of internal stresses *(Russian)* 77−73290
B films, prep. by H reduction of BCl_3, struct. and hardness 80−54543
B modifications, exam. of physical props. and electron structure 79−94954
B pellets preparation from powder, high-pressure testing appl. 80−50569
B, zone melting, solar energy appl., struct. and elec. props. 77−16492
B-B_4C materials, hot-pressed lattice constants determ. 79−79018
B-Si, (0 to 14.3 at.%), phase charact., regions of existence *(French)* 80−104117
B_4C, melting and phase homogeneity range 80−20911
BN, contact reactions with Ti and WC-Co at high pressures 80−61029
BN, conversion of wurtzite into cubic form, stress state effect 80−64943
BN, cubic, growth pressure-temp. region in system BN-Mg 79−66053
BN, cubic single crysts., dislocations and other defects, X-ray topography study 79−99207
BN, cubic struct. form. from hexagonal struct. at high press., catalytic effects *(Japanese)* 77−90308
BN, dislocation tilt boundaries, Laue photograph exam. 77−11562
BN, structural changes occurring during shock compression in presence of H_2O 80−16301
BN, superhard, dynamic charact. *(Russian)* 77−80593
BN, wurtzite-type, lattice distortions 77−11636
B_2O_3, vitreous, struct. obs. using small-angle X-ray scatt. 79−41966
B_2O_3-K_2O-Na_2O-Rb_2O-Cs_2O glass, small angle X-ray scatt. exam. of struct. 80−38922
B_2O_3-Li_2O-Fe_2O_3, prep. by quenching methods, exam. of microcrystalline precipitates of Li_2O-Fe_2O_3 *(French)* 79−20019
B_2O_3-NaF-$NaBF_4$, crystalline compounds and glasses 78−11210
BP coatings, on Mo by CVD and their composition and microhardness 79−28942
B_2S_3-Tl_2S system, phase diagram and verification 80−35165
B_2Se_3-Tl_2Se_3 system, phase diagram 80−35165
Ba hectorite, Ba ion position, water effect *(French)* 77−72593
Ba-Se(Te) systems, phase diagrams 77−36472
$BaAl_{12}O_{19}$, Czochralski cryst. growth, quality examination by polarisation microscopy, etching and X-ray topography 79−24428
$Ba_2Co_{2x}Zn_{2-2x}Fe_{12}O_{22}$, mechanically oriented, topotactic prod. technique, mag. props. 80−35140
BaF_2-MnF_2-FeF_3 system, X-ray investigation, struct. relations, liquid-solid equilibria diagram, study by DTA *(French)* 79−34017
BaF_2-NiF_2-CrF_3, X-ray crystallography study, phase identification at 700°C, cryst. symm. *(French)* 78−95733
BaF_2-YF_3 system, phase diagram 78−35363
$BaFe_{12}O_{19}$, Ca^{2+} substitution effect on hexaferrite lattice and mag. props. 80−60243
$BaFe_{12}O_{19}$, powder, milled and annealed, phase composition, lattice conts. and crystallite size 80−71677
$BaFe_{12}O_{19}$ powders, fast reaction presintering 80−97445
$BaFe_2O_4$ amorphous film, prep. by RF sputtering, crystallisation 80−76183
β-$BaFe_2S_4$, cryst. struct., X-ray diffr. obs. 80−84153
$Ba_3FeTa_2O_9$, Mossbauer and X-ray diffr. studies 80−103905

X-ray diffraction examination of materials continued
$BaGd_4X_5O_{17}$ (X=Si,Ge), cell consts., luminesc. of various rare-earth activators 80−93376
$BaHPO_4$, high temp. conversion to $Ba_2P_2O_7$, X-ray diffr. meas. 78−44371
$BaMnF_4$, phase transitions review 79−78378
$BaMnF_4$, spectroscopy near ferroelec. transition, dielec. anomalies near mag. ordering temp. 80−75965
$BaMoO_4$-CdO(PbO)(ZnO) and $BaMoO_4$-$CdMoO_4$($PbMoO_4$)($ZnMoO_4$) systems, phase diagrams 77−25034
$Ba(NO_3)_2$, isomorphous crysts., growth defects, X-ray topography 80−70188
$Ba_2NaNb_5O_{15}$, incommensurate refls. near ferroelastic transition, neutron and X-ray precession obs. 80−70395
$BaNb_2O_6$, solid-phase formation reaction, thermographic, X-ray phase and chemical anal. 77−12783
$Ba_3Nb_{10}O_{28}$, diffuse ferroelec. phase transition, dielec. const. and X-ray diffr. meas. 78−23419
BaO-B_2O_3-V_2O_5 glass, oxidation-reduction of V, thermodynamics 80−85169
BaO-Fe_2O_3-B_2O_3 glass, splat cooled, low temp. micromagnetism 80−34660
BaO-Fe_2O_3-Na_2O glass, mag. props. 78−88123
BaO-In_2O_3 system, stability of synthesized compounds 77−36487
BaO-SiO_2-Fe_2O_3 permanent mag. ceramics, exam. of phase diagram, using X-ray analysis, optical microscopy, electron probe anal., and thermal analysis *(German)* 79−29012
BaO-TiO_2-Al_2O_3 system, subsolidus equilibria, X-ray powder diffr. 80−108413
BaO-TiO_2-Cr_2O_3, new compound, phase relations *(Japanese)* 78−6911
BaO.$6Fe_2O_3$, solubility of CaO 80−100333
BaS, press. induced phase transform., X-ray diffr. study 80−39283
BaS-CaS:Cu phosphors, X-ray diffr. and fluoresc. spectra 80−40148
$BaSi_2$, trimorphic, transform. of three-connected Si nets, press.-temp. phase diagram, 40 kbar and 1000°C 80−75198
$Ba_3SiAl_{10}O_{20}$, Ce^{3+} activated, X-ray diffr. and luminesc. props. 80−49199
$BaSi_{2-y}Ge_y$, solid solution with type $SrSi_2$ struct., lattice parameters at high press. 80−54203
Ba_2SiO_4 cement, hardened, H_2SO_4 resistance *(Japanese)* 77−77602
(BaSrCa)O, cathodes, thermionic emission charact., X-ray struct. obs. 78−48270
$Ba_xSr_{1-x}Nb_2O_6$ crystals, defects and their characteristic features 80−88138
$(Ba_xSr_{1-x})SO_4$:Eu mixed crystal series, X-ray diffr. study of miscibility 80−2168
(BaTi) citrates, thermal decomp., thermal anal., IR and X-ray diffr. obs. 79−24735
$BaTiO_3$, 90° electric domain processes, mech. stress, X-ray diffr. 78−72478
$BaTiO_3$ ceramics, calcination effects, TiO_2 powder eval. *(Japanese)* 78−64516
$BaTiO_3$, epitaxial vacuum condensates struct. 79−95290
$BaTiO_3$, ferroelec., crit. X-ray scatt. 79−33636
$BaTiO_3$, ferroelec., X-ray diffr. topographic study of polarisation reversal 79−38442
$BaTiO_3$, ferroelec. domain form., X-ray topography 79−78638
$BaTiO_3$, ferroelec. thin films, r.f. sputtering, X-ray and microprobe obs. 79−47627
$BaTiO_3$, ferroelectric domain struct. and cryst. struct. changes, X-ray diffr. 77−24803
$BaTiO_3$, ferroelectric domains, X-ray topography 79−65815
$BaTiO_3$, polycryst., phase transition obs. in −170 to 220°C range *(Russian)* 80−103474
$BaTiO_3$, surface layer exam. 78−43805
$BaTiO_3$, synthesis by solid-solid reactions 79−38776
$BaTiO_3$, X-ray diffr. intensities, anomalous temp. depend. *(Russian)* 79−1484
$BaTiO_3$:Co, tricritical point, X-ray diffr. meas. 80−71341
$Ba(Ti_xSn_{1-x})O_3$ thick film, ferroelec., phase transitions and dielec. props. 80−97215
$Ba_{0.15}VO_2$, electrical cond., thermo-EMF, and lattice consts. 80−54685
$BaVS_3$, exam. of ferromagnetic, antiferromagnetic behaviour, depending on stoichiometry 78−52233
$BaY_4X_5O_{17}$ (X=Si,Ge), cell consts., luminesc. of various rare-earth activators 80−93376
$BaZrO_3$, cryst. growth and thermoluminesc. *(Russian)* 78−23604
Be, charge-density from X-ray structure factors 77−19893
Be, core electron distribution, X-ray diffr. and γ-ray Compton profile obs. 80−1958
Be metaphosphate glass, crystallization *(Japanese)* 77−72566
Be, thick film, amorphous, RF magnetron sputtering 80−80971
BeO-Al_2O_3-SiO_2-MF_2 (MF) glasses, M=Mg, Ca, Sr, Ba, Li, Na, fluoride ion role during crystn. 79−65176
Be_4TeO_7, cryst. growth by solid-state reaction and struct. *(German)* 78−18603
Bi film, structure and electronic props. 80−70562
Bi film, vap. deposited, effect on deposition parameters and substrate condition on crystallinity 78−10290
Bi film, X-ray diffr. anal., {001} textured growth 78−72016
Bi foil, splat quenched, preferred orientation 80−40381
Bi, low-temp. phase diagram, using diamond anvil pressure cell and X-ray diffr. 78−1951
Bi, thin film, oxidation process rel. to X-ray diffraction *(Japanese)* 79−29273
Bi:N film, ion-implanted, struct., X-ray obs. 77−76692
$Bi_2Al(Ga)_4O_9$, fluoresc. and X-ray data 78−80403
$Bi_3B_5O_{12}$, crystal growth from melt, exam. of growth kinetics 78−72717
$BiCo_{1-x}Fe_xO_3$, $x \leq 0.7$, X-ray powder diffr. data, configuration 79−64956
$BiCoO_3$, X-ray powder diffr. data, configuration 79−64956
$Bi_{24}CoO_{37}$, in Bi_2O_3-CoO system, X-ray diffr., thermal anal. and metallography obs. 80−24598
$Bi_{12}GeO_{20}$, cryst. chirality and optical rotation sense 79−61327
$Bi_{12}GeO_{20}$, X-ray sensitive ceramic, sintering 80−25621
Bi_3GeVO_9, dielec. props. and twin struct. 77−12350
$BiH(PO_3)_4$, condensed, thermal behaviour and IR spectra 80−19912
Bi_2O_3-$AlPO_4$, phase equilib. 80−35168
Bi_2O_3-CdO system, phase diagram 77−25032
Bi_2O_3-CoO system, X-ray diffr., thermal anal. and metallography obs. 80−24598

X-ray diffraction examination of materials continued
Bi_2O_3-SrO, solid state phase diagram, thermal and high temp. X-ray anal. *(French)* 79−65190
Bi_2O_3-TiO_2-Nb_2O_3, subsolidus phase equilibria 77−55954
EGa-Bi_2O_3+KCL, quantitative anal. of multcomponent powders, full-profile refinement of Guinier-Hagg X-ray film data 79−39249
BiP_5O_{14}, condensed, thermal behaviour and IR spectra 80−19912
$Bi_{0.9}Sb_{0.1}$, epitaxial film, defect struct. and galvanomagnetic props. 77−89889
$Bi_2(SeO_4)_3$, single cryst. growth in silica gels, X-ray diffr., IR and emission spectroscopy study 79−74075
$Bi_{12}SiO_{20}$, cryst. chirality and optical rotation sense 79−61327
$Bi_2Sn_2O_7$, polymorphic phase transition, X-ray, DSC, SHG, dielec. and optical obs. 80−44163
$BiTaO_4$, X-ray and ESR study of phase changes 78−72476
Bi_2Te_3 single crystals, melt grown, structural perfection 80−15101
$Bi_2W_2O_9$-$BiVO_4$, solid soln., X-ray diffr. study 80−2001
C, amorphous, diffraction intensities, chem. bonding effects 77−72557
C, amorphous, X-ray and electron diffr. intensities, model struct. 78−26441
C fibre, coated with pyrolytic SiC 78−60857
C fibre reinforced glassy C composite, graphitisation 79−15643
C fibre reinforced Ni, struct. and strength change at high annealing temp. *(Russian)* 79−66076
C fibres, fibril dimension estimation, using lubricostatic structural models 80−54171
C fibres, PAN based, structural parameters obtained by electron microscopy and X-ray diffr., comparison 77−47353
C fibres, surface treatment with tetra-(octadecyl) titanate, X-ray and electron microscope study *(Japanese)* 79−74280
C fibres struct. and physical props. effects of B additions and heat treatment temp. 78−68715
C, glassy, struct. evolution due to thermal treatment at 1000 to 2700°C, layers evolution 77−68923
C, glassy, struct. evolution due to thermal treatment at 1000 to 2700°C, tridimens. config. 77−68924
C, glassy, struct. parameter var. with heat treatment temp. 77−11488
C, graphite content, quantitative X-ray phase analysis 79−52820
C, graphitisation, cooperative accelerating effect of $CaCo_3$ and N_2 80−55429
C microneedles, grown on W wires under intense elec. fields, X-ray diffr. and AES 80−54580
C, non-graphitic, two-dimensional X-ray reflections, anal. 80−24308
C, nongraphitizable, catalytic graphitization by Cr_2O_3, MnO_2 80−97440
C, prod. from solid-state reduction of carbonate ions, X-ray diffr. 78−56594
C, pyrolised non-graphitising, modified struct. model, interference function 78−67681
C, structure change, during thermal ordering, radiation disordering 80−54283
C, turbostratic, formed in phenolic resin C by catalytic graphitisation of dispersed Ni, TEM study 79−77466
C-S-H gel, formed in hydration of C_3S pastes, chem. comp. 79−79346
$C_{12.6}AuCl_3$, intercalation compound, struct. *(French)* 78−42982
CC Al-Zn-Mg (4.5,1(2)(3) at.%), decomposition during ageing, preageing and cooling rate influence 80−20938
$C_{12}^{2+}PtF_6^-$, struct. and elec. props. 80−70183
CU_2O high press. phase transforms, optical and X-ray studies 80−44313
$CaAl_2O_4$, phase transform. accompanying hydration, US and X-ray obs. 79−39115
$CaCO_3$ single crystals, effect of defect struct. charact. on X-ray diffr. 79−65089
$CaCO_3$+SiO_2, in presence of NaF, thermal decomposition of Ca_2SiO_4 formation 78−68889
$CaEuAl_3O_7$, mechanism of solid-phase reactions of formation and physicochem. props. 77−52622
CaF_2, etching in H_2SO_4, etch pit morphology and $CaSO_4$ growth 80−6408
CaF_2, polished crysts., rocking curve meas. *(German)* 78−2347
CaF_2-(Y,R)F_3 (R=any lanthanide except Pm, Eu), phase diagrams 78−84783
CaF_2-AlF_3-Na_3AlF_6(-Al_2O_3), phase equilibria, X-ray diffr. and DTA meas. 80−108409
CaF_2-ScF_3, phase relationships at 100 kbar and 1200°C 77−43335
CaF_2+SiO_2+$Mg(OH)_2$ matrix, quantitative anal. of multcomponent powders, full-profile refinement of Guinier-Hagg X-ray film data 79−39249
Ca_2GeO_4-$Ca_4(PO_4)_2$ system, phase equil. 77−36469
$CaHPO_4.2H_2O$, gel grown crysts., quality study by X-ray topography 79−87572
$CaLaFeO_4$, X-crystallog. and Mossbauer spectrum *(French)* 77−66447
$Ca_4La_6Si_4P_2O_{26}$, and derivatives, synthesis, physicochemical props. 77−21066
$CaLn_4(SiO_4)_3O$ silicate oxyapatites, prep. and props. of single crystals 77−28704
$CaMg(CO_3)$, dolomite, kinetics and thermodynamics of decomposition to metastable solid product 78−80740
CaO and $CaO:Gd^{3+}$, crystal growth from molten solvent LiF-20 mole % CaF_2 77−77358
CaO, produced from $CaCO_3$ powder decomp. in vac. and in CO_2 80−45255
CaO-Al_2O_3-SiO_2 diffusion triangular diagram, diffusion between lime and sintered kaolinite *(French)* 79−69296
CaO-B_2O_3-Fe_2O_3 glasses, effect of heat treatment on electronic props. 78−2480
CaO-P_2O_5-H_2O system, phase diagram at 200°C 80−45286
CaO-SiO_2, melt, effect of cooling rate upon glass transition, X-ray analysis 79−27920
CaO-SrO-Fe_2O_3 system, phase relations, Sr hexaferrite field occurrence 80−93545
7CaO-V_2O_3-$2SiO_2$, X-ray diffr. data 80−81037
β-(CaO_2)-SiO_2-H_2O, SEM and X-ray diffr. exam. of structure, crystallisation props. 78−73012
3CaO.Al_2O_3-$CaSO_4.2H_2O$-CaO-H_2O, citric acid effect on reactions 78−27725
3CaO.Al_2O_3+$CaSO_4.2H_2O$, effects of prehydration on liq. hydration 79−100354
ZCaO.SiO_2-2CaO.$Na_2O.P_2O_5$ system, polymorphism and solid soln. 78−19731
CaO.$3B_2O_3$, form. by dehydration of hydrated calcium borates *(Japanese)* 79−74378

X-ray diffraction examination of materials continued
CaO.$6Al_2O_3$, thermodynamic stability, reaction with Ti, Cr and Zr oxides 80−92687
$Ca_{10}(PO_4)_6(OH)_2$, hydroxyapatite, prep. by hydrotherm. recrystn., composition and props. study 79−33913
$Ca_5(PO_4)_3OH$, prep. from sulphate, X-ray diffr. and IR spectrosc. 80−29893
$CaSO_4$, thermal expsn., 22-1000°C 80−6530
$CaSO_3.1/2H_2O$-$CaSO_4$ solid solution, prepared by coprecipitation from solns., exam. 79−20034
$CaSiO_3$, structural transform. during hydration, IR spectra and X-ray diffr. meas. 77−76548
Ca_2SiO_4, structural transform. during hydration, IR spectra and X-ray diffr. meas. 77−76548
Ca_2SiO_4, structurally related phases, high-temp. X-ray powder diffr. 80−81050
β-Ca_2SiO_4, very reactive powder, prep. 77−55924
Ca_3SiO_5, structural transform. during hydration, IR spectra and X-ray diffr. meas. 77−76548
$Ca_6Si_6O_{18}.4H_2O$, tobermorite synthetic crysts., hydrothermal growth, TEM and X-ray diffr. characterisation 79−43122
$Ca_{0.15}VO_2$, electrical cond., thermo-EMF, and lattice consts. 80−54685
$CaZrO_3$-$CaHfO_3$, solid soln. formation obs. 77−86003
$Ca[B_3O_4(OH)_3].H_2O$, differential thermal X-ray anal. of phase transitions in non isothermal conditions 79−52205
$Ca[B_3O_3(OH)_5].4H_2O$, differential thermal X-ray anal. of phase transitions in non isothermal conditions 79−52205
Cd, anharmonic interactions, elastic X-ray scatt. 78−75755
Cd films, struct. and props., X-ray diffr. spectra anal. 80−80119
Cd foil, splat quenched, preferred orientation 80−40381
Cd, single cryst., root-mean-square atom displacement, X-ray meas. 78−75624
Cd-As system, phase diagram, $CdAs_4$ struct. 79−74138
Cd-Ge-As system, quenched samples, phase diagram, DTA after annealing 79−69226
Cd-Zn alloys, splat-quenched, X-ray diffr., SEM and TEM study of struct. 79−66077
Cd_3As_2, amorphous to crystalline transform. 79−77519
Cd_3As_2, vapour phase single cryst. growth, X-ray topographic obs. of perfection 78−9976
$CdCO_3$, topotactic decomp., X-ray diffr. obs. 77−44478
$Cd_{1-x}Cu_xCr_2Se_4$ solid solution, spinel struct., X-ray investigation 79−78940
$CdGa_2Se_4$-$CdIn_2Se_4$ solid solutions, order-disorder transition 79−19181
$CdGeAs_2$, amorphous, thermal gradient expts., recrystn. 80−55438
$CdGe_{1-x}M_xAs_2$ (M=Si,Sn,Pb), (x=0.0,0.1,0.2), amorphous struct. 78−22651
$CdGe_{1-x}Sn_xAs_2$, amorphous, radial distrib. anal. and mag. susceptibility meas. 77−43152
$Cd_{65}Hg_{35}$ and $Cd_{55}Hg_{45}$, X-ray study of cryst. struct. and thermal expansion 80−24405
$Cd_xHg_{1-x}Te$, vac. evap. film struct. rel. to carrier scatt. 77−85116
CdI_2, 2H to 4H structural change, X-ray diffr. study 78−75614
CdI_2 crystals, growth conditions effect on polytypism, X-ray diffr. study 80−28942
CdI_2, hexagonal-rhombohedral polytypic transformation, electron diffr. and X-ray diffr. obs. 80−49163
CdI_2 polytypes, vapour growth mechanism 80−84124
$CdI_{2-x}Br_x$, vapour grown mixed cryst., growth and polytypism 79−69044
$CdIn_2S_4$ film, vac. deposited, growth, struct., optical and photoelectronic props. 80−10831
$CdIn_2Se_4$, needle-like cryst. X-ray exam. 79−42031
CdLn(TiNb)O_7, Ln=La-Lu, synthesis physicochem. props. 77−43186
$Cd_2(NH_4)_2(SO_4)_3$, X-ray and optical studies of ferroelec. phase transition 79−38495
$Cd_2Nb_2O_6S$, pyrochlore struct., ferroelec., dielec. and structural study 79−38488
CdO, X-ray determ., Debye-Waller factors, Debye temp. and vibration amplitudes 78−55928
CdO-B_2O_3-GeO_2 system, phase equilibria at 800°C, X-ray powder diffr. anal. 79−4956
$Cd(OH)_2$ decomposition, martensitic character of struct. transition, CdO crystallite shape determ. *(French)* 78−10194
$CdPS_3$, layered, organometallic intercalates, X-ray diffr., optical absorpt. and mag. props. 80−45103
$Cd_3(PS_4)_2$, synthesis by roasting, and exam. of props. 79−4926
CdS, chemically sprayed film, prod. by centrifugal disk atomizer, struct. 79−65343
CdS, deposited anthraquinone, decoration patters 77−1137
CdS, dry process formation from CdO and S *(Spanish)* 78−56607
CdS, epitaxial layers on Cd single crystal, direct synthesis and struct. 78−68628
CdS film, on Si, structural and transport props. 78−6463
CdS film, prep. by hot wall technique, morphology and semicond. props. 79−95292
CdS, film, X-ray diffr. and elec. cond. 78−64149
CdS layers, struct. investigation by electron and X-ray diffr., and electron microscopy, growth mechanism 79−56094
CdS, vacuum epitaxial growth on $CuInSe_2$ 78−92193
CdS, X-ray diffr. investig. of high-press. polymorphism 77−43324
CdS, X-ray diffuse scattering 80−14964
CdS:Cu(Se)(Zn), heavily doped, defect struct. 78−22756
CdS:In, flash evaporated films, struct. anal. 80−20792
CdS:Mn, vacuum deposited film, Mn migration, EPR and X-ray study 80−65411
CdS_xSe_{1-x}, flash evaporated films, struct. anal. 80−20792
CdSe (1120), surface electronic struct. and chem. struct. 78−14788
CdSe film, struct. props., influence of O_2 partial press. and substrate temp. during vapour deposition 77−39751
CdSe film, vac. deposited, elec. resist. and surface changes by laser annealing 80−2491
CdSe, hexagonal, anharmonicity, X-ray intensity meas. 77−43286
CdSe, X-ray diffuse scattering 80−14964
$CdSe_xTe_{1-x}$ film, polycrystalline, deposition and physical props. 77−4741
$CdSn_xO_y$, DC reactively sputtered film, elec. and optical props. 79−87022
Cd_2SnO_4, film, spinel struct., X-ray diffr. study 78−75644
CdTe, grown by chem. transport, morphology, struct. and microhardness *(Russian)* 78−22729

X-ray diffraction examination of materials continued
CdTe layers, on CdS substrate, cryst. perfection and defects, X-ray diffr. obs. 79−56081
CdTe, temp.-depend. of root-mean-square dynamic displacements, characteristic temp., X-ray study 78−83895
CdTe, thermal cond. and X-ray topography investig. of cryst. defects 77−39706
CdTe-In system, equilib. phase diagram and liq. phase epitaxial growth of CdTe from In soln. *(Japanese)* 80−71634
$(CdTe)_{1-x}$-$(ZnSe)_x$ system, mutual solubility and band gap energy *(Japanese)* 77−51501
$CdTe_{1-x}Se_x$ solid solution films, prep., struct., and photocond. 80−54541
$Cd_{1-x}Zn_xS$:In, film, technical data, for low cost solar cell 79−48127
Ce-Co-Al (0-33.3 at.% Ce), isothermal section, X-ray study *(Ukrainian)* 80−39002
Ce-M intermetallic cpds., M=3d transition metal, sorption of H_2, structural charges 80−88429
Ce-Nd-Si, phase diagram, X-ray anal. *(Ukrainian)* 79−38792
Ce-Pr powder, DHCP⇄FCC transition, X-ray, DTA and resistivity studies 80−50629
CeAsS, and homologs, struct. determ. *(French)* 77−51361
$CeCo_{5-x}Cu_x$, $0 \leq x \leq$ internal oxidation kinetics, oxide struct., X-ray study 80−104329
$Ce_6(MoO_4)_8(Mo_2O_7)$, X-ray examination crystal struct. 78−67687
$CeNH_4P_4O_{12}$ and $Ce(NH_4)_2(PO_3)_5$, synthesis by solid-phase reaction, characts. 80−60778
$CeNbO_{4+x}$, oxidation-reduction reactions 78−39930
Ce_3NbO_x, $CeNbO_x$ and $CeNb_3O_x$, redox processes, elec. resist., phase anal., mag. suscept., thermogravimetric meas. 78−34482
$CeNiC_2$, struct. determ. using X-ray diffraction *(Ukrainian)* 80−33949
CeO-SiO_2, molten and glassy state, X-ray diffr. determ. of struct. *(Japanese)* 78−9936
CeO_2, plasma deposition of crysts. and their characterisation 80−20800
CeO_2-rare earth oxides, complexes of the 'two impurity ions-vacancy' type 79−95004
Ce_2O_5-P_2O_5 glass, crystallisation 77−51326
$CePd_3$ single crystal Czochralski growth and characterisation 80−60767
$CeRu_2$, H absorption induced Ce valence change, mag. and supercond. props. 80−50042
$Ce_4Si_2O_7N_2$, lattice consts., X-ray diffr. anal. 80−28986
$CeTaO_{4+x}$, oxidation-reduction reactions, phase equilibrium, thermogravimetry and magnetic susceptibility meas. 78−39930
CfO_x-O_2 system, for $1.50<O/Cf<1.72$, temp., press. and stoichiometry depends. 77−28009
Cm-O system, phase obs. in $CmO_{1.50}$-$CmO_{1.71}$ region 77−36490
CmAs(N)(P)(S)(Sb)(Se)(Te), lattice consts., X-ray diffr. study 80−33953
$(Co,Fe)_{0.75}B_{0.25}$ metallic glasses, annealed, equilib. crystalline phases 80−3019
Co complex, $[Co(NH_3)_6]I_3$, enantiotropic phase transition obs. 80−107412
Co, corrosion in Ar-SO_2 atmospheres, scale struct. obs. *(Japanese)* 80−55568
Co evaporated film, X-ray diffr. study 80−6663
Co ferrite, growth on fine acicular γ-Fe_2O_3 particles 80−29871
Co film, evaporated, texture and columnar struct. 80−54566
Co film, on Si substrate, laser irrad., cellular struct. and silicide form. 80−10710
Co, reactive cathodic sputtering *(French)* 77−63519
Co, transformation from FCC to HCP struct *(Russian)* 77−47570
Co-Al, band struct. and density of states, KKR method and X-ray meas. 80−10863
Co-Al, mag. struct. of Co rich intermetallic cpd., neutron scatt , cluster model 78−80130
Co-Al alloy, multilayer martensite phases, illustration of polytype structures 80−84932
Co-B alloys, amorphous, saturation magnetisation, mag. moments, X-ray diffr. obs. 79−4704
Co-CoAl eutectic, invariant composition redeterm. 78−3099
Co-Cr system, phase diagram re-determ. from thermodynamic data 78−76631
Co-Cr-Al, exam. of cyclic oxidation resistance at 1100 and 1200°C, comparison with Ni-Cr-Al system 78−88572
Co-Cr-Ni-Ta-Al-Y (25, 10, 5, 3, 0.5 wt%), exam. of hot corrosion 79−20251
Co-Cu, electrodeposited alloy, struct. and physicochem. props. 78−35327
Co-Cu alloy, multilayer α'-phase form. during martensitic transform. *(Russian)* 77−59785
Co-Fe epitaxial films, singularities of $\gamma \rightarrow \alpha$ transform., X-ray diffr. obs. *(Russian)* 79−52198
Co-Ge binary system, phase diagram rel. to that of Ni-Ge *(French)* 80−97463
Co-Ni-Cr-Nb, effect of Fe addition on precipitation behaviour 80−29962
Co-Os, short-range order parameters, ordering energy on first coordination sphere *(Russian)* 79−69058
Co-P, amorphous electrodeposited foils, struct. characterisation by X-ray scatt. 79−77932
Co-P, amorphous foil, complex permeability and eddy currents, annealing induced short-range order 77−8360
Co-P, electrodeposited alloys, heat-induced structural changes *(Japanese)* 80−89263
Co-Pt, struct. and mag. props. rel. to degree of order 78−72368
Co-Si film system, interaction kinetics 78−79823
Co-Ti, multilayer and imperfect martensitic phases form. 78−19754
Co-V (10 to 23 wt.%) system, phase constitution, X-ray and elec. resist. meas. 80−3007
Co-W-C system, η-carbide linear expansion coeff., X-ray diffr., 30-1500°C 77−25021
$CoAl_2O_4$, cation distribution, Mossbauer and X-ray diffr. obs. 78−95532
CoB-based boride coatings on Co base alloys, microstruct. and mech. props. 78−11427
$Co_{67}Er_{33}$ amorphous alloy, sputtered, local order and amorphous struct. 80−88061
$Co_{0.91}Fe_{0.09}$, X-ray scatt. factor 79−41907
$CoFe_2O_4$ mag. fluid particles, comp., struct., and mag. props. 80−60374
β-CoGa, Cu addition effects on defect struct. *(German)* 77−11546
$Co_2Ga_{2-x}M_x$ (M=V, Cr, Mn, Fe), mag. props. and order 77−12093
Co_5Ge_3, phase and struct. characts. 77−36450
Co_xMM, (MM+mischmetal), coercive force, effect of preparation conditions 78−95467
CoO on Co_3O_4, oriented growth following Co_3O_4 pyrolysis 78−80739

X-ray diffraction examination of materials continued
CoO, under controlled atmosphere, exam. of composition and temp. dependence, of lattice parameter *(French)* 79−19214
CoO-MgO-Al_2O_3-Cr_2O_3-TiO_2, form. and colour of spinel solid soln. *(Japanese)* 77−32550
CoO-MgO-Cr_2O_3-Fe_2O_3-TiO_2, form. and colour of spinel solid soln. *(Japanese)* 80−16059
CoO-ZnO-Al_2O_3-Cr_2O_3-TiO_2 system, form. and colour of spinel solid soln. *(Japanese)* 77−25001
$Co_{0.9}P_{0.1}$ noncrystalline ferromagnet, electroless deposited, struct. and microscopic mag. props. 80−88063
$Co(S_xSe_{1-x})_2$, $(0 \leq x \leq 1)$, mag. props. and elec. resist. 79−65657
$CoSe_2$, bulk mag. susceptibility, anomalous temp. depend., NMR and X-ray diffr. meas 79−87229
$CoSeO_4.4H_2O$, cryst. chemical and X-ray powder data 79−51073
$Co_{75}Si_{15}B_{10}$, amorphous, crystallisation study *(Japanese)* 78−9959
$CoTe_2$-GeTe, phase diagram, from thermal, X-ray, microstructural analyses 80−55367
$CoTi_{1-x}Al_x$, form. of mag. moment of Co atom, X-ray diffr., mag. meas. and NMR 77−43819
$Co_{90}Zr_{10}$, ferromag. amorphous alloy, crystn. and domain struct. study 80 107056
$Co_{0.83}[Pt(C_2O_4)_2].6H_2O$, quasi-one-dimens. conductor, Peierls distortion and superlattice, X-ray study 80−29397
Cr, corrosion in SO_2, 700-1000°C 80−97642
Cr, crystal structure below Neel temp., X-ray diffr. study 78−83772
Cr electrodeposit on steel, stress meas., X-ray methods 79−29298
Cr electrodeposits, hardness estimation 77−36708
Cr, evap. film, refl. and struct. 78−72021
Cr film, preparation by decomp. of bis-arene cpds., struct. and phys. props 80−60785
Cr film, residual stress meas. by X-ray diffr. using $\sin^2\psi$ method 79−15059
Cr, interaction with dense stream of N ions, metallography, microhardness, specific volume *(Russian)* 80−15169
Cr-Al, band struct. and density of states, KKR method and X-ray meas. 80−10863
Cr-Al alloys, antiferromag., charge and spin density, neutron and X-ray diffr. 77−31971
Cr-Cr_2O_3, black chrome electroplating for solar energy photothermal conversion, prep. and struct. 79−74544
Cr-Fe-Ga system, phase obs. at 800 and 820°C *(Russian)* 78−23662
Cr-Ge liquid and amorphous alloys, struct. props., cond., viscosity, surface tension *(Russian)* 80−54119
Cr-Ge system, phase diagram, thermal anal., X-ray diffr., microhardness, and electron probe anal. *(French)* 80−97462
Cr-Ge system, XPS, X-ray and neutron diffr. and mag. meas. to study chem. bonding and electronic struct. 80−60749
Cr-Mo-N system, at high-pressure, temp., X-ray anal., phase diagram 80−50607
Cr-Ni(Co)-Ga, phase equilibria diagrams at 800 and 600°C *(Ukrainian)* 78−92236
Cr-Pt alloy, mag. props., effect of atomic environment 78−23247
Cr-Pt thin film couple, diffusion, new Cr-Pt phases obs. 79−42319
Cr-rare earth, dil., oxidation of Cr, effect of rare earth impurities 79−79160
Cr-SiO films, sputtered, elec. and struct. props. 80−39694
$Cr_{1-x}Fe_xS$, metal-dielec. transition, X-ray, thermal anal., elec. cond. temp. depend. 78−67942
Cr_2O_3, hydrostatic compression, X-ray diffr. meas. 79−99269
Cr_2O_3 powder, activation and sintering 77−21078
Cr_2O_3-Mo_2O_3, catalyst, effect of Al_2O_3 additives on catalytic activity, in oxidation of methanol to formaldehyde *(Russian)* 79−66346
$Cr_2O_3.SH_2O$, heat-treated, narrow particle size distrib., surface props. 78−85210
CrS_xTe_{1-x} (x=0 to 0.2), magnetic props. study 80−11194
$CrSe_2$, layered, phys. and elec. props. 80−44594
Cr_3Si, charge distrib. X-ray diffr., rel. to supercond. V_3Si 77−68944
Cr_3Si, single cryst. growth by floating zone method, X-ray and neutron diffr. study 79−74084
$Cr_{2.8}V_{0.7}Fe_{3.4}C_3$, stacking fault study, morphology, comp. and struct. 80−84190
Cs, accurate struct. factor determ. by X-ray and neutron diffr. 79−51046
Cs graphite, structural ordering in intercalation compounds 78−26539
Cs-SiO_2-Al_2O_3 system interactions, getter development for radiocaesium 80−83208
$CsAg_3Se_2$, crystal struct., X-ray study *(German)* 78−83795
CsAu, semicond. and metallic, NMR line shape, Knight shift, X-ray diffr. study 78−68402
CsCl, twin form. by compressive stress during phase transform. 80−49358
CsCl:Fe, defect struct., Mossbauer spectra and X-ray diffr. obs. 80−7237
$CsCuCl_3$, Jahn-Teller effect induced phase transitions 79−47439
$Cs(D_xH_{1-x})_2AsO_4$, phase transition exam. 77−12340
$CsFeF_4$, struct. phase transition at 250K 80−10663
$CsFeF_4$, two dimensional structural phase transitions, sp. ht., optical, dielec., X-ray diffr. meas. 79−69240
CsH_2PO_4, ferroelec., X-ray and dielec. studies on phase transition 79−38477
CsH_2PO_4, ferroelec., X-ray struct. study at room temp. 80−88113
CsI:Tl, precipitation of Tl solid solns. 80−70419
$Cs_2LiFe(CN)_6$, struct., phase transformations, temp. depend. Raman spectra 79−11416
$CsNO_3$, single cryst., γ-irradiated, X-ray diffr. effects 79−46704
$Cs_2NaLn(III)Br_6$, prep., cryst. genesis, and charact. by X-ray powder diffr. *(French)* 79−43135
$Cs_2NaM^{3+}Cl_6$ (M^{3+}=Bi,Nd,Pr), ferroelastic phase transitions, thermal expansion, elasticity, and X-ray anal. 80−70393
$Cs_2Ni_3(P_2O_7)_2.nH_2O$, thermal dehydration 80−35513
Cs_2NpBr_6, prep., cryst. struct. and enthalpy of formation 78−10014
Cs_2O-SiO_2(-GeO_2) system glasses, electron radial distrib. curves 78−87622
$CsPO_3$-$Sr(PO_3)_2$ system, physicochem. investigation 77−35666
$CsPbCl_3$, lattice thermal expansion, X-ray powder technique 80−19965
$Cs_2PbCu(NO_2)_6$, incommensurate Jahn-Teller transition, Huang scatt. 80−70401
$Cs_2PbCu(NO_2)_6$, one-dimensional stacking order 80−28941
$Cs_2PbCu(NO_2)_6$, successive Jahn-Teller phase transitions, neutron and X-ray diffr. 78−95154

X-ray diffraction examination of materials continued
$Cs_5Sn_3X_{3(5)(6)}$ (X=Cl, Br, I), single cryst. gel growth, X-ray diffr. study 80−29870
Cs_3VF_4, structural phase transitions above room temp. 80−29167
$Cs_9(XeO_3Cl_2)_4Cl$, neutron and X-ray diffr. struct. determ., Xe-Cl bonding 78−30591
$Cs_{1.75}[Pt(CN)_4].xH_2O$, one-dimensional, X-ray diffuse scatt. meas. 77−19937
Cu annealed and cold rolled, with bamboo structure, exam. of grain boundaries as vacancy sources in diffusional creep 78−88508
Cu, commercial pure, creep-rupture props., vacuum,, SEM and X-ray diffr. meas. *(Japanese)* 78−72843
Cu complex, bis-(alkylammonium) (11) tetrachloride, perovskite, lattice perfection 78−87633
Cu complex, $Cu(en)_3Cl_2.0.75$ en, X-ray and ESR data, Jahn-Teller distortions 78−80206
Cu crystals, floating zone method growth, X-ray diffr. study of preferred growth 80−7490
Cu, Debye Waller determ. from modified Cheveau model 78−59918
Cu, deformation band, role in fatigue crack nucleation and propag. 79−24585
Cu, dislocation substructure formation under hydrostatic extrusion 78−56696
Cu electrodeposits, collagen and chloride additions effects obs., on morphology and crystal orientation 78−51852
Cu, electron irradiated, small-angle X-ray scatt. investig. of stage III recovery 77−7763
Cu film, electrodeposited, recrystallisation kinetics, X-ray scatt. *(Russian)* 78−60045
Cu film and filings, interrelation between dynamic and static distortions, X-ray diffr. meas. *(Russian)* 77−43305
Cu, Frenkel defects, diffuse X-ray scatt. obs. *(German)* 79−23600
Cu layers, grown by ion plating method on Si wafers and glass plates *(Japanese)* 77−21039
Cu, neutron irradiation induced dislocation loops and point defects, temp. depend., 316 to 483K 77−51410
Cu, plastically deformed, lattice strain distrib. *(German)* 80−85012
Cu, positron lifetime changes and X-ray particle size meas. during cyclic fatigue 79−43060
Cu, self interstitial struct. determ., and vacancy clustering, X-ray exam. 78−47351
Cu, stress strain anal. of single crystal induced by absorbed H_2 *(Japanese)* 78−11276
Cu, vacuum deposited on Al substrate, recrystallisation 78−60044
Cu whiskers, Bragg case diffr. curves by X-ray triple cryst. diffr. method 79−51461
Cu, wire, axial texture after electroplastic drawing, X-ray struct. investigation *(Russian)* 80−104177
Cu wire, electroplastic drawing X-ray diffr. anal. and mech. props. exam. *(Russian)* 79−29138
Cu/Ni interface, diffr. studies of conc. variations 79−42322
Cu-Ag (3 at.%), plastically deformed, lattice strain distrib. *(German)* 80−85012
Cu-Ag interface, interdiffusion, X-ray and electron microprobe data 77−4225
Cu-Ag-Ge, Hume-Rothery glass form. 80−96449
Cu-Ag-P(6-14, 11-14 wt.%) amorphous, crystn. and elec. props., X-ray diffr., elec. resist. and DTA meas. *(Japanese)* 80−84088
α- Cu-Al (6 to 17 at.%), short-range order investigated by diffuse X-ray scatt. *(Russian)* 80−104187
Cu-Al system, high temp. lattice parameters by X-ray diffr. 80−28950
Cu-Al-Ni, formation of martensitic phases during deform. by extension 79−20048
Cu-Al-Ni, long period martensite phases, X-ray diffr obs. 80−7571
Cu-Al-Ni (13.8, 7.9 wt.%), cooling rates effect on internal friction *(Japanese)* 80−39217
Cu-Au film, short wavelength composition modulation, interdiffusion exam. 77−72723
Cu-Be-Co, discontinuous reaction, analytical TEM 80−100842
Cu-Be(Al)(Mg)(Ti), study of internal oxidation using central diffusion of X-rays *(French)* 79−37839
Cu-Cd alloys obtained by electrolysis, struct. 78−91552
Cu-Cl boracite, ferroelec., X-ray study on phase transition 79−33622
Cu-Ge, thermal expansion, X-ray determ. 78−26697
Cu-M alloys (M=Zn,Al,Sn,Mn,Pb), diffusive redistrib. during friction *(Russian)* 78−52999
Cu-Ni, powder mixtures, form. using electric discharge sintering 77−12563
Cu-Ni alloys 706 and 715, corrosion in flowing sea water, dissolved sulfide effect 80−35379
Cu-Ni crystals, growth, H_2 reduction of CuI-$NiBr_2$ mixture, habit study by X-ray difr., optical and SEM 79−60665
Cu-Ni-Be-(Al) (30,0.5,(0.2-2) wt.%), Al addition effect on grain boundary reaction *(Japanese)* 80−54254
Cu-Ni-Sn, thermal decomposition after prior cold work 78−15427
Cu-Ni-Ti system, phase equilibria in Cu rich region and Cu-T quasi-binary constitution *(Japanese)* 80−89203
Cu-Ni-Ti system, reactions with melt in Cu-rich region *(Japanese)* 80−89202
Cu-Pd alloy, pressure effect on β-phase transition by elec. resist. meas., X-ray diffr. meas. 79−15660
Cu-Sb alloy, splat-quenched, energy dispersive X-ray diffr. 78−23728
Cu-Si (16.5 wt.%) alloy, X-ray diffr. patterns, stress induced martensite from γ phase 79−70066
Cu-Si alloy, FCC→HCP transition mechanism 77−77479
Cu-Sn (15 at.%), temp. depend. of elastic consts. above martensitic transition temp., US exam. 78−76695
Cu-Sn-Al, deform at high temps. *(Polish)* 80−89284
Cu-Ti (Zr), strength improvement by thermomechanical treatment *(Japanese)* 78−48426
Cu-W, powder, prod. by controlled reduction in H_2O/H_2 mixture of $CuWO_4$ 79−24458
Cu-W composite powder, prod. by H_2 reduction of $CuWO_4$ 79−20006
Cu-W sintered materials, porous, mech. and X-ray elastic const. *(German)* 77−81288
Cu-W(Fe)(Ag), biphase material X-ray stress determ. *(Russian)* 79−5097
β_1-Cu-Zn mixed crystal, metastable structural Umklapp process, isothermal phase transform. *(German)* 78−22798
Cu-Zn-Al wire, made from pendant drop melt extraction technique from bulk material, X-ray diffr. and thermal anal. 79−43227

X-ray diffraction examination of materials continued
Cu-Zr (50 or 54 at.%), splat-quenched, glass transition and crystn. temps. determ. 78−22659
Cu-Zr alloys, amorphous, struct. X-ray scatt., rel. to Ni-P alloys 77−51324
Cu-Zr amorphous alloy, splat cooled, local order and amorphous struct. 80−88061
$Cu_xAg_{1-x}I$ crystals, layer structs., X-ray diffr. studies 80−96457
$CuAl_2$, Kossel interferences of proton-induced Alk_α radiation 77−43112
Cu_3Au, heterophase fluctuations near order-disorder transform., X-ray and neutron diffr. 77−73272
Cu_3Au, ordering process, cluster size evolution 78−39766
Cu_3Au, X-ray and inelastic neutron scatt. investig. of spinodal ordering 77−77473
$Cu_3Au(-xCo)$, x=0.64 and 1.5 at.% Co, LRO 78−18584
CuBr-$PbBr_2$ system, phase diagram, DTA and X-ray diffr. analysis 77−47552
CuCl, anharmonic thermal vibr. X-ray diffr. exam. 78−30728
CuCl, optical microscopic, X-ray diffr. and elec. resist. studies at high press. 80−11051
CuCl, photosensitive film formation on Cu 77−9105
CuCl-TlCl system, phase diagram and high ionic cond. obs. 78−79802
$CuCr_2O_4$ and $CuCrO_4$, IR spectrometry and EPR study *(French)* 79−47452
$CuCr_2O_4$-$MgCr_2O_4$, phase analysis 77−44224
$CuCr_2Se_4$, crystal growth from melt, exam. of props. 80−55283
$CuFeO_2$-Fe_2O_3, decomposition kinetics and mechanism of spinel solid soln., composition and precipitation effects *(Japanese)* 77−77489
$CuFe_2O_4$-$CuGa_2O_4$, physicochem. props. *(French)* 77−44233
$CuGaSe_2$, thermal expansion obs. 80−70432
$(CuGaTe_2)_{1-x}$-$(2CdTe)_x$, phase diagram and microstruct. DTA and X-ray diffr. 77−59762
CuI solid electrolyte α-phase stabilisation 80−29209
CuI-PbI_2 system, phase diagram, DTA and X-ray diffr. analysis 77−47552
$CuInS_2$ films, RF sputtered, growth and props. 80−80124
$CuInS_2$ films prod. by RF sputtered Cu-In films exposure to H_2S 79−95926
$CuInS_2$, homogeneity region and intrinsic dopant mechanism 78−34630
$CuInS_2$, region of existence, determ. by quenching and X-ray anal., phase transition 79−66054
$CuIn_5S_8$, single crystn. phase, CVD prep., X-ray cryst. struct. determ. 79−65990
$CuInS_2(Se_2)$-$GeS_2(Se_2)$, degree of solid solubility and phases charcts. 78−35377
$CuInS_2(Se_2)(Te_2)$, film, electron and X-ray diffr. 77−11819
$CuInSe_2$ amorphous thin film, flash evaporation, struct., stoichiometry 80−89150
p-$CuInSe_2$ film, prep. from vac. evaporation of $CuInSe_2$, optical and elec. props. 79−82697
$Cu_2MnIn_{1-x}Sn_x$ alloys compositional SRO, hyperfine interactions 80−71065
$Cu_xMo_3S_4$, chevrel phase, charge transfer and valence electron conc. 78−6029
$Cu_{40}Nb_{30}X_{30}$ (X=Ti, Zr, Hf), superconductors with metastable ordered structs. 80−108484
CuO-Ag film solar absorbers, mechanism of high-temp. instability 78−22971
Cu_2O-CuO-MoO_3, subsolidus phase diagram, mag. props. 80−50615
$(Cu_3Pt)_{1-c}Mn_c$, mag. suscept. and effect of atomic order and disorder 77−24669
Cu_2S, high temp. X-ray diffractometry, polymorphic transition mechanism study 79−55692
Cu_2S, polycryst. thin films, struct., optical and elect. props. for solar energy appl. 80−10837
$Cu_2S+Ln_2S_3$, powdered mixtures, reaction rate, production of ionic semiconductors 80−93741
$Cu_{2-x}S$, digenite, X-ray determ. of structural transitions 80−92474
Cu_xS, layers produced by reactive RF sputtering, struct., elec. and optical props. 79−90908
Cu_3SbS_3, skinnerite, polymorphism, X-ray diffr. and NQR meas. 80−49165
$Cu_{60}Zr_{40}$, stability, crystallisation, ductility meas. 78−47246
D NaCl:Fe, defect struct., Mossbauer spectra and X-ray diffr. obs. 80−7237
Dy, crystal structure, P-T phase diagram 78−84776
$Dy_3Ni_7B_2$, struct., space groups, X-ray study *(Ukrainian)* 80−39029
$DyRh_{1.1}Sn_{3.6}$, new supercond./mag. cpds., X-ray powder diffr. data 80−100215
$Dy_2[Pt(CN)_4]_3.21H_2O$, phase transitions, X-ray study and spectroscopic study 79−60506
Er, film, reaction with H_2O vapour, spectroscopic and X-ray diffr. obs. 77−40575
$(ErCo_2)_x(ErAl_2)_{1-x}$, mag. and struct. investigations of intermetallic systems 78−95440
ErD_2, thin film, reaction with H_2O vapour, spectroscopic and X-ray diffr. obs. 77−40575
$Er(Fe_{1-x}Co_x)_3$, spin reorientation, easy axis of magnetisation 80−25144
$Er_6Ga_{1.5}Ni_{2.5}$, struct. determ. by X-ray powder method *(Ukrainian)* 80−39001
$3Er_2O_3$-Ta_2O_5 refractories, prep. and anal. 77−48384
$ErRh_4B_4$, film, sputter deposition and low temp. props. 80−2948
$ErRh_{1.1}Sn_{3.6}$, new supercond./mag. cpds., X-ray powder diffr. data 80−100215
$ErRh_{1.1}Sn_{3.6}$, synthesis, supercond. and mag. props. 80−100547
C-$Er_2Si_2O_7$, single cryst. flux growth, polymorphic forms study by X-ray methods 79−52097
$Er_2[Pt(CN)_4]_3.21H_2O$, phase transitions, X-ray study and spectroscopic study 79−60506
Es compounds, X-ray powder diffr. 80−2002
Eu selenides, X-ray phase anal. 77−11514
EuB_6, simple crystal, prep., floating zone technique 77−85934
EuB_6, thermal expansion, X-ray method, room temp. to 1300 C 80−96670
EuC_6, intercalation cpd. with graphite, synthesis and struct. 80−44184
$EuFe_4Al_8$, mag. ordered, mixed valency of Eu, X-ray, susceptibility and Mossbauer spectra studies 79−19728
EuM_2Ge_2, M=Mn, Fe, Co, Ni, Cu, magnetism and hyperfine interactions 78−76228
EuO:Yb(Sm), electron transition and valence state of impurities, X-ray spectroscopy and structural anal. 78−39064

X-ray diffraction examination of materials continued
Eu_2O_3, C→B transformation 77−11688
Eu_2O_3, cubic to monoclinic transform. 77−8815
Eu_2O_3-Gd_2O_3-Ta_2O_5 system at 25, 50 and 75 mole.% Ta_2O_5, cross section investig. 77−12607
Eu_2O_3-R_2O_3-Ta_2O_5, R=La, Gd, Y, quasibinary cross sections 77−90333
Eu_2O_3-Y_2O_3-Ta_2O_5, struct., phase form., luminesc. and X-ray diffr., obs. *(Russian)* 78−6765
$Eu_5(PO_4)_3OH$, prep. from sulphate, X-ray diffr. and IR spectrosc. 80−29893
EuPd, mech. of H absorption, Mossbauer, mag. and X-ray diffr. meas. 78−38846
$EuRh_2$, mech. of H absorption, Mossbauer, mag. and X-ray diffr. meas. 78−38846
EuS:Yb(Sm), electron transition and valence state of impurities, X-ray spectroscopy and structural anal. 78−39064
$Eu_{0.8}Y_{0.2}S$, Debye-Waller factor, X-ray diffr. meas. 77−11659
$Eu_{1-x}Yb_xO$, solid soln., ferromag. semicond., increase of exchange interaction 78−88109
$Eu_{1-x}Yb_xS$, solid soln., ferromag. semicond., increase of exchange interaction 78−88109
β-FEOOH, Mossbauer spectra obs., chemical and thermal anal., X-ray diffr., saturation magnetisation 80−88896
(Fe, Ni, Co)-Si-B, amorphous, compositional effect on struct. changes, after heating up to 700°C, exam. *(Japanese)* 78−48433
Fe and related compounds, hdyrostatic compression expts. 78−83862
Fe, Armco, borided surface layers, Mossbauer and metallographic anal. 80−50769
Fe, Armco, ground, residual stresses, X-ray evaluation 80−79863
Fe, Armco, sleeve, deformed by cold drawing, exam. of surface and texture *(Russian)* 79−34057
Fe, bonding of Al, growth of intermediate phases, effect of O and N impurities 78−27680
Fe, cast, graphite content determ. by X-ray diffr. method 80−100977
Fe, casting, fatigue strength, section size and surface struct. effect *(Japanese)* 79−20170
Fe complex, $FeOCl[(ethyltetramethylcyclopentadienyl)_2Fe]_{0.16}$ synthesis and struct. 80−44176
Fe complex, iron 4,7-$(CH_3)_2$-(1,10-phenanthroline)$_2(NCS)_2$, spin state transition, X-ray and Mossbauer obs. 80−7195
Fe, ductile, with different secondary struct., abrasive wear *(German)* 80−25871
Fe electrodeposited foils, microstruct., internal stress and mech. props. 80−20807
Fe film, thermally evaporated, contamination effects obs. 80−49545
Fe, interaction with dense stream of N ions, metallography, microhardness, specific volume *(Russian)* 80−15169
Fe, isochronous annealing recovery, in cold rolled and explosively formed samples 79−100166
Fe, lattice distortions due to H, X-ray diffr. exam. 78−79629
Fe microcrystals, dislocation struct. singularities in early deform. stage *(Russian)* 77−55284
Fe, nitrided, X-ray and Mossbauer study of surface 78−48568
Fe ore, water bearing mineral effects on X-ray fluorescence analysis 77−12866
Fe, oxidised aerosoled ultrafine particles, X-ray and Mossbauer examination 80−21183
Fe powder, passivating oxide layer comp. 78−31558
Fe, single cryst., lattice parameter determ., ratio method 77−43106
α-Fe single crystal whiskers, controlled growth by H reduction of ferrous halides, X-ray and SEM exam. of crystals 78−60554
Fe, stress strain anal. of single crystal induced by absorbed H_2 *(Japanese)* 78−11276
Fe surface, laser doping with V *(Russian)* 78−95065
α-Fe, textured, residual stress evaluation by X-rays *(German)* 80−40670
Fe whisker crystals, domain walls, interaction with dislocation bundle, X-ray topography obs. 79−87282
Fe whiskers, elongation induced struct. distortion, X-ray topographic investig. 77−85121
Fe whiskers, undeformed, X-ray topographic study 77−80716
Fe/Fe-Cr composite powder, X-ray diffr. exam. of densification during rolling 80−40289
Fe/ZrB_2, metal-like cpd. form. in diffusion layer during solid phase saturation 80−19994
Fe-Al, band struct. and density of states, KKR method and X-ray meas. 80−10863
Fe-Al (1 to 4 wt.%), effect of nitriding on surface structure and props., and on diffusion layer *(Russian)* 79−34197
Fe-Al (up to 7.2%), oxidation process 78−85022
Fe-Al-C alloys, C migration and mag. aftereffect, mag. permeab. disaccommodation and long-range order meas. 79−8020
Fe-Al-Cr (10, 5 to 10, wt.%), corrosion by coal char, SEM and X-ray diffr. exam. 78−88573
Fe-Al(Cr)(Mn)(Pt)(V), X-ray exam. of dynamic characts. *(Russian)* 77−62608
Fe-Al(Si), disordered, obs. of Kohn singularities in X-ray diffuse scatt. 79−27874
Fe-Al(25 at.%), mag. anisotropy induced by plastic deform., dislocations, long-range order 77−4544
Fe-B, amorphous alloy, mag. props. 80−84618
Fe-B, amorphous alloys, compositional study on short-range struct. 80−84095
Fe-B metallic glass, X-ray diffr. meas., semi-empirical struct. model 80−107059
Fe-B metallic glasses, density, mech. and thermal props. 78−31432
Fe-B_4C powder mixtures, phase changes and struct. of sintered materials *(Russian)* 78−6872
Fe-B-C amorphous alloys, atomic struct., energy dispersive X-ray diffr. meas. 79−73100
α-Fe-Be(Ti)(Mo)(P)(Sb), effect of mag. transition on solubility of alloying elements, X-ray diffr. and microprobe anal. *(Japanese)* 79−42256
Fe-C, liquid, C content effect on short-range order struct., X-ray diffr. obs. 80−6351
Fe-C-Ti (0.2 to 1.8, 0.1 to 1.7 wt.%), crystallisation and microstruct. *(Russian)* 77−66632
Fe-Co, isothermal compression and BCC→HCP phase transition, up to 300 kbar, at room temp. 77−90346
Fe-Cr, oxidation, in H_2/H_2O vapour mixtures, epitaxial oxide phase formation, effect on oxidation 78−88568

X-ray diffraction examination of materials continued
Fe-Cr (20 wt.%), high temperature oxidation resistance, effect of rare earth and reactive element additions *(Japanese)* 79−20271
Fe-Cr alloys and Fe, lattice parameters, 293 to 1273K, α to γ phase transform., X-ray diffr. exam. *(Russian)* 80−50625
Fe-Cr-Al-Y (Y-Al_2O_3)(Y_2O_3), preparation and exam. of mech. props. 78−52720
Fe-Cr-Co-Al(V)-(Nb)(Ti), phase equilib., X-ray diffr. meas. *(Russian)* 79−47658
Fe-Cr-Co-Mo alloys, struct. transform. and mag. props. *(Russian)* 77−76543
Fe-Cr-Mn-C, high temp. oxidation, X-ray and weight gain meas. *(Russian)* 78−15571
Fe-Cr-Mo-C, X-ray investigation after friction and oxidation 78−52997
Fe-Cr-Ni-Nb-C, austenitic, splat quenching 78−72798
Fe-Cr-Y, Y addition effect on high temp. oxidation resistance *(Japanese)* 79−70223
Fe-Cu (4.54 wt.%) alloy, scaling behaviour, 700-1000°C, 1 atm. O_2 80−93679
Fe-Fe_2O_3 composite films, structural props., microhardness, 250 to 700K 78−84095
β-Fe-Ge, mag. props. from X-ray, magnetisation and Mossbauer meas. 79−42755
Fe-graphite, intercalate, prod. by slow electrochemical reduction *(French)* 78−27437
Fe-Mn, annealed, α-γ phase transformation obs. 78−75831
Fe-Mn (15(24)(30)wt.%), high hydrostatic pressure influence on stress-strain curve 80−25805
Fe-Mn-C, γ→ε→α′ martensitic transform. 79−24523
Fe-Mn-C (11.5, 0.2 to 1.6 wt.%), water quenched, effect of C on phase composition, abrasion, plasticity *(Russian)* 78−35445
Fe-Mn-Ti alloys, austenitic, precipitation strengthened 80−25714
Fe-Ni, martensitic transform. dynamic, quasi-static atomic displacements, NGR, X-ray and electron scatt. meas. *(Russian)* 78−68688
Fe-Ni, oxidation, Mossbauer spectroscopy, metallography, SEM and X-ray diffr. anal. 78−15577
Fe-Ni, quenched irreversible alloy, zero or negative thermal dilatation, para-process mag. susceptibility 79−4419
Fe-Ni, taenite, superstruct. in Fe meteorites 78−61820
Fe-Ni (30 wt.%), Ni segregation singularities during dendrito-cellular solidification *(Russian)* 80−7542
Fe-Ni (31 at.%), austenitic, ageing, absence of at. order 77−11502
Fe-Ni alloy, fluorination kinetics and fluoride film form., chem. nature obs. 80−101035
Fe-Ni alloys, mag. state of austenite and γ→α transform. *(Russian)* 80−40350
Fe-Ni electrodeposit, sectional analyses and impurities *(Japanese)* 80−21350
Fe-Ni films, scatt. of homogeneous spin waves by anisomeric oriented plane, ferromag. reson. 78−19336
γ-Fe-Ni Invar alloy, phase mixture produced by long annealing 79−5065
Fe-Ni meteorite, STEM/X-ray microanalysis across α/γ interface 80−105212
Fe-Ni superstructure in metal particles in chondrites 80−12713
Fe-Ni-Al alloys, ordering X-ray and neutron diffr. obs. *(Russian)* 79−20038
Fe-Ni-B metallic glass, X-ray diffr. meas., semi-empirical struct. model 80−107059
Fe-Ni-C (30, 0.5 wt.%) single cryst., stress induced martensitic transform. 80−60860
Fe-Ni-C-Mn (3.56, 3.25, 0.6 wt.%), solid soln., quenched, changes during annealing to crystal structure, mech. props. *(Russian)* 79−34076
Fe-Ni-Cr, Elinvar, struct. and mag. props., singularities during tempering *(Russian)* 80−50627
Fe-Ni-Cr, vapour-deposited film, effect of condensation temp. on form. of metastable phases and mag. props. 79−65700
Fe-Ni-Cr coating, electrodeposited, exam. of passivity 78−80655
Fe-Ni-Mo (16.4, 8.1 wt.%), effect of substituting Mo by W during ageing 80−29991
Fe-Ni-Ti, preaged martensite, shear strain magnitude, X-ray diffr. method 80−93592
Fe-Ni-Ti (31.2, 5.3 wt.%), γ-phase ageing effect on martensitic transform. *(Russian)* 77−28814
Fe-Ni-V alloy, ageing of martensite *(Russian)* 78−39808
Fe-Ni(Mn)-Al-C, form. of ductile Ni_3Al by split quenching, mech. props. 79−100197
Fe-P alloys, X-ray exam. of amorphous structure *(Japanese)* 77−84661
Fe-P-C amorphous alloy, small angle X-ray scattering study of struct. and crystallisation 79−50999
Fe-Pd Invar, low temp. FCT phase obs. 80−93538
Fe-Sb-Ti(V)(Cr)(Mn)(Co)(Ni), interactions and segregations, Mossbauer and X-ray diffr. study 80−70415
Fe-Si, plastic deform., synchrotron X-ray topography dynamic expts. 78−67621
Fe-Si, single cryst., lattice parameter determ., ratio method 77−43106
Fe-Si, single cryst., mag. domain wall motion, X-ray topography study 80−65953
Fe-Si (2-8 wt.%), single crysts., growth striations, X-ray studies 80−79774
Fe-Si (2.35 wt.%), misorientation dependence of grain boundary segregation, Auger spectroscopy exam. 78−76629
Fe-Si (3 wt.%), polycryst. (110), synchrotron radiation topographs and mag. domain obs. 78−67620
Fe-Si (3.72 wt.%) fatigue failure in vacuum and air 78−68789
Fe-Si(Cr)(Ni)(Mn)(C), alloy layers formed by reaction with molten Al, X-ray, EPMA anal., hardness meas. *(Japanese)* 78−72926
Fe-Ti-C, rapidly quenched by splat-cooling 80−84923
Fe-Ti-S-(C), sulphide phases *(Russian)* 77−25017
Fe-W-Cr-Mo system, mag. and mech. props. rel. to production methods *(Japanese)* 80−71107
Fe-Zn, crystallographic relations by X-ray diffr. 80−24408
Fe-Zn, phase diagram, DTA, EDAX, X-ray diffr. study 80−50602
FeB thin films, produced by ion bombardment on Fe and plain steel, X-ray struct. anal. *(French)* 79−73413
$Fe_{100-x}B_x$, mag. and struct. props., comp. depend. 78−60314
Fe_2B thin films, produced by ion bombardment on Fe and plain steel, X-ray struct. anal. *(French)* 79−73413
$Fe_{80}B_{20}$, amorphous to cryst. transorm. 80−34188
$Fe_{80}B_{20}$ amorphous wire, crystn. by annealing at 780°C 80−100177
$Fe_{80}B_{20}$, crystallisation of amorphous alloys, TEM and X-ray diffr. exam. of struct., growth characts. 78−79539

X-ray diffraction examination of materials continued
$Fe_{80}B_{20}$, Metglas 2605, Young's modulus meas. using piezoelectric US composite oscillator technique 80−108656
$Fe_{84}B_{16}$, amorphous, struct., X-ray diffr. meas. 79−4252
$FeCl_2$-graphite, intercalation compound, formation by reduction of Fe(III) compounds with $Fe(CO)_5$ 78−63721
FeCo, isothermal annealing effect on lattice const. *(Japanese)* 79−20076
$Fe_{3-x}Co_xSi$, structural, mag. moment, and hyperfine field behaviour, local environment model 79−65762
$(Fe_{1-x}Co_x)_{77}Si_{10}B_{13}$ alloys, amorphous, induced mag. anisotropy by mag. annealing 79−4671
$Fe_{65.4}Cr_{20.5}Al_{10.7}V_{3.4}$, effect of Al and V on form. of $L2_1$ superstructure and stratification 77−77474
$Fe^{2+}{}_{1+x}Cr_{2-2x}Ti_xO_4$ spinel, low temp. crystallographic transitions 77−15589
$Fe_xCu_{1-x}Cr_2Se_4$, crystallographic and image props. 80−39049
FeF_3, amorphous, characterisation by thermal, mag. and Mossbauer study 79−42782
FeF_3 thin film prep. and charact. *(French)* 78−64470
$Fe(Li_{0.5}Fe_{1.5-x/8}Mn_{x/8})O_4$ $0 \leq x \leq 2$ spinel system, X-ray diffr. anal. of loss of order on Cr substitution 79−73178
$Fe_{1.4}Mg_{1.3-x}Zn_xTi_{0.3}O_4$ spinel system, X-ray diffraction, Fe Mossbauer effect 80−88900
$(FeMn)_3$ Si alloys, L2,A struct. of single phase alloy 77−59393
$(Fe_{1-x}Mn_x)_3Al$, mag. moments determ. from magnetisation and neutron and electron diffr. expts. 79−56520
$Fe_{3-x}Mn_xAl$, ordering of Fe atoms, X-ray diffr. meas. and mid gamma reson. anal. *(Russian)* 80−96469
$(Fe_{0.45}Nb_{0.53})O_2$, rutile, cation distrib. and mag. ordering *(German)* 80−107116
$(Fe_{0.6}Ni_{0.4})_{100-x}B_x$ and $(Fe_{100-x}Ni_x)_{80}B_{20}$ amorphous alloys, X-ray diffr. struct. determ. 80−64906
$(Fe_{100-x}Ni_x)_{100-y}B_y$, metallic glass, embrittlement and crystn. 80−7685
$Fe_{40}Ni_{40}B_{20}$ alloys, crystalline and amorphous, resistivity minimum, X-ray, Mossbauer studies 79−73489
$Fe_{50}Ni_{30}B_{20}$, crystallisation of amorphous alloys, TEM and X-ray diffr. exam. of struct., growth characts. 78−79539
$Fe_{65}(Ni_{1-x}Mn_x)_{35}$, H solid solutions magnetisation behaviour in pulsed mag. fields 79−65674
$Fe_{40}Ni_{38}Mo_4B_{18}$, amorphous, mag. anisotropy, Mossbauer study 80−65864
$Fe_{40}Ni_{40}P_{14}B_6$, amorphous ribbon, cold rolling, annealing mag. props. 77−8958
$Fe_{40}Ni_{40}P_{14}B_6$, amorphous alloy, structural relaxation kinetics, X-ray diffr. exam. 78−38627
$Fe_{40}Ni_{40}P_{14}B_6$, amorphous, energy dispersive X-ray diffr. study of structural relaxation 79−14689
$Fe_{40}Ni_{40}P_{14}B_6$ glass, struct. relax., ferromag. reson. and X-ray scatt. 79−90566
$Fe_{40}Ni_{40}P_{14}B_6$, Metglas 2826, stability, crystallisation, ductility meas. 78−47246
FeO, wustite, simultaneous solubilities of Na and Ca *(French)* 78−31392
α-Fe_2O_3 (haematite), X-ray diffr. compression studies under hydrostatic isothermal conditions 78−85539
α-Fe_2O_3, crystalline grain growth during heat treatment 78−11252
β-Fe_2O_3 film, CVD and characterisation 77−44172
α-Fe_2O_3 film, prep. by reactive condensation and mag. props. 78−64241
Fe_2O_3 films, DC reactively sputtered, for selectively semitransparent photomasks, struct., mech. and chem. props. 80−59835
α-Fe_2O_3, hydrostatic compression, X-ray diffr. meas. 79−99269
Fe_2O_3, pelletised, internal stresses, X-ray investigation *(Russian)* 78−19684
Fe_2O_3, plasma sputtered coatings, oxide dissociation, coating props., struct. and composition *(Russian)* 80−54577
γ-Fe_2O_3 recording tapes, orientation, Mossbauer, X-ray and electron microscope meas. 77−16219
γ-Fe_2O_3, small particles, vacancy sintering 77−65975
γ-Fe_2O_3, struct. vacancy distrib., effect on $\gamma \rightarrow \alpha$ transform. heat 78−6051
α-Fe_2O_3, X-ray diffr. exam. at phase transition from weakly ferromag. to pure antiferromag. state 77−51904
Fe_2O_3:Mn, surface props. 79−65302
xFe_2O_3-$(1-x)PbO$-$3B_2O_3$ glass, Mossbauer study of Fe cations 79−91325
α-Fe_2O_3-Li_2O, structural and thermal phase behaviour from mag., spectral and thermal studies 80−2673
Fe_2O_3-PbO-B_2O_3 glass, X-ray and electron microscope studies, mag. and Mossbauer effect meas. 80−28919
Fe_2O_3-TiO_2 system, high temp. intergrowth struct., metal atom ordering in intergrowth boundaries 78−79573
Fe_3O_4, effect of Al ion on formation and structure *(Japanese)* 77−59727
Fe_3O_4 film, prep. by reactive condensation and mag. props. 78−64241
Fe_3O_4 film prep. and form. by Fe naphthenate thermal decomposition *(Japanese)* 77−32519
Fe_3O_4 mag. fluid particles, comp., struct., and mag. props. 80−60374
Fe_3O_4, magnetite, oxidation kinetics, influence of cryst. size 78−79778
Fe_3O_4, magnetite, phase transition, X-ray diffr. meas. 80−15238
Fe_3O_4, orientation on α-Fe_2O_3 after low-temp. reduction, X-ray texture analysis *(French)* 77−39738
Fe_3O_4 powder, oxidation to γ-Fe_2O_3, coercivity changes 80−44864
Fe_3O_4, substituted magnetite, correl. between IR spectra, X-ray diffr., and struct. vacancy distrib. 80−84753
Fe_xO_y film, thermally evaporated, contamination effects obs. 80−49545
$Fe_3O_{4-x}F_x$, specific heat in neighbourhood of Verwey temp. 79−33500
$Fe(OH)_3$ thin films, Mossbauer spectra obs., chemical and thermal anal., X-ray diffr., saturation magnetisation 80−88896
δ-FeO(OH) and its solid solns. synthesis, X-ray diffr. and TEM studies 80−29891
FeOOH, crystal growth in $FeSO_4$ solution with NaOH or NH_4OH as precipitant, phase diagrams *(Chinese)* 80−44158
FeOOH, ferric hydroxide gel, struct. determ. 79−11832
δ-FeO(OH), study of thermal decomp. by X-ray diffr., electron diffr. and TEM 80−66790
$Fe_2O(OH)_4$, Mossbauer spectra obs., chemical and thermal anal., X-ray diffr., saturation magnetisation 80−88896
$(Fe_2O_3)_x(3B_2O_3.PbO)_{1-x}$ glass, X-ray diffr. struct. obs. 79−32915
$20Fe_2O_3.80[3B_2O_3.(1-x)PbO.xGeO_2]$ glass, phys. props. 80−49119
Fe_2P, grown in liq. Cu medium, composition and mag. props. 79−11313

X-ray diffraction examination of materials continued
$Fe_{80}P_{13}C_7$, amorphous and crystalline, electrochemical and semicond. behaviour *(Russian)* 80−101021
$Fe_{80}P_{16}C_3B_1$ amorphous filament, produced by glass coated melt spinning, mech. props. 78−15483
$Fe_{25}Pd_{50}Au_{25}$, atomic ordering influence on mag. props. and elec. resistance *(Russian)* 80−7551
FePt lattice, symmetry, state of order, vibration, temp. effects *(German)* 77−4067
Fe_3Pt, atomic thermal vibr. anisotropy, martensitic transform. model *(French)* 80−70355
FeS_2, oxidation, Mossbauer spectroscopic and magnetokinetic studies, 400-500°C 80−44880
$FeSO_4$, anhydrous, γ, β and γ-phases, Mossbauer spectra and X-ray diffr. 77−12287
$FeSi_2$ films, structural and Anderson transitions, cond. and IR reflectance meas. 79−15200
$Fe_3Si_{1-x}Al_x$, hyperfine interactions and structural disorder, spin echo, X-ray and magnetisation meas. 77−32289
$Fe_{78}Si_{10}B_{12}$, amorphous alloy crystallisation study *(Japanese)* 78−9959
$FeSiF_6.6H_2O$, phase transform. exam. by X-ray and DSC methods 78−83948
Fe_2SiO_4, fayalite, single crystal growth by floating zone method, exam. 78−60570
$Fe_{2-x}SiO_4$, fayalite, oxidation kinetics and growth of Fe_2O_3 whiskers 78−84113
$FeSnO(OH)_5$, mag. props. and cryst. struct. 78−43574
$(Fe_{0.5}Ta_{0.5})O_2$, rutile, cation distrib. and mag. ordering *(German)* 80−107116
ε-FeTi, Ce addition effect on H_2 absorption capacity 79−61899
$(Fe_{1-x}V_x)_3Ge$, magnetic and X-ray studies 80−1966
Fe_xVS_2 $(0.20<x<1.00)$, phase diagram and order-disorder transition of vacancies 80−81039
Ga, amorphous film, X-ray diffr. 79−51451
Ga metastable states, supercooling and polymorphism *(French)* 78−14325
Ga whisker growth from GaN/Ga layered films 80−92800
Ga-Ni-R, (R=Dy, Ho, Er, Tm, Lu), struct. determ. by X-ray powder method *(Ukrainian)* 80−39001
Ga-rare earth alloys, phase diagram determ. 78−15366
$Ga_{0.64}Al_{0.36}As$, plasma grown oxide, phys. and elec. props. 78−48550
$Ga_{0.65}Al_{0.35}As$ epitaxial layer on GaAs, two-dimensional lattice mismatch parallel to interfacial boundary 79−51439
$Ga_{1-x}Al_xAs$, epitaxial layers, on GaAs substrates, X-ray double-cryst. diffractometry, state of strain 79−19480
$Ga_{1-x}Al_xAs$ LPE layer on GaAs, lattice mismatch using X-ray source 79−82470
$Ga_{1-x}Al_xAs$ VPE layers, X-ray diffr. 80−29296
$Ga_{1-x}Al_xAs$-GaAs, heteroepitaxial layers on GaAs(001), misfit dislocation asymmetry 77−47694
$Ga_{1-x}Al_xAs$-GaAs heterojunctions grown by metallorganic CVD 80−15599
$Ga_xAl_{1-x}As$-GaAs heteroepitaxial layer distortion characterisation by X-ray multiple diffr. 80−96754
$Ga_{1-x}Al(In)_xAs$, $GaAs_{1-x}P_x$, substit. solid solns., comp. determ. from X-ray integral intensities 77−84584
GaAs (111) substrate, and homoepitaxial layers, characterisation by divergent X-ray beam diffr. 78−31352
GaAs, anodic oxide for device application, crystallisation dynamics 79−66190
GaAs, anomalous scatt. factors and integrated intensities near K-absorpt. edges 77−19834
GaAs, anomalous scattering factors determ. near absorpt. edges, by one-intensity-ratio method 80−1888
GaAs, chem. bond, modulation X-ray diffr. obs. 80−96464
GaAs, Czochralski growth, melting and regrowth, inclusion density and dislocation generation 77−21016
GaAs, fast neutron irrad., effect on cryst. lattice period, X-ray diffr. meas. 79−37743
GaAs, intrinsic surface gratings, low-angle X-ray diffr. obs. 77−85035
GaAs LPE layers, X-ray topographic studies of defects 77−62772
GaAs, LPE layers, X-ray topographic exam. of defects 78−30844
GaAs, proton-bombarded, lattice strain, precision X-ray meas. 77−27922
GaAs, temp. depend. of X-ray reflection intensity near absorpt. edge 80−1889
GaAs thin films, reactively sputtered, ESCA/XPS study 80−97430
GaAs, X-ray diffraction, integrated intensity meas. near absorption edge with synchrotron radiation 77−76253
GaAs:Sn, proton implantation and annealing behaviour *(Chinese)* 80−44224
GaAs-Al interface, struct. study by X-ray total-external-refl.-Bragg diffr. 80−34321
GaAs-AlAs, one-dimensional superlattice, X-ray diffr. 77−27860
GaAs-AlAs layered films, MBE prep., struct., rel. to optical props. 79−77950
GaAs-AlGaAs DH laser, rapid degradation caused by process-induced defects 77−71985
GaAs-$Ga_xIn_{1-x}P$ heterostructure, elastic stresses and substrate/epitaxial film mismatch, X-ray diffr. method 80−92794
GaAs-Pd junction, contact reactions 79−56308
$(GaAs)_n(AlAs)_m$ multilayers, MBE, interdiffusion, X-ray diffr. study 80−70474
GaAs(Sb), two-phonon diffuse scatt. of X-rays 78−26374
$GaAs_xSb_{1-x}$ solid solution epitaxial layer, morphology and defect structure 77−1330
$GaAs_ySb_{1-y}$, miscibility gap, rel. to LPE 79−33090
$GaCO_3$, calcite, hydrothermal growth processes revealed by defects 77−55250
$Ga_xIn_{1-x}As_yP_{1-y}$/GaAs structure, LPE growth and lattice consts. matching conditions 80−59822
$Ga_xIn_{1-x}P$, diffuse X-ray scatt. investig. of cation distrib., segregation 77−24409
$Ga_xIn_{1-x}P$ MBE layers, comp., Rutherford scatt. and X-ray diffr. meas. 80−75457
$Ga_{1-x}In_xSb$, press.-induced structural phase transition 78−30751
$Ga_xIn_{1-x}Sb$, growth by LPE 78−27421
$Ga_{1-x}In_xSe$, energy spectrum and struct., X-ray diffr. and light absorption 79−11437
$(Ga_xIn_{1-x})_2Se_3$, $1 \geq x \geq 0$, phases, lattice parameters and thermal expansion between room temp. and melting point 80−39031
GaN, elastic constant calc., elastic wave propag. vel. 78−87734

X-ray diffraction examination of materials continued
GaN, epitaxial growth on sapphire substrates, elec. props., X-ray diffr. anal., photoluminescence spectra 79−4919
GaN epitaxial layers for LED, X-ray diffr. topography and cryst. characterisation 79−65336
GaN, VPE, on sapphire, crystallographic aspects 78−2387
$GaNbO_4$, polymorphic transition under high press. 80−100835
Ga_2O_3 film, growth by reactive vapour deposition, optical and elec. props. 77−48347
Ga_2O_3-R_2O_3:Nd^{3+} glass, prep., characts., X-ray diffr., absorpt. and thermal anal. obs. *(French)* 78−19704
GaP, 1 MeV proton bombardment, lattice deformation investigation by Kossel effect 78−22775
GaP, growth and props. of LPE layers on Si substrates 78−6864
GaP, growth of dislocation free crysts. from stoichoometric melt. 77−81212
GaP, heteroepitaxial growth on Si substrate by MBE 78−64481
GaP, LEC growth of dislocation-free crysts., microdefects and striations 78−9974
GaP VPE layers, precision lattice parameter meas. by Umweganregung method, using triple reflection 79−65047
GaP-GaAlP-GaP LPE layers, lattice matched, X-ray diffractometer traces 79−51445
GaP_xAs_{1-x} ($0 \leq x \leq 0.32$) epitaxial film, one-dimens. superlattice, X-ray spectrometer scanning, struct. variations 78−47681
GaP_xAs_{1-x}-GaAs one dimens. superlattice, possibility of X-ray and electron diffr. struct. determ. 80−54560
$GaPO_4.2H_2O$, orthorhombic, thermal dehydration 79−79234
$(GaP)_x(ZnSe)_{1-x}$, solid solution, reaction of Zn with Se during Czochralski growth and LPE 79−8238
GaS, lattice dynamics parameters, X-ray diffr. study *(Russian)* 80−29146
GaS_xSe_{1-x}, grown by iodine vapour transport, X-ray struct. studies 79−4411
GaSe, basal plane orientation determ. in vertical Bridgman grown single crysts. 78−19658
GaSe, lattice dynamics parameters, X-ray diffr. study *(Russian)* 80−29146
$\alpha(\beta)$-Ga_2Se_3, cryst. growth, optical, X-ray diffr. and SEM study 80−71587
Ga_2Se_3-FeSe, phase diagram, elec. cond., mag. susceptibility 80−88301
Ga_2Se_3-In_2Se_3 solid solution system, X-ray diffr. exam. 77−63639
Gd, crystal structure, P-T phase diagram 78−84776
Gd-Ag, vap. quenched alloys, struct. and mag. props. 78−84461
Gd-Ag (0-16 at.%), vapour-quenched, struct. and mag. props. 78−38980
Gd-C-N system, isothermal section at 1200°C, X-ray investigation *(German)* 80−93543
Gd-Co-Mo, amorphous, sputtered very thin film struct. 77−15707
Gd-Fe(Co) film, amorphous, preferential resputtering effect induced anisotropic distrib. of atomic pairs 78−63950
Gd-Mg, X-ray determ. of Debye temp., mean amplitude of vibr. 78−38802
Gd-Zn, X-ray determ. of Debye temp., mean amplitude of vibr. 78−38802
$GdAl_2$-$GdCo_2$ system, EPR and mag. props. 79−33478
$GdCl_3.6H_2O$, X-ray emission luminesc. *(Japanese)* 80−55763
GdF_3, chemically reacted film on ferroelectric-ferroelastic $Gd_2(MoO_4)_3$, characterisation 79−15057
GdF_3-RF_3, R=Tb, Ho, Er, Yb, stabilisation of rhombic β-YF_3 type struct. 78−67700
$GdFe_2$ films, electron beam deposited, amorphous and cryst., mag. and struct. props. 79−4710
$Gd_3Ga_5O_{12}$ crystal growth from melt, X-ray topography meas. *(Hungarian)* 80−11556
$Gd_3Ga_5O_{12}$, garnet substrate, surface polishing, damage, abrasion, brittle fracture model *(German)* 77−73357
$Gd_3Ga_5O_{12}$, high energy heavy ion irrad., lattice strain 80−49278
$GdH_{2.92}$, electrical resistance anomalies at high pressures 80−29381
GdM_2Ge_2, M=Mn, Fe, Co, Ni, Cu, magnetism and hyperfine interactions 78−76228
$(GdMn_2)_x(GdAl_2)_{1-x}$, mag. and struct. investigations of intermetallic systems 78−95440
$GdNi_2H_4$, effect of absorbed H_2 on struct. and mag. behaviour 78−2682
$GdNi_2H_4$, effect of H_2 absorption on struct. and mag. behaviour 78−10685
Gd_2O_3-Al_2O_3 glasses, crystallization 79−50998
GdS, Debye-Waller factor, X-ray diffr. meas. 77−11659
Gd_6WO_{12}, thermodynamic and X-ray investig. at 1200-1400K 77−36778
Ge, (111, 400, 311), anomalous X-ray passage for four-wave diffr. *(Russian)* 77−35437
Ge, amorphous layer on Ge bulk, photoemission during X-ray Bragg diffr. 78−47209
Ge, cross-slip of single dissociated screw disclocations, double etching and X-ray topography studies 80−15104
Ge, cryst., deformed, diffr. effects obs. during X-ray transmission 79−4310
Ge, diffractive focusing of spherical X-rays *(Russian)* 79−4207
Ge, dislocation free single crysts., six wave diffr. of X-rays, anomalous transmission 79−14650
Ge, electrodeposited, X-ray, electrochem., and electrorefl. characterisation 78−14624
Ge, epitaxial, in situ X-ray topography, misfit dislocations 78−47671
Ge epitaxial layer on GaAs tetragonal distortion in heteroepitaxial layer, X-ray diffr. exam. 78−67922
Ge, film, elec. props., prep. by DC sputtering *(Japanese)* 79−78237
Ge, four-wave X-ray diffraction, intensification of Borrmann effect 77−39501
Ge, lattice parameter determ. by X-ray multiple diffr. study *(Russian)* 80−10460
Ge particles, homogeneously nucleated, production and props. 77−56252
Ge, Pendellosung fringe shape depend. on specimen-film distance *(Russian)* 80−87994
Ge, polycrystalline epitaxial film, exam. of growth kinetics and props. 80−55304
Ge, screw dislocation loops, shrinkage vel. and cross slip freq., activation energies *(German)* 78−43028
Ge, shaped crystals, grown by Stepanov method, struct. perfection 78−2123
Ge single crystal, dislocation free, swinging fringes, six wave diffr. of X-rays 79−14649

X-ray diffraction examination of materials continued
Ge, six-beam anomalous transmission, interpretation from eigensolns. 77−19832
Ge surface, line tension induced dislocation motion, obs. by etching and X-ray topography 79−82212
Ge, X-ray anomalous transmission at three-wave diffraction (220;202) *(Russian)* 78−34393
Ge, X-ray anomalous transmission at three-wave diffraction (220;202) *(Russian)* 78−34394
Ge, X-ray diffraction, effect of dislocations on temp. depend. of integrated intensities 77−39513
Ge:Ga, heavily doped, structure defect evolution during heating *(Russian)* 78−43026
Ge:Li, dislocation free, anomalous transmission of X-rays *(Russian)* 77−15286
Ge-Au-Ni(Pt)(Pd) trilayered films, annealing, interdiffusion 78−22902
Ge-GaSb, metastable continuous solid solutions 79−8284
Ge-S glasses, Cu doped, thermal, structural and dielectric props. 79−60283
Ge-S-In, chalcogenide glass, determ. of glass phases, phys. props. meas. 79−23526
Ge-Si, solid phase heteroepitaxy 80−6670
Ge-Te, exam. of new compound, using light microscopy and X-ray diffr. exam. 78−48383
Ge-Te alloy films, amorphous, semicond. props., refr. index, struct. study 78−26978
$Ge_{1-x}(GaAs)_x$, metastable solid solution, fine struct. *(Russian)* 79−27960
$Ge_{1-x}(GaSb)_x$, metastable solid solution, fine struct. *(Russian)* 79−27960
$Ge_{1-x}H_x$, amorphous, atomic struct., X-ray study 80−49106
GeO_2, amorphous, obtained by hydrolysis of $GeCl_4$, exam. of props. 79−95956
GeO_2 particles used for optical fibre fabrication, struct. props. 80−89167
GeO_2-CdO system, phase diagram anal. by differential thermal, X-ray anal. 77−8805
GeS-GeSe, limits of solid soln. region, microstructural, X-ray and DTA meas. 78−47530
GeSe, amorphous, pair distrib. function, anomalous X-ray scatt. 80−49126
$GeSe_2$ amorphous semicond., DC conductivity, calorimetric, and X-ray diffr. meas. 79−78107
$GeSe_2$-Te, phase diagram and vitrification region determ. by DTA, SEM, X-ray diffr. *(French)* 77−72565
Ge_xSe_{1-x}, $0<x<0.2$, crystallisation in amorphous bulk and thin films 78−55813
Ge_xSe_{1-x}, amorphous, X-ray diffr. and local order modelling 80−49125
$Ge_{20}Se_{40}Te_{40}$ amorphous alloys, thermal crystn. study 78−26789
GeTe, antistructural disordering 77−15402
GeTe, machining effects on electrophys. props. 77−86199
GeTe-As_2Te_3 system, phase diagram, eutectic comp., thermographic and X-ray anal. *(Russian)* 77−63646
$Ge_xZn_{1-x}Fe_2O_4$, ferrimagnetism and ion distrib. 77−12103
H_2, metallic and mol. crysts., X-ray scatt. factors, Hartree-Fock calc. 79−60219
H_2, solid, crystallographic transformation below 1.5K, X-ray study 79−73374
H_2, solid, structure transition below 1K 79−56024
β-$H_2O.11Al_2O_3$, conversion from β-$Na_2O.11Al_2O_3$ and characterization 78−3069
$HUO_2AsO_4.4H_2O$ and $HUO_2PO_4.4H_2O$ layered cpds., struct. investigs. below antiferroelec. transition temps., H bond ordered structs. 80−107416
$HUO_2PO_4.4H_2O$, H^+ ion cond., struct. mechanism, X-ray diffr. obs. 78−34651
Hf-Al-C, phase diagram and lattice constants, X-ray diffr. method 80−89207
Hf-C-N-O-H, solid solns. of H, exam. of props. 80−29172
Hf-Co, phase diagram, X-ray diffr., thermal anal. and metallography obs. 78−60652
Hf-Nb (30 to 50 at.%) exam. of beta phase decomposition processes 78−76674
HfB_2, oxidation in O_2 atmosphere, exam. 80−11814
$Hf_{1-x}Fe_x$ amorphous alloys, formation, crystallisation and electrical resistivity 80−96838
$HfFe_{2-x}Si_x$, Laves pseudo-binary compound, cubic C15 phase stabilisation 77−39559
HfO_2 film, CVD growth, struct., elec. and optical prop. characterisation 77−55891
HfO_2, plasma deposition of crysts. and their characterisation 80−20800
HfO_2-CeO_2, solid solutions 77−16549
HfO_2-La_2O_3 system, phase form. and relations, phys. props. 79−43218
HfO_2-PrO_x, phase equilibria and physicochem. props. in range 1000 to 1800°C 79−100117
HfO_2-R_2O_3 solid solns., prep., crystn., R=Nd,Sm,Dy,Yb 78−42909
HfO_2-Sm_2O_3, X-ray diffr. obs. of phase relations 79−61566
HfO_2-Y_2O_3, solid soln., diffuse X-ray scatt. by vacancies 78−71728
$Hg_{3-x}AsF_6$, one-dimens. lattice dynamics, X-ray scatt. study 80−75317
$Hg_{1-x}Cd_xTe$, LPE growth and characterisation 80−50565
Hg_2Cl_2, high press. induced phase transitions, X-ray study 79−69242
Hg_2Cl_2, low temp. phase transition, X-ray diffr., Raman spectra 78−22849
HgTe-CdTe, mixing energy and short-range order, diffuse X-ray scatt. 77−28006
Ho, phase transition along mag. field, X-ray obs., 77-292K *(Russian)* 77−4504
C-$Ho_2Si_2O_7$, single cryst. flux growth, polymorphic forms study by X-ray methods 79−52097
I, metallic solid, high press. struct., phase transition, X-ray diffr. study 78−87647
I_2, solid, press.-induced struct. phase transition, X-ray obs. 79−65192
In, film, vac. deposited, influence of ion bombardment during condensation 79−82483
In-Bi (2-33.3 at.%), phase diagram DTA, X-ray diffr. and supercond. T_c meas. 79−38795
In-Ga-As-P, phase diagram rel. to lattice matched LPE 78−39708
In-Tl, exam. of magnetic susceptibility in solid and liquid states, and X-ray data *(Russian)* 79−28503
In-Tl alloy, FCC→FCT martensitic transformation, on cooling, enthalpy meas. and X-ray exam. 78−39773

X-ray diffraction examination of materials continued
In-Tl single crystal, phase transform. X-ray topographic study *(Japanese)* 78−31405
InAs, thermal diffuse scattering measurements of [100] and [111] phonon dispersion curves 79−77701
InAs-CdTe quasi-binary system, temp.-comp. diagram, physicochem. and thermodynamic analysis 80−104127
$InAs_{1-x}Sb_x$, organometallic VPE growth on InAs 80−45233
$In_{1.9}As_{0.1}Se_3$, growth by chem. vap. transport, characterisation as photoelectrode 78−43994
$InBO_3$, thermal expansion, up to 610°C, X-ray determ. 77−43352
InGaAs-GaAs heterojunction with low misfit, misfit dislocation struct. 77−62783
$In_xGa_{1-x}As$, MBE layers on InP substrates, elec. props., photoluminesc., X-ray and Auger obs. 79−51450
$In_xGa_{1-x}As$ MBE layers on InP substrate, lattice deformation, misorientation 79−90896
$In_{0.9}Ga_{0.1}As_{0.3}P_{0.7}$, short-range order parameters, X-ray diffr. determ. 80−38875
InGaPAs, LPE-grown on (001)-InP, lattice mismatch study using X-ray double-cryst. diffr. 79−99440
$In_{1-x}Ga_xP_{1-y}As_y$ lattice-matched epitaxial layers, LPE growth on GaAs(100), characterisation 80−75465
$In_xMo_3S_4$, chevrel phase, charge transfer and valence electron conc. 78−6029
$In_xMo_{15}Se_{19}$, new ternary Mo(II) compounds, containing Mo_6Se_8 and Mo_9Se_{12} units, X-ray diffr. study 79−65056
InN, epitaxial layer prep. and X-ray analysis 79−38747
InN film growth by reactive sputtering in Ar-N_2 discharge, mechanism 80−89107
InO_3:Sn film, prep. by spray hydrolysis, struct., elec. and optical props. *(Japanese)* 79−42678
In_2O_3, lattice defects, optimum prep. conditions w.r.t. stoichiometry 79−27974
In_2O_3, thermally evaporated film, struct. and elec. props. 80−104066
In_2O_3, thin film, sputter deposition form., optical and elec. props. 80−60123
In_2O_3:Sn, sputtered film, optical and elec. props. 78−76177
In_2O_3-InN film growth by reactive sputtering in N_2-O_2 discharge, mechanism 80−89108
In_2O_3-SnO_2, X-ray and optical meas. of solubilities 79−55894
$In(OH)_3$, cubic, cryst. struct., X-ray and neutron diffr. obs. 79−77568
InP (111) substrate, and homoepitaxial layers, characterisation by divergent X-ray beam diffr. 78−31352
InP film, heteroepitaxial, deposited on GaAs substrate *(Czech)* 77−15710
InP, liquid encapsulated Czochralski cryst. growth, X-ray study 79−47619
InP-Au contacts, conditions of fabrication that control interfacial microstruct. 79−42643
InSb, acoustoelectric phonon attenuation of X-ray anomalous transmission 77−4160
InSb, amorphous, pressure induced struct. transform., X-ray diffr. obs. 77−11690
InSb, single crystal, stress induced phase change 79−23719
InSb, sputtered NaCl-type compression 79−46751
InSb, two-phonon diffuse scatt. of X-rays 78−26374
InSb:Se, exam. of defects in crystal 80−6423
InSb-GaSb superlattice, interlayer diffusion 77−85086
α-In_2Se_3, X-ray diffr. line broadening 80−49047
In_4Se_3 layer crystal, three-dimensionalization of transport effects and X-ray diffr. anal. 79−73514
$In_xSi_yO_z$, thin film, sputter deposition form., optical and elec. props. 80−60123
$(In_{1-x}Sn_x)_2O_{3-y}$, pyrolytic selective coating, Sn additions effect 78−43499
$In_{2-x}Sn_xO_{3-y}$ film, magnetron DC reactive sputtering, X-ray diffr. meas. 77−44160
InTe, In_2Te_3, molten III-VI semiconductors, SRO 77−65945
$InVO_4$, synthesis and thermal props. *(French)* 80−97443
Ir_3Cr, yield stress and saturisation magnetisation 80−16389
$IrSi_x$, formation, Ir films on Si, He ion backscatt. X-ray diffr. study 79−82471
K, accurate struct. factor determ. by X-ray and neutron diffr. 79−51046
K-La-NH_3 system, cpd. formation, phase analytical and X-ray expts. *(German)* 79−66043
K-rare earth double sulphates, $K_{6+3n}R_{4-n}(SO_4)_9$, ($n\approx0.4$), cryst. struct. 80−28985
$K_2Ag_4Se_3$, crystal struct., X-ray study *(German)* 78−83795
$KAlSi_3O_8$, orthoclase, impact structs., peak shock press., X-ray diffr. investig., lunar rock bombard. appls. 78−7002
$(K_{3/4}Bi_{1/4})(Zn_{1/6}Nb_{5/6})O_3$, cation disordered perovskite, elastic consts. and thermal expansion 80−96587
KBr, additively dyed, amplitude-phase holograms *(Russian)* 80−1152
KC_{24}, intercalated graphite, struct. phase transitions, X-ray diffr. 79−65189
KC_{24}, press. induced staging transition 80−79938
$KC_8H_{2/3}$, struct., X-ray anal. *(French)* 78−26538
$KCaCl_3$, form. of equilib. pseudocubic phase from supersaturated solid soln. based on NaCl *(Russian)* 77−63681
$KCdF_3$, structural phase transitions, X-ray diffr. and differential type thermal analysis 77−80620
KCl melt, effect of cooling rate upon glass transition, X-ray analysis 79−27920
KCl, pure and Ba doped, symm. of elastic fields due to defect displacements, diffuse X-ray scatt. 80−70256
KCl, X-ray integrated intensities in Bragg and Laue geometries 77−31553
KCl:Ba, γ-irradiation, defect struct., X-ray and chemical etching exam. 77−84793
KCl:Ba, structural changes due to γ-irradiation *(Russian)* 77−76460
KCl:Ba (0.005 at.%), spatial diffuse X-ray scatt. intensity distrib. 77−7757
KCl:Pb^{2+}, highly doped, state of dispersion of Pb^{2+} 77−1144
KCl-NaCl-K_2NaVF_6, phase diagram 77−48416
$KClO_4$, cryst. growth from gelatin gels, exam. of growth and morphology 80−7488
$KCoF_3$, antiferromag. domain wall motion under external stress 80−80583
$KCoF_3$, $KFeF_3$ and $KNiF_3$, crystal growth from flux, degree of perfection and dislocation density 77−77359
X-ray diffraction examination of materials continued
$KCoF_3$, lattice parameter temp. depend., phase transitions and thermal expansion coeff. 80−1988
$K_2Cr_2O_7$, polymorphic behavior, depend. on thermal and prep. history 80−34184
$K_2Cr_2O_7$, thermal props. thermal anal. and X-ray diffr. obs. 78−30752
$K_2Cu_{1-x}Mn_xF_4$ system, ($0\leq x\leq0.2$), prep., cryst. chem., and ferromag. props., X-ray and neutron diffr. study 79−24162
KD_2PO_4, transparent dielec., thermal analysis of laser-induced damage 80−66336
KD_2PO_4, X-ray topography of single crysts. grown on KDP seeds 78−23594
$KEuHP_3O_{10}$, synthesis of K_2CO_3, Eu_2O_3 and phosphoric acid, exam. of structure 79−1837
$KEu(PO_3)_4$, synthesis of K_2CO_3, Eu_2O_3 and phosphoric acid, exam. of structure 79−1837
KF, high press. B1 to B2 phase transition, X-ray diffr. obs. 79−23722
KF-BeF_2-DyF_3 system, KBe_2F_5-DyF_3 cross section phase diagram, vitreous phases struct. 77−24383
KF-ErF_3, phase diagram 80−92645
KF-NaF-K_2NaVF_6, phase diagram 77−48416
$KFeF_4$, struct. phase transitions obs. by dielec. const. and X-ray diffr. studies 79−95161
K_2GeF_6, first order phase transition, X-ray diffr. and IR spectra 79−73945
$KH_{2(1-x)}D_{2x}PO_4$, X-ray topographic study of growth strains in single crystal 78−91279
KH_2PO_4, struct. memory effects in low temp. changes 79−28700
KH_2PO_4, under electrostatic field, mechanism of enhancement of neutron diffr. *(Chinese)* 79−51907
$KH_3(SeO_3)_2$, ferroelastic, lattice consts. and thermal expansion tensors, X-ray diffr. meas. 79−37856
$KH_3(SeO_3)_2$, phase transition, acoustic phonon softening 77−27997
$KIO_3.HIO_3$, I atom electronic struct. in X-ray-neutron difference synthesis 79−90595
$K_xLi_{1-x}NbO_3$, epitaxial growth of single-cryst. films on $K_2BiNb_5O_{15}$ substrate by RF sputtering 79−15041
$K_x(M_yTi_{2-y})O_4$, ($M=Mg,Zn,Ni,Cu,Fe^{III},Mn^{III}$), ($0.7\leq x\leq0.9$), new layer struct. *(French)* 80−84149
$K_{1.54}Mg_{0.77}Ti_{7.23}O_{16}$, hollandite, cationic short range order, ion-ion interaction 77−11729
$K_{1.54}Mg_{0.77}Ti_{7.23}O_{16}$, one-dimens. superionic cond., ionic order, defect cond. 78−87815
$KMnF_3$, lattice parameter temp. depend., phase transitions and thermal expansion coeff. 80−1988
$KMn_{0.9}M_{0.1}F_3$, ($M=Co,Ni$), lattice parameter temp. depend., phase transitions and thermal expansion coeff. 80−1988
KNO_3, orientations and twinning in the struct. transform. aragonite-type to calcite-type 77−24284
$KNbO_3$, cubic, temp. depend. of intensity of X-ray interference 80−59613
$KNbO_3$ powder synthesis, unit cell determ. 78−11168
$KNbO_3$, X-ray diffr. before and after high temp. phase transition 77−11694
$KNiF_3$, antiferromag. domain behaviour 77−69607
$KNiF_3$, antiferromag. domain wall motion obs. by X-ray synchrotron topography 78−88139
$KNiF_3$, lattice parameter temp. depend., phase transitions and thermal expansion coeff. 80−1988
$KNiF_3$, magnetostriction, X-ray diffractometry and strain gauge meas. 80−65997
$K_2Ni_3(P_2O_7)_2.nH_2O$, thermal dehydration 80−35513
K_2O high temp. X-ray anal. using special cell for reactive substances *(French)* 79−68978
K_2O-Al_2O_3-B_2O_3, subsolidus compatibility relations determ. *(Japanese)* 79−4957
K_2O-B_2O_3-Fe_2O_3 glasses, nonbridging O formation, Mossbauer spectroscopy 80−55001
K_2O-SiO_2(-GeO_2) system glasses, electron radial distrib. curves 78−87622
KOH-KO_2, phase diagram *(French)* 80−107177
$K_2O.SiO_2$ glass, X-ray diffr. *(Japanese)* 80−19720
KPO_3-$Pb(PO_3)_2$, phase diagram of binary system 77−21114
$K_2PbCu(NO_2)_6$, incommensurate Jahn-Teller phase transition 78−79730
$K_2PbCu(NO_2)_6$, incommensurate Jahn-Teller transition, Huang scatt. 80−70401
$K_2PbCu(NO_2)_6$ Jahn-Teller phase transitions, X-ray and neutron measurements 78−91438
K_2ReCl_6-K_2ReBr_2 solid soln., mixed ligand complexes 77−72585
$K_2SO_4.Al_2(SO_4)_3.24H_2O$, stirring effect on crystalline quality of soln. grown crystals 78−91281
K_2SnCl_6, phase instabilities and mode softening X-ray and neutron diffr. 77−7830
$KTiF_4$, struct. phase transitions obs. by dielec. const. and X-ray diffr. studies 79−95161
$K_2Ti_3O_7$ fibres, synthesis by kneading, drying, calcination process *(Japanese)* 79−38779
$K_2Ti_6O_{13}$, crystallographic study 77−72601
KVF_3, antiferromag. ordering points, thermal anal. and X-ray diffr. meas. *(French)* 78−84421
KVF_4, struct. phase transitions obs. by dielec. const. and X-ray diffr. studies 79−95161
$KYbHP_3O_{10}$, thermal decomp., thermogravimetric and X-ray obs. 80−101013
$K_4Zn(MoO_4)_3$, domain struct. and phase transition, ferroelastic behaviour 77−62581
$K_{1.75}[Pt(CN_4)].xH_2O$, one-dimensional, X-ray diffuse scatt. meas. 77−19937
Kr adsorbed on graphite, X-ray diffr. from 2-D solid 78−75498
Kr, monolayer on graphite, commensurate-incommensurate transition, X-ray scatt. 79−73382
Kr, solid, density at melting and isochoric equations of state 78−83915
Kr, submonolayer, adsorbed on graphite, melting, X-ray scatt. obs. 78−95234
$Kr.2SiO_2$, props. of vitreous deposits 78−22664
La-Al amorphous alloys, internal friction, relaxation process 80−92607
La-Au, splat-quenched, Mossbauer effect and elec. resist., amorphous struct. 80−84676
La-Ge-B, X-ray investigation of phase equilibrium 79−99294
LaB_6, thermal expansion, X-ray method, room temp. to 1300 C 80−96670

X-ray diffraction examination of materials continued

$LaBO_3$ (B=V, Cr, Mn, Fe, Co, Ni), chem. stability X-ray and thermal anal. 79−79242
$La_xCa_{1-x}RuO_3$, metallic, mag., electronic and structural props., ^{99}Ru Mossbauer spectroscopy 77−48107
$LaCoO_3$, conducting oxide powder prod. by freeze drying 79−95984
$LaCoO_3$, synthesis and characterisation by powder X-ray diffr. 78−79580
La_2CoO_4, synthesis and characterisation by powder X-ray diffr. 78−79580
$La_4Co_3O_{10}$, synthesis and characterisation by powder X-ray diffr. 78−79580
LaF_3-$La(OH)_3$, high pressure phases, X-ray diffr. and IR spectroscopic anal. 79−47679
$LaFe_4P_{12}$-type structure ternary arsenides, synthesis and cryst. struct. 80−84154
$LaH_{2.98}$, electrical resistance anomalies at high pressures 80−29381
$LaLi_{0.5}Ir_{0.5}O_3$, perovskite, prep. and mag. study 80−80486
$LaNi_{4.4}B_{0.6}$, H_2 absorpt. props. 80−88432
$LaNiC_2$, struct. determ. using X-ray diffraction *(Ukrainian)* 80−33949
La_2O_3, thermal expansion, 100 to 300K, X-ray method 79−99335
La_2O_3-Y_2O_3, phase diagram at high temps. *(Japanese)* 77−70038
La_2O_3-Y_2O_3 phase, diagram at high temps. *(Japanese)* 77−1218
LaOF-LaF_3, high pressure phase transitions 80−55368
$La(OH)_3$, thermal decomposition, TGA, DTA, X-ray diffr. study *(Japanese)* 77−36436
$La(OH)_2Br$, hydrothermal phase equilib., cryst. struct. 78−35372
$La_7(OH)_{18}Br_3(I_3)$, hydrothermal phase equilib., cryst. struct. 78−35372
$(LaO)_2S$-$(LnO)_2S$ system (Ln=Y or Lu), TEM, X-ray diffr. and fluorescence spectroscopy 79−64957
La_2O_2S-Ga_2S_3 system, phase diagram determ. by DTA and X-ray diffr. *(French)* 77−43309
La_2O_2S-R_2O_2S (R=rare earth), solid solubility, differences in ionic radii 77−15593
$LaRu_2$, H absorption induced Ce valence change, mag. and supercond. props. 80−50042
$La_3Ru_3O_{11}$, crystal struct., X-ray diffr. study 78−67688
$La_4Si_2O_7N_2$ single cryst. growth by floating zone method with SiO_2-Si_3N_4 additions 80−93481
$La_{0.5}Sr_{0.5}CoO_3$, conducting oxide powder prod. by freeze drying 79−95984
$La_{1-x}Sr_xCoO_3$ ($0.5 \leq x \leq 1.0$), rel. between comp. and lattice parameters 79−24154
$La_{0.75}Sr_{0.25}CrO_3$, struct. refinement by X-ray powder diffr. profile analysis 77−84721
$La_xSr_{1-x}RuO_3$, metallic, mag., electronic and structural props., ^{99}Ru Mossbauer spectroscopy 77−48107
$La_2Zr_2O_7$-$La_2Hf_2O_7$ system, cryst. struct., phase diagram 78−83806
Li aluminosilicate, formation of glass-ceramic in $LiCl_3$ vapour 77−16536
Li, X-ray scatt. factor, solid state effect 80−70163
Li-Co ferrite, mag. anisotropy induced by thermomag. treatment, ionic order effect, magnetostriction meas. 80−103830
Li-graphite intercalation compounds, synthesis, elec. and optical props. 79−74108
Li-Pd, phase diagram and mag. props. 77−90321
Li-Pt, phase diagram for comp. range 0-40 at.% Pt, mag. and elec. props. *(German)* 80−84912
$Li_2Ag_{2-x}In_x$, optical props., struct., energy bands, interband transitions 78−72539
$LiAl_xFe_{5-x}O_8$, IR spectra, ionic ordering in absence of fine struct. 77−8583
β-$LiAlO_2$, reindexing X-ray powder diffr. pattern 79−51069
$LiAl_5O_8$, ordered single cryst., struct. determ. *(French)* 80−15074
$LiAlSiO_4$, β-eucryptite, of Li, one dimens. co-operative diffusion 78−2294
$Li_2Cd_{2-x}In_x$, optical props., struct., energy bands, interband transitions 78−72539
$LiCd_{1-x}Tl_x$, intermetallic, X-ray and Knight shift meas. of ^{205}Tl and ^{113}Cd 79−42851
LiCl:Fe, defect struct., Mossbauer spectra and X-ray diffr. obs. 80−7237
$LiClO_4.3H_2O$, absolute sign of piezoelec. d_{33} and pyroelectric p_3 coeffs. 78−43793
$LiCr_xFe_{5-x}O_8$, IR spectra, ionic ordering in absence of fine struct. 77−8583
Li_2CrO_4-K_2CrO_4, phase diagram determination by DTA and X-ray diffr. 78−31391
LiF, deformed by conc. loading, X-ray beam scattering *(Russian)* 78−35430
LiF, neutron-irrad., X-ray diffr. profiles 77−84803
LiF, single crystal, neutron and gamma irradiation, SEM and Bragg profile anal. 80−15158
LiF, X-ray integrated intensities in Bragg and Laue geometries 77−31553
LiF-AlF_3-Na_3AlF_6-Al_2O_3 system, phase equilibrium, X-ray diffr., DTA, quenching, optical microscopy study 80−50610
LiF-$Al(PO_3)_3$ glass, phase decomp., X-ray diffr. and IR spectra study 80−30003
$Li_{0.5}Fe_{2.5}O_4$-$CuFe_2O_4$-$ZnFe_2O_4$, order-disorder transition, quadratic transformation *(French)* 78−76447
$Li_{0.5}Ga_{0.85}Cr_{1.625}O_2$ spinel, tetrahedral coordination of Cr^{3+} ion, electronic spectra, X-ray and neutron diffr. *(French)* 79−65031
$Li_2Gd_4(MoO_4)_7$, Czochralski growth, struct. and optical props. 78−27397
α-$LiIO_3$, in electrostatic field, X-ray double cryst. spectrometric investigation *(Chinese)* 78−67666
$LiIO_3$, phase transitions obs. by DTA, heat treatment, X-ray diffr. *(Chinese)* 78−2249
$LiInS_2$ single cryst. growth by directional solidification, X-ray diffr. study 79−61514
Li_2MgSiO_4-Li_2ZnSiO_4, form. of solid soln. *(Japanese)* 77−25037
$LiNH_4SO_4$, ferroelectric phase transition, lattice parameters and thermal expansion coeffs. 80−40074
Li(Nb,Ta)O_3 solid solution, LPE growth of thin film waveguides on $LiTaO_3$ substrates, X-ray examination on growth conds. 79−41467
$LiNbO_3$, amorphous ribbons, prep., electron and X-ray diffr. obs., dielec. const. temp. depend. 79−50993
$LiNbO_3$, cleaved, crystallographic and electrooptic props. 80−59575
$LiNbO_3$, twinning systems produced by plastic compression 77−1135
$LiNbO_3$ waveguide, diffusion of Ti, exam. by electron probe anal. and X-ray diffr. 78−47588
$LiNbO_3$, X-ray determ. of piezoelec. coeff. 77−8511

X-ray diffraction examination of materials continued

$LiNbO_3$, X-ray diffr. study of lattice dynamics parameters *(Russian)* 79−65156
$LiNbO_3$, X-ray diffuse scatt., temp. depend., 20 to 750°C 79−37800
$LiNbO_3$:Fe, lattice-strains induced by light, X-ray topography 77−76458
$LiNbO_3$:Fe, local photodeformation 79−42932
$LiNbO_3$:Na^+(Co^{2+},Zr^{4+}) films, LPE growth from Li_2O-V_2O_5 flux, X-ray and acoustic characterisation 80−15383
$Li(Nb_{1-x}Ta_x)O_3$, $0 \leq x \leq 1$, LPE thin film growth on $LiTaO_3$ substrate, high temp. X-ray spectrometry of lattice mismatches 79−56087
$LiNdP_4O_{12}$, grown by top seeded pulling technique, possible laser material 80−25542
LiO_2-Al_2O_3-SiO_2, glass containing ZrO_2, cryst. process 80−103253
LiO_2-Al_2O_3-SiO_2-TiO_2:Sn^{3+}, ESR and X-ray phase anal. 79−99752
Li_2O pellets, sintered, reaction with Mo and Ho alloys 79−47913
Li_2O-Al_2O_3-SiO_2 glass, crystallised, grain size and internal strain 80−103259
Li_2O-Al_2O_3(Ga_2O_3)(Bi_2O_3), quenched glasses, crystn. and ionic cond. 80−33899
Li_2O-Fe_2O_3-siO_2 glass, struct. and crystallisation behaviour 78−83738
Li_2O-GeO_2 glass, synthesis, Ge coordination state 77−24271
Li_2O-LiX-B_2O_3 glass, X=halogen, high anionic cond. of new solid electrolytes 80−107546
Li_2O-MgO-Al_2O_3 system, subsolidus phase equilibria 80−81036
Li_2O-SiO_2 glass, crystallisation study 79−90567
Li_2O-SiO_2 glasses, crystn. kinetics from amorphous X-ray scattering study 80−38919
Li_2O-TiO_2, pseudobinary phase rotations, DTA and X-ray anal. 80−108411
LiOH, electron distrib. of OH^- 78−75973
$Li_{x+2}P_xO_{3x+1}$, polyphosphate, melting and crystallisation 80−70376
Li_2SO_4 based solid electrolytes, FCC phase transport mechanism studies and uses 80−107525
Li_2SO_4, fast ion conductors, X-ray diffr., neutron diffr., and Brillouin scatt. study 80−107170
$LiTaO_3$, single crysts., temp. depend. of diffuse X-ray scattering intensity 79−61318
$LiTaO_3$, X-ray diffr. study of lattice dynamics parameters *(Russian)* 79−65156
$LiTaO_3$, X-ray diffuse scatt., temp. depend., 20 to 750°C 79−37800
$LiTaO_3$-$CaZrO_3$, struct. and dielec. props. 78−80298
$LiTaO_3$-$NaTaO_3$-$KTaO_3$, quenched metastable glassy and crystalline phases 79−61568
LiTi, substituted ferrite, cation distribution, Mossbauer, X-ray, neutron diffr. study 80−28975
$LiTi_2O_4$, prep., characterisation and supercond. props. 77−40010
$Li_{1-x}Ti_{2-x}O_4$, struct. phase transition and thermal expansion 78−14465
$Li_{1+x}Ti_{2-x}O_4$, high temp. spinel-Ramsdellite transform. 80−70407
Li_2TiO_3-MgO (20 to 40 at.%), order-disorder transitions, DTA and X-ray anal. 79−29050
Li_xTiS_2, electrochemically intercalated, ion ordering, X-ray diffr. meas. 80−44177
LiV_2O_5, needle cryst. form. by reduction of molten Li_2O-V_2O_5, semicond. props. *(Japanese)* 78−3030
$Li_xV_2O_5$ ($0.1 < x < 1.0$), phase relationship in ambient temperature system 80−20912
$Li_2VS_2(Se_2)$ based topochemical cells, low voltage behaviour 79−92069
Li_2W0_4, type II polymorph. crys. struct. determ. 80−15073
$LiY_{1-x}Er_xF_4$, structure, constitution and melting behaviour 77−39665
LiZn, substituted ferrite, cation distribution, Mossbauer, X-ray, neutron diffr. study 80−28975
Li_2ZnGe, single cryst. growth, by normal freezing method, X-ray diffr. study 79−28908
Li_2ZnSiO_4, tetahedral struct., polymorphic α-β transform. kinetic obs. and method 79−90778
$LixTiS_2$, mechanism of Li intercalation, optical and X-ray studies 79−100394
$Lu_2Si_2O_7$, charact., synthesis and spectroscopic study 80−84846
$Lu_4Si_2O_7N_2$, lattice consts., X-ray diffr. anal. 80−28986
$M_{1-x}Sr_xSi_2$ (M=Ca, Eu, Ba), solid solution with type $SrSi_2$ struct., lattice parameters at high press. 80−54203
metal, FCC, X-ray Debye-Waller factors, CGW vs. DAF models 79−37794
Mg ferrite, crystal lattice defectiveness and degree of inversion, effect of synthesis temp. 77−11501
Mg films, struct. and props., X-ray diffr. spectra anal. 80−80119
Mg powder, temp. depend. of Debye-Waller factor, by energy dispersive X-ray method 79−51208
Mg, X-ray Debye charact. temp., powder specimens 77−84876
Mg-Al (25 wt.%) powder, reaction with high press. H_2, MgH_2 form. and decomposition *(Korean)* 78−11554
Mg-Y-Zn (20, 30 wt.%), phase equilibria investigation *(Russian)* 79−74131
Mg-Zn alloy, aged, one dimensional transition phase β'_2, crystallographic obs. *(Chinese)* 80−60865
$MgCa(CO_3)_2$, dolomite, partial thermal decomp. into MgO and $CaCO_3$, product cryst. growth 80−108706
Mg_3Cd, effect on order, of compression deformation 78−52924
$MgCr_2O_4$-TiO_2, porous ceramics, humidity-sensitive electrical conduction 80−107782
$MgCu_{2-x}Ni_2$, X-ray and neutron diffr. investigation of Laves phases of $MgCu_2$-type *(German)* 80−15050
$MgCu_{2-x}Zn_x$, X-ray and neutron diffr. investigation of Laves phases of $MgCu_2$-type *(German)* 80−15050
MgF_2 (rutile), high-pressure phase transformations 79−44181
$MgFe_{2-y}Al_yO_4$, with added Co, effect of Na_2O admixture on props. 77−36423
$Mg_xFe_{3-x}O_4$, cation redistribution, effect of composition and thermal treatment 79−27966
Mg_2GeO_4-Mg_2SiO_4 system, struct. similar solid soln. obs. and charact. 80−108403
MgIn, X-ray diffr. exam. of compressibility 78−51610
MgMn ferrite, reaction during ferrite form. X-ray phase and mag. anal., contact volt. amperometry 77−21068
$Mg(NH_3)_6(ClO_4)_2$, phase exam. by adiabatic calorimetry and X-ray diffr. methods 78−63854
$Mg(NO_3)_2.6H_2O$, crystal structure changes due to substitution of Mg^{2+}, by Co^{2+} or Ni^{2+} *(German)* 80−24428
$MgNi_{2-x}Zn_x$, X-ray and neutron diffr. investigation of Laves phases of $MgCu_2$-type *(German)* 80−15050

X-ray diffraction examination of materials continued
MgO, hot-pressed, elasticity props. of polycrystals and single crystals 80−54301
MgO, lattice defects., calcination temp. effect 80−15091
MgO, solid solubility of Sc_2O_3, Al_2O_3, Cr_2O_3, SiO_2 and ZrO_2 80−15247
MgO, strength under confining press. of 250 kbar, brittle-ductile transition 77−47510
MgO, thermal expansion, 500-1800°C, X-ray diffr. 77−35723
MgO:Mn^{2+}(Fe^{2+})(Cr^{2+}), redox behaviour of ions, ESR and X-ray diffr. 78−52341
MgO-Al_2O_3-SiO_2, exam. of microstructure and crystallisation kinetics 78−80501
MgO-Al_2O_3-SiO_2, melt and glass crystn. with ZrO_2-TiO_2 nucleants 77−31599
MgO-Al_2O_3-SiO_2: ZrO_2, TiO_2, glass, phase separation *(German)* 80−38932
MgO-$MgCl_2$-H_2O, cement paste, reaction products, X-ray diffr. study 78−23689
MgO-NiO, crystalline soln., microstrain rel. to lattice energy and strain energy 77−24411
MgO-SiO_2, melt, effect of cooling rate upon glass transition, X-ray analysis 79−27920
$(MgO)_x$-$(Al_2O_3)_y$ formation of nonstoichiometric spinel on heating hydrous $MgAl_2O_4$ 78−76672
$MgO(Al_2O_3)_{1.8}$ spinel, Berg-Barrett method, dislocation substructure during creep form. *(French)* 78−68737
$Mg(OH)_2$, sintering, IR spectra, X-ray anal. 80−66452
$Mg_3(OH)_4(NO_3)_2$, nitrate based cement binder formed from MgO powder 79−15634
(Mn,Co)O⇌(Mn,Co)Al_2O_4, and (Mn,Co)O⇌(Mn,Co)Cr_2O_4, ion exchange equilib., 1100°C 77−32566
Mn aluminosilicate, ganophyllite, cryst. struct. 78−75633
Mn coated BN powder particles, X-ray investig. of thermal stresses generated in vac. deposition 77−40455
Mn pyrophosphates, physicochem. charact. 77−39562
Mn-Al-C, ferromag., transform. kinetics 80−34627
Mn-Al-C anisotropic permanent mag., cryst. orientation and form., X-ray diffr. anal. 79−82778
γ-Mn-Au(Pd), magnetic struct. for compositions near onset of antiferromag. ordering 77−63111
γ-Mn-Fe, FCC→FCT transform. temp. and Neel temp., X-ray and neutron diffr. expts. *(Russian)* 78−84797
Mn-Ga (24.1 wt.%), reversible memory of form, X-ray diffr. expts. *(Russian)* 79−5006
Mn-Ge (10.3 to 15.5 wt.%), reversible memory of form, X-ray diffr. expts. *(Russian)* 79−5006
Mn-H(D), ferromag., thermal, struct. mag. props. 78−88145
Mn-Sb two layer film, cpd. formation kinetics, ion backscatt., X-ray diffr. and mag. meas. 77−72801
Mn-Si (62.5 to 63.8 wt.%), phase anal. and cryst. struct. *(Japanese)* 80−15049
$Mn_{1.11}Al_{0.89}$, unit cell parameters, temp. depend. 79−55697
MnAs, single cryst. whiskers, morphology and cryst. orientation, SEM and X-ray diffr. study 79−60664
$MnAs_{1-x}P_x$, high spin-low spin transition 77−20591
$Mn_{46}Co_{54}$, amorphous alloy prep. by high-rate sputtering, struct. and prop. characteris. 79−24462
MnF_2, rutile type, polymorphism at high press., distorted fluorite phase 79−69050
MnF_2, X-ray diffr. investig. of high-press. polymorphism 77−43324
Mn_3Ga, formation of DO_{22} superstruct. and para-antiferromag. transition 79−19737
Mn_3In, antiferromag., mag. susceptibility, X-ray and neutron diffr. 79−11314
MnMg ferrite, products of reaction with ferrogel with $MnCl_2$ solution 77−12582
$Mn_{1-x}Mg_xSe$, mag. and struct. phase transitions, mag. susceptibility and X-ray diffr. study 80−71022
Mn_3O_4, hausmannite, tetragonal-cubic transform., X-ray anal. 80−103288
α-MnS, polycryst. and oriented single cryst., phase transition at 131K 78−6157
MnS, X-ray determ., Debye-Waller factors, Debye temp. and vibration amplitudes 78−55928
MnS-$CuInS_2$, phase relations, 400 to 1300°C, X-ray and microscopic exam. 79−1853
α-MnSe, mag. and struct. phase transitions, mag. susceptibility and X-ray diffr. study 80−71022
MnSi-Si system, striations and cryst. struct. of matrix 80−103292
$MnSi_{\sim 1.73}$ crystal growth and characterisation 80−93474
$Mn_{15}Si_{26}$, growth by Bridgman method and chemical transport, X-ray structural analysis 79−100043
MnTe, effect of press. on Neel temp. and lattice parameter 79−95594
Mo, borosilicate cladding compatibility *(Russian)* 77−66741
Mo, dislocation structure evolution near electro-eroded crater *(Russian)* 80−100237
Mo, evap. film, refl. and struct. 78−72021
Mo film, cc preparation by H_2 reactive sputtering *(Japanese)* 79−95929
Mo film, electron beam deposition on Si, X-ray obs. of silicide form., diffusion processes *(German)* 77−1341
Mo film, on Si, silicide formation obs. 78−43261
Mo film, on Si substrates, laser irrad., cellular struct. and silicide form. 80−10710
Mo film, silicide formation during growth by electron beam evaporation *(German)* 78−84717
Mo film deposited by low temp. carbonyl pyrolysis, struct. 78−72039
Mo, neutron irradiated, influence on X-ray diffr. patterns *(Russian)* 78−22764
Mo oxides, low-grade, soda roasting study *(Korean)* 80−93508
Mo powder, struct. changes under action of high-powder pulses 79−70018
Mo, superconducitng, isotopic vol. effect confirmation by energy-dispersive X-ray diffr. 77−36019
Mo, thin film fabrication for photothermal solar convertors 80−11573
Mo-Al-Ge, phase equilibria, X-ray and microstructural anal. 80−93536
Mo-Mn powder mixture, X-ray diffr. exam. of reaction between Mo and Mn, during sintering 80−16242
Mo-Mn-Fe-Si/Al_2O_3 ceramic seal, interfacial phases 78−72011
Mo-Si film-substrate interface, reaction on heat treatment, silicide formation 80−79999

X-ray diffraction examination of materials continued
Mo-SiO_2-Si, Mo-Si pelicular structures, struct. transitions during vacuum thermal treatment *(Russian)* 78−95238
Mo-Ti, internally nitrided, lattice expansion by precipitation 78−68700
Mo-W bilayer films on Si substrates, silicides formation, marker expt., X-ray diffr. obs. 79−99376
$Mo_6Cl_{10}S$, struct., dielec. and diamag. props. *(French)* 78−67691
$Mo_6Cl_{10}Se$, struct., dielec. and diamag. props. *(French)* 78−67691
$Mo_6Cl_{10}Te$, struct., dielec. and diamag. props. *(French)* 78−67691
MoF_6-graphite intercalation cpds. 78−27441
Mo_5GaS_6, struct. and mag. anomalies, 15 to 300K *(Russian)* 77−7864
MoO_3, film, colour centre studies, optical absorpt. spectra 78−71724
MoO_3 topotactic transform into MoO_2, electron microscopy, X-ray anal. 80−107417
MoO_{3-x}, single cryst. growth and vapour phase transport, X-ray phase determs. study 79−28903
$(Mo_{0.6}Ru_{0.4})_{82}B_{18}$, supercond. metallic glass, neutron irrad. effects 80−29060
MoS_2, prep. and mag. props. *(French)* 80−93072
2H-MoS_2, thermal expansion between 10 and 320K, cell dimensions meas. 79−65222
MoS_3, amorphous struct., X-ray radial distrib. anal. and XPS 80−49115
MoSCl, thermal expansion and thermal transform. 78−26696
$MoSCl_3$, prep. and characterisation 77−59705
$MoSe_2$ coating, on Mo, support annealing influence on orientation, texture and hardness *(Russian)* 80−20961
$MoSe_2$, evaporation, mass spectroscopic investigation 77−76530
$MoSi_2$, integrated intensities and lattice parameters, X-ray anal. 78−63733
$MoSi_2$ refractory formation by As^+ ion beam bombardment 80−107286
Mo_xSi_y films, magnetron DC reactive sputtering, struct. and props. 80−80966
β-$MoTe_2$, low-temperature structural phase transition, X-ray meas. 79−14928
N_2 ($^1\Sigma_g^+$), charge density, X-ray scatt. factors, gas phase electron diffr. 78−930
N_2, X-ray structure factors, mapping of electrostatic props. 79−94841
NB-H(D), lattice expansion due to interstitially dissolved impurity 77−39600
$(NH_4)_2BeF_4$, paraelec. and ferroelec. phases, X-ray diffuse scatt. and superlattice struct. *(Japanese)* 77−43189
$(NH_4)_2BeF_4$, phase transition at 185K, X-ray scatt. obs. 77−36186
NH_4F, electron distribution and charge transfer in NH_4^+ ion 78−91291
$(NH_4)_3H(SO_4)_2$, successive phase transitions, dilatometric and X-ray expts. 80−11348
α-NH_4HgCl_3, thermal expansion, lattice constants between 302 and 364K 80−15268
$((NH_4)_xK_{1-x})_2SnCl_6$, mixed cryst., spectroscopic study 79−33712
NH_4NO_2, thermal anal. by energy-dispersive X-ray diffr. 78−91440
$(NH_4)_2Ni_3(P_2O_7)_2.nH_2O$, thermal dehydration 80−35513
$5(NH_4)_2O.12\ WO_3$, thermal decomp., 100-500°C, thermogravimetric, evolved gas, X-ray and SEM expts. 77−56223
$(NH_4)_2SO_4$ ferrielectric, X-ray anal. of sub-lattice order parameters 78−92035
$(NH_4)_2SO_4$, paraelec. phase, X-ray diffuse scatt., soft mode model 77−31744
$(NH_4)_2S_2O_3$, cryst. and X-ray powder data 79−51074
NI_3Al, structural order and homogeneity, X-ray, mag. susceptibility and Mossbauer meas. 77−63663
$^{15}N_2$, solid struct., and thermodynamic props. *(Russian)* 80−88083
Na, accurate struct. factor determ. by X-ray and neutron diffr. 79−51046
$NaAlSi_2O_6$ melts quenched at high press., Al K-radiation data rel.to struct. 79−32907
$NaBrO_3$, cryst. chirality and optical rotation sense 78−10026
NaCN, diffuse scatt., hard-core correl., weak-graph method 80−49137
$NaCaPO_4$-Ca_2SiO_4 partial system, phase diagram 78−35364
NaCl, deformed by conc. loading, X-ray beam scattering *(Russian)* 78−35430
NaCl, dislocation ordering influence on integrated X-ray coeff. 80−103357
NaCl, integrated intensity of X-ray diffr. by polygonization walls 77−89447
NaCl melt, effect of cooling rate upon glass transition, X-ray analysis 79−27920
NaCl, plastically deformed, glide on {111} planes 79−82234
NaCl, single cryst., shock wave compression, flash X-ray diffr. obs. 78−83877
NaCl, strength under confining press. of 250 kbar, brittle-ductile transition 77−47510
NaCl-$BaCl_2$ 1%, oriented growth of $BaCl_2$ phases, morphology 77−80627
NaCl-CsCl-$CrCl_3$ system, phase struct. anal. by X-ray method *(Russian)* 78−3112
NaCl-kCl melt, reaction with LiO_2-$2SiO_2$ X-ray, IR exam. 80−55706
NaCl-KCl mixed crystal, growth, X-ray exam. and microstruct. 78−44001
NaCl-KCl-CuCl system diagram investig. *(Russian)* 79−96015
NaCl-KCl-$NiCl_2$ system diagram investig. *(Russian)* 79−96014
$NaClO_3$, cryst. chirality and optical rotation sense 78−10026
NaCl. deform. in steel band, X-ray investig. *(Russian)* 78−68727
NaF, isothermal compression at 673K, up to 10 GPa, X-ray diffr. study 80−59565
NaF, X-ray intensity, extinction wavelength depend. 79−27956
NaF-Al_2O_3, β-Al_2O_3 form. *(Japanese)* 78−6912
NaF-YF_3 system, fusibility diagram, quasibinary section of NaF-YF_3-YOF system charact. 80−55371
$NaFeF_2$, Mossbauer and low-temp. dilatometry study *(French)* 80−80662
$(Na_xKy)_2CO_3$, non-stoichiometric, cryst. struct. *(French)* 80−79761
$(Na_{0.5}La_{0.5})_xBa_{1-x}TiO_3$, dielec. and IR spectra exam., ferroelec. transition 78−23418
$Na_{1-x}Li_xNbO_3$, dielec. const. and X-ray diffr., for Curie temp. and phase diagrams 78−72768
$Na_3Mg_2P_3O_{16}$, cryst. and X-ray powder data 79−51072
$Na_2Mg_6Si_8O_{22}F_2$, fluoramphibole, fibrous, crystn. from gas phase, mechanism 78−34451
$NaNO_2$, 163°C phase transition, thermal history effects on range of modulated struct. 78−95563
$NaNO_2$, ferroelec., crit. X-ray scatt. 79−33636

X-ray diffraction examination of materials continued
$NaNO_2$, ferroelec., electron distrib., X-ray and neutron diffraction study 80−24411
$NaNO_2$, ferroelec., X-ray diffr. topographic study of polarisation reversal 79−38441
$NaNO_2$, ferroelec., X-ray obs. during polarisation reversal 79−51921
$NaNO_2$, modulation of intermediate antiferroelectric phase 79−38462
$NaNO_2$, polarisation reversal by time-resolved X-ray diffr., NO_2 radical rot. 77−63382
$NaNO_2$, X-ray crit. scatt. 78−52461
$NaNO_2(NO_3)$, linear compressibility to 27 kbar, X-ray diffr. obs. 80−34125
$NaNbO_3$, antiferroelec., primary order parameter, X-ray scatt. 79−51919
$NaNbO_3$-based ferroelec. solid solns., morphotropic transitions and elec. props., enhanced vacancy conc. 80−55048
$NaNbO_3$-$SrNb_2O_6$, phase diagram, props. meas. 79−11576
$Na_2Ni_3(P_2O_7)_2.nH_2O$, thermal dehydration 80−35513
Na_2O-$2SiO_2$, melt, effect of cooling rate upon glass transition, X-ray analysis 79−27920
Na_2O-Ag_2O-B_2O_3 glass, Ag^+ ion distrib., X-ray diffr. study 80−84076
Na_2O-Bi_2O_3-TiO_2, subsolidus phase equilibrium at 1000 degrees C 78−48384
Na_2O-CaO-Al_2O_3-SiO_2-F-B_2O_3-ZrO_2 glaze, crystallisation, MgO, ZnO, BaO and SrO effects 79−60279
Na_2O-GeO_2 glass, X-ray diffr. study of Ge coordination number 80−10503
Na_2O-GeO_2 glasses, struct. changes, X-ray diffr. study *(Japanese)* 78−91254
Na_2O-GeO_2-Yb_2O_3, glass struct., Yb^{3+} ion segregation 78−87620
Na_2O-NaF-CaO_xZnO_{1-x}-Al_2O_3-SiO_2, opal glasses, strength, surface composition 80−30066
Na_2O-SiO_2 glass, internal and surface struct. by X-ray scatt. 80−84074
Na_2O-SiO_2 glass, stability at high press., X-ray diffraction obs. *(German)* 78−92251
Na_2O-SrO-Nb_2O_5 system, solid state equil., 800°C *(Italian)* 77−47549
$Na_2O.y(Al_{1-x}Fe_x)_2O_{3-m}$, β''-Al_2O_3 phase stability, lattice constants 80−45283
Na_3PO_4-$Ni_3(PO_4)_2$ system, phase equilibrium diagrams, crystallographic study, double orthophosphates *(French)* 80−93546
Na_2SO_4, pure and K-doped, phase transforms., X-ray, DSC and elec. cond. obs. 79−33082
Na_2SO_4, topotaxic phase change obs. 77−51340
$Na_3Sc_2P_3O_{12}$, fast-ion conductor, struct. phase transition 80−88362
$NaTb(MoO_4)_2$, lattice thermal expansion, rel. to temp. 79−77782
Na_xTiS_2, electrochemically intercalated, ion ordering, X-ray diffr. meas. 80−44177
β-$Na_xV_2O_5$, Bridgman and Czochralski single cryst. growth, X-ray diffr. anal. 79−47618
$Na_3Zr_2Si_2PO_{12}$, NASICON, phase transition, X-ray diffr., ionic cond. and sp. ht. meas. 80−19979
$Na_2[B_4O_6(OH_4)].8H_2O$, differential thermal X-ray anal. of phase transitions in non isothermal conditions 79−52205
Nb A15 compounds, preferential order-disorder 77−84702
Nb, borosilicate cladding compatibility *(Russian)* 77−66741
Nb CVD coatings on graphite, grain struct. depend. on temp. 80−25574
Nb complex, prep. by halide reaction with tetramethylurea and tetramethylthiourea, and characterisation 79−15972
Nb film, sputtered, comparison with electron diffr. and AES *(Czech)* 79−51448
Nb film on Si, Ar ion bombard., $NbSi_2$ form. 80−10709
Nb, plastically deformed single crystal, low temp. thermal cond. 79−28336
Nb, strain profile of plastic zone in dislocation-free single cryst. by X-ray topography 79−14876
Nb, X-ray and neutron diffuse scatt. intensities comparison, thermal vibrs. 77−43294
Nb/Cu layered ultrathin coherent struct. 80−80122
Nb-Al-C, phase diagram and lattice constants, X-ray diffr. method 80−89207
Nb-C-N-O-H, solid solns. of H, exam. of props. 80−29172
Nb-Ga, phase system form. and stability of A15 phase 77−90347
Nb-Ga-Fe ternary system, phase equilib. at 1000°C, supercond. transition temp. 80−35158
Nb-Ga-Ir, phase equilib. at 1000°C, cryst. data for intermediate phases 78−52763
Nb-Ga-Ir system, phase equilib. at 1000°C and supercond., Nb-rich portion 77−36480
Nb-Ga-Y system, X-ray and microprobe anal., isothermal section and supercond. transition temp. *(Ukrainian)* 79−38793
Nb-Ge, supercond. A-15 phase, supercond. transition temp. after ion implantation 80−49972
Nb-Ge system, phase diagram determ. 79−38796
Nb-Ge-Cu, phase equilib. and supercond. props. *(Russian)* 80−40332
Nb-Ge-Si film, CVD, struct., comp., stability and homogeneity 80−15421
Nb-H system, Huang diffuse scatt. of X-rays from displacement field 77−15446
Nb-H(D), H ordering, review 80−60850
Nb-H(D) system, incoherent phase transition 79−73304
Nb-N, superconducting layers, sputtering in high vacuum apparatus *(German)* 80−89147
Nb-Ni, glassy alloy, struct. anal. using X-ray diffr. 79−51004
Nb-Ni glasses, struct. factor temp. depend. 80−28920
Nb-Os, phase diagram exam. 77−21103
Nb-Sn(Al)(Ga)(Ge)(Si)-C, phase equilib. and supercond. 80−50593
Nb-Ta system, short-range order exam. by diffuse X-ray scatt. *(Russian)* 77−31644
Nb-V system, short-range order exam. by diffuse X-ray scatt. *(Russian)* 77−31644
Nb-Zr (1 wt.%), internal oxidation state of O_2, dispersion hardening by diffusion alloying, X-ray diffr. and internal friction *(Russian)* 79−70102
NbC, deformation behaviour during rubbing in wide temp. range 80−16486
NbC, diffuse, superconductive props. obs. *(Bulgarian)* 80−80467
$Nb_xCr_{1-x}O_2$, ($x \geq 0.5$), cryst. growth by chem. transport and phase transitions 78−35281
Nb_3Ga, supercond. crit. temp. and struct., heat treatment and stoichiometry effects 77−43769
$Nb_3(Ge,Si)$ A15 film, supercond. and structural props. 79−87177
X-ray diffraction examination of materials continued
Nb_3Ge film, CVD, thermal expansivity, X-ray diffr. meas. 78−6166
Nb_3Ge film, supercond., electron beam codeposition in O_2, Cl_2 or air, phase diagram 77−28728
Nb_3Ge films, prep. by DC sputtering and solid state diffusion, supercond. props. and struct. 79−38212
Nb_3Ge, supercond. film, amorphous content, X-ray diffr. study, rel. to transition temp. 80−75668
Nb_3Ge, supercond. film, determ. of lattice consts. 78−6470
Nb_3Ge supercond. thin films, He- and Ar-irradiated, X-ray diffr. studies 80−29503
Nb_3Ge superconducting film, struct. 77−32123
Nb_3Ge superconducting film, Nb_5Ge_3 and NbO content, X-ray diffr. obs. 80−2515
Nb_3Ge tape, prepared continuously by CVD, props. 78−60257
$Nb_3Ge(Si)$, RF sputtered films, amorphous atomic scale struct. 80−84064
NbH_x, coherent α-α' phase transition 80−71641
NbH_x, structural transform. rel. to order-disorder transform. 80−60858
NbN, diffuse, superconductive props. obs. *(Bulgarian)* 80−80467
NbN, Nb_4N_3-NbN, Nb_2N-Nb_4N_3, Nb_2N, cryst. growth parameters and morphology of chem. vapour deposition, X-ray diffr. and SEM study 79−23861
NbN single crystal preparation, zone melting and nitriding techniques 80−60776
NbN, supercond. RF reactively sputtered films, deposition parameter effects on props. 80−80972
Nb_2N, supercond. props. and structural phase transform. induced by C^+ and N^+ implantation 80−107942
$Nb_{60}Ni_{40}$, metallic glass, obs. of temp. depend. of struct. factor 78−87624
NbO, single cryst. with 25% vacancies, neutron damage 77−15459
Nb_2O_5, carbothermal reduction in N_2 intermediate phases 79−11773
$NbSCl_3$, prep. and characterisation 77−59705
$NbSe_3$, incommensurate CDW, X-ray scatt. and elec. field studies 79−42471
$NbSe_x$, x=1.48-2.0, nonstoichiometric, press.-comp.-temp. rel. determ. by annealing 79−74139
Nb_3Si, supercond. props., effect of neutron irrad. 79−38211
Nb_3Sn diffusion layer material, characterisation 79−38213
Nb_3Sn film, electron beam codeposited, growth morphology and tensile props. 78−10301
Nb_3Sn, lattice microstrain induced metastable phase, low temp. struct. and props. 77−8482
Nb_3Sn, vap. deposited supercond. film, effect of N_2 and tape heating 78−34939
Nb_3Sn, X-ray study of fission fragment induced structural damage 78−51589
Nd, crystal structure, P-T phase diagram 78−84776
Nd, magnetic-structure, neutron and X-ray diffr. study 80−60197
Nd, triple-q magnetic structure, neutron and X-ray diffr. investig. 79−73687
Nd-Cr-B system, phase equil. at 800°C, boride lattice parameters *(Russian)* 78−31388
Nd-Ga alloy, phase diagram, DTA, X-ray and metallographic obs. 79−24494
Nd-Ni-Al, isothermal section, 600°C, X-ray struct. anal. *(Ukrainian)* 80−33929
Nd-Sn (0 to 50 at.%), phase equilibria diagram *(Ukrainian)* 79−34001
Nd-Tl phase diagram, intermediate phases 78−60653
$NdAl_3(BO_3)_4$, LPE for thin film miniature lasers 79−74101
$NdFeTiO_5$, magnetic props. and crystal growth 78−92185
$Nd(Ga,Cr)_3(BO_3)_4$, cryst. growth by LPE, Nd^{3+} fluorescence, lattice constants 80−29883
$NdGa_3(BO_3)_4$ crystal structure by X-ray spectral microanalysis 79−46621
$Nd(OH)_2Br$, hydrothermal phase equilib., cryst. struct. 78−35372
$Nd_7(OH)_{18}Br_3(I_3)$, hydrothermal phase equilib., cryst. struct. 78−35372
$Nd_2O_3.4TiO_2$, growth from soln., struct. 78−83794
NdP_5O_{14}, ferroelastic, hydrostatic press. effect on phase transition temp. 80−70293
$Nd_xPr_ySm_zCo_5$ permanent magnets, coercive force, low-temp. annealing influence *(Russian)* 80−39812
$NdRh_{1.2}Sn_{4.1}$, new supercond./mag. cpds., X-ray powder diffr. data 80−100215
$NdTlO_3$, physicochem. props. 80−25625
$Nd_xY_{1-x}Zn$ system, solid soln., mag. susceptibility, 77 to 600K *(Russian)* 80−65776
$(Ni,Cr)_3Py$, layer formed on phosphidation of Ni-Cr alloy in P vapour, 700°C 80−25906
$Ni_{75}Si_8B_{17}$, amorphous alloy, crystallisation study *(Japanese)* 78−9959
Ni, cold-rolled, anomalous effects during X-ray stress meas. *(German)* 80 104184
Ni complex, 1,2-benzoquinonedioximates, refl. spectra, 0.5-2.5 eV, Young's modulus and internal friction 78−39562
Ni complex, $[Ni(en)_2Cl]_2Cl_2$, heat capacity, X-ray diffraction and mag. meas., phase transition 78−47515
Ni, corrosion, high temp., SO_4 induced, studied at 900°C in O_2+4.2% SO_2 80−97639
Ni, Czochralski grown single cryst., X-ray topography, mag. domains 77−12147
Ni, Czochralski grown single crystal, crystal perfection, X-ray topography 78−47252
Ni, Debye Waller determ. from modified Cheveau model 78−59918
Ni, dislocation structure parameter determ. due to plastic deformation *(Russian)* 80−54242
Ni, dislocation substructure formation under hydrostatic extrusion 78−56696
Ni electrodeposits, struct., electrolyte anions influence 80−20056
Ni filings, interrelation between dynamic and static distortions, X-ray diffr. meas. *(Russian)* 77−43305
Ni film, electrodeposited, recrystallisation kinetics, X-ray scatt. *(Russian)* 78−60045
Ni, magnetostriction, lattice parameter changes, direct X-ray obs. 78−15001
Ni, Ni-Fe, X-ray study of occluded H_2 77−16586
Ni, oblique mag. domain walls, obs. by X-ray topography 78−6540
Ni precipitates, isothermal annealing influence on structural state, X-ray diffr. anal. *(Russian)* 80−100849
Ni, self-ion irradiated, defect clusters, annealing 78−18687

X-ray diffraction examination of materials continued
Ni superalloy, STEM microanal. of precipitates and their nuclei 80−81067
Ni/Pt double layers on Si substrate, silicide formation 78−84010
Ni-Al, band struct. and density of states, KKR method and X-ray meas. 80−10863
Ni-Al-Si, β-phase stability *(Russian)* 78−39738
Ni-C system, satellite structs. of intermed. phases in diamond synthesis using Ni catalyst *(German)* 77−32538
Ni-C-Ce, overmodification *(Russian)* 80−40432
β-Ni-Co-Al, martensitic transform., metallographic, X-ray diffr., and elec. resist. obs. *(Russian)* 78−19748
Ni-Co-Al alloys, continuous precip., SEM, TEM, X-ray diffr. study 80−89220
Ni-Co-Mo alloys, electrodeposition, struct. 79−28970
Ni-Co-P, ferromag. film, amorphous to cryst. transition, diffr. and resistivity meas. 78−60587
Ni-Co-W, electrodeposition, surface morphology and cryst. struct. 80−71602
Ni-Cr, solubility limit determ., X-ray method 79−43199
Ni-Cr-Fe-Mo-Co (21.41, 19.28, 8.64, 2.16 wt.%), Hastelloy alloy X, exam. of thermal stability 78−84865
Ni-Cr-Ta system, phase equilib. of Ni rich region at 1523 and 1273K 80−93541
Ni-Fe alloy, FCC, density, lattice parameters, X-ray diffr. and hydrostatic weighing 78−55904
Ni-Fe-Ce superalloy, vacuum melted, Ce effects on microstruct. 77−36552
Ni-Fe-Nb-Al(-Mo), wear resisting mag. head material, mag. props. and struct. 80−35350
Ni-ferrite powders, form. in presence of Li_2SO_4-Na_2SO_4 molten salts, prep. and characts. 80−84869
Ni-Ge binary system, phase diagram rel. to that of Co-Ge *(French)* 80−97463
Ni-Nb (5, 10 at.%), oxidized specimen study using SEM, HEED X-ray diffr. and ion backscattering anal. *(Japanese)* 79−24651
Ni-Nb alloys, oxidation at high temp., high energy ion backscattering anal. *(Japanese)* 80−35405
Ni-Ni_2B eutectic, high temp. X-ray anal. 80−71639
Ni-Os, short-range order parameters, ordering energy on first coordination sphere *(Russian)* 79−69058
Ni-P, amorphous, low P, struct. study using high-angle X-ray diffr. 80−107055
Ni-P, amorphous, reversible effects of temp. on struct. 78−34442
Ni-P, amorphous, struct., X-ray scatt., rel. to Cu-Zr alloys 77−51324
Ni-P, amorphous electrodeposited alloys, phase-separation *(Japanese)* 80−54140
Ni-P, electroless deposition on Al 79−90907
Ni-P(B), amorphous, thermal anal. and X-ray diffr., solidification struct. development *(French)* 78−91253
Ni-Pd-Mn ternary alloys, mag. characts., use for thermoseed 80−107995
Ni-S, defect control by heat-treatment in S atmos. 79−43293
Ni-Ta (70, 30 wt.%) metallic glass, struct. and crystn. *(Russian)* 80−70136
Ni-Ta-Al system, phase equilibria and diagram, electron probe, X-ray diffr. anal. 80−29927
Ni-Ta(7 at.%), short-range order, pseudopot. calc. and diffuse X-ray scatt. *(Russian)* 77−28008
Ni-Ti (1.6, 7.64 wt.%), monophase high temp. scaling, metallography study 80−21159
Ni-W (20 to 50 at.%), phase distrib. var. with annealing time, metastability of hexagonal phase *(Russian)* 77−8851
Ni-W sintered powder pressings, intermetallic phases *(Russian)* 80−55349
Ni-Zn ferrite, electrical cond., Seebeck coeff. and saturation magnetisation 77−20315
β′-NiAl, single cryst., quenched and annealed, ω-like diffr. effects, TEM and X-ray diffr. study 79−60216
β-$Ni_{1\pm x}Al_{1\pm x}$, defect struct. and Debye Waller factors vs. composition 77−31658
$Ni_{66}B_{34}$, morphological, structural and phys. props. *(French)* 80−44444
NiF_2 film preparation and characterisation 80−59815
NiF_2, tetragonal to orthorhombic transition at high press., possible mag. ordering 78−18765
Ni_3Fe, Debye temp. determ. from elastic consts. and X-ray meas., effect of configurational order 78−30727
Ni_3Fe, long range order, Mossbauer spectra comparison 78−10810
Ni_3Fe, X-ray diffraction investig. of order-disorder transform. *(Russian)* 77−70043
$NiFe_{2-t}Al_tO_4$, cryst. and mag. props. 78−14940
$Ni_{40}Fe_{40}B_{20}$ glass alloy, rapidly quenched, explosive welding to A516-70 steel and to itself 78−39954
$Ni_xFe_yCr_{1-x-y}$ films, struct., mag. props., and corrosion resist. 80−34706
$Ni_{36}Fe_{32}Cr_{14}P_{12}B_6$, metallic glass, crystallisation 79−77520
$NiFe_2O_4$ epitaxial film on NdGG, structural and ferromagnetic reson. meas. 77−1574
$NiFe_2O_4$ mag. fluid particles, comp., struct., and mag. props. 80−60374
$Ni_xFe_2O_4$ series, chem. and mag. transformation, X-ray diffr. and mag. susceptibility study 79−51774
$(Ni_{1-x}Fe_x)S$, solid solns., electronic props., X-ray, thermal and Mossbauer study 79−78376
NiH_x, formation and decomp. studies 80−71626
Ni_2MnIn, Heusler alloy, order-disorder phase transitions, X-ray diffr. meas. 77−66640
$Ni_2Mn(Mn_xSn_{1-x})$, Heusler alloy, antiferromagnetic order, X-ray and neutron diff. 78−64189
Ni_4Mo, order-disorder phase transform., X-ray diffr. *(Russian)* 79−1855
$Ni_2Mo_6S_6O_2$, O-containing Chevrel phases, synthesis and props. 80−108368
$Ni(NH_3)_6(BF_4)_2$, enantiomorphic transition, X-ray powder diffr. meas. 78−30574
$Ni(NH_3)_6(ClO_4)_2$, X-ray powder diffr. exam. of enantiomorphic transitions 78−2054
$0.5Ni(NO_3)_2 \times 1.5Ni(OH)_2$ form., X-ray parameters 77−16519
$Ni_{60}Nb_{40}$, stability, crystallisation, ductility meas. 78−47246
NiO, lattice parameters, microstrains, non-stoichiometry, comparison between mosaic microcrysts. and quasi-perfect single microcrysts. 80−24414
NiO samples, colour difference, X-ray line broadening study 80−100206

X-ray diffraction examination of materials continued
NiO, temp. depend. of thermal expansion and IR lattice vibrational mode 77−84950
NiO, under controlled atmosphere, exam. of composition and temp. dependence, of lattice parameter *(French)* 79−19214
NiO:Cr, effect of Cr additives on structure parameters *(Bulgarian)* 80−44319
NiO-MgO-ZnO, solid soln. form and colour *(Japanese)* 77−63647
$Ni_{77}P_{23}$ metallic glass, struct. relax., X-ray expts. 79−1400
$Ni_{80}P_{20}$, amorphous, struct. factor temp. depend., X-ray diffr. study *(Japanese)* 79−51005
$Ni_{80}P_{20}$ amorphous alloy, liquid-quenched structure 77−1082
$NiPS_3$-Li, chemical and electrochemical intercalation *(French)* 78−38679
$(Ni_5Pd_5)_{82}P_{18}$, phase separated, exam. of crystallisation by differential thermal analysis 78−87623
NiS, struct. mechanism of low-temp. phase transition in hexagonal modification 78−71855
$Ni_{1-x}S$, metal-semimetal transition, lattice dynamics and thermodynamic props. 80−29324
β-Ni_3S_2, defect struct. 78−63754
β-Ni_3S_2, formation during Ni sulphidation in H_2S-H_2 mixtures 78−3257
β-Ni_3S_2, formed during sulphidation of Ni, defect struct. and chemical diffusion 78−2115
$Ni_{78}Si_{10}B_{12}$, amorphous, struct. factor temp. depend., X-ray diffr. study *(Japanese)* 79−51005
NiTi, premartensitic transformation of B2 phase, shape memory 80−84931
$Ni_{40}Ti_{60}$, amorphous, chem. short-range-order, X-ray and neutron scatt. obs. 80−96447
$NiTiO_3$, synthesis from products of soln. spray drying, kinetics 77−16519
$Ni_{62}Ti_{29}Zr_9$, amorphous, H-sorption, X-ray and DSC obs. 80−49526
Ni_4W, order-disorder phase transition, X-ray struct. exam. *(Russian)* 78−64532
NiZn ferrites, comp., X-ray diffr. and saturation magnetisation obs. 78−18617
$Ni_{0.25}Zn_{0.75}Fe_2O_4$, structural phase transition, X-ray and neutron diffr. study 80−79735
$Ni_xZn_{1-x}Mn_2O_4$, mag. props. 78−43573
$Ni_{64}Zr_{36}$, amorphous and cryst., H-sorption, X-ray and DSC obs. 80−49526
Np_6Fe, existence and cryst. chemistry 77−51349
NpO_2 single crystal growth, gas phase chemical transport method *(French)* 80−60760
O_2 ($^3\Sigma_g^-$), charge density, X-ray scatt. factors, gas phase electron diffr. 78−930
O_2, solid, transformation charact. and orientation relations 80−33917
P, amorphous, prepared by chem. transport in low-press. H_2 plasma, radial distrib. function 80−64899
P_xAs_{1-x}, periodic structs. characts. determ. by means of satellite Bragg reflections 79−46510
PCl_5, sublimed phase studied by ^{31}P NMR, Raman spectra and X-ray diffr. 80−100209
PLZT ceramics, ferroelectric and struct. transitions, crystallographic, thermal, and dielec. anal. 80−29693
PLZT ferroelectric thin films, epitaxial growth and optical props. 80−70543
PLZT film, epitaxial growth by RF sputtering, and characterisation 77−85937
PLZT film, growth by RF sputtering, struct. and ferroelec. props. 77−48340
PLZT, thin film epitaxial growth and characteris. 79−28918
PLZT, thin film prep. by RF sputtering, struct. and ferroelec. props. *(Japanese)* 77−69992
(PLZT)(PLZN) system, ferroelec. transparent, prep. and study 79−42911
Pb compounds identification in urban aerosols, rel. to health hazard 78−44991
Pb, film, deposited on Si substrate, residual strains 78−18915
Pb film, thermal strain, strain relax. mech. 79−42427
Pb film, vac. deposited, thermal strain depend. on thickness and grain size 79−90926
Pb, high-press. superconducting transitions determ. at liquid He temps. 77−11442
Pb:O, thin film, microstruct. and thermal stress, doping effects 80−88458
Pb/Ag-Pd, sequentially deposited, thin film reaction kinetics, X-ray diffr. expts. 77−89594
Pb-Au (0-0.0918 at.%), lattice parameter changes due to Au dissolution 79−77558
$(Pb_{1-y}Ba_y)_{1-x}La_xNb_{2-x/5}O_6$, ferroelec., phase transitions 79−38487
Pb_2CoWO_6, antiferroelectric substruct. 79−38489
$2PbFe_{1/2}Nb_{1/2}O_3$-Pb_2FeReO_6, comp., struct., dielec. and mag. props. 80−2704
$2PbFe_{1/2}Ta_{1/2}O_3$-Ba_2FeReO_6, comp., struct., dielec. and mag. props. 80−2704
$2PbFe_{1/2}Ta_{1/2}O_3$-Pb_2FeReO_6, comp., struct., dielec. and mag. props. 80−2704
$Pb(Fe_{2/2}U_{1/3})O_3$-$PbZrO_3$ solid solns., phase transition 77−48138
$PbFe_{2/3}W_{1/3}O_3$-$BaTiO_3$ system ferroelec., antiferromag., ESR and dielec. props. meas. 77−40172
$Pb_3(Ge,Si)_2O$, growth from melt, struct. and dielec. props. 77−44148
$Pb_5Ge_3O_{11}$ bonded Pb(Zr,Ti)O_3 composites, piezoelec. props. 79−78629
$Pb_5Ge_3O_{11}$, lattice dynamics parameters anisotropy, X-ray diffr. study 80−59612
$Pb_5Ge_3O_{11}$, sputtered ferroelec. films, prep. struct. and dielec. props. 80−75452
$Pb_{1-x}Ge_xTe$, solubilities, elec. and optical props. 77−35940
PbI_2 crystal, gel-grown AgI impurity effects on struct. transformations during growth 77−76339
PbI_2 film, photolyzed, refr. index change 78−11010
PbI_2, polytypic change, 5 new polytypes, X-ray diffr. anal. 79−37648
PbI_2, Raman spectra, phonon dispersion curves, vibrational props., lattice parameters 79−69211
$Pb_5I_2Br_8$, form., cryst. symmetry, X-ray diffr. obs. 79−23570
$Pb_5I_4Br_6$, form., cryst. symmetry, X-ray diffr. obs. 79−23570
$Pb_2Li_{1/2}Nb_{3/2}O_6$, antiferroelec. cryst. growth and props. 77−36189
$Pb(Mg_{1/3}Nb_{2/3})O_3$-$PbTiO_3$-$PbZrO_3$, piezoelec. PCM ceramic, formation process *(Japanese)* 77−85978

X-ray diffraction examination of materials continued
- $Pb_xNb_yO_6$ pyrochlore phases, three odd superstructures *(French)* 77−68946
- PbO layers, crystal platelets orientation and thickness, X-ray diffr. obs. 78−87890
- PbO, reactively evaporated, photocond., H_2O induced phase transform. 80−60122
- PbO/TeO_2 system, central region of phase diagram, X-ray and thermal anal. 79−70046
- PbO-GeO_2 glass, synthesis, Ge coordination state 77−24271
- PbO-ZnO-B_2O_3, Corning 7575 seal glass, devitrification 78−79532
- $PbO_{1.57}$, thermal expansion tensor, phase transitions, X-ray diffr. obs. *(French)* 79−1515
- PbO_2, thermal decomposition, heating rate effect, kinetics, mechanism, struct. 78−92473
- 4PbO.GeO_2, X-ray phase and thermal anal., new antiferroelectric 79−1744
- $Pb_3(PO_4)_2$, ferroelastic transition, X-ray diffr. and scatt. *(French)* 77−31769
- $Pb_5(PO_4)_3OH$, prep. from sulphate, X-ray diffr. and IR spectrosc. 80−29893
- PbS, epitaxial film, struct. perfection, two cryst. X-ray spectrometry 78−26792
- PbS film, polycryst., chem. deposition from soln. and characterisation 78−72743
- PbS film, soln. grown on Si, struct. and comp. of heterojunction 80−54530
- PbS films, polycryst. and epitaxial, small-angle X-ray scatt. and electron density inhomogeneities 80−96758
- n-PbS, natural galenite, (200), (400), (600) planes observed 79−42975
- PbS, oxidation, $PbSO_4$ distrib. in products *(Polish)* 80−25883
- PbS, X-ray determ., Debye-Waller factors, Debye temp. and vibration amplitudes 78−55928
- PbS-Si heterojunction, PbS film growth and struct. 80−96762
- PbS_xSe_{1-x} film, prep. by co-evaporation method *(Japanese)* 78−64477
- $PbSbO_2Cl$, nadorite, thermal expansion, X-ray determ. 78−18802
- $PbSc_{2/3}Te_{1/3}O_3$-$PbSc_{2/3}W_{1/3}0_3$($PbFe_{2/3}Te_{1/3}O_3$) ferroelec. props. and lattice consts. 80−60520
- PbSe, X-ray diffr. exam. of struct., and luminescence props. 80−55209
- $PbSnF_4$, allotropic transformations 80−84926
- $PbSnF_4$, anionic conductor *(French)* 79−1523
- $Pb_{1-x}Sn_xSe(Te)$ single crystals, Bridgeman grown, X-ray exam. 79−56926
- $Pb_{1-x}Sn_xTe$, VPE crystals, X-ray diffr. data interpretation 77−15712
- $Pb_{1-x}Sn_xTe$:In epitaxial layers, growth, elec. props., and luminesc. 80−54542
- $Pb_{1-x}Sn_xTe$-PbTe heterojunction, Sn diffusion and elec. effects of dislocations, elec. and metallurgical expts. 77−89839
- $Pb_{1-x}Sn_xTe$-PbTe heterojunction, Sn diffusion profile, X-ray diffr. data interpretation 78−51832
- Pb_2TaMnO_6, reaction of form. from oxides, ferroder. props. 80−55326
- PbTe, crystallite size in epitaxial layers by X-ray diffraction rocking curves 80−20052
- PbTe, undoped, nature of defects, X-ray diffr. and optical absorption meas. 77−43211
- PbTe-Ga_2Te_3, phase interaction, DTA, XPA and microstructural anal. 80−96625
- PbTe-InTe system, phase interactions and solid soln. form., physicochem. and elec. characteris. 80−104129
- $PbTe_{1-x}Se_x$, epitaxial layers synthesis, cryst. struct. perfection and elec. characts. 79−87587
- Pb(Ti, Zr)O_3, piezoelectric-ferroelectric ceramic, polarisation processes, X-ray obs. 80−34847
- $PbTiO_3$, $(PbTiO_3)_{0.9}(B_2O_3)_{0.1}$ amorphous ribbons, prep., electron and X-ray diffr. obs., dielec. const. temp. depend. 79−50993
- $PbTiO_3$, X-ray interference intensity temp. depend., lattice ion vibr. *(Russian)* 80−20601
- $PbTiO_3$-La_2O_3.3TiO_2, struct. and dielec. props. 80−54200
- $PbTiO_3$-$PbZrO_3$-based multicomponent ferroelec. solid solns., morphotropic transitions and comp.-temp. phase diagrams 80−55047
- $PbWO_4$, thermal expansion tensor, phase transitions, X-ray diffr. obs. *(French)* 79−1515
- Pb_2WO_5, phase transformation study by high temp. X-ray diffr. and differential scanning calorimetry 79−43244
- Pb(Zr,Ti)O_3 ceramic, X-ray investigation before and after polarisation *(Chinese)* 80−2712
- Pb(Zr,Ti)O_3, doped, Goldschmidt factors and ferroelec. antiferroelec. transition 77−12332
- Pb(Zr,Ti)O_3 film, prep. by electron beam evaporation technique 77−1809
- Pb(Zr, Ti)O_3, formation 79−43185
- Pb(Zr,Ti)O_3, phase transform. at 163K *(Ukrainian)* 77−69082
- Pb(Zr,Ti)O_3, prep. and reactivity from butoxide precursors 78−84749
- Pb(Zr,Ti)O_3, tetragonal ferroelec. ceramic, 90° domain-rot. fraction after polarisation, X-ray determ. 80−75992
- Pb(Zr,Ti)O_3 thin film, ferroelec., fabrication by RF sputtering *(Japanese)* 80−25560
- Pb(Zr,Ti)O_3, X-ray study in tetragonal-rhombohedral phase-transition composition area 79−42921
- Pb(Zr,Ti)O_3:Cr_2O_3 ceramics, reson. freq. comp. and temp. depend. 80−70413
- $PbZrO_3$, elec. field induced phase transitions 77−62643
- $PbZrO_3$, phase transitions, X-ray, dielec., and thermal anal. 80−45020
- $PbZrO_3$, struct. phase transition 79−61312
- 1-x$PbZrO_3$-x$PbSc_{0.5}Nb_{0.5}O_3$, $0 \leq x \leq 1$, phase transitions, X-ray, dielec., and thermal anal. 80−45020
- $PbZr_xTi_{1-x}O_3$ ceramics, morphotropic phase boundary 80−81035
- $Pb(Zr_xTi_{1-x})O_3$ films, ion beam deposition, struct., dielec. and ferroelec. props. 80−20788
- $PbZr0_3$, X-ray interference intensity temp. depend., lattice ion vibr. *(Russian)* 80−20601
- Pd complex, 1,2-benzoquinonedioximates, refl. spectra, 0.5-2.5 eV, Young's modulus and internal friction 78−39562
- Pd film, on Si substrate, laser irrad., cellular struct. and silicide form. 80−10710
- Pd film on Si, Xe ion beam induced form. of PdSi 80−10800
- Pd-Ag-Au, lattice parameters and thermal expansion coeffs., X-ray diffr. meas. 79−99121
- Pd-Ag-Au, temp. effect on lattice parameters and thermal expansion 78−51473

X-ray diffraction examination of materials continued
- Pd-Cu-Ga, cold work and annealing-induced hardening, X-ray diffr. anal. and metallographic exam. *(Russian)* 79−38844
- Pd-D, crystallite size effects, simultaneous sorption and X-ray study 80−65237
- Pd-Ni-Si amorphous alloys, crystn. process during isothermal ageing 80−89275
- Pd-Si, amorphous, compositional study on short-range struct. 80−84095
- Pd-Si, amorphous, neutron irradiated, small angle X-ray scatt. study 79−14850
- Pd-Si, amorphous metallic glass, with defined local coordination, struct. model 80−84092
- Pd-Si amorphous alloy, neutron irradiation effects *(Japanese)* 77−84806
- Pd-Si layers, form. by laser irrad. of Pd film on Si substrate 79−99438
- Pd-V, alloy and bilayer, silicide form. solid phase reaction with Si 80−6568
- Pd-Zn, $L1_0$ type intermetallic phase, X-ray diffr. study of lattic compression 80−49182
- $(Pd_{80}Au_7Si_{13})/Fe_{30}$, compositionally modulated amorphous film, diffusion, struct. relax. 80−103518
- $Pd_{1-x}M_xSe_2$ (M=Ru,Co,Ni), high pressure phase transformation studies, lattice constants and densities 79−65187
- $Pd_2MnIn_{1-y}Sb_y$, Heusler alloy, mag. order obs. 80−29528
- $Pd_2MnIn_{1-x}Sn$, and $Pd_2MnIn_{1-y}Sb$, Heusler alloys, mag. order, disorder effects 80−88723
- $Pd_2MnIn_{1-x}Sn_{1-x}$, mag. order exam. 77−40036
- Pd_2MnSb, ferromag. Heusler alloy, mechanical and heat treatment effects 79−78582
- $Pd_{2-x}MnSb$, struct., appl. as improved neutron polariser 80−60199
- $Pd_2MnSn_{1-x}Sb_x$, mag. order exam. 77−40036
- $Pd_{0.8}Si_{0.2}$, amorphous, He^{2+} ion irradiation effect on structure 79−42120
- Pd_2Si and PdSi films, on Si, stress obs. 80−80145
- $Pd_{80}Si_{20}$, amorphous, structural changes by neutron irradiation, X-ray scatt. meas. 78−6104
- $Pd_{80}Si_{20}$, amorphous, struct. factor temp. depend., X-ray diffr. study *(Japanese)* 79−51005
- $Pd_{80}Si_{20}$, amorphous, structural changes with neutron irrad., X-ray scatt. obs. 80−33898
- $Pd_{80}Si_{20}$, amorphous alloy crystn., high press. effect 78−95001
- $Pd_{80}Si_{20}$, amorphous alloy, partial struct. functions, X-ray, electron and neutron diff. studies *(Japanese)* 80−88050
- $Pd_{80}Si_{20}$ metallic glass, struct. relax., X-ray expts. 79−1400
- $Pd_{82.5}Si_{17.5}$, amorphous and liq. alloys, struct. 77−24275
- $(Pd_{85}Si_{15})_{61}/(Fe_{85}B_{15})_{39}$, compositionally modulated amorphous film, diffusion, struct. relax. 80−103518
- $Pd_{100-x-y}Si_xFe_y$, amorphous, ^{57}Fe Mossbauer spectra, X-ray diffr., ageing behaviour 79−28651
- (1,10-phenanthroline-2-carbaldehyde phenylhydrazone) iron perchlorate, high spin to low spin transition, X-ray diffr. and Mossbauer obs. 79−38418
- Pr-Cr-B system, phase equil. at 800°C, boride lattice parameters *(Russian)* 78−31388
- Pr-Ni-Al system, Pr (0 to 33.3 at.%), isothermal section at 800°C *(Ukrainian)* 79−34002
- $Pr_{1-x}Ca_xMnO_3$, struct. and magnetisation study 80−65804
- $PrNiC_2$, struct. determ. using X-ray diffraction *(Ukrainian)* 80−33949
- $Pr(OH)_3$, thermal decomposition, exam. 80−55640
- $Pr(OH)_2Br$, hydrothermal phase equilib., cryst. struct. 78−35372
- $Pr_7(OH)_{18}Br_3(I_3)$, hydrothermal phase equilib., cryst. struct. 78−35372
- $PrRh_x$, Sny, crystallography X-ray powder diffr. study 80−100217
- PrS, isothermal compressibility 79−99262
- PrSe, isothermal compressibility 79−99262
- $Pr_4Si_2O_7N_2$, lattice consts., X-ray diffr. anal. 80−28986
- Pt chain compounds, one dimens. conductors, Fermi wavevector determ., X-ray scatt. obs. 80−44187
- Pt complex, 1,2-benzoquinonedioximates, refl. spectra, 0.5-2.5 eV, Young's modulus and internal friction 78−39562
- Pt complex, $(C(NH_2)_3)_2Pt(CN)_4Br_{0.23}.H_2O$, pseudo-one-dimens. cpd., solitary wave excitations, and cryst. struct. 78−6307
- Pt complex, $[C(NH_2)_3]_2[Pt(CV)_4]Br_{0.23}.H_2O$, one-dimensional, X-ray diffuse scatt. meas. 77−19937
- Pt complex, $Mg_{0.82}Pt(C_2O_4)_2.xH_2O$, X-ray diffuse scatt., 1-D Peierls-Kohn anomaly and struct. transforms. 78−14680
- Pt-GaAs contacts, sintered, eval. of W, Ti, Mo and Hf barrier metals 77−8193
- Pt-Ni vacuum condensates on Si and SiO_2, thermally treated, X-ray anal. *(Russian)* 80−70559
- Pt-Si contact, silicide layer struct., sputter etching and annealing ambient effects 77−62991
- Pt-Si layers, form. by laser irrad. of Pt film on Si substrate 79−99438
- PtO, existence 78−18923
- PtO_x, thin film, sputtering deposition, XPS and X-ray diffr. chracterisation 79−78878
- PtSi films, on Si, stress obs. 80−80145
- PtSi, growth under protective layers on Pt covered Si substrates, X-ray diffr. and Rutherford backscattering anal. 78−22965
- Pu-Pt(Rh)(Pt-Rh), exam. of phases and crystal structure 78−80518
- PuO_2-UO_2-Na aerosol, from LMFBR HCDA conditions, characterisation 78−94104
- $RbAg_3Se_2$, crystal struct., X-ray study *(German)* 78−83795
- RbAu, NMR line shape, Knight shift, X-ray diffr. study, struct. props. 78−68402
- $RbCaF_3$, cubic to tetragonal phase transform., X-ray, neutron, Mossbauer diffr. study 80−49360
- $RbCaF_3$, influence of domains on struct. phase transition 79−28097
- $RbCaF_3$, lattice consts. temp. depend., X-ray examination, 194K transition *(French)* 78−10184
- RbCl/KCl interface, diffr. studies of conc. variations 79−42322
- RbCl-CuCl, solid electrolyte, AC cond. and phase relations meas. 77−72713
- RbCl-KCl powder blends, diffusional homogenisation, X-ray diffr. exam. 78−18847
- $RbCrI_3$, radiocrystallographic and mag. study *(French)* 79−46632
- $Rb_4Cu_{16}I_7Cl_{13}$ in CuCl-CuI-RbCl system, high Cu ion cond. solid electrolyte, elec. props. and powder X-ray diffr. anal. 80−15295
- RbF, high press. B1 to B2 phase transition, X-ray diffr. obs. 79−23722
- $RbFeF_4$, two dimensional structural phase transitions, sp. ht., optical, dielec., X-ray diffr. meas. 79−69240
- $RbHSeO_4$, ferroelec. phase transition, X-ray study 80−7309
- $RbH_3(SeO_3)_2$, ferroelec. phase transition, X-ray study 79−38479

X-ray diffraction examination of materials continued
RbI, single cryst., press.-induced B1-B2 phase transition, X-ray diffr. meas. 78−63852
RbI, vaporisation thermodynamics, mass-loss Knudsen effusion, mass spectrometry 79−28093
$RbLiSO_4$, field induced ferroelec. phase 79−78633
$RbLiSO_4$, successive struct. transitions, X-ray diffr. 80−10521
$RbNO_3$, cubic to rhombohedral transition, X-ray diffr. obs. 78−22681
$RbNbWO_6$, pyrochlore struct., tetragonal to cubic phase transition 80−75355
$Rb_2Ni_3(P_2O_7)_2.nH_2O$, thermal dehydration 80−35513
Rb_2O, high temp. X-ray anal. using special cell for reactive substances *(French)* 79−68978
$RbPO_3$-$AgPO_3$ system, phase diagram 77−25033
$Rb_2PbCu(NO_2)_6$, incommensurate Jahn-Teller phase transitions 79−65185
$Rb_2PbCu(NO_2)_6$, incommensurate Jahn-Teller transition, Huang scatt. 80−70401
$RbSnX_{3(5)(6)}$ (X=Cl, Br, I), single cryst. gel growth, X-ray diffr. study 80−29870
$RbVF_3$, antiferromag. ordering points, thermal anal. and X-ray diffr. meas. *(French)* 78−84421
RbV_2F_6, X-ray powder diffr. data 79−78861
$Rb_9(XeO_3Cl_2)_4Cl$, neutron and X-ray diffr. struct. determ., Xe-Cl bonding 78−30591
$Rb_{1.75}[Pt(CN)_4].xH_2O$, one-dimensional, X-ray diffuse scatt. meas. 77−19937
Re, thermal expansion, X-ray determ., 113-1700K 78−67838
Re-Hg-O system, solid state synthesis of 5 crystn. compounds, thermal and X-ray anal. *(French)* 79−66281
ReO_3, lattice parameters, thermal expansion 291 to 464K, Bond technique meas. 78−75617
ReO_3, phase transition at high press., Fermi surface and X-ray studies 79−65188
Rh_2ReO_6, preparation, X-ray powder diffractograms 78−76615
RuS_2 amorphous, prep. at ambient temp., magnetic structure 80−35119
S, monoclinic, order-disorder transition, X-ray struct. determ. 78−30750
$(SN)_x$, linear compressibilities, X-ray determ. 78−34565
$(SN)_n$* radicals polymerisation to $(SN)_x$ in thin films, optical spectra 80−16656
Sb cryst. struct. appl. of 50 kbar gasketed diamond anvil cell for single cryst. diffractometer 77−31560
Sb film, X-ray diffr. anal., {001} textured growth 78−72016
Sb-Bi, X-ray diffr. investig. of high-press. polymorphism 77−43324
Sb-O-Cl(Br)(I), glass-forming regions 80−88057
Sb_2O_3 glass, X-ray diffr. anal. of struct. 78−87621
Sb_2O_3-$SiO_2(GeO_2)$-Na_2CO_3-H_2O, crystallisation 77−12605
Sb_2S_3, vacuum deposited films, struct. and photoelec. props. 77−85092
SbSI, diffuse X-ray scatt., anisotropy in phonon dispersion relations 77−84866
$SbTaO_4$, X-ray and ESR study of phase changes 78−72476
Sc, thermal expansion anisotropy, 78-783K, X-ray determ. 78−83983
Sc-Fe-Si system, phase obs. at 800°C *(Russian)* 78−23661
Sc-Rh-Si system, partial phase diagram, X-ray diffr. and microprobe anal. 80−25659
$Sc_{0.995}Gd_{0.005}H_{1.9}$, low temp. anomaly, Gd^{3+} EPR linewidth and X-ray meas. 77−69687
$Sc_2Re_3Si_4$, X-ray struct. determ. *(Russian)* 79−27958
Sc_xS, high temp. vaporisation, enthalpy, atomisation, dissoc. energies 77−1223
$ScSbO_4$, polymorphism at high pressure, X-ray phase anal. 79−46804
Se, amorphous, struct., DSC and X-ray diffr. expts. 78−22662
Se amorphous layer structure, influence of vacuum deposition conditions *(German)* 78−63957
Se film, noncryst., ageing and crystn. obs., tentative struct. model 80−2295
Se, monoclinic to trigonal transform., DTA, X-ray diffr. and optical microscopy meas. 78−14461
Se, monoclinic to trigonal conversion, thermodynamic stability and associated investigs. 80−24592
Se powder compacts, sintered, electrical cond. 80−70693
Se-Te solid solutions, ordering, diffuse X-ray scatt. 77−65965
$(Se)_x$, crystn. and melting 80−40241
$Se_{1-x}Te_x$, film, struct. and props. 79−99079
Si, 5 MeV α-particle irrad., X-ray exam. of surface layer struct. changes 78−6114
Si, 60° dislocation, X-ray diffraction contrast, section topography 78−83819
Si amorphous, diffraction intensities, chem. bonding effects 77−72557
Si, amorphous film, RF plasma deposition from $SiCl_4$-H_2, characterisation 80−66435
Si, amorphous film, sputtering by 0.5 to 5 keV Ar^+ ions 79−91550
Si, B implanted layers, damage obs. by X-ray double refl. 77−15463
Si, B ion irradiated, long-range damage to crystallinity, X-ray diffr. meas. 78−2171
Si bent crystal, X-ray Laue diffraction, integrated intensity 79−23492
Si, Bragg-case X-ray thin cryst. rocking curves, theory and expt. comparison 78−55785
Si, CVD epitaxial film, stacking fault nucleation and growth 78−10064
Si, cross-slip of single dissociated screw disclocations, double etching and X-ray topography studies 80−15104
Si crystal, Czochralski grown, enhanced Borrmann effect 80−70191
Si crystal surface, adsorbed Br, X-ray standing waves obs. 80−96417
Si, crystalline struct. and lattice imperfections 80−24398
Si, Czochralski-grown, oxide precip. form. process 80−49364
Si, Czochralski-grown cryst., swirl defect formation and defect migration 77−76405
Si, diffuse scatt. close to reciprocal lattice points, high-resolution technique 77−39511
Si, diffusion-induced lattice strain and dislocation obs. by X-ray diffraction *(Japanese)* 77−84753
n-Si, dislocation free, memory effect associated with appearance of prismatic dislocation loops 77−1130
Si, dislocation-free single crystals, microdefect type by anomalous X-ray transmission 79−95019
Si, elastically bent, strain canc. determ. by microfluorescent densitometry of X-ray topography 80−79245
Si, elastically bent cryst., intensity of diffracted beams in general case of diffr. 79−50935
Si, film, CVD, low press., struct. and stability, X-ray diffr. and TEM obs. 78−91559

X-ray diffraction examination of materials continued
Si, film, chemically deposited on amorphous SiO_2, influence of substrate temp. and SiH_4 to N ratio on struct. 79−65346
Si film, deposited on quartz and MgO substrates, by double cathode sputtering system *(Japanese)* 77−55889
Si film, low press. CVD prep., struct., elec. and optical props. 80−70548
Si film, polycrystalline, struct. thickness relationships 77−62779
Si film on sapphire, quality evaluation using soft X-ray rocking curve 77−80711
Si, film on Si substrate, stress meas., X-ray topography technique 78−5710
Si films, polycryst., glow discharge deposited below 250°C, struct. and morphology 80−49535
Si, growth and melting processes, origin of swirl defects 77−76407
Si, heavily implanted, lattice defects and strains after high temp. annealing 78−10077
Si, implantation induced strains, X-ray interferometry and topography 78−43039
Si, influence of temp. and alloying on integral X-ray intensities *(German)* 77−69066
Si, initial stage of plastic flow 78−64602
Si, ion implantation, investigation of radiation damage by pendellosung topography 79−51125
Si, ion implanted by high energy C ions structural and optical props. 80−107292
Si, ion-implanted, defect struct., SEM, TEM and X-ray topography expts. 77−51399
Si, lattice constant, press. depend., X-ray diffr. meas. effect of nonhydrostaticness of press. 77−35439
Si, lattice constants anomalous temp. depend. 79−46821
Si, lattice damage, influence of laser annealing 79−23608
Si, lattice parameter determ. by X-ray multiple diffr. study *(Russian)* 80−10460
Si, lattice parameters and perfection *(Japanese)* 79−4300
Si, local mechanical defects, annealing and effect on autoepitaxial growth *(Russian)* 80−7701
Si, MBE growth, X-ray topography study 79−83141
Si, meas. of dynamical and kinematical components with triple cryst. diffractometer 79−50948
Si, multiple diffr., Bragg. refl. theory 79−94842
Si, multiwave Bormann effect, expt. detect. 79−14648
Si, neutron irrad. effects on lattice parameter and anomalous X-ray transmission 79−86821
Si, neutron irradiated, changes in lattice period, X-ray meas. 77−7767
Si, oxidation-induced stacking faults, refl. X-ray topography 77−84767
Si, oxide scale microstruct. of oxidised single cryst. 80−108613
Si, oxidised on one side, elastically flexed, dynamic X-ray scatt. *(Russian)* 77−43115
Si, Pendellosung fringes in synchrotron X-ray topographs 79−32858
Si, perfect cryst., X-ray acoustic reson. 79−27873
Si, perfect crystal, dispersion surface of X-ray radiation, X-ray acoustic resonance method 79−41908
Si, photoelectron emission due to Bragg diffr. of X-rays 79−69960
Si, polycryst. film on Si, disloc. config. obs. 78−10312
Si, polymorphism under high press. *(Russian)* 78−59947
Si, precipitation of O, 1000°C TEM, IR absorpt. and X-ray studies 80−34194
Si, ribbon, edge-defined film-fed grown, orientation depend. of defect struct. 77−1134
Si, scratches on near (111) slices, X-ray topographs 77−12726
Si single crystal, X-ray photoelectron yield, effect of asymm. Bragg diffr. *(Japanese)* 77−43110
Si, strip-type crystals, growth mechanism, morphology 79−7559
Si substrate, silicide formation with large bilayers of Pd-Pt, Pd-Ni and Pt-Ni 79−51444
Si surface, line tension induced dislocation motion, obs. by etching and X-ray topography 79−82212
Si surface electron beam deposited silicide formation using scanning CW laser beam 80−66862
Si, surface layer, thin, density meas. by total external X-ray reflection 78−14635
Si, transmission topograph recording, of large cryst. slices, geometrical conditions 80−38869
Si wafer, bending by thin polycrystalline Si film deposition and by film doping using B diffusion 79−95276
Si wafer, Czochralski grown, precipitation during high temp. oxidation 78−11381
Si wafer, heat treatment behaviour of microdefects and residual impurities, X-ray diffr. and IR absorpt. study 80−49214
Si wafer creep testing using stress provided by deposited Si_3N_4 film 77−66000
Si, with various dislocation densities, ang. depend. of X-ray polarisation of curve of 111 Bragg reflection 79−46509
Si, X-ray acoustic reson., Borrmann effect reson. suppression by transverse US vibrs. 79−32852
Si, X-ray diffraction characterisation, highly collimated beam 78−9912
Si, X-ray intensity anomalously transmitted, ϵ_{220} values 78−83650
Si, X-ray rot. polarisation, absorpt. crystal orientation effects 78−47206
Si, X-ray section topography in the Bragg case 80−79637
Si:Au(P)(B) whiskers, impurity inhomogeneity 80−39145
Si:B, detection of atomic plane displacement in near-surface layers, ang. depend. of photoemission during X-ray Bragg diffr. 78−47207
Si:B, implanted laser annealed, lattice strain, X-ray study 80−96554
Si:B, implemented laser annealed samples, unidirectional contraction 78−71747
Si:B, inhomogeneous surface layer, diffusion and implanted, X-ray rocking curves 80−6603
Si:B ion implanted, strain profiles from X-ray rocking curves 80−107290
Si:B ion implanted, X-ray topographical images at different absorption conditions 80−2052
Si:B_2O_3, analytic study of Si-B phase formed 79−19269
Si:B(P)(Ge), strain distributions rel. to dopant conc., accurate determ. by X-ray Bragg reflection 77−19835
Si:Ge B, strain compensation, X-ray Bragg reflexion 80−39137
Si:H film, amorphous, plasma-deposited, small angle X-ray and neutron scatt. studies 80−59826
Si:O film, thermally deposited, semi-insulating, crystallographic study 78−75954
Si:P, shallow strain distrib. near cryst. surface, asymmetric X-ray Bragg reflexion 77−76252

X-ray diffraction examination of materials continued
Si:P epitaxial layer, strain distrib. at interface with substrate, obs. by X-ray double cryst. method 79−99461
p-Si:P p-n junctions, dislocations investig. rel. to P diffusion, SEM, X-ray topography techniques 77−76433
Si:P^+, highly implanted, two step annealing effect on crystallinity 77−31683
Si:Sb, ion implanted, annealing behaviour of stress 78−63778
Si/Pd-W, contact reactions, backscattering, X-ray diffr. meas. 80−20040
Si-B system, DTA, X-ray diffr. and metallographic study *(German)* 80−66484
Si-Cr interfaces, metallurgical and electrical props. 80−60081
Si-Fe, ferromagnetic domains and their junctions, simulation of X-ray topographs 79−78434
Si-Ge heteroepitaxial layers on Si substrate, lattice const. meas. 79−69382
Si-H, amorphous, struct. and press. induced transition 80−44131
Si-Na-B-O-N glass, synthesis and characterisation 80−108381
Si-Ni(Pd)(Pt) film struct., silicide form. He^+ back scatt. and X-ray diffr. obs. 79−51442
Si-Pd-Ti, silicide form. in evaporated films 80−80006
Si-saphhire, Si ion implanted wafer, laser annealing 79−99989
Si-SiN mixtures, X-ray diffr. powder anal. method, integrated intensities peak height approx. 77−56323
Si(-H), amorphous, H atom effect on Si-Si atomic short-range order, X-ray diffr. obs. 79−64996
SiAlON, prepared from siliceous sand and Al powder, hot pressing, steatite contamination effects *(Japanese)* 80−93528
SiC, 2H disordered single crystal, X-ray diffr. stacking fault exam. 77−89452
SiC, 2H→6H transform. mechanism, X-ray diffr. theory 78−30575
SiC coating on C fibre, chemical vapour deposition, relation between surface morphology and coating conditions *(Japanese)* 78−39704
SiC coating on Mo, CVD and stability under thermal cycle conditions 80−7500
SiC coatings for first-wall candidate materials by RF sputtering 80−25563
SiC coatings for HTR nuclear fuels, characterisation by small-angle X-ray scatt. 80−44451
α-SiC, corrections for crystal-to-film distance variations in Laue photographs 77−43114
SiC, dissociation in silicate bonded refractories, X-ray obs. *(German)* 79−47893
α-SiC, epitaxial layer, impurity macroincorporation, distrib. of Al, B, N and P 77−69192
SiC, epitaxial layer polytypism 77−62781
SiC fibres, reinforced complex alloy, influence of TiN coating on fibre matrix interaction *(Russian)* 78−95820
SiC filamentary crystals, dia. determ. by X-ray extinction method 79−97343
SiC film synthesis by plasma deposition process 78−11127
SiC, further polytypes discovered using Laue diffraction *(Chinese)* 80−10535
SiC, high period polytype at interface of two interacting spirals 80−20041
SiC, monocrystalline bars, grown from gas phase, exam. of growth process 79−95912
β-SiC, oxidation in CO-CO_2 mixture *(German)* 78−23844
SiC, oxide scale microstruct. of oxidised single cryst. 80−108613
β-SiC, polytype stability, α→β phase transformation during growth 78−6028
SiC polytypes, quantitative calcs. from X-ray diffr. peak intensities 79−82174
β-SiC, powder, synthesis by chemical vapour phase reaction from methylsilane, exam. of props. *(German)* 79−4938
SiC, pyrolytic particles for high temp. reactor fuel, X-ray and SEM study *(French)* 78−22734
β-SiC, sintering, B transport and lattice parameter change 80−108370
SiC, synthesis by ion implantation of diamond and silicon, struct. characts. 77−76434
B-SiC, X-ray diffr. study of anisotropic layers in twinned seams 80−107274
SiC, X-ray diffuse scattering 80−14964
SiC:B(Be), dislocation induced deceleration of impurity diffusion 77−28043
SiC-2H, structure parameters and polarity, X-ray diffr. meas. 80−19781
SiC+CeO_2(Pd), high temp. chem. reactions, products obs. by X-ray diffr. 78−17312
$Si_{0.92}Ge_{0.08}$ film on Si, elastic strain, misfit dislocation density 77−85119
$Si_{1-x}H_x$, amorphous, atomic struct., X-ray study 80−49106
SiN_x film, d.c. reactive sputtering, and characterisation 78−3047
β-Si_3N_4, β′-$Si_2Al_4N_4O_4$, combined X-ray and IR analyses 78−79579
Si_3N_4, CVD amorphous film, X-ray diffr. 79−87013
Si_3N_4, consolidation by hot isostatic pressing 80−11605
α-Si_3N_4, exam. of chemical vapour deposition, and IR transmission and reflectance 79−19993
Si_3N_4, film on Si substrate, stress meas., X-ray topography technique 78−5710
Si_3N_4, growth of α and β phases 78−95717
Si_3N_4, hot-pressed, strength anisotropy origins 80−89330
Si_3N_4, pyrolytic, prep. by CVD, bulk and coatings, exam. of electrical, optical and physical props. 79−95935
Si_3N_4, reaction bonded, creep, internal oxidation effects 78−56701
Si_3N_4, reaction-bonded, hexagonal (wurtzite) form of Si 77−1112
Si_3N_4, reaction-bonded, internal oxidation processes role in high-temp. mech. props. 79−38915
β-Si_3N_4-AlN-Al_2O_3-MgO, insolubility of Mg in β-Si_3N_4 79−10953
Si_3N_4-AlN-SiO_2-Al_2O_3 solid-liquid equilibria 78−92247
Si_3N_4-CeO_2 additive, hot-pressing and oxidation behaviour 80−71618
Si_3N_4-Y_2O_3-Al_2O_3-SiO_2, X-ray diffr. exam., phase equilib. at 1400 degrees C *(Japanese)* 78−44113
α,β-Si_3N_4+C, powders, high temp. reactions *(Japanese)* 77−48685
SiO_2, amorphous, very small angle X-ray scatt. before and after thermal neutron irrad. 80−75270
SiO_2 colloidal sol, particle size distrib., small-angle X-ray scatt. obs. 77−44516
SiO_2, crystobalite form. in evacuated silica ampoules, cryst.-amorphous transform. 77−68933
SiO_2 fabric, structural stability rel. to brittleness, X-ray diffr. and IR spectrosc. studies 80−96634

X-ray diffraction examination of materials continued
SiO_2, film on Si substrate, stress meas., X-ray topography technique 78−5710
SiO_2 gel, internal and surface struct. by X-ray scatt. 80−84074
SiO_2, molten, struct., X-ray radial distrib. anal. 78−67651
SiO_2, synthesized tridymite, thermal changes, X-ray and optical studies 79−65020
SiO_2, vitreous, quant. X-ray anal. of cristobalite 80−88049
SiO_2:TiO_2, prep., amorphous struct., effect of roasting, bonds 78−44061
SiO_2-Al_2O_3 mixture, depend. of phase comp. on nuclei available 79−11584
SiO_2-Al_2O_3-CaO-MgO-NaO-K_2O-B_2O_3-ZrO_2, glaze, exam. of zircon crystallisation 79−19155
SiO_2-Al_2O_3-Fe_2O_3-CaO, basalt glass ceramics, crystallite form. due to heat treatment 80−38917
SiO_2-Al_2O_3-K_2O-Na_2O, exam. of leucite crystal growth 79−19496
SiO_2-base cores, for superalloys, high temp. characterisation 80−10640
SiO_2-C mixture, nitridation to form. Si_3N_4 additives effects, exam. 78−44068
SiO_2-glass fibres, struct. anal. using X-ray diffr. and optical microscopy 77−65952
SiO_2-Li_2O-K_2O-ZnO glass ceramic, prep., phase transformations and physical props. 80−45299
SiO_2-Na_2O-CaO glass, phase separation characts., melting atmosphere effect 80−44141
SiO_2-Na_2O-CaO-MgO glasses, surface and near surface struct. 78−87850
SiO_2-TiO_2 system, true solid soln. existence obs. 77−36475
SiO_x, powder and vac. deposited, amorphous struct., X-ray diffr. meas. 80−1931
Si_2O_3-TiO_2 system, phase transform. at high temp. 77−84926
Si_2ON_2-Y_2O_3-Al_2O_3 phase relations at 1400°C *(Japanese)* 79−38811
Sm, crystal structure, P-T phase diagram 78−84776
Sm-Cr-B system, phase equil. at 800°C, boride lattice parameters *(Russian)* 78−31388
Sm-Pr-Co, added Fe_2Sn, permanent magnets, demagnetisation curves, X-ray obs. 78−91900
Sm(-Pr)-Co, sintered, cryst. phases *(Russian)* 80−39004
$SmCo_5$ based alloys, dissociation process *(Russian)* 78−27542
$SmCo_5$ based solid soln., X-ray diffr. obs. of decomp. *(Russian)* 77−81264
$SmCo_5$, high coercivity isotropic plasma-sprayed magnet, eutectoid decomp. 80−80568
$SmCo_5$ isotropic plasma sprayed magnet, high coercivity 78−68295
$SmCo_5$, isotropic plasma-sprayed high coercivity magnet, eutectoid decomp. 80−75810
Sm_xCo_y, mag. and struct. investigations of intermetallic systems 78−95440
$Sm_xDy_{1-x}Co_5$, temp. compensated magnetic material, mag. and struct. characterisation 78−68177
$Sm_xEr_{1-x}Co_5$, temp. compensated magnetic material, mag. and struct. characterisation 78−68177
SmF, vaporisation, sublimation, Knudsen effusion method 80−6508
$Sm_{0.85}Gd_{0.15}S$, metal-semicond. transition, X-ray diffr. obs. 90-473K 79−95333
SmH_x [x=2.78, 2.85, 2.91], electrical resistance anomalies at high pressures 80−29381
$Sm_xLa_{1-x}B_6$, solid solns., exam. of structure, elec. props. 80−39290
$Sm_6Mn_{23-x}Fe_x$, magnetic behaviour, temp. and comp. depend. 80−93090
$Sm_3Ni_6Ga_2$, X-ray struct. determ. *(Russian)* 79−27959
SmS, Debye temps., vibr. amplitudes, X-ray diffr. determ. 78−2222
SmS, Debye-Waller factor, X-ray diffr. meas. 77−11659
SmS, semicond.-metal transition, phase struct. determ. 78−91618
SmSe, Debye temps., vibr. amplitudes, X-ray diffr. determ. 78−2222
$Sm_xTb_{1-x}Co_5$, temp. compensated magnetic material, mag. and struct. characterisation 78−68177
SmTe, Debye temps., vibr. amplitudes, X-ray diffr. determ. 78−2222
$Sm_{0.7}Y_{0.3}S$, Debye-Waller factor, X-ray diffr. meas., evidence of optic phonon softening 77−11659
Sn, film, vac. deposited, influence of ion bombardment during condensation 79−82483
Sn, sputtered film, exam. of frictional props. 79−15814
Sn ternary intermetallic systems, new supercond./mag. cpds., X-ray powder diffr. data 80−100215
Sn, white, anharmonicity in diffraction intensities 78−71626
Sn, white, forbidden Bragg maxima 78−63638
Sn, white, forbidden Bragg maxima 78−63639
Sn, white, lattice vibrations anharmonicity, X-ray meas. 78−51624
Sn/CU electroplated bimetallic films, interfacial reaction 80−96765
Sn-Bi alloy, splat-quenched, energy dispersive X-ray diffr. 78−23728
Sn-Ni electrodeposit, metastable, transform. kinetics, X-ray and SEM meas. 78−38979
$Sn_xGe_{1-x}Te$, ferroelec. semicond. structural phase transition, X-ray study 79−37836
SnI_2-SnF_2 system, phase diagram construct. *(French)* 80−50605
$Sn_xMo_3S_4$, chevrel phase, charge transfer and valence electron conc. 78−6029
$Sn_xMo_6S_6$, supercond. props., effect of W and Re alloying additions, Mossbauer and X-ray diffr. meas. *(Russian)* 79−15245
SnO chlorination, Mossbauer and X-ray phase anal. 80−21266
SnO-GeO_2 system, glass form., compound anal. 77−35486
SnO-SiO_2 glass, struct., X-ray density, IR obs. 79−46574
SnO_2, film, effects of Sb and In additions on struct. and resist. 77−20469
SnO_2, transparent conductive film, prep. by magnetron sputtering and elec., optical and structural props. *(Japanese)* 79−8247
SnO_2:Sb, transparent cond. film prep. by thermal decomp. of Sn salt of organic acid *(Japanese)* 77−90269
SnO_2-Si solar cells, electron-beam deposited, struct., photovolt. props. 80−50956
SnO_2-TiO_2 solid solns., X-ray diffr. and thermogravimetric meas. 79−90792
SnO_x films, non-stoichiometric, DC reactively sputtered, elec. props. 80−80415
SnO_x films reactive DC sputtering prep., phase comp., X-ray diffr. and Mossbauer meas. 79−90914
$Sn_2P_2S_6$ ferroelectric semicond., polarisation Raman scatt. spectra, X-ray struct. study 79−95778
$Sn_{1-x}Pb_xTe$, epitaxial layers synthesis, cryst. struct. perfection and elec. characts. 79−87587

X-ray diffraction examination of materials continued
SnSe-Sb_2Se_3 system, phase diagram, differential thermal, microstruct., X-ray phase and microstructure anal. 77−16555
SnSe-Tl_2Se, phase diagram, DTA and X-ray diffr. peritectic decomposition *(French)* 77−51471
$Sn_xTi_{(1-x)}O_2$, solid soln., thermal reaction with V(V), Cr(III), Cr(VI), Mn(II), Fe(III), Co(II), NI(II), Cu(II), Sb(III) 80−16674
Sr Nb_2O_6, crystallography, polymorphism and isomerism, X-ray diffr. and DTA study 80−100216
$Sr_5(PO_4)_3OH$, prep. from sulphate, X-ray diffr. and IR spectrosc. 80−29893
$SrAl_2O_4$, X-ray powder diffr. data 79−51071
$SrB_{0.5}B'_{0.5}O_4$, where B=Ln, Y, Sc, Fe, In, Rh and B′=Nb, Ta, synthesis and characterisation 79−69087
$(SrCaR)_2(Cr_xGa_{1-x})O_4$, R=La or Sm, mag. 2-D oxide, phys. props. 78−47974
$Sr(Ca_{1/3-x}Sr_xNb_{2/3})O_3$, perovskite, X-ray and electron diffr. study *(French)* 79−99161
$Sr_2Co_2O_5$, characterisation and mag. props. *(French)* 79−90619
$SrFe_{12}O_{19}$, Ca^{2+} additives effect on hexaferrite lattice and mag. props. 80−60243
$Sr_3FeTa_2O_9$, Mossbauer and X-ray diffr. studies 80−103905
$Sr(NO_3)_2$, isomorphous crysts., growth defects, X-ray topography 80−70188
$Sr(No_3)_2$, lattice parameter, 261-740K, thermal expansion and Gruneisen coeff. determ. 77−35720
SrO-SiO_2-Fe_2O_3, permanent mag. ceramics, exam. of phase diagram, using X-ray analysis, optical microscopy, electron probe anal., and thermal analysis *(German)* 79−29012
SrS:Ho phosphor, prep. methods, X-ray diffr. appraisal 77−51350
$Sr_3SiAl_{10}O_{20}$, Ce^{3+} activated, X-ray diffr. and luminesc. props. 80−49199
SrSn, Sr_2Sn, prep. by melting, characterisation *(French)* 77−70017
$Sr_6Ti_2Nb_4O_{20}$, new class of layer ferroelectrics. X-ray anal. and permittivity meas. 77−16266
$SrTiO_3$, cubic, temp. depend. of X-ray reflection intensities 80−107021
$Sr_{0.15}VO_2$, electrical cond., thermo-EMF, and lattice consts. 80−54685
steel, Hadfield, hollow cathode sputtering 78−11433
Ta complex, prep. by halide reaction with tetramethylurea and tetramethylthiourea, and characterisation 79−15972
Ta epitaxial layers, formation conditions influence on struct. *(Russian)* 80−20045
Ta film, reactively sputtered, N content determ. from Fourier anal. of X-ray diffr. profile 77−76693
Ta, lattice parameter, X-ray meas. 77−89406
Ta powder, extraction of N_2 by vacuum hot extraction method, effect of graphite *(Japanese)* 78−84729
Ta-Al-C, phase diagram and lattice constants, X-ray diffr. method 80−89207
Ta-H alloy, high conc., Huang diffuse X-ray scatt. from lattice strains 78−38746
Ta-H(D), H ordering, review 80−60850
Ta-H(D), lattice expansion due to interstitially dissolved impurity, isotope effect 77−39600
Ta-O solid soln., interstitial ordering and precipitation at 100 to 270°C, exam. 78−52813
Ta-V system, short-range order exam. by diffuse X-ray scatt. *(Russian)* 77−31644
TaC_x, solubility of H, X-ray diffr. exam. 80−44318
Ta_2C_x, solubility of H, X-ray diffr. exam. 80−44318
$Ta_2C_xO_y$, solubility of H, X-ray diffr. exam. 80−44318
1T-TaS_2, nearly commensurate phase stabilisation 77−15588
TaS_3, Peierls superstruct., low temp. X-ray diffr. obs. 78−59793
$TaSCl_3$, prep. and characterisation 77−59705
$TaSe_2$, 1T and 2H superstruct., cryst. struct. using X-ray diffr. 80−39044
$TaSe_2$, 4Hb polytype, CWD induced atomic shifts 80−39045
$TaSe_2$ (2H), broken hexagonal symm., incommensurate charge-density wave struct. 80−96646
$TaSe_2$ (2H), thermal and elastic props., X-ray diffr. exam. 79−37754
$TaSe_2$, (2H) CDW, reentrant lock in transition at high press. 80−88320
$TaSe_2$, evaporation, mass spectroscopic anal. 77−76530
$TaSi_2$ refractory formation by As^+ ion beam bombardment 80−107286
TaS_2(pyridine)$_{1/2}$, pyridine orientation, X-ray diffr. meas. 79−55679
Tb, press. induced polymorphic transition 77−59113
Tb-Sn-Se system, cross section Tb_2Se_3-$SnSe_2$ phase diagram, physicochem. anal. 79−87621
Tb-Y, single crystal growth from melt, X-ray obs., props. *(Russian)* 78−95689
$TbCo_2$, rhombohedral distortion at low temp. 80−34743
TbIG, X-ray topographic obs. of domain evolution in mag. field 77−69600
$TbRh_xSny$, crystallography X-ray powder diffr. study 80−100217
$Tb_2[Pt(CN)_4]_3.21H_2O$, phase transitions, X-ray study and spectroscopic study 79−60506
Te, anisotropic thermal motion of atoms, X-ray exam. 78−18730
Te film, evaporated, crystallinity and electronic props., annealing effect 77−85107
Te-Sn (20 at.%), amorphous, exam. of crystallisation by DTA, X-ray diffr. and TEM 78−47242
TeO-V_2O_5 glass system, X-ray diffr. study 79−10805
TeO_2-Cr_2O_3 system, phase diagram and vitrification 79−83182
TeO_2-GeO_2 system, phase diagram, X-ray phase analysis, DTA and electron microscopy 77−15545
TeO_2-MoO_3-V_2C_5, phase comp. determ. using X-ray diffr., electron microscopy and DTA *(German)* 80−88046
TeO_2-NiO system, phase diagram and vitrification 79−83182
TeO_2-V_2O_5-$Li_2O(Na_2O)(K_2O)(Cs_2O)(Ag_2O)$, glass, IR spectra of crystalline phases 79−38536
Te_xSi_y, (x=78,87, y=22,13), amorphous, struct., X-ray diffr. study 80−6362
Th-C-N system, existence of new β'ThCN' phase, struct. and thermodynamic study *(French)* 80−92499
$ThFe_5$, mag. props., ferrimag. moment arrangement 79−33475
ThO_2, particle size of crystallites in soln. by line-broadening meas. 78−18488
ThO_2, plasma deposition of crysts. and their characterisation 80−20800
ThO_2, thermal expansion, 500-1800°C, X-ray diffr. 77−35723
thermogravimetric and X-ray phase investig., synthesis by solid-phase reactions 77−21067

X-ray diffraction examination of materials continued
Ti alloy, BT22 quenched from 850-1200°C, X-ray study of structure *(Ukrainian)* 80−24402
Ti alloys, type VTZ-1 and VT8, high-temp. X-ray diffr. study of dissociation process *(Russian)* 79−74152
α-Ti alloys VT1 and VT5, struct. and phys. props., H_2 effect 80−108576
Ti coated BN powder particles, X-ray investig. of thermal stresses generated in vac. deposition 77−40455
Ti complex, TiOCl[Co(cyclopentdienyl)$_2$]$_{0.16}$, sxnthesis and struct. 80−44176
Ti, exam. of oxidation kinetics, and oxide film structure 78−56822
Ti, fatigue damage, SEM, X-ray diffr. and surface trace anal. 80−85040
Ti, recrystallised, dislocation obs. and characterisation by X-ray topography *(French)* 78−22722
Ti, vacuum deposited, cryst. struct. and elec. props. 78−79908
α-Ti, X-ray Debye charact. temp., powder specimens 77−84876
Ti/Cu/(Au) thin films thermocompression bonds degradation by thermal ageing 80−66546
Ti-Al alloy system, quenched from β-region, struct. obs. *(Russian)* 77−21146
Ti-Al film, struct. and elec. props. 80−7002
Ti-Al-Cr-Mo-V alloy VT-22, effect of heating rate on phase recrystallisation *(Russian)* 79−34077
Ti-Al-Mo, type BT22, phase transformations under step-by-step heat treatment *(Russian)* 80−108436
Ti-Al-Sn (5, 2.5 wt.%), electron microscope and X-ray diffr. exam., of basal and near basal hydrides 78−80550
Ti-Al-V-(Sn), surface finishing effect on internal stresses, X-ray study *(German)* 79−34210
Ti-Al-Zr, TA6Zr5D, oxidation at high temp. *(French)* 78−23860
Ti-Al-Zr (6,5 wt.%), alloy IMI 685, SEM exam. of crack growth 78−72849
Ti-alloy, VT16, volume and phase changes during continuous heating *(Russian)* 77−77470
Ti-Be-Si glass ribbons, physical and mech. props. 78−95767
Ti-C-N-O-H, solid solns. of H, exam. of props. 80−29172
Ti-Cu thin films, oxidation kinetics in air at 100 to 300°C, meas. 80−40590
Ti-Cu-Si alloy system, transforms. in Ti-Ti_3Si_3-TiCu region, 800-1600°C *(Russian)* 77−21099
Ti-H, deposited on carriers, synthesis, structure and catalytic props. 80−29890
Ti-Mo, metastable β-phase, stress induced products formed by cold rolling *(Japanese)* 78−84843
Ti-Mo (20 at.%), incommensurate struct., stacking soliton 80−107109
Ti-Mo alloys, structural stability under high-pressure soaking 80−104151
Ti-Mo-Fe (3, 0.13 at.%), metastable phases, Mossbauer study 80−7243
Ti-Mo-Zr-Sn (11.5, 6, 4.5 wt.%), β III, mech. props. rel. to heat treatment 80−84961
Ti-Mo-Zr-Sn (11.5, 6.0, 4.5 wt.%) alloy, struct. as affected by processing history 80−84972
Ti-Nb (4.32 wt%), high temp. oxidation kinetics under 1 bar pressure, 1255-1471K 80−89410
Ti-Nb-Zr-Ta, superconducting props. comp. depend., stress effects and precipitation behaviour, X-ray scatt. 80−93059
Ti-Permalloy films, interdiffusion, Auger anal. and X-ray diffr. obs., degradation of mag. props. 80−34251
Ti-S, pressure-temp.-comp. phase diagram, TiS_2 growth by chem. vapour transport 77−59764
Ti-Si cosputtered films, silicide form., X-ray diffr. and resist. study 80−54546
Ti-Si film thin film interaction, metallisation, X-ray diffr. and sheet resist. 80−54442
Ti-Ta (4.37 wt%), oxidation kinetics, 1258-1473K, and at pressure of 0.013, 0.133 and 1.0 bar 80−89411
Ti-Ta-Co system, phase stability, X-ray anal. 79−61580
Ti-V, metastable β-phase, stress induced products formed by cold rolling *(Japanese)* 78−84843
Ti-V-Mo alloy system, phase equilibria and interstitial effects, TEM and X-ray diffr. study 79−43204
Ti-V-Ru alloy system, metastable phases form. *(Russian)* 77−21098
Ti_3Al, phase transitions and physical props. 77−25068
$Ti_{0.75}Al_{0.25}H_x$, $x<1.5$, metastable hydride form. 78−51682
TiB_2 coatings, prep. by CVD and interaction with substrate 79−24680
TiB_2, erosion resistant boride coating on Ti and Ti alloys 79−20290
TiB_2-(Ni) (20 wt.%), initial stage sintering under high press., lattice strain 77−55905
$Ti_{50}Be_{40}Zr_{10}$ glass, mech. props., X-ray diffr. exam. 78−11292
$Ti_{50}Be_{40}Zr_{10}$, Metglas 2204, stability, crystallisation, ductility meas. 78−47246
TiC, ageing and ordering phenomena *(Russian)* 78−39807
TiC base hard metals, N_2-containing surface wear resistant layers, struct. anal. *(German)* 78−92405
TiC coating thickness meas. using X-ray diffr. 80−21243
TiC coatings, RF sputtered, on 440-C steel, adherence, friction, and wear props. 79−47823
TiC, deformation behaviour during rubbing in wide temp. range 80−16486
TiC, frictional characts. and contact-zone deform. in homogeneity range 80−66673
TiC, oxidation at various O_2 pressures 79−96172
TiC, X-ray diffraction study of struct. of ordered phase and phase transform. *(Ukrainian)* 79−37660
TiC-Au film, prep. by activated reactive evaporation, struct. and mech. props. *(Japanese)* 78−3252
TiC-B, struct. and mech. props. 80−55461
TiC-Kh6V3M steel alloy, reaction during sintering and heat treatment 78−60617
TiC_x film, formation by hollow cathode discharge reactive deposition process, on mild steel sheet 79−24451
TiC_x-TiN double-layer films, on C steel, CVD in US field, X-ray and SEM characterisation 79−65338
Ti(CN) coating for steel, abrasion resist., CVD parameter depend. 77−40471
TiC_xN_y monolayer films, on C steel, CVD in US field, X-ray and SEM characterisation 79−65338
TiC_xN_y, powder preparation, physical, chemical props. *(Russian)* 80−76212
$TiCl_4$-$MgCl_2$, high activity catalyst for polyethylene, struct. and mechanism investig. 80−11951

X-ray diffraction examination of materials continued
$TiCr_{1.8}$, H and D soln., enthalpy, solubility and mol. vibr. determ., comparison with soln. in metals and binary alloys 80−79951
TiN film, magnetron DC reactive sputtering, X-ray diffr. and SEM 77−44160
TiN film, struct. and elec. props. 78−26788
TiN, gaseous phase, crystallisation, effect of temp., vapour-gas mixture conc., and deposition time 79−33910
TiN, synthesised in SHF discharge plasma, exam. of props. *(Russian)* 80−7524
TiN-Ti_2N, activated reactive evaporation formed deposits, microstructure, transformation depend. on depositing conditions 80−24761
TiN_2, ultrafine synthesis in RF plasma, X-ray diffr. chem. and electron microscopy anal. 79−70026
TiN_x film, reactively sputtered in Ar-N_2 atm., elec. and struct. props. 80−15636
TiN_2-TiO_y, thermal expansion, 23-1000°C, X-ray obs. 78−91454
TiO+$BaCO_3$, react., mechanism, effect of polymorphic transitions 79−11605
$TiO_{0.42}$, diffuse X-ray and neutron scatt. due to out-of-step configurations of O atoms 77−62518
TiO_2 film, RF sputtering, dielec. props. and X-ray phase analysis 78−80288
TiO_2 films, deposition by electron beam evap. chem. comp., refr. index, struct. *(Japanese)* 77−62777
TiO_2, formed by Ti oxidation in air 79−11730
TiO_2, reactive- and chemical-sputter deposition from Ti and TiC target 79−100051
TiO_2, rutile, reduction by C, thermodynamic and struct. study, 1400 to 1600K 79−52650
TiO_y, thermal expansion of cubic phase at low temp. X-ray diffr. anal. 79−1514
Ti_2O_3, structural changes associated with semicond.-metal transition 77−15583
TiO_yH_m, thermal expansion of cubic phase at low temp. X-ray diffr. anal. 79−1514
$TiO_{1.95}$iFe, quenched near melting point, transverse composition waves 79−99220
$Ti_{1+x}S_2$, polytypic struct., Ti ordering, two-dimensional model, X-ray diffuse scatt. intensity, computer simulation 79−14776
$Ti_{1+x}S_2$, short-range ordering, electron and X-ray diffuse scatt. 77−19936
$Ti_{1+x}Se_2$, superlattice form., phase transform., electron and X-ray diffr. meas. 77−15383
$TiSi_2$, crystal atomic struct., X-ray diffr. exam., lattice parameters and integrated intensities 78−75647
$(Ti_{1-x}V_x)_2O_3$, spin glass and metallic antiferromagnetism 78−68268
$(Ti_{1-x}V_x)_4O_7$, metal-insulator transition investig. by resist., sp. ht. and X-ray diffr. 77−43497
$Ti_{1-x}Zr_xCr_{2-y}Mn_y$, C14 type alloy, hydride form. *(Japanese)* 78−19944
Tl-Bi system, phase transitions near Tl_3Bi, elec. props. meas. 80−35181
Tl-Bi-Sb-Te system, peritectic reactions in $TlBiTe_2$-$TlSbTe_2$ cross section, crystn. character 80−108406
Tl-Pb-S system, phase diagram quasibinary Tl_2S-PbS section obs. 80−55372
Tl-Sn-Te system equilibria, polythermal and isothermal cross sections obs., ternary cpd. form. 80−104128
TlBS, synthesis, struct., optical, spectral props. 79−15631
$(TlBiS_2)_{1-x}$-$(2PbS)_x$ system, phase diagram 77−36471
TlBr-TlI, KRS-5, periodic strain anisotropy, optical and X-ray diffr. study 80−54167
TlCl, Debye-Waller factors of Tl^+ and Cl^- 77−31742
TlCl, thermal vibr. amplitudes, 296-534K 77−35656
$TlGaS_2$-$TlGaSe_2$, phase and composition-property diagrams 80−55366
TlI films, polymorphic, double epitaxy and growth on KCl, X-ray and optical obs. 79−77944
$TlInS_2$-$TlInSe_2$, phase and composition-property diagrams 80−55366
$TlNO_3$, boiling and melting pts., heats of transformation, solid-solid transformation 78−91441
$Tl_2PbCu(NO_2)_6$, incommensurate Jahn-Teller phase transitions 79−65185
$Tl_2PbCu(NO_2)_6$, incommensurate Jahn Teller phase transitions 79−95156
$Tl_2PbCu(NO_2)_6$, incommensurate Jahn-Teller transition, Huang scatt. 80−70401
$TlR(MoO_4)_2$ (R=La to Ho), polymorphism, X-ray diffr., thermographic anal. 78−47269
TlS_2, amorphous, struct. and origin of crystn. process 77−76322
TlS_x, amorphous, struct. from radial electron density distrib. curves 79−23527
Tl_2S-SnS, phase equilibria exam. 80−55369
$Tl_2S(Se)$, molten III-VI semiconductors, SRO 77−65945
$(Tl_2Se)_{3x}$-$(Sb_2Se_3)_{1-x}$ system, phase diagram 77−16558
Tl_5Te_3-Tl_4SnTe_3-Tl_4PbTe_3, phase equilib., DTA, SPA and microhardness meas. 80−96628
$TlVO_4$, synthesis and thermal props. *(French)* 80−97443
TmSe, Debye temps., vibr. amplitudes, X-ray diffr. determ. 78−2222
TmSe, nonstoichiometry, high temp. chem. and valence instability *(German)* 79−23743
$Tm_4Si_2O_7N_2$, lattice consts., X-ray diffr. anal. 80−28986
U-C-N system, high temp. X-ray diffr. exam. of structure *(French)* 78−72765
U-Hg system, phase relations determ. 79−91624
U-O system, phase equilibrium, thermal, X-ray and cond. meas. 78−35371
U-UNi_2-UCo_2, system, phase equilibria, lattice constants *(German)* 80−50598
U-Y-C FBR nuclear fuels, phase anal., 1400°C 80−66485
UAl_2-UNi_2, phase relationships, thermal, microscopic and X-ray exam. *(German)* 78−88447
UAs, search for lattice distortions at low temps. 80−79759
U_3As_4, rhombohedral distortion of low temp. 77−7828
UAs_xSe_{1-x}, lattice distortion below Curie temp. 77−63252
UC, miscibility with rare earth nitrides *(German)* 80−96654
UC-PuC, carbothermal synthesis *(German)* 77−18661
UC-UC_2, alloyed, electron bombarded, enhancement of U_2C_3 deposition 77−27911
UMn_2, cubic to monoclinic struct. transition obs. 78−75833
UN, search for lattice distortions at low temps. 80−79759
$U_{1-x}Nd_xS$, mag. phase diagram 80−71027

X-ray diffraction examination of materials continued
UO_2 and UO_2-Gd_2O_3 solid soln., high temp. thermal expansion, 298-1700K 78−83979
UO_2 pellet surfaces, β-$UO_{2.33}$ formation in air at 229 to 275°C, X-ray diffr. study 80−35362
UO_2-$20CeO_2$ mixed powder, X-ray and microprobe exam. of homogenisation 80−25609
UO_2-PuO_2 powder compacts, homogenization kinetics study by X-ray diffr. technique 79−37883
UO_2-UC_2-C microspheres, carbothermic prep., rate-controlling preps. 80−45257
UO_{2+x}-ThO_2-MgO system, in air, phase rel., X-ray diffr., electron probe and metallography anal. 79−74137
U_3P_4, rhombohedral distortion of low temp. 77−7828
$U_{1-x}Pr_xS$, mag. phase diagram 80−71027
$U_{0.75}Pu_{0.25}O_{2-x}$, variation in O_2 potential with simulated burnup 78−70597
US-UC_2, solution studies 77−21120
US-UC-UC_2 system, potential nuclear fuels, phase solid soln. studies, prep. and props. exam. 79−40996
USb, search for lattice distortions at low temps. 80−79759
USb_2, single crystal growth, structural perfection 80−15024
U_3Si for heavy-water-cooled reactor, arc melting and hydrogenation methods comparison *(Chinese)* 79−85721
V complex, VOCL [Co(cyclopentadienyl)$_2$]$_{0.16}$, synthesis and struct. 80−44176
V, film, vac. deposited, influence of ion bombardment during condensation 79−82483
V, oxidation in low press. O_2 at high temp. *(Japanese)* 80−71807
V, single cryst., (110) scatt. factor, absolute meas. 78−71706
V-Al, band struct. and density of states, KKR method and X-ray meas. 80−10863
V-C system, ordering and phase equilibrium processes 79−99311
V-C(N) system, mutual phase orientation, X-ray diffr. exam. *(Russian)* 77−62498
V-H(D), hydrogen ordering, review 80−60850
V-Mn, equiatomic, ordering kinetics and antiphase domain coarsening 80−7559
V-Mn-Cr, disordered BCC state, mag. phase diagram, mag. and elec. props. 77−63185
V-N system, ordering and phase equilibrium processes 79−99311
V-N system, X-ray determ. of phase equilibria *(Russian)* 77−55952
V-Os system, equilib. phase fields, X-ray diffr., elec. resist., DTA, and EPMA meas. 79−47661
V-Re system, discovery of supercond. A-15 phase 78−88060
V-Rh alloy system, constitution diagram 77−44216
V-Sn(Al)(Ga)(Ge)(Si)-C, phase equilib. and supercond. 80−50593
$V_{0.985}Al_{0.015}O_2$, insulating T-phase cation disproportionation and V-V pairing 77−62825
$V_{0.985}Al_{0.015}O_2$, struct. aspects of metal insulator transitions 78−18965
$V_{1-x}Al_xO_{2\pm y}$, mag. and struct. props. meas. 78−2658
VC-TiC coating, high rate deposition by activated reactive evaporation, and characterisation 78−11372
$V_{3-x}Cr_xSi$, x=0 to 3, struct., supercond. and mag. props. 80−1962
V_2D, BCC α-phase, metal atom-induced diffuse X-ray scatt. from short range order 79−60358
V_2D, short-range interstitial order above crit. temp., diffuse X-ray scatt. obs. 79−95159
V_2D, single cryst., superstruct. modulation and long range order obs. 78−71712
V_3Ga, long-range order parameter variations determ. and correls. with supercond. T_c 77−11504
$V_{1-x}Ga_xO_2$, M1→T phase transition, X-ray and mag. meas. 77−11692
V_3Ge, forbidden Bragg refls., rel. to supercond. transition temp. 79−15251
V_2H, long-range order and β to β' transition, X-ray scatt. obs. 79−95160
VO_2, diffuse X-ray scatt. due to lattice instability near metal-semiconductor transition 78−56074
VO_2, X-ray determ. of lattice constants and thermal expansion coeffs. near transition temp. 79−86747
VO_x, defect struct., local ionic arrangements in disordered phase 80−10532
VO_x, diffuse scatt., relation to curvature of free energy surface 79−99025
V_2O_3, hydrostatic compression, X-ray diffr. meas. 79−99269
V_2O_3, impurity doping effects, elec. props. obs. 80−75609
V_2O_3, thermal expansion tensor, phase transitions, X-ray diffr. obs. *(French)* 79−1515
V_2O_3:Al, struct., props., rel. to V_2O_3:Cr, X-ray diffr. and elec. resist. obs. 78−2531
V_2O_3:Cr, anomalies in X-ray diffuse scatt. at high temp. metal-insulator transition 79−87042
V_2O_5, amorphous semicond., solubility and fibrous texture 80−75162
V_2O_5 bronze catalysts, α- and β-phase, rel. to decomp. mechanism determ. for isopropanol 78−11553
V_2O_5, thermal expansion tensor, phase transitions, X-ray diffr. obs. *(French)* 79−1515
V_2O_5-CsV_2O_5 system, phase comp. and phase diagram for conditions of inert atmosphere 77−25030
V_2O_5-Fe_2O_3-LiO_2 system, physical properties 78−84503
V_2O_5-MoO_3 system, X-ray diffr., IR absorption spectra, NMR and thermal analysis 77−24379
V_2O_5-TiO_2 interface, role of struct. props. in interfacial reactions 78−31688
V_3O_5, high-temp. phase transition, resistivity, valence photoelectron spectra 80−49357
V_3O_5, increase of X-ray refl. intensities and profile widths at phase transition temp. 79−69052
V_3O_5, phase transition, X-ray diffr. and DTA meas. 77−28001
V_3O_5-Ti_3O_5, DTA, mag. susceptibility and X-ray diffr. study 80−70970
V_xO_y film, prep. by thermal decomp. of vanadium naphthenate, and elec. props. *(Japanese)* 78−88425
V_xO_y, film, preparation by calcining vanadium naphthenate, formation process exam. *(Japanese)* 78−30849
$(V_2O_5)_{0.93}(MoO_3)_{0.07}$ solid soln., struct. transform. in oxidizing and reducing gas atm. 79−23740
$V_{1+x}P_{1-x}O_{5-c/2}$, density and struct. from X-ray scatt. meas. 77−89380
$V_{1-x}Re_xO_2$ ($0\leq x\leq 0.15$), insulator-metal transition, DTA, X-ray, mag. and elec. meas. 78−10353
VS_2, non-stoichiometric phase, physico-chemical props. 80−29532

X-ray diffraction examination of materials continued
- $V_{1+x}S_2$, local moment formation, X-ray, mag. susceptibility and NMR meas. 77−69511
- V_8S_8, non-stoichiometric phase, physico-chemical props. 80−29532
- V_8S_8, paramag. cryst., struct. factors using polarised neutron diffr. 80−15691
- VSe_2 (1T), incommensurate periodic lattice distortion, X-ray diffraction study 80−107414
- V_3Si, d-spacing fluctuations above Martensitic phase transition 80−7570
- V_3Si plastically deformed cryst., lattice transform., Kossel technique 78−95153
- V_3Si, powdered, Debye-Waller factors and lattice consts., 25-1000K *(German)* 79−33060
- V_3Si, single cryst., anharmonicity determ. from X-ray refl. intensities 79−73284
- $(V_{1-x}Ti_x)_2O_3$, solid solution, phase transition exam. 77−15590
- $V_2Zr(Hf)$, struct. transform. at low temp., X-ray diffr. anal. *(Russian)* 80−45298
- Ve-Fe-Ga system, phase obs. at 800 and 820°C *(Russian)* 78−23662
- W, borosilicate cladding compatibility *(Russian)* 77−66741
- W film, electron beam deposition on Si, X-ray obs. of silicide form., diffusion processes *(German)* 77−1341
- W film, silicide formation during growth by electron beam evaporation *(German)* 78−84717
- W film deposited by low temp. carbonyl pyrolysis, struct. 78−72039
- W, from $WO_{2.96}$ reduction 77−28744
- W/α-Al_2O_3 heteroepitaxy, orientation relationships, X-ray diffr. study 79−60661
- W-Hf-C, phase equilib. 80−55348
- W-Mo powder mixtures, form. using electric discharge sintering 77−12563
- W-Ru based refractory transition metal-metalloid glass, struct. 80−1938
- W-Ti(Zr)(Hf)-C, cubic solid soln., form. and props. 78−48348
- WAl_4, diffusive interaction of solid W and Al melt *(Russian)* 78−26735
- WC base alloys, uncoated and TiC or Al_2O_3 coated, wear charact. 78−92365
- WC, deformation behaviour during rubbing in wide temp. range 80−16486
- WC, fine powder prod. from $WO_3+C+Co_3O_4$ *(Japanese)* 78−92226
- WC, powder form. from WO_3-Co_3O_4-C powder mixture *(Japanese)* 78−92227
- WC-Co DC and RF sputtered coatings, bias effect, struct., X-ray-Auger study 80−70565
- WC-Co powder, prep. by direct carburisation of WO_3 in presence of Co_3O_4 80−50573
- WC-Co sputter deposited film, struct. and comp. 78−72023
- WC-Co sputter deposited film, friction and wear 78−72918
- WC_x (3×5) struct. on W (110) surface, at. beam diffr. and scatt., surface characteris. 79−78819
- WF_6-graphite intercalation cpds. 78−27441
- $W_{50}Fe_{50}$ glassy alloy, refractory, triode sputtered 80−75185
- $W_9Nb_8O_{47-x}$ polycrystalline film as electrochromic material 79−65949
- $W_{1-x}Nb_xSe_2$, packing defects, correl. with diffr. pattern changes 77−15429
- WO_3, acoustic instability near monoclinic orthorhombic phase transition, X-ray scatt. 80−65215
- WO_3 film, amorphous, electrochromism and local order 77−59553
- W_xO_y, carburisation/reduction with CO, morphological study 79−47977
- WS_3, amorphous struct., X-ray radial distrib. anal. and XPS 80−49115
- $WSCl_3$, prep. and characterisation 77−59705
- 2H-WSe_2, thermal expansion between 10 and 320K, cell dimensions meas. 79−65222
- WSi_2 refractory formation by As^+ ion beam bombardment 80−107286
- Xe monolayer, adsorbed on graphitised spheron, X-ray diffr. patterns 77−43433
- $(Y,Sm,Lu,Cu)_3(Fe,Ge)_5O_{12}$, ion implanted, hard bubble suppression 80−11238
- Y-Ge-B, X-ray investigation of phase equilibrium 79−99294
- Y-M intermetallic cpds., M=3d transition metal, sorption of H_2, structural charges 80−88429
- Y-Ni-Al ternary system, 800°C isothermal section in range 0 to 33.3 at.% Y *(Russian)* 77−70028
- YAG, production of densely sintered ceramic, exam. of recrystallisation during sintering 80−11609
- $YAlO_3$ and $Y_3Al_5O_{12}$, influence of flux on cryst. growth, X-ray powder diffr. meas. 77−24950
- $Y_2(CO_3)_3.nH_2O$, tengerite, single cryst. hydrothermal growth 80−97417
- $(YEuYbCa)_3(FeGe)_5O_{12}$ bubble films, Ne^+-implanted, cryst. and mag. props., X-ray diffr. obs. 79−38362
- $Y_3F_5O_{12}$, X-ray determ. of deformed surface layer thickness 78−53119
- $YFe_{1-x}Ga_xO_3$, zone refined, exam. of Curie point and magnetisation 79−4673
- YIG and Ga-substituted YIG, high energy heavy ion irrad., lattice strain 80−49278
- YIG, film, LPE, annealing-induced relief of compressive misfit strain 78−2386
- YNi_2 amorphous alloy, at. struct. 80−19704
- Y_2O_3 hydroxy salt binder phase form., X-ray, thermal anal. obs. 79−28999
- Y_2O_3 sintered body, luminous pipe of high press. Na discharge lamp, corrosion resistivity *(Japanese)* 78−19915
- Y_2O_3, thermal expansion, 500-1800°C, X-ray diffr. 77−35723
- Y_2O_3-Nb_2O_5, solid state reactions, 1275 to 1350°C, electron microscopy, EPMA, X-ray diffr., dilometry *(Japanese)* 78−63883
- YOF-YF_3, high pressure phase transitions 80−55368
- $Y(OH)_3$-α-FeOOH, physicochem. props. rel. to growth of $Y_3Fe_5O_{12}$ 77−40418
- $Y(OH)CO_3$, ancylite like phase, hydrothermal cryst. growth *(French)* 80−108340
- $Y_2[Pt(CN)_4]_3.21H_2O$, phase transitions, X-ray study and spectroscopic study 79−60506
- Yb, film, energy-scanning X-ray diffr. technique, stacking faults and coherent domains *(French)* 78−43264
- YbC_6, intercalation cpd. with graphite, synthesis and struct. 80−44184
- $ZiSiO_4$, natural and synthetic, X-ray dilatometry 77−51522
- Zn alloys, anodic corrosion in seawater 77−77628
- Zn, anharmonic lattice vibr., 'forbidden' X-ray reflections obs., 300K 78−34586
- Zn, electron irradiated, diffuse X-ray scatt. exam. of self interstitials 79−73213

X-ray diffraction examination of materials continued
- Zn, electron irradiated, diffuse X-ray scatt. exam. of interstitial clustering during thermal annealing 79−73214
- Zn ferrite, production by mechanochemical reactions by grinding in ball mill 79−20014
- Zn foil, splat quenched, preferred orientation 80−40381
- Zn hexagonal films, residual stress meas. from X-ray peak shift anal. 77−72807
- Zn, microrupture singularities in low stress range at elevated temp. *(Russian)* 79−29172
- Zn, RMS atomic displacement meas., anisotropic extinction correction 77−62606
- Zn single cryst., diffuse X-ray scatt. determ. 78−11255
- Zn, single cryst., mean square vibr. amplitudes X-ray diffr. 77−35640
- Zn, vacancy conc., lattice parameters meas. 78−10040
- Zn-Al, unidirectional eutectic, FCC phase, preferred orientation 80−29973
- Zn-As system, homogeneity range of $ZnAs_2$ and electrophys. props. 80−60833
- Zn-Sb diffusion couple, ZnSb phase layer growth kinetics, 240-320°C, up to 30 kbar 78−10229
- $Zn_xCd_{1-x}S$ film, prep. and use as heterojunction optical energy converters 79−95488
- ZnF_2, X-ray diffr. investig. of high-press. polymorphism 77−43324
- $ZnFe_2O_4$-Fe_3O_4 solid solns., form. of α-Fe_2O_3 during oxidation 80−25889
- $ZnIn_2S_4$, III(a) polytype, absorpt. spectrum tail changes due to microstresses 80−2788
- ZnO fibre reinforced elastomer, X-ray diffr. exam. of filamentary crystal distrib. 80−7738
- ZnO film, RF sputtered, characterization for SAW transducers 80−80138
- ZnO film, sputtering using Zn target, technique and characterisation 78−3040
- ZnO films, DC reactive magnetron sputtering technique, quality study 79−78877
- ZnO, ground powder, X-ray Fourier anal. *(Japanese)* 78−39727
- ZnO piezoelectric films, RF planar-magnetron sputtered, characterisation 80−96751
- ZnO powder, effect of dry grinding in EPR and catalytic activity *(Japanese)* 80−84640
- ZnO RF sputtered films, post deposition annealing behaviour 80−100416
- ZnO, structure parameters and polarity, X-ray diffr. meas. 80−19781
- ZnO, wurtzite structure, hydrothermally grown exam. of thermal expansion coefficient 78−75854
- ZnO, X-ray diffuse scattering 80−14964
- ZnO-Al_2O_3-SiO_2 glass, crystalline phase precipitation, crystallisation *(Japanese)* 79−32916
- ZnS, 4H and 6H polytypes, struct. changes on plastic deform. 77−43328
- ZnS crystal, inhomogeneous, microscopic struct. investig. using synchrotron radiation 77−76424
- ZnS, crystal, layered struct. microscopic observations *(Japanese)* 78−38725
- ZnS, deposited anthraquinone, decoration patterns 77−1137
- ZnS film, RF sputtered, characterization for SAW transducers 80−80138
- ZnS, sphalerite modification, polysynthetic cryst., struct. changes due to uniaxial compression 77−15482
- ZnS vapour grown crystals, morphology and structure 78−42937
- ZnS, X-ray diffuse scattering 80−14964
- ZnS:Ag phosphor prep., physicochemical investigation of processes 78−11170
- ZnS:Cu, Cl luminophor, photoluminesc. and struct. props. 77−32414
- ZnS-$CuInS_2$, phase relations, 400 to 1300°C, X-ray and microscopic exam. 79−1853
- ZnS-MnS, phase relations, 400 to 1300°C, X-ray and microscopic exam. 79−1853
- ZnSb, dynamical props. and thermal expansion, 78-300K *(Russian)* 77−7833
- ZnSe, thermal expansion, 20 to 1100°C *(Russian)* 79−95188
- $ZnSiP_2$, 1 MeV proton bombardment, lattice deformation investigation by Kossel effect 78−22775
- $ZnSiP_2(As_2)$, thermal expansion coeffs. meas. *(Russian)* 80−65258
- $ZnSnP_2$-$ZnSiP_2$, heterocombination simultaneous crystallisation 78−60560
- ZnTe films, grown on glass using atomic layer evaporation 80−44453
- ZnTe, polymorphism at elevated temp., elec. resist. and X-ray diffr. under press. 80−49359
- ZnTe:Cu films, high cond., elec. and optical props. 80−88651
- Zr alloys, crystallographic texture, quantitative charact., review 78−21647
- Zr sheet, elasticity coefficient computation by use of pole figure data 77−77521
- Zr-Al-C, phase diagram and lattice constants, X-ray diffr. method 80−89207
- Zr-C-N-O-H, solid solns. of H, exam. of props. 80−29172
- Zr-Co(Ni) amorphous alloy, thermal stability and electronic props. 79−73487
- Zr-Cr (1.9 wt.%), β-quenched and tempered, X-ray diffr. phase identification 79−66061
- Zr-Cu, glassy alloy, struct. anal. using X-ray diffr. 79−51004
- Zr-H, deposited on carriers, synthesis, structure and catalytic props. 80−29890
- α-Zr-H, volumetric changes, and thermal expansion, dilatometric and X-ray analysis exam. *(Russian)* 79−11665
- β-Zr-Mo oxidised alloys, high temp. deformation, X-ray study 79−79045
- Zr-Nb alloy, isothermal decomposition at elevated temp. 78−27470
- Zr-Nb-Fe (13 wt.%, 5 wt.%), struct. changes during decay of BCC β solid solution 79−15669
- Zr-Nb-Fe(Mo) alloys, decomp. of β solid soln., metastable and equilib. phases 79−11632
- Zr-Nb-V-Fe (12 wt.%, 6 wt.%, 4 wt.%), struct. changer during decay of BCC β solid soln. 79−15669
- ZrB_2, oxidation in O_2 atmosphere, exam. 80−11814
- ZrB_2-Nb, reactions between components 80−100812
- $Zr(Ca,Y)O_{2-x}$, local ionic arrangement, X-ray diffr. study 80−100203
- $Zr_{70}Co_{30}$, $Zr_{70}Fe_{30}$, $Zr_{70}Ni_{30}$ and $Zr_{70}Pd_{30}$ amorphous alloys, struct. factors and radial distrib. functions 80−84096
- $Zr(HPO_4)_2H_2O$, ^6Li loaded, α-radiation damage, X-ray Guinier powder reflection study *(German)* 78−47437

X-ray diffraction examination of materials continued
ZrI_4, high-temp. enthalpy, X-ray powder diffr. data 80−107446
$ZrMF_6$ (M=Co, V, Mn), X-ray powder diffr. data 79−78861
ZrN, in homogeneity range, high-temp. thermodynamic characts. 77−77464
ZrO_2, crystallisation from $Zr(OH)_4$, effect of water vapour, heat treatment and grain size *(Japanese)* 79−19170
ZrO_2 film, CVD from organometallic cpds. and characterisation 78−23626
ZrO_2 gels, calcination 80−11964
ZrO_2, monoclinic, variation of lattice strains *(Japanese)* 77−72600
ZrO_2, neutron irrad., monoclinic to cubic transform. 78−87720
ZrO_2, plasma deposition of crysts. and their characterisation 80−20800
ZrO_2, polymorphism at high press., X-ray diffr. obs. 79−73311
ZrO_2, porous, sintered stabilised microspheres, strength and fracture studies 80−85019
ZrO_2, stabilised, fabrication by hot petroleum drying method, X-ray diffr. and thermal anal. study 80−40297
ZrO_2 thin film, optical props. rel. to cryst. struct. 80−97357
ZrO_2-Nd_2O_3(Sm_2O_3)(Dy_2O_3) eutectic, unidirectional solidification, microstruct. and crystallographic characterization 80−35176
ZrO_2-R_2O_3 solid solns., prep., crystn., R=Nd,Sm,Dy,Yb 78−42909
ZrO_2-Sc_2O_3-Yb_2O_3 system, order-disorder phenomena, Raman spectra study 80−97254
ZrO_2-TiO_2 solid solns., X-ray diffr. and thermogravimetric meas. 79−90792
ZrO_2-UF_4, orthorhombic struct., X-ray and electron diffr. study *(French)* 78−67689
ZrO_2-Y_2O_3, solid soln., diffuse X-ray scatt. by vacancies 78−71728
ZrO_2,SiO_2-αAl_2O_3 mixed powders, solid state reactions 80−40337
$ZrSiO_4$, Fe_2O_3 and TiO_2 additions effect on stability 77−48377
$ZrSiO_4$, mechanochemical effect by mechanical grinding *(Japanese)* 78−84754
$ZrSiO_4$, synthesis, influence of rare-earth additives on props. 80−20868
$ZrSiO_4$-Fe_2O_3, pink colour form. kinetics 79−60360
ZrV_2, supercond., structural distortion obs. 79−11654
Zr_xWO_3, perovskite-type, stability in ZO_2-WO_2-WO_3 phase diagram 77−15582

X-ray diffraction examination of microstructure
see also crystal microstructure
A15 compounds, neutron irrad., X-ray scatt. theory 79−37740
absorbing crystals, dislocation contrast in the case of anomalous X-ray transmission 80−100240
alite paste, mature, microstructure study by SEM, TG and X-ray diffr., corrosion 78−92381
alkali halide single crystals, mosaic struct. determ., rapid X-ray method 79−37584
alloy, with correlated system of second phase particles, X-ray and electron scatt. *(Russian)* 77−59738
alloy steel, complex, X-ray diffr. determ. of fine struct. changes during quenching and tempering 77−56004
aluminosilicate glass, phase separated, phase characterization by STEM and X-ray microanal. 80−50643
aluminosilicate refractories, X-ray struct. determ. of quantitative phase contents 77−52707
asymmetric Bragg condition for thick real crysts., applic. to dislocation networks *(German)* 78−67607
Au film growth on Si(100), LEED and X-ray texture anal. 79−99452
austenite, hot-worked, struct., post-deform. ht. treatment effects *(Russian)* 77−8859
austenite, hot-worked, subgrain struct., X-ray diffr. and electron microscope obs. *(Russian)* 79−15698
Berg-Barrett single crystal substructure exam. using microfocus X-ray source 79−52495
biological specimens, multilayered structures, planar, small-angle X-ray data processing, theory 79−37582
block copolymers, as ideal model system for a pseudo two phase solid texture, small-angle X-ray scatt. 79−14693
bone china body, MgO effect on vitrification mech. props. *(Japanese)* 79−78922
boride coatings on Ni alloy, thermal stability, exam. of coating 78−44271
borosilicate glass, birefringent, X-ray small-angle scatt. study 80−103937
brass, γ-phase region, X-ray and electron diffr. obs. 79−61562
α-β brass, cold-rolled, energy dispersive X-ray diffr. studies 80−40379
brass, high-speed strain effect on struct. and props. *(Russian)* 77−59855
brass, plastically deformed, phase transforms. and diffusion phenomena *(Russian)* 79−20115
α-brass, stress corrosion cracking, X-ray study *(Czech)* 78−85043
brass, textured thin specimens, fracture 78−60816
bronze-steel, phase composition and struct. of diffusional interlayer in fusion zone, X-ray analysis 78−56821
Burgers vector sign determ. for nearly screw dislocations, X-ray dynamical theory applic. 80−59467
$Ca_3(VO_4)_2$-$Zn_3(VO_4)_2$, exam. of phase composition and phase diagrams 79−1851
calcite rocks, experimentally deformed, texture development 79−83230
carnauba wax, electret states, role of crystallites 80−2686
cast iron, hypereutectic, transform. of cementite to austenite 77−52318
cellulose, comparison of conclusions from small-angle X-ray scattering and electron microscope obs. 79−86717
cement, hot-pressed paste, strength, X-ray diffr., DTA, Ir spectra, microstruct. exam. 77−8864
ceramics, crack propagation, microstructural aspects 79−15771
ceramics acid-resistant, based on Artemov clay and obsidian 80−20852
coal tar and petroleum pitches, pyrolysis, press. effects on coke yield and microstruct. form. 77−70289
coke, anisotropic spheres obtained during needle coke form., struct. obs. 77−63573
coke, pressure effects on structure, polymorphic transitions X-ray diffr. anal. 79−1859
cordierite, synthesis rel. to WC addition 77−8787
corundum, subjected to thermal shock, study of substruct. and surface morpholoy, X-ray diffr. and TEM study 79−43292
corundum single crystal, premetallizing with Mo-Mn-SiO_2 79−47792
crystallite, cylindrical, layer disorder, X-ray diffr. intensity effect 80−39113

X-ray diffraction examination of microstructure continued
crystallite dimensions determ. using synchrotron radiation X-ray diffr. photographs 80−24313
crystallite orientation distribution function, determ. from isolated axis density values 77−48612
crystallites, curved, cluster with layer shift, X-ray diffr. intensities 80−39114
crystallites, elliptical 79−19122
crystallites, with step displacement, particle sizes and distortion determ. *(German)* 80−14960
deep-drawing curves, cryst. microstruct. during deform. *(French)* 79−20066
diamond, natural, (110) and (210) defects, X-ray diffr. pattern weak extra reflections 79−82257
diamond, natural, defect struct., recent obs. by new methods 78−30628
diamond, natural, impurity complexes, shape and dimens., diffuse X-ray scatt. obs. 78−47398
diamond, natural, $N_{S(111)}$ impurity segregation on diffuse X-ray scatt. 79−95046
diamond, synchrotron electron beam damage, study by optical, cathodoluminesc. and X-ray topography 80−39155
diamond, synthetic, carbonado type, struct. and microhardness 78−84994
diamond, synthetic disorientation of crystallite subgrains *(German)* 77−68939
diamond, synthetic grits, crystal morphology of cyclic twins 80−2037
diffusional homogenisation in compacted powder blends, X-ray diffr. line profile analysis 78−80491
dislocation contrast in X-ray synchrotron topographs 77−76408
dislocation distrib. function *(German)* 78−63767
dislocation microstress fields, study by X-ray dynamic focusing 79−23613
dislocation outcrop, extra equal-thickness fringes obs. with X-ray plane wave 80−39084
dislocation stress field computation method 78−30624
dislocation velocity, thermal activation exam. of applied stress and temp. depend., expt. methods *(French)* 80−59474
dislocation X-ray-diffraction image fine struct. using single-crystal interferometer 77−62537
dislocations, TV system for visualisation of X-ray diffraction topographic patterns 77−58925
electric steel, induction above magnetisation curve knee from pole density texture 77−12151
energy dispersive diffractometry for quantitative determination of texture 79−87818
epitaxial thin films, structural characterisation 80−3451
exploding wire unduloids, preferred grain orientations, lattice distortions, zonal texture 77−36568
fatigue crack, macroscopic residual stress at tip, X-ray obs. and finite element anal. *(Slovak)* 78−19885
FCC metal, origin of dislocations during microdeformation tests, X-ray topography 79−82226
feldspar, dislocation image contrast in electron microscopy and X-ray topography 78−26573
ferritic alloy, reinforced by dispersed oxide, mech. props., modification by recovery heat treatment *(French)* 77−59837
ferromagnetic alloy, 35KFN10, X-ray diffr. investig. after thermomech. treatment *(Russian)* 77−48457
fibre texture volume part determ. *(German)* 77−48595
fluorophosphate system glasses alkali free and crystn. products, struct. and IR spectra 79−94913
FORTRAN program for Fourier coeffs. of assoc. generalised Legendre polynomials of generalised spherical harmonics in texture analysis *(French)* 77−15279
geikielite, solid soln., phase transform. during reduction *(Russian)* 78−44042
glass, crystallisation and opacity, exam. by high temp. viscometry and X-ray diffr. *(Polish)* 78−84875
glass, decomposition, phase separation processes, diffusion coeffs. determ. *(Germany)* 78−39736
glass-ceramic second-order microstresses 78−27468
grain boundary sliding model 80−75237
grain orientation nonuniformity across wire specimen sections, anal. of X-ray patterns 78−23886
graphite, pressure effects on structure, polymorphic transitions, X-ray diffr. anal. 79−1859
graphite intercalation compound with SbF_5, texture 78−31355
Guinier-Preston ellipsoidal zone model *(French)* 77−84568
H_2O:HF ice, single crystal, velocity of individual dislocations by X-ray topography *(French)* 78−87677
heteroepitaxial surface morphologies and misalignments *(Japanese)* 80−15411
hexamine, BCC, dislocation slip initiation 77−43222
ice bicrystal, anisotropy of migration and faceting of grain boundaries 79−60381
II-VI semiconductors, lattice defects, X-ray diffr. and electron microscopic study 80−15088
II-VI semiconductors, thin foils, electron microscopic investigations 79−32864
ilmenite, solid soln., phase transform. during reduction *(Russian)* 78−44042
ilmenite ore, liquid, behaviour above 1500°C, X-ray obs. *(French)* 79−70100
4,5-iminophenanthrene, polymorphism, X-ray diffr. and photoluminesc. obs., 77 to 300K 77−63449
Incoloy, oxide-dispersion-strengthened, pulsed YAG laser welding 79−70075
Incoloy 800 Fe base heat resistant alloy oxidation 77−86231
Incoloy 800H, high temp.-low cycle fatigue, ageing and cold working effect on initial stress/strain curve 79−47720
internal stresses, calc. with integration methods, X-ray stress meas. 79−32415
Invar N36 melt, cast metal struct. depend. on heat treatment, subgrain struct. *(Russian)* 80−40343
ketone-paraffin solid soln., dielec. relax., temp. and lattice const. depend. *(German)* 78−76383
Kevlar 29 and 49, aramid fibres, microvoid obs. 80−38960
Kh20N40 alloys, phase composition after quenching, tempering 78−60650
lattice defects, convolution relations for X-ray line breadth calcs. 78−51394
lattice distortion, X-ray moire pattern fine struct. study 80−79775

X-ray diffraction examination of microstructure continued
lattice period determ. by axial X-ray camera 79−68974
line broadening, polyphase or non-cubic materials, thermally induced strains 77−4809
metal, atomic defect config. from X-ray and neutron scattering studies 78−47322
metal, fatigue damage examination using two-crystal X-ray spectrometer method 79−52481
metal, FCC, cavitation erosion 77−86191
metal, FCC, with fibre texture, X-ray method of twin fault probability determ. 79−87817
metal, friction pair, seizure centres on contacting surface *(Russian)* 77−70185
metal, oxidation of high temp. material, lattice vacancy effect 77−70203
metal, plastic deform. effects from X-ray diffr. data, moment method *(Czech)* 78−31593
metal, textures and collective props. of lattice defects, external surfaces, grain boundaries 77−62543
metal coating, prep. by plasma arc spraying and characterisation 79−23873
metal dislocation structures, X-ray diffr. exam. by vibrating crystal method *(Russian)* 78−34519
metal substructure exam. by astigmatic X-ray microbeam method 78−85076
metal-C system, spheroidal graphite formation, role of high angle boundaries *(Russian)* 80−81065
metals, FCC, plane shock wave loading, microdistortion X-ray anal. *(Russian)* 77−52399
metamorphic plagioclases from Japan, modulated microstructure 79−96760
microcrack enlargement in heterogeneous materials, conc. criterion 80−11769
misfit boundary, X-ray diffr., general soln. 78−51562
misfit boundary, X-ray diffr., special cases 78−63776
Mo, slip line study of pure single crystal compressively deformed at low temps. 79−43361
multialkaline antimonides, (Sb, Na, K, Cs) type, photoemission rel. to chem. struct. *(French)* 78−39655
nepheline concentrate, low Fe, phase composition 77−21110
neutron-irrad., void annealing, positron annihilation obs. 77−76469
Nimonic type, elastic interphase strains on ageing effects on extinction *(Russian)* 77−66646
nondestructive subsurface distrib. meas., polychromatic X-ray technique *(Japanese)* 77−48600
nonisothermal devitrification kinetics 80−92465
nuclear track detectors, microcrystallite nucleation and detection threshold 80−890
nylon 6, microfibril dimensions, from small-angle X-ray scattering 79−37574
nylon 6, notched sheet, deform. mech., fracture, X-ray obs. *(Japanese)* 77−59863
Nylon 6 gut yarn, fine struct. change in twisting, annealing and untwisting, microbeam X-ray obs. 80−81026
Nylon 6 gut yarn, fine struct. change in twisting, annealing and untwisting, X-ray and electron microscopy obs. 80−84904
Nylon-6, injection moulded, struct. and morphology 80−38949
octadecanol, normal, single cryst., lattice defects, X-ray topographic obs. 78−18650
ordered alloys, long period antiphase structs. 79−95027
ordered superlattices, X-ray studies, rel. to microstructure 79−94844
oriented polyethylene film, deformation band studies 77−52420
oxide eutectics, directionally solidified, crystallography and microstruct. 79−78950
oxide systems, exam. of techniques used to determine phase diagrams and equilibria, and effects on equilibria 79−8415
PAN fibres, heat treatment, structural changes *(Polish)* 77−28835
pentacene, evaporated on quartz, optical absorption, substrate temp. depend. 78−2932
PET, densification, cryst. perfection, mechanism 79−66082
petroleum feedstocks and cokes, graphitisability 80−93580
phase equilibria at 500°C *(Russian)* 78−56612
plagioclase, labradorite, Al/Si distrib. in An_{66}, superstructure in An_{54} 79−94970
plagioclase feldspars, modulated structs., X-ray diffr. and electron microscopy obs. 79−95031
PMMA, notched, sheet, deform. mech., fracture, X-ray obs. *(Japanese)* 77−59863
polethylene-polypropylene blend, extruded, thermal swelling and mech. characterisation 80−81110
poly(vinylidene fluoride) orientation, solid state deformation by coextrusion 80−40394
poly-1,3-pentadiene, microstruct., IR, NMR, X-ray determs. 79−37637
polyamide, directionally solidified, X-ray diffr. 79−10809
polyamide fibres, crystallinity and crystallite size meas. 78−30549
polybutylene terephthalate, hysteresis of stress-induced cryst. phase transition 78−31404
polycarbonate, notched sheet, deform. mech., fracture, X-ray obs. *(Japanese)* 77−59863
polycrystals, deformed, particle sizes and mean square strains *(German)* 78−3284
polycrystals, X-ray substructure anal. *(German)* 77−68895
polyester fibres, crystallinity and crystallite size meas. 78−30549
polyethylene, from the melt, small-angle X-ray scatt. study of crystn. 79−14692
polyethylene, high density, hydrostatic extrusion conditions effect 77−63722
polyethylene, high-density, lamellar sep. during deform. 78−23775
polyethylene, hot-stretched, small angle X-ray scatt., computer anal. 79−14699
polyethylene, linear, bulk-crystallised, morphology study 79−32918
polyethylene, linear, struct. and relax. transitions, pulsed NMR and X-ray diffr. *(Russian)* 77−47357
polyethylene, melt crystallised, chain defects distrib. and microstruct. 79−10818
polyethylene, notched sheet, deform. mech., fracture, X-ray obs. *(Japanese)* 77−59863
polyethylene, one dimens. synthesis of SAXS pattern 78−75589
polyethylene, oriented, partially crystalline, amorphous component obs., X-ray diffr. *(Russian)* 79−23534
polyethylene, oriented, shear strain, effect on stuct., props. *(Russian)* 80−7656

X-ray diffraction examination of microstructure continued
polyethylene, ultradrawn linear, kink bands by compression, interfibrillar motion 79−24581
polyethylene, uniaxially stretched, density fluctuations 78−75587
polyethylene terephthalate, oriented amorphous phase 78−95003
polyethylene terephthalate fibres, high freq. US effects on physical and chem. structs. *(Polish)* 78−51446
polyhexamethylene terephthalate/polyoxytetramethylene block copolymers, supramolecular texture 78−91261
polymer, coorientation with low molecular organic substances *(Russian)* 77−21089
polymer, melt-crystallised, one-dimensional characterisation of microstruct. 78−75588
polymer crystalline structure stability *(Russian)* 77−19880
polymers, X-ray diffr., lateral grain boundaries 79−14700
polymide, elasticity of crystal lattice 78−3164
polypropylene, cold-drawn isotactic bars and thin films, microstruct. and annealing 78−95760
polypropylene, notched sheet, deform. mech., fracture, X-ray obs. *(Japanese)* 77−59863
polystyrene, glassy atactic, struct. anal. from small-angle X-ray scattering 79−73109
polytetramethyl-p-silphenylenesiloxane, degree of crystallinity 78−26453
polytetramethylene terephthalate, injection-moulded, struct. depend. of fracture behaviour 77−8912
polytrioxane, γ-irrad., layer-like void formation 78−22760
polyurethane, segmented, struct. changes on annealing, small-angle X-ray meas. 77−4052
polyurethaneurylenes, segmented, structural features *(Russian)* 77−47356
polyvinylidene fluoride, poling process effect on fine struct. 80−7285
polyvinylidene fluoride, polycryst. ferroelec., microstruct., piezoelec. and pyroelec. props. 80−7303
polyvinylidene fluoride films, corona-charged, struct. changes, piezo- and pyroelec. props. 79−11389
porcelain enamel panels, TiO_2-opacified, quantitative X-ray diffr. anal. of anatase, rutile 79−32857
portland cement paste, microstructure study by SEM, TG and X-ray diffr., corrosion 78−92381
preferred orientation, quantitative determ. by energy-dispersive X-ray diffr. 77−25241
PTFE, heat shrinkable tubing, crystallite orientation 77−4795
PVC, highly syndiotactic, X-ray diffr. and IR studies of annealed material, crystallinity 78−2022
PVC, plasticised, processing-morphology-mech. props. relation 79−8264
pyrocarbon, X-ray anal. of porosity, effect on radiation stability 77−79464
pyrocarbon coatings on HTGR fuel particles, Bacon anisotropy factors meas. technique 79−13418
quartz, crystal growth in fluoride environment, growth features and props. 80−6373
quartz, defects growth, study by X-ray diffr. topography *(French)* 80−39095
quartz, piezo quasi-mosaic struct. effect obs. on X-ray diffr. *(Russian)* 77−89349
quartz, resonator, X-ray double crystal topographic assessment of defects 79−50943
quartz, strain amplitude depend. of internal friction, role of dislocations 77−27939
quartz, synthetic, discoloration rel. to lattice deform. 77−24872
α-quartz, synthetic, growth, defects induced by seed orientation 80−96454
rare earth germantes, flux-grown, X-ray topography 80−64939
rare earth oxide (R_2O_3)-M_xO_y glassy systems (M=Ti,Nb,Ta), rapid quenching by laser beam, exam. of composition and crystallization 78−52856
rare earth-Au-In, Fe_2P type phases 77−70033
refractory oxide coating, prep. by plasma arc spraying and characterisation 79−23873
sapphire ribbon crysts., grown by edge-defined film-fed growth technique, X-ray topography study of dislocations 79−4305
section topography as single-cryst. interferometry 78−47208
self-lubricating, struct. and props. 79−100267
semiconductor film, heteroepitaxial, on insulating substrates, characterisation, book contrib. 79−82497
Si, X-ray step scanning section topography, lattice imperfection characterisation, automatic Bragg angle control 79−60221
siloxane, temp. transitions, linear dilatometry and X-ray diffr. obs. *(Russian)* 80−59404
single crystals for devices with multiple crystal arrangement, X-ray characterisation 78−83651
small-angle scattering, rel. to elec. resist. 79−19125
solid-solid interface chemistry, characterisation, theory 80−75448
spinel-type lattice, determ. of stacking faults, diffr. effects, in presence of dislocations 77−55290
stacking fault contrast, variation with phase shift value in X-ray topography 77−65986
stacking faults, X-ray imaging in cryst. with Bragg geometry 78−59821
steel, 30KhG and 30KhN, carbide formation, Mo alloying effects *(Russian)* 78−48402
steel, AISI 4340, positron lifetime and X-ray particle size meas. during high cycle fatigue 79−5053
steel, Al, quenched, tempered, orientation of precipitated Fe_xC particles, X-ray obs. *(Russian)* 79−29063
steel, alloy, fretting corrosion, exam. of secondary structures 79−100292
steel, alloy, Mn (Ni), Mossbauer, X-ray and electron microscope studies of martensite 78−56621
steel, alloy, type 11Kh18M, eutectic carbide composition change due to heating 80−16353
steel, alloy, type ST.5, structural and phase changes after high temp. heating *(Russian)* 80−55439
steel, alloy, V-W-Mo-Cr, exam. of carbide transformation 80−16299
steel, alloy and C, ion nitrided and ion-softnitrided, comparison of compound layers *(Japanese)* 79−8386
steel, and alloy, austenitic transformation, temp.-conc. range of product formation 79−100135
steel, austenite to martensite transformation, orientation relationships 79−78964
steel, austenitic, 16H2NMB, struct., texture and mech. props. of product of transform. 78−92273

X-ray diffraction examination of microstructure continued
steel, austenitic, Cr-Ni-Mn-V, X-ray anal. of carbide phases formed during ageing *(Russian)* 80−20936
steel, austenitic, deform., struct., transform. kinetics hot working effects *(Russian)* 77−52361
steel, austenitic, Kh12N20T3R, ageing, submicroscopic struct. role in dispersion hardening *(Russian)* 78−64549
steel, austenitic, martensitic transform., mechanism and kinetics, TEM, X-ray and optical obs. *(Rumanian)* 78−19746
steel, austenitic, metastable, alloy 000Kh18N10 creep at low temps. 77−1861
steel, austenitic Cr-Mn, $M_{23}C_6$ carbide precipitates comp., heat and thermomech. treatment influence *(Russian)* 80−40361
steel, austenitic stainless, ferritic, single phase ferritic solidification in welds, exam. 80−7546
steel, austenitic stainless, hydride study by X-ray diffr., rel. to martensitic transform. *(Japanese)* 77−81263
steel, austenitic stainless, welds, exam. of austenitic solidification mode 80−7545
steel, austenitic stainless, X-ray line profile analysis 77−86048
steel, austenitic-ferritic Ni-Cr, 12Kh21N5T, phase and struct. transform. *(Russian)* 78−95748
steel, austenito-martensitic, struct. changes during plastic deform., mutual influence of phases *(Russian)* 80−30015
steel, C, decomposition of supercooled austenite, exam. of carbide formation *(Russian)* 78−35388
steel, C, explosively fractured, struct. of white etching band 79−61722
steel, C, transform. kinetics, heat cond. and elastic-plastic stresses during quenching *(Japanese)* 80−25688
steel, C, wear charact. of worn surface layer under lubrication *(Japanese)* 78−35526
steel, C, X-ray line fitting by Gram-Charlier distrib., appl. to tension test *(French)* 79−15689
steel, C and alloy, nitriding, effect on struct. and internal stresses 80−30162
steel, C and alloys, ion-softnitriding effects on metallurgical props. of nitrided layer *(Japanese)* 79−5079
steel, C type U10A, X-ray diffr. investig. of carbide residues after deform. and tempering *(Russian)* 77−81275
steel, C-Mn, corrosion cracking, role of microstresses and crystal lattice stresses *(Russian)* 77−25190
steel, cast structural, heat treatment and mech. working influence on mech. props. *(Russian)* 80−40392
steel, CC Cr-Mo-V (1,1,.25 wt.%), Mo_2C-V_4C_3 precipitation, creep rupture test *(Japanese)* 79−70070
steel, cold strained, defects interaction with carbide strengthening phases, carbide decomp. degree *(Russian)* 80−84955
steel, cold-rolled, recovery of lattice defects in cementite 77−90370
steel, complex alloy, exam. of temper brittleness 78−44209
steel, Cr and Ni-Cr, cyclic re-austenitizing 80−35222
steel, Cr bearing, carbide phase precipitation during tempering, Mossbauer, X-ray diffr. studies *(Russian)* 79−87636
steel, Cr-C, (2.14, 1.08 at.%) tempered, resistance to small plastic deformation, strain relaxation *(Russian)* 78−56698
steel, Cr-C (13, 0.15 wt.%), bainitic transform. *(German)* 78−11218
steel, Cr-C (18, 0.9 wt.%), cavitation, abrasion resistance, effect of unstable austenitic struct. *(Russian)* 77−16695
steel, Cr-Mn, non-metallic inclusions anal. with increased N content *(Bulgarian)* 79−82259
steel, Cr-Mn, unstable austenite, martensitic transform., effect of alloying, heat treatment, and deform. 78−19751
steel, Cr-Mn type, martensite struct. after quenching and HTMT 80−84975
steel, Cr-Mn-W(Mo), W and Mo addition effect on carbide form. in type 30 KhG *(Russian)* 79−87638
steel, Cr-Mo(-V), ductility and heat resistant prop. prediction rel. to fine struct. and solid soln. state 79−15751
steel, Cr-Mo (2.25, 1 wt.%), decarburization, carbide effects in high temp. Na *(Japanese)* 78−15403
steel, Cr-Mo (2.25, 1 wt.%), in high temp. Na, heat treatment and metallurgical struct. effects 77−16619
steel, Cr-Ni-Mo-V-Nb (12,8,1,1.5,0.4 wt.%) Ce addition effects on strength and hardness *(Russian)* 78−15454
steel, Cr-Ni-W(Mo), W and Mo addition effect on carbide form., X-ray obs. *(Russian)* 79−87639
steel, Cr-Si-Mn-ΔV-Ti-Nb-Mo, effect of V, Ti, Mo, Nb additions on substructure, mech. props. *(Russian)* 79−34108
steel, Fe-Mn-(Cr)-C, intermediate phase form. during martensite form. 77−12626
steel, hardened, martensite struct. charact., Cu and Al additions effect *(Russian)* 78−19709
steel, high C, investigation of transformations during tempering by nuclear gamma resonance method *(Russian)* 80−76256
steel, high speed, R18 and R6M5, rolled and annealed carbide phase investigation 77−90374
steel, high speed tool rapidly quenched, exam. of solidification struct. 78−39758
steel, high V-W-Mo, high speed, phase composition and struct. of atomized powders 77−90323
steel, hypoeutectoid, C22, recrystn., influence of carbides distrib., X-ray exam. *(German)* 79−38850
steel, induction hardened, static bending strength and correlation between static strength and endurance limit *(Japanese)* 77−70108
steel, ion-softnitriding of type S15C with N_2-H_2-CH_4 mixture, mech. props. of surface *(Japanese)* 79−61780
steel, low alloy, low C grain boundary proeutectoid ferrite formation, direct obs. method 80−3074
steel, low alloy, SMCM 8, tempered, fractographic study of stress corrosion cracking *(Japanese)* 79−66214
steel, low alloy, type 10KhN1M, heat-treated, struct. and resist. to thermal embrittlement 79−15788
steel, low alloy composite, ferrite-carbide struct., cold plastic deform. 77−90408
steel, low C, cold rolled sheet, Cu effect on recrystallization texture *(Chinese)* 79−74173
steel, low C, deform. form effect on texture *(Russian)* 78−3141
steel, low C, gas nitrocarburized, cyclic stressing 79−57098
steel, low C, high C, bainite transform. heat treatment effects *(Czech)* 77−63661
steel, low-C, Al-stabilised, texturing during annealing *(Russian)* 78−19777

X-ray diffraction examination of microstructure continued
steel, maraging, ageing kinetics and struct. of N12K7M5TYu, effect of high temp. deform. of austenite *(Russian)* 80−84960
steel, maraging, hardening mechanism of quenched samples, tempering *(Czech)* 79−78989
steel, martensite, partially disintegrated X-ray anal., appl. of method of moments 79−52223
steel, martensitic, low C without Ni, for deep-well sucker rods, corrosion fatigue 80−55588
steel, martensitic, obtained by deform. of austenite 70Kh5G4 *(Russian)* 78−88464
steel, martensitic, retained austenite study by X-ray diffr. *(Korean)* 78−44143
steel, medium C, microalloying with V and Ti, effect on hardness and structure 80−11750
steel, medium C 80−11752
steel, mild, Al-Zn alloy coated, interface struct. 79−52466
steel, mild, plastic deform. around fatigue cracks, X-ray microbeam and recrystn. studies 80−35258
steel, mild, plate, explosive hardening of one end 77−36531
steel, Mn, H_2 embrittlement mechanism *(Korean)* 78−68774
steel, Mn, tempered, sementite crystals, carbide phase segregation, X-ray study *(Russian)* 78−35391
steel, Mn-Cr-V, structural changes during solution annealing *(Czech)* 78−84864
steel, N-Cr-Mn, influence of nitride phase on corrosion behaviour *(Bulgarian)* 79−61798
steel, NC6, cementite network separation, kinetics *(Polish)* 80−25698
steel, Ni, martensite decomposition *(Russian)* 79−1841
steel, Ni (17 wt.%), martensitic deform. temp., cryst. struct. effect *(Russian)* 80−66576
steel, Ni-Cr, temper embrittled, electron microscope and X-ray microstruct. obs. 79−38870
steel, Ni-P plated, electroless, fatigue strength and plated layer microstruct. *(Japanese)* 80−93645
steel, Pb and MnS inclusions 77−77685
steel, problems of X-ray determ. of dislocation density from one diffraction line *(German)* 78−2129
steel, recrystn., structural inheritance charact., X-ray and friction obs. 79−57017
steel, stainless, 18-8, stress corrosion cracking, in H_2SO_4-NaCl soln. *(Japanese)* 77−21315
steel, stainless, alloyed with C, magnetron-sputtered, microstruct., and cryst.-amorphous transition 80−19719
steel, stainless, carbide and intermetallic phases, quantitative anal. by X-ray diffr. 80−66514
steel, stainless, Cr-Ni (18, 8 wt.%) average inclusion size and contents exam. measurements using optical microscopy and Br-Methanol methods *(Korean)* 79−66080
steel, stainless, deoxidation in melting with Si *(Korean)* 78−19947
steel, stainless, metastable, determ. of strain-deform. martensite content 78−3282
steel, stainless, oxidation in melting *(Korean)* 78−19946
steel, stainless, sensitized, direct evidence of Cr depletion near grain boundaries 77−90358
steel, stainless, type 316, cast, precipitation kinetics of χ phase and $M_{23}C_6$ carbide 78−88469
steel, stainless 18-8, stress corrosion cracking in H_2SO_4-NaCl soln., martensite form. *(Japanese)* 78−92396
steel, stainless 304, elevated temp. low cycle fatigue, heat treatment effect 78−27626
steel, stainless SUS 316, creep fracture at elevated temps. vacuum environment effect *(Japanese)* 77−8942
steel, structural, strained in tension after tempering, compression effects on struct. changes *(Russian)* 80−66577
steel, structural recrystallisation, phase and struct. transformations during heating 77−55990
steel, thermally and thermomechanically treated, struct. and decomposition of martensite 78−19784
steel, tool, W-Mo, heat treatment effect on props. 80−50656
steel, tool type M2, surface hardening and microstruct. refinement by laser melting, electron beam melting, heat treatment *(Korean)* 79−70093
steel, type 1Kh17N2, white zone formation and props. during friction in vac. *(Russian)* 80−40542
steel, W-Co-Mo-Cr-V-C (8.5, 8.1, 4.5, 3.5, 2.2, 1.02 wt.%), phase composition, struct. and props. 80−104163
steel, with 4% Al, κ'-martensite struct. and $\kappa' \rightarrow \alpha_m$ transform., X-ray diffr. *(Russian)* 77−59786
steel, X-ray and microhardness meas. at high strain rates *(German)* 78−3184
steel 1095, quenched, Mossbauer study of surface martensite 77−32578
steel 12Kh1MF, fine struct., effect of isothermal transform. temp. 77−21137
steel 15Kh1M1F, microstruct. changes rel. to creep and fracture *(Russian)* 79−24572
steel 18 Gps, ductile fracture, rel. between plastic deform. in fracture zone and fracture charact. *(Russian)* 77−52457
steel alloys, low and medium C content, relaxation phenomena in volume changes during tempering *(Russian)* 79−100176
steel fibre reinforced Mg, fibre-matrix interfacial reactions 80−20043
steel fine structure after heat treatment, X-ray diffr. exam. 80−60890
steel Kh18N9T, fractographic features of rupture, rel. to struct. changes 77−63801
steel mild, plastically deformed, X-ray meas. of stress and TEM 77−48496
steel Ni-Cr-Ti-C (2.8, 0.9, 0.2, 0.73 wt.%), ferrite, orientation in pearlite, rel. to austenite *(Russian)* 80−81072
steels, 110G13 and 40Kh10G10, hardening and structural transformations during friction *(Russian)* 77−52527
steels, hypereutectoid, 120G4 and U15 type, with initially pearlitic struct., mechanism of structural inheritance *(Russian)* 77−52329
steels, tool, type U10A and R6M5, phase comp. and phys. props. after hydrostatic extrusion 79−96053
structural transitions in single crysts., diffractometry use 79−52483
subgrain boundary, X-ray misorientation contrast 77−27780
swirl defects in single crysts. 80−44200
TBBA liquid crystal, monoclinic cell parameters of solid, smectic and metastable phases, temp. dependence 80−70122
tetramethyl-p-silphenylenesiloxane-dimethyl siloxane copolymers, degree of crystallinity 78−26453

X-ray diffraction examination of microstructure continued
texture, evaluation by X-ray and neutron diffr. anal., comparison *(French)* 79−91882
textured material, X-ray quantitative phase anal. *(Chinese)* 80−21195
thin dust layers, particle size effects automatic correction, computer appls. in spectrometry 79−83539
three-dimensional texture analysis, data processing, subroutines 77−25240
Ticonal-type alloys, struct. after quenching from 800-850°C *(Russian)* 77−59822
topography, oscill. technique for cryst. coarse perfection investigs. 78−30518
transition metal carbides, X-ray investig. of abrasive action 77−52497
TTF-TCNQ crystals, X-ray topographic study of cryst. perfection 80−96525
very perfect crystals, topography and goniometry 78−30516
vitrinite, in bituminous coal, microporosity and micromineralogy, small-angle X-ray scatt. study 79−12117
wide-angle analysis, plastic deformation appl., alloys behaviour obs. *(German)* 80−3283
Zircaloy-4, microstrain and particle size meas. by Warren-Averbach method 80−55420
Zircaloys, I_2 induced stress corrosion cracking 79−8381
$3PbO.GeO_2$, X-ray and electron diffr. exam. *(German)* 80−11632
Ag film, ion plated on AT-cut quartz crystal 80−2280
Ag film, lattice defects, convolution relations for X-ray line breadth calcs. 78−51394
Ag, recrystallisation texture development after plane-strain deform. 77−48448
Ag, vapour-deposited on rotating substrate at oblique angle, X-ray struct. anal. 77−62775
Ag-Cd (45 at.%), morphology and struct. of bainite plates in β' phase 79−52213
Ag-Cd (47 at.%), crystal struct. and internal defects of thermoelastic martensite 77−48438
Ag-Cu (6.2 at.%), tricrystalline specimen, discontinuous precipitation, specific grain boundary energy *(German)* 77−86039
α-Ag-Ge, cold-worked, lattice imperfections, X-ray diffr. study 78−38732
Ag-Ge (4.5 at.%), FCC, vapour-deposited, lattice imperfections, X-ray diffr. 78−72032
Ag-In alloys, rapidly quenched from melt, stacking faults, TEM and X-ray diffr. meas. 77−59768
Ag-In-Sn, internal oxidation, precipitation behaviour of oxide *(Japanese)* 80−66515
Ag-Sb, cold-worked, lattice defects, convolution relations for X-ray line breadth calcs. 78−51394
Ag-Sm system, phase diagram, eutectic temps., microstruct. *(German)* 80−104119
Ag-Sn, splat-quenched, X-ray diffr. study 80−81094
Ag-Sn (6,11 at.%) alloy, splat-quenched, X-ray diffr. study of microstruct. 77−8860
Ag-Sn-Cu-Hg, constitution of quaternary amalgam at 37°C *(German)* 77−81250
Ag-Sn-Te phase equilib. 79−29033
Ag-Zn, cold-worked, lattice defects, convolution relations for X-ray line breadth calcs. 78−51394
$AgAsS_2$-$AgSbS_2$ system, thermal, microstructural X-ray phase anal. 77−32565
$Ag_3Au_{1-x}Cu_x$, phase relations, X-ray diffr. and differential thermal anal. 80−108395
AgI-Ag_2O-MoO_3 system, glass form. with high ionic conductivity 77−89379
AgI-BiI_3, phase equilib. study *(French)* 79−66047
Ag_2Te, Ag movements, X-ray microanal. by SEM *(French)* 79−42304
AgZn, $\beta' \rightarrow \zeta$ transformation, effect of additional elements 80−66507
AgZn-AgMg quasibinary alloy, phase relation and superlattice form. 78−3097
Al alloy, fretting corrosion, exam. of secondary structures 79−100292
Al alloy 7075, precipitation hardening, toughness and microstruct. *(Japanese)* 78−15509
Al, and Al-Cu(Pb) dil. alloys, pulsed ruby laser irrad., noncryst. phase form 80−35012
Al, annealed and neutron irrad., exam. of positron lifetimes in voids and other defects 78−47426
Al, annealing twin growth, obs. by synchrotron radiation X-ray topography 79−55753
Al, anodic layers, coloured, prep. by ultramicrotome without embedding, for TEM and X-ray obs. 79−39074
Al, cast, testing of castings and die casting machines 78−53097
Al, creep and rupture, in torsion, mech. *(Russian)* 79−5030
Al, defect structure after plastic deformation 78−31467
Al, defects formed during cryst. growth or by plastic deform., X-ray transmission topography obs. *(Russian)* 80−25761
Al, deformed, nucleation and recrystallisation at second phase particles 78−6941
Al, dislocation density, prep. of high-purity cryst. by strain-anneal method 78−48314
Al, energy-dispersive diffr., preferred orientation influence 78−22603
Al, fatigue crack propag., grain size effect *(Japanese)* 78−39889
Al film, meas. of stress gradients generated by electromigration, X-ray topography and SEM 77−51541
Al, plastically deformed single crystal, X-ray diffr. by defects 77−68976
Al, plate, explosive hardening of one end 77−36531
Al single crystal nonstop uniaxial tensile tests, electro-optical image intensifier 79−34277
Al single crystals, crystal orientation effect on their cutting mechanism 79−34193
Al, struct. changes during cyclic deform. *(Russian)* 77−25127
Al, struct. changes in single cryst. under influence of static and dynamic stresses *(Russian)* 78−92300
Al, wire, determ. of incomplete axial texture by X-ray diffr. 78−23720
Al-Ag (up to 4 wt.%), creep, 570-630°C, influence of Ag addition *(Russian)* 79−5003
Al-Ag alloy mirror for use as solar reflector, co-sputtering 80−20789
Al-Cr, rapidly solidified, crystalline and amorphous structures 77−44274
Al-Cu (Mg)(Zn), corrosion of chill zone, solidification microstruct. effect 77−36687
Al-Cu (1.7 at.%), EXAFS study of precipitation 79−100151
Al-Cu (3 wt.%), stress aged, GP zone struct. by X-ray diffuse scatt. meas. *(Japanese)* 80−71653

X-ray diffraction examination of microstructure continued
Al-Cu (4 wt.%), aged to contain Guinier Preston zones, crystallographic fatigue crack growth 78−60832
Al-Cu (4 wt.%), reversion charact. *(Japanese)* 77−21150
Al-Cu (4 wt.%), single cryst., small angle X-ray scatt. map after spinodal decomp. 79−15645
Al-Cu (4 wt.%) alloy, reversion charact. *(Japanese)* 79−56989
Al-Cu (5 wt.%), ageing, extinction effects *(Russian)* 77−81283
Al-Cu (5 wt.%) alloy, ageing during relax. of elastic stresses, X-ray diffr. expts. *(Russian)* 77−59821
Al-Cu-Mg alloy, struct. of Guinier-Preston zones *(Russian)* 79−1870
Al-Cu-Mg-Mn-Fe-Si, alloy D16, effect of mechanisothermal treatment on mech. props. 78−56674
Al-Cu(Zn, Ag, Mg_2Si), intermediate precipitates, stability, X-ray, elec. resist. and hardness study 80−3063
Al-Ge alloy, effect of high press. on phase equilibrium *(Russian)* 79−1844
Al-Ge alloy, Ge particle size, determ. by small- and wide-angle X-ray scatt. 78−19966
Al-Li (10 at.%), struct. changes on annealing, 25-500°C, Li atoms role 80−35183
Al-Li (6.72 at.%), δ' coherent solvus determ. on ageing at 20 to 200°C, X-ray scatt. 77−25056
Al-Li system, δ' coherent miscibility gap determ. by small-angle X-ray scatt. 77−77483
Al-Mg (33 at.%), liquisol quenched, decomposition 79−61622
Al-Mg cold drawn wires with FCC lattice, texture and structure 77−70067
Al-Mg supersaturated solid soln., spinodal decomposition at 20°C *(French)* 77−85987
Al-Mg-Si alloys, dendritic non-homogeneity 78−56641
Al-Mn, cooling after recrystallisation, phase transform., X-ray and thermal anal. *(Russian)* 77−66663
Al-Mn (1.8 wt.%), cold-rolled, precipitation and recrystallisation 78−27540
Al-Mn alloys, study of solidification by rapid cooling *(Japanese)* 78−88459
Al-Ni mixed-powder-based plasma-sprayed coatings, strength charact. 77−12548
Al-Pt (2 wt.%), rapidly solidified alloy, metastable phase formation and decomposition 79−52194
Al-Si, deformed, local lattice rotations at second phase particles 80−25709
Al-Si, inoculated with NaCl+KCl+NaF, effect on morphology of eutectic columns *(Russian)* 79−15684
Al-Si-Cn-Mg, alloy AL32, ageing of castings produced by pressure die castings 78−56650
Al-Si-Sr phase diagram *(Russian)* 78−15363
Al-silicide-Si systems with $CoSi_2$, $Pt_xNi_{1-x}Si$, and $MoSi_2$ as silicide, diffusion, compound form., and microstructure 80−34253
Al-Ti-B alloys, phase comp. and distrib. of components, X-ray obs. *(Russian)* 79−52164
Al-Zn, ageing alloy, zonal decomposition stage, new effects in X-ray diffr. anal. *(Russian)* 79−4982
Al-Zn, dil. alloy, ageing and reversion, annealing curves, X-ray obs. 78−88485
Al-Zn, GP zones, effect of Si, Ag, Mg on transport props. 77−16588
Al-Zn, Guinier-Preston ellipsoidal zone model of X-ray scatt. *(French)* 77−84568
Al-Zn, metastable solvus curve, struct. changes 77−55950
Al-Zn, precipitation struct. and phys. props. effect of miscibility gap *(German)* 78−92265
Al-Zn, resistivity calc. for age-hardened alloy 77−73284
Al-Zn, X-ray diffr. after omnidirectional compression *(Russian)* 80−88262
Al-Zn 6.8 at.%, Guinier-Preston zones *(French)* 79−87640
Al-Zn (10 wt.%), ageing at low temp., solute conc. fluctuation effects *(Japanese)* 79−4969
Al-Zn (15,16,18 at.%) alloys, coherency spinoidal curve position determ. 77−52281
Al-Zn (18 at.%), position of coherency spinodal curve 78−23660
Al-Zn (2 and 4 wt.%), ageing and elec. cond. reversion *(Japanese)* 79−4983
Al-Zn (22 at.%), X-ray scatt. obs. of segregation *(French)* 79−96032
Al-Zn (30 wt.%), metastable phases, transformation kinetics, quenching rate effects meas. 77−55960
Al-Zn (30 wt.%), precipitation sequences and transformation kinetics, X-ray diffr. and TEM obs. 77−55959
Al-Zn (6.8 at.%), synchrotron radn. use in X-ray scatt. *(French)* 79−47723
Al-Zn (7 at.%), liquid quenched, early stage phase separation, exam. 78−68698
Al-Zn alloy, metastable phases formed at 200°C, room temp. stability 80−16315
Al-Zn alloy, resist. and X-ray small angle scatt. during GP zone form., theory *(French)* 79−29070
Al-Zn alloys, relation between microhardness and average radius of Guinier-Preston zones 78−95811
Al-Zn alloys, room temp. decomp. of metastable phases precipitated at 200°C 78−84814
Al-Zn-Cu (22, 0-3 at.%) alloys, coherent spinodal curve 79−87605
Al-Zn-Fe-Si, Fe and Si effects on precip., TEM and X-ray diffr. obs., ageing at 90°C 77−48439
Al-Zn-Mg, Guinier-Preston zones, comp. and contrib. to elec. resist. 80−16316
Al-Zn-Mg, solid soln. decomp., 20 to 200°C 79−38830
Al-Zn-Mg (3.2, 2.2 wt.%) alloy, GP zone reversion, η' of formation, quant. investig. 77−4784
Al-Zn-Mg (3.6, 1.95 wt.%), ageing and plastic deform., effect on structure, electron microsc. and X-ray diffr. study *(Russian)* 80−81108
Al-Zn-Mg (4.8, 1.2 wt.%), quenched, Guinier Preston zones formation 80−45273
Al-Zn-Mg alloy 7075, effect of thermal and mechanical pretreatments, on Guinier-Preston zone 78−39817
Al-Zn-Mg alloys, extra-resistivity of coherent precipitates calc. using X-ray small angle scattering intensities 80−3050
Al-Zn-Mg alloys, precipitation behaviour *(German)* 78−39780
Al-Zn-Mg-Cu alloy 7075, SCC from T6 to overaged T7X 77−90487
Al-Zn-Mg(3.2, 2.2 wt.%), deform. strengthened by Guinier Preston zones 77−52343
Al-Zn(Ag)-Mg, metastable T′ phase 77−21151

X-ray diffraction examination of microstructure continued
Al-Zn(10 at.%), supersaturated solid soln., structural charact. of decomposition 77−70027
$Al_2Be_3(Si_6O_{18})$, beryl single crysts., dislocations obs., X-ray topography *(French)* 79−37709
$Al_2Be_4(Si_6O_{18})$, beryl single crysts., growth defects study using X-ray topography *(French)* 79−37710
AlN, prep. and charact. of ultrafine powders 80−2983
AlO_2, corrosion resistance of phosphate bonded castable, and dense fired types in steam CO at 199°C 79−20222
α-Al_2O_3, adsorption of $H(H_2)$, microweighing and X-ray obs. *(German)* 78−51825
Al_2O_3 and Al_2O_3-Y_2O_3, plasma spraying, microstruct., porosity and adhesion 77−32710
α-Al_2O_3 CVD and Czochralski grown crysts., imperfection anal. comparison 79−78868
Al_2O_3, detonation coating, porosity, electrical strength, phase anal. *(Russian)* 77−69204
Al_2O_3, layer, obtained by reactive evap., surface struct. and morphology *(Polish)* 79−28242
Al_2O_3 plasma-sprayed, struct. and thermal diffusivity 79−86932
Al_2O_3, powder, phase composition, sintering, effect of explosive treatment 77−21079
Al_2O_3 refractories, stability of refractory bond phases in steam-CO atmosphere 79−24634
Al_2O_3 sintered surfaces, premetallizing with Mo-Mn-SiO_2 79−47792
Al_2O_3 sintering in liq. phase presence, particle rearrangement 79−29004
Al_2O_3, sintering with $SrTiO_3$ admixture *(Polish)* 78−19699
Al_2O_3 substrates, tape-casted, fracture strength analysis 80−60948
Al_2O_3-B_2O_3 system, phase comp. and sorption props., Al salts chem. nature influence 79−51426
Al_2O_3-$Eu_2O_3(Gd_2O_3)$, phase diagrams at high temps. exam. 78−44114
Al_2O_3-SiO_2 glasses, phase decomp., small-angle X-ray and neutron scatt. study 79−14688
Al_2O_3-Sm_2O_3, phase diagram at high temps. *(Japanese)* 78−19732
Al_2O_3-TiO_2 coating, prep. by plasma arc spraying and characterisation 79−23873
Al_2O_3-TiO_2-MgO.$2TiO_2$, exam. of solid solutions by X-ray phase analysis 79−95981
β-Al_2O_3.Na_2O, ceramic tube fabrication, crystallite preferred orientation, ionic cond. 77−8781
$AlPO_4$, twinning and phase transform., X-ray diffr. obs. 77−47466
Al_2TiO_5, eutectoid decomposition, kinetic study *(Japanese)* 77−55941
AlZn alloys, ageing zone stage duration depend. on quenching temp. *(Russian)* 77−55993
Am, polymorphic transform. exam. by hot stage X-ray diffr. anal. *(Russian)* 79−24518
Am, polymorphic transforms. obs. *(Russian)* 78−6153
Au bicrystal, grain boundary thickness, meas. using X-ray techniques 80−34011
Au, bicrystals, large-angle twist grain boundaries, X-ray diffr. obs. 79−90672
Au, electron irradiated, interstitials and their clusters, diffuse X-ray scatt. study 80−33997
Au quenched single crysts., vacancies, diffuse scatt. and resist. obs. 80−33994
Au, tilt boundary, small- and large-angle [001], X-ray diffraction study 79−82238
Au/Ti thin film, temp. and humidity effect on interdiffusion 79−51317
Au-Ag-Cd, martensitic transformation, preceding struct. anomaly 78−68692
Au-Co electrodeposits, heating effect on microstruct. and surface topography 77−43456
Au-Cu, dil., electron irradiated, interstitials and their clusters, diffuse X-ray scatt. study 80−33997
Au-Fe, polygonisation, recrystallisation, precipitation microstruct. without external plastic deform. 79−43276
Au-Ge, liquid quenched, exam. of phase decomposition 78−48371
Au-In-Pb, $AuIn_2$-In-Pb portion of phase diagram 77−32562
Au-Ni (30 at.%), singularities of struct. state, diffuse electron and X-ray scatt. *(Russian)* 79−4945
Au-Pt-Pd-Ag-Cu, commercial dental alloy, age-hardening charact. 80−89235
$Au_3Cu_{1-x}Ag_x$, phase relations, X-ray diffr. and differential thermal anal. 80−108395
Au_3Zn(Cd), long-range ordered, periodic antiphase domain boundary struct., X-ray diffr. obs. 79−95028
B fibre reinforced Mg, fibre-matrix interfacial reactions 80−20043
B-C system, region of existence of B_4C phase 78−76636
B_4C, effect of fast neutron irradiation on struct. 78−26597
BN, hardness rel. to temp., phase compositions 78−60752
BN, polycryst. cubic, props. 80−21013
BN powder, wurtzite sphalerite struct. phase transition, effect on substruct. 80−25690
BN, wurtzite type, phase and struct. changes at high temps. 77−12618
BN/BN composites, prep., mech. props. 77−21080
Ba-Al-Si system, phase diagrams construction by simplex designing method 78−6899
Ba-Nd, phase diagram, microstruct., X-ray, chemical and thermal diffusion anal. *(Russian)* 78−52761
BaO-La_2O_3-GeO_2, exam. of glass forming region, properties and crystallisation 78−88454
BaO-TiO_2-Nd_2O_3, exam. of compositional and dielectric props. 79−33601
$BaTiO_3$, polycrystalline, X-ray diffraction, Curie temp., lattice defects, phase changes 79−99830
$BaTiO_3$-CeO_2 liquid immiscibility region, X-ray diffr. anal. 80−50611
$BaTi_4O_9$ effect of chemical treatment on loss quality, at microwave wavelengths 79−34159
$Ba_2Ti_9O_{20}$, effect of chemical treatment on loss quality, at microwave wavelengths 79−34159
$Ba_3(VO4)_2$, determination of enthalpies of formation, from heats of solution 80−2182
Be bronze BrB2, quenched deformed, substruct. and props., effect of prerecrystallisation annealing *(Russian)* 78−60677
Be, phase struct. *(Russian)* 78−15401
Be-Co (0-50 at.%) alloys, thermal, metallographic and X-ray anal., phase diagram *(Russian)* 78−56611
Be-Si-O-N polytypes, X-ray study 78−27496
Be_2SiO_4, phenakite, flux grown single crysts., twinning study by hydrothermal etching and X-ray diffr. 80−107271

X-ray diffraction examination of microstructure continued
Bi-Sb, conditions for dendritic crystallisation, accompanying rapid cooling *(Russian)* 79−34020
$Bi_4Ti_3O_{12}$ ceramics, ferroelectric, hot-forged, grain orientation and dielectric props. 80−40076
C fibre, prep. from benzene, struct. changes with stepwise heat treatment up to 3000°C 77−12649
C fibres, from mesophase pitch, resist. magnetoresist., EPR and mech. props. rel to struct. 79−78116
C fibres with large breaking strain, prep., mech. props., struct., appl. 78−44077
C, glassy, LMSC process prepared, exam. of props. by TEM and X-ray anal. 78−63675
C pyrolytic, paracrystn. nature, bimodal statistics anal. 79−77451
Ca-Sb, phase diag. 77−52284
$CaAl_2O_5$, form by interdiffusion of CaO and Al_2O_3 79−28998
$CaCO_3$, growth dislocations obs. using Lang X-ray topography 78−2133
CaF_2-AlF_3, phase equilibria, DTA and X-ray diffr. study 78−27493
CaF_2-LaF_3, solid soln. with fluorite struct., phase diagram 79−100119
CaO-Al_2O_3-SiO_2-ZnO, continuous unidirectional crystn. of fibrous metasilicates from melt 78−95739
CaO-MgO-Al_2O_3-SiO_2-ZnO, continuous unidirectional crystn. of fibrous metasilicates from melt 78−95739
CaO-MgO-CeO_2, fired, phase equilibrium diagram, 1700 to 1200°C 78−92248
CaO-SiO_2-ZnO continuous unidirectional crystn. of fibrous metasilicates from melt 78−95739
$(CaO)_3SiO_2$, effects of polymorphism on hydration, X-ray and TEM obs. *(Japanese)* 79−20046
$Ca_{10}(PO_4)_6(OH)_2$, synthesis and characterisation in dense polycryst. form 77−4749
$Ca_3(VO_4)_2$-$Mg_3(VO_4)_2$, exam. of phase composition and phase diagrams 79−1851
Cd films, vacuum deposited, microstruct. exam., X-ray diffr. profile anal. 79−46973
Cd, single cryst., Burgers vector determ. of perfect dislocations obs. by X-ray topography 79−37711
Cd, thin film, vac.-deposited, X-ray diffr. struct. obs., props. 79−37937
Cd, vacuum evaporated film, HCP, microstruct., X-ray obs. 80−10827
$Cd_xHg_{1-x}Te$, correlation between structural and chemical inhomogeneity *(Russian)* 80−49484
$Cd_xHg_{1-x}Te$, X-ray topographic assessment 79−37716
$Cd(OH)_2$, highly dispersed precipitate, microstruct. and exchange props. 77−36793
CdS, single cryst., surface treatment effects on photoluminesc., struct. and optical props. *(Russian)* 78−15224
CdS sprayed film, prep., optical props., struct. and comp. 79−78875
CdS:Cu, In, Ga, spray deposited films 78−71713
CdS-CdTe double layers on various GaAs surfaces, morphology and crystallography 80−34326
CdSe evaporated films, struct. and epitaxy, TEM, RHEED, and X-ray diffr. obs. 79−77939
CdSe, X-ray topography 77−89441
CdTe, single cryst. sublimation growth, X-ray topographic characterisation 80−29866
CdTe-ZnS ternary mutual system, phase diagram 80−20904
Ce, cold working, deform. induced struct. effects 80−25719
Ce-Ga, phase diagram *(Russian)* 78−27478
Ce-Mn-Co, temp. conc. limits of homogeneous compounds *(Russian)* 78−23666
Co allotropic transformation, X-ray diffr., analysis exam. *(Russian)* 79−34027
Co film, evaporated, columnar struct. depend. on degree of texture 80−54567
Co film, texture and adsorption of CO *(German)* 77−24485
Co-Al-Nb, monovariant directionally solidified eutectics, struct. and mech. props. *(Russian)* 78−92254
Co-B-Si ternary system, partial phase diagram, Co rich region 77−52293
Co-Cr-Ni superalloy Mar-M509 standard and Mo modified, phase anal. 77−63675
Co-Fe (2.92 to 30.05 wt.%), determination of phase equilibrium diagram *(Japanese)* 78−48374
Co-Ga-B, phase diagram, metallographic, X-ray and electron probe anal. 78−92241
Co-Ge-Te system, phase equilib. 80−20908
Co-mischmetall system, phase relations, microstruct., mag. props. 80−104118
Co-Mo-Cr-Si Laves phase, sputter deposited, struct. and wear props. 77−40477
Co-Ni alloys, electrodeposited, struct., internal stress, and mag. props. 78−95471
Co-Ni-Cr-Mo, mech. props., effect of twinning and FCC to HCP transform. 77−4779
Co-Pt, mag. annealing, form. of ordered phase, study using X-ray scatt. *(Russian)* 80−81052
Co-rare earth permanent magnet, grain alignment, metallographic method using eutectoid transform, of Co_5R 77−9003
Co-Sb-Te ternary system, crystn., heat treatment and phase equilib. 79−52156
Co-Se, P-T diagram and structural study 78−56622
Co-Si-Ge system, X-ray diffr. exam., band struct. *(Russian)* 78−56623
Co-Sm permanent magnet, grain alignment determ., metallographic method using eutectoid transform. of Co_5Sm 77−9003
Co-Ti-C, secondary precipitation and allotropic transform., TEM obs. 80−108453
$CoFe_2O_4$ synthesis, chem., thermal histories rel. to fine cryst. struct. 79−43186
CoS-MnS(ZnS)(CdS), phase study by X-ray obs., lattice const. 79−1854
$Co_2Ti_{2-2x}Fe_{2x}O_{6-x}$ solid solution, extended defect model, X-ray diffr. and electron microscopy *(French)* 77−47446
Cr, antiferromagnetic spin-density-wave domain and size and behaviour, X-ray and neutron topography 79−42793
Cr bronze Sn, recrystn. props., hot rolling, annealing, polygonisation *(Russian)* 80−55419
Cr, CVD on Ni, reaction mechanism, growth rate and struct. obs. 80−39476
Cr, deposited by high rate sputtering, mech. props. 77−36630
Cr foil, laser irradiated, low-angle X-ray scatt., angular block misalignment and hardness *(Russian)* 80−103413

X-ray diffraction examination of microstructure continued
Cr-C(N) coating, deposited by hollow cathode discharge, characterisation 78−11371
Cr-Fe (30 wt.%) alloys, refined fine comminution 78−60598
Cr-$NdAlO_3$, dielectric films, phase composition and structure 80−39464
Cr-Sm-Pr, Sm and Pr additions and plastic deform. effects on texture *(Russian)* 77−55983
Cr-W-O, phase relations, thermodynamic props. of $CrWO_4$ and Cr_2WO_6 80−104120
Cr_2O_3, active, block growth in crystallisation 77−85972
Cr_2O_3 polycrystalline powder, crystallite sizes and surface areas 77−66086
Cr_2O_3 X-ray diffr. studies, crystallite size, phase transformation 77−21138
Cr_2O_3-MoO_3, physicochem. investig. of phase struct. 77−8807
Cr_2O_3-WO_3, phase relations 78−92249
Cu alloy, fretting corrosion, exam. of secondary structures 79−100292
Cu alloys, microconductors, cast, struct. and physical props. exam 78−44232
Cu, bright galvanic coatings, crystallite size determ. 79−66221
Cu, crack nucleation and stage I propag. in high strain fatigue, mechanism 78−52937
Cu, cross-slip at low stresses 77−11564
Cu crysts., thick imperfect, dynamical X-ray diffr., topographic effects 77−68898
Cu, diffracted beam-transmitted beam Borrmann X-ray topography 79−86795
Cu, dislocation-free melt growth conditions, and perfection obs. 78−3025
Cu, electron irradiation, vacancy clustering study by small angle X-ray scatt. 79−14845
Cu, fibre texture of filament produced by glass coated melt spinning 77−85966
Cu foil, laser irradiated, low-angle X-ray scatt., angular block misalignment and hardness *(Russian)* 80−103413
Cu, plastically deformed, containing dislocation distribs., X-ray diffr. line broadening 77−43218
Cu plates, thin, dislocation-dislocation interaction inducing cross-slip, X-ray topographic anal. 80−49233
Cu, prismatic dislocation loops revealed by X-ray topography and etching 77−11563
Cu, rolled at room temp. and 200°C, variation in props., hardness and X-ray meas. *(Russian)* 77−73285
Cu, single crysts., cyclically and unidirectionally deform. X-ray diffr. study 80−89319
Cu, struct. changes in single cryst. under influence of static and dynamic stresses *(Russian)* 78−92300
Cu, whiskers, Ar^+ ion implanted, X-ray study on lattice defects *(Japanese)* 79−99230
Cu, X-ray and microhardness meas. at high strain rates *(German)* 78−3184
Cu, X-ray studies of fusion energy neutron damage 78−51593
Cu, zigzag stress-induced, X-ray topography obs. dislocations 79−99205
α_2-Cu-Al, antiphase period and tetragonality 78−15374
Cu-Al, α_2 phase form. process 77−48464
Cu-Al, heavily deformed martensites, annealing 79−38873
α-Cu-Al, short range ordered, struct. and new superlattice phase 78−52756
Cu-Al (11.47 wt.%), high temp. phase transforms., effect of pre-exposure to neutrons 79−20045
β'Cu-Al martensite, stacking order, disorder anal. by continuous Fourier transformation of diffracted intensities 80−39115
Cu-Al-Fe-Mn (10,3,2 wt.%), phase comp. struct., continuous cooling from β-phase effect 79−24499
Cu-Al-Ni, phase diagram associated with stress induced martensitic transform. 79−8272
Cu-Au, long-range ordered, periodic antiphase domain boundary struct., X-ray diffr. obs. 79−95028
Cu-Bi (0.02 wt.%) alloy, intergranular fracture, Kossel X-ray diffr. in SEM obs. 80−108579
α-Cu-Ga (3.4-15 at.%) alloy, cold-worked, lattice imperfections obs. 77−55291
Cu-Ga porous solid formed by shock compression 80−29905
Cu-Ge, primary coplanar slip, role in deform. of FCC crystals *(Japanese)* 77−52412
Cu-Ge (10-12 wt.%), intermediate ξ'-phase form. during deform. *(Russian)* 78−19747
Cu-Ge single cryst. containing heavily faulted regions, X-ray diffr. profiles 80−24462
Cu-Mg(Sn) precipitating phase nuclei, diffuse X-ray scattering intensity determ. *(Russian)* 77−86031
Cu-Ni, diffusional homogenisation in compacted powder blends, X-ray diffr. line profile analysis 78−80491
Cu-Ni, sintered, props. and degree of nonhomogeneity 80−20848
Cu-Ni, sulphidation between 653 to 770K, exam. of scale morphologies, using X-ray diffr., and electron microprobe anal. 78−88559
Cu-Ni alloy, dislocation density during deform., comparison of electron microscopy and X-ray diffr. *(Russian)* 79−5002
Cu-Ni bicrystals, epitaxial growth, chemical interdiffusion, X-ray diffr. line profile anal. 79−1527
Cu-Ni-Al, ageing charact., optical TEM, X-ray, hardness obs. 79−29079
Cu-Ni-Al, grain boundary reaction under isothermal ageing at 623 to 973K *(Japanese)* 79−70090
Cu-Ni-Be (30, 0.5 wt.%), grain boundary reaction after ageing and quenching, obs. *(Japanese)* 79−70089
Cu-Ni-Mn (20,20wt.%), structural transform., X-ray and hardness study *(French)* 78−39760
Cu-Ni-Sn (10, 6 wt.%), spinodal decomposition, X-ray and electron diffr. study 80−81063
Cu-Ni-Sn (15, 8 wt.%), prior deform. effect on spinodal age hardening 80−108465
Cu-Ni-Sn (15, 9 wt.%), age hardening accompanying phase transition 78−64551
Cu-Ni-Zn alloy, FCC, cold-worked, comp. effects 78−3143
Cu-Pt, quenched, microdomain model anal. of diffuse X-ray scatt. 79−52276
Cu-SiO_2, deformed, lattice rotations at second phase particles 80−25709
Cu-Sn (25 wt.%), liq., struct. from thermodynamic and diffr. studies 80−6350
Cu-Ti, lattice parameter change during ageing *(Japanese)* 78−35411
Cu-Ti (4 wt.%), ageing, X-ray study 77−56012
Cu-Ti alloys (0.5 to 4.0 wt%) ageing charact. determ. 79−20089

X-ray diffraction examination of microstructure continued
α-Cu-Zn, whiskers, X-ray topography, substruct. 77−11831
Cu-Zn-Al, reversible shape memory effect associated with $\beta_1 \rightleftarrows \beta_1' \rightleftarrows \alpha_1'$, transform. *(Japanese)* 79−43242
Cu-Zn-Sn (24-34, 1.0 wt.%), cold-worked microstruct., X-ray diffr. obs. 80−3088
$Cu_3Ag_{1-x}Au_x$, phase relations, X-ray diffr. and differential thermal anal. 80−108395
$CuAl_2$, constitutional defect struct., from X-ray and density meas. proposed substitutional-vacancy model 79−37696
Cu_3Au, ordered and disordered, cavitation induced erosion 77−16743
CuAu(Pt), quenched, short-range order X-ray diffuse scatt., microdomain model anal. 79−96043
$Cu_2{}^{I}B^{II}C^{IV}X_4$, ($B^{II}$=Zn, Mn, Fe, Co; C^{IV}=Si, Ge, Sn; X=S, Se), X-ray elec. and mag. meas. 79−65660
$Cu_{0.5}Fe_{2.5}O_4$, ferrite, determination of specific heat at 298-800K 80−2579
Cu_2MnAl, plastically deformed, domain struct., X-ray diffr. and electron microscope obs. *(Russian)* 79−20110
Cu_2O, creep substruct. under compression, X-ray diffr. study 78−95785
CuPt alloy, equiatomic, ordering processes, anisothermal annealing exam. *(Japanese)* 78−39765
Cu_2S, molten, oxidation, exam. of product phase composition by X-ray anal. *(Russian)* 79−34166
Cu_2S-Tl_2S system, phase diagram 80−20906
CuZn32 bands, mechanical props. anisotropy after annealing at variable heating rates 77−90364
Dy, magnetoplastic deform., 70-90 kOe, 4.2K 77−8376
Dy, single crystal, plastic and magnetoplastic deform. 77−63713
$ErFe_2$, Czochralski growth, and cryst. quality determ. 77−8742
Er_2O_3-ZrO_2, subsolidus phase relations, X-ray diffr. and thermal expansion exam. 78−31382
Eu-Te, chalcogenides, exam. of crystal-chemical charact. 79−1407
Fe, 90° walls, stable orientations, theory and X-ray observations *(Japanese)* 80−60359
α-Fe, $(\bar{1}\,\bar{1}2)$ $[\bar{1}\,\bar{1}\,\bar{1}]$ anti-twinning slip system, low temp. strengthening, dislocation struct. 77−21164
Fe alloy, (110) [001] texture development by recrystallization and normal grain growth 77−32594
Fe alloy, oxide dispersed, mech. alloying, microstruct. 77−25063
Fe alloy, surface layers examination, X-ray method 78−35606
Fe, Armco, inter- and intragranular sulphidation 80−55570
Fe, Armco, recrystn., structural inheritance charact., X-ray and internal friction obs. 79−57017
Fe, armco, X-ray diffractometrical sub-structure analysis *(German)* 77−68894
Fe, cast, Ce hypoeutectic, new phase formation sequence during crystallisation, X-ray obs. *(Russian)* 78−95731
Fe, cast, high Mg content (0.33%), exam. of phase composition charact. 78−84780
Fe, cast, inoculated with Ce, exam. of phase composition 78−56620
Fe, cast, Mg, despheroidising effect of Bi, Sn on graphite in alloy 78−56670
Fe, cast, Mg-Sb, despheroidising composition and distribution of phases, X-ray obs. *(Russian)* 78−95732
Fe, cast, white, high Cr, phase composition, B effect 80−104172
Fe, cast, with Mn, high S, exam. of sulphide phases, cocrystallisation during solidification 78−56646
Fe, cold rolled, struct., transmission Kossel patterns obs. 77−48451
Fe, creep, effect of H_2 on struct. 77−16652
Fe, creep at 77, 295K, formation of five struct. 80−60926
Fe, electrolytic, oxidation in melting *(Korean)* 78−19946
Fe, fibre texture of filaments produced by glass coated melt spinning 77−85966
Fe film, evaporated at oblique incidence, columnar and textural struct. *(Japanese)* 77−62776
Fe films, vacuum evaporated, exam. of texture for various vapour beam incidence angles *(Japanese)* 78−48318
Fe, granular film, microstructure using X-ray, electron diffr. and TEM 79−65344
Fe, high-purity single crystals, X-ray topography and double-crystal diffraction 80−92534
Fe, liquid, N solubility and AlN precipitation 79−11630
α-Fe, nitrided, aging at room temp. 80−71679
Fe, pure, initial grain boundaries effect on cold-rolling and annealing textures *(Japanese)* 80−35205
Fe, wear of surface due to friction, surface hardening 78−44227
Fe whiskers, cryst. morphology and dislocation struct. study using optical and SEM, X-ray diffr. topography 79−23876
Fe, whiskers, high strength, polycrystalline, microstruct. obs. 79−33214
Fe whiskers, struct., dislocations, mag. domains *(Polish)* 79−33210
Fe, zone refined, strained, substructural changes during annealing *(Slovenian)* 78−84845
Fe-Al, single crystals, deform. at high temps. 80−81125
α-Fe-Al(Zn), (111) fibre texture development through diffusion process without α-γ transform 79−100170
Fe-B_4C sintered material, mech. props. and struct. charact. 79−100084
Fe-Be (16.5 or 19.5 at.%), four-phase model of struct. in initial ageing stages *(Russian)* 78−48430
Fe-C solid solution, martensite, carbide decomposition, electron microscopy and X-ray diffr. obs., review *(Russian)* 79−33998
Fe-C-Si, struct. and constitution on quenching from liquid state *(Russian)* 77−52309
Fe-C(0.47 wt.%) austenite, obs. of morphology and crystallography of proeutectoid ferrite 77−8837
Fe-Co-Cr, alloy K25Kh15, phase tranforms., nucl. gamma reson. and X-ray diffr. meas. *(Russian)* 77−44241
Fe-Co-Cr, Cr effect on struct. of ordering 78−35407
Fe-Co-Cr, magnetic, phase transform. obs. *(French)* 79−47676
Fe-Co-Cr, solid state phase equilib., isothermal sections determ. 800-1300°C 79−91623
Fe-Co-Ta for semipermanent magnets *(French)* 79−47675
Fe-Co-V(-Ni), annealing effect on microstruct. rel. to mag. and mech. props. 80−89267
Fe-Cr-Al-Ce, Ce effect on high temp. oxidation 79−100301
Fe-Cr-Al-Ce, high temp. oxidation *(Japanese)* 78−11413
Fe-Cr-Al-TaC (13.5, 3.7, 9 wt.%) eutectic alloy, directionally solidified, thermal cycling effects on microstruct. 77−32686
Fe-Cr-C system at 870°C 77−28782
Fe-Cr-Co hard-mag. alloys, fine cryst. struct. *(Russian)* 77−66706

X-ray diffraction examination of microstructure continued
Fe-Cr-Mo-Ti (13, 1.5, 3.5 wt.%), equilibrium studies on chi-phase strengthening 79−24496
Fe-Cr-N (5.9, 0.5 wt.%), martensitic, tempered, fine struct. 77−25079
Fe-Cr-Nb-C, X-ray microanal. of carbide phases rel. to Nb conc. *(Russian)* 78−88467
Fe-Cr-Ni, textured ($\alpha+\gamma$) alloy, α' lath martensite formation 78−95749
Fe-Cr-Ni(Mn)(Ni-Mn)-C alloy, carbide-austenite equilibria, 1173 to 1373K, microscopic and X-ray obs. 78−44085
Fe-Cr-O system, phase relations at 1200°C using diffusion couple technique 80−89205
Fe-Cr-V-C, X-ray microanal. of carbide phases rel. to V conc. *(Russian)* 78−88467
Fe-Cr-(C), oxidation, grain size and growth effects *(Japanese)* 77−48583
Fe-Cr-(Co), decomposition of solid soln. in mag. field, neutron and X-ray diffr. study *(Russian)* 78−68694
Fe-Ga, constitution between 10 and 50 at.% Ga, heat treatment depend., BCC phases *(German)* 77−90325
Fe-Ga, solid soln., order-disorder transform. *(French)* 78−3121
Fe-Mn, ε-martensite, preferred orientation and constitution, reverse pole figures *(Russian)* 80−104178
Fe-Mn, γ to ε phase transform. induced by high press. and plastic deform. 78−68686
Fe-Mn (10 to 14 at.%), martensitic transforms., dilatometric effects and X-ray diffr. meas. *(Russian)* 78−6922
Fe-Mn alloy, splat-quenched, martensite formation obs. 77−44247
Fe-Mn alloys, quantitative phase anal., correction factor for texture 79−52528
Fe-Mn-C, anomalous changes in austenite and martensite lattice parameters 80−50636
Fe-Mn-Cu-C, Cu effect on ε'-martensite, X-ray obs. of heating effects *(Russian)* 79−87667
Fe-Mn-Nb-V, high Mn, dispersion strengthening 77−16602
Fe-Mn-Ni base maraging alloys, age hardening 79−74170
Fe-Mo (13-20 at.%) binary alloys, spinodal decomp. on ageing, TEM and X-ray diffr. study 80−97503
Fe-Mo alloys, spinodal decomp. and modulated struct. form. on ageing *(Japanese)* 79−100184
Fe-Mo-Cr(Ni)(Mn)-C, carbide-austenite equilibria, 1173 to 1373K, microscopic and X-ray obs. 78−44085
Fe-Mo(V), nitrided by const. activity ageing, X-ray studies 77−32720
Fe-N (10 at.%), structural transforms., expt. investig. *(Russian)* 77−12613
Fe-Ni, α to γ transformation, changes in Young's modulus and electrophysical props. *(Russian)* 79−20042
Fe-Ni base amorphous alloy, crystallisation 77−84660
Fe-Ni single crystal, pseudo-Kossel study of fibrous substruct. 77−1835
Fe-Ni-Al-Co-Cu-Ti alloy YuNDKT, nature of X-phase heat treatment effect on microstruct. 77−90380
Fe-Ni-C alloy, splat-quenched, martensite formation obs. 77−44247
Fe-Ni-C austenitic alloy, banded struct. formed by deform. 80−71713
Fe-Ni-Mn martensitic alloy, precipitation 77−12630
Fe-Ni-Mo, small angle X-ray scatt. study, pre-precipitation phenomenon obs. *(French)* 78−19757
Fe-Ni-Ti, martensite, tetragonality, X-ray obs. 77−63665
Fe-Ni-Ti (30, 3 wt.%), reverse martensitic transform. and memory effect *(Russian)* 79−87627
Fe-Ni-Ti (30, 6 wt.%), austenitic, discontinuous coarsening of lamellar cellular precipitates, morphology 79−78967
Fe-Ni-V, nitrided austenitic alloys, modulated substitutional interstitial solute atom clustering 79−74160
Fe-Ni-WC hard alloy, struct. and props. 79−79007
Fe-P-C, amorphous alloy, crystallisation 79−100112
Fe-Si, recrystallization, in situ studies, appl. of X-ray synchrotron topography 78−35610
Fe-Si (2.4 wt.%), simulation of X-ray topographies of ferromag. domains *(French)* 77−77070
Fe-Si (3 wt.%), grain oriented, mag. domain movements 79−82815
Fe-Si (3 wt.%), hysteretic losses, domain struct. and cryst. defects 79−19747
Fe-Si (3 wt.%), mag. domain wall contrast in synchrotron X-ray topographs 80−75792
Fe-Si (3.1 wt.%), anisotropy of electromigration of substructure of polygonisation *(French)* 77−28047
Fe-Si (3.25 wt.%), single crystals and polycrystals, cutting surface texture 79−20291
Fe-Si (3.5 wt.%) plastic deform., slip initiation, X-ray topography study 79−47750
Fe-Si as grown crystal, dislocation study by etching and X-ray topography 78−47377
Fe-Si single crysts., interaction of {110} 90° walls with lattice imperfections 80−39807
Fe-Si-N alloy, BCC→FCC transform., martensitic character obs. *(Russian)* 78−48397
Fe-W-C, eta carbides at 1250°C 77−36506
Fe-W-C-Cr, eta carbides at 1250°C 77−32581
Fe-WO_3 system, struct. phase exam. by optical microscopy and X-ray diffr. 78−31389
Fe-Zn, homogeneous intermetallic cpd., synthesis and charact., δ_1-phase 79−87616
Fe-Zn, phase diagram, ferrite-austenite phase boundaries, X-ray diffr. exam. *(German)* 78−80510
Fe_3Al, vacancy conc. and ordering conc. 78−18639
FeB_x coatings on steel, formed by B diffusion, pack cementation process, microstruct. and mech. props. 78−15592
FeC_x ($x\leq0.05$), splat-quenched, struct., elec. and mag. props. 77−21187
$FeGe_2$, single cryst. perfection depend. on growth rate and direction 80−55284
$Fe_{1.67}Ge$, Mossbauer and X-ray expts. 79−1734
β-Fe_5Ge_3 formation in isothermal sintering, phase transition kinetics 80−89197
Fe_2MnAl, plastically deformed, domain struct., X-ray diffr. and electron microscope obs. *(Russian)* 79−20110
Fe_2O_3 haematite platelets, growth and cross-connection in consolidation of haematite pellet *(Chinese)* 80−104186
α-Fe_2O_3, hematite, weakly ferromag. domain struct., X-ray topography obs. 79−28551
α-Fe_2O_3, prep. by evaporative decomposition of $Fe(NO_3)_3.6H_2O$ soln. 79−20011

X-ray diffraction examination of microstructure continued
α-Fe_2O_3, single cryst., hematite, X-ray topographic obs. of domain struct. changes in external mag. field 80−88785
Fe_2O_3, X-ray diffr. studies, crystallite size, phase transformation 77−21138
Fe_2O_3-Al_2O_3 mixed oxide, X-ray diffr. and elec. cond. 80−79954
Fe_2O_3-Cr_2O_3, crystalline size and phase transform. study by X-ray diffr. 77−21138
γ- Fe_2O_3-Fe_3O_4, lodestone, microstructure and mag. props., source of mag. hardening 79−82828
Fe_2O_3-WO_3, phase relations 78−92249
Fe_3O_4, magnetite crysts., skull melter growth 79−24430
$Fe_{80}P_{13}C_7$, amorphous, rapidly quenched, magnetic props., effect of annealing 77−16701
Fe_3Pt austenite, long range order parameter, temp. depend. discussion 80−97481
Fe_3Pt, premartensitic phenomena *(French)* 79−8297
$Fe_{1-x}S$, NC-type, wave distrib. of vacancies 79−99178
FeSi-Fe_2Si_5 eutectic, $FeSi_2$ formation, annealing temp. and time effects 79−24512
Ga, dislocation structure on melting of nearly perfect crysts., Borrmann topography 77−31663
Ga-As-Se, exam. of phase diagram, rel. to LPE of GaAs:Se 79−1849
Ga-Cu, fast quenching of A15-phases *(German)* 77−36014
$Ga_{1-x}Al_xAs$-GaAs, grown by LPE, direct obs. of dislocations 79−65087
$Ga_{1-x}Al_xAs_{1-y}P_y$-GaAs quaternary heterojunction, misfit dislocation charact. by synchrotron radiation white beam topography 78−63771
$Ga_{1-x}Al_xAs_{1-y}P_y$-GaAs heterojunctions, light-induced misfit dislocation motion, photoluminesc. and X-ray diffr. meas. 79−11200
GaAs, dislocation density effect on polarisation and intensity of reflected $CuK_{\alpha1}$ radiation 77−1131
GaAs, implanted amorphous layer reordering 77−76435
GaAs:Si, stacking fault prod. during heat treatment in As vapour 80−96547
GaAs/AlGaAs DH wafers and lasers, defect struct., X-ray topography 79−50312
GaAs-$Ga_{1-x}Al_xAs$ DH lasers, X-ray topographic obs. of lattice defects rel. to degradation 77−15420
GaInAsP-InP DH layers, lattice deform. and misfit dislocations 79−19473
$Ga_xIn_{1-x}P_yAs_{1-y}$, 111-A and 111-B faces, defect struct., etching and X-ray diffr. obs. 80−2026
GaP, Be-Au and Si-Au ohmic contacts, metallurgical struct. 77−1485
GaP epitaxial layer, crystal defects influence on luminesc. obs. 79−87511
GaP film, deposited by RF sputtering *(Czech)* 78−52667
GaS-YbS system, phase diagram, reacts., thermal, mag. and elec. meas. 79−11578
GaSe, excitation spectra and structural props., X-ray Laue diagrams and optical transmission *(French)* 80−50358
GaTe, hexagonal, vacuum deposited, physical parameters and substruct. 78−2393
Gd, texture formation during cold rolling *(Russian)* 78−92275
Gd-Co based amorphous sputtered films, microstruct. variability and mag. anisotropy, implanted ion effects 80−88459
Gd-Fe-Si, phase diagram 79−52158
$Gd_3Al_5O_{12}$ phase obtained by crystallisation of amorphous $Gd_2O_3.5/3Al_2O_3$ by quenching 78−92224
$GdCrO_3$-$GdAlO_3$ solid solutions 80−20887
$GdFe_2$, Mossbauer sample, X-ray diffr. obs. 78−22737
$Gd_3Ga_5O_{12}$, planar defects, X-ray topography obs. *(French)* 80−2008
$Gd_3Ga_5O_{12}$, X-ray topography and double-crystal diffraction 80−92534
Ge, dislocation motion near surface 79−82219
Ge epitaxial film, misfit dislocations, determination of Burgers vector *(Russian)* 79−33207
Ge, evaporated film, lattice parameters and phase transition temp., surface influence of glass substrates 78−94996
Ge, hot microdeformation and simultaneous X-ray topography apparatus *(French)* 80−38871
Ge monocrystal, dynamic interaction of screw dislocations with flat clusters of dislocations on other slip planes *(Russian)* 79−86800
Ge, single cryst., proton irradiated, defect study using X-ray diffuse scattering 79−95048
Ge single crystals, constitutional supercooling growth conditions, structural and chem. inhomogeneities 80−93473
Ge:As, containing dislocation loops, dynamic scatt. of X-rays, extinction effect 78−47384
Ge-As, supersaturated solid soln., dislocation form. during thermocyclic treatment *(Russian)* 80−3057
Ge-Si-Sb solid soln., struct. peculiarities and mech. props. under weightlessness *(Russian)* 78−23693
Ge-Sn-As system alloys, microstruct., X-ray phase and thermal anal. 77−32564
GeO_2 glass, nonisothermal devitrification kinetics 80−92465
GeTe, quenched, phase transitions and electrophysical props. 79−51250
GeTe-MnTe, heat treatment effect on struct., elec. props. 80−54725
H_xMoO_3, ($0<x\leq2.0$), phase relationships, X-ray diffr. exam. of microstruct. 78−76639
Hf-Co-Ga system, crystal atomic struct. and phase equilibria *(Ukrainian)* 78−84772
Hf-Mo-C, isothermal section of phase diagram at 1400°C, X-ray phase analysis determ. 79−34006
Hf-Mo-C, phase diagram, crystallisation patterns of partial system Mo-HfC-Hf 77−12598
Hf-Nb-Ga, phase equilibria X-ray study at 800°C *(Ukrainian)* 79−95998
Hf-Ni(Cu)-Ge, alloys, phase diagrams and cryst. struct. *(Russian)* 80−25658
Hf-V, superconductivity, X-ray and optical metallography 79−4610
Hf-Zr-Ga, phase equilibria X-ray study at 800°C *(Ukrainian)* 79−95998
HfO_2-Eu_2O_3, phase composition in HfO_2-rich region, X-ray anal. 77−12609
HfO_2-Eu_2O_3, phase equilibrium, 960 to 1900°C, X-ray anal. 78−23688
HfO_2-Gd_2O_3, phase relations 78−72769
HfO_2-MgO system, intermediate phases existence, X-ray diffr. and IR obs. 79−38805
HfO_2-TiO_2, phase relations and thermal expansion 77−21121
$Hg_{1-x}Cd_xTe$, segregation, compositional characterisation 80−107434
$HgCr_2Se_4$:Cd, precipitations during growth by chem. transport method 80−55409

X-ray diffraction examination of microstructure continued
$Hg_{1-x}Fe_xTe$, struct. invest. using X-ray diffr. and electron microscopy 80−75365
Ho-Ga, exam. of phase diagram, using differential thermal and X-ray phase anal. *(Russian)* 79−11555
$HoFe_2$, Czochralski growth, and cryst. quality determ. 77−8742
In, dislocation obs. by X-ray topography *(French)* 79−46661
In-Cd, shape memory *(Japanese)* 79−43243
In-Cd alloy crystal, phenomenological study of FCC⇄FCT transform. *(Japanese)* 79−100140
In-Sn alloy crystals, phase changes and shape memory effect *(Japanese)* 80−108502
In-Tl, electrodeposition from aq. sulphate soln., X-ray struct. 78−84722
In-Tl, single crystal containing Li, X-ray study of FCC⇄FCT transform. *(Japanese)* 80−108435
InP, and InP_xAs_{1-x}, 111-A and 111-B faces, defect struct., etching and X-ray diffr. obs. 80−2026
InP:Zn heavily doped X-ray topography, cathodolum., and TEM obs. 79−99197
InSb, X-ray topographic evidence of asymmetrical pre-yield behaviour 80−75229
InSb:Te, Czochralski cryst. growth, strain configuration study using X-ray anomalous transmission topography 79−23552
β-In_3Sn, decomposition, X-ray powder diffr. study 80−89196
$IrGe_{1.5}S_{1.5}(Se_{1.5})$, new skutterudite relation compounds, prep. and charact. 78−52700
$IrSn_{1.5}S_{1.5}$, new skutterudite relation compounds, prep. and charact. 78−52700
KCl, mosaic struct. 77−7740
KCl, pure and Ba-doped, γ-irrad. effects on intensity distrib. of diffuse X-ray scatt. 77−24329
KCl, spontaneous cleavage, step line propag., macroscopic defects 78−87662
KCl:TlCl, lattice defects, X-ray line profile obs. 80−24455
$KCoF_3$, flux-grown cryst., direction of dislocations, X-ray topography obs. 77−35565
$K_2CrO_4+La_2(NoO_4)_3$, $(Nd_2(NoO_4)_3)$, X-ray phase analysis, IR absorption spectra, and thermogravimetric anal. 79−1944
$KEuHP_3O_{10}$ acid, exam. of thermal decomposition 80−55638
KH_2PO_4, Burgers vector sign determ. for nearly screw dislocations, X-ray obs. 80−59467
$K_2Mg_4Mo_4O_{16}(OH)_2(H_2O)_2$ study of non-stoichiometry *(French)* 78−30604
$KNiF_3$, flux-grown cryst., direction of dislocations, X-ray topography obs. 77−35565
K_2O-Fe_2O_3-SiO_2, subsolidus sector of phase diagram, X-ray obs. 80−40335
$K_2O.4TiO_2$, new fibrous phase 80−20917
La-Fe, liquid quenched, X-ray diffr. and Mossbaeur effect exam. of structure 78−76678
La-Re-B, annealed and quenched, X-ray structural and phase anal. 78−11207
La-Si-As ternary cpd., synthesis, stoichiometry 80−104083
$LaNi_{5-x}Fe_x(Cr_x)$, Fe and Cr electron hydride formation, X-ray and SEM obs. *(Japanese)* 79−43202
La_2O_3-CeO_2, microstruct. of La_2O_3 rich crystallites, electron microscopy and diffr. *(French)* 78−35374
$(LaO)_2S$-$(LnO)_2S$ system (Ln=Y or Lu), TEM, X-ray diffr. and fluorescence spectroscopy 79−64957
(Li,Na,K) $(Nb,Ta)O_3$, pseudo-binary and ternary systems quenched metastable glassy and cryst. phases 80−29935
$LiBa_3Nb_3(Ta_3)(Sb_3)Ti_5O_{21}$, insertion of Li, X-ray and neutron diffr. study *(French)* 78−91324
LiCl-$AlCl_3$, phase diagram determ. by DTA and X-ray anal. *(Japanese)* 78−92250
LiF, plasic deform., cleavage-crack propag., X-ray topography 77−39625
LiF, strong reorientation resulting from creep, X-ray obs. 79−100228
LiF:Co^{2+}, X-ray and electron microscope obs. of CoF_2 precip. morphology 77−31777
$Li_{0.5}Fe_{2.5}O_4$, antiphase domains, broadened X-ray diffr. line anal. 78−26578
Li_2O-BeO-SiO_2, X-ray diffr. exam. of phase equilibrium 78−80522
$LiTaO_3$-SiO_2-Al_2O_3, transparency in relation to microstruct. 78−53005
$Li_{0.44}Zn_{0.09}Fe_{2.47}O_4$, ordering, elect. of V_2O_5 additions 77−35532
Mg cast iron, effect of heat treatment on phase comp., microstruct., wear resistance 77−56006
Mg film, influence of isothermal and thermal cycling on porosity vacuum deposited coatings *(Russian)* 78−87884
Mg, HCP lattice, Huang diffuse scatt. from interstitials 80−88142
Mg, melt grown by Bridgeman method, X-ray topography 78−59770
Mg, recrystallisation after straining by rolling, −25 to 100°C *(French)* 77−59815
Mg, vacancy loop behaviour on high-temp. oxidation, X-ray topography 77−76414
Mg-Ag-Cd, X-ray diff. exam. of phase fields *(Russian)* 79−56957
Mg-Cu(Ni), binary system, nonstoichiometry, of Laves phases, $MgCu_2$ and $MgNi_2$ *(French)* 78−52770
Mg-Ga (6 wt.%), precipitation, lattice const., ageing effects *(Chinese)* 79−43279
Mg-Si (5 wt.%), thermally induced strains, X-ray line broadening 77−4809
Mg-Y-Al alloys, phase equilib. *(Russian)* 80−20890
Mg-Y-Cd, phase equilibria and mech. props. *(Russian)* 80−20894
Mg-Zn (5 wt.%), age hardening, X-ray diffr. anal. *(Chinese)* 80−104173
Mg-Zn-Zr, cast, exam. of phase composition, mech. props. 79−100217
$Mg_{(x+2)/3}T_{(x-2)/3}O_x$ (T=Si, Mg), 145 Å superstructure 79−99143
$Mg_{0.8}Mn_{0.2}Fe_{1.8}Al_{0.2}O_4$, grade 6SChl ferrite, milling conditions effect on fine cryst. struct. and activity 79−24483
MgO, adsorption of $H(H_2)$, microweighing and X-ray obs. *(German)* 78−51825
MgO briquets, prep. by shock compaction and characteris. 79−43178
MgO, Cr bearing basic refractory, prod. from brine MgO 79−83158
MgO, lattice misorientation and displaced vol. for microhardness indentation 78−64617
MgO polycrystals, hot-pressed, changes in preferred orientation on annealing 79−34073
MgO, substructure, X-ray diffraction study, rel. to preparation by thermal decomposition 77−12581
MgO, X-ray and electron diffr. crystallite size determ. *(Polish)* 79−100153

X-ray diffraction examination of microstructure continued
MgO-Al_2O_3-Cr_2O_3 refractory system, phase conversion and props., X-ray anal. 77−90336
MgO-Al_2O_3-Fe_2O_3-SiO_2, cordierite, in ceramic, effect of heat treatment on cordierite content 79−20039
$MgTi_2O_5$, formation of solid solutions, on chemical reduction, X-ray analysis of phases *(Russian)* 79−33072
$Mg_3(VO_4)_2$, determination of enthalpies of formation, from heats of solution 80−2182
Mn cast Fe, W effect on transform. in thin surface layers during dry sliding friction 77−21289
Mn-Al-C, ferromag. alloy, transform. kinetics 80−76229
Mn-Ga (19 to 30 at.%), phase equilib. diagrams, X-ray diffr., thermal expansion, and mag. meas. *(Japanese)* 78−39743
Mn-Ga (19.0 to 31.2 at.%), exam. of phase diagram, using X-ray diffr., thermal expansion and mag. meas. 78−76634
$Mn_xCr_{3-x}O_4$ spinels, miscibility gap boundaries, annealing expts. 77−86012
MnZn ferrites, impurity induced exaggerated grain growth 78−92222
Mo alloys, fractography of deformed samples *(Russian)* 78−19889
Mo, BCC, struct. singularities rel. to solid solution behaviour *(Russian)* 77−11696
Mo, C and Ir impurities in single cryst. growth, effect on fine struct. *(German)* 77−28714
Mo, dislocation structure inhomogeneity in electromachining crater zone *(Russian)* 80−16326
Mo, dislocation structure of diffusional welding zone *(Russian)* 80−96531
Mo film, on Si, X-ray line-shape anal., simplifications using Fourier series 79−82123
Mo film, on SiO_2/Si substrate, effect of heat treatment after deposition on internal stress 78−22973
Mo film, sputtered on Si, annealing effect on uniform and nonuniform strains 79−82504
Mo, fracture and crack propag. tested in tension along [001] axis *(Russian)* 80−50697
Mo, monocrystalline, density change during plastic deformation *(Russian)* 79−87689
Mo, neutron irradiated, small angle X-ray scatt. and TEM study of voids 79−14849
Mo, single crystal, subjected to plastic deform., substruct. using X-ray diffr. 79−70083
Mo single crysts., substruct. variation during fatigue, kinetics *(Russian)* 78−60742
Mo-(Zr+V+C) (1.1 wt.%) alloy, phase composition, carbide phase microhardness *(Russian)* 80−60834
Mo-Cu-Al, phase equilibrium *(Russian)* 78−15361
Mo-Ti (up to 5.48 wt.%), internal nitriding, hardness, nitride type, precipitation *(Japanese)* 79−79157
Mo-Zr-C (0.12, 0.002 wt.%), prep. of diffusion metal coating on alloy, oxidation rates *(Russian)* 78−56816
Mo-Zr-C (0.63, 0.06 wt.%), quenched and deformed, structural changes during heating to ageing temp. *(Russian)* 79−1879
Mo-Zr-Nb-C, polythermal sections *(Russian)* 78−15365
Mo-Zr-Nb-C alloys, phase diagram and comp., Zr and Nb influence *(Russian)* 79−52167
Mo-Zr-Nb-C and Mo-Zr-C, carbide precip. hardening kinetics, ageing singularities *(Russian)* 77−25059
$NH_4H_2PO_4$, defects, X-ray topographic study 78−26580
$(NH_4)H_2PO_4$, single cryst., X-ray diffr. contrast at twin boundaries, computer simulation 79−33000
$NH_4H_2PO_4$, X-ray interference fringes due to diffraction effect at grown-in twin boundary 78−38728
NaCl, plastic deform., cleavage crack propag., X-ray topography 77−39625
NaCl, plastically deformed [001] orientated single crystal, glide props. and X-ray topography 77−21228
NaCl, plastically deformed, containing dislocation distribs., X-ray diffr. broadening 77−43218
NaCl, plastically deformed, integrated X-ray reflection coeff. determ. 77−65981
NaCl single crystal, stained by abrasion, struct. defects *(Russian)* 79−74262
NaCl:Ca, precipitate form., transform. after annealing, critical flow stress 78−38848
NaCl:Ni single crystals, VUV spectrum, ionic conductivity, X-ray diffr. 78−92097
NaCl-$AlCl_3$, phase diagram determ. by DTA and X-ray anal. *(Japanese)* 78−92250
$NaClO_3$, dislocations rel. to growth mechanism from aq. soln., X-ray topography 80−59464
Na_2CoGeO_4 hydrothermal single crystals, X-ray topographic study of growth defects rel. to growth conds. 79−19166
Na_2O-Al_2O_3-P_2O_5, exam. of subsolidus structure 79−4954
Na_2O-CaO-Al_2O_3-SiO_2 glass, crystn. for the purpose of obtaining vitroceramics *(French)* 80−75163
Na_2O-MgO-P_2O_5, subsolidus struct. 77−63640
Na_2WO_4-$CsWO_4$-WO_3, system form., melting point 79−43222
Nb, BCC, struct. singularities rel. to solid soln. behaviour *(Russian)* 77−11696
Nb, dislocation-free single crystal, deformed at 180K, X-ray topographic obs. 79−24587
Nb, low temp. annealing effect, precip. of Nb_2O_5 *(Russian)* 77−52456
Nb, oxidation kinetics, abnormal, at high temp. 79−29289
Nb, plastically deformed single crystal, foil, damage free prep. for TEM and X-ray topography *(German, English)* 80−30200
Nb single crystals, growth by pulling from a melt on a pedestal, charact. arrangement of dislocations 79−4911
Nb-Al(Ga)(Ge), fast quenching of A15-phases *(German)* 77−36014
Nb-Ga-Cu, fast quenching of A15-phases *(German)* 77−36014
Nb-Ga-Cu, phase diagram, metallographic and X-ray study, annealed and as-cast supercond. crit. temp. *(Russian)* 78−56617
Nb-Ge alloys, stoichiometry and phase equilibria, X-ray diffr. study *(French)* 79−70040
Nb-H(D) system, single cryst. prep. and characterisation 79−95910
Nb-Mo, BCC, struct. singularities rel. to solid solution behaviour *(Russian)* 77−11696
Nb-Pd constitution diagram, metallographic and X-ray diffr. anal. 80−89204
Nb-Pt alloy, superconducting parameters of A15- and σ-phases 78−39242

X-ray diffraction examination of microstructure continued
Nb-Sn alloys, stoichiometry and phase equilibria, X-ray diffr. study *(French)* 79−70040
Nb-Ti-O system, phase equilib., microstruct., thermal, and X-ray anal. 77−8806
Nb-Ti(Zr)(Hf)-N, exam. of phase equilibrium using electron microscopy and X-ray analysis *(Russian)* 79−15654
Nb_3Ge amorphous films, microstruct. X-ray small angle scatt. study 79−14685
Nb_3Ge amorphous films, X-ray diffr. analysis of microstruct. 78−72035
NbO, cryst. growth and microstructure 79−95913
NbO_2, cryst. growth and microstructure 79−95913
NbO_2, slightly substoichiometric, microstructure 77−47584
$Nb_{12}O_{29}$, cryst. growth and microstructure 79−95913
Nb_2O_5, cryst. growth and microstructure 79−95913
Nb_3Sn, diffusion-processed layer, texture meas. 79−82726
Nb_3Sn, neutron irrad., X-ray scatt. theory 79−37740
Nb_3Sn, powder metallurgically produced, microstruct. characts. 80−89233
Nd-Ga, phase diagram *(Russian)* 78−27478
$NdAlO_3$, dielectric films, phase composition and structure 80−39464
Ni, 109° and 71° walls, stable orientations, theory and X-ray observations *(Japanese)* 80−60359
Ni base alloys, hot corrosion in coal conversion system atmos. 79−96200
Ni base alloys, oxidation reaction investigation by X-ray diffr. and fluorescence *(German)* 79−57345
Ni base heat resistant casting alloy, fatigue resistance, microstruct. obs. 79−66159
Ni, carbonyl powder, dislocation density sintering 80−108372
Ni, cavitation-erosive wear in surface-active media, dislocation struct. and fracture study by FMR *(Russian)* 79−52384
Ni, change in twin faults during growth of ⟨100⟩ texture electrodeposits 79−65334
Ni, creep at 77, 295K, formation of five struct. 80−60926
Ni, crysts., thick, imperfect, dynamical X-ray diffr., topographic effects 77−68898
Ni, deformed, work-hardening, dislocation and mosaic struct., X-ray and electron microscopy 77−35625
Ni, deformed by filing, fine struct. obs. *(Russian)* 77−21309
Ni, dislocation structure evolution after hydroextrusion *(Russian)* 80−96530
Ni, electrolessly deposited, structural comparison with electroplated films 79−23869
Ni, growth direction orientation effect on impurity distrib. 78−47261
Ni heat resistant alloys, orientational correspondence between γ solid solution, and $\gamma+\gamma'$ eutectic precipitation *(Russian)* 79−11621
Ni layers, fibre texture volume part determ. by quantitative X-ray diffr. *(German)* 77−48595
Ni, mag. domain walls, X-ray surface reflection and transmission topography 77−20630
Ni, rolling texture, athermal softening *(Russian)* 77−66655
Ni, splat quenched, gaseous impurities effect on struct. 77−4042
Ni, texture nonhomogeneity during rolling 79−91670
Ni, textured galvanic layers, grain size determ., matrix and twinning orientations *(Russian)* 77−43461
Ni, transformed into hydride and decomposed, dislocation density and dislocation profile depth, positron annihilation and X-ray estimation 78−38711
Ni, variation in dislocation density during creep, determ. by X-ray diffr. analysis *(Russian)* 80−76302
Ni, Voigt function fit, of X-rays and neutron powder diffr. profiles 79−86651
Ni/Au-Ge/GaAs contact system, alloying behaviour, microprobe AES and X-ray diffr. 80−54548
β_1-Ni-Al, elastic softening and electron diffr. anomalies prior to martensitic transform. 77−8825
Ni-Al film, co-evaporated, comp.-depend. struct. and morphological changes 79−87020
Ni-Be bronze, Fe and Si alloying addition effect on phase composition *(Russian)* 78−15360
Ni-Cr, high temp. thermomech. treatment effect on tensile diagrams of KhN77TYuR *(Russian)* 80−60884
Ni-Cr, ordering in the vicinity of Ni_2Cr 79−38819
Ni-Cr alloy, structural changes, during thermal stress cracking, X-ray and microhardness meas. *(Russian)* 78−35496
Ni-Cr-Ce, Ce effect on oxidation 79−43484
Ni-Cr-Fe, high temp. corrosion and creep in carburizing and oxidising atmos. 79−11727
Ni-Cr(Mo), solid soln., US effect on mech. props. *(Russian)* 78−23819
Ni-Cu-Si, Si effect on structural changes during ageing, TEM and X-ray obs. 78−15438
Ni-Fe alloys, electrodeposited, electron microscope investig. *(Russian)* 77−43442
Ni-Fe-Nb (Mo), magnetic alloy, TEM and X-ray obs. *(Chinese)* 80−24401
Ni-Fe-Nb-Al (11.2, 8.09, 79.66 wt.%), modulated struct. growth process rel. to ageing *(Chinese)* 80−66541
Ni-NiAl solid soln., high temp. transforms *(Russian)* 79−56973
Ni-P, struct. obs. by X-ray diffr., low temp. annealing and deform. effects 79−56995
Ni-P alloy, electrodeposited, heat induced struct. changes *(Japanese)* 78−15433
Ni-Si, intergranular segregation of Si, electron energy loss spectrometers, X-ray anal. *(French)* 79−8388
Ni-Ta-C, composites of γ+TaC 77−85965
Ni-Ti (10 wt.%), X-ray study of ageing of plate and powder 77−1847
Ni-Ti (60 at.%) alloy, high stress effects on struct. and props. *(Russian)* 78−19838
Ni-Ti (8 and 10 wt.%) alloy, aged, precipitation behaviour at 550 to 950°C, X-ray and electron microscopy exam. 78−39785
Ni-Zn, γ-phase region, X-ray and electron diffr. obs. 79−61562
Ni-ZrO_2, dispersed inclusions, effect on recovery and recrystallisation 77−25064
β-NiAl, omega-like structural defects, diffuse X-ray scatt. obs. 79−95005
Ni_3Al, cold-worked 77−59806
$Ni_{40}Fe_{40}P_{14}B_6$, amorphous alloy, microstruct. study of crystallisation 77−86062
NiH_n thin film, X-ray phase analysis *(Russian)* 77−59124
$Ni_{65}Mo_2Fe$, O_2 effect on secondary recrystallisation and mag. props. 80−35201

X-ray diffraction examination of microstructure continued
NiO-CdO-Fe_2O_3 system, phase equilibria 79−11582
NiPt, quenched, ordering kinetics and domain struct. form. during isothermal tempering *(Russian)* 80−66502
NiTa, exam. of oxidation 79−96221
NiTiCu, shape memory alloys, electron microscope and X-ray diffr. study of struct. 79−82179
Pb film, monocryst., heteroepitaxial growth, struct. defects, and elec. props. *(Russian)* 80−84403
Pb films, vapour deposited FCC, normal and oblique incidences, microstructure, X-ray diffr. study 80−20048
Pb-Bi alloy, fine powder electrodeposition and X-ray struct. obs. 78−11163
Pb-Rb, phase diagram *(Russian)* 78−19720
$Pb_3Ge_2O_7$, dielectric thin film, obtained by sedimentation, exam. of dielectric props. and structure 80−2282
$Pb_5Ge_3O_{11}$, Czochralski growth, secondary phase formation 78−3027
PbO, polycrystalline layers, influence of prep. conditions on phase comp., texture and struct. 79−4495
Pb_3O_4, phase transition, texture of tetragonal and orthorhombic phases *(French)* 79−23726
PbS, vap. deposited film, island growth obs. by optical diffr. from electron micrograph 78−10291
$Pb_{0.8}Sn_{0.2}Te$ crysts., Bridgman grown, X-ray perfection study 80−107018
$PbTiO_3$, crysts., X-ray investigation of 90° domain struct. 79−15426
Pd, low temp. lattice parameter meas. 78−26496
Pd-Ag-Cu (35,25 at.%), determ. of ageing transformations by resist. meas., metallography, TEM and X-ray diffr. 79−4967
Pd-H alloys, low temp. lattice parameter meas., β and mixed ($\alpha+\beta$) phases study 78−26496
Pd-Si, struct. obs. by X-ray diffr., low temp. annealing and deform. effects 79−56995
Pd-Zn, γ-phase region, X-ray and electron diffr. obs. 79−61562
Pd_3Fe, X-ray and electron microscope obs. of antiphase domains and superdislocations *(Russian)* 77−86017
PdGe, Pd_2Ge, growth kinetics and structure on Ge substrate 79−11514
Pt-Cu (49.37 at.%), coexistent phases in homogeneous ordering 79−29052
Pt-Zr(Hf), high temp. thermodynamic props. 77−63633
Pu-Pt(Rh)(Pt-Rh), exam. of phases and crystal structure 78−80518
Re-Al-Si , X-ray determ.of system *(Russian)* 78−19763
Re-Cu-Al phase diagram, X-ray structural and microscopic anal. *(Russian)* 80−20895
Re-Fe-Al, physical-chemical investigation *(Russian)* 78−15362
Re-Zr-V, constitutional diagram *(Russian)* 79−56956
$RhGe_{1.5}S_{1.5}$, new skutterudite relation compounds, prep. and charact. 78−52700
RuO_2-TiO_2 coatings for Ti anodes, microstructural investigations 79−43469
Sb-Se-I, phase diagrams of various cross-sections 78−44093
Sc-[Co,Ni,Cu]-Ga, phase equilibria, diagrams of state, X-ray, microstructural study *(Russian)* 80−55356
Sc-Co(Ni)(Cu), phase diagram determination, using X-ray diffr., metallography and DTA techniques *(Russian)* 79−34004
Sc-Fe-Ga system alloys, isothermal sections of phase diagram *(Ukrainian)* 78−92235
Sc-Mn-Ga system alloys, isothermal sections of phase diagram *(Ukrainian)* 78−92235
$Sc_{(x+2)/3}T_{(x-2)/3}O_x$ (T=Si, Mg), 145 Å superstructure 79−99143
Sc_2O_3:MgO, defect struct., X-ray diffr. and pyrometric density 78−34524
Si, amorphous, hydrogenated, small angle X-ray scatt., void distrib. 80−15087
Si, Bragg diffraction from crysts., Mo K_α radiation polarisation 80−1893
Si, crack-tip dislocation pattern, X-ray topography *(French)* 80−107253
Si crystal limited topogram technique for investigation of dislocation distrib. 79−23496
Si crystal microscopic inclusions 79−55749
Si crysts., deformed, strain distrib. characterisation, annealing response 77−70140
Si defects in surface due to oxidation, exam. using double crystal back reflection topography *(German)* 79−51098
Si, dislocation dipole lattice image, stacking fault energy 79−60375
Si, dislocation motion near surface 79−82219
Si, dislocation-free single crystals, growth microdefects, etching and X-ray expts. 78−47385
Si, edge dislocation, crystal surface interception, X-ray diffr. obs. in Bragg case 80−49228
Si, elastically bent crystal, with large strain gradient, X-ray diffraction study 80−44073
Si, epitaxial, on sapphire, characterisation, X-ray rocking curves 80−75458
Si epitaxial layer, on Si ribbon substrate, dislocation density, X-ray topography obs. 77−85102
Si epitaxial layers, X-ray topographic study using Berg-Barrett techniques 79−28221
Si, high-dose Ar implantation, X-ray topographic obs. of strains and damage 80−59496
Si, ion-implanted, laser irrad., characterisation by X-ray topography 79−74026
Si, low temp. relax. of local stresses, dislocation behaviour, X-ray obs. 79−69110
Si, mechanical strength, origin of difference in Czochralski grown and float-zone-grown cryst. 80−44212
Si, microdefect obs., using double cryst. X-ray topography 77−4105
Si, microdefects, diffuse X-ray scatt. obs. 80−34014
Si, microdefects, X-ray topography 79−86797
Si n^+-p solar cells, degradation mechanisms associated with Ti impurities 80−81465
Si, near (III) surface, dislocation movement at annealed scratches, X-ray topography obs. 80−2029
Si, nearly perfect crysts., point defect aggregates, high resolution diffuse X-ray scattering study 80−49211
Si, new materials properties achievable by ion implantation doping and laser processing 79−69127
Si, oxidation stacking faults and microdefects, growth behaviour during high temp. annealing 78−72901
Si, oxidation-induced Frank sessile dislocation loops, struct. change 80−75228

X-ray diffraction examination of microstructure continued
Si particle reinforced Al, internal stresses, X-ray diffr. meas. *(Russian)* 78−23765
Si, plastically deformed, dislocation reactions obs. by X-ray topography 78−75691
Si, plastically deformed monocrystal, X-ray topographical study *(German)* 78−59813
Si, precipitation of O, 650°C, IR absorpt. and X-ray diffr. 80−76258
Si, single cryst., observation of dislocation by X-ray plane wave topography 78−91342
Si single crystals, nearly perfect, high resolution diffuse X-ray scattering study 79−32854
Si, small-diameter cryst. grown by pedestal technique, investigation of microdefects using X-ray topography 79−55683
Si, snowflake defect due to annealing in H at 1000°C, X-ray topography study *(Chinese)* 80−49227
Si, thermally induced microdefect form., C and O role 80−11439
Si wafer, anomalously transmitted X-ray intensity enhancement by asymmetric diffr., appl. to microstructure 79−14647
Si wafer, Cu-decoration technique for characterising lattice imperfections *(Japanese)* 79−65069
Si, wafer, suppression of oxidation stacking fault generation by preannealing in N_2 atm. 78−30648
Si, X-ray channeling technique anomalous transmission, appl. to microdefects induced by heat treatment 79−19124
Si, X-ray topography and double-crystal diffraction 80−92534
Si:As, ion-implanted, dislocation loops and etch pits, X-ray diffr. and TEM obs. 79−42068
Si:B, ion implanted, laser annealed, thermal annealing effect 79−73191
Si:B, ion implanted, radiation defect accumulation and annealing, X-ray diffr. obs. 79−37726
Si:B(Sb)(P), microdefect formation depend on doping, Cu decoration, X-ray transmission topography, preferential etching 79−69120
Si:Cu extinction of X-ray topographic images of Cu precipitates 80−45310
Si:P, high dose implantation, outside dislocation generation 78−87672
Si:P polycrystalline layer, role in lattice defect reduction assoc. with P predeposition 80−70229
Si:P^+ ion-implanted, annealing characts. 78−14372
Si-Al-O-N, mullite like cpd. comp., EPMA, X-ray and chem. anal. obs. *(Japanese)* 80−35175
Si-Al-O-N sintered ceramic, microstruct., phase composition and transformation mech., mech. props. 80−40309
Si-Al-O-N system, exam. of compounds and properties 78−48387
Si-Li(Au)(Cu), diffusion-induced defects, X-ray triple cryst. diffractometry 80−2213
SiC (2H), vapour grown, growth and deform. faults, X-ray obs. 78−30650
SiC crystals, 2H to 6H solid-state transformation, X-ray diffraction study 80−28943
α-SiC, plastic deform. 77−12673
SiC, polytypic transform. during hot pressing 78−52739
SiC, reaction bonded, microstruct. characterisation 78−48353
SiC, subjected to thermal shock, study of substruct. and surface morpholoy, X-ray diffr. and TEM study 79−43292
SiC:N, impurity effect on stress gradients and dislocation development 77−4116
SiC-B eutectic alloys, struct. of crystallising graphite 79−38829
SiC(6H), ion-implanted, laser-induced recrystallization and defects 80−44221
Si_3N_4, hot pressed, Y_2O_3 fluxed, microstruct. 78−64512
Si_3N_4, hot-pressed with crystn. grain boundary phases, prep. 78−95715
Si_3N_4, oxidised, with Y_2O_3 densification aid, temp. and compositional stability of $Y_6Si_6O_{21}$ 78−27664
Si_3N_4, phase content determ., using X-ray diffr. anal. 78−44281
Si_3N_4, prep. and charact. of ultrafine powders 80−2983
Si_3N_4, reaction bonded, effect of Si powder grain size on microstructure, and mech. props. *(German)* 79−4998
Si_3N_4, reaction bonded, exam. of Na_2SO_4 induced heat corrosion 79−20224
Si_3N_4, reaction bonded, pore size and distrib. effect on strength 79−29165
Si_3N_4, reaction-bonded, microstructural analyses 77−8782
Si_3N_4, reaction-bonded, struct., form. mechanisms and kinetics 77−4760
Si_3N_4 with Y_2O_3 and Al_2O_3 additions, hot pressed, exam. of mech. props., grain boundary crystallization 79−20009
Si_3N_4:$(MgO+Al_2O_3)(Y_2O_3)$, hot-pressed and sintered, microstruct. and impurity distrib. 80−49261
Si_3N_4-Al_2O_3, hot-pressed with crystn. grain boundary phases, prep. 78−95715
Si_3N_4-Al_2O_3-Y_2O_3, sintered, observation of a noncrystalline phase 78−64536
Si_3N_4-AlN-Al_2O_3-SiO_2-Y_2O_3, phase equilibrium study by X-ray diffr. and optical microscopy 80−50614
Si_3N_4-SiO_2-MgO, phase relations and interrelation with mech. strength, and oxidation 78−48386
Si_3N_4-SiO_2-ZrN-ZrO_2, X-ray diffr. phase anal. and reactions $Si_3N_4+ZrO_2$, SiO_2+ZrN 80−50613
α-SiO_2, adsorption of H(H_2), microweighing and X-ray obs. *(German)* 78−51825
SiO_2-CaO-ZnO-B_2O_3-Na_2O-S, SrO effect on crystallisation 80−54135
SiO_2-Na_2O-CaO (13, 11 wt.%) glass, phase separation, SiO_2 purity effect 80−44144
SiO_3-Na_2O-CaO-MgO-Al_2O_3 charge, silicate formation during heating 80−55342
Sm-Co, decomp. kinetics when aged, X-ray mag. props. and metallography study *(Russian)* 78−56644
Sm-Cu phase diagram *(Russian)* 78−27477
Sm-Ga, phase diagram *(Russian)* 78−27478
$SmCO_5$ based permanent magnets, props. and cryst. orientation *(Russian)* 80−20431
$SmCo_5$ alloy, orientability and texture, milling time effect 79−100168
$SmCo_5$, remanence and energy product, X-ray method of planar orientation 77−8342
$SmCo_5$ sintered magnets, eutectoid decomp. 80−89219
$SmCo_5$, vacuum-deposited, eutectoid decomp. *(Russian)* 77−66621
$SmCo_{5-x}Cu_x$ magnet alloy, metallurgical study *(Korean)* 77−8853
Sn, X-ray diffraction study of thermal motion of atoms in β-Sn 80−39243
Sn-Ni, electrodeposited, thermal stability 77−52319
Sn-Pb, dil., undercooled alloy, solidification 78−3120

X-ray diffraction examination of microstructure continued
SnO_2:Sb, and pure cryst., microstruct., X-ray diffr., optical and electron microscope studies 78−79619
$(SnTe)_{1-x}(PbSe)_x$ films on glass-ceramics, struct. and elec. props. 77−52251
Sr-Al-Nd phase diagrams *(Russian)* 78−27480
Sr-Al-Si system, phase diagrams construction by simplex designing method 78−6899
Sr-Nd, phase diagram, microstruct., X-ray, chemical and thermal diffusion anal. *(Russian)* 78−52761
Sr-Ti-O system, perovskite oxides, nonstoichiometry rel. to dielectric const. 77−80628
$SrNb_2O_6$-$NaNbO_3$-$LiNbO_3$ pseudo-ternary system, DTA, heat treatment and X-ray diffr. obs. *(Chinese)* 79−52175
$SrTeO_3$, X-ray diffractional and optical studies, ferroelectric properties 79−65805
$Sr_3(VO_4)_2$, determination of enthalpies of formation, from heats of solution 80−2182
Ta, film, CVD on silica, struct. and mech. props. 77−24965
Ta-H(D) system, single cryst. prep. and characterisation 79−95910
Ta-N (0.6 to 6.5 at.%), supersaturated solid soln., precipitation 79−96028
Ta-O supersaturated solid solution, precipitation processes, hardness change meas. 80−25712
Ta-Pd system, phase diagram exam. of composition by X-ray diffr., electron microprobe anal., and metallography 78−76632
TaC-TaB_2, exam. of high temp. friction and wear, and deformation behaviour 79−34152
Tb-Dy-Ho, phase diagram, alloy struct. *(Russian)* 77−25016
$TbCo_2$, spontaneous distortion, mag. props. due to cryst. field, exchange field, magnetoelastic energy 79−61096
$Tb_2Ge_2O_7$, flux-grown, X-ray topography 80−64939
Te, c-slip, asymmetry and orientation depend. 77−27888
Te, hexagonal film vac.-evaporated at normal incidence, X-ray Fourier line shape anal. 79−99454
Te-Pb (20 at.%) alloy, amorphous, obtained by rapid cooling from liq. state, crystn. behaviour 78−26445
$(Th,U)O_2$, burnup simulated, high O_2 pot., chem. state 80−91220
Th-Fe (20 to 70 at.%), amorphous alloy, electrical resistivity and thermal stability 80−33901
β-Ti alloy, rolling orientation pattern form. *(Russian)* 77−21161
Ti alloy, VT16, decomp. of α″ martensite during continuous heating *(Russian)* 78−48370
Ti alloy, VT16, decomposition of metastable β-phase *(Russian)* 78−68710
Ti alloy, X-ray diffr. anal. of hydrides 77−12628
Ti alloy VT20 and VT22, yield strength anisotropy and durability after cyclic loading *(Russian)* 78−27565
α,α+β Ti alloys, structural instability during prolonged periods of heating *(Russian)* 78−56664
Ti alloys, X-ray phase analysis, quantitative description of new method 79−52222
Ti and Ti-Al (4,6,9 wt.%), X-ray line profile anal. 77−47459
Ti, single crystals, recrystallised, dislocations obs. 78−10054
Ti, Ti recrystallisation texture from neutron diffr., cf X-ray diffr. *(French)* 77−84593
Ti-Al, phase diagram in Ti rich region *(Russian)* 77−25013
Ti-Al alloys, α_2 phase obs. using microscopy and X-ray diffr. 79−52497
Ti-Al-Mo-Zr (Cr-Fe), effect of heating on thermal stability of phases, lattice constants and chem. comp. 78−56672
Ti-Al-Mo-Zr alloy, VT9, decomp. kinetics of metastable β-phase, X-ray and mech. props. obs. *(Russian)* 78−48368
Ti-Al-V (6,4 wt.%), microstruct. improvement by cyclic heating *(Japanese)* 79−100185
Ti-Al-V (6,4 wt.%), phase transformation after hydrogenation 80−7560
Ti-Al-V-Cr-Zr-Mo (3, 8, 6, 4, wt.%), phase transforms. 79−100113
Ti-Al-V-Fe-Si, alloy VT6, phase transform. kinetics and Young's modulus *(Russian)* 77−81258
Ti-Al-(Mo), phase relations 80−108398
Ti-alloy, VTZ-1 and VT8, decomposition of metastable phases, effect of plastic deform. *(Russian)* 78−39770
Ti-B-W(Mo), annealed at 1400°C, exam. of phase diagram, using X-ray phase and metallographic analysis 79−1847
Ti-Cr-Zr, martensite formation, chemical composition effect 80−50634
β-Ti-Fe, (7.1 wt.%) exam. of ω phase formation, by X-ray diffr. and Mossbauer spectroscopy 78−52800
α-Ti-Fe(0.22 wt.%), ω phase form. during ageing 77−52355
Ti-Mn, fine cryst. struct. by diffuse X-ray and electron scatt. *(Russian)* 79−99329
β-Ti-Mo, alloy, struct. changes during deformation and ageing *(Russian)* 78−39791
Ti-Mo, fine cryst. struct. by diffuse X-ray and electron scatt. *(Russian)* 79−99329
Ti-Mo, phase diagram investigation *(Japanese)* 77−63632
Ti-Mo, structure associated with BCC to omega transform. *(Russian)* 80−108432
Ti-Mo binary system, solid state phase transform. and miscibility gap, phase diagram 79−8298
Ti-Nb, phase transformation due to shock wave treatment *(Russian)* 79−91641
Ti-Nb-Al, decomposition during isothermal annealing 80−25653
Ti-Nb-V(25 wt.%, 15 wt.%), precipitation of β and ω phases during ageing at 350°C 77−8838
Ti-Nb-W, 20 to 1000°C, isothermal section, X-ray anal., microstruct., hardness, cond., transform. *(Russian)* 77−55947
Ti-Nb-Zr (35, 3 wt.%), martensitic τ phase, X-ray diffr. obs. 80−16300
Ti-Si amorphous alloy, melt-quenched, transform. studies and mech. props. 80−100838
Ti-TiC-TiN system, phases 80−20905
Ti-V-Si, equlibrium silicide, X-ray and electron diffr. obs. 78−27483
Ti-Zr-W-(Al) alloys, phase struct. and props. *(Russian)* 80−16270
Ti_2AlN, prep. and props. 77−28745
TiC-WC-TaC carbide mixture in plasma reactor *(German)* 77−1819
$TiC_{0.93}$-$TiN_{0.818}$, structural parameters, and X-ray and pycnometric densities in homogeneity range 77−90311
TiCu intermetallic compounds, decomposition reaction by H_2 absorption *(Japanese)* 78−23668
TiN, precipitation of ordered δ′-phase *(Russian)* 78−6929
TiN-VN alloys, synthesis in low-temp. plasma, phys.-chem. props. *(Russian)* 79−38761

X-ray diffraction examination of microstructure continued
TiO-ZrO_2, pseudo binary system, effect of Ti addition on struct. and props. of zirconia 79−11583
TiO_2-Ga_2O_3 system, phase relations and microstructs. 78−3107
$TiS_{1.7}$, screw dislocs., X-ray topography 77−47460
Tl-B-Se system, vitrification region, primary crystallisation fields 77−15321
Tl-Bi-Hg alloys, phase diagrams and equilib. *(Russian)* 79−52166
Tl-Te, phase equilibrium exam., using DTA, X-ray diffraction, and hardness 79−1846
Tl_2S-Tl_2Se(Tl_2Te), exam. of phase equilibria, using DTA, X-ray phase analysis and microhardness 79−4953
Tl_2Se-SnSe(PbSe) systems, phase equilib. 79−52181
Tl_2Te-HgTe(HgSe) systems, phase diagrams 79−87620
U-Fe(Ni)(Co)-B, isothermal section of phase diagram, X-ray obs. 79−52157
U-Re-C, crystalline struct. of a compound 77−25023
U_3O_8, λ-type heat capacity anomalies 77−20080
V, structural changes in single crystal under single electric impulse discharge *(Russian)* 79−65086
V-C alloys, low carbides struct. rel. to ht. treatment 77−48458
V-Ga-Cu, phase diagram *(Russian)* 77−25014
V-Ga-Sc, phase diagram, metallographic and X-ray meas., solubility boundaries *(Russian)* 78−56618
V-Ga(Ge)(Si), fast quenching of A15-phases *(German)* 77−36014
V-H(D) system, single cryst. prep. and characterisation 79−95910
V-N, BCC solid soln., superperiodicity of lattice in quenched ordered struct. *(Russian)* 78−56662
V-N α-solid solution, struct. transform. during annealing and quenching *(Russian)* 77−81257
V-Ni-Mo, structure in alloy crystallisation region, peritectic equilibria *(Russian)* 80−50622
V-Ni-Mo alloy, annealed at 1150°C, isothermal section *(Russian)* 79−52154
V-O system β phase BCT, X-ray diffr. study of additional scatt. effect *(Russian)* 80−10537
V-S system, quenched, order-disorder transition of metal vacancies, DTA and X-ray analysis 78−30576
V-Se system, quenched, order-disorder transition of metal vacancies, DTA and X-ray analysis 78−30576
V_3Ga, diffusion-processed layer, texture meas. 79−82726
V_3Ga superconducting tape, diffusion-processed, cryst. textures, X-ray pole figures 79−11266
V_2O_5 and lower oxides, defect structures and related props. 80−59454
V_4O(β-phase), X-ray study of precipitated phase *(Ukrainian)* 78−6928
$V_{2-x}Sb_xO_4$, defect struct. exam. 78−18635
W, BCC, struct. singularities rel. to solid soln. behaviour *(Russian)* 77−11696
W, deformed, surface layer struct. effect on polygonisation and recryst., X-ray diffr. anal. and metallographic exam. *(Russian)* 80−84948
W fibre reinforced Ni-Cr steel, TiN coated fibre, protective props. *(Russian)* 79−66201
W, polygonisation critical stage in single crystals deformed in compression 79−4979
W powder, effect of prep. temp. on fine structure, X-ray diffr. anal. 79−33971
W, texture and grain boundary struct., primary misorientation function, expt. deform. 79−1876
W tube, CVD, study of preferred orientation *(Korean)* 77−8761
W, vapour deposited, dislocation struct., rel. to texture *(Russian)* 80−65394
WC powder, effect of prep. temp. on fine structure, X-ray diffr. anal. 79−33971
WC-Co, prep. temp. effect on fine struct. of WC phase, X-ray obs. 79−33971
WC-Co compacts and sintered alloy, fine struct. of carbide phases, preforms re-pressing under high press. effect 79−28987
WC-Co molten Zn reaction, lamellar struct. form. 79−33964
WS_2, single crysts., growth by direct vapour transport method, X-ray and electron diffr. study 79−28904
Y, texture formation during cold rolling *(Russian)* 78−92275
Y-Fe-Si alloy, phase diagram 79−52158
Y-Ni-B, X-ray and microstruct. anal., phase composition 77−16539
Y-Re-B, annealed, and quenched X-ray structural and phase anal. 78−11207
$YAlO_3$, with perovskite structure comparative assessment of methods of prep. 79−95980
Y_2O_3, translucent ceramic, prep. effect on struct. and props. 79−87601
$Y_2Ti_2O_7$, precipitation from oxalates, carbonates, exam. 80−55641
Yb-Ga, phase diagram, differential thermal and X-ray analysis *(Russian)* 78−56615
$YbCr_{1-x}Al_xO_3$ solid solutions 80−20887
Yb_xSy, synthesis and mag. props. 78−23242
Zn film, vac. deposited, X-ray diffr. study of microstruct. 78−26796
Zn, film, vac. deposited, X-ray diffr. study of microstruct. 78−75966
Zn, HCP lattice, Huang diffuse scatt. from interstitials 80−88142
Zn, single cryst., Burgers vector determ. of perfect dislocations obs. by X-ray topography 79−37711
Zn-Al, unidirectionally solidified eutectic, morphology and crystallography 77−48421
Zn-Sn-Hg, diagram of state, melting temp., peritectic and eutectic phases *(Russian)* 80−55350
ZnO based varistors, evolution and role of chem. constituents rel. to prep. method, influence on elec. props. *(French)* 78−31367
ZnO ceramics, microstructural evaluation 79−55750
ZnO heteroepitaxial films, grown on Al_2O_3 substrates, X-ray topographic study of struct. 79−15048
ZnO heteroepitaxial film, orientation relations for growth on Al_2O_3 substrates, X-ray diffr. anal. 79−15049
ZnO triode sputtered film elastic props. rel. to structure and composition 79−46988
ZnO triode-sputtered film crystallite structure, X-ray evaluation 79−46987
ZnO-Al_2O_3-SiO2, transparent glass ceramics, heat treatment effect on microstruct. 78−56667
ZnO-Bi_2O_3-Sb_2O_3-Co_2O_3-MnO_2-Cr_2O_3, nonohmic ceramic, microstruct. exam. 78−47292
ZnO-La_2O_3-GeO_2, exam. of glass forming region, properties and crystallisation 78−88454
ZnO-TiO_2 system, heat treated, X-ray anal. of phase form. sequence 79−1850

X-ray diffraction examination of microstructure continued
ZnO.$ZnCl_2$.H_2O cement, phase equilibrium diagram 77−86013
ZnS, crystals with stacking faults, Laue method study 79−94847
ZnS, polymorphic transition, (β→α) effect of mech. deformation 79−1858
ZnS:Mn, dopant conc. effect on stacking fault energy 80−2041
ZnS-MgS, solid solution, prep. of single crystals with wurtzite structure, exam. 79−1821
ZnSe, twinning on melt-growth under pressure 77−80515
ZnSe:I, I vapour transport prep., conductive and photolum. cryst. 79−100035
ZnSe+CeTe⇄CdSe+ZnTe ternary mutual system, phase equilib. 79−52179
ZnTe film, prepared by single-source vacuum deposition method *(Japanese)* 80−6664
$Zn_3(VO_4)_2$, determination of enthalpies of formation, from heats of solution 80−2182
Zr base alloys, formation of phases precipitated from β solid solutions *(Russian)* 79−1869
α-Zr monocrystal perfection using Berg method and diffractometer with omega device *(French)* 80−2035
Zr, structural changes during plastic deform. *(Russian)* 77−8880
Zr-Al (14 wt.%), transformation sequence from Zr-Al martensite to Zr_3Al phase 80−3027
β-Zr-Nb(Cb) alloys, anneal hardening and flow softening 79−78993
Zr-V, superconductivity, X-ray and optical metallography 79−4610
ZrC-Ni, refractory-liquid metal, interfacial reactions, C effect, electron microprobe analysis 77−12829
$Zr_{50}Co_{50-x}Ni_x$, transform. and deform. studies 79−1864
ZrO_2, destabilisation by phosphoric acid, cubic to monoclinic transition, effect of temp., grain size, chemical composition 79−20037
ZrO_2, optimum sintering characts., density, X-ray diffr., IR spectrum, UV spectrum obs. 78−76617
ZrO_2-CaO, stabilised microspheres, structure, mechanical props. *(Russian)* 80−100379
ZrO_2-CaO(MgO)($YO_{1.5}$), partially stabilised, growth morphology of tetragonal phase 79−4968
ZrO_2-$GdO_{1.5}$ (80 mol.%), X-ray diffr. exam. of continuous transition 78−68684
ZrO_2-MgO system, intermediate phases existence, X-ray diffr. and IR obs. 79−38805
ZrO_2-P_2O_5, hydrated, heat treatment and coprecipitation, phase transitions 77−90335
ZrO_2-Sc_2O_3, phase system, X-ray and thermal anal. 78−27494
ZrO_2-SiO_2 (11 to 13 wt.%), X-ray phase anal. 80−35195
ZrO_2-ThO_2, high temp. study of phase diagram using X-ray and thermal anal. *(French)* 79−70049
ZrO_2-TiO_2 refractories, TiO_2 effect on props. and phase composition 79−38809
ZrO_2-Y_2O_3, stabilised microspheres, structure, mechanical props. *(Russian)* 80−100379
ZrO_{2-x}, high temp. phase diagram, exam. of lower phase boundary 78−76638

X-ray diffraction examination of molecular structure
see also molecular configurations
antibodies, conformation in presence and absence of antigen, small angle X-ray studies 79−11890
bacteriophage S shape determ. from small-angle X-ray scatt. 79−39347
biological structural determinations using synchrotron X-rays 80−46112
biopolymers, X-ray struct. study using synchrotron radiation and multichannel detector 78−47210
bis(diethylamino)dithiaboretane, cryst. struct., bond lengths and angs. X-ray diffr. obs. 78−18628
4-bromophenoxyacetyl-4-ethylbenzene, single crystal, X-ray struct. determ. 79−1426
ceruloplasmin, human, mol. wt. determ. by hydrodynamic methods and low-angle X-ray scatt. 78−15761
cholesteryl ethyl carbonate, long periods in sol. state, X-ray diffr. study 80−96503
chromatin, low-angle X-ray and neutron diffr., interparticle effects 80−72134
coke, anisotropic spheres obtained during needle coke form., struct. obs. 77−63573
collagen, interpretation of small-angle X-ray diffr. using α1 chain primary struct. 77−66792
collagen fibrils, in connective tissue, preferred orientation and orientation distrib. function determ., high-angle X-ray diffr. patterns 79−62177
copolymer, semicryst. random, characterisation by small angle neutron and X-ray scatt. 80−75189
dectran hydrolyzates in soln., branching assessment using small-angle X-ray scatt. 79−41926
diacetate-nitrocellulose, long period struct., 180-265°C, X-ray diffr. obs. *(Russian)* 79−24556
dibromomaleic acid thioanhydride, mol. and cryst. structs., X-ray obs. *(German)* 80−44199
diiodomaleic acid thioanhydride, mol. and cryst. structs., X-ray obs. *(German)* 80−44199
1,8-dinitronaphthalene, orthorhombic 22, and 97°C 78−6048
N,N′-diphenyl-m-phenylenediamine, crystal and mol. struct., X-ray diffr. 78−47312
CsDNA, absorpt. factor, X-ray diffr. study using 1.2 Å synchrotron radiation 78−76988
DNA, circular superhelical 300-10000 Å resolution 77−9168
DNA, polymorphism, X-ray diffr. and computerised model building study 78−27894
DNA compact form, tertiary struct., small angle X-ray scatt. 80−72129
DNA with heavy atom, X-ray struct. study using synchrotron radiation and multichannel detector 78−47210
elastase, globule, atomic density distrib. 79−79458
epoxide compound, polymerisation in non-uniform magnetic field, exam. of structural changes 80−7791
ferredoxin, S. platensis [2Fe-2S], struct. and evolution of chloroplast-type ferredoxins 80−94165
formamide, comparison of theoretical and experimentally determined electron density distrib. 78−82634
globular protein struct., large angle X-ray diffuse scatt. exam. 78−3444
glycogen phosphorylase b activity, struct. of cryst. and complexes 78−80830
gummosine, cryst. and mol. structs., and absolute config., X-ray expts. 78−79602

X-ray diffraction examination of molecular structure continued
heart, review of studies, book contrib. 80−109079
histidine decarboxylase quarternary struct. 79−92129
histidine-decarboxylase, molecular weight and form determ. by low angle X-ray scatter 78−76987
isotactic polystyrene gel, anomalous X-ray diffraction effects, rel. to chain conformation and isomeric homogeneity 77−50576
keratin, mammalian, organisation of polypeptide chains 77−4981
lysozyme and complex with trisaccharide inhibitor, struct. in soln. and in cryst. 77−81465
macromolecular structure, linked-atom least-squares reciprocal-space refinement system, LALS, incorporating stereochemical restraints 78−26377
macromolecules, partially oriented specimens, numerical deconvolution procedure 78−75497
melanostatin, correl. between X-ray struct. and conform. in soln. 77−48752
N-methyl-piperidinium-acet-meta-chloro-anilide-iodide, crystallisation from water, X-ray exam. of cryst. struct., mol. config. *(German)* 79−51095
mucopolysaccharides in collagen, small angle studies, rat tail tendon 79−16132
muscle, contracting, dynamic structure, X-ray scatt., time resolved, rapid data collection systems 80−61740
muscle contraction, single, high-time resolution X-ray investigation method 80−81777
muscle contraction, time resolved studies using small angle X-ray diffr., design of data collection system 79−12052
myelin lattice swelling kinetics study 80−21436
one-electron density functions, many-centred finite multipole expansions 78−71624
organosilicon ladder polymers, struct. and phys. props., book contrib. 79−65012
oxymyoglobin structure determ. by X-ray diffr. 78−56950
phosphoglycerate kinase, sequence, struct. and activity, hingee-bending enzyme 79−74595
plasma low-density lipoprotein, human, molecules organisation of central core 77−90722
PMMA, molecular alignment 78−14299
PMMA isotactic, syndiotactic stereocomplex formation in soln., composition, struct. 79−66292
poly(cis 1,4-isoprene), cryst. phase, elastic modulus 79−57037
poly γ-methyl L-glutamate films, thermal motion of α-helical mols. 79−64133
polyamide single crysts., struct. *(Russian)* 77−43158
polyamidoimide film, thermomech. props. rel. to mol. struct. *(Russian)* 79−57029
polyethylene, chlorinated, semicryst. random, characterisation by small angle neutron and X-ray scatt. 80−75189
polyethylene, supermolecular structure study, IR spectroscopy *(Spanish)* 79−77532
β-polyethylene oxybenzoate, cryst. struct. and mol. conformation 79−55674
polyglucosan, soluble, single crystals from Acetobacter xylinum, internal structure resemblance to Cellulose Hydrate II *(Japanese)* 79−94121
polymer, FSGO model, X-ray diffr. struct. factor calcs. 77−46660
polymer surface, supramol. struct. characterisation, use of C X-radiation 80−79705
polymers, structure elucidation, model construction and X-ray methods *(German)* 80−103267
polyoma virion and capsid crystal structures 80−8011
polypeptides, poly-L-lysine based, comb-like, struct., physicochem. props. *(Russian)* 79−55644
polypeptides, structured, nature of 4.5 Å max. on X-ray diffuse scatt. curves 78−31769
polystyrene, atactic, structure elucidation, model construction and X-ray methods *(German)* 80−103267
polystyrene, conform. and near all-trans extended-chain model relevant in gels, X-ray diffr. patterns interpret. 80−79707
polystyrene, molecular alignment 78−14299
polytetramethylene terephthalate, monofilaments, chain conform. rel. to strain 77−4055
polytrimethylene terephthalate single crystals, X-ray and electron diffr. obs. of cryst. struct., packing analysis 79−94924
polyvinylidine fluoride, corona charging at 12.5 kV, obs. 78−92027
prealbumin, human, struct., X-ray diffr., amino acid sequence, circular dichroism meas., comparison 77−42450
prealbumin, protein-DNA and protein-hormone interactions rel. to model of thyroid hormone nucl. receptor 77−66793
prealbumin-DNA-hormone interactions, X-ray studies, review 78−53322
protein, X-ray diffraction data collection, FORTRAN program 77−51279
protein, X-ray struct. study using synchrotron radiation and multichannel detector 78−47210
protein structural dynamics, temp.-depend. X-ray diffraction 79−92133
proteins, globular, struct. anal. in soln. by large-angle diffuse X-ray scatt. 77−86723
proteins, nature of 4.5 Å max. on X-ray diffuse scatt. curves 78−31769
pyridinium manganese (II) chloride monohydrate, crystal struct. and mag. susceptibility 79−19239
quinolinium manganese (II) chloride monohydrate, crystal struct. and mag. susceptibility 79−19239
rare earth ions, aquo complex form., in aq. chloride soln., coord., X-ray diffr. obs. 79−64975
retinal photoreceptors, small angle X-ray data processing 80−81536
ribulose bisphosphate carboxylase, two-layered square-shaped mol. 77−56336
sarcoplasmic reticulum membranes, small angle X-ray data processing 80−81536
Schiff's base compounds, double axis, Siamese Twin type liq. crysts., thermal and X-ray obs. 80−39312
solution X-ray scattering, review of recent developments, book contrib. 80−109077
styrene-vinylpyrrolidone block copolymer soln., conform. props., light-, X-ray scatt. and viscometry obs. *(Russian)* 78−37779
subtilysin, globule, atomic density distrib. 79−79458
TCNQ complex with 5-phenyl-[1-thiol]-3-selenol-2-thione, charge-transfer salt, cryst. and mol. struct. 80−33986
tolan-mercury diphenyl, energy charact. determ. of mol. interaction and short range order parameters 79−14794
transition metal complexes, mol. dissymmetry, book 80−27057

X-ray diffraction examination of molecular structure continued
triacetate-nitrocellulose, long period struct., 180-265°C, X-ray diffr. obs. *(Russian)* 79−24556
1,3,5-trioxane-1, 3-dioxolane copolymer, semicryst. random, characterisation by small angle neutron and X-ray scatt. 80−75189
two-electron density functions, total X-ray scatt. 78−70889
viscose, long period struct., 180-265°C, X-ray diffr. obs. *(Russian)* 79−24556
$AlPO_4$, amorphous, struct. determ. by radial distrib. functions derived from X-ray diffr. 77−43151
$BaVO(EDTA).6H_2O$, cryst. and mol. struct., X-ray diffr. obs. *(Russian)* 78−30601
C-C bonds, single, double, triple, electron density distrib., X-ray diffr. data accuracy rel. to ab initio calcs. 79−89805
CN^-, electron density distrib., theoretical and expt. determ. 77−61683
CO ($^1\Sigma^+$), X-ray and electron diffr. scatt. intensities, electron correlation effects 78−17577
Cd complex, $(Cd[SC(CH_3)_2CH_2NH_2]_2CdCl_2)_2.2H_2O$ cryst. and mol. struct. 78−74787
Cl_2, solid, electron density distrib. using X-ray diffr. meas. 79−42006
Cu complex, [Cu(1,4,7,10-tetrabenzyl-1,4,7-10-tetraazacyclododecane)Cl]NO_3, cryst., struct. 80−64966
Cu complex, Cu (II)-substituted ethylenediamines and monocarboxylates, cryst. and mol. struct., X-ray diffr. obs. 79−82182
N_2, elec. field gradient electronic contrib., using generalised X-ray scatt. factors 77−75321
Ni complex, Ni (II)-substituted ethylenediamines and monocarboxylates, cryst. and mol. struct., X-ray diffr. obs. 79−82182
SCN^-, electron density distrib., theoretical and expt. determ. 77−61683
B-trichloro-m-carborane, cryst. electrophilic chlorination of 9, 10-dichloro-m-carborane, cryst. and mol. struct. from X-ray diffr., cryst. struct. 78−9268

X-ray diffractometers
angle and energy-dispersive diffractometry system, design, operation and appls. 80−47163
APD 3600 automatic X-ray powder diffractometer, sophisticated derivative method appls., JCPDS data base 80−107017
attachment for cryst. growth from liq. 78−71641
attachment for large-crystal structural imperfection control 79−68975
autoclave attachment for Philips instrum. 80−31959
automated, state-of-art 77−19833
automated powder diffractometer, computerised control 80−3453
automatic attachment for punching DRON diffractometer data to tape 78−34385
automatic four-circle, for high-press. struct. investig. 79−23495
Bond, for precise meas. of single cryst. lattice parameters and thermal expansion 79−23498
Bonse-Hart X-ray diffractometer, asymmetrically cut, comparison with Kratky camera 80−77917
Bonse-Hart X-ray diffractometer, asymmetrically cut, for SAXS, design and performance 80−77916
Bragg X-ray intensities, collected on single cryst. diffractometer with graphite monochromator, assessment 80−57448
Bragg-type X-ray diffractometer, narrow beam, interference phenomena by plates 79−41909
broad beam technique with increased resolution 79−86650
characteristic absorption of X-rays, diffractometer study 80−20733
cryostat design for X-ray diffractometry of solid He 77−53921
crystal centering, and diffractometer alignment errors calcs., appl. to high pressure crystallography 80−22494
dead time, correction for counting losses in single cryst. X-ray diffractometry *(French)* 79−37587
diamond anvil cell adaption to automatic for circle X-ray diffractometer 78−75501
diamond-anvil high pressure cell used in automatic diffractometer up to 90-kilobars 78−54387
diffraction pattern parallel meas. 79−94848
diffractometer, two-circle SSD, appls. in angle dispersive mode 79−14641
double-crystal, design features, appl. 78−49948
DRON-0.5 X-ray diffractometer, low-temp. attachment 78−343
dual detector diffractometer for residual stress meas. 78−5716
elemental analyser, diffractometer based 80−318
energy-dispersive diffractometry, optimum resolution 78−42857
Enraf-Nonius CAD-4 diffractometer, mechanical design, computer control and system performance 80−24318
external crystal adjustment, for Lang topography *(German)* 78−59719
fast X-ray diffractometer based on a spherical drift multiwire proportional chamber with digital position encoder 80−90969
four-circle, solid-state detector, for white X-ray diff. work *(Japanese)* 80−1897
four-circle diffractometers, simple methods of aligning with crystal reflections 80−22493
four-circle single-cryst. diffractometer, interchangeable Si(Li) detector fitment 77−51278
four-circle single-crystal diffractometer, mechanical devices for aiding alignment 80−99029
furnace, temp. calibration using eutectic transitions of alloys *(Japanese)* 79−6128
goniometer, zero deviation *(German)* 79−58854
heating equipment, gas-flame, temps. up to 2600K for 4-circle diffractometer 79−60222
high angle double crystal diffractometry, improvement for meas. temp. depend. of lattice constants, pt.I 80−1890
high angle double crystal diffractometry, temp. depend. of lattice constants, pt.II 80−1891
high-pressure-low-temp. type, appl. 78−82089
high-resolution energy-dispersive, using synchrotron radiation 79−14640
high-temperature attachment 79−49355
high-temperature chamber attachment for roentgenography of hollow cylindrical specimens 79−21883
horizontal axis θ-θ diffractometer with cryostat *(French)* 77−84575
HZG 4 universal X-ray diffractometer 79−54242
HZG 4/A universal instrument, applic. versatility of basic software 80−52375
instrumental line broadening with non-ideal standard specimen, anal. 78−41391
laser thermonuclear fusion, shell target parameters meas. using X-ray schlieren method 80−14942
line broadening, due to instrumental conditions 78−86399

X-ray diffractometers continued
linear position sensitive proportional counter tests *(French)* 77−31557
low-temperature X-ray diffractometer for work with actinide metals and compounds 80−316
microcomputer controlled system 80−317
microprocessor-based, features 80−70082
monitor arrangements *(German)* 80−52374
multiple counter diffractometer with equatorial geometry 77−27779
orientation of single cryst., small spherical, nonabsorbing, and large extended face 78−42856
oscillation apparatus, description *(Japanese)* 78−82086
Philips PW 1100, used for crystal struct. research at high pressure 80−38873
Picker FACS-I diffractometer, microprocessor-controlled optical incremental angle encoder system 80−18058
polarisation ratio of crystal monochromators, method eliminating its relevence 78−55775
polythermal attachment for powder diffractometers to allow operations in range −150 to +900°C 80−311
portable flash X-ray diffr. system 77−62445
portable X-ray analyser for residual stresses, design, operation and testing 78−53058
position-sensitive detector, employed in diffractometer, geometrical problems, stress measurement use 79−85205
proportional counter detector system for powder diffractometry appl., digital read-out 78−4751
residual stress measurement, X-ray diffr. equipment, comparison 80−82858
scanning block modernisation by scaler adjustment 80−31958
sealed cell for examination of powder specimens 79−35906
secondary fluorescer coupler in combined spectrometer/diffractometer system and stand-alone spectrometer system 77−41746
single crystal diffraction, heating device construction 78−74116
single-crystal diffractometry, peak searching, crystal setting and determining automatic cell constants 80−6319
slit unit, for PW1100, computer controlled 80−37135
soft X-ray spectrometer, for gaseous studies 78−24911
specimen cell for recording powder patterns of solid-state-stable coordination compounds at low temp. *(French)* 78−54515
specimen holder for reactive and toxic materials 79−63863
stress meas. in different ψ directions, X-ray diffractometer 78−5715
temperature monitor for PW1100 diffractometer 78−67617
temperature scanning X-ray diffraction camera for liquid crystals 77−31558
time-resolved X-ray diffraction counter and data acquisition system 78−45758
triple crystal, for high resolution X-ray diffuse scattering meas. 79−9267
triple crystal diffractometer, for scatt. close to reciprocal lattice pts. 79−77455
URS-50I and 50IM attachment for radiography of thin films 77−76247
weak X-ray scatt. interpretation by automated diffractometer 79−68977
white beam, X-ray energy dispersive diffractometry using synchrotron radiation, special features 78−66019
X-ray anal., conf., Denver, USA (Aug. 1976) 77−70382
X-ray powder diffractometer, APD3600, file searching techniques 80−24319
Cu-target diffr. tubes, K_α charact. radiation rel. intensities calc. 78−4754
Si(Li) solid state detector appl. on modern single cryst. X-ray diffractometer 79−58855

X-ray effects
see also biological effects of X-rays
actomyosin, X-irradiated ENDOR and ELDOR obs. 80−63689
L-alanine:Cr^{3+}, X-irrad., thermoluminesc., ESR, UV photobleaching 77−9104
β-alanine, cryst., X-irrad. producting radicals, ESR and ENDOR 79−56612
alcohol glasses, X-irradiated, electron scavenging mechanism 77−56235
alkali borate binary glass, energy storage behaviour studied by thermoluminesc. 80−50432
alkali halide, X-ray induced strain effects rel. to time of irrad. 78−6120
alkali halide crystals, X-ray irradiated, luminescence during release of pressure 79−65939
alkali halides, ^{14}N impurities, molecular point defects, EPR isotropic hyperfine triplets 80−2636
alkali metal halides, X-ray induced colour centre and halogen aggregate form. 80−96565
alkaline earth fluorides, radiation damage and photochromism in doped and undoped crysts. 79−51148
alkane:toluene, radiolysis at 77K, luminesc., excited singlet toluene form., energy transfer mechanism 77−16846
alkoxy free radicals, produced by X-irrad. of hydroxy containing cpds., characterisation by ESR and ENDOR 78−95938
ammonium acetate, irrad. crysts., freq. swept ELDOR obs. at 77K, resolution of spin packets 79−95686
anthracene, single cryst., X-radiation damage recovery, using triplet state exciton probe 78−75694
anthracene, single cryst., X-ray radiation damage, delayed fluoresc. meas. *(Japanese)* 79−37736
aromatic ethers, comparative study of X-ray and γ-induced photolysis and radiolysis *(German)* 78−64854
L-asparagine.H_2O, X-irrad. at room temp., ESR and ENDOR 77−40131
1,2-bis(p-tolysulphonyloxymethylen)-l-buten-3-inylen, ESR of X-irrad. cryst., 77K 79−11806
calcium tartrate tetrahydrate, X-ray irrad. single cryst., free radical EPR 77−63936
cell morphologic transformation by UV, effect of X-irrad. and chem. carcinogens 77−1981
chloroacetamide, X-irrad., ESR of $CH_2ClCO^{\cdot}$ radical 78−76882
5-chlorodeoxyuridine, X-irrad., α-chloro radical ESR and ENDOR 77−4916
cryostat for low temperature X-irradiation and electron paramagnetic resonance 80−86321
cyclohexane, liq. and solid, mobility of excess charge carriers 78−2489
deoxycytidine 5′-phosphate, H_2O, X-irrad., 3αH radial. form., ENDOR, ESR 77−73453
dielectric, surface vac. breakdown by ultrasoft X-rays 80−43989
diffusion equation model for kilovolt electron transport at X-irradiated interfaces 79−24388

X-ray effects continued
dimethyl sulfone, X-irrad. cryst., ESR spectrum 78−3351
dipotassium glucose-1-phosphate, X-irrad., ESR-ENDOR obs 80−60419
doped-silica optical fibres, nuclear radiation effects 80−33172
dulcitol, X-irrad., 4.2K, electron traps, alkoxy hyperfine coupling, ENDOR obs. 80−50863
ethane, X-irradiated, 4.2K, pairwise radical trapping mechanism, EPR obs. 79−100412
ethanol, glassy matrix, absorpt. spectra after X-irrad., solvated electrons 79−65903
fusion reactor, first wall, thermal response to X-rays, effect of inert gases 79−85776
glass, Libyan Desert Glass, redox form. conditions, EPR obs. of as-received and irrad. samples 78−28228
glassy organic matrices, electron spin-lattice relax. of radiation-produced Ag atoms, temp. depend., tunnelling relax. 79−34331
glycine-d_2 crystal, X-irrad., H-D exchange reactions 77−16837
5-halouracils, solid, radiation damage, free radicals in 5-fluorouracil single crysts. 80−71926
s-halouracils, solid, radiation damage obs., deoxyribose ring opening in single crysts. 80−71929
hydroxyproline HCl, X-irrad., free radical products, ENDOR meas. 78−76883
ice, X-irradiated, EPR spectra, obs. of thermally reversible radical, g-value 79−5144
ice matrices, polycryst., electron spin-lattice relax. of radiation-produced Ag atoms, temp. depend., tunnelling relax. 79−34331
imidazole, EPR study of H exchange 80−40718
inositol, X-irrad., deuteration effects, ENDROR and ESR meas. 78−73067
inositol, X-irrad., radical form. detection by ESR and ENDOR, oxidation process 78−27797
insulating film, electric charging by X-radiation *(Japanese)* 79−61488
insulating materials, high energy radiation effects 80−19835
ionisation gauge, hot cathode type, improvement on soft X-ray limit *(Japanese)* 77−140
laser-fusion reactor, surface heating of 1st wall by pulsed photon and ion irrad. 78−89979
methane, X-irradiated, 4.2K, pairwise radical trapping mechanism, EPR obs. 79−100412
methanol, glassy matrix, absorpt. spectra after X-irrad., solvated electrons 79−65903
α-methyl-D-glucopyranoside, X-irrad. cryst., radical form., EPR-ENDOR study 79−56613
6-methylmercaptopurine riboside, S-substituted nucleoside, ESR and ENDOR obs. 77−36766
MOST, short channel, output conductance, effect of ionising radiation 80−70836
multiple radiography overexposures anal. 79−49877
myosin, X-irradiated ENDOR and ELDOR obs. 80−63689
N-acetyl-L-leucine, single crysts., X-ray induced free radicals 80−45525
neopentane:n-butane, electron mobility and electron-ion recombination rate const. 79−73557
nitromethyluracil, radiation-induced oxidation and reduction 77−32816
1-phenyl-3-thiosemicarbazide, X-irrad., radical prod., ESR, ENDOR 77−36770
photographic film, fogging effects diagnosis, use of granularity meas. 79−47952
photographic film, props. of latent image formed by X-ray exposure 79−20407
2,5-piperazinedione, X-ray damaged, ENDOR, δ proton hyperfine interaction 77−9103
PMMA, X-ray irrad., thermoluminescence emission, exam. of kinetic order 79−43046
PMMA, X-ray irradiated, thermolum. glow peaks 77−90204
poly-p-xylylene films, carrier traps, X-ray induced TSC, thermolum. and dielec. loss study 80−88570
polycrystalline dipeptides, X-irradiated ENDOR and ELDOR obs. 80−63689
polyethylene, high density, carrier trapping, X-ray induced TSC 80−11005
polyethylene, high density, trapped carriers, thermally stimulated currents, influence of oxidation 77−80792
polystyre, irrad, thermoluminesc. 78−2931
polystyrene, X-ray irrad., thermoluminescence emission, exam. of kinetic order 79−43046
polyvinylidene fluoride, X-ray induced TSC 80−75578
potassium hydrogen bisphenylacetate, X-irrad., ENDOR of trapped benzyl radical 77−10695
pyrrole, free radicals produced by X-irrad. and decay of tritium atom, EPR study 78−48676
α-quartz:Ag, Ag atom paramagnetic centre, $A_{Ag\text{-}Si}$ 78−76308
quartz:Cu(Ag), paramagnetic centre formation after α-irradiation *(French)* 77−69690
α-quartz, hydrogenic trapped hole species, EPR studies 80−44915
quartz, photocond., X-ray and other irrad. effects 78−76103
quartz, surface damage by X-rays, γ-rays, neutrons, SEM study 80−79837
quartz, synthetic, connection between lattice deform. and coloration pattern 78−10930
quartz, thermoluminescence output intensity depend. on γ- and ξ-irrad. temp. 77−59623
α-quartz, uncompensated Ti^{3+} centre, annealed, EPR meas. 79−65731
α-quartz, X-irrad., paramag. Ag_2^+/AlO_4 centre, EPR obs. 79−28612
quartz crystal, oscillating characts., nucl. and X-irrad. effects 79−78626
radiography, rare-earth screens, effect of P X-rays 80−30867
rhamnose, single cryst., X-irrad. at 4.2K, trapped electrons and electron traps characts. 79−78037
Rochelle salt, refractive index, X-ray radn. effect on dispersion and temp. depend. 78−72480
Rochelle salt, X-irrad., radical II struct. and location, ENDOR 77−51991
ruby colouring due to specific growth, annealing and irrad., exam. of visible, infrared and UV spectra 79−11440
sapphire, pure and doped, luminesc. centres 79−33791
satellite shielded cables, hardening techniques for reducing X-ray response 79−23642
semiconductor, ionization and subthreshold effects in defect creation and annihilation 77−84811
silicate glasses, effect of high-dose X-rays and reactor radiation 80−19838

X-ray effects continued
solid-electron and X-ray interaction *(Chinese)* 80−70253
solids, interaction with electrons and X-rays *(Chinese)* 80−80896
sorbitol, X-irrad., 4.2K, electron traps, alkoxy hyperfine coupling, ENDOR obs. 80−50863
SOS structure, radiation dose at interface due to electron beam aluminisation 78−68089
spinel transparent glass ceramics, colour centre form. due to alkali metal vapour and X-ray irradiation 79−87316
steel, stainless, X-ray induced desorption of gases from surface 77−35813
succinamic acid, X-irrad., primitive radn. damage, ESR, ENDOR 78−3352
sucrose, single cryst., X-irrad. at 4.2K, trapped electrons and electron traps characts. 79−78037
system-generated EM pulse boundary layer, time-dependent, scaling behaviour 79−23641
TGS, cryst. struct. exam. after X-irradiation/field treatment 77−11531
TGS, cryst. struct. exam. at low radiation doses 77−11530
TGS, ferroelec., negative ENDOR study of radiation damage 78−19373
TGS, internal field prod. in layer periodical domain struct. by X-ray irrad. 80−71359
TGS, polarisation reversal, cryst. defects effect 78−27156
TGS, pyroelec. IR detectors, permanent polarisation due to X-rays, optimum non-ferroelec. behaviour 77−41684
TGS, X-irrad., thermal diffusivity, cooling const. and heat transmission coeff. 79−86935
TGS deuterated, X-irrad., negative ENDOR, collective motion 79−47357
TGS X-irradiated, paramag. relax, spin-echo study 80−7168
trifluoroacetamide, single cryst., X-irrad., transient radical form., INDO and ESR calcs. 77−12814
trifluoroacetamide, X-irrad., CF_3...F radical ESR 78−73066
triphenylseleniumchloride, X-irrad. cryst., forming Ph_2SeCl, ESR study 79−39167
TTF-TCNQ, anisotropic cond., X-ray effects 80−96855
TTF-TCNQ, X-ray irrad., transverse cond. 80−6432
tungstate phosphors, thermoluminesc. and afterglows 79−38681
X-ray image sensor, charge-coupled, radiation damage effects 77−74565
xylitol, X-irrad., 4.2K, electron traps, alkoxy hyperfine coupling, ENDOR obs. 80−50863
zircon, natural and synthetic crysts. Hf and Tb activated, capture centres and luminescence mechanism *(Russian)* 77−28626
α-quartz:Ge, Ge^{3+} centres, dynamic interchange, EPR obs. 79−19776
Ag cluster growth on AgBr microcrystals after X-ray and low-temp. light exposure 79−83485
AgCl, AgCl:AgBr, exciton creation, ODMR 78−79933
AgCl, irradiated, surface defect center, XPS study 79−28894
$Al(NO_3)_3.9D_2O$, X-irradiated, ENDOR and ESR of radicals 77−50455
α-Al_2O_3, crystal defects from X-ray irradiation, F-centres, X-ray luminesc. obs. 80−55176
Al_2O_3, X-irrad., electron and hole traps, TSC and optical bleaching meas. 79−28356
Al_2O_3, X-ray induced desorption of gases from surface 77−35813
α-Al_2O_3:Er(Cr), crystal defects from X-ray irradiation, F-centres, X-ray luminesc. obs. 80−55176
β-Al_2O_3-$K_2O(Na_2O)(H_3O^+)$, ESR of paramag. defects in cond. planes 80−29617
β-Al_2O_3-Na_2O, EPR and optical absorpt. studies of X-ray produced defects 78−95517
β-Al_2O_3-Na_2O, X-ray induced defects, EPR and ENDOR study 80−60456
Ar, solid, X-ray induced point defects 80−59514
As_2S_3, glassy, X-ray induced paramag. colour centres 78−19327
$As_2S_3(Se_3)$, X-ray induced paramag. states and luminesc. 78−95520
As_2Se_3, glassy, X-ray induced paramag. colour centres 78−19327
Au, X-ray induced desorption of gases from surface 77−35813
B_2O_3-Li_2O-LiCl, EPR of Cl_2^- colour centres *(French)* 79−47333
$[(100-x)B_2O_3.xLi_2O]_{98}.2CdO$, glass, X-ray irrad., EPR study of Cd^+ centres *(French)* 78−43638
$BaBr_2:K^+$, X-irradiated, perturbed F-centre, EPR and optical absorption 77−68966
$BaF_2:Cd^{2+}$, irrad., ESR of Cd^+ centres 77−59459
BaFBr, X- and γ-irrad., thermolum. and optical absorpt. spectra 79−95857
BaFCl crystals, F-centres, X- and γ-irradiation, thermoluminescence and optical absorption spectra 80−45155
BaO-Al_2O_3-B_2O_3:Ce^{3+} glass, EPR spectra, before and after X-irrad. 78−19320
$BaSO_4$, X-ray irrad., electron and holes traps, g-factors, ESR obs. 80−50183
$BaTiO_3$, ferroelectric semicond. anomalous photovoltaic effect due to ionising radiation 80−29437
$BaTiO_3$, X-ray irrad. effect on dielec. props. 78−15082
$BaWO_4$ crystals, X-irradiated, EPR, TSC and thermoluminescence spectra meas. 79−1791
BeO, ceramic and single cryst., EPR-ENDOR study of [Li]° centre 77−85569
Ca fluorapatites, carbonated, B-type, EPR of F^+-centre after X-irrad. *(French)* 80−108065
$CaCO_3$, calcite, X-ray irrad., luminesc. and dielec. loss decays 77−12431
$CaCO_3$:Li, CO_3^{2-}-Li^+ centre, irradiated synthetic single crystal, bond angle and wave function 77−81006
$CaCO_3$:Li, synthetic calcite, $(CO_3Li)^{2-}$-Li^+ defect after X-irrad., EPR study 80−75852
CaF_2: Ni crystals, X-irradiated, EPR study of Ni^+ and Ni^{3+} 80−75849
$CaF_2:Cd^{2+}$, irrad., ESR of Cd^+ centres 77−59459
CaF_2:Co, X-irrad., F-centre form., optical absorpt. spectra and dichroism obs. 79−42998
CaF_2:Co, X-irrad., luminesc. spectra 79−28801
CaF_2:Co, X-irradiated, optical absorption spectrum 78−35173
CaF_2:M, M=Mn, Fe, Co, Ni, X-irrad., impurity effects on defect prod. 80−92525
CaF_2:Mn, EPR and optical absorpt. spectra 80−93171
CaF_2:Mn, low temp. X-irrad., Mn centres, optical absorpt. and emission props. 80−60635
CaF_2:Mn(Co)(Ni), X-irrad., thermolum. 80−60686
CaF_2:Na, single cryst., X-irrad., optical absorpt. and thermoluminesc. 80−34952
CaF_2:Ni, X-irrad., optical absorpt. spectra and dichroism meas. 80−108239

X-ray effects continued
CaF_2:Ni, X-irradiated, optical and EPR meas. 80−108235
$CaFPO_3$, colour centre form., X-ray and electron bombardment *(Russian)* 77−19948
$CaMoO_4$, scheelite struct., intrinsic hole centres, EPR study 78−64274
CaO, doped, thermal stability of hole centres and hole recombination luminescence *(Russian)* 78−72614
$Ca(OH)_2$, V-centres, EPR obs. 77−48051
$Ca(OH)_2$:Ni^{2+} single cryst., X-irrad., Ni^+ EPR, g-factors and point-charge model 80−2626
$Ca_3(PO_4)_2$-$CaCl_2$:F^-, EPR of electron excess centres 78−10772
$Ca_{10}(PO_4)_6Cl_2$, nonstoichiometry effect on X-irrad. induced electron-excess centres 77−62525
$Ca_{10}(PO_4)_6(OH)_2$:Mn, thermoluminesc. 77-500K, X-irrad. at 77K *(French)* 78−15234
CaS:Tb,Eu phosphors, fluoresc. spectra under X-ray excitation 80−16083
$CaSO_4$, thermoluminesc. spectra, X-irrad. effect 78−35210
$CaSO_4$:Dy, phosphor, X-irrad., thermoluminesc., role of Na_2SO_4 as charge compensator 79−78764
$CaSO_4$:Sm phosphors, X-irrad., thermoluminesc., charge compensation effects 80−97351
$CaWO_4$, scheelite struct., intrinsic hole centres, EPR study 78−64274
$Cd(ClO_3)_2$, irrad., bleaching and annealing expts., EPR and optical absorpt. 79−91476
$Cd(ClO_3)_2$ irradiated single crystal, ESR and annealing, trapped defect centre 80−55141
CdS, acoustoelectric mobility measurement for X-ray excited carriers 77−15916
CdS, photocond. on supplementary X-irrad. *(Russian)* 77−28212
CdS single crystals, Roentgenoluminescence, exciton interactions *(Russian)* 80−2853
n-CdS:Cu, Si, photocond., carrier lifetime, X-ray effects 77−59300
Co melt, struct. charact. time depend. in X-ray studies *(Russian)* 80−24350
CsBr, irradiated with ultrasoft X-rays, thermolum. meas., surface energy losses 77−16408
CsBr, X-irradiated, release of stored energy 78−38753
CsBr:Cu^+, X-ray irrad., thermoluminesc. 80−16107
$CsCdBr_3$:Cr^{3+}(Cr^+), EPR of impurities, charge compensation, X-ray effects 80−60407
CsCl:Cu^+, X-ray irrad., thermoluminesc. 80−16107
CsI:Na, X-ray irradiated, optical and ESR studies in IR absorption band 80−80828
$CsMgCl_3(Br_3)$:Cr^{3+}(Cr^+), EPR of impurities, charge compensation, X-ray effects 80−60407
$Fe_{0.5}Co_{0.5-x}Cr_x$ films, vacuum-deposited cryst. and mag. struct. *(Russian)* 80−93081
Ge surface, slow relaxation of surface states 77−62980
GeO_2, hexagonal and glassy, X and γ-irrad., thermolum. and paramag. centres 77−63472
GeO_2:Sc^{3+}(Y^{3+})(In^{3+}), trapped-hole centres, ESR meas. 79−77597
H_2SO_4, frozen soln., EPR of trapped H-atoms produced by UV and X-irrad. 80−3369
H_2SO_4, glass, trapped H spin-lattice relax., modulation, saturation ESR 77−9095
KBr and KBr:Sr X-irradiated, optical investig. of Br_3^- centres 77−16348
KBr, cation defects creation mechanism 80−75224
KBr, efficiency of creation of X_3^- centres in X-rayed alkali halides *(Russian)* 78−71731
KBr, excitation of thermolum. near liq. He temp. 80−40171
KBr, pure and Sr^{2+} doped, X-irrad., hole Br_3^- centre creation and destruction 77−15411
KBr, single crystal, preirradiation and radiation defects, electron microscopic estimation *(Russian)* 78−75695
KBr, stored energy after X-irrad. at low temp., 10-50K 77−76459
KBr whisker, X-irrad., defect form., thermolum. and ionic cond. obs. *(Russian)* 78−84666
KBr, whiskers, F-centre accummulation and track effects due to X-ray irrad. 80−39484
KBr, X-irrad., F-centre role in thermoluminescence 80−20720
KBr, X-irrad. crysts., halogen aggregation, absorpt. spectra obs. *(Russian)* 80−66234
KBr, X-irradiated, at 80K, interstitial K ions associated with interstitial Br ions *(Russian)* 78−75655
KBr:Ca, X-ray re-irradiation effects on Z_1 centres 78−75664
KBr:NO_2, X-irrad., paramag. and nonparamag. hole centres 77−16176
KBr:Na, X-irrad., luminesc. from self-trapped excitons 77−28614
KBr:Rb, H-centre interaction with Rb^+ ion 78−75662
KBr:Sr, X-irradiated, first-stage F-centre production 77−76395
KBr(Cl), X-ray irrad., tunnelling recomb. luminesc. 80−2873
KBr(Cl):Sr^{2+},Cu^+, thermolum. response, extension of two-step reaction model 80−89075
K_2CO_3-D_2O, glassy matrix, absorpt. spectra after X-irrad., solvated electrons 79−65903
KCl (Br) crystals, thermally stimulated luminescence accompanying recombination of V_F and F centres 80−55201
KCl, cryst., colour centres, ionic cond., X-ray effects, thermoluminesc. *(Russian)* 78−6056
KCl, doped with alkaline earth ions, Z_1-centres form. under X-ray irrad. 79−24338
KCl, efficiency of creation of X_3^- centres in X-rayed alkali halides *(Russian)* 78−71731
KCl, pure and Pb^{2+}-doped, X-irrad., quenching effects on thermal glow curves 78−27333
KCl, room temp. X-irrad., first stage F-centre form. 78−67709
KCl, single crystal, preirradiation and radiation defects, electron microscopic estimation *(Russian)* 78−75695
KCl single crystals, F-band absorpt. and thermolum. under DC field and X-ray irrad. 79−65910
KCl, whiskers, F-centre accummulation and track effects due to X-ray irrad. 80−39484
KCl, X-irrad. induced deform. effects, glow curves *(Russian)* 79−52022
KCl, X-irradiated, formation of cation defects 78−91359
KCl, X-irradiated, release of stored energy 78−38753
KCl, X-ray irrad., thermoluminescence, TSC and thermal stability 79−95859
KCl, X-ray irradiated, first-stage F-centre prod. 80−107231
KCl, X-ray irradiated, vacancy conc. determ., thermal expansion meas. 80−79782

X-ray effects continued
KCl:Ag, X-irrad., thermoluminesc. study of Ag centres 80−80874
KCl:Ca^{2+}, Z_1-centre thermolum. 80−80879
KCl:Eu^{2+}, cation impurity-vacancy pairs, effect of X-rays 79−55778
KCl:Ga(In), ESR of impurity centres, impurity optical absorpt. bands 80−29618
KCl:Ga(Tl,Pb), X-irradiated, EPR spectra 79−28613
KCl:Hg^{+}, X-irradiated, ESR meas. 77−1588
KCl:I crystals, V-band development using X-rays 78−88337
KCl:Li, X-irrad., F_A centres, thermolum. studies 80−80878
KCl:Pb^{2+}, X-ray irrad., electron-trapped centres, Pb^{+} and Pb^{0}, optical absorpt. spectra 80−71461
KCl:Sn^{2+}, EPR exam. of struct. and prod. of $Sn^{-}(5p^3,4S)$ defects 79−61215
KCl:$SnCl_2$, photostimulated hole recombination luminesc. *(Russian)* 80−80833
KCl:$SnCl_2$, X-ray irrad., polarised luminesc. and EPR study of Sn^{3+} centres 80−39868
KCl:Sr, thermally pre-treated, glow curves 80−25470
KCl:Sr^{2+}, X-irrad., thermolum., impurity aggregation, trapping centre form. 78−88367
KCl:Sr^{2+}, X-irradiated, thermolum. decay, effect of impurity aggregation 77−85814
KCl:$SrCl_2$, H_{Na} annealing, X-ray irrad., H centre capture by IV dipoles 78−10927
KCl:Tl, ESR of trapped electron and hole centres 79−78516
KCl:Tl, thermal glow of trapped electron and hole centres 79−78762
KCl:Tl and KCl, F-centre production by positive ions and X-rays 78−38760
KCl:Tl^{+}, optical absorpt. spectra following X-irrad., F- and V-centres 79−99912
KCl:Tl^{+}, Na, X-irrad., activator-impurity association *(Russian)* 77−85761
KCl-Ba, X-ray irrad. cryst., thermoluminescence spectra 80−20719
KCl-$BaTiO_3$, composite cryst., F-centres, thermoluminesc., DC field and X-irrad. effects 78−2926
KCl-KBr, mixed cryst., radiation hardening 79−99238
KCl-KH cryst. stimulated by X-radiation, spatial redistribution of F and U centers 79−14804
KCl-Mg, X-irrad. and F-bleached, optical and ESR spectra 77−48052
$KCl_{0.5}Br_{0.5}$:Ca, X-ray irrad., Z_1-centres, thermoluminesc. and optical absorpt. meas. 80−16108
$KClO_4$, ClO_3^{-} detection by EPR of ClO_3 radicals created by X-irrad. 78−76311
$KClO_4$, X-irrad., ESR spectra of O_3^{-} and ClO_3 exchange-coupled to O_2 78−64856
$KClO_4$, X-irrad. induced paramag. defects, ESR study 80−24493
$K_2Cr_2O_7$ single crystals, X-irrad., EPR spectra 80−2638
KF:U, EPR of U^{5+} centre charge compensation mechanism 77−90030
KH_2PO_4:KH_2AsO_4, X-irrad., EPR 77−32257
$KHSO_4$:SO_3^{-}, X-irradiated, ESR saturation 78−80220
KI, efficiency of creation of X_3^{-} centres in X-rayed alkali halides *(Russian)* 78−71731
KI, V-centres, Raman spectra 79−91429
KI(Br), irradiated at room temp., thermolum. and F-centre thermal stability 78−84669
KI(Br), X-irradiated cryst., luminesc. during press. release 80−20722
$KMg_3[AlSi_3O_{10}].F_2$ with excess Al, synthetic fluorphlogopite, radiation-induced paramag. O^{-} centres 80−60417
KN_3, X-irradiated, N defect, EPR obs. 79−82870
K_2SO_4:$(NH_4)SO_4$, X-irrad., EPR of NH_3^{+} 80−11272
Kl:Tl^{+}, X-irrad., absorpt. spectra investig. of Tl_2^{+} centres 77−20887
Li disilicate glass, radiation induced centres, EPR exam. 78−35033
LiD:Mg^{2+}, X-irrad., dielec. loss 80−55024
LiF, X-irradiated cryst., luminesc. during press. release 80−20722
LiF:Mg, dependence of optical absorpt. on temp. during X-ray irrad. 80−66237
LiF:Mg, X-irrad., colour centres, ESR and UV asborpt. meas. 80−108069
LiF:Mg, X-irrad. induced sensitisation mechanism, optical absorpt. spectra 80−60637
LiF:Mg, X-irradiated, thermoluminesc. of Z_3-centres 78−15236
LiF:Mg, X-ray irrad., trapping processes, Z-centres and dipoles, two models 80−49222
LiF:$Mg^{2+}(CO^{2+})$, X-ray induced UV absorpt., band shapes, F- and Z-centers 77−20889
LiF:OH crystals, X-irradiated, H centres formation and annealing 80−54226
LiF:U, EPR of U^{5+} centre, charge compensation mechanism 77−90030
LiF:U, X-ray and γ-ray irrad., EPR of U^{5+} centres 79−91295
LiF:U_3O_8, irrad., U^{5+} luminesc. molecular centres, optical and ESR expts. 77−48224
LiH, defect form. at low temp., EPR, thermolum. and TSC study 80−107222
LiH, formation and annihilation of Li colloids and H bubbles 80−107228
$LiNbO_3$ crystals, polaron character of colour centres produced by X-rays 80−2013
$LiNbO_3$, optical damage induced by X-irradiation 77−20814
$LiNbO_3$, two-photon and X-ray induced Nb^{4+} and O^{-} small polarons, ESR and optical absorpt. 78−76306
$LiNbO_3$, X-ray photovoltaic effect and its correl. with ESR 79−82639
$LiNbO_3$:Fe, impurity valence state charge on X-ray irrad., Mossbauer meas. 80−7235
$LiNbO_3$:Fe, optical damage induced by laser light, X-ray irrad., carrier mobility effects 79−33657
$LiNbO_3$:Fe, X-ray and γ-ray irradiation effects on Fe charge state, Mossbauer study 80−40013
Li_2O-LiCl-B_2O_3 system, fast Li^{+} ion vitreous superconductors, EPR study *(French)* 80−11269
MgF_2, X-irradiated, radiation conductivity 79−69555
MgF_2:Mn(Co), photoluminesc. due to X-rays, colour centre thermal breakdown 79−24359
$Mg(NH_4)_2(SO_4)_2.6H_2O$:Cr_2O^{2-}, optical absorption study, $Cr_2O_7^{-}$ and CrO_4^{3-} centres 80−55128
MgO, doped, thermal stability of hole centres and hole recombination luminescence *(Russian)* 78−72614
MgO, pure and doped crysts., X-ray stimulated luminesc. 79−28802
MgO, single crystal, thermal and optical stimulation processes of V-centres *(Japanese)* 80−11485
MgO, thermally stimulated exoelectron emission *(German)* 80−66404

X-ray effects continued
MgO:Al(Li)(F)(Sn), hole processes in photostimulated luminesc., electron emission, X-ray irrad., ESR relaxation 79−69889
MgO:Fe^{3+}, Mn^{2+}, X-irrad. induced anion Frenkel defects, stabilisation by Fe^{3+}, optical and ESR obs. 77−68969
Mg_2SiO_4:Tb TLD, response to X-ray and electron irrad. 79−3285
$NH_4Al(SO_4)_2.12H_2O$, CrO_4^{3-} centres, EPR and optical absorption spectra 79−91475
NH_4ClO_4, formation of colour center by X-irradiation, optical absorption spectra 79−19247
$(NH_4)_2SO_4$:MnO_4^{-}, X-ray irrad. damage, optical absorpt. spectra study 80−66246
$NaAl_3(PO_4)_2(OH)_4$, EPR of at. H caused by X-rays 79−28614
$Na_8Al_6Si_6O_{24}.Cl(Br)(I)$, cathodochromic sodalites, coloured crysts., tunnel and recomb. luminesc., temp. depend. *(Russian)* 80−66261
$Na_6Al_6Si_6O_{24}.NaX_{(2-n)}$, (X=Cl, Br, I), X-ray irrad., thermal-erase cathodochromism and dihalide mol. centres *(Russian)* 80−66236
NaBr-U-centre containing cryst., X-ray radiation induced cation vacancy generation 80−39078
$NaBrO_3$, single crystals, thermolum., optical absorpt., X-ray effect 79−95858
NaCl crystals with dipole O colour centres, radiation colouring and holographic recording 80−48187
NaCl, efficiency of creation of X_3^{-} centres in X-rayed alkali halides *(Russian)* 78−71731
NaCl, F-thermal bleaching 77−89433
NaCl, filamentary crystal, vacancy-enriched surface layers 78−51536
NaCl, irradiated, at 80K, thermolum. processes 80−34990
NaCl, irradiation-induced energy transfer from bulk to surface, luminesc. meas. 78−92132
NaCl, optically bleached and X-irrad., relation between F- and C-centres 77−72613
NaCl, positron trapping by X-ray produced defects, A-centre form. 77−48273
NaCl, pure and doped, 20K X-ray irradiation, thermolum. and recovery processes 80−93412
NaCl, thermal expansion meas. after X-ray irrad., F-centre bleaching 80−44338
NaCl, thermoluminesc. and optical absorpt., simultaneous DC field and X-irrad. 79−99956
NaCl whiskers, X-irrad., stress oriented dislocation loop nucleation 79−33213
NaCl, X-irrad. dose depend. of dislocation charge 77−47464
NaCl, X-ray irrad., F-centre accumulation and rad. hardening *(Russian)* 78−51538
NaCl, X-ray irrad., vacancy conc., thermal expansion meas. 80−6431
NaCl:Ag^{+}, X-irrad., B-centres, thermal annealing, monomolecular and bimolecular sequence of kinetics 78−47373
NaCl:AgCl, positron annihilation characts., positronium state form., X-irrad. effects 77−4700
NaCl:Ca, X-irradiated, Z_1-centre form. kinetics, thermolum. investig. 77−4693
NaCl:Ca, Z_1 centre thermoluminescence study 80−16109
NaCl:Ca^{2+}, X-ray induced luminescence 78−23516
NaCl:Ca(Mg), X- and gamma-irrad., thermostimulated electrons and luminesc. 79−91505
NaCl:Cu, X-irrad., thermoluminesc., F-centres 79−33849
NaCl:Cu^{+}, X-irrad., anisotropic Cu centre anal. 79−78714
NaCl:Cu^{+}, X-irrad., thermoluminesc. centre, EPR anal. 79−43045
NaCl:Cu^{+}, X-irrad. at room temp., ESR of Cu^{2+} centres 78−52343
NaCl:Cu^{+}, X-ray irrad., role of Cu^{+} in thermoluminesc. 78−56526
NaCl:Ga(In), ESR of impurity centres, impurity optical absorpt. bands 80−29618
NaCl:Ga(Tl,Pb), EPR spectra 79−28613
NaCl:Hg^{+}, X-irradiated, ESR meas. 77−1588
NaCl:Mn^{2+}, radiation-induced colouring, room temp. kinetics 79−55736
NaCl:Mn^{2+}, X-irrad., thermoluminesc. and EPR 79−61444
NaCl:Mn^{2+}, X-ray irradiated, thermolum. and EPR 77−81161
NaCl:V^{2+}, X-irrad. and unirrad., EPR of isolated V^{2+} ions 79−15347
NaCl:$V^{2+}(Ca^{2+})(Mn^{2+})$, X-irrad. effects on divalent metal aggregates, EPR and ionic cond. meas. 79−82263
NaCl:Zn^{+}, X-irrad., EPR and optical absorpt. 78−43642
NaCl-O^{2-} X-ray irrad., defect generation during radiolysis 80−7831
NaCl(Br), X-ray or UV irradiated, cation defects creation mechanism 80−75224
NaCl(F), irradiated at room temp., thermolum. and F-centre thermal stability 78−84669
$NaClO_3$ trapped O species in irradiated samples, low-temp. X-ray photoelectron spectroscopy 78−27799
$NaClO_4$, aq. glass, formation of trapped H-atoms and electrons 80−35559
$NaClO_4$, frozen soln., EPR of trapped H-atoms produced by UV and X-irrad. 80−3369
$NaClO_4$-D_2O, glassy matrix, absorpt. spectra after X-irrad., solvated electrons 79−65903
NaF, X-irrad., colour centres and thermolum. 80−84790
NaF:U, EPR of U^{5+} centre, charge compensation mechanism 77−90030
NaI colour centre formation and accumulation *(Russian)* 77−65978
NaI(Tl) scintillation detectors, temp. depend. of radiation-induced coloration 79−72204
$NaMgF_3$, defects induced by X- and vacuum UV irrad., optical and elec. study 80−107319
NaN_3, X-irrad., EPR of N_2^{-} 77−66421
$NaNO_2$, X-irradiated IR, UV and visible absorption 79−95811
Na_2O-Al_2O_3-B_2O_3-SiO_2:Ag, photochromic glass, EPR of Ag^{0} and Ag_2^{+} centres 77−24741
Na_2O-GeO_2, glass, thermolum. rel. to coordination number 77−16405
Na_2O-SiO_2:Au+CeO_2, Au particle nucleation 80−81066
NaOH, frozen soln., EPR of trapped H-atoms produced by UV and X-irrad. 80−3369
NaOH-D_2O, glassy matrix, absorpt. spectra after X-irrad., solvated electrons 79−65903
Ni melt, struct. charact. time depend. in X-ray studies *(Russian)* 80−24350
$PbMoO_4$, defect electron centres after X-irrad. 79−55738
PbO:Ag film, X-ray stimulated diffusion, current-voltage characts. 77−80653
$PbWO_4$, EPR of radiation induced MoO_4^{3-} centres 78−80217
$Pb(WO_4)_{1-x}(MoO_4)_x$ mixed crystals, X-irrad., EPR and thermoluminesc. 79−15352
RbCl:Cu, X-irrad., ESR of noncentral Cu^{0} atoms, 20-180K 77−24739

X-ray effects continued
RbCl:Sn crystals, effect an absorption spectra 78−76500
RbCl(Br), cation defects creation mechanism 80−75224
S photoelectret produced in polycrysts. in elec. field 78−31147
S, polycryst., photoelectret state following X-irrad. 80−60485
SbSI, ferroelectric semicond. anomalous photovoltaic effect due to ionising radiation 80−29437
Se, electrical conductivity after X-ray irradiation 79−51567
Se, electroconductivity *(Russian)* 80−15519
Se xeroradiography films, photosensitivity recovery from X-ray induced fatigue 77−2709
p-Si, subthreshold defect prod., Hall meas. of carrier conc. and photocond. spectra 77−89470
Si, X-irrad., photocond. spectrum 77−15903
p-Si, X-ray bombard. effects on elec. resist., and carrier density, annealing effect 77−4125
Si/Au interface, X-ray dose enhancement, Monte Carlo calcs. 79−22484
Si-Au(Rh)(In), Schottky diode, X-ray effects on elec. props., irrad. induced diffusion 77−4439
Si-In(Rh)(Au) Schottky diodes, X-ray irradiated, radiation-accelerated diffusion of impurities in Si 78−26952
SiC, radiation resistant substrate materials, for X-ray gratings 80−90960
SiO, doped, thermal stability of hole centres and hole recombination luminescence *(Russian)* 78−72614
SiO_2 in FET, electron trapping due to electron beam deposited Al 78−80060
SiO_2 in MOS struct., location of positive charged generated by UV and X-irrad. 77−51820
SiO_2, vitreous, X-ray compaction efficiency 80−65044
SiO_2:Ag, cryst. and glassy, X-ray induced EPR and luminesc. centre 80−65043
$SrCl_2$, F-centre production mechanism, radiolysis exam. 79−23602
$SrF_2:Cd^{2+}$, irrad., ESR of Cd^+ centres 77−59459
SrF_2:Ni, X-irrad., optical absorpt. spectra and dichroism meas. 80−108239
SrFCl, thermolum. and optical absorption spectra 80−66309
$SrSO_4$, celestite, colouring mechanisms 79−82998
Sr0, x-irradiated, intrinsic V^- and V^0 centres, ESR exam. 77−40126
Tb_2O_3-P_2O_5-MO system glasses, (M=Mg, Ca, Sr, Ba or Pb), photoluminesc. under X-ray excitation 80−89060
TiO_2, thermally stimulated exoelectron emission *(German)* 80−66404
TiO_2, X-irrad., adsorpt. of O_2, EPR meas. 78−80211
V_2O_5, thermally stimulated exoelectron emission *(German)* 80−66404
YAG, colour centres conceived as bound polarons 78−63990
$YAl_3(BO_3)_4$, thermolum. anal. 79−87514
YIG, influence of X-ray radiation on mag. props. 77−8337
$Y_2O_3:Zr^{3+}$, F-centre charge state, ESR and thermally stimulated luminesc. obs. 80−60418
ZnO, thermally stimulated exoelectron emission *(German)* 80−66404
ZrO_2, Y_2O_3-stabilised, X-irrad., thermoluminesc. 77−48259
ZrO_2-Y_2O_3:M^{3+}, M=transition metal, X-ray luminesc. 77−44063
$ZrSiO_4$, X-irrad., trapping and emission centres, OH^- ion contribution 80−80876

X-ray emission spectra
see also appearance potential spectra; conversion electron spectra
actinide compounds, spectroscopic techniques for electronic props. meas. 80−11427
actinide fission product X-rays in micas, comparison with superheavy elements K- and L-shell ionisation estimates 77−50581
actinides, 3d X-ray spectra, 4f and 5f states 78−84681
actinides, expt. and theoret. binding and transition energies, review 78−50497
actinides, K X-ray energies, natural widths and intensities 80−37768
air/glass interface, ns. grazing discharge, X-ray emission 80−33846
Al, one-electron calcs. of X-ray absorpt. and emission, jellium model 78−56543
alkali halide, irrad. stability obs. using X-ray emission meas. *(Russian)* 80−66326
alkali silicate glasses, struct. and thermal props. 80−84075
alkaline earth metals, atomic interaction effects in X-ray emission spectra *(Russian)* 79−69905
alkaline earth oxide, irrad. stability obs. using X-ray emission meas. *(Russian)* 80−66326
aluminosilicate minerals, X-ray spectral study, emission bands, quantum yield, tetrahedra valence band 77−28660
antiprotonic atoms, X-ray transition energies, strong interaction and $\bar{p}$ mass meas. 78−25759
antiprotonic atoms of light nuclei and isotopes, $\bar{p}$-n strong interaction effects 78−29867
antiprotonic H atoms, first obs. of L X-rays 78−90111
archaeological artifacts, particle induced X-ray emission anal. 77−70398
astronomical, X-ray sources, emission mechanisms, detection techniques 77−22061
astrophysical X-ray spectra, limitations, comments and reply 77−56824
astrophysical X-ray spectra, usefulness 77−56823
atom, $20 \leq Z \leq 90$, $K\alpha_2$ intrinsically inverted transitions 77−61701
atom, Compton profile asymmetry obs., Al, Ti, Fe, Cu, using $K\alpha$ fluoresc. 77−57937
atom, electron impact ionis., X-ray and Auger spectra, ang. distrib., polaris. 77−75305
atom, electron impact ionisation, characteristic X-radiation ang. distrib. obs. 80−1069
atom, inner-shell ionisation, fluoresc. X-ray ang. depend. 77−10649
atom, inner-shell photoionis., anisotropy of X-rays and Auger electrons 78−58633
atom, K_η hypersatellite ratio, intermediate coupling 77−3296
atom, K_α/K_β ratio for X-ray transitions in collisions 80−27972
atom, K_α/K_β X-ray intensity ratio, depend upon energy of incident proton 80−47934
atom, $K\beta/K\alpha$ ratio anomalies, K-capture rel. to bremsstrahlung excitation 77−18825
atom, K lines, chem. shifts, free-at. approximation interpretation 77−50395
atom, multielectron, correlated transitions in decay of two inner-shell vacancies 80−37799
atom, outer shell ionisation, ang. distribs. and polaris. of charact. X-rays and Auger electrons 79−10205
atom, pionic, π^- rest mass determ. 77−268
atom, reson. Raman X-ray scatt., K-vacancy excited state widths, appl. to Zr, Mo, Rh, Ag and Sn 79−45661

X-ray emission spectra continued
atom, satellite line spectra, spin doublet emission, common doublet levels 77−10621
atom, Slater transition-state calculations of multi-electron X-ray transition energies 78−90110
atom, Sommerfeld screening parameter σ_1, Z=13 to 103 78−25463
atom, transition array and energy level distribs. variance, Mo VX-XIV appl. 80−37767
atom, X-ray lines involved in K-capture, hyperfine struct. *(Russian)* 79−85931
atom, X-ray satellites, $L\beta'_1$ and $L\beta''_1$ 77−42266
atom+H^+ ion collisions, Z=35 to 56, L X-rays, Coster-Kronig threshold effects 77−18831
atom+ion collisions, continuum photon emission, radiative electron capture, mol. orbital emission 77−42401
atom+ion collisions, KK-vacancy sharing, X-ray emission 78−42190
atom+ion collisions, MO, radiative electron capture X-ray emission 77−19043
atom Breit interaction between electrons, calc. angular coeffs., computer program 80−18779
atom-atom collisions, X-ray continua from coalescing atoms 77−530
atom-ion collision, X-ray cross-sections, plane wave Born approx. 77−68094
atomic, Z=20 to 90 $K\alpha_1/K\beta_1$ X-ray intensity ratio rel. to at. number 77−23457
atomic inner shell electron props., relativistic effects 77−18803
atomic inner shell ionisation by electrons, positrons, protons and α-particles 77−46643
atomic inner shell ionisation phenomena, conf., Freiburg, West Germany (Mar.-Apr. '76) 77−27040
atomic inner shells, multiply ionised, satellite spectra, energy levels 77−18833
atomic K and L X-ray line widths determ. 77−42265
atomic K-shell ionisation by relativistic electron impact, X-ray emission 77−23565
atomic radiative and radiationless yields, K and L shell 79−76376
atomic screening model for solid-state effects 77−73194
atomic spectral line shifts for heavy quark atoms 78−62965
atomic X-ray spectra, parity violation, from electron-nucleus weak currents *(Russian)* 79−22642
atoms, electronegativity scale determ. from effective nuclear charges and X-ray spectra 77−75037
atoms, excited, collisionally aligned, angular correl. of autoionisation electrons, photons 77−14385
atoms, Z=46-54, $L_{\gamma 2,3}$ emission spectra, breadth, dynamical effects 80−32645
beam-foil projectile K X-rays, configuration rearrangement effects 77−46634
benzene free and coordinated mols., X-ray and X-ray electron spectra 77−27087
blood plasma, X-ray emission anal. by proton excitation 79−84054
book on X-ray spectroscopy 80−2899
borides, MB_{12}, exam. of electronic structure, using X-ray emission spectra *(Russian)* 79−33865
bremsstrahlung spectra computation rel. to Ge(Li) detect. meas. spectra 79−52047
bremsstrahlung spectra stripping up to 300 kVp on desk type computer 79−83846
cadmium, $L\alpha$ X-ray spectra, $_{40}$Zr to $_{48}$Cd, linewidths 79−41131
carbon tetrachloride, low-energy X-ray emission spectra, MO anal., ionis. pot., rel. to CH_4 and $CHCl_3$ 79−85975
cellulose, proton and photon induced X-ray emission anal., depth sensitivity 78−23988
chain method appl. to electron emission 78−43983
chemical shift meas. using automated X-ray fluoresc. spectrometer system 78−4750
chemical shifts of hard X-ray lines, applicability of Koopmans' theorem, HF calcs. 80−74145
compound nucleus prompt K X-rays from heavy ion reactions 79−67768
Cr, double K-shell ionisation by electron impact, X-ray spectra 78−62928
crystal, coherent X-ray generation by relativistic charged particle 78−60531
crystals, biatomic, charact. X-ray intensities, depend. on cryst. orientation 77−63488
crystals, electron spin correlation, gamma-ray and X-ray production 79−11486
Cu_cNi_{1-c}, soft X-ray emission spectra 78−95620
cyclotron X-ray spectroscopic analysis of elements from Ti to Cs 79−100474
diborides of light metals, X-ray emission spectra and transition probability calcs. *(Russian)* 77−52203
dielectronic recombination spectra, appls. in astronomy 80−46391
disordered systems, study by EXAFS, limitations 79−43065
dynamical calculations 80−55227
electron and positron relativistic channelled beams, X-ray and γ-ray emission 77−36304
electron backscattering, X-ray prod., transport eqn. soln. 79−38698
electron probe X-ray microanalysis, quantitative investigation of thin specimens 80−101068
electron rearrangement in K X-ray spectra due to heavy ion bombardment 77−85846
electron-beam sliding spark device, C^{4+} plasma, soft X-ray emission, no superradiant gain 78−79444
elements, high Z, photoelectric L-shell cross-sections, 37, 74 keV 77−57950
emission energies calc., evaluation of mathematical expressions 77−29065
energy-dispersive, radiative Auger-like satellites 78−5168
energy-dispersive fluorescence spectra, interpretation 77−36820
ethylene free and coordinated mols., X-ray and X-ray electron spectra 77−27087
EXAFS, fluorescence detection, sensitivity enhancement for dil. species and thin films 77−85843
exploded-wire plasmas, spatial resolution techniques 78−14188
fast heavy particle collisions, radiative ionisation 77−14562
ferricyanide, X-ray spectral study of electronic struct. 77−28652
ferrocyanide, X-ray spectral study of electronic struct. 77−28652
fission fragment X-rays from $^{235}U(n,f)$ 3.5 MeV 77−18638
fluorapatite, proton and photon induced X-ray emission anal., depth sensitivity 78−23988

X-ray emission spectra continued
fluorescence spectra, energy dispersive, least-squares anal., detector response function approach 80−3457
fluorescence spectra, resolution by weighted least squares computer program 80−3459
fluorescence spectra of light elements by using synchrotron orbital radiation 78−39630
fluorescent X-ray source for study of radiographic imaging systems 78−24132
fourth-row elements, Pd to Xe, XPS, XES, dynamical effects 80−52924
graphite, X-ray emission and absorption, XPS, electronic struct. 77−16431
grazing incidence concave grating spectrometer for ultra soft X-ray emission spectra 78−62273
hard X-ray energy and flux meas. for 50 keV to 10 MeV range 80−48992
heavy elements, $74<Z<93$, L-subshell vacancy relative radiative decay rates 78−55137
heavy ion+at. collisions using GSI linear accelerator, X-ray production, appls. 77−19041
heavy ion+atom, $3d\pi$-$2p\pi$ radial coupling, symm. and near symm. collisions 77−71857
heavy ion+atom, double K-shell vacancy sharing 79−45809
heavy ion+atom, radiative electron capture, target thickness depend. 78−58778
heavy ion+atom collisions, accelerators and X-ray emission spectra *(Norwegian)* 78−22013
heavy ion+atom collisions, K X-ray transition energies, two electron-one photon mechanism 77−18828
heavy ion+atom collisions, mol. M-X-rays, self-consistent relativistic HF-Slater many electron correl. diagrams 77−14567
heavy ion+atom collisions, quasimol. X-ray line tails 77−14564
heavy ion beam-foil spectra, ion equilib. excitation, density effect 77−19056
heavy ion bombardment, swift, X-ray prod. *(Japanese)* 77−23540
heavy ion collisions, Doppler shift of continuum X-rays from quasimols. 79−22808
heavy ion collisions, electron EM field interaction, quantised field formalism 80−83478
heavy ion collisions, electronic states in rot. two-centre Coulomb systems 77−14561
heavy ion collisions, molecular-orbital X-rays yield 78−13587
heavy ion collisions, quasimol. KX-ray spectra, Doppler shift 77−19044
heavy ion collisions, radiative electron capture, line profiles 77−14565
heavy ion produced, K_β/K_α intensity ratios 78−78658
heavy ion-atom collisions, inner shell ionis. X-ray emission and Auger spectra obs., appls. *(Japanese)* 78−9240
heavy ions passing through gas or solid target, electron capture effect on X-ray emission 77−27169
heavy-ion collision, azimuth angle depend. of quasimolecular anisotropy 79−68298
heavy-ion collision, quasimolecular L X-rays, relativistic self-consistent correlation diagram 78−5247
heavy-ion collisions, intermediate L-K mol. orbital radn. spectral distrib. 77−50511
heavy-ion collisions, K-vacancy prod., K-L level matching 78−42196
heavy-ion collisions, X-ray transitions induced by nuclear charges movement 77−50510
heavy-ion collisions, $Z\geq35$ projectiles, 12 to 470 MeV, K-vacancy cross sections 77−19026
heavy-ion impact on solid targets, mol. orbital X-rays 77−69957
highly ionised atoms, L-shell refilling rate in solid 77−12469
II-IV-V_2 semiconductor, electronic struct. determ. 77−76751
III-V semiconductor, electronic struct. determ. 77−76751
implanted ion detection by X-ray emission anal. in TEM 78−51575
impurity atom position determ. from ion-excited characteristic X-ray emission *(Russian)* 78−47408
inert gas atoms, double ionisation by electron impact, soft X-ray emission *(Russian)* 77−34766
inert gas binary mixture, μ-capture, near 5 atm., X-ray yield 80−58419
inorganic compounds, chemical bonds using $K\alpha_1$ line chem. shifts, Mossbauer isomer shifts 77−27089
interband transition probabilities calc. based on muffin tin potential 80−104014
ion, in exploded-wire plasma, inner-shell X-ray spectra 77−27720
ion+atom, low vel., X-ray emission ang. distrib., MO calc. 79−54803
ion+atom (molecule), slow collisions, K-shell excitation, impact parameter depend. 79−72388
ion+atom collision, electron spin coupling in rot. frame, X-ray emission 79−36724
ion+atom collisions, mol. X-ray anisotropy 77−19046
ion+atom collisions, X-ray polarisation 79−45810
ion excitation, review 79−49976
ion-atom collisions, X-ray prod. and detection, book contrib. 78−74757
ion-induced X-ray prod., solid-effects 77−77326
ion-induced X-rays, review 79−96405
ion-surface impact, MO X-ray spectra, recoil effects 80−25510
ions, highly charged, impact excit. dielectronic satellites 78−62762
ions, two vacancies in K shell, 2 electron 1 photon, and hypersatellite transition probabilities 78−46294
ions backscattered from solid surfaces, radiative electron capture 78−11057
ions moving through solids, charge states determined by X-ray spectra 79−83061
ions moving through solids, X-ray emission 79−83062
K_β X-ray width meas. with bent crystal spectrom. 77−30697
K_β/K_α X-ray intensity ratio used to obtain efficiency curve of planar Ge(Li) detector 80−880
$K\alpha\alpha^h$ emission, method for L-shell config. calc. 77−42269
$K\alpha\alpha$ and $K\alpha\beta$ transitions obs., following ion+atom double ionis. 77−57918
$K\beta/K\alpha$ rel. intensity obs., $33\leq Z\leq57$ 80−32665
K level X-ray lines, relative transition probability 80−935
K shell prod. cross section of Ti, Cr, Fe, Ni, Cu, Zn for 75 to 150 keV p and e excitation 79−47552
K-satellites, screening effect 80−999
K-shell emission at satellite altitude from proton precipitation 78−61641
K-shell prod. cross-sections of Sc, Ti, V, Mn, Fe, Co, Ni for 4-38 MeV B ions 77−69958
K-spectra, origin of low-energy satellites, α-region 80−55229

X-ray emission spectra continued
kaonic hydrides (deuterides), Z=3, 6, 8, 11, 20, X-ray intensities, comparison with the atoms 77−58212
kinematic dipole model for the anisotropy of quasimolecular X-rays 79−13814
L shell prod. cross section of Zr, Mo, Ag, Cd and In for 75 to 150 keV p and e excitation 79−47552
L X-ray spectrum, L_1 subshell yield from ^{181}W electron capture decay 79−49608
L-shell X-rays of elements Z=35 to 56, Coster-Konig threshold effects 77−18831
L-vacancy production, near symmetric heavy ion collisions, projectile and target X-ray spectra 79−89768
lanthanide atom+H^+, L-subshell ionisation cross-section, 150-400 keV 79−45665
large M0 K X-ray, anisotropy from Ne on Al foil 78−55254
laser plasma, electron density determ. from X-ray spectra of multiply charged K ions 78−94938
light elements ($Z=15$ to 28), $_5{}^{10}B$ ion bombardment, K-shell ionisation, X-ray obs. 78−95619
light metal, soft X-ray emission spectra, renormalisation theory 78 52595
line emission from single and multiple exploding wires 77−84519
line profiles evolution due to Comptonisation, Monte Carlo computations 79−66916
liquid alloys, magnetic properties, review, soft X-ray emission spectra 79−51741
low alloy steel, alloying constituents, XES determ. 78−73126
lutetium diphthalocyanine, solid-state anion migration in anodic oxidation 80−60994
M shell prod cross section of Au, Pb and U for 75 to 150 keV p and e excitation 79−47552
M-subshell direct Coulomb ionisation, X-ray emission, PWBA calcs. 79−45664
many body effects 78−27374
meson transfer reactions in solids, surface struct. effects 80−104015
metal, 3d, X-ray emission and XPS broadening, many-body effects and intra-atomic exchange 77−44090
metal, bandwidths from characteristic electron energy loss values 79−83057
metal, core spectra, independent-electron metal calc. 79−83056
metal, effects of correlation interaction of electrons with deep holes in X-ray spectra 78−31279
metal, narrow-band extra-atomic relax. and X-ray spectra 77−24928
metal, renormalised first order theory 77−8688
metal, soft X-ray emission spectra and Fermi surface, contrib. of John Bardeen 80−57057
metal, valence band Auger spectra, effect of edge anomaly 79−69908
metal, X-ray emission edges, effect of incomplete phonon relaxation 78−35227
metal film, thickness meas., using nondestructive radioisotopic technique 80−68179
metal with finite lifetime of deep hole 77−85845
metallic film, single layer and multilayer, thickness determ. by X-ray fluoresc. 80−68180
metallic film, X-ray production by H^+ and $H_2{}^+$ impact, search for cluster effects 78−43961
metals, X-ray spectra, final state pot., one-electron theory 80−55230
metals and alloys, review of X-ray spectroscopy 77−55849
methane, C X-ray spectrum meas. by soft X-ray spectrometer 78−24911
methane, electron impact, Balmer-α emission Doppler profile energy depend. 77−42423
methane, low-energy X-ray emission spectra, MO anal., ionis. pot., rel. to CCl_4 and $CHCl_3$ 79−85975
Mg, K X-ray emission spectra, double plasmon high energy satellite 80−11510
microanalysis, sample sandwiched between anode and converter *(French)* 79−74471
microchemical analysis, optimising conditions, analytical electron microscopy 80−101067
mild steel, alloying constituents, XES determ. 78−73126
minerals, $K\alpha_{1,2}$ emission spectra, chem. shift, effective charges of Al,Si,Fe and O atoms 77−28659
mixtures, quantitative analysis using PES and XES 77−90678
molecular, collision dynamic effects 77−19045
molecular fluorescence, ultrasoft region, 5M grating spectrograph eval. for high resolution spectra prod. 79−27117
molecular orbital K X-ray anisotropy peaks, Z-depend. 77−58043
molecular orbital X-ray emission, from primary exciting collision 77−50449
molecular orbital X-rays, scaling law derivation 79−18284
molecular orbital X-rays from atomic and molecular impact on solid targets 79−36750
molecular X-ray fluorescence polarisation 78−1003
molecular X-ray fluorescence spectra, observation using 5 m grating spectrograph 80−86538
molecular X-ray transitions in heavy ion-atom collisions 80−43170
molecule, free, ultra-soft X-ray emission spectroscopy, correl. with electron spectroscopy 78−50558
monazite inclusions in mica, proton-induced X-ray emission, evidence for primordial superheavy elements 77−9429
multielement anal., proton-induced X-ray emission 78−85272
multiply charged ions, multiply charged, laser plasmas, 1.5-15 Å 78−13462
muonic atom cascade program, X-ray calcs. and cataloguing 78−90323
muonic atoms, X-ray emission polarisation *(German)* 80−69268
muonic atoms, X-ray meas., vac. polarisation test 78−29287
Muonic atoms, X-ray vacuum corrections, nuclear moments, transitions and deformation parameters 80−37912
muonic K_β/K_α ratios from pure elements 79−68335
muonic X-ray intensities in low-Z elements and their hydrides 80−9761
muonic X-rays, circular polarisation *(German)* 80−69266
muonic X-rays, formation and expts. 80−43215
$Na_2[Fe(CN)_5NO]$, valence levels, X-ray photoelectron and X-ray spectra 77−88500
narrow band metals, extra-atomic relax., X-ray spectra 77−36312
neutron induced X-ray atomic excitation 80−23510
niobium, Lα X-ray spectra, $_{40}Zr$ to $_{48}Cd$, linewidths 79−41131
nuclear excitation by electron transition (NEET) 77−34256
nuclear K-X-ray satellites, Z=50-83, by α-bombard, 17.5-22.5 MeV 80−42984

X-ray emission spectra continued
organic compounds O emission spectra Kα line from carbonyl compounds 77−28653
organometallic compounds containing hydrocarbon π ligands, X-ray spectral study of electronic struct. 77−27088
oxide target, MeV ion bombard., multiple inner-shell ionisation 77−8686
oxides, muonic X-ray spectra, empirical intensity correls. 78−90326
oxides of third-row elements, Auger LVV transitions, X-ray photoelectrons and emission spectra 78−21978
paradichlorobenzene, electronic struct., X-ray emission obs. 78−5246
perovskites, $(AA')(BB')O_6$, ion valency pairs determ. from lattice consts. 77−43195
pionic atom, X-ray intensity, at. no. variation, Z=5-90 80−43212
pionic atom broadened X-ray lines, appl. of absorpt. edge technique 78−70976
pionic atoms, strong interaction effect, pionic X-rays 79−76535
PIXE, 3 parameters determ. of depth profile of foreign atoms in bulk material 79−4331
PIXE, medium and heavy element anal. by K X-ray fluorescence, 20 to 50 MeV protons 79−57312
PIXE, sensitivity of high energy anal. in different matrix materials 79−16086
PIXE, single photon emission in double K-shell ionisation 77−71864
PIXE appl. to trace element anal. 77−48717
PIXE high intensity sub-kV source for detector calib. 77−71714
plasma, electron temp. and spatial distrib., soft X-ray meas. *(Russian)* 77−47260
plasma, laser induced, X-ray camera development 77−54031
plasma, laser initiated, X-ray diagnostics appl., review 77−55176
plasma, laser-produced, X-ray spectra 80−75075
plasma diagnostics with EUV and X-ray high resolution spectra 77−84522
plasma dielectronic satellite spectra, electron collisions, corona model theory 80−59188
plasma focus, hard X-rays indicating electron beam 79−14613
plasma focus, microinstabilities, current driven, suprathermal microwave emission and soft X-rays obs. 77−89328
plasma spectra, errors in differential emission measure solns. 79−12397
plasma XUV transition Doppler broadening suppression, collisional-radiative model 80−19614
polycrystalline luminophors, energy yield of X-ray luminesc. *(Russian)* 77−48280
polyethylene, C muonic X-ray spectra, H(D) isotope effects 77−75344
polyethylene, X-ray emission spectra of CO_2 laser-irrad. targets, nonlinear processes 80−33793
proton-induced X-ray, human diseases and trace elements 77−70547
proton-induced X-ray emission and proton elastic scatt., atmospheric particles anal. 77−70399
protonium, atomic X-ray yields 1s and 2p level shifts and widths, cascades, calc. 80−78730
α-quartz, valence electron states and X-ray emission spectra, pseudopot. and OPW calcs. 77−35866
α-quartz, valence electron states calc. by pseudopotential method 77−20239
α-quartz electron states, self-consistent pseudopot. calc. 77−62823
quasimolecular X-ray emission in heavy-ion collisions, electron slip effects 77−19040
quasimolecule as atomic collision intermediate, superheavy, X-ray emission empirical scaling rule 79−76502
Quasimolecule formation in heavy ion collisions *(Russian)* 78−33568
quasimolecules, superheavy, M-like X-ray transitions 79−6951
radiography, diagnostic, X-ray spectra determ., high intensity 80−41217
radiography, diagnostic X-ray beam photon energy distrib. 77−70530
rare earth germanides, X-ray emission, absorption and photoelectron spectra *(Russian)* 80−11509
rare earth metals, atomic interaction effects in X-ray emission spectra *(Russian)* 79−69905
rare earth metals, X-ray 5p emission bands, valence energy band 80−104016
rare earth metals, X-ray $N_{IV,V}$ emission spectra in region of 5p→4d transitions *(Russian)* 78−6815
rare earth monophosphides, K-emission bands, electronic struct. 78−15250
rare earth vanadites, X-ray fluoresc., IR and UV spectra 77−77206
rare earths, 3d X-ray spectra, 4f and 5f states 78−84681
rare earths, compounds, K X-ray line shift associated with valency change and isomorphous phase transitions 79−47553
rare-earth metal tetraborides, electronic structure and bonding determ. 77−59646
refractory metal compounds, electronic structure and chem. bonding 79−27948
relative orbital electron capture probabilities, experimental techniques, review 77−18893
resonance fluorescence, in X-ray K-spectra *(Russian)* 78−37587
resonant X-ray Raman scattering, IR divergence of Compton effect 78−21873
satellite peaks, relationship between X-ray emission and X-ray photoelectron spectra 78−66492
scanning proton microprobe in atmospheric environment 77−70394
second-row elements, K-shell X-ray prod. by H(He) ion bombardment 79−47550
silicate binary glasses, SiKα and SiKβ X-ray emission spectra 77−24272
silicate minerals, X-ray spectral study, emission bands, quantum yield, tetrahedra valence bands 77−28660
simple metals, effect of core hole on X-ray emission spectra 80−20737
simple metals, X-ray threshold anomaly, exponents in theory 77−85838
single crystals, use of polarised radiation 78−8481
soft X-ray appearance pot. spectra, deconvolution 79−56886
soft X-ray transition radiation observation from medium energy electrons 80−76104
solid, appl. to studies of band struct. *(Polish)* 79−56887
solids, X-ray prod. range by 2 to 15 keV electrons, thin film and bulk targets 79−19298
spark source (RF), of mass spectrometer, analysis of hard X-ray emission 79−90480
spectral line breadth, anal. method using Voigt function 78−34387
spectrometer for soft X-ray emission studies of liquid metals and metallic vapours 80−73564
stainless steel, alloying constituents, XES determ. 78−73126
steel, stainless, proton and photon induced X-ray emission anal., depth sensitivity 78−23988

X-ray emission spectra continued
superdense plasma, X-ray emission, plasma diagnosis *(Russian)* 78−30487
superheavy and intermediate atomic collision systems, UNILAC expts. 80−63751
superheavy element data from monazite, background re-evaluation 77−33077
superheavy elements, L and M spectra 77−38631
superheavy elements, Z=114, 126, 134, 145, 164, 173, electronic transition rate calc. 77−26999
superheavy elements in monazite crystals, proton induced X-ray spectra 77−17106
superheavy quasimolecules, Bang Hansteen scaling rule, $Kα_1$ line anal. 79−10126
superradiance, criteria 77−88680
surface bombardment, by electrons, protons and heavy ions, characterisation of materials 79−96406
surface electron states, valence band spectroscopy in ultrasoft X-ray region 77−55852
surface layers, methods, results of studies of atomic states and elemental composition 77−29063
surface plasmon obs. 78−92146
symmetrical molecule, interference effects in electron impact induced X-ray emission spectra 77−83640
target, ion beam heated, soft X-ray and VUV spectra 80−2907
techniques and spectral interpretation, rel. to XPS, book contrib. 80−11514
theory, techniques, and appl., book 80−8748
thin film, electron-induced X-ray spectrometry anal. *(French)* 79−43067
thin film, sputter profiling, combined Auger-X-ray anal. 80−66909
thin films, thickness meas. anal. characterisation using proton-induced X-ray emission 80−35618
third-row elements, at. K-shell X-ray prod. by $^{14}N^+$ bombardment 80−91482
third-row elements, L-shell X-ray prod. by H(He) ion bombardment 79−47548
time-resolved X-ray spectroscopy of laser-produced plasmas 80−84004
TiO, local density of states, X-ray spectra, Hartree-Fock and Xα calcs. discrepancies 79−77980
Tokamak plasma confinement systems, soft X-ray meas. 80−48959
transition elements, first-group, K-emission satellites, quasi-stationary states and origin 80−80903
transition metal, effect of correl. interaction of electrons with core holes 78−92178
transition metal, energy band structure and X-ray emission spectra, calc. *(Russian)* 77−1763
transition metal, many-config. approx. in X-ray and electronic spectra interpret. 80−32615
transition metal atom+O ion, K X-ray prod. 77−23554
transition metal carbide, X-ray emission band exam. and electronic struct. 77−8689
transition metal carbonitrides, carboxides and oxynitrides, electronic struct., theoretical approach 80−54584
transition metal compounds, chem. shifts of X-ray emission K-lines of transition elements, free-atom approx. applic. 80−11513
transition metal compounds, valence band struct., X-ray spectroscopic study 80−29319
transition metal germanides, X-ray emission, absorption and photoelectron spectra *(Russian)* 80−11509
transition metal nitrides, X-ray emission band exam. and electronic struct. 77−8689
transition metal sulphides, electronic struct. from X-ray emission spectra 77−28661
transition metal-Al, X-ray spectra, electronic structure 79−78793
transition metal-oxygen compounds, salts, X-ray Lα emission spectra, excited states calcs. 79−59488
transition metals, 3d, electron impact excited soft X-ray spectra, resonances and many body effects 80−50468
transition metals, 3d-, 4d-, 5d-, band struct. from spectral data and theoret. calcs. *(Russian)* 77−8013
transition metals, electronic struct. and X-ray emission spectra calc. 77−28105
transition metals, high spin compounds, X-ray and photoelectron spectra, one-config. approx. 78−92145
transition metals, resonant Raman scatt. and fluoresc. near K-absorpt. edge 79−52042
transition metals and alloys, appl. of X-ray spectroscopy to band struct. study *(Polish)* 79−56887
transition metals and compounds, L_l and L_η X-ray emission spectra 78−39631
transition radiation, spectrum and energy depend. meas. 78−68577
transition radiation freq. spectrum from 5, 9 GeV electrons on multiple foils 77−27907
trichloromethane, low-energy X-ray emission spectra, MO anal., ionis. pot., rel. to CCl_4 and CH_4 79−85975
ultrarelativistic charge collision with atom or diatomic mol. *(Russian)* 78−70776
weakly inductive vacuum discharge, multiply ionised Fe ion spectra *(Russian)* 77−76224
X-ray and electron spectra excited by atomic collisions, beats mechanism *(Russian)* 79−94075
X-ray energies meas. by soft X-ray spectrometer 78−24911
X-ray intensity ratio $Lβ/Lα$, atomic number dependence 80−62818
X-ray lasers, plasma, production, optical transitions of multiply charged ions, population inversion, review 77−19227
XUV region, spectral and time-based anal. using streak camera *(Italian)* 78−54513
Z=132 quasi-atom, I-Au system, X-ray spectra 77−14177
Z=13 to 92, inner shell ionis., by ultrarelativistic electrons, scaling law 77−54615
Z=8-50 kaonic atoms, X-rays, strong interaction effects 80−9763
Z-dependence of the intensity of $|\Delta n|=2$ pionic X-rays 79−94111
zeolites, coordination of Al and Si from X-ray spectra 78−11021
ZnO-based varistor, grain-boundary segregation, thin film X-ray spectroscopy obs. 80−35185
Zr, X-ray emission spectrum, K-satellites 80−40188
μ^- K-shell X-ray transitions in F, Na, Al, Si, P, S, K, nuclear charge radii 78−66195
$\mu^\pm$ spin rotation, μ relaxation and repolarisation, muonic X-rays 80−42644

X-ray emission spectra continued
μXe muonic atoms, vanishing muon transfer effect 80−9765
$\pi^+\pi^-$ atomic bound states and $\pi\pi$ scatt. lengths in H_2 gas target, X-ray spectra 77−27206
A15 compounds, electronic struct., XPS and SXE spectra calc. 79−42437
Ag, electron impact ionis., X-ray obs., 3000 to 6000 keV, measuring system 77−68116
Ag halide photochromic glass:Cu^{2+}, characterisation of Cu ions 78−5530
Ag halides, tetrahedrally coordinated, semiempirical band struct. model 77−51655
Ag, K-shell ionis., X-ray prod. cross section for incident H^+, ^4He and ^{14}N ions 78−70923
Ag, K-shell X-ray prod. by H^+ and He^+ bombardment, cross sections, energy depend. 78−5337
Ag, K-shell X-ray spectra, $K\beta_2/K\beta_1$ determ. 77−23456
Ag, $K\beta_3/K\beta_1$ and $K\beta_2/K\beta_1$ relative intensities 77−75088
Ag, L-X-ray emission spectra, hypersatellite origin 79−89629
Ag, L-series X-ray spectrum, anal. Coster-Kronig calcs. 77−75091
Ag, Lα X-ray spectra, $_{40}$Zr to $_{48}$Cd, linewidths 79−41131
Ag photoelec. cross sections, 5-40 keV photons, X-ray emission spectra 77−18866
Ag plasma, laser produced soft X-ray spectra, transitions 77−15171
Ag, X-ray prod. by 5 MeV/amu deuterons (oxygen ions), projectile Z depend. 80−42982
Ag-Ge(Si) eutectic alloy, X-ray spectral exam. *(Russian)* 77−63489
Ag+Ag symmetric collisions, MO-2pσ radiation anisotropy, quasimolecular nature 78−70924
$Ag+H^+$, characteristic X-ray emission polaris. *(Russian)* 79−59394
$Ag+H^+$, excited X-ray polarisation, Born approx. calcs. *(Russian)* 80−78566
$Ag+H^+$, X-ray emission, optical transition radn. 78−58618
$Ag+H^+(O^{5+})$, L-shell X-ray prod. cross-section determ. 77−6913
$Ag+I^+$, impact parameter depend. of K X-rays 78−94308
$Ag^{+14}N^{n+}$, 7-35 MeV, K-shell X-ray production cross sections 77−75090
^AAg, A=97, 98 and $99^{g,m}$ decay spectral meas. 78−93976
Al, bremsstahlung isochromat beyond Duane Hunt limit 77−73188
Al, bremsstrahlung spectra, 10 to 30 keV, thick target expts. 77−8687
Al, chem. environment effect on Kα satellites intensity, heavy-ion collisions 77−54527
Al coated glass microballoon targets for laser implosion expt., search for shell disintegration 80−33792
Al, energy bands, densities of states and X-ray spectra, superposed self-consistent pots. 78−39010
Al, incomplete phonon relax. in X-ray emission calc. 77−52202
Al, ion beam bombardment, $(1s^{-1}2p^{-1})^1P_1$ state nonstatistical population, X-ray spectrum 78−62894
Al, K X-ray absorption, K-emission spectrum, band struct. using APW method 80−97380
Al laser plasma, high-Z, temp. meas. from bremsstrahlung emission 80−87914
Al, many-body response in X-ray absorption, emission and photoemission spectra 80−16124
Al, muonic atoms formed by muon transfer free μp and μd systems, isotope effect on Lyman series 79−86090
Al, muonic X-rays following μ^- transfer from muonic H 78−55259
Al, range of 100 keV Pr^{2+} and Tb^{2+}, M-shell X-ray cross-sections 77−35614
Al, soft X-ray emission and absorpt. edges, self-absorpt. studies 80−40183
Al, Soft X-ray emission edge self absorption and effect of exciting voltage 77−90220
Al, soft X-ray emission edge, temp. depend. 80−89090
Al, soft X-ray spectrum, Al core state transition probabilities, band struct. calc. 77−77325
Al, surface, proton bombarded at 450 keV, X-ray bremsstrahlung, 2.5-8.5 keV 78−80436
Al targets, C contamination, in high vacuum electron excitation X-ray tube 79−44996
Al, thin film, K X-ray production due to ^{16}O ions, 0.25-2.25 MeV/amu 79−69906
Al ultrasoft X-rays, phys. props. and Chinese hamster cell expts. 77−86542
Al, X-ray absorpt. and emission edges, one-electron and many-body effects 80−25484
Al, X-ray continua emission, proton and ^{14}N bombard. 78−23559
Al, X-ray emission spectra, high energy plasmon satellite intensities 78−64430
Al, X-ray emission spectra of CO_2 laser-irrad. targets, nonlinear processes 80−33793
Al XIII, hot pinched plasma, Lyman series Stark profiles, electron density determ. 78−51348
Al^{10+}, $^4p^0_{5/2}$ state excitation energy, X-ray spectra 77−27017
Al^{n+} foil-excited ion, X-ray spectra and satellite classification 80−95567
Al-Cu, disordered, electron energy struct. and X-ray emission bands, average t-matrix approx. *(Russian)* 80−24779
Al-Ge eutectic alloy, X-ray spectral exam. *(Russian)* 77−63489
Al-Mg alloy, charge transfer, X-ray emission spectra exam. 77−47774
Al+Al, (Cl)(F), molecular K X-ray transitions, mol. radiative electron capture effect 78−58802
$Al+H^+(^3He)$ ion collisions, K-shell ionisation cross sections 77−23555
$Al+He^+$, X-ray spectra, two-electron one-photon transition in solid target, 2 MeV 78−94209
$Al+He^+(H^+)$, 1.9 MeV, Kα X-ray polaris. and line strengths 77−30983
Al+He(C)(N)(O), inner-shell multiple ionisation systematics, X-ray obs. 80−63790
Al+He(C)(O)(Ne), K-shell ionising collisions, average L-shell ionisation probability, K_α spectra 79−72408
Al+heavy ion, X-ray spectra, one-photon two-electron rearrangements 77−6712
$Al+N^{4+}$, Kα and Kβ X-ray spectra for 84 MeV incident energy 77−50517
$Al+N^{n+}(O^{n+})(F^{n+})$, X-ray prod. and electron transfer cross-section 79−45790
AlIX-XII, plasma, X-ray line radiation, radiation transport eqns., calc. method 80−64777
AlN, X-ray Kα satellite struct., target chemical effects, 38 MeV F ion bombardment 77−24910

X-ray emission spectra continued
Al_2O_3, irrad. stability obs. using X-ray emission meas. *(Russian)* 80−66326
Al_2O_3, Kα X-ray satellite struct., target chemical effects, 38 MeV F ion bombardment 77−24910
Al_2O_3-SiO_2-$Na_2O(Li_2O)$, coordination number study by AlK_α fluorescence X-ray spectra *(Japanese)* 77−73190
Al_2S_3, X-ray Kα satellite struct., target chemical effects, 38 MeV F ion bombardment 77−24910
Ar, 250 to 270 eV, new interpretation 78−33460
Ar, electron impact, L X-ray spectrum, radiative Auger transitions 80−58227
Ar, electron impact, struct. near $L_{2,3}$ edges 77−75083
Ar, free ats. electron bombard., subsequent X-radiation ang. distrib. 80−53144
Ar IX, Ne I like reson. and Na I-like satellite lines, relativistic HF calc. and expt. 78−94210
Ar, inner shell alignment calc. in electron impact ionisation 77−14586
Ar ion+target collisions, two-electron-one-photon transitions, X-ray spectra 77−19068
Ar, Kα X-ray satellite spectra, gas phase meas. 78−66496
Ar L-shell, X-ray emission spectra prod. by 0.3-3 keV electron impact, line intensities 79−45666
Ar, L-spectrum X-ray energies meas. by soft X-ray spectrometer 78−24911
Ar, lifetimes of L and LM vacancy states, X-ray emission linewidth 78−17621
Ar, multiply excited, inner level X-ray emission spectra, line widths and Auger transition rates 79−36575
Ar, pionic, X-ray ang. distrib. meas. 77−3496
Ar, single-K multiple L-shell vacancy prod. in ion collisions, X-ray spectra 79−22809
Ar, single-photon decay of ion states with two intrinsic $L_{2,3}$ vacancies *(Russian)* 77−6716
Ar supersonic jet, ultrasoft X-ray emission following electron excitation 77−27015
Ar, two-electron one-photon transition rate 77−71772
Ar XIII, Ar XIV in solar flares, atomic data rel. to XUV electron density diagnostics 79−88633
Ar^{15+} and Ar^{16+}, beam-foil obs. of lifetimes of metastable states 80−14116
Ar^{x+}, high resolution spectroscopy of prompt and metastable decaying levels 78−33462
Ar+Ar, K-X-ray excitation, 2.5-8 MeV, impact parameter depend. 78−50628
Ar+Ar low energy collisions, K X-ray excitation, impact parameter depend. 80−23539
$Ar+C^{4+}(C^{6+})$, K-shell X-ray prod. at high energy, charge state independ. 77−6905
$Ar+Cu^{x+}(11\leq x\leq 22)$, 1 MeV/amu, X-ray production cross-sections 78−37714
$Ar+H^+$ ions, K-Auger spectra, relative satellite line intensities, X-ray spectra 77−19066
$Ar+Li^{+1,2,3}$, K-shell ionisation depend. on projectile charge state 77−34743
Ar+N ion, Kα X-ray satellites prod. 80−9541
Ar^++Ar, L-shell X-ray cross sections, 0.2-1.5 MeV, fluoresc. yield 78−1068
Ar^{2+}+Al(Sn), impact-parameter depend. of K- and L-X-rays 79−76501
Ar^{x+}+Sn(Sb)(Xe), vacancy sharing between K and L shells in 3dσ mol. orbital 79−22807
As, L-shell soft X-ray emission spectra, oscillator strengths 80−32651
As-S glasses, spectral variation of SKβ emission with S content 79−8209
As_2O_3, density of valence states, photoemission meas. 77−72808
As_2O_3, electronic struct., X-ray emission, XPS, UPS obs., CNDO cluster calc. 78−52638
As_2O_3, X-ray emission spectrum and XPS, electronic struct. calcs. using scattered wave method 79−11502
As_2S_3, electronic struct., X-ray emission, XPS, UPS obs. 78−52638
^{33}As, origin of high and low freq. K-satellites in X-ray emission spectra 80−50466
Au, electron impact L-shell ionis., 300-600 keV 77−50542
Au, energy band structure, X-ray N-emission spectra, relativistic APW calcs. 80−70596
Au, energy band structure, X-ray emission spectra, APW calc. 80−92811
Au, inner-shell ionis. by relativistic electron and positron impact 77−6933
Au, L$_\beta$ emission band, surface plasmons in X-ray emission bands 78−92146
Au, L-X-ray production by 9.5 to 41.8 MeV Fl ions 77−85847
Au, L-shell electron impact ionisation, X-ray production cross sections 77−19095
Au, L-subshell ionisation cross-section ratio determ. by ion beam impact 77−6920
Au, Lα X-rays produced by surface impact of F^{n+} and Si^{n+} 79−69907
Au single cryst., thin films and bulk, anisotropic X-ray emission 80−108303
Au, X-ray cross sections, L-shell, proton induced, 1 to 3 MeV range 79−1799
Au-M (M=Cd, In, Sn, Sb, Te), charge-transfer and valence-band behaviour using ^{197}Au Mossbauer and X-ray photoemission spectra 79−60695
$Au+{}^4He^{2+}$, L-shell ionis. probability, X-ray prod. 79−18276
$Au+H^+$, atomic K-shell ionis., X-ray emission 79−18280
$Au+H^+$, L X-ray production cross sections, 0.3-1.8 MeV, expt. rel. to PWBA prediction 80−53115
$Au+H^+$, L-shell ionis., 0.5-3.5 MeV, X-ray emission obs. 77−54528
$Au+H^+$, L-subshell ionisation cross-sections, X-ray meas. 77−46520
$Au+H^+$, L-subshell X-ray prod., cross-section meas. 77−46575
$Au+H^+$ ionisation, induced L-shell alignment 80−32813
Au+I, noncharacteristic X-ray emission, self-consistent relativistic many-electron correl. diagram 77−19023
Au+I collisions, average ionisation probability of Au meas. 77−68005
^{79}Au, electron impact, relativistic, L-shell ionis., Lβ/Lα branching ratio energy depend. 79−98228
$^{79}Au+{}^{19}F(^{28}Si)$, target L$\alpha$ X-ray prod., projectile charge state depend. 79−47549
$^{197}Au(^6Li,xn)$, 75, 85, and 95 MeV, K X-ray multiplicity 79−76019
B, B K X-ray, chemical bonding and multiple ionis. effects 78−50630
B, evaporated, electronic struct., XPS, SXS and isochromat investig. 80−76143

X-ray emission spectra continued
B III, IV, laser produced plasma, satellite spectra 78−5165
B, K-shell ionis., double and single, cross section meas. by ion bombardment 78−50629
B, Kα, rel. to structure of rare earth tetraborides 77−59646
B, muonic X-ray transitions, nuclear charge radii 80−99589
B, X-ray spectral line broadening in solid and gas targets 77−6713
B+C(N)(O) ions, 10-40 MeV, soft X-ray spectra 77−75089
B+H$^+$(He$^+$), double K-shell ionis., projectile Z depend. 78−25680
BF, vibrational structure in X-ray spectra, calcs. 77−30884
BF_3, X-ray fluorescence, electronic struct. determ. 78−86887
BN, B K X-ray, chemical bonding and multiple ionis. effects 78−50630
BN, electronic energy band struct., X-ray spectra, pseudopotential calcs. 79−78008
BN, hexagonal, anisotropic emission of the X-ray K-emission band 78−23557
BN, hexagonal, electronic struct. from X-ray emission and XPS 79−47009
BO_3^{3-}, X-ray fluorescence, electronic struct. determ. 78−86887
B_2O_3, microprobe state anal. by X-ray OK and BK emission band spectra *(Japanese)* 78−19606
BP-BAs, quasi-binary system, X-ray emission and electron spectra of solid soln. *(Russian)* 77−1764
BP-BAs solid solns., electronic struct. of valence bands and nature of interatomic interaction 78−34764
BP_xAs_{1-x} system, electron struct. and interatomic interactions, X-ray spectroscopy 80−20736
$_5^{10}B^{n+}$+Cu to Rb, 4-38 MeV, K-shell ionis., X-ray obs. 79−59549
BaO, atomic interaction effects in X-ray emission spectra *(Russian)* 79−69905
$BaTiO_3$, O Kα X-ray emission band spectra *(Russian)* 79−15563
^{133}Ba decay data and standardisation 77−88081
^{137m}Ba, internal conversion decay, double K-hole creation 77−18887
Be and BeO, K X-ray spectra produced by heavy ion bombard., chem. effects 77−36314
Be, anisotropy, theoretical investigation by K-emission, APS, and Compton profiles 78−63970
Be, Be K X-ray, chemical bonding and multiple ionis. effects 78−50630
Be, Doppler effects in X-ray spectra excited by accelerated ions 78−86808
Be, effect of short range order and deep vacancy screening, multiple-screening theory 77−28651
Be, HCP metals, K-emission valence bands, structure and bonding 80−7438
Be II, III, laser produced plasma, satellite spectra 78−5165
Be, K-shell ionis., double and single, cross section meas. by ion bombardment 78−50629
Be, kaonic X-ray meas., strong interaction widths, shifts, yields 77−58210
Be muonic X-ray transitions, nuclear charge radii 80−99589
Be, polarised K-emission valence bands 77−16429
Be, soft X-ray emission and absorpt. edges, self-absorpt. studies 80−40183
Be, Soft X-ray emission edge self absorption and effect of exciting voltage 77−90220
Be, soft X-ray emission edge, temp. depend. 80−89090
Be, X-ray emission spectrum, double plasmon high energy satellite 78−72639
Be, X-ray K emission spectrum, high energy double plasmon satellite intensity calcs. 78−2944
Be, X-ray spectra, separation of K-emission and absorpt. edges 79−33864
Be-like ions, multiply charged, laser plasmas, 1.5-15 Å 78−13462
Be+H$^+$(He$^+$), double K-shell ionis., projectile Z depend. 78−25680
BeF_2, K-emission spectra, optical effects 78−64431
BeO, Be K X-ray, chemical bonding and multiple ionis. effects 78−50630
BeO, K-emission spectra, optical effects 78−64431
BeO, X-ray emission spectra, double plasmon high energy satellites 80−29829
Bi, keV electron impact, L X-ray prod. cross section 79−18293
Bi, L-X-ray production by 9.5 to 41.8 MeV Fl ions 77−85847
Bi, L-subshell ionisation cross-section ratio determ. by ion beam impact 77−6920
Bi+H$^+$, L X-ray production cross sections, 0.3-1.8 MeV, expt. rel. to PWBA prediction 80−53115
Bi+H$^+$, L-shell ionis., 0.5-3.5 MeV, X-ray emission obs. 77−54528
Bi_2O_3, electronic struct., X-ray emission, XPS, UPS obs. 78−52638
^{83}Bi, electron impact, relativistic, L-shell ionis., Lβ/Lα branching ratio energy depend. 79−98228
^{209}Bi, charge distrib. from elastic electron scatt. and muonic X-ray data anal. 78−54681
^{209}Bi, pionic 4f→3d transition, pionic 3d state strong interaction level shift and width 79−98251
^{209}Bi/^{208}Pb isotone pair, charge distrib. polarisation from e$^-$ scatt. and muonic X-ray data consistency 77−22873
^{209}Bi+^{209}Bi collisions, 1 GeV, mol. orbital X-rays 79−49978
^{210}Bi→^{210}Po→^{206}Pb, decay chain, L-shell ionisation investig., X-ray emission during β, α decay 77−18891
Br, 12-60 MeV, ion-atom collision, K-vacancy prod., mol.-orbital model 77−68095
Br ion+target collisions, K-X-ray yields, 1sσ excitation 77−19051
Br, ion+target collisions, X-ray yields, K-L level matching 77−19052
Br ions+target collisions, K-X-ray yields, K-vacancy sharing 77−23548
Br K-X-ray yields, 2pσ excitation 77−23549
Br, L-shell soft X-ray emission spectra, oscillator strengths 80−32651
Br+Br, symmetric collisions, MO-2pσ radiation anisotropy, quasimolecular nature 78−70924
Br+O ion, K X-ray prod. 77−23554
Br+target atom, 12-60 MeV, K-vacancy cross sections, target depend. 77−19026
Br^{25+}+Br^{25+}, correlation diagrams, inner-shell vacancy prod., characteristic X-rays 77−83503
C IV, V, laser produced plasma, satellite spectra 78−5165
C, K-shell X-ray yield, following H$^+$ bombardment of foil 77−10624
C, muonic X-ray transitions, nuclear charge radii 80−99589
C, pionic X-ray intensities in graphite 80−32858
C, proton impact X-ray emission, ang. distrib. and polarisation fraction 78−56546
C-bearing gases, K-shell X-ray yields, proton-induced, chem. effects 80−37820
X-ray emission spectra continued
C+C(N)(O) ions, 10-40 MeV, soft X-ray spectra 77−75089
C+C(N)(O) ions, 4 to 40 MeV, beam-foil K-shell X-ray prod. cross sections 78−33461
C+H$^+$, absolute C K X-ray production cross sections, 18-26 MeV 77−83719
C^{x+}+He, electron capture, K X-ray emission ang. distrib. 77−57919
$(C)_n$, cryst. struct. determ. from X-ray photoelectron and X-ray spectra 78−88384
$CH_2(CD_2)$, pionic X-ray intensities in polyethylene$(-d_n)$ 80−32858
CO, core hole energy curve determ. 79−41186
CO, vibr. struct. of K_α emission spectra 78−86886
CO, vibrational structure in X-ray spectra, calcs. 77−30884
CO_3^{2-}, electronic struct., X-ray spectra obs. 78−55185
CO_3^{2-}, molecular orbital anal., anisotropic X-ray emission obs. of components 80−18786
CO_3^{2-}, X-ray fluorescence, electronic struct. determ. 78−86887
CS_2, high resolution X-ray emission, valence electron struct. and chemical bonding 79−31545
^{12}C+X, X=Ti-Pb, atomic K-vacancy production 77−23543
Ca to Zn series, K-shell ionisation on ^{14}N-ion bombardment 77−54526
Ca, two-electron one-photon transition rate 77−71772
Ca, X-ray production by protons by 0.5 to 2.0 MeV energy 78−66646
Ca XV, Ca XVI in solar flares, atomic data rel. to XUV electron density diagnostics 79−88633
Ca-Ca symmetric collisions, molecular-K-X-ray anisotropy spectra, discrete struct. 77−14560
Ca+H$^+$, K X-ray production, 0.2-0.5 MeV, ionis. cross-section 79−31459
$CaAl_2$, Laves phase, soft X-ray spectrum, band struct. calc. 77−77325
CaO, atomic interaction effects in X-ray emission spectra *(Russian)* 79−69905
CaO-(CaF_2)-Al_2O_3, IR absorption spectra and X-ray emission spectra obs. *(Japanese)* 77−52075
$CaSi_2$, X-ray spectra, valence band struct. *(Russian)* 79−1798
$CaTiO_3$, O K_α X-ray emission band spectra *(Russian)* 79−15563
^{A}Ca, A=40, 42-44, 48, pionic X-rays, strong interaction and isotope shifts, π-nuclear optical pot. 80−53169
Cd, A=110, 116, difference in nuclear charge radius, X-ray isotopic shift meas. 77−18382
Cd, K-shell X-ray spectra, $K\beta_2/K\beta_1$ determ. 77−23456
Cd, $K\beta_3/K\beta_1$ and $K\beta_2/K\beta_1$ relative intensities 77−75088
Cd, proton-induced L-shell ionisation cross-sections 80−100707
Cd-P compounds, X-ray emission bands intensity distrib., influence of chem. bonds 77−28658
$CdGeP_2$, electronic struct. at cryst./vitreous transition, X-ray K-absorpt. and emission 78−15248
CdO-Bi_2O_3-Al_2O_3, glass formation and IR transmission *(Japanese)* 80−54146
$CdP_{2?}$ role of metal d states in valence band formation 79−65380
CdP_4, role of metal d states in valence band formation 79−65380
Cd_2P_3, role of metal d states in valence band formation 79−65380
Cd_3P_2, band struct., X-ray spectra determ. 78−35225
Cd_3P_2, role of metal d states in valence band formation 79−65380
$CdSiP_2$, electronic struct., X-ray spectroscopic investigation 80−108300
p-CdTe diodes, X-ray escape peak variations 77−71723
CdTe, trace anal. by heavy ion induced X-ray emission and SIMS 80−55755
Cd(π$^-$, X), A=111, 112, 0 MeV, E2 nuclear resonance effects, γ and X-ray meas. 78−41774
CeS, atomic interaction effects in X-ray emission spectra *(Russian)* 79−69905
^{252}Cf spontaneous fission, element yields from X-ray multiplicities meas. 77−26812
^{252}Cf spontaneous fission, element yields from meas. X-ray multiplicities 77−50179
^{252}Cf spontaneous fission, prompt element yields determ. from X-ray multiplicities 77−30643
Cl, chem. environment effect on Kα satellites intensity, heavy-ion collisions 77−54527
Cl, foil excitation, K-vacancy bearing metastable states yield, 30-50 MeV 77−54600
Cl ion+target collisions, two-electron-one-photon transitions, X-ray spectra 77−19068
Cl, Kα X-ray satellite spectra, gas phase meas. 78−66496
Cl, L X-ray emitting levels, lifetimes 78−66493
Cl, single-photon decay of ion states with two intrinsic $L_{2,3}$ vacancies *(Russian)* 77−6716
Cl VII, in laser heated plasma, emission intensity anomalies, 58-78 Å *(Russian)* 77−46521
Cl VIII, Ne I like reson. and Na I-like satellite lines, relativistic HF calc., beam-foil spectra 78−94210
Cl X-ray emission spectra, detect. from Alcator-A Tokamak 80−92389
Cl+Al, molecular K X-ray transitions, mol. radiative electron capture effect 78−58802
Cl+Cl collisions, impact parameter dependence of emitted noncharacteristic rad. 77−14563
Cl+He(C)(O)(Ne), K-shell ionising collisions, average L-shell ionisation probability, K_α spectra 79−72408
Cl$^+$+Ar, L-shell X-ray cross sections, 0.2-1.5 MeV, fluoresc. yield 78−1068
Cl^{5+}+Ca(Sc)(Ti) thick targets, 30 MeV, near symmetry collisions, double-K-vacancy sharing 79−3391
Cl^{n+}+Ar, K X-ray cross sections, 15 and 30 MeV, impact parameter depend. 77−19032
Cl^{n+}+Cu, effect on projectile charact. X-rays and REC of target thickness 79−45662
Cl^{n+}+Cu film on C foil, X-ray production, radiative electron capture 77−19063
Cl^{n+}+Ne(SiH$_4$)(H_2S)(HCl)(Ar), K X-ray cross section, projectile charge depend. 77−19029
Cl^{n+}+Ti(Ni), 35 MeV, K-shell vacancy sharing, impact parameter depend., X-ray obs. 77−71858
Cl^{x+}+Cl(Ti)(Ni), K-shell ionization probability in energetic nearly symmetric heavy-ion collisions, 35 MeV 79−27078
Cl^{x+}+Sn(Sb)(Xe), vacancy sharing between K and L shells in 3dσ mol. orbital 79−22807
ClO_2^-, Cl $L_{II,III}$ fluoresc. X-ray spectra, mol. orbital struct. 78−70848
ClO_3^-, Cl $L_{II,III}$ fluoresc. X-ray spectra, mol. orbital struct. 78−70848
ClO_4^-, Cl $L_{II,III}$ fluoresc. X-ray spectra, mol. orbital struct. 78−70848
^{36}Cl, beta decay, K-shell electron ejection 77−18888

X-ray emission spectra continued
Co, α and β phases, L_{III} emission bands *(Russian)* 80−25491
Co, electron bombard., 300 to 600 keV, K_α/K_β X-ray intensity ratios, K-shell ionis. cross sections 78−37747
Co, ferromag., energy band struct. X-ray emission spectra *(Russian)* 79−15564
Co, K X-rays, chemical bonding and multiple ionis. effects 78−50630
Co, $K\beta_{1,3}$ X-ray emission spectra, low energy plasmon satellites 80−19560
Co, liq., soft X-ray band spectra 77−52199
Co-Ge eutectic alloys, X-ray spectral investig. of electron struct. 77−44087
Co-like ions, multiply charged, laser plasmas, 1.5-15 Å 78−13462
Co-Si-Ge system, X-ray diffr. exam., band struct. *(Russian)* 78−56623
CoAl, bonding, self-consistent energy bands 78−91610
$CoCl_2$, energy spectrum of valence electrons, X-ray emission spectra 77−16430
CoGe, and TiCoGe, electronic struct., X-ray K- and L-spectra obs. *(Russian)* 78−11022
CoGe, Co_2Ge and $CoGe_2$, X-ray spectrum analysis, energy band struct. *(Ukrainian)* 77−52200
$CoGe_x$, Co emission spectra *(Russian)* 78−21942
CoSi, and TiCoSi, electronic struct., X-ray K- and L-spectra obs. *(Russian)* 78−11022
CoSi, electronic struct. determ. by XPS and X-ray emission spectra 77−85147
CoSi, X-ray emission spectra obs. of valence band states *(Ukrainian)* 77−69935
Cr, AES meas. of soft X-ray emission threshold potential *(Russian)* 79−33866
Cr, band structure, emission band shape, self-consistent calc. 77−28104
Cr compounds, multiplet spectra in XPS and K-emission 77−63527
Cr, double K-shell ionisation by electron impact 78−62929
Cr, K X-rays, chemical bonding and multiple ionis. effects 78−50630
Cr, K_β/K_α following K-electron capture and X-ray excitation 78−13031
Cr, $K\alpha^h$ hypersatellite spectra and K-shell double photoionisation cross-section 78−21874
Cr, $K\beta$ X-ray emission, plasmon satellite 77−28662
Cr, $K\beta_{1,3}$ X-ray emission spectra, low energy plasmon $K\beta'$ satellite 79−74020
Cr, oxidation, combined AES and threshold potential spectroscopy 78−11026
Cr, X-ray emissive short-wave satellite lines in K-series, mech. of formation *(Russian)* 79−91538
Cr, X-ray fluoresc., $K\alpha$ hypersatellites 77−18830
Cr, X-ray K_β emission spectrum, unpaired electrons and plasmon correlation 78−88383
Cr, X-ray prod. by 5 MeV/amu deuterons (oxygen ions), projectile Z depend. 80−42982
Cr, X-ray production by protons by 0.5 to 2.0 MeV energy 78−66646
Cr XXII, spectra from laser plasma comparison with solar corona and vacuum spark 78−17596
Cr-SiO_2-Si structure, solid-phase interaction between Cr and SiO_2, X-ray spectral obs. 78−10560
$Cr+H^+$, K X-ray production, 0.2-0.5 MeV, ionis. cross-section 79−31459
$Cr+H^+$ ion collisions, K-shell ionisation cross sections 77−23556
$Cr+N^{4+}$, $K\alpha$ and $K\beta$ X-ray spectra for 84 MeV incident energy 77−50517
CrO_3, $K\beta_{1,3}$ X-ray emission spectra, low energy plasmon $K\beta'$ satellite 79−74020
CrO_4^{2-}, electronic struct. determ. from X-ray spectra 78−86885
Cr_2O_3, electron structures calc. using models, ESCA and X-ray spectral data 77−35863
Cr_2O_3, low energy X-ray emission satellite, unpaired election and plasmon effects 80−35007
^{54}Cr, K_β/K_α intensity ratios, chem. effects 79−63949
Cs L-shell X-ray prod. by H(He) ion bombardment 79−47548
Cs, soft X-ray outer-shell absorption and emission, one-electron calc. 79−69904
Cu, 15-33 MeV electron bombardment, X-ray ang. distrib. meas. using ETL quantameters 80−91367
Cu (111), final state band gap effects in UPS 80−89120
Cu, bremsstrahlung spectra, 10 to 30 keV, thick target expts. 77−8687
Cu, CC $K\beta_{1,3}$ emission spectrum, double vacancy transitions 79−59393
Cu, channelling of Xe ions, Xe(M) radn. yield 79−73234
Cu crystal, X-radiation generation via electrons, nonlinear rise and line-narrowing, book contrib. 79−28865
Cu, electron bombard., 300 to 600 keV, K_α/K_β X-ray intensity ratios, K-shell ionis. cross sections 78−37747
Cu halides, tetrahedrally coordinated, semiempirical band struct. model 77−51655
Cu, K_β/K_α following K-electron capture and X-ray excitation 78−13031
Cu, K-shell ionis., X-ray prod. cross section for incident H^+, ^4He and ^{14}N ions 78−70923
Cu, K-shell X-ray prod. by H^+ and He^+ bombardment, cross sections, energy depend. 78−5337
Cu K-shell X-ray production, projectile Z, energy and incident charge state depend. 79−78794
Cu, K-shell X-ray yield, following Cl^{n+} bombardment, residual vacancy effects 77−10623
Cu, $K\alpha$ hypersatellite spectrum, double K ionis. 77−18829
Cu, $K\beta_{1,3}$ X-ray emission spectra, low energy plasmon satellites 80−19560
Cu, L-shell soft X-ray emission spectra, oscillator strengths 80−32651
Cu $L\alpha_{1,2}$ radiation, test of ESCA apparatus used as soft X-ray spectrometer *(French)* 77−13832
Cu, polycryst., X-ray intensity, microfocus source, non-linear rise studies 80−77927
Cu, proton impact X-ray emission, ang. distrib. and polarisation fraction 78−56546
Cu, proton-induced K-shell ionis., probability ang. depend. 77−14553
Cu, two-electron one-photon transition rate 77−71772
Cu, valence band splitting, X-ray K-emission spectroscopy 80−40189
Cu, X-ray prod. by 5 MeV/amu deuterons (oxygen ions), projectile Z depend. 80−42982
Cu, XX 80−100707
Cu XXII, X-ray spectra in laser plasma, $2p^6\ ^1S_0 \rightarrow 2s2p^5\ ^1P_1$ 79−1340
Cu/Ni film counter, surface counting method for diffusion study, based on X-ray fluoresc. 79−42321

X-ray emission spectra continued
Cu-Mn alloys, Mn K X-ray emission and XPS lines, width and asymm. 78−19605
Cu-Ni, soft X-ray emission and local densities of states 79−83059
$Cu+Cl^{q+}$, X-ray cross sections, projectile fluoresc. yields 78−74751
Cu+Cu collisions, $K\alpha$ X-ray energy shifts, target thickness depend. 80−83311
$Cu+H^+$, 4 MeV beam-foil X-ray production cross-section 79−7003
$Cu+H^+$, atomic K-shell ionis., X-ray emission 79−18280
$Cu+H^+$, X-ray emission, optical transition radn. 78−58618
Cu+Ni foil target, 50-65.5 MeV, K-vacancy production, impact parameter depend. 79−54958
Cu+O ion, K X-ray prod. 77−23554
$Cu+X^{n+}$, X=F, Al, Si, S, K X-ray production, target thickness depend. 77−75280
$CuAl_2$, Kossel interferences of proton-induced Alk_α radiation 77−43112
CuCl, band struct., OPW calc. and X-ray spectra meas. 80−75506
^{64}Cu β^- and β^+-decays, K-shell ionisation probabilities, X-ray spectra 80−42592
D, muonic atom, initial population of 2S metastable state 77−27207
D_2, electron impact, Balmer-α emission Doppler profile energy depend. 77−42423
Dy atom K-shell ionisation and X-rays from $^{158}Gd(\alpha,xn)$ 79−93960
Dy, X-ray cross sections, L-shell, proton induced, 1 to 3 MeV range 79−1799
$Dy+H^+$ ionisation, induced L-shell alignment 80−32813
^{160}Dy anomalous γ-L X-ray directional correlations from ^{160}Tb decay 80−52610
Er, kaonic atom, radiationless mixing, even-even X-ray yield *(Russian)* 77−61880
Er, keV electron impact, L X-ray prod. cross section 79−18293
Er, L-X-ray emission, new satellite 77−10620
Er, L-line emission spectrum diagram line 80−84808
Er, X-ray emission spectrum, electronic quadrupole transition $L_2M_3(\beta_{17})$ 79−98018
ErT_2, film, surface oxide form. and interfacial metal loss, AAS, XES 78−31733
^{165}Er decay parameters and whole-body dose, for radioisotope scanning 77−70529
Eu, K-shell X-ray energy, excitation mode depend. 79−26926
Eu, $K\alpha$ line widths, precise meas. 78−62761
Eu, $L_{II}N_{II}$ forbidden transition obs. 77−23451
Eu, L_1 X-ray fluoresc. and Coster-Kronig yields 77−30814
$Eu+H^+$, atomic K-shell ionis., X-ray emission 79−18280
EuSe, atomic interaction effects in X-ray emission spectra *(Russian)* 79−69905
^{152}Eu, X-ray emission probabilities per decay 80−14027
F ion+solid target collisions, K-shell ionisation, X-ray emission cross sections 77−19069
F ions, moving in Ne, Ar, Kr gases and C foils and slabs 77−69020
F ions+Ne(Ar)(Kr) and C foil and slab, K shell X-ray spectra 78−17599
F isoelectronic sequence, spectra and energy levels 79−93948
F, isoelectronic sequence, X-ray spectra 80−87071
F K_α X-ray satellite struct. and KLL Auger electron spectra, solid-state effects 80−89089
F, K-shell X-ray spectra from light ion bombard. studies 80−71518
F-bearing gases, K X-ray yields induced by proton bombardment 79−45736
F+Al, molecular K X-ray transitions, mol. radiative electron capture effect 78−58802
$F+N^{4+}$, bonding effect on $K\alpha$ satellite struct. 79−59392
F^{6+}+He, 10 to 40 MeV, F^{6+} K-vacancy production, role of excitation 80−37859
$F^{7+,8+}+H_2$(He), 20-56 MeV, F K X-ray cross sections, inner shell Coulomb excitation 77−19025
F^{8+}+He, X-ray prod. cross sections resulting from electron capture and electron excitation of F^{8+} ions 79−3557
F^{n+}+Ag foil, 10-40 MeV, Ag L-shell X-ray production 77−71856
F^{q+}+He, (q=1-9), X-ray prod. by electron excitation, ionisation and capture 79−76379
F^{q+}+Ne, MO X-ray prod. obs. 79−45663
F^{q+}+Ne, radiative electron capture X-ray profiles from fast collisions, calcs. 79−49975
F^{x+}+He, electron capture, K X-ray emission ang. distrib. 77−57919
$^{19}F+Z$, Z=22 to 57, 2 to 28 MeV, prod. of target atom K-shell X-rays 79−18285
$(Fe,Cr)_3C$, reln. between bond energy and X-ray emission line shifts 78−50555
Fe alloys, ion-implanted, depth profile and diffusion coeff., X-ray emission study 80−54277
Fe atoms in chem. compounds, $K\beta$ X-ray spectra, struct. similarities 77−28655
Fe compounds, radiative Auger transition, $K \rightarrow M^2$ weak X-ray emission lines 78−33556
Fe, double K-shell ionisation by electron impact, X-ray spectra 78−62928
Fe, double K-shell ionisation by electron impact 78−62929
Fe, electron bombard., 300 to 600 keV, K_α/K_β X-ray intensity ratios, K-shell ionis. cross sections 78−37747
Fe F2 (Fe F3), electronic struct., binding energy, X-ray emission and photoelectron spectra obs. 80−35008
Fe, highly ionised, 1s to 3p $K\beta$-like X-ray spectrum 77−50394
Fe I $K\alpha$ fluorescence in solar flares, photospheric Fe abundance probe 79−75192
Fe, inner-shell vacancies, cascade decay, multiple ionisation and X-ray emission calcs. 80−87072
Fe ion+Fe(Ni) collisions, X-ray spectra, two-electron transitions 77−19050
Fe, K X-rays, chemical bonding and multiple ionis. effects 78−50630
Fe, K_β/K_α following K-electron capture and X-ray excitation 78−13031
Fe, $K_{\beta 1,3}$ X-ray emission spectra, low-energy plasmon satellites 79−65957
Fe, $K\alpha$ hypersatellite spectrum, double K ionis. 77−18829
Fe, $K\alpha$ satellite lines following electron bombardment 80−69097
Fe, $K\alpha^h$ hypersatellite spectra and K-shell double photoionisation cross-section 78−21874
Fe, $L\alpha_{1,2}$ and $L\beta$ X-ray emission spectrum, determ. using modified photoelectron spectrometer 78−50557
Fe, liq., soft X-ray band spectra 77−52199
Fe oxide films, anodically formed, compositions 79−90898

X-ray emission spectra continued
Fe, two-electron one-photon transition rate 77−71772
Fe X, $3p^4 4s$ levels, population processes 80−47926
Fe, X-ray fluoresc., Kα hypersatellites 77−18830
Fe, X-ray line emission in Cygnus X-3, crystal spectrometer obs. 78−8153
Fe, X-ray prod. by 5 MeV/amu deuterons (oxygen ions), projectile Z depend. 80−42982
Fe, X-ray production by protons by 0,5 to 2.0 MeV energy 78−66646
Fe XIX and isoelectronic ions $2p^4$-$2p^3 3d$ transition array 77−42267
Fe XVII, X-ray spectra due to n=3 and 4 quantum nos. 79−22641
Fe XVII to Fe XXI spectra, 8 to 18 Å, emitted from plasma after laser heating 78−25464
Fe XVIII and XIX $2s^2 2p^n$-$2s^2 2p^{n-1}$4d classification, for laser produced plasmas and solar spectra 77−42268
Fe XXI and isoelectronic spectra $2p^2$-2p3d transition array 77−38632
Fe XXV, spectra from laser plasma, comparison with solar corona and vacuum spark 78−17596
Fe-Al, X-ray emission spectra 80−25489
Fe-Al alloy, soft X-ray emission 77−32471
Fe-Al alloys, cond. electron wave function, lattice symm. depend. 77−85844
Fe-Al compounds, X-ray emission investig. of electron localisation in valence zone *(Russian)* 77−48277
Fe-group elements, L spectra interpretation 77−27013
Fe-like ions, multiply charged, laser plasmas, 1.5-15 Å 78−13462
Fe-Ni alloys, thermal expansion rel. to X-ray emission spectra *(Russian)* 77−32470
Fe+Fe, symmetric collisions, MO-2pσ radiation anisotropy, quasimolecular nature 78−70924
Fe+Fe symmetric collisions, molecular-K-X-ray anisotropy spectra, discrete struct. 77−14560
Fe+H^+, K X-ray production, 0.2-0.5 MeV, ionis. cross-section 79−31459
Fe+H^+ ion collisions, K-shell ionisation cross sections 77−23556
Fe+I, Fe K-α X-ray emission, high-resolution meas. 80−37871
Fe+N^{4+}, Kα and Kβ X-ray spectra for 84 MeV incident energy 77−50517
Fe+Ni, two electron one-photon X-ray transitions, Dirac-Fock calcs. 78−17600
FeAl B2 struct., band struct. and density of states, KKR calc. 78−63969
FeAl, bonding, self-consistent energy bands 78−91610
$Fe_{70}Cr_{30}$, disordered, X-ray spectra study of electronic struct. 77−77324
$Fe(NH_4)_2.(SO_4)_2.6H_2O$, Kβ′ satellite of $Kβ_1$ X-ray emission line, plasmon oscill. theory 78−23556
Fe_2O_3, $K_{β1}$ X-ray emission line, optical effects 79−91534
FeS_2, diatomic crysts. electron induced X-ray emission, channelling effects 79−56888
$Fe_{1-x}S$, soft X-ray emission and AES study 79−91535
Fe_3Si(Al), electronic structure, X-ray spectra comparison with band struct. calcs. 80−97383
Ga, L-shell soft X-ray emission spectra, oscillator strengths 80−32651
GaAs, use of ion induced X-rays for lattice location of S and Mn implanted in single crystals 79−4332
GaAs, X-ray and Rutherford backscatt. yields from channelled $^4He^+$ ions 79−46730
GaP, 1 MeV proton bombardment, lattice deformation investigation by Kossel effect 78−22775
GaP:Sn(Sb), lattice location of implanted atoms, ion backscatt. and ion-induced X-ray obs. 77−84785
^{31}Ga, origin of high and low freq. K-satellites in X-ray emission spectra 80−50466
$Gd(Al_{1-x}Mn_x)_2$, alloys soft X-ray emission spectra investigation 79−91537
$GdCl_3.6H_2O$, thermal decomp., X-ray emission luminesc. *(Japanese)* 80−55763
$GdF_3(Br_3)$, chem. binding, 4d X-ray spectra obs. 79−69910
$Gd_3Ga_5O_{12}$, chem. binding, 4d X-ray spectra obs. 79−69910
Gd_2O_3 79−69910
^{155}Gd $L_{2,3}$ subshell X-ray fluorescence and Coster-Kronig yields from ^{155}Eu decay 80−69102
Ge, heavy ion impact, meas. of life-time of inner-shell vacancy in recoiled Ge atoms 77−63513
Ge K X-ray prod. for Br ions 79−47547
Ge, X-ray emission spectra formation, role of nonequilibrium electron density *(Russian)* 77−63490
Ge, X-ray spectra and energy band struct. 79−69407
Ge XXIV, $2p^5$-$2p^4 3s(2p^4 3d)$ transitions in laser produced X-ray spectra 78−13460
Ge-rare earth alloys, nature of chemical interaction, X-ray emission, absorpt. and photoelectron study *(Russian)* 80−55261
Ge-Si alloys, electronic struct. comp. depend., X-ray spectral obs. 77−81178
Ge+$^{14}N^{n+}$, 7-35 MeV, K-shell X-ray production cross sections 77−75090
Ge+Ge, quasimolecular K X-ray anisotropy and ang. distrib. 78−1073
Ge+Ge, symmetric collisions, MO-2pσ radiation anisotropy, quasimolecular nature 78−70924
Ge+O ion, K X-ray prod. 77−23554
GeO_2, photoemission and X-ray emission spectra calc. 77−89866
GeP, thin films, vacuum-deposited, struct. characterisation 77−47691
GeS(Se)(Te)(O_2), K X-ray spectra, Ge atoms effective charge, energy-gap widths 77−28657
Ge_xSi_{1-x}, Si X-ray emission spectra obs. *(Russian)* 77−1767
GeTe, X-ray emission spectra, amorphous and cryst. struct. *(Russian)* 78−88385
^{32}Ge, origin of high and low freq. K-satellites in X-ray emission spectra 80−50466
H kaonic atom X-ray observation, energy shift 79−55008
H, mesic, atomic X-ray yields 1s and 2p level shifts and widths, cascades, calc. 80−78730
H, muonic atom, initial population of 2S metastable state 77−27207
H-like ions, multiply charged, laser plasmas, 1.5-15 Å 78−13462
H^++X, X=Nb through to Gd, 0.6 to 2.4 MeV 78−13586
H_2, electron impact, Balmer-α emission Doppler profile energy depend. 77−42423
H_x^++Al surface, x=1,2,3, relative K X-ray yields 77−75282
HCl, emission K spectra, vibronic and core hole effects, nonempirical orbital defreezing calc. 78−5200
HCl, K-emission and -absorpt. spectra, vibr. struct., ab initio calcs. 77−79629
HF, emission K spectra, vibronic and core hole effects, nonempirical orbital defreezing calc. 78−5200
HF, K-emission and -absorpt. spectra, vibr. struct., ab initio calcs. 77−79629
H_2O (D_2O), O muonic X-ray spectra, H(D) isotope effects 77−75344
H_2O, ESCA and soft X-ray emission, vibr. excitation 80−23433
$H_2S+O^+(Cl^+)$, S highly stripped core ion outer shell rearrangement, Kα X-ray spectra 77−3451
He, electron impact excitation of $1^1S \rightarrow 2^1P(3^1P)$, excitation cross section and polarisation fractions, XUV emission 79−22841
He, electron impact excitation rel. to photon interactions 80−27985
He, L-X-ray production by 9.5 to 41.8 MeV Fl ions 77−85847
He^+ Lamb-shift measurement by the quenching-radiation anisotropy method 80−18824
He-like ions, multiply charged, laser plasmas, 1.5-15 Å 78−13462
He+B(C)(N)(O)(F) bare nuclei, electron capture to excited states, X-ray cross-sections 77−71814
$He^{2+}(H^+)$+X, (X=Nb to Gd), K-shell X-ray prod. cross-sections 77−71865
^{3}He, liquid, pionic atoms, X-ray energies, Lorentzian widths, relative intensities 78−46470
^{3}He, liquid, pionic K X-ray transition energies and Lorentzian widths 80−78727
^{4}He, kaonic and pionic X-rays, strong interaction widths and shifts 79−98253
^{4}He-$\bar{p}$, X-ray spectrum, energies and relative intensities for 3d and 2p levels 78−70979
Hf, electron structure and soft X-ray emission spectrum, RAPW calcs. 79−91536
Hf+H^+(He^+), L-subshell ionisation cross section, branching ratios, fluoresc. yield, Coster-Kronig factors 80−43166
Hg doubly K ionised, energy shift between $K_α$ X-ray and its hypersatellite line 78−9107
Hg+H^+, L-subshell ionisation cross-sections, X-ray meas. 77−46520
Hg+H^+, L-subshell X-ray prod., cross-section meas. 77−46575
Hg+Xe^{x+}, single and multiple collisions, charact. and quasimolecular X-rays 77−83713
^{A}Hg, A=198-202 and 204, nuclear charge radii variations from K X-ray isotope shifts 78−70441
Ho, K X-rays, energy shifts, role of atomic struct. 78−70777
Ho, keV electron impact, L X-ray prod. cross section 79−18293
Ho, Lα X-rays produced by surface impact of F^{n+} and Si^{n+} 79−69907
Ho, soft X-ray APS of 4f states 77−24911
^{67}Ho-^{19}F(^{28}Si), target Lα X-ray prod., projectile charge state depend. 79−47549
^{155}Ho $L_{2,3}$ subshell X-ray fluorescence and Coster-Kronig yields from ^{165}Er decay 80−69102
^{165}Ho(π^-,X), 175 MeV/c, monopole and quadrupole strong interaction effects in pionic atoms 78−41777
H^+(spin polarised)+atom, inner-shell ionis., subsequent radiation ang. distrib. 80−53114
I, 15-80 MeV, ion-atom collision, K-vacancy prod., mol.-orbital model 77−68095
I ion+target collisions, K-X-ray yields, 1sσ excitation 77−19051
I ion+target collisions, K-X-ray yields, K-vacancy sharing 77−23548
I ion+target collisions, K-X-ray yields, 2pσ excitation 77−23549
I ion+target collisions, X-ray yields, K-L level matching 77−19052
I+Au, slow collision, M MO radiation anisotropy 79−72269
I+target atom, 15-80 MeV, K-vacancy cross sections, target depend. 77−19026
I^++$_z$A, Z≥47, inner shell X-ray prod., vacancy configurations and cross sections 79−13815
I^{25+}+Te^{24+}, I^{43+}+Au^{69+}, I^{25+}+Au^{51+}, correlation diagrams, inner-shell vacancy prod., characteristic X-rays 77−83503
In, K-shell X-ray spectra, $Kβ_2/Kβ_1$ determ. 77−23456
In, $Kβ_3/Kβ_1$ and $Kβ_2/Kβ_1$ relative intensities 77−75088
In, L X-ray yields from double-vacancy states 79−49977
In, Lα X-ray fluoresc. spectra, natural linewidth meas. 79−85934
In, X-ray cross sections, L-shell, proton induced, 1 to 3 MeV range 79−1799
In, X-ray prod. by 5 MeV/amu deuterons (oxygen ions), projectile Z depend. 80−42982
In+I^{10+}, double K-shell vacancies obs., $K_α$ hypersatellite transitions, shift, shared double vacancies 79−72268
InP, III-V semicond., electronic struct. of valence and conduct. bands 77−28110
^{114m}In, K-shell internal conversion, $Kα_1$ hypersatellite line energies, intensities 77−18885
Ir, energy band structure, X-ray emission spectra, APW calc. 80−92811
K, incomplete phonon relax. in X-ray emission calc. 77−52202
K, soft X-ray emission and absorpt. edges, self-absorpt. studies 80−40183
K, Soft X-ray emission edge self absorption and effect of exciting voltage 77−90220
K, soft X-ray emission edge, temp. depend. 80−89090
K, soft X-ray outer-shell absorption and emission, one-electron calc. 79−69904
K+O ion, K X-ray prod. 77−23554
KCl, doublet intensity ratio meas. for efficiency of planar solid state detectors at very low energies 79−3286
K_2CrO_4, $Kβ_{1,3}$ X-ray emission spectra, low energy plasmon Kβ′ satellite 79−74020
K_2CrO_4, X-ray Lα emission spectra, excited states calcs. 79−59488
$K_2Cr_2O_7$, $Kβ_{1,3}$ X-ray emission spectra, low energy plasmon Kβ′ satellite 79−74020
$KMnO_4$, X-ray emission spectra, plasmon satellites 79−99985
K_2O-AlF_3-B_2O_3 glass, Al atom bonding mode, optical absorption of VO^{2+} and $AlK_α$ spectrum *(Japanese)* 78−11023
$K_2Pt(CN)_4$, muonic X-ray radiation anisotropy *(German)* 80−69267
K_2SO_4, doublet intensity ratio meas. for efficiency of planar solid state detectors at very low energies 79−3286
Kr, 202-330 MeV, ion-atom collision, K-vacancy prod., mol.-orbital model 77−68095
Kr, electron impact, struct. near $M_{4,5}$ edges 77−75083
Kr, free ats. electron bombard., subsequent X-radiation ang. distrib. 80−53144
Kr, inner shell alignment calc. in electron impact ionisation 77−14586
Kr, ion+target collisions, K-X-ray yields, 1sσ excitation 77−19051
Kr ion+target collisions, X-ray yields, K-L level matching 77−19052
Kr ion+target collisions, K-X-ray yields, 2pσ excitation 77−23549

X-ray emission spectra continued
Kr, ultrasoft X-ray emission near $M_{4,5} \rightarrow N_{2,3}$ transition 79−76377
Kr+Cu^{q+}, ($16 \leq q \leq 23$), 1.4 MeV/amu, X-ray emission, charge state dependence 78−37713
Kr+Kr(Xe), X-ray prod. cross sections for Kr L-shell vacancies 79−10190
Kr+target atom, 200-330 MeV, K-vacancy cross sections, target depend. 77−19026
Kr^{24+}+Ge, K X-ray prod., impact parameter depend. 78−58800
Kr^{n+}+Ta(W)(Pt)(Au)(Pb)(Bi)(Th)(U), K-L level matching, X-ray obs. 79−63948
^{84}Kr ions+target collisions, K-X-ray yields, K-vacancy sharing 77−23548
La, diagram lines in X-ray L emission spectrum obs. 77−6715
La, electron impact excited soft X-ray spectra, resonances and many body effects 80−50468
La, $N_{IV,V}$ emission spectrum in energy zone below $N_{IV,V}$-potentials of ionisation *(Russian)* 77−77322
La, X-ray reson. emission, appearance pot. and charact. electron energy loss spectra 80−16126
La_2O_3, 4f states of La, diagram lines in L-spectrum obs. 77−20959
La_2O_3, atomic interaction effects in X-ray emission spectra *(Russian)* 79−69905
LaOBr:Tm X-ray emission spectra and screen-film system design 78−11024
Li, Auger widths of core levels calc. using diagrammatic many-body technique 77−43544
Li, emission spectra in 10 to 25 nm range excited by electron-atom collision *(Russian)* 77−83526
Li film, temp. depend. of K X-ray emission edge 77−32472
Li I-like spectra, energy struct., accurate semiempirical formulae 79−49970
Li, incomplete phonon relax. in X-ray emission calc. 77−52202
Li, kaonic X-rays meas., strong interaction widths, shifts, yields 77−58210
Li like ions, oscillator strength calc. for inner shell transitions 77−30821
Li, one-electron calcs. of X-ray absorpt. and emission, jellium model 78−56543
Li, Soft X-ray emission edge self absorption and effect of exciting voltage 77−90220
Li, X-ray absorpt. and emission edges, one-electron and many-body effects 80−25484
Li, X-ray edge spectra, phonon broadening 77−77279
Li, X-ray emission and absorpt. edges, temp. depend. 78−31282
Li, X-ray emission spectrum, one-electron band approx. calcs. 78−80437
Li, X-ray K-edge transitions, band theory 77−16426
Li-like ions, multiply charged, laser plasmas, 1.5-15 Å 78−13462
Li-like ions K...Fe, survey table of wavelengths in X-ray region 77−79569
LiF, Kα-satellites of F^- *(German)* 79−28864
LiF, N^+ and Ne^+ irradiation, MO X-ray intensity meas. 78−82831
LiH, kaonic X-rays meas., strong interaction widths, shifts, yields 77−58210
LiO_2-Al_2O_3-SiO_2, bonding of Si-O exam. by X-ray emission spectra 78−52594
Lu, calc. of soft X-ray emission spectra by relativistic APW method 79−78792
Lu, K-shell X-ray energy, excitation mode depend. 79−26926
Lu, L-shell satellite, $L_2M_4 \rightarrow M_4M_4$ transition 77−79565
^{71}Lu, L_2M_3 electric quadrupole transition detect., L X-ray spectrum 77−3294
^{175}Lu, muonic, nuclear spectroscopic ground state quadrupole moments from X-rays 79−98252
$^{175}Lu(\pi^-,X)$, 230 MeV/c, monopole and quadrupole strong interaction effects in pionic atoms 78−41777
Mg, Doppler effects in X-ray spectra excited by accelerated ions 78−86808
Mg, HCP metals, K-emission valence bands, structure and bonding 80−7438
Mg I, Mg II autoionisation state radiative decay *(Russian)* 80−5509
Mg, $K\alpha_1$ and $K\alpha_2$ wavelengths 80−50464
Mg, $K\alpha^h$ hypersatellite spectra and K-shell double photoionisation cross-section 78−21874
Mg, $K\alpha^h$ hypersatellite spectrum, K-shell electron double ionisation cross section, binding energy 79−36577
Mg, one-electron calcs. of X-ray absorpt. and emission, jellium model 78−56543
Mg, room temp. meas. using HgI_2 detector 78−78049
Mg, soft X-ray emission and absorpt. edges, self-absorpt. studies 80−40183
Mg, Soft X-ray emission edge self absorption and effect of exciting voltage 77−90220
Mg, soft X-ray emission edge, temp. depend. 80−89090
Mg, X-ray absorpt. and emission edges, one-electron and many-body effects 80−25484
Mg, X-ray fluoresc., Kα hypersatellites 77−18830
Mg XII, resonance line, atomic parameters calc. for dielectronic satellite lines 80−42983
Mg^{9+}, beam-foil excited, spin orbit-forbidden X-ray transition obs. 80−23537
Mg^{n+}, foil-excited ion, X-ray spectra and satellite classification 80−95567
Mg-Cu alloy, electronic struct. obs. 77−16428
Mg+heavy ion, X-ray spectra, one-photon two-electron rearrangements 77−6712
$MgAl_2O_4$, irrad. stability obs. using X-ray emission meas. *(Russian)* 80−66326
MgF_2:Mn, X-ray luminesc., activator flash 79−65958
$MgO.Al_2O_3$-$MgO.nAl_2O_3$ spinel, coordination state of atoms, charact. X-ray emission *(Japanese)* 78−6816
Mn, doublet struct. of Kα-hypersatellite 78−5167
Mn, K X-rays, chemical bonding and multiple ionis. effects 78−50630
Mn, $K\alpha^h$ hypersatellite spectra and K-shell double photoionisation cross-section 78−21874
Mn, $K\beta_{1,3}$ X-ray emission spectra, low energy plasmon $K\beta'$ satellite 79−74020
Mn, X-ray emissive short-wave satellite lines in K-series, mech. of formation *(Russian)* 79−91538
Mn, X-ray fluoresc., Kα hypersatellites 77−18830
Mn, X-ray $K_{\alpha 1,2}$ and $K_{\beta 1}$ lines, photon excitations of Mn and K-capture in ^{55}Fe *(Russian)* 77−77321
X-ray emission spectra continued
Mn, X-ray K_β emission spectrum, unpaired electron and plasmon effect 77−12468
Mn, X-ray production by protons by 0.5 to 2.0 MeV energy 78−66646
Mn+H^+, K X-ray production, 0.2-0.5 MeV, ionis. cross-section 79−31459
Mn+H^+ ion collisions, K-shell ionisation cross sections 77−23556
$MnCl_2$, energy spectrum of valence electrons, X-ray emission spectra 77−16430
MnO, $K_{\beta 5}$ X-ray emission spectrum, low energy plasmon satellite A 78−2945
MnO, $K\beta_{1,3}$ X-ray emission spectra, low energy plasmon $K\beta'$ satellite 79−74020
MnO, X-ray Kβ emission spectra, unpaired electron and plasmon effects 78−19603
MnO_2, $K\beta_{1,3}$ X-ray emission spectra, low energy plasmon $K\beta'$ satellite 79−74020
MnO_2, X-ray emission spectra, plasmon satellites 79−99985
MnO_2, X-ray Kβ emission spectra, unpaired electron and plasmon effects 78−19603
MnO_4^-, electronic struct. determ. from X-ray spectra 78−86885
MnP, metallic, band struct., X-ray spectral obs. 78−11019
Mn_3Si, electronic structure, X-ray spectra comparison with band struct. calcs. 80−97383
MnZn ferrites, thin struct. of $K\beta_5$ and $L\alpha_{1,2}$ emission bands of Fe *(Ukrainian)* 79−78790
Mo, band structure, emission band shape, self-consistent calc. 77−28104
Mo, bremsstrahlung spectra, 10 to 30 keV, thick target expts. 77−8687
Mo complexes, electronic struct., XPS and X-ray emission spectra 77−42336
Mo IX, 4p-5d,6d and 4p-6s,7s transitions, grazing incidence spectrograms 79−36576
Mo ions, X-ray emission spectra, from laser produced plasma, line identification via HF calcs. 78−33459
Mo, K-shell X-ray spectra, $K\beta_2/K\beta_1$ determ. 77−23456
Mo, $K\alpha_{1,2}$ $K\beta_{1,3}$ using diffractional focusing X-ray spectrometer 78−5988
Mo, $K\beta_3/K\beta_1$ and $K\beta_2/K\beta_1$ relative intensities 77−75088
Mo, proton-induced L-shell ionisation cross-sections 80−100707
Mo X-ray emission spectra, detect. from Alcator-A Tokamak 80−92389
Mo, X-ray Mζ energy, revised values 80−14102
Mo XLI, Mo XL, X-ray emission from vacuum-spark plasma 78−41991
Mo XV to Mo XXXIII identification in soft X-ray spectrum of TFR Tokamak 77−72504
Mo^{33+}, X-ray spectra, $2p^5$-$2p^4$3d, laser plasma 78−86806
Mo+Nb, K-shell vacancy prod., impact parameter depend. 80−14225
MoS_2, struct., XES and XPS obs. 80−43105
Mo_3Si, Mo_5Si_3 and $MoSi_2$, ultrasoft X-ray emission bands, empirical band schemes 78−15249
^AMo, A=92, 94-98, 100, muonic atom X-ray transitions, nuclear charge radii 80−27545
N, muonic X-ray transitions, nuclear charge radii 80−99589
N V, VI, laser produced plasma, satellite spectra 78−5165
N^++N, 35-200 keV, K MO X-rays, production mechanism, spectral distrib. 78−42183
N^++N_2, 35-200 keV, X-ray spectrum, rel. to N^++N mechanism 78−42183
N^++N_2, X-ray emission ang. distrib., MO calc. 79−54803
N^++$NH_3(H_2O)$(Ne) symmetric collisions, double K-shell ionisation, two-electron-one-photon transitions 77−19067
N^{x+}+He, electron capture, K X-ray emission ang. distrib. 77−57919
N_2, core hole energy curve determ. 79−41186
N_2, vibr. struct. of K_α emission spectra 78−86886
N_2+N^+, molecular-orbital X-rays, recoil effects 78−66645
NH_3, ESCA and soft X-ray emission, vibr. excitation 80−23433
NH_3, vibr. excitation in soft X-ray emission and core ESCA spectra 80−69163
NH_3+N^+, 35-200 keV, X-ray spectrum, rel. to N^++N mechanism 78−42183
NO, core hole energy curve determ. 79−41186
NO_2^-, electronic struct., X-ray spectra obs. 78−55185
NO_3^-, electronic struct., X-ray spectra obs. 78−55185
NO_3^-, X-ray fluorescence, electronic struct. determ. 78−86887
N_2O, X-ray fluoresc. obs., ionis. pot., fine struct., LCAO SCF calc. 77−68055
Na, Auger widths of core levels calc. using diagrammatic many-body technique 77−43544
Na compounds, muonic X-ray intensities, Lyman series 80−23578
Na, impurities and photoexcited ions 80−39523
Na, incomplete phonon relax. in X-ray emission calc. 77−52202
Na K_α X-ray satellite struct. and KLL Auger electron spectra, solid-state effects 80−89089
Na, KK vacancy prod. in Na^++Ne collisions 78−17781
Na, $K\alpha_1$ and $K\alpha_2$ wavelengths 80−50464
Na, one-electron calcs. of X-ray absorpt. and emission, jellium model 78−56543
Na, room temp. meas. using HgI_2 detector 78−78049
Na, Soft X-ray emission edge self absorption and effect of exciting voltage 77−90220
Na, soft X-ray L_{23} emission and absorpt. spectra 79−43064
Na, X-ray absorpt. and emission edges, one-electron and many-body effects 80−25484
Na, X-ray edge shape, band struct. role 77−16425
Na, X-ray emission spectra, double plasmon high energy satellites 80−29829
Na-like ions, Kr-Mo, 2-3 transitions, plasma X-ray spectra classification 79−37544
Na-like ions, transition probabilities for reson. transitions 78−66494
Na^++Ti(Ni)(Zn)(Fe), 0.2-3.0 MeV, united-at. limits, mol.-orbital continua 77−19030
$Na_6Al_6Si_6O_{24}$, zeolite, luminescence and coloration *(Russian)* 78−72578
$Na_8Al_6Si_6O_{24}F_2$(Cl)(Br)(I), sodalite, luminescence and coloration *(Russian)* 78−72578
Na_2O-TiO_2-SiO_2 glass, co-ordination of Ti, X-ray emission spectra study 80−84072
$Na_2O(K_2O)$-P_2O_5 glasses, P K-band X-ray emission spectra, state anal. 80−40190
NaV_6O_{15} monocrystal, electronic struct. and X-ray emission spectra anisotropy 80−84807
Na_3VO_4, X-ray Lα emission spectra, excited states calcs. 79−59488
Nb, band structure, emission band shape, self-consistent calc. 77−28104

X-ray emission spectra continued
Nb, L-spectra, influence of temp., liq. N_2 temps. *(Russian)* 80−80907
Nb, pure and metal-like compounds, $L\beta_2$ bands at room and liquid N temps. 77−28654
Nb, X-ray $M\zeta$ energy, revised values 80−14102
Nb XXXIX and XL, X-ray spectrum weak line detection 80−5497
Nb-Co, X-ray emission spectra investigation of electron struct. of Laves phases *(Russian)* 78−23554
Nb-Cr(Mn)(Mo)(Zr), internal impurity adsorption effect on bond type of intercrystallite zones 77−16684
Nb-Fe, X-ray emission spectra study of electron struct. of Laves phases *(Russian)* 78−23555
Nb-V, negative muon Coulomb capture ratio and Lyman series intensities 80−14255
Nb-V alloy, valence bands, X-ray M- and L-emission bands obs. *(Russian)* 78−19602
Nb-Zr-C (0.1, 0.01 wt.%) plastic deform. influence on electronic state of Nb atoms 80−40463
Nb+Kr, excitation of 1sσ and 2pσ quasimolecular radiation 78−78801
Nb+Nb, 67 MeV, Doppler shift and anisotropy of quasimolecular X-rays 77−3048
Nb+Nb, selected MO X-ray coincidence with separated at. K X-rays 80−43148
Nb+Nb, X-ray ang. distrib., 35-75 MeV 2 pΣ MO calc. 79−76380
Nb+Nb symmetric collisions, MO-2pσ radiation anisotropy, quasimolecular nature 78−70924
NbC, band struct. and X-ray emission spectra, APW and Xα calc. 80−70605
NbC, chemical bonding and X-ray emission spectral analysis 77−44088
NbC, interpretation in terms of relativistic elec. dipole transition probabilities 79−3459
NbC, valence band struct. *(Russian)* 78−6268
$Nb_3Ga(So)(Ir)(Pt)(Au)$, X-ray $M_{IV,V}$ emission bands *(Russian)* 80−45170
$Nb_{0.5}Mo_{0.5}$, soft X-ray spectra, theoretical considerations 80−11511
NbN, chemical bonding and X-ray emission spectral analysis 77−44088
NbO chemical bonding and X-ray emission spectral analysis 77−44088
NbO, electronic struct. from photoelec.- and X-ray emission spectra and X_α calcs. of NbO_6^{-10} cluster 79−23892
NbO, photoemission and X-ray emission spectra 78−64442
NbO_2, rutile phase, energy levels, momentum density, and Compton profile, embedded cluster model 80−50453
Nb_4Si, Nb_5Si_3 and $NbSi_2$, ultrasoft X-ray emission bands, empirical band schemes 78−15249
Nb_3(Sn-Al) system, X-ray spectroscopic studies of electronic struct. of A15 cpds. 80−2900
^{95}Nb, beta decay, K-shell electron ejection 77−18888
^{95}Nb, K-shell autoionisation in β-decay 77−298
^{93m}Nb disintegration rate meas. for fast neutron flux determ. *(German)* 77−38579
^{93m}Nb, radioactive decay period meas. *(French)* 77−79341
Nd, Lα X-rays produced by surface impact of F^{n+} and Si^{n+} 79−69907
Nd, threshold pot. spectra, $N_{4,5}$ absorpt. widths 79−69578
Nd, X-ray cross sections, L-shell, proton induced, 1 to 3 MeV range 79−1799
^{60}Nd, L-emission spectrum, new lines obs. 78−86809
^{60}Nd, L-emission spectrum, new lines obs. 77−79566
$^{60}Nd+^{19}F(^{28}Si)$, target Lα X-ray prod., projectile charge state depend. 79−47549
Ne, Auger rates, X-ray transition energies and fluoresc. yield calcs. 77−6714
Ne, charge-state distributions and the population of X-ray emitting states 79−68311
Ne filled glass microballoons, laser imploded, compressed core density meas. by X-ray continuum edge shift 79−10705
Ne, gaseous and in solid target, X-ray spectra 77−23452
Ne I isoelectronic sequence, X-ray spectra, K X to Fe XVII 79−22641
Ne II-VIII L-shell excit. by highly ionised heavy ion impact 78−1074
Ne, isoelectronic sequence, X-ray spectra 80−87071
Ne, K_α X-ray transition energies 79−98017
Ne, Kα satellite lines meas. by soft X-ray spectrometer 78−24911
Ne, Li-like X-ray and Auger populations and line intensities from Cl^{13+} collisions 77−10625
Ne post-foil Kalpha X-ray emission, correlation with empirical charge state distribs. 78−15252
Ne recoil ion, highly charged, K X-ray emission 80−91649
Ne spectral line broadening as diagnostic for compressed laser fusion targets 79−98979
Ne, two-electron one-photon transition rate 77−71772
Ne, X-ray emission spectrum, multiplet struct. 78−82678
Ne, X-ray line shift for high density laser produced plasma diagnostics 80−64778
Ne, X-ray spectral line broadening in solid and gas targets 77−6713
Ne^{7+}, $1s2l3l'$ config., Auger and radiative deexcitation, intermediate coupling 77−79567
Ne-like ions, Kr-Mo, 2-3 transitions, plasma X-ray spectra classification 79−37544
Ne-like ions, multiply charged, laser plasmas, 1.5-15 Å 78−13462
Ne^{n+}-Ne, K-shell vacancy prod. cross section, X-ray and Auger electron prod. fluoresc. yield 78−13582
Ne+Al foil, projectile K-vacancy production cross section, X-ray production rel. to target thickness 77−19059
$Ne+Ar^{12+}(Xe^{24+})(Pb^{40+})$, X-ray transitions 78−66641
$Ne+Cl^{12+}(S^{14+})$ soft X-ray emitting slow multiply charged ion prod., recoil ion spectroscopy 77−50516
Ne+heavy ion, few-electron states prod. K X-rays obs. 80−9718
$Ne+Li^{+1,2,3}$, K-shell ionisation depend. on projectile charge state 77−34743
$Ne+N_2$, K-X-ray spectrum, collisional configuration-rearrangement 78−82816
Ne^++Kr, low vel. collision, enhanced K-L vacancy sharing ratios, X-ray prod. cross section 78−78790
$Ne^++NH_3(H_2O)(Ne)$ symmetric collisions, double K-shell ionisation, two-electron-one-photon transitions 77−19067
$Ne^{n+}+Ne$ collisions, n=1 to 4, K-X-ray production, projectile charge state dependence 77−14570
Ni (001) surface, initial oxidation, RHEED and X-ray emission meas. 77−31885
Ni (110), oxidation, initial stage kinetics, RHEED and X-ray emission 78−15588

X-ray emission spectra continued
Ni, AES meas. of soft X-ray emission threshold potential *(Russian)* 79−33866
Ni, crystal spectroscopy to small quantum energies, $M_{2,3}$ spectrum 77−69938
Ni, electron bombard., 300 to 600 keV, K_α/K_β X-ray intensity ratios, K-shell ionis. cross sections 78−37747
Ni, highly dispersed, K_β emission spectra, cluster effects 77−28650
Ni ion+Ni(Fe) collisions, X-ray spectra, two-electron transitions 77−19050
Ni, $K_{\beta 1,3}$ X-ray emission spectra, low-energy plasmon satellites 79−65957
Ni, Kα hypersatellite spectrum, double K ionis. 77−18829
Ni, L_{III}-binding energy, absolute determ. from self-absorpt. meas. 80−71519
Ni, liq., soft X-ray band spectra 77−52199
Ni, oxidation, electron beam influence, disappearance potential spectroscopy obs. 77−1766
Ni photoelec. cross sections, 5-40 keV photons, X-ray emission spectra 77−18866
Ni, proton-induced L-shell ionisation cross-sections 80−100707
Ni, Si ion projectile bound s electron polaris. rel. to transient mag. fields 79−33023
Ni, X-ray absorption and emission K and L spectra, APW calc. 78−68579
Ni, X-ray intensity reson. near 2p threshold 80−60717
Ni XXI, X-ray spectra in laser plasma, $2p^6\ ^1S_0 \rightarrow 2s2p^5\ ^1P_1$ 79−1340
Ni-like ions, multiply charged, laser plasmas, 1.5-15 Å 78−13462
Ni-P alloy, electrodeposited, heat induced struct. changes *(Japanese)* 78−15433
Ni+Mn(Pb), inner shell vacancy prod., impact parameter depend. 77−6906
$Ni+N^{4+}$, Kα and Kβ X-ray spectra for 84 MeV incident energy 77−50517
Ni+Ni, 12-90 MeV, molecular orbital K X-rays ang. distrib. 79−10125
Ni+Ni, 39 MeV, X-ray emission spectra, nonLorentzian shape of atomic line tail 78−21872
Ni+Ni, beam-foil collisions, X-ray transitions between correl. many electron quantum states 77−79689
Ni+Ni, continuum X-ray radiation, collision broadening 80−9539
Ni+Ni symmetric collisions, molecular-K-X-ray anisotropy spectra, discrete struct. 77−14560
$Ni+Ni^+$, with nuclear sticking, molecular orbital and compounds nucleus X-ray emission 80−1048
$Ni+Ni^{x+}$, K X-rays, two-electron-one-photon excitation 78−13589
Ni+Ni(Nb), Doppler shift of continuum X-rays from quasimols. 79−22808
NiAl, bonding, self-consistent energy bands 78−91610
NiGe, Ni_2Ge and Ni_3Ge, X-ray spectrum analysis energy band struct. *(Ukrainian)* 77−52200
$NiGe_x$, Ni emission spectra *(Russian)* 78−21942
^{58}Ni+p, K-shell X-ray photon proton coincidences, nucl. time delay 79−18281
$_{28}{}^{58}Ni^{n+}+{}_{25}Mn(_{50}Sn)(_{82}Pb)$, 45, 94, and 138 MeV Ni inner shell vacancy production, impact parameter depend. 79−41130
Np, M-series X-rays, energies and widths 77−75092
^{237}Np, nuclear excitation by electron transition (NEET) 77−34256
O I, isoelectronic sequence, X-ray spectra 80−87071
O ions, moving in Ne, Ar, Kr gases and C foils and slabs 77−69020
O, K-shell ionis., double and single, cross section meas. by ion bombardment 78−50629
O, Kα spectrum, intensity of high energy peak as function of oxide layer thickness 80−936
O VII, laser produced plasma, satellite spectra 78−5165
O VII line intensity ratios depend. on temp. and ionization balance 79−16903
O-bearing gases, K X-ray yields induced by proton bombardment 79−45736
$O+H^+(He^+)$, double K-shell ionis., projectile Z depend. 78−25680
O^++Al, Al K-vacancy cross sections, 0.15 to 91 MeV, recoil effects and mechanisms 77−19033
$O^++NH_3(H_2O)(Ne)$ symmetric collisions, double K-shell ionisation, two-electron-one-photon transitions 77−19067
O^{x+}+He, electron capture, K X-ray emission ang. distrib. 77−57919
O_2, core hole energy curve determ. 79−41186
O_2, X-ray K emission spectra, band interpretation and satellites 77−88464
$O^{7+}(O^{8+})$+He, p-state alignment, X-ray emission polaris. obs. 79−50123
^{188}Os, muonic resonance spectra, deduced isomer shifts and electric moments 80−18948
^{191}Os, K-shell internal conversion, $K\alpha_1$ hypersatellite line energies, intensities 77−18885
^{194}Os beta decay, X-ray/gamma relative intensities, L_1 subshell yields 78−4919
P allotropic modifications, muonic X-ray intensities, computer analysis 80−23577
P, muonic allotropes muonic Roentgen intensities *(German)* 80−53168
PH_3, K-fluoresc. obs. of electronic struct. 80−37818
PO_4^{3-}, synchrotron radiation excited fluoresc., O K-emission spectrum, electronic struct. 77−42335
^{31}P, muonic, 3d-2p X-ray transition 80−9764
Pb, 15-33 MeV electron bombardment, X-ray ang. distrib. meas. using ETL quantameters 80−91367
Pb, 90-110 MeV, ion-atom collision, K-vacancy prod., mol.-orbital method 77−68095
Pb, A=204-208, charge distrib. from elastic electron scatt. and muonic X-ray data anal. 78−54681
Pb, double-vacancy states, L X-ray fluoresc., K Auger electrons 77−27016
Pb, electron impact L-shell ionis., 300-600 keV 77−50542
Pb, K-shell ionis. probability, 25- 40-and 74-MeV α particles 77−528
Pb, L-X-ray production by 9.5 to 41.8 MeV Fl ions 77−85847
Pb, L-shell electron impact ionisation, X-ray production cross sections 77−19095
Pb, LL-vacancy states produced by KLL Auger transitions, X-ray fluoresc. yield 77−18832
Pb, X-ray emission spectra of CO_2 laser-irrad. targets, nonlinear processes 80−33793
Pb, X-ray L shell emission spectra *(Spanish)* 79−98016
$Pb+H^+$, L-shell ionis., 0.5-3.5 MeV, X-ray emission obs. 77−54528

X-ray emission spectra continued
Pb+H^+ (L_α, L_β, L_γ) X-ray emission probability, impact parameter dependence 77−23553
Pb+Pb K-MO spectrum, impact parameter depend. 80−5613
Pb+Pb quasimolecules ab initio calc. of K X-ray spectra 78−21941
Pb+target atom, 90-110 MeV, K-vacancy cross sections, target depend. 77−19026
Pb^++Z (42≤Z≤92), 1sσ MO excitation probability and binding energy, X-ray coincidence 78−94316
PbO, microprobe state anal. by X-ray OK and BK emission band spectra *(Japanese)* 78−19606
PbO-B_2O_3 glass, X-ray emission spectra of Fe and Cu 77−44089
PbO-B_2O_3-SiO_2, molten mixture, microprobe state anal. by X-ray OK and BK emission band spectra *(Japanese)* 78−19606
PbO-Bi_2O_3-Al_2O_3, glass formation and IR transmission *(Japanese)* 80−54146
PbO.SiO_2 film, formation mechanism on Si, X-ray spectral anal. 79−87008
$PbTiO_3$, O K_α X-ray emission band spectra *(Russian)* 79−15563
^{82}Pb, electron impact, relativistic, L-shell ionis., $L\beta/L\alpha$ branching ratio energy depend. 79−98228
^{205}Pb, decay, orbital electron capture ratios 77−18894
^{208}Pb, charge distrib. polarisation from e^- scatt. and muonic X-ray data consistency 77−22873
^{208}Pb+^{208}Pb collisions, 1 GeV, mol. orbital X-rays 79−49978
^{208}Pb+Ag(Au), 5.8 MeV/amu, Pb K-shell excitation probability 78−5338
^{208}Pb(^{6}Li,xn), 75, 85, and 95 MeV, K X-ray multiplicity 79−76019
Pd, circular polarisation of muonic K_α X-rays 78−9284
Pd, circular polarisation of muonic X-rays, strange μ^- depolarisation 78−25758
Pd, electronic structre, Compton scatt., soft X-ray emission and X-ray photoelectron spectra 79−77999
Pd, K-shell X-ray spectra, $K\beta_2/K\beta_1$ determ. 77−23456
Pd, $K\beta_3/K\beta_1$ and $K\beta_2/K\beta_1$ relative intensities 77−75088
Pd, L-spectra, influence of temp., liq. N_2 temps. *(Russian)* 80−80907
Pd, Lα X-ray spectra, $_{40}$Zr to $_{48}$Cd, linewidths 79−41131
Pd, proton-induced L-shell ionisation cross-sections 80−100707
Pd+H^+(O^{3+}), L-shell X-ray prod. cross-section 77−6913
^{105}Pd muonic X-rays, nuclear charge parameters, quadrupole moments 78−29377
^{147}Pm decay, K-orbital shake off electrons and X-ray spectra 77−46141
^{208}Po, L-shell ionisation in α-decay 78−78324
Pr, L-X-ray production by 9.5 to 41.8 MeV Fl ions 77−85847
Pr_2O_3, atomic interaction effects in X-ray emission spectra *(Russian)* 79−69905
^{141}Pr, double K-hole creation in 145 keV internal conversion 77−18823
^{141}Pr, internal conversion decay, double K-hole creation 77−18887
Pt compounds, L X-ray spectra and X-ray electron spectra, influence of chem. bonds 77−28656
Pt, energy band structure, X-ray emission spectra, APW calc. 80−92811
Pt, laser produced plasma, Ni-like X-ray spectrum 80−43983
Pt, X-ray cross sections, L-shell, proton induced, 1 to 3 MeV range 79−1799
Pt+H^+, L-subshell ionisation cross-sections, X-ray meas. 77−46520
Pt+H^+, L-subshell X-ray prod., cross-section meas. 77−46575
^{A}Pt(^{6}Li,xn), A=194, 198, 75, 85, and 95 MeV, K X-ray multiplicity 79−76019
α-Pu, 5f electron distrib. analysis 77−28663
Pu, M-lines 78−15251
^{239}Pu, highly deformed, muonic X-rays, nuclear charge distrib., elec. quadrupole moment 78−70440
Rb, L-shell soft X-ray emission spectra, oscillator strengths 80−32651
Rb, soft X-ray outer-shell absorption and emission, one-electron calc. 79−69904
Rb+$^{14}N^{n+}$, 7-35 MeV, K-shell X-ray production cross sections 77−75090
Rb+H^+, atomic K-shell ionis., X-ray emission 79−18280
Re, pionic 4f→3d transition, pionic 3d state strong interaction level shift and width 79−98251
Rh, L-spectra, influence of temp., liq. N_2 temps. *(Russian)* 80−80907
Rh, Lα X-ray spectra, $_{40}$Zr to $_{48}$Cd, linewidths 79−41131
Rh, proton-induced L-shell ionisation cross-sections 80−100707
Ru complexes, $K_{\alpha 1}$ lines chem. shift, donor-acceptor capacity of ligands 79−33867
Ru electrodes, adsorption and surface reactions, cyclic voltammetry and X-ray emission spectrometry 78−61018
Ru, electronic struct. and X-ray emission band intensities 77−20960
Ru, Lα X-ray spectra, $_{40}$Zr to $_{48}$Cd, linewidths 79−41131
S adsorption in coal, content meas., using X-ray radiometric analysis 80−26077
S, chem. environment effect on Kα satellites intensity, heavy-ion collisions 77−54527
S, concentration and valence state in pollution samples, X-ray fluoresc. anal. 79−48027
S, foil excitation, K-vacancy bearing metastable states yield, 30-50 MeV 77−54600
S, He-like, 2^3P_1 state lifetime, X-ray emission 77−18851
S, He-like ions, X-ray emission passing through thin foils 77−3293
S, in CoS, CdS, ZnS, MnS, $BaSO_4$ and K_2SO_4, X-ray L-emission spectra *(Japanese)* 78−15254
S ion+target (Z=4-40), single and double K-shell excitation, X-ray satellites, hypersatellites 77−19058
S ion+target collisions, two-electron-one-photon transitions, X-ray spectra 77−19068
S ions, multiplet state equilib. population in beam-foil excitation 77−19057
S, Kα satellite, hypersatellite X-ray emission spectra, yield ratios 78−86810
S, Kα X-ray satellite spectra, gas phase meas. 78−66496
S, L X-ray emitting levels, lifetimes 78−66493
S to Br, $O^{2+,3+,4+,5+}$ induced K-shell ionis., 7 to 24 MeV X-ray production cross section 77−61850
S_x X-ray and Auger transition probabilities to 2p level 78−17640
S^{4+}, travelling in solids, Kα X-ray spectra 80−100706
S+Ar, 32 MeV, $K_\alpha^h/K_{\alpha\alpha}$ branching ratios, S projectile charge state depend. 79−63947
S^++Ar, double K-vacancy prod., X-ray X-ray coincidence and fluoresc. yields obs. 78−55230
S^{n+}+Ar, molecular K-X-ray production, projectile charge depend. 78−90188

X-ray emission spectra continued
S^{n+}+Ne(SiH_4)(H_2S)(HCl)(Ar), K X-ray cross section, projectile charge depend. 77−19029
SF_4+O^+(Cl^+), S highly stripped core ion outer shell arrangement, Kα X-ray spectra 77−3451
$(SN)_x$, X-ray and optical props. 78−39632
^{32}S ions+Be(C)(Ni), radiative electron capture, X-ray ang. distrib. 77−38729
Sb, $K\beta_3/K\beta_1$ and $K\beta_2/K\beta_1$ relative intensities 77−75088
Sb_2O_3, density of valence states, photoemission meas. 77−72808
Sb_2O_3, electronic struct., X-ray emission, XPS, UPS obs., CNDO cluster calc. 78−52638
Sb_2S_3, electronic struct., X-ray emission, XPS, UPS obs. 78−52638
^{113}Sb mean nuclear lifetime from X-ray spectrum in ^{112}Sn(p,p′) 80−9267
Sc, electronic struct. and X-ray emission band intensities 77−20960
Sc, X-ray production by protons by 0.5 to 2.0 MeV energy 78−66646
Sc+H^+, K X-ray production, 0.2-0.5 MeV, ionis. cross-section 79−31459
ScGa and Sc_5Ga_3, exam. of X-ray K spectra of pure Sc, Ga in alloys *(Russian)* 79−15562
Se allotropic modifications, muonic X-ray intensities, computer analysis 80−23577
Se, circular polarisation of muonic K_α X-rays 78−9284
Se, Doppler effects in X-ray spectra excited by accelerated ions 78−86808
Se, electron bombard., 300 to 600 keV, K_α/K_β X-ray intensity ratios, K-shell ionis. cross sections 78−37747
Se film, metal ion diffusion during memory switching 78−26976
Se, K-emission satellites, HF and LF, origin 80−50465
Se, muonic allotropes, muonic Roentgen intensities *(German)* 80−53168
Se XXVI, $2p^5$-$2p^43s(2p^43d)$ transitions in laser produced X-ray spectra 78−13460
Sf_6, high resolution X-ray emission, valence electron struct. and chemical bonding, LCAO comparison 79−31545
Si, amorphous and cryst. K X-ray spectra of band struct. 79−87525
Si, chem. environment effect on Kα satellites intensity, heavy-ion collisions 77−54527
Si, F^{q+} ion impact, X-ray emission and fluoresc. yields 79−83060
Si, foil excitation, K-vacancy bearing metastable states yield, 30-50 MeV 77−54600
Si, He-like, 2^3P_1 state lifetime, X-ray emission 77−18851
Si, in laser-irradiated glass shell plasma, electron density and temp. diagnostics *(Chinese)* 80−38718
Si ions, H-like, He-like and Li-like, X-ray spectra after foil excitation 79−59545
Si ions, multiply-charged, beam-foil obs. of $1s2p^3P_1$ lifetime 80−14114
Si, K_α X-ray emission spectra chemical shifts, linewidths and intensities 78−13461
Si, K-shell ionis., X-ray prod. cross section for incident H^+, ^{4}He and ^{14}N ions 78−70923
Si, K-spectra, fine struct. intensity, temp. depend. *(Ukrainian)* 77−55850
Si, Kα X-ray satellite spectra, gas phase meas. 78−66496
Si, L X-ray emitting levels, lifetimes 78−66493
Si, positron channelling, possible tunable X-ray source 79−69167
Si, range of 100 keV Pr^{2+} and Tb^{2+}, M-shell X-ray cross-sections 77−35614
Si, relativistic electron channelling spectra 10-130 keV 80−24516
Si, solid, electron rearrangement after inner shell ionisation by heavy charge particle impact 80−87043
Si, struct. of $L_{2,3}$VV-Auger line, rel. to soft X-ray spectra 78−2953
Si, two electron one photon transitions, K$\alpha\alpha$ X-rays 77−30813
Si, X-ray continua emission, proton and ^{14}N bombard. 78−23559
Si, X-ray emission spectra, high energy plasmon satellite intensities 78−64430
Si, X-ray emission spectra formation, role of nonequilibrium electron density *(Russian)* 77−63490
Si, X-ray $L_{2,3}$ emission spectrum, high energy plasmon satellite 79−82538
Si, X-ray resonance Raman scattering, solid target, proton bombarded 79−61465
Si^{n+}, foil excited, satellite lines in X-ray spectrum 79−85929
Si:B(P)(As), ion implantation, 20-2800 keV, obs. of X-rays produced 78−14367
Si+F^{q+}, q=3-9, Si K-shell ionis., electron transfer cross sections, solid targets 79−10192
Si+H^+(^{3}He) ion collisions, K-shell ionisation cross sections 77−23555
Si+He^4, X-ray spectra, two-electron one-photon transition in solid target, 2 MeV 78−94209
Si+He(C)(O)(Ne), K-shell ionising collisions, average L-shell ionisation probability, K_α spectra 79−72408
Si+heavy ion, X-ray spectra, one-photon two electron rearrangements 77−6712
Si+$Li^{+1,2,3}$, K-shell ionisation depend. on projectile charge state 77−34743
Si^{12+}+He, K X-rays for population in $^3S_1$ metastable state, Si^{12+} from C, Au foils 78−17776
Si^{q+}+He, q=2-11, K-shell fluoresc. yields, charge-state depend. 78−55231
SiC, struct. of $L_{2,3}$VV-Auger lines, rel. to soft X-ray spectra 78−2953
SiF_4+O^+(Cl^+), Si highly stripped core ion outer shell rearrangement, Kα X-ray spectra 77−3451
SiH_4+F^{n+}, X-ray emission from gaseous target, q=4-9, 1 and 2 MeV/amu 79−83060
SiH_4+O^+(Cl^+), Si highly stripped core ion outer shell rearrangement, Kα X-ray spectra 77−3451
SiH_4(SiF_4), electron rearrangement after inner shell ionisation by heavy charge particle impact 80−87043
Si(Li) energy dispersive X-ray spectra, computer anal. 79−1981
SiO_2, amorphous and α-cristobalite cryst., band struct., photoelectron and X-ray spectra interpret. 80−24787
SiO_2, microprobe state anal. by X-ray OK and BK emission band spectra *(Japanese)* 78−19606
SiO_2, orthosilicates, mica, soft X-ray spectra and photoelectric yield spectra 78−72640
SiO_2, photoemission and X-ray emission spectra calc. 77−89866
SiO_2, proton induced ionisation, energy dependence of K_β/K_α intensity ratio 80−60716
SiO_2 stishovite, electronic struct., Si, $L_{II,III}$ emission, quantum yield spectra, and X-ray spectra of O 79−8210

X-ray emission spectra continued
SiO_2, struct. of $L_{2,3}VV$-Auger line, rel. to soft X-ray spectra 78−2953
SiO_2-$Na_2O(Li_2O)$ glasses, bonding of Si-O exam. by X-ray emission spectra 78−52594
SiO_2.B_2O_3.(Al_2O_3) film, formation mechanism on Si, X-ray spectral anal. 79−87008
SiP_2, pyrite structure, density of states 77−15733
Si_3Si_5, X-ray spectra, valence band struct. *(Russian)* 79−1798
SiX_4 (X=Cl,H,F), chemical shifts, relax., X-ray spectra, SCF Xalpha calcs. 80−27928
^{28}Si, $3d_{5/2}$-$2p_{3/2}$ muonic X-ray transition, energy, wavelength meas. 78−66695
$^{28}Si^{n+}$+Sc(Ti)(Cu)(Ge), K-shell ionisation, projectile charge state depend., theory 78−17786
Sm, keV electron impact, L X-ray prod. cross section 79−18293
Sm, L-X-ray production by 9.5 to 41.8 MeV Fl ions 77−85847
Sm, X-ray prod. by 5 MeV/amu deuterons (oxygen ions), projectile Z depend. 80−42982
Sn, $K\beta_3/K\beta_1$ and $K\beta_2/K\beta_1$ relative intensities 77−75088
Sn, $L\alpha$ X-ray fluoresc. spectra, natural linewidth meas. 79−85934
Sn, X-ray cross sections, L-shell, proton induced, 1 to 3 MeV range 79−1799
Sn+H^+(O^{5+}), L-shell X-ray prod. cross-section determ. 77−6913
Sn+He(C)(N)(O), inner-shell multiple ionisation systematics, X-ray obs. 80−63790
$^{122}Sn(K^-, X)$, 0 MeV, E2 nuclear resonance effects, γ and X-ray meas. 78−41774
Sr, L-shell soft X-ray emission spectra, oscillator strengths 80−32651
SrO, atomic interaction effects in X-ray emission spectra *(Russian)* 79−69905
$SrTiO_3$, O K_α X-ray emission band spectra *(Russian)* 79−15563
Ta, bremsstrahlung emission meas., using vac. UV isochromat spectrometer 77−74521
Ta, K X-ray energy, excitation mode depend. 78−17597
Ta, K X-ray energy, excitation mode depend. 78−17598
Ta, K-shell X-ray energy, excitation mode depend. 77−18824
Ta, K-shell X-ray energy, excitation mode depend. 79−26926
Ta, KLL Auger emission, de-excitation of double L vacancy states 77−18886
Ta, $K\alpha$ line widths, precise meas. 78−62761
Ta, L-subshell ionisation cross-section ratio determ. 77−6920
Ta, X-ray fluoresc. yields in KLL Auger emission 77−54525
Ta XLVI(XLVII), $3d^k$-$3d^{k-1}$npnf transitions in laser plasma 78−9108
Ta-Fe, X-ray emission spectra study of electron struct. of Laves phases *(Russian)* 78−23555
Ta+H^+(He^+), L-subshell ionisation cross section, branching ratios, fluoresc. yield, Coster-Kronig factors 80−43166
^{181}Ta, pionic 4f→3d transition, pionic 3d state strong interaction level shift and width 79−98251
^{181}Ta, pionic X-rays, effective quadrupole moment determ. 78−66200
$^{181}Ta(^6Li,xn)$, 75, 85, and 95 MeV, K X-ray multiplicity 79−76019
^{182}Ta, decay scheme, conversion electron spectra, K-line transitions 78−13025
Tc, $L\alpha$ X-ray spectra, $_{40}Zr$ to $_{48}Cd$, linewidths 79−41131
Te, $K\beta_3/K\beta_1$ and $K\beta_2/K\beta_1$ relative intensities 77−75088
Te, valence-band X-ray emission spectrum 78−84682
^mTe, A=125,127,129, internal conversion of M4 transitions at 109.27, 88.26, 105.50 keV 77−65214
Th, L and M X-ray emission following H and O ion impact, parameter depend. 80−66327
Th, X-ray L shell emission spectra *(Spanish)* 79−98016
Th+H^+, L-shell ionis., 0.5-3.5 MeV, X-ray emission obs. 77−54528
ThF_4, 5d X-ray spectra 78−88382
ThO_2, 5d X-ray spectra 78−88382
^{231}Th, L2/L3 vacancy ratio for internal conversion by γ-X-ray coincidence technique *(Spanish)* 79−97682
^{232}Th, highly deformed, muonic X-rays, nuclear charge distrib., elec. quadrupole moment 78−70440
Ti, AES meas. of soft X-ray emission threshold potential *(Russian)* 79−33866
Ti, electronic struct. and X-ray emission band intensities 77−20960
Ti, K_β/K_α following K-electron capture and X-ray excitation 78−13031
Ti, $K_{\beta 5}$ emission band, effect of struct. change on alloying *(Russian)* 77−59645
Ti, K-shell ionis., X-ray prod. cross section for incident H^+, ^4He and ^{14}N ions 78−70923
Ti, K-shell ionisation probability, for 150 keV protons, impact-parameter depend. 79−10189
Ti, $K\beta$ X-ray emission, plasmon satellite 77−28662
Ti $K\beta_{1,3}$ line width and $K\beta_5$ band 78−2946
Ti, X-ray continua emission, proton and ^{14}N bombard. 78−23559
Ti, X-ray production by protons by 0.5 to 2.0 MeV energy 78−66646
Ti XXI, spectra from laser plasma comparison with solar corona and vacuum spark 78−17596
Ti-Co, X-ray emission spectra investigation of electron struct. of Laves phases *(Russian)* 78−23554
Ti-Ni alloys, energy band structures *(Ukrainian)* 77−32469
Ti-Zr alloy, valence bands, X-ray M- and L-emission bands obs. *(Russian)* 78−19602
Ti+H^+, K X-ray production, 0.2-0.5 MeV, ionis. cross-section 79−31459
Ti+H^+ ion collisions, K-shell ionisation cross sections 77−23556
Ti+He^{2+}(C^{4+})(O^{5+})(N^{4+})(N^{5+}) atom-ion collisions, ratio of single K-shell ionisation cross section to double K-shell ionisation cross section 80−53119
Ti+N^{4+}, $K\alpha$ and $K\beta$ X-ray spectra for 84 MeV incident energy 77−50517
TiC, soft X-ray emission, excitation pot. spectra, excited level binding energy 80−35009
TiC, X-ray emission spectra and chem. bonding 77−20958
TiCo, and TiCoSi(Ge), electronic struct., X-ray K- and L-spectra obs. *(Russian)* 78−11022
TiF_2, TiF_4, X-ray emission, core level chem. shift calcs. 80−53010
$TiGa$, $TiGa_2$, Ti_5Ga_3, X-ray K- and L-bands, electronic struct. *(Russian)* 79−1797
TiGe, and TiCoGe, electronic struct., X-ray K- and L-spectra obs. *(Russian)* 78−11022
TiGe, $TiGe_2$, Ti_5Ge_3, X-ray K- and L-bands, electronic struct. *(Russian)* 79−1797
Ti_xGe_y, interrelationship of X-ray charact. with physical props. *(Russian)* 77−1765

X-ray emission spectra continued
TiH_4, X-ray emission, core level chem. shift calcs. 80−53010
TiH_3F, X-ray emission, core level chem. shift calcs. 80−53010
TiN, soft X-ray emission, excitation pot. spectra, excited level binding energy 80−35009
TiN, X-ray emission spectra and chem. bonding 77−20958
TiNi, electronic charge transfer, binding energies 77−44091
TiO, soft X-ray spectra and XPS, $X\alpha$ and Hartree-Fock calcs. discrepancies 79−77979
TiO, X-ray emission spectra and chem. bonding 77−20958
TiO_2, core levels, cryst.-field splitting, X-ray emission study 80−66328
TiO_X, $K\beta_{1,3}$ line width and $K\beta_5$ band 78−2946
TiO_x, X-ray Ti K spectra and band struct. 77−77320
Ti_2O_3, electron structures calc. using models, ESCA and X-ray spectral data 77−35863
TiP, metallic, band struct., X-ray spectral obs. 78−11019
$TiPd_3$, valence band struct. *(Russian)* 77−40304
TiSi, and TiCoSi, electronic struct., X-ray K- and L-spectra obs. *(Russian)* 78−11022
$Ti_xV_{1-x}C$, electronic struct. and X-ray emission spectra, cluster MO calc. 80−65444
^ATi, A=46, 48, 50, pionic X-rays, strong interaction and isotope shifts, π-nuclear optical pot. 80−53169
Tl, A=205,203, charge distrib. from elastic electron scatt. and muonic X-ray data anal. 78−54681
Tl+H^+, L-shell ionis., 0.5-3.5 MeV, X-ray emission obs. 77−54528
Tm, $K\alpha$ line widths, precise meas. 78−62761
^{169}Tm, double K-shell vacancy creation by internal conversion in ^{169}Yb, EC decay 77−57627
U, A=235, 238, highly deformed, muonic X-rays, nuclear charge distrib., elec. quadrupole moment 78−70440
U, L-subshell ionisation cross-section ratio determ. 77−6920
U, M-shell X-ray emission obs. by photoelectron spectrosc. 77−54529
U, X-ray and Auger transition probabilities to 2p level 78−17640
U, X-ray L shell emission spectra *(Spanish)* 79−98016
U+H^+, L X-ray production cross sections, 0.3-1.8 MeV, expt. rel. to PWBA prediction 80−53115
U+H^+, L-shell ionis., 0.5-3.5 MeV, X-ray emission obs. 77−54528
U+H^+(He^+), 2-18 MeV, L-subshell ionis. cross section, projectile energy depend. 77−19031
UO_2, 5d X-ray spectra 78−88382
UO_2, electronic distributions by X-ray spectroscopy 80−97407
UO_3, 5d X-ray spectra 78−88382
^{236}U, populated in (n, γf), X-ray prefission yield depend. on fission width 77−10453
^{238}U, muonic, non-axiality effects in quadrupole hyperfine splitting 77−46107
V, atom and ions, shell energy struct., SCF calc. by Dirac-Fock-Slater method 80−52877
V, band structure, emission band shape, self-consistent calc. 77−28104
V, electronic structure, X-ray spectra and XPS meas. 77−85842
V, K_β/K_α following K-electron capture and X-ray excitation 78−13031
V, $K_{\beta 1,3}$ X-ray emission spectra, low-energy plasmon satellites 79−65957
V, $K_{\beta 5}$ emission band, reinterpretation *(Russian)* 77−59645
V, $K\alpha^h$ hypersatellite spectra and K-shell double photoionisation cross-section 78−21874
V, X-ray band spectra calcs. 79−33860
V, X-ray fluoresc., $K\alpha$ hypersatellites 77−18830
V, X-ray production by protons by 0.5 to 2.0 MeV energy 78−66646
V XXII, He-like ion resonance line satellites 79−10064
V XXII, spectral from laser plasma, comparison with solar corona and vacuum spark 78−17596
V-Mo, X-ray K-emission spectra *(Russian)* 77−55851
V-Nb, X-ray K-emission spectra *(Russian)* 77−55851
V-Re, X-ray K-emission spectra *(Russian)* 77−55851
V-Ta, X-ray emission spectra *(Russian)* 77−55851
V-W, X-ray K-emission spectra *(Russian)* 77−55851
V+H^+, K X-ray production, 0.2-0.5 MeV, ionis. cross-section 79−31459
V+H^+ ion collisions, K_α satellite intensity meas. 77−23550
V+H^+ ion collisions, K-shell ionisation cross sections 77−23556
VC, interpretation in terms of relativistic elec. dipole transition probabilities 79−3459
VC, soft X-ray emission, excitation pot. spectra, excited level binding energy 80−35009
VC, valence band struct. *(Russian)* 78−6268
V_3Ga, structure effects on supercond. props. and electron spectrum *(Russian)* 77−80862
VH, electronic struct. and X-ray emission spectra 77−52201
VN, soft X-ray emission, excitation pot. spectra, excited level binding energy 80−35009
VO_4^{3-}, electronic struct. determ. from X-ray spectra 78−86885
V_2O_3, electron structures calc. using models, ESCA and X-ray spectral data 77−35863
V_2O_5, core levels, cryst.-field splitting, X-ray emission study 80−66328
V_2O_5 energy band struct. rel. to expt. studies 80−70603
V_2O_5, X-ray $L\alpha$ emission spectra, excited states calcs. 79−59488
V_xO_y, $L\alpha$ emission spectra of V 78−2947
VRu, soft X-ray emission, photoelectron spectra and electron structure 79−37978
V_3Si, band struct. and core levels 77−48278
V_3Si, electronic struct., charge distrib. and X-ray emission spectra 79−51481
^{51}V, K_β/K_α intensity ratios, chem. effects 79−63949
W, axial to planar channelling transition, proton induced X-ray yield meas. 77−31704
W, bremsstrahlung spectra, 10 to 30 keV, thick target expts. 77−8687
W, electron impact ionisation, L-subshell cross-sections, X-ray obs. 79−76519
W ion emission from PLT Tokamak, W ion soft X-ray emission effects 78−83537
W, $K\alpha_1$ X-ray line wavelength determ. 79−41132
W, N-shell ionisation by proton impact 78−78800
W, proton-induced L-shell ionisation cross-sections 80−100707
W XX to XXXV spectra and spatial distrib. in PLT Tokamak 78−55747
W+H^+(He^+), L-subshell ionisation cross section, branching ratios, fluoresc. yield, Coster-Kronig factors 80−43166
^{74}W, L-emission spectrum, forbidden lines 77−3295
$^{260}X_{105}$, prod., L X-ray spectra, decay 78−8780

X-ray emission spectra continued
Xe, 326-470 MeV, ion-atom collision, K-vacancy prod., mol.-orbital method 77−68095
Xe compounds, Xe chemical and isomer shifts, electron valence struct. *(Russian)* 80−53056
Xe, electron impact, L-shell excitation, characteristic X-ray spectra, relative cross sections 77−19094
Xe, electron impact, struct. near $N_{4,5}$ edges 77−75083
Xe, free ats. electron bombard., subsequent X-radiation ang. distrib. 80−53144
Xe ion+Au foil (Hg vapour) collisions, quasimol. M-radiation 77−14566
Xe isotope shifts of 1s electron in K-X-rays following electron capture 77−23454
Xe, K X-ray energy shifts following electron capture beta decay, role of nucl. hyperfine struct. 78−5166
Xe, L-shell fluorescence yields 77−79568
Xe like ions (I^-, Cs^+, Ba^{2+}, La^{3+}) $3d^94f$ config., collapse of 4f electron, X-ray spectral obs. *(Russian)* 80−58204
Xe+Bi, Bi Kα X-ray lines, Doppler broadening 78−62759
Xe+Cu^{q+}, ($16 \leq q \leq 23$), 1.4 MeV/amu, X-ray emission, charge state dependence 78−37713
Xe+H^+, ionisation, induced L-shell alignment 80−32813
Xe+Pb, 4.6 MeV/amu, 1 sσ vacancy production, impact parameter depend. 79−72393
Xe+target atom, 326-470 MeV, K-vacancy cross sections, target depend. 77−19026
Xe^++Ag, quasimolecular L and Ag L X-ray excitation thresholds, electron correl., calc. and expt. 78−78793
^{136}Xe ion+target collisions, K-X-ray yields, 1sσ excitation 77−19051
^{136}Xe ion+target collisions, X-ray yields, K-L level matching 77−19052
^{136}Xe ion+target collisions, K-X-ray yields, K-vacancy sharing 77−23548
^{136}Xe ion+target collisions, K-X-ray yields, 2pσ excitation 77−23549
Y, electron bombard., 300 to 600 keV, K_α/K_β X-ray intensity ratios, K-shell ionis. cross sections 78−37747
Y, electronic struct. and X-ray emission band intensities 77−20960
Y, M-series emission bands *(Russian)* 77−81177
Y Mζ radiation source for ESCA, 132.3 eV, continuously deposited anode 77−4958
Y, X-ray Mζ energy, revised values 80−14102
Y^{30+}, X-ray spectra, $2p^5$-$2p^43d$, laser plasma 78−86806
Y+$^{14}N^{n+}$, 7-35 MeV, K-shell X-ray production cross sections 77−75090
Y_2O_3, M-series emission bands *(Russian)* 77−81177
YOF, electronic stuct. calcs. from XPS and X-ray emission spectra 80−35056
YS, band struct. and X-ray emission spectra, APW and Xα calc. 80−70605
YVO_4, X-ray Lα emission spectra, excited states calcs. 79−59488
Yb, electron impact L-shell ionis., 300-600 keV 77−50542
Yb+Yb^+, with nuclear sticking, molecular orbital and compounds nucleus X-ray emission 80−1048
^{70}Yb L-shell X-ray emission spectrum investigation 77−3297
^{70}Yb, L X-ray emission spectrum, new satellites 78−46293
^{169}Yb, K-shell internal conversion, Kα_1 hypersatellite line energies, intensities 77−18885
^{172}Yb, muonic resonance spectra, deduced isomer shifts and electric moments 80−18948
Zn, core levels, cryst.-field splitting, X-ray emission study 80−66328
Zn film, hexagonal struct., vacuum deposited, X-ray peak shift anal. 79−65335
Zn, HCP metals, K-emission valence bands, structure and bonding 80−7438
Zn, K_β/K_α following K-electron capture and X-ray excitation 78−13031
Zn, Kβ X-ray spectra and autoionisation following β-decay of ^{64}Cu 78−13029
Zn, L-shell soft X-ray emission spectra, oscillator strengths 80−32651
Zn, Lβ_1 and L$\alpha_{1,2}$ lines, atom comparison with metal 78−74604
Zn photoelec. cross sections, 5-40 keV photons, X-ray emission spectra 77−18866
Zn, proton-induced L-shell ionisation cross-sections 80−100707
Zn XXII, $2p^5$-$2p^33s(2p^43d)$ transitions in laser produced X-ray spectra 78−13460
Zn+O ion, K X-ray prod. 77−23554
$ZnGeP_2$, cryst., electronic struct., X-ray K-absorpt. and emission 78−15248
ZnS, diatomic crysts. electron induced X-ray emission, channelling effects 79−56888
ZnSe, diatomic crysts. electron induced X-ray emission, channelling effects 79−56888
$ZnSiP_2$, 1 MeV proton bombardment, lattice deformation investigation by Kossel effect 78−22775
$ZnSiP_2$, electronic struct., X-ray spectroscopic investigation 80−108300
^{30}Zn, electron bombardment, Kα satellites 80−47932
^{68}Zn, 2s-2p muonic X-ray transition obs. 80−74264
^{68}Zn muonic atom, dynamical E0 excitation, E0 resonances, muonic X-rays 80−95749
Zr, electronic struct. and X-ray emission band intensities 77−20960
Zr, Lα X-ray spectra, $_{40}$Zr to $_{48}$Cd, linewidths 79−41131
Zr photoelec. cross sections, 5-40 keV photons, X-ray emission spectra 77−18866
Zr, X-ray Mζ energy, revised values 80−14102
Zr XII, energy level system, spectrum obs. 70 to 630 Å 80−37766
Zr-H alloy, soft X-ray emission spectra, electronic struct. 79−65959
Zr-Ni, energy spectra of valence electrons *(Ukrainian)* 78−6814
Zr-Ni alloys, energy spectra, X-ray emission obs. *(Russian)* 78−19604
Zr+$^{14}N^{n+}$, 7-35 MeV, K-shell X-ray production cross sections 77−75090
$ZrAl_2$, X-ray energy spectrum of valence electrons *(Russian)* 80−108304
Zr_2Al, X-ray energy spectrum of valence electrons *(Russian)* 80−108304
Zr_4Al_3, X-ray energy spectrum of valence electrons *(Russian)* 80−108304
ZrC, valence band struct. *(Russian)* 78−6268
ZrH_x (x=1.55, 1.7), synthesis and electron structure 80−29889
ZrN_yH_x (y=0.81 or 0.84, x=0.19 or 0.16) synthesis and electron structure 80−29889
$ZrPd_2$, valence band struct. *(Russian)* 77−40304
ZrSi and $ZrSi_2$, ultrasoft X-ray emission bands, empirical band schemes 78−15249
ZrX_2 alloy, Laves phases with $MgZn_2$, $MgCu_2$ structs., X-ray emission Zr spectra *(Russian)* 80−71517

X-ray fluorescence analysis
absolute determinations and matrix corrections, high con. method 80−81379
absorption correction, effective wavelength calc. 79−24855
additional excitation, evaluation 77−52700
advances, techniques and instrumentation, conference, Denver, USA (Aug. 1978) 80−3447
aerosol loaded filters, X-ray fluoresc. anal., absorpt. corrects. calcs. 78−7311
aerosol loaded filters, X-ray fluoresc. anal., filter absorpt. correction 77−60166
aerosol samples energy-dispersive X-ray fluoresc. anal. 78−85269
aerosols, atmospheric, X-ray fluoresc. anal., filter attenuation corrections 78−35740
aerosols in atmosphere, detection and measurement 77−41152
air, particulate matter, suspended, X-ray fluoresc. anal., semicond. detector X-ray spectrometer construction, calibration 77−56321
air particulate emissions from automobiles, containing H_2SO_4, X-ray fluoresc. anal. technique 77−60173
air pollutants, Zn and Pb, radioisotope-induced X-ray fluoresc. analysis 77−17214
air pollution, particulate matter, analysis 77−41150
air pollution, particulate matter, heavy metal analysis 77−41151
air pollution analyser using Harwell 6000 series electronics 79−5649
airborne mineralogical dusts, metallic elements determ. by energy dispersive X-ray fluorescence anal. 80−76569
airborne particulates, in industrial Greek city, X-ray fluoresc. 78−27857
allanite, metamict, phase changes on heating, age determ., x-ray fluoresc. anal. 77−51493
alloys, X-ray fluoresc. anal. using matrix correctional procedure 78−80817
alpha-induced X-ray spectrometry, element determination 78−53275
alpha-particle induced energy dispersive soft X-ray fluorescence anal. 77−48728
analytical physico-chem. methods, charact. *(French)* 79−48033
ancient pottery, origin determ. *(German)* 77−29064
anodic oxide superficial layer, X-ray emission spectrometry and ion backscattering *(French)* 80−49482
applications, conf., Denver, CO, USA, July-Aug. 1979 80−90613
archaeology, Unexplored Mansion, Knossos, anal. of Cu and bronze artefacts 77−34066
atmospheric aerosol sampling and anal. system for particulate S monitoring 79−21029
atmospheric aerosols, Israel, pollution sources detection by X-ray fluoresc. 79−52975
atmospheric particulates, X-ray fluoresc. anal., self-absorpt. effects, Monte Carlo simulation 77−60165
atmospheric particulates collected on filters, X-ray fluoresc. anal., least-squares method appl. 77−60168
atmospheric sampling filters, charged particle induced X-ray fluorescence anal. *(French)* 78−27852
automated fusion device for making fusion tablets *(German)* 77−90512
automated process, motor vehicle air pollution analysis *(French)* 77−41234
background determination by simple check ratios 80−3435
background reduction in secondary target energy dispersive spectrum 79−100471
bauxite, determ. of Sr, Y, Zr, Ga, X-ray fluoresc. method 77−36849
bauxites, analysis, comparison of atomic absorpt., X-ray fluoresc. and other classical methods 80−89551
binary alloy films, anal. by X-ray fluorescence *(Chinese)* 79−48035
biological samples, importance of geometry 79−5430
biological samples, lateral distrib. of trace elements, proton induced X-ray fluoresc. using microbeam scanner 79−5431
biological samples, multichannel analyser spectroscopy using XRF, minicomputer appls. 78−20106
biological X-ray microanalysis 80−41349
blood, human, X-ray fluorescence spectroscopy for trace element anal. 78−20248
blood presence on Shroud of Turin, spectroscopic and chem. tests 80−102875
blood serum, trace element anal. of thick samples, photon excited X-ray fluoresc. 78−3423
bone, in vivo technique for determ. of Pb conc. 79−25084
borate fusion buttons with unknown sample/flux ratio 79−24851
borate glass, Al^+ ion coordination study by $AlK_{\alpha 1,2}$ X-ray fluorescence spectra *(Japanese)* 78−7308
botanic reference materials, candidate standards, homogeneity testing, anal. methods 78−11594
Bragg reflected polarised X-rays, energy dispersive fluoresc. anal. 77−40619
brine, spectrometric anal., applying theoretical matrix corrections 78−88690
cereal, proton-induced X-ray emission and nuclear reactions for determ. of protein quality 78−20321
chrome ores, rapid anal. by X-ray fluoresc. 79−16065
chrome-magnesia, rapid anal. by X-ray fluoresc. 79−16065
coating thickness gauge, spectrometer channel with Si(Li) detector 79−35671
coatings, gamma thickness meter based on NaI scintillation counter, performance improvement 79−35670
coins, Septimius Severus denarii, reproducibility 77−34067
complex anion electronic struct., outer sphere cation effects, X-ray fluoresc. spectra 78−86884
component particle size analyser, using X-ray fluorescence *(Japanese)* 78−15615
components mutual effect, exam. by calibration method during analysis 80−21339
computer operating system for X-ray diffr., fluoresc. anal. and electron microprobe anal. 80−322
computer-controlled analyser 78−23982
conference, Denver, USA (Aug. 1975) 77−56307
conference, Denver, USA (Aug. 1976) 77−70382
Conference, nuclear materials, safeguards and accountability meas., Williamsburg, USA (May 1978) 79−81045

X-ray fluorescence analysis continued
correction procedures, accurate coeff. method 77−56311
correction procedures, mathematical, review 77−56308
crystalline solids, electronic industry, chem. anal. instrumental methods progress 80−66903
data interpretation, online system using multivariate statistical anal. and pattern recognition 80−3461
data reduction, anal. using QUAN computer program 77−56267
detectors and electronics 77−46452
dosimetry film evaluation by neutron activation and X-ray fluoresc. anal. 79−63820
dosimetry film exposure determ., comparison of X-ray fluoresc. and optical density 78−24137
double monochromator systems for fluoresc. X-ray anal. 78−62280
electronic materials, analysis by fluorescent X-ray spectroscopy *(Japanese)* 77−86417
elemental concentration of geological samples 78−85268
emission spectrophotometry, review of data processing systems *(Japanese)* 78−88685
empirical influence coefficient methods, review 80−3455
energy dispersive, calibration standards, vacuum deposits 77−60177
energy dispersive, erroneous peaks, removal 77−56314
energy dispersive, least squares, Monte Carlo methods, mathematical anal. techniques 78−85243
energy dispersive, matrix correction method for environmental samples, X-ray scatt. calcs. 77−70352
energy dispersive, pulsed tube excitation, resolution recovery by digital processing 77−56313
energy dispersive, pulsed-tube counting rate performance 78−4752
energy dispersive, trace elements in rock determ. 77−44565
energy dispersive analysis, without need for standards, empirical table for fluoresc. yields 77−44543
energy dispersive X-ray spectra, peak separation from background 78−7310
energy selective X-ray anal. in TEM 80−84036
energy-dispersive, appl. of mathematical techniques 79−11837
energy-dispersive, direct meas. of net peak areas 79−1989
energy-dispersive, external reference signal 77−21433
energy-dispersive, tissue trace element anal., mass determ. by scatt. 77−48971
energy-dispersive, using X-ray tubes in combination with secondary targets, spectrometer optimisation 80−30316
energy-dispersive fluorescence spectra, interpretation 77−36820
energy-dispersive X-ray fluorescence analysis of highly radioactive samples with small tubes and pyrographite crystals 78−92578
environmental anal., energy dispersive X-ray fluoresc. spectrometry using pulsed X-ray excitation 77−56319
environmental particulates, anal., X-ray techniques 77−56322
environmental samples, book 77−41217
environmental samples, multielement anal. 78−69513
environmental samples, X-ray fluoresc. anal., particle size correction method 78−48705
environmental samples, X-ray fluoresc. anal. absorpt. corrections 77−60169
epitaxial thin films, chemical structure 80−3451
equations of bond, review 80−66898
erythrocytes labelled with stable Rb, survival determ. by fluoresc. excitation anal., rabbits 80−81788
EXAFS, detection with X-ray filter assembly 80−31961
excitation by accelerated ions *(Russian)* 79−61933
external standard variant method, construction of analytical curve 80−21338
ferrites, composition determination, interelement effects 78−85259
film, simultaneous determ. of comp. and mass thickness 77−90655
film thin, limits of observation of X-ray fluoresc. anal. 79−24857
filter assembly for fluorescence EXAFS meas. 80−90971
filters, metal foil, electrolytic production method 79−95947
fish stock discrimination, X-ray fluoresc. tissue anal., pattern recognition technique 77−60330
flexible scanning industrial X-ray/fluoroscopic inspection 80−89459
fluorescence spectra, nonlinear least squares anal. 77−48731
fracture surfaces, quantitative analysis problems in energy dispersive X-ray spectrometry with Si(Li) diodes *(French)* 80−89571
frame recording method for intermittent X-ray TV to reduce exposure dose in fluoroscopy *(Japanese)* 78−89607
fully-automatic analyser with minicomputer *(German)* 78−88677
geochemical haloes analysis using X-ray radiometric methods 77−53231
geochemical specimens, energy dispersive X-ray fluoresc. anal. 77−48702
geological samples, element analysis by fluorescence spectrometry *(Rumanian)* 77−33217
germanate glass, Al^{+} ion coordination study by $AlK_{\alpha 1,2}$ X-ray fluorescence spectra *(Japanese)* 78−7308
glass, ancient, X-ray fluoresc. anal., importance of sample prep. 77−34064
glass, structural analysis, using fluorescence excitation *(German)* 80−38923
glass fibre reinforced cement, glass content meas. by X-ray fluorescence anal. 79−52840
glass fragments, classification into window and non-window types 80−81401
glasses, high vol. low cost, as solar reflectors, compositions and weathering effects 80−106589
grain legumes, proton-induced X-ray emission and nuclear reactions for determ. of protein quality 78−20321
hair, biopsy material for trace elements in human body 79−83955
heterogeneous materials, expt. geom. effect on local analysis results 79−52819
high intensity polarised X-rays, excitation, improved X-ray fluoresc. capabilities 80−3468
high intensity source of polarised X-rays, for medical diagnosis 77−60238
high-alumina materials, analysis accuracy 77−60163
hydrochemical prospecting, APDC coprecipitation and X-ray spectrometry for trace element determ. 77−37445
industrial X-ray inspection systems for welded seams in heavy engineering, Philips MG 420 and MG 300 79−93269
intensity due to photoelectrons, calc. 80−26075
intensity measurements in X-ray fluorescence analysis 80−16759
intensity model for X-ray fluorescence, for wavelengths up to 3 angstroms 78−56934
intensity-concentration modelling in energy dispersive systems 80−3464
X-ray fluorescence analysis continued
interactive regression anal., computer program 80−3463
interelement correction, models, computer program, appls. to alloys 77−56315
ion-exchange resin kinetics 77−60111
joint inflammation, radioisotope X-ray fluoresc. technique obs. 80−56184
K X-ray fluoresc. anal. 77−81449
K X-ray fluorescent multi-strip probe for accelerator beam studies 80−102362
kaolinite-mullite reaction sequence, spectroscopic anal. of Al coordination changes 78−48719
laterites, Venezuelan, analysis, comparison of atomic absorpt., X-ray fluoresc. and other classical methods 80−89551
least squares anal., detector response function approach 80−11989
line intensities calc., computer program, appls. 78−61107
liquid sample holder for radioactive solutions 79−24867
liquid/solid nondestructive anal., fundamentals *(German)* 78−20125
logarithmic intensities and matrix corrections 78−88669
lunar surface elemental composition, analytical determ. from Apollo X-ray and γ-ray spectrometer data 79−2495
magnesia-chrome, rapid anal. by X-ray fluoresc. 79−16065
marine sediment, ferromanganese nodules, use of semiconductor detectors *(Russian)* 79−29887
marine sediment analysis and pollutant detection 77−5361
Martian soil, proportional counters for Viking Lander spectrometer 78−40792
Martian soil, Viking lander expt., anal. methods and results 78−20703
mass absorption coeffs., meas. using X-ray diffractometers and fluoresc. spectrometers 80−18063
matrix correct., FORTRAN IV program 78−7313
matrix correction, computer program *(German)* 80−3427
matrix correction methods using scattered radiation 80−3456
matrix effects, corrections calc. method 77−52699
matrix effects, mathematical correction methods 78−61080
matrix effects, reduction by Monte Carlo, fundamental parameters method 80−3460
medical samples small size, X-ray fluoresc. anal. system, computerised target changer 77−60249
medical technique for static or dynamic organ studies *(French)* 77−37033
metal, near absorpt. threshold *(Russian)* 77−4704
metal, oxidation, Auger electron, X-ray fluoresc. spectroscopy appls. 77−44412
metal coating, foil thicknesses, X-ray fluoresc. meas. method, appls. *(Russian)* 78−56582
metal compounds on microfilters, X-ray fluoresc. spectrometry anal. 80−30315
metal sample preparation furnace for remelting prior to spectrochem. analysis 77−44556
metals industry, chemical analysis using simultaneous X-ray fluorescence spectrometer 79−93268
method with corrections for absorption 80−85239
mica, stress-induced K^{+} ion migration, X-ray fluoresc. anal. 77−4221
micro co-precipitation technique for trace elements 79−57339
microanalyser, MAR-2, operation in two-channel mode with spectrum standardisation 77−52703
microanalysis, sample sandwiched between anode and converter *(French)* 79−74471
minerals, anal. of small samples using X-ray quantometer 78−61112
minicomputer appl. *(German)* 77−90702
mixed oxide fuel pellets, close coupled X-ray anal. 79−11876
monazite, from South Indian beach sand, superheavy element search, K X-ray fluoresc. anal. 80−61801
monazite from South India beach sands, superheavy elements search using X-ray fluorescence 78−16017
monolithic integrated circuits, digitised layouts and impurity profiles, particle induced X-ray fluoresc. obs. 79−52804
Monte Carlo simulation, inter-element effects determ. 80−26080
Moon, surface chem., appl. of weighted-filter imaging technique 78−12124
multielement anal., sample dispersion into film-forming polymer soln. 77−56316
multielement apparatus using semiconductor detector and X-ray tube 80−22488
multiphase systems, fluorescent excitation in phase boundary vicinity effect on local spectral analysis results 79−52813
Naval Research Laboratory Programme, 1965-75, progress rpt. 78−3425
nondestructive testing review including X-ray methods *(German)* 77−77724
nonlinear least squares anal. of full energy peaks 77−88328
Nottingham clay tobacco pipes, chronological groups, chemical analysis 79−29422
nuclear fuel reprocessing plant, remotely controlled computer-guided preparation facility for X-ray fluoresc. anal. *(German, English)* 78−17399
nuclear fuels, nondestructive measurement of U and Th conc. and quantities using XFA and gamma spectrometry 80−71877
nuclear materials, nondestructive element and isotope assay of Pu and U 80−71870
nuclear materials safeguards, assay of dissolver solns. by totally sampled wavelength dispersive X-ray fluorescence 80−83160
nuclear materials safeguards, nondestructive, energy-dispersive, X-ray fluorescence analysis of product-stream concentrations from reprocessed nuclear fuels 80−83163
nuclear target thickness meas. 77−18728
observation limit, relationship with atomic number 80−18057
optical emission and X-ray spectrometry developments *(French)* 80−68263
ore-flux mixtures, automatic X-ray fluorescence monitoring of major components 77−87887
ores, appl. of semiconductor spectrometer 79−87902
organic compounds, light elements, determ., matrix composition effects on line intensity 78−7257
organic specimens, thick, trace element anal., photon excited X-ray fluoresc. 78−3423
oxide film characterisation, using low energy electron induced X-ray spectroscopy *(French)* 78−41386
particle induced X-ray fluorescence emission, moving target mechanism 80−73562

X-ray fluorescence analysis continued
particulate reference sample on membrane filters for X-ray fluoresc. spectrometer standardisation 77−60176
particulate sample X-ray fluoresc. anal., multichannel spectrometer, computerised 77−60170
petroleum products, X-ray fluoresc. anal. with solid and aqueous standards 77−60145
pewter, English and Scottish measures 78−347
phosphate glass, Al^{+} ion coordination study by $AlK_{\alpha 1,2}$ X-ray fluorescence spectra *(Japanese)* 78−7308
phosphosilicate glass, IC protective coating, technique for P determ. 77−40612
pigments of Minoan painted pottery, XRF-XRD analysis method 80−35586
PIXE, elemental trace anal. in serum 77−48974
PIXE, trace element anal., comparison with XRF 77−48737
PIXE anal., conc. profile determ. using beam energy variation 78−76965
PIXE of thick samples in air, trace element analysis 79−24866
PIXE trace element anal., new method to determ. concentrations 78−76966
plant trace element anal. by X-ray fluoresc. for environmental pollution study 78−3690
polarised radiation for anal. of elements with Z=47-57 78−85271
pollution, environmental 77−41161
pollution control appl. 78−15882
polymer blends, interdiffusion, meas. method 79−69271
portable analyser for bore hole and powder meas. 78−45759
pottery, archaic Greek 77−34068
powder sample isoformation for X-ray fluoresc. anal. 79−87930
powdered samples, additivity of effective coeffs. for X-ray absorpt. 79−24856
preconcentration using ion exchange and precipitation, for trace anal. 77−12864
proportional counter with slight pulse amplitude shift for X-ray detection *(German)* 78−46213
proton induced, ancient pottery anal. 77−48734
proton induced, elemental trace anal. of biological and air pollution samples 77−36831
proton-induced X-ray emission anal. for mass determ., spectrum decomp. code 79−11845
proton-induced X-ray emission anal. of roadway aerosol filter sample 77−41233
pseudobinary alloy, use of parallel and monochromatic beams for comp. determ. by X-ray fluorescence 79−48000
pulp streams, X-ray fluoresc. element anal., conc. calcs., iterative method 78−61109
pulsed X-ray spectrometry using fluorescence 77−18149
PVC-poly-ε-caprolactone, interdiffusion, meas. method 79−69271
quantitative, using fundamental parameter technique 77−56309
quantitative ultratrace elemental analysis by X-ray fluoresc. spectrometry 79−34376
α-quartz, correlation between cryst. perfection and refl. intensity for analyser cryst. 78−48259
radioactive, comparison with neutron activation using low intensity ^{252}Cf source 77−16885
radioactive waste, X-ray fluorescence anal. for solns. and slurries, feasibility study 79−81051
radioisotope, sensitivity, portable units 77−16886
radioisotope excited X-ray analysis of environmental samples, calibration procedure and applications 79−20491
radioisotope sources, development, charact. 78−15741
radioisotope X-ray fluoresc. analysis of trace elements in biological specimens 80−12240
radioisotopic analysis of Zr, Nb and Ta in industrial samples 77−52702
radiometric, using Ge detector 77−52701
Rasberry Heinrich equation, extended, appl. 79−16060
reactor fuel for LMFBR, pilot plant based on X-ray fluoresc. chem. anal. 78−5006
rock samples, fused, X-ray fluoresc. anal., fundamental parameter method 77−77820
rock samples, major-element data processing, SORT, REORD and MW programs in FORTRAN 77−86398
rocks, anal. of small samples using X-ray quantometer 78−61112
rocks, silicate, carbonate, trace element anal. using computerised automatic X-ray fluoresc. spectrograph 77−56320
sample preconcentration, using ion exchange filter membranes 78−7228
sample-sequenced fluorescence spectrometer, appls. *(German)* 78−93787
scattering contribution to fluorescence spectra intensity 77−90677
Schartz's ineqality applic. to equiv. wavelength variation analysis *(French)* 80−50894
secondary excitation correction 80−30317
SEM energy dispersive X-ray imaging techniques and appls. 78−48740
sensitive analysis of small samples 77−40618
Shroud of Turin, scientific investigation 80−87576
silicate rock X-ray fluorescence analysis 78−88945
silicate rocks, X-ray spectral fluoresc. anal. 78−3762
simultaneous determ. of three elements 80−40786
slurries, solids content determ. by X-ray scatt. 80−3467
spectra, energy dispersive, least-squares anal., detector response function approach 80−3457
spectra, resolution by weighted least squares computer program 80−3459
spectral analysis, nonlinear least-squares fitting program 79−1987
spectrometer for industrial quality assurance 79−70398
spectrometer system, PW1400, microprocessor controlled *(German)* 80−16758
spectrometry, single and multielement anal., optimum excitation conditions, automated determ. 80−323
spectrometry, XRF and emission, equipment developments 79−20486
statistics, appl. in X-ray fluoresc. anal. 77−56310
steel, C, wear of Cr, Zn protective coatings, exam. using nuclear radiation excited X-ray fluorescence 80−21206
steel, carbon content in surface layers and in bulk 80−3466
steel, dual phase HSLA, compositional anal., TEM 80−85253
steel, galvanised coatings, thickness meas. using X-ray fluorescence radiation, apparatus design 80−21202
steel, mild, AISI 1009 and 1018, corrosion incipient processes in hypersaline geothermal brine at 90°C 80−50753
steel, stainless, 300 and 400 series, quantitative anal. 80−3465
steel, standard, energy dispersive X-ray fluoresc. spectrometry, computer directed optimisation 80−45585

X-ray fluorescence analysis continued
steel, tool and high speed samples, emission spectral and X-ray fluorescence anal. *(Japanese)* 79−43232
steel, tool and high-speed, high freq. induction melting and centrifugal casting in instrumental anal. 80−84886
steel, X-ray fluorescence thickness meas. for Zn and Sn coatings 77−55884
steel foil, microanalysis by energy dispersive X-ray spectrometry *(French)* 80−85250
steel for nucl. reactors, trace element anal., implications for decommissioning 78−54833
steel products, production line X-ray fluoresc. anal., coating thickness meas. 77−54029
steels, alloying element determ. by computer-controlled X-ray spectrometry 77−56318
steels, stainless and low-alloy, X-ray fluorescence anal., matrix corrections, minicomputer program 80−3458
steels, X-ray spectral anal., theoretical correction parameters rel. to chem. composition 78−61108
surface and bulk microanalysis, electron spectroscopy apparatus *(French)* 80−47151
surface chemical anal. using RHEED-solid state detector method 80−108760
surfaces and thin films, combined ion, electron and X-ray beams for anal. and struct. determ. 77−86412
synchrotron radiation, props. and appls., review 79−36830
synchrotron radiation applications, review 79−67448
synchrotron radiation applications 79−48009
synthetic calibration standards 79−24850
target preparation of aqueous samples 79−87915
teeth, in situ, determ. of Pb exposure 77−64128
Terra Sigillata from La Peniche, Switzerland, chem. comp., mineralogy and porosity 79−26198
thickness meas. of Au and Ni layers on Cu substrates simultaneously 80−13041
thin dust layers, particle size effects automatic correction, computer appls. in spectrometry 79−83539
thin film calibration standards 80−22496
thin specimens, X-ray spectra characteris. in TEM 78−35788
thyroid fluorescent scanning system of concentric source-detector design 77−40738
thyroid I measurement by X-ray fluoresc. scanning, effect of background radiation change 78−73216
tomofluorographic camera with lens objective and angular tube 79−57750
tomography, X-ray fluorescence techniques, I distrib. in thyroid gland 80−61664
total reflection X-ray fluorescence analysis *(German)* 80−30314
trace element anal., comparison of PIXE and XRF methods 77−48737
trace element anal., polarised X-radiation excitation source 78−7314
trace element anal. with low power monoenergetic X-ray tube 78−70686
trace element analysis by ion-induced X-ray fluorescence *(German)* 77−86399
trace element meas., comparison of charged particle and photon excited fluorescence 77−52716
trace element meas. in air water and organic materials *(Norwegian)* 78−53278
trace elements, calibration consts. *(French)* 78−61095
trace elements in light element matrices, direct determ. using incoherent scattered radiation as internal standard 80−11970
UNO_3, gravimetric standards, best fit calibration curve parameters, error estimates 79−87931
Viking experiment on Mars, sampling strategy, lab. simulation 78−20704
water, elemental anal. using PIXE 78−20127
water, mineral type, Na, Cl, I and S determ. by neutron activation and X-ray fluoresc. analyses 78−3428
water, natural, trace metals, energy dispersive X-ray fluoresc., at absorpt. anals., comparison 77−60175
water, preconc. technique using ion exchange resins 78−61620
water, trace metal anal. by energy dispersive X-ray fluoresc., enrichment procedures 77−60174
water pollution by metals monitoring, instrument survey 79−74580
wavelength and energy dispersive X-ray fluorescence spectrometers compared 80−89573
wavelength dispersive X-ray fluorescence analysis, rel. to energy dispersive X-ray fluorescence anal. 80−7885
working curves linearisation for all matrices 78−53281
X-ray emission and critical absorpt. energies calc., evaluation of mathematical expressions 77−29065
X-ray excited, trace element anal., comparison with PIXE 77−48737
(pX,X) expt., partial sensitivity enhancement in trace element anal. 78−61128
Ag film, vac. deposited, thickness meas. using X-ray fluoresc. technique 79−90911
Ag thin film, X-ray fluoresc. spectroscopy of surface using RHEED-solid state detector method 80−108760
Al alloys, energy dispersive X-ray fluoresc. spectrometry, computer directed optimisation 80−45585
AlBi, X-ray fluorescence analysis *(Japanese)* 78−88663
$Al_xGa_{1-x}P$, proportional ingredient content determ. by X-ray fluoroscopy 80−97747
Al_2O_3-SiO_2 glasses, X-ray spectral fluorescent analysis, standard function method, chemical analysis of glasses 79−52822
Al_2O_3-supported catalysts, X-ray fluoresc. anal. using matrix correctional procedure 78−80817
AlSi alloys, method *(Dutch)* 79−96394
Au artifacts from Sarawak, X-ray fluorescence and at. absorpt. analysis 80−85229
Au coins, surface anal. by X-ray fluoresc., SEM and scanning Auger spectroscopy 80−89552
Au trace anal. with portable X-ray analyser 78−49160
Ba plaster, X-ray absorption coefficients, from 100 to 400 keV 78−31283
$Cd_{1-x}Zn_xS$, use of parallel and monochromatic beams for comp. determ. by X-ray fluorescence 79−48000
Co, determ. in NBS standard alloy steels, X-ray fluoresc. method 78−31734
Co/Na zeolite, -A and -Y type, local coordination of Co(II) ions studied by X-ray absorpt. fine struct. spectroscopy 80−93434

X-ray fluorescence analysis continued
Cr-Mo-N system, at high-pressure, temp., X-ray anal., phase diagram 80−50607
Cu content of Rumanian ores, analysis method *(Rumanian)* 77−29508
Cu film, vac. deposited, thickness meas. using X-ray fluoresc. technique 79−90911
Cu ore processing materials, nondispersive X-ray fluoresc. anal. 78−92575
Cu-Ag film, vac. deposited, thickness meas. using X-ray fluoresc. technique 79−90911
Cu-Ga, binary alloy constituent EDS anal., secondary fluorescence, SEM study *(Chinese)* 80−85231
ErD_2 thin film, degradation during film processing, investigation 80−101047
Fe ore, water bearing mineral effects on X-ray fluorescence analysis 77−12866
Fe-Si (3wt.%), grain-oriented, secondary recryst., grain growth inhibition 80−89245
$FeCr_2S_4$, vapour grown, struct. and stoichiometry, X-ray fluoresc. anal. 79−4263
Fe_3O_4-$FeAl_2O_4$-$FeTiO_3$ titaniferous magnetite, chlorination, 1273 to 2273K 80−55752
GaAS, binary alloy constituent EDS anal., secondary fluorescence, SEM study *(Chinese)* 80−85231
Ge low energy X-ray detectors, entrance windows 77−71718
Hf and Zr, trace elements, simultaneous determ. in soln. using X-ray fluorescence anal. 80−97752
HgI_2 detectors, room temp. X-ray spectra of Na and Mg 78−78049
HgI_2, soft γ-ray detector fabrication and props. 77−3208
I^-, anal. in groundwater by X-ray fluorescence spectrometry 80−45829
$In_xAl_{1-x}P$, proportional ingredient content determ. by X-ray fluoroscopy 80−97747
$In_xGa_{1-x}P$, proportional ingredient content determ. by X-ray fluoroscopy 80−97747
InSb, films, X-ray fluoresc. anal. method, long-term stability 80−61212
K_2O-TiO_2-SiO_2 glass, Si-O bonding, Si$K\beta$ X-ray fluorescence and IR spectra 80−10500
La, determination by X-ray fluorescence 78−61127
LiF focusing array for fluoresc. EXAFS in dilute samples 80−99028
Mg, inclusions, types and size distrib. *(German, English)* 80−97492
Mn, Pb and V in waste water, coprecipitation method *(Japanese)* 80−21333
MnZn ferrite, quantitative anal., using X-ray fluorescence 78−40090
MnZn ferrites, thin struct. of $K\beta_5$ and $L\alpha_{1,2}$ emission bands of Fe *(Ukrainian)* 79−78790
$NH_4H_2PO_4$, correlation between cryst. perfection and refl. intensity for analyser cryst. 78−48259
Na determ. in rock, mineral samples, X-ray fluoresc. quantometer modification 78−61589
Na_2O-TiO_2-SiO_2 glass, Si-O bonding, Si$K\beta$ X-ray fluorescence and IR spectra 80−10500
Nd, determination by X-ray fluorescence 78−61127
Nd_2O_3, and oxalate, X-ray fluoresc. spectrometric anal. of trace rare earth impurities 79−24853
Ni base alloys, oxidation reaction investigation by X-ray diffr. and fluorescence *(German)* 79−57345
Ni-Cr-B-Si-Fe alloy, Cr content by X-ray fluoresc. 79−43654
NiZnCo ferrite, quantitative anal., using X-ray fluorescence 78−40090
Pb content of children's teeth, in situ meas. 77−16976
$Pb_5Ge_3O_{11}$, Czochralski growth, secondary phase formation 78−3027
Pr, determination by X-ray fluorescence 78−61127
PtI_4, aerosol, X-ray fluoresc. anal., particle size correction method 78−48705
$(Pu,U)O_2$ mixed oxide pellet assay, using automated X-ray spectrometer 79−81066
Rb-Sr, ratio determ., by X-ray fluoresc., for radiometric age meas. 77−70356
S determ. in environmental samples 78−85270
S, determ. in fuel oil, by radioisotopic energy dispersive X-ray fluoresc. anal. 78−61122
S, in atmosphere, meas. using compact X-ray fluoresc. analyser 78−68971
S meter, model XA-300, for laboratory use 80−26085
S, SO_4^{2-} and related species, sampling and anal. of atm. aerosols 78−96283
Si, film on Al-Cu, ellipsometric meas. technique, comparison to X-ray fluoresc. anal. 78−51840
Si(Li) gas cooled detector for in situ XFA spectrometer 80−18055
Si(Li) spectrom. with ^{71}Ge source for energy dispersive X-ray fluorescence anal. *(German)* 77−86429
Sm, determination by X-ray fluorescence 78−61127
Ti, in laterite samples, using ^{55}Fe, energy dispersive X-ray fluoresc. 78−76955
TiO_2 paper filler, quantitative determination, using radioisotope X-ray fluorescence anal. 78−56935
$Tm_{1-x}Y_xTe$, $(0 \leq x \leq 1)$, single cryst. growth and characts. 78−23603
U in geological samples, rapid determ. using X-ray fluorescence anal. methods 79−88479
U, isotopic anal., apparatus construction and testing *(Czech)* 77−50244
U ore, radioisotopic X-ray anal. by K-shell fluorescence 79−79353
$UO_2(NO_3)_2$, preparation of uranium nitrate standards for X-ray fluoresc. anal. 79−81053
WC-Co cemented carbides, effect of Co form and distrib. in prep. starting mixture 78−44072
YIG:La,Ga, film, LPE-grown, Ga incorporation, depend. of magnetisation on growth rate 80−84627
Zn coating on continuous galvanising line, mass meas. and control 78−19960
ZnO triode sputtered film elastic props. rel. to structure and composition 79−46988
ZnSe:Ga,As, characts. of simultaneous incorporation, by Mn^{2+} ESR and X-ray fluoresc. anal. 80−34017
Zr and Hf, trace elements, simultaneous determ. in soln. using X-ray fluorescence anal. 80−97752
Zr, thin film, trace element determ. by X-ray fluoresc. anal. 78−40107

X-ray fluorimetry *see X-ray fluorescence analysis*

X-ray lasers
alkaline earth vapour, soft X-ray gain 77−23655
amplification by ion accel. in plasma by steady state fields 80−28187
artificial layered media 77−71989
atomic collision processes and X-ray and UV lasers 80−64787
bremsstrahlung laser possibility in soft X-ray region 77−646
charge exchange, swept-focus scheme for ion beams 77−38848
coherent emission, population inversion basic physical concepts, review 79−31850
coherent X-ray generation from CO_2 laser backscattered relativistic electron beam 80−53252
Compton laser, scatt. stimulation by decelerated EM waves, semiclassical theory 78−29926
confined plasma column, soft X-ray lasing action conditions 80−74346
electron beam-sliding spark plasma device, props. and laser appls. 78−5974
electron pumping of C and He like ions, for lasing below 1000 Å 77−65589
electron-beam sliding spark device, C^{4+} plasma, soft X-ray emission, no superradiant gain 78−79444
excimer laser systems appls., book contrib. 79−81441
feasibility *(Japanese)* 77−31086
feasibility considerations 77−71967
flash X-ray sources, characteristics 78−41392
gas lasers, review 77−7099
holography using X-ray lasers pumped by synchrotron radiation 78−55322
ion beam, lens system using toroidal mag. field for intense ion beam 77−34053
ion beam production, intense, in toroidal mag. lens, appl. to fusion ignition, X-ray laser 77−67535
ion beam pumped X-ray laser, progress report 79−45920
micro-resonators, high flux, for X and γ-ray lasers 79−7151
multicomponent laser plasma, soft X-ray population inversion by resonant photoexcitation 79−10680
multicomponent laser plasmas, soft X-ray population inversion by resonant photo-excitation 77−7050
multiply charged laser plasma, rapid cooling, possible short-wavelength radiation generation 79−41852
optically excited soft X-ray laser technique development, travelling wave lens 78−59016
parametric non-threshold amplification, three-frequency interaction *(Russian)* 77−79902
periodic stratified medium, birefr., phase matching, X-ray lasers 77−65566
phototube detector, interchangeable cathodes, Fe, Al *(German)* 77−10107
plasma, production, optical transitions of multiply charged ions, population inversion, review 77−19227
plasma population inversion evidence 78−74893
population inversion in FM-1 spherator 77−7048
pumping and charge transfer, book contrib. 79−31852
pumping with synchroton radiation and low-energy photons 79−41371
quantum theory of spontaneous and stimulated emission of channelled electrons and positrons *(Russian)* 78−49999
relativistic ion beam laser, continuously IR to X-ray tunable, in negative temp. state *(Chinese)* 80−87373
resonator based on successive refls. of surface wave 80−99021
review, power requirements 77−38849
short wavelength sources, book 79−31921
short-wave emission, initial plasma parameters 80−99692
soft X-ray population inversion in laser plasmas, reson. photoexcitation, photon-assisted processes 80−87378
stimulated Compton scatt., X-ray regime, growth time limitation 77−7049
superradiance, criteria 77−88680
travelling wave source pumping, numerical anal. 77−83864
tunable, using high energy accelerator beam of one-electron atoms 79−86154
XUV lasing, gain-verification problem 78−71086
Al, laser-produced plasma, population inversion between Al^{11+} levels, X-ray lines obs. 78−38539
Al XII, multiple photoexcitation in optically thick Si-Al plasma, lasing at 44 Å 79−3684
B, X-ray laser, inner-shell photoionis. pumped, practicability 77−58319
Be III, X-ray lasers pumped with synchroton radiation and low-energy photons 79−41371
C ion, extended plasma source for short-wavelength amplifiers 78−79447
C ion impurity in linear Z-pinch He plasma, outer 2s-shell electron excitation emission 78−22113
C VI, laser produced plasma, pumping by C VII+Ar III charge exchange 78−5462
C VI, XUV gain in expanding cylindrical plasma 77−15170
C VI laser produced plasma, transient population inversion at 18.2 nm 79−41876
Cl VII, transitions in laser heated plasma, intensity anomalies obs. 58 to 78 Å 78−1214
$Cs+H^+$, charge transfer processes with plasma gun, Lyman-α radiation exam. 78−46573
Cu crystal, X-radiation generation via electrons, nonlinear rise and line-narrowing, book contrib. 79−28865
Ge complanar X-ray resonator circulating beam, high symm. multiple wave configurations *(Russian)* 80−78875
H like ions, shock tube generated, lasing on Balmer-α line 77−58317
$He^{2+}+Li$ collisions, soft X-ray emission obs. 80−83591
KrF* laser, generation of high-spectral-brightness tunable XUV radiation at 83 nm 80−91846
Li I laser, 207 Å, oscillator strengths 80−83598
Li II, III, X-ray lasers pumped with synchroton radiation and low-energy photons 79−41371
Li ion soft X-ray laser, 199 Å, autoionising state effect 77−34876
Li laser, 207 Å, proposal for construction 80−43324
N ion impurity in linear Z-pinch He plasma, outer 2s-shell electron excitation emission 78−22113
$Na+H^+$, charge transfer processes with plasma gun, Lyman-α radiation exam. 78−46573
Ne like ions, population inversion, gain estimate for 40 to 80 nm range transitions 77−75482
Ne like multiply charged ion transitions, stimulated emission possibility in far UV 79−10292
Ne-like multicharged ions, vacuum UV lasing action 78−1213
O ion impurity in linear Z-pinch He plasma, outer 2s-shell electron excitation emission 78−22113

X-ray monochromators
BESSY SX/700: a monochromator system covering the spectral range 3 eV $\lesssim \hbar\omega \lesssim$ 700 eV 80−90952
Borrmann principle based monochromatisation of primary beam in low-angle camera 78−−5985
channel-cut, identification of spurious reflections 80−90959
complex material atomic structure study, laboratory extended X-ray absorpt. fine structure technique 79−17589
conference on synchrotron radiation instrumentation, Orsay, France (Sept. 1977) 78−62999
crystal monochromator for high-angle double-cryst. diffr. 77−43111
crystal monochromators, determ. of polarisation ratio 80−99018
curved, X-ray synchrotron rad. focusing, expt. data interpretation 78−75496
curved monochromators, X-ray diffr. characts. for synchrotron rad. 79−9268
curved-crystal, X-ray monochromatising and focusing efficiency 79−55612
cyclic X-ray monochromators, with perpendicular dispersion planes, emission coherence 80−90974
Daresbury SRS, VUV and soft X-ray 80−90942
development for synchrotron radiation facilities 80−91351
diffracted-beam monochromator, in single-cryst. diffractometry, a performance assessment 80−57448
doubly curved crystal point focusing X-ray monochromator 77−82657
fixed wavelength, with removable Soller collimators 80−6318
(n,m) focusing position, to create monochromator for synchrotron radiation 80−87989
geometry for focusing synchrotron radiation above 10 keV 80−90958
graphite, X-ray monochromator crystal, TDS, Mossbauer obs. *(German)* 77−16230
graphite bonded channel design of simple construction 77−15282
grasshopper monochromator, improved high resolution, 10 to 1000 eV 80−90939
grazing incidence for UV monochromators using toroidal holographic gratings 80−90946
grazing incidence monochromator, ultra high vac., SSRL, design considerations and operating experience 78−62269
grazing incidence monochromator FLIPPER, ultra high vac., for synchrotron radiation 78−62237
grazing incidence monochromators, optimisation for synchrotron radiation 80−90943
grazing incidence monochromators with holographic toroidal gratings, 10 to 150 eV 80−90947
grazing incidence soft X-ray spectrometer with concave grating without entrance slit 77−45926
high flux grazing incidence monochromator based on holographic grating for synchrotron radiation 78−62271
high vacuum two crystal monochromator for soft X-ray synchrotron radiation 78−62272
holographic grating monochromator for 5 to 1000 eV synchrotron radiation 78−18049
holographic transmission diffraction gratings for soft X-rays 80−90965
holographic transmission gratings appl. to UV and X-ray synchrotron radiation monochromators 78−63186
integration scan, ω/θ, restricted detector slits 78−9908
LURE grazing incidence spectromonochromator, soft X-ray synchrotron radiation, 2 years operating experience 78−62270
LURE Rowland circle grazing incidence monochromator, performance 110 to 280 eV 80−90945
MAXIMOC grazing incidence monochromator for XUV investigations with synchrotron radiation 78−62238
mirror monochromator, modified, for rotation photography of large-unit-cell crysts. 79−9269
monolithic crystal monochromators for synchrotron radiation with order sorting and polarizing properties 80−31963
monolithic monochromators for synchrotron radiation, 1 to 4 Å, order sorting, focusing and polarising 80−90955
normal incidence monochromator for synchrotron radiation, charact. modification using holographic concave gratings 78−62236
normal incidence monochromators for synchrotron radiation sources, experimental uses 78−62235
optical adjustment of bent-crystal monochromators 79−14645
polarisation ratio, of two graphite monochromators, use of jig for X-ray beam polarisation 79−37588
scattering at grazing incidence from optical surfaces, effect of surface topography 80−90968
section topography, high resolution, using asymmetrically reflecting plane crystal monochromator 80−57449
soft X-ray interference mirror 78−41385
straight groove toroidal grating monochromators, 10 to 500 Å, design optimisation for synchrotron radiation 80−90944
synchrotron radiation, separated function focusing monochromator system 78−62278
synchrotron radiation, X-ray optics and monochromators 77−54027
synchrotron radiation collection mirrors, soft X-ray throughput 78−62275
synchrotron radiation monochromatisation by crystal diffraction 78−62277
synchrotron radiation source, X-ray monochromatisation, phase space analysis 78−62276
synchrotron radiation source for X-ray spectroscopic studies, SPEAR storage rings 77−41745
synchrotron VUV and X-radiation, polarising effect of monochromators 78−66732
total external reflection and β filter combination for monochromatization 78−4745
transmission diffraction gratings for synchrotron rad. sources, modelling 80−90964
UHV beam line at SSRL for spectral range 4-4000 eV, monochromatised radiation 78−62673
ultra-high-vacuum double crystal monochromator beam line for studies in the spectral range 500-4000 eV 80−90957
wave packet polarisation, in X-ray monochromators, dynamic theory *(Russian)* 80−64826
white beam X-ray diffr., synchrotron radiation 78−62279
Wisconsin Synchrotron Radiation Center, UHV Seya-Namioka and adjustable slit 'Grasshopper' monochromators 78−62234
X-ray curve-crystal monochromator system 78−66017
XUV monochromator design for use with synchrotron radiation sources 80−90940

X-ray monochromators continued
LiF focusing array for fluoresc. EXAFS in dilute samples 80−99028
Si, harmonic-free single cryst., neutron and X-ray physics appl. 78−75493
Si impurity-doped cryst. plate, as an X-ray monochromator, strain distribs. for 220 reflection 80−100126

X-ray photoeffect *see X-ray photoelectron spectra*

X-ray photoelectron spectra
4f substances, rel. to electronic props. at config. crossover 77−47775
accuracy, factors affecting 78−7249
acetylene, vibr. fine struct. accompanying core ionis., STO calcs. 78−62844
acetylene adsorbed on Fe containing segregated C, hydrogenation, C-1s XPS spectra obs. 80−84366
achromatic X-ray source, spectrum iterative deconvolution 78−72689
acid oxygen carbon electrodes, electrochemical measurements and surface studies, ESCA method appl. 78−31651
actinide compounds, spectroscopic techniques for electronic props. meas. 80−11427
actinide cpds., ESCA spectra, intense shake-up satellites, model 78−50589
actinides, XPS, many-electron effects, comparison with rare earths 80−7466
adhesion, surface anal. techniques appl. 80−65381
adsorbate core-level spectra, spectral function calculation, time depend. approach 79−43096
adsorbate relaxation energies in XPS, calc. 78−15283
adsorbates, core level spectra, correlation effects 78−68605
adsorbates, line shapes and multiple lines 78−84702
adsorbates, plasmon effects on core level spectra 78−60547
adsorbates, surface plasmon effects on satellites in XPS 79−61493
adsorbed atoms, soluble relax. model for core level spectroscopy 79−8226
adsorbed atoms and molecules, core level spectroscopy, surface relax. energies, theory 77−89830
adsorbed atoms and molecules XPS, many-body effects 80−55266
adsorbed atoms on metal surface, XPS satellite spectra 77−20993
adsorbed layer, core photoelectron spectra, shape 79−47596
adsorbed layers, core photoelectron spectra, shake up and relaxation effects 79−47595
adsorbed layers, photoelectron spectra, review 79−52072
adsorbed molecules, core ionisation, negative shake-up energy 80−100749
adsorbed species, plasmon versus shake-up satellites in XPS 78−48286
adsorbed species, relax. shifts, line shapes and satellites in XPS and X-ray absorption spectra 77−90242
adsorption layers, core level photoemission, book contrib. 78−95673
air pollution, X-ray photoelectron spectroscopy *(French)* 77−36837
Al-Mn(Fe)(Co)(Ni)(Cu), alloy, dil., electronic states, XPS meas. 77−44117
alkali halide dibenzo-18-crown-6 complex, ESCA, binding energy 78−50584
alkali halides, XPS, trapped electrons at F-centres and anion defects, photoionis. cross sections 77−90249
alkali metaborates, vapour over heated solid, XPS, obs. 80−87171
alkali silicate glass, appl. of XPS *(Japanese)* 79−34416
alkaline earth fluorides, orbital binding energy and ionicity relations, XPS meas. 80−97399
n-alkanes, solid, core electron relax. energies and valence band form., XPS exam. 77−36372
alkyl cadmium, valence and core electron energies, photoelectron spectra, ab initio calc. 78−25613
alloy core electrons, spectra asymmetry *(Ukrainian)* 78−2982
amino acid overlayers, on Ag, XPS and SIMS study 79−86986
amino acid overlayers, static SIMS exam. 79−83074
amorphous semiconductor, local order as determined by electronic and vibrational spectroscopy 79−37627
analytical potential, book contrib. 80−16761
angle resolved, energy distrib. *(German)* 78−60543
angle resolved UPS and XPS disorder effects 78−15287
angle-resolved, role of electron diffraction 78−64446
angle-resolved XPS, interpretation 78−72696
angular dependent, depth profile determ., appl. to Cs film on Mo substrate 78−88404
anthracene, solid, electronic struct., comparative ESCA study of polyacenes 78−52631
aromatic organic macromolecules, energy-gain satellite in C(1s) XPS 79−1813
N-aryl ylides, obs. of satellite lines 78−37680
atom, deep level X-ray absorption cross section modulation by optical field 77−14399
atom, Tl 5d XPS comparison with TlI 80−43099
atom, X-ray photoelec. effect in presence of laser radiation 78−37615
atomic screening model for solid-state effects 77−73194
atoms, natural line widths, K and L X-rays, XPS and KLL Auger lines 79−76383
atoms, X-ray Compton and photo-effect in laser field 79−13688
Auger lines, generation by bremsstrahlung 80−87174
Auger peaks, bremsstrahlung-induced, utility in spectroscopy 79−30618
benzene, solid, electronic struct., comparative ESCA study of polyacenes 78−52631
benzene, solid, electronic struct., XPS 77−73213
benzene, X-ray photoelectron spectra, C 1s shake-up struct., PPP CI calc. 78−42126
benzene free and coordinated mols., X-ray and X-ray electron spectra 77−27087
binding energy determ. without retarding pot., relativistic mass increase 78−41377
book on X-ray spectroscopy 80−2899
borate glasses, appl. of XPS *(Japanese)* 79−34416
boride RF sputtered wear-resistant coatings, XPS study of adherence 79−34191
brass, cold worked, surface composition anal. oxidation, sulphidation by X-ray photoelectron spectroscopy 78−11423
brass coated steel wire, surface composition, oxidation, sulphidation, study by XPS 78−11423
bremsstrahlung isochromat spectroscopy using a modified XPS apparatus 79−35912
bremsstrahlung-induced Auger peaks 80−45199

X-ray photoelectron spectra continued
2-bromostearic acid, photoelectron escape depths determ. from X-ray photoelectron spectra 78−27368
cadmium arachidate, monolayer, electron mean free path length, XPS obs. 79−74051
carbide RF sputtered wear-resistant coatings, XPS study of adherence 79−34191
-carotene, valence bands, XPS obs. 78−24030
catalyst struct., binding energies, ESCA, applic. to MoS_2, MoS_3, ultramarine 77−21420
cathode workshop, conf., Washington, DC, USA (Jan.-Feb. 1978) 79−43068
chalcogenide glass, optical transitions and electronic struct., review 77−76741
charge corrections, comparison of use of different spectrometers 77−20989
charge effects on insulator sample current *(French)* 78−41376
charging effect, elimination in ESCA *(French)* 79−97474
chemical shift of spectrum c.g., valence electron distrib. distortion 77−27084
chemical states at surfaces exposed to high-temp. vapours 78−11559
chemisorbed species, core level XPS, shake-up and relax. effects 79−56910
chrysotile, adsorpt. of organic micropollutants, XPS and gas solid elution chromatography exam. 78−80790
CO, dissoc. sorption on Pt, XPS obs. 77−16863
coating chemical characterisation by surface and near-surface sensitive techniques 79−15053
cobalt stearate, monomolecular layer, electron escape depth, XPS *(Japanese)* 80−11532
cobalt stearate, monomolecular multilayers, XPS escape length depend. on emission angle, elastic scatt. role *(Japanese)* 80−84833
computer controlled ESCA for nondestructive surface characterization utilizing a TV-type position sensitive detector 78−76969
contamination layers, XPS meas. 78−31301
coordination compounds, ligands studied by XPS 78−62842
core level ligand field splittings 80−43106
core line asymmetries in muffin tin approximation 79−69953
core-hole lifetime effects in deep-level spectroscopies 78−48283
corrosion science, review of use of XPS 78−15586
crocidolite, adsorpt. of organic micropollutants, XPS and gas solid elution chromatography exam. 78−80790
cross section calculation, from X-ray absorption data 78−56562
crystal, single or poly-, XPES struct., one-electron approx., transition metals, dielectrics, semiconds. 78−64445
crystals, electron spectroscopy, book 80−36786
d^6-complexes and oxides, spin-state transitions, PES study 79−100014
data acquisition, rapid, using multichannel electro-optical detector 79−93263
development (1900-1960) 79−12560
diamond, Ar ion induced struct. changes, depth profiles, from XPS 78−34554
diamond, valence bands, strong-coupling method 77−28679
diamond, valence electrons XPS spectrum, OPW calc. 77−4715
differential subshell photoionisation cross-sections, for elements Li-U 79−10150
difluorobenzenes, X-ray and UV photoelectron spectra, ionis. pots., ab initio GO calcs. 77−61795
difluoroethylenes, plasma polymerisation, ESCA characterisation of polymers 80−21283
dimethyl ether, condensed multilayers, electron bombard. effects, AES line-shape anal., XPS, and desorption meas. 80−7450
dimethyl zinc, valence band and Zn 3d levels, electric field gradients 77−88495
dynamical calculations 80−55227
edge singularities of relaxed-out bound states and relaxed-in band states 78−92173
electron binding energies accurately determined by X-ray photoelectron spectroscopy *(Chinese)* 79−54821
electron energy loss spectra in core-level XPS, intrinsic and extrinsic plasmons 77−63532
electron rest energy, using X-ray photoelectron spectrometer, student expt. 79−25802
electron spectroscopy, for bulk and surface microscopy and microanal. 80−52367
electron transport Monte Carlo calcs., orthogonal function expansion technique 77−26248
electron velocity distribution in semi-infinite targets 77−28688
electronic levels, appl. of XPS *(French)* 80−45200
electronic material and device characterisation using surface-sensitive analytical techniques 80−65341
electronic structure exam. by soft X-ray and X-ray photoelectron spectroscopy 77−85136
elements, high Z, photoelectric L-shell cross-sections, 37, 74 keV 77−57950
elements with $Z \leq 30$, core electron binding energies in free and standard state 77−43168
energy distribution of X-ray photoelectrons 78−88405
energy spectra generated by low-energy X-rays from intense plasmas, meas. using mag. spectrometer 78−31298
ESCA, chem., technical and industrial appls., lecture 78−27875
ESCA, conf., Uppsala, Sweden (May 1977) 78−53297
ESCA, quantitative surface anal., limitations, depth profiling, catalyst surface anal. 78−53298
ESCA 36 spectrometer, advanced data anal. 77−90684
ESCA apparatus, calibration and use as soft X-ray spectrometer *(French)* 77−13832
ESCA apparatus *(Dutch)* 79−1982
ESCA chemical shifts and modified Sanderson electronegativity calcs. 77−83656
ESCA expt., charging and rotational dependence of time position 78−21970
ESCA expt., photoconducting effect on charging 78−21971
ESCA shifts and effective charges 80−78648
ESCA spectra automatic analysis by top down method *(Japanese)* 77−40598
ESCA using X-ray photons >1500 eV, Au M_α X-rays (2123 eV) 78−72683
ethylene, valence XPS spectrum satellite struct., C(2s) region, correlation states 78−5278
X-ray photoelectron spectra continued
ethylene free and coordinated mols., X-ray and X-ray electron spectra 77−27087
ethylene oxide-d_0, -d_4, ion chemistry, photoionisation and ion cyclotron reson. obs. 77−21373
EXAFS in photoelectron yield spectra 80−16123
EXAFS in photoelectron yield spectra and optimisation of the photon glancing angle 78−80435
EXAFS-Auger process for surface struct. anal. 77−51580
excited by MG Kα radiation, X-ray satellite line removal 77−77343
ferrocyanide ion, electronic struct. and related props., calc. by SCF Xα-scattered wave method 77−15809
film, reduction in thickness D/λ, evaluated using XPS data *(German)* 79−1558
fixed-orientation atomic orbitals, rel. to plane-wave final state approx., angle-resolved photoemission 79−28891
fluorides, meas. *(Japanese)* 80−16154
fluoropolymer adhesive joints, fracture and surface anal. by SEM and ESCA 77−55434
fluoropolymers, linear, valence electronic struct., LCAO cryst. orbital calcs., ESCA 78−5384
fly ash, depth composition determ. by XPES 78−68943
formaldehyde, adsorbed on W(100) single cryst., XPS obs. of decomp. 77−4927
formaldehyde, O and C 1s ionis. pots., shakeup XPS spectra electron spin coupling depend. 77−30925
fourth-row elements, Pd to Xe, XPS, XES, dynamical effects 80−52924
fuel particles, HTR, surface anal. by XPS 78−33252
furan, gas, X-ray photoelectron spectra, satellite struct. 78−5281
gabbro-anorthosite, reduction of Fe, Ti, Si in H atm., X-ray photoelectron spectra 79−25527
germanates, meas. *(Japanese)* 80−16154
glass fibres, types E and A, surface composition, effect of ageing, reduction, exam. using X-ray photoelectron spectroscopy 79−20223
glasses and ceramics, characterisation with analytical electron microscope 80−84068
grain boundary segregation, critical assessment 80−75362
graphite, high energy cond. and valence band states 78−39664
graphite, photoelectron escape depths determ. from X-ray photoelectron spectra 78−27368
graphite, surface alteration by interaction with Ar^+ and Xe^+ beams 78−91347
graphite, X-ray emission and absorption, XPS, electronic struct. 77−16431
graphite, X-ray photoelectron diffraction, influence of radiation damage 79−19970
graphite, XPS and Auger KVV valence band spectra 78−11028
graphite fibre, surface anal. by XPS and polar/dispersive free energy anal. 80−65340
graphite intercalation compounds with K and Cs, low temp. specific heat meas. and XPS 78−26693
graphite monofluoride, surface alteration by interaction with Ar^+ and Xe^+ beams 78−91347
graphite plate sample holders 80−11972
graphite-alkali metal intercalation cpds., electronic props. 80−45202
graphite-AsF_5 intercalated species, fractional ionisation and identification 80−97397
graphite-$SbF_5(Cl_5)$ intercalation compounds, compacts, elec. resistivity, C fluorination 80−34493
group IV, V and VI elements, XPS, bond ionicity, struct. stability and charge transfer 77−44127
halogens in transition metal coordinate compounds, binding energies from XPS data 78−21973
hexatriacontane, polycryst., UPS, 11.4-21.2 eV, polyethylene model compound 77−66570
historical development, 1900 to 1960, review 77−82359
homopolymers, ESCA methods, core levels of simple homopolymers 78−88673
hydroxide surface, XPS exam. of chemical changes induced by Ar^+ ion bombardment 79−14993
ice, electronic structure investig. by XPS, UPS and UV absorpt. spectra 77−16452
imperfect surfaces, XPS *(Russian)* 78−35252
Incoloy 600 and 800, surface film in hot conc. NaOH, XPS study 80−11824
Inconel 600, nuclear reactor boiler corrosion, XPS 80−66709
Inconel 600, nuclear reactor boiler corrosion, XPS 80−71816
Inconel 600, XPS exam. of initial growth of oxide films 79−20240
inorganic compounds, XPS chem. anal., chem. shift, core binding energy 78−20134
insulating film, electric charging by X-radiation *(Japanese)* 79−61488
insulating films, chemical shift meas. by ESCA *(Japanese)* 79−4891
insulators, chemical state identification, Auger and photoelectron lineshapes and chem. shifts 77−32855
insulators, soft X-ray induced secondary-electron emission, models and meas. 79−74034
insulators, XPS, binding energy, surface pot. and work function calcs. 80−89113
interface composition determ. methods 79−70396
intermediate valence materials, autocorrelation, line shapes, power spectrum due to occupancy variations 78−47742
Invar, electronic structure, influence of temp. 77−28681
Invar, XPS of valence electrons, temp. effects, 122-580K *(Russian)* 77−8727
ion beam-surface impact effects, ESCA obs. 79−33020
ion bombarded surfaces, energy analysed SIMS with Auger and XPS meas. 79−4457
ion-etch profiles, interface position determ., nomographic method 77−89658
iron oxides, core line X-ray photoelectron spectra 78−7263
IV-VI compounds, XPS, bond ionicity, struct. stability and charge transfer 77−44127
lanthanides, core-hole screening, 3-d XPS, multiplet splitting 79−43095
layered materials, in powder form, thickness meas. by XPS and ion sputtering 79−88913
lepidolite, quantitative anal. by XPS 78−35742
lifetime broadening in electron spectroscopy of core levels in solids 80−80938
light metal, surface effects on X-ray level widths 79−47147
lineshape transformations for Fourier transform resolution enhancement 77−90250

X-ray photoelectron spectra continued
localised levels near surfaces, photoelectron spectroscopy, scatt. effects and relax. shifts 78−15291
lunar regolite, Fe reduction on heating in vacuum, XPES spectra 80−41740
lunar regolite characterisation 79−21206
lunar regolith, reduction of Fe, Ti, Si in H atm., X-ray photoelectron spectra 79−25527
many body effects 78−27374
metal, 3d, X-ray emission and XPS broadening, many-body effects and intra-atomic exchange 77−44090
metal, conduction band X-ray photoemission, intrinsic plasmons effects 78−39661
metal, d-band, shake-off reduction of single particle spectrum in XPS 79−1812
metal, dynamic screening of core hole, semiclassical model 79−69445
metal, free-electron-like, lineshape asymmetries 78−14681
metal, independent electron, soln. of X-ray edge problem, recoil spectrum of suddenly perturbed Fermi sea 80−80932
metal, narrow-band extra-atomic relax. and X-ray spectra 77−24928
metal, passivation termination, ESCA study 79−20267
metal, ultrasoft XPS, plasmon satellite intensity 80−35058
metal, XPS and X-ray absorption spectra, thermal broadening of core levels, many-electron effects 78−31284
metal, XPS angular depend. *(Russian)* 79−38722
metal electron response to local fields, X-ray processes 78−23584
metal halide intercalated graphite, acceptor site, XPS study 80−49218
metal oxide powder, quantitative surface meas., XPS method and appl. 78−40104
metal surface, 10 eV ion impact, chem. modification, ESCA obs. 77−24916
metal surface, electron bombardment sample evaporation source for cleaning, ESCA 77−90248
metal surface, reactivity, review of electron spectra 77−62748
metal surface, with adsorbed at., XPS intrinsic plasmon satellites, dispersion and lifetime effects 79−56151
metal surfaces, characterisation by SIMS and XPS 79−16054
metal with finite lifetime of deep hole 77−85845
metal with incomplete shell, spin-depend. final-state interactions in core photoelectron spectra 77−20981
metal with incomplete shell, spin-depend. final-state interactions in core photoelectron spectra 77−20982
metal-bromide, satellite of Br 4s line in XPS 78−56556
metal-containing plasma polymerised fluorocarbon films, deposition, struct., and polymerisation mechanism 79−78928
metal-InP contacts, intermediate adsorbed layer effect on electronic props. 80−39674
metal-semiconductor thin film preparation under UHV conditions 78−72733
metallic glass, bulk and surface properties, review 80−44147
metallic glasses, electronic structure, neutron scatt., elec. resist., Hall coeff., mag. susceptibility and XPS 78−23013
metallic substances, retention and exchange of 4f electrons *(Dutch)* 79−1587
metallic system, X-ray line shapes for core levels, phonon broadening 77−12464
metalloporphyrin, Z-ray photoelectron spectra satellites 80−5582
metals, free-electron, model-independent constraints on many-electron XPS asymmetries 77−52219
metals, narrow-band, and simple, edge singularities in spin-depend. final-state interactions 78−6810
metals, photoelectron spectroscopy of surface states 79−56909
metals, X-ray edges theory, review 77−66556
metals, X-ray photoemission line shape, Fermi surface excitations, book contrib. 79−61499
metals, X-ray photoemission spectroscopy, anomalous, frequency dependence of exponents 80−71563
metals, X-ray spectra, temp. broadening 77−69936
metals and alloys, electrodeposited on Au foil 77−81196
metals and alloys, review of X-ray spectroscopy 77−55849
methane, core 1s shakeup study, XPS and Xalpha calcs. 80−69064
methane, photoelectron spectra, 21.2-151.4 eV and soft X-ray, ionis. cross-section 78−37683
methanol, condensed multilayers, electron bombard. effects, AES lineshape anal., XPS, and desorption meas. 80−7450
microanalysis, sample sandwiched between anode and converter *(French)* 79−74471
microanalysis and microscopy applics. *(French)* 77−36835
microbeam anal., conf., Ann Arbor, MI, USA (June 1978) 79−39258
MIS solar cells, interface problems, AES, SIMS and XPS study 80−89627
mixed valence inorganic compounds with inequivalent atoms, XPS 80−2918
models for X-ray induced emission of photoelectrons, Auger electrons and secondary electrons 77−59669
molecular inner-shell photoabsorpt., shape resonances, extended X-ray absorpt. fine struct. 77−18979
molecules containing 1st row atoms, K-shell binding energy shifts, NDDO MO calcs. 80−58413
molecules or clusters, interpretation of data from Mossbauer, ESR, susceptibility, optical and XPS meas. 80−37825
monofluoromethane, X-ray photoelectron spectral linewidth of F core, ab initio HF calc. 78−62841
monohalobenzenes, inner shell excitation and ionis., electron energy loss spectra, XPS, assignments 78−62934
muscovite, quantitative anal. by XPS 78−35742
Mycenaean pottery from Megiddo, X-ray photoelectron spectroscopic analysis 79−29421
$Na_2[Fe(CN)_5NO]$, valence levels, X-ray photoelectron and X-ray spectra 77−88500
naphthalene, solid, electronic struct., comparative ESCA study of polyacenes 78−52631
narrow band metals, extra-atomic relax., X-ray spectra 77−36312
nearly free electron metal, simple model for quantitative evaluation of XPS line shape asymmetries 77−21002
Nilomag alloy 771 coloured, X-ray photoelectron spectroscopy of surface film 78−64899
nitrides, meas. *(Japanese)* 80−16154
p-nitroaniline, binding energy, XPS obs. 80−37833
p-nitroanilines, intramol. charge transfer satellites, XPS 80−78650

X-ray photoelectron spectra continued
nitronaphthylamines, ESCA and UV photoelectron spectra, assignments 78−50588
noble metal, XPS of valence bands, ang. depend. 77−44122
noble metals, many-body effects in X-ray photoemission 77−28684
noble metals, simple model for quantitative evaluation of XPS line shape asymmetries 77−21002
organo-tin polymer films, glow discharge prep., comp. determ. by XPS and AES 80−35109
organometallics, group V, XPS spectra interpretation, pot. model 78−50587
oxide, binding energies 77−44121
oxide surface, XPS exam. of chemical changes induced by Ar^+ ion bombardment 79−14993
oxides, surface microphases investigation by X-ray electron spectral anal. 79−51269
oxides of third-row elements, Auger LVV transitions, X-ray photoelectrons and emission spectra 78−21978
oxidised Iconel surface, quantitative anal. by XPS and rastered ion bombardment 77−40604
passivation films, on Sn plate, lacquer adhesion, ESCA exam. of constitution and effects 80−40776
PDX vacuum vessel, glow discharge conditioning 80−79607
Permalloy film, oxidation, quartz cryst. microbalance, AES and XPS obs. 78−27676
Permalloy film oxidation, microbalance, AES, ESCA and sputter profiling 78−15600
Permalloy films, oxidation effects on atmospheric corrosion, AES, XPS and ion sputtering anal. 80−11829
Permalloy-Rh, film, influence of Rh on corrosion resist. and mag. props. 80−3235
perovskites, d-band, model for X-ray photoelectron distrib. 79−61491
phlogopite, quantitative anal. by XPS 78−35742
phonon broadening of XPS line shapes and independence of hole state lifetimes 77−48313
phosphides of Cu,Ag,Zn,Cd,Ga,In, d electrons of metals, participation in chem. bonds 77−28682
photoelectric cross-section at K-edge measurements 78−2983
phthalocyanine compounds, XPS and change transfer 80−95681
plasmon effects in electron spectroscopies and chemisorption 79−33190
plasmon satellite struct., intrinsic versus extrinsic processes 77−77342
pollutant particles, characterised by AES and XPS 79−43694
poly(p-xylylene), electron MFP as function of kinetic energy, XPS 78−52114
polyacetylene:AsF_5, AES, XPS, UPS, and X-ray induced 80−66400
polyacetylene:AsF_5, thermal decomp. kinetics, elec. cond., ESCA and mass spectra 80−50830
polyacetylene:I, electronic structure, XPS and UPS meas. 80−66385
polyacetylene:I charge transfer complex, struct. 79−74052
polyacetylene : AsF_5 X-ray and UV photoemission spectra, Auger spectra 79−98150
polyacetylene X-ray and UV photoemission spectra, Auger spectra 79−98150
polyacetylene-I_2, highly conducting, Raman, XPS and X-ray diffr. obs. 78−80454
polyatomic system, multiple scattering method for photoelectron and absorpt. spectra 77−88501
polydiacetylene-bis(toluenesulphonate), XPS valence band obs., binding energies 77−77339
polyethylene, melting against Al, XPS obs. 77−32700
polyethylene, melting on Al, XPS meas. 78−15556
polyethylene, valence electronic struct., LCAO cryst. orbital calcs., ESCA 78−5384
polyethylene films, adhesive props. improvement by corona discharge appl. *(French)* 78−92438
polymer, angular-dependent studies on some prototype vertically and laterally inhomogeneous samples 78−95655
polymer, ESCA investigation of struct., reactivity and bonding, O_2 (inert gas) surface modification 78−3438
polymer, ESCA investigations on selected systems, struct. and bonding obs. 78−14302
polymer, surface modification by RF plasma, difference ESCA spectra 77−63529
polymer films on Au, ESCA, sample charging phenomena 80−20764
polymer primary structures ESCA and EHCO methods 78−52630
polymer surface, plasma treatment in O, ESCA and XPS obs. 78−72910
polymer surface, struct., bonding and reactivity, ESCA meas. 79−52073
polymer surfaces, appl. of ESCA to struct. and bonding 79−57344
polymers, photoelectron escape depths determ. from X-ray photoelectron spectra 78−27368
polyphenylene oxide thin films, electrochem. prep., impurity effects on cond., electroforming 80−88655
polypropylene, isotactic, conformational origin of peak struct. in XPS spectrum 79−89819
polysiloxane-metal oxide interfaces, bonding mechanism, surface anal. by XPS and static SIMS 78−15643
polystyrene, form. of Cu-O-polymer complex 78−92372
polystyrene, O treated, interaction with vapour-deposited Cr and Ni atoms 80−3407
polysulphur nitride:bromine, struct. and phase transition 80−24382
polyvinyl alcohol-Cu interface, XPS study 79−83093
powder specimens, oxidised and unoxidised layers, X-ray irradiated electron emission intensities, Monte Carlo calc. *(Russian)* 78−6825
primary and secondary yields using low-energy monochromatic X-rays, standard surfaces 80−35053
PTFE+metal, fluoride prod., DSC and XPS anal., rel. to polymer wear 80−11889
pure elements, line intensity meas. 78−56563
PVC, chlorinated, X-ray photoelectron spectra investig. 80−3469
PVC surfaces, natural and stabilised, composition, ageing, oxidation and weathering, ESCA obs. *(French)* 80−61139
pyrrole, gas, X-ray photoelectron spectra, satellite struct. 78−5281
quantitative, parameters, appls. 79−43697
quantitative, rel. to subshell photoionis. cross-sections and electron mean free path 80−81389
quantitative surface anal., comparison of XPS results with model 78−40091
α-quartz, electronic struct., local disorder influence 80−59870
α-quartz surface, XPS study 80−93451
quick frozen solutions, apparatus and technique for study *(German)* 77−44119

X-ray photoelectron spectra continued
rare earth alloys, RBe_{13}, XPS, resist. and susceptibility study 80−71565
rare earth compound, valence fluctuation type, replicate core level XPS probe 80−25521
rare earth compounds, intermediate valence states 79−33887
rare earth compounds, magneto-optical effects rel. to 4f electron excitation energies, XPS 77−52222
rare earth cpds., ESCA spectra, intense shake-up satellites, model 78−50589
rare earth germanides, X-ray emission, absorption and photoelectron spectra *(Russian)* 80−11509
rare earth metal, 4f levels, obs. by bremsstrahlung isochromat and XPS spectroscopy 79−24411
rare earth metal films, reactions with O_2 and water, XPS obs. 77−31888
rare earth metals, 3d core electron XPS spectra, low-binding-energy satellites, exception of Eu 80−104040
rare earth metals, core electron binding energy study 77−48309
rare earth metals, density of 4f states below and above Fermi level, XPS and bremsstrahlung isochromat spectroscopy 80−76140
rare earth metals, electronic structure rel. to valence, chem. bonding 80−54601
rare earth metals, XPS and bremsstrahlung isochromat spectra of f^{n+1}, f^{n-1} states 80−40220
rare earth mixed valence compounds, spin dynamics, mag. neutron scatt., Mossbauer effect, XPS studies 80−39786
rare earth oxides, core electron binding energy study 77−48309
rare earth oxides, electronic structure rel. to valence, chem. bonding 80−54601
rare earth oxides, XPES final state struct., 4d electron ionis. 78−25616
rare earth oxides, XPS, 4f-electron ionisation 77−14493
rare earth tris-dipivaloylmethide chelates, XPS, 4f-electron ionisation 77−14493
rare earth vanadates, electron energy loss spectra, primary excitation processes in cathodolum. 79−11490
rare earths and their cpds., XPS satellites, screening of 3d holes 78−76586
recoil effects in light atom mols., X-ray photoelectron induced vibr., rot. excitation 78−42129
refractory compounds, RF sputtered, comp. by XPS 78−51839
relative intensities, elastic scatt. in solid effect on free path and ang. distrib. 80−11531
resolution enhancement by deconvolution *(German)* 78−82087
retinal$_1$, all-trans, valence bands, XPS obs. 78−24030
review of literature, 1975-1977 78−85225
rubber to metal bonding 78−15648
rubber-brass interface, adhesion failure, XPS study 80−40671
rubber-metal interface, adhesion mechanism, XPS study 80−65382
satellite lines in solids, review *(French)* 77−36363
satellite peaks, relationship between X-ray emission and X-ray photoelectron spectra 78−66492
scanning ESCA, operation and limitations 77−36818
self-consistent charge calcs. of core-electron binding energy shifts 80−69084
semiconductor, core electron line shapes 78−11082
semiconductor, surface final-state effects on core electron transition energies 78−91745
semiconductors, soft X-ray induced secondary-electron emission, models and meas. 79−74034
semimetal, core electron line shapes 78−11082
silicate, fundamental study on quantitative anal. of O^0, O^-, O^{2-} ions by XPS *(Japanese)* 77−48710
silicate minerals, X-ray photoelectron diffr., quantitative anal. 80−66912
silicates, core-level XPS peak intensity ratio ang. variations rel. to surface anal. and chemisorption 80−40225
silicide RF sputtered wear-resistant coatings, XPS study of adherence 79−34191
simple metals, photoemission theory, book contrib. 80−16159
SIMS-AES-X-ray photoelectron spectral analysis system, for solids anal. 79−39268
single crystal and polycrystalline samples, comparison 77−12493
soft X-ray spectra, meas. by photoelectron anal. 80−73557
solid, Auger effect theory, plasmon effects in electron spectroscopies of valence state 78−56098
solid, struct. of XPS *(Russian)* 77−63544
solid characterisation *(French)* 77−36367
solid surface and thin film anal. methods, review 79−34410
solid-state and adsorbate shifts, equivalent cores calc. 79−28888
solid-state effects in XPS 80−55264
solids, electronic states determ. using synchrotron radiation 77−20882
solids, quantitative anal. by XPS 78−35742
source area minimisation, appl. to 30μm trachelomonas cell surface anal. 79−48037
spectrometer, consistent calibration method, rel. to Pd Fermi level 77−16458
spectroscopy resolution with Mg Kα radiation 80−18888
sputtered refractory carbides, adhesion to metal substrates, improved 80−76481
stearic acid, photoelectron escape depths determ. from X-ray photoelectron spectra 78−27368
steel, austenitic, Cr-Ni, ion-implanted N, chem. state study by AES and XPS 80−79825
steel, austenitic stainless, Cr-Ni-Mo (21,6,9 wt.%), N_2-strengthened, surface segregation of B, Auger and XPS spectra 79−90854
steel, cold-rolled sheet, surface chemistry 80−61146
steel, galvanised, with paint coating, adhesion failure, XPS study 80−40671
steel, industrial, surface chem. characterisation by SIMS, glow discharge spectrometry and other techniques 80−66907
steel, low alloy Mn-Sb(2, 0.12 wt.%), reversibility of temper embrittlement, studied by XPS and AES 77−32667
steel, mild, surface analysis rel. to annealing *(French)* 77−32857
steel, stainless, coloured, X-ray photoelectron spectroscopy of surface film 78−64899
steel, stainless, Cr-Ni-Mo, surface, scraping, mech. (electrolytic) polishing, ion etching, effects on ESCA 78−53037
steel, stainless, ferritic, passivity in 1N HCl, X-ray photo-electron spectroscopic study 80−11817
steel, stainless, passive layers, X-ray photoelectron spectroscopy analysis 77−32715
steel, stainless, surface treatment, X-ray photoelectron spectrosc. study 80−50764

X-ray photoelectron spectra continued
steel, stainless, type 430, Ni^+-implanted, struct., comp. and electrochem. anal. of surface alloy 80−16603
steel, stainless, wear in dibenzyl disulphide-containing oil, X-ray photoelectron spectroscopy of surface chemistry 78−64736
steel, wear testing in oils containing organosulphur cpds., XPS obs. of surface comp. rel. to wear 77−36668
steels, free-machining, fractography and X-ray photoelectron spectroscopy 80−7673
steels, stainless, surface characterisation rel. to adhesive bonding chem. etching, SEM, AES, XPS and electron probe microanal. 80−88416
Stellite-6, XPS obs. of aqueous oxidation, surface comp. and gaseous oxidation effect 80−81238
p-substituted polystyrene, shake-up phenomena, ESCA studies 77−54638
sulphides of Cu,Ag,Zn,Cd,Ga,In, d electrons of metals, participation in chem. bonds 77−28682
surface (100), atomic struct., angle-resolved XPS, LEED and ISS investigation 80−10765
surface analysis, in space exploration, analytical appls. of Auger and XPS 78−35756
surface analysis, spectroscopic methods, review *(Chinese)* 79−34414
surface analysis techniques, AES, ESCA, and photoelectron spectroscopy 79−95252
surface analysis techniques 79−70411
surface analytical techniques, quantification, review 80−65342
surface characterisation, physical methods, review *(French)* 80−7889
surface characterisation, XPS and AES techniques 77−32495
surface chemical analysis through even derivatives 79−100463
surface electron state characterisation by X-ray techniques 77−55868
surface layer, ion beam-modified, ESCA obs. 78−52612
surface layers, methods, results of studies of atomic states and elemental composition 77−29063
surface problems, in materials science and technology, conference, Gothenburg, Sweden, June 1979 80−51950
surface quantitative analysis *(French)* 77−36836
surface segregation, effect on metallurgical props, SIMS, XPS and AES *(French)* 80−80045
surface struct. anal. using extended X-ray absorpt. fine struct.-Auger process 77−11768
surface techniques, AES, ESCA and SIMS 77−56187
synchrotron radiation, appls. 78−74825
synchrotron radiation, props. and appls., review 79−36830
synchrotron radiation techniques for studying atomic physics 80−63583
systems Ni ions anal. by ESCA *(Japanese)* 80−40787
TCNQ and its salts, XPS meas. surface effects 78−11075
TCNQ salts, IR, X-ray electron spectra, tetrathiotetracene $(TCNQ)_2$ cond. investig. 77−44005
$TCNQF_4$, charge transfer complexes and salts, C(1s) and N(1s) XPS anal. of shake-up satellites 77−14492
Teflon, surface alteration by interaction with Ar^+ and Xe^+ beams 78−91347
tetracene, solid, electronic struct., comparative ESCA study of polyacenes 78−52631
11,11,12,12-tetracyanonaphthoquinodimethane, XPS of solid and mol., ionis. pot. 79−31593
tetrafluoromethane, X-ray photoelectron spectral linewidth of F core, ab initio HF calc. 78−62841
tetraphenylcobalt porphyrin, XPS, valence electron levels 78−82785
tetraphenylcopper porphyrin, XPS, valence electron levels 78−82785
tetraphenylnickel porphyrin, XPS, valence electron levels 78−82785
tetraphenylporphyrin, XPS, valence electron levels 78−82785
tetraphenylzinc porphyrin, XPS, valence electron levels 78−82785
tetraselenotetracene, electronic structure, conductivity studied by ESCA 79−4889
tetrathionaphthalene, electronic structure, conductivity studied by ESCA 79−4889
tetrathiotetracene, electronic structure, conductivity studied by ESCA 79−4889
tetrathiotetracene salts, IR, X-ray electron spectra, tetrathiotetracene $(TCNQ)_2$ cond. investig. 77−44005
thin film, and surface anal., modern methods 80−54486
thin foil microanalysis using XPS and STEM, surface film effects 78−35789
thionine-coated electrode for photogalvanic cells, electrochem. and XPS anal. 80−72071
thorium compounds, 4f level XPS shake-up satellites, assignments 78−1023
TiO, local density of states, X-ray spectra, Hartree-Fock and Xα calcs. discrepancies 79−77980
transition metal, 3d, electron-electron interaction, X-ray excited Auger spectra 78−91631
transition metal, 3d, superatomic relax. and positions of inner levels 78−11069
transition metal, effect of correl. interaction of electrons with core holes 78−92178
transition metal, surface electronic structure calculations 78−95329
transition metal borides, charge state of B, core electron binding energies *(German)* 78−10391
transition metal borides, silicides and germanides, binding energies from X-ray photoelectron spectra 80−49170
transition metal borides, XPS meas. and chem. bond 80−20761
transition metal carbides, charge transfer from XPS core level chem. shift anal. 77−72837
transition metal carbides and borides, electronic structures calc. in conjunction with X-ray photoelectron spectroscopy *(Japanese)* 79−15074
transition metal carbonyl complexes, UV and X-ray photoelectron spectra, effect of adsorbed CO 79−4897
transition metal clusters, particle size rel. to bulk metallic props. 80−44490
transition metal compounds, satellites in XPS 77−12488
transition metal compounds, valence band struct., X-ray spectroscopic study 80−29319
transition metal compounds, XPS, anal., approx. mol. orbital theories 77−18975
transition metal cpds., ESCA spectra, intense shake-up satellites, model 78−50589
transition metal cyanides, octahedral, electronic struct., multiple scatt. mol. orbitals calcs., ESCA satellites 77−14488
transition metal elements of fifth period, core level binding energies 80−71564

X-ray photoelectron spectra continued
transition metal germanides, X-ray emission, absorption and photoelectron spectra *(Russian)* 80−11509
transition metal monosulphides of first-row, XPES and UV PES 80−20760
transition metal oxide and hydroxide surfaces, chem. changes induced by Ar^+ bombardment, XPS obs. 79−83084
transition metal oxides, O(1s) peaks 77−16457
transition metal oxides, second and third-row, XPES 80−87170
transition metal oxides, XPS, trapped electrons at F-centres and anion defects, photoionis. cross sections 77−90249
transition metal phosphides, valence electron energy spectrum, deduced from X-ray spectra and XPS 79−99984
transition metal phosphides, valence-level struct., X-ray spectra and X-ray photoelectron spectra calcs. 79−64044
transition metal sulphides, ion bombardment damage, XPS obs. 80−97404
transition metal surface (adsorbate), intermediate UPS/XPS synchrotron radiation study 78−52633
transition metals, 3d, electron delocalisation and characterisation of L_3MN Auger spectra 77−48315
transition metals, 3d, XPS of valence bands 78−35249
transition metals, 3d-, 4d-, 5d-, band struct. from spectral data and theoret. calcs. *(Russian)* 77−8013
transition metals, alloys, and cpds., XPS asymmetry of core electrons and electronic struct. parameters 80−93460
transition metals, high spin compounds, X-ray and photoelectron spectra, one-config. approx. 78−92145
transition metals XPS, asymmetric, due to electron-hole interactions, theoretical model *(Russian)* 79−33901
transition potentials, for ESCA and Auger spectra, equiv. cores and Hellmann-Feynman calcs. 77−61724
transition-metal compounds, effects of electron transfer on shake-up satellites, model calc. 78−95650
transition-metal perovskitelike compounds, covalency effects, partial densities of p- and d-states photoelectron spectra 79−38718
transiton metal oxide perovskites, UPS, XPS, X-ray absorpt. spectra, band struct. study 79−56885
triamino-trinitrobenzene, UV and shock-induced decomp. XPS obs. 79−31595
1,3,5-trinitro 1,3,5,-triazacyclohexane, shock-induced intramol. bond breaking, XPS and EPR study 80−76512
trinitrotoluene, shock-induced intramol. bond breaking, XPS and EPR study 80−76512
TTF-TCNQ, XPS, surface electronic struct. 78−52627
TTF-TCNQ complexes, charge transfer, X-ray photoelectron spectra determ. 77−73210
underpotential deposition on Pt electrodes, XPS and AES 77−77770
uniform depth profiling, in XPS, using saddle field ion source 78−48708
vacuum dependent scientific instruments, hydrocarbon contamination 79−63259
valence ionisation pots., SCF-MS-Xα calcs., mol. space partitioning 79−36529
water, condensed multilayers, electron bombard. effects, AES line-shape anal., XPS, and desorption meas. 80−7450
X-ray source, Cu lines in achromatic Mg X-ray source 79−75667
Y-type zeolites, rare earth ion exchanged, XPES obs. 80−83421
zinc blende structured semiconductor surface analysis *(Japanese)* 78−88672
A15 compounds, electronic struct., XPS and SXE spectra calc. 79−42437
Ag, 30-90 keV, electron yield 77−8726
Ag, 4d spectrum, high resolution X-ray photoelectron spectra, comparison with APW calc. 77−1784
Ag (110), adsorption of O_2 and coadsorpt. of Na and O_2, XPS and UPS obs. 77−69183
Ag (110) surface, photoelectron spectroscopy and surface order, UPS and XPS obs. 78−56568
Ag (111), adsorbed layers of $O_2(N_2)(S)$, electronic props., XPS and UPS 78−10279
Ag (111) surface, ethylene adsorption, XPS and UPS investigation 80−103573
Ag, adsorption and surface reaction of formic acid 80−40741
Ag, adsorption of O, surface species identification by XPS, high press. 79−28191
Ag, angular depend. of X-ray photoelectrons *(German)* 78−72679
Ag, atomic cross-section effects in soft X-ray photoemission from valence bands 77−1783
Ag, Auger spectra, 4d bandwidth effect 80−89093
Ag, contact material, contamination layer thickness, resist., ESCA study *(German)* 80−55561
Ag, core level binding energies 80−71564
Ag cpds., valence electron spectrum, SRO and LRO effects 78−52639
Ag, N-shell vacancy state widths, X-ray photoelectron, Auger spectra 77−18875
Ag, nature of 3.8 eV plasmon in XPS 79−78838
Ag on Pt electrode, underpotential deposition, XPS and AES 77−77770
Ag photoelec. cross sections, 5-40 keV photons, X-ray emission spectra 77−18866
Ag, photoemission spectra and total primary yields for exploding wire radiator source 80−32773
Ag, photoemission spectrum from d-bands, ang. depend. obs. 77−12492
Ag surface, CO chemisorption, SIMS, XPS study 80−84382
Ag underpotential deposition, on Pt substrate, XPS 77−59672
Ag, XPS and $M_{4,5}N_{4,5}N_{4,5}$ Auger spectra 79−61472
Ag-Cd, α and β phase, XPS, effects of atomic order on band struct. 79−42440
α-Ag-Cd, dil., electronic struct. determ. from thermoreflectance and XPS 78−39011
Ag-Cu (10 wt.%), contact material, contamination layer thickness, resist., ESCA study *(German)* 80−55561
Ag-Mn, dil., valence and core level spectra, XPS study 80−84838
Ag-Mn (20 at.%), mag. virtual bound state alloys, XPS of core states 79−47588
Ag-O-Cs surface, oxidation, role of Cs suboxides in low work function surface layers, XPS 80−76131
Ag-Pb (30 wt.%), contact material, contamination layer thickness, resist., ESCA study *(German)* 80−55561
Ag-Ru(Rh)(Pd) film, valence band spectra, XPS meas. 78−52618
AgBr, photographic emulsions, adsorpt. of thiolic antifoggants, chem. struct., ESCA investig. 78−32907

X-ray photoelectron spectra continued
$Ag_{0.5}Cd_{0.5}$, Cd 4d band apparent splitting, cryst. field and d-d overlap influence XPS obs. 79−78825
AgCl, irradiated, surface defect center, XPS study 79−28894
AgCl-AgBr, microcryst., halide comp. profiles, XPS 77−12850
AgCl(Br), thermal shifts in energy level separations, ESCA 77−8723
AgCuSe, X-ray photoelectron and Auger spectra 78−56561
$AgGaSe_2$, and Ag_9GaSe_6, XPS, Auger and direct electron spectra 78−52620
Ag_2HgI_4, XPES, lattice instability 79−33904
AgI, lattice instability, XPS 79−11500
AgI, XPES, lattice instability 79−33904
$AgInSe_2$, reflectvvity and XPS meas. 78−35165
$AgNO_3$, ESCA contrib. to X-ray struct. determ. *(French)* 77−62508
AgO and Ag_2O, ESCA spectra, Auger effect, initial and final states effect 78−15280
Ag_2S, XPES, lattice instability 79−33904
Ag_2S-K_2SO_4 mixtures, surface comp., AES and XPS obs. 80−81386
Ag_2Se, X-ray photoelectron and Auger spectra 78−56561
Al, 30-90 keV, electron yield 77−8726
Al (111), chemisorpt. of O 78−14593
Al, achromatic X-ray source, spectrum iterative deconvolution, 2p spectrum 78−72689
Al, adsorpt. of O_2 (NO), 80 to 290K, 10^{-6} to 10^{-2} Pa, XPS study 78−95657
Al, adsorption and decomp. of methanol, UPS, XPS and thermal desorption obs. 79−82441
Al, adsorption and decomp. of NH_3 and hydrazine, XPS obs. 80−92783
Al, adsorption of O_2, AES, XPS, and LEED obs. 79−46938
Al, adsorption of O_2, intrinsic and extrinsic plasmon coupling, XPS of adsorbed atoms core states 78−10278
Al, adsorption of small molecules, photoelectron spectra, surface plasmon spectroscopy 79−47148
Al, ang. depend. of plasmon loss features in XPS 78−43987
Al, angle-resolved XPS from valence levels, Brillouin zone averaging 78−48285
Al, anodic behaviour in NO_3^-/Cl^- solns., electrochemical and XPS meas. 80−16694
Al, atomized powder, metallic contact for hot rolling in air 77−73294
Al brass condenser tubes, XPS study of protective layers 80−35383
Al, bulk and surface plasmon loss intensities in XPS, Auger and electron energy loss spectra 79−38012
Al, core-level XPS, electron energy loss spectra, intrinsic and extrinsic plasmons 77−63532
Al, corrosion-protective chromate coatings, characterisation 79−47798
Al film, XPS lineshapes, many body processes 78−39663
Al, many-body response in X-ray absorption, emission and photoemission spectra 80−16124
Al, oxidation by exposure to O_2 and H_2O, soft XPS exam. 78−80683
Al, photoelectron spectral yields from monochromatic soft X-radiation 79−22757
Al, photoemission spectrum for exploding wire radiator source, Boltzmann eqn. soln. 79−26949
Al, plasmon struct. of core lines in XPS meas. 77−63530
Al sheet surfaces, chem. characterisation by SIMS, glow discharge spectrometry and other techniques 80−66907
Al surface, oxidation, synchrotron radiation photoelectron obs. 78−52634
Al, ultra soft X-ray photoelectron energy loss study, angle and energy dependence 78−23582
Al, X-ray induced electron emission, secondary electron energy distrib. 77−59669
Al, XPS theory, core level spectra, plasmon creation 78−72701
Al-Ag alloy, ageing exam. by X-ray electron spectroscopy and electron diffr. exam. *(Russian)* 78−60685
Al-Al_2O_3, local struct. and interface states using surface soft X-ray absorpt. and photoemission spectroscopy 79−69595
Al-M, dil. alloy, electronic states of 3d-transition metal (M) impurities 78−64005
Al-Mg, alloy, surface activity of Mg, XPS and AES meas. 79−86975
Al-Mn(Fe)(Co)(Ni)(Cu)(La)(Ce)(Gd), dil. virtual bound state 78−15285
Al-Mn(Ni)(Cu), dil., core and valence band spectra, XPS study 80−84837
Al+NO_3^-, reactions between metal and aq. nitrate solns., XPS 77−12825
AlAg, Auger spectra, 4d bandwidth effect 80−89093
$AlAsO_4$, XPS of cryst., inner shell binding energies of elements 79−43092
$AlAsO_4.2H_2O$, XPS of cryst., inner shell binding energies of elements 79−43092
AlN, interatomic interactions from XPS 80−49171
Al_2O_3, dense, exposed to steam, influence of Ca migration on strength reduction 80−11797
Al_2O_3, electronic struct., XPS meas. 77−73217
γ-Al_2O_3, fluorided, appl. of XPS method for surface anal. 78−40104
Al_2O_3, interatomic Auger transitions XPS exam. 77−8692
Al_2O_3, quantitative surface anal., comparison of XPS results with model 78−40091
α-Al_2O_3, rapid firing, XPS study of cryst. struct. 78−68663
Al_2O_3 thin film used in inelastic electron tunnelling spectroscopy, X-ray photoelectron spectrum 80−108319
$AlPO_4$, XPS of cryst., inner shell binding energies of elements 79−43092
$AlPO_4.2H_2O$, XPS of cryst., inner shell binding energies of elements 79−43092
AmO, and AmO_2, electronic struct. and chem. bonding and XPS line shape calcs. 79−33264
AmO_2, XPS meas. 77−48314
Ar, ESCA spectra from 132.3 eV YMζ radiation source 77−4958
Ar, photoelectron spectra, 21.2-151.4 eV and soft X-ray, ionis. cross-section 78−37683
Ar, photoemission angular distribution, atomic pseudopotentials for soft X-ray excitations 77−23478
Ar, photoionisation, Auger processes, decay lifetime, line shift, profile, X-ray photoelectron spectra 80−37798
As, amorphous, electron and phonon density of states calcs., comp. to XPS 78−56066
As film, sputtered, density of valence states by XPS and UPS 77−24926
As, K shell photoelectric cross section, at 74.409 keV 79−72288
AsF_3 X-ray and UV photoemission spectra, Auger spectra 79−98150
AsF_5 X-ray and UV photoemission spectra, Auger spectra 79−98150
As_2O_3 crystalline and amorphous, EXAFS study of struct. 80−19776

X-ray photoelectron spectra continued
As_2O_3, density of valence states, photoemission meas. 77−72808
As_2O_3, electronic struct., X-ray emission, XPS, UPS obs., CNDO cluster calc. 78−52638
As_2S_3, amorphous, density of valence states, XPS and UPS obs. 77−48308
As_2S_3, amorphous, XPS, electronic struct. calcs. using scattered wave method 79−11502
As_2S_3, amorphous semicond., photo-induced optical and structural changes *(Japanese)* 78−47244
As_2S_3, crystalline and amorphous, surface charging effects on valence band spectra in XPS 77−8725
As_2S_3, electronic struct., X-ray emission, XPS, UPS obs. 78−52638
As_2S_3 layered crystal and amorphous analogues, XPS valence band spectra, electronic struct. 77−52218
$As_2S_{2.66}Se_{0.34}$, X-ray photoelectron spectra, electron binding energy, effect of Ag alloying 79−11499
$As_2(Se,Te)_3$ glasses, X-ray absorption and photoelectron spectroscopy study 80−7463
As_2Se_3 amorphous film, comp. ratio variation by annealing and laser irrad., ESCA meas. 79−99447
Au, 30-90 keV, electron yield 77−8726
Au, achromatic X-ray source, spectrum iterative deconvolution, doublet and valence band 78−72689
Au, ang.-depend. XPS meas. 77−40329
Au, angle resolved XPS, temp. independence 79−19975
Au, angle-resolved XPS from valence levels, Brillouin zone averaging 78−48285
Au, angular depend. of X-ray photoelectrons *(German)* 78−72679
Au, angular-dependent studies on some prototype vertically and laterally inhomogeneous samples 78−95655
Au clusters on alkali halide surface, size depend. of valence bands, XPS study 80−65647
Au, core level binding energy and density of states from first atomic layer, XPS meas. 79−87563
Au, Coster-Kronig N_{45}-$N_{67}X$ transitions, semi-empirical Auger electron model and obs. 77−85889
Au, D-orbital directed emission 77−40328
Au, ESCA spectra for outermost electronic shells 77−1970
Au laterally inhomogeneous sample, ang. and spatial depend. intensity 79−74468
Au organometallics, ESCA core binding energies 78−50586
Au, photoemission spectrum form d-bands, ang. depend. obs. 77−12492
Au, photoemission spectrum for exploding wire radiator source, Boltzmann eqn. soln. 79−26949
Au, surface atoms, XPES, core level binding energy, density of states 79−8224
Au surface electronic structure, XPS study 80−55259
Au, X-ray induced electron emission, secondary electron energy distrib. 77−59669
Au, XPS, electronic struct. 80−7464
Au/GaSb (110) interface, heat-treated, struct. and chem. state, angle-resolved XPS 80−97400
Au-Al/GaAs interfaces, atomic interdiffusion, soft XPS studies 80−65302
Au-Cs(Mg)(Rb)(Zn), charge transfer, Mossbauer effect ^{197}Au isomer shifts, XPS valence-band spectra 80−2676
Au-Fe (20 at.%), mag. virtual bound state alloys, XPS of core states 79−47588
Au-Fe(Co)(Ni), dil., valence and core level spectra, XPS study 80−84838
AuSn, XPS, electronic struct. 80−7464
B, evaporated, electronic struct., XPS, SXS and isochromat investig. 80−76143
B-S compounds, relative antiwear efficiency 78−35532
$BAsO_4$, XPS of cryst., inner shell binding energies of elements 79−43092
BN, hexagonal, electronic struct. from X-ray emission and XPS 79−47009
BN, interatomic interactions from XPS 80−49171
B_2O_3, chem. bonding, electronic struct., ESCA, Auger, and SIMS spectra 80−50512
BPO_4, XPS of cryst., inner shell binding energies of elements 79−43092
Ba, electron-correlation satellites, selective reson. enhancement 80−9569
Ba, photoelectron spectra, strong many electron effects from core levels 77−18862
Ba, XPS, in BaS and $BaSO_4$ 80−43104
Ba^{2+}, on calcite surface, ESCA, calibration 77−81432
BaF_2, core-electron peaks, satellite and loss structs. 77−66571
BaH_2, XPS spectra, crystalline potentials 77−77344
BaO, electron energy loss and secondary emission mechanisms, plasmon losses 78−76565
BaO, XPS valence bandstruct. 80−89117
$BaTiO_3$, band struct. calc., interpretation of XPS and UPS spectra 80−70597
$BaTiO_3$, electronic props., SCF-MS-Xα calc. 80−54607
$BaTiO_3$, electronic struct., XPS and band struct. calc. 79−38708
$BaTiO_3$, photoelectron and optical spectra derived from self-consistent charge MO and band calcs. 80−96785
$BaTiO_3$, XPS, band struct., density of states, photoionisation cross sections 78−52629
$BaTiO_3$, XPS and UPS from surface defects 80−76136
$BaTiO_3$, XPS satellite spectra, mol. orbital study 80−43100
Be, conduction electron hole coupling, XPS obs. 77−28135
Be, electronic density of states 78−6829
Be inorganic compounds, chemical binding and surrounding symm. effect on Be photoelectric yield 77−27086
Be, plasmon struct. of core lines in XPS meas. 77−63530
Be, XPS theory, core level spectra, plasmon creation 78−72701
Bi, L-shell X-ray photoelectric cross sections, fluorescence spectra 78−58636
Bi, photoionisation cross section of d-core level synchrotron radiation study of spin-orbit branching ratio 79−74057
Bi, solid and liq., core-level line shape, high-resolution XPS meas. 77−59668
Bi, solid and liq., valence band structure, XPS meas. 77−32504
Bi surface, detection of high mass cluster ions by SIMS and XPS surface monitoring 77−16442
Bi, XPS, electronic struct. 80−7464
BiI_3, layered semicond., valence bands UPS and XPS obs. 78−11078
Bi_2O_3, electronic struct., X-ray emission, XPS, UPS obs. 78−52638
X-ray photoelectron spectra continued
Bi_2O_3, oxide film on polycrystalline Bi, exam. of oxide film growth rate using XPS *(German)* 79−11041
Bi_2X_3 (X=O,S,Se,Te), electronic struct. 77−32493
BkO, and BkO_2, electronic struct. and chem. bonding and XPS line shape calcs. 79−33264
BkO_2, XPS meas. 77−48314
Br, ESCA, lifetime broadening, CI resonances 77−18853
Br_2, extended X-ray absorption fine struct. amplitude attenuation, rel. to XPS satellites 80−37821
Br_2, K shell photoelectric cross section, at 74.409 keV 79−72288
C, adsorbed on Fe(100), adsorbate coverage determ. by LEED, AES and XPS 80−103566
C, bombardment by Ar and ^{57}Fe ions, effects anal. by XPS 77−11769
C bonding to Tokamak walls, XPS studies 80−80942
C film, diamond-like, produced in butane plasma, XPS anal. and elec. props. 79−82484
C, photoemission spectra and total primary yields for exploding wire radiator source 80−32773
C:Ni, X-ray photoemission studies 80−76138
$(C)_n$, cryst. struct. determ. from X-ray photoelectron and X-ray spectra 78−88384
$C_{6.6}FeCl_3$ intercalation compound, charge transfer, acceptor sites, XPS study 80−49218
CO adsorbed on Ni (001) surface, XPS for adsorbate geometry 79−65314
CO, chemisorbed on Cu(100), XPS shake-up satellites, Xα-SW cluster model calcs. 79−95899
CO, hydrogenation on Fe foil, AES and XPS study 80−7858
CO oxidation by NO on Ir surface XPS and UPS 78−15702
CO, photoelectron spectra, 21.2-151.4 eV and soft X-ray, ionis. cross-section 78−37683
CO, vibr. struct. of K_α emission spectra 78−86886
CO_2, photoelectron spectra, 21.2-151.4 eV and soft X-ray, ionis. cross-section 78−37683
Ca, photoelectric cross sections at 52.4, 60, 72.2 and 84.4 keV 80−69187
CaF_2, core-electron peaks, satellite and loss structs. 77−66571
CaF_2 laser window surface O_2 detection 79−14056
CaH_2, XPS spectra, crystalline potentials 77−77344
CaO, XPS valence bandstruct. 80−89117
Cd, AES and XPS, vapour-metal electron energy shifts 80−16142
Cd, core binding energies, gas phase X-ray photoelectron spectra 78−37611
Cd, core level binding energies 80−71564
Cd, electron binding energy and shift, core level XPS 80−87088
Cd, N-shell vacancy state widths, X-ray photoelectron Auger spectra 77−18875
Cd, photoelectric cross sections at 52.4, 60, 72.2 and 84.4 keV 80−69187
Cd, XPS and $M_{4,5}N_{4,5}N_{4,5}$ Auger spectra 79−61472
Cd, XPS line intensity ratios for outer electron shells 79−100018
Cd-Co(-Mo), amorphous films, thermal stability of mag. props. *(Japanese)* 79−47307
CdF_2, UPS and XPS spectra, rel. to optical props. 80−66386
CdI_2, valence-band XPS meas. 77−12487
$CdIn_2S_4$, valence band densities of states, XPS meas. 79−28892
$Cd_{0.6}Mn_{0.6}Te$ crystals, Mn($3d^5$) band, photoemission evidence 80−11535
CdO, ESCA spectra, Auger effect, initial and final states effect 78−15280
CdS, XPS, secondary illumination effects, band bending, level shifts 80−108324
CdS-Al(Au) interfaces, bonding and interdiffusion, XPS obs. 80−80000
CdSe photoanodes, S substitution during operation and mech. of surface protection XPS study 80−107906
CdSe photoelectrode, immersed in polysulphide soln., S/Se substitution, XPS obs. 79−19656
CdTe, clean and oxidised surfaces, O_2 sticking coeff., ionicity effects 77−85887
CdTe surface, sputter cleaning and dry oxidation, XPS and LEED study 80−108618
CdTe, surface layers formed by etchants, XPS meas. 78−44240
Ce and Ce-Al alloys, XPS valence band spectra meas. 77−48306
Ce, oxidation, ESCA and UPS meas., core levels 77−63542
γ-Ce, photoelectron spectra, 4f level position 80−25519
γ-Ce, valence band exam. by XPS and UPS 79−37977
CeAs, XPS for electronic struct. determ. 79−33888
CeB_6, thermionic emission rel. to surface state 78−39654
$CeBe_{13}$, intermediate valence state, XPS, resist. and susceptibility study 80−71565
CeN, electronic struct., XPS exam. 78−6269
CeN, XPS for electronic struct. determ. 79−33888
CeO_2-La_2O_3 system, surface microphases investigation by X-ray electron spectral anal. 79−51269
CeO_2-Y_2O_3 film, surface characterisation, XPS, ESCA, and AES expts. 78−72028
$Ce(OH)_3$, mol., XPES, satellite phenomena 79−27035
CeP, XPS for electronic struct. determ. 79−33888
$CePd_3$, mixed-valence, 3d and 4d core levels, XPS study 80−89111
Ce_2S_3, 4d absorpt. edge region, chem. binding effects 77−12467
CeSb, XPS for electronic struct. determ. 79−33888
Cf_xO_y, XPS meas. 77−48314
Cl compounds, chemical shifts of X-ray electron and Auger lines 78−86912
Cl, in Ir catalysts, determ. by X-ray photoelectron spectroscopy 77−9146
Cl_2, chemisorpt. on Ag (110), XPS and UPS meas. 78−31293
Cl_2, interaction with H_2SO_4 and water, surface reactions at low temps. 79−79288
ClF_3, ESCA chemical shift, energy levels, SCC-MO calcs. 79−64045
CmO, and CmO_2, electronic struct. and chem. bonding and XPS line shape calcs. 79−33264
CmO_2, band struct., cryst. binding and ESCA spectra, X_α cluster calc. 78−64443
CmO_2, XPS meas. 77−48314
Co (0001), adsorption of O_2 and CO, XPS and UPS study 79−74050
Co, adsorption of CO 77−35818
Co, adsorption of O_2, CO and CO_2 *(French)* 77−36362
Co base amorphous alloys, alloying elements influence on corrosion behaviour, XPS obs. 80−89422
Co, clean surface, interaction with O_2 and air, XPS 77−16466

X-ray photoelectron spectra continued
Co complex, oxygenated CoII amino acid-imdazole, XPS 78−21968
Co II acetylacetonate, XPS 80−74196
Co, monolayer, oxidation, quasisimultaneous SIMS, AES, XPS 78−72919
Co, oxidation, XPS obs. of epitaxial CoO form. 80−66396
Co, polycryst. surface interaction with O_2, CO and CO_2 *(French)* 77−73219
Co^{3+} d^6-complexes and oxides, spin-state transitions, PES study 79−100014
Co-Al_2O_3 catalysts, reducing and sulphiding treatments, XPS obs. 78−85196
Co-Sn alloy, electroplated, oxide films, XPS/AES expts. 79−15862
CoAl, bonding, self-consistent energy bands 78−91610
Co_3B, crystalline, photoemission and electronic struct. 80−2926
CoF_2, valence-electron density of states, XPS meas. 77−69963
$CoFe_2O_4$, core line X-ray photoelectron spectra 78−7263
$CoFe_2O_4$, thermally induced surface chemistry and struct., XPS 78−22939
Co(III) compounds, XPS exam., struct. of 2p lines 78−19631
$Co(NH_3)_4Cl_2Cl$, cis and trans isomers, XPS, shake-up satellites 78−82783
CoO and Co_3O_4, XPS interpretation, valence band structure 77−12497
CoO, ESCA and Auger lines, chem. shifts 78−6817
CoO, electronic struct., XPS and UPS expts. *(French)* 79−38711
CoO, valence band struct., cryst. field anal., photoelectron data 79−47007
Co_3O_4, ESCA and Auger lines, chem. shifts 78−6817
Co_3O_4, electronic struct., XPS and UPS expts. *(French)* 79−38711
$Co_{78}P_{14}B_8$, amorphous, photoemission and electronic struct. 80−2926
$CoS_2(Se_2)$, core-level and valence-band XPS 80−93450
$CoS_2(Se_2)$, electronic struct., UPS and XPS study 80−80935
CoSb, electronic struct., XPS meas. 78−2990
CoSi, electronic struct. determ. by XPS and X-ray emission spectra 77−85147
$Co(ethylenediamine)_3(ClO_4)_3$, ESCA chem. shift meas., internal standards 78−50585
Cr, adsorption of O, photoemission exam. 79−19976
Cr alloys, ESCA meas. of oxide layer 78−15584
Cr, atoms, vapour deposited on polystyrene, core-level spectra 79−56911
Cr compounds, multiplet spectra in XPS and K-emission 77−63527
Cr film, reversal etching in gas plasma, reaction mechanism, AES and XPS obs. 80−16564
Cr oxides, XPS study, electron binding energies, spin orbit splittings, exchange splittings 79−78839
Cr/polymer interface, electronic struct., XPS study 80−45204
Cr^{6+}/Cr^{3+} colloidal SiO_2 surface films on Al, TEM/XPS study 80−85090
Cr-Cr_2O_3, black chrome films, surface microstruct. rel. to optical props. in solar absorbers 79−52036
Cr-Cr_2O_3, black chrome electroplating for solar energy photothermal conversion, prep. and struct. 79−74544
Cr-Cr_2O_3 composite mixture, preferential sputtering, XPS expts. 79−87544
Cr-Ge system, XPS, X-ray and neutron diffr. and mag. meas. to study chem. bonding and electronic struct. 80−60749
Cr-O system, initial oxidation, combination anal. using ESCA, AES and SIMS 78−72924
$CrMoO_4$, ESCA on H_2 reduction *(French)* 77−36365
$Cr(NO)_4$, bonding, shake-up intensities and shake-up energies, SCF Xα multiple scatt. calc. 80−74121
$Cr(NO)_4$, XPS and UV photoelectron spectra, compared to NO data 80−58317
CrO_2, particulate, proton donor adsorption effect on mag. moment, XPS anal. 80−71117
CrO_2, valence states of Cr, XPS obs. 80−40216
CrO_4^{2-}, electronic struct. determ. from X-ray spectra 78−86885
Cr_2O_3, $Cr(OH)_2.0.4H_2O$, CrO_3, X-ray photoelectron spectra 77−73483
Cr_2O_3, electron structures calc. using models, ESCA and X-ray spectral data 77−35863
Cr_2O_3, electronic struct. study by XPS 80−25518
Cr_2O_3 films, black, microstruct. depend. of optical props., SEM, XPS, and sputter depth-profiling 79−43049
Cs, atom, XPS, free atom core binding energy 78−74699
CsAu, electronic struct., XPS meas. 79−69403
CsAu, photoelectron spectroscopy and energy bands calc. 78−76581
$CsBO_2$, vapour over heated solid, XPS, obs. 80−87171
CsI, depth of emission of secondary photoelectrons 79−8228
Cs_3Sb vacuum deposited photoemitter, XPS study 80−89122
$CsSnBl_3$, electronic struct., XPES and band theory calc. semimetallic behaviour 79−78837
$CsSnCl_3$, electronic struct., XPES and band theory calc. semimetallic behaviour 79−78837
Cu, 30-90 keV, electron yield 77−8726
Cu (001), adsorbed O c(2×2), surface geometry determ. by deep-core-level XPS 80−40224
Cu (001), with adsorbed O, core-level XPS, azimuthal anisotropy 79−19969
Cu (100), adsorbed layers of N, O and S, electronic props., UPS, XPS and Auger spectra 77−66088
Cu (100), adsorpt. of CO, UV and X-ray photoelectron spectra, LEED 78−56037
Cu (100), XPS of chemisorbed CO 79−15589
Cu, (100) crystal, angle resolved core level XPS calc. 79−33895
Cu (111), adsorbed Cs, XPS exam. of Cu surface state and Cs valence electrons 79−19647
Cu (111), hydroxylation and dehydroxylation, XPS obs. 80−7850
Cu, AES excited by X-rays, satellite lines 79−33893
Cu adhesion to Au, surface treatments and surface impurities 77−15701
Cu, adsorption and surface reaction of formic acid 80−40741
Cu and Cu alloys, corrosion inhibitor study by XPS, adsorbed benzotriazole 78−35554
Cu, ang. depend. XPS valence-band spectra meas. 77−21006
Cu, angle resolved photoemission, thermally induced breakdown of direct-transition model 77−77346
Cu, angular depend. of X-ray photoelectrons *(German)* 78−72679
Cu, chem. aspects of corrosion inhibition by benztriazole 80−16545
Cu complexes, paramag., XPS, temp. depend. 79−15582
Cu compounds, chemical shifts of X-ray electron and Auger lines 78−86912

X-ray photoelectron spectra continued
Cu compounds, ESCA shake-up satellites, spin density intensity ratio relation 78−50590
Cu, corrosion inhibition, chem. nature and struct. of protective films 77−60001
Cu, corrosion inhibitive films formed by corrosion determination of thickness by X-ray photoelectron spectra 79−15845
Cu, D-orbital directed emission 77−40328
Cu, film, growth on amorphous C, electronic props., UPS and XPS obs. 79−82476
Cu film, valence bands, XPS excited by Zr Mζ radiation 80−40236
Cu, K shell photoelectric cross section, at 74.409 keV 79−72288
Cu, $L_3M_{23}M_{23}$ Auger energy calc. using XPS, effect of 3d-4s admixed screening on relax energies 77−1782
Cu, LMM Auger spectra, rel. to L_{23} photoelectron spectra 77−77348
Cu, LMM Auger spectra, transition probabilities, term splittings and effective Coulomb interaction 77−44126
Cu molybdates, valence band X-ray induced Auger spectra and XPS 78−80813
Cu, on polystyrene, unusual core level spectra, XPS obs. 79−24415
Cu oxides, valence band X-ray induced Auger spectra and XPS 78−80813
Cu, photoemission angular dependence, direct transition interpretation 77−21004
Cu, single cryst. and polycryst. comparison 77−12493
Cu surface, (110), methanol adsorption, XPS, UPS and thermal desorpt. study 80−84388
Cu, surface, d-band narrowing, obs. using angle-resolved XPS 80−11062
Cu, surface d-band narrowing, angle resolved XPS 78−19635
Cu, surface film of 2-mercaptobenzothiazole and 2-mercaptobenzimidazole, XPS and X-ray induced Auger spectra obs. 80−40600
Cu, underpotential deposition, on Pt substrate, XPS 77−59672
Cu, XPS, angle-resolved, valence band density of states distrib. 77−44123
Cu/polymer interface, electronic struct., XPS study 80−45204
Cu-Be, dynamic segregation, ESCA obs. 77−8718
Cu-Fe(Co)(Ni), dil., valence and core level spectra, XPS study 80−84838
Cu-Mn alloys, Mn K X-ray emission and XPS lines, width and asymm. 78−19605
Cu-Ni alloys, XPS apparatus appls. *(Dutch)* 79−1982
Cu-Sn-P (5, 1-5 wt.%), effect of P on friction and wear characts. 80−16494
Cu-Zn alloy, surface layer composition determ. by XPS 79−43682
Cu-Zr, metallic glasses, valence band struct. investigation 80−11533
$CuAl_2O_4$, pure and NiO promoted catalysts, surface oxidation state and comp., XPS study 80−76134
$CuAlS_2$, reflectvvity and XPS meas. 78−35165
CuCl, XPS and Auger spectroscopy, elec. struct. 80−29852
$CuCl_4^-$, ESCA satellite intensity, ab initio SCF calcs. 80−74103
$CuFe_2O_4$, thermally induced surface chemistry and struct., XPS 78−22939
$CuFeS_2$, superficial degradation in air and water, XPS obs. *(French)* 80−89110
$CuGaS_2$, reflectvvity and XPS meas. 78−35165
Cu_2HgI_4, XPES, lattice instability 79−33904
CuInSe, reflectvvity and XPS meas. 78−35165
$Cu_xMg_{1-x}Al_2O_4$, spinel solid solns., solid-state and surface props. 77−66415
$CuMn_2O_4$, ionic config., re-exam. of expt. evidence 77−19897
$(Cu_xNi_{1-x})S_2$, XPS of valence band meas. 77−85885
CuO, solid, XPS satellite struct. 79−56908
CuO-Cr_2O_3 based oxide, catalyst, adsorption of fluorobenzene, binding energy of F 1s electrons *(French)* 79−69346
$Cu_{12}O$, solid, XPS satellite struct. 79−56908
CuP_2, Cu_3P, electronic struct. of valence bands, X-ray spectra and XPS 78−92176
Cu_2S, XPES, lattice instability 79−33904
$CuS_2(Se_2)$, electronic struct., UPS and XPS study 80−80935
CuSe, X-ray photoelectron and Auger spectra 78−56561
Cu_2Se, X-ray photoelectron and Auger spectra 78−56561
CuZr, photoemission study 80−104046
$Cu_{60}Zr_{40}$ glassy metal, photoemission and mag. susceptibility 79−28896
Cu(001), adsorbed O, deep core level XPS anisotropy 78−72690
Cu(110), photoemission, bulk versus surface effects 78−52626
Cu(111), (100), temp. depend. of bulk and surface energy bands using angle-resolved photoemission 79−69572
Cu(111) frequency depend. photoelectric surface state cross section periodic oscills., PES study 80−50522
Dy_2O_3, XPS, charging effects on core-level binding energies 79−24409
ErH_2, synchrotron XPS obs., rel. to theory for metal dihydrides 80−55275
Er_2O_3, XPS, charging effects on core-level binding energies 79−24409
Eu, X-ray photoabsorpt. near 3d edges 77−38645
$EuCu_2Si_2$, XPS studies, valence band, 4-f region 78−6831
$Eu_xLa_{1-x}Al_2$, binding energy and workfunction charges using XPES 80−33928
$Eu(OH)_3$, mol., XPES, satellite phenomena 79−27035
$EuRh_{2-x}Pt_x$, intermediate-valance state, XPS obs. 77−28687
F Kα X-ray line, from KF, for excitation of electron spectra 78−29865
Fe (11O), coadsorption of K and 0_2, XPS, UPS, AES, and LEED study 80−80084
Fe (110), adsorption of K, LEED, AES, UPS and XPS meas. 79−77919
Fe (110), K promoted, adsorption of CO, UPS, XPS, AES, and flash desorption obs. 79−82463
Fe, adsorption and surface reaction of formic acid 80−40741
Fe, adsorption of acetic acid and ethylenediamine, XPS study 80−76132
Fe, adsorption of CO and O_2 79−15003
Fe, adsorption of ethoxysilanes 77−89639
Fe, adsorption of N_2 and NH_3, 80-290K, XPS and UPS obs. 77−31901
Fe, adsorption of O_2, oxide formation, XPS/UPS obs. 77−85074
Fe alloy, corrosion inhibition, chem. nature and struct. of protective films 77−60001
Fe base amorphous alloys, alloying element role in improving corrosion resist., ESCA study 80−50754
Fe complex, $[Fe(CN)_6]^{3-}$, electronic struct., optical transitions, XPS, Mossbauer isomer shift, valence ionisation pot., SCF-MSX calc. 79−6864
Fe complexes, paramag., XPS, temp. depend. 79−15582
Fe, desorption of $O_2(N_2)$, surface anal., XPS appl. 79−24875

X-ray photoelectron spectra continued
Fe, electronic structure, influence of temp. 77−28681
Fe, evaporated, adsorbed acetylacetone, XPS study 80−76133
Fe, excitation of 1s core-level photoelectrons with synchrotron radiation 78−19632
Fe F2 (Fe F3), electronic struct., binding energy, X-ray emission and photoelectron spectra obs. 80−35008
Fe film, chemisorption of O_2 and water vapour, XPS obs. 77−48587
Fe industrial catalysts for NH_3, XPS studies 79−70370
Fe, inner level ESCA spectra, many particle effects *(Russian)* 79−91560
Fe, K shell photoelectric cross section, at 74.409 keV 79−72288
Fe, molecular adsorption and dissociative chemisorption of N_2, XPS obs. 79−99427
Fe, oxide and benzoic acid film exam. by X-ray photoemission spectroscopy 78−88561
Fe oxides, interatomic interaction by XPS 80−7474
Fe surface, form. and decomp. of nitrides 79−24831
Fe, XPS line intensity ratios for outer electron shells 79−100018
Fe, XPS obs. of Fe 2p states 78−52625
Fe^{2+} d^6-complexes and oxides, spin-state transitions, PES study 79−100014
Fe-Al (8 at.%), XPS investig. of cond. band region 77−16456
Fe-Al(Si)(Ga)(Ge)(As)(Sn)(Sb), dil., XPS meas. 77−63538
Fe-B amorphous alloys, valence band spectrum, XPS study 80−50534
Fe-Cr, mechanically polished, XPS determ. of comp. of surface and surface oxide 78−7074
Fe-Cr, nondestructive in-depth surface anal. by XPS with different excitation X-ray energies 79−20328
Fe-Cr, passivity in H_2SO_4, XPS study 78−44256
Fe-Cr, surface composition change caused by heating in high vacuum, XPS obs. 78−44254
Fe-Fe_2O_3 composite mixture, preferential sputtering, XPS expts. 79−87544
Fe-Ni, and Fe-Ni-Cr alloys, preferential sputtering, XPS expts. 79−87544
Fe-Ni, XPS obs. of Fe 2p states 78−52625
Fe-Ni alloys, electronic struct. by XPS obs. 79−33226
Fe-Ni alloys, electronic struct., XPS study 80−29842
Fe-Ni alloys, XPS of valence electrons *(Russian)* 77−77340
Fe-O system, initial oxidation, combination anal. using ESCA, AES and SIMS 78−72924
Fe+H_2O, clean surface oxidation and passivation by H_2O vap. 77−81424
FeAl, bonding, self-consistent energy bands 78−91610
$FeAsO_4$, XPS of cryst., inner shell binding energies of elements 79−43092
FeB and Fe_2B, ESCA and mag. spin data, electronic struct., isomer shifts, valence bands and chemical bonding 80−75489
FeB and Fe_2B, multiplet splitting of ESCA Fe 3s core levels 80−29847
$Fe_{80}B_{20}$, metallic glass, high-resolution XPS study, electronic state struct. 80−29846
FeF_2, valence-electron density of states, XPS meas. 77−69963
Fe_xGe_{1-x} amorphous film, XPS and Mossbauer exam. 79−56577
$Fe_{32}Ni_{36}Cr_{14}P_{12}B_6$, metallic glass, high-resolution XPS study, electronic state struct. 80−29846
$Fe_{40}Ni_{40}P_{14}B_6$, metallic glass, high-resolution XPS study, electronic state struct. 80−29846
FeO, valence band XPS and UPS, LCAO-MO calcs. 80−45197
FeO, XPS and UPS 79−91565
$Fe_{1-x}O$, surface struct., XPS study 80−20759
Fe_2O_3, core and valence level XPS spectra meas. 78−15290
Fe_2O_3, Fe_3O_4, α-FeOOH, γ-FeOOH, X-ray photoelectron spectra 77−73483
Fe_2O_3, XPS and UPS 79−91565
Fe_3O_4, core and valence level XPS spectra meas. 78−15290
Fe_3O_4, XPS and UPS 79−91565
Fe_xO, core and valence level XPS spectra meas. 78−15290
Fe_xO, wustite, width of d-level final-state struct. obs. in XPS 78−19633
FeOOH, core and valence level XPS spectra meas. 78−15290
αFeOOH, core line X-ray photoelectron spectra 78−7263
$Fe_{1-x}(P,B)_x$, amorphous and crystalline, photoemission and band structure 80−60754
$FePO_4$, XPS of cryst., inner shell binding energies of elements 79−43092
$Fe_{1-x}Pd_x$ film, air-exposed, comp. profiles by AES, ESCA and ion sputtering 78−95245
$Fe_{1-x}Pd_x$ film, vac. deposited, oxidation and corrosion, AES, XPS and STEM obs. 79−100286
FeS_2, core-level and valence-band XPS 80−93450
FeS_2, superficial degradation in air and water, XPS obs. *(French)* 80−89110
FeSi and $FeSi_2$, inner level ESCA spectra, many particle effects, hole lifetime *(Russian)* 79−91560
FeSi, $FeSi_2$, valence shell XPES 79−43105
FeTi, surface and mag. props., heat treatment and hydrogenation effects 80−75447
FeTi, surface segregation and catalytic effect on hydrogenation, AES and XPS study 79−11626
Fe(100), CO and H_2 adsorption and desorption, C, O, S and K adlayer effects 80−71573
Fe(111) surface, interaction with hydrazine, UPS and XPS 79−46956
Fu-polymer composite foils, fracture surface exam. *(German)* 78−84992
Ga, effect of $L_1L_{2,3}M$ Coster-Kronig processes on $L_{2,3}MM$ Auger spectrum 78−72681
Ga, LMM Auger spectra, rel. to L_{23} photoelectron spectra 77−77348
Ga, LMM Auger spectra, transition probabilities, term splittings and effective Coulomb interaction 77−44126
GaAs (110), adsorption of O_2, oxide form., XPS/UPS study 80−49497
GaAs (110), coadsorption of Cs and O_2, initial oxidation, soft XPS obs. 80−10793
GaAs (110), initial oxidation, XPS and AES study 80−11542
GaAs (110), with ultrathin Al and Cs overlayers, O_2 adsorption, comparative studies 80−50740
GaAs (110) cleaved surface, oxidation, XPS exam. 78−31551
GaAs (110) surface, chemisorption of O_2, electronic struct. theory, oxidation, electron spectra interpretation 79−42376
GaAs (110) surface oxidation process, XPS study 79−15585
GaAs (110) surfaces, ordered and disordered, O_2 adsorption, XPS meas. 80−49498

X-ray photoelectron spectra continued
GaAs (110)-Al interface, XPS study of interface interaction, Al proximity effects and replacement reaction 79−100019
GaAs (111) and $(\bar{1}\bar{1}\bar{1})$ surfaces, XPS study 79−83102
GaAs anodic films, XPS study 80−71562
GaAs, anodic oxide layers, chem. depth profiles, XPS determ. 80−3222
GaAs, $CO(O_2)$ interactions, surface electronic struct. (surface chem.) using synchrotron radiation 78−53254
GaAs, chem. prep. of surfaces, and AES and XPS characterisation 77−90477
GaAs, clean and oxidised surfaces, O_2 sticking coeff., ionicity effects 77−85887
GaAs film, RF sputtered, ESCA, surface chemistry suitability for photovolt. appl. 80−7476
GaAs interface with anodic and thermal oxides, comparison of AES and ESCA 78−95980
GaAs, LMTO self consistent band struct. calc. 80−20078
GaAs, oxidation, water vapour and O_2 excitation effects, XPS obs. 79−100274
GaAs oxide film, thermal and anodic, in-depth profiles, XPS expts. 78−84086
GaAs oxide films, anodically and thermally grown, XPS study 80−16141
GaAs oxide layers prepared by anodic, thermal and plasma oxidation, in-depth profiles and annealing effects 79−61768
GaAs, polycryst., wet and dry oxides, comparative study by AES, SIMS and XPS 80−80116
GaAs, shallow core level spectra 80−104037
GaAs solar cell, polycryst., grain boundary passivation by oxidation, AES, SIMS and XPS obs. 80−81467
GaAs surface, O_2 sorption and excitonic effects, photoemission expts. 77−85055
GaAs, surface (111), $(\bar{1}\bar{1}\bar{1})$, (110), XPS, photo-Auger ionisation cross section, electron mean free paths 78−56558
GaAs, surface cryst. regularity by X-ray photoelectron diffr. 80−89112
GaAs surface states obs. by XPS 80−50515
GaAs, surface states XPS 80−25528
GaAs, surface studies during MBE growth 79−90899
GaAs thin films, reactively sputtered, ESCA/XPS study 80−97430
GaAs, XPS, secondary illumination effects, band bending, level shifts 80−108324
GaAs-Au(Ag) Schottky barrier solar cells, interface problems, AES, SIMS and XPS study 80−89627
GaAs-metal Schottky barrier contacts, interface chemistry 79−74049
GaAs-oxide interfaces, local atomic and electronic struct., high resolution XPS 80−49927
$GaAsO_4$, XPS of cryst., inner shell binding energies of elements 79−43092
GaAs(111), O bonding, thermodesorption and ESCA meas. 77−86206
GaN, electron struct., ESCA study 80−89116
GaN, interatomic interactions from XPS 80−49171
GaN on Si, form. with GaCl-NH_3-H_2(He), ESCA and RHEED meas. 79−90909
GaP (110), initial oxidation, XPS and AES study 80−11542
GaP (110) surface oxidation process, XPS study 79−15585
GaP, oxidation, water vapour and O_2 excitation effects, XPS obs. 79−100274
GaP, photoemission from (111) and $(\bar{1}\bar{1}\bar{1})$ surfaces 79−91562
GaP surface, quantitative XPS meas. 78−56559
$GaPO_4$ film growth on GaP, XPS exam. 78−31552
$GaPO_4$, XPS of cryst., inner shell binding energies of elements 79−43092
GaS, shallow core level spectra 80−104037
GaS, XPS and valence band density of states, tight binding approx. 78−63974
GaSb surface, quantitative XPS meas. 78−56559
GaSb-Au structure, metal-semicond. interaction, soft XPS meas. 78−60203
GaSe, shallow core level spectra 80−104037
GaSe, spatial symm. of valence band struct. by angularly resolved XPS 77−69961
Gd and Gd-Al alloys, XPS valence band spectra meas. 77−48306
Gd, X-ray photoabsorpt. near 3d edges 77−38645
$GdCoO_3$, spin state of Co^{3+} ion, X-ray photoemission line broadening 79−82751
GdFe, amorphous films, thermal stability of mag. props. *(Japanese)* 79−47307
GdFe(Co), amorphous film, XPS meas. 79−87295
$Gd(OH)_3$, mol., XPES, satellite phenomena 79−27035
Ge, amorphous and crystn. films, contamination behaviour, XPS examin. 79−1815
Ge, chemisorption of O(1s) 77−69170
Ge, electron scattering, inelastic, 70-1400 eV, mean free path 78−84696
Ge film, amorphous, vac. deposited, XPS and elec. props., evidence for polycryst. phase 77−28691
Ge, inelastic mean free path in 700 to 1200 eV range, bulk method 80−20763
Ge, ion implanted, cond. and valence bands study by X-ray bremsstrahlung and photoelectron spectra 80−2360
Ge, LMM Auger spectra, rel. to L_{23} photoelectron spectra 77−77348
Ge, LMM Auger spectra, transition probabilities, term splittings and effective Coulomb interaction 77−44126
Ge, valence band relaxation energies during XPS 78−39657
Ge, valence electrons, XPS, LCAO and OPW calc. 77−12496
Ge/GaAs (110) heterojunction, valence band discontinuity in XPS spectra, precise determ. 80−84834
Ge-GaAs abrupt interface, orientation depend. of interface dipole energies, XPS expts. 78−39196
Ge-GaAs interface, XPS obs. of electronic struct. 78−95341
Ge-rare earth alloys, nature of chemical interaction, X-ray emission, absorpt. and photoelectron study *(Russian)* 80−55261
GeAsS, X-ray photoelectron spectra, valence electrons density of states *(Russian)* 79−15583
GeS, amorphous, UPS and XPS, valence band struct. 77−90247
GeS(Se)(Te), XPS investig. of valence band struct. 77−48311
GeSe, amorphous, UPS and XPS, valence band struct. 77−90247
GeTe, amorphous, UPS and XPS, valence band struct. 77−90247
H_3BO_3, chem. bonding, electronic struct., ESCA, Auger, and SIMS spectra 80−50512
HCN, vibr. fine struct. accompanying core ionis., STO calcs. 78−62844
HCl, mol., XPS and KLL Auger effect, line shifts 79−31602

X-ray photoelectron spectra continued
$H_{1.6}MoO_3$, electronic props., mag. susceptibility and spectra 80−80266
H_2O, core 1s shakeup study, XPS and Xalpha calcs. 80−69064
H_2O, photoelectron spectra, 21.2-151.4 eV and soft X-ray, ionis. cross-section 78−37583
H_2O, trace element anal. by ESCA 77−66779
H_2O_2, gas phase XPS, binding energy 77−34689
H_2S, gas-phase, states in valence photoelectron spectrum 78−94284
H_2S, gaseous 1s binding energy and S $KL_2L_3(^1D_2)$Auger energy, XPS obs. 77−3416
H_2S, mol., XPS and KLL Auger effect, line shifts 79−31602
$H_2W_{12}O_{40}^{6-}$, XPS spectra, oxidation states 78−6824
H_xWO_3 bronzes, Anderson transition, XPS 80−107705
H_xWO_3, crystalline, band struct., XPS meas. 77−59667
He(I), 80−63599
He(II), 80−63599
Hf, valence band XPS, correl. to supercond. 79−65980
HfC_xN_{1-x}, X-ray valence photoelectron spectrum, 4f signal calc. 80−66391
$HfC_xN_yO_z$, valence band XPS, correl. to supercond. 79−65980
Hg, ESCA spectra from 132.3 eV YMζ radiation source 77−4958
Hg, electron binding energy and shift, core level XPS 80−87088
Hg, L-shell X-ray photoelectric cross sections, fluorescence spectra 78−58636
Hg-As-S system glasses, photoelectron X-ray spectroscopy study 80−29858
$Hg_{0.8}Cd_{0.2}Te$ surface, sputter cleaning and dry oxidation, XPS and LEED study 80−108618
HgTe surface, sputter cleaning and dry oxidation, XPS and LEED study 80−108618
$HoCoO_3$, spin state of Co^{3+} ion, X-ray photoemission line broadening 79−82751
Ho_2O_3, XPS, charging effects on core-level binding energies 79−24409
I compounds, XPS, binding energies and bond orders 77−18976
I, photoelectron spectra, strong many electron effects from core levels 77−18862
I_2, $M_{4,5}N_{4,5}X$ Auger electron spectra, many-body effects 79−59415
In, chemisorption of O_2, XPS and static SIM spectral study 80−80055
In, core level binding energies 80−71564
In film, oxidation, XPS excited by Zr Mζ radiation 80−40236
In film, oxidized polycrystalline, spectra obtained from combined XPES and SIMS investigation of surface 80−52377
In film, RF plasma oxidised, surface analysis using ESCA 80−50742
In, outer core d level linewidths determ. using synchrotron radiation 77−44118
In, oxidised surface, bonding of Cd arachidate monolayers, XPS 79−15011
In, photoelectric cross sections at 52.4, 60, 72.2 and 84.4 keV 80−69187
In, photoionisation cross section of d-core level synchrotron radiation study of spin-orbit branching ratio 79−74057
In, quantitative surface anal., comparison of XPS results with model 78−40091
In surface, impurity precipitation and resolution at melting point 78−14553
In, ultra soft X-ray photoelectron energy loss study, angle and energy dependence 78−23582
In, XPS and $M_{4,5}N_{4,5}N_{4,5}$ Auger spectra 79−61472
InN film growth by reactive sputtering in Ar-N_2 discharge, mechanism 80−89107
InN, thin film, characterisation using XPS electron energy loss spectra 79−87561
In_2O_3, thin film, characterisation using XPS electron energy loss spectra 79−87561
In_2O_3-InN film growth by reactive sputtering in N_2-O_2 discharge, mechanism 80−89108
In_2O_3-SnO_2 film, XPS expts., energy band model accounting for phys. props. 77−90241
InO_xN_y, thin film, characterisation using XPS electron energy loss spectra 79−87561
InP interface with anodic and thermal oxides, comparison of AES and ESCA 78−95980
InP surface, interaction with Cl, electron spectroscopic obs. 78−56036
In_2S_3, valence band densities of states, XPS meas. 79−28892
InSb (110), initial oxidation, XPS and AES study 80−11542
InSb (110) surface oxidation process, XPS study 79−15585
InSb, oxidation, water vapour and O_2 excitation effects, XPS obs. 79−100274
InSb, single crystal, chem. and ion etching, surface changes *(French)* 80−108614
InSb, surface analysis, X-ray photoelectron spectra, surface oxidation-etchant correlation 78−56029
InSe, band structure, XPS, UPS and tight-binding calc. 77−47727
InSe thin film, sputter growth and chem. anal. by XPS/ESCA 80−80976
InSe, two-dimensional band struct., XPS meas. and tight-binding calc. 78−2419
InSe, X-ray photoemission intensity, nearest-neighbour backscatter 79−65977
Ir (111), chemisorption of CO, UPS and XPS obs., comparison with Pt 78−38942
Ir (111) surface, chemisorption of O_2, dynamics, XPS meas. 77−59211
Ir (111) surface, kinetics of CO oxidation reaction, appl. of XPS 77−31886
Ir (111) surface with preadsorbed O, titration by CO, XPS investigation 79−91994
Ir, chemisorbed CO, XPS and UPS 77−16450
IrO_2, electronic struct., XPES obs., rel. to TiO_2, RuO_2 78−52632
Ir(111), O_2 chemisorption, XPS obs. 77−20190
K, adsorbed on Fe(100), adsorbate coverage determ. by LEED, AES and XPS 80−103566
K adsorbed on Fe(110), UPS and XPS meas. 80−95675
K adsorbed on Pt(111), UPS and XPS meas. 80−95675
K, atom, XPS, free atom core binding energy 78−74699
K surface, clean and O_2-exposed, X-ray and UV photoelectron spectra 78−52636
KBO_2, vapour over heated solid, XPS, obs. 80−87171
$KCoF_3$, multiplet struct. in XPS spectra of 3p and 3s subshells 78−43981
$KCoF_3$, XPS of band struct. 77−11851
$KCuF_3$, multiplet struct. in XPS spectra of 3p and 3s subshells 78−43981
X-ray photoelectron spectra continued
$KCuF_3$, XPS of band struct. 77−11851
$KFeF_3$, multiplet struct. in XPS spectra of 3p and 3s subshells 78−43981
$KFeF_3$, XPS of band struct. 77−11851
K_2FeO_4, XPS of hexavalent iron binding energies calcs. 80−43013
KH_2PO_4 and related substances, electronic structures study *(Japanese)* 79−87463
KH_2PO_4, electronic struct., UV reflection spectra and XPS 79−38558
KH_2PO_4:AsO_4^{4-}-(SeO_4^{2-}), ferroelec., low freq. fluctuations, isotope effects, EPR, ENDOR, ESCA 77−73118
KI, mean free paths of 200-1500 eV electrons, XPS determ., model calc. 79−38715
KMF_3, M=Mg, Mn, Ni, band struct., excitons 77−20871
$KMnF_3$, multiplet struct. in XPS spectra of 3p and 3s subshells 78−43981
$KMnF_3$, XPS of band struct. 77−11851
$KNbO_3$, electronic props., SCF-MS-Xα calc. 80−54607
$KNbO_3$, electronic struct., XPS and band struct. calc. 79−38708
$KNbO_3$, XPS, band struct., density of states, photoionisation cross sections 78−52629
$KNiF_3$, multiplet struct. in XPS spectra of 3p and 3s subshells 78−43981
$KNiF_3$, XPS of band struct. 77−11851
K_2SO_3-Ag_2SO_4 mixtures, surface comp., AES and XPS obs. 80−81386
$KTaO_3$, electronic props., SCF-MS-Xα calc. 80−54607
$KTaO_3$, electronic struct., XPS and band struct. calc. 79−38708
K_2UF_6, electronic structure 77−32491
KX, (X=F, Cl, Br), photoelectron spectra using Zr Mζ, Al Kα and other X-ray lines, photoionis. cross sections ratios 77−90246
$KZnF_3$, multiplet struct. in XPS spectra of 3p and 3s subshells 78−43981
$KZnF_3$, XPS of band struct. 77−11851
$K[Fe_4S_3(NO_7)]$, valence levels, X-ray photoelectron and X-ray spectra 77−88500
Kr, 3p X-ray photoelectron spectrum, many-electron effects 78−50513
Kr, atomic, XPS calc. 78−958
Kr, ESCA, lifetime broadening, CI resonances 77−18853
La and La-Al alloys, XPS valence band spectra meas. 77−48306
La^{2+}, XPS in oxide and chromite, multicomponent struct. of 4d orbital 78−74620
La-Sm-Au, amorphous, surface effects on Sm valence, XPS and X-ray absorption meas. 80−108325
LaB_6 (001) surface, struct., initial oxidation, XPS, UPS, LEED, AES, work function meas. 79−99403
LaB_6, (001) surface struct., XPS, LEED meas. 78−63909
LaB_6 (100), (110), and (111), surface structs. and work functions 80−70512
LaB_6 (210) surface, work function, struct. and chemisorpt. stability, XPS, UPS and LEED 80−65344
LaB_6, surface (100), atomic struct., angle-resolved XPS, LEED and ISS investigation 80−10765
LaB_6, synthesis and props., review *(Japanese)* 80−40255
LaB_6, thermionic emission rel. to surface state 78−39654
LaB_6, UPS and XPS of valence band 78−84703
LaB_6(001) surface, struct. and initial oxidation, UPS, XPS and work functions meas. 77−86195
$LaCo_5N_n$, formation by N_2 absorpt. by $LaCo_5$ 80−24599
$LaCoO_3$, spin states, XPS meas. 78−68599
$LaCrO_3$, spin states, XPS meas. 78−68599
$LaFe_{1-x}Co_xO_3$, UPS, XPS, X-ray absorpt. spectra, band struct. study 79−56885
$La_{1-x}M_xCrO_3$, M=Mg, Sr, electronic struct. study by XPS 80−25518
$LaNi_{1-x}Fe_xO_3$, UPS, XPS, X-ray absorpt. spectra, band struct. study 79−56885
$LaNi_{1-x}Co_xO_3$, UPS, XPS, X-ray absorpt. spectra, band struct. study 79−56885
La_2O_3, electronic struct. study by XPS 80−25518
LaOF, features of formation of band structure 79−33232
$La(OH)_3$, mol., XPES, satellite phenomena 79−27035
La_2O_2S:Tb, cathodoluminesc. efficiency changes due to processing, XPS meas. of surface changes 79−99951
$La_{1-x}Pb_xMnO_3$, spin polarised XPS and UPS, elec. struct. 77−8717
$LaTiO_3$, spin states, XPS meas. 78−68599
Li electrode, in lithium perchlorate-propylene carbonate solution, surface anal. *(French)* 80−50859
Li film, XPS lineshapes, many body processes 78−39663
Li, soft X-ray spectra, phonon broadening calc. 77−63526
Li, surface characterization of film growth 80−81240
$LiBrO_3$, radiation damage, XPS obs. 80−29844
LiC_6, intercalation compound, electronic struct., XPS meas. 80−59850
LiCl, photoelectron spectra using Zr Mζ, Al Kα and other X-ray lines, photoionis. cross sections ratios 77−90246
$LiClO_4$, radiation damage, XPS obs. 80−29844
$LiCoO_2$, XPS of low spin Co (III) 78−31300
LiF, photoelectron spectra using Zr Mζ, Al Kα and other X-ray lines, photoionis. cross sections ratios 77−90246
LiH, valence band struct., XPS exam. 79−69416
$LiIO_4$, radiation damage, XPS obs. 80−29844
$LiNO_3$, electron irrad. damage, XPS obs. 78−64444
$LiNbO_3$, optical waveguide, Ti diffusion, XPS 77−11014
$LiNbO_3$ surfaces, ion and electron bombard., photoelectron spectroscopy and electronic props. 80−71559
$LiNbO_3$, XPS and UPS from surface defects 80−76136
$LiNbO_3$, XPS core line intensities, electron escape depth 79−100025
Li_2SO_4, electron irrad. damage, XPS obs. 78−64444
Li_2WO_4, electron irrad., reduced species form., XPS 79−11498
Li_xWO_3, band struct., XPS meas. 77−59667
LuH_2, synchrotron XPS obs., rel. to theory for metal dihydrides 80−55275
Lu_2O_3, XPS, charging effects on core-level binding energies 79−24409
Lu_2S_3, XPS, binding energies 79−15586
Lu_3S_4, XPS, binding energies 79−15586
Mg, adsorption of O_2, at 100 and 300K, XPS, UPS and X-ray AES meas. 78−18901
Mg, atom, XPS, free atom core binding energy 78−74699
Mg, core-level XPS, electron energy loss spectra, intrinsic and extrinsic plasmons 77−63532
Mg, electronic density of states 78−6829
Mg film, XPS lineshapes, many body processes 78−39663
Mg, plasmon struct. of core lines in XPS meas. 77−63530

X-ray photoelectron spectra continued
Mg, plasmon-loss intensities in XPS, EELS and Auger spectra 80−10902
Mg, polycryst., adsorpt. of O_2 at 100 and 300K, XPS, UPS, XAES 78−18906
Mg, XPS, plasmon gains as monitor of incomplete relax., interference effects and sudden to adiabatic limits transition 80−66390
Mg, XPS theory, core level spectra, plasmon creation 78−72701
Mg-Cd, plasmon loss and plasmon gain, X-ray photoemission and AES 79−23918
MgAg, Auger spectra, 4d bandwidth effect 80−89093
$MgCl_2$, partially hydrated powder surface, electron beam effects, XPS obs. 79−33900
Mg_2Cu polycrystals, surface study by AES, XPES and X-ray induced AES 80−65346
MgF_2, core-electr peaks, satellite and loss structs. 77−66571
MgF_2, interatomic Auger transitions, XPS exam. 77−8692
MgO, catalytic behaviour, rel. to XPS obs. 79−24820
MgO, electronic struct., XPS meas. 77−73217
MgO, XPS valence bandstruct. 80−89117
MgO:M^{2+}, M=Co, Ni, Cu, next-nearest-neighbour ion effects on impurity 2p levels 77−20987
MgO-Al_2O_3 system, surface microphases investigation by X-ray electron spectral anal. 79−51269
MgO-ZnO, solid soln., surface comp., Auger and XPS investig. 78−51806
Mn oxides, XPS study, electron binding energies, spin orbit splittings, exchange splittings 79−78839
Mn-Ag, XPS meas., Fermi level to 1000 eV below it 80−66389
MnAg alloys, XPS meas. 80−60751
MnF_2, d-orbital directed photoemission using AlK_α radiation 79−95901
MnF_2, valence-electron density of states, XPS meas. 77−69963
MnO_2, UV irradiated, XPS rel. to Viking gas exchange reaction on Mars 80−72831
MnO_4^-, electronic struct. determ. from X-ray spectra 78−86885
$MnS_2(Se_2)$, core-level and valence-band XPS 80−93450
MnS(Se)(Te), core level binding energies and valence band spectra, XPS meas. 78−80455
MnSb, electronic struct., XPS meas. 78−2990
MnSi, Mn_5Si_3, valence shell XPES 79−43105
Mo complexes, dinitrogen type and derivs., XPS 77−75216
Mo complexes, electronic struct., XPS and X-ray emission spectra 77−42336
Mo film on Si surface, $MoSi_2$ form. conditions *(French)* 78−43270
Mo halides and complexes, low oxidation state, XPS 77−75215
Mo, monolayer, oxidation, quasisimultaneous SIMS, AES, XPS 78−72919
Mo X-ray electron spectra, paramag. susceptibility, depend. on plastic deform. for single crystals 77−28683
Mo-Al_2O_3, catalysts, reducing and sulphiding treatments, XPS obs. 78−85196
Mo-O system, initial oxidation, combination anal. using ESCA, AES and SIMS 78−72924
MoN, interatomic interactions from XPS 80−49171
MoO_2, photoelectron spectra, X-ray and UV polycrystalline 79−28889
MoO_3, ESCA of surface composition changes under ion bombardment 77−20974
MoO_3, ESCA on H_2 reduction *(French)* 77−36365
MoO_3 film, electrochromism, X-ray electron spectra 78−48146
MoO_4^{2-}, valence level electron struct. by XPS 77−4712
MoS_2 film, adhesion to oxidised metal surfaces, XPS meas. 78−22972
MoS_2, spatial symm. of valence band struct. by angularly resolved XPS 77−69961
MoS_2, struct., XES and XPS obs. 80−43105
MoS_3, amorphous struct., X-ray radial distrib. anal. and XPS 80−49115
N containing molecules, N NMR, nuclear mag. shielding, X-ray photoelectron spectra 78−17695
N_2, core photoelectron line shape, localisation role 79−59512
N_2, ESCA spectra from YMζ radiation source, 132.3 eV 77−4958
N_2, NO, N_2O, dry air, chemisorbed on transition metals at high pressures, XPS 77−20990
N_2, photoelectron spectra, 21.2-151.4 eV and soft X-ray, ionis. cross-section 78−37683
N_2, shake-up peak positions and intensities calcs. using eqns. of motion Green's function method 78−86910
N_2, valence electron spectra, excited by YMζ and $AlK\alpha$ ESCA sources 78−53301
N_2, vibr. struct. of K_α emission spectra 78−86886
N_2^++first row transition metal surface reactions 79−96363
N_2^++Group IV elements and oxides, XPS and UPS prod. determ. 78−73084
NH_3, core 1s shakeup study, XPS and Xalpha calcs. 80−69064
NH_3, photoelectron spectra, 21.2-151.4 eV and soft X-ray, ionis. cross-section 78−37683
NH_3, solid, AES excited by X-rays 79−33894
NH_3, vibr. excitation in soft X-ray emission and core ESCA spectra 80−69163
$NH_4H_2PO_4$, electronic struct., UV reflection spectra and XPS 79−38558
$NH_4H_2PO_4$, ferroelec., electronic struct. study *(Japanese)* 79−87463
$NH_4H_2PO_4$:AsO_4^{4-}(SeO_4^{3-}), antiferroelec., low freq. fluctuations, isotope effects, EPR, ENDOR, ESCA 77−73118
NH_4NO_3, shock-induced intramol. bond breaking, XPS and EPR study 80−76512
NO, core photoelectron line shape, localisation role 79−59512
N_2O, photoelectron spectrum, vibronic interaction and autoionis. effects 80−95680
Na, atom, XPS, free atom core binding energy 78−74699
Na, core-level XPS, electron energy loss spectra intrinsic and extrinsic plasmons 77−63532
Na, electronic density of states 78−6829
Na film, XPS lineshapes, many body processes 78−39663
Na, KLV Auger line shape, one-orthogonalised plane wave calc. 77−48316
Na, plasmon struct. of core lines in XPS meas. 77−63530
Na, soft X-ray spectra, phonon broadening calc. 77−63526
Na, XPS, plasmon gains as monitor of incomplete relax., interference effects and sudden to adiabatic limits transition 80−66390
Na, XPS theory, core level spectra, plasmon creation 78−72701
NaA-zeolites, analytical and struct. information 77−90239
NaBr-H_2O, quick-frozen aq. soln., XPS 79−38713
NaCl-H_2O, quick-frozen aq. soln., XPS 79−38713

X-ray photoelectron spectra continued
$NaClO_3$, radiation damage, XPS obs. 80−29844
$NaClO_3$ trapped O species in irradiated samples, low-temp. X-ray photoelectron spectroscopy 78−27799
NaF, interatomic Auger transitions, XPS exam. 77−8692
NaF-H_2O, quick-frozen aq. soln., XPS 79−38713
NaI-H_2O, quick-frozen aq. soln., XPS 79−38713
NaNCO, val. band electronic struct., XPS meas., MOC and INDO calc. 80−95520
$NaNO_3$-H_2O, quick-frozen aq. soln., XPS 79−38713
Na_2O-P_2O_5 glass, XPS quantitative struct. anal. 80−2917
Na_2O-SiO_2 glass, bridging to non-bridging ratio and correl. to glass density and refr. index, ESCA study 80−84832
Na_2O-SiO_2-NiO systems Ni ions anal. by ESCA *(Japanese)* 80−40787
Na_2SO_4-H_2O, quick-frozen aq. soln., XPS 79−38713
Na_xWO_3, band struct., XPS meas. 77−59667
Na_xWO_3 bronze, oxidation state of W, oxidation by air exposure 77−8719
Na_xWO_3 bronze, XPS of W 4f levels 78−95648
Na_xWO_3, cubic, final-state effects in XPS 77−90251
Na_xWO_3, metallic, XPS, initial and final states, WO_3 binding energy 79−95898
NaX, (X=F, Cl, Br), photoelectron spectra using Zr Mζ, Al Kα and other X-ray lines, photoionis. cross sections ratios 77−90246
Na(1s), X-ray photoelectron spectrum, binding energy, at. compared with metal 78−70800
$Na_2[Fe(NO)_2(S_2O_3)]_2$, valence levels, X-ray photoelectron and X-ray spectra 77−88500
Nb electrode, surface changes induced by strong cathodic polarisation 79−100388
Nb film, sputter-deposited on stainless steel, electron microscopy and ESCA 77−52554
Nb films, oxidation, XPS study 80−80944
Nb, K shell photoelectric cross section, at 74.409 keV 79−72288
Nb, oxide growth and oxide coatings, XPS and AES studies 80−50765
Nb oxides, XPS study, electron binding energies, spin orbit splittings, exchange splittings 79−78839
Nb-NbO_x-Pb superconductive tunnel junctions, oxide tunnelling barriers, ESCA characterisation 80−65745
NbC, valence band struct. *(Russian)* 78−6268
NbC, valence band XPS meas., comparison with X-ray emission spectra and band struct. spectral calcs. 80−50535
Nb_3Ge, superconducting hybridisation and bonding, XPS exam. 78−2988
NbN, interatomic interactions from XPS 80−49171
NbO_2, photoelectron spectra, X-ray and UV polycrystalline 79−28889
$Nb_3Os(Ir)(Pt)(Au)$, XPS of valence electrons meas. 77−21003
$Nb_3Se_5Cl_7$, preparation, struct. and props. 79−65040
Nd, photoelectric cross sections at 52.4, 60, 72.2 and 84.4 keV 80−69187
$Nd(OH)_3$, mol., XPES, satellite phenomena 79−27035
Ne, photoelectron spectra, 21.2-151.4 eV and soft X-ray, ionis. cross-section 78−37683
Ni (001), adsorbed CO c(2×2), surface geometry determ. by deep-core-level XPS 80−40224
Ni (001), photoelectron diffr. effects in core-level photoemission 80−76144
Ni (001)/CO(O) system, adsorbate geometries determ. from final state scattering in X-ray photoemission 80−54488
Ni (100), adsorption of CO, SIMS and XPS meas. 79−42378
Ni (100), adsorption of water $(O_2)(H_2)(CO)$, combined XPS/LEED/SIMS exam. 79−83075
Ni (100), chemisorption of O_2, SIMS and XPS 79−15019
Ni, adsorption of acetic acid and ethylenediamine, XPS study 80−76132
Ni, Ar ion implantation $1S_{1/2}O$, $1S_{1/2}t$ and $2P_{3/2}Ni$ states 80−16149
Ni, band struct. and multielectron excitations, angle-resolved photoemission determ. 80−76147
Ni, bound hole pairs, XPS study, satellite peaks 80−40218
Ni, chemisorption of NO, XPES meas. 79−77922
Ni, clean; chemisorpt. of S-containing alkanes, XPS and thermal desorpt. with mass spectrometric anal. 78−14595
Ni, electronic structure, influence of temp. 77−28681
Ni, electronic structure, photoelectron spectra, theory 80−80168
Ni, evaporated, adsorbed acetylacetone, XPS study 80−76133
Ni films, HCP and amorphous, RF sputtered, O_2 incorporation, ESCA obs. 80−10832
Ni, growth on amorphous C, electronic props., UPS and XPS obs. 79−82476
Ni halides, XPS, multiplet struct. and multielectron excitations, in 3 p and 2p shells 80−78649
Ni II acetylacetonate, XPS 80−74196
Ni intermetallics and oxide, interatomic interaction by XPS 80−7474
Ni, K shell photoelectric cross section, at 74.409 keV 79−72288
Ni, $L_3M_{23}M_{23}$ Auger energy calc. using XPS, effect of 3d-4s admixed screening on relax energies 77−1782
Ni, $M_{II,III}$ spectrum, ab initio calculation 80−83276
Ni, oxidation study by X-ray photoelectron spectroscopy 79−61787
Ni, passive film, XPS study 79−100469
Ni photoelec. cross sections, 5-40 keV photons, X-ray emission spectra 77−18866
Ni, photoelectric cross sections at 52.4, 60, 72.2 and 84.4 keV 80−69187
Ni, quasi-particle energies, two-hole XPS satellite 80−66399
Ni, surface, d-band narrowing, obs. using angle-resolved XPS 80−11062
Ni, vapour deposited on polystyrene, core-level spectra 79−56911
Ni, XPS for band struct. 79−33889
Ni, XPS line intensity ratios for outer electron shells 79−100018
Ni, XPS valence band spectra 77−21007
Ni/Al_2O_3 catalysts, coprecipitated methanation type, metal-support interaction, XPS obs. 80−80936
Ni/polymer interface, electronic struct., XPS study 80−45204
Ni-Al alloys, XPS for band struct. 79−33889
Ni-Cr/$MgSiO_3$, methanation catalysts, S resistant, XPS characterization 79−83506
Ni-Cr(Fe)(Cu) alloy, matrix effect in SIMS anal. using O_2^+ primary beam 80−76576
Ni-Cu alloy, asymmetry of XPS of shell electrons *(Russian)* 78−76579
Ni-Fe, (100) surface, O interaction, LEED and XPS studies 79−82437
Ni-NiO composite mixture, preferential sputtering, XPS expts. 79−87544
Ni-O system, initial oxidation, combination anal. using ESCA, AES and SIMS 78−72924

X-ray photoelectron spectra continued
Ni-P amorphous alloys, electrodeposited and melt-quenched atomic and electronic structures 80−88062
Ni-Pd surfaces, electrochem. passive film form. and comp. determ. by SEM, SIMS, XPS 80−39401
Ni-Zn alloys, XPS for band struct. 79−33889
NiAl, bonding, self-consistent energy bands 78−91610
β'-NiAl, density of states, XPS meas. 78−48284
Ni_3C formation and decomposition during evaporation of Ni onto graphite 79−15055
NiF_2, ESCA, charge transfer satellite struct., hole state localisation intensity depend., MS-MO calc. 77−66139
NiF_2, valence-electron density of states, XPS meas. 77−69963
$NiFe_2O_4$, core line X-ray photoelectron spectra 78−7263
$NiFe_2O_4$, thermally induced surface chemistry and struct., XPS 78−22939
NiO film, formed by Ni galvanic oxidation in borate buffer soln., struct. 80−100948
NiO single crystals, ang. distrib. of X-ray photoelectrons anal. of satellites *(German)* 79−11497
NiO:C, surface charge, O(1s), C(1s) and Ni(2p) XPS 80−45196
NiO/SiO_2, catalyst, XPS for surface struct. and composition 79−43093
$NiO-Al_2O_3/SiO_2$ catalyst, XPS for surface struct. and composition 79−43093
NiO-MgO solid solns., surface comp. study by XPS 80−104035
NiS, semiconductor-metal transition, UPS and XPS 79−23896
$NiS_2(Se_2)$, core-level and valence-band XPS 80−93450
$NiS_2(Se_2)$, electronic struct., UPS and XPS study 80−80935
NiSb, electronic struct., XPS meas. 78−2990
$Ni_{0.96}Sb_{0.04}$, surface segregation, XPS and AES obs. 80−76135
NpO, and NpO_2, electronic struct. and chem. bonding and XPS line shape calcs. 79−33264
NpO_2, XPS meas. 77−48314
NpO_2, XPS of 5f electrons 77−73216
O, adsorbed on Fe(100), adsorbate coverage determ. by LEED, AES and XPS 80−103566
O bonding to Tokamak walls, XPS studies 80−80942
O_2, core photoelectron line shape, localisation role 79−59512
O_3, core electron binding energies, XPS, Xα scatt. wave calcs. 77−75332
OF_2, core electron binding energies, XPS spectra 77−3417
Os, ESCA on in situ cleaned surface 79−83101
OsO_4^{2-}, valence level electron struct. by XPS 77−4712
P, amorphous, stability in air, XPS study, comparison with cryst. polymorphs 80−25517
P, amorphous, XPS anal. of stability, form. of oxidised layer *(German)* 79−11496
P_4, core and mol. orbital XPS spectra, binding energies 77−65508
PF_5, ESCA chemical shift, energy levels, SCC-MO calcs. 79−64045
PH_3, mol., XPS and KLL Auger effect, line shifts 79−31602
P_4S_3, XPS spectra, binding energies, differential photoelec. cross sections ratios 77−65508
Pb (100) and (110) surfaces, oxidation and sulphidation, LEED and XPS obs. 78−20070
Pb and compounds, outer core d level linewidths determ. using synchrotron radiation 77−44118
Pb, inelastic mean free path in 700 to 1200 eV range, bulk method 80−20763
Pb, L-shell X-ray photoelectric cross sections, fluorescence spectra 78−58636
Pb overlayers, on Cu substrate, oxidation, AES and XPS obs. 79−47833
Pb, photoionisation cross section of d-core level synchrotron radiation study of spin-orbit branching ratio 79−74057
Pb, quantitative surface anal., comparison of XPS results with model 78−40091
Pb surface, oxidation, XPS and SIMS study 79−15873
Pb^{2+}, on calcite surface, ESCA, calibration 77−81432
Pb-In(-Au) base electrode film Josephson junctions, tunnel barrier oxide struct. 80−65750
$PbCl_2(Br)(I_2)$, valence band electronic struct., XPS and UPS obs. 78−6826
PbI_2, layered semicond., valence bands UPS and XPS obs. 78−11078
PbI_2, valence-band XPS meas. 77−12487
PbInAu film, RF plasma oxidised, surface analysis using ESCA 80−50742
PbS, superficial degradation in air and water, XPS obs. *(French)* 80−89110
PbS(Se)(Te), chemisorption of O_2, room temp., UPS and XPS obs. 78−91529
PbS(Se)(Te), XPS investig. of valence band struct. 77−48311
PbSe surface, clean and O_2-exposed, XPS (UPS) obs., electronic struct. 78−52637
$Pb_{0.8}Sn_{0.2}Te$ surfaces, oxidation in air and thermal desorption, XPS and LEED meas. 79−47830
$Pb_{1-x}Sn_xTe$ IR detector, ESCA meas., surface leakage currents 77−20402
$Pb_{1-x}Sn_xTe$, MBE, O_2 uptake, AES, XPS and UPS expts. 78−95227
PbTe (111), adsorption of O_2, UPS and XPS exam. 78−71962
PbTe surfaces, oxidation in air and thermal desorption, XPS and LEED meas. 79−47830
Pd, adsorbed CO, photoelectron spectra, 40-180 eV, adsorbate sensitivity enhancement 78−80453
Pd at. N-shell vacancy state widths, X-ray photoelectron, Auger spectra 77−18875
Pd catalytic clusters, electronic structure, XPS obs. 77−77345
Pd, electronic structre, Compton scatt., soft X-ray emission and X-ray photoelectron spectra 79−77999
Pd, film, growth on amorphous C, electronic props., UPS and XPS obs. 79−82476
Pd surface, CO chemisorption, SIMS, XPS study 80−84382
Pd surface, segregated S state, AES, EELS, UPS and XPS study 80−93452
Pd, XPS, electronic struct. 80−7464
Pd, XPS line intensity ratios for outer electron shells 79−100018
Pd-Ag, ion bombarded, surface segregation, XPES obs. 79−77885
Pd-Ag alloy, asymmetry of XPS of shell electrons *(Russian)* 78−76579
Pd-Cu alloy, asymmetry of XPS of shell electrons *(Russian)* 78−76579
Pd-H system, many-body contrib. to XPS line asymm. 77−66575
Pd-H system, XPS line shape asymmetry, role of electron screening 77−21001
Pd-Si, metallic glasses, XPS and UPS studies 79−74062
Pd-Zr, metallic glasses, valence band struct. investigation 80−11533

X-ray photoelectron spectra continued
PdAg surface, CO chemisorption, SIMS, XPS study 80−84382
PdO, electronic struct., XPS and UPS study 80−35061
PdSb, XPS, electronic struct. 80−7464
$Pd_{0.81}Si_{0.19}$, amorphous, partial densities of states, XPS, UPS and AES meas. 79−95315
$Pd_{80}Si_{20}$ metallic glass, high-resolution XPS study, electronic state struct. 80−29846
PdZr, photoemission study 80−104046
$Pr(OH)_3$, mol., XPES, satellite phenomena 79−27035
Pt, 5d band structure effects on line shapes and intensities of core electron excitations 78−92177
Pt (100), adsorption of NO, 40-400°C LEED, AES, XPS and UPS obs. 77−35820
Pt-(100) unreconstructed surface, CO chemisorption 78−38962
Pt (111), adsorption of CO using XPS, UPS, TDS and dynamic meas. of work function 79−65322
Pt (111), adsorption of CO, XPS, UPS, thermal desorption, and work function meas. 79−77905
Pt (111), chemisorption of mol. O_2, XPS, UPS, EELS, and work function meas. 80−76139
Pt (111), interaction with water, thermal desorption, UPS, and XPS study 80−80088
Pt (111) and Pt (S)-12(111)X(111)surfaces, adsorption of 0, thermal desorption, AES, XPS, and LEED study 80−70534
Pt, angle resolved XPS, temp. independence 79−19975
Pt, CO absorbed on (111) surface, 40-150 eV 77−16465
Pt, $CO(O_2)$ interactions, surface electronic struct. (surface chem.) using synchrotron radiation 78−53254
Pt catalytic clusters, electronic structure, XPS obs. 77−77345
Pt compounds, L X-ray spectra and X-ray electron spectra, influence of chem. bonds 77−28656
Pt film, RF diode sputtered, thickness distrib., XPS determ. 77−39743
Pt film, RF sputtered, thickness distribution function 78−11083
Pt oxidation, XPS spectra study 80−3254
Pt, reactive sputtering in Ar-O_2 mixtures, glow discharge mass spectrometric meas. 79−91552
Pt surface, electrochem. oxidation and reduction, XPS obs. 78−95653
Pt, XPS, 4f core threshold effects 79−83096
Pt, XPS, electronic struct. 80−7464
Pt-Cu, ESCA study 80−2923
Pt-Cu, surface composition, XPS *(Portuguese)* 80−24722
Pt-Cu alloy, asymmetry of XPS of shell electrons *(Russian)* 78−76579
Pt-Cu alloys, ESCA determ. of electronic struct. 80−34352
Pt-Ni alloys, XPS d bands and core levels 77−32498
Pt-Rh alloys, surface behaviour on heating in air, XPS and SIMS *(French)* 77−40327
Pt-$SrTiO_3$ (100) interface, Auger and photoemission studies, relax. and chem. shift effects 80−54749
PtBi, XPS, electronic struct. 80−7464
$PtCl_4^{2-}$, electronic struct., SCF Xalpha ESCA spectrum assignment 80−23339
Pt(IV), reduction to Pt(II), X-ray irrad., Ar ion bombardment, XPS obs. 80−35573
PtO_x, thin film, sputtering deposition, XPS and X-ray diffr. chracterisation 79−78878
Pu, oxidation, binding energies, Auger and X-ray photoelectron spectra study 80−76550
PuO, and PuO_2, electronic struct. and chem. bonding and XPS line shape calcs. 79−33264
PuO_2, XPS meas. 77−48314
PuO_2, XPS of 5f electrons 77−73216
rare earth oxides, XPS 80−87170
Rb, atom, XPS, free atom core binding energy 78−74699
RbAu, photoelectron spectroscopy and energy bands calc. 78−76581
$RbBO_2$, vapour over heated solid, XPS, obs. 80−87171
RbCl(Br)(I), thermal shifts in energy level separations, ESCA 77−8723
Re, dissociative and mol. adsorption of NO and H_2O, XPS, AES and SIMS study *(French)* 79−69344
Re, ESCA on in situ cleaned surface 79−83101
Re, electronic struct. and CO adsorption characts., XPS, UPS, and thermal desorption study 80−71571
Re surface, interaction with N_2^+ beam, reaction dynamics studied by XPS and thermal desorpt. spectrometry 80−93797
ReO_4^-, valence level electron struct. by XPS 77−4712
Re(0001), adsorption of O_2, CO, NO, and H_2O, XPS, UPS and temp. programmed desorption 80−71574
Rh (110), chemisorption of CO and NO, LEED, AES, XPS, UPS, and desorption obs. 79−77899
Rh, oxidised surface, bonding of Cd arachidate monolayers, XPS 79−15011
Rh-Co (20 at.%), mag. virtual bound state alloys, XPS of core states 79−47588
Rh-Fe (25, 20 at.%), mag. virtual bound state alloys, XPS of core states 79−47588
Ru (001), adsorption of NO, KPS, UPS, and X-ray AES meas. 80−6655
Ru (001), adsorption of SF_6, XPS exam. 77−55866
Ru (001), physically adsorbed SF_6, XPS expts. 77−69178
Ru (10$\bar{1}$0) surface, oxide form., thermal desorption and ESCA obs. 79−82442
Ru, physisorbed SF_6, XPS interpretation 77−89830
Ru-Cu catalyst, electron spectroscopy exam. 78−44405
RuO_2, electronic struct., XPES obs., rel. to TiO_2, IrO_2 78−52632
RuO_2, photoelectron spectra, X-ray and UV polycrystalline 79−28889
S, adsorbed on Fe(100), adsorbate coverage determ. by LEED, AES and XPS 80−103566
S, XPS, in BaS and $BaSO_4$ 80−43104
S-N system, inorganic, electronic struct. obs. by photoemission XPS and UPS, CNDO calcs. 80−78653
S_8, X-ray photoelectron spectra, S2s and 2p levels binding energies 77−6844
SF_4, ESCA chemical shift, energy levels, SCC-MO calcs. 79−64045
SF_6, gaseous 1s binding energy and S $KL_2L_3(^1D_2)$ Auger energy, XPS obs. 77−3416
$(SN)_x$, calc. using photoionisation cross sections 78−72697
$(SN)_x$, electronic struct., X-ray and UV photoemission obs., OPW and pseudopot. calcs. 78−6832
$(SN)_x$, film, brominated, XPS, electronic struct. 78−72678
$(SN)_x$, LCAO band struct. calc. for one-dimens. chain and three-dimens. cryst. 77−76723

X-ray photoelectron spectra continued
S_2N_2, gas phase and solid state core level XPS 80−66401
S_2N_2, XPS, solid-state polymerisation 78−19630
S_4N_4, film, brominated, XPS, electronic struct. 78−72678
S_4N_4, solid state core level XPS 80−66401
$(SNBr_{0.04})_x$ and $(SNBr_{0.25})_x$, solid state core level XPS 80−66401
SO_2, adsorption on Fe surface, X-ray photoelectron spectra 78−27370
SO_2, gaseous 1s binding energy and S $KL_2L_3(^1D_2)$ Auger energy, XPS obs. 77−3416
Sb, core level binding energies 80−71564
Sb, XPS, electronic struct. 80−7464
Sb_2O_3, density of valence states, photoemission meas. 77−72808
Sb_2O_3, electronic struct., X-ray emission, XPS, UPS obs., CNDO cluster calc. 78−52638
Sb_2S_3, amorphous, density of valence states, XPS and UPS obs. 77−48308
Sb_2S_3, electronic struct., X-ray emission, XPS, UPS obs. 78−52638
Sc, core level binding energies, plasmon peaks 78−6828
Sc, oxidation by O_2 and H_2O, XPS obs. 79−47827
ScH_2, core level binding energies, plasmon peaks 78−6828
ScH_2, synchrotron XPS obs., rel. to theory for metal dihydrides 80−55275
Sc_2O_3 core level binding energies, plasmon peaks 78−6828
Se compounds, chemical shifts of X-ray electron and Auger lines 78−86912
Se film on brass, ESCA interface study 78−43269
Se, K shell photoelectric cross section, at 74.409 keV 79−72288
Se_8, monoclinic, XPS and valence band struct., comparison with trigonal form and S_8 77−44124
Si (111), chemisorbed O_2 electronic struct. tight-binding calc., XPS and UPS meas. 80−49845
Si (111), intermediate oxidation state, core photoelectron absorpt. vs. chemical shifts 80−81220
Si (111) 7×7 surface, giant core-exciton effects, electron energy loss spectra and XPS 77−24600
Si (111) surface, clean, ESCA obs., Ni(Au) surface impurities 78−52640
p-Si, achievement of negative electron affinity 78−2980
Si, adsorption of O_2, early stages, AES, LEED, and XPS obs. 79−46937
Si, amorphous, hydrogenated bonding 78−19636
Si, CF_3^+ ion bombardment, XPS and Auger study 79−70367
Si, chemisorption of O(1s) 77−69170
Si, chemisorption of XeF_2 and SiF_4, XPS and Auger spectra, surface chemistry 80−81358
Si, dry etching induced surface contamination, SIMS, AES, and XPS obs. 80−11810
Si KLL Auger peaks, bremsstrahlung-induced 80−45199
Si layer, on buried SiO_2 layer formed by high-dose, O ion implantation, TEM, AES, and XPS obs. 80−88172
Si, oxidised, angular-dependent X-ray photoemission at low X-ray incidence angles 77−32492
Si, oxidised surface, bonding of cadmium arachidate monolayers XPS 79−15011
Si, photoelectron escape depths determ. from X-ray photoelectron spectra 78−27368
Si, photoelectron yield variation under asymmetric diffr. condition of X-rays 79−65972
Si, semi-insulating polycrystalline CVD layers, AES and XPS characterisation 80−16129
Si, single cryst. and polycryst. comparison 77−12493
Si single crystal, X-ray photoelectron yield, effect of asymm. Bragg diffr. *(Japanese)* 77−43110
Si surface, before and after N_2^+ bombardment at 500 eV, chem. reactions 78−48265
Si surface, oxide overlayer, angular-depend. XPS exam. 77−55864
Si, thermally oxidized, chemical shift meas. by ESCA *(Japanese)* 79−61761
Si, valence band relaxation energies during XPS 78−39657
Si, valence bands, strong-coupling method 77−28679
Si, valence bands, XPS excited by Zr $M\zeta$ radiation 80−40236
Si, valence electrons XPS spectrum, OPW calc. 77−4715
Si:H, amorphous, 2p level shift, XPS obs. 80−97401
Si-O compounds 77−18971
Si-SiO_2, angular-dependent X-ray photoelectron spectra 77−12485
Si-SiO_2, bonding at (111) interface, stoichiometry and kinetics, synchrotron radiation photoemission spectroscopy 80−24744
Si-SiO_2 interface, chem. struct. of transitional region 78−95824
Si-SiO_2 interface, ESCA and ellipsometric study 79−82678
Si-SiO_2 interface, local at. struct., XPS obs. 80−20042
Si-SiO_2 interface, N_2 gas reaction, elec. and structural characts. 77−39950
Si-SiO_2 interface study by XPS 80−50507
Si-SiO_2 interfaces, local atomic and electronic struct., high resolution XPS 80−49927
Si-SiO_2 interfacial transition layer thickness, XPS obs. 80−11540
Si+NH_3, surface nitride form., XPS excited by Zr $M\zeta$ radiation 80−40236
$Si_{1-x}C_x$:H glow discharge films, local atomic struct., XPS and AES study 80−93448
Si_xC_{1-x}:H reactive sputtering deposition, compositional and structural props. 79−99077
$Si_xGe_{1-x}O_2$, $0 \leq x \leq 1$, XPS and UPS, electronic struct. 77−48318
SiH_4, mol., XPS and KLL Auger effect, line shifts 79−31602
SiN, interatomic interactions from XPS 80−49171
Si_3N_4 film, with varying refr. index, AES and XPS 78−72029
SiO film, binding energy meas. 77−7989
SiO surface, before and after N_2^+ bombardment at 500 eV, chem. reactions 78−48265
SiO_2, amorphous, local at. struct., XPS obs. 80−20042
SiO_2, amorphous and cryst., electronic band struct. interpret. 77−16454
SiO_2, dry etching induced surface contamination, SIMS, AES, and XPS obs. 80−11810
SiO_2 film, thermally grown, thickness, XPS obs. 80−11540
SiO_2 layer, on Si, XPS, data evaluation 79−65975
SiO_2, orthosilicates, mica, soft X-ray spectra and photoelectric yield spectra 78−72640
SiO_2, quantity anal. of O ions, meas. of chemical shift in Si2p binding energy, using ESCA *(Japanese)* 78−48274
SiO_2 surface, before and after N_2^+ bombardment at 500 eV, chem. reactions 78−48265
SiO_2:Ag, implanted atom, X-ray photoemission obs. 78−39050

X-ray photoelectron spectra continued
SiO_2:Au, implanted atom, X-ray photoemission obs. 78−39050
SiO_2:Au(Ag)(Cu), XPS line broadening and extra-atomic relax. energies 80−71561
SiO_2:Cu(Ag)(Au), isolation matrix, XPS, atomic electronic struct. 79−89655
SiO_2/InP film/substrate system, interface formation during CVD, modelling 80−24764
SiO_2-Na_2O-CaO-MgO float glass, surface SnO_2 distrib., ellipsometry and XPS study 80−84346
SiO_2-Si interfacial regions obs., ultrathin oxide films 79−15039
SiO_x, chem. shift of Si 2p core level, relax. contrib. 79−47141
SiO_x, core level shifts, nature of bonding 77−84698
SiON/GaAs film/substrate system, interface formation during CVD, modelling 80−24764
Sm metal, valence transition at surface of Sm 80−70652
Sm metal, XPS evidence for weak surface divalent component 77−39808
Sm surface, electron spectroscopy of 4f energy shift 80−2925
Sm surface electronic structure, XPS study 80−55259
Sm, surface mixed valence, XPS study 80−60753
Sm, XPS, 50-250 eV, 4d→4f transition and surface mixed valence 79−15588
Sm, XPS, electronic struct. determ. for surface 80−20765
Sm-Au, amorphous, surface effects on Sm valence, XPS and X-ray absorption meas. 80−108325
SmB_6, surface mixed valence, XPS study 80−60753
SmB_6, valence mixing, XPS 77−21000
SmB_6, XPS of 4f-levels, Sm^{2+}/Sm^{3+} valence ratio 77−63537
$Sm_{1-x}Ca_xS$, XPS, electronic struct. excitonic effects, insulator to metal transition 78−43988
$SmCo_5$, electronic struct., X-ray photoelectron spectra 77−20992
$Sm_{1-x}Gd_xS$, XPS, electronic struct. excitonic effects, insulator to metal transition 78−43988
$Sm(OH)_3$, mol., XPES, satellite phenomena 79−27035
$SmS_{1-x}P_x$, valence changes, XPS and UPS study 80−97402
$Sm_{1-x}Th_xS$, XPS, electronic struct. excitonic effects, insulator to metal transition 78−43988
$Sm_{1-x}Y_xS$, XPS, electronic struct. excitonic effects, insulator to metal transition 78−43988
Sn, at. N-shell vacancy state widths, X-ray photoelectron, Auger spectra 77−18875
Sn compounds, Sn(II) valency config., Mossbauer and X-ray electron determ. *(Russian)* 77−8483
Sn, core level binding energies 80−71564
Sn electrodes, potentiostatic polarisation in NaOH soln., XPS 77−90608
Sn, electron inelastic MFP from photoionisation cross sections and ang. var. studies 77−66572
Sn, inelastic mean free path in 700 to 1200 eV range, bulk method 80−20763
Sn organometallic cpds., chem. shifts in ESCA and Mossbauer spectra *(French)* 77−28685
Sn, outer core d level linewidths, determ. using synchroton radiation 77−44118
Sn, oxidised surface, bonding of cadmium arachidate monolayers, XPS 79−15011
Sn, photoionisation cross section of d-core level synchrotron radiation study of spin-orbit branching ratio 79−74057
Sn plate, passivated by cathodic dichromate treatment, nature of Cr 77−56139
Sn plate surface, ion-bombardment conditions effect on chem. profile 80−54287
Sn, XPS, electronic struct. 80−7464
Sn, XPS and $M_{4,5}N_{4,5}N_{4,5}$ Auger spectra 79−61472
Sn-Ni metastable alloy, surface film comp., time depend., XPS 78−60870
$SnCl_2$, valence band electronic struct., XPS and UPS obs. 78−6826
SnO_2 electrodes, dye-modified, erythrosin, attachment, X-ray photoelectron, photocond. investigs. 79−43600
SnO_2-NiO(ZnO)(Nb_2O_5), activated sintering mechanism 80−60810
SnS, X-ray photoemission intensity, nearest-neighbour backscatter 79−65977
SnS_2, X-ray photoemission intensity, nearest-neighbour backscatter 79−65977
SnS(Se)(Te) XPS investig. of valence band struct. 77−48311
$SnSe_2$, single crystal, reflectivity, XPS, UPS, and band struct. 78−6701
$SnSe_2$ spatial symm. of valence band struct. by angularly resolved XPS 77−69961
SnTe surfaces, oxidation in air and thermal desorption, XPS and LEED meas. 79−47830
Sr, K shell photoelectric cross section, at 74.409 keV 79−72288
$SrCoO_{3-x}$, XPS spectra, shake-up satellite of Co2p 78−52617
SrF_2, core-electron peaks, satellite and loss structs. 77−66571
SrF_2, UPS and XPS spectra, rel. to optical props. 80−66386
SrH_2, XPS spectra, crystalline potentials 77−77344
SrO, electronic struct., XPS meas. 77−73217
SrO, XPS valence bandstruct. 80−89117
$Sr_2(SbCo)O_6$, spin state of Co^{3+} ion, X-ray photoemission line broadening 79−82751
$SrTiO_3$ (111), O_2, H_2 and H_2O chemisorption, UPS and XPS studies, illum. effects 80−71572
$SrTiO_3$ electrode, surface comp. changes during photoelectrolysis, XPS obs. 79−7894
$SrTiO_3$, electronic struct., XPS meas. 77−73217
$SrTiO_3$, XPS, band struct., density of states, photoionisation cross sections, theoretical determ. 78−52629
TL, L-shell X-ray photoelectric cross sections, fluorescence spectra 78−58636
Ta film, photoemiss. from conduction band and core levels 77−16464
$Ta_{0.97}Hf_{0.03}S_2$ (1T), charge density waves, ESCA, XPS investigs. 77−12490
TaO_6^{7-}, octahedral cluster, ionisation energies and atomic populations, XPS and SCFMS Xα calc. 79−93923
TaO_n, combined SIMS, AES and XPS investigation 79−33199
Ta_2O_5, preferential sputtering by Ar^+ ions, XPS obs. 79−83083
Ta_2O_5, XPS, low energy ion backscatt. spectra 78−72660
TaS_2 (1T), charge density waves, ESCA, XPS investigs. 77−12490
$TaSe_2$ (1T and 2H), charge density waves, ESCA, XPS investigs. 77−12490
$TbCrO_4$, valence states of Cr, XPS obs. 80−40216
Tb_4O_7, XPS, charging effects on core-level binding energies 79−24409
Te coating of PbTe surfaces, struct. and junction characts. 80−50743

X-ray photoelectron spectra continued
Te compounds, X-ray photoemission, core level binding energy shifts rel. to Mossbauer isomer shifts 78−2984
Te, core level binding energies 80−71564
Te, film, AES, LEED, XPS, energy loss spectra studies oxidation effects 78−73086
Te, photoelectron spectra, strong many electron effects from core levels 77−18862
Te, relax. energies for photoionisation 77−20988
TeO_2, film, AES, LEED, XPS, energy loss spectra studies 78−73086
Th, absorption coefficients, near O_{IV} O_V thresholds, 5d cross sections calc. 78−90134
Th, adsorption of O_2, XPS study 80−7473
Th cpds., configuration interaction satellites in core level ESCA spectra 77−30923
Th, valence and 5f states, XPS and bremsstrahlung isochromat spectroscopy 80−66393
Th, XPS of 5p level, screening and configuration interaction effects 80−54633
ThO_2, satellites in XPS, cf UO_2 and La_2O_3 77−4711
$ThO(NO_3)_4.xH_2O$, satellites in XPS 77−4711
ThPt, valence bands, XPS spectra 80−50520
thiophen, gas, X-ray photoelectron spectra, satellite struct. 78−5281
Ti (0001), valence band struct. and chemisorption, XPS and UPS study 80−35062
Ti (10$\bar{1}$1), of CO, XPS, UPS, flash desorption mass spectra, and active ion bombard. obs. 79−11822
Ti compounds, XPS, p-shell, multiplet struct. 78−76580
Ti, electronic structure of omega and alpha phases, nonrelativistic APW method and XPS study 79−90952
Ti film, ultra-thin, AES and XPS anal. 78−91573
Ti, monolayer, oxidation, quasisimultaneous SIMS, AES, XPS 78−72919
Ti, nitriding, ESCA study *(Japanese)* 80−11833
Ti, oxidation, ESCA and UPS meas., core levels 77−63542
Ti, oxidation in monolayer range, SIMS, AES and XPS meas. 77−86215
Ti oxides, XPS study, electron binding energies, spin orbit splittings, exchange splittings 79−78839
Ti, polycryst., adsorpt. of O at room temp. 77−89645
Ti, X-ray photoelectron appearance potential spectrum 79−65973
Ti, XPS exam. *(French)* 78−23858
Ti:N surface, ion nitriding by a DC glow discharge method, surface anal. 78−80672
Ti-H, deposited on carriers, synthesis, structure and catalytic props. 80−29890
Ti-Ni, electron phase transition XPS, optical spectra and mag. susceptibility meas. 80−19943
$TiBr_4$, X-ray photoelectron spectra 79−22759
TiC coatings, RF sputtered, on 440-C steel, adherence, friction, and wear props. 79−47823
TiC, electronic struct. and XPS, cluster method and band struct. 79−60710
TiC reactively sputtered coatings on Ni-Cr-Mo-Ti (19,11,3 wt.%), adherence, XPES and wear study 80−25565
TiC sputtered coatings on Ti-Al-V (6,4 wt.%), adherence, XPES and wear study 80−25565
TiC, valence X-ray photoelectron spectrum, density of states 77−81197
TiC_x refractory layers on steel surfaces, ESCA obs. 80−39471
TiC_x, single cryst., core level shifts, valence band struct., ESCA 77−32499
TiC_x^{n-}, nonstoichiometric, ESCA spectra, MO LCAO calcs. 79−59513
$TiCl_4$, X-ray photoelectron spectra 79−22759
TiF_4, X-ray photoelectron spectra 79−22759
TiH_x and $TiD_{0.9}$, surface characts., AES, EELS, SIMS, and XPS study 80−65343
TiH_x film electrode, oxidation, electrochem. and surface analytical characterisation 79−39034
TiI_4, X-ray photoelectron spectra 79−22759
TiN, interatomic interactions from XPS 80−49171
TiO, Hartree-Fock and local exchange energy bands, disagreement of results 77−76724
TiO, soft X-ray spectra and XPS, Xα and Hartree-Fock calcs. discrepancies 79−77979
TiO_{1+x}, conduction band determ. 78−60055
TiO_2, clean and hydrated, surface sites, XPS 80−35052
TiO_2, ESCA, charge transfer satellite struct., hole state localisation intensity depend., MS-MO calc. 77−66139
TiO_2, electronic struct., XPS meas. 77−73217
TiO_2, electronic struct., XPES obs., rel. to RuO_2, IrO_2 78−52632
TiO_2 powder, $SiO_2(Al_2O_3)$ coated, thickness meas. of coating, XPS and ion sputtering 79−88913
TiO_2, sputtering defects, associated surface electron states, UPS, XPS and AES obs. 80−60755
TiO_2, Ti^{4+} XPS, band struct. investig. 79−38707
TiO_2, XPS satellite spectra, mol. orbital study 80−43100
TiO_2:Cu, anodic, effect of Cu on optical props., rel. to possible appl. in solar energy conversion 80−16115
TiO_2-Ni (100) interface, electronic props., struct., comp., chemical bonding 80−84499
TiO_2-Ta_2O_5 system, surface microphases investigation by X-ray electron spectral anal. 79−51269
TiO_x, interstitial alloy, electronic state, XPS, mag. susceptibility and elec. resist. 77−12486
Ti_2O_3, electron structures calc. using models, ESCA and X-ray spectral data 77−35863
Ti_2O_3, XPS, band states 77−20986
Ti_2O_3:V_2O_3, XPS, band states 77−20986
Ti_xO_x on Ti film electrodes, AES, XPS and electrochem. characterisation 78−7086
TiP, TiP_2, electronic struct. of valence bands, X-ray spectra and XPS 78−92176
$TiS_2(Se_2)$, modelling contrasting semimetallic characters 78−43393
TlBr, polymorphism, XPS obs. 80−97398
TlBr, XPS, valence bands 78−76578
TlCl, polymorphism, XPS obs. 80−97398
TlCl, valence band electronic struct., XPS and UPS obs. 78−6826
TlCl, XPS, valence bands 78−76578
TlI, Tl 5d XPS comparison with Tl 80−43099
TlI, XPS, valence bands 78−76578
TlI, XPS and UPS study of phase transforms. 80−45210

X-ray photoelectron spectra continued
Tl(III) organocompounds, XPS study *(French)* 79−64047
Tm_2O_3, XPS, charging effects on core-level binding energies 79−24409
TmTe, f^{12} and f^{13} config. photoemission fractional parentage coeffs., intermediate and LS coupling calc. 80−84829
U, absorption coefficients, near O_{IV} O_V thresholds, 5d cross sections calc. 78−90134
U, adsorption of water and O_2, XPS study 80−7473
U, core and valence band spectra, XPS obs. 80−50530
U in transition metal coordinate compounds, binding energies from XPS data 78−21973
U, L-shell X-ray photoelectric cross sections, fluorescence spectra 78−58636
U, valence and 5f states, XPS and bremsstrahlung isochromat spectroscopy 80−66393
$UAl_2(Co_2)$, surface comp. and electronic struct., photoemission study 80−66382
UAs, U 4f ESCA spectra 80−16148
UCu_5, core and valence band spectra, XPS obs. 80−50530
β-UD_3, electronic props., metallic character 80−6693
UF_3, $4f_{7/2}$ electron XPS obs., in condensates and ion-bombarded UF_4 79−45763
UF_4, condensate and ion-bombarded powder, $4f_{7/2}$ electron XPS obs., spectra of UF_3 79−45763
UF_4, electronic structure 77−32491
UN, U 4f ESCA spectra 80−16148
UNi_5, core and valence band spectra, XPS obs. 80−50530
$UNi_{0.5}Cu_{4.5}$, core and valence band spectra, XPS obs. 80−50530
UO_2, electronic distributions by X-ray spectroscopy 80−97407
UO_2, electronic struct. and Coulomb correl. energy, XPS and bremsstrahlung spectra 80−55272
UO_2, electronic transitions, crystal field effects and phonons, phase transition 80−97303
UO_2, Mg Kα and He(II) photoelectron spectra, origin from multiconfigurational Dirac-Fock calcs. 80−66387
UO_2, U_2O_5, U_3O_8 and UO_3, bonding and valence obs. 77−28696
UO_2, U_3O_8, U_2O_5, shake-up satellites and band struct. 77−55861
UO_2, uranyl cpds., electronic struct. obs. 77−28695
UO_2, valence electronic configuration determ. by photoelectron spectroscopy 78−15284
UP, U 4f ESCA spectra 80−16148
UPt, valence bands, XPS spectra 80−50520
US, U 4f ESCA spectra 80−16148
USb, UPS and XPS, surface oxidation 80−7465
V compounds, XPS, p-shell, multiplet struct. 78−76580
V, electronic structure, X-ray spectra and XPS meas. 77−85842
V oxides, XPS and AES study, electron correl. effects, semicond.-metal transition 80−7467
V oxides, XPS study, electron binding energies, spin orbit splittings, exchange splittings 79−78839
V, photoelectric cross sections at 52.4, 60, 72.2 and 84.4 keV 80−69187
V, surface state, XPS investigation 78−11070
V_3Au, effect of atomic ordering on XPS of valence bands 77−52224
V_3Au, XPS of valence electrons meas. 77−21003
VC, valence band struct. *(Russian)* 78−6268
VC_x electron band struct. and X-ray spectra *(Ukrainian)* 79−51482
VC_x, surface state, XPS investigation 78−11070
VN, interatomic interactions from XPS 80−49171
VN_{x1} surface state, XPS investigation 78−11070
VO_4^{3-}, electronic struct. determ. from X-ray spectra 78−86885
VO_x, surface state, XPS investigation 78−11070
V_2O_3, electron structures calc. using models, ESCA and X-ray spectral data 77−35863
V_2O_3:Cr, metal-insulator transitions, XPS and UPS 79−33236
V_2O_4 films, characterisation using XPS, metal-semiconductor transition 79−28900
V_2O_5, (001) surface modification, during catalytic oxidation of propene *(French)* 80−45557
V_2O_5 and lower oxides, defect structures and related props. 80−59454
V_2O_5 and lower oxides, electronic, optical, structural and surface props., review 80−88120
V_2O_5 energy band struct. rel. to expt. studies 80−70603
V_2O_5 film, electrochromism, X-ray electron spectra 78−48146
V_3O_5, high-temp. phase transition, resistivity, valence photoelectron spectra 80−49357
V_3Si, band struct. and core levels 77−48278
V_3Si, XPS and APS of valence band 77−20994
W (110), adsorpt. of N_2, N_2O, and NO_2/N_2O_4, 300K and 100K, XPS, UPS, and XAES 79−28203
W (110), adsorpt. of NO, 300K and 100K, XPS, UPS and XAES 79−28204
W (110), chemisorption of CO, LEED, XPS and Auger meas. 77−89647
W, L-shell X-ray photoelectric cross sections, fluorescence spectra 78−58636
W surface, (110), X-ray photo emission spectra, bulk atom 4f splitting 79−100020
W, XPS, angle-resolved, from valence bands, obs. of strong temp. depend. and direct-transition effects 80−60752
W:Os coated dispenser cathode, chemical and physical process obs. 79−28885
WC-Co hard alloys, machined with polycryst. superhard materials, surface struct. using X-ray photoelectron spectroscopy 80−25919
$W_xMo_{1-x}O_3$, reduction and temp. effect on electronic core levels, XPES 79−91564
WO_3, amorphous coloured film, charge transfer, XPS 77−12491
WO_3, band struct., XPS meas. 77−59667
WO_3 film, electrochromism, X-ray electron spectra 78−48146
WO_3 films, electron struct. changes during electrocoloration, XPS obs. 80−40217
WO_3, reduction and temp. effect on electronic core levels, XPES 79−91564
WO_4^{2-}, valence level electron struct. by XPS 77−4712
WO_x, nonstoichiometric, XPS meas. 77−48307
WS_3, amorphous struct., X-ray radial distrib. anal. and XPS 80−49115
W(110), adsorbed CO, adsorbate characterisation by UPS, XPS and X-ray AES 77−15683
Xe, $4d_{5/2}/4d_{3/2}$ intensity ratio, Cooper minimum region 79−31481
Xe, 5s→ep photoelectron ang. distrib., interchannel and spin-orbit coupling 77−3329
Xe, $M_{4,5}N_{4,5}X$ Auger electron spectra, many-body effects 79−59415

X-ray photoelectron spectra continued
Xe, photoelectron spectra, strong many electron effects from core levels 77−18862
Xe, satellites in 304 Å photoelectron spectrum 78−17627
Y, photoelectric cross sections at 52.4, 60, 72.2 and 84.4 keV 80−69187
Y, XPS relative intensity and photoionisation cross-section 80−63599
$YCoO_3$, spin state of Co^{3+} ion, X-ray photoemission line broadening 79−82751
YH_3, synchrotron XPS obs., rel. to theory for metal dihydrides 80−55275
YOF, band structure formation, valence band 79−33232
YOF, electronic stuct. calcs. from XPS and X-ray emission spectra 80−35056
Y_2O_2S:Tb, cathodoluminesc. efficiency changes due to processing, XPS meas. of surface changes 79−99951
Yb, 4f levels, hole lifetime and chemical shift, UHV study 80−20762
Yb-Al mixed valent film form., XPS study 80−80943
$YbAl_3$, XPS studies, valence band, 4-f region 78−6831
$YbAu_2$, surface electronic structure, XPS study 80−55259
$YbAu_2$, valence transition at surface of Yb 80−70652
Yb_2O_3, XPS, charging effects on core-level binding energies 79−24409
Zn, AES and XPS, vapour-metal electron energy shifts 80−16142
Zn, atomic and metallic, photoelectron and L_{23}-MM Auger spectra, binding energies 77−90238
Zn, core binding energies, gas phase X-ray photoelectron spectra 78−37611
Zn, electron binding energy and shift, core level XPS 80−87088
Zn, Fermi surface-Brillouin zone interaction, XPS obs. 79−52078
Zn, K shell photoelectric cross section, at 74.409 keV 79−72288
Zn, $L_3M_{23}M_{23}$ Auger energy calc. using XPS, effect of 3d-4s admixed screening on relax. energies 77−1782
Zn, LMM Auger spectra, rel. to L_{23} photoelectron spectra 77−77348
Zn, LMM Auger spectra, transition probabilities, term splittings and effective Coulomb interaction 77−44126
Zn photoelec. cross sections, 5-40 keV photons, X-ray emission spectra 77−18866
Zn, photoelectric cross sections at 52.4, 60, 72.2 and 84.4 keV 80−69187
Zn, XPS and Auger spectra, many-body calcs. 79−49995
ZnF_2, valence-electron density of states, XPS meas. 77−69963
$ZnGeP_2(As_2)$, reflectvvity and XPS meas. 78−35165
ZnO, powder, adsorption of methanol, electron spectrosc. obs. 79−52076
ZnO powder, with adsorbed methanol, appl. of XPS method for surface anal. 78−40104
ZnO, thin Zn or O rich layers, thermolysis, photolysis, SEM, XPS 77−11821
ZnO-Si(SiO_2) interface, XPS and Auger LMM anal. 79−90893
ZnO{1010} surface, clean, preparation, XPS meas. 78−39933
ZnP, Zn_3P_2, electronic struct. of valence bands, X-ray spectra and XPS 78−92176
ZnS, RF sputtered film, stoichiometry, chem. comp. 78−34727
ZnS, superficial degradation in air and water, XPS obs. *(French)* 80−89110
ZnS:MnF_2 films, effect of Mn conc., XPS obs. 79−33886
ZnS_2, XPS of valence band meas. 77−85885
ZnS(Se)(Te), clean and oxidised surfaces, O_2 sticking coeff., ionicity effects 77−85887
ZnSe surface, quantitative XPS meas. 78−56559
ZnTe films, grown on glass using atomic layer evaporation 80−44453
Zr complex of glycine, XPS study of glycine binding 79−41196
Zr, electronic structure of omega and alpha phases, nonrelativistic APW method and XPS study 79−90952
Zr photoelec. cross sections, 5-40 keV photons, X-ray emission spectra 77−18866
Zr, valence-band meas. using XPS 79−69958
Zr, XPS relative intensity and photoionisation cross-section 80−63599
Zr:N surface, ion nitriding by a DC glow discharge method, surface anal. 78−80672
Zr-Co, amorphous and crystalline, d-band struct., alloying effects 80−59862
Zr-H, deposited on carriers, synthesis, structure and catalytic props. 80−29890
Zr-Ni, amorphous and crystalline, d-band struct., alloying effects 80−59862
ZrB_2, band struct. and XPS 77−90253
ZrB_2, self-consistent band struct., XPS, reflectance, NQR, Hall effect and density of states meas. 80−107689
ZrC, electronic struct. and XPS, cluster method and band struct. 79−60710
ZrC, valence band struct. *(Russian)* 78−6268
$ZrH_{1.65}$, valence-band meas. using XPS 79−69958
ZrH_2, synchrotron XPS obs., rel. to theory for metal dihydrides 80−55275
ZrN, plasma-formed, ESCA and supercond. transition temp. 78−19697
ZrO_2:Y_2O_3 film, preferential sputtering, Auger and XPS spectra obs. 79−52071
ZrO_2-Y_2O_3 film, surface characterisation, XPS, ESCA, and AES expts. 78−72028
ZrS, electronic struct., bonding effects, photoelectron spectroscopic and low temp. heat capacity cal. 80−96780
Zu, K shell photoelectric cross section, at 74.409 keV 79−72288

X-ray production
see also X-ray tubes
AURORA machine studies of air chem., cond. and boundary layer 78−32144
BESSY, a 800 MeV storage ring dedicated to synchrotron radiation, review 79−68021
betatron 5 MeV, design and performance, X-ray prod. 80−63421
biological sample analysis, nanosec. X-ray diffr. pattern techniques 80−26429
BNL National Synchrotron Light Source, 2.5 GeV X-ray ring, design status 79−68023
Borrmann effect, production of nearly monoenergetic X-rays 77−61170
bremsstrahlung filtered spectral source for radiological studies 77−77969
bremsstrahlung intensity distrib. at origin in thick W target by attenuation anal., 60 to 140 kV 77−34060
calibration sources for proportional counters using radionuclides 79−705
Cherenkov radiation as intense X-ray source *(Russian)* 77−5971
CHESS synchrotron radiation facility, high energy tunable X-ray source 80−68984

X-ray production continued
coherent X-ray emission from relativistic electron beam 80−91739
Daresbury 2 GeV synchrotron radiation source, X-rays and VUV, progress report 78−62666
diamond type IIb, soft X-ray source for high resolution X-ray lithography 79−97481
DORIS double storage ring, synchrotron radiation source in X-ray and UV regions 78−62668
electron beam X-ray source, X-ray spectral distribs. FLASH code 79−22524
electron probe anal., corrections, quantitative, effect of electron incidence angle 79−39270
flash techniques, review 79−49356
flash X-ray machine, distributed pulse power system anal. using SCEPTRE circuit code techniques 80−68336
flash X-ray sources, characteristics 78−41392
generator design, with thyristor based power supply, bell shape pulses generation 80−57446
high brilliance sources and generators, soft and pulsed X-ray generators, book contrib. 78−42861
high power microsecond electron beam, soft X-ray prod. 80−52378
K-shell ionisation, X-ray or Auger-electron prod. by ion impact, cross section tables 79−54947
laser produced plasma, X-ray generation, mag. field effect 77−19740
laser-plasma source, for pulsed X-ray lithography 79−30636
N-16 source, exposure rate and absorbed dose meas. for 6-7 MeV photons 79−26766
nanosecond impulse generation, using HV decaying discharge *(Russian)* 77−34061
nanosecond pulse electron and bremsstrahlung generator 78−21308
Penning source, continuous discharge, with 50 Å to 300 Å emission lines 79−50363
plasma, laser produced, as soft X-ray source 78−14213
plasmas, laser produced, as X-ray source for synchrotron radiation research and microradiography 80−320
positrons, planar channelled, radiation characts. 79−55797
pulsed high intensity monoenergetic low energy source and absolute monitor 77−38531
radiological safety standard for industrial X-ray equipment, USA 78−29223
rotary anode X-ray generators, comparison of characteristics of X-ray and γ-ray sources 80−14030
scanning microsource, for photolithography and microprobe appl. 79−9266
soft X-rays from plasma mirror of electroionisation CO_2 laser , test of X-ray mirror objectives 78−85850
solar flares, hard X-rays from confined hot electrons 79−96982
SPEAR storage ring, initial operation of mag. wiggler 79−68025
standard monoenergetic source development and appl. 77−38078
synchrotron radiation, review of props., facilities, and source parameters and optimisation 79−68018
synchrotron radiation and its applications 79−44997
synchrotron radiation for VUV and X-ray spectroscopy, lecture 78−24870
synchrotron radiation from helical wiggler, orbits and fields 77−79203
synchrotron radiation from short period helical wiggler 77−79202
synchrotron radiation source, book contrib. 80−5421
synchrotron radiation source, Daresbury 2 GeV storage ring with 600 MeV booster synchrotron, review 79−68022
synchrotron radiation sources and utilisation, review 78−41390
syncyrotron orbital radiation appl. *(Japanese)* 78−25941
target thickness dependence of X-ray production from ion impact 77−85846
TEM, analytical, sources of background X-radiation 80−101908
TEM/STEM systems, spurious X-ray production 79−17573
template modulated coherent light for X- and γ-ray production, energy spectra, freq., polarisation 77−13833
Therac 6 linear accelerator, field elongation effects on depth-dose curves, central-axis output of X-rays 79−5361
tomographic application X-ray generators 79−16288
tomography, ultra high speed, X-ray source 79−66541
transition radiation source 80−69303
ultrarelativistic charge, X-ray prod., stack of plates with absorption and allowance for multiple scattering *(Russian)* 77−83450
undulator linac, electron dynamics, coherent radiation source 78−82539
VUV source, laser induced two photon blackbody radiation from He atoms in glow discharge 78−58102
X-ray synchrotron source, design status 79−68024
Ag, electron (positron), impact, K- and L-shell ionisation, Kα and L X-rays meas. 80−99575
Au, X-ray production cross sections for protons, fluoresc. obs. 80−102476
Au+light and heavy ions, L-shell X-ray production and subshell ionisation cross sections meas. 80−91637
Cl^{9+}+Cu, K X-ray production and radiative electron capture, fluoresc. yield determ. 80−99553
^{55}Fe, X-ray source, parameter determ. 78−5081
^{71}Ge source for energy dispersive X-ray fluorescence anal. *(German)* 77−86429
He^{2+}+Li, electron capture, ionis. cross section, low-vel. He^+(3l) production, X-ray production 79−22822
Pb, X-ray production cross sections for protons, fluoresc. obs. 80−102476
^{103}Pd decay, 357 keV γ:K X-ray abundance ratio obs. 79−498

X-ray protection *see radiation protection*

X-ray reflection
absorptive single crystal, X-ray refl. coeff. 78−9898
beam-foil spectra, Doppler shifted X-ray refl. 77−18821
catoptrical crossed-mirror imaging at grazing incidence 80−77923
circular waveguides, transmission in curved Pb glass capillaries 78−86395
crystal defect observation by X-ray reflection topography *(Chinese)* 80−44074
curved-crystal, numerical computation of X-ray reflectance 79−55612
diamond structure crystals, forbidden Bragg refl., electron distrib. 77−51265
EXAFS and surface EXAFS from X-ray refl. meas 80−71512
glass, polished surfaces, depend. on refr. index distrib. of superficial layer *(French)* 77−28643
intensifying screen, role of reflective layer 80−62816

X-ray reflection continued
interface co-ordinate determ. by X-ray backscatt., signal-noise ratio 80−77925
metal density measurement, using X-ray total external reflect. and double crystal spectrometer 80−64831
metal films, X-ray interferences obs., energy dispersive method 78−79499
metallic thin film, refr. index for X-rays, elec. current density influence *(Spanish)* 79−78784
mirror profile meas. machine 80−69496
monochromatic images of X-ray emitting sources, hot plasma diagnostics appl. 80−64772
multilayer mirrors, for X-ray and far UV radiation 78−1313
neutron star surfaces, X-ray refl. theory and appl. to Hercules X-1 78−28716
optical image reducing system using crystal reflection of X-rays, for sub-micrometre dimens. 79−58859
paracrystalline materials, weakly absorbing, method for normalising diffr. spectra 79−60220
polished surfaces, depend. on refr. index distrib. of superficial layer *(French)* 77−28643
quartz, ion-implanted layers, total X-ray reflection investig. of clustering 78−6081
reflectometer, for optical efficiency and scatter meas. 79−17590
resonator based on successive refls. of surface wave 80−99021
review of X-ray optics in 1 to 300 Å wavelength range 78−29221
rough surface, X-ray total external refl. 80−2896
specular reflection, from interface between two media, transition-layer model 78−83647
stearic acid salts, pseudocryst. integral X-ray reflectance coeff., cation depend. 77−11437
surface roughness influence on X-ray propag. through capillaries 79−49349
Takagi-Taupin equations, boundary conditions in numerical integration, appl. to Bragg and Laue cases 80−1886
thick crystals, X-ray diffr. process, layer model, reflectivity, polarisation *(German)* 77−51262
thick crystals, X-ray diffr. process, layer model, reflectivity, polarisation *(German)* 77−51263
total external reflection and β filter combination for monochromatization 78−4745
total external reflection of X-rays, differential eqn. calcs. 78−71625
X-ray fluorescence anal. by total reflection *(German)* 80−30314
$BaTiO_3$, pot. functions of ions 80−19885
Co, X-ray refl. near $L_{2,3}$ absorpt. edge 80−71513
InGaAs-$In_{1-x}Ga_xAs_yP_{1-y}$ DH laser, LPE fabrication, electroluminesc., lasing characts. 79−3709
$LiNbO_3$, imaging of photorefractive effects by double cryst. X-ray refl. topography 78−39521
Nb, cold-rolled, deform. zone geometry and texture gradients 77−48452
Si ion-implanted layers, total X-ray reflection investig. of clustering 78−6081
Si, surface layer, thin, density meas. by total external X-ray reflection 78−14635
Si, thermoreflectance near $L_{2,3}$ soft X-ray threshold, temp. depend. 78−35224
Si, with various dislocation densities, ang. depend. of X-ray polarisation of curve of 111 Bragg reflection 79−46509
Ti, X-ray refl. near $L_{2,3}$ absorpt. edge 80−71513

X-ray scattering
see also Compton effect; X-ray diffraction
aerosol loaded filters, X-ray fluoresc. anal., absorpt. corrects. calcs. 78−7311
anomalous, from K absorption edge of free atoms and mols., Kramers-Heisenberg dispersion calc. 79−89628
anomalous X-ray scattering 80−54075
anomolous scattering factors 80−9540
atom, K-shell electron elastic photon scatt., high-energy calcs. 77−431
atom, neutral, with Z up to 54, coherent scatt. factors *(Japanese)* 77−43103
atomic systems, elastic X-ray scatt. intensity, rel. to average electron density, isoelectronic changes 80−91424
atoms, mols., total X-ray scatt., two-electron density functions 78−70889
biopolymer soln., low angular scatt. of synchrotron radiation, use of proportional chambers 78−65155
bremsstrahlung backscattering from semi-infinite reflectors, spectral composition 77−54028
C, valence electron radial and momentum distribs., X-ray form factors and Compton profiles 79−65956
caesium hydrogen tartrate, Cs L_{III}-edge anomalous X-ray scatt., meas. by synchrotron radiation 79−24389
cosmic X-ray bursts tails, interstellar dust scatt. model refuted 79−12546
critical angles in total reflection of, Compton, X-ray and fluoresc. scatt. 80−59343
crystal, coherent scatt., photon model 80−24309
crystal, Compton X-ray scatt., electron binding energy effect 77−59639
diatomic mol., X-ray scatt. intensities, vibr. averaging 78−74722
disordered multicomponent solid solutions conc. fluctuation waves, microscopic theory 80−44327
dispersion factors f′ and f″, for scatt. near K absorpt. edge 79−65954
distorted crystal, X-ray intensity mode oscills., two wave WKB approx. calcs. 80−28876
DNA, circular superhelical, X-ray scatt. calcs. 80−56109
DNA compact form, tertiary struct., small angle X-ray scatt. 80−72129
dynamic scattering, asymm. Laue case, attenuation effects calcs. 77−7633
elastic scatt., electron density and ionisation pots., Thomas-Fermi and Hartree Fock anal. 79−52041
elastic X-ray scattering, by thermodynamic average electron-charge density 80−100123
by electrons, bound and free, X-ray scatt. in presence of strong laser field 78−58148
EM radiation in media with spatial dispersion, spatial coherence formation and polarisation increase 80−106442
environmental samples, X-ray fluoresc. anal. absorpt. corrections 77−60169
film adsorbed on graphite, two-dimensional phase transitions 80−107653
film-screen characteristics effects on threshold detectability of small low-contrast objects 78−53487

X-ray scattering continued
film-screen characteristics effects on threshold detectability of small low-contrast objects 78−53488
fluorescence, matrix correction methods using scattered radiation 80−3456
graphite, pyrolitic, oriented ellipsoidal voids, small-angle X-ray scatt. 78−64429
graphite, X-ray scatt. from small particles at zero k 80−11505
graphite, X-ray spectrum in region of Raman band 80−7436
grazing incidence scattering, from optical surfaces, effect of surface topography 80−90968
Guinier-Preston zones, X-ray small angle scattering, for extra-resist. calcs. 80−92873
Hercules X-1, reson. Compton cyclotron scatt. rel. to cyclotron line form. 80−8711
ideal anharmonic crystal, X-ray diffuse scatt. asymm. *(Russian)* 77−47300
ideal crystal, anharmonicity contrib. 77−58920
imaging system, surface roughness and scatt. effects 80−77921
inelastic scatt. in crystals, review 78−39625
intensity errors due to TDS, effects on atomic parameters and electron density distrib. 77−19819
liquid crystals, temp. stabilised sample cell system for small-angle scatt. expts. 77−13830
low-angle scattering with C Kα radiation 77−84579
mammographic image quality improvement by scattered radiation grids 79−92332
mammography, backscatt. factors, var. with field diameter and half-value layer 78−3593
metal, electronic X-ray Raman scattering, many-body suppression 77−20953
metal, X-ray excitation of surface plasmons on spherical voids 77−11974
metals, reson. scatt. of X-ray theory 78−11017
methanol-H_2O, liq., zero-angle X-ray scatt., conc. depend. 79−27897
neutron star magnetospheres, Thomson scatt. rel. to hard X-ray spectra of Centaurus sources 77−2493
noncrystalline state structure determ. techniques, phase retrieval methods 78−22656
one-dimensionally disordered cryst., X-ray scatt. intensities, disorder parameter reduction 77−84569
parallel cylinders, radial size distrib., modified Riseman integral transform method 78−83648
particle size distribution functions determ. by small-angle X-ray scatt., calc. methods 77−16420
photon resonance scattering by relativistically channelled electrons, enhancement coeff. 80−39190
plasma scattering, influence of electron exchange energy 80−50458
plasmon excitation during X-ray scatt. 80−108297
plasmon X-ray scatt. by solids, electron exchange energy influence 79−56884
polydisperse system of platelets, randomly oriented, independently scatt., thickness distrib. 77−60132
proteins, small angle X-ray scattering using sychrotron radiation, mol. wts. determ. 78−66700
radiographic intensifying screen information content and contrast, comparison of rare earth with $CaWO_4$ 78−73232
radiography, X-ray, antiscatter grid exptl. evaluation method 78−53485
Raman scattering edge, atomic struct. and extended modulation 79−99031
random stacking model scatt. intensity, appl. to tetrahedrally bonded amorphous semicond. 78−9953
reverberation and time-dependent Comptonisation in X-ray sources, rel. to rapid time variability 80−86013
rotating aperture wheel device for radiographic contrast improvement 80−56202
semiconductor, valence electron crystal pot. and pseudopot. components determ. from X-ray scatt. factors 79−65032
slit-height correction in small-angle scatt. without spherical symmetry, numerical calc. 78−18490
small angle scattering, radial electron density distrib. calcs. indirect Fourier transform method 77−76246
small angle scattering camera for synchrotron radiation X-rays, description and results 78−66020
smectic B, liq. cryst., scatt. predicted by bond orientational order model 79−10790
solid surface, optically polished, X-ray scatt. 78−83652
by sound wave in coherent state 77−84860
spectroscopy, book 80−2899
spherical X-ray wave, dynamics theory of diffr. 78−26372
synchrotron radiation, props. and appls., review 79−36830
synchrotron radiation camera and data acquisition system for time resolved X-ray scattering studies 80−99023
thermodynamic data determ. by X-ray and neutron scatt. 78−83974
tissue equivalent phantom, scatt. obs. 80−94279
tissue sample mass determ. for energy-dispersive X-ray fluoresc. anal. 77−48971
tissue-maximum ratios for high-energy X-rays 78−3609
transition metals, resonant Raman scatt. and fluoresc. near K-absorpt. edge 79−52042
TTF-SCN, quasi one-dimens. conductor, CDW phase transform., X-ray scatt. study 80−24594
TTF-TCNQ, $4k_F$ anomaly, density correlation of classical dimensional electron gas 77−80744
TTF-TCNQ, interpretation of the $2k_F$ and $4k_F$ X-ray scatt. 77−63487
weak X-ray scatt. interpretation by automated diffractometer 79−68977
β-AgI, phonon-induced X-ray scatt. from lattice dynamical model 79−37790
Al alloys, age-hardenable, precipitation and dissolution processes, positron annihilation and X-ray small-angle scattering comparison 80−89238
Al, incoherent scatt. factors calc. by direct integration over impulse approx. Compton profiles 80−102475
Al-Ag (16 wt.%) alloy, quenched, early stages of decomposition, small-angle X-ray scatt. meas. 77−59740
Al-Zn, age hardenable precipitation and dissolution, positron annihilation and X-ray scatt. 80−16314
Al-Zn, isothermal preprecipitation, small angle X-ray scatt. expts. 80−35186
Ar, incoherent scatt. factors calc. by direct integration over impulse approx. Compton profiles 80−102475
Ar, incoherent X-ray scatt., statistical atom model 78−29747

X-ray scattering continued
BC, X-ray scatt., polarised radiation excitation source for X-ray fluoresc. anal. 78−7314
BF, X-ray and high-energy elastic electron scatt., vibr. averages 79−81279
Be, X-ray plasmon scatt., electron exchange energy influence 79−56884
Be, X-ray scattering, Wannier function calcs. 80−87988
C fibres, pitch and lignite based, exam. of microvoids by X-ray scatt., heat treatment and stretching effects 79−20091
C, first-principles pseudopotential in the local-density-functional formalism 79−59328
CO, X-ray and high-energy elastic electron scatt., vibr. averages 79−81279
$CaWO_4$ and rare-earth X-ray intensifying screen sensitivity to scattered radiation 78−7450
Ce-Co, liq., charge transfer effect 78−94967
Ce-Cu, liq., charge transfer effect 78−94967
Cr, single cryst., Compton X-ray scatt., electron binding energy effect 77−59639
Cu, atom and ions, isoelectronic sequence, coherent photon scatt. cross section calc. 78−5177
Cu extended X-ray fine struct., lattice consts. 80−89085
FH, X-ray and high-energy elastic electron scatt., vibr. averages 79−81279
Ge, inelastic X-ray scatt. cross section accompanied by intermediate momentum transfer 79−24387
Ge, inelastic X-ray scattering cross sections, in case of small momentum transfer 77−27786
Ge, valence electron radial and momentum distribs., X-ray form factors and Compton profiles 79−65956
Ge:Li, dislocation free, anomalous transmission of X-rays *(Russian)* 77−15286
H_2, synchrotron radiation scattering cross sections 78−55213
$(H_2O)_2$, coherent X-ray scatt. profile calcs. 77−61765
He, synchrotron radiation scattering cross sections 78−55213
InAs, intensity of 3-phonon diffuse scattering of X-rays 80−84027
KCl, aq. soln., zero-angle X-ray scatt., 25°C, conc. depend. 78−83713
Kr, incoherent scatt. factors calc. by direct integration over impulse approx. Compton profiles 80−102475
$Li(H_2O)^+$, coherent X-ray scatt. profile calcs. 77−61765
Mo, reson. Raman X-ray scatt., evidence for K-M scatt. 79−61466
N_2, X-ray and high-energy elastic electron scatt., vibr. averages 79−81279
Na, incoherent scatt. factors calc. by direct integration over impulse approx. Compton profiles 80−102475
Na, thermal diffuse X-ray scatt. meas. in longitudinal and transverse branches 78−19598
$NaNbO_3$, energy width of central peak near phase transition 78−79724
$NbSe_3$, quasi one-dimens. conductor, CDW phase transform., X-ray scatt. study 80−24594
Si, energy-integrated inelastic X-ray scattering cross sections, energy-integrated, separation of components 78−38587
Si, inelastic X-ray scatt. cross section accompanied by intermediate momentum transfer 79−24387
Si, inelastic X-ray scattering cross sections, in case of small momentum transfer 77−27786
Si, valence electron radial and momentum distribs., X-ray form factors and Compton profiles 79−65956
Si, X-ray resonance Raman scattering, solid target, proton bombarded 79−61465
Si, X-ray rot. polarisation, absorpt. crystal orientation effects 78−47206
$SrTiO_3$, energy width of central peak near phase transition 78−79724
VO_x, diffuse scatt., relation to curvature of free energy surface 79−99025
W, first-principles pseudopotential in the local-density-functional formalism 79−59328
ZnO, valence electron states, X-ray Compton profile 79−65955
ZnS, valence electron states, X-ray Compton profile 79−65955
Zr, anomalous dispersion corrections using scanning interferometer 77−48274

X-ray sources (astronomical)
see also X-ray astronomical observations
2A 0311−227, optical counterpart identification and spectroscopic obs. 79−25762
3U 1700−37 (HD 153919), X-ray binary, uvby photometry 77−17624
1732−303, 1745−248, new X-ray burst sources, discovery and identifications with globular clusters (Terzan 1, 5) 80−98739
1909+048 (Stephenson-Sanduleak 433), new type of radio star, possibly supernova stellar remnant 79−17117
HR 1099, RS Canum Venaticorum type binary, light and colour curve meas. 80−73004
4U 1608−52, steady X-ray source assoc. with Norma X-ray burst source, Uhuru obs. 77−5593
25 1702−363, IR candidate in error box, JHKL photometry 78−61934
γ195+5, >100 MeV γ-ray source, X-ray emission obs. 79−97101
A0535+26, 1978 August outburst of recurrent transient, Ariel 5 obs. 78−86038
A0535+26, SAS-3 obs. of strong outburst (1977, May) 77−49498
A0535+26, transient slow X-ray pulsar, spectrophotometric survey 78−4263
A0535+26 (HDE 245770), Hβ var., general props., spectral obs. of optical counterpart 78−4247
A0535+26 (HDE 245770), spectroscopy and orbital periods 78−93306
A0535+26 (HDE 245770), UBV photometry during X-ray outburst 79−67024
A0538−66, outbursts and proximity to LMC X-4 position, Ariel 5 obs. 77−82321
A0538−66, recurrent X-ray transient source in LMC 78−54085
A0620−00, intensity variations and evidence for 8 day period 77−13496
A0620−00, transient source, optical counterpart, visible and IR obs. 80−101653
A0620−00, transient X-ray source, spectrophotometry 78−4400
A0620−00, X-ray nova, Ariel V crystal spectrometer/polarimeter obs. 77−2494
A0620−00, X-ray nova, distance determ. from reddening 77−2495
A0620−00, X-ray nova, spectroscopic obs. 77−87417
A0620−00 (V616 Monocerotis=Nova 1975), 8-day modulation 77−87442
A0620−00 (V616 Monocerotis=Nova 1975), spectral characts. 77−87443

X-ray sources continued
A0620−00 (V616 Monocerotis=Nova 1975), spectroscopic obs. 77−82257
A0620−00 (V616 Monocerotis=Nova 1975), X-ray and visible light curves 77−82331
A0620−00 and A0535+26, spectroscopic obs. of X-ray novae 77−87577
A0620-00, Nova Monocerotis 1975, spectrophotometry 77−33684
2A0 120−591, obs. of assoc. galaxy/quasar, (ESO 113-IG45) 78−28782
A1540−53, X-ray pulsator near 3U 1538−52 77−33696
A1742−28, transient source, optical counterpart, visible and IR obs. 80−101653
2A 0042+323 (3U 0042+32), optical candidate obs. 78−54088
2A 0042+323 (3U 0042+32), periodic behaviour rel. to binary nature 78−54089
2A 0251+413, identification as AWM 7 galaxy cluster by HEAO 1 80−90573
2A 0311−227, AM Herculis type binary star, IR photometry and polarimetry 80−77517
2A 0311−227, AM Herculis type X-ray binary, optical counterpart, radial vel. obs. 80−94890
2A 0311−227, complex emission line structure of spectroscopic binary 80−51915
2A 0311−227, high-speed photometry of AM Herculis-type binary 80−41912
2 A 0311−227, IR flickering obs. 79−40298
2A 0311−227, new AM Herculis-type system, optical identification 79−101211
2A 0311−227, optical counterpart, AM Herculis type eclipsing binary, V-band obs. 80−101617
2A 0311−227, optical counterpart high speed photometry 80−82547
2A 0311−227, optical counterpart identification as AM Herculis type star 79−30149
2A 0311−227, optical counterpart spectroscopic and photometric obs. 79−101222
2A 0311−227, orbital period and polarisation obs. of optical counterpart 79−30151
2A 0311−227, simultaneous optical photometric and spectroscopic obs. 80−90572
2A 0311−227, soft X-ray emission from AM Herculis-type system 79−101219
2A 0311−227, variable soft X-ray source discovery 79−35434
2A 0311−227, X-ray flux modulation period from HEAO obs. 80−77516
2A 0311−227 optical counterpart, binary star, light curve Fourier anal. 80−82549
2A 0335+096, identification with galaxy cluster Zw 0335.1+0956 80−90574
2A 0526−328, high speed optical photometry 80−51917
2A 0526−328, optical counterpart, eclipsing binary, visible emission line variability 80−73075
2A 0526−328, optical counterpart position and spectrum 79−5925
2A 0526−328, optical counterpart radial vel. meas. and orbital period 80−90579
2A 0526−328, spectroscopic obs. of optical counterpart 80−77515
2A 0526−328, X-ray emitting cataclysmic variable, optical and X-ray obs. 79−97103
2A 0526-328, location and identification with blue emission line star 80−22118
2A 0526-328, optical photometry of assoc. star 80−22120
A 0535+26, near IR photometry of optical counterpart HDE 245770 OBe star 79−48826
A 0535+26, transient source, possible RR Tauri relationship 80−26853
A 0535+26, transient X-ray source, flare obs. by (Prognoz 6) *(Russian)* 80−51920
A 0535+26, variable source, line and continuum vars. of possible optical counterpart (HDE 245770) 80−17600
A 0535+26, X-ray pulsar, optical counterpart HDE 245770 spectral type and luminosity 80−72976
ZA 0536−328, AM Herculis-like star identification confirmed 79−40296
A 0538−66, recurrent transient LMC X-ray source, precise position, supergiant star counterpart 79−62933
A 0538−66, X-ray burster position and optical candidate in LMC 80−73076
A 0620−00 (V616 Monocerotis=Nova 1975), UBV photometry *(Russian)* 79−58360
2A 0946−310, spectroscopic obs. of possible galaxy counterpart 78−45404
2A 1052+606, location and identification with late type emission line star (SAO 015338) 80−22118
2A 1052+606, spectroscopic obs. of counterpart SAO 015338, RS Canum Venaticorum binary 79−21352
2 A 1052+606, X-ray and optical variability of RS CVn star 80−31331
2A 1052+606 (BD+61°1211), RS Canum Venaticorum binary star, spectroscopic obs. 80−36663
2A 1052+606 (SAO 015338), analysis of possible identification 78−32608
2A 1102+384, soft X-ray emission obs. 78−49564
2 A 1102+384 (Markarian 421=B2 1101+38), soft X-ray flux discovery 79−25721
2A 1102+384 (Markarian 421) BL Lacertae object, low-energy X-rays detect. 78−54083
2A 1219+305, high latit. X-ray source identification with BL Lacertae object 79−48960
2A 1251−290, high-latit. X-ray source, X-ray spectrum and variability 78−32611
2A 1348+700, 1415+255, 1410−029, Seyfert galaxies, X-ray spectra and variability 78−32611
A 1710−34, X-ray, optical and radio obs. 79−71158
2A 1822−371, galactic X-ray source, position and identification 79−12545
A 1909+04 (SS 433), radio and optical obs. 79−88661
2A 2151−316, BL Lacertae object, optical counterpart, spectral slope from far UV obs. 80−82509
2A 2251−179, X-ray quasar, UBV photometry 80−82349
3A 2252−035, optical counterpart, proper motion and radial vel. determ. 80−82395
2A 2315−428 (NGC 7582), narrow emission line X-ray emitting nucleus, UV spectra 80−101640
2A catalogue, review 78−73659

X-ray sources continued
2A catalogue and supplementary results from Ariel 5 sky survey 79−58276
A non 0945−30, galaxy, X-ray detect. and intermediate luminosity X-ray galaxies contrib. to background 79−2578
Abell 1060 galaxy cluster, X-ray spectrum obs. by (HEAO A-2) 80−82518
Abell 2029 galaxy cluster, radio and SAS 3 X-ray obs. 80−82519
Abell 2142, spectroscopic obs. of X-ray cluster (40 1556+27) 79−48940
Abell 2241, candidate X-ray cluster of galaxies, redshifts 77−17699
Abell 2256, rich cluster, steep-spectrum radiosource obs. 79−9016
Abell 2256, X-ray cluster of galaxies, radio props. 80−36726
Abell 376, 2319, clusters of galaxies, Westerbork obs. of fields 78−96549
Abell 399/Abell 401, X-ray binary galaxy cluster, mass 80−90546
Abell 401, X-ray cluster of galaxies, radio emission distrib. 80−98731
Abell 401 cluster, lunar occultation obs. at 327 MHz, survey 80−73052
Abell 401 cluster of galaxies vel. dispersion meas. rel. to X-ray luminosity 77−26072
Abell 478, cluster of galaxies, X-ray and radio obs. 78−8133
Abell 478, X-ray cluster of galaxies, redshift and optical struct. 78−8134
Abell 754, cluster of galaxies, extended radio emission from X-ray source 79−25737
Abell clusters 401 and 399, possible gravitationally bound system, diffuse X-ray emission 79−25736
Abell clusters and superclusters, search for X-ray emission 78−54091
Abell clusters of galaxies, X-ray luminosity function 78−36704
Abell clusters of galaxies, X-ray survey, HEAO 1 1-10 keV obs. 80−51882
accreting compact object, axisymmetric accretion theory 77−33334
accreting compact object in binary system, magnetosphere theory, X-ray sources 80−46394
accreting magnetic degenerate dwarfs, X-ray and UV emission 80−41826
accreting magnetised neutron stars, normal mode anal. of interchange instability at magnetopause 77−13376
accreting nonmagnetic degenerate dwarfs, X-ray and UV radiation 79−40184
accreting pulsars, role of Alven surface in X-ray pulses form. 77−78899
accretion column of X-ray pulsar, cyclotron line formation 80−67901
accretion disc, polarisation effects in emission 79−35128
accretion disc interaction with stellar mag. field, plasma diffusion across Alfven surface 78−93461
accretion discs, secondary winds and evaporation 77−64751
accretion discs, structure in mag. field, MHD eqns. approach 80−8714
accretion discs, turbulent energy transport 78−28661
accretion discs in X-ray binaries, structured coronae, model 79−48852
accretion disk model, gas flow above alpha disk 80−62161
accretion disks, theoretical review *(Polish)* 80−26739
accretion magnetospheres, general solns. 77−45400
active galactic nuclei, X-rays from inverse Compton refl. 79−48920
active galactic nuclei X-ray sources, hard X-ray emission mechanism 79−97080
ζ Andromedae, spectroscopic binary, photometric and spectroscopic obs. *(Russian)* 78−57588
anticorrelated spectral var. in black hole candidate and other sources 77−53709
Aquila X-1, intense X-ray flare obs. 77−33687
Aquila X-1, nature of X-ray outbursts 78−20909
Aquila X-1, optical counterpart spectrum 78−77626
Aquila X-1, photometry and spectroscopy of optical counterpart, model 78−32614
Aquila X-1, recurrent X-ray outbursts, Ariel V ASM obs. 77−26088
Aquila X-1, UBV photometry during 1978 X-ray outburst *(Russian)* 79−101224
Aquila X-1, X-ray outburst obs. (1978 June 14 to 22) 78−65721
Aquila X-1, X-ray outburst of recurrent transient, 1979 March 79−44638
Aquila X-1 (3U 1908+00), faint flare star optical candidate 77−67141
Aquila X-1 (3U 1908+00), flaring activity obs. 77−22332
Aquila X-1 (3U 1908+00), optical counterpart for flaring source 78−41089
Aquila X-1 (4U 1908+00), 1978 summer X-ray and optical outburst 80−73068
Aquila X-1 (4U 1908+00), optical outburst, obs. 78−69911
Aquila X-1 (4U 1908+00), optical outburst obs. 80−67909
Aquila X-1 (4U 1908+00), X-ray outburst obs. 80−77514
Ariel 0327+43 new X-ray source near Nova Persei 1901, discovery 78−69910
Ariel 0535+26, flaring X-ray source, 2 cm obs. 78−54081
Ariel 0535+26, periodic transient source, hard X-ray pulse profile 77−29951
Ariel 0535+26, spectroscopic obs. of optical counterpart HDE 245770 77−45450
Ariel 0535+26, transient source, refined position meas. and pulse period data 79−44635
Ariel 0535+26, X-ray outburst on 1978 April 10, SAS-3 obs. 78−45433
Ariel 0535+26 (HD 245770), photoelectric UBV photometry 78−36592
Ariel 0535+26 (HDE 245770), 1977 spectrum, objective prism study 78−61866
Ariel 0535+26 (HDE 245770), recurrent X-ray transient, further outburst 79−40300
Ariel 0535+26 (HDE 245770), UBV photometry during X-ray flare-up 78−28705
Ariel 0620−00, optical light curve and periodicity 77−13497
Ariel 0620−00, spectroscopic obs. of optical counterpart V616 Monocerotis 77−45450
Ariel 0620−00, transient source, X-ray spectra obs. with Bragg crystal spectrometer 79−12542
Ariel 0620−00, transient X-ray source, obs. using OSO-8 Bragg cryst. spectrometer 78−12426
Ariel 0620−00, transient X-ray source, spherical model 78−12415
Ariel 0620−00 (Nova Monocerotis 1976), Ariel 5 obs. of decay 77−29950
Ariel 0620-00, distance from interstellar colour excess 77−64744
Ariel 0620-00 (Nova Monocerotis 1975), photographic photometric obs. 78−36587
Ariel 0620-00 (V616 Monocerotis), UBV photometry 80−56846
Ariel 0620-00 (V616 Monocerotis), visible light curve 77−64777
Ariel 1353-40, transient source, relation to young cluster (NGC 5367) 77−82294
Ariel 1524=61, transient X-ray source optical identification 77−45611
Ariel 1540−53, eclipsing X-ray binary pulsator 78−8151
Ariel 1540−53, X-ray flux 8.8 min periodic var. obs. 77−49502
Ariel 1850−08, identification with NGC 6712 globular cluster 77−13414
Ariel 5 clusters, optical morphology and galaxy density 78−8135
Ariel 5 hard X-ray observations 79−58444
Ariel 5 obs. of Circinus X-1 and galactic plane sources (1976 Nov.) 77−9818
Ariel V (SSI) catalogue, of high galactic latit. (|b|>10°) X-ray sources 78−32362
Ariel V rotation modulation collimator experiment, 10 new X-ray sources obs. 77−49501
UX Arietis (H0324+28), RS Canum Venaticorum system as coronal X-ray source 79−16979
KR Aurigae, X-ray source nearby, X-ray, IR and visible obs. 80−67742
α Aurigae (Capella), intense line emission in soft X-ray spectrum 78−93228
AWM 4, poor galaxy cluster, extended X-ray emission detect. surrounding cD galaxy (NGC 6051) 80−51884
B-type stars, optical counterparts of X-ray sources, luminosity class from O I 7773 Å triplet absorpt. 79−71031
background, hot clumpy intergalactic medium emission contrib. 80−62335
background contribution from young galaxies 80−82550
background data from Ariel V, universal large scale shearing 80−62352
background irregularities 80−62331
background radiation, detection of quasar contrib. 80−62323
background radiation fluctuations and X-ray source counts at high galactic latit. 79−67119
background radiation isotropy, 2-18 keV energy range 80−46709
background radiation origin 77−33703
BD+61°1211, optical counterpart of 2A 1052+606, RS Canum Venaticorum binary system 79−92803
Be stars, review 79−84809
binaries, Fe line emission from Alfven shell 80−98737
binaries, limitations on nature and evolution 77−82273
binaries, neutron star free precession, role of vortex pinning 77−49420
binaries, optical radiation polarization *(Russian)* 79−58450
binaries in dense stellar clusters, dynamical effects 79−97098
binarity, detection via Doppler effect *(Russian)* 78−77623
binary pulsating X-ray sources, spin-up due to accretion from Keplerian disc 80−67904
binary sources, distortion of absorpt. line vel. curves due to X-ray heating 77−29878
binary sources, effect of vacuum birefringence on X-ray polarisation 78−4408
binary sources, observational constraints on neutron star masses 77−5543
binary sources rel. to OB stars and pulsars, tugboat model for evolution 77−56915
binary sources with OB supergiant companions, possible mass transfer mechanism 77−9809
binary star systems, Roche lobe formation 80−41858
binary stars, cyclotron line feature identification 80−90577
binary stars, observational evidence for black holes 77−57007
binary stars, review *(Italian)* 78−32516
binary stars, short period, X- and γ-ray bursts from mag. reconnection 78−81654
binary stars and neutron star spin down *(Chinese)* 78−28857
binary stars linear radial and nonradial modes of oscillation 78−4213
binary systems, accretion discs, observational appearances *(Russian)* 77−87477
binary systems, radiation pressure force influence on critical surfaces 78−96505
binary systems, spherically symm. accretion near Eddington limiting luminosity 79−16809
binary systems, variable optical polarization rel. to black hole secondary component 78−20910
binary systems, X-rays polarisation from mag. accretion disc *(Russian)* 77−87575
binary X-ray pulsars, continuum optical pulsation from companions 79−30147
binary X-ray pulsars, review 77−29869
binary X-ray pulsars, rot. history 79−62871
binary X-ray source in stellar wind, variable spectral features interpretation 77−17716
binary X-ray sources, accretion disc coronae 78−16569
binary X-ray sources, accretion of plasma onto neutron stars 80−109452
binary X-ray sources, anomalous periastron positions 79−25756
binary X-ray sources, cyclotron emissivity in accreting neutron stars 80−90463
binary X-ray sources, double core evolution 79−84816
binary X-ray sources, effects of libration on light curves 78−57579
binary X-ray sources, evolutionary history 78−12431
binary X-ray sources, fate of matter and ang. momentum in disc accretion onto magnetised neutron star 78−28715
binary X-ray sources, lifetimes 77−9812
binary X-ray sources, matter supply mechanisms 77−9813
binary X-ray sources, models of supercritical accretion discs around black holes 80−105272
binary X-ray sources, orbital precession and nutation 77−13392
binary X-ray sources, properties and models 77−41419
binary X-ray sources, radiative effects in supersonic accretion 78−40978
binary X-ray sources, recurrent transients model 80−109565
binary X-ray sources, relation of type I supernovae 77−57021
binary X-ray sources, review 77−17631
binary X-ray sources, review of new developments 77−71154
binary X-ray sources, review of optical obs. 78−12429
binary X-ray sources, review of types and props. 80−109564
binary X-ray sources, Roche-lobe overflow model 78−32601
binary X-ray sources, spin up as indicator of normal component evolution *(Russian)* 77−74100
binary X-ray sources, stability of non-synchronous stars in close binary systems 79−40223
binary X-ray sources, X-ray spectral lines rel. to neutron star struct. 77−78812

X-ray sources continued
binary X-ray sources evolution, accretion onto ZAMS stars and contact binary stage 79−66994
binary X-ray sources light and velocity curves simultaneous solution, eccentric orbit generalisation 80−36664
binary X-ray sources stellar parameters of early type companions 78−36564
binary X-ray system, Fe fluoresc. line struct. 77−78889
binary X-ray systems, accretion flows 78−12432
binary X-ray systems, evaporative winds 77−78888
binary X-ray systems, evidence of noncircular orbits 79−12541
binary X-ray systems, K-fluorescence lines in spectra 78−93456
binary X-ray systems, massive, gas streams and accretion discs 78−93464
binary X-ray systems, models, X-ray transfer, Monte Carlo study 78−93463
binary X-ray systems, twisted accretion discs 78−4283
black hole, massive, radiation spectrum of gas debris from tidally disrupted star 80−90467
black hole accretion discs, Lightman-Eardley instabilities rel. to disc thickening 80−31324
black hole candidates *(Czech)* 80−31325
black holes, electron-positron pair production in hot unsaturated Compton accretion models 80−36658
black holes, high-freq. EM waves propag. through magnetised plasma in curved space time 80−48894
black holes, theory, of rapid X-ray variability and dying pulse trains 80−56872
black holes, X-ray radiation polarisation features 80−46700
η Bootis, soft X-rays detect. with imaging X-ray telescope 79−48953
burst, spectral evolution 77−29958
burst of X-rays propag. through interstellar dust, small-angle scatt. effects 78−57433
burst source model, He flashes on accreting neutron star 79−17008
burst source near galaxy MCG-5-9-22, possible assoc. with supernova 78−81644
burst sources, appl. of sinking filaments model of accretion onto magnetised neutron stars 80−51798
burst sources, average props. of 10 objects 78−81710
burst sources, effects of thermal limit for spherical accretion 78−45430
burst sources, galactic distribution 77−49507
burst sources, matter accretion from magnetopause of neutron star 77−49419
burst sources, model, accreting rot. neutron star, burst energy histograms 79−35428
burst sources, model, substorm process at accreting neutron star 79−17132
burst sources, neutron star thermonuclear runaway model 80−22032
burst sources, neutron-star thermonuclear flahses model 78−12417
burst sources, nuclear burning on accreting neutron stars 78−36724
burst sources, obs. and models *(Danish)* 80−12830
burst sources, obs. of assoc. optical flashes 77−41420
burst sources, optical monitoring 78−77622
burst sources, persistent emission rel. to nature of galactic bulge X-ray sources 79−84871
burst sources, properties, binary systems *(Russian)* 78−93477
burst sources, radiation spectrum rel. to neutron stars mass-radius relation 80−77444
burst sources, radiative heat transfer in mag. neutron stars surface layers 80−94826
burst sources, rel. to neutron stars nonstationary accretion of stellar wind *(Russian)* 78−69825
burst sources, review 78−12416
burst sources, review 78−41084
burst sources, review 78−49566
burst sources, SAS 3 obs. (1977, July and August) 77−74160
burst sources, search for correlated X-ray and radio emission 78−57695
burst sources, simple physical model 77−29960
burst sources, summary of available information 77−45614
burst sources, thermonuclear flashes in envelope of accreting neutron star 80−109455
burst sources in Aquila, discovery 77−13500
burst sources in globular clusters, neutron stars hypothesis *(Russian)* 78−16480
burster phenomenon, mathematical simulacrum 77−87570
bursters, models 80−4460
bursters, radius and mass, general relativistic effects 80−8712
bursters, spectroscopic study of optical counterparts 80−46699
bursters, time dependent accretion by magnetic neutron stars 78−4401
bursters, X-ray satellite availability for obs. programs 79−40297
bursts, 2-20 keV, OSO-8 obs. 77−5601
bursts, Ariel V RMC expt. sky coverage and sensitivity 77−13204
bursts, atmospheric fluorescence in near UV as means of detection 77−9663
bursts, possibly from black holes in globular clusters *(Russian)* 77−17721
bursts, review 77−37669
bursts of hard X-rays, SAS-3 detect. 1976, Nov. 77−2499
3C273, gamma-radiation, X-ray source size limitations 79−30143
3C273, HEAO 1 (A4) obs. of 13-120 keV X-rays 79−44633
3C 120, Seyfert galaxy, X-ray emission detect. 77−78890
3C 273, quasar, second-order Compton interpretation of X-rays and γ-radiation 80−22106
3C 273, X-ray variability, spectrum and position 79−62929
3C 273, X-ray variability of quasar 79−67112
3C 390.3, 3C 273, 3C 111, 3C 129, extragalactic radio sources, search for hard X-ray emission 77−29939
CA 0340−538 (3U 0328−523), southern cluster of galaxies, vel. dispersion and global parameters 78−36705
α Canis Majoris (Sirius B), EUV obs., evidence against photospheric origin of 0.25 keV flux 78−49481
α Canis Majoris B (Sirius B), effective temp. rel. to soft X-ray obs. 79−44477
α Canis Majoris B (Sirius B), minimum flux H coronal model rel. to X-ray emission 80−8626
α Canis Majoris B (Sirius B), search for far UV emission 79−5821
α Canis Majoris B (Sirius B) corona model constraints rel. to X-ray emission 79−2543
RS Canum Venaticorum binary stars, introduction to series of papers 79−21329
X-ray sources continued
RS Canum Venaticorum stars, Hα line variability, visible spectra obs. 80−105277
RS Canum Venaticorum systems, candidate list for southern HD stars 80−4395
RS Canum Venaticorum systems, X-ray emission progress report 79−21345
RS Canum Venaticorum systems, X-ray obs. and coronal model development 80−56873
η Carinae, soft X-ray results from OSO-8 Wisconsin Expt. 78−36722
ν Carinae, X-ray emission obs. from star and surrounding nebula 80−26876
γ Cassiopeiae, Be star, coordinated IR and optical obs., (in late 1976) 79−25616
γ Cassiopeiae, UV and optical spectral var. rel. to coronal emission 78−93251
catalogue of 517 objects 80−56720
CD −33°12119, 3U 1727−33 candidate, UBV photometry 78−12251
proxima=V645 Centauri, dMe flare star, quiescent corona, transition region, and chromosphere obs. 80−56850
α Centauri, soft X-ray emission 79−16951
Centauris X-4, possible new outburst, identification with optical novalike object 79−62842
Centaurus A, X-ray variability, OSO-8 obs. 78−41082
Centaurus A (NGC 5128), detect. of X-ray emission from giant radio lobes 78−41055
Centaurus A (NGC 5128), radio and X-ray var. of nucleus 78−36711
Centaurus A (NGC 5128), slowly varying flux component, 22 GHz confirmation 80−56939
Centaurus galaxy cluster, X-ray spectrum obs. by (HEAO A-2) 80−82518
Centaurus transient source, 1979 May obs. and possible Cen X-4 identification 79−53938
Centaurus X-3, accretion disk evidence from month-long X-ray obs. 79−44636
Centaurus X-3, binary star, cyclotron line feature identification 80−90577
Centaurus X-3, long-term studies with Ariel 5 All-Sky Monitor 79−30146
Centaurus X-3, neutron star charact. from correlated spin-up and X-ray luminosity meas. 80−101648
Centaurus X-3, periodicity of extended lows 78−24526
Centaurus X-3, pulsation period and orbital elements 77−49494
Centaurus X-3, search for X-ray polarization 80−4457
Centaurus X-3, spectroscopic obs. of Krzeminski's star 79−53934
Centaurus X-3, stellar wind vel. change during transition 80−12829
Centaurus X-3, X-ray binary, tidal friction effects 77−57013
Centaurus X-3 and related binary X-ray sources, origin 77−29954
Centaurus X-4, magnitude of optical counterpart 1979 June 14 79−75220
Centaurus X-4, novalike transient source, radio detect. 79−67026
Centaurus X-4, SIT Vidicon spectra 79−80370
Centaurus X-4, spectroscopic obs. of visual counterpart, companion type 80−82545
Centaurus X-4, transient X-ray burster, optical counterpart discovered 80−67906
Centaurus X-4, X-ray burst from novalike object 79−62935
Centaurus X-4 (V748 Centauri), high-latit. eclipsing system, VBLUW photometry 79−44529
Centaurus XR-4, bright transient X-ray source, assoc. with NGC 5824 globular cluster 78−12420
VW Cephei, W Ursae Majoris star, identification with faint X-ray source 80−51913
π Ceti, late B-type star, X-ray emission obs. 79−101160
CG 176-7, 189+1 and 195+4, X-ray emission associated with γ-ray source 80−31393
characteristics and evolution, from radio, X-ray, and γ-ray obs. 77−37611
Circinus X-1, Ariel 5 X-ray and IR brightness meas. 77−82325
Circinus X-1, binary model, orbital eccentricity from X-ray and radio obs. 80−98735
Circinus X-1, binary model, radio emission 80−98736
Circinus X-1, changes in optical, IR and radio emission 80−67910
Circinus X-1, continuation of anomalous X-ray behaviour 78−32606
Circinus X-1, distance 78−12413
Circinus X-1, intense X-ray flares obs. 77−33687
Circinus X-1, IR magnitude drop (1978 March-April) 78−54080
Circinus X-1, JHKL photometry and IR brightness decline 77−74162
Circinus X-1, JHKLM photometry and light curve 78−54086
Circinus X-1, ms X-ray bursts, possible black hole 78−4404
Circinus X-1, nature and binary star model 79−75296
Circinus X-1, peculiar flaring episode detect., 1979 Jan. 79−21465
Circinus X-1, periodic X-ray emission, COS-B obs. 77−53705
Circinus X-1, position meas., radio and optical identifications 77−91671
Circinus X-1, radio flare obs. at 2.1 cm wavelength 79−9035
Circinus X-1, radio flare phenomena Dec. 1979 and Jan. 1980 obs. 80−36731
Circinus X-1, radio source obs. at 408 MHz 79−53940
Circinus X-1, semiperiodic pulsations 79−48963
Circinus X-1, X-ray and radio flux meas. 77−2498
Circinus X-1, X-ray flare obs., 1977, Sept. 77−82328
Circinus X-1 (3U 1516−56), obs. of optical and radio counterpart 78−12414
Circinus X-1 and Cygnus X-1, time variability comparison 80−56974
Circinus X-1 and galactic plane sources, 1976 Nov., Ariel 5 obs. 77−9818
Circinus X-1 as gamma-ray source, eccentric orbit binary model 79−97100
Cirinus X-1, simultaneous radio and optical obs. during outbursts 79−17137
close binaries accretion processes rel. to binary X-ray sources 77−57034
close binary sources, ellipsoidality effects and linear polarisation 77−78898
close binary stars with black hole circumstellar gas motion 77−17628
cluster X-ray sources, luminosity-temp. relation 79−44622
clusters of galaxies, Compton scatt. of microwave background by intracluster gas 78−24575
clusters of galaxies, detection of large X-ray halos 79−5909
clusters of galaxies, evidence for gas stripping from spirals 78−32586
clusters of galaxies, evolution rel. to origin and distrib. of intracluster gas 78−28770

X-ray sources continued
clusters of galaxies, Fe-enriched gas origin and evolution 78−93390
clusters of galaxies, hot gas X-ray emission rel. to radio sources props. 78−12398
clusters of galaxies, implications of galactic coronae model for intracluster medium origin 80−31355
clusters of galaxies, intergalactic hot gas distrib. 79−17089
clusters of galaxies, intergalactic matter rel. to X-ray emission interpretation 80−109543
clusters of galaxies, intracluster gas flow patterns and X-ray emission 78−65705
clusters of galaxies, intracluster gas heating by relativistic electrons rel. to X-ray and radio emission 78−57655
clusters of galaxies, intracluster hot gas temp. and entropy 80−17660
clusters of galaxies, intracluster relativistic electrons hard X-ray spectra and gas heating 79−25735
clusters of galaxies, large-scale struct. 80−82524
clusters of galaxies, large-scale X-ray struct. 80−8700
clusters of galaxies, numerical models for X-ray line emissions 78−8149
clusters of galaxies, origin of X-ray emission 78−57660
clusters of galaxies, OSO 8 X-ray spectra discussion 79−25734
clusters of galaxies, radial distrib. of morphological types of galaxies 78−8129
clusters of galaxies, radial vel. dispersions 80−8696
clusters of galaxies, radiative regulation of gas flow, X-ray source model 78−4371
clusters of galaxies, radio and X-ray emission, review 77−64862
clusters of galaxies, radio limits on ionised gas 78−89243
clusters of galaxies, rich X-ray emitting clusters, VHF obs. 80−62294
clusters of galaxies, search for extended hot gas halos in Perseus, Virgo and Coma clusters 80−56953
clusters of galaxies, source structure and spectra 79−58448
clusters of galaxies, spatial distrib. of Compton-produced X-ray flux 77−33686
clusters of galaxies, spatial distrib. of heavy elements 77−91654
clusters of galaxies, thermal bremsstrahlung model rel. to intracluster Faraday rot. obs. 79−75285
clusters of galaxies, unborn, microwave and X-ray emission 78−8131
clusters of galaxies, vel. dispersions 77−9804
clusters of galaxies, X-ray and optical study 78−28805
clusters of galaxies, X-ray emission, Compton and thermal models 78−12378
clusters of galaxies, X-ray emission rel. to intracluster hot gas 78−12374
clusters of galaxies, X-ray emitting gas evolution 79−40266
clusters of galaxies, X-ray luminosity rel. to richness 78−65704
clusters of galaxies, X-ray luminosity-richness relation 78−93431
in clusters of galaxies, X-ray props. 78−96565
clusters of galaxies, X-ray sources evolution 79−17133
clusters of galaxies, X-ray spectra and relationship to other cluster props. 80−22093
clusters of galaxies, X-ray spectra in 2-20 keV range, OSO 8 obs. 79−5908
clusters of galaxies, X-ray struct. and spectra 78−12387
clusters of galaxies, X-ray temps. meas. rel. to other cluster props. 77−91668
clusters of galaxies, X-rays energy spectra 77−13472
clusters of galaxies observed by HEAO 1 scanning modulation collimator, X-ray locations and sizes 79−97090
clusters of galaxies rel. to infalling intergalactic matter 78−93487
clusters of galaxies subsonic accretion of cooling gas 77−74151
clusters of galaxies. X-ray luminosity correl. with galactic content 78−32585
collapsed stars, accretion magnetosphere stability, polar cap dripping motion 78−4194
colliding stellar winds, X-ray emission upper limits 78−65607
Coma, Perseus and Virgo clusters, X-ray emitting intracluster gas models 77−45577
Coma cluster, X-ray emission monitoring by Ariel V Sky Survey 77−2491
Coma cluster of galaxies, hydrostatic struct. of hot plasma 77−17697
Coma cluster of galaxies, spatial distrib. of Compton-produced X-ray flux, theory 77−33686
Coma cluster of galaxies, structure of diffuse X-ray emission 79−92874
Coma cluster X-ray source, X-ray brightness distrib. prediction 79−92896
Coma galaxy cluster, low energy X-ray absorpt. obs. 78−86025
compact binary X-ray sources, model for galactic bulge sources 79−35430
compact source, intensities from stellar wind flow past compact object 80−22116
compact sources, Ariel 5 and Copernicus obs. 79−58443
compact sources, self-consistent spherical accretion 79−53936
compact sources, time-depend. spherically symmetric accretion 79−21462
compact X-ray sources, as cosmic laboratories for study of neutron stars and hadron matter 80−77442
compact X-ray sources, form. from evolution of mass-accreting white dwarfs 80−77281
compact X-ray sources, masses 78−12430
compact X-ray sources, spectra form. 80−22115
Compton and synchrotron processes in spherically-symmetric non-thermal sources 79−88583
Comptonisation of Fe X-ray spectral features 78−20908
Comptonization and radiation spectra, Monte Carlo calc. *(Russian)* 79−80372
Comptonization of X-rays by low-temp. electrons, Monte Carlo calc. 80−12653
Comptonization of X-rays by low-temperature electrons, rel. to X-ray sources spectra 79−35108
convective accretion discs and X-ray sources 78−16568
cool stars, HEAO 1 search for coronal soft X-ray emission 79−101140
σ Coronae Borealis (H 1613+33), spectroscopic binary, soft, X-ray obs. with (HEAO-1) 80−56886
COS-B γ-ray sources, nearby faint X-ray sources detect. 78−54093
cosmic exploration by X-rays, 1978 Bakerian lecture 79−48964
cosmic X-ray bursts, mechanism assoc. with max. mass of neutron stars 77−33545
cosmic X-ray bursts, OGO-5 satellite obs. 77−13492
cosmic X-ray bursts tails, interpretation 79−12546
cosmic X-ray sources, multiple Compton scatts. effects on X-ray emission spectrum 78−96389

X-ray sources continued
Crab Nebula, imaging by balloon-borne X-ray telescope *(Japanese)* 79−80220
Crab nebula, model for pulsed γ-ray and X-ray emission 80−62230
Crab Nebula, obs. by gamma-ray telescope with modulating anticollimator *(Russian)* 79−16832
Crab Nebula, optical and X-ray surface brightness from supernova remnant physical theory supernova 80−51834
Crab Nebula, polarimetry with OSO-8 X-ray polarimeter 78−12426
Crab Nebula, possible line feature at 73 keV, intensity and width 79−92829
Crab Nebula, search for thermal X-ray line emission 78−8095
Crab Nebula, shock waves hydrodynamics rel. to diffuse soft X-rays 78−85997
Crab Nebula, X-ray polarization, precision meas. without pulsar contamination 78−41086
Crab Nebula X-ray source lunar occultation obs. by balloon *(Japanese)* 77−82319
Crab pulsar, high-energy photon spectrum rel. to energetic particles momentum distrib. 78−73727
critical accretion flow of gas into compact stars, rel. to X-ray sources 78−20817
cyclotron self-absorption in accretion columns of magnetic degenerate stars, X-ray sources appl. 80−12760
SS Cygni, dwarf nova, ANS detection of both soft and hard X-ray emission 78−36579
SS Cygni, dwarf nova, identification as hard X-ray source by HEAO 1 scanning modulation collimator 79−2548
SS Cygni, dwarf nova, soft X-ray pulsation obs. 80−46563
SS Cygni, dwarf nova, X-ray polarisations discovery 78−65628
Cygnus A, giant cD radio galaxy, extended X-ray source 79−67109
Cygnus Loop, supernova remnant, X-ray spectra var. with position 80−82472
Cygnus Loop, X-ray image 79−25663
Cygnus OB2 association (V1 Cygni), soft X-ray emission sources discovery 80−26918
Cygnus region, soft X-ray sources and supernova remnants 78−4397
Cygnus superbubble 80−105323
Cygnus X-1, 39 day polarization period, Thomson scatt. 78−8166
Cygnus X-1, (Cygnus X-1), in optical counterpart V1357 Cygni 80−41861
Cygnus X-1, (HDE 226868), IUE UV spectrum obs. 78−96569
Cygnus X-1, absence of 39 day period in non-UV data 78−8167
Cygnus X-1, accretion disc corona 78−16569
Cygnus X-1, accretion disc temp. rel. to spectrum 77−45479
Cygnus X-1, accretion disk round black hole, temp. var., X-ray obs. 80−109561
Cygnus X-1, anomalous light curve during X-ray increase of 1975 April-May 78−28850
Cygnus X-1, bimodal behaviour of accretion disc 77−60850
Cygnus X-1, binary system model 78−81706
Cygnus X-1, black hole candidate, review 78−16577
Cygnus X-1, brightness var. rel. to subphotospheric layers *(Russian)* 79−25764
Cygnus X-1, correlated X-ray-radio transition, 1976 February 77−17719
Cygnus X-1, critique of polarimetric evidence on physical parameters and orbital inclination 80−109486
Cygnus X-1, discovery of synchronous binary polarization 78−41087
Cygnus X-1, distortion of absorpt. line vel. curves due to X-ray heating 77−29878
Cygnus X-1, evidence for 39 day period 78−8165
Cygnus X-1, evidence for new variabilty in hard X-ray emission 80−27011
Cygnus X-1, extended secondary envelope with eclipsing region, V-polarization obs. 79−35433
Cygnus X-1, extended-bandwidth X-ray obs. 80−17689
Cygnus X-1, hard X-ray intensity and spectrum short term changes 77−9814
Cygnus X-1, hard X-ray spectrum 79−71156
Cygnus X-1, hard X-ray spectrum during 1975 November transition 77−2496
Cygnus X-1, HEAO-1 pointed obs. 78−7856
Cygnus X-1, high-energy X-ray spectra, 0S0-8 obs. 79−71151
Cygnus X-1, intensity transitions obs. by OSO 8 77−64886
Cygnus X-1, inverse Compton model 80−51918
Cygnus X-1, line blending effects rel. to black hole candidacy 77−64878
Cygnus X-1, linear optical polarisation obs. *(Russian)* 77−64880
Cygnus X-1, mean blue light curve feature 77−17718
Cygnus X-1, model of neutron star surrounded by massive disc 80−36736
Cygnus X-1, neutron star model from bi-metric theory of gravitation 80−90466
Cygnus X-1, new period in X-ray binary system *(German)* 78−81712
Cygnus X-1, obs. during high state (1980 June 11 to 27) 80−86017
Cygnus X-1, obs. in energy range 100 keV-3 MeV 78−20907
Cygnus X-1, optical and X-ray evidence for 78/39-day period 78−89274
Cygnus X-1, optical polarisation orbital vars. rel. to binary system inclination 78−54077
Cygnus X-1, orbital period and Hβ light curve 79−48952
Cygnus X-1, physical reality of millisecond bursts questioned, shot noise effects 78−45429
Cygnus X-1, polarimetry with OSO-8 X-ray polarimeter 78−12426
Cygnus X-1, possible black hole, astronomical background to speculations *(French)* 78−77624
Cygnus X-1, possible existence of black hole 79−48842
Cygnus X-1, possible remnant of SN 1408, from Chinese historical records *(Chinese)* 79−80343
Cygnus X-1, radio source, variable binary system, SHF obs. 80−73071
Cygnus X-1, rapid X-ray flaring obs. 77−57105
Cygnus X-1, rotating black hole existence, obs. test 77−33699
Cygnus X-1, Salyut-4 obs. in 0.2-10 keV range *(Russian)* 77−57109
Cygnus X-1, search for rapid optical periodicities 78−24573
Cygnus X-1, search for X-ray polarisation 78−4406
Cygnus X-1, short-term time variability, shot noise model 78−36721
Cygnus X-1, short-term time variability 78−93466
Cygnus X-1, short-term variability in hard X-ray region *(Japanese)* 79−80369
Cygnus X-1, shot noise model for short-term variability 78−93474
Cygnus X-1, status report 78−77618
Cygnus X-1, submillisecond meas. of low state 77−45607
Cygnus X-1, temporal and spectral var., X-ray rocket obs. 78−8163

X-ray sources continued
Cygnus X-1, transition from high X-ray state to low X-ray state, 1980 June to July 80−98738
Cygnus X-1, UV shot noise upper limit 80−4458
Cygnus X-1, variable circular polarisation obs. 77−29952
Cygnus X-1, X-2 and X-3, long-term-studies with Ariel 5 All-Sky Monitor (ASM) 80−17688
Cygnus X-1, X-ray and UV spectra from HEAO 2 and IUE 80−82543
Cygnus X-1, X-ray emission rel. to disc accretion onto black hole 77−64791
Cygnus X-1, X-ray flux time variability struct. *(Russian)* 80−51921
Cygnus X-1, X-ray variability in high state 78−28855
Cygnus X-1 (HDE 226868), 78.4 day period search in X-rays and optical polarisation 79−75297
Cygnus X-1 (HDE 226868), accretion disk size 80−51910
Cygnus X-1 (HDE 226868), Hα emission in (1977) 80−51919
Cygnus X-1 (HDE 226868), long-term circular polarisation variability 79−9031
Cygnus X-1 (HDE 226868), optical photometry, (1972-1976) 78−32609
Cygnus X-1 (HDE 226868), orbital period and inclination 78−16579
Cygnus X-1 (HDE 226868), variable linear polarisation, 1974-1975 obs. 77−9810
Cygnus X-1 (HDE 226868), variable UV polarisation 77−37622
Cygnus X-1 (HDE 226868) He II 4686 Å emission in spectrum 79−21328
Cygnus X-1 (HDE 226868) system, search for third star 77−45606
Cygnus X-1 (V1357 Cygni), narrow-band photoelec. obs. *(Russian)* 79−88767
Cygnus X-1 (V1357 Cygni), optical light curve vars. rel. to X-ray vars. 80−109560
Cygnus X-1 (V1357 Cygni), optical photometry (1980 May 25 to July 7) 80−90578
Cygnus X-1 (V1357 Cygni), UBVR obs. and accreting disk radiation *(Russian)* 79−25645
Cygnus X-1 (X-2, X-3), X-ray polarisation obs. from OSO 8 80−90571
Cygnus X-1 and Circinus X-1, time variability comparison 80−56974
Cygnus X-1 and X-3, search for 1-20 MeV gamma rays, balloon-borne obs. 80−67912
Cygnus X-1 possible existence of black hole in binary system 78−16457
Cygnus X-2, Ariel 5 SSI obs., modulation rel. to 79−21464
Cygnus X-2, binary, radial vel. and orbital elements from visible spectra obs. 80−77519
Cygnus X-2, high-speed photometry optical candidate 77−13494
Cygnus X-2, optical magnitude variation *(Russian)* 77−26093
Cygnus X-2, optical variability upper limits 78−96564
Cygnus X-2, polarimetry with OSO-8 X-ray polarimeter 78−12426
Cygnus X-2, rapid UV flux vars., IUE obs. 80−12833
Cygnus X-2, spectroscopic obs., orbital period, spectral-type var., X-ray heating 79−9036
Cygnus X-2, spectroscopic obs. *(Russian)* 77−26092
Cygnus X-2, TV photometer obs. of optical counterpart *(Russian)* 78−57697
Cygnus X-2, variable optical flickering 78−73773
Cygnus X-2, X-ray and optical obs., (1973 to 1977) 79−30148
Cygnus X-2, X-ray binary, optical variability in UBV 77−26027
Cygnus X-2 (V1341 Cygni), halo population binary 79−97099
Cygnus X-2 (V1341 Cygni), possible 82-minute quasi-periodic bursts obs. *(Russian)* 79−17140
Cygnus X-2 (V1341 Cygni), shortest optical variability *(Russian)* 80−17695
Cygnus X-2 (V1341 Cygni), UBV photometry and light vars. 79−5833
Cygnus X-2 as spherically accreting nonmagnetic degenerate dwarf 80−46703
Cygnus X-3, 1974 EAS obs. of high-energy gamma-ray source *(Russian)* 77−64881
Cygnus X-3, 34.1 day period, 2-12 keV obs. by COS-B 80−94897
Cygnus X-3, 4.8 hour modulation period change disproved 80−8713
Cygnus X-3, 4.8 hour periodicity in spectra 79−5920
Cygnus X-3, 50-400 keV obs., power law spectrum 80−41913
Cygnus X-3, γ-ray flux meas. above 10^{12} eV 77−53706
Cygnus X-3, binary puisar age and activity *(Russian)* 78−4413
Cygnus X-3, cocooned X-ray binary pulsar model 78−36723
Cygnus X-3, continuous period change obs. in 2-12 keV range 79−9033
Cygnus X-3, COS-B X-ray obs., 4.8 hour modulation 78−28856
Cygnus X-3, efficient particle acceleration 80−31391
Cygnus X-3, evidence for X-ray Fe line emission obtained with cryst. spectrometer 78−8153
Cygnus X-3, gamma radiation during radio outburst 77−64884
Cygnus X-3, gamma-ray emission from mag. accretion disc 77−78894
Cygnus X-3, gamma-ray emission periodicity 79−62932
Cygnus X-3, gamma-ray obs. with 4.8 hr periodicity 77−26086
Cygnus X-3, hard X-ray spectrum obs. 80−31388
Cygnus X-3, inverse Compton γ rays 77−41421
Cygnus X-3, model for quiescent radio emission 77−33689
Cygnus X-3, observational constraints, on models 78−16567
Cygnus X-3, period derivative 79−48955
Cygnus X-3, period derivative and asymmetric X-ray light curve from HEAO 2 obs. 80−105394
Cygnus X-3, period stability 77−2489
Cygnus X-3, periodic γ-ray emission obs. *(Russian)* 77−91672
Cygnus X-3, periodic gamma flux *(Russian)* 77−26090
Cygnus X-3, search for gamma ray emission 77−74159
Cygnus X-3, X-ray Fe line emission meas. with Bragg crystal spectrometer 79−12544
Cygnus X-3, young pulsar in binary system model 77−29955
Cygnus X-6, X-7, part of large X-ray superbubble, X-ray obs. 80−90575
Cygnus X-I, main energy release region, plasma temp. determ. 80−85850
Cygnus X-ray superbubble, existence and power source, X-ray obs. 80−90575
Cygnus X-Z rel. to old novae 77−87576
degenerate dwarf stars, X-rays from spherically symm. accretion 77−78781
HR Delphini (Nova 1967), simultaneous X-ray, UV and optical obs. 80−109440
dense clouds and X-ray burst origin 77−78896
detection of cosmological objects 80−62323
diffuse background, active galactic nuclei contrib. 78−36733
diffuse background radiation, origin, primaeval hot gas clouds fragmentation 78−28861

X-ray sources continued
diffuse background spectrum, 20 keV spectral index change determ. 78−69916
diffuse soft X-ray background, three-band obs. rel. to thermal emission models 77−45604
diffuse soft X-ray background enhancements 77−29953
diffuse soft X-ray sky, astrophysics rel. to 0.1-2.0 keV cosmic X-rays 78−16581
diffuse soft X-ray sources, obs. via Bragg cryst. spectrometer 77−5440
diffuse X-ray background, implications of Hubble const. for discrete source models 79−101226
diffuse X-ray background, source 78−8168
diffuse X-ray background, spectrum from 3 to 50 keV 80−41916
disc accretion onto magnetised compact objects, theory *(Russian)* 79−44467
discrete source model for cosmic X-ray background, search for correl. with light of galaxies 80−56977
Dopplers, Hα line freq. depend. general relativistic formula, appl. to (SS 433) 79−97010
AD Draconis, flare star, coronal soft X-ray emission obs. by (HEAO 1) 79−101140
dwarf novae, EUV obs. from Apollo-Soyuz Test Project 78−93252
dwarf novae, soft X-ray emission 77−45457
dynamical evolution of hot intracluster gas from galaxies, Fe abundance in X-ray clusters 79−12530
effects on ionospheric VLF propag. 79−53649
Einstein Observatory sources fields, RI photometry with CCD camera 80−62315
emission mechanism involving accretion onto compact bodies 80−90459
emission mechanisms, detection techniques 77−22061
emission-line galaxies, high-excitation, HEAO 1 X-ray obs. 79−62907
40 Eridani A(=o^2 Eridani), evidence of corona on X-ray image 80−105282
40 Eridani C, X-ray image of dM4e flare star 80−105282
ESO 103-G35, Seyfert galaxy and possible X-ray source 79−88741
EUV/soft X-ray background, Apollo-Soyuz sky survey results 79−71160
EXP 0520−66, flaring X-ray pulsar, recurrent gamma-ray bursts obs. *(Russian)* 80−36741
extragalactic, review *(Polish)* 79−101223
extragalactic compact sources, observational consequences of synchrotron self-Compton models 77−29961
extragalactic sources, deep X-ray surveys predictions and strategies 78−96567
extragalactic sources, positional and spectral data, HF obs. 80−86019
extragalactic sources, review 78−73776
extragalactic sources and diffuse X-ray background 79−58447
extragalactic sources correl. with radiosources from 26.3 MHz survey 78−65707
extragalactic sources in 2A catalogue, optical identifications 78−89273
extragalactic X-ray sources, luminosity function and variability time scale 78−57701
extragalactic X-ray sources, radio emission problems *(Dutch)* 77−67133
Fairall 9, X-ray emitting Seyfert galaxy 78−28790
Feige 24, white dwarf, intense soft X-ray source in Cetus 77−9746
flare-up of X-ray source, SAS-3 obs. 78−20915
flaring X-ray pulsar in Dorado, gamma-ray bursts *(Russian)* 79−88765
FXP 0520−66, flaring X-ray pulsar, nature and optical identification *(Russian)* 80−77521
FXP 0520−66, flaring X-ray pulsar in Dorado, Venera 11 and 12 obs. 80−27018
galactic, anticorrelation with radio sources, plasma cloud interpretation 80−82514
galactic, IR photometric obs., identifications, reddening 79−71155
galactic, photoionization of interstellar gas causing UV absorpt. lines 77−13439
galactic and extragalactic, review of current knowledge in 0.5 to 10 keV range 78−69915
galactic bulge sources, radio continuum obs. at 2.7, 4.8 and 10.7 GHz 80−101619
galactic bulge X-ray sources, black hole and orbital disk model 80−17691
galactic bulge X-ray sources, models, binary systems 78−81706
galactic bulge X-ray sources, precise positions from SAS-3 obs. 78−16575
galactic centre, Prognoz-6 obs. of X-ray fluxes and energy spectra *(Russian)* 80−109562
galactic centre, search for X-ray pulsations 79−44617
galactic centre, X-ray activity 79−58419
galactic centre, X-ray point source flux rel. to central black hole mass 80−90467
galactic centre and Cygnus region, spectral characts. of X-ray sources 78−54079
galactic centre region, high-energy X-ray detection 80−67854
galactic centre sources, positions meas. by Ariel-5 RMC expt. 78−4407
galactic centre X-ray burst sources 77−13499
galactic clusters, X-ray emission energy sources 79−44574
galactic diffuse soft X-ray emission, brightness distrib. 79−53942
galactic distrib. 80−67905
galactic hard and soft X-ray sources, space distrib. and physical nature 80−62316
galactic nuclei, compact X-ray sources model rel. to giant elliptical galaxy (M87) 78−28847
galactic nucleus, high-resolution 2-10 keV rocket obs. of discrete X-ray sources 78−65692
galactic soft X-ray background rel. to coronal gas O VI absorpt. 78−36653
galactic source distrib. 78−93462
galactic sources, Ariel 5 positions 79−58446
galactic sources, review 77−29962
galactic sources, unidentified, positions with HEAO-1 scanning modulation collimator 80−105395
galactic structure rel. to weak low-latitude source studies 79−84858
galactic X-ray sources, $320° < l^{II} < 340°$, positions 78−28860
galactic X-ray sources, $55° < l^{II} < 320°$, positions 78−61938
galactic X-ray sources, −20° to +6° galactic longit., positions 78−54094
galactic X-ray sources, classification and Ariel 5 obs. 79−58445
galactic X-ray sources, constraints on apsidal motion 77−87571
galactic X-ray sources, correl. between hardness and pulsation 78−4399
galactic X-ray sources, distrib. in Milky Way 78−28851
galactic X-ray sources, large-scale distrib. 79−48954

X-ray sources continued
galactic X-ray sources, long-term variability 79−2579
galactic X-ray sources, obs. from on board (Salyut 4) 77−91665
galactic X-ray sources, optical identifications 77−87573
galactic X-ray sources, OSO-7 obs. 78−32600
galactic X-ray sources, precise positions 77−87574
galaxies, active nuclei, theories and X-ray production 79−58421
galaxies, compact nuclei, scattered X-ray flux 78−4363
galaxies, normal, contrib. to diffuse X-ray background 79−17141
galaxies, primeval, appearance in X- and γ-ray regions, contrib. to background rad. 80−8692
galaxies, review of compact sources and Seyferts 79−58422
galaxies, X-ray luminosity limit of nearby normals 80−4443
galaxies active nuclei, models of unsaturated Compton accretion discs around supermassive black holes 80−22033
galaxies compact groups, X-ray emission obs. 80−90574
galaxies in MKW-AWM poor clusters, optical props. 80−94878
galaxies in nearby superclusters, X-ray source clustering rel. to hot gas 78−41065
Galaxy, diffuse soft X-rays distrib. and energy spectrum 78−28853
galaxy cluster relaxation effect on intergalactic gas and X-ray emission 80−46684
galaxy cluster X-ray sources, luminosity function evolution 80−62314
galaxy cluster X-ray sources evolution, subcluster collisions 79−53915
galaxy clusters, nonspherical, hydrostatic struct. of hot plasma and X-ray morphology, rel. to Perseus cluster rot. 79−35406
galaxy clusters, X-ray brightness distrib., gravitational potentials 79−12529
galaxy clusters, X-ray luminosity function, predictions from thermal bremsstrahlung model 79−101208
galaxy clusters, X-ray luminosity function 79−40277
galaxy clusters, X-ray spectra 80−26996
Galaxy contrib. to diffuse X-ray flux in 2 to 7 keV range 80−98745
galaxy coronae, hot gas dynamics simulation 80−82481
galaxy rich clusters and superclusters, and clusters extended halos, X-ray emission search 80−26988
galaxy superclusters, X-ray emission, Uhuru meas., intergalactic gas 78−41064
U Geminorum, soft X-ray emission and visual magnitude estimates 77−91544
giant X-ray pulses, mass transfer in eccentric binary model 77−33690
globular cluster X-ray source, evolution of 100 M⊙ black hole in binary 78−61932
globular cluster X-ray source formation by collisions of compact and normal stars 78−28854
globular cluster X-ray sources, review 78−12428
globular clusters, appl. of QSO black tide model to X-ray sources 77−78884
globular clusters, central X-ray binary stars 78−20916
in globular clusters, close binary X-ray sources origin 79−44530
globular clusters, evidence for H II in cores 78−8065
globular clusters, gas content upper limits rel. to X-ray emission 80−22047
globular clusters, incidence of close binary stars, rel. to nature of cluster X-ray sources 77−41396
globular clusters, nova-driven winds rel. to X-ray source models 78−57596
globular clusters, star counts 77−33578
globular clusters, UBV photometry 78−16468
globular clusters, X-ray obs. with ANS 77−26029
globular clusters, X-ray sources locations 79−97102
gravitationally redshifted γ-rays, neutron star mass constraints 78−4274
GX304−1 (4U 1258−61), shell spectrum of optical counterpart 80−46582
GX9+1, lunar occultation position 77−45612
GX 13+1 (3U 1811-17), X-ray and radio obs. 78−41081
GX 17+2 (3U 1813−14), photometry of optical candidate 78−28849
GX 17+2 (3U 1813-14), optical search 77−2485
GX 17+2 (3U 1813-14), radio and optical identification 78−45428
GX 17+2 (3U 1813-14), X-ray and radio obs. 78−41081
GX 1+4, galactic centre source, X-ray obs. periodicity 80−105399
GX 1+4, search for Hα pulsations 78−86037
GX 1+4 optical counterpart, symbiotic star, spectrophotometry 77−33498
GX 301−2, binary star, cyclotron line feature identification 80−90577
GX 301−2, spectra and pulse period vars. 77−2486
GX 301−2 (4U 1223−62), SAS-3 obs. of 1978 January brightening 78−28858
GX 304−1, shell star optical counterpart 78−93471
GX 304−1 (3U 1258−61), discovery of 272 second period var. 78−8152
GX 326.3−1.8≡MSH 15-56, soft X-ray emission detect. 79−44639
GX 339−4, black hole candidate 79−48962
GX 339−4, variable X-ray source identification with faint blue object 79−40294
GX 339−4 (4U 1658−48), possible black hole binary, optical studies 79−101220
GX 3+1, X-ray bursts obs., (1980 July 19 to August 18) 80−98739
H0118+067, identification with RS Canum Venaticorum star UV Piscium, X-ray obs. 80−101654
H0405−08 (40 Eridani), X-ray emission discovery 79−97035
H0630+82, identification with RS Canum Venaticorum star SV Camelopardalis, X-ray obs. 80−101654
H1122−59 (G292.0+1.8), supernova remnant, optical identification and spectrum 79−84839
H1122−59 (G292.0+1.8), young supernova remnant, high vel. material obs. 80−22064
H1122−59 near Centaurus X-3, new source, MSH 11−54 coincidence 78−28859
H1207−52, soft X-ray emission detect. from southern SNR 78−77620
H1616−51, soft X-ray emission detect. from southern SNR 78−77620
H1-36 (3U 1746-37), emission line object, radio spectrum 77−82239
H2027+19, extended soft X-ray source in Delphinus, discovery 80−90576
H2155−304 (PKS 2155−304), newly discovered BL Lacertae object, X-ray and optical props. 80−36702
H2309+59 near Cassiopeia A, new source, V Cassiopeia coincidence 78−28859
H 0523−00 assoc. with Arakelyan 120, X-ray obs. of Seyfert 1 galaxy 80−105344
H 0544-665, optical candidate for LMC X-ray source 80−36737

X-ray sources continued
H 0622−529, obs. of highly variable source 79−48959
H 1538−32, new extended soft X-ray source detect., possible old supernova remnant 80−51912
H 1743−32, transient source, detect. 78−45431
H 1743-32, transient X-ray source, HEAO-1 position obs. 77−87572
H 1834−653, spectral obs. of optical counterpart ESO 103-G35 Seyfert galaxy 78−96547
H 1901+43, soft X-ray emission from nova-like object 79−92787
H 1908+050 (SS 433), X-ray obs. 79−71153
H 2155−304, highly luminous BL Lacertae object, spectral obs. 80−4459
H 2155−304, optical candidate spectrophotometric obs. 79−25761
H 2155−304, positions and optical counterpart identification 78−93478
H 2155−304, Very Large Array obs., radio source discovery 79−44643
H 2156−304, intense high-latit. soft X-ray source and possible new BL Lacertae object 79−92891
H 2208-47, possible identification with S0 Seyfert galaxy (NGC 7213) 78−86024
H 2252−035, optical counterpart photometry and spectrum 80−101651
H 2252−035, spectrophotometry, no periodic linear polarization (1980 Sept.) 80−105401
H 2252−035, X-ray flux modulation, compact star rotation 80−101652
hard X-ray sources, obs. by spectrometer on Kosmos 428 satellite 77−64640
hard X-ray sources discovered by HEAO A-2 expt. 80−17690
HB3, supernova remnant, X-ray emission obs. 78−81679
HB 3, supernova remnant, soft X-ray obs. 80−56915
HD 152667 (V861 Scorpii), eclipsing binary X-ray source, possible black hole 79−53858
HD 152667 (V861 Scorpii), phys. props. and orbital parameters, supergiant star with black hole companion model 79−71067
HD 153919, Of supergiant, X-ray binary 3U 1700−37 optical counterpart, light curve anal. 78−32470
HD 153919, Of X-ray binary, narrow band photoelectric photometry 77−60761
HD 153919 (3U 1700−37), X-ray binary, UV photometric obs. 77−45490
HD 153919 (3U 1700−37), X-ray eclipsing binary, VBLUW photometric obs. 79−17135
HD 226868 (Cygnus X-1), periodicity in optical light curve during X-ray flare 78−81652
HD 64740, He variable star, X-ray source 4U 0750−49 optical candidate 78−36584
HDE 245770 (Ariel 0535+26), optical spectrum of Be star 78−4227
Hercules X-1, 23 day low state, Uhuru obs. 77−5594
Hercules X-1, 2-6 keV pulse profiles, Uhuru data 79−17129
Hercules X-1, 64 keV line feature in X-ray spectrum 77−78895
Hercules X-1, (HZ Herculis), optical and UV obs. 80−109487
Hercules X-1, accretion disc viscosity determ. using slaved disc model 80−62110
Hercules X-1, binary star, cyclotron line feature identification 80−90577
Hercules X-1, cyclotron line form. by reson. Compton cyclotron scatt. 80−8711
Hercules X-1, cyclotron self-absorpt. in accretion column of mag. degenerate star 80−12760
Hercules X-1, eclipsing binary, X-ray spectra from Ariel V satellite 80−90580
Hercules X-1, eclipsing binary system obliquity 77−13390
Hercules X-1, energy transport by circulation from illuminated region of HZ Herculis 79−71070
Hercules X-1, evidence for 35 day precession in orbit 77−37667
Hercules X-1, Fe line emission discovery in low-state spectrum by (HEAO-1) 79−5922
Hercules X-1, hard X-ray line feature obs., cyclotron emission 78−81709
Hercules X-1, hard X-ray pulsation obs. 78−12293
Hercules X-1, hard X-ray spectrum, strong cyclotron line emission 78−41085
Hercules X-1, heliocentric pulse period, OSO 8 obs. 77−91573
Hercules X-1, high-energy pulsed X-ray spectrum from OSO 8 obs. 79−92888
Hercules X-1, high-energy X-ray spectrum 78−93473
Hercules X-1, implications of cyclotron features in X-ray spectrum 80−86015
Hercules X-1, linear optical polarisation obs. *(Russian)* 77−64880
Hercules X-1, long-term studies with Ariel 5 All-Sky Monitor 79−30146
Hercules X-1, mag. neutron star, cyclotron emission and beaming mechanisms 78−36726
Hercules X-1, orbital precession 78−65718
Hercules X-1, orbital precession from Doppler modulation of pulsation arrival times 77−13398
Hercules X-1, precessing accretion disc with 70 day period 77−33693
Hercules X-1, precessing twisted accretion disks 80−56973
Hercules X-1, pulse phase spectroscopy, 6-60 keV 79−84870
Hercules X-1, pulse profile in hard X-rays 77−9811
Hercules X-1, search for X-ray polarization 80−4457
Hercules X-1, X-ray binary, X-ray refl. from neutron star surface 78−28716
Hercules X-1, X-ray emission behaviour 77−87569
Hercules X-1, X-ray lines and magnetic field 78−24574
Hercules X-1, X-ray pulsation obs. by SAS-3 during 1975, July 77−60793
Hercules X-1, X-ray spectra, Fe line fluoresc. from subrelativistic shell 78−4405
Hercules X-1, X-ray spectra, pulse phase depend. in high-energy continuum 79−17128
Hercules X-1, X-ray spectra near turn-on in 35 day cycle 77−60794
Hercules X-1, X-ray spectrum of pulse 78−8154
Hercules X-1 (HZ Hercules), 70 day period refuted 80−56975
Hercules X-1 (HZ Herculis), 1978 UBV photometry of active state 80−62189
Hercules X-1 (HZ Herculis), 35 day clock mechanism 80−73070
Hercules X-1 (HZ Herculis), 35 day cycle investigation 78−32509
Hercules X-1 (HZ Herculis), abnormal N III emission lines in 1978 Aug. spectrum 78−81661
Hercules X-1 (HZ Herculis), Bowen fluorescence mechanism evidence 78−53985
Hercules X-1 (HZ Herculis), coordinated optical and X-ray pulsations obs. 80−51909
Hercules X-1 (HZ Herculis), Copernicus and Ariel V obs. 77−45609

X-ray sources continued
Hercules X-1 (HZ Herculis), eclipsing binary, light curve interpretation rel. to disclike envelope struct. 78−65658
Hercules X-1 (HZ Herculis), hard X-ray obs. 78−36728
Hercules X-1 (HZ Herculis), IUE Obs., spectrum and light var. 80−73069
Hercules X-1 (HZ Herculis), IUE UV spectrum obs. 78−96569
Hercules X-1 (HZ Herculis), light curve, radiation pressure effects 80−105280
Hercules X-1 (HZ Herculis), mass from optical pulsation calcs. 78−57580
Hercules X-1 (HZ Herculis), multiperiod variable star 78−28848
Hercules X-1 (HZ Herculis), optical behaviour in (1976) 78−32603
Hercules X-1 (HZ Herculis), optical pulsations rel. to accretion disc/mag field interaction *(Russian)* 80−51799
Hercules X-1 (HZ Herculis), periodic mass transfer rel. to X-ray light curve 80−51911
Hercules X-1 (HZ Herculis), soft X-ray results from OSO-8 Wisconsin Expt. 78−36722
Hercules X-1 (HZ Herculis), Sonneberg photographic obs. 77−37618
Hercules X-1 (HZ Herculis), X-ray binary, tidal friction effects 77−57013
Hercules X-1 (HZ Herculis), X-ray continuum and Fe line emission during X-ray low state 80−105393
Hercules X-1 (HZ Herculis) binary system, pre-supernova parameters 80−62318
Hercules X-1 (HZ Herculis) mass determ. 77−78891
Hercules X-1 binary system, possible third star existence 77−33572
Hercules X-1 spectrum, struct. and higher harmonics of cyclotron lines 78−20912
Hercules X-1/HZ Herculis, evaporative winds 77−78888
AM Herculis, 1.2 and 2.2 μm light curves interpretation, model parameters 79−8949
ϕ Herculis, Ap star, X-ray emission obs. 79−101160
AM Herculis, evidence on nature of soft X-ray source from HEAO 1 obs. 79−17134
AM Herculis, hard X-ray spectrum 79−17022
AM Herculis, highly magnetised, accreting white dwarf 77−49396
AM Herculis, IR and visual monitoring, model constraints 79−17018
AM Herculis, IR spectroscopy, period, mass function 79−71066
AM Herculis, IUE UV obs. 79−67051
AM Herculis, multicolour photometry, slow optical pulsar 78−28693
AM Herculis, narrow-band photoelectric obs. *(Russian)* 78−77565
HZ Herculis, nonperiodic optical flickering obs. 78−53988
HZ Herculis, optical props. of accretion disc 78−28729
AM Herculis, OSO-8 hard X-ray obs. 78−4409
AM Herculis, OSO-8 X-ray obs., 2-250 keV energy range 79−71075
HZ Herculis, refl. effect turn-off *(Russian)* 78−69840
AM Herculis, spectroscopic obs., H lines and He II 4686 Å line intensities 78−57589
AM Herculis, UBVRI light curves 78−85972
AM Herculis, visual magnitude estimates (1980 March-June) 80−82428
AM Herculis, X-ray binary, emission lines, radial vel. var. 77−33567
AM Herculis, X-ray binary, obs., slow rotator model 78−12408
AM Herculis, X-ray binary, optical light curve 77−33566
AM Herculis, X-ray binary, polarization obs., mag. compact star discovery 77−33569
AM Herculis, X-ray binary, spectroscopy and photometry, model 77−33568
AM Herculis, X-ray binary, vel. curves for emission lines broad and sharp components 78−32513
DQ Herculis, X-ray obs. from Ariel 5 satellite 77−37671
AM Herculis (3U 1809+50), IR light curves 78−28727
AM Herculis (3U 1809+50), multicolour linear and circular polarisation obs. and geometrical model 78−8053
AM Herculis (3U 1809+50), soft X-ray results from OSO-8 Wisconsin Expt. 78−36722
AM Herculis (4U 1813+50), binary source, optical variability 78−53952
AM Herculis (4U 1813+50), narrow-band photoelec. obs. *(Russian)* 79−88767
HZ Herculis (Hercules X-1), optical behaviour, 1976 Aug.-1977 Nov. 79−53855
HZ Herculis (Hercules X-1), optical pulsations spectrum meas. 77−33685
HZ Herculis (Hercules X-1), UBVR photometry during 1977 Jul.-Aug. *(Russian)* 79−17028
AM Herculis type binaries, cyclotron self-absorption in accretion columns of magnetic degenerate stars 80−12760
AM Herculis/3U 1809+50 X-ray binary, rot. mag. white dwarf model 77−33571
High Energy Astrophysics Division of Am. Astron. Soc., meeting (Cambridge, MA, 28-30 Jan. 1980) 80−36761
high galactic latitude sources, identifications with southern clusters of galaxies 78−49553
high-latitude sources, Uhuru satellite obs. of 3U and MX objects 77−9808
high-sensitivity X-ray survey, discrete source contrib. to extragalactic background 80−27016
hot corona around black hole accretion disc and Cygnus X-1 model *(Russian)* 77−22265
hot degenerate stars in steady-state accretion, thermal stability 78−40929
hot plasma, X-ray emission and radiative transfer effect 78−36451
hot white dwarf, radial oscill. mode nonlinear calc. 80−67713
hot white dwarfs as EUV and soft X-ray sources, space density 78−61856
hot white dwarfs as thermal soft X-ray sources 78−57553
HR 1099, RS Canum Venaticorum star, 4U 0336+01 optical counterpart 78−32475
HR 1099 (V711 Tauri), RS Canum Venaticorum star, Hα line variability, visible spectra obs. 80−105277
HR 5110, Algol type RS Canum Venaticorum star, Hα, yu photometry obs. 80−105276
HR 976, Am-type star, soft X-ray source obs. 78−81634
EX Hydrae, soft X-ray emission during optical quiescence, HEAO-A2 obs. 79−71054
EX Hydrae, spectra of dwarf nova 80−98670
HZ 43, ultra soft X-ray spectrum of hot white dwarf 78−85941
IC 4329 A, X-ray obs. of extreme type 1 Seyfert 79−12515
IC 443, supernova remnant, X-ray spectrum and structure 77−49453

X-ray sources continued
imaging by HEAO-2 satellite, obs. 79−92892
induced surrounding clouds 79−67117
information sources for neutron star, dense matter and gravitational collapse physics 80−36657
intensity and spectral variability of strong galactic X-ray sources observed by ANS 79−17127
intergalactic collapsed objects, gas accretion, source of cosmic X-ray background 80−90581
inverse Compton reflection, time-depend. theory, X-ray sources appl. 80−12652
ionisation effects in ionospheric D-region 79−35048
ionising background radiation, influence on H at periphery of galaxies 78−65729
Kepler's supernova remnant, X-ray obs. from Einstein Observatory 80−82465
Kerr black hole, low-freq. radiation from infalling particle 80−62176
Klemola 44, cluster of galaxies, X-ray, optical and radio obs. 77−74150
Klemola 44, X-ray cluster of galaxies, redshifts and vels. 78−45414
BL Lacertae objects, high-energy X-ray obs. 80−31353
BL Lacertae objects, X-ray emission obs. by HEAO 1 scanning modulation collimator expt. 79−48921
late-type main-sequence and subgiant stars, HEAO 1 obs. of active coronae 80−72925
Liller I/MXB 1730−333, IR burst detection 79−97105
line spectra, prod. by nonthermal ions 78−36725
linear optical polarisation obs. *(Russian)* 77−64880
LMC, X-ray survey using HEAO 1 scanning modulation collimator 80−17648
LMC bar, soft X-ray source identification 80−82491
LMC N 49, X-ray source 0525.9-66.1, gamma-ray burst obs. *(Russian)* 80−36739
LMC X−1, luminous extended X-ray source obs. 78−16570
LMC X-1, optical candidate spectrum and semi-accurate position 80−67908
LMC X-1, X-2 and X-3, positions from HEAO 1 modulation collimator 79−5923
LMC X-1 region (MC76 and 77), 2 cm obs. 80−51875
LMC X-2, optical candidate UBV photometry and variability 79−17136
LMC X-2, spectrogram confirms optical counterpart 79−21463
LMC X-4, Ariel 5 obs. of eclipses and identification confirmation 77−74161
LMC X-4, binary nature of optical candidate 77−64879
LMC X-4, discovery of X-ray eclipses 78−24572
LMC X-4, identification with eclipsing binary system, review *(German)* 78−81713
LMC X-4, obs. of X-ray eclipses 78−24571
LMC X-4, possible OB star optical candidate 77−9820
LMC X-4, possible optical counterpart 77−13502
LMC X-4, possible optical counterpart OB star 77−29959
LMC X-4, spectroscopic obs. and orbit 79−9028
LMC X-4, X-ray variability obs. 78−4398
LMC X-4 optical counterpart, photometric and spectroscopic obs. 77−49431
LMC X-ray source light curves, Ariel V obs. 77−74164
Loop I, X-ray features, SNR model 80−22066
LS I+61°303, radio, optical, X-ray, gamma-ray Be star, optical and radio obs. 79−88755
LS I+61°303, variable binary radio star (B1 Ib), X-ray emission detect. 80−105400
lunar occultation dates during next decade 77−33697
lunar occultations of X-ray sources, first and last dates (1980 to 1985) 80−77513
RU Lupi, T Tauri star, chromosphere and corona parameters and expected X-ray fluxes *(Russian)* 80−51770
Lupus flare source, Ariel 5 ASM obs. (1979 October 25) 80−8715
AY Lyrae, soft X-ray emission detect. from dwarf nova, H1839+37 79−75227
α Lyrae, soft X-rays detect. with imaging X-ray telescope 79−48953
M15, globular cluster, dynamical models without black hole 78−32536
M15, globular cluster, optical struct. of core 77−13412
M15, globular cluster, search for radio emission from ionized H 77−13410
M15, nucleus brightness profiles of X-ray globular cluster 78−69848
M15, X-ray globular cluster, search for O III 5007 Å forbidden line emission 78−36644
M31, extended H I regions rel. to interpretation of X-ray obs. 78−12354
M31, X-ray sources, obs. 80−26979
M42 (Orion Nebula), X-ray obs. by Astronomical Netherlands Satellite 78−28852
M86, elliptical galaxy, X-ray evidence for hot gas retention 80−90535
M87, central giant galaxy in Virgo cluster, excess X-ray emission 80−41907
M87, elliptical galaxy, enormous mass rel. to extended X-ray source model 78−28775
M87, Faraday rot. in radio/X-ray halo 80−67844
M87, search for hard X-ray emission 77−29939
M87/Virgo cluster X-ray source spectrum, 1.1 keV Fe line emission discovery 79−25758
in Magellanic Clouds, high luminosity rel. to galactic X-ray sources 78−49559
magnetic X-ray binaries, synchronous rotation appl. to AM Herculis 79−62867
magnetised accretion discs, X-ray burst sources model 77−53702
magnetoactive plasma, cyclotron absorption effects 80−8533
magnetospheric accretion model for repeatedly bursting X-ray sources 77−5597
Markarian 421, optical and radio obs., identification with 2A 1102+384 X-ray source 79−5899
massive binaries, evolution review 80−82343
massive binary stars, X-ray induced shocks in stellar winds 80−94784
massive binary X-ray sources, evolution in conservative case 78−49479
massive black holes, X-ray luminosity 77−33547
massive black holes, X-ray spectrum from disc accretion 78−40985
massive close binary systems, late evolutionary stages 77−57023
massive X-ray binaries, evolution of optical components 80−41857
massive X-ray binaries, lifetimes 77−45608
massive X-ray binaries, OB stars, evolutionary influence of stellar wind 79−101172
massive X-ray binary systems, pulsars rot. history 77−49412

X-ray sources continued
Maxwellian synchrotron sources, spectral characts., model for 3C 273 radio and X-ray spectra 79−35107
MCG−6-30-15, type 1 Seyfert galaxy, X-ray and optical obs. 80−82479
MCG 5-23-16, galaxy, X-ray emission detect. 78−41052
MCG 8-11-11, Seyfert galaxy inside error box of 2A0551+466, optical spectra 77−74130
MCG 8-11-11, X-ray Seyfert galaxy, recent optical activity in nucleus 79−25701
MCG -6-30-15, X-ray emission in 2-10 keV range 78−45405
MIT/OSO 7 catalogue of X-ray sources, intensities, spectra, long-term vars. 79−80243
Mk 421, BL Lacertae-type object, X-ray emission detect. from 2A 1102+384 optical counterpart 78−57698
MKW 3s, poor galaxy cluster, extended X-ray emission detect. surrounding cD galaxy (NGC 5920) 80−51884
models, rel. to solar flare physical mechanisms 77−17499
MR2251−178, X-ray QSO discovery, 2 Ariel 2251−179 optical counterpart 78−24567
MR 2251−178, X-ray QSO, spectrophotometric obs. 79−17122
MR 2251−178, X-ray quasar, companion galaxies redshift data 79−84861
MR 2251−178, X-ray quasar, IR obs. 79−44642
MSH 11-54 (H1122−59), supernova remnant, X-ray obs. 80−82463
MSH 14−63, probable remnant of A.D. 185 supernova, X-ray emission obs. 78−45427
MX0053+60, possible identification with Be star γ Cassiopeiae 77−49401
MX 1406−61, possible X-ray counterpart of γ-ray source (CG 312−1) 78−54092
MXB0512-40, X-ray burst obs. 77−71153
MXB1637−53, 9 X-ray burst obs. 77−9822
MXB1637−53, X-ray burster, optical candidate 77−67140
MXB1730−335, MXB1728−34 rapid bursters, SAS 3 obs. 77−91666
MXB1730−335, rapid burster, turn-off obs. 1977, May 24 77−57107
MXB1730−335, rapid X-ray burster, dual charact., X-ray bursts classification 78−32613
MXB1730−335, SAS-3 obs. on 1978 Apr. 15-16, no burst activity 78−49563
MXB1730−335, X-ray bursts, Ariel 5 obs. 77−57106
MXB1730-335, rapid X-ray burster, turn-on 77−82330
MXB1916−05, X-ray burst obs. 77−64883
MXB 1636−53, simultaneous radio and X-ray obs. of X-ray burst source 79−48961
MXB 1636−53, X-ray burst source, SAS-3 obs. 78−8156
MXB 1636−53, X-ray burst source, simultaneous X-ray and optical bursts obs. 79−92893
MXB 1636-536, binary nature from simultaneous X-ray and optical obs. 80−82548
MXB 1659−29, identification with faint UV stellar object 78−61936
MXB 1659−29, nearby single burst on 1978 March 8 analyzed 78−36731
MXB 1659−29, persistent X-ray emission obs., (1978 March 6 to 9) 78−41090
MXB 1659-29, burst source identification with faint blue object 79−40294
MXB 1706−43, X-ray bursts obs. 78−8161
MXB 1728−34, bursts spectra, intensity and repetition rate 77−49504
MXB 1728−34, type I X-ray burst obs. by (HEAO-1) 80−17692
MXB 1728−34, X-ray burster, search for optical counterpart 77−33694
MXB 1728−34, X-ray bursts obs., (1978 March 8 to 10) 78−41091
MXB 1728-34, X-ray bursts discovery 77−5596
MXB 1730−333, no burst activity in 1980 July-Sept. period 80−105402
MXB 1730−333, Rapid Burster, possible X-ray emission 79−84868
MXB 1730−333, rapid X-ray burster, accreting rot. magnetised neutron star model 79−84866
MXB 1730−333 (Liller I), unusual burst in K-band (2.2 μm) 80−62319
MXB 1730−335, 2.2 μm flashes from X-ray rapid burster 80−46706
MXB 1730−335, 4100 MHz obs. of microwave bursting pattern 80−46705
MXB 1730−335, bursts obs. by SAS-3, 1978 March-April 78−45434
MXB 1730−335, comparison with dwarf novae rel. to neutron star model 78−12410
MXB 1730−335, further analysis of SAS 3 obs. 79−30145
MXB 1730−335, HEAO obs. of X-ray burst 79−17139
MXB 1730−335, IR bursts detect. from Liller 1 optical candidate 79−44640
MXB 1730−335, magnetised accretion disc model for X-ray bursts 77−53702
MXB 1730−335, microwave bursts detect. from rapid X-ray burster 79−48957
MXB 1730−335, new mode of X-ray bursts 80−41915
MXB 1730−335, Rapid Burster, IR bursts detect. confirmation 80−27020
MXB 1730−335, rapid burster, position determ., HEAO 1 obs. 78−49561
MXB 1730−335, rapid burster, SAS-3 obs., (1979, March 3 to 4) 79−40299
MXB 1730−335, rapid burster, search for X-ray bursts, (1978 March 8 to 10) 78−41091
MXB 1730−335, rapid X-ray burster, long-term behaviour 78−32602
MXB 1730−335, rapid X-ray burster, SAS-3 obs. 79−9037
MXB 1730−335, rapid X-ray bursts obs. by SAS-3 77−53707
MXB 1730−335, SAS-3 obs. of 1978 March burst activity 78−45432
MXB 1730−335, SAS-3 obs. of burst activity, 1978 Oct. 78−96573
MXB 1730−335, variability of X-ray burst source 78−77621
MXB 1730−335, X-ray rapid burster, unsuccessful search for IR bursts 80−98740
MXB 1730−335 (Rapid Burster), microwave bursts obs. 80−62320
MXB 1730−335 (Rapid Burster), steady X-ray emission obs. 80−22119
MXB 1730−33, X-ray burster, globular cluster as possible optical counterpart 77−33694
MXB 1730-335, anomalous bursts obs. from rapid X-ray burster 77−49496
MXB 1730-335, rapid-burst source, IR obs. of assoc. globular cluster 77−9776
MXB 1735−44, optical bursts discovery 78−81708
MXB 1735−44, optical bursts obs. 78−61937
MXB 1735−44, rapid X-ray bursts obs. by SAS-3 77−53707

X-ray sources continued
MXB 1735−44, X-ray burst sources, 3 s delay in optical burst 79−58442
MXB 1837+05, optical monitoring 78−77622
MXB 1837+05, X-ray bursts obs. by SAS-3 77−49500
MXB 1837+05(Serpens X-1), simultaneous optical and X-ray bursts obs., 1978 Sept. 79−35435
MXB 1837+05 (Serpens X-1), detect. of optical burst coincident with X-ray burst 80−27013
MXB 1837+05 (Serpens X-1), optical obs. of X-ray bursts 79−30153
MXB 1837+05 (Serpens X-1) simultaneous radio and X-ray obs. 79−21467
MXB 1916−05, optical monitoring 78−77622
N49, supernova remnant in LMC, possible assoc. with gamma ray burst (1979, March 5) 79−58441
N-galaxies as new class of X-ray sources 79−2572
NAB 0137−01, spectrophotometry of possible X-ray quasar 77−13490
nearby main sequence and subgiant stars, XUV radiation upper limits 79−12471
neutron star, accreting, magnetopause struct. 78−65647
neutron star, magnetised, X-ray radiation and cyclotron line form. 79−48839
neutron star, thermal X-ray emission 80−41849
neutron star models 80−62175
neutron star spherical accretion, X-ray spectra and luminosity 77−82271
neutron stars, burst source from He burning shell 80−85968
neutron stars, Eddington luminosity limit and supercritical accretion, time-independ. calcs. 80−67768
neutron stars, effects of superfluidity on X-ray emission 80−77441
neutron stars, electrodynamics of disk acrretion, magnetic field structure 80−85973
neutron stars, highly magnetised, thermal radiation 80−56869
neutron stars, in close binary systems, X-ray source model *(German)* 79−84814
neutron stars, luminosity enhancement following X-ray bursts 78−32502
neutron stars, nonequilibrium shells, role in X-ray emission and nucleosynthesis, review 80−67774
neutron stars, nuclear energy release and X-ray emission 77−78814
neutron stars, rotating, magnetic, accretion flow inside magnetosphere rel. to rot. rate 78−8037
neutron stars, thermonuclear flashes in envelopes of accreting objects 80−67772
neutron stars, X-ray emission assoc. with supercritical time-dependent accretion 80−85967
neutron stars, X-ray spectra from accretion column, optically thick region inc. 80−67767
neutron stars, X-rays from accretion as signals from extraterrestrial civilisations 77−53432
neutron stars surface radiation, detectability rel. to cooling and heating processes 80−31323
NGC 1275, central giant galaxy in Perseus cluster, excess X-ray emission 80−41907
NGC 1275, X-ray emission rel. to Perseus cluster soft X-ray struct. 79−9009
NGC 1851, globular cluster, radial vel. of evolved star UV5 as X-ray source candidate 77−74158
NGC 1851, globular cluster, unsuccessful search for H I 79−5873
NGC 1851, X-ray globular cluster, central region struct. 77−45501
NGC 1851, X-ray globular cluster, UV energy distrib. from OAO photometry 80−73009
NGC 2110, Seyfert 2 X-ray galaxy, optical studies 80−22071
NGC 3783, possible X-ray emitting Seyfert galaxy 77−13467
NGC 4151, OSO 8 X-ray obs. of flare in Seyfert galaxy 79−17093
NGC 4151, Seyfert galaxy, repeated X-ray flaring obs. 80−90534
NGC 4151, Seyfert galaxy, Uhuru obs. 78−12411
NGC 4151, X-ray emission, two-component model for Seyfert galaxy 78−45399
NGC 4151, X-ray emission monitoring by Ariel V, evidence for flare 77−2491
NGC 4151, X-ray flares in Seyfert, thermal model and central black hole 78−93407
NGC 4151 (4U 1206+39), Seyfert galaxy, hard X-ray spectrum 78−49537
NGC 5128 (Centaurus A), X-ray structure 78−24569
NGC 5128 (Centaurus A), X-ray variability, Ariel V Sky Survey obs. 78−16574
NGC 5506, IR obs. of X-ray Seyfert-like galaxy 78−65696
NGC 5506, Seyfert 2 galaxy, detect. of flare in X-ray emission 80−17656
NGC 5506, X-ray Seyfert, spectra 78−93411
NGC 5506 (3U 1410−03), probable X-ray galaxy, optical spectrum and morphology 77−13466
NGC 6221 and NGC 7213, optical spectrophotometry of X-ray galaxies 79−35377
NGC 6224, X-ray globular cluster, photometry of nucleus 77−37628
NGC 6440 (MX 1746−20), globular cluster, surface photometry of cluster core 80−82436
NGC 6624, optical counterparts of X-ray burster in core of globular cluster 80−67801
NGC 6624, optical studies of X-ray globular star cluster 78−93335
NGC 6624, UBV photometry of X-ray globular cluster 78−93337
NGC 7078 (M15), globular cluster, spectra of two-hour variable UV-bright star (M15-K1082) 79−88681
NGC 7213, IR photometry of lenticular Seyfert X-ray galaxy 78−89262
non-thermal sources, constraints rel. to X-ray background synthesis constraints rel. to X-ray background synthesis 80−27021
Norma, novalike source, refined SAS 3 position 77−78893
Norma nova-like source, search for optical candidates 77−82322
Norma X-ray burster, Uhuru obs. 77−2487
North Polar Spur (Radio Loop 1), X-ray obs. 80−105370
nova at $\alpha=1^h14^m$, $\delta=+64.4°$, discovery obs. 78−24515
Nova Monocerotis 1975 (Ariel 0620−00), linear polarisation obs. 77−13351
Nova Ophiuchi 1977, identification with X-ray transient 77−91540
Nova Ophiuchi 1977 (H1705−25), X-ray light curve 78−49453
Nova Ophiuchi 1977 (H1705−25), X-ray nova, HEAO 1 obs. 78−49452
novae, optical and X-ray events, comparison 79−58350
novae, spectroscopic obs. of optical counterparts 77−45450
novae, transient thermal X-ray emission from shocked circumstellar gas 77−45437

X-ray sources continued
novalike object in Centaurus, possibly Centaurus X-4, X-ray obs. and optical identification 79−62842
novalike source in Norma, SAS-3 obs. 77−67142
NP 0532, Crab pulsar, optical and X-ray pulses, Compton effect 79−53849
NP 0532, Crab pulsar, search for X-ray polarisation 79−5851
NP 0532, Crab pulsar, transient structure of high-energy X-ray emission 77−33541
NP 0532, Crab pulsar, X-ray and gamma-ray radiation 80−41885
OAO 1653−40=HD 152667 (V861 Scorpii) physical parameters 79−17021
OAO 1653−40, HEAO obs. of X-ray pulsations 79−44637
OAO 1653−40, identification with eclipsing binary V861 Scorpii 78−69838
OAO 1653−40, pulsating hard X-ray source detect. 79−67118
OAO 1653−40 38 s pulsating X-ray source position and optical search 80−73072
OAO 1653−40 area, 38.22 second X-ray pulsations discovery 80−27014
OAO 1653-40 (V861 Scorpii?), simultaneous UV and X-ray obs. 80−17616
OAO 1653-40 (V861 Scorpii), near IR obs. of single line spectroscopic binary 80−8652
OB supergiant X-ray binaries, line distortion effects 78−7995
objective prism spectrophotometry of UV and X-ray sources 78−8150
observations and models, review, 1960-1980 period 78−49567
of giant black holes *(French)* 80−94828
V843 Ophiuchi (Kepler supernova 1604) remnant, soft X-ray emission detect. 79−40244
Ophiuchus flare source near 4U 1708-23, Ariel 5 obs. 77−82323
optical and X-ray simultaneous obs. proposed for 1979 78−77627
optical counterparts, appl. of simultaneous fast double head UBV photometer 80−72775
optical spectral line emission bursts in X-ray heated medium *(Russian)* 80−77286
optical spectrum of high temp. gas, emission line formation *(Russian)* 80−36740
particles accelerated by Alfven waves, distrib. function self-similar solns. 79−32757
period vars. in pulsating sources, X-ray timing obs. 79−5917
periodic modulation search in three galactic X-ray sources 77−5592
periodic polarization variations in rotating astrophysical systems 79−88585
periodic pulsating X-ray sources discovery, Ariel 5 obs. 77−64885
periodicity investigation at 21 cm 80−82529
periods, review 78−12424
X Persei, 580 day and other periodicities 78−16435
X Persei, Be star, coordinated IR and optical obs., (in late 1976) 79−25616
X Persei, BV magnitudes 77−91542
X Persei, distance determ., 3U 0352+30 optical counterpart *(Chinese)* 78−69836
X Persei, energy distrib., light vars. 1972-76 period 78−16437
X Persei, photometric behaviour, 1964 to 1979, and binary star model 79−53820
β Persei, soft X-ray image 77−53627
X Persei, V-band polarization variability 78−49455
GK Persei, X-ray outburst detect. from old nova 79−67033
X Persei, X-ray spectra, binary model 79−25757
X Persei (2U 0352+30), photoelec. obs., light vars. 78−40999
X Persei (2U 0352+30), spectral line variations *(Russian)* 78−65655
X Persei (3U 0352+30), photometry, search for optical 13.9 minute period 78−16426
X Persei (3U 0352+30), reality of massive companion questioned 77−13495
X Persei (3U 0352+30), simultaneous X-ray and ground-based optical obs. 80−17591
X Persei (4U 0352+30), absence of ellipsoidal light vars. 79−80337
X Persei (4U 0352+30), balloon obs. of hard X-ray flux variability 79−48803
X Persei (4U 0352+30), light vars., tidal distortion by massive unseen companion 78−36640
X Persei (A 0535+26), Prognoz-6 obs. of X-ray fluxes and energy spectra *(Russian)* 80−109562
β Persei (Algol), hard X-ray obs. 77−13493
β Persei (Algol), orbital period, 1964 to 1978, rel. to radio and X-ray activity 79−58377
β Persei (Algol), X-rays detect. 77−9773
Perseus Cluster, compact and diffuse X-ray sources in core 78−49545
Perseus cluster, hard X-ray obs. 77−13493
Perseus cluster of galaxies, energy-dependent map of X-ray emission, SAS 3 obs. 78−65702
Perseus cluster of galaxies, soft X-ray map 77−5579
Perseus galaxy cluster, low energy X-ray absorpt. obs. 78−86025
Perseus X-ray cluster, form. of optical filaments in cooling gas round NGC 1275 galaxy 80−67862
PKS 0548−322, BL Lacertae object, X-ray spectrum 80−17654
PKS 0548-322, possible BL Lacertae object, low-energy X-rays detect. 78−89270
PKS 0548-322, surface photometry of X-ray emitting BL Lacertae object 80−22069
PKS 2155, BL Lacertae object, UV flux meas. by IUE 80−12833
PKS 2155−304, BL Lacertae object, rapid X-ray variability obs. 80−73035
plasma clouds, comptonisation of X-rays, radiation spectra 80−85850
point X-ray source, imaging via automodulation collimator telescope *(Russian)* 80−62018
point-like X-ray sources, lunar occultations anal. for source positions 79−88567
point-like X-ray sources positions determ., lunar occultation optimisation 79−92652
polarized radiation transfer in X-ray pulsars, analytical solns. 80−94894
position determ., parameter estimation method 78−61748
positions, meas. by scanning modulation collimator on (HEAO 1) 78−93459
primaeval giant elliptical galaxies, observable props. 78−89260
properties, general description *(Danish)* 77−67106
PSR 0531+21 X-ray pulse ground-based obs. 77−91444
PSR 1913+16, X-ray and timing meas. correlations, grav. radiation, gas cloud friction 80−62171
pulsar binary, X-ray reflection effects on timing obs. of pulses 79−53935

X-ray sources continued
pulsars, effect of vacuum birefringence on X-ray polarisation 78−4408
pulsars, pair form. above polar caps rel. to X-ray and gamma-ray emission 79−92790
pulsating binary X-ray sources, periodic timing residual 78−65718
pulsating sources, appl. of high-luminosity He-burning degenerate stars theory 77−5519
pulsating X-ray sources, accretion disc mag. field calc. for oblique mag. dipole configuration 80−94895
pulsating X-ray sources, accretion torques 77−49505
pulsating X-ray sources, mag. neutron stars disc accretion model 78−93294
pulsating X-ray sources, neutron stars accretion disc and rot. mag. field interaction 80−62173
pulsating X-ray sources, period changes due to rot. mag. neutron stars accretion torques 80−31320
pulsating X-ray sources, radiating accretion column model 77−53710
pulsating X-ray sources, radiation polarisation and beaming, vacuum birefringence effect in mag. field *(Russian)* 78−93476
pulsating X-ray sources, secular period changes 77−45613
pulsating X-ray sources, strongly magnetised plasma collisional relax. of ion beam 80−33785
pulsating X-ray sources period vars., torque vars. and stellar response 79−9029
pulsating X-ray sources spectra, possible vacuum signature 80−27015
pulsing X-ray sources, long-period, neutron stars spindown in close binary systems 79−40210
VV Puppis, dwarf nova, visible spectroscopic obs. rel. to possible X-ray emission 79−80322
CP Puppis (Nova 1942), soft X-ray emission detect. 79−80325
Puppis A, X-ray and Fe XIV 5303 Å emission 80−26962
Puppis A, X-ray struct. from Copernicus data 79−8982
Puppis A supernova remnant, X-ray spectra var. with position 80−82472
QSO 0241+622, nearby X-ray quasar, extended radio emission search 80−31382
quasar 0241+622, IR obs. 79−44642
quasar 0241+622, very high resolution radio obs. 79−88758
quasar-like objects, black hole model for X-ray emission 78−20905
quasars, Comptonised spectrum, Monte Carlo simulation 80−90566
quasars, discrete evolving sources contrib. to X-ray background 80−82551
quasars, low redshift X-ray selected, visible spectra and UBVRI photometry 80−105397
quasars, models of unsaturated Compton accretion discs around supermassive black holes 80−22033
quasars, new obs. 79−62930
quasars, possible source for X-ray background 80−94898
quasars, uniformity of radial distrib. in chronometric cosmology rel. to X-ray background 80−105409
quasars, X-ray emission from accreting stellar debris clouds 78−32597
quasars and active galactic nuclei, magnetic flare model, magnetised accretion disc around massive black hole 80−22113
radiative transfer of X-rays through optically thick shell 78−65488
radio binary systems, X-ray emission model 77−33700
radio continuum obs. of southern X-ray sources 77−17573
radio emission from point X-ray sources, origin 80−62317
radio identifications at 2 cm wavelength 79−53939
radio quasars, deep search for X-ray emission by Ariel V 78−12402
rapid time variability, role of time-dependent Comptonisation and X-ray reverberations 80−86013
red dwarf stars, X-ray flares rel. to galactic X-ray background 77−9755
relativistic astrophysics, pulsars, supernovae, and X-ray sources *(German)* 79−101060
relativistic electron spectra, inference from meas. of inverse Compton radiation 80−90339
resonant X-ray lines, freq. redistrib. and radiation diffusion, Voigt profile, thermalisation length *(Russian)* 79−5747
review 77−78892
review of X-ray sources 78−32604
reviews, galactic and intergalactic astronomy *(Russian)* 77−57061
Roche-lobe overflow and massive X-ray binary systems 79−35301
2S0921−630, discovery and optical stellar identification 79−21466
2S1728−337 vicinity, 5 IR sources detected by K-band photometry 78−54076
2S 0114+650, OB star optical candidate and spectral var. 78−16578
2S 0114+650, X-ray source discovery obs. 78−12423
2S 1553−542, possible X-ray counterpart of γ-ray source (CG 327−0) 78−54092
2S 1636−536 (MXB 1636−53), X-ray burst source, position 78−12419
2S 1702−363, optical counterpart UBV photometry 80−82349
2S 1702−363, possible optical counterpart discovery 78−54082
2S 1702−363, spectroscopic obs. of possible optical candidate, red variable star 78−77566
2S 1702−363 field, IR object identified as Mira variable 78−81705
2S 1728−337 (MXB 1728−34), X-ray burst source, position 78−12419
2S 1735−444 (MXB 1735−44), X-ray burst source, position 78−12419
2S 1822-371, optical photometry of assoc. star 79−92894
Sagittarius, Ariel V obs. of X-ray nova (1979 October-November) 80−12834
satellite obs. of various objects 77−26087
V861 Scorpii, IR obs. of black hole candidate 79−44538
V861 Scorpii (HD 152667), X-ray binary, behaviour of Hα 79−101171
V861 Scorpii (OAO 1653−40), Hα emission features vars. 78−77579
Scorpius X−1, interstellar extinction and UV flux distrib. 79−25754
Scorpius X-1, binary star, X-ray spectrum 20-75 keV, high sensitivity determ. 80−98741
Scorpius X-1, binary star X-ray obs. from 20 to 250 keV 80−94893
Scorpius X-1, binary system model 78−81706
Scorpius X-1, emission var., Salyut 4 obs. in 0.2-2 keV range *(Russian)* 77−33702
Scorpius X-1, extended X-ray obs. with Bragg crystal spectrometer 79−12543
Scorpius X-1, high energy X-ray and SHF radio obs. 80−73067
Scorpius X-1, high energy X-ray obs. with Ariel V 80−17694
Scorpius X-1, light and colour curve of periodic variation 77−49497
Scorpius X-1, linear optical polarisation obs. *(Russian)* 77−64880
Scorpius X-1, linear X-ray polarisation obs. 79−101221
Scorpius X-1, linear X-ray polarisation upper limit 77−49503
Scorpius X-1, linear X-ray polarisation upper limit 78−49557
Scorpius X-1, low-energy γ-rays, Dec. 1974 balloon obs. in 0.2-5 MeV range *(Portuguese)* 78−57702

X-ray sources continued
Scorpius X-1, mag. field determ. via linear polarisation spectrum *(Russian)* 80−90344
Scorpius X-1, mass-exchange binary characts. 77−57046
Scorpius X-1, optical magnitude variation *(Russian)* 77−26093
Scorpius X-1, Prognoz-6 obs. of X-ray fluxes and energy spectra *(Russian)* 80−109562
Scorpius X-1, rapid variability simultaneous X-ray and optical obs. 80−62322
Scorpius X-1, Salyut-4 X-ray spectrometry *(Russian)* 77−26091
Scorpius X-1, SAS-3 obs. 1979 March 79−30150
Scorpius X-1, semiopaque plasma model of X-ray source 77−13501
Scorpius X-1, UV, visible, IR and X-ray obs., X-ray obs. 80−82541
Scorpius X-1, variability analysis, method of time histograms 78−20652
Scorpius X-1, worldwide study plan (1980 April) 79−97104
Scorpius X-1, X-ray binary, spectrum calc. 77−29881
Scorpius X-1, X-ray energy spectrum in 0.2-50 keV range, rocket obs. 78−57696
Scorpius X-1, X-rays effect on equatorial lower mesosphere ionisation 78−36233
Scorpius X-1 and similar sources, Compton scattering effects 79−84869
Scorpius X-1 rel. to old novae 77−87576
Scorpius X-1 review 78−16576
Serpens X-1, Ariel 5 obs. and models of spectrum and time var. 78−81707
Serpens X-1, no IR bursts assoc. with Type I X-ray burst 80−98742
Serpens X-1 (4U 1837+04), burster optical binary counterpart visible spectra and photometry 80−94891
Serpentis X-1, possible identification with MXB 1837+05 77−49500
Seyfert 1 galaxies, HEAO 1 scanning modulation collimator, obs. 80−51859
Seyfert 1 galaxy nuclei, luminosity function and implications for X-ray background 80−8682
Seyfert 1 X-ray emitting galaxies, HEAO 1 spectra 80−51860
Seyfert 2 X-ray galaxies, nucleus spectra and photometry obs. 80−98712
Seyfert galaxies, type 1, nuclei props., UV emission, colour index *(French)* 79−48923
Seyfert galaxies, Type 1, obs. with HEAO-1 scanning modulation collimator 79−92864
Seyfert galaxies detected as X-ray sources by Ariel V satellite 78−49540
Seyfert galaxies X-ray emission, Uhuru obs. 78−93392
SMC, atlas of variable stars, clusters, emission regions and supergiant stars, book 79−44619
SMC X-1, distortion of absorpt. line vel. curves due to X-ray heating 77−29878
SMC X-1, HEAO-1 pointed obs. 78−7856
SMC X-1, observational constraints on mass 77−29957
SMC X-1, pulsation period and orbital period decrease 77−49499
SMC X-1, pulse profile and refined orbital elements 78−8148
SMC X-1, soft X-ray emission detection, 2-day flaring period 79−35432
SMC X-1, spin-up rate meas. 78−41083
SMC X-1, spin-up rate of X-ray pulsar 77−29956
SMC X-1, VBLUW photometry, evidence for accretion disc 78−12409
SMC X-1, VBLUW photometry of optical counterpart Sk 160 77−82277
SMC X-1, X-ray binary, 5 colour photometry 77−17622
SMC X-1 (Sanduleak 160), binary system, orbital elements and masses 77−9815
SMC X-1 (SK 160), spectroscopic orbit and masses 78−4285
SMC X-2, 14th magnitude OB star 0.5′ from source position 78−4411
SMC X-2, Be-type optical candidate 78−77619
SMC X-2, colours, spectral type and position of optical candidate 78−12421
SMC X-2, obs. of optical candidate 78−8162
SMC X-2, optical identification with main sequence Be-star 79−40301
SMC X-2, SMC X-3, discovery, hard spectra, high luminosity rel. to galactic X-ray sources 78−49559
SMC X-2, SMC X-3, optical counterparts spectra 78−93469
SMC X-2, UBV photometry of proposed optical counterpart 79−67116
SMC X-2 and SMC X-3, variable X-ray sources, SAS-3 obs. 78−20914
SMC X-2 and X-3, SAS 3 discovery of new sources 77−91667
SMC X-3, colours, spectral type and position of optical candidate 78−12421
SMC X-3, obs. of optical candidate 78−8162
SMC X-ray sources, deep survey results and max. luminosities 79−25702
SN 1006 remnant, X-ray emission models 77−17646
SNR in Cygnus, soft X-ray emission detection 78−54013
soft (0.15-2 keV) sources, review 77−26094
soft X-ray background, spatial struct., OSO-8 obs. 78−16580
soft X-ray background 78−16582
soft X-ray emission from unidentified high galactic latit. source 77−5598
soft X-ray emission origin *(Russian)* 77−74165
soft X-ray transient and X-ray bursters, different phenomena from some objects 79−25755
solar flares, acceleration mechanisms, implications for hard X-ray burst models 80−72912
source counts at high galactic latitude 78−49565
source counts rel. to cosmological models 79−40305
sources similar to Scorpius X-1, observational study 77−13498
southern Milky Way sources, Ariel V obs. 77−2492
space distrib. of galactic sources using Uhuru catalogue 78−8159
spectral lines profile evolution due to Comptonisation, Monte Carlo computations 79−66916
spectroscopic observations, review *(German)* 77−60854
spectroscopy and polarimetry from Spacelab 78−32314
spherical accretion, luminosity thermal limit 80−82546
spherically symmetric accretion flows, stability anal., X-ray sources appl. 80−46387
SS 433, 10 GHz variability and thermal radio emission hypothesis 80−31307
SS 433, 164^{d} period as precessional motion, massive black hole and pulsar models 80−62138
SS 433, 180 mm interferometric obs. of triple structure 80−105259
SS 433, 1978 spectrograms reanalyzed and emission spectral feature ephemeris 79−58345
SS 433, 1979 May-June radio flare, 3.24 GHz obs. 80−46567
SS 433, 6.55 day periodicity in emission line wavelengths 80−51784
SS 433, accreting black hole model 80−85958

X-ray sources continued
SS 433, accretion disc viscosity determ. using slaved disc model 80−62110
SS 433, associated filamentary optical nebulosity detect. 79−88723
SS 433, B V photometry and short-term light vars. (1979 July 23 to September 17) 79−101165
SS 433, beam acceleration, radiation and precession theory 80−72971
SS 433, beam models, energetics anal., possible triple system 80−90433
SS 433, binary star model including mag. white dwarf 80−4385
SS 433, change in radio struct., 1980 January to June, from VLBI obs. 80−109557
SS 433, deviations from standard model 80−98669
SS 433, discrepancy between optical and radio positions 80−31303
SS 433, disk-driven precession 80−94803
SS 433, dissipative infall model 80−67749
SS 433, early-type binary model 80−56843
SS 433, emission line radical vels. and no periodic signals 79−80327
SS 433, emission line wavelength changes 79−48816
SS 433, emission regions and black hole accretion disk 80−67746
SS 433, enormous periodic Doppler shifts obs. 80−17593
SS 433, evidence for association with supernova remnant (W50) 80−51851
SS 433, general spectral features 80−77421
SS 433, Hα emission object, 21.6 and 43 GHz obs. 79−92783
SS 433, Hα radial vel. obs. (1979 July) 79−88674
SS 433, H I absorption obs. and distance 80−56848
SS 433, IR and visible obs., IR excess and emission processes 80−4387
SS 433, IR energy distrib. obs. 80−31312
SS 433, IR light curves from BVIJHK photometry, period and ephemeris 80−8642
SS 433, IR photometry, and search for short period variability 79−58346
SS 433, IR spectral obs., reddening and emission 80−4388
SS 433, IR variability obs. 80−98676
SS 433, light curves, double peak and binary-like period, photometry 80−94804
SS 433, light minimum epoch and period 80−26886
SS 433, line posn. vars. interpretation 79−75218
SS 433, magnetic X-ray binary model 80−109447
SS 433, mass accel. and collimation mechanisms 80−4368
SS 433, mass loss rates and lifetime from W50 optical filaments 80−12804
SS 433, models of supercritical accretion discs around black holes 80−105272
SS 433, nature and evolutionary state *(Russian)* 80−36647
SS 433, near IR (600 to 1100 nm) spectra, 1979 June and September 79−97009
SS 433, near IR spectrum obs. 79−84803
SS 433, nearby faint, highly-contorted nebular filament discovery 80−94855
SS 433, no 6-day periodicity in 1978 June-1980 Feb. obs. period 80−62150
SS 433, Of star orbited by neutron star, model 80−22025
SS 433, photometric and astrometric obs. 79−84801
SS 433, photometry, 1979 July to October, and 6.5 day period identification 80−8643
SS 433, precessing ring model, test by spectral line obs. 79−101152
SS 433, radial vel. curve low amplitude section, visible spectra anal. 80−67737
SS 433, radio and optical positions coincidence 80−56840
SS 433, radio jet discovery 80−31381
SS 433, reality of 6-day periodicity in spectral lines wavelengths var. 80−67743
SS 433, relativistic beam interaction with interstellar matter, mass loss rate, visible obs. 80−101629
SS 433, review of obs. and theories 80−72987
SS 433, search for radio spectral lines in UHF 80−109556
SS 433, short term Hα central intensity increases 80−4375
SS 433, spectral features interpreted a precessing neutron star with jets, possible binary 80−90447
SS 433, spectroscopic obs. and probable binary nature 80−51780
SS 433, UV spectral search and 8 GHz linear polarization 79−71048
SS 433, V band photometry and broad min. prediction (1980 April-May) 80−82390
SS 433, visible and IR photometric and polarisation obs. 79−80321
SS 433, visible and JHKL photometry and light vars. periodicity 79−53821
SS 433, VLBI detect. and ang. struct. 80−31304
SS 433 (4U 1908+05), kinematic model for line wavelengths vars. 79−75226
SS 433 (W50), assoc. optical supernova remnant discovery 80−56916
SS 433 as veiled pulsar 80−41842
SS 433 inside SNR, unique spectrum 80−82381
SS 433 model, precessing jets in ultra-close binary system 80−4384
stars in X-ray source fields, transmission grating spectroscopy, optical candidates 79−21283
steady accretion disk, with magnetic field, basic equations 79−40179
stellar coronae, evidence for existence from X-ray and UV obs. 80−12756
stellar wind flow, heating by X-rays and bow shock form. *(Russian)* 77−60855
stellar wind in H II regions, X-ray flux rel. to narrow radio recomb. lines 79−8972
stellar X-ray sources at high galactic latit., location with HEAO 1 scanning modulation collimator 80−22118
Stephenson-Sanduleak 433, 1.2-2.5 μm spectroscopy, photometry and polarimetry 80−41838
Stephenson-Sanduleak 433, anomalous emission lines, gas around central massive black hole 79−53831
Stephenson-Sanduleak 433, emission-line star/X-ray source/radiosource assoc. with W50 SNR 79−8930
Stephenson-Sanduleak 433, massive black hole hypothesis 79−71057
Stephenson-Sanduleak 433, model, precessing ring around massive black hole 79−88678
Stephenson-Sanduleak 433, moving emission features, dynamical models 79−67034
Stephenson-Sanduleak 433, possible double jet struct. 79−48827
Stephenson-Sanduleak 433, spectral variability 79−62839
Stephenson-Sanduleak 433, Thomson scatt. lines in spectrum, relativistic gas motions 80−22019
Stephenson-Sanduleak 433, X-ray emission obs. 79−12480

X-ray sources continued
strong sources, graphite cryst. spectrometer obs., sensitivity to line emission 77−13238
subcritically accreting black holes, model for X-ray sources in globular cluster cores and X-ray burster sources 80−12779
Sun, microwave radiation from thermal, hard X-ray sources 79−8892
Sun possible compact companion, identification with X-ray source 79−2490
superclusters, X-ray emission, matter infall 79−67106
supercritical accretion discs winds struct. and appearance, numerical models 80−21984
supercritical accretion onto unmagnetized neutron stars rel. to galactic bulge X-ray sources 79−80331
supernova γ- and X-rays, recorded by Antarctic ice NO_3^- content 80−31314
supernova remnants, adiabatic phase, thermal X-ray spectra 80−82475
supernova remnants, obs. of X-ray emissions 79−58404
supernova remnants, two-fluid blast-wave model 79−80345
supernova remnants, X-ray emission rel. to evolutionary phases 77−87521
supernova remnants, young, thermal X-rays theoretical spectra 78−73751
supernovae, extragalactic, X-ray bursts search using HEAO-1 satellite 80−46585
supernovae, soft X-ray flux prediction method 79−71060
supernovae, type II, nonequilib. processes in evolution 80−46586
supernovae, Type II, X-ray bursts 78−93287
supernovae remnants, parameter determ. from X-ray data and known age, blast model *(Chinese)* 80−77471
young supernovae remnants, X-ray props. rel. to neutron stars cooling 80−77443
V711 Tauri (HR 1099), Lyman α H I and D I interstellar absorption 80−8658
T Tauri stars, infall model and X-ray emission 77−13329
T Tauri stars, X-ray emission from outflowing envelopes, prediction 78−96482
transient events with precursor pulses, SAS 3 obs. 78−49562
transient short-lived source at high galactic latitude, ANS obs. 78−96563
transient soft X-ray sources, identification with flare stars 78−45337
transient soft X-ray sources, identification with supposed flare stars questioned 78−96485
transient source in Norma, precise position determ., HEAO 1 obs. 78−49560
transient source in Pictor, HEAO-1 A-2 expt. obs. 78−32607
transient source near galaxy MCG-5-9-22, probably not associated with new supernova 78−81643
transient sources, discoveries and obs., review *(Polish)* 77−17720
transient sources, energy storage and release, model constraints 78−65491
transient sources, high-latit., optical counterpart identification using proper motion data 78−93457
transient X-ray sources, eccentric orbit binary model 77−53703
transient X-ray sources, galactic distrib. and physical nature 79−84867
transient X-ray sources, rel. to neutron stars thermal/timing instability 79−92795
transient X-ray sources, review 77−33695
transient X-ray sources, review 78−12425
transient X-ray sources in the galactic plane 78−93460
transrelativistic plasmas, relevance of photon pair prod. 78−20632
Triangulum Australe, X-1, position meas., radio and optical identifications 77−91671
turbulent disc αω dynamo theory for mag. field generation 80−46663
twisted accretion discs, time-dependent eqns., X-ray binary systems appl. 79−12395
Tycho supernova remnant, Type I SNR, elemental abundances from X-ray spectrum 80−46635
Tycho supernova remnant, X-ray line emission obs. 80−46636
4U0134−11, galaxy supercluster candidate, no X-rays from hot gas 78−8164
4 U1145−61, two X-ray periodicities from Ariel V obs. 78−81711
4U 0026−73, identification with SMC globular cluster (Kron 3) 79−5919
4U 0041+32, hard X-ray outburst, 1970 obs. 80−56976
3U 0042+32, SAS-3 meas. of position during flaring activity 77−37670
3U 0042+32, variable mid-latitude X-ray source, accurate position 77−78897
3U 0042+32 and 1728−16, optical counterparts 77−74163
3 U 0055−79, possible identification with Seyfert 1 galaxy (ESO 012-G21) 80−8695
4U 0115+634, X-ray binary, 1980 Aug. photometry and spectroscopy 80−101650
4U 0115+63, 3.6s X-ray pulsations discovery 78−61939
4 U 0115+63, absorption line in pulsed hard X-ray spectrum, HEAO 1 obs. 80−27017
4U 0115+63, orbital elements and nature of hard X-ray transients 78−93470
4U 0115+63, transient X-ray binary, absorpt. feature discovery at 20 keV 78−69909
4U 0115+63, transient X-ray source, accurate positions 78−24570
4U 0115+63, transient X-ray source, obs. 79−92890
4U 0115+63, transient X-ray source, optical and X-ray obs. 78−32605
4U 0115+63, X-ray transient, position and pulse profile 78−93467
4U 0115+63 transient near G126.2+1.6 SNR 80−8668
4U 0223+31, identification with NGC 931, interacting Seyfert galaxy 79−25716
4U 0241+61, optical and radio identification, luminous low-redshift QSO 78−61940
4U 0241+61, possible X-ray counterpart of γ-ray source (CG 135+1) 78−54092
4U 0241+61 (QSO 0241+622), spectrum and luminosity of low redshift object 78−93451
4U 0241+62, identification with QSO or Seyfert nuclei-like object 78−16572
4U 0241+62, nearby quasar, radio props. 79−25752
3U 0258+60, flux from assoc. γ-ray source 77−2497
3U 0328−52 region, X-ray emission from galaxies, Ariel V sky survey obs. 77−5599
3U 0352+30, 13.9 minute periodicity of optical counterpart X Persei 77−22247
X-ray sources continued
3U 0352+30, evidence for 581 day modulation in X-ray pulse period 77−53708
4U 0352+30 (X Persei), Be star, evidence for 6-year photometric periodicity 80−109446
3U 0352+30 (X Persei), eccentric close binary model 77−29879
3U 0352+30 (X Persei), OSO-7 hard X-ray obs. 77−26085
3 U 0352+30 (X Persei), UBVRI photometry 78−8049
3U 0527−05, improved position and possible optical identifications 77−33691
4U 0531−05, Copernicus obs. of θ^2 Orionis A optical candidate 79−67050
3U 0614+09, case for X-ray burst 78−32610
2U 0832-45, extended X-ray source centred on Vela pulsar 78−41095
3 U 0833−45, assoc. with Vela pulsar, nature 79−17138
3U 0833−45, Vela pulsar X-ray flare obs. 77−22260
4U 0833−45, X- and gamma-ray emission from Vela SNR and pulsar *(Russian)* 80−94861
4U 0900−40, pulsating X-ray binary, search for periodic behaviour 79−84865
4 U 0900−40 (HD 77581), apsidal motion test 80−51908
4U 0900−40 (HD 77581) optical pulsations from eclipsing binary 79−48951
4U 0900−40 and 1700−37, polarimetric obs. of massive X-ray binaries 80−98688
3U 0900-40 (HD 77581), binary X-ray source, spectroscopic orbit and masses of components 78−16461
3U 0900-40 (HD 77581), increase in pulsational period 77−64877
3U 0901-09, obs. of radio counterpart 77−26089
4U 0945−30, spectroscopic obs. of possible galaxy counterpart 78−45404
4U 1043−59, possible assoc. with supernova remnant G287.8−0.5 77−2488
3U 1118−60 (Centaurus X-3), hard X-ray obs. 77−2493
4U 1145−61, bright active source, SAS-3 monitoring 78−57699
4U 1145−61, optical counterpart HD 102567, atm. model from UV obs. 80−105396
4U 1145−61 (HD 102567), X-ray periodicity and orbital motion 78−8160
4U 1145−61 (Henize 715), Be-type star, colour and luminosity vars. (1976-1980) 80−72979
4U 1206+39 (NGC 4151), hard X-ray variability of Seyfert galaxy 80−17647
3U 1207+39 (NGC 4151), Seyfert galaxy, high-energy X-ray obs. with balloon-borne telescope 77−45610
3U 1223−62, binary X-ray pulsar, Ariel V obs. 78−96566
4U 1223−62, binary X-ray pulsar, optical counterpart Wray 977, spectra 80−72984
4U 1223−62, high-speed UV photometry of periodic modulation of WRA 977 (Feb.-Mar. 1977) 78−16442
4U 1223−62, pulsating X-ray binary, search for periodic behaviour 79−84865
4U 1223−62 (GX 301−2, WRA 977), binary star orbit determ. from X-ray obs. 80−90570
3U 1223-62 (GX 301-2), hard X-ray obs. 77−2493
3U 1223-62 (Henize 788=Wray 977), five colour photometry 77−29846
4U 1232+07, HEAO 1 obs. 80−12832
4U 1240-05 rel. to Seyfert NGC 4593, Ariel V obs. 79−84856
3U 1247-41, Centaurus X-ray cluster, vel. dispersion 77−74148
4U 1249−28, location and identification with dwarf nova EX Hydrae 80−22118
4U 1249-28, possible identification with EX Hydrae (U Geminorum type star) 78−36729
3U 1252−28, evidence for assoc. with single galaxy 78−32586
3U 1254−69, hard X-ray obs. 77−2493
4U 1258−61, spectrum change in optical counterpart 79−71154
3U 1258−61 and 1626−67, X-ray obs. from satellites 77−37671
4U 1322−42 (Centaurus A, NGC 5128) nucleus, radio and X-ray variability model 80−90522
4 U 1325−31, X-ray emission in 2-10 keV range from MCG -6-30-15 Seyfert galaxy counterpart 78−45405
4U 1326+11, identification with galaxy cluster MKW 11 80−90574
3U 1538−52, Ariel 5 obs. 77−49498
4U 1538−52, binary X-ray pulsar, early B-type supergiant as counterpart 78−93472
3U 1538−52, binary X-ray pulsar, orbital elements 78−16573
4U 1538−52, eclipsing binary pulsating system, position meas. by HEAO-1 78−96570
4 U 1538−52, eclipsing X-ray source, corrections to ephemeris and revised period 79−25760
4U 1538−52, obs. of optical candidate 78−41093
4 U 1538−52, optical light curve of X-ray binary 79−35431
4U 1538−52, spectrograms of optical candidate, confirmation of identification 78−41094
4U 1538-52, binary X-ray source, spectral type of possible optical counterpart 78−36727
3U 1538-52, optical candidates 78−12412
4U 1538-52, optical counterpart spectroscopy and system parameters 79−5924
4U 1543−62, optical candidate obs. 78−77625
4U 1608−52, 1977 Oct. decline, all-sky-monitor obs. 78−4412
4U 1608−52, 3-6 keV flux during 1977, Sept. 77−82329
4U 1608−52, burst activity since Hakucho launch (1980 April) 80−62321
4U 1608−52, obs., identification with MXB 1608−52 78−69914
4U 1608−52, optical identification and transient source outburst 78−41088
4 U 1608−52, recurrent transient, possible X-ray flare obs. 79−30152
4U 1608−52, X-ray bursts obs. 79−48958
4U 1626−67, 7.7-second X-ray pulsar, simultaneous X-ray and optical obs. 80−51914
4U 1626−67, discovery of optical pulsations from proposed candidate faint blue star 79−9034
4U 1626−67, light pulses from optical counterpart 80−51916
4U 1626−67, optical counterpart photometry 79−67120
4U 1626−67, pulsed optical emission detect. 79−62934
4U 1626−67, UBV photometry of X-ray pulsar candidate 79−17130
3U 1626−67, X-ray pulsar, 7.68 sec. periodicity, SAS-3 obs. 78−8157
4U 1626−67, X-ray pulsar, HEAO 1 obs. 79−92889
4U 1626−67, X-ray pulsar, optical candidate photometry 78−12418

X-ray sources continued
3U 1626−67, X-ray pulsar, X-ray position and optical candidate 77−67139
3U 1626−67, X-ray pulsar as accreting neutron star in compact binary 78−49470
4U 1626-67, optical candidate light pulsations discovery 78−65720
3U 1626-67, position meas., radio and optical identifications 77−91671
4U 1630−47, emission-line object candidate investigations 77−82324
4U 1630−47, obs. of recurrent transient source 78−41092
4U 1630−47, recurrent transient, Ariel 5 SSI obs. of 1978 May-June flare 78−61935
3 U 1630−47, recurrent transient source, Uhuru and Ariel V obs. 77−5595
4 U 1630−47, recurrent transient X-ray source flaring episode obs. 79−2580
4U 1636−53 (MXB 1636−53), X-ray burster, optical candidate photometry 78−12418
4U 1642−45, possible assoc. with G 339.6−0.1 H II region 79−71143
4U 1642−45 and 1630−47, X-ray flare detect. 78−12422
4U 1651+39, identification with BL Lacertae object Markarian 501 by HEAO 1 modulation collimator 79−5918
4U 1658−48, optical counterpart identification and X-ray flare obs. 78−69908
4U 1700−37, 97 minute periodicity discovery 79−5921
3U 1700−37, further Copernicus X-ray obs. 78−96568
4U 1700−37, SAS-3 obs. of 97 minute periodicity 78−36730
4U 1700−37, search for X-ray flux short time-scale periodicity 79−71157
3 U 1700−37(HD 153919), coronal emission line search 79−35302
4U 1700−37 (=HD 153919), eclipsing binary, X-ray obs. 80−86016
4 U 1700−37 (=HD 153919) eclipsing binary, supergiant-neutron star, optical variability 80−82419
3U 1700−37 (HD 153919), binary X-ray source, radial vel. data in blue spectral region 78−61888
3U 1700−37 (HD 153919), forbidden Fe XIV 5303 Å emission detect. 78−16571
3U 1700−37 (HD 153919), further spectroscopic obs. 80−4358
4U 1700−37 (HD 153919), IUE UV spectrum obs. 78−96569
4U 1700−37 (HD 153919), optical oscills. obs. 78−96572
4U 1700−37 (HD 153919), X-ray binary, high-energy X-ray obs. 80−86014
3U 1700−37 (HD 153919), X-ray binary, spectrum variations 78−8158
3U 1700-37 (HD 153919), binary X-ray source, radial vels. in blue spectral region 78−49556
4U 1700-37 (HD 153919), uncertainty of 97 min. periodicity 79−40295
3U 1700-37 (HD 153919), X-ray binary, five colour photometry 77−29877
4U 1702-36, Scorpius X-1 like source, high energy X-ray obs. with Ariel V 80−17694
3U 1727−33, X-ray flux periodic behaviour 77−9816
3U 1735−44, optical identification 77−60852
3U 1735−44, spectral obs. of optical counterpart 77−64882
4U 1735−44 (MXB 1735−44), optical identification and similarity to (Scorpius X-1) 78−93468
4U 1735−44 (MXB 1735−44), X-ray burster, optical candidate photometry 78−12418
3 U 1743−29, galactic centre, X-ray emission 79−17102
4U 1746-37, nearby X-ray bursts, 1977 August SAS 3 obs. 77−74160
4U 1755−33, exclusion from flaring transient source error box 77−82326
4U 1755−33, optical candidate obs. 78−77625
3U 1805+50 (AM Herculis) eclipsing binary, UV and visible spectra anal. 80−109563
3U 1809+50, X-ray light curve of optical counterpart AM Herculis 77−45491
3U 1809+50 (AM Herculis), eclipsing binary, review of obs. 77−71155
3U 1809+50 (AM Herculis), light curves and Fourier analysis 78−49483
3U 1809+50 (AM Herculis), low-mass X-ray binary, radial vels. and line intensities 77−78826
3U 1809+50 (AM Herculis), near IR and violet mag. obs. 77−53643
3U 1809+50 (AM Herculis), polar, IR photometric obs. 80−98687
3U 1809+50 (AM Herculis), polarimetry and spectrophotometry rel. to mag. field 80−94835
3U 1809+50 (AM Herculis), simultaneous three-channel photometry rel. to optical flickering mechanism 80−82411
3U 1809+50 (AM Herculis), single accretion column model 78−57578
3U 1809+50 (AM Herculis), spectrophotometric obs. at min. light 80−98692
3U 1809+50 (AM Herculis), UV spectrum obs. 80−67782
3U 1809+50 (AM Herculis), X-ray eclipsing binary, multicolour photometry 77−78887
3U 1809+50 (AM Herculis) accretion onto highly magnetised white dwarf 79−92764
3 U 1809+50 (AM Herculis) system nature, general *(Russian)* 78−4295
4U 1813+50 (AM Herculis), rapid light variability obs. *(Russian)* 80−8662
4U 1814+50 (AM Herculis), X-ray emitting mag. white dwarf binary, review of props. 80−105403
3U 1820−30, giant X-ray pulses, mass transfer in eccentric binary model 77−33690
3U 1820−30, magnetised accretion disc model for X-ray bursts 77−53702
3U 1820−30 in globular cluster NGC 6624, binary star model for recurrent X-ray bursts 77−33701
3U 1820−30 in globular cluster NGC 6624, recurrent X-ray bursts 77−60806
3U 1820-30, X-ray burster, accretion disc with hot corona model 77−17717
3U 1820-30 (NGC 6624), globular cluster, optical, IR and X-ray obs. 77−45498
4U 1822−37, 2129+42, X-ray fluxes modulation periods from HEAO obs. 80−77516
4U 1825+33, identification with variable radio galaxy (3C 382) 78−86031
4U 1837+04, UBR plates of Davidson optical counterpart 78−81714
4U 1837+04 (Serpens X-1), obs. of optical candidate 78−41093
4U 1837+04 (Serpentis X-1), absorption spectrum of counterpart 78−69912

X-ray sources continued
4U 1907+09, optical identification using HEAO-1 scanning modulation collimator position 80−82542
4U 1907+09, X-ray flare obs. during 1980 Jan. period 80−41914
3U 1915−05, X-ray burst source discovery 78−8155
4U 1916−79, high-latit. X-ray source, X-ray spectrum and variability 78−32611
3U 1921+43 in Abell 2319, cluster of galaxies, X-ray and radio obs. 77−53692
3U 1956+11, optical counterpart photometry and spectrum 78−49554
3U 1957+40 (Cygnus A region), X-ray obs. with ANS 77−53700
3U 1959−69, possible identification with EUV source in Pavo region 78−28675
4U 2129+12, in M15, proximity to variable emission line star 79−5840
4U 2129+12, in M 15, nature of emission-line variable in cluster core 80−77458
4 U 2129+47, position and optical identification, evidence for X-ray heating and binary period 80−17693
4U 2129+47, X-ray light curve and binary model 80−46704
4U catalogue of X-ray sources 79−40088
Uhuru sources, energy spectra of 43 objects, 2-20 keV 77−60851
UKS 1751−241, globular cluster near galactic centre, IR studies 80−82434
ultrasoft X-ray background, obs. in S galactic hemisphere 77−45615
AN Ursae Majoris, soft X-ray flux detected 80−4400
SU Ursae Majoris, soft X-ray halo around dwarf nova 80−98677
3V 1223-62 (WRA 977) B-type supergiant, spectroscopic obs. 79−101148
vacuum polarisation by mag. field effect on EM wave propag. in plasma *(Russian)* 79−77392
variable sources, Ariel 5 obs. 77−82320
Vela supernova remnant, X-ray maps 80−51838
Vela X-1, long-term studies with Ariel 5 All-Sky Monitor 79−30146
Vela X-1, OSO 8 extended obs. 78−49555
Vela X-1 (3U 0900−40), Ariel V Sky Survey instrument obs. 77−45495
Vela X-1 (3U 0900−40), X-ray obs. and UBV photometry 78−65722
Vela X-1 (HD 77581), binary source, spectral obs., UV, visible and X-ray 80−94892
Vela X-1 (HD 77581), binary X-ray source, photometric obs. 77−41392
Vela X-1 (HD 77581), discovery of optical pulsations 77−82327
Vela X-1 (HD 77581), four colour photometric obs. and light curve anal. 77−17621
Vela X-1 (HD 77581), optical pulsations discovery 78−20911
Vela X-1 (HD 77581), radial vel. curve distortions due to tidal deform. 77−53640
Vela X-1 (HD 77581), X-ray binary, uvby obs. 77−37668
Vela XR-1 (3U 0900−40), balloon obs. 78−69913
Vela-Puppis, low-luminosity X-ray source obs. 78−93458
Virgo cluster, structure of extended X-ray source 78−4410
Virgo cluster X-ray source, struct. 78−54090
Virgo galaxy cluster, low energy X-ray absorpt. obs. 78−86025
VV Puppis, 3470 Å emission as cyclotron line 80−36673
weak, variability analysis, method of time histograms 78−20652
weak X-ray sources, ANS meas. 80−46701
white dwarf binary systems, hard X-ray obs. 78−36732
white dwarf with mass accretion, H shell flashes and X-ray emission 78−57550
white dwarfs, highly magnetised, accretion theory 79−92764
Wolf-Rayet close binaries, X-ray production 77−13401
Wray 977 (4U 1223−62), B-type supergiant, spectral classification 79−80305
X-ray bursters, 1980 plans for simultaneous optical/X-ray obs. 80−8716
X-ray bursters, props. and model 77−71154
X-ray bursts, review 78−12427
X-ray pulsars, relativistic accretion 79−9032
XB 1724−31, X-ray burst source, identification with globular cluster (Terzon 2) 79−5919
III Zw 2, X-ray emitting Seyfert galaxy, VLBI obs. 79−5903
Cygnus X-2, linear optical polarisation obs. *(Russian)* 77−64880
H I deficient region in Hercules, O VII emission line obs. in diffuse soft X-rays 79−25759
Si XIII and Si XIV line emission search with ANS crystal spectrometer 79−17131

X-ray spectra
see also X-ray absorption spectra; X-ray chemical analysis; X-ray emission spectra
acid phthalate curved crystal spectrograph, diffraction efficiency calc. method 80−79630
actinides, K-shell fluorescence yields from Auger electrons and X-rays, precision meas. 79−31462
asbestos fibre, identification techniques 77−60018
atom, mean wavelength and spectral width of transition arrays 79−6913
atom, reson. Raman X-ray scatt., K-vacancy excited state widths, appl. to Zr, Mo, Rh, Ag and Sn 79−45661
atom, sommerfeld screening parameters for $S_{1/2}$ terms in X-ray spectra 78−66495
atomic, relative intensity of $K\alpha_1$, $K\beta_1$, and $K\beta$ lines, non-orthogonal wavefunction calc. 77−83477
atomic line shape broadening anal., least squares method 80−63588
atomic X-ray satellites, multiple inner shell vacancies from collision processes 77−83527
atoms, natural line widths, K and L X-rays, XPS and KLL Auger lines 79−76383
Bragg-type X-ray diffractometer, narrow beam, interference phenomena by plates 79−41909
bremsstrahlung backscattering from semi-infinite reflectors, spectral composition 77−54028
chemical shift of spectrum c.g., valence electron distrib. distortion 77−27084
coherent Roentgen radiation prod. from channelled charged particles in a monocrystal *(Russian)* 78−92138
edge theory, extension to entire X-ray spectrum 77−12465
edge theory, extension to entire X-ray spectrum 77−12466
effective atomic charge rel. to electronegativity and ionicity 77−24287
electron beam X-ray source, X-ray spectral distribs. FLASH code 79−22524
electron-probe computerisation development 79−11859
elements, configurational interaction effects in region of 4f and 3d shell built up 77−27012

X-ray spectra continued
energy dispersive, computer-aided analysis 80−3433
energy dispersive peak separation from background 78−7310
energy dispersive spectroscopy, quantitative, computer program 79−43689
energy-dispersive detector, simplex method for fitting Gaussian profiles 79−722
fluorescence, energy-dispersive, direct meas. of net peak areas 79−1989
foil, surface density meas. method using charact. X-rays *(Czech)* 77−50323
n-GaAs, semidegenerate, acoustoelec. gain and lattice attenuation, X-ray Brillouin scatt. and elec. meas. 79−15193
gas proportional counter, for X-ray analysis, atomic K-lines *(Czech)* 79−31323
half-value-layer measurement, 5 to 40 MV, rel. sensitivites of water, Al, Cu, Sn and Pb 77−45927
hydrogenic atoms, Compton profile and X-ray scatt. factors, elec. field and elec. field gradient effects 79−31458
ion-atom collisions, two-electron rearrangement X-ray transitions, theory 77−38633
ion-neutral atom, in foil, inner-shell processes, oscill. X-ray spectra excitation 77−54565
ions, highly ionised, review 78−62755
kaonic H atom X-rays obs. 79−86088
lectures on interaction of radiation with condensed matter, Trieste, Italy (Jan.-March 1976) 78−27172
lineshifts in nonrelativistic and relativistic approxs. 78−951
mammography, simulation of X-ray spectra 80−76826
measurement, interpretation and comparison from various industrial units *(German)* 78−7149
measurement standards, National Bureau of Standards (USA) 80−90807
mesic atom, X-ray radiation anisotropy, suppression coeffs. *(Russian)* 78−22058
metal, electron inelastic scatt., interaction effect in final state 79−69454
metallic system, X-ray line shapes for core levels, phonon broadening 77−12464
metals, method of effective non-Hermitian Hamiltonian in theory of X-ray phenomena *(Russian)* 77−77323
metals, X-ray spectra, temp. broadening 77−69936
model uncertainty and bias in evaluation, smoothest consistent baseline theory 78−11591
molecules, chemical shift, influence of inner level vacancy 77−27085
Moseley's expts.: Kα line freqs., rel. to at. number, reinterpretation 80−82616
multiple Compton scatterings effect on X-ray emission spectrum, Monte Carlo calcs. 78−96389
muonic atom, nucl. charge distrib. meas. 78−54679
muonic atoms, transition potential of muonic X-rays, unique parameterisation 79−31745
muonic atoms, X-ray emission 79−86087
one- and two-dimensional spatial resolution recording by spherical crystal analyser 78−74114
phosphides of Cu,Ag,Zn,Cd,Ga,In, d electrons of metals, participation in chem. bonds 77−28682
plasma diagnostics appl., using Ross filters and Si detectors 80−59273
radiochemical analysis by coincidence spectrometry, minicomputer system 79−11864
radiographic inspection, spectra and angular distrib. meas. of scattered X-radiation *(German)* 78−7148
radiography, computerised tomography, correction for spectral artifacts in cross-sectional reconstruction 77−21621
scattering near K absorpt. edge, dispersion factors f′ and f″ 79−65954
semiconductor, crystal-glass transition influence on local struct., Mossbauer and X-ray spectra 77−36163
Sommerfeld screening parameters for the K level in X-ray spectra 79−68208
spark spectra, doublet formation 79−22639
spectral distribution, evaluation of method of estimation from attenuation data *(Japanese)* 80−95207
spin doublets in X-ray satellite spectra 80−58203
sulphides of Cu,Ag,Zn,Cd,Ga,In, d electrons of metals, participation in chem. bonds 77−28682
synchrotron radiation collection mirrors, soft X-ray throughput 78−62275
threshold, role of ferromag. exchange interaction 77−90219
transition energy data, rel. to theory 79−76378
transition metal phosphides, valence-level struct., X-ray spectra and X-ray photoelectron spectra calcs. 79−64044
transition metal silicides, elec. struct. *(Russian)* 77−28106
transition radiation in stack of plates 78−9044
X-ray transition radiation, eikonal approx. 79−49422
X-ray tube with thermionic cathode in pulsed mode, spectra 78−4744
Z=100 to 173, Dirac-Fock-Slater calcs. of energy eigenvalues and total eigenvalues 77−71739
Z=11 to 103, theoretical, L-shell Coster-Kronig energies 77−83524
Z=95 to 130, calc. of K- and L-X-rays binding energies 77−83525
μ^- induced instantaneous fission, mesoatomic X-ray radiation *(Russian)* 79−30869
Σ^- atoms, meas. of strong interaction effects 78−42251
Al, condensed film, phase and struct. nonuniformity *(Russian)* 80−54536
Al plasma, laser-prod., X-ray spectrum time depend. *(Russian)* 77−55173
Al XII, intercomb. line obs., in laser-produced plasma 78−9106
Ar, radiative decay of collective levels, X-ray spectra *(Russian)* 77−6717
Au, K-shell X-rays, energy shifts and excitation mechanism 78−41990
Ba, X-ray spectra, high energy Lγ satellites 80−102474
Bi, pionic 4f→3d X-ray transition 79−86085
C-bearing gases, K X-ray yields induced by proton bombardment 79−45736
CO, X-ray and electron scatt. first Born approx. calcs. 77−61867
Ca, in brine, routine anal. by X-ray fluoresc. spectrometry applying matrix corrections 78−88690
Ca ions, dielectronic recombination excitation in solar X-ray lines 80−51725
Cd, photon interactions, energy role 77−36305
CdTe detectors, X-ray fluorescence escape peaks in X-ray spectra 80−9448

X-ray spectra continued
Cl, in brine, routine anal. by X-ray fluoresc. spectrometry applying matrix corrections 78−88690
Cl XVI, intercomb. line obs., in laser-produced plasma 78−9106
Co(VIII), resonance transitions, classification 80−42985
Cr-Fe-Ga system, phase obs. at 800 and 820°C *(Russian)* 78−23662
Cs^{2+} formation during electron-ion collisions, ultrasoft X-ray spectroscopic study *(Russian)* 80−43193
Cu, K$\beta_{1,3}$ intensity distribution, line strength calcs., single vacancy scheme 80−32650
CuP_2, Cu_3P, electronic struct. of valence bands, X-ray spectra and XPS 78−92176
Cu(X), resonance transitions, classification 80−42985
Eu, mag. and struct. transitions, X-ray K-line shift, 77-1000K *(Russian)* 77−4518
$Eu_{1-x}La_xS$, electron struct., lattice consts., X-ray spectral study *(Russian)* 80−100432
^{19}F, pionic 2p-1s X-ray transitions 79−18319
Fe IX lines in solar corona, appl. as plasmas density indicators 79−44429
Fe XX and isoelectronic ions, $2p^3$-$2p^23d$ transition array 77−65434
Fe XXIII, Fe XXIV, new line obs. in laser-produced spectra 79−81175
Fe XXIV, XXV, line wavelengths in 1.85 to 1.87 Å region in solar flare X-ray spectra 80−21973
Fe XXV-XXVI resonance lines region, laboratory reproduction of solar flare X-ray spectra 80−18819
$Gd_xSm_{1-x}S$ K X-rays chem. shifts, electronic phase transition, semicond.-metal transition 77−28116
H-like ions (Mg XII to S XVI), anal. of satellites to reson. lines in X-ray region 77−88421
He like ions Z=12-19, $1s^2\ ^1S_0$-$1s3p\ ^1P_1$ lines satellites obs. in laser 79−22640
He-like ions, X-ray form factors and total scatt. X-ray intensities 79−10063
I+Z (total Z≥100) adiabatic collision, inner shell X-ray prod., vacancy prod. 79−31675
^{123}I source sumpeak calibration absolute activity 77−57785
K, in brine, routine anal. by X-ray fluoresc. spectrometry applying matrix corrections 78−88690
Li, X-ray inelastic scatt. for $k \gtrsim 2k_F$ plasmon dispersion relation 79−15557
LiF curved crystal spectrograph, diffraction efficiency calc. method 80−79630
Li_2O-BaO-Al_2O_3-SiO_2-xTiO_2 glass, X-ray spectra, Ti ion electron config. *(Russian)* 77−8674
Mg XI, intercomb. line obs., in laser-produced plasma 78−9106
Mg XI resonance lines, dielectronic satellite lines atomic parameters calcs. 80−78567
Mg-Ga(Ge), electronic struct. *(Russian)* 77−48279
MgO-CaO-FeO(Fe_2O_3)-Al_2O_3-SiO_2 glass, X-ray spectra Fe ion electron config. *(Russian)* 77−8674
MnZn ferrites, effect of In additives on electron-ionic struct. *(Ukrainian)* 79−52046
Mo, X-ray spectra, Kα hypersatellites 80−63576
Mo XXXIII, XXXIV, XXXV, transition identification X-ray spectra 80−32648
Mo-Zr alloys, TsM-6, Zr segregation at grain boundaries, carbide precipitation, X-ray spectral anal. *(Russian)* 79−74154
N IX to Ni XII, wavelengths of transitions between lower configurations 80−99474
N_2, X-ray and electron scatt. first Born approx. calc. 77−61867
NaI, isoelectronic sequence, X-ray spectra 80−87071
$NaNO_3$, fine structure changes on interaction with weak shock waves *(Russian)* 80−54313
^{23}Na, pionic 2p-1s X-ray transitions 79−18319
Nb XXXII, XXXIII, XXXIV, transition identification X-ray spectra 80−32648
Nb_3Si, Nb_3Sn, Nb_3Ge, Nb_3Ga, Nb_3Al, electronic struct., electron-phonon interactions, X-ray spectra 78−91613
$Nd_xSm_{1-x}S(Se)$, K X-rays chem. shifts, electronic phase transition, semicond.-metal transition 77−28116
Ne atom with 1s-hole, wave function calcs. using radial orbitals, orthogonality 77−67971
Ni XXV, Ni XXVI, line classifications in laser-produced spectra 79−81175
$Ni_{13}(O_h)$ cluster, electronic states and X-ray spectra in Xα approx. of multiple scatt. theory 77−28645
O_2, X-ray and electron scatt., first Born approx. calcs. 77−61867
P XIV, intercomb. line obs., in laser-produced plasma 78−9106
^{103}Pd, K-electron capture decay, double K-shell vacancy creation 80−22773
Rb^{2+} formation during electron-ion collisions, ultrasoft X-ray spectroscopic study *(Russian)* 80−43193
Re, pionic 4f→3d X-ray transition 79−86085
S, in CS_2 and SCO, $L_{II,III}$-absorption spectra 78−86807
S XV, intercomb. line obs., in laser-produced plasma 78−9106
SO_4, in brine, routine anal. by X-ray fluoresc. spectrometry applying matrix corrections 78−88690
Se, meas. of K-edge dispersion anomalies using X-ray interferometry 80−90956
Si (2p) optical transitions, final state effects, soft X-ray electroreflectance study 77−66553
Si, thermoreflectance near $L_{2,3}$ soft X-ray threshold, temp. depend. 78−35224
Si(Li), analytic fitting of full energy peaks 77−71716
SiO_2, amorphous forms, surface struct. ESCA, X-ray line shift meas. *(Russian)* 77−66775
SiO_2, electronic struct., review of spectroscopic and theoretical data 77−76749
Sm, mag. and struct. transitions, X-ray K-line shift, 77-1000K *(Russian)* 77−4518
$Sm_{1-x}Gd_xS$, electron mechanism of high temp. phase transform., X-ray K-line shift obs. *(Russian)* 77−89704
$Sm_{1-x}La_xS$, electron struct., lattice consts., X-ray spectral study *(Russian)* 80−100432
SmS, electron mechanism of high temp. phase transform., X-ray K-line shift obs. *(Russian)* 77−89704
$Sm_{1-x}Yb_xS$, simultaneous Sm^{2+}-Sm^{3+} and Yb^{2+}-Yb^{3+} electron transitions *(Russian)* 79−60711
^ASm, A=150, 152, muonic, X-ray spectra meas. and anal., charge radii, multipole moments 79−3600

X-ray spectra continued
Ta, pionic 4f→3d X-ray transition 79−86085
TiC, energy schemes 77−39778
$TiH_x(D_x)$, electron-positron annihilation and X-ray K-spectra *(Russian)* 77−1761
TiN_{1-x}, substoichiometric, electronic density of states, CPA method calcs., X-ray spectra calc. 80−88464
TiP, TiP_2, electronic struct. of valence bands, X-ray spectra and XPS 78−92176
^{235}U (n,f), fission by fast neutrons, fragment K X-ray spectra, $\bar{\nu}$ energy depend. in heat balance method 78−17260
$^{238}U^{n+}+Z$, Z=6 to 92, 3.6 to 5.9 MeV/amu K-vacancy prod. 79−31672
V-Ti-C, high temp. carbide form., electron microscopy study 80−89228
VC, energy schemes 77−39778
V_3Si, V_3Sn, V_3Ge, V_3Ga, V_3Al, electronic struct., electron-phonon interactions, X-ray spectra 78−91613
Ve-Fe-Ga system, phase obs. at 800 and 820°C *(Russian)* 78−23662
W, $L_{\alpha 1}$ line width meas. *(French)* 77−50393
Y, X-ray fluorescence of L_α spectrum *(Russian)* 77−63491
Yb vapour, Mα line width 77−27014
YbB_{12}, valence state and mag. props. 80−50031
ZnP, Zn_3P_2, electronic struct. of valence bands, X-ray spectra and XPS 78−92176
Zr XXXI, XXXII, XXXIII, transition identification X-ray spectra 80−32648

X-ray spectrometers
see also X-ray crystallography apparatus
5 m grating spectrograph for studying molecular X-ray fluorescence spectra 80−86538
acid phthalate crystals, diffr. props., 0.1-2 nm 77−41740
active-recording X-ray crystal spectrometer for laser induced plasmas 77−3993
APS, soft X-ray, with Al foil in front of photocathode *(Japanese)* 80−13193
Ariel 5 Bragg spectrometer, crysts. preparation and calibration 77−5441
astronomical graphite crystal X-ray spectrometer on OSO-8 satellite 77−13238
astronomical Hadamard X-ray spectrometer with wide field-of-view 78−53829
automated, anal. of large samples in geochem. oceanography 79−16711
automated, qualitative anal. 80−22497
automation of Philips 1220 X-ray spectrometer 77−196
basic oxygen furnace, process monitoring 79−17586
bent crystal, for solar X-ray spectroscopy 78−7881
bent crystal spectrom., instrumental line width, meas. of K_β X-ray width 77−30697
bent crystal spectrom. geom. with shadow source 77−34507
Bent Crystal Spectrometer for solar X-ray spectroscopy 79−25489
bent crystal X-ray scanning spectrometer 77−45925
biaxial optical guider for rocket-borne solar obs. *(Polish)* 78−61744
body radioactivity measurement, SABRE 3 computer system 78−85425
Bragg crystal spectrometer, on line, step scan control and data accumulation system *(Japanese)* 78−5088
bremsstrahlung isochromat spectroscopy using a modified XPS apparatus 79−35912
Cauchois focusing with oblique-cut quartz analyser cryst. 79−52815
chemical anal., spectrometer control, interactive program for data collection, manipulation 78−7312
coincidence intensity meas., tailing convections 79−81141
concave grating grazing incidence mounting, use of curved slits 79−58858
constrained model-based representations of X-ray detector efficiency curves 79−49897
control system, automatic control of pitch motion 80−69012
convex curved crystal X-ray spectrograph, ray tracing 79−35900
crystal 2d value determ., isochromat spectroscopic method 77−65933
crystal analyser optical alignment for X-ray fine spectral structure study 77−18148
crystal diffraction spectrometers 79−72183
crystal spectrograph with active readout 80−4826
crystal spectrometer, new type, for cosmic X-ray studies 77−5443
curved crystal spectrometer for pionic X-ray measurements 80−78487
curved crystal X-ray spectrometer, for HEAO-B satellite 78−49331
curved-cryst. spectrometer, principle and performance 80−99026
curved-crystal, continuous angular scanning meas. system 79−6787
detector, photodiode array, self-scanning, direct X-ray response 77−54032
diffraction grating for X-ray microanalyzer 78−4746
diffractional focusing 78−5988
dispersive crystal spectrometers, geometric accuracy *(Chinese)* 80−22495
double axis, two-crystal X-ray spectrometer 78−66023
double crystal, appl. in density meas. of metals using X-ray total external reflect. 80−64831
double-beam triple-crystal X-ray spectrometer, high sensitivity, for lattice parameter and topographic meas. 80−77915
double-crystal, stabilised by dynamic feedback system 79−97482
DRON-1, valve voltmeter for examination of heterogeneous structures and textures 77−39504
electron probe anal., X-ray energy dispersive spectrometer appl., data collection, review 77−56312
electron probe microanal. in SEM by means of X-ray spectrometers, review 80−95194
electronics for X-ray focal plane spectrometer 78−40826
energy and wavelength dispersive spectrometers, minimum detection limits comparison 78−24002
energy and wavelength dispersive types comparison 78−21312
energy dispersive, quantitative elemental anal. 80−104840
energy dispersive, using pulsed X-ray excitation, for X-ray fluoresc. anal. 77−56319
energy dispersive, using semicond. detectors, for anal. of ferrous metals, report *(French)* 78−85281
energy dispersive spectrometer, for quantitative electron microprobe anal. *(German, English)* 77−63994
energy dispersive X-ray fluoresc., calibration standards development 77−60177
equipment development 79−20486
ESCA apparatus, calibration and use as soft X-ray spectrometer *(French)* 77−13832

X-ray spectrometers continued
EUV spectroheliographic, in Apollo Telescope Mount experiment S082A 77−60597
excitation-potential spectrometer for excitation potentials of soft X-rays 80−101912
FET, drain feedback preamplifier 77−38074
flat and convex curved crystal spectrographs, wavelength calibration 79−40649
fluorescence analyser for in situ Au trace anal. 78−49160
fluorescence detectors and electronics 77−46452
fluorescence quantometer, modification for Na determs. in geological samples 78−61589
fluorescence S analyser, for atmospheric particulate effluent meas. 78−68971
fluorescence spectra in secondary target energy dispersive spectrom., background reduction 79−100471
fluorescence spectrometer for industrial quality assurance 79−70398
fluorescence spectrometer system, automated for chem. shift meas. 78−4750
fluorescence spectrometer system, PW1400, microprocessor controlled *(German)* 80−16758
fluorescence spectrometer with sample loader, meas. sequence flexibility increase, electronic modification 80−77926
focusing Fe line crystal spectrometer for Spacelab 79−25500
focusing gas scintillation proportional counter 77−83461
focusing spectrograph for laser plasma X-radiation recording 78−1891
four-crystal, single-crystal plates deformation meas. 80−49048
gas scintillation counter, for high count rate X-ray detection 80−14052
gas scintillation counter for spectral line studies in X-ray astronomy 77−13247
gas scintillation counter X-ray spectrometer performance figures astronomy appl. 79−48673
gas scintillation proportional counter of large area for X-ray astronomy 79−80222
gas scintillation proportional counter using a photomultiplier tube array 79−76294
gas scintillation proportional counters, props. in soft X-ray detection 79−13600
gas scintillation spectrometer for X-ray astronomy, performance characteristics 80−56709
grating spectrograph, eval. for high resolution mol. X-ray fluoresc. in ultrasoft X-ray region 79−27117
grazing incidence, crossed optics 80−314
grazing incidence concave grating spectrometer for ultra soft X-ray emission spectra 78−62273
grazing incidence spectrometer, 10 m, for soft X-ray mol. appls. 80−18062
grazing incidence spectrometer, astigmatism correction method 77−82659
Hard X-Ray Burst Spectrometer on Solar Maximum Mission 80−51658
Hard X-ray Imaging Spectrometer on Solar Maximum Mission 80−51659
HEAO-B, focal plane crystal X-ray spectrom. 78−40825
HEAO-B, imaging proportional X-ray counter 78−40823
HEAO-B, solid state X-ray spectrom. 78−40824
HEAO-B monitor proportional counter instrument 78−40822
HEAO-B X-ray telescope, gas control system 78−40827
HEAO-B X-ray telescope, high resolution imaging instrument 78−40821
HEAO-B X-ray telescope 78−40820
high pressure gas scintillation spectrometers for X-ray astronomy 80−105166
imaging collimator for hard region spectroscopy of solar active area 77−5437
International Sun-Earth Explorer C spacecraft X-ray expt. 78−85787
isochromat vacuum UV spectrometer using Geiger Muller phonon counter 77−74521
Leicester solar coronal Bragg spectrometer, wavelength calibration and resolution 77−5442
light element detection, meas. near detectability limits with a horizontal cryst. spectrometer 79−21877
linear pulse amplifier, cct., features 78−78595
Lixiscope with good energy resolution 20 to 200 keV 80−99401
low energy X-ray fluoresc. spectrometer for air suspended particulate matter anal. 77−56321
low noise preamplifier with continuous drain negative feedback for X-ray spectrometer 79−26072
low noise preamplifier with pulsed drain negative feedback for X-ray spectrometer 79−26071
low temp. cooling device with DRON or URS-50 spectrometers 78−24910
low-energy high-fluence refl.-refr. spectrometer 78−49946
LURE grazing incidence spectromonochromator, soft X-ray synchrotron radiation, 2 years operating experience 78−62270
matrix correction coeff. derivation by Siemens P88/MAR 320 programs 77−65412
metal compounds on microfilters, X-ray fluoresc. spectrometry anal. 80−30315
monochromator for grazing incidence soft X-ray spectrometer without entrance slit 77−45926
MOS diode as low energy Xand γ-ray spectrum 79−36462
multichannel, thin dust layers, particle size effects automatic correction, computer appls. in spectrometry 79−83539
multichannel analyser for quantitative image processing with SEM, surface meas. appls. *(French)* 78−41379
multichannel fixed and sequential X-ray fluoresc. spectrometer system for air particulate anal. 77−60170
multicrystal, device for producing small rotation angles 79−35905
multicrystal with independent standard sample, for internal stresses determ. in single crysts. 80−64832
MWPC, anode modulation effects of X-ray beam positions 79−76282
MWPC, modulation of anode signal in soft X-ray detection 79−18081
MWPC X-ray drift chamber for soft X-ray detection 79−18071
nanosecond spectrometer, for 5 to 200 keV range 77−26447
optimisation, for energy-dispersive XFA using X-ray tubes in combination with secondary targets 80−30316
ore dressing X-ray spectrometric analysis centre 80−86541
OSO-8, high-energy celestial X-ray instrument 78−28522
p-i-n photodiodes as low-energy photon spectrometer, resolution, efficiency, for ~22 keV X-rays 78−17471
parallel plate imaging proportional counter and its performance with different gas mixtures 79−45533

X-ray spectrometers continued
PIN-photodiodes, comparison for X-ray spectrom. 78−74531
PIXE, appl. of wavelength dispersive spectrom. 77−48735
PIXE spectra, wavelength dispersion anal. 77−48736
plasma diagnostics using multichannel high-speed spectrometer, bremsstrahlung of hot electron component obs. 80−57445
plastic scintillation fast-slow coincidence spectrom., K-shell photoelectric cross section meas. 78−86754
pollution detection and anal. appl. 79−48027
position sensitive gas scintillation proportional counter for X-ray astronomy 80−58053
position-sensitive low-intensity X-ray imaging scope 80−86539
proportional counters, X-ray spectrometer appl. 79−18088
proportional counters and counting electronics *(French)* 77−74564
proportional counters for energy dispersive X-ray spectrometry, resolution 77−34504
proportional counters for Viking Lander spectrometer, fluoresc. anal. of Martian soil 78−40792
quality control, operational stability and reliability 79−54240
reference voltage supply using high-voltage source 78−21307
remote sensing, data analysis system for planetary mission appl. 79−12411
Rowland circle focusing spectrometer with concave diffr. grating 77−54030
sample-sequenced fluorescence spectrometer, appls. *(German)* 78−93787
scanning X-ray projection microscopy, using energy dispersive spectrometer 79−17593
scintillation proportional large area gas counter for X-ray astronomy 78−49321
scintillation proportional large area gas counter for X-ray astronomy 78−49322
scintillators, organic, temporal characteristics and saturation effects for low energy X-rays 79−81125
secondary fluorescer coupler in combined spectrometer/diffractometer system and stand-alone spectrometer system 77−41746
Seeman type with position sensitive detector, optimum geometry 78−4749
semiconductor, appl. to X-ray spectral anal. of ores 79−87902
semiconductor, features 79−80733
semiconductor detectors, use in high energy physics *(Russian)* 77−50325
semiconductor radiation detector, cooled preamplifier systems *(Slovak)* 78−21813
semiconductor X-ray spectrometer with optical feedback 79−68124
Si(Li) detector efficiency for 0.7-6 keV X-ray energy region 79−97928
simultaneous fluorescence spectrometer for use in metals industry 79−93268
single crystal absorption spectrometer 79−89052
Skylab Apollo Telescope Mount XUV spectrographs, optical contamination prevention 77−60603
soft X-ray emission studies of liquid metals and metallic vapours 80−73564
soft X-ray spectra, meas. by photoelectron anal. 80−73557
soft X-ray spectrometer, for diffuse cosmic sources 77−5440
soft X-ray spectrometer, for gaseous studies 78−24911
soft X-ray spectrometer, use of gas tube as radiation source 77−18152
soft X-ray spectrometry at high count rates 79−31310
soft X-rays, calibration and use of ESCA apparatus *(French)* 77−13832
solar X-ray imaging techniques, past and future, review 79−25495
solar X-ray spectrograph, cylindrical-crystal, design and characteristics 79−29990
solar XUV, grazing incidence spectrograph on Skylab 77−60601
solid-state detector for X-ray fluoresc. anal. of steel products in production lines 77−54029
spatial resolution function effect on beam-foil lifetime meas. 77−23580
spectrograph 5 m, with holographic, classical grating optics, construction 77−54034
spectrograph for single pulse detection 78−846
standardisation for air particulate anal. using reference sample on membrane filters 77−60176
steel, standard, energy dispersive X-ray fluoresc. spectrometry, computer directed optimisation 80−45585
streak camera electrode design using plasma simulation code 79−30632
synchrotron, Si crystal wavelength calibrator 79−89051
synchrotron radiation spectrometer for 100 to 130 nm 80−90953
telescope-X-ray spectrometer system for solar corona studies 80−105168
thermostatic control, Diapazon temperature variator 80−47160
three-crystal spectrometer for crystal perfection study 77−19837
threshold-potential, based on Auger electron solid surfaces meas. appl. 80−52365
topography settings, white beam X-ray, for cryst. defects, synchrotron radiation 2-axis spectrometer 78−67619
toroidal grating spectrometer for soft X-ray region, 16 to 625 Å 80−90948
transmission gratings for 7-304 Å operation, efficiency and resolution 80−82195
true volume steam content in thin channels at high pressures meas., spectrometric method 79−13585
two crystal, small angle scattering obs. 80−54077
two-crystal method for fatigue damage exam. of metals 79−52481
wavelength and energy dispersive X-ray fluorescence spectrometers compared 80−89573
wavelength dispersive X-ray fluorescence analysis, rel. to energy dispersive X-ray fluorescence anal. 80−7885
wavelength-dispersive, combined with SEM for elemental anal. 79−12917
wavelength-dispersive X-ray anal., developments in instrumentation 78−82090
X-ray fluoresc. anal. system, small sample, for medical appls. 77−60249
X-ray fluorescence, anal. of brine, applying theoretical corrections 78−88690
XRF, for classification of small glass fragments into window and non-window types 80−81401
Al alloys, energy dispersive X-ray fluoresc. spectrometry, computer directed optimisation 80−45585
4π-CaF_2(Eu) spectrum for X-ray and electron meas. 77−398
CdTe detectors, geometry variations 77−61663
CdTe detectors, international workshop 78−41887
CdTe detectors, use in spectrometers, physical and electronic factors *(Czech)* 80−23259

X-ray spectrometers continued
CdTe, MIS contacted small portable detector head for X-ray spectrometry 77−61662
CdTe n-type low resistivity detectors, advantages and limitations 78−41890
CdTe sensors, review of medical appl. 77−64147
CdTe spectrometers for hard X-ray astronomy 77−13206
n-CdTe surface barrier detectors, energy resolution 77−71724
CdTe X-ray detectors, energy resolution 77−71722
Cu $K\alpha_{1,2}$ spectrum, detection of multiplet struct. by monolithic double cryst. spectrometer 78−8482
Ge detector, intrinsic, for meas. of soft X-ray spectra of Tokamak plasma 77−51232
Ge detectors appl., high-purity, preparation and properties 78−86723
Ge intrinsic detector appl. to determ. of photon energy distrib. of diagnostic X-ray beams 77−70530
Ge low energy X-ray detectors, entrance windows 77−71718
Ge spectrometers, cooled, for X-ray and gamma-ray astronomy 77−5438
HgI_2 detectors, fabrication, appl. to X- and gamma-ray detection 77−83459
HgI_2 detectors, γ- and X-ray detection, solution grown crystals 80−63452
HgI_2 detectors, international workshop 78−41887
HgI_2, resolution limit in room temp. low energy X-ray spectrom. 78−37479
LiF dispersing crystal, X-ray source, synchrotron-like intensities, EXAFS expts. 78−86398
$(Pu,U)O_2$ mixed oxide pellet assay, using automated X-ray spectrometer 79−81066
Si detectors, high resistivity p-type, for β-ray and X-ray spectrometry, advantages 77−88329
Si high-resolution X-ray spectrocopy, portable system 79−81117
Si:Li detector system for X-ray astronomy rocket expt. 77−5439
Si/Li, cooled with Peltier elements *(Czech)* 78−49947
Si-Li surface-barrier detectors for electron and soft X-ray spectrometry 80−882
Si(Li), analytic fitting of full energy peaks 77−71716
Si(Li) detector, appl. to Am and Pu low conc. meas. in earth samples 78−58505
Si(Li) detector, β-ray background removal in X-ray meas. 78−55091
Si(Li) detector, improvement of time depend. instabilities by IR and γ-irradiation 79−36477
Si(Li) detector, low power monoenergetic X-ray tube for trace element anal. 78−70686
Si(Li) detector, preamplifier with drain feedback 78−66448
Si(Li) detector efficiency meas. 78−55108
Si(Li) detector for energy dispersive analysis *(French)* 77−26445
Si(Li) detector system, discrepancies in X-ray excitation efficiencies 80−9450
Si(Li) detector system response to microphonics 79−31333
Si(Li) detector window of aluminised mylar for X-ray fluorescence meas. 80−27894
Si(Li) detectors, operational possibilities from −90°C to −60°C 80−73555
Si(Li) detectors, X-ray detection efficiency at off centre point 77−57811
Si(Li) gas cooled detector for in situ XFA spectrometer 80−18055
Si(Li) gas cooled high resolution mini-probe 79−22550
Si(Li) high resolution spectrometer, with thermoelectric cooling 79−26813
Si(Li) non-dispersive spectrom. with high precision dead-time correction 77−54392
Si(Li) photopeak efficiency meas., 0.52-8.04 keV 80−27889
Si(Li) solid state detector appl. on modern single cryst. X-ray diffractometer, fluorescence anal. 79−58855
Si(Li) spectrom. with ^{71}Ge source for energy dispersive X-ray fluorescence anal. *(German)* 77−86429
Si(Li) X-ray detector, efficiency calib. in range 1-5 keV 77−79504
Si(Li) X-ray detector, efficiency calibration in 1.5 to 60 keV energy range 80−47823
Si(Li) X-ray spectrom., dead-time meas. system 77−79503
Si(Li) X-ray spectrometer, development, and interdisciplinary appl. *(Hungarian)* 80−18056
Si(Li)-NaI spectrometer, L X-rays, meas. of trace radionuclides in soil 80−58020
Xe gas hard X-ray detector, risetime discrimination 78−90031

X-ray spectroscopy
see also appearance potential spectroscopy; X-ray crystallography; X-ray diffraction; X-ray spectra
aerosol sampling, chemical heterogeneity revealed by X-ray photoelectron spectroscopy 80−55970
ammonium hydrogen tartrate, struct. refinement using X-ray diffractometer equipped with Si(Li) detector 79−58855
analyser for soft X-ray spectroscopy of excitation potentials 79−21882
analytical and quality control techniques, review 80−98989
artifacts, obs. in energy dispersive X-ray spectrometry in SEM 79−21888
astronomy, spectroscopic and photometric facilities of 80 cm X-ray telescope *(German)* 80−109358
Bragg mode analyser potassium acid phthalate, Bragg refl. coeff. obs. 80−95204
broadband X-ray excitation, quasi-fundamental correction methods 80−321
calibration, numerical procedure 77−48742
calibration facility of Lawrence Livermore Laboratory 79−49354
calibration materials for X and γ-ray spectrometers, decay data 80−106221
calibration sources for proportional counters using radionuclides 79−705
CAMAC, 2-D anal. of spectroscopic data, electronics 80−5460
coal ash characterisation with X-ray photoelectron spectroscopy 79−1977
cosmic X-ray spectroscopy, prospects 77−71009
cosmic X-ray spectroscopy, transmission grating behind grazing incidence telescope 77−64654
curved cryst. X-ray diffr. spectrometry, image formation 80−99025
data interpretation, online system using multivariate statistical anal. and pattern recognition 80−3461
DESY absorption spectroscopy set-up 80−74069
dual parameter list mode for anal. by crystal spectrometers 77−10153
electron bombardment induced X-ray emission, for chem. analysis *(French)* 77−36838

X-ray spectroscopy continued
electron induced X-ray spectroscopy, detect. sensitivity anal. 79−5229
element analysis, using nuclear-physical methods *(German)* 77−25347
emission, trace element analysis appl., small proton accelerator suitability obs. *(German)* 77−25348
energy dispersive, technique, appls. *(Japanese)* 80−57450
energy dispersive, ultramicroanalysis of biological fluids 78−92768
energy dispersive filtration for simultaneous energy and wavelength dispersive analysis 79−12918
energy dispersive microanalysis, in SEM, artifacts *(German)* 80−73561
energy dispersive X-ray diffraction method, annotated bibliography (1968-78) 80−36794
energy dispersive X-ray spectrometry using proportional counters, resolution 77−34504
energy-dispersive, data interpretation and quantitative treatment *(French)* 77−36839
energy-dispersive, nongaussian peak overlap problem 78−78050
excitation potentials of soft X-rays, meas. using spectrometer with channel electron multiplier 80−101912
failure analysis tools comparison and selection 80−71865
flow analysis using X-ray image contrast evaluation 78−344
fluorescence coating-thickness gauge, channel with Si(Li) detector 79−35671
fluorescence in pulsed X-ray spectrometry 77−18149
fluorescence spectra, nonlinear least squares anal. 77−48731
fluorescence spectrometry, single and multielement anal., optimum excitation conditions, automated determ. 80−323
focusing X-ray spectrograph for laser fusion expts. 80−31962
fracture surfaces, quantitative analysis problems in energy dispersive X-ray spectrometry with Si(Li) diodes *(French)* 80−89571
gas scintillation proportional large area counter, X-ray astronomy appl. 79−45556
gas-filled electroluminescent detector for soft X-rays, constr. and charcts. 80−32569
heavy ion induced X-ray emission anal. 77−48727
heterostructures, effect of primary electrons scattering on results of X-ray spectral microanal. 80−20735
high energy resolution X-ray spectroscopy, review 80−14959
high-efficiency low-energy spectroscopy, 100-500 eV 78−49944
high-pressure and low-temp. cell for X-ray diffuse scattering studies 80−86336
inhomogeneities analysis in metals and ceramics, use of STEM field emission gun 80−59354
interference X-ray spectroscopy 77−5970
International Committee for Radionuclide Metrology, report 77−23357
iterative deconvolution, effect of errors on convergence 77−53849
L-spectra line width, meas. method *(French)* 77−50393
laser plasma X-ray spectroscopic diagnostics using high-quality quartz and Si crystals 79−68953
light elements, ultrasoft X-ray spectroscopy, local anal., electron-microprobe excited radiation 80−99027
Lorentzian broadened K-series X-ray peaks of heavy elements, fitting algorithm 77−57799
metal film, mass absorption coeff. meas. using proton induced X-rays 78−2942
metallic supported film, thickness determ. using ^{63}Ni radioactive source 78−22989
metals and alloys 77−55849
microcomputer automatic control of double-crystal X-ray spectrometer *(Polish)* 80−32563
microscopic equipment, methods, appls. and related topics, bibliography 80−73124
microscopy, high resolution, with synchrotron radiation, for chem. microanal. 80−81416
moire interferometric pattern, analyser B diffusion effect *(Russian)* 79−44994
Mossbauer gamma-X-ray coincidence meas. 80−14041
multichannel analysers *(Hungarian)* 80−95205
mussel trace element monitoring appl. 80−30954
nonlinear least squares anal. of full energy peaks 77−88328
optical emission and X-ray spectrometry developments *(French)* 80−68263
photoactivation ratios, 15 to 40 MV, for specification of radiotherapy beam spectral quality 77−21619
photoactivation ratios, 4 to 15 MV, for specification of radiotherapy beam spectral quality 77−21620
photoelectron, combination with SIMS for surface studies 80−52377
photoelectron spectroscopy, resolution enhancement by deconvolution *(German)* 78−82087
photographic system, dispersive, for recording X-ray spectrum in 0.1-1.9 nm range 79−35904
PIXE, anal. of S and trace metals in nonurban and marine aerosols 77−49136
PIXE, impurity depth determ. 77−48725
PIXE, influence of matrix effects on absolute anal. 77−48721
PIXE, trace element anal., medical appl. 77−48865
PIXE, trace element anal. with triggered beam pulsing 77−46453
PIXE, use of external proton beam for multielement anal. 77−48719
PIXE anal., appl. to environmental samples 77−48730
PIXE anal., enhancement 77−48722
PIXE anal., review of target backings and specimen preparation 77−48979
PIXE anal. of aerosol elemental composition in particle size fractions, human respiratory uptake 77−48726
PIXE anal. of thick and thin targets of biological materials 77−48723
PIXE anal. with REX computer program 77−52714
PIXE applications, conf. 77−48715
PIXE meas. at Univ. of Manitoba 77−46650
PIXE spectra, computer code trace 77−52713
PIXE spectroscopy, trace element analysis 77−48718
PIXE system, automated anal. of environmental samples 77−48716
PIXE system for air pollution meas. in South America 77−49157
plasma electron temp. meas. by soft X-ray energy anal., pulse pileup effects 79−64910
plasma focus X-ray spectra meas. with time resolution 77−43064
polynuclear aromatic hydrocarbons, analysis by X-ray excited optical luminescence technique 80−66891
processor X- and γ-ray, active zero-pole cancellation feedback loop 79−9972
proton induced X-ray spectroscopy, detect. sensitivity anal. 79−5229
quantitative, comparison of mathematical models 79−17587
radiography, diagnostic, Compton-scatter method 77−2044
regression line derivation, low stability conditions 77−73486
remelting process anal. appl. 78−23560
review, energy spectrum analysis, Si(Li) probes *(Chinese)* 79−30635
review *(Japanese)* 79−26142
self-absorption, method for unoccupied valence states obs. in metals and alloys *(Russian)* 77−81175
SEM imaging techniques, and X-ray microanal. 80−57432
SEM microanalysis techniques, review 80−71995
single crystals, use of polarised radiation 78−8481
soft X-ray and EUV spectroscopy techniques *(Japanese)* 77−65058
solar and cosmic high resolution spectroscopy, instrumentation 77−13243
solar and cosmic X-ray spectroscopy, symposium, England (May 1975) 77−5433
solid state spectroscopy using synchrotron radiation, book contrib. 80−7375
Spacelab facility for X-ray source spectroscopy and polarimetry 78−32314
spherically symmetric objects, reconstruction from slit-imaged emission, appl. to spatially resolved spectroscopy 78−78930
steel foil, microanalysis by energy dispersive X-ray spectrometry *(French)* 80−85250
surface sensitive analytical techniques, eval. 78−27876
surface valence band spectroscopy in ultrasoft X-ray region 77−55852
surfaces and thin film studies by combined system of SIMS, AES and XPS 80−86536
synchrotron radiation, application to EXAFS and angle resolved photoemission spectros. *(Korean)* 80−74453
synchrotron radiation, spectroscopic appls., review 77−58239
synchrotron radiation, X-ray optics and monochromators 77−54027
synchrotron radiation applications 77−51283
synchrotron radiation appls., including extended X-ray absorpt. fine struct. technique 78−32963
synchrotron radiation as intensity reference 79−75619
synchrotron radiation for VUV and X-ray spectroscopy, lecture 78−24870
synchrotron radiation research, developments 78−78051
synchrotron radiation source for X-ray spectroscopic studies, SPEAR storage rings 77−41745
synchrotron radiation spectroscopy instrumentation and appls., book contrib. 80−4782
time resolved spectroscopy with synchrotron radiation 80−31902
trace element analysis, absorpt. edge method of charact. filters 79−8461
transmission grating, facet-type, aberrations for cosmic X-ray and XUV spectroscopy 78−85851
undulator radiation source, specified spectrum 79−10251
AgCuAg sandwich target, proton induced K-shell X-ray yield ratios 77−48724
Al intermetallides, multicomponent, spectral microanalysis by accel. voltage variation method *(Bulgarian)* 79−16093
Bi-MnBi eutectic region, of Bi-Mn phase diagram 80−81034
Cu electrodeposition on Su, reliability anal. 78−24901
Cu, valence band splitting, X-ray K-emission spectroscopy 80−40189
Cu-Ga, binary alloy constituent EDS anal., secondary fluorescence, SEM study *(Chinese)* 80−85231
Fe-Si (3wt.%), grain-oriented, secondary recryst., grain growth inhibition 80−89245
GaAS, binary alloy constituent EDS anal., secondary fluorescence, SEM study *(Chinese)* 80−85231
Hg-As-S system glasses, photoelectron X-ray spectroscopy study 80−29858
HgI_2 detectors, room temp. X-ray spectra of Na and Mg 78−78049
HgI_2, resolution limit in room temp. low energy X-ray spectrom. 78−37479
HgI_2 thin sections with Peltier-cooled preamplification for X-ray spectrosc. 80−324
$Mg_{1.86}Al_{1.67}Si_{2.47}O_{3.19}N_{3.81}$, 12H polytype, intergranular phases and compositional variations 80−79645
Si Kα source, sensitivity factors, cross section and resolution data 80−77920
Si:Li X-ray astronomical spectroscopy 77−5460
Si(Li) energy dispersive X-ray spectra, computer anal. 79−1981
Si(Li) solid state detector appl. on modern single cryst. X-ray diffractometer, fluorescence anal. 79−58855
Zr, anomalous dispersion corrections using scanning interferometer 77−48274
$ZrO_2.SiO_2$-αAl_2O_3 mixed powders, solid state reactions 80−40337

X-ray transport *see photon transport theory*

X-ray tubes
acquisition time reduction in pulsed X-ray tubes 79−54239
anode voltage compensation under dropping power condition, digital compensation system *(Bulgarian)* 79−35902
biomedical, target angle and inferential kilovoltage meas. 80−30843
calibration system, tubes and generators 79−17583
cathode heating transition processes *(Bulgarian)* 79−93264
ceramic for half-weight portable NDT X-ray apparatus 79−57193
computerised tomography scanner tubes 79−66537
computerised tomography spectral artifact correction 78−35953
current fall-off during an exposure, investigation and explanation 80−56203
dental, improvements 78−65129
dental X-ray unit kVp meas. 77−40767
diagnostic system compatible with DHEW standards 78−7445
diagnostic tubes, meas. of focal spot size 80−89831
Dynalyzer II, application to X-ray quality control 78−77896
education, Poisson statistics demonstration using X-ray tube, electronic 'shot noise' 80−73129
electroluminescent memory screens, evaluation of X-ray defectoscopic parameters 78−72992
energy dispersive X-ray fluoresc. systems, pulsed-tube counting rate performance 78−4752
expandable flash type, with 0.5 mm source size, features 79−21887
filament lifetimes, in rotating-anode X-ray machines, increasing using beam-deflecting magnet 80−77918
flash, for diffraction studies on 2-stage light gas gun 80−86537
flash techniques, review 79−49356
flash X-ray tubes with new type of cathode 78−58101
fluorescent excitation anal., high intensity source of polarised X-rays 77−60238

X-ray tubes continued
fluorescent X-ray intensifying screen, efficiency determ., standard method 80−37140
fluorescent X-ray source for study of radiographic imaging systems 78−24132
fluoroscopic installations with undertable X-ray tubes, survey form and techniques 77−73597
fluoroscopy, kVp variable, with automatic brightness stabilisation, X-ray tube pot. var. 78−69202
focal site lengthening, in Elliott rotating-anode X-ray sets 80−77919
focal spot size determ. from pinhole camera images 79−79627
focal spot size meas., systematic error in pinhole camera system 79−75666
focal spot size measurement, optical simulation, for correction factor determ. 77−26449
focal spots, effective size of transverse dimension 77−71414
gas-filled tube, as radiation source for soft X-ray spectrometer 77−18152
grid control type, diagnostic, quality improvements 78−11733
heavy-duty rotating anode X-ray tubes 80−73568
high brilliance sources and generators, soft and pulsed X-ray generators, book contrib. 78−42861
high potential X-ray generator, PD150L, standardisation of exposure factors *(Japanese)* 77−73577
high tension unit, HD150G-40, for X-ray diagnosis *(Japanese)* 77−73576
high vacuum electron excitation X-ray tube, rate of C contamination, on Al targets 79−44996
image convertor with video signal output 80−36125
image intensifier, magnetic interferences *(German)* 80−105761
image intensifier tube, 14 in 79−16285
image quality, MTF anal. of influencing factors *(Japanese)* 77−73580
imaging properties of X-ray focal spots 77−21596
incandescent light bulb, conversion to X-ray tube 77−33755
for industrial applications, essential components 77−38068
industrial hard X-ray channel-plate image intensifier 78−54517
Kvant-60 miniature pulsed X-ray unit 77−38076
kVp indirect determ. using digital readout device 78−53486
laser driven 3 kA X-ray source 78−41389
laser-fusion diagnostics, subpicosecond X-ray streak camera 78−42822
line focus, rapid slit alignment procedure 77−26448
lithography laboratory apparatus *(Polish)* 79−89050
low power Ag anode X-ray tube for air suspended particulate matter anal. 77−56321
low powered transmission tube with transparent anodes, for exciting fluorescence 79−21881
medical diagnostic tubes, vacuum technology *(German)* 79−30634
microfocus, electron source with single pole mag. lens and novel focusing system 78−32964
microfocus source, non-linear intensity rise studies 80−77927
microfocus source in Berg-Barrett single crystal substructure exam. 79−52495
modulation effectiveness, electron gun considerations 80−73554
MTF of X-ray tube focus rel. to current *(Japanese)* 77−70545
multielement system with regenerative monochromatic filters, for photoelec. diode calibrations 77−54033
operation, guide 79−49350
optoelectronic revolution counter for X-ray tube anodes *(German)* 78−12678
p-i-n photodiode meas. of X-ray tube kVp *(German)* 79−232
penetrameter cassette calibration to 400 kV and extra-focal radiation effects in X-ray tube filtration meas. 78−20242
performance characteristic rel. to radiologic image quality 80−17125
Philips PW 1360 X-ray diffraction tube shield, mechanical safety interlock device 78−36989
picosecond X-ray chronoscopy 78−38546
pulsating potential X-ray machines, filter method for peak volt. and inherent filtration meas. 78−73201
pulse generator of 1-10 Å, X-rays for calibration and adjustment of X-ray pulse detectors 79−2902
pulsed high-power subnanosec. X-ray source 80−73565
pulsed soft X-ray source of nanosecond duration 77−41742
pulsed X-ray thermionic tube intensity and dose angular distrib. obs. 79−67450
quality and output determ. in diagnostic range, TLD method 77−60241
radiation spectra contamination determ. by spectrometer with Si(Li) detector 77−45924
radiographic phototimers, acceptance testing and performance monitoring 77−5071
radiographic testing equipment, device charact. *(German)* 80−76438
radiographic X-ray tube current, effect of electron evaporation 78−69204
radiography, diagnostic, X-ray spectra determ., high intensity 80−41217
radiography, falling load technique, performance evaluation 78−69201
radiography, focal spot meas. for quality control, using random object distrib. 77−2047
rapid process recording using type RTR-1 tube 80−9080
ROTANODE, heavy duty X-ray tube for diagnotic use 79−44999
rotary anode, C by transition metal carbides *(German)* 80−105759
rotary anode, HV insulation, discharges due to back scattered electrons elimination *(German)* 80−105758
rotary anodes, high continuous power, with Rh-W disc bonded to graphite *(German)* 80−105760
rotating anode, increased loadability 79−12915
rotating anode, upper limitation of output, radiographical appls. 79−30631
rotating anodes, temperature distribution, physical props. 78−29222
rotating anodes temp. distrib., compound anodes numerical anal. 78−62285
rotating-anode X-ray tube apparatus 78−58100
sharp-focus pulsed X-ray tube with plasma electron sources 79−93265
shielding device, Pb glass, for use with ceiling mounted tube 79−92397
single- and three-phase generator performance comparison *(Japanese)* 79−92354
spectral purity, for diffr. anal. appls., quantitative determ. *(Chinese)* 80−57444
standard monoenergetic source development and appl. 77−38078
status monitor, for Elliot rotating-anode X-ray source 79−35908
streak camera, high time resolution, with X-ray microscope *(French)* 78−42823
student laboratory, improved light bulb X-ray tube 79−62971

X-ray tubes continued
subnanosecond X-ray framing camera, fibre array technique 78−41394
Super Rotalix Ceramic, new type of X-ray tube 80−104749
support, for serial cerebral angiography in stereoscopic magnification *(Japanese)* 77−73574
survey of operating conditions 77−11441
technological and philosophical changes over a decade 80−37136
Tel-X-Ometer apparatus for educational demonstrations 80−8763
thermal monitoring system, LOADIX, features 78−3658
thermionic cathode in pulsed mode, spectra 78−4744
tomofluorographic camera with lens objective and angular tube 79−57750
topogram visualisation raster tube with shoot-through target 80−31956
TV chain MTF and image quality determ. factors 80−36126
variable focus, aerospace industry use in NDT 79−80734
vidicon tube appl. *(German)* 79−26050
vidicon tube for low level X-ray and γ-ray imaging 77−81561
voltage error effects on image quality of roentgenograms 78−57060
voltage meas. in high security system 79−35794
X-ray anal., conf., Denver, USA (Aug. 1976) 77−70382
X-ray fluoresc. anal., polarised radiation excitation source 78−7314
X-ray fluoresc. spectrometry using pulsed X-ray excitation, for environmental anal. 77−56319
X-ray fluorescence anal., pulsed tube excitation 77−56313
X-ray source, industrial, use for electronic component radiation effects work, calibration 80−63402
CsI:Na phosphor screen, absolute efficiency under fluoroscopy conditions 78−82084
Cu-target diffr. tubes, K_α charact. radiation rel. intensities calc. 78−4754
Mg X-ray source, achromatic, Cu lines in defective or worn tube 79−75667
Rh X-ray tube for silicate rock X-ray fluorescence analysis 78−88945

X-rays
see also cosmic ray X-rays; photons
80 years progress in techniques *(Dutch)* 80−82859
atmosphere, X-rays from electron precip. event on (1974 November 14) 77−87182
channelling positron (electron), coherent radiation 77−76476
classically forbidden region, molecular-orbital X-rays, spectral distrib. 79−72334
demonstration using Tel-X-Ometer apparatus 80−8763
gravitational effects on polarised radiation from vicinity of black hole 77−82440
history of discovery *(Danish)* 77−64912
linear accelerator beam energy at off-axis points, calc. technique for correct. 80−81742
linear accelerator X-ray beams, off-axis beam quality change 80−78461
medical accelerator high energy X-ray beams, neutron dosimetry 79−83942
Rontgen's discovery of X-rays, accidents role in scientific enterprise 80−4502
signal backscattered from semi-infinite reflector, quantitative analysis of intensity controlling factors 77−54371
T-10 Tokamak, plasma X-ray emission 80−28840
Cu-Si(Sb), dil., chemical etching and X-ray topography obs. of cellular struct. *(French)* 79−96249

X-Y model
2-D spin correlation function above T_c 79−2734
Abelian Higgs-Kibble model on lattice, spontaneous magnetisation 78−57870
anisotropic, quasi-one-dimens. system, with spin Peierls phase transition, tricritical point 80−25142
anisotropic linear spin chain, two-magnon problem with arbitrary interaction radius 78−72320
anisotropic magnet, low-temperature properties 79−65633
anisotropic spin 1/2 chains, transverse correlation function, results at $T=\infty$ 77−32145
antiferromagnet, low-dimensional, Neel temp. in mag. field 77−32200
antiferromagnet, one-dimens., nonlinear dynamics 80−80521
antiferromagnet, two-dimensional, approx. to susceptibilities 78−47928
antiferromagnetic insulator, one-dimens., Friedel type oscills. 78−60296
biquadratic, spin one, variation of Curie temp. 80−97102
classical, absence of long range order 79−63162
classical, comparison of plane rotor with Ising ferromag. 80−60348
classical, high-temperature expansion, correl. length and transition temp. 79−33447
classical, Monte Carlo study 79−63168
classical, random system, absence of long range order 77−30103
classical confluent-singularity anal. of thermodynamic functions, planar-rotator model on FCC lattice 79−69686
classical one-dimensional, free energy in mag. field 77−4484
classical XY spin dynamics far from equilibrium 78−68136
computer simulations of classical one-dimens. X-Y model 79−78396
continuous spin systems, position-space renormalisation group study 79−38350
continuous symmetry breaking in Ising, XY- and Heisenberg model 79−82787
correlation functions, dynamical, zero temp., critical exponents 78−72324
correlation functions in X-Y models and step free energies in roughening models 78−67675
Coulomb gas, 2-dimens., dissociation at low temp. 77−31748
critical behaviour, high temp. susceptibility and internal energy series 78−34987
critical behaviour of effective nonintegral space dimensionality infinite lattice 77−49688
critical phenomena, real space renormalisation group 78−56338
critical properties, review 77−66326
critical properties near Lifshitz point, Monte Carlo study 79−28543
dialkylammonium iron tetrachloride, antiferromag., mag. susceptibility meas. 80−60220
(1+1/N)-dimensional, Ising model in 2+1/N dimensions 79−93071
dimethylamine iron tetrachloride, antiferromag., mag. susceptibility meas. 80−60220
discrete Abelian spin and gauge systems, phase struct. 79−85232
discrete and Abelian lattice gauge theories 79−9279
disordered, two-dimens., phase transition 79−82789
disordered spin systems, crit. dynamics 77−43844

X-Y model continued
DOBAMBC, chiral smectic C-phase ferroelectric liq. crystal film, classical X-Y system, props. 80−44123
domain wall, phase transition, three-dimensional XY model 79−51805
double scaling limit of one-dimens. XY model in monodromy preserving deformation theory 80−47194
duality props. and phase diagrams of general discrete planar models 80−60286
FCC lattice, phase transitions of fully frustrated models 80−29517
Fermi system, 1-D, and plane xy model, behaviour of correlation functions 78−56091
ferromagnet, anisotropic, in external mag. field, continuous phase transition existence 80−108011
ferromagnet, critical behaviour at field-induced transition at mag. displacive limit 77−66335
ferromagnet, Ising-Heisenberg-XY crossover, bicritical-point, partial differential approximants for susceptibility series 77−85466
ferromagnet, magnetically dilute, two dimens. lattices 77−63056
ferromagnet, one-dimensional planar, in external field, static props. 79−51735
ferromagnet, phonon thermal cond., crit. anomalies *(Russian)* 78−80159
ferromagnet, S=1, with uniaxial anisotropy, Curie temp. 79−78425
ferromagnet, S=1/2, on triangular lattice, ground state props. 80−60165
ferromagnet, spin X-Y, correl. functions 79−47221
ferromagnet, zero temp. props. in 3 dimens. 79−61032
ferromagnetic, anisotropic, Green-function theory 77−16025
ferromagnetic coupling, finite magnetisation 78−43541
free energy calc. in new approx. scheme 77−41547
frustrated two-dimensional planar model, spin-spin correl. 80−11212
frustration effect in s=1/2 XY and Heisenberg models 80−15677
frustration network, phase transitions 80−2596
gauge theory analogue, 4-D self-dual gauge model, phases and transitions 80−27399
generalised, Lie algebra appl. 78−77806
ground state energy, renormalisation calc. 79−61150
ground state energy density 78−12651
ground state props., in three dimensions 79−15274
Heisenberg-Ising spin chain quantum inverse scatt. method, Jordan-Wigner transformation 80−93068
helicity modulus at low temperatures 78−70052
high-temperature representation of anisotropic rotator, XY and Heisenberg models for dimensions D≥2 80−11146
inequalities for classical spin vector models, X-Y and Heisenberg models 77−91
insulating systems, magnetic, review of expts. 78−68240
interactions, spirals and phase transitions with and without long range order 80−60350
interface roughening and tricritical points 78−23286
isotropic, alternating, homogeneous, time and frequency depend. correlation functions 80−36953
isotropic spin 1/2, phase transitions in quantum spin systems 78−84434
isotropic two-dimensional magnetism, long range forces effect 78−52291
isotropic X-Y chain, static spin correl. functions at zero temp., boundary effects 77−43802
Josephson junction array, granular supercond., phase transition 80−88684
lattice spin systems, matching conditions for crit. props., group struct. of block transforms 80−22305
Lifshitz point region, crit. exponents 80−65898
linear chain in random fields, thermal properties, appl. to praseodymium ethyl sulphate 79−65679
linear magnetic chain, struct. transition under external mag. field and stress 77−12126
magnetic resonance *(Russian)* 77−80992
magnetisation, time dependent autocorrelation function, of x-component, for 1D S=$^1/_2$ X-Y model 77−77018
magnetisation of ground-state 79−65629
mean-field theory of Peierls and spin-Peierls instabilities−commensurability, harmonics and dimerized-state pinning 80−108014
meron and meron pair analogs in XY model 80−32010
Migdal recursion eqns., existence of long range order 79−67231
migdal renormalization group approach to quantum spin systems 79−38333
Migdal-like approximation, quantum spin systems 80−34649
Monte Carlo simulation, phase transition with vortices 77−43799
Monte Carlo simulation of quantum spin systems, two dimens. X-Y model 78−27011
Mori continued fraction truncation for spectral function 78−6496
noncollinear magnetic order and spin wave spectrum in presence of competing exchange interactions 80−65834
nonlinear excitations by numerical determination 79−71372
nonuniversal dynamic scaling in two dimens. degenerate systems 78−6497
one dimens., transverse correl. function at zero temp. 79−40493
one dimensional, with anisotropic interaction, high freq. props. *(Russian)* 77−80902
one dimensional spin-1/2 XY model, finite temp. transverse autocorrelation function 80−50024
one particle reduced density matrix of impenetrable bosons in one dimension at zero temperature 80−17863
one-dimens., transverse correls. 79−40492
one-dimens. alternating X-Y model time-depend. spin correl. functions and ergodic props. 78−31031
one-dimens. time-depend. xx correl. function 78−31030
one-dimensional, crossover scaling function at zero temp. 79−15273
one-dimensional, many-spin correlation functions at zero temp. and in presence of mag. field 79−7956
one-dimensional, time-dependent correl. functions in high-temp. limit 79−73727
one-dimensional, transverse time-depend. spin correl. functions, zero temp. 78−65876
one-dimensional, with symmetry-breaking fields, thermodynamics and static props. 79−73742
one-dimensional classical and quantum chains, spin-Peierls transition theory 77−66375
one-dimensional isotropic, dynamics 80−71057
one-dimensional magnetic models, fluctuations in energy-energy correlation function 79−73726
X-Y model continued
order parameter, fluctuation, high temp. series expansion, simple hypercubic and face-centred hypercubic lattices, spin 1/2 80−50098
order-disorder transitions in gauge and spin systems 78−70072
paramagnet, approxs. for Mori continued fraction 77−20529
partition function 79−151
percolation in three-dimens. model 78−80113
phase transition in 2D Coulomb gas, sine-Gordon theory and XY model, renormalisation group anal. 80−36950
phase transition in X-Y model, singular bounds on free energy and susceptibility 78−43595
phase transitions, rigorous existence theorems 79−58649
phase transitions in quantum X-Y and Heisenberg models 80−25141
planar spin two-dimens. model, mag. correlation function, self-consistent calc. 80−29563
praseodymium ethyl sulphate, one-dimensional X-Y model, hyperfine contrib. to specific heat 79−1678
praseodymium ethyl sulphate, specific heat, electric suscept. and thermal cone., one-dimens. electric dipolar XY system 77−32148
praseodymium ethylsulphate:Sm, one-dimens. X-Y system, spin dynamics, electron spin echo meas. 80−66031
praseodymium ethylsulphate:Sm, XY system, mag. relax. and spin dynamics 79−61211
quantum, S=$^1/_2$, zero temp. renormalisation group method in transverse field 80−108025
quantum effects and dynamics at low temps., path integral approach 80−84584
quantum effects in crit. props., crossover scaling near zero temp. 79−28535
quantum effects in critical props., in transverse magnetic field 78−2689
quantum one-dimensional model, renormalisation group method anal. 80−17887
quantum spin chains with X-Y symmetry, anharmonic effects and IR singularity 77−32146
quantum spin system, two-dimens., frustration, renormalisation group study 80−80535
quantum systems, one-dimens. isotropic model, zero temp. renormalisation group method 79−82800
random isotropic dipolar magnet, absence of ferromag. long range order 79−28546
random magnetic systems, gauge symmetries, Ising and X-Y models anal. 79−38295
relaxation function for 3-dimens. system 77−69666
renormalisation group transformation for quantum spins 78−47984
renormalization group approach to two-dimensional XY and Heisenberg spin 1/2 models 79−42727
rigorously solvable, numerical computations 77−1534
screw spin ordered state through dipole-dipole interaction 78−39337
second order Green's function theory 80−54913
sequential term prediction 78−57866
sine Gordon theory, equivalence to z-dimens. ferromag. classical X-Y model low temp. behaviour 77−13873
smectic A-nematic transition, defect model, derivation from X-Y model 79−14916
smectic liquid cryst. film, ferroelec., two-dimens. X-Y crit. behaviour 79−77497
smectic liquid crystal, ferroelec., two-dimensional X-Y crit. behaviour 79−77514
solid on solid model rel. to XY model and Coulomb gas 77−84684
solid-on-solid representation, planar model Monte Carlo simulation 80−96727
soliton-like features of two-dimens. model with quartic anisotropy 79−78429
solitons, coupled linear chain system 77−43463
spin, 1/2, ground state energy, pair correl. 78−72321
spin 1/2, ground state energy, long-range order determ. by variational method 78−72322
spin 1/2, high temp. longitudinal susceptibility 79−87275
spin 1/2, phase transitions at T=0, z-field renormalisation group method 80−71051
spin 1/2, renormalisation group method, triangular lattice 77−26247
spin 1/2 dimerized XY chain, equivalence with Ising chains in transverse field 79−19713
spin 1/2 model, time depend. correlations in high density limit 79−54071
spin 1/2 X-Y inequalities, proof 79−73660
spin 1/2 X-Y model, thermodynamic props., high temp. series expsn. 78−47929
spin 1/2 X-Y model, thermodynamic props. in three dimens., high temp. series expsn. 78−47930
spin complexes, occurrence in model with anisotropic biquadratic exchange interaction 77−28356
spin dynamics for classical X-Y model in one and two dimens. 78−34997
spin dynamics of one-dimens. system 77−4486
spin glass, high-temperature series for order-parameter susceptibility 79−28534
spin glass, infinite ranged models 78−80166
spin glass, low temp. renormalisation, crit. temp. 78−10688
spin glass, mean field theory and ε-expansion 78−10705
spin glass, quantum, frustration, 2-D lattice, functional integration technique *(French)* 80−39789
spin glass, rel. between isotropic X-Y model and mobility edge problem 78−88138
spin glass, two-level system, three-dimensional model and mag. field effect 78−39331
spin glass, X-Y and Heisenberg, below four dimensions, vanishing of Edwards-Anderson order parameter 80−60347
spin glass phase transitions, instability 78−23285
spin glass with non-random interactions, mag. susceptibility 77−55673
spin glasses, quartic operators in Ising, X-Y, and Heisenberg systems 79−33498
spin glasses, recent developments 78−68264
spin glasses, time translation, spatial scaling and nonexponential relaxation 80−97110
spin model, one-dimensional, high power terms, spectral and thermodynamic props. 77−80900
spin operators, general commutator eqn. 79−4638
spin Peierls transition, gap eqns. 80−24801
spin Peierls transition temperature in magnetic field 79−56537
spin wave theory of spin 1/2 X-Y model 80−7068

X-Y model continued
spin XY one dimensional system containing impurities, static mag. props. *(Russian)* 80−65826
spin-$^1/_2$ system, X-Y model and self avoiding walk approximation 77−4488
spin-$^1/_2$ XY model, thermodynamic quantities, high-temp. series expansions anal. 80−7067
spin-glass, two-level system, general formalism and two-dimens. model 78−19257
spin-S XY model on FCC lattice, high-temp. fluctuation expansions, spin depend. 79−95596
spin-S XY-model, susceptibility series expansions 79−28540
spontaneous magnetisation in d-dimensional models for d≥2 78−72319
square lattice, ground state energy 77−80904
superfluid density in two-dimens. 79−95242
superfluidity and the two dimensional XY model 79−28498
susceptibilities of S=1/2 XY model on the square lattice at T=0 80−88732
tetragonal XY-like antiferromagnet, multicritical behaviour, global phase diagrams 79−42779
thermal excitations in Heisenberg-xy systems 80−97047
thermodynamic limit asymptotic equivalence of three 1D disordered models 77−77019
TMMC, linear antiferromag., mag. phase diagram, expt. and theoretical study 80−71038
TMMC, symmetry crossover in spin dynamics, proton spin lattice relax. calc. 77−40147
TMMC, XY-Ising crossover transition, quasi-elastic neutron scatt. obs. 80−44826
TMMC one-dimens. antiferromagnet, effect of mag. field on correl. length 79−91244
transition metal layer compounds, mag. model, 0K phase diagram, spin wave spectrum 79−87273
transverse correlations, eqns. of motion of finite temp. 80−105581
transverse correlations, infinite temp., inhomogeneous 1-dimens. spin-1/2 X-Y model 78−65877
two dimensional, Monte Carlo simulation and phenomenological theory of phase transition 78−6534
two-dimens. isotropic spin system, phase transition 79−42716
two-dimens. XY magnet and Heisenberg antiferromagnet, ground state anal. 79−42728
two-dimens. XY spin glass 79−42729
two-dimensional, disordered, finite susceptibility phase 79−61031
two-dimensional, physical realisation, surface reconstruction 80−15351
two-dimensional, with quartic anisotropy, mol. dynamics study 78−75739
two-dimensional planar magnet, crit. slowing down in transverse autocorrel. function 78−95448
two-dimensional spin 1/2 XY model, temp. marginality by linear renormalisation transform. 79−38341
two-dimensional spin system on square lattice, exact duality-decimation transform. 80−17890
two-dimensional systems, phase transitions 78−68241
two-dimensional X-Y magnets with annealed non-mag. impurities 79−78391
two-point correlation function, analogy with screw dislocations in solid-on-solid model 78−63691
vortex formation in Monte Carlo calcs. 77−63224
vortices and low temp. struct. 78−49777
zero temperature crit. behaviour in transverse mag. field 80−29555
$BaCo_2(AsO_4)_2$, planar X-Y model, mag. ordering 77−66256
$BaCo_2(AsO_4)_2$, quasi 2D XY helimag., sp. ht. meas. 79−61151
$BaCo_2(PO_4)_2$, quasi 2D XY helimag., sp. ht. meas. 79−61151
Co complex, $Co(C_5H_5NO)_6(ClO_4)_2$ and $Co(C_5H_5NO)_6(BF_4)_2$, S=$^1/_2$ XY magnet, sp. ht. below 1K 77−55682
Co complex, $Co(C_5H_5NO)_6I_2$, simple cubic X-Y mag., specific heat, mag. exchange anisotropy meas. 78−39346
Co complex, Co(II)(1,2,4-triazole)$_2$(NCS)$_2$ quasi two-dimens. canted S=1/2 antiferromag. 80−70976
$CoBr_2.6[(D_2O)_{0.48}(H_2O)_{0.52}]$, antiferromag. ordering, quasi-elastic neutron scatt. study 79−61068
$Co(C_5H_5NO)_6(ClO_4)_2$ [$(BF_4)_2$], X-Y antiferromagnet, Neel temp., spin correlation functions 80−60345
$Co_{1-x}Zn_x$hexa(pyridine-N-oxide)$(ClO_4)_2$, dilute cubic S=1/2 XY antiferromag., sp. ht. data 77−66358
Cs_2CoCl_4, heat capacity below 1K, rel. to S=1/2 linear chain XY model 77−59415
Cs_2CoCl_4, paramag. mag. exchange rel. to low temp. mag. characts. 77−55669
$Cs_2Co_{1-x}Zn_xCl_4$, mag. sp. ht., effect of dilution, comparison with linear XY antiferromag. 77−66354
$CsMnF_3$, isotropic antiferromag., crossover behaviour of mag. phase boundaries 79−78370
$CsMnF_3$, mag. phase boundaries, XY to Ising crossover, virtual bicritical point 80−50095
$CsMnF_3$, specific heat, crossover from Heisenberg to XY like behaviour 77−85461
$CsNiF_3$, one-dimensional ferromagnet, optical absorpt. and static spin correlation functions 80−71415
Cu compounds, layered, anisotropic and dipolar interaction terms effect on mag. phase transition 77−63210
Cu-Mn, spin glass, meas. of order parameter 80−34642
$Cu(NO_3)_2.5H_2O$, spin-pair system, spin ordering, XY-model in external field 77−73033
^{3}He-^{4}He mixtures, two-dimens., phase diagram of dil. classical X-Y model 79−60593
^{4}He film, superflow onset, 2-dimens. XY model 78−47623
K_2CuF_4, 2-dimens. ferromagnet, low-temp. mag. struct. *(Japanese)* 79−33461
$KNiF_3$, isotropic antiferromag., crossover behaviour of mag. phase boundaries 79−78370
$PrCl_3$, one-dimensional X-Y system, far IR absorpt. spectra, cooperative spin excitations 78−95584
$RbMnF_3$, isotropic antiferromag., crossover behaviour of mag. phase boundaries 79−78370

Xalpha calculations
ab initio-LCAO-Xα-SCF, atoms in mols., theory and appl. 77−57869
alkali dithioferrates (III), electronic struct. and hyperfine interactions, Xα calcs. 80−100448
alkali metal binary intermetallic cpds., OPW calc. of struct., bonding and stability 77−43169

Xalpha calculations continued
alkali metals, liq., electrical resistivity and thermoelec. power, Harrison's method 79−78066
all electron pseudopotential method 80−83282
angle resolved photoemission, multiple scatt. approach 78−72693
atomic clusters, muffin-tin potential and SW Xα SCF calcs. for core levels *(German)* 78−82874
atomic independent particle pots. comparison 80−52846
atomic ionisation potential, X_α eigenvalues and Slater transition state 79−31394
atomic multiplet struct. obtained from HF, statistical exchange and local spin density approx. 80−32619
atomic orbital, optimised STO exponents 78−62721
atoms, first ionis. potential, Slaters transition-state method 78−46269
chlorofluoromethanes, MS Xα calcs., ionis. pots., electron affinities 77−79540
Compton profile as criterion for choice of local exchange parameter α 78−33410
conjugated systems, nonparametric resonance energies, graph theory and MO 77−61681
copper porphine, Xα multiple scatt. calcs., EPR and electronic spectra 78−13426
cyclobutane, MS-Xα-MT study 80−52906
diamond, energy band calcs. using intersecting spheres model 77−66110
diatomic homonuclear molecule, of 1st row, canonical exchange energy modulation parameters, MTXα calc. 79−97997
diatomic molecules of 1st row, total Xα energy, LCAO calc., rel. to local density models 80−32607
diatomic mols., one electron props., SCF-Xalpha scattered wave method 80−83279
dicyanomethane, multiple scatt. Xα calc. of electronic struct. 78−78626
difluoromethane, binding energy, ionisation pots., overlapping sphere MS Xα 77−83499
discrete variational Xα cluster calculations, applic. to metal clusters 78−90332
electronegativity, spin-orbital, and catalytic activity 78−73078
enzymes, chem. active sites 79−52757
ethane, rot. barriers, MS-SCF-X_α calcs. 80−106267
ethylene, and perfluoro derivatives, negative ion states, electron affinities, ionisation pots., overlapping spheres Xα calc. 79−26885
ethylene, ionisation energy, LCAO Xα calcs. 77−50353
ethylene cation, state geometries, electronic vibr. coupling consts., HF calcs., comparison with Xalpha calcs. 80−27946
exchange potential, elimination in multiple scatt. method 80−103652
excimer laser, electronic structure, pot. energy curves, radiative transition probabilities, quantum mech. calcs. 79−10284
ferrocyanide ion, electronic struct. and related props., calc. by SCF Xα-scattered wave method 77−15809
ferroelectric, band struct. calc. 78−15106
film, appl. of extended rigorous cellular method 78−52055
first-row atoms, atomic X_α calcs. 80−83280
first-row elements, s-shell spin polarisation calcs. 77−75318
fluoromethane, binding energy, ionisation pots., overlapping sphere MS Xα 77−83499
fluoromethane, LCAO-Xα-SCF, atoms in mols. theory and appl. 77−57869
fluoromethanes, ionisation pots., SCF-multiple scatt.-Xα calcs. 78−5141
fluoromethanes, Xα calcs. using ΔSCF formalism 79−6861
Hartree-Fock formalism, fractional occupation, local Xα pot. calcs. 80−95538
hexafluorides, MS Xα calc. 77−30778
hexafluoroethane, rot. barriers, MS-SCF-X_α calcs. 80−106267
inelastic electron tunnelling spectroscopy, multiple-scatt. theory of intensities 79−68285
interface modelling, Xα-scatt. wave cluster approach 80−49851
ionisation, Xalpha transition state and transition operator method calcs. 78−70743
magnetic impurities and Kondo effect, theoretical model 79−33455
metal atom cluster compounds, bonding calc. using d-orbital overlap model, SCF-Xα-SW calc. 80−102595
metal cluster, H site, SCF-Xα-MS calc. 78−47730
metal clusters, electronic states and mag. props., MO calc. 77−20219
metal phthalocyanine, vap., photoelectron spectra 79−64043
metal surface, chem. active sites 79−52757
methane, core 1s shakeup study, XPS and Xalpha calcs. 80−69064
model potential Xα method for electronic struct. calcs. 80−102446
molecular α values determ. 79−10032
molecular multicentre potential, X_α scattered waves method and Schrodinger eqn. soln. 80−37740
molecules, spheroidal config. region in scattered-wave method 78−25437
dimolybdenum tetraformate, metal-metal bond energy, SCF-Xα-SW calcs. 80−78538
MS-Xα method, single centre secular eqns. 79−36528
MTXα_R method, semiempirical MSXα scheme, applic. to Li_2 77−10593
multiple scattering, appl. to props. of metal clusters *(Russian)* 78−38996
multiple scattering X_α treatment, of scattering states of clusters 77−30747
organometallic compounds, chem. active sites 79−52757
oriented molecules, inelastic low energy electron scatt. 78−72653
overlapping muffin tin multiple scattering wave X_α method 79−13638
parabenzoquinone, and perfluoro derivatives, negative ion states, electron affinities, ionisation pots., overlapping spheres Xα calc. 79−26885
piezoelectric, band struct. calc. 78−15106
polydiacetylenes, electronic structure, bond length variations effect, Xα SCF calc. 78−5378
porphine, semiempirical Xα calcs. 79−26886
potential variation between atomic spheres in SW method 78−86764
rare earth orthovanades, $LnVO_4$:R^{3+}, R=Nd, No, Tm, Sm, Dy, Er, Eu, Tb, electronic struct. and spectra of VO_4, RO_8 clusters 78−10953
SCF-Xα scattered wave method, computer program 78−50453
SCF-Xα-scatt. wave calcs. for photoionisation cross sections and asymmetry parameters 80−63542
SCF-Xα-SW model, mol. interactions, secular matrix contraction 77−26960
second-row atoms, atomic X_α calcs. 80−83280
second-row elements, s-shell spin polarisation calcs. 77−75318
secular equation, appl. to SW method using general form pot. 79−31396
self-consistent charge Xα method, appl. to small mols. 80−91449
self-consistent charge Xα method, theory 80−91448

Xalpha calculations continued
small, medium and large systems, ab initio and approx. rigorous calcs. 78−62714
spherical system, relativistic pseudopotential 78−82653
stable negative ions instability, Xalpha calcs. 80−99452
statistical exchange calcs. 77−30766
TC, internal conversion, scattered-wave cluster technique 80−107696
technetium hexahalides, X_α-SW-calc. of chemically induced decay const. variation of ^{99m}Tc in TcO_4^- and hexahalides 79−54769
tetrabiomethane, electronic struct., Xα SW calcs. 80−102447
tetracyanomethane, multiple scatt. Xα calc. of electronic struct. 78−78626
tetracyanoquinodiamine, LCAO-Xα-SCF atoms in mols., theory and appl. 77−57869
tetrafluoromethane, Auger transition energies, transition state approx. SCF Xα calc. 77−65426
tetrafluoromethane, electronic struct., Xα SW calcs. 80−102447
tetrahedrally coordinated covalent semiconductor point defects, multiple scatt. Xα model 80−54636
tetrathiofulvalene, LCAO-Xα-SCF atoms in mols., theory and appl. 77−57869
TiO, local density of states, X-ray spectra, Hartree-Fock and Xα calcs. discrepancies 79−77980
transition metal clusters, particle size rel. to bulk metallic props. 80−44490
transition metal complexes, discrete variational Xα cluster calcs. 80−15444
transition metal fluorides, electron affinities and ionis. pots. MS Xα calcs. 79−10031
3d-transition metal ions, s-doublet struct., appl. of exchange correlation mass operator approx. 80−106266
transition metal-oxygen compounds, salts, X-ray Lα emission spectra, excited states calcs. 79−59488
transition metals, Fe series, interstitial H, cluster model for bonding mechanism 79−60753
TTF-TCNQ, dimers and trimers, Xα scattered wave calc. 78−10326
valence ionisation pots., SCF-MS-Xα calcs., mol. space partitioning 79−36529
work function theory, comparison of Hartree Fock and X_α formalism 77−76900
Ag (111) surface, adsorption of I, cluster calc. with Xα scattered wave method 77−31894
Ag_n, n=7,10,13,19, atom clusters, local density of states, Xα scattered wave calcs. 78−18989
AgBr, vapour, photoelectron spectrosc., interpretation 80−95679
AgCl, vapour, photoelectron spectrosc., interpretation 80−95679
AgI, vapour, photoelectron spectrosc., interpretation 80−95679
Al (100), O chemisorption , mol. orbital cluster calc. 78−14582
Al, chemisorption of O_2, orbital resons., Xα cluster model calcs. 77−72774
Al_5, chemisorpt. of Na, Si and Cl, core hole induced electronic relax. 79−90874
AlF_6^{3-}, octahedral complex, ionis. energy, SCF-Xα study 78−70967
AlF_6^{3-}, SCF Xα SW calcs., ionis. pot. 79−26887
α-Al_2O_3, chemisorbed water, binding energy, SCF-Xα-SW calc. 77−69169
α-Al_2O_3, chemisorbed water binding energy, SCF-Xα-SW calc. 77−69169
β-Al_2O_3-Na_2O, adsorption of Na, surface electronic struct. calcs. 80−75431
Al(111), chemisorption of O_2, SCF X_α scatt. wave MO calc. 79−42374
Ar, Compton profiles, Xalpha wavefunctions 80−106265
Ar, solid, lattice dynamics calc. using energy band theory 80−49320
Ar:H crystalline matrix, Xα scattered wave cluster model 79−73468
As, band structure and cryst. energy, pseudopot. calc. 79−90954
BaF_2, F-centres, muffin-tin approx. inadequacy 78−63761
BaF_2, U-centre, electronic struct. and optical transition energies, SCF MS Xα calc. 79−4532
$BaTiO_3$, electronic props., SCF-MS-Xα calc. 80−54607
Be_2, ground state, multiple scatt. Xα calcs. 80−58149
BrF, He(I) photoelectron spectra, interpretation 79−13766
BrF_3, electronic struct. and ionisation pot., SCF DV Xalpha method 80−69057
BrF_5, electronic struct. and ionisation pot., SCF DV Xalpha method 80−69057
C_2, ground state potential energy, non-muffin tin MS Xα calcs. 77−14355
CO and $(CO)_6$, electronic struct. and bonding, SCF-Xα-MSW calcs. 78−25431
CO, chemisorbed on Cu(100), XPS shake-up satellites, Xα-SW cluster model calcs. 79−95899
CO, ground state potential energy, non-muffin tin MS Xα calcs. 77−14355
CO, LCAO-Xα method calcs., comparison with Hartree Fock and MS Xα methods 80−95539
CO, oriented molecules, vibrationally inelastic electron scatt. 78−67907
CO_2, ionisation energy, LCAO Xα calcs. 77−50353
CO_2+$H_2(D_2)$, ab initio LCAO-MO-SCF intermolecular pot. energy surface, V→T transfer 77−50489
C_3S_2, electronic struct., optical and photoelectron spectra 78−70745
C_3S_2, electronic struct., optical and photoelectron spectra 78−70982
Ca_2, ground state, multiple scatt. Xα calcs. 80−58149
CaF_2, F-centres, muffin-tin approx. inadequacy 78−63761
CaF_2, U-centre, electronic struct. and optical transition energies, SCF MS Xα calc. 79−4532
CaF_2:O^-, Jahn-Teller distortion, electronic struct., MS Xα calc. 78−23057
CeF_3, CeF_3+, MS Xα electronic struct. calc., inner shell photoelectron spectra 77−10594
CeF_3, ionisation energies, satellite struct., photoelectron spectra, MS Xα calcs. 78−13425
ClO_4^-, dummy spheres in SCF Xalpha calcs. 80−69056
ClO_4^-, ionisation energies, SCF-Xα transition state calcs. 80−74115
CmO_2, band struct., cryst. binding and ESCA spectra, X_α cluster calc. 78−64443
CoAl, bonding, self-consistent energy bands 78−91610
$Co(CN)_6^{3-}$, electronic struct., photochem. props., MS Xα calcs. 79−22600
$CoCl_4^{2-}$, electronic energy levels calc. by conventional and Xα Hartree-Fock methods 78−66470
$Cr(CO)_6$, electronic struct. and bonding, SCF-Xα-MSW calcs. 78−25431
$CrCl_4$, ligand field states, multiple scatt. Xalpha calcs. 80−47891
$Cr(NO)_4$, bonding, shake-up intensities and shake-up energies, SCF Xα multiple scatt. calc. 80−74121
$Cr(NO)_4$, XPS and UV photoelectron spectra, compared to NO data 80−58317
Cs, electronic transition from self consistent APW Xα calcs. 78−51884
$CsNpF_6$, optical spectrum anal. 79−26963
Cu, chemisorption of CO, electronic struct. of $(M)_5CO$ clusters 78−95948
Cu, chemisorption of N atoms, electronic struct. of Cu_5N cluster, Xα scattered-wave calcs. 79−60902
Cu, chemisorption of O, S, Se, NO and O_2, discrete variational Xα cluster method 80−29264
Cu-Ni(Fe)(Mn)(V), dil., local mag. moments and Kondo effect, theoretical model 79−69651
Cu_4 clusters, electronic structures, SCF-Xα-SW method 80−88468
$CuCl_4^{2-}$, electronic energy levels calc. by conventional and Xα Hartree-Fock methods 78−66470
$CuCl_2(Cl_4^{2-})(Cl_6^{4-})$, electronic struct. studies by SCF, MSXα and INDO method 80−74119
$CuF_2(F_6^{4-})$, electronic struct. studies by SCF, MSXα and INDO method 80−74119
Cu_3Zn clusters, electronic structures, SCF-Xα-SW method 80−88468
EuO, electronic structure, octahedral clusters, determ. by X_α method 78−10350
F^-, Xα method predicting unstable state 78−82640
F_2, LCAO-GTO Xα calc., rel. to other LCAO calcs. 80−52871
F_2, MSXα calc., partial wave expansion, binding energy and orbital energy 80−37738
$F_4S_4N_4$, SCF-Xα-CNDO/BW calcs., comparison 78−25435
Fe complex, $[Fe(CN)_6]^{3-}$, electronic struct., optical transitions, XPS, Mossbauer isomer shift, valence ionisation pot., SCF-MSX calc. 79−6864
Fe, hyperfine interaction parameters, effect of local exchange, Xα and HF calcs. 78−78622
Fe-Al systems, band struct. and cluster calcs. 79−51480
$FeAl_3$ bonding, self-consistent energy bands 78−91610
FeO_4^{2-} ion, electronic struct., hyperfine interactions, SCF Xα calcs. 79−37951
Fe_3O_4, SCF X_α calcs. of one-electron energy levels 78−47727
FeS_6^{10-}, electronic struct., SCF-Xα scatt. wave calcs., rel. to spectra of FeS, FeS_2 78−5138
GaAs, electronic struct., mol. cluster model, SCF multiple scatt. method 79−42446
GaAs, vacancies Xalpha cluster model, electronic dangling bond effect elimination 79−99504
GaAs:Cr, impurity electron states by Xα scattered wave cluster method, electron-electron interactions 80−6767
GaAs:Cu, multiple scatt. Xalpha cluster model, impurity electronic states, dangling bond effect elimination 79−99504
GaAs:O, electronic struct., multiple-scatt. Xα mol. cluster model 80−15445
GaAs:Se, multiple scatt. Xalpha cluster model, impurity electronic states, dangling bond effect elimination 79−99504
$GeBr_4$, electronic struct., Xα SW calcs. 80−102447
GeF_4, electronic struct., Xα SW calcs. 80−102447
Ge_2H_6, rot. barriers, MS-SCF-X_α calcs. 80−106267
H_2, ground state, pot. curves, MTXα_R method 80−5482
H_2, ground state potential energy, non-muffin tin MS Xα 77−14355
H_2, oriented molecules, vibrationally inelastic electron scatt. 78−67907
H_2, $X_{\alpha\beta}$ statistical exchange calc. rel. to multiple scatt. calc. without exchange 79−85883
H_2, Xα theory appls. approximations 80−9510
H_2^+, SCF multiple scatt. calc. 80−916
HF, ionisation energy, LCAO Xα calcs. 77−50353
H_2O, Compton profile, H-bond contrib., HFS Xα model 78−17726
H_2O, core 1s shakeup study, XPS and Xalpha calcs. 80−69064
H_2O, one-electron props., SCF Xα SW functions 78−62719
H_2O, pot. energy surface by MS Xα method 79−13656
H_2O^-, states geometries, electronic vibr. coupling consts. HF calcs., comparison with Xalpha calcs. 80−27946
H_2O_2, ionisation energy, LCAO Xα calcs. 77−50353
H_2S, valence and Rydberg excited states, SCF-Xα-SW mol. oribtal study 79−36550
He^+, Xα statistical exchange method, orbital energies, HF method comparison 78−9071
I_2, FCC metallic, self-consistent APW Xα electron-band calc., up to 22000K 77−39762
IF, He(I) photoelectron spectra, interpretation 79−13766
inert gases, solid, Compton profiles, APW-Xα calc. 80−80894
Ir, hyperfine interaction parameters, effect of local exchange, Xα and HF calcs. 78−78622
KC_8, intercalated graphite, electronic and cryst. struct. 80−44472
$KNbO_3$, electronic props., SCF-MS-Xα calc. 80−54607
$KTaO_3$, electronic props., SCF-MS-Xα calc. 80−54607
LaB_6, metallic, energy band structure and Fermi surface, self-consistent APW method 77−69221
$LaBr_3$, ionisation energies, satellite struct., photoelectron spectra, MS Xα calcs. 78−13425
$LaCl_3$:Pr^{3+}, crystal field parameters using multiple-scatt.-X_α method 78−95271
LaF_3, ionisation energies, satellite struct., photoelectron spectra, MS Xα calcs. 78−13425
LaF_3, MS Xα electronic struct. calc., inner shell photoelectron spectra 77−10594
LaO_4^{5-}, ionisation energies, satellite struct., photoelectron spectra, MS Xα calcs. 78−13425
Li, liq., temp. and density depend. of struct., improved pseudopot. theory 79−14669
Li_2, potential curve calc. using MTXα_R method 77−10593
Li_2Br_2, UPS of dimeric mol., expt. and Xα calc. 80−9640
LiCl, aqueous soln., self consistent wavefunctions, HFS Xα pot. in cluster model, Compton profile calc. 79−78783
Li_2Cl_2, UPS of dimeric mol., expt. and Xα calc. 80−9640
Li_2F_2, UPS of dimeric mol., expt. and Xα calc. 80−9640
LiH, ground state, pot. curves, MTXα_R method 80−5482
LiH, numerical calc. of one-electron props. from SCF-Xα-SW calcs. 77−6688

Xalpha calculations continued
LiH, one electron props., Xα multiple scattering wave functions 80−42945
Li_2I_2, UPS of dimeric mol., expt. and Xα calc. 80−9640
$LiNbO_3$, band struct. and spontaneous polarisation calcs. 78−95261
$MNbO_3$, orthorhombic, electronic struct., SCF-MS-Xα calc. 80−70600
Mg_2, ground state, multiple scatt. Xα calcs. 80−58149
MgO, ionic cryst., surface electronic struct., discrete variational Xα cluster method 79−4591
$MnCl_4^{2-}$, electronic energy levels calc. by conventional and Xα Hartree-Fock methods 78−66470
MnF_2, SCF-Xα MO calcs. of core photoelectron shake-up satellites 77−20991
$MnF_2(I_2)$, SCF-Xα MO calcs. of core photoelectron shake-up satellites 77−20991
MnI_2, SCF-Xα MO calcs. of core photoelectron shake-up satellites 77−20991
Mo complex, hexadimethylamino molybdenum, electronic description of triple bonds and verification by photoelectron spectroscopy 78−41949
Mo, localised electronic states near dislocations 79−33257
Mo, localized electronic states near ⟨100⟩ edge dislocation compared with perfect lattice 78−30888
Mo_2 metal-metal bond energy, SCF-Xα-SW calcs. 80−78538
$Mo_2Cl_8^{4-}$, low lying states, weak electronic coupling, Xα valence band theory 79−72237
$Mo_2Cl_8^{4-}$, metal-metal bond energy, SCF-Xα-SW calcs. 80−78538
$Mo_2Cl_9^{3-}$ complexes, cluster exchange coupling consts. SCF-Xα-SW calcs. 80−74120
$Mo_6Cl_{14}^{2-}$, cluster ground state electronic struct. SCF Xα SW calc. 79−3607
$Mo_2(NH_2)_6$, electronic description of triple bonds and verification by photoelectron spectroscopy 78−41949
MoO_6^{6-}, electronic struct., discrete variation and scatt. wave X_α methods 80−917
$Mo_2(OH)_6$, electronic description of triple bonds and verification by photoelectron spectroscopy 78−41949
$Mo_6X_8^{4+}$ cluster cpds. (X=F, Cl, Br, I), SCF-SW-Xα calcs. 80−74276
N^{3-}, in crysts., X-ray scattering factors using Xα method 79−7521
N_2, ground state potential energy, non-muffin tin MS Xα calcs. 77−14355
N_2, MSXα calc., partial wave expansion, binding energy and orbital energy 80−37738
N_2, oriented molecules, vibrationally inelastic electron scatt. 78−67907
N_2, Xα theory appls. approximations 80−9510
NH_3, core 1s shakeup study, XPS and Xalpha calcs. 80−69064
NH_3, pot. energy surface by MS Xα method 79−13656
NO, ionis. pot. and electron affinity, overlapping sphere MS Xα calc. 78−41948
$NO_2(NO_2^-)$, ionis. pot. and electron affinity, overlapping sphere MS Xα calc. 78−41948
$NO_3(NO_3^-)$, ionis. pot. and electron affinity, overlapping sphere MS Xα calc. 78−41948
$N_3P_3Cl_6$, ionisation energy and electronic struct., UV photoelectron spectra and Xα calcs. 78−94281
$N_3P_3F_6$, ionis. energies, Xα scatt. wave calcs. 77−42242
$N_4P_4F_8$, ionis. energies, Xα scatt. wave calcs. 77−42242
Na clusters, electronic relaxation energies in $KL_{2,3}L_{2,3}$ Auger transitions, SCF-Xα-SW calcs. 78−90334
Na-Li, liq., Knight shift calc. by multiple scatt. Xα method 80−54961
Na_2, ground state, pot. curves, $MTX\alpha_R$ method 77−71762
$Na_8(Al_6Si_6O_{24})Cl_2$, sodalite, electronic struct. of F-centre 80−2356
NaCl, electronic struct., SCF cryst. cluster model 80−24792
NaH, ground state, pot. curves, $MTX\alpha_R$ method 80−5482
NaLi, ground state, pot. curves, $MTX\alpha_R$ method 77−71762
$Na_7MoO_4(S_4)(Se_4)$ crystals, charge transfer spectra of MoX_4^{2-} complexes 80−54658
$NaNO_2$, band struct., polarisation and piezoelec. consts. calc. 78−52448
Nb clusters, scattered wave Xα calcs. 79−15068
Nb_8 clusters, electronic struct., scattered wave-Xα calc. 79−11053
NbC, band struct. and X-ray emission spectra, APW and Xα calc. 80−70605
NbC, self consistent APW-Xα calc., electronic struct. 77−20237
NbN, self consistent APW-Xα calc., electronic struct. 77−20237
NbO, electronic struct. from photoelec.- and X-ray emission spectra and X_α calcs. of NbO_6^{-10} cluster 79−23892
NbO, photoemission and X-ray emission spectra, X_α cluster calc. 78−64442
NdF_3, ionisation energies, satellite struct., photoelectron spectra, MS Xα calcs. 78−13425
Ne, Compton profiles, Xalpha wavefunctions 80−106265
Ne, solid, lattice dynamics calc. using energy band theory 80−49320
Ne_2, total energy MS and LCAO Xα calcs., non-muffin-tin corrections, overbinding 78−46266
Ni (001), chemisorpt. of O_2, MSXα total energy calcs. with non-muffin-tin corrections 77−72795
Ni, chemisorpt. of CO, catalytic activity, SCF-Xα-SW calcs. 78−15711
Ni, chemisorption of CO, electronic struct. of $(M)_5CO$ clusters 78−95948
Ni, chemisorption of H, Xα cluster calcs. *(Japanese)* 78−72002
Ni, chemisorption of O, S, Se, NO and O_2, discrete variational Xα cluster method 80−29264
Ni, chemisorption of S and Se, Xα cluster model calcs. 79−65313
Ni cluster-H, electronic struct. calc., H-metal bonding 77−89823
Ni clusters local densities of states 80−88466
Ni, Xα theory appls. approximations 80−9510
Ni-H system, cluster calc. of electronic struct. of interstitital H 78−43326
NiAl, bonding, self-consistent energy bands 78−91610
$Ni(CO)_4$, back donation, multiple scatt. Xalpha calcs. 79−36527
$Ni(CO)_4$, back donation, multiple scatt. Xalpha calc. 79−63913
$Ni(CO)_4$, bonding, shakeup energies, and shakeup intensities for photoelectron spectra 80−50528
$Ni(CO_4)$, ionisation energies, approx. SCF Hartree-Fock-Slater calcs. 77−75334
Ni_3Ti, electronic struct., Xα calc., photoelectron and AES spectra 80−20769
Ni(001), adsorbed c(2×2)-CO, struct. by LEED, self-consistent scatt. pot. 80−70536
$NpAl_4$ clusters, band struct., variational Xα calc. 79−4508
$NpAl_4$, clusters, X_α calculations *(Japanese)* 79−82519
NpF_6, electronic struct. and transitions, SCF-Xα-SW calcs. 78−78627

Xalpha calculations continued
O^-, Xα method predicting unstable state 78−82640
O_2, MSXα calc., partial wave expansion, binding energy and orbital energy 80−37738
O_3, core electron binding energies, XPS, Xα scatt. wave calcs. 77−75332
OsO_4, MS Xα calc., ionis. pots., energy levels, atomic spheres radii effect 77−18789
PF_4, MS Xα calcs., pot. energy surface, electronic struct. 77−57877
PF_6^-, octahedral complex, ionis. energy, SCF-Xα study 78−70967
PO_4^{3-}, ionisation energies, SCF-Xα transition state calcs. 80−74115
PbS, first-principles calc. of eqn. of states 80−49649
PbS, relativistic electronic mol. struct., calcs. 79−761
PbS, thermomech. props., SCF Xα scatt. wave theory 78−71704
PbSe, relativistic electronic mol. struct., calcs. 79−761
Pd, chemisorption of O_2 and CO, catalytic activity, SCF-Xα-SW calcs. 78−15711
Pd cluster-H, electronic struct. calc., H-metal bonding 77−89823
Pd, metal cluster, calculated structural stability 78−95268
Pd-H system, cluster calc. of electronic struct. of interstitial H 78−43326
PrF_3, ionisation energies, satellite struct., photoelectron spectra, MS Xα calcs. 78−13425
Pt, chemisorpt. of O_2, catalytic activity, SCF-Xα-SW calcs. 78−15711
Pt, chemisorption of O_2 and CO, SCF-Xα cluster calcs. 80−65365
Pt cluster-H, electronic struct. calc., H-metal bonding 77−89823
$PtCl_4^{2-}$, electronic struct., SCF Xalpha ESCA spectrum assignment 80−23339
$PtCl_2(NH_3)_2$, cis- and trans-isomers, electronic struct., SCF-Xα study 80−18795
$PuAl_4$ clusters, band struct., variational Xα calc. 79−4508
$PuAl_4$, clusters, X_α calculations *(Japanese)* 79−82519
PuF_6, electronic struct. and transitions, SCF-Xα-SW calcs. 78−78627
$Re_2Cl_8^{2-}$, spectral assignment, metal-metal bonds, SCF Xα SW calcs., relativistic corrections 80−53006
$Re_3Cl_{12}^{3-}$, cluster ground state electronic struct. SCF Xα SW calc. 79−3607
Re_3Cl_9, cluster ground state electronic struct. SCF Xα SW calc. 79−3607
Re_3Cl_9 metal cluster complexes, He(I) photoelectron spectrum, SCC DV Xα calcs., $Re_2Cl_8^{2-}$ comparison 80−28063
Ru, hyperfine interaction parameters, effect of local exchange, Xα and HF calcs. 78−78622
RuO_4, SCF Xα SW calcs. of ground state 78−90081
S_4^x, x=2−, 0, 2+, struct. differences explained, SCF Xα scatt. wave MO calcs. 78−74784
S_8, cyclic, electron deformation density distrib., SCF-Xalpha-scatt. wave method 78−33425
SF_6, ionisation pot., discrete variational Xα calc., Slater-type orbitals in Hartree-Fock basis 78−78837
SF_6, MS Xα calc. 77−30778
SF_6, octahedral complex, ionis. energy, SCF-Xα study 78−70967
SF_6, valence levels, photoionisation cross-sections, MS Xα calcs. 79−54923
SMS, band struct. and semicond. metal phase transition 80−80180
$S_4N_4H_4$, SCF-Xα-CNDO/BW calcs., comparison 78−25435
SO_4^{2-}, ionisation energies, SCF-Xα transition state calcs. 80−74115
ScP, electronic struct., self-consistent Hedin-Lundqvist and Xα APW calcs. 80−29322
ScP, energy band struct., exchange-correl. pot. effects, APW calcs. 80−29321
Se, trigonal reflectivity and density of states press. depend., self-consistent pseudopotential calc. 77−31931
SeF_6, MS Xα calc. 77−30778
Si (111), with chemisorbed Cl and F, electronic energy struct. calcs. 79−78144
Si, amorphous, hydrogenated, electronic struct., SCF Xα calc. 80−49580
Si, band structure selfconsistently determined with X_α potentials using MAPW method 79−33227
Si, solid, electron rearrangement after inner shell ionisation by heavy charge particle impact 80−87043
Si:O, A centre, theoretical study 80−75521
Si:transition metal, electronic states of impurities 77−43531
Si_2, SCF Xα calcs. using pseudopots. and PW basis set 77−34558
$SiBr_4$, electronic struct., Xα SW calcs. 80−102447
SiF_4, electronic struct., Xα SW calcs. 80−102447
SiF_4, photoelectron spectra, bonding, MS Xα calcs. 79−18116
SiF_6^{2-}, octahedral complex, ionis. energy, SCF-Xα study 78−70967
SiF_6^{2-}, SCF Xα SW calcs., ionis. pot. 79−26887
SiH_4, $L_{II,III}$ continuous absorpt. spectrum of Si 80−95645
SiH_4, photoelectron spectra, bonding, MS Xα calcs. 79−18116
Si_2H_6, rot. barriers, MS-SCF-X_α calcs. 80−106267
Si_2H_6, tetrahedral edge sharing, distortions, MO calcs. 77−14380
SiH_3Br, mol. ionis. and excitation energy, Xalpha calc. 79−41105
SiH_3Cl, mol. ionis. and excitation energy, Xalpha calc. 79−41105
SiH_3F, mol. ionis. and excitation energy, Xalpha calc. 79−41105
$SiH_{4-n}F_n$ (n=1 to 3), photoelectron spectra, bonding, MS Xα calcs. 79−18116
SiH_3I, mol. ionis. and excitation energy, Xalpha calc. 79−41105
$SiH_4(SiF_4)$, electron rearrangement after inner shell ionisation by heavy charge particle impact 80−87043
SiO^+, vac. UV photoelectron spectra, ab initio mol. orbital and Xα calcs., $(X^1\Sigma^+)$ state 78−46395
Si_2O_2, tetrahedral edge sharing, distortions, MO calcs. 77−14380
Si_2S_2, tetrahedral edge sharing, distortions, MO calcs. 77−14380
SiX_4 (X=Cl,H,F), chemical shifts, relax., X-ray spectra, SCF Xalpha calcs. 80−27928
SrF_2, F-centres, muffin-tin approx. inadequacy 78−63761
SrF_2, U-centre, electronic struct. and optical transition energies, SCF MS Xα calc. 79−4532
$SrTiO_3$ (100) surface electronic structure, DV-Xα cluster method 80−39646
TaO_6^{7-}, octahedral cluster, ionisation energies and atomic populations, XPS and SCFMS Xα calc. 79−93923
$Tc_2Cl_8^{3-}$ ion, visible spectra, electronic struct. 78−5240
TcO_4^-, X_α-SW-calc. of chemically induced decay const. variation of ^{99m}Tc in TcO_4^- and hexahalides 79−54769
Te, trigonal, self-consistent ground state 80−54604
TeF_6, MS Xα calc. 77−30778
$ThAl_4$ clusters, X_α calculations *(Japanese)* 79−82519
$ThF_4(Cl_4)$, electronic struct., MS-SCF-Xα calcs. and VUV photoelectron spectra 80−63710

Xalpha calculations continued
Ti-H system, cluster calc. of electronic struct. of interstitial H 78−43326
Ti_2, electronic structure of five and ten atom chains SCF-Xα-SW calcs. 80−5483
TiC, electronic struct. and XPS, cluster method and band struct. 79−60710
TiC, TiC_6^{20-} cluster electron state, MS Xα calculations 77−8037
$TiCl_4$, optical and Ti 2p core photoemission spectra, SCF Xα anal. 79−94032
TiH, electronic structure of five and ten atom chains SCF-Xα-SW calcs. 80−5483
TiO, Hartree-Fock and local exchange energy bands, disagreement of results 77−76724
TiO, soft X-ray spectra and XPS, Xα and Hartree-Fock calcs. discrepancies 79−77979
TiO_2, clusters, surface electron struct. and defect states, DV-Xα calc. 80−20268
TiO_2, OH^- adsorption on defect site, electronic struct. 79−47150
TiO_2, surface electronic struct. by discrete variational Xα cluster calc. 78−43449
U, valence energy levels, SCF relativistic Xalpha calc. 79−85912
UAl_4, clusters, band struct., variational Xα calc. 79−4508
UAl_4, clusters, X_α calculations *(Japanese)* 79−82519
UC, electronic struct., comparison with photoemission spectra 80−91450
UC, partially filled f bands, configurational and relativistic effect sensitivity 79−78002
UCl_6, electronic struct., photoelectron spectra and SW Xα calcs. 79−72355
UF_6, electronic struct., relativistic MS Xα calc. 79−85911
UF_6, electronic struct. and transitions, SCF-Xα-SW calcs. 78−78627
UF_6, MS Xα calc. 77−30778
UF_6, valence energy levels, SCF relativistic Xalpha calc. 79−85912
$UF_4(Cl_4)$, electronic struct., MS-SCF-Xα calcs. and VUV photoelectron spectra 80−63710
UN, electronic struct., comparison with photoemission spectra 80−91450
UO_2^{2+}, valence energy levels, SCF relativistic Xalpha calc. 79−85912
UO_2^{2-}, relativistic X_α scatt. wave calcs. 78−46268
UO_6^{6-}, electronic struct., discrete variation and scatt. wave X_α methods 80−917
$(UO_8)^{12-}$, electronic struct., variational Xalpha cluster calc. 80−39499
US, optical props. and electronic struct. 80−25410
$(UX_6)^{n-}$, X=N,O,S, electronic struct., variational Xalpha cluster calc. 80−39499
VO, octahedral clusters, electronic struct., Xα discrete variation and SW methods 78−63976
VO_2 clusters in metallic and semiconductor phases, electronic struct., Xα calcs. 78−63977
V_3Si, electronic struct., charge distrib. and X-ray emission spectra 79−51481
WF_6, electronic structure, SCF-Xα-SW calcs. 77−26974
WO_6^{6-}, electronic struct., discrete variation and scatt. wave X_α methods 80−917
Xe, solid, zero temp. isotherm, APW calc. 79−73128
$XeCl_2$, electronic structure, MSW-SCF-Xα method 80−78539
XeF_x, x=2, 4, 6, electronic structure, MSW-SCF-Xα method 80−78539
YOF, electronic stuct. calcs. from XPS and X-ray emission spectra 80−35056
YPO_4:Ce(Tb), luminesc. and optical spectra 79−65921
YS, band struct. and X-ray emission spectra, APW and Xα calc. 80−70605
YVO_4:Eu, cluster electron struct., X-alpha calc., emission spectra 78−2898
YZn, self-consistent energy bands and Fermi surface 77−72814
YbF_3, MS Xα electronic struct. calc., inner shell photoelectron spectra 77−10594
Zn_4 clusters, electronic structures, SCF-Xα-SW method 80−88468
ZrC, electronic struct. and XPS, cluster method and band struct. 79−60710

xenon
see also nuclei with .....
^{123}Xe, production in $^{127}I(p,5n)^{123}Xe$ 79−79651
AC Stark effect, on saturated absorption line shape in partially Doppler-compensated system 79−45669
adatom-graphite surface interaction, polarisation energy from opt. data 77−72792
additive gas in CO lasers 79−18407
adsorbate levels, substrate split localised, spin polarisation effects in photoemission 79−19971
adsorbed layer, on $NiCl_2$, phase transition identified as 2D polymorphic transform. 78−56040
adsorbed layer of Ag, lateral compression effects calc. 80−6641
adsorbed layers on Pd (100), lateral interactions, effect on work function, UPS, and IR spectra 79−77904
adsorbed layers on Pd-Pt, Ir, and Ru, 5p photoemission, local surface struct. influence 80−2920
adsorbed monlayer, two-dimens. Lennard-Jones system, melting 79−28071
adsorbed monolayers, thermodynamic props. and lattice const., quasiharmonic theory 79−42380
adsorbed on (0001) surface of graphite, monolayer liquid and solid struct. 80−65400
adsorbed on Au and Ti, electronically excited atoms coupling to cond. states 77−89642
adsorbed on carbon black, effect on further He adsorption 77−59172
adsorbed on Cu, NaCl, stepped and disordered surfaces, two-dimens. phase transformations 80−103580
adsorbed on Pd (110), anomalous 5p photoemission, electron binding energies 80−100750
adsorbed on Pd (110), anomalous 5p photoemission 80−7471
adsorbed on W, UPS, $P_{3/2}$ level splitting mechanism 77−31880
adsorbed on W (110), mobility and two-dimens. compressibility, field emission current fluctuation method 80−80089
adsorption, on Ni (100) or Fe (110), UPS obs. 79−33897
adsorption, on W(110), 77 to 90K, LEED study 79−42382
adsorption and coadsorption with O on W, work function and thermal desorption meas. 80−39448
adsorption and desorption on graphite (0001), kinetics using AES 77−72782
adsorption on activated C, equil. adsorption coeffs. at low partial press. 77−52673

xenon continued
adsorption on Ag(111), structural and thermodynamic studies 80−6640
adsorption on Au (100), LEED, AES, EELS, surface pot. 77−15691
adsorption on BN_3 and graphite 79−73397
adsorption on Cu (311), electron energy loss spectra 77−63507
adsorption on Ge (111) plane, adsorpt. pot. 78−26768
adsorption on graphite, finite size effect and temp. depend., multicritical phase diagrams 79−42372
adsorption on graphite, substrate deform. meas. 80−54520
adsorption on graphite (0001), 2-dimens. condensed layer, isothermal desorption spectroscopy 77−69181
adsorption on hexagonal BN_3 79−73395
adsorption on Ir (100), local surface struct., UPS study 80−39429
adsorption on Ir and Pt, field emission meas. 77−24479
adsorption on Na (100) surface, AES and LEED meas. 77−11792
adsorption on Pd(110) surface, AES, UPS, LEED, work function, flash desorption 80−6633
afterglow, $6s_{12}$ metastable atom density decay rate 78−63612
afterglow, metastable atom deactivation, electron collision effects 77−23441
afterglow, radiative and collisional deexcitation of reson. states, absorpt. and emission obs. 80−38742
afterglow $6s'(^1/_2)_0$, $6s'(^1/_2)_1$ at. states, collisional relax., population decay 78−63617
Allende meteorite, fission Xe rel. to ^{244}Pu in early solar system 77−29663
Allende mineral grain inclusion, excess ^{129}Xe meas., chronological information 80−67675
anomalous isotope composition at Oklo natural reactor deposit 77−56630
arc, wall-stabilised, dynamic analysis, radiation transport 80−44066
arc lamp, acoustical resonances and instabilities 77−58907
arc lamp versatility 79−23036
atom, 11 photon ionisation probability in 1 μm beam 77−46548
atom, 1.4 to 5.9 MeV/u, K-shell ionisation cross-section meas. 79−31671
atom, 3.41 μm line press. broadening 77−14390
atom, 3.51 μm broadening due to velocity-changing collisions 78−37597
atom, 3.51 μm laser transition, phase-changing broadening, inert gas perturbers 78−82949
atom, $4d^{10}$ shell, photoionisation cross sections, electron shell alterations determ. *(Russian)* 80−58144
atom, $4d^{10}$ subshell photoionisation cross section, electron shell rearrangement 77−14400
atom, 4d ionis, photoelectron spectrum, post-collision interaction 77−30837
atom, 4d reson. line excitation, Auger decay 78−70804
atom, $5d_{7/2} \rightarrow 6p_{5/2}$ transition, struct., laser spectrosc. and double reson. obs. 78−1210
atom, $5d\{3/2)_1$ photoexcited state radiative decay 78−74605
atom, $5p^55s$ state, electron excitation fine struct. neg. ion reson. 77−14585
atom, $5p^5ns$, $5p^5np$, $5p^5nd$ and $5p^54f$ config., HF calc. 77−23468
atom, $5p^6$ subshell, photoelectron ang. distrib., ionisation cross section 77−14401
atom, 5p shell photoelectron branching ratio, energy depend. 77−88435
atom, 5p subshell photoelectron branching ratio, Dirac-Fock calcs. 78−42021
atom, $5s^2$ shell, oscillator strength determ. *(Russian)* 80−58144
atom, $5s^2$ subshell, discrete excitations, generalised oscill. strength calcs. 77−65441
atom, 5s, 5p ESCA spectrum, photoionisation many electron description 78−50516
atom, $5s \rightarrow \varepsilon p$ photoelectron ang. distrib., interchannel and spin-orbit coupling 77−3329
atom, $5s \rightarrow \varepsilon p$ photoelectron ang. distrib. near Cooper minimum 80−18834
atom, 5s electron photoionisation cross section with synchrotron radiation 78−5180
atom, 5s photoelectron ang. distrib. 78−33482
atom, 5s photoelectron satellite spectrum 79−13690
atom, 6s-6p emission, following vac. UV irrad., press. depend. 79−63950
atom, $^3P_1$ resonance state, three photon excitation, fluoresc. obs. 78−13481
atom, $^3P_1$ state, reson. fluoresc., Zeeman beats, time-resolved VUV spectra using synchrotron radiation 78−33454
atom, $^1P_2$ metastable, deexcitation by slow electrons *(Russian)* 78−13607
atom, ab initio effective core pot., Dirac-Hartree-Fock and Hartree-Fock calcs. 78−33426
atom, absolute photoionis. cross sections of spin-orbit components of 4d electron 77−38646
atom, approximate relativistic Hartree-Fock eqns., soln. using Slater-type functions 80−58168
atom, Autler-Townes effect, i.r. laser transitions 77−425
atom, autoionising reson., Stark effect 80−58198
atom, collective excitation spectra, schematic model 78−41981
atom, doppler-free two-photon spectroscopy using degenerate four-wave mixing 79−31490
atom, double ionisation by electron impact, soft X-ray emission *(Russian)* 77−34766
atom, elastic electron scatt., 2-300 eV, ang. distrib. 80−43179
atom, elastic positron scatt., phaseshifts and elastic, diffusion and annihilation cross section 80−53134
atom, elastic scattering of electrons, expt. 79−857
atom, elastically scattered electrons spin polarisation 5-300 eV, 30-120° 80−23548
atom, electron energy loss spectra, energy-depend. multichannel quantum defect theory anal. 77−61860
atom, electron impact, near threshold UV-emitting level excitation 78−25711
atom, electron impact, struct. near $N_{4,5}$ edges 77−75083
atom, electron impact autoionisation, cross-section parametrisation 77−6932
atom, electron impact ionis. of inner shells, coincidence expt. theory 78−58837
atom, electron impact ionisation, cross section ratios 78−94326
atom, electron impact polaris. and excitation functions 78−66665
atom, electron inelastic interaction, two-grid thyratron expts. 77−83747
atom, electron ionis. cross section, Born approx. 77−83745

xenon continued
atom, electron ionisation and excitation coeffs. in low E/N region 80−48090
atom, electron pulse radiolysis, 2p levels formation and decay kinetics 78−31665
atom, electron scattering, elastic, low-energy, polarised-orbital calcs. 80−37882
atom, excited double hole state, single photon decay probability 77−34606
atom, excited levels Lande factors *(French)* 79−68326
atom, Feshbach reson. classification, relation to ionis. pots., appl. Ne, Kr, Ar, Xe 77−54519
atom, first excited config., intermediate coupling coeff. 80−83450
atom, fluoresc. lifetimes, time resolved VUV spectra 78−17601
atom, g-factors meas. by optical pumping and mag. reson. 80−14246
atom, ground state, two-photon excitation spectra, fluoresc. decay 77−75115
atom, GTO basis sets, Hartree-Fock-Roothaan calcs. 79−97973
atom, Hanle effect, lifetimes and cross sections of laser levels 77−75480
atom, Hanle effect expt. on $6p_{01}$ level, peculiar signal 78−25487
atom, high Rydberg states, radiative lifetimes and transition probabilities 78−86817
atom, independent particle pots. comparison 80−52846
atom, intershell correlation, double electron ejection from outer shell 78−42019
atom, ionisation of high Rydberg states by collision with molecules 77−88545
atom, K X-ray energy shifts following electron capture beta decay, role of nucl. hyperfine struct. 78−5166
atom, L-shell electron impact excitation, characteristic X-ray spectra, cross sections 77−19094
atom, L-shell fluorescence yields 77−79568
atom, laser light irrad. in mag. field, light modulation expt. 78−82699
atom, laser light irrad. in mag. field, light modulation theory 78−82698
atom, line strength calcs. for 8s-7p and 5d-6p transitions 77−14384
atom, line transition probabilities, in afterglow plasma, light absorpt. obs. 77−30807
atom, low-energy 5s-εp photoionization, relativistic effects 78−50515
atom, $M_{4,5}N_{4,5}X$ Auger electron spectra, many-body effects 79−59415
atom, metastable, photoionisation rel. to laser development 78−13476
atom, multiphoton ionisation spectrum, interatomic effects in multiphoton transitions 78−29764
atom, N-shell Coster-Kronig transitions 79−13691
atom, noncoplanar symmetric (e,2e) reaction, factorised distorted-wave approx., 0.4-2.5 keV 78−55245
atom, ns→εp photoelectrons, spin polarisation 80−37792
atom, outer shell photoionisation, relativistic RPA calcs. 80−9571
atom, perturbation of Cs 6s-9p doublet, simultaneous additive effect on multiple satellite lines 79−76389
atom, photoelectron asymmetry parameters 80−95684
atom, photoelectron branching ratio in 4d subshell 79−18164
atom, photoelectron spectra, intershell correl. effects 77−18863
atom, photoelectron spectra, many-electron interactions from 4s and 4p core levels 77−18861
atom, photoelectron spectra, strong many electron effects from core levels 77−18862
atom, photoelectron spectrum ang. distrib. abnormality in strong mag. field 78−50666
atom, photoelectron studies of 5p branching ratio 80−37793
atom, photoelectron-Auger electron post collision interaction, Auger peak-shift obs. 77−27039
atom, photoioinisation, expt. techniques, processes, theory, review 77−14402
atom, photoionis., $\sigma 3/2{:}\sigma 1/2$ branching ratio in $5s5p^6 6p(^1P_1)$ resonance 77−42292
atom, photoionis. collective level existence RPA with exchange calc. 78−42025
atom, photoionis. from excited states 79−10078
atom, photoionisation, correl. satellites and subshell cross-sections, electron spectrosc. obs. 79−31485
atom, photoionisation, spin-polarised photoelectrons angular distrib. 80−106306
atom, plane polarised VUV irrad., emitted photoelectron polarisation, ang. depend. 80−47952
atom, polarisation effects in photoionisation *(Russian)* 79−3420
atom, polarisation of elastically scatt. electrons, 150-1200 eV 77−38734
atom, polarisation transfer collision with Rb atom, NMR of Xe 78−33453
atom, polarised photoelectron ejection by unpolarised light 79−72289
atom, population inversion, intershell transitions, photoionisation, from UV irradiation *(Russian)* 78−70803
atom, primary ionisation by ~2 MeV relativistic electrons *(Russian)* 77−75309
atom, produced by vac. UV irrad., near IR emissions 79−3393
atom, radiation imprisonment of $1s_4$ resonance line 79−82115
atom, recently enhanced multiphoton ionisation and third harmonic generation 80−91526
atom, relativistic Hartree-Fock calcs. using spherical Gaussian basis sets 80−32595
atom, reson. levels relax. consts. determ. by alignment method in discharge 79−26936
atom, resonantly enhanced multiphoton ionis., photoelectron energy anal. 80−63597
atom, s-p transitions, Stark consts. and oscill. strengths, shock tube meas. 80−18822
atom, scatt. from Pt(111), direct inelastic scatt. with trapping-desorption scatt., vel. and ang. distribs. 80−16140
atom, self-broadening of first reson. line 79−26933
atom, six-photon ionis., electron energy spectra 79−54824
atom, spontaneous emission, fluctuation spectroscopy 77−434
atom, subshell photoionisation, multichannel k-matrix calc., spin orbit interactions 80−63600
atom, term dependence of position of 4f electron in $4d^9 4f$ configuration 77−26973
atom, three level systems, obs. of isotope shifts 78−82670
atom, transition oscill. strengths, electron spectrometric obs. 77−10769
atom, unpolarised, spin polarisation of ejected electrons 78−78765
atom, visible lines, absolute transition probabilities 80−69108
atom, VUV fluoresc. under monochromatic excitation 78−9237
atom, X-ray photoelectron spectrum, 304 Å, satellites 78−17627
xenon continued
atom, XPS, $4d_{5/2}/4d_{3/2}$ intensity ratio, Cooper minimum region 79−31481
atom, XPS and XES, dynamical effects 80−52924
atom+H(D), ion pair formation, curve crossing model 80−87216
atom+Li(Na)(K)(Rb), quenching cross sections of alkali n^2P states, 5-100 eV 79−76505
atom and ions, electronic struct., relativistic Dirac-Fock-Slater calc., fluoresc. yield, X-ray energies shift 78−25450
atom-atom collision with Rb, disorientation cross-section temp. depend. 77−23546
atom-diatom paradox, phenomenological description of spectroscopic props. 78−78766
atomic electron scatt., optical model for electron spin polaris. 78−50646
atomic electron scattering, 20-300 eV, total cross sections 79−36778
atomic extravalence excitations, VUV spectra, solvent perturbations 77−50386
atomic high Rydberg state, ionis. by collision with organic mols. 78−50620
atomic photoionisation, ion alignment, many electron correl. effect 78−74622
atomic structure, Hartree-Fock electron density, kinetic energy functional 79−26879
atomic structure, Thomas-Fermi model with Fermi-Amaldi correction 79−81156
atomic three-body collision-induced light scatt. spectrum moments 78−9226
atomic three-level system, collisional effects on optical coherence 79−93954
atoms, free, electron bombard., subsequent X-radiation ang. distrib. 80−53144
atoms, inner-shell level energies, absorpt. spectroscopy with synchrotron radiation 80−99583
atoms in Ne matrix, radiative and nonradiative lifetimes in excited states 80−69106
Auger transitions, K-MM, atom, calc. within intermediate coupling framework 77−34601
brain, Xe regional kinetics meas., imaging methods in transmission computerised tomography 80−98131
carbonaceous chondrite fission Xe, elimination of ^{248}Cm as possible progenitor 77−37581
carbonaceous chondrite fission Xe, Q1 carrier phase rel. to Fe-Ni sulphides 79−58303
carbonaceous chondrites, fission Kr and Xe origin 79−35199
carbonaceous chondrites, superheavy element fission hypothesis for Xe origin 77−78726
chloropentafluoroethane-Xe, multiphoton dissoc., ^{13}C enrichment factor, CO_2 laser wavelength and fluence depend. 80−58331
compressed, electron beam excited, VUV radn. emission 79−27089
computerised tomography, expt. dual XE detectors for quantitative CT and spectral artifact correct. 80−76825
concentration effect, on ^{114}Cd NMR line contour 79−63945
condensed at high press., electron-band theory and fluid theory calcs. 80−59875
condensed electron beam excited, exciton radiative lifetimes 80−6727
condensed phases, emission coeff. of cond. electrons, depend. on elec. field intensity *(Russian)* 79−78855
continuum absorption coefficient, in shock tube, determ. 77−39463
convective instabilities in closed vertical cylinder heated from below 79−77072
cosmogenic Xe ratios, lunar rocks cosmic ray exposure ages and burial depths 77−57661
critical fluid, ratio of sound dispersion to attenuation 79−55826
critical region, thermodynamic properties, correlation experimental data 78−6139
cryogenic distillation from gaseous effluents in nucl. fuel reprocessing 80−5309
crystal, edge hot emission, free exciton luminesc. *(Russian)* 79−15520
crystal, elastic consts. determ. by Brillouin scatt., comparison with neutron scatt. data 77−39622
crystal, exciton exam. 78−51898
crystal, photoelectron spectroscopy, hole-electron valence bound state 77−36369
crystal, X-ray and photoluminesc. 79−87480
crystalline, lattice constant at insulator-metal transition 80−107706
crystalline, photoluminesc. lifetime meas. 78−19548
crystalline, polariton effects, reflectivity, absorpt., and resonant luminesc. spectra calcs. 80−20095
crystallite on Be substrate, crystallite dimensions determ. using synchrotron radiation X-ray diffr. photographs 80−24313
crystals, internal energy, Monte Carlo calcs. 77−72577
DC arcs, with and without focal spot, electric behaviour *(German)* 80−64800
decay chain expansion significance 79−9712
deep-sea basalts, He and Xe as measure of magmatic differentiation 80−31040
desorption, on Pt (111), gas surface interactions, 3-D generalised Langevin model appl. 80−107637
determination, extraction from granite, fission component investig. 78−96216
diamond:^{129}Xe, implanted, elec. quadrupole interaction, integral perturbed ang. correlation study 79−11364
diamond:Xe, quadrupole interaction of implanted Xe 79−61279
diffusion, sorption, solubility, permeation in polyvinyltrimethylsilane *(Russian)* 80−6564
diffusion and solubility in PTFE 80−6561
diffusion coefficients and mobilities of F^- ions in Kr and Xe 80−100048
diffusion of Kr, diffusion coeff. density expansion, search for log. term 79−82024
dilute gas, kinetic-hydrodynamic transition obs., Brillouin scatt. 77−7508
dilute gas, transport props., simple pair pot. model 80−87835
discharge, Blumlein-type transverse fast, voltage meas discharges (electric) 80−19642
discharge, energy balance, optical meas. 78−1935
discharge, HF, with propag. EM wave, isotope distrib. *(Russian)* 77−76235
discharge, microwave, energy characts. 78−5979
discharge, pulsed, visible line afterglow emission obs., excimer form. 80−38754
discharge lamp, RF excited electrodeless, atomic fluoresc. spectrometry 77−86395

xenon continued
discharge lamp, tubular, with short discharge, characts. *(Russian)* 79−32019
discharge lamp switching, transfer processes from thyristor rectifiers *(Russian)* 78−94421
discharge lamps, 147 nm resonance line production 77−39497
discharge lamps, large, electrode temp. meas. by photographic method *(Russian)* 80−47057
discharge plasma spectral and integral characteristics calc. 78−71583
discharges, electrodeless, UHF in waveguide rel. to DC characts. 80−38762
dye-Xe vapour mixture, electron beam pumping 77−42535
EBR-II cover-gas cleanup system 79−97874
electric breakdown, anode-directed streamer propagation simulation 78−67591
electrical conductivity beyond critical point, intermediate density between gas plasma and solid *(Russian)* 80−20265
electroluminescence, electron resonance trapping, temp. effects 78−14130
electron mobilities in various phases, density, elec. field and temp. effects, quasilocalisation 78−59535
electron scattering, Ramsauer effect enhancement in mag. field 80−53137
equation of state and thermodynamic properties formulation, 161.36 to 800K and 0 to 350 MPa 77−51468
equation-of-state of high temp. and pressure, rel. to fission gas behaviour in fast reactor 79−67860
excimer laser, atm. press. and low e-beam excitation rates, expt. studies 80−78863
excimer laser, efficient vac. UV, 172 nm at 6 atm 78−50793
excimer laser, high-power repetitive, tunable, VUV 80−5758
excimer laser, near atm. press. operation 78−17905
excimer laser, VUV fluoresc. study, electron beam excitation 80−87379
excimer radiation excited by radial electron beam 79−94239
excimers and excimer lasers 80−48217
excitation by low energy electrons, IR spectra obs. 80−27974
excited levels, lifetimes, measurement by photon-photon delayed coincidence technique 79−89640
expt. determ. of temp. depend. of thermal diffusion factors *(Russian)* 79−60095
field ion appearance potential spectroscopy, temp. effects 79−19978
fissiogenic isotopes in CO_2 well gas 78−73374
fission gas, bonded radial distrib. in mixed carbide fuel pins, electron probe anal. 79−36318
fission gas release from $(U,Pu)C_{1-x}N_x$ LMFBR MX-type fuels 80−73921
fission gas release from UO_2-Zr high burnup nuclear fuel rods 80−57846
fission product, separation from ^{85}Kr by distillation for industrial use *(German, English)* 77−61516
fission products formation and behaviour, Kr and Xe separation and processing *(Czech)* 79−49707
fission reactor mixed carbide fuels, radial distrib. of bonded fission gas 80−57844
fission reactor transient processes optimisation 78−17295
fission waste product, distribs. and concs. in reactor core 78−58322
fission Xe isotope dating technique 79−21043
flash lamp for pumping Nd:glass Mikron laser system 80−91815
flashlamp, discharge channel evolution 77−84559
flashlamp with interf. coating, laser pumping efficiency improvement 79−10316
fluid, high density behaviour, extrapolated $P\rho T$ surfaces and critical density 80−87834
fluid, near crit. point, correl. range and Rayleigh linewidth 80−93352
fluorescence, K-shell, yield determ., by proportional counter method 77−27023
fusion reactor first wall, hydrodynamic response of Xe protective buffer gas after absorbing target debris 79−85777
gas, atoms, electron thermalization time and position distribution meas. 80−93771
gas, diffusion enhanced by radioactivity 79−60094
gas, ion mobility and longit. diffusion coeff. of Na^+ 80−106866
gas, ionized shock wave, equilibrium zone behind shock wave *(Russian)* 77−89154
gas, Kerr effect virial coeffs. 79−50843
gas, liquid, solid, refractive index, density and dielectric const. 80−66138
gas, proportional scintillation mechanism 79−81131
gas, refraction, determ. by phase vel. matching method *(Russian)* 78−30406
gas, streamer breakdown parameters 77−80388
gas, supersonic radiation waves generated by CO_2 laser radiation 79−10593
gas, third harmonic generation, bandwidth limitations in Lyman-α vicinity 79−81482
gas, two-body time correls., Van Hove scatt. function meas. 80−100053
gas discharge, laser beam polarisation plane rot. near reson. 77−1024
gas mixtures for gas-filled particle detectors 80−74089
gas scintillation proportional counter, UV emission spectrum, prod. mech. 77−26935
gas-liquid crit. pt. region, depolarised light scatt. 78−34612
gaseous adsorption in fission reactor fuel reprocessing 79−31094
gaseous fission product, continuous determ. of content in reactor loop 79−30905
gaseous reactor waste treatment in PWR and BWR 79−54570
high power pulse gas discharges development, photographic obs. 80−14954
high pressure lamp for polymer spectral sensitivity determ. *(German)* 80−61119
HTGR, large pebble bed, Xe oscillations detection 80−22988
HTGR, pebble-bed, computational procedure for xenon stability 77−61501
HTR, Xe dynamics, 2D reactor models, axially collapsing methods *(German)* 80−68731
HTR individual coated fuel particles, gas anal., optimum heating and crushing 77−56294
HTR individual coated fuel particles, mass spectrum. determ. of Xe, Co and Kr gases 77−56293
hydrostatic medium for diamond anvil cells to 300 kbar press. 79−97402
impurities in alkali metal films, optical excitation spectra obs. 77−24876
incommensurate overlayer on Ag (111), dynamical calc. of LEED 78−30828

xenon continued
inner electron energy characteristics, validity of Hartree-Fock-Pauli approx. 80−42957
ion, γ-γ PAC following nucl. electron capture, cascades perturbed by hyperfine coupling 78−37303
ion, highly charged, prod. in electron beam superconducting ion source 77−23333
ion+Au foil (Hg vapour) collisions, quasimol. M-radiation 77−14566
ion bombardment of polycryst., kinetic energy reflection 77−85869
ion collisions, 326-470 MeV, K-vacancy production, multiple and single collisions in mol. orbital excitation 77−83717
ion impact on C foil, energy loss 78−55902
ion implantation defect introduction in ZnTe, cathodolum. studies 80−75250
ion source, HF, proton yield increase, influence of various admixtures to H_2 obs. 80−57422
ion-atom collision, K-vacancy prod., mol.-orbital method 77−68095
ionisation detector in liquid, signal amplification by optical pumping 79−54746
ions, 300 keV, InSb implantation, dose rate and orientation dependence of radiation damage 77−89482
ions, prod. of isotope-resolved beams of highly charged ions 79−93858
IR lasers pumped by U fission fragments 80−28198
isoelectronic series, $3d^9 4f$ config., collapse of 4f electron, X-ray spectral obs. *(Russian)* 80−58204
isotope abundance of Te ores, geochem. test of nucleon stability 78−8667
isotope separation, centrifuge in RF discharge, rot. mag. field 79−10737
isotope separation, HF stationary discharge, travelling mag. field, barodiffusion separation 80−44049
isotope separation, plasma ion cyclotron reson. 77−10787
isotope separation in Hf discharge, thermodiffusion *(Russian)* 77−46649
isotope separation in RF discharge, light inert gas admixture effects 79−41250
isotope separation using SIDONIE and PARIS separators 77−14269
isotope shifts of 1s electron in K-X-rays following electron capture 77−23454
isotopic abundances, s-process contributions 79−5739
isotopic composition anomaly in Murchison meteorite, reply 79−44425
isotopic composition anomaly in Murchison meteorite 79−44424
Kerr effect in gas, statistical theory 79−50842
lamp, pulsed, effect of gas heat capacity on characts. 78−42838
lamp, ultrahigh-pressure, Soviet-made DKSSh lamp spectral characts., in pulsed regime 80−48371
lamp spectral radiation density, 400 to 1000 nm obs. 79−14072
laser, and associated high gain phenomena, expt. and theory 79−10280
laser, electron beam excited, form. of multiply-charged ions *(Russian)* 78−25853
laser, He-Ne-Xe mixture, hollow cathode, internal anode system, CW 78−9396
laser, high gain, ang. multiplexing for short pulse amplification 79−36924
laser, new IR laser transitions, 3.725 to 17.233 μm 80−87374
laser, pulsed ion, pump for open dye stream laser 79−81448
laser, pumping by relativistic electron beam, energy transfer theory 77−31089
laser, recombination, in expanding CO_2 laser prod. plasma 77−88698
laser, simple VUV high press., with coaxial electron beam pumping 79−974
laser, waveform analysis of 3.5 μm self-mode-locked pulse 78−1290
laser 3.5 μm transition, quasi-Gaussian pulse propagation, effect on lineshape parameter anal. 78−55333
laser amplifiers, spectral narrowing and saturation induced rebroadening optical heterodyne obs. 80−63976
laser discharge tube, radial variation meas. at 3.51 μm gain 77−54694
laser induced gas breakdown threshold at 1.06 micron 80−28594
laser line ionic assignment at 3306 Å 78−1209
laser oscillation obs. in transversely initiated laser-produced plasma 77−88696
laser oscillator, gain switched, analytic modelling 77−7052
laser pump source for blue laser dyes 78−46621
laser pumped dye laser, construction and performance of laser and pumping source *(Japanese)* 77−58341
lattice heat capacity, thermal vibrations, Lindeman parameter, lattice dynamic model *(Russian)* 80−29141
Lennard Jones (12,6) pot. distance parameter, transport props. calc. 80−79423
light scattering, in crit. region, scaling interpretation 79−46420
light scattering, multiple scattering contribs. to depolarisation 80−87842
liquid, α-particle and electron excited luminesc., time depend., specific ionisation density effect 80−71495
liquid, μ, ρ and T-surfaces, global behaviour, rel. to catastrophe theory 78−26226
liquid, acoustic nonlinearity parameters *(German)* 79−77685
liquid, comparison on interaction induced light scatt. and IR absorption 80−60561
liquid, electron mobility, role of shallow traps 80−34440
liquid, high-field electronic conduction obs. 79−4587
liquid, ionisation and scintillation, application to radiation detectors, review *(Japanese)* 78−35206
liquid, principle of corresponding states for viscosity 77−84959
liquid, Ramsauer-Townsend minimum in electron scatt. cross section 77−89821
liquid, recomb. and self-trapped exciton luminesc., free electron dynamics, excited states 80−25463
liquid, recomb. luminesc. 78−60521
liquid, scintillation counter for imaging of positron emitters 77−2042
liquid, struct. factor calc., perturbation treatment using Lennard Jones (6, 12) pot. 80−10483
liquid, T_c, P_c, V_c, from eqn. of state 78−2228
liquid, triplet state of self-trapped exciton states, evidence of existence, luminescence meas. 78−72608
liquid, UV reflection spectra, density depend., excitonic band evolution 77−77246
liquid and solid, γ-irrad., average energy expended per ion pair *(Russian)* 80−5438
liquid independent structure model, critical point, liquid-vapour equilib., second virial coeff. *(Spanish)* 77−4031
liquid ionisation chamber media, review of physical props. 79−41071
liquid radial distrib. functions and structural parameters 79−55640

xenon continued
liquid-vapour coexisting densities, nonlinear crossover, scaling corrections 77−84913
liquid-vapour crit. exponents, NMR 78−18759
Mars, atmospheric Kr and Xe, Viking obs. 77−56856
Mars, regolith adsorption rel. to atmosphere Xe relative conc. 78−49358
mass spectroscopic chemical anal. using quadrupole mass spectrometer for fissile material accounting 80−63300
matrix isolated CO and N_2, rel. to solid UPES 79−45762
matrix isolated NO $3s\sigma(A^2\Sigma^+)$ Rydberg state 'bubbles', reson. fluoresc. obs. 77−83636
metallic state of static press., elec. cond. meas. 79−33313
metallic state transition under high press., supercond. *(Russian)* 79−60713
metastable ions, $5d^4D_{7/2}$ state, laser induced fluoresc. 77−14387
metastable ions, fast beam, high resolution spectra 77−42274
meteorites, isotope anomalies rel. to extinct radioactivities and presolar grains 77−45367
meteorites Xe anomaly, fission origin implications for astrophysical r-process 78−93204
molecule, photoelectron spectra, $X^1\Sigma^+_{(1/2)g}$ ground state pot. 78−5280
molecule excited state lifetimes time-resolved spectra 78−17704
molecule near metal surface, proximity effects 79−36797
molecules, time-resolved excitation using synchrotron radiation *(French)* 77−88483
monolayer, on graphite, misfit dislocations and lattice parameters, model 78−34708
monolayer, on graphite (0001), liq. state model appl. 77−69185
monolayer, physisorbed on Pd (100), angular-resolved photoemission 79−43102
monolayer adsorbed on graphitised spheron, X-ray diffr. patterns 77−43433
monolayer adsorption on Ag(111) surface, lateral struct. and Xe-Xe interactions 77−1311
monolayer adsorption on Ag (111), LEED obs. 77−1307
monolayer adsorption on Ag (111), statistical mech. 80−34306
monolayer adsorption on Cu(100), thermodynamics and kinetics, LEED and AES obs. 79−99423
monolayer on graphite, phase transition from localised to nonlocalised solid 77−11787
MSBR, transient Xe anal. 78−54843
Murray (C-2) carbonaceous chondrite, I-Xe age and trapped Xe components 80−98618
nuclear reactor, one dimens. slab, optimal control of Xe oscills., computer program *(German)* 77−61529
nuclear reactor, Xe poison, optimal control *(Korean)* 77−54323
optical discharge radiation source 78−87116
organ blood flow measurements, effect of instantaneous partition coeff. of Xe 80−101256
oscillation suppression, reactor system reciprocity props. 80−27773
outer $p_{1/2}$ subshell photoionisation, polarised electrons, relativistic RPA calcs. 80−83331
P ρ T surfaces, butterfly catastrophe 79−86546
photoabsorption, local field effects 80−74151
photoelectrons, 5s→εp, ang. distrib. and spin polarisation 78−58634
physisorbed layer, UPS spectra, lateral interaction 78−92174
physisorbed monolayer on graphite, dynamical and thermal props. 80−34292
physisorbing on Ni and Cu, stay time meas. 78−56044
physisorption on W (100), Lennard-Jones model, mol. dynamics study 80−34308
plasma, dense, nondegenerate, electron transport, thermal cond. *(Russian)* 79−98865
plasma, dense, photoionisation absorption spectra, photorecombination radiation 78−26252
plasma, dense, shock-heating, calc. of equilibrium props. *(Japanese)* 80−79513
plasma, electron energy distrib. function, Coulomb collision effects 80−38532
plasma, electron-ion pairs, correlated pairs, effect on conductivity 78−26249
plasma, emission and absorption coeff. at high electron density 80−103121
plasma, energetic binary collisions 79−77337
plasma, high-press. arc discharge, elec. cond. 80−59181
plasma, laser prod., fast ionis. wave *(Russian)* 78−22528
plasma, low threshold supersonic emission waves and effect on laser beam 79−27780
plasma, photodetonation and supersonic radiation wave propag. *(Russian)* 80−10385
plasma, primary electron effective MFP meas. in multidipole device 77−24183
plasma, ruby laser radiation effects *(Russian)* 78−22514
plasma, shock-compressed, thermophysical and gasdynamic characts. 77−43016
plasma, shock-heated, dense, continuum radiation and optical transmittance diagnostics 80−24202
plasma, shock-heated, high-density, elec. cond. 80−38557
plasma, thermodynamic functions, composition, and elec. cond., calc. method 79−32738
plasma, thermodynamics of nonideal low-temperature multicomponent plasma: chemical model 79−41796
plasma, total emission coeff., line contrib. 79−77346
plasma, wall-stabilised, temp. and press. of high press. plasma *(German)* 79−23450
plasma, Z-pinch heating efficiency 78−47152
plasma afterglow, spectral features, 450-900 nm 79−23404
plasma column in flashtube, characts. and parameters 80−54053
plasma jet, radiating, bulk energy distrib. 80−75107
plasma shock front, elementary processes 80−19581
plasma Tokamak discharge, impurity emission spectra for diagnostics 77−11403
plasma-recombination laser, CO_2 laser prod. using periodic pumping 79−45927
poisoning transient anal. in fission reactors using XESAMO code *(Spanish)* 80−52749
positron annihilation in rare gases, Doppler broadening meas., electron mom. distribs. 78−55131
o-positron quenching rate crit. slowing down near gas-liquid transition 77−24907
positronium formation in Xe gas near crit. pt. 79−86091
xenon continued
power reactor parameter identification in Xe oscillation model using maximum likelihood method 80−18466
prebreakdown elec. cond. of nearly saturated Xe vapour 80−48841
precursors, associative ionisation and photoionisation, relative contrib., electron density prediction 80−43858
probe for radiation contamination monitoring 80−27826
pulse discharge regime, time-depend. of radiation *(Russian)* 77−84548
pulse gas discharge, high-intensity, energy storage and temp. in channel 78−1926
pulsed arc lamp with adjustable plateau slope 79−68422
pulsed discharge, superheating instability, effect of secondary ionisation 77−55189
pulsed high frequency discharge, energy spectrum and electron density meas. *(Russian)* 78−26354
pulsed light source, programmed command unit 77−79163
PWR, Xe-induced spatial flux transient, anal. and control, parameter identification 80−18441
radiation-induced porosity of Ni, effect of 2 MeV Xe^+ ion irradiation on pore distribution and size 79−71898
radioactive, adsorbed on charcoal, release in spill accident 77−50262
radioactive ion implantation using Lublin separator 79−82251
rarefied plasma, emission characts. 80−103122
refractive index meas. using low temp. refractometer 77−57382
resonance lamp in vac. UV, new developments 79−32017
retained in advanced nuclear fuels, meas. by microprobe anal. 79−40997
Rydberg atoms, field ionisation, 300K background radiation effects 79−68271
satellite lines in 5s-5p photoelectron spectrum 78−25493
scintigraphy, estimation of regional ventilatory clearance 80−30854
scintillation detectors appl. *(Czech)* 78−86727
second continuum fluoresc. excited by synchrotron radn. 78−90113
secondary scintillation under mag. fields, effect in gas proportional counters 80−58055
self-diffusion coefficient, radioactive tracer meas. 77−13534
separation performance from Ar binary mixture, in thermal diffusion column 77−42192
shock wave, strong, piston struct. and gas distrib. 80−10265
short-arc lamp, current modulated, arc forms and instability 80−96399
single crystal, photoemission exam. 79−78845
single crystal, Pockel coeffs. and short-range-interaction parameters 79−73962
solid, absorption spectra of self-trapped excitons 78−43879
solid, core excitons, integral eqn. formalism, isolated atoms and cryst. 78−47704
solid, elastic consts., thermodynamic props., Monte Carlo simulation 77−62575
solid, electronic struct. of self-trapped excitons 79−19525
solid, enthalpy of sublimation, internal energy, determ. from vapour pressure 78−91435
solid, H_2 and D_2 CoM freq. matrix shifts calc. 79−6969
solid, HCP, vap. phase grown thin films 78−18917
solid, high press. equation of state 79−37809
solid, improved unsymmetrised SCF approx. for strongly anharmonic crysts. 78−75791
solid, lattice dynamics calc. using Kihara hard core pot. 77−1193
solid, lattice vibrs., heat capacities 79−42169
solid, liquidus lines in liq. air component mixtures *(German)* 77−84915
solid, luminesc. from self trapped excitons (excimers) 79−1785
solid, n=1 surface excitons and LO-TO splittings of bulk excitons 79−73445
solid, phonon densities of states and dispersion curves, unpaired elastic force model 79−51220
solid, phonon dispersion, many body pot. assuming variable at. polarisability, mech. props. 79−55840
solid, self-trapped exciton, pseudopotential method 79−82529
solid, self-trapped exciton emission bands 80−20697
solid, surface excitons 77−76892
solid, synchrotron irradiation pulse excitation photoluminesc. decay, exciton generation 78−6746
solid, two-phonon difference scatt. 80−60588
solid, zero temp. isotherm, APW calc. 79−73128
solid film, decay times meas. of 1750 Å intrinsic luminesc. band 77−59619
solid film, electron MFP, vacuum UV photoemission data 77−28690
solid matrix, optical excitation of rotational transition of methane, 6K 78−60494
solubility in liq. scintillator solvents, meas. using radioactive tracers 77−57808
solution, mean force of two atoms dissolved in water 80−54114
sorption, diffusion, solubility in polyvinyltrimethylsilane rel. to temp. *(Russian)* 80−6565
sound propag. near critical pt. 79−82285
sound propagation, near crit. point, theoretical anal. 77−69046
spatial Xe oscillation time-optimal control in PWR 79−628
sputtering gas, improved economy using getter pumping 77−40371
St. Severin chondrite, fission Xe rel. to U and Pu distrib. 80−72889
sticking coefficients on W (110) and (100) planes 79−82464
superheated liquid, nucleation rates 79−23741
supersonic radiation waves, excitation by CO_2 laser 79−90433
surface, desorption of He, appl. of simplified continuum model 78−87860
temperature fixed point suitability 78−77838
tetracene-Kr(Xe), intramol. intersystem crossing in supersonic beam, external heavy atom effect 80−14167
tetrafluoro-dibromo-ethylene-Ar-Xe mixture, experimental study of stimulated emission 79−98347
tetramethyldioxetane, collisional dissoc. by supersonic Xe beam, chemiluminesc. 78−40029
thermal conductivitiy, 170-1300K and press. to 200 Mpa 79−82025
thermal conductivity, 500 to 2400K, interatomic pots. 77−39393
thermal conductivity, 500 to 5000K 77−58833
thermal conductivity, at high press. 80−103099
thermal conductivity, law of corresponding states *(Russian)* 78−87426
thermal conductivity, Lennard-Jones (12-6) pot. parameters calcs. 80−28591
thermal conductivity calc., law of corresponding states and interatomic pots. 79−7437
thermal conductivity coeff. meas. 1100-2200K range, differential technique 77−33989
time resolved spectra, UV and near UV continuums 78−78653

xenon continued
Townsend discharge, electron energy distrib. functions 79−4198
Townsend discharge electron energy distrib. obs. 78−67549
triple light scatt. along crit. isochore 77−58838
two-scale factor universality near crit. point 78−55936
united atom rare gas spectra analogy with mol. Rydberg states 80−32700
valence orbital, electron impact ionisation, absolute cross-section 80−69241
viscosity meas., 170-1300K, up to 1000 bar 78−42698
whole-body counting and dose determs. 80−89853
α scintillation kinetics in condensed Xe 79−26828
μXe muonic atoms, vanishing muon transfer effect 80−9765
^{133}Xe custom trapping and holding system for animal research, design and evaluation 80−30950
Al-Xe film, ion implanted radiation enchanced Xe outdiffusion, Rutherford backscatt. 77−76609
Ar:Xe, liq. 0-1.4 g cm^{-3}, vac. UV absorpt. spectra, Wannier impurity states 77−77232
Ar:Xe film, solid, competition between electronic energy transfer and relax., photoelectron spectra 77−24929
Ar:Xe:Cl_2, photochem. XeCl prod., ESR 77−18947
Ar:Xe^+, 0.1-1.4 gm cm^{-3}, adiabatic electrostatic polarisation energy, calc. 77−85640
Ar-Xe, liq., Zwanzig perturbation expansion convergence, free energy 77−76274
Ar-Xe, low-threshold nuclear pumped laser, generation characts. 80−19018
Ar-Xe gaseous mixtures, collision-induced microwave absorpt. 78−78680
Ar-Xe high press. transverse discharge laser using Xe IR transitions 80−63978
Ar-Xe high-press. neutral IR laser emission from Xe 79−86159
Ar-Xe IR laser pumped by electron beam stabilised discharge, lasing parameters 80−102698
Ar-Xe mixture, microwave absorption, collision-induced 79−22626
Ar-Xe-NF_3, mixture in XeF laser, discharge stabilised by short-pulse electron beam 80−14358
Ar-Xe-NF_3 mixture, fluorescence from e-beam excitation at low temp. and high press. *(French)* 78−58727
Ar-Xe-tetrachloromethane, self-sustained electrophotoionised discharge in compressed gas 80−38003
Ar-Xe-tetrachloromethane excimer discharge laser 79−13957
Ar+Xe, relaxation processes of Xe*($^3P_2$) metastable atoms 78−50624
Ar+Xe($^3P_2$), flowing afterglow metastable decay rates, diffusion, two- and three-body rate consts. 78−73027
Ar+Xe(F_2), proton excited mixtures, energy transfer processes 78−66647
Ar+Xe→Xe*, electronic energy transfer, emission spectra, electron beam excitation 77−38722
Ar*($4s'_{2,0}$)+Kr(Xe), elastic and reactive scatt., ang. distribs. 77−6919
Ar($4s'^3P_{2,0}$)+Xe, specific channel rate construction 77−46627
B+Xe(Kr), reson. radn. quenching 77−30820
Ba+Xe, spectral line contour meas. determ. of potentials 78−25477
CO-He-Xe, laser, Xe effect on gas temp. 77−19238
CO-Xe-N_2-He gas laser power rel. to mixture composition *(Russian)* 79−7114
CO_2-Xe laser, sealed-off, high efficiency, low impedance 77−3614
CO_2+H+Xe plasma, elec. parameters, Xe effects *(Russian)* 77−84507
Ca-Xe charge exchange system, optical gain meas. 79−10285
CdTe:Xe, anomalous Xe^+ ion implantation defect introduction, cathodolum. obs. 77−62554
Cl^--Ne(Ar)(Kr)(Xe), longitudinal diffusion coeff., generalised Einstein relation 79−86552
Co:^{129m}Xe, mag. hyperfine field determ. by Mossbauer effect 77−8460
Cs, Xe perturbed emission lines, satellites in square well pot. approx. 78−46303
Cs:Xe, optical absorption by rare gas, cluster Bethe lattic calc. 77−8612
Cs:Xe film, metal-insulator transition, cond. and optical absorption meas. 77−24598
Cs-Xe, oscill. strength, for induced dipole transitions, pot. energy curves 77−75100
Cs-Xe molecular bands, time-resolved fluoresc., lifetimes 77−58068
Cs-Xe solar-pumped MHD excimer laser, modelling 80−95873
Cs-Xe vapour mixture, possibility of solar direct energy conversion into laser radiation 79−59688
Cs+Xe, broadened Cs principal series lines, absorption meas., Cs-Xe pots. 77−79584
Cs+Xe, collision-induced 6s-ns transitions in absorpt. spectrum 78−9101
Cs+Xe, effect on Cs $^2P_{1/2}$ and $^2P_{3/2}$ levels lifetimes 77−3307
Cs+Xe (neopentane), Cs line shape broadening, satellite data inversion, interaction pot. 78−74608
CsCl(Cs_2Cl_2)+Ar(Kr)(Xe), collision-induced ion-pair form., absolute cross sections 78−73029
Cs($6^2P_{3/2}$)+He(Ne)(Ar)(Xe), collisional depolaris., nucl. spin depend., by Zeeman scanning 77−19012
Cs(8^2P)+He(Ar)(Xe), fine-struct. transition cross sections, semiclassical calcs. 77−30972
Cu-Xe film, metal-nonmetal transition, optical and resist. meas. 77−89818
F+Xe, differential scatt. cross sections, crossed beam study, interaction pot. 79−3517
F+Xe, enhanced quenching in intense KrF laser light, computer modelling 78−55232
F+Xe(H)$^+$(H_2), ($^2P_{3/2}$) state quenching, Franck-Condon approach 78−66640
Fe:^{129m}Xe, mag. hyperfine field determ. by Mossbauer effect 77−8460
Fe:^{133}Xe, heavy ion implantation, recovery, Mossbauer effect meas. 78−52393
Fe:Xe, gyromagnetic ratios of first 2^+ states in Xe, implantation PAC 78−12966
Fe:Xe, interaction of impurities with point defects, Mossbauer spectroscopy exam. 78−47414
Fe:Xe, isotope ion implantation control *(Flemish)* 78−79623
Ga-Xe film, metal-nonmetal transition, optical and resist. meas. 77−89818
H+Xe, electron-loss cross section struct., 0.05-4 MeV 78−9236
H^-+Kr(Xe), electron capture into 3s state, cross-section meas. 78−42209
H_2-Ar(Kr)(Xe) mixtures, intermol. forces 78−62867
H_2-Xe, bound complex form., anisotropic intermol. pot., IR spectra anal. 78−37634
xenon continued
H_2^++He(Kr)(Xe), collisional dissociation, ion-pair prod., negative ion prod., cross sections 77−14529
HBr-Xe, thermodynamics of binary liquid mixtures 78−64876
HCl-Xe, liq., enthalpy of mixing, calorimetric meas. 80−59661
He:Xe, liq., 0.04-0.1 g cm^{-3}, vac. UV absorpt. spectra, Wannier impurity states 77−77232
He-Ar(Kr)(Xe), 208 and 707K, intermol. forces, virial, diffusion, and viscosity coeffs. 77−75256
He-CO_2-Xe electrical discharge laser pumped by crossed electric and mag. fields 78−42320
He-Co_2-Xe plasma discharge electron conc. and temp., optical diagnostics method 79−41871
He-Kr(Xe), scaling parameters for thermal diffusion factors, viscosity, mutual diffusion coeff. calcs. 77−35292
He-Ne-Xe, ion laser transitions, hollow cathode excitation 80−1184
He-Ne-Xe ion lasers, hollow cathode, CW operation and excitation mechanism 80−69363
He-Xe, eqn. of state, Monte Carlo calcs. 80−59158
He-Xe, H_2CO-stabilised laser, freq. stability in axial mag. field 79−22991
He-Xe, high-press. neutral IR laser emission from Xe 79−86159
He-Xe, ion laser transitions, hollow cathode excitation 80−1184
He-Xe, low-threshold nuclear pumped laser, generation characts. 80−19018
He-Xe, Xe I TEA lasers, energy characteristics 80−63977
He-Xe 3.51 μ laser mode competition in axial mag. field 80−63974
He-Xe laser, 3.51 μm, mode competition in axial mag. field 78−25850
He-Xe laser, freq.-offset-locked at 3.51 μm 79−98400
He-Xe laser, nuclear pumping by vol. source of fission fragments 79−36879
He-Xe laser, Zeeman tuned *(Korean)* 79−7145
He-Xe mixtures, high temp. heat conduction 79−14509
He-Xe mixtures, US vel. meas., phase separation 79−27738
He-Xe optical amplifier, high gain coeff., noise characts. 80−43365
He-Xe optical amplifier, striation form. for DC discharge plasma, noise anal. 80−43366
He-Xe plasma, in mag. field, effect of CO_2 mol. addition on plasma parameters 77−42965
He-Xe recombination lasers, CO%d2 laser-produced plasma-initiated 80−48286
He-Xe-F_2 mixture, pulsed avalanche discharge at high gas press., homogeneous form. conditions 80−49027
He-Ze laser, freq. stability at 3.51 μm 79−98401
He+Ar(Kr)(Xe), He*(2^1S) scatt., low energy repulsion systematic struct. 78−22000
He+Ne(Ar)(Kr)(Xe), energy transfer, time-resolved VUV spectra 77−19028
He+Xe, electron-loss cross section struct., 0.05-4 MeV 78−9236
He^++Xe, internal energy distrib. at 100 eV 80−99564
He^++Xe charge transfer, optical emission cross sections 77−61853
^{3}He-Xe, direct nuclear pumped lasers using ^{3}He(n,p)^{3}H reaction 79−31863
^{3}He-Xe, nucl. lasing, population inversion mechanism 80−63980
^{3}He-Xe, nucl. pumped laser plasma, distrib. functions 79−36880
^{3}He-Xe laser, direct nucl. pumping via ^{3}He(n,p)^{3}H 77−71972
^{3}He-Xe laser, direct nuclear pumping by protons and tritons 78−5458
^{3}He-Xe laser, nucl. pumping by volumetric ^{3}He(n,p)^{3}H reaction 77−10886
^{3}He-Xe nuclear pumped laser, small signal gain coeff. and power output, theory comparison with expt. 80−63983
^{3}He-Xe nuclear pumped laser, electron distrib. function role 80−63984
^{3}He-Xe volume pumped nuclear laser survey of lasing 80−63979
^{4}He stopping cross sections, 1-8.5 MeV 78−58558
He*+Ar(Kr)(Xe), elastic scatt., repulsive rainbows and optical pots. 79−840
Hg/Xe films, optical study of metal-insulator transition 79−65947
Hg-Xe, mixtures, prebreakdown discharges, discharge current depend. on electron mobility 79−77433
Hg-Xe film, random mixtures, superconducting transition temp. and metal-nonmetal transition 80−29498
Hg-Xe solid films, optical absorpt., localised states 79−61452
Hg-Xe solid mixture, optical criterion for Mott transition 78−75996
Hg-Xe system, metal-insulator transition temp.-coeff. of cond. 77−66188
Hg-Xe vapour deposited films, cond. transitions, effect of disorder on supercond. 80−88659
Hg-Xe(Kr)(Ar), fluoresc. emission, high press., electron beam excitation, laser appl. 77−34676
Hg+He(Xe), collisionally induced coherence, orientation and alignment, transfer among 6s6d levels 78−74747
Hg+Xe, pressure broadened absorption profiles *(French)* 79−98033
I+Ar(Xe), collision-induced $^2P_{1/2}$→$^2P_{3/2}$ emission 77−83528
K-He(Ne)(Ar)(Kr)(Xe), oscill. strengths, for induced dipole transitions, pot. energy curves 77−75100
K^++Xe, differential elastic cross-section meas. *(German)* 77−58130
Kr, thermal diffusion factors, isotopic 78−22450
Kr-Xe, absorpt. spectra line-narrowing, with reson. excitation transfer 79−89973
Kr-Xe, glow discharges, AC cataphoresis meas. using light spectrometry 79−60096
Kr-Xe, isotopic mixtures, separation in high-freq. discharge in mag. field *(Russian)* 77−75317
Kr-Xe, phase matched, generation of Lyman-α radiation 80−91845
Kr-Xe-F_2 excimer laser, kinetics of excimer formation 80−14328
Kr-Xe-F_2 mixtures, excimer emission bands *(Russian)* 77−71885
Kr+Kr(Xe), X-ray prod. cross sections for Kr L-shell vacancies 79−10190
Kr+Xe, nonresonant excitation transfer, Doppler profiles, donor levels *(French)* 77−30824
Kr^++$H_2(N_2)(O_2)(CO)$, near-resonant charge transfer, 4-45 keV 77−27176
KrCl*+Xe, substitution efficiency during excitation in transverse AC electric discharge 80−50850
KrF+He(Ne)(Xe)(NF_3), quenching rate consts. meas. 79−24718
Mo:Xe, BCC, heavy ion implanted, vacancy recovery, Mossbauer spectroscopy 79−82896
N_2-Kr-Xe, liquefaction, retention of ^{85}Kr from fission exhaust gases, separation technique *(German)* 80−27753
NH_3-$N_2(H_2)$(Ne)(Ar)(Kr)(Xe), as R(1,1) vibr-rot. line parameters, ν_2 band, using CO_2 laser light 79−3444

xenon continued
Na-(Ne)(He)(Ar)(Kr)(Xe), oscill. strengths, for induced dipole transitions, pot. energy curves 77−75100
Na-Hg-Xe cylindrical high pressure arc discharge, acoustic resonance 78−67454
Na-Xe, high-pressure discharge, electron density, interferometric meas. 78−75415
Na-Xe, multiphoton ionisation in third harmonic generation by mode locked Nd:YAG laser 78−94413
Na-Xe discharge kinetic model for visible lasers 78−63088
Na-Xe excimer lasers, high-power discharges, models 80−69373
Na-Xe vapour, high power discharge, potential excimer laser 78−82957
Na+Xe, nonreson. two-photon absorpt., 4s excited states and pot. energy curves, close coupled eqns. 80−48068
Na+Xe+$\hbar\omega$, collisions in presence of nonresonant lasers 80−99567
Ne, solid, doped with Xe and benzene, energy transfer 77−32416
Ne:Xe, electronic relax. cascades in Wannier and Frenkel type exciton states 79−33759
Ne:Xe, liq., 0.1-0.65 g cm^{-3}, vac. UV absorpt. spectra, Wannier impurity states 77−77232
Ne:Xe, luminesc. in vacuum UV 79−15519
Ne:Xe film, solid, competition between electronic energy transfer and relax., photoelectron spectra 77−24929
Ne-Xe gas discharge, LF oscillations, modulation by gravitation and inertia forces 77−11429
Ne-Xe gaseous mixtures, collision-induced microwave absorpt. 78−78680
Ne-Xe mixture, microwave absorption, collision-induced 79−22626
Ne-Xe-F_2(NF_3), excited states quenching 79−18406
Ne-Xe-HCl, transient optical absorpt. meas. for XeCl laser 79−55115
Ne+Xe and Ne+Kr+Xe glow discharge, Kr^+ and Xe^+ excitation in negative luminesc. *(Russian)* 77−68883
Ne^{2+}+He(Ne)(Ar)(Xe)(Kr), cross sections for electron capture, 60 to 200 keV 78−46442
Ni:^{129m}Xe, Mossbauer obs. of mag. hyperfine field 77−8460
$O^{4,5,6,7+}$+Ne(Ar)(Kr)(Xe), 10-30 MeV, charge exchange 77−34757
O_2-^{85}Kr-Xe, liquefaction, retention of ^{85}Kr from fission exhaust gases, separation technique *(German)* 80−27753
O(^{3}S)+Ne(Ar)(Kr)(Xe), total cross sections 78−42188
Pb-Xe film, struct., electron diffr. meas., rel. to metal-nonmetal transition 77−51626
Rb^+, ionic mobility in Ar, Kr and Xe, interaction pot. determ. 79−18991
Rb-Xe mixture, nonreson. third harmonic generation of I laser radiation 79−3746
Rb-Xe mixture, third harmonic generation with Nd:glass mode-locked laser 77−27318
Rb+Xe, interatomic spectrum, theoret. and exptl. obs. 78−9112
Rb+Xe system, reson. fluoresc., quasimol. states *(Russian)* 79−85935
Rb*+He(Xe), thermal, 5p $^2P_{1/2}$ state depolarisation cross-sections 77−71852
Rb*+Xe+Xe, mol. form., eikonal approx. calcs. 77−14531
Rb(6^{2}P)+He(Ar)(Xe), fine-struct. transition cross sections, semiclassical calcs. 77−30972
$S_2(B^3\Sigma_u^-\nu=4)$+He(Ar)(Xe), collision-induced transfer rates 79−94062
Se^{2+}+inert gas, low energy reactions, SIFT and drift tube obs. 80−97705
Si surface-barrier detectors, characts. in Xe ion beam 78−78571
Si:O, Xe, ion implanted, Xe retention, Rutherford backscatt., comparison with SiO_2+Xe 79−4320
Si:Xe, ion implantation, high fluence retention 79−23627
SiO_2:Xe, ion implanted, Xe retention, Rutherford backscatt., comparison with Si-O, Xe 79−4320
Sr-Xe, resonant third harmonic generation anal. 78−90460
Sr+He(Xe), Sr reson. line width, 4607 Å, press. effects, pot. well depths 79−89643
Ta:Xe, BCC, heavy ion implanted, vacancy recovery, Mossbauer spectroscopy 79−82896
Tl-Xe, electric discharge excitation of Tl in high-press. Xe 80−49025
Tl-Xe, excimer band emission from electron beam initiated discharge in Tll-Xe 80−78840
Tl+Xe, broadening of Tl 377.5 nm line 77−71781
W:Xe, attachment of mobile particles to non-saturable traps 80−39418
W:Xe, BCC, heavy ion implanted, vacancy recovery, Mossbauer spectroscopy 79−82896
^{133}X calibration of environmental and personal dosimeters 80−86992
Xe 5s, photoelectron ang. distrib., relativistic Dirac-Fock calc. 79−59411
Xe, adsorbed monolayer, THEED intensity meas. 78−84075
Xe arc discharge, radiative characts. computational model requirements 80−64812
Xe fission gas release and microscopic swelling in LMFBR highly-rated MX-type fuels 80−57848
Xe I, 147 nm resonance line, wavelength stability 77−17948
Xe I, arc spectrum, press. shifts and broadenings in visible and near i.r. 77−440
Xe I, electron impact excitation in 18-24 eV autoionis. region 77−58171
Xe I, indirect level population in electron excitation *(Spanish)* 77−3461
Xe I, laser line observations in Cu(Ag) hollow cathode discharges 79−68383
Xe I level deviation from Boltzmann population in steady-state plasma 78−67605
Xe I spectra, theoretical transition probabilities and lifetimes, data tables 79−54793
Xe I three-level system, level splitting within natural width, saturation spectrum 80−106291
Xe I-III, hollow cathode discharge, excitation and ionis. mechanisms, spectra obs. 77−15261
Xe II, 5d^{4}D$_{7/2}$-6p^{4}P$_{5/2}^0$ transition, isotope shift, h.f.s., laser-ion beam expt. 79−93945
Xe II, 5p^{4}6s and 5p^{4}5d configs., config. interaction effects 78−66478
Xe II, excited states lifetime meas., photon-photon delayed coincidence technique 77−68011
Xe II, influence of relativistic effects, excited states 79−72274
Xe II, optical and Auger spectra, discrepancies anal. 79−93944
Xe II, radiative lifetimes, beam-foil spectroscopy 80−18825
Xe II, transition probabilities for 5p^{4}6p to 5p^{4}6s array 77−436
Xe II 5s5p^6 $^2S_{1/2}$ state, lifetime meas. 79−13670
Xe III, 5s^{2}5p^3(^{4}S)nl levels, ionis. pot., from spectral data 80−47920
Xe IV laser excited by long current pulse discharge, double-pulsed output 80−37993
Xe, in gas discharge, collisional excitation, radiation lifetimes, macroscopic alignment obs. 80−33734
xenon continued
Xe in inert gases at high press., extravalence excitation solvent perturbation 77−75099
Xe, plasma, optical props., wall erosion products effects calcs. 78−47164
Xe prod. cross sections with protons of 320-590 MeV, nuclear medicine appl. 80−36133
Xe VI, emission spectral lines, classification 80−95563
Xe VII, VUV line classifications and energy levels in triplet system 80−37763
Xe VIII, beam-foil lifetime meas. using ANDC anal. for reson. doublet 79−93964
Xe VIII, beam-foil lifetime meas., cascading problem 80−14249
Xe VIII, one-electron spectrum in theta pinch discharge, line identification 80−32640
Xe^-, electron capture expts. to search for long lived states 79−72410
Xe^+, 5p^{4}5d^{4}D$_{7/2}$ and 5p^{4}6p^{4}P$^0_{5/2}$ levels, HFS, ion-beam laser fluoresc. 77−75319
Xe^+, absolute electron impact ionisation cross section 80−83496
Xe^+, beam metastable fraction determ., by W surface impact, secondary electron obs. 79−28873
Xe^+, metastable, electron impact cross section, laser fluoresc. 77−3465
Xe^+, symmetric charge transfer reaction cross section, selected kinetic energies 77−16813
Xe^+, UPS by threshold photoelectron spectrosc. by electron attachment method 79−89708
Xe^+, Xe_2^+, $^2P_{1/2}$ and $^2P_{3/2}$ states, mobilities in Xe, spin state depend. 77−3913
Xe^{2+}, beam metastable fraction determ., by W surface impact, secondary electron obs. 79−28873
Xe^{2+}, energy level radiative lifetimes using 1-5 MeV ions 80−47947
Xe^{2+}, mobility in He gas, drift-tube meas. 78−66657
Xe^{2+}, mobility in parent gas 79−7439
Xe^{24+}, impact on highly-ionised Ne target, selective target electron capture effects 80−14202
Xe^{3+}, molecular electron impact ionisation 80−102582
Xe^{4+}, molecular electron impact ionisation 80−102582
Xe^{5+}, molecular electron impact ionisation 80−102582
Xe: ^{57}Co, solid, ion implantation for rare gas matrix isolation, Mossbauer spectroscopy study 80−54271
Xe:^{138}Ba, 6$^+$ state, nucl. g-factor and nucl. spin relax. in gas phase 77−22884
Xe:He binary gas mixture convective instabilities in closed vertical cylinder heated from below 79−72880
Xe:methane, impurity rotational states, inelastic neutron scatt. study 79−51020
Xe:N_2O, photoluminesc. from XeO (^{1}D) excimers 78−68544
Xe-^{3}He plasma, plasma parameters determ. 80−54047
Xe-Ar, 3547 to 1182 Å conversion efficiency limited by Kerr-induced dispersion 78−37940
Xe-Ar, mol. interactions, thermodynamic props., mol. dynamics calcs. 77−61044
Xe-Br_2 discharge, atomic state density determ. 79−36573
Xe-Br_2(Cl_2)(HCl) mixtures, low-press. excimer form. and quenching by e-beam excitation 79−50071
Xe-Cl_2(Br_2)(I_2), UV transient absorption following flash photolysis 79−61879
Xe-Cs^+, ion mobility and interaction pot., drift tube meas. at 300K 78−59537
Xe-D plasma, shock-wave struct., heavy doping effects *(Russian)* 77−11343
Xe-F two module discharge laser, gain and temporal characts. 80−87385
Xe-Freon, saturation curve 1 to 8 atm., for ionography ionisation chambers 77−12997
Xe-He, 3.51 μm laser amplifiers, spectral narrowing and saturation induced rebroadening optical heterodyne obs. 80−63976
Xe-He source, intensity fluctuations of amplified spontaneous emission at 3.51 μm 80−32957
Xe-He-I_2(anthracene), gaseous mixture with one low conc. component, thermal diffusion calcs. 77−19661
Xe-He(Ne), gas mixture, element and isotope separation in impulse plasma centrifuge *(Russian)* 80−38725
Xe-I dating of silicate and troilite in Fe meteorites group IAB 80−17554
Xe-I_2 mixtures, electron beam excitation, XeI* emission spectrum 77−6843
Xe-induced flux oscillations in PBHTR *(German)* 78−82430
Xe-inert gas mixtures, far UV spectra, press. (temp.) depends., interaction consts. 77−61698
Xe-Kr, gas, diffusion coeffs. meas., 350-1200K 80−14869
Xe-Kr binary mixture, expt. determ. of temp. depend. of thermal diffusion factors *(Russian)* 79−60095
Xe-Kr gas mixture, vapour-liq. equilib. data *(German)* 77−84915
Xe-Kr mixtures for gas proportional scintillation counters 77−83464
Xe-Kr-Ar mixtures, VUV continuous spectrum prod. in low volt. lamp *(Russian)* 78−75451
Xe-Kr(Ar), UV absorption spectra, induced lines and line-shift meas. *(French)* 77−61697
Xe-like ions, 3d photoabsorpt. spectra, continuum and discrete states 79−81176
Xe-MF_6, M=W, Mo, U, Re, Ir, charge transfer interactions, VUV and IR obs. 78−50664
Xe-methane, mol. relax., optoacoustic reson. meas. 80−27351
Xe-Mg discharge and MgXe excimer band, emission intensities and excited-state densities meas. 80−92413
Xe-Mg plasma, near reson. charge exchange spectra *(German)* 77−31425
Xe-N_2, afterglow, 6s$_{12}$ metastable atom density decay rate 78−63612
Xe-Ne, equilibrium of coexisting phases 80−87197
Xe-Ne, interatomic pots., Ne adatom on Xe-plated graphite 78−18904
Xe-Ne-He hollow cathode discharge, laser oscill. at 5314 Å Xe II line 79−3679
Xe-Xe(Kr), glory structure in total cross section, crossed supersonic atomic beam, n(x)-6 potential 80−48060
Xe+ inert gas, Xe three level system, collisional transfers, disalignment cross section 80−53098
Xe+^{4}He^{2+}, optical transition excitation function and cross sections 80−63787
Xe+^{75}As, slowing down of atoms/ions with KE≤5 eV by inert gases 79−31650
Xe+^{75}As^{n+}, slowing down of atoms/ions with KE≤5 eV by inert gases 79−31650

xenon continued
Xe+acetylene, vibr. relax. study using laser-induced fluoresc. 80−74219
Xe+$Ar^+(Ar^{2+})(Ne^+)(Ne^{2+})$, thermal energy charge transfer reaction rates, mass spectrometric obs. 78−61000
Xe+$Ar^{2+}(Ne^{2+})$, single electron capture excitation, photon emission, VUV spectroscopy 80−58379
Xe+Ar^{6+}, collisional excitation, excitation cross sections 79−98209
Xe+Ar^{x+}, multiple scatt., combined ang. and lateral spread 78−46441
Xe+$Ar^{x+}(Cl^{x+})$, vacancy sharing between K and L shells in 3dσ mol. orbital 79−22807
Xe+Ar(He)(Ne)(Kr), thermal cond., 800 to 2000K from Wassiljewa's expression 79−27736
Xe+Ar(Kr), collision induced microwave absorpt. spectra 80−74216
Xe+Ar(Kr), total scatt. cross-sections, glory undulations 77−10732
Xe+Au, meas. of shape and absolute value of 1sσ excitation probability 79−13816
Xe+Bi, Bi Kα X-ray lines, Doppler broadening 78−62759
Xe+$Br_2(CCl_4)$, excitation functions and rotational polarisation, chemiluminesc., crossed beam study 80−76491
Xe+$Br_2 \rightarrow XeBr^* + Br$, rot. polaris. in chemiluminesc. 79−8432
Xe+C_2H_4 liquid mixtures, intermol. forces effect on phase diagram and excess props., perturbation theory 80−39287
Xe+CHF_3, vibr. relax. times at 298K 77−525
Xe+CO, intermol. pot. energy surfaces from electron gas model, ang., distance, and vibr. depend. 79−3520
Xe+CO_2 (methane), ^{13}C-mag. shielding density depend. 78−9173
Xe+$CO(N_2)$, ^{129}Xe chem. shielding, second virial coeff. 78−66563
Xe+Ca collision-induced dipole transition due to long range interaction, absorpt. obs. 80−63779
Xe+Cl, elastic scatt. for interaction pot., $Cl(^2P)+Xe(^1S)$ 79−27059
Xe+Cl_2, classical trajectory calcs., energy threshold for collision induced dissoc. determ., 80−95709
Xe+$Cl_2(F_2)$, XeCl(XeF) form., relax. and quenching 80−81314
Xe+Cl^-, elastic differential cross-section, 250-500 eV, well depth of $XeCl^-$ 79−86027
Xe+$Cl^{4+}(I^{5+})$, 20 MeV, electron loss cross sections, pot. model data anal. 79−27082
Xe+ClF, thermal and photochem. reactions investig. 80−61117
Xe+Cl(F), coupled channel study, rel. to elastic approx. 79−81255
Xe+Cs, Cs spectral line profile and absorpt. transitions 80−47944
Xe+Cs, shift, halfwidth, satellite and absorpt line in square-well pot. 80−42993
Xe+CsF_3 sudden, body-fixed and semiclassical approx. calcs. 78−42164
Xe+Cu^{q+}, ($16 \leq q \leq 23$), 1.4 MeV/amu, X-ray emission, charge state dependence 78−37713
Xe+D^+, double charge exchange to produce D^- *(French)* 79−94080
Xe+F, collision in laser field, ang. momentum anal., quantum mech. theory 78−74733
Xe+F_2, collision induced photoabsorpt. indicating $Xe+F_2+H\nu \rightarrow XeF^*+F$ 78−27786
Xe+F_2, transient species, matrix isolation spectra 78−48635
Xe+F^-, elastic differential cross-section, 250-500 eV, well depth of XeF^- 79−86027
Xe+$F(^2P_{1/2})$, nonadiabatic collision processes, electronic degrees of freedom, classical model 79−64062
Xe+Fe^{4+}, 20 MeV, gaseous targets, electron loss, charge state yields 79−54957
Xe+H, 20-500 eV, ion pair and free electron production, integral cross sections 78−46437
Xe+H, low energy elastic scatt. cross section MCSCF calc., van der Waals forces 78−70897
Xe+H, simultaneous ionisation investig. 80−32815
Xe+H_2 79−98211
Xe+H^-, 1 to 5 keV, production cross sections for 3d,3s,4s,5s states of H 78−33603
Xe+H^+, electron capture, 4-20 keV, production of highly excited H atom 79−54963
Xe+H^+, electron capture, charge-state distrib. 80−32814
Xe+H^+, electron capture cross sections 79−86061
Xe+H^+, M-subshell ionisation cross section, binary encounter approx. 78−62890
Xe+H^+ charge exchange, H spin polarisation 77−61688
Xe+H^+ ionisation, induced L-shell alignment 80−32813
Xe+HCl, infrared line shape, rotational lines, influence of collision duration 80−43110
Xe+HCl, spectral line shift of vibr.-rot. lines. press. shift 79−18237
Xe+HCl(HBr), liquid mixtures, intermol. forces effect on phase diagram and excess props., perturbation theory 80−39287
Xe+H(D), free electron production, integral cross-sections determ. 79−89754
Xe+$H(H_2)$, orbiting resons., van der Waals pots., beam scatt. obs. 79−89739
Xe+H(2S), metastable atom total quenching 77−46628
Xe+He, 2^1S and 2^3S assoc. and Penning ionisation cross sections vel. depend. 79−3551
Xe+He, saturated absorpt. of 3.51 μm line, vel. changing collisions by line width 78−86819
Xe+He(Ne)(Ar)(Kr), binary mixture viscosity and diffusion coeffs. 78−38443
Xe+He($2^1S,2^3S$), Van der Waals forces, one-electron model pot. calcs. 80−14094
Xe+ion ($1 \leq Z_1 \leq 90$), 2.5-400 keV, 1-6°, effective interat. pots. 80−23492
Xe+K, K 5^2P level broadening and collisional relax., quantal, semiclassical and expt. comparison 80−18903
Xe+K, photon emission polarisation anal., coincidence studies 80−5614
Xe+Kr, excitation transferred populations, absorpt. profile analysis 78−74748
Xe+$Li^*(2^2P_J)$, collision induced fine struct. transition rate coefficients determ. 80−74220
Xe+$NH_3(H_2S)(SO_2)(HCl)$, ionis. cross sections calc. 77−68103
Xe+NO, angle depend. intermolecular pot., crossed beams study 80−9682
Xe+Na, 3^3P-3^2D line broadening obs. 80−78684
Xe+Na, excimer bands, multiperturber interactions 78−66497
Xe+Na, non-Lorentzian spectral line shape 80−106297
Xe+Na, reson. line broadening, press. depend. 78−66596
Xe+Na_2, rot. energy transfer, scaling law 78−90272
Xe+Na_2, rot. inelastic collision, rate correls., scaling theory 79−36736
Xe+Na_2*, rot. energy transfer, level-to-level dynamics, laser fluoresc. obs. 79−64029
xenon continued
Xe+Na_2*, rot. energy transfer, vel. depend. 80−95715
Xe+Ne, elastic scatt. absolute total cross section, long range interaction 78−58768
Xe+Ne, fluoresc. spectra, mol. bands, 0.1 to 6 atm., 3000-8200 Å 79−3394
Xe+Ne_2 quenching of excited $Xe^*(^3P_2, ^3P_1, ^1P_1)$ states 80−63578
Xe+Ne^{2+}, electron capture collisions, 15 to 50 keV, excitation 80−102566
Xe+Ne*, chemiionis. in metastable state collisions 79−68306
Xe+Ne*, quenching rate const. for metastable $Ne(^3P_2)$, flowing afterglow 78−46295
Xe+Nx_2 rate consts., energy corrected scaling laws 80−69225
Xe+O, magnetically selected $O(^3P)$ state scatt. 80−99543
Xe+O_3, collisional energy transfer in unimol. reaction, classical trajectory calcs. 78−62882
Xe+$O^{n+}(Xe^{n+})(Pb^{n+})$, 50 keV, multiple scatt., target at.+energetic ion spatial correlation influence 79−27062
Xe+$O(^1D)$, deactivation rate consts., 110-330K 78−88628
Xe+$O(^1D)$, inelastic collisions, spin-orbit coupling 80−5605
Xe+Pb, 4.6 MeV/amu, 1 sσ vacancy production, impact parameter depend. 79−72393
Xe+Rb(Cs), metal atom spectral line breadth and shift, Van der Waals pot. calc. 78−90126
Xe+S, collision-induced emission of $S(^1S)$, 232 and 425K 79−81264
Xe+S_2, fluoresc. quenching and lifetimes of S_2 78−46386
Xe+target atom, 326-470 MeV, K-vacancy cross sections, target depend. 77−19026
Xe+TlF(Tl_2F_2), collision-induced ion-pair formation 78−17749
Xe+Xe, near threshold collision, UV emission 79−54799
Xe+Xe, potential well depth estimation method 79−86034
Xe+Xe, relativistic effects in variable-screening model 77−14516
Xe+Xe_2, Thomas-Fermi-Dirac interaction pots. 77−75253
Xe+Xe^+, 0.3-1.2 MeV, multiple N- and M-shell excitation, inelastic energy loss meas. 79−852
Xe+Xe^+, differential cross section, pot. curve fitting reson. electron exchange 77−58118
Xe+Xe^+, XeI reson. line excitation 80−87220
Xe+Xe^{10+} depend. of charge transfer on ionisation pot. of atoms 79−64096
Xe+Xe^{2+}, charge transfer from ground and metastable states 79−31677
Xe+XeF*, quenching rates for XeF in (B) state 78−58730
Xe+XeF*+F_2 temp. dependent quenching rate constants 80−63701
Xe+Xe(6s'(1/2)), (6p(1/2)), energy transfer, rate coeffs. 78−33573
$Xe^+ + 2Xe \rightarrow Xe_2^+ + Xe$, gas phase reaction rate const. calc. 78−92457
Xe^++Ag, quasimolecular L and Ag L X-ray excitation thresholds, electron correl., calc. and expt. 78−78793
Xe^++Ar, $XeAr^+$ form., dissoc. energy, reaction equilib. and rate consts. 80−61071
$Xe^+ + Cl^- +$Ne, three body ion-ion recombination probability, Monte Carlo simulation 80−85160
Xe^++Cs, total charge-transfer cross-section meas. 77−50527
Xe^++ethylene (haloethylenes), 2-stage ion beam mass spectrometric obs. 77−9061
Xe^++molecules, $^2P_{3/2}(^2P_{1/2})$ doublet ground state reactions at 300K 80−108702
$Xe^+ + NF_3$ reaction, XeF^+ form., $Xe^+(^2P_{1/2})$ radiative deactivation 78−27737
$Xe^+ + O_2 \rightarrow O_2^+ + Xe$, $O_2^+ + Xe \rightarrow Xe^+ + O_2$, charge transfer, photoionisation mass spectra 77−16793
Xe^++Xe, quasi-resonant charge transfer at thermal energies 80−48082
Xe^++Xe, symmetric charge exchange, below 1 keV, cross sections calcs. 77−532
Xe^++Xe, XeI reson. line excitation 80−87220
Xe^++Xe collisions, Auger electron ionisation, inelastic energy loss meas., multiple inner shell excitation 77−19055
$Xe^+ + Xe^+$, charge transfer and ionisation Xe^{2+} prod. 80−91659
Xe^++fluoromethanes, thermal energy charge transfer reactions mechanism 77−63889
Xe^{10+}+He(Ne)(Ar)(Kr)(Xe)(Cd)(Na)(Cs), depend. of charge transfer on ionisation pot. 79−64096
Xe^{2+}+Ar(Xe)$(H_2)(N_2)(O_2)(CO_2)$, charge transfer from ground and metastable states 79−31677
Xe^{2+}+$H_2(N_2)(O_2)$ (inert gas), charge transfer reaction rate consts. 80−7779
Xe^{2+}+Xe, radiative charge transfer coeffs. 79−7010
Xe^{2+}+Xe, symm. reson. double charge transfer, 0.04-20 eV 78−66657
Xe^{24+}+Ne, highly charged very slow Ne recoil ions, K X-ray transition 80−91649
Xe^{31+}+Ne, 200 MeV collision, Auger emission 77−57952
Xe^{n+}+gas target, 50 keV, multiple scatt., target at.+energetic ion spatial correlation influence 79−27062
Xe^{n+}+H, (H_2), electron capture by heavy multicharged ions at low velocities total cross sections meas. 80−99548
Xe^{n+}+Xe, electron transfer cross-sections, 15 keV to 1.6 MeV 79−59557
Xe^{x+}+Hg, single and multiple collisions, charact. and quasimolecular X-rays 77−83713
Xe_2 coaxial-diode tunable vacuum UV excimer laser systems 77−54738
Xe_2, collision-induced Raman spectra, absolute cross sections 78−46351
Xe_2, dispersion damping functions and interaction energy calcs. 80−78673
Xe_2, e-beam excited, 193 nm absorpt. studies 80−43323
Xe_2, effective core pot., Hartree-Fock calc., relativistic and nonrelativistic effects 78−46281
Xe_2, electron beam excited, 193 nm absorpt. meas. rel. to 172 nm laser pulse termination 80−28200
Xe_2, electron impact ionisation, relative cross-sections, mass spectrometric meas. 79−86078
Xe_2, electron-beam pumped, visible absorpt. rel. to laser development 79−59671
Xe_2, excimer laser action in coaxial field emission diode, comparison with Ar_2, Kr_2 80−28201
Xe_2 excimer laser pulse temporal evolution, cavity mirror depend. 79−76732
Xe_2 excimer lasers, review *(Japanese)* 78−33723
Xe_2, fluoresc. decay of O_u^+ and 1_u states, rad. decay consts. 79−86009
Xe_2, large-scale laser, gas purity 78−87063
Xe_2, laser performance for atm. press. and microsecond electron beam excitation 80−28199

xenon continued
Xe_2, near IR absorpt. spectra 78−66547
Xe_2, performance as photolytic driver at low electron beam excitation rates 80−32963
Xe_2, population inversion in high press. short discharge 77−71974
Xe_2, time and energy resolved fluorescence, radiative lifetime, collisional mixing, pulsed synchrotron radiation obs. 79−98136
Xe_2, VUV radn. emission, radiative lifetimes 79−27089
Xe_2, van der Waals mol., photoionisation 77−18991
Xe_2, van der Waals mol., photoelectron spectra 78−66599
Xe_2, vibr. level spacings calc. from Lennard-Jones pot. 77−42369
Xe_2^*, $A^2\Sigma_{1/2u}^+ \rightarrow D^2\Sigma_{1/2g}^+$ system, theoretical absorption spectrum 80−32734
Xe_2^+, dimer ions, electronic struct., chem. binding 79−31376
Xe_2^+, dissoc. recomb. in afterglow, rate coeff., excited state prod. 77−46647
Xe_2^+, effective core pot., Hartree-Fock calc., relativistic and nonrelativistic effects 78−46281
Xe_2^+, electronic states, pot. curves, with/without spin-orbit interaction 78−33443
Xe_2^+, electronic struct., pot. energy curves, spectroscopic consts. 79−18114
Xe_2^+ excimer form. in pulsed discharge, visible emission obs. 80−38754
Xe_2^+, near UV absorption spectra, config. interaction methods 78−17680
Xe_2^+, photodissoc. cross sections at 3.0 and 3.5 eV 78−62861
Xe_2^+, photodissoc. cross-section, 6200-8600 Å 78−78761
Xe_2^+, photodissociation cross sections, 3500-5400 Å 79−81243
XeF*(B), nuclear pumped laser, buffer effects 80−37617
XeI, transition probabilities of optical lines 79−89626
XeI*, emission spectrum, from $Xe-I_2$ 77−6843
$Xe^+(^2P)$+Ca(Sr), collisional quenching of metastable states, excitation transfer cross sections 78−66653
$Xe(^3P_{0,2})+Br_2 \rightarrow Xe^*+Br$, excitation function 78−40028
$Xe(^3P_2)$, quenching mechanisms and rate consts. 79−13801
$Xe(^3P_2)$+F donor reagent, quenching, excimer form. 79−63953
$Xe(^3P_2)$+fluorine containing molecules, quenching rate consts., XeF* formation branching ratios 77−9072
$Xe(^3P_2)+XeF_2 \rightarrow XeF^*$, mechanisms 77−30897
$Xe(^1S_0)+HF(^1\Sigma^+)$, expt. and computational study, 0.044 and 0.153 eV 79−89748
Xe(XeNe)(XeAr), obs. in Xe-rare gas far UV spectra, press. (temp.) depends, interaction consts. 77−61698
$Xe^{2+}(Xe^{3+})(Xe^{4+})(Xe^{5+})$, molecular electron impact ionisation 80−102582
Xe_2(−Kr,He), time-resolved excitation spectra, 1500 Å region, fluoresc. lifetime 77−75195
^{A}Xe, A=124, 126, 128, 129, appl. for PWR gas tagging 79−59222
^{A}Xe, A=133,135, interference with low-energy meas. systems 80−89872
^{122}Xe-^{122}I short-lived positron emitter generator 79−100740
^{123}Xe production by 1 GeV proton spallation on Cs, Ba, La 79−63676
^{125}Xe production by 1 GeV proton spallation on Cs, Ba, La 79−63676
^{127}Xe, health physics, dose calcs. 80−98142
^{127}Xe, production in $^{127}I(d,2N)^{127}Xe$ 79−79651
^{127}Xe whole-body retention for dosimetry calcs. 77−60257
^{129}Xe and ^{131}Xe, HFS of 6p, 7p, 4f and 5f levels *(French)* 79−68211
^{129}Xe, chem. shift in CH_4, CF_6 and SiF_4, chem. shielding 77−6707
^{129}Xe, chem. shift in NO gas, chem. shielding 77−6706
^{129}Xe, excesses in Hawaii lavas olivine phenocrysts and xenolithic dunites 79−34814
^{129}Xe, in meteorites, rel. to extinct radioactivities and presolar grains 77−49342
^{129}Xe, in mineral grains from Allende inclusions, chronological information 80−67675
$^{129}Xe^+$, hyperfine struct., ion-beam mag reson., laser induced fluoresc. for signal detect and state selection 78−41986
^{129}Xe+nonspherical molecule, interaction pots., effect on mag. shielding, NMR meas. 77−71816
^{131}Xe, KLM- and KLN-Auger transitions 77−18884
^{131}Xe+Rb, spin-exchange cross section, ^{131}Xe nucl. spin relax. obs. 80−37868
^{131}Xe*, hyperfine struct., ion-beam mag reson., laser induced fluoresc. for signal detect and state selection 78−41986
^{133}Xe air contamination, meas. technique 80−41255
^{133}Xe, atmos. separation technique, preliminary results *(German)* 78−16222
^{133}Xe charcoal traps, simple leak tests, nuclear medicine appl. 80−104734
^{133}Xe clearance, meas. of pig cerebral blood flow 80−94421
^{133}Xe clearance for cerebral regional blood flow meas. 79−83912
^{133}Xe, diffusion behaviour in SiC, 1650 to 1850°C 78−79814
^{133}Xe diffusion through frog skin, toad bladder and water boundary layer 77−66803
^{133}Xe, energy spectra and spectral resolution in Xe-filled multiwire chamber 79−49901
^{133}Xe in a plastic catheter, diffusion dynamics obs. 80−79973
^{133}Xe inhalation technique in stroke management, computerised system 79−79626
^{133}Xe, muscular hyperemia study technique 79−5351
^{133}Xe, myocardial blood flow studies, theoretical, technical and practical aspects 80−94355
^{133}Xe, nuclear moments and optical isotope shift 78−33118
^{133}Xe, probability distrib. for release in PWR steam generator tube rupture 80−13668
^{133}Xe, quantitative assessment of ventilation-perfusion mismatch in the lung 79−16279
^{133}Xe radio-spirometric measuring system for regional respiration function testing 77−90889
^{133}Xe retention in hepatic steatosis rel. to biopsy 80−17069
^{133}Xe, simple method of air monitoring 79−83949
^{133}Xe solubility coefficients in water, saline, dog blood and organs 80−56331
^{133}Xe storage and dispensing device for nuclear medicine *(Czech)* 79−43986
^{133}Xe trapping and re-use system for nucl. medicine 78−28051
^{133}Xe, use in quantitative meas. of skin perfusion 80−81707
^{133}Xe washout method for meas. of bone blood flow and obs. 80−72288
^{133}Xe washout rel. to single-breath imaging for ventilation abnormalities detect. 80−41183
^{133}Xe waste storage and retrieval, clinical use 77−86649

xenon continued
$^{133}Xe/^{133}Cs$, implanted in various hosts, isomer shift values, Mossbauer spectra 80−7240
^{135}Xe, determ. of fission gas degassing constant from liquid Na to cover gas 79−41009
^{135}Xe isotopes, production by ^{135}I decay in liq. Na in fission reactor, degassing behaviour 77−34410
^{136}Xe +Au(Pb)(Bi)(Th), 625 MeV, probability of forming 1sσ vacancies 78−25681
^{136}Xe $7p[3/2]_1$ level, cascade alignment in discharge 80−44057
^{136}Xe ion+target collisions, K-X-ray yields, 1sσ excitation 77−19051
^{136}Xe ion+target collisions, X-ray yields, K-L level matching 77−19052
^{136}Xe ion+target collisions, K-X-ray yields, K-vacancy sharing 77−23548
^{136}Xe ion+target collisions, K-X-ray yields, 2pσ excitation 77−23549
^{136}Xe laser amplifier, pressure shifts of 3.51 μm line 79−76669
$^{136}Xe+^{238}U$, nuclear Coulomb excitation, inner shell ionisation and internal conversion, quasimol. formation 78−94026
Xe*+Xe, $^3P_2$ state, metastability-exchange and depolarisation, press. broadening of mag. reson. curves 77−71853
Xe_2*, form. and UV fluoresc. under monochromatic excitation and collision processes 78−9237
Xe_2*, laser, electron beam excitation 77−711
Xe_2*, synchrotron radiation excited, time resolved spectroscopy 80−69092
Xe_2*, Xe_2^+, Xe_2, pot. energy curves, relativistic ab initio effective core pots. 78−86800
$^{131}_{54}$Xe, K-Auger transitions 77−18883
$Xe(6s,^3P_2)+Cl_2(PCl_3)(CCl_4)(COCl_2)$, vibr. energy disposal from XCl* spectrum 79−100345
$Xe(6s,^3P_2)$+RCl, reactive quenching, XCl* emission spectrum obs. 79−100344
$Xe^+(7s^2P_{1/2,3/2})$, charge exchange excitation in Ne-Xe glow discharge 80−38857
Xe(nf)+NH_3, at. Rydberg state further excitation by rot. transfer, field ionis. obs. 78−58795
Xe(nf)+SF_6, l-changing collisions obs. 80−91633
Xe(nf Rydberg state)+NH_3, n- and l-changing and ionising collisions 80−58360
Ze+Na, excited state, collisional depopulation cross-sections meas. 79−86057

xenon compounds
chemical and isomer shifts, electron valence struct. *(Russian)* 80−53056
hydrate, reorientation and diffusion of H_2O, PMR and dielectric relax. 77−36142
ArXe, continuous VUV emission spectrum 80−43066
ArXeF*, gain meas. at 4416 Å 78−50758
CsXe excimer, laser-excited fluoresc. in Cs-Xe mixture, pumping, level scheme 78−86909
K(5S)Xe, K(5S)Kr, excimer, visible emission band, exptl. results relative to theory 78−82779
KrX, (X=He, Ne, Ar, Xe), VUV absorpt., van der Waals mols. props. 78−13513
Na(4S)Xe, Na(4S)Kr, excimer, visible emission band, exptl. results relative to theory 78−82779
Xe-Ar system, band formation exam. by photoelectron spectroscopy 77−66116
$XeAr^+$, dissoc. energy, reaction equilib. and rate consts. 80−61071
XeAr(XeKr) photoionisation spectra of ground and excited states 78−5297
XeBr, B and C states, energy ordering from temp. depend. of emission spectra 80−78837
XeBr electric discharge pumped laser *(Chinese)* 80−102701
XeBr, emission and form. kinetics, sequential two-photon absorpt. expt. 80−32767
XeBr, high-energy lasing in elec. discharge 78−55340
XeBr laser, electron beam excited, experimental study 79−98347
XeBr laser, energy decrease mechanism 80−28243
XeBr, matrix isolated, absorpt. and emission spectra 77−14446
XeBr, UV bound-free emission after electron excitation 77−27279
XeCl 80−53323
XeCl avalanche discharge laser, D and B state coupling, population depletion 80−28214
XeCl, B and C states, energy ordering from temp. depend. of emission spectra 80−78837
XeCl, B-X and D-X band systems, vibr. anal. 79−59482
XeCl discharge, KrF laser induced preionization 80−84020
XeCl discharge laser, energy characts. 80−48228
XeCl effective laser performance with combined pumping, discharge stability by short electron beam 79−94250
XeCl, efficient laser output at 308 nm, electron-beam excitation 79−59678
XeCl, electric discharge excimer laser with intense preionisation 80−63991
XeCl electroionisation laser, energetic, threshold and spectral characts. 80−99705
XeCl, electron-beam pumped excimer laser *(Japanese)* 79−64208
XeCl, energy curves and transition moments 80−28210
XeCl, excimer emission band at 235.5 nm 77−18935
XeCl excimer laser, efficient Raman conversion of radiation in Ba vapour 78−79069
XeCl excimer laser, electron beam controlled discharge, construction and operation 78−63125
XeCl excimer laser, electron-beam pumped, emission spectrum, saturation intensity, optical absorpt. 79−927
XeCl excimer laser, excited by discharge stabilised by electron beam 80−63992
XeCl excimer laser, high power, discharge pumped 78−55375
XeCl excimer laser, long-life operation 79−41366
XeCl excimer laser, using chlorinated hydrocarbons as Cl donors 78−79007
XeCl excimer laser radar, stratospheric O_3 layer meas. 79−16681
XeCl, excimer UV discharge laser, emission spectra 77−79809
XeCl, excimers and excimer lasers 80−48217
XeCl, form., relax. and quenching 80−81314
XeCl frequency-tuned laser, coherent tunable vacuum UV near H Ly-β transition 80−99798
XeCl high specific power long-pulse supersonic flow laser at 308 nm 80−48221
XeCl, high-energy subnanosecond pulse amplification 80−99770

xenon compounds continued
XeCl, in Ar, ESR spectrum at 4.2K 77−18947
XeCl, intense lasing with HCl halogen donor 78−90411
XeCl laser, B→X, form. and quenching kinetics 80−74341
XeCl laser, closed cycle characts. 80−33030
XeCl laser, closed cycle flow type, operating characts. 80−43349
XeCl laser, discharge excited, preionisation technique 80−23714
XeCl laser, discharge stabilisation with 50 nsec electron beam 80−23716
XeCl laser, efficient discharge pumping, 3080 Å emission 77−42524
XeCl laser, electron beam excitation *(Russian)* 78−22115
XeCl laser, electron beam, beam-stabilized discharge and fast discharge excitations 80−28204
XeCl laser, lifetime extension by H addition 80−91773
XeCl laser, pumping for dye lasers 79−59691
XeCl laser, transient optical absorpt. meas. 79−55115
XeCl laser, UV picosecond pulse amplification 80−74372
XeCl laser pulse backward Raman compression in Pb vapour 80−19068
XeCl lasing performance using Ar, Ne diluents 79−94212
XeCl, matrix isolated, absorpt. and emission spectra 77−14446
XeCl mini-laser operation at high repetition rate 80−74396
XeCl molecule excited by electron beam, stimulated emission obs. 80−32966
XeCl, relax. and quenching rate consts., emission spectra modelling 80−28211
XeCl, UV preionised discharge pumped laser, improved performance 78−37906
XeCl UV preionised simple compact laser, elec. and gain characts. 80−28206
$XeCl^-$, well depth of mol., $Xe+Cl^-$ elastic cross-section expt. 79−86027
XeCl+HCl (inert gas atom), ground state destruction, quenching rate consts. meas. 80−63758
$XeCl_2$, electronic structure, MSW-SCF-Xα method 80−78539
Xe_2Cl, triatomic excimer, transient gain meas. at 488.0, 497.6, 514.5 nm 80−58511
Xe_2Cl triatomic excimer laser in visible 80−64048
XeCl(B) formation in electron beam assisted Xe/HCl laser discharge 80−63988
XeCl(F), inert gas halide lasers, 60-ns electron beam excitation 80−74340
XeCl*, elec. discharge excimer lasers, stimulated emission 79−31884
XeCl* emission spectrum obs., in $Xe(6s,^3P_2)+RCl$ reactive quenching 79−100344
XeCl* excimer laser, electron-beam-excited discharge in Ar-Xe-CCl_4 79−18408
XeCl* spectra, for $Xe(6s,^3P_2)+RCl$ vibr. energy disposal assignment 79−100345
XeCl*+Kr, substitution efficiency during excitation in transverse AC electric discharge 80−50850
XeF, 1 μsec pulse lasing, cold cathode electron beam initiation 78−63079
XeF 2 kHz repetition rate laser action at 351, 353 nm 79−59714
XeF, 3500 Angstrom band, vibr. anal. 78−70843
XeF, (B,C) state prod. and kinetics, XeF_2 photolysis with VUV radiation 80−32975
XeF, B and C-state kinetics with self-sustained discharge pumping 80−28212
XeF, B- and C-state fluoresc. rel. to laser efficiency 79−41368
XeF, B-X transition vibr. anal., flash photolysis UV absorpt. spectroscopy 78−42088
XeF, broadband emission origin 80−38007
XeF, C-A blue-green band, gain meas. at 488 and 475.9 nm 79−45929
XeF, C-state radiative lifetime meas. 77−46598
XeF, covalent and ionic states, ab initio CI calcs. 78−78634
XeF, diffraction-limited laser, with negative branch unstable resonator 77−38937
XeF, direct pumping by electron beam pulses, gain and laser oscill. obs. in blue-green 80−102699
XeF, discharge excited laser operation at elevated temps., transitions, output power 80−43359
XeF discharge laser, gain and fluorescence meas. at high energy loading 77−79844
XeF discharge pumped laser at 490 nm 79−89893
XeF discharge-excited laser, high repetition rate operation with gas recycling 79−973
XeF, double discharge laser amplifier, small signal gain meas. 77−79807
XeF, double discharge laser, operating parameters, discharge characts. 77−88704
XeF, double pulse fast discharge driven laser, optimal timing and power enhancement 78−63132
XeF, effective core pot., Hartree-Fock calc., relativistic and nonrelativistic effects 78−46281
XeF, electric discharge pumped laser, model for UV preionisation 77−23658
XeF electric discharge laser, energy and spectral characts. changes on press. increase 79−64214
XeF electric discharge laser at 490 nm 79−89890
XeF, electric discharge excimer laser with intense preionisation 80−63991
XeF electroionisation laser, energetic, threshold and spectral characts. 80−99705
XeF, electron beam controlled Ne stabilised laser 79−972
XeF, electron beam pumped multiatmosphere laser, Ne diluent 77−88705
XeF, electron beam pumped laser, gain, fluoresc. and laser output at 351, 488 nm 80−28215
XeF electron beam pumped laser, energy, time and spectral characts. 80−38005
XeF, electron beam sustained discharge excitation, threshold power density meas. 78−63078
XeF, electron impact deexcitation, low energy cross-sections and rate consts. 80−1071
XeF, electron impact deexcitation cross sections and rate consts. calcs. 80−32848
XeF, electron quenching rate consts. meas. by fluoresc. anal., laser implications 80−32969
XeF electron-beam pumped laser at 486 nm 79−89892
XeF electron-beam-pumped laser, characts., 300-600K 80−78839
XeF, energy curves and transition moments 80−28210
XeF, energy ordering of excited states, rel. to fluoresc. and laser action 78−74887

xenon compounds continued
XeF excimer laser, electron beam controlled, output power, efficiency 78−82951
XeF excimer laser, excited by discharge stabilised by electron beam 80−63992
XeF excimer laser, high-repetition rate operation, gas recycling 77−58337
XeF excimer laser, providing high-power stimulated radiation in Ar and F lines 77−83858
XeF excimer laser, self-sustained discharge pumping 80−28219
XeF, excimer laser pumped dye laser *(Chinese)* 80−1234
XeF excimer lasers, review *(Japanese)* 78−33723
XeF, excimer UV discharge laser, emission spectra 77−79809
XeF, excimers, power superluminesc. in elec. discharge *(Russian)* 77−7621
XeF, form., relax. and quenching 80−81314
XeF, formation and quenching of electronic excited states 77−673
XeF, from photodissoc. of XeF_2, $B(1/2)$-$X^2\Sigma^+$ transition, stimulated emission 78−71097
XeF, ground state dissoc. vibr. equilibrium 80−9652
XeF, ground state kinetics, multilevel model of energy transfer 80−99707
XeF ground-state dynamics in laser discharge 79−18404
XeF high power lasers, const. E/N pumping 77−88711
XeF, high press. discharge, UV ps. pulse amplification 77−88768
XeF, high press. UV laser, electron beam excited *(Russian)* 77−14696
XeF, high pulse repetition freq. laser action, appl. of multiple-circuit pulse generator 78−94399
XeF, high repetition rate transverse flow laser 78−46620
XeF, high-intensity short pulse generation, oscillator-optical gate-amplifier system 80−38038
XeF high-power electron-beam pumped lasers, optical performance 78−46640
XeF high-pressure supersonic flow electronic transition laser, with pulsed blowdown and electron gun facility 79−59723
XeF, in Ar and Ne matrices, reson. fluoresc., ground $X^2\Sigma^+$ state pot. well 77−14482
XeF, kinetics simulation of high-power gas lasers 79−59676
XeF laser, 1 μs pulse production electron beam excitation 77−14692
XeF laser, active mode locking 77−23656
XeF laser, C-A blue-green, multipass amplification and tuning 80−43346
XeF laser, closed cycle characts. 80−33030
XeF laser, closed cycle flow type, operating characts. 80−43349
XeF laser, discharge-pumped, spectroscopic study at high resolution 78−37873
XeF laser, efficient operating conditions with electron beam stabilisation 80−38006
XeF, laser, efficient Raman conversion of output, 351 to 585 nm 77−58377
XeF laser, electron beam controlled discharge pumping 77−23657
XeF laser, electron beam stabilised discharge *(Russian)* 78−25894
XeF laser, electron beam excited, long pulse operation 78−50794
XeF laser, electron beam excitation, kinetics scheme 78−78999
XeF laser, electron beam, beam-stabilized discharge and fast discharge excitations 80−28204
XeF laser, electron beam excited, gain measurements using amplified spontaneous emission 80−37986
XeF laser, electron-beam sustained discharge excitation, threshold power density meas. 77−88699
XeF laser, excitation by microsecond electron beam 79−59686
XeF laser, excited states quenching of electron beam excited media 79−18406
XeF, laser, influence of diluent gas 78−9365
XeF, laser, injection locking, cross relax. rates 78−17909
XeF laser, nuclear pumping possibility 78−17916
XeF laser, optically excited by incoherent Xe_2* radiation, B→X band emission 78−87044
XeF laser, output control by injection locking 80−74405
XeF laser, photoionization-stabilised self-sustained, energy extraction efficiencies 79−41369
XeF laser, temp. depend. absorpt. processes in Ne-Xe-NF_3 mixtures 80−1188
XeF laser, transverse discharge in $Xe+He+NF_3$, time and energy characts. *(Russian)* 78−25861
XeF laser, UV preionised discharge pumped, 10 kHz repetition rate 80−33029
XeF, laser action on C→A transition, pumping mechanisms, kinetics and efficiencies 80−32967
XeF laser efficiency improvement at elevated temps. 79−45957
XeF, laser emission, ab initio config. interaction calcs. on electronic states 78−63083
XeF laser excited by proton beam, stimulated emission at 351, 353 nm 79−98344
XeF laser line, 353 nm, picosecond gain and saturation meas. 78−17910
XeF laser performance, ground state population effect 80−63987
XeF laser using Ar-Xe-NF_3 mixture, discharge stabilised by short-pulse electron beam 80−14358
XeF laser using XeF_2 photodissociation, fluoresc. and laser performance 80−32976
XeF laser wavelength transient absorpt. in electron beam excited inert gases 80−32644
XeF lasers, discharge and electron beam pumped, review 78−71083
XeF linac-excited gas mixture, UV fluoresc. meas. 80−28216
XeF, long pulse electron beam excited laser 79−940
XeF, long pulse UV laser emission in electron beam excited supersonic flow 78−66801
XeF, matrix-isolated, search for IR fundamental 77−58017
XeF molecule formed by XeF_2 photodissociation, laser action due to bound-free C(3/2)-A(3/2) transition 80−14334
XeF, photodissociation by Xe_2*, excimers inducing blue-green excimer lasing, laser spectra 79−68382
XeF, ps laser pulse amplifier 77−14736
XeF pumped Tm:$LiYF_4$, excimer excited storage laser 80−33003
XeF, relax. and quenching rate consts., emission spectra modelling 80−28211
XeF, scalable multiatmosphere high power laser 77−71995
XeF, self-sustained discharge laser, kinetic processes 78−74888
XeF, simple high-power TEA laser operating in UV 79−94251
XeF, spark-preionised large-vol. discharge laser 78−1218
XeF, spontaneous emission lifetime meas. of C→A band 79−31874

xenon compounds continued
XeF superradiance laser excited by electric discharge 77−19236
XeF, superradiant laser, gain saturation effects 78−66808
XeF, supersonic expansion jet, B←X system rot. and vibr. anal., isotope intervals, fluoresc. spectra 80−14174
XeF, transfer and quenching rate constants for (III, 1/2) and (II, 3/2) states 79−16003
XeF, transient species, matrix isolation spectra 78−48635
XeF, transverse-discharge laser, increased efficiency 79−72595
XeF, UV laser, longit. elec. discharge *(Russian)* 78−1220
XeF, UV preionized discharge pumped laser 77−10889
XeF waveguide laser operation on 351, 353 nm transitions 79−22942
XeF, X, B, and D-states, spectra, vibr. and rot. consts. 78−70844
XeF, $X^2\Sigma^+$, energy curve calcs. 77−10719
XeF^-, well depth of mol., Xe+F^- elastic cross section expt. 79−86027
XeF^+, selected valence-electron split-shell MO calc., ground state props. 79−22585
^{136}XeF in polycrystalline XeF_2 or XeF_4, ESR spectra, struct. and dynamic parameters of radical sites determ. 80−84652
XeF+He(Ne)(Xe)(F_2)(NF_3), radiative lifetime and collisional quenching kinetics 78−94289
XeF_2 chemisorption of Si surface, chemistry, XPS and Auger spectra 80−81358
XeF_2, dissociative electron attachment, rate const., flowing afterglow obs. 77−6946
XeF_2, dissociative electron attachment, 0-20 eV 79−72430
XeF_2, photodissoc. to XeF, stimulated emission 78−71097
XeF_2, photodissoc. yield in solid Xe and Kr, time-resolved photolum. excitation obs. 80−3372
XeF_2 photodissociation forming XeF, laser action due to bound-free C(3/2)-A(3/2) transition 80−14334
XeF_2 photodissociation for XeF laser 80−32976
XeF_2, photolysis, lifetime and collisional quenching meas. of XeF*(B) 78−33545
XeF_2 photolysis with VUV radiation, XeF (B,C) state prod. and kinetics 80−32975
XeF_2, pseudopotential SCF-MO studies, equilib. struct., stretch-stretch interaction force const. 80−95525
XeF_2, pure rot. Raman spectrum 78−94254
XeF_2, stereochem. of structs. and valence bonds 79−69066
XeF_2 vapour, etching of Si, adsorption/desorption process 79−43449
XeF_2→XeF*, vac.-UV photolysis, B→X fluoresc. and quenching 77−58061
XeF_2+Si, surface reaction, IR chemiluminesc. 79−43633
XeF_2+Si(SiO_2)(Si_3N_4), plasma etching, electron or ion bombardment, Ar^+ enhancement 79−82073
$2XeF_2+Si \rightarrow SiF_4+2Xe$, surface reaction, IR chemiluminesc. 79−83504
XeF_4, pseudopotential SCF-MO studies, equilib. struct., stretch-stretch interaction force const. 80−95525
XeF_4, stereochem. of structs. and valence bonds 79−69066
XeF_4, vibr. force consts. calc. 78−58655
XeF_5^+, pseudopot. SCF MO studies, steric aspects of struct. and force fields, Jahn-Teller effect 80−99444
XeF_6, energy levels, nonrigid mol. effects 78−41931
XeF_6 molecules with Jahn-Teller pseudo-effect, ang. depend. of inelastic scatt. of electrons 80−69246
XeF_6, monomeric charact., electron ionisation mass spectra 77−75322
XeF_6, pseudopot. SCF MO studies, steric aspects of struct. and force fields, Jahn-Teller effect 80−99444
XeF_6 seeded mol. beam, transverse ionisation, space charge, mass spectra and vel. 80−78725
XeF_6, UV absorpt. band shape 78−5289
$Xe_2F_3^+$, 6-electron 5-centre bonding units, increased valence theory calcs. 77−46500
XeF(B) nuclear pumping, candidate laser fusion driver 79−86171
XeF_2(C) state lifetime, quenching rate consts., photolysis in inert gas atmospheres 80−66816
XeF(Cl)(Br), discharge pumped multiwavelength lasers *(Chinese)* 80−102703
XeF(Cl)(Br) excimer lasers, lasing action *(Chinese)* 79−59682
XeF(Cl)(Br)(I), covalent and ionic states, spectroscopic props., ab initio CI calc. 78−90092
XeF* ($C_{3/2}$), radiative lifetime meas. 78−63087
XeF*, $B^2\Sigma^+$ and $C^2\Pi_{3/2}$ states, fluoresc. decay dynamics, collisional quenching and radiative lifetimes 80−58306
XeF*, broadband emission origin 80−28202
XeF*, elec. discharge excimer lasers, stimulated emission 79−31884
XeF*, electron impact excitation, temp. depend. quenching rate consts. 80−63701
XeF*, fluoresc. intensity, two- and three-body quenching by Ar, Xe 77−58053
XeF*, formation and quenching in Ne-Xe-F_2 laser mixtures 78−42324
XeF*, formation by XeF_2+Ar(Kr)(Xe) metastable states reaction, mechanisms 77−30897
XeF* gas-discharge excimer laser, kinetics 80−48226
XeF* laser mixture, Ne- and Ar-rich, absorption 78−63062
XeF* laser system, trimer form. rates 80−50831
XeF*, lifetime and collisional quenching meas., XeF_2 photolysis 78−33545
XeF* nuclear pumped laser obs. 80−63996
XeF*, optical excitation device 78−13629
XeF*, pressure depend. of C to B state ratios 79−24731
XeF*, waveguide laser excited by capacitively coupled discharge 78−94391
XeF*+F_2+Xe, temp. dependent quenching rate constants 80−63701
XeF*+He(Xe)(NF_3)(F_2), quenching rates for XeF in (B) state 78−58730
XeF*(C1/2), excited state radiative lifetime meas. 77−34671
XeH^+, pot. energy curves, VB calcs. 77−61688
XeHCl, microwave and RF spectra, mol. beam elec. reson. meas. 79−72302
XeI, B(1/2)-A(1/2) system, emission spectra 79−6934
XeI, UV bound-free emission after electron excitation 77−27279
Xe(II, IV, VI and VIII) compounds, Mossbauer study 79−65772
XeI*, production via laser absorpt. processes at 193 nm, quenching kinetics 80−91466
XeO, Ar-matrix-isolated, UV absorpt. spectra 77−3375
XeO, $d^1\Sigma^+ \rightarrow a^1\Sigma^+$($b^2\Pi$), green band emission spectroscopic anal., RKR pot. curves, bond lengths and dissoc. energies 79−41181
XeO, emission kinetics 77−34684
xenon compounds continued
XeO, excited state spectra, subpicosec. predissoc., solvation, in solid rare gas hosts 77−68050
XeO, laser, optical pumping, ^1S-^1D transition, 0.54 μm emission 77−667
XeO, lasing, low-lying electronic states, ab initio config. interaction calcs. 78−63084
XeO, low lying state characterisation 80−99543
XeO, luminesc. meas. of O(^1S) absolute quantum yield in photolysis of CO_2, N_2O 80−35561
XeO, photochem. laser performance, 0.54 μm stimulated emission 79−45938
XeO photochemical laser, energy characts., kinetic model of physicochem. processes 80−28228
XeO^+, $X^4\Sigma^-$ state, pot. energy curves and correl. effects, elastic scatt. cross sections 80−23502
XeO_3, stereochem. of structs. and valence bonds 79−69066
XeO_4, mol. vibrs. and reaction pathways, min. energy coords. and compliance consts. 77−57966
XeO_2F_2, mean amplitudes of vibr. and molar thermodynamic functions 78−17649
XeO_3F_2, mol. consts., general valence force field calcs. 78−21906
XeOH exciplex, UV emission 78−37653
XeO*, mol. laser emitting at green wavelengths, population inversion kinetics 77−23661
XeO* production through collisional electronic energy transfer from two-photon excited Xe atoms 78−62775
XeS, photoluminesc. in rare gas matrices 80−5568
XeX, (X=F,Cl,Br,I), Ar matrix isolated, MCD, low temp. depend., spectroscopic parameters calc. 77−38682
XeX, (X=He, Ne, Ar, Kr), VUV absorpt., van der Waals mols. props. 78−13513
^{A}Xe, A=129, 131, Mossbauer isomer shifts, book contrib. 79−87360
xeCl excimer laser, lasing action *(Chinese)* 79−55126

xerography *see electrophotography; reproduction (copying)*

xeroradiography *see electrophotography*

XPS *see X-ray photoelectron spectra*

Yang-Mills theory
0(4) eqns., soln. reln. to Einstein field eqns. 78−8521
β-function in noncovariant Yang Mills theory from perturbation theory 79−247
ζ-function regularisation of fluctuations around Yang-Mills pseudoparticle 78−16919
ν-dimensional Yang-Mills and (ν-1)-dimens. nonlinear σ-model connection, quark confinement, dual strings 80−90978
σ model representation as a spontaneous violation *(Russian)* 80−13220
σ-model supersymmetric dynamics on pre-QCD level with elementary quarks and composite gluons 80−82886
't Hooft's mag. monopole unicity 78−16908
't Hooft electromagnetic tensor for Higgs fields of arbitrary isospin 80−68364
't Hooft-Polyakov monopole interactions, Prasad-Sommerfield limit, Yang-Mills-Higgs system 79−251
Abelian field configurations, instability 80−344
allowed supersymmetric vacuums 78−4783
angular momentum in non-Abelian gauge field theory 77−71446
asymptotic behaviour of 't Hoofts mag. monopole 78−32974
asymptotic behaviour of classical Yang-Mills fields in Minkowsi space, Gribov ambiguities 78−93800
asymptotic freedom, vacuum polarisation of unstable mode 79−9278
asymptotic freedom in the infinite-momentum frame, SU(N) Yang-Mills theory renormalisation 80−22519
asymptotic scattering states of colored classical particles 80−397
asymptotic Yang-Mills pot., symmetry props. of multicharged instanton solns. 79−21946
asymptotically free models and the G_2-group 80−18072
asymptotically free models with Yang-Mills fields, symplectic groups framework 79−2940
asymptotically non-free Yang-Mills theory, IR divergences 80−37166
Atiyah-Singer index theorem, local version for vector fields 78−58128
axial anomalies and index theorems on open spaces 78−93821
axially symmetric multi-instanton solutions generated by conformal mappings in SU(2) Yang-Mills field 80−42337
Backlund transforms and symmetries of Yang eqns. 80−52393
bag and multimeron solutions of the classical Yang-Mills equation 80−4853
Belavin Yang-Mills pseudoparticle soln., metric representation, isotropic Universe relation 80−27404
bifurcation solutions of cylindrically symmetric Yang-Mills equations 80−99034
black holes as Yang-Mills field source 78−8280
bounded solutions 80−105764
BPST instanton uniqueness 78−12811
broken symmetry soln., Higgs fields and Einstein gravity action 80−101746
caloron importance in high-temp. Yang-Mills gas 80−95221
canonical, with invariant gauge families, renormalisation scheme 79−12944
canonical, with invariant gauge families 78−74140
canonical quantisation, interaction Lagrangian *(Chinese)* 79−21950
canonical Yang-Mills theory with invariant gauge families 78−74140
Cauchy problem for the Yang-Mills equations 80−13206
Chern classes, Pontrjagin forms and classification of gauge fields 79−67461
chiral SU(2) supergroup for Yang-Mills fields, Baker-Campbell-Hausdorff formula 79−49414
chromodynamics, SU(n), classical noncommuting quark source charges 78−78144
chronos principle and interactions of fields of spin 0 and 1 78−8286
classical, screening solns., state external source 78−62302
classical and prequantised mechanics without Lagrangians or Hamiltonians for relativistic particles 78−74126
classical eqns., singular pots. and analytic regularisation 80−334
classical Euclidean field configurations and charge confinement 78−54557
classical Euclidean Yang Mills theory, zero action complex solns. 78−62308
classical Euclidean Yang-Mills theory, self dual SU(2) solutions 79−2945
classical field classification using spinor methods 77−78990

Yang-Mills theory continued
classical field theory geometrisation, applied to Yang-Mills field theory 80−46841
classical gauge field theory eqns. with arbitrary value of topological charge 79−21954
classical particle in external Yang-Mills field and SU(2) coherent states 78−74150
classical particle in Yang-Mills field, eqns. of motion and general covariance 78−74125
classical point charges, interaction, rel. to quark confinement *(Russian)* 78−32995
classical pseudoparticle solutions in general relativity 78−89390
classical scalar and spinning particles interacting with external field 77−67557
classical second order Yang-Mills field eqns., twistor space formulation 78−86415
classical soln. to Yang-Mills gauge theory in colour meson model 78−45780
classical solution of Yang-Mills field eqns., asymptotic form 77−10181
classical solutions of SU(2) Yang-Mills theories, historical development and general introduction 79−93295
classical SU(2) gauge theory, exact multipseudoparticle solutions 77−22649
classical SU(2) Yang-Mills field, ignorable variables extraction from Hamiltonian 80−328
classical SU(2) Yang-Mills field eqns., periodic solns. in Minkowski space-time 80−4854
classical theory, glueball non-existence 77−74569
classical theory as chiral field on path, integrability 79−97492
classical Yang Mills field decay in 4-dimens. Minkowski space 79−35914
classical Yang Mills fields, cylindrical config., symmetrical props. 78−62309
classical Yang Mills potentials, massless charged scalar fields, stability 77−34089
classical Yang-Mills eqn., multiple meron solns. 78−32987
classical Yang-Mills eqns., multimeron solns., existence theorem 79−92960
classical Yang-Mills eqns., soln. method 80−77970
classical Yang-Mills equations, static spherically symm. solns., SU(2) gauge group 79−2914
classical Yang-Mills field equations, with static external sources 79−21930
classical Yang-Mills field of a quark source 78−78077
classical Yang-Mills fields in a Robertson-Walker universe 79−2692
classical Yang-Mills solns., W meson condensation, superdense matter composition symmetry 79−93292
classical Yang-Mills theory, local harmonicity of Wilson loop integral 79−75684
classical Yang-Mills theory, screening solns., state external source 78−62302
classification of SU(3) mag. monopole 78−364
classification of Yang-Mills fields, Lorentz invariant and gauge invariant methods 79−97495
closed string as source of Yang-Mills field, gluon gauge field vortex 78−41413
colour confining pot., upper bound, Yang-Mills theory and lattice QCD 79−2992
colour spin and path ordered phase factor, path integrals 80−4932
colour-screening by Yang-Mills instability 77−45951
coloured theory, string like phase 78−32990
configuration constraint 80−82903
confinement and the consistency of Yang-Mills theory 80−62852
confinement in Z_n lattice gauge theories implies confinement in SU(n) lattice Higgs theories 79−58930
conformal properties of fields 80−32024
conformally flat space-times of divergence free Riemann tensor 78−41220
conformally flat spaces and solutions to Yang-Mills equations 80−57481
conservation-law violation at high energy by anomalies 80−62855
conserved axial vector currents and self-forces 77−30264
conserved flux, elimination of colour charge from gauge field 78−89659
conserved quantities in classical theories 80−350
conversion of isospin degree of freedom into spin degree of freedom 78−89617
cosmic matter-antimatter asymmetry and gravitational force 80−90586
Coulomb gauge ambiguity, instanton solns. 78−8514
Coulomb gauge description of large Yang-Mills fields 78−54555
Coulomb gauge fixing degeneracy 79−30655
Coulomb guage vacua of (2+1) dimensionsl Yang-Mills theory 80−90997
Coulomb solution of Yang-Mills eqns. with external sources 80−27407
coupling of O(2) supergravity with vector multiplets, Yang Mills field appl. 78−33020
covariant canonical formulation of Yang-Mills theories, phys. S-matrix unitarity, phys. state subsidiary conditions 78−37141
covariant gravitational theory *(German)* 79−21615
covariant path integral formalism in presence of Gribov ambiguities 79−54261
covariant theory of gravitation, curvature quantities, Yang-Mills type field *(German)* 77−53816
CP^{n-1} model, embeddings of classical solns. of O(2p+1) nonlinear σ-models, instantons 80−86562
critical principal connections and gauge-invariance 79−6287
cut vertices and their renormalisation, generalisation of Wilson expt. 79−21929
cylindrically symmetric Yang-Mills eqns., some aspects of their solns. 79−35921
defect dynamics, field equations, four dimensional space-time setting 80−96521
dense and dilute instanton-anti-instanton pair configurations 80−52424
distorted gauge invariant theory, renormalisation props. 77−45967
double well oscillator, nonlinear contribs. to the partition function 79−12963
dual models, ambiguous relationship to Yang-Mills fields 79−49495
dual spinor model, low energy region, supersymm. Yang-Mills theory, supergravity theory 77−49923
dual strings, interaction, correspondence between gauge group and dual model 80−42432
dual-charges, self-dual Yang-Mills pseudoparticles *(Chinese)* 77−82684
Yang-Mills theory continued
duality equation, many-dimens. method based on inverse scatt. problem *(Russian)* 77−74600
duals of gauge field tensors, representations 79−89057
dynamical spontaneous symmetry breaking, in scalar electrodynamics and Yang-Mills fields, scalar particles 79−97536
dyon field, extended Yang-Mills formalism, Mandelstam's path depend. formalism 78−62288
dyon solns. and symmetry, elec. and mag. charge conservation 77−26183
dyon solns. for classical Yang-Mills field eqn. 78−54560
dyons, mag. charge and Pontryagin index equality in SU(2) 80−57562
dyons, spatial volume integral of Tr F(tilde) F, Yang-Mills theory 80−77943
Dyson equations, Ward identities, and the infrared behavior of Yang Mills theories 80−42353
effective Lagrangian for nonAbelian plane waves, one loop quantum correction 79−67472
effective potential in intense fields, gauge non-fixing calc. 80−52397
effective potentials in gauge field theories containing scalar bosons 78−21330
Einstein's matter free theory of gravit. construction using Yang Mills theories 78−70026
Einstein's nonsymmetric unified field theory extension, geom. props. 79−44833
Einstein field equations, covariant splitting, spherical symmetry models *(German)* 79−21616
Einstein-Maxwell and Einstein-Yang-Mills space-times, infinitesimal holonomy group structure 80−12976
Einstein-Yang-Mills equation, soln. for gravity coupled to non-Abelian plane waves 79−35602
Einstein-Yang-Mills equations, canonical connections on Riemannian symmetric spaces 80−95004
Einstein-Yang-Mills pseudoparticles and electric charge quantization of dyon black hole 79−12703
Einstein-Yang-Mills system, Feynman-quantised, null-gauge functional measures 79−12702
Einstein-Yang-Mills system in six dimensions, static solution 80−8883
Einstein-Yang-Mills theory, gauge theory and symmetry 77−22464
electric vortex lines from unstable Yang-Mills field mode 79−9291
elliptic function methods 80−4829
elliptic solns. of classical Yang-Mills theory 77−74586
embedding classical fields in QFT, electrodynamics, Yang-Mills theories, gravit. appls. 78−54223
embeddings of gauge groups in Yang-Mills theory, SU(3) case 78−93802
equations of motion finite range classical solns., confinement 80−57474
equivalence of vacuum Yang-Mills gravitation and vacuum Einstein gravitation 79−25924
Euclidean, four-dimens. SU(2) Yang-Mills theory, natural guage condition ambiguities 79−2934
Euclidean, multiply charged mag. monopoles, SU(3) pseudoparticles, gravitational pseudoparticles 77−45960
Euclidean, vanishing of energy-momentum tensor 80−77961
Euclidean eqns., self-dual solns. 79−26230
Euclidean functional determinant, bounds 80−32019
Euclidean lattice Yang-Mills theory in two spacetime dimensions *(German)* 80−37157
Euclidean self-dual Yang-Mills field configurations, set of linear algebraic eqns. 80−73587
Euclidean SU(2) Yang-Mills theory, degrees of freedom in pseudoparticle systems 77−45954
Euclidean SU(2) Yang-Mills theory, pseudoparticle solns. 79−35931
Euclidean Yang Mills eqns., instantons 77−45950
Euclidean Yang Mills theory, pseudoparticle parameters for arbitrary gauge groups 78−24955
Euclidean Yang-Mills fields, instantons and monopoles 78−4760
euclidean Yang-Mills theory, exact classical solns. 79−45001
Euclidean Yang-Mills theory with spherical symmetry, explicit classical solns. 79−12966
extended supersymmetric Yang-Mills theories, superfield formulation, auxiliary component fields 80−90995
extended system, pseudoparticle solns. 78−4764
extension to include two types of self-coupling 78−16926
factorisation, Reggeisation, spontaneously broken Yang Mills theories, high energy gauge meson exchange reactions 77−18172
Faddeev-Popov determinant in Yang-Mills theories, geometrical interpretation 79−85220
Faddeev-Popov ghost field, explicit classical construction, Yang-Mills field 80−82874
Fermi weak interaction theory, consistent renormalisation scheme, Yang-Mills theory parallel 78−66071
fermion Green's functions in presence of Yang-Mills pseudoparticles 78−54548
fermion-boson puzzle, coupled Yang-Mills isovector Higgs system, canonical formalism 78−41415
fermion-fermion high energy scatt., transverse momentum cut-off hypothesis, Yang-Mills theory 80−86575
fermion-meron interactions in Minkowski space-time, classical Yang Mills fields 79−2913
fermions in background pseudoparticle field in O(5) formulation 77−41761
Feynman diagram theory, finite, analogy with space-time approach 80−52400
Feynman path integrals, conference, Marseille, France, 1978 80−31422
fibre bundle topology, classification of monopoles and vortices 77−22635
fibre bundles, internal affine symm. of Dirac fields 78−24697
field equation, soln. 77−30265
field propagation, Lagrangian gauge fixing terms 79−40652
field strength and gauge pot. *(Chinese)* 77−13841
field strengths, sources, and gauge potentials *(Chinese)* 79−35920
field strengths, sources and gauge potentials *(Chinese)* 78−29231
field strengths and gauge potentials *(Chinese)* 77−71436
finite local gauge transformation 80−31968
finite local gauge transformations 79−12943
finite-band solutions to the duality equation on S^4 and two-dimensional relativistically invariant systems 80−42349
flux quantisation and angular momentum in nonAbelian gauge field theories 77−74594
fluxon solutions in non-abelian gauge models 79−9287
formal linearisation of eqns. 80−335

Yang-Mills theory continued
frequency splitting, gauge invariant, of continuum Yang-Mills field 77−87905
gauge ambiguities and nonlinear σ-model relations in Yang-Mills vacuum sector 80−105767
gauge ambiguity in $n.A^a = C_2^a(x)$ 79−75679
gauge conditions for the Yang-Mills field 79−93296
gauge dependence in the Yang-Mills S matrix 80−351
gauge field masses and degenerate pots., Yang-Mills and Higgs field unification 79−17647
gauge field theory formulation in quantum field theory framework 79−21908
gauge fixing ambiguities, flux strings, and the unconstrained Yang-Mills theory 79−35927
gauge invariance for effective action of source-free field *(Russian)* 77−61181
gauge invariance of spontaneously broken non-Abelian theories in Bogoliyubov-Parsyuk-Hepp-Zimmermann method 77−49861
gauge invariance on space of Bose and Fermi coordinates 77−45958
gauge invariant gluons, Hamiltonian operator 80−105843
gauge invariant operators, renormalisation, S-matrix elements 79−256
gauge invariant S-matrix elements with Yang-Mills SU(2) instantons and antiinstanton 80−22511
gauge symmetries, perturbation theory 78−359
gauge symmetry, max. 4-dimens., and general covariance, implications 79−63115
gauge theories, an introduction for experimental particle physicists 78−82119
gauge theories, facts and prospects, conf., Schladming, Austria (Feb.-Mar. 1978) 79−26203
gauge theories and strong gravity 79−58869
gauge theory, renormalisation of ghost and Goldstone fields and ghost symmetries 80−90987
gauge theory of gravity, gravit. field of spherically symm. matter distribs. 78−4773
gauge theory of gravity, SO(1,3), self-gravitating cosmons 77−82431
gauge zero modes, treatment methods 80−62840
general relativity, SL(2,C)Yang-Mills field theory description, in curved twistor space 79−21602
general Taub-NUT-De Sitter metric, self-dual Yang-Mills soln. of gravity 80−46946
generalised Einstein eqn., field eqn. for EM field and Yang-Mills instantons 80−8872
generalised vector field equations, symmetry group *(Russian)* 77−79206
geometrical gauge conditions, nonexistence results 80−47166
geometrical setting for Yang-Mills type gauge fields, review 80−32014
ghost free axial gauge, infrared gravitons 79−67214
gluon field condensation, instability of Yang-Mills level *(Russian)* 78−70289
gluon propagation in non-Abelian gauge theories, IR props. 79−2983
grand unified schemes and spontaneous compaction 77−87896
gravitation, geom. of first quantised theories 77−37799
gravitation theory, homogeneous cosmological models 79−17304
gravitational and strong interactions, unified gauge theory 80−95016
gravitational dynamics, Yang-Mills formulation 78−24721
gravitational field, compact internal symmetry groups 80−95022
gravitational field of spherically symm. matter distribs. 78−4773
gravitational instanton, CP^2 props. compared with SU(2) Yang-Mills instanton 78−81909
gravitational instanton contribution to spin 3/2 axial anomaly 79−17321
gravitational instantons, self-dual soln. to Euclidean gravity 80−68118
gravitationally coupled classical fields, decomposition method extension 78−127
gravitons, Einstein eqn. soln., on nonsingular positive definite metric 79−49150
gravity, microscopic, as Yang-Mills field 79−44829
gravity dynamics, homogeneous and isotropic world models 78−45543
gravity Lagrangian with ghost-free curvature-squared terms 79−21640
gravity theory bases on internal translation group 80−42134
guage fixing problem around classical solns. of Yang-Mills theory 78−70260
hadron bags, interactions under strict quark-line rule 78−41495
hadronic matter, Pomeron and critical temp. 80−22566
hadrons, Yang-Mills pots., Van der Waals force and fermion motion 80−52465
Hamiltonian dynamics, interacting gravit. gauge and Higgs fields, spherical symm. appls. 77−54051
heavy quark effective potential, non-perturbative semi-classical calc. 79−13053
Higgs field zeros for axially symmetric multi-monopole configurations 80−82887
Higgs fields and the determination of the Weinberg angle 79−40709
Higgs Kibble model on basis of canonical Yang-Mills field theory 80−105781
Higgs-Kibble-Yang-Mills field eqns., axially symm. solns. 78−368
high energy meson elastic scatt. amplitude, leading term approx. in SU(2) Yang-Mills theory 80−5017
high-energy scatt. amplitudes to arbitrary perturbative orders 77−67571
higher-derivative theory, ghost problem 80−31970
Hopf fibrings, associated with solns. of Yang-Mills and Maxwell eqns. 78−37129
indefinite-metric QFT of general relativity 78−89391
index symmetry of classical Yang-Mills fields 79−71631
infra-red struct., QCD mag. mom. anal. 77−13859
infrared behaviour, low energy theorem for renormalised proper vertices 77−65094
infrared behaviour of pure Yang-Mills fields, fermionic representation 77−71445
infrared singularities of self energy functions in axial gauge 77−2746
infrared struct., perturbative study, quark confinement 77−38089
instability, simple proof 78−45793
instability of constant Yang-Mills fields 80−343
instantaneous Coulomb interaction in SU(2) Yang-Mills QCD 80−396
instantaneous Coulomb interaction in SU(2) Yang-Mills QCD 80−22574
instanton construction 78−37138
instanton effects in pure Yang-Mills theory, perturbation theory rules 78−58125
instanton effects on axion mass 78−58127
instanton gas, bag-to-vacuum phase transition, mean field approx. 80−9097
Yang-Mills theory continued
instanton gas, first order phase transition existence conditions *(Russian)* 80−62866
instanton in Taub-NUT space 79−2691
instanton plasma in O(3) nonlinear σ model 78−16912
instanton sector renormalisation, zeroth sector comparison, pure Yang-Mills perturbation theory 80−105775
instanton solutions, Penrose twistor transform and methods of algebraic geometry 80−73612
instanton solutions to reduced eqns., F=*F review 80−32021
instanton statistical mechanics in QCD 80−57567
instanton-like solns., vanishing of energy-momentum tensor 78−74143
instantons, description in self-dual Euclidean Yang-Mills fields 79−6256
instantons, differential geometry and global anal., appl. to Yang-Mills equations 79−30641
instantons, local supersymmetry transf. and fermion solns. 78−74177
instantons, multi-, quantum fluctuations, Seeley coeffs. 80−77934
instantons, space-time topology 78−8522
instantons, topological props., non-Abelian group, SU(3) group *(Russian)* 78−45801
instantons, variational anal. 78−24934
instantons, virial theorems, variational arguments 77−49857
instantons and antiinstanton forces in sigma model and Yang-Mills theory 77−26462
instantons and characters in non-Abelian Yang-Mills theory 79−63345
instantons and Higgs fields 79−21957
instantons and merons in Euclidean space solns. *(Russian)* 80−42344
instantons and monopoles in Yang-Mills gauge field theories 80−91003
instantons and renormalisation for Yang-Mills effective Lagrangians with trace anomaly 79−85221
instantons and restoration of symmetries 78−66033
instantons and the index theorem 79−21951
instantons in two and three dimens. 78−4781
instantons of Yang-Mills eqn., rank 2 stable vector bundles 78−45774
instantons with fractional topological charge 78−21336
integral formulation divergence elimination, connecting const. renormalisation *(Russian)* 80−68369
invariance of Yang Mills theory, hypertorus solns. 78−24960
invariants and classification of Yang-Mills field 77−45971
inverse scatt. in higher dimensions 80−47165
inverse scatt. problem, self-duality eqns. 78−29247
IR divergence cancellation in pure theory 77−38091
IR divergences, real and virtual 77−45943
IR divergences and zero mass limit 80−32025
IR divergences in Yang-Mills theories, Feynman diagram labelling 78−54547
IR stability in zero-instanton sector 77−30244
isotopic spin sources, motion, gauge theories 80−12977
k-instantons in Sp(1) Yang-Mills theory, calculation method 80−13223
Kinoshita's theorem in Yang-Mills theories 77−6030
Klein-Gordon eqn., two dimensional model anomalously slow stochastisation *(Russian)* 79−89068
Lagrangian and Hamiltonian descriptions of Yang-Mills particles 78−78089
Lagrangian in winding number space, kinetic and potential energy, band structure of θ-vacuum *(Chinese)* 80−62860
Landau gauge in euclidean Yang-Mills theories, pathological features 78−89623
large order calcs. 78−8511
lattice, convergence of strong coupling expansion and linear pot. 78−45847
lattice approx. of gauge field theories 78−29225
lattice gauge theories, comparison with gauge groups SU(2) and Z_2 80−31966
lattice gauge theory, Gaussian transformation into string field theory 80−32003
lectures given at CERN School of Physics (6-19 June 1976) 77−61173
Lie group framework for soliton eqns., Lund-Regge model generalisations 79−17605
Lienard-Wiechert type of solution in SU(2) 80−4879
line space construction of non-self-dual Yang-Mills fields 80−9103
linear field equations on self-dual spaces 80−42328
linear plane wave solns. 78−74151
linearisation stability of Yang-Mills and Einstein-Yang-Mills eqns. 79−49142
linearised constraint equations for Yang-Mills field, elliptic complex 79−45008
little-group classification of gauge fields 79−58879
secret long range force in QFT with instantons 79−9283
long-range quantum effects in IR stable Yang-Mills system 77−67565
low energy quanta emission in nonAbelian gauge theories, coloured gluons 77−79223
magnetic charge of Yang-Mills fields, in terms of Higgs fields, SO(4), SU(4) 77−45935
magnetic fields, flux string and monopole, geometric configuration, compared to O(3) nonlinear σ-model 80−57527
magnetic monopole solns. in Yang-Mills and unified gauge theories 78−21320
magnetic monopoles, non-Abelian, stability analysis, Yang-Mills equations 80−31987
magnetic monopoles in the presence of quark sources 80−13213
manifestly covariant canonical formulation, general formalism 79−35932
manifestly gauge invariant gluon eqns. from Yang-Mills fields 80−86681
many-instanton problem, Euclidean supersymmetry 77−74615
mass shell amplitudes, gauge invariant, definition by dimensional regularisation 77−10179
mass singularities, cancellation mechanism 77−82676
mass singularities in certain quark prod. processes 77−26459
mass spectrum for integral isospin monopoles, bag model as high isospin limit 78−24935
massive, appl. of path integrals to non-perturbative study 80−32020
massive Lagrangian, separation of non-renormalisable divergences 77−49854
massive Schwinger model, consistency and Lorentz invariance 78−89613
massive theory, S-matrix unitarity in zero-mass limit 77−2732
massive Yang-Mills fields, minimal coupling and unitarity 77−22640
massless propagator, IR bound 80−73581
massless theory, exponentiation of leading IR divergences 77−13847
massless theory solutions representing nonlinear massive plane waves *(Russian)* 79−71641
massless Yang-Mills field and many-body pot. 78−29258

Yang-Mills theory continued
massless Yang-Mills theory, exponentiation of leading IR divergences 78−32988
Maxwell eqns., null solns., generalised to Yang-Mills theory 80−27388
Maxwell form. of Yang-Mills eqns. 79−17606
meron pair, introduction, motivation and formalism 80−82861
meron pairs, bare activity 80−82862
mesons, deformations and spectral props. 80−13203
metastable vacuum states in SU(2) Yang-Mills theory, quantum decay process 79−250
minimal coupling, symplectic mechanics of classical particle in Yang-Mills field 78−74136
Minkowski space, classical soln. 78−29263
Minkowski space, four dimensional, general theorem for absence of finite energy nonsingular solns. 78−21318
monopole classification in SU(2) and SU(3) gauge field theory 77−38082
monopole soln. 77−67566
monopole system, equivalence with Yang-Mills field, 't Hooft monopolar solution 80−9084
multi-instanton solution, new compact form 78−24971
multimeron field configurations, numerical computation 79−258
multiple direct exchange in Yang Mills theory, high energy behaviour of Feynman diagrams sum 77−34088
multipseudoparticle configuration, compact form 78−54558
multipseudoparticle solns. 78−74152
multireggeon processes, Yang-Mills theory *(Russian)* 77−2808
N=4 supersymmetric Yang-mills theory, 3-loop β function zero value 80−105783
n-pseudoparticle solns., small variations 78−66042
non Abelian gauge theories in external electromagnetic fields *(Russian)* 80−57533
non-Abelian gauge fields, prepotentials 77−87912
non-Abelian gauge theories, high energy behaviour, reggeon field theory, QCD 80−62822
non-Abelian gauge theories, local covariant operator formation, quark confinement 80−47190
non-Abelian gauge theory, Yang-Mills phase factor renormalisability 80−95211
non-Abelian mag. charges, quark confinement 77−49849
non-Abelian massless fields, discussion of Schrodinger equation 79−17614
non-Abelian phase factors, Yang-Mills Hamiltonian 80−73575
non-Abelian solution energy in presence of external source 79−89062
non-Abelian structure, IR finite asymptotic states 79−265
non-Abelian vector potls., existence instability 78−70264
non-Abelian Yang Mills field, infrared behaviour, gluon decoupling 79−85215
non-perturbative quantum field theory, lattice renormalisation construction 80−9098
non-relativistic scattering by stationary external metrics and Yang-Mills potentials 80−101938
non-self-dual gauge fields 79−9282
nonAbelian, nonlinear Yang-Mills field eqns., self-duality, helicity, coherent states 80−31988
nonAbelian gauge model, Becchi-Rouet-Stora invariant, superfield struct. 78−74121
nonAbelian gauge theories, ambiguous fields, Yang-Mills potentials *(Russian)* 79−93297
nonAbelian gauge theory with spontaneous symm. breaking *(Russian)* 77−6038
nonleading IR divergences in QCD, renormalisation group function 77−71422
nonlinear models, gauge theory formulation 79−71627
nonlinear Yang-Mills pseudoparticle solns., quantisation, conformal group contraction 79−67464
nonsingular gravitational collapse, Yang-Mills cosmos 79−21621
nonstatic solns. of sourceless equation for SO(4) and SO(3,1) 77−65101
nonzero temperature case, spherically symm. solns. 79−2941
null tetrad formulation of Yang Mills field eqns. 78−74135
O(2) symmetric connections in an SU(2) Yang-Mills theory 80−4839
O(3)-symmetric merons in SU(N) gauge theory 80−82904
O(4) Yang-Mills, Higgs system, topologically stable solns. 80−52382
observation, calcs. using relativistic quantum field theory 78−24933
octonions and exceptional groups in field theory, unified interaction model *(Russian)* 79−67491
operator ordering and Feynman rules in gauge theories 80−101926
over-critical point source 80−4846
$P(\phi)_2$ gauge invariant massive theory 78−41403
pairing theory of Yang-Mills field and string phase 79−13047
particle motion in classical gauge field, variational derivation and uniqueness of equations of motion 79−40658
path dependent phase factors, functional eqns. 79−85219
path-depend. approach to coloured mag. monopoles 78−37127
Pauli-Villars regularization for non-Abelian gauge theories 79−21956
peeling theorem in asymptotic limit 79−259
periodic solutions of massive ϕ^4 and Yang-Mills theories 79−12935
perturbation Feynman rule, gauge-nonfixing method 80−57462
planar diagrams, SU(N) asymmetric model, semiclassical approach 80−77957
potential determination from field strength 80−32011
potentials and field strengths 77−41774
Prasad-Sommerfield dyon (monopole) soln. of SU(2) Yang-Mills field with Higgs multiplet 80−339
Prasad-Sommerfield monopole, time depend. soln. of SU(2) Yang-Mills-Higgs system 79−273
projective invariance in general space times with spinor, torsion and Yang-Mills fields 78−57832
pseudoparticle, O(5) formalism, ghost propagators 78−8531
pseudoparticle configurations, conformal props. 77−41772
pseudoparticle methods for toplogical invariants greater than one 78−45789
pseudoparticle physical mechanism for quark confinement, Yang-Mills theory confinement 79−49463
pseudoparticle soln. of 4-D Euclidean Yang-Mills eqns. *(Chinese)* 78−86419
pseudoparticle solns. in extended systems 78−4764
pseudoparticle solns. on O(5,1) light cone 78−24952
pseudoparticle solution, O(5) formalism, ghost formalism 78−8531
pseudoparticles and sine-Gordon solitons, transformations 77−65100
pseudoparticles with any integer dual charge *(Chinese)* 77−82669
Yang-Mills theory continued
QCD, energy levels of 1+1 dimensional lattice gauge theory 78−4828
QCD, hadronic and supersymm. string states 79−75724
QCD, semiclassical methods, hadron struct. theory 79−97594
QCD, struct. functions, perturbation theory *(Russian)* 78−8595
QCD and Weinberg-Salam model for strong and electro-weak interactions 80−73638
QCD development from classical Yang Mills theory, a qualitative critique 79−80804
QCD vacuum in strong external gauge fields, spontaneously, broken chiral symmetries 80−57555
QED, perturbation series, asymptotic estimates and guage invariance 77−87925
quantisation, Ward identities and Green's function eqns. 77−67552
quantisation, without fixing gauge, functional technique 80−57471
quantisation by separation of gauge variables 79−67474
quantisation of gauge fields avoiding path-integral formalism 77−13863
quantisation of Yang-Mills field and Mandelstam's theory in gauge-independent path-dependent formalism 77−30249
quantisation of Yang-Mills theory around classical solns. 78−29245
quantisation of Yang-Mills theory in Coulomb gauge 78−54546
quantisation problems, in lectures on functional methods in quantum field theory 77−57458
quantisation using asymptotic field theory formalism 77−22653
quantisation without fixing gauge 80−13207
quantised strings and chromodynamic IR behaviour, Yang-Mills electric flux lines 77−30316
quantised topological charge, implications of zero field tensor 80−31983
quantum action method in quantum field theory 79−40659
quantum chromodynamics, field strength formulation 78−16924
quantum collective field method, planar limit appl., SU(N) theory and harmonic oscillators 80−57468
quantum dual string wave functional in Yang-Mills theories 79−21921
quantum scattering by external metrics and Yang-Mills potentials 80−31535
quantum string representation, SU_2 gauge group 80−57465
quark confinement, absence of localised coloured/charged physical states, coherent photon states 80−57573
quark confinement, saturated Euclidean vacuum functional, instanton distrib. 79−22029
quark confinement and Gribov ambiguities in Coulomb gauge 78−62297
quark confinement and observables in covariant canonical formalism 79−6322
quark field quantum fluctuation computation in arbitrary Yang-Mills instanton background 80−13268
quark fragmentation in gauge theories 78−21340
quark mass shell gauge in Kondo-Yang-Mills theory 77−30309
quark pair condensation and confinement 79−17677
quaternion quantum mechanics as the description of tachyons and quarks 79−30273
radiation gauge calc. of high-energy scatt. amplitudes 77−38111
radiative corrections, vacuum state instability 78−8515
Regeisation of scalars and dual model struct. 78−16927
relativistic string model generalisation in geometrical approach, Yang-Mills approx. 80−383
relativity, seven-dimensional, 4-D gravity coupled to Yang-Mills fields 80−82699
renormalisation in two-loop approx. for arbitrary gauge *(Russian)* 77−49865
renormalisation of four dimensional operators 78−16929
renormalisation of massive two-dimens. theory, nonrenormalisability of four-dimens. theory 77−45945
renormalisation of theory developed around instanton 80−32027
renormalisation scheme 79−12944
renormalisation theory, perturbative, general features, quantum action principles, pure Yang-Mills theory 80−105794
renormalised eqns. and renormalisation constants, Abelian gauge invariance 77−65093
renormalization of Yang-Mills theory developed around an instanton 79−45009
review of gauge theories of weak, EM and strong interactions 77−13835
rotating plane-fronted waves and their Poincare-invariant differential geometry 80−332
rotational covariance and Yang-Mills monopole 77−13870
rotationally invariant solutions of Yang-Mills-Higgs system for general gauge group, mag. monopoles 78−29235
S_3-symmetrical model, use of permutation symmetry 79−26280
S-matrix for interaction of gravitational and Yang-Mills fields 80−42315
scalar field coupled to Yang-Mills field, decay 79−67459
scalar field interacting with Yang-Mills field, higher order perturbation theory *(Russian)* 78−62316
scalar field solutions to Yang-Mills and Vierbein field theories 79−12682
scattering amplitudes, sixth-order, Yang-Mills fields, finite-diagram theory 80−73585
Schrodinger particle as the source of a Yang-Mills field 80−57494
self dual Euclidean Yang Mills theories, Atiyah-Singer index theorem 78−54541
self dual fields on S^4, local stability of deformations 78−74153
self dual SU(2) fields in multicentre spaces 80−73600
self dual SU(N) Yang-Mills fields, nonlocal continuity eqns. 80−9096
self dual Yang Mills theory, general solns. for O(n), SU(n) and Sp(n) gauge groups 79−6281
self duality in 4-dimens. Riemannian geometry, Yang-Mills eqns. 78−78073
self-coupled vector fields, calcs. using Dirac quantisation procedure 78−89610
self-dual gauge field, Green function 78−82099
self-dual propagating wave solns. for sourceless field eqns., superposition props. 79−85227
self-dual solns. and a superposition principle 78−82096
self-dual SU(2) gauge fields, Backlund transform. and Atiyah-Ward ansatze 78−21339
self-dual Yang Mills fields in Minkowski space 80−18078
self-dual Yang-Mills fields, complex, in Minkowksi space time 78−41424
self-screening of classical Yang-Mills fields *(Russian)* 79−6289
Sikivie-Weiss magnetic dipole soln. 80−22523
single particle theory, g-2 calc., charged spin-one Yang-Mills particle appl. 77−13872
singular SU(2) symmetric potentials, bound states *(Russian)* 79−30665

Yang-Mills theory continued
six-dimensional approach to Weinberg-Salam model, Higgs particle 80−4905
skeleton expansion, free of overlapping divergences 77−65092
Slavnov-'t Hooft identities in Mandelstam's formalism 78−45776
SO(1,3)-gauge theory of gravity 79−129
SO(3,1) gauge theory, classical solns., mag. and electric charge 78−54550
SO(3) gauge invariant theory, quantisation, spontaneous broken gauge theory, S-matrix gauge independ. 79−269
SO(4,1) de Sitter gauge theory, general relativity as gauge theory limit 79−58598
SO(4) Yang-Mills model, classical solns. with both instantons and anti-instantons 77−79211
SO(4)-symmetric solutions of Minkowskian Yang-Mills field equations 78−4780
SO(5) Yang-Mills eqns., class of pseudoparticle solns. 78−371
SO (1,3) gravity, post-Newtonian, strong equivalence principle 80−68113
solitons in 2+1 dimens., Coleman's rules 77−82678
solutions of Yang-Mills eqns. with external sources, colour charged particles 78−89624
source-free Yang-Mills theories 79−12956
source-free Yang-Mills theory, absence of static solns. 77−2744
sourceless eqns., exact classical solns. 77−41759
sourceless field eqn., self duality and energy of solns. 78−66032
sourceless SO(4) and SO(3,1) eqn. spherically symmetric soln. 77−65103
sourceless Yang-Mills eqns., eqns. of motion, holonomy functional formulation *(Chinese)* 79−80760
space-time independent potentials for SU(2), SU(1,1) and E(2) gauge theories 79−49381
spherically symm. Einstein-Yang-Mills-Higgs system, canonical formalism 77−87892
spherically symm. Yang-Mills Euclidean solns. 78−8533
spherically symmetric fields in gauge theories, Yang Mills eqns., mag. monopoles 78−16914
spherically symmetric solutions of Yang-Mills equations in Riemann spaces *(Russian)* 79−30666
spin glass, local exchange invariance concept 78−60288
spinning solutions of classical Yang-Mills theory 80−101937
spinor analysis of Yang-Mills theory 78−8532
spinor functional determinate in Yang-Mills potential, upper bound of 1 79−311
spinor Yang-Mills superfield 78−12825
spontaneously broken, reggeon field theory appl. 78−8512
stability and bifurcation in Yang-Mills theory 80−52417
stability and gap phenomena 80−18073
stability in system with external source 79−9286
stability of solitons, Poincare stability, gauge theories, nonlinear Schrodinger equation 80−4881
static Euclidean anti-self-dual SU(2) eqns., small deformation of Prasad-Sommerfield soln. 79−71633
static gauge fields, singularities and sources 79−49401
static magnetic SU(2) Yang-Mills-Higgs system, static axial and mirror symmetric monopoles 80−90992
static monopole fields, propagation functions, Yang-Mills instanton equivalence 79−35928
static quark forces in classical chromodyanamics, bag models, SU(2) Yang-Mills field 79−2990
static quark potentials from Yang-Mills equations 79−45056
static solutions of 4-dimens. eqns. of Yang-Mills gauge fields with mass 80−82872
static sources in classical Yang-Mills theory 79−97513
static SU(2) Yang Mills eqns., with external charge sources, T-invariant 79−71638
static Yang-Mills fields with sources 79−97512
string theories 77−79216
string type solns., in classical gauge field theories, broken gauge symmetry 78−62317
strong Backlund transformations, generalisation and existence in ≥4 dimens. 79−30316
SU_2 Yang Mills theory, high energy scatt. amps. 79−63346
SU(2), Coulomb gauge fixing 79−26235
SU(2), in Coulomb gauge, quantisation 78−54546
SU(2), local uniqueness theorem for (anti) self dual solns. 78−70263
SU(2), Yang-Mills field eqn. configurations in curved spacetimes 80−18076
SU(2) 4-dimens. Yang-Mills theory, noninteger topological number and infiniteness of action 79−246
SU(2) classical gauge field eqn., self-dual static solns. 78−45792
SU(2) classical Yang-Mills eqn., multimeron solns. 80−57477
SU(2) classical Yang-Mills equations, exact solutions 79−40667
SU(2) colour Yang-Mills theory, quark source charge screening, confinement 80−22565
SU(2) eqns. in compactified Minkowski space, invariance conditions 79−63342
SU(2) field equations, props. of O(4)×O(2) symm. solns. 78−24931
SU(2) finite-temp. Yang-Mills gas, periodic Euclidean soln. 78−66041
SU(2) gauge group, solns. for Yang-Mills eqns. *(Russian)* 77−79226
SU(2) gauge theory, external charges, topological classification for Yang-Mills eqns. 80−90977
SU(2) Higgs-Kibble model with spontaneous symmetry breaking, covariant-formulation of Yang-Mills theories 79−54256
SU(2) instanton, physical interpretation of degrees of freedom 78−62312
SU(2) instantons, Yang's self-duality eqns. *(Chinese)* 78−78099
SU(2) Landau gauge Yang Mills theories, nonsingular spherically symmetric separable copy 79−71619
SU(2) lattice Yang-Mills fields, strong coupling expansion, recursive eqns. 79−245
SU(2) pseudoparticle soln., quantum field theory studied in O(5) covariant formalism 77−30256
SU(2) supergroups, Yang-Mills, Lie groups, chiral coeffs., Baker-Campbell-Haussdorff formula 80−68355
SU(2) theory, 1st and 2nd order eqn. equivalence 80−90979
SU(2) theory, role of surface variables in vac. struct. 77−30242
SU(2) theory deformation of instantons 78−45786
SU(2) theory in 1+1 dimensions, lattice model calcs. 77−41752
SU(2) theory in transverse gauge, single meron configuration 78−74145
SU(2) Yang Mills multi-instanton paths, tunnelling pots. and WKB wave functionals 79−248
Yang-Mills theory continued
SU(2) Yang Mills theory, field-strength description of non-Abelian gauge theories 80−62856
SU(2) Yang-Mills eqns., classical solns. 80−4875
SU(2) Yang-Mills eqns., complex and Lienard-Wiechert solns. in Minkowksi spacetime 79−2938
SU(2) Yang-Mills eqns., elliptic generalization of the one-meron configuration 80−62854
SU(2) Yang-Mills field, 't Hooft monopole, Julia-Zee dyon, stable solns. 79−26229
SU(2) Yang-Mills field, pure gauge forms 79−26228
SU(2) Yang-Mills field equation instability, removal by (1+1) dimens. Higgs mechanism, SU(N) generalisation 79−58924
SU(2) Yang-Mills fields, coupled to (2s+1) dimens. Higgs field, classical soln. 78−41430
SU(2) Yang-Mills fields, quasi-metric with nonself-dual curvature 79−26213
SU(2) Yang-Mills gauge theory, two meron configurations in transverse gauge 79−71637
SU(2) Yang-Mills invariants, polynomial basis 79−17609
SU(2) Yang-Mills quantum field theory, meron pairs and quark confinement 78−37174
SU(2) Yang-Mills theory, finite field eqn. 80−62830
SU(2) Yang-Mills theory, ground state 80−101939
SU(2) Yang-Mills theory, self duality of solns. 78−37143
SU(2) Yang-Mills theory, topological and differential geometric techniques 79−71586
SU(2) Yang-Mills theory, transverse pure gauge fields 79−26227
SU(2) Yang-Mills theory, vacuum struct. 79−71588
SU(2) Yang-Mills theory, vacuum struct. 80−57501
SU(2) Yang-Mills theory with potentials invariant under U(1) gauge subgroup 79−54255
SU(2) Yang-Mills-Higgs system, classical finite energy solns. embedding in supersymmetric extension 79−2950
SU(2) Yang-Mills-Higgs system, soliton solns. 79−26218
SU(3) classical gauge theory, dyons and new topologically conserved quantity 77−6014
SU(3) theory of Yang-Mills-Higgs fermion-monopole system, topologically stable soln. 77−13888
SU(3) Yang-Mills theory, study of O(3) symmetric merons 79−30651
SU(4) supersymmetric, charge renormalisation 78−24929
sU(4) Yang-Mills field solution 79−71584
SU(N) 2-D theory in leading 1/N expansion 78−8516
SU(N) field, self-dual, parametric Backlund transformation 79−97503
SU(N) lattice gauge model, weak coupling, monopole condensation and quark confinement 79−75683
SU(N) massive Yang-Mills field theories, struct. and renormalisability, Higgs field 79−6279
SU(N) Yang-Mills field eqns., constant classical solns. for N=∞ 80−73589
super Yang-Mills theory, anomalies and supersymmetric regularisation by dimensional reduction 80−82916
superdense material, crystallisation of Yang-Mills fields *(Russian)* 78−54562
supergauge invariant Yang-Mills eqns., exact solns. 79−67471
supergravity, auxiliary fields and UV divergences, supersymmetric Yang-Mills-Einstein system 78−78127
supergravity, gauge group and geometry 80−8888
supergravity, SU(4) invariant theory 78−41471
supergravity and gravity, BRS gauge and ghost field supersymmetry 77−38116
supergravity and gravity as gauge theories on group manifold 78−41469
supergravity and Yang-Mills theory unification 77−46011
superspace gauge theories, superspace Maxwell and Yang-Mills actions 80−86582
superspace geometry in supergravity, Riemannian theory reduction, Yang-Mills connections 80−57156
supersymmetric, absence of induced spontaneous supersymmetry breaking in first order 77−211
supersymmetric, point-splitting derivation of anomalous divergence for the spinor current 78−74148
supersymmetric, Ward identity, one-loop level, renormalisation 80−73597
supersymmetric cancellation of supercurrent anomaly 78−8518
supersymmetric extension, OSp(1,4), superfield formulation in anti-de Sitter space 80−57508
supersymmetric theories 77−45944
supersymmetric Yang-Mills field theory, point splitting regularisation, superformal anomaly 80−91014
supersymmetric Yang-Mills theory, mag. monopoles and dyons, quantum corrections 78−62334
supersymmetric Yang-Mills theory in superspace 79−12979
supersymmetric Yang-Mills theory in Wess-Zumino gauge, supersymmetric regulators and supercurrent anomalies 80−86614
supersymmetry, review of principles and historical development 77−18197
supersymmetry and classical solns. 78−8549
supersymmetry and instantons 78−32986
superunified field theories, geometrical transformation laws 79−63117
superunified theories, geometry of gauge invariance 78−24723
symmetry breaking and space-time geometry 78−54533
tachyon bound state, vac. instability 78−29244
temporal gauge, quantisation and asymptotic freedom 79−80754
temporal gauge struct. by Feynman propagation kernel 80−37162
tensor field, infinitesimal connection extension *(French)* 77−82664
tensor mesons mass, model Lagrangian, SU(3) Yang-Mills fields, tensor fields 77−13874
theories without spontaneous symmetry breaking 79−54263
thermodynamics of Yang Mills gas, contrib. of instantons 79−12964
time-independent Yang-Mills statics 79−12957
timelike gauge, physical states 78−21335
topological aspects of Yang-Mills theory 78−78060
topological setting for axial anomalies and index theorems on open spaces 79−303
transverse lattice QCD, hadron mass spectrum 80−57568
twistor programme, self dual solns. to reduced equations 79−26231
two-dimensional SU(2) Yang-Mills theory 78−24942
two-dimensional Yang-Mills theory in the leading 1/N expansion 79−26242
U(2) invariant solutions to Yang-Mills equations in compactified Minkowski space 78−70262

Yang-Mills theory continued
U(N) lattice Yang-Mills theory, Schwinger-Dyson eqns., string model equivalence 80−4855
U gauge in Abelian and non-Abelian gauge theory, Gribov ambiguities 78−45788
unconstrained temporal gauge 78−45790
unification of Maxwell, Dirac and Yang-Mills eqns., octave algebra 79−2967
unified spatial and isotopic symmetry 79−21952
unified theories of weak and electromagnetic interactions 78−81908
unified theory of gravity and strong interactions, quark confinement 77−22681
unified Yang-Mills-Einstein-Higgs gauge theory, hadron struct., quark confinement 79−9275
uniqueness of potentials determ. 77−45972
unitarity of S-matrix in Yang-Mills theory 77−82681
unitary gauge in SU(2) Yang-Mills-Higgs system 77−30229
universal phase space for particles in Yang-Mills fields 79−21902
UV infinity suppression in gravity modified field theories 80−105787
vacuum gauge field for Yang Mills theory in Landau gauge 78−70259
vacuum in the Coulomb gauge 78−24932
vacuum polarisation, one-loop contributions *(Russian)* 77−74605
vacuum polarisation under external field, renormalised scalar Euclidean functional determinant 78−78061
vacuum spontaneous magnetisation in quantum Yang-Mills theory and magnetostatics 79−6268
vacuum stability and singlet pair condensation 79−2926
vacuum structure, time-like gauge $A_0=0$, Hamiltonian struct. 79−26211
vacuum structure of SU(2) Yang Mills theories, in Coulomb gauge 78−49971
vacuum symmetries of gauge supersymmetry, quantum effects 79−17634
vacuum tunneling, gauge ambiguity role in Yang-Mills theories 79−17604
vacuum wave functional calc. 80−13212
vacuum-to-vacuum amplitude, one-loop contrib., manifestly 0(5)-invariant calc. 78−24945
vector boson model from SL(2,C) gauge theory of gravitation and Yang-Mills theory 79−322
vector meson scatt., two to three body, high energy 78−17051
vertex functions, triple-gluon, gauge invariance in non-Abelian gauge theories 80−42326
vortex condensation, quark confinement mechanism 79−6272
Weinberg angle determ. in reformulation of Weinberg model to Yang-Mills theory 79−35984
Wong eqns. of motion for spinning Yang-Mills particle 78−24946
Wu-Yang soln., stability of S-wave perturbations 78−24944
Yang's K gauge, solns. to self-dual SU(2) gauge field 79−12965
Yang's R gauge for self-dual SU(3) gauge fields 78−78088
Yang equations, invariance props. 80−62836
Yang-Mills equations, SL(3,C) self dual instanton solns. 79−63369
Yang-Mills field, isodoublet-scalar field coupled, large order estimates for perturbation theory 79−71632
Yang-Mills fields, instantons, tensor products of instantons *(Russian)* 79−67477
Yang-Mills instantons in self-dual spacetimes 79−35939
Yang-Mills theory, instantons and algebraic geometry 77−74570
Yang-Mills-Einstein eqn. pseudoparticle solns., gravit. effect on Yang-Mills topology 77−82682
Yang-Mills-Higgs eqns., topological cohesion 78−62295
Yang-Mills-Higgs model, axially symm. monopole-type soln. 78−54561
Yang-Mills-Higgs SO(3,1) gauge theory, classical solns. 78−54550
Z(N) topological excitations in Yang-Mills theories: duality and confinement 79−12938
zero frequency modes in perturbation expansion about classical field theory configs. 77−18169
zeta-function regularization and multi-instanton determinants 80−13215
$e^+e^-\rightarrow W^+W^-\gamma(e^+e^-W^+W^-)$, Yang-Mills coupling 80−68443
NN scattering in nonAbelian gauge theory, π-, ρ-, and ω-exchange, scalar Pade approx. 79−67573
$\rho\pi$ system effective Lagrangian *(Russian)* 77−6036

yield point
see also yield strength; yield stress
alloy with dispersion precipitate of ordered phase, yield limit theory surmountable pair mech. *(Russian)* 77−1855
alloys, $L1_2$-type superstruct., anomalous temp. depend. of deform. charcts. *(Russian)* 79−20109
annular plates, minimum weight design *(Russian)* 79−10498
biaxial testing machine, for flat specimens, study of specimen shape *(Japanese)* 77−70268
brass, low-temperature testing, −196°C to +20°C 79−61692
α-brass, single crystal, obstacle strength variation during stress relaxation 78−68723
cement mortar, deform. charact., expt. study *(Japanese)* 78−56704
composite, fibre reinforced 77−59871
composite superconductor, flux jumps and training 80−70911
concrete slabs, subjected to biaxial moments, optimum design of steel bars reinforcement, using analytical and graphical methods 80−50664
continuous casting cylindrical ingot, development of elastic-plastic temp. stresses and deformations *(Russian)* 79−29151
Corson alloys, AE during tensile deform. *(Japanese)* 79−61654
cracked bodies, plane stress to plane strain thickness dependent transition, anal. model 78−67126
dislocation mech. study of yield surfaces 77−14916
elastic body, inhomogeneous yielding, slip plane intersection with stress free boundary 78−5667
elastic springback in beams and plates, bending 80−38256
epoxy-polyglycol elastomers, fracture strength under compression 79−38929
eutectic alloy, yield point analysis 77−8875
failure beyond linear elastic regime 78−67141
fatigue crack growth, model prediction, two coupled differential equations 78−67103
FCC metal, polycrystalline, computer simulation of rolling texture *(Japanese)* 77−63686
fission reactor fuel rod ballooning prevention 78−17290
fracture, Griffith type, analysis for large scale yield conditions 77−3771
fracture, post-yield, numerical investigation 78−18249
glass (roving cloth) fibre reinforced plastics, yielding behaviour of plate with circular hole *(Japanese)* 79−8323
glass fibre reinforced plastics, relation between matrix vol. changes and mech. props. 80−11715
glass reinforced fabric, low-temperature testing, −196°C to +20°C 79−61692
hypoelastic materials with internal variable, work-hardening, hysteresis, fracture law 77−62177
J-integral determ. under elastic-plastic strain 79−64515
leucosapphire single cryst., W grid reinforced, growth 77−16530
membrane action effect on plastic collapse load of circular orthotropic slabs with fixed edges 78−79225
metal, anisotropic, continuum description of anomalous yielding 79−11677
metal, plasticity at very low temperature, dislocation motion, rel. to supercond. and tunnelling *(Czech)* 77−32630
metal sheets, yield locus prediction using texture data 79−86347
metal-H systems, anelastic and plastic props., review 80−49298
metallic glasses manufacture, struct. and stability *(Norwegian)* 79−14687
metals, FCC, yield threshold at 4.2K, effect on strain-hardening curve *(Russian)* 80−50671
metals, transversely isotropic plastic props., yield charact. 78−60707
Mohr-Coulomb material, yield condition for axisymmetric compression around circular hole 79−57914
multimaterial impact, dynamic yield point 77−32731
Ni alloy KhN45Yu, strength properties, dispersity of struct. effect 80−55486
oil shales, review of thermophysical properties 79−100479
oriented polyethylene film, deformation band studies 77−52420
orthorhombic symmetry, yield surface charact. 80−64405
oxides, interaction between point defects and dislocations, cryst. plasticity 80−15149
Ozhennite, yield point, effect of ageing stress 77−21223
plastic anisotropy, Bauschinger effect, general formulation, comparison with expt. yield curves *(German)* 77−20006
plasticity, polycrystalline, probabilistic approach, appl. 78−26622
plate, simply supported circular, transverse shear and rot. inertia, dynamic plastic response 80−79175
plate weakened by equal-armed cross-shaped crack, plastic strain and fracture 80−69740
plates, rectangular, hinge-supported, eccentrically applied, ultimate point load, kinematic solutions 80−53638
plates with random strength, conditional collapse prob. under given loads 77−3754
PMMA, plastic deform. by crazing *(Japanese)* 80−93619
poly-n-benzamide, lyotropic liq. cryst., structural orientation *(Russian)* 77−31593
polyamide, test pipes, static tensile strength, equipment effect on tension-extension diagram *(German)* 78−35453
polycarbonate, amorphous, yield behaviour in oriented and unoriented condition, effect of temp. 80−97537
polycarbonate, craze morphology, 77 to 375K, gaseous environment effect 77−63819
polycarbonate, glassy, rolled, craze initiation *(Japanese)* 77−8969
polycarbonate, rigid plastic, yield behaviour *(Japanese)* 80−93620
polycarbonate of bisphenol A, neck form. and propag., strain anal. 80−16376
polychlorotrifluoroethylene, tensile deform. in He, N_2, Ar, O_2 and CO_2 gaseous environments 77−56040
polyethylene, high density, crystalline, flat stressed state, yield point time-temp. factors 78−64601
polyethylene, linear, crystallised from melt, effect of crystallisation time on density, mech. props., X-ray scattering 80−25680
polyethylene, linear, strain rate effects on ratio of recoverable to nonrecoverable strain 78−27566
polyethylene, linear role of recovery forces in deformation 78−48459
polyethylene spherulites, high density, microstruct. and mech. props. 78−42921
polyethylene terephthalate film, deformation band studies 77−52420
polyisobutylene, undiluted, mol. wt. influence on creep behaviour 80−45370
polyolefins, plastic flow, yield limit rel. to press. *(Russian)* 80−7657
polypropylene, crystalline, yield behaviour in oriented and unoriented condition, effect of temp. 80−97537
polypropylene, mech. behaviour rel. to combined press.-temp. effects 77−16648
polypropylene nonfilaments, highly drawn, plastic deform. 78−44174
polystyrene-poly(styrene-b-butadiene-b-styrene) polyblends, mech. props. 78−52919
polystyrol, test pipes, static tensile strength, equipment effect on tension-extension diagram *(German)* 78−35453
porous rigid-plastic material containing rigid inclusions, yield function, plastic potential, void nucleation 78−64612
post yield fracture criteria assessment 77−35092
post yield solutions for fracture mechanics analyses of cracks emanating from elliptic holes 79−68643
prismatic bar hysteretic behaviour, yield condition under repeated axial loading 77−62167
PVC, rigid plastic, yield behaviour *(Japanese)* 80−93620
PVC, stress relaxation in macrodeformation range 80−16370
PVC, tensile tests, post-yield phenomena 79−91752
PVC, test pipes, static tensile strength, equipment effect on tension-extension diagram *(German)* 78−35453
PVC block copolymers, physical props. and morphology 79−82166
PVC sheet, notched, yielding 78−56708
ruby, temp.-time dependence of yield point by compression and extension 78−6988
shell, deposited in vacuum, elastic charcts. meas. by short time static extension *(Russian)* 78−39961
shell, rectangular flexible elastoplastic, yield theory and deformation theory appl. 80−74773
solid mechanics, yield criteria and constitutive eqn. of elastic-plastic material *(Japanese)* 79−59933
steel, alloy, temp. profile, IR obs. during pull tests 77−44427
steel, austenitic, ageing and plastic deform. effect on struct. and mech. props. of N15Kh5G3T3 *(Russian)* 80−71691
steel, austenitic, high tensile X 3 CrNiMoNbN 23 17, creep at room temp., effect of Bauschinger effect *(German)* 77−1852
steel, austenitic, metastable, hardening by cycling of martesitic transform. during rapid heating, in 30N24M4 and 50N21M3 *(Russian)* 79−20074

yield point continued
steel, austenitic, undergoing martensitic transform. during deform., temp. depend. of yield point *(Russian)* 77−66677
steel, austenitic stainless Kh18N10T, strength properties, dispersity of struct. effect 80−55486
steel, austenitic stainless sheet, texture anisotropy influence on deformation forming limits 79−91706
steel, C, fatigue damage accumulation and nonuniform microscopic strains, development features 79−91770
steel, C, plastic deform., study of loading surface 77−44322
steel, C, predeformed, anisotropy temp. effect on yield point 78−39878
steel, C, tensile props. in high press. H_2 at room temp. *(Japanese)* 80−108501
steel, C, yield point determ. rel. to grain size, deform., ageing and temp., dislocation theory *(Serbian)* 79−34120
steel, comp. and ferrite grain size influence on Ludwik eqn. constants *(German)* 80−81107
steel, correlation links between mech. props. controlled rolling effect 80−35234
steel, Cr-C, (2.14, 1.08 at.%) tempered, resistance to small plastic deformation, strain relaxation *(Russian)* 78−56698
steel, Cr-Mo, press. vessel material, yield surface behaviour, investigation techniques 79−61658
steel, Cr-Mo (2.25, 1 wt.%), strain hardening shakedown load during bending 80−20958
steel, Cr-Mo-Ni-Nb, Nb effect on mech. props. *(German)* 80−30012
steel, Cr-Mo-V (1.35, 1.0, 0.25 wt.%) exam. of mech props, comparison with mathematical model predictions *(Czech)* 79−91740
steel, CrMoV, failure in post yield regime using single edge notched tension specimens 78−68765
steel, data reduction for samples under high ambient press. and axial tension 78−3181
steel, deformation anisotropy in yield point, precompression effects *(Russian)* 78−11268
steel, fatigue strength, statistical prop. *(Japanese)* 79−20169
steel, for pressure tanks, yield point influence on brittle fracture, tensile strength *(German)* 80−40539
steel, fracture toughness determ., rel. to mech. props. 77−21277
steel, H_2 effect 78−15474
steel, heat resistant 15Kh1M1FL, cast, crack development at various stages of fracture, prolonged load 77−63802
steel, heat-resistant, 12Kh1MF, yield point rel. to dislocation density and cryst. lattice spacing *(Russian)* 77−44291
steel, hot rolled strip formability, mech. testing and mech. props. *(German)* 79−66089
steel, low C, creep, prestrain effects *(Korean)* 77−21227
steel, low C, plastic props., fracture, effect of strain rate in static tensile tests *(Czech)* 77−59866
steel, low C, pressurised, strain rate sensitivity prior to serrated yielding onset 78−48482
steel, low C, yield point, effect of ageing stress 79−96091
steel, low-alloy, plastic deform. mechanisms under dynamic loading 80−100883
steel, low-alloy, props. with nitride and Cu hardening at low temps. *(Russian)* 80−40372
steel, low-alloy structural, rel. to radiation hardening and embrittlement *(Russian)* 77−21243
steel, low-C, fully pearlitic, struct. and mech. characts. rel. to cooling conditions *(French)* 80−40425
steel, martensitic transform. critical temp. determ. 77−90349
steel, Mg effect on precipitation of C and or N, and mech. props., during strain ageing *(German)* 78−35387
steel, mild, AC effect on fatigue and static props. 80−45372
steel, mild, fracture toughness meas. with reinforced-double-cantilever-beam specimen 77−4842
steel, mild, microbehaviour of notch tip during increasing load in brittle fracture beyond general yield 78−35487
steel, mild, yield point, effect of neutron irrad. and N_2 conc. 80−45365
steel, mild cylindrical shells, limit loading under loop bending moment 78−80581
steel, Mn, H_2 embrittlement mechanism *(Korean)* 78−68774
steel, Ni-Cr-Mo, quenched and tempered, notched bar tensile tests *(German)* 80−35247
steel, plane C, nonstrain-ageing state 77−52349
steel, plastic flow area, determ. of relative elongation and rel. to yield point 78−23769
steel, precipitation hardening, strength and struct. *(German)* 79−47701
steel, quench ageing effect of Mn content on C and N precipitation and mech. props. *(German)* 78−31409
steel, quenched, tempering treatment, ultimate tensile strength and yield point *(Russian)* 77−32599
steel, reinforcement, low, high temp. static strength testing 79−15902
steel, research of Cottrell and Bilby, (1945-55) 80−62444
steel, S45C and SS41 types, dynamic yield condition under dynamic torsion and static tension 79−34214
steel, sorbitic, yield point rel. to average carbide particle size *(Russian)* 78−6967
steel, spring wire and springs, type 60S2A and 50KhFA, stress tempering effect on mech. props. 79−66085
steel, stainless, martensitic, ageing, strength/structural charact. relationship 77−90426
steel, stainless type 03Kh13AG19, deformation temp. influence on dislocation struct *(Russian)* 80−11698
steel, structural, C10, C15 and St52-3, grain size dependence of low yield point *(German)* 78−56689
steel, structural, exam. of mech. props. when under impulsive loading *(Czech)* 79−91742
steel, structural, susceptibility to brittle fracture criteria, comparison of notch impact and fracture toughness testing *(German)* 77−70237
steel, structural, wide plate tensile testing eval. *(German)* 80−100969
steel, toughness, review of joint tests *(German)* 80−65142
steel, VNS-5, damping capacity 77−1849
steel, yield point charact., grain size effect *(German)* 78−72810
steel (0.45 and 0.8 wt.%), strength, fracture, effect of H_2 *(Russian)* 77−25129
steel A-106, yield point suppression by H_2 79−8368
steel alloy, low-temperature testing, −196°C to +20°C 79−61692
steel alloys, low and medium C content, relaxation phenomena in volume changes during tempering *(Russian)* 79−100176
steel fire simulation, determ. method of critical value in case of nonstationary heating *(German)* 77−86268
yield point continued
steel OKh18N10T, subjected to low temp. thermal cycling, temp. depend. of yield point *(Russian)* 78−48489
steel plates, explosively clad, fatigue crack propagation behaviour *(Japanese)* 80−104262
steel U8, struct. and mech. props., effect of hydrostatic extrusion *(Russian)* 77−56022
steels, austenitic stainless, stress corrosion cracking, correl. between electrochem. and mech. parameters 80−97613
steels, wide plate and V-notch bending tests evaluation on basis of materials mechanics *(German)* 80−66571
steels, with yield pt. of about 420 to 720 N/mm^2, correlation between yield pt./tensile strength ratio and toughness *(German)* 80−66615
tensors of anisotropic component of yield condition *(German)* 77−23901
textile insulation tapes low-temperature testing, −196°C to +20°C 79−61692
textured aggregates, theoretical plasticity, anisotropy and yield function 79−32298
thermo-plasticity of irradiated metals 77−4146
thick walled tube, incremental collapse criterion, including yield point stress temp. depend. 79−98625
tuff, deform. charact., expt. study *(Japanese)* 78−56704
unified theory of elasticity and plasticity using rate theory type constitutive eqns. 78−9571
viscoplastic kinematic hardening model, cyclic loading appl., yield surface 80−79162
yield zone form., fracture resistance, influence of specimen configuration 78−68817
Zircaloy-2, yield pts. obtained by ageing at two stresses 80−81091
Zircaloy-4, exam. of plastic props. at elevated temps. in air 77−4811
Ag and Ag-Sn(In)(Sb) dil. alloy, single crystals, dynamic dislocation behaviour 77−4108
Ag, yield point, 4.2 to 300K, depend. on cryst. purity *(Russian)* 79−20116
Ag, yield point, temp. depend., 2 to 300K *(Russian)* 80−45346
Ag-Ni (10 wt.%) wire, plastically deformed, fracture struct. *(German)* 80−71744
AgMg, deform. at high temp., yield pts. 79−61674
Al alloy, fracture toughness determ., rel. to mech. props. 77−21277
Al alloy, PA2N (AlM2), yield surface, effect of 2-D cyclic loading 79−34097
Al alloy 7075-T6, notched sheet under tensile loaded, notch tip opening/contraction, J-integral relationship *(Japanese)* 77−4840
Al, bicrystal having Σ7 and Σ21 coincidence tilt boundary, plastic deform. *(Japanese)* 79−66116
Al, isotropic hardened, yield condition 79−61653
Al, polycrystalline, acoustic emission energy release, grain size and flow stress depend. 80−11722
Al, strength changes on US treatment in programmed loading *(Russian)* 77−32583
Al, yield surfaces from dislocation mechanics 77−14917
Al-Be, two-layer foils, mech. props. *(Russian)* 78−51858
Al-Mg-Si, Portevin-Le Chatelier effect, effect of precipitation hardening 77−32585
Al-Mn profiled alloy components pulled from melt, physicomech. props. 78−3175
AlMg5, memory effect of plastically deformed alloy under complex loading 79−38891
C steel, crack initiation lives at stresses near endurance limit, probability distribs. 77−86127
$CdO-WO_3-H_2O$, interconnection between kinetics of structure formation and chem. reactions 78−53198
CsI, mechanical props., effect of impurities 77−69034
CsI, yield point, obstacles to dislocation motion 77−43270
Cu, creep resist., yield point and hardening under alternating torsional strains *(Russian)* 77−32587
Cu, filament produced by glass-coated melt spinning, tensile strength 77−48508
Cu, isotropic hardened, yield condition 79−61653
Cu, low-temperature testing, −196°C to +20°C 79−61692
Cu, neutron irrad. cryst., slip bands in yield region, high-speed cinematographic recording 79−7607
Cu, plastically deformed, lattice strain distrib. *(German)* 80−85012
Cu, single cryst., deform. process, effect of surface layer 79−8315
Cu, strain hardening parameters, 4.2 to 300K *(Russian)* 79−20063
Cu-Ag (3 at.%), plastically deformed, lattice strain distrib. *(German)* 80−85012
Cu-Ag(Se)(Sn)(Ag-SeSn), Ag, Se, and Sn effects, singly and together, on recrystallisation 79−100164
α-Cu-Al (0.5 to 10 at.%), latent hardening and dislocation density 78−19853
Cu-Al (7.5 at.%), single crystal, etched under load, slip bands 77−89446
Cu-Al alloys, strain hardening parameters, conc. and temp. depend., 4.2 to 300K *(Russian)* 79−20063
Cu-Al-Ti-Zr, internally oxidized, morphology of precipitates and dispersion hardening *(Russian)* 79−52217
Cu-Be alloy props. obs., dependence on heat treatment *(Czech)* 80−55448
Cu-Cd (1.0 wt.%), yield stress and flow stress 80−97524
Cu-Si(Ge), dissoc. dislocations pinning by Suzuki effect *(French)* 79−100223
Cu-Zn-Si, deform. close to martensitic transform. temp. 77−63714
Fe, Armco, Bauschinger effect, computerised evaluation method 80−93625
Fe, Armco, strength, fracture, effect of H_2 *(Russian)* 77−25129
Fe, Armco, struct. and mech. props., effect of hydrostatic extrusion *(Russian)* 77−56022
Fe, cast, thermal treatment influence on mechanical props. *(German)* 80−29980
Fe, filament produced by glass-coated melt spinning, tensile strength 77−48508
Fe, H_2 effects 78−15474
Fe, isotropic hardened, yield condition 79−61653
Fe, quenched-in hydrogen, yield stress decrease of prestrained specimens 80−16454
Fe, relaxation process effect on initial stages of flow *(Russian)* 79−74189
Fe, sintered, porous, yield point *(Czechoslovakian)* 77−28748
Fe, var. in mag. moment of ferromags. during plastic deform. *(Russian)* 77−66401

yield point continued
α-Fe, yield point behaviour for extremely inhomogeneous deformation *(German)* 80−55453
α-Fe, yield point behaviour in homogeneous plastic deformation *(German)* 80−35248
Fe-Cr-Ni alloy, deforming stresses anomalous temp. depend. *(Russian)* 77−81296
Fe-Ni single crystals, stress induced martensite 77−8827
Fe-refractory compound condensate, struct. and mech. props., disperse particle content depend. *(Russian)* 78−19772
Fe-Si, glissile and twinning dislocation motion temp. depend., influence of grain boundaries *(Russian)* 77−47452
Fe-Si (2.6 wt.%) single cryst., crack propag., controlled plastic crack tip opening rate 80−60943
Fe-Si (3 wt.%), singularities in geometry of slip, point temp. depend. *(Russian)* 79−24574
Fe-Si (3 wt.%), yielding phenomena at high temp. *(Japanese)* 77−48489
InP single crystals, uniaxial compression deform. characts. 80−84991
InSb, X-ray topographic evidence of asymmetrical pre-yield behaviour 80−75229
KCl, US plastic deform., dislocation struct. 80−19809
LiF, electron irradiated, mech. characts. 78−26595
MgF_2, single cryst., tensile strength and yield point, temp. depend. 77−14785
Mo, mag. field effect on mech. props. and dislocation struct. *(Russian)* 79−42818
Mo, mechanical props. and dislocation struct., mag. field effect 80−54935
Mo-V-C, hot-worked, substructural hardening and high-temp. strength *(Russian)* 80−25731
NaCl, dislocation struct. of slip bands, hydrostatic press. effect 80−54249
NaCl, strain ageing exam. 78−56661
NaCl:Ca^{2+} crystals, influence of dipoles and dipole complexes on yield point 80−39208
Nb, cold-worked, Snoek-Koster relaxation transient period, comparison with Schoeck's theory 79−34086
Nb, mag. field effect on mech. props. and dislocation struct. *(Russian)* 79−42818
Nb, mechanical props. and dislocation struct., mag. field effect 80−54935
Nb single crystal, yield point and dislocation struct. temp. depend. *(Russian)* 77−81290
Nb-Mo solid soln., single cryst., yield point and dislocation struct., temp. depend. *(Russian)* 77−81290
Nb-Zr-C, (1, 0.1 wt.%) alloy, mech. characts. structral sensitivity in strained state *(Russian)* 79−52301
Nb_3Sn, hot isostatically pressed, plastic deform. 80−108510
Ni 200, C interstitial effect of yield point develop. during static strain ageing, model 78−88498
Ni, deformation in const. mag. field, 4.2K *(Russian)* 80−29591
Ni, magnetised mono- and polycryst., activation vol. var. during low temp. deform. *(Russian)* 78−3178
Ni, yield point, effect of alloying elements *(Russian)* 80−50670
Ni-Cr machine steel, austenite grain size effects on mech. props. *(Russian)* 77−44292
Ni-ZrO_2, thin layers, vapour deposited, dispersion strengthened, exam. of struct., mech. props. 78−80554
Ni_3Al and $Ni_3(Al,Ti)$, deformation characts., temp., strain rate and orientation depend. 77−44320
Pb-Sb, influence of quench deform. on precipitation *(German)* 77−86064
PbS single crystals, plastic deform. thermal activation anal., dislocation behaviour, point defect influences 79−65095
$Pd_{80}Si_{20}$, plastic flow, fracture, slanted necking and elongation at high temps. 79−57057
$SbS_xSe_{1-x}I$ layer elec. and ferroelec. props., mech. stress effects *(Russian)* 80−50279
Si, dislocation dynamics in plastic deform., theoretical anal. 79−42077
Si, plastic deformation, dislocation density in yield point area *(German)* 78−38720
Sn-Sb (0.57 at.%) solid soln., yield point for cold-worked and annealed specimens *(Russian)* 78−48448
Sn-Zn (0.4 at.%) solid soln., yield point for cold-worked and annealed specimens *(Russian)* 78−48448
Ti alloy, fracture toughness determ., rel. to mech. props. 77−21277
α+β Ti alloys, fracture, influence of phase comp. in VT16 and VT9, quenching effects *(Russian)* 78−56665
Ti, commercial, creep behaviour, 25 to 400°C, role of impurities and/or alloying elements *(French)* 80−45354
α-Ti, commercial purity, static strain ageing 77−86061
Ti, commercial purity, stress relaxation expt. 77−48472
Ti, yield pts. obtained by ageing at two stresses 80−81091
Ti-Al-V-Sn(Mo-Fe), heavy section extrusion, fabrication and mech. props. 78−6985
β-Ti-Mn, exam. of reloading yield points 78−72822
W, strength, temp. depend. 77−1871
α-Zircaloy, strain ageing at 1000K 79−47725
Zn single cryst., dislocation velocity and plastic deform. 80−64998
Zn, single cryst., plastic deform., 1.5-300K *(Russian)* 77−77533
Zr, neutron irradiated, yield point phenomenon 79−52304
α-Zr, strain ageing at 1000K 79−47725
Zr, yield pts. obtained by ageing at two stresses 80−81091
Zr-Nb (2.5 wt.%), nuclear fuel channels, neutron effects on ultimate fracture strength, 293 to 573K 80−85054
Zr-O-N system, struct. and plastic deform. *(Russian)* 78−80588

yield strength
ageing alloys, single cryst., deform. and hardening 78−23716
alloy, strain rate sensitivity rel. to ductility, anomalies 77−36590
alloys, two-phase, coarse microstructs., structural approach to yield strength 80−7634
bar (tube), compressible, combined loading, elastic-plastic problem 78−63311
brass, cold rolling, inhomogeneous texture 80−89251
α-brass, concentrated single crystal, yield region investigation, CRSS, slip 77−48478
α-brass stress corrosion cracking in nontarnishing ammoniacal environment, fractography, chemical anal. 77−40466

yield strength continued
bronze P, heavily cold rolled, yield strength enhancement mech. 77−36539
butt joint, tensile bond strength, effect of aspect ratio 80−50823
composites, unidirectional, micromech. prediction of initial yield surfaces 80−25777
convexity of yield bodies of isotropic and anisotropic media *(German)* 79−98624
crack opening displacement, interrelation with J-integral 79−50648
deep circular notches, plane strain general yielding under loads and bending 79−18809
dental restorative materials, empirical eqn. including fracture toughness for friction 78−61283
diamond, compressive strength for [111] loading 79−79036
diamond, high press. appl. by spherical diamond indentor, plastic deform. obs. method 78−35619
diamond, sintered compact, stress-strain curves using ultrahigh-pressure apparatus 79−43322
diamond, yield stress from Hugoniot elastic limit and elastic consts., compressive yield strength 79−83261
elastomers, rel. between relax. behaviour and tensile strength *(German)* 80−66604
elastoplastic solid, fracture and yield conditions 79−14344
ELN-1 alloy, prestrain effects on strength *(Russian)* 78−11267
endosseous implant material, radiation processed alumina-polyacrylic acid composite 77−60308
epoxide resin, tensile, compressive and shear yield strengths, pyramidal criteria 77−8884
ethylene-base ionomers, impact tensile props. *(Japanese)* 79−96120
fatigue crack propagation, crack closure, effective stress range factors 80−100924
ferritic alloy, reinforced by dispersed oxide, mech. props., modification by recovery heat treatment *(French)* 77−59837
fracture toughness screening using sharp notch tension 77−56169
glass fibre reinforced polyester, epoxy-polyamide, single lap joint, tension-shear strength *(Japanese)* 78−11494
glass fibre reinforced polyester, single lap joint, tension-shear strength *(Japanese)* 78−11494
heat resistant weld seam metal, tensile strength, thermophysical characts. 79−91769
heat treatment, struct. and mech. props. 78−52864
heat-resistant alloys, installation for mech. tests under superplasticity conditions 80−55603
Incoloy 800, mech. props. above 600°C 79−43370
Inconel alloy 718, exam. of struct., properties and continuum synthesis of ductile fracture 78−76736
metal, deformation heat during forming, eqn. *(German)* 79−66105
metal, diffusional relaxation of stress conc. at second phase particles 79−1889
metal mechanical property effects on frictional behaviour 80−55548
metal structures, collapse load and energy absorpt., matrix anal. methods 77−35050
metallic glasses, friction coeff. determ. using sliding friction rig 80−89355
metallic materials, erosion resistance, eval. of role of mech. props. 79−83328
metals, constitutive model at high strain-rate, shear modulus, yield strength 80−75292
metals, determ. of yield strength 80−25937
metals, plastic yield criteria, interpolation scheme 80−64400
metals and alloys, fracture toughness determ. in conditions of similarity to local fracture *(Russian)* 78−31505
metals and alloys, strength/ductility relation *(Japanese)* 79−29145
metals and alloys, stress-strain time dependence based on nonlinear heredity, delayed yielding 78−48452
microstruct. and tensile props. 80−34077
mild, plastic flow under proportional and non-proportional straining at controlled rates 79−57084
montmorillonite, mech. props. at high press., rel. to fault behaviour 79−84234
Nimonic 115, superalloy, critical strain model for creep fracture 77−32648
notch-tip geometry, influence on stress and strain distrib. 80−33535
Nylon 6, unidirectionally reinforced, mech. props. and fracture 77−21252
1-nylon polymers, stress-strain curve 80−60938
obstacle controlled, theory, workshop 77−32645
optical ceramic KO-1 strain, yield limit, and stress relaxation obs. 79−46018
pipeline girth welds, NDT of defects 78−27704
plastic constitutive equations with work hardening *(Japanese)* 80−25718
plastic deform., generalised constitutive eqns. 80−104219
poly(2,6-dimethyl-1,4-phenylene oxide)/poly(styrene-co-p-chlorostyrene) blends, tensile props. modelling 80−19868
poly(β-methylalanine), methacrylamide polymerisation by H transfer, catalyst sodium-napththalene *(Japanese)* 78−95726
polyacetal, stress-strain relations, effect of strain rate and static outer press. *(Japanese)* 77−52418
polycarbonate, plastic insulation for cryogenic power cable, exam. of dielectric, tensile props. 80−25823
polycarbonate, stress-strain relations, effect of strain rate and static outer press. *(Japanese)* 77−52418
polyester (Mylar), plastic insulation for cryogenic power cable, exam. of dielectric, tensile props. 80−25823
polyethylene: (Dy_2O_3), mech. props. and transfer to steel surfaces 80−16496
polyethylene, branched, frictional props., normal force/shear for relationship 79−47785
polyethylene, photodegradation mechanism, from yield strength, elongation and mol. wt. studies *(Japanese)* 80−76311
polyethylene, photodegradation study by Fourier transform IR spectroscopy *(Japanese)* 79−24772
polyethylene, plastic insulation for cryogenic power cable, exam. of dielectric, tensile props. 80−25823
polyethylene ribbons, flow-induced crystn. from melt, in dies fed by single screw extruder 80−84110
polymer, failure, book 78−92361
polypropylene, flow-induced crystn. from melt, in dies fed by single screw extruder 80−84110

yield strength continued
polypropylene, fracture toughness eval. with surface crack specimens 79−15777
polypropylene, oriented, compressive elastic modulus and yield strength 80−16385
polypropylene, plastic insulation for cryogenic power cable, exam. of dielectric, tensile props. 80−25823
polystyrene, coarse shear bands and fracture, SEM study, craze fracture surfaces 79−29191
polystyrene, fracture toughness eval. with surface crack specimens 79−15777
polysulphone, plastic insulation for cryogenic power cable, exam. of dielectric, tensile props. 80−25823
polyvinylidene fluoride, γ-ray irradiation effect on mech. props., in presence of triallyl trimellitate *(Japanese)* 77−86091
powder, triaxial test procedure and num. calc. method for flow props. 77−60028
PVA carbonisation process and carbonised block props., high temp. resistant materials *(Russian)* 79−8268
PVC, rubber-modified, stress whitening and yield mechanism 79−8324
reinforced concrete containment model behaviour under thermal gradients and internal pressure 80−42837
rock, deformation and fracture under general triaxial stress states, anisotropic dilatancy *(Japanese)* 78−56750
sand, triaxial test, bifurcation anal. 79−70783
sheet material, method for strength meas. under biaxial tension 80−66717
shells of revolution, plastic, limit anal., lower bound numerical method 78−63337
single crystals, dislocation mobility under conc. loads at indentations 79−95015
sludge, cohesive, dynamic props. *(Japanese)* 80−45580
solid solution hardening, statistical behaviour analysis, with aid of computer *(Japanese)* 80−11658
spinodal alloys characterisation techniques, props. and appls., review 80−50588
steel, 12Kh18N9T-TiB_2, eutectic alloy, high temp. props. 78−84931
steel, 24Kh2NMFA, crack resistance, yield strength, ductile-brittle transition temp., optimum tempering of 24Kh2NMFA 77−63787
steel, 4140 compact, fatigue crack growth delay, yield strength, neg. stress ratio depend. 78−3210
steel, Al-killed, sheets, effect of strain path changes on formability 79−43347
steel, alloy, 300M, fracture toughness and strength, effect of heat treatment on microstruct. 78−15436
steel, alloy, Mn-Cr-Cu, exam. of ductility when deformed, alloying addition effects 78−44175
steel, alloy, toughness evaluation inconsistency of AISI 4340 austenitised at increasing temp. 78−52982
steel, alloy, type 4340, fracture toughness, effect of partially dissociated N_2 78−80642
steel, alloy 18G2AV, residual stress distrib. effect on fatigue crack growth 79−57111
steel, alloy 4340, fracture and high temp. props., 533K to 1255K 78−60821
steel, austenitic, 800H, effect of hardening processes on initial stress-strain curve 78−84846
steel, austenitic, corrosion-resistant, strengthening by alloying with N_2 78−95757
steel, austenitic, Mn-base, as LNG storage and transportation system material 79−70133
steel, austenitic, tensile strength, elec. current impulse effect down to 4.2K 80−81131
steel, austenitic stainless, 316, surgical implant ion beam textured, stress/strain relations, fatigue characts. 78−73297
steel, austenitic stainless, biphase, ferritic, ageing and thermomech. treatment effects on struct. and props. 80−35226
steel, austenitic stainless, Cr-Ni, Mn and Mo effect on mech. props. rel. to treatment 79−96039
steel, austenitic stainless, martensitic transform. effect during static and fatigue loading 77−52325
steel, austenitic stainless, mech. props. correl. methodology development for fusion environments 80−29068
steel, austenitic stainless, porous fibre, sintered and compacted, mech. props. 79−15623
steel, austenitic stainless, strain hardened containing N_2, low temp. props. 79−66128
steel, austenitic stainless, supercond. magnets, mech. and phys. props. at 4K 80−86976
steel, austenitic stainless, type 321S12, fatigue cycling in R = −1 loadings 80−35317
steel, austenitic stainless, yield strength, effect of N_2 additions and grain size, solid soln. strengthening 77−52430
steel, austenitic stainless JIS type 304, tensile test at elevated temp., high velocity 77−73302
steel, austenitic stainless SUS 301, stress corrosion cracking susceptibility, effect of strain-induced α′-martensite *(Japanese)* 80−104335
steel, austenitic stainless tensile ductility in air and H_2 77−66687
steel, austenitic stainless types 304 and 316, environment effect on crack growth, under creep and fatigue conditions 80−85035
steel, austenitic-martensitic, yield strength rel. to struct. and phase comp. 79−66127
steel, C, bainitic, microstruct. and cleavage resistance 77−52481
steel, C, cumulative damage rule, based on reduction in fatigue limit, experimental confirmation 78−92358
steel, C, type 1792AF 79−38966
steel, C, US exam. of yield and breaking strength 79−15755
steel, C-Mn, pressure vessel usage, elevated temp. mech. beahviour 78−35462
steel, C-Mn-(Cr), structural changes during stress cycling after heat treatment and cold rolling *(Russian)* 78−19787
steel, C-Mn-V-Cb-N, high strength low alloy, controlled-rolled 80−100803
steel, cast automatic couplings, yield strength, crack propag. resistance and ductile-brittle transition temp. 80−104281
steel, CC Ti-C, threshold fatigue behaviour, effect of grain size and yield strength 79−91790
steel, cold rolled, high strength, mech. props. 77−36527
steel, cold rolled high strength sheet, with high drawability, fabrication process 77−73288
yield strength continued
steel, comp. and processing effects on microstruct. and props. rel. to low temp. applic. 77−52365
steel, constructional, struct., props., isothermal thermomechanical working *(Russian)* 77−25076
steel, Cr (12 wt.%), thermomechanical treatment, high temperature, effect on props. and struct. *(Czechoslovakian)* 77−32603
steel, Cr-Mo, cast and forged, difference in mech. props. 77−48465
steel, Cr-Mo, effect of Mo on high-temp. props. 80−85005
steel, Cr-Mo, grain size effect on ductile brittle transition 79−24615
steel, Cr-Mo (10-14, 2-6 wt.%), heat-resist., creep-rupture strengths 80−104271
steel, Cr-Mo-V pressure vessel, microstruct. parameters and yielding rel. to plastic deform. 80−89318
steel, die, with high heat resist. and toughness 78−84989
steel, duplex ferrite-martensite, microstructure resistance optimisation 80−40482
steel, effect of H_2 on phys. and mech. props. 80−101657
steel, eutectoid, mech. behaviour, thermomech. treatment effects 80−84970
steel, fatigue and cyclic plasticity rel. to struct. inhomogeneity 80−81184
steel, fatigue crack propagation rate in types 15KP, ST3, 15G and 10G251 with different yield strengths 78−52987
steel, Fe-Mn, improvement of cryogenic mech. props. through thermal/mech. treatments 79−79098
steel, ferritic stainless, embrittlement 80−85041
steel, ferritic-martensitic, fatigue crack tip plastic zone *(Japanese)* 80−71738
steel, fracture toughness, temp. and loading rate effect 77−36663
steel, H_2 assisted cracking equilibrium and kinetic studies 78−3201
steel, high alloy Cr-Mo-W, splat quenched, formation of metastable austenite 80−84974
steel, high speed type M-50 and 18-4-1, fracture and fatigue 80−16457
steel, high strength, fatigue crack growth 78−64697
steel, high strength, low alloy, mech. props. 78−60739
steel, high strength, low C, with N_2, yield strength, Mo effects 77−90410
steel, high strength, Nb(C, N) precipitation in austenite, effect on mech. props. *(Japanese)* 77−21186
steel, high strength, press. depend. yield and plastic vol. change 78−19810
steel, high-speed, quenched and tempered notch toughness, ultimate and yield strength in tension and compression 78−95782
steel, high-strength, dynamic yield strengths, phase transition press. and Hugoniot parameters 80−75331
steel, high-strength, gun barrel, fracture mechanics 77−77569
steel, high-strength plate with soft cladding layer, failure resistance during repeated static banding 77−44406
steel, hot rolled, low C, low alloy, bainitic alloying addition effects on microstruct. and props. 77−36546
steel, HSLA, V effect on mech. props. *(Korean)* 80−29987
steel, hypereutectoid type HF-1, microstruct. effects on fracture toughness, ductility, strength 79−74255
steel, irradiation by neutrons, damage function for mech. props. 78−13228
steel, low alloy, exam. of fatigue crack growth, and Paris Law parameter relationship 78−92343
steel, low alloy, ferritic-pearlitic, carbonitride hardening 80−104174
steel, low alloy, hot deform. behaviour and modified ausforming *(Japanese)* 78−11244
steel, low alloy, impurity and strength effect on H_2 induced cracking 78−27625
steel, low alloy, microstruct. effects on fatigue at intermediate and high crack growth rates 79−74247
steel, low alloy, naval, stretch zone width meas., COD for ductile crack initiation 78−68813
steel, low alloy, strengthening by strain tempering, deform. effects 78−15424
steel, low alloy, type 10KhN1M, heat-treated, struct. and resist. to thermal embrittlement 79−15788
steel, low alloy, type 3sp, effect of temp. at end of rolling on mech. props., and coercive force 78−72799
steel, low alloy, type 4340, quenched and tempered, effect of plastic strain followed by ageing, on torsion fatigue resistance 78−92360
steel, low C, annealed, fatigue crack propag. law under elastic-plastic and general yield conditions *(Japanese)* 77−48538
steel, low C, fatigue crack propag. prestrain effect *(Japanese)* 79−96116
steel, low C, ferritic, static yield prop. changes during fatigue cycling 77−52427
steel, low C, P, plastic anisotropy and mech. prop. dynamic strain ageing effect 78−64608
steel, low C, rephosphorised static strain ageing 77−70079
steel, low C, rimmed, structural damage in sheet metal forming 78−64614
steel, low C, strain ageing, effect of prestrain *(Korean)* 77−8865
steel, low C, tempered, lath martensite, Ni (5 wt.%), microstruct./yield strength relationship 77−21234
steel, low C, unnotched specimens, brittle fracture beyond general yielding tensile-torsional stresses 77−56096
steel, low-C, fatigue strength, low-cycle, effect of shock wave press. 79−29205
steel, low-C martensitic, Ni addition influence on toughness and ductile-brittle transition 80−30099
steel, maraging, (18 wt.% Ni), solution annealed, exam. of cryogenic tensile, fatigue, and fracture props. 78−92311
steel, maraging, hardening mechanism of quenched samples, tempering *(Czech)* 79−78989
steel, maraging, high strength, gaseous H_2 embrittlement 77−86147
steel, maraging, influence of microstructure, strain rate and temp., on tensile props. 80−11733
steel, maraging, steady state unidirectionally solidified, austenite reversion and determ. 77−25118
steel, martensite and ferrite-pearlite, fatigue crack growth rates, stress ratio dependence 79−70148
steel, martensitic, as LNG storage and transportation system material 79−70133
steel, microalloyed, precipitation effect on microstruct. and mech. props. *(French)* 80−25708
steel, microalloyed, types V1599, V1600, V1286, NbCN precipitation in undeformed austenite 80−89230

yield strength continued
steel, mild, yield strength and fracture toughness, microstruct. effect, heat treatment 78−27615
steel, Mn-Cr-Mo, Mn-V-Mo, high-strength heat-treatable sintered 80−50575
steel, Mn-Si, St 52-3, cleavage fracture toughness, temperature and notch sharpness influence *(German)* 80−35291
steel, Mn-Si, St 52-3, fracture toughness determ. from yield strength and cleavage fracture strength *(German)* 80−35292
steel, Mn-Te, structural, brittle fracture resistance, Ti addition effect *(Czech)* 80−45392
steel, Mn-V reinforcing type, strain ageing characts. rel. to mech. props. 80−84969
steel, Nb-Va microalloyed, mech. props. *(French)* 80−35252
steel, Ni, welded joints on LNG carriers mech. props. and fracture toughness 80−85017
steel, Ni-Cr-Mo, cleavage fracture toughness, temperature and notch sharpness influence *(German)* 80−35291
steel, Ni-Cr-Mo, fracture toughness determ. from yield strength and cleavage fracture strength *(German)* 80−35292
steel, normalised, C-Mn-P, P effect on mech. props. 77−63745
steel, pearlitic, strength, fracture, microstructure effect 77−40449
steel, quenched and tempered, environmentally assisted fatigue crack propag. 77−44403
steel, rail, toughness, effect of Sn, SEM exam. 80−97569
steel, sheet, rapid test for props. assessment 80−40650
steel, silchrome, thermomech. hardening 78−23736
steel, stainless, 10Kh18N9TL, S, Se, Te and Bi additions effect on mech. props. 79−83312
steel, stainless, 316, 304, LMFBR primary piping materials, mech. props., review 77−25151
steel, stainless, C-Cr-Ni-Mn-V , non mag., aged, struct. and mech. props. *(Russian)* 78−56666
steel, stainless, cold-worked, 316, chem. comp. effects on rupture life, tensile props. 77−25152
steel, stainless, Cr-Ni-Co (13, 4.5, 0 to 13.8 wt.%), Co effect on martensite ageing *(Russian)* 77−66660
steel, stainless, deformation temp. determ. for high yield strength 78−44177
steel, stainless, ferritic, mech. props., impurity effects *(Russian)* 77−52403
steel, stainless, fracture toughness, −20 to +22°C, of type UNS-S 15500 79−70145
steel, stainless, sulphide stress corrosion cracking resistance, improvement by heat treatment 78−7076
steel, stainless, type 304, description of deformation induced plastic anisotropy 79−43268
steel, stainless, type 316, 20% cold worked, exam. of creep 78−72817
steel, stainless, type 316, modelling effects of fast neutron irradiation in mech. behaviour 80−84234
steel, stainless AISI 316, fatigue crack growth, effect of grain size on threshold stress intensity 78−44216
steel, stainless type 316, neutron irradiated, transient mech. response prediction 79−74207
steel, stainless type XM-19, influence of recrystn. behaviour on mech. props. 79−83213
steel, statistical treatment of experimental data 80−53644
steel, strength, acoustic monitoring 80−35479
steel, structural, classification according to ductile-brittle transition temp. 78−11298
steel, structural, sharp notched bending specimens, fracture stress, temp. depend. anal. 77−56062
steel, tempered, high strength, internal stresses and mech. props. 80−3200
steel, Ti, hot-rolled, inhomogeneity of mech. props. *(Chinese)* 80−55455
steel, tool, high-strength, mech. props. in compression, tempering temp. effect 79−83240
steel, type 10G2SAF, yield strength, influence of deform. rate *(Bulgarian)* 80−89315
steel, type IN-787, for use in Arctic, low temp. effects on mech. props. 80−76310
steel, V and V-N , high strength, mech. props. and strain ageing, processing variables effects 77−59819
steel, V high-strength low-alloy, for low temp. use, tensile and yield strength 79−70118
steel, VN precipitation after heat treatment 79−29067
steel, yielded pipeline, fracture resistance changes, impact tests 77−16667
steel 17G1S, magnetic method of mech. prop. determ. of thick sheet 78−48600
steel bimetallic tube with internal Cu coating segmental specimens, tensile testing 79−70255
steel H-beams, tensile samples shape influence on results of mech. props. determ. 77−52569
steel Kh, work hardening under nonisothermal loading 79−57005
steel St.3kp, ductile-brittle transition temp., variation with grain size 78−27640
steel tubing, cold rolled, nondestructive mag. method for determ. of mech. props. 78−23903
steel/Cu bemetallic pipe, determ. of yield, tensile strength 80−25771
steels, wide plate and V-notch bending tests evaluation on basis of materials mechanics *(German)* 80−66571
structural reliability, using chance-constrained programming, appl. to reinforced silo 78−63338
superconducting magnets, pulsed, hysteretic and mechanical loss calcs. 79−80649
suspension, conc., of aggregable particles, viscosity calc. 79−7362
tensile machines, temperature control of suspended electric furnaces 77−82523
TZM-Mo alloy, mech. props., effect of exposure to high temp. He containing O_2, room temp. study 80−93639
wedge shaped notches with large flank angles, plane strain general yielding under loads and bending 79−18808
wire in torsion, installation for automated determination of yield strength 80−21221
Zircaloy, in-pile temp. depend of yield strength and growth, under neutron irrad. 79−73219
Zircaloy cladding, irrad., tensile props., effects of temp., strain rate and annealing 77−48463
Zircaloy tubes, yield loci, evaluation based on texture data and mech. testing 79−91695

yield strength continued
Zircaloy-2, effect of simulated fission products on elongation fractography and metallography 80−649
Zircaloy-2 cladding tubes, heat treatment influence on texture and mech. anisotropy 79−91694
Zircaloy-4, H_2 effect on mech. props. *(Korean)* 79−70123
Zircaloy-4 tubes, texture influence on anal. of thermoelastic/plastic anisotropy and initial yielding 80−35260
Ag, cold rolling, inhomogeneous texture 80−89251
Ag-Cu-Zn-(Cd)(Mn), solder, UTS, room temp. to 4.2K 79−57064
Al 6061-T6 alloy, shock-compressed, reshock and release 77−32732
Al alloy, crack opening displacement, expt. and FEM study 78−68811
Al alloy, mechanical properties, correlation with elect. cond. 79−34114
Al alloy, particle strengthened, yield drop and creep minimum *(German)* 78−39881
Al alloy, yield surface of material subjected to combined cyclic loadings 78−84905
Al alloy 01205, mech. props. at cryogenic temps. 79−29206
Al alloy 2024-T3 77−56049
Al alloy 6061, thermomechanically treated elev. temp. mech. props. 79−8310
Al alloy 6061-T6, yielding of tubing under dynamic biaxial loading 80−16377
Al alloys, (5083, 6061, 2219), supercond. magnets, mech. and phys. props. at 4K 80−86976
Al alloys, cryogenic, AMg5 and AMg6, mech. props. at −196°C 77−63748
Al, cold rolling, inhomogeneous texture 80−89251
Al, commercially pure, prestrained, yield criteria and stress-strain relations anal. 79−57051
Al foils, high strength, vapour deposited on curved surfaces, quantitative characterisation 80−80144
Al, high purity 6061, thermomechanical treatment 77−44277
Al, non-elastic deformation, phenomenological model with solute strengthening effect incorporation 78−39832
Al, recovery and recrystallisation during temperature strain *(Czech)* 77−73287
Al, recrystallisation and recovery during temperature strain *(Czech)* 77−70071
Al, use in design of composite superconductors in elasto-plastic region 77−28851
Al/Al_xO_y vacuum deposited laminates, struct. and mech. props. 79−28219
Al-(Mg)(Fe), pure (dilute), large wire drawing plastic deform. 80−108508
Al-Ag, thin-layered laminates, yield strength rel. to dislocation generation and motion 79−20137
Al-Al_3Ni, aligned, eutectic alloy, mech. behaviour at high strain rates 78−39855
Al-Cr (3 to 11 at.%), cooling rate effect on solidification struct. and mech. props. *(Japanese)* 78−39755
Al-Cu, thin-layered laminates, yield strength rel. to dislocation generation and motion 79−20137
Al-Cu (2.6 wt.%), sheets, effect of strain path changes on formability 79−43347
Al-Cu (4 wt.%), relationship between enthalpy, yield strength, and size of Guinier-Preston zone *(French)* 78−19767
Al-Cu (4.6 wt.%), cold work and ageing influence on ductility and fracture behaviour *(Japanese)* 80−89295
Al-Cu-Mg, type 2036, deformation at ageing temp., effect on struct. and props. 80−7605
Al-Cu-Mg-Zn, Mg and Zn addition effects on dendrite struct. and mech. props. *(Korean)* 77−28796
Al-Cu-Mn (1-5.2, 0-0.6 wt.%), N alloying and comp. effect on mech. props. *(Bulgarian)* 80−71719
Al-$CuAl_2$ aligned, fracture, effect of growth speed, orientation, environment 77−28907
Al-Li-Mn (2.8, 0.3 wt.%), recrystallised sheet, fracture behaviour, SEM and TEM study 80−97566
Al-Mg-Cu-Si-Cr (1,2.7,0.6,0.2wt.%), laser shock hardening of weld zones 78−39800
Al-Mg-Li-Zr alloys, struct., mech. props. 79−24498
Al-Mg-Mn-Cr (4, 0.45, 0.15 wt.%), laser shock hardening of weld zones, exam. 78−39800
Al-Mg-Si, type 6061-T6, 6063-T6, effective stress range factor in fatigue 80−100924
Al-Mg-Si (0.7, 0.4 at.%), effect of precipitation hardening on strain rate behaviour and yield behaviour 79−29075
Al-Ni (6 wt.%), fine-grained, deform. in tension and torsion 80−85008
Al-Si eutectic, directionally solidified, tensile props. 78−64531
Al-Si(9.3, 12) with graphite particles seizure resistance study using Hohman wear tester 80−89360
Al-Zn eutectoid, superplasticity, test machine rigidity effect 79−70250
Al-Zn-Mg alloys, role of dispersed transition metal intermetallic compounds 79−96088
Al-Zn-Mg-Cu, optimum treatment combination for thermochemical processing 77−44278
Al-Zn-Mg-Cu alloys, heat treatment optimisation 80−60888
Al_2O_3, vacuum condensate, struct. and mech. props., second phase effect *(Russian)* 80−71705
BaF_2, formation and growth of oxidation centres result of O^{2-} diffusion 80−7706
Be bronze, struct. and props. after ageing under load 78−84932
Be fibre reinforced Ti-Al-V (6.4 wt.%), synthesis and mech. props. 77−32544
Be, polycryst., yield strength, struct. factors effects 77−63749
Be-Cu high-strength alloy characteristics for electrical components 78−48547
C evaporated films, nucl. appl. 80−23214
C fibre reinforced composites, kinking as structural degradation mode 78−52893
C fibre reinforced polyethylene, for medical appls., tensile and flexural props. 78−31969
C steel, yield strength, anisotropy in relation to temp. of deformation 78−80612
CU-Zr-(Cr), powder metallurgical alloys, thermomech. treatment effect on props. 80−50660
CaF_2, press forged, mech. and optical props. 80−38079
Cd, warm rolled, texture and grain size depend. of tensile props. 80−71720

yield strength continued
Co based metallic glass, B and P glass former additions, elastic consts., flow behaviour correlations 78−44154
Co-base superalloy, machine thixocast, mech. prop. deficiencies 79−74244
Co-Fe-V-Ni, mag. and mech. props., heat treatment and stress effects 80−60363
Co-Ni-Cr superalloys, γ′-precipitation-strengthened, yielding 77−8894
Co-Ti-Fe (3, 1 to 2 wt.%), spinodal decomposition 80−100839
Co-W-Cr (15,20 wt.%), surgical implant ion beam textured, stress/strain relations, fatigue characts. 78−73297
Cu alloys, flat spring, mechanical props. in bending, stress relax. test, 23 to 232°C 78−72806
Cu based materials, sputter deposited at high rate, microstruct. and props. 78−22988
Cu, cold rolled sheet, anisotropy of elastic and strength props. 80−81077
Cu, cold worked, grain size effects on short-term strength *(Russian)* 78−56693
Cu high purity, grain boundaries as dislocation sources in premacroyield strain region 79−34096
Cu, polycryst., grain size and high-temp. yield strength 80−7641
Cu powder compacts, yield curve comparison, different loading paths *(Japanese)* 80−93621
Cu, recrystallisation and recovery during temperature strain *(Czech)* 77−70071
Cu, recrystallisation and recovery during temperature strain *(Czech)* 77−73287
Cu, thick sputter deposit, microstruct., tensile props. 77−40461
Cu-Al martensite, temper hardening, study by TEM, DTA, microhardness and yield strength meas. 79−43260
Cu-base alloy formed by high rate sputtering 78−11368
Cu-Be (2 at.%), plastic deform. and dislocation substruct. 80−76307
Cu-BeCo (1.85, 0.29 wt.%), type CA172 (TH04), strengthened by spinodal decomp., stress relax. in bending 80−7616
Cu-Cd (1.0 wt.%), yield stress and flow stress 80−97524
Cu-Cr (0.75 wt.%), deformation characts., fully reversed cyclic strain with fatigue cracks and dislocation struct. 80−81148
Cu-Cr alloys, isothermal decomp. diagrams 79−38791
Cu-Ge (0.44 to 7.3 wt.%), concentrated single crystal, yield region investigation, CRSS, slip 77−48478
Cu-Ge(Zn), conc. single crystal, yield region investigation, flow stress and obstacle charact. 78−3173
Cu-In, thermally cycled, effect on mech. props. and microstruct. 79−4987
Cu-Ni, powder, sintered, effect of cold and hot dynamic pressing, upon structure and props. 79−33970
Cu-Ni-Fe, age hardened, yield strength correlation with internal coherency strains 77−44254
Cu-Ni-Fe, spinodal alloy, heat treatments for improved mech. props. 79−5024
Cu-Ni-Sn (15, 9 wt.%), age hardening accompanying phase transition 78−64551
Cu-Sn(5 wt.%), electrical resistivity, annealing, cold rolling 77−8070
Cu-Ti-Fe (0.7, 0.9 wt.%) film, dispersion-strengthened, form. by high rate magnetron/plasmatron sputtering, and props. 80−25715
Cu-Zn-Be, precipitation hardening 77−16599
Fe based dispersion strengthened thick condensates, struct., mech. props. 77−90361
Fe based metallic glass, B and P glass former additions, elastic consts., flow behaviour correlations 78−44154
Fe, cast, increase in yield strength, after phase transformations 78−44125
Fe, cast, spheroidal graphite, graphite size effect on mech. props. *(Korean)* 78−11278
Fe, casting, fatigue strength, section size and surface struct. effect *(Japanese)* 79−20170
Fe, commercial, ductile-brittle transition temp., variation with grain size 78−27640
Fe, sintered, strength and elongation, rel. to density 80−30047
Fe-Ag (50 vol.%), two-phase system, plastic deformation *(French)* 78−39831
Fe-Al-C, low C, yield strength changes during carbide precip. 78−52814
Fe-Co, damping capacity of Gentalloy, internal friction meas., mech. and mag. depend. *(Japanese)* 78−52875
Fe-Co-V alloy, Remendur, heat treatment effects on mech. and struct. props. 77−8846
Fe-Cr-Al (7, 5 wt.%), expt. stainless alloys, phys. and mech. props. 80−97637
Fe-Cr-Mn (11.5, 3 wt.%), microduplex ferritic-martensitic steel, exam. 78−39862
Fe-Cr-Ni-Ti-Al, superalloy, Ti, Ni, Al, H_2 variations effect on mech. props. 78−3188
Fe-Cu-C, fatigue behaviour for tempering at 500°C, precip. hardening 77−40442
Fe-Cu-Ti, improvement of irradiation-enhanced Cu embrittlement by Ti addition 79−43393
Fe-Mn, warm rolled, rel. contribs. of texture and grain shape to props. 79−91705
Fe-Mn (up to 8 wt.%), microstructure, mech. props. and fracture *(Japanese)* 80−35304
Fe-Mn-Ti alloys, austenitic, precipitation strengthened 80−25714
Fe-Ni, brittle transgranular and intergranular fatigue crack growth rate, yield strength effect 78−68786
Fe-Ni, reactive metal alloy, effects of thermomechanical processing on strength and toughness 79−70112
Fe-Ni (15, 25 at.%), longitudinal forces in the hot torsion test *(German)* 79−38889
Fe-Ni (25 wt.%), and single phase, solidified from undercooled melt, mech. props. 77−48540
Fe-Ni austenite, precipitation hardened, transform. strengthening 79−24531
Fe-Ni heterogeneous alloys, ferrite, martensite and austenite phase distrib., effect on mech. props. 80−45363
Fe-Ni-Al-(Cu) (12, 0.5, 0.5 to 3 wt.%), Cu addition strengthening at 77K, mech. props. 80−60875
Fe-Ni-C (10, 0.6 wt.%), effect of austenite yield strength on martensitic transformation 78−39772
Fe-Ni-Cr-C, effect of austenite yield strength, stacking fault energy, on martensite morphology 78−80546
Fe-Ni-Cr-Ti, superalloy A286, powder, exam. of microstruct. and mech. properties 78−52979
yield strength continued
Fe-Ni-Ti-(Cu) (12, 0.25, 2 wt.%), Cu addition strengthening at 77K, mech. props. 80−60875
Fe-Ni-V-(Cu) (12, 2, 2 wt.%), Cu addition strengthening at 77K, mech. props. 80−60875
Fe-Ni-(Cu) (12, 0.5 to 3 wt.%), Cu addition strengthening at 77K, mech. props. 80−60875
α-Fe-P, static strain ageing 77−70079
Fe-Si (3 wt.%), electron irradiated, yield strength and elongation 80−76325
Fe-TiB_2, eutectic alloy, high temp. props. 78−84931
Fe-Ti(Nb), internally nitrided, mech. props. 77−44307
Fe-W system, damping capacity of Gentalloy, internal friction, mech. and mag. props. 79−77679
Ge, high press. appl. by spherical diamond indentor, plastic deform. obs. method 78−35619
Ge, ultimate yield strength calc. 78−43062
Ge, yield stress from Hugoniot elastic limit and elastic consts., compressive yield strength 79−83261
KCl, pure and Sr doped crystals, strengthening effects rel. to IV-dipoles and aggregates 78−55907
KCl-KBr single crysts., yield strength and dislocation mobility, solid soln. hardening model 77−72649
LiF mech. and optical props. rel. to forging conditions 80−33101
LiF, press forged, mech. and optical props. 80−38079
Mg-Y-Nd-Zn-Zr (2,2,0.3, 0.7 wt.%), heat treatment effect on casting dimensional stability, alloy mech. props. 78−44146
Mg-Zn-Zr, cast, exam. of phase composition, mech. props. 79−100217
MgO, cryst. preliminary processing rel. to deform. curve parameters, slip line struct. 77−52421
MgO crystal, yield strength and dislocation mobility 80−93601
$MgZn_2$, single cryst., yield strength 77−44318
Mo alloy, precipitation hardened, yield stress in tension and compression, SD-effect *(Ukrainian)* 77−56021
Mo alloys, fusion reactor first wall and blanket material, props. for struct. appl. 80−30071
Mo, mech. props., effect of exposure to high temp. He containing O_2, room temp. study 80−93639
Mo-C-Zr (0.03, 0.17 wt.%), thermal treatment effect on yield drop 77−90382
Mo-C-Zr-B (0.004, 0.12, 0.002 wt.%) effect of grain size, cellular dislocation structure, on mech. props. *(Russian)* 79−34105
Mo-Mn alloy, plasticity, fracture, strength depend. on C content *(Russian)* 80−35257
Mo-Ti-Zr alloy TZM, fatigue and plastic flow, irradiation effects 77−52466
NaCl, pure and Sr doped crystals, strengthening effects rel. to IV-dipoles and aggregates 78−55907
Nb alloys, fusion reactor first wall and blanket material, props. for struct. appl. 80−30071
Nb, fusion neutron damage effects on mech. props., simulation by 16 MeV protons 78−71768
Nb, neutron irrad., microstruct. and tensile props. 80−34077
Nb, neutron irrad., microvoid form., ang. correl. and yield strength meas., TEM obs. 78−88381
Nb, radiation hardening and yield strength correlations for 16 MeV H^+ and (D,T) neutron effects 78−14389
Nb-low alloys, strength and ductility at high temp. and different strain rates 80−16401
Nb-Ti alloy, supercond., low-temp. plasticity 77−15992
Nb-Ti-Ta alloys, metallurgical anal. and crit. current densities 79−38286
Nb-Zr-C alloy, strengthening phase, particle distrib. anal. *(Russian)* 79−15685
NbC, vacuum condensate, struct. and mech. props., second phase effect *(Russian)* 80−71705
Nb_3Sn fatigue effects in unidirectional composites, computer simulated model 80−35289
Ni alloy, fatigue and cyclic plasticity rel. to struct. inhomogeneity 80−81184
Ni, fusion neutron damage effects on mech. props., simulation by 16 MeV protons 78−71768
Ni, neutron irrad., microstruct. and tensile props. 80−34077
Ni, oxide dispersion strengthened materials, effect of prior creep at 1365K on room temp. tensile props. 78−39857
Ni, radiation hardening and yield strength correlations for 16 MeV H^+ and (D,T) neutron effects 78−14389
Ni, thick sputter deposit, microstruct., tensile props. 77−40461
Ni-Al bronze, fracture resistance of tubes 78−19867
Ni-Co (10 wt.%), cast single phase, solidified from undercooled melt, mech. props. 77−48540
Ni-Co electrodeposit, strength, heat treatment and comp. var. effects 77−32660
Ni-Cr-Al-Ti-Mo, low temp. mech. behaviour, precipitation 78−39860
Ni-Cr-Mn-Fe-Nb (20,3,3,2.5 wt.%), short-range order effects on tensile behaviour 80−25793
Ni-Cr-(Al), oxide dispersion strengthened materials, effect of prior creep at 1365K on room temp. tensile props. 78−39857
Ni-Cu (30 wt.%), cast single phase, solidified from undercooled melt, mech. props. 77−48540
Ni-Fe-Cr (18, 18 wt.%) superalloy, mech. props., 4-295K 77−44327
Ni-H, thermally charged, serrated yielding 80−85007
Ni-Nb-Al (21,2.5 wt.%), eutectic aligned alloy, mech. behaviour at high strain rates 78−39855
Ni-TaC, eutectic alloy, fibre reinforced, directionally solidified, anisotropic yielding behaviour 79−11675
Ni-Ti mech. memory alloys, tensile props. *(Korean)* 77−63724
Ni-ZrO_2, dispersion-strengthened condensate, density and mech. props. 77−44196
$Ni_3(Al,W)$, temp. and orientation depend. 77−28857
Ni_3Al-B, $L1_2$ type intermetallic cpd. room temp. ductility improvement by B addition *(Japanese)* 80−35263
Ni_3GA single crystals, anomalous temp. depend. of strength, dislocation struct., optical and TEM 79−74228
Pb(Ag) alloys, effect of Ag content on yield strength 80−76322
Pb−(Au) (0.1 and 0.2 wt.%), single crysts., yield strength depend. at 77K on Av conc. 80−55479
Pd-Cd eutectic, unidirectionally solidified, tensile and compressive props. 78−27567
α-Pu and δ-stabilised Pu-Ga alloy, strain rate effect on tensile props. 77−21284

yield strength continued
Si, high press. appl. by spherical diamond indentor, plastic deform. obs. method 78−35619
Si, ultimate yield strength calc. 78−43062
Si, yield stress from Hugoniot elastic limit and elastic consts., compressive yield strength 79−83261
Sn plate, rapid test for props. assessment 80−40650
α-β Ti alloy, fracture toughness rel. to microstruct. 77−16673
Ti alloy, X-ray diffr. anal. of hydrides 77−12628
Ti alloy VT20, phase composition and structure effect on mech. props. 79−38958
Ti alloy VT20 and VT22, yield strength anisotropy and durability after cyclic loading *(Russian)* 78−27565
Ti alloys, AT3 and AT6, tensile props. prolonged oxidation effects 78−85050
$\alpha+\beta$ Ti alloys, fracture, influence of phase comp. in VT16 and VT9, quenching effects *(Russian)* 78−56665
α-βTi alloys, high strength, heat-treated weldments, intergranular fracture 80−21097
Ti, neutron effects on thermally activated tensile props. 77−62567
α-Ti, solid soln., strain ageing *(Japanese)* 78−6953
Ti-Al-H, H effect on mech. props. and lattice constants 80−21036
Ti-Al-V (6, 4 wt.%), hot isostatically pressed casting, fatigue crack initiation 79−79078
Ti-Al-V (6, 4 wt.%), void formation and growth, tensile fracture, exam. 78−80637
Ti-Al-V (6,4 wt.%), age hardened, deform. charact. 77−36608
Ti-Al-V (6,4 wt.%), α/β interface phase influence on tensile props. 80−30034
Ti-Al-V (6,4 wt.%), strongly textured, influence of crystallographic orientation on tensile behaviour 80−7633
Ti-Al-V (6,4 wt.%), surgical implant ion beam textured, stress/strain relations, fatigue characts. 78−73297
Ti-Al-V-Cr-Zr-Mo-Fe (3.4, 8.3, 5.8, 3.9, 4.2, 0.06 wt.%), shock loaded, residual strength 77−36589
Ti-Be-Si glass ribbons, physical and mech. props. 78−95767
β-Ti-Mo-Zr-Sn (10.2, 5.8, 4.7 wt.%) heat treated, tensile yield, fracture behaviour, primary deform. mode, exam. 78−60724
Ti-Mo-Zr-Sn (11.5, 6, 4.5 wt.%), β III, mech. props. rel. to heat treatment 80−84961
TiB_2, TiC, vacuum condensate, struct. and mech. props., second phase effect *(Russian)* 80−71705
α-U, polycrystalline, compressive deform. at low temps. 77−28856
U-Mo-Nb-Zr-Ti (0.75, 0.75, 0.75, 0.5 wt.%), heat treatment effect on microstruct. and mech. props. 78−23729
UO_2, strain rate and temp. depend. of yield stress 77−46281
V alloys, fusion reactor first wall and blanket material, props. for struct. appl. 80−30071
V-low alloys, strength and ductility at high temp. and different strain rates 80−16401
V-Ti-O single crystal alloy, mech. props. 77−25112
V_3Si single cryst., A-15 compound supercond., plastic deform., at high temp. 79−20104
W fibre reinforced epoxy resin, strength of metal-polymer adhesive contact, time-temp. depend. 78−68753
W, high temp. strength and ductility 77−52406
W, with different microstructs., temp. depend. of yield strength 80−16404
WC, cemented carbide, deformation, high temp., stress relaxation, and strain rate depend. 78−39854
WC-Co, cemented carbide, deformation, high temp., stress relaxation, and strain rate depend. 78−39854
WC-Co cemented carbide, stress-strain curves using ultrahigh-pressure apparatus 79−43322
WC-Co cemented carbides, irreversible deformation, yield stress, SEM study 79−70110
WC-Co-Ta(Ta-Ti-Nb), cemented carbide, deformation, high temp., stress relaxation, and strain rate depend. 78−39854
Zn, nitrided, yield strength, influence of deform. rate *(Bulgarian)* 80−89315
Zn particulate composite, mech. props., microstruct. correlation, at low and high temps. 77−32624
Zr alloys, neutron irrad., yield strength changes and radiation hardening, damage annealing *(Italian)* 77−65269
Zr-CR (1.9 wt.%), β-quenched and tempered, tensile props. rel. to tempered conditions, SEM study 79−66109
Zr-Nb (2.5 wt.%), nuclear fuel channels, neutron effects on ultimate fracture strength, 293 to 573K 80−85054
Zr-Nb (2.5 wt.%) pipe, fracture resistance, hydrogenation effect 80−104279
Zr_3Al, cold worked, annealing effects 77−36535
Zr_3Al, $L1_2$ phase yield strength 78−19811
Zr_3Al, ordered, strengthening by fast neutron irrad. 78−84838
ZrO_2, ZrB_2, vacuum condensate, struct. and mech. props., second phase effect *(Russian)* 80−71705

yield stress
see also yield point; yield strength
acrylonitrile-styrene copolymer melts, rheological behaviour *(German)* 77−51012
alkaline silicate glass, surface layers, plasticity and microcrack formation, electron microscopy *(German)* 80−40469
alloy, $L1_2$ ordered 77−52392
alloys, precipitation hardening, yield stress *(Russian)* 79−56990
alloys, with ordered domains and disordered regions, critical shear stress *(Russian)* 80−107237
alloys of two ductile phases of unequal strength, deform. *(Japanese)* 78−11284
anisotropic plasticity, theory development, expt. results 79−27553
anisotropic polycrystal, yield and tensile test meas. of plastic behaviour 77−32631
axially loaded butt joints, stress strain behaviour 79−74209
beams, influence of transverse shear on plastic yielding 79−32287
bifurcation in elastic-plastic solids, perturbed motion of stress axes 78−90730
bone, anelastic deform. and friction stress 78−19871
α-brass, bicrystal, grain boundary fracture at intermediate temp. *(Japanese)* 79−15774
brass, M63, yield stress decrease in compression, rel. to previous elongation *(Polish)* 80−50665
β-brass, quenched single crystal, deform. and slip 79−79026

yield stress continued
αbrass, single cryst., yielding behaviour rel. to low temp. annealing treatment *(Japanese)* 80−93582
α-β brass, two phase bicrystal, deform. and fracture at 450K 80−16409
brittle materials, abrasion, size effect 79−34131
carboxyl terminated butadiene nitride-diglycidyl ether of bisphenol A epoxy resin, struct. and mech. props. 78−52901
ceramic nuclear fuels, mech. props. at compressive deformation 80−651
composites, two phase, depend. of texture and microstruct. on yield stresses of components 79−91697
compressed bar, secondary plastic deformation influence beyond yield stress *(Russian)* 79−37199
compressible materials, flow behaviour 78−55573
concretes, further development of 2 point test for workability and extension of its range 80−66728
crack opening displacement and stress intensity factor relationship, appl. of modified Dugdale model 79−41615
crack tips, blunt, elastic-plastic stress fiield, plane stress and plane strain *(Chinese)* 80−64469
crack tips, yielding on inclined planes 80−33525
cracks, penny-shaped, ductile, dynamic effects in propagation, Hankel and Laplace transform methods 80−87741
creep, anisotropic, phenomenological descriptions 77−24347
cylindrical shell, pressurized, containing long part-through notch plane strain general yielding 78−18199
deformation behaviour contrib. in rod drawing *(German)* 80−11684
diamond, yield stress from Hugoniot elastic limit and elastic consts. 79−83261
disc, nonhomogeneous, accelerating, with varying thickness and density with radial loading, yielding 78−63322
dislocation, straight line, motion in conc. solid soln. computer simulation 77−81268
dislocation motion, effect of anisotropic elastic medium, appl. to martensitic transform. 77−28811
dislocation motion, straight line, in concentrated solid soln., computer simulation 77−15413
dislocation movement, in volume dispersion of obstacles, stochastic model, low temp. anomalies rel. to yield stress 79−60367
disperse system, plastoviscous, cone plastometer for strength props. determ. 80−76426
dispersion hardened alloy, load type effect on yield stress 78−35458
dispersion-hardened single crystals, theory of high-temp. strength 77−48445
dolomite, yield stress inferred from impact and static compression studies 77−44977
double-layer lattice plate yield surfaces, anisotropic continuum treatment *(Japanese)* 78−22261
edge dislocation thermally activated motion, appl. to KCl-KBr solid soln., computer simulation 79−19249
effect of pressurisation on acoustic emission characts. during tensile testing 78−92304
elastic body, inhomogeneous yielding, slip plane intersection with stress free boundary 78−5667
epoxy resin, effect of environment on stability of cracking 78−95807
epoxy resin, plastic deform. mechanism 80−97534
epoxy resin systems, synthesis review, phys. and mech. props. at low temps. 80−25650
epoxy resins, correlation between valence energies and low temp. flexibility 80−25815
eutectic alloy, yield point analysis 77−8875
eutectics, single grained, directionally solidified, anisotropic yielding behaviour 80−103412
fatigue crack, macroscopic residual stress at tip, X-ray obs. and finite element anal. *(Slovak)* 78−19885
FCC alloy, hardening by spinodal modulated structure 80−60874
fibre-reinforced rigid-plastic plates transverse impact anal. 78−38211
fracture, plane strain cumulative, criterion, high yield stress promotion 79−60432
fracture stress obtained from the elastic crack tip enclave model 80−71730
gabbro, long-term creep, large and small specimen results obtained over 20 and 3 years respectively *(Japanese)* 78−56705
glassy polymer, Robertson eqn. modification 77−36574
granite, long-term creep, large and small specimen results obtained over 20 and 3 years respectively *(Japanese)* 78−56705
granular materials, invariants depend. models 78−34026
hexagonal polycrystals, creep and plasticity, rel. to single crystal slip 78−13920
high-pressure anvils, relationship of yield stress to press. attained at yielding and ultimate attainable press. 79−54150
hot metal, dynamic yield characts. during multistage deform., plastometer design 80−85135
I-beams under shear, and shear and axial loading 77−35049
ionic crystals, structurally modulated, elasticity and its limits, yielding and melting 80−49295
iron, pure, tensile deformation behaviour under high pressure *(Japanese)* 80−16381
mechanical anisotropy evaluation, using hardness test *(Polish)* 78−48575
metal, BCC, polycrystalline aggregate, prediction of plastic props., deformation by ⟨111⟩ pencil glide 80−11731
metal, hot deformability test methods, comparative evaluation *(German)* 77−36713
metal, microstructure and strength *(German)* 77−70138
metal film bonded to rigid substrate, yield stress 79−99463
metal rods, static mech. props. rel. to impulse stress 78−95779
metal/glass fibre reinforced plastic vessel, with damaged reinforcing layer, carrying capacity 78−39876
metallic glasses, structures based on disclination-dislocation model 79−82159
metals, aspects of impact testing effect of grain size on yield and fracture stresses 79−79111
metals, BCC, low temp. softening 79−34113
metals, radiation effects on elasticity and elastic moduli, yield stress 80−2078
metals, transversely isotropic plastic props., yield charact. 78−60707
metals, work-hardening, dislocation multiplication model 79−61608
metals and alloys, temp. depend. *(Russian)* 78−56691
metals and alloys, yield criterion, rheological interpretation *(Russian)* 80−21014
microstruct. and tensile props. 80−34077

yield stress continued
multilayered composite soft interlayer, limiting stressed state and carrying capacity 78−30201
Nimonic cylinder, stress redistribution obs. 77−4831
Nimonic PE 16, γ' particle dispersion rel. to yield stress 79−29153
non-Newtonian fluids, rheological props., pressure induced change of yield stress 80−53736
non-Newtonian viscoelastic liquid, flow with allowance for yield stress 77−84280
nonlinear material and structural behaviors, soln. procedure, theoretical basis for program composite−III 78−30204
nonsteady-state mechanism 78−48481
Nylon 6, injection moulded, yield stress and fracture toughness 80−38951
olivine, hardness var. with temp., rel. to polycryst. yield stress 80−26500
opposed anvils, yield stress calc. 77−57343
oriented transversely isotropic solid, yielding and failure 78−13915
orthotropic strip, stress intensity factors and crack opening displacements 80−53710
PET, crystallised by nonreactive liquids, exam. of mech. props. 79−43338
pipeline girth weld, determ. of acceptable defect level 79−34143
plane stress crack problems, fully plastic soln. and large scale yielding estimates 77−19573
plastic anisotropy theory based on yield function of fourth order 78−31457
plastic deformation, inhomogeneous, reference degree of deform. definition *(German)* 80−99936
plastic flow in thick-walled cylindrical shell, non-homogeneity effect, numerical calc. 80−19248
plastic material, rate type, with kinematic work hardening 78−15450
plastic material, strain hardened, yield criteria 79−14282
plasticised cellulose acetate sheet, post-yield fracture 80−25859
plate, notched, plane strain general yield due to combined axial force and bending 78−18197
plate, symmetrically notched, plane-strain general yield due to combined axial force and bending 78−18198
PMMA, craze zones at crack tips at different temps., meas. correl. with Dugdale model 78−23826
polycarbonate, delayed yiedling under const. load 79−38906
polycarbonate, effect of rolling on mech. props. 78−52837
polycarbonate, glassy state, rel. between thermal pre-treatment and viscoelastic behaviour 79−79038
polycarbonate, impact behaviour, effects of thermal pre-treatment and mol. wt. 78−95798
polycarbonate, rigid plastic, yield behaviour *(Japanese)* 80−93620
polycarbonate, viscoelastic ductile, delayed yielding of plane stress viscoelastic Dugdale model 78−27569
polycarbonate, yielding and crazing behaviour in torsion under superimposed hydrostatic press. 78−52898
polycarbonate blends, yield and deform. behaviour, impact modification 77−36572
polycrystalline material, plasticity analysis using stat. model *(Russian)* 78−26619
polycrystalline metal, FCC, plastic stress-strain rels. under proportional loading 77−32627
polyester model material, optical response and yield behaviour 78−31453
polyether sulphone, effect of rolling on mech. props. 78−52837
polyethylene, correlation between valence energies and low temp. flexibility 80−25815
polyethylene, high density, impact yielding, flow stress rel. to temp. 77−32653
polyethylene, high molecular weight, effect of density on properties 77−90403
polyethylene, high-density, deform. resistance and flow curve 77−90405
polyethylene, orientated, var. of yield stress with orientation, yield criteria exam. 78−52900
polyethylene, solid-state extruded, exam. of props. 80−11669
polymer, glassy, power law relationship between yield stress and shear modulus 78−15467
polymer, oriented, macroscopic yielding 77−90397
polymer, viscoelastic ductile, delayed yielding of plane stress viscoelastic Dugdale model 78−27569
polymer, yield behaviour, interpret. w.r.t. correlated motion 78−6973
polymer, yield stress and elastic modulus power law relationship 79−47752
polymeric systems, rheology, review 78−87317
polymers, cryst., hard-elastic fibres, morphology mech. props., mechanisms, review 77−32612
polymers, glassy, viscoelastic relaxation processes role in macrodeformation 79−72825
polymers, solid, mech. deform., model 79−20120
polymers, yield stress estimation at high strain rate using Taylor's impact technique 79−64605
polymers, yield stress estimation from relaxation data 78−64594
polyoxymethylene, effects of hydrostatic press. on shear deform. 78−15457
polyoxymethylene, yielding behaviour under complex triaxial stress conditions 77−56030
polypropylene, effects of hydrostatic press. on shear deform. 78−15457
polypropylene, glassy state, macrodeformation stresses, anelastic characteristics 79−52289
polypropylene, metallic glass filled, mech. props. rel. to temp., strain rate filler content *(Japanese)* 79−15742
polypropylene, shear stress/strain behaviour, press. effect 78−84936
polypropylene, yielding behaviour under complex triaxial stress conditions 77−56030
polystyrene, glassy state, macrodeformation stresses, anelastic characteristics 79−52289
polystyrene, rubber-modified, fracture mechanics anal. of effect of rubber content, craze formation 79−29190
polystyrene latex, ordered monodisperse, lyotropic liq. cryst., mech. props. 79−98676
polystyrene melt, carbon-black filled, rheological study 80−48665
polysulphone, effect of rolling on mech. props. 78−52837
polytetramethylene terephthalate, injection-moulded, struct. depend. of fracture behaviour 77−8912
polyurethane foam, SiO_2 particulate filled, mechanical props. 79−11666
polyvinyl acetate, torsional stress/strain meas., press. effect 78−84937
porous ductile media, rupture by void nucleation and growth, criteria and flow rules 77−52492
yield stress continued
porous material, wedge indentation hardness, slip line field theory 77−86128
porous metal, yield stress variation during cold deformation 80−16395
porous metals, plasticity, stress-strain curves, yield stresses, strain vectors 80−83738
propylene-butene-1 copolymers, thermal and mech. props. 79−34091
prosthesis block copolymers, non-thrombogenic, struct. and mech. props. 77−52925
PTFE, crystalline, subject to simple plane loading, limiting resistant, time and temp. factors 78−23794
PVC, glassy state, macrodeformation stresses, anelastic characteristics 79−52289
PVC, oriented mouldings, struct. order 80−60896
PVC, rigid plastic, yield behaviour *(Japanese)* 80−93620
radiation blistering, fracture model, stress fields around lenticular bubble 79−86823
reactor fuel pin tubes 79−47755
reinforced concrete slabs, generalised yield lines 79−83265
rod of rate-sensitive material, elastic-plastic tension-torsion analysis 80−83741
ruby single crystal, compression tests, temp.-time depend. 78−48484
shock-loaded material, self-consistent technique for estimating dynamic yield strength 78−80692
silica paricle filled epoxy resin, mech. props., fracture by slow crack growth 77−40443
solid soln. strengthening, conc. computer simulation 78−31420
splint making materials, comparative study 79−39606
stability of thin-walled pressure vessels of elastic-plastic linear hardening material 80−92075
steel, Al-killed rolled sheet, plastic anisotropy theory based on yield function of fourth order 78−31458
steel, alloy, ultrahigh-strength, near threshold fatigue crack propag., microstructure effects 77−86168
steel, alloy 36NKhTYu, deformation resistance, grain size effect *(Russian)* 78−11271
steel, annealed, limit stress, effect of specimen length 77−44357
steel, austenitic, 45Kh2N12GS, post deformation holding at deform. temp. effect on struct. and strength of austenite and martensite *(Russian)* 79−1880
steel, austenitic stainless, cold worked, 20%, heat treatment effects on mech. state, load-relaxation expts. 77−52350
steel, brass clad plate/roll bonded Ni clad, fatigue crack growth behaviour 80−40484
steel, C, deformation strength and strain rate depend. under plain strain state *(Japanese)* 80−30028
steel, C, rotating bending fatigue strength, high tensile load effect during stress cycling *(Japanese)* 77−52477
steel, C, strain ageing contribution to fatigue hardening 78−23817
steel, Cr (13 wt.%), sintered, organometallic complex addition effects on mech. props. 80−25595
steel, Cr-C (3.74, 0.86 wt.%), stress assisted bainitic transform. *(Czechoslovakian)* 77−32573
steel, Cr-Mo (2.25, 1.00 wt.%), bainitic, strain rate effects on elevated temp. tensile behaviour 78−35461
steel, Cr-Mo (2.25, 1 wt.%) annealing, high strain rate tensile props. 77−25117
steel, Cr-Mo-V, press. vessel, fracture, effect of tempering 78−60799
steel, Cr-Ni-Nb, containing controlled particle dispersions, creep strength 77−52425
steel, Cu-Zn, brass clad, fatigue crack growth behaviour 80−40484
steel, eutectoid, mech. behaviour, thermomech. treatment effects 80−84970
steel, fatigue crack propag., single overload effect 77−86170
steel, ferritic, cleavage fracture toughness, temp. and strain rate depend. 80−85028
steel, ferritic, static yield props., changes during fatigue cycling 78−23790
steel, lamellar pearlite, containing proeutectoid cementite, brittle fracture study *(Japanese)* 80−93648
steel, low alloy, reactor pressure vessel, effect of Mn and C content on irrad. response 79−20196
steel, low and medium C, dynamic and static strength, strain rate and temp. depend. of flow stress 80−85139
steel, low C, cold rolled sheet, strain rate effect on yield *(Japanese)* 79−96084
steel, low C, lower yield stress, grain size effects, Petch slope, temp. depend. *(Japanese)* 78−39852
steel, low C, plastic deformation by pencil glide, r-values and yield loci 80−7654
steel, low C, relation between low yield behaviour and tensile speed, preloading and temp. effect *(Japanese)* 78−6982
steel, low-C martensitic, Ni addition influence on toughness and ductile-brittle transition 80−30099
steel, maraging, and HY-80, deform., hydrostatic pressure effect 77−36596
steel, martensitic-bainitic, lath morphology effect on yield stress, martensitic and ductile-brittle transition temps. 79−100215
steel, microalloyed, types V1599, V1600, V1286, NbCN precipitation in undeformed austenite 80−89230
steel, mild, elastic-plastic analysis of yield process 77−36571
steel, mild, fatigue crack initiation 77−86163
steel, mild, plate, effect of striking velocity on perforation energy 78−68818
steel, mild, tensile deformation, behaviour under high pressure *(Japanese)* 80−16381
steel, Mn-Mo-Ni-Cr, bainitic, microstructures and mechanical properties *(French)* 80−16362
steel, Nb, controlled-rolled into ferrite temp. range, soln. temp. and rolling effects 80−11678
steel, Ni, welded joints on LNG carriers mech. props. and fracture toughness 80−85017
steel, Ni-Cr-Mo, type 4340, equivalence of K_{Ic} and J_{Ic} fracture toughness meas. for range of yield stress 79−38934
steel, nuclear pressure vessel, type A533B-1, three point bending, yield stress, exam., Charpy V-notch and precracked specimens 78−92310
steel, pearlite, interlamellar spacing effect on yield stress *(Czech)* 79−43341
steel, stainless, 304, creep fracture propag., elongation, tensile strength, yield stress meas. applicability of fracture mechanics parameters 78−35508

yield stress continued
steel, stainless, Cr-Ni type, low temp. plasticity, effects of deform. rate and cooling conditions 77−70099
steel, stainless, effects of material properties on the dynamic response of pressure-loaded core subassembly wrappers 79−49756
steel, stainless, neutron irradiation effect on low cycle fatigue and tensile props. at 298K 80−30059
steel, stainless 18-8, stress corrosion cracking in H_2SO_4-NaCl soln., martensite form. *(Japanese)* 78−92396
steel, stainless 304, deformation twins contribution to yield stress Hall-Petch law for inter-twin spacing 79−24588
steel, stainless type 316, monotonic and cyclic biaxial loading at room temp. 78−52928
steel, stainless type XM-19, influence of recrystn. behaviour on mech. props. 79−83213
steel, structural, grain size depend. of yield stress in homogeneous deformation range *(German)* 80−30013
steel, structural, influence of deform. heat on the mech. props. *(German)* 78−84904
steel, structural, St37-2, crack tip displacement and flow curves *(German)* 79−47747
steel, ultrahigh strength, monotonic and cyclic stress strain curves 80−35268
steel, unalloyed, brittle fracture, effect of prestrain and ageing *(German)* 78−19857
steel, V containing dual-phase, yielding and strain ageing, early stages 80−25794
steel, V strengthened dual phase, deform. and fracture props. 78−48467
steel 10GN2MFA, yield stress increase as result of decrease in temp. 79−57027
steel 45, fatigue strength determ. apparatus, in corrosive environment under complex stress *(Russian)* 77−77657
steel stainless, plastic deform. of single crystal, contribution of $\gamma \rightarrow \varepsilon$ transform. 77−52394
steel-concrete composite T-beam, third point loading tests, ultimate flexural strength determ. 77−86252
steels, C, quenched and tempered, struct.-prop. relationships 80−7599
steels, structural St 37-2, cleavage fracture, report 80−25868
stress/strain relation, rate and temp. depend., analytic formulation 80−40466
Ta, single crystals, microyielding, high amplitude damping 77−52396
tensile tests, standardization from metal physics viewpoint *(German)* 80−93711
thermo-plastic materials, polarisable, constitutive eqns. *(Japanese)* 78−67062
thermo-plasticity of irradiated metals 77−4146
thermoplastic rectangular parallelepiped pressure vessel, photoelastic coating anal. 79−59950
thermoplastics, homogeneous, fracture under plane strain and plane stress conditions 78−52941
three point bending tests, calc. of yield stress, review 78−92310
tip of blunt notch, plastic yielding during static and fatigue loading 79−77010
Tresca type plastic material, simple shear deform. with combined work hardening *(Japanese)* 80−35206
trigonal monocrystals, classes 3 and $\bar{3}$, elastic potential and yield condition *(Russian)* 80−29108
trigonal monocrystals, classes 3 and $\bar{3}$, plastic potential and yield stress *(Russian)* 80−29109
virus solid, low density, yield stress model 78−88725
wood, yield stress, strain-rate theory, moisture effects 77−16646
work hardening, indentation hardness to yield stress ratio glide processes 77−40426
work hardening and solid solution hardening model 79−34051
work hardening material indentation analysis 79−8308
yield surface motion and loading surface 78−15449
Zircaloy-2, neutron irradiated, inhomogeneous deformation behaviour 80−50679
Zircaloy-4, β-transformed, flow stress and dynamic strain ageing 80−3101
Ag and Ag alloys, yield stress temp. variation hysteresis *(Russian)* 78−52905
Ag single cryst., effects of impurities and prestraining, 2-300K *(Russian)* 77−47506
Al alloy, yield surface after proportional preloading, Tresca-type strss-strain rel. 77−32628
Al alloy, yield surfaces, effect of preloading under combined axial load and torsion 77−25091
Al alloy 2024-T351, fatigue crack propag., residual stress distrib. 79−70146
Al alloy sheet, anisotropic, yield strsses and plastic strain rates, directionality correl. 78−23760
Al bronze, BA 1032, deformation at high temp. *(Polish)* 79−79023
Al, cold rolled, annealed, fatigue crack propag. rate, temp. effect 78−39904
Al, isoaxial bicrystal, deformation behaviour, study by photoelastic coating and moire methods *(Japanese)* 78−11294
Al, polycrystalline, movement of 3-fold nodes of boundaries in high temp. creep 80−89317
Al, prestrained, isotropic hardening rule, rel. to stress/strain curve 78−23772
Al, single cryst., latent hardening *(Japanese)* 78−44135
Al, superconducting, an anomalous strain-rate sensitivity of flow stress 79−43313
Al, tensile flow stress at room temp., grain size and strain effect 77−77528
Al tube, thin-walled statically pre-tensioned, torsional impact loading 78−27557
Al, yield surface motion and loading surface 78−15449
Al/Cu laminates, vapour deposited, strength enhancement 79−24576
Al-Bi(Cd)(Pb)-Ti, containing low-melting pt. inclusions, mech. props. 80−93632
Al-Cu-Mg-Ni-Fe alloy RR 58, creep resistance at elevated temps., thermomechanical treatment effects 77−59836
Al-Cu-Zr (6, 0.4 wt.%), superplastic deformation characts. 80−16387
Al-$CuAl_2$ eutectic, heat treatment and interlamellar spacing effect on tensile deformation 80−29979
Al-Ge (2 wt.%), averaged, plastic flow mechanism 77−48507
Al-Mg, superconducting, an anomalous strain-rate sensitivity of flow stress 79−43313
yield stress continued
Al-Mg (2 wt.%), hardening and fracture characts., β-phase dissolution role 80−81178
Al-Ni (6 wt.%), fine-grained, deform. in tension and torsion 80−85008
Al-Ni(Cd)(Fe)(Si), cold worked, struct. and props. 80−71666
Al-SiO_2 interface, stress and microstruct. via TEM 78−26797
Al-Zn (6.5 at.%), fatigue props., effect of ageing and thermomech. treatment 78−27620
Al-Zn alloy, flow stress, Zn content effect 79−38913
Al-Zn-Mg, solid soln. decomp., 20 to 200°C 79−38830
Al-Zn-Mg-Cu, age hardened, effect of strain rate, temp. and environment on ductility 80−45368
α-Al_2O_3:Cr^{3+}(Ti^{3+})(Ti^{4+}), solid soln. hardening, yield stress conc. depend. 77−28823
AlZnMg alloy, precipitation hardened, strength 78−39786
BaF_2:Y^{3+},Gd^{3+} production and mech. props. 79−72638
α-brass, serrated yielding, tensile tests and TEM obs. 79−34110
C mixes, rheological props. at very low shear rates using capillary rheometer 77−65691
C mixes, rheological props. using capillary rheometer, binder content depend. 77−65692
C-fibre reinforced epoxy resin, laminated structs. mech. props. 80−50672
CdTe, crysts., mech. behaviour, yield stress function of temp., stress relaxation 79−60427
Co-Cr-Al-C eutectic alloy, thermal cyclic loading, exam. 78−48496
CoO single crystals, strain rate deform. characts., yield stresses and work hardening 77 to 1400K 80−60939
CsI, annealing effects on mech. and microstruct. props. 77−66686
CsI:Na^+(K^+)(Cu^{2+})(Tl^{3+})(Eu^{3+}), crysts., influence of impurities on yield stress 79−15748
Cu, annealed, positron lifetime changes during cyclic fatigue 79−43060
Cu crystal, Cr-plated, const. strain rate tests, yield stress 79−83276
Cu, cyclic strain hardening under deform. at various temps. 79−43273
Cu, dispersion hardened, mobile dislocation density and length of slip lines 77−51387
Cu, fatigued high-purity polycrystals, temp. depend. of flow stress 77−44316
Cu, fatigued polycrystals, impure, temp. depend. of flow stress 77−44317
Cu fatigued polycrystals, point defect cluster rel. with yield stress temp. depend. 78−6989
Cu, M1E, yield stress decrease in compression, rel. to previous elongation *(Polish)* 80−50665
Cu powder compacts, yield curve comparison, different loading paths *(Japanese)* 80−93621
Cu, pure, cross-slipping, stress orientation depend. 79−95022
Cu, pure, dynamic stress strain relations in combined tension and torsion, testing device 80−21197
Cu, recrystallised, inhomogeneous deform. due to texture changes *(German)* 79−29158
Cu, soft crystal, US irrad. induced dislocation distrib. 77−32584
Cu, stress hardening anal. 78−56652
Cu, stress-strain behaviour over large strain range 79−15745
Cu, yield stress of electron irrad. cryst., isochronal annealing effects 79−79037
Cu-Al, two-phase Cu-rich alloy, influence of microstruct. on stress-strain behaviour 80−7631
Cu-Al (10 at.%) alloy, work hardening at high temp. 77−32589
Cu-Al (<3 at.%), new type of discontinuous slip at low temps. 77−12676
Cu-Al(Si), single crysts., latent hardening study by meas. of flow stress on secondary systems *(Japanese)* 79−24538
Cu-Be, dynamic strain age hardening 77−52375
Cu-Cd (1.0 wt.%), yield stress and flow stress 80−97524
Cu-Cr(-SiO_2), single crysts., yield and pre-yield behaviour rel. to aging time 80−81103
Cu-Fe, single crystal with coherent γ-Fe particles, precipitation hardening 78−31416
Cu-H, rolled sheet, plastic anisotropy theory based on yield function of fourth order 78−31458
Cu-Mn (3 to 20 at.%), high temp. steady state tensile deform. *(Japanese)* 78−52917
Cu-Nb multifilamentary composites, in situ formed, anomalous strength increase 79−43323
Cu-Ni-Sn (10, 6 wt.%), temp. depend of yield stress and work hardening 80−21026
Cu-SiO_2 single crystals, dispersion hardened, exam. of yield stress between 77 to 1200K 78−76720
Cu_3Al-Al_2O_3 dispersion hardenend, short range order, quenching effect on yield stresS 78−35399
Cu_3Au, dislocation slip band mobility, critical stress 80−2032
β-CuZn, yield stress and operative slip systems, orientation depend. 77−48498
CuZnAl, martensitic, ordering effect on yield stress 79−100133
β-Cu(ZnMn), orientation, temp. depend. 78−10056
Fe and Fe alloys, fast neutron irradiated at high temps., mech. props. 79−51157
Fe based dispersion strengthened thick condensates, struct., mech. props. 77−90361
α-Fe, dislocation density determ. after quenching, internal friction meas. 78−18658
Fe electrodeposited foils, microstruct., internal stress and mech. props. 80−20807
Fe, high purity single crysts., thermally activated slip deformation between 4.2 and 300K 80−25801
Fe, irradiation softening in single crystal, temp. and orientation depend. 77−86113
Fe, Luder's band form. high speed camera obs. 80−16410
Fe, Ni-plated, surface film softening in single slip orientation 77−32719
Fe, plastic deform. and fracture, H_2 effect, studied by electron microscopy and Auger spectrography *(French)* 77−77545
Fe, polycrystalline, exam. of Luders deformation 78−84893
Fe, pure, tensile deform., sources of acoustic emission 78−19814
Fe single crystals, size effect on slip deformation ability at very low temps. 80−21049
Fe-Al-Si (6.22, 9.63 wt.%), bending test under high press., high temp. 80−85057
Fe-C-Cu (0.21, 0.2 wt.%), neutron irradiated, torsional props. effect of Cu additions and annealing temp. 78−56699
Fe-Cu alloy, effect of ε-Cu phase on strain ageing *(Japanese)* 80−7582

yield stress continued
Fe-MoS_2, exam. of props., using differential thermal analysis, and metallography *(Russian)* 79−15653
Fe-N, neutron irrad. effects on mech. props. 79−4338
Fe-N, single cryst., solid soln. softening, effect of interstitial N 80−97496
Fe-Nb-C (0.04, 0.02 wt.%), strengthening, hot rolling *(Chinese)* 79−100154
Fe-Ni, dilute, irradiation softening effect on yield stress 80−76319
Fe-Ni-C (9, 0.1 wt.%), effect of intercritical tempering on impact energy, exam. of mech. props. 78−52861
Fe-Ni-C austenite, effects of strain rate grain size, temp., on yield stress 78−72821
Fe-Ni-C austenite, metastable, influence of prior deform. on yield stress 78−15461
Fe-Ni-Mo alloy, high-strength ferritic, for cryogenic service, mech. characteris. 77−70143
Fe-Ni(Mo), solid soln., cyclic stress-strain props., depend. of fatigue crack growth rate 77−4853
Fe-refractory compound condensate, struct. and mech. props., disperse particle content depend. *(Russian)* 78−19772
Fe-Si, dilute, irradiation softening effect on yield stress 80−76319
Fe-Si (10 wt.%), effect of short range order on yield stress *(German)* 78−52932
Fe-V, dilute, irradiation softening effect on yield stress 80−76319
Fe-V-N, precipitation study, 550 to 600°C *(German)* 77−90350
Fe-V(Nb)-N, precipitation study, 550 to 600°C *(German)* 77−90350
GaAs:Si, hardening by solute-vacancy pairs 77−4794
Ge, doubly deformed, dislocation interaction obs. 79−73172
Ge, ultimate yield strength calc. 78−43062
Ge, yield stress from Hugoniot elastic limit and elastic consts. 79−83261
GeTe, effect of phase transition on mech. and elec. props. 77−51746
GeTe, stoichiometry deviations influence on mech. props., 25-500°C 80−103410
H embrittlement cracking at notches, model, based on stress induced diffusion of H atoms 78−39897
H embrittlement cracking at notches 78−84985
Ir_3Cr, yield stress and saturisation magnetisation 80−16389
K, device for press. variation of yield stress, elastic constants 78−53047
KCl, pure and Sr doped crystals, strengthening effects rel. to IV-dipoles and aggregates 78−55907
KCl:Pb, lead aggregation effect on yield stress, incoherent precipitates, solubility determ. method 80−50645
KCl-KBr conc. solid soln., edge dislocation motion in stress field *(Japanese)* 78−2138
KCl-KBr solid soln., highly conc., computer simulation of dislocation motion *(Japanese)* 77−68972
KCl-KBr solid solution, yielding model on plateau stress 78−27568
LiF, dislocation structure, influence of variable deform. temp. 80−70211
LiF:Mg, slip band struct. changes with temp. 78−47390
$MgAl_2O_4$, spinel materials press forged, mech. props., IR appl. 78−39722
MgO, compressive stress-strain behaviour at high temps. 80−25774
MgO crystal, yield strength and dislocation mobility 80−93601
MgO crysts., plastic deform. activation parameters, rel. between macroscopic and in-situ HVEM expts. 80−103355
MgO, single crysts., work hardening and creep 79−43262
Mo alloys, precip. hardened, yield stress in tension and compression, SD-effect *(Ukrainian)* 77−56021
Mo, exam. of H_2 embrittlement mechanisms, effect on mech. props. 78−39891
Mo, high purity single crystal doped with C, low temp. mech. props. 77−77544
Mo, neutron irrad., radiation anneal hardening mechanism 80−71678
Mo, neutron irradiated, radiation softening and hardening 80−34083
Mo, polycrystalline, fracture and ductile-brittle transition, hydrostatic press. effects 78−60735
Mo-Ti-Zr, alloy TZM, polycrystalline, anal. of elastic anisotropy and microyielding 80−30050
NaCl, pure and Sr doped crystals, strengthening effects rel. to IV-dipoles and aggregates 78−55907
NaCl:X (X=Ca, Sr, Ba, Mg, K, Li, Tl, Ag), impurity conc. effect on mech. and elec. props. 78−47469
NaCl+Pb, Pb aggregation effect on yield stress, incoherent precipitates, solubility determ. method 80−50645
Na_2O-CaO-SiO_2, dynamic hardness testing, pendulum attenuation, yield stress obs. 79−24699
Nb, anodic oxide coating effects on mechanical behaviour 77−32659
Nb, H_2 embrittlement, macroscopic behaviour at low temps. 77−32665
Nb, low temp. neutron irradiation 77−27915
Nb, neutron irrad., embrittlement, yield stress, fracture stress and strain *(Japanese)* 77−76472
Nb, neutron irrad., microstruct. and tensile props. 80−34077
Nb, neutron irrad., yield stress and activation vol. 77−90418
Nb, neutron irrad. effects on mech. props. 78−91361
Nb wire, neutron irrad., yield stress as function of anneal temp. 79−70077
Nb-N (0.3 to 300 at. ppm), deform. 77−48477
Nb-O, yield stress as function of neutron damage and O conc. 79−42117
Nb-O system, solid soln. hardening and softening 80−71665
Nb-T alloy, effect of T on low temp. yield stress of Nb, comparison with Nb-H alloy behaviour 78−39863
Nb-Y, and Nb, mech. props., neutron irrad. and Y scavenging effects 77−90394
$(Ni,Co)_3Ge$, Co effect on temp. depend. of yield stress 78−31487
$(Ni,Co)_3Ge$, single cryst., Co effects on temp. depend. of yield stress 77−4812
Ni 200, static strain ageing, 373 to 473K 77−36558
Ni, deformation twins contribution to yield stress, Hall-Petch law for inter-twin spacing 79−24588
Ni, low-temp. fracture, electron fractography obs. *(Russian)* 77−90437
Ni, neutron irrad., microstruct. and tensile props. 80−34077
Ni, quenched vacancies, effect of oxidation *(French)* 78−27686
Ni, sintered carbonyl type and with dispersed ZrO_2 inclusions, struct. effect on high-temp. ductility 77−63757
Ni wire reinforced epoxy resin, and cement paste matrices, debonding and pull-out of wires 79−29142
Ni-SiO_2 composite film, influence of hardening phase on yield stress *(Russian)* 79−5001
yield stress continued
Ni_2 (Al, Nb) single crystals, orientation and temp. depend. of yield stress 80−25791
Ni_3 (Al.Ti), flow stress and work hardening, exam. of temp. depend. by tensile tests 78−84839
Ni_3(Al, Nb) single crystal, yield stress, orientation and temp. depend. 80−108511
γ'-Ni_3(Al,Ti), single crystal, dislocation movement, HVEM obs. *(Japanese)* 80−108503
Ni_3(Al,W), yield stress, orientation depend. 78−39830
Ni_3Al, ductility, tensile and compressive tests *(Japanese)* 77−52414
Ni_3Al, ductility in poly- and single crystals, compressive and tensile tests 78−56715
Ni_3Al, irrelevance to long range order 77−27849
Ni_3Al, substitutional soln. and defect hardening mechanisms 77−21155
Ni_3(Al.Ti), single crysts., flow and fracture behaviour tested in tension 79−79075
$Ni_{49}Fe_{29}P_{14}B_6Si_2$ glass, flow and failure 80−40438
Ni_3GA single crystals, anomalous temp. depend. of strength, dislocation struct., optical and TEM 79−74228
Ni_3Ga, temp. depend. of mech. props. *(Russian)* 79−38895
Ni_3Ge single crystal, yield stress, temp. and orientation depend. 77−90432
Ni_3Ge, temp. depend. of mech. props. *(Russian)* 79−38895
NiO, doped and pure single crystals, plastic deform. 77−36578
Ni_3V, ordered, domain size effect on mech. props. 79−79027
Pb, dislocation inertial effects, internal-friction meas. on normal and superconducting states 79−38883
Pb, film, hillock formation by grain boundary sliding 80−107673
Pb, strain hardening and recovery, during primary creep 78−39799
Pb-Sn, dil., dislocation inertial effects, internal-friction meas. on normal and superconducting states 79−38883
Pb-Sn(Ag), dil. alloys, dislocation motion and electron-dislocation interactions 77−7728
Pb(Ag) alloys, effect of Ag content on yield strength 80−76322
Pb−(Au) (0.1 and 0.2 wt.%), single crysts., yield strength depend. at 77K on Av conc. 80−55479
$Pd_{80}Si_{20}$ amorphous alloy, skip deform. and crit. shear stress, using tensile testing machine 80−89321
$Pd_{80}Si_{20}$, glass, deform. localisation, plastic instabilities and fracture 80−89320
$^{239}PuO_2$, stoichiometric, high-temp. deformation 80−81111
$^{239}PuO_2$, hypostoichiometric, high temp. deformation rel. to cryst. microstruct. 79−79041
Si thin ribbon grown at high speed, thermal stresses, reduced thermal buckling 80−107078
Si, ultimate yield strength calc. 78−43062
Si, yield stress from Hugoniot elastic limit and elastic consts. 79−83261
Sn, white, single crystal, dislocation movement in pre-yield region, etch hillock technique 79−60371
Ta, evidence for slow strain-rate embrittlement due to O_2, SEM study 79−79109
Ta, flow stress, temp. and strain rate depend. 77−77534
Ta, oxide coating effects on mechanical behaviour 77−32659
Ta, single crystal, microyielding microflow parameters 77−52395
Ta, Ta-Re, Ta-Re-N, deformed at 77K, dislocation substruct. 77−32647
Te, c-slip, asymmetry and orientation depend. 77−27888
α-Ti, determination of microflow parameters from compression tests 80−66584
Ti, dynamic annealing, effect on dynamic strain ageing phenomena 80−7594
Ti, grain size effect on yield stress and work hardening at 295 and 575K 78−64593
Ti, neutron effects on thermally activated tensile props. 77−62567
Ti-Al, age-hardened, deform., order effects in Ti_3Al and temp. effects 77−25111
Ti-Al, hardening of Ti by addition of Al *(French)* 78−23715
Ti-Al (14 at.%), with precipitate free zones, tensile props., grain size effects 77−16690
Ti-Al-Sn (5, 2.5 wt.%) alloy, fatigue under combined alternating bending and torsional stresses 77−8923
Ti-Er(Y), effects of Er and Y additives on deformation behaviour 80−81121
βTi-V-Si (40, 1 at.%), Si effect of precipitation and age hardening 77−63676
Ti-Y(Er), dispersoid effect on deform. 79−24530
TiC, mech. props., 1073 to 2273K *(Japanese)* 79−15732
UO_2, strain rate and temp. depend. of yield stress 77−46281
V, different grain sizes, room temp. microstrain *(German)* 77−36614
V, neutron irrad., yield stress and activation vol. 77−90418
V, polycrystalline, strength, ductility, 4.2 to 400K, O_2 effect 77−36529
W wire reinforced Cu, microfield, flow stress 78−27575
WC-Co cemented carbides, irreversible deformation, yield stress, SEM study 79−70110
WC-Co sintered hard alloy, yield stress, internal thermal stress effect 79−100230
Zn-22 wt.% Al superplastic eutectoid alloy tensile deformation obs. *(Japanese)* 79−90714
Zr and Zircaloy-4, tensile props., room temp. to 900K 77−70104
Zr, neutron irradiated, yield point phenomenon 79−52304
Zr polycrystalline, low-temp. alternating deformation and annealing, yield stress, elec. cond. variation *(Russian)* 79−74199
Zr-Al (8.0 wt.%), tensile props. and fracture toughness after fast neutron irradiation 80−3198
Zr-Al (8.6 wt.%), dimensional stability struct. and mech. props, effects of neutron irrad. 80−92563
Zr-Al (8.6 wt.%), neutron irradiation effect on tensile props., swelling 77−7768
Zr-Al(8.6 wt.%), mech. props., corrosion and fast neutron irrad. influence 78−84948
Zr-Nb (2.5 wt.%), cold-worked, pressure tubing, metallography and mech. props. 80−89269
Zr-Sn-Mo (4.5,1 wt.%) and (4.5,2 wt.%), creep behaviour at room temp. *(Czech)* 79−24590

yielding *see plastic deformation*

Young's modulus
acrylourethane coatings, radiation curable, tensile, elongation and modulus props. appl. techniques 80−66847
Al-Cu(4wt.%), θ' precipitation, effect on Young's modulus, electron microscope obs. *(French)* 79−47689

Young's modulus continued
bagasse fibre reinforced phenol formaldehyde, tensile strength and Young's modulus, SEM study 80−60952
biomembrane elasto-viscous properties determined from bilayer meas. 80−30671
bone, anisotropy, US meas. 78−11687
bone, elastic props. of cortical bone of female human femurs, noninvasive meas. 77−21552
bone anisotropy, fibre-reinforced composite model 80−35944
bones, long, struct. anal., appl. to human tibia 77−21551
β-brass bicrystals, shear-incompatible, grain boundary contrib. to Bauschinger effect 80−97550
brittle materials, abrasion, size effect 79−34131
brittle materials, internal friction and Young's modulus meas. apparatus 77−27499
canine aorta Young's modulus, 10 MHz US meas. 79−57836
cell wall, Acetabularia, deform. rel. to genetic and geometric factors 77−56348
ceramic layers on metallic substrates, mech. props. meas. *(French)* 80−104375
chrysotile asbestos fibres, texture rel. to mech. props. 77−81300
collagen, reconstituted, mech. props. drug release support appl. 78−3666
column, non-uniformly compressed, optimal shape and non-homogeneity 80−10145
complex Young's modulus determ. by resonant rod vibrs. *(German)* 78−18259
composite, 2-phase linearly elastic, moduli by differential scheme 77−39227
composite, elastic props. meas., reliability establishment 77−52574
composite bar technique for Young's modulus and internal friction meas., multiple reson. 78−35612
composite material, structural anisotropy in viscoelasticity 77−86073
composites, elastic modulus and expansion coeff., approx. method *(Russian)* 77−39681
coral skeleton US velocity and Young's modulus anisotropy obs. 79−57837
cord reinforced rubber laminate, interlaminar-shear-strain meas. 79−57043
crack weakened bodies, modulus of elasticity *(Russian)* 77−14898
cylindrical tubes, compressible, wire-layer reinforced, inflation and extension 79−3922
determination from microimpression tests 77−86281
1,6-dicarbazolyl hexadiyne, solid-state polymerisation, monomer to polymer phase transformations 80−38948
eddy current determination 80−65116
education, Young's modulus meas. using audio generator amplifier and speaker 80−62427
elasticity and damage, interrelation *(French)* 79−90182
epoxy impregnated superconducting composites, mech. props., strain effect at 4K 80−25822
epoxy polymer, with low thermal expansion coeff., Young's modulus under tension 78−3094
epoxy resin, glass bead filled, elastic moduli, interfacial slippage effect anal. 78−76688
epoxy resin, glass bead filled, particle size effect on Young's modulus *(Japanese)* 78−60694
epoxy resin, low temp. fatigue, tensile strength, Young's modulus *(German)* 78−76748
epoxy resin, plastic deform. mechanism 80−97534
fatigue cracks, steady state growth rate, empirical formulations for anal. and prediction trends 77−90450
fibre reinforced composites, transverse plane, elastic, failure behaviour *(Japanese)* 78−48510
fibre-reinforced materials, slender, non-dilute, thermal and mechanical props. 80−103524
fibrous composite materials, models for composites with different props. in tension and compression 78−35417
filled polymer, elastic moduli, effect of particle shape 78−15444
fracture toughness, J-integral rel. to crack tip opening displacement *(Japanese)* 78−42569
glass, determination, using static compression, tension, and dynamic loading 78−83867
glass, laser, elastic, elasto-optic consts. and extinction coeffs., Brillouin scatt. meas. 79−11429
glass, stress in working zone under biaxial compression, Moire-band method 77−81369
glass bead-reinforced epoxy resin composite, bulk and shear elastic props. 78−6959
glass fibre epoxy cross-ply laminates, multiple transverse cracking 78−95800
glass fibre reinforced Al alloy, formed by hot extrusion, mech. props. 77−24987
glass fibre reinforced cement, durability in wet and dry conditions, fibre length and content effect 80−71726
glass fibre reinforced composite, random short fibres, elastic props. 77−70090
glass fibre reinforced epoxy filler shape, orientation distrib. and interaction effects on Young's modulus *(Japanese)* 78−39735
glass fibre reinforced epoxy resin, dynamic Young's modulus and internal friction 80−25754
glass fibre reinforced plastics, exposed to liq. media, dynamic high-speed Young's modulus determ. *(German)* 80−85123
glass fibre reinforced plastics, heat treatment and heating temp. effect on Young's modulus 80−35233
glass wool reinforced polymer, relationship between Young's modulus and dissipation of energy *(German)* 79−96064
glass-ceramic, machinable, elastic const. temp. depend. 80−79852
glass-plastic, Young's modulus, expt. study 77−52389
glass/C fibre reinforced plastic, hybrid effects between interlaminar and translaminar config., mech. props. 79−52351
graphite, nucl. grade, unirrad. and neutron irrad., compressive stress effect on Young's modulus 77−61503
graphite structures in PBR, neutron radiation damage, mech. props., stress fields *(German)* 77−34387
gypsum, strength changes on setting *(Japanese)* 77−36619
HCP metals, and alloys, anisotropy of phys. props. rel. to texture 79−91700
hexagonal crystal, anisotropic behaviour of Poisson's ratio, Young's modulus, shear modulus 77−11622
high-temperature US apparatus for elasticity characts. and thermal cond. meas. of materials 78−5705
hot-pressed with crystn. grain boundary phases 78−95716
insulating thin films, Young's modulus measurement by micromechanics 80−33548
isotropic materials, Young's modulus determ., kinematic excitation of resonance oscillations 80−25958
isotropic solid, viscoelastic characterisation using harmonic dispersion of longit. reson. 79−10538
Jahn-Teller system, thermodynamic properties, internal stress effects 80−59679
Kevlar fibres, effect of crystallinity and orientation on mech. props. *(Japanese)* 79−38952
Kevler fibre, mech. props. in aq. H_2SO_4 soln. *(Japanese)* 79−47753
Kroner limits of technically important materials, low order limit comparison *(German)* 79−33029
laminates, exposed to liq. media, dynamic high-speed Young's modulus determ. *(German)* 80−85123
laser window materials, optical suitability 77−58361
lecithin membrane, depend. of Young's modulus in plane of membrane on deform. 78−80894
magnetostriction materials, effect of compression 77−40109
magnetostrictive ferrites, magnetising field influence on amplitude depend. of Young's modulus rel. var. 78−2723
measurement, laboratory instrument design and construction 77−82350
measurement, laser-target technique, for glass, over wide temp. range 77−27497
measurement using automated Marx's composite oscillator method 80−37151
mechanical anisotropy of texture effect on X-ray stress measurement *(German)* 79−29091
metal, FCC, ratio of shear and Young's moduli 77−25088
metal under Shoenberg effect conditions, Young modulus anomalies *(Russian)* 78−35018
metallic glass, struct. relax. effects 78−72804
metallic glasses, amorphous, Young's modulus, using impulse induced resonance method 80−30008
metallic glasses, small samples, Young's modulus meas. by impulse induced resonance technique 80−40411
metallic glasses, strength and stiffness 77−8899
metallic glasses, Young's modulus/thermal props. correlation 78−6961
metals, HCP exam. of texture and Young's modulus anisotropy, developed during deformation *(Russian)* 79−15694
metals, polycryst., relations between shear modulus, bulk modulus and Young's modulus 80−97540
metals, radiation effects on elasticity and elastic moduli, yield stress 80−2078
mullite fibre reinforced mullite, in vitro degradation, bending strength, Young's modulus, density meas. 78−85011
multilayer film, intrinsic and thermal stress modelling and interferometry 79−14059
muscle dynamic stiffness rel. to crossbridge action 78−48819
Nimonic 115, superalloy, critical strain model for creep fracture 77−32648
non-homogeneous stratum, hyperbolic variation 77−868
nuclear fuel compacts for HTR, irrad.-induced creep 78−44168
nylon 6, effect of moisture content on glass transition temp. and Young's modulus 79−4401
nylon-1 polymers and copolymers, mech. props. rel. to glass transition 77−11625
optical glass strength limit rel. to Knoop microhardness 79−72641
optical waveguide blanks, thermal and elastic stresses in a cylinder 80−14447
organosilicon ladder polymers, struct. and phys. props., book contrib. 79−65012
PAN fibres, neutron irradiated, struct. and props. *(Russian)* 80−25763
paper, in-plane elastic moduli depend. on basis weight *(Japanese)* 77−77523
particulate reinforced epoxy resin model specimens, Young's modulus, expt. study *(Japanese)* 78−56683
PET, crystallised by nonreactive liquids, exam. of mech. props. 79−43338
phenol-formaldehyde resin, thermodynamic props. 78−91452
photopolymer, biaxial stress-strain test 80−40417
piezoelectric transducer automatic setup, for continuous meas. of internal friction and elastic moduli of solids 80−108652
plastic, glass-reinforced bottoms with a filler, rigidity 80−15183
plate, orthotropic, rotationally retrained, buckling under uniaxial compression 77−84169
polethylene-polypropylene blend, extruded, thermal swelling and mech. characterisation 80−81110
poly(2,6-dimethyl-1,4-phenylene oxide)/poly(styrene-co-p-chlorostyrene) blends, tensile props. modelling 80−19868
poly-4-methylpentene-1, elastic parameters, US velocity meas. at 2.1-240K 80−40415
polyamide, hydrogen bonding rel. to mech. props. 77−4053
polycarbonate, craze morphology, 77 to 375K, gaseous environment effect 77−63819
polychlorotrifluoroethylene, tensile deform. in He, N_2, Ar, O_2 and CO_2 gaseous environments 77−56040
polycrystal, elastic deform., effect of Young's modulus, shear modulus, Poisson's ratio 77−24344
polyester, unsaturated, glass bead filled, particle size effect on Young's modulus *(Japanese)* 78−60694
polyester laminates, glass fibre-reinforced, due to natural weathering 79−66107
polyester polymer concrete, longitudinal deform. modulus study is creep conditions *(Bulgarian)* 80−71685
polyether-polyester elastomer, fine structure and mech. props. 77−59844
polyethylene, crystallised from oriented melt, mech. and thermomech. props., framework struct. 77−63756
polyethylene, drawn polymer, fibre composite model 78−76719
polyethylene, filled with glass particles, uniaxially drawn, elastic constants, filler addition effect *(Japanese)* 78−95780
polyethylene, highly oriented, fibre composite model 78−3183
polyethylene, highly oriented 78−47614
polyethylene, linear, crystallised from melt, effect of crystallisation time on density, mech. props., X-ray scattering 80−25680
polyethylene, linear, draw temp. and mol. wt. effect on draw ratio and Young's modulus 80−84998
polyethylene, of low density, determ. of avoiding of tensile cracks *(German)* 80−19874

Young's modulus continued
polyethylene, oriented chain-extended, Young's modulus, fracture and compression behavior 80−11747
polyethylene, ultra-high modulus, drawing behaviour, effect of drawing temp. 80−35232
polyethylene, ultra-high-strength filaments, soln. spun/drawn, mech. and thermal props. 80−40440
polyethylene, ultrahigh modulus linear, annealing effects on mech. stiffness and struct. 79−91717
polyethylene, Young's modulus, crystallite thickness 78−76689
polyethylene fibre, high-strength high-modulus, morphology and tensile prop. relations 80−103264
polyethylene filaments, ultrahigh-strength, from soln. spinning and hot drawing 80−45268
polyethylene oxide blends, thermal and mechanical props. 79−11679
polyethylene terephthalate, extruded, elastic consts. meas., mech. anisotropy 78−44155
polyethylene terephthalate, mech. props., influence of cryst. arrangement and noncryst. region struct. 78−76707
polyethylenes, ultra-high modulus, manufacture by drawing through conical die 80−66583
polymer, foamed, rigidity 78−95769
polymer, precision meas. using reson. method *(German)* 78−76823
polymer, semicryst., and filled, elastic modulus, strength, rel. to crystallite shape 80−45335
polymer complex dynamic Young's modulus measurement equipment 78−1615
polymers, anal. of mechanics of solid phase extrusion 80−39204
polymers, cryst., hard-elastic fibres, morphology mech. props., mechanisms, review 77−32612
polymers, testing using Rayleigh surface waves 79−70249
polyoxymethylene, ultra-high modulus, prod. by high temp. tensile drawing 79−43352
polyoxymethylene, ultrahigh modulus oriented, exam. of true crystal modulus, from −150 to 20°C 80−11687
polypropylene, audio freq. shear and Young's modulus determ. from torsional vibr. of laminated bar 77−62218
polypropylene, drawn polymer, fibre composite model 78−76719
polypropylene, extruded, elastic consts. meas., mech. anisotropy 78−44155
polypropylene, mech. behaviour rel. to combined press.-temp. effects 77−16648
polypropylene, ultrahigh modulus, tensile drawing, mol. wt. effect 80−104211
polypropylene rods, prep. by die-drawing 80−45327
polystyrene, amorphous, failure in methanol and ambient air 80−3165
polystyrene, glass bead-filled, elastic moduli, interfacial slippage effect anal. 78−76688
polystyrene, oriented high-molecular, physicocomech. props. *(Russian)* 79−33028
polystyrene spheres, crystallised suspension, gravitational compression 78−23975
polystyrene-polyethylene(ethylene-propylene) blends, copolymer modified, mech. props., morphology 79−57088
polytetramethyl-p-silphenylene siloxane, morphology and mech. behaviour 78−84885
polyvinylidene fluoride, piezoelec., nonlinear dynamic response 80−75946
precipitate vol. fraction with ellipsoidal morphology estimation method using Young's modulus data 78−39781
propylene-butene-1 copolymers, thermal and mech. props. 79−34091
prosthesis block copolymers, non-thrombogenic, struct. and mech. props. 77−52925
PVC, film, uniaxially stretched, effect of mol. orientation on anisotropy of Young's modulus 77−86076
pyrocarbon, fuel particle coating, strength and Young's modulus meas., brittle ring test 77−8868
pyrocarbon coating of Biso fuel, neutron effects on stress and strain 77−79437
pyrocarbon coating of Biso fuel, neutron effects on stresses and strains 77−79436
pyroceramic, stress in working zone under biaxial compression, Moire-band method 77−81369
rare earth alloys, highly magnetostrictive props. 77−12180
rare earth Co Laves phase cmpds., elastic props. rel. to temp., mag. field 79−51834
rare earth-Fe_2, magnetomech. coupling and Young's modulus 78−84472
raw kaolin, acoustical investigations of the effect of additives on elastic props. 80−66559
reinforced plastic, elastic orthotropic cylindrical shell, axisymmetric contact problems, shell interaction with tires 78−1569
rock, mech. props. rel. to cooling *(Japanese)* 80−31036
rubber, dynamic mechanical properties models *(Polish)* 79−43349
rubber compounds, measurement using automatic progressive wave apparatus 79−91866
rubber stress/strain relations, uniaxial extension and compression 78−80578
running crack tip, effect of strain rate depend. Young's modulus on stress and strain fields 78−75097
sandstone, mech. props. rel. to water content *(Japanese)* 77−44980
sea ice in Gulf of Bothnia, Young's modulus from flexural waves meas. *(Japanese)* 78−96225
shell, deposited in vacuum, elastic characts. meas. by short time static extension *(Russian)* 78−39961
silica paricle filled epoxy resin, mech. props., fracture by slow crack growth 77−40443
silicate glasses, elastic moduli calc. 78−60696
softwoods, transverse Poisson's ratio and Young's modulus *(Japanese)* 80−2111
spinal cord, dog, in vivo dynamic material props. 77−40706
steel, 300 grade maraging low temp. elastic props. 78−27555
steel, austenitic, age-hardening kinetics, study by resistivity, Young's modulus and internal friction *(Czech)* 80−29970
steel, austenitic stainless, N-alloyed 80−108490
steel, Cr-Mn (13, 19 wt.%), elastic const. behaviour, anomalous, low temp. 80−97521
steel, elastic consts., meas. app. 77−33739
steel, elastic moduli, temp. depend. *(Japanese)* 77−59840
steel, fibre reinforced Al, fracture mechanics under fatigue *(Czech)* 78−64629
steel, low C, apparatus for elevated temp. meas. *(Polish)* 79−96279

Young's modulus continued
steel, maraging, steady state unidirectionally solidified, austenite reversion and determ. 77−25118
steel, stainless, Cr-Ni-Mn, N strengthened, low-temp. elastic props. 79−70109
steel, stainless type 304, elastic const. variability, US vel. meas. 80−55446
strain intensity criterion for crack branching in brittle mats. 78−55592
stretch zone width and striation spacing. The comparison of theories and experiments 80−85051
Stycast-1266, mechanical props. at low temps. 80−57286
styrene-butadiene triblock copolymer films, mech. props., effect of casting solvent 79−11651
surface layers and microvolumes, physical and mechanical props., continuous indentation calcs. *(Russian)* 80−40629
TCNQ salt, $(N(CH_3)_3H)(I)(TCNQ)$, elastic props., semicond. transitions 79−95072
TCNQ salt, $Cs_2(TCNQ)_3$, elec. cond. and elastic const., mol. bending *(Korean)* 78−23090
tetragonal crystal, elastic moduli, anisotropic behaviour, cryst. symmetry effects 78−51604
tetramethyl-p-silphenylene siloxane/dimethyl siloxane, block copolymer, morphology and mech. behaviour 78−84885
thin plate, meas. by composite vibrator method *(Japanese)* 79−50599
thin plate, measurement by composite vibrator method *(Japanese)* 78−11463
transparent materials, low-modulus, mech. props. determ. method 78−5704
trigonal crystal, elastic moduli, anisotropic behaviour, cryst. symmetry effects 78−51604
TTF-TCNQ, phason and metal-insulator microdomain model, Young's modulus temp. depend. anal. 77−31964
TTF-TCNQ, sound vel. in a a dand b directions, 0-300K 77−84851
TTF-TCNQ, temp. depend., rel. to transition points 77−15475
urethane elastomers, rheo-optical const., Young's modulus *(Polish)* 79−70108
ventricular myocardium plastic cast global Young's mod., calc. from angiograms 77−48827
viscoelasticity, instantaneous moduli, determ. from long-term static test results 80−38286
wire reinforced Al, stress-deformed state, elastic, strength props. *(Russian)* 80−76303
wood, stress distrib. in cell wall subject to tensile force in transverse direction *(Japanese)* 77−77539
Zerodur, glass-ceramic, thermoelastic props. 78−27550
zirconosilicate glass fibre, effect of cement environment 77−44335
Ag, film, vacuum deposited, differential technique 77−1340
Ag, Young's modulus depend. on temp. and mech. action *(Russian)* 80−92584
Ag-Pd-Cu alloys, contact-spring props. and age hardening 78−88473
Al 2024 alloy, Young's modulus under shock loading, heat treatment effects 77−32611
Al alloy, 2024, shock-loaded, recovery of Young's modulus 78−23751
Al alloy, elastic moduli, temp. depend. *(Japanese)* 77−59840
Al alloy, precipitation hardened 2014 and 2219, temp. depend. of elastic constants 77−66673
Al alloy AMg6, preliminary plastic deform., effect on stability of compressed rods 77−81305
Al, changes after plastic deforms. at room and cryogenic temps. 78−23747
Al-Cu (2-5 wt.%), precipitation total surface influence on resistivity *(French)* 80−71650
Al-Cu (4 wt.%), θ'-phase precipitation, characterisation of stages 79−56984
Al-$Fe_{78}Mo_2B_{20}$ wire composite, mech. props. 80−40441
Al-Si alloy, rod, tensile loaded, internal friction and Young's modulus measuring equipment, inelastic phenomena exam. *(Hungarian)* 79−52546
Al-SiC cermet elasticity, porosity meas. by US means 80−81101
Al-Zn-Hg alloy, cathodic protection characts., surface free energy, lattice struct. 79−29281
Al-Zn-Mg alloys, decomp. kinetics from Young's modulus obs., microprocesses *(German)* 78−64522
Al-Zn-Mg plasma sputtered, mech. props. rel. to heat treatment *(Russian)* 80−40387
Al_2Cu crystal, Young's modulus, Poisson ratio, elastic consts. determ. by extensometry and US meas., anisotropy discussion *(French)* 79−50683
Al_2O_3 ceramics, elastic props. meas. in 100 to 300°C range 80−55445
α-Al_2O_3 fibre FP, manufacture, strength and modulus 80−81013
Al_2O_3 refractories, fracture, J-integral meas. 80−108537
β-Al_2O_3-Na_2O, hot pressing and phys. props. 79−4940
β-Al_2O_3-Na_2O, Young's modulus and internal friction obs. 77−35624
Al_2O_3-Y_2O_3-SiO_2 containing TiO_2, La_2O_3, exam. of elastic moduli and refractive indices 78−80502
$Al(PO_3)_3$-LiF system glasses, microhardness and US vel. 79−99274
$Al(PO_3)_3$-NaF system glasses, microhardness and US vel. 79−99274
a-As, second and third order elastic consts., ultrasonic velocity meas. 80−103408
As_2S_3 glass fibre, elongation, force depend., deviations from linearity 80−45334
Au, rod, tensile loaded, internal friction and Young's modulus measuring equipment, inelastic phenomena exam. *(Hungarian)* 79−52546
B fibre, prep. by closed CVD system, mech. props. and surface defects 79−52311
B fibre reinforced Al, dynamic Young's modulus and internal friction 80−25754
B fibre reinforced epoxy, dynamic Young's modulus and internal friction 80−25754
B-fibre reinforced Al, elastic props., 300-4K 77−86066
B_4C, mech. and thermal props. 80−21083
B_2O_3 glass fibre, elongation, force depend., deviations from linearity 80−45334
B_6O, mech. and thermal props. 80−21083
Ba hexaferrites, mech. and mag. props. 79−70151
$BaTiO_3$:Al, 0.05-0.3 wt.%, ceramic dielectric, dielec. and mech. props. 79−8091
Bi, Young's modulus and internal friction, 20°C to melting point *(Russian)* 80−89278
β-brass, effective Young's modulus, in isoaxial bi- and tri-axial crystals 77−90391
C fibre, high temp. obs. 79−20139

Young's modulus continued
C fibre derived from mesophase-pitch, Young's modulus and tensile strength, struct. flow elimination 80−80995
C fibre reinforced C, processing, room temp. mech. props., and low temp. expansion 80−25820
C fibre reinforced epoxy, dynamic Young's modulus and internal friction 80−25754
C fibre reinforced plastic, Young's modulus, depend. on cross-sectional area of fibre 77−4804
C fibre reinforced plastic, laminate, non Hookean behaviour in fibre direction, effect of fibre waviness on tensile props. 78−19804
C fibre reinforced plastics, prep. with large breaking strain C fibre 78−44077
C fibres, durability, elastic props. and struct., heat treatment temp. effect, US meas. methods 80−40446
C fibres, from mesophase pitch, resist. magnetoresist., EPR and mech. props. rel to struct. 79−78116
C fibres, mech. props., thermal stability up to 2000°C 80−60929
C fibres, oxidation by NO_2, struct., props. modification 78−44237
C fibres with large breaking strain, prep., mech. props., struct., appl. 78−44077
C, heat-treatment and neutron irrad. effects on US atten. and Young's modulus 79−11644
C-fibre reinforced epoxy resin, laminated structs. mech. props. 80−50672
$CaSO_4.2H_2O$, Young's modulus in (010) plane, dynamical meas., natural cryst. 78−38768
Cd, Young's modulus and internal friction, 20°C to melting point *(Russian)* 80−89278
$CeH_{1.98}$, $CeH_{2.98}$, elastic props. at high press. 77−84825
Co, internal friction anomalies in spin reorientation temp. range *(Russian)* 80−49299
Co-Fe, internal friction anomalies in spin reorientation temp. range *(Russian)* 80−49299
Co-powder, isostatic compaction, mech. and elec. props. *(French)* 80−40285
$Co_xZn_{1-x}Fe_2O_4$, elastic behaviour, mag. field and temp. depend. 79−87301
Cr-Fe, elastic moduii, electron conc., pulse echo overlap meas. 80−59550
Cr-Fe alloys, polycrystalline, antiferromag., elastic moduli and thermal expansion meas. 77−43860
$CsNiF_3$, one-dimensional mag., Young's modulus softening along linear-chain direction 77−62578
Cu alloy, precipitation hardened, anomalous elastic props. 77−86071
Cu, cold rolled sheet, anisotropy of elastic and strength props. 80−81077
Cu, dislocation damping strain amplitude depend. on 1 MeV electron irrad. and quenching 79−95023
Cu, dislocation pinning rate, neutron and electron irrad., meas. by internal friction method 80−96570
Cu, rod, tensile loaded, internal friction and Young's modulus measuring equipment, inelastic phenomena exam. *(Hungarian)* 79−52546
Cu wires, electrolytic, Young's modulus, working temp. effects 80−50667
Cu, Young's modulus depend. on temp. and mech. action *(Russian)* 80−92584
Cu-Al-Ni (13.8, 7.9 wt.%), cooling rates effect on internal friction *(Japanese)* 80−39217
Cu-Be alloy props. obs., dependence on heat treatment *(Czech)* 80−55448
Cu-$Fe_{78}Mo_2B_{20}$ wire composite, mech. props. 80−40441
Cu-Ti, ageing effect on internal friction and elastic props. *(Russian)* 77−28842
Cu-Zr amorphous alloys, mech. props. *(Japanese)* 77−86179
Er-Tb, elasticity modulus, ΔE-effect, internal friction, magnetic transformations *(Russian)* 79−91723
Eu_2O_3, mech. and physical props. rel. to reactor control rod appl. 78−21641
Fe alloy, cast, Young's modulus and microstructure *(German)* 77−25090
Fe, and its alloys, Young's modulus of Fe_3C phase *(Russian)* 80−76297
Fe base amorphous alloys, Invar and Elinvar charact. 80−29592
Fe, porous, density, elec. cond., Young's modulus, toughness 78−64645
Fe, powder, consolidated, exam. of mech. and electrical props. 78−56599
Fe-B, binary alloys, giant ΔE effect and Elinvar charact. 78−76291
Fe-B amorphous Invar alloy, elastic props., Elinvar charact. and ΔE effect 79−56595
Fe-B metallic glasses, density, mech. and thermal props. 78−31432
Fe-B phase ferromag. amorphous alloys, stiffening below Curie temp., pole effect *(Japanese)* 80−84632
Fe-B-Si amorphous ribbons, effect of annealing conditions on magneto-mechanical props. 80−34740
Fe-B(P) amorphous alloys, anomalous thermal expansion, ΔE effect, Invar and Elinvar charact., delay time 80−80589
Fe-C, effect of H on elastic props., due to internal microcracking *(Russian)* 79−24561
Fe-Cr-B, amorphous, Elinvar and Invar charact. *(Japanese)* 80−11832
Fe-Cr-B amorphous alloys, corrosion resistance, Invar and Elinvar characts. *(Japanese)* 79−96213
Fe-Cr-Co, elastic props. anisotropy at room temp. *(Russian)* 80−89279
Fe-Cr-b amorphous Invar alloy, elastic props., Elinvar charact. and ΔE effect 79−56595
Fe-Ni, α to γ transformation, changes in Young's modulus and electro-physical props. *(Russian)* 79−20042
Fe-Ni, FCC, anomalous props. at high temp. and new phase *(Japanese)* 78−80520
Fe-Ni alloys, XPS of valence electrons rel. to decrease in Young's modulus *(Russian)* 77−77340
Fe-Ni based metallic glasses, search for Invar-like magnetoelastic behaviour 79−56596
Fe-Pd Invar alloy, Young's modulus, magnetostriction, Curie temp. 80−65988
Fe-Si (3 wt.%), magnetisation variation during bending oscills., rel. to ΔE effect *(Russian)* 80−65983
Fe-Si-B ferromagnetic amorphous alloys, Young's modulus and delay time charact. *(Japanese)* 77−85543
Fe-W-Cr-Mo-Co with austenitic phase, magnetic and mech. props., cold working and ageing effects *(Japanese)* 78−60678
$Fe_{80}B_{20}$ amorphous ribbons, magnetomechanical coupling constant and Young's modulus, mag. annealing 79−15333
$Fe_{80}B_{20}$, elastic, magnetoelastic and thermal props. 79−19759
$Fe_{80}B_{20}$, Metglas 2605, Young's modulus meas. using piezoelectric US composite oscillator technique 80−108656
Young's modulus continued
$(Fe_xCo_{1-x})_{78}Si_8B_{14}$, amorphous, saturation magnetostriction, strain modulated FMR obs. 80−75863
$Fe_{32}Ni_{36}Cr_{14}P_{12}B_6$, elastic, magnetoelastic and thermal props. 79−19759
$Fe_{0.49}Ni_{0.415}Mo_{0.095}$, Vibralloy, high-temp. vibrating reed meas. 79−55811
$Fe_{40}Ni_{38}Mo_4B_{18}$ and $Fe_{78}Mo_2B_{20}$ amorphous ribbons, magnetoelastic effects in as-quenched and stress-relieved states 80−80588
$Fe_{40}Ni_{40}P_{14}B_6$, bending tests, evidence of ideal elastic-plastic deform. 80−97543
$Fe_{40}Ni_{40}P_{14}B_6$, elastic, magnetoelastic and thermal props. 79−19759
$Fe_{1-x}O$, IR reflectivity obs. 77−43996
$Fe_{80}P_{13}C_7$, amorphous ribbon, giant ΔE effect, magnetomech. coupling factor 77−8379
$Fe_{80}P_{16}C_3B_1$ amorphous filament, produced by glass coated melt spinning, mech. props. 78−15483
Fe_3Pt, Invar alloy, elastically stressed, ^{57}Fe effective field, anomalous behaviour, Mossbauer obs. *(Russian)* 77−8485
$Fe_{78}Si_{10}B_{12}$ amorphous ribbons, magnetomechanical coupling constant and Young's modulus, mag. annealing 79−15333
$Fe_2(Tb_{0.2}Dy_{0.22}Ho_{0.58})$, highly magnetostrictive alloy, vibrating-reed meas. of ΔE effect and internal friction 79−42819
GaP, elastic moduli, 80-700K, and elastic consts. 79−73245
GaS, elastic prop. anisotropy, Debye temp. *(Russian)* 80−88244
GaS(Te)(Se), elastic characteristics, Debye temp., ultrasonic study *(Russian)* 80−79872
Gd-Tb, elasticity modulus, ΔE-effect, internal friction, magnetic transformations *(Russian)* 79−91723
Gd-Y (40 wt.%) alloy, magnetic phase transitions, elastic consts. meas. 78−14957
Ge, amorphous, random network model, calc. 78−6119
Ge film, amorphous, LF vel. of sound for Young's modulus mode 77−35636
Ge-As-Se glasses, US vel. and reson. freq. meas. 78−23756
GeO_2 glass fibre, elongation, force depend., deviations from linearity 80−45334
HFO_2, polycrystalline, monoclinic, elastic props. at room temp. 78−27548
$(Hf_{1-x}Zr_x)V_2$, supercond., Young's modulus and internal friction meas. 79−11654
In-Cd alloys, elastic-phase transition, US study 78−6919
K_2O-PbO-SiO_2, glass, mech. and optical props. *(Russian)* 77−20860
K_2O-SrO-SiO_2, glass, elastic constants 77−16630
$LaH_{2.96}$, elastic props. at high press. 77−84825
LiF, inverse moduli, up to temp. of 650°C 78−14397
Li_2O-Na_2O-B_2O_3-Al_2O_3-SiO_2 glass, Young's modulus and density, ion exchange effects 80−84982
Mg-Al(Sn)(Ni)(Cu), damping capacity 77−48474
Mn-Bi mictomagnetic alloy, mag., elec. and elastic props. *(Russian)* 80−108028
Mn-Ni alloys, γ-phase antiferromag., lattice distortion and elastic props., ΔE effect interpret. 77−20671
Mn-Ni-Ti (Zr) systems, and mech. props. thermal expansion for different heat treatments *(Japanese)* 79−29123
Mn-Ni-Ti(Zr), non-ferromagnetic Elinvar-type alloys 79−24566
Mn-Ni-V(Nb)(Ta), nonferromagnetic Elivar type, mech. props. meas. 77−48473
Mn-Pt, Elinvar props., −150 to 500°C *(Japanese)* 77−52385
Mn-Pt, exam. of Elinvar props., from −150 to 500°C 78−76684
γ-MnAu, antiferromag., phase diagram, X-ray diffr. and Young's modulus meas. 80−71024
MnBi, mictomag. alloys, elastic props. *(Russian)* 80−7141
Mo, pure, temp. depend. of Young's modulus, and shear modulus 78−27553
Mo-Ti-Zr, alloy TZM, polycrystalline, anal. of elastic anisotropy and microyielding 80−30050
NbC, elastic modulus, porosity factor 77−21207
NbC, physicomechanical props. within the homogeneity range 77−1848
$Nb_{0.55}Ir_{0.45}$ metallic glass, Young's modulus meas. by impulse induced resonance technique 80−40411
$NbSe_3$, Young's modulus meas. 78−48443
Nb_3Sn, Young's modulus, 4.2-300K, behaviour near martensitic transition 80−66564
NbTi filament reinforced Cu, superconducting composite, elastic const., temp. depend. 78−68717
Ni, Bordoni peak struct., evolution of Young's modulus 79−82282
Ni complex, 1,2-benzoquinonedioximates, refl. spectra, 0.5-2.5 eV, Young's modulus and internal friction 78−39562
Ni powders, stereological appl. in study of compacting process, elec. and mech. props. *(French)* 80−40286
Ni, pure, temp. depend. of Young's modulus, and shear modulus 78−27553
Ni, self interstitial migration and crowdion conversion, dislocation pinning expts. 77−84762
Ni, thermal expansion anomaly near Curie temp. 77−85474
Ni-Al (15 wt.%), temp. depend. of Young's modulus 79−83236
Ni-Zn ferrite, elastic moduli temp. and composition depend. 78−26617
β_2-NiAl alloys, Young's modulus, −196 to 800°C, effect of martensitic transforms. 79−83253
Ni_3Al, elastic moduli changes at Curie point 77−66406
$(Ni_{1-x}Cu_x)Ti$, martensitic, shape memory effect kinetics and thermodynamics 80−3021
$Ni_{1-x}Fe_x$, short range order exam. allowing for formation of structural domains *(Russian)* 78−6888
$Ni_{36}Fe_{32}Cr_{14}P_{12}B_6$ metallic glass, mech. props. and thermal stability 80−76362
NiTi, martensitic, shape memory effect kinetics and thermodynamics 30−3021
Pb, Young's modulus and internal friction, 20°C to melting point *(Russian)* 80−89278
Pb-Bi, elastic moduli, internal friction from US velocity meas. 79−15717
Pb-Sn eutectic, superplastic, anelasticity effect on stress relaxation 78−31443
PbO-B_2O_3-ZnO solder glass, with admixtures, crystallisation and thermal expansion 80−24364
Pd complex, 1,2-benzoquinonedioximates, refl. spectra, 0.5-2.5 eV, Young's modulus and internal friction 78−39562
Pd:H, elastic props. of dilute solid solutions 78−75706
Pd-Si, amorphous alloys, elastic props. and temp. coeff. of delay time, appl. to US delay lines *(Japanese)* 79−96069

Young's modulus continued
Pd-Si amorphous alloy, neutron irradiation effects *(Japanese)* 77—84806
Pt complex, 1,2-benzoquinonedioximates, refl. spectra, 0.5-2.5 eV, Young's modulus and internal friction 78—39562
Pt, pure, temp. depend. of Young's modulus, and shear modulus 78—27553
Pt, rel. to high temp. dilation correction to sp. ht. at const. vol. 79—14940
Pu-Ga (1 wt.%) alloy, polycryst. consts. calc. from single cryst. data 77—20005
$(SN)_x$ single crystal, mech. props. 79—24580
$(SN)_x$, tensile and piezoresist. expts. 78—15447
$SbGe_xSe_y$ glasses with const. Sb content, heat capacity, thermal expansion, US vel. and elastic moduli 77—76574
Sc_2O_3, polycrystalline, elastic props., porosity and temp. depend. 77—52384
Se, vitreous, elastic coeffs. about glass transition temp. US study *(French)* 80—19865
Si , amorphous, random network model, calc. 78—6119
Si film, amorphous, LF vel. of sound for Young's modulus mode 77—35636
Si whisker, amorphous, meas. of Young's modulus 78—83865
SiB_4, mech. and thermal props. 80—21083
SiC, continuous fibre synthesis with high tensile strength and Young's modulus 79—15633
SiC fibres, continuous, tensile strengths and Young's moduli, 600-1400°C 77—59885
SiC, fuel particle, coating meas. of strength and Young's modulus, brittle ring test 77—8868
SiC, strength assessment by Young's modulus meas. up to 1400°C *(German)* 78—11253
Si_3N_4, reaction-sintered, elastic moduli, fracture mechanics parameters, and strength 77—28889
Si_3N_4-Al_2O_3, hot-pressed with crystn. grain boundary phases 78—95716
Si_2N_2O, elastic props. 79—29122
SiO_2 fibres, plastic deformation and Young's modulus *(French)* 78—23746
SiO_2 glass fibre, elongation, force depend., deviations from linearity 80—45334
$SiO_2B_2O_3$-K_2O-Al_2O_3-As_2O_3 glass fibres containing metallic granules, tensile strength, Young's modulus, DC conductivity 80—30023
Sn, Young's modulus and internal friction, 20°C to melting point *(Russian)* 80—89278
$SrGa_2Si_2O_8$-$SrGa_2Ge_2O_8$, solid solution, exam. of elastic and electrical props. 79—96057
$Tb_{0.27}Dy_{0.73}Fe_2$, LF magnetoelastic effects 78—68348
$Tb_{0.3}Dy_{0.7}Fe_2$, US velocity and attenuation obs. 77—28423
Ti alloys, precipitate vol. fraction estimation from elastic modulus data 79—61595
β IIITi alloys solution treated and aged, estimation of precipitate volume fraction using Young's modulus 78—39781
Ti, hot-rolled, anisotropy of Young's modulus calc. *(Russian)* 78—23749
Ti sheet, anisotropy and texture, effect of plastic deform., recovery and recrystallisation *(Russian)* 77—8850
Ti-Al-V (6,4 wt.%), age hardened, deform. charact. 77—36608
Ti-Al-V (6,4 wt.%), heat treated and rolled, texture instability 77—63689
Ti-Al-V-Fe-Si, alloy VT6, phase transform. kinetics and Young's modulus *(Russian)* 77—81258
Ti-Mo alloys, elasticity moduli, 80-300°C *(Russian)* 78—80574
Ti-Mo-V-Al-Cr-Fe (4.8, 4.7, 5.2, 1.1, 1.0 wt.%), structural changes during heating up to 1000°C, DTA study *(Russian)* 80—93552
Ti-V, elastic moduli, electron conc., pulse echo overlap meas. 80—59550
Ti-V-H system, BCC, hydrogen effects on anisotropic elastic props. 79—24565
$Ti_{50}Be_{40}Zr_{10}$ glass, mech. props., X-ray diffr. exam. 78—11292
TiC, frictional characts. and contact-zone deform. in homogeneity range 80—66673
TiC_xO_y, elastic characts. 77—80568
$Ti_{0.60}Ni_{0.40}$ metallic glass, Young's modulus meas. by impulse induced resonance technique 80—40411
TiO_2-Fe_2O_3, comp. waves, Young's modulus minima rel. to crystallographic shear orientations 78—43034
$TiSe_2$ Young's modulus and internal friction obs., 1.3 to 300K 79—46750
Tm_2O_3, polycrystalline, elastic props., porosity depend. 77—52384
UAl_2-Al dispersion fuel, effect of reactions on Young's modulus and rupture strength *(German)* 78—62596
UFe_2, giant magnetoelastic deform. of cryst. struct. mag. props. *(Russian)* 80—93159
UN-ZrN, antiferromagnetic anomaly 80—92583
UO_2, computer model of Young's modulus 78—31450
V-H single crysts., elastic consts., temp. depend., H effects 80—66563
W_2C and WC, plastic deform. under bending, 800-2200°C *(French)* 80—55482
Zn particulate composite, mech. props., microstruct. correlation, at low and high temps. 77—32624
ZnO-$Al_2O_3SiO_2$, transparent glass-ceramic, microstruct., physical props., crystallisation ht. treatment depend. 78—80506
ZnSb, thermodynamic props. and elastic moduli 79—77767
ZnSe, elastic moduli, temp. depend., 293-973K, electrostatic reson. determ. 78—59850
α-Zr, 4.2 to 1133K *(Russian)* 79—57034
Zr alloy, elastic props. of fuel cladding and press. tubing material 79—15711
Zr_3Al, ordered, exam. of Young's modulus and thermal expansion coeff. 78—72805
ZrC, elastic modulus, porosity factor 77—21207
$Zr_{0.35}Cu_{0.65}$ metallic glass, Young's modulus meas. by impulse induced resonance technique 80—40411
ZrN, physicomechanical props. with the homogeneity range 77—1848
ZrO_2, partially stabilized, props. and appl. to extrusion dies 80—97507

ytterbium
see also nuclei with .....
$4f^{14}6s6p\ ^3P_1$ and $^1P_1$ levels, Stark effect, tensor polarisabilities 80—87080
amorphous metal films, crystallisation with and without mag. field 80—70570
atom, 4f states, soft X-ray apperance pot. spectra 79—47551

ytterbium continued
atom, autoionisation and Auger decay, collective excitation effect 80—43008
atom, electron impact excitation cross section, Born and Ochkur approx. 80—87230
atom, electron impact L-shell ionis., 300-600 keV 77—50542
atom, emission spectrum, extended anal. 79—85923
atom, excited state lifetime meas. using cw dye-laser 79—89636
atom, highly excited levels, odd and even parity spectra, multichannel quantum defect anal. 80—58133
atom, highly excited levels, reson., visible two photon absorpt. spectra obs. 80—58228
atom, highly selective multistep ionisation by laser radiation 79—59408
atom, isomers and hyperfine struct., selective detection through Rydberg states 80—52903
atom, L X-ray emission spectrum, new satellites 78—46293
atom, method for studying X-ray spectra 77—27014
atom, optical isotope shifts and hyperfine splittings 79—93943
atom, photoabsorpt. spectra 77—88417
atom, photoionisation cross-section of $^3P_1$ excited state, laser isotope separation *(Russian)* 78—25496
atom, Rydberg states, optically pumped, electric field ionis. *(Russian)* 79—27095
atom, scalar relativistic approximation 79—26899
atom, Schumann region absorpt. spectrum, oscill. strengths, line profiles, collisional and autoionis. broadening 77—18818
atom, two-photon absorption spectra of highly excited states 78—70806
atom, two-photon laser spectra, hybrid resonances 79—31489
atom, UV photoelectron spectra, config. interaction effects 77—50413
atom, VUV absorpt. spectrum, $4f^{14}$ subshell excitation 79—76373
atom, Zeeman quantum beats in $6s6p\ ^3P_1$-$6s^2\ ^1S_0$ transition 79—13682
atom detection by selective laser excitation and field ionisation from Rydberg states 79—18159
atomic energy level classification, ground state to two-electron level 77—68003
atomic HFS in $6s6p\ ^1P_1$ state, level-crossing and anticrossing spectroscopy 77—27036
atomic spectra, 1060-1700 Å 78—82675
atomic spectra, $6s^2$ shell excitation 79—72265
atoms, electron impact excitation, 40 to 120 nm, 5p ionisation 78—82845
chemi-ionisation reactions of Ca, Sr, Ba, and Yb with halogens and interhalogens 77—32791
electrical resistivity of solid and liquid phases, thermopower, melting temp. 80—59955
electron and positron multiple scatt. 80—15171
electron radiation damage, elec. resistivity change rates 80—59954
EXAFS, white lines, interatomic distances 77—40302
FCC, Fermi surface parameters, de Haas-van Alphen effect, press. depend. 77—28092
FCC, nucl. orientation of 3d impurities and magnetisation meas. 78—64280
FCC phase, low temp. mag. props., impurity effects 80—20387
film, amorphous and cryst., transport props., rel. to band struct. *(Russian)* 77—12026
film, energy-scanning X-ray diffr. technique, stacking faults and coherent domains *(French)* 78—43264
film, O_2 and H_2 contamination effect on elec. resist. 77—80856
film, vapour-quenched, unsuccessful search for supercond. above 0.3K 77—12053
fluorite type crystal: Yb^{3+}, axial g-values of $4f^{13}$ ions with trigonal symmetry *(Korean)* 79—24135
glass:Yb^{3+},Er^{3+}, stimulated emission 77—50675
hole lifetime and chemical shift of 4f-levels, XPS study 80—20762
impurity in nonmag. host, anisotropic exchange Hamiltonian, rel. to ESR spectrum 77—20696
isotope shifts and high resolution laser fluoresc. spectroscopy in deep blue spectral region 77—82622
isotopic and elemental abundances in meteorites and terrestrial samples 78—32419
liquid, divalent, electrical resist. 79—38039
liquid, resist. and thermoelec. power, t-matrix calc. 78—26840
metaphosphate glass: Nd^{3+}, Yb^{3+}, luminesc., energy transmission and migration between Nd^{3+} and Yb^{3+} 80—66297
phosphate glass:Yb^{3+}, excitation migration in inhomogeneous line profile, energy gap depend. 80—7407
phosphate glass:Yb^{3+}, impurity centres, migration of excitations, math. modelling 78—48225
phosphate glass:Yb^{3+}, luminesc. band struct., chronoscopic study at 4.2K 80—60663
phosphate glass:Yb^{3+}, migration of electronic excitations, manifestation in reson. luminesc. 77—8642
phosphate glass:Yb^{3+}, nonreson. interaction parameters, luminesc. kinetics obs. *(Russian)* 78—31246
photoemission, valence-charge-induced Fano reson. 80—55267
piezoresistance gauge, lateral compressive stresses meas. in shock-loaded PMMA 80—103007
rare earth oxysulphide, R_2O_2S:Yb^{3+},Ho^{3+}, anti-Stokes emission band assignments, energy transfer mechanism 77—40277
recrystallisation of wires and filings by thermal processing encapsulated in metal tubulation 77—59810
semiconducting phase, resistivity behaviour at high temps. semimetal-semiconductor transition 78—14727
semimetal-semicond. transition at high press., Seebeck coeff. meas. 77—62956
shock compressed, elec. cond. behaviour and transitions, up to 220 kbar *(Russian)* 77—80761
stress transducer, piezoresistive effects 77—68539
structural and electronic changes under 200 kbar press. and above 80—24588
yttrium ethyl sulphate:Yb, spin refrigerator, proton polarisation 77—83435
BaF_2:Yb^{3+}, trigonal centres, point-charge approx. 78—39072
BaY_2F_8:Yb^{3+}, ESR spectra and spin-lattice relax. 80—11263
$Bi_4Ge_3O_{12}$:Yb^{3+} crystal growth, spectral and laser props. 80—45115
CaF_2:Mn^{2+},Yb^{3+}, efficient luminesc. energy transfer from Mn^{2+} to Yb^{3+} 78—19536
CaF_2:Mn^{2+},Yb^{3+}, luminescent energy transfer efficiency obs. 78—6777
CaF_2:Yb^{2+}, cryst., stress polarisation of luminesc. and emitting states struct. 77—69897
CaF_2:Yb^{2+}, divalent ion radiative state, magneto-optical obs. 77—69893

ytterbium continued
- CaF_2:Yb^{2+}, luminesc. polarisation, elastic uniaxial compression effect, radiative state model 78−6739
- CaF_2:Yb^{2+}, spectra, kinetics and polarisation of luminesc. 77−69892
- CaF_2:Yb^{3+}, cryst. field at O_h sites 77−35899
- CaF_2:Yb^{3+}, Er^{3+}; and CdF_2-CaF_2:Yb^{3+}, Er^{3+}, IR to visible upconverting system 77−44035
- CaF_2:Yb^{3+}, point-charge approx. tetragonal centres 77−47778
- CaF_2:Yb^{3+}, trigonal centres, point-charge approx. 78−39072
- CaF_2:Yb^{3+} vacuum UV absorpt. spectrum, rel. to other rare-earth ions 79−43001
- CaF_2+Yb^{3+}, evidence for covalency 77−85180
- CaF_2+Yb^{3+}, Stark level Zeeman energies, mag. susceptibiltiy, Schottky specific heat, crystal field splitting 78−26831
- $CaWO_4$:Yb^{3+}, phase relaxation electron spin echo spectra 80−29613
- $CaWO_4$:Yb^{3+}, phase relax. time rel. to g-factor anisotropy, electron spin echo obs. 80−29615
- CdTe, Yb^{3+} implantation, nonstoichiometry effect 77−15440
- CdTe:Yb, exciton emission, cathodoluminescence 78−39033
- CeO_2:Yb^{3+}, ENDOR, evidence for covalency 78−80247
- CeO_2:Yb^{3+}, trigonal centres, point-charge approx. 78−39072
- CeO_2:Yb^{3+}, trigonal sites of Yb^{3+}, ENDOR meas. 79−95677
- Cs_2NaYCl_6:Yb^{3+} electron spin-lattice relax. 77−63274
- $DyAlO_3$:Yb^{3+}, Mossbauer relax. 80−15875
- Er^{3+}, Yb^{3+}:glass, Nd laser radiation energy conversion *(Russian)* 77−62013
- Er^{3+}:Yb^{3+} in liq. media, luminesc. cooperative sensitisation 80−2827
- EuO:Yb, electron transition and valence state of impurities, X-ray spectroscopy and structural anal. 78−39064
- EuS:Yb, electron transition and valence state of impurities, X-ray spectroscopy and structural anal. 78−39064
- Fe:^{169}Yb, lattice location and hyperfine field of implanted Yb, annealing temp. depend. 77−48100
- Fe:^{172}Yb, hyperfine mag. field, TDPAC meas. 78−52394
- Fe:Yb, ^{18}O, interaction between implants 77−27921
- Fe:Yb,O, interaction between impurities, perturbed ang. correlation meas. 77−1628
- Fe:Yb(Au), radiation-damage evolution, influence on lattice-location meas. 80−6426
- GaP:Yb, magnetic susceptibility, impurity states 79−61044
- GaSb:Gd(Yb), elec. props., dopant effects 79−87115
- H, and He, stopping powers meas. 80−42904
- $HoAlO_3$:Yb^{3+}, Mossbauer relax. 80−15875
- K halide, Yb^{2+} activated, X-ray and intracentre luminesc. 78−6737
- KBr:Eu(Yb), electron-irrad., photostimulated luminesc., ionic processes 78−52561
- KCl:Yb, Z_2 and Z_2^+ centres, excited state, magnetooptical spectra 80−108233
- KCl:Yb, Z_2-centres, optical absorpt. and ESR spectra 79−91481
- $KMgF_3$:Yb^{3+}, ^{19}F hyperfine interaction, anisotropic Fermi and isotropic dipolar interactions 79−78056
- $KMgF_3$:Yb^{3+}, cryst. field parameters, optical, EPR spectra, spin-lattice relax. time 77−51950
- $KMgF_3$:Yb^{3+}, perovskite type cryst., ENDOR meas. 80−80638
- $KMgF_3$:Yb^{3+}, transferred hyperfine interaction of Yb^{3+}, ENDOR meas. 78−19375
- KYF_4, KY_2F_7, KY_3F_{10}, Er^{3+} and Yb^{3+} doped, IR excitation curves for visible luminesc. 79−33795
- $KZnF_3$:Yb^{3+}, cryst. field parameters, optical, EPR spectra, spin-lattice relax. time 77−51950
- $KZnF_3$:Yb^{3+}, perovskite type cryst., ENDOR meas. 80−80638
- La_2O_2S:Yb^{3+}, charge transfer type luminesc. 79−33797
- La_2O_2S:Yb^{3+},Er^{3+}, IR excited visible luminesc. of Er^{3+} 78−2910
- $LaPO_4$:Yb^{3+}, charge transfer type luminesc. 79−33797
- $LaRh_2$, ESR of Yb^{3+} 79−87315
- LiCl-KCl:Ln^{n+}, fused eutectic, electrolytic behaviour *(Japanese)* 79−16009
- $LiYF_4$:Yb^{3+}, ESR, nonlinear effect of elec. field 80−2635
- $LiYF_4$:Yb^{3+}, Ho^{3+}, sensitised anti-Stokes luminesc., theory 77−66537
- $(Lu,Yb)_3Al_5O_{12}$:Yb^{2+}, stimulated emission 77−52135
- Lu_2O_2S:Yb^{3+}, charge transfer type luminesc. 79−33797
- $LuPO_4$:Yb^{3+}, charge transfer type luminesc. 78−64392
- $LuPO_4$:Yb^{3+}, charge transfer type luminesc. 79−33797
- Na_2O-B_2O_3-SiO_2:Yb(Tb), luminesc. cooperative processes, glass struct. and comp. effect 80−16101
- Na_2O-TeO_2:Yb^{3+} glass, luminesc. quenching by OH and OD *(Russian)* 79−28839
- $Na_3Sc_2V_3O_{12}$:Yb^{3+}, EPR of Yb^{3+} in octahedral sites 80−54948
- $NaYF_4$:Ho, Yb, two photon anti-Stokes effect, excited by 2 μm radiation 78−50852
- Nd^{3+}-Yb^{3+}:glass, excitation transfer, selective filling of levels in inhomogeneous contour 77−69898
- Ni:^{172}Yb, hyperfine mag. field, TDPAC meas. 78−52394
- $POCl_3$-$ZrCl_4$:Yb^{3+}, Er^{3+}, energy transfer from Yb^{3+} to Er^{3+}, agglomeration formation 78−64405
- PbF_2:Yb^{3+}, superhyperfine interaction, ENDOR and RF discrete saturation expts. 79−73856
- PrSb:Yb, ESR of non S-state ions 77−43881
- Si:Yb, impurities behaviour 79−78568
- SrF_2:Yb, superhyperfine interaction of trigonal Yb^{3+} centres 78−27117
- SrF_2:Yb^{3+}, trigonal centres, point-charge approx. 78−39072
- SrF_2:Yb^{3+}, trigonal centres, superhyperfine interaction, model 78−88114
- Tb^{3+}:Yb^{3+} in liq. media, luminesc. cooperative sensitisation 80−2827
- $TbAlO_3$:Yb^{3+}, Mossbauer relax. 80−15875
- ThO_2:Yb^{3+}, trigonal centres, point-charge approx. 78−39072
- ThO_2:Yb^{3+}, trigonal sites of Yb^{3+}, ENDOR meas. 79−95677
- $TmAlO_3$:Yb^{3+}, mag. relax., Mossbauer expts. 79−8078
- $Tm_3Al_5O_{12}$:Yb^{3+}, g-shift meas., EPR 78−56376
- $(Y,Yb)_3Al_5O_{12}$:Yb^{3+}, stimulated emission 77−52135
- YAG, influence of facial growth effect on Yb ion incorporation 79−10822
- YAG:Yb, US attenuation 77−89500
- YAG:Yb^{3+}, cryst. field, Schottky sp. ht., paramag. susceptibility 77−11882
- $YAlO_3$:Yb^{3+}, absorption and luminescence spectra, electron-phonon resonances, Stark splitting *(Russian)* 80−20674
- $Y_3Al_5O_{12}$:Yb^{3+}, one-phonon satellites in luminesc. spectra, rel. to effective phonon density 78−6730
- YB^++inert gas, ($^2P_{3/2}$) states relax. cross sections 78−13595
- YF_3:Er^{3+}, Yb^{3+}, IR excitation curves for visible luminesc. 79−33795
- YF_3:Yb,Er, IR to visible light conversion, effect of temperature on efficiency *(Russian)* 77−28628
- YF_3:Yb,Er, IR to visible radiation transform., limit yield *(Russian)* 79−28838
- YF_3:Yb,Er, limit efficiency of transformation of IR to visible radiation 80−29784
- YF_3:Yb^{3+}, Tm^{3+}, IR to blue up-converting phosphor 79−83004
- YGa garnet:Yb^{3+}, cryst. field, Schottky sp. ht., paramag. susceptibility 77−11882
- $Y_{1.3}GdYb_{0.7}GaO_{12}$, epitaxial film, ferromagnetic reson. exam. 77−85579
- YIG:Yb, magnetoelastic coupling of Yb ions, ferromag. reson. meas. 77−69698
- YOCl:Yb,Er, anti-Stokes luminesc., temp. depend. *(Russian)* 78−6764
- YOCl:Yb^{3+}, Er^{3+}, anti-Stokes luminesc., 4.2 to 293K 77−59609
- Y_2O_2S:Ho, Yb, two photon anti-Stokes effect excited by 2 μm radiation 78−50852
- Y_2O_2S:Yb^{3+}, charge transfer type luminesc. 79−33797
- YPO_4:Yb^{3+}, charge transfer type luminesc. 78−64392
- YPO_4:Yb^{3+}, charge transfer type luminesc. 79−33797
- Y_2SiO_5:Yb^{3+}, EPR and spin-lattice relax. 80−108063
- YVO_4:Er^{3+}, Yb^{3+}, IR excitation curves for visible luminesc. 79−33795
- ^{169,175}Yb electrosorption on anodically polarised Pt surface 79−52684
- Yb I, high Rydberg levels of $4f^{14}$ 6snd configs., very high resolution obs. 80−106300
- Yb I, Yb II, excited states radiative lifetimes 79−76386
- Yb I isotope shift studies in 3900 to 6500 Å region 80−74144
- Yb II, 6s $^2S_{1/2}$-6p $^2P^o_{1/2,3/2}$ transition, relativistic oscillator strengths, influence of core polarisation 80−58132
- Yb^{2+}, broadband luminesc. in fluorite struct. crysts. 79−65923
- Yb^{3+} doped phosphors, IR excitation and absorpt. and emission spectra *(Russian)* 79−52021
- Yb^{3+}, in dessicated (nondessicated) and protonated (deuterated) solvents, photoluminesc. energy degredation 78−19544
- Yb^{3+} in paramagnet, cryst. field effects on EPR and NMR *(Japanese)* 77−43880
- Yb^{3+}, in soln., non-radiative transitions as Forster's energy transfer to solvent vibrations 80−1014
- Yb^{3+}, local symmetry in frozen aq. solns., EPR and local electric field effect 77−16169
- Yb^{3+}, luminesc. sensitisation of Er^{3+}, Tb^{3+} in liq. efficiency *(Russian)* 78−90116
- Yb^{3+}, spectrum and energy levels 79−26916
- Yb:glass, luminesc., low temp. energy transfer 80−2837
- Yb^{3+}:phosphate glass, relation between absorption and equilib. luminesc. spectra 77−85754
- Yb-Cu_2O Schottky-barrier solar cells, surface anal. using AES 79−43759
- Yb+H^+, K-shell ionisation, 7-15 MeV, relativistic effects 78−82830
- Yb+O_2→YbO+O, crossed mol. beam expt. 77−44468
- Yb+Yb^+, with nuclear sticking, molecular orbital and compounds nucleus X-ray emission 80−1048
- YbI, first spectrum, wavelengths and intensities, Zeeman effect 79−3389
- ^{A}YbI, A=170,171,173, 6s6p $^1P_1$-6s^2 $^1S_0$ transition, spectrosc., isotope shifts and hyperfine structure 80−23368
- ^{70}Yb L-shell X-ray emission spectrum investigation 77−3297
- ^{169}Yb, K-shell internal conversion, Kα_1 hypersatellite line energies, intensities 77−18885
- ^{170}Yb in some metal and metal-like compounds, Mossbauer study, isomer shift and intermediate valence state 79−33569
- ^{170}Yb, Mossbauer line shape, Liouville relax. supermatrices 79−28649
- ^{172}Yb, muonic resonance spectra, deduced isomer shifts and electric moments 80−18948
- ^{173}Yb, 6s6p $^1P_1$ state, level crossing with additional pumping of ground state 77−34595
- Yb(6^3P_1), Zeeman splitting, high-resolution time-resolved quantum beat spectra 78−58640
- ZnO:Yb, electro- and photoluminesc. 79−83024
- ZnO:Yb, electrolum. brightness, field strength and freq. depend. 80−100696
- ZnS:Yb^{3+}, spin-lattice relax. times meas. 78−19324
- $ZrSiO_4$:Yb, anisotropic mag. susceptibility meas. 77−43806

ytterbium alloys
- Kondo system, crystal field effects on thermopower and Kondo effect 77−66163
- magnetic susceptibility, 1.4 to 1060K, investig. of Yb valency 77−20543
- Magnico alloy, with Si, Nb, Ti effect of Ub on mag. props. and grindability 77−63811
- transition metal-Yb alloys, valence state of Yb 79−77545
- $Ag_{1-x}Au_xYb_y$, thermopower and resistivity 79−65457
- Au-^{171}Yb, dil., nuclear induced resistivity drop 78−10431
- Au-^{174}Yb, dil., nuclear induced resistivity drop 78−10431
- Au-Yb, dil., conduction electron-local moment interactions using dHvA waveshape anal. 79−77981
- Au-Yb, dil., EPR at 100 mK to 1K 80−66028
- Au-Yb, dil. alloy, high field nuclear relax. of ^{173}Yb, anisotropic cond.-electron exchange 77−8434
- Au-Yb alloys, dil., nucl. reson. of ^{173}Yb local moments 79−65763
- Au-Yb dilute, NMR investig. of anisotropic cond. electron exchange 77−63309
- Au-Yb thin films, ESR spectra, strain effects 80−71172
- Ba-Yb, phase diag. *(Russian)* 78−80514
- $CePd_3$-Yb, dil., EPR 80−25201
- Gd-Yb, Curie temp. and saturated mag. moment, nonmag. solute effects 78−39301
- Gd-Yb, dil., mag. hyperfine field of ^{176}Yb, Mossbauer effect meas. 79−24242
- Gd-Yb, magnetocrystalline anisotropy, magnetisation and torque curve meas. 80−65859
- Mg-Yb, dil., Kondo scatt. from Yb, low temp. elec. resist. meas. 80−44578
- Tb-Yb, mag. ordering temps., susceptibility meas. 80−25136
- $Y_2(Fe_{1-x}Co_x)_{17}$, hyperfine interactions, Mossbauer spectra 78−2780
- Yb-Al, valence changes during autoionisation and Auger electron emission 80−50475
- Yb-Al mixed valent film form., XPS study 80−80943
- Yb-Eu alloys, mag. ordering, magnetisation meas. 80−7081
- Yb-Ga, phase diagram, differential thermal and X-ray analysis *(Russian)* 78−56615
- Yb-Ga system, phase diagram, cryst. structs. of phases 79−52169

ytterbium alloys continued
YbAg, mag. susceptibility, thermally excited interconfiguration crossover 77−16042
$YbAl_2$ and $YbAl_3$, intermediate valency cpds., paramag. susceptibility, 1.4 to 1060K 77−63079
$YbAl_2$-Gd(Er)(Dy)(Nd), dil., EPR and mag. susceptibility 80−15797
$YbAl_3$, Mossbauer effect obs. of induced hyperfine field 78−52396
$YbAl_3$, susceptibility, sp. ht. and magnetisation 79−28512
$YbAl_3$, unstable valence system, model for thermodynamic props. 77−69487
$YbAl_3$, valence instabilities 79−78546
$YbAl_3$, XPS studies, valence band, 4-f region 78−6831
$YbAl_2Ga_2$, synthesis, NMR and X-ray absorpt. studies 80−108083
YbAu, mag. susceptibility, thermally excited interconfiguration crossover 77−16042
$YbAu_2$, surface effects on valence 78−91746
$YbAu_2$, surface electronic structure, XPS study 80−55259
$YbAu_2$, valence transition at surface of Yb 80−70652
$YbAuNi_4$, mag. props. 77−20595
$Yb_2Co_{17-x}Fe_x$, magnetisation, Curie temp., anisotropy 77−89947
YbCu, mag. susceptibility, thermally excited interconfiguration crossover 77−16042
YbCuAl, intermediate valency cpds., paramag. susceptibility, 1.4 to 1060K 77−63079
YbCuAl, intermediate-valent, nucl. reson. and relax. 79−78550
YbCuAl, mixed valence behaviour, mag. props. 78−68150
YbCuAl, mixed valence cpd., dynamic susceptibility, neutron inelastic scatt. 80−65807
YbCuAl, mixed-valence behaviour, mag. susceptibility and sp. ht. 77−80939
YbCuAl, mixed-valent cpd., thermal expansion and magneto-volume effects 80−66005
YbCuAl, phase diagrams, lattice props., electron hole symmetry 79−91002
YbCuAl, susceptibility, sp. ht. and magnetisation 79−28512
$YbCu_2Si_2$, interconfiguration fluctuation, NMR expts. 80−66069
$YbCu_2Si_2$, mag. 4f Zeeman-level power spectrum using diffuse mag. neutron scatt. 79−60775
$YbCu_2Si_2$, tunnelling anomalies due to intermediate valence phenomenon 77−62873
$YbCu_2Si_2$, valence fluctuation and temp. depend. of Cu nuclear quadrupole interaction 80−15818
$YbFe_2$, cryst. elec. field and exchange interac., ^{170}Yb Mossbauer obs., magnetostriction contrib. 80−108124
$YbFe_2$, Curie temp., elec. quadrupole couplings, Mossbauer study 80−39949
$YbFe_2$, high field Mossbauer study 80−75893
$YbFe_2$, Laves phase compounds, synthesis, mag. props., ^{57}Fe Mossbauer effect 78−10807
$YbFe_2$, Mossbauer spectra, cryst. elec. field and exchange interaction 79−47368
$YbFe_2$, preparation and mag. props. 80−25259
$YbFe_4Al_8$, mag. props. 78−52250
$Yb_2Fe_4Si_9$ and $YbFeSi_3$, cryst. struct. and mag. suscept., temp. depend. *(Russian)* 78−34957
$YbGa_2$, intermediate valency cpd., paramag. susceptibility, 1.4 to 1060K 77−63079
$YbInAu_2$, intermediate valence cpd., mag. susceptibility expts., 4.2-280K 78−39288
$YbNi_2$-$YbCu_2$ system, valency state, Yb behaviour *(French)* 80−45277
$YbNi_2Ge_2$, intermediate valence cpd., mag. susceptibility expts., 4.2-280K 78−39288
$YbNiSi_3$, mag. susceptibility, 80-1200K *(Russian)* 77−66281
YbPd-YbAg system, valency state, Yb behaviour *(French)* 80−45277
YbPt-YbAu system, valency state, Yb behaviour *(French)* 80−45277
$Yb_xSc_{1-x}Al_3$, valence fluctuation system, suscept. meas. 78−68149
$YbSn_3$, powdered, de Haas-van Alphen effect 80−59857
$Yb_{1-x}Y_xCuAl$, disordered extended Anderson model, CPA-alloy analogue treatment 80−65506
$Yb_{1-x}Y_xCuAl$, intermediate Yb valence states, mag. props. 79−51743
YbZn, mag. susceptibility, thermally excited interconfiguration crossover 77−16042

ytterbium compounds
see also ytterbium alloys
chalcogenides, multiphonon inelastic light scatt., hot recomb. 77−8559
ethyl sulphate, crystal field effects on mag. and hyperfine props. of Yb^{3+} 80−97101
etioporphyrin, electronic energy transfer with porphines and metalloporphyrins, luminesc. 77−474
ferrite aluminates, prep. 77−85970
formate, IR spectra and phase transitions, under pressure 78−31179
ions, 4f photoelectron spectral intensity, relativistic calc. 79−54816
mixed valence compounds, charge dominated fluctuation props. comparison, mag. moments and ordering 80−54659
mixed valence compounds, mag. props. 79−78048
monochalcogenides, multiphonon inelastic light scatt. 77−90144
monochalcogenides, Raman light scatt., phonons and valence fluctuations, review 77−63415
Mossbauer spectrum of ^{172,174,176}Yb, appl. of in-beam implantation method 78−25372
phthalocyanine solutions, bleaching by ruby laser beam 78−30030
silicate: Yb_2O_3 glassy film, Yb laser spectral microanalysis 80−76585
triphenyl phosphonium ytterbium chloride, $Yb^{3+}(4f^{13})$ absorpt. spectrum, cryst. electric field splitting 77−73151
YIG, bulk, convolution with magnetoelastic Rayleigh waves 79−64404
$(BaF_2)_{1-x}(YbF_3)_x$, crystal growth and struct. 77−12520
$Bi_xYb_{3-x}Fe_5O_{12}$ LPE film, phase grating integrated optic coupler-modulator 77−11048
C_6Yb intercalation compounds, three dimensional continuous melting 80−59631
CaF_2:YbF_3, clustering, defect struct., NMR study 78−80229
CaF_2-YbF_3 system, phase relationships *(German)* 79−24501
CdF_2:YbF_3, conversion processes into semiconductor 78−14730
CdF_2:YbF_3, photoconversion from insulating to semicond. state, IR absorption and elec. cond. 78−14759
$Cs_2NaYbCl_6$, electronic struct., paramag. susceptibility and electronic Raman spectrum, cryst. field parameters *(German)* 77−63072
$(Eu,Yb)_3Fe_5O_{12}$, low temp. CVD epitaxial film growth and mag. props. 79−42406

ytterbium compounds continued
$Eu_{1-x}Yb_xO$, solid soln., ferromag. semicond., increase of exchange interaction 78−88109
$Eu_{1-x}Yb_xS$, solid soln., ferromag. semicond., increase of exchange interaction 78−88109
$Eu_{1-x}Yb_xTe$, ($0<x<1$), mag. semicond., elec., mag. and optical props. 80−97070
$Fe_{0.76}Yb_{2.16}S_4$, cryst. struct. determ. 78−26533
GaS-YbS system, phase diagram, reacts., thermal, mag. and elec. meas. 79−11578
GdF_3-YbF_3, stabilisation of rhombic β-YF_3 type struct. 78−67700
HfO_2-Yb_2O_3 solid solns., prep., crystn. 78−42909
KF-YbF_3, phase analysis 78−44101
$KYbHP_3O_{10}$, thermal decomp., thermogravimetric and X-ray obs. 80−101013
Kb_2S_3, condensates, struct. and optical transmittance 80−20727
LaB_6-YbB_6 exam. of secondary ion-ion emission, due to bombardment by 8 keV Ar ions 79−33882
$LiYbF_4$:Ho^{3+}, laser converter for 2.06 μm radiation, Nd primary laser 79−18427
$(Lu,Yb)_3Al_5O_{12}$:Yb^{3+}, stimulated emission 77−52135
Na_2O-GeO_2-Yb_2O_3, glass struct., Yb^{3+} ion segregation 78−87620
$NaYb(WO_4)_2$, thermal expansion, X-ray determ. 80−39323
$SbCu_3Si_2$, mixed valence system, X-ray absorption spectroscopic study 80−80906
$Sm_{1-y}Yb_yB_6$, valence transition, lattice parameter and mag. susceptibility meas. 80−59929
$Sm_{1-x}Yb_xS_x$ optical investig. of substitution effects on metal-semicond. transition 77−63427
$Sm_{1-x}Yb_xS$, simultaneous Sm^{2+}-Sm^{3+} and Yb^{2+}-Yb^{3+} electron transitions *(Russian)* 79−60711
$Sm_{1-x}Yb_xS$, valence transition under high press. 79−73551
(Y, Eu, Yb, Ca)$_3$(Ge, Fe)$_5O_{12}$, bubble film, LPE on $Gd_3Ga_5O_{12}$, mismatch and faceting 77−20657
(Y,Gd,Yb,Bi)$_3$(Fe,Al,Ga)$_5O_{12}$ films, magnetic bubble domains, domain wall motion examined 78−19294
(Y,Gd,Yb,Bi)$_3$(Fe,Al)$_5O_{12}$ film, nonreciprocal effects in domain boundary motion in inhomogeneous field 77−24726
(Y, Gd, Yb, Bi)$_3$(Fe, Al)$_5O_{12}$ epitaxial film, domain wall motion and oscill. 80−2616
(Y,Gd,Yb,Bi)$_3$(Ga,Al,Fe)$_5O_{12}$, bubble conversion to anomalous behaviour 78−23309
(Y,Gd,Yb)$_{3-x}$Bi$_x$(Fe,Al)$_5O_{12}$, garnet single cryst. film, possible bubble appl. 78−6552
(Y,Gd,Yb)$_{3-x}$Bi$_x$(Fe,Al)$_5O_{12}$, LPE, for magneto-optical appls. 78−48341
(Y,Gd,Yb)$_3$(Fe,Ga)$_5O_{12}$ film, magnetisation processes and domain struct. near compensation temp. 78−14996
(Y,Yb)$_3$Al$_5O_{12}$:Yb^{3+}, stimulated emission 77−52135
(Y,Gd,Yb)$_{3-x}$Bi$_x$(Fe,Al)$_5O_{12}$ film growth on $Gd_3Ga_5O_{12}$ substrates 79−78623
(YCaEuYb)$_3$(FeGe)$_5O_{12}$, LPE, stripe end motion, effect of in-plane field 78−68330
(YCdYbBi)$_3$(FeAl)$_5O_{12}$, cylindrical domain wall vel. anisotropy *(Russian)* 77−59440
(YEuYbCa)$_3$(FeGe)$_5O_{12}$, ion-implanted, in-plane mag. field effects on bubble props. 77−85521
(YEuYbCa)$_3$(FeGe)$_5O_{12}$ film, mag. σ-bubbles, automation props. 78−88150
(YEuYbCa)$_3$(FeGe)$_5O_{12}$ bubble films, Ne^+-implanted, cryst. and mag. props., X-ray diffr. obs. 79−38362
(YEuYbCa)$_3$(FeGe)$_5O_{12}$ film, isolated straight stripe domain dynamic props. 79−33514
(YEuYbCa)$_3$(FeGe)$_5O_{12}$, garnet film, isolated straight stripe domain, dynamic behaviour 80−39809
(YEuYbCa)$_3$(GeFe)$_5O_{12}$ bubble film with ion-implanted layer, FMR study 80−2643
(YEuYb)$_3$(FeGa)$_5O_{12}$, LPE, stripe end motion, effect of in-plane field 78−68330
YFe_2O_4, extra electron relfections 80−100139
(YGdYbBi)$_3$ (FeAl)$_5O_{12}$ epitaxial film, diffuse domain wall, bubble domain expansion 80−25170
(YGdYbBi)$_3$(FeAlGa)$_5O_{12}$ film, motion of mag. bubble domains in inhomogeneous pulsed mag. field 78−27064
(YGdYbBi)$_3$(FeAl)$_5O_{12}$, epitaxial garnet film, with mag. compensation point, behaviour of 'compromise' phase boundary 78−60321
(YGdYbBi)$_3$(FeAl)$_5O_{12}$, garnet, epitaxial film, interior domains 79−91268
(YGdYbBi)$_3$(FeAl)$_5O_{12}$ ferrite-garnet films, effect of in-plane field on dynamics of domain walls 80−65979
(YGdYbBi)$_3$(FeAl)$_5O_{12}$ epitaxial garnet film, uniaxial ferromagnet domain struct., phase transition *(Russian)* 80−108044
(YGdYbBi)$_3$.(FeAl)$_5O_{12}$ films, substrate orientation influence on max. vel. of domain boundaries 79−15330
$Y^{16}O$ and $Y^{18}O$, vibr. anal. of blue and red system 79−809
(YYbBi)$_3$(FeAl)$_5O_{12}$ films, Faraday effect in transverse mag. field, orientation depend. 80−88971
$Y_{1-x-y}Yb_xEr_yOCl$, Er ion excited state decay and population *(Russian)* 80−100694
Yb complex, fluorescein dye(-Yb^{3+}), triplet state energy transfer, fluoresc. quenching obs. 79−54897
Yb complexes, lanthanide-induced NMR shifts, temp. depend. 77−68061
Yb-H system, phase transforms. at high H_2 press. 78−63853
Yb-S system, L-X-ray absorpt. spectroscopy, conc. of ions with various numbers of f electrons 77−28646
YbAG, cryst. field parameters calc., exchange charge model 78−47747
YbAG, electrostatic model of cryst. field 80−59945
$YbAlO_3$, and mag. ordering 79−8078
$YbAlO_3$, single crysts., prep. and phys. props., X-ray struct. anal. 79−4298
$YbAl_3[BO_3]_4$, thermal stability, X-ray struct. anal., refractive indices 79−4297
$YbAsO_4$, ferroelectricity, dielec. meas. 80−60515
YbB_{12}, mag. props., cryst. struct., valence of Yb *(Russian)* 78−60263
YbB_{12}, valence state and mag. props. 80−50031
YbB_4, mag. and elec. props., metallic character 80−20386
YbB_4, mag. props. *(French)* 77−20566
YbB_6, ^{11}B nucl. quadrupole interaction, NMR meas. 80−2660
YbB_6, growth by soln. method, struct. and mech. props. 80−16168
YbB_6, resistivity press. variation, lattice consts. 80−100456
$YbB_{6-x}C_x$, pure and doped, mag. and transport props. 80−54689
$YbBO_3$, cryst. struct. reappraisal 77−47427

ytterbium compounds continued
$YbBe_{13}$, mag. props. and EPR meas. 80−11175
YbBr, emission spectra in arc discharge, vibr. anal. 78−74670
YbC_6, intercalation cpd. with graphite, synthesis and struct. 80−44184
YbCl, chemiluminesc., vibr. anal. 77−30917
YbCl, emission spectra in arc discharge, vibr. anal. 78−74670
$YbCl_2$, mag. props., 77-292K 78−52197
$Yb(ClO_4)_3$, osmotic coeffs. 80−45556
$YbCl_3.6H_2O$, paramag. relax., Mossbauer spectra 80−20536
$YbCl_3.6H_2O:Gd^{3+}$, spin Hamiltonian parameters EPR meas. 77−36128
$YbCl_3.6H_2O:Gd^{3+}$, EPR, temp. depend., spin-lattice relax. time 80−93173
$YbCoO_3$, ^{59}Co NMR, quadrupolar and hyperfine interactions 79−15366
$YbCr_{1-x}Al_xO_3$ solid solutions 80−20887
$Yb_{0.5}Eu_{0.5}Fe_2O_4$, rhombohedral oxides, symmetry group *(French)* 80−84157
YbF, chemiluminesc., vibr. anal. 77−30917
YbF_2, thermal props. *(German)* 80−81355
YbF_3, MS Xα electronic struct. calc., inner shell photoelectron spectra 77−10594
YbF_3, mol. force, compliance and Coriolis consts. 79−31726
YbF_3 single-layer film 2.8 μm, 3.8 μm absorpt. meas. 78−90463
YbF_3, standard enthalpies of formation 79−24810
YbF_3-alkali fluoride binary liquid mixtures, thermochemistry 80−45538
$YbF(^2\Sigma^+)$, matrix isolated ESR spectra 78−86890
YbFX mixed halides, synthesis and lattice parameters 78−30594
$YbFe(CN)_6.5H_2O$, powder, elec. transport props. obs. 80−70701
$YbFe_xMo_6S_8$, singularities in mag. and supercond. props. 79−51710
$YbFeO_3$:Co, mag. struct. factors, neutron diffr. study 79−47248
$YbFe_2O_4$, rhombohedral oxides, symmetry group *(French)* 80−84157
$Yb_2Fe_3O_7$, extra electron relfections 80−100139
$Yb_3Fe_4O_{10}$, extra electron relfections 80−100139
$Yb_3Fe_4O_{10}$, struct. image by a 1 MeV high resolution electron microscope 79−37671
YbGaG, mag. props. between 44-600 mK 80−80517
$YbGa(In)_2X_4$, X=S,Se,Te, prep. and props. 77−85214
$Yb_3Ga_5O_{12}$, dipolar magnet, sp. ht. and magnetisation meas. 80−60344
YbH^+, YbH_2, relativistic (non-relativistic) HF one-centre expansion calcs. 80−52908
YbH(YbD), and isotopic forms, optical and EPR matrix isolated spectra, HFS, bonding 77−83613
YbI, emission spectra in arc discharge, vibr. anal. 78−74670
YbIG, H parallel to (100), transition between canted phases, liquid-vap.-like critical point 77−80938
YbIG, IR Faraday rotation meas. 77−43978
YbIG, mag. permeability, Faraday rotation expts. 77−16287
YbIG, mag. transitions at low temp., soft mode existence 77−69557
YbIG, mean field phase diagrams 78−23269
$YbMn_2As_2(Sb_2)$, pnictides with Ce_2O_2S-type struct. 79−65055
$YbMo_6S_8$, low temp. Mossbauer study and mag. susceptibility 80−80656
$YbMo_6S_8$, supercond., low temp. thermal and mag. props. 78−14904
$YbMo_6S_8$, ternary superconductor, paramagnetic relax. effects 78−68112
$Yb_{1.0}Mo_6S_8$, Chevrel phase supercond., compressibility and vol. depend. of Tc 78−31008
$Yb_{1.0}Mo_6Se_8$, Chevrel phase supercond., compressibility and vol. depend. of Tc 78−31008
$Yb_xMo_6Se_8$, supercond., mag. props., 0.7 to 295K 77−32113
YbN, vaporization enthalpy, Knudsen cell vaporization of rare earth nitrides 79−10936
$YbNbO_4$, ^{93}Nb NQR spectra, 77 to 450K 79−38401
$YbNbO_4$, ferroelastic phase transition exam. 77−27934
$YbNbO_4$-$CaWO_4$, phase transitions of fergusonite-scheelite *(French)* 80−19942
YbO, cryst. field parameters due to $4f^{N-1}5D$ configs. 80−80230
YbO, Yb_3O_4, form. at high press. from $Yb+Yb_2O_3$ 78−85192
Yb_2O_3, 300 to 900K, mag. susceptibility and Curie temp. meas. 78−56288
Yb_2O_3, activator in Na_2O-B_2O_3-SiO_2 glass, exam. of distribution by absorption study 79−4832
Yb_2O_3, EXAFS and chemical shift 77−81176
Yb_2O_3, electronic cond. rel. to partial press. of O_2 of high temp. *(French)* 80−59979
Yb_2O_3 film, amorphous, electron beam deposited, dielec. props. 79−91339
Yb_2O_3 film, struct., electron microscope and diffr. obs. 79−11028
Yb_2O_3, M-series soft X-ray appearance pot. spectroscopy 79−54866
Yb_2O_3, merohedral twins, many beam diffr. contrast 78−83829
Yb_2O_3 thin film on Cr substrate, refr. index depend. on thin film thickness 80−108290
Yb_2O_3, XPS, charging effects on core-level binding energies 79−24409
Yb_2O_3-based ceramic, preparation, mech. props. 77−24998
Yb_2O_3-GeO_2-NaOH-H_2O, hydrothermal crystallisation 77−40344
Yb_2O_4, extra electron relfections 80−100139
$YbOsB_4$, mag. susceptibility meas., paramag. Curie-Weiss behaviour 79−61041
$YbPO_4$, IR and Raman spectra 80−34904
$YbPO_4$-$Pb_2P_2O_7$, solubility curves for high temp.-melts for growth of single crysts. 78−95687
YbP_5O_{14} and $Yb_{0.9}Tb_{0.1}P_5O_4$, IR absorpt. and luminesc. spectra 80−55079
$Yb_4(P_4O_{12})_3$, X-ray struct. characts. 80−54202
YbPrBiIG, wave props. of domain wall 78−48011
$YbRuB_4$, mag. susceptibility meas., paramag. Curie-Weiss behaviour 79−61041
YbS, multiphonon processes and exciton-LO phonon interaction 79−95784
YbS, Raman spectra reson., reflectance spectra, multiphonon processes 78−84581
$YbS_{1.387}$, magnetic and thermal props. 80−34586
YbS_x, thermo-EMF, elec. and thermal cond., 300 to 1000K, comp. depend. 79−38111
YbSb, forbidden band gap and electrotransfer parameters 80−39497
YbSe, crystn. by chem. transport reaction with I_2 77−24935
YbSe, formation and crystallographic charact. of thin film phase 78−91574
Yb_2Se_3, elec. resist., thermoelectromotive force, temp. depend., 300 to 1400K *(Russian)* 78−84243
ξ-Yb_2Se_3, mag. susceptibility and cryst. field parameters 80−65510
$Yb_2(SeO_4)_3.8H_2O$, thermal decomp. and IR spectra 80−3319
$YbSi_{1.8}$, valence fluctuation cpd., X-ray anal., mag. susceptibility and linear expansion coeffs. 79−77569

ytterbium compounds continued
Yb_3Si_5, valence fluctuation cpd., X-ray anal., mag. susceptibility and linear expansion coeffs. 79−77569
$Yb_2Si_2O_7$, crystal struct. of X form, polymorphism under press. *(French)* 77−47430
$Yb_2Si_2O_7$, IR and Raman spectra, internal and external modes 79−61365
$Yb_2Si_2O_7$, polymorphic transforms. and phase diagram under press. *(French)* 77−15573
$Yb_2Si_2O_7$, polymorphism under press., cryst. struct. 77−35692
$Yb_{1-x}Sm_xS$, electron config. of Sm ions, X-ray L-absorpt. spectroscopy 80−60715
$YbTaO_4$, heat of form. by adiabatic calorimetry 79−83494
YbTe, high-temperature evaporation and reactivity 80−103469
Yb_2Te_3, films, prep., elec. props. 78−43494
$Yb_2Ti_2O_7$, cryst. field props., Yb^{3+} hyperfine spectra, Mossbauer effect meas. 78−67990
$Yb_2Ti_2O_7$, crystal field props., ^{170}Yb Mossbauer spectroscopy 79−4750
$YbVO_4$, ^{51}V NMR, nucl. quadrupole coupling const., chem. shift 77−90055
$Yb_2V_2O_7$, physical props. 78−39320
$Yb_2V_2O_7$ prep., cryst. chem. and chem. anal. 79−41986
$Yb_2V_2O_7$, pyrochlore struct., mag. props. 78−72335
$Yb_2(WO_4)_3$, mag. props., 300 to 900K 79−28510
Yb_2WO_6, growth from soln. in melt 77−1806
ZrO_2-Yb_2O_3 solid solns., prep., crystn. 78−42909

yttrium
see also nuclei with .....
abundance in Ap and Am stars 77−33505
addition to Cr_3C_2 fibre reinforced Ni-based composite, effect on oxidation and creep 80−66685
adsorbed on 4d or 5d metal, work function, O_2 coadsorpt. effects, thermionic emission obs. 78−11064
adsorption on anodised Al, prep. of radiation sources 79−36454
atom, electron bombard., 300 to 600 keV, K_α/K_β X-ray intensity ratios, K-shell ionis. cross sections 78−37747
atom, in Y_2O_3, study of 4d excited states 77−26989
atom, integral Compton scatt. cross sections, of γ-rays from K-shell electrons 78−58643
atom, K-shell photoelectric cross section 79−22676
atom, Mζ radiation source for ESCA, 132.3 eV, continuously deposited anode 77−4958
atom, oscill. strength absolute value, collision broadened absorpt. linewidth method 77−10639
atom, XPS relative intensity and photoionisation cross-section 80−63599
charged particle stopping power meas. by 100 keV proton induced X-ray emission 79−45593
core level binding energies 80−71564
de Haas-van Alphen effect, Fermi surface 80−15435
determination, in Ta-Re-Y-La alloy, spectrochem. method 79−16076
determination in bauxite, X-ray fluoresc. method 77−36849
determination in PuO_2, PuO_2-UO_2, by chem. separation, at. emission anal. 77−52723
diffusion of C, radiographic meas. *(Russian)* 77−31809
diffusion of Fe, Mossbauer exam. 78−27138
diffusion of H, neutron scatt. and absorpt. study 79−60556
elastic consts., 4 to 300K 80−39200
electric field gradient, at ^{181}Ta substitutional atoms, press. depend. 78−52385
electron and positron multiple scatt. 80−15171
electron radiation damage, elec. resistivity change rates 80−59954
electronic excitations, charact. energy loss meas. up to 50 eV 80−60723
Fermi surface and de Haas-van Alphen effect 78−75983
film, ion plating deposition system using electron beam evaporation *(French)* 80−20802
film, optical absorption meas. using synchrotron radiation, 20-250 eK 77−12457
film, prepared in ultrahigh vac., optical meas. 6 to 14 eV 79−78767
film, temp., thickness and comp. depend. of elec. resist. 79−78221
film, thickness dependent polymorphism rel. to resistivity 78−39232
HCP, elec. field gradient 78−14698
HCP, nonlocal effects in lattice dynamics 78−91397
implantation on Cr-Ni Nb stabilized austenitic stainless steel surface, effect on oxidation behaviour 80−71791
implementation of Fe-Cr-Al Fecralloy stainless steel surface, effect on oxidation behaviour 80−71790
interband, collective and atomic (p,d) excitations, Z-160 eV, fast EELS 80−93443
K-satellite origin, Hayasi model of quasi-stationary states 77−1762
Knight shift meas. at low temp. 77−28466
M-series emission bands *(Russian)* 77−81177
magnetic and elec. props., 100 to 900K *(Russian)* 80−25077
magnetic form factors, neutron diffr. study 79−47234
mean excitation energy based alpha particle stopping power meas. 78−30678
metal-oxide-electrolyte systems, Y_2O_3 anodic glow 77−12447
normal spectral emittance above 1000K 77−28028
nuclear dipolar magnetic ordering, dipole-dipole interactions, review 77−85475
phonon dispersion, phenomenological model 79−7660
phonon dispersion relations and dielectric screening 77−35646
photoabsorption spectra, at. ionisation, band struct. mechanisms, electron energy loss investig. 77−24909
photoelectric cross sections at 52.4, 60, 72.2 and 84.4 keV 80−69187
plastic deformation, at different deform. speeds, dislocation glide *(Russian)* 80−93598
plastic deformation props., deformation ageing, plastic flow, dislocation-impurity interactions *(Russian)* 80−66582
recrystallisation *(Russian)* 77−24946
reflectivity spectrum, 3.5 to 30 eV, dielectric function and plasmons 77−44014
silicide thin film formation on (100) and (111)Si substrate, backscattering study 80−70542
solubility in U at 1700K 77−89545
solubility of H_2 and D_2 *(Japanese)* 78−18784
solubility of T, 250-400°C, rel. to possible appl. for T recovery from molten Li blanket in fusion reactor 79−90784
sorption of H_2, tritium recovery in D-T fusion reactor *(Japanese)* 78−29646
sorption of T from liq. Li fusion reactor blanket 80−95434

yttrium continued
spin-spin relaxation times, pH depend. 80−66059
sputtered particles from D bombardment, ion fraction and energy anal. 77−36345
surface implantation in stainless steel, effect on oxidation resistance at high temp. 77−8977
texture formation during cold rolling *(Russian)* 78−92275
thermal and elastic props. 79−33027
thermal diffusivity, T>1100K 77−24548
thermionic emission work function of single cryst. 78−2971
thermoelectric power anisotropy at high temp. 79−23952
thermophysical properties at high temps., exam. *(Russian)* 79−28105
transport props., anisotropy, high temp. obs. 78−26843
X-ray emission spectra and electronic structure 77−20960
X-ray fluorescence of L_α spectrum *(Russian)* 77−63491
X-ray Mζ energy, revised values 80−14102
X-ray production, K-shell, on N^+ impact 77−75090
α-induced X-ray anal. of Y, La, Ce, Nd content of apatite minerals 79−16084
Au-Y_2O_3-Y junctions, migration of Au rel. to voltage-controlled negative resist., SIMS obs. 79−91157
BaF_2:Y^{3+}, diffusion of bound and free $F_{(i)}^-$ interstitials, NMR meas. 79−78542
BaF_2:Y^{3+}, phonon reson. and IR absorpt. 80−84752
BaF_2:Y^{3+},Gd^{3+} production and mech. props. 79−72638
$Ba_{0.54}Sr_{0.46}Nb_2O_6$:Y, dielectric and electrooptic props. 78−68466
CaF_2:Y, absorpt. spectra, radiation defect formation energy, F to M centre conversion kinetics 79−65079
CaF_2:Y, dielec. relax. spectrum, ion size trends 78−72460
CaF_2:Y, natural fluorite colouring, effect of impurities on absorpt. spectra 79−56822
CaF_2:Y^{3+}, DC cond., high Y concs. influence 78−22887
CaF_2:Y^{3+}, diffusion of bound and free $F_{(i)}^-$ interstitials, NMR meas. 79−78542
CaF_2:Y^{3+}, ionic cond. and thermal depolarisation obs. of defect clustering 80−71298
CaF_2:Y^{3+},O^{2-}, thermal depolarisation obs. of defect clusters 80−71299
$CaMoO_4$:Y, luminescence props., emission decay time 79−95835
CaO:Y phosphor, chemical instability, thermoluminescence study 79−38682
$CaSO_4$:Y, ESR, thermolum. correlation studies following gamma irradiation 77−59628
$CaWO_4$:Y, luminescence props. 79−95835
CdF_2:Mn, Y, deconversion due to vacuum heat treatment, elec. resist. and electron probe meas. 79−24025
CdF_2:Mn,Y, in MIS struct., blue-green electrolum. 79−52025
CdF_2:Mn^{2+},Y^{3+}, thermal stability under vacuum, effect of heat treatment on resist. 79−23969
CeO_2:Y, slow transient phenomenon 80−107550
Cr-Y coatings, spectral determ. of Y content 77−90681
Cu-rare earth oxide-Y composite coatings, oxide and Y effect on coating precipitation 80−55554
Fe:Y, ion implanted, deep D traps due to Y-vacancy complex 80−103372
GeO_2:Y^{3+}, trapped-hole centres, ESR meas. 79−77597
He(2^3S, 2^1S)+Ba(Y)(Ce), Penning process, double ionisation 77−3439
LaB_6:Y, Sc effects of impurities thermionic emission 78−60542
Ni:^{86}Y, mag. hyperfine field determ. by DPAC 77−8458
O_2+La(Y)(Sc), crossed beam chemiluminescence reaction, spectral simulation, hyperthermal energy meas. 78−80732
Si:Y, photoelectric props. 80−107860
SrF_2:Y^{3+}, diffusion of bound and free $F_{(i)}^-$ interstitials, NMR meas. 79−78542
$^{90}Sr/^{90}Y$ radioisotope generator, educational aid 78−78535
T sorption from K and Li onto Y, fusion reactor breeder blanket 78−66411
TiO_2:Y, polycrystalline photoanode, improved solar efficiency 79−96479
Y I, Y II, lifetimes of excited states, rel. to solar abundance determ. 78−86815
Y III, $4p^64d$-$4p^54d5s$ transitions, level assignments 79−22631
Y Mζ, 132 eV X-ray source of ESCA 78−53301
Y VI, 4p-5s transition 77−27010
Y VI, VII, VIII, 4p-4d transitions obs. 78−82669
Y VII (VIII), 4p-5s transitions 77−23453
Y^{10+}, spectrum and energy levels 80−32639
Y^{30+}, X-ray spectra, $2p^5$-$2p^43d$, laser plasma 78−86806
Y-F_2(ClF)(Cl_2)(SF_6)(Br_2)(IBr), visible chem. laser development from reactions yielding visible chemilum. 78−63111
Y-Y_2O_3-Au junction, defect struct. and local conduction 78−26970
Y-Y_2O_3-metal junction, electroforming and conduction 78−26969
Y+H_2O(D_2O)(alcohols), O atom abstraction, product internal state distrib., fluoresc. study 78−48643
Y+H_2(D_2)(T_2), high temp. equilib. meas. 80−66780
Y+O_2(NO_2)(N_2O)(O_3), oxidation, single collision chemiluminesc. 77−25267
Y+O_2(NO)(SO_2), nascent product state distribs., laser fluoresc. detect. 78−7187
Y+O_2→YO+O, $A^2\Delta$-$X^2\Sigma^+$ transition 77−1927
YIG film, shallow groove, magnetostatic surface wave reflectivity 77−73055
Y_2O_3 plasma, eqn. of state investig. 80−75027
^{90}Y 25 Ci generator, preparation and use 77−40768
^{90}Y, adsorption on anodised Al, oxide layer thickness, Al purity, temp. depend. studies 79−82458
^{90}Y, appl. to cancer therapy of liver 80−17098
^{90}Y electrosorption on anodically polarised Pt surface 79−52684
^{90}Y extraction and determ. in acidic media 79−16025
^{90}Y, interstitial radiation therapy, results for infant haemangiomas 79−88156
^{90}Y, radiation dose-response curves, hazard function method of resolution 79−66556
^{91}Y, radiation dose-response curves, hazard function method of resolution 79−66556
^{91}Y, removal rate in lower stratosphere, seasonal vars. 80−55957

yttrium alloys
see also yttrium compounds
mixed valence compounds, mag. props. 79−78048
Nichrome based dispersion hardened material, Ti, Y, Zr addition effects on crystallisation *(Russian)* 79−74143
pseudobinary Laves phases, mag. reson. 79−87323

yttrium alloys continued
rare earth alloys, mag. phase diagram 78−10684
rare earth Y alloys, Neel temps., mag. susceptibility meas. 77−73025
steel, austenitic stainless, hot plasticity, Y additions effect 79−83270
steel, stainless, Fecralloy, creep-rupture props., 650-800°C 80−97535
steel, stainless, ferritic, alloyed with Y, high temp. scaling 79−47834
transition metal intermetallics ESR of Nd^{3+} and Gd^{3+} 79−87315
YMg, exchange coulombic contrib. of cond. electrons to cryst. elec. field 79−95376
Ag-Y, dil., virtual bound states, transport props. obs. 80−70667
Al-Si-Y alloy, phase equilibria in Al rich region *(Russian)* 80−93537
Al-Y, dil., hyperfine interactions, $^{87}Y^m$ nuclear orientation meas. 78−43715
Al-Y, specific elec. resist., variation with Y conc. 80−84455
Al-Y foil, alloying effect on strength characts. and weldability 80−55475
Au-Y, dil., conduction electron-local moment exchange interaction meas. 80−60191
Au-Y, dil., Friedel d-reson. scatt. and elec. resists. 80−44566
Au-Y, dil., hyperfine interactions, $^{87}Y^m$ nuclear orientation meas. 78−43715
Au-Y, dil., virtual bound states, transport props. obs. 80−70667
Be-Y, plastic deform., flow stresses, fracture *(Russian)* 80−108496
(Ce,Y)Al_2, collective phenomena 80−65933
$Ce_x(La_yY_{1-y})_{1-x}Al_2$, local mag. moments, neutron scatt. study 79−61058
$Ce_x(La_{0.76}Y_{0.24})_{1-x}Bi$, mag. phase diagrams 79−56535
$Ce_x(La_{0.76}Y_{0.24})_{1-x}Sb$, mag. phase diagrams, exchange interaction variation-thermodynamic model 79−65673
$(Ce_xY_{1-x})Fe_2$, mag. susceptibility and Mossbauer meas., lattice parameters 80−97068
Co-Cr-Al-Y, high temp. oxidation 78−11432
Co-Cr-Al-Y, low temp. hot corrosion, Na_2SO_4-induced, mechanism, burner rig tests 80−40610
Co-Cr-Al-Y, turbine blade coating, hot corrosion by Na_2SO_4 and vaporous NaCl 78−19941
Co-Cr-Al-Y coated turbine airfoils, effect of electron beam deposition rate on struct. 79−23870
Co-Cr-Al-Y coating, Pt-modified, oxidation and hot corrosion resist. 78−11437
Co-Cr-Al-Y coatings, hot corrosion resist., thermal expansion coeffs. 79−24674
Co-Cr-Al-Y protective coating for combustion turbines, hot corrosion evaluation 80−40608
Co-Cr-Ni-Ta-Al-Y (25, 10, 5, 3, 0.5 wt%), exam. of hot corrosion 79−20251
CoCrAl-Y, Y effect on oxidation 78−44275
$(Co_{1-x}Fe_x)_2Y$, substitutional Fe atoms effect on mag. and elec. props., paramagnon scatt. 77−36054
Co_2Y, Laves phase, elec. resist. rel. to mag. props. 77−59282
$Co_{35}Y_{65}$, metallic glass, internal friction peaks 80−25753
Cr-V-B-Y system, fatigue strength and fatigue fracture at 20 and 1100°C, SEM study 80−3194
Cr-Y, cast, B additions effect on struct. and props. *(Russian)* 78−19891
γ-γ'-Cr_3C_2-Y eutectic, Y addition effect on oxidation during thermal cycling 79−74310
Cu-Cu_6Y eutectic alloy, cast and directionally solidified, struct. and props. *(Russian)* 80−104138
Cu-Y, effect of alloying additions on electrical cond., and mech. strength 78−44233
Dy-Y, magnetisation and hysteresis, temp. depend. 79−69673
Dy-Y, paramag. susceptibility in basal plane and hexagonal axis 77−20548
Dy-Y, scatt. of cond. electrons by spin disorder 78−47778
$Dy_{0.9}Y_{0.1}Al_2$, hyperfine field, NMR spectra 80−15811
$Dy_{1-x}Y_xAl_2$, cryst. field quenching of Dy^{3+} 4f shell, Mossbauer effect meas. 78−39480
$Dy_{1-x}Y_xAl_2$, ordered alloys, ^{163}Dy NMR, hyperfine field 78−10801
$Dy_xY_{1-x}Al_2$, domain wall dynamics, NMR 77−69614
$(Er_xY_{1-x})Al_2$, cryst. field splitting, inelastic neutron scatt. data 80−44551
$Er_xY_{1-x}Al_2$, mag. props. meas. and neutron diffr. data 80−7126
$Er_xY_{1-x}Cu$, antiferromagnetic, mag. and resist. behaviour 80−34412
Fe, cast, influence of Y and Sb on microhardness and lattice spacing of ferrite *(Russian)* 80−19748
Fe, cast, Y effect on graphite nodularisation *(Japanese)* 77−55999
Fe, cast, Y effect on struct. 80−29967
Fe-Cr-Al-Y, high temp. corrosion depend. on Y, oxidation, stress growth *(Russian)* 80−40588
Fe-Cr-Al-Y, influence of Y additions on oxide-scale adhesion 77−8993
Fe-Cr-Al-Y, oxidation resistance, heat treatment and Al^+ ion implantation 80−71785
Fe-Cr-Al-Y, oxide grain morphology and growth mechanism 80−3239
Fe-Cr-Al-Y, scales, α-Al_2O_3, early stages development at high temp. 80−89413
Fe-Cr-Al(-Y), isothermal oxidation behaviour at 1200°C, SEM 80−50755
Fe-Cr-Al(-Y), thermal cycling influence on oxidation behaviour at 1200°C, SEM 80−50756
Fe-Cr-Y, Y addition effect on high temp. oxidation resistance *(Japanese)* 79−70223
Fe-Cr-Y-Al, La or Y with Al addition effect on high-temp. oxidation 79−100302
Fe-Ni-Cr-Al-Y, oxidation mechanism, Y addition effect on kinetics and oxide adherence 80−97623
Fe-Ni-Cr-Y, oxidation at 800 to 1300°C, Y addition effects, comparison with Ni-Cr-Y alloy *(French)* 79−43481
Fe-Ni-Cr-Y, Y addition effect on selective oxidation/diffusion phenomena relationship *(French)* 80−108623
Fe-Y, amorphous, charge transfer and mag. props., ^{57}Fe Mossbauer spectra 79−19719
Fe-Y, amorphous, resist. and magnetoresist. meas., local moment system 78−68018
Fe-Y, dil., hyperfine interactions, $^{87}Y^m$ nuclear orientation meas. 78−43715
Fe-Y amorphous films, mag. props., Mossbauer effect and magnetisation meas. 79−69701
Gd-Fe-Y, amorphous film, thermomagnetic writing 78−84428
Gd-Y, Curie temp. and saturated mag. moment, nonmag. solute effects 78−39301

yttrium alloys continued
Gd-Y, Kaufman approach to calc. of intra-rare earth phase diagrams 80−25657
Gd-y, magnetic-field variations of velocity of sound 79−90101
Gd-Y (40 wt.%) single crystal, elastic, magnetic props. 78−14957
Gd-Y alloy, anomalous thermal expansion, interferometric meas. 78−52333
Gd-Y alloy, metal sphere prod. by spark erosion technique 78−81956
Gd-Y alloys, mag. crit. temp. gap 80−60260
$Gd_{0.5}Dy_yY_{0.5-y}Ir_2$, effect of dil. Dy substitution on Gd ESR 79−82868
$Gd_{1-x}Y_x$, Mossbauer spectra, hyperfine interactions 80−15923
$Gd_xY_{1-x}Al_2$ ($x<0.05$), Hall effect measurements 80−44569
$(Gd_xY_{1-x})Al_2$, ferromag. and spin glass like behaviour, magnetisation meas. 80−75734
$(Gd_xY_{1-x})Co_2$, mag. interactions, effects on moments *(Rumanian)* 79−15296
$Gd_xY_{1-x}Co_2$, transferred hyperfine interactions, ^{155}Gd Mossbauer effect and ^{165}Ho NMR expts. 77−63339
$(Gd_xY_{1-x})_4Co_3$, Curie temp. and resist.-temp. curves, comp. depend. 80−71020
$Gd_xY_{1-x}Fe_2$, effective g-values, ferromag. reson. meas. 77−20720
$(Gd_xY_{1-x})Fe_2$, Fe mag. behaviour, FMR measurements, mag. props., Vangsness relation anal. 79−78336
$(Gd_xY_{1-x})Fe_2$, high temp. mag. behaviour 77−1538
$Gd_xY_{1-x}Fe_2$, s-d exchange interaction integral, change due to hydrostatic compression 78−88199
$Gd_xY_{1-x}Fe_3$, saturation magnetisation, magnetostriction, Curie temp., ferrimag. ordering, exchange field *(Russian)* 78−68343
$Gd_xY_{1-x}Ir_2$, ESR meas., bottleneck and relax. rates 79−38369
$(Gd_{0.5}Y_{0.5})Ni$, FeB struct., cryst. field effects on mag. struct. 78−52226
$Gd_{1-x}Y_xNi$, FeB-CrB type stacking variations, cryst. struct. 80−64952
$Gd_xY_{1-x}Zn$, ferromag., mag. susceptibility and magnetisation, temp. depend. 80−70975
$(Ho,Y)Co_2$, first order phase transitions 78−84426
$(Ho,Y)Co_2$, mag. props., elec. resist. and thermal expansion 78−76246
$Ho_{0.01}Gd_{1-x}Y_xNi_2$, spin echo meas. on ^{165}Ho, limited quenching of Ho moment by cryst. field 79−73851
$Ho_xY_{1-x}(Fe_{0.1}Co_{0.9})_2$, ^{57}Fe hyperfine interaction, mag. props., Mossbauer study 80−39951
$Ho_{1-x}Y_xNi$, ferromag. behaviour, struct., Curie temp. 79−99677
$Ho_cY_{1-c}Sb$ system, magnetisation, elec. resist., and sp. ht. meas. 80−60213
Ir-Y eutectic alloy, supercond. transition enhancement due to lattice softening 80−103775
(La,Y)Ce, dil., Kondo supercond., transition temp., susceptibility and resist. 80−65733
La-Y/AlO_x/Al tunnel junctions, cond. meas., cryst. field effects 80−88694
LaCeY, three normal supercond. transitions 78−26989
$La_{1-x}Y_x$ alloys, PAC obs. of hyperfine field fluctuation at ^{140}Ce, Kondo effect interpret. 77−20761
$(La_{0.80}Y_{0.20})Ce$, three superconducting crit. point behaviour 78−10625
$La_{1-y}Y_y(Ce)$ system, mag. impurities in supercond., supercond. transition temp. and sp. ht. 78−39244
$(La_{1-x}Y_x)_{1-y}Ce_yAl_2$, resistivity meas., Kondo temp. enhancement 77−62917
$Mg-Mg_{17}Y_{13}$, high temp. hydrides for vehicular H storage 80−45793
Mg-Y-Al alloys, phase equilib. *(Russian)* 80−20890
Mg-Y-Cd, phase equilibria and mech. props. *(Russian)* 80−20894
Mg-Y-Nd-Zn-Zr (2,2,0.3, 0.7 wt.%), heat treatment effect on casting dimensional stability, alloy mech. props. 78−44146
Mg-Y-Zn (20, 30 wt.%), phase equilibria investigation *(Russian)* 79−74131
Mg-Y-Zn alloys, phase equilib. *(Russian)* 80−16271
Mg-Y-Zn-Nd-Cd alloys, influence of Zr addition on struct. and mech. props. *(Russian)* 80−40370
Mg-Y-Zr, phase equilib. and props. *(Russian)* 77−66626
Mn-Y-Zn-Cd alloy,phase equilibria, plastic deformation, microhardness *(Russian)* 80−40334
$Mn_{23}Y_6D_x$, D atom location, neutron diffr. study *(French)* 80−24426
Nb-Ga-Y system, X-ray and microprobe anal., isothermal section and supercond. transition temp. *(Ukrainian)* 79−38793
Nb-Y, cold plastic deform., oriented microdistortions *(Russian)* 78−39840
Nb-Y mech. props., neutron irrad. and Y scavenging effects 77−90394
Nd-Y, elec. resist. temp. depend. 78−2462
Nd-Y, mag. character of stable and metastable phases 79−38329
$Nd_2Y_{1-x}Co_5$, saturation magnetisation and anisotropy, 4.2K-T_c 77−85427
$Nd_xY_{1-x}Zn$ system, solid soln., mag. susceptibility, 77 to 600K *(Russian)* 80−65776
Ni-Al-Cr_3C_2-Y, eutectic alloy, directionally solidifed, oxidation resistance, influence of Y 80−89409
Ni-based superalloys, hot workability, effect of S, Ca, Mg, Y and Zr minor elements 80−66552
Ni-Co-Cr-Al-Y, plasma-arc-sprayed, metallurgical characts. and oxidation behaviour 80−40618
Ni-Co-Cr-Al-Y coating, electron beam evap., low press. gas scatt. 77−40474
Ni-Co-Cr-Al-Y coating, electron beam deposited, for Ni-base superalloy, fatigue crack initiation and propag. 78−11438
Ni-Co-Cr-Al-Y protective coating for combustion turbines, hot corrosion evaluation 80−40608
Ni-Cr-Al-Y coating for oxidation protection of Ni base TaC eutectics 77−40475
Ni-Cr-Al-Y/ZrO_2-Y_2O_3, NASA two-layer thermal barrier coating, for gas turbine engines, test results 80−40617
Ni-Cr-Y, oxidation at 800 to 1300°C, Y addition effects, comparison with Fe-Ni-Cr-Y alloy *(French)* 79−43481
Ni-Cr-Y, Y addition effect on intergranular and volumetric diffusion, oxidation reduction *(French)* 79−83382
Ni-Y, amorphous, elec. resist., press. depend. 80−96841
Ni-Y, amorphous, resist. and magnetoresist. meas., weak itinerant ferromagnet 78−68018
(NiCo)-Cr-Al-Y/ZrO_2-Y_2O_3 plasma sprayed ceramic coating for turbine engine components 80−40616
NiCr-AlY sintered fibre metal struct. abradable seal material, friction and wear 78−56785
NiCrAlY, mechanically alloyed, maintaining elongated grain struct. after deform. 77−36534

yttrium alloys continued
$(Ni_{1-y}Y_y)_3Al_{1-x}Sc_x(Ti)_x$, quarternary gamma prime ($L1_2$) pseudobinary props. revealed by ionicity modified pair model 78−19725
Pd-Y (8 at.%), H_2 permeability and solubility, comparison with other Pd solid soln. alloys 79−23738
$Sc_xY_{0.95-x}Sm_{0.05}$, ^{153}Eu isomer shift, at. vol. depend. 77−43915
$Sm_{1-x}Y_xCo_5$, mag. props., domain boundary pinning on statistical conc. heterogeneities *(Russian)* 79−99728
Sn-Y system, heats of form. 80−89517
Sr-Y, phase diag. *(Russian)* 77−59745
TMg, direct coulombic contrib. of cond. electrons to cryst. elec. field 79−91005
Ta-Re-Y-La alloy, Y, La determ., spectrochem. method 79−16076
Tb-Gd, mag. ordering temp. and indirect exchange integrals *(Russian)* 79−95590
Tb-Y, Fermi surface topology var., mag. and elec. props. *(Russian)* 77−80723
Tb-Y, helicoid antiferromag. ferromag. transition, magnetostriction and magnetocaloric effect *(Russian)* 77−80937
Tb-Y, mag. anisotropy, contrib. from single-ion cryst. anisotropy and anisotropic exchange *(Russian)* 80−29546
Tb-Y, mag. ordering temps., susceptibility meas. 80−25136
Tb-Y, magnetostriction, mag. and elec. props. 78−27068
Tb-Y, single cryst., magnon component of elec. resist. 77−15827
Tb-Y, single crystal growth from melt, X-ray obs., props. *(Russian)* 78−95689
Tb-Y, spin wave dispersion, spiral mag. struct., neutron scatt. study 79−47268
Tb-Y alloy, mag. hysteresis in antiferromag.-ferromag. transition *(Russian)* 79−33508
Tb-Y solid solution, X-ray diffraction obs. of magnetostriction and phase transitions 77−73068
Tb-Y-Zn, magnetic props. conc. and temp. depend. *(Russian)* 77−47989
$Tb_{0.76}Y_{0.24}$, spin waves rel. to cond. electron susceptibility 78−68195
$Tb_{1-x}Y_x$ alloy, helicoidal antiferromag. to ferromag. transition 78−10687
$(Tb_{1-x}Y_x)_3Co$, mag. props. and transitions, conc. depend. *(Russian)* 78−10671
$Tb_xY_{1-x}Co_{5+0.1x}$, exchange interactions and magnetocrystalline anisotropy 80−34618
$Tb_cY_{1-c}P(As)$, singlet ground state systems, resistivities 77−62912
$Tb_cY_{1-c}Sb$, elec. resist., cryst. field and exchange interaction contribs. 80−39556
Th-Y, absolute thermoelec. power values 77−20303
Th-Y-Ce, supercond., magnetisation of Ce impurities, sp. ht. meas. 78−47904
Th-Y-H, hydride form. and supercond. 77−36007
$Th_{1-x}Y_xCo_{5-y}Fe_y$, lattice consts., magnetisation, and anisotropy fields 79−78364
Ti-Er(Y), effects of Er and Y additives on deformation behaviour 80−81121
Ti-Y, dispersoid effect on deform. 79−24530
V-Zr-C-Y alloy weld metal, hardening phase precipitates examination, TEM appl. 80−7576
$(Y,Er)Al_2$, cryst. field parameters, inelastic neutron scatt. study 79−23937
Y-B, amorphous, B-rich, low freq. modes, Raman scatt. obs. 80−108202
Y-Cd, dil., electric field gradient, γ-ray ang. correl. meas. 79−56632
Y-Ce, dilute alloy, cryst. fields and Kondo effect 77−43809
Y-Ce, Kondo system, spatial extent of Ce moment, neutron diffr. meas. 78−68159
Y-Co, amorphous, thermal stability, crystn., DSC and elec. resist. study 80−107060
Y-Co, amorphous alloy film, spin reson. meas., exchange stiffness 78−68389
Y-Co, CPA calcs., moments and transition temps. 78−52252
Y-Co, Curie temp. determ. 79−65672
Y-Co, ferromagnet, first and second order transitions 80−34631
Y-Co, hyperfine fields, NMR spin echo 77−63318
Y-Co alloy, mag. anisotropy origin 79−38319
Y-Er, surface, high-freq. elec. cond. dispersion function, effects of polishing and annealing 78−19506
Y-Fe, amorphous, thermal stability, crystn., DSC and elec. resist. study 80−107060
Y-Fe, evap. amorphous alloys, thermomag. history effects 77−66389
Y-Fe alloy amorphous thin films, anisotropic mag. and microstruct. props. 78−95487
Y-Fe alloys, mag. interactions, effects on moments *(Rumanian)* 79−15296
Y-Fe amorphous alloy film, mag. props. 77−16121
Y-Fe film, amorphous, microstruct. and magnetism 78−64230
Y-Fe-O system, O-stabilised intermetallic $Y_{12}Fe_{32}O_2$, prep. and characterisation 77−8956
Y-Fe-Si, phase diagram 79−52158
Y-Fe(Co), mag. interactions, exchange fields, mol. field model 77−4498
Y-Gd, de Haas-van Alphen effect, Fermi surface 80−15435
Y-Gd, dil., reverse resist. anomaly and negative magnetoresist. 80−84459
Y-Gd, spin glasses, low temp. sp. ht. and magnetisation 80−65913
Y-Gd spin glass, sp. ht., 0.3-10K 80−25145
Y-H, degree of positron localisation on components 77−85833
Y-H film, temp., thickness and comp. depend. of elec. resist. 79−78221
Y-H system, positron localisation *(Russian)* 77−66555
Y-Ir, dil., elec. field gradient at ^{193}Ir, Mossbauer meas. 80−66090
Y-M intermetallic cpds., M=3d transition metal, sorption of H_2, structural charges 80−88429
Y-Mn alloy, mag. props. and effect of H_2 absorpt. 78−19250
Y-Mn(-Co), amorphous, paramag. props. and Hall effect 79−73692
Y-Ni, liquid alloys, enthalpy struct. *(Russian)* 78−27474
Y-Ni amorphous alloy, spontaneous magnetisation, Curie temp. and paramag. susceptibility 78−68189
Y-Ni-Al ternary system, 800°C isothermal section in range 0 to 33.3 at.% Y *(Russian)* 77−70028
Y-Ni-B, X-ray and microstruct. anal., phase composition 77−16539
Y-rare earth, dil., cryst. fields 78−80127
Y-rare earth, dil. alloy, cryst. field parameter determ. 78−10650
Y-rare earth, dil. alloy, cryst. field determ. 78−10651
Y-rare earth metal, mag. susceptibility, 4.2 to 300K, Neel temps. 79−19735

yttrium alloys continued
Y-Re-B, annealed, and quenched X-ray structural and phase anal. 78−11207
Y-Ru, elec. field gradient and temp. depend. TDPAC meas. 80−60477
Y-Sb compounds, heat of form. meas. 77−36783
Y-Si melts, enthalpy of formation and dissolution, microinhomogeneous struct., interatomic interactions *(Russian)* 80−34206
Y-Zr-H, phase diag. *(Russian)* 77−59749
YAl_2, de Haas-van Alphen effect 78−91590
YAl_2-Er, dil., EPR, $Er^{3+}\Gamma_8$ ground state 80−15798
YAl_2-Er(Dy)(Bd), dil., EPR and mag. susceptibility 80−15797
Y_2Au, mag. props., 4.2-300K 79−7972
$Y_3Au_3Sb_4$, cryst. struct., X-ray diffr. meas. 77−47378
YBe_{13} lattice spacings and susceptibilities 80−65778
YBe_{13}-Mo, solid state reaction, 1000 to 1400°C *(Russian)* 78−18845
YCo_2, anomalous high-field magnetisation 78−47958
YCo_2, density of states, mag. props. 79−90936
YCo_2, high-field magnetisation, Fermi liquid model 79−11303
YCo_3, amorphous ferromagnet, exchange dominated surface modes 78−52359
YCo_3 amorphous film, domain struct., influence of planar anisotropy 79−78472
YCo_3 amorphous films, ^{59}Co spin echo study 80−80636
YCo_3 film, amorphous, DC sputtered, easy axis and easy plane magnetisation 78−64237
YCo_3 film, amorphous, induced and surface anisotropies, ferromag. reson. and static meas. 77−85507
YCo_3 film, amorphous, impurity like relaxation mechanism 79−73820
YCo_3 film, amorphous, sputtered, in-plane anisotropy induced by rare gas annealing 78−84458
YCo_3, hydride phase synthesis, thermal stability and struct. 80−59438
YCo_5, coercivity, random substitution of Y by Co *(Chinese)* 77−8343
YCo_5, covalent electron number, from chem. shift of Co X-ray absorption spectra 77−59641
YCo_5, NMR enhancement of modulating field due to anisotropic component of hyperfine field 77−55729
YCo_5, spin polarised energy band struct., APW calc. 78−10342
YCo_5, substituted, magnetocryst. anisotropy, different contribs. of two Co sites 77−8301
YCo_5, uniaxial intermetallic, large magnetisation anisotropy 80−71011
YCo_x, mag. interactions, effects on moments *(Rumanian)* 79−15296
$Y_{1-x}Co_x$, amorphous, conc. depend. of Co moment 78−56300
$Y_{1-x}Co_x$, amorphous, mag. props. 80−84590
$Y_{1-x}Co_x$, CPA calcs., mean mag. moments 77−72997
$Y_{1-x}Co_x$, temp. depend. of magnetisation 77−77043
$Y_{2+x}Co_{17-2x}$ single crystal, magnetocrystalline anisotropy 79−38320
Y_2Co_{17}, and $Y_{2x}Dy_{2(1-x)}Co_{17}$, magnetocryst. anisotropy, 77-383K 77−89949
Y_2Co_{17}, NMR spin echo meas., dipolar field anisotropy 80−71236
Y_xCo_y, NMR meas. of ^{59}Co 77−85585
$Y_2(Co_{1-x}Al_x)_{17}$, low-temperature sp. ht. meas. 79−56541
$Y(Co_{1-x}Cu_x)_5$, neutron diffr., thermal expsn. *(French)* 80−19749
$Y(Co_{1-x}Cu_x)_5$, neutron diffraction study *(Chinese)* 80−39000
$Y_2(Co_{0.31}Fe_{0.69})_{19.2}$, statistical site occupancy deviations, neutron diffr. investig. 77−7717
$Y_2(Co_xFe_{1-x})_{17}$, mag. anisotropy assoc. with Fe substitution 78−76240
Y_3Co_3Ga, crystal struct., X-ray determ. *(Russian)* 79−27951
$Y_2(Co_{1-x}M_x)_{17}$, bulk magnetisation and magnetocryst. anisotropy interpretation 77−40055
$Y_2(Co_{1-x}M_x)_{17}$, M=Al, Cu, single crystal, mag. props. 77−47993
$Y_2(Co_{1-x}M_x)_{17}$, magnetocryst. anisotropy 77−40054
$Y(Co_{1-x}Ni_x)_5$, distrib. of Co and Ni atoms, neutron diffr. obs. *(Russian)* 80−64954
$Y(Co_{1-x}Ni_x)_5$, mag. heterogeneities and coercive force, neutron scatt. study 80−2553
$Y(Co_{1-x}Ni_x)_5$, mag. props. and mag. reversal phenomena *(Russian)* 77−51924
$Y(Co_{1-x}Ni_x)_5$, spontaneous magnetisation mag. anisotropy, spin reorientation transformation *(Russian)* 80−7082
$YCo_5(Ni_5)$, H_2 solubility *(Russian)* 78−15356
$Y_{0.98}Dy_{0.02}$, spin glass, calorimetric exam. 78−68270
$Y_{1-x}Dy_xCo_5$, NMR meas. of ^{59}Co 77−85585
$Y_{1-x}Er_x$, dil., cryst. field interactions, neutron scatt. spectra 80−50048
$Y_xEr_{1-x}Al_2$, paramag. anisotropy 80−39737
$Y_2(Fe,Co)_{17}$, mag. anisotropy fields by singular pt. detection 79−24156
$Y_2(Fe,Co)_{17}$, magnetic anisotropy meas. by singular point detection method 77−63170
$Y_6(Fe, Mn)_{23}$, itinerant ferromagnet, magneto-volume, expts. 77−66404
YFe_2, amorphous, mag. order, cluster phenomena, hyperfine struct. 77−16079
YFe_2, amorphous, small angle neutron scatt. study of mag. order and mag. microstruct. 79−15283
YFe_2 amorphous, spin-glass and mag. blocking transitions, low field DC susceptibility meas. 79−61141
YFe_2, amorphous, surface ferromag. layer, spin wave reson. Rutherford backscatt., and magnetisation meas. 79−73819
YFe_2, amorphous concentrated spin glass, susceptibility, Mossbauer and neutron scatt. meas. 80−39783
YFe_2, crit. phenomena, Mossbauer effect 78−52403
YFe_2, density of states, mag. props. 79−90936
YFe_2, $ErFe_2$-YFe_2 (30, 70 wt.%), mag. props., 80-1300K *(Russian)* 80−75750
YFe_2, ferromagnetic cpds., mean field exchange consts., Stoner itinerant model calcs. 80−50084
YFe_2, magnetostrictive material, changes in vibr. modes near mag. phase transition 79−90736
YFe_2, phonon softening below Curie temp., Mossbauer effect 77−4589
YFe_x film, ($x\simeq 2$), magnetoelastic excitations obs. 78−68307
$Y_{1-x}Fe_x$, amorphous, Mossbauer spectra, appearance of magnetism 78−52401
$Y_{1-x}Fe_x$, amorphous, spin resonance exam. 79−51860
$Y_{1-x}Fe_x$, mean mag. moment calc. 79−82761
Y_2Fe_{17}, hyperfine interactions, Mossbauer effect, 5 to 300K 77−85634
Y_6Fe_{23}, magnetostriction, temp. depend., 20 to 350K 80−65994
Y_xFe_{1-x} amorphous films, microstruct. and mag. anisotropy 79−82838
YFeAl, scatter order cpd., mag. props. 77−51891
$Y(Fe_{1-c}Al_c)_2$, local model for mag. behaviour 77−63135
$Y(Fe_{1-c}Al_c)_2$, mag. and Mossbauer study, local environment effects 78−27033
$Y(Fe_{1-x}Al_x)_2$, Laves phase, mag. props. and Mossbauer effect 77−85632
$YFe_{2-x}Al_x$, magnetisation behaviour, mag. scatter order 77−28373
yttrium alloys continued
YFe_4Al_8, mag. props. 78−52250
$Y(Fe_cAl_{1-c})_2$, mag. props. 79−38308
$Y(Fe_xAl_{1-x})_2$, mag. order in pseudobinary systems down to millikelvin temps. 78−19251
$Y(Fe_xAl_{1-x})_2$, Mossbauer spectra and mag. props. 80−39950
$Y_6(Fe_{1-x}Al_x)_{23}$, cryst. struct. and mag. props. 79−82180
$(Y_{65}Fe_{35})_{100-x}B_x$ glasses, mag. props. 79−73693
$Y(Fe_xCO_{1-x})_2$ model, Co, mean mag. moment composition depend.; reciprocal susceptibility, thermal var. 78−47945
$Y(Fe_{0.022}Co_{0.978})_2$, ferromag. relax. model, Mossbauer spectra 80−15853
$Y(Fe_{0.022}Co_{0.978})_2$ mag. props., Mossbauer expts., 0.15-4.2K 78−43712
$Y(Fe_{1-x}Co_x)_2$, mag. hyperfine field, conc. depend., Mossbauer expts. 77−63337
$Y(Fe_{1-x}Co_x)_2$, magnetic saturation moment, Co conc. depend., NMR exam. 78−15037
$Y(Fe_{1-x}Co_x)_2$, NMR study 80−75882
$Y(Fe_xCo_{1-x})_2$, $0.5\geq x\geq 0.2$, Mossbauer effect meas., 5 to 300K *(German)* 77−24771
$Y(Fe_xCo_{1-x})_2$, compositional dependence of Co's mean mag. moment, local environment model anal. 78−43560
$Y(Fe_xCo_{1-x})_2$, ferromag. reson. of pseudobinary cubic compounds 78−91961
$Y(Fe_xCo_{1-x})_2$, Mossbauer effect at 78 and 300K, ^{57}Fe hyperfine fields 80−2677
$Y(Fe_xCo_{1-x})_2$, $x\leq 0.2$, mag. props. and Mossbauer meas. 80−75798
$Y(Fe_{1-x}Ir_x)_2$, magnetisation, mag. hyperfine field 80−20531
$Y(Fe_{1-x}Mn_x)_2$, mag. order onset 80−25135
$Y(Fe_{1-x}Mn_x)_2$, Mossbauer spectra and mag. props. 80−39952
$YFe_{2x}Mn_{2-2x}$, mag. props. and FMR 79−95581
$Y_6(Fe_{1-x}Mn_x)_{23}$, ferro- to paramag. transition, press. depend. 77−73028
$Y_6(Fe_{1-x}Mn_x)_{23}$, Mn-rich compounds, Mossbauer effect study 80−71276
$Y_6(Fe_{1-x}Mn_x)_{23}$, struct. and mag. props. 80−25083
$Y_6(Fe_xMn_{1-x})_{23}$, mag. order in pseudobinary systems down to millikelvin temps. 78−19251
$Y_2(Fe_{1-x}N_x)_{17}$, magnetic properties, Mossbauer spectra *(Chinese)* 78−95433
$Y(Fe_{1-x}Ni_x)_2$, Laves phase, mag. props. and Mossbauer effect 77−85632
$YFe_{3-x}Ni_x$, electronic sp. ht., saturation magnetisation and lattice parameter meas. 78−68261
$Y_2(Fe_{1-x}Ni_x)_{17}$, Mossbauer spectra, hyperfine field interactions 78−6614
$Y(Fe_xRh_{1-x})_2$, mag. props., Mossbauer spectra 80−25108
YFe_2Si_2, mag. props. 4.2 to 950K, diamag. Fe atoms 77−20544
$Y(Fe_xT_{1-x})_2$, Mossbauer spectra, mag. props. 80−20563
$Y(Fe_{1-x}Co_x)_2$, electronic sp. ht. meas., rel. to mag. props. 77−63197
$Y_{1-x}GdCo_5$, exchange interactions and magnetocrystalline anisotropy 80−34618
$Y_{1-x}Gd_xCo_2$, NMR meas. of ^{59}Co 77−85585
$Y_{1-x}Gd_xCo_2$, NMR of ^{59}Co 78−52376
$(Y_{1-x}Gd_x)Co_2$, spin echo NMR of mag. states 80−7190
$(Y_{1-x}Gd_x)_2Co_{17}$, ^{59}Co NMR, hyperfine fields and contrib. of 4f electrons 77−20727
$Y_{1-x}Gd_xCo_5$, ferrimag., magnetisation, exchange interactions, mag. anisotropy 80−80565
YGe_2 film, supercond. obs. 77−72939
$Y_{1-x}Ho_xCo_5$, NMR meas. of ^{59}Co 77−85585
Y_2In, mag. props., 4.2 to 270K 79−56512
Y_5Ir_2, cryst. struct. 80−96473
$YIr_2(Rh_2)$, ESR of Nd^{3+} and Gd^{3+} 77−85564
YM_2:Nd^{3+}, M=Rh, Ir, Pt, ESR investigation 79−78514
YM_2-Gd, M=transition metal, correl. between g-shift and stability, EPR study 80−88874
YM_4Al_8 (M=Cr, Mn, Fe, CU), magnetism and hyperfine interactions 80−25256
YMg, direct Coulomb contrib. of cond. electrons to crystalline elec. field 77−76784
YMg, Pauli paramagnet, mag. susceptibility, nonlinear band behaviour 80−75706
YMn_2, lattice consts. and mag. props. before and after H_2 absorption 77−36061
YMn_2, Y_6Mn_{23}, H_2 absorption effect on mag. props. 77−89931
Y_6Mn_{23}, ferrimag., mag. interactions, polarized neutron diffr. meas. 79−78322
Y_6Mn_{23}, lattice consts. and mag. props. before and after H_2 absorption 77−36061
Y_6Mn_{23}, low temp. specific heat determ. 80−65896
Y_6Mn_{23}, magnetic moments, magnetisation 80−25094
$YMn_{2-x}Co_x$, mag. order in pseudobinary region 79−99689
$Y_6(Mn_{0.75}Fe_{0.25})_{23}$, mag. scatter state, hysteresis loops 78−56350
$Y_6(Mn_{1-x}Fe_x)_{23}$, hydriding characts. and mag. props. 77−69527
$YMn_{2-x}Fe_xH_2$, mag. props., ordering temps. 80−71028
$Y_6Mn_{23}H_x$, influence of absorbed H on mag. behaviour 77−85423
$Y_{0.25}Nd_{0.75}Co_5$, basal plane anisotropy 77−8295
$Y_{1-x}Nd_xCo_5$, exchange interactions and magnetocrystalline anisotropy 80−34618
$Y_{1-x}Nd_xCo_5$, ferrimag., magnetisation, exchange interactions, mag. anisotropy 80−80565
YNi_2 amorphous alloy, at. struct. 80−19704
YNi_2, density of states, mag. props. 79−90936
YNi_3, loss of ferromagnetism after H_2 absorpt., Pauli paramag. props. 80−34588
YNi_3, magnetism resurgence, neutron diffr. and mag. props. study 80−65819
YNi_5, Haucke compounds, low temp. heat capacity, Debye temp. 80−96663
$Y_{0.22}Ni_{0.78}$ amorphous alloy, low temp. sp. ht. 79−65680
Y_2Ni_{17}, ferromag. struct., neutron diffr. expt., cryst. field calcs. 77−73001
Y_3Ni_2, crystal struct., tetragonal type 78−14309
Y_xNi_{1-x}, amorphous, high press. magnetisation and Curie temp. 80−20442
$YNi_{5-x}Al_x$, Al addition effects on structural and H_2 absorpt. props. 79−52761
$YNiSi_3$, mag. susceptibility, 80-1200K *(Russian)* 77−66281
Y_3Os, cryst. struct. 80−96474
Y_5Os, cryst. struct. 80−96475
YPd_3, rare earth impurities, magnetostriction 79−4714
YPd_3-Gd, ultralow interaction temp. and cryst. field effects for Gd impurities 79−61100
Y_3Pd, cryst. struct. 80−96474

yttrium alloys continued
Y_3Pd_2, structure determ., rhombohedral Er_3Ni_2 type 77−80443
Y_5Pd_2, mag. props. 77−20547
Y_5Pt_4, isotypic with Pu_5Rh_4, X-ray cryst. struct. refinement anal. 79−4271
YRh, electronic struct., susceptibility, sp. ht. and Knight shift meas. 77−43485
Y_3Ru, cryst. struct. 80−96474
$Y_{1-x}Sm_xCo_2Ni_3$, giant intrinsic magnetic hardness 78−56347
$Y_{1-x}Tb_xCo_5$, spontaneous magnetisation anisotropy, spin reorientation transforms. *(Russian)* 80−7082
$Y_{1-x}Tb_xCo_{5+0.1x}$, ferrimag., magnetisation, exchange interactions, mag. anisotropy 80−80565
$Y_{1-x}Tb_xPd_3$, magnetisation, magnetostriction, and inelastic neutron spectra 80−65998
$Y_{1-x}Th_xFe_3$, saturation magnetisation, fields up to 120 kOe, comp. depend. 77−8283
$Y_{1-x}Th_xFe_3$ system, elec. resist. meas., 77-300K 80−34413
YZn, self-consistent energy bands and Fermi surface 77−72814
$(Y_{1-x}2Co_x)Co_5$, anisotropy fields, coercivities, annealing effects 78−91898
$YbCu_2Si_2$, local mag. moments, neutron scatt. study 79−61058
$Yb_{1-x}Y_xCuAl$, disordered extended Anderson model, CPA-alloy analogue treatment 80−65506
$Yb_{1-x}Y_xCuAl$, intermediate Yb valence states, mag. props. 79−51743
Yfe_3, NMR investig. of Y hyperfine field temp. depend. 77−4567
Zn-Y alloys, thermodynamic props. *(Russian)* 79−70041
Zn_2Y, magnetostatic volume waves, magnetocrystalline anisotropy effects, group delay 79−78355
$ZnY_{0.95}R_{0.05}$ resist. anisotropy due to impurities 77−62902
Zr-Y (15 wt.%) solid solution, decomp., during heating and cooling cycles *(Russian)* 78−92267

yttrium compounds
see also yttrium alloys
alkali metal-yttrium oxides, MYO_2, synthesis and physicochem. props. 77−48216
carbonates, standard ht. of formation determ. 78−53239
crystal growth from fused oxides, flow method, simple and economical apparatus *(Italian)* 80−80960
Czochralski crystal growth 79−95920
dihydirdes, structs. and stabilities 80−107146
domain boundary mobility, effect of easy magnetization axis inclination 78−19293
ethylsulphate, rare earth doped, NMR of protons adjacent to impurity 77−85589
garnet, inhomogeneous collective magnon oscill. excited by RF field *(Russian)* 80−100582
garnet, magnetoelastic wave, propagation characts. obs. 77−40107
garnet film, ion-implanted, bubble collapse field, in-plane mag. field effect 77−73060
garnet film, wall velocity at high drive fields 77−85518
garnet preparation, novel Li_2MoO_4-$Y_2(MoO_4)_3$ flux sytem 77−48359
germanates, cryst. struct. and cryst. chemistry 77−39571
horizontally dipped LPE film, inhomogeneities, spin wave reson. meas. 79−91298
large growth-induced anisotropy to preferential occupation of Fe sites 80−75754
LPE growth, saturation magnetisation, collapse field, bubble diameter 78−95703
metaphosphate glasses, $n(M_2O.P_2O_5).(1-x)Y_2O_3.xTb_2O_3.3P_2O_5$, M=Li, Na, K, excitation and emission spectra 80−40150
orthoferrite, magneto-optical controlled transparencies, page composers 78−50932
perovskite-like oxides, synthesis, struct., elec. props. 80−65554
plasma sprayed ceramic coating for turbine engine components 80−40616
silicates, cryst. struct. and cryst. chemistry 77−39571
silicides, valence band struct. *(Russian)* 79−15076
sintering at Si_3N_4-Al_2O_3-Y_2O_3 *(Japanese)* 78−19703
sulphides, RR'_3S_6, where R,R'=rare earth, Sc or Y, struct. organisation *(French)* 77−11519
system, oxyorthophosphates form. 79−78942
ternary metal oxides, DC electrolum. 77−77300
tetrabutylammonium europium yttrium isothiocyanate, conc.-depend. electron-phonon coupling, and self-quenching 80−60657
YAG, crystal orientation determ. by Laue method, computer calc. *(Chinese)* 79−32853
YAG crystals, EPR spectra of V^{2+} ions, ion energy levels 80−7157
YAG powder, X-ray K_α doublet diffr. peak position rel. to lattice const. precision 77−68891
YAG synthetic, cryst. growth, review *(German)* 79−33926
YIG, cryst. growth from high-temp. soln., book contrib. 79−69973
YIG, energy location of mag. Fe levels, spin polarised photoemission 79−24413
YIG, hot spraying to give fine, free flowing, sinterable powder 80−20865
YIG, optical absorption and magneto-optic spectra 79−99860
YIG, reson. magnetostatic modes, spectrum in inhomogeneous mag. field 79−28621
YIG, thermal cond. at low temps. 80−2222
$(YSmEuCa)_3(FeGe)_5O_{12}$, garnet film, ion implanted, bubble domain props. 78−88152
Yttralox, chem. laser window material 77−46769
yttrium ethyl sulphate:Yb, spin refrigerator, proton polarisation 77−83435
$3Y_2O_3.5Al_2O_3$, garnet, synthesis by firing mixed oxides 79−61545
Al_2O_3-Y_2O_3, melting behaviour and metastability determ. by optical DTA 80−92648
Al_2O_3-Y_2O_3, plasma spraying, microstruct., porosity and adhesion 77−32710
Al_2O_3-Y_2O_3, sintering kinetics, influence of minor additions of Y_2O_3 80−84868
Al_2O_3-Y_2O_3 ceramics, corrosion protective W coating 80−35367
Al_2O_3-Y_2O_3-SiO_2 containing TiO_2, La_2O_3, exam. of elastic moduli and refractive indices 78−80502
$AlPO_4$-Y_2O_3, system, oxyorthophosphates form. 79−78942
Au-Y_2O_3-Y junctions, migration of Au rel. to voltage-controlled negative resist., SIMS obs. 79−91157
BaF_2-YF_3 system, phase diagram 78−35363
$(BaF_2)_{1-x}(YF_3)_x$, crystal growth and struct. 77−12520

yttrium compounds continued
$BaGeO_3$-$(0.25MgF_2.0.75YF_3)$-Ga_2O_3 glass, synthesis and props. 80−25648
$Ba(PO_3)_2$-YF_3 glasses, pseudobinary, elec. cond. and dielec. losses 77−7890
$Ba_{0.50}Sr_{0.50}Nb_2O_6$:$Y_2O_3$, Raman spectra 79−78678
BaY_2F_8:Nd^{3+}(Ho^{3+})(Er^{3+})(Yb^{3+}), ESR spectra and spin-lattice relax. 80−11263
Ba_2YRuO_6, perovskites, prep., struct., emission control catalysts 77−68957
$(Ba_{1-x}Y_x)TiO_3$ ceramic, resistivity rel. to donor dopant content 79−65474
$BaY_4X_5O_{17}$ (X=Si,Ge), cell consts., luminesc. of various rare-earth activators 80−93376
δ-$(Bi_2O_3)_{1-x}(Y_2O_3)_x$, thermoelectric power rel. to fast ionic conduction 80−107549
CaF_2-$(Y,R)F_3$ (R=any lanthanide except Pm, Eu), phase diagrams 78−84783
CaF_2-$(Y,R)F_3$ systems (R=rare earth), phase diagrams, limiting solubilities and non-stoichiometry 79−47665
CaF_2-YF_3, fluorite- and tysonite-related ordered phases *(German)* 79−23725
CaF_2-YF_3:Er^{3+}, stimulated emission 77−52135
CaF_2-YF_3:Nd^{3+}, selective excitation of activator centres, time resolved luminesc. 78−15223
CaF_2-YF_3:Nd^{3+}, spectral migration of electronic excitation, selective laser excitation *(Russian)* 78−80417
CaS-Y_2S_3 (1 wt.%), solid electrolyte, elec. cond. under low partial pressures of S *(Japanese)* 80−49409
$CaYAl_3O_7$, type of melting, crystallisation from melt 77−12515
$Ca_{1-x}Y_xF_{2+x}$, fast ionic conduction of F^- ions 79−99360
$Ca_{1-x}Y_xF_{2+x}$, solid anionic conducting electrolytes, struct., elec. props. 77−84977
$CaY_2Ge_3O_{12}$:Nd, energy levels and laser action, fluoresc. meas. 79−81438
$Ca_3Y_2Ge_3O_{12}$:Eu^{3+}, garnets, prep., struct., luminesc., absorpt. spectra, Eu^{3+} localisation 77−69884
$Ca_{0.5}Y_{0.5}H_n$, H_2 dissociation press., phase behaviour and struct. 78−2260
$CaY_2Mg_2Ge_3O_{12}$:Nd, CW room temp. laser operation, 0.941 and 1.059μm 78−66842
$CaY_2Mg_2Ge_3O_{12}$:Nd^{3+}, optical absorpt. and fluoresc. intensities 80−29793
$CaY_4(SiO_4)_3O$:Nd^{3+}, absorpt. and luminesc. spectra 77−85755
CdF_2:YF_3, photoconversion from insulating to semicond. state, IR absorption and elec. cond. 78−14759
CdF_2-YF_3, thermal ionisation energy of monovalent centres 80−80207
$Ce_x(La,Y)_{1-x}Sb$, and $Ce_x(La,Y)_{1-x}Bi$, antiferromag. spin arrangement, neutron diffr. obs. 77−63106
CeO_2:Y_2O_3, bias sputtering, film growth and characts. 77−40366
CeO_2:Y_2O_3, O ion cond. and defect struct. 80−107553
CeO_2-Y_2O_3 film, surface characterisation, XPS, ESCA, and AES expts. 78−72028
CeO_2-Y_2O_3 solid soln. phases, synthesis 80−104132
$Ce_{0.08}Y_{0.92}Sb$, dilute f-electron system in cluster regime, crystal field and exchange splittings 80−97062
$^{57}CoY_2O_4$, after effects of orbital electron capture 79−73870
Cr-Y_2O_3 dispersion hardened, oxidation and nitridation resistance, embrittlement 78−44267
$CrPO_4$-Y_2O_3, system, oxyorthophosphates form. 79−78942
Cs_2NaYCl_6, Raman spectrum 77−59567
Cs_2NaYCl_6:Bi^{3+}, luminesc., cryst. growth, Stockberger method 79−8174
$Er_xY_{3-x}Fe_5O_{12}$, garnet, mag. anisotropy and magnetostriction 80−11189
$Er_xY_{3-x}Fe_5O_{12}$, spin reorientation transitions 78−2686
$Er_xY_{1-x}Rh_4B_4$, mag. and supercond. transitions 80−70874
$Er_xY_{1-x}Rh_4B_4$, supercond. phase transitions, recentering temp. to normal ferromag. state 80−7024
$(Eu,Y)_3Fe_5O_{12}$, low temp. CVD epitaxial film growth and mag. props. 79−42406
EuGaYIG film, bubble dynamics, anisotropy depend., ferromag. reson. expts. 77−63240
EuGaYIG:Cr, epitaxial garnet film, interaction pot. of domain walls with localised stress fields 80−44889
Eu_2O_3-R_2O_3-Ta_2O_5, R=La, Gd, Y, quasibinary cross sections 77−90333
Eu_2O_3-Y_2O_3 solid soln. phases, synthesis 80−104132
Eu_2O_3-Y_2O_3-Ta_2O_5, struct., phase form., luminesc. and X-ray diffr., obs. *(Russian)* 78−6765
$(EuY)_3(FeGa)_5O_{11}$, ferrite garnet film, mag. bubble motion delay 79−91269
$Eu_{0.6}Y_{2.4}Ga_{1.26}Fe_{3.74}O_{12}$ garnet film, Walker oscills., detection by mag. bubble collapse 78−68318
$Eu_{0.6}Y_{2.4}Ga_{1.26}Fe_{3.74}O_{12}$ garnet film, dynamic bubble-collapse determ. of domain wall motion oscillation 79−78454
$Eu_zY_{3-z}Ga_tFe_{5-t}O_{12}$, epitaxial garnet films, props. at compensation points 80−39823
EuYIG:Sb, growth from PbO-B_2O_3 based flux, prop. depend. on Pb content 80−39824
$Eu_{0.8}Y_{0.2}S$, Debye-Waller factor, X-ray diffr. meas. 77−11659
Ga-YIG, accelerated crucible rotation technique effect on cryst. growth by induced striation method 77−63553
GaYIG, magnetoelastic surface wave attenuation 77−20667
$(Gd,Tm,Y)_3(Fe,Ga)_5O_{12}$ film, magnetocrystalline anisotropy 79−78450
$(Gd,Tm,Y)_3(Fe,Ga)_5O_{12}$ LPE garnet thin films, magnetocrystalline anisotropy 80−93147
$(Gd,Tm,Y)_3(Ga,Fe)_5O_{12}$, bubble domain gradient propag., elliptical distortion and bias compensation 78−19292
$Gd_{1.8}Y_{1.2}Fe_5O_{12}$, nucl. gamma reson., anomalous behaviour of intensity 77−12289
$Gd_xY_{1-x}Rh_4B_4$, mag. and supercond. transitions 78−68127
$Gd_{0.9}YTm_{1.1}Ga_{0.44}Fe_{4.56}O_{12}$, ion implanted, ferromag. reson. meas. 78−68385
HfO_2 single crystals, Y_2O_3 stabilised, optical props., impurities and annealing conditions influence 79−52399
HfO_2:Y_2O_3, elastic props., sonic reson. meas. 80−7612
HfO_2-Y_2O_3, solid soln., diffuse X-ray scatt. by vacancies 78−71728
$(HfO_2)_{0.9}(Y_2O_3)_{0.1}$:$Cu^{2+}$, ESR at room temp., spin Hamiltonian parameter determ. 77−16167
HgO_2-Y_2O_3, solid soln., elastic and photoelastic props., Mendelstam-Brillouin scatt. 78−6693
Ho-YIG, magnetic props. in strong fields at low temp., Ising approx. calcs. *(Russian)* 80−54920

yttrium compounds continued
$Ho_xY_{1-x}F_3$, calc. of $Ho^{3+} \rightarrow Ho^{3+}$ energy transfer rates *(French)* 78−79966
HoYIG, level intersection and instability of mag. struct. *(Russian)* 77−43816
$Ho_xY_{1-x}Sb$, mag. props. 80−34634
$KY(WO_4)_2:Ho^{3+}$, stimulated emission at low temps. 80−106526
(La, Y, Sc)B_6 solid solns. electron work function, thermal emission technique 80−20755
(La,Y)B_6, (Eu,Y)B_6, single crystal growth for thermionic emission 78−92183
LaB_6-YB_6-ScB_6, thermionic emission 78−11068
La_2O_3-Cr_2O_3-Y_2O_3 ceramics, fireproof, direct energy conversion appl. *(Czech)* 79−70455
La_2O_3-Y_2O_3, phase diagram at high temps. *(Japanese)* 77−70038
La_2O_3-Y_2O_3 phase, diagram at high temps. *(Japanese)* 77−1218
La_2O_3-Y_2O_3-Al_2O_3-SiO_2, coloration by transition metal oxides, absorpt. bands *(Japanese)* 80−55148
$La_{1-x-y}Pr_xY_yCl_3$, satellite lines in optical absorpt. spectra, Zeeman effect 79−65912
$LiTb_{0.5}Y_{0.5}F_4$, mag. susceptibility, dilution effect on critical behaviour of dipolar uniaxial ferromagnet 80−34635
$LiTb_{0.5}Y_{0.5}F_4$, uniaxial dipolar ferromag., critical behaviour, mag. susceptibility meas., effect of Y^{3+} dilution 80−80528
$LiY_{0.416}Er_{0.5}Tm_{0.067}Ho_{0.017}F_4$, Stockbarger single cryst., charact. of solidification behaviour 77−24948
$LiYF_4$:Ce, tunable UV laser at 325, 309 nm, KrF laser excitation 80−38022
$LiYF_4:Ce^{3+}$, UV laser at 325 nm, stimulated emission obs. 79−72574
$LiYF_4$:Ho laser, TEM_{00} mode and Q-switched operation 80−74395
$LiYF_4:Ho^{3+}$, optical absorpt. and luminesc. spectra 79−4844
$LiYF_4:Pr^{3+}$, spectroscopic determ. of ground config. energy levels 80−34969
$LiYF_4$:Tm, XeF pumped, excimer excited storage laser 80−33003
$LiYF_4$-HO^{3+}, 1.392, 1.673 and 3.914 μm stimulated emission, laser cascades 80−9886
$LiYSiO_4$, cryst. struct. determ. 77−58997
$LiY_{1-x}Tb_xP_4O_{12}$, and $LiY_{1-x}Eu_xP_4O_{12}$ phosphors, prep. and fluoresc. 77−48219
$Li_6Yb(BO_3)_3$, cryst. struct. determ. 78−18621
(Lu, La, Y, Ca)$_3$(Ge, Fe)$_5O_{12}$, temperature compensated high mobility bubble garnet, LPE and props. 77−20656
MnS-Y_2S_3, chem. twinning, electron microscopic study 79−46678
$Mn_{23}Y_6D_x$, D atom location, neutron diffr. study *(French)* 80−24426
$MoSi_2$-Y_2O_3, ceramics, fireproof, direct energy conversion appl. *(Czech)* 79−70455
NaF-YF_3 system, fusibility diagram, quasibinary section of NaF-YF_3-YOF system charact. 80−55371
Na_2O-P_2O_5-Y_2O_3-Tb_2O_3 glass, conc. quenching of luminesc. in disordered system with dipolar interaction 80−89059
Na_2SO_4-$Y_2(SO_4)_3$, solid solution, effect of defect concentration on ionic conductivity 78−75870
$Na_6YSc[SiO_7]_2$, crystal struct., atom coordinates, X-ray study 80−59446
$NaYSiO_4$, crystal structure refinement, X-ray anal. 80−79764
$Na_5YSi_4O_{12}$, high Na^+ ion conduct. 78−91479
$NaY_{1-x}Sm_xF_4$, luminesc. expt. suggesting Sm^{3+} ion pairing 80−76065
$Na_xY_xZr_{1-x}S_2$, ionic cond. and NMR mobility obs., comp. depend. *(French)* 80−70459
$Nb_xY_{3-x}Fe_5O_{12}$, low-temp. magnetocrystalline anisotropy study 79−95586
Nd:Y_2O_3 single crystal fibre laser, room temp. CW operation at 1.07 and 1.35 μm 78−63121
Nd:YAG, high repetitive picosecond laser system and broad range wavelength tuning *(Japanese)* 79−3698
Nd:YAG, solid-state formation 80−35121
Nd:YAG lasers, sun-pumped and lamp-pumped, for space communications 79−86194
Nd_2O_3-Y_2O_3 film, segregation obs. by EELS 80−79953
Nd_2O_3-Y_2O_3-As_2O_5 glass, spectroscopic props., rel. to possible appl. in lasers 78−84624
$Nd_{0.14}Y_{0.86}P_5O_{14}$ epitaxial layer an $Gd_{0.33}Y_{0.67}P_5O_{14}$, growth lasing 77−46722
$Nd_{1-x}Y_xP_5O_{14}$, laser emission at 1.32 μm, Ar laser pump source 79−31909
$Nd_xY_{1-x}P_5O_{14}$, conc. quenching 79−61435
$Nd_xY_{1-x}P_5O_{14}$, fluorescence quenching 77−69903
$Nd_xY_{1-x}P_5O_{14}$, fluoresc. conc. quenching, decay rate consts. 78−64404
$Nd_xY_{1-x}P_5O_{14}$, laser material, flux evaporation growth dislocation etch tunnels 77−35560
$Nd_xY_{1-x}P_5O_{14}:Nd^{3+}$, radiationless decay processes, laser photoacoustic spectroscopy meas. 80−84766
$Pr_xY_{3-x}Fe_{5-y}O_{12}$ film, IR absorpt. and Faraday rot. spectra 77−52093
Sc_2O_3, solid and liq. phases, thermophysical and electrophysical props. 80−103495
Sc_2O_3-Y_2O_3, phases and phase transitions at high temp. *(French)* 79−100126
Si-Y-Al-O-N glasses, compositional anal., hardness depend. on N_2 content 79−34129
Si_3N_4, hot pressed, Y_2O_3 fluxed, microstruct. 78−64512
Si_3N_4, Y_2O_3 doped, hot pressed, improved high temp. strength 79−61613
Si_3N_4:($MgO+Al_2O_3$)(Y_2O_3), hot-pressed and sintered, microstruct. and impurity distrib. 80−49261
Si_3N_4-Al_2O_3-Y_2O_3, sintered, observation of a noncrystalline phase 78−64536
Si_3N_4-AlN-Al_2O_3-SiO_2-Y_2O_3, phase equilibrium study by X-ray diffr. and optical microscopy 80−50614
Si_3N_4-SiC-Y_2O_3, reactively sintered, microstruct. and strength 80−25631
Si_3N_4-SiO_2-Y_2O_2, subsolidus phase relations 80−60845
Si_3N_4-SiO_2-Y_2O_3 pseudoternary system, phase relations and stability 77−86015
Si_3N_4-Y_2O_3, hot pressed, sintered, microstruct., flexural strength and fractographic anal. 80−40293
Si_3N_4-Y_2O_3, hot-pressed, oxidation kinetics 80−16520
Si_3N_4-Y_2O_3 ceramic, thermal degradation, C impurity effect 80−50708
Si_3N_4-Y_2O_3-Al_2O_3-SiO_2, X-ray diffr. exam., phase equilib. at 1400 degrees C *(Japanese)* 78−44113
Si_3N_4-Y_2O_4-Al_2O_3 (4-17, 4 wt.%), sintering 80−81009
Si_3N_4.Y_2O_3 prepared by hot press, cryst. struct. 80−10534
SiO_2-Al_2O_3-Y_2O_3-La_2O_3-TiO_2 glasses with high elastic moduli, alkaline durability 80−85071

yttrium compounds continued
Si_2ON_2-Y_2O_3-Al_2O_3 phase relations at 1400°C *(Japanese)* 79−38811
$(Sm,Y)_3(Fe,Ga)_5O_{12}$, epitaxial mag. layer, LPE, growth rotation rate, effect on props. 78−56053
Sm-YIG garnets, implanted and Permalloy coated, comparison between planar domain walls in bubbles 77−85520
$Sm_{0.3}Lu_{0.2}Tm_{0.2}Y_{1.45}Ca_{0.85}Fe_{4.15}Ge_{0.85}O_{12}$, LPE growth, saturation magnetisation, collapse field, bubble diameter 78−95703
$(SmLuYCa)_3(FeGe)_5O_{12}$ film, ion implant profile 79−78477
$(SmYCa)_3(FeGe)_5O_{12}$ epitaxial layer, growth kinetics and struct. as functions of cryst. lattice parameter mismatch 80−6677
$(SmY)_3(FeGa)_5O_{12}$, LPE on $Gd_3Ga_5O_{12}$, growth kinetics, 920-980°C 78−3064
$Sm_{0.4}Y_{2.6}Fe_{3.8}Ga_{1.2}O_{12}$, LPE. improved method of stirring 78−68641
$Sm_{0.4}Y_{2.6}Fe_{3.8}Ga_{1.2}O_{12}$ epitaxial films, uniaxial mag. anisotropy, ferrimag. reson. study 80−80577
$Sm_xY_{3-x}Fe_5O_{12}$, magnetostriction comp. depend., 78 to 300K 77−77082
$Sm_xY_{3-x}Fe_5O_{12}$, spin reorientation transitons 78−2686
SmYGa garnet, bubble motion depend. on wall pinning 79−78455
$Sm_{0.4}Y_{2.6}Ga_{1.1}Fe_{3.9}O_{12}$, LPE, growth rate anisotropy and kinetic coeffs. of vicinal faces 78−51846
$Sm_{0.4}Y_{2.6}Ga_{1.2}Fe_{2.8}O_{12}$, H^+ implanted film, epitaxial, mag. bubbles, walls and fine struct. 77−63241
$Sm_{0.25}Y_{0.75}S$, phonon anomalies and electron-lattice coupling 80−39490
$Sm_{0.7}Y_{0.3}S$, Debye-Waller factor, X-ray diffr. meas., evidence of optic phonon softening 77−11659
$Sm_{0.75}Y_{0.25}S$, intermediate-valence-state system, phonon dispersion meas. 79−19342
$Sm_{0.75}Y_{0.25}S$, intermediate valence system, mag. excitations 79−60771
$Sm_{0.75}Y_{0.25}S$, intermediate valence compound, phonon investigation by neutron scatt. 80−6476
$Sm_{0.75}Y_{0.25}S$, mixed valence, phonon dispersion theory 80−34153
$Sm_{0.75}Y_{0.25}S$, mixed-valence, electron-lattice correlations, EXAFS studies 80−76103
$Sm_{0.76}Y_{0.24}S$, induced magnetic form factor, polarised neutron studies 80−25078
$Sm_{0.76}Y_{0.24}S$, mixed valence, induced mag. form factor 78−68163
$Sm_{1-x}Y_xS$, anomalies in phonon dispersion 79−73268
$Sm_{1-x}Y_xS$, CPA calc. of rare-earth impurity, valence change 77−63096
$Sm_{1-x}Y_xS$, effect of valence fluctuations on lattice dynamics 78−47493
$Sm_{1-x}Y_xS$, electronic config., Mossbauer spectra meas. 77−16228
$Sm_{1-x}Y_xS$, magnetoresist. in semicond. and metallic phases 80−96914
$Sm_{1-x}Y_xS$, metal-semicond. isomorphous transition curve, low temp. crit. point, lattice parameter changes 79−95334
$Sm_{1-x}Y_xS$, mixed valence system, electron-phonon coupling, theory 80−70343
$Sm_{1-x}Y_xS$, mixed valence, phonon softening and linewidths, calc. 80−75319
$Sm_{1-x}Y_xS$, press.-induced semicond.-metal transition, refl. and lattice compression meas. 77−62826
$Sm_{1-x}Y_xS$, valence transitions, theoretical model 79−69474
$Sm_{1-x}Y_xS$, XPS, electronic struct. excitonic effects, insulator to metal transition 78−43988
SrF_2-(Y,R)F_3, R=rare earth, phase equilibria, X-ray charact. of phases 79−61570
Sr_2YRuO_6, perovskites, prep., struct., emission control catalysts 77−68957
$Tb_xLa(Y,Gd)_{1-x}$.DAM.SaI_3, DAM=diantipyrylmethane, luminesc. *(Russian)* 77−55830
TbY ferrite garnet, Tb^{3+} energy level inversion, Faraday effect *(Russian)* 79−47418
$Tb_xY_{1-x}As$, anomalous resistivity maxima in metallic magnetic system 78−79977
$Tb_pY_{1-p}AsO_4$, crystallographic, mag. phase transition as function of temp. and Tb conc. 78−43334
$Tb_cY_{1-c}As(P)(Sb)$, singlet ground state systems, microwave resist. data 77−47843
$Tb_{0.2}Y_{2.8}Fe_5O_{12}$, Mossbauer investigation of spin-reorientation transition 78−88243
$Tb_{0.26}Y_{2.74}Fe_5O_{12}$, anomalous props., 200-250K 79−28527
$Tb_{0.26}Y_{2.74}Fe_5O_{12}$ garnet, mag. transition, mag. props. anomaly 80−93120
$Tb_xY_{3-x}Fe_5O_{12}$ hysteresis in spin-orientation phase transitions 79−73761
$Tb_xY_{3-x}Fe_5O_{12}$, spin reorientational phase transitions *(Russian)* 78−39349
$Tb_xY_{3-x}Fe_5O_{12}$, spin-reorientation phase transitions, neutron depolarisation factor 78−27037
$Tb_xY_{3-x}Fe_5O_{12}$, anomalies of magnetisation and magnetostriction obs. in strong fields, 4.2K 77−1581
$Tb_xY_{1-x}PO_4$, H_2 VUV laser excitation, fluoresc. decay charact. 78−60510
ThO_2 ceramics, CaO and Y_2O_3 stabilised density, elec. cond., permittivity 78−47838
ThO_2:Y_2O_3, electrochem. cell, complex impedance, temp. and freq. depends. 77−1458
ThO_2-$YO_{1.5}$, solid solns., defective oxides, ionic cond. 80−107548
ThO_x:Y_2O_3 solid electrolyte high-temp. vaporisation obs. 78−14456
TiB_2-Y_2O_3, thermal stability of composite materials 78−60638
TiO_2-Y_2O_3 system, dislocation mechanism of diffusion processes 79−77837
$Tm_y(La,Y)_{1-y}S$, microwave resistivity 77−11949
$Tm_y(La,Y)_{1-y}Te$, microwave resistivity 77−11949
$Tm_xY_{1-x}Se$, Kondo effect, Van Vleck behaviour 80−25085
$Tm_{1-x}Y_xTe$, ($0 \leq x \leq 1$), single cryst. growth and charact. 78−23603
(U,Y)C, U self-diffusion 80−92711
U-Y-C FBR nuclear fuels, phase anal., 1400°C 80−66485
UIG, Ga-substituted, computer simulation of temp. and field depend. of sublattice magnetisation and spin-flip transition 79−11300
UO_2, Y_2O_3 stabilised, O self diffusion 79−28135
U_3O_8-Y_2O_3, solid soln. electrode, high temp. electrochem. appl. 80−6828
US, electronic struct. calc. 78−91615
US, phonon anomalies 79−7663
$(U_{0.3}Y_{0.7})O_{2-x}$, ionic cond. 80−6828
$(Y,Ca)_3(Fe,Ge)_5O_{12}$ LPE layer, exchange stiffness coeffs., 20-300K 79−78464
$(Y,Ca)_3(Fe)_2(FeGe)_3O_{12}$ film, exchange const., ferromag. reson. meas. 79−8023
$(Y,Eu,Lu,Ca)_3(Fe,Ge)_5O_{12}$, bubble memory chip, dynamic conversion comparison with $(Y,Sm,Lu,Ca)_3(Fe,Ge)_5O_{12}$ 78−68319
$(Y,Eu,Sm)_3(Ga,Fe)_5O_{12}$ film, mag. loss and bubble dynamics 77−8371

yttrium compounds continued
$(Y,Eu,Tm,Ca)_3(Fe,Ge)_5O_{12}$, Ca, Ge substituted garnet LPE films, elec. props., charge imbalance, Seebeck effect 78−68101
$(Y,Eu,Tm,Ca)_3(Fe,Ge)_5O_{12}$ garnet film coercivity, new annealing method 78−84459
$(Y, Eu, Yb, Ca)_3(Ge, Fe)_5O_{12}$, bubble film, LPE on $Gd_3Ga_5O_{12}$, mismatch and faceting 77−20657
$(Y,Eu)_3(Fe,Ga)_5O_{12}$, epitaxial, cylindrical mag. domain struct., radial wall motion effect *(Russian)* 77−8373
$(Y,Eu)_3(Fe,Ga)_5O_{12}$, LPE growth from molybdate fluxes, bubble props. 78−68322
$(Y,Eu)_3(Ga,Fe)_5O_{12}$ film, bubble wall state stability obs. 77−20651
$(Y,Gd,Tm)(Fe,Ga)_5O_{12}$, cylindrical mag. domain behaviour in external mag. field *(Russian)* 78−6553
$(Y,Gd,Yb,Bi)_3(Fe,Al,Ga)_5O_{12}$ films, magnetic bubble domains, domain wall motion examined 78−19294
$(Y,Gd,Yb,Bi)_3(Fe,Al)_5O_{12}$ film, nonreciprocal effects in domain boundary motion in inhomogeneous field 77−24726
$(Y, Gd, Yb, Bi)_3(Fe, Al)_5O_{12}$ epitaxial film, domain wall motion and oscill. 80−2616
$(Y,Gd,Yb,Bi)_3(Ga,Al,Fe)_5O_{12}$, bubble conversion to anomalous behaviour 78−23309
$(Y,Gd,Yb)_{3-x}Bi_x(Fe,Al)_5O_{12}$, garnet single cryst. film, possible bubble appl. 78−6552
$(Y,Gd,Yb)_{3-x}Bi_x(Fe,Al)_5O_{12}$, LPE, for magneto-optical appls. 78−48341
$(Y,Gd,Yb)_3(Fe,Ga)_5O_{12}$ film, magnetisation processes and domain struct. near compensation temp. 78−14996
$(Y,Gd)BO_3:Eu^{3+}$, phosphor, vac. UV excitation spectra, appl. to gas discharge display 80−2816
$(Y,Gd)_3(Fe,Ga)_5O_{12}$, thin film lightguide, noninteracting mode conversion *(Russian)* 78−1347
$(Y,Ho)VO_4$:^{165}Ho, enhanced NMR meas. 77−66428
$(Y,La)B_6$, superconducting transition temps., impurity effects 80−20341
$(Y,Lu)_3(Fe,Sc)_5O_{12}$ LPE layer, exchange stiffness coeffs., 30-300K 79−78464
$(Y,Re)_{3-x}Ca_xGe_{5-x}Ge_xO_{12}$, garnet films, LPE growth for bubble memory appls. 77−11813
$(Y,Sm,Ca)_3(Fe,Ge,Si)_5O_{12}$ single-crystal films, props. 78−64247
$(Y,Sm,Ca)_3(Fe,Ge)_4O_{12}$, garnet thin film, mag. anisotropy, Faraday effect meas. 79−42812
$(Y,Sm,Ca)_3(Fe,Ge)_5O_{12}$, domain wall, radial motion, method of dynamic collapse of mag. bubbles 79−8026
$(Y,Sm,Ca)_3(Fe,Ge)_5O_{12}$ epitaxial films, mag. props., growth condition effects 80−97124
$(Y,Sm,Ca)_3(Ge,Fe)_5O_{12}$ film, bubble wall state stability obs. 77−20651
$(Y,Sm,Ga)_3(Fe,Ge,Si)_5O_{12}$ film, static and dynamic mag. props., 20-160°C 77−24725
$(Y, Sm, Lu, Ca)_3(Fe, Ge)_5O_{12}$:$Ne^+$, film, S=1 bubbles dynamic props., temp. depend. 77−20658
$(Y,Sm,Lu,Ca)_3(Fe,Ge)_5O_{12}$, bubble memory chip, dynamic conversion comparison with $(Y,Eu,Lu,Ca)_3(Fe,Ge)_5O_{12}$ 78−68319
$(Y,Sm,Lu,Ca)_3(Fe,Ge)_5O_{12}$ garnet film coercivity, new annealing method 78−84459
$(Y,Sm,Lu,Ca)_3(Fe,Ge)_5O_{12}$ bubble magnetic garnet film, LPE grown, props., $CaCO_3/GeO_2$ molar ratio influence 80−50152
$(Y, Sm, Lu, Ca)_3(FeGe)_5O_{12}$ LPE films, factors affecting coercivity 79−91267
$(Y,Sm,Lu,Ca)_3(Ga,Ge,Fe)_5O_{12}$, film growth and mag. props. for bubble-memory appl. 79−87297
$(Y,Sm,Lu,Cu)_3(Fe,Ge)_5O_{12}$, ion implanted, hard bubble suppression 80−11238
$(Y,Sm,Lu,Tm,Ca)_3(Fe,Ge)_5O_{12}$, epitaxial garnet film, temp. depend. mag. props. 80−39825
$(Y,Sm,Lu)_3(Fe,Ga)_5O_{12}$, LPE mag. film, suitability for 1 to 3 micron bubble devices 78−68323
$(Y, Sm, Tm)_3(FeGa)_5O_{12}$ LPE films, factors affecting coercivity 79−91267
$(Y,Sm)_3(Fe,Ga)_5O_{12}$ film, static and dynamic mag. props., 20-160°C 77−24725
$(Y,Sm)_3(Fe,Ga)_5O_{12}$, garnet LPE films, growth rate anisotropy 80−54558
$(Y,Sm)_3(Fe,Ge)_5O_{12}$, Ca, Ge substituted garnet LPE films, elec. props., charge imbalance, Seebeck effect 78−68101
$(Y,Sm)_3(Ga,Fe)_5O_{12}$ epitaxial layers, annealing effect on mag. props. 79−61191
$(Y,Sm)_3(Ga,Fe)_5O_{12}$ film, domain boundary mobility, effect of easy magnetization axis inclination 78−19293
$(Y,Sm)_3(Ga,Fe)_5O_{12}$ films, growth from melt, growth property control 78−27395
$(Y,Sm)_3(Ga,Fe)_5O_{12}/(Eu,Er)_3(Ga,Fe)_5O_{12}$ double-layer self-biasing garnet films, dynamic behaviour of domain walls 80−34722
$(Y,Yb)_3Al_5O_{12}$:Yb^{3+}, stimulated emission 77−52135
$(Y,Gd,Yb)_{3-x}Bi_x(Fe,Al)_5O_{12}$ film growth on $Gd_3Ga_5O_{12}$ substrates 79−78623
Y ferrite-garnet, porous polycrystal, law of approach to saturation *(Russian)* 78−47956
Y porphyrin complexes, luminesc. 77−18958
Y-Fe-O, phase equilib. and thermodynamics, solid state high temp. electrochem. obs. 79−56967
Y-Ge-B, X-ray investigation of phase equilibrium 79−99294
Y-H, degree of positron localisation on components 77−85833
Y-H, exam. of electron structure 80−29306
Y-H film, temp., thickness and comp. depend. of elec. resist. 79−78221
Y-H system, solid soln. phase, wide-line PMR 80−25226
Y-Re-Si system, phase diagram at 800°C 79−38806
Y-Si-Al-O-N ceramic, phase assemblages, relationships with props. 80−60848
Y-Si-Al-O-N glass, prep. and props. 80−25647
Y-Si-Al-O-N solid soln., based on α-Si_3N_4 struct., comp. and struct. 79−74136
Y-Si-O-N system, behavioural diagrams 79−24507
Y-Sm ferrogarnet *(Russian)* 80−71140
Y-W(Mo)-B, phase equilibria, struct. of crysts. 77−21122
$Y_{0.7}$ $Th_{0.3}C_{1.58}$, specific heat 78−91813
YA-O_3:Er^{3+}, pulsed laser action, $^4S_{3/2}$ to $^4I_{9/2}$ transition laser action, optical and luminescence spectra 80−16082
YAG, as substrate for $Er_3Al_{5-x}Ga_xO_{12}$ LPE film for solid laser 80−93419
YAG, brilliance, sparkliness and fire of diamond simulants 78−90363
YAG brittleness anisotropy, microcrack formation due to surface treatment 80−40526
yttrium compounds continued
YAG, colour centres conceived as bound polarons 78−63990
YAG crystal with rare earth ion impurities, active medium reson. pumping method for Nd laser freq. conversion 80−1206
YAG, crystallization kinetics and growth mechanism on oriented seeds in melt-solns. 79−14717
YAG crystals, dislocations and inclusions, birefringence topography obs. 80−107248
YAG, Czochralski grown crystals, interface shape change 78−83760
YAG Czochralski grown crysts., growth of facets and vicinal interfaces *(Chinese)* 79−90578
YAG, electrostatic model of cryst. field 80−59945
YAG, exposed to ultrasoft X-rays, thermal luminesc. and electron emission 79−8192
YAG, facet formation 78−63687
YAG, high temp. soln. growth using accelerated crucible rotation 79−100039
YAG, high-resolution many beam lattice image anal. 80−14979
YAG, influence of facial growth effect on Yb ion incorporation 79−10822
YAG, interrelationship between mech. props. and elec. relief on surface layer 79−23821
YAG laser, resonator length effects on loss coeffs. and ouptut energy *(German)* 78−66849
YAG laser single pulse formation kinetics with self-modulation of quality factor *(Russian)* 77−27312
YAG, melting behaviour and metastability determ. by optical DTA 80−92648
YAG, molten, complexity in solidification behaviour, SEM electron images 79−43229
YAG, neutron diffr. determ. of O coordinates 77−1117
YAG, optical absorption of hole centres, polaron model 80−97314
YAG, optical films, high quality growth 79−46984
YAG, phonon spectrum, incoherent inelastic neutron scatt. meas. 77−66006
YAG, production of densely sintered ceramic, exam. of recrystallisation during sintering 80−11609
YAG rods, thermally induced birefringence in (001) direction, transmission loss *(Chinese)* 77−77166
YAG, simulated mol. images, point models and kinematical struct. amplitudes 80−103223
YAG single crystal growth by flux method *(Japanese)* 78−19655
YAG single crystal growth, by vertical directed crystn., thermal characts. 80−2944
YAG single crystals, derivation of cryst. parameters and orientation by X-ray topography *(Chinese)* 79−46622
YAG, single crysts., kinetic characts. of growth from melt-solns. on oriented seeds 79−14719
YAG, single crysts., melt growth using heat exchange method 79−52106
YAG, solubility in solvent $PbO_{-x}PbF_2$, phase form. in system Y_2O_3-Fe_2O_3-PbO-PbF_2-B_2O_3 78−95247
YAG solution, in $PbO/PbF_2/B_2O_3$ solvent systems, density, surface tension and expansivity data, effect of B_2O_3 conc. 79−19985
YAG, stress fields of dislocation arrays *(German)* 79−23615
YAG, surface grating relief pattern profile altering, oblique shadow deposition technique 79−68451
YAG, temp. distribution in growth from Czochralski method 79−65998
YAG, thermoelastic stress distribution in single cryst. pulling by Czochralski technique 78−63681
YAG, transient colour centres caused by UV radiation 77−84744
YAG, traps, energy spectra, X-irrad. effects and thermoluminesc. *(Russian)* 77−20940
YAG, undoped and Ce^{3+}-doped, cathodolum. intensity and decay time, 10-480K 79−99952
YAG, Yb^{3+} crystalline field, Schottky specific heat, paramagnetic susceptibility temp. depend. 77−11882
YAG:$^{154}Gd^{3+}$, hyperfine interactions, PAC 77−43909
YAG:Ce, γ-irradiated elec. cond. meas. 77−43601
YAG:Ce phosphors, luminesc. efficiency, prep. and dopant effects 80−45151
YAG:Ce^{3+}, new fast scintillator for SEM 78−86394
YAG:Ce^{3+}, photoluminescence excitation energy, crystal field and temp. effects 80−11460
YAG:Ce^{3+}, scintillation detector, in SEM, electro-optical props. 80−52819
YAG:Ce^{3+}(Eu^{3+})(Gd^{3+})(Tb^{3+}), cathodoluminesc. efficiency rel. to activator conc. 80−11479
YAG:Ce^{3+}(Tb^{3+}), recomb. processes, spectral, kinetic and relative quantum intensity meas. 79−61443
YAG:Cr_i optical detection of phonons 80−92630
YAG:Cr^{3+}, absorption and luminesc., spectra, Cr conc. depend. 77−12435
YAG:Cr^{3+}, electronic states interactions with crystal odd vibrs., R-lines vibr. recurrences 78−84639
YAG:Cr^{3+}, optical absorption, cryst. field pot. expansion 77−36268
YAG:Cr^{3+}, radiation colour centres, absorpt. and thermolum. spectra 78−48206
YAG:Cr^{3+} 80−2740
YAG:Dy(Er)(Tm)(Tb)(Yb), US attenuation 77−89500
YAG:Er, elastic wave damping, 300 to 1500 MHz, impurity effects 80−92602
YAG:Er^{3+}, 3 μm stimulated emission at room temp. 77−42541
YAG:Er^{3+}, crystal field theory, Er^{3+} behaviour in tetragonal field 77−8259
YAG:Er^{3+}, laser active media, nonradiative losses due to $^4I_{11/2}$-$^4I_{13/2}$ transition 79−31911
YAG:Er^{3+}(Ho^{3+}), stimulated radn., electron-phonon interaction *(Russian)* 77−8605
YAG:Er^{3+}(Ho^{3+})(Tm^{3+}), oscillator strengths of impurities, 5000 to 30000 cm^{-1} 79−4830
YAG:Eu^{3+}, reson. fluoresc. spectra, showing multiple Eu^{3+} sites 80−2812
YAG:Gd^{3+}, EPR absorpt. spectrum 78−76305
YAG:Ge^{3+}, excited state absorpt. loss, 5d→4f rare earth lasers 78−90417
YAG:Ho^{3+}, low-lying cryst. field levels 79−91007
YAG:Ho^{3+}, spectroscopy, stimulated emission 80−93374
YAG:Ho^{3+}, stimulated emission at low temps. 80−106526
YAG:M^{3+}, ESR absorption spectra, line broadening of Fe^{3+}, Cr^{3+}, Gd^{3+} 78−91940

yttrium compounds continued
YAG:Mn, impurity-induced O^- colour centres, absorpt. and fluoresc. spectra 77−1709
YAG:Nd, laser cryst., dislocations density and propag., rel. to Czochralski growth *(Chinese)* 77−11552
YAG:Nd, laser material, linear expansion coeff. and r.i., temp. depend. 77−733
YAG:Nd, pumped laser rod, quantum efficiency 77−88724
YAG:Nd, single crysts., melt growth using heat exchange method 79−52106
YAG:Nd, with improved fluoresc. lifetime of $^4F_{3/2}$ state 77−687
YAG:Nd,Ce,Cr, effect of γ-rays, fast electrons on optical props., annealing and colour centre destruction 77−8608
YAG:Nd crystal, orientation influence on thermally induced birefringence *(Chinese)* 80−88958
YAG:Nd garnet, heat capacity and thermal diffusivity meas. 80−19956
YAG:Nd glass clad fibre laser, 1.3 μm operation with LED end pumping 77−7120
YAG:Nd laser, kinematic mode synchronisation *(Russian)* 77−34892
YAG:Nd laser, radiation characts. rel. to pumping intensity in long-time operation *(Russian)* 77−68214
YAG:Nd laser pulses, mutual exchanges with plasma *(German)* 80−48918
YAG:Nd^{3+}, Ce^{2+}, sensitisation, luminesc., absorpt. and emission spectra *(Russian)* 78−10982
YAG:Nd^{3+}, cryst. field parameters calc., exchange charge model 78−47747
YAG:Nd^{3+}, cryst. field anal. 78−64013
YAG:Nd^{3+}, energy transfer between Nd^{3+} ions, laser-excited time-resolved site-selection spectroscopy 79−95839
YAG:Nd^{3+}, many-phonon nonradiative transition probabilities 79−95842
YAG:Nd^{3+}, multiplet splitting, effective ligand point-charge model calcs. 77−76779
YAG:Nd^{3+}, nonradiative multiphonon relaxation of isolated impurity level, transition probability calcs. 79−56853
YAG:Nd^{3+}, photon echo form. 77−23720
YAG:Nd^{3+}, radiationless decay processes, laser photoacoustic spectroscopy meas. 80−84766
YAG:Nd^{3+} and free Nd^{3+} ion, energy levels, absorption spectra 79−11076
YAG:Nd^{3+} crystal, zero-phonon linewidths, in $^4I_{9/2} \rightleftarrows {}^4F_{3/2}$ luminesc. band calc. 79−28834
YAG:R^{3+}, CRT and X-ray phosphor lattice-activator energy transfer model 78−6792
YAG:R^{3+}, R=Nd, Er, (Er, Ga), LPE and luminesc. 78−64408
YAG:rare earth, phonon impurity scatt., lattice thermal cond. and US attenuation meas. 78−87748
YAG:rare earth ion, laser freq. conversion by reson. pumping *(Russian)* 79−10314
YAG:rare earth metal, US absorpt. meas., relax. model 80−24539
YAG:Ti, crysts., colour centres, optical absorpt. spectra 79−65080
YAG:Ti, growth conditions from melt 79−95924
YAG:V_2O_5, CaO, V^{4+} ion impurity spectral anal. 79−78719
YAG-Ce^{3+}(Eu^{3+})(Tb^{3+})(Gd^{3+}), cathodolum. intensity, temp. depend., comparative study 79−99953
YAG-Ti, polarised luminescence 79−95843
$Y_3(Al,Fe)_5O_{12}$, optical anisotropy and stress birefringence assoc. with growth striations 79−42940
$YAl_3(BO_3)_4$, and $(Y,Er)Al_3(BO_3)_4$, crystallisation and growth characts., density and composition 80−35080
$YAl_3(BO_3)_4$, cryst. growth rate determ. 79−86731
$YAl_3(BO_3)_4$, crystallisation from solution in a melt, solvent composition 80−38976
$YAl_3(BO_3)_4$, solubility in fused potassium trimolybdenate and seeded cryst. growth 77−43330
$YAl_3(BO_3)_4$ solubility in $K_2Mo_3O_{10}$ melt 80−65211
$YAl_3(BO_3)_4$, thermolum. anal. 79−87514
$YAl_3(BO_3)_4$-$NdAl_3(BO_3)_4$, substitution of Nd for Y in $YAl_3(BO_3)_4$, exam. 80−11551
$YAl_3B_4O_{12}$:Bi^{3+}, luminesc., vibr. struct., energy transfer 79−38584
$Y_3(Al_{0.5}Ga_{0.5})_5O_{12}$:$Nd^{3+}$, radiationless decay processes, laser photoacoustic spectroscopy meas. 80−84766
$Y_3(Al_{1-x}Ga_x)_5O_{12}$:Nd, fluoresc. energy transfer and radiationless relax. 79−38625
$Y_3(Al_{1-x}Ga_x)_5O_{12}$:$Nd^{3+}$, time-resolved site-selection spectroscopy, energy transfer 80−2814
$YAlO_3$, cryst. growth with $Y_3Al_5O_{12}$ by flux method 77−24950
$YAlO_3$, melting behaviour and metastability determ. by optical DTA 80−92648
$YAlO_3$ perovskite, elasticity meas. to 6 kbar 77−51428
$YAlO_3$, rare earth doped, intra- and inter-ionic multiphonon transitions 80−34973
$YAlO_3$, with perovskite structure comparative assessment of methods of prep. 79−95980
$YAlO_3$, $YAlO_3$:Nd, colour centre form. rel. to growth conditions, absorpt. spectra 79−90652
$YAlO_3$:Ce, fast decay UV phosphor 80−71471
$YAlO_3$:Co, Ti, effects of Co and Ti ions on cryst. growth 77−28711
$YAlO_3$:Cr^{3+}, electronic states interactions with crystal odd vibrs., R-lines vibr. recurrences 78−84639
$YAlO_3$:Cr^{3+}, fluorescence R-lines anisotropy, effective Hamiltonian parameters 77−16368
$YAlO_3$:Er^{3+}, free-ion-model cryst.-field calc. 77−43545
$YAlO_3$:Ho^{3+}, stimulated emission at low temps. 80−106526
$YAlO_3$:Nd, refractive index determ. 78−80311
$YAlO_3$:Nd^{3+}, thermal broadening and shift calcs. of Nd^{3+} energy levels 77−48208
$YAlO_3$:Nd^{3+} biaxial laser cryst., anisotropy of spectral characts. 79−50303
$YAlO_3$:Nd^{3+} laser, $^4F_{3/2} \rightarrow {}^4I_{13/2}$ transition, stimulated emission wavelength, continuous tuning 77−58334
$YAlO_3$:Pr, hyperfine interaction in lowest levels of $^3H_4$ and $^1D_2$ states 79−78065
$YAlO_3$:Pr^{3+}, ultrahigh resolution photon echo spectroscopy 80−28285
$YAlO_3$:Tm^{3+}, cryst. field parameter determ. 77−15800
$YAlO_3$:Yb^{3+}, absorption and luminescence spectra, electron-phonon resonances, Stark splitting *(Russian)* 80−20674
$YAlO_3$:Yb^{3+}, mag. relax., Mossbauer expts. 79−8078
$Y_3Al_3O_{12}$ crystal growth from melt, gas bubble capture theory 80−64941

yttrium compounds continued
$Y_3Al_5O_{12}$, cryst. growth with $YAlO_3$ by flux method 77−24950
$Y_3Al_5O_{12}$ crystals, variation of microhardness anisotropy with heat treatment 79−56053
$Y_3Al_5O_{12}$, laser cryst., struct. inhomogeneity obs. by vac. decoration 77−35701
$Y_3Al_5O_{12}$, layer structuresrevealed by decoration method and electron microscopy 77−27902
$Y_3Al_5O_{12}$, Mollwo-Ivey relation between peak-colour absorption energy and average O ion spacing 77−90179
$Y_3Al_5O_{12}$:Er^{3+}, stimulated emission 77−52135
$Y_3Al_5O_{12}$:Nd^{3+}, single crystal, $^4F_{3/2}$ level splitting and spectra dependence on press. *(Russian)* 77−52183
$Y_3Al_5O_{12}$:Tb^{3+}, mechanism of $^5D_3$-$^5D_4$ cross-relax. 77−4656
$Y_3Al_5O_{12}$:Yb^{3+}(Nd^{3+}), one-phonon satellites in luminesc. spectra, rel. to effective phonon density 78−6730
$YAl_3[BO_3]_4$ crystals, capture centres, thermoluminesc. study 79−65935
$YAl_3[BO_3]_4$, thermal stability, X-ray struct. anal., refractive indices 79−4297
YAsS, struct. determ. *(French)* 77−51361
YB_{12}, exam. of electronic structure, using X-ray emission spectra *(Russian)* 79−33865
YB_{12}, mag. susceptibility, 90-1200K 80−50032
YB_6, metallic, energy bands and bonding 77−43486
YB_6, thermophys. props., 700 to 1200K 79−37850
YB_{68}, melt grown, props. meas. 77−11518
YBO_3, cryst. struct. reappraisal 77−47427
YBO_3:Bi^{3+},Eu^{3+}, vacuum UV excitation spectra and quantum efficiencies 79−28811
$Y_{1.6}Bi_{1.0}Ca_{0.4}Fe_{4.4}In_{0.4}V_{0.2}O_{12}$, cation distrib. 79−19211
$(YBi)_3Fe_{5-x}Ga_xO_{12}$ film, ferrimag., splitting of domains into layers 77−28420
$Y_{1-4}BiFe_{3.8}Ga_{1.2}O_{12}$ garnet films, bistable bubble domain 79−15331
$Y_2BiFe_{3.8}Ga_{1.2}O_{12}$ film, colour contrast between different domains 77−12166
$Y_2BiFe_{3.8}Ga_{1.2}O_{12}$ film, magnetooptic interference of light 77−32458
$Y_2BiFe_{3.8}Ga_{1.2}O_{12}$, film, dynamics of domain walls 78−27065
$Y_{2.7}Bi_{0.3}Fe_{3.8}Ga_{1.2}O_{12}$ epitaxial film, mag. domains in microwave mag. field, Faraday obs. 78−19295
$Y_{3-x}Bi_xFe_{5-y}Ga_yO_{12}$, epitaxial film, domain wall dynamics *(Russian)* 78−2718
$Y_{3-x}Bi_xFe_{5-y}Ga_yO_{12}$-PbO-$B_2O_3$-$Bi_2O_3$ system, crystn. fields 78−43996
$Y_2BiFe_5O_{12}$ garnet films, magnetooptical interference 79−28724
$Y_{3-x}Bi_xFe_5O_{12}$, ferrite-garnet formation 78−52737
$(YBiSmCa)_3(FeGe)_5O_{12}$ epitaxial layer, growth kinetics and struct. as functions of cryst. lattice parameter mismatch 80−6677
$YBiTe_3$, prep., elec. props., and crystallographic date 80−59981
$(YBi)_3.(FeGa)_5O_{12}$ film, interaction between Bloch walls and dislocations *(Russian)* 79−61196
YC_2-DyC_2, solid solution, antiferromag. props. 79−91230
$Y_2(C_2O_4)_3$, roasting effect of temp. on props. of Y_2O_3 77−8790
$Y_2(CO_3)_3.nH_2O$, tengerite, single cryst. hydrothermal growth 80−97417
YCa garnets, solid soln., mag. and cryst. chem. props. 77−16057
$(YCaEuYb)_3(FeGe)_5O_{12}$, LPE, stripe end motion, effect of in-plane field 78−68330
$Y_{3-x}Ca_{2x}Fe_{2-y}In_yFe_{3-x}V_xO_{12}$, first magnetocryst. anisotropy const., ferrimag. reson obs. 78−68218
$(Y_{3-x}Ca_x)(Fe_{2-x}Sn_x)(Fe_3)O_{12}$, long and short range magnetic order 79−38419
$Y_{3-2x}Ca_{2x}Fe_{5-x}V_xO_{12}$, single cryst., Faraday effect and opt. props. 77−1660
$Y_{3-y}Ca_yFe_{2-y}Zr_yFe_3O_{12}$, first magnetocryst. anisotropy const., ferrimag. reson obs. 78−68218
YCaSmTmGeIG, epitaxial layer with submicron bubbles, mag. props. 77−12172
$YCa_3Zr_2Fe_{2.75}Ga_{0.25}O_{12}$, mag. ordering and bond geometry rel. to tetrahedral Fe^{3+} 77−32163
$(Y_{3-x}Ca_x)[Fe_{2-x}Sn_x](Fe_3)O_{12}$, Mossbauer spectra of Fe^{27} and Sn^{119} nuclei 79−95578
$Y_{3-x}Ca_x[Fe_{2-x}Sn_x]Fe_3O_{12}$, Mossbauer spectra, Sn hyperfine mag. field 80−15893
$(YCdYbBi)_3(FeAl)_5O_{12}$, cylindrical domain wall vel. anisotropy *(Russian)* 77−59440
YCl supersonic mixing flame, spontaneous emission, electronic transition chem. laser pot. 78−66817
YCl_3, Raman spectrum 77−59567
YCl_3:$^{143}Nd^{3+}$($^{145}Nd^{3+}$), EPR and ENDOR spectra 79−78515
YCl_3-MCl melt, M=Cs, K, Li, Raman spectra 77−59567
YC_{n+}(n=2, 3, 4, 5, 6), atomisation energies, Knudsen cell mass spectrometric obs. 80−58409
$YCoO_3$, ^{59}Co NMR, quadrupolar and hyperfine interactions 79−15366
$YCoO_3$, anomalous $^{57}Fe^m$ charge states, Mossbauer study 80−40017
$YCoO_3$, spin state of Co^{3+} ion, X-ray photoemission line broadening 79−82751
YCo_2Si_2, mag. props. 80−107988
$YCrO_3$, antiferromag., exciton absorption lines obs. during field induced spin-reorientation 77−63397
$YCrO_3$, antiferromag., mag. domain walls, ^{53}Cr NMR study 79−11327
$YCrO_3$, bubble domain struct. temp. depend. 80−71137
$YCrO_3$, EPR linewidth, Neel point to 700K 80−39849
$YCrO_3$, exchange interactions 78−60279
$YCrO_3$, mag. circular dichroism and Faraday rotation in R-lines region 79−28725
$YCrO_3$, magnetisation, NMR freq. temps. depend. weak ferromagnetic-antiferromagnetic spin reorientation transition 80−29631
$YCrO_3$-Cr (40 wt.%) cermet, effect of Cr preoxidation on props. 79−87603
$YCrO_3$-$MgCr_2O_4$ sintered ceramics, elec. cond. 80−24927
$YCrO_3$-W(Mo)(Cr) eutectics, prep. and microstruct. 80−108380
$Y_2Cr_2O_7$, $Y_2Mn_2O_7$, pyrochlore type, synthesis and physical props. 80−33963
$YCu_3Mn_4O_{12}$, synthesis, structure and mag. props. of perovskite-like oxides 77−68960
$YCu_3Mn_4O_{12}$, synthesis and mag. props. 80−75717
YD, electronic spectra *(French)* 77−14442
$YD_{1.96}$, cryst. struct. by neutron diffr. 80−70179
YE+AG:Er^{3+}, laser material, radiative and nonradiative transitions, conc. quenching 77−16391
$(YErCa)_3(Fe\ Ge)_5O_{12}$, mag. loss and domain wall mobility 80−65980
$(YErCa)_3(Fe_{5-x}Ge_x)O_{12}$ film, high g, for mag. bubble applics. 77−85529

yttrium compounds continued

$(YEuCa)_3(FeGeSi)_5O_{12}$, mag. loss and domain wall mobility 80−65980
$(YEu)_3(FeGa)_5O_{12}$ rigid magnetic bubble transition to normal behaviour 78−95501
$(YEu)_3(FeGa)_5O_{13}$, LPE growth, uniaxial magnetocryst. anisotropy 77−8766
$Y_{2.45}Eu_{0.55}Fe_{3.8}Ga_{1.2}O_{12}$, hard bubble conversion in in-plane field 78−14998
$Y_{2.35}Eu_{0.65}Ga_{1.2}Fe_{3.8}O_{12}$, bubble translation vel., ion-implantation effects 78−68327
$(YEuLuCa)_3(FeGe)_5O_{12}$ film, stable state of bubbles containing Bloch lines 78−76281
YEuLuCaGe garnets, 7 μm-period bubble devices 80−44887
YEuLuGa garnets, 7 μm-period bubble devices 80−44887
$Y_{1-x}Eu_xP_3O_9$ phosphor, prep. and fluoresc. 77−48219
YEuTmCa garnet bubble films, domain wall transition 79−56584
$(YEuTmCa)_3(FeGe)_5$ bubble garnet films, ion-implanted, mag. susceptibility meas. 79−47311
YEuTmCaGe garnets, 7 μm-period bubble devices 80−44887
$(YEuTmCa)_3(GeFe)_5O_{12}$ film, Bloch loop punch-through in mag. bubbles 77−59437
$Y_{1.52}Eu_{0.3}Tm_{0.3}Ca_{0.88}Ge_{0.88}Fe_{4.12}O_{12}$, bubble translation vel., ion-implantation effects 78−68327
$(YEuTm)_3(FeGa)_5O_{12}$ film, dynamic props. of bubble domains by high speed photography 80−15771
$(YEuTm)_3(FeGa)_5O_{12}$ garnet film, bubble domain steady state motion on a circle 80−29589
YEuTmGa garnet bubble film, dynamic diffuse wall deform. 80−54927
YEuTmGa garnets, 7 μm-period bubble devices 80−44887
$(YEuTm)_3(GaFe_5)O_{12}$ ferrite garnet films, mag. bubbles, translational motion, mechanism for inertial effects 80−100606
$Y_{1.57}Eu_{0.78}Tm_{0.65}Ga_{1.05}Fe_{3.95}O_{12}$, bubble garnet, low drive stripe head vel. 77−32225
$Y_{1.57}Eu_{0.78}Tm_{0.65}Ga_{1.05}Fe_{3.95}O_{12}$ film, gradient propagation, overshoot and creep 78−19291
$(YEuYbCa)_3(FeGe)_5O_{12}$, ion-implanted, in-plane mag. field effects on bubble props. 77−85521
$(YEuYbCa)_3(FeGe)_5O_{12}$ film, mag. σ-bubbles, automation props. 78−88150
$(YEuYbCa)_3(FeGe)_5O_{12}$ bubble films, Ne^+-implanted, cryst. and mag. props., X-ray diffr. obs. 79−38362
$(YEuYbCa)_3(FeGe)_5O_{12}$ film, isolated straight stripe domain dynamic props. 79−33514
$(YEuYbCa)_3(FeGe)_5O_{12}$, garnet film, isolated straight stripe domain, dynamic behaviour 80−39809
$(YEuYbCa)_3(GeFe)_5O_{12}$ bubble film with ion-implanted layer, FMR study 80−2643
$(YEuYb)_3(FeGa)_5O_{12}$, LPE, stripe end motion, effect of in-plane field 78−68330
YF, $^3\Phi-{}^3\Delta$ system, rot. anal. 78−9149
YF, Franck-Condon factors and R-centroids, rot.-vibr. effects 78−50596
YF^+ emission, 3400 to 3700 Å, rot.-vibr. anal., electronic struct. 77−6839
YF_3, crystal field parameters acting on rare earth ions 79−69475
YF_3, force consts., Coriolis coupling consts., vibr. amplitudes 78−17650
YF_3, mol. consts., kinetic consts. and L-approx. methods 80−18839
YF_3:Er^{3+}, Yb^{3+}, IR excitation curves for visible luminesc. 79−33795
YF_3:Nd, Ce, energy transfer between 5d electronic states 80−2808
YF_3:Nd^{3+}(Er^{3+})(Tm^{3+}), VUV fluorescence and tunable coherent sources from 1650 to 2600 Å 77−688
YF_3:Tb^{3+}, cryst. fields, luminesc. spectra 78−19563
YF_3:Tm, Nd, energy transfer between 5d electronic states 80−2808
YF_3:Tm^{3+}(Nd^{3+})(Er^{3+}), vacuum-UV excitation spectra 78−80381
YF_3:Yb,Er, IR to visible light conversion, effect of temperature on efficiency *(Russian)* 77−28628
YF_3:Yb,Er, IR to visible radiation transform., limit yield *(Russian)* 79−28838
YF_3:Yb,Er, limit efficiency of transformation of IR to visible radiation 80−29784
YF_3:Yb^{3+}, Tm^{3+}, IR to blue up-converting phosphor 79−83004
YF_3-alkali fluoride binary liquid mixtures, thermochemistry 80−45538
$Y_3F_5O_{12}$, amorphous, magnetic props. *(French)* 80−80490
$Y_3F_5O_{12}$, X-ray determ. of deformed surface layer thickness 78−53119
$Y(Fe, Ga)_5O_{12}$, garnet film, strip domain struct. behaviour in applied field 78−68341
$YFe_{5-x}Al_xO_{12}$, impurity redistrib. kinetics, temp. depend., vacancy effects 80−75263
$Y_3Fe_{5-x}Al_xO_{12}$, linear expansion 77−48024
$Y_3Fe_{5-x}Al_xO_{12}$, permeability spectra rel. to microstruct. 80−71100
$Y_3Fe_{5-x}Al_xO_{12}$, mixed garnet, cation distrib., temp. depend., magnetisation study 80−79831
YFe_2B_2, compounds with $CeAl_2Ga_2$ structure type *(Ukrainian)* 79−32970
$YFe_3(BO_3)_4$, solubility in Bi_2O_3-B_2O_3 melt and crystallisation 80−19736
$Y_3Fe_{5-x-y}Co_xGe_yO_{12}$, anisotropy and magnetostriction, ferromag. reson. expts., 4.2-500K 78−27030
$YFe_{1-x}Co_xO_3$, reorientation transitions, neutron diffr., mag. behaviour *(Russian)* 77−24678
$Y_3Fe_{5-x}Co_{x/2}Si_{x/2}O_{12}$, spin reorientation, NMR and ferromag. reson. meas. 80−65890
$YFe_{1-x}Co_{x/2}Ti_{x/2}O_3$, anomalous decrease of spontaneous magnetisation in spin reorientation region 77−36059
$YFe_{1-x}Co_{x/2}Ti_{x/2}O_3$, magnetostriction meas. in spin reorientation region 78−2721
$YFe_{1-x}Co_{x/2}Ti_{x/2}O_3$, orthoferrite, anisotropy of Faraday rotation 79−61341
$YFe_{0.62}Cr_{0.38}O_3$, compensation of weakly ferrimag. moment 79−8035
$YFe_{1-x}Cr_xO_3$, reorientational transitions, mag. and neutron diffr. exam. 77−12097
$YFe_{1-x}Cr_xO_3$, weak ferrimagnet, anomalous mag. props. explained by exchange interactions *(Russian)* 77−69538
$YFe_{1-x}Ga_xO_3$, zone refined, exam. of Curie point and magnetisation 79−4673
$YFe_{4.5}Ga_{0.5}O_{12}$ domains, neutron dpolarisation and Faraday rotation study 80−93137
$YFe_{5-x}Ga_xO_{12}$, impurity redistrib. kinetics, temp. depend., vacancy effects 80−75263
$Y_3Fe_{4.2}Ga_{0.8}O_{12}$, LPE grown thin film, ferromag. reson. 78−35041
$Y_3Fe_{4.5}Ga_{0.5}O_{12}$, domain struct., neutron depolarisation and Faraday rot. 80−71084
$Y_3Fe_{4.6}Ga_{0.4}O_{12}$ film, surface spin wave reson. 77−85576

yttrium compounds continued

$Y_3Fe_{5-x}Ga_xO_{12}$ garnet, spin wave parametric excitation threshold anisotropy in second region 80−29542
$Y_3Fe_{5-x}Ga_xO_{12}$ epitaxial layers grown from soln., prep. and props. *(German)* 78−52691
$Y_3Fe_{5-x}Ga_xO_{12}$, garnet, magnetically inequivalent positions of cations in external mag. field 80−11307
$Y_3Fe_{5-x}Ga_xO_{12}$, inhomogeneous stress effect on ferromagnetic resonance 79−24219
$Y_3Fe_{5-x}Ga_xO_{12}$ layers, current-induced soln. growth 77−48358
$Y_3Fe_{5-x}Ga_xO_{12}$, mag. domains and cryst. defects 80−75789
$Y_3Fe_{5-x}Ga_xO_{12}$, refr. index spectrum, visible region 79−73894
$Y_3Fe_{5-x}Ga_xO_{12}$, substituted garnet, floating zone grown, FMR line width, saturation magnetisation 80−29626
$Y_3Fe_{5-z}Ga_zO_{12}$, mixed garnet, cation distrib., temp. depend., magnetisation study 80−79831
$Y_3Fe_{5-x}Gd_xO_{12}$, permeability spectra rel. to microstruct. 80−71100
$Y_3Fe_{5-x}In_xO_{12}$, K absorpt. and Mossbauer spectra *(Russian)* 77−32467
$YFe_{1-x}Mn_xO_3$ orthoferrite, spin reorientation, mag. torque meas. 78−47979
$YFeO_3$, Bloch, Neel and head to head domain wall mobilities 77−1562
$YFeO_3$, Bloch, Neel and head to head wall vels. 78−68287
$YFeO_3$, bubble domain struct. temp. depend. 77−69647
$YFeO_3$, Co^{2+} substituted, reorientational transitions 77−59419
$YFeO_3$, domain boundary inertia during mag. reversals *(Russian)* 80−88776
$YFeO_3$, domain wall motion, magnetoelastic coupling 79−78435
$YFeO_3$, domain walls vel. *(Russian)* 79−28553
$YFeO_3$, exchange interactions 78−60279
$YFeO_3$, Faraday rotation anisotropy 77−20837
$YFeO_3$, floating zone method growth, interface shapes 80−60775
$YFeO_3$, hydrothermal synthesis, mag. struct. 77−47972
$YFeO_3$, induced spin reorientation near Neel point 78−19267
$YFeO_3$, influence of mag. field on Faraday effect 78−27196
$YFeO_3$, influence of photomagnetic effects on ^{57}Fe NMR 78−52365
$YFeO_3$, mag. anisotropy in cryst. field approx. 80−60241
$YFeO_3$, mag. bubble stray field distrib. meas. using micro Hall element 77−40097
$YFeO_3$, mag. domain walls, photomagnetic effects, ^{57}Fe NMR obs. 78−95464
$YFeO_3$, magneto-optical near UV reflection-spectra, meridional and polar intensity effects *(Russian)* 78−39572
$YFeO_3$ monocrystalline, mag. field depend. of magnetic domain *(Korean)* 78−68337
$YFeO_3$, orthoferrite, vel. of planar domain wall 78−72363
$YFeO_3$, orthoferrite, domain boundary vel. exceeding limiting vel. *(Russian)* 79−24192
$YFeO_3$ orthoferrite, weak ferromagnet domain struct. near Neel temp. 79−99739
$YFeO_3$, orthoferrite, crit. domain wall vel. 80−71135
$YFeO_3$ photoanode for photoelectrolysis of water 77−81409
$YFeO_3$ plate, anisotropy of domain wall velocity, magneto-optical obs. 79−99725
$YFeO_3$ platelets, domain wall mobility, dynamic coercivity 78−91884
$YFeO_3$, Raman scatt. from magnons, anisotropy consts. determ. 80−66178
$YFeO_3$, skew bubble domains, stripe domains 77−89999
$YFeO_3$, solubility in aq. KOH under hydrothermal conditions 77−39677
$YFeO_3$, spin-wave damping of domain walls 79−42795
$YFeO_3$, thermodynamic study of form. 78−48685
$YFeO_3$, thermomag. recording in surface layer of orthoferrite 79−24165
$YFeO_3$, transit time meas. of domain-wall mobilities, magnetostatic and magnetoacoustic effects 79−42794
$YFeO_3$, weak ferromagnet, domain wall motion and velocity *(Russian)* 80−54917
$YFeO_3$, weak-ferromagnet, domain boundary dynamics *(Russian)* 79−73768
$YFeO_3$:Co, NMR of ^{57}Fe, spin echo 78−91987
$YFeO_3$:Co^{2+}, Ti^{4+}, spin reorientation, Faraday rot. meas. 77−8547
$YFeO_3$:Co^{2+}, weak ferromagnetism, single ion anisotropy contrib. 80−25126
YFe_2O_4, low temp. phase transitions and mag. props. 80−7106
YFe_2O_4, Mossbauer spectra of ^{57}Fe in antiferromag. and paramag. states 80−15834
YFe_2O_4, parasitic ferrimagnetism 79−4703
YFe_2O_4, two-dimensional spin ordering, neutron diffr. study 80−29530
$Y_3Fe_5O_{12}$, amorphous, mag. moments, susceptibility, Mossbauer studies 79−78345
$Y_3Fe_5O_{12}$, formation mechanism from metallic oxides 77−48376
$Y_3Fe_5O_{12}$, growth rel. to physicochem. investig. of $Y(OH)_3$-α-FeOOH system 77−40418
$Y_3Fe_5O_{12}$ LPE growth on $Gd_3Ga_5O_{12}$ substrates, substrate orientation effect 80−66438
$Y_3Fe_{5-x}Sc_xO_{12}$, garnets, magnetooptical spectra, 15000-21000 cm^{-1} 77−90131
$Y_3Fe_{5-x}Sc_xO_{12}$, local spin struct., Mossbauer obs. 77−32305
$Y_2Fe_4Si_9$ and $YFeSi_3$, cryst. struct. and mag. suscept., temp. depend. *(Russian)* 78−34957
$Y_3Fe_{5-x}Si_xO_{12}$, charact. of photoinduced mag. effects in weak magnetising field 78−27071
$Y_3Fe_{5-x}Si_xO_{12}$, photoinduced change of mag. permeability *(Russian)* 77−1560
$Y_3Fe_{5-x}Si_xO_{12}$, photoinduced jumps of permeability 79−28564
YGa garnet, Yb^{3+} crystalline field, Schottky specific heat, paramagnetic susceptibility temp. depend. 77−11882
$Y_{10}Ga_3Co_7$, X-ray cryst. struct. determ. 80−33977
$Y_3GaFe_4O_{12}$, mag. props. meas. in high mag. fields, review *(Japanese)* 78−52303
$Y_3Ga_xFe_{1-x}O_{12}$, film growth conditions rel. to memory element props. 77−66399
$Y_3Ga_xFe_{5-x}O_{12}$, Faraday rot., 1.06 μm, 100-300K 77−52059
$Y_3Ga_xFe_{5-x}O_{12}$ film, growth kinetics of film with cylindrical mag. domains 77−1577
$Y_3Ga_xFe_{5-x}O_{12}$, HF Faraday light modulator, optical charcts. crystal struct. depend. 77−39052
$Y_3Ga_xFe_{5-x}O_{12}$, spin struct. obs. by Faraday rotation expts. in fields up to 200 T 77−69809
YGaIG, Faraday effect and IR radiation modulation 79−10403
YGaIG, magnetoelastic wave propagation time dispersion reduction 80−75836
$YGaO_3$:Nd^{3+}, spectroscopic charcts. 77−12427

yttrium compounds continued
$Y_3Ga_5O_{12}$, rare-earth doped garnet, high temp. mag. susceptibility 79−78347
$Y_3Ga_5O_{12}:Er^{3+}$, laser active media, nonradiative losses due to $^4I_{11/2}$-$^4I_{13/2}$ transition 79−31911
$Y_3Ga_5O_{12}:Fe^{3+}$, impurity absorpt. spectra to 5.5 eV 77−20892
$Y_3Ga_5O_{12}:Fe^{3+}$, spin Hamiltonian parameters, g-factors, temp. depend. EPR obs. 77−48038
$Y_3Ga_5O_{12}:Ho^{3+}$, low-lying cryst. field levels 79−91007
$Y_3Ga_5O_{12}:Nd^{3+}$, cryst. field parameters calc., exchange charge model 78−47747
$Y_3Ga_5O_{12}:Nd^{3+}$, cryst. field anal. 78−64013
$Y_3Ga_5O_{12}:Nd^{3+}$, energy transfer between Nd^{3+} ions, laser-excited time-resolved site-selection spectroscopy 79−95839
$Y_3Ga_5O_{12}:Nd^{3+}$, radiationless decay processes, laser photoacoustic spectroscopy meas. 80−84766
$Y_3Ga_5O_{12}:Nd^{3+}$, spectroscopic characts. 77−12427
$Y_3Ga_5O_{12}:Tb^{3+}$, fluoresc. and absorption spectra 77−32422
$Y_3Ga_5O_{12}:Tb^{3+}$, luminesc. 77−48251
$Y_3Ga_5O_{12}$-$Y_3Fe_5O_{12}$ garnets, EPR spectra of ferric ions 77−66414
$(Y_{0.8}Gd_{0.2})AlO_3:Er^{3+}$, spectroscopic props. 77−85791
$Y_{1-x}Gd_xAlO_3:Ho^{3+}$, stimulated emission of Ho^{3+} ions 77−81126
$Y_3Gd_3Bi_3(FeAlGa)_5O_{12}$, epitaxial film, thermomag. recording *(Russian)* 77−1571
$Y_{1.4}Gd_{0.6}BiFe_{3.8}Ga_{1.2}O_{12}$ film, bistable bubble domains, static, dynamic and optical props. 79−28574
$Y_{3-3x-2z}Gd_{3x}Ca_{2z}Fe_{5-z-u}V_zSi_uCo_uO_{12}$, mag. props., effect of V substitution 77−20582
$Y_{2.3}Gd_{0.6}Fe_{4.7}Al_{0.4}O_{12}$ garnet, effect of Gd on magnetite exsolution in a garnet matrix 79−11624
$Y_{3-x}Gd_xFe_{5-y}Al_yO_{12}$, solid solns., IR absorpt. spectra, physical props. 80−55082
$Y_{2.6}Gd_{0.4}Fe_{3.9}Ga_{1.1}O_{12}$, epitaxial uniaxial film, mag. phase diagram, optical expts. *(Russian)* 77−48022
$Y_{2.01}Gd_{0.99}Fe_{4.925-x}Mn_xO_{12}$, comp. depend. of mag. props., and stress sensitivity control 78−27057
$Y_{3-x}Gd_xFe_5O_{12}$, FMR, influence of Gd^{3+} substitution on linewidth 77−8416
$Y_{3-x}Gd_xFe_5O_{12}$, field depend. of susceptibility *(Russian)* 78−68176
$Y_{3-x}Gd_xFe_5O_{12}$, linear expansion 77−48024
$Y_{3-x}Gd_xFe_5O_{12}$, mag. phase diagrams, mag. transitions, exchange interaction *(Russian)* 80−54896
$Y_{3-x}Gd_xFe_5O_{12}$, solid solns., IR absorpt. spectra, physical props. 80−55082
(YGd)$(GaFe)_5O_{12}$ epitaxial film, nonlinear magnetoelastic effects *(French)* 80−34745
$Y_{2.55}Gd_{0.45}GaFe_4O_{12}$, garnet thin films, magnetisation orientation, temp. depend. 80−71125
YGdIG, with various domain wall orientations, natural spin reson. 80−66040
Y_2GdIG film, amorphous, mag. bubbles obs. and structural transformation 80−75824
$Y_{1-x-c}Gd_xNd_cScO_3$, crystal, absorption, luminescence, stimulated emission spectra 78−15220
$Y_{1-x}Gd_xRh_4B_4$, mag. supercond., anomalous temp. depend. of upper crit. fields 80−29510
$Y_{1-x}Gd_xRh_4B_4$, supercond., phase diagrams and upper crit. fields 80−2531
$Y_{1-x}Gd_xSiO_3:Ho^{3+}$, stimulated emission of Ho^{3+} ions 77−81126
$YGdTmFe_{4.3}Ga_{0.7}O_{12}$ epitaxial films, bubble-domain lattices with specified parameters 80−60386
$(YGdTm)_3(FeGa)_5O_{12}$ epitaxial film, formation of lattice of cylindrical mag. domains from stripe domains *(Russian)* 80−80579
$(YGdYbBi)_3$ $(FeAl)_5O_{12}$ epitaxial film, diffuse domain wall, bubble domain expansion 80−25170
$Y_{0.9}Gd_{1.1}Yb_{0.7}Bi_{0.3}Al_{0.9}Ga_{0.2}Fe_{3.9}O_{12}$ films, cylindrical mag. domain form. *(Russian)* 77−40098
$(YGdYbBi)_3(FeAlGa)_5O_{12}$ film, motion of mag. bubble domains in inhomogeneous pulsed mag. field 78−27064
$(YGdYbBi)_3(FeAl)_5O_{12}$, epitaxial garnet film, with mag. compensation point, behaviour of 'compromise' phase boundary 78−60321
$(YGdYbBi)_3(FeAl)_5O_{12}$, garnet, epitaxial film, interior domains 79−91268
$(YGdYbBi)_3(FeAl)_5O_{12}$, epitaxial film, 360° domain walls with periodically distrib. Bloch lines 80−7127
$(YGdYbBi)_3(FeAl)_5O_{12}$ ferrite-garnet films, effect of in-plane field on dynamics of domain walls 80−65979
$(YGdYbBi)_3(FeAl)_5O_{12}$ epitaxial garnet film, uniaxial ferromagnet domain struct., phase transition *(Russian)* 80−108044
$(YGdYbBi)_3.(FeAl)_5O_{12}$ films, substrate orientation influence on max. vel. of domain boundaries 79−15330
$Y_{1.3}GdYb_{0.7}GaO_{12}$, epitaxial film, ferromagnetic reson. exam. 77−85579
$Y_4GeO_6(OH, F)_4$, cryst. struct. 79−19229
YH, $^1\Sigma$ state, Dirac-Fock one-centre calcs. 80−23301
YH, electronic spectra *(French)* 77−14442
YH, YD, 3800-9000 Å negative glow spectra, triplet and singlet systems 77−79608
$YH_{1.92}$, tensile strength and creep 80−55459
$YH_{1.98}$, cryst. struct. by neutron diffr. 80−70179
YH_2, electronic struct., band theory 79−78006
YH_2, electronic struct., photoelectron spectra study 80−50527
YH_2 film, struct. and elec. resist., electron diffr. meas. 78−87888
YH_2, location of H, PMR rigid-lattice second moment meas. 80−71198
YH_2, self-consistent energy bands, KKR method with Hedin-Lundqvist approx. 80−49593
YH_2, synchrotron XPS obs., rel. to theory for metal dihydrides 80−55275
YH_3:Er, Mossbauer spectra of Er^{3+}, gyromagnetic ratios and cryst. field parameters determ. 78−19388
YH_x (x=1.92 to 1.98), magnetic and elec. props., 100 to 900K *(Russian)* 80−25077
YH_x, mech. props. 77−44333
YH_x, positron localisation *(Russian)* 77−66555
YH_x:Er, proton distrib. and site energies, ESR meas. 80−59509
$YHfTaO_6$, powder X-ray diffr. data 79−99155
YI, IR $^1\Pi\rightarrow{}^1\Sigma$ system, Fourier spectrometry, rovibrational anal. 80−83360
YIG, Al substituted, transferred hyperfine fields, Mossbauer effect meas. 79−1726

yttrium compounds continued
YIG, Al- and Ga-substituted, floating zone method growth, interface shape and horizontal variations of Al and Ga contents by electron pulse anal. 79−33929
YIG, amorphous, ionic glass, hard-sphere random-packing model 80−24369
YIG, and Ga-substituted YIG, mag. birefringence rel. to sublattices 79−28723
YIG and Ga-substituted YIG, high energy heavy ion irrad., lattice strain 80−49278
YIG, anisotropic elastic waveguide normal-mode anal., appl. to Rayleigh-Love wave mode converter 79−23113
YIG, anisotropic linear mag. birefr., light modulation 77−8548
YIG, anomalous subsidiary absorpt. butterfly curves at 9.16 GHz and 300K 79−82875
YIG, Barkhausen effect *(German)* 78−14986
YIG, Bi-substituted, LPE film, optical absorpt. changes due to impurity incorporation 77−1702
YIG, Bi-substituted, LPE, domain wall reson. 80−60387
YIG, Bloch line mass and mobility in a domain boundary *(Russian)* 80−93138
YIG, Bloch wall mobility, effect of dynamic change in wall struct. *(Russian)* 78−2698
YIG, Brillouin-Mandelstam scattering from thermal and excited magnons 80−70980
YIG bubble films, light scatt. from spin waves, hysteresis meas. by Voigt effect 80−15770
YIG, bulk, low mag. domain wall mobility 78−95463
YIG, CVD defect free epitaxial growth, conditions depend. 77−16502
YIG, cation sites distrib. and valence states 79−99167
YIG ceramic, transient flash effect on permeability 78−27024
YIG, computer optical isolator for near IR region 78−83104
YIG, corrugated slab, magnetostatic surface wave propagation 78−27072
YIG, crit. behaviour, Mossbauer and magnetisation meas. *(Russian)* 79−61106
YIG, crystal and static mag. props. 79−99166
YIG crystals, bulk growth from high temp. solns., props. 80−66413
YIG, cylindrical mag. domains, translational motion 80−108043
YIG, deformed at high temp., subgrain boundaries and dissociations of dislocations, TEM obs. 79−90658
YIG, demagnetising factor meas., magnetoelastic Rayleigh wave convolution 77−10072
YIG, diamagnetic substituted, anal. of polar Kerr rot. spectra 78−68485
YIG, diamagnetically substituted, annealing effects on cation distrib. 79−1455
YIG dielectric layered struct. magnetostatic bulk wave steering 80−25166
YIG, diffr. of laser radiation by parametrically excited elastic and magnetoelastic waves 78−19338
YIG, dilute, magnetoacoustic surface wave excitation by RF field on Bloch walls 80−25178
YIG, dissociation press. and Gibbs energy of form. 79−11816
YIG, distrib. of easy magnetisation axes near edge dislocation *(Russian)* 80−44891
YIG, domain boundary nuclear spin echo excitation, NMR domain freq. capture effect *(Russian)* 80−44955
YIG, domain wall mobility and mass meas. method *(Russian)* 80−108033
YIG, domain wall size and mag. losses in freq. spectra 77−85481
YIG, double layer struct., LPE growth from molybdate and Pb borate fluxes 80−39827
YIG, dynamic characts. of domain walls, low temp. behaviour 77−69598
YIG, elastic and thermoelastic consts., US meas. *(German)* 77−59061
YIG, elec. props. 79−99552
YIG, elec. props. meas., 600-1500K 77−8098
YIG, electron and γ-irrad., photomagnetic effect 80−103877
YIG, electrostatic model of cryst. field 80−59945
YIG, empirical formula for lattice const. calc. 79−27968
YIG, energy dispersive X-ray microanalysis, improved reproducibility by normalization to the background 78−48727
YIG, epitaxial, temp. stabilisation of ferrimag. reson. field by Ga, La substitution 77−77104
YIG epitaxial film, strong in-plane ang. depend. of spin-wave intensities 77−69521
YIG epitaxial film, magnetostatic volume wave propag. 78−10736
YIG epitaxial film and cryst., bound magnetostatic waves controlled by field gradients 78−95425
YIG epitaxial films, substituted, floating bubble domains, effect of structural stratification 80−2615
YIG, epitaxial layer, n and p-type, UPS, elec. struct. 77−4710
YIG epitaxial layers grown from soln., prep. and props. *(German)* 78−52691
YIG, FMR line broadening, two-magnon scatt. contribs. 77−20711
YIG, Faraday effect, influence of mag. field on sublattice contributions 80−88975
YIG, Faraday rot. rel. to sublattice magnetisation 79−33675
YIG, ferrimagnet, one-magnon light scatt. effect of quadratic magneto-optical coupling 79−11407
YIG, ferromag. film on nonmag. substrate, magnetoelastic wave propag. 79−99744
YIG, ferromag. reson. of unclamped specimen, magnetoreson. force effects *(Russian)* 77−32264
YIG, ferromag. reson., press. up to 6.5 kbar 77−51956
YIG ferromagnetic film, quasi surface spin wave giant oscills. *(Russian)* 80−15767
YIG, ferromagnetic resonance and magnetostatic waves in inhomogeneous internal field *(Russian)* 80−54954
YIG film, Ca, Ge-substituted, having mag. bubbles, LPE growth 78−31350
YIG film, calc. of magnetostatic mode freq. 78−68313
YIG film, dielec. layered struct., magnetostatic volume wave propag. 78−95426
YIG film, dielec. layered struct., magnetostatic bulk wave power flow and energy distrib. 80−34610
YIG film, domain struct., influence of planar anisotropy 79−78472
YIG film, ferrimag., determ. of freq. of magnetostatic modes 77−36104
YIG, film, LPE, annealing-induced relief of compressive misfit strain 78−2386
YIG film, low field microwave excitations of mag. domain walls 79−78456

yttrium compounds continued
YIG, film, magnetoelastic Lamb wave velocity changes, theory 78−91923
YIG, film, magnetostatic surface wave refl. at shallow groove 78−19283
YIG film, magnetostatic surface wave propag. 79−4661
YIG film, magnetostatic forward volume wave excitation 79−82775
YIG film, magnetostatic surface wave propag. in nonuniform mag. field, anal. 80−20437
YIG film, magnetostatic surface and forward volume wave oblique incident at shallow groove 80−34704
YIG film, magnetostatic surface wave propag. in nonuniform mag. field 80−80574
YIG film, microwave generation and manipulation of magnetic domains 78−39378
YIG film, oblique incidence of magnetostatic waves on metallic grating 78−19229
YIG film, on GdGaG, mag. excitations, diffusion layer effects 78−31112
YIG film, periodically corrugated, insertion loss, reson. linewidth effect 80−80614
YIG, film, photoinduced mag. surface anisotropy spin wave reson. 77−4560
YIG film, shallow groove effect on magnetostatic forward volume wave reflection 78−84473
YIG, film, spin wave reson., complex mag. surface energies 77−4561
YIG, film, spin-wave spectra in terms of mag. boundary conditions 79−78532
YIG film, stripe domain struct. with two periods 79−69706
YIG film, surface effects in spin wave reson. 77−16182
YIG film, surface pinning parameter, symm. props. 79−28570
YIG film, tangentially magnetised, magnetoelastic Lamb wave propag. 79−82856
YIG film filter, theory of characts. 79−42808
YIG film tangentially magnetised, magnetostatic surface wave excitation 80−29586
YIG, film waveguide, magnetooptical effects 77−3650
YIG film-dielectric layer-conductor struct., magnetostatic bulk wave propag. dispersion relations 80−54925
YIG films, deposition by DC sputtering from two facing targets 78−31341
YIG films, MCD spectrum 79−28722
YIG, floating zone method growth, interface shapes 80−60775
YIG, forced magneto-optical rot. 79−61347
YIG, Ga and Al substituted, single cryst. growth by the travelling solvent float zone technique 79−43138
YIG, garnet, high temp. solns., shear viscosity meas., rel. to LPE 80−10697
YIG, growth from molten soln., improved crucible shapes *(German)* 77−1800
YIG, heat transport by magnons, effect of magnon-phonon thermal relax., calc. 77−39705
YIG, Hf response and thermodynamic props. *(Russian)* 78−72338
YIG, high field magneto-optical study 77−85749
YIG, homogeneous crit. relax. in dipole region *(Russian)* 78−10782
YIG, homogeneous mag. relax. near phase transition *(Russian)* 78−23351
YIG, hyperfine interaction determ. from Mossbauer spectra in applied mag. field 77−28497
YIG, hyperfine parameters, Huckel theory calc. 80−39542
YIG, impurity absorpt. spectra to 5.5 eV 77−20892
YIG, in multilayer planar structure, magnetostatic propag. 77−16120
YIG, influence of X-ray radiation on mag. props. 77−8337
YIG, interaction force between 180° domain wall and edge dislocation 77−28408
YIG, intrinsic microwave emission, coupling to waveguide system, magnon system cooling 77−24912
YIG, LPE and CVD films, boundary effects, spin wave reson. meas. 79−78447
YIG, LPE film, magnetostatic wave to exchange resonance coupling 79−82774
YIG, LPE film, non-Ohmic currents 78−68099
YIG LPE film, optical waveguide in mag. strip domains *(French)* 77−83979
YIG, LPE grown, FMR linewidth, Pb incorporation effects 77−8407
YIG, La- and Ga-substituted, inhomogeneous epitaxial films, spin wave reson. 79−99773
YIG, light diffr. by banded domain struct. *(Russian)* 78−15150
YIG, light scatt. by parametric spin waves with longit. pumping *(Russian)* 78−43648
YIG, localised high-Q ferromag. reson. in nonuniform mag. fields 77−85575
YIG, MCD meas. by retardation modulation technique 80−16014
YIG, MW dielectric losses, causes and reduction *(Chinese)* 80−75930
YIG, mag. and magneto-optic props., temp. and exchange field depend. 77−24824
YIG, mag. domain walls, Lorentz microscopy 79−91249
YIG, mag. linear double refr., two-sublattice model *(Russian)* 79−28728
YIG magnetic bubble domain grating, light diffr. *(German)* 79−95737
YIG, magnetic domain wall motion in high drive fields 80−65955
YIG, magnetic relaxation phenomena 79−99776
YIG, magnetisation density, polarized neutron expts. 78−52215
YIG, magnetised in raised cosine profile magnetostatic surface wave propag. 80−2567
YIG, magneto-optical coeffs. induced by elec. and mag. dipole transitons 77−52060
YIG, magneto-optical near UV reflection-spectra, meridional and polar intensity effects *(Russian)* 78−39572
YIG, magneto-optical Kerr effect, reflectivity spectra 80−66157
YIG, magnetocrystalline surface anisotropy energy, one-ion mechanism 79−42756
YIG, magnetocrystalline surface anisotropy energy, one-ion mechanism 79−78362
YIG, magnetoelastic wave dispersion rels. and normal modes 77−55694
YIG, magnetoelastic wave propagation time dispersion reduction 80−75836
YIG, magnetooptical spectra, polar Kerr rotation, dielectric tensor elements spectra 80−40091
YIG, magnetoresistance of bulk and epitaxial films 78−91706
YIG, magnetostatic precession modes, optical investigation 78−19337
YIG magnetostatic surface wave dispersion rel. to mag. saturation diffusion 78−2671

yttrium compounds continued
YIG, magnetostatic volume waves, magnetocrystalline anisotropy effects, group delay 79−78355
YIG, magnetostatic wave linewidth, wave no. depend., mag. relax., rods and films *(Russian)* 78−2667
YIG, magnetostriction meas. with recording rot. field magnetostrictometer 78−12733
YIG, magnon high amplitude collective oscills., double parametric reson. *(Russian)* 77−28451
YIG, monocrystal film growth by chem. transport in closed system 77−77392
YIG monocrystals, echo of magnetoelastic waves 77−55697
YIG, mulitiple mag. layer structures, magnetostatic surfacewave propag. 80−88839
YIG multilayered film, magnetostatic spectrum 78−23350
YIG, Neel point behaviour in stoichiometry vicinity 80−88750
YIG, nonreciprocal attenuation of elastic surface waves 77−55696
YIG, nonreciprocal attenuation of magnetoelastic Rayleigh waves 80−60399
YIG nonreciprocal thin film acoustic device, design, appl. of cct. theory of elastic waveguides 77−85042
YIG, nonstoichiometry and electronic defects, thermogravimetric expts. and anal. of elec. data 78−6050
YIG, normally magnetised disc, reson. modes of magnetostatic waves 77−81015
YIG octa- and tetra-sublattices, anisotropy of effective mag. field at ^{57}Fe *(Russian)* 80−10929
YIG, one-magnon light scatt. with and without compensation temps. 78−31062
YIG, one-magnon Raman scatt., Faraday rot. 80−66156
YIG, open die hot pressing, spin wave and FMR line width 80−89170
YIG, optical detection of scatt. of homogeneous precession of magnetisation by defects 79−69728
YIG, optical spectroscopic exam. of ferromag. reson. *(Russian)* 77−48057
YIG, parallel microwave pumping threshold, RF modulation of mag. field 78−88195
YIG, parametric excitation of spin waves in single-domain and polydomain states 77−12206
YIG, parametrically excited spin waves, spectral density *(Russian)* 79−4667
YIG, parametrically excited reson. magnetostatic modes of spin, elastic and magnetoelastic waves 79−56523
YIG, parametrically excited wave discrete structure obs., light diffr. and modulation *(Russian)* 79−95650
YIG periodic film layer, magnetostatic surface wave propag. 80−2607
YIG, permeability, domain rot. and wall displacement contrib. 80−80564
YIG, permeability spectra rel. to microstruct. 80−71100
YIG, perpendicular pumping, spin wave instabilities, laser probing 77−43889
YIG, phonon inelastic scatt. by magnons 77−20570
YIG, phonon viscosity effect on dislocation motion 80−24450
YIG, photomagnetic effects, irreversible 79−99719
YIG, plastic deform. and mag. props 77−40087
YIG, plastically deformed, TEM, dislocation Burgers vectors 77−11557
YIG, polar Kerr rotation spectra, 2-5.7 eV, comparative study with $Li_{0.5}Fe_{2.5}O_4$ 79−47413
YIG, polarised neutron diffr. and extinction models 77−1046
YIG, polarised neutron expts., extinction models 80−24322
YIG, polariser neutron study of covalency effects 80−2552
YIG, polycryst., initial and reversible parallel susceptibilities, hydrostatic press. effects 80−75835
YIG, polycrystalline, microwave relax. at low power levels 78−39409
YIG, polycrystalline, microwave relax. at high power levels 79−61231
YIG, porous, parallel-pump spin-wave instability temp. depend. 79−78531
YIG, porous and fine grain polycrystalline, temp. depend. of effective linewidth 77−85574
YIG, precipitation of Fe_3O_4 78−84815
YIG, prep. and imperfections, rel. to props. 79−100031
YIG, press. depend. of effective mag. fields on ^{57}Fe nuclei 78−52383
YIG, pseudo-surface magnetoelastic waves, damping *(Russian)* 78−23320
YIG, pure and Ga-substituted diffuse refl. and thermorefl. spectra near Curie point 80−40131
YIG, refr. index, isotropic exchange and higher-order anisotropic mag. contribs. 77−69808
YIG, relax. after spin wave excitation in ferrite *(Russian)* 79−19783
YIG, resonant phonon-magnon scatt., phonon spectroscopy obs. 79−65150
YIG rod, inhomogeneously magnetised, propag. characts. of magnetoelastic wave 78−15006
YIG, SAW transducers, approximate theory 79−68533
YIG sandwiched between grounded dielectric layers, magnetostatic bulk wave propagation 80−60380
YIG, second group of spin waves, parametric excitation 79−99694
YIG, Si substituted, spin reorientation, Mossbauer spectroscopy obs. 80−44989
YIG, single cryst., high temp. dislocation mobility 79−19255
YIG, single cryst., Neel lines, Faraday effect obs. 78−64216
YIG, single cryst., spin-wave linewidth influence on spin wave propagation direction for parallel pumping 79−1660
YIG, single cryst. film, pinning effects on magnetostatic modes 78−31111
YIG, single cryst. growth by floating zone method 78−19656
YIG, single cryst. growth from high temp. soln. 78−31315
YIG single crystal growth in Na_2O-B_2O_3 flux system in air 77−81207
YIG, single crystal., domain wall struct. and cryst. orientation 77−16104
YIG single crystals, liq. flux growth, obs. 80−66416
YIG, single crysts. grown by floating zone method, quality eval. of etching and optical microscopy, ferromag. resonance linewidth meas. 79−19990
YIG slab, corrugated, magnetostatic surface-wave propagation 78−19228
YIG slab, magnetostatic forward vol. waves delay characts. 79−99691
YIG slab, partially magnetised, expt. obs. of group delay of magnetostatic waves 80−7100
YIG, sound vel., temp. depend., phonon scatt. processes 80−96598
YIG spheres, anomalously low saturation threshold of magnetostatic modes 79−69729
YIG, spin and magnetoelastic waves on longit. mag. pumping, optical obs. *(Russian)* 80−29727

yttrium compounds continued
YIG, spin struct. obs. by Faraday rotation expts. in fields up to 200 T 77 69809
YIG, spin wave and magnetostatic wave echo 77−43887
YIG, spin wave instability, parametrically excited spin waves distribs. *(Russian)* 79−38317
YIG, spin wave instability theory 79−73825
YIG, spin wave parametric excitation threshold at low temp. 80−97084
YIG, spin waves, nonlinear spectroscopy studies 79−99696
YIG, spin-wave and magnetostatic mode attenuation, double-pulse echo method 79−82874
YIG, spinwave dispersion curves 78−19230
YIG, subsidiary absorpt. spin-wave instability threshold, anomalous struct. 80−34776
YIG, substituted, effect of electron bombardment on mag. and elec. props. 79−42103
YIG, substituted, magnetite nucleation in transitional zone, ionic process, lattice imaging 80−107424
YIG substituted film waveguides, TE→TM mode conversions 78−66904
YIG substrate magnetoacoustic modes, meander-line excitation 77−20670
YIG substrates, magnetoelastic surface waves, magnetostatic reson. anal. 80−20441
YIG, superexchange and applied field depend. of Faraday rot. induced by elec. dipole transitions 77−36206
YIG, surface spin waves, microscopic theory, mag. field effects 78−35044
YIG target and DC glow discharge sputtered film compositions compared 77−55886
YIG, thermal attenuation of US waves, 500-1000 MHz 77−84854
YIG, thermodynamic props. 77−36078
YIG, thermomag. anal. by electron diffr. 80−108035
YIG, thermoreflectance spectra 80−20616
YIG, thick epilayer, unpinned magnetostatic modes 77−63290
YIG, thin ferromagnetic resonators, intermodulation distortion, spin waves 78−48048
YIG, thin ferromagnetic film, exchange interaction constant, from paramag. resonance spectra of spin waves 79−42811
YIG, thin film, Brillouin scattering from spin waves 80−65843
YIG thin film, metal film effect on mag. boundary conditions, spin wave reson. obs. 79−78527
YIG thin film gyromag. waveguide, on GGG substrate, optical propag. props. Faraday effect 80−74513
YIG, thin films, magnetostatic modes at Q-band freq. 80−65828
YIG, transparent, domain struct. realignment in external mag. field 78−10739
YIG, universal hysteresis loop for soft ferrimag. polycryst. 77−69620
YIG, vitreous electric-field-gradient distrib., Mossbauer quadrupole splitting meas. 80−75901
YIG: Ca,(Mg), films, microwave losses induced by Fe^{4+} ions, ferromag. reson. study 79−1715
YIG: Ca^{2+} epitaxial films, Fe^{4+} centres, MCD, optical absorpt., and thermoelectric power meas. 78−95595
YIG: Si single crysts., mag. props. 80−107981
YIG:$^{154}Gd^{3+}$, hyperfine interactions, PAC 77−43909
YIG:B,Pb, IR spectrum, localised modes, rel. to impurities and O vacancies 80−50377
YIG:Be^{2+} LPE film, microwave relaxation props. 79−65741
YIG:Ca, epilayer, reversible oxidation, ferromag. reson. 78−76781
YIG:Ca, O diffusion depend. on defect conc. 78−67857
YIG:Ca, oxidising effects of high temp. annealing in reducing atmosphere 80−66696
YIG:Ca eddy current damping 80−39876
YIG:Ca film, strong mag. reson. of Fe^{4+} 78−48047
YIG:Ca films, rapid O diffusion at 25 to 250°C 77−85120
YIG:Co film, influence of stress induced anisotropy on domain struct. 80−100605
YIG:Co LPE films, with rectangular bubble domains, prep. and props. 79−82848
YIG:Co^{2+}, mag. permeability, illumination and impurity depend. *(Russian)* 78−64220
YIG:Eu,Pb, bubble domain film, magnetocrystalline anisotropy coeff. reduction, by Pb addition 79−11329
YIG:Fe^{2+}, magnetocrystalline anisotropy, effect of high hydrostatic press. 77−43831
YIG:Fe^{2+}, magnetostriction const. temp. depend., ferromag. reson. meas. 77−40103
YIG:Ga, crystal growth from high temp. soln., induced striation method 77−1802
YIG:Ga(Sc), magneto-optical Kerr effect, reflectivity spectra 80−66157
YIG:Gd, Ga, optical probing of magnetoelastic Rayleigh waves 79−78495
YIG:Gd^{3+}, mag. relax., hyperfine field interactions, PAC expts. 78−27128
YIG:Ho(Er), magnetisation anomalies in strong mag. fields *(Russian)* 77−43854
YIG:Ir, Ir on tetrahedral sites, contrib. to mag. anisotropy, optical absorpt. meas. 77−69867
YIG:La,Ga, film, LPE-grown, Ga incorporation, depend. of magnetisation on growth rate 80−84627
YIG:La,Ga film, uniaxial anisotropy, variation along growth direction 77−28416
YIG:La film, for microwave applics., growth and ferromag. reson. meas. 78−3008
YIG:La(Ga) films, ferromagnetic resonance, ion implantation effect 80−97145
YIG:Nb, tetrahedral Fe^{2+} detect. by induced anisotropy ang. variation 79−11311
YIG:Pb, valence of Pb in Fe-garnets 77−47480
YIG:Pb(Si) film, (111) LPE, in-plane mag. anisotropy and ferromag. reson. meas. 78−2706
YIG:Pr^{3+} influence of Pr^{3+} ions on spin-wave damping 79−28625
YIG:Ru, optical absorpt. and MCD obs. of Ru^{4+} site occupancy 80−71456
YIG:Ru(Ru,Zn), mag. anisotropy 77−69544
YIG:Si, EM wave effects on mag. and optical props., lecture 78−27031
YIG:Si, enhanced photoinduced mag. circular and linear dichroism 77−52053
YIG:Si, photo-induced low freq. mag. permeab. *(Russian)* 78−39368
YIG:Si, relative Fe^{2+} ion conc. depend. 77−48150

yttrium compounds continued
YIG:Si, thermomagnetic processing and illum. effects on mag. props. *(Russian)* 77−8410
YIG:Si single crystals, liq. flux growth, obs. 80−66416
YIG:Si^{4+}, mag. permeability, illumination and impurity depend. *(Russian)* 78−64220
YIG:Si(Ge), effects of nontrigonal cryst. field on spectroscopic props. of Fe^{2+} ions 80−92864
YIG:Si(Ge), Fe^{2+} spectroscopic props., nontrigonal cryst. field effects 80−44553
YIG:Sm^{3+}, mag. anisotropy, effect of Sm^{3+} ferromag. reson. study 80−80615
YIG:Sn, IR absorpt. and MCD 78−19447
YIG:Tb garnet, Faraday effect in strong mag. field *(Russian)* 80−100651
YIG:V, mag. anisotropy and magnetostriction, effect of V 78−27029
YIG:Yb, magnetoelastic coupling of Yb ions, ferromag. reson. meas. 77−69698
YIG:Zr, near IR absorpt. and magnetic circular dichroism 80−60580
YIG/n-GaAs layered structure, magnetostatic surface wave amplification 78−88107
YIG-dielectric layered structure, magnetostatic surface wave propag., finite width effects 77−20668
YIG-Ge layer structure, amplification of bulk magnetostatic waves 78−34972
YIG-Ge layered struct., anisotropy of EMF under nonlinear ferromag. reson. conditions 77−8417
YIG-Ge structure, profile and position of reson. galvanomag. effect curve 78−72242
YIG-InSb system, surface magnetostatic wave interaction with drift electrons *(Russian)* 77−12185
YIG-LiF film system, ATR, substrate surface polaritons reson. effect *(Russian)* 77−32384
YIG-rare earth garnet solid solutions, magnetisation temp. depend. calcs. 80−20388
YIG-semiconductor coupled system, magnetostatic surface wave amplification, energy anal. 77−55699
YIG-semiconductor coupled system, magnetostatic surface wave amplification, ferromag. loss 77−85434
YIG-semiconductor-dielectric-metal layered structure, amplification characts. of magnetostatic surfaces waves 78−23321
YIGaG, magnetoelastic wave propag. time and total loss, freq. depend. *(Russian)* 77−43859
YIr_4B_4, $NdCo_4B_4$ type struct., mag. behaviour 80−20375
$Y_{1-x}LaAlO_3:Ho^{3+}$, stimulated emission of Ho^{3+} ions 77−81126
$(YLaBi)_3(FeGa)_5O_{12}$, pure and In^{3+} doped, near IR absorpt. and Faraday rot. 78−95580
$Y_{2.85}La_{0.15}Fe_{3.75}Ga_{1.25}O_{12}$ epitaxial film, magnetostriction consts., microwave reson. meas. 77−24716
$Y_{2.85}La_{0.15}Fe_{3.75}Ga_{1.25}O_{12}$, inhomogeneous bubble film, spin wave reson. 77−32265
$Y_{2.85}La_{0.15}Fe_{3.75}Ga_{1.25}O_{12}$ epitaxial film, spin wave reson. spectrum 77−69703
$Y_{2.85}La_{0.15}Fe_{3.75}Ga_{1.25}O_{12}$ LPE films, ion implantation effect on spin waves 80−71124
$Y_{2.85}La_{0.15}Fe_{3.85}Ga_{1.15}O_{12}$ garnet, mag. props., ion implantation effect, Mossbauer study 80−97166
$Y_{3-x}La_xFe_{5-y}Ga_yO_{12}$, mag. bubble film, low freq. ferrimag. reson. 78−31110
$Y_{3-x}La_xFe_{5-y}Ga_yO_{12}$ film, horizontally dipped LPE grown, FMR, anisotropy field obs. 79−78449
$Y_{3-y}La_yFe_{5-x}Ga_xO_{12}$, garnet film, radial oscillation of bubble lattice 79−73787
$Y_{3-x}La_xFe_5O_{12}$, mag. props. rel. to ionic struct. 80−75756
$Y_{1-x}LaScO_3:Ho^{3+}$, stimulated emission of Ho^{3+} ions 77−81126
$YLiF_4$, rare earth doped, intra- and inter-ionic multiphonon transitions 80−34973
$YLiF_4$:rare earth, spin-lattice relax. and nuclear polarisation *(Russian)* 79−8049
$Y_xLu_{1-x}Ir_4B_4$, supercond., magnetism and metastability 80−29501
$(YLuSmCa)_3(FeGe)_5O_{12}$ garnet film, bubble domain expansion, fuzzy wall struct. 80−71128
$(YLuSmCa)_3(GeFe)_5O_{12}$ bubble garnet film, coercivity 79−78459
$(YLuSmCa)_3(GeFe)_5O_{12}$ garnet films, bubble expansion saturation vel., sampling optical photography 80−75820
$(Y_xLu_{1-x})_2V_2O_7$ semiconducting ferromag. pyrochlore, mag. props. 80−29547
$Y_2M_3(BO_3)_4$, M=Ba,Ca, thin-film capacitor mat. synthesis and props. 77−48128
$YMnO_3$, solid phase synthesis mechanism 80−21268
Y_2MoO_5, cryst. struct., IR spectra, elec. and mag. props. 80−33954
Y_2MoO_6, growth from soln., struct., props. 77−28705
$Y_2Mo_2O_7$, pyrochlore compounds, sp. heat meas. 80−107438
YMo_6X_8 (X=S, Se), supercond., sp. ht., 1 to 14K 79−51720
YN, and YN-UN, decomp. press.-temp. relations 78−52780
$YNO_3(Se_2O_5).3H_2O$, X-ray cryst. struct. determ. 80−1972
$YNbTiO_6:Eu^{3+}$ emission under UV excitation 78−6770
YNi_5Si_3, X-ray crystal struct. determ. 77−7701
YO, $A^2\Pi$-$X^2\Sigma^+$ photoluminesc. 78−55195
YO, $A^2\Pi-X^2\Sigma^+$ and $B^2\Sigma^+-X^2\Sigma^+$ systems, Fourier transform spectroscopy anal. 79−22718
YO, absorption spectra, in flame, optogalvanic spectrosc. obs. 79−18202
YO, chemiluminesc. from Sc+O_2 reaction 77−1927
YO, fluoresc. spectra, atom+ROH O atom abstraction reactions, fluoresc. study 78−48643
YO, spectra, 4500-6900 Å, mol. consts. 78−50551
YO, temp. depend. of chemilum. reactions, activation energies for excited state form. 78−66818
$YO_{1.5}$-PrO_x, phase relns. and electrophys. props. of solid solutions 78−23686
YO_x-ZrO_2, YO_x-rich, phase equilibria 77−21117
Y_2O, Y_2O_2, atomisation energies and stand. ht. of formation 77−54622
Y_2O_3 and double oxides, photon multiplication and secondary electron-hole pairs generation *(Russian)* 80−66262
Y_2O_3, autolocalised excitons *(Russian)* 79−19523
Y_2O_3 barrier layer, for good high-temp. stability, BN in contact with W 79−70194
Y_2O_3 binder, sintering 79−24469
Y_2O_3, calorimetric meas. of enthalpy, heat of fusion, heat of high temp. phase transition 77−28020

yttrium compounds continued
- Y_2O_3 capillary discharge plasma, temp., radiation screening elimination 80−64682
- Y_2O_3 cathodes, thermionic emission, 1000-1800K 77−48302
- Y_2O_3 ceramic, elec. resistance rel. to density 79−82594
- Y_2O_3, ceramic structs., thin-walled fabrication, plasma spraying technique 79−33978
- Y_2O_3 ceramics, strength under mech. and thermal actions 80−97554
- Y_2O_3 coated Ag mirror for the 0.5 to 14 μm region 80−87456
- Y_2O_3, coating for graphite crucible used in melting U 77−32712
- Y_2O_3, cooling rate in melt-growth effect on struct. perfection 77−85925
- Y_2O_3, corrosion resist. in fused Li rel. to phase and microstruct. changes 77−44378
- Y_2O_3, crucible material, Cu-Nb alloy prep. 80−84879
- Y_2O_3, crystal growth by floating zone method, using thermal imaging system 77−77373
- Y_2O_3, digital pyrometry in solar furnace *(Japanese)* 78−32821
- Y_2O_3, dislocation and plasticity dissociation 80−107247
- Y_2O_3, dislocation density depend. on crystal pulling rate 77−81210
- Y_2O_3, effect of roasting temp. of $Y_2(C_2O_4)_3$ on crushing, compressibility, sintering props. 77−8790
- Y_2O_3, effect on elec. cond. of fused CaF_2 78−43157
- Y_2O_3, elec. cond. components 77−85272
- Y_2O_3, electrical conductivity of mono- and poly-crystalline substances 77−20322
- Y_2O_3, electron and hole migration distances determ. 78−19526
- Y_2O_3, electron irrad., dislocations *(French)* 80−2076
- Y_2O_3, electronic excitations, charact. energy loss meas. up to 50 eV 80−60723
- Y_2O_3, film, anodic glow in Y-Y_2O_3-electrolyte system 77−12447
- Y_2O_3 film, struct. and elec. resist., electron diffr. meas. 78−87888
- Y_2O_3 film in Y-Y_2O_3-metal junction, electroforming and conduction 78−26969
- Y_2O_3 film in Y-Y_2O_3-Au junction, defect struct. and local conduction 78−26970
- Y_2O_3, fission and phase transition enthalpies 79−99299
- Y_2O_3, formation and changes in point defects, EPR, optical transitions and thermolum. spectra 78−2118
- Y_2O_3 fused single crystals, struct. 80−19804
- Y_2O_3, grain size depend. of fracture energy, SEM study 79−34130
- Y_2O_3, high temp. sintering *(Japanese)* 77−55928
- Y_2O_3, hot cast ceramic, prod., used as dielectric 78−11181
- Y_2O_3, hot pressing charact. 78−27456
- Y_2O_3 hydroxy salt binder phase form., X-ray, thermal anal. obs. 79−28999
- Y_2O_3, in MIM struct., electroforming props. 80−65705
- Y_2O_3, interband, collective and atomic (p,d) excitations, Z-160 eV, fast EELS 80−93443
- Y_2O_3 laser coating, UV damage obs. 80−33056
- Y_2O_3, laser heated pellet, melting point determ., secondary melting point standard 78−37011
- Y_2O_3, liq. and solid phase elec. cond., high temp. meas. 80−84468
- Y_2O_3, M-series emission bands *(Russian)* 77−81177
- Y_2O_3, Mandelshtam-Brillouin spectra, transverse phonon contrib., elastic and photoelastic consts. 77−81115
- Y_2O_3, nonstoichiometry study, thermal emission of electrons 80−108317
- Y_2O_3, photoabsorpt. spectra, at ionisation, band struct. mechanisms, electron energy loss investig. 77−24909
- Y_2O_3, plastic deform. tests, under compression, creep testing, exam. 78−48458
- Y_2O_3, plastically deformed, dislocations obs. by TEM *(French)* 78−51545
- Y_2O_3, plastically deformed monocryst., HV electron microscopy obs. of dislocation config. *(French)* 79−55747
- Y_2O_3, plasticity, microhardness testing, indentation, plastic deform. temp. depend. *(French)* 78−56713
- Y_2O_3, polycrystalline, high temp. O ion bombard., TEM microstruct. investig. 77−27923
- Y_2O_3 powder, active, sintering 80−20870
- Y_2O_3, prep. of transparent ceramic, exam. of light transmission preps. 79−20013
- Y_2O_3 protected Al mirror, high refl. 8 to 12 μm, normal to high incident angles 78−79090
- Y_2O_3, rare earth activated, cathodolum., use of internal reference 77−44071
- Y_2O_3 reactions with Cr surface, IR spectroscopy 79−100297
- Y_2O_3, reduction in Li vapour, 1800-2500K, thermodynamics 77−90595
- Y_2O_3, reflection spectra, Kramers-Kronig anal. of optical charact. 79−8161
- Y_2O_3, secondary ref. stand., MP 77−45821
- Y_2O_3, secondary standard investigation, melting point *(French)* 78−41271
- Y_2O_3 sintered bodies, thermal cond. and diffusivity *(Japanese)* 79−55944
- Y_2O_3 sintered body, blackness study thermoluminescence anal. *(Japanese)* 78−23541
- Y_2O_3 sintered body, luminous pipe of high press. Na discharge lamp, corrosion resistivity *(Japanese)* 78−19915
- Y_2O_3 sintered pieces, optical transmittance 80−40561
- Y_2O_3 sintered-ceramic separator plate development, LiAl/LiCl-KCl/FeS battery applications 80−61321
- Y_2O_3 sintering activator, effect on α-Al_2O_3 mineralisation, alumina heat treatment 80−89186
- Y_2O_3, sintering of granular masses of ZrO_2, stabilisation 78−44064
- Y_2O_3, specific elec. cond., m.p. to 3200K, activation energy 78−43383
- Y_2O_3 stabilised ZRO_2 and HfO_2 single crystals, optical props., impurities and annealing conditions influence 79−52399
- Y_2O_3 stabilised ZrO_2, ultrafine grained, fabrication and flexural strength 77−1829
- Y_2O_3 stabilised ZrO_2, synthesis and eval. for H_2 prod. 77−85976
- Y_2O_3 stabilized ZrO_2, thermal diffusivity meas. 77−28021
- Y_2O_3 stabilized ZrO_2 heat-resistant granular artifacts, procedure for making 80−35148
- Y_2O_3, stacking fault energy calc. *(French)* 77−62549
- Y_2O_3, strength-controlling fracture energy depend. on flaw-size to grain-size ratio 80−81152
- Y_2O_3, synthesis at high-press and temp., supercond. 80−2513
- Y_2O_3, thermal expansion, 500-1800°C, X-ray diffr. 77−35723
- Y_2O_3, thermoluminesc., in H_2O vap. atm., temp. depend., time decay *(Russian)* 77−44074
- Y_2O_3, translucent ceramic, prep. effect on struct. and props. 79−87601

yttrium compounds continued
- Y_2O_3 transparent ceramic, transmittance, grain size and dopant effects *(Japanese)* 80−19083
- Y_2O_3, U, C interactions, thermal anal. 78−85154
- Y_2O_3, US comminution of refractory compound powders 78−23656
- Y_2O_3, vacuum UV luminesc., excitation by X-ray synchrotron radiation 79−8168
- Y_2O_3:Eu, cathodoluminesc. investig., appl. to cathode ray tube screening 80−108282
- Y_2O_3:Eu, fluoresc., cathodoluminesc. and thermal quenching 79−47488
- Y_2O_3:Eu, surface luminesc. centres excitation charact. 78−52560
- Y_2O_3:Eu sintered slice, DC electroluminesc., impact excitation 79−47522
- Y_2O_3:Eu^{3+}, absorpt. spectra, fluoresc., electron beam excitation 78−92093
- Y_2O_3:Eu^{3+}, cubic, laser-induced polarised fluoresc., Stark levels and cryst. field parameters 79−95838
- Y_2O_3:Eu^{3+}, quantum yield in candoluminescence process by low energy H^+ ion bombard. 79−65930
- Y_2O_3:Eu^{3+}(Sm^{3+}), rel. band intensities in luminesc. spectra *(Russian)* 77−48238
- Y_2O_3:Eu(Tb)(Tm), powder layer, electrolum., comparison with La_2O_3 and Y_2O_2S 77−20927
- Y_2O_3:Fe^{3+}, EPR obs. of non-cubic phase 78−19316
- Y_2O_3:HfO_2, elec. cond. and O ion mobility 80−34490
- Y_2O_3:Nd^{3+}, absorpt. spectra, hypersensitivity of $^4I_{9/2}$ to $^4G_{5/2}$ $^2G_{7/2}$ transition 80−97309
- Y_2O_3:Tb^{3+}(Dy^{3+}), conc. quenching of X-ray and UV-excited luminesc. *(Russian)* 77−55829
- Y_2O_3:ThO_2, IR absorpt., 2-4 μm 77−55805
- Y_2O_3:Zr^{3+}, ESR spectrum 79−69716
- Y_2O_3:Zr^{3+}, F-centre charge state, ESR and thermally stimulated luminesc. obs. 80−60418
- Y_2O_3-2Y_2O_3.Al_2O_3 two-phase refractory, fracture 80−21080
- Y_2O_3-Al_2O_3, thin film, electron diffraction exam. of phase transformations *(Russian)* 79−34025
- Y_2O_3-AlN, creep 77−21235
- Y_2O_3-AlN-SiO_2 oxynitride glasses, elec. props. 80−80267
- Y_2O_3-Fe_2O_3 systems, solid-phase reacts., $Y_3Fe_5O_{12}$ form. 78−44062
- Y_2O_3-Fe_2O_3-Ga_2O_3-PbO-P_2O_5, primary crystallisation regions 77−44222
- Y_2O_3-Gd_2O_3-Nd_2O_3 solution phase diagrams and thermal conductivity *(Russian)* 78−88448
- Y_2O_3-HfO_2(ZrO_2) systems, solid soln. form. mechanisms 79−11579
- Y_2O_3-Lu_2O_3-Eu_2O_3-CaO-GeO_2-Fe_2O_3-PbO-B_2O_3 system, garnet crystn. fields 78−43995
- Y_2O_3-Mn_2O_3, solid-phase reactions 77−48405
- Y_2O_3-Nb_2O_5, solid state reactions, 1275 to 1350°C, electron microscopy, EPMA, X-ray diffr., dilometry *(Japanese)* 78−63883
- Y_2O_3-P_2O_5-M_2O(M′O), (M=alkali metal, M′=alkaline earth), metaphosphate glass phosphors, fluoresc. props., activation conc. effect 80−89058
- Y_2O_3-R_2O_3, (R=La,Nd,Sm,Gd and Dy to Yb), cryst. growth by Verneuil method 77−1803
- Y_2O_3-Sc_2O_3 fused powders, production of ceramics of good thermal strength 77−63607
- Y_2O_3-SiO_2-Al_2O_3 system, composition depend. of refractive index in vitrification region 77−24812
- Y_2O_3-TiB_2, ceramic, production by sintering in vacuo, or hot moulding at 1500°C 78−60629
- Y_2O_3-TiO_2 system, elec. cond. at 700-1000°C 79−78100
- Y_2O_3-ZrO_2 (HfO_2), cubic solid soln., lattice parameters 79−82186
- Y_2O_3-ZrO_2 refractory, sublimation *(Russian)* 78−47513
- Y_2O_3+Li_2O, ionic cond., effects of moisture and LOOH on elec. and struct. props. 79−69283
- Y_2O_3(:Nd) single crystal growth, floating zone method with Xe arc lamp imaging furnace 80−60777
- YOCl:Yb,Er, anti-Stokes luminesc., temp. depend. *(Russian)* 78−6764
- YOCl:Yb^{3+}, Er^{3+}, anti-Stokes luminesc., 4.2 to 293K 77−59609
- YOF, band structure formation, valence band 79−33232
- YOF, electronic stuct. calcs. from XPS and X-ray emission spectra 80−35056
- YOF, trigonal, NMR of F^{19} to detect paired formations 79−14788
- YOF:Eu^{3+}(Sm^{3+}), rel. band intensities in luminesc. spectra *(Russian)* 77−48238
- YOF:Tb^{3+}, conc. quenching of X-ray and UV-excited luminesc. *(Russian)* 77−55829
- YOF-YF_3, high pressure phase transitions 80−55368
- $Y(OH)_3$, dynamical effects of interaction between 4f electrons and optical phonons 80−108196
- $Y(OH)_3$:Er^{3+}, g-values and hyperfine interaction parameters, calc. for Er^{3+} 79−15123
- $Y(OH)_3$:Tb^{3+}, excited state relax., ns time resolved spectroscopy 77−61140
- $Y(OH)_3$:Tb^{3+}, spin-lattice relax. at high gap energies using pulsed tunable dye laser 77−48047
- $Y(OH)_3$-α-FeOOH, physicochem. props. rel. to growth of $Y_3Fe_5O_{12}$ 77−40418
- $Y(OH)CO_3$, ancylite like phase, hydrothermal cryst. growth *(French)* 80−108340
- $YOHCO_3$, cryst. struct., X-ray diffr. meas. 77−4079
- $YOHCO_3$, synthesis of rare earth carbonates under hydrothermal conditions 78−72714
- Y_2O_2S, compact specimen prep. 77−85951
- Y_2O_2S:Eu, high press. effect on luminesc. efficiency and lifetime, charge transfer absorpt. 80−66266
- Y_2O_2S:Eu, phosphor, temp. meas. by line shift method 77−13750
- Y_2O_2S:Eu phosphor, luminescence saturation effects due to N_2 laser and cathode-ray excitation 80−40151
- Y_2O_2S:Eu phosphor, particles of different sizes, prep. by flux method 77−44140
- Y_2O_2S:Eu^{3+}, luminesc. props., charge transfer effects 78−15214
- Y_2O_2S:Eu^{3+}, luminesc., excitation spectra, cooperative phonon sidebands 79−33771
- Y_2O_2S:Eu(Tb)(Tm), powder layer, electrolum., comparison with La_2O_3 and Y_2O_3 77−20927
- Y_2O_2S:Ho, Yb, two photon anti-Stokes effect excited by 2 μm radiation 78−50852
- Y_2O_2S:Tb, cathodoluminesc. efficiency at low electron energy 78−6790
- Y_2O_2S:Tb, cathodoluminesc., nonlinear depend. on activator concs. 79−8190
- Y_2O_2S:Tb, cathodoluminesc. efficiency changes due to processing, XPS meas. of surface changes 79−99951

yttrium compounds continued
Y_2O_2S:Tb_3 recomb. processes and emission spectra *(Russian)* 78−6797
Y_2O_2S:Tb^{3+},Eu^{3+}, energy transfer mechanism 78−6793
Y_2O_2S:Tb^{3+} (Eu^{3+}) temp. and viscosity depend. of colour coords. 80−40149
Y_2O_2S:Tb^{3+} (Pr^{3+}), enhancement of cathodolum. efficiency 79−69891
Y_2O_2S:Yb^{3+}, charge transfer type luminesc. 79−33797
Y_2O_2S:Yb^{3+},Ho^{3+}, anti-Stokes emission band assignments, energy transfer mechanism 77−40277
Y_2O5d3 films, preparation, electrophys. props. in metal-oxide-metal structs. 77−24956
$Y_2O_3.2SiO_2.Al_2O_3$ glass, thermal stability 77−44502
YP(As)(Sb)(Bi), coupling between Gd 4f electrons and conduction electrons, EPR linewidth 78−52347
$Y(PO_3)_2$, vitreous, microhardness 80−25864
YPO_4, cryst., IR spectra, complex anions internal vibrs. resonance splitting 80−34907
YPO_4 phosphor, ionisation of capture centres, thermolum. spectra 80−11487
YPO_4:Ce(Tb), luminesc. and optical spectra 79−65921
YPO_4:Eu^{3+}, vac. UV luminesc.-excitation spectra 77−85774
YPO_4:Gd^{3+}, mag. susceptibility, cryst. field calc. 78−76035
YPO_4:Gd^{3+}, zircon struct. EPR investig., rel. to radiation resistance 80−97138
YPO_4:Pb^{3+}, EPR, hyperfine interactions 80−108050
YPO_4:Yb^{3+}, charge transfer type luminesc. 78−64392
YPO_4:Yb^{3+}, charge transfer type luminesc. 79−33797
YPO_4-Cr_2O_3, system, oxyorthophosphates form. 79−78942
YPO_4-$Pb_2P_2O_7$, solubility curves for high temp.-melts for growth of single crysts. 78−95687
YPO_4-Y_2O_3 system, oxyorthophosphates form. 79−78942
$YP_{0.99}V_{0.01}O_4$, luminesc. spectra in visible region, vanadate group 78−43921
$Y_xPb_{1\pm x}Mo_{6+y}S_8$, sputtered supercond. props. 80−50019
YPo, X-ray struct. anal., FCC struct. and unit cell const. 77−15363
$Y_{2.5}Pr_{0.5-x}Ca_xFe_5O_{12}$, magnetic aftereffect exam. 78−23304
$Y_{2.8}Pr_{0.2}Fe_5O_{12}$, magneto-optical props. 78−72489
Y_3RB_7 and analogues, rare earth, cryst. struct. *(Ukrainian)* 77−31642
YRBiFe garnets, epitaxial films, R=Gd+Yb, Faraday effect and phys. props. 77−69928
$(YRBi)_3(FeAl)_5O_{12}$ films, R=Gd, Yb, Faraday effect in transverse mag. field, orientation depend. 80−88971
$Y_{1-x-y}R_xEr_yAlO_3$, $Y_{1-x-y}R_xEr_yScO_3$, stimulated emission of Er^{3+} ions 78−6705
$(Y_{1-x}R_x)_3Fe_5O_{12}$, photoinduced decrease in permeability, 77K 77−85497
$Y(ReO_4)_3.4H_2O$, ^{187}Re HQR freq. temp. depend. 80−25245
YRh, gaseous, dissociation energies, high temp. mass spectrometric determ. 80−93790
YRh_4B supercond., re-entrant magnetism, energy band calc. 78−52140
YRh_4B_4, cryst. struct., X-ray diffr. 77−89423
YRh_4B_4, high supercond. transition temp. 77−89893
YRh_4B_4, NMR and sp. ht. in supercond. and mag. ordered phases 80−7037
YRh_4B_4, supercond., anomalous cond.-electron polaris. 80−25047
YRh_4B_4, supercond., electronic struct. and reentrant magnetism 78−10340
$Y(Rh_{0.85}Ru_{0.15})_4B_4$, mag. ordering and supercond. 78−14861
$YS_{1.5}Ru_2$, Mn_5C_2-type struct., X-ray cryst. struct. determ. 80−96483
$Y_2Ru_2O_7$, pyrochlore compounds, sp. heat meas. 80−107438
YS, $A^2\Pi$-$X^2\Sigma$ and $B^2\Sigma$-X^2Sigma transitions vibr. anal. and B-X(0,) band rot. anal. 79−31537
YS, band struct. and X-ray emission spectra, APW and Xα calc. 80−70605
YS, electronic instability and phonon softening, APW calc. 80−29323
YS, electronic struct., appl. of fast self-consistent cluster calc. for large systems 79−82513
YS, phonon anomalies and electron-lattice coupling 80−39490
YS, soft-mode behaviour in phonon dispersion, inelastic neutron scatt. meas. 78−38807
YS, supercond., phonon anomalies, inelastic neutron scatt. 78−59901
YS, supercond. transition temp. and lattice dynamics 79−56361
YS, superconductor, resonances in generalised susceptibility and phonon anomalies 79−60443
Y_2S_3, elec. cond. and thermoelectric power, p-n transition *(French)* 78−84264
Y_2S_3, polymorphic transforms. on impact compression 77−47575
δ-Y_2S_3:Nd^{3+}, spectroscopic props. from absorpt., photoluminesc. and excitation spectra 80−34968
Y_2S_3-Ga_2S_3 system, phase diag. *(French)* 78−3108
$YSbO_4$, high temp. modifications, cryst. chem. identification X-ray anal. 79−65059
$Y_3Sc_2Al_3O_{12}$:Nd^{3+}, cryst. field parameters calc., exchange charge model 78−47747
YScIG, expitaxial film, magneto-spatial interaction, conversion coeffs. 77−55774
$YScO_3$ dielectric thin films from vaporisation by cathode ray and HF ion-plasma methods 77−77380
$YScO_3$, synthesis and lattice const. 78−30593
Y_3Se_4 powder, prep. and optical props. 77−28771
YSeF, crystal atomic struct. *(French)* 78−10001
YSeF, direct lattice imaging of polytypes 77−4087
YSeF, modulated struct. phenomena, survey 79−95033
YSeF, orthorhombic polytype 140, struct. study *(French)* 80−88102
YSeF, ten-layer polytype 10M, cryst. struct., X-ray diffr. meas. *(French)* 77−47409
$Y_2(SeO_4)_3.8H_2O$, thermal decomp. and IR spectra 80−3319
$Y_x(Si,Al)_{12}(O,N)_{16}$, α'-Sialon ceramics, prep. and characterisation 78−84750
YSi_n, electronic struct., calc. and X-ray obs. *(Russian)* 79−13634
Y_5Si_3, $YSi_{3.56}$ solubility of Re 79−38806
Y_2SiO_5:Ce^{3+}(Nd^{3+})(Er^{3+})(Yb^{3+}), EPR and spin-lattice relax. 80−108063
Y_2SiO_5:Ho^{3+}, single cryst luminesc. and stimulated emission 77−69895
Y_2SiO_5:Nd^{3+}, stimulated emission 77−52135
$Y_6Si_6O_{21}$ in oxidised Si_3O_4, temp. and compositional stability 78−27664
$Y_3Si_2O_8Cl$; Ce phosphor, prep. and luminescence props. 78−52740
$YSiO_3F(Cl)(Br)$, phosphor host, luminesc. and struct. props. 78−48212
YSi_2O_2N, cryst. struct. determ. 77−47427
$Y_{1.62}Sm_{0.21}Lu_{0.27}Cu_{0.9}Ge_{0.9}Fe_{4.1}O_{12}$, implanted bubble garnet, anisotropy profile, FMR study 80−7103

yttrium compounds continued
$(YSmCa)_3(FeGe)_5O_{12}$ mag. bubble garnets, ion implantation induced stress influence on props. 79−91274
YSmCaFeGe, mag. garnet films, segregation of Ca and Ge in LPE growth 80−29959
$(YSmCa)_3(FeGe)_5O_{12}$ LPE films, optimum growth conditions for low coercivity 78−95499
$(YSmCa)_3(FeGe)_5O_{12}$ LPE film, growth and coercivity 79−4707
$(YSmCa)_3(FeGe)_5O_{12}$ films, cc $(YSmLuCa)_3(FeGe)_5O_{12}$ films, mag. bubble props. mag. bubble props. and LPE conditions 79−74107
$(YSmCaLu)_3(FeGe)_5O_{12}$, bubble film inhomogeneity, spin wave reson. meas. 80−44439
$Y_{2.2}Sm_{0.4}(Fe,Ga)_5O_{12}$, garnet film, strip domain struct. behaviour in applied field 78−68341
$(YSm)_3(FeGa)_5O_{12}$ film, LPE on $Gd_3Ga_5O_{12}$, interface processes, horizontal dipping obs. 80−49552
$(YSm)_3(FeGa)_5O_{12}$, growth rate anisotropy and kinetic coefficients of vicinal faces 78−63954
$Y_{2.6}Sm_{0.4}Fe_{3.8}Ga_{1.2}O_{12}$, garnet films, LPE growth, mag. anisotropy field control 77−69642
$Y_{3-y}Sm_yFe_{5-x}Ga_xO_{12}$ film, LPE process exam. by induced striation 77−69643
$Y_{3-y}Sm_yFe_{5-x}Ga_xO_{12}$ film, LPE growth induced mag. anisotropy 78−2709
$Y_{3-y}Sm_yFe_{5-x}Ga_xO_{12}$ epitaxial layers grown from soln., prep. and props. *(German)* 78−52691
$Y_{2.6}Sm_{0.4}Fe_{5-x}Ga_xO_{12}$, epitaxial; domain wall crit. vel., effect of material parameters 79−99740
$Y_{3-x}Sm_xFe_5O_{12}$, cubic and induced anisotropy, temp. depend., 100-300K, ferromag. reson. obs. *(Russian)* 78−39313
$Y_{3-x}Sm_xFe_5O_{12}$:^{57}Fe film, ion implanted, Mossbauer conversion spectra study 80−80663
$Y_{2.6}Sm_{0.4}Ga_{1.2}Fe_{3.8}O_{12}$ film, ion-implanted, bubble domain behaviour 77−12177
$(Y_{1.5}Sm_{0.3}Lu_{0.3}Ca_{0.9})(Fe_{4.1}Ge_{0.9})O_{12}$, growth reproducibility, static bubble props. 77−16130
$(YSmLuCa)_3(FeGaGe)_5O_{12}$, reproductibility in bubble garnet LPE growth 78−92204
YSmLuCaFeGe garnets, growth and temp. characts. of small bubbles 78−80183
$(YSmLuCa)_3(FeGe)_5O_{12}$, mag. props. and growth of 2 μm bubbles 78−91910
$(YSmLuCa)_3(FeGe)_5O_{12}$, LPE growth, growth reproducibility of bubble props. 78−92208
$(YSmLuCa)_3(FeGe)_5O_{12}$ films, mag. bubble props. and LPE conditions 79−74107
$(YSmLuCa)_3(FeGe)_5O_{12}$ film, bubble propagation direction effects on high frequency bias margin 79−78480
$(YSmLuCa)_3(FeGe)_5O_{12}$, double layer struct., LPE growth from molybdate and Pb borate fluxes 80−39827
$(YSmLuCa)_3(FeGe)_5O_{12}$, bubble material, dynamic characterisation, comparison between transport and FMR methods 80−39833
$(YSmLuCa)_3(FeGe)_5O_{12}$, mag. loss and domain wall mobility 80−65980
$(YSmLuCa)_3(FeGe)_5O_{12}$, epitaxial films, LPE grown, annealing effects on mag. anisotropy 80−66548
YSmLuCaGe garnets, 7 μm-period bubble devices 80−44887
$(YSmLuCa)_3(GeFe)_5O_{12}$, garnet film, refractive index dispersion 78−88273
$(YSmLuCa)_3(GeFe)_5O_{12}$, LPE low defect density films, prep. for mag. bubble device fabrication 79−87590
$(YSmLuCa)_3(GeFe)_5O_{12}$, stripe domain wall, form. and punch-through of horizontal Bloch line 79−99723
$YSm_{0.5}Lu_{0.7}Ca_{0.8}Ge_{0.8}Fe_{4.2}O_{12}$ film, magnetic bubble propagation with 8 μm period ion implanted propagation patterns 79−78475
YSmLuCaGeIG, mag. props. and defects, depend. on B_2O_3 conc. on growth in PbO-B_2O_3 solvents 78−68321
YSmLuCaGeIG films, epitaxial growth with 3 μm magnetic bubbles 79−61518
$(YSmLu)_3(FeGaSc)_5O_{12}$, submicron mag. bubble garnet 80−54929
YSmLuGa garnets, 7 μm-period bubble devices 80−44887
YSmTmCaGe garnets, 7 μm-period bubble devices 80−44887
$(YSmTmCa)_3(GeFe)_5O_{12}$ film, YY pattern racetrack discrimination and state stability of S=1 and 0 bubbles 78−91908
$(YSmTm)_3(FeGa)_5O_{12}$, small-bubble appl. 79−82845
YSmTmGa garnets, 7 μm-period bubble devices 80−44887
$Y_xSn_xMo_6S_8$, supercond. props. 80−97023
YTa_7O_{19}, crystal struct., isomorphism with rare earth tantalates 77−7698
Y_3TaO_7, non-stoichiometric phase struct. 79−55716
$Y_{1-x}Tb_xAl_3B_4O_{12}$ phosphors, cathodoluminesc. 77−73177
$Y_{1.5}Tb_{1.5}Al_{0.65}Fe_{4.35}O_{12}$, garnet thin films, magnetisation orientation, temp. depend. 80−71125
$Y_{1-x}Tb_xP_3O_9$ phosphor, prep. and fluoresc. 77−48219
$Y_{0.7}Th_{0.3}C_{1.55}$, superconducting crit. mag. field curve, initial slope 77−28318
$YThNbTiO_8$, synthesis and cryst. struct. *(French)* 78−83799
$Y_2Ti_2O_7$, ferroelec., layer type struct., cryst. growth 80−108348
$Y_2Ti_2O_7$, ferroelec., temp. depend. of SHG intensity 79−24267
$Y_2Ti_2O_7$, precipitation from oxalates, carbonates, exam. 80−55641
$Y_2Ti_2O_7$:Nd^{3+}, spectroscopic props. 77−69866
$YTiTaO_6$, powder X-ray diffr. data 79−99155
$Y_{0.8}Tm_{0.2}Se$, sp. ht. meas., 1.6 to 20K, mag. contrib. 80−65934
Y_6UO_{12}, energy transfer, cryst. struct. and chemical composition effect 80−108248
$YV_{1-x}M_xO_3$ (where M=Cr or Fe), solid solns., elec. and mag. props 79−23967
YVO_4, ^{51}V NMR, nucl. quadrupole coupling const., chem. shift 77−90055
YVO_4, electron energy loss spectra, primary excitation processes in cathodolum. 79−11490
YVO_4, luminesc. spectra in visible region, vanadate group 78−43921
YVO_4 phosphor, ionisation of capture centres, thermolum. spectra 80−11487
YVO_4, pure and Bi^{3+} doped, absorpt. and emission props., excitons 79−38592
YVO_4, soft X-ray APS study of empty electron states, VO_4^{3-} cluster model 80−25488
YVO_4, X-ray Lα emission spectra, excited states calcs. 79−59488
YVO_4:Er^{3+}, Yb^{3+}, IR excitation curves for visible luminesc. 79−33795
YVO_4:Eu, cathodoluminesc. investig., appl. to cathode ray tube screening 80−108282

yttrium compounds continued
YVO_4:Eu, cluster electron struct., X-alpha calc., emission spectra 78−2898
YVO_4:Eu, fluoresc., cathodoluminesc. and thermal quenching 79−47488
YVO_4:Eu^{3+}, absorption and fluoresc. spectra, SU(2) chain *(French)* 78−28912
YVO_4:Eu^{3+}, absorpt. spectra, fluoresc., electron beam excitation 78−92093
YVO_4:Eu^{3+}, laser site-selection spectroscopy investigation 78−68556
YVO_4:Eu^{3+}, ligand field parameters, computed from fluoresc. and absorption data 78−2453
YVO_4:Eu^{3+} phosphor, cathodoluminesc. and photon statistics 77−59621
YVO_4:Eu^{3+}(Er^{3+}), energy transfer, laser time-resolved spectroscopy 78−27306
YVO_4:Eu^{3+}(Sm^{3+}), rel. band intensities in luminesc. spectra *(Russian)* 77−48238
YVO_4:Ho^{3+}, CW and pulsed laser emission at 2.0412 μm 77−19254
YVO_4:Nd, stimulated emission cross-sections at 1064 and 1342 nm 78−39575
YVO_4:Nd^{3+}, absorption and fluoresc. spectra of laser states 77−38900
YVO_4:Nd^{3+}, energy transfer processes, laser-excited time-resolved spectroscopy 80−84765
YVO_4:Nd^{3+}, fluoresc. lifetime of $^4F_{3/2}$ state 79−87494
YVO_4:Nd^{3+}, optical absorption intensities 79−24335
YVO_4:Nd^{3+}, radiationless decay processes, laser photoacoustic spectroscopy meas. 80−84766
YVO_4:Nd^{3+}, zircon struct., cryst. field analysis 80−80232
YVO_4:R^{3+}, R=Nd, No, Tm, Sm, Dy, Er, Eu, Tb, electronic struct. and spectra of VO_4, RO_8 clusters 78−10953
YVO_4:Tm^{3+}, cryst. field parameters, appls. 77−20277
$YVO_5$4-$NaVO_3$, solubility curves for high temp.-melts for growth of single crysts. 78−95687
$Y_2V_{10}O_{28}.24H_2O$, cryst. struct. by X-ray diffr. 78−43005
$Y_2V_{10}O_{28}.24H_2O$, cryst. struct. determ. by vector subsystems method 79−60340
$Y_2V_{10}O_{28}.24H_2O$, X-ray cryst. struct. anal. 80−39060
$Y_2(V_{4/3}W_{2/3})O_7$ pyrochlore, synthesis and elec. props. 80−29914
Y_2WO_6, growth from soln. in melt 77−1806
Y_2WO_6, new structural type, unit cell, space group, fluorescence spectra 79−1420
Y_2WO_6:Eu, noncontinuum model for energy transfer 79−33800
Y_2WO_6:Eu^{3+}, luminesc., rel. to crystallographic data 79−33793
Y_2WO_6:U^{6+}, luminesc. 77−55816
Y_6WO_{12}:Eu^{3+}, crystal struct., fluorescence spectra, exam. 78−52558
Y_6WO_{12}:ZrO_2(MgO)(CeO)(SrO)(BaO), polycryst., elec. cond., 800-7400°C 80−15517
$(Y_{0.80}Yb_{0.19}Er_{0.01})F_3$ phosphors, IR to visible conversion 78−48210
$Y_{1-x-y}Yb_xEr_yOCl$, Er ion excited state decay and population *(Russian)* 80−100694
$(Y_{0.80}Yb_{0.19}Ho_{0.01})F_3$, IR to visible conversion 78−48210
$Y_2[Pt(CN)_4]_3.21H_2O$, phase transitions, X-ray study and spectroscopic study 79−60506
$Y_2[Pt(CN)_4].21H_2O$, energy band calcs. 77−39780
$YaI_3[BO_3]_4$, impurity incorp. on growth from soln. 77−52242
Yb_xSy, synthesis and mag. props. 78−23242
YiG-Bi layer struct., Landau electron absorpt. mechanism, spin wave amplification 78−72344
ZRO_2 single crystals, Y_2O_3 stabilised, optical props., impurities and annealing conditons influence 79−52399
ZrO_2, Y_2O_3 stabilised, hydrothermal growth 78−15302
ZrO_2:Y_2O_3, bias sputtering, film growth and characts. 77−40366
ZrO_2:Y_2O_3, cryst., IR refl., refr., absorpt. 77−12382
ZrO_2:Y_2O_3, in contact with $YCrO_3$, electrical cond. meas. 78−76071
ZrO_2:Y_2O_3, low-temp. specific heat, oxygen vacancy effects 80−49376
ZrO_2:Y_2O_3, solid electrolytes, charge carrier conc. and diffusion 77−11930
ZrO_2:Y_2O_3 film, preferential sputtering, Auger and XPS spectra obs. 79−52071
ZrO_2-CaO-Y_2O_3, formation, stability and elec. props. of fluorite-like solid solutions 77−16550
ZrO_2-Y_2O_3, Faradaic reaction kinetics, impedance dispersion anal., electrode/electrolyte interface process 79−11798
ZrO_2-Y_2O_3, phase equilibria and ordering 78−48385
ZrO_2-Y_2O_3, solid electrolyte, cond. maximum 78−47577
ZrO_2-Y_2O_3, solid solns., density meas. rel. to O vacancy model 78−2113
ZrO_2-Y_2O_3, solid soln., elastic and photoelastic props., Mendelstam-Brillouin scatt. 78−6693
ZrO_2-Y_2O_3, solid soln., diffuse X-ray scatt. by vacancies 78−71728
ZrO_2-Y_2O_3, stabilised, struct. of single crysts. 77−35527
ZrO_2-Y_2O_3, stabilised, reaction with Cr_2O_3 77−36438
ZrO_2-Y_2O_3, stabilised, light scatt. spectrum 79−73954
ZrO_2-Y_2O_3, stabilised microspheres, structure, mechanical props. *(Russian)* 80−100379
ZrO_2-Y_2O_3, ZrO_2-CaO system, fluorite related ordered compd, prep., struct. 77−68958
ZrO_2-Y_2O_3 (10 mole%), electron transport, elec. induced p-n junction 77−43597
ZrO_2-Y_2O_3 (6 mol.%), neutron irrad. damage 77−84804
ZrO_2-Y_2O_3 ceramic powder, in situ deposition of metal coating, cermet form. 77−32713
ZrO_2-Y_2O_3 ceramic with graining structure, props., effect of heating to 2000°C 80−104194
ZrO_2-Y_2O_3 film, surface characterisation, XPS, ESCA, and AES expts. 78−72028
ZrO_2-Y_2O_3 microspheres, stabilised, from HF air plasma, struct. 79−78917
ZrO_2-Y_2O_3 monocrystalline solid solutions, struct. and phase form. 79−52188
ZrO_2-Y_2O_3 powder, prep. for plasma spheroidisation, sputter drying *(Russian)* 80−55324
ZrO_2-Y_2O_3 superionic cond. cell, complex impedance 80−10702
ZrO_2-Y_2O_3:M^{3+}, M=transition metal, X-ray luminesc. 77−44063
ZrO_2-Y_2O_3/Ni sputtered multilayered ceramic/metal coatings, props. 80−40620
ZrO_2-Y_2O_3/Pt interface, electrode kinetics, complex impedance dispersion anal. 79−96325
ZrO_2-Y_2O_3/(Cr-Ni) sputtered multilayered ceramic/metal coatings, props. 80−40620
ZrO_2-Y_2O_3-CaO(MgO), long term firing effect at 2100 to 2200°C on solid soln. conc. and microstruct. 77−90309
ZrO_2-Y_2O_3-Nd_2O_3, high-temp. thermophys. props. 78−26663
yttrium compounds continued
ZrO_2-Y_2O_3-Nd_2O_3, spectral determ. of crystal stabilisation 78−27203
ZrO_2-Y_2O_3-Nd_2O_3(CeO_2), solid solns., form. by coprecipitation, struct., X-ray, electron diffr. anal. 77−12583
ZrO_2-Y_2O_3-Ta aligned eutectic composite, solidification and fracture behaviour 77−48387
ZrO_2-$YO_{1.5}$, partially stabilised, growth morphology of tetragonal phase 79−4968
ZrO_2-$YO_{1.5}$, solid solns., defective oxides, ionic cond. 80−107548
ZrO_2-$YO_{1.5}$ solid solutions, ZrO_2 rich side, X-ray spectroscopic study 78−95617
ZrO_2-$YO_{1.5}$-$TaO_{2.5}$, cubic fluorite phase, elec. cond. 80−107551
$(ZrO_2)_{0.9}(Y_2O_3)_{0.1}$:Cr, Mn, stabilised single crystal, EPR of Mn^{2+} and Cr^{3+} obs. 80−66024
$(ZrO_2)_{0.9}(Y_2O_3)_{0.1}$:Ti, γ-irrad., ESR of trigonal centres, attributed to Ti^{3+} at cation sites 77−24740
$(ZrO_2)_{0.9}(Y_2O_3)_{0.1}$:$VO^{2+}$, ESR of V^{4+} at room temp., spin Hamiltonian parameter determ. 77−16167
$ZrO_2Y_2O_3$/Ni-Cr-Al-Y, NASA two-layer thermal barrier coating, for gas turbine engines, test results 80−40617
$((ZrO_2)_{0.92}(Y_2O_3)_{0.08})_{1-x}(Fe_2O_3)_x$, Fe solubility and elec. cond. 79−99354

Yukawa potential *see meson field theory; nuclear forces*

Z-centres
alkali halides, irradiated, formation of Z centre 80−103326
alkali halides, Z_1-centres, peculiarities of thermolum. 80−103999
$BaTiO_3$:Eu(Sm), absorption spectra, Ti^{3+} ion and Z-centre formation 77−24871
CsCl(Br)(I), doped F_{Z1}-centre exam. 78−14341
KBr:Ca, F→Z_1 colour centre conversion, hologram recording appls. 78−17877
KBr:Ca, X-ray re-irradiation effects on Z_1 centres 78−75664
KBr(Cl):Eu, Z_2-centre investig. by EPR and optical absorpt. 77−16177
KCl, doped with alkaline earth ions, Z_1-centres form. under X-ray irrad. 79−24338
KCl, ion processes in F→Z_1 transition, photocond. meas. 77−15412
KCl, luminesc. of Z_4 centres 79−24355
KCl, Z_2 centres in triplet state, EPR study 80−108068
KCl:Ba, negative photoplastic effect, photodestruction of Z-centres 77−43272
KCl:Ba(Sr), Z-centre, luminesc. and absorpt. spectra obs. 80−49221
KCl:Ca, additively coloured, spectral and temp. depend. of initial yield of Z_3-centre form. 79−78716
KCl:Ca, F→Z_1 colour centre conversion, hologram recording appls. 78−17877
KCl:Ca, optical studies of Z_4 centres 79−24336
KCl:Ca, thermolum. and optical absorpt. spectra of Z_1 centres 79−52029
KCl:Ca, vol. holographic grating, modulation characts. using F to Z_1 colour centre conversion 79−94197
KCl:Ca, Z_2-centres, optical absorpt. and ESR spectra 79−91480
KCl:Ca^{2+}, Z_1-centre thermolum. 80−80879
KCl:Ca(Ba)(Mg)(Sr), microcrystalline powders, role of Z-centres in stabilizing coloration 80−54227
KCl:Ca(Yb), Z_2 and Z_2^+ centres, excited state, magnetooptical spectra 80−108233
KCl:Eu, luminescence and absorption of color centres in RbCl:Cu and KCl:Eu crystals 78−92118
KCl:Eu crystallophosphores, aggregation of $Eu^{2+}v_c^-$ centres *(Russian)* 78−43909
KCl:Sr, thermally pre-treated, glow curves 80−25470
KCl:Sr, triplet state of F_z-centres, ESR spectra 80−29616
KCl:Sr crystal, Z_4 colour centre, luminesc. study 80−64993
KCl:$SrCl_2$, Z_1-centres, dipolar relax., ITC meas. 78−75660
KCl:Yb, Z_2-centres, optical absorpt. and ESR spectra 79−91481
KCl-Mg, thermolum. of Z-centre, optical absorpt. 80−55203
KCl-$SrCl_2$, photoluminescence of Z_4-centre and associated Z type colour centre *(Russian)* 79−4851
$KCl_{0.5}Br_{0.5}$:Ca, X-ray irrad., Z_1-centres, thermoluminesc. and optical absorpt. meas. 80−16108
LiF, restored thermoluminescence mechanism 78−19580
LiF, TLD phosphor, Z_3 centre, thermolum. and optical absorption spectra 79−24374
LiF, thermolum., trapping mechanism based on Z-centres 80−76089
LiF:Mg, dependence of optical absorpt. on temp. during X-ray irrad. 80−66237
LiF:Mg, X-irrad. induced sensitisation mechanism, optical absorpt. spectra 80−60637
LiF:Mg, X-irradiated, thermoluminesc. of Z_3-centres 78−15236
LiF:Mg, X-irradiated, Z_1-centre exam. 77−68968
LiF:Mg, X-ray irrad., trapping processes, Z-centres and dipoles, two models 80−49222
LiF:Mg, Z_2- and associated Z-centres, elec. cond., ionic thermocurrent, and optical absorpt. meas. 80−107229
LiF:Mg,Ti, optically induced dichroism of Z_2-centres 79−28710
LiF:Mg,Ti, thermolum. related Z-centres, optical absorpt. bands 78−23540
LiF:Mg,Ti crystals, Z_3-centres, correlation of thermoluminescence and optical absorption 80−45154
LiF:Mg^{2+}(CO^{2+}), X-ray induced UV absorpt., band shapes, F- and Z-centers 77−20889
NaCl, gamma irradiation, optical and thermal bleaching of colour centres, trapped electron centre form. 79−95814
NaCl:Ca, X-irradiated, Z_1-centre form. kinetics, thermolum. investig. 77−4693
NaCl:Ca, Z_1 centre thermoluminescence study 80−16109
NaCl:Mg^{2+}(Mn^{2+})(Ni^{2+})(Cd^{2+})(Pb^{2+}), Z_4-like centre, absorpt. spectra obs. 78−76498
NaCl:V^{2+}, elec. field effect on Z-like centres spectrum 80−2802
RbCl:Ca^{2+}, thermolum. and optical absorption studies 80−104002
RbCl:Eu, luminescence and absorption of color centres in RbCl:Cu and KCl:Eu crystals 78−92118
$SrTiO_3$:Eu(Sm), absorption spectra, Ti^{3+} ion and Z-centre formation 77−24871

Z pinch *see pinch effect*

Z transforms
see also sampled data systems
chirp, for constant-Q spectral analysis of loudspeakers 79−64407
modular chirp Z transform equivalent to two-lens optical Fourier transform 78−78943

Z transforms continued
sonar beamforming by CCD scan conversion for SAW chirp-Z transform 80−43552
sonar system, CCD implementation of chirp Z-transform 79−18626
TeO_2 time-integrating acousto-optical correlator for chirp spectrum analyses 80−106474

Zeeman effect
see also atomic spectra; Hanle effect; spectral line breadth
$^1\Sigma$ state, anomalous Zeeman effect, Doppler-free standing wave saturated resonance, book contrib. 78−9279
^{3}He-^{20}Ne stabilised transverse Zeeman laser, tuning characts., freq. fluctuation 80−48273
alkali halides, spin lattice relax. and g-shift 80−15799
alkali metal, ground state coherence, transversal relaxation rates, Zeeman shifts 77−6888
alkali metal atoms, Zeeman coherences relaxation in ground state by spin-exchange and sudden collisions 77−50402
alkali metal modulated optical absorption transients weights, Zeeman frequency shift effects 77−6887
aminobenzonitrile, para- and meta-, NQR linewidth, Zeeman effect, mol. config., H bonding, cryst. struct. 77−51986
Ap-stars, magnetic intensification of spectral lines *(Russian)* 78−4254
application to atomic absorption spectroscopy 80−76567
arc spectra, Zeeman effect *(French)* 77−83521
aromatic radical ion recomb., mag. field modulation, Liouville eqn. soln. 77−28995
atmospheric pollutants spectra, Zeeman tuning for laser perturbation spectroscopy 78−69526
atom, coherent transients, spherical tensor treatment 79−26940
atom, many-electron, in external mag. field, Hamiltonian and classical electrodynamics 77−79576
atom, selection rules, EM transitions in strong coherent light field 77−447
atom+atom collisional intense-field fluoresc., Zeeman degeneracy effects 80−99477
atomic, two-level system, absorption spectrum, intense two-photon excitation obs. *(Russian)* 78−33465
atomic absorpt. spectroscopy, RF-excited hollow cathode lamps as Zeeman-modulated sources 78−85275
atomic absorption analysis, Zeeman effect appls. 80−85245
atomic absorption spectrometry, background correction, Zeeman effect based methods 78−27831
atomic absorption spectrometry, theory 79−43677
atomic absorption spectrometry, Zeeman modulated technique, appls., detect. limits 79−24876
atomic absorption spectrophotometer using Zeeman effect and polarisation characts. 77−90651
atomic absorption spectrosc. anal. curve shapes 80−22437
atomic absorption spectroscopy, Zeeman effect, appls. *(Japanese)* 80−35600
atomic absorption spectroscopy, Zeeman effect method, calibration curves 77−32866
atomic absorption spectroscopy, Zeeman effect method, mag. field strength determ. 77−63997
atomic absorption spectroscopy, Zeeman modulated, quantitative sensitivity *(Japanese)* 78−20124
atomic absorption spectroscopy, Zeeman modulation technique, line interferences 79−24877
atomic absorption spectroscopy using capacitively coupled RF spectral sources 77−61135
atomic gas with resonant levels, mag. rot. of ellipse of polarisation of propagating rad. 79−50340
atomic hyperfine transitions in buffer gas, quantum theory *(Russian)* 78−21881
atomic RF spectroscopy, nonlinear and parametric effects, review 80−18816
atomic spectra and radiative transitions, book 80−22159
atomic transition, Zeeman degeneracies effect on reson. fluoresc. *(French)* 77−61703
atoms interacting with polarised light, resonant Voigt effect, analysis 79−76390
backward Raman amplifier for excimer laser pulse compression, parasitic superfluoresc. suppression 80−69453
benzene, photoexcitation, triplet factor group states assignment 77−85741
benzophenone $^3(n,\pi^*)$, and isotopic forms, in 4,4′-dibromodiphenylether, level anticrossings, ODMR obs. 78−2772
bibliography at. energy levels and spectra, (July 1971-June 1975) 77−71764
biomolecular EPR and saturation transfer EPR spectra at high microwave field intensities 79−34488
blackbody radiation interaction with LF atomic transitions, Zeeman, Stark and stimulated emission 79−41127
BPM 25114, southern mag. white dwarf, Zeeman effect in higher Balmer lines 79−92765
1-bromo-2, 4-dinitrobenzene, cryst., ^{79}Br NQR Zeeman effect 78−2765
caesium perfluoro-octanoate/D_2O system, ^{2}H NMR quantum orders, RF pulses 80−103892
carbonyl chlorofluoride, rot. Zeeman effect, g-factors and mag. suscept. anisotropies, microwave meas. *(German)* 77−57993
cascade effects on Zeeman quantum beats 79−89631
chloranil, phase transition, Zeeman effect of ^{35}Cl NQR 78−59944
6-chloro 2,4-dimethoxypyrimidine, ^{35}Cl NQR, Zeeman effect 80−18874
1-chloro-9,10-anthraquinone crystal, electronic structure of lowest triplet state *(Japanese)* 79−8158
m-chloroacetanilide, cryst., ^{35}Cl NQR, Zeeman effect 77−8443
chromocene, mag. suscept., zero-field splitting, ligand field, 1-303K 77−89924
collisional excitation transfer in high mag. fields, theory 80−9688
copper porphin, Zeeman expt. on phosphoresc. triplet and quartet states 79−33786
β Coronae Borealis, Ap star, transverse Zeeman effect, oblique rotator model 77−13361
coronene, solution in bromobutane, Zeeman effect in phosphoresc. at laser $T_1 \leftarrow S_0$ excitation 78−37679
cross-relaxation between Zeeman and spin-spin degrees of freedom *(Russian)* 77−32237
trans-crotonaldehyde, rot. Zeeman effect, microwave spectra, mol. parameters 79−3491

Zeeman effect continued
cubic crystal Zeeman anisotropy in absorpt., emission and MCD, eigenfunctions 77−55773
cubic semiconductor, long-range exchange splitting of excitons 77−51671
cubic semiconductor, Zeeman split acceptor levels, calc. method 79−28322
cumulative resonance in atomic ground state induced by modulated light field 78−66518
3-cyanopyridine, NQR Zeeman obs., crystal packing 80−54978
1,1-cyclobutanedicarboxylic acid, X- and γ-irrad. cryst., EI-EPR overlapping spectra resolution 77−16179
V1057 Cygni, OH line Zeeman splitting and stellar mag. field 80−36629
dark clouds, H I 21 cm Zeeman effect obs., magnetic fields 79−8977
data collected using high mag. field installation *(Dutch)* 78−252
diatomic molecule, numerical diagonalization of perturbation matrix approach 77−14486
diatomic molecules, $^2\Pi$ states, $^2\Delta$ states, $^2\Pi$ ground state, g-factor, Zeeman effect 79−98149
diatomic molecules, calc. for doublet transitions 78−58740
diatomic molecules, laser-induced predissoc., surface mag. field effect 80−106365
2,6-dichloroacetanilide, NQR, cryst. struct., band character 78−6596
p-dichlorobenzene, ^{35}Cl powder Zeeman NQR, injection and phase locked NQR spectrometer 80−54979
4,4′-dichlorodiphenylsulphide, NQR line, Zeeman effect 77−59481
3,5-dichloronitrobenzene, NQR line, Zeeman effect 80−28034
1,8-dichlorooctane, quadrupolar relax. centres, limited spin diffusion 80−100649
4,6-dichloropyrimidine, ^{35}Cl NQR, Zeeman effect 80−18874
1,1′-diethyl-2,2′-cyanine iodide, neat and mixed crysts., visible absorption and emission spectra assignments 77−1692
1,3difluorobenzene, rot. Zeeman effect, g-tensor, mag. susceptibility 77−497
1,2-difluorotetrachloroethane, mol. motions and Zeeman-quadrupole cross relax., NMR obs. 79−65751
dilatation transformation and Stark-Zeeman effect 79−3398
Dirac equation in Kerr space-time, anomalous Zeeman splitting of energy level 77−74081
duraldehyde, S_1-T_1 nonradiative transition mechanism, double reson. obs. 77−30893
education, plane rotator, degenerate perturbation theory, Zeeman and Stark effects 79−9059
EM wave propagation near combined resonance 79−99772
energy interval measurement by obs. Zeeman transition in microwave spectra 80−69274
EPR and saturation transfer EPR, fast computation, master supermatrix eqn. soln. 78−62213
EPR and saturation transfer EPR, fast computation, perturbation approach 78−62212
EPR and saturation transfer EPR, fast computation, perturbation approx. extension for overmodulation 78−82754
EPR and ST-EPR spectra of nitroxide spin labels in rigid-lattice limit, rapid computer simulation 79−93189
ESR saturation, influence on magnetooptical effects, allowance for dipole-dipole reservoir of electron spins 79−15442
ethyleneoxide, elec. dipole moment, g-values, mag. susceptibility, moments and charge distrib. 77−58077
excited atomic and molecular states in strong electromagnetic fields 79−49955
exciton luminescence, RF coherence and polarisation 78−10937
Feige 7, mag. white dwarf, spectroscopic studies 79−25603
ferroelectric semiconductor, magnetic field influence, ferroelectric transitions 80−55049
fluoroacetylene, and -d_1, vibr. Zeeman effect, g-factors 78−46391
fluoroform, Zeeman effect, mag. moments and susceptibility, nuclear shielding 79−13764
formyl chloride, rot. Zeeman effect of low-J transitions 78−25519
formyl radical, laser mag. reson. spectrum at 5.3 micron 80−47981
formyl radical-d_0,-d_1, microwave spectroscopy, high field Zeeman effect 78−37631
free atoms in high magnetic fields, review 77−50383
free radicals, rot. Zeeman spectroscopy, mag. field splitting of hyperfine components 78−25610
free-base porphin, Zeeman shift meas. by photochem. hole-burning 80−83416
fulminic acid-d_0, -d_1, rot. Zeeman effect and nucl. quadrupole coupling 78−78683
gas laser, induced polarisation anisotropies, direct meas. 77−19234
gas ring laser, nonlinear Zeeman effect 78−71123
gas superluminescence in high-current discharge, polarisation due to Zeeman splitting 80−100060
GD 229, mag. white dwarf, spectroscopic studies 79−25603
glyoxal, mag. quenching of fluoresc. 79−31582
glyoxal, singlet-triplet radiationless processes in mag. field 80−106347
ground state Zeeman splittings, reson. Raman spectra and mag.-optical activity 80−5579
Heisenberg's work on anomalous Zeeman effect and multiple spectra of atoms 78−70784
heme-proteins, general spin Hamiltonian for determ. of ligand nucl. Zeeman and hyperfine interactions 77−85617
AM Herculis (3U 1809+50), polarimetry and spectrophotometry rel. to mag. field 80−94835
highly excited atoms, review of recent expts. 80−23325
W Hydrae, long-period variable, suspected Zeeman splitting in OH masers 80−36632
III-V semiconductor, acceptor levels, anisotropy of Zeeman splitting and polarization of luminesc. in mag. field 79−24365
interdoublet EPR spectrum ang. depend. for ions with arbitrary electron and nuclear spins in strong axial cryst. field 80−93164
interstellar dense cloud complexes, H I lines Zeeman splitting rel. to mag. fields determ. 79−5757
ions in uniaxial crystals, transverse Zeeman effect, theory 77−4628
irreducible tensor operator methods in strong-field coupling 79−7811
isothiazole, rot. Zeeman effect, localised susceptibilities 80−91600
laser, mobile resonances, appl. to freq. stabilisation and tunability 77−7138
laser gyro, Zeeman, beat-note sensitivity 80−53340
laser modes selection, expts. with He-Ne laser *(Russian)* 80−1251
laser or amplifier, Zeeman systems, bistability and intensity fluctuations 80−53254

Zeeman effect continued
line profile, mag. field determ., appl. of radiative transfer problem soln. 80−82221
LP 790-29, mag. degenerate star, C_2 Swan bands broadening and shifting 79−5815
LP 790-29, southern mag. white dwarf, Zeeman effect in C_2 spectrum 79−92765
magnetic stars 77−45442
methane, $F_2^{(2)}$ doublet Zeeman effect obs., nonlinear reson. *(Russian)* 77−38027
methane, hyperfine struct. of $F_2^{(2)}$ line, appl. of laser spectrometer 77−58201
methane, rotational state, avoided-crossing molecular beam spectroscopy 80−63730
methane(-^{13}C), absorpt. spectra. optoacoustic laser meas. 78−37635
methoxy free radical, laser mag. reson. submillimetre spectrum, linear Zeeman effect 77−46579
methyl bromide, rot. Zeeman effect 79−54909
methyl chloride, Zeeman effect, mag. moments and susceptibility, nuclear shielding 79−13764
methyl groups, reorientation in solids, nonexponential Zeeman relax. 78−6589
methyl hypochlorite-d_0, -d_3, microwave Zeeman spectra, dipole moment, nuclear quadrupole tensor 77−459
methyl vinyl ether, rot. Zeeman effect, g-values, mag. susceptibility, quadrupole moments 77−490
methyl-d groups, reorienting or tunnelling spin-lattice relax. 80−97156
3-methylfurane, rot. Zeeman effect, g-tensor, mag. susceptibility 77−497
molecule, complex, Zeeman effect in phosphoresc. at laser $T_1 \leftarrow S_0$ excitation 78−37679
molecule, diatomic, Zeeman effect, relativistic corrections 77−83646
molecules, orthorhombic, triplet-singlet transitions, rot. structure 77−61790
molecules, with low internal rot. barrier, effective rotorsional Hamiltonian 79−26970
monochloroacetic acid single crystal, Zeeman and ^{35}Cl NQR investig. 80−66066
muonium, ground state, muon mag. moment and HFS, Zeeman transition obs. 77−75345
muonium hyperfine Zeeman freq. meas. via Ramsey reson. 77−14620
naphthalene: quinoxaline, anisotropic spin lattice relax. of triplet mols. in high mag. field 77−81141
naphthalene:quinoxaline, spin-lattice relax. of triplet states of high mag. fields 79−19933
naphthalene-tetrabromophthalic anhydride, complex cryst., visible spectra, singlet-triplet absorpt. 79−19897
naphthalene-tetrachlorophthalic anhydride, complex cryst., visible spectra, singlet-triplet absorpt. 79−19897
1,4-naphthoquinone, $T_1 \leftarrow S_0$ transition, elec. and mag. field spectra 78−88322
nematic liquid crystal, ESR of symmetrical three-spin systems, slow motional spectra 77−36135
neutron stars, X-ray emission lines Zeeman splitting by mag. field 78−4275
NMR in rotating frame, effect of nonresonant oscillating field, modification of Zeeman energy 77−28454
NQR, electronics appls. 80−63668
nuclear magnetic double resonance spectroscopy, review *(Rumanian)* 79−15380
nuclear resonance scattering of gamma rays, line inversion 80−39919
Orion Nebula, Zeeman splitting in OH masers 78−16493
orthorhombic rot. mols., doublet-doublet transitions 78−74608
orthorhombic rotating molecules, doublet-quartet transitions, Zeeman effect calcs. 78−94280
α-oxalic acid dihydrate, low-lying excited states, ODMR and optical obs. 79−41188
palladium porphin, in n-alkane crystal, Zeeman and crystal field effects, absorpt. vibr. anal. 80−7372
palladium porphin, triplet state, optically detected EPR and Zeeman meas. 79−19809
palladium porphin, Zeeman expt. on phosphoresc. triplet and quartet states 79−33786
palladiumporphin in n-octane cryst., lowest triplet state, ESR-optical detect. 77−58050
paramagnetic system with quadrupole splitting, magneto-optical effects, magnetic resonance saturation 80−60404
Paschen-Back effect in reson, radiation field 78−17607
perchloro-3cyclopentenone, ^{35}Cl NQR Zeeman obs. 80−54981
perovskite:Er^{3+}, ESR spectrum, higher order Zeeman effects 79−99766
phonon scattering by paramagnetic ions, Zeeman levels in absence of zero field splitting 77−15508
platinum phthalocyanine single cryst., triplet state Zeeman effect, phosphoresc. 78−6747
polar semiconductors, chemical shift of Zeeman masses 78−10338
polarization problem of the Zeeman effect *(Chinese)* 79−54808
polycrystalline samples, ^{14}N NQR, Zeeman effect, second-order theory 80−20503
polycrystalline solids, Zeeman spectra 78−68487
polyethylene, molecular motion and spin-lattice relaxation 78−48071
porphins orientation in n-alkane Shpolskii hosts, spectra 80−48035
positronium, ground state, fine struct. interval, NMR meas. 77−34787
propanediol, behaviour of nucl. spins near highly polarised paramag. centres 77−77127
pyridine, elec. dipole moment, g-values, mag. susceptibility, moments and charge distrib. 77−58077
quadrupole spin echo, effect of mag. field in polycrystalline materials 77−12245
quadrupole spin echo envelope EFG tensor axisymmetry in mag. field 80−20497
quadrupole-Zeeman cross-relax. between two nucl. spin species, appl. to difluorotetrachloroethane 79−65766
quantum dynamical semigroups and spin multipole relaxation in isotropic surroundings 78−86813
α-quartz, hydrogenic trapped hole species, EPR studies 80−44915
radiation problems, semiclassical theory 78−74684
rare earth elements, atomic energy levels, data tables 78−86805
relativistic correction to the linear Zeeman effect in a Coulomb field 80−102484
resonance lineshapes, motional narrowing, analytical results 77−46524
resonance lineshapes, motional narrowing, expt. 77−46525

Zeeman effect continued
resonance lineshapes, motional narrowing, lineshape in absence of motion 77−38636
resonance lineshapes, motional narrowing, Monte Carlo simulation 77−38635
resonance lineshapes, motional narrowing 77−38634
ring laser, four-mode operation 80−19053
ring Zeeman laser, interaction of modes characterized by orthogonal circular polarizations 80−48306
rotator, low loss, and appl. for isolator design 77−58447
ruby, Cr^{3+} ion doped, R-line region, absorpt. spectrum, dispersion rel. to mag. field 80−2732
ruby, double electron-nuclear resonance at Cr^{3+} B1, B2 absorpt. lines, optical detection *(Russian)* 80−7194
ruby, E, 2A levels, laser excitation, Zeeman spectra 78−43908
ruby, ESR of Cr^{3+} excited state as function of delay time, Zeeman levels explained 78−43695
ruby, far IR to visible conversion for tunable quantum counter 77−5909
ruby, high mag. field spin-lattice relaxation rate of Cr^{3+} 78−52340
ruby, optical pumping, bottlenecked 29 cm^{-1} phonon spectral width 77−12425
ruby, optically excited, diffusion of bottlenecked 29 cm^{-1} phonons 80−6472
ruby, optically induced two-phonon processes connecting ^{2}E states 80−25443
ruby, phonon bottleneck of direct decay within $\bar{E}(^2E)$ state, optical detection 80−10608
ruby, Zeeman effect in $^4A_2{}^2E$ pair states in first nearest neighbour Cr (III) pair 79−15440
ruby, Zeeman effect of R-absorpt. lines 79−47416
ruby, Zeeman splitting, MG field production and appls. 79−71491
Rydberg spectra, Landau standing wave form. 80−102466
saturated absorption, Zeeman coherence 77−46527
scheelite:Er^{3+}, ESR spectrum, higher order Zeeman effects 79−99766
semiconductor, magnetic circular dichroism at E_1 edges 78−92051
single axial mode laser, degenerated by mag. field, light props. *(Japanese)* 79−64254
small molecules, detect. by magnetically tuned freq.-modulated at. line sources 79−59508
sodium uranyl acetate, absorpt. spectra, MCD and natural dichroism, UV and visible 79−69853
solar spectra, small line shifts meas. via automatic comparator 77−82123
solar spectrum, multi-dimensional non-LTE transfer of polarised radiation 78−69673
solid, dipole-dipole ordering in nuclear spin system by acoustic pulse, temp. of Zeeman subsystem 79−11333
solid, relativistic corrections and very small g-shifts 78−72393
spectral line components with hyperfine structure, line strengths and splittings 78−77482
spectrophotometer, Zeeman effect appl., development of spectral-line sources 80−76583
spin 3/2 nuclei, Zeeman NQR powder spectra 80−20502
spin Hamiltonian diagonalisation, theory and appls. of generalised operator transforms 77−4546
spin-orbit coupled system in mag. field, evolution operator factorisation 77−14376
SS Cr, g-factor of J=2 states, interacting Rydberg series 78−17609
Stark splitting, optical dynamic, Zeeman degeneracy 80−37774
state reduction in passage of mol. beam through Stern-Gerlach apparatus, calculational example 79−36696
stellar atmosphere, non-LTE line formation in mag. field, two-level atom with freq. independent source function 78−61726
stellar spectrograms, relative Zeeman and Doppler shifts determ. via statistical approach 78−36467
Stern-Gerlach quantum-like behaviour of a classical charged particle 79−85913
subDoppler Stark spectroscopy in crossed elec. and mag. field 78−948
Sun, magnetosensitive line contours in active regions *(Russian)* 80−51718
sunspot penumbrae, line shifts and asymmetries 80−51715
sunspot umbrae, mag. field gradient from echelle spectrograms 77−33456
TBBA, smectic, freq. dispersion of proton Zeeman relax. time and quadrupole reson. of ^{14}N 77−62468
TCNQ salt, Rb-TCNQ, ^{14}N NQR, Zeeman perturbation study, charge transfer 78−39438
terbium ethyl sulphate, mag. and thermal props. 79−7971
tetrachlorobenzene, in durene, 1.6K, $S_1 \sim\!\!\rightarrow T_1$ relax. mechanism, Zeeman phosphoresc. and PMDR obs. 77−30912
tetrahedral four spin $^1/_2$ systems, Zeeman and tunnel system reson., coupled and uncoupled relax. 80−50214
tetramer clusters, ESR spectra, spin Hamiltonian analysis 77−28429
tetramethyl pyrazine in durene, phosphorescent mols., quantum beats in triplet states 80−58312
tetramethylgermanium, Zeeman spin-lattice relaxation rate maxima 80−84666
thiazole, rot. Zeeman effect, localised susceptibilities 80−91600
thioformic acid, g-values, mag. susceptibility, quadrupole moments, rot. Zeeman effect, isomer effects 78−25520
three-spin systems in nematic liq. cryst., EPR 77−14463
transient ESR line profiles, $S=I=^1/_2$ system, calcs. 78−88170
travelling-wave Zeeman gas laser operating at high radiation intensities, theory 80−9912
trinuclear exchange clusters, Dzyaloshinsky coupling effects in Mossbauer spectra *(Russian)* 80−108142
triphenylmethyl, in triphenylamine, photon-echo decay, in lowest doublet-doublet electronic transition 77−79903
two step reson. photoionisation, multimode and level degeneracy effects 80−78583
two-level atom, spin-$^1/_2$ RF spectroscopy, saturation effects, semiclassical calcs. 77−67998
two-level system, strongly coupled, induced transition probabilities and energy 78−66598
two-photon spectroscopy, Doppler-free *(Dutch)* 79−50167
type II superconductor, spin diffusion in inhomogeneous mag. fields 78−2618
vanishing electric dipole transition moment, appl. to fluoresc. 79−59397
vibronic splitting and Zeeman effect for $^4A_{2g} \rightarrow {}^2E_g$ transition 78−60495
vinyl formate, rot. Zeeman study, g-factors, mag. susceptibility, quadrupole moments 78−50572

Zeeman effect continued
white dwarfs, Hα polarisation and line profiles in strong mag. fields 77−2427
xanthione, large zero-field splitting of lowest triplet state 80−58171
Zeeman atomic absorpt. spectroscopy, absorpt. max. in analytical curves 80−86442
Zeeman laser, two-transitions with common upper level *(Japanese)* 79−55112
zinc chlorophyll b, triplet state population at 4.2K, magnetic field effects 77−30915
zinc porphin, in n-alkane crystals. at 4.2K, Zeeman spectra for Jahn-Teller instability 78−27256
Ag_3AsS_3, proustite, structural changes in low temp. phase transition, NQR study 80−19935
AgBr, photoluminesc. study of excitons in high mag. fields 80−80843
Al particles, small supercond. nuclear spin-lattice relax. meas. 80−88681
Al particles, supercond., Zeeman crit. field, NMR spin echo meas. 79−56453
$Al_2O_3:Ni^{3+}$, Jahn-Teller effect for Ni^{3+}, EPR 79−82564
Ar, cascade effects on Zeeman quantum beats 79−89631
As I, level identification and Zeeman effect obs. 80−95571
BO_2, $A^2\Pi_u$-state, Hanle effect, press. and Zeeman broadening 79−18239
BO_2, gas, optically detected mag. reson. spectrum, $X^2\Pi$ rovibronic sublevels 78−82756
$^{12}B \rightarrow B^- + {}^{12}C$, second-class current search, alignment correlation meas. by Zeeman technique 78−37313
$^{12}B \rightarrow \beta^- + {}^{12}C$, alignment correlation meas. by Zeeman technique, vector currents and form factors 78−37312
Ba, diamagnetic Zeeman effect, 20-40 kG, induced config. mixing 78−17608
Ba, quadratic Zeeman effect, diamagnetic shift, Rydberg series, strong field mixing 78−946
BaF_2, rare earth and transition ion doped, far IR absorption and Zeeman effect 77−40246
BaF_2: rare earth, far IR electronic transitions 77−4657
$BaF_2:R^{3+}$, far IR Stark and Zeeman splitting 77−48190
Bk, emission spectrum, 2540-9800 Å, electrodeless lamp source 80−27970
^{81}Br NQR in MAl_2Br_7 crysts. (M=Li, Na, K, Cs, NH_4, $(CH_3)_4N$), Zeeman effect 78−6597
C II, Zeeman splitting of high-n recomb. lines 80−58210
CO, elec. and mag. props., mol. beam elec. reson. spectroscopy 77−61791
CO_2, anomalous Zeeman effect, nonlinear optical techniques, book contrib. 78−9279
CO_2 IR Zeeman spectra utilizing copropag. wave reson., diamag. shift obs. 80−53055
CS_2, mag. quenching of fluoresc. 79−31582
CaF_2, rare-earth and transition ion doped, far IR absorption and Zeeman effect 77−40246
CaF_2, spin-diffusion const. 77−66432
$CaF_2:Ce^{3+}$, ENDOR meas. on Ce^{3+} photochromic centre 78−19372
CaF_2:Er, hydrogenated and deuterated, optical and EPR specra 79−61209
$CaF_2:R^{3+}$, far IR Stark and Zeeman splitting 77−48190
$CaF_2:Tm^{3+}$, 8.2 keV excited state, mag. props., Schottky ht. capacity, nucl. quadrupole splitting 78−76037
CaF_2+Yb^{3+}, Stark level Zeeman energies, mag. susceptibiltiy, Schottky specific heat, crystal field splitting 78−26831
CaO:Fe^{2+}, octahedral symm., vibronic effects from Zeeman field induced Mossbauer spectra 77−8477
$CaSnCl_6$, Cl NQR anomalous temp. depend., crystal struct. and phase transitions 80−54977
$CdBr_2:Co^{2+}$, exchange-coupled Co^{2+} pairs, optical absorpt. and Zeeman studies 80−66242
$CdCl_2:Co^{2+}$ Zeeman spectra meas. 78−6712
CdF_2, rare earth and transition ion doped, far IR absorption and Zeeman effect 77−40246
$CdF_2:R^{3+}$, far IR Stark and Zeeman splitting 77−48190
$Cd_{1-x}Mn_xTe$ mixed cryst., giant exciton Faraday rotation 78−27260
CdS:Ni^{2+}, Zeeman effect at Ni impurities 80−60633
CdTe, exciton magnetoreflectance spectra, multicomponent polaritons, Zeeman splitting 80−88974
CdTe, luminescence and reflect. investig. of excitons, stress and Zeeman splitting 77−40281
CdTe, shallow donors, excited state transitions 78−6710
^{113}Cd, two-level system, absorption spectrum, intense two-photon excitation obs. *(Russian)* 78−33465
$CeCl_3$, doubly degenerate phonon states, mag. field dependent splitting 77−16320
Cl_2, matrix isolated, Zeeman effect and magnetically polarised luminesc. 78−46379
ClF, mol. beam Zeeman effect, dipole moment sign, coupling const. 77−75208
ClO_2, gas-phase electron g-tensor, magic doublet rot. Zeeman spectra 78−90212
ClO_2, laser mag. reson. spectra tuned by Zeeman level crossing avoidance, perp. spectra 79−68229
ClO_2, laser mag. reson. spectra tuned by Zeeman level crossing avoidance, high-field spectra 79−76424
^{244}Cm, emission spectrum, 2400-11200 Å, wavelengths, rel. intensities, Zeeman effect 77−46514
$Co_x^{2+}Fe_{1-x}^{2+}Fe_2^{3+}O_4$, Mossbauer parameters, effect of Fe^{2+}, Zeeman patterns 79−28647
$Co_cZn_{1-c}F_2$, Raman scatt. from Zeeman split levels 77−66243
Cr-Ta, mixed SDW and Zeeman hyperfine interactions, TDPAC calc. 79−99797
CrO_3^- radical in K_2CrO_4 and $KCrO_3Cl$, g-factor anisotropy 78−67994
Cs, $6S_{1/2}$-$7P_{1/2}$ transition, photon echo polarisation rotation in mag. field 78−22180
Cs, $7P_{3/2}$-$6S_{1/2}$ transition, photon-echo quantum beats obs. 80−23373
Cs, coherence of HFS excitations in optically oriented ats. mag. field modulation *(Russian)* 77−54530
Cs, optically oriented, RF coherency on HFS transition excitation by AM UHF mag. field *(Russian)* 77−42278
$^{133}Cs^+/Cs$ g-factor ratio, NMR and zeeman transition freqs. 78−17817
$CsCdCl_3:Co^{2+}$, Zeeman Raman scatt. and Zeeman IR absorpt. spectra 79−56782
Cs_3CoBr_5, optical anisotropies of mechanism of vibronic transitions in spectra 77−12372
Zeeman effect continued
Cs_3CoCl_5, optical anisotropies of mechanism of vibronic transitions in spectra 77−12372
$Cs_3Cr_2Br_9$, Cr (III) trigonal pair, exchange interactions, absorpt., MCD and Zeeman spectra 78−19009
$Cs_2Cr_2Cl_9$, Cr (III) trigonal pair, exchange interactions, theory 78−19008
$Cs_2GeF_6:Mn^{4+}$, magnetically circularly polarised emission and MCD of vibronic lines 77−16377
$CsMgCl_3:Co^{2+}$, Zeeman Raman scatt. and Zeeman IR absorpt. spectra 79−56782
$CsSiF_6:Mn^{4+}$, splitting of vibronic levels 78−60496
$Cs_2SiF_6:Mn^{4+}$, Jahn-Teller effect in $^4T_{2g}$ state, Zeeman meas. 80−29367
$Cs_2TiF_6:Mn^{4+}$, spin-orbit and field splitting, Jahn-Teller effect, Zeeman meas. 80−80234
$CsUO_2(NO_3)_3$, absorpt. spectra, MCD and natural dichroism, UV and visible 79−69853
$Cs(6^2P_{3/2})$+He(Ne)(Ar)(Xe), collisional depolaris., nucl. spin depend., by Zeeman scanning 77−19012
$(Cu,Zn)Cs_2(SO_4)_26(H,D)_2O$, thermal contact between nucl. Zeeman and electron dipole-dipole interaction system 77−90065
Cu complex, $Cu(H_2O)_6^{2+}$, ligand hyperfine interactions, orbital angular momentum contrib. 80−96833
$CuBr_4^{2-}$, ground state Zeeman splittings, reson. Raman spectra and mag.-optical activity 80−5579
Cu(I) complexes, cuprous halide triphenylphosphines, NQR, Zeeman effect 80−54980
DO_2, ν_2 fundamental band, 9.8 micron, laser mag. reson. spectroscopy 79−85961
$Dy_2O_2SO_4$, antiferromag., mag. props. and Zeeman effect meas. 79−33464
$Dy_2O_2SO_4$, mag. ordering, magnetisation, AC susceptibility and Zeeman effect meas. 80−60205
$Dy_2O_2SO_4$, magnetic struct. in antiferromag. and ferrimag. states 80−15695
$ErCrO_3$, mag. field induced spin reorientation, optical Zeeman absorpt. spectra 79−61398
Eu absorption spectrum, 2100-7200 Å, wavelengths, intensities, J- and g_J-values determ. 77−14383
Eu, spin relaxation of $^8S_{7/2}$ ground state in noble gases 77−58131
$Eu_2Mg_3(NO_3)_{12}.24H_2O$, Zeeman effect in absorpt. spectrum 77−63402
Fe Zeeman tuned mag. confined arc lamp, appl. to U 78−17593
Fe^{2+}, in octahedral symm., vibronic effects from Zeeman field induced Mossbauer spectra 77−8476
$FeCO_3$, siderite, Fe^{2+} Mossbauer spectrum, ligand field theory 77−16212
$FeNiBO_4$, mag. and Mossbauer studies 79−65661
$FeNi_2BO_5$, mag. and Mossbauer studies 79−65661
Fe_3O_4:^{119}Sn, magnetic interactions, Mossbauer spectra, Zeeman line, depend. on temp. 79−15301
Ga, ground-state hyperfine struct., differential Stark effect 80−42990
GaAs, conduction band effective mass, influence of high uniaxial stress 80−80162
GaAs, shallow acceptor states exam. by far IR Fourier transform spectroscopy 78−31185
GaAs, shallow donors, excited state transitions 78−6710
GaAs, trace element conc. meas. by Zeeman atomic absorpt. spectroscopy 80−29046
GaAs:Al, optical detection of NQR 79−69752
GaAs:C, Zeeman effect of effective mass acceptor, polarised luminesc. 79−4541
GaAs:Co VPE layers, bound-exciton luminesc., Zeeman anal. 79−95818
GaAs:Cr, semi-insulating, Zeeman studies of 0.839 eV emission 80−103987
$GaCl_3$, cryst. struct., Zeeman split fine struct. lines, FT NQR obs. 80−54982
GaP, complex form of donor energy levels, optical spectra anal. 78−23045
GaP:Co, optical spectra and Zeeman anal. of Co $3d^7$ state 80−66247
GaP:Ni, optical and EPR study of two-electron-trap state 79−73806
GaP:S(Se)(Te), pot.-depend. g-values and quenched diamag., props. of donor states 77−62861
GaP:S(Se)(Te), pot.-depend. g-values and quenched diamag., pseudoacceptors D^0, X 77−62862
GaP:Zn, Raman spectra of Zn acceptor 77−77187
GaSe, magnetoluminesc. at 4.2K 79−61345
$Gd_2(MoO_4)_3$, low temp. optical absorpt., external mag. field influence 78−43896
$GdVO_4:Ho^{3+}$, optically excited doublet splitting in magnetically ordered state 78−19238
Ge, excitation spectra of shallow acceptors, Zeeman effect, expt. 80−7381
Ge, impurity spectral linewidth meas., free electron effects 80−71463
Ge:Al, acceptor levels, Zeeman splitting, far IR photoconductivity spectrum 78−43444
Ge:Al, Zeeman effect in excitation spectra, photoelectric spectroscopy 79−82633
Ge:Ga, magnetoacoustic resonance attenuation, Zeeman splitting of acceptor ground state 77−47869
Ge:Sb, excited donor states, double optical transitions, reson. absorpt. meas. 80−93371
GeO_2:Al, tetragonal, $[Al]^0$ centre, nuclear Zeeman and quadrupole effects 78−35035
H ($1^2S_{1/2}$) to ^4He (2^3S_1) electronic g-factor ratio from Zeeman resonance meas. 78−13467
H atoms, Stark and Zeeman effects in parabolic coordinates 79−63957
H, Balmer-α line profiles and polarisations in strong mag. field 77−6729
H, dispersion relations 80−27978
H II, Zeeman splitting of high-n recomb. lines 80−58210
H II regions, search for Zeeman effect in RF recomb. lines 77−60809
H lines, integrated polarisation in strong magnetic field 77−17563
H maser response to coherent Zeeman perturbations 78−58972
H, nonrelativistic high order perturbation theory corrections to energy levels, infinite series representation 77−34564
H, quadratic Zeeman effect, perturbative approach 79−22649
H, quantum mechanical atom in mag. field 77−79577
H, spin-aligned atoms, theoretical props., expt. prep. 80−42969
H, Stark-Zeeman effect, dilatation transformation 79−3398
H, uniform mag. field, low lying levels below 10^9 G, adiabatic approx. 79−72235

Zeeman effect continued
H, Zeeman levels orientation by reson. radn. in turbulent plasma *(Russian)* 79−98028
H-like atom, fine struct. and HFS levels, Zeeman effect, relativistic corrections 80−37776
H_2, 3d-triplet complex, Zeeman effect, eigenvectors and g-factors, rovibronic states 79−72353
H_2, Bender-Wu formula, SO(4,2) dynamical group and Zeeman effect, perturbation coeffs. determ. 80−95674
H_2, Zeeman effect in 3d singlet states, g-values 78−50571
H_α and H_β spectral profiles from neutral beams and plasmas in high mag. fields 80−83999
HCO, ν_2 fundamental band, laser mag. reson. spectra 78−5256
H_2O_2, Zeeman effect and mol. quadrupole moment, beam maser spectrosc. 78−90152
He, 1s3d config., Zeeman sublevel energies, anticrossing and degeneracy 77−23417
He, high-L states, laser driven forbidden transitions, line shapes 79−22638
He II, Zeeman splitting of high-n recomb. lines 80−58210
He-Ne, ring laser, influence of reson. radiation trapping 77−75574
He-Ne laser light polarisation in transverse mag. field, Zeeman effect *(Dutch)* 78−29997
He-Ne laser mode locking by three-level reson., Zeeman tuning of intracavity Ne absorber 79−89943
He-Ne ring laser, influence of pressure on Zeeman effect 80−19056
He-Ne ring laser, nonlinear Zeeman effect 78−71123
He-Ne ring laser, operating well above lasing threshold Zeeman effect 80−33039
He-Ne stabilised transverse Zeeman laser, light source for optical meas. 80−48272
He-Ne two-mode travelling-wave laser, Zeeman beats 78−50827
He-Xe 3.51 μ laser mode competition in axial mag. field 80−63974
He-Xe laser, Zeeman tuned *(Korean)* 79−7145
^{3}He, BCC, Zeeman exchange cross relax. time 78−22930
^{4}He (2^3S_1) to H ($1^2S_{1/2}$) electronic g-factor ratio from Zeeman resonance meas. 78−13467
^{4}He, laser mag. reson., 7^1S-9^1P energy separation, motional Stark effect, Zeeman tuning parameters 79−6911
HfI, at spectrum, g-values, Zeeman effect, LS-coupling, ionisation pot. 77−3292
$HfSiO_4:U^{4+}(U^{5+})$, opt. spectra 78−88334
Hg 6^3P_1 collisional transfer rate between m-sublevels mag. field depend. 80−32802
Hg, 8^3S_1 level, Lande factor *(French)* 77−430
Hg lamp, line crossing obs. in 2537 Å line 78−9129
Hg, two photon excitation, time resolved spectroscopy 80−87075
$HgCl_2$, ^{35}Cl powder Zeeman NQR, injection and phase locked NQR spectrometer 80−54979
$^{185}Hg^m$, and $^{186m-191m}$Hg, nucl. spins, on-line quantum beat spectrosc. determ. 80−9562
$Hg(6^3P_0)$, $^3P_1$-$^2P_0$ fine struct. obs., CO_2 laser mag. res. 77−61696
$Hg(6^3P_1)+Hg(6^1S_0)$, collisional excitation transfer in high mag. fields, fluoresc. obs. 80−9689
$HoCrO_3$, magneto-optical investig. of Ho-Cr and Ho-Ho interactions 77−52055
$Ho_2O_2SO_4$, antiferromag., mag. props. and Zeeman effect meas. 79−33464
$Ho_2O_2SO_4$, mag. ordering, magnetisation, AC susceptibility and Zeeman effect meas. 80−60205
$Ho_2O_2SO_4$, magnetic struct. in antiferromag. and ferrimag. states 80−15695
$HoVO_4$, first excited doublet, zero field splitting 77−20870
I photodissociation laser, tuning using Zeeman effect 79−50316
I switch, active modulation of transmission based on Zeeman effect 79−22994
InP, excitons bound to neutral donors in VPE layers, luminesc. and absorpt. obs. 79−42460
Ir II, term anal. of spectrum 79−6902
$IrCl_6^{2-}$, ground state Zeeman splittings, reson. Raman spectra and mag.-optical activity 80−5579
K, $4^2P_{1/2}$ resonance substate, disorientation cross-section, Zeeman scanning obs. 80−42988
K, diamag. Zeeman shift of S,D Rydberg states, two-photon absorpt. 77−23461
K+He, 4^2P state $j_1m_1 \rightarrow j_2m_2$ Zeeman transition, total cross section energy depend. 80−83475
$KCdCl_3:Co^{2+}$, Zeeman Raman scatt. and Zeeman IR absorpt. spectra 79−56782
$KCl:PO_2^-$, triplet state pseudonuclear Zeeman effect, optical detections *(Russian)* 79−78571
$KCl:PO_2^-$, triplet state, level anticrossing and pseudonuclear Zeeman effect, microwave ODIMR 80−39896
$KMgF_3:Eu^{2+}$, Zeeman absorpt. and luminesc. spectra *(Russian)* 77−69872
$KMgF_3:Fe^{2+}$, octahedral symm., vibronic effects from Zeeman field induced Mossbauer spectra 77−8477
$KMgF_3:Fe^{2+}$, super hyperfine struct., Zeeman splitting and dynamic Jahn-Teller effect 77−85555
$KMgF_3$:Ni, Ni-Ni pair optical spectra 80−45042
$KMgF_3:Sm^{2+}$, absorpt. spectra and Zeeman effect, 3000-12000 Å, 4.2-295K 79−24341
$KMgF_3:Sm^{2+}$, luminesc. spectra 4.2, 77 and 295K and Zeeman spectra, 4.2K 77−81146
^{39}K, ground-state g-factor, rel. to ^{87}Rb, spin-exchange optical pumping meas. 77−34596
^{41}K vapour, optically pumped, RF shift for one quantum transitions 79−26930
Kr, $^3P_1$ state, reson. fluoresc., Zeeman beats, time-resolved VUV spectra using synchrotron radiation 78−33454
$LaBr_3:Pr^{3+}$, laser-induced fluoresc. line-narrowing, hyperfine struct. and Zeeman effect 77−85789
$LaCl_3:Pr_I$ optical absorpt. and Zeeman spectra, zero mag. field splitting 79−91482
$LaCl_3:Pr^{3+}$, hyperfine Zeeman effects, fluorescence line-narrowing technique 77−62881
$LaCl_3:Pr^{3+}$, satellite lines in optical absorpt. spectra, Zeeman effect 79−65911
$LaCl_3:Pr^{3+}$, second order Zeeman hyperfine effect *(French)* 77−52162
$LaCl_3:Pr^{3+}$, Zeeman second-order effects, fluoresc. line narrowing technique 80−16103
Zeeman effect continued
$LaF_2:Pr^{3+}$, ultraslow optical dephasing for $^3H_2$-$^1D_2$ transition 79−64290
$LaF_3:Er^{3+}$, optically excited, direct-process spin-lattice relaxation 80−93378
$LaF_3:Pr^{3+}$, optical line narrowing by nuclear spin decoupling, photon echo meas. 80−48353
$LaF_3:Pr^{3+}$, ultraslow optical dephasing 80−58648
$LaF_3:Pr^{3+}$, ultraslow opt. dephasing at 2K 80−91864
$La_2O_3:Mn^{2+}$, position and intensity of forbidden hyperfine lines, ESR spectra, nucl. Zeeman term 79−19775
$(La_{1-x-y}Pr_xA_y)Cl_3$ (A=Ce, Gd, Y), satellite lines in optical absorpt. spectra, Zeeman effect 79−65912
$LaRh_2:Nd^{3+}$ cubic metallic host, spin-lattice relaxation, ESR obs. 79−1710
$La_{1-x}Tb_xAg(Sn_3)(Al_2)$, paramag. anisotropy of Tb^{3+} in cubic cryst. field 80−15687
LiF, behaviour of nucl. spins near highly polarised paramag. centres 77−77127
LiF, NMR, thermodynamic effects of RF pulse pair on system with two spin species 77−66433
$MgCl_2:Co^{2+}$, Zeeman electronic Raman scatt. spectra 79−42962
MgO, powder, positronium fine struct. interval meas. by Zeeman transitions 78−95616
$MgO:Fe^{2+}$, $^5T_{2g} \rightarrow {}^5E_g$ adsorption, Zeeman effect meas. 77−12405
$MnCl_2.2H_2O$, magnetically ordered phase, $^6A_{1g}$ to $^4T_{2g}$ transition absorpt. lines, Zeeman effects 78−6699
$MnCl_2.2H_2O$, ordered, paramag. phases, optical absorpt. spectra, V-lines, Zeeman effects 78−6698
$MnCl_2.2H_2O$, paramag. phase, external mag. field depend. of $^4T_{2g}$(II) Kramer doublets of Mn^{2+} 78−6700
MnF_2, MCD spectrum, Zeeman splitting of purely excitonic lines 77−40262
$Mn_{1+x}Sb_{1-x}Sn_x$, nuclear Zeeman effect, Mossbauer meas. 79−28654
N, reson. lines shapes determ. by Zeeman scans 77−6723
NH_2, ν_2 band, laser mag. reson. 80−83523
NH_4ClO_4, with 0.015% and 0.1% D, proton Zeeman relaxation 78−6592
$(NH_4)_2HAsO_4$, Zeeman perturbed NQR spectra, EFG tensors and antiferroelectric ordering 77−43898
$NH_2(X^2B_1)$, laser mag. reson. spectra, Zeeman and hyperfine effects, rot. consts. 77−30892
NO, $^2\Pi_{1/2}$ and $^2\Pi_{3/2}$ band centre freqs., opto-acoustic detection 77−58108
NO, intracavity Zeeman modulation detect., passive Q-switching, CO IR laser obs. 80−9597
NO, Zeeman modulation IR spectroscopy using spin-flip Raman laser 79−18181
NO, Zeeman modulation spectroscopy, line shape analysis 80−74197
NO, Zeeman spectrum, mol. beam elec. reson. spectrosc. 80−91621
NO, Zeeman spectrum with magnetospectrophone 77−83647
NO_2, EPR, mag. dipole transitions, Zeeman parameters 78−17697
NO_2, rot. Zeeman spectroscopy, 8_{08} to 7_{17} rot. transition 78−25610
N_2O, anomalous Zeeman effect, nonlinear optical techniques, book contrib. 78−9279
$^{14}N^{16}O$, $^{15}N^{16}O$ isotopic species determ. using Zeeman scanning of atomic line, vibr.-rot. line profiles 79−49983
Na, $3^2S_{1/2}$-$3^2P_{3/2}$, spectral distrib. and collisional depolarisation of laser light, D_2-fluorescence 80−58209
Na D_1 line profile, Zeeman scanning 80−47928
Na, Rydberg states, fine struct. and Zeeman beats 79−14044
Na, vap., sum frequency generation, via reson. quadrupole transition, theory 78−42385
Na vapour, laser induced population grating 80−69466
Na vapour, Zeeman coherence, transient and stationary, polarisation spectroscopy 80−58212
NaF, F_3^+ centre zero-phonon line, photochem. and population hole burning 79−42997
$NaMgF_3:Eu^{2+}$, Zeeman absorpt. and luminesc. spectra *(Russian)* 77−69872
$NaMgF_3:Sm^{2+}$, absorpt. spectra and Zeeman effect, 3000-12000 Å, 4.2-295K 79−24341
$NaMgF_3:Sm^{2+}$, luminesc. spectra 4.2, 77 and 295K and Zeeman spectra, 4.2K 77−81146
$Na_2O.2Al_2O_3.5SiO_2:Fe^{3+}$, Mossbauer effect and magnetometric exam. 78−6613
$Na_3Pr(C_4H_4O_5)_3.2NaClO_4.6H_2O$, single cryst., forbidden $A_1 \rightarrow A_1$ transition, mag. field induced intensification 80−50302
$Na_3Pr(C_4H_4O_5)_3.2NaClO_4.6H_2O$, absorpt., circular dichroism, and mag. circular dichroism spectra 80−97243
^{23}Na, ground state g_J factor, meas. from weak-field Zeeman spectra 78−33469
$Na(3^2P_J)+Na(3^2S_{1/2})$, collisional excitation transfer, pot. symm. rules and cond. function 80−9690
NdF_3, Zeeman splitting in mag. fields up to 100 kG 78−52483
Ne, fine struct. obs. by beam-gas spectroscopy, level crossing resonances 80−9719
Ne, g-factors meas. by quantum beat spectroscopy 79−93955
Ne, high resolution Zeeman spectroscopy by mode crossing 77−71776
Ne I, $2p^56d$ config. in mag. field, energy levels 79−63955
Ne, optical-optical double reson., $2p_4$ and $2s_2$ level g_J-values by mode crossing 77−50411
Ne, reson. level lifetimes, Zeeman coherence radiative and collisional transfer between excited states 77−23466
Np I, spectrum, 4000-40000 cm^{-1}, term analysis 77−38629
O 2.53 mm line, Zeeman splitting rel. to geomagnetic field vars. 80−77124
O_2, high precision effect 79−3492
O_2, rot. struct. in Zeeman effect 79−50078
O_3, mol. beam electric resonance, electric and mag. props. determ. 77−27055
O_3, mol. beam Stark, Zeeman effects, polarisability, moments, mag. susceptibility anisotropy 77−79649
OD, $^2\Pi_{3/2}$ state EPR spectra 78−21949
OH, $^2\Pi$ states, $^2\Delta$ states, $^2\Pi$ ground state, g-factor, Zeeman effect 79−98149
OH, interstellar, new main line maser obs. with probable Zeeman pattern 80−56908
OH, isotope effects, Zeeman effect, far IR laser mag-reson. spectra obs. 80−63674
OH maser emission from W3 (OH), Zeeman effect 78−93377
OH radical, gas phase EPR, rot. states electronic struct. and Zeeman parameters 78−86896

Zeeman effect continued
ONF, J transitions, rot. Zeeman effect 80−63707
Pb traces in human blood plasma, atomic absorpt. anal., nonspecific absorpt. correction using Zeeman effect 80−76881
$Pb_3(PO_4)_2$:Gd^{3+} (Eu^{2+}), EPR spectra of α- and β-phases 80−11261
Pd-Ni, dil., Zeeman splitting of cond. electrons 77−11884
Pr^{3+} aquo ion spectra, MCD of $^3P_0 \leftarrow {}^3H_4$ transition 80−7331
Pt porphin in n-alkane single cryst. ^3E_u-$^1A_{1g}$ transition, Zeeman expts. at 4.2K 80−78645
Rb, lowest metastable autoionising level identification by RF spectroscopy 77−426
Rb, maser response to coherent Zeeman perturbations 78−58972
Rb, optical pumped magnetometer *(Japanese)* 79−21790
Rb, Zeeman resonance lineshapes, motional narrowing 77−46525
$RbFeCl_3$, singlet ground state 1-D ferromag., far IR Zeeman spectra 77−52098
RbKr, magnetic resonance meas. of spin-rotational interaction 78−33528
Rb_2MnCl, layer antiferromag., optical absorpt., temp. and mag. field depend. 80−20661
^{85}Rb, hyperfine struct., diamag. shift obs. 77−61717
^{87}Rb, ground state g-factor, rel. to ^{39}K, spin-exchange optical pumping meas. 77−34596
S^-, photodetachment in mag. field 79−41143
SO, and isotopic forms, $X^3\Sigma^-$ state, CO_2 laser mag. reson. spectroscopy 80−9602
SO, high precision effect 79−3492
$SbCl_3$, cryst. struct., Zeeman split fine struct. lines, FT NQR obs. 80−54982
Se_2, Lande factor meas. by Zeeman quantum beats *(French)* 79−45761
SeH($X^2\pi_{3/2}$), far IR LMR spectrum 78−66564
SeO, $X^3\Sigma^-$ state mol. parameters, Zeeman and EPR spectra 79−6966
$^{80}Se_2$, B $^3\Sigma_u^-$ state, Lande factor meas., mol. perturbations 79−45756
Si, exciton-impurity complexes, emission spectra, Zeeman splitting *(Russian)* 78−64413
Si:Al, localised exciton bound to isoelectronic trap 80−66283
Si:Au, EPR spectrum, strong nucl. quadrupole effect 80−93172
Si:B(P), recombination spectra of bound multiexciton complexes, Zeeman splitting *(Russian)* 79−38526
Si:K, bound exciton luminescence in mag. field *(Russian)* 80−108278
Si:Li, photolum. of bound exciton and bound multiexciton complex, Zeeman effect 80−108265
Si:Mg, Zeeman effect of excitation spectrum of neutral donors 77−63439
Si:P, acceptor bound multiexciton complex recomb., shell model, luminesc. line splitting 78−6275
Si:P, Zeeman and stress-induced spectra, shell model for bound multiexciton complexes 77−31953
Si:P^+, Zeeman energy transfer at surface layer 80−11247
SiC, (6H), radiation damaged, luminesc. 80−25462
β-SiC, cubic, conduction band minima location and shape determ. 77−85141
SiH_3Br, rot. Zeeman effect 79−54909
SiH_3NCS, microwave spectrum, rot. Zeeman effects 79−54847
SiO_2, glass, irrad., EPR of Al E_1' centres 80−11268
SiO_2, powder, positronium fine struct. interval meas. by Zeeman transitions 78−95616
Sm, coherent ground state transients, beat meas. 80−948
SmI, Zeeman coherence, transient and stationary, polarisation spectroscopy 80−58212
$SnCl_2.1.5H_2O$ single cryst., ^{35}Cl NQR, cryst. struct. 80−60449
Sr, quadratic Zeeman effect, diamagnetic shift, Rydberg series, strong field mixing 78−946
Tb II, Zeeman patterns, g-factors 79−22651
Tb^{3+} in rare earth ion cryst. field in YF_3 struct., spectra 78−19563
$ThSiO_4$:U^{4+}(U^{5+}), opt. spectra 78−88334
$UFe_3B_2(B_4)$, Mossbauer effect of ^{57}Fe nuclei, mag. props. 80−103907
Xe, $^3P_1$ state, reson. fluoresc., Zeeman beats, time-resolved VUV spectra using synchrotron radiation 78−33454
Xe I three-level system, level splitting within natural width, saturation spectrum 80−106291
Xe+ inert gas, Xe three level system, collisional transfers, disalignment cross section 80−53098
YAG:Gd^{3+}, EPR absorpt. spectrum 78−76305
YAG:M^{3+}, ESR absorption spectra, line broadening of Fe^{3+}, Cr^{3+}, Gd^{3+} 78−91940
YIG:Si(Ge), effects of nontrigonal cryst. field on spectroscopic props. of Fe^{2+} ions 80−92864
YIG:Si(Ge), Fe^{2+} spectroscopic props., nontrigonal cryst. field effects 80−44553
Yb, Zeeman quantum beats in $6s6p\ ^3P_1$-$6s^2\ ^1S_0$ transition 79−13682
$YbCu_2Si_2$, mag. 4f Zeeman-level power spectrum using diffuse mag. neutron scatt. 79−60775
YbI, emission spectrum, extended anal. 79−85923
YbI, first spectrum, wavelengths and intensities, Zeeman effect 79−3389
Yb(6^3P_1), Zeeman splitting, high-resolution time-resolved quantum beat spectra 78−58640
ZnO, Zeeman splitting of A1-exciton emission lines, k-linear term effects 78−52563
ZnO:Cu, excited state, zero phonon lines in emission and Zeeman spectra 79−38026
ZnO:Ni^{2+}, Zeeman effect at Ni impurities 80−60633
ZnS:Cu^{2+}, motional averaging in excited state 77−66137
ZnS:Mn^{2+}, $^4T_2$ level, Zeeman splittings, Jahn-Teller effect 80−40141
ZnS:Ni^{2+}, Zeeman effect at Ni impurities 80−60633
ZnSe, cubic, magnetoreflection of s-excitons 78−60426
ZnSe, valence-band parameters and g-factors from free-exciton magnets reflectance 79−73905
ZnTe, I_4 bound exciton, magneto-optical meas. 77−20836
ZnTe:Li, Zeeman splitting of ground and excited acceptor states, selective pair luminesc. 80−84780
$ZrSiO_4$:U^{4+}(U^{5+}), opt. spectra 78−88334

Zener breakdown *see Zener effect*

Zener diodes
breakdown voltage, electron irrad. effects 79−95472
dosimeter, for high-level electron dose meas. 77−50331
junction breakdown voltage, temp. effects 79−7882
radiation dose measurement using radiation induced changes *(Japanese)* 78−78504
sample heater, high vacuum, using Zener diode 78−12690
tunnelling and negative resistance phenomena in p-n junction devices, book 78−26947

Zener effect
see also Zener diodes
semiconductor, Zener tunnelling in mag. and elec. fields 79−91082
$Ga_{0.47}In_{0.53}As$ p-n junctions, band-to-band tunnelling current 80−107895
InGaAsP avalanche photodiodes, breakdown mechanism, donor conc. effect 80−70710
InSb, Zener tunnelling in mag. and elec. fields 79−91082

Zener relaxation
plate, deform. vibrs., acoustic thermal relax. method for thermophys. props. determ. of group V metals at high temp. 79−85143
Ag-Sn(In)(Cd), Zener relaxation, valency and dimensional effects *(Russian)* 78−19802
Ag-Zn (30 at.%), electron irrad. exam. of defect supersaturation by elasticity, and creep meas. 78−47366
Ag-Zn (30 at.%), neutron irrad., at. mobility enhancement, Zener relax. meas. 77−1157
Al-Ag, precipitation study by internal friction *(French)* 80−35190
Au-Ag alloy, vacuum-deposited monocryst., rel. to internal friction, 200-3000 Hz, 20-850°C *(Russian)* 77−21197
Cu-Zn-Al, Zener relaxation *(Russian)* 77−21198
α-CuNiZn alloys, Zener-relaxation effect 80−3121
n-Ge, US attenuation by impurities 77−69047
Pd-Ag-H(D), elastic energy dissipation peak 80−60905
Pd-H system, α and $\alpha+\beta$ phases, annealed and deformed, anelastic effects 80−66567
Pd-H(D), elastic energy dissipation peak 80−60905
Pd-Pt-H(D), elastic energy dissipation peak 80−60905
p-Si, US attenuation by impurities 77−69047

zero gravity experiments
acoustic levitation and manipulation method for controlling liquid samples 80−74666
alloy, solidification mechanisms, contribution of microgravity expts. 78−88457
Atmospheric Cloud Physics Laboratory on Space Shuttle, image dissector for size and position of statically suspended particles 80−26616
Atmospheric Cloud Physics Laboratory on Spacelab 80−4090
binary fluid layer heated from below, thermal diffusion, instability 78−75860
biological expts. on Cosmos 782 satellite, results 78−85818
biological materials separation in space environment, electrokinetic phenomena and electrophoresis 79−48351
biorheology 80−3659
biosatellite Cosmos-782, biological expts. 80−61710
blood sedimentation rate free from gravity influence, rapid determ. from density meas. *(German)* 78−81085
blood viscosity and red cell aggregation at zero and 1G, instrumentation for Space Lab 3 80−61716
blood viscosity and red cell aggregation under near-zero gravity 80−3660
body fluid volume changes induced by spaceflight 80−61715
bone formation inhibition in rat during space flight 79−48350
bubble detachment from wall, mech. at zero and negative gravity 77−3863
bubble thermal migration, internal heat transport effects in weightless liquids 80−24075
bubble with adsorbed film, migration in Hele-Shaw cell, rel. to materials processing in space 79−28912
bubbles with adsorbed films, motion through viscous fluid 79−18933
capillary shaper under conditions of weightlessness 78−2038
cardiovascular system, early adaption to simulated zero gravity 80−3827
casting, dendrite remelting and macrosegregation in low-gravity 79−47669
ceramics and glasses, materials science applications in space environment 79−47885
combustion and fluid dynamics, possible space environment expts. 79−46402
composite materials, porsibility of production under conditions such that effects of grvitx forcer balnce ott 78−31363
composite materials preparation under microgravity conditions, stability during melting, thermal soak, solidification *(German)* 80−7521
convection, surface-tension induced, at reduced gravity 78−83374
critical phenomena experiments, gravity effects in fluids near the gas-liquid critical point 79−58667
critical phenomena experiments in space 79−67278
crystal growth, future research 79−47607
crystal growth, Polish technological experiments in space *(Polish)* 79−56920
crystal growth, preparatory experiments for first Spacelab flight 78−88414
crystal growth, thermomolecular fluid flow effects in low-g 79−73117
crystal growth and materials processing, future fluid flow research 79−47622
crystal growth from solutions in low gravity 78−84706
crystal growth in space, past and future, rel. to spacelab 78−80462
crystal growth in space environment 79−47605
crystal growth in Spacelab 78−52647
cylindrical slab of fluid, in weightlessness condition, surface-tension driven convection *(Russian)* 78−90872
drop vibration analysis, at near zero gravity 77−7426
droplet growth and initial dew point temp. accuracy in cloud chamber on space shuttle 78−96268
dynamic stabilization of multiphase media subjected to vibrations under low gravitation conditions 80−7511
education, soap film on wire frame in zero gravity, variation problem branching 79−9057
electronic materials growth technology, possibilities for low-g expts. 79−47606
electrophoresis, deflected-lamina, biological materials fractionation in space 78−85397
electrophoretic separator, continuous flow, for biological materials on sounding rocket 78−85398
European Space Agency cyrogenic programme and superfluid He cryostat for spacelab 79−63239
exercise response to simulated weightlessness 80−61713
floating zone, under reduced gravity, Marangoni convection 80−66425

zero gravity experiments continued
floating zone melting, microgravity simulation of Marangoni convection 79−28911
floating zone melting using reduced gravity environment, floating zone structure 79−28909
flow processes in microgravity environments 80−1720
fluid behaviour in space environment, review 79−46410
fluids, ph 77−39658
fluorocarbon monomers, plasma polymerisation 78−35304
glass technology, optical and magnetic materials *(German)* 80−40317
haemorheology in near zero gravity environment 80−3661
heat pipe, mathematical model including transport-opposing body forces 79−41552
heat transfer under reduced gravity conditons 77−4192
Hele-Shaw cell, bubble motion, study of 2 phase flows under reduced gravity 79−14457
human, haematological response, math. and exptl. simulation 80−61714
laser host glass, outer space formation 77−21084
liquid metal thermal conductivity meas. in Spacelab *(German)* 80−57303
long duration exposure facility, utilisation of vacuum developed in wake zone 78−36433
low gravity solidification expts., use of metallic analogue materials 80−71635
lung, human, radiographic comparison of shape during normal gravity and weightlessness 80−67260
material charging in space environment 80−109327
material processing facilities and expts. and Spacelab 78−36431
material sciences in space, proposals for first Spacelab mission, review 77−36377
materials processing, expt. capabilities in space 79−47882
materials processing, expt. capabilities in Space Shuttle/Spacelab 79−47883
materials processing in space 78−35296
materials processing in Spacelab. 78−35295
materials research and processing programme for Spacelab by German Federal Republic 78−88620
materials science and technology, space flight appl., conf., Gaithersburg, USA (April 1977) 79−47881
materials science in space, crystal growth, prod., and rare earth synthetic mag. materials *(French)* 79−83111
MBE experiments on Space Shuttle 78−35317
metal adhesion experiment for Spacelab 78−88621
metal foam solidification, fluid flow effects 79−47674
metallurgical studies in Skylab and Apollo-Soyuz 79−47700
metals, phenomena and priorities for research in space 79−47884
microgravity experiments, physical basis *(German)* 79−67277
narrow band gap semiconducting alloy layers, electron beam microzoning 78−35325
nonequilibrium systems, effect of gravity on pattern formation 79−70302
optical glass, melting, fining, surface tension, diffusion, nucleation in microgravity 80−81016
phase transformations, second order, critical phenomena and condensation 79−46783
pool boiling in very low gravity, proposed spacelab expt. 78−63849
powder reinforced metal composite with glass microsphere filler prod. in space 78−52726
pulmonary ventilation and perfusion distrib. during short weightlessness periods 79−83951
purification and thermodynamics 79−46816
relativity experiments, control requirements 80−8896
skin technology, industrial appl. of space processing 79−28991
Skylab, review of manned expts. in space 78−36429
sled programme, Spacelab, weightlessness expts. on man 80−94381
smelting, metallurgy and electrolysis, ERNO space research, with vertical Skylark rocket *(German)* 79−19980
solidification, direct obs. as function of gravity level 77−36494
solidification, properties for space environment expts. 79−46787
solidification in space environment, bubbles thermal migration and interaction with solidification interfaces 79−47670
solidification interface in reduced gravity, bubble interactions 78−84787
space laboratory, crystal growth, techniques *(Hungarian)* 79−47603
space research impact, 1981 Spacelab era influence forecasting 79−19981
Space Shuttle, expts. on mol. and atomic beam interactions with surfaces 78−35243
Space Shuttle, use for science and engineering, Symposium, California (May 77) 78−36426
Space Shuttle orbiting molecular beam laboratory 78−35242
Spacelab, biomedical expts. 77−16999
Spacelab, ESA material science experiments 78−88618
Spacelab, Federal Government of Germany promotion 78−53790
Spacelab, material processing facilities and expts. 78−53789
Spacelab, use of ion beams in near-surface anal. 78−35755
Spacelab and artificial satellites appls., conf., Rome, Italy (Mar. 1978) 78−96384
Spacelab as orbiting atmospheric laboratory 77−21941
Spacelab crystal growth expts. 78−52648
Spacelab metallurgical experiments, possible influence on current procedures 78−88619
Spacelab optical techniques for liquid flow and temp. meas. 79−82007
Spacelab project, zero gravity physics 77−29619
superconductivity, space applications 80−41694
surface analysis, in space exploration, analytical appls. of Auger and XPS 78−35756
thermodynamics and dynamics of pure interfaces, rel. to Spacelab 79−28910
transport processes in fluids 79−46825
vapour growth in microgravity environment 79−83131
vitroceramic-metal composite materials development, Spacelab appl., mech. props. *(French)* 78−92229
wake of space vehicles, use of vacuum for conducting expts. 78−74013
weightless liquid systems, acoustic manipulation in space 77−49716
weightless zone recrystallization, stability of a singly connected molten zone 79−78874
zone crystallisation, double-ellipsoid mirror furnace for expts. in Spacelab 79−78872
Ag composite, SiC whisker-reinforced, prep. aboard Skylab. 78−84741
Al-Cu (33 wt.%) eutectic, solidification under reduced gravity, behaviour of suspended Al_2O_3 particles *(German)* 80−60853

zero gravity experiments continued
Al-In (40, 70 wt.%), liq. phase immiscible system, solidification in microgravity 78−84770
Al-In alloys within miscibility gap, agglomeration in space environment 79−47672
Al-In emulsion, solidification mechanisms at zero gravity, review 78−88458
Al_2O_3, Czochralski bulk flow, in microgravity, digital simulation 80−28934
AlPb alloy prod. under microgravity *(German)* 79−38766
AlSb, gravitational influences on liquid-state homogenisation and solidification 79−78864
Be casting produced in zero gravity environment, BeO particles uniform distrib. 78−72753
Be, containerless grain refinement using BeO in space environment, melting and solidification 79−47673
Be, containerless melts in terrestrial and space environment, thermodynamic props. calc. from solidification and cooling curves 79−70052
CBr_4, low gravity solidification, bubble behaviour 80−15219
GaAs (110) surface, exposed to O and O_2 photoemission spectra meas., Space Shuttle expt. 78−35246
Ge, crystal growth and segregation under zero gravity 79−43130
Ge-S-Sb glasses, microgravity effect on recrystn., optical and elec. props. 80−49127
Ge-Si-Sb solid soln., components distrib., influence of conditions for Universal Furnace expt. in Soyuz-Appollo programme *(Russian)* 78−31381
^{3}He, superfluid, behaviour in zero gravity 79−55987
^{4}He, superfluid, behaviour in zero gravity 79−55987
^{4}He, superfluid, props., expts. in zero gravity 77−31822
^{4}He, superfluid film 80−54464
Mn-Bi alloy, melting and solidification under microgravity, mag. props. *(German)* 80−45296
NH_4Cl-H_2O, solidification microstructs., effect of reduced gravity 80−96632
Pb-Sb eutectic alloys, solidification in space environment 79−47671
PbTe single crystals, growth from vapour phase under micro-gravity conditions 80−80957
W, containerless melts in terrestrial and space environment, thermodynamic props. calc. from solidification and cooling curves 79−70052

zero sound
see also liquid helium sound propagation
classical liquid, excitation, damping, memory function approach 78−67771
dense neutron matter, zero sound propag., Landau theory 78−53977
exciton dielectric type system with doping, low freq. excitations *(Russian)* 80−15459
Fermi liquid, normal, transition from first sound to zero sound 77−89609
ferromagnet, excitonic, zero-sound excitations, Fermi liq. model 80−93101
kinetic theory of normal Fermi liquids 78−87841
Landau F_2 calc. from zero sound velocity 78−91500
nuclear matter collective excitation stability with Skyrme interaction *(Russian)* 79−13239
Cu, zero to first sound transition, inelastic-neutron scatt. data 77−31738
He II-^{3}He degenerate soln., spin waves and zero sound possibility *(Russian)* 77−35789
^{2}He, liq., 0.015K, elementary excitations, neutron scatt. study 79−46874
^{3}He, incipient superfluidity, above superfluid transition temp. 78−79846
^{3}He, liq., elementary excitations, RPA model using extended Landau theory 78−14527
^{3}He, liq., interface with nonmag. solid, Kapitza resist., quantum perturbation treatment 80−88385
^{3}He, liq., longitudinal zero-sound dispersion, thermal cond., and Landau F_2 78−2327
^{3}He, liq., neutron scattering, dynamical form factor, RPA calc. 77−7938
^{3}He, liq., normal phase, Landau Fermi liquid theory and low temp. props., book contrib. 79−99386
^{3}He liquid, zero sound lifetime, neutron inelastic scatt. study 80−65329
^{3}He, liquid, zero sound with velocity less than Fermi velocity *(Russian)* 80−92747
^{3}He, neutron inelastic scattering, zero sound and spin-fluctuation peaks 78−79836
^{3}He, normal liquid, elementary excitations, density and spin density, zero sound mode, press. depend. RPA model calcs. 80−59749
^{3}He, normal phase, spin-zero-sound solns. of the quasi-particle Boltzmann equation 79−77856
^{3}He, normal phase, suppression of transverse zero sound by mag. field *(Russian)* 78−59995
^{3}He, normal phase, transverse acoustic impedance meas., 0.015-1.0K 77−59167
^{3}He, superfluid, zero sound attenuation from order parameter fluctuations 78−79845
^{3}He, superfluid, zero sound and spin waves coupling near T_c 79−69309
^{3}He, superfluid A-phase, absence of orientational elec. field effect 79−19417
^{3}He, superfluid A-phase, attenuation of zero sound 77−24461
^{3}He, superfluid A-phase, spin relax. and zero sound attenuation at low temp. 80−107595
^{3}He, superfluid B-phase, HF sound propag. meas. 80−88391
^{3}He, superfluid B-phase, transverse zero sound 77−31829
^{3}He, superfluid B-phase, zero sound attenuation peak obs. 80−88390
^{3}He, superfluid B-phase low freq. zero sound attenuation, satellite peak struct. press. depend. 78−75901
^{3}He, transverse zero sound *(Russian)* 79−95240
^{3}He under pressure, inelastic neutron scatt., zero sound mode nature 79−55998
^{3}He/solid interface, refl. of transverse zero sound *(Russian)* 80−70492

zeros *see poles and zeros*

zeta-potential *see electrokinetic effects*

zinc
see also nuclei with .....
3p vacancy state radiationless deexcitation, exchange and relax. effects 79−3396
acoustic emission during twinning of single crystal 78−11468
adiabatic to sudden regime transition for $M_3M_{4,5}M_{4,5}(^1G)$ Auger excitation 80−45176
adsorption-desorption on GaAs, thermal desorpt., at. beam adsorpt., AES, SEM, RHEED 78−14591

zinc continued
aerosol, condensation in heat-pulse cloud chamber, prismatic and spherical particle form. 77−9135
AES and XPS, vapour-metal electron energy shifts 80−16142
air pollutant, radioisotope-induced X-ray fluorescence analysis 77−17214
alpha-particle irradiation, 6.1 MeV, stage III and IV recovery kinetics, defect diffusion 77−76474
alternating bending of single crysts., shear strain accumulation and microstrain distrib. *(Russian)* 78−60706
anharmonic lattice vibr., 'forbidden' X-ray reflections obs., 300K 78−34586
anisotropic thermal expansion 79−23750
atom, 3p-3d^2 super Coster-Kronig and 3p-3d4s Coster Kronig transitions 78−50522
atom, ^{1}S, ^{3}P, ^{1}P states, dipole polarisabilities from compact variational trial functions 80−63568
atom, (ns nd)^{1}D$_2$ states, Hanle effect, alignment destruction by collisions *(French)* 78−5324
atom, and Zn^+, excitations, comparison of gas-phase, plasma, sputtering and beam-foil 80−32820
atom, core binding energies, gas phase X-ray photoelectron spectra 78−37611
atom, electron bombardment, Kα satellites 80−47932
atom, electron impact ionisation cross sections, 40 eV 77−3472
atom, excited states, collisional quenching cross sections and exit channels, fluoresc. quenching obs. 80−18919
atom, Fermi correlation, for parallel-spin electrons in momentum space 77−10602
atom, ground state correl., photoelectron spectra, multiconfig. Hartree-Fock calcs. 77−50471
atom, highly ionised, spectral classifications below 55 Å 79−13658
atom, inner core neutral binding energies, relaxed orbital relativistic Hartree-Fock-Slater calc. 78−13433
atom, Kβ X-ray spectra and autoionisation following β-decay of ^{64}Cu 78−13029
atom, Kβ/Kα ratio anomalies, K-capture rel. to bremsstrahlung excitation 77−18825
atom, L_{23}-$M_{4,5}M_{4,5}$ principal and satellite Auger spectra 78−42030
atom, L and M Auger spectra, CI effects, anomalies 78−33488
atom, L-shell soft X-ray emission spectra, oscillator strengths 80−32651
atom, low energy electron scatt., shape resonances, electron affinity 77−14581
atom, metastable state depopulation, diffusion coeff. in Zn afterglow determ. 77−23542
atom, $O^{2+,3+,4+,5+}$ induced K-shell X-ray production cross section, 7 to 24 MeV 77−61850
atom, oscillator strengths of reson. transitions 79−22666
atom, photoelectric cross sections, 5-40 keV photons, X-ray emission spectra 77−18866
atom, quadrupole antishielding factors, Hartree-Fock perturbation theory 78−62723
atom, Rayleigh scattering at 59.34 keV through 60° to 150° 77−83547
atom, reson. X-ray Raman scattering, IR divergence of Compton effect 78−21873
atom, self-broadened 3075.9 Å line, temp. effects 77−3318
atom, simultaneous excitation of two electrons 78−21867
atom, Stark interaction in nspz^{1}P$_1$ levels, optical double resonance obs. 79−63941
atom, triplet state lifetimes, (4s6s), (4s5d), (4s6d) configs. *(French)* 78−5175
atom, UV photoelectron spectra, wavelength depend. of satellite struct. 77−34597
atom, XPS and Auger spectra, many-body calcs. 79−49995
atom+H^+(D^+), K shell ionisation, nuclear Coulomb effect 80−91650
atom+O ion collisions, A=16, 18, K-X-ray production 77−23554
atomic and metallic, photoelectron and L_{23}-MM Auger spectra, binding energies 77−90238
atomic electron collision cross sections 77−42410
atomic spectral line breadth optimisation, pulsed supply hollow cathode discharge 78−33471
atomic vibr. and fermion behaviour of HCP metals 80−6474
atomic vibrations, antisymmetric, from elastic neutron scattering data 79−33046
atomic vibrations, mean square displacements in cryst. lattice, rel. to sp. ht. *(German)* 80−79902
atomisation, for graphite furnace AAS, using graphite platform 78−32877
atoms, electron binding energy and shift, core level XPS 80−87088
atoms and ions, photon coherent scatt., cross sections 77−50410
Auger effect, K→M^2 radiative, low energy satellites meas. 80−45174
Auger electron spectra, electron impact excited, vap. and solid state differences 78−52603
Auger energy calc. using XPS, effect of 3d-4s admixed screening on relax energies 77−1782
Auger LMM spectra, transition probabilities, term splittings and effective Coulomb interaction 77−44126
Auger spectra, comparison with multiplet struct. calc. 78−31287
Auger spectra, $L_{2,3}M_{4,5}M_{4,5}$, solid state and oxidation effects 77−63501
Auger spectra, LMM, rel. to L_{23} photoelectron spectra 77−77348
Auger spectra MVV during oxidation, line shape, relax. energies 77−73195
Auger spectrum, multiplet struct. 77−48285
background damping in vicinity of grain boundary peak 77−28843
band structure, density of states and Fermi surface, APW calc. 77−20232
basal dislocation-prismatic dislocation ring interactions by method of moments *(Russian)* 80−10550
basal forest dislocation as source of pyramidal, dislocations *(Russian)* 77−84759
basal screw dislocation, exptl. determ. of line energy 80−88154
basal slip, early stages in single crystal 77−72623
bicrystal, ⟨10$\bar{1}$0⟩ tilt, misorientation depend. of grain boundary sliding 80−15119
bicrystal, compatible, plastic deform. *(Japanese)* 78−31460
bicrystal, diffusionless motion of grain boundaries, 200-405°C 79−19264
bicrystals, galvanomagnetic phenomena at common boundary, electric field potential distribution *(Russian)* 80−29388
bicrystals, grain boundary slip in deform. 80−34008
bicrystals grown by modified Bridgman technique 78−60563
black Zn-dust pigmented solar selective coatings for solar photothermal conversion 80−66997
zinc continued
British coastal waters, Zn pollution and photosynthesis inhibition 79−24921
brittle fracture, temp.-time depend. of strength in embrittlement region *(Russian)* 77−25125
Burgers vector determ. of perfect dislocations obs. by X-ray topography of single cryst. 79−37711
cataphoretic laser, transverse separation dynamics 77−38865
cathodic pretreatment 78−19929
cavitation induced multiple slip, twinning and fracture 78−39872
chelation with aspartic acid, US study 77−44464
chromated, electroplate on steel, corrosion, effect of chromate content 79−20286
cleavage fracture, hydrostatic tension effect, pure polycrystalline specimens 78−52990
coated steel sheet, chromate passivation protection against wet-storage stain 78−95854
coating for steel products, thickness meas. by X-ray fluoresc. 77−54029
coating on Cu crystal, effect of coating on Cu fatigue behaviour 78−72850
coating on steel, cold rolling influence on struct. and deform. of diffusional layer *(Russian)* 80−55465
coating on steel, fast reactions in hot galvanising rel. to props. 79−43486
coating on steel strip, plastic deform. 77−90368
cold rolling texture development 80−25720
comparison with conventional Leclanche cells 80−35660
complexation with aspartic acid, free metal, ligand conc. determ. 79−87892
compressive strength of polycryst., temp. and strain rate effects 80−16616
concentration in a.c. arc, during interruption, time depend. *(Russian)* 78−22597
concentration in atmospheric sedimentable powder, in Vizcaya, Spain *(Spanish)* 78−57265
concentration in snow of Mt. Blanc rel. to air pollution 78−81258
conduction-electron elec. field gradient, probe valence effects 78−47749
contact area, effect of loading time *(Japanese)* 78−6230
contact with electrolyte, current-potential characts. 77−1482
core levels, cryst.-field splitting, X-ray emission study 80−66328
corrosion, by applied alternating currents 79−70205
corrosion in de-aerated 0.1 M NaCl pH range 1.6 to 13.3 78−19921
corrosion in HCl and H_2SO_4, alkaloid inhibitor effectiveness 79−57146
corrosion in HCl under forced convection 80−35426
corrosion inhibition, role of thiocyanate ion in perchloric acid with n-decylamine 79−96223
corrosion inhibition by n-decylamine, synergistic effect of halide ions 80−11819
corrosion inhibition by surface active substances 80−40589
corrosion rate, electrochem. meas. using differential pulse polarograph 77−59980
corrosion rate meas. by differential pulse method 78−19962
corrosion rate monitoring, automatic, in near-neutral soln., using a microcomputer 80−50749
Cottrell-Stokes law, 4.2 to 300K, forest dislocations and other obstacles 77−43269
crack form. at grain and twin boundaries at low temp. *(Russian)* 80−66620
crack intermittent growth during strain in single crystal in contact with liq. Hg and Ga 79−87757
creep, compression anisotropy effects 79−83275
creep, low-temp., thermal heating and quantum mechanisms 80−79868
creep, press. effect *(Russian)* 79−29134
creep in temp. range of dynamic recovery *(Russian)* 77−81294
creep mechanism at low temps. *(Russian)* 79−11659
critical temp. determ. by exploding wires method, liquid metal enthalpy 78−6149
crystal, mean square vibr. amplitudes, X-ray diffr. 77−35640
crystal growth, Bridgman method *(Japanese)* 80−40252
crystal subgrain misorientations, X-ray diffr. microscopy technique 77−70272
cutting mechanism of large crystals *(Japanese)* 77−48523
cutting of bicrystal to compare mechanism for large crystals and polycrystals *(Japanese)* 78−60871
cyclotron mass and superconducting energy gap calc. as a function of Fermi surface position 79−69625
de Haas-van Alphen effect, oscill. freq., 1-140 bar *(Russian)* 79−19506
de Haas-van Alphen effect under press., Fermi surface and pseudopot. form factors 77−43475
Debye-Sears cell lattices, DSC-1 and DSC-2, computation of coincident and near-coincident cells 77−84746
deep drawing behaviour *(French)* 79−52325
defect recovery after low temp. electron irrad. 78−10090
deformation twin form. kinetics, Rose channel form. and interactions, twin growth rate *(Russian)* 79−60378
deformed, internal friction meas. 77−86067
deformed single crystals, stacking faults and dislocation dissoc. 77−31681
deforming stress and dislocation density depend. in slip system {11$\bar{2}$2}⟨11$\bar{2}$3⟩ *(Russian)* 80−103353
deforming stress under basal slip, contrib. of forest and primary dislocations 78−3186
deposits, layers in South Niger, geological features *(Croatian)* 79−29772
Derwent Reservoir, N.England, Zn, Cd and Pb in water, sediments and submerged plants 79−25286
determ., in seawater, graphite furnace atomic absorption spectroscopy 80−40768
determ. in water and organic materials, flameless atomic absorpt. spectrometry with wire loop atomiser 80−45586
determination, by dithizone complex extraction and isotope substitution anal. 78−95983
determination, in acetone, by AAS using W filament electrothermal atomiser 78−86346
determination, in beef extract, by NAA 78−27856
determination by proton-induced X-ray emission anal. in blood and liver tissue 79−53291
determination in Cu, Fe, at. absorpt. spectrometer performance appl. 77−77825
determination in Cu alloys, by at. absorpt. spectroscopy *(Russian)* 78−23998

zinc continued
determination in ore, by universal backscattered gamma method 79−1984
die pressed powder, green strength 77−59876
die-cast, substrate temp. effects on microstruct. and stresses in evaporated Cr film 78−10304
differential cathode ray polarograph, exam., determination of Cd, Zn 78−56930
diffusion, in Al, isotope effect 78−84006
diffusion along grain boundaries of Al, effect of grain boundary struct. *(Japanese)* 77−15628
diffusion and solubility in Pd, press. effects 77−43385
diffusion behaviour in $Al_xGa_{1-x}P$, device appls. 77−11741
diffusion coefficient in Al, resistometric determ. 79−51313
diffusion in $Al_{0.7}Ga_{0.3}As$, comparison with GaAs 78−26589
diffusion in Al and Al-Zn-Mg (5, 2 wt.%), 165 to 645°C and 165 to 560°C respectively 77−11743
diffusion in Al whiskers, temp. depend. 77−85122
diffusion in Al-$CuAl_2$ lamellar eutectic, two dimensional, computer simulation 78−30799
diffusion in Cu and Ag 79−77825
diffusion in $Ga_{1-x}Al_xAs$, depend. on Al content 78−59981
diffusion in $Ga_xIn_{1-x}P$, epitaxial film, effect of intrinsic impurities 78−87825
diffusion in GaAs, interimpurity interaction effect on distrib. profiles of impurities diffusing simultaneously 77−76451
diffusion in GaAs and GaP, low-temp.-selective process using anodic oxides 78−47399
diffusion in GaAs under open tube conditions 80−84326
diffusion in GaAs-AlGaAs half-ring laser 78−17960
diffusion in GaInAsP-InP planar stripe lasers, sputtered SiO_2 diffusion mask 80−48249
diffusion in GaP, interimpurity interaction effect on distrib. profiles of impurities diffusing simultaneously 77−76451
diffusion in GaP, P addition effect on induced dislocation density 77−19955
diffusion in $In_xGa_{1-x}As$, diffusion coeff. and surface conc. 80−39122
diffusion in ion implanted GaAs, profiles 80−24681
diffusion in $LiNbO_3$, and its effect on acoustic velocity 77−84847
diffusion into n-type GaP, p-n junction depth 77−89841
diffusion into SnO_2 films *(Japanese)* 79−95218
diffusion of C, radiographic meas. *(Russian)* 77−31809
diffusion of III-V semicond. by isoconc. technique, anal. of 'up-hill' region 77−35755
diffusion parameters in Ni whiskers 750 to 950°C 77−66101
diffusivity along Al grain boundaries, grain boundary struct. effects 77−20128
discontinuous creep, in single cryst., under singlet slip conditions *(Russian)* 77−81292
dislocation damping on $\{\bar{1}2\bar{1}2\}\langle\bar{1}2\bar{1}3\rangle$ slip system above Debye temp. 77−62538
dislocation etch on (0001) surface of single crystal 79−65091
dislocation etch pits on (0001) surface of single crystal *(Japanese)* 78−59811
dislocation interaction with 'forest' dislocations, TEM exam. 77−89440
dislocation internal friction, orientation depend., for single crysts. 78−52882
dislocation mechanism of Rose channel formation under impact loading conditions *(Russian)* 79−79073
dislocation mobility, pyramidal edge and screw, compressional stress pulse technique 77−19957
dislocation mobility under action of current pulses, selective etching meas. 79−19259
dislocation struct. stability, effect of deformational and thermal annealing 78−64567
dislocation structure, high press. effects, plastic deform. *(Russian)* 80−88159
dislocation structure control after prep. low angle boundary decomp. *(Russian)* 78−3142
dislocation velocity and plastic deform., single crysts. 80−64998
distribution in waters of Yarra River estuary 79−16552
dopant for GaP, behaviour on crystallisation from melt 77−84772
ductile-brittle transition pressure, grain size effect *(Japanese)* 78−60745
dust, O_2 determ. by 14 MeV neutron activation anal. *(Japanese)* 80−11977
EFG sign at ^{69m}Zn site 77−59492
elastic constants, diffuse X-ray scatt. determ., single cryst. 78−11255
elastic properties, compilation and review 78−27551
electric field gradient, magnitude and sign 77−80755
electric field gradient, naive model 78−91650
electric field gradient at nucleus calc. 78−39079
electric field gradient on Cd, press. depend., TDPAC expts. 78−48092
electric field gradients of recoil-implanted ^{19}F via $^{9}Be(^{12}C, np)^{19}F$ 77−8471
electrical and thermal resist. calc. 79−69489
electrical resistivity, low temps., Matthiessen's rule deviations *(Croatian)* 79−11099
electrical resistivity and anisotropy coeff. at press. up to 80 kbar 77−43554
electrocrystallisation, on Cu single cryst. planes, under influence of asymm. AC 77−28731
electrocrystallisation, reaction mechanism, appl. of impedance meas. *(French)* 80−103597
electrocrystallisation noise, phenomenological model 78−51845
electrode, dispersed, for primary and secondary cells, electric vehicles appl. *(French)* 80−72023
electrode, evaporation rate from cathode spot in vacuum arcs 79−37566
electrode, passive film form. by chrono-ellipsometry *(Japanese)* 78−68900
electrode, single crystal, fracture surface charge density effect 78−68787
electrode in alkaline soln., exam. of surface state by potentiodynamic voltammetry 80−85187
electrodeposit dendritic growth control using impedance meas. 78−84721
electrodeposit formation from various electrolytes 79−57242
electrodeposit structure, rel. to electrochem. noise 78−67916
electrodeposited, planar stress relaxation 79−24563
electrodeposited, residual stresses, effect of triacetylpyridine and polyethylene glycol additives to NH_4Cl electrolytes 80−21190
electrodeposited coatings, residual stress diagrams 80−16588
electrodeposited on polished Fe, reaction rate in solid state *(Japanese)* 78−15322
zinc continued
electrodeposited on steel with Cu cladding, bond strength through intermediate Zn layer *(Korean)* 79−66213
electrodeposition, inhibited, electrode kinetics and deposit morphology 79−56089
electrodeposition, on Ni surface, nondendritic granular, deposit form. 77−59968
electrodeposition from high purity industrial acid sulphate electrolyte, effects of Cd on deposit structures 79−56091
electrodeposition from high purity synthetic and industrial acid sulphate electrolytes, Pb effect on deposit structures 79−56090
electrodes, porous, concentration changes during cycling 80−35666
electrolytic deposition, on Pt single crystal spheres, critical overvoltage 80−104080
electrolytic Zn coatings on steel, adhesion strength determination by centrifugal method 77−56149
electron emission depend. on surface mechanical treatment *(Russian)* 80−100945
electron impact ionisation efficiency curve, threshold of 12.7 eV 79−50137
electron irrad. effect on electrolum., defects form. and quenching obs. 80−55194
electron irradiated, diffuse X-ray scatt. exam. of interstitial clustering during thermal annealing 79−73214
electron irradiated, diffuse X-ray scatt. exam. of self interstitials 79−73213
electron momentum distrib., neutron-induced defects, positron annihilation study, for single cryst. 80−71508
electron motion, Hall effect and Fermi surface 77−47793
electron radiation damage, determ. of threshold displacement energy 78−59837
electron radiation damage in HVEM, nature of defect clusters 78−59838
electron-phonon interaction anisotropy, microcontact spectroscopy *(Russian)* 78−43372
electron-phonon interaction anisotropy, microcontact spectroscopy *(Russian)* 79−37786
electron-phonon mass enhancement, anisotropy and temp. depend. 77−15745
electronic band struct., pseudopotential calcs. 79−19510
electronic surface states, (001) surface, Brillouin zone 79−24047
electroplastic deformation, stress relax. meas. *(Russian)* 79−38894
electroplated coatings internal stresses, theory and meas. review *(German)* 78−56049
electroplating process, optimisation 79−43452
electrowinning, use of organic additives, eval. 78−44048
erosion by laser beam, in self-consistent mode *(Russian)* 77−69945
estuarine river water, particulate heavy metal content, Cochin backwater, India 80−7964
evaporation rate, effect of inert gas 80−84285
EXAFS, obs. of single cryst. 78−2943
extraction with 2-(2-thiazolylazo)-4-methyl phenol 77−60063
extractive metallurgy, developments, review 80−20820
extruded, continuum mech. anal. of flow curve anisotropy and plastic strain *(German)* 78−84947
faceting of interstitial loops 78−47381
failure under hydrostatic press., kinetics 78−52944
fast separation by ion exchange resin *(Rumanian)* 78−23922
fatigue failure at low temp. under low-freq. cyclic loads for single crysts. *(Russian)* 79−61697
Fermi surface, stress-induced changes 79−82516
Fermi surface changes under uniaxial compression 78−51876
Fermi surface stress induced changes calcs., principal cross sectional areas 79−60684
Fermi surface-Brillouin zone interaction, XPS obs. 79−52078
field gradients, temp. depend., electronic and lattice contribs., ab initio study 79−42501
film, deposition props. on specially prepared substrate, desorption energy and surface diffusion 79−90917
film, hexagonal struct., vacuum deposited, X-ray peak shift anal. 79−65335
film, RF sputtered, ageing processes 78−84322
film, RF sputtered, electrical conduction 79−42674
film, thickness meas., using nondestructive radioisotopic technique 80−68179
film, vac. deposited, X-ray diffr. study of microstruct. 78−26796
film, vac. deposited, X-ray diffr. study of microstruct. 78−75966
film deposition on Al, TEM and electron diffr. obs. 80−75460
film growth, HEED and projection microscope obs., surface orientation depend. on deposition parameters 77−32523
film growth on C, conductance meas. 79−82495
films, hexagonal, residual stress meas. from X-ray peak shift anal. 77−72807
fine powder, electrodeposition 80−60802
flow stress during cutting 77−59881
foil, splat quenched, preferred orientation 80−40381
forest dislocation effect on single twin layer development in single crystals 78−63775
fracture stress of single crysts. 80−104269
free-electrons momenta distribution, anisotropy, positron annihilation meas. 77−36309
p-GaAs:Zn, diffusional doping, photoluminesc. in mag. field 77−16384
galvanic couple with Al alloys, velocity effect on corrosion 78−35566
galvanisation, hot, production components, installation and power supply *(French)* 80−66686
gamma ray generation of microwaves *(Russian)* 78−2939
geochemistry, chemical speciation in mixed freshwater, seawater and bine solns. 78−20409
geochemistry in sediments of Gulf of St. Lawrence and estuary 78−92855
glide dislocations, second order pyramidal band, etch pit obs. of pure single cryst. *(Japanese)* 78−38716
grain boundaries, activationless motion, group co-operative transition mechanism 80−2039
grain boundary detachment from adsorbed impurity, conc. depend. 78−2144
grain boundary diffusion in Al, nonvacancy mechanism *(Russian)* 80−24669
grain boundary nonactivated motion vel., orientation depend. *(Russian)* 80−84180

zinc continued
growth from melt, conditions influencing dislocation struct. *(Russian)* 80−97424
Hall effect, analysis at high temp. 78−2465
Hall effect and elec. resist., temp. depend. 78−64030
Hall effect and phonon scattering in pure crystal 79−23948
Hall effect coeffs., linearised Boltzman eqn. solved 79−1595
HCP, lattice dynamics, local pseudopotential approach, dielectric functions 80−34151
HCP lattice, Huang diffuse scatt. from interstitials 80−88142
HCP metals, K-emission valence bands, structure and bonding 80−7438
HCP structure, selection rule, electron momentum distrib. rel. to positron annihilation 80−39495
heat capacity meas. by computer-interfaced differential scanning calorimetry 78−65935
hexagonal, temp. depend. anisotropy of phonon scatt. resist. 78−51967
hexagonal lattice equilibrium, electron gas model with noncentral forces, lattice dynamics 78−95123
hexagonal networks in basal plane, TEM exam. 78−2132
hot dip galvanising, texture of δ-Fe-Zn layer formed 77−9001
hot rolled, grain boundary fine structures, TEM exam. 78−76680
human dietary absorption, radionuclide study technique 79−5349
hydrostatically compressed single crystal, work hardening studied by stress relax. method 79−20069
ice nucleating material 78−49093
impact strength, exam. with pulsed drop impact loading 78−84944
impurity in Al, PIXE anal., conc. profile determ. using beam energy variation 78−76965
incompatible bicrystals, effect of grain boundaries on mech. props. *(Japanese)* 78−39798
incorporation into B modifications, struct. changes 78−79596
interface, Zn(0001)-Zn(0001), local and nonlocal contribs. to adhesive energies 77−85085
interface, Zn (0001)-Zn (0001), self-consistent electronic densities and adhesive energies 78−72005
internal friction anomalies in temp. initiated brittle-plastic transition *(Russian)* 80−96648
ion bombardment, energy distrib. of positive secondary ions and sputtered atoms 77−32485
ion etching, dispersion coeff. determ. *(German)* 80−40597
ions, XVII to XX, relativistic Dirac-Fock-Slater orbital binding energies, one-electron transition energies 79−25778
α-irradiation damage and stage I recovery 78−38759
isoelectronic sequence, 4s-4p reson. transition in highly charged ions 77−75087
isoelectronic sequence, electron impact excitation of reson. transitions 80−63825
isoelectronic sequence, oscill. strength and MCHF wavefunctions, outer correl. 80−91505
isoelectronic sequence, RRPA calcs. of resonance transitions from $4s^2\ ^1S_0$ 78−17612
isoelectronic series, $4s4d\,^1D$-$4p^2\,^1D$ interaction, multiconfig. Hartree-Fock calcs. 79−76351
isoelectronic series, theoretical oscillator strengths for resonance transitions 78−74616
isomer shift values of implanted $^{133}Xe/^{133}Cs$, Mossbauer spectra 80−7240
isothermal annealing effect at 400-410°C, on dislocation struct. in monocrystals *(Russian)* 79−20082
isotopic enrichment during zone melting process *(Russian)* 77−10522
K shell photoelectric cross section, at 74.409 keV 79−72288
K shell prod. cross section of Ti, Cr, Fe, Ni, Cu, Zn for 75 to 150 keV p and e excitation 79−47552
K-shell X-ray prod. by $^{14}N^+$ bombardment 80−91482
laser CW oscillation, Zn^+ transitions in He-ZnB_2, He-$ZnCl_2$ and He-ZnI_2 discharges 78−50765
lattice dynamics 77−15513
lattice Hg location and quadrupole interaction, gamma-spectral study 80−80227
lattice vibrations, anharmonicity, elastic neutron scatt. 77−51454
Lindemann's rule and X-ray Debye temp., anisotropic single crysts. 79−28076
liquid, electron component of entropy *(Russian)* 79−23747
liquid, electron energy states calc. *(Russian)* 79−4506
liquid, hot galvanising of Fe, Fe-Zn compound form. *(French)* 79−20275
liquid, interference function temp. depend. from X-ray diffr., elec. resist. calc. 77−47332
liquid, isothermal compressibility, harmonic pot. model calc. 79−14870
liquid, Knight shift, temp. depend. 78−80232
liquid, NMR and relax. 79−8061
liquid, reaction with Cu 77−9127
liquid, reaction with solid Fe, interdiffusion exam. *(Japanese)* 78−39944
liquid, resist. and thermo-electric power using corrected parameters of Shaw model 79−19566
liquid, structure factor, 460 to 650°C, by neutron diffr., elec. resist. temp. coeff. 77−47333
liquid, surface tension, temp. depend. *(Russian)* 80−15336
liquid, thermal conductivity meas. in Spacelab, measuring cell design and testing *(German)* 80−57303
liquid, thermoelectric power, pseudopotential calc. 80−59959
liquid, US wave velocity *(Japanese)* 79−60438
liquid, viscosity calc. using microinhomogeneous struct. model *(Russian)* 80−15284
liquid, viscosity determination by oscillating vessel method *(Japanese)* 80−70439
liquid, X-ray diffraction analysis 79−4232
liquid metal embrittlement 78−64653
liquid metal embrittlement 79−83375
magnetic susceptibility behaviour *(Russian)* 77−80912
magnetoresistance anisotropy change under stress, $2^1/_2$ order phase transition *(Russian)* 77−62907
marine pollution determ. in Gulf of Fos, NW Mediterranean 79−12141
mechanical twins in single crystals *(German)* 79−33004
melt density, temp. depend. *(Russian)* 79−69174
metallic precipitates, crystallography dendritic origin of hexagonal prisms 79−66366
microcrack propagation and plastic strain 80−81187
microplastic deformation, basal dislocation generation, glide and locking, X-ray topography study 80−88156
zinc continued
microrupture singularities in low stress range at elevated temp. *(Russian)* 79−29172
minerals suspended in ocean waters 79−74904
molten, reaction with WC-Co, lamellar struct. form. 79−33964
molten, struct. investig. by neutron diffr. 79−4233
molten, surface tension, positive temp. coeff. 77−72751
monomer/dimer vapour equilib. mixture, flow through porous barrier 77−31383
mosaic single cryst., neutron integrated reflectivities 79−86656
Mossbauer spectra, 2nd-order Doppler shift, 1-100K 79−91317
Mossbauer spectra, quadrupole interaction 80−7206
muscle membrane, insect, permeation of Mn, Cd, Zn and Be through Ca channels 77−56357
natural waters, radiotracer methods for speciation study 79−88490
neutron diffraction, site symmetrized Fourier invariant treatment of anharmonic temperature factors 79−33040
neutron irradiated, recovery of c-axis spacing and elec. resist. 80−34081
nitrided, yield strength, influence of deform. rate *(Bulgarian)* 80−89315
NMR of HCP metal, pulsed ^{67}Zn NMR studies at 4.2K 79−91315
noncubic crystal, temp. depend. of elec. field gradient 79−99515
NQR, pure, obs. 79−47354
nuclear quadrupole interaction, theory 78−10412
nuclear quadrupole interaction theory of ground state of ^{67}Zn nucleus 79−73481
ocean concentrations in NE.Pacific 78−36200
ore, leaching, effects of ultrasonics and their appls. 78−92214
oriented polycrystals, tensile behaviour under hydrostatic press. *(Japanese)* 77−52417
oscilloscopic polarography determ. in environmental pollution anal. *(Chinese)* 79−53002
oxidation, UPS study 79−100296
oxide film growth on (0001) surface, at. and electronic struct. 78−15587
N.Pacific, trace metal vertical profiles 80−67381
paint, zinc-rich, for protection of mild steel, dust particle size effect 78−95840
paint, zinc-rich, for protection of mild steel, Zn content effect 78−95842
paint, zinc-rich, for protection of mild steel, ZnO addition effect 78−95843
paint, zinc-rich for protection of mild steel, exposed area ratio effect 78−95841
particulate composite, mech. props., microstruct. correlation, at low and high temps. 77−32624
phonon density of states calc. from neutron diffr. data 77−24369
phonon density of states determ. from heat capacity *(Russian)* 80−29131
phonon dispersion relations, first-principles calc. 79−60448
phosphate coating, effect of grain size on film formation kinetics 79−34203
phosphating processes and additives 79−79147
phosphidation in P vapour, kinetics and associated diffusion coeffs. 80−3405
photoelectric cross sections at 52.4, 60, 72.2 and 84.4 keV 80−69187
photoemission relax. energies *(French)* 77−36357
pionic atom, 2p level shifts and widths 78−46469
planar diffusion in InP, p-n junction formation 78−43040
plasma, electron beam in Zn vapour, plasma prod. and beam interaction 78−47133
plasma arc srapying, chem. reaction with plasma gases 80−66427
plastic anisotropy of extruded bars *(German)* 77−86126
plastic deform., strain rate history and temp. effects depend. 79−11684
plastic deform after pinch effect *(Russian)* 78−27563
plastic deform. and fracture obs. by acoustic emission of single crysts. in metal melt *(Russian)* 78−56737
plastic deformation, 1.5-300K *(Russian)* 77−77533
plastic deformation effect of hydrostatic press. stress relax. meas. *(Russian)* 79−96102
plasticity under hot deform. conditions, temp. depend. *(Russian)* 79−29133
plate, thick infinite, transversely isotropic, containing circ. hole, end effects 79−27510
plating C steel nails, barrel plating efficiency 80−100964
plating electrolyte, ion-exchange chromatography of Zn, Cd and Al salts 77−16890
plating thickness meas. with MIP-10 78−53144
point contacts, electron-phonon coupling, microcontact spectroscopy investig. *(Russian)* 78−38796
pollution levels in Belfast Lough 80−3539
polycrystals, deformation, grain sizes effect at room temp. *(Czech)* 80−45359
polycrystals with axial texture, heterogeneity of props. *(Russian)* 80−29192
polyethylene/Cu(Zn) adhesion, role of surface topography 80−35500
polythioglycolate passivation 79−70217
positron annihilation, 4.2-500K, Doppler broadening meas. 78−43957
positron annihilation, external electric field effect on ang. distribs. 77−77317
positron annihilation, high current densities, ang. distrib. of annihilation quanta *(German)* 77−12462
positron annihilation in plastically deformed sample, electric field effect 79−69899
positron-electron annihilation spectra, Doppler broadened 79−65953
positron-vacancy interactions, equilib. temp. depend. of positron annihilation 78−76547
power law creep, exam. of whether creep is diffusion controlled 78−52890
preferred crystal orientations, rot. mill device investig. 79−57006
protective coating on C steel, durability obs. using nuclear radiation excited X-ray fluoresc. 80−21206
proton-induced L-shell ionisation cross-sections 80−100707
quadrupole interaction, ^{67}Zn Mossbauer expt. 78−27120
quadrupole interaction, Mossbauer spectra 78−92004
quadrupole interaction at ^{181}Ta in Zn, TDPAC meas. 78−52392
quadrupole interaction for ^{129}I, ^{131}I and ^{132}I, PAC expts. 78−48087
quadrupole interaction of ^{12}B and ^{12}N 78−47750
quadrupole interaction of ^{67}Ge and ^{71}Ge, TDPAC meas. 78−43740
quadrupole interactions, nuclear quadrupole alignment of $^{69}Zn^m$ 78−48090
quantum oscillations of thermal EMF under mag. breakdown conditions *(Russian)* 77−69305
radionuclide dosimetry standards and crit. organs 78−35961

zinc continued
Raman scattering, TO optical phonon, anharmonicity 77−15520
recovery after 6.1 MeV α-particle irradiation at 4.2K 78−47441
recovery from Zn_2SiO_4 ores, hydrometallurgical treatment 77−52263
recovery from Zn_2SiO_4 ores, review 77−48365
recycling, effect on comp. 80−66455
residual electrical resistance of single crysts., contrib. of basal dislocations *(Russian)* 80−75539
resonant two hole bound state at 3p core threshold 80−60750
roadside soil and plants in Alexandria district, Egypt, contamination with Cd, Ni, Pb and Zn 78−81171
rolling texture formation, computer simulation in HCP and orthorhombic metals 80−3095
secondary batteries, props. of alternate electrolytes 80−104502
serum, human, trace elements determ. by proton activation 80−81731
shaped single crystal prod. from melt, twinning 78−2040
sherardising process development 79−78998
single cryst. stress relax. depend. on elec. current, electron plastic effect 79−79021
single crystals, positron trapping by edge dislocations, produced by bending 78−80606
skin lesion Mn, Cu and Zn conc. meas. by neutron activation 80−17063
slip, density of basal dislocations, rel. to deforming stress, 1.5-300K *(Russian)* 80−29028
slip band theory, model for creep based on dislocation climb at grain boundaries, comparison with expt. data 79−37756
small-core approx. and structural phase stability 79−99498
smoke-particle aggregates, long-range correlations 79−46369
soil-water system interfacial reactions and heavy metal adsorption 78−3832
solar photosphere abundance, discrepancy with meteorite abundance 80−72897
solid-liquid and solid-solid interfacial tensions 77−36452
solubility and cosolubility in InAs 77−16552
solutions, conc. changes, proton induced X-ray emission obs. 77−25325
spin-orbit interac. contrib. to mag. susceptibility of interacting electrons 77−63084
sputtered atom radiative emission, geometry depend. 77−28669
sputtered excited states, secondary photon emission, role of transition probability 80−102483
sputtered film, thermal ageing, thickness dependent effects 78−6462
sputtering, binding energies 80−108312
sputtering by Ar^+ bombardment, ionised and excited particle production, validity of thermodynamic models 79−52062
sputtering efficiency ang. distrib. meas. using thermal particle detector 77−28671
sputtering in inert atm., with uncooled cathode, oxidation of metallic coatings, X-ray diffr. obs. 78−3041
stacking faults, plastic deformation, due to laser beam irrad. *(Russian)* 80−15121
steel, X-ray fluorescence thickness meas. for Zn and Sn coatings 77−55884
steel, Zn coated strips, plastic deform. influence on struct. and quality *(Russian)* 80−40377
steels, types SS41, SB42, SM50A, STK55, liq. Zn embrittlement *(Japanese)* 80−81164
stopping power for 0.3-1.5 MeV protons 79−55801
stopping power for 6.75 MeV protons 80−34107
stopping power of 0.5-2.0 MeV ^4He ions, elastic backscatt. meas. 78−87730
strength of single crystals, temp. and strain rate effects 80−16373
strengthening by electroplastic strain, surfactant effect *(Russian)* 80−20953
structure sensitive props., temp. hysteresis after melting and crystallisation *(Russian)* 79−29036
substrate for polystyrene film, electrode effect on carrier injection, TSC, I-V characts. 80−34463
superconducting, ultrasonic attenuation 78−88071
superconducting film, SAW US attenuation 79−73633
superconducting film for energy selective phonon detection 80−92621
superconducting transition temp., electron-phonon mass enhancement, pseudopot. calcs. 78−2604
superconducting transition temp., perturbative corrections, direct and indirect ladder diagrams 80−49979
superconductive fixed points for temperatures above 0.5K 79−63221
surface, (0001), Cu ordered monolayer, electronic struct., photoelectron spectra 78−39660
surface, (0001), interaction with water, UPS meas. 78−76585
surface, isotope effects in ion-scattering double spectroscopy curves for He^+ 77−59658
surface, O_2 interaction, chemisorpt. and oxidation 78−64886
surface, Q-switched ruby laser irrad., recoil momentum 79−65961
surface (0001), adsorption of Te, UPS investigation 79−91563
surface layer of Ge, heterodiffusion due to H atom surface recombination stimulation *(Russian)* 80−59726
surface oxidation, Auger spectrosc. obs. 80−97388
surface props., Rayleigh-Ritz variational calcs. 79−69570
surface sliding damage, no lubrication, materials depend. *(Japanese)* 78−56780
tension cycle close to soft loading, accumulation of damages, theory 77−14968
thermal expansion, temp. depend., vacancy effects 80−79962
thermal fatigue, low-temp., fracture and plastic deform. 77−28837
thermal neutron cross sections, in single crysts. 80−19672
thermal recovery and stress-strain relations 78−11266
thermal sprayed coating on steel substrate, cavitation and corrosion resist. in sea water 80−35427
thermally stimulated exo-electron emission 80−11547
thin metal primer systems for steelwork 79−79148
tracer concen. profiles in GaP 78−95189
transfer from galvanised wire to stainless steel, type AISI 316 at 550°C, effect on steel props. 78−88527
tropospheric fallout fluxes in Antarctica and Greenland 79−58007
twin boundaries, computer simulation 80−39109
twinning, influence of dislocation drag, mag. field effects 80−59472
twinning dynamics of single crystal 77−4115
ultrafine particle, positron annihilation exam. 78−56542
US attenuation due to conduction electrons 79−46754
US attenuation of conduction electrons, shear waves calc. 78−91589
US attenuation of conduction electrons calc. 78−91588

zinc continued
US attenuation under high hydrostatic press., dislocation mechanism 77−43284
US hardening kinetics rel. to dislocations 80−50644
US vibrations, anomalous damping under hydrostatic press. 79−14890
US vibrations, damping under high hydrostatic press. 77−55324
vacancy concentration meas., lattice parameter and length changes, form. parameters 79−37697
vapour, diffusion-limited condensation meas. rel. to vacuum processing of metallurgical melts 77−8775
vapour, reaction with solid Fe, Zn chem. potential effect on interaction layers 78−11416
vapour laser, operation by dissoc. of metal complex 77−54702
water, natural, trace metals, energy dispersive X-ray fluoresc., at absorpt. anals., comparison 77−60175
wave formation during oblique collision *(Russian)* 77−89494
wear resistant coating, effect of surface-active substances in electrodeposition on props. *(Russian)* 78−11359
wear under reversed friction, temp. effect 80−108588
whisker, supercond. crit. temp. stress depend. 77−39989
whiskers, quantum oscills. of mag. moment 79−15280
wire, elastically bent, elec. resist. in mag. field 80−44568
work hardened crystal, jump-like plastic deform. dislocation struct. instability 79−96094
X-ray diffraction meas. of RMS at. displacement, anisotropic extinction correction 77−62606
X-ray emission $L\beta_1$ and $L\alpha_{1,2}$ lines, atom comparison with metal 78−74604
X-ray emission spectra, L_l and L_η 78−39631
X-ray K-absorpt. edge shifts, plasmon energies correlation 80−20734
XPS escape depths and relative photoionisation cross section for 3p subshell 77−73212
Z dependence of thick target β-ray backscattering 80−76118
zincating of Be, deposition conditions, film characts. 77−40397
zone melting by electron beam, isotope fractionation enhancement 80−45229
(Al,Ga)As:Zn planar stripe lasers with deep Zn diffusion, guiding mechanisms controlled by impurity concs. 80−78853
Al:Zn, impurity low-field galvanomag. coeffs., 4 OPW calcs. 77−69304
Al:Zn, ion implanted, electron beam annealing 80−59500
Al-Zn alloy, dil., electron-irradiated, impurity-interstitial interactions 77−15449
AlGaAs, Zn diffused window structure laser, high optical power density emission 79−98394
p- (AlGa)As:Zn, MBE grown, elec. props., shallow junction solar cell use 79−91175
$Al_xGa_{1-x}As$ MBE layers, ionized beam doping, elec. and optical characts. 79−37721
$Al_xGa_{1-x}As$:Ge(Te)(Zn), photo- and cathodolum., comp. depend. *(Russian)* 77−48215
$Al_xGa_{1-x}As$:Zn DH laser, stripe geometry, horizontal transverse mode stabilisation, lasing characts. 77−19313
$Al_xGa_{1-x}AsZn$-GaAs solar cells by LPE, open circuit voltage, fill factor 80−101108
$Al_xGa_{1-x}P$:Zn, solution-grown single crysts., photo- and electrolum. at 77K 79−52004
$Al_xGa_{1-x}Sb$:Zn, doping of solid solns. during LPE *(Russian)* 77−85087
$Al_xGa_{1-x}Sb$:Zn, impurity diffusion, p-n junction depth 80−24678
BP:Zn, epitaxial layers, ion implantation, defects and lattic locations, channelling obs. 80−88179
$BaTiO_3$:Zn, annealed in H_2 and O_2, valence change in phase stability 80−20600
Be:Zn, lattice location of implanted Zn, ion-beam channelling meas. 77−68992
Bi-Zn, light ion large angle scatt. in weakly screened Rutherford region 80−84823
CaS:Zn phosphor, photoluminesc. meas. 77−20913
Cd, nuclear quadrupole antishielding effects, ab initio theory 78−34814
Cd UV subshell photoionisation cross section, expt. and GIPM theory 78−21887
Cd:^{67}Ge, quadrupole interaction temp. depend. 77−12264
Cd:^{67}Zn elec. quadrupole interaction temp. depend., PAC meas. 79−42877
CdP_2:Bi,Zn, photolum. and photocurrent stationary characts. 78−27317
CdS:Zn, heavily doped, defect struct. 78−22756
CdTe:Zn, TSC, carrier traps, depth and quenching by IR radiation 78−56420
Cu/Zn galvanic couple, potential distrib. meas. technique, appl. to corrosion study, apparatus *(Japanese)* 78−53049
Cu-Zn bilayer system, optical mechanical and corrosion properties 77−32707
Cu-Zn heterocontacts, microcontact spectra *(Russian)* 80−34502
Cu-Zn multilayer condensate, diffusion process, brass formation 78−43186
Cu-Zn thin film couples, room temperature interactions 80−96699
$CuInSe_2$, Zn implantation profiles by AES 77−31692
$CuInTe_2$:Zn, donor impurity in diffusion, elec. and optical props. 78−68504
Cu_2S:Zn, effects of doping on elec. and optical props. 78−38743
electrodes, shape change resulting from cell cycling, quantitative study 79−43591
Fe_3O_4:Zn, and pure, influence of mag. order on charge delocalisation, Mossbauer spectra 78−68423
Fe_3O_4:Zn^{2+}, Verwey transition 80−6513
Ga+:N,Zn, interimpurity recomb., acceptor binding energies 78−34796
(GaAl)As, Zn diffused DH laser with twin transverse junctions, low threshold current 79−98393
(GaAl)As, Zn diffused proton bombarded stripe laser 79−98392
GaAlAs:Zn recombination radiation drift, charge carrier photon induced drift in varigap semicond. 80−50418
GaAlAs/GaAs solar cells, Be and Zn behaviour 80−101111
GaAlAs-GaAs heterojunction prep., Zn conc. effect in epitaxial layer, high-power IR emission *(Spanish)* 77−39932
$Ga_{1-x}AlAs$:Zn, acceptor energy level and elec. props. 80−65482
GaAs:Cr, Zn, shallow impurity implantation, elec. props. after annealing 80−24465
GaAs:Cr,Zn, implanted, doping profiles after laser annealing, elec. props. 80−2058
GaAs:n, ion implantation, hole conc. and mobility profile meas. 78−23082
p-GaAs:Zn, carrier drag by photons, rel. to IR detection 79−11185

zinc continued
GaAs:Zn, diffused, depth profile by photoluminesc., LED applic. 78−72587
GaAs:Zn, diffusion during LPE, impurity gradients and annealing effects 80−29882
GaAs:Zn, diffusion of Zn by two-temp. method, LED fabrication 80−49416
GaAs:Zn, dislocation-free, TEM study of microdefects 79−82213
GaAs:Zn, distribution of radiative recombination efficiency 79−78725
GaAs:Zn, dopant influence on hardness 77−84777
GaAs:Zn, heavily doped, photolum. obs., above gap 80−29796
GaAs:Zn, high surface conc. Zn diffusion for good ohmic contact 77−11575
GaAs:Zn, implanted, furnace annealed, electrical, Rutherford backscattering and TEM meas. 80−100272
GaAs:Zn, implanted, hole conc. and mobility profiles meas. 78−23081
GaAs:Zn, implanted, laser annealing, elect., Rutherford backscattering and SEM meas. 80−100273
GaAs:Zn, implanted, low temp. photolum. spectra 78−39583
GaAs:Zn, ion implanted, TEM study after laser and furnace annealing 80−70234
GaAs:Zn, LPE, and doping characts. 79−33948
GaAs:Zn, laser annealing of implanted layers 77−55296
p-GaAs:Zn, luminescent, ion doped MBE growth 80−44436
GaAs:Zn, MBE with ionized beam doping 77−77418
p-GaAs:Zn, Mn, degenerate, tunnel p-n junction and semicond.-metal struct., I-V characts. 78−72252
p-GaAs:Zn, optical absorpt. spectra and photocond. after 2 MeV electron irrad. *(Russian)* 77−69859
GaAs:Zn, pulsed laser annealing, expt. 78−34828
p-GaAs:Zn, Raman scatt. by LO phonon-plasmon coupled modes, wave vector non-conservation 80−16033
GaAs:Zn, recrystn. of implanted amorphous layers, TEM and channelling obs. 77−89459
GaAs:Zn, Se, double doping during LPE, exam. of elec. cond. and Hall effect 79−4923
GaAs:Zn, sign inversion of the linear photogalvanic effect *(Russian)* 80−80321
GaAs:Zn, surface conc. control 79−55758
n-GaAs:Zn, VPE, deep-level transient spectroscopy 80−34383
GaAs:Zn (110), spin polarised electron production by photoemission from Cs-O overlayer 79−95903
GaAs:Zn films, VPE growth and photoluminesc. props. 79−38642
GaAs:Zn ion implanted ionic alloy, electrophysical props., annealing 80−39133
GaAs:Zn MBE layers, ionized beam doping, elec. and optical characts. 79−37721
GaAs:Zn optically pumped ribbon-whisker laser, picosecond pulses 80−99771
GaAs:Zn polycrystalline film, Hall effect, resistivity meas. 80−96911
n-GaAs:Zn substrate, ion implantation as predeposition process 79−19268
GaAs:Zn waveguide, light coupling at fundamental absorption edge 79−23082
GaAs:Zn-$Al_{0.5}Ga_{0.5}As$ p-n junction, surface layer effect on surface recombination current 79−69585
GaAs:Zn-GaAs n-p junction, ion implanted, residual radiation defect influence on characts. *(Russian)* 78−84287
GaAs-Zn, spreading resist. meas. 79−28343
$GaAs_{0.1}P_{0.9}$:Zn, shallow Zn diffusion profile determ. using anodic oxidation and double radioactive tracer method 77−43239
$GaAs_{0.6}P_{0.4}$:Zn, control of Zn diffusivity by multiple implantation 78−38877
$GaAs_{1-x}P_x$:Zn, diffusion profile determ., $^{32}P/^{65}Zn$ double tracer technique 78−55888
$GaAs_{1-x}P_x$:Zn implanted, Zn diffusion 77−84993
$GaAs_{1-x}P_x$-SiO_2:N,Zn ion-implanted multiple layers, ion range distribs., secondary ion microprobe meas. 79−42129
GaInAsP/InP, DH laser, low threshold current density, 1.3 μm emission 79−94249
GaInAsP-InP Zn diffused stripe geometry DH diode laser fabrication 79−98386
GaN:Zn, cathodolum. obs., recomb. model 79−11474
GaN:Zn, cathodoluminesc., photocapacitance 79−38679
GaN:Zn, epitaxial film lumins. 78−10955
GaN:Zn, epitaxial growth on sapphire substrates, elec. props., X-ray diffr. anal., photoluminescence spectra 79−4919
GaN:Zn, epitaxial layer, effective electroluminesc., blue regime *(Russian)* 77−77302
GaN:Zn, heavily doped, photocond. spectra 77−72887
GaN:Zn, LED, blue, yellow and green emission, temp. depend. 77−8658
GaN:Zn, low voltage LED, epitaxial layer, growth and electrolum. *(Russian)* 77−77297
GaN:Zn, n-i struct., anomalous luminesc. 80−80865
GaN:Zn, polarised electroluminescence, mag. field intensity depend. *(Russian)* 79−91502
GaN:Zn, temp. and press. depends., electrolum. 78−19567
GaN:Zn, VPE grown, optical cross sections, photoluminesc. and optical absorpt. meas. 80−55160
GaN:Zn, VPE growth, photoluminesc. rel. to doping conditions 80−55159
GaN:Zn, violet bipolar LED 79−38190
GaN:Zn epilayers, growth parameters effect on props., device struct. 78−26975
GaN:Zn epitaxial films, luminesc. spectra separation into individual bands by impurity absorpt. region excitation 79−74002
GaN:Zn epitaxial layers, doping effect on cathodoluminesc. 77−20935
GaN:Zn LED, electrolum. centres, rel. to growth morphology, Zn conc. and etch patterns 77−1733
GaN:Zn LED, I-V characts., elec. cond. mechanism 77−55614
GaN-Zn, lattice parameters, variation with stoichiometry and doping 79−73153
GaP:Zn, diffusion in SSD crystals for green LED fabrication 77−81208
GaP:Zn, diffusion profile determ., $^{32}P/^{65}Zn$ double tracer technique 78−55888
GaP:Zn, dopant diffusion profiles at 900°C, radiotracer meas. 77−59147
GaP:Zn, doping from gas phase during LPE 80−55312
GaP:Zn, excited acceptor state investig. by photoluminesc. 77−8632
GaP:Zn, growth, I-V characts., electroluminesc. *(Korean)* 78−52653
GaP:Zn, Hall effect and elec. cond., 80-400K 78−91705

zinc continued
p-GaP:Zn, Hall effect determ. of hole mobility temp. depend., scatt. mechanisms 77−4364
GaP:Zn, IR photocond. response spectra 79−56257
GaP:Zn, implanted, elec. profiling using anodic oxidation in N-methylacetamide 80−54690
GaP:Zn, isolated Ga vacancy due to electron irrad., EPR study 78−95519
GaP:Zn, light attenuation by impurity precipitates 79−11441
GaP:Zn, luminesc., acceptor-bound multiple excitons 80−11476
GaP:Zn, multiple bound excitons, photoluminesc. obs. 79−95837
GaP:Zn, O, influence of impurity-absorbed illumination on luminesc. 80−93395
GaP:Zn, O LED, neutron irrad. effects on capacitance, I-V and electrolum. characts. 77−66543
GaP:Zn, Raman spectra of Zn acceptor 77−77187
GaP:Zn, shallow Zn diffusion profile determ. using anodic oxidation and double radioactive tracer method 77−43239
GaP:Zn, Sn doped epitaxial layers, Hall const., hole mobility and conc. 80−15143
GaP:Zn, Te, epitaxial layers, determ. of Zn conc. 79−77614
GaP:Zn, thermodynamics of Zn doping by liquid phase expitaxy 78−83832
GaP:Zn,O, Auger coeff. from luminesc. decay and Hall effect 77−48226
GaP:Zn,O, Auger coeff. from luminesc. efficiency and Hall effect 77−48227
GaP:Zn,O, bulk electrolum. degradation in LEDs 77−81156
GaP:Zn,O, degradation of bulk luminesc. induced by laser excitation 77−1715
GaP:Zn,O, kinetics of X-ray luminesc. 78−10984
GaP:Zn,O, photodiodes, high temp. emission spectra *(Russian)* 77−66545
GaP:Zn,O, red LED, deep-level changes associated with degradation 77−1472
GaP:Zn,O LED, 76K electrolum, spectrum, γ-irrad, and forward bias effects 79−78756
GaP:Zn,S, donor-acceptor pair luminesc., excitation spectroscopy 80−25440
p-GaP:Zn,S, spin polarisation of donors and acceptors in mag. field, optical and microwave study 80−93393
plGaP:Zn-electrolyte interface, electrochemical LED, luminescence obs. 80−84507
GaSb:Te,Zn(Te,Mn), prep. and electrophys. props. 79−87116
GaSb:Zn, carrier density dependence on impurity conc., rel. to solubility limit 77−8047
p-GaSb:Zn, hole transport props. from 77 to 300K 79−73530
GaSb:Zn, thermal sensitivity, −170 to +180°C, resist. meas. 77−39906
p-GaSb:Zn film, epitaxial, lifetime of nonequilib. carriers, determ. from circular polarisation of luminesc. 77−24898
p-Ge:Nz, Sb, influence of electron irradiation in elec. props. 77−20318
Ge:Zn, Sb, photoelec. props., 70 to 300K 80−65621
p-Ge:Zn,Au,Sb, radiation-defect form., Au influence 80−92911
Ge:Zn photoresistor, current responsivity rel. to nonequilib. hole lifetime 80−60035
p-Ge:Zn^-, deep levels, optical-phonon-assisted capture of carriers 79−51597
Ge:Zn^-, G and D lines, stress induced components 80−71447
Ge:Zn^{II} carrier lifetime, nonequilibrium, phase method for determ. 80−65629
He-Zh laser, hollow cathode type, oscillation characts. improvement by inert gas additions *(Japanese)* 77−65590
He-Zn, coaxial type hollow cathode laser, oscillation charact. *(Japanese)* 78−13692
He-Zn, hollow cathode laser discharge, selective excitation of 5894, 7479 Å transitions by Ar 77−27280
He-Zn, hollow cathode laser, gain meas. for 7588, 4924, 7479 and 5894 Å Zn^+ transitions 77−88713
He-Zn, hollow cathode laser tube, with direct current excitation *(Japanese)* 79−76704
He-Zn hollow cathode laser, electron density, excited ions radial profiles 78−29937
He-Zn hollow cathode laser, 7588 Å in ZnII, operating characts. and upper level operating mech. 78−63071
He-Zn hollow cathode laser, upper level decay rate, mag. field tuning dip meas. 78−87043
He-Zn hollow cathode laser discharge, comparison with He-$ZnCl_2$ discharge 80−28203
He-Zn hollow cathode laser discharge, radiative cascade excitation effect on upper laser levels 80−102697
He-Zn hollow-cathode discharge, excitation processes, rel. to Zn II laser 79−98342
He-Zn II laser, 0.4924 μm oscill. spectra meas. using scanning interferometer *(Japanese)* 80−9864
He-Zn laser, 7588 Å, He metastable atoms effect on power 78−33722
He-Zn laser, negative glow and positive column discharges comparison 78−1217
Hg+Zn(Cd), sensitized fluoresc., orientation and alignment transfers *(French)* 79−13808
$In_{1-x}Al_xP$:Zn,O, radiative recombination at isoelectronic centres 79−52027
InAs:Zn, optical absorpt. and refl. spectra 79−91479
InAs:Zn,S,(Se)(Te), exam of microhardness, Hall effect as function of dopant 79−95038
InAs:Zn,S(Se), solubility and donor-acceptor interaction 80−54263
p-$In_{0.53}Ga_{0.47}As$:Zn on InP, elec. and optical props. 80−75662
$In_xGa_{1-x}As$:Zn, lattice matching to InP, LPE growth conditions 80−70541
InGaAsP:Zn, LPE growth, influence of growth-solution dopants on distrib. coeffs. 79−47640
$In_{1-x}Ga_xP$:Te,Zn, photolum. and electrolum., direct transition region 77−8659
$In_{1-x}Ga_xP$:Zn,O, radiative recombination at isoelectronic centres 79−52027
$In_{1-x}Ga_xP_{1-z}As_z$:Zn, x∼0.12, z∼0.26, LPE, DH lasers, tunnelling involving defects 77−65594
InP:Zn, avalanche photodiode characts., impurity diffusion effects 80−70709
InP:Zn, dislocation-free, TEM study of microdefects 79−82213
p-InP:Zn, electrical meas., doping levels hole conc. 78−14745
InP:Zn, isoconcentration diffusion of Zn at 800°C 78−6186
p-InP:Zn, single cryst. growth by temp. gradient method 79−28907

zinc continued
InP:Zn, substitutional dopant and hole conc. meas. 80−75260
p-InP:Zn, vapour grown, prep. and props. 80−54268
InP:Zn heavily doped X-ray topography, cathodolum., and TEM obs. 79−99197
p-InP-Zn, ohmic contact formation on InP by laser photochemical doping 80−80369
InSb:Cr,Zn, transport props. meas. 77−1424
InSb:Cr:Zn, magnetic freeze-out electrons at deep Cr level 79−15169
InSb:Zn, heat treatment effects on elec. props. 78−43411
InSb:Zn, impurity centre behaviour, impurity conc. and Hall coeff. meas. 80−65490
InSb:Zn, ion-irrad., p-n conversion during heat treatment 80−96558
n-InSb:Zn, Zn diffusion out of implanted layers 79−10984
p-InSb:Zn film, heavily doped, ionized impurity scatt., Hall effect and DC cond. meas. 79−99643
InSb:Zn p-n junctions, ion implantation and diffusion spreading, elec. and photoelec. props. 79−73573
KCl(Br)(I):Zn^+, optical absorpt. bands rel. to charge transfer 80−66245
K_2MnF_4:Zn, mag. effects of impurities 80−65869
K_2MnF_4:Zn(Mg)(Ni), local magnetisation, NMR and Green's function study 80−65870
Li_2SO_4:Zn^{2+}, monoclinic-cubic transform., effect of impurities 79−52744
liquid, polyvalent, electrical resistivity by harmonic model potential 80−54668
MnF_2:Zn, shift and broadening of optical transitions 79−38579
Na^++Ti(Ni)(Zn)(Fe), 0.2-3.0 MeV, united-at. limits, mol.-orbital continua 77−19030
NaCl:Zn^+, interpretation of optical absorption spectra 79−51993
NaCl:Zn^+, X-irrad., EPR and optical absorpt. 78−43642
NaCl:Zn^{2+}, electrolytically coloured, CESR 77−16174
NaCl-NaF:Zn^{2+}, point defects, ionic thermal current and optical meas. 80−6403
Ne^++Zn, charge exchange and Penning ionisation in pulsed discharge afterglow 79−7007
Ni electrochem. deposition on Zn surfaces 80−29885
Pb-Zn belts and their origin 79−48427
Pb-Zn-Ag, liquid system, 450-750°C, phase boundaries *(French)* 77−69081
PbTe:Zn, defect struct., Hall effect and solubility meas. 77−11572
p-PbTe-Zn, barrier props. 79−7898
Sb, optical phonon anharmonicity and melting, light scatt. study 80−60621
Si:Zn, deep-level impurities, insulating props. 78−39124
Si:Zn, diffusion mechanism of fast impurities, distrib. in surface layers 77−11735
Si:Zn, electronic states of impurities 77−43531
Si:Zn, ground state of impurities 79−28313
Si:Zn, implanted atom diffusion during laser annealing 79−37725
Si:Zn, impurity states, localised orbital approach 80−92851
Si:Zn, minority carrier lifetime investigation 80−80292
Si:Zn, n^+-n-n^+ structure, photocond. lifetimes, deep level occupancy in exclusion region 78−72253
Si:Zn, P^+-n-n^+ struct., deep doubly ionized centres, impedance calc. 79−11202
Si:Zn, photoionisation of deep impurity levels 80−34386
Si:Zn, recombination waves threshold parameters in microwave field 77−28206
Si:Zn, resist. inhomogeneity effects on photoelec. props. 77−8151
Si:Zn, reson. characts. of impedance near excitation threshold of recomb. waves 80−20301
Si:Zn, surface characterised by negative electrochemical pot., electronic props. 80−44695
Si:Zn, trapping struct., analysis of TSC meas. 77−8045
n-Si:Zn,P, local deform. of cryst. lattice, charact. parameters or recomb. waves 77−4386
Si:Zn p-n junction diode, computer-aided study of carrier lifetimes 80−24999
Si:Zn p-n junctions, I-V characts. using exact DC circuit model 79−95476
p-Si:Zn , deep levels, optical-phonon-assisted capture of carriers 79−51597
Si_3N_4-SiO_2:N,Zn ion-implanted multiple layers, ion range distribs., secondary ion microprobe meas. 79−42129
TiO_2:Zn^{2+}, reduced by H_2, photoconductive props. 77−55558
Zn, elec. field gradient at ^{111}Cd, effects of high press., TDPAC meas. 80−25266
Zn electrodeposition, on Zn and Al single crysts., from H_2SO_4 bath, SEM obs. *(Japanese)* 80−93502
Zn I, absorpt. spectra, line and total absorpt. comparison 80−11991
Zn I, relative populations in arc, sputtering and gas phase collisions 80−934
Zn I,II, excited state lifetimes, electron-photon delayed coincidence meas. 78−25478
Zn II, beam excited levels, population inversion 79−18161
Zn II, Hanle effect, $^2P_{3/2}$ lifetime determ. 77−18852
Zn II, lifetime extraction from beam-foil decay curves 80−14107
Zn I(II), low lying level lifetimes, beam foil spectra 79−36751
Zn island films, effect of surface press. on lattice spacings 79−11045
Zn isoelectronic sequence, resonance oscill. strengths 79−3413
Zn ore dust, pollution analyser using Harwell 6000 series electronics 79−5649
Zn XIX, XX, spectral lines 20 to 50 Å 77−18822
Zn XX, electron impact excitation, transition probabilities, oscill. and collision strengths 78−25718
Zn XX, energy levels and one electron transitions, relativistic calculations 80−87051
Zn XXII, 2p-4d and 2p-4s transition arrays, wavelengths and oscillator strengths 80−47933
Zn XXII, $2p^5$-$2p^4$3s($2p^4$3d) transitions in laser produced X-ray spectra 78−13460
Zn, XXII, spectra and energy levels of F isoelectronic series 79−93948
Zn XXVIII, spectra calcs., fine struct., transition energies 77−42260
Zn^+ laser in He-halide discharge, CW oscill. 78−17913
Zn^+, transport in cation-exchange membranes 78−96033
Zn^{2+} binding to nucleic acid bases, ab initio SCF (pseudopot.) calcs. 80−12052
Zn^{2+}, closed shell ion, 3d electron pair correl. energies calcs. 79−31417
Zn^{2+}, electron pair correlation energies 79−93927
zinc continued
Zn^{2+} ions, adsorpt. by doped MnO_2, ^{65}Zn γ-ray scintillation investig. 80−70529
Zn^{2+}, quadrupole antishielding factors, Hartree-Fock perturbation theory 78−62723
Zn^{2+}, sorption from HCl solns. by cation exchange resin Dowex 50 W×8, temp. depend. *(Bulgarian)* 79−87004
Zn^{28+}, ^1P and ^3P energy levels, relativistic RPA calc. 80−47913
Zn:^{115}In, 828 keV state, elec. quadrupole interaction meas. 77−8484
Zn:^{67}Ge, elec. quadrupole interaction temp. depend., PAC meas. 79−42877
Zn:^{67}Ge, quadrupole interaction temp. depend. 77−12264
Zn:^{69}Ge, quad. interac., rad. damage effs. during PAC obs. 77−27918
Zn:^{99}Ru, quadrupole interaction temp. depend., PAC method, electric field gradients 77−73105
Zn:Al, ion implantation, temp. and time depend. 80−65013
Zn:Al, ion implantation of Al, defect flow induced outdiffusion 78−63779
Zn:Al, residual resistivity, numerical calc., Fermi surface and multiple plane wave band struct. 77−51722
Zn/Cu film system, UPS during atomic diffusion 79−43097
Zn/$ZnSO_4$/Zn system, laser interferometric study of corrosion of coated and uncoated metals, technique standardisation 79−35815
Zn-AgO cell, Zn electrode slurry-paste fabrication optimisation 79−96430
Zn-barium stearate-Zn structs., internal voltage work function meas. 79−82684
Zn-Cu-Zn system, galvanic corrosion, anal. for coplanar electrodes with one electrode infinitely large 79−8398
Zn-GeS-Zn structure, current-voltage characts., thermionic electron emission model 77−28260
Zn-GeS-Zn system, Schottky and Poole-Frenkel cond. mechanisms 80−54799
Zn-glass, friction, loading time effect *(Japanese)* 78−34095
Zn-H_2(He)(Ar) mixtures, binary diffusion coefficients, 1 atm., 720-1120K 80−1725
Zn-HgO, primary battery, self-discharge rates using microcalorimeter 79−61963
Zn-Hg(Ga) metal/liquid metal, exam. of crack propag. in liquid metal environment 78−60766
Zn-like ions, 4s-4p reson. lines and transitions obs. by means of laser prod. plasma, appl. to Tokamaks 80−99468
Zn-Pb proximity sandwiches, tunnelling characts. 79−56396
Zn-pore electrodes and cells, operation 80−26126
Zn-S system, Zn-rich liquidus, 1000-1300°C 78−18747
Zn-Sb diffusion couple, layer growth of ZnSb phase at high press., elec. meas. 80−2218
Zn-Sb diffusion couple, ZnSb phase layer growth kinetics, 240-320°C, up to 30 kbar 78−10229
Zn^+-He, positive column laser discharge, upper and lower state densities, Penning collision 80−32964
Zn+H^+, K-shell ionisation calcs. 80−23534
Zn+H^+, K-shell ionisation cross-sections calcs. 80−43165
Zn+H^+(He^{2+}), L- and M-shell Auger electrons 79−27076
Zn+He, Penning ionisation cross section of target atom, for He(2^3S_1) 80−63777
Zn+He^+, thermal energy charge transfer reaction, ion states, relative yields 79−45840
Zn+He^+(He_2^+), inelastic collisions, 2-800 eV, excited state form. 78−94312
Zn+N_2, $A^3\Sigma_u^+$ state, vibr. excitation 80−1054
Zn+N^+, X-ray production cross section, Kβ/Kα ratio, 0.5-2.5 MeV/amu 77−54526
Zn+O_3, matrix reactions, IR, Raman and visible spectra in Ar and N_2 matrices 80−87110
Zn+P reaction mechanism and kinetics, effect of Ag and Mn impurities 77−21416
Zn+Se, π capture, radioactivity meas. 80−47831
Zn^++He(Ne)(Ar), 1-500 keV, Zn^+ excitation, reson.-line emission and polaris. 80−18911
Zn^++He(Ne)(Ar), Zn^+ collision-induced alignment, reson.-line emission polaris. obs. 80−18912
Zn^{2+}+H, electron capture by slow ions, pseudo-crossing 80−43176
Zn_2, ab initio SCF LCAO MO calcs., contracted basis set effects 77−83495
Zn_2, electronic states, CI calcs., rel. to Hg_2 77−10601
Zn_2, in Ar and Kr matrices, 10K, UV spectrum, vibr. assignments 77−58038
Zn_2, matrix isolated, Raman spectra 79−50024
Zn_2, pot. energy curve of low-lying states, MO theory 79−89624
Zn_2, quenching and predissociation, possible excimer laser 80−32770
Zn_4 clusters, electronic structures, SCF-Xα-SW method 80−88468
$ZnAs_2$, thermodynamic functions 79−10961
$ZnCl_2$-Zn chemically deposited photosensitive cells, photovoltaic characts. 79−39303
ZnI, II, excited states, radiative lifetimes, multi-channel delayed-coincidence method 80−32669
Zn($^1P_1$)+NO($X^2\Pi$)→Zn($^1S_0$)+NO($A^2\Pi^+$, v=0,1), near-resonant electronic energy transfer, fluoresc. quenching 77−14549
Zn($^1P_1$)+NO($X^2\Pi$)→Zn($^1S_0$)+NO($A^2\Sigma^+$), near reson. electronic energy transfer, initial rot. state population 79−68304
ZnP_2, cathodoluminesc. 4.2 to 200K 79−52028
Zn(^1S), dipole polarisability, relativistic effective core pot. calc. 79−76362
ZnTe:O,Zn, dual ion implantation, luminesc. spectra obs. 78−87697
Zn(0001)-Zn(0001), metallic adhesion 79−73463
^{62}Zn/^{62}Cu generator, source of ^{62}Cu for radiopharmaceuticals 80−67248
^{64}Zn isotope, fractionation during zone recrystn. 80−2946
^{65}Zn behaviour in sediments in laboratory-scale aquatic ecosystem 78−3831
^{65}Zn, sediment-bound, absorpt. through digestive tract of marine demersal fish 79−92400
^{65}Zn, uptake of gamma-emitting activation products in plants 80−30614
^{65}Zn whole-body retention in pregnant mice, and secretion into milk 79−88200
^{67}Zn, ^3D, ^1D, $^3P_1$ and $^1P_1$ levels, quadrupole coupling consts. 80−23434
^{68}Zn, 2s-2p muonic X-ray transition obs. 80−74264
^{68}Zn muonic atom, dynamical E0 excitation, E0 resonances, muonic X-rays 80−95749
Zn(g)+H_2O(g)=ZnO(s)+H_2(g), standard Gibbs free energy of reaction 79−11815

zinc alloys
see also brass; zinc compounds
admiralty brass, stress corrosion cracking, aqueous $CuSO_4$ 77−59961
Admiralty Metal, transgranular stress corrosion crack propag. 80−89402
Al-Zn-Mg (5,1 wt.%), decomp. process, TEM study 80−71660
Al-Zn-Mg (6, 3 wt.%), water vapour embrittlement and H_2 bubble form 78−15564
anodic corrosion in seawater 77−77628
binary substitutional solutions, thermodynamics 80−44337
brass, corrosion protection in chlorosubstituted acetic acids, use of 2-methyl benzothiazole corrosion inhibitor 79−57149
brass (70/30), interaction of annealing twins in fcc metals and alloys 78−68712
brazing, flux adhesion, and spreading coefficient 80−15379
Cu-Zn-Mn, de-alloying props. 80−104332
deep drawing behaviour, exam. in binary and ternary alloys *(French)* 79−52325
dilute binary alloy, residual resistivity 77−1406
ζ-Fe-Zn layer formed during hot dip galvanizing, texture 79−29287
high strength Al-Zn-Mg-Cu alloys, mechanical props. *(Japanese)* 79−91654
intergranular dissolution of sacrifical anode in seawater at elev. temps. 79−96181
internally deformed struct. as source of homogeneous linear struct. 78−26497
Kondo alloys, with magnetic breakdown, anal. of de Haas-van Alphen effect 78−34751
liquid amalgams mixing, excess entropy, vibr. contrib. *(Russian)* 79−51263
liquid metal embrittlement, eval. by quasistatic crack propag. technique 79−29262
$Mg_{70}Zn_{30}$, amorphous alloy 77−27835
mutual alloying behaviour of the elements straddling the line Li-Mg-Cu-Au in the long periodic table 78−84769
Ni-Zn ferrites, mag. param. 78−35005
phosphor bronze, beam, cylindrical, flexurally vibrating, Timoshenko's shear coeff. 78−83866
phosphor bronzes, surface Cs^+ impact, 5.5 keV negative secondary ion emission obs., rel. to Cu *(French)* 77−66562
positron annihilation expts., electronic struct. and Fermi surface studies 80−54594
precipitate free zones, X-ray microanal. 80−108768
preferred crystal orientations, rot. mill device investig. 79−57006
rare earth alloys, ferromag., parastriction and magnetoelastic coeffs. 80−65996
rare earth alloys, RZn_{12}, mag. struct. and interactions 80−25092
rare earth alloys, RZn, ordered, NMR determ. of hyperfine fields 78−84180
rare earth intermetallics, RZn, magnetoelastic consts. 78−15005
rare earth-Zn_{12}, mag. props. and structs. 78−84393
rare earth-Zn, mag. coupling mechanism 79−4655
rare earth-Zn alloys, existence and cryst. struct. 79−77555
rolled and press. die-cast, creep and deformation behaviour *(German)* 80−66611
slip band theory, model for creep based on dislocation climb at grain boundaries, comparison with expt. data 79−37756
steel, Cu-Mn-Zn, Zn addition effects in powder forgings produced by liquid solid alloying 78−11157
steel, galvanized, Fe-Zn phases, Mossbauer study 80−50233
steel, stainless wire reinforced Al-Zn-Mg system, resistance to crack propagation 79−43409
Ag Zn system, β-β′ order-disorder phase transition 79−47678
Ag-Cu-Zn, effect of additions on eutectic and peritectic temp., of binary alloys 78−84801
Ag-Cu-Zn-Cd solid metal lubricant in self lubricating composite steels 78−11340
Ag-Cu-Zn-(Cd)(Mn), solder, UTS, room temp. to 4.2K 79−57064
α-Ag-Zn, atomic short-range order determ., X-ray scatt. and pseudopot. calc. 78−2067
Ag-Zn, α-phase alloy, thermopower at low temps. 78−84196
Ag-Zn, cold-worked, lattice defects, convolution relations for X-ray line breadth calcs. 78−51394
Ag-Zn, dil., elec. quadrupole interactions on ^{111}Cd probe nuclei, time differential PAC meas. 78−15066
α-Ag-Zn, electron irrad., atomic mobility enhancement by defects, dynamic characts. 79−37871
Ag-Zn, electron irrad. self-interstitials, migration and elimination characts. 79−37872
Ag-Zn, interdiffusion coeff. in ε phase *(Japanese)* 79−14969
Ag-Zn, internally oxidized, elec. contact characts., alloying additions effect *(Japanese)* 80−88619
Ag-Zn, liquid, thermodynamic props. *(German)* 79−87615
Ag-Zn, molten, EMF meas. of activities using ZrO_2 solid electrolytes *(Japanese)* 80−88339
Ag-Zn, negative muon capture ratios 80−55007
Ag-Zn, production and annealing of radiation defects 78−47362
α-Ag-Zn, short-range order calc. by pseudopotential method *(Russian)* 77−43175
Ag-Zn, temp. depend. of elec. field gradient, TDPAC meas. 77−32304
Ag-Zn, thermopower at low temp., Fe impurities 79−65440
Ag-Zn, vacancy prod. rate by displacement cascades, anelastic meas. during neutron irrad. 80−19794
Ag-Zn (2 to 12 wt.%) containing several metals, internal oxidation *(Japanese)* 80−16570
Ag-Zn (24 at.% Zn), γ-irradiated, freely migrating defects, rate of production *(French)* 79−10877
Ag-Zn (27-48 wt.%), interphase β′-ζ transform., thermal expansion exam. 77−63630
Ag-Zn (30 at.%), electron irrad., mobilities of self-interstitials and vacancies 77−84795
Ag-Zn (30 at.%), electron irrad. exam. of defect supersaturation by elasticity, and creep meas. 78−47366
Ag-Zn (30 at.%), electron irradiated, atomic mobility, elastic after-effect meas. *(French)* 78−63874
Ag-Zn (30 at.%), neutron irrad., at. mobility enhancement, Zener relax. meas. 77−1157
Ag-Zn (38 at.%), morphological and struct. studies of thermoelastic martensites 77−63669
Ag-Zn (50 at.%), BCC β phase, high temp. creep, existence of master curve 80−55473

zinc alloys continued
Ag-Zn electrodeposition, controlled-potential, spontaneous transformations obs. 78−51853
Ag-Zn equiatomic, creep of β phase *(French)* 78−48477
Ag-Zn-Te(-Sn)(-In), internally oxidised, oxide particle size control *(Japanese)* 80−89480
$Ag_xAu_{1-x}Zn$, resistivity and X-ray diffr. 78−47283
AgCd-AgZn, quasibinary alloys, phase relations 79−8273
AgZn, B2 intermediate phase, slip system, ordering energy and atomic size ratio depend. 80−59471
AgZn, β′ to ζ_0 and β to ζ_0 phase transform. 79−34026
AgZn, β′→ζ transformation, effect of additional elements 80−66507
AgZn-AgMg quasibinary alloy, phase relation and superlattice form. 78−3097
γ-Ag_5Zn_8, high pressure effect on brass struct. 80−107108
Ag_xZn_y, TDPAC meas. of ^{111}Cd 77−28492
Al bronze, BA 1032, deformation at high temp. *(Polish)* 79−79023
Al-Ag-Zn, ring diffuse X-ray scatt. phenomena *(Russian)* 77−16538
Al-Ca-Zn (5,5 wt.%) superplastic sheet alloy, mechanical properties, superplastic forming behaviour 80−60920
Al-Cu-Mg-Mn-Zn-Cr, low temp. deformed, ageing and mech. props. 79−1881
Al-Cu-Mg-Zn, Mg and Zn addition effects on dendrite struct. and mech. props. *(Korean)* 77−28796
Al-Cu-Mn-Mg-Fe-Si-Zn alloy D16, surface layers chem. composition rel. to fatigue resist., corrosion-fatigue resist. 79−29275
Al-Cu-Zn alloy, ageing, X-ray and electron diffr. meas. *(Russian)* 78−39806
Al-Cu-Zn system, solid-phase reactions, phase diagram 80−50603
Al-Cu-Zr (6, 0.3 wt.%), superplastic, mech. anisotropy and deformation mechanisms 79−83254
Al-Mg-Zn, granulated, degassing atm. effect on mech. props. of semifinished products 80−7720
Al-Mg-Zn, interdiffusion 78−51751
Al-Mg-Zn, neutron small angle scatt. study 79−43255
Al-Mg-Zn, O_2^+ ion bombard., SIMS and photon emission spectra, local thermodynamic equilib. model 80−20751
Al-Mg-Zn alloy, surface Be migration, depth profiling by ion microprobe with high mass resolution 79−46894
Al-Mg-Zn alloy 7179-T651, reduced ductility under tensile after exposure to water 80−11835
Al-Mg-Zn alloys, Al-rich, weld metal comp. effect on microsegregation and eutectic phase segregation *(German)* 80−108455
Al-Mg-Zn alloys, evaporation effect of alloying elements Mg and Zn in in-situ EM studies 80−103388
Al-Mg-Zn alloys, liq./solid phase equilibria determ. *(German)* 80−50601
Al-Mg-Zn solid solution, thermophysical props., 0-400°C *(Russian)* 77−89548
Al-Mg-Zn-Cu, type 7050, calorimetric study of fatigue induced microstructural changes 80−85034
Al-Mg-Zn(-Cu) exam. of precipitation struct. by neutron scattering 78−92270
Al-Mn-Zn, fatigue cracks, in NaCl, oil and water vapour *(Japanese)* 78−11414
Al-Ni(Pt)(Zn), rapidly solidified, twinned dendrites 80−70572
Al-Si-Zn alloy, creep rates, pre-torsional deformation effect 79−96096
Al-Zn, age hardenable precipitation and dissolution, positron annihilation and X-ray scatt. 80−16314
Al-Zn, ageing alloy, zonal decomposition stage, new effects in X-ray diffr. anal. *(Russian)* 79−4982
Al-Zn, binary metallic melt, deviation from the Kopp law, specific heat *(Russian)* 80−39305
Al-Zn, coating on mild steel, interface struct. 79−52466
Al-Zn, cold working causing preprecipitation, thermoelec. power *(French)* 79−8306
Al-Zn, comparison between very-slow-neutron transmission and small-angle neutron scatt. expts. 80−19677
Al-Zn, corrosion of chill zone, solidification microstruct. effect 77−36687
Al-Zn, dil, deviation from Matthiesen's rule, 4-OPW approx. calc. 79−19574
Al-Zn, dil., Dingle temp. calc. 78−39005
Al-Zn, dil., electronic transport coeffs. for point defect scatt., 4-OPW calc. 79−42531
Al-Zn, dil., grain boundary diffusion 78−91475
Al-Zn, dil., magnetoresist., temp. depend. 80−70682
Al-Zn, dil. alloy, ^{65}Zn diffusion 77−51540
Al-Zn, dil. alloy, ageing and reversion, annealing curves, X-ray obs. 78−88485
Al-Zn, discontinuous decomposition *(Polish)* 78−52808
Al-Zn, effects of temp. on order-depend. elec. resist. 77−31992
Al-Zn, electrical resist. and magnetoresist., 2 to 40K, Matthiessen rule deviations *(Russian)* 77−31996
Al-Zn, electrical resist. of Guinier-Preston zones during age hardening 77−72848
Al-Zn, electron probe microanalysis, depleted zone formation in air and vacuum 79−57013
Al-Zn, flow stress, Zn content effect 79−38913
Al-Zn, formation of Guinier-Preston zones, and their limit temp. *(Japanese)* 78−84861
Al-Zn, GP zones, effect of Si, Ag, Mg on transport props. 77−16588
Al-Zn, G.P. zone form., temp. limit 80−16317
Al-Zn, grain boundary reaction sites, determ. of struct. aspects, by electron microscopy 80−103359
Al-Zn, Guinier-Preston ellipsoidal zone model of X-ray scatt. *(French)* 77−84568
Al-Zn, Guinier-Preston zone form. kinetics study using linear localisation probe *(French)* 78−15413
Al-Zn, Guinier-Preston zone reversion, thermoelectric power meas. *(French)* 79−20058
Al-Zn, Guinier-Preston zone struct., absolute SAXS meas. *(Japanese)* 79−70072
Al-Zn, interdiffusion meas. by elec. resist. 80−49433
Al-Zn, isothermal preprecipitation, small angle X-ray scatt. expts. 80−35186
Al-Zn, liq., physical props. study by electrodiffusion method *(Czech)* 77−84956
Al-Zn, liq. solutions, thermodynamic properties *(Polish)* 80−49380
Al-Zn, low temperature lattice parameters 78−38658

zinc alloys continued
Al-Zn, metastable phases formed at 200°C, room temp. stability 80−16315
Al-Zn, metastable solvus curve, struct. changes 77−55950
Al-Zn, miscibility gap, spinodal region, thermodynamic data transferability *(German)* 79−20027
Al-Zn, neutron small angle scattering from above critical point 79−1840
Al-Zn, neutron small angle scatt. study 79−43255
Al-Zn, nonhomogeneity of deform. 78−84888
Al-Zn, pitting potential 78−35550
Al-Zn, plastic deform. effect on struct. transform. at elev. temp. *(Czech)* 79−79044
Al-Zn, precipitation struct. and phys. props. effect of miscibility gap *(German)* 78−92265
Al-Zn, rapid quenching, struct. and decomp. 80−76244
Al-Zn, recrystallization texture 79−91679
Al-Zn, resistivity anomalies in Guinier Preston zones *(French)* 78−6937
Al-Zn, resistivity calc. for age-hardened alloy 77−73284
Al-Zn, short range order, many electron effects, pseudopotential method 78−79954
Al-Zn, short-range order, electronic theory, pseudopotential approach 77−80717
Al-Zn, small-angle neutron scatt. in crit. point regions, 324-435°C *(German)* 77−85993
Al-Zn, solid soln., exam. of evolution by thermo EMF meas. *(French)* 78−52862
Al-Zn, spinodally decomposing, main wavelength of conc. fluctuations calc. 80−97459
Al-Zn, tension deformed superplastic specimens, instantaneous strain rate variation *(Russian)* 79−79033
Al-Zn, type 7075-T6, coldworked hole specimens, residual stresses, fracture mech. anal. 80−97587
Al-Zn, work hardening under tension at 1.6-900K 79−38842
Al-Zn, X-ray diffr. after omnidirectional compression *(Russian)* 80−88262
Al-Zn 6.8 at.%, Guinier-Preston zones *(French)* 79−87640
Al-Zn (0.041 to 4.4 at.%), clusters, electrical resistivity meas. *(Japanese)* 77−21168
Al-Zn (0.14 at.%), nuclear acoustic reson., 20-80K 79−8058
Al-Zn (10 at.%), ring diffuse X-ray scatt. phenomena *(Russian)* 77−16538
Al-Zn (10 at.%), short-range order parameter calc. in pseudopot. approx. *(Russian)* 80−49183
Al-Zn (10 wt.%), ageing at low temp., solute conc. fluctuation effects *(Japanese)* 79−4969
Al-Zn (10 wt.%), ageing at low temp., effects of fluctuation of solute conc. 80−76287
Al-Zn (10 wt.%), ageing at low temp., effects of fluctuation of solute conc. 80−76288
Al-Zn (10 wt.%), ageing behaviour, calorimetric study 80−45328
Al-Zn (10 wt.%), solid soln., decomposition meas. by resistivity meas. under isothermal conditions *(French)* 79−20025
Al-Zn (10 wt.%), solute conc. fluctuation effects on ageing at low temp. 79−57023
Al-Zn (11 wt.%), stress depend. of strain rate at elev. temps. 78−23757
Al-Zn (11.8 at.%), growth and dissolution of metastable precipitates, neutron scatt. study 79−15671
Al-Zn (12.5 wt.%) retardation of precip. reaction by DC stress 77−55969
Al-Zn (15,16,18 at.%) alloys, coherency spinoidal curve position determ. 77−52281
Al-Zn (15 at.%), structural changes during post ageing between 125°C to 215°C 80−40399
Al-Zn (15 at.%), supersaturated alloy, growth and decomposition kinetics 80−29965
Al-Zn (15 wt.%), calorimetric ageing study 80−45330
Al-Zn (18 at.%), position of coherency spinodal curve 78−23660
Al-Zn (1.9 at.%), 1 MeV electron irradiated, induced homogeneous precipitation 79−77638
Al-Zn (2 and 4 wt.%), ageing and elec. cond. reversion *(Japanese)* 79−4983
Al-Zn (20 (30) (35) (40) (60) at.%), effect of UTS on cyclic creep strength *(Korean)* 80−25778
Al-Zn (21.8 at.%), elec. conductivity and α'-precipitates, 276-302°C 77−80758
Al-Zn (22 at.%), X-ray scatt. obs. of segregation *(French)* 79−96032
Al-Zn (22 wt.%), superplastic strain rate sensitivity, rel. to ductility 78−31478
Al-Zn (30 wt.%), metastable phases, transformation kinetics, quenching rate effects meas. 77−55960
Al-Zn (30 wt.%), precipitation sequences and transformation kinetics, X-ray diffr. and TEM obs. 77−55959
Al-Zn (30 wt.%), precipitation ageing plastic deform. effects 77−66645
Al-Zn (38 at.%), alloy, TEM study of precipitation processes or different microstructures during ageing 80−93561
Al-Zn (3.9 wt.%), single crysts., fatigued age-hardenable, dislocation structure *(German)* 80−54247
Al-Zn (40 at.%), resistance of homogenization in micro-segregation 79−100180
Al-Zn (40 wt.%), grain refinement by thermal cycling 78−3149
Al-Zn (40 wt.%), mechanical properties after thermal cycling 78−3150
Al-Zn (40(50)(65) wt.%), deformed, free energy changes in process of discontinuous precipitation 80−3054
Al-Zn (40(50)(65) wt.%), plastic deform. effect on discontinuous precipitation 80−3053
Al-Zn (5.05 at.%), comparison of X-ray and neutron small-angle scatt. 79−15647
Al-Zn (60 or 71 wt.%), natural ageing *(Russian)* 78−48367
Al-Zn (6.5 at.%), fatigue props., effect of ageing and thermomech. treatment 78−27620
Al-Zn (6.8 at.%), decomposition, electron microscope study *(French)* 77−40422
Al-Zn (6.8 at.%), hardening during spinodal decomposition *(French)* 79−66035
Al-Zn (6.8 at.%), neutron small angle scatt., interparticle interference 77−77514
Al-Zn (6.8 at.%), synchrotron radn. use in X-ray scatt. *(French)* 79−47723
Al-Zn (6.8 at.%) alloy, elec. resist. temp. depend. rel. to ageing processes 77−77486

zinc alloys continued
Al-Zn (6.8 wt.%), effects of ageing temps. on microhardness and resistivity *(Japanese)* 78−35408
Al-Zn (6.8 wt.%), Guinier Preston zones internal struct., study by X-ray diffusion, α_R phase comparison *(French)* 80−66472
Al-Zn (7 at.%), liquid quenched, early stage phase separation, exam. 78−68698
Al-Zn (70, 30 wt.%), decomp. study, 25-160°C *(Czech)* 80−89225
Al-Zn (8-25 wt.%), solid solns., residual resist. during clustering 80−97483
Al-Zn alloy, resist. and X-ray small angle scatt. during GP zone form., theory *(French)* 79−29070
Al-Zn alloy, solid state eutectoid transformation 79−74146
Al-Zn alloy, type 7010, die-forged, tensile props. after heat treatment, stress corrosion 79−66103
Al-Zn alloy cladding materials, corrosion behaviour under vacuum heating *(Japanese)* 79−91845
Al-Zn alloys, anisotropy function determ. 77−43565
Al-Zn alloys, cast, Zn diffusion during homogenization *(Polish)* 79−33108
Al-Zn alloys, interfacial stability of planar solid-liq. interface during solidification 80−104145
Al-Zn alloys, interfacial holes distrib. at beginning of interfacial instability in solidification 80−104146
Al-Zn alloys, preprecipitation, elec. resist., microhardness meas., dislocation-growth distortion interactions *(Japanese)* 77−25053
Al-Zn alloys, recrystallisation and superplasticity, HVEM straining 80−39207
Al-Zn alloys, relation between microhardness and average radius of Guinier-Preston zones 78−95811
Al-Zn alloys, room temp. decomp. of metastable phases precipitated at 200°C 78−84814
Al-Zn alloys, spinodally decomposing, resistivity behaviour 80−45271
Al-Zn changes in inner-electron binding energies during ageing, electronic spectra study 77−28816
Al-Zn coated steel sheet, chromate passivation protection against wet-storage stain 78−95854
Al-Zn eutectic, mechanism of lamellar spacing adjustment 78−31395
Al-Zn eutectoid, superplastic, fracture, electron microscope obs. 78−31533
Al-Zn eutectoid, superplasticity, test machine rigidity effect 79−70250
Al-Zn eutectoid alloy, sensitivity analysis of torsion method in evaluating superplasticity indicators 77−56179
Al-Zn ingots, solidified, formation of equiaxed eutectic grains *(Japanese)* 78−39756
Al-Zn melt, electrotransfer *(Russian)* 77−66034
Al-Zn solid soln., controlling creep mechanisms, role of diffusion 78−31469
Al-Zn solid soln., controlling creep mechanisms role of diffusion 78−31470
Al-Zn system, R-phase, mixing free enthalpy approx. calc. 77−1832
Al-Zn thin film, prep. using Sn-Zn evaporant source 80−100789
Al-Zn-Cu (22, 0-3 at.%) alloys, coherent spinodal curve 79−87605
Al-Zn-Cu-Mg (V95T1), subcritical crack growth under static plane stress 80−55528
Al-Zn-Fe-Si, Fe and Si effects on precip., TEM and X-ray diffr. obs., ageing at 90°C 77−48439
Al-Zn-Hg alloy, cathodic protection characts., surface free energy, lattice struct. 79−29281
Al-Zn-In-Mg, substitution for Mg in Mg-MnO_2 short-circuited cell, performance 79−61964
Al-Zn-Mg, acoustic emission meas. during tensile testing, reproducibility of results 80−50782
Al-Zn-Mg, age-hardenable, precipitation and dissoluton processes, positron annihilation and X-ray small-angle scattering comparison 80−89238
Al-Zn-Mg, atmosphere effect on fatigue crack propag. *(Japanese)* 80−81161
Al-Zn-Mg, cavitation during superplastic deform. *(Japanese)* 78−15464
Al-Zn-Mg, crack-arrest markings on integranular stress corrosion fracture surfaces 80−89405
Al-Zn-Mg, decomp. kinetics and ageing mechanism *(Russian)* 80−45269
Al-Zn-Mg, decomposition calorimetric study *(German)* 79−74165
Al-Zn-Mg, ductile intercrystalline fracture obs. 77−77554
Al-Zn-Mg, duplex ageing effect on tensile props. 79−91721
Al-Zn-Mg, effect of microstruct. on localised shear failure 78−52996
Al-Zn-Mg, effect of microstruct. and corrosive environments on stress corrosion cracking *(Japanese)* 79−79159
Al-Zn-Mg, elec. resist. of η' precipitates 77−48441
Al-Zn-Mg, electron probe microanalysis, depleted zone formation in air and vacuum 79−57013
Al-Zn-Mg, fatigue crack propag., stage I 77−36653
Al-Zn-Mg, fractographic stage I fatigue facets 77−16680
Al-Zn-Mg, grain boundary surfaces, plasmon loss satellites in Auger spectra 78−15261
Al-Zn-Mg, grain boundary segregation, AES meas. 78−72781
Al-Zn-Mg, Guinier-Preston zones, comp. and contrib. to elec. resist. 80−16316
Al-Zn-Mg, heat treatment and inversion processes, elec. resist. study *(Hungarian)* 77−25078
Al-Zn-Mg, long term strength and creep 80−60925
Al-Zn-Mg, metastable miscibility gap determ. by small angle scatt. 77−28781
Al-Zn-Mg, metastable T′ phase 77−21151
Al-Zn-Mg, O transport during fatigue crack growth 78−52981
Al-Zn-Mg, oriented growth of precipitates on dislocations, model 80−108448
Al-Zn-Mg, plastic deform. influence on structural transform. and mechanical props. *(Russian)* 80−7623
Al-Zn-Mg, plastic instability rel. to grain boundary failure at low temps. 78−56702
Al-Zn-Mg, polygonized struct. in extrusions, thermal stability and mech. props. 80−50659
Al-Zn-Mg, precipitation mechanism, effect of Mg additions *(French)* 77−52330
Al-Zn-Mg, precipitation of η' phase, heat treatment, electron microscope obs. 78−68699
Al-Zn-Mg, precipitation strengthened, Bauschinger effect 77−36585
Al-Zn-Mg, role of dispersed transition metal intermetallic compounds 79−96088
Al-Zn-Mg, solid soln. decomp., 20 to 200°C 79−38830

zinc alloys continued
Al-Zn-Mg, stress conversion cracking based on micromech. surface reactions 80−7716
Al-Zn-Mg, TEM and calorimetric study 80−76290
Al-Zn-Mg, TEM characteris. of precipitates 80−104166
Al-Zn-Mg, type 7075, strain rate effects on H embrittlement 80−3190
Al-Zn-Mg, type 7075-T651 plate, thickness direction inhomogeneity of mech. props. and fracture toughness 80−100892
Al-Zn-Mg, type V-95, ultimate tensile strength for brief impact 80−70309
Al-Zn-Mg, weldable, microstruct. and intercrystalline fracture 77−48550
Al-Zn-Mg, welded section stress in rolled plate edges, mechanical surface treatment and environment effects 80−21193
Al-Zn-Mg, zone composition change during ageing 79−29110
Al-Zn-Mg (Fe), dil. alloy, ^{65}Zn diff. 77−51540
Al-Zn-Mg (2.1, 1.3 wt.%), single crysts., fatigued age-hardenable, dislocation structure *(German)* 80−54247
Al-Zn-Mg (3,1.5 wt.%), precipitation hardened and fatigued alloys, solute loss at fracture surface, EPMA exam. 78−39893
Al-Zn-Mg (3.2, 2.2 wt.%) alloy, GP zone reversion, η' of formation, quant. investig. 77−4784
Al-Zn-Mg (3.6, 1.95 wt.%), ageing and plastic deform., effect on structure, electron microsc. and X-ray diffr. study *(Russian)* 80−81108
Al-Zn-Mg (3.87, 1.79 wt.%) TEM exam. of early stage precipitation, on dislocation lines 79−4972
Al-Zn-Mg (3.87, 1.79 wt.%), oriented growth of precipitates on dislocations, TEM obs. 80−108447
Al-Zn-Mg (4.5, 2 to 3 at.%) solid state reactions by interrupted continuous heating 80−25737
Al-Zn-Mg (4.5, 2 wt.%), stress corrosion resist., vac. heat treatment effect 79−96203
Al-Zn-Mg (4.5, 2.5 wt.%), fatigue crack propag. 77−86171
Al-Zn-Mg (4.5, 2.5 wt.%), composition effect on stress corrosion and mech. behaviour 78−27684
Al-Zn-Mg (4.5 at.%, 2 or 3 at.%), decomposition behaviour during continuous cooling, XSAS and TEM examination 80−16264
Al-Zn-Mg (4.5 at.%, 2 to 3 at.%), decomp. behaviour during continuous heating 80−29922
Al-Zn-Mg (4.8, 1.1 wt.%), second phase dissolution, calorimetry study 79−100193
Al-Zn-Mg (4.8, 1.2 wt.%), quenched, Guinier Preston zones formation 80−45273
Al-Zn-Mg (5, 1 wt.%), age hardening, conditions leading to localised plastic deform. and fracture in slip bands during fatigue 78−64670
Al-Zn-Mg (5, 1 wt.%), relation between mech. props., SCC and dislocation struct. *(German)* 77−81345
Al-Zn-Mg (5, 2 wt.%), diffusion of ^{65}Zn, 165 to 560°C 77−11743
Al-Zn-Mg (5,2 wt.%), TEM of early stages of precipitation 77−40423
Al-Zn-Mg (5,2.5 wt.%) observation of stress corrosion cracking 78−60868
Al-Zn-Mg (5.9, 2.9 wt.%), ageing effects on microstruct. 80−16306
Al-Zn-Mg (6, 2.5 wt.%), fracture toughness-transgranular fracture relation 77−52447
Al-Zn-Mg (6, 2.5 wt.%) alloy, intergranular fracture mechanism due to ledge formation 79−57089
Al-Zn-Mg (6,1.5%), influence of ageing and cold work on tensile and fracture props. *(Japanese)* 78−52842
Al-Zn-Mg (6,3 wt.%), hydrogen embrittlement and trapping 80−55490
Al-Zn-Mg (6,3 wt.%) high-strength alloy, dislocations distrib., corrosive environment influence *(Russian)* 79−52442
Al-Zn-Mg (6.0, 2.5 wt.%), aged, grain, size depend. of fracture toughness 78−48495
Al-Zn-Mg (6.27, 2.94 wt.%), single crystals, effect of environment on liquid-metal embrittlement, stress corrosion cracking and corrosion fatigue 78−64676
Al-Zn-Mg (9, 1 wt.%), superplastic flow, relative motion of grains 77−52426
Al-Zn-Mg (91, 6, 3, wt.%), H embrittlement and trapping, HVEM obs. 80−76364
Al-Zn-Mg alloy, Ag addition and pre-precipitation treatment, influence on GP zone growth 80−71658
Al-Zn-Mg alloy, microstruct. obs. by optical and electron microscopy *(German, English)* 77−52601
Al-Zn-Mg alloy, stress corrosion cracking, exam. *(Japanese)* 78−53026
Al-Zn-Mg alloy, thermomech. treatment, precipitation and strengthening 79−24527
Al-Zn-Mg alloy, welded, solute profiles at weld bead/parent metal interface 78−19942
Al-Zn-Mg alloy 1915, stress corrosion cracking, protective anodic film *(Russian)* 78−35572
Al-Zn-Mg alloy 7075, effect of thermal and mechanical pretreatments, on Guinier-Preston zone 78−39817
Al-Zn-Mg alloy 7075, unstable shear failure 77−48516
Al-Zn-Mg alloy (6, 3 wt.%), grain boundary segregation, AES exam. 78−39783
Al-Zn-Mg alloy AA-7039, stress corrosion cracking, SEM obs. 80−104323
Al-Zn-Mg alloy V95, two-stage ageing kinetics, mech. props. effects 79−83238
Al-Zn-Mg alloys, decomp. kinetics from Young's modulus obs., microprocesses *(German)* 78−64522
Al-Zn-Mg alloys, decomposition kinetics, resistivity meas., extended jump model 78−84766
Al-Zn-Mg alloys, extra-resistivity of coherent precipitates calc. using X-ray small angle scattering intensities 80−3050
Al-Zn-Mg alloys, grain boundary segregation, implications to stress corrosion cracking 80−84936
Al-Zn-Mg alloys, H_2 bubbles in embrittlement 78−19868
Al-Zn-Mg alloys, precipitation behaviour *(German)* 78−39780
Al-Zn-Mg alloys, stress corrosion cracking *(Japanese)* 77−25194
Al-Zn-Mg alloys stress corrosion 80−35395
Al-Zn-Mg granules and bands rolled from them, heat treatment 80−100862
Al-Zn-Mg plasma sputtered, mech. props. rel. to heat treatment *(Russian)* 80−40387
Al-Zn-Mg powder, selected-area electron diffr. ring patterns 80−50642
Al-Zn-Mg superplastic alloy, cavity growth under creep conditions 80−60940
Al-Zn-Mg type 7N01-T4, weld, SCC in NaCl-H_2O_2 soln. *(Japanese)* 80−108631

zinc alloys continued
Al-Zn-Mg type 7017 and 7018 alloy plate, fractographic study of stress-corrosion crack propag. 79−57158
Al-Zn-Mg-Ag, detection of small amounts of Ag by energy dispersive X-ray anal. 77−60154
Al-Zn-Mg-B fibre reinforced composite, packet rolling, thermodeform. process parameters *(Russian)* 80−55433
Al-Zn-Mg-Co, crazing tendency *(Russian)* 80−30068
Al-Zn-Mg-Cu, age hardened, effect of strain rate, temp. and environment on ductility 80−45368
Al-Zn-Mg-Cu, alloy 7075, hydrostatic pressure effects on ductile fracture 78−60779
Al-Zn-Mg-Cu, alloy 7075, fatigue, loading sequence, normal and reversed sequence effect 78−68791
Al-Zn-Mg-Cu, alloy 7075, effect of purity level, dispersoid type, heat treatment, on fracture toughness 78−80636
Al-Zn-Mg-Cu, alloy 7075-T6, corrosion in halide solutions, exam. of anion dependency 78−60867
Al-Zn-Mg-Cu, alloy 7075-T6, fatigue crack closure with negative stress ratio, following single tensile overloads 78−64687
Al-Zn-Mg-Cu, flaw growth in stress corrosion environment 79−66198
Al-Zn-Mg-Cu, fracture toughness 78−7044
Al-Zn-Mg-Cu, inclusions, oriented distrib. metallography and effects on anisotropy *(Russian)* 78−80589
Al-Zn-Mg-Cu, optimum treatment combination for thermochemical processing 77−44278
Al-Zn-Mg-Cu, type 7075, microstruct. role in hydrogen assisted fracture 80−30091
Al-Zn-Mg-Cu 7075, extraction and phase anal. 79−15673
Al-Zn-Mg-Cu (6, 2.5, 1.5 wt.%), deform. simulation using torsional test, elastoplastic constitutive eqn. 80−93594
Al-Zn-Mg-Cu (6,2, xwt.%) type alloy, fatigue crack propag., Cu content and recryst. effect 80−60960
Al-Zn-Mg-Cu (6.76, 2.37, 1.80 wt.%), cyclic SCC in salt water *(Japanese)* 80−45435
Al-Zn-Mg-Cu age-hardened alloys, fatigue crack propagation rel. to grain size in vac. and NaCl soln. 80−16538
Al-Zn-Mg-Cu alloy, laminated, adhesively bonded alloy 7075-T6, exam. of fracture resistance 78−76754
Al-Zn-Mg-Cu alloy, stress corrosion cracking mechanisms, rel. to micrographic obs. *(French)* 77−73376
Al-Zn-Mg-Cu alloy, type 7050 and AZ 74.61, engineering props. 79−70219
Al-Zn-Mg-Cu alloy, X-ray microanalysis in scanning transmission electron microscope, limitations 78−20122
Al-Zn-Mg-Cu alloy 7075, SCC from T6 to overaged T7X 77−90487
Al-Zn-Mg-Cu alloy 7075, overaged, precracked stress corrosion specimen, incubation effects 79−91832
Al-Zn-Mg-Cu alloy 7075-T651, adiabatic shear localisation and erosion 79−96157
Al-Zn-Mg-Cu alloys, effect of alloying elements as stress corrosion failure using regression analysis 78−80669
Al-Zn-Mg-Cu foil, STEM-microanal., specimen thickness effect on X-ray count rates 77−70374
Al-Zn-Mg-Cu type 7XXX, Cu effect and recrystallisation, low cycle corrosion fatigue 79−91852
Al-Zn-Mg-Cu type 7075, heat treatment optimisation 80−60888
Al-Zn-Mg-Cu-Co (6.5, 2.5, 1.5, 0.4 wt.%), fatigue crack propag. 80−55521
Al-Zn-Mg-Cu-Co-Fe-Si, powder alloy, fatigue crack tip plasticity, from load interactions 80−21066
Al-Zn-Mg-Cu-Cr, (5.6, 2.5, 1.6, 0.3 wt.%), laminates, 8 and 22 layers, adhesively bonded exam. of fatigue crack propag. 78−92345
Al-Zn-Mg-Cu-Cr, (5.6, 2.5, 1.6, 0.3 wt.%), alloy 7075, plates, adhesively bonded, exam. of fatigue crack growths 78−92348
Al-Zn-Mg-Cu-Cr, shot peened, positron annihilation meas. 77−63833
Al-Zn-Mg-Cu-Cr-Zr, high strength Cr and Zr addition effects 77−59820
Al-Zn-Mg-Li alloys, effect of Li on thermal props. 79−24515
Al-Zn-Mg-Mn, correlation of microscopic features, with macroscopic crack propagation 78−60800
Al-Zn-Mg-Ti, Ti effect on microstructure during ageing 78−64568
Al-Zn-Mg-Zr (6.45, 2.08, 0.11 wt.%), exam. of cyclic stress strain response in corrosion fatigue 78−64788
Al-Zn-Mg-(Zr), low cycle fatigue, grain refinement effect 77−44345
Al-Zn-Mg-(Zr) alloy, microstruct. effect on fatigue crack growth 80−3164
Al-Zn-Mg(Mg-Ti), TEM exam. of early stage ageing behaviour, exam. of precip. kinetics 78−56645
Al-Zn-Mg(3.2, 2.2 wt.%), deform. strengthened by Guinier Preston zones 77−52343
Al-Zn-Si, thermodynamic props., meas. by EMF method *(Czech)* 77−59753
Al-Zn-Ti(Mn), mech. props., Ti or Mn addition effect *(Korean)* 80−93613
Al-Zn-(Mg), age hardenable single crystal, fatigue and fatigue cracks *(German)* 77−16689
Al-Zn(0.1 at.%), μ^+ depolarisation 79−56697
Al-Zn(10 at.%), supersaturated solid soln., structural charact. of decomposition 77−70027
Al-Zn(11 wt.%), dynamic recovery during and after steady state deform. 77−1842
(Al-Zn):Cd eutectic system, cellular growth, unidirectional solidification investig. *(Korean)* 77−28805
AlZn alloys, ageing zone stage duration depend. on quenching temp. *(Russian)* 77−55993
AlZn, disordered, residual resistivity due to clustering, ageing effects 80−65521
AlZn, homogenization processes, dendritic struct. 79−15700
AlZnMg alloy, precipitation hardened, strength 78−39786
AlZnMg, corrosion cracking *(Czech)* 79−43478
AlZnMgCuO.5, crack propag. under monotone and cyclic load 78−7006
AlZnMgCuO.5, static crack growth, stress state effect, elec. pot. meas. 78−7007
Au/Zn/InP Schottky barrier diode, fabrication and elec. props. 79−33348
β-Au-Cu-Zn, martensitic transformation temps. ageing and quenching effect 79−47687
Au-Cu-Zn-Ni (13, 3.4, 8.5 wt.%), white gold, metallographic structure after cold rolling, effect of heat treatment, recrystallisation *(French)* 79−52238

zinc alloys continued
Au-Ni-Cu-Zn, white gold, metallographic struct., heat treatment and plastic working effect 80−40403
Au-Pd-Zn system, quasibinary section phases investig. 77−12596
Au-Zn, (55 to 88 at.%), equilib. diagram, X-ray diffr. obs. 80−25660
Au-Zn, charge transfer, Mossbauer effect ^{197}Au isomer shifts, XPS valence-band spectra 80−2676
α-Au-Zn, disordered, shaft range order diffuse scatt., electron diffr., interpretation 77−84596
Au-Zn, liq., thermodynamic props. *(German)* 80−49386
Au-Zn, molten, EMF meas. of activities using ZrO_2 solid electrolytes *(Japanese)* 80−88339
α-Au-Zn, superconducting transition temp. depend. on electron per atom ratio, lattice deform. 77−8222
Au-Zn/p-$Ga_xIn_{1-x}PyAs_{1-y}$, specific contact resist. 80−84509
Au-Zn(Cu), electrolytic thinning for use in transmission electron microscopy 78−57918
$Au_2(MnZn)_2$, Heusler alloy, magnetic order and coupling 79−38303
Au(Pd)-Zn, martensitic transformation, Hall coeff., specific elec. resistivity and X-ray powder diffraction 78−72774
$Au_{50-x}Pd_xZn_{50}$, ($0 \leq x \leq 15.02$) β′-phase, Hall effect and elec. cond. 80−107768
$Au_{100-x}Zn_x$, ($47 \leq x \leq 52$), β′-phase, Hall effect and elec. cond. 80−107768
Au_3Zn, long-range ordered, periodic antiphase domain boundary struct., X-ray diffr. obs. 79−95028
Au_3Zn, R_2-phase, long period domains, transmission, scanning and optical microscopy obs. 79−38801
Au_4Zn, electropolishing for electron microscopic examination 78−35589
Au_4Zn, long period ordered alloy, selective radiation damage in electron microscopy 78−10092
Au_4Zn, modulated struct. phenomena, survey 79−95033
Au_4Zn, ordered alloy, long period superstructure study, electron microscopy, diffr. 78−10059
Au_4Zn, ordered alloy, long-period antiphase boundary struct., growth mechanism 79−19262
Bi-Zn, alloy absolute thermoEMF temp. and conc. depend. *(Russian)* 80−39561
Bi-Zn, liquid, interstitial index, definition and variation with temp. *(French)* 80−2011
CC Al-Zn-Mg (4.5,1(2)(3) at.%), decomposition during ageing, preageing and cooling rate influence 80−20938
Ca-Zn liquid alloys, thermodynamics 79−52173
$CaZn_3$, struct. with mixed $BaLi_4$- and $CeCu_2$-like ordering 80−107106
Cd-Ag-Zn (96, 3, 1 wt.%.) soldering alloy powder, atomised, prod. and appl. 79−100073
Cd-Zn, annealed, work softened, exam. of crystallographic texture, hardness 78−80559
Cd-Zn, binary metallic melt, deviation from the Kopp law, specific heat *(Russian)* 80−39305
Cd-Zn, cryst., internal friction, dislocation interactions 79−87673
Cd-Zn, directionally solidified lamellar eutectics, specimen prep. for TEM *(German, English)* 78−95885
Cd-Zn, polycryst. wire, cold worked, resistivity changes 78−68827
Cd-Zn, solidification in mag. field, crystallite obs. *(Russian)* 77−4770
Cd-Zn (1.5 wt.%), warm worked, effect of grain size, texture, on mech. props. 79−4988
Cd-Zn (up to 1.57 at.%), single cryst., precip. hardening, 77-300K 78−60675
Cd-Zn alloys, splat-quenched, X-ray diffr., SEM and TEM study of struct. 79−66077
Cd-Zn binary systems, melts, elec. resist., 0-700°C 80−65517
Cd-Zn eutectic, microstruct. degradation, role of temp. fluctuations 77−4766
Cd-Zn eutectic and off-eutectic alloys, stability 77−25077
Cd-Zn eutectics, microstruct. after solidification, heat pipe influence 80−76243
Cd-Zn single crystal, plasticity, 4 to 50K 79−43362
Cd-Zn single crystals, crit. resolved shear stress at low temps. 80−3138
Cd-Zn-Hg, liq., comp. and temp. depend. of Hg VP, activity, free energy and enthalpy *(Russian)* 77−20087
Ce-Zn, liquid, solubility and thermodynamic props. *(Russian)* 78−19717
CeZn, cryst. field and exchange effects, inelastic neutron scatt. study 80−24855
CeZn, mag. struct. and cryst. field effects 78−52223
CeZn, magnetic struct. and cryst. field, neutron diffr. exam. 78−72328
Cn-Sn, dil., magnetic susceptibility, impurities effect, free electron gas model 79−91206
Co-Ni-Zn, diagram of state, crystalline lattice consts., microhardness *(Russian)* 80−66479
γ-Co-Zn, inversion antiphase domains, formation and stabilisation, electron conc. effect 78−14363
Co-Zn, physical-chemical metallurgy *(German)* 80−108390
γ-Co-Zn, struct. obs. 77−24290
Co-Zn melt, Zn activity determ. *(German)* 78−19715
CoZn β- and γ-intermetallic compounds, thermodynamics *(German)* 78−92242
Cu-Ag-Zn, exam. of phase diagrams and thermodynamics props. 79−8275
Cu-Al-Zn, period of periodic antiphases, quant. metallography *(French)* 79−100111
Cu-Al-Zn, structural phenomena preceding martensitic transform. 77−12624
Cu-Ni-Zn, Cu rich, penetration tendency model for diffusion 77−39701
Cu-Ni-Zn, diffusion couples, zero-flux planes and flux reversals 80−15313
Cu-Ni-Zn, microduplex, superplastic deform., cavitation and fracture 78−64640
Cu-Ni-Zn, multiphase couples, diffusion paths and struct. at 775°C 77−62666
Cu-Ni-Zn, Portevin-Le Chatelier effect during tensile deform. *(German)* 79−8330
Cu-Ni-Zn (18, 27 wt.%), surface comp., Auger electron spectroscopy study, manufacture and storage influence 80−65348
Cu-Ni-Zn alloy, at 775 degrees C, diffusional and thermodynamic interactions 78−38883
Cu-Ni-Zn alloy, FCC, cold-worked, microstruct., X-ray obs. 78−3143
Cu-Ni-Zn alloy, surface comp., outdoor exposure influence 80−59770
Cu-Ni-Zn system, tie lines in a two phase region 80−24404

zinc alloys continued
Cu-Ni-Zn-Mn fine grained precipitation-hardenable alloy, high strength and ductility 80−100805
α-Cu-Ni-Zn-Pb, fire cracking and ordering *(German)* 78−60760
α-Cu-Ni-Zn-Pb, fire cracking, effect of pores and impurities 79−29207
Cu-O-Zn dilute liquid alloy, Zn-O interaction parameter 80−55694
Cu-Si-Zn wire, silicon bronze, magnetoresist. upper limit 77−43567
Cu-Sn alloy, surface comp., outdoor exposure influence 80−59770
Cu-Zn, α-phase, photoelectron meas. 78−35247
Cu-Zn, charge transfer, core-electron binding-energy shift 80−2676
Cu-Zn, cohesive props., augmented-spherical-wave calcs. 79−94952
Cu-Zn, cold worked solid solution, flow stress and activation volume 80−16393
Cu-Zn, conc. single crystal, yield region investigation, flow stress and obstacle charact. 78−3173
Cu-Zn, cyclic stress/strain curves in monocrystalline and polycrystalline samples, cold work and Zn addition effects 78−95786
Cu-Zn, de-alloying props. 80−104332
Cu-Zn, diffusive redistrib. during friction *(Russian)* 78−52999
Cu-Zn, dil., impurity electron struct., self-consistent KKR Green's function calc. 79−78040
Cu-Zn, dil., magnetic susceptibility, impurities effect, Fermi surface effects 79−91207
Cu-Zn, dil., Matthiessen's rule deviations above room temp. 79−91023
Cu-Zn, dil., optical props. and electronic struct. 78−35164
Cu-Zn, dil. alloy, thermopower and resistivities, validity of Nordheim-Gorter relation 78−91671
Cu-Zn, dilute solid soln., exam. of recrystallisation and stored energy 78−52836
Cu-Zn, interface sliding of FCC and BCC boundaries 80−104240
Cu-Zn, magnetic susceptibility, comp. and temp. depend., melting effects 78−52202
Cu-Zn, microconductors, cast, struct. and physical props. exam 78−44232
Cu-Zn, optical composition modulation spectra, dielec. const. var., Fermi surface and electronic level shifts 80−6707
Cu-Zn, order-disorder transform, influence of strain energy 78−84796
Cu-Zn, phase boundary motion kinetic during interdiffusion *(Russian)* 79−60559
Cu-Zn, solid soln., rheological study of crystallographic order on creep *(French)* 80−97548
β_1Cu-Zn, structural Umklapp processes at low and high temp. lattice kinetics of phase transformation isotherms *(German)* 78−30707
Cu-Zn, thermally stimulated exo-electron emission 80−11547
Cu-Zn, wear, effect of Mn_5Si_3 content *(Japanese)* 78−35525
α-Cu-Zn, whiskers, X-ray topography, substruct. 77−11831
Cu-Zn, Zn effect on stainless steel embrittlement during soldering 79−47773
Cu-Zn (2 at.%), stacking fault energies, weak beam method of electron microscopy 77−19971
Cu-Zn (30 wt.%), rolled, electron microscope exam. of recrystallisation 78−76663
Cu-Zn (30 wt.%), single crysts., quantitative anal. of stress relax., obstacle strength and athermal stress variation 80−89277
Cu-Zn (36 wt.%), hardness-flow stress rel. during strain-controlled bending fatigue 79−74245
Cu-Zn (38.9 wt.%), β-brass, spinodal decomposition, electron microscope and diffr. study 79−78930
Cu-Zn (4 at.%), anneal hardening mechanism 80−60879
Cu-Zn (47.3 wt.%), spinodal decomposition, electron microscope and diffr. study 79−78930
Cu-Zn (50 at.%), BCC β phase, high temp. creep, existence of master curve 80−55473
α-Cu-Zn (5.3 to 21.8 wt.%), single crystals, effect of stacking fault energy on extrusion and intrusion development 78−72826
Cu-Zn alloy, α-phase, lattice sp. ht. calcs. 80−65246
Cu-Zn alloy, molecular dynamic exam. of perfect and imperfect cryst. 77−39647
Cu-Zn alloy, surface layer composition determ. by XPS 79−43682
Cu-Zn alloys, surface comp., outdoor exposure influence 80−59770
β-Cu-Zn elec. resist. change with degree of order *(Japanese)* 78−34817
β_1-Cu-Zn mixed crystal, metastable structural Umklapp process, isothermal phase transform. *(German)* 78−22798
Cu-Zn-Al, β_1' martensite crystal crossing rel. to reversible shape memory effect *(Japanese)* 80−108499
β-Cu-Zn-Al, diffr. effects., obs. and interpretation of extra maxima 80−44173
β-Cu-Zn-Al, electron microscope exam. of premartensitic state 78−72801
Cu-Zn-Al, internal friction, temp. and amplitude depend. 78−11262
Cu-Zn-Al, internally faulted martensite, TEM obs. 78−3124
Cu-Zn-Al, martensitic phase transformation effect on low cycle fatigue behaviour 80−7666
Cu-Zn-Al, martensitic transform., short range order effect 79−61586
Cu-Zn-Al, memory alloy wire and ribbon reversible martensitic transformation, ageing effect, review 80−7564
β-Cu-Zn-Al, ordering, TEM obs. 78−39768
β-Cu-Zn-Al, ordering 78−68687
Cu-Zn-Al, polycrystn., β-phase, fatigue life, intergranular cracking 79−38974
Cu-Zn-Al, pseudoelastic alloy, exam. of fatigue props. 78−76744
Cu-Zn-Al, reversible shape memory effect associated with $\beta_1 \rightleftarrows \beta_1' \rightleftarrows \alpha_1'$, transform. *(Japanese)* 79−43242
Cu-Zn-Al, reversible shape memory effect obtained by heating under constraint *(Japanese)* 79−43335
Cu-Zn-Al, reversible shape memory effect *(Japanese)* 80−108500
Cu-Zn-Al, single cryst., stress induced martensitic transformation 80−45308
Cu-Zn-Al, TTT diagrams *(German)* 79−43208
β-Cu-Zn-Al, US elastic const. meas. near martensitic transform. temp. 78−39827
Cu-Zn-Al, Zener relaxation *(Russian)* 77−21198
α-Cu-Zn-Al (18, 7 at.%), deform. and mech. props. 79−29159
Cu-Zn-Al (19.3, 13.0 wt.%), effect of hydrostatic or uniaxial stress on elastic consts., near martensitic transformation point 78−76697
Cu-Zn-Al (19.5, 6.35 wt.%), martensitic, static stresses influences on damping behaviour 80−10594
Cu-Zn-Al (26, 4 wt.%), martensitic transform. temp. variation after low temp. ageing 79−15666
β-Cu-Zn-Al (27.5, 4.0 wt.%), strain induced martensite, exam. of structure, microstructure 80−7648

zinc alloys continued
Cu-Zn-Al (35.45, 1.72 wt.%), memory effect and martensitic transform. *(Russian)* 79−43320
Cu-Zn-Al alloy, lattice dynamical study of premartensitic state, phonon meas. 79−77696
Cu-Zn-Al alloys, dendritic struct. obs. 77−8810
Cu-Zn-Al cubic alloy, phonon sp. ht. near martensitic transform. 79−60521
Cu-Zn-Al Marmem alloy, β_1 phase superstruct. obs., rel. to transform. mode 78−39776
Cu-Zn-Al martensite, β-phase, single cryst., elastic waves behaviour as function of temp. 79−55807
Cu-Zn-Al martensite, lattice dynamics, neutron scatt. meas. 80−88286
Cu-Zn-Al martensite, the rubber effect 79−47684
Cu-Zn-Al martensites, model for rubber like behaviour 79−47685
β-Cu-Zn-Al pseudoelasticity 79−29126
Cu-Zn-Al wire, made from pendant drop melt extraction technique from bulk material, X-ray diffr. and thermal anal. 79−43227
Cu-Zn-Be, precipitation hardening 77−16599
Cu-Zn-Fe, Mossbauer effect of Fe impurities 78−31131
Cu-Zn-Ga martensite, thermally produced large single crystals 77−12615
Cu-Zn-Ga(Al), martensites, internally faulted, shape memory mechanism 80−30010
Cu-Zn-Gu, configs. of martensite variants, shape deform. matrices 77−12620
Cu-Zn-Mn, steady-state diffusion of Zn and Mn 80−70445
Cu-Zn-Si, deform. close to martensitic transform. temp. 77−63714
β-Cu-Zn-Si, premartensitic instability 77−12625
Cu-Zn-Sn (24-34, 1.0 wt.%), cold-worked microstruct., X-ray diffr. obs. 80−3088
Cu-Zn-Sn-Pb (5, 5, 5 wt.%) analysis in glow discharge lamp and in ion microprobe, sputtering processes 77−52730
β-Cu-Zn(-Ni)(-Mn), order-disorder transformation temperature effect on quench hardening 78−95745
Cu-Zn(30 at.%), electron irrad., positron annihilation, defect recovery 79−74018
β- Cu-Zn(47.4 wt.%), heat content between 300.05 and T (T from 400 to 1000K) drop calorimetry *(French)* 80−10682
α-$Cu_{0.7}$ $Zn_{0.3}$, point-geometry ang. correl. curves, enhancement in positron annihilation 79−95873
Cu_x Zn_{1-x}, sputtering, binding energies 80−108312
α-CuNiZn alloys, Zener-relaxation effect 80−3121
β-(CuNi)Zn, anomalous strengthening 77−48503
Cu_2NiZn, atomistic approach to ordering 79−94944
Cu_2NiZn, characterisation of superlattice dislocations by TEM 79−55748
Cu_2NiZn, comparison between different theories predicting stacking fault energy from extended nodes 80−75240
Cu_2NiZn, separation of partials of superlattice dislocations, anisotropic elasticity theory, ordering 79−65082
Cu_2NiZn, stacking fault energy determ. from extended nodes 80−107280
Cu_2NiZn, superlattice dislocations 78−83816
β-CuZn, acoustic emission rel. to stress induced martensitic transformation 80−81061
CuZn, omega phase, roles of electron microscopy and electron diffraction *(French)* 78−27524
CuZn, planar faults, faint electron microscopic image contrast obs. 80−107283
Cu_3Zn clusters, electronic structures, SCF-Xα-SW method 80−88468
Cu_xZn_{1-x}, disordered alloy, muffin-tin model, electronic struct. and density of states calc. 80−29302
Cu_xZn_{1-x}, positron annihilation and Mossbauer effect exam. 79−65775
CuZnAl, martensitic, ordering effect on yield stress 79−100133
CuZnAl single crystal, thermodynamic anal. of martensitic transform. under stress 79−87635
$Cu_{3-x}Zn_xSn$, one-dimens. long period superstructs. with Zn and Ni additions 78−83777
$Cu_{66}Zr_{34}$, amorphous metallic glass, differences caused by preparation technique *(French)* 80−103247
DyZn, direct Coulomb contrib. of cond. electrons to crystalline elec. field 77−76784
DyZn, direct coulombic contrib. of cond. electrons to cryst. elec. field 79−91005
DyZn, exchange coulombic contrib. of cond. electrons to cryst. elec. field 79−95376
ErZn, magnetoelastic and quadrupolar couplings 78−52328
ErZn, preferred mag. domain orientation, and microstructural defects, magnetostriction meas. 79−73769
$EuNi_xZn_{5-x}$, mixed valency of Eu, Mossbauer expts. 78−52407
$EuZn_5$, cond. electron spin polarisation 77−63136
FE-Zn, prep. and phase diagrams *(French)* 80−76231
solid Fe/liquid Zn, interdiffusion reaction 79−77845
Fe-C-Zn (0.45 wt.% C, 1.56 wt.% Zn), pearlite transformation during continuous cooling 78−80538
Fe-Cu-Zn, high-temperature phase diagrams *(German)* 80−108390
Fe-Mn-Zn, high-temperature phase diagram *(German)* 80−108390
Fe-Si-Zn, influence of trace elements on morphology *(German)* 80−108390
α-Fe-Zn, ⟨111⟩ fibre texture development through diffusion process without α-γ transform 79−100170
Fe-Zn, chemically induced grain boundary motion 78−38724
Fe-Zn, coating on low C rimming steel, effect of addition of Al on phase composition and morphology *(Polish)* 78−53014
Fe-Zn, coercive force anisotropy after cold plastic deform. *(Bulgarian)* 80−75809
Fe-Zn, crystallographic relations by X-ray diffr. 80−24408
Fe-Zn, diffusion coefficients in δ_1 phase *(Japanese)* 78−14512
Fe-Zn, dil., size effects on mag. hyperfine fields at non-mag. impurities 78−43586
Fe-Zn, δ-phase, X-ray analysis 77−59758
Fe-Zn, galvanised coating appl., metallurgy review 79−96199
Fe-Zn, galvanization study *(French)* 80−66447
Fe-Zn, homogeneous intermetallic cpd., synthesis and charact., ξ-phase 79−83177
Fe-Zn, homogeneous intermetallic cpd., synthesis and charact., δ_1-phase 79−87616
Fe-Zn, homogeneous phases, Gibbs free energies of form., Knudsen effusion method 80−66481

zinc alloys continued
γ-Fe-Zn, inversion antiphase domains, formation and stabilisation, electron conc. effect 78−14363
Fe-Zn, layer formed in diffusion couple, effect of small alloying element addition *(French)* 77−43388
Fe-Zn, liquid-solid reaction in Zn bath, effect of Fe concentration, alloy layer growth, exam. *(Japanese)* 78−85037
Fe-Zn, multiphase diffusion 78−79822
Fe-Zn, phase diagram, DTA, EDAX, X-ray diffr. study 80−50602
Fe-Zn, phase diagram, ferrite-austenite phase boundaries, X-ray diffr. exam. *(German)* 78−80510
Fe-Zn, phase diagram Zr aggregated effect on Fe corrosion *(Dutch)* 78−48571
Fe-Zn, physical-chemical metallurgy *(German)* 80−108390
Fe-Zn, quenched, martensite struct. and hardness, electron microscope exam. *(Russian)* 80−66619
Fe-Zn, stable and metastable alloys, order-disorder, mag. interactions and corrosion behaviour 78−68422
Fe-Zn alloys, electrochem. corrosion of ζ, δ_1 phases *(French)* 79−20274
Fe-Zn compound form. after hot galvanising Fe with liquid Zn and by diffusion *(French)* 79−20275
Fe-Zn couple, Zn electrodeposited on polished Fe, reaction rate in solid state *(Japanese)* 78−15322
Fe-Zn intermetallides, initial stages of form. *(Russian)* 80−20889
δ-Fe-Zn layer formed on hot dip galvanising, texture 77−9001
Fe_4Zn_9, γ-brass with I cell, ordering 77−24290
Ga-Ge-Zn ternary alloys, thermodynamic props., EMF meas. 80−81033
Ga-Zn, dil., elec. resist., temp. and impurity depend., deviation from Matthiessen's b-axis crystals 78−51970
Ga-Zn, eutectic system, diffusion coeff. depend. on composition *(Russian)* 80−59695
Ga-Zn, liquid binary alloys, magnetic susceptibility *(Russian)* 77−24671
Gd-Zn, X-ray determ. of Debye temp., mean amplitude of vibr. 78−38802
$GdCu_{1-x}Zn_x$, mag. struct. determ. 79−87238
$Gd_xLa_{1-x}Zn$, magnetisation and paramag. suscept. 78−88101
$Gd_xNd_{1-x}Zn$, ferromag., mag. susceptibility and magnetisation, temp. depend. 80−70975
$Gd_xY_{1-x}Zn$, ferromag., mag. susceptibility and magnetisation, temp. depend. 80−70975
Hg-In(Tl)-Zn, liquid alloys, thermodynamic props., 25 to 75°C *(German)* 77−73259
Hg-Zn, dil. liq. amalgams, expanded, cond. at high temps. and press. 77−20287
$Hg_{1-x}Zn_xCr_2Se_4$, magnetic struct., neutrongraphic and mag. investigation *(Russian)* 80−88726
Ho-Zn, crystal field parameters from neutron spectra, rel. to mag. props. in ordered state 77−43546
HoZn, mag. excitations near spin rot. temp., neutron scatt. study 79−19731
HoZn, magnetic excitations 80−25115
HoZn, magnetoelastic and quadrupolar couplings 78−52328
HoZn, spin wave spectrum, Green function analysis 78−2666
In-Zn, liq., Zn activity meas. by Knudsen torsion-effusion method 79−10950
In-Zn binary system, melts, elec. resist., 0-700°C 80−65517
In-Zn/p-InP ohmic contact evaluation 77−24619
$La_{1-x}Gd_xZn$, NMR ^{139}La 78−15038
LiZn, elastic moduli and Debye temp., US meas. 79−91724
Mg-Al-Zn, anelastic creep and recovery 77−63709
Mg-Al-Zn, solute-vacancy binding energies from hardness meas. 78−39789
Mg-Al-Zn (3, 1 wt.%), alloy AZ31, mech. props. of extruded and welded pipe and sheet, optical microscopy exam. 79−34065
Mg-Al-Zn (94.3, 3.9, 1.8 wt.%), pricip. on dislocations, weak-beam TEM 80−76264
Mg-Al-Zn (9wt.%Al), sand cast, preferred orientation and mechanical props. *(Japanese)* 80−20979
Mg-Al-Zn-Mn (8, 0.5, 0.3 wt.%) casting alloy, penetration resistance 80−100901
Mg-$MgNi_2$-Zn, diagram of state, Zn solubility, initial phase precipitation *(Russian)* 80−66478
Mg-Nd-Zn dilute alloy, metallography and precip. kinetics 80−71655
Mg-Y-Nd-Zn-Zr (2,2,0.3, 0.7 wt.%), heat treatment effect on casting dimensional stability, alloy mech. props. 78−44146
Mg-Y-Zn (20, 30 wt.%), phase equilibria investigation *(Russian)* 79−74131
Mg-Y-Zn alloys, phase equilib. *(Russian)* 80−16271
Mg-Y-Zn-Nd-Cd alloys, influence of Zr addition on struct. and mech. props. *(Russian)* 80−40370
Mg-Zn, amorphous sputtered film, elec. props. 78−68006
Mg-Zn, metallic glass, stability, microscopic calcs. 79−32914
Mg-Zn (5 wt.%), age hardening, X-ray diffr. anal. *(Chinese)* 80−104173
Mg-Zn alloy, aged, one dimensional transition phase β'_2, crystallographic obs. *(Chinese)* 80−60865
Mg-Zn metallic glass, hardness, elastic moduli, density, cryst. temp., mech. props., for flywheel appl. *(Dutch)* 78−52878
Mg-Zn-Zr, cast, exam. of phase composition, mech. props. 79−100217
Mg-Zn-Zr rare earth alloy, mech. props., effect of microshrinkage during solidifaction 79−43234
Mg-Zn-Zr-Cd-Nd, Lawes phase separation using acetate electrolyte, Cd and Nd effects 79−70237
$MgCu_2$-$MgZn_2$ system, heats of form. of Laves phases *(German)* 79−66337
$MgCu_{2-x}Ni_2$, X-ray and neutron diffr. investigation of Laves phases of $MgCu_2$-type *(German)* 80−15050
$Mg(Cu_{1-x}Zn_x)_2$, crystal struct. and lattice spacing under high press. comp. depend. 77−72581
$MgNi_{2-x}Zn_x$, X-ray and neutron diffr. investigation of Laves phases of $MgCu_2$-type *(German)* 80−15050
$MgZn_2$ Laves phase, deformation-mechanism maps 79−29150
$MgZn_2$, single cryst., yield strength 77−44318
$MgZn_2$, solid soln. softening in homogeneity range, dislocation density and velocity *(German)* 77−44264
$MgZn_2$, struct. exam. using Shaw's model potential calc. 77−19906
$MgZn_2$, two-layer, Friauf-Laves phases, stacking variants 80−96468
$MgZn_2$-$MgAg_2$, Friauf-Laves phase, long-period stacking variants, electron conc. depend. 77−80444
$Mg_{70}Zn_{30}$ metallic glass, struct. and dynamics 79−37632

zinc alloys continued
$Mg_{74}Zn_{26}$, glass, exam. of crystallisation 78−71681
Mn-Cu-Zn system, optimum heat-treatment routine for max. damping 79−87670
Mn-Y-Zn-Cd alloy,phase equilibria, plastic deformation, microhardness *(Russian)* 80−40334
Mn-Zn ferrite single crystals, mech. polishing effect on mag. props. *(Japanese)* 80−16569
β_1-MnZn, ferromag., spin wave contrib. to nucl. spin-lattice relax. time meas. 77−36147
Mn_3ZnN, sp. ht., 6 to 350K, mag. and crystallographic phase transitions 80−71060
Mo-Ni-Fe-Co-Zn alloys, Ni, Fe, Co and Zn distrib. using neutron-activation anal. 79−52531
Nb_3Ge-Zn, synthesis from thermalised sputtering and changes in Tc and depend. of H_{c2} on temp. 79−56350
$Nd_{0.2}La_{0.8}Zn$, cryst. field, neutron diffr. meas. 78−34810
$Nd_xY_{1-x}Zn$ system, solid soln., mag. susceptibility, 77 to 600K *(Russian)* 80−65776
Ni-Al bronze, fracture resistance of tubes 78−19867
β-Ni-Cu-Zn, electron microscopy of premartensitic state 79−66059
α-Ni-Zn, continuous precipitation kinetics *(Russian)* 78−76652
Ni-Zn, dil., ferromagnetic, hyperfine field and relax. time obs. of impurity heavy nuclei 80−75533
β-Ni-Zn, eutectoid decomposition kinetics *(German)* 77−8819
Ni-Zn, γ-phase region, X-ray and electron diffr. obs. 79−61562
Ni-Zn, implantation damaged, crit. behaviour, perturbed ang. distrib. meas. anal. 80−60476
Ni-Zn, physical-chemical metallurgy *(German)* 80−108390
α-Ni-Zn, solid soln. diffusion annealing effect *(Japanese)* 80−34255
Ni-Zn alloy electrodeposition from acetate bath 77−52257
Ni-Zn alloys, XPS for band struct. 79−33889
Ni-Zn diffusion couple, annealing and reaction diffusion *(Japanese)* 78−51749
Ni-Zn liquid alloys, Zn activity obs., 1100 to 1300K 78−40072
Ni-Zn melt, Zn activity determ. *(German)* 78−19715
Ni-Zn solid soln., lamellar spacing in discontinuous precipitation, expt. proof of Gaussian distrib. *(German)* 77−36517
α'_2-Ni-Zn-Cu martensite, thermoelastic, microscope obs., TEM 77−55966
Ni-Zn-Mn-Fe spinel, crystn. from soln. in melt 80−2945
NiZn β- and γ-intermetallic compounds, thermodynamics *(German)* 78−92242
NiZn with γ-brass struct., superstructures and defect obs. 80−107284
$Ni_{1-x}Zn_xFe_2O_4$, statistical model and phase transform. *(German)* 77−85473
Pb-Zn, liquid phase immiscibility determ., DTA 78−64523
Pb-Zn, off-eutectic alloys, controlled grain growth *(Japanese)* 77−55958
Pb-Zn, pressure effect on solubility and diffusion of Zn 77−43385
Pb-Zn, unmixing alloys, mathematical model for solidification process *(Russian)* 80−81047
Pd-Zn, γ-phase region, X-ray and electron diffr. obs. 79−61562
Pd-Zn, $L1_0$ type intermetallic phase, X-ray diffr. study of lattic compression 80−49182
Pd-Zn system, phase characterisation *(German)* 78−60654
Pd-Zn system, struct. stability of B2 and $L1_0$ phases 78−26495
$Pr_{0.25}La_{0.75}Zn$, cryst. field, neutron diffr. meas. 78−34810
β_1-PtZn, defect struct., lattice parameter meas. 78−43009
β-PtZn nonstoichiometric Ll_0 phase, thermodynamic activity of Zn 77−90320
Sb-Zn, electronic work function, contact pot. difference meas. 77−85299
SmZn, ferromag., cond. band antiparallel polarisation exceeding 4f moment 80−60207
SmZn, unusual form factor, polarised neutron scatt. 79−99684
Sn-Zn, ingots, solidified, formation of equiaxed eutectic grains *(Japanese)* 78−39756
Sn-Zn, molten, struct. investig. by neutron diffr. 79−4233
Sn-Zn, planar and cellular solidification interfaces, distrib. coeffs. and conc. profiles *(German)* 77−32568
Sn-Zn, thermodynamic quantity meas. by quantitative thermal anal. of heating process 78−19730
Sn-Zn (0.4 at.%) solid soln., yield point for cold-worked and annealed specimens *(Russian)* 78−48448
Sn-Zn (9.8 wt.%), eutectic superplasticity 77−36582
Sn-Zn dilute alloys, thermo EMF *(Russian)* 79−33285
Sn-Zn eutectic, liq., appl. to drilling of steel, cutting conditions rel. to tool parameters *(Russian)* 79−34187
Sn-Zn melts, plasticising action in deform. hardening of medium C steel 80−55415
Tb-Cu-Zn, mag. props. *(Russian)* 77−51905
Tb-Y-Zn, magnetic props. conc. and temp. depend. *(Russian)* 77−47989
$TbAg_{1-x}Zn$, solid solns., mag. props. *(Russian)* 77−77049
TbZn, elec. resist., behaviour at mag. crit. points 80−65901
TbZn, ferromag., elec. resist., just below crit. temp., effect of mag.-domains 80−39557
TbZn, ferromag., thermoelec. power, temp. depend. and crit. behaviour 80−96852
TbZn, ferromag. transition, transport coeffs. critical behaviour 80−15498
TbZn, mag. excitations meas. 80−70979
Th_2Zn_{17}, constant axial ratio of the hexagonal cell 79−69056
Tm-Zn, paramagnetism, mag. excitations, exchanges interactions 80−88718
$Tm_{1-x}Lu_xZn$, third-order mag. susceptibility, quadrupolar effects 79−99674
TmZn, cooperative Jahn-Teller effect 78−67998
TmZn, magnetic-ion-lattice interactions, cryst. elec. field 77−4540
TmZn, parastriction, magnetoelastic and quadrupolar exchange coeffs. 79−19758
TmZn, quadrupolar phase transitions, magnetoelastic and quadrupolar coupling consts. 80−15744
TmZn, struct. phase transition driven by quadrupolar pair interaction 79−61583
TmZn, US attenuation in cooperative Jahn-Teller system 79−78053
$TmZn_2$, Mossbauer effect meas. in antiferromag. and paramag. states 80−71265
γ-Vi-Zn, inversion antiphase domains, formation and stabilisation, electron conc. effect 78−14363
YZn, self-consistent energy bands and Fermi surface 77−72814

zinc alloys continued
YbZn, mag. susceptibility, thermally excited interconfiguration crossover 77−16042
Zn-^{54}Mn, nuclear orientation meas. 79−65644
Zn-22 wt.% Al superplastic eutectoid alloy tensile deformation obs. *(Japanese)* 79−90714
Zn-Ag, anisotropic, dislocation interaction with tetragonal impurity, mobility 77−19953
Zn-Ag, dil., dislocation-point defect interactions in slip systems 78−47417
Zn-Ag, dil., elec. field gradient, temp. depend. 78−39481
Zn-Ag, dil., polycryst., amplitude-depend. internal friction *(Polish)* 79−96079
Zn-Ag-Cu alloy powder, brazing solder, production using electrodeposition and heating in reducing atm. 79−100079
Zn-Al, dil., impurity quasi-particle lifetimes and pseudopotential form factor 78−47734
Zn-Al, dil., isotherm of internal adsorption at dislocations 79−37733
Zn-Al, dislocation slip peculiarities during superplastic deform. 79−20102
Zn-Al, electroless plating of Ni, baths and activating solns. *(Japanese)* 80−71604
Zn-Al, high strength superplastic alloy, exam. of precise forging method 79−4929
Zn-Al, impure and pure, as cast, endogenous-exogenous freezing 78−19736
Zn-Al, liq., partial interference functions, short range chem. order effects 79−7541
Zn-Al, near eutectoid alloy, deformation kinetics analysis 79−29161
Zn-Al, splat quenched and bulk specimens, eutectoid decomposition 77−63628
Zn-Al, unidirectional eutectic, FCC phase, preferred orientation 80−29973
Zn-Al, unidirectionally solidified eutectic, morphology and crystallography 77−48421
Zn-Al (0.4 wt.%), grain size effect on acoustic emission generated during plastic deformation 78−80609
Zn-Al (0.4 wt.%), intergranular slip during in situ superplastic deform. 80−96538
Zn-Al (10,22,50wt.%), low temp. mech. props. plastic deformation, glissile dislocation nucleation *(Russian)* 80−11695
Zn-Al (15 wt.%), thermal sprayed coating on steel substrate, cavitation and corrosion resist. in sea water 80−35427
Zn-Al (1.1 wt.%) superplastic alloy, grain size determ. *(Czech)* 80−81118
Zn-Al (20 wt.%) superplastic alloys, Zn diffusion, strain influence *(Russian)* 79−37870
Zn-Al (22 at.%), heat treatment and straining effect on fracture and corrosion 79−87672
Zn-Al (22 at.%) eutectic, superplastic, microscopic examination of internal void formation 80−16383
Zn-Al (22 wt.%), activation energy for superplasticity 77−86112
Zn-Al (22 wt.%), eutectoid, low stress and superplastic creep behaviour 80−81120
Zn-Al (22 wt.%), meas. of plasticity parameters under superplastic flow 78−60710
Zn-Al (22 wt.%), positron diffusion and trapping at grain boundaries 80−39157
Zn-Al (22 wt.%), superplastic eutectoid cavitation evidence 77−63741
Zn-Al (22 wt.%), superplastic deform. mechanism, electron microscope obs. 78−3167
Zn-Al (22 wt.%), superplastic deform. rate rel. to flow stress, determ. methods 78−60709
Zn-Al (22 wt.%), superplastic, eutectoid alloy, ductility and fracture 78−60819
Zn-Al (22 wt.%), superplastic, of very high purity, cavitation 79−24586
Zn-Al (22 wt.%), superplastic eutectoid, concurrent grain growth and deformation mechanism 79−74222
Zn-Al (22 wt.%), texture effect on superplasticity 79−20103
Zn-Al (22 wt.%) eutectoid, superplastic, factors affecting ductility 77−86097
Zn-Al (22 wt.%) eutectoid, superplastic, grain size effect on plastic deform. at room temp. *(Japanese)* 78−31462
Zn-Al (22 wt.%) superplastic alloy, cavitation and neck form. 80−30022
Zn-Al (22 wt.%) superplastic alloy, grain growth texture 80−81075
Zn-Al (40 wt.%), superplastic deform., dislocation effects 77−48515
Zn-Al alloys, comp. effects on intergranular slip during superplastic deform. *(Russian)* 77−32633
Zn-Al alloys, dislocations obs. in superplastic deformation 78−51549
Zn-Al dilute alloy, Kondo effect anisotropy 77−43578
Zn-Al eutectic alloy, uni-directionally solidified, damping capacity *(Japanese)* 80−16364
Zn-Al eutectoid, superplasticity, study by electron microscopy 77−48479
Zn-Al eutectoid alloy, straining at elev. temp., whisker crystal 79−29087
Zn-Al eutectoid alloy sheets, creep bulging 80−1439
Zn-Al eutectoid superplastic alloy, fatigue, microstruct. obs. and frequency effect 77−36659
Zn-Al superalloy, transform. kinetics 79−100114
Zn-Al superplastic eutectoid alloy, low strain rate behaviour 80−40458
Zn-Al-Cu (18, 4 wt.%), plastic deform. at room temp., superplastic props., tensile strength *(Czech)* 80−45360
Zn-Al-Cu (18, 5 wt.%) alloy, superplasticity *(Russian)* 77−59856
Zn-Al-Cu casting alloys, mech. props. and dendritic morphology, Al content effect *(Korean)* 80−93612
Zn-Al-Cu-Mg (22, 0.5, 0.01 wt.%), superplastic alloy, strengthening mechanism *(Japanese)* 77−55975
Zn-Al-Cu-Mg (4.1, 3.1, 0.05 at.%), thermal cond. and sp. ht. meas. below 4.2K 77−20081
Zn-Al-Cu-Mg-Pb-Sn, Cu, Mg, Pb, Sn effects on corrosion in wet steam 77−48585
Zn-Al-Cu-Mg-Pb-Sn (12, 1, 0.02, 0.01, 0.015, wt.%), combined effects of Pb and Sn additions on corrosion, in wet steam 78−39952
Zn-Al-Mg alloy, annealed, recrystallised, influence of strain and purity on orientation *(Russian)* 79−52234
Zn-Al(Cu), dil. alloy, creep ductility 79−38899
Zn-Al(Cu), mech. and technological props. *(Polish)* 80−89286
Zn-Al(Mg) alloys, cold-rolled, texture formation rel. to Zn purity *(Russian)* 77−59804
Zn-Al(22 wt.%), alloy sheet, superplastic, cold-rolling effects on mech. props. and microstructure *(Japanese)* 80−71671

zinc alloys continued
Zn-As system, homogeneity range of $ZnAs_2$ and electrophys. props. 80−60833
Zn-Bi, liquid, inconsistent conjugated liquidus 80−76232
Zn-Bi, specific elec. resist., temp. and conc. depend., 20-800°C 79−82571
Zn-Bi alloys, morphology and mechanism of formation of eutectic *(Russian)* 78−6916
Zn-Bi liquid alloy, surface tension and surface adsorpt. determ. *(French)* 79−69325
Zn-Ca, liquid alloy, exam. of thermodynamic props., using EMF method *(Russian)* 79−34003
Zn-Cd, anisotropic, dislocation interaction with tetragonal impurity 77−19953
Zn-Cd, dil., dislocation-point defect interactions in slip systems 78−47417
Zn-Cd, three-dimensional microstruct. analysis, appl. of basic topological concepts 77−59739
Zn-Cd (1.4 at.%), crystallisation kinetic diagram appl. *(Russian)* 78−15384
Zn-Cd alloys, liq. and solid, ultrasound speed and compressibility meas. 80−102941
Zn-Cd liquid alloy, activity meas. by transportation method *(Japanese)* 78−35358
Zn-Cd liquid/Fe-Ni-Al mag. powder, effective viscosity of composites *(Russian)* 80−54424
Zn-Cd-Bi, appl. of computational techniques for treatment of thermodynamic data, phase diagram calc. 78−10172
Zn-Cd-Bi-Sn phase diagram with liquid-liquid immiscibility, computer calc. 77−36463
Zn-Cr, dil., mag. anisotropy, 0.001 to 2K 78−68157
Zn-Cr, Kondo alloys, spin and phonon resistivity independ. 78−47777
Zn-Cu, thermal conductivity, data anal. and synthesis 78−95284
Zn-Cu system, sputtering during atomic diffusion, UPS meas. 78−92159
Zn-Fe, dil., ^{57}Fe Mossbauer effect meas. 78−95534
Zn-Fe alloys, dil., positron-electron annihilation spectra, Doppler broadened 79−65953
Zn-Ga, temp. regime of crystn. on rapid cooling *(Russian)* 80−66495
Zn-Ga liquid soln., thermodynamic props. determ., invariant method appl. 77−59742
Zn-Ge, eutectic, stereomorphology using SEM, TEM and optical microscopy *(Russian)* 79−52187
Zn-Hg, dil., anomalously high elec. field gradients below 0.05K 78−72442
Zn-In alloy, solid-liq. equilib. roughening transition 80−96630
Zn-In-Cd, anal. calc. of phase diagram 79−91631
Zn-In-Cd soln., liquid, thermodynamic props. 79−83176
Zn-In(Bi) interfacial tension and microstruct. 79−74132
Zn-Mn, dil., Kondo effect and impurity interactions in resist., 0.05-14K 78−14721
Zn-Mn, Kondo alloys, spin and phonon resistivity independ. 78−47777
Zn-Mn, Kondo-system, ion implantation as method for study 80−70241
Zn-Mn, supercond., thermal cond. compared with Shiba's theory 77−8228
Zn-Mn dilute alloy, Kondo effect anisotropy 77−43578
Zn-Mn(Cr), dil, mag. anisotropy, Hartree-Fock calcs. 80−11162
Zn-Mn(Cr), dil., mag. anisotropy below 1K, low field magnetisation meas. 80−20382
Zn-Pb composite, production under conditions when gravity forces are balanced out by EM forces 78−31363
Zn-Pb melt, immiscible component distrib. in crossed EM fields *(Russian)* 77−48396
Zn-Pb(Bi), liquid, surface tension, size effect *(French)* 80−15341
Zn-Sb system, phase interactions and phase diagram 79−87607
Zn-Sn, binary metallic melt, deviation from the Kopp law, specific heat *(Russian)* 80−39305
Zn-Sn, specific elec. resist., temp. and conc. depend., 20-800°C 79−82571
Zn-Sn alloys, morphology and mechanism of formation of eutectic *(Russian)* 78−6916
Zn-Sn and Zn-Sn-Pb, intergranular and solid-liquid interfacial tensions 77−36452
Zn-Sn-Bi, ternary phase diagrams, interactive computer program 80−71629
Zn-Sn-Hg, diagram of state, melting temp., peritectic and eutectic phases *(Russian)* 80−55350
Zn-Sn-Hg amalgam, liq., thermodynamic props. *(Russian)* 77−66624
Zn-Sn(Bi), discrete eutectic formation mechanism *(Russian)* 77−66634
Zn-Ti, environmental factors affecting pitting corrosion potential in NaOH solns. 80−45423
Zn-transition metal, residual resistivity, effect of 4d and 5d transition metal impurities 79−60791
Zn-Y alloys, thermodynamic props. *(Russian)* 79−70041
ZnAl (18.75 wt.%), supercooling phase β break up kinetics *(Polish)* 80−25654
$Zn_{13}Fe$, ^{57}Fe Mossbauer effect meas. 78−95534
ZnMn, dil., magnetoresist. meas., temp. depend. anisotropy 80−65532
Zn_2Y, magnetostatic volume waves, magnetocrystalline anisotropy effects, group delay 79−78355
$ZnY_{0.95}R_{0.05}$ resist. anisotropy due to impurities 77−62902
Zr-Cu-Ti (2.5, 0.15 wt.%), indentation irregularity at elastic limit after heat treatment *(French)* 79−79004
$Zr_{1-x}Nb_xZn_2$, microscopic mag. props., NMR investigation 80−15807
$ZrZn_2$, de Haas-van Alphen effect, Fermi surface, theory 80−103614
$ZrZn_2$, high press. study of Curie temp. and mag. susceptibility 80−84600
$ZrZn_2$, high purity, mag. props., pulsed fields up to 17 T 78−64198
$ZrZn_2$, itinerant electron ferromag., NMR exam. of effect of spin fluctuations 77−16192
$ZrZn_2$, itinerant electron ferromag., nucl. spin-lattice relax. time meas. 77−63308
$ZrZn_2$, itinerant electron ferromagnet, magnetovolume effects 80−60397
$ZrZn_2$, phonon contrib. to Stoner enhancement factor, ferromag. and possible superconductivity 80−25070
$ZrZn_2$, weak itinerant electron ferromagnet, resistivity 77−72850
$ZrZn_2$, weak itinerant magnetism as inhibited superconductivity 79−51715
$ZrZn_2$:^{57}Fe mag. props. from Mossbauer effect obs. *(Japanese)* 80−15933
$ZuCuZn_2$, martensitic transition, shear elastic const. meas. 77−28810

zinc compounds
see also zinc alloys
additives to MnZn ferrites, effect on X-ray spectra *(Ukrainian)* 79−52046
alkylammonium zinc tetrachloride cpds., high temp. phase transitions 80−54372
binary, with chalcogenides and pnictides, at. vol. and semicond. props. 77−20089
bis-tetraethylammonium tetrachlorozincate, heat capacity, structural transitions 79−65209
$Ca_3(VO_4)_2$-$Zn_3(VO_4)_2$, exam. of phase composition and phase diagrams 79−1851
cathodoluminescence, bibliography of papers till 1977 79−21482
chalcogenide, extra-atomic photoemission relax. energies, ionicity depend. *(French)* 77−36357
chalcogenide spinels, thermal stability, thermochemical, thermodynamic and crystallochemical props. 77−51519
chalcogenides, electronic polarisabilities of ions 78−79559
chalcogenides, film, on NaCl, preferential epitaxy induced by electron bombard. or elec. field 80−10824
chalcogenides, thin films, VPE, needle-like cryst. growth 80−80148
chalcopyrites, refr. index dispersion 80−55057
dialkylammonium zinc dichlorobromides, long chain cpds., phase transitions, calorimetric study 80−70390
dialkyldithiophosphate surface film, prep. and nature 80−104300
duplex struct. formation during sintering, grain growth study 79−11541
elbaites, Zn-Fe, γ-irradiated, Mossbauer study 80−44990
etioporphyrin I anion radical, photoreduction obs. *(Russian)* 78−23958
ferrite, hexagonal, with M, W and Y structures containing Fe^{2+} and Fe^{3+} mag. ions, saturation moment and anisotropy 80−71009
ferrite, production by mechanochemical reactions by grinding in ball mill 79−20014
ferrite, spinel type catalytic oxidation of CO, role of mag. exchange interactions 78−56916
formate dihydrate:Co, spin lattice relax. of Co^{2+} ions 80−75847
formate dihydrate, 2-D Heisenberg antiferromag., sp. ht. 78−14965
formate dihydrate, Co^{2+}-doped, EPR spectrum, g-factor anisotropy for A- and B-sites 77−77089
halide, extra-atomic photoemission relax. energies, ionicity depend. *(French)* 77−36357
halide interaction with vulcanisable resins, IR spectrometry *(Bulgarian)* 79−33993
halides, matrix isolation, vibr. spectra, isotope effects, force consts. and geometry 78−46337
halides-He discharge, CW ion laser oscill. 78−17913
malonate dihydrate, cryst. struct., X-ray refl. obs. 78−75652
manganese zinc formate dihydrate, two-dimens. antiferromag., anomalous crit. phenomena, neutron scatt. and PMR obs. 80−50104
metal-ZnO-SiO_2-Si structures, charge injection 80−49919
methylzinc methoxide, tetrameric, X-ray cryst. struct. determ. 80−107197
nitroprussides, Mossbauer spectra, dehydration effects 79−24237
octaethylporphin, radiationless transitions, fluoresc. and phosphoresc., isotope effects 77−65502
orthovanadates:rare earth ions, spectroscopic props. 77−16363
oxalate, crystal growth in silicate gel, X-ray diffr. and i.r. spectrum 77−4724
oxalate, crystallisation kinetics, specific surface energy at cryst.-soln. interface 78−26471
oxalate, effect of supersaturation on crystallisation kinetics, turbidimetry meas. 78−30569
oxalate, isothermal crystallisation from soln. 80−108336
paste, direct tensile tests and tied crack model 78−11178
phthalocyanine, electrochromism and oxidation 80−93768
phthalocyanine, photovoltaic effects, dark elec. props. of rectifying cells 79−4604
phthalocyanine, photovoltaic effects, illuminated thin-film cell props. 79−4605
phthalocyanine film, between Au or Ag layers, microstruct. characterisation by TEM method 78−95241
phthalocyanine film, surface photovoltage, central ligand effect 79−78231
piezo-birefringent zinc blende crystals, optical filters using coupled polarised waves *(French)* 78−33896
polyphosphinate, bulk compressibility meas. to 30 kbar 80−76306
porphin ($-d_4$,d_8,d_{12}), nonradiative transition probabilities, deuteration effects 79−3485
porphyrins, anion radicals and dianions, reson. Raman spectra 77−471
portland cement, doped with ZnO, struct. and props. 80−60914
protoporphysin, solns., anal. by fibre optic filter fluorometer 77−36813
pyrochlorophyllide in nematic liq. cryst., oriented photoexcited triplets, EPR study 80−84636
silicates:Mn, sintered, photocond. *(German)* 79−51627
silicates, entropy estimates at 298K from molar vols. 77−1243
solid solns., determ. of degree of imperfection 77−80624
sphalerite, dissolution in ferric chloride soln. 79−47919
sphalerite, hydrothermal single crysts., feasibility of optical methods for quality control 80−89065
sphalerite, kinetic study of pressure leaching for Zn prep. 78−44050
sphalerite, kinetic study on press. leaching 77−4893
stearate, addition to atomised Fe powder, effect on processing props. 79−100077
stearate, additive to UO_2 green pellet fuel, effect on sintering 80−68908
tetramethylammonium tetrachlorozincate, ferroelec., incommensurate-commensurate transition, neutron scatt. study 80−40073
tetramethylammonium tetrachlorozincate, incommensurate phase study, ferroelectric-paraelectric phases *(French)* 80−88318
tetramethylammonium tetrachlorozincate, low temp. phases, superstruct., X-ray study 80−39065
tetramethylammonium zinc tetrachloride, ^{13}C NMR and PMR study of incommensurate phase transition 80−34863
tetramethylammonium zinc tetrachloride, incommensurate phase transitions, ^{13}C NMR study 80−75968
tetramethylammonium zinc tetrachloride, Raman spectra near incommensurate phase transitions 80−76013
triple orthoarsenates, $KZnCr_2(AsO_4)_3$ and $NaZnCr_2(AsO_4)_3$, prep. by high temp. synthesis, and cryst. struct. 79−66028
vanadates, elec. and mag. props., stoichiometry 78−51991
zinc bisdiethyldithiocarbamate:Cu^{2+}, exchange interaction of Cu^{2+}-Cu^{2+} pairs, spin-lattice relax. 78−48034
zinc blende type crystals, internal displacements 80−34127

zinc compounds continued
zinc octaethyl porphin, soln., photochem. ionogenesis 80−61116
zinc phthalocyanine, resonant two hole bound state at 3p core threshold 80−60750
zinc porphin, in n-alkane crystals. at 4.2K, Zeeman spectra for Jahn-Teller instability 78−27256
zinc stearate lubricant, admixed, effect on Fe sintered compact, shrinkage and mech. props. 80−45402
zinc stearate lubricant effect on Fe powder compact, apparent density, mixing, and friction 80−45403
$Zn_3B_7O_{13}Br$, ferroelec. 43m-mm2 phase transition, molar heat capacity meas. 80−93249
Zn_3P_2, UV photoconductive detectors 80−4766
α-$ZnIn_2S_4$, and related polytypes, electron band struct. 79−51485
ZnO, film, reactively RF sputtered, anal. of texture 78−67921
ZnO-resin electrophotographic photosensitive layers, dark decay mechanism of corona charge *(Japanese)* 79−24002
ZnO/Si acoustoelectric devices 80−80332
ZnS:Mn,Cu, thin-film phosphors, LV DC electroluminescence 79−11472
ZnS:V^{2+}, impurity states by Green's function method 80−92855
ZnS single crystals, O content determ. by fast neutron activation anal. 80−15142
β-ZnS-graphite electrode, interfacial impedance with graphite in acidic aq. soln. *(Japanese)* 77−52648
ZnS-Mn, Cu film, ZnS-Cu_xS films, electroluminescence, joule heating 78−2599
n-ZnSe:In, highly compensated, freq. depend. of cond. 79−99548
Al-ZnS-Au structure, coulombic centres, thermal ageing, cond. and photovoltaic charact. *(French)* 77−43741
$Al_2O_3.3H_2O-H_3PO_4$-ZnO, phase equilib., $AlPO_4$ solid soln. 79−11586
Au-ZnO-In metal-semicond. diode, electrolum. spectra 79−99948
Au-ZnSe:Ga(Al), Schottky diode, wavelength modulated photoresponse spectra 78−6714
B_2O_3-ZnO, glass-ceramic-cement composites, review 79−38783
$Ba_2Co_{2x}Zn_{2-2x}Fe_{12}O_{22}$, mechanically oriented, topotactic prod. technique, mag. props. 80−35140
$BaFe_2O_4$-Fe_2O_3-$ZnFe_2O_2$ system, phase relations at 1200°C 78−72767
$BaMoO_4$-ZnO and $BaMoO_4$-$ZnMoO_4$ systems, phase diagrams 77−25034
BaO-K_2O-Na_2O-ZnO-SiO_2, corrosion and microhardness, effect of detergents 80−16518
$BaZn_{1.38}Co_{0.62}Fe_{16}O_{27}$, W-type hexaferrite cryst., first order magnetisation processes 78−95472
$Ba_2Zn_{2-2(x+y)}Cu_{2x}Cd_{2y}Fe_{12}O_{22}$, mag. props. and Mossbauer spectrum 80−75765
$Ba_2Zn_{2-2x}Cu_{2x}Fe_{12}O_{22}$, hexagonal ferrites, prep. and mag. characterisation 79−1727
$BaZn_2Fe_{16-x}Al_xO_{27}$, saturation magnetisation, anisotropy field and Mossbauer meas. 77−69508
$BaZn_2Fe_{16-x}M_xO_{27}$ (M=Al, Ga, In, Sc), mag. props. and Mossbauer effect 80−75766
$Ba_2Zn_2Fe_{12}O_{22}$, anisotropic magnetisation and susceptibility 78−84411
$Ba_2Zn_2Fe_{12}O_{22}$, model for low mag. moment, magnetisation meas., 5-1375K 78−2655
$Ba_3Zn_2Fe_{24}O_{41}$, ferromag. reson., low power nonlinear effects 80−75861
Ba_2ZnS_3, prep. by solid state reaction and melt growth, X-ray anal. 77−73226
(BaZnSr)TiO_3 ferroelectric film, parameters at upper end of centimetre band *(Russian)* 77−40185
Bi_2O_3-ZnO, elec. cond., dielec. const., mag. susceptibility meas., effect of melting transition 77−7849
Bi_2O_3-ZnO, phase diag. 77−40416
$CaZn(SiO_4).H_2O$, clinohedrite, cryst. struct., H bonds 78−79593
$Ca[ZnSiO_4].H_2O$, clinohedrite, cryst. struct., comparison with $(Mn,Mg)Mg(OH)_2[ZnSiO_4]$, herstmannite 79−19228
$CdCr_2Se_4$-$ZnCr_2Se_4$, single cryst., mag. props. 79−28526
CdO-ZnO-Al_2O_3-Fe_2O_3-SiO_2 system glass, ESR spectra 79−65711
CdO-ZnO-P_2O_5 glasses, prep., density, elec. and optical props. 79−70033
n-CdS/p-$ZnIn_2Se_4$ thin film solar cell, photovoltaic props. 80−89628
CdS-ZnS(CdSe), film, light transmittance spectra, comparison with Schott GG 495 glass filter 78−33838
CdSb-ZnSb, crystallisation characts., phase diagram 80−55383
CdTe, electrodes for photochemical production of H_2, a comparison 77−70311
CdTe-ZnS system, phase diagram and solid solubility 80−20909
CdTe-ZnS ternary mutual system, phase diagram 80−20904
CdTe-ZnS(Se) solid solns., optimal synthesis conditions for single cryst. growth 80−100776
CdTe-ZnSe pseudobinary system, phase diagram and equil., Bridgman single cryst. growth method 79−43213
$(CdTe)_{1-x}$-$(ZnSe)_x$ system, mutual solubility and band gap energy *(Japanese)* 77−51501
$Cd_{3-x}Zn_xAs_2$, cryst., two-band and impurity conduction, 1.8 to 370K 78−19057
$Cd_{3-x}Zn_xAs_2$ press. and temp. depend. of Hall coeff. 77−69349
$Cd_{3-x}Zn_xAs_2$ solid soln., US wave prop. vel., composition depend. 77−20013
$Cd_{1-x}Zn_xCr_2Se_4$, ferromag. semicond., surface magnetism, magneto-optical meas. 77−20831
$Cd_{1-x}Zn_xCr_2Se_4$, mag. semicond., neutronographic obs. *(Russian)* 79−11297
CdZnS thin films, growth and evaluation for fabrication of high performance photovoltaic solar cells 80−93501
(CdZn)S-Cu_2S solar cell, film form. and characts. 78−68080
$Cd_{1-x}Zn_xS$ 10 μm film optical and electrical characterisation *(French)* 78−64153
$Cd_{1-x}Zn_xS$, electro-optical multilayer film, for data storage and display 78−71176
$Cd_{1-x}Zn_xS$, electroless film deposition with variable comp. and polymorphic structs. 79−95952
$Cd_{1-x}Zn_xS$, epitaxial growth of single crystal layers on (111) GaAs substrate, close-space geometry 78−92198
$Cd_{1-x}Zn_xS$, film, technical data, for low cost solar cell 79−48127
$Cd_{1-x}Zn_xS$ films, thermal evaporation prep., phys. props. 80−84410
$Cd_{1-x}Zn_xS$ heteroepitaxial single-cryst. layers, photoluminesc. props. 80−100692
$Cd_{1-x}Zn_xS$, RF sputtered electro-optical film for data storage and display 78−83047
$Cd_{1-x}Zn_xS$ reactively sputtered phtoconductive films for high field applications *(German)* 78−39154
zinc compounds continued
$Cd_{1-x}Zn_xS$ solar cell thin films, microprobe characterisation *(French)* 80−61349
$Cd_{1-x}Zn_xS$ spray deposited film, for low cost solar cells 79−7915
$Cd_{1-x}Zn_xS$, use of parallel and monochromatic beams for comp. determ. by X-ray fluorescence 79−48000
$Cd_{1-x}Zn_xS/Cu_2S$ thin film heterojunction solar cells, operational charact. 80−45687
$Cd_{1-x}Zn_xS$-p-GaAs heterojunctions, elec. and photovolt. props. rel. to growth technique 80−29466
$Cd_{1-x}Zn_xS$-PbS heterojunctions prepared by spray pyrolysis 79−60917
$Cd_xZn_{1-x}S$ film, vacuum evaporated, struct. 78−38985
$Cd_xZn_{1-x}S$ films, chem. sprayed, carrier density and mobility 80−60121
$Cd_xZn_{1-x}S$, vibr. spectra, microscopic theory 79−73949
$Cd_xZn_{1-x}S$-Cu_2S solar cell, interface chemistry modification of current-voltage charact. 79−100523
$Cd_{1-x}Zn_xSe$, epitaxial layer growth with Zn content from doping to solid soln. formation 77−85094
$Cd_{1-x}Zn_xTe$, solid soln., vibr. spectra restructuring anomalies 79−4803
(Co,Zn)Cr_2S_4 and (Co,Zn)S solid soln. equilib. composition *(German)* 77−36486
$(Co,Zn)SiF_6.6H_2O$, phase transition at low temp., IR spectra 79−24302
CoNiZn ferrites, Fe excess, complex permeab. var. with annealing temp. 77−89979
CoO-ZnO-Al_2O_3-Cr_2O_3-TiO_2 system, form. and colour of spinel solid soln. *(Japanese)* 77−25001
CoO-ZnO-MgO ternary systems, solid solns., struct. charact. 80−60629
CoS-ZnS, phase study by X-ray obs., lattice const. 79−1854
CoZn, complex, $Co_pZn_{1-p}(C_5H_5NO)_6(CPO_4)_2$, dilute simple-cubic antiferromag., sp. ht. near crit. conc. 79−38336
CoZn ferrite, chemical shift in X-ray absorpt. spectra, effective changes 78−6811
$Co_{1-x}Zn_xF_2$, antiferromag. crit. props., neutron scatt. obs. 80−88749
$Co_xZn_{1-c}F_2$, Raman scatt. from Zeeman split levels 77−66243
$Co_{1-x}Zn_xFe_{2(1-y)}Cr_{2y}O_4$ spinels, solid solns., struct. 80−19764
$Co_xZn_{1-x}Fe_2O_4$, elastic behaviour, mag. field and temp. depend. 79−87301
$Co_xZn_{1-x}Fe_2O_4$, ferrite, DC cond., dielec. props., lattice consts. 80−80272
$Co_{0.0031}Zn_{0.5676}Ni_{0.4293}Fe_2O_4$, single phase ferrite powder, from solid solution of schoenite-type salt 77−16524
$(Co_{0.001}Zn_{0.189}Ni_{0.143}Fe_{0.667})SO_4.(NH_4)_2SO_4.6H_2O$, schoenite-type salt, formation of single phase ferrite powders 77−16524
$Co_xZn_{1-x}Rh_2O_4$, mag. props., EPR spectra, antiferromag. order 80−75736
$Co_xZn_{1-x}Rh_2O_4$ spinel, crit. conc. for long range mag. order, expt. evidence 79−47239
$Co_{2-y}Zn_yTiO_4$, cation distrib. and mag. props. 78−14939
$Co_{2-y}Zn_yTiO_4$, spinel series, exchange integrals, mag. struct. and coercive force, magnetisation meas. 77−69507
$Co_{1-x}Zn_x$hexa(pyridine-N-oxide)$(ClO_4)_2$, dilute cubic S=1/2 XY antiferromag., sp. ht. data 77−66358
$CsZnCl_4:Cu^{2+}$, electron spin echo, 35 GHz 80−13113
$(Cu,Zn)Cs_2(SO_4)_26(H,D)_2O$, thermal contact between nucl. Zeeman and electron dipole-dipole interaction system 77−90065
$(Cu,Zn)Cs_2(SO_4)_2.6(H,D)_2O$, proton spin-lattice relax. exam., rel. to EPR 77−90064
$(Cu,Zn)Cs_2(SO_4)_2.6(H,D)_2O$ Tutton salt, proton spin-lattice relax. time, proton conc. depend. and spin diffusion role 80−71221
$(Cu,Zn)_3Pb(A_3O_4)_2(OH)_2$, bayldonite, struct. chem., complex layer struct. 79−46609
Cu complex, hexakis pyridine-N-oxide cuprate ion, pure and Zn doped, EPR, Jahn-Teller effect 78−10754
Cu^{2+} ions influence on $PbSO_4$ flotation, with sodium hexadecyl sulphate, metallurgical waste treatment appl. *(Japanese)* 80−55701
$(Cu_xAn_{1-x})_2AsO_4(OH)$, olivenite-adamite solid soln., ordering 78−42962
$Cu_{0.5}Fe_{2.5}O_4$-$ZnFe_2O_4$, cation distrib., mag. moment, Mossbauer spectra, chem. anal. 80−75210
$CuGa_{0.5}In_{0.5}Se_2/Zn_{0.29}Cd_{0.71}S$ heterojunction solar cell, preparation and props. 80−101110
$(CuInTe_2)_{1-x}$-$(2ZnTe)_x$, phase diagram and cryst. growth of $CuZn_2InTe$ from $ZnCl_2$ flux 80−16287
CuO-ZnO-Fe_2O_3, sintered ferrite, preparation, mag. susceptibility, DC resistivity 80−34598
Cu_2S-Zn_xCd_{1-x}, heterojunction, composition meas. near interface using aqueous ion-exchange 80−29465
Cu_2S-$Zn_xCd_{1-x}S$ and Cu_2S-CdS thin film solar cells by solid state reaction, comparison 80−101109
Cu_2S-$Zn_xCd_{1-x}S$ heterojunction, improved model of electro-optic behaviour 80−94023
$(Cu_2SnS_3)_x$-$(3ZnS)_{1-x}$, diamond-type semiconductor, Mossbauer spectrum of ^{119}Sn 80−44991
$(Cu_2SnS_3)_x(3ZnS)_{1-x}$, second co-ordination sphere atoms effect on ^{119}Sn Mossbauer spectra *(Russian)* 77−63348
$Cu_xZn_{1-x}SiF_6.6H_2O$, heat capacities and thermodynamic props., 14 to 300K, cooperative Jahn-Teller transition 80−21314
$Cu_xZn_{1-x}ZrF_6.6H_2O$, distortions of nearest Jahn-Teller $[Cu(H_2O)_6]^{2+}$ centres 78−68000
$Fe_{1.985}Ni_{0.975-x}Zn_xCo_{0.04}O_{4+\gamma}$, elementary coupling energy of Co^{2+} to lattice 77−1549
$Fe_{1-x}O$-ZnO at 900°C, some peculiarities *(French)* 77−70037
Fe_2O_3-NiO-ZnO-CoO (15.1, 17.6, 0.6 wt.%) ferrite, effect of electron beam machining on surface layer 79−34178
Fe_3O_4-$ZnFe_2O_4$, spinel type solid soln., thermodynamic study by EMF meas. 78−15379
$Fe_{1-x}Zn_xF_2$, dil. antiferromag., Raman scatt. expts. 79−78666
$Fe_{1-x}Zn_xF_2$, dil. antiferromag., electronic and mag. props., Raman scatt. and optical absorpt. study 80−108207
$Fe_{1-x}Zn_xF_2$, electronic Raman scatt., mag. anisotropy 80−66184
$Fe_xZn_{1-x}F_2$, Neel point and short range order, dilution effects, mag. birefr. obs. 80−71019
$Fe_xZn_{1-x}F_2$, Neel temp., CPA calc. 78−68233
$Fe_{1-y}Zn_{3y/2}O_3$, solid soln. prep., struct. and mag. moment 78−52228
$Fe_{3-x}Zn_xO_4$ low temp. Mossbauer spectra, electron transfer and spin density distribution 78−52404
GaAs-ZnSe, solid solution crystals, grown by Bridgman method, exam. of resistivity and Hall effect 79−95919
GaAs-ZnSe, X-ray cond. 5.4 to 17.5 keV, spectral and dosimetric charcts. *(Russian)* 77−35964
GaAs-ZnSe system, phase diagram 77−28785

zinc compounds continued
$(GaAs)_x(ZnSe)_{1-x}$ single crystal, visible cathodoluminesc. spectra 80−20716
p-$(GaAs)_x(ZnSe)_{1-x}$-nn$^+$.GaAs, avalanche heterojunctions, inverse branch of volt ampere characts. *(Russian)* 80−6974
GaP:ZnO, LED, degradation, temp. and current depend. 79−87144
GaP-ZnS, solid solns., microstruct. investig. 78−2128
GaP-ZnSe solid solutions, spectral studies *(Russian)* 79−91498
$(GaP)_x(ZnS)_{1-x}$ solid solutions, X-ray fluorescence spectra, photoluminescence *(Russian)* 79−74003
$(GaP)_x(ZnSe)_{1-x}$, solid solution, reaction of Zn with Se during Czochralski growth and LPE 79−8238
$(GaP)_x(ZnSe)_{1-x}$/GaP, epitaxial heterostructures, chem. microinhomogeneity 77−80831
GaSb-Zn(Cd)Te, quasibinary system, phase equilibrium, intermol. interaction 77−12601
Ge-ZnSe, (100) interface, electronic struct. calc. 80−49861
Ge-ZnSe p-n heterojunctions, effect of interfacial condition on optoelectronic props. 79−24061
$Ge_xZn_{1-x}Fe_2O_4$, ferrimagnetism and ion distrib. 77−12103
$HCl.2ZnCl_2.2H_2O$, struct. refinement 78−51488
He-$ZnCl_2$ hollow cathode laser discharge, comparison with He-Zn discharge 80−28203
$Hg_{0.8}Cd_{0.2}Te$-ZnS MIS struct., nonparabolic bond semicond., surface state studies, capacitance measurements 79−78190
HgTe-ZnTe solid solns. form., equil. vacancy conc. changes 77−43208
$Hg_xZn_{1-x}Cr_2Se_4$, absorption spectra near the absorption edge 78−80340
In-ZnO-Al metal-semicond. diode, electrolum. and photoluminesc. spectra 79−99948
In-ZnSe:Al-In, MSM structure, mechanism of current flow *(Russian)* 79−78208
$In_{2-x}Sn_xO_{3-y}$-ZnS:Mn thin film structure, surface morphology and electro-optical props. *(Russian)* 80−49554
$K_2Cu_{1-x}Zn_xF_4$, two-dimens., ferromag., spin wave excitations 78−80140
$K_2Cu_xZn_{1-x}F_4$, Curie temp., Cu conc. depend. 80−60255
$KMn_{0.18}Zn_{0.82}F_3$, excitation of Mn^+ clusters, neutron scatt. 78−68200
$K_2Mn_xZn_{1-x}F_4$, 2-dimens. antiferromag., sidebands on EPR lines 78−56370
$3KNO_3-2ZnCl_2$, glass form. from liq., struct. transform., Raman spectrum obs. 80−64916
K_2O-PbO-ZnO-B_2O_3-SiO_2, corrosion and microhardness, effect of detergents 80−16518
K_2O-ZnO-P_2O_5, exam. of chemical durability, glass transformation temp. 79−20221
K_2SO_4-$ZnSO_4$ glass, transition metal ion doped, visible spectra 79−51990
K_2SO_4-$ZnSO_4$ system, glass formation and phase diagram study, physical props. 78−27500
K_2SO_4-$ZnSO_4$:Cu II, glass, O basicity, ESR study 78−80199
K(Zn,Mn,Co)F_3, crysts., Mn, Co distrib., as function of cryst. region *(German)* 78−14375
$K_2Zn_2Be_2(SiO_4)(Si_2O_7)$, cryst. struct. determ. 80−88121
$K_2Zn(CN)_4$, third order elastic consts. 80−84231
K_2ZnCl_4, ^{35}Cl NQR study of incommensurate phase transition 80−60450
K_2ZnCl_4, ferroelec. props. 79−4772
$KZnF_3$, exchange interactions of transition metal ions in orbitally degenerated excited states 80−65512
$KZnF_3$:Mn^{2+}, Cu^{2+}, exchange coupled, luminesc. props. 79−33781
$KZnF_3$:Ni^{2+}, Mn^{2+}, interference transition electric dipole mechanism 80−34896
$KZnF_3$:Ni^{2+}, temp. depend. of luminesc. 79−83016
$KZn_2H(PO_4)_2$, X-ray cryst. struct. determ. *(French)* 79−69080
$K_4Zn(MoO_4)_3$, cryst. struct., cohesion 77−31641
$KZn_4(PO_4)_3$, X-ray cryst. struct. determ. *(French)* 79−19205
$K_xZn_{x/2}Ti_{8-x/2}O_{16}$, ionic cond., K mobility rel. to struct. and bonding *(French)* 77−76594
$K_xZn_{x/2}Ti_{8-x/2}O_{16}$, ionic cond., rel. to struct. and chemical bonding *(French)* 78−18824
$K_xZn_{x/2}Ti_{8-x/2}O_{16}$, ionic cond. meas. 78−67856
$K_2Zn(ZrF_6)_2.6H_2O$, EPR of Cu^{2+}, temp. depend. 78−80201
$K_2Zn(ZrF_6)_2.6H_2O$:CO^{2+}, anisotropic exchange interactions between Co^{2+} ions, ESR spectra 79−95637
(Li,Na,Cu,Zn) ferrites, nonceramic synthesis, electrochem. investig. 78−35339
Li-Zn ferrite, magnetic props., effect of V_2O_5 addition *(Japanese)* 77−28415
Li-Zn ferrites, (Li, Zn, Ti, Cr substituted), Mossbauer spectrometry, effect of supertransferred hyperfine fields and relaxation *(French)* 80−80654
$Li_{0.5}Fe_{2.5}O_4$-$CuFe_2O_4$-$ZnFe_2O_4$, order-disorder transition, quadratic transformation *(French)* 78−76447
Li_4GeO_4-Zn_4GeO_4, solid electrolyte system, phase diagram 80−66489
LiMnZn ferrites, elementary coupling energy to lattice of Mn^{3+} ions, depend. on T_c 77−69534
Li_2O-ZnO-P_2O_5, exam. of chemical durability, glass transformation temp. 79−20221
LiTiZn ferrites, elec. resist., mag. props., effect of Bi addition 78−95474
LiTiZn microwave ferrites, effects of Mn and Bi additives, expt. *(German)* 77−28411
LiZn ferrite, dielec. const. and loss meas., 50-10^6 Hz 77−77135
LiZn ferrite, Mossbauer study, relax. and supertransferred hyperfine fields 80−39941
LiZn ferrospinel, sequence of mag. transforms. *(Russian)* 78−19252
LiZn ferrospinels, mol. field. coeff. conc. depend. 80−97114
LiZn, substituted ferrite, cation distribution, Mossbauer, X-ray, neutron diffr. study 80−28975
$Li_{0.44}Zn_{0.09}Fe_{2.47}O_4$, ordering, elect. of V_2O_5 additions 77−35532
$Li_{0.5-z/2}Zn_xFe_{2.5-z/2}O_4$, field magnetisation and susceptibility 79−82762
$Li_{0.5(1-x)}Zn_xFe_{2.5-0.5x}O_4$, cryst. struct., neutron and X-ray diffr. obs. *(Russian)* 77−31645
$Li_{0.5(1-x)}Zn_xFe_{2.5-0.5x}O_4$, canted spin struct., neutron diffr. study 78−68175
$Li_{12}Zn_2(GeO_4)_4$ LISICON system, Li ionic conductivity *(Chinese)* 80−88350
$Li_{14}Zn(GeO_4)_4$, crystal struct. and ionic conductivity 78−51728
$Li_{14}Zn(GeO_4)_4$, LISICON, AC meas. of ionic cond., 298 to 573K 80−107526
$Li_4Zn(GeO_4)_4$, ionic cond. 79−55922
$Li_4Zn(PO_4)_2$, cryst. struct. determ. 77−15386
zinc compounds continued
Li_2ZnSiO_4, tetahedral struct., polymorphic α-β transform. kinetic obs. and method 79−90778
$LiZnVO_4$, high press. spinel modification, vibr. spectra 78−35124
MgF_2-ZnS multilayers, high vacuum deposition for cold light mirror prod. *(German)* 80−53486
$MgFe_2O_4+ZnO$, powders, cation mutual diffusion coeffs. calc. 77−15635
MgMnZn ferrite, ultrafine powder, prod. by cryochemical, freeze drying, spray drying or soln. techniques 80−55336
MgO-ZnO, solid soln., surface comp., Auger and XPS investig. 78−51806
MgO-ZnO-Fe_2O_3, sintered ferrite, preparation, mag. susceptibility, DC resistivity 80−34598
MgO-ZnO-Fe_2O_3 ternary system, phase equilibria 77−21116
MgO-ZnO-Fe_2O_3-Cr_2O_3 system spinels, IR absorpt. spectra, short-range order 79−42957
$Mg_{0.25}Zn_{0.75}Fe_2O_4$, ferrite, DC cond., dielec. props., lattice consts. 80−80272
$Mg_xZn_{1-x}Te$, band struct. refl. spectra meas. 80−80813
$Mg_xZn_{1-x}Te$, comp. profile, second derivative wavelength modulation 80−103967
$Mg_xZn_{1-x}Te$, high purity, luminesc. and band gap 78−68553
$Mg_xZn_{1-x}Te$, long wavelength optical phonon replica 78−60468
$Mg_xZn_{1-x}Te$, spin orbit splitting, of electron energy levels, reflectivity meas. 79−69479
$Mg_xZn_{1-x}Te$, temp. depend. of energy gap, near band gap reflectivity spectra 79−28786
(Mn,Mg)$Mg(OH)_2[ZnSiO_4]$, herstmannite, comparison with $Ca[ZnSiO_4].H_2O$, clinohedrite 79−19228
(Mn,Ni,Zn) ferrite single cryst., flame fusion cryst. growth, conc. change 77−77369
(Mn,Zn)Cr_2S_4 and (Mn,Zn)S solid soln., equilib. composition *(German)* 77−36486
(Mn,Zn)Fe_2O_4:Si, Ca, Ti, second phase effect on elec. and mag. props. 80−60986
Mn-Zn ferrite, domain struct. and initial permeability, effect of O nonstoichiometry 78−35001
Mn-Zn ferrite, extraordinary Hall effect 79−51615
Mn-Zn ferrite, oxidation-reduction equilib. and struct. defects 77−20189
Mn-Zn ferrite, single crystal, electrolytic buffing studies *(Japanese)* 77−86259
Mn-Zn ferrite, single crystal, surface damaged layer study *(Japanese)* 77−86260
Mn-Zn ferrite powder, spray dried calcination 77−12558
Mn-Zn ferrites, grain boundary exam. using TEM and AES 80−107268
Mn-Zn ferrites, mag. parameters, determ. from RF susceptibility 79−82769
Mn-Zn ferrites, permittivity anal. and meas. *(Russian)* 79−15391
Mn-Zn ferrites, single-crystal, machining effect obs., on magnetisation curves *(Japanese)* 77−21295
Mn-Zn ferrospinels, carrier transfer phenomena 80−54727
Mn-ZnF_2, crit. neutron scatt. 78−52249
MnO-ZnO, solid solns. prep., struct. 78−95157
MnO-ZnO-MgO-Fe_2O_3 ferrites, effect of Fe^{2+} ion on initial permeability 77−8357
$(Mn_xSn_{1-x})Fe_2O_4$ thin film LPE on Bridgman grown Zn_2TiO_4 substrate 79−100065
MnZn ferrite, appreciable SiO_2 content, origin of core losses, microstructure and mag. props. 78−64225
MnZn ferrite, combined Sn-Ti substitutions, improved props. *(German)* 77−20644
MnZn ferrite, combined Bridgeman-zone levelling cryst. growth technique 80−35076
MnZn ferrite, gas phase fluorination for improved props. 78−52306
MnZn ferrite, high cond., magneto-microwave Kerr effect 77−43888
MnZn ferrite, initial mag. permeability rel. to mag. anisotropy 80−80557
MnZn ferrite, laser drilling and cutting, anal. of results using computer model 79−70180
MnZn ferrite, mag. anisotropy, effect on recording head characts. 80−39765
MnZn ferrite, mag. loss accommodation depend. on freq. and amplitude of mag. field *(Russian)* 80−34686
MnZn ferrite, mag. permeability spectra, 0.001-100 MHz range *(Russian)* 77−8355
MnZn ferrite, mag. permeability accommodation depend. on mag. field *(Russian)* 80−34685
MnZn ferrite, mag. relax., permeability and loss tangent determ. at 4.2 to 300K 77−32263
MnZn ferrite, mag.-mechanical-microstruct. interaction 77−1578
MnZn ferrite, mechanically induced anisotropy, effect on mag. permeability 78−47970
MnZn ferrite, MoO_3 addition effect on grain growth kinetics and densification 79−61550
MnZn ferrite, natural, intrasite cation ordering and clustering 77−12259
MnZn ferrite, nonstoichiometric, neutronographic determ. of cation distrib. *(Bulgarian)* 78−83656
MnZn ferrite, O_2 stoichiometry effect on fracture 80−25826
MnZn ferrite, optical refl. and electroreflection spectra obs. 78−27262
MnZn ferrite, polycrystalline, doped, DC resist. 78−47788
MnZn ferrite, polydispersive spin relax. near Curie temp., mag. susceptibility meas. 77−69513
MnZn ferrite, prep. and magnetic props. 78−19254
MnZn ferrite, props. rel. to raw materials *(German)* 77−21074
MnZn ferrite, quantitative anal., using X-ray fluorescence 78−40090
MnZn ferrite, spray dried agglomerates, compaction response, fracture, deform. 79−43172
MnZn ferrite, surface damaged layer, mag. domain obs. by taper section SEM 77−59423
MnZn ferrite, temperature dependence of Hall mobility 78−30944
MnZn ferrite, thermal cond. of single crystals 77−36079
MnZn ferrite, Ti substituted, vacancy contents and phase equilibria 80−29012
MnZn ferrite, wall topography change induced by external press. 80−34734
MnZn ferrite, weak mag. losses, microcalorimetric meas. 77−51926
MnZn ferrite disc, excitation of radial mode vibration due to AC 79−69708
MnZn ferrite fabricated by hot isostatic pressing, recording head appl. 80−35139

zinc compounds continued
MnZn ferrite fillers for elastic mag. materials, prep. and props. 79−52143
MnZn ferrite particles, mag. filtration from air streams 77−4945
MnZn ferrite powder prep., wet method 80−89180
MnZn ferrite powders, reactive, mag. materials obtained by compaction 80−89182
MnZn ferrite single cryst., Bridgman growth and appl. *(Chinese)* 79−33928
MnZn ferrite single cryst., high temp. phase transform. characts., growth techniques *(Chinese)* 79−33927
MnZn ferrite single crystals, growth by Bridgman technique, book contrib. 79−69977
MnZn ferrites, cationic distrib. and Curie temp. *(Russian)* 79−91232
MnZn ferrites, doped; determ. of grain boundary composition, using Auger spectroscopy *(German)* 79−23618
MnZn ferrites, elec. cond. mechanism in paramag. and ferrimag. phases 80−15524
MnZn ferrites, field depend. of mag. permeability accommodation *(Russian)* 79−69694
MnZn ferrites, form. of comp. heterogeneity during high-temp. sintering 80−60818
MnZn ferrites, hot pressed, mechanism of protective action of ZnO coating *(Russian)* 79−15822
MnZn ferrites, impurity induced exaggerated grain growth 78−92222
MnZn ferrites, initial mag. permeabilities under low temp. reactor irrad. 77−36093
MnZn ferrites, internal friction and ΔE effect depend. on demagnetisation method 80−80584
MnZn ferrites, low loss, highly stable, study *(Slovene)* 78−27055
MnZn ferrites, mag. domains on worked surfaces 79−99722
MnZn ferrites, mag. susceptibility freq. spectrum, effect of pressure 78−95420
MnZn ferrites, neutron diffr. exam. of influence of technology on mag. and cryst. parameters 79−42741
MnZn ferrites, post sinter-cooling rates effects 80−89369
MnZn ferrites, spinel use of phase equilibria in manufacture 79−11596
MnZn ferrites, thin struct. of $K\beta_5$ and $L\alpha_{1,2}$ emission bands of Fe *(Ukrainian)* 79−78790
MnZn ferrites, Ti substituted, mag. permeab. meas., grain boundary comp. AES obs. 78−95473
MnZn ferrous ferrite, initial mag. permeability second-order magnetocrystalline anisotropy influence 80−88820
MnZn ferrous ferrites, mag. permeability stress depend. 80−88822
MnZn polished ferrite worked layer magnetic characts. changes meas. *(Japanese)* 78−10742
MnZn, pressing powders, spray dried, pressing behaviour and props. 80−11617
MnZn soft ferrites, commercial grade, microstruct. rel. to mag. props. 80−34009
MnZn-ferroferrites, sintered, microstruct., TEM study *(Dutch)* 80−2036
$Mn_{1.18}Zn_{0.06}Co_{0.01}Fe_{1.75}O_4$, transport props. near Curie points 78−88100
$Mn_{1-c}Zn_cF_2$, antiferromag. reson., far IR spectrum, CPA calc. 77−20716
$Mn_{1-c}Zn_cF_2$, Heisenberg antiferromag., linear mag. birefringence meas. 77−16277
$Mn_{1-x}Zn_xF_2$, antiferromagnetic reson. freq. from far IR transmittance spectra 77−69695
$Mn_{1-x}Zn_xF_2$, linear mag. birefr., crit. behaviour 77−52061
$Mn_cZn_{1-c}F_2$, crit. neutron scatt. near percolation threshold 78−2693
$Mn_xZn_{1-x}F_2$, antiferromag. spin flop crit. field 79−24218
$Mn_xZn_{1-x}F_2$, CPA estimate for Neel temp. 78−76245
$Mn_xZn_{1-x}F_2$, Neel point and short range order, dilution effects, mag. birefr. obs. 80−71019
$Mn_xZn_{1-x}F_2$, three dimens. Heisenberg-Ising antiferromag., fluctuations near percolation threshold 79−78390
$Mn_{0.4}Zn_{0.42}Fe_{2.16}O_{4+x}$, permeability, rel. to intrinsic mag. props. 79−4702
$Mn_{0.510}Zn_{0.417}Fe_{2.073}O_{4+\delta}$ relationship between magnetic permeability and stoichiometry 79−42799
$Mn_{0.53}Zn_{0.35}Fe_{2.12}O_4$, and Ti substituted, acoustic losses 79−24207
$Mn_{0.7}Zn_{0.1}Fe_{2.2}O_4$, temp. depend. of microwave resistivity 79−69540
$(Mn_{0.7}Zn_{0.3})_xFe_yO_4$, electromag. props. rel. to Fe content 78−43613
$Mn_{1-x}Zn_xFe_2O_4$, noncollinear mag. structure, Mossbauer spectrum 77−69501
$Mn_{1-x}Zn_xFe_2O_4$, prepared by wet method, neutron diffr. and high field Mossbauer expts. 80−75719
$(ND_4)_2Zn(SO_4)_2.6D_2O:Cu^{2+}$, EPR exam. 77−24735
$(NH_4)_2Zn(SO_4)_2.6H_2O:VO^{2+}$, γ-irradiated NH_3^+ ESR, N hyperfine coupling tensor 79−69722
$(NH_4)_2ZnCl_4$, ferroelectricity and incommunsurate-commensurate phase transitions 80−60523
NH_4ZnF_3, rot. motion of NH_4^+ in lattice, neutron scatt. 79−37773
$(NH_4)_2Zn(SO_4)_2:Ni^{2+}$, optical absorpt. spectrum, room and liq. air temp. 79−15499
NaBaZn glass, Eu^{3+} centre symm. 80−100447
Na_2O-ZnO-P_2O_5, exam. of chemical durability, glass transformation temp. 79−20221
$Na_2TiZn_2[GeO_4]O_3$, cryst. struct. determ. 78−63734
$Na_{2-x}Zn_xFe_3(PO_4)_2(OH)_{2-x}O_x$, x=0.1, X-ray struct. anal. 77−84733
$Na_2Zn(SO_4)_2.4H_2O:VO^{2+}$, EPR spectra at X-band, spin-Hamiltonian parameters 79−56606
$Na_2Zn(SO_4)_2.4H_2O$:Ni, optical absorpt. and EPR. obs. 78−76501
$Na_2Zn_3(SiO_4)_2$, cryst. struct. anal. 79−19222
$Nd_2Zn_3(NO_3)_{12}.24H_2O$, EPR of Mn^{2+}, Gd^{3+} doped single crystal 79−24212
Ni-Co-Zn ferrite, exam. of electromag. characteristics 79−1409
Ni-Zn ferrite, elastic moduli temp. and composition depend. 78−26617
Ni-Zn ferrite, electrical cond., Seebeck coeff. and saturation magnetisation 77−20315
Ni-Zn ferrite, grain size depend. of grain boundary sliding *(Japanese)* 80−15120
Ni-Zn ferrite, high temp. behaviour of grain boundaries under bending stress *(Japanese)* 77−1875
Ni-Zn ferrite, neutron irrad., mag. spectra, domain wall behaviour 77−48006
Ni-Zn ferrites, comp., lattice imperfections, sintering 78−3080
Ni-Zn ferrites, mag. recording head props. rel. to manuf. from schoenite-type solid solns. 77−85496

zinc compounds continued
Ni-Zn ferrites, polycrystalline, grain boundary slip *(Japanese)* 77−63764
Ni-Zn ferrites 600 NN and M450 NNI, Curie point radiative shift due to neutron irrad. *(Russian)* 80−39775
Ni-Zn-Co ferrites, synthesis from solid solns. of schoenite-type salts 80−93511
$Ni_{0.5-x}Co_xZn_{0.5}Fe_2O_4$ ferrospinal solid solutions, cryst. lattice defects and props. 80−19796
$NiFe_2O_4+ZnO$, powders, cation mutual diffusion coeffs. calc. 77−15635
NiO-MgO-ZnO, solid soln. form and colour *(Japanese)* 77−63647
NiO-ZnO, solid solution, exam. of mechanism and kinetics of reaction with Fe_2O_3 ferrite formation 80−3309
NiZn complexes with hydrazine, X-ray diffr. expts. *(Rumanian)* 79−73149
NiZn ferrite, dielec. props., Jahn-Teller ion effects 80−97181
NiZn ferrite, effect of reactor radiation on mag. props. 77−32215
NiZn ferrite, exchange integrals, magnetisation data and mol. field theory 78−19241
NiZn ferrite, laser drilling and cutting, anal. of results using computer model 79−70180
NiZn ferrite, mag.-mechanical-microstruct. interactions 77−1578
NiZn ferrite, magnetic props., porosity and grain size effects 77−36095
NiZn ferrite, magnetic field effect on Rayleigh wave attenuation 78−6557
NiZn ferrite, prep. of single crystal by chem. transport with $TeCl_4$ 80−104051
NiZn ferrite, wall topography change induced by external press. 80−34734
NiZn ferrite, ZrO_2 additions influence on sintering and physicochem. props. 80−108369
NiZn ferrite quarter wave type absorber 79−38386
NiZn ferrites, comp., X-ray diffr. and saturation magnetisation obs. 78−18617
NiZn ferrites, internal friction and ΔE effect depend. on demagnetisation method 80−80584
NiZn ferrites, mag. head props., technical possibilities and limitations 80−88803
NiZn ferrites, mag. susceptibility freq. spectrum, effect of pressure 78−95420
NiZn ferrites, Mossbauer effect and IR spectra 78−64300
NiZn ferrites, nonstoichiometric, initial susceptibility and microstruct. 80−84591
NiZn ferrites, substituted ferrospinel, spin configuration determ. *(Russian)* 77−32162
NiZn ferrites, V_2O_5induced mag. aftereffects 80−60379
NiZn ferrites under high press., grain growth *(Chinese)* 78−52825
NiZnCo ferrite, excess Fe type, saturation magnetostriction meas., oxidation effects 79−82852
NiZnCo ferrite, model of photomagnetic effect 77−43853
NiZnCo ferrite, quantitative anal., using X-ray fluorescence 78−40090
NiZnCo ferrites, switching time and coeff., hydrostatic press. effect 80−88802
NiZnCo ferrites, temp. stability, effect of Fe content and processing conditions 79−28993
NiZnCo ferrites, voltage response under sinusoidal and pulse magnetisation effected by hydrostatic press. 80−88846
$Ni_{0.25}Zn_{0.75}Fe_2O_4$, Mossbauer study, spin fluctuations 80−60471
$Ni_{0.25}Zn_{0.75}Fe_2O_4$, Mossbauer study, noncollinear spin struct. 80−60472
$Ni_{0.25}Zn_{0.75}Fe_2O_4$, structural phase transition, X-ray and neutron diffr. study 80−79735
$Ni_{0.32}Zn_{0.68}Fe_2O_4$ ferrites microstructure and magnetic props., effects of silica content, sintering temp. and sintering time 79−87746
$Ni_{0.32}Zn_{0.68}Fe_2O_4$, mag. props. and neutron damage 77−47973
$Ni_{0.36}Zn_{0.64}Fe_2O_4$, normal grain growth 78−72796
$Ni_{0.38}Zn_{0.62}Fe_2O_4$, preparation, Mossbauer study 80−50231
$Ni_{0.4}Zn_{0.6}Fe_2O_4$, conditions for max. resistivity 77−21065
$(Ni_{0.47}Zn_{0.53})_{1-x}Fe_{2+x}O_4$, recording head medium 77−86187
$Ni_{0.5}Zn_{0.5}Fe_2O_4$ coarse grain polycryst. ferrite, diffusional creep *(Japanese)* 80−104238
$Ni_{0.5}Zn_{0.5}Fe_2O_4$, Hall mobility, elec. cond. and carrier conc., 30 to 180°C 77−51765
$Ni_{0.8}Zn_{0.2}Fe_2O_4$, twisted tubular polycryst. sample in axial mag. field, circular magnetisation 77−32230
$Ni_{0.85}Zn_{0.15}Fe_2O_4$, ferrite, mag. anisotropy compensation under neutron irrad. 80−75807
$Ni_{1-x}Zn_xFe_2O_4$, LPE growth, film quality, mag. meas. 78−11136
$Ni_{1-x}Zn_xFe_2O_4$, polycryst., domain wall energy rel. to anisotropy 80−71090
$Ni_{1-x}Zn_xFe_2O_4$ spinel, low-temp. transitions and spin configurations, Mossbauer study 78−27144
$(Ni_xZn_{1-x})_{0.5}Fe_2O_4$, spontaneous vibr. modes excited by reversible magnetostriction 79−56587
$Ni_xZn_{1-x}Fe_2O_4$, catalytic oxidation of CO, mag. props., kinetic parameters and composition depend. 80−16723
$Ni_xZn_{1-x}Fe_2O_4$, crystal growth from $BaO-B_2O_3-ZnO-NiO-Fe_2O_3$ melt, exam. of crystal props. 80−40249
$Ni_xZn_{1-x}Mn_2O_4$, mag. props. 78−43573
$Ni_{1-x}Zn_xO$, reaction with Fe_2O_3, microstruct. 79−87834
$Nz(ClO_4)_2.6H_2O:Mn^{2+}$, EPR obs. of high temp. phase transition 79−28598
Pb-Zn-SiO melt, mathematical model of thermal C reduction *(Russian)* 78−15663
$PbCl_2-ZnCl_2$, thermodynamic quantity meas. by quantitative thermal anal. of heating process 78−19730
PbF_2-ZnSe multilayer 16 μm dichroic mirror, 16 μm region, mech. stress compensation 80−74465
$PbO-B_2O_3-SiO_2-Al_2O_3-ZnO-CuO-Bi_2O_3$ solder glass, crystallisation prevention by Cu addition 80−11654
$PbO-B_2O_3-SiO_2-LiO_2-ZnO$, glass enamel, chemical durability and microstruct., ZnO addition effect 79−29255
$PbO-B_2O_3$-ZnO solder glass, with admixtures, crystallisation and thermal expansion 80−24364
$PbO-ZnO-B_2O_3$, glass ceramic cements, crystallisation kinetics and character 77−85982
$PbO-ZnO-B_2O_3:TiO_2$ glass, circuit corrosion protection on alumina substrates 79−29236
$PbS-CuS_{1.8}$-ZnS, phase equilib. *(Russian)* 77−28786
PbTe-ZrO_2 (SiO_2), epitaxial MIS struct., fabrication and elec. props. 80−2472

zinc compounds continued
$Pb_{1.8}Zn_{0.15}Na_{0.05}Nb_2O_{6.95}F_{0.05}$, electric cond. and dielect. props. of cathodic-sputtered films *(French)* 79−33371
Rb_2ZnBr_4, dielectric const. and ferroelectric hysteresis 78−84535
Rb_2ZnBr_4, incommensurate phases, neutron scattering study 79−15417
Rb_2ZnBr_4, modulation phase transitions, neutron scatt. 79−95712
Rb_2ZnCl_4, ^{35}Cl NQR, incommensurate struct. phase transition 79−47401
Rb_2ZnCl_4, NQR exam. of noncommensurate superstructures produced by phase transitions 79−69791
Rb_2ZnCl_4, phase transitions, soft mode, Raman scatt. meas. 79−4389
Rb_2ZnCl_4, phase transitions, thermal expansion coeff. 80−100638
Rb_2ZnCl_4 type ferroelectrics, phase transitions and physical props. *(Japanese)* 79−78636
Rb_2ZnCl_4, US vel. and attenuation at normal-incommensurate phase transition pt. 79−55833
n-Si-SiO_2-ZnO-Al, SAW convolver in monolithic MIS struct. 77−23791
SiO_2-Al_2O_3-CaO-BaO-SrO-ZnO-Na_2O-K_2O-B_2O_3, glaze effect of P_2O_5 additions 80−60824
SiO_2-CaO-ZnO-B_2O_3-Na_2O-S, SrO effect on crystallisation 80−54135
SiO_2-K_2O-Na_2O-BaO-SrO-ZnO system glass, props. optimisation 79−91611
SiO_2-Li_2O-K_2O-ZnO-P_2O_5, glass ceramic, phase changes and crystn. processes 80−7562
SiO_2-Li_2O-K_2O-ZnO glass ceramic, prep., phase transformations and physical props. 80−45299
SiO_2-ZnO-Na_2O-Li_2O, glass-ceramic coating, optimisation of props. by selective oxide action 80−55552
$Sm_2Zn_3(NO_3)_{12}.24H_2O:Gd^{3+}$, EPR X-band, fine struct., low field lines 79−15351
$Sn_{2.8}Li_{1.6}Sn_{1.6}O_8$, four layer hexagonal close packing, cryst. struct. determ. *(French)* 80−28999
SnO_2-Cu,S-ZnS:Mn,Cu-Al_2O_3-Al, light-emitting struct., cond. and electrolum., heat treatment 80−97345
SnO_2-ZnO, activated sintering mechanism 80−60810
SnO_2-ZnS:Mn thin film structure, surface morphology and electro-optical props. *(Russian)* 80−49554
SnZ films, from thermal decomp. or organometallics, growth kinetics and struct. 79−78895
$Sr_6Fe_{10}O_{22}$-Fe_2O_3-$ZnFe_2O_4$ system, phase relations at 1100°C 78−68676
Ta-Ta_2O_5-ZnS:TbF_3-Au thin films, MIS struct., DC electrolum. obs., Poole-Frenkel effect 78−88038
TiO-ZrO_2, pseudo binary system, effect of Ti addition on struct. and props. of zirconia 79−11583
V_2O_5-B_2O_3-ZnO semiconductivity glasses, optical and modulated absorpt. spectra in band gap region 77−48189
V_2O_5-BaO-K_2O-ZnO glasses, elect. props. and struct. 80−15547
V_2O_5-V_2O_4-$BaZnO_2$ glass, V ion states, mag. and elec. props. 80−88556
V_2O_5-ZnO-B_2O_3 glass, sputtered, optical absorpt., band gap and Urbach tail 77−8597
ZNSe, surface, energy-minimisation approach to atomic geometry 78−95213
(Zn, Cd, Hg)S:Cu,In, electroluminesc. temp. depend. 77−1732
(Zn,Cd,Hg)S:Cu,In, electroluminesc., brightness waves 77−59616
(Zn,Cd)Cr_2S_4 and (Zn,Cd)S solid soln. equilib. composition *(German)* 77−36486
(Zn,Cd)S:Cu,Al, luminesc. efficiency deterioration due to surface oxidation by $(NH_4)_2Cr_2O_7$ thermal decomp. 80−29810
(Zn,Fe)S (sphalerite), FeS content as geobarometer, experimental extension to 10 kbar 78−85703
(Zn, Hg)S:Cu, Cl, effect of superposition of two sinusoidal fields and freq. on electroluminesc. 78−39606
$(Zn,Mg)_2GeO_4:Mn^{2+}$ phosphor, for low press. fluoresc. lamps, luminesc. characts. 78−10960
$(Zn,Mg)_3(PO_4)_2:Mn^{2+}$, cathodoluminescence obs. 80−71492
Zn (II) complex, β-diketonate, 5-coord. adducts, Cu^{2+}, ground state ion wavefunction calcs. 78−895
Zn $(OH)_2$, physio-chemical behaviour in Garonne-Gironde river estuary system, radioactive tracing *(French)* 80−7994
Zn complex, aminoacetate, proton spin-lattice relaxation, temp. depend. 78−31119
Zn complex, aspartic and chelation, US obs. 77−44464
Zn complex, β-diketonate complexes, CNDO calcs. 79−59358
Zn complex, monopyrazine zinc sulphate trihydrate:Cu^{2+}, ESR meas. 78−84478
Zn complex, Zn-DTPA, comparison with Ca-DTPA for ^{241}Am removal from beagles 77−73599
Zn complex, Zn-DTPA treatment schedules for ^{239}Pu decorporation from simulated wounds 77−64137
Zn complex, Zn-DTPA vs. ca-DTPA as chelate in removal of ^{242}Cm from rat 77−64141
Zn complex, Zn-TMP-pyridine, burning out of valleys in absorpt. spectra 79−76440
Zn complex, Zn-tetraphenylporphine, absorption spectra fine struct., hole-burning method 77−88594
Zn complex, ZnS_2O_4.pyridine, cryst. struct., nature of S-S bonds 78−55847
Zn complex, Zn(1,2,4-triazole)$_2$$(NCS)_2$:Co, quasi two-dimens. canted S=1/2 antiferromag. 80−70976
Zn complex, Zn(l-spartein)Cl_2, IR circular dichroism spectra, vibr.-electronic interaction 80−55074
Zn complexes, bis(methylammonium) tetrachlorozincate and bis(methylammonium) tetrabromozincate, cryst. data 77−39567
Zn complexes, pheophytins a and b, dual phosphorescence molecular splitting 79−89706
Zn complexes, Zn(detc)$_2$ and Zn(desc)$_2$, spin-lattice relax. of Cu^{2+} 77−59453
Zn diethyldithiocarbamates, use in liquid-liquid extraction of corrosion and fission products 80−18459
Zn II complex, hexaimidazole-zinc(II) dichloride tetrahydrate:Cr(III), D-tensor orientation, charge-compensation vacancies 80−50172
Zn porphin, in triphenylene, single site fluoresc. and visible spectra, vibr. assignments 77−58031
Zn S-CdS:Ag(Cu), cathodoluminesc. investig., appl. to cathode ray tube screening 80−108282
Zn^{2+} ions in electrolyte solns., pulse polarography, polarographic current const. 77−25338
Zn/$ZnSO_4$/Zn system, laser interferometric study of corrosion of coated and uncoated metals, technique standardisation 79−35815
Zn-As-S chalcogenide glass system, prod. and acoustooptic props. *(Russian)* 78−63158

zinc compounds continued
Zn-As-Te system, phase diagram, As_2Te_3-ZnTe cross section investig. 77−36473
Zn-astrakhanite single crysts., EPR spectra of ion radicals SO_4^-, PO_4^{2-} and SeO_4^{3-} 79−51845
Zn-B system, interactions, product chem., phase, struct. anal., book contrib. 78−47305
Zn-Cl boracite, reinterpretation of EPR expt. on Cu^{2+} rel. to struct. 79−38372
Zn-Cl boracite, X-ray powder spectra of structure 79−37828
Zn-Cu-Se system, condensed phase equilibria, 800-1000°C, vapour pressures of Zn, Se_2 77−16553
Zn-Cu-Se system, region of existence of ZnSe phase 77−16554
Zn-Fe-O ferrite system, thermodynamic stability, dissociation and phase relations *(Japanese)* 80−55378
Zn-Fe-S-O, sulfide ore, use of phase equilibria in pyrometallurgy 79−11588
Zn-Ga-P-S quaternary system, p-type conductive alloys 78−39105
Zn-In-S thin layers, ternary phases, optical props. near long-wavelength intrinsic absorpt. edge 80−80887
Zn-In-S ultraviolet detector *(Russian)* 80−18014
Zn-Li silicates, cryst. struct. and phase transform. 79−65036
Zn-nucleotide, triphosphate complexes, ^{35}Cl NMR obs. 80−63661
Zn-S system, Zn-rich liquidus, 1000-1300°C 78−18747
Zn-Sb system, phase diagram, struct. and stability of phases *(German)* 78−60661
Zn-Sn-P, phase diag. rel. to $ZnSnP_2$ growth 77−44225
Zn-Te-O, partial pressure diagrams 77−36681
Zn-tetraphenylporphine/metal electrode, photocurrent generation mechanism 78−76868
Zn-Ti-Fe-O, spinel solid solns. 77−48409
Zn^{2+}-Cl^- system, ion exchange, complex form. studied using radiotracer, effect of macroelectrolyte cation 80−16659
Zn^{2+}-H_2O clusters, solvation, Monte Carlo simulation 80−44102
$ZnAl_2O_4$ spinel powder prod. 77−52271
$ZnAl_2O_4:Cr^{3+}$, luminesc. spectra, N-lines and Cr^{3+} pairs 78−2896
$ZnAl_2O_4:Cr^{3+}$, Raman effect to probe dynamical processes of Cr^{3+} photoexcited states 80−2740
$ZnAl_2S_4$, thermodynamic stability, enthalpy of form. 79−52737
$ZnAl_2S_4$:Fe(Mn), superhyperfine interaction of Fe and Mn ESR spectra 77−63271
$ZnAl_2S_4$-$ZnCr_2S_4$, nonstoichiometric spinel solid solns., synthesis and cryst. chemistry 77−35526
$ZnAl_2S_4$-$ZnIn_2S_4$, phase relationships, 800 to 1050°C 79−1852
$ZnAs_2$, homogeneity region and electrophys. props. 80−60833
$ZnAs_2$, λ-modulated photoemission spectra 79−87565
$ZnAs_2$, monoclinic, lattice vibr. symm., IR and Raman active frequencies *(Russian)* 77−69055
$ZnAs_2$ Schottky diodes, elec. and photoelec. props., excitons 80−65653
$ZnAs_2$, single crystals, growth from vapour phase 78−88416
Zn_3As:Cu(Te), single crysts., gas phase growth, elec. props. 79−15598
Zn_3As_2 and $ZnAs_2$, molten, thermal expansion and atomic bond strength parameters 80−65257
Zn_3As_2, determ. of ionicity by X-ray absorption method 78−31278
Zn_3As_2, optical band-gap, absorption meas. 80−25372
Zn_3As_2, oxidation, hardness and electromechanical polishing response 80−71776
Zn_3As_2, p-type semiconductor, absorption edge spectra, energy gap 79−56793
Zn_3As_2, phys. props. 78−26527
Zn_3As_2, solubility in Bi, LPE on $(Cd_xZn_{1-x})_3As_2$ 78−35324
Zn_3As_2, sp. ht., thermodyn. props. 78−22863
Zn_3As_2, synthesis and layer growth 78−15312
Zn_3As_2-2ZnTe, solid soln., sphalerite-antifluorite struct. stability, cation distrib. 77−43334
Zn_3As_2-ZnSe(ZnTe) solid solutions, single cryst., phase equilib. and props. 80−16283
Zn_2AsO_4OH, paradamite, X-ray cryst. struct. determ. H bond strengths 79−42016
$Zn_2(AsO_4)(OH)$, paradamite, crystal struct., anisotropic temp. factors 80−84145
$ZnB^4C^5_2$, chalcopyrite struct., surface energy and compressibility, rel. to glass form. 79−51417
$Zn(BF_4)_26H_2O$:Ni, phase transition study, EPR of diluted Ni^{2+}, 98-298K 80−75846
ZnB_2O_4-RF_2, R=Mg, Ca, Sr, Ba, glass form., struct. and props. 80−84077
$Zn_3(BO_3)_2:Sm^{3+}$, photoluminescence obs. *(Spanish)* 79−73986
$Zn_4B_6O_{13}:Tb^{3+}$, fluoresc. and thermophosphoresc. spectra *(Spanish)* 77−90188
$Zn_3B_7O_{13}Cl$, boracite, single cryst. prep. and phys. props. 80−100763
$Zn_2BaFe_{12}O_{22}$, mag. phase transitions, magnetostriction temp. depend. *(Russian)* 78−34983
$Zn_2Ba_2Fe_{12}O_{22}$, phase transition, mag. props. *(Russian)* 79−51837
$ZnBr_2$, ^{81}Br NQR line width obs. 80−50219
$ZnBr_2$, aq. solns., EXAFS meas. 80−60714
$ZnBr_2$, XPS, satellite of Br 4s line 78−56556
$Zn(BrO_3)_2.6H_2O:Cu^{2+}$, Jahn-Teller system, EPR and spin-lattice relax. 78−10760
$Zn(CH_3)_2$, valence mol. orbital energy, nonempirical pseudopot. 79−22592
$Zn(CN)_4^{2-}$, mol. vibrs. and reaction pathways, min. energy coords. and compliance consts. 77−57966
$ZnCO_3:Fe^{2+}$, electronic relaxation, Mossbauer effect 78−19385
$ZnC_2O_4.2H_2O$, crystn. kinetics by precipitation 80−50884
ZnCaSO, struct. and phase analysis *(Russian)* 77−58995
ZnCdS:(Cu+Ag) binder layer for electrophotography 80−4797
ZnCdS:Ag, phosphor screen, electron beam excited, light ang. distrib., modulation transfer function 80−45150
(ZnCd)S:Ag phosphor, absolute efficiency under fluoroscopy conditions 78−73203
ZnCdS:Ag screen, electron beam excited, light emission spectra 80−25466
ZnCdS:Cu, binders effect on electrophotographic characts. 79−80712
ZnCdS:Cu, high field photoconduction in binder layer 79−47121
ZnCdS-Ag binder layers, electrophotographic characts. eval. for use in charge transfer electrophotography 77−41714
n-ZnCdS-PTA, photosensitive powder mixed with electrochromic material, photoinduced coloration and electrochem. bleaching 77−81082
$Zn_{0.1}Cd_{0.9}S$, two-photon and two-step absorption of light 80−7389

zinc compounds continued
$Zn_{0.1}Cd_{0.9}S$:Cu, doping effect on two-photon absorpt. spectra, deep levels 77−69870
$Zn_{0.1}Cd_{0.9}S$-CdTe p-n junction, prep. by spray pyrolysis, photovoltaic props. 78−60196
$Zn_{0.35}Cd_{0.65}S$ binder layers, doped and undoped, xerographic charact. 79−56288
$Zn_{1-x}Cd_xS$ films, polycryst., reactively sputtered, MSM struct. obs. of dielec. props. and cond. mechanism *(French)* 78−14841
$Zn_{1-x}Cd_xS$, graded comp. semicond., tunable narrow-band filter, 4272 to 4584 Å 77−31128
$Zn_{1-x}Cd_xS$ mixed crystals, Raman spectra between frequencies LO(Γ) to TO(Γ) 78−2854
$Zn_{1-x}Cd_xS$, reactively sputtered polycryst. film, cond. mechanism and grain boundary barriers *(French)* 77−76972
$Zn_{30}Cd_{70}S$ ceramic, electroluminesc., stationary thermostimulated cond. 79−87120
$Zn_xCd_{1-x}S$, bound-exciton lines, compositional fluctuation-induced broadening 80−2846
$Zn_xCd_{1-x}S$ epitaxial layers, elec. resist. and luminescence obs. 78−19540
$Zn_xCd_{1-x}S$ film, optimal synthesis conditions for single cryst. growth 80−100776
$Zn_xCd_{1-x}S$ film, prep. by soln. spray method, and struct., optical and elec. props. 78−52666
$Zn_xCd_{1-x}S$ film, prep. and use as heterojunction optical energy converters 79−95488
$Zn_xCd_{1-x}S$, film, single-thermal-source form. 80−2492
$Zn_xCd_{1-x}S$, film for heterojunction solar cell 77−8208
$Zn_xCd_{1-x}S$ films, spray pyrolysis, elec. props. 80−75657
$Zn_xCd_{1-x}S$, forbidden band width, exciton refl. and luminesc. meas. 78−10947
$Zn_xCd_{1-x}S$, graded single crysts., laser or electron beam excited, luminesc. 77−85792
$Zn_xCd_{1-x}S$, granulated films, optical reson. 79−4863
$Zn_xCd_{1-x}S$ laser beam spontaneous action *(Russian)* 77−88820
$Zn_xCd_{1-x}S$, laser damage, self-focusing influence 78−50844
$Zn_xCd_{1-x}S$, lasing modes and spatial distrib. under one-photon excitation, cavity model 78−74913
$Zn_xCd_{1-x}S$ layers on ZnS substrate, VPE growth 77−77420
$Zn_xCd_{1-x}S$ monocrystal, optical and nonlinear optical charact. *(Russian)* 79−98442
$Zn_xCd_{1-x}S$ monocrystal petal lasers, single-photon excitation *(Russian)* 80−99736
$Zn_xCd_{1-x}S$, platelet single cryst. one-photon optical excitation, spatial distrib. and mode struct. of laser emission 79−31912
$Zn_xCd_{1-x}S$, reflectivity spectrum, excitons and energy band struct. 77−55804
$Zn_xCd_{1-x}S$, resonance Raman scatt. involving exciton complexes 80−16039
$Zn_xCd_{1-x}S$ solid soln. film by spray pyrolysis 77−81214
$Zn_xCd_{1-x}S$ solid soln. films, reactive cosputtering, struct., comp. and opt. absorpt. edge *(French)* 78−6237
$Zn_xCd_{1-x}S$ substrate, rough, lattice mismatch with Cu_2S and InP films 78−43263
$Zn_xCd_{1-x}S$, thin solid soln. films, vapour deposited, elec. and optical characts. 80−60110
$Zn_xCd_{1-x}S$:Cl, $Cu^+(Ag^+)$, high pressure luminesc. 78−19533
$Zn_xCd_{1-x}S$:Cu, photoluminesc., Birman effect *(Russian)* 79−28837
$Zn_xCd_{1-x}S$:Cu, photoluminescence 80−29783
$Zn_xCd_{1-x}S$:Cu, thermoemission of positive ions in simple gas atmos. *(Russian)* 77−28676
$Zn_xCd_{1-x}S$:Cu crystallophosphors, spectra of IR electrophotographic sensitivity *(Russian)* 80−50423
$Zn_xCd_{1-x}S$:In, low resist. film for solar cell window 78−71200
$Zn_xCd_{1-x}S/Cu_2S$ heterojunction solar cells, fabrication and performance 79−79397
$Zn_xCd_{1-x}S/Cu_2S$ heterojunction solar cells, junction anal. 79−92080
$Zn_xCd_{1-x}S/GaAs$ heterojunction solar cells, meas. of minority carrier diffusion length 80−26158
$Zn_xCd_{1-x}S$-Cu_2S heterojunction solar cells, props., comp. meas. of interfacial region 80−81472
$Zn_xCd_{1-x}S_ySe_{1-y}$, energy bandgap and lattice constant contours 80−103622
$Zn_xCd_{1-x}S$(Te), solid soln., broadening of exciton states, depend. on conc. 79−73449
$Zn_xCd_{1-x}S_yTe_{1-y}$, energy bandgap and lattice constant contours 80−103622
p-$Zn_{0.1}Cd_{0.9}Sb$, thermoelec. anisotropic semicond., carrier kinetics at low temps. 80−92893
$Zn_{0.1}Cd_{0.9}Sb$, thermoelectrically isotropic semicond., carrier kinetics in intrinsic cond. range 80−92894
$Zn_{1-x}Cd_xSe$, mixed crystals, antireson. in phonon spectrum, Raman spectroscopy 80−88992
$Zn_xCd_{1-x}Se$, exciton reflection spectra anomalies *(Russian)* 80−97304
$Zn_xCd_{1-x}Se$, vacuum condensates, forbidden band width determ. from transmission spectra 77−8670
$Zn_xCd_{1-x}Se_yTe_{1-y}$, energy bandgap and lattice constant contours 80−103622
$Zn_{1-x}Cd_xTe$ p-n junctions, LPE growth process, elec. props. 77−7981
$Zn_xCd_{1-x}Te$, absorpt. edge luminesc. on high-intensity excitation 78−6745
$Zn_xCd_{1-x}Te$ films, absorpt. spectra in 3.0 to 5.8 eV range 79−52034
p-$Zn_xCd_{1-x}Te$, negative photocond. excited by fundamental absorpt. region light 77−15905
$Zn_xCd_{1-x}Te$, reflection spectra, energy band struct. comp. depend. *(Russian)* 78−56500
$Zn_xCd_{1-x}Te$, relaxation processes, emission spectra *(Russian)* 78−72598
$Zn_xCd_{1-x}Te$, reson. Brillouin scatt. meas. using injected acoustic domains 78−27243
$Zn_xCd_{1-x}Te$, reson. Brillouin scatt., acoustic domain injection 79−38557
$Zn_xCd_{1-x}Te$, reson. Raman scatt. of light by longitudinal optical phonons 77−28577
$Zn_xCd_{1-x}Te$, resonant Brillouin scattering *(Japanese)* 79−15474
$Zn_xCd_{1-x}Te$-P, vibr. modes of defects, IR absorpt. expts. 77−62601
$ZnCl_2$, ^{35}Cl NQR freqs. meas. 80−58285
$ZnCl_2$, aq. soln., Raman spectrum, local order 78−84563
$ZnCl_2$, aq. soln., structural transition, neutron diffr. study 80−64872
$ZnCl_2$, aq. solns., complex IR refr. indices, IR spectra, mechanisms, spectrometer system 78−43831
$ZnCl_2$, deformation densities, relativistic effect 80−42928
zinc compounds continued
$ZnCl_2$ glass, glass transition temp. and thermal expansion 80−64902
$ZnCl_2$ glass, potential ultralow loss optical fibre material 78−74955
$ZnCl_2$, glassy and liq, EXAFS obs. of struct., comparison with vitreous GeO_2 80−70133
$ZnCl_2$ hydrocracking of solvent refined coal for petroleum prod. 80−30333
$ZnCl_2$ in H_2O, complexity investigation using US method 80−33326
$ZnCl_2$ in methanol-water mixtures, thermodynamic props. from EMF meas. 79−52735
$ZnCl_2$, liq., glass, cryst., sp. ht. meas., glass transition temp. rel. to press. 77−66029
$ZnCl_2$, liq. solutions in NaCl and KCl, solubility of Co_2 79−90785
$ZnCl_2$, polymorphism, Raman spectra 78−80332
$ZnCl_2$, pseudopot. calcs. of mol. electronic props. 77−30779
$ZnCl_2$ solution, solvent stress cracking of nylons 78−27594
$ZnCl_2$ steam hydrolysis, for thermochem. H prod. using ZnSe cycle 80−35782
$ZnCl_2$ transport in cation-exchange membranes 78−96033
$ZnCl_2$, UPS, cryst. field splitting 79−83103
$ZnCl_2$ with $FeCl_3$ impurity, removal by zone melting 79−52111
$ZnCl_2$:NO_2^-, aqueous solns., luminesc., absorpt. and Raman spectra *(Russian)* 77−36291
$ZnCl_2$-$CdCl_2$ melt, Raman spectra, struct. anal. 79−38549
$ZnCl_2$-KCl-NaCl, molten system, containing Ni^{2+} ions, appl. to electrorefining, polarographic study 80−66810
$ZnCl_2$-LiCl(NaCl)(KCl)(CsCl), molten, density meas. *(Japanese)* 79−19383
$ZnCl_2$-LiCl(NaCl)(KCl)(CsCl), molten, US velocity, thermodynamic quantities and struct. *(Japanese)* 80−88270
$ZnCl_2$-LiCl(NaCl)(KCl)(CsCl), molten, US absorption coeffs. and bulk viscosity coeffs. *(Japanese)* 80−88271
$ZnCl_2$-Li(Na)(K)(Cs)Cl, molten, viscosity, 260 to 560°C *(Japanese)* 77−51537
$ZnCl_2$-MCl, (M=Li,Na,K,Cs), melt, viscosity meas. by oscillating cylinder method *(Japanese)* 80−10696
$ZnCl_2$-MCl_2 (M=Cd,Pb,Sn,Ba) system, molten, viscosity coeff. meas. *(Japanese)* 79−77662
$ZnCl_2$-oil system, simulation of steel-slag, macrophotographic method of diagnosing disperse system 80−25952
$ZnCl_2$-$PbCl_2$, molten, US velocity and absorpt., thermodynamic quantities and bulk viscosity *(Japanese)* 80−84249
$ZnCl_2$-Zn chemically deposited photosensitive cells, photovoltaic charact. 79−39303
$ZnCl_2$-$ZnBr_2$ melt, Raman spectra, struct. anal. 79−38549
$ZnCl_2(Br_2)(I_2)$ glassy aqueous solutions, Raman spectral study 80−84738
$ZnCl_2(NCR)_2$, R=CH_3 or C_2H_5, thermal decomp., thermogravimetric and differential thermal anal. *(Chinese)* 80−81291
$Zn(ClO_4)_2$, thermodynamic irreversible parameters, Onsager reciprocal relationship verification 79−47960
$Zn(ClO_4)_2$, $ZnCl_2$ self complexing comparison 79−47961
$Zn(ClO_2)_2.2H_2O$, X-ray cryst. struct. determ. 80−19759
$ZnCl_2$; thermodynamic irreversible parameters, Onsager reciprocal relationship verification 79−47961
$Zn_xCn_{0.1}Fe_{2.9}O_4$, Cu, Zn substituted magnetite, domain wall resonance, mag. props. 80−15756
$Zn_{1-x}Co_xF_2$, Raman scatt. by mag. excitations 77−55775
$Zn_{0.2}Co(Ni)_{0.8}O$. $1.1Al_2O_3$ powders, ZnO vaporisation from 80−16675
$(Zn_{0.2}Co_{0.8}(Ni_{0.8}))O.Al_2O_3$, ZnO evaporation in vac. 80−59640
$ZnCo_2O_4$, Mossbauer spectra and cryst. struct. determ. 79−56637
$ZnCrFeO_4$, ferrite spinel, unsupported and SiO_2 supported, structural and catalytic studies 80−44191
$ZnCr_xFe_{2-x}O_4$, Mossbauer spectra, quadrupole splitting, Debye temp. 80−93218
$ZnCrO_4$, diffuse reflectance spectra 78−88326
$Zn(CrO_4)_2$ solar absorber surface spectral selectivity rel. to temp. and UV ageing 79−62027
$ZnCr_2O_4$, antiferromag. spinel, absorpt. and luminesc. spectra 80−66225
$ZnCr_2O_4$, mag. phase with short range order *(French)* 77−63203
$ZnCr_2O_7$ coating on Zn electroplate on steel, corrosion rel. to chromate content 79−20286
$ZnCr_2O_4(S_4)(Se_4)$, magnetic exchange interactions 77−24690
$ZnCr_2S_4$, thermodynamic stability, enthalpy of form. 79−52737
$ZnCr_2Se_4$, EPR linewidth, 100-300K, spin-lattice relax. 77−51942
$ZnCr_2Se_4$, electroconductivity, thermoelectromotive force, Hall effect *(Russian)* 80−70694
$ZnCr_2Se_4$, magnetoelastic coupling, mag. suscept. meas. 78−76288
$ZnCr_2Se_4$, screw spin struct., neutron diffr. exam. 78−27019
$ZnCr_2Se_4$, screw spin structure, method of controlling the sense, polarised neutron diffr. study 80−70944
$ZnCr_2Se_4$, screw spin structure, magnetoelectric effect 80−75827
$ZnCr_2Se_4$:In, magnetoresist. and elec. resist. above and below Neel temp. *(Russian)* 80−88576
$ZnCr_2Se_4$:Mn, paramagnetic, giant cubic anisotropy 80−7073
$ZnCs_2(SO_4)_2.6H_2O$:VO^{2+}, single cryst., X-band EPR meas. 77−90024
$ZnCs_2(SO_4)_2.6H_2O$:Mn^{2+} EPR, 298K, spin-Hamiltonian parameters, cryst. fields 78−27086
$ZnCs_2(SO_4)_2.6H_2O$:VO^{2+}, optical absorpt. spectra obs. 80−40146
$Zn_xCu_{0.1}Fe_{2.9-x}O_4$, ferromag. relax. 80−60422
$Zn_xCu_{0.1}Fe_{2.9-x}O_4$, ferromag. reson., g-factors, Jahn-Teller ion effects 80−66043
$Zn_xCu_{1-x}Fe_2O_4$, mag. props., Mossbauer spectra 79−87344
$Zn_{1-x}Cu_xGeF_6.6H_2O$, depression of dynamic Jahn-Teller effect 77−16164
ZnF, mol., ESR spectra in inert gas matrix 79−76455
ZnF_2, ^{67}Zn Mossbauer spectroscopy with 93 keV reson. 80−66095
ZnF_2, 93.3 keV Mossbauer transition in ^{67}Zn, isomer shifts 80−39978
ZnF_2, elastic constant determ. by US pulse echo overlap 79−14874
ZnF_2, elastic moduli, press. depend., 0-10 kbar 78−10117
ZnF_2, elastic props., 4.2-300K, incipient ferroelec. transition 78−30691
ZnF_2, electronic structure of outermost levels, UPS study 80−7468
ZnF_2, high temp. polymorphism and thermal props. 80−75199
ZnF_2, long-wavelength lattice vibr. modes, symmetry coordinates 78−43081
ZnF_2, melting curve, press. up to 40 kbar, rel. to high press. melting systematics 77−51475
ZnF_2 powder, preferred orientation, X-ray intensity corrections 80−1880
ZnF_2, UPS, cryst. field splitting 79−83103
ZnF_2, valence-electron density of states, XPS meas. 77−69963
ZnF_2, X-ray absorpt. spectrum polarisation depend. 80−104012

zinc compounds continued
ZnF_2, X-ray diffr. investig. of high-press. polymorphism 77−43324
$ZnF_2:Co^{2+}$, Raman tensor calcs. of isolated impurity in diamagnetic matrix 80−76025
ZnF_2:Mn, thin films, electroluminescence, brightness voltage charact. hysteresis 80−20709
$ZnF_2:Mn^{2+}$, zero-field splitting, appl. of complete d-electron calc. 77−15799
ZnF_2-He positive column discharge cataphoretic distrib. of Zn and F atoms 77−68886
ZnF_2-NaF-CrF_3, solid-liquid equilib. diagram *(French)* 77−1216
ZnFCl, existence and vibr. characterisation, IR and Raman matrix isolation obs. 78−78706
$ZnF_2(FCl)(FBr)$, matrix isolated IR and Raman spectra, assignments, force consts., isotope effects and thermodynamic props. 80−63631
$Zn_xFe_yMn_zFe_2O_4$, ferrite, production from Fe_2O_3, effect of impurities on props. *(German)* 79−4925
$ZnFeO_4$, ferrite spinel, structural and catalytic studies 80−44191
$ZnFe_2O_4$, cation distrib., preference energy determ. by neutron irrad. method 77−15384
$ZnFe_2O_4$, heat capacity investigation of dopant effects on mag. disordering temp. 80−25143
$ZnFe_2O_4$, LPE growth, film quality, mag. meas. 78−11136
$ZnFe_2O_4$, neutron damage effects, superparamag. state replacement cascades 77−16051
$ZnFe_2O_4$, single cryst. prep. by chemical transport 77−16482
$ZnFe_2O_4$-Fe_3O_4 solid solns., form. of α-Fe_2O_3 during oxidation 80−25889
$ZnFe_2O_4$+NiO_2(MgO) powders, cation mutual diffusion coeffs. calc. 77−15635
$Zn_{0.005}Fe_{2.995}O_4$, phase transitions, neutron elastic scatt. and resist. meas. 77−28000
$Zn_xFe_{0.85-x}O$, prep. and struct., mag. and semicond. props. *(French)* 78−51506
$Zn_xFe_{3-x}O_4$, collective electron states, ^{57}Fe Mossbauer meas. 77−69748
$Zn_xFe_{3-x}O_4$, cond. mechanism, collective electron description 77−4588
$Zn_xFe_{3-x}O_4$ ferrite, mag. struct., Mossbauer spectra and magnetisation study, 4.2K 80−103818
$Zn_xFe_{3-x}O_4$, ferromag. reson., g-factors, Jahn-Teller ion effects 80−66043
$Zn_xFe_{3-x}O_4$, mag. ordering and domain wall relax. 77−8336
$Zn_xFe_{3-x}O_4$, Mossbauer exam. of relax. phenomena 77−8479
$Zn_xFe_yO_4$, heat capacity investigation of dopant effects on mag. disordering temp. 80−25143
$Zn_2Fe(PO_4)_2.4H_2O$, phosphophyllite, chem., optical and X-ray data 77−15366
(ZnFe)S, marmatite, optical properties 78−39555
$ZnGa_2$, excimer visible emission spectra in RF discharge, vibr. struct. 79−18201
$ZnGa_2O_4:Cr^{3+}$, weak exchange interaction determ., ESR study 80−93107
$ZnGa_2O_4:Fe^{3+}(Mn^{2+})$, EPR, spin Hamiltonian parameters 80−25195
$ZnGa_2S_4$, band struct., pseudopot. method 80−92816
$ZnGa_2S_4(Se_4)(Te_4)$, sp. ht., low temp. 77−35705
$ZnGa_2Te_4$, cryst. struct., and melting point 78−35360
$ZnGa_2X_4$, X=S,Se, Fourier IR and Raman spectra, cryst. struct. and symm. *(German)* 79−24313
$ZnGeAs_2$, elec. cond. in solid and liq. state 77−11912
$ZnGeAs_2$, photoelectron spin polarisations, electron level struct. 79−87557
$ZnGeAs_2$, reflectvvity and XPS meas. 78−35165
$ZnGeAs_2$-$GdGeAs_2$, material distrib., possibility of heterostructure *(Russian)* 78−30979
$ZnGeF_6.6H_2O:Mn$ (II), phase transition, ESR meas. 77−62636
$Zn_{1-x}Ge_xFe_{2-x}{}^{3+}Fe_{2x}{}^{2+}O_4$, double exchange magnetism, Mossbauer study 80−66087
$Zn_{1-x}Ge_xFe_2O_4$, spinel series, obs. by Mossbauer spectroscopy of electron hoppings 78−43754
$ZnGeO_3$, HP phase transform. 80−19941
Zn_2GeO_4 single crystals, vapour growth 79−87571
$ZnGeP_2$ bandgap absorption edge, spectra, electron transitions *(Russian)* 80−97305
$ZnGeP_2$, birefringence, effects on hydrostatic pressure and temp. 80−45033
$ZnGeP_2$, Br_2-methanol etching soln. for crystallographic axes determ. 78−35541
$ZnGeP_2$, cond. compensation by electron bombardment 79−15151
$ZnGeP_2$, cryst., electronic struct., X-ray K-absorpt. and emission 78−15248
$ZnGeP_2$, crystal, polarisation of recombination radiation 78−19562
$ZnGeP_2$ dissoc. press., vapour comp. and press., thermodynamic charact. 77−24934
$ZnGeP_2$, electron irrad., elec. and optical props. 79−33743
$ZnGeP_2$, IR radiation parametric conversion to visible range 79−94297
$ZnGeP_2$ layers, growth on Ge substrates, using chemical vapour deposition 79−52122
$ZnGeP_2$, one- and two-phonon Raman scatt. 79−78681
$ZnGeP_2$, P vacancies, lattice parameters, optical props. depend. on thermal treatment *(Russian)* 78−71729
$ZnGeP_2$ p-n homodiode, polarisation photosensitivity and photopleochroism spectra 80−107866
p-$ZnGeP_2$, photoluminescence of crystals with varying comp. and dopants 77−32431
$ZnGeP_2$, pseudodirect bandgap semiconductor, natural birefringence 79−65834
$ZnGeP_2$, reflectvvity and XPS meas. 78−35165
$ZnGeP_2$, single cryst., polarised light photocond., optical transparency anisotropy *(Russian)* 78−2518
$ZnGeP_2$, synthesis, charact., applic. to laser windows *(French)* 78−80467
$ZnGeP_2$, temp. depend. Sellmeier coeffs. and coherence lengths for chalcopyrite crystals 79−76752
$ZnGeP_2$, temp. depend. phase-matched nonlinear optical devices 80−99794
$ZnGeP_2$ thermo-optic coefficient, dispersion 80−71396
ZnH, lifetime, Λ-doubling and hyperfine struct. of $A^2\Pi$ excited states 77−58083
ZnH^+, ZnH_2, relativistic (non-relativistic) HF one-centre expansion calcs. 80−52908
$Zn(H_2PO_2)_2$, X-ray cryst. struct. determ. and refinement, heavy-atom method 79−19194
zinc compounds continued
$Zn(H_2PO_2)_2.H_2O$, X-ray cryst. struct. determ. and refinement, heavy-atom method 79−19194
$ZnHPO_4.H_2O=(H_3O)ZnPO_4$, cryst. struct. determ. 78−63739
$Zn(HSeO_3)_2.2H_2O$, neutron diffr. cryst. struct. determ. 80−33983
ZnHg excimer, optical pumping of Zn reson. line, optical and kinetic props. 78−58991
$(Zn_{0.877}Hg_{0.116}Fe_{0.002})_{0.995}S$, unit cell dimensions *(Chinese)* 79−90616
ZnHg(Mg), Ar matrix absorpt. spectra, vibronic spacing and bonding 79−3453
$Zn_{0.1}Hg_{0.9}Se$ type alloy, dispersion law of cond. band *(Russian)* 77−1366
$Zn_xHg_{1-x}Se$, band struct. and scattering mechanism, determ. from transport coeffs. 77−59254
$Zn_xHg_{1-x}Se$, band struct. from Shubnikov de Haas effect and hydrostatic press. meas. 80−49599
$Zn_xHg_{1-x}Se$, current carrier scattering mechanism 80−65546
$Zn_xHg_{1-x}Se$, galvanomagnetic effects, Shubnikov-de Haas oscill. determ. of band struct. 80−6884
$Zn_xHg_{1-x}Se$ semimetal-semicond. transition, thermo-EMF in mag. field and Hall expts. *(Russian)* 77−15881
$Zn_xHg_{1-x}Se(Te,S)$ film preparation and props. *(Russian)* 78−11122
$Zn_xHg_{1-x}Te$, impurity influence on thermomagnetic effects and elec. cond. 79−60856
$Zn_xHg_{1-x}Te$, vacancy electron states, acceptor behaviour, electron mobility 80−70193
$Zn_xHg_{1-x}Te$, vacancy mech. of resorption of Hg droplets 80−39070
ZnI_2, ^{127}I NQR freqs. meas. 80−58285
ZnI_2 aqueous solution, US study of apparent molar compressibility 78−10125
ZnI_2, cryst. struct. determ., X-ray anal. *(French)* 79−7585
ZnI_2, vapour, excited by photodissociation, fluoresc. yields 78−55138
Zn(II) complexes with gluconate ions, reduction, polarographic behaviour 78−92568
$Zn(IO_3)_2$, complex salts, phase transitions, cryst. struct. *(Chinese)* 80−70171
$ZnIn_2S_4$ (I) film, one-packed polytype, resist., photocond. and luminesc. 79−1608
$ZnIn_2S_4$, and $ZnIn_2S_4$-In_2S_3 alloys, SCL currents, trap distrib. 78−52000
$ZnIn_2S_4$, cond. and valence band states, photoemission study 80−35054
$ZnIn_2S_4$ crystals, switching effect, electric field distribution 80−107872
$ZnIn_2S_4$ diode struct., photoelec. props. *(Russian)* 77−43720
$ZnIn_2S_4$, electronic props. of polytypic forms, pseudopot. calc. 80−38997
$ZnIn_2S_4$ film, photoluminesc. and photocond. 78−52677
$ZnIn_2S_4$, fund. optical consts., Kramers-Kronig analysis, reflectivity spectra 78−39573
$ZnIn_2S_4$, fund. reflectivity, 2 to 6 eV, band struct. implications 78−39574
$ZnIn_2S_4$, III(a) polytype, absorpt. spectrum tail changes due to microstresses 80−2788
$ZnIn_2S_4$, IR refl. spectra and cryst. struct. 79−56777
$ZnIn_2S_4$, lattice dynamics, IR and Raman spectra 77−81106
$ZnIn_2S_4$ layered compound, phonon freqs., IR refl. and transmission spectra 77−77210
$ZnIn_2S_4$, layered semicond., wavelength modulated reflectivity spectra 79−8155
$ZnIn_2S_4$ layered semiconductor, fundamental optical constants, comparison with band structure calcs. and PES 79−56757
$ZnIn_2S_4$, nonlinear susceptibility, SHG 78−30019
$ZnIn_2S_4$, photoluminesc., reson. Raman scatt. 78−48179
$ZnIn_2S_4$, Raman and IR spectra 78−48181
$ZnIn_2S_4$, Raman scatt., hydrostatic press. effect 80−84745
$ZnIn_2S_4$, recomb. process of photoexcited carriers 77−44042
$ZnIn_2S_4$, S-type negative resist. and switching effects 80−65581
$ZnIn_2S_4$ single cryst., intense radiation effect on optical transmission, absorpt. saturation 80−53385
$ZnIn_2S_4$ switching investigation, negative resistance state instability, resistivity transitions 80−6920
$ZnIn_2S_4$, valence band photoemission spectroscopy 78−56569
$ZnIn_2S_4$, vibr. spectrum, Raman study 80−97278
$ZnIn_2S_4:Er^{3+}$, cryst. field parameters, thermal and mag. props. calc. 77−20540
$ZnIn_2S_4$-Ni diode, electric and photoelectric charact. 77−12005
$Zn_xIn_2S_{3+x}$, residual cond. 78−56185
$ZnIn_2Se_4$ defect tetrahedral semiconductor, band structure, charge density 77−11850
$ZnIn_2Se_4$, luminescence spectra, recomb. processes and energy level scheme 77−1726
$ZnIn_2Te_4$ defect tetrahedral semiconductor, band structure, charge density 77−11850
$ZnIn_2X_4$, X=S,Se, Fourier IR and Raman spectra, cryst. struct. and symm. *(German)* 79−24313
$ZnK_4(P_3O_9)_2.4H_2O$, cryst. struct. determ. *(French)* 78−26503
$ZnK_2(SO_4)_2.6H_2O:Mn^{2+}$, EPR spectra, spin-Hamiltonian anal. 77−77088
$Zn_cM_{1-c}Fe_2O_4$, M=Ni^{2+}, Co^{2+}, Fe^{2+}, $Zn_cMFe_{2-c}O_{4-c}F_c$, M=Ni^{2+}, Co^{2+}, calc. of saturation magnetisation by cluster components 77−43817
$Zn_2Mg(PO_4)_2$, cation distrib. from X-ray profile-fitting refinement 77−76376
$Zn_{1-x}Mg_xTe$ alloys, high purity, metallurgical and analytical methods of prep. 80−40247
$Zn_{1-x}Mg_xTe$ alloys, luminesc. and elec. props. 80−2813
$Zn_{1-x}Mg_xTe$, growth from melt, luminesc. *(French)* 77−21019
$Zn_{1-x}Mg_xTe$, long wavelength optical phonons, IR ref. and Raman obs. *(French)* 78−60433
$Zn_{1-x}Mg_xTe$, variation of fundamental edge, wavelength modulated reflectivity meas. *(French)* 77−81124
ZnMn ferrites, prepared by wet chemical and ceramic methods, comparison of struct. and mag. props. *(German)* 79−24470
$ZnMn_{1-x}Cr_xFeO_4$, Mossbauer effect, quadrupole splitting 80−29664
$Zn_{0.8}Mn_{0.2}Fe_2O_4$, spin interaction, neutron diffr. and Mossbauer effect meas. 77−4501
$Zn_xMn_{1-x}Fe_2O_4$, Mossbauer spectra exam. 77−40155
$Zn_xMn_{1-x}Fe_2O_4$, substitution effect on mag. struct. and exchange interaction *(Russian)* 78−47949
$Zn_{0.3}{}^{2+}Mn_{0.7}{}^{2+}Mn_y{}^{3+}Fe_{2-y}{}^{3+}O_4$, Mossbauer hyperfine field meas. 77−81033
$(ZnMn_2O_4)_{1-x}(MgAl_2O_4)_x$, $0<x<1$, mixed oxide spinels, chemical shifts of Mn K-absorpt. edge 80−29828

zinc compounds continued
$Zn_xMn_{2-x}Sb$, anti-PbFCl type, cryst. struct. and ferromag. ordering 77−84723
$Zn^{2+}Mo^{4+}O_3$, defect spinel struct., elec. and mag. props. 80−70176
$ZnMo_2Re_2S_8$, cubic structure, mixed tetrahedral cluster *(French)* 77−15372
$Zn(Mo_2Re_2)S_8$, synthesis and electrical props. of mixed tetrahedral cluster phases 80−2971
$ZnMo_6S_8$, mixed Chevrel phases, crystallography 80−39038
$ZnMo_5S_6(Se_6)$, Chevrel-phase, low temp. struct. instability rel. to super-cond. 77−47919
$Zn_xMo_3S_4(Se_4)(Te_4)$, chevrel phase, anomalous elec. resist. 79−56221
β-$Zn(NCS)_2$, cryst. struct. 77−65972
$Zn(NH_3)_4(ClO_4)_2$:Mn, EPR study of Mn^{2+} detection of structural transition 79−87308
$ZnNH_4H_3(PO_4)_2.H_2O$, X-ray cryst. struct. determ. *(French)* 80−88104
$Zn(NH_4)_2(SeO_4)_2.6H_2O$:$Mn^{2+}$, EPR spectra 80−100608
$Zn(NO_3)_2$, aq. electrolyte, apparent molar heat capacity and volume, of 298.15K 79−65208
$Zn(NO_3)_2$-$Cu(NO_3)_2$ glass forming melts, density and viscosity 79−77794
$Zn(NO_3)_2.4H_2O$, high press. phase behaviour, dehydration and congruent melting 79−78947
$Zn(NO_3)_2.6H_2O$, high press. phase behaviour, dehydration and congruent melting 79−78947
$Zn_2NaP_3O_{10}.9H_2O$, cryst. struct. determ. *(French)* 77−47406
$ZnNa_6(SO_4)_4$, vanthoffite cryst. sruct., lattice parameters and thermal behaviour 77−19929
$ZnNa_2(SO_4)_2.4H_2O$:Mn^{2+}, EPR, 300K 79−51848
$ZnNb_2O_6$, bonding characterisation 78−38680
$ZnNb_2O_6$, columbite struct., normal coord. anal. 78−964
$ZnNb_2O_6$, columbite struct., IR and Raman spectra *(French)* 78−19485
$ZnNb_2O_6$, force fields rel. to cryst. struct. *(French)* 80−107104
$Zn_{1-x}Ni_xCr_2S_4$, spin struct., mag. props. meas. 77−85428
$Zn_{0.7}Ni_{0.3}Fe_2O_4$ film, epitaxial deposition, comp. and mag. prop. obs. using Mossbauer effect 79−38748
$Zn_{0.75}Ni_{0.25}Fe_2O_4$, mixed ferrite-spinel, helicoidal struct. 79−47242
$Zn_{1-x}Ni_xFe_2O_4$, heat treatment and sintering effect on porosity 80−25610
$Zn_xNi_{1-x}Fe_2O_4$, magnetic props. rel. to localised canting model 77−32161
$Zn_xNi_{1-x}Fe_2O_4$, Mossbauer spectra, mag. hyperfine struct. 80−15877
ZnO, ^{67}Zn Mossbauer spectroscopy with 93 keV reson. 80−66095
ZnO $10\bar{1}0$ surface, reaction of O_2, AES, LEED, EPR, desorpt., surface cond. and work function expts. 78−95950
ZnO, 93.3 keV Mossbauer transition in ^{67}Zn, isomer shifts 80−39978
ZnO (0001), (000$\bar{1}$) and ($10\bar{1}0$), UPS rel. to elec. struct. 78−15288
ZnO (000$\bar{1}$), adsorption of alkali metal, anomalous behaviour of Na 78−79883
ZnO (000$\bar{1}$) and (0001), Ar field ion microscopy 79−47601
ZnO (0001) and (000$\bar{1}$) polar surfaces, 6-fold LEED patterns 78−71920
ZnO (000$\bar{1}$) and ($10\bar{1}0$) surfaces, clean and contaminated, reactivity to Cl_2 79−61904
ZnO, (0001) surface, clean and O adsorbed, AES and refl. electron energy loss spectra 79−46927
ZnO (0001) surface, hardness, electrolyte pH and bias voltage effect 78−47654
ZnO (000$\bar{1}$) surface, surface and bulk excitations, reflection electron energy loss spectroscopy 77−20389
ZnO ($10\bar{1}0$), LEED anal. of atomic geometry 77−69149
ZnO ($10\bar{1}0$), surface struct. from LEED anal., matrix inversion method 79−46897
ZnO ($10\bar{1}0$) and ($11\bar{2}0$) surface, atomic geometry from elastic LEED intensities 77−20170
ZnO ($10\bar{1}0$) prismatic surfaces, nonstationary sublimation *(German)* 78−60035
ZnO ($10\bar{1}0$) surface bias voltage effect on hardness, charge exchange near dislocations 78−52078
ZnO, absolute work function determ. 77−28697
ZnO absorbers, ^{67}Zn isomer shift 80−39920
ZnO, accumulation layer, ESR and NMR studies of adsorbed H_2 *(Japanese)* 80−50186
ZnO accumulation layers, Hall mobility and work function, correl. 78−60185
ZnO accumulation layers, electrolytic contact quantisation effects, self consistent quantum calcs. 79−60920
ZnO, acoustic phonon intensity fluctuations after strong nonlinear amplification 78−59909
ZnO, additive for activated sintering of SnO_2 77−36415
ZnO additive for celsian ceramics, props. obs. *(Bulgarian)* 80−50579
ZnO, additive to Zn-rich paint for protection of mild steel 78−95843
ZnO, additives effects on sintering and grain growth 78−80497
ZnO, adhesion deterioration between Ni-SiC coating and Al alloy *(Russian)* 80−66697
ZnO, adsorbing p- and n-type dyes, surfaces pot., UV light illum. effect 80−75624
ZnO, adsorpt. of H_2O vapour, annealing and grinding effects 78−68656
ZnO, adsorption of Br_2 and I_2, γ-irrad. induced centres 80−54513
ZnO, adsorption of ethylene, adsorption rate spectra, freq. response method 78−51817
ZnO, adsorption of H, space charge accumulation layers effect on secondary ion yields, H conc. meas. 79−83087
ZnO, adsorption of isopropyl alcohol, (acetone), decomp., IR and kinetic obs. 80−59780
ZnO, adsorption of N_2, 76.8 to 87.3K, expt. isotherms 77−31869
ZnO, adsorption of rhodamine B on (0001) face of single cryst. electrode 78−31645
ZnO, and ZnO-Al_2O_3, surface spark discharge, channel spreading and substrate vaporisation 77−89336
ZnO, ang. depend. of reflection spectra and directional dispersion of anisotropic exciton polaritons 78−31216
ZnO, antireflective coating, semiconductor laser, transverse modes, mirror reflectivity dependence 79−68404
ZnO, aqueous-deposited films, struct. and electronic props. for solar cell appls. 80−100797
ZnO, attenuation of transmitted light in exciton region, polarisation, coherence, scatt. 77−69852
ZnO, band gap depend. on energy of zero-point vibrs., luminesc. obs. 79−73436
ZnO based films, photographic props. *(Russian)* 77−71401
zinc compounds continued
ZnO based varistor, analysis of highly nonlinear current-voltage characts. 77−11983
ZnO based varistors, evolution and role of chem. constituents rel. to prep. method, influence on elec. props. *(French)* 78−31367
ZnO based varistors, nonlinear cond. theory 79−78192
ZnO, biexciton levels, luminescence-assisted two-photon spectra 80−29795
ZnO binder electrophotography, tone reproduction and copy quality *(German)* 78−62259
ZnO binder layers, regeneration of sensitising dyes 78−21241
ZnO, black, possible use as spectrally selective coating for low temp. solar collectors 79−994
ZnO, Bleustein-Gulyaev wave transmission characts. at corner 77−59197
ZnO, bulk and surface plasmons, single and multiple excitation 77−12474
ZnO, c-direction cryst. growth and crystallographic polarity 79−28902
ZnO CVD epitaxial layer, highly conductive layer, cond. and Hall coeff. obs. 79−51696
ZnO, CVD films on sapphire substrates, use as optical waveguide 78−90500
ZnO, CVD of epitaxial films on sapphire, SAW interdigital transducer fabrication 80−66430
ZnO, catalytic effect on thermal transitions of $Na_2S_2O_8$ and $K_2S_2O_8$ 79−15983
ZnO ceramic, nonohmic, drift phenomena of capacitance and current 80−39587
ZnO, ceramic, nonohmic props. 77−85229
ZnO ceramic, with additives, nonohmic thermally stimulated current meas. 77−20325
ZnO ceramic containing rare earth metal oxides and Co_3O_4, non-ohmic props. 77−76833
ZnO, ceramic varistor, physical props. of elec. barriers by AES and electron microscopy 77−20326
ZnO ceramic varistors, I-V characts., single grain junction meas. 79−15225
ZnO ceramic varistors, trapping by localized states, effect on dielec. and elec. props. *(Russian)* 79−28671
ZnO ceramic varistors, thermal breakdown 80−88928
ZnO ceramics, heat treatment effect on cryst. phases, microstruct. and elec. props. 79−100268
ZnO ceramics, microstructural evaluation 79−55750
ZnO ceramics, non-Ohmic, cond. mech. 78−68034
ZnO ceramics, non-Ohmic transient cond. phenomena, current-voltage overshoots 79−91057
ZnO ceramics, nonohmic, cryst. phases 78−26530
ZnO, change in exciton-phonon mechanism due to defects 78−71804
ZnO, charged dislocations, flow of charge with plastic deform. 80−85010
ZnO, chemical effect, influence on stopping power 80−47830
ZnO, chemisorpt. of pyridine, acetone, dimethyl sulphoxide, UPS, mol. orbitals effect on bonding 78−72699
ZnO, chemisorpt. of water, cond. and ESR meas. 79−56072
ZnO, chemisorption of CO_2, NH_3, differential heat 79−52759
ZnO, chemisorption of H_2O, differential heat of chemisorption 78−84052
ZnO, chemisorption of O_2, charge transfer, obs. by surface piezoelec. effect, contact. pot., and surface photovoltage 77−89824
ZnO, chemomechanical effects 79−82431
ZnO, combination light scattering *(Russian)* 77−85739
ZnO, condensates, growth from vapour, morphological comparison with, MgO, AlN 78−34450
ZnO, cryst. growth using $K_2S_2O_7$ as flux material 80−71582
ZnO crystal, adsorption of merocyanine dye, spectral sensitisation of photocond. 77−47854
ZnO crystalline films, deposition techniques *(Japanese)* 79−74098
ZnO, crystallising in double HCP lattice, microstruct., TEM and electron diffr. obs. 77−31655
ZnO crystals, adsorbed dye laser, charge transfer, field effect and spectrally sensitised photocond. meas. 80−49815
ZnO crystals, SEM study *(German)* 80−33860
ZnO, cubic cryst., lattice dynamics, overlap shell model and bond charge model 79−42156
ZnO, defect struct. calc., doping effects 80−107218
ZnO deposition for metal-ZnO-SiO_2-Si struct., SAW appl., fabrication related deterioration 78−14829
ZnO, dielec. theory of interacting exciton reson., wave-vector polariton dispersion relation 78−14673
ZnO, diffusion of excitons due to scatt. by optical phonons, photoluminesc. 77−24521
ZnO, dislocation loop nucleation on prismatic faults in high voltage electron microscope 77−72620
ZnO, dislocation motion, in situ TEM obs. 77−19961
ZnO, doped, dielec. losses 77−81049
ZnO, dye adsorption, contact pot. difference 80−27365
ZnO, EPR spectra, g∼1.96 signal intensity var. 77−63264
ZnO, E1 and A1 polaritons, spectra, optical meas. system 77−38018
ZnO, effect of crystallisation of Na_2O-CaO-Al_2O_3-SiO_2-F-B_2O_3-ZrO_2 glaze 79−60279
ZnO, effect on elastic modulus temp. depend. of silicate glass 79−61637
ZnO, effect on PbO activity in molten PbO-SiO_2 system 78−60663
ZnO, effect on props. of PbO containing cryst. glass 80−24637
ZnO, effect on viscosity of PbO containing crystal glasses 80−19973
ZnO, elastic, piezoelec. and dielec. props. 80−108157
ZnO, elec. cond. and oxidation kinetics of Zn in O_2-CO_2-SO_2 gas mixture 80−34448
ZnO, elec. cond. at high fields 80−80287
ZnO, electric field dependence of photoconductivity *(Russian)* 80−49821
ZnO electrode, in aq. soln., phototransition at 380 nm, anodic photocurrent obs. 78−19145
n-ZnO electrode, photoelectrochemical behaviour in acetonitrile solns. 78−31644
ZnO electrode, reson. Raman spectra of adsorbed rose bengal 78−76446
ZnO electrode, role of triplet states in xanthene dye sensitisation 78−76869
ZnO electrode surface, dye sensitisation mechanism, from reson. Raman spectrum obs. 78−42066
ZnO, electron beam induced decomposition and desorption, AES and contact pot. difference meas. 78−79893
ZnO, electron irrad., vacancies and interstitials, EPR meas. 79−14803

zinc compounds continued
ZnO, electron irrad. damage, orientation depend. 80−2075
ZnO, electron-exciton elastic scatt. cross sections, central field and exchange approxs. 77−62919
ZnO, electron-exciton inelastic collision cross sections 79−90967
ZnO, electron-hole liq., optical gain meas. 77−85794
ZnO, electron-hole liquid theory, generalised RPA 78−87914
ZnO, electron-hole plasma, gain and refl. spectra study 80−66227
ZnO, electron-hole recombination emission, temp. depend. and phonon repetitions *(Russian)* 79−15521
ZnO, electronic struct. calc., appl. of O nonlocal ionic pseudopot. 77−51659
ZnO, electrophotographic layer, fatigue recovery 79−63321
ZnO, ellipsometric spectroscopy of nonpolar (1$\bar{1}$00) surface 79−33651
ZnO epitaxial film, ionized-cluster beam and reactive ionized-cluster beam deposition, cathodolum. characterisation 80−16202
ZnO epitaxial film, nonuniform cond. due to H chemisorption *(Russian)* 80−65723
ZnO epitaxial film, UV luminesc. due to one-, two-photon excitation, laser possibility 79−11468
ZnO epitaxial film electrical props. rel. to substrate orientation and growth conditions 79−56339
ZnO epitaxial film on Al_2O_3 substrate, recombination radiation in intense single photon excitation 80−7410
ZnO epitaxial film with smooth surface from CVD onto a sputtered ZnO film on sapphire, waveguide appl. 78−56588
ZnO, epitaxial layers, influence of deposition conditions on luminescence, electrical props. 79−99924
ZnO epitaxial layers, rel. between elec. and photoluminesc. props. and their deposition conditions 79−95530
ZnO, excited states of bound excitons, photoluminesc. obs. 80−44513
ZnO, exciton luminesc., 16 to 77K 80−97329
ZnO, excitonic mol. emission, strain induced splitting 77−44060
ZnO, excitonic mol. transitions, optical gain and induced absorpt. spectra 80−11438
ZnO, excitonic molecule transitions, M-band emission 79−78742
ZnO, existence of biexcitons, reson. two-photon Raman scatt. 79−19889
ZnO, F^+-centre exam., ground and first excited energy level 77−39800
ZnO, F-centre exam., pseudopotential calc. 78−43328
ZnO, fatigue of electrophotographic layers 79−63320
ZnO fibre reinforced elastomer, X-ray diffr. exam. of filamentary crystal distrib. 80−7738
ZnO, field emission energy distrib., surface state emission obs. 78−35258
ZnO, field-effect mobility in accumulation layers on polar surfaces 79−73509
ZnO, film, adsorpt. of O_2, logarithmic law 79−42392
ZnO film, chemisorption of H, electrical cond. exam. adsorption centres 78−67913
ZnO film, elastic-surface-wave device with zero first-order temp. coeff. 77−88987
ZnO film, etching, for SAW transducers, Al electrode micro-fabrication technique 77−80042
ZnO film, growth rate and defectiveness, rel. to deposition conditions and substrate orientation 78−3057
ZnO film, high-resist., band and hopping cond., AC cond. and capacitance meas. 77−72928
n-ZnO film, highly degenerate, IR absorption by free polarons 77−4697
ZnO film, longit. elastic wave attenuation, 9.4 GHz 78−18888
ZnO film, low energy ion capture, elec. cond. increase *(Russian)* 77−12034
ZnO film, optical measure of acoustic quality 80−80893
ZnO film, optical waveguide fabrication, CVD on sputtered ZnO film on sapphire 79−86269
ZnO film, prep. by reactive ionized cluster beam deposition, and characterisation 80−10829
ZnO film, pyroelectric effects, origin 78−88258
ZnO, film, SAW resonators 78−83199
ZnO film, sputtering using Zn target, technique and characterisation 78−3040
ZnO film acousto-optical props. for integrated optical Bragg cell 79−55251
ZnO film concave transducer, for focusing microwave ultrasound 77−7276
ZnO film concave transducers for scanning acoustic microscopes 80−74663
ZnO, film for solar cell appl. structural, optical and elec. props. 80−2294
ZnO film on glass substrate, unidirectional SAW transducers 77−68355
ZnO film on glass substrate, high-rate deposition using DC reactive magnetron sputtering 80−80978
ZnO film on Si convolver, with surface-controlling junctions 77−88988
ZnO, film waveguide, Bragg electrostriction, power balance approach 77−75660
ZnO films, amorphous and cryst., CVD growth and elec. props. 77−76973
ZnO films, DC reactive magnetron sputtering technique, quality study 79−78877
ZnO films, RF sputtered single-cryst., on sapphire, struct. and SAW props. 80−80105
ZnO films, texture and grain size rel. to chem. spray deposition parameter 77−31921
ZnO films preparation using spray pyrolysis 80−96985
ZnO, freq. depend. of TO phonon decay parameter, and phonon-phonon interaction mechanisms 77−59084
ZnO, fully dense, grain growth 80−93526
ZnO, green luminesc. band, UV irrad. photocond. and quantum yield 77−36284
ZnO, ground powder, X-ray Fourier anal. *(Japanese)* 78−39727
ZnO, growth by recrystallisation of ZnO in H_2O vapour and H_2 77−85913
ZnO, growth rate, sublimation rate and etching behaviour along polar axis 80−24387
ZnO, heteroepitaxial, for SAW and electro-optic device appl., prep. and props., book contrib. 79−83134
ZnO heteroepitaxial film, orientation relations for growth on Al_2O_3 substrates, X-ray diffr. anal. 79−15049
ZnO heteroepitaxial films, grown on Al_2O_3 substrates, X-ray topographic study of struct. 79−15048
ZnO, hexagonal spot pattern production with light source and electron beam 77−69148
zinc compounds continued
ZnO, high field Faraday rotation, 6.5K 79−38522
ZnO, high rate epitaxy on sapphire by planar magnetron RF sputtering 79−28916
ZnO, high-field cond. charcts. calcs. 79−91056
ZnO, highly excited, biexciton states, M-band luminescence 79−78744
ZnO, hollow crystals, growth by oxidation of ZnSe vapour, mechanism 78−34733
ZnO, hot-electron microwave conductivity, hot-electron, high DC field 79−38113
ZnO, IR spectra, surface phonon modes 79−78668
ZnO in opaque glazes, microstruct. 79−60281
ZnO, in silicate glass, thermal capacity 80−88335
ZnO, influence on frequency-temp. coeff. of SAW devices 80−79066
ZnO integrated optical transducer arrays 79−50444
ZnO, intensity fluctuations of nonlinearly amplified phonons, Brillouin scatt. meas. 77−90163
ZnO interdigital transducer, efficient bulk-wave excitation in layered media 77−69156
ZnO, ion implantation effect on luminesc. and cryst. damage 78−6758
ZnO, irradiation in high voltage electron microscope dislocation loops study 80−88157
ZnO, isoelectric point meas. 80−88609
ZnO, L_l and L_η X-ray emission spectra 78−39631
ZnO, laser thresholds and stimulated emission, intrinsic recomb. processes 79−15489
ZnO layers, electrophotographic processes 80−4802
ZnO, light sensitivity rel. to local internal fields *(Russian)* 78−49932
ZnO, low energy cathodolum., surface effects 78−60522
ZnO, low-energy-electron transmission, optical modulation 79−83070
ZnO low-loss optical waveguides on amorphous substrates 80−58793
ZnO, luminesc. due to exciton-electron scatt., calc. 77−16379
ZnO, luminescent, phonon detection by shallow electronic trap states 79−14902
ZnO MIS structure, Al-ZnO-SiO_2-Si, charge-transfer device using SAW 79−11229
ZnO, MVV Auger spectra, line shape relax., energies 77−73195
ZnO, microcryst., surface microscopic modes, IR detection 79−38527
ZnO microcrystals, morphology, formed by Zn anodic electrocrystn. 77−80432
ZnO monocrystal and RF sputtered heteroepitaxial film, SAW attenuation comparison 79−56063
ZnO monolithic SAW device, separation of storage effects 79−18611
ZnO, multiparticle exciton complexes, luminesc. spectra *(Russian)* 80−16090
ZnO, near-forward Raman scatt. intensity of E_1(TO) polariton mode 78−23462
ZnO, negative photocond. by excitation of exciton-impurity complexes, recomb. mechanism *(Russian)* 79−28379
ZnO non-ohmic ceramic, degradation props. under AC and DC bias 80−80262
ZnO, nonhomic ceramic, current oscillation phenomena 79−69515
ZnO, nonohmic ceramic, current creep 79−69514
ZnO nonohmic ceramic, formation mechanism 80−60813
ZnO, nonpolar surface, interaction with CO and CO_2 79−65321
ZnO on Zn (0001), oxide film growth, at. and electronic struct. 78−15587
ZnO, optical gain and induced absorption from excitonic mols. 78−84609
ZnO, optical gain spectra, direct recording using laser modulation 78−66834
ZnO, optical second-order nonlinear polarisability 78−25919
ZnO, optical surface phonon modes, far IR transmission 77−31863
ZnO particles, average dielectric const. generalised theory, appl. to IR spectra 79−28667
ZnO, particulate, Dember effect, rel. to electrography 78−95314
ZnO particulates, Dember effect 79−20380
ZnO pellets, and ZnO:Li single crysts., photo-induced AC impedance meas., photodielec. effect 78−52034
ZnO phosphor fired with Zn, luminesc. in green and red region 80−66265
ZnO, phosphors, emission spectra, impurity effects 77−32420
ZnO phosphors, origin of UV emission 78−64400
ZnO, photocond., spectral sensitisation mechanism 77−43651
ZnO, photodesorption of CO_2, rel. to surface cond. and AES, band-bending model 77−47671
ZnO, photodesorption of $H_2O(NH_3)(NO)$(acetone), photoion emission, quantum yield limit 78−79896
ZnO, photodesorption of CO_2, pulsed-laser-dynamic-mass-spectrometer study 80−35568
ZnO, photodielectric effect, improved model including effect of traps 77−1445
ZnO, photodielectric effect, space-charge polaris. 79−60872
ZnO, photoelastic consts., absolute sign determ. by Biegelsen method 79−1749
ZnO, photoelectret, nonisothermal relax. 77−12306
ZnO photoelectret, recomb. and trapping kinetics determ. 79−38083
ZnO photoelectret, TSC reversals 77−8493
ZnO piezoelec. film, fabrication and appl. *(Japanese)* 78−23616
ZnO, piezoelec. films produced by gas transport reaction, US excitation efficiency 80−2700
ZnO, piezoelec. powder, dynamic polarisation echoes 78−52443
ZnO piezoelectric films formed by RF reactive ion-plating 79−83140
ZnO piezoelectric films, RF planar-magnetron sputtered, characterisation 80−96751
ZnO, piezoelectric powder, RF dynamic polarisation echo obs. 77−16254
ZnO, plasmochemical synthesis, oxidised from metals, exam. of props. 80−2984
ZnO, polar (000$\bar{1}$) surface, annealing and Ar^+ bombard. effects on conductivity, LEED obs. 79−51653
ZnO, polar faces, space charge layers, anomalous electron mobility 77−62981
ZnO, polar semiconductor, electron-hole liquid, electron-phonon interactions 80−6739
ZnO, polar surface, clean (O_2-H-exposed), reflection energy loss spectra, 2-30 eV 78−64434
ZnO polar surfaces, H and O_2 exposed, ion irrad., and heat treated, cond., EELS study 80−71525
ZnO, polar surfaces (0001), (000$\bar{1}$) specificity, field emission, H adsorption 77−21009
ZnO, polariton dispersion, IR reflection spectroscopy 80−11415

zinc compounds continued
ZnO, polycryst., γ-radiolysis, O_2 radiation yield, mechanism 77−36772
ZnO powder, adsorption of O_2, H_2, light effects *(Japanese)* 78−95230
ZnO, powder, adsorption of methanol, electron spectrosc. obs. 79−52076
ZnO powder, CO_2 desorption during electron irrad. and interaction with atomic H 77−89638
ZnO powder, effect of dry grinding in EPR and catalytic activity *(Japanese)* 80−84640
ZnO powder, Hall effect, O_2 partial press. and illumination effects 79−51607
ZnO, powder, sintering, surface area reduction, exam. 78−44039
ZnO, powder, surface cond., effects of O_2 chemisorption and CO_2 photodesorption 77−11980
ZnO powder, with adsorbed methanol, appl. of XPS method for surface anal. 78−40104
ZnO powder layer, adsorption of Rose Bengal dye, effect on surface potential and photovoltage obs. *(Japanese)* 79−24003
ZnO, powder layers, conductivity, O_2 chemisorpt. and photodesorpt. effects 78−43441
ZnO powders, direct meas. of intrinsic cond., using emulsion 79−99595
ZnO powders, electron-beam-induced desorption, phase-sensitive detection 80−54502
ZnO powders, UV luminesc. spectral distrib., comparison with single crysts., excitons role 80−55167
ZnO, precipitation from gas phase 78−6025
ZnO, prereduced surfaces, room temp. activity for oxygen isotopic exchange 79−91998
ZnO, prismatic surface, O_2 interaction obs. 77−31899
ZnO, pure and rare earth doped, photo- and electroluminesc. 79−28803
ZnO, RF sputtered epitaxial film, appl. to integrated optics 77−14821
ZnO RF sputtered films for SAW transducers, X-ray characterisation 80−80138
ZnO RF sputtered films, post deposition annealing behaviour 80−100416
ZnO, rate of deposition and morphology 78−84719
ZnO reaction with Fe_2O_3, microstruct. 79−87834
ZnO, red, electronic and opt. props., electrographic props. 77−57419
ZnO, reflection spectra, exciton reflection at high excitation levels 77−69853
ZnO resin layer leakage current in corona charging *(Japanese)* 78−24877
ZnO, reson. Raman scatt. 78−35137
ZnO, segregation of Li_2O at grain boundaries 78−64513
ZnO, self-activated phosphor, band width and shift, temp. depend. 77−8623
n-ZnO, semicond. electrode, electrolum. due to hole injection from electrolytes 77−20926
ZnO sensitized photolayer, overall spectra of local electronic levels 79−23933
ZnO Sezawa mode pn-diode array memory correlator 79−78178
ZnO, single cryst., photo- and thermoluminescence 80−66311
ZnO single cryst., UV laser, electron beam excited 80−53304
ZnO, single cryst. and film, absorpt., emission and photocurrent spectra in visible and near infrared *(Russian)* 77−52133
ZnO, single cryst. growth in $ZnO-H_2-H_2O-O_2$ vapour, morphology, electrophys. and opt. props. 78−52649
ZnO, single crystal, excess Zn atom conc. and elec. cond. determ. 78−3435
ZnO, single crysts., photocond. lifetimes, Zn^+ hole traps 80−75581
ZnO single crysts. with stoichiometry deviations, intrinsic defects, thermodynamic analysis 79−42485
ZnO single csytals quantised accumulation layers, Hall mobility of electrons 79−60909
ZnO, sintered, impurity ion effects on crystalline state *(Japanese)* 77−28768
ZnO sintered electrode, for dye-sensitive solar photocell 80−16816
ZnO, sintering, isothermal, surface area reduction 77−8779
ZnO, slow-electron-stimulated desorption 79−60623
ZnO, small crystal, optical surface phonon modes 78−71940
ZnO, small crystal, surface phonon modes, IR transmission spectra 80−11398
ZnO solar absorber surface spectral selectivity rel. to temp. and UV ageing 79−62027
ZnO, spacecraft thermal control material, low-energy proton effects 80−70288
ZnO, spray coated, reaction with Si, IR investig. 79−39197
ZnO sputtered films, undoped and Ga doped, props. rel. to deposition conditions 80−107935
ZnO sputtered films, vertical electrode config. to avoid contamination 79−69982
ZnO, stimulated two-photon emission from excitonic molecules 79−28815
ZnO, strong accumulation layers, negative magnetoresistance 78−6428
ZnO, structure parameters and polarity, X-ray diffr. meas. 80−19781
ZnO substrate, for Ni films, band bending, UPS study 80−7472
ZnO surface, adsorbed acetonitrile IR spectrum, species identification *(French)* 79−82967
ZnO surface, adsorption of O_2 and CO, electron energy loss spectra meas. 78−14601
ZnO surface, photocell, enhancement of photoelec. effect by organic additives 79−57437
ZnO surface, quantised accumulation layer magnetoresistance, spin scattering model 79−69529
ZnO, surface charge transfer in presence of photosensitising dyes 78−68049
ZnO, surface electron donor sites and acid-base props., adsorbed radical ESR 77−21417
ZnO surface electron states, appl. of surface photovoltage spectroscopy 77−69391
ZnO, surface exciton dispersion relations, additional boundary conditions 77−43687
ZnO, surface exciton polariton, nonlinear optical excitation 77−59259
ZnO, surface exciton polaritons, ATR obs., book contrib. 79−42620
ZnO, surface exciton polaritons, nonlinear optical excitation and dispersion relation 79−82657
ZnO surface extreme accumulation layers due to He^+ ions 77−72909
ZnO surface layers, high-field electrolysis during field emission 79−52084
ZnO, surface phenomena, interpretation by compensation model 78−95323
ZnO, surface phonon-plasmon coupling (surface plasmarons) 80−54497
zinc compounds continued
ZnO, surfaces, charge transfer in presence of photosensitising dyes, photovoltage spectra 78−72193
ZnO surfaces, work function, band bending, and electron affinity 79−47145
ZnO, temp. depend. elec. cond. 79−91041
ZnO, theory of photoelastic effect 77−55769
ZnO, thermally stimulated exoelectron emission *(German)* 80−66404
ZnO, thermoemission of positive ions in single gas atmos. *(Russian)* 77−28676
ZnO thin film opt. waveguide, collinear acousto-optic interaction and appl. to tunable opt. filter 80−74509
ZnO thin film SAW device manufacture, sputtering system and film characterisation 78−95692
ZnO thin film SAW devices, for HF range *(Japanese)* 80−53598
ZnO thin film SAW filters 79−23157
ZnO thin films, surface acousto-optic interaction, diffr. 77−3685
ZnO, thin Zn or O rich layers, thermolysis, photolysis, SEM, XPS 77−11821
ZnO thin-film loading of $LiNbO_3$, suppression of SAW harmonic generation 80−84355
ZnO thin-film transducer, bulk wave generation due to nonlinear interaction of SAW 79−42359
ZnO, third order nonlinear optical difference frequency generation 78−22176
ZnO transparent films for conductor-insulator-semiconductor (CIS) solar cells 80−93947
ZnO triode sputtered film elastic props. rel. to structure and composition 79−46988
ZnO triode-sputtered film crystallite structure, X-ray evaluation 79−46987
ZnO, two photon spectra, quantitative investigation temp. depend. 80−50373
ZnO, two-photon-excitation, tunable laser emission, luminesc. processes 80−55127
ZnO UV laser, electron-beam pumped 80−99753
ZnO, uniaxial pyroelectric, nonlinear optical susceptibility 77−23705
ZnO, valence electron states, X-ray Compton profile 79−65955
ZnO vaporisation from defective spinel powders, in vac. 80−16675
ZnO, vaporization from spinel solid solns. 77−76541
ZnO, varistor, low temp. AC props. 79−38434
ZnO, varistor action, homojunction breakdown mechanism 78−60193
ZnO varistor ceramics, current-voltage characts., inhomogeneities and single barriers 80−80273
ZnO varistors, barrier voltage determ. 79−56306
ZnO varistors, cond. model 78−14736
ZnO varistors, statistics and grain size effects on breakdown characts. 80−34010
ZnO, vol. depend. of refr. index 78−88275
ZnO, with adsorbed metal, photoexcited ions and electron emission *(Russian)* 77−40324
ZnO, with chemisorbed neutral red, photocond. meas. *(Japanese)* 79−42572
ZnO, wurtzite structure, hydrothermally grown exam. of thermal expansion coefficient 78−75854
ZnO, wurtzite type cryst., temp. depend. of one phonon Raman spectra, Gruneisen parameters 77−66500
ZnO, X-ray diffuse scattering 80−14964
ZnO, Zeeman splitting of A1-exciton emission lines, k-linear term effects 78−52563
ZnO, Zn 3d core-level transition in electron energy loss spectra, rel. to ZnSe (111) surface 78−68584
ZnO:$^{31}P^+$ implanted nonlinear resistor production and characteristics *(Russian)* 80−49252
ZnO:Ba, Co, rare earth metal varistors, microstructure-prop. relations 80−100249
ZnO:Bi, Sb, Co, second phase effect on elec. and mag. props. 80−60986
ZnO:Ce(Sm) phosphors, electrolum. 79−99946
ZnO:Ce(Tb) phosphors, electrolum. brightness, voltage and freq. depend. 80−60681
ZnO:Co ions, impurity distrib. from EPR 77−51401
ZnO:Co^{2+}, polarised optical absorpt. spectrum, crystal field transitions 77−48206
ZnO:Cu, excited state, zero phonon lines in emission and Zeeman spectra 79−38026
ZnO:Cu, H(D), IR absorpt. line spectra, OH and OD vibr., optical excitation 79−15498
ZnO:Cu, H(D), OH and OD centres, IR-active absorpt. line spectra 79−15496
ZnO:Cu, O, Fe(Co)(Ni) photocond., electron escape probabilities and trap depths 77−32041
ZnO:Cu,H, motional effects in EPR spectra 78−80207
ZnO:Cu^{2+}, electronic struct., optical absorpt. and ESR 79−87312
ZnO:Dy(Nd)(Sm), phosphor, electroluminesc., photoluminesc. spectra 78−80421
ZnO:Dy(Yb)(Nd)(Sm)(Pr)(Gd)(La)(Er), electrolum. brightness, field strength and freq. depend. 80−100696
ZnO:Er, phosphors, photo- and electroluminesc. 77−12428
ZnO:Er(Ag), photoluminescence and electroluminescence 78−27327
ZnO:La phosphor, electrolum. brightness waves, −168 to +85°C 78−52580
ZnO:Li, effect of LiOH mineraliser on struct. and optical props. 77−8737
ZnO:Li, electron irrad., F^+ centre, photosensitivity of e.p.r. spectrum 77−1594
ZnO:Li, luminesc. donor-acceptor pairs, exchange broadened optically detected EPR spectra 78−23373
ZnO:Li, optically detected ESR, donor-acceptor pairs, line broadening 78−80256
ZnO:Li_2O single crystal, triboelectric charge and photodischarge obs. 79−82663
ZnO:Li(Na), band-edge emission obs. 77−20933
ZnO:Nd, electrolum. brightness waves, 93 to 363K 79−33839
ZnO:Ni^{2+}, Zeeman effect at Ni impurities 80−60633
ZnO:Ni^{2+} tetrahedral ion config. interaction and crystal field spectra intensity 78−43335
ZnO:Pr(Gd)(Er), phosphors, photoluminesc. and electroluminesc. spectra 79−11457
ZnO:Yb(Nd)(Pr)(Sm), electro- and photoluminesc. 79−83024
ZnO/Al_2O_3, microstratified mixing of suspensions, viscosity dependence 79−70023

zinc compounds continued
ZnO/quartz for SAW device appls., expt. study of props. 80−80050
ZnO/SOS monolithic SAW amplifier 78−6205
ZnO/Si SAW structs., anal. of charge injection 80−80049
ZnO/substrate higher order mode SAW propagation obs. 79−46909
ZnO-Al_2O_3, isoelectric point meas. 80−88609
ZnO-Al_2O_3-SiO_2 glass, crystalline phase precipitation, crystallisation *(Japanese)* 79−32916
ZnO-Al_2O_3-SiO_2:Cu, Cu film self-generation for low-expansion IR laser mirrors 79−14127
ZnO-Al_2O_3-SiO2, transparent glass ceramics, heat treatment effect on microstruct. 78−56667
ZnO-$Al_2O_3SiO_2$, transparent glass-ceramic, microstruct., physical props., crystallisation ht. treatment depend. 78−80506
ZnO-Au-epoxy resin, and ZnO-Au-fused quartz transducers, λ/4-mode operation, theory *(Japanese)* 78−30145
ZnO-B_2O_3, glass, ESR exam. of paramagnetic centres formed during mech. destruction by grinding 78−88188
ZnO-B_2O_3, glass, refraction, refractive index from 0.365 to 2.50 μm 80−88953
ZnO-B_2O_3 glass, structure toughness-composition relationship 80−104257
ZnO-B_2O_3:Cu^{2+}, glasses, ESR and optical absorpt. 80−34760
ZnO-B_2O_3-SiO_2 glass-ceramic-cement composites, review 79−38783
ZnO-based binary semiconductor system nonlinearity prognosis *(Russian)* 78−43406
ZnO-based ceramic microstructure and nonlinear props., B diffusion effects *(Russian)* 80−49423
ZnO-based ceramic varistors, current-voltage charact., leakage and breakdown regions, 100 to 1300°C 79−56231
ZnO-based nonohmic ceramic, dielec. dispersion and equiv. circuit 77−73110
ZnO-based varistor, grain-boundary segregation, thin film X-ray spectroscopy obs. 80−35185
ZnO-Bi_2O_3, ceramic semiconductor, injection currents 79−11141
ZnO-Bi_2O_3, heterojunction, current-voltage charact. 79−56291
ZnO-Bi_2O_3 varistor, grain boundary segregation, STEM study 79−78980
ZnO-Bi_2O_3-CoO-MnO-Sb_2O_3 (97.5, 0.5, 0.5, 1.0 mole%), exam. of elec. props. at different annealing temps. 80−3099
ZnO-Bi_2O_3-Sb_2O_3-Co_2O_3-MnO_2-Cr_2O_3, nonohmic ceramic, microstruct. exam. 78−47292
ZnO-Bi_2O_3-ZnO structure, injection currents, SCL and TSC obs. *(Russian)* 77−32068
ZnO-binder system, reciprocity failure, photoconductivity 78−39151
ZnO-CdSe than film n-n heterojunctions, prep. elec. and optical props. *(Korean)* 77−28244
ZnO-CdTe heterojunctions preparation using spray pyrolysis 80−96985
ZnO-Co_3O_4(Fe_2O_3), ceramics, impurity at. states, elec. cond. 79−11130
ZnO-Cr_2O_3, crystal structure, valence of chromium ion rel. to variation of Cr/Zn ratio *(Rumanian)* 79−65057
ZnO-Cs, fabrication, UPS meas. 78−15279
ZnO-Cu_2O heterojunction solar cells, prop. by RF sputtering 80−93945
ZnO-electrolyte contact, current-potential charact. 77−1482
ZnO-electrolyte contact, electrolytic decomposition and photodecomposition 78−95357
ZnO-electrolyte interface, electron transfer sensitisation by salt additions 78−34894
ZnO-Fe_2O_3, isoelectric point meas. 80−88609
ZnO-GeO_2-MnO-B_2O_3 wideband cathodoluminescent phosphor 80−55196
ZnO-glass layered system, charact. of phase-velocity dispersion and struct. of surface waves 80−59775
ZnO-glass-ZnO structure, with Bi_2O_3-based glass and granular ZnO layers, current-voltage charact. *(Russian)* 77−69404
ZnO-grainboundary-ZnO junction in ceramic varistor, capacitance-voltage charact. 80−65689
ZnO-La_2O_3-B_2O_3, glass, refraction, refractive index from 0.365 to 2.50 μm 80−88953
ZnO-La_2O_3-GeO_2, exam. of glass forming region, properties and crystallisation 78−88454
ZnO-Nb_2O_5 system, Czochralski growth, phase relations and cryst. data 78−9975
ZnO-NiO:Li_2O n-p heterojunction, contact resist., effects of water vapour 80−34506
ZnO-on-Si SAW convolver development 77−27430
ZnO-P_2O_5 glass, ESR of VO^{2+} ions 80−100610
ZnO-P_2O_5-SiO_2 glasses, photoelastic consts. and polarisability 79−65839
ZnO-PbF_2-SiO_2 glass, shear wave velocity and its temp. depend. *(Japanese)* 78−30702
ZnO-PbO electroluminesc. phosphors, AC field excitation green and yellow emission 77−59617
ZnO-PbO-B_2O_3, exam. of glass formation and its props. 79−8283
ZnO-Pd Schottky-barrier diode, H_2 sensitivity 80−11085
ZnO-polystyrene photoreceptors sensitised by β-Cu phthalocyanine 79−17552
ZnO-resin electrophotographic layers, light decay curve empirical eqn., reciprocity law failure *(Japanese)* 79−39158
ZnO-resin photoconductive layers, impedance-freq. charact. meas. *(Japanese)* 79−38120
n-ZnO-rubrene, radical cation reduction, triplet state formation, luminesc. 77−16825
ZnO-Sb_2O_3-O_2 system, cpd. forming reactions 78−52699
ZnO-Si p-n diode monolithic storage correlator 78−18119
ZnO-Si structure, MIS and SAW propag. charact. 78−30988
ZnO-SiO_2 layered system, charact. of phase-velocity dispersion and struct. of surface waves 80−59775
ZnO-SiO_2 system, struct. and phase comp. of luminescent Zn orthosilicate 80−19951
ZnO-SiO_2-Si layered structure, SAW props., anal. 77−62729
ZnO-SiO_2-Si monolithic convolver, long time storage of surface-acoustic-wave signals 77−1287
ZnO-SiO_2-Si SAW device, interface transduction 80−102949
ZnO-Si(SiO_2) interface, XPS and Auger LMM anal. 79−90893
ZnO-SnO_2-M_xO_y, M_xO_y=glass-forming additive, I-V charact., heat treatment effects 77−43595
ZnO-TeO_2, cryst. chem. study, X-ray diffr. powder data *(French)* 80−15080
ZnO-TeO_2 glass, struct. and props. *(Japanese)* 79−32917
ZnO-Ti transparent type MIS solar cells 80−45662
ZnO-TiO_2 system, heat treated, X-ray anal. of phase form. sequence 79−1850
zinc compounds continued
ZnO-WO_3, phase rels. and cryst. struct. 80−108410
ZnO-Zn_2TiO_4, solid soln. formation 78−27490
ZnO-ZnS powder mixtures, elec. cond. and Hall effect meas., percolation effects 79−7828
ZnO-ZnS powder mixtures, Hall effect and elec. cond. 79−51607
ZnO+Li_2O, ionic cond., effects of moisture and LOOH on elec. and struct. props. 79−69283
ZnO_2, polycrystn., determ. of crystallographic orientation of grains 79−69049
ZnO_x, O(1s) XPS energies, oxidised metal surfaces, powders 77−16457
$Zn_{1+x}O$, nonstoichiometry investig., 400 to 1200°C 77−11543
(ZnO-ZnS)Cu:I, double band electroluminophors, form., props. 78−19568
$Zn_4O(BO_2)_6$, phonon coupling exam. by Raman spectroscopy 78−30719
$Zn_4O(BO_2)_6$:Tb, phosphoresc. study *(Spanish)* 80−16105
$Zn_4O(B_6O_{12})$, skeletal cubic cryst., refinement of cryst. struct. 79−86765
ZnOHF (I), single cryst., X-ray cryst. struct. determ. 79−60344
$(Zn(OH)(NH_3)_2)^+$, model for biological active sites, ab initio calcs., comparison with Be complex 80−104551
$Zn_3(OH)_4(NO_3)_2$, sp. ht., 5-300K, thermodynamic props. 79−55900
$Zn(OH)(NO)_3.H_2O$, sp. ht., 5-300K, thermodynamic props. 79−55900
$Zn_5(OH)_8(NO_3)_2.2H_2O$, sp. ht., 5-300K, thermodynamic props. 79−55900
$Zn(OH_2)_6(SiF_6)$, phase transitions, spectrometric exam. *(French)* 78−88291
ZnO(S), spectrally selective EM wave absorber, solar energy collector material, props. *(Dutch)* 78−50872
$Zn_3O(SO_4)_2$, cryst. struct. 77−27863
ZnO(S)(Se)(Te) 79−19906
ZnO(S)(Se)(Te), cryst., ionic radii and electronic polarisabilities 77−1091
$(ZnO)_nV_2O_5$, (n=1, 2, 3), elec. and mag. props. 79−78094
ZnO{10$\bar{1}$0} surface, clean, preparation, XPS meas. 78−39933
4ZnO.K_2O.4Cr_2O_3.3H_2O, corrosion inhibitor of mild steel 78−95839
ZnO.$ZnCl_2.H_2O$ cement, phase equilibrium diagram 77−86013
ZnO.6Bi_2O_3, IR and Raman spectra, vibr. anal. 78−76464
ZnP glass heavy-ion track detectors 3 to 120 MeV 80−91389
ZnP, Zn_3P_2, electronic struct. of valence bands, X-ray spectra and XPS 78−92176
ZnP_2, 442 class gyrotropic crysts., self-induced rot. of light polarisation plane 80−99810
ZnP_2, α-β heterojunction, I-V charact. and photoresponse 78−64105
ZnP_2, birefringence, circ. dichroism, temp. depend. *(Russian)* 79−1748
ZnP_2, birefringence and optical activity, dispersion 78−2821
ZnP_2, birefringence dispersion *(Russian)* 77−85686
ZnP_2, Brillouin scattering and optical props. meas. 80−76041
ZnP_2, cryst., tetragonal, 2-phonon IR absorpt. 80−66176
ZnP_2, d-electron participation in chem. bonds 77−28682
α-ZnP_2, doped, single crystal, electrical properties 80−92892
ZnP_2, large tetragonal single cryst. growth from vap. 77−69976
α-ZnP_2, lattice parameters and thermal expansion, 80-320K, X-ray obs. 80−75373
ZnP_2, light polarisation, self-induced optical rotation 79−19860
α-ZnP_2, local centre parameters, photoelectron transition scheme, recomb. process anal. 80−44654
ZnP_2, monoclinic, cathodoluminesc. spectra exam. 79−15534
ZnP_2, monoclinic, lattice vibr. symm., IR and Raman active frequencies *(Russian)* 77−69055
ZnP_2, polarised spectra of IR absorption and emission of single crysts., oscillatory states *(Russian)* 77−28583
ZnP_2, pure and doped, carrier mobility and conc., donor and acceptor energy levels, 190 to 380K 78−84217
ZnP_2, Raman light scatt. efficiency for He-Ne laser light *(Russian)* 77−52104
ZnP_2, reson. interaction of vibr. states, polarised Raman spectra meas. 77−15521
ZnP_2, resonance Raman scatt. singularities *(Russian)* 80−89007
α-ZnP_2, resonant Brillouin scatt. near indirect band gap 80−93350
ZnP_2, rotation of plane of polarisation of light 79−15432
ZnP_2 Schottky diodes, elec. and photoelec. props., excitons 80−65653
ZnP_2, second-order vibr. spectra and dispersion of phonon branches 80−25376
ZnP_2, sublimation 80−34181
ZnP_2, surface destruction by ruby laser irrad. *(Russian)* 77−20964
ZnP_2, tetragonal, interband Faraday effect *(Russian)* 78−72490
ZnP_2, tetragonal, one and two phonon states using second order Raman spectra 78−43874
ZnP_2, tetragonal bright red crysts., natural optical activity 77−16276
ZnP_2 tetragonal crystals, polarisation study of photocond. 80−96942
ZnP_2 tetragonal crysts., light scatt. by optic phonons 80−55116
ZnP_2, trapping levels, TSC and thermolum. meas. 79−15115
ZnP_2, two-photon light absorpt. dispersion, allowed-forbidden transition *(Russian)* 78−15193
ZnP_2, Zn_3P_2, polymorphic transitions 78−23699
ZnP_2:As, local vibrs. of impurity ions, Raman study 80−29745
ZnP_2:In(Ga)(Ge)(S)(Se), doped and undoped, optical absorpt. spectra in range 0.5 to 2.2 eV 80−66250
p-ZnP_2:S(Se)(Te), photocond., carrier generation and recomb. at high excitation levels *(Russian)* 78−64059
Zn_3P_2, ^{31}P multiple pulse NMR, chem. shift anisotropy 78−52369
Zn_3P_2, absorption edge meas. 78−80380
Zn_3P_2 bulk and thin film, UV reflectivity spectra, photovoltaic effects, optical consts. 80−25472
Zn_3P_2, characteristics for photovoltaic appl. 79−7839
Zn_3P_2, cryst., gas phase growth, morphology 79−10821
Zn_3P_2, determ. of ionicity by X-ray absorption method 78−31278
Zn_3P_2, direct and indirect optical transitions, metal-Zn_3P_2 contact photovoltage response 80−25402
Zn_3P_2, elec. cond., Hall effect, P interstitial effects 80−84465
Zn_3P_2, evaporated metal contact barrier heights 80−80375
Zn_3P_2, high press. phase relns. and cryst. structs. 78−59792
Zn_3P_2 large crystal growth, vapour transport perforated capsule technique, prototype solar cell appls. 80−93464
Zn_3P_2, multiphonon absorption in IR spectra 78−39554
Zn_3P_2, optical props., transition energies from transmission and refl. meas. 80−60532
Zn_3P_2, photocond. and Dember effect meas., 0.5 to 1.2 μm, possible detector appl. 78−91721
Zn_3P_2, photoluminesc. spectra 79−87502

zinc compounds continued
Zn_3P_2 photovoltaic material and Schottky diode characteristics 78−64066
Zn_3P_2, phys. props. 78−26527
Zn_3P_2, polycryst. thin film photovoltaic materials, photon loss anal., expt. determ. 80−93888
Zn_3P_2, single crystal, growth, electronic and device props. 80−25551
Zn_3P_2, sp. ht., thermodyn. props. 78−22863
Zn_3P_2, stoichiometry deviation from phase diagram 80−35164
p-Zn_3P_2, temp. dependence of resistivity and Hall constant 77−35937
Zn_3P_2, thermoluminescence glow curve method for radiation induced traps 80−60689
Zn_3P_2 thin polycrystalline films for solar photovoltaic cells 80−97797
Zn_3P_2-Al(Mg)(Be), diode, spectra response meas. of minority carrier diffusion length 79−78131
Zn_3P_2-Au Schottky diodes, influence of additional laser illumination on photoresponse spectra 77−89852
Zn_3P_2-Au surface barrier diode, wavelength-modulated photoresponse spectra 77−12004
Zn_3P_2-metal contacts, photoelectric props. 80−92930
$Zn(PO_3)_2$, vitreous, microhardness 80−25864
$Zn_3(PO)_2$, thermoluminescence glow curve method for radiation induced traps 80−60689
$Zn_3(PO_4)_2$:Mn, cathodoluminophor, nature of ageing 78−10994
$Zn_3(PO_4)_2.4H_2O$, hopeite, cryst. struct. redeterm. 78−75640
$Zn_3(PO_4)_2.4H_2O$, thermal transitions, thermographic investig. 77−9063
$Zn_3(PS_4)_2$, synthesis, structural and thermodynamic props. 77−24304
$Zn_4(P_2S_6)_3$, cryst. struct. *(French)* 78−34474
$Zn_4(P_2S_6)_3$, monoclinic system *(French)* 78−59791
Zn_2PdO_4, cryst. struct. and mag. props. meas. *(French)* 77−15381
$ZnRb_2(SO_4)_2.6H_2O:Mn^{2+}$, EPR, 298K, spin-Hamiltonian parameters, cryst. fields 78−27086
$ZnRb_2(SeO_4)_2.6H_2O:Mn^{2+}$, EPR spectra 80−100608
Zn(S,Se), large single crystals, vapour growth and defect characterisation 80−25540
ZnS 80−35096
ZnS, ^{57}Co gamma source, time depend. Mossbauer spectra 80−50245
ZnS, ^{67}Zn and ^{33}S nuclear magnetic shielding, chemical shifts and linewidths 80−60434
ZnS, ^{67}Zn Mossbauer spectroscopy with 93 keV reson. 80−66095
ZnS, 4H and 6H polytypes, struct. changes on plastic deform. 77−43328
ZnS, 93.3 keV Mossbauer transition in ^{67}Zn, isomer shifts 80−39978
ZnS, (110) cleavage stratigraphic etch patterns, displacements 77−7680
ZnS, (111) face, flux-grown cryst. dissolution charact. 77−59014
ZnS, additively coloured or neutron irradiated, near IR emission 77−90199
ZnS, antireflection coating, 100 ns pulsed laser damage at 2.7 and 3.8 μm 80−33057
ZnS antireflection coatings on solar cells 80−43414
ZnS, appl. of orthogonalised augmented plane wave method, appl. to ZnS 77−66105
ZnS, band structure calcs. by modified orthogonalised plane wave (MOPW) method 80−54609
n-ZnS based heterojunctions, epitaxial, elec. props. *(Russian)* 78−88023
ZnS, Bridgeman growth under pressure, macroscopic inclusions and defects 80−45226
ZnS, broadband dielectric mirror interference coatings, scatter losses 79−50365
ZnS bulk and surface states anal. using synchrotron radiation 77−66574
ZnS CVD IR material specifications 80−48364
ZnS CVD IR window, optical and physical characteristics 80−106620
ZnS, CVD sample, refractive index var. with temp., 22° and 34°C 79−14053
ZnS CVD window, IR lattice absorption, phonon assigments and image spoiling 80−33104
ZnS CVD windows for forward looking IR radar systems 78−46816
ZnS, cathodolum. emission spectra, exciton lines 80−76084
ZnS, charged dislocations, flow of charge with plastic deform. 80−85010
ZnS, chem. laser window material 77−46769
ZnS, chemisorption of O_2 after illumination and in presence of CO and O_2 78−87877
ZnS, clean surface, AES and LEED exam. 80−10762
ZnS, Compton profile, state of valence electrons 78−11018
ZnS, cryst. grown from melt under press., microstruct. 77−59019
ZnS crystal, inhomogeneous, microscopic struct. investig. using synchrotron radiation 77−76424
ZnS, crystal, layered struct. microscopic observations *(Japanese)* 78−38725
ZnS crystals, luminescence kinetics, centre discrimination exam. 78−15215
ZnS crystals, structural change under plastic deform., partial dislocation movement 80−79736
ZnS crystals in electrolyte, electrolum. and elec. props. 80−93407
ZnS, crystals with stacking faults, Laue method study 79−94847
ZnS, cubic, compression 80−107358
ZnS, cubic, direct and modulated refl. spectra, 165-360 nm 77−13807
ZnS, cubic, gel growth, expt. conditions 78−68614
ZnS, cubic, IR-active phonons obs. 80−55084
ZnS, cubic, thermal vibr. temp. depend., anharmonic models 80−92618
ZnS, cubic and hexagonal, lattice coupling with BiOCl, ErOCl and LaOCl for heterojunctions 79−60919
ZnS, cubic crysts., having substitutional elastic distortion centres, diffuse X-ray scattering 80−24302
ZnS cubic single crystals, growth by double decomposition reaction in melt 78−60557
ZnS, current and refractive index oscills. in electric fields due to barrier instability 79−91372
ZnS, current oscills., 300K, 1-6 s period *(Russian)* 77−80819
ZnS, d-electron participation in chem. bonds 77−28682
ZnS, decomposition in H_2 atmosphere, electron-hole mechanism *(Russian)* 77−16409
ZnS, defect form. in single crysts. during implantation of Zn, S, and Ar *(Russian)* 78−14369
ZnS, defect struct., dark-field microscopy, anal. of decoration patterns 79−23506
ZnS, dependence of hexagonal layer formation on dopant conc. 79−19265
ZnS, deposited anthraquinone, decoration patterns 77−1137
ZnS, diatomic crysts. electron induced X-ray emission, channelling effects 79−56888
ZnS diffraction mode selector for He-Ne laser 79−89951

zinc compounds continued
ZnS, effect of temp. var. on light transmission 78−79136
ZnS, elastic moduli of polytypic modifications 79−51187
ZnS, elec. struct., piezoelec. consts. *(Chinese)* 79−56122
ZnS, electroless film deposition with variable comp. and polymorphic structs. 79−95952
ZnS, electrolum. phosphors, surface phenomena occurring during ageing *(Russian)* 79−33842
ZnS, electroluminesc. and photoluminesc. spectra, fine struct. *(Russian)* 78−84661
ZnS electroluminescent films, low energy Mn implantation system 78−30658
ZnS, electroluminescent emission, UV excitation after effects 80−45144
ZnS, electroluminophor, ageing rate, voltage effects *(Russian)* 78−84662
ZnS electroluminophors, ageing effects *(Russian)* 78−15231
ZnS, electron irrad., ESR 79−91293
ZnS, electronic struct. from X-ray emission spectra 77−28661
ZnS, energy levels of Mott excitons 78−6282
ZnS, epitaxial film, CVD growth, photolum. spectra *(French)* 77−36403
ZnS, epitaxial growth, appl. to electronic devices, review *(Japanese)* 80−55281
ZnS epitaxial growth, in H_2, mass transport processes and effects of bypass flow 79−23860
ZnS, epitaxial growth by Zn-S-H_2 CVD method 78−27413
ZnS epitaxial layers, growth kinetics on CaF_2 by vapour phase transport *(French)* 80−54572
ZnS, epitaxial layers on Ge and GaAs substrates, exam. of growth 79−1828
ZnS, epitaxy in quasiclosed volume 77−85093
ZnS, equation of state 79−82310
ZnS evaporated film, refl. loss on UV irrad., ZnO form. 80−99813
ZnS evaporated film optical props. 160 to 2000 A 79−15544
ZnS, excited phosphor, IR stimulation and quenching of luminesc., review *(Russian)* 80−11455
ZnS, exciton-ionised donor complex, binding energy 78−67949
ZnS, F-centre exam., pseudopotential calc. 78−43328
ZnS, Fe^{3+}-Cu^+ complexes and A-centres, g-factor anisotropy *(Russian)* 77−20271
ZnS film, and ZnS-MgF_2 film system, Rayleigh scatt., 441.6 nm, scatt. losses correl. with deposition parameters 79−78782
ZnS film, defect form. and development 80−96759
ZnS film, doubly silvered, light interferometry, refr. index, film thickness and phase shift determ. 78−276
ZnS film, epitaxial growth on Si in ultrahigh vacuum, source nonstoichiometry effects 77−77387
ZnS film, evaporated amorphous, mechanism of memory phenomena *(Japanese)* 78−23140
ZnS film, intrinsic stress meas. 80−71696
ZnS film, ion beam deposition 77−70008
ZnS, film, laser evaporation synthesis, surface struct. 79−28954
ZnS, film, on semicond. substrates, early stages of growth, electron microscope obs. *(Russian)* 78−38976
ZnS film, optical inhomogeneity, rel. to struct. 79−83047
ZnS film, photovoltaic effects under illum. from above and below 78−52031
ZnS film, struct. electron microscopy 77−59226
ZnS, film, vac. deposition onto NaCl cryst. in H_2S environment 78−63945
ZnS, film, vac. sputtering deposition by CW CO_2 laser beam *(Russian)* 77−21024
ZnS film, vac.-deposited, origin of mech. stress 79−90925
ZnS film deposition using radiation-heated tubular-type evaporator 80−76191
ZnS film free carrier absorption for laser beam modulation *(Japanese)* 79−7164
ZnS film on Si, fused quartz substrates, H_2O absorpt., IR anal. 80−75446
ZnS film production, for luminophors, method and apparatus *(Bulgarian)* 80−7499
ZnS films, electrolum., bistable excitation 80−93406
ZnS films prepared by thermal evaporation in vac., nature of defects 80−10835
ZnS, four-photon transitions, perturbation theory calc. 80−96786
ZnS, gas, identification by high-temp. mass spectrometry 80−45593
ZnS, glide plane of dislocations 79−46667
ZnS, granulated films, optical reson. 79−4863
ZnS, green-blue luminesc. characts., model of luminesc. centres 79−73999
ZnS, ground state of electron subsystem, quasimolecular model 79−69055
ZnS, growth of cubic single crystal by I_2 transport 79−91572
ZnS, growth rate, sublimation rate and etching behaviour along polar axis 80−24387
ZnS, heteroepitaxial growth on GaP by closed space technique 79−28939
ZnS, heterogeneous birefringence 79−95728
ZnS, high field Faraday rotation, 6.5K 79−38522
ZnS, high purity, prep. from ZnO *(Rumanian)* 80−76206
ZnS, high temp. annealing effects on photoluminescence 78−19564
ZnS, high-level photocurrent excitation and carrier recombination expt. *(Russian)* 79−95446
ZnS, high-resist., optical transmission thermal processing effects 77−63431
ZnS, high-voltage photovoltaic effect in polycryst. layers 79−42573
ZnS, highly transparent semicond. crysts., multiphonon IR absorpt. 78−10885
ZnS, horizontal epitaxial growth systems, transport kinetics 79−4920
ZnS, hot pressed, water drop impact damage, SEM exam., IR transmission 78−88543
ZnS hot pressed microcryst. compact, Irtran 2, refr. index meas. 78−66877
ZnS, IR transmitting semicond., dn/dT, wavelength depend. 77−77163
ZnS IR window refractive index var. with temp., −180° to +200°C obs. 79−14052
ZnS, in thin film polarising beam splitter 77−19422
ZnS, inhomogeneous interface laser mirror coatings 80−1252
ZnS, interaction between charged dislocations and luminesc. centres *(Russian)* 79−56860
ZnS, interference filter, solar radiation resistance 77−39015

zinc compounds continued
ZnS interference layers on Fe whiskers, optimisation of magnification of magneto-optic Kerr effect 79−51808
ZnS, interimpurity high press. luminesc. 78−19532
ZnS ion beam etching, topographic changes, amorphisation, luminescence study 80−76078
ZnS, ion implantation effects on luminesc., thermo-EMF 80−88178
ZnS, large single crystals, vapour growth and defect characterisation 80−25540
ZnS, laser evaporated film, microstruct. TEM obs. 79−82479
ZnS, laser irradiated, in-depth and surface temp. meas. by Moire-Schlieren technique 80−53392
ZnS, laser radiation initiated electron emission, evidence for photoelec. mechanism 77−69970
ZnS, laser residual lattice absorpt., freq. and temp. depend. 78−25910
ZnS, lattice dynamics, deformable-ion model 78−91396
ZnS, lattice dynamics, phonon freq., bond bending force model calcs. 80−70335
ZnS layer, spectrophotometer-type filters of highest possible performance, 2.5-40 μm 80−14438
ZnS leaky waveguide electro-optic modulator limitations 78−22218
ZnS, linear electrooptic coeff. dispersion 80−71380
ZnS, linear thermal expansion coeffs. meas., room temp. to 250°C 78−55416
ZnS, low resistivity, ohmic contact noise characts. and contact resistance 78−14827
ZnS, low resistivity, prep. and characterisation for blue LEDs 77−81209
ZnS, low temp. equilibrium compensation limit of intrinsic-defect hole conductivity *(Russian)* 79−1598
ZnS, low voltage cathodoluminescence 78−52585
ZnS, low-temp. trap anal. thermally stimulated luminesc. model extension 80−80877
ZnS, luminesc. data. statistical anal. *(Russian)* 78−68559
ZnS, luminescence of M-centre 80−29779
ZnS, microregions disorientation degree anal. by birefringence, ESK and decoration methods 79−60389
ZnS monocrystalline substrate, influence of struct. on CdS epitaxial growth and nucleation 80−88455
ZnS, multilayer interference film, mass production by roll coating *(Japanese)* 79−81577
ZnS, multispectral aircraft window materials, production processes 77−73237
ZnS, natural and artificial appl. of cathodolum. microscopy and spectrometry 77−69919
ZnS, natural and stress induced birefringence dispersion 78−6651
ZnS, ODMR of Zn vacancy obs. 80−108121
ZnS, optical coating in liquid, laser damage 77−61994
ZnS, optical film cross sections SEM and TEM 77−19387
ZnS, optical material, thermal expansion, 60-300K 78−33791
ZnS, oxidation, hardness and electromechanical polishing response 80−71776
ZnS, oxidation in fluidised bed 77−4929
ZnS, phase diagram of electron-hole liqs. in polar semicond. 77−89706
ZnS, phonon dispersion under extreme press. and metallic transform., Raman spectra meas. 78−10895
ZnS, phonon spectra calc. by recursion method 80−59596
ZnS phosphor, exciton struct. in luminesc. excitation spectra 77−52176
ZnS, phosphor, optical flash stimulation, optical absorption, MCD, thermally stimulated luminescence expts. 78−10951
ZnS phosphor, powdered, in host material, solar cells wavelength shifting 80−85286
ZnS, phosphor, voltage and temp. dependence of pre-breakdown electroluminescence 80−45147
ZnS, phosphor, voltage depend. of electrolum. brightness 80−45148
ZnS phosphorescent tracer method for fluid film lubrication, velocity profile meas. 78−94866
ZnS phosphors, Gudden-Pohl effect, temp. depend. and decay rate 77−44070
ZnS phosphors, Gudden-Pohl effect, field ionis. of trapping centres 77−73170
ZnS phosphors, synthesis under unidirectional pressure and roasting in vacuum 77−32547
ZnS, photocell, transient photoelec. phenomena 79−82687
ZnS photocells, thickness depend. of interband transition photovoltaic voltage and short circuit photocurrent 77−76871
ZnS, photocond. excited with laser radiation near fundamental absorpt. edge 77−76867
ZnS photoconductors, spectral sensitisation, role of local centres *(Russian)* 80−90924
ZnS, photoelasticity, exchange charge polaris. effect 77−81046
ZnS, photoluminesc. quenching by weak alternating field 77−85778
ZnS, plastic deform. induced luminesc., dislocations role *(Russian)* 78−10985
ZnS, plastically deformed, anisotropic cond. 78−56143
ZnS platelets, cathodolum. analysis using STEM 78−32950
ZnS, polarisation of self-activated luminesc. 77−73159
ZnS, polycryst., laser window material, IR thermooptic coeff. meas. 77−36208
ZnS, polymorphic transition, ($\beta \rightarrow \alpha$) effect of mech. deformation 79−1858
ZnS, polytype relative stabilities, entropy contribs. 80−100197
ZnS, polytypism, phase and growth aspects 78−83764
ZnS, post field recomb. in pulsed electrolum. 80−71488
ZnS, powder phosphor, IR-induced changes in emission spectra 78−80389
ZnS powder phosphors electroluminescent cells, AC electrolum. characts. *(Japanese)* 80−71489
ZnS, prebreakdown electrolum., domain form. and negative resist. effects 80−84788
ZnS, pulsed optically detected resonance, time depend. recomb. processor study 79−38411
ZnS, RF sputtered film, stoichiometry, chem. comp. 78−34727
ZnS RF sputtered films for SAW transducers, X-ray characterisation 80−80138
ZnS, Raman scatt. by phonon polaritons 80−103959
ZnS, rare earth activated phosphor, scintillation mechanism *(Russian)* 78−48231
ZnS, reflective coatings, refr. index, UV polariser mirror coating appl. *(Russian)* 77−34928
ZnS, refr. index oscills, in strong. elec. field 79−28720
ZnS, reson. Brillouin scatt., acoustic domain injection 79−38557
zinc compounds continued
ZnS, reson. Brillouin scatt. and piezobirefringence 80−93348
ZnS, S annealed, IR enhancement and quenching of photocond. 78−14763
ZnS, Schottky barrier, semiempirical light-binding calcs. 79−28408
ZnS Schottky-barrier diodes, blue light emission 79−38671
ZnS scintillator with faster decay 77−42217
ZnS, second order Raman scatt., lattice dynamical calc. and expt. 80−25370
ZnS, secondary electron emission coeffs. for multiply charged ion bombard. 78−11051
ZnS, self activated emission, spin depend. donor acceptor pair recombination, ODMR exam. 79−42870
ZnS, self energy effects of valence and conduction electrons 79−37980
ZnS, self-activated, IR sensitivity 78−6742
ZnS, self-activated, orientation of luminesc. centre 78−27307
ZnS, self-activated, trap distrib. and photoelectronic effect due to UV, IR and visible excitation 77−36282
ZnS, shallow traps, thermolum. glow curves obs. 79−91508
ZnS, single cryst., grown from melt distrib. coeffs. of transition metals, Pb and Sn 77−55298
ZnS single cryst., linear electro-optical props., temp. depend. 80−71376
ZnS, single cryst., radiation emission, stimulation by IR light *(Russian)* 77−66542
ZnS single cryst., UV laser, electron beam excited 80−53304
ZnS, single cryst. plate, photovoltaic spectra, intensity depend. 78−14762
ZnS, single cryst. vap. growth by sublimation and chem. transport 78−27390
ZnS, single crystal, effect of elec. field on cond. 78−84228
ZnS, single crysts. excited by laser beam and elec. field, streamer luminesc. and photolum. obs. 80−34986
ZnS, single electron excitation study, cathodoluminescence image contrast using STEM 80−89072
ZnS, solution growth, using Te solvent 79−65993
ZnS, sphalerite, struct. of twin seam obs. by optical microscopy 77−39596
ZnS, sphalerite modification, polysynthetic cryst., struct. changes due to uniaxial compression 77−15482
ZnS, sphalerites, in-determ. by nondestructive neutron activation anal. 79−87929
ZnS sputtered film, interband photocond. edge *(French)* 77−8212
ZnS, Stark-Ladder current theory 78−68035
ZnS striated platelets, SEM studies of local variations in cathodolum. 78−15232
ZnS structure, evaluation of finite strain eqns. of state using lattice models 80−96620
ZnS, superficial degradation in air and water, XPS obs. *(French)* 80−89110
ZnS surface, nonpolar, electronic struct., tight-binding calc. 77−20383
ZnS, surface, work function and luminesc. phenomena, effect of H,H_2,O and O_2 adsorpt. 78−10538
ZnS, surface acoustic wave modes 78−2352
β-ZnS, suspension-electrolysis leaching in 1N H_2SO_4 soln., anodic impedance of PbO_2(Pb) electrode *(Japanese)* 79−43594
ZnS, temp. coeffs. of charact. reflectivity struct. 77−85745
ZnS, temp. depend. of edge emission band shape 77−20934
ZnS, theory of photoelastic effect 77−55769
ZnS, thermal expansion and lattice dynamics under press. 80−100316
ZnS, thermoluminescence at different excitation levels 80−93413
ZnS, thin film deposition, by low pressure, high freq. induction plasma *(Russian)* 79−69992
ZnS thin films, effect of fabrication parameters on electroluminescence and related props. *(Japanese)* 80−76083
ZnS thin-film waveguide SHG phase-matching obs. with tunable parametric oscillator 77−58390
ZnS, tight binding calc., F-centres, and isoelectronic defects 77−20266
ZnS, tight-binding model of F-centre 77−89729
ZnS, time differentiated Mossbauer spectra from ^{57}Co impurities, relaxation processes *(Russian)* 80−34834
ZnS, time resolved ODMR, electron-hole recombination 79−42872
ZnS, twist boundary struct., atomic scale electron microscopy obs. 80−107276
ZnS, two-photon absorpt. in crossed elec. and mag. fields 77−85693
ZnS type lattices, luminescence, constants, temperature dependence, activation energies 79−99923
ZnS type structure solids, contrib. of many body forces to elastic consts. 78−2188
ZnS UV laser, electron-beam pumped 80−99753
ZnS, ultra-microhardness testing for vacuum deposited film and bulk specimen 78−79910
ZnS, uncoated and liq. layer coated, vaporisation mechanism, surface morphology 77−35683
ZnS underlayer for Cr film on glass substrate, thermal strength, recrystn. influence 79−87748
ZnS, VPE on GaP in open tube system 79−28938
ZnS, vacuum-evaporated conducting films, prep. and props. 79−66007
ZnS, valence electron states, X-ray Compton profile 79−65955
ZnS, vaporisation, negative whisker form. by solid-liq.-vapour mechanism 77−35684
ZnS vapour grown crystals, morphology and structure 78−42937
ZnS, vol. depend. of refr. index 78−88275
ZnS, wavelength-modulated refl. spectra, 2.5 to 8 eV 77−20877
ZnS with Au film coating, calc. of defect conc. 78−95052
ZnS with cation impurity, first order transitions in Raman spectra 78−88310
ZnS, with CdS or Cu_2S addition, phase transform. during crystn., 850 or 1150°C 77−48362
ZnS with substitutional impurity, dipole and weak-dipole vibr. 79−14904
ZnS, work done and heat evolved in plastic deform., stacking fault energy 77−80573
ZnS, wurtzite, ZnO solubility, 1444-1240°C 80−15248
ZnS, wurtzite type cryst., temp. depend. of one phonon Raman spectra, Gruneisen parameters 77−66500
ZnS, X-ray diffuse scattering 80−14964
ZnS, X-ray L-emission spectra of S *(Japanese)* 78−15254
ZnS, zinc blende-wurtzite-zinc blende, optical quenching of photocond. *(Russian)* 77−28240
ZnS, ZnS-CeF_3, single-layer vac. antirefl. coatings for near IR spectral region 80−33099
ZnS:^{57}Co Mossbauer sources, Fe^{1+} transient charge state 80−108128

zinc compounds continued
ZnS:^{90}Sr, continuously acting luminous solid for photoelec. meas. over 300-800 nm range 79−3757
ZnS:(Cu, Cl), electroluminesc., voltage effect on ageing rate 79−95848
ZnS:Ag, Al and ZnS:Cu, Al, LV cathodoluminesc. 79−33844
ZnS:Ag, Al(Cu), trap parameters, thermostimulated luminesc. and cond. meas. *(Russian)* 77−72868
ZnS:Ag, cathodoluminescence. yield, calorimetric method determ. *(Russian)* 77−20938
ZnS:Ag, cathodoluminesc. investig., appl. to cathode ray tube screening 80−108282
ZnS:Ag, cryst. struct., electron traps and glow curves 79−61437
ZnS:Ag, electroluminesc., surface barriers *(Russian)* 78−2919
ZnS:Ag, luminesc. efficiency deterioration due to surface oxidation by $(NH_4)_2Cr_2O_7$ thermal decomp. 80−29810
ZnS:Ag, Ni thermographic phosphor luminesc. screen, for IR laser pulse recording 79−64342
ZnS:Ag, phosphor, luminesc. of surface glow centres 80−29782
ZnS:Ag, phospors, nature of fluorescent centres and traps 79−91484
ZnS:Ag, photon counting statistics of cathodoluminesc. light emission 79−24371
ZnS:Ag, single crystal, ionisation mechanism of field trapping centres 80−45156
ZnS:Ag, struct. and mech. props. 78−22753
ZnS:Ag, TSC and induced impurity photoconductivity, existence of two electron trapping centres 80−44655
ZnS:Ag,Al, computer calc. of band model for luminesc. and photocond. *(Russian)* 78−52542
ZnS:Ag,Cl, embedded in HBO_3-glass matrix, blue electrolum. 80−55195
ZnS:Ag,Sm, recomb. centre interaction, luminesc. quenching 78−10946
ZnS:Ag film, evaporated, IR quenching of photocapacitance, deep levels obs. 78−56180
ZnS:Ag film, photocapacitance IR quenching, hole photoionisation energy and spectral distrib. 79−87127
ZnS:Ag phosphor prep., physicochemical investigation of processes 78−11170
ZnS:Ag phosphors, luminesc. of glow surface centres *(Russian)* 79−28836
ZnS:Ag^{2+}(Cu^{2+}), absence of EPR spectra due to strong spin-lattice coupling of Kramers doublets 77−85181
ZnS:Al, IR studies of Al complexes 79−33741
ZnS:Al, signal enhancement by field modulation, ODMR expts. 78−56406
ZnS:Al,Cu(Ag)(Au) phosphors, luminesc. excitation spectra and exciton struct. 80−55164
ZnS:Al(Te) phosphors, luminesc. excitation spectra and exciton struct. 80−55165
ZnS:Au, phosphor, 'blue' and 'green' centre form. *(German)* 79−38665
ZnS:B, new luminesc. centre 79−38635
ZnS:Be, far IR lattice absorpt., Green's function calc. 78−43865
ZnS:Be, impurity modes and IR absorption 78−76506
ZnS:Cl, self-activated, blue emission band 79−38633
ZnS:Cl, shape of self-activated cathodoluminesc. band 80−34987
ZnS:Cl, single cryst., deep centre study by impurity electroabsorpt., photocond. meas. 77−12411
ZnS:Cl, spectral distrib. of photocond., effect of powerful UV illumination 78−14767
ZnS:Cl^-, Cu^+(Ag^+), phosphor, high press. effect on thermoluminesc. 78−64419
ZnS:Co, impurity luminescence no phonon line depend. on temp., Debye temp. 80−66273
ZnS:Co, Jahn-Teller interaction energy determ., piezospectroscopic expt. *(Russian)* 77−4623
ZnS:Co Mossbauer source, Fe^{2+} abnormal populations and vibronic props. 80−15912
ZnS:Co^{2+}, EPR and spin-lattice relax. of Co^{2+} centres *(Russian)* 79−1706
ZnS:Co^{2+}, spin-lattice relax., phonon heating effect *(Russian)* 78−19317
ZnS:Co(Fe)(Mn)(Ni), impurity-induced Raman scatt., central force const. reduction 77−32379
ZnS:Cr, anomalous temp. depend. of near IR absorption 79−28794
ZnS:Cr^+, Fe^{2+}, luminesc., cond. and paramag. centre conc. parameters 78−6724
ZnS:Cr^{2+}, absorpt. and luminesc. of Cr^{2+}(d^4), cryst. field theory interpretation 79−83000
ZnS:Cr^{2+}, Cr^{2+} $^5T_2$ and ^5E states, Jahn-Teller effect calcs. 80−39539
ZnS:Cr^{2+}, excitation spectrum of IR emission 77−12421
ZnS:Cr^{2+}, Jahn-Teller interaction energy calc. 78−2455
ZnS:Cr^{2+}, Jahn-Teller coupling 78−67997
ZnS:Cr^{2+}, photoionisation, lattice relaxation energy 80−6778
ZnS:Cr(Mn)(Fe)(CoXVi), vibr. modes of transition element impurities 78−76472
ZnS:Cu, Al phosphors, mechanism of IR stimulated and quenching 77−69881
ZnS:Cu, Br based electroluminesc. cells, light, const. field effects on electroluminesc. 78−84658
ZnS:Cu, Cl, I, anisotropy of blue Cu luminesc. centres 77−81137
ZnS:Cu, Cl, Mn film, AC electrolum. 80−60680
ZnS:Cu, Cl luminophor, photoluminesc. and struct. props. 77−32414
ZnS:Cu, Co, deep traps and stationary luminescence *(Russian)* 78−48227
ZnS:Cu, current pulses stimulated by elec. field at low temp. 78−39121
ZnS:Cu, deep transition metal impurity states, SCF CNDO cluster calcs. 80−100442
ZnS:Cu, effect of elec. field on photoluminescence, model of luminogen centre 78−76522
ZnS:Cu, electroluminesc. spectra fine struct. 79−95847
ZnS:Cu, Er, Na, phosphor, mechanism of sensitisation effect of Cu and Na ions 77−16369
ZnS:Cu, film effect of Cu valency on cond. 79−11246
ZnS:Cu, Gudden-Pohl effect, flash kinetics 79−24367
ZnS:Cu, H, double band phosphor, electrolum., −100 to +100°C 78−10987
ZnS:Cu, halogen, electroluminescent cells, visible light and DC voltage effects on ageing 77−69914
ZnS:Cu, Mn DC electroluminescent powder panels, bulk and junction effects 80−89068
ZnS:Cu, O(Fe,Co,Ni) photoconductors, killer impurities effect on electron escape probabilities and trap depths 77−4392

zinc compounds continued
ZnS:Cu, Pb, phosphors, ruby laser stimulated time delayed emission spectra 77−69874
ZnS:Cu, polycryst. electret, electroluminesc. light flash character *(Russian)* 77−55833
ZnS:Cu, polycryst. phosphor, excitation storage, recombination barrier participation 78−27316
ZnS:Cu, spectral distrib., rise and decay behaviour *(German)* 80−60625
ZnS:Cu,Al, anisotropy of blue-Cu luminescence centres 78−64390
ZnS:Cu,Al phosphor, shallow hole traps 78−31237
ZnS:Cu,Cl, electrolum. brightness wave, effect of square pulses 77−52184
ZnS:Cu,Cl, electrolum. voltmeter design, accurate high-voltage meas. 78−24813
ZnS:Cu,Cl, exciton refl. spectra, hexagonal struct. 77−44021
ZnS:Cu,Cl phosphor, effect of charged imperfections on electrolum. 77−32443
ZnS:Cu,Cl(Br)(I), green luminesc., interimpurity phototransitions investig. *(Russian)* 77−66541
ZnS:Cu,Co, phosphor luminesc. screen, spectral characts. determ. of IR pulsed lasers 79−10341
ZnS:Cu,Er,Cl film, ageing and forming, DC electroluminesc., impact excitation 79−47522
ZnS:Cu,O, photocurrent spectral distrib., Fe, Co and Ni impurity effects 77−8135
ZnS:Cu,Pb, thermoemission of positive ions in simple gas atmos. *(Russian)* 77−28676
ZnS:Cu,Pb film, sublimated, pulse electrolum. meas. *(Russian)* 77−85806
ZnS:Cu,Pt phosphors, photoluminesc., thermoluminesc. 78−43915
ZnS:Cu 79−24350
ZnS:Cu AC electroluminescent patterns and polytypic transformations 78−6784
ZnS:Cu crystal, powder, epitaxial film, luminescence anomalous thermal 80−76077
ZnS:Cu crystallophosphors, spectra of IR electrophotographic sensitivity *(Russian)* 80−50423
ZnS:Cu phosphor, electric field quenching of photoluminesc. and flashlike rise in luminesc. 78−2911
ZnS:Cu powder exam. of dielectric constant anomaly, in terms of polarisation catastrophe phenomena 79−51897
ZnS:Cu^{2+}, Jahn-Teller effect, stacking faults and formation of polytypes, absorption and emission spectra 77−4660
ZnS:Cu^{2+}, motional averaging in excited state 77−66137
ZnS:Cu(Cl), electroluminesc. and photoluminesc. spectra, fine struct. *(Russian)* 78−84661
ZnS:Cu(Pb), phosphor, photocapacitive effect, Gudden-Pohl effect 79−65520
ZnS:Er diodes, electrolum. 79−33840
ZnS:Er^{3+}, ion-implanted, annealing, cathodolum. obs. 80−2868
ZnS:Er^{3+}, luminesc. centres with cubic symmetry 79−38636
ZnS:Eu^{3+}, origin of red fluoresc., occurrence of rare earth oxysulphide inclusions *(French)* 77−69875
ZnS:Fe, luminesc. and ESR investigations 80−2822
ZnS:Fe, piezospectroscopic effect on electron-vibr. lines of Fe^{2+} 78−27269
ZnS:Fe^{2+}, impurity electron-phonon reson. relax. time, thermal cond. 77−59085
ZnS:Fe^{2+}, low temp. Mossbauer spectra, in source and absorber expts. 77−28500
ZnS:Fe^{2+}, relax. meas. from Mossb auer absorber and source expts. 80−39956
ZnS:Fe^{2+}, reson. relax. time for impurity electrons and localised phonons interaction, appl. to thermal cond. 80−59590
ZnS:Fe^{2+}, thermal expansion and heat capacity, effect of Fe^{2+} 77−31782
ZnS:Fe^{3+}, spin-lattice relax., expt. evidence for optical phonons 80−20451
ZnS:Ga, self-activated emission, A-centre ODMR 79−95685
ZnS:Ga(Cl), deep traps, impurity electroabsorpt. and photocond. meas. 78−6707
ZnS:In, polarisation of deep centre electroabsorpt., effect of random electric fields 77−48148
ZnS:In, recombination emission by optically detected magnetic resonance 80−66272
ZnS:M, M=substitutional impurities, lattice dynamics and local mode freqs. *(French)* 77−66011
ZnS:Mn, AC thin film electroluminesc., filamentary emission and memory effect 79−38672
ZnS:Mn, AC thin-film electrolum. devices, electrolum. efficiency profiles 79−65931
ZnS:Mn, Cu, Cl films, AC electrolum. 80−60679
ZnS:Mn, Cu powder devices, DC electroluminesc. 79−38674
ZnS:Mn, dopant conc. effect on stacking fault energy 80−2041
ZnS:Mn, electrolum. film, direct impact excitation of Mn centres 77−24900
ZnS:Mn, electrolum. films, activating impurity diffusion coeff. *(Russian)* 77−84995
ZnS:Mn, electroluminescent film, stimulated emission *(Russian)* 77−19255
ZnS:Mn, phosphor, surface changes following interaction with H *(Russian)* 78−72602
ZnS:Mn, Raman spectrum, luminesc. rejection 77−18100
ZnS:Mn, self-activated and Mn^{2+} emission, high press. action 80−16093
ZnS:Mn AC thin film devices, domain electrolum. 80−66303
ZnS:Mn AC thin film electrolum. device, filament behaviour 80−20712
ZnS:Mn co-deposited electrolum. thin film device, phys. and elec. characterisation 80−20713
ZnS:Mn electroluminescent films, amplification factor during electric field excitation, population inversion *(Russian)* 79−78757
ZnS:Mn film, AC electrolum., memory effect 78−15228
ZnS:Mn film, AC electrolum., memory effects 79−38673
ZnS:Mn film, current conduction and light emission, physical mechanism 78−14840
ZnS:Mn film, electroluminescence theory 79−11470
ZnS:Mn film, emission centres of DC electrolum. 78−68564
ZnS:Mn film, luminesc. of highly efficient DC diodes 77−8630
ZnS:Mn film, spectral and electro-optical props. 77−1736
ZnS:Mn film device, laser modulation of electrolum. 78−52576
ZnS:Mn film in SnO_2-ZnS-Cu_xS-ZnS:Mn-Al_2O_3-Al struct., electrolum. 79−33837

zinc compounds continued
ZnS:Mn films, photoluminesc. and electroluminesc., excitation mechanism of luminesc. centres 79−11459
ZnS:Mn films, surface struct., microrelief rel. to morphology of SnO_2 transparent cond. support 79−56092
ZnS:Mn on SnO_2/glass transparent conductive base, surface morphology effects on electroluminesc. *(Russian)* 78−48238
ZnS:Mn Schottky diodes, reverse-biased, electroluminescence, hot electron impact excitations 80−25005
ZnS:Mn-H atom systems, surface physiochem. changes, radical recombination luminesc. investig. 79−56863
ZnS:Mn^{2+}, $^4T_1$ excited state, absorpt., MCD, Jahn-Teller model 78−43907
ZnS:Mn^{2+}, $^4T_1$ state, magneto-optical meas. 77−20833
ZnS:Mn^{2+}, $^4T_2$ level, Zeeman splittings, Jahn-Teller effect 80−40141
ZnS:Mn^{2+}, cubic, EPR, ENDOR 77−77093
ZnS:Mn^{2+}, heavily doped, anomalies in reflectivity 77−20891
ZnS:Mn^{2+}, Jahn-Teller effect in fluorescent level 78−52566
ZnS:Mn^{2+}, spin-lattice coupling coeffs. of Mn^{2+} ions in stacking faults 77−20690
ZnS:Mn^{2+}, spin-lattice relax. time, continuous saturation expts., spin diffusion 77−36120
ZnS:Mn^{2+}, spin-lattice relaxation, EPR, optical phonons 80−39852
ZnS:Mn^{2+} phosphors, luminesc. excitation spectra and exciton struct. 80−55164
ZnS:MnF_2 films, effect of Mn conc., XPS obs. 79−33886
ZnS:Mn(Al)(Te), luminesc., exciton struct. 79−33801
ZnS:Na, and undoped, thermoemission of positive ions in simple gas atmos. *(Russian)* 77−28676
ZnS:Ne, implanted single crysts., photolum. and bombardment effect, thermolum. curve obs. 80−55166
ZnS:Ni, IR luminesc. and absorpt. spectroscopy 80−108261
ZnS:Ni, optical absorpt., impurity ionisation, optical phonon coupling 80−88505
ZnS:Ni^{2+}, Zeeman effect at Ni impurities 80−60633
ZnS:Pb, blue luminesc., photoexcited EPR spectrum 80−108070
ZnS:Pb, luminescence, polaris. emission 79−38634
ZnS:Pb current pulses due to elec. field liberation of electrons from trapping centres by tunnel processes 79−28378
ZnS:Pb phosphor, electrolum. brightness, temp. depend. 77−48249
ZnS:Pb phosphor, ionisation mechanism of field trapping centres 80−45156
ZnS:Pb phosphor mech. of elec. field liberation of electrons from traps 78−72616
ZnS:Pb^{2+}(Mn^{2+}), high press. luminesc., localised excitations 78−19534
ZnS:RF_3 film, AC electrolum., memory effects 79−38673
ZnS:RF_3 in Ta-Ta_2O_5-ZnS:RF_3-Au struct., electrolum. and cathodolum. meas. *(French)* 77−16398
ZnS:S, photoconductivity and negative differential photo-effect 78−39156
ZnS:Tb, Cu(Ag) phosphors, luminesc. props. 80−100690
ZnS:Tb^{3+}, NdF_3 film, vac. deposited, electrolum. energy transfer 80−2861
ZnS:Tb^{3+}, sputtered film, DC electroluminesc. and host-excited photoluminesc., Tb^{3+} content depend. 77−85807
ZnS:TbF_3, photoelectroluminescence, effect of electron-hole pairs 78−27328
ZnS:TbF_3 film between semicond. Y_2O_3 layers, bright green electrolum. 80−2859
ZnS:Te, single crysts. grown from Te soln., photolum. props. 79−52005
ZnS:Tl(Al)(Zn), UV spectra of donor-doped single crysts. 77−12404
ZnS:Tm, cathodoluminesc. yield, calorimetric method determ. *(Russian)* 77−20938
ZnS:Tm^{3+}, charge compensation and polytypism influences on fluorescence 80−89051
ZnS:Tm(Er)(Nd) phosphors, optical scintillation mechanism 79−56867
ZnS:V (d^3), absorption and luminesc. spectra 78−15203
ZnS:Yb^{3+}(Nd^{3+}), spin-lattice relax. times meas. 78−19324
ZnS/ZnSe composite window, erosion-resistant, fabriction and evaluation 78−71211
ZnS-Ag, broad band visible heat reflecting mirror 77−39017
ZnS-Ag-ZnS coating on glass, structure, optical props. 77−46781
ZnS-Al_2S_3, phase relationships, 720 to 1110°C 79−1852
ZnS-Au electrolum. Schottky barrier diode, S^+-implanted, blue emission 80−76082
ZnS-based phosphor, microstruct. and luminesc. efficiency 78−10959
ZnS-BiOCl, electroluminesc. heterojunction phys. props. 77−66198
ZnS-CdS, equimolar solid soln. formation kinetics 80−39289
ZnS-CdS, fluorescent screens for thermophotography 77−171
ZnS-CdS films, prep. by atomisation 80−16176
ZnS-CdS system, IR luminesc. and absorpt. centres, donor-acceptor pair model 77−44043
ZnS-CdS system, solid soln. form. mechanism 79−43177
ZnS-CdS:Ag, cathodoluminesc. yield, calorimetric method determ. *(Russian)* 77−20938
ZnS-CdS:Ag, Ni, Co, thermoluminesc. glow curves 78−95611
ZnS-CdS:Ag, Ni, Co phosphor, thermoluminesc. 77−66547
ZnS-CdS:Ag, Ni luminophor, temp. sensitive, biological effects of microwaves determ. appl. 80−36186
ZnS-CdS:Ag, phospors, nature of fluorescent centres and traps 79−91484
ZnS-CdS:Ag(Cu), cryst. struct., electron traps and glow curves 79−61437
ZnS-CdS:Ag(Ni)(Co), electron-irradiated phosphors, void formation mechanism 79−55780
ZnS-CdS:Tm,Ni, recomb. centre interaction, luminesc. quenching 78−10946
ZnS-Cu, comet shaped electroluminesc. lines 78−52578
ZnS-Cu, polycryst., influence of alternating elec. field and UV light on struct. defects, electrolum. expts. 79−43041
ZnS-$CuGaS_2$ heterodiodes, LPE, emission spectra 79−33335
ZnS-$CuGaS_2$ n-p heterojunction, for LED appl., prep. and characterisation 79−1831
ZnS-$CuInS_2$, phase relations, 400 to 1300°C, X-ray and microscopic exam. 79−1853
ZnS-GaAs, n-p heterojunction, struct., multibeam electron microscopy obs. 79−11031
ZnS-GaAs solar cell structs., photolum. props. 80−50958
ZnS-metal interface, metal-induced chem. reactions and surface states 80−20311
zinc compounds continued
ZnS-metal interface in MIM struct., photoexcitation level assignment *(French)* 80−15622
ZnS-metal Schottky barrier height rel. to chem. reactivity 80−25008
ZnS-MgF_2 alloy films, struct. and optical props. 79−90910
ZnS-MgF_2 dielectric film, laser irrad. and microscopic inhomogeneities 78−2157
ZnS-MgF_2 mirror, dielectric, Rayleigh scatt. at 441.6 nm 80−97367
ZnS-MgF_2 mixtures, triple-layer broad band antireflection coatings 79−32011
ZnS-MgF_2/MgF_2, homogeneous mixed dielecs. as antirefl. coatings effective at two visible wavelengths 79−76770
ZnS-MgF_2/MgF_2 double-layer antireflection coatings, transmittance meas. 79−36967
ZnS-MgF_2(SrF_2), dielec. films, transparent, microscopic inhomogeneities and optical breakdown 78−10844
ZnS-MgS, exam. of piezoelectric props. and elastic compliances, as function of MgS conc. 79−95709
ZnS-MgS, solid solution, prep. of single crystals with wurtzite structure, exam. 79−1821
ZnS-Mn crystal, polarisation meas., luminesc. and Raman spectra 79−8138
ZnS-Mn sublimated phosphor films, annealing effects *(Russian)* 78−43949
ZnS-MnS, phase relations, 400 to 1300°C, X-ray and microscopic exam. 79−1853
ZnS-MnS-$CuInS_2$, sobsolidus equilib., phase diagrams 80−3016
ZnS-Na_2O-K_2O-SiO_2, form. using electric furnace, furnace design 80−11620
ZnS-Na_3AlF_6 Fabry-Perot interference filter, neutron irrad. effects on props. 79−76867
ZnS-Na_3AlF_6 layer achromatic interference polarizers, design, fabrication 79−55222
ZnS-Na_3AlF_6 multilayer dielectric optical filter, irreversible thermal effect 77−7195
ZnS-Na_3AlF_6 multilayer films, thermally evaporated, dispersion characts. 77−59629
ZnS-O, single cryst., fast neutron irrad., optical props. 78−27331
n-ZnS-p-Cu_2S heterojunction, I-V characts., photocond. and electrolum. 78−72251
ZnS-SiO_2 multilayer reflector, reflectance under slight absorpt. conditions 80−83655
ZnS-SrF, multilayer dielec. coatings, radiation breakdown and microinhomogeneities 80−7294
ZnS-SrF_2 dielectric film, laser irrad. and microscopic inhomogeneities 78−2157
ZnS-ZnO, solid solns., edge emission and exciton spectra *(Russian)* 77−24899
ZnS-ZnSe mixed powders, hot-pressed polycrystalline, photolum. and electrolum. 77−32426
ZnS-ZnSe single cryst. grown from melt, anisotropy of mech. props. and struct. 77−24303
ZnS_2, mag. props. rel. to Hubbard model 79−78373
ZnS_2, XPS of valence band meas. 77−85885
(ZnS-ZnSe):Cu, H systems, electrolum. 77−4690
$(ZnS)_{0.2}(CdS)_{0.8}$, elec. props. effect of wurtzite-sphalerite boundary 77−55531
$ZnSO_4$, aq. solns., viscosity meas., viscous flow activation energy, entropy *(Japanese)* 77−43363
$ZnSO_4$, cubic H-cristobalite struct. *(German)* 79−51089
$ZnSO_4$, effect of press. on ion pair dissoc., cond. of aq. solns. 78−53218
$ZnSO_4$, electrolyte evaluation by cyclic voltammetry and SEM 77−29076
$ZnSO_4$ electrolytes containing Ge and Co, polarisation charact., exam. by cyclic voltammetry 80−104444
$ZnSO_4$, LMFBR, boiling pools with internal heat generation, void distrib. 78−21626
$ZnSO_4$, rate constant of reaction, determ. from overall crystal growth coeff. 78−59773
$ZnSO_4.H_2O$, hydrate librational modes in IR spectra 78−48161
$ZnSO_4.7H_2O$ impurity meas. using digital instrument *(Polish)* 78−31653
$ZnSO_4.7H_2O$, meas. of water physically adsorbed rel. to water of crystallisation *(Japanese)* 80−6622
$ZnSO_4.7H_2O$:Mn^{2+}, EPR 77−16165
$ZnSO_4.7H_2O$:VO^{2+}, single cryst., struct., EPR 78−15014
ZnS(Se), highly transparent semicond., multiphonon IR absorpt. 78−60461
ZnS(Se), ionicity trends in diamagnetism and its temp. depend. 79−19717
ZnS(Se), reaction with Sn chalcogenides, thermodynamic anal. 80−40728
ZnS(Se), stress-induced birefringence meas., 1-12 μm 77−24818
ZnSSe:Cu, Br, SCL currents and electrolum. via rad. recomb. 77−44065
ZnS(Se):Mn^{2+}, ^4E levels, orbit-lattice interaction and Jahn Teller effect 80−24860
$ZnS_{1-x}Se_x$, electroluminescence with In and Au contacts, comp. depend. 77−59618
$ZnS_{1-x}Se_x$:Cu,Br ceramic, current oscills. and electrolum. under high elec. fields 79−38677
ZnS_xSe_{1-x}, band gap, comp. depend., exciton refl. spectrum obs. 78−56071
ZnS_xSe_{1-x}, electron trap associated with anion vacancy, DLTS study 80−80210
ZnS_xSe_{1-x}, epitaxial film, CVD growth and characterisation *(French)* 77−36403
ZnS_xSe_{1-x}, epitaxial film on CaF_2, comp. and temp. depend. of fund. band gap 80−11115
ZnS_xSe_{1-x}, growth of cubic single crystal by I_2 transport 79−91572
ZnS_xSe_{1-x} laser, electron-beam pumped, end-pumped config., 415-430 nm emission 77K 77−14745
ZnS_xSe_{1-x} layer on ZnS, ZnSe, growth by solid-state diffusion technique 78−56578
ZnS_xSe_{1-x}, phonon spectra calculations by recursion method, mixed crystals 80−103430
ZnS_xSe_{1-x}, VPE, characterisation of defect centres by photoelectronic meas. 80−10914
ZnS_xSe_{1-x}, VPE on CaF_2 substrate, in flowing H_2, growth and characterisation *(French)* 80−107678
ZnS_xSe_{1-x}:Fe, photolum. meas. 79−19921
ZnS_xSe_{1-x}:Mn(Cu), luminesc. obs. 78−60519

zinc compounds continued
ZnS(Se)(Te), clean and oxidised surfaces, O_2 sticking coeff., ionicity effects, XPS expts. 77−85887
ZnS(Se)(Te), relative supersaturation, formula valid for different technological conditions *(Russian)* 78−84081
ZnS(Se)(Te):Co^{2+}, IR luminesc. quenching, Co^{2+} level position, ionisation energy 80−16079
$ZnS_{1-x}Te_x$, polytype single cryst. grown from melt 79−14762
ZnS.CdS, flux growth, processes accompanying roasting of CdS+NaCl 78−23590
ZnSb, band struct. calc. 78−39015
ZnSb, enthalpy of formation *(Russian)* 80−35564
ZnSb, epitaxial films, growing conditions effect on elec. cond., thermo-EMF 80−39687
ZnSb, layer growth in Zn-Sb diffusion couple at high press., elec. meas. 80−2218
ZnSb, orientated crystn. conditions during reaction diffusion *(Russian)* 80−70558
ZnSb phase in Zn-Sb diffusion couple, layer growth kinetics, 240-320°C, up to 30 kbar 78−10229
ZnSb, thermodynamic props. and elastic moduli 79−77767
ZnSb, thermoelec. anisotropic semicond., carrier kinetics at low temps. 80−92893
ZnSb, X-ray diffr., 78-300K, dynamical props. and thermal expansion *(Russian)* 77−7833
Zn_3Sb_2, phys. props. 78−26527
$ZnSb_2O_4$, isomorphous with Pb_3O_4, cell parameters evolution with temp. *(French)* 78−75642
$ZnSb_2O_6$, force fields rel. to cryst. struct. *(French)* 80−107104
$ZnSc_2O_4$ spinel, cryst. struct. 79−32963
$ZnSc_2S_4$, IR and Raman spectra, force consts. 78−68503
ZnSe 79−38457
ZnSe, ^{67}Zn Mossbauer spectroscopy with 93 keV reson. 80−66095
ZnSe, ^{67}Zn nuclear magnetic shielding, chemical shifts and linewidths 80−60434
ZnSe, 10.6 μm absorption meas. using thermal emission 77−1649
ZnSe, 93.3 keV Mossbauer transition in ^{67}Zn, isomer shifts 80−39978
ZnSe (100) surface, electronic struct., scattering-theory formulation 79−42607
ZnSe (100) surfaces, surface states meas. by LEED, AES and EELS *(Japanese)* 79−99599
ZnSe (110), LEED intensity anal. and electron spectroscopy 77−43678
ZnSe (110) surfaces, obs., by low-energy-electron loss spectroscopy *(Japanese)* 79−83071
ZnSe (111), low-energy electron loss spectra, bulk and surface transitions 78−11042
ZnSe, absorpt. modulation of light, and its appl. to page composer 77−40258
ZnSe, absorpt. modulation of light, and its appl. to page composer *(Japanese)* 78−83083
ZnSe, ambipolar diffusion meas. using nonlinear transient gratings 78−80000
ZnSe, amorphous thin film, prep. and electronic props. 77−85350
ZnSe and ZnSe:Sb, photoconduction under Nd laser irrad., local level distrib. 77−55580
ZnSe, Anderson-Gruneisen parameter, bulk modulus temp. depend. 78−10154
ZnSe, attenuated total refl. spectra of surface exciton polariton 77−36262
ZnSe, band-edge photoluminesc., far-below band-gap excitation 80−76063
ZnSe, blende type struct., luminesc. under high excitation 79−19928
ZnSe, blue photoluminesc. excited with strong laser radiation 80−93391
ZnSe, Bridgeman growth under pressure, macroscopic inclusions and defects 80−45226
ZnSe, Bridgman growth under Ar press., temp. distrib. in furnace 78−11100
ZnSe, bulk and surface states anal. using synchrotron radiation 77−66574
ZnSe, CVD, delayed failure 79−99462
ZnSe, CVD, laser window material, refr. index, temp. and stress effects 77−46771
ZnSe, CVD, laser window material, impurity absorpt. meas. 78−25909
ZnSe CVD IR material specifications 80−48364
ZnSe, carrier mobility and deform. pot. const. determ. 79−91051
ZnSe, cathodoluminesc. in SEM, spatial resolution anal. *(Russian)* 77−32448
ZnSe, charged dislocation motion mechanism *(Russian)* 78−79820
ZnSe, charged dislocations, flow of charge with plastic deform. 80−85010
ZnSe, clean and oxidised surfaces, surface states, low-energy EELS study 80−11522
ZnSe coated CaF_2 trapezoid, IR characterisation by internal-refl. spectra 78−71161
ZnSe, coated/uncoated, effect of sand erosion on optical absorption 77−72037
ZnSe coatings on CaF_2 laser windows, photoacoustic spectroscopy 80−33052
ZnSe cold pressing 77−52258
ZnSe, commercial feasibility for optical ceramic manufacture 79−87598
ZnSe, cryst., elec. cond., dislocation motion effects 80−54710
ZnSe cryst., IR absorpt., annealing effect 80−80774
ZnSe crystal, difference freq. generation of 2 CO_2 lasers 79−10362
ZnSe crystal, exciton reflection spectra, control of exciton-free surface layer thickness 80−7373
ZnSe, crystal, new polytype structure 78−14319
ZnSe crystal, refr. index temp. increments meas. 80−33098
ZnSe crystal and film, refr. index, 10.6 μm ellipsometric meas. 78−24847
ZnSe, crystallographic polarity and etching behaviour 77−85030
ZnSe crystals, degenerate four-wave interaction, nonlinear optics effects 80−91856
ZnSe crystals, doped and undoped, optical absorption edge 80−60626
n-ZnSe crystals, electron scatt. mechanisms, high mobility 80−34433
ZnSe, cubic, anomalous photovolt. effect in absorpt. tail 79−42583
ZnSe, cubic, magnetoreflectance of Γ_6-Γ_8 exciton ground state 78−23495
ZnSe, cubic, magnetoreflection of s-excitons 78−60426
ZnSe, cubic, valence band parameters, magnetoreflectance of Γ_6-Γ_8 exciton 78−60056

zinc compounds continued
ZnSe, cubic and hexagonal, lattice coupling with BiOCl, ErOCl and LaOCl for heterojunctions 79−60919
ZnSe, cubic cryst., optical birefringence obs. 77−4616
ZnSe, cubic cryst. lattice dynamics, overlap shell model and bond charge model 79−42156
ZnSe, cubic monocrystal, electron-phonon interaction, low temp. luminesc. *(Russian)* 80−25451
ZnSe, deep centres, photolum., photocapacitance and photocurrent expts. 78−39053
ZnSe, diatomic crysts. electron induced X-ray emission, channelling effects 79−56888
ZnSe, dielec. const. strain depend., spectral behaviour by acousto-optic method 77−48147
ZnSe, direct gap semicond., exciton energy at 300K from reabsorption of luminesc. 79−78728
ZnSe, dislocation motion, influence on elec. cond. 79−15149
ZnSe, donor-acceptor pair emissions charact. *(French)* 80−108249
ZnSe, EXAFS amplitudes, many-body effects 80−97379
ZnSe, elastic moduli, temp. depend., 293-973K, electrostatic reson. determ. 78−59850
a-ZnSe, elec. and optical meas., Mott-type model for amorphous semicond. 78−2414
ZnSe, elec. props. efect of wurtzite-sphalerite boundary 77−55531
ZnSe, electric charge transport by dislocations 80−103709
ZnSe electrode, electrochem. behaviour *(French)* 79−52676
ZnSe, electroluminesc. exam. high voltage pulses 79−15533
ZnSe electroluminescent diode, ageing effects 77−8660
ZnSe, electroluminescent MIS diodes, surface state density determ. 77−35993
ZnSe, electron beam induced current study of grain boundaries by SEM 80−59479
ZnSe, electron irrad., dislocation climb, TEM obs. 79−1461
ZnSe, electron irrad., short-lived optical absorpt. 79−51989
ZnSe electron irradiation induced displacement defects 77−80543
ZnSe, electron trap associated with anion vacancy, DLTS study 80−80210
ZnSe, electron-beam-controlled transmission of 10 μm radiation 79−81466
ZnSe, electronic struct. of charged Zn vacancy, cluster model 77−47764
ZnSe, electronic structure, self consistent local description 80−20067
ZnSe, empty surface states and surface order effects on sorption 77−85281
ZnSe, energy levels of Mott excitons 78−6282
ZnSe, epitaxial, organometallic CVD, on GaAs, and photolum. 79−8249
ZnSe, epitaxial growth, orienting semiconductive substrate effects 77−47688
ZnSe, epitaxial growth by vapour flow method 78−64482
ZnSe, epitaxial growth on Ge substrate 80−75469
ZnSe, epitaxial layers, close-spaced technique, preparation and optical props. 79−47637
ZnSe epitaxial layers, organometallic CVD prop., growth kinetics and luminescent props. 79−51458
ZnSe epitaxial layers, prep. by chem. transport reactions 80−16192
ZnSe epitaxial layers, growth kinetics on CaF_2 by vapour phase transport *(French)* 80−54572
ZnSe etalon, temp. controlled, multiline oscillation charact. of TEA CO_2 laser 80−74334
ZnSe, evap. onto electron bombarded NaCl substrates, epitaxial growth and charact. 79−28948
ZnSe, exciton emission, halfwidths, thermal and optical activation energies obs. *(French)* 80−66268
ZnSe, exciton energy determ., electron beam excited luminesc. 79−38680
ZnSe, exciton refl. spectra, temp. depend. 80−59886
ZnSe, exciton-impurity complex, electroabsorption meas. 79−15484
ZnSe, Faraday effect visible optical isolator 77−75657
ZnSe film, grown on sapphire substrate, stimulated emission 79−78708
ZnSe, film, hopping cond. 80−2499
ZnSe film, MBE and resistivity 79−100059
ZnSe film, on semicond. substrate, early stages of growth, electron microscope obs. *(Russian)* 78−38976
ZnSe film, rare earth fluoride doped, electrolum. meas. 77−16397
ZnSe film, strain induced anisotropy, ellipsometer and reflector meas. 79−33856
ZnSe film, struct., influence of laser beam 79−7761
ZnSe film, surface polaritons, thermostimulated emission *(Russian)* 78−10904
ZnSe film, thermostimulated polariton emission 78−2436
ZnSe film on GaAs substrate, transition layer form. kinetics 79−87007
ZnSe films, long wavelength IR polariton emission band thermal shift and broadening 80−92833
ZnSe films, reson. Raman spectra 80−80888
ZnSe, grown from Ga soln., near band-edge luminesc. 79−69881
ZnSe, growth centres, crystallographic parameters and etching patterns study *(French)* 79−41998
ZnSe, growth of cubic single crystal by I_2 transport 79−91572
ZnSe, Gudden-Pohl effect, release of electrons from traps 80−45149
ZnSe, heat-treated in controlled partial press. of Zn or Se, TSC 80−59910
ZnSe, high conductivity films appl. to p.n. heterojunctions 78−68100
ZnSe, high field Faraday rotation, 6.5K 79−38522
ZnSe, high transparency IR material 77−27326
ZnSe, high-resistance layers, effect of electrode materials on switching 79−65549
ZnSe, highly transparent semicond. crysts., multiphonon IR absorpt. 78−10885
ZnSe, hot-pressed powder LED fabrication and charact. 78−23639
ZnSe, IR absorpt., temp. depend. 78−48155
ZnSe, IR laser window coating absorption rel. to deposition conditions 79−14061
ZnSe, IR transmitting semicond., dn/dT, wavelength depend. 77−77163
ZnSe, IR transparent materials, forward and backward scatt. data 78−59099
ZnSe IR window refractive index var. with temp., −180° to +200°C obs. 79−14052
ZnSe, impact ionisation electroluminesc. 77−44066
n-ZnSe, impurity band, Hall effect, elec. cond., mobility and magnetoresist. expts. 77−35888
ZnSe, impurity effects on two-photon absorpt. spectrum 77−59597

zinc compounds continued
ZnSe in insulator-semicond.-insulator struct., induced birefr., influence of kinetics of transient processes 79−24294
ZnSe, inhomogeneous interface laser mirror coatings 80−1252
ZnSe, ionisation energy of H-like impurities 80−20120
ZnSe LED, p-n and MOS structs., blue electrolum. 77−32441
ZnSe, LPE from Zn-Ga soln., charcts. 79−28965
ZnSe, LPE growth on ZnTe, characterisation of heterojunction 77−4745
ZnSe, laser damage threshold at 10.6 μm, up to 10^{10} W/cm^2 77−50707
ZnSe, laser induced modulation of opt. absorpt. 78−88324
ZnSe, laser irradiated, in-depth and surface temp. meas. by Moire-Schlieren technique 80−53392
ZnSe, laser residual lattice absorpt., freq. and temp. depend. 78−25910
ZnSe laser window, laser induced thermal stresses 77−46747
ZnSe, laser window material, multiphonon absorpt. temp. depend., calorimetric meas. 78−25907
ZnSe, laser window material, absorpt. at CO wavelengths, calorimetric meas. 78−25911
ZnSe, laser window material, surface and bulk absorpt., photoacoustic meas. 78−25912
ZnSe laser window photoacoustic spectroscopy 80−33052
ZnSe laser windows, AR coated, photoacoustic chopping freq. studies using CO_2 laser 80−83629
ZnSe laser windows, photoacoustic signal var. with chopping freq. 80−75309
ZnSe, lattice vibration, thermal expansion and pressure effect 80−39233
ZnSe layers, cond. type determ. by pot. profiling 80−73387
ZnSe layers, LPE growth from Zn-Ga soln., photoluminesc. 79−56840
ZnSe, linear electro-optic coeff. dispersion, relation to reson. Raman scatt. 78−56459
ZnSe, linear thermal expansion coeffs. meas., room temp. to 250°C 78−55416
ZnSe, liq. drop collisions, simulation of erosion in rainfield 77−56113
n-ZnSe, long persistent cond. relax. and frozen cond. 80−54735
ZnSe, low resist. single crysts., radiative recomb. mechanism, photolum. and electrolum. 78−6744
ZnSe, low resistance ohmic contacts using In-Ga liquid alloy, LED fabrication appl. 80−70823
a-ZnSe, low temp. photocond., increase of activation energy as temp. decreases 78−26902
ZnSe, luminesc., hot electron effects 80−66277
ZnSe, luminesc., reson. Raman scatt. due to excitonic mols. 79−33816
ZnSe, MBE growth, elec. and optical props. 80−75462
ZnSe MBE growth, growth rate and sticking coeff. 77−32532
ZnSe MIS diode, blue electrolum., heat treatment effects 78−19569
ZnSe MIS diode, forward-bias electrolum. 78−23532
ZnSe MIS LED, donor density calc. from C-U meas. 78−47878
ZnSe MOS diodes, injection type electrolum. 77−59614
ZnSe MOS diodes, injection luminesc., edge emission 79−28842
ZnSe, mech. of electroplastic effect 79−28035
ZnSe, mid IR laser window materials, absorption props. 77−46770
ZnSe, minority carriers diffusion length by surface photovoltage method 80−60003
ZnSe, moments of phonon spectra from specific heats 80−15203
ZnSe multilayer film, intrinsic and thermal stress modelling and interferometry 79−14059
ZnSe, multiphonon ionisation of deep point centres in a charged dislocation field *(Russian)* 80−100281
ZnSe, multispectral aircraft window materials, production processes 77−73237
ZnSe, NMR, chemical shift and linewidth determ. 79−19792
ZnSe, nature of large electric charges of moving dislocations *(Russian)* 78−39065
ZnSe, near band edge photoluminescence, electron-hole recombination 80−80835
ZnSe, nonlinear optical effects in rotationally twinned crysts., phase matching 77−42570
ZnSe, nonstoichiometry, Zn and Se press. meas., up to 1400K 78−87664
ZnSe, ODMR expts., A and V^--centres, origin of emission bands 78−80255
ZnSe, optical axes for birefringence *(French)* 77−20819
ZnSe, optical material, thermal expansion, 60-300K 78−32791
ZnSe, optically detected mag. reson., donor g-factor 77−69732
ZnSe, optically detected mag. reson. of V^- centre and donors 78−10805
ZnSe, optically pumped stimulated emission at 4580 Å, near band edge luminesc. 78−71105
ZnSe, oxidation by atmos. O_2 and SeO_2 vapour 77−52520
ZnSe, P-T diagram, cryst. struct. stability 78−51886
ZnSe, parasitic birefringence dispersion induced by lattice plane defects 77−4617
ZnSe, phase transition, differential thermal analysis 77−7863
ZnSe, phonon dispersion under extreme press. and metallic transform., Raman spectra meas. 78−10895
ZnSe, phonon dispersion relations, eight-parameter bond-bending forces model 80−70334
ZnSe, photocurrent, temp. depend. and extinction, elec. inhomogeneity effects *(Russian)* 77−32037
ZnSe, photoelastic and elastic constants determ. using thermal Brillouin scatt. *(Japanese)* 79−51974
ZnSe, photoexcited hot electrons at 2K, photolum. meas. 79−78741
ZnSe, photolum. and blue electrolum. in MIS structs. 77−20928
ZnSe, photolum. excitation spectra of tightly bound holes, valence band contrib. 80−60658
ZnSe, photoplasticity and photocond., excitation energy conc. near dislocations, hardening 77−24346
ZnSe, piezobirefringence in opaque region 80−60541
ZnSe, polar semicond., radiative recomb., electron-phonon interaction effects, calc. 80−49631
ZnSe, polaritons, reson. Brillouin scatt., heavy and light excitons 79−99898
ZnSe, polycryst., laser window material, IR thermooptic coeff. meas. 77−36208
ZnSe, positron annihilation study 80−60713
ZnSe pulses and single crystals, oxidation in air 77−12724
ZnSe, pure and Cu doped, elec. props. after heat treatment in Zn or Se vapour 79−99505
n-ZnSe, purified by annealing in molten Zn, Hall mobility and polaron coupling 77−85243
ZnSe, RF bias-sputtered CVD films on CaF_2 79−14060
ZnSe, reabsorpt. of excitonic luminesc. in direct band gap semiconds. 77−63469
zinc compounds continued
ZnSe, reactor irrad., opt. props. 77−90137
ZnSe, recrystallisation during hot pressing 77−85952
ZnSe, refr. index meas. and nonlinear moment parameters 77−85681
ZnSe, refr. index meas. at 3.8 μm, 10.6 μm, 80 to 300K 79−82938
ZnSe, relaxation processes in Raman scattering and exciton luminescence under resonant excitation 80−25386
ZnSe, residual cond., recomb. of photoexcited carriers, Hall coeff. 80−75605
ZnSe, reson. absorpt. of coherent IR radn. by acceptors, photocurrent and emission spectra 79−73974
ZnSe, reson. Brillouin scatt., lifetime broadening 79−51971
ZnSe, reson. Brillouin scatt., dispersion curves, piezobirefringence anal., electronic state lifetime broadening effects 79−61390
ZnSe, reson. Brillouin scatt., quasi-static anal. 79−65887
ZnSe, reson. Raman scatt. meas. 77−66510
ZnSe, resonance Raman scatt., exciton-polariton luminescence *(Russian)* 80−97287
ZnSe, resonant Brillouin scatt. by injected acoustic waves 77−12394
ZnSe, Schottky barrier, semiempirical ligt-binding calcs. 79−28408
ZnSe, second order Raman scatt., lattice dynamical calc. and expt. 80−25370
ZnSe, self-compensation, role of impurities 80−92850
ZnSe, self-consistent localised electronic struct. 79−42445
ZnSe, single cryst., electron-hole drops, boundary luminesc. *(Russian)* 78−80412
ZnSe single cryst., lasing action excited by ruby laser picosecond pulses 80−64035
ZnSe single cryst., linear electro-optical props., temp. depend. 80−71376
ZnSe, single cryst. and film, long wave IR emission by lattice vibrs. 77−51528
ZnSe, single cryst. film, MBE, quality obs. using photoluminesc. 77−77419
ZnSe single cryst. for LED, heat treatment effects on elec. props. 80−29406
ZnSe, single cryst. ingot., laser screen for CRT 77−75561
ZnSe, single cryst. vap. growth by sublimation and chem. transport 78−27390
ZnSe single crystal, exciton photolum. and refl. spectra, 4-90K *(Russian)* 77−66540
ZnSe single crystal, nonlinear optical coeff. and SHG coherence length 77−79893
ZnSe single crystals, birefringence due to native defects and electro-optic effect *(French)* 79−24293
ZnSe, single crysts., grown from melt under Ar pressure, defects form. 79−4312
ZnSe, single crysts., opt. band gap and Mn^{2+} EPR, effects of prep. conditions 77−47730
ZnSe single-layer film 2.8 μm, 3.8 μm absorpt. meas. 78−90463
ZnSe solar spectrum convertor for GaAs solar cells 80−101117
ZnSe, solution growth, using Te solvent 79−65993
ZnSe sphere extinction cross section, Mie theory with spatial dispersion 79−98284
ZnSe sputtered laser window coatings, prep. and evaluation 77−50739
ZnSe, streamer laser 77−79831
ZnSe substrate, beam splitter and reflection reducing coatings for 3 to 14 μm 79−76811
ZnSe surface, nonpolar, electronic struct., tight-binding calc. 77−20383
ZnSe surface, quantitative XPS meas. 78−56559
ZnSe, surface (110) atomic struct. 79−69331
ZnSe surface barrier diode, hot charge carriers, elec., photoelec., and electroluminesc. props. *(Russian)* 79−33841
ZnSe, surface exciton polaritons, attenuated total reflection spectra 77−24867
ZnSe surface states, electron interaction characterisation, by low energy electron transmission photovoltaic modulation 79−60896
ZnSe, temp. coeffs. of charact. reflectivity struct. 77−85745
ZnSe, thermal expansion, 20 to 1100°C *(Russian)* 79−95188
ZnSe, thermal expansion and lattice dynamics under press. 80−100316
ZnSe, thermally treated crystals, photoluminesc. 80−60661
ZnSe thermochem. cycle for H prod., chemical and process design studies 80−35782
ZnSe, thermoelec. power meas. 78−52021
ZnSe, transport props., effect of In-doping and Zn-annealing 78−76075
ZnSe, twinning effect on electro-optical props. 78−68478
ZnSe, twinning on melt-growth under pressure 77−80515
ZnSe, two photon absorpt. by envelope-hole coupled exciton states, polarisation depend. 77−66522
ZnSe, two photon absorption relative to Raman cross sections 78−87098
ZnSe, two-photon absorpt., envelope-hole coupled exciton states 77−52124
ZnSe, two-photon absorpt., effect of polarisation of laser radiation 77−69856
ZnSe, two-photon and two-step absorption of light 80−7389
ZnSe, undoped and doped, pair spectra, edge emission and shallow acceptors 77−28617
ZnSe, VPE on GaAS, role of interaction between gas and solids *(French)* 77−62769
ZnSe, valence-band parameters and g-factors from free-exciton magnets reflectance 79−73905
ZnSe, vapour phase single crystal growth 79−91573
ZnSe visible-IR window assembly for ultrahigh vacuum systems 78−54380
ZnSe, wavelength-modulated refl. spectra, 2.5 to 8 eV 77−20877
ZnSe, with wurtzite-sphalerite boundaries, LF photofluctuations 79−69560
ZnSe, X-ray cond. 5.4 to 17.5 keV, spectral and dosimetric charcts. *(Russian)* 77−35964
ZnSe:Ag, low-temp. photolum. meas. 77−20912
ZnSe:Ag^{2+}(Cu^{2+}), absence of EPR spectra due to strong spin-lattice coupling of Kramers doublets 77−85181
ZnSe:Ag(In)(Cu), melt growth, dopant partition coeffs. 79−14837
ZnSe:Al, current switching mechanism *(German)* 79−28385
n-ZnSe:Al, free carrier absorpt., 80-300K 77−63432
ZnSe:Al, thermally stimulated transients, new approach 79−38086
ZnSe:Al, vapour phase doped, thermodynamics 79−90686
ZnSe:Al single crysts., photoluminescence spectra *(Russian)* 77−28627
ZnSe:Al(As), and pure single cryst., defect struct., Hall effect and Zn self-diffusion meas. 79−1427
ZnSe:Al(As), high temp. electron mobility, lattice scatt. and ionized impurity scatt. 79−91042

zinc compounds continued
ZnSe:Al(Ga)(In), single cryst., doping, blue luminesc. 78−39584
ZnSe:Al(Mn), elec. and luminesc. props. 77−39844
p-ZnSe:As, ion implantation and heat treatment 78−87700
ZnSe:B(F), ion implantation, photocond. and cathodoluminesc. meas. 78−26586
ZnSe:Co, effect of in-band position of states on photoelec. props. 78−23132
ZnSe:Co, impurity luminescence no phonon line depend. on temp., Debye temp. 80−66273
ZnSe:Co, optical props. in near IR 78−43924
ZnSe:Co^{2+}, depression of vibronic levels, transition of Jahn-Teller states from dynamic to static 78−43337
ZnSe:Cr, piezodichroism due to reorientation of Jahn-Teller centres 80−11363
ZnSe:Cr^{+}, Fe^{3+}, luminesc. cond. and paramag. centre conc. parameters 78−6724
ZnSe:Cr^{2+}, absorpt. and luminesc. of $Cr^{2+}(d^4)$, cryst. field theory interpretation 79−83000
ZnSe:Cr^{2+}, Cr^{2+} $^5T_2$ and ^5E states, Jahn-Teller effect calcs. 80−39539
ZnSe:Cr^{2+}, excitation spectrum of IR emission 77−12421
ZnSe:Cr^{2+}, Jahn-Teller coupling 78−67997
ZnSe:Cr^{2+}, photoionisation, lattice relaxation energy 80−6778
ZnSe:Cr^{2+}, spin Hamiltonian parameters and wave function coeffs., LCAO theory 77−39804
ZnSe:Cr^{2+}, stress-induced alignment of Jahn-Teller centres 79−78651
ZnSe:Cu, Al, single cryst., low-voltage red cathodolum. 78−80423
ZnSe:Cu, Cl, high press. luminesc. 78−19532
ZnSe:Cu, deep energy levels 80−6774
ZnSe:Cu, discovery of bound exciton, electroabsorption 80−45038
ZnSe:Cu, I, ceramic, electroluminesc., electric field induced switching effect under illum. 77−1460
ZnSe:Cu, I ceramic, injection electroluminesc. of p-n microjunctions 80−40163
ZnSe:Cu, luminescence and diffusion behaviour of Cu impurities 78−35188
ZnSe:Cu,Al, LV cathodoluminesc. 79−33844
ZnSe:F, signal enhancement by field modulation, ODMR expts. 78−56406
ZnSe:Ga, defect struct., Hall effect and resist. meas. 79−1428
ZnSe:Ga, P, optically detected mag. reson. of P_{Se}-centre 79−33566
ZnSe:Ga,As, characts. of simultaneous incorporation, by Mn^{2+} ESR and X-ray fluoresc. anal. 80−34017
ZnSe:Ga(As), edge luminesc. 80−20699
ZnSe:I crystals, I vapour transport prep. 79−100035
ZnSe:I/aqueous electrolyte junction, electrochem. behaviour in dark and under illum. 80−25003
ZnSe:In, heavily compensated, galvanomag. props. and thermopower 79−51600
ZnSe:In, heavily compensated, negative magnetoresistance 79−91079
ZnSe:In, heavily doped, Hall effect and DC cond. expts., compensating acceptors 78−52013
ZnSe:In, heavily doped, impurity band cond., Hall coeff. and cond. expts. 78−72147
n-ZnSe:In, heavily doped, high field DC cond. 79−65490
ZnSe:In, highly compensated single crystals, thermally initiated current breakdown, current-voltage characts. 80−65579
ZnSe:In, Li, binding energy of excitons bound to donor-acceptor pairs, electron-phonon coupling 77−4689
ZnSe:In, optical absorpt. spectrum, 0.4 to 0.7 μm 77−81136
ZnSe:In, single crysts., new vapour phase growth method, elec. cond. props. and photoluminesc. spectra 79−19982
ZnSe:In films, MBE growth, doping effect on photoluminesc. 80−10818
n-ZnSe:Li, semicond. selective pair luminesc., excited impurity state investigation 79−61439
ZnSe:Li diodes, electroluminescence and fabrication, expt. *(Japanese)* 77−28633
ZnSe:Li(Na), shallow acceptor excited states, luminescence spectra, Rydberg energy 79−78750
ZnSe:Li(Na)(Ga) doped and pure cryst., donor-acceptor bands 80−11465
p-ZnSe:Li(Na)(N)(P), LPE layers, photocapacitance and photocond. meas. 79−99572
ZnSe:Mg, local vibrations of impurities, IR absorpt. spectra exam. 77−7815
ZnSe:Mn, single crysts., associated pt. defects, EPR method 77−48040
ZnSe:Mn thin film, AC electrolum. 79−47519
ZnSe:Mn/n-GaAs low threshold thin film DC electrolum. cell, pulse-excited characts. 80−76081
ZnSe:Mn^{2+}, ligand HFS calcs., EHT-SCCC, scattered-wave, LCAO methods, comparison with expt. 77−55501
ZnSe:Mn^{2+}, refined spin Hamiltonian parameters *(French)* 77−63268
ZnSe:Mn^{2+} Schottky barrier diodes, spin depend. cond. and photovoltage 79−91141
ZnSe:Mn^{2+}-n-Ge thin film electrolum. cell with low-threshold voltage 80−84786
ZnSe:Mn^{3+}, Jahn-Teller effect in fluorescent level 78−52566
ZnSe:Mn-n-GaAs, single cryst. substrate low threshold DC electrolum. 77−63465
ZnSe:Mn(Al)(I), Schottky diode, direct excitation of luminescent centres 79−7900
ZnSe:N, ion implanted cond. type conversion on annealing *(Korean)* 78−18668
ZnSe:Na, characterisation of edge emission 78−27312
ZnSe:Ni, evidence for exciton binding at Ni impurity sites, photolum. excitation spectrum 80−45135
ZnSe:Ni, optical absorpt., impurity ionisation, optical phonon coupling 80−88505
ZnSe:Ni, photocapacitance meas. of impurity level 77−69372
ZnSe:Ni, photolum. excitation spectroscopy 80−80841
ZnSe:P(Ga), 1.91 eV red emission, optically detected mag. reson. study 79−69750
ZnSe:Pb, luminescence photocond. 79−38634
ZnSe:Ti^{2+}, EPR meas. 80−80594
ZnSe:V (d^3), absorption and luminesc. spectra 78−15203
ZnSe/metal, dielectric phonon-metal electron interaction, effect on optical props. *(Russian)* 79−19663
ZnSe/water, interface, laser-induced damage in ZnSe 80−102746
ZnSe-BiOCl, electroluminesc. heterojunction phys. props. 77−66198
ZnSe-CdTe, and ZnSe-ZnTe n-p heterojunction, photovoltaic props. 77−55600
zinc compounds continued
ZnSe-CdTe heterojunction, radiative recomb., electrolum. obs. 77−32445
ZnSe-CdTe heterojunction, cathodolum. and electrolum. 78−6782
ZnSe-CdTl, epitaxial film, cond. transition, laser switched memory *(Russian)* 77−8182
ZnSe-electrolyte boundaries, photo e.m.f. meas., semicond. energy bands 77−1481
ZnSe-electrolyte junction, current photoresponse 79−82669
ZnSe-GaAs (110) interface, electronic struct., self-consistent calc. 79−95486
ZnSe-GaAs heterojunction, LF noise, I-V and C-V characts., illumination effects *(Russian)* 77−66200
ZnSe-GaAs narrow junction lasers 80−43334
ZnSe-GaAs solid solns., chem. transport cryst. growth, struct. 78−43991
ZnSe-GaAs system, heterovalent substitutionary solid solns., prep. and props. 77−24553
ZnSe-Ge (100) interface, electronic struct., self-consistent pseudopot. calc. 78−91747
ZnSe-Ge (100) interface, electronic struct. calc., scattering theoretic approach 80−6940
ZnSe-Ge abrupt (110) interface, electronic struct. 78−95339
ZnSe-Ge heterojunction, change in interfacial microstruct. on high temp. annealing 77−28242
ZnSe-Ge(GaAs)(GaP) heterojunctions, elec. and photoelec. props. *(Russian)* 77−32070
ZnSe-Ge(GaAs)(mica) epitaxial heterostructs., growth struct. 78−43257
ZnSe-HCl-H_2, vapour phase chemical kinetics in open tube horizontal furnace *(French)* 77−63909
ZnSe-HgSe, solid soln., defect distrib., elec. props., Hagemark's theory 78−64040
ZnSe-In system, residual conductivity, cathode quenching 79−7902
ZnSe-metal contact, elec. props. 78−14826
ZnSe-metal Schottky barrier height rel. to chem. reactivity 80−25008
ZnSe-Si, IR segmented composite window design 80−106621
ZnSe-Si heterojunctions, IR quenching of photocapacitance 80−92968
ZnSe-Si n-n heterojunction photovoltaic effect, freq. meter in visible wavelength *(Korean)* 79−60915
ZnSe-ZnS semiconductor waveguide laser, electron beam excited, blue emission 79−18447
ZnSe-ZnTe amorphous thin-film p-n heterojunction, fabrication and characts. 79−47154
ZnSe-ZnTe heterojunction, cathodolum. and electrolum. 78−6782
ZnSe-ZnTe heterojunction, epitaxial, photosensitive, photoelec. props. 79−11203
ZnSe-ZnTe heterojunction, prep. and props. 79−95483
ZnSe+CeTe⇄CdSe+ZnTe ternary mutual system, phase equilib. 79−52179
ZnSe+Mn^{2+}, LCAO calc. of d-orbital splitting 77−28148
ZnSe(:Ga)(Al), effect of thermal treatment and doping on elec. props. 77−85223
$(ZnSe)_x(CdTe)_{1-x}$, low temp. photoluminesc. *(Russian)* 78−43931
ZnSeCu, double comet shaped electroluminesc. 78−52577
$(ZnSe)_{1-x}(GaAs)_x$ solid solns., photoluminescence spectra 80−40159
$(ZnSe)_x(GaAs)_{1-x}$, LPE growth, resist., Hall effect and cathodoluminesc. meas. 77−28270
$(ZnSe)_{1-x}(GaP)_x$, two-photon absorpt. at ruby laser freq., clarification *(Russian)* 79−15505
$ZnSeO_4.6H_2O:Cu^{2+}$, crystal struct. orientational degeneracy removal scheme, space groups, ESR spectra 78−47267
$ZnSe_{1-x}S_x$, luminescence, polaris. emission 79−38634
$ZnSe_xS_{1-x}$, melt grown, 10K, band edge photoluminesc. 78−84628
ZnSe(Te), fine structure of lowest exciton state *(Russian)* 80−96801
ZnSe(Te), Raman-luminescence problem, interference analogy and expt. discrimination by polarisation correl. 79−95764
$ZnSe_xTe_{1-x}$, MBE, comp. ratio control 79−28947
n-ZnSe−p-GaAs heterojunction high-detectivity threshold photodetectors 79−6181
ZnSe(100) surface, anomalous oxidation props. 78−15558
ZnSe(110), surface struct., kinematical LEED calcs. 77−85034
$ZnSiAs_2$, birefringence, effects on hydrostatic pressure and temp. 80−45033
$ZnSiAs_2$, cryst. growth and elec. props. *(French)* 77−76815
$ZnSiAs_2$, electron irrad., defects, elec. and optical props. 79−19282
p-$ZnSiAs_2$, electron irrad. elec. props. annealing, lattice defects 80−100465
n-$ZnSiAs_2$ photodiode, fabrication and photoelec. props. 77−8146
$ZnSiAs_2$, photoelectron spin polarisations, electron level struct. 79−87557
$ZnSiAs_2$, pseudodirect bandgap semiconductor, natural birefringence 79−65834
$ZnSiAs_2$, synthesis and layer growth by CVD in open flow system 78−15312
$ZnSiAs_2$, thermal expansion coeffs. meas. *(Russian)* 80−65258
p-$ZnSiAs_2$:Au(Tl)(S), photoluminesc., radiative recombination 77−24883
$ZnSiF_6:Cu^{2+}$, spin-spin interactions of impurity pairs *(Russian)* 78−72397
$ZnSiF_6 6H_2O:Mn^{2+}$, ESR spectrum, effect of uniaxial compression 80−29609
$ZnSiF_6.6H_O:Co^{2+}$, spin Hamiltonians and pair interactions 77−36119
$ZnSiF_6.6H_2O$, aq. soln. growth 77−63554
$ZnSiF_6.6H_2O$, dielec. props., 100-270K, rel. to $NiSiF_6.6H_2O$ 78−35088
$ZnSiF_6.6H_2O$, spin-phonon interaction between Ni^{2+} ions, phonon bottleneck effects, splitting parameters *(Russian)* 80−15796
$ZnSiF_6.6H_2O:Co$, influence of hydrostatic press. on Co^{2+} EPR spectrum 78−27084
$ZnSiF_6.6H_2O:Ni^{2+}$, EPR 77−59451
$ZnSiF_6.6H_2O:Ni^{2+}$, cryst. field, uniaxial compression method *(Russian)* 78−35027
$ZnSiF_6.6H_2O:Ni^{2+}$, spin-lattice relax. at press. up to 6.5 kbar 78−48033
$ZnSiF_6.6H_2O:V^{2+}$, paramagnetic impurity ion spin multiplet initial splitting parameter, immediate environments distortion influence on sign 79−65720
$ZnSiF_6.6H_2O:V^{2+}$, spin-lattice relax. at normal and high press. 80−2632
$ZnSiF_6.6H_2O(.6D_2O)$, near IR spectrum, 80K, assignments 78−48164
$ZnSiO_3$, HP phase transform. 80−19941
Zn_2SiO_4, cryst. growth from PbO-SiO_2 flux 77−16484
Zn_2SiO_4, determ. of electronic polarisabilities of ions 79−7570
Zn_2SiO_4 ore, processing review 77−48365
Zn_2SiO_4 ores, hydrometallurgical treatment for Zn recovery 77−52263
Zn_2SiO_4, willemite, cryst. struct. 78−83804

zinc compounds continued
Zn_2SiO_4, Willemite, single crysts., X-ray evaluation of atomic parameters for study of optical props. 79−4283
Zn_2SiO_4:As,Mn, enhanced luminesc. stimulation, 20-320K *(German)* 77−20900
Zn_2SiO_4:Mn, cathodoluminesc. yield, calorimetric method determ. *(Russian)* 77−20938
Zn_2SiO_4:Mn, cathodoluminophor, nature of ageing 78−10994
Zn_2SiO_4:Mn, energy storage effect and retrieval 80−100684
Zn_2SiO_4:Mn, phosphoresc. decay into second-order components 77−20907
Zn_2SiO_4:Mn film, electron beam depth-dose functions, cathodoluminesc. 80−2867
Zn_2SiO_4:Mn luminescent film on Si, electron injection 78−23176
Zn_2SiO_4:Mn phosphor, luminesc. saturation under intense vac. UV irrad. 79−56841
Zn_2SiO_4:Mn phosphor, efficiency enhancement by $AlPO_4$ substitution 80−11452
Zn_2SiO_4:Mn^{2+}, quantum yield in candoluminescence process by low energy H^+ ion bombard. 79−65930
Zn_2SiO_4:Mn^{2+} phosphor, for low press. fluoresc. lamp, luminesc. characts. 78−10960
Zn_2SiO_4-Mg_2SiO_4, melt solidification behaviour 77−90337
Zn_2SiO_4-SiO_2 dielectric, struct. exam. by optical, photoemission electron and SEM 78−80706
$Zn_4Si_2O_7(OH)_2H_2O$, hemimorphite, polarised IR refl., vibr. modes *(French)* 77−85698
$Zn_4(Si_2O_7)(OH)_2.H_2O$, calamine-hemimorphite, cryst. struct. determ. 77−76380
$Zn_4Si_2O_7(OH)_2.H_2O$, X-ray and neutron diffr. study 79−99159
$Zn_4Si_2O_7(OH)_2.H_2O$, hemimorphite, phase-angle determ. by anomalous X-ray scattering with 4-circle SSD diffractometer 80−49188
$ZnSiP_2$, 1 MeV proton bombardment, lattice deformation investigation by Kossel effect 78−22775
$ZnSiP_2$, band struct. calc., empirical pseudopotential method 77−1362
$ZnSiP_2$, birefringence, effects on hydrostatic pressure and temp. 80−45033
$ZnSiP_2$, chem. inhomogeneities, X-ray lattice parameter meas. *(German)* 77−72693
$ZnSiP_2$, conc. profiles during gas phase transport *(German)* 78−64452
$ZnSiP_2$ crystal growth, DTA obs. of Sn-Zn-$ZnSiP_2$ phase diagram 80−24394
$ZnSiP_2$, crystallisation from gas phase *(German)* 77−69977
$ZnSiP_2$ crysts., imperfect struct. anal. using divergent X-ray beam technique 77−76259
n-$ZnSiP_2$, deep impurity levels, Schottky TSC meas. 79−95419
$ZnSiP_2$, effect of crystal growth method, on physical props., effect of doping on physical props. *(German)* 79−52094
$ZnSiP_2$, electronic struct., X-ray spectroscopic investigation 80−108300
$ZnSiP_2$, first- and second-order Raman scatt. 78−35151
$ZnSiP_2$, growth under nonstoichiometric conditions in gas phase, microanalytical investig. *(German)* 79−33909
n-$ZnSiP_2$, IR absorption 77−12377
n-$ZnSiP_2$, lattice limited Hall mobility, nonpolar optical scatt. mechanism 79−51579
$ZnSiP_2$ monocryst., impurity induced photoluminescence *(Russian)* 79−4850
$ZnSiP_2$, one- and two-phonon Raman scatt. 79−78681
$ZnSiP_2$, photocond. and photolum. spectra, optical anisotropy 78−72200
$ZnSiP_2$, photocond. under laser excitation *(Russian)* 78−84258
$ZnSiP_2$, proton induced Kossel effect *(German)* 77−84601
$ZnSiP_2$, pseudodirect bandgap semiconductor, natural birefringence 79−65834
$ZnSiP_2$, pseudodirect chalcopyrite semicond., electronic band struct. 80−20079
$ZnSiP_2$, reflectance spectra at 300K 80−25407
$ZnSiP_2$ Schottky diode, electrolum. under forward and reverse bias conditions 77−63466
p-$ZnSiP_2$, single cryst., recomb. processes, photoelec. props. *(Russian)* 78−68053
$ZnSiP_2$, thermal expansion coeffs. meas. *(Russian)* 80−65258
$ZnSiP_2$:Ga, effect of doping conc. on elec. cond. and Hall coeff. 78−76077
n-$ZnSiP_2$:Ga, elec. cond. and Hall meas., 77 to 1000K, scatt. mechanisms 79−11153
$ZnSiP_2$-Au(Ni) Schottky contact, production and props. 79−7901
$ZnSiP_2$-In Schottky diode, photovoltaic spectra 80−2423
p-ZnSnAs, LPE, electronic struct. obs. by laser excited photolum. 80−60654
$ZnSnAs_2$, LPE in open tube system 78−92206
$ZnSnAs_2$-$CdSnAs_2$, material distrib., possibility of heterostructure *(Russian)* 78−30979
$ZnSnAs_2(P_2)$ single crysts., refl. spectra, band struct., dielec. consts. 77−44022
$ZnSnCuO_4$, cryst., struct., mag. susceptibility obs. 78−2085
Zn_2SnO_4, form. by vapour phase method, form. reaction, effect of starting materials *(Japanese)* 77−32514
Zn_2SnO_4, vap. phase needle cryst. growth from ZnO-Sn mixture 77−12509
p-$ZnSnP_2$, photolum. anisotropy, 77K 78−19557
$ZnSnP_2$-$ZnSiP_2$, heterocombination simultaneous crystallisation 78−60560
ZnTE, MBE growth, elec. and optical props. 80−75462
ZnTE, relaxation processes in Raman scattering and exciton luminescence under resonant excitation 80−25386
$Zn_2Ta_2O_6$, metastable orthorhombic variety, crystallographic characts. *(French)* 79−82185
p-ZnTe 79−43028
ZnTe, ^{67}Zn Mossbauer spectroscopy with 93 keV reson. 80−66095
ZnTe, ^{67}Zn nuclear magnetic shielding, chemical shifts and linewidths 80−60434
ZnTe, 1.5 to 30K, thermal expansion and Gruneisen parameter meas. 80−59681
ZnTe, 93.3 keV Mossbauer transition in ^{67}Zn, isomer shifts 80−39978
ZnTe (110) and (111) surfaces, electron energy loss spectra, bulk and surface losses 79−43080
ZnTe (110) and (111) surfaces, O_2 adsorption, electron energy loss and Auger spectra 79−47568
ZnTe (110) surface, elastic LEED anal. 79−86967
ZnTe (110) surface struct. determ. by LEED, UPS, and EPR 80−49475
zinc compounds continued
ZnTe, adsorpt. of CO_2, H_2, CO_2-H_2, manometric and mass-spectroscopic investig. 77−35808
ZnTe, Anderson-Gruneisen parameter, bulk modulus temp. depend. 78−10154
ZnTe, anomalous penetration of implanted ^{65}Zn and compensation zone build up 77−19975
ZnTe, band parameters from bound exciton, donor-acceptor pair excitation luminescence 78−92111
ZnTe based metal-semicond. struct., spectral photosensitivity obs. 79−95492
ZnTe, blende type struct., luminesc. under high excitation 79−19928
ZnTe, Brillouin scatt. spectra, elastic and photoelastic consts. 77−59585
ZnTe, bulk and surface states anal. using synchrotron radiation 77−66574
ZnTe, charged dislocations, flow of charge with plastic deform. 80−85010
ZnTe clean and adsorbed O_2 (110) surfaces, UV photoemission spectra *(Japanese)* 80−93456
ZnTe, clean and oxidised surfaces, surface states, low-energy EELS study 80−11522
ZnTe, cryst. growth under thermodynamically controlled conditions 77−48327
ZnTe crystals, polariton effects in luminesc. 80−103988
ZnTe crystals, secondary radiation polarization and relaxation of optical excitation 80−11399
p-ZnTe, cyclotron resonance from photoexcited electrons 79−69723
ZnTe, diamond-like semicond., Mossbauer isomer shift meas. 77−16233
ZnTe, dominant acceptors, annealing and quenching 80−24463
ZnTe, donor acceptance pairs, photoluminesc. excitation spectra *(Japanese)* 78−64409
p-ZnTe, doped and pure, photoluminesc. and photocond. spectra 77−55826
ZnTe doped with group I impurities, fluorescence spectra meas. 78−10949
ZnTe, doping and intrinsic stoichiometric defects, self-compensation 80−59918
ZnTe, edge luminesc. excited by electron bombard. 80−66308
ZnTe, effect of quenching on electrical props. 79−1920
ZnTe, effects of Zn anneals in 400-550°C range on acceptor conc. 80−10571
ZnTe, elec., SEM and TEM studies of impurity segregation during long annealing 80−30001
ZnTe, elec. active intrinsic defects, Hall meas. of carrier conc. 77−51700
ZnTe, elec. field and impurity conc. effects on ionisation energy of impurities, appl. to acceptors 80−88514
ZnTe, electro- and cathodoluminesc., impurity segregation 79−43042
ZnTe, electro-optic suscept. dispersion curve 77−3620
ZnTe electrode, redox reaction due to complex $M(CN)_6^{3-/4-}$ *(French)* 80−89482
ZnTe electrodes for photochemical production of H_2, a comparison 77−70311
ZnTe, electron-phonon coupling, donor-acceptor pairs selective excitation 80−11475
ZnTe, electronic and optical parameters of O related centre 77−24534
ZnTe, energy levels of Mott excitons 78−6282
ZnTe, epitaxial film growth initial stages 77−80707
ZnTe epitaxial growth on NaCl by ion deposition 77−32533
ZnTe, epitaxial growth on GaAs by closed-tube chemical vapour transport method, elec. props. 79−99449
ZnTe, excited acceptor, donor states, luminesc. 78−72604
ZnTe, exciton localisation at impurity pairs 79−37999
ZnTe, excitonic complexes, stress splitting of luminesc. lines 77−4672
ZnTe, excitonic effects at E_0 and E_1 gaps, wavelength modulated reflectivity spectroscopic study 79−61400
ZnTe, extrinsic luminesc., bands, temp. injection level, and freq. depend. 80−20714
ZnTe film, conduction mechanisms in non-ohmic off-state 77−72932
p-ZnTe film, current-voltage characts. 77−66214
ZnTe film, electron irrad. effect on electrophys. props., prep. conditions depend. 79−28421
ZnTe film, exciton spectra, press. and temp. depend. 80−80886
ZnTe film, grown on sapphire substrate, stimulated emission 79−78708
ZnTe film, LF oscills. of dark current obs. 78−19093
ZnTe film, on semicond. substrate, early stages of growth, electron microscope obs. *(Russian)* 78−38976
ZnTe film preparation and props., by single-source vacuum deposition method *(Japanese)* 80−6664
ZnTe films, grown on glass using atomic layer evaporation 80−44453
ZnTe films, internal stress effect on fund. refl. spectra 80−60701
ZnTe films, residual conductivity, Kikuchi lines of electron diffr. pattern 79−91173
ZnTe films, simple and modified Poole-Frenkel cond. 80−97017
ZnTe, free exciton refl., surface layer effects 78−76493
ZnTe, free-exciton emission band under high-intensity photoexcitation 79−73993
ZnTe, gas, identification by high-temp. mass spectrometry 80−45593
ZnTe, growth from In solvents, self-compensation 77−28144
ZnTe growth from vapour, growth interruption 80−97416
ZnTe, high purity acceptor bound and free exciton states 79−99941
ZnTe, high quality p-type cryst., predominant acceptors 78−60504
ZnTe high-purity single cryst. growth by sublimation travelling heater method 79−28901
ZnTe, I_4 bound exciton, magneto-optical meas. 77−20836
p-ZnTe, interface impedance in KOH electrolyte soln. *(French)* 77−51814
ZnTe, ion implantation defect introduction, cathodolum. studies 80−75250
ZnTe ion implanted planar waveguides, refr. index profiles 77−62039
ZnTe, irradiation induced radiative centers obs. 80−66290
ZnTe, LPE growth on ZnSe, characterisation of heterojunction 77−4745
ZnTe, laser thresholds and stimulated emission, intrinsic recomb. processes 79−15489
ZnTe, lattice dynamics and phonon parameters, bond bending force model lattice dynamics and phonon parameters bond bending force model 80−59595
ZnTe, lattice vibration, thermal expansion and pressure effect 80−39233
ZnTe, low temp. vapour growth, closed tube transport technique 77−85914

zinc compounds continued
ZnTe, low voltage green LED, struct. double diffusion procedure 80−100697
ZnTe, luminesc., donor-acceptor-pair excitation spectroscopy 80−25456
ZnTe, luminescence spectra struct. surface and volume polaritons *(Russian)* 80−16089
ZnTe, MBE growth, growth rate and sticking coeff. 77−32532
ZnTe MBE thin film growth, elec. and optical props. 78−47887
ZnTe, magneto-optical effect, I_2 bound exciton 77−12432
ZnTe, magnetoreflectance meas. on Γ_6-Γ_8 exciton 78−6656
ZnTe, moments of phonon spectra from specific heats 80−15203
ZnTe, NMR, chemical shift and linewidth determ. 79−19792
ZnTe, nonlinear absorpt., temp. depend. *(Russian)* 77−20899
ZnTe, nonlinear magnetoelec. susceptibility, three-dimens. model 80−39845
ZnTe, nonlinear optical effects in rotationally twinned crysts., phase matching 77−42570
ZnTe, optical identification of substitutional acceptors by low temp. photoluminescence 79−99940
ZnTe, phonon dispersion under extreme press. and metallic transform., Raman spectra meas. 78−10895
ZnTe, photoinduced dielec. loss and capacitance changes, rel. to space charge polarisation 80−2417
ZnTe, photolum. excitation spectra of tightly bound holes, valence band contrib. 80−60658
ZnTe, photoluminesc., donor and acceptor excited states 79−38622
ZnTe, photoreflection exciton spectra *(Russian)* 77−20874
ZnTe, polymorphism at elevated temp., elec. resist. and X-ray diffr. under press. 80−49359
ZnTe, pure and P(As) doped, shallow-acceptor, donor, free-exciton, and bound-exciton states 80−60667
ZnTe, radiative recombination involving free particle scatt. 79−38648
ZnTe, Raman scatt. and exciton luminesc. under reson. excitation 79−38617
ZnTe, real structure effect on luminescence and absorption spectra, dislocations 80−16085
ZnTe, refined, undoped, Cu acceptor, optical absorption and photoluminesc. meas. 80−34970
ZnTe, reflectivity meas., double beam wavelength modulated technique *(Korean)* 80−50365
ZnTe, relax. processes at high excitation levels, Bose-Einstein condensation of excitons 78−48219
ZnTe, relax. times of secondary radiations, circular polarisation correlation 79−28816
ZnTe, relaxation processes, emission spectra *(Russian)* 78−72598
ZnTe, reson. Brillouin scatt., injected acoustic domains obs. 78−19493
ZnTe, reson. Brillouin scatt., acoustic domain injection 79−38557
ZnTe, reson. Brillouin scatt., lifetime broadening 79−51971
ZnTe, reson. Brillouin scatt., quasi-static anal. 79−65887
ZnTe, reson. secondary radiation 79−99886
ZnTe, resonance Raman scatt. of excitonic polaritons by LO and acoustic phonons 79−65879
ZnTe, resonance Raman scatt. at high excitation levels *(Russian)* 80−55109
ZnTe, SEM and luminesc. study of Li segregation 79−38657
ZnTe, second order Raman scatt., lattice dynamical calc. and expt. 80−25370
ZnTe, secondary emission, transient behaviour under band-to-band excitation 80−108266
ZnTe, self-diffusion profile and trapping of Zn 80−75381
ZnTe, semi-insulating, acoustoelectric domain injection from CdS 77−51778
ZnTe, single cryst., anomalous struct. of exciton refl. spectra 77−44020
ZnTe, single cryst., electron-hole drop conc. *(Russian)* 79−11460
ZnTe single cryst., lasing action excited by ruby laser picosecond pulses 80−64035
ZnTe, single cryst. vap. growth by sublimation and chem. transport 78−27390
ZnTe single crystal, excitonic reflectance 90 to 300K 79−11430
ZnTe single crystal, power depend. of photocurrent on excitation intensity, sublinear behaviour 78−43442
ZnTe single crystal, Schottky-barrier diodes and ohmic contacts props. 80−96987
p-ZnTe, single crystal *(Russian)* 78−23488
ZnTe single crystal electrodes, non-intentionally doped, electrochem. props. *(French)* 79−96326
ZnTe, spin flip scatt. of laser light 77−43976
ZnTe, spin flip scatt. of laser light 77−43977
ZnTe, spin-flip plus phonon scatt., line shape and shift in peak position 79−73907
p-ZnTe, spin-flip Raman scattering, review 80−108209
ZnTe surface, nonpolar, electronic struct., tight-binding calc. 77−20383
ZnTe, surface (110) atomic struct. 79−69331
p-ZnTe surface barrier structures, photo-EMF 77−89851
ZnTe, TEM obs. of precipitates, shape of Te solidus line 80−25703
ZnTe, temp. depend. of Raman scatt. and exciton luminesc. spectra 78−39586
ZnTe, thermal expansion and lattice dynamics under press. 80−100316
ZnTe, thermoreflectance spectra, at energies from absorption edges to 9 eV *(Japanese)* 79−11436
ZnTe, thick sample, atomic comp. determ., H^+ and He^+ induced X-ray anal. 79−5223
ZnTe thin film, model for off-on transition 80−54742
ZnTe, thin film, stopping power for protons and alpha particles, proton energy straggle values 77−89489
ZnTe, two-photon absorpt. line shape near direct band gap and critical point 79−65898
ZnTe, unalloyed, photoluminesc., mechanism of radiative transitions 80−50405
ZnTe, undoped, electroreflectance of fundamental edge, exciton levels *(Japanese)* 80−20612
ZnTe, vacuum deposited on Al alloy for optical contrast enhancement 78−44301
ZnTe, valence band parameters and free exciton reduced mass, free exciton magnetoreflectance 80−45046
ZnTe, vapour growth by closed tube method 78−39703
ZnTe, wavelength modulated reflectivity spectra *(Japanese)* 79−11435
ZnTe, wavelength-modulated reflectance spectrum, electron-phonon and exciton-phonon interactions 79−11434
ZnTe: group I element, absorption saturation *(Russian)* 78−35183

zinc compounds continued
ZnTe:Ag, containing dislocation loops, optical absorption-edge fine struct. 78−43905
ZnTe:Ag, dislocation loops creation in region of interface 79−82210
ZnTe:Ag, doped during frowth and by diffusion, defect form. 80−15129
ZnTe:Ag, real structure effect on luminescence and absorption spectra, dislocations 80−16085
ZnTe:Ag^{2+}(Cu^{2+}), absence of EPR spectra due to strong spin-lattice coupling of Kramers doublets 77−85181
ZnTe:Al,Cl, photolum., complex acceptor, ionization energy 80−20693
ZnTe:As(Li), donor-acceptor pair excitation and recomb., photoluminesc. obs. 80−20691
ZnTe:As(P), spin flip acceptor scatt. 78−92072
ZnTe:As(P)(Li), binding energy of shallow acceptors from photoluminesc. excitation spectra for donor-acceptor pairs 79−95809
ZnTe:As(P)(Li), electronic Raman scatt. and IR absorpt. spectra of shallow acceptors 79−73978
ZnTe:Au, impurity identification and characterisation, capacitance, luminescence and IR absorption 80−60639
ZnTe:B^+ native and implant-created defects 77−76446
ZnTe:Bi, laser annealing, channelling, reflectivity spectra 80−66215
ZnTe:Co, impurity luminescence no phonon line depend. on temp., Debye temp. 80−66273
ZnTe:Cr^{2+}, absorpt. and luminesc. of Cr^{2+}(d^4), cryst. field theory interpretation 79−83000
ZnTe:Cr^{2+}, Cr^{2+} $^5T_2$ and ^5E states, Jahn-Teller effect calcs. 80−39539
ZnTe:Cr^{2+}, Jahn-Teller coupling 78−67997
ZnTe:Cr^{2+}, spin Hamiltonian parameters and wave function coeffs., LCAO theory 77−39804
ZnTe:Cr(Mn)(Fe), exciton refl. spectra 80−2806
ZnTe:Cu, doping behaviour, SEM in cathodoluminesc. and photoluminesc. exam. 79−65927
ZnTe:Cu, elec. and optical identification of persistent acceptor 79−60764
ZnTe:Cu, precipitates, electron microscopic investigation 80−45312
ZnTe:Cu, red centre, electric and optical props. 80−20239
ZnTe:Cu, voltage depend. on precip. contrast 79−1433
ZnTe:Cu films, high cond., elec. and optical props. 80−88651
ZnTe:In(Al), pure and doped, Zn vacancy energy levels, elec. and optical props. 79−4827
ZnTe:Li, bleaching by green laser radiation 77−62015
ZnTe:Li, diffusion investigation by SEM and TEM 80−10706
ZnTe:Li, electron-phonon interactions in Raman scatt. 80−60594
ZnTe:Li, impurity segregation during short annealing and quenching, SEM, TEM and elec. meas. 80−10676
ZnTe:Li, Li in Te precipitates, diffusion during thermal anneal 80−39358
ZnTe:Li, O, Hagemark theory, O modification isoelectronic trap 80−75517
ZnTe:Li, Zeeman splitting of ground and excited acceptor states, selective pair luminesc. 80−84780
ZnTe:Li(As), electronic Raman scatt., mag. field depend. 79−73928
ZnTe:Li(Cl)(Al)(In), ion implanted and annealed, photoluminesc. meas. 78−15208
ZnTe:Mn, exciton refl. band, giant mag. splitting *(Russian)* 78−56079
ZnTe:Mn, mag. field splitting α n=2 exciton state *(Russian)* 78−79940
ZnTe:Mn, ordering mechanism 80−2572
ZnTe:Mn, spin-lattice coeffs. of Mn^{2+} 80−84646
ZnTe:Mn^{2+}, forbidden transitions of Mn^{2+} induced by hyperfine interactions 80−60458
ZnTe:Na(Li), spin flip acceptor scatt., transition selection rules, gyromagnetic ratios 79−61380
ZnTe:O, deep centres, photocapacitance detection 79−95362
ZnTe:O, Ne or Al implantation, electronic and optical parameters of O-related centre 78−6399
ZnTe:O,Zn, dual ion implantation, luminesc. spectra obs. 78−87697
ZnTe:P, excitations spectra of donor-acceptor pair photoluminesc. 78−23522
ZnTe:P, pure and doped, electron and exciton excited states of neutral donor 80−34393
p-ZnTe:P, semicond. selective pair luminesc., excited impurity state investigation 79−61439
ZnTe:P, spin flip scatt., shallow acceptor states 77−8587
ZnTe:P(As), g-values, spin temp., determ. from Raman spectra 78−43856
ZnTe:P(As), ion implanted, cathodoluminescence emission spectrum 80−108281
ZnTe:P(Li), luminesc. transitions, quantum efficiency 79−1783
ZnTe:Sb film, elec. props. 78−76172
ZnTe-CdS(Se)(S_xSe_{1-x}) heterojunctions, prep. and electrolum. characts. 77−24610
ZnTe-CdSe, solid soln. formation and effects 78−27489
ZnTe-CdSe heterojunction, radiative recomb., electrolum. obs. 77−32445
ZnTe-CdSe single cryst. film heterojunctions, prep. and props. 79−19652
ZnTe-CdSe solid solutions, phase equilib. *(Russian)* 79−43224
ZnTe-electrolyte boundaries, photo e.m.f. meas., semicond. energy bands 77−1481
ZnTe-electrolyte interface, electrochem. behaviour of single crysts. 79−91138
ZnTe-Ga_2Te_3, phase diagram 78−35360
ZnTe-In Schottky diodes, photocapacitance determ. of electron-hole recomb. *(French)* 79−47119
ZnTe-metal structures, photosensitivity spectrum *(Russian)* 78−76147
p-ZnTe-n-GaN, electroluminescent hetero-junctions, memory effect, I-V characts. *(Russian)* 77−40289
ZnTe-ZnSe, and ZnTe-CdSe(Te) p-n heterojunction, photovoltaic props. 77−55600
$(ZnTe)_x$-$(ZnSe)_{1-x}$, diamond-type semiconductor, Mossbauer spectra, quadrupole interaction of ^{125}Te 80−44992
ZnTe(:In), single cryst. film, MBE, quality obs. using photoluminesc. 77−77419
ZnTe(S), semiconductor-metal transition, press. calibration above 100 kbars fixed points 80−77808
ZnTe(Se), optical circular polarisation correl. in secondary radiation, resonant light excitation 77−69885
$ZnTe_xSe_{1-x}$, phonon spectra calculations by recursion method, mixed crystals 80−103430
$ZnTe_xSe_{1-x}$, Raman phonon spectra, resonance interaction effect 80−25375
ZnTi ferrites, electron exchange between Fe^{2+} and Fe^{3+}, paramag., Mossbauer spectra and susceptibility meas. 77−63327

zinc compounds continued
$ZnTiF_6.6H_2O$ and $ZnTiF_6.6D_2O$, ^{19}F NMR, phase transition 79−19790
$ZnTiO_3$, ceramic channel electron multiplier, detect. efficiency in vacuum UV 78−12759
$ZnTiO_3$, HP phase transform. 80−19941
Zn_2TiO_4 crysts., grown by Bridgman techniques, as substrate for $(Mn_xZn_{1-x})Fe_2O_4$ growth 79−100065
$ZnTl_2(SO_4)_2.6H_2O:Mn^{2+}$, EPR, 300K 79−51848
$Zn(UO_2AsO_4)_2.8H_2O$, prep. cryst. struct. characterisation 78−30589
$ZnU_2.nH_2O$, cryst. struct. *(German)* 80−1987
$Zn_2V_2O_7$, elec. props. and EPR meas. 79−11114
$Zn_2V_2O_7$, V-O-V bridge stretching freq. correl. with bond angle 78−74636
$Zn_3(VO_4)_2$, determination of enthalpies of formation, from heats of solution 80−2182
$Zn_3(VO_4)_2$, luminesc. spectra in visible region, vanadate group 78−43921
$(ZnV_2O_4)_c(MgFe_2O_4)_{1-c}$, struct. parameters, IR spectra, cluster-component analysis 77−47425
$ZnWO_4$, luminesc. and capture centres *(Russian)* 78−52543
$ZnWO_4$, scintillation charcts. 80−66256
$ZnWO_4:Ni^{2+}$, luminescence rel. to Ni concn. 79−24352
ZnX_2, (X=Cl, Br, I), spectroscopic parameters of mols. from vibr. isotopic effects 78−74798
ZnX_2, ZnXY, X and Y=halogen, matrix isolation IR and Raman spectra 78−55171
$ZnX_4^{2-}(IO_4^-)$, (X=Cl,Br, I), force consts., compliance and Coriolis consts. calcs. 78−42242
ZnXY, (X, Y=Cl, Br, I), spectroscopic parameters of mols. from vibr. isotopic effects 78−74798
ZnY_2O_4, cryst. struct. 80−100207
ZnO based varistor, analysis of highly nonlinear current-voltage characteristics 77−39917
$Zn_3[Co(CN_6)_6]_2.12H_2O$, X-ray cryst. struct. determ. 79−14751
$Zn^{2+}.CO_2-H_2O$ clusters, solvation, Monte Carlo simulation 80−44102
$Zn(g)+H_2O(g)=ZnO(s)+H_2(g)$, standard Gibbs free energy of reaction 79−11815
Zns, vacuum deposited, destruction props. obs., suitability for integrated optics assessment *(Slovak)* 80−33224
ZrO_2-$ZnAl_2O_4$ transparent glass-ceramic, microstruct. and props. 78−59960

zirconium
see also nuclei with .....
γ attenuation coeffs. meas. for burn-up determ. correction *(Russian)* 78−82597
abundance determ. in silicate rocks, meteorites and lunar samples by neutron activation 78−20547
abundance in stony meteorites 79−92731
acoustic emission during deformation, expt. 77−73425
adsorption and absorpt. of CO, NO, N_2, O_2, and D_2, dissoc. and diffusion 80−80085
adsorption on W(Ta) (Re), low-temp. mobility, surface struct. 77−20197
adsorption on W (100), AES, LEED, thermal desorption, and work function meas. 80−39444
allotropic transform. BCC⇆HCP 77−36496
alloying addition in Mg-Y-Zn-Nd-Cd alloy, influence on struct. and mech. props. *(Russian)* 80−40370
amplitude depend. damping 77−32617
anelastic relaxation and O_2 diffusion in α-phase 77−4219
annealed, high-temp., kinetics *(Russian)* 80−21166
annealed, neutron irradiated, 573 to 923K, damage struct. 79−99247
anodic oxidation, growth and morphology of ZrO_2 films 77−16717
anodic oxidation, growth stresses of ZrO_2 film 77−16716
anodic oxidation, typical valve metal behaviour 77−21311
anodic oxidation in 0.05 M Na_2SO_4 electrolyte 79−57144
anodisation, use of nucl. reaction to trace source of O 79−52683
anomalous self diffusion in β-phase, temp. depend. of isotope effect 79−86918
atom, elastic scatt. of 145 keV gamma rays 79−13680
atom, in catapleiite, study of 4d excited states 77−26989
atom, integral Compton scatt. cross sections, of γ-rays from K-shell electrons 78−58643
atom, K-shell photoelectric cross section 79−22676
atom, Lα X-ray spectra, $_{40}$Zr to $_{48}$Cd, linewidths 79−41131
atom, magnetic hyperfine struct. 78−934
atom, photoelectric cross section, derived from total absorpt. cross sections 77−10646
atom, photoelectric cross sections, 5-40 keV photons, X-ray emission spectra 77−18866
atom, photoelectric cross sections for 323 keV gamma rays 77−88432
atom, reson. Raman X-ray scatt., K-vacancy excited state widths 79−45661
atom, total to K-shell photoelectric cross section ratios, 145 to 662 keV γ-rays 77−54545
atom, XPS relative intensity and photoionisation cross-section 80−63599
atoms, absorption spectra, isolated in rare gas matrices 78−78652
band structure and X-ray emission spectra calcs. 77−28105
band structure correlation with ZrC, APW calc. *(Japanese)* 78−23017
BCC, lattice dynamics, 1400K, phase transform. 79−19337
BCC, phonon vibrs., pseudopot. method 80−15204
BCC β phase, anomalous diffusion behaviour 78−91474
blistering, by 2 MeV He^+ ions, optical microscopy and SEM obs. 79−42119
blistering and exfoliation by 2 MeV He^+ beam 79−46722
breakaway oxidation, at 573K, SEM study 79−74305
breakaway oxidation kinetics at 623K, SEM study 80−97633
calibration sample proposal, long wavelength neutron scatt. meas. 78−29722
cast iron-steel mixture, interaction of Zr, formation reaction thermodynamics *(Russian)* 80−55645
cathodic behaviour in conc. hot H_2SO_4 79−52423
chemical analysis of C and N by photon and proton activation *(French)* 79−43666
coadsorption with O_2 on W (100) 80−6653
cold-rolled, textural transform. *(Russian)* 78−39790
combustion, laser-initiated, time-resolved spectroscopy 77−77765
core level binding energies 80−71564
corrosion by molten alkali metal hydroxides and liquid Li 77−44414
corrosion protection, oxidation kinetics of ZrC_xN_{1-x} coating, 450-600°C, 50-400 Torr O_2 press. *(French)* 77−25171

zirconium continued
corrosion protection, oxidation kinetics of ZrN coating, 550-700°C, 50-500 Torr O_2 press. *(French)* 77−25170
corrosion resistant pure metal, passivity and pitting in chloride solutions 78−44258
corrosion studies of materials for nucl. reactor applic. 77−34402
cracking, H_2 induced delay, strain energy effect on H_2 solubility 78−92364
creep, optical and electron metallographic anal., 473 to 873K 78−39986
creep, stress charcts., 300 to 900K, α-phase 77−66675
creep and growth, radiation induced, fundamental mechanisms 80−92596
creep in α-phase, stress change effects *(Czech)* 79−96085
crept single crystal, nature of γ-hydride 77−21147
crystal structure, computed X-ray powder diffr. patterns and densities 77−43172
crystalline anisotropy in α-phase, charact. by thin oxide film form. *(French)* 79−20269
crystalline anisotropy of α-phase, determ. by hardness meas. *(French)* 79−20157
cyclic deform. of polycrystalline α-phase *(Japanese)* 78−68757
damping, amplitude dependent at high temp. 77−52383
de Haas-van Alphen studies in high mag. fields, Fermi surface model 80−6702
defect solute atom interaction investigation using channelling techniques 78−47442
deformation at high press. of α-phase, α-ω transform. obs. *(Russian)* 79−74147
deformation texture during rolling in sequential passes 79−11674
depth profiling of ^3He ion implantation 78−59830
determination in bauxite, X-ray fluoresc. method 77−36849
deuteron implanted, temp. depend. depth profile of deuterons 78−95076
deuteron irradiated, 10 keV, retention and precipitation 80−34099
diffusion and solubility of H in β-Zr, above 1000°C and below 1×10^{-4} mm Hg *(Russian)* 80−24671
diffusion in Cu, microstruct. and microanal. study of coating formed *(Rumanian)* 78−19917
diffusion in Nb bulk cryst., diffusion coeff., effect on Nb self diffusion isotope effect 78−47602
diffusion of C, 620 to 830°C *(Russian)* 79−46842
diffusion of H, NMR study 80−108088
diffusion of O in α-phase, 290 to 1500°C 77−76613
diffusion of O in α-phase, O stabilisation 78−51737
dislocation-point defect interactions, anisotropic elasticity theory 77−11588
dissolution of γ-ZrH, in situ study, HVEM obs. 78−55951
elastically deformed, positron annihilation, Doppler broadening study 79−69900
elasticity coefficient computation by use of pole figure data 77−77521
elasticity moduli, 4.2 to 1133K *(Russian)* 79−57034
electric field gradients at substitutional Ta atoms, TDPAC high-pressure study, ω phase 78−52384
electrochemical pitting in alkaline chloride soln., H_2 evolution and anodic disintegration 80−16553
electromigration effective charge for ^3H, H conc. depend. 77−51545
electron extinction distances for twenty two lowest order reflections 78−47213
electron induced irradiation creep, dislocation process obs. 77−47483
electron irradiated, interaction of self-interstitials with O_2 atoms 79−65118
electron irradiation damage, direct obs. 80−84212
electronic excitations, charact. energy loss meas. up to 50 eV 80−60723
electronic structure calc. and obs., by APW method and X-ray photoelectron spectroscopy *(Japanese)* 79−15074
electronic structure of omega and alpha phases, nonrelativistic APW method 79−90952
embrittlement in I_2, environmental purity effect 80−30149
emittance at 400 to 850K and normal spectral reflectance at room temp. 77−20813
excited state radiative lifetime, sputtering technique 78−17602
fatigue, 20 to 700°C 77−70154
field evaporation, search for high ionic charges 78−35269
film, optical absorption meas. using synchrotron radiation, 20-250 eK 77−12457
film, reactive ion beam sputtering 78−19666
FIM, specimen prep. and results 77−11449
foil, convergent beam thickness determ. 79−4215
foil, dislocation loop nucleation and growth during 1 MeV electron irrad. 80−88152
foil, naturally passivated, ESCA, sputter etching 77−70218
foil bending by in situ ion irrad., neutron damage simulation, room temp. oxide growth 80−107342
foils, dehydrogenation of V by annealing 80−96736
gamma-ray attenuation coeff. meas., 1115, 1173, 1332 keV 77−55303
gamma-ray elastic scatt. cross section at 279 keV 79−26421
gettering of H, mass spectrometry and microgravimetry study, rel. to HTGR gas purification 80−73374
HCP, elec. field gradient 78−14698
HCP, neutron-irradiated, Frenkel defect spontaneous recomb. volumes 79−60355
HCP, nonlocal effects in lattice dynamics 78−91397
HCP, normal vibr. modes, temp. depend. 79−19339
HCP, temp. depend. of C-axis phonon dispersion curves 78−59884
high temperature thermophysical properties 78−91404
hydride precipitation and growth at crack tips, electron optical obs. 80−108449
integral emittance, during high temp. heating and oxidation *(Russian)* 80−39327
internal friction and O_2 pair diffusion 77−16634
ion implantation, comparison with thermal oxidation of Ti 77−8976
ion implantation, oxidation mechanisms study 77−8980
ion implanted, ranges of implanted 10-30 keV D^+ 78−83858
ion nitriding by a DC glow discharge method, surface anal. 78−80672
ion-implanted polycryst., thermal oxidation 80−71786
irradiation creep in simple crystal 77−42081
irradiation growth, influence of microstructure and test conditions 80−92561
irradiation growth, reaction rate theory calcs. 80−88212
irradiation induced defects, electron microscope images 78−83854
isotope abundances in S-type stars R Cygni and V Cancri 78−53957

zirconium continued
isotopic composition, at. wt., rock standards, chondrite composition 79−3591
K-edge photoabsorption spectra, linear APW calc. 78−43960
L shell prod. cross section of Zr, Mo, Ag, Cd and In for 75 to 150 keV p and e excitation 79−47552
laser microprobe damage, metallographic exam. of craters formed 78−39988
liquid, viscosity at melting point, free energy *(Russian)* 80−92699
low temp. deformed, O_2 effect on production and recovery of defects, elect. resist. meas. 79−47705
LWR fuel-cladding gap, Cs-U-Zr-H-I-O system, chemical thermodynamics 78−82440
magnetic form factor, field-induced, polarised neutron scatt. meas. 80−50044
magnetic susceptibility, plastic deform. effect *(Russian)* 80−65984
martensite, furnace cooled and water quenches, strength and deform. 79−20101
microstructure exam. by electron microscopy, oxide film appl. 79−70243
monitoring, in ^{113m}I eluates from ^{113}Sn generator 77−5078
monocrystal perfection using Berg method and diffractometer with omega device for α-phase *(French)* 80−2035
neutron induced displacement damage anal., program DISPKAN 79−14854
neutron irradiated, dislocation loop nature 77−47489
neutron irradiated, faulted loops 78−10094
neutron irradiated, low temp. deform. studies 79−47757
neutron irradiated, twinning deformation 79−14848
neutron irradiated, yield point phenomenon 79−52304
neutron irradiated at 573 to 923K, damage struct. 80−107334
neutron irradiation, effect on deformation twinning in Zr deformed at 77K 79−37741
neutron irradiation damage characterization by TEM 79−42110
neutron thermal capture cross-section var. with time, calc. 77−61505
nitride formation in RF discharge 77−86222
nuclear fuel element sheathing, reliability, including hydration process, probabilistic model *(Russian)* 80−52742
nuclear steam superheating, design tests of Zr channels 80−5211
oxidation, in O_2-N_2 atmospheres 80−104353
oxidation in flow conditions at 1000 to 6000K 78−11445
oxide film texture determ., corrosion in air and water vapour 77−56163
$\beta \rightarrow \alpha$ phase transformation, cooling rate effects 80−7565
phonon density of states, scatt. law in thermal neutron field 77−72663
phonon dispersion, modified Sharma-Joshi model 80−100311
phonon dispersion relations, d-electron contrib. to Cauchy discrepancy 80−92628
photoelectric cross section, total to K-shell ratios 78−5188
photoelectric cross sections, from total absorption cross sections, 5 to 130 keV 79−26947
photoelectric cross-section at K-edge measurements 78−2983
photon emission due to Ar^+ ion bombard., adsorbed and recoil-implanted O effect 80−80872
photon emission from inert gas-surface impact 78−11059
plasma arc srapying, chem. reaction with plasma gases 80−66427
point defect migration into dislocation loops, finite difference calc. 80−54225
point defect props., effect on irradiation behaviour of Zr alloys 78−30609
polarisation in high temp. water 77−52540
polycrystalline, low-temp. alternating deformation and annealing, yield stress, elec. cond. variation *(Russian)* 79−74199
polycrystals with axial texture, heterogeneity of props. *(Russian)* 80−29192
positron annihilation in α phase 77−68999
powder heap, thermal cond., effect of temp., press., and atmospheric composition, sintering appls. 78−80487
proton irradiation, 10 to 16 MeV, isochronal annealing meas. 80−2083
proton irradition, 10 to 16 MeV, resistivity changes 80−2082
PWR fuel dissolution process remote maintenance cell 79−9838
quantitative anal., for D, by ion microanalysis 78−56945
radiation induced creep, yielding creep theory, time depend. of irrad. growth 77−26845
radioisotopic X-ray fluorescence determ. in industrial samples 77−52702
range distributions for 25-200 keV $^{14}N^+$ ions 80−103405
rare metal ores, quantitative relns. between Ta, U, Th and Zr 77−56629
reactive, trapping of energetic 18 keV deuterons 78−10096
reactive diffusion with graphite, interaction kinetics 79−42318
reactive sputtering, O_2 press. depend. 77−12530
reactor cooling and heat recovery appl. *(Italian)* 78−4978
RF sputter deposition, ion bombardment and ion implanation 80−25564
ribbon filament lamp, calibrated source for IR radiometer 80−83653
rolling and recrystallisation texture formation *(Russian)* 77−59802
rolling texture formation, computer simulation in HCP and orthorhombic metals 80−3095
scattering and radiation damage for 14 MeV neutrons and 10 to 20 MeV protons 77−15458
separation from fission products, fast chem. methods 77−16856
separation from Hf, new process 78−6875
solid state phase transformation $\alpha \rightarrow \omega$, exam. of phase transformation kinetics under static, and dynamic pressures 78−80541
solubility in Mo-W solid soln. 77−25025
solubility of H optical metallography, internal friction meas. 78−83962
solvent extraction and complex formation with tridentate organophosphorous compounds 78−76853
sorption of H_2, tritium recovery in D-T fusion reactor *(Japanese)* 78−29646
source for ultrahigh vacuum surface expts. 79−12810
specific heat, lattice, temp. depend. calc. 79−37851
sputtered film, compressive stress transition 78−10310
sputtered ion fraction meas. using matrix isolation spectroscopy 80−60738
strain ageing at 1000K in α-phase 79−47725
structural changes during plastic deform. *(Russian)* 77−8880
substrate, contact angle with low melting metals 79−77864
superconductivity enhancement obs. after H(D) implantation 80−70884
surface structure, (0001) face, HCP phase, LEED study 80−20017
TEM obs. of irradiation damage, critical review 79−10879
tensile deformation behaviour, neutron irrad. effects, dislocations, twinning inhibition 77−90393
tensile props., room temp. to 900K 77−70104
thermo EMF, effect of H diffusion 79−23950

zirconium continued
thin film, TEM, sources of background X-radiation 80−101908
thin film, trace element determ. by X-ray fluoresc. anal. 78−40107
tracer diffusion in α-phase, atom size effect 78−84005
twin interfaces {10$\bar{1}$2}, serrated 80−84182
UPS constant final state energy spectra direct emissions and Auger decay from multiplet final states 77−44131
vacancy recovery following 1.5 MeV electron irrad., positron annihilation meas., α-form. 77−47485
vacuum technology appl., melt processing and appl. *(Hungarian)* 80−55318
valence-band meas. using XPS 79−69958
void swelling during electron irrad., HVEM study 80−92559
X-ray anomalous dispersion corrections using scanning interferometer 77−48274
X-ray emission spectra and electronic structure 77−20960
X-ray emission spectrum, K-satellites 80−40188
X-ray fluorescence analysis, simultaneous determ. of Zr and Hf trace elements in soln. 80−97752
X-ray K-absorption spectra 78−76558
X-ray Mζ energy, revised values 80−14102
X-ray production, K-shell, on N^+ impact 77−75090
X-ray reflection intensities, charact. temps. and Debye-Waller factors, 100-370K 78−18731
yield points, obtained by ageing at two stresses 80−81091
Zircaloy 2 irradiation creep strain meas. technique 77−42084
Zn-salt, molten system, separation of Hf and Zr 80−11884
Al_2O_3:Zr ceramic, elec. props., additives effect, and interaction with steel melt 80−104305
(Br,Zr) quasimolecular system, 1 s σ orbital, variational calc. 78−37707
CaS:Zr, Gd phosphors, thermoluminesc., trap distrib., activator effects 78−2929
CaS:Zr phosphors, photoluminesc. 79−28806
CaS:Zr phospors, photoluminesc. 79−28805
Cu coated, thickness monitoring by back scattering of single energy electrons, density meas. 79−97362
Cu-Al-Ti-Zr, internally oxidized, morphology of precipitates and dispersion hardening *(Russian)* 79−52217
Ga_2O_3:Zr single crystals, quenched, ionic and elec. props. 78−30922
H terminal solid solubility, in α-Zr, optical metallographic study 80−34195
LMFBR, U-Pu-Zr fuelled breeding potential assessment 79−9685
$LiNbO_3$:Co^{2+}, Zr^{4+} films, LPE growth from Li_2O-V_2O_5 flux, X-ray and acoustic characterisation 80−15383
$LiNbO_3$:Co^{2+}, Zr^{4+} film, improvement in temp. stability and SAW device appls. 80−75939
$NbSe_3$:Zr, dopant effect on supercond. transition temp. rel. to CDW 80−39699
Ni_3Zr, cryst. struct. and stability 79−90597
Si_3N_4/Zr joint, solid state bonded, exam. of bond fracture strength 78−76826
Si_3N_4/Zr laminates, metal to ceramic joints, adherence props. 80−45386
SrS:Mn, Zr phosphor, photodielectric effect 80−107848
SrS:Zr(Zr,Mn), yellow and red-fluoresc. mechanism 77−32419
T diffusion coeff. deter. 80−15306
TiO_2:Zr, electronic conduction, temp. depend. 77−8099
UO_2-Zr fuel performance evaluation in power ramp tests 79−26544
V-Ga-Zr, multifilamentary supercond. wire, crit. current props. 79−61013
W-Zr field emitter, time-of-flight atom-probe study 80−80949
W(100) coating, TF electron emitters props. obs. 80−66403
YIG:Zr, near IR absorpt. and magnetic circular dichroism 80−60580
YIG:Zr^{4+}, X-ray induced change in initial permeability 78−19280
Y_2O_3:Zr^{3+}, ESR spectrum 79−69716
Y_2O_3:Zr^{3+}, F-centre charge state, ESR and thermally stimulated luminesc. obs. 80−60418
β-Zr, Cr diffusion rates in temp. range 914 to 1240°C 80−15304
α-Zr, electrolytic polishing optimal condition determ. from anodic impedance meas. *(French)* 80−3250
α-Zr, grain-boundary sliding component in high temp. fatigue 80−50706
Zr I, lifetimes of excited states, rel. to solar abundance determ. 78−86815
Zr II and III, oscillator strengths for certain transitions 79−18143
Zr IV, $4p^64d$-$4p^54d5s$ transitions, level assignments 79−22631
Zr IV, energy levels, spectrum obs. 440 to 2670 Å 80−99470
Zr IX, $4s^24p^2$-$4s4p^3$ transitions, in VUV 80−91480
α-Zr, some stress change expts. on creep 80−3125
Zr V, energy levels, spectrum obs. 200 to 2670 Å 79−54798
Zr VII, 4p-5s transition 77−27010
Zr VII, energy levels, $4s^24p^4$ to $4s4p^5$ transitions obs. 77−3288
Zr VII, VIII, IX, 4p-4d transitions obs. 78−82669
Zr VIII, reson. transitions in UV 80−91479
Zr VIII (IX), 4p-5s transitions 77−23453
Zr XI and XV, spectra, perturbation theory with model pot. 78−58579
Zr XII, energy level system, spectrum obs. 70 to 630 Å 80−37766
Zr XIII, electronic struct. of complex ion, relativistic perturbation theory 79−22610
Zr XXXI, XXXII, XXXIII, transition identification X-ray spectra 80−32648
α-Zr:H, energy of interstitial H calc. 79−23596
Zr:He, diffusion of He studied by thermal evolution spectrometry 77−69120
Zr:N, difference in conc. distribs. between implanted N^+ and N_2^+ ions 77−80529
Zr/Al, getter for TFTR Flexibility Modification, in-torus surface pumping 80−95451
Zr-H, inhomogeneous system, time changes of Hall voltage 79−87080
Zr-H system, H location in HCP phase 78−18637
Zr-O-N system, struct. and plastic deform. *(Russian)* 78−80588
Zr-O-W (100) thermal field emitters, operational experience 80−71576
Zr-O(2.85 at.%), Pr effect on internal friction of single crystal 77−4155
Zr-ZrO_{2-x} composite, wetting charact. 77−44207
Zr+H^+, K-shell ionisation cross-section determ. 80−48077
Zr+H^+, K-shell ionisation cross-section, 85 to 790 keV 80−106390
ZrC, solid-phase reacts., effect of nonstoichiometry, thermodynamic evaluation 78−60632
$ZrH_{1.5}$ and $ZrH_{1.75}$, low temp. phase transitions in H sublattice 77−24405
ZrO_2-Zr cermet composite, hot pressed, fracture toughness 78−27604
ZrSi/$ZrSi_2$ coating on Ar, exam. of oxidation behaviour by O_2, H_2O *(French)* 79−20284

zirconium continued
^{89}Zr, electron capture to positron emission ratios determ. 77−18896
^{91}Zr, hyperfine struct. and nucl. elec. quadrupole moment. at. beam mag. reson. meas. 78−55133
^{94}Zr, in silicate samples, neutron activation anal. 78−76951
^{94}Zr(n,α)^{91}Sr, fast n, fission spectrum averaged cross section 80−63177

zirconium alloys
see also zirconium compounds
absorption of H_2 79−77754
acoustic emission during tensile testing 77−90433
advanced reactors, materials and design 78−78452
bronze, sintered, Zr addition effects on struct., hardness, wear resistance *(Russian)* 77−70019
cathodic behaviour in conc. hot H_2SO_4 79−52423
cladding, new material development 77−50242
core materials development for water cooled reactor systems 77−46296
corrosion props. rel to exoelectronic emission props. and energy-band parameters of ZrO_2 layers 79−91571
corrosion resistance and mech. parameters of sheaths and tubes for nuclear power appl. 79−97813
corrosion stability, effect of steel presence 77−56162
corrosion studies of materials for nucl. reactor applic. 77−34402
cracking, H_2 induced delay, strain energy effect on H_2 solubility 78−92364
creep, steady state creep rate, stress depend. at low stress *(Czechoslovakian)* 77−32640
creep and growth, irradiation induced, microstruct. depend. 80−93602
creep and growth, irradiation induced, rate theory approach 80−89294
crystallographic texture, quantitative charact., review 78−21647
decomposition of BCC β solid solns., X-ray and electron diffr. *(Russian)* 79−1869
diffusion coefficient of O, 675-1800°C, α and β alloys 77−62680
diffusion of H_2 at room temp. 79−51312
diffusion of H, NMR study 80−108088
domain struct. of diffuse ω-phase formed in quenching, 1D model 78−27523
elastic props. of fuel cladding and press. tubing material 79−15711
embrittlement in I_2, environmental purity effect 80−30149
fission reactor fuel cladding, strain reduction by changing pellet configurations 79−81008
foil, dislocation loop nucleation and growth during 1 MeV electron irrad. 80−88152
irradiation creep anisotropy, and growth 79−83255
irradiation growth, dislocation model 78−51595
irradiation props., point defect struct. of α-Zr effect 78−30609
neutron irradiated, in-pile dimensional changes 77−24331
neutron irradiated, yield strength changes and radiation hardening, damage annealing *(Italian)* 77−65269
Nichrome based dispersion hardened material, Ti, Y, Zr addition effects on crystallisation *(Russian)* 79−74143
Ozhennite, yield point, effect of ageing stress 77−21223
phase reflex calc. on theoretical roentgenograms of immobile monocrystals 79−23491
β→α phase transformation, cooling rate effects 80−7565
plasma-sprayed thermal barrier coatings, evaluation 80−40619
pressure tubes, cracking due to high residual tensile stresses 78−29585
pseudo-binary alloys, $Zr(A_xB_{1-x})_2$ (A=V, Cr, Mn; B=Fe, Co), H_2 absorpt. capacity 80−88433
reactor fuel sheath mat., thermophys. props. 77−46280
steel, austenitic, phase composition of Kh14N16 with Zr, Ti, Nb and N additions after quenching and tempering 77−90378
steel, low-C, structural, grain boundaries, AES 79−24524
steel, R6M6, micro-alloying effect 78−6939
steel, stainless, oxidation effect of Zr 80−35394
stress relaxation, in-reactor study at low temps. 80−93588
TEM obs. of irradiation damage, critical review 79−10879
TZM-Mo alloy, mech. props., effect of exposure to high temp. He containing O_2, room temp. study 80−93639
wear due to fretting and periodic impacting 80−16509
XL alloy, thermal neutron capture cross-section var. with time, calc. 77−61505
β-Zircalloy, creep charact. 79−8317
Zircalloy, H diffusion, neutron scatt. and absorpt. study 79−60556
Zircalloy in thermal gradient, calc. of supercharging effect of H_2 and hydride distrib. 78−21639
Zircalloy-4 fuel sheathing, inverted primary creep 78−86615
Zircaloy;UO_2 fuel design, LOWI 78−70600
Zircaloy, accelerated corrosion in BWR and high temp. high press. steam, correlation 77−3104
Zircaloy, annealed, neutron irradiated, inhomogeneous deform. behaviour 80−85014
Zircaloy, breakaway mechanism, corrosion kinetics in steam 80−61030
Zircaloy, cladding in fuel rods, stress corrosion fracture on power increase 79−47818
Zircaloy, claddings for irradiated UO_2 fuel, stability during long-term storage 79−26588
Zircaloy, creep and growth, radiation induced, fundamental mechanisms 80−92596
Zircaloy, deformed, positron annihilation and electron microscopy 77−8898
Zircaloy, deposits on inside surface in LWR cladding, SEM obs. 79−6741
Zircaloy, design and performance evaluation of All-Zircaloy fuel assemblies for PWR 80−13560
Zircaloy, effect of dispersion and spheroidisation treatment of δ ZrH 79−76073
zircaloy, effect of reactor irradiation on H diffusion 77−14231
Zircaloy, fatigue crack propag., environmental effects *(French)* 77−66711
Zircaloy, foil, dislocation loop nucleation and growth during 1 MeV electron irrad. 80−88152
Zircaloy, H absorption, Sn(Fe)(Cr)(Ni) effect 80−49527
Zircaloy, hydriding reaction kinetics, oxidised specimens 78−26728
zircaloy, in-pile creep measuring rig 77−42083
Zircaloy, in-pile temp. depend of yield strength and growth, under neutron irrad. 79−73219
Zircaloy, in-reactor creep meas. appl. in design of PWR fuel 77−42073
Zircaloy, irrad. behaviour, chemical process, densification, corrosion *(Japanese)* 77−83033
Zircaloy, irradiated spent fuel cladding, annealing effects 79−89382

zirconium alloys continued
Zircaloy, irradiation growth in annealed and cold worked samples 77−88225
Zircaloy, LWR cladding, I_2 stress corrosion cracking 79−89380
Zircaloy, LWR fuel rod cladding, damage accumulation during I_2-induced stress corrosion cracking 80−71810
Zircaloy, micrograin superplasticity at 850°C 78−23758
zircaloy, nuclear microprobe methods for investigating oxidative corrosion 80−71787
β-Zircaloy, O_2 diffusion 78−6181
Zircaloy, O diffusion during UO_2-Zircaloy interaction 79−10986
Zircaloy, polarisation in high temp. water 77−52540
Zircaloy, post irradiation recovery of growth 79−46711
Zircaloy, PWR fuel induced cladding deformation, creep correl., in-pile meas. 80−97547
Zircaloy, PWR primary corrosion products 80−13578
Zircaloy, steam oxidised, partitioning behaviour of O_2 78−68839
Zircaloy, textural model for stress corrosion crack susceptibility 79−47825
Zircaloy, textured, interactive creep and growth, upper-bound evaluation 80−89293
Zircaloy, unirrad., stress corrosion cracking, I_2-induced, effect of test temp., alloy comp. and heat treatment 80−97632
zircaloy 2, annealed, corrosion fatigue in aqueous soln. at 575K 78−64789
Zircaloy 2 and 4, oxidation kinetics appl. to loss of coolant accidents, data review 78−19958
Zircaloy 2/I_2 system, stress corrosion crack growth for short cracks 78−80685
Zircaloy 4, creep anal. and appl. in prediction of residual stress relaxation 79−43325
Zircaloy 4 tubing, cold-worked and annealed, stress relaxation behaviour 77−57717
Zircaloy clad fuel rod burst behaviour in simulated PWR LOCA 79−36337
Zircaloy clad UO_2 fuel elements, irrad. effects 80−666
Zircaloy cladding, effects of stress biaxiality on ballooning behaviour 79−30919
Zircaloy cladding, embrittlement and failure during reactor power-cooling-mismatch 78−21688
Zircaloy cladding, enhanced steam oxidation by deformation under LWR LOCA 80−73917
Zircaloy cladding, internally pressurized, effect of temp. nonuniformity on diametral expansion during transient heating in steam 79−30920
Zircaloy cladding, irrad., tensile props., effects of temp., strain rate and annealing 77−48463
Zircaloy cladding, stress corrosion cracking, inner surface texture effect 80−66695
Zircaloy cladding, stress corrosion cracking due to I and Cs redistrib. in LWR fuel rods 80−32343
Zircaloy cladding, stresses due to pellet cladding interaction 80−42762
Zircaloy cladding ballooning, analytical model for transient gas flow in LWR 80−18499
Zircaloy cladding fabrication, review, charact. which impact fuel manufacture 79−59241
Zircaloy cladding stress corrosion cracking due to I *(Japanese)* 80−78361
Zircaloy cladding thermal failure and UO_2 fuel melting during LWR PCM transient 80−42834
Zircaloy cladding tubes, under internal and external overpressure in FRG-2 in-pile creep 77−42082
zircaloy cladding tubes of irrad. fuel, flattening test *(Japanese)* 77−42054
Zircaloy claddings, PWR fuel assemblies, LOCA behaviour in multirod burst tests 80−27739
zircaloy corrosion, in-reactor, effects of water radiolysis 77−12817
Zircaloy corrosion in water reactors, comparison of uniform and nodular forms 79−47817
Zircaloy creep collapse, hot cell examination 78−86596
Zircaloy fuel cladding, azimuthal temp. distrib. during LOCA 80−662
Zircaloy fuel cladding, irrad. capsule design for continuously monitoring creepdown 79−54513
Zircaloy fuel cladding, irradiation-induced in-reactor corrosion in CANDU reactors 80−104352
Zircaloy fuel cladding, O embrittlement obs. 78−89947
zircaloy fuel cladding tubes, prod. and inspection *(Japanese)* 79−26518
Zircaloy fuel claddings, multirod burst tests following PWR LOCA 80−777
Zircaloy fuel sheathing, NIRVANA high temp. creep model 79−87704
Zircaloy heated surface, FeO deposition in boiling water 78−58353
Zircaloy hulls, conversion to zirconate ion exchange materials for waste stabilisation 78−702
Zircaloy LWR cladding, modeling of deform. and fracture in SPEAR code system 79−93729
Zircaloy oxidation, improved evaluation model 80−32349
Zircaloy pressure tubes, effect of microstruct. on irradiation creep 79−74208
Zircaloy PWR fuel cladding, balloon deformation during LOCA 80−659
Zircaloy PWR fuel cladding deformation tests under mainly convective cooling conditions 80−57862
Zircaloy reactor fuel cladding tubes, high temp. deformation model with nonlinear temps. 80−661
Zircaloy sheath, fission gas absorpt. following irrad., power history effects 80−78395
Zircaloy sheath tube, oxidation calc. *(German)* 77−346
Zircaloy sheathed UO_2 combustibles, CEA expt. on transient behaviour *(French)* 80−18417
Zircaloy sheaths, oxidation rate calc. method 80−78394
Zircaloy solid wastes from fuel reprocessing plant, management 77−61591
Zircaloy tubes, yield loci, evaluation based on texture data and mech. testing 79−91695
Zircaloy tubing, I_2 stress corrosion cracking, pellet cladding interaction mechanism *(German)* 80−16565
Zircaloy-2, anisotropic irradiation creep 79−8333
Zircaloy-2, annealed, neutron irradiation growth 79−42109
Zircaloy-2, anodic oxidation kinetics, in 0.05M oxalic acid (aq. and alcoholic) 80−104331
zircaloy-2, anodisation, cladding appl. 77−81341
Zircaloy-2, Cd metal embrittlement in 300-340°C 77−16747

zirconium alloys continued
Zircaloy-2, cold worked, temp. cycling effects on irradiation growth 80−2079
Zircaloy-2, deformation instability and tensile elongation 77−32655
Zircaloy-2, effect of simulated fission products on elongation fractography and metallography 80−649
Zircaloy-2, effects of simulated fission products on mechanical props. 80−52740
Zircaloy-2, elastic const. determ. 78−11257
Zircaloy-2, electrochemical pitting in alkaline chloride soln., H_2 evolution and anodic disintegration 80−16553
Zircaloy-2, exposed to I_2 vapour, stress corrosion crack initiation sites 78−92324
Zircaloy-2, fatigue, 20 to 700°C 77−70154
Zircaloy-2, fretting corrosion in water-cooled nucl. reactor 77−79431
Zircaloy-2, hot-pressed, influence of diffused C on structure and oxidation 80−61016
Zircaloy-2, hydride precipitation and growth at crack tips, electron optical obs. 80−108449
Zircaloy-2, I_2 stress corrosion cracking, Cs_2O and Cs influence, in- and out-of-pile 80−3252
Zircaloy-2, inelastic deformation, generalised strain rate dependent constitutive eqn., load relaxation tests 79−11655
Zircaloy-2, iodine environment, plane strain tension test 80−22944
Zircaloy-2, irradiation creep under H^+ bombardment at 5.5 MeV 78−14392
Zircaloy-2, irradiation growth, influence of microstructure and test conditions 80−92561
Zircaloy-2, irradiation growth, reaction rate theory calcs. 80−88212
Zircaloy-2, irradiation growth, shape and volume changes 80−92562
Zircaloy-2, irradiation induced creep in reactor claddings under biaxial stress conditions 79−30912
Zircaloy-2, irradiation-induced creep following 4 MeV H^+ bombardment 78−14390
Zircaloy-2, martensitic transform. contrib. to strength and work hardening, and martensite flow props. 78−84842
Zircaloy-2, mech. props. after exposure to I_2-methanol solutions, SEM study 80−93689
Zircaloy-2, neutron irrad., low temp. deform. studies 79−47757
Zircaloy-2, neutron irrad. at 573 to 923K damage struct. 80−107334
Zircaloy-2, neutron irrad. damage, TEM characts. 80−107332
Zircaloy-2, neutron irradiated, inhomogeneous deformation behaviour 80−50679
Zircaloy-2, neutron irradiation damage characterization by TEM 79−42110
Zircaloy-2, oxidation, protective oxide layer stress accumulation and perturbation of parabolic kinetics 79−5076
Zircaloy-2, oxide coating thermal cond. meas. 80−80009
Zircaloy-2, plastic deform. generalised constitutive eqns. 80−104219
Zircaloy-2, polycrystn., thermal history effect on tensile props. 79−74204
Zircaloy-2, polycrystn., thermal history effect on tensile props., comment 79−74205
Zircaloy-2, pressure tube, fragmentation on failure 78−72863
Zircaloy-2, pressure tubes, irrad. creep and growth, anisotropy factors 80−97536
Zircaloy-2, radiation and isotope effects on corrosion in H_2O/D_2O mixture 77−21314
Zircaloy-2, radiation induced creep, yielding creep theory, time depend. of irrad. growth 77−26845
Zircaloy-2, reaction with UO_2-PuO_2 79−17982
Zircaloy-2, reactor cladding, delta-wrinkly zone near crack edge obs. 79−3203
Zircaloy-2, recoverable plastic strain 77−63708
Zircaloy-2, reversible embrittlement in CH_3OH/HCl 79−91833
Zircaloy-2, role of oxide plasticity in oxidation behaviour 77−36680
Zircaloy-2, TEM and SEM of anodically formed oxides 77−21313
β-Zircaloy-2, tensile creep and creep rupture props. under vacuum 78−52915
Zircaloy-2, thermal neutron capture cross-section var. with time, calc. 77−61505
Zircaloy-2, tritium diffusion 80−32341
Zircaloy-2, yield pts. obtained by ageing at two stresses 80−81091
zircaloy-2 and 4, tubing, rel. between contractile strain ratio R and texture 79−61607
Zircaloy-2 and -4, ⟨c⟩ component dislocations from TEM contrast expts. 80−6412
Zircaloy-2 and associated oxide layers, thermal property meas. 77−8063
Zircaloy-2 anodic oxidation in 0.05 M Na_2SO_4 electrolyte 79−57144
Zircaloy-2 cladding, beta-phase creep and creep rupture props., 1000 to 1500°C 78−78470
Zircaloy-2 cladding, bonding to UO_2 fuel, mechanisms determ. by SEM and EPMA 78−17317
Zircaloy-2 cladding, fracture in iodine environment 78−31581
Zircaloy-2 cladding, stress corrosion cracking in iodine vapour, 250-450°C 78−17313
zircaloy-2 cladding tube, fission cutting *(Japanese)* 77−67808
Zircaloy-2 cladding tubes, heat treatment influence on texture and mech. anisotropy 79−91694
zircaloy-2 cladding tubes, post neutron irrad. ring-tensile props. pre-hydriding effect 77−42053
Zircaloy-2 claddings, oxidation reaction kinetics in steam environment in temp. range 1273-1673K 80−35401
Zircaloy-2 fuel tube, thermal conductivity of oxide deposit 79−63745
Zircaloy-2 fuel tubes, cumulative damage fatigue tests at room temp. and 300°C 80−93638
Zircaloy-2 fuel tubes, low cycle fatigue studies at room temp., 300 and 350°C 80−93637
Zircaloy-2 irradiation growth at 353 and 553K, texture and temp. cycling effect 79−46709
Zircaloy-2 pressure tube, elongation in Douglas Point CANDU reactor 80−78398
Zircaloy-2 pressure tube elongation, neutron induced creep and growth, meas. and anal. 80−93628
Zircaloy-2 thin walled large diam. tubes in CANDU reactors 79−13429
Zircaloy-2 tube, external pressure creep behaviour 79−57083
Zircaloy-2 tubing, quantitative charact. of crystallographic texture 78−21647
Zircaloy-4, ^{51}Cr bulk diffusion 79−73347
Zircaloy-4, β-transformed, flow stress and dynamic strain ageing 80−3101
zirconium alloys continued
Zircaloy-4, accelerated corrosion in high temp., high press. steam, effect of heat treatment 78−44263
Zircaloy-4, anomalous oxide growth during transient temp. oxidation 80−50773
Zircaloy-4, CANDU irrad. fuel bundles storage, long-term stability investig. 80−13774
Zircaloy-4, creep damage at LWR temp. 79−52312
Zircaloy-4, creep rupture at monotonous stress and temp. ramp loading 79−74241
Zircaloy-4, creep rupture at superimposed non-stationary stress and temp. loading 80−66630
Zircaloy-4, cyclic nature of corrosion in 633K water, optical and electron microscope study 79−66207
Zircaloy-4, damping, amplitude dependent, at high temp. 77−52383
Zircaloy-4, diffusion bonding with 304 stainless steel 78−34658
Zircaloy-4, elastic props., O additions effect 80−66565
Zircaloy-4, exam. of plastic props. at elevated temps. in air 77−4811
Zircaloy-4, failure strain prediction under non-stationary loading conditions 80−93640
Zircaloy-4, fuel cladding, burst criteria under LOCA conditions 80−73931
Zircaloy-4, fuel cladding, steady-state creep from 940 to 1873K 79−74206
Zircaloy-4, H_2 effect on mech. props. *(Korean)* 79−70123
Zircaloy-4, heat treatment in SiO_2 capsules, vapour transport of Zr and Si 80−55437
Zircaloy-4, in-pile PWR creep meas., comparative eval. of 10 creep correl. 80−652
Zircaloy-4, interdiffusion with Ni 79−42320
Zircaloy-4, load relaxation and tensile tests 79−20093
Zircaloy-4, microstrain and particle size meas. by Warren-Averbach method 80−55420
zircaloy-4, Nb additions, corrosion behaviour 77−40469
α-Zircaloy-4, O stabilized, O diffusion using ^{18}O tracer 78−51737
Zircaloy-4, oxidation at 900 and 1100°C in high pressure steam 79−66208
zircaloy-4, oxidation in high temp. steam atm. effect on cladding ductility 79−26515
Zircaloy-4, oxidation in steam, 900-1500°C, kinetics 80−3241
Zircaloy-4, oxidation in steam, 900-1500°C, O diffusion in oxide and α-phases 79−100288
Zircaloy-4, oxide coating effect on ductility 79−47819
Zircaloy-4, plain strain ductility dependent of struct. and texture 77−8885
Zircaloy-4, Poisson's ratio determ. at several temp. levels 78−52874
Zircaloy-4, polytype struct. of intermetallic precipitates, electron microscope obs. 79−43250
Zircaloy-4, PWR tubes, ZrO_2 scales formed in steam, microstruct. 77−6524
Zircaloy-4, quenched, strain ageing behaviour, ageing time and temp. effects 78−56657
Zircaloy-4, quenched and annealed, strain ageing 77−25071
Zircaloy-4, resistance-welded, microstruct. of weld region 80−66549
Zircaloy-4, strain rate dependent mech. response 77−21254
Zircaloy-4, strain rate sensitivity parameter measurement, from expt. load vs. time curves, superplastic range 79−8406
Zircaloy-4, stress relaxation specimens, thermally induced strain recovery causing microstruct. changes 77−25057
Zircaloy-4, stress-relieved and cold-worked, stress relaxation in bending at 673K 80−93609
Zircaloy-4, techniques of impact and sliding wear study 79−74337
Zircaloy-4, tensile props., room temp. to 900K 77−70104
Zircaloy-4, tensional stress cycling 80−3168
Zircaloy-4 BWR channels, corrosion resistance 80−104351
Zircaloy-4 clad UO_2 fuel, long term storage in water and stress corrosion cracking 79−93737
Zircaloy-4 cladding, creep transients, plastic hoop strain meas. 79−57068
Zircaloy-4 cladding, irrad. growth prediction using crystallographic texture model 77−46300
Zircaloy-4 cladding, steady-state creep, 940 to 1873K 79−15759
Zircaloy-4 cladding deformation under LOCA transient heating conditions, analytical modelling 80−104236
Zircaloy-4 cladding rubes, burst strain and stress corrosion cracking, I influence 80−3248
Zircaloy-4 cold worked, strain ageing behaviour with varying O_2 content 77−48455
Zircaloy-4 fuel cladding axial deform. in PWR LOCA 80−13585
Zircaloy-4 fuel sheaths, ballooning behaviour at heating rate 0.5°C s^{-1} 79−24593
Zircaloy-4 PWR cladding, effect of oxide coating on ductility 79−89381
Zircaloy-4 spent fuel cladding, tensile props. and annealing characts. 79−22392
Zircaloy-4 tubes, I stress corrosion cracking *(Korean)* 79−34195
Zircaloy-4 tubes, texture influence on anal. of thermoelastic/plastic anisotropy and initial yielding 80−35260
Zircaloy-4 tubing, unirradiated, under internal pressurisation, threshold conditions for I-induced stress corrosion cracking 79−66206
Zircaloy-4-O alloys, rapidly heated and quenched, transform. charact. 79−20041
Zircaloy-4/stainless steel, diffusion bonding in presence of Fe intermediate layer 79−10987
Zircaloy-4/stainless steel type 304 diffusion junction, hydriding behaviour 79−65200
Zircaloy-O_2 phase diagram 80−3003
Zircaloy-UO_2 fuel rods, eddy-current testing of claddings using encircling and probe coils 80−21245
Zircaloy-Z, thermal diffusion of H, numerical soln. with computer *(Korean)* 80−19989
Zircaloys, fractographic distinction between hydride cracking and stress corrosion cracking 78−92363
Zircaloys, I_2 induced stress corrosion cracking 79−8381
Zircaloys, stress corrosion cracking 77−63824
Zirconium-4, oxidation reaction kinetics in unlimited steam environment 77−8988
Ag-Zr, optical props., DC resist. and thermoelec. power 77−85824
Al alloy 7075, $CrAl_7$ form., effect of V and Zr 78−44132
Al-Cr-Zn (2.5, 1.5 wt%), phase equilibrium, solubility *(Russian)* 78−19723
Al-Cr-Zr, calc. of phase equilibria 79−11569

zirconium alloys continued
Al-Cu-Mn-Zr-Fe-Si (6,0.3,0.18,0.3,0.1 wt.%) experimental evidence of Mn enrichment in Al_2Cu precipitates by EDS in TEM 78−15415
Al-Cu-Zr, superplastic alloy Supral, solidification and recrystallisation 80−7550
Al-Cu-Zr (6, 0.3 wt.%), superplastic, texture studies 79−83210
Al-Cu-Zr (6, 0.4 wt.%), superplastic flow activation energy 80−11701
Al-Cu-Zr (6, 0.4 wt.%), superplastic deformation charact. 80−16387
Al-Mg-Li-Zr alloys, struct., mech. props. 79−24498
Al-Mg-Ti-Zr alloy AL23-1, nucleating cellular dendritic crystallisation *(Russian)* 79−70055
Al-Mg-Zr, phase diagram *(Russian)* 78−11205
Al-Mg-Zr, struct. and factors determining brittle intermediate compound form. 78−52817
Al-Mn-Zr (0.9, 0.4%), strain induced continuous recrystn., rel. to superplastic behaviour 78−84915
Al-Mn(Cu)-Zr, particle stabilized structures, hot deform. 79−47733
Al-Mn(0.6 wt.%), supersat. solid solns., isothermal decomp., Zr addition effects 77−63626
Al-Si-Cu-Zr, ageing kinetics *(Russian)* 80−76274
Al-Zn-Mg-Cu-Cr-Zr, high strength Cr and Zr addition effects 77−59820
Al-Zn-Mg-Zr, low cycle fatigue, grain refinement effect 77−44345
Al-Zn-Mg-Zr (6.45, 2.08, 0.11 wt.%), exam. of cyclic stress strain response in corrosion fatigue 78−64788
Al-Zn-Mg-(Zr) alloy, microstruct. effect on fatigue crack growth 80−3164
Al-Zr, cast, precipitation and solidification *(German)* 77−36519
Al-Zr, dilute, vacancy-impurity interaction investig. by tempering method *(French)* 77−68995
Al-Zr, interphases, formed during precipitation and solidification *(German)* 79−29062
Al-Zr, simultaneous recrystallisation and precipitation *(French)* 80−16313
Al-Zr, solidification and precipitation, Zr effect on cast struct. *(German)* 77−36518
Al-Zr (0.22 wt.%), hardness and struct. changes during prolonged ageing at 350, 400 450°C *(Japanese)* 79−52281
Al-Zr (0.8 and 1.5 wt.%), hyperperitectic, non equilibrium solidification 78−3113
Al-Zr (1-13 wt.%), rapidly quenched, extended solid solubility, grain refinement and age-hardening 80−76266
Al-Zr solid soln., discontinuous precipitation of metastable Al_3Zr 78−3130
$Al_{20}Cu_{25}Zr_{55}$ metallic glass, inelastic deform., free energy spectra 80−71699
Ar-Re, phase diagram between 1866 to 1913K 79−100115
Au-Zr, dil., Friedel d-reson. scatt. and elec. resists. 80−44566
Be-Nb-Zr, glassy and partially crystalline, supercond. T_c and struct. props. 78−60239
Be-Zr, glassy, quenched from melt, supercond. props. 78−26983
$Be_{40}Ti_{50}Zr_{10}$, metallic glass, thermoelectric power and resist. 78−95289
CU-Zr-(Cr), powder metallurgical alloys, thermomech. treatment effect on props. 80−50660
$Ce_{1-x}Gd_xRu_2Zr_2Co$, spin-pairing state investig. via Josephson effect 77−47942
Co-Cr-Zr, phase diagram calc. 79−1848
Co-Cr-Zr, thermodynamically calculated phase diagram 79−91617
Co-Cr(Si)-Zi, eutectic alloys, charact. by melting, oxidation resistance and composition 78−52768
Co-Zr, amorphous phase form. in Zr-poor region, hardness and fracture strength *(Japanese)* 80−84914
Co-Zr, dendritic segregation 80−76260
Co-Zr, dil., mag. annealing effect, depend. of uniaxial mag. anisotropy on Zr conc. 80−39772
Co-Zr-Er alloys, mag. annealing effect, effect of Er on induced uniaxial mag. anisotropy 80−39771
Co_2Zr, $CoZr_2$, and $CoZr_3$, mag. susceptibility, 77-500K *(Russian)* 77−80911
Co_2Zr, Laves phase, elec. resist. rel. to mag. props. 77−59282
$Co_{90}Zr_{10}$, ferromag. amorphous alloy, crystn. and domain struct. study 80−107056
Co_2ZrAl, Heusler alloy, paramag. state NMR and susceptibility meas. 79−65643
Co_2ZrSn-Fe, dil., Heusler alloy, Fe hyperfine fields, Mossbauer obs. 78−68424
Co_2ZrSn(Al), ferromag., hyperfine fields meas. by NMR 77−63315
Cr-M, optimum alloying with rare earth metals, Ti, Zr, Hf, Nb, Ta 78−68651
Cr-Zr evaporation source improvement, diffusion barrier layer deposition for IC metallurgy 80−76163
Cu-Be-Ni-Zr, anodic behaviour of intermetallic phase 78−72895
Cu-Cr-Zr-Mg (0.5, 0.1, 0.03 wt.%), exam. of low cycle fatigue props. at elevated temp. 78−64674
Cu-Cr-Zr-Ti-B alloy system, solidification cracks formed during welding, reduction by microalloying with B 79−96148
Cu-Cu Zr eutectic composite, struct. and props., heat treatment and crystn. rate influence *(Russian)* 79−38813
Cu-Ti, Zr effects on cellular precipitation 77−16587
Cu-Ti-Zr, strength improvement, using thermomechanical treatment *(Japanese)* 78−48426
Cu-Zn, amorphous, viscoelastic behaviour *(Japanese)* 77−86110
Cu-Zr, amorphous, struct., X-ray scatt., rel. to Ni-P alloys 77−51324
Cu-Zr, amorphous, viscoelastic behaviour *(Japanese)* 77−86110
Cu-Zr, intermediary phases of equilib. diagram 78−84771
Cu-Zr, metallic glasses, valence band struct. investigation 80−11533
Cu-Zr, vapour quenching prod. (thermal evaporation and r.f. sputtering), amorphous film for electron microscopy 78−6851
Cu-Zr (50 or 54 at.%), splat-quenched, glass transition and crystn. temps. determ. 78−22659
Cu-Zr alloys, isothermal transformation diagram 80−20902
Cu-Zr amorphous alloy, splat cooled, local order and amorphous struct. 80−88061
Cu-Zr amorphous alloys, mech. props. *(Japanese)* 77−86179
Cu-ZrO_2, dispersion hardened, electrical cond. and mech. props. 78−44133
Cu-ZrO_2, internally oxidised, orientational relationships of precip. oxide phase 77−4783
$Cu_{40}Nb_{30}X_{30}$ (X=Ti, Zr, Hf), superconductors with metastable ordered structs. 80−108484

zirconium alloys continued
$Cu_{40}Zr_{60}$, $Cu_{56}Zr_{44}$, and $Cu_{60}Zr_{40}$ metallic glass, inelastic deform., free energy spectra 80−71699
CuZr, photoemission study 80−104046
$CuZr_2+H_2$, 550 to 850°C, absorption isotherms, thermodynamics 79−87841
$Cu_{0.57}Zr_{0.43}$, amorphous, partial struct. factor, TOF pulsed neutron 79−14684
$Cu_{0.57}Zr_{0.43}$ amorphous alloy, neutron diffr. obs. of struct. 80−88060
$Cu_{40}Zr_{60}$, amorphous alloys, supercond. transition temp., press. depend. 80−84524
$Cu_{46}Zr_{54}$, devitrification effect on mech. props. 80−30082
$Cu_{46}Zr_{54}$, metallic glass, dynamical struct. factor and freq. distrib. meas. 80−54136
$Cu_{50}Zr_{50}$, amorphous and cryst. alloy, corrosion rates and anodic polarisation curves 79−24650
$Cu_{50}Zr_{50}$, metallic glass, internal friction peaks 80−25753
$Cu_{56}Zr_{44}$ metallic glass, devitrification and its effect on mech. props. 80−33893
$Cu_{57}Zr_{43}$, amorphous alloy, computer simulation of atomic structure 80−70125
$Cu_{60}Zr_{40}$, amorphous, ductility and stress relief, low-temp. annealing effects 80−76296
$Cu_{60}Zr_{40}$, amorphous, elec. resist. calc. and temp. coeff., using t-matrix 78−72130
$Cu_{60}Zr_{40}$, amorphous powder, production using gas-water atomisation unit 80−7518
$Cu_{60}Zr_{40}$ glassy metal, photoemission and mag. susceptibility 79−28896
$Cu_{60}Zr_{40}$, metallic glass, composition, mech. props., simulation 80−49117
$Cu_{60}Zr_{40}$, stability, crystallisation, ductility meas. 78−47246
Fe, cast Zr effect on graphite nodularisation *(Japanese)* 77−55999
Fe-Co-Ni-Al-Zr magnetically hard alloys, reduction *(Russian)* 78−43614
Fe-Zr, amorphous, charge transfer and mag. props., ^{57}Fe Mossbauer spectra 79−19719
Fe-Zr, amorphous phase form. in Zr-poor region, hardness and fracture strength *(Japanese)* 80−84914
Fe-Zr, dilute solid solution, surface segregation, AES exam. 77−43413
Fe-Zr amorphous films, mag. props., Mossbauer effect and magnetisation meas. 79−69701
$GdZrFe_2$, hyperfine field at Gd, TDPAC meas. 80−93214
$(Hf,Zr)V_2$, phase transition, sp. ht. anomalies meas., 70-150K 77−35691
Hf, 0.3 wt.% Zr, melting pt. and radiance temp. meas. by pulse heating method 77−53914
Hf-Zr, binary continuous solid solution, elec. resist. and thermoelec. power behaviour 79−69492
Hf-Zr (3 wt.%), $\alpha \rightarrow \beta$ transform. temp. and entropy, emissivity 77−48424
Hf-Zr-Ga, phase equilibria X-ray study at 800°C *(Ukrainian)* 79−95998
Hf_xZr_{1-x}, elec. quadrupole interactions at ^{181}Ta impurities, TDPAC meas. 78−76364
$(Hf_xZr_{1-x})_{80}Nb_{20}$, influence of Hf additions to $Zr_{80}Nb_{20}$, beta decomposition anal. 79−8304
$Hf_{1-x}Zr_xV_2$, lattice consts. at 4K and room temp., phase division at x=0.4 78−51474
$Hf_{0.5}Zr_{0.5}V_2H_x(D_x)$, enhanced supercond. transition temp. on H(D) additions 78−80083
Mg-Nd-Zr, phase diagram, Mg rich region, microscopic anal. and elec. resistivity meas. *(Russian)* 78−56619
Mg-Y-Nd-Zn-Zr (2,2,0.3, 0.7 wt.%), heat treatment effect on casting dimensional stability, alloy mech. props. 78−44146
Mg-Y-Zr, phase equilib. and props. *(Russian)* 77−66626
Mg-Zn-Zr, cast, exam. of phase composition, mech. props. 79−100217
Mg-Zn-Zr rare earth alloy, mech. props., effect of microshrinkage during solidifaction 79−43234
Mg-Zn-Zr-Cd-Nd, Lawes phase separation using acetate electrolyte, Cd and Nd effects 79−70237
Mg-Zr, cavitation during diffusion creep 77−44296
Mn-Ni-Zr, and mech. props., thermal expansion, for different heat treatments *(Japanese)* 79−29123
Mn-Ni-Zr, non-ferromagnetic Elinvar-type alloys 79−24566
Mn-Zr-S, phase equilibrium *(German)* 78−72764
Mo-(Zr+V+C) (1.1 wt.%) alloy, phase composition, carbide phase microhardness *(Russian)* 80−60834
Mo-C-Zr-B (0.004, 0.12, 0.002 wt.%) effect of grain size, cellular dislocation structure, on mech. props. *(Russian)* 79−34105
Mo-Ti-Zr, alloy TZM, polycrystalline, anal. of elastic anisotropy and microyielding 80−30050
Mo-Ti-Zr, D trapping in fusion reactor materials, temp. dependence 80−37577
Mo-Ti-Zr, diffusion and solubility of C *(French)* 79−55932
Mo-Ti-Zr, fusion reactor first wall material, compatibility with impure He 80−32469
Mo-Ti-Zr, TZM, corrosion behaviour in high temp. impure He gas 80−76402
Mo-Ti-Zr (TZM), fusion reactor materials, radioactivity minimization by elemental substitution and isotopic tailoring 79−22463
Mo-Ti-Zr (0.5, 0.1 wt.%), neutron irradiated, void swelling and shrinkage, TEM study 80−34079
Mo-Ti-Zr (0.5, 0.7 wt.%) alloy TZM, props. and appl. *(German)* 80−21040
Mo-Ti-Zr alloy, neutron radiation-induced shrinkage of voids 79−51158
Mo-Ti-Zr alloy TZM, fatigue and plastic flow, irradiation effects 77−52466
Mo-Ti-Zr alloys TZM and TZC, superior powder metallurgy die alloys for isothermal forging mech. props. 79−74201
Mo-Ti-Zr-C, stress cycling at room temp. *(Russian)* 77−25148
Mo-Zr, electron beam melted, alloying addition effects on brittleness and ductility 79−61728
Mo-Zr, heavy ion irradiated, void swelling, phase instability 80−29084
Mo-Zr, interaction with $MoSi_2$ diffusion coating, at elevated temps. *(Russian)* 79−28150
Mo-Zr, nitride form. in N_2 atmos. *(Russian)* 78−19938
Mo-Zr, nucleation conditions, effect on formation of oxide phase during internal oxidation *(Russian)* 80−81064
Mo-Zr (0.15 wt.%), wrought, fracture, characteristic features 80−104278
Mo-Zr (6 wt.%), absorption of N_2 in induction and plasma-arc heating *(Russian)* 77−16732

zirconium alloys continued
Mo-Zr alloys, TsM-6, Zr segregation at grain boundaries, carbide precipitation, X-ray spectral anal. *(Russian)* 79−74154
Mo-Zr-B, neutron irrad. at 780-1080°C, porosity, hardening and embrittlement *(Russian)* 80−29062
Mo-Zr-B, porosity and mech. props. after neutron bombard., 780-1080°C *(Russian)* 80−24502
Mo-Zr-B-C, dil. alloy, struct. changes under prolonged high temp. annealing *(Russian)* 78−6944
Mo-Zr-C, deformed, singularities of fragmented structs. *(Russian)* 77−44289
Mo-Zr-C (0.063, 0.06 wt.%) alloys, ageing, effect of cold deform. by hydrostatic extrusion 79−57001
Mo-Zr-C (0.08, 0.02 wt.%), struct. and banding tendency, thermomechanical treatment effects 77−86063
Mo-Zr-C (0.12, 0.002 wt.%), prep. of diffusion metal coating on alloy, oxidation rates *(Russian)* 78−56816
Mo-Zr-C (0.63, 0.06 wt.%), quenched and deformed, structural changes during heating to ageing temp. *(Russian)* 79−1879
Mo-Zr-C alloys, carburising and annealing effects *(Russian)* 77−59828
Mo-Zr-C-B, dilute, electron microscope obs. of planar defect diffr. contrast patterns 77−43227
Mo-Zr-N, exam. of phase equilibria *(Russian)* 79−29018
Mo-Zr-Nb-C, polythermal sections *(Russian)* 78−15365
Mo-Zr-Nb-C alloys, phase diagram and comp., Zr and Nb influence *(Russian)* 79−52167
Mo-Zr-Nb-C and Mo-Zr-C, carbide precip. hardening kinetics, ageing singularities *(Russian)* 77−25059
Mo-Zr-Ti-C(0.1, 0.15, 0.004 wt.%), alloy TsM2A, cavitation failure mechanism 77−70169
Mo-ZrC, eutectic formation of regular struct., crystn. *(Russian)* 80−66496
Mo-ZrC, internal oxidation, struct. formation law, microstruct. examination 78−84836
Mo-ZrC, phase diagram *(Russian)* 78−27476
Mo-ZrO_2 dispersion hardened, rolled, grain struct. and props. 77−77492
$(Nb,Zr)_3Sn$, effect of Zr alloy element on growth kinetics *(Chinese)* 79−90579
Nb-Mo-Ti-Zr, influence of C content on creep charact. and creep-rupture strength *(Russian)* 77−48483
Nb-Mo-Ti-Zr-C, work function temp. and phase depend. *(Russian)* 80−2449
Nb-Mo-Zr-Ti, Zr and Ti effects on struct. and mech. props. 77−70061
Nb-Ti-Zr, electrical resist. at low temp., enhancement due to short-range supercond. order 77−28157
Nb-Ti-Zr, supercond. wire, anomalous increments of AC losses due to flux jumps 77−28289
Nb-Ti-Zr, superconducting, ageing effect on critical current density *(Japanese)* 79−61747
Nb-Ti-Zr, superconducting, critical current density and microstruct. correlation *(Japanese)* 79−61748
Nb-Ti-Zr, superconducting wire, coil simulation, class and instability meas. 79−71487
Nb-Ti-Zr, superconducting wire, coil simulation meas. of losses and instabilities 80−37050
Nb-Ti-Zr, wire, anomalous crit. AC 77−16014
Nb-Ti-Zr ternary alloy wires, flux jumping 79−60965
Nb-Ti-Zr ternary system, high-field supercond. 80−97045
Nb-Ti-Zr wire, supercond., longit. critical currents in AC mag. field 77−72958
Nb-W-Mo-Zr, long-term strength props., vac. level effect 80−55484
Nb-W-Mo-Zr (5, 2, 1 wt.%), surface-layer struct. and mech. props., effect of O_2 diffusion saturation 79−5087
Nb-W-Mo-Zr (5, 2.1, 0.92 wt.%), creep resist., high temp. ageing in vacuum 80−71716
Nb-W-Mo-Zr-C, strength and ductility, prolonged high-temp. soaking effect 80−55483
Nb-W-Mo-Zr-C(5,2,1,0.02 wt.%) alloy 5 BMTs, short-time tensile strength in liquid Bi and Li *(Russian)* 77−25186
Nb-W-Zr-C, quenched from liquid state, formation of nonmetallic inclusions *(Russian)* 79−57007
Nb-W-Zr-N alloy, with dispersed second phase, ductile-brittle transition 80−93653
Nb-W-Zr-Ta, long-term strength props., vac. level effect 80−55484
Nb-W-Zr-Ta (90, 4.5, 3.5, 2 wt.%) creep and creep limit in super vac. at 1100°C, heat treatment effect 80−81133
Nb-Zn-N alloys, Zr-N complex formation, internal friction temp. depend. *(Russian)* 80−54311
Nb-Zr, (10 at.%), optical props., 0.1-25 eV, band models 78−10892
Nb-Zr, acoustic phonon anomalies and superstructure, neutron inelastic scatt. meas. 80−19892
Nb-Zr, BCC phase, elastic consts., 4.2-300K 77−81285
Nb-Zr, cold plastic deform., oriented microdistortions *(Russian)* 78−39840
Nb-Zr, crit. current, flow-flow resist. depend., allowance for superheating *(Russian)* 80−93061
Nb-Zr, deformed, α-peak, internal friction meas. between 90 and 300K 79−100205
Nb-Zr, deformed strip, pinning force, widely varied j_c, temp. and mag. field variations *(Russian)* 79−7948
Nb-Zr, diffuse neutron scatt. 78−71816
Nb-Zr, diffusion of N, effect of Zr and struct. defects 79−55938
Nb-Zr, diffusion of O_2 78−2298
Nb-Zr, dil., neutron irradiation at 4.6K, influence of impurities on defect prod. 79−55790
Nb-Zr, effect of band structure on elastic constants and superconductivity 79−8313
Nb-Zr, elastic constants, 0K to melting point 79−38882
Nb-Zr, fusion reactor first wall materials, compatibility with impure He 80−32469
Nb-Zr, internal impurity adsorption effect on bond type of intercrystallite zones 77−16684
Nb-Zr, nitriding, diffusive saturation, lattice spacing and activation coeffs. *(Russian)* 80−21168
Nb-Zr, single cryst. elastic consts. 77-298K 78−84879
Nb-Zr, thermoelec. power, 4.2 to 300K 80−70683
Nb-Zr, ty-pe II superconductor, mech. behaviour and stress effects 77−86083
Nb-Zr, type II supercond., radiation-induced flux pinning 78−80106
Nb-Zr, vacuum heat treatment effects on gas content and elec. and mech. props. *(Russian)* 79−43281

zirconium alloys continued
Nb-Zr (1 at.%), annealed, TEM study of ion implanted irregular He bubbles 80−15164
Nb-Zr (1 wt.%), corrosion behaviour in high temp. impure He gas 80−76402
Nb-Zr (1 wt.%), D_2 diffusion coeffs., 923-1148K 77−84991
Nb-Zr (1 wt.%), fusion reactor blanket struct. material, low cycle fatigue behaviour 80−30073
Nb-Zr (1 wt.%), He bubble growth, α-particle effects 78−67749
Nb-Zr (1 wt.%), high temp. creep, under O_2 stream pressure *(Russian)* 77−52404
Nb-Zr (1 wt.%), internal oxidation state of O_2, dispersion hardening by diffusion alloying, X-ray diffr. and internal friction *(Russian)* 79−70102
Nb-Zr (1 wt.%), ion irradiated, void ordering 78−22770
Nb-Zr (1%), He bubbles and voids with ringed images SEM and TEM exam. 78−51529
Nb-Zr (1.5 wt.%) alloy, field ion microscopy investigation, surface struct. 80−45220
Nb-Zr (3 wt.%), neutron-irradiated, positron annihilation ang. correl. meas. 80−93430
Nb-Zr alloy, 5VMTs1, thermal expsn., 1261-2289K 78−43150
Nb-Zr alloy, BCC-ω phase transition, electronically driven nature 80−103433
Nb-Zr film, amorphous, temp. stability 78−63948
Nb-Zr sputtered films on Ta, struct. and supercond. props. *(Japanese)* 78−52138
Nb-Zr-Al superconductor, struct. determ. by optical microscopy and electron diffraction *(Russian)* 77−16628
Nb-Zr-C, (1, 0.1 wt.%) alloy, mech. charact. structral sensitivity in strained state *(Russian)* 79−52301
Nb-Zr-C, dispersion-hardened with carbide phase, influence of hydrostatic extrusion on struct. and props. *(Russian)* 77−52338
Nb-Zr-C, effect of ageing on high temp. strength *(Ukrainian)* 79−52249
Nb-Zr-C, phase comp. and precip. after heat treatment 79−57020
Nb-Zr-C, plastic deform. and annealing, dislocation struct. *(Russian)* 80−20951
Nb-Zr-C, strengthening phase struct. and morphology after prolonged high temp. stress in vacuum *(Russian)* 77−25065
Nb-Zr-C, structural depend. of elasticity limit fracture features *(Russian)* 79−29171
Nb-Zr-C (0.1, 0.01 wt.%) plastic deform. influence on electronic state of Nb atoms 80−40463
Nb-Zr-C alloy, creep in vacuum, prolonged high-temp. ageing effects *(Russian)* 78−56692
Nb-Zr-C alloy, long term strength rel. to carbide precipitate geometry *(Ukrainian)* 78−92266
Nb-Zr-C alloy, long term loading at high temps. effect on struct. and morphology of carbide phase 79−15754
Nb-Zr-C alloy, strengthening phase, struct. and morphology after stress ageing *(Russian)* 78−31454
Nb-Zr-C alloy, strengthening phase, particle distrib. anal. *(Russian)* 79−15685
Nb-Zr-C alloy, struct. changes during stressed and unstressed ageing at 900, 1100°C *(Russian)* 79−29064
Nb-Zr-C welding solid solutions, ageing kinetics, influence of inclusion elements *(Russian)* 80−100853
Nb-Zr-C(N), phase comp. after casting and annealing, precip. 79−56983
Nb-Zr-N, deformed and annealed, internal friction, rel. to structural state *(Russian)* 78−6957
Nb-Zr-N, exam. of phase equilibrium using electron microscopy and X-ray analysis *(Russian)* 79−15654
Nb-Zr-N biphase alloy, recrystallization annealing 80−104180
Nb-Zr-O, corrosion resistance in molten Li *(Russian)* 78−31567
Nb-Zr-Si, ductile amorphous, superconductivity 80−60131
Nb-Zr-Ti, needle field emitter, ion bombardment effects, field emission microscope obs. 77−55869
Nb-Zr-Ti alloys, scale formation 77−44229
Nb-ZrN alloy, high temp. hardness and short duration tensile strength *(Russian)* 77−44266
Nb_3Sn strip, made by diffusion method, crit. curent anisotropy, Zr alloying addition effects *(Russian)* 78−47921
Nb_3Sn-Zr (0.8%), supercond. tape, crit. current, two stage annealing effect *(Russian)* 77−63046
NbZr, energy anal. of diffuse ω-reflections, Mossbauer, X-ray scatt. 78−60369
NbZr, thermally activated flux creep, effect on AC response 79−33416
$Nb_{0.75}Zr_{0.25}$, effect of force constant, disorder on Eliashberg function 80−29504
$Nb_{0.75}Zr_{0.25}$, supercond. energy gap, proximity tunnelling method determ. 79−56404
$Nb_{1-x}Zr_x$, supercond., McMillan-Rowell tunnelling spectroscopy 79−60985
$(Nb_{1-x}Zr_x)_3$ Sn, bronze-processed tape, AC losses between 5 and 16K 79−82727
$Nb_{20}Zr_{80}$, supercond., US attenuation 80−44766
$Nb_{20}Zr_{80}$, supercond. and normal, sp. ht. meas., 2-20K 80−70893
$(Nb_{0.99}Zr_{0.01})_{1-x}Ge_x$, supercond. transition temp. and crit. field 79−38220
$(Nb_{0.99}Zr_{0.01})_{1-x}Ge_x$, supercond., mag. field props. 80−54822
$(Nb_{1-y}Zr_y)_{1-x}Ge_x$, transition metal atom stabilised superconductivity 79−7924
$(Nb_{0.99}Zr_{0.01})_3Sn$, AC power losses in parallel AC and DC mag. fields 80−97041
Ni-based superalloys, hot workability, effect of S, Ca, Mg, Y and Zr minor elements 80−66552
Ni-Cr-Si (10, 1.8 wt.%), Zr, Hf, La or Sm alloying additions effect on oxidation resist. 77−63831
Ni-Cr-Zr, degradation after exposure to 1% H_2S/H_2 gas mixture at 1000°C 80−89408
Ni-Cr-Zr, eutectic alloy charact. by melting temp., composition and oxidation resistance 78−52771
Ni-Zr, amorphous phase form. in Zr-poor region, hardness and fracture strength *(Japanese)* 80−84914
Ni-Zr, wetting of AlN, effect of alloys exam. 78−80710
Ni-Zr-C (1, 0.1 wt.%), safe-life testing strengthening phases evolution and influence on heat resist. *(Russian)* 79−52476
Ni-ZrB_2 powders, densification by hot pressing 80−25604
Ni_3Al-Zr, powder, X-ray spectral analysis exam. 80−16239

zirconium alloys continued
- $Ni_{62}Ti_{29}Zr_9$, amorphous, H-sorption, X-ray and DSC obs. 80−49526
- $Ni_{100-x}Zr_x$, (x=34-40) metallic glass, cryst., isothermal annealing behaviour 80−6367
- $Ni_{11}Zr_9$, cryst. struct., X-ray obs. 79−65035
- $Ni_{64}Zr_{36}$, amorphous and cryst., H-sorption, X-ray and DSC obs. 80−49526
- Ni_xZr_{1-x} metallic glass, crystallisation kinetics, elec. resist. and mag. susceptibility meas. 80−103659
- Pd-Zr, metallic glasses, valence band struct. investigation 80−11533
- Pd-Zr alloy, activity coeff. rel. to electronic props. *(German)* 77−20084
- PdZr, amorphous, supercond., US props. 80−44765
- PdZr, photoemission study 80−104046
- $Pd_{30}Zr_{70}$, amorphous alloys, supercond. transition temp., press. depend. 80−84524
- $Pd_{35}Zr_{65}$, mag. susceptibility meas. 80−75740
- Pt-Zr, high temp. thermodynamic props. 77−63633
- Pt-Zr, solid soln., magnetic props. and lattice parameters *(German)* 79−87236
- Pt-Zr alloy, activity coeffs. rel. to electronic props. *(German)* 77−20084
- Pu-Zr, BCC, self-diffusion activation volumes, melting-diffusion correl. validity 77−20122
- ζ-Pu-Zr, X-ray powder diffr. cryst. struct. determ. 79−19187
- Re-Zr-V, constitutional diagram *(Russian)* 79−56956
- Sc-Zr, binary continuous solid solution, elec. resist. and thermoelec. power behaviour 79−69492
- Sc-Zr, low-temp. heat capacity 80−75370
- SiC fibre reinforced Ti, effect of Al, Zr and Mo alloying additions on reaction rate of Ti with fibres 80−16249
- Sm-Co-Cu-Fe-Zr, reversible changes in coercive force and struct. state during heat treatment 400-800°C *(Russian)* 80−29574
- Sm-Co-Cu-Fe-Zr magnet, production and mag. props. 77−40085
- $Sm_2(Co, Cu, Fe, Zr)_{17}$, permanent magnet, improved props. 77−89978
- $Sm_2Cu_{1.6}Zr_{0.16}Fe_{3.3}Co_{12}$, enhancement of mag. props. 79−82825
- $Sm_{0.91}Zr_{0.09}(Co_{0.68}Cu_{0.10}Fe_{0.22})_{6.7}$, alloy permanent magnet, coercive force *(Russian)* 80−65966
- $Sr_2(Co_{1-x}Ti_x)_{17}$, powders, influence of substitutes on mag. props. 80−100601
- TZM, D^+ impact, surface blistering, SEM study 78−71774
- TZM, diffusion of Cs, AES, SIMS depth profile study *(German)* 78−84008
- TZM, fatigue and threshold behaviour under high cycle fatigue 80−40487
- Th-Pu-U-Zr (20, 4, 8 wt.%) metal fuels, compatibility with cladding alloys for FBR appls. 80−102242
- Th-Zr, BCC phase, supercond. props. 79−87178
- Th-Zr, supercond. transition temp. depend. on constitution 78−88056
- Th-Zr-H, hydride form. and supercond. 77−36007
- α+β Ti alloy VT9, influence of phase comp. on fracture *(Russian)* 78−56665
- Ti-(Al)-Zr-Si (5, 0.5 wt.%), creep 77−36595
- Ti-Al-Cr-Mo-Zr, effect of structure and heat treatment on tensile strength, ductility, fatigue limit and notch sensitivity 78−56711
- Ti-Al-Cr-Mo-Zr hard alloy VK15, shot blasting in strength improvement 77−81272
- Ti-Al-Mo-Cr-Fe, distrib. of Sn, Zr between phases, temp effect. 80−55357
- Ti-Al-Mo-Zr, compressor disk, surface plastic deform., optimal method 80−60924
- Ti-Al-Mo-Zr, effect of heating on thermal stability of phases, lattice constants and chem. comp. 78−56672
- Ti-Al-Mo-Zr alloy, VT9, decomp. kinetics of metastable β-phase, X-ray and mech. props. obs. *(Russian)* 78−48368
- Ti-Al-Mo-Zr alloy VT9, Cu-Cr(Ni) coated, plastic deform. and diffusion annealing effect on props. *(Russian)* 78−35425
- Ti-Al-Mo-Zr SiC fibre reinforced composites, matrix selection *(Russian)* 80−35192
- Ti-Al-Mo-Zr-Si (6.6, 3.3, 1.8, 0.3 wt.%)-SiC fibrous composite, component interaction kinetics *(Russian)* 80−55364
- Ti-Al-Sn-Zr, Ti-680, O contamination under high temp. *(Chinese)* 80−66688
- Ti-Al-Sn-Zr (6.19, 1.92, 1.43 wt.%), fatigue cracking characteristics of β annealed microstruct. 79−5051
- α-βTi-Al-Sn-Zr-Mo (6, 2, 4, 6 wt.%), interface struct. 77−44212
- α-βTi-Al-Sn-Zr-Mo (6, 2, 4, 6 wt.%), deformation associated with surface cracks and α particles 79−79107
- Ti-Al-Sn-Zr-Mo (6,2,4,6 wt.%), α-β type 6246, fusion zone fracture behaviour in weldments 80−30093
- Ti-Al-Sn-Zr-Mo (6,2,4,6 wt.%) fusion weldment, substruct. characts. 80−84183
- Ti-Al-Sn-Zr-Mo (6,2,45 wt.%), surface cracking under unidirectional loading 78−56753
- Ti-Al-Sn-Zr-Mo alloy, Ti-6242, α+β, creep property improvement by Pt ion plating 80−16408
- α+β-Ti-Al-Sn-Zr-Mo-Cr, low cycle fatigue crack nucleation and early growth 79−8354
- Ti-Al-Sn-Zr-Mo-Si (6, 2, 4, 2, 0.1 wt.%), effect of elevated temperature and environment on fatigue crack growth 80−40486
- Ti-Al-Sn-Zr-Mo-Si-O-H, Si, O, H effects on fatigue, fracture and creep charact. 79−11697
- Ti-Al-V (6, 4 wt.%) cylinders, residual stresses introduced by quenching elastoplastic anal. *(French)* 80−45355
- Ti-Al-V-Cr-Mo-Zr (3,8,6,4,4 wt.%), beta-C, microstruct. effect on mech. props. 78−27577
- Ti-Al-V-Cr-Zr-Mo (3, 8, 6, 4, wt.%), phase transforms. 79−100113
- Ti-Al-V-Cr-Zr-Mo-Fe (3.4, 8.3, 5.8, 3.9, 4.2, 0.06 wt.%), shock loaded, residual strength 77−36589
- Ti-Al-V-Sn-Zr alloy TS5, annealing effect on ductility and strength *(Russian)* 78−35427
- αTi-Al-Zr, embrittlement due to ageing 78−56673
- Ti-Al-Zr, environmental effects in alloy fretting, effect on fatigue props. 78−56787
- Ti-Al-Zr, TA6Zr5D, oxidation at high temp. *(French)* 78−23860
- Ti-Al-Zr (3,3 wt.%), W alloying addition effects on mech. props. *(Russian)* 77−59860
- Ti-Al-Zr (6,5 wt.%), alloy IMI 685, SEM exam. of crack growth 78−72849
- α-Ti-Al-Zr (6.16, 5.23 wt.%), alloy IMI 685, electron microscope observations of strain induced hydrides 78−72828
- Ti-Al-Zr alloy, TA6Zr5D, structural evolution during continuous cooling at different rates *(French)* 80−45300

zirconium alloys continued
- Ti-Al-Zr system, room temp. elec. resist. and thermal EMF *(Russian)* 77−20290
- Ti-Al-Zr-Mo alloy 685, phase at α/β interface *(French)* 80−25661
- Ti-Al-Zr-Mo-Si (6, 5, 0.5, 0.25 wt.%), β-processed, fatigue props., hold time effect 80−60961
- Ti-Al-Zr-Mo-Si (6,5,0.5,0.25 wt.%), fracture toughness and crack propag. 78−39892
- Ti-Be-Zr, coupled phase diagrams and thermochemical descriptions 80−25656
- Ti-Be-Zr, struct. and form. of metastable phase m-TiBe 78−48375
- Ti-Be-Zr base, glassy, temp. depend. of resist., rel. to resist. thermometer appl. 77−82532
- Ti-Cr-Zr, martensite formation, chemical composition effect 80−50634
- Ti-Cu-Zr, heat treatable alloys, effect of alloying on strength, tensile props. 78−56671
- Ti-Mg-ZrC, sintered, friction and wear props. 79−70019
- Ti-Mo-Zr-Al (15,5,3 wt.%), phase transform. kinetics study by X-ray diffr. 79−56960
- Ti-Mo-Zr-Sn, alloy, βIII, struct. transform. in thermally affected zones after electron beam welding 78−23919
- β-Ti-Mo-Zr-Sn (10.2, 5.8, 4.7 wt.%) heat treated, tensile yield, fracture behaviour, primary deform. mode, exam. 78−60724
- Ti-Mo-Zr-Sn (11.5, 6, 45 wt.%), plastically strained regions, decoration 77−28864
- Ti-Mo-Zr-Sn (11.5, 6, 4.5 wt.%), metastable beta III phase, recrystallization and grain growth 80−3091
- Ti-Mo-Zr-Sn (11.5, 6.0, 4.5 wt.%), mech. property, microstruct. relationships 80−84961
- Ti-Mo-Zr-Sn (11.5, 6.0, 4.5 wt.%) alloy, struct. as affected by processing history 80−84972
- Ti-Mo-Zr-Sn-Fe-C-Si alloy, β-III, cold deform. and annealing, effect on struct. and mech. props. *(Russian)* 79−24533
- β-Ti-Mo-Zr-Sn(11.5, 6, 4.5 wt.%), metastable phase III, microstruct. and age hardening response 80−84945
- Ti-Mo-Zr(-Al) (15, 5 (3) wt.%), quenched and aged metastable β-phase, crystallography, morphology and decomposition 80−76262
- Ti-Nb-V-Zr, superconductors, struct. determ. by optical microscopy and electron diffraction *(Russian)* 77−16628
- Ti-Nb-Zr (35, 3 wt.%), martensitic τ phase, X-ray diffr. obs. 80−16300
- Ti-Nb-Zr-Fe, supercond. and paramag. props., effect of Fe additions *(Russian)* 80−65730
- Ti-Nb-Zr-Fe-Mo-V, cold worked, struct. and phase transform. during ageing 78−3153
- Ti-Nb-Zr-Ta, superconducting props. comp. depend., stress effects and precipitation behaviour, X-ray scatt. 80−93059
- $Ti-TiO_2-ZrO_2$-Mo, sintered struct. and mech. props. 78−60618
- Ti-Zr, binary continuous solid solution, elec. resist. and thermoelec. power behaviour 79−69492
- Ti-Zr, equiatomic, allotropic transform., metal purity and N_2 effects *(French)* 77−59782
- Ti-Zr, sintered, manufacture and exam. of props. 79−95975
- Ti-Zr, valence bands, X-ray M- and L-emission bands obs. *(Russian)* 78−19602
- Ti-Zr-Cr-Mn/$LaNi_5$ hydriding alloy mixtures for H energy storage 80−45788
- Ti-Zr-Hf disordered solid solns., thermal cond. 79−15132
- Ti-Zr-Mo alloy, effect of O_2 on elec. resistivity, microhardness, mech. props. 77−56092
- Ti-Zr-Mo-V, alloy VT20, exam. of plasticity in temp. range 20 to 1000°C 78−56712
- Ti-Zr-Nb-Si, Nb and Si surface alloying effects on wear and corrosion resistance *(Russian)* 77−25191
- α-Ti-Zr-W, effect of W impurity on mech. preps. 80−16392
- Ti-Zr-W-(Al), phase struct. and props. *(Russian)* 80−16270
- α-β TiAl-Sn-Zr-Mo (6,2,4,6 wt.%), age hardening 79−61604
- Ti_3Al-Sn-Zr, alloy, Sn and Zr alloying influence on creep and scaling resist. *(Russian)* 79−52302
- $Ti_{50}Be_{40}Zr_{10}$, amorphous, thermopower meas., Nordheim-Gorter relations 79−99535
- $Ti_{50}Be_{40}Zr_{10}$, amorphous, crystn. temp., press. and heating rate depend. 80−70132
- $Ti_{50}Be_{40}Zr_{10}$ glass, mech. props., X-ray diffr. exam. 78−11292
- $Ti_{50}Be_{40}Zr_{10}$, Metglas 2204, stability, crystallisation, ductility meas. 78−47246
- Ti(Zr,Hf)-Gd-B system, phase equilib. 80−11629
- $Ti_{1-x}Zr_xCr_{2-y}Mn_y$, C14 type alloy, hydride form. *(Japanese)* 78−19944
- $Ti_{1-x}Zr_xMn_2$, hydride formation, hydriding characts. of reversible uptake 78−44402
- $Ti_{1-x}Zr_xMn_{2-y-z}Cr_yV_z$, hydrogen storage appl. *(Japanese)* 80−61443
- $Ti_xZr_{1-x}{}_{70}Nb_{30}$, ω phase precipitation 79−34042
- U/(Zr-Cu-Mo alloy) welded joints, mech. characts. determ. 20 to 750°C 79−29113
- U-Mo-Nb-Zr-Ti (0.75, 0.75, 0.75, 0.5 wt.%), heat treatment effect on microstruct. and mech. props. 78−23729
- U-Mo-Zr, ductile-brittle transition *(French)* 77−66693
- U-Mo-Zr and U-Nb-Zr, shear martensitic transform. during quenching, plastic deform. and annealing 77−28815
- U-Nb-Zr (16.6, 5.6 wt.%), stability of BCC phase 79−66039
- U-Nb-Zr (7.5, 2.5 wt.%), elastically bent, ageing induced shape instability 77−16622
- U-Pu-Zr metal fuel remote alloying and casting 79−89477
- U-Pu-Zr(-Th) LMFBR metal fuel elements, development and performance 80−57856
- U-$Q^4(Q^5)$, Q^4=quad, Q^5=quint, stress corrosion cracking in moist air, salt water, salted moist air 78−35562
- U-Zr, absolute thermoelec. power values 77−20303
- U-ZrH low enrichment fuel for TRIGA and plate-type reactors 80−22950
- UO_2 fuel rod, Zircaloy clad, chemical activity determ. of fission product 79−49682
- UO_2 pellets-graphite-Zircaloy cladding, evaluation of graphite lubrication 80−32342
- UO_2/Zircaloy pellet/cladding interaction, eval. of lubrication of graphite 79−67857
- UO_2-Zircaloy fuel element behaviour in PWR power plants 80−631
- UO_2-zircaloy-4, reaction kinetics at high temps., O_2 diffusion 80−16667
- δ-UZr_2, computed X-ray powder diffr. patterns and densities 77−43172
- V-Hf-Zr, multifilamentary, superconducting props. improvement 79−38267

zirconium alloys continued
V-Ti-Zr, 4 MeV Ni^{++} irrad., He gas bubble form. 80−29085
V-Zr, strengthening by internal oxidation 80−55424
V-Zr (2 wt.%), internally oxidised, neutron irradiated, annealing effect on mech. props., elec. cond. and electron microscope obs. *(Japanese)* 79−15701
V-Zr-C, radiation hardening and plastic instability *(Russian)* 78−39842
V-Zr-C-Y alloy weld metal, hardening phase precipitates examination, TEM appl. 80−7576
V-Zr-N quasi-binary section, long term hardness to compare heat resistance 78−3223
V-Zr-Nb alloy, rel. between density of states and martensitic and superconducting phase transition temps. 78−10594
V_2(Hf,Zr), Laves phase compounds, electrical resistivity, temperature dependence 78−76047
V_2(Hf,Zr), NMR and mag. susceptibility, density of states determ. *(Russian)* 80−66053
V_2Hf, NMR meas., mag. susceptibility, Knight shift and elec. field gradient determ. *(Russian)* 78−23359
V_2HfZr, C-15 cryst. struct. supercond. props. 78−64173
$V_2Hf_{1-x}Zr_x$, normal and supercond. state, transition temps., mag. susceptibility and specific heat determ. *(Russian)* 80−60132
V_2Ta, NMR meas., mag. susceptibility, Knight shift and elec. field gradient determ. *(Russian)* 78−23359
V_2Zr, NMR meas. mag. susceptibility, Knight shift and elec. field gradient determ. *(Russian)* 78−23359
V_2Zr, struct. transform. at low temp., X-ray diffr. anal. *(Russian)* 80−45298
W-C-Zr, vacuum melted, phase composition, struct. and props. 78−31403
W-Cu-Zr exam. of mech. props. as function of temp., composition, and oxidation props. 80−16472
W-Zr, Zr addition effect on heat resistance and radiative props. *(Russian)* 80−25515
W-Zr (2.92, 7.42 and 10.02 wt.%), and W_2Zr, thermal expansion, elec. resistance, 100-900°C, crystallisation 78−91455
W-Zr system, kinetics of interdiffusion process *(Russian)* 79−69298
W-Zr-C, cubic solid soln., form. and props. 78−48348
W-Zr-C, Zr and C addition effect on heat resistance and radiative props. *(Russian)* 80−25515
W-ZrC(-Re) eutectic alloy, Re effect on breaking stress, lattice parameters, electron struct. *(Russian)* 79−1845
Y-Zr-H, phase diag. *(Russian)* 77−59749
zircalloy-2, annealed, neutron irradiated, 573 to 923K, damage struct. 79−99247
Zircaloy 2, mechanical equation of state, stress relax. meas. 78−52880
Zircaloy, dispersion and spheroidisation treatment of δ ZrH, effect on corrosion resistance 79−76072
Zircaloy, I_2 stress corrosion cracking, temp. and stress depend., threshold press. determ. 80−16595
α-Zircaloy, strain ageing at 1000K 79−47725
Zircaloy-2, effect of simulated fission products on mech. props. 80−73922
Zircaloy-2, electron irradiation damage, direct obs. 80−84212
Zircaloy-4, deformation behaviour between 77 and 900K 80−71686
$(Zr,Hf)Fe_2$, mag. hyperfine field at Hf sites, TPDAC meas. 79−82901
Zr,Nb (2.5 wt.%), interaction of hydride, stress, and crack growth at 600K, metallographic obs. 77−12695
Zr base alloy, fatigue crack propag., role of adsorption in H_2S, Hg and moist air *(French)* 78−15580
Zr TA6V6E2, tensile and toughness props. after isothermal quenching and continuous cooling *(French)* 77−59833
Zr-Al, diffusion welding with Al_2O_3 and ZrO_2, 1000 to 1300°C *(German)* 79−33122
Zr-Al (14 at.%), martensitic, discontinuous precipitation, TEM obs. 79−34040
Zr-Al (14 wt.%), transformation sequence from Zr-Al martensite to Zr_3Al phase 80−3027
Zr-Al (4.6 wt.%), microstruct. effect on mech. props. 79−20080
Zr-Al (4.6 wt.%) martensite, precipitation of Zr_3Al_2, TEM study 79−74156
Zr-Al (8.0 wt.%), tensile props. and fracture toughness after fast neutron irradiation 80−3198
Zr-Al (8.6 wt.%), dimensional stability struct. and mech. props, effects of neutron irrad. 80−92563
Zr-Al (8.6 wt.%), effect of fast neutron irradiation on irradiation growth of Zr_3Al 78−55896
Zr-Al (8.6 wt.%), fast neutron irradiated, tensile props. and fracture toughness 80−84994
Zr-Al (8.6 wt.%), neutron irradiation effect on tensile props., swelling 77−7768
Zr-Al alloy, selective gettering action for partial H_2 press. meas. 77−87775
Zr-Al getter modules, transient getter scheme for Tokamak fusion test reactor 80−79584
Zr-Al getter pump, for fusion reactor 77−57748
Zr-Al getter pumping in beam driven Tokamaks 78−50401
Zr-Al intermetallic compounds in SAES ST101 getter, surface anal. during stimulated pumping 79−67945
Zr-Al martensite, DO_{19} phase formation, selected area diffr. obs. 78−84779
Zr-Al-C, phase diagram and lattice constants, X-ray diffr. method 80−89207
Zr-Al-Cr H sorption props. for H storage, influence of Al 80−45794
Zr-Al-Fe (8.9, 0.001 to 0.006 wt.%) Fe partitioning to Zr_2Al during peritectoid transformation 78−39784
Zr-Al-V, H sorption props. for H storage, influence of Al 80−45794
Zr-Al-(Fe,Co), H sorption props. for H storage, influence of Al 80−45794
Zr-Al(8.6 wt.%), mech. props., corrosion and fast neutron irrad. influence 78−84948
Zr-Al(8.6 wt.%), neutron irradiated, irradiation growth and recovery, annealing 80−15162
Zr-Au (0.3 and 0.2 wt.%), irradiated, backscattering meas. of Zr self-interstitial atom trapping by Au 77−69014
Zr-B, abrasive props. 80−16489
Zr-B (1.3 wt.%), investigation of swelling due to neutron irrad. *(Russian)* 79−60404
Zr-base alloy as reactor core material, microstruct., deform. and fracture 78−4988
Zr-base alloys, annealed specimens, irradiation growth 80−49276

zirconium alloys continued
Zr-Be, coupled phase diagrams and thermochemical descriptions 80−25656
Zr-Be, metallic glass form. and props. 80−16219
Zr-C, exam. of metastable phase diagrams, at high temp. and pressure *(Russian)* 79−56955
Zr-Co, amorphous alloy film, spin reson. meas. 78−68389
Zr-Co, amorphous and crystalline, d-band struct., alloying effects 80−59862
Zr-Co-Ga, mag. susceptibility in phases of structural type Th_6Mn_{23} *(Russian)* 79−24130
Zr-Co(Ni) amorphous alloy, thermal stability and electronic props. 79−73487
Zr-Cr, role of oxide plasticity in oxidation behaviour 77−36680
Zr-Cr (1.9 wt.%), β-quenched and tempered, optical and TEM study 79−66061
Zr-Cr (1.9 wt.%), β-quenched and tempered, $ZrCr_2$ precipitation, TEM study 79−66062
β-Zr-Cr (1.9 wt.%), decomposition 79−87604
Zr-Cr-B system, self-propagating high temp. synthesis, crystallochemical and mech. props. 80−20861
Zr-Cr-Cu, phase diagram in Zr corner *(Russian)* 78−19721
Zr-Cr-Fe, irradiation damage, metallurgical struct. effect 77−51412
Zr-Cu, amorphous alloy, sheet production by plasma spray quenching 77−44193
Zr-Cu, dil. martensites, struct. and strength 79−29077
Zr-Cu, glassy alloy, struct. anal. using X-ray diffr. 79−51004
Zr-Cu, metallic glasses, glass transition temp., crystallisation temp., exothermal relaxation effect 79−52747
Zr-Cu, optical elements, US cleaning, deleterious effects 77−42631
Zr-Cu, role of oxide plasticity in oxidation behaviour 77−36680
Zr-Cu (1.6 wt.%), mechanical equation of state, stress relax. meas. 78−52880
Zr-Cu (1.6 wt.%), near eutectoid, active eutectoid decomposition ageing and quenching effects 80−2993
Zr-Cu amorphous alloys, glass transition and ductility, O additions effect 80−75168
Zr-Cu-Ga, mag. susceptibility in phases of structural type Th_6Mn_{23} *(Russian)* 79−24130
Zr-Cu(Ni)(Co)(Fe) metallic glasses, glass form. and thermal stability 80−75177
Zr-Dy dil. alloys, plastically deformed, mech. props. and microstruct. *(Russian)* 79−20112
Zr-Fe, amorphous alloy film, spin reson. meas. 78−68389
Zr-Fe, amorphous alloy quenched by levitation method, crystallisation 79−55669
Zr-Fe, Mossbauer spectra parameters of Zr_2Fe particles *(Russian)* 80−29654
Zr-Fe, role of oxide plasticity in oxidation behaviour 77−36680
Zr-Fe-Cu-W, Mossbauer spectra parameters of Zr_2Fe particles *(Russian)* 80−29654
Zr-Fe(Co)(Ni)(Cu), oxidation of intermetallic phases 79−100298
Zr-Ge-B system, phase equilibria 78−35356
Zr-H, diffusion in hydride phase, exam. 80−29204
Zr-H, effect of neutron irrad. on electrical resistance, magnetic susceptibility 80−29063
Zr-H, inhomogeneous system, time changes of Hall voltage 79−87080
Zr-H, precip. of γ-ZrH, shear mechanism 80−104170
Zr-H, soft X-ray emission spectra, electronic struct. 79−65959
α-Zr-H, volumetric changes, and thermal expansion, dilatometric and X-ray analysis exam. *(Russian)* 79−11665
Zr-H formation, of $\delta \rightarrow \gamma$ transformation 80−84929
Zr-H formation, the $\delta \rightarrow \epsilon$ transformation 80−84930
Zr-H phase diagram, auto-radiographic and metallographic study of γ-phase *(Russian)* 78−56616
Zr-Hf, dil., ^{178}Hf Mossbauer transition, electric quadrupole interaction 80−39928
Zr-Hf, mag. susceptibility, elec. cond., Hall conc. thermoEMF conc. depend. *(Russian)* 80−39551
Zr-Hf (2.2 wt.%), high temp. oxidation in flowing O_2, 873-1173K 80−93687
Zr-Hf (2.2 wt.%), oxidation kinetics in flowing CO_2, 873 to 1173K 80−16596
Zr-Hf(2.2 wt.%), oxidation kinetics in flowing CO_2 at high temp. 80−47575
Zr-Ir, $\alpha \rightleftarrows \beta$ transform. *(Russian)* 78−80540
Zr-Ir, dil., elec. field gradient at ^{193}Ir, Mossbauer meas. 80−66090
Zr-Ir, high temp. modification, X-ray diffr. obs. *(Ukrainian)* 79−32947
Zr-Ir hardened alloys, metastable phases *(Ukrainian)* 79−34000
Zr-M-H (M=V, Cr, Mn, Fe, Co, Ni), synthesis at high pressure, props 80−29924
Zr-Mn (up to 0.3%), high-magnetic field magnetisation and magnetoresistance 78−10652
Zr-Mn alloys, impurity and self-diffusion 79−60540
Zr-Mo, high temp. phase diagrams 77−44217
Zr-Mo (3 wt.%), β-phase stability 78−39742
β-Zr-Mo oxidised alloys, high temp. deformation, X-ray study 79−79045
Zr-Mo-Al (3, 1 wt.%), β-phase stability 78−39742
Zr-Mo-Nb-V-Sn (1,2,2,2 wt.%), heat treatment, transform. reactions and mech. props. 79−24545
Zr-Mo-Sn (3,2 wt.%), heat treatment, transform. reactions and mech. props. 79−24545
β-Zr-Mo-(Al)(Ti)(La), metastable, deform. induced transform. 78−52805
Zr-Mo(Co)(Fe)(Cu)(Ni-Cu)-H, catalytic props. 80−30274
Zr-Mo(Ru) film, amorphous, temp. stability 78−63948
Zr-N system, hydrogenation, phases form. 79−43200
Zr-Nb, (2.5 wt.%), cold-worked pressure tubing for CANDU reactors, slit burst testing 79−26532
Zr-Nb, fracture resistance, atomic reactor material *(Russian)* 77−25140
Zr-Nb, phase transformation sequences, prediction using free energy composition diagrams 79−4951
Zr-Nb, pressure tube alloy, initiation COD as fracture criterion 78−72862
Zr-Nb, role of oxide plasticity in oxidation behaviour 77−36680
Zr-Nb, singularities of $\beta \rightarrow \omega$ transform. in alloy, with high content of β-stabiliser *(Russian)* 78−76644
Zr-Nb, stacking solitons in ω-phase systems and quasielastic scatt. 79−38822

zirconium alloys continued
Zr-Nb, structure associated with BCC to omega transform. *(Russian)* 80−108432
Zr-Nb (0.1, 2.5 wt.%), foil, dislocation loop nucleation and growth during 1 MeV electron irrad. 80−88152
Zr-Nb (1 and 2.5 wt.%), annealed, thermal expansion, α/β transition *(Russian)* 78−26702
Zr-Nb (1 at.%), high-temp. nitriding, chemical and metallographic anal., disintegration test 79−24668
Zr-Nb (1 wt.%), corrosion in water at 285°C 77−56161
Zr-Nb (1 wt.%), static strain ageing between 295 to 773K, TEM obs. of plastic strain 79−38855
Zr-Nb (1 wt.%), tensile props., 295 to 773K 79−8318
Zr-Nb (1 wt.%) exam. of creep behaviour, 373 to 773K 78−80599
Zr-Nb (1 wt.%) high-temp. reaction with UO_2 78−66344
Zr-Nb (20 wt.%), ω-phase form., diffuse Mossbauer scatt. 80−25324
Zr-Nb (20 wt.%) ω-phase transform., structural model, intensity distrib. in neutron diffr. 77−77472
Zr-Nb (20%), low-j_c supercond. vortex pinning *(Russian)* 77−80885
Zr-Nb (2.25 wt.%), oxidation kinetics in flowing CO_2, 873 to 1173K 80−16596
Zr-Nb (2.3 and 5.5wt.%) martensite, precipitation 77−8836
Zr-Nb (2.5 at.%), thermal neutron capture cross-section var. with time, calc. 77−61505
Zr-Nb (2.5 wt.%), annealed, irradiation growth at 353K 79−46710
Zr-Nb (2.5 wt.%), annealed and quenched-and-aged, neutron irradiated, 573 to 923K, damage struct. 79−99247
Zr-Nb (2.5 wt.%), channel tubes, in-reactor creep and irrad. growth 80−93604
Zr-Nb (2.5 wt.%), cold worked, in reactor oxidation of crevices and cracks 78−23865
Zr-Nb (2.5 wt.%), cold worked, press. tubes, secondary cracking obs. 78−80630
Zr-Nb (2.5 wt.%), cold-worked, pressure tubing, metallography and mech. props. 80−89269
Zr-Nb (2.5 wt.%), crack resistance, influence of ZrH_x fracture toughness 80−16444
Zr-Nb (2.5 wt.%), effect of irradiation on stability of precipitates 77−69007
Zr-Nb (2.5 wt.%), effect of pre-irradiation on oxidation 78−88580
Zr-Nb (2.5 wt.%), fractographic aspects of H_2 induced delayed cracking 79−47767
Zr-Nb (2.5 wt.%), fuel cladding, anisotropy after creep and irradiaton 78−7001
Zr-Nb (2.5 wt.%), H_2 induced subcritical crack growth meas., application of potential drop method 78−27645
Zr-Nb (2.5 wt.%), heat treatment effects on slow crack growth, cold working effects 77−28836
Zr-Nb (2.5 wt.%), high temp. oxidation in flowing O_2, 873-1173K 80−93687
Zr-Nb (2.5 wt.%), hydride forming materials, H_2 induced delayed cracking 78−27623
Zr-Nb (2.5 wt.%), hydride TEM obs. in pressure tubing 79−8338
Zr-Nb (2.5 wt.%), hydride induced crack growth, effect of stress, temp. and H_2 content 80−3178
Zr-Nb (2.5 wt.%), hydride precipitation and growth at crack tips, electron optical obs. 80−108449
Zr-Nb (2.5 wt.%), meas. of crack growth at elevated temp. by holographic interferometry 79−38933
Zr-Nb (2.5 wt.%), memory effect in hydride precipitation 78−11227
Zr-Nb (2.5 wt.%), neutron irrad. at 573 to 923K, damage struct. 80−107334
Zr-Nb (2.5 wt.%), nuclear fuel channels, neutron effects on ultimate fracture strength, 293 to 573K 80−85054
Zr-Nb (2.5 wt.%), oxidation kinetics appl. to loss of coolant accidents, data review 78−19958
Zr-Nb (2.5 wt.%), pressure tubes, irrad. creep and growth, anisotropy factors 80−97536
Zr-Nb (2.5 wt.%), seam welding tubing, microstruct. in weld region 79−61621
Zr-Nb (2.5 wt.%), strain ageing 77−77511
Zr-Nb (2.5 wt.%), superplasticity 77−12669
Zr-Nb (2.5 wt.%), superplastic and strain rate depend. plastic flow, 873 to 1373K 80−30052
Zr-Nb (2.5 wt.%), tensile specimen, stress corrosion cracking by stray contamination 77−70215
Zr-Nb (2.5 wt.%), transforms. during annealing of welded joint, after thermal cycling *(Russian)* 80−29984
Zr-Nb (2.5 wt.%) alloys, microstruct investigation by electron microscopy using oxide films 79−70243
Zr-Nb (2.5 wt.%) neutron effects on oxidation kinetics 78−690
Zr-Nb (2.5 wt.%) pipe, fracture resistance, hydrogenation effect 80−104279
Zr-Nb (2.5 wt.%) pressure type rel. between stess intensity factor, crack opening displacement and J-integral 80−100920
Zr-Nb (97.5, 2.5 wt.%) nuclear reactor pressure tube material, H embrittlement study by TEM 80−76363
Zr-Nb alloy, direct imaging of point defects using TEM 77−35453
Zr-Nb alloy, isothermal decomposition at elevated temp. 78−27470
Zr-Nb microduplex alloys, struct. and props. 78−3170
Zr-Nb pressure tubes of PWR reactor, cracks identification and avoidance 78−82472
Zr-Nb solid solutions, BCC, direct imaging of linear defect using diffuse scatt. 78−22726
Zr-Nb-Cr (0.5, 0.5 wt.%), TEM study on intermetallics in Zr alloys 79−11622
Zr-Nb-Fe (13 wt.%, 5 wt.%), struct. changes during decay of BCC β solid solution 79−15669
Zr-Nb-Fe(Mo) alloys, decomp. of β solid soln., metastable and equilib. phases 79−11632
Zr-Nb-Ga, phase equilibria 800°C *(Ukrainian)* 80−35157
Zr-Nb-Ge, singularities of $\beta \rightarrow \omega$ transform. in alloy, with high content of β-stabiliser *(Russian)* 78−76644
Zr-Nb-H_2, exam. of phase diagram, using modified format 79−8280
Zr-Nb-Mo, phonon spectra anomalies, lattice dynamics calculations, superconductivity parameters 79−7655
Zr-Nb-Mo-Re, alloying effect on dislocation core struct., determ. by discrete lattice modelling 78−30618
Zr-Nb-Sn (3,1 wt.%), corrosion resist. depend. on mech. and heat treatments 80−653

zirconium alloys continued
Zr-Nb-Sn (3.0, 1.0 wt.%), oxidation kinetics in flowing CO_2, 873 to 1173K 80−16596
Zr-Nb-Sn (3.0, 1.0 wt.%), high temp. oxidation in flowing O_2, 873-1173K 80−93687
Zr-Nb-Sn(3 wt.%, 1 wt.%), oxidation kinetics in flowing CO_2 at high temp. 80−47575
Zr-Nb-V-Fe (12 wt.%, 6 wt.%, 4 wt.%), struct. changer during decay of BCC β solid soln. 79−15669
Zr-Nb-V-Si superconductor, struct. determ. by optical microscopy and electron diffraction *(Russian)* 77−16628
β-Zr-Nb(Cb) alloys, anneal hardening and flow softening 79−78993
Zr-Nb(2.5 wt.%), irradiation growth, influence of microstructure and test conditions 80−92561
Zr-Nb(2.5 wt.%), oxidation kinetics in flowing CO_2 at high temp. 80−47575
Zr-Nb(2.5 wt.%), tensile props., strain rate and temp. effects 77−73307
Zr-Ni, amorphous and crystalline, d-band struct., alloying effects 80−59862
Zr-Ni, diffusion of H_2, 900 to 1080°C *(Korean)* 80−19988
Zr-Ni, energy spectra of valence electrons *(Ukrainian)* 78−6814
Zr-Ni, surface layer, segregation of ferromag. Ni, magnetooptic investigation 80−2256
Zr-Ni (65 to 80 at.%), phase diagram and cryst. struct. of intermediate phases 79−52170
Zr-Ni alloy, H_2 storage in form of capsules *(French)* 79−92091
Zr-Ni alloys, energy spectra, X-ray emission obs. *(Russian)* 78−19604
Zr-Ni-Cu-H_2 catalytic activity, exam. by conversion of toluene, and bicyclic aromatic hydrocarbons 80−30276
Zr-Ni-Ga, mag. susceptibility in phases of structural type Th_6Mn_{23} *(Russian)* 79−24130
Zr-Ni-H, catalytic activity, exam. by conversion of toluene, and bicyclic aromatic hydrocarbons 80−30276
Zr-Ni-H_x($x=2.8$ to 3), surface layer, segregation of ferromag. Ni, magnetooptic investigation 80−2256
Zr-Ni(Fe,Ci,Cr,Ti) powder based composite, high temp. strength of W reinforcing fibres 79−70021
Zr-Os, $\alpha \rightleftarrows \beta$ transform. *(Russian)* 78−80540
Zr-Os quenched alloys, metastable phases *(Ukrainian)* 78−84804
Zr-Pd, metallic glasses, electronic props. and supercond. 79−73486
Zr-Rh, absorbed interstitial H_2 energy 79−82198
Zr-Rh, $\alpha \rightleftarrows \beta$ transform. *(Russian)* 78−80540
Zr-Rh, high temp. modification, X-ray diffr. obs. *(Ukrainian)* 79−32947
Zr-Rh alloys, amorphous, thermal relax. effects on electronic and supercond. props. 79−65575
Zr-Rh-H(D), superconducting transition temp., effect of H(D) conc. 80−84532
Zr-Ru, alloy Zr rich, Ru solubility, eutectic decay, $\alpha \rightleftarrows \beta$ transform., struct. *(Russian)* 80−65227
Zr-Ru(Pd), heat treated, mech. props. and struct. 78−80571
Zr-Sc-Ga, phase equilibria 800°C *(Ukrainian)* 80−35157
Zr-Sn, grain-boundary migration during fatigue at 600 to 775°C 80−16443
Zr-Sn, oxide film texture determ., corrosion in air and water vapour 77−56163
β-Zr-Sn, zircaloy-2, exam. of grain boundary sliding 78−79616
Zr-Sn, Zircaloy-2 and 4, high temp. oxidation in steam 78−80676
Zr-Sn (1.5 wt.%), electron irradiation damage, direct obs. 80−84212
Zr-Sn (1.5 wt.%), martensitic transform. contrib. to strength and work hardening, and martensite flow props. 78−84842
Zr-Sn alloys, mathematical models for transient deform. 78−86616
Zr-Sn-Fe-Ni (1.5, 0.1, 0.15 wt.%), electron irradiation damage, direct obs. 80−84212
Zr-Sn-Mo (4.5,1 wt.%) and (4.5,2 wt.%), creep behaviour at room temp. *(Czech)* 79−24590
Zr-Sn-Mo (6, 1 wt.%), creep and creep rupture 78−23778
Zr-Sn-Mo-(Nb), creep and creep fract. at 623 to 823K *(Czechoslovakian)* 77−32643
Zr-Sn-Mo-(Nb), fracture in creep 77−36581
Zr-Sn-Mo(Nb), creep and creep fracture, 623 to 823K *(Czech)* 77−59916
Zr-Sn-No-(Nb), steady state creep 77−36580
Zr-Sn(Fe)(Ni) (0.15 wt.%), electron irradiation damage, direct obs. 80−84212
α-Zr-Sn(Mo), creep characts., influence of Sn and Mo *(Czech)* 80−81119
ω-Zr-Ta, electric field gradients at substitutional Ta atoms, TDPAC high-pressure study 78−52384
Zr-Ta (5 wt.%), β-precipitation in martensitic struct., tempering temp. effect 79−34045
Zr-Ta (5 wt.%), martensitic transform. by rapid cooling, non-equilib. precipitation 79−34075
Zr-Ta (5 wt.%) martensite, β_1 precipitation, thermodynamics 79−74164
Zr-Ti, alloy, mag. susceptibility, elec. cond., Hall conc. thermoEMF conc. depend. *(Russian)* 80−39551
Zr-Ti, oxide film texture determ., corrosion in air and water vapour 77−56163
Zr-Ti martensites, furnace cooled and water quenched, strengh and deform. 79−20101
Zr-Ti-Be metallic glass, phase separation 80−97464
Zr-Ti(Hf)(Sc), thermopower composition depend. 79−65445
Zr-V, superconductivity and metallurgy of C15 materials 79−4610
Zr-V foil, rapidly quenched and heat treated, supercond. props. 80−54852
Zr-W-Cr, Zr-rich corner of phase diag. *(Russian)* 78−80517
Zr-Y (15 wt.%) solid solution, decomp., during heating and cooling cycles *(Russian)* 78−92267
Zr-Zr_2Al_3, diffusion weldings between 1000 and 1300°C, electron microprobe anal. *(German)* 78−84011
Zr-ZrC, eutectic formation of regular struct., crystn. *(Russian)* 80−66496
$ZrAl_2$, X-ray energy spectrum of valence electrons *(Russian)* 80−108304
Zr_2Al, X-ray energy spectrum of valence electrons *(Russian)* 80−108304
Zr_3Al, Ar^+ ion and electron irradiation, irradiation swelling, lattice parameter changes 79−65123
Zr_3Al base alloy, forming press. tubes 77−8784
Zr_3Al, cold worked, annealing effects 77−36535

zirconium alloys continued
- Zr_3Al, deformed and irrad., lattice defects obs., superlattice dislocations and defect clusters 80−107261
- Zr_3Al, disordering by 1 MeV electron irradiation 78−51583
- Zr_3Al, hyperperitectoid, tensile strength, effect of fast neutron irrad. 77−52408
- Zr_3Al, ion beam prod. damaged regions 79−60409
- Zr_3Al, irradiation 78−6111
- Zr_3Al, $L1_2$ phase, work hardening 78−23718
- Zr_3Al, $L1_2$ phase yield strength 78−19811
- Zr_3Al, neutron irrad. effect on tensile props. 80−3156
- Zr_3Al, ordered, elec. resist. of LI_2 phase as function of temp. 79−19572
- Zr_3Al, ordered, exam. of Young's modulus and thermal expansion coeff. 78−72805
- Zr_3Al, ordered, notch sensitivity, neutron suppression 78−23779
- Zr_3Al, ordered, oxidation, weight gain and metallography 80−89398
- Zr_3Al, ordered, review of physical metallurgy 78−15419
- Zr_3Al, ordered, strengthening by fast neutron irrad. 78−84838
- Zr_3Al ordered alloy, ion bombardment damage, TEM 80−100287
- Zr_3Al, ordered polycrystals, hardness and flow stress relationship 77−44309
- Zr_3Al, ordered polycrystals, ductile fracture 78−64641
- Zr_3Al, tensile props., surface preparation depend. 80−3155
- Zr_3Al, thermal neutron capture cross-section var. with time, calc. 77−61505
- Zr_4Al_3, X-ray energy spectrum of valence electrons *(Russian)* 80−108304
- $ZrAlC_{2-x}$, lattice constants, X-ray powder diffr. method 80−89207
- $Zr_2Al_3C_{5-x}$, lattice constants, X-ray powder diffr. method 80−89207
- Zr_5Al_3C, lattice constants, X-ray powder diffr. method 80−89207
- $Zr(Al_xCo_{1-x})_2$, Laves phase, H_2 absorption capacity meas. 78−87866
- $Zr(Al_xFe_{1-x})_2$, Laves phase, H_2 absorption capacity meas. 78−87866
- ZrB_2-Nb, reactions between components 80−100812
- Zr_xBe_{1-x} noncrystalline alloy, phonon-electron scatt., superconducting temp. 80−54330
- ZrC-C, CVD, microhardness and microstruct. 77−8916
- ZrC-NbC-MoC_{1-x} alloys, physicomech. props., comp. depend. 79−66097
- ZrC-Re, in H_2, thermionic emission residual gas effects 78−48269
- ZrC-Re, spectral emissivity, 1400 to 2500K, surface relief and composition 77−24420
- ZrC-W, thermionic emission current density, cathode operating time and comp. depend. 77−8714
- ZrC-W (75 wt.%) eutectic refractory alloys, smelting in suspended states, components distrib. *(Russian)* 80−19913
- ZrC-ZrB_2, friction characts., comp. depend., 20-1400°C 80−3203
- ZrC-ZrB_2, preparation and high temp. antifriction props. 79−1918
- ZrC-ZrB_2, wear in vacuum, role of boride phase 80−21113
- ZrC_x, x=0.99 to 0.13, elec. cond., supercond. state 78−43504
- $Zr_{1-x}Co_x$, amorphous, conc. depend. of Co moment 78−56300
- $Zr_{1-x}Co_x$, amorphous alloys, thermal stability, elec. cond. enthalpy 80−100172
- $Zr_{70}Co_{30}$ amorphous alloys, struct. factors and radial distrib. functions 80−84096
- $Zr_{70}Co_{30}$, metallic glass, low temp. resist., supercond. T_c 79−38235
- Zr_2CoGa_3, crystal struct. determ. by single crystal method *(Ukrainian)* 79−51049
- $Zr(Co_xM_{1-x})_2$ (M=V,Cr,Mn) H absorption and desorption props. 77−55448
- $Zr_3Co_{1-x}M_x$, M=Cu, Ni, Fe, Mn, Ag, and Ru, phase stability and supercond. T_c 78−80519
- $Zr_{50}Co_{50-x}Ni_x$, transform. and deform. studies 79−1864
- ZrCoSi, crystal struct. *(Ukrainian)* 78−83774
- $ZrCr_2$, mag. props. H absorpt. effect 80−88821
- $Zr(Cr_xCo_{1-x})_2$, Laves phase, phenomenological model for H_2 absorption capacity 77−84935
- $Zr(Cr_xCo_{1-x})_2$, mag. props. H absorpt. effect 80−88821
- $ZrCr_2D_x$, site occupation modes and cryst. struct., neutron diffr. study 80−59440
- $Zr(Cr_xFe_{1-x})_2$, Laves phase, phenomenological model for H_2 absorption capacity 77−84935
- $Zr(Cr_xFe_{1-x})_2$, mag. props. H absorpt. effect 80−88821
- ZrCu, constitutional and struct. studies, by mag. susceptibility, metallography and X-ray diffr. 80−70166
- $Zr_{0.35}Cu_{0.65}$ metallic glass, Young's modulus meas. by impulse induced resonance technique 80−40411
- $Zr_{65}Cu_{35}$, metallic glass, low temp. resist., supercond. T_c 79−38235
- $Zr_{40}Cu_{50}Fe_{10}$, magnetically dil. glass, 3d moments, mag. susceptibility and magnetisation meas. 79−95574
- $Zr_{40}Cu_{60-x}Fe_x$, electronic and mag. props. 77−8271
- $Zr_{40}Cu_{60-x}Gd_x$, magnetically dil. glass, 4f moments, mag. susceptibility and magnetisation meas. 79−95575
- $Zr_{0.475}Cu_{0.475}M_{0.05}$, glass transition temp., comp. depend. 80−79702
- $Zr_{40}Cu_{60-x}M_x$ (M=Fe,Mn,Gd,Tb), amorphous, mag. ordering and local random anisotropy 78−68273
- $Zr_{40}Cu_{60-x}M_x$, (M=Gd, Tb, Fe or Mn), amorphous alloy, mag. interactions 78−95432
- $Zr_{40}Cu_{50}Mn_{10}$, magnetically dil. glass, 3d moments, mag. susceptibility and magnetisation meas. 79−95574
- $Zr_{40}Cu_{60-x}Tb_x$, magnetically dil. glass, 4f moments, mag. susceptibility and magnetisation meas. 79−95575
- $(Zr_{1-x}Er_x)_3Rh$, amorphous, influence of mag. ordering on supercond. props. 80−29511
- $Zr(Fe,Al)_2$, weak itinerant ferromag., mag. anisotropy effects on mag. isotherms 80−11187
- $Zr(Fe, Co)_2$, itinerant ferromagnet, magneto-volume expts. 77−66404
- $ZrFe_2$, lattice dynamics, Mossbauer spectra 80−19888
- $ZrFe_2$, Mossbauer diffr., combination type maxima, hyperfine interactions on nuclei 80−25263
- $Zr_{70}Fe_{30}$ amorphous alloys, struct. factors and radial distrib. functions 80−84096
- $Zr(Fe\text{-}Co)_2$, itinerant electron ferromagnet, magnetovolume effects 80−60397
- $Zr(Fe_{1-x}Al_x)_2$, Curie temp., magnetisation, and cryst. struct., conc. depend. 80−75730
- $Zr(Fe_{1-x}Al_x)_2$, Laves phase, mag. props. and Mossbauer effect 77−85632
- $Zr(Fe_{1-x}Al_x)_x$, transition region, spin glass or long range mag. order 80−44841
- $Zr(Fe_{1-x}Co_x)_2$, density of states estimation from magnetisation and resistivity meas. 78−84119
- $Zr(Fe_{1-x}Co_x)_2$, ferromag. and mictomag., thermal expansion and forced volume magnetostriction 80−75830
- $Zr(Fe_{1-x}Co_x)_2$, low temp. sp. ht. and mag. props. 79−61153
- $Zr(Fe_{1-x}Co_x)_2$, mag. props. and Mossbauer effects 79−91322
- $Zr(Fe_{1-x}Co_x)_2$, magnetic saturation moment, Co conc. depend., NMR exam. 78−15037
- $Zr(Fe_{1-x}Co_x)_2$, magnetovolume effects, thermal expansion and forced vol. magnetostriction meas. 80−29595
- $Zr(Fe_{1-x}Co_x)_2$, mictomagnetism 80−15863
- $Zr(Fe_{1-x}Co_x)_2$, NMR study 80−75882
- $Zr(Fe_{1-x}Co_x)_2$, press. effects on ferromag. to paramag. transition 77−66302
- $Zr(Fe_{1-x}Co_x)_y$, transition region, spin glass or long range mag. order 80−44841
- $Zr(Fe_xCo_{1-x})_2$, mag. order in pseudobinary systems down to millikelvin temps. 78−19251
- $Zr(Fe_xM_{1-x})_2$, (M=V,Cr,Mn), H absorption and desorption props. 77−55448
- $Zr(Fe_{1-x}Ni_x)_2$, Laves phase, mag. props. and Mossbauer effect 77−85632
- ZrGe, film, supercond. obs. 77−72939
- $ZrGe_2$, RF sputtered, supercond. crit. temp. 78−14853
- $ZrH_{1.5}$ and $ZrH_{1.75}$, low temp. phase transitions in H sublattice 77−24405
- $ZrH_{1.97}$, FCT, elec. quadrupole interaction at ^{181}Ta, TDPAC obs., 20-588K 79−33574
- ZrH_x, two-phase ($\delta+\varepsilon$), homogenisation during neutron bombard. *(Russian)* 78−18684
- $Zr_xHf_{1-x}V_2$, polycrystalline superconductor, resist. and mag. susceptibility, transition temp., temp. depend. 80−25113
- Zr_3In, Ll_2 ordered alloy, positive temp. depend. on strength, phase destabilization 80−81203
- $ZrMn_2$, Curie-Weiss law depend. of susceptibility, mag. props. *(Russian)* 79−65655
- $ZrMn_2$, mag. props. H absorpt. effect 80−88821
- $Zr(Mn_xCo_{1-x})_2$, Laves phase, phenomenological model for H_2 absorption capacity 77−84935
- $ZrMn_2D_3$, deuterated hexagonal Laves-phase, D atoms interstices and diffusion paths, positional disorder 79−73334
- $Zr(Mn_xFe_{1-x})_2$, Laves phase, phenomenological model for H_2 absortion capacity 77−84935
- $ZrMn_2H_x$, proton NMR relax. time and Knight shifts, diffusional activation energies meas., sorption props. 80−75871
- ZrNb, ω-phase, diffuse neutron scatt. meas. 78−14311
- ZrNb, pressure tube, fragmentation on failure 78−72863
- ZrNb, supercond. thermal cond. meas. 79−60970
- $(Zr_{1-x}Nb_x)Fe_2$, antiferromag. spin struct., Mossbauer effect study 80−66086
- $(Zr_{1-x}Nb_x)Fe_2$, magnetovolume effects and Invar characters 80−15773
- $Zr_{1-x}Nb_xZn_2$, microscopic mag. props., NMR investigation 80−15807
- ZrNi, surface segregation of Ni, influence on catalytic activity 80−30275
- $ZrNi_5$, methanation catalyst, AES and characteristic energy loss spectra 78−56915
- Zr_2Ni, search for soft phonon modes, neutron scatt. 79−23686
- Zr_2Ni, spin-pairing state investig. via Josephson current between weakly-coupled superconductors 77−47942
- $Zr_{70}Ni_{30}$ amorphous alloys, struct. factors and radial distrib. functions 80−84096
- $Zr_{70}Ni_{30}$, metallic glass, low temp. resist., supercond. T_c 79−38235
- $ZrPd_2$, valence band struct., X-ray emission spectra *(Russian)* 77−40304
- $Zr_{0.7}Pd_{0.3}$, amorphous supercond., sp. ht. and thermal cond., 0.1-10K 78−26991
- $Zr_{70}Pd_{30}$ amorphous alloys, struct. factors and radial distrib. functions 80−84096
- $ZrPt_3$, corrosion resist. and elec. cond., bulk and film samples 78−72285
- $Zr_{75}Rh_{25}$, amorphous, evidence for short wavelength cutoff in fluctuation spectrum 78−68113
- $Zr_{75}Rh_{25}$, amorphous superconductor, high-κ, upper and lower crit. fields 79−4629
- $ZrRh_{3-x}Pd_x$, electronic and cryst. struct. comparison 78−84398
- $ZrRh_{3-x}Pd_x$, powdered alloys, catalytic behaviour correlation with electronic struct., lattice struct. and surface comp. 79−82181
- ZrSi and $ZrSi_2$, ultrasoft X-ray emission bands, empirical band schemes 78−15249
- $ZrSi_2$-Si interfaces, chemical state, AES expts. 78−91767
- $Zr_xTb_{1-x}Fe_2$, Laves phase alloys, magnetostriction *(Russian)* 77−51932
- $Zr_xTb_{1-x}Fe_2$, props. of near magnetostrictive material 77−51934
- $Zr(V,Al)_2$, struct., supercond. props., elec. resist. and mag. susceptibility, 4.2 to 300K *(Russian)* 79−15246
- ZrV_2, supercond., dielec. phase transition *(Russian)* 78−64168
- ZrV_2, anomalous softening at martensitic transform. 80−93630
- ZrV_2, C-15 struct., phase transitions, elec. cond., crystal lattice parameters *(Russian)* 80−54826
- ZrV_2, C15 supercond., dielec. transitions, temp. depend. of resist. and mag. susceptibility, 4.2-300K 79−38136
- ZrV_2, dielectric phase transition, elec. resist. temp. depend. 79−65525
- ZrV_2, elec. resist. and mag. suscept., anomalous temp. depend. 79−69491
- ZrV_2, Knight shift vs. susceptibility plot 80−75712
- ZrV_2, latent heat of structural transform. 80−24589
- ZrV_2, Laves-phase, cubic to rhombohedral transition, lattice electron instability 78−92261
- ZrV_2, supercond., Young's modulus and internal friction meas. 79−11654
- ZrV_2, supercond. rel. to struct. instability *(Russian)* 78−23196
- $Zr(V_{1-x}Co_x)_2$, relation between electronic struct. and H_2 storing props. 80−76662
- $Zr(V_xCo_{1-x})_2$, Laves phase, phenomenological model for H_2 absorption capacity 77−84935
- $ZrV_2D_{4.5}$, deuterated cubic Laves phase, D atom distrib., neutron diffr. anal. 80−29006
- $ZrV_2D_x(H_x)$, site occupation modes and cryst. struct., neutron diffr. study 80−59440
- ZrX_2 alloy, Laves phases with $MgZn_2$, $MgCu_2$ structs., X-ray emission Zr spectra *(Russian)* 80−71517
- $ZrZn_2$, de Haas-van Alphen effect, Fermi surface, theory 80−103614
- $ZrZn_2$, high press. study of Curie temp. and mag. susceptibility 80−84600

zirconium alloys continued
$ZrZn_2$, high purity, mag. props., pulsed fields up to 17 T 78−64198
$ZrZn_2$, itinerant electron ferromag., NMR exam. of effect of spin fluctuations 77−16192
$ZrZn_2$, itinerant electron ferromag., nucl. spin-lattice relax. time meas. 77−63308
$ZrZn_2$, itinerant electron ferromagnet, magnetovolume effects 80−60397
$ZrZn_2$, phonon contrib. to Stoner enhancement factor, ferromag. and possible superconductivity 80−25070
$ZrZn_2$, weak itinerant electron ferromagnet, resistivity 77−72850
$ZrZn_2$, weak itinerant magnetism as inhibited superconductivity 79−51715
$ZrZn_2$:^{57}Fe mag. props. from Mossbauer effect obs. *(Japanese)* 80−15933

zirconium compounds
see also zirconium alloys
baddeleyite-corundum refractories, fused, elec. resist., 1300-2300°C 79−28345
baddeleyite-corundum refractories, thermophysical props. 79−82398
binary oxides fluorite related struct., order-disorder phenomena, Raman spectra 77−65960
borozirconia glazes, low-melting, struct. and liq.-phase separation 79−60282
carbide interstitial phases, elec. and mag. props., neutron radiation effects 79−77640
ceramics containing metastable tetragonal ZrO_2, grinding induced tempering 80−89260
cordierite, dense ceramic prep. with sintered condition over 300°C interval 79−33983
cordierite glass ceramics, effect of TiO_2 and ZrO_2 content on phase sequence during heat treatment 78−48381
bis-π-cyclopentadienylzirconium dichloride, struct. parameter refinement 78−87660
gels, thermal and related studies 80−71937
halides, XY_4 molecules, force consts. by modified Redington and Aljibury method 80−69261
hot pressing aids for Si_3N_4 powders, effect on oxidation resist. 77−8971
hydride interstitial phases, elec. and mag. props., neutron radiation effects 79−77640
hydrides, computed X-ray powder diffr. patterns and densities 77−43172
MgO-ZrO_2 ceramic reinforced with filamentary crystals, mech. and thermal props. 80−45262
orthovanadates:rare earth ions, spectroscopic props. 77−16363
oxide film, anodic, photodepolarisation *(Russian)* 77−32316
polymer filled ceramic, ZrO_2 stabilised, fracture mechanism *(Russian)* 80−100895
potassium zirconium oxalate, X-ray K-absorpt. spectra 78−76558
rare earth $Zr_{1-x}O_{2-x/2}$, growth from skull melting, directional solidification 78−60567
refractory carbides, borides and nitrides, wetting by and interactions with liq. metals 80−54473
tetrahalides, struct., force field and Coriolis const. calcs. 78−86843
tetrahalides of Gp.IV elements, M-X bond flexibility, by compliance scheme 80−37805
thermoluminescence, traps and emission centres 79−24373
zeolites, type Y, catalytic activity, NMR, mechanism 79−29405
Zircaloy 4, stress relaxation in bending 78−68719
Zircaloy clad defective fuel rods, behaviour under continued reactor operation 79−30915
Zircaloy-2, deformation and fracture behaviour, uniaxial tension test in I_2 environment 80−13580
zircon, dissociated, form. in plasma furnace, comp. and microstruct. 77−36429
Zircon, fine ground, mechanised method of cleaning with acid 79−83357
zircon, natural and synthetic crysts. Hf and Tb activated, capture centres and luminescence mechanism *(Russian)* 77−28626
zircon, rate of dissolution in molten Fe_3O_4, porosity effects *(Japanese)* 77−11699
zircon bricks, thermal conductivity meas. up to 1200°C *(Japanese)* 78−95193
Zircon ceramic, exam. of development and fabrication 80−11608
zirconate-titanate ceramics, K_{IC} eval. by double torsion technique 77−90444
zirconium hexacyanoferrate, possible agent for removal of radioactive Cs from contaminated water *(Slovak)* 78−24319
zirconosilicate glass fibre, effect of cement environment 77−44335
$ZrC_{0.98}$, porosity influence on high temp. creep. *(Russian)* 80−25764
$ZrH_{1.66}$, thermal neutron inelastic scatt. phonon spectra determ. *(Chinese)* 79−10906
ZrO_2, high temperature interactions with Re 80−16665
α-ZrO_2, projection of Zr and O packings, computer program 79−14707
ZrO_2 powders, stabilised, for plasma spray-coatings 80−20869
$2ZrSiO_4 3Al_2O_3$, identification of stages in reactive hot-pressing 79−11542
Ag-Zn, molten, EMF meas. of activities using ZrO_2 solid electrolytes *(Japanese)* 80−88339
$AgZr_2(PO_4)_3$ system, phase charact. at different temps. 80−29936
Al_2O_3-MgO/ZrO_2-CeO_2/MgF_2 triple layer antirefl. coating for crown glass in visible region 78−13777
Al_2O_3-Mo (20 wt.%) cermet, ZrO_2 crystal addition effect on thermal fatigue resistance 80−40528
Al_2O_3-SiO_2-ZrO_2, liquidus surface, discussion 77−44231
Al_2O_3-SiO_2-ZrO_2 refractories, corrosion behaviour in glassmelting furnaces *(Polish)* 80−71783
Al_2O_3-ZrO_2, dispersion hardened, fracture toughness improvement by induced microcracking *(German)* 78−31501
Al_2O_3-ZrO_2, microstructure effect on friability 78−64515
Al_2O_3-ZrO_2, multiphase ceramics, mech. strengthening due to dispersion of non-metallic particles *(German)* 78−60674
Al_2O_3-ZrO_2, tetragonal to monoclinic transform. of ZrO_2 particles *(German)* 79−43240
Al_2O_3-ZrO_2 cast refractories, nucleation processes reconstruction by SEM, TEM and STEM 78−35380
Al_2O_3-ZrO_2 composite, fracture toughness increase by microcracking in energy dissipative zone near crack tip 79−20156
Al_2O_3-ZrO_2 dispersed system, thermal diffusivity/conductivity, effect on microcracking resulting from phase transform. 78−10231
Al_2O_3-ZrO_2 dispersed system, fracture toughness, inclusion induced microcracking effect 78−11296

zirconium compounds continued
Al_2O_3-ZrO_2 mixture, stress induced transformation of tetragonal ZrO_2, exam. 78−48392
Al_2O_3-ZrO_2-SiO_2, fusion cast refractory, effects of glassy phase on thermal cycling resist. 78−84956
Al_2O_3-$ZrSiO_4$, granular corundum-zircon refractory, development 80−66462
Al_2O_3-$ZrSiO_4$ mixture, reaction sintering, correlation between densification and reaction 80−29911
$3Al_2O_3.2SiO_2$-ZrO_2 composites, sintered, in situ-reacted, fracture props. 80−81158
ArC, nondifferentiated Auger electron spectrum 79−69929
ArO_2-ScO_3 solid electrolytes, thermoEMF 78−95184
Au-Zn, molten, EMF meas. of activities using ZrO_2 solid electrolytes *(Japanese)* 80−88339
$BaTiO_3$:ZrO_2, dielec. loss tangent and const. 79−4769
$BaTiO_3$-ZrO_2 mixture, exam. of liquid phase sintering, densification 79−33979
CC ZrS:O_4, X-irradiated, trapping and emission centres, thermolum. meas. 80−89076
Ca-Mg-Zr combustion sensor, pipe-form ceramics appl. *(Japanese)* 80−55761
CaO-MgO-Cr_2O_3-Al_2O_3-ZrO_2-SiO_2 system, subsolidus region charact. 80−97466
CaO-MgO-ZrO_2-SiO_2, phase study, SiO_2 compatibility relationship 78−95734
CaO-MgO-ZrO_2-SiO_2, phase study, ZrO_2 compatibility relationship 78−95735
CaO-MgO-ZrO_2-SiO_2 refractories, phase diagram 80−11634
CaO-ZrO_2 solid soln., thermodynamic investig., by EMF method 77−36485
$(Cr,Al)_2O_3$-$ZrSiO_4$ refractories, glass resist. and corrosion mechanism 79−61757
Cr_2O_3-Al_2O_3-$ZrSiO_4$, exam. of microstructure by optical microscopy 79−29073
Cr_2O_3-Al_2O_3-$ZrSiO_4$ system, electrosmelted refractories, phase comp., corrosion and glass resist. Cr^{3+} conc. depend. 79−33982
Cr_2O_3-CrO_3-$ZrO_2.CrO_3H_2O$, exam. of thermal transitions 79−100116
Cr_2O_3-ZrO_2 granules, from spray drying of suspensions 80−104100
$Cu_xIn_xZr_{1-x}S_2$ system, struct. and cond. meas. *(French)* 80−88354
$Cu_xZn_{1-x}ZrF_6.6H_2O$, distortions of nearest Jahn-Teller $[Cu(H_2O)_6]^{2+}$ centres 78−68000
Dy_2O_3-ZrO_2 phase diagram and long range ordering 80−93542
Er_2O_3-ZrO_2, subsolidus phase relations, X-ray diffr. and thermal expansion exam. 78−31382
Eu_2O_3-ZrO_2, phase decay 77−86002
Fe/ZrB_2, metal-like cpd. form. in diffusion layer during solid phase saturation 80−19994
Fe-ZrB_2, dispersion strengthened, thick vacuum condensate, control of struct. and mech. props. 80−16324
Fe-ZrB_2 condensate, struct. and mech. props., disperse particle content depend. *(Russian)* 78−19772
Fe-ZrB_2-MoS_2, self lubricating coatings, exam. of props. 79−96217
Fe-ZrO_2, dispersion strengthened, thick vacuum condensate, control of struct. and mech. props. 80−16324
Fe-ZrO_2 condensate, struct. and mech. props., disperse particle content depend. *(Russian)* 78−19772
Fe-ZrO_2 granular film, interface props., Mossbauer spectroscopy 80−34336
Fe-ZrO_2 granular films, superparamag., Mossbauer effect 80−7131
Fe-ZrO_2-MoS_2, self lubricating coatings, exam. of props. 79−96217
Fe_xZrSe_2, intercalation compound, IR spectra 78−88300
GdF_3-BaF_2-ZrF_4 glass fibres, IR transmission, losses, fabrication 80−87516
$Gd_xZr_{1-x}O_{2-x/2}$, elec. cond. of ceramic solid solutions 80−107554
$Gd_xZr_{1-x}O_{2-x/2}$, fluorite and pyrochlore solid solutions, electrical conductivity meas. 80−65287
HfF_4-BaF_2-ThF_4-(ZrF_4) glass system, IR transmitting, synthesis and props. 80−71623
$K_3Zr(MoO_4)_3$, synthesis and struct. 77−36386
$K_8Zr(MoO_4)_6$, X-ray structural investigation 78−79597
$K_4Zr_5O_{12}$, cryst. struct., X-ray study 80−33957
K_xZrS_2, intercalation cpd., X-ray K absorption edges 78−39627
LaF_3-BaF_2-ZrF_4(-MF), M=Na, Li, glassy transition, refr. index, density and molar refr. 80−1937
La_2O_3-GeO_2-ZrO_2, vitrification, crystn. 77−15559
$La_2Zr_2O_7$-$La_2Hf_2O_7$ system, cryst. struct., phase diagram 78−83806
$Li_{1-x}Zr_{2-x}Ta_x(PO_4)_3$, new solid ionic conductors 77−35953
MgO-Al_2O_3-SiO_2: ZrO_2, TiO_2, glass, phase separation *(German)* 80−38932
MgO-Al_2O_3-ZrO_2, wetting with liquid Fe and Al 78−22936
MgO-ZrO_2, dispersion hardened, fracture strength and texture, rel. to temp. *(German)* 79−43378
MgO-ZrO_2 ceramic sublimation at optical furnace focal spot *(Russian)* 79−95983
MnO-SiO_2-ZrO_2 molten slag system-molten steel interface, wetting angles, surface tension *(Czech)* 79−19432
$Na_xIn_xZr_{1-x}S_2$, ionic conduction of phases *(French)* 77−47620
$NaLiZrSi_6O_{15}$, zektzerite, silicate mineral with six-tetrahedral-repeat double chains 78−63719
Na_2O-Al_2O_3-ZrO_2-SiO_2 glass, chemical stability in NaOH and Na_2CO_3 solns. 80−16532
Na_2O-CaO-Al_2O_3-SiO_2-F-B_2O_3-ZrO_2 glaze, crystallisation, MgO, ZnO, BaO and SrO effects 79−60279
Na_2O-SnO_2-ZrO_2-SiO_2 glass, chemical stability in NaOH and Na_2CO_3 solns. 80−16532
Na_2O-ZrO_2-SiO_2 glass, density, refractive index, thermal expansion hardness, IR spectra, DTA *(Japanese)* 78−15535
Na_2O-ZrO_2-SiO_2 glass, treated with 2 N solns. of $NaCO_3$ and NaOH, surface layer comp. 80−35366
Na_2O-ZrO_2-SiO_2 system, glass, corrosion in NaOH and Na_2CO_3 solns. at 90-150°C 79−66187
$Na_xY_xZr_{1-x}S_2$, ionic cond. and NMR mobility obs., comp. depend. *(French)* 80−70459
$Na_4Zr_2Ge_3O_{12}$, cryst. struct., X-ray diffr. 79−19224
$Na_{1+x}Zr_{2-x}In_x(PO_4)_3$, three-dimens. solid soln., comp. depend. of ionic cond. *(French)* 80−34230
Na_2ZrSiO_5, scintillation props., excited by α particles 80−29809
Na_2ZrSiO_5:Ln^1,Ln_2, scintillation, α-excited *(Russian)* 79−28841
$Na_4Zr_2Si_3O_{12}$, struct. analysis at 300 and 600°C, rel. to ionic cond. 80−107189

zirconium compounds continued
$Na_{1-x}Zr_2Si_xP_{3-x}O_{12}$, press. and comp. effect on fast Na^+ ion transport 80−107516
$Na_3Zr_2Si_2PO_{12}$, NASICON, ionic cond. temp. depend., comparison with β-Al_2O_3-Na_2O 80−107520
NaZr[Si_2O_6OH], keldyshite, X-ray structural anal. 79−14779
Nb-ZrN, BCC solid soln., nitride solubility, alloying effects *(Russian)* 79−51262
Nb_2O_5-TiO_2-ZrO_2, quasiternary system 77−44229
Nb_2O_5-ZrO_2 sputtered thin layer structure and optical props. 79−28851
$Nd_xZr_{1-x}O_{2-x/2}$, elec. cond. of ceramic solid solutions 80−107554
$Nd_xZr_{1-x}O_{2-x/2}$, fluorite and pyrochlore solid solutions, electrical conductivity meas. 80−65287
Ni-ZrO_2, dispersed inclusions, effect on recovery and recrystallisation 77−25064
Ni-ZrO_2, dispersion strengthened, thick vacuum condensate, control of struct. and mech. props. 80−16324
Ni-ZrO_2, dispersion-strengthened condensate, density and mech. props. 77−44196
Ni-ZrO_2, electron-beam-evaporated condensate, cold deform. and annealing effects on microstruct. 80−16331
Ni-ZrO_2, thin layers, vapour deposited, dispersion strengthened, exam. of struct., mech. props. 78−80554
Ni-ZrO_2 compact cermet cathode for high temp. water vapour electrolysis *(French)* 79−74399
$NiZrF_6.6H_2O$, uniaxial ferromagnetism 78−80143
Ni_xZrS_2, fundamental optical absorption edge 79−99904
$NpBa_6Zr_{12}F_{64}$ glass, Mossbauer spectrum, evidence for charge states 3+ and 4+ *(French)* 78−88231
$POCl_3$:$ZrCl_4$:Nd^{3+}(Er^{3+}), radiative transition probabilities within 4f configs. 77−8617
$POCl_3$-$ZrCl_4$, splitting of Sm^{3+} near IR absorpt. bands 80−2750
$POCl_3$-$ZrCl_4$:Nd^{3+} free-running liquid laser, design and performance 77−14706
$POCl_3$-$ZrCl_4$:Yb^{3+}, Er^{3+}, energy transfer from Yb^{3+} to Er^{3+}, agglomeration formation 78−64405
PZT, ferroelec. film, elec. props., composition anal., AES 78−84530
PbO-B_2O_3-SiO_2-Li_2O-ZrO_2-CdO(CoO)(CuO), glass enamel, chemical durability, microstruct., CuO, CdO and CoO addition effects 79−29256
PbO-B_2O_3-SiO_2-ZrO_2, glass enamel, chemical durability and microstruct., ZrO_2 addition effect 79−29255
Pb(Zr,Ti)O_3 fibre arrays in epoxy cement, ferroelectric ceramic-plastic composites 80−81015
Pb(Zr, Ti)O_3 internal struct., prep. effect, ionic shadowing obs. *(Polish)* 80−11612
Pb(Zr,Ti)O_3 polycrystalline ceramic, fracture and strength, surface treatment effects 80−11704
$PbZrO_3$-$PbCd_{0.5}W_{0.5}O_3$, phase transitions 78−43817
$PbZrS_3$, cryst. struct. refinement using neutron diffr. powder data 79−4294
Pb($ZrTi$)O_3 ceramic transducer for generation and detection of unipolar stress pulses 80−64328
$PbZr_xTi_{1-x}O_3$, ferroelec. phase transition under high press. 79−99833
PuC-ZrC, solubility study 78−83956
Rb_xZrS_2, intercalation cpd., X-ray K absorption edges 78−39627
Sc_2O_3-ZrO_2, cubic solid soln., lattice parameters 79−82186
Si-Al-Zr-O-N, calc. of phase diagrams from data set 80−55362
Si_3N_4/ZrO_2, hot-pressed, compressive surface stresses developed by oxidation induced phase change 80−60992
Si_3N_4-SiO_2-ZrN-ZrO_2, X-ray diffr. phase anal. and reactions $Si_3N_4+ZrO_2$, SiO_2+ZrN 80−50613
Si_3N_4-ZrO_2, sintered and hot pressed, exam. of mech. props. 78−48509
Si_3N_4-ZrO_2, tetragonal to monoclinic transform. of ZrO_2 particles *(German)* 79−43240
SiO_2-Al_2O_3-CaO-MgO-NaO-K_2O-B_2O_3-ZrO_2, glaze, exam. of zircon crystallisation 79−19155
SiO_2-Al_2O_3-Li_2O:ZrO_2,Fe_2O_3, pyroceramic glass, coloration, absorpt. spectra obs. 77−8615
SiO_2-CaO-Na_2O-ZrO_2 system, water, alkali, acid resist., chem. durability 79−34162
SiO_2-ZrO_2, noncrystalline film form., IR study *(Japanese)* 77−59634
SiO_2-ZrO_2 adsorbents, coprecipitated, porous struct. rel. to form. conditions 78−53263
SiO_2-ZrO_2-Al_2O_3-CaO-Na_2O-K_2O-Li_2O, chemical resistant glass for glass fibres 80−21128
SiO_2-ZrO_2-Li_2O-Na_2O based crystallisable glasses composition and properties 80−50731
$Sn_xZr_{1-x}Se_2$, growth by I_2 vap. transport, cryst. struct. 77−73223
SrN, impurity activated whisker growth by CVD 79−66010
SrO.ZrO_2, US comminution of refractory compound powders 78−23656
$SrZr_{0.8}Yb_{0.2}O_{2.9}\square_{0.1}$, $SrZr_{0.8}Mg_{0.2}O_{2.8}\square_{0.2}$, ionic conductivity 77−20119
$Ta_{1-x}Zr_xSe_2$ (1T), CDW stacking order, interlayer interactions and impurity effects 77−7699
Th-Zr-C, phase diagram *(German)* 77−48413
(Ti,Zr)B_2 on graphite, CVD coatings, hardness meas., SEM study 80−24760
Ti-Zr-B system, CVD 78−60581
TiB_2-ZrB_2, refractory compound, direct evaporation deposition, struct. and props. 77−44392
TiC-ZrC, mag. susceptibility, elec. cond. and thermoelec. props. 80−50033
TiC-ZrC, pseudobinary systems, phase diagrams, computer calcs. 78−44092
TiC-ZrC, solid soln., conc. and temp. dependence of props. 80−39736
TiC-ZrC carbide alloys, thermophys. props., temp. depend., specific elec. resist. 79−86908
TiO_2-ZrO_2, submicron powders, vapour phase production from $TiCl_4$-$ZrCl_4$-O_2 system 80−40301
TiO_2-ZrO_2 sputtered thin layer structure and optical props. 79−28851
TiO_2-ZrO_2-SiO_2 amorphous film, alkali resistance, refractive index, IR spectra *(Japanese)* 78−23546
(U,Zr)C, U self-diffusion 80−92711
U-ZrH fission reactor fuel options for TRIGA Mk.III 80−5235
U-ZrH system, neutron spectrum in critical pile 79−45322
UC-ZrC and UC-ZrC-NbC, solid soln. strengthening rules, physicomech. prop. changes 77−28826
UC_2 and (8Th, 1U)O_2 fuel kernel, experimental containing CVD ZrC coatings, irradiation behaviour 77−3103
UN-ZrN, Young's modulus antiferromagnetic anomaly 80−92583
$U_xZr_{1-x}Fe_2$, Curie temp. and saturation moment at 4.2K 80−70966

zirconium compounds continued
W-ZrC (25 wt.%), eutectic alloy, thermionic emission and adsorption props. 79−69951
YO_x-ZrO_2, YO_x-rich, phase equilibria 77−21117
Y_2O_3-ZrO_2, cubic solid soln., lattice parameters 79−82186
Y_2O_3-ZrO_2 system, solid soln. form. mechanisms 79−11579
Y_6WO_{12}:ZrO_2(MgO)(CeO)(SrO)(BaO), polycryst., elec. cond., 800-7400°C 80−15517
Z+C, band struct. correlation with Zr, APW calc. *(Japanese)* 78−23017
Z_2B, abrasive, effect on machinability of Ti alloys *(Russian)* 80−97593
Z_2C, abrasive, effect on machinability of Ti alloys *(Russian)* 80−97593
ZI_4, interaction with U_3Si, 700 to 800°C, exam. using metallographic and local X-ray spectral anal. 79−90831
$ZiSiO_4$, natural and synthetic, X-ray dilatometry 77−51522
Zr complexes, X-ray K-absorption edge, shift and width meas. 77−8683
Zr double arsenates, $M^IZr_2(AsO_4)_3$, $M^{II}Zr_4(AsO_4)_6$, (where M^I=Li, Na, K, Rb, Cs and M^{II}=Ca, Sr, Ba, Mn, Co, Cu, Zn), cryst. characts. 79−55726
Zr double phosphates, $M^{II}Zr_4(PO_4)_6$, (where M^{II}=Ca, Sr, Ba, Mn, Co, Cu, Zn), cryst. characts. 79−55726
Zr-Al_2O_3 couple, diffusion welding, 1000 to 1300°C *(German)* 79−28155
Zr-Al-O system, diffusion welding, 1000 to 1300°C, Al_2O_3-(Zr-Al) alloy, ZrO_2-(Zr-Al) alloy, Al_2O_3-ZrO_2 couples *(German)* 79−33122
Zr-C disordered systems, Hall effect depend. on composition conc. 79−95459
Zr-C-N-O-H, solid solns. of H, exam. of props. 80−29172
Zr-H, deposited on carriers, synthesis, structure and catalytic props. 80−29890
Zr-H, diffusion in hydride phase, exam. 80−29204
Zr-H, effect of neutron irrad. on electrical resistance, magnetic susceptibility 80−29063
Zr-H, exam. of electron structure 80−29306
Zr-H, tensile strength and creep 80−55459
Zr-H system, δ and ε phases, neutron irrad., radiation swelling investigation 78−18685
Zr-H system, low temp. NMR 78−72431
Zr-M-B systems (M=Rh,Ir), phase equilib. and cryst. structs. 80−15072
Zr-N_2, condensate formed by plasma flow precipitation in vacuum, cryst. and surface props. *(Russian)* 80−100788
Zr-Nb (1 wt.%), stress drop expt. during creep 79−29152
Zr-Ni-H, surface segregation of Ni, influence on catalytic activity 80−30275
Zr-O, high temp. phase diagram 78−11211
Zr-ZrO_{2-x} composite, wetting charact. 77−44207
ZrB_{12}, exam. of electronic structure, using X-ray emission spectra *(Russian)* 79−33865
ZrB_2, band struct. and XPS 77−90253
ZrB_2, coating on rapid steel, surface modification 79−66203
ZrB_2 coatings, deposited by electron evaporation, struct. and props. 79−23871
ZrB_2 dispersion strengthened Fe condensates, struct., mech. props. 77−90361
ZrB_2, electric arc melting prep. and oxidation props. 80−20860
ZrB_2 electronic structures calc. and obs., by APW method and X-ray photoelectron spectroscopy *(Japanese)* 79−15074
ZrB_2, etching method using H_3PO_4 and H_2SO_4, effect of Pt 78−44339
ZrB_2, Fermi surface, de Haas-van Alphen effect meas. 78−84134
ZrB_2, hot pressing, applied press. effect *(Japanese)* 79−38780
ZrB_2, hyperfine interactions from β-ray spectra of recoil nuclei polarised by fast polarised beams 77−28502
ZrB_2, impurity content, effect of synthesis conditions 80−21344
ZrB_2, microhardness and charact. hardness 79−52376
ZrB_2, oxidation in O_2 atmosphere, exam. 80−11814
ZrB_2 powders, synthesis and impurities 80−55329
ZrB_2, prod., oxidation rate, corrosion resistance 77−52274
ZrB_2, pure, vacuum hot-press sintering and microstruct. *(Japanese)* 78−23649
ZrB_2, reactions with Ti-Al-Cr-Mo alloy VT3-1 80−16585
ZrB_2, refractory compound, direct evaporation deposition, struct. and props. 77−44392
ZrB_2, self-consistent band struct., XPS, reflectance, NQR, Hall effect and density of states meas. 80−107689
ZrB_2, single cryst., quadrupole coupling const. of ^{12}B 78−37279
ZrB_2, single crystal growth *(Japanese)* 79−65987
ZrB_2, vacuum condensate, struct. and mech. props., second phase effect *(Russian)* 80−71705
ZrB_2-SiC-C(-V)(-Nb), refractory cermet, hot pressing and oxidation resist. 80−3231
ZrB_2-Ta composite, vacuum hot-press sintering and microstruct. *(Japanese)* 78−23649
ZrB_2-TiB_2 solid solns., prod., oxidation rate corrosion resist. 77−52274
ZrB_2-ZnS:Ag(Ag,Ni)-glass binder, thermally stable, comp. 77−63617
$ZrB_{\sim 51}$, X-ray powder profile refinement 79−23574
$Zr(BH_4)_4$, and d_{16}, mol. vibr. amplitude, normal coord. anal., T model 79−59433
$Zr(BH_4)_4$ catalytic reactions on Al_2O_3, inelastic electron tunnelling spectra 80−75425
$Zr(BH_4)_4$, mol. vibr., T_d model and force field 79−801
ZrBr, electronic struct., self-consistent and non-self-consistent band calcs. 80−44499
$ZrBr_4$, X-ray K-absorpt. spectra 78−76558
$ZrBrH_n$, (n=0.5, 1), ^1H NMR, shielding tensors 79−69731
$ZrBrH_x$, PMR exam. of H-location and diffusion 78−56382
Zr(C,N), coating on Zr substrate, oxidation by water vap., kinetics, 0.2-20 torr, 500-600°C *(French)* 78−44266
Zr(C,N), hydrolysis 78−15713
ZrC, abrasive action X-ray investig. 77−52497
ZrC, adsorption of Cs(K), adsorpt. energy, thermionic emission 77−7978
ZrC, and TiC-ZrC coatings, deposited by electron evaporation, struct. and props. 79−23871
ZrC and ZrC-Re alloys, adsorption of H 79−19467
ZrC based cermets, strength and gas-abrasive wear resistance 77−25163
ZrC, bond energy and ionization efficiencies from SIMS 79−24400
ZrC, brittle mat. discs, ultimate thermal stresses 77−4210
ZrC CVD coated fuel particles, diffusion of ^{137}Cs, ^{90}Sr and ^{144}Ce 80−13582
ZrC, CVD on reactor fuel elements 77−74941
ZrC coated emitters, thermionic emission props. *(Japanese)* 77−40322

zirconium compounds continued
ZrC coating, vapour deposition, phys. and chem. props. 77−40456
ZrC, coating on C fibre, mech. props. 77−70197
ZrC coating on refractory metal fibre, diffusion barrier, deposition 77−4759
ZrC coating on refractory fibre, effect on high-temp. strength *(Russian)* 77−52536
ZrC crystals, electron energy spectra 80−49568
ZrC deposit on C steel surface, exam. of composition *(Russian)* 79−34201
ZrC, deposition with vapor-gas phase circulation in closed circuit 77−55927
ZrC, destruction delay time under laser impact 79−38976
ZrC, determ. in cementite by annealing in moist H_2 *(German)* 79−39231
ZrC, diffusion of W, correl. with self-diffusion 77−24437
ZrC dispersion hardened Mo alloy, thermally activated plastic deform. *(Russian)* 77−36612
ZrC, elastic modulus, porosity factor 77−21207
ZrC, electronic struct. and XPS, cluster method and band struct. 79−60710
ZrC electronic structures calc. and obs., by APW method and X-ray photoelectron spectroscopy *(Japanese)* 79−15074
ZrC, exam. of brittle fracture props., using Hertzian indentation 79−11686
ZrC, factors affecting CVD 77−8760
ZrC, film, solar selective surface *(Japanese)* 78−90465
ZrC, fracture by laser beams, macrocrack propag. 79−15789
ZrC, generalised susceptibilities and electronically driven phonon anomalies 79−42208
ZrC high-temp. plastic deform. effects on elec. props. 77−44370
ZrC, high-temp. strength, affecting factors 77−63794
ZrC, high-temp. supercond., role of electronic struct. in obs. phonon anomalies 77−24363
ZrC, in H_2, thermionic emission, residual gas effects 78−48269
ZrC, isothermal sintering kinetics 79−66032
ZrC, kinetics of growth on graphite via activated cementation *(French)* 77−52552
ZrC, low-temp. reactor irrad., calorimetric investig. 77−80547
ZrC, microhardness and charact. hardness 79−52376
ZrC, micropowder, abrasive props. 77−63821
ZrC, NbC-ZrC, right-through sat. prep., strength and plasticity, temp. depend. 77−40432
ZrC, negative surface ionisation 77−77335
ZrC powder, plastic strain of particles under vibratory milling 77−90423
ZrC powder, struct. after vibratory milling 77−28840
ZrC powders, synthesis and impurities 80−55329
ZrC powders produced by various methods, impurities 80−11615
ZrC, prep. by impregnation, strength, surface submicrocracks 77−16661
ZrC, prep. from $ZrCl_4$+C *(Russian)* 78−19682
ZrC, pure and with Y additions, thermionic emission, hot pressed or CVD 77−12484
ZrC, reactions with Ti-Al-Cr-Mo alloy VT3-1 80−16585
ZrC, recrystallisation 78−11251
ZrC, rupture mechanism due to internal heat evolution 77−8922
ZrC, single cryst. growth by modified hot-filament method, cryst. morphology and microhardness 79−19983
ZrC single crystals, synthesis and impurities 80−55329
ZrC, sintering 78−19700
ZrC, sintering shrinkage, effect of struct. vacancies in interstitial phases 78−60630
ZrC, solubility, diffusion and permeation of Cs 78−51684
ZrC, stoichiometric, emissibility, integral hemispherical and monochromatic, N_2 content effect 78−91457
ZrC, supercond. transition temp. and lattice dynamics 79−56361
ZrC, thermal stress cracking, neutron radiation effects 79−77641
ZrC, thermionic emission current density, compared with ZrC-W alloys 77−8714
ZrC, true heat capacity meas. by pulse method 80−19953
ZrC, US comminution of refractory compound powders 78−23656
ZrC, valence band struct. *(Russian)* 78−6268
ZrC, whiskers, CVD on Ni, catalytic effect 78−51865
ZrC, work function, effect of H_2 adsorpt., thermionic emission expts. 78−2970
ZrC work function, sorbed O_2 effect, thermionic emission and thermal desorption obs. 79−56285
ZrC, X-ray K-absorpt. spectra 78−76558
ZrC, ZrC-ZrB_2, refractory compounds, direct evaporation deposition, struct. and props. 77−44392
ZrC-C, disordered, Hall const. anomalies 79−56277
ZrC-C composite system, electrical resist. meas., percolation theory anal. 78−84269
ZrC-C composite system, negative magnetoresist. 80−60008
ZrC-C composites, hot pressed, thermophys. props. at high temps. 80−59675
ZrC-C mixtures, gas composition effect on CVD, bromide process 79−24448
ZrC-HfC, pseudobinary systems, phase diagrams, computer calcs. 78−44092
ZrC-NbC, kinetic characteristics, review 78−47613
ZrC-NbC, prep. by impregnation, strength, surface submicrocracks 77−16661
ZrC-NbC-MoC_{1-x} system, thermal expansion coeff. up to 2500°C 79−69267
ZrC-NbN, mag. susceptibility, zone struct., conc. and temp. depends. 77−8788
ZrC-Ni, refractory-liquid metal, interfacial reactions, C effect, electron microprobe analysis 77−12829
ZrC-Re, spectral emissivity, 1400 to 2500K, surface relief and composition 77−24420
ZrC-TaC solid solns., high-temp. creep 79−11661
ZrC-TiC, phase diag. calc. 77−90329
ZrC-W(Mo), thermionic emission, surface structural charact. after prolonged use, work function variation 80−20758
ZrC-ZrB_2, strength and antifriction props. over wider range of concs. 80−50673
ZrC-ZrN system, solid solns., elec. resist., thermo EMF, thermal cond., expansion coeffs. 78−60176
ZrC+$CeO_2(UO_2)$(SrO), high temp. reactions 80−3320
ZrC+$NaCO_3$, flame, optical and temp. charact. meas. method, light scatt. ZrO_2 particles *(Russian)* 78−56894

zirconium compounds continued
$ZrC_{0.84}$, single crystal work function, thermionic emission and contact pot., microhardness and binding 79−19649
$ZrC_{0.91}$, sintered, strength charact. effect of struct. and substruct. 80−16260
$ZrC_{0.97}$-$NbN_{0.93}$, $Zr_{0.5}Nb_{0.8}C_xN_{0.98-x}$, solid solns., elastic props. expansion and hardness 77−52380
ZrC_n^+, clusters, electronic props., mass spectra obs. *(French)* 79−45877
ZrC_x, change in lattice const. in region of homogeneity 77−25029
ZrC_x, complex phases with NaCl struct., microhardness rel. to electronic structure 77−90438
ZrC_x, creep-comp. curves for homogeneous region 78−52911
ZrC_x, micro X-ray spectral anal. of boundary zones 79−8301
ZrC_x, monocrystal, work function anisotropy of electrons *(Russian)* 79−73568
ZrC_x, static distortions and Debye temp. determ., neutron diffr. exam. *(Russian)* 77−80482
ZrC_x, thermophysical props. at high temp., thermal vacancies form. 78−43141
ZrC_x whiskers, nonstoichiometric, synthesis by CVD 79−28941
ZrC_x, x=0.99 to 0.13, elec. cond., supercond. state 78−43504
ZrC_x+Be→Be_2C layer, limiting stage investig. 77−36786
ZrC_xN_{1-x} coating, on Zr, oxidation kinetics, 450-600°C 50-400 Torr O_2 press. *(French)* 77−25171
$ZrC_xN_zO_y$, H_2 solubility 77−84930
ZrC_xO_y, C-stabilised low temp. cubic phase 77−36478
ZrC_xO_y, H_2 solubility 77−84930
$ZrC_xO_xN_z$, homogeneity and struct. vacancies 77−84937
$Zr(Ca,Y)O_{2-x}$, local ionic arrangement, X-ray diffr. study 80−100203
$Zr(Ca,Y)O_{2-x}$, X-ray diffr. study of average struct. 79−99123
$Zr(Ca)O_{2-x}$, internal, external distortion mechanisms, neutron diffr. study 78−83946
$Zr(Ca)O_{2-x}$, lattice shear distortions 79−99221
ZrCl, electronic struct., self-consistent and non-self-consistent band calcs. 80−44499
$ZrCl_3$ disproportionation reaction sequence, and Zr lower halide formation enthalpies 79−15973
$ZrCl_4$, cryst., melt, gas, Raman spectra interpretation *(German)* 79−28753
$ZrCl_4$ reaction with $POCl_3$ in O_2, for ZrP_2O_7 prep. 80−21272
$ZrCl_4$-CsCl melt, equilib. phase diagram and vapour press., equilib. reaction 77−66764
ZrClH, ^{1}H NMR shielding anisotropy 80−20466
$ZrClH_n$, (n=0.5, 1), ^{1}H NMR, shielding tensors 79−69731
$ZrClH_x$, PMR exam. of H-location and diffusion 78−56382
$ZrCo_2Si_2$, X-ray cryst. struct. anal. 79−60342
ZrD, electrodes with externally ignited vacuum arc source of D^+ ions 80−33845
$ZrD_{1.82}$, and $ZrD_{1.96}$, struct. and phase equilib., neutron diffr. obs. *(Russian)* 78−92244
$Zr_3Er_4O_{12}$, cryst. struct. determ., powder X-ray diffr. exam. 77−4083
ZrF_4 based glass, elec. and dielec. props. in freq. and temp. ranges 5-500 kHz and 130-280°C *(French)* 79−23772
ZrF_4 based glasses, solid electrolyte, conductivity and activation energy 80−70464
ZrF_4 glasses, elec. props. *(French)* 78−75868
ZrF_4, mol. struct. and vibr. freqs., gaseous electron diffr. obs. 80−32836
ZrF_4, muon Coulomb capture ratio 78−62959
ZrF_4:Eu^{3+} glass, luminesc. of Eu^{3+}, transition probabilities 80−80845
ZrF_4-BaF_2-MF_n (M=Na, Ca, Ln, Th, n=1, 2, 3, 4), vitreous phases, network formers, modifiers and stabilisers *(French)* 80−64909
ZrF_4-BaF_2-NdF_3 glass, vitreous domain, prep. and optical props. 78−27304
ZrF_4-BaF_2-ThF_4-NaF(RF_3) (R=rare-earth) glass system, anion cond. 80−70460
ZrF_4-BaF_2-ThF_4(LaF_3)(NdF_3)(PrF_3), F^- ion cond. glasses, cond. process 80−107477
ZrF_4-based glasses, elec. transport props. 80−79983
ZrF_4-THF_4-BaF_2 glass, IR-transparent, synthesis using reactive atm. processing technique 80−100826
ZrF_4-ThF_4-BaF_2:V^{3+}(Cr^{3+}) glasses, absorpt. spectra *(French)* 79−99918
ZrF_4-ThF_4-NdF_3(LaF_3), phase equilibrium, vitreous phase struct., charact. temp., optical props. *(French)* 79−11587
(ZrF_4-BaF_2-ThF_4)-EuF_2 system, glass forming region, prep. and props. 79−91633
$Zr_2F_8(H_2O)_6$, cryst. struct. refinement 78−18592
ZrF_4ThF_4-BaF_2 system, new fluoride glass, optical props. *(French)* 77−36443
$Zr_{0.9}Fe_{0.1}V_2$, NMR and mag. susceptibility 78−95527
Zr_3Ge, superconducting transition temp. 78−47898
$ZrGeO_4$, cryst. growth from PbO-GeO_2 flux 77−16484
γ-ZrH, precipitation in Zr, exam. of precipitation mechanism due to shears, electron microscope exam. 78−84809
$ZrH_{1.65}$, valence-band meas. using XPS 79−69958
$ZrH_{1.8}$, radiation-induced defects in hydrogen sublattice 79−37739
$ZrH_{1.9}$, neutron irrad. induced defects, nature and thermal stability 77−50246
$ZrH_{1.92}$, plasticity 77−36569
$ZrH_{1.92}$, total neutron cross section of protons at 77.4K 79−60444
$ZrH_{1.97}$, FCT, elec. quadrupole interaction at ^{181}Ta, TDPAC obs., 20-588K 79−33574
ZrH_2, H positions by neutron quasi-elastic scatt. 79−42042
ZrH_2, non-secular part of nucl. dipolar broadening detected by μ^+ zero-field spin relaxation 80−7250
ZrH_2, synchrotron XPS obs., rel. to theory for metal dihydrides 80−55275
ZrH_4, Dirac-Fock one-centre calcs. 77−88380
ZrH_x, fracture toughness, influence on crack resistance of Zr alloys 80−16444
ZrH_x (x=1.55, 1.7), synthesis and electron structure 80−29889
ZrH_x, laser irrad. effect on interstitial phases, metallographic obs. 79−37734
ZrH_x, mech. props. 77−44333
ZrH_x, self-diffusion of T, autoradiographic study, energy of soln. in H sublattice *(Russian)* 80−2194
ZrH_x, soft X-ray emission spectra, electronic struct. 79−65959
ZrH_x, two-phase (δ+ε), homogenisation during neutron bombard. *(Russian)* 78−18684
ZrH_x:Er, (x=1.5 and 1.85), Mossbauer spectra 80−20527
δ-Zr_xH_y, diffusion of H_2 *(Korean)* 77−20118

zirconium compounds continued
$ZrH_mCe_n(PO_4)_2.XH_2O$, cryst., self-diffusion of Ce^{3+} ions 78−34648
α-$ZrH_{0.74}La_{0.42}(PO_4)_2.4.6H_2O$ cryst., self-diffusion of La^{3+} ions 78−34648
$Zr(HPO_4)_2$, amorphous, crystalline, enthalpy of formation 80−6518
$Zr(HPO_4)_2$, cryst., heat treated, acid strength distrib. 78−92377
$Zr(HPO_4)_2H_2O$, ^6Li loaded, α-radiation damage, X-ray Guinier powder reflection study *(German)* 78−47437
$Zr(HPO_4)_2.H_2O$, Na^+ transport, gas-solid and solid-solid reaction kinetics 80−61086
$Zr(HPO_4)_2.H_2O$-Kynar membranes, struct., ion mobility 78−76915
γ-$Zr(HPO_4)_2.2H_2O$, form. region and struct. model 79−46615
ZrI, gaseous, generated by HI+Zr reaction, enthalpies of formation 79−20458
ZrI_2, gaseous, generated by HI+Zr reaction, enthalpies of formation 79−20458
ZrI_3, disproportionation 77−89546
ZrI_3, gaseous, generated by HI+Zr reaction, enthalpies of formation 79−20458
ZrI_4, gaseous, generated by HI+Zr reaction, enthalpies of formation 79−20458
ZrI_4, high-temp. enthalpy, X-ray powder diffr. data 80−107446
ZrI_4, thermodynamics of vaporisation and high temp. enthalpy 78−91432
ZrI_4, thermodynamics of vaporisation from substoichiometric solid Zr iodides 80−3393
ZrI_4, X-ray cryst. struct. refinement, new AB_4 struct. type *(German)* 79−32950
$Zr_{1-x}In_{2x}O_{2-x}$, ionic conductivity, lattice const. 80−96688
$ZrIr_3Br_{\sim 4}$, cryst. struct. 78−42963
$Zr(KPO_4)_2$, cryst., ionic cond., layered struct. 80−92710
$Zr(LiPO_4)_2$ cryst., ionic cond., layered struct. 80−92710
$ZrMF_6$ (M=Fe, Cr, Ni, Co, Mn, V), flux growth of crystal 79−78861
ZrN, absorption spectra, isolated in rare gas matrices 78−78652
ZrN coating, on Zr, oxidation kinetics, 550-700°C, 50-500 Torr O_2 press. *(French)* 77−25170
ZrN, coating on Zr substrate, oxidation by water vap., kinetics, 0.2-20 torr, 550-700°C *(French)* 78−44266
ZrN, form. in RF discharge 77−86222
ZrN high-temp. plastic deform. effects on elec. props. 77−44370
ZrN, in homogeneity range, high-temp. thermodynamic characts. 77−77464
ZrN, microhardness and resist. to brittle fracture 79−87715
ZrN, opt. consts. and physicochem. spectra 77−85677
ZrN, optical props. and charact. electron energy loss spectra 79−52056
ZrN, optical props. at 300K 78−19466
ZrN, phonon dispersion curve anomalies, inelastic neutron scatt. obs. 79−86858
ZrN, physicomechanical props. with the homogeneity range 77−1848
ZrN, plasma-formed, ESCA and supercond. transition temp. 78−19697
ZrN, RF sputter deposition, ion bombardment and ion implanation 80−25564
ZrN, sintering in vacuum and in N_2 77−12586
ZrN, thermodynamic props. of vacancies 77−11539
ZrN, vibr. IR spectrum, mol. consts. 79−68230
ZrN, whisker growth in CVD 80−59843
ZrN-Al_2O_3, effect of N on sintering 79−33991
ZrN-Al_2O_3, exam. of sintering and densification kinetics, and physical props. 79−95986
ZrN-Al_2O_3, sintering reaction thermodynamics 80−2989
ZrN-Al_2O_3 composites, strength rel. to solid-, liquid-phase sintering 80−100823
ZrN-AlN, composite, erosion resist. in electron stream 78−11365
ZrN-AlN composites, struct. and props. 77−40413
ZrN-coated C fibres in Ni, diffusion barrier effectiveness 78−60624
ZrN-Mo, cermet, sintering reaction thermodynamics 80−2989
ZrN-NbC solid solns., mag. susceptibility and elec. resist. in 300-1300K range 77−24670
ZrN-NiO, solid-phase reactions 79−11774
ZrN+SiO_2, X-ray diffr. phase anal. of reaction products 80−50613
ZrN+W reaction, high-temp. compatibility 79−39132
ZrN_x, $0.71 \leq x \leq 0.79$, ^{15}N tracer diffusion, short cct. mechanism 77−24429
ZrN_x, MP N press. depend. 77−35669
ZrN_x spectral reflectance, selective solar absorber appl. 77−79954
ZrN_x, thermal diffusivity in region of homogeneity, 1000-1800°C 78−71892
ZrN_x:Cs, thermionic emission, metallic sublattice vacancy effects 78−68597
Zr_3N_4, powder, form. by vapour phase reaction of $ZrCl_4$-NH_3-H_2-N_2 system *(Japanese)* 77−73247
ZrN_yH_x (y=0.81 or 0.84, x=0.19 or 0.16) synthesis and electron structure 80−29889
ZrN_2O_y, H_2 solubility 77−84930
$Zr(NO_3)_4.5H_2O$, X-ray K-absorpt. spectra 78−76558
$Zr(NaPO_4)_2$, cryst., ionic cond., layered struct. 80−92710
$Zr_{0.5}Nb_{0.5}C_xN_{1-x}$, mag. susceptibility, zone struct., conc. and temp. depends. 77−8788
$ZrNi_{1.4}Si_{3.6}$, X-ray determ. of crystal struct. *(Russian)* 77−76361
ZrO, $B^3\Pi$ state radiative lifetimes, transition rates and oscillator strengths, reson. fluoresc. decay 80−28053
ZrO, band identifications in $^1\pi$-$X^1\Sigma^+$ system 77−18931
ZrO bands, integrated intensity meas. and effective vibr. temp. 80−43111
ZrO, brilliance, sparkliness and fire of diamond simulants 78−90363
ZrO, $C^3\Delta$-$X^3\Delta$ system, electronic transition moment depend. on internuclear dist. 77−68079
ZrO corrosion layer, specimen preparation for TEM by ion beam thinning *(German, English)* 80−11861
ZrO, Franck-Condon factors rot. depend. 80−58319
ZrO, γ system anal., isotopic band shifts in stellar spectra calc. 79−50029
ZrO, in Ne matrix, laser photoluminesc. 77−14481
ZrO, predicted IR spectrum and possible presence in S-type stars 80−62124
ZrO, singlet-triplet separation meas. 80−78623
ZrO spectrum, new $^3\Pi$-$^3\Delta$ system identification 80−23414
ZrO, vibr.-rot. interaction influence on band intensity parameters 79−49999
ZrO, $X(^1\Sigma)$ state, vibrational IR spectrum using microwave powered molecular source, rotational analysis 80−9596

zirconium compounds continued
ZrO^+ spectrum, $^2\Pi$-$^2\Sigma$ system identification 80−23413
$^{90,92,94}ZrO^+$, rot. anal. in near IR 80−74162
ZrO_2 $1.6H_2O$, anion defect formation and annealing during thermal decomp. in vacuum 77−51366
ZrO_2, abrasive grains, single, wear on steel, exam. *(Japanese)* 78−44230
ZrO_2, addition to $SrTiO_3$, effect on sintering kinetics 78−44037
ZrO_2 additions in NiZn ferrite, influence on sintering and physicochem. props. 80−108369
ZrO_2, additive for sintered TiO_2 ceramics, effect on props. 78−35329
ZrO_2, adsorption of electron acceptors, strength and distrib. of electron donor sites, ESR meas. 78−84055
ZrO_2 amorphous film, alkali resistance, refractive index, IR spectra *(Japanese)* 78−23546
ZrO_2 anodic film, ionic incorporation 79−57160
ZrO_2, anodic films, growth stresses 77−16716
ZrO_2, anodic films, growth and morphology 77−16717
ZrO_2, arc spot heat impact degradation *(Japanese)* 78−39819
ZrO_2, baddeleyite, high-press. phase transform., Earth mantle appl. 80−8296
ZrO_2 based solid electrolyte, use for study of O_2 solubility and diffusivity in liq. metals 80−59669
ZrO_2, CW CO_2 laser deposited dielect. thin film, optical and struct. props. 80−7506
ZrO_2, CaO stabilised, exam. of O_2 permeability and p-type electronic cond. 79−10980
ZrO_2, CaO stabilised, preferred slip system 80−66585
ZrO_2, CaO stabilized, O_2 permeability at low O_2 partial press. 79−47980
ZrO_2, CaO- or Y_2O-stabilised, crystal growth by floating zone method using thermal imaging system 77−77373
ZrO_2, cell electrolysis of H_2O at 800° to 1000°C *(French)* 80−26024
ZrO_2 ceramic, dense nonstabilized, fabrication by hydrothermal reaction sintering 80−97451
ZrO_2 ceramics, microstruct. and props., monoclinic to tetragonal transition 80−3035
ZrO_2 ceramics fireproof, direct energy conversion appl. *(Czech)* 79−70455
ZrO_2 coating, pore size distrib. and permeability 79−24641
ZrO_2, coating on Cu, thermal shock performance 78−7081
ZrO_2 coating on Zircaloy-4, effect on ductility 79−47819
ZrO_2 coating on Zircaloy-2, thermal cond. meas. 80−80009
ZrO_2 coatings, prod. by low-temp. oxidation, props. 78−23856
ZrO_2, containing metastable tetragonal phase, stress induced phase transform. effect on props. 78−68683
ZrO_2, correcting coatings, u.v. transmission cutoff 77−760
ZrO_2 crystalline particles, TEM and electron diffr. meas. 77−21350
ZrO_2, crystallisation from $Zr(OH)_4$, effect of water vapour, heat treatment and grain size *(Japanese)* 79−19170
ZrO_2, crystallisation from $Zr(OH)_4$, influence of water vapour *(Japanese)* 79−78865
ZrO_2 crystallite growth from oxide plasmas, growth morphology 80−59417
ZrO_2, cubic, anion vacancy form. during electrolysis, density change 77−80648
ZrO_2, cubic, nitride stabilised 78−92223
ZrO_2, cubic single crystal, colour centres 77−15410
ZrO_2, decomp. of $CaO.6Al_2O_3$ 80−92687
ZrO_2, destabilisation by phosphoric acid, cubic to monoclinic transition, effect of temp., grain size, chemical composition 79−20037
ZrO_2, dielec. and thermophys. props. 77−52009
ZrO_2, digital pyrometry in solar furnace, freezing point *(Japanese)* 78−32821
ZrO_2, dispersed phase in sintered Ti-Al, effect on mech. props. 77−12636
ZrO_2 dispersion strengthened Fe condensates, struct., mech. props. 77−90361
ZrO_2, doped, ionic cond., theoretical model 80−107552
ZrO_2, effect on crystn. in Li_2O-Al_2O_3-SiO_2 glasses 77−16534
ZrO_2, effect on hot pressing of Si_3N_4 *(Japanese)* 77−55929
ZrO_2, elec. cond. at high temps. 78−6380
ZrO_2, elec. cond.-nonstoichiometry relationship, direct determ. 78−76079
ZrO_2, electrochemical cells for O_2 sensing, EMF oscills. 79−47999
ZrO_2, electrode fabrication for MHD generator by plasma deposition 77−39474
ZrO_2 electrolyte cells, elec. props. 79−24477
ZrO_2 electrolyte cells, sintering 79−24476
ZrO_2, electronic excitations, charact. energy loss meas. up to 50 eV 80−60723
ZrO_2, enthalpy and heat capacity at 1100-2500K 80−103472
ZrO_2 film, 1064 nm 150 ps laser pulse damage rel. to OH^- content and refr. index 79−14016
ZrO_2 film, CVD from organometallic cpds. and characterisation 78−23626
ZrO_2 film, electron beam deposition, refr. index and microporosity 78−90467
ZrO_2 film, growth by thermal decomp. of β-diketonate complexes, characts. 79−100055
ZrO_2 film, refr. index and struct., deposition temp. depend. 79−4857
ZrO_2, film, stability, high temp. and electron irrad. effects 77−39747
ZrO_2 films on Zr alloys, model of stress distrib. 79−49694
ZrO_2 films on Zr alloys, exoelectronic emission props. and energy-band parameters 79−91571
ZrO_2 foils, production for TEM 79−74087
ZrO_2 gels, calcination 80−11964
ZrO_2 glass, melting depend. on minute components, surface crystallisation 80−84278
ZrO_2, glaze, liq. phase separation rel. to cryst. in glassy phase 80−103252
ZrO_2, high pressure polymorphism 80−59429
ZrO_2, high temp. compatibility with BN 77−24995
ZrO_2 high-frequency sputtered optical coatings 79−76900
ZrO_2, hydrous, prep. from $ZrOCl_2$ soln. and cryst. texture determ. *(Japanese)* 77−89398
ZrO_2, hydrous particles, crystal texture *(Japanese)* 77−25002
ZrO_2, in LiO_2-Al_2O_3-SiO_2 glass, cryst. process 80−103253
ZrO_2 induction furnace for precision silica optical fibre drawing 78−1446
ZrO_2, isoelec. points, effect of pH on electrophoretic mobility 80−35548
ZrO_2 laser coating, UV damage obs. 80−33056

zirconium compounds continued
ZrO_2, metastable, tetragonal, erosive damage depth, martensitic transform. effect 79−61738
ZrO_2, metastable, tetragonal, strengthening by surface grinding 80−71777
ZrO_2, MgO partially stabilized, microstruct. development during ageing 79−91710
ZrO_2 microsphere stabilised ceramic, fracture characts., thermal stability *(Russian)* 80−76335
ZrO_2, monoclinic, variation of lattice strains *(Japanese)* 77−72600
ZrO_2, near-surface phase transforms., effect of grinding and polishing 78−15557
ZrO_2, neutron irrad., monoclinic to cubic transform. 78−87720
ZrO_2, obtained by coprecipitation with different oxides, props. 78−64514
ZrO_2, obtained by vapo-condensation, exam. of structure and phase props. *(French)* 79−19489
ZrO_2, optical coating in liquid, laser damage 77−61994
ZrO_2, optical coatings, laser damage resist., spectral depend. 77−62022
ZrO_2, optical layer form. from $ZrOCl_2$ in alcoholic soln. 77−88877
ZrO_2, optimum sintering characts., density, X-ray diffr., IR spectrum, UV spectrum obs. 78−76617
ZrO_2, partially stabilised, toughening mechanism 77−56084
ZrO_2, partially stabilised, high temp. effect on strength *(German)* 79−43316
ZrO_2, partially stabilised ceramics, strengthening, post-sintering heat treatment 80−97518
ZrO_2, partially stabilized, precipitation hardening effect on fracture mode 77−90353
ZrO_2, partially stabilized, precipitation effects on fracture mode 77−90354
ZrO_2, partially stabilized, transform. toughened, fracture toughness 79−91775
ZrO_2, partially stabilized, props. and appl. to extrusion dies 80−97507
ZrO_2, partially stabilized, processing defects 80−97558
ZrO_2 particles, influence of ionic treatment on formation of Al coatings *(Russian)* 80−50552
ZrO_2, perovskite type, X-ray K-absorpt. edge, chem. shift 79−91529
ZrO_2, plasma deposited, porosity, gas permeability and dielectric strength 79−52125
ZrO_2, plasma deposition of crysts. and their characterisation 80−20800
ZrO_2, plasma sprayed coatings, elec. cond. and gas permeability 79−82478
ZrO_2, polycrystalline, tetragonal phase, stabilisation 78−15392
ZrO_2, polymorphism at high press., X-ray diffr. obs. 79−73311
ZrO_2, polymorphism rel. to stabilisation *(Rumanian)* 78−59946
ZrO_2, porous, sintered stabilised microspheres, strength and fracture studies 80−85019
ZrO_2, powder, preparation technique for highly sinterable powder 78−39714
ZrO_2 powders, vapour phase reaction production 78−68660
ZrO_2, produced by coprecipitation with stabiliser, sintering 77−66614
ZrO_2 products from granules, props., prep. method effect 80−25628
ZrO_2, R_2O_3-stabilised (R=La, Gd, Y or Yb), solid soln., Raman scatt. anal. of struct. transform. 78−88312
ZrO_2, Raman spectra, temp. depend. 78−6668
ZrO_2, rate of dissolution in molten slag of polycomponent systems *(Japanese)* 78−22859
ZrO_2, reaction with dolomite, mineralisation during roasting 79−43180
ZrO_2, reactive sputtering, O_2 press. depend. 77−12530
ZrO_2 refractories, elec. cond. variation, gas flow effect 80−39581
ZrO_2 refractories, high-temp. induced porosity increase 80−35146
ZrO_2 refractories, wettability with Fe and Al melts 77−89619
ZrO_2, semisintered, shear strength at high press. 80−76308
ZrO_2 shock wave treatment of powders *(Russian)* 77−44186
ZrO_2 single crystals, Y_2O_3 stabilised, optical props., impurities and annealing conditions influence 79−52399
ZrO_2, sintering of granular masses, stabilized with CaO and Y_2O_3 78−44064
ZrO_2, sintering response with const. rate of heating, depend. on processing related pore distrib. 79−28992
ZrO_2 solid electrolyte, electrochem. reduced, electrocatalytic decomp. of NO 80−61113
ZrO_2 solid electrolyte cell for high temp. water vapour electrolysis *(French)* 79−74399
ZrO_2, solid solubility in MgO 80−15247
ZrO_2, spray dried agglomerates, compaction response, fracture, deform. 79−43172
ZrO_2, stabilised, coating for turbine components, degradation due to internal stresses 79−24671
ZrO_2, stabilised, fabrication by hot petroleum drying method, X-ray diffr. and thermal anal. study 80−40297
ZrO_2, stabilised, ionic mech. of charge transport 79−10976
ZrO_2, stabilised, low temp. induced centres, ESR meas. 78−72409
ZrO_2, stabilised microspheres, sintered, temp. depend. of strength, 20 to 1700°C *(Russian)* 78−23766
ZrO_2, stabilised voltage-current-time charact. with point contact Pt electrode in Ar gas ambient 77−1461
ZrO_2 stabilised with lime, electrical conductivity at high temp. *(Rumanian)* 80−65575
ZrO_2 stabilised with Nd_2O_3, refractories prod. and long-term high-temp. behaviour 77−59725
ZrO_2 stabilised with Y_2O_3, ultrafine grained, fabrication and flexural strength 77−1829
ZrO_2, stabilised with Y_2O_3 synthesis and eval. for H_2 prod. 77−85976
ZrO_2, stabilized, protective coating for blast furnace tuyeres *(German)* 79−66193
ZrO_2, stabilized, thermal barrier coating system, spectral emission and absorpt., 300 to 1590K 79−24672
ZrO_2, stabilized by Y_2O_3, corrosion and thermal shock resist. in diesel engines 79−24675
ZrO_2, stabilized porous refractory, mech. strength 80−35322
α-ZrO_2, structure factor determ. using crit. voltage effect, comments 77−1102
ZrO_2, substoichiometric, thermodynamic props. at lower phase boundary 80−29185
ZrO_2, surface spark discharge, channel spreading and substrate vaporisation 77−89336
ZrO_2, synthesis by solid state reaction 80−100821
ZrO_2, synthetic, cryst. growth, review *(German)* 79−33926
ZrO_2 TLD using stabilised single cryst., for high gamma doses 77−56476

zirconium compounds continued
ZrO_2, technical grade containing CaO, polymorphic transform. up to 1200°C 78−64539
ZrO_2, tetragonal polycryst., sintering and props. 79−29008
ZrO_2, tetragonal to monoclinic phase transf. by ball-milling 80−25687
ZrO_2, thermal anal. using solar heating *(Ukrainian)* 79−77725
ZrO_2, thermolum., UV and γ-ray effects 78−2930
ZrO_2, thermoluminesc., in H_2O vap. atm., temp. depend., time decay *(Russian)* 77−44074
ZrO_2 thin film, optical props. rel. to cryst. struct. 80−97357
ZrO_2, thin film coated sample, absorptive laser damage analysis by Weibull distrib. 80−33061
ZrO_2, transformation toughened, localised impact damage 80−7665
ZrO_2 transparent film thickness and refractive index calc. 79−15547
ZrO_2, vacuum condensate, struct. and mech. props., second phase effect *(Russian)* 80−71705
ZrO_2, wear chart, exam. *(German)* 78−35521
ZrO_2, wet vibro-grinding with surfactants, superhigh density sintering suitability 79−33989
ZrO_2, X-ray K-absorpt. spectra 78−76558
ZrO_2, Y_2O_3 stabilised, hydrothermal growth 78−15302
ZrO_2, Y_2O_3 stabilized, thermal diffusivity meas. 77−28021
ZrO_2, Y_2O_3 stabilized, neutron irrad. damage 77−84804
ZrO_2, Y_2O_3 stabilized, heat-resistant granular artifacts, procedure for making 80−35148
ZrO_2, Y_2O_3-stabilised, X-irrad., thermoluminesc. 77−48259
ZrO_2, ZrO_2-HfO_2, soft phonon modes and monoclinic-tetragonal phase transition 77−62638
ZrO_2:^{89}Zr electron captive decay lifetime, struct. environment effects 77−28523
ZrO_2:CaO, polycrystalline, grain boundary enhanced interdiffusion, flux density eqn. 80−29220
ZrO_2:Cu, point defects, electrochem. characterisation 80−35599
ZrO_2:Nd_2O_3, in contact with $NdCrO_3$, electrical cond. meas. 78−76071
ZrO_2:Y_2O_3, bias sputtering, film growth and characts. 77−40366
ZrO_2:Y_2O_3, cryst., IR refl., refr., absorpt. 77−12382
ZrO_2:Y_2O_3, in contact with $YCrO_3$, electrical cond. meas. 78−76071
ZrO_2:Y_2O_3, low-temp. specific heat, oxygen vacancy effects 80−49376
ZrO_2:Y_2O_3, solid electrolytes, charge carrier conc. and diffusion 77−11930
ZrO_2:Y_2O_3 film, preferential sputtering, Auger and XPS spectra obs. 79−52071
ZrO_2/Al clad powder prep. and physicomech. props. 79−29010
ZrO_2/Pt solid electrolyte/porous electrode system, interface polarisation effects 80−61114
ZrO_2/SmF_3 mirror coatings, light scatt. and optical strength in UV range 80−106595
ZrO_2-Al_2O_3, cooling effects on mech. props. *(Russian)* 79−78999
ZrO_2-Al_2O_3-SiO_2, subsolidus equilibria and stabilization of tetragonal ZrO_2 78−27497
ZrO_2-Al_2O_3-SiO_2 fusion cast ceramics, crystn., microstructures rel. to conditions 80−11638
ZrO_2-based solid solutions, effect of added B_2O_3 and Nb_2O_5 on sintering and stability 77−40410
ZrO_2-CaO, and ZrO_2-$YO_{1.5}$, solid solns., defective oxides, ionic cond. 80−107548
ZrO_2-CaO, microstruct., ordering, elec. props. 77−15374
ZrO_2-CaO, phase equilibria and ordering 78−27498
ZrO_2-CaO, stabilised microspheres, structure, mechanical props. *(Russian)* 80−100379
ZrO_2-CaO (12-19 mole%), AC elec. behaviour, 300-900°C, grain size, electrode material, and sintering effects 78−34649
ZrO_2-CaO ceramics fireproof, direct energy conversion appl. *(Czech)* 79−70455
ZrO_2-CaO RF sputtered film, solid electrolyte, comp., struct. and AC cond. 77−39741
ZrO_2-CaO solid electrolyte, for O_2 flow regulator 80−57301
ZrO_2-CaO system, fluorite related ordered compd. prep., struct. 77−68958
ZrO_2-CaO thin film O_2 sensor, ionic transference number, cell design 77−70360
ZrO_2-CaO:Mn^{2+}, EPR spectra, impurity substitution behaviour in various phases 77−16160
ZrO_2-CaO-SiO_2, relationship between texture parameters, and sintering, elec. cond. and mech. strength props. *(German)* 79−24474
ZrO_2-CaO-Y_2O_3, formation, stability and elec. props. of fluorite-like solid solutions 77−16550
ZrO_2-CaO(MgO)($YO_{1.5}$), partially stabilised, growth morphology of tetragonal phase 79−4968
ZrO_2-CaO(Y_2O_3) ceramics with grainy structure, props., effect of heating to 2000°C 80−104194
ZrO_2-CeO_2, semiconducting ceramics, electronic conductivity and oxido-reduction *(French)* 78−26919
ZrO_2-CeO_2 ceramic fireproof, direct energy conversion appl. *(Czech)* 79−70455
ZrO_2-Cr_2O_3 system, react., phase diagram 1600-2400°C 79−11580
ZrO_2-Gd_2O_3, solid solution with fluorite and pyrochlore structure; exam. of elec. conductivity *(German)* 79−23766
ZrO_2-$GdO_{1.5}$ (80 mol.%), X-ray diffr. exam. of continuous transition 78−68684
ZrO_2-HfO_2, monoclinic solid soln., ceramic prep. and use 80−55338
ZrO_2-HfO_2-CaO, cubic solid solutions, thermal expansion 77−15598
ZrO_2-HfO_2(Y_2O_3) solid soln. complex refractories, sublimation *(Russian)* 78−47513
ZrO_2-$KInO_2$($KScO_2$), ionic cond., lamellar struct. *(French)* 77−1257
ZrO_2-La_2O_3 system, phase form. and relations, phys. props. 79−43218
ZrO_2-MgO system, intermediate phases existence, X-ray diffr. and IR obs. 79−38805
ZrO_2-Nd_2O_3 system, solid solns., evaporation, mass spectroscopy investig., thermodynamics 79−10938
ZrO_2-Nd_2O_3(Sm_2O_3)(Dy_2O_3) eutectic, unidirectional solidification, microstruct. and crystallographic characterization 80−35176
ZrO_2-P_2O_5, hydrated, heat treatment and coprecipitation, phase transitions 77−90335
ZrO_2-R_2O_3 solid solns., prep., crystn., R=Nd,Sm,Dy,Yb 78−42909
ZrO_2-rare earth oxide, cubic solid soln., lattice parameters 79−82186
ZrO_2-Sc_2O_3, phase system, X-ray and thermal anal. 78−27494
ZrO_2-Sc_2O_3 system, high-temp. phase transitions, elec. cond., thermal props. 77−16573
ZrO_2-Sc_2O_3-Yb_2O_3 system, order-disorder phenomena, Raman spectra study 80−97254

zirconium compounds continued
- ZrO_2-SiO_2, liquid immiscibility, microstruct. of plasma dissociated $ZrSiO_4$ 80−107429
- ZrO_2-SiO_2, protective antirefl. coatings, electron beam evaporation on glass 77−31143
- ZrO_2-SiO_2 (11 to 13 wt.%), X-ray phase anal. 80−35195
- ZrO_2-SiO_2 glass fibre prep. form metal alcoholates 78−6886
- ZrO_2-SiO_2 powder mixture for optical glass polishing 80−28367
- ZrO_2-SiO_2(-Na_2O) glass fibres, prep. from metal alkoxides, resistance to NaOH soln. 80−97454
- ZrO_2-SiO_3, layer for dielectric mirror, for KrF excimer laser *(Japanese)* 79−72588
- ZrO_2-Ta and ZrO_2-Y_2O_3-Ta aligned eutectic composites, solidification and fracture behaviour 77−48387
- ZrO_2-ThO_2, high temp. study of phase diagram using X-ray and thermal anal. *(French)* 79−70049
- ZrO_2-TiO_2 refractories, TiO_2 effect on props. and phase composition 79−38809
- ZrO_2-TiO_2 solid solns., X-ray diffr. and thermogravimetric meas. 79−90792
- ZrO_2-TiO_2 system, adsorption of electron acceptors, strength and distrib. of electron donor sites 78−84055
- ZrO_2-TiO_2 system, Z *(Ukrainian)* 79−96007
- ZrO_2-UF_4, orthorhombic struct., X-ray and electron diffr. study *(French)* 78−67689
- ZrO_2-UO_2, differential thermal anal. of irradiated material 79−62484
- ZrO_2-V(Ta), eutectic system, metallography *(Russian)* 77−66629
- ZrO_2-W, eutectic microstruct. 78−27499
- ZrO_2-Y_2O_3, Faradaic reaction kinetics, impedance dispersion anal., electrode/electrolyte interface process 79−11798
- ZrO_2-Y_2O_3, phase equilibria and ordering 78−48385
- ZrO_2-Y_2O_3, solid electrolyte, cond. maximum 78−47577
- ZrO_2-Y_2O_3, solid solns., density meas. rel. to O vacancy model 78−2113
- ZrO_2-Y_2O_3, solid soln., elastic and photoelastic props., Mendelstam-Brillouin scatt. 78−6693
- ZrO_2-Y_2O_3, solid soln., diffuse X-ray scatt. by vacancies 78−71728
- ZrO_2-Y_2O_3, stabilised, struct. of single crysts. 77−35527
- ZrO_2-Y_2O_3, stabilised, light scatt. spectrum 79−73954
- ZrO_2-Y_2O_3, stabilised microspheres, structure, mechanical props. *(Russian)* 80−100379
- ZrO_2-Y_2O_3, ZrO_2-CaO system, fluorite related ordered compd, prep., struct. 77−68958
- ZrO_2-Y_2O_3 (10 mole%), electron transport, elec. induced p-n junction 77−43597
- ZrO_2-Y_2O_3 ceramic powder, in situ deposition of metal coating, cermet form. 77−32713
- ZrO_2-Y_2O_3 film, surface characterisation, XPS, ESCA, and AES expts. 78−72028
- ZrO_2-Y_2O_3 microspheres, stabilised, from HF air plasma, struct. 79−78917
- ZrO_2-Y_2O_3 monocrystalline solid solutions, struct. and phase form. 79−52188
- ZrO_2-Y_2O_3 powder, prep. for plasma spheroidisation, sputter drying *(Russian)* 80−55324
- ZrO_2-Y_2O_3 superionic cond. cell, complex impedance 80−10702
- ZrO_2-Y_2O_3:M^{3+}, M=transition metal, X-ray luminesc. 77−44063
- ZrO_2-Y_2O_3/Ni sputtered multilayered ceramic/metal coatings, props. 80−40620
- ZrO_2-Y_2O_3/Pt interface, electrode kinetics, complex impedance dispersion anal. 79−96325
- ZrO_2-Y_2O_3/(Cr-Ni) sputtered multilayered ceramic/metal coatings, props. 80−40620
- ZrO_2-Y_2O_3/(NiCo)-Cr-Al-Y plasma sprayed ceramic coating for turbine engine components 80−40616
- ZrO_2-Y_2O_3-CaO(MgO), long term firing effect at 2100 to 2200°C on solid soln. conc. and microstruct. 77−90309
- ZrO_2-Y_2O_3-Nd_2O_3, high-temp. thermophys. props. 78−26663
- ZrO_2-Y_2O_3-Nd_2O_3, spectral determ. of crystal stabilisation 78−27203
- ZrO_2-Y_2O_3-Nd_2O_3(CeO_2), solid solns., form. by coprecipitation, struct., X-ray, electron diffr. anal. 77−12583
- ZrO_2-Y_2O_3(Nd_2O_3)(Ce_2O_3), stabilised, reaction with Cr_2O_3 77−36438
- ZrO_2-$YO_{1.5}$ solid solutions, ZrO_2 rich side, X-ray spectroscopic study 78−95617
- ZrO_2-$YO_{1.5}$-$TaO_{2.5}$, cubic fluorite phase, elec. cond. 80−107551
- ZrO_2-$ZnAl_2O_4$ transparent glass-ceramic, microstruct. and props. 78−59960
- ZrO_2-Zr cermet composite, hot pressed, fracture toughness 78−27604
- ZrO_2-ZrO_2, multiphase ceramics, mech strengthening due to dispersion of non-metallic particles *(German)* 78−60674
- ZrO_2-$ZrTiO_4$, optical film material 77−753
- ZrO_3+$BaCO_3$ react., mechanism, effect of polymorphic transitions 79−11605
- ZrO_2+Si_3N_4, X-ray diffr. phase anal. of reaction products 80−50613
- ZrO_{2-x}, high temp. phase diagram, exam. of lower phase boundary 78−76638
- ZrO_4^{4-}, normal vibr. freqs., force consts., calc. *(Russian)* 77−6759
- Zr_7O_3 microcrystals, tetragonal struct. stabilisation, crystallite size effect 78−51670
- $ZrOCl_2.8H_2O$, X-ray K-absorpt. spectra 78−76558
- $(ZrO_2)_x(In_2O_3)_{1-x}$ ceramic, bulk resistivity 77−35936
- $ZrOS_2O_3.8H_2O$, IR and Raman spectra, possibility of nonexistence of cpd. of given formula *(French)* 77−24279
- $(ZrO_2)_{0.9}(Y_2O_3)_{0.1}$:Cr, Mn, stabilised single crystal, EPR of Mn^{2+} and Cr^{3+} obs. 80−66024
- $(ZrO_2)_{0.9}(Y_2O_3)_{0.1}$:Ti, γ-irrad., ESR of trigonal centres, attributed to Ti^{3+} at cation sites 77−24740
- $(ZrO_2)_{0.9}(Y_2O_3)_{0.1}$:$VO^{2+}$, ESR of V^{4+} at room temp., spin Hamiltonian parameter determ. 77−16167
- $ZrO_2Y_2O_3$/Ni-Cr-Al-Y, NASA two-layer thermal barrier coating, for gas turbine engines, test results 80−40617
- $((ZrO_2)_{0.92}(Y_2O_3)_{0.08})_{1-x}(Fe_2O_3)_x$, Fe solubility and elec. cond. 79−99354
- $4.26ZrO_2.Nb_2O_5$, elec. cond. meas. 80−100463
- $ZrO_2.SiO_2$-αAl_2O_3 mixed powders, solid state reactions 80−40337
- $6.14ZrO_2.Ta_2O_5$, elec. cond. meas. 80−100463
- $ZrO_2.nH_2O$, possible agent for removal of radioactive Cs from contaminated water *(Slovak)* 78−24319
- ZrO_{2-x}(cubic)-ZrO_{2-x}(cubic+tetragonal), phase boundary 80−81038
- $Zr_{11}Os_4$, cubic struct. type described by cluster concept, X-ray determ. 80−33933
- Zr_3P, superconducting transition temp. 78−47898

zirconium compounds continued
- $Zr(PO_3)_4$, modification I, cryst. struct. determ. 77−15390
- ZrP_2O_7, prep. from $ZrCl_4$ reaction with $POCl_3$ via O_2 80−21272
- $Zr_{0.99}Pt_{0.99}V_2$, NMR and mag. susceptibility 78−95527
- ZrS, electronic struct., bonding effects, photoelectron spectroscopic and low temp. heat capacity cal. 80−96780
- ZrS, equilibria, nonstoichiometry and elec. props. temp. depend. *(French)* 78−64053
- ZrS_2, charge densities, X-ray form factors, and bonding props. 79−94950
- ZrS_2, core states, energy bands, and valence densities of states 79−95322
- ZrS_2, intercalation-induced shift of absorpt. edge 79−82999
- ZrS_2 layer compound, electronic ground state, band struct. calcs. 77−51651
- ZrS_2, layer compound, expansivities and thermal degradation 77−89554
- ZrS_2, nonstoichiometry 78−75841
- ZrS_2, one T-polytype overlap matrix, Slater-Koster interpolation 79−7766
- ZrS_2, vacuum UV reflectivity spectra, cond. band model 77−44012
- ZrS_2, valence density of states 80−44465
- ZrS_2, valence density of states, Gilat-Raubenheimer method 80−88465
- ZrS_3, excitonic transition, reson. Raman spectra, Franck-Condon factors 80−97252
- ZrS_3, one-dimensional semicond., Raman spectra 79−87447
- ZrS_3, paired-anion ligand effects in valence band, photoemission spectrosc. obs. 80−87173
- ZrS_3, phonon study of chemical bonding 80−20645
- ZrS_3, photolum. from excitons 80−66274
- ZrS_3, quasi one-dimens., optical phonon anisotropy, IR spectra study 80−40112
- ZrS_3, quasi one-dimens. semicond., elec. transport props. 80−107790
- ZrS_3, Raman spectra and cryst. symm. 80−34922
- ZrS_3 synthesis 80−35142
- ZrS_3, thermomodulated reflectivity and transmission 80−50357
- $Zr_{1-x}S$, short- and long-range ordering of vacancies, rel. to supercond. transition temp. 77−19945
- $ZrS_2Cs_{0.37}$, lamellar cpd., gas absorpt. 80−44418
- ZrS_2Cs_x, adsorpt. of H_2, mol. sieving effect *(French)* 79−65305
- $Zr(SO_4)_2.4H_2O$, X-ray K-absorpt. spectra 78−76558
- Zr_3Sb, superconducting transition temp. 78−47898
- $Zr_3Sc_4O_{12}$, cryst. struct. determ., powder X-ray diffr. exam. 77−4083
- $Zr_3Sc_4O_{12}$, n-beam struct. images, expt. observations and computer calc. 78−38593
- $ZrSe_2$, charge densities, X-ray form factors, and bonding props. 79−94950
- $ZrSe_2$, core states, energy bands, and valence densities of states 79−95322
- $ZrSe_2$, intercalation with K, struct. and phase limits *(French)* 77−35536
- $ZrSe_2$, layer type cpd., reflectivity meas., 6-40 eV 77−55801
- $ZrSe_2$, nonstoichiometry 78−75841
- $ZrSe_2$, optical phonon modes and localised effective charges, reflection spectra 78−76453
- $ZrSe_2$, photo-intercalation: possible application in solar energy devices 80−108803
- $ZrSe_2$, vacuum UV reflectivity spectra, cond. band model 77−44012
- $ZrSe_2$, valence density of states, Gilat-Raubenheimer method 80−88465
- $ZrSe_3$, electronic props, variation with struct. 79−42438
- $ZrSe_3$, long wavelength optical phonons, Raman scatt. and IR refl. 80−34921
- $ZrSe_3$, paired-anion ligand effects in valence band, photoemission spectrosc. obs. 80−87173
- $ZrSe_3$, phonon study of chemical bonding 80−20645
- $ZrSe_3$, quasi one-dimens., optical phonon anisotropy, IR spectra study 80−40112
- $Zr(SeO_4)_2.4H_2O$, cryst. struct., X-ray powder diffr. meas. 78−34483
- $ZrSi/ZrSi_2$ coating on Ar, exam. of oxidation behaviour by O_2, H_2O *(French)* 79−20284
- $ZrSi_2$, self-propag. high-temp. synthesis 80−2988
- $ZrSi_2$, thermal expansion, microhardness, Debye temp. meas. 77−35717
- $ZrSi_2$, work function rel. to phys. props. 77−47887
- Zr_3Si, superconducting transition temp. 78−47898
- $ZrSiO_4$, body centered matrix basis 80−79765
- $ZrSiO_4$, compression to 8 GPa, meas. with WC-anvil X-ray apparatus and epoxy press. medium 77−89496
- $ZrSiO_4$, cryst. growth from PbO-SiO_2 flux 77−16484
- $ZrSiO_4$, determ. of electronic polarisabilities of ions 79−7570
- $ZrSiO_4$, Fe_2O_3 and TiO_2 additions effect on stability 77−48377
- $ZrSiO_4$, heavy ion irrad., metamict zircon form. 80−2088
- $ZrSiO_4$, isomorphous replacement of Zr^{4+} by Tb^{3+}, charge compensation 77−47424
- $ZrSiO_4$, mechanochemical effect by mechanical grinding *(Japanese)* 78−84754
- $ZrSiO_4$, natural, radiation defect centre, EPR obs. 80−75853
- $ZrSiO_4$, natural zircon, nucl. radiation effect on elastic moduli 77−11616
- $ZrSiO_4$, plasma dissociated, quenching rate effect on microstruct. 79−38854
- $ZrSiO_4$, plasma dissociated, improved thermal shock resistant refractories 79−52350
- $ZrSiO_4$, single cryst. growth from soln. in melt, solvent system selection 80−55285
- $ZrSiO_4$, sintering, effect of grinding and additives 78−48356
- $ZrSiO_4$, synthesis, influence of rare-earth additives on props. 80−20868
- $ZrSiO_4$, synthetic Raman spectrum and lattice vibrs. 77−48160
- $ZrSiO_4$, X-irrad., trapping and emission centres, OH^- ion contribution 80−80876
- $ZrSiO_4$, zircon, (sand), thermolum., UV and γ-ray effects 78−2930
- $ZrSiO_4$, zircon, cryst. struct. and compressibilty at high press. 79−82184
- $ZrSiO_4$, zircon, high-press. phase transform., Earth mantle appl. 80−8296
- $ZrSiO_4$, zircon, Indian, fission track dating and annealing, U content determ. 79−57891
- $ZrSiO_4$, zircon, resonance splitting of internal vibr. freq. of complex anion 80−55080
- $ZrSiO_4$, zircon, thermoluminesc. glow curve and spectrum 79−33847
- $ZrSiO_4$, zircon, U content estimation using plastic track detector *(French)* 77−64445
- $ZrSiO_4$ zircon ceramic with glass-forming additives, sintering and mech. props. 80−60814

zirconium compounds continued
$ZrSiO_4$, zircon yellow pigment, synthesis *(Polish)* 80−66466
$ZrSiO_4$:Er(Yb), anisotropic mag. susceptibility meas. 77−43806
$ZrSiO_4$:U^{4+} (U^{3+}), opt. spectra 78−88334
$ZrSiO_4$-Al_2O_3 (SiO_2) suspensions for slip casting, prep. and props. 80−104103
$ZrSiO_4$-Al_2O_3 mixture, reaction hot pressing 79−38775
$ZrSiO_4$-Al_2O_3 system, particle rearrangement kinetics due to densification 80−25626
$ZrSiO_4$-Fe_2O_3, pink colour form. kinetics 79−60360
$Zr(SiO_4)_{1-x}(OH)_{4x}$, synthetic hydroxyled zircon, influence of OH^- on thermoluminescent emission *(French)* 78−6795
$ZrTe_3$, phonon study of chemical bonding 80−20645
$ZrTe_5$, giant resistivity anomaly 80−107794
$ZrTiO_4$, form. mechanism from spray drying of solns., precip., of hydroxides and reactions of hydrates and solns. 79−43182
ZrV_2, NMR and mag. susceptibility 78−95527
Zr_xWO_3, perovskite-type, stability in ZO_2-WO_2-WO_3 phase diagram 77−15582
ZrX_4, (X=Cl,Br,I), He I and He II photoelectron spectra, ionis. energy, chem. bonding 78−46394
$Zr(Y)O_{2-x}$, internal, external distortion mechanisms, neutron diffr. study 78−83946
$Zr_3Y_4O_{12}$, δ-phase cryst. struct., X-ray diffr. 77−19925
$Zr_{0.8}Yb_{0.2}F_{3.2}O_{0.3}(MX_{3.5})$ anion excess ReO_3 phases, non-stoichiometry 79−60322
$Zr_3Yb_4O_{12}$, cryst. struct. determ., powder X-ray diffr. exam. 77−4083
$ZrZn_2$, Laves phase separation using acetate electrolyte, Cd and Nd effects in Mg-Zn-Zr-Cd-Nd alloys 79−70237
^{95}Zr-^{95}Nb, diffusion behaviour in SiC, 1650 to 1850°C 78−79814
Zrc, whisker growth in CVD 80−59843

zodiacal light
see also sky brightness
1550 Å intensity, upper limit 79−16882
brightness, depend. on helioecliptic coords. 80−72878
brightness distrib. rel. to dust near 1 AU, Helios 1 and 2 obs. 78−36511
brightness integral, phase function isotropy, scatt. from particles *(French)* 78−45279
brightness integral inversion, three-dimensional eqn. 79−75155
brightness integral inversion 79−48738
brightness rel. to galaxies apparent magnitudes estimation *(Russian)* 78−93389
charged dust particles, motion in interplanetary space 80−4299
circular polarisation of zodiacal light, interplanetary mag. field 77−53474
colour and polarization from UV to near IR, rocket-borne obs. 79−48737
dark patches, caused by interplanetary dust patches 78−93153
dust, large fluffy particles as explanation of optical props. 78−57499
dust, light scatt. intensity, theory 80−109324
dust cloud, thermal emission at 11 and 20 microns 80−90367
dust free zone around Sun, search with Helios 1 solar probe 78−45277
Fabry ten-colour photometer on Skylab for gegenschein and zodiacal light obs. 77−60610
far UV radiation background at high galactic latits., D2B-Aura satellite obs. 79−17143
Fraunhofer lines Doppler shift, interplanetary dust dynamics 78−45278
gegenschein, brightness correl. with Danjon relation *(French)* 79−96968
Gegenschein, vars. in polarisation 77−71060
Helios 1 and 2 obs. 78−24483
Helios probe data processing and analysis 77−78650
Helios zodiacal light expt., data processing and evaluation 79−80235
indicator of interplanetary dust 78−57500
International Solar Polar Mission, predictions for zodiacal light and local interstellar dust obs. 79−92717
interplanetary dust, solar flare protons interaction, γ-ray and X-ray lines prod. 79−53771
interplanetary dust, spatial distribution *(German)* 79−80268
interplanetary dust concentration toward Venus orbital plane, zodiacal light obs. 79−21228
IR photometric obs. using balloon-borne telescope 78−36453
IR radiance model and meas. 78−81588
meteor streams, sunlight scatt. rel. to meteor shower assoc. nightglow 80−94761
meteoroid stream widths, rel. to zodiacal light interp. 78−4156
night sky model for artificial satellite search systems 77−73923
photometric axis, prediction from theoretical model 78−20727
photopolarimetry, brightness annual vars. rel. to zodiacal cloud symmetry plane 78−45276
scattering by irregular absorbing particles, new model 80−67543
scattering matrices, Mueller, for nonspherical particles 78−90366
source function from Helios A and Pioneer 10 photometric obs. 78−36539
spectrum, Doppler shifts meas. 78−85904
spectrum in middle UV 77−29720
sub-micron interplanetary dust 77−13284
surface brightness meas. by AE-C satellite 80−17548
UV brightness excess from interplanetary dust motion obs. 80−101555
UV observation, from D2B-Aura satellite 79−58299
UV observations by Astro 7 rocket expt., reddening 78−96427
UV polychromator appl., Astro 7, absolute radiometric calibration 78−49336
UV spectroscopy at 20° elongation 78−20728
UV zodiacal light, TD-1 satellite obs. 77−13504
wavelength dependent model, 1500 Å to 60 μm, Mie scatt. and thermal emission 78−81587

zonal heating *see atmospheric thermodynamics*

zone melting
binary alloy, numerical calc. and simulation of nonsteady mass transfer by moving phase boundaries *(German)* 77−8811
bubble with adsorbed film, migration in Hele-Shaw cell, rel. to materials processing in space 79−28912
bytownite megacrysts., study of trapped basaltic melts, petrogenetic process study 78−95688
cd CdTe, growth from In solvents, self-compensation 77−28144
concentration profile during zone melting, radiometric determ., slot method *(Czech)* 80−55289
control for floating-zone melting with viscous torque 80−89140
crystn. parameters optimisation using temp. distrib. calcs. *(German)* 79−43140

zone melting continued
p-dichlorobenzene, NQR study of zone melting purification 79−91583
distribution coeffs., techniques for calculating, from expt. data 78−75606
float glass, Sn penetration in bottom surface, synthesis 80−79993
floating zone, exam. of power required to form, and zone shape 78−60568
floating zone melting, microgravity simulation of Marangoni convection 79−28911
floating zone melting using reduced gravity environment, floating zone structure 79−28909
floating zone method growth, interface shapes 80−60775
furnace, for zone refining and cryst. growth for materials with melting point between 60-500°C 79−52110
high melting pt. cpds., single cryst. growth *(Japanese)* 80−16175
high-melting metal multicrystal hollow ingot growth 79−69978
horizontal levitation zone melting method of single crystal growth 78−64468
II-VI semiconductors, optimal synthesis methods for single cryst. growth 80−100764
interfaces, pure, thermodynamics and dynamics rel. to Spacelab 79−28910
lamp image type floating-zone furnace for cryst. growth *(Japanese)* 79−74085
LPE kinetics, zone recrystallisation with moving temp. gradient *(Russian)* 77−48354
Marangoni convection, floating zone, under reduced gravity 80−66425
Marangoni number, critical, for the onset of oscillatory flow in crystal growth melts 79−23555
metal, isotope enrichment by combined elec. migration and zone melting 78−76600
molten zone shape and stability, theory 78−30568
optical fibre crystals floating zone growth, for IR optical waveguides 80−79019
rare earth ditatantes, $R_2Ti_2O_7$, crystal synthesis and SHG, solid laser freq. manipulation 79−41421
(rare-earth)$_2$ Ti_2O_7, (RE=La-Nd, Sm, Gd, Y), ferroelec., layer type struct., cryst. growth 80−108348
refining, theory, mathematical treatments, current state-of-the-art, and possible developments *(Spanish)* 80−76172
refractory metal, heat treatment and zone melting installation 80−20959
refractory oxide crystallisation by floating-zone method using thermal imaging system 77−77373
ribbon-to-ribbon growth method and sample characterisation Si 78−11103
rotating container melt growth, crystallisation parameters calcs. 80−103285
ruby fibre, sapphire-clad, single-crystal, growth by floating-zone technique 77−90268
ruby fibre laser, room temp. continuous operation without cooling, crystal growth, heating effects 78−66833
sapphire, float zone growth, maximum stable zone length 79−91582
sapphire constant diameter cryst., laser heated float zone growth, meniscus angle meas. 80−108347
sapphire filament, cryst. growth by laser-heated floating zone technique 77−32518
semiconductor, math. simulation of zone melting process *(German)* 79−28913
semiconductor growth, process parameters influence on radial scatter of resist. 80−16174
shaped crystal growth from melt, meniscus-controlled process 80−107075
skin technology, industrial appl. of space processing 79−28991
solute redistribution, theoretical, during modified form of zone refining-cascade purification 79−74083
solution-melt drops, periodic instability of motion over crystal surface 78−47260
Spacelab crystal growth expts. 78−52648
thermocapillary convection, in floating zone melting, influence of zone geometry and Prandtl no. at zero gravity 79−66002
thermodynamics of phase transition intensity in crystn. processes *(Russian)* 78−38636
toroidal ellipsoid furnace, narrow zone heating by new radiation focusing 78−88424
transition metal borides, refractory, single cryst. prep. methods and characterisation, book contrib. 78−48296
weightless zone recrystallization, stability of a singly connected molten zone 79−78874
X-ray diffractometer attachment for cryst. growth from liq. 78−71641
zone crystallisation, double-ellipsoid mirror furnace for expts. in Spacelab 79−78872
Al-Cu, liq. diffusion coeff. meas. using temp. gradient zone melting 78−26710
$Al_xGa_{1-x}As$, epitaxial layer, distribution of Te and Ge impurities 78−43046
$Al_xGa_{1-x}As$ thick epitaxial layer production, by zone recrystn. in temp. gradient 79−15619
Al_2O_3, floating zone melting, forced convection, computer simulation 78−88422
Al_2O_3, floating zone melting, forced and free convection, computer simulation 78−88423
$Al_6Si_2O_{13}$, mullite, crystal growth by floating zone method using thermal imaging system 77−77373
B, electron beam non-crucible zone remelting prep., anal. of gaseous inpurities 80−20785
β-B, electron beam zone melting growth, crystn. and defect form. 80−15020
B modifications, polymorphism, cryst. chem., struct., growth, book contrib. 78−47278
B, physical characterisation *(French)* 80−16189
B, zone melting, solar energy appl., struct. and elec. props. 77−16492
B-Si alloys, B-rich, prep., anal. and cryst. growth *(French)* 80−104091
Bi-Sb, cryst., hopper growth 78−18564
Bi-Sb (1 at.%) alloy single cryst. growth solid-liq. interface study 80−107073
$Bi_{1-x}Sb_x$, growth by horizontal zone refining, low charge carrier conc. 77−21020
p-Bi_2Se cryst. growth, elec. props. 77−8748
$Ca_2Al_2SiO_7$, single cryst. growth by floating zone method, opt. microscopy charact. 79−47623
$Ca_2MgSi_2O_7$, single cryst. growth by floating zone method, opt. microscopy charact. 79−47623

zone melting continued
$Ca_2Nb_2O_7$, crystal synthesis and SHG, solid laser freq. manipulation 79−41421
CaO, crystal growth by floating zone method, using thermal imaging system 77−77373
Cd isotope enrichment, by refining and pulsed currents 78−3032
Cd, isotopic enrichment during zone melting process *(Russian)* 77−10522
$CdIn_2S_4$ single crystal growth by two-zone horizontal Bridgman technique 78−27400
CeB_6, crystal preparation, elec. resistance, phase transitions 80−97427
Co, growth of single crysts. by electron-beam floating zone method 78−68624
Cr, floating zone-melting prep., activation anal. 80−29875
CrB_2, crystal growth by floating-zone method, elec. and mag. props. 77−1801
Cr_3Si, single cryst. growth by floating zone method, X-ray and neutron diffr. study 79−74084
$CuGaSe_2$, single cryst. growth from melt, doping 77−12522
$CuInTe_2$, grown from near stoichiometric comp., elec. and optical props. 78−68504
Cu_2O, growth by melting, photocond. spectra 78−52029
Cu_2O, prep. rel. to defect levels by TSC 77−66138
EuB_6, simple crystal, prep., floating zone technique 77−85934
Fe, high purity, prep. and recrystallisation temp. 77−55911
Fe, purification, recrystn. temp. and elec. resistivity *(Japanese)* 80−100780
Fe-Si (3 wt.%), single crystal growth by floating zone melting at various rates, growth striation obs. 79−95914
Fe_2SiO_4, fayalite, single crystal growth by floating zone method, exam. 78−60570
$FeTiO_3$, single cryst. growth by floating-zone method 79−19991
GaAs, melted zone displacement by current *(Russian)* 78−26727
$Ga_{1-x}In_xSb$, temp. gradient zone melting 80−50550
GaP:Te, struct. imperfections, prep. and doping effects 77−89451
GdB_6, crystal preparation, elec. resistance, phase transitions 80−97427
Ge p-n junction, high-grade, temp. gradient zone melting in production 77−4747
HfC, single crystal growth by plasma heating 78−60569
HgTe, high purity cryst. grown from soln. by travelling heater method 77−52243
InBi, single cryst. zone melting growth and etching 79−34189
InP, molten stoichiometric, surface tension 78−39684
InSb, horizontal zone melting in vacuum 79−47624
KBr, single crystal, preirradiation and radiation defects, electron microscopic estimation *(Russian)* 78−75695
KBr(Cl), prep. of crysts. containing impurities of specified amounts *(Russian)* 80−66424
KCl, single crystal, preirradiation and radiation defects, electron microscopic estimation *(Russian)* 78−75695
LaB_6, arc floating zone prep. technique 77−12521
LaB_6, single crysts., growth by laser heated floating zone method 77−81213
LaB_6, synthesis and props., review *(Japanese)* 80−40255
$La_4Si_2O_7N_2$ single cryst. growth by floating zone method with SiO_2-Si_3N_4 additions 80−93481
Li_2O, single crysts., growth by floating zone method 79−43139
$Lu_{2-x}Si_2O_7$:Eu_x, synthesis and spectroscopic study 80−84846
$MgAl_2O_3$, crystal growth by floating zone method using thermal imaging system 77−77373
Mg_2TiO_4 single crystals, growth by floating zone method 79−78873
MnZn ferrite, combined Bridgeman-zone levelling cryst. growth technique 80−35076
Mo, doped, surface tension driven flow in electron beam floating zone expts. 80−19731
Mo, single crystal growth by plasma heating 78−60569
$NaNO_3$ floating zone melting, surface tension driven flow 78−48313
Nb, single crystal growth by plasma heating 78−60569
NbN, γ- and δ-forms, cryst. growth and supercond. transition temp. 80−107946
NbN single crystal preparation, zone melting and nitriding techniques 80−60776
$NbN_{0.7}C_{0.3}$, cryst. growth and supercond. transition temp. 80−107946
$NbN_{0.7}C_{0.3}$, single cryst., zone melting growth 79−8246
$Nd_3Ga_5O_{12}$, floating zone method growth, interface shapes 80−60775
Ni, growth of single crysts. by recrystallisation 78−68626
Ni single crystal, preferred growth direction in floating zone method 80−25555
NiO, oriented bicrystal growth by floating zone and Verneuil's method *(French)* 78−92186
PbTe-SnTe, solid soln. single crysts., TSM growth and elec. characts. 78−68625
Rh, single crystal growth by plasma heating 78−60569
Si, crucible-free growth, zone melting in combined heating system 78−3031
Si crystal, shape stability in float zoning 77−47362
Si, crystal growth by float zone melting, limitations in using KHz radio frequencies 79−19989
Si, crystal growth conditions effect, on microdefect distrib. 80−50549
Si crystals, temp. distrib. anal. in floating-zone method 79−74082
Si, deformed crystal, Czochralski and float zone growth, Luder's bands 79−79025
n-Si, dislocation free, process induced cryst. defects 80−24392
Si, failure in strong melt grown single crysts. 78−3205
Si, float zone crystal, dislocation creation and elimination 80−107072
Si, float zone crysts., large diameter, growth parameters 78−31336
Si, float zone grown, low ohmic seeds and dislocations 78−27398
Si, float zone growth, maximum stable zone length 79−91582
Si, float-zone cryst. growth, shape of melt interfaces and radial P distrib. 77−24952
Si, floating zone melting, forced convection, computer simulation 78−88422
Si, floating zone melting, forced and free convection, computer simulation 78−88423
Si, floating zone structural perfection changes by high temp. treatment, dendrites, dislocation interactions 80−29049
Si, growth conditions rel. to cryst. struct. perfection *(Russian)* 80−38971
Si, influence of imperfections on microplasma formation in p-n junctions 77−8177
n-Si, irrad. with 1.2 GeV electrons, form. of radiation defects 79−51156
Si multicrystalline solar cell material prep., fast-pulled float zone, CZ and cast ingot and foil methods 80−93483
Si purification, plasma melting zone technique *(French)* 80−89141
Si purification, plasma melting zone technique, optimisation *(French)* 80−89142
Si ribbon growth by laser zone melting 80−93482
Si, single cryst., temp. gradient meas. by photoelec. pyrometer 77−40359
Si single crystal growth advances 78−6842
Si, small defects in Czochralski grown and zone-floated monocrystals, TEM identification 79−95001
Si, small-diameter cryst. grown by pedestal technique, investigation of microdefects using X-ray topography 79−55683
Si solar cell, fabrication using zone melting of CVD Si on graphite, and performance 77−85945
Si solar cells, capacitance transient spectra of processing- and radiation-induced defects 80−61340
Si, swirl defects, formation by agglomeration of self interstitials 77−80507
Si, swirl defects A-type as source of dislocation generation on macroscopic scale 80−25554
Si, swirl type defects in float-zone and Czochralski single crysts. 79−27992
Si, temp. distrib. in working zone of composite heater, heat transfer calc. 78−3016
Si wafer, stresses generated by thermomigration of liquid inclusions 79−37875
Si:In extrinsic IR detector material with high responsivity compensated by neutron transmutation, float-zone growth 80−75597
Si:O, C, impurity conc. profiles and process-induced defects 78−6094
n-Si:P, doping, by zone melting using solid dopant source 78−43035
Si:P, effect of annealing on charge carrier conc. on floating zoned crystals 78−47805
Si-Ge, variable-gap cryst. made from solid soln. 79−66003
Si-Ge single crystals, solid solutions, growth by electron-beam zone melting without crucible 79−4917
SiC, diffusion tracer deposition, using travelling solvent zone 78−51742
SiC, growth from soln. in fused Si, temp. gradient method in Tb vap. 78−35301
SmB_6, crystal preparation, elec. resistance, phase transitions 80−97427
^{119}Sn isotope, fractionation during zone recrystn. 80−2946
$Sr_2Nb_2O_7$, crystal synthesis and SHG, solid laser freq. manipulation 79−41421
TaB_2, single cryst. growth, floating zone and Al soln. methods 79−86729
TaC, single crystal growth by plasma heating 78−60569
β-Ta_2N-εTaN, prep. by exothermic reaction and by zone melting, cryst. struct. 77−35533
TiC single crystal, prep. by floating zone technique *(Japanese)* 78−23607
TiC_x single cryst. with homogeneous composition, preparation by floating zone technique 79−100049
TiO_2, rutile, crystal growth by floating zone method using thermal imaging system 77−77373
δ-VN, cryst. growth by floating zone and zone annealing techniques 77−69983
V_3Si, single cryst. growth by electron beam melting 78−64467
W, single crystal growth by plasma heating 78−60569
$Y_3Fe_{5-x}Ga_xO_{12}$, substituted garnet, floating zone grown, FMR line width, saturation magnetisation 80−29626
$YFeO_3$, floating zone method growth, interface shapes 80−60775
YIG, Al- and Ga-substituted, floating zone method growth, interface shape and horizontal variations of Al and Ga contents by electron pulse anal. 79−33929
YIG, floating zone method growth, interface shapes 80−60775
YIG, Ga and Al substituted, single cryst. growth by the travelling solvent float zone technique 79−43138
YIG, single crysts. grown by floating zone method, quality eval. of etching and optical microscopy, ferromag. resonance linewidth meas. 79−19990
Y_2O_3, crystal growth by floating zone method, using thermal imaging system 77−77373
Y_2O_3(:Nd) single crystal growth, floating zone method with Xe arc lamp imaging furnace 80−60777
Zn, isotopic enrichment during zone melting process *(Russian)* 77−10522
Zn, zone melting by electron beam, isotope fractionation enhancement 80−45229
$ZnCl_2$ with $FeCl_3$ impurity, removal by zone melting 79−52111
ZnTe, growth from In solvents, self-compensation 77−28144
^{64}Zn isotope, fractionation during zone recrystn. 80−2946
ZrO_2, CaO- or Y_2O-stabilised, crystal growth by floating zone method using thermal imaging system 77−77373
ZrO_2-Ta and ZrO_2-Y_2O_3-Ta aligned eutectic composites, solidification and fracture behaviour 77−48387

zone plates (optical) *see optical zone plates*

zone refining
p-dichlorobenzene, NQR study of zone melting purification 79−91583
electron beam zone refiner, improved emission current control 78−6844
furnace, for zone refining and cryst. growth for materials with melting point between 60-500°C 79−52110
inclusion emersion in vertical zone refining 78−52663
metal, isotope enrichment during zone refinement *(Russian)* 77−59686
metal refining in superhigh vacuum, condensation from vap. and zone recrystallization *(Russian)* 79−15604
narrow band gap semiconducting alloy layers, electron-beam microzone refining, in space 78−35325
organic compound *(Japanese)* 78−48312
organic material six-sample zone refiner with built-in stirring 77−28715
oven for material purification *(Spanish)* 78−44009
rare earth metal refining *(Russian)* 77−59687
recrystallisation *(Russian)* 77−24946
semiconductor, doping reduction using zone recrystn. with temp. gradient 80−104062
theory, mathematical treatments, current state-of-the-art, and possible developments *(Spanish)* 80−76172
trimethylacetic acid, multizone refiner, continuous purification to very high purities 77−55883
Al 77−8750
$Al_xGa_{1-x}As$ solid soln., epitaxial layer growth on GaAs by zone recrystallisation with temp. gradient 77−16510

zone refining continued
B, effect of Ni doping on conductivity type, microhardness and metallographic obs. 77−31682
β-B, electron beam zone refining, crucibleless, crystn. front shape 79−78871
Bi-Sb solid soln., crystallisation in capillaries *(Russian)* 78−44006
$Bi_{1-x}Sb_x$, growth by horizontal zone refining, low charge carrier conc. 77−21020
ρ-BiSe, single crystal, synthesis and elec. props. 77−16490
Cd isotope enrichment, by refining and pulsed currents 78−3032
$CdAs_2$, thermoelec. props., anisotropy 80−34470
CdTe, crystal growth by sealed ingot zone refining technique 77−40360
CdTe, growth from soln. in fused $CdCl_2$ 77−44138
CdTe, purification, efficiency for extraction of Cu and Ag impurities, impurity scatt. meas. 77−8749
Cr, floating zone-refining, activation anal. 80−29875
Cu crystals, floating zone method growth, X-ray diffr. study of preferred growth 80−7490
Dy, recrystallisation *(Russian)* 77−24946
Fe, free surface and grain boundary O_2 and S chemistry 80−75410
Fe, high purity prep. by electron beam floating zone melting under ultra high vacuum 77−28751
Fe, high-purity, notch toughness 77−44353
GaAs, epitaxial layer, partition coefficients of impurities 77−15443
GaAs-AlAs, epitaxial layer, partition coefficients of impurities 77−15443
GaP:Te, struct. imperfections, prep. and doping effects 77−89451
Ge detector preparation, high-purity, for X-ray and gamma-ray spectroscopy 78−86723
Ge, molten zone movement under influence of Peltier effect 78−44007
Ge purification 78−39683
Ge:Sb crystals, purification by zone recrystallisation with temp. gradient 79−4916
GeTe, nonstoichiometric, homogenisation 78−44004
KCl, zone refined single crystal growth for high power CO_2 laser optics 78−22181
LaB_6 crystals, zone refined, chem. characterisation 80−93821
Mo, impurity interactions with C, N, and O, struct., mech. props. and purification 79−52277
Mo, rolled and annealed, zone-refining effect on recryst. grain orient. 77−36532
Nb, impurity conc. monitoring during single cryst. production, use of nuclear phys. methods 78−31337
Nb-Th, eutectic composition 80−100828
Ni, distribution coefficient of Ir, Os, Rm between liquid and solid phase, zone fusion *(French)* 77−77374
$NiCl_2$, zone sublimation 78−52664
Pb, by electron transfer *(Russian)* 78−19662
PbFBr(Cl), dehydration, zone refining and Bridgman cryst. growth 77−36395
PbS, liquid encapsulation zone-refining, source material for sublimation growth 78−27399
Pd, float zone purification, residual resistivity ratio 78−44008
Si crystal production and perfection for photodetectors 78−11107
Si, monocryst. plates, purification by thermal diffusion, impurity migration anal. 80−25553
Si, zone refined, prep. of solar cells 78−64475
Si:Pt, implanted and laser annealed, segregation and increased dopant solubility 80−65016
Si-Al-Si, isothermal version of the moving solvent method 79−1824
Si_xGe_{1-x}, Ge distrib. in single crysts. grown by zone refining without crucible 78−22754
Sn_xO_y films, semiconducting, equipment for deposition on cylindrical objects 77−40378
Ta, rolled and annealed, zone-refining effect on recryst. grain orient. 77−36532
$Te-(Bi_xSb_{1-x})_2Te_3$ eutectic, electrophys. props., directed crystn. conditions influence and comp. depend. 80−107827
Te-based eutectics, crystn. rate effect on electrophys. props. mutual solubility effect 80−60774
Ti-Th, eutectic composition 80−100828
V, zone-refined, deform. behaviour, stress relax. and slip plane patterns 79−29163
W, high purity, zone-refining growth, radial distrib. of structural defects *(Russian)* 79−19250
W, impurity interactions with C, N, and O, struct., mech. props. and purification 79−52277
W, single cryst. wire fabrication using electron beam zone-refining system modification 78−6845
W, zonal electronic purification, mass spectra of contaminants *(Polish)* 80−25552
$YFe_{1-x}Ga_xO_3$, zone refined, exam. of Curie point and magnetisation 79−4673

zoology
2.45 GHz irradiation effect on rat digestive transit *(French)* 80−3723
915 MHz prenatal irradiation effect on rat foetal and postnatal development 80−3722
animal behaviour, as earthquake precursor 79−39673
animal behaviour before earthquakes, produced by aerosol anomalies 79−16407
animals, small, nose-only inhalation exposures to $^{106}RuO_4$, system 80−41346
anthozoans, pennatulacea, colonial coordination 80−94197
Aplysia, restoration of transmission in synapses inactivated by habituation 80−56009
aquatic animals swimming in scombroidal way, hydrodynamic theory *(Ukrainian)* 77−32928
aqueous organisms, swimming parameters determination by cine recording *(Russian)* 77−32921
auditory primary neurons, comparative physiology 80−94224
baikal grayling, oxygen debt and swimming efficiency *(Russian)* 77−64168
Baikal grayling, skeletal muscle ultrastructure *(Russian)* 77−29240
Baikal grayling, swimming efficiency and optimum velocity *(Russian)* 77−32924
bee, thermoregulation by evaporative cooling of head (honeybee) 80−61515
behaviour patterns in cod released by elec. stimulation of olfactory tract bundlets 80−97951
bird skulls, struct. anal. using mammography techniques 80−36209
bird song spectrum anal. rel. to Western musical scales 77−50840

zoology continued
bull, intestinal-prostatic impedance at ejaculation 78−40458
clam from Galapagos Rise hot spring field, growth rate using natural radionuclide ratios 79−84300
cone pigment ecology in teleost fish 78−69041
conference, Tokyo, Japan (June 1979) 80−31412
coral, off Florida, ^{14}C meas. in annual rings 79−16513
coral reef epifauna, susceptibility to UV irrad. 80−98037
deep-sea animals trapping, pressure vessel with simply actuated closure 78−3821
distributed trigger system, non-linear stability, biological barrier 79−92117
dolphin, hydrodynamic swimming characteristics *(Russian)* 77−32922
dolphin, lung collapse and intramuscular circulation during diving 80−81643
dolphin acoustorespiratory system, morphology and function *(Russian)* 77−64060
dolphin swimming, leaping for efficiency at high speed 80−61619
ECG in veterinary science 79−83969
elephant, hearing freq. range 80−104596
firefly larva, bioluminesc. exhibiting circular polarisation 80−94441
fish, endoepithermal secretions rel. to swimming speed *(Russian)* 77−32967
fish, fast swimming, drag reduction by slimy secretions into boundary layer *(Russian)* 77−32915
fish, flow velocity meas. at olfactory organ nares *(German)* 78−69262
forces in animal joints 80−94251
gastopod photosynthesis with incorporated algal chloroplast, Placobranchus sp. 80−61522
gastropod locomotion, role of pedal mucus 80−76780
genetic and physiological process control by magnetic methods *(Russian)* 79−2088
geomagnetic field sensitivity in animals, ferromag. coupling to muscle receptors as basis 80−72185
hummingbird colour vision to near UV light 80−97914
insect colour vision, effected by one visual pigment and filters 80−94212
instrumentation of zoologists 79−96720
lizard jaw action, mechanical significance of streptostyly 80−51143
locust, proprioceptors with central cell bodies 80−51132
marine cephalopods, radioactive trace elements obs. 80−94379
Murray-Darling river system, Australia, symposium (Melbourne, 13 October 1977) 79−92556
Peracarida, burrowing, temp. effects on emergence rhythms *(French)* 80−94174
pigeon magnetic field sensing capability 80−56076
rat, female, sexual behaviour and US vocalisations 78−40208
rat brain ATP, ADP and AMP levels after 2.45 GHz whole-body irradiation 80−3718
rat EEG activity depression by 2.45 GHz whole-body irradiation 80−3720
rat sleep patterns under chronic low-power microwave irradiation *(French)* 80−3716
rat thermoregulatory behaviour when subject to microwave irrad. 80−81547
ratfish, electroreception, obs. 80−94442
ray, Black Sea, electric organ discharge structure 78−64969
reptile epidermis, water permeability rel. to lipid content 80−97875
Ross Ice Shelf project, scientific sampling 79−88366
salmon in spawning migration, swimming velocity and efficiency *(Russian)* 77−32925
sea creatures, hydrodynamic mechanisms associated with cutaneous mantle structures *(Russian)* 77−32917
sharks, red muscle structure rel. to swimming velocity *(Russian)* 77−64172
spider, web vibr. sensed by Argyrodes elavatus kleptoparasite 80−61595
thermal energy balance in leaves, crops, hot and cold blooded animals 77−32875
turtle, sex determination during embryo development, temp. depend. 80−81546
turtle retina, chromaticity horizontal cells, synapse mechanisms 80−51079
ungulate cardiac electrical activity peculiarities and evaluation methods 79−39394
whale biothermal mathematical model 80−12059
whales, southern right, sound playback expts. 80−89772
wildlife biotelemetry, reviews 80−30966

zoosemiotics *see biocommunications*
Zr *see zirconium*